NAT'L INST. OF STAND & TECH R.I.C.
A11105 158109

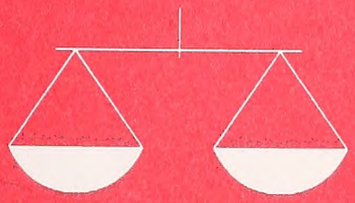
REFERENCE

NIST
PUBLICATIONS

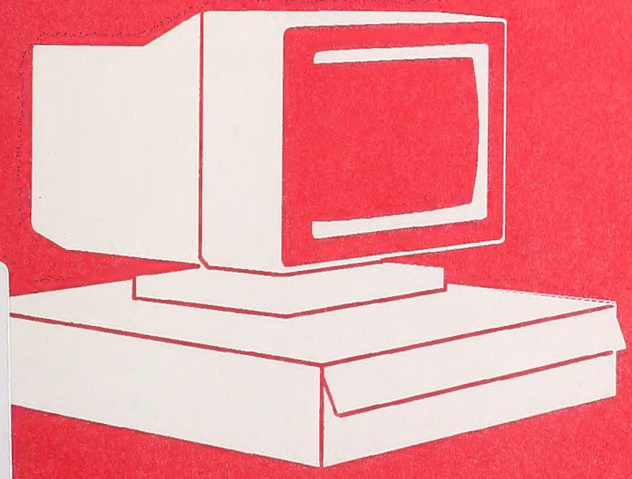
NIST Special Publication 305—Supplement 26

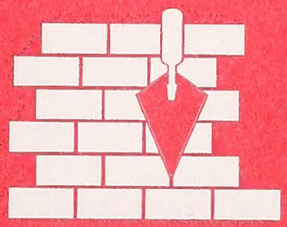
Publications of the National Institute of Standards and Technology 1994–1996 Catalog













QC
100
.U57
NO.305
Supl.26
1997

NIST
U.S. Department of Commerce
Technology Administration
National Institute of Standards and Technology

The National Institute of Standards and Technology was established in 1988 by Congress to "assist industry in the development of technology . . . needed to improve product quality, to modernize manufacturing processes, to ensure product reliability . . . and to facilitate rapid commercialization . . . of products based on new scientific discoveries."

NIST, originally founded as the National Bureau of Standards in 1901, works to strengthen U.S. industry's competitiveness; advance science and engineering; and improve public health, safety, and the environment. One of the agency's basic functions is to develop, maintain, and retain custody of the national standards of measurement, and provide the means and methods for comparing standards used in science, engineering, manufacturing, commerce, industry, and education with the standards adopted or recognized by the Federal Government.

As an agency of the U.S. Commerce Department's Technology Administration, NIST conducts basic and applied research in the physical sciences and engineering, and develops measurement techniques, test methods, standards, and related services. The Institute does generic and precompetitive work on new and advanced technologies. NIST's research facilities are located at Gaithersburg, MD 20899, and at Boulder, CO 80303. Major technical operating units and their principal activities are listed below. For more information contact the Publications and Program Inquiries Desk, 301-975-3058.

Office of the Director
- National Quality Program
- International and Academic Affairs

Technology Services
- Standards Services
- Technology Partnerships
- Measurement Services
- Technology Innovation
- Information Services

Advanced Technology Program
- Economic Assessment
- Information Technology and Applications
- Chemical and Biomedical Technology
- Materials and Manufacturing Technology
- Electronics and Photonics Technology

Manufacturing Extension Partnership Program
- Regional Programs
- National Programs
- Program Development

Electronics and Electrical Engineering Laboratory
- Microelectronics
- Law Enforcement Standards
- Electricity
- Semiconductor Electronics
- Electromagnetic Fields[1]
- Electromagnetic Technology[1]
- Optoelectronics[1]

Chemical Science and Technology Laboratory
- Biotechnology
- Physical and Chemical Properties[2]
- Analytical Chemistry
- Process Measurements
- Surface and Microanalysis Science

Physics Laboratory
- Electron and Optical Physics
- Atomic Physics
- Optical Technology
- Ionizing Radiation
- Time and Frequency[1]
- Quantum Physics[1]

Materials Science and Engineering Laboratory
- Intelligent Processing of Materials
- Ceramics
- Materials Reliability[1]
- Polymers
- Metallurgy
- NIST Center for Neutron Research

Manufacturing Engineering Laboratory
- Precision Engineering
- Automated Production Technology
- Intelligent Systems
- Fabrication Technology
- Manufacturing Systems Integration

Building and Fire Research Laboratory
- Structures
- Building Materials
- Building Environment
- Fire Safety Engineering
- Fire Science

Information Technology Laboratory
- Mathematical and Computational Sciences[2]
- Advanced Network Technologies
- Computer Security
- Information Access and User Interfaces
- High Performance Systems and Services
- Distributed Computing and Information Services
- Software Diagnostics and Conformance Testing

[1] At Boulder, CO 80303.
[2] Some elements at Boulder, CO.

NIST Special Publication 305—Supplement 26

Publications of the National Institute of Standards and Technology 1994–1996 Catalog

Debby King, Editor

Office of Information Services
National Institute of Standards and Technology
Gaithersburg, MD 20899-0001

Issued July 1997



U.S. Department of Commerce
William M. Daley, Secretary

Technology Administration
Gary R. Bachula, Acting Under Secretary for Technology

National Institute of Standards and Technology
Robert E. Hebner, Acting Director

National Institute of Standards and Technology Special Publication 305 Supplement 26
to accompany National Bureau of Standards / NIST Special Publication 305 and its Supplements 1 through 25
Natl. Inst. Stand. Technol. Spec. Publ. 305 Suppl. 26, 1,147 pages (July 1997)

CODEN: NSPUE2

U.S. GOVERNMENT PRINTING OFFICE
WASHINGTON: 1997

For sale by the Superintendent of Documents, U.S. Government Printing Office, Washington, DC 20402-9325.

CONTENTS

About the National Institute of Standards and Technology ..... inside front cover

Catalog structure and use iv

Availability and ordering information iv

NIST publications announcements 1

Indexes
- Personal author PA-1
- Keyword KW-1
- Title TI-1
- NTIS order/report number OR-1

Appendixes
- A List of depository libraries in the United States A-1
- B List of district offices of the U.S. Department of Commerce B-1

Order forms F-1

NIST technical publications program ..... inside back cover

NTIS subject categories ..... back cover

CATALOG STRUCTURE AND USE

Full bibliographic citations including keywords and abstracts for National Institute of Standards and Technology (NIST) papers published and entered into the National Technical Information Service (NTIS) collection are cited in the "NIST Publications Announcements" section of this catalog. (Also included are papers published prior to 1994 but not reported in previous supplements of this annual catalog.) Entries are arranged by NTIS subject classifications which consist of 37 broad subject categories (see back cover) and over 350 subcategories. Within a subcategory, entries are listed alphanumerically by NTIS order number.

Four indexes are included to allow the user to identify papers by personal author, keywords, title, and NTIS order/report number. Each entry lists the appropriate title, the NTIS order number, and the abstract number.

Papers may also be identified by searching the NTIS database either online via commercially available *systems such as DIALOG, or in the issues of NTIS's Government Reports Announcements and Index* and its *Government Reports Annual Index.*

AVAILABILITY AND ORDERING INFORMATION

The highest quality and least expensive copies of NIST publications published as Government documents are available from the Superintendent of Documents, U.S. Government Printing Office, Washington, DC 20402. Publications cited with stock numbers (SN) should be ordered by these numbers. GPO will accept payment by check, money order, VISA, MasterCard, or deposit account. For availability and price, write to the GPO or telephone (202) 783-3238. Should a NIST publication be out of print at the GPO, its continued availability is assured at NTIS which sells publications in microfiche or paper copy reproduced from microfiche.

If an entry has a price code, such as PC A04/MF A01, the publication may be ordered from NTIS in paper copy (PC) or microfiche (MF) or both if both codes are given. Order from the National Technical Information Service, 5285 Port Royal Road, Springfield, VA 22161. A copy of the latest price code schedule is available from NTIS. NTIS will accept payment by check, money order, VISA, American Express, MasterCard, or deposit account. NTIS is the sole source of Federal Information Processing Standards (FIPS), Interagency Reports (IRs), and Grant/Contract Reports (GCRs). For more information call (703) 487-4650.

Papers noted "Not Available NTIS" may be obtained directly from the author or from the external publisher cited. Such papers are not for sale by either the GPO or NTIS.

Two other sources for NIST publications are depository libraries (libraries designated to receive Government publications) and Department of Commerce District Offices. The depository libraries listed in Appendix A receive selected NIST publications (see inside back cover for a description of the various NIST publication series). While not every Government publication is sent to all depository libraries, certain depositories designated as Regional Depositories receive and retain one copy of all Government publications made available. Contact the depository library in your area to obtain information on what is available and where.

Department of Commerce District Offices listed in Appendix B provide ready access at the local level to publications, statistical data and summaries, and surveys. Each District Office serves as an official sales agency of the Superintendent of Documents, U.S. Government Printing Office. A wide range of Government publications can be purchased from these offices. In addition, the reference library of each District Office contains review copies of many Government publications.

NIST PUBLICATIONS ANNOUNCEMENTS

SAMPLE ENTRY

BUILDING INDUSTRY TECHNOLOGY — **NTIS Subject Category**

Building Equipment, Furnishings, & Maintenance — **NTIS Subcategory**

00,123 — *Abstract Number*

PB94-194339 PC **A03**/MF **A01** — **NTIS order number** Availability **Price Codes**

National Inst. of Standards and Technology (BFRL), Gaithersburg, MD. Fire Science Div. — Corporate or performing organization

Performance Parameters of Fire Detection Systems — **Report Title**

R. L. Smith. Jun 94, 20p — Personal authors Report date Page count

NISTIR-5439 — Report Number

Contract or grant number

Keywords: *Fire detectors, *Buildings, Fire prevention, Parameters, Fire extinguishers, Warning systems, Probability theory, Smoke detectors, Mathematical models, Fires.

Keywords: * indicates keyword index entry

This report is a formal, functional analysis of fire detection systems' requirements. The performance parameters of fire detection systems are given as conditional probabilities. These parameters are identified by the objective analysis of the functions of a fire detection system. It is demonstrated that using the false alarm rate to specify the malfunctioning of a threshold detection system is inadequate. The principal function of fire detection systems is identified as the notification of anti-fire agents of the probability of an unwanted fire. The evaluation of the information provided by a detector system is central to its worth.

Abstract

ADMINISTRATION & MANAGEMENT

Management Information Systems

00,001
PB94-163383 PC A06/MF A02
National Inst. of Standards and Technology, Gaithersburg, MD.
Putting the Information Infrastructure to Work: Report of the Information Infrastructure Task Force Committee on Applications and Technology.
Special pub.
May 94, 114p, NIST/SP-857, ISBN-0-16-043188-3.
Also available from Supt. of Docs. as SN003-003-03267-1.

Keywords: *Information systems, *National interests, Commerce, Manufacturing, Industries, Health care, Education, Environmental monitoring, Libraries, Government agencies, Public participation, Citizen participation, *NII(National Information Infrastructure), Information superhighways.

The goal of this document is to express how improvements in the technical foundation upon which modern communications rests can benefit all Americans. The authors call this platform the National Information Infrastructure (NII), meaning the facilities and services that enable efficient creation and diffusion of useful information. They wish to focus the public debate on the uses of the NII and the benefits to be derived by applications of advanced computing and communications technologies.

00,002
PB96-146360 PC A04/MF A01
National Inst. of Standards and Technology (CSL), Gaithersburg, MD. Systems and Software Technology Div.
Open System Environment (OSE): Architectural Framework for Information Infrastructure.
Special pub.
F. Schulz. 1995, 54p, NIST/SP-500/232.
Also available from Supt. of Docs. as SN003-003-03380-4.

Keywords: *Computer networks, *Information systems, *Systems management, Distributed processing, Computer applications, Application program(Computers), Computer architecture, Software engineering, Operating systems(Computers), Communication networks, Information services, Computer program portability, Computer program transferability, Systems engineering, Information management, Electronic security, Human-computer interface, *Open System Environment, National Information Infrastructure.

This document identifies a set of interfaces, services, and formats which are to be provided to users of an information infrastructure, and the methods for accessing these services. This document provides a context and guidance for standards selection, but does not identify standards for use within an information infrastructure. The document may, however, refer to standards in order to illustrate aspects of the services which are important in making selections among the candidate specifications. This discussion will provide a basic set of terminology and concepts to support discussion and resolution of policy issues. Finally, technical guidance is provided to agencies which intend to use information infrastructure for exchange of government information and services within government, and to deliver government information and services to citizens and organizations outside of government.

00,003
PB96-165915 PC A05/MF A01
National Inst. of Standards and Technology (CSL), Gaithersburg, MD.

ADMINISTRATION & MANAGEMENT

Management Information Systems

Manager's Guide for Monitoring Data Integrity in Financial Systems.
Special pub.
R. Sies. Feb 96, 72p, NIST/SP-500-233.
Also available from Supt. of Docs. as SN003-003-03387-1. See also PB95-216602.

Keywords: *Financial management, *Monitoring, *Accounting, *Automation, Data integrity, Computer security, Data processing security, Electronic data exchange, Management information systems, Software tools, Federal information systems.

This guide will enable the manager to identify and justify inclusin of software tools and techniques into new or existing financial systems. The result would be a Monitoring Module consisting of a set of software routines and an easy-to-use report generator. The users of financial and accounting systems and the users of systems that feed data into financial and accounting systems could use the Monitoring Module in a proactive way to ensure the accuracy, completeness, and timeliness of input to the financial systems. The Monitoring Module if included in new or existing systems would help ensure consistency of data across the organization, and provide management with more ability to test and report the level of success with which their management goals are being met. In an environment where most financial transactions are automated, there may be no 'paper trail.' Furthermore, implementation of highly automated financial systems may expose organizations to increased risks of waste, fraud, or abuse if system controls fail to be effective. It is imperative, therefore, that automated monitoring capabilities as sophisticated as the automated financial operations themselves be available to managers. This guide is a step in that direction.

Management Practice

00,004
PB95-126025 Not available NTIS
National Inst. of Standards and Technology (NEL), Gaithersburg, MD. Applied and Computational Mathematics Div.
Development and Validation of Multicriteria Ratings: A Case Study.
Final rept.
S. I. Gass, and S. R. Torrence. 1991, 10p.
Pub. in Socio-Economic Planning Sciences 25, n2 p133-142 1991.

Keywords: *Ratings, Conferences, Complexity, Costs, Services, Decision making, Criteria, Calibrating, Models, Reprints, *Multicriteria, AHP(Analytic Hierarchy Process), US NIST.

Using the hierarchical structure and methodology of the Analytic Hierarchy Process (AHP), a procedure was developed for the rating of conferences in terms of their complexity that enabled the Public Information Division of the National Institute of Standards and Technology to assess the cost of its staff's services. A meeting's complexity is measured by a multicriteria process that involves both the time and expertise of the Division's staff. The validity of the model, that is the calibration of the weights of the decision criteria, was established by showing that the weighting procedure of the AHP replicated the previous year's decisions.

00,005
PB96-161237 Not available NTIS
National Inst. of Standards and Technology (CSL), Gaithersburg, MD.
Guidance of the Legality of Keystroke Monitoring.
Final rept.
S. M. Radack. 1993, 4p.
Pub. in Computer Systems Laboratory Bulletin, p1-4 Mar 93.

Keywords: *Keyboards, *Data processing terminals, *Monitoring, Man machine systems, Human-computer interface, Users, Legal aspects, Liability, Computer security, Electronic security, Reprints, *Legality.

This bulletin advises federal system administrators that keystroke monitoring during computer sessions may be found illegal in certain circumstances and that notice of such monitoring should be given to users.

Productivity

00,006
PB97-124135 PC A99/MF E08
National Inst. of Standards and Technology, Gaithersburg, MD.
Standards Activities of Organizations in the United States.
Special pub. (Final).
R. B. Toth. Sep 96, 788p.
Contract NIST-43NANB514538
Also available from Supt. of Docs. as SN003-003-03427-4. See also PB91-177774.

Keywords: *Standardization, *Organizations, *United States, *Directories, Sources, Standards, Trade associations, National government, Specifications, Military organizations, Technical societies, Recommendations, Test methods, Coding.

The directory is a guide to mandatory and voluntary standards activities in the United States at the Federal level and by nongovernment (trade associations, technical and other professional societies). It excludes proprietary (company) standards and those of local levels of government. Superseding the 1991 edition (NBS SP 806), 'Standards Activities of Organizations in the United States', it includes standards distributors, libraries, and information centers. It also lists organizations that no longer develop standards or have become defunct since the previous directory was issued. Over 700 current descriptive commentaries are formatted, with subject headings to facilitate access to specific information. The main sections cover developers of formal and informal nongovernment studies; Federal agencies which develop standards; sources of standards documents and information; a subject index and related listings covering acronyms and initials, defunct bodies, and those organizations with name changes. Organizations have been included if they develop standards or contribute to the standardization process, whether voluntary of mandatory, or are sources of standards documents or information. An introductory section provides general information on Federal (including military) standards activities, a list of 20 major nongovernment standards developers, and an overview of U.S. (National) standardization activities.

Public Administration & Government

00,007
PB95-216602 PC A03/MF A01
National Inst. of Standards and Technology (CSL), Gaithersburg, MD. Systems and Software Technology Div.
Self Monitoring Accounting Systems.
Special pub.
R. F. Sies. Mar 95, 18p, NIST/SP-500/226.
Also available from Supt. of Docs. as SN003-003-03324-3.

Keywords: *Financial management, *Auditing, *National government, Computer systems programs, Chief Financial Officers(CFO) Act of 1990.

The Federal Government is in need of financial systems that provide more complete, consistent, reliable, and timely information. This report recommends a service for use by management in performing self audits of financial systems. Tools used in the past by Electronic Data Processing Auditors to audit accounting systems are examined, and the similarities between these tools and the service. The use of this service is then described, as it would be used, within the accounting system. How the service can provide more internal control and financial information usually obtained from analysis performed by financial consultants is explained.

Research Program Administration & Technology Transfer

00,008
DE94-017162 PC A05/MF A02
Department of Energy, Washington, DC.
Economic, Energy, and Environmental Impacts of the Energy-Related Inventions Program.
M. A. Brown, C. R. Wilson, C. A. Franchuk, S. M. Cohn, and D. Jones. 31 Jul 94, 100p, ORNL/CON-381.
Contract AC05-84OR21400

Keywords: *Economic impact, *Inventions, Inventions/Environmental impacts, Commercialization, US DOE, Grants, Patents, Program evaluation, ERIP (Energy Related Inventions Program), US NIST.

The report provides information on the economic, energy, and environmental impacts of inventions supported by the Energy-Related Inventions Program (ERIP)--a program jointly operated by the US Department of Energy and the National Institute of Standards and Technology (NIST). It describes the results of the latest in a series of ERIP evaluation projects that have been completed since 1980. The period of interest is 1980 through 1992. The evaluation is based on data collected in 1993 through mail and telephone surveys of 253 program participants, and historical data collected during previous evaluations for an additional 189 participants.

00,009
PB94-157831 PC A12/MF A03
Bio En-Gene-Er Associates, Inc., Wilmington, DE.
Opportunities for Innovation: Biotechnology.
R. M. Busche. Sep 93, 275p, NIST/GCR-93/633.
Grant NANB2D1219
Sponsored by National Inst. of Standards and Technology (CSTL), Gaithersburg, MD. Biotechnology Div.

Keywords: *Biotechnology, *Technology innovations, *Commercial development, *US NIST, Health care, Farm crops, Chemical industry, Electronics industry, Mining, Pollution control, Plastics industry, Drug industry, Small businesses, Research and development, Government/industry relations, Food processing, Animal husbandry, Genetic engineering, Renewable resources, Ethanol fuels, Biodegradability, Biomass, Synthetic fuels, Bioconversion, Agribusiness.

The basic purpose of this project is to help small businesses get on the fast track in biotechnology research and development leading to the spin off of viable commercial businesses, probably with the help of larger companies having the resources for commercialization that are lacking in a small enterprise. Such resources could include financing, and positions in marketing, manufacturing, regulatory affairs, and raw material supply, to name a few. In general, biotechnology can be expected to have a major impact on fundamental human needs engendered in the market segments of: health care, agriculture, forestry, food ingredients, industrial chemicals, plastics, energy, mining, pollution control, and bioelectronics.

00,010
PB94-166212 PC A08/MF A02
National Research Council, Washington, DC. Commission on Engineering and Technical Systems.
Learning to Change: Opportunities to Improve the Performance of Smaller Manufacturers.
G. Markovits, W. J. Brill, J. P. Cooper, S. P. Garretson, H. G. Hall, B. E. Hamilton, A. L. Heald, D. F. Kocaoglu, J. H. Mize, R. D. Nelson, R. A. Pritzker, P. D. Rimington, W. B. Rouse, I. Feller, and B. M. Fossum. 1993, 154p, ISBN-0-309-04982-2.
Contract NIST-50SBNB2C7187
Library of Congress catalog card no. 93-86600. Sponsored by National Inst. of Standards and Technology, Gaithersburg, MD.

Keywords: *Manufacturing, *Small businesses, *Public policies, Technology transfer, Performance evaluation, Technology assessment, Advisory services, Regulations, Government/industry relations, US NIST, National government, State government, Operating costs, Quality, Improvement, Competition, Industrial sector, Technical assistance, *Modernization, MTC(Manufacturing Technology Centers), Manufacturing extension centers.

State and local governments have created industrial assistance services, the federal government has multiple programs aimed at helping small businesses, and there is strong interest in the Clinton administration in creating a national network of industrial assistance centers (Clinton and Gore, 1993). Expanding the National Institute of Standards and Technology (NIST) Manufacturing Technology Centers (MTCs) program is one mechanism for creating such a national assistance network. Given this context--rapid changes in manu-

facturing, growth in the numbers of smaller manufacturers, and their apparent lag in modernization effort--NIST asked the Manufacturing Studies Board to form a committee to examine the barriers to manufacturing improvement in smaller firms and to identify the appropriate role of the MTCs in addressing those barriers. In addition to discussing barriers facing smaller manufacturers, both company representatives and assistance providers discussed opportunities to help firms overcome these barriers and to improve significantly their production costs, quality, and market responsiveness. The recommendations of the committee reflect the changed circumstances that have resulted from the emergence in early 1993 of substantial additional federal funding for industrial assistance activities, as well as President Clinton's proposals for the creation of a national network of manufacturing extension centers.

00,011
PB94-185360 Not available NTIS
National Inst. of Standards and Technology (EEEL), Gaithersburg, MD. Electronics and Electrical Engineering Lab. Office.
Transfer of Technology from Defense to Civilian Sectors.
Final rept.
R. Hebner. 1994, 3p.
Pub. in Institute of Electrical and Electronics Engineers Power Engineering Review, p9-11 May 94.

Keywords: *Technology transfer, *Defense industry, *Government/industry relations, Reprints, Civilian population, Economic development, Technology utilization, Science, Electricity.

Changes occurring today within government with respect to its science and technology policies reflect the close linkage that has existed between technology and defense. In the past, the best minds of the times were set to solve technology problems at the government's behest to provide for national defense. Today, the Cold War has ended. The situation provides the U.S. with a window of opportunity to redefine its technology investment strategy. New forms of government-industry interaction are being explored to help technology make a difference in the civilian economy like it has in national defense.

00,012
PB94-207750 PC A04/MF A01
National Inst. of Standards and Technology (CSL), Gaithersburg, MD. Computer Security Div.
Preliminary Functional Specifications of a Prototype Electronic Research Notebook for NIST.
S. J. Chang, E. Fong, J. Foti, and B. Rosen. Apr 94, 65p, NISTIR-5395.

Keywords: *Research and development, *Information management, *Data storage, *Multimedia, Information retrieval, Computer security, Digital techniques, Requirements, Technology assessment, ERNs(Electronic Research Notebooks), US NIST.

This report is a preliminary study on the feasibility and possible use of electronic research notebooks (ERNs) at the National Institute of Standards and Technology (NIST). The goal of this project is to determine the requirements for ERN and to assess current technologies for the design of a prototype ERN for NIST scientists. The project involves the determination and specifications of functional requirements of the ERN. NIST scientists were interviewed to survey current notekeeping practices and identify specific needs for the ERN. The survey identified a set of basic and enhanced ERN features. Current technologies and products were also assessed in order to see how these requirements may be met. A potential system configuration is proposed where functional specifications for a basic ERN are defined.

00,013
PB94-211836 Not available NTIS
National Inst. of Standards and Technology, Gaithersburg, MD. Office of the Director.
Differences in Competitive Strategies between the United States and Japan.
Final rept.
H. Hellwig. 1992, 2p.
Pub. in Institute of Electrical and Electronics Engineers Transactions on Engineering Management 39, n1 p77-78 1992.

Keywords: *Technology innovation, *Competition, *United States, *Japan, Technology transfer, Research and development, Commercialization, Businesses, Product development, Human resources, Production, Reprints.

The subject is introduced with a taxonomy (called product genesis) of the process of bringing an idea from the laboratory to the marketplace. A discussion of the competitive threshold follows: in a competitive fashion, the traditional strategic approach in both countries is discussed in the areas of human resources, production processes, and business objectives. These strategies are mapped against the various stages of product genesis. The hypothesis is developed that the competitive threshold for Japanese firms is much further downstream than the onset of competitive worries in U.S. companies; i.e., U.S. companies already protect their applied research activities whereas their Japanese counterparts still cooperate at this stage and become protective only before design or prototyping of products and processes takes place.

00,014
PB95-200747 PC A17/MF A04
National Inst. of Standards and Technology (TS), Gaithersburg, MD. Office of Information Services.
Publications of the National Institute of Standards and Technology 1992 Catalog.
Special pub.
D. I. King. Mar 95, 388p, NIST/SP-305/24.
Also available from Supt. of Docs. as SN003-003-03323-5. See also report for 1991, PB92-217579.

Keywords: *Catalogs(Publications), *Bibliographies, Sciences, Technologies, Research management, *National Institute for Standards and Technology.

The 24th Supplement to Special Publication 305 contains full bibliographic citations including key words and abstracts for National Institute of Standards and Technology (NIST) 1992 papers published and entered into the National Technical Information Service (NTIS) collection. (Also included are NIST papers published prior to 1992 but not reported in previous supplements of this annual catalog.) Four indexes are included to allow the user to identify NIST papers by personal author, key words, titles, and NTIS order/report number.

00,015
PB95-209854 PC A05/MF A01
National Inst. of Standards and Technology (MEL), Gaithersburg, MD. Office of Manufacturing Programs.
Automated Manufacturing Research Facility 1994 Annual Report.
D. C. Stieren, and C. F. Albus. Nov 94, 78p, NISTIR-5613.
Sponsored by Office of Naval Research, Arlington, VA. Manufacturing Science and Technology Div.

Keywords: *Computer aided manufacturing, *Research facilities, US NIST, Navy, Reporting requirements, Robotics, Annual reports.

The Automated Manufacturing Research Facility (AMRF) was created at the National Institute of Standards and Technology (NIST) in 1982 in order to provide a national testbed for research and development in computer integrated manufacturing. Since its founding, the AMRF has achieved several significant accomplishments. Among these include the development of over 25 commercial products, roughly 20 patents, and more than 25 national and international standards. Most of the AMRF efforts have been jointly funded by NIST, the Navy ManTech Program, other agencies, and industry. AMRF technical projects are conducted primarily within the Manufacturing Engineering Laboratory (MEL) of NIST.

00,016
PB96-182266 PC A14/MF A03
National Research Council, Washington, DC. Computer Science and Telecommunications Board.
Unpredictable Certainty. Information Infrastructure through 2000.
c1996, 298p, ISBN-0-309-05432-X.
Grant NSF-IRI-9421465
Library of Congress catalog card no. 96-67383. Sponsored by National Science Foundation, Arlington, VA., Advanced Research Projects Agency, Arlington, VA. and National Inst. of Standards and Technology, Gaithersburg, MD.

Keywords: *Computer networks, *Telecommunication, *Government policies, *Meetings, Technology assessment, Technology transfer, Trends, Information technology, Economic models, Financing, Television, Investment, Electronics industry, Communication networks, United States, Telephones, Wireless communications, Public sector, Private sector, *NII(National Information Infrastructure), Internet.

The authors have available an impressive array of information technology. They can transmit literature, movies, music, and talk. Government, businesses, and individuals are eager to go on-line to buy, sell, teach, learn, and more. The Unpredictable Certainty explores the national information infrastructure (NII) as the collection of all public and private information services. How will more and better services reach the home, small businesses, and remote locations. The Unpredictable Certainty examine swho will finance the NII, exploring how technology companies decide to invest in deployment and the vain search of 'killer apps' (applications that drive markets). It discusses who will pay for ongoing services and how they will pay, looking at past cost/price models relevant to the future. The Unpredictable Certainty discusses the underlying technologies, appliances, and services needed before the NII becomes a reality; reviews key features of important technologies, and analyzes current levels of deployment in telephone, cable and broadcast television, and wireless systems, and the difficulties in interconnection. The volume explores the challenge of open interfaces that stimulate new applications but also facilitate competition, the trend toward the separation of infrastructure from specific services, the tension between mature services and new contenders, the growth of the Internet, and more.

00,017
PB96-183215 PC A11/MF A03
National Inst. of Standards and Technology (TS), Gaithersburg, MD. Office of Information Services.
Publications of the National Institute of Standards and Technology 1993 Catalog.
D. I. King. Apr 96, 216p, NIST/SP-305/25.
Also available from Supt. of Docs. as SN003-003-03409-6. See also report for 1992, PB95-200747.

Keywords: *Catalogs(Publications), *Bibliographies, Sciences, Technologies, Research management, Materials, Chemistry, Electronics, Physics, Manufacturing, Buildings, Fire research, Computer systems, Engineering, *National Institute of Standards and Technology.

The 25th Supplement to Special Publication 305 contains full bibliographic citations including key words and abstracts for National Institute of Standards and Technology (NIST) 1993 papers published and entered into the National Technical Information Service (NTIS) collection. (Also included are NIST papers published prior to 1993 but not reported in previous supplements of this annual catalog.) Four indexes are included to allow the user to identify NIST papers by personal author, key words, titles, and NTIS order/report number.

00,018
PB96-210059 PC A07/MF A02
National Inst. of Standards and Technology, Gaithersburg, MD.
Working Conference on Global Growth of Technology: Is America Prepared. Held in Gaithersburg, Maryland on December 7, 1995.
Special pub.
G. Mulholland, J. Fassett, and C. Ehrlich. Jun 96, 108p, NIST/SP-897.
Errata sheet inserted. Also available from Supt. of Docs. as SN003-003-03413-4. Prepared in cooperation with President's Council on Competitiveness, Washington, DC.

Keywords: *Technology innovation, *United States, Economic growth, Government policies, Government/industry relations, Meetings, International trade, Investments, Productivity, Living standards, *Global economy.

The purpose of this conference 'Global Growth of Technology: Is America Prepared' - was to articulate the issues behind the question and to address these issues from the broadest range of perspectives. The impetus for the conference was provided by the National Institute of Standards and support of the Council on Competitiveness (CoC) for organizing this meeting. NIST and the CoC are appropriate partners to host this conference: NIST's programs are defined by its core mission of promoting U.S. economic growth by working with industry to develop technology, measurements, and standards; the CoC focuses on the key issues related to competitiveness such as trade, productivity, investment, and the U.S. standard of living.

AERONAUTICS & AERODYNAMICS

Aerodynamics

00,019
PB94-213170 Not available NTIS
National Inst. of Standards and Technology (CAML), Gaithersburg, MD. Statistical Engineering Div.
Recent Approaches to Extreme Value Estimation with Application to Wind Speeds. Part 1. The Pickands Method.
Final rept.
J. A. Lechner, S. D. Leigh, and E. Simiu. 1992, 11p.
Pub. in Jnl. of Wind Engineering and Industrial Aerodynamics 41-44, p509-519 1992.

Keywords: *Wind velocity, *Wind pressure, *Estimating, *Extreme-value problems, Statistical analysis, Wind effects, Functions(Mathematics), Dynamic loads, Wind measurement, Reprints, *Extreme value estimation.

The last 15 years have seen the development of a new body of theory and of a new generation of statistical estimation procedures applicable to extreme data. Essentially these approaches emphasize the primacy of the information concerning the largest of the extremes (the tails), as opposed to information inherent in the bulk of the extreme data (the body of the distribution). We consider the application of a terminal CME (conditional mean exceedance) slope estimator, inspired by Bryson (1974), to yearly extreme wind data samples obtained from more than 100 stations in the conterminous United States. Next we apply our own implementation of the Pickands method, serially fitting exponential and Generalized Pareto (or Generalized Extreme Value) Distribution models to the conditional exceedance CDF's of the wind data, starting with each ordered sample value in turn, and plotting the fitted tail index versus the order number.

Aeronautics

00,020
PB95-180279 Not available NTIS
National Inst. of Standards and Technology (BFRL), Gaithersburg, MD. Fire Science Div.
Suppression Effectiveness of Extinguishing Agents under Highly Dynamic Conditions.
Final rept.
G. Gmurczyk, W. Grosshandler, and D. Lowe. 1994, 12p.
Sponsored by Department of the Air Force, Wright-Patterson AFB, OH.
Pub. in Proceedings of International Symposium on Fire Safety Science (4th), Ottawa, Ontario, Canada, June 13-17, 1994, p925-936.

Keywords: *Fire extinguishing agents, *Fire suppression, *Aircraft fires, Effectiveness, Fire protection, Fire fighting, Ignition, Combustion, Aviation safety, Fire safety, Reprints, Halon 1301.

Alternatives to halon 1301 are sought which are effective fire suppressing agents and which do not create unacceptable safety, environmental, or systems compatibility problems. Investigations of eleven chemical compounds using a deflagration/detonation tube have revealed a great potential for the technique to study the fire suppression process. The facility is used to evaluate new suppressants, establishing their dynamic characteristics as well as elucidating complex suppression mechanisms occurring in fires under highly dynamic conditions typical of fast turbulent flames, explosions and detonations. The deflagration/detonation tube arrangement has been successfully employed to clearly discriminate among the dynamic characteristics of the eleven alternative agents, revealing new unexpected effects. The results have been used to help select among the alternatives for full-scale testing in simulated aircraft dry bay fires.

00,021
PB95-181095 Not available NTIS
National Inst. of Standards and Technology (BFRL), Gaithersburg, MD. Fire Science Div.
Suppression of Elevated Temperature Hydraulic Fluid and JP-8 Spray Flames.
Final rept.
I. Vazquez, W. Grosshandler, W. Rinkinen, M. Glover, and C. Presser. 1994, 11p.
Sponsored by Department of the Air Force, Wright-Patterson AFB, OH.
Pub. in Proceedings of the International Symposium on Fire Safety Science (4th), Ottawa, Ontario, Canada, June 13-17, 1994, p1255-1265.

Keywords: *Hydraulic fluids, *JP-8 jet fuel, *Fire extinguishing agents, *Aircraft fires, Fire suppression, Fire fighting, Aviation safety, Aviation fuels, Fire safety, Concentration(Composition), Fire protection, Fuel sprays, Flames, Combustion, Reprints, Halon 1301.

A coaxial turbulent spray burner was used to determine the suppression characteristics of twelve different fire fighting agents in elevated temperature hydraulic fluid and jet fuel (JP-8) spray flames. The effectiveness of the gaseous agents, being considered as alternatives to halon 1301, was compared based upon the mass required for suppression and the equivalent storage volume, normalized by the amount of halon 1301 required to suppress the flame. The elevated temperature results were compared to measurements previously obtained with the incoming air and JP-8 at ambient temperature. No statistically significant difference in relative agent performance was found between the heated hydraulic flame and the previous JP-8 experiments.

00,022
PB95-202420 Not available NTIS
National Inst. of Standards and Technology (BFRL), Gaithersburg, MD. Fire Science Div.
Flow of Alternative Agents in Piping.
Final rept.
T. G. Cleary, W. L. Grosshandler, and J. C. Yang. 1994, 11p.
Sponsored by Department of the Air Force, Wright-Patterson AFB, OH.
Pub. in Proceedings of Halon Options Technical Working Conference, Albuquerque, NM., May 3-5, 1994, p105-115.

Keywords: *Fire extinguishing agents, *Fire suppression, *Fluid flow, *Nacelles, *Aircraft fires, Engine inlets, Flow measurement, Aircraft safety, Fire fighting, Piping systems, Two phase flow, Fire protection, Pressure gradients, Reprints, HFC-227ea, Halon 1301.

As part of the USAF, Army, Navy and FAA sponsored halon replacement project, the pipe flow characteristics of selected alternative agents for engine nacelle fire protection are being studied. Due to the remote location of the agent storage bottle, piping is required to transport the agent to various locations in an engine nacelle. The pipe flow from an agent bottle is characterized as a transient, two-phase flow. Since the selected alternative agents have thermophysical properties different from halon 1301, the flow characteristics will be different, which may require system design changes. An experimental apparatus to study the flow characteristics of the alternative agents was designed and is described. Preliminary results on the flow characteristics of HFC-227ea and halon 1301 are presented.

Aircraft

00,023
PB94-203403 PC A99/MF E08
National Inst. of Standards and Technology (BFRL), Gaithersburg, MD. Fire Science Div.
Evaluation of Alternative In-Flight Fire Suppressants for Full-Scale Testing in Simulated Aircraft Engine Nacelles and Dry Bays.
Special pub.
W. L. Grosshandler, R. G. Gann, and W. M. Pitts.
Apr 94, 857p, NIST/SP-861.
Also available from Supt. of Docs. as SN003-003-03268-9. Sponsored by Department of the Air Force, Wright-Patterson AFB, OH., Naval Air Systems Command, Washington, DC., Aviation and Troop Command (Army), St. Louis, MO., and Federal Aviation Administration Technical Center, Atlantic City, NJ.

Keywords: *Aircraft fires, *Halon alternatives, *Fire suppression, Fluorocarbons, Thermodynamic properties, Fluid dynamics, Combustion chemistry, Reaction kinetics, Fire research, *Halon 1301, HCFCs(Hydrochlorofluorocarbons), FCs(Fluorocarbons), HFCs(Hydrofluorocarbons), Discharge rate, National Institute of Standards and Technology.

Civilian and military aircraft suppliers and operators are searching for alternatives to the discontinued chemical Halon 1301 (CF3Br) for protecting aircraft against in-flight fires. This study identifies the best two or three candidates from among a list of twelve fluorocarbons (FCs), hydrofluorocarbons (HFCs), and hydrochlorofluorocarbons(HCFCs) for full-scale testing in the engine nacelle and dry bay simulators at Wright-Patterson Air Force Base. An assessment of the potential for a powder, sodium bicarbonate (NaHCO3), and other realistic gaseous candidates was also requested. The primary recommendations for the dry bay application were FC-218 and HFC-125; partial testing of CF3I was also recommended. Details of all aspects of the research program and the rationale for making these recommendations are provided in this special publication.

00,024
PB95-242368 PC A03/MF A01
National Inst. of Standards and Technology (MSEL), Gaithersburg, MD. Metallurgy Div.
Fracture Testing of Large-Scale Thin-Sheet Aluminum Alloy.
R. deWit, R. J. Fields, S. R. Low, D. E. Harne, and T. Foecke. May 95, 32p, NISTIR-5661.
Sponsored by Federal Aviation Administration, Washington, DC.

Keywords: *Aluminum alloys, *Fracture tests, *Aircraft, Toughness, Fracture properties, Crack propagation, Plastic properties, Models, Fuselages, Monocoque construction, Aircraft panels, R-curve, MSD(Multiple Site Damage), US FAA.

A series of fracture tests on large-scale, pre-cracked, aluminum alloy panel was carried out to examine and to characterize the process by which cracks propagate and link up in this material. Extended grips and test fixtures were specially designed to enable the panel specimens to be loaded in tension in a 1780-kN-capacity universal testing machine. Using existing information, a test matrix was set up to explore regions of failure controlled by fracture mechanics, with additional tests near the boundary between plastic collapse and fracture. In addition, a variety of multiple site damage (MSD) configurations were included to distinguish between various proposed linkage mechanisms. All tests but one used anti-buckling guides. The data were analyzed by two different procedures, (1) the plastic zone model based on the residual strength diagram, and (2) the R-curve. The first three tests were used to determine the basic material properties, and these results were then used in the analysis of the subsequent tests with MSD cracks.

00,025
PB96-160601 Not available NTIS
National Inst. of Standards and Technology (BFRL), Gaithersburg, MD. Fire Science Div.
Computer-Aided Molecular Design of Fire Resistant Aircraft Materials.
Final rept.
M. R. Nyden, and J. E. Brown. 1993, 93p.
Also available as N94-10779 (Order as N94-10766).
Pub. in International Conference for the Promotion of Advanced Fire Resistant Aircraft Interior Materials, Atlantic City, NJ., February 9-11, 1993, p147-158.

Keywords: *Computer-aided design, *Aircraft construction materials, *Flammability testing, *Fire resistant materials, Aircraft fires, Honeycomb structures, Ignition, Burning rate, Commercial aircraft, Nonflammable materials, Molecular structure, Heat treatment, Heat transmission, Flame calorimeters, Reprints.

Molecular dynamic simulations and Cone Calorimeter measurements were used to assess the effects of electron beam irradiation and heat treatments on the flammability of the honeycomb composites used in the sidewalls, ceilings and stowage bins of commercial aircraft. The irradiation of this material did not result in any measureable changes. A dramatic reduction in the peak rate of heat release, however, was observed in samples that had been heated overnight at 250 deg C.

Avionics

00,026
AD-A278 782/8 PC A03/MF A01
National Bureau of Standards, Gaithersburg, MD.
Handbook Preferred Circuits Navy Aeronautical Electronic Equipment. Supplement Number 3.
1 Apr 60, 18p.
See also Supplement 2, AD-A278 783.

Keywords: *Circuits, *Electronic equipment, *Handbooks, Navy, Aeronautics, Standardization, Vacuum apparatus, Transistors, Direct current, Power supplies, Cathode followers, Amplifiers, Multivibrators, Trigger circuits, Pulses, Automatic frequency control, Noise reduction, Crystal oscillators, Silicon, Tubes, Regulators, Squelch, Servoamplifiers, *Preferred circuits, N-44599.

No abstract available.

00,027
AD-A278 783/6 PC A03/MF A01
National Bureau of Standards, Gaithersburg, MD.
Handbook Preferred Circuits Navy Aeronautical Electronic Equipment. Supplement Number 2.
1 Apr 59, 46p, BUAER-16-1-519-SUPP-2.
See also Supplement No. 3 AD-A278 782 and Supplement No. 1, AD-A278 784.

Keywords: *Circuits, *Electronic equipment, *Transistors, *Handbooks, Navy, Aeronautics, Power supplies, Receivers, Airborne, Fire control computers, Crystal oscillators, Trigger circuits, Delay circuits, Cathode followers, Automatic frequency control, Cathode ray tubes, *Preferred circuits, N44599, Blocking oscillators, Frequency dividers, Distance mark generators, Video mixers.

No abstract available.

00,028
AD-A278 784/4 PC A05/MF A01
National Bureau of Standards, Gaithersburg, MD.
Handbook Preferred Circuits Navy Aeronautical Electronic Equipment. Supplement Number 1.
1 Aug 58, 94p, BUAER-16-1-519-SUPP-1.
See also Supplement No. 2, AD-A278 783 and Supplement No. 3, AD-A278 782.

Keywords: *Circuits, *Electronic equipment, *Handbooks, Navy, Aeronautics, Direct current, Video amplifiers, Oscillators, Noise reduction, Airborne, Fire control computers, Regulators, Multivibrators, *Preferred circuits, N-44599.

No abstract available.

00,029
PB94-145711 PC A05/MF A01
National Inst. of Standards and Technology (EEEL), Boulder, CO. Electromagnetic Fields Div.
Aperture Excitation of Electrically Large, Lossy Cavities.
Technical note.
D. A. Hill, J. W. Adams, M. T. Ma, M. L. Crawford, R. T. Johnk, A. R. Ondrejka, and B. F. Riddle. Sep 93, 81p, NIST/TN-1361.
Also available from Supt. of Docs. as SN003-003-03238-7.

Keywords: *Electromagnetic interference, *Electromagnetic shielding, *Apertures, Cavities, Q factors, Reverberation, Transmission, Mathematical models, Scaling, Absorption, Polarization(Waves), Computer software, US NIST, Avionics, Lossy materials, *Aircraft electronics, *Cavity Q.

The document presents a theory based on power balance for aperture excitation of electrically large, lossy cavities. The theory yields expressions for shielding effectiveness, cavity Q, and cavity time constant. In shielding effectiveness calculations, the incident field can be either a single plane wave or a uniformly random field to model reverberation chamber or random field illumination. The Q theory includes wall loss, absorption by lossy objects within the cavity, aperture leakage, and power received by antennas within the cavity. Extensive measurements of shielding effectiveness, cavity Q, and cavity time constant were made on a rectangular cavity, and good agreement with theory was obtained for frequencies from 1 to 18 GHz.

00,030
PB94-210051 PC A04/MF A01
National Inst. of Standards and Technology (EEEL), Boulder, CO. Electromagnetic Fields Div.
Measurements of Shielding Effectiveness and Cavity Characteristics of Airplanes.
D. A. Hill, M. L. Crawford, R. T. Johnk, A. R. Ondrejka, and D. G. Camell. Jul 94, 63p, NISTIR-5023.

Keywords: *Avionics, *Electromagnetic shielding, *Electromagnetic interference, *Electromagnetic measurement, Electromagnetic fields, Time domain, Electromagnetic wave propagation, Leakage, Frequencies, Electronic warfare.

We present measured data for shielding effectiveness, cavity Q, and cavity time constant of three small (twin-engine) airplanes for frequencies from 400 MHz to 18 GHz. Both cw and time-domain measurement methods were used, and the time-domain method yields higher values of cavity Q. Both methods yield Q values below a theoretical upper bound determined by window leakage losses. The measured shielding effectiveness is quite variable, but averages about 15 dB. The measured time constants are also variable and average about 15 ns. This short time constant is a result of the low Q of the aircraft cavities.

00,031
PB95-175675 Not available NTIS
National Inst. of Standards and Technology (EEEL), Boulder, CO. Electromagnetic Fields Div.
Aperture Excitation of Electrically Large, Lossy Cavities.
Final rept.
D. A. Hill, M. T. Ma, A. R. Ondrejka, R. Johnk, B. F. Riddle, and M. L. Crawford. 1994, 10p.
Pub. in Institute of Electrical and Electronics Engineers Transactions on Electromagnetic Compatibility 36, n3 p169-178 Aug 94.

Keywords: *Cavities, *Apertures, *Electromagnetic shielding, *Lossy media, Avionics, Polarization(Waves), Electromagnetic interference, Electromagnetic wave transmission, Electromagnetic absorption, Q factors, Reverberation, Reprints.

We present a theory based on power balance for aperture excitation of electrically large, lossy cavities. The theory yields expressions for shielding effectiveness, cavity Q, and cavity time constant. In shielding effectiveness calculations, the incident field can be either a single plane wave or a uniformly random field to model reverberation chamber or random field illumination. The Q theory includes wall loss, absorption by lossy objects within the cavity, aperture leakage, and power received by antennas within the cavity. Extensive measurements of shielding effectiveness, cavity Q, and cavity time constant were made on a rectangular cavity, and good agreement with theory was obtained for frequencies from 1 to 18 GHz.

AGRICULTURE & FOOD

Agricultural Equipment, Facilities, & Operations

00,032
PB94-154390 PC A03/MF A01
National Inst. of Standards and Technology (MSEL), Gaithersburg, MD. Metallurgy Div.
Corrosion Resistance of Materials for Renovation of the United States Botanic Garden Conservatory.
E. Escalante, and R. E. Ricker. Jan 94, 29p, NISTIR-5360.
Sponsored by Architect of the Capitol, Washington, DC.

Keywords: *Greenhouses, *Renovating, *Corrosion resistance, Washington DC, Botany, District of Columbia, Trusses, Steel structures, Moisture, *United States Botanic Garden.

The purpose of the report is to evaluate the corrosivity of the greenhouse environments and their effect on materials considered for restoration of the Botanic Garden Conservatory. On the basis of this evaluation, recommendations are made on materials which will provide the best performance in these environments. To accomplish this goal of materials selection, the range of conditions anticipated in the greenhouses, in combination with the various herbicides, pesticides, and fertilizers normally used are considered. Special corrosion control considerations, where necessary, are pointed out. The information presented here is intended to serve as a general guideline to the architects and engineers responsible for designing the details of the botanic garden conservatory. Within the time limits of the review, the authors can only address the major problems that the designers will encounter and some of the more important details that will lead to a successful design.

Animal Husbandry & Veterinary Medicine

00,033
PB94-200524 Not available NTIS
National Inst. of Standards and Technology (CSTL), Gaithersburg, MD. Organic Analytical Research Div.
Individual Carotenoid Content of SRM 1548 Total Diet and Influence of Storage Temperature, Lyophilization, and Irradiation on Dietary Carotenoids.
Final rept.
N. E. Craft, S. A. Wise, and J. H. Soares. 1993, 6p.
Pub. in Jnl. of Agricultural and Food Chemistry 41, n2 p208-213 1993.

Keywords: *Animal feed, *Food analysis, *Carotenoids, *Food storage, Liquid chromatography, Temperature, Lyophilization, Reprints, *Standard reference materials.

A modified version of the AOAC procedure for the extraction of carotenoids from mixed feeds was coupled with an isocratic reversed-phase liquid chromatography (LC) method to measure individual carotenoids in SRM 1548 total diet and in a high-carotenoid mixed diet (HCMD). The major carotenoids identified in SRM 1548 were lycopene, beta-carotene, lutein, alpha-carotene, and zeaxanthin in descending order of concentration. The concentration of all carotenoids in SRM 1548 decreased as storage temperature increased. Significant differences in carotenoid concentrations occurred between -80 and 4 C storage temperatures. Lyophilization of the HCMD significantly decreased beta-carotene and lycopene concentrations and produced an apparent increase in xanthophyll concentrations. Exposure to gamma-irradiation significantly decreased alpha-carotene and beta-carotene concentrations and led to an apparent increase in beta-cryptoxanthin. SRM-1548 was found to be unsuitable for use as a reference material for carotenoid measurements, while HCMD has greater potential as a reference material.

Fisheries & Aquaculture

00,034
PB94-198157 PC A03/MF A01
Environmental Research Lab., Gulf Breeze, FL.
Histopathology, Blood Chemistry, and Physiological Status of Normal and Moribund Striped Bass ('Morone saxatilis') Involved in Summer Mortality ('Die-Off') in the Sacramento-San Joaquin Delta of California.
Journal article.
G. Young, C. L. Brown, R. S. Nishioka, J. R. Cashman, H. A. Bern, L. C. Folmar, and M. Andrews. c1994, 22p, EPA/600/J-94/339.
Pub. in Jnl. of Fish Biology 44, p491-512 1994. Prepared in cooperation with California Univ., Berkeley., Crockett Sports Fishing Center, CA., and IGEN Research Inst., Seattle, WA.

Keywords: *Striped bass, *Animal physiology, *Blood chemical analysis, *Mortality, Reprints, Marine fishes, Marine biology, Toxicology, Histology, Pathology, Pacific Ocean, Assays, Statistical analysis, *Sacramento(California), *Carquinez Strait, *San Francisco Bay, Summary die-off, Morone saxatilis.

Summer mortalities of juvenile and adult striped bass (Morone saxatilis) occur annually in the San Francisco

Bay-Delta system, most commonly in the lower delta area. Preliminary work identified pathological changes in the liver of moribund animals. This study represents a comprehensive survey of tissue pathology, blood chemistry and physiological status of moribund animals in comparison to wild and hatchery-reared bass.

Food Technology

00,035
PB94-198322 Not available NTIS
National Inst. of Standards and Technology (TS), Gaithersburg, MD. Standard Reference Materials Program.
Recently Developed NIST Food Related Standard Reference Materials.
Final rept.
R. Alvarez. 1990, 3p.
Pub. in Fresenius Jnl. of Analytical Chemistry 338, n4 p466-468 1990.

Keywords: *Food analysis, *Chemical composition, *Toxic substances, *Food contamination, *Nutrients, Reprints, Chemical analysis, Certification, Cholesterol, Vitamins, Quality control, Trace elements, Organic compounds, Inorganic compounds, *Standard reference materials, NIST(National Institute of Standards and Technology), Recommended Dietary Allowances.

NIST issues food related, chemical composition Standard Reference Materials (SRMs) for validating food analyses. SRMs certified for inorganic constituents are: Non-Fat Milk Powder (SRM 1549), Oyster Tissue (SRM 1566a), Bovine Liver (SRM 1577a), Wheat Flour (SRM 1567a), Rice Flour (SRM 1568a), and Total Diet (SRM 1548). The certificate of analysis for the total diet SRM also provides a certified concentration for cholesterol. Oyster tissue, a renewal SRM, is certified for 25 elements including 6 (Al, Cl, I, P, S, and V) that had not been certified in the previously issued SRM 1566. The elemental certified concentrations are based on concordant results of two or more independent analytical methods. The chemical compositions of the six food matrix SRMs are tabulated. Three food matrix SRMs certified for organic constituents are: Cholesterol and Fat-Soluble Vitamins in Coconut Oil (SRM 1563), Cholesterol in Whole Egg Powder (SRM 1845) and Organics in Cod Liver Oil (SRM 1588). Serum and urine matrix SRMs are also available that may be useful for metabolic and bioavailability studies.

00,036
PB94-199650 Not available NTIS
National Inst. of Standards and Technology (NML), Gaithersburg, MD. Ionizing Radiation Div.
Estimation of the Absorbed Dose in Radiation-Processed Food. 2. Test of the EPR Response Function by an Exponential Fitting Analysis.
Final rept.
M. F. Desrosiers. 1991, 3p.
Pub. in Applied Radiation and Isotopes-International Jnl. of Radiation Applications and Instrumentation 42, n7 p617-619 1991. See also Part 3, PB94-199684.

Keywords: *Food processing, *Dosimetry, *Ionizing radiation, Meat, Electron paramagnetic resonance, Dose-response relationships, Reprints.

The use of electron paramagnetic resonance (EPR) spectrometry to accurately estimate the absorbed dose to radiation-processed bones (and thus meats) is examined. Additive re-irradiation of the bone produced a dose response which was used to determine the initial dose by back-extrapolation. It was found that an exponential fit (versus linear or polynomial) to the data provided improved accuracy of the estimated dose. These data as well as the protocol for the additive dose method are presented.

00,037
PB94-199684 Not available NTIS
National Inst. of Standards and Technology (PL), Gaithersburg, MD. Ionizing Radiation Div.
Estimation of the Absorbed Dose in Radiation-Processed Food. 3. The Effect of Time of Evaluation on the Accuracy of the Estimate.
Final rept.
M. F. Desrosiers, and F. G. Le. 1993, 4p.
Pub. in Applied Radiation and Isotopes 44, n1/2 p439-442 1993. See also Part 2, PB94-199650.

Keywords: *Food processing, *Ionizing radiation, *Dosimetry, Durapatite, Electron paramagnetic resonance, Meat, Chickens, Bones, Dose-response relationships, Reprints.

Electron paramagnetic resonance (EPR) spectrometry is evaluated as a method to retrospectively assess the absorbed dose to radiation-processed chicken (containing bone). Decay of the hydroxyapatite paramagnetic center EPR signal intensity was monitored at three different dose levels (0.5, 3.0, 7.0 kGy) up to 20 days, and the dose was assessed for each level at 1, 8, and 20 days after irradiation. It was determined that the time of evaluation (up to 20 days post-irradiation) did not adversely affect the estimate for 0.5 and 3.0 kGy bone, and only moderately affected the 7.0 kGy estimates.

00,038
PB94-199692 Not available NTIS
National Inst. of Standards and Technology (PL), Gaithersburg, MD. Ionizing Radiation Div.
Estimation of the Absorbed Dose in Radiation-Processed Food. 4. EPR Measurements on Eggshell.
Final rept.
M. F. Desrosiers, F. G. Le, P. M. Harewood, E. S. Josephson, and M. Montesalvo. 1993, 5p.
Pub. in Agricultural Food Chemistry 41, p1471-1475 1993. See also Part 3, PB94-199684.

Keywords: *Food processing, *Ionizing radiation, *Dosimetry, Egg shell, Electron paramagnetic resonance, Salmonella, Dose-response relationships, Eggs, Reprints.

Fresh whole eggs were treated with ionizing radiation for Salmonellae control testing. The eggshell was then removed and examined by electron paramagnetic resonance (EPR) spectroscopy to determine if EPR could be used to (1) distinguish irradiated from unirradiated eggs and (2) assess the absorbed dose. No EPR signals were detected in unirradiated eggs, while strong signals were measurable for more than 200 days after irradiation. Although a number of EPR signals were measured, the most intense resonance ($g = 2.0019$) was used for dosimetry throughout the study. This signal was observed to increase linearly with dose (up to approximately 6 kGy), which decayed approximately 20% within the first 5 days after irradiation and remained relatively constant thereafter. The standard added-dose method was used to assess, retrospectively, the dose to eggs processed at 0.2, 0.7, and 1.4 kGy. Relatively good results were obtained when measurement was made on the day the shell was reirradiated; with this procedure estimates were better for shell processed at the lower doses.

00,039
PB94-199718 Not available NTIS
National Inst. of Standards and Technology (NML), Gaithersburg, MD. Ionizing Radiation Div.
Estimation of the Absorbed Dose in Radiation-Processed Food. 1. Test of the EPR Response Function by a Linear Regression Analysis.
Final rept.
M. F. Desrosiers, G. L. Wilson, C. R. Hunter, and D. R. Hutton. 1991, 4p.
Pub. in Applied Radiation and Isotopes-International Jnl. of Radiation Applications and Instrumentation 42, n7 p613-616 1991. Sponsored by Monash Univ., Clayton (Australia). Dept. of Physics.

Keywords: *Food processing, *Bones, *Dosimetry, *Cesium 137, Electron paramagnetic resonance, Chickens, Meat, Regression analysis, Reprints.

Free radicals produced in chicken bone tissue by (137)Cs gamma rays were measured using electron paramagnetic resonance (EPR) spectroscopy. The yield of radicals was proportional to the absorbed dose. Additive re-irradiation of previously irradiated bones is the basis of a method to estimate the absorbed dose in radiation-processed foods. The ability of the method to accurately provide estimates for a range of doses (0.5 - 7.4 kGy) is tested here. It was determined that a linear fit to the data yielded good dose estimates for bone irradiated < 2 kGy, but failed at the higher doses using a linear approximation to the dose response. These data and their implications are discussed.

00,040
PB95-175204 Not available NTIS
National Inst. of Standards and Technology (CSTL), Boulder, CO. Thermophysics Div.
Supercritical Fluid Extraction of Biological Products.
Final rept.
T. J. Bruno, C. A. Nieto de Castro, J. F. Hamel, and A. M. F. Palavra. 1993, 52p.
Pub. in Recovery Processes for Biological Materials, Chapter 11, p303-354 1993.

Keywords: *Separation processes, *Biotechnology, *Pharmacology, Materials recovery, Supercritical fluids, Solubility, Bioprocessing, Extraction, Food processing, Drugs, Reprints, *Supercritical fluid extraction, *Bioproducts.

In this review, the application of supercritical fluid extraction to biological products is discussed. The review begins with a general discussion of the supercritical fluid state, covering pure fluid and mixture properties, solubility, transport phenomena, and phase diagram modeling. The major experimental measurement are discussed, especially the determination of solute solubility in supercritical fluids. Some recent applications in the areas of pharmaceuticals and foods are described in detail. Finally, an overview of current work and future prospects is presented.

00,041
PB95-180675 Not available NTIS
National Inst. of Standards and Technology (PL), Gaithersburg, MD. Ionizing Radiation Div.
Food Irradiation Dosimetry.
Final rept.
W. L. McLaughlin. 1994, 4p.
See also PB88-175179.
Pub. in Transactions of the American Nuclear Society 71, p8-11 1994.

Keywords: *Radiation dosage, *Food irradiation, *Dosimetry, Gamma rays, X rays, Absorption, Dose-response relationships, Reprints.

Measurements of absorbed dose, dose rate, and dose distribution in food products are vital to the success of treatment of food by ionizing radiation (x- and gamma radiation and electron beams). Dosimetry is used not only for regulatory purposes and quality control, but as documentation of research leading to each food treatment process and for setting proper doses and acceptable dose limits. For regulatory purposes as well as for economic viability of food irradiation, such documentation is thoroughly dependent on dosimetry. It must include process characterization, dosimeter calibration data, dose mapping results, routine dosimetry data and associated process parameters and control for each run, readout equipment maintenance and standard operating procedures, statistical data, product loading and dosimeter locations, dose uniformity, and evaluations of probability that the process specifications have (or have not) been met.

00,042
PB96-161690 Not available NTIS
National Inst. of Standards and Technology (PL), Gaithersburg, MD. Ionizing Radiation Div.
Inter-Laboratory Trials of the EPR Method for the Detection of Irradiated Meats Containing Bone.
Final rept.
M. F. Desrosiers, F. G. Le, and W. L. McLaughlin. 1994, 7p.
Pub. in International Jnl. of Food Science and Technology, v29 p153-159 1994.

Keywords: *Food, *Labelling compliance, *Meats, Reprints, Test evaluation, Irradiaton, Bone, *Foreign technology, *Electron paramagnetic resonance.

Three international trials on the use of electron paramagnetic resonance (EPR) to detect irradiated meats containing bone were sponsored as part of a coordinated research programmed by the International Atomic Energy Agency. In these trials, 11 laboratories used EPR to examine a total of 154 bone samples from three different meats. In one of the trials food irradiation processing conditions were simulated. The results were 100% successful for identifying both irradiated and unirradiated bones. A protocol for the EPR method is provided.

00,043
PB96-164124 Not available NTIS
National Inst. of Standards and Technology (PL), Gaithersburg, MD. Ionizing Radiation Div.

Commentary on 'Optimization of Experimental Parameters for the EPR Detection of the Cellulosic Radical in Irradiated Foodstuffs'.
Final rept.
M. Desrosiers, D. Bensen, and D. Yaczko. 1995, 6p.
Pub. in International Jnl. of Food Science and Technology, v30 p675-680 1995.

Keywords: *Food processing, Reprints, Standards, Protocols, *Foreign technology, *EPR, Spectrometer parameters.

After many interlaboratory trials, several EPR methods for the detection of irradiated foods are being prepared as standard protocols. The works of Goodman et al. (1994) and Raffi et al. (1992) present conflicting general recommendations for optimum parameter sets in the EPR protocols. Here we demonstrate that shortcomings of recommending general parameter sets for the varying types of food samples and the different spectrometer configurations employed to examine them.

ASTRONOMY & ASTROPHYSICS

General

00,044
PB96-123278 Not available NTIS
National Inst. of Standards and Technology (PL), Boulder, CO. Quantum Physics Div.
Goddard High Resolution Spectrograph: Instrument, Goals, and Science Results.
Final rept.
J. L. Linsky. 1994, 19p.
Pub. in Publications of the Astronomical Society of the Pacific, v106 p890-908 Aug 94.

Keywords: *Spaceborne astronomy, *Ultraviolet astronomy, Spectrographs, Spectral resolution, Stellar physics, Stellar activity, Stellar spectra, Sky surveys(Astronomy), Hubble Space Telescope, Reprints, *Goddard High Resolution Spectrograph.

The Goddard High Resolution Spectrograph (GHRS), currently in Earth orbit on the Hubble Space Telescope (HST), operates in the wavelength range 1150-3200 A with spectral resolutions of approximately 2 x 10 to the 3rd power, 2 x 10 to the 4th power, and 1 x 10 to the 5th power. The instrument and its development from inception, its current status, the approach to operations, representative results in the major areas of the scientific goals, and prospects for the future are described.

00,045
PB96-123328 Not available NTIS
National Inst. of Standards and Technology (PL), Boulder, CO. Quantum Physics Div.
Scientific Rationale and Present Implementation Strategy for the Far Ultraviolet Spectrograph Explorer (FUSE).
Final rept.
J. L. Linsky. 1993, 11p.
Pub. in International Workshop on 'Space Project to Probe the Internal Structure and Magnetic Activity of the Sun and Sun-like Stars', Catania, Italy, November 5-8, 1991, p323-332.

Keywords: *Spectrographs, *Sky surveys(Astronomy), *Ultraviolet astronomy, Cool stars, Far ultraviolet radiation, Ultraviolet spectra, High resolution, Project administration, Reprints, *FUSE(Far Ultraviolet Spectrograph Explorer), *Far Ultraviolet Spectrograph Explorer.

FUSE will observe a broad range of astrophysical sources, including cool stars, with high sensitivity and high spectral resolution in the far ultraviolet (912-1205A). It will also observe the 100-1600A region with high throughput and modest resolution. The author summarizes the development and present status of FUSE.

Astrophysics

00,046
AD-A278 521/0 PC A05/MF A02
National Bureau of Standards, Boulder, CO.
Aerodynamic Phenomena in Stellar Atmospheres - A Bibliography.
Technical note.
R. N. Thomas. Sep 59, 98p.

Keywords: *Aerodynamics, *Stellar atmospheres, *Bibliographies, Spectroscopy, Bibliographies, Gas dynamics, Interstellar matter, Sun.

This is an attempt to provide a working bibliography for particular use in preparation for the Fourth Symposium on Cosmical Gas Dynamics: Aerodynamic Phenomena in Stellar Atmospheres.

00,047
AD-A280 291/6 PC A03/MF A01
National Bureau of Standards, Gaithersburg, MD.
Papers on the Symposium on Collision Phenomena in Astrophysics, Geophysics, and Masers.
M. J. Seaton, A. Dalgarno, and C. Pecker. Dec 61, 35p, NBS-TN-124.

Keywords: *Astrophysics, Symposia, Solar atmosphere, Particle collisions, Nebulae, Earth atmosphere, Upper atmosphere.

This publication comprises three papers on astrophysical and geophysical problems that were presented at a special symposium at the National Bureau of Standards Boulder (Colo.) Laboratories in June 1961. The speakers spoke on the question: What are the most important atomic and molecular data needed by theoreticians for progress in astrophysics, geophysics, and gas lasers. The papers are entitled 'Astrophysical problems' by Michael Seaton; 'Collision processes in the high atmosphere' by A. Dalgarno; and 'Some problems connected with the analysis of the structure of the solar atmosphere' by Charlotte Pecker.

00,048
PB94-185212 Not available NTIS
National Inst. of Standards and Technology (PL), Boulder, CO. Quantum Physics Div.
Four Years of Monitoring alpha Orionis with the VLA: Where Have All the Flares Gone.
Final rept.
S. A. Drake, J. A. Bookbinder, D. R. Florkowski, R. E. Stencel, J. L. Linsky, and T. Simon. 1992, 3p.
Pub. in Proceedings of Cambridge Workshop on Cool Stars, Stellar Systems, and the Sun (7th), Tucson, AZ., October 1991, p455-457 1992.

Keywords: *Supergiant stars, *Red giant stars, Stellar chromospheres, Stellar winds, Radio astronomy, Reprints, *Alpha Orionis star, Very large array(VLA).

We observed this prototypical M supergiant using the VLA at centimeter wavelengths about once a month over a 4-year period from July 1986 to September 1990, resulting in a cumulative exposure time of about 120 hours. There is no evidence for radio flaring at any of the observing wavelengths. Low-level variability (about = or < 25%) does appear to be present at the shorter wavelengths (2 and 3.6 cm) and may be also occurring at 6 cm, and is usually in the form of temporary decreases of the radio flux densities from their usual levels. The timescale for these radio dips is not well-determined by the present data set, but significant variability on a timescale of = or < 1 month is observed on occasion. There is no correlation between the variations observed at the different wavelengths.

00,049
PB94-185220 Not available NTIS
National Inst. of Standards and Technology (PL), Boulder, CO. Quantum Physics Div.
Distant Future of Solar Activity: A Case Study of Beta Hydri. 3. Transition Region, Corona, and Stellar Wind.
Final rept.
D. Dravins, P. Linde, T. R. Ayres, T. Simon, F. Wallinder, J. L. Linsky, and B. Monsingnori-Fossi. 20 Jan 93, 14p.
Contract NASA-NAG5-82
Pub. in Astrophysical Jnl. 403, p412-425, 20 Jan 93. Sponsored by National Aeronautics and Space Administration, Washington, DC.

Keywords: *Solar activity, *Stellar evolution, Stellar coronae, Stellar winds, Ultraviolet spectra, X-ray spectra, Atmospheric models, Late stars, IUE, Reprints, *Beta Hydri star.

The secular decay of solar-type activity with age is studied through a detailed comparison of the present Sun (G2 V) with the very old (9-10 Gyr) solar-type star beta Hydri (G2 IV), taken as a proxy of the future Sun. Analyses of successive atmospheric layers are made, and this Paper III in the series treats the outermost parts. The far-UV emission lines from the transition zone are among the faintest so far seen in any solar-type star. The significance of the deduced fluxes for the weak and marginally detected lines is tested through two independent reductions of IUE data. The coronal soft X-ray spectrum was measured through different filters on EXOSAT and compared to simulated X-ray observations of the Sun seen as a star. The flux from beta Hydri is weaker than that from the solar corona and has a different spectrum.

00,050
PB94-185626 Not available NTIS
National Inst. of Standards and Technology (PL), Boulder, CO. Quantum Physics Div.
Rotational Modulation and Flares on RS Canum Venaticorum and BY Draconis Stars. XVI. IUE Spectroscopy and VLA Observations of C1182(=V 1005 Orionis) in October 1983.
Final rept.
M. Mathioudakis, J. G. Doyle, M. Rodono, S. Avgoloupis, J. L. Linsky, D. Gary, L. N. Mavridis, P. Varvoglis, D. M. Gibson, and P. B. Byrne. 1991, 11p.
Pub. in Astron. Astrophys. 244, p155-165 1991.

Keywords: *Stellar flares, Ultraviolet spectra, Microwave spectra, Radiative transfer, IUE, Reprints, Very large array (VLA).

A large flare was detected simultaneously with IUE and VLA on GI 182 on 5 October 1983, this event showing the largest C IV flare enhancement yet observed by IUE. A smaller flare was also detected on 4 October, although only with the IUE satellite. We use line ratio and emission measure techniques to derive various physical parameters of the flares, i.e., the electron pressures and the dimensions of the emitting plasma. The radio data suggest that the flare was an optically-thick gyro-resonance or gyro-synchrotron event. There is no evidence that the event was circularly polarized.

00,051
PB94-185915 Not available NTIS
National Inst. of Standards and Technology (PL), Boulder, CO. Quantum Physics Div.
High Sensitivity Survey of Radio Continuum Emission in Herbig Ae/Be Stars.
Final rept.
S. L. Skinner, A. Brown, J. Linsky, and R. T. Stewart. 1992, 3p.
Contract NASA-W-17772
Pub. in Proceedings of Cambridge Workshop on Cool Stars, Stellar Systems, and the Sun (7th), Tucson, AZ., October 1991, p331-333 1992. Sponsored by NASA Center for AeroSpace Information, Baltimore-Washington International Airport, MD.

Keywords: *Pre-main sequence stars, Radio sources(Astronomy), Radio emission, High sensitivity, Surveys, Reprints, Very large array(VLA).

We present results of a high sensitivity VLA/Australia Telescope survey of radio continuum emission from the 57 Herbig Ae/Be stars (and candidates) cataloged by Finkenzeller and Mundt (1984). Twelve stars were detected at the primary observing wavelength of 3.6 cm, with an additional five stars possibly detected. Upper limits for undetected stars are typically 0.1 mJy (3 sigma). Follow-up observations in the wavelength range 2 - 20 cm give spectral index estimates for 9 stars. Preliminary analysis suggests that the radio emission is of thermal origin in most cases, although nonthermal emission is a possibility for TY CrA and MWC 137.

00,052
PB94-198652 Not available NTIS
National Inst. of Standards and Technology (PL), Boulder, CO. Quantum Physics Div.
Discovery of an X-Ray Selected, Radio-Loud Quasar at z=3.9.
Final rept.
R. H. Becker, D. J. Helfand, and R. L. White. 1992, 4p.
Pub. in Astronomical Jnl. 104, n2 p531-534 Aug 92. Sponsored by Department of Energy, Washington, DC. Office of Energy Research.

Keywords: *X-ray sources, *Quasars, Radio sources(Astronomy), Emission spectra, Red shift, Reprints.

A flux-limited catalog of radio sources in the northern sky has been used to select about 600 weak x-ray sources from a database of about 10(sup 5) 2-4 sigma fluctuations derived from Einstein Observatory Imaging proportional counter x-ray images. Optical spectroscopy of only six of these sources resulted in the discovery of a quasar with an emission-line redshift of 3.87, the highest redshift x-ray source yet discovered. Subsequent VLA observations reveal the source to have a flat-spectrum radio core plus an unresolved radio lobe 2.5 seconds away with a spectral index of alpha=-1.45. The lobe is connected to the core by a weak jet. The integrated flux density of the source at 20 cm is 0.66 Jy. The V magnitude of the quasar in 19.5, and the tentative x-ray source has a very soft spectrum. The authors discuss the properties of the object in the context of known high-redshift radio sources and existing x-ray selected quasar samples, and comment on the potential of our discovery technique for exploring the properties of very distant active galaxies.

00,053
PB94-199437 Not available NTIS
National Inst. of Standards and Technology (PL), Boulder, CO. Quantum Physics Div.
IUE Observations of Solar-Type Stars in the Pleiades and the Hyades.
Final rept.
J. P. Caillault, O. Vilhu, and J. L. Linsky. 20 Dec 91, 8p.
Contracts NASA-NAG5-82, NASA-INT-89-00202
Pub. in Astrophysical Jnl. 383, p594-601, 20 Dec 91. Sponsored by NASA Center for AeroSpace Information, Baltimore-Washington International Airport, MD. and National Science Foundation, Arlington, VA.

Keywords: *Pleiades cluster, *F stars, *G stars, Stellar chromospheres, Stellar spectra, Satellite observation, Ultraviolet spectra, Late stars, Magnesium ions, Carbon ions, IUE, Reprints, *Hyades cluster.

The authors have made the first extensive set of IUE observations of solar-type stars (spectral types F5-G5) in the Pleiades. Spectra were obtained in 1988 January and August for both the transition region (C IV 1550 A; low-resolution) and chromospheric (Mg II 2800 A; high-resolution) emission wavelength regions, respectively. The Pleiades solar-type stars lie at the extreme limit of what IUE can observe in very long exposures. The authors were able to detect Mg II fluxes for two out of three Pleiades stars and interesting C IV upper limits for two of these stars. Long-wavelength, high-resolution spectra were also obtained for previously unobserved solar-type stars in Hyades. With the inclusion of spectra of additional Hyades stars obtained from the IUE archives, they have calculated surface fluxes and fractional luminosities for both clusters' solar-type stars. These values provide a better estimate for the Mg II saturation line for single (as opposed to contact-binary) stars.

00,054
PB94-199528 Not available NTIS
National Inst. of Standards and Technology (PL), Boulder, CO. Quantum Physics Div.
First Results from the Goddard High-Resolution Spectrograph: The Chromosphere of Tauri.
Final rept.
K. G. Carpenter, R. D. Robinson, G. M. Wahlgren, J. L. Linsky, A. Brown, F. M. Walter, T. B. Ake, and D. C. Ebbets. 1991, 4p.
Contract NASA-S-56460-D
Pub. in Astrophysical Jnl. 377, pL45-L48, 10 Aug 91. Sponsored by NASA Center for AeroSpace Information, Baltimore-Washington International Airport, MD.

Keywords: *Stellar chromospheres, Stellar winds, Stellar spectra, Ultraviolet spectra, Emission spectra, Late stars, K stars, Copper ions, Silicon ions, Iron ions, Nickel ions, Cobalt ions, Reprints, Alpha Tavri star.

The K5 III star alpha Tau was observed with the Goddard High Resolution Spectrograph on 1990 November 27 as part of the Science Assessment Program for the Hubble Space Telescope. The observations include spectra in both the Large and Small Science Apertures in modes G270M at 2345 A and echelle B at 2325 A. The spectra show intersystem and permitted chromospheric emissions lines of C II (right bracket), Si II (right bracket), Fe II, Fe I, Ni II, and Co II. Resolved profiles of the C II (right bracket) lines indicate a complex chromospheric turbulent velocity distribution with mean value of approx. 24 km/s (right bracket), while their observed wavelengths indicate a 4 km/s downflow of the CII (right bracket) plasma. Twenty-five new emission lines have been found in the 2320-2370 A region, 17 of which have been identified with the aid of Skylab data obtained above the solar limb, including four lines from Co II (UV 8) and an Fe I (UV 12) line.

00,055
PB94-199601 Not available NTIS
National Inst. of Standards and Technology (PL), Boulder, CO. Quantum Physics Div.
ROSAT All-Sky Survey of Active Binary Coronae. 2. Coronal Temperatures of the RS Canum Venaticorum Systems.
Final rept.
R. C. Dempsey, J. L. Linsky, J. H. M. M. Schmitt, and T. A. Fleming. 1993, 6p.
Contract NASA-NAG5-1797
Pub. in Astrophysical Jnl. 413, p333-338, 10 Aug 93. Sponsored by NASA Center for AeroSpace Information, Baltimore-Washington International Airport, MD.

Keywords: *Binary stars, *Stellar coronal, *Stellar temperature, X-ray spectra, ROSAT mission, Reprints, Sky surveys(Astronomy).

The authors present the results from an analysis of X-ray spectra of 44 RS CVn systems obtained during the ROSAT All-Sky Survey with the Position Sensitive Proportional Counter (PSPC). Thermal plasma models with two temperature components are found to reproduce the observations better than single or continuous temperature models. The authors typically find that a bimodal distribution of temperatures centered near 2 x 10(sup 6) and 1.6 x 10(sup 7) K fit the data best. They show that the PSPC temperatures agree well with those from similar low-resolution measurements, although differences exist, primarily due to differing detector bandpasses. After comparing coronal characteristics--temperature or emission measure--with stellar parameters including rotation period and dynamo number, the authors find no compelling relationship. Including a gravity term, as suggested by previous investigators, leads to a deceptive relationship, because gravity is a strong function of rotation period for these systems. Similarly, the height integrates emission measures of the components in the two-temperature models, including a gravity term, are found to be well correlated with temperature.

00,056
PB94-211067 Not available NTIS
National Inst. of Standards and Technology (PL), Boulder, CO. Quantum Physics Div.
Dynamic Phenomena on the RS Canum Venaticorum Binary II Pegasi in August 1989. 1. Observational Data.
Final rept.
J. G. Doyle, B. J. Kellett, C. J. Butler, A. Brown, D. Fox, J. E. Linsky, P. B. Byrne, and J. E. Neff. 1992, 23p.
Pub. in Astronomy and Astrophysics Supplement Series 96, p351-373 1992.

Keywords: *Binary stars, *Stellar flares, X-ray spectra, Visible spectra, Balmer lines, GINGA satellite, IUE, Reprints, RS CVn stars, Raymond-Smith models.

Results are presented for two flares detected by the X-ray satellite GINGA, the International Ultraviolet Explorer satellite, ground-based Johnson U-band photometry, and optical spectroscopy from the Isaac Newton telescope for the RS CVn star II Peg.

00,057
PB94-211083 Not available NTIS
National Inst. of Standards and Technology (PL), Boulder, CO. Quantum Physics Div.
Radio Continuum and X-Ray Properties of the Coronae of RS Canum Venaticorum and Related Active Binary Systems.
Final rept.
S. A. Drake, T. Simon, and J. L. Linsky. 1992, 11p.
Contract NASA-W-17777
Sponsored by NASA Center for AeroSpace Information, Baltimore-Washington International Airport, MD.
Pub. in Astrophysical Jnl. Supplement Series 82, n1 p311-321 Sep 92.

Keywords: *Binary stars, *Stellar coronae, Radio emission, Continuous radiation, Circular polarization, X rays, Reprints, RS CVn stars.

We present some new radio continuum and X-ray data on the coronae of RS CVn and related active binary systems which complement those included in the previous Drake, Simon, and Linsky study of the radio emission properties of these stars. The bulk of these new radio data consists of 6 cm circular polarization measurements of 28 binaries for which we can set significant constraints (approx = or < 25%) on this quantity. Seven sources showed definite circular polarization at levels from 2% to 13%, and two others showed possible circular polarization. We also present 2 cm flux density and circular polarization measurements for 29 Dra, lambda And, and sigma Gem on dates for which we also have 6 cm observations.

00,058
PB94-211802 Not available NTIS
National Inst. of Standards and Technology (PL), Boulder, CO. Quantum Physics Div.
Interstellar Disk-Halo Connection in Galaxies: Review of Observational Aspects.
Final rept.
C. Heiles. 1991, 16p.
Pub. in Proceedings IAU Symposium 144, v51 p433-448 1991.

Keywords: *Galactic halos, Interstellar space, Magnetic fields, Cosmic rays, Neutral gases, Ionized gases, Reviews, Reprints.

The review is organized as follows. First, the author discusses the various gas components in rough order of increasing scale height. Section 1 discusses neutral gas, section 2 the 'warm' and 'not-so-warm' ionized gas, section 3 the T approx = 10(sup 5) K component at higher z that is detected in UV absorption and emission, section 4 the high-velocity neutral gas, section 5 the cosmic-ray halo as revealed by synchrotron emission, and section 6 the magnetic field. Next, section 7 covers the interaction between the low-z gas and the halo, which is the main topic of this symposium; and finally, section 8 discusses some aspects of the interstellar medium that are relevant to this interaction, with emphasis on the uncertainties.

00,059
PB94-212214 Not available NTIS
National Inst. of Standards and Technology (PL), Boulder, CO. Quantum Physics Div.
Opacity Project and the Practical Utilization of Atomic Data.
Final rept.
D. G. Hummer. 1991, 9p.
Contract NASA-NAGW-766, Grant NSF-AST88-02937
Sponsored by NASA Center for AeroSpace Information, Baltimore-Washington International Airport, MD. and National Science Foundation, Washington, DC.
Pub. in Stellar Atmospheres: Beyond Classical Models, p431-439 1991.

Keywords: *Stellar envelopes, *Stellar atmospheres, *Radiative transfer, Ionization cross sections, Transition probabilities, Computer applications, Photoionization, Reprints, Opacity project, Atomic data.

The Opacity Project was organized to compute new opacities for stellar envelopes, but has produced as a secondary product a vast amount of atomic radiative data for almost all elements of astrophysical interest. The photoionization cross sections in many cases show extensive resonance structure, which introduces complications when they are used in stellar modeling. Possible ways of dealing with this problem are discussed. Finally, a method of presenting atomic data in standardized subroutines in order to eliminate the need for large, special purpose data sets is proposed.

00,060
PB94-213022 Not available NTIS
National Inst. of Standards and Technology (PL), Boulder, CO. Quantum Physics Div.
Radiation-Driven Winds of Hot Luminous Stars X. The Determination of Stellar Masses Radii and Distances from Terminal Velocities and Mass-Loss Rates.
Final rept.
R. P. Kudritzki, D. G. Hummer, A. W. A. Pauldrach, J. Imhoff, J. Puls, and F. Najarro. 1992, 8p.
Pub. in Astronomy and Astrophysics 257, p655-662 1992.

Keywords: *Hot stars, *Stellar mass, *Stellar winds, Stellar mass ejection, Massive stars, Terminal velocity, Reprints, *Stellar distances, *Stellar radii.

A new, purely spectroscopic method to determine masses, radii and distances of massive, luminous hot

stars is presented. This method is based on the theory of radiation-driven winds and uses terminal velocity, mass-loss rate and effective temperature as observational quantities determined from the spectrum. The potential of this method is discussed.

00,061
PB94-213287 Not available NTIS
National Inst. of Standards and Technology (PL), Boulder, CO. Quantum Physics Div.
Astrophysical Aspects of Neutral Atom Line Broadening.
Final rept.
E. L. Lewis. 1990, 12p.
Pub. in Proceedings of International Conference on Spectral Line Shapes (10th), Austin, TX., June 25-29, 1990, p541-552.

Keywords: *Atom-atom collisions, *Line broadening, Resonance lines, Spectral lines, Neutral atoms, Hydrogen, Reprints, Redistribution functions.

Recent work on aspects of line shapes which are relevant to astrophysical spectra are discussed, namely (i) the impact broadening of strong resonance lines by atomic hydrogen, (ii) the effects on line profiles of collisional redistribution of radiation in the impact region and (iii) the influence of velocity changing collisions on impact region redistribution.

00,062
PB94-213402 Not available NTIS
National Inst. of Standards and Technology (PL), Boulder, CO. Quantum Physics Div.
Atomic Data Needed for Far Ultraviolet Astronomy with HUT and FUSE.
Final rept.
J. L. Linsky. 1993, 10p.
Pub. in Atomic and Molecular Data for Space Astronomy: Needs and Availability, Chapter 3, p33-42 1993.

Keywords: *Ultraviolet astronomy, Extreme ultraviolet spectra, Far ultraviolet radiation, Spaceborne astronomy, Astronomical satellites, Electron collisions, Oscillator strengths, Cross sections, Photoionization, Wavelengths, Reprints, Atomic data, FUSE satellite.

The author will summarize the spectroscopic capabilities of existing and planned space experiments, including HUT and FUSE, that will obtain spectra of astronomical sources at wavelengths shorter than Lyman-alpha. The important atomic and molecular data needed to analyze far and extreme ultraviolet spectra that will be obtained with these instruments include accurate wavelengths, oscillator strengths, photoionization cross sections for six important molecules, and, especially, electron collisional excitation cross sections for both low and high stages of ionization.

00,063
PB94-213410 Not available NTIS
National Inst. of Standards and Technology (PL), Boulder, CO. Quantum Physics Div.
FUSE: The Far Ultraviolet Spectrograph Explorer.
Final rept.
J. L. Linsky. 1992, 7p.
Pub. in Proceedings of Cambridge Workshop on Cool Stars, Stellar Systems, and the Sun (7th), Tucson, AZ., October 1991, p622-628 1992.

Keywords: *Astronomical satellites, Extreme ultraviolet spectra, Far ultraviolet radiation, Ultraviolet astronomy, Cool stars, Satellite observation, Spaceborne astronomy, Reprints, *FUSE satellite, FUSE project.

The author will summarize the past developments and present status of the FUSE Project. FUSE will observe a broad range of astrophysical sources, including cool stars, with high sensitivity and high spectral resolution in the far ultraviolet (912-1250A). It will also study broad band spectra (100-1600A) with high throughput and modest resolution.

00,064
PB94-213428 Not available NTIS
National Inst. of Standards and Technology (PL), Boulder, CO. Quantum Physics Div.
Ultraviolet Observations of Stellar Coronae: Early Results from HST.
Final rept.
J. L. Linsky. 1992, 13p.
Contract NASA-S-56500-D
Sponsored by NASA Center for AeroSpace Information, Baltimore-Washington International Airport, MD.
Pub. in Proceedings of IAU Joint Commission Meeting on Solar and Stellar Coronae, Buenos Aires, Argentina, July 31, 1991, p577-589 1992.

Keywords: *Stellar coronae, *Ultraviolet spectra, Hubble Space Telescope, Stellar spectra, Giant stars, Late stars, Binary stars, Emission spectra, Electron density, Stellar chromospheres, Reprints, *Capella star, *Gamma Draconis star.

I report on the first GHRS (Goddard High Resolution Spectrograph) spectra of two very different late-type giant stars - Capella and gamma Dra. Capella is a 104 day period binary system consisting of two stars (G9 III and G0 III) each of which shows bright emission lines formed in solar-like transition region and coronae. By contrast, gamma Dra is a hybrid-chromosphere star with very weak emission lines from high-temperature plasma. Low-dispersion spectra of these stars covering the 1160 to 1717 A spectral range show unresolved emission lines from neutral species through N V. The very different surface fluxes detected in the spectra of these stars suggest different types of heating mechanisms.

00,065
PB94-213436 Not available NTIS
National Inst. of Standards and Technology (PL), Boulder, CO. Quantum Physics Div.
X-rays from Stellar Flares.
Final rept.
J. L. Linsky. 1991, 14p.
Contract NASA-NAGW-1480
Sponsored by NASA Center for AeroSpace Information, Baltimore-Washington International Airport, MD.
Pub. in Mem. Soc. Astron. Ital. 62, n2 p307-320 1991.

Keywords: *Stellar flares, X-ray sources, Binary stars, Algol, Reprints, *Stellar x-rays, RS CVn stars.

I will summarize the x-ray observations of flares on dMe, active spectroscopic binaries, and young stars. Questions of particular interest include the energy associated with the x-ray emission and its relation to other components of the flare energy budget, the time behavior of the flaring plasma as revealed by the x-ray emission, and comparisons of stellar flare parameters with solar compact and two ribbon flares.

00,066
PB94-213444 Not available NTIS
National Inst. of Standards and Technology (PL), Boulder, CO. Quantum Physics Div.
Goddard High-Resolution Spectrograph Observations of the Local Interstellar Medium and the Deuterium/Hydrogen Ratio along the Line of Sight Toward Capella.
Final rept.
J. L. Linsky, A. Brown, K. Gayley, T. R. Ayres, W. Landsman, S. N. Shore, S. R. Heap, A. Diplas, and B. D. Savage. 1993, 16p.
Contract NASA-S-56500-D
Sponsored by NASA Center for AeroSpace Information, Baltimore-Washington International Airport, MD.
Pub. in The Astrophysical Jnl. 402, p694-709, 10 Jan 93.

Keywords: *Interstellar matter, Far ultraviolet radiation, Hubble Space Telescope, Ultraviolet spectra, Binary stars, Line of sight, Giant stars, Late stars, Hydrogen, Deuterium, Magnesium ions, Iron ions, Ratios, Reprints, Capella star.

We analyze HST Goddard High-Resolution Spectrograph observations of the 1216, 2600, and 2800 A spectral regions for the spectroscopic binary system Capella, obtained at orbital phase 0.26 with 3.27-3.57 km/s resolution and high signal-to-noise ratio. We infer the column densities of H I, D I, Mg II, and Fe II for the local interstellar medium along the 12.5 pc line of sight, together with estimates of the temperature and turbulent velocity. If we assume that the intrinsic Ly(alpha) lines of the component stars in the Capella system can be approximated as scaled solar lines (with self-reversals), which is consistent with the observed Ly(alpha) profile of the high radial velocity star delta Lep, then the average interstellar neutral hydrogen number density = 0.047/cc.

00,067
PB94-213451 Not available NTIS
National Inst. of Standards and Technology (PL), Boulder, CO. Quantum Physics Div.
Class of Radio-Emitting Magnetic B Stars and a Wind-Fed Magnetosphere Model.
Final rept.
J. L. Linsky, S. A. Drake, and T. S. Bastian. 1992, 3p.
Contract NASA-W-17772, Grant NGL-06-003-057
Sponsored by NASA Center for AeroSpace Information, Baltimore-Washington International Airport, MD.
Pub. in Proceedings of Cambridge Workshop on Cool Stars, Stellar Systems, and the Sun (7th), Tucson, AZ., October 1991, v26 p325-327 1992.

Keywords: *Magnetic stars, *Radio stars, Radio sources(Astronomy), Stellar magnetospheres, Stellar winds, Peculiar stars, B stars, A stars, Reprints.

We have detected a total of 16 magnetic Bp-Ap stars at 6 cm, out of 61 observed, including both He-strong and He-weak/Si-strong stars with log L(6) = 14.7 to 17.9, but none of the classical (SrCrEu-type) Ap stars at a detection limit of log L(6) < 14.9. We believe that the radio-emitting CP (chemically peculiar) stars form a distinct class of radio stars that differs from both the hot star wind sources and the active late-type stars. For the detected CP stars, we find that L(6) is proportional to M(sup 0.5) B(rms), produced by optically thick nonthermal gyrosynchrotron emission. In our model, the electrons are accelerated in current sheets located 10-20 radii from the star.

00,068
PB94-213469 Not available NTIS
National Inst. of Standards and Technology (PL), Boulder, CO. Quantum Physics Div.
Radio Emission from Chemically Peculiar Stars.
Final rept.
J. L. Linsky, S. A. Drake, and T. S. Bastian. 1992, 16p.
Sponsored by NASA Center for AeroSpace Information, Baltimore-Washington International Airport, MD.
Pub. in The Astrophysical Jnl. 393, n1 p341-356, 1 Jul 92.

Keywords: *Magnetic stars, *Radio stars, Radio sources(Astronomy), Stellar magnetospheres, Radio emission, Electron trajectories, Stellar winds, Peculiar stars, B stars, A stars, Very large array(VLA), Reprints.

We have extended the initial survey of radio emission from magnetic Bp-Ap stars by Drake et al, in five subsequent very large array (VLA) observing runs. A total of 16 sources have been detected at 6 cm out of 61 observed, giving a detection rate of 26%. Of these stars, three are also detected at 2 cm, four at 3.6 cm, and five at 20 cm. In addition to the three He-strong and two He-weak/Si-strong stars previously reported as radio sources, we have detected 11 new stars as radio sources with spectral types B5-A0 that are He-weak and Si-strong. We have not yet detected any of the classical (SrCrEu-type) Ap stars despite many attempts. We find a wide range of high 6 cm radio luminosities for the detected stars, with log L(6) = 14.7-17.9. We show that all of the observed properties of radio emission from these stars may be understood in terms of optically thick gyrosynchrotron emission from a nonthermal distribution of electrons. We propose a model in which the electrons are produced in current sheets forming 10-20 radii from the star. In this model the electrons travel along magnetic fields to smaller radii and higher magnetic latitudes where they mirror and radiate microwave radiation.

00,069
PB94-213477 Not available NTIS
National Inst. of Standards and Technology (PL), Boulder, CO. Quantum Physics Div.
First Results from a Coordinated ROSAT, IUE, and VLA Study of RS CVn Systems.
Final rept.
J. L. Linsky, D. Fox, A. Brown, J. H. M. M. Schmitt, T. Fleming, M. Rodono, I. Pagano, J. E. Neff, G. Bromage, R. Dempsey, and C. Schmitt. 1992, 3p.
Contracts NASA-W17-772, NAG5-82
Sponsored by NASA Center for AeroSpace Information, Baltimore-Washington International Airport, MD.
Pub. in Proceedings of Cambridge Workshop on Cool Stars, Stellar Systems, and the Sun (7th), Tucson, AZ., October 1991, p106-108 1992.

Keywords: ROSAT mission, Ultraviolet spectra, X ray spectra, Radio emission, Binary stars, IUE, Very large array(VLA), Reprints, *RS CVn stars.

This is a preliminary report on our extensive set of coordinated observations of RS CVn systems obtained during the ROSAT all-sky survey. Simultaneous with the PSPC and WFC observations, we observed five RS CVn systems with IUE and 15 systems with the VLA, typically at three wavelengths. We list the times of the coordinated observations and show our derived fluxes for one system - TY Pyx.

00,070
PB94-216033 Not available NTIS

National Inst. of Standards and Technology (PL), Boulder, CO. Quantum Physics Div.
Rapid Decline in the Optical Emission from SN 1957D in M83.
Final rept.
K. S. Long, P. F. Winkler, and W. P. Blair. 1992, 5p.
Pub. in Astrophysical Jnl. 395, p632-636, 20 Aug 92.

Keywords: *Supernova remnants, Emission spectra, Oxygen ions, Sulfur ions, H alpha line, Nucleosynthesis, Reprints, *Supernova 1957D.

As part of a search for the supernova remnants in M83, we have obtained new interference filter images of the site of SN 1957D and new spectra of the young supernova remnant (SNR) itself. Images were obtained in the light of H(alpha) (O III), (S II), and several continuum bands using the prime focus CCD camera on the CTIO 4 m telescope. An inspection of the images shows that the flux from the SNR, as observed through the (O III) filter, has decreased by at least a factor of 5 compared with observations made at Las Campanas 4 years earlier. There is no indication of a change in the emission from the SNR in any other filter. Spectroscopic observations conducted at the position of the SN yield an (O III) flux in 1991 April, down by a factor of 3 from measurements with the same instrument 2 years earlier.

00,071
PB95-125738 Not available NTIS
National Inst. of Standards and Technology (NML), Gaithersburg, MD. Molecular Physics Div.
Infrared Spectra of van der Waals Complexes of Importance in Planetary Atmospheres.
Final rept.
G. T. Fraser, A. S. Pine, and W. J. Lafferty. 1990, 5p.
Pub. in Proceedings of International Conference on Laboratory Research for Planetary Atmospheres (1st), p64-68 May 90.

Keywords: *Planetary atmospheres, *Infrared spectra, *Complexes, Van der Waals forces, Near infrared radiation, Vibrational spectra, Venus atmosphere, Mars atmosphere, Predissociation, Argon complexes, Trimers, Dimers, Reprints, *Carbon dioxide complexes.

It has been suggested that (CO2)2 and Ar-CO2 are important constituents of the planetary atmospheres of Venus and Mars. Here, we present recent results on the laboratory spectroscopy of CO2-containing van der Waals complexes which may be of use in the modeling of the spectra of planetary atmospheres. Sub-Doppler infrared spectra have been obtained for (CO2)2, (CO2)3, and rare-gas-CO2 complexes in the vicinity of the CO2 Fermi diad (nu(1) + nu(3), 2nu(2) + nu(3)) at 2.7 micrometers using a color-center-laser optothermal spectrometer. From the spectroscopic constants, the geometries of the complexes have been determined and van der Waals vibrational frequencies have been estimated. The equilibrium configurations are C(2h), C(3h), and C(2v), for (CO2)2, (CO2)3, and the rare-gas-CO2 complexes, respectively. The linewidths of the rovibrational transitions are = or < 22 MHz, indicating that predissociation is as much as four orders of magnitude faster than radiative processes for vibrational relaxation in these complexes.

00,072
PB95-152070 Not available NTIS
National Inst. of Standards and Technology (NML), Boulder, CO. Quantum Physics Div.
IRAS Spectroscopic Observations of Young Planetary Nebulae.
Final rept.
C. Y. Zhang, and S. Kwok. 1990, 16p.
Pub. in Astronomy and Astrophysics 237, p479-494 1990.

Keywords: *Planetary nebulae, *Interstellar matter, *Cosmic dust, Intermediate infrared radiation, Infrared astronomy, Infrared Astronomy Satellite, Stellar evolution, Silicates, Oxygen, Carbon, Reprints.

The 18 micrometer silicate dust feature is detected in 11 young planetary nebulae selected from radio properties. The presence of the 18 micrometer silicate feature suggests that oxygen-rich planetary nebulae are more common than previously believed. The silicate dust probably originates from the remnants of the circumstellar envelopes of the nebulae's asymptotic-giant-branch progenitors and remains visible in young planetary nebulae. Most interestingly, there are six young planetary nebulae that show both oxygen- and carbon-rich dust features. It is possible that a planetary nebula that descends from an oxygen-rich progenitor star will be classified as carbon rich as the silicate feature diminishes and the ultraviolet-excited polycyclic aromatic hydrocarbon bands become more prominent as the nebula ages. We suggest that a true chemical origin of planetary nebulae can only be reliably determined from young planetary nebulae.

00,073
PB95-152195 Not available NTIS
National Inst. of Standards and Technology (NML), Gaithersburg, MD. Time and Frequency Div.
Laboratory Measurements for the Astrophysical Identification of MgH.
Final rept.
L. R. Zink, D. A. Jennings, K. M. Evenson, and K. R. Leopold. 1990, 2p.
Pub. in Astrophysical Jnl. 359, n2 pL65-L66 1990.

Keywords: *Magnesium hydrides, *Rotational spectra, Electron transitions, Interstellar matter, Reprints.

The frequencies of the N = 1 <-- 0 transition of MgH are reported. They will serve as a basis for astrophysical searches for the molecule.

00,074
PB95-153441 Not available NTIS
National Inst. of Standards and Technology (PL), Boulder, CO. Quantum Physics Div.
Distant Future of Solar Activity: A Case Study of beta Hydri. 3. Transition Region, Corona, and Stellar Wind.
Final rept.
D. Dravins, P. Linde, T. R. Ayres, T. Simon, F. Wallinder, J. L. Linsky, and B. Monsingnori-Fossi. 1993, 14p.
Contract NAG5-82
Sponsored by NASA Scientific and Technical Information Facility, Baltimore, MD.
Pub. in Astrophysical Jnl. 403, p412-425, 20 Jan 93.

Keywords: *Solar activity, *Stellar evolution, *Stellar coronae, Stellar winds, Ultraviolet spectra, X-ray spectra, Atmospheric models, Late stars, EXOSAT satellite, IUE, Reprints.

The secular decay of solar-type activity with age is studied through a detailed comparison of the present Sun (G2 V) with the very old (9-10 Gyr) solar-type star beta Hyi (G2 IV), taken as a proxy of the future Sun. Analyses of successive atmospheric layers are made, and this Paper III in the series treats the outermost parts. The far-UV emission lines from the transition zone are among the faintest so far seen in any solar-type star. The significance of the deduced fluxes for the weak and marginally detected lines is tested through two independent reductions of IUE data. The coronal soft X-ray spectrum was measured through different filters on EXOSAT and compared to simulated X-ray observations of the Sun seen as a star. The flux from beta Hyi is weaker than that from the solar corona and has a different spectrum. Implications are discussed.

00,075
PB95-202263 Not available NTIS
National Inst. of Standards and Technology (PL), Boulder, CO. Quantum Physics Div.
Hydrogen Lyman-alpha Emission of Capella.
Final rept.
T. R. Ayres, A. Brown, K. G. Gayley, and J. L. Linsky. 1993, 11p.
Contract NASA-S-56500
Sponsored by NASA Scientific and Technical Information Facility, Baltimore, MD.
Pub. in Astrophysical Jnl. 402, p710-720, 10 Jan 93.

Keywords: *Lyman alpha radiation, Lyman spectra, Emission spectra, Ultraviolet spectra, Binary stars, IUE, Reprints, *Capella star.

We describe the hydrogen Ly(alpha) emission of the spectroscopic binary Capella (G8 III + G0 III) recorded at 0.1 A resolution by the International Ultraviolet Explorer (IUE). The overt changes in the composite line shape with orbital phase are controlled by the active G0 III star and permit a dissection of the stellar components despite the obliteration of the central portion of the profile by atomic hydrogen and deuterium absorption along the 12.5 pc sightline. The Ly(alpha) line shape of the active G0 III star is surprisingly asymmetric and possibly is variable. Both characteristics suggest a stellar wind of moderate excitation, a key component of the coronal evolution scenario of Simon and Drake for the Hertzsprung-gap giants.

00,076
PB95-202321 Not available NTIS
National Inst. of Standards and Technology (PL), Boulder, CO. Quantum Physics Div.
Observations of 3C 273 with the Goddard High Resolution Spectrograph on the Hubble Space Telescope.
Final rept.
1993, 16p.
Pub. in Astronomical Jnl. 105, n3 p831-846 Mar 93.

Keywords: *Quasars, Hubble space telescope, Spaceborne astronomy, Interstellar matter, Absorption spectra, Ultraviolet spectra, Nickel ions, Galaxies, Reprints, *3C 273 radio source.

The observations of the quasar 3C 273 taken with the Goddard High Resolution Spectrograph in February 1991 are presented here. We have included both the reduced raw data, and smoothed and deconvolved spectra. Also, a list of observed absorption lines is presented. The data comprise 11 spectra, including 1 low resolution observation and 10 medium resolution observations. The wavelength region covered ranged from about 1,150 to 2,820 A, but was not all inclusive. The procedures used to obtain and reduce the data, including corrections for fixed pattern noise, compensation for the effects of spherical aberration in the HST primary mirror, and objective detection of weak absorption lines, are described. We have also included a short discussion on the detection of galactic Ni II and Virgo cluster metal lines.

00,077
PB95-202479 Not available NTIS
National Inst. of Standards and Technology (PL), Boulder, CO. Quantum Physics Div.
ROSAT All-Sky Survey of Active Binary Coronae. 1. Quiescent Fluxes for the RS Canum Venaticorum Systems.
Final rept.
R. C. Dempsey, J. L. Linsky, T. A. Fleming, and J. H. M. M. Schmitt. 1993, 11p.
Contract NASA-NAG5-1797
See also Part 2, PB94-199601. Sponsored by NASA Scientific and Technical Information Facility, Baltimore, MD.
Pub. in Astrophysical Jnl. 86, n2 p599-609 Jun 93.

Keywords: *Binary stars, *Stellar coronae, X ray astronomy, Spaceborne astronomy, ROSAT mission, Sky surveys(Astronomy), Reprints.

We present observations of 136 RS CVn active binary systems obtained with the ROSAT Position Sensitive Proportional Counter (PSPC) during the all-Sky Survey phase of the mission. Of this sample, 112 targets were detected in exposures of about 600 s or less. This represents the largest sample of RS CVn systems observed to date at any wavelength, including X-rays. Furthermore, since the entire sky was surveyed, these data do not suffer from any biases other than those present in the methods used to discover the RS CVn binaries. Comparison of the X-ray properties of the RS CVn systems with 6 cm radio and C IV ultraviolet emission is also presented.

00,078
PB95-202669 Not available NTIS
National Inst. of Standards and Technology (PL), Boulder, CO. Quantum Physics Div.
Sobolev Approximation for Line Formation with Partial Frequency Redistribution.
Final rept.
D. G. Hummer, and G. B. Rybicki. 1992, 10p.
Contract NASA-NAGW-766, Grant NSF-AST88-02937
See also PB85-226058. Sponsored by National Science Foundation, Washington, DC. and National Aeronautics and Space Administration, Washington, DC.
Pub. in Astrophysical Jnl. 387, p248-257, 1 Mar 92.

Keywords: *Spectral lines, Radiative transfer, Reprints, Sobolev approximation, Expanding atmospheres.

The formation of a spectral line in a uniformly expanding infinite medium is investigated in the Sobolev approximation with particular attention to the various mechanisms for frequency redistribution. Numerical and analytic solutions of the transfer equation are presented for a number of redistribution functions and their approximations, including type I and type II partial redistribution, coherent scattering and complete redistribution, and the Fokker-Planck and uncorrelated ap-

proximation to the R(II) function. The solutions for the mean intensity are shown to depend very much on the type of redistribution mechanism, while for the frequency-weighted mean intensity J(bar), which enters the rate equations, this dependence is weak. This implies that the use of Sobolev escape probabilities based on complete redistribution can be an adequate approximation for many calculations for which only the radiative excitation rates are needed. However, it is shown that the criteria for applicability of Sobolev theory may be difficult to meet when transfer occurs primarily in the Voigt wings, especially for complete redistribution.

00,079
PB95-202677 Not available NTIS
National Inst. of Standards and Technology (PL), Boulder, CO. Quantum Physics Div.
Recombination Line Intensities for Hydrogenic Ions-III. Effects of Finite Optical Depth and Dust.
Final rept.
D. G. Hummer, and P. J. Storey. 1992, 14p.
Contract NASA-NAGW-766
See also Part 2, PB89-107148. Sponsored by NASA Scientific and Technical Information Facility, Baltimore, MD.
Pub. in Monthly Notices of the Royal Astronomical Society 254, p277-290 1992.

Keywords: *Hydrogen, Lyman lines, Cosmic dust, Element abundance, Universe, Radiative recombination, Radiative transfer, Radio astronomy, Helium, Reprints.

We explore systematically the effect on the recombination spectrum of hydrogen arising from: (i) finite optical thickness in the Lyman Lines; (ii) the overlapping of Lyman lines near the series limit; (iii) the absorption of Lyman lines by dust or photoionization, and (iv) the long-wave radiation emitted by dust. Full account is taken of electron and heavy particle collisions in redistributing energy and angular momentum. We find that each of these deviations from the classical Case B leads to observable effects, and that dust influences the recombination spectrum in characteristic ways that may make possible new observational constraints on dust properties in nebulosities. On the basis of these calculations, we believe the uncertainty in the determination of the helium-to-hydrogen abundance ratio in the Universe may be larger than currently claimed.

00,080
PB95-202834 Not available NTIS
National Inst. of Standards and Technology (PL), Boulder, CO. Quantum Physics Div.
Stellar Coronal Structures.
Final rept.
J. L. Linsky. 1994, 10p.
Sponsored by National Aeronautics and Space Administration, Washington, DC.
Pub. in IAU Colloq. 144 'Solar Coronal Structures', Tatronska Lomnica, Slovak Rep., September 20-24, 1993, p641-650 1994.

Keywords: *Stellar coronae, Stellar winds, Binary stars, Dwarf stars, Peculiar stars, Magnetic fields, Reprints.

Large magnetic structures in the coronae of stars containing gas at a wide variety of temperatures are now being studied in X-rays, radio wavelengths, and H(alpha). Here the author summarizes what we are learning about coronal structures in three types of stellar systems: the magnetic chemically peculiar stars, the RS CVn binary systems containing G- and K-type subgiants, and active solar-type dwarfs like V471 Tauri and AB Doradus.

00,081
PB95-202842 Not available NTIS
National Inst. of Standards and Technology (PL), Boulder, CO. Quantum Physics Div.
Deuterium in the Local Interstellar Medium: Its Cosmological Significance.
Final rept.
J. L. Linsky, A. Diplas, B. Savage, C. Andrulis, and A. Brown. 1994, 4p.
Contract NASA-S-56500-D
Sponsored by National Aeronautics and Space Administration, Washington, DC.
Pub. in Frontiers of Space and Ground-Based Astronomy, p301-304 1994.

Keywords: *Interstellar matter, *Deuterium, *Hydrogen, *Isotope ratio, Hubble space telescope, Lyman alpha radiation, Line of sight, Galactic evolution, Cosmology, Reprints, Procyon star.

We report on our ongoing program to measure the deuterium/hydrogen (D/H) ratio and interstellar gas properties along many lines of sight through the local interstellar medium using the Hubble Space Telescope (HST) Goddard High-Resolution Spectrograph. For the line of sight towards Capella (12.5 pc) we had previously found D/H = 1.65(+ 0.07, -0.18) X 10(exp -5), T = 7,000 K, and turbulent velocity 1.66 km/s. These quantities were determined by modeling the interstellar hydrogen and deuterium Lyman alpha lines and the resonance lines of Fe II and Mg II against the background stellar emission-line profiles. We now report on our preliminary analysis of these spectral lines for the line of sight toward Procyon (3.5 pc). We find that D/H = 1.40 + or - 0.05 X l0(exp -5). Further analysis of this and other lines of sight are planned to determine whether the D/H ratio varies within the local interstellar medium. We infer the primordial value of D/H from Galactic evolution models and comment on the derived baryon density of the Universe.

00,082
PB95-202859 Not available NTIS
National Inst. of Standards and Technology (PL), Boulder, CO. Quantum Physics Div.
Peeking Through the Picket Fence: What Astrophysical Surprises May Be Present in the 100-1200 Angstrom Region.
Final rept.
J. L. Linsky, and D. G. Luttermoser. 1991, 10p.
Contracts NASA-NAG5-82, NASA-H-80531
Sponsored by NASA Scientific and Technical Information Facility, Baltimore, MD.
Pub. in Advances in Space Research 11, n11 p(11)5-(11)14 1991.

Keywords: *Ultraviolet astronomy, Extreme ultraviolet radiation, Far ultraviolet radiation, Ultraviolet spectrometers, Ultraviolet spectra, Spaceborne astronomy, Stellar coronae, Flare stars, G stars, Reprints.

In anticipation of more sensitive EUV and FUV spectroscopic instruments, we simulate spectra, including interstellar absorption, of solar-like, RS CVn, and flare stars as folded through the instrument parameters of the Extreme Ultraviolet Explorer (EUVE), Lyman/Far Ultraviolet Spectroscopic Explorer (FUSE) Phase A, and a desirable next-generation spectrometer. We find that even the relatively insensitive EUVE spectrometer will be able to detect sufficient spectral lines from many active binary and dMe stars to determine their coronal emission measure distributions. The Lyman/FUSE or next-generation spectrometers are needed to study solar-type stars or flaring stars with high time resolution. The high throughput and effective area of a next-generation spectrometer is needed for Doppler imaging studies, stellar wind and downflow measurements, and high time and spectral resolution of stellar flares.

00,083
PB95-203501 Not available NTIS
National Inst. of Standards and Technology (PL), Boulder, CO. Quantum Physics Div.
New High-Redshift Damped Lyman-alpha Absorption Systems and the Redshift Evolution of Damped Absorbers.
Final rept.
R. L. White, A. L. Kinney, and R. H. Becker. 1993, 14p.
Pub. in Astrophysical Jnl. 407, n2 p456-469, 20 Apr 93.

Keywords: *Lyman alpha radiation, Galactic evolution, Absorption spectra, Red shift, Cosmology, Galaxies, Reprints.

We have discovered two high-redshift (Z(abs) = 3.388 and 2.908) damped Ly(alpha) absorption systems and a third possible damped system (Z(abs) =3.080) while obtaining spectra of optical counterparts from a sample of flat spectrum radio sources. These three systems all have higher redshifts than any previously known damped Ly(alpha) absorption systems in the spectra of radio-loud quasars, and they are among the highest redshift damped Ly(alpha) systems known. This is the first good statistical evidence for evolution in the number (or size) of damped Ly(alpha) absorbers at high redshift. We argue that the most likely explanation for the rapid disappearance of damped Ly(alpha) absorbers between z = 3.5 and z = 3 is that we are observing the epoch of galaxy formation.

00,084
PB95-203527 Not available NTIS
National Inst. of Standards and Technology (PL), Boulder, CO. Quantum Physics Div.
CCD Mosaic Images of the Supernova Remnant 3C 400.2.
Final rept.
P. F. Winkler, T. M. Olinger, and S. A. Westerbeke. 1993, 11p.
Sponsored by National Science Foundation, Washington, DC. and National Aeronautics and Space Administration, Washington, DC.
Pub. in Astrophysical Jnl. 405, p608-613, 10 Mar 93.

Keywords: *Supernova remnants, Charge coupled devices, H alpha radiation, Nitrogen ions, Oxygen ions, Sulfur ions, Planetary nebulae, Reprints.

We have constructed CCD mosaic images of the old Galactic supernova remnant 3C 400.2 in lines of H(alpha) + (N II), (S II), and (O III), plus a continuum band. These are the first CCD images covering the full extent of this remnant, and they reveal significantly more nebulosity than the deepest photographic plates. Comparison with radio and X-ray images indicates dramatically different morphology in the three regimes. The optical images both in H(alpha) + (N II) and in (S II) show an almost complete, irregular shell of emission, with a diameter of about 16', little over half that of the radio shell, while the X-ray structure is a centrally peaked ellipsoid. We also report a previously uncataloged planetary nebula southwest of 3C 400.2.

00,085
PB95-203535 Not available NTIS
National Inst. of Standards and Technology (PL), Boulder, CO. Quantum Physics Div.
G203.2-12.3: A New Optical Supernova Remnant in Orion.
Final rept.
P. F. Winkler, and B. Reipurth. 1992, 6p.
Pub. in Astrophysical Jnl. 389, pL25-L28, 10 Apr 92.

Keywords: *Supernova remnants, H alpha radiation, Sulfur ions, Nebulae, Reprints.

We report the discovery of what appears to be a supernova remnant at unusually high latitude near the Galactic anticenter. CCD images in the light of both (S II) and H(alpha) show patchy filaments scattered over a 3' region, but with relative strengths in the two lines which vary by a factor of 20 from one filament to another. Spectra confirm the line identifications and variable intensities. The most extreme filaments have line flux ratios (S II)/H(alpha) approx = 5, among the highest observed in remnants. The position of G203.2-12.3 coincides with that of a 'guest star' recorded by Chinese astronomers in A.D. 483.

00,086
PB96-102033 Not available NTIS
National Inst. of Standards and Technology (PL), Boulder, CO. Quantum Physics Div.
Far-Ultraviolet Flare on a Pleiades G Dwarf.
Final rept.
T. R. Ayres, J. R. Stauffer, T. Simon, G. S. Basri, J. A. Bookbinder, A. Brown, G. A. Doschek, J. L. Linsky, L. W. Ramsey, F. M. Walter, R. A. Stern, and S. K. Antiochos. 1994, 4p.
Sponsored by National Aeronautics and Space Administration, Washington, DC.
Pub. in Astrophysical Jnl. 420, pL33-L36, 1 Jan 94.

Keywords: *Stellar flares, *G stars, *Dwarf stars, *Brightness, Stellar mass ejecta, Ultraviolet spectra, Far ultraviolet radiation, Stellar luminosity, Luminous intensity, Stellar magnetosphere, Pleiades cluster, Reprints.

The HST/FOS recorded a remarkable transient brightening in the C IV (gamma-gamma) 1548,50 emissions of the rapidly rotating Pleiades G dwarf H II 314. on the one hand, the 'flare' might be a rare event luckily observed; on the other hand it might be a bellwether of the coronal heating in very young solar-mass stars. If the latter, flaring provides a natural spin-down mechanism through associated sporadic magnetospheric mass loss.

00,087
PB96-102249 Not available NTIS
National Inst. of Standards and Technology (PL), Boulder, CO. Quantum Physics Div.
Search for Radio Emission from the 'Non-Magnetic' Chemically Peculiar Stars.
Final rept.
S. A. Drake, J. L. Linsky, and J. A. Bookbinder. 1994, 4p.
Sponsored by National Aeronautics and Space Administration, Washington, DC.

Pub. in Astronomical Jnl. 108, n6 p2203-2206 Dec 94.

Keywords: *Peculiar stars, *Radio emission, *Stellar magnetic fields, Radio sources(Astronomy), Stellar magnetosphere, Steller luminosity, Stellar temperature, Very large array(VLA), Reprints.

The authors observed 23 members of the Am and HgMn subclasses of chemically peculiar (CP) stars with the VLA to search for nonthermal radio emission at levels comparable to those found for the Si and He peculiar subclasses of the CP stars be Linsky et al. (ApJ, 393, 341 (1992)). The authors detected none of the Am and HgMn stars as radio emitters with upper limits typically < 0.20 mJy. Applying a correlation between radio luminosity, surface magnetic field, and effective temperature derived from previous radio studies of the Si and He peculiar CP stars, the authors find that the predicted radio luminosities of alpha-And (an HgMn star) and Sirius (a hot Am star) are more than an order of magnitude larger than the observed upper limits, indicating that these stars lack magnetospheres, and, by inference, surface magnetic fields.

00,088
PB96-102256 Not available NTIS
National Inst. of Standards and Technology (PL), Boulder, CO. Quantum Physics Div.
X-ray Emission from Chemically Peculiar Stars.
Final rept.
S. A. Drake, J. L. Linsky, J. H. M. M. Schmitt, and C. Rosso. 1994, 5p.
Contract NASA-W-17772
Sponsored by NASA Scientific and Technical Information Facility, Baltimore, MD.
Pub. in Astrophysical Jnl. 420, p387-391, 1 Jan 94.

Keywords: *X ray emission, *Peculiar stars, *Stellar magnetic fields, Binary stars, Companion stars, Steller magnetospheres, X ray sources, Radio sources(Astronomy), Steller luminosity, X ray astronomy, Rosat mission, Reprints.

The authors have searched the ROSAT All-Sky Survey (RASS) database at the positions of approximately 100 magnetic Bp-Ap stars of the helium-strong, helium-weak, silicon, and strontium-chromium subclasses. The authors detect X-ray sources at the positions of 10 of these stars; in four cases the X-ray emission presumably arises from an early-type companion with a radiatively driven wind, while the authors believe that the magnetic chemically peculiar (CP) star is the most likely X-ray source (as opposed to a binary companion) in at least three and at most five of the six remaining cases. The authors discuss the X-ray and radio emission properties of their sample of CP stars, and argue that both types of emission may be magnetospheric in origin; however, there is clearly not a simple one-to-one correspondence between them, since many of the magnetic stars that are detected radio sources were not detected as X-ray sources in the present survey.

00,089
PB96-102322 Not available NTIS
National Inst. of Standards and Technology (PL), Boulder, CO. Quantum Physics Div.
Rotational Modulation and Flares on RS Canum Venaticorum and BY Draconis Stars. XVIII. Coordinated VLA, ROSAT, and IUE Observations of RS CVn Binaries.
Final rept.
D. C. Fox, J. L. Linsky, A. Veale, J. E. Neff, I. Pagano, M. Rodono, G. E. Bromage, M. Kurster, J. H. M. M. Schmitt, R. C. Dempsey, and A. Brown. 1994, 14p.
See also PB94-185626. Sponsored by National Aeronautics and Space Administration, Greenbelt, MD. Goddard Space Flight Center.
Pub. in Astronomy and Astrophysics 284, p91-104 1994.

Keywords: *Binary stars, *Steller flares, *Radio sources(Astronomy), *X ray sources, Radio emission, Stellar coronae, Stellar chromospheres, Stellar radiation, Radio spectra, Ultraviolet spectra, Variable stars, Rosat mission, Very large array(VLA), IVE, Radio astronomy, Reprints.

As part of a coordinated program of multi-wavelength observations of RS CVn close binary systems, the authors observed 15 systems with the VLA and 10 systems with IUE, simultaneously or nearly simultaneously with the ROSAT All Sky Survey observations of these stars. Of the 22 systems observed with ROSAT, three were observed both by IUE and the VLA. The prinicipal aim of this program was to check the validity of the existing empirical correlations between the radio and soft X-ray emissions of their coronae, and between the chromospheric/transition region and coronal emissions.

00,090
PB96-102504 Not available NTIS
National Inst. of Standards and Technology (EEEL), Boulder, CO. Electromagnetic Technology Div.
Extended CO(7 yields 6) Emission from Warm Gas in Orion.
Final rept.
J. E. Howe, D. T. Jaffe, E. N. Grossman, G. J. Stacey, W. F. Wall, and J. G. Mangum. 1993, 9p.
Pub. in Astrophysics Jnl., v410 p179-187, 10 Jun 93.

Keywords: *Orion nebula, *Interstellar gas, *Molecular clouds, Carbon oxides, Interstellar matter, Cosmic dust, Cosmic gases, Stellar luminosity, Brightness temperture, Line spectra, Emission spectra, Reprints.

We mapped the quiescent emission from the 807 GHz J=7 yields 6 transition of CO in Orion along a strip in R.A. extending from 0.7 pc west to 1.2 pc east of Theta(sup 1) C Orionis. Orion KL outflow shows that the luminosity of shock-excited CO(7 yields 6) emission in Orion is only a few percent of the luminosity of the widespread quiescent CO(7 yields 6) emission.

00,091
PB96-102694 Not available NTIS
National Inst. of Standards and Technology (PL), Boulder, CO. Quantum Physics Div.
High-Velocity Plasma in the Transition Region of AU Microscopii: Evidence for Magnetic Reconnection and Saturated Heating during Quiescent and Flaring Conditions.
Final rept.
J. L. Linsky, and B. E. Wood. 1994, 9p.
Contract NASA-S-56500-D
Sponsored by National Aeronautics and Space Administration, Washington, DC.
Pub. in Astrophysical Jnl. 430, p342-350, 20 Jul 94.

Keywords: *Flare stars, *Ultraviolet spectra, *Chromospheres, Reprints, Emission spectra.

We analyze high-resolution HST spectra of the dM0e flare star AU Mic, including the profiles of the C IV 1548.2 A, 1550.8 A and Si IV 1393.8 A, 1402.8 A lines obtained with the G160M grating of the Goddard High-Resolution Spectrograph. The quiescent profiles of the C IV and Si IV lines are broad, and not simple Gaussian in shape. Flux in the C IV and Si IV lines, for example, can be measured reliably out to about + or - 200 km s-1 from line center. Each of the C IV and Si IV profiles can be fitted accurately by two Gaussians (one narrow and the other broad) centered on nearly the same wavelength, with the narrower component accounting for roughly 60% of the total integrated flux. The narrow components have similar line widths to those observed in solar active and quiet region. The broad Gaussian components of the AU Mic line profiles are reminiscent of the broad C IV profiles observed in solar transition region explosive events, which are thought to be associated with emerging magnetic flux regions where field reconnnection occurs.

00,092
PB96-102777 Not available NTIS
National Inst. of Standards and Technology (PL), Boulder, CO. Quantum Physics Div.
Observing Stellar Coronae with the Goddard High Resolution Spectrograph. I. The dMe Star AU Microscopii.
Final rept.
S. P. Maran, R. D. Robinson, S. N. Shore, B. E. Woodgate, J. L. Linsky, A. Brown, P. B. Byrne, M. R. Kundu, S. White, J. C. Brandt, J. W. Brosius, and K. G. Carpenter. 1994, 9p.
Sponsored by National Aeronautics and Space Administration, Washington, DC.
Pub. in Astrophysical Jnl. 421, p800-808, 1 Feb 94.

Keywords: *Stellar coronae, *Stellar spectra, *Spectral resolution, Noise reduction, Emission spectra, Stellar flares, Stellar chromospheres, Ultraviolet spectra, Late stars, Reprints, HST(Hubble Space Telescope), High Resolution Spectrography.

The authors report on an observation of AU Mic taken with the Goddard High Resolution Spectrograph, aboard the Hubble Space Telescope. The data consist of a rapid sequence of spectra covering the wavelength range 1345-1375 Angstroms with a spectral resolution of 10,000. The observations were originally intended to search for spectral variations during flares. No flares were detected during the 3.5 hr of monitoring. A method of reducing the noise while combining the individual spectra in the time series is described which resulted in the elimination of half of the noise while rejecting only a small fraction of the stellar signal. The resultant spectrum was of sufficient quality to allow the detection of emission lines with an integrated flux of 10(exp -15) ergs/sq cm/s or greater. Lines of C I, O I, O V, Cl I, and Fe XXI were detected, This is the first indisputable detection of the 1354 Angstroms Fe XXI line, formed at T about 10(exp 7)K, on a star other than the Sun. The line was well resolved and displayed no significant bulk motions or profile asymmetry.

00,093
PB96-103189 Not available NTIS
National Inst. of Standards and Technology (PL), Boulder, CO. Quantum Physics Div.
Volume-Limited ROSAT Survey of Extreme Ultraviolet Emission from all Nondegenerate Stars within 10 Parsecs.
Final rept.
B. E. Wood, A. Brown, J. L. Linsky, S. T. Hodgkin, J. P. Pye, B. J. Kellett, and G. E. Bromage. 1994, 21p.
Contracts NAGW-2904, NAG501792
Sponsored by National Aeronautics and Space Administration, Washington, DC.
Pub. in Astrophysical Jnl. Supplement Series 93, p287-307 Jul 94.

Keywords: *Extreme ultraviolet radiation, *Sky surveys(Astronomy), *Late stars, Ultraviolet emission, Ultraviolet spectra, Emission spectra, Stellar luminosity, Stellar coronae, M stars, X ray stars, Binary stars, Rosat mission, Ultraviolet astronomy, Reprints, *Nondegenerate stars.

We report the results of a volume-limited ROSAT Wide Field Camera (WFC) survey of all nondegenerate stars within 10 pc. Of the 220 known star systems within 10 pc, we find that 41 are positive detections in at least one of the two WFC filter bandpasses (S1 and S2), while we consider another 14 to be marginal detections. We compute X-ray luminosities for the WFC detections using Einstein Imaging Proportional Counter (IPC) data, and these IPC luminosities are discussed along with the WFC luminosities throughout the paper for purposes of comparison. Extreme ultraviolet (EUV) luminosity functions are computed for single stars of different spectral types using both S1 and S2 luminosities, and these luminosity functions are compared with X-ray luminosity functions derived by previous authors using IPC data.

00,094
PB96-112016 Not available NTIS
National Inst. of Standards and Technology (PL), Boulder, CO. Quantum Physics Div.
GHRS Observations of Cool, Low-Gravity Stars. 1. The Far-Ultraviolet Spectrum of alpha Orions (M2 Iab).
Final rept.
K. G. Carpenter, R. D. Robinson, G. M. Wahlgren, J. L. Linsky, and A. Brown. 1994, 16p.
Pub. in Astrophysical Jnl., v428 p329-344, 10 Jun 94.

Keywords: *Far ultraviolet radiation, *Cool stars, *Ultraviolet spectra, *Stellar spectra, M stars, Supergiant stars, Red giant stars, Late stars, Stellar chromospheres, Stellar atmospheres, Stellar temperature, Line spectra, Ultraviolet astronomy, Reprints, *Alpha Orionis star.

We present far-UV (1200-1930 A) observations of the prototypical red supergiant star alpha Ori, obtained with the Goddard High Resolution Spectrograph (GHRS) on the Hubble Space Telescope. The observations, obtained in both low- (G140L) and medium- (G160/200M) resolution modes, unambiguously confirm that the UV 'continuum' tentatively seen with IUE is in fact a true continuum and is not due to a blend of numerous faint emission features or scattering inside the IUE spectrograph. This continuum appears to originate in the chromosphere of the star, at temperatures ranging from 3000-5000 K, and we argue that it is not related to previously reported putative companions or to bright spots on the stellar disks.

00,095
PB96-119474 Not available NTIS
National Inst. of Standards and Technology (PL), Boulder, CO. Quantum Physics Div.

Stars, Atmospheres, Radiative Transfer.
Final rept.
D. G. Hummer. 1992, 2p.
Pub. in Astronomy and Astrophysics Encyclopedia, p703-704 Mar 92.

Keywords: *Stellar atmospheres, *Radiative transfer, *Transition probabilities, Stellar spectra, Stellar winds, Stellar temperature, Stellar mass, Gases, Radiation, Stars, Flow rate, Stellar models, Reprints.

Radiative transfer in stellar atmospheres refers to the quantitative treatment of the flow of radiant energy through the outer layers of stars and the interaction of radiation with the gas in these regions. In addition to radiant energy, in certain types of stars a small amount of energy is transported through the atmosphere by the large-scale motion of the gas itself; both forms, of course, arise ultimately from thermonuclear processes deep inside the stars. The division between these two modes is not fixed, as radiation can transfer momentum to the gas, causing outflows known as stellar winds, and flow energy can be transformed into radiation by shocks. Radiation undergoes repeated interactions with the gas, which collectively determine the rate at which it can escape from the atmosphere. Because the rate at which energy is produced deepin the star is essentially fixed. These interactions establish the equilibrium distribution of temperature and density in the atmosphere. In addition to this constructive role, radiative transfer also plays a diagnostic role, for the spectrum of the escaping radiation carries with it all that we can possibly learn about the internal physical conditions of the atmosphere and the underlying layers.

00,096
PB96-119532 Not available NTIS
National Inst. of Standards and Technology (CAML), Gaithersburg, MD. Statistical Engineering Div.
Discussion: Statistical Signal Processing of Quasiperiodicities.
Final rept.
W. Liggett. 1992, 3p.
Pub. in Statistical Challenges in Modern Astronomy, Chapter 16, p378-380 1992.

Keywords: *Binary stars, *Stellar mass accretion, *X ray spectra, Stellar spectra, Signal processing, X ray astronomy, Statistical analysis, Stellar physics, Reprints.

The authors summarize what has been inferred about the physics of binary stars through a variety of statistical signal processing techniques. They affirm certain aspects of the most widely accepted model for accreting binary stars, conclude that clumps of matter must accrete at more than 400 per second, and point to aspects of the observed x-ray intensities that seem unexplained.

00,097
PB96-119540 Not available NTIS
National Inst. of Standards and Technology (PL), Boulder, CO. Quantum Physics Div.
Relationship between Radiative and Magnetic Fluxes for Three Active Solar-Type Dwarfs.
Final rept.
J. L. Linsky, C. Andrulis, S. H. Saar, T. R. Ayres, and M. S. Giampapa. 1994, 3p.
Pub. in Cool Stars, Stellar Systems, and the Sun, Cambridge Workshop (8th), ASP Conference Series, Athens, GA., October 1993, p438-440 Sep 94.

Keywords: *Dwarf stars, *Stellar magnetic fields, *Radiative transfer, *Magnetic flux, Stellar activity, Stellar magnetospheres, Stellar radiation, Magnetic field configurations, Functional analysis, Reprints, Spatial analysis.

We present some preliminary results from our coordinated campaign of IUE and McMath Telescope magnetic field measurements of three active solar-type dwarf stars: 59 Vir, xi Boo A , and HD 131511. We observed the three stars mearly every day from May 9 to May 25, 1993, covering between 1 and 3 rotations. We explore the functional and spatial relationship between magnetic and radiative fluxes.

00,098
PB96-122817 Not available NTIS
National Inst. of Standards and Technology (PL), Boulder, CO. Quantum Physics Div.
Sleuthing the Dynamo: HST/FOS Observations of UV Emissions of Solar-Type Stars in Young Clusters.
Final rept.
T. Ayres, G. Basri, T. Simon, S. Antiochos, J. Bookbinder, A. Brown, G. Doschek, J. Linsky, L. Ramsey, F. Walter, J. Stauffer, and R. Stern. 1994, 3p.
Pub. in Proceedings: Cool Stars, Stellar Systems, and the Sun Workshop (8th), ASP Conference Series, Athens, Georgia, October 1993, v64 p53-55 Sep 94.

Keywords: *Ultraviolet spectra, *Stellar spectra, *Late stars, Stellar coronae, Stellar chromospheres, Emission spectra, Open clusters, Hubble Space Telescope, Reprints, Stellar evolution.

HST/FOS spectra of young solar-type stars are providing new clues to the early evolution of subcoronal activity.

00,099
PB96-122882 Not available NTIS
National Inst. of Standards and Technology (PL), Boulder, CO. Quantum Physics Div.
Efficient Way of Identifying New Active Stars: A VLA Survey of X-ray Selected Active Stellar Candidates.
Final rept.
S. A. Drake, T. Simon, J. L. Linsky, and N. E. White. 1994, 3p.
Contract NASA-NAG5-2075
Sponsored by National Aeronautics and Space Administration, Washington, DC.
Pub. in Cool Stars, Stellar Systems, and the Sun, Cambridge Workshop (8th), ASP Conference Series, Athens, GA., October 1993, v64 p690-692.

Keywords: *X ray sources, *Stellar radiation, *Sky surveys(Astronomy), Binary stars, Stellar coronae, Radio sources(Astronomy), Very large array(VLA), X ray astronomy, Radio astronomy, Reprints.

Source confusion makes it difficult to identify active stars, such as the RS CVn binaries, with X-ray sources detected in low angular resolution surveys. Short (15 minute) VLA radio continuum observations of candidates having appropriate spectral types and X-ray to visual flux ratios obtained from an X-ray selected sample, combined with other information, has enabled us either to confirm or rule out proposed late-star counterparts for 27 out of 32 X-ray sources selected from the Einstein Slew Survey.

00,100
PB96-123005 Not available NTIS
National Inst. of Standards and Technology (PL), Boulder, CO. Quantum Physics Div.
Magnetic Fields in Star-Forming Regions: Observations.
Final rept.
C. Heiles, A. A. Goodman, C. F. McKee, and E. G. Zweibel. 1993, 25p.
Pub. in Protostars and Planets III, p279-326 1993.

Keywords: *Magnetic fields, *Orion nebula, *Spectral lines, Interstellar gas, Cosmic gases, Molecular clouds, Interstellar clouds, Cosmic dust, Zeeman effect, Polarization, Emission spectra, Reprints.

The authors review the observational aspects of magnetic fields in dense, star-forming regions. First the authors discuss ways to observe the field. Next, they discuss selected observational results, focusing on detailed discussions of a small number of points rather than a generalized discussion that covers the waterfront. Next the authors discuss the derivation of the complete magnetic vector, including both the systematic and fluctuating component, from a large sample of Zeeman and linear polarization measurements for the L204 dark cloud. Third, they discuss the virial theorem as it applies to dark clouds in general and one dark cloud. Finally the authors critically discuss the numerous claims for alignment of cloud structural features with the plane-of-the-sky component of the magnetic field and find that many of these have not been definitively established.

00,101
PB96-123286 Not available NTIS
National Inst. of Standards and Technology (PL), Boulder, CO. Quantum Physics Div.
A-type and Chemically Peculiar Stars.
Final rept.
J. L. Linsky. 1993, 10p.
Contract NAG5-1797
Sponsored by NASA Scientific and Technical Information Facility, Baltimore, MD.
Pub. in Physics of Solar and Stellar Coronae, p257-266 Sep 93.

Keywords: *Peculiar stars, *A stars, *Stellar temperature, Stellar spectra, Emission spectra, Radio emission, X ray emission, Stellar luminosity, Stellar coronae, Steller magnetospheres, Reprints.

The authors will show that the magnetic chemically peculiar (CP) stars hotter than about spectral type A2 display many of the phenomena seen in the most active late-type stars. In particular, many CP stars are luminous nonthermal radio sources and ROSAT confirms that many are also luminous coronal x-ray sources like the RS CVn systems. A wind-fed magnetosphere model has been proposed to explain both the nonthermal radio and the x-ray emission. In this model, the stellar wind plays the role of a mechanical energy source analogous to the role played by convection in the active late-type stars.

00,102
PB96-123294 Not available NTIS
National Inst. of Standards and Technology (PL), Boulder, CO. Quantum Physics Div.
High Velocity Plasm in the Transition Region of Au Mic: A Stellar Analog of Solar Explosive Events.
Final rept.
J. L. Linsky, and B. E. Wood. 1994, 3p.
Contract NASA-S-56500-D
Sponsored by National Aeronautics and Space Administration, Washington, DC.
Pub. in Cool Stars, Stellar Systems, and the Sun, Cambridge Workshop (8th), ASP Conference Series, Athens, GA., October 1993, v64 p441-443.

Keywords: *Late stars, *Stellar mass ejecta, *Ultraviolet spectra, Stellar flares, Line spectra, Emissions spectra, Stellar intensity flux, Carbon isotopes, Silicon isotopes, High resolution, Reprints.

High-resolution GHRS spectra of the dMOe flare star AU Mic shows C IV and Si IV line profiles that are unexpectedly broad and can be fit accurately by two Gaussians (one narrow and the other broad), The broad Gaussian components of the AU Mic line profiles resemble closely the C IV profiles observed in solar explosive events in emerging flux regions (EFRs). The authors therefore propose that the EFR is the solar analog of the most active component of the transition region of this and presumably other dMe flare stars.

00,103
PB96-123302 Not available NTIS
National Inst. of Standards and Technology (PL), Boulder, CO. Quantum Physics Div.
Radio and X-ray Emissions from Chemically Peculiar B- and A-Type Stars: Observations and a Model.
Final rept.
J. L. Linsky. 1993, 10p.
Contracts NASA-W17772, NASA-H-04630
Sponsored by NASA Scientific and Technical Information Facility, Baltimore, MD.
Pub. in Peculiar versus Normal Phenomena in A-Type and Related State P, IAU Colloq. 138, Trieste, Italy, July 1993, v44 p507-516.

Keywords: *Peculiar stars, *A stars, *Stellar temperature, Magnetic stars, Radio stars, Stellar spectra, Radio emission, X ray emission, Stellar luminosity, Stellar coronae, Stellar magnetosphere, Reprints.

The author argues that the magnetic chemically peculiar (CP) stars hotter than about spectral type A2 display many of the activity phenomena seen in the most active late-type stars. In particular, many CP stars are luminous nonthermal radio and coronal x-ray sources like the RS CVn systems. A wind-fed magnetosphere model has been proposed to explain both the nonthermal radio and the x-ray emission. In this model the stellar wind plays the role of a mechanical energy source analogous to the role played by convection in the active late-type stars.

00,104
PB96-123310 Not available NTIS
National Inst. of Standards and Technology (PL), Boulder, CO. Quantum Physics Div.
Redshifts in Stellar Transition Regions.
Final rept.
J. L. Linsky, B. E. Wood, and C. Andrulis. 1994, 3p.
Contract NASA-S-56560-D
Sponsored by National Aeronautics and Space Administration, Washington, DC.
Pub. in Cool Stars, Stellar Systems, and the Sun, Cambridge Workshop (8th), ASP Conference Series, Athens, GA., October 1993, v64 p59-61.

Astrophysics

Keywords: *Red shift, *Stellar spectra, *Spectral resolution, Stellar chromospheres, Stellar coronae, Late stars, Ultraviolet spectra, Emission spectra, Transition probabilities, Reprints.

The authors present moderate resolution GHRS spectra of the stars Procyon (F5 IV-V), AU Mic (MO Ve), Beta Gem (K0 III), Capella (G0 III + G8 III), alpha TrA (K2 II-III), and Beta Dra (G2 II-Ib) to study the phenomenon of redshifted transition region lines first observed by IUE. The authors' GHRS data show redshifts for all of these stars except alpha TrA, but they find no correlation between redshift and stellar activity.

00,105
PB96-123336 Not available NTIS
National Inst. of Standards and Technology (PL), Boulder, CO. Quantum Physics Div.
Transition Regions of Capella.
Final rept.
J. L. Linsky, B. E. Wood, A. Brown, T. R. Ayres, C. Andrulis, and P. Judge. 1994, 3p.
Contract NASA-S-56460-D
Sponsored by National Aeronautics and Space Administration, Washington, DC.
Pub. in Cool Stars, Stellar Systems, and the Sun, Cambridge Workshop (8th), ASP Conference Series, Athens, GA., v64 p62-64 Oct 93.

Keywords: *Binary stars, *Transition probabilities, *Stellar chromospheres, *Ultraviolet spectra, Emission spectra, Low resolution, Moderate resolution, High resolution, Red shift, Electron density, Hubble Space Telescope, Reprints, *Capella star.

The authors report on an extensive set of observations of Capella obtained with GHRS on HST at orbital phase 0.26. The data set consisting of low, moderate, and high resolution spectra, allows the authors to separate the contributions of each star to many of the emission lines and to measure line centroid redshifts. The authors estimate the electron density in the transition region of the hotter star and construct an emission measure distribution.

00,106
PB96-135264 Not available NTIS
National Inst. of Standards and Technology (PL), Boulder, CO. Quantum Physics Div.
Recalibration for the Final Archive of the International Ultraviolet Explorer (IUE) Satellite.
Final rept.
J. L. Linsky, and J. Nochols-Bohlin. 1993, 8p.
Pub. in Proceedings of the Workshop on the Vacuum Ultraviolet Calibration of Space Experiments (9th), Boulder, CO., March 1993, p197-204.

Keywords: *IUE, *Ultraviolet spectra, *Calibration, *Data storage systems, Flux density, Signal to noise ratio, Ultraviolet radiation, Ultraviolet astronomy, Astronomical satellites, Reprints.

For the past several years, the IUE Project has been developing the software needed to reprocess the entire data set into a form suitable for its Final Archive. The object of the Final Archive Project is to produce a uniform archive of all spectra, including enhanced signal-to-noise and corrections for fixed pattern noise and scattered light, and new algorithms for sensitivity changes with time and spectrography temperature. The Final Archive will use the new Signal Weighted Extraction Technique (Kinney, Bohlin, and Neill 1991) to extract spectra with the highest feasible signal/noise and will use the bet available absolute flux calibration. The present brief report will summarize the absolute flux calibration approach used in preparing the Final Archive.

00,107
PB96-176706 Not available NTIS
National Inst. of Standards and Technology (PL), Boulder, CO. Quantum Physics Div.
Developments in Stellar Coronae.
Final rept.
J. L. Linsky. 1995, 4p.
See also PB87-223798.
Pub. in Transactions of IAU, Theory of Stellar Atmospheres, p414-417 Sep 95.

Keywords: *Stellar coronas, *Observation, *Radio sources(Astronomy), *X ray sources, Binary stars, Extraterrestrial radiowaves, X ray spectra, X rays, Astronomical observatories, Spaceborne astronomy, ROSAT mission, Hubble Space Telescope, Extreme Ultraviolet Explorer Satellite, Astro missions(STS), Japanese spacecraft, HEAO 2, Reprints.

The report summarizes the major developments (observational and theoretical) in the study of stellar coronae driven in large part by the analysis of the new data sets from ROSAT, EUVE, ASCA, Yohkoh, and HST, together with the continuing analysis of Einstein data and radio observations.

00,108
PB96-176714 Not available NTIS
National Inst. of Standards and Technology (PL), Boulder, CO. Quantum Physics Div.
Transition Regions of Capella (1995).
Final rept.
J. L. Linsky, B. E. Wood, P. Judge, T. R. Ayres, A. Brown, and C. Andrulis. 1995, 20p.
Contract NASA-S-56500-D
See also PB96-123336. Sponsored by National Aeronautics and Space Administration, Washington, DC.
Pub. in Astrophysical Jnl., v442 p381-400, 20 Mar 95.

Keywords: *Binary stars, *Transition probabilities, *Stellar chromospheres, *Ultraviolet spectra, Emission spectra, High resolution, Red shift, Electron density, Hubble Space Telescope, Stellar coronas, Normal density functions, Reprints, *Capella star.

The authors have used the Goddard High Resolution Spectrometer (GHRS) to observe the spectroscopic binary system Capella (G8 III + G1 III).

00,109
PB96-200217 Not available NTIS
National Inst. of Standards and Technology (PL), Boulder, CO. Quantum Physics Div.
Riass Coronathon: Joint X-ray and Ultraviolet Observations of Normal F-K Stars.
Final rept.
T. R. Ayres, T. A. Fleming, A. Brown, R. C. Dempsey, and J. L. Linsky. 1995, 32p.
Pub. in Astrophysical Jnl. Supplement Series, v96 p223-259 Jan 95.

Keywords: *X ray astronomy, *Ultraviolet astronomy, *Sky surveys(Astronomy), *Stellar atmospheres, X ray stars, Late stars, F stars, G stars, K stars, Stellar coronas, Chromosphere, Extreme ultraviolet radiation, Ultraviolet emission, Emission spectra, ROSAT mission, IUE, Reprints.

Between 1990 August and 1991 January the ROSAT/IUE All Sky Survey (RIASS) coordinated pointings by the International Ultraviolet Explorer with the continuous X-ray/EUV mapping by the Roentgensatellit. The campaign provided an unprecedented multiwavelength view of a wide variety of cosmic sources. We report findings for F-K stars, a large proprtion of the RIASS targets. Forty-eight of our 91 'Coronathon' candidates were observed by the IUE during the campaign. For stars missed by the IUE, we supplemented the ROSAT survey fluxes with archival UV spectra and/or follow-on observations. In addition to the coordinated work, we examined the UV emission histories of the Coronathon stars.

00,110
PB96-200621 Not available NTIS
National Inst. of Standards and Technology (PL), Boulder, CO. Quantum Physics Div.
Accurate Measurements of the Local Deuterium Abundance from HST Spectra.
Final rept.
J. L. Linsky. 1996, 4p.
Contract NASA-S-56460-D
Sponsored by National Aeronautics and Space Administration, Washington, DC.
Pub. in Examining the Big Bang and Diffuse Background Radiations, p529-532 1996.

Keywords: *Deuterium, *Abundance, *Ultraviolet stars, Hydrogen, Isotope ratio, Interstellar matter, Intergalactic media, Line spectra, Absorption spectra, Baryons, H lines, D lines, Lyman alpha radiation, Line of sight, Cosmology, Galactic evolution, Hubble space telescope, Reprints.

An accurate measurement of the primordial value of D/H would provide a critical test of nucleosynthesis models for the early universe and the baryon density. I briefly summarize the ongoing HST observations of the interstellar H and D Lyman-alpha absorption for lines of sight to nearby stars and comment on recent reports of extragalactic D/H measurements.

00,111
PB96-200639 Not available NTIS
National Inst. of Standards and Technology (PL), Boulder, CO. Quantum Physics Div.
Deuterium and the Local Interstellar Medium: Properties for the Procyon and Capella Lines of Sight.
Final rept.
J. L. Linsky, A. Diplas, B. E. Wood, B. D. Savage, A. Brown, and T. R. Ayres. 1995, 17p.
Contract NASA-S-56500-D
See also PB95-202842. Sponsored by National Aeronautics and Space Administration, Washington, DC.
Pub. in Astrophysical Jnl., v451 p335-351 Sep 95.

Keywords: *Deuterium, *Ultraviolet star, *Line of sight, *Interstellar matter, Stellar spectra, Line spectra, D lines, H lines, Hydrogen, Stellar composition, Abundance, Isotope ratio, Lyman alpha radiation, Emission spectra, Absorption spectra, Reprints, Pryocyon star, Capella star.

We present Goddard High-Resolution Spectrograph observations of the interstellar H I and D I Ly(alpha) lines and the Mg II and Fe II resonance lines formed along the lines of sight toward the nearby stars Procyon (3.5 pc, l=214 degrees, b=13 degrees) and Capella (12.5 pc, l=163 degrees, b=5 degrees). New observations of Capella were obtained at orbital phase 0.80, when the radial velocities of the intrinsic Ly(alpha) emission lines of each star were nearly reversed from those of the previous observations at phase 0.26 (analyzed by Linsky et al.). For the analysis of the Procyon line of sight we assumed that (D/H)(sub LISM) = 1.6 x 10 to the -5th power, the same value as for the Capella line of sight, and we modified the broadened solar profile to achieve agreement between the simulated and observed line profiles.

00,112
PB97-122295 Not available NTIS
National Inst. of Standards and Technology (CSTL), Gaithersburg, MD.
Experimental Determination of the Rate Constant for the Reaction of C2H3 with H2 and Implications for the Partitioning of Hydrocarbons in Atmospheres of the Outer Planets.
Final rept.
A. Fahr, P. S. Monks, L. J. Stief, and A. H. Laufer. 1995, 8p.
Pub. in ICARUS, v116 p415-422 1995.

Keywords: *Gas giant planets, *Planetary atmospheres, *Hydrocarbons, Atmospheric chemistry, Chemical reaction kinetics, Partition, Absorption spectroscopy, Gas chromatography, Hydrogen ions, Vinyl radicals, Jupiter atmosphere, Photolysis, Laser pumping, Reprints, Rate constants.

The reaction between C2H3 and H2 has been suggested to be potentially important in accounting for observational data on the abundance of low-molecular weight hydrocarbons in the atmospheres of the giant planets. In the work, the room temperature rate constant for the reaction of the vinyl radical with molecular hydrogen has been determined by employing laser photolysis coupled to a kinetic-absorption spectroscopic technique and separately via a gas chromatographic product analysis technique.

ATMOSPHERIC SCIENCES

General

00,113
PB96-175666 PC A07/MF A02
National Inst. of Standards and Technology, Gaithersburg, MD.
Journal of Research of the National Institute of Standards and Technology, January/February 1996. Volume 101, Number 1.
1996, 115p.
See also PB96-175674 through PB96-175690 and PB96-159215. Also available from Supt. of Docs. as SN703-027-00068-7.

Keywords: *Marine atmospheres, *Experimental mechanics, *Electron beams, *Calibration, Reprint.

Contents:
An International Marine-Atmospheric 222Rn Measurement Intercomparison in Bermuda Part I:
NIST Calibration and Methodology for Standardized Sample Additions;
An International Marine-Atmospheric 222Rn Measurement Intercomparison in Bermuda Part II:
Results for the Participating Laboratories;
Theory of Electron Beam Moire.

00,114
PB96-175674 (Order as PB96-175666, PC A07/MF A02)
National Inst. of Standards and Technology, Gaithersburg, MD.
International Marine-Atmospheric (222)Rn Measurement Intercomparison in Bermuda. Part 1. NIST Calibration and Methodology for Standardized Sample Additions.
R. Colle, M. P. Unterweger, P. A. Hodge, and J. M. R. Hutchinson. 1996, 19p.
Included in Jnl. of Research of the National Institute of Standards and Technology, v101 n1 p1-19 Jan/Feb 96.

Keywords: *Marine atmospheres, *Calibration, Environment, Reprints, Intercomparison, Measurement, Standards, Radium-226, Radon-222.

As part of an international 222Rn measurement intercomparison conducted at Bermuda in October 1991, NIST provided standardized sample additions of known, but undisclosed ('blind') 222Rn concentrations that could be related to U.S. national standards. The standardized sample additions were obtained with a calibrated 226Ra source and a specially-designed manifold used to obtain well-known dilution factors from simultaneous flow-rate measurements. The additions were introduced over sampling periods of several hours (typically 4 h) into a common streamline on a sampling tower used by the participating laboratories for their measurements. The standarized 222Rn activity concentrations for the intercomparision ranged from approximately 2.5 Bq.m-3 to 35 Bq.m-3 (of which the lower end of this range approached concentration levels for ambient Bermudian air) and had overall uncertainties, approximating a 3 standard deviation uncertainty interval, of about 6% to 13%. This paper describes the calibration and methodology for the standardized sample addition.

00,115
PB96-175682 (Order as PB96-175666, PC A07/MF A02)
National Inst. of Standards and Technology, Gaithersburg, MD.
International Marine-Atmospheric (222)Rn Measurement Intercomparison in Bermuda. Part 2. Results for the Participating Laboratories.
R. Colle, M. P. Unterweger, J. M. R. Hutchinson, B. Ardouin, J. G. Kay, J. P. Friend, B. W. Blomquist, W. Nadler, T. T. Dang, R. J. Larsen, A. R. Hutter, S. Whittlestone, and G. Polian. 1996, 25p.
Prepared in cooperation with Australian Nuclear Science and Technology Organisation, Sutherland., Centre des Faibles Radioactives, Gif-sur-Yvette (France)., Drexel Univ., Philadelphia, PA. Dept. of Chemistry. and Department of Energy, New York. Environmental Measurements Lab.
Included in Jnl. of Research of the National Institute of Standards and Technology, v101 n1 p21-46 Jan/Feb 96.

Keywords: *Marine atmospheres, Environment, Air, Reprints, Intercomparison, Measurement, Radon-222.

As part of an international 222Rn measurement intercomparison of instruments used to measure atmospheric 222Rn, four participating laboratories made nearly simultaneous measurements of 22Rn activity concentration in commonly sampled, ambient air over approximately a 2 week period, and three of these four laboratories participated in the measurement comparison of 14 introduced samples with known, but undisclosed ('blind') 222Rn activity concentration. The exercise was conducted in Bermuda in October 1991.

Aeronomy

00,116
AD-A292 039/5 PC A01/MF A01
National Bureau of Standards, Washington, DC. Inst. for Basic Standards.
Comparison of Meteor Activity with Occurrence of Sporadic E Reflections.
V. C. Pineo. 14 Jul 50, 2p.
Pub. in Science, v112 n2898 p50-51, 14 Jul 50.

Keywords: *Meteors, *Ionization trails, *Meteor burst communications, Ionosphere, Reprints, Electromagnetic wave reflections, E region, Sporadic e layer.

In a previous paper, the writer presented evidence to show that the character of the echo obtained from a trail of ionization produced by a meteor is different in character from the echoes frequently obtained on ionosphere recorders and described as sporadic E reflections. Since the presentation of that paper a statistical study has been carried out on the frequency of reflections obtained with the meteor equipment in operation by the Central Radio Propagation Laboratory of the National Bureau of Standards, and the frequency of occurrence of sporadic E reflections observed over the same hiterval with the automatic multifrequency ionosphere recorder operated by the laboratory. By sporadic E, also sometimes called abnormal E, is meant what Lovell referred to as long duration abnormalities in the E region as distinguished from what Appleton and Naismith referred to as ionization bursts. In the scaling of sporadic E data from the vertical incidence ionosphere records, extreme eare was taken to see that only reflections of the sporadic E type were scaled. (MM).

00,117
PB96-148101 Not available NTIS
National Inst. of Standards and Technology (CSTL), Gaithersburg, MD. Chemical Kinetics and Thermodynamics Div.
Free Radical Chemistry of the Atmospheric Aqueous Phase.
Final rept.
R. E. Huie. 1995, 46p.
See also PB90-218207.
Pub. in Free Radical Chemistry of the Atmospheric Aqueous Phase, Chapter 10, p374-419 1995.

Keywords: *Atomspheric chemistry, *Free radicals, Electron transfer, Ionizing radiation, Aerosols, Fog, Clouds(Meteorology), Chemical reactions, Reprints, *Aqueous phase, Gas phase.

The chemical environment of the atmospheric aqueous phase: clouds, fogs, aerosols, and raindrops, has a rich chemistry strongly dependent upon the surrounding gas phase. For many atmospheric species, this environment is quite different than the gas phase; in water, they may hydrate, protonate, deprotonate, or dissociate. Most important, the aqueous phase opens up the possibility of an entirely new class of chemical reaction: electron transfer. In this review, the author will discuss the aqueous-phase chemistry of a number of free radicals of possible importance to the aqueous phase of the atmosphere.

00,118
PB97-112577 Not available NTIS
National Inst. of Standards and Technology (CSTL), Gaithersburg, MD. Chemical Kinetics and Thermodynamics Div.
Atmospheric Lifetimes of HFC-143a and HFC-245fa: Flash Photolysis Resonance Fluorescence Measurements of the OH Reaction Rate Constants.
Final rept.
V. L. Orkin, R. E. Huie, and M. J. Kurylo. 1996, 6p.
Pub. in Jnl. of Physical Chemistry, v100 p8907-8912 1996.

Keywords: *Atmospheric chemistry, *Chemical reaction kinetics, *Hydroxyl radicals, *Hydrofluorocarbons, Photolysis, Fluorescence, Temperature, Arrhenius equation, Error analysis, Constants, Reprints.

Rate constants for the reactions of hydroxyl radicals with Ch3CF3 (HFC-143a) and CHF2CH2CF3 (HFC-245fa) have been measured using the flash photolysis resonance fluorescence technique over the temperature range 273-370 K. A data analysis procedure is presented which should minimize rate constant errors introduced by the possible effects of radical diffusion.

Dynamic Meteorology

00,119
PB94-143427 PC A03/MF A01
Massachusetts Inst. of Tech., Cambridge. Dept. of Mechanical Engineering.
Computational Model for the Rise and Dispersion of Wind-Blown, Buoyancy-Driven Plumes. Part 2. Linearly Stratified Atmosphere.
Final rept.
X. Zhang, and A. F. Ghoniem. Dec 93, 49p, NIST-GCR-93-637.
Contract 60NANB0D1036
Sponsored by National Inst. of Standards and Technology (BFRL), Gaithersburg, MD.

Keywords: *Wind direction, *Dispersions, *Plumes, *Buoyancy, Mathematical models, Atmospheric composition, Stratification, Dynamics, Atmospheric density, Vorticity, Height, Lagrangian functions, Baroclinic vorticity.

A multi-dimensional computational model of wind-blown, buoyancy-driven flows is applied to study the effect of atmospheric stratification on the rise and dispersion of plumes. The model utilizes Lagrangian transport elements, distributed in the plane of the plume cross section normal to the wind direction, to capture the evolution of the vorticity and density field, and another set of elements to model the dynamics in the atmosphere surrounding the plume. Solutions are obtained for a case in which atmospheric density changes linearly with height. Computational results show that, similar to the case of a neutrally stratified atmosphere, the plume acquires a kidney-shaped cross section which persists for a long distance downstream the source and may bifurcate into separate and distinct lumps.

00,120
PB95-220471 PC A03/MF A01
National Inst. of Standards and Technology (BFRL), Gaithersburg, MD. Structures Div.
Extreme Wind Estimates by the Conditional Mean Exceedance Procedure.
J. L. Gross, N. A. Heckert, J. A. Lechner, and E. Simiu. Apr 95, 20p, NISTIR-5531.

Keywords: *Wind velocity, *Estimating, Functions(Mathematics), Mathematical models.

We describe work aimed at improving procedures for the estimation of non-tornadic extreme wind speeds, regardless of their direction, in regions not subjected to hurricanes. Using the Generalized Pareto Distribution (GPD) approach and the Conditional Mean Exceedance (CME) estimation method, we analyze 115 17-year to 52-year sets of largest annual speeds and sets drawn from 48 15-year to 26-year records of maximum daily wind speeds. Based on this analysis we attempt an assessment of the widely held belief that the Gumbel distribution with site-dependent location and scale parameters is a universal model of extreme wind speeds. Some of our results suggest that the reverse Weibull distribution is a more appropriate model. This would result in more reasonable estimates of wind-induced failure probabilities and wind load factors than the corresponding estimates based on the Gumbel distribution. However, our assessment is so far only tentative owing to uncertainties inherent in our results. Future work based on lower thresholds (larger data samples) and alternative estimation methods is planned.

Meteorological Data Collection, Analysis, & Weather Forecasting

00,121
AD-A295 319/8 PC A02/MF A01
National Bureau of Standards, Gaithersburg, MD.
Low-Temperature Performance of Radiosonde Electric Hygrometer Elements.
Research paper.
A. Wexler. Jul 49, 8p, RP2003.
Pub. in Jnl. of Research of the National Bureau of Standards, v43 p49-56, Jul 49.

Keywords: *Radiosondes, *Hygrometers, Reprints, Low temperature, Electric power, Calibration, Range(Extremes), Humidity, Atmospheric sounding.

The performance of radiosonde electric hygrometer elements was investigated in the temperature range

from 0 to 400 C. It was found that an element indicated relative humidity with an average deviation of + 2.4-percent relative humidity from the average calibration for all of the elements tested. The maximum deviation in indication of any element did not exceed 10.5-percent relative humidity. The lag in response was found to increase markedly with decrease in temperature, to depend upon the magnitude and direction of relative humidity change, and the relative humidity from which the change was made.

00,122
PB95-108791 Not available NTIS
National Inst. of Standards and Technology (NEL), Gaithersburg, MD. Fire Measurement and Research Div.
Global Climatic Effects of Aerosols: The AAAR Symposium.
Final rept.
J. E. Penner, and G. W. Mulholland. 1991, 2p.
Pub. in Atmospheric Environment A 25, n11 p2433-2434 1991.

Keywords: *Meetings, *Aerosols, *Climatic changes, *Global aspects, *Air pollution, Nuclear war, Global warming, Ozone depletion, Reprints, *American Association of Aerosol Research.

The American Association of Aerosol Symposium on global climatic effects of aerosols included papers on the aerosol-related phenomena for the following three topics: Climatic Effect of Nuclear War; Global Warming; and The Ozone Hole. This introduction to the symposium volume highlights key findings presented at the meeting.

Meteorological Instruments & Instrument Platforms

00,123
AD-A278 851/1 PC A03/MF A01
National Bureau of Standards, Gaithersburg, MD.
Methods of Measuring Humidity and Testing Hygrometers.
A. Wexler, and W. G. Brombacher. 28 Sep 51, 22p, NBS-512.

Keywords: *Humidity, *Hygrometers, *Measuring instruments, Water, Test and evaluation, Gases, Atmospheres, Calibration, Dew point, Mechanical properties, Electrical properties, Gravimetry, Thermal conductivity, Pressure, Volume, Dielectrics, Psychrometers, Meteorology, Earth sciences, Climate, Index of refraction.

No abstract available.

00,124
PB95-150132 Not available NTIS
National Inst. of Standards and Technology (BFRL), Gaithersburg, MD. Fire Science Div.
Radiometric Model of the Transmission Cell-Reciprocal Nephelometer.
Final rept.
G. W. Mulholland, and N. P. Bryner. 1994, 15p.
Pub. in Atmospheric Environment 28, n5 p873-887 1994.

Keywords: *Nephelometers, *Aerosols, *Light scattering, *Radiometric correction, *Atmospheric scattering, Aerosol generators, Microspheres, Polystyrene, Absorptivity, Optical measuring instruments, Atmospheric optics, Reprints.

A radiometric model has been developed to assess the effects of angular truncation, finite size of the detector, and angle response characteristics of the cosine sensor on the measurement of the total scattering coefficient by a transmission cell-reciprocal nephelometer. These effects are computed for monodisperse polystyrene spheres over the size range 0.02-8 micrometers based on Mie theory and for smoke agglomerates ranging from 10 to 10(exp 7) primary units based on the Fisher-Burford approximation. The accuracy of the model calculations is determined by comparison with exact solutions for the case of a detector with an infinitesimal area and for a finite area detector with a diffuse scattering function. The predicted results are compared with measured results for six different sizes of monodisperse polystyrene sphere aerosols with particle diameters in the range 0.1-2.35 micrometers. The measurements were carried out as a function of the distance between the laser beam and detector for 1.3 and 2.7 cm diameter cosine sensors. A table of design parameters for making accurate total scattering measurements is obtained for both spheres and agglomerates. An accuracy of + or - 5% was obtained for spherical particles with diameters less than or equal to 1.1 micrometers with our TCRN, and we estimate that similar performance would be obtained for smoke agglomerates with up to 3 x 10(exp 3) primary spheres per agglomerate.

00,125
PB96-214648 PC A04/MF A01
National Inst. of Standards and Technology (PL), Gaithersburg, MD. Optical Technology Div.
Report on USDA Ultraviolet Spectroradiometers.
E. A. Early, and A. Thompson. Jul 96, 36p, NISTIR-5871.

Keywords: *Spectroradiometers, *Ultraviolet spectroradiometers, Radiometers, Linearity, Responsivity, Slit-scatter, Stray-light, Wavelength.

Two ultraviolet spectroradiometers manufactured by Research Support Instruments, Inc., and the Atmospheric Science Research Center for the U.S. Department of Agriculture monitoring network were characterized. From measurements of the linearity of the instruments, the dead time of the photon counting system was approximately 12 ns. From spectral scans of the emission lines of a Hg lamp, the wavelength precision of the instrument of 0.02 nm, while the accuracy is 0.04 nm. Spectral scans of the 325 nm line of a HeCd laser showed that the bandwidth of the instruments is 0.3 nm and that the monochromators have a stray light rejection of 10 to the minus 8 power. The spectral irradiance responsivity, determined with FEL-type irradiance standards lamps, changes both with movement of the instruments and with time.

Physical Meteorology

00,126
PB94-198215 Not available NTIS
National Inst. of Standards and Technology (NML), Gaithersburg, MD. Chemical Thermodynamics Div.
Thermodynamic Properties of Gas Phase Species of Importance to Ozone Depletion.
Final rept.
S. Abramowitz, and M. W. Chase. 1991, 6p.
Pub. in Pure and Applied Chemistry 63, n10 p1449-1454 1991.

Keywords: *Ozone depletion, *Thermodynamic properties, *Vapor phases, *Atmospheric chemistry, *Spectrum analysis, Chlorine oxides, Reaction kinetics, Stratosphere, Air pollution, Reprints.

Thermodynamic and spectroscopic data have been evaluated for several chlorine-oxygen gas phase species of interest in the study of ozone depletion models. The evaluated data have been used to compute JANAF Thermochemical Tables for these species. The data will be discussed and applied to several proposed models for ozone depletion. The recent catalytic cycle involving ozone loss by ClO and Cl2O2 in the Antarctic stratosphere is discussed.

00,127
PB95-219416 PC A05/MF A01
National Inst. of Standards and Technology (BFRL), Gaithersburg, MD. Structures Div.
Extreme Wind Distribution Tails: A 'Peaks Over Threshold' Approach.
Building science series.
E. Simiu, and N. A. Heckert. Mar 95, 80p.
Also available from Supt. of Docs. Prepared in cooperation with Johns Hopkins Univ., Baltimore, MD. Dept. of Civil Engineering. Sponsored by National Science Foundation, Arlington, VA.

Keywords: *Wind velocity, *Extreme value problems, Wind effects, Wind pressure, Wind loads, Dynamic Loads, Winds, Structural engineering, Statistical analysis, Weibull distribution, Graphs(Charts), *Peaks over threshold methods, Load factors, Extreme winds, Probabilistic models.

The authors seek to ascertain whether the reverse Weibull distribution is an appropriate extreme wind speed model by performing statistical analyses based on the 'peaks over threshold' approach. The data are taken principally from records of the largest daily wind speeds obtained over periods of 15 to 26 years at 44 U.S. weather stations in areas not subjected to mature hurricane winds. From these records the authors create samples with reduced mutual correlation among the data. In our opinion, the analyses provide persuasive evidence that extreme wind speeds' are described predominantly by reverse Weibull distributions, which unlike the Gumbel distribution have finite upper tail and lead to reasonable estimates of wind load factors. Instructions are provided for accessing the data and attendant programs.

BEHAVIOR & SOCIETY

General

00,128
FIPS PUB 10-4 PC E05
National Inst. of Standards and Technology (CSL), Gaithersburg, MD.
Countries, Dependencies, Areas of Special Sovereignty, and Their Principal Administrative Divisions. Category: Data Standards and Guidelines; Subcategory: Representation and Codes.
6 May 93, 56p.
Supersedes FIPS PUB 10-3.

Keywords: *Geocoding, *Geography, *Classification, *Foreign countries, Territories, Data processing, Data elements, Data codes, Administrative divisions, Dependencies, Provinces, Data standards and guidelines, Representation and codes, Federal Information Processing Standards.

This Standard provides a list of the basic geopolitical entities in the world, together with the principal divisions that comprise each entity. Each basic geopolitical entity that was listed in FIPS PUB 10-3, Countries, Dependencies, and Areas of Special Sovereignty, as updated, is included; it is represented by the same two-character alphabetic, country code. Each principal administrative division is identified by a four-character code consisting of the two-character country code followed by a two-character administrative division code.

00,129
PB95-502563 CP T05
National Inst. of Standards and Technology (CSL), Gaithersburg, MD.
Codes for Named Populated Places, Primary County Divisions, and Other Locational Entities of the United States (FIPS PUB 55-3) (on Magnetic Tape).
Data file.
Nov 94, mag tapes.
This product contains text only. Customers must provide their own search and retrieval software. Also available in paper copy, order as FIPS PUB 55-3-DC. Supersedes PB87-142436.
Available in 9-track, ASCII character set tape, 1600 bpi, 6250 bpi, or 3480 cartridge. Documentation included; may be ordered separately as FIPS PUB 55-3.

Keywords: *Data file, *Communities, *Counties, *Federal information processing standards, United States, Coding, Urban areas, Villages, Census tracts, Reservations, Airports, Military facilities, National parks, Postal service, Geographic areas, Magnetic tapes.

This guideline implements ANS X3. 47-1993, Information Systems-Codes, Structure and Data Requirements for the Identification of Named Populated Places, Primary County Divisions, and Other Locational Entities of the United States and its Outlying and Associated Areas for Information Interchange, as amplified herein, as a Federal Information Processing Standard (FIPS). This publication, which supersedes FIPS PUB 55-2 and 55DC-4, provides a 2-character FIPS State code and a 5-character FIPS numeric code to uniquely identify each entity contained in a list of names of incorporated places, other communities and

settlements, primary county divisions (such as townships, New England towns, and census county divisions), American Indian and Alaska Native areas, airports, military bases, national parks, post offices, and other locational entities (except natural or physical features). A 2-character class code distinguishes the different types of geographic entities. The purpose of the codes is to promote the interchange of formatted, machine-sensible data.

00,130
PB95-503504 Diskette $30.00
National Inst. of Standards and Technology, Gaithersburg, MD.
Countries, Dependencies, Areas of Special Sovereignty, and Their Principal Administrative Divisions (for Microcomputers).
Data file.
Sep 95, 1 diskette.
This product contains text only. Customers must provide their own search and retrieval software. WordPerfect 5.1 can be used but is not contained on diskette. Supersedes PB87-222859.
The datafile is on one 3 1/2 inch DOS diskette, 1.44M high density. File format: ASCII text. Also available as paper copy, order number FIPSPUB 10-4.

Keywords: *Data file, *Geocoding, *Geography, *Classification, *Foreign countries, Territories, Data processing, Diskettes, Data elements, Data codes, Administrative divisions, Dependencies, Provinces, Data standards and guidelines, Representation and codes, Federal Information Processing Standards.

This standard provides a list of the basic geopolitical entities in the world, together with the principal divisions that comprise each entity. Each basic geopolitical entity that was listed in FIPS PUB 10-3 'Countries, Dependencies, and Areas of Special Sovereignty', as updated, is included; it is represented by the same two-character alphabetic, 'country code.' Each principal administrative division is identified by a four-character code consisting of the Two-character 'country code' followed by a two-character 'administrative division code.' This Standard supersedes FIPS 10-3 in its entirety.

Education, Law, & Humanities

00,131
ED-376 823 Not available NTIS
National Inst. of Standards and Technology, Gaithersburg, MD.
Information Infrastructure: Reaching Society's Goals. A Report of the Information Infrastructure Task Force Committee on Applications and Technology.
Sep 94, 160p, NIST-S-PUB-868.
Available from ERIC Document Reproduction Service (Computer Microfilm International Corporation), 3900 Wheeler Ave., Alexandria, VA 22304-5110.

Keywords: *Computer mediated communication, *Policy formation, *Public policy, *Technological advancement, Access to information, Computer networks, Copyrights, Criminology, Disabilities, Emergency programs, Government role, Humanities, Physical environment, Social change, Standards, Traffic safety, Transportation, *National Information Infrastructure, Electronic Libraries, Internet, Telecommuting.

Intended for public comment and discussion, this document is the second volume of papers in which the Information Infrastructure Task Force has attempted to articulate in clear terms, with sufficient detail, how improvements in the National Information Infrastructure (NII) can help meet other social goals. These are not plans to be enacted, but the material with which the citizens and their government may have a structured conversation, a purposeful interaction, and deliberation on the issues raised in the evolution of more capable means of information processing and human communications. Eight papers are presented in this volume: (1) NII: An Investment in People with Disabilities; (2) Supply and Demand of Electric Power and the NII; (3) Improving Transportation: The NII and Intelligent Transportation Systems; (4) Promoting Telecommuting: An Application of the NII; (5) The Effect of NII on Local, State, and Federal Emergency Management; (6) Public Empowerment with Environmental Information; (7) Arts, Humanities, and Culture on the NII; and (8) Public Safety and the NII: Supporting Law Enforcement and Criminal Justice. Six of the papers include references. (BBM).

00,132
PB94-173028 Not available NTIS
National Inst. of Standards and Technology (MEL), Gaithersburg, MD. Precision Engineering Div.
Investing in Education to Meet a National Need for a Technical-Professional Workforce in a Post-Industrial Economy.
Final rept.
D. A. Swyt. 1990, 10p.
Pub. in Keynote Paper NATO Advanced Research Conference, Eindhoven, Netherlands, October 9-12, 1990.

Keywords: *Education, *Fixed investment, *Labor force, Technology, Productivity, Economy, United States, Reprints.

Workforce data show that the U.S. is shifting from blue-collar production to technical-professional service as the basis of its post-industrial economy. The lesson of increased effectiveness with increased capital per person has not been lost on U.S. service industries which have for the last decade lead the U.S. economy in capital spending. In contrast, what may be the most important service industry -- basic public education -- has undergone a steep fifteen-year-long decline in its growth in capital investment per student. This suggests that means to focus on capital spending in basic education, such as instituting capital-equipment budgets, are in order.

00,133
PB94-188463 PC A03/MF A01
National Inst. of Standards and Technology (CSL), Gaithersburg, MD. Systems and Software Technology Div.
User Profile for Researchers Studying Objects: Implications for Computer Systems.
J. Moline. Apr 94, 25p, NISTIR-5415.
See also PB-235 952.

Keywords: *Humanities, *Information processing, *User needs, Artifacts, Computers, Information systems, Data acquisition, Requirements, Research projects, Imaging, Data base management, Computer communications, Documents, Information retrieval, Guidelines, Numismatics.

A group of twenty-five researchers who study objects was observed over a four year period. A variety of methods of data collection was used: observation, interview, questionnaires, and analysis of published materials. This report identifies the features needed in computer systems to facilitate the research of those who study objects. The researchers need to link objects with text, work with a variety of data types, and collaborate with colleagues over a computer network.

00,134
PB96-159769 Not available NTIS
National Inst. of Standards and Technology (TS), Gaithersburg, MD. Director's Office Technology Services.
Montgomery Education Connection and Resource Education Awareness Partnership Making Connections between Local Schools and NIST Volunteers.
Final rept.
D. R. Johnson. 1991, 8p.
Pub. in Editorial in R and D Magazine.

Keywords: *Information resources, Cooperation, Information dissemination, Resource assessment, Schools, Education, Reprints, *US NIST, *Public-private partnerships, Montgomery Education Connection, Montgomery County(Maryland).

Established in the Spring of 1984, the Montgomery Education Connection (MEC) is a non-profit public-private partnership formed specifically to link Montegomery County Public Schools and the county's employers. The mission is simply to share private sector resources to improve the education of our children and future employees. The objectives of the organization are to identify the school system needs, to identify community resources to meet those needs, and to identify business needs to which the school system can respond. The Resource Educational Awareness partnership (REAP) is the NIST in-house program that works with the MEC. The goal is to share NIST resources through presenters who visit the schools, through science kits and materials to loan, and through lab visits and special activities.

00,135
PB96-160874 Not available NTIS
National Inst. of Standards and Technology (CSL), Gaithersburg, MD. Systems and Software Technology Div.
Using a Multi-Layered Approach to Representing Tort Law Cases for Case-Based Reasoning.
Final rept.
B. B. Cuthill, and R. McCartney. 1993, 7p.
Pub. in Case-Based Reasoning Papers from the 1993 Workshop, Washington, DC., July 11-12, 1993, p41-47.

Keywords: *Litigation, *Information retrieval, Lawsuits, Comparisons, Knowledge representation, Information systems, Integrated systems, Reprints, *Case-based reasoning, Case indexing, Case representation, Case retrieval, Multi-layer systems.

This paper presents a multi-layered case representation for addressing the problem of comparing and indexing cases in a case-based reasoning system using both the facts and the underlying themes associated with those cases. In many domains, experts discuss problems in terms of multiple layers of abstract principles, classifying problems by conflicts, strategies, or themes important to the domain. Representing the case as a single flat frame does not support reasoning about the underlying themes in the case because it does not represent interconnections among the facts and themes of the case. Instead, a case-based reasoner should use a multi-layered representation including both these facts and interconnections.This representation has implications for much of the case-based reasoning process including case comparison, selection and retrieval mechanisms. The paper will describe the CHASER case-based reasoning system which uses a multi-layered case representation approach to reason about tort law cases.

00,136
PB96-179502 Not available NTIS
National Inst. of Standards and Technology (TS), Gaithersburg, MD. Office of Standards Services.
Consensus Process in Standards Development.
Final rept.
B. L. Collins. 1995, 17p.
Sponsored by National Center for Education Statistics, Washington, DC.
Pub. in Proceedings of Joint Conference on Standard Setting for Large-Scale Assessments, Washington, DC., October 5-7, 1994, v2 p203-219 Oct 95.

Keywords: *Education, *Standards, *Agreements, Procedures, Requirements, Process control, Product development, Systems engineering, Quality assurance, ISO, Reprints, US NIST, American National Standards Institute.

The American National Standards Institute (ANSI), all major standards developers in the United States, the National Institute of Standards and Technology (NIST), and the International Organization for Standardization (ISO) have each defined procedures for developing consensus. Although these procedures are generally applied to the development of product and process standards to ensure quality, safety, health, and/or environmental integrity, they may provide a useful model for evaluating the effectiveness of procedures and standards developed in the field of education. The general consensus process is described with particular focus on relevance for developing standards for education.

Job Training & Career Development

00,137
PB96-123161 Not available NTIS
National Inst. of Standards and Technology (CSL), Gaithersburg, MD. Systems and Software Technology Div.
Proposed International Interactive Courseware Standard.
Final rept.
W. F. Thode, L. A. Welsch, J. Keck, and S. Lewis. 1991, 10p.
Pub. in International Training Equipment Conference (ITEC) (2nd), Maastricht, Netherlands, April 15-17, 1991, 10p.

Keywords: *Video recording, *Training aids, *Standards, *Computer assisted instruction, Teaching

methods, Computer programs, Computer graphics, Military training, Interoperability, Interactive systems, Man computer interface, Reprints.

Millions of dollars are invested in the development of interactive courseware training to be delivered by microcomputer-based training systems, often with interactive video included. Significant development and delivery costs can be avoided if new interactive courseware materials can be made to operate on multiple delivery platforms. A standard that uses a virtual device interface is a flexible approach to interactive courseware portability. The US Department of Defense is adopting this standard as a requirement for future purchases of interactive courseware by the uniformed services. The interface is also under study by the US National Institute for Standards and Technology as a potential component of a general multimedia courseware architecture.

BIOMEDICAL TECHNOLOGY & HUMAN FACTORS ENGINEERING

Biomedical Instrumentation & Bioengineering

00,138
PB94-172012 Not available NTIS
National Inst. of Standards and Technology (MSEL), Gaithersburg, MD. Polymers Div.
Influence of Tempering Method on Residual Stress in Dental Porcelain.
Final rept.
K. Asaoka, N. Kuwayama, and J. Tesk. 1992, 5p.

Keywords: *Dental materials, *Residual stress, *Porcelain, Thermophysical properties, Cooling curves, Computer simulation, Metal strips, Reprints.

The porcelain component of a porcelain-fused-to-metal restoration is strengthened by residual (tempering) stresses which are induced by cooling procedures followed in dental laboratories. The thermophysical properties of materials and cooling rate are the main factors which determine the residual stress. In this paper, the temperatures in the midplane of body-porcelain disks were measured from a heat-soak temperature (1000 C) to room temperature during two different cooling procedures: slow cooling in air and forced-air cooling. Experimental results approximated exponential cooling wherein the cooling rates could be represented by a linear equation of temperature. Residual stresses, as affected by the tempering method and thickness of a porcelain disk, were calculated by computer simulation for regions away from the edges. The cooling rate dependencies of the glass transition temperature and the temperature distribution during cooling were also included. The cooling rates used in this simulation were derived from the tempering data.

00,139
PB94-172608 Not available NTIS
National Inst. of Standards and Technology (MSEL), Gaithersburg, MD. Polymers Div.
Adsorption of Low-Molecular-Weight Sodium Polyacrylate on Hydroxyapatite.
Final rept.
D. N. Misra. Oct 93, 5p.
Pub. in Jnl. of Dental Research 71, n10 p1418-1422 Oct 93. Sponsored by American Dental Association Health Foundation, Chicago, IL.

Keywords: *Molecular weight, *Polyacrylates, *Hydroxyapatites, *Adsorption, *Dental cements, Minerals, Electrostatics, Osmolar concentration, Phosphates, Teeth, Isotherms, Reprints.

Adsorption of low-molecular-weight sodium polyacrylate from aqueous solution onto synthetic hydroxyapatite was studied at room temperature so that the mechanism of adhesion of polyacrylate cements to tooth mineral could be elucidated. The adsorption isotherm of sodium polyacrylate was Langmuirian in shape and was thus qualitatively different from that of polyacrylic acid (Misra, 1991), which exhibited an adsorption maximum. The self-association of the molecules that probably causes the maximum to occur with polyacrylic acid was effectively absent for the relatively well-ionized, electrostatically repelling polyacrylate ions of the salt. With the adsorption of acrylate ions, the concentration of phosphate ions increased monotonically, while the concentration of calcium ions showed a minimum. The adsorption of sodium polycrylate was irreversible, as it was for polyacrylic acid.

00,140
PB94-172616 Not available NTIS
National Inst. of Standards and Technology (MSEL), Gaithersburg, MD. Polymers Div.
Interaction of Some Coupling Agents and Organic Compounds with Hydroxyapatite: Hydrogen Bonding, Adsorption and Adhesion.
Final rept.
D. N. Misra. 1994, 13p.
Pub. in Jnl. of Adhesion Science and Technology, v8 n2 p87-99 1994. Sponsored by American Dental Association Health Foundation, Chicago, IL.

Keywords: *Hydroxyapatites, *Adsorption, *Hydrogen bonding, *Organic compounds, *Adhesion, *Dental materials, Solutions, Cross-linking reagents, Bone cements, Dental cements, Osmolar concentration, Reprints.

Adhesion to hydroxyapatite (which is the structural prototype of bone or tooth mineral) is a first step towards the efficacious application of restorative composites and bone cements to teeth and bones. The key medium to effect chemical adhesion between the mineralized substrate and a composite resin is a coupling agent. On the basis of many adsorption studies, primarily by the author, which are reviewed in this paper, it is proposed that a potential coupling agent suitable for dental adhesion can develop strong and durable bonds with a substrate through its hydrogen-bonding functional groups. The coupling agents must also be polyfunctional or possess some hydrophobic moieties to be hydrolytically stable. The criterion defining the capability for adhesion of a compound to hydroxyapatite is determined through a study of its adsorption characteristics from a particular solvent. The stability of this bond in aqueous environments may be determined by desorbing the adsorbed compound with water. The surface orientation of a coupling agent and whether it is reversibly or irreversibly adsorbed from a solvent primarily depend on the balance between the type, location, and number of hydrophilic and hydrophobic moieties in the agent molecule. In the case of water-soluble ionic compounds as coupling agents, the uptake of the compounds will also be influenced by the concentrations of calcium, phosphate, and hydrogen ions in the solution.

00,141
PB94-172723 Not available NTIS
National Inst. of Standards and Technology (MSEL), Gaithersburg, MD. Polymers Div.
Effect of Two Initiator/Stabilizer Concentrations in a Metal Primer on Bond Strengths of a Composite to a Base Metal Alloy.
Final rept.
N. D. Richards, F. Eichmiller, S. V. Dickens, and F. V. Simoni. Mar 93, 4p.
Pub. in Dental Materials 9, p91-94 Mar 93. Sponsored by American Dental Association Health Foundation, Chicago, IL.

Keywords: *Dental materials, *Chemical bonds, *Composite materials, *Alloys, Additives, Amines, Peroxides, Stabilizers(Agents), Polymers, Polymerization, Adhesives, Reprints, Peroxide/benzoyl, Toluidine/N-N-dimethyl, Butylated hydroxytoluene, Pyrometallic glycerol dimethacrylate.

The study examined the effect of three additives, amine, peroxide and stabilizer, in two concentrations in a metal primer on the adhesion between a cast metal alloy and a resin composite using a 23 factorial statistical design. The additives, benzoylperoxide (BPO) used at 1% or 2% w/w and N,N-dimethyl-p-toluidine (DMPT) at 0.5% or 1.8% w/w, are polymerization initiators. The third additive, butylated hydroxytoluene (BHT) at 0.01% or 0.03% w/w, is used as a stabilizer. BPO and BHT were dissolved in an acetone solution containing 20% of the adhesive resin pyromellitic glyceroldimethacrylate (PMGDM). DMPT was in a separate acetone solution. Bonding resin and composite were applied over the primer and stored overnight in water. Bond strengths were determined by shearing the composite from the metal at a cross head speed of 0.5 mm/min.

00,142
PB94-172871 Not available NTIS
National Inst. of Standards and Technology (MSEL), Gaithersburg, MD. Polymers Div.
Dental Materials.
Final rept.
J. A. Tesk, J. M. Antonucci, F. C. Eichmiller, R. W. Waterstrat, A. C. Fraker, L. C. Chow, L. A. George, J. W. Stansbury, E. E. Parry, J. R. Kelly, and N. W. Rupp. 1993, 77p.
Pub. in Kirk-Othmer Encyclopedia of Chemical Technology, (Fourth Edition), v7 p946-1022 1993.

Keywords: *Dental materials, *Equipment and supplies, Dentistry, Composites, Porcelain, Metals, Glasses, Ceramics, Alloys, Polymers, Dental cements, Temporary dental restoration, Permanent dental restoration, Cost analysis, Reprints.

Dental therapy includes the replacement of hard and soft oral tissues lost through disease using inert materials that may be metallic, ceramic, or organic, or composites employing combinations of these three classes. The operative restorations and prostheses are made of amalgam, precious and nonprecious alloys, special cements, synthetic polymers, porcelain, and glass-ceramics. All must withstand the rigors of the oral environment. The accessory materials needed in the fabrication procedures include synthetic polymers, synthetic and natural gums and waxes, hydrocolloids, gypsums, and refractories. The total value of dental supplies and equipment manufactured in the United States in 1992 is estimated at about $1.2 billion. These materials are used by about 170,000 practicing dentists (1992) and >8,500 commercial dental laboratories employing about 40-50,000 technicians. The dental materials market is limited because the public does not buy directly except for toothpastes, mouthwashes, tooth brushes, denture aids, etc.

00,143
PB94-198397 Not available NTIS
National Inst. of Standards and Technology (MSEL), Gaithersburg, MD. Polymers Div.
Effect of Transformation of Alloy on Transient and Residual Stresses in a Porcelain-Metal Strip.
Final rept.
K. Asaoka, and J. A. Tesk. 1992, 6p.
Pub. in Residual Stresses - III, Science and Technology, v1 p626-631 1992.

Keywords: *Dental materials, *Phase transformations, *Alloys, *Stress analysis, *Computer simulation, *Composite materials, Thermal expansion, Residual stress, Porcelain, Metal strips, Ceramics, Transient loads, High strength, Reprints.

High strength dental alloys are usually strengthened by phase transformations which affect their coefficients of thermal expansion. These transformations can affect the stresses developed in porcelain-fused-to-metal (PFM) restorations. In order to aid the understanding of these effects, we conducted computer simulations of stresses developed in a PFM strip. Pd alloys were chosen as Pd-based alloys form the basis for some major alternatives to high cost gold alloys, yet can maintain many of the desirable characteristics. The Pd-Cu alloy system which has a super lattice at 40.3 atomic % Cu displays a typical first-order transformation feature. The transient stresses in the porcelains and alloy thermal contraction and curvature of a PFM beam were computed for cooling from a heat soak temperature to room temperature. The residual stress distribution in the composite was also computed. Effects of the transformation of the alloy on transient and residual stresses were revealed from the results of the simulations.

00,144
PB94-199049 Not available NTIS
National Inst. of Standards and Technology (MSEL), Gaithersburg, MD. Polymers Div.
Adhesion of Composites to Dentin and Enamel.
Final rept.
R. L. Bowen, and W. A. Marjenhoff. 1993, 4p.
Pub. in California Dental Association Jnl. 21, n6 p19-22 Jun 93. Sponsored by American Dental Association Health Foundation, Chicago, IL.

Keywords: *Adhesives, *Dental materials, *Dentin, *Enamels, Teeth, Composite materials, Oral hygiene, Reprints.

Extrapolations based on the history of the development of composites and an adhesion system for bonding dental resins and composites to hard tooth tissues can rightfully be the basis for strong optimism regarding future improvements in esthetic and conservative treatment modalities. Improved understanding of mechanisms of action and the clinical application steps common to current adhesion systems will certainly lead to improved oral health care.

00,145
PB94-199056 Not available NTIS
National Inst. of Standards and Technology (MSEL), Gaithersburg, MD. Polymers Div.
Development of an Adhesive Bonding System.
Final rept.
R. L. Bowen, and W. A. Marjenhoff. 1992, 6p.
Pub. in Operative Dentistry, Supplement 5, p75-80 1992. See also PB91-236539. Sponsored by American Dental Association Health Foundation, Gaithersburg, MD. Paffenbarger Research Center.

Keywords: *Acid bonded reaction cements, *Adhesives, *Dental materials, Enamels, Dentin, Teeth, Inorganic silicates, Composite materials, Aqueous solutions, Reprints.

Building on findings concerning adhesion to enamel, R. L. Bowen and his colleagues at the Paffenbarger Research Center, National Institute of Standards and Technology, began addressing and solving problems associated with (1) silicate cements and unfilled resins, (2) bonding in an aqueous environment, and (3) the development of an adhesion system for both dentin and enamel that could withstand various stresses. This article reviews the development of an adhesion system for bonding dental composites to dentin and enamel.

00,146
PB94-211240 Not available NTIS
National Inst. of Standards and Technology (MSEL), Gaithersburg, MD. Polymers Div.
Clinical Perspective on Dentin Adhesives.
Final rept.
F. C. Eichmiller. 1993, 3p.
Pub. in Jnl. of Indiana Dental Association 72, n5 p22-24 1993. Sponsored by American Dental Association Health Foundation, Chicago, IL.

Keywords: *Dental materials, *Adhesive bonding, *Dentistry, *Polymers, Dentin, Monomers, Acids, Surfaces, Reprints, Restorative materials.

The newer generation of dentin adhesives has changed the practice of restorative dentistry. Two features common to most of the bonding restorative materials are the ability to alter, through the use of acidic etching agents, the surface of the dentin and the ability to completely wet and re-infiltrate the altered dentin surface with a hydrophilic polymerizable monomer. The acidic etchants remove or break up the smear layer, partially demineralize and/or alter the mineral in the first few microns of the dentin surface, and expose the collagen fibril network. The hydrophilic adhesive monomers that contain both acidic and methacrylate groups on the same molecule are bifunctional in nature. These monomers are able to infiltrate the demineralized dentin due to their hydrophilic nature and polymerize to encapsulate the exposed collagen fibers. Available products can be divided into two broad categories: systems that contain a low concentration of adhesive monomer diluted in a volatile solvent and systems that use adhesive resins of moderate to high viscosity. Knowledge of the features and properties of dentin adhesives provides the needed rationale for the protocol of application and the proper choice of materials in restorative dentistry.

00,147
PB94-211257 Not available NTIS
National Inst. of Standards and Technology (MSEL), Gaithersburg, MD. Polymers Div.
Selective Inhibition of Crystal Growth on Octacalcium Phosphate and Nonstoichiometric Hydroxyapatite by Pyrophosphate at Physiological Concentration.
Final rept.
N. Eidelman, W. E. Brown, and J. L. Meyer. 1991, 10p.
Sponsored by American Dental Association Health Foundation, Chicago, IL.
Pub. in Jnl. of Crystal Growth 113, p643-652 1991.

Keywords: *Calcium phosphates, *Pyrophosphates, *Crystal growth, *Inhibitors, Apatites, Hydroxy compounds, Dental materials, Reprints, Hydroxyapatite, Biominerals.

Octacalcium phosphate, Ca8H2(PO4)6(dot)5H2O (OCP), appears to be a precursor in biomineral formation. The formation of OCP as the precursor is supported by the observation that stoichiometric hydroxyapatite, Ca5(PO4)3OH (OHAp), cannot form directly because of the presence of its growth inhibitors in serum. Therefore, the effects of the physiological concentration of pyrophosphate (P2O7(4-)), one of the most important calcium phosphate growth inhibitors in blood, on calcium phosphate growth rates on OCP and nonstoichiometric OHAp (apatite) seeds were measured. The amounts of seed crystals used to initiate the growth were adjusted by trial and error so that the control growth rates (in the absence of P2O7(4-)) were the same on both OCP and apatite seeds at a given supersaturation. The crystal growth on both kinds of seed crystals from supersaturated solutions in the presence of I microM P2O7(4-) added once ('one-time' addition) at constant pH (7.4) and 25 C was determined by KOH titration and decreases in Ca and PO4 concentrations in the solutions. Crystal growth on OCP seed crystals in the presence of a constant concentration of I microM P2O7(4-) was measured. The results of this study show that: (1) P2O7(4-) ions inhibited the growth on the apatite seeds more than on the OCP seeds; (2) apparently OCP precipitated on both types of seeds, followed by its hydrolysis to a more apatite-like phase; (3) slower crystal growth was observed on OCP seeds in the presence of a constant physiological concentration of P2O7(4-) (I microM) than in the 'one-time' addition of P2O7(4-).

00,148
PB94-211513 Not available NTIS
National Inst. of Standards and Technology (NEL), Gaithersburg, MD. Automated Production Technology Div.
NIST Power Reference Source.
Final rept.
S. E. Fick. 1993, 15p.
Pub. in Ultrasonic Exposimetry, Chapter 6, p169-183 1993.

Keywords: *Laboratory equipment, *Ultrasonic tests, Clinical medicine, Ultrasonic wave transducers, Reprints, *Power reference sources, Standard reference materials.

This chapter addressed ways in which laboratory instruments used to evaluate clinical ultrasonic equipment can themselves be characterized using a source of well known levels of ultrasonic power. A detailed presentation of the design and working characteristics of NIST SRM 1855, an ultrasonic absolute power transfer standard, is preceded by an exposition of methods by which clinical and research ultrasonic equipment should be tested before being put into service.

00,149
PB94-212008 Not available NTIS
National Inst. of Standards and Technology (MSEL), Gaithersburg, MD. Polymers Div.
Periapical Tissue Reactions to a Calcium Phosphate Cement in the Teeth of Monkeys.
Final rept.
Y. C. Hong, J. T. Wang, C. Y. Hong, W. E. Brown, and L. C. Chow. 1991, 14p.
Sponsored by American Dental Association Health Foundation, Chicago, IL.
Pub. in Jnl. of Biomedical Materials Research 25, p485-498 1991.

Keywords: *Dental materials, *Calcium phosphates, *Biocompatible materials, *Biological effects, *Root canal filling materials, Laboratory animals, Monkeys, Tissues(Biology), Dental pulp cavity, Comparison, Performance evaluation, Reprints, Grossman sealer, Sargenti N2.

A calcium phosphate cement, Grossman sealer, and Sargenti N2 were compared under conditions where root canals of monkey incisors were deliberately overfilled and the apical tissue responses were evaluated histologically. The periapical tissues exposed to Sargenti N2 revealed severe irritation at all times through the 6-month experimental period. The reactions to Grossman sealer were milder but persisted throughout the observation period. The calcium-phosphate-cement treated animals showed mild tissue irritation after 1 month, but thereafter the adverse tissue reactions were minimal. The compatibility of calcium phosphate cement with the periapical tissue suggests that the cement may have other applications in dentistry and medicine.

00,150
PB94-216090 Not available NTIS
National Inst. of Standards and Technology (MSEL), Gaithersburg, MD. Polymers Div.
Effect of Three Sterilization Techniques on Finger Pluggers.
Final rept.
W. D. Luper, F. C. Eichmiller, W. Doblecki, D. Campbell, and S. H. Li. 1991, 4p.
Sponsored by American Dental Association Health Foundation, Chicago, IL.
Pub. in Jnl. of Endodontics 17, n8 p361-364 Aug 91.

Keywords: *Sterilization, Dental materials, Fatigue(Materials), Fracture(Materials), Autoclaving, Heat, Steam, Reprints, *Finger pluggers.

The effects of different sterilization methods on fatigue life of finger pluggers was investigated. Four sizes (A, B, C, D) of finger pluggers were subjected to 1, 8, or 15 cycles of steam autoclave, dry heat, or bead sterilization. Controls were not sterilized. Finger pluggers were subjected to cyclic bending until fracture. Only the autoclave 8-cycles subgroup of the A finger pluggers had a significantly lower number of cycles to failure compared to controls. The following subgroups had significantly greater cycles before failure when compared to their controls: autoclave 15-, bead 1-, and bead 15-cycles subgroups of B finger pluggers; autoclave 1-, 8-, and 15-, dry heat 1-, and bead 15-cycles subgroups of C finger pluggers; and the bead 15-cycles subgroup of D finger pluggers. The others were not different. Since all but one sterilized group had cyclic lifetimes that were not significantly shorter than nonsterilized controls, clinicians can generally use any of the 3 sterilization methods without a detrimental effect on fatigue life of finger pluggers.

00,151
PB94-216355 Not available NTIS
National Inst. of Standards and Technology (MSEL), Gaithersburg, MD. Polymers Div.
Paffenbarger Research Center: The Cutting Edge of Dental Science.
Final rept.
W. A. Marjenhoff, and L. A. George. 1992, 4p.
Sponsored by American Dental Association Health Foundation, Chicago, IL.
Pub. in Jnl. of the American College of Dentists 59, n4 p6-9 1992.

Keywords: *Dental materials, *Dentistry, *Technology innovation, Adhesion, Dental cements, Dentin, Dental enamel, Licenses, Protective coatings, Calcium phosphates, Composite resins, Reprints, *Paffenbarger Research Center, National Institute of Standards and Technology.

Science Research (CEMSR) and Paffenbarger Research Center (PRC) at the National Institute of Standards and Technology (NIST) has been in the forefront of transferring new and improved dental technologies to the profession since 1928. The list of PRC/NIST innovations is long and impressive. During the past five years, dentistry has seen the commercialization of a PRC adhesion system for bonding composites to dentin and enamel simultaneously and glass-ceramic inserts that improve the properties of composite restorations. Licenses are currently being negotiated with dental manufacturers for a variety of other products based on American Dental Association Health Foundation (ADAHF) patents. Current research includes the further development of calcium phosphate cements for various dental and medical applications; resins that exhibit minimal dimensional change on hardening; protective coatings for dentin, as well as enamel; and synthetic dentin.

00,152
PB94-216561 Not available NTIS
National Inst. of Standards and Technology (MSEL), Gaithersburg, MD. Polymers Div.
Crystal Structure of Dicalcium Potassium Trihydrogen Bis(pyrophosphate) Trihydrate.
Final rept.
M. Mathew, L. W. Schroeder, and W. E. Brown. 1993, 5p.
Sponsored by American Dental Association Health Foundation, Chicago, IL.

Pub. in Jnl. of Crystallographic and Spectroscopic Research 23, n8 p657-661 1993.

Keywords: *Crystal structure, *Calcium phosphates, *Pyrophosphates, *Potassium phosphates, Dental materials, Layers, X-ray diffraction, Reprints.

The crystal structure of Ca2KH3(P2O7)2 3H20 has been determined by single crystal X-ray diffraction. Crystals are monoclinic, space group P2(sub 1)/n with a = 10.518(3), b = 19.253(9), c = 7.340(3)A, Beta = 90.07(2) deg, and Z = 4. The structure was refined to R = 0.048 and R(sub w) = 0.044 for 1,839 reflections with I > than or = 3 sigma(I). The structure consists of a compact assembly of Ca, K, HP2O7, and H2P2O7 ions and three water molecules arranged in layers perpendicular to the b-axis. The two independent Ca ions and the HP2O7 ion comprise one layer; K and H2P2O7 ions and the three water molecules form an interstitial layer. Coordinations of the two independent Ca ions are quite similar, but the environments of HP2O7 and H2P2O7 ions are quite different, probably due to their locations in different layers. The general structural features are quite similar to those of Ca(NH4)HP2O7.

00,153
PB94-216579 Not available NTIS
National Inst. of Standards and Technology (MSEL), Gaithersburg, MD. Polymers Div.
Crystal Structure of Calcium Adipate Monohydrate.
Final rept.
M. Mathew, S. Takagi, and H. L. Ammon. 1993, 5p.
Sponsored by American Dental Association Health Foundation, Chicago, IL.
Pub. in Jnl. of Crystallographic and Spectroscopic Research 23, n8 p617-621 1993.

Keywords: *Crystal structure, Dental materials, X-ray diffraction, Polymers, Chemical bonds, Layers, Monocrystals, Hydrates, Least squares method, Reprints, *Calcium adipate monohydrate, *Calcium dicarboxylate.

The crystal structure of calcium adipate monohydrate, Ca(C6H8O4) (H2O), has been determined by single crystal X-ray diffraction study. The structure was refined by full-matrix least-squares techniques to R = 0.040, R(sub w) = 0.058 for 1,283 reflections with I > or = 3 sigma(I). Ca is coordinated to seven oxygen atoms and the coordination polyhedron is best described as pentagonal bipyramid. The coordinations of the two carboxylate groups in adipate ion are quite different. One carboxylate group binds three different Ca ions forming a four-membered chelate ring with one Ca ion and unidentate bridge bonds to two other Ca ions. The other carboxylate group links to two Ca ions through unidentate bonds. The structure is highly polymeric, but with a layer-type structure parallel to (001) with the hydrocarbon chains sandwiched between the polar regions consisting of Ca, carboxylate and water molecules.

00,154
PB95-125613 Not available NTIS
National Inst. of Standards and Technology (MSEL), Gaithersburg, MD. Polymers Div.
Evaluation of Fracture Toughness and Residual Stress in Dental Porcelain by Indentation-Microfracture Method.
Final rept.
K. Asaoka, J. A. Tesk, and J. R. Kelly. 1994, 6p.
Pub. in International Conference on Residual Stresses (4th), Baltimore, MD., June 8-10, 1994, p854-859.

Keywords: *Dental materials, *Porcelain, *Residual stress, *Fracture strength, Surfaces, Toughness, Study estimates, Crack propagation, Reprints, *Indentation-microfracture method.

The indentation-microfracture (IM) method was applied to estimate both the fracture toughness, K(sub Ic), and residual stress in the surface of 2.0 x 10.0 mm disks of two dental porcelains (A and B) that were either slowly cooled or tempered by two different treatments. The shape parameter, m, for Weibull plots of the K(sub Ic)'s that were measured by IM method, was calculated to be within the range of 7.1 to 9.1 for the slowly cooled specimens. Tempering had no significant effect on the Weibull shape parameters. The surface residual stresses for porcelain A were estimated to be 26-28 and 64-88 MPa in compression for specimens cooled in ambient air and with forced air, respectively, as calculated from the median/radial crack length after indentation. The estimated residual stresses were in good agreement with the results of computer simulations by Asaoka et al. It was concluded that the IM method can be applied for measurement of the fracture toughness and residual stress in the near surface region (100-400 micrometers deep) for dental metal-ceramic porcelains that have a micro structure that is unaffected by cooling rate.

00,155
PB95-126173 Not available NTIS
National Inst. of Standards and Technology (PL), Gaithersburg, MD. Ionizing Radiation Div.
Image Information Transfer Properties of X-Ray Intensifying Screens in the Energy Range from 17 to 320 keV.
Final rept.
A. Ginzburg, and C. E. Dick. 1993, 9p.
Pub. in Medical Physics 20, n4 p1013-1021 Jul/Aug 93.

Keywords: *Biomedical radiography, *Fluorescent screens, *X-ray fluorescence, KeV range 10-100, KeV range 100-1000, X-ray absorption, Image intensifiers, Quantum efficiency, Calcium tungstates, Rare earths, Phosphors, Reprints.

The image information transfer properties of a number of x-ray fluorescent screens have been measured for x-ray energies from 17 to 320 keV. The detective quantum efficiency of the screens at each x-ray energy has been determined by separate measurements of the x-ray absorption efficiency and the statistical factor associated with the emission of optical photons upon absorption of an incident x ray. Data have been recorded for both rare-earth phosphor screens and calcium tungstate screens. The value of the statistical factor for optical photon emission tends toward a constant value as the incident energy increases. Comparisons of the image information transfer properties are presented for several screens, which have been measured over a ten year interval. The utility of the screens for high-energy radiography is discussed.

00,156
PB95-140448 Not available NTIS
National Inst. of Standards and Technology (MSEL), Gaithersburg, MD. Polymers Div.
Effects of Surface-Active Resins on Dentin/Composite Bonds.
Final rept.
G. E. Schumacher, F. C. Eichmiller, and J. M. Antonucci. 1992, 5p.
Sponsored by National Inst. of Dental Research, Bethesda, MD.
Pub. in Dental Materials 8, p278-282 Jul 92.

Keywords: *Dentin, *Dental materials, *Surfactants, *Chemical bonds, Polymerization, Monomers, Feasibility studies, Reprints, *Pyromellitic dianhydride, *Methacrylate/hydroxyethyl, Chemical reaction mechanisms.

Effective dentin bonding systems based on para-PMDM diadduct of pyromellitic dianhydride and 2-hydroxyethyl methacrylate (HEMA) have been developed. Para-PMDM, a solid of limited solubility, is usually applied from an acetone solution to dentin that has been preconditioned with acid and N-phenylglycine. The feasibility of using a liquid, surface-active bonding resin to substitute for or to supplement para-PMDM was explored. The results suggest that solutions based on Mono(2-methacryloyloxy)ethyl phthalate (MMEP) and/or para-PMDM in acetone or in other monomers, especially those containing HEMA, can effectively promote bonding to dentin. A new mechanism for the observed self-polymerization of MMEP or para-PMDM with N-phenylglycine is proposed.

00,157
PB95-151080 Not available NTIS
National Inst. of Standards and Technology (MSEL), Gaithersburg, MD. Polymers Div.
Effects of Calcium Phosphate Solutions on Dentin Permeability.
Final rept.
M. S. Tung, H. J. Bowen, G. Derkson, and D. H. Pashley. 1993, 5p.
Sponsored by American Dental Association Health Foundation, Chicago, IL.
Pub. in Jnl. of Endodontics 19, n8 p383-387 Aug 93.

Keywords: *Calcium phosphates, *Dentin permeability, *Dental materials, Precipitation(Chemistry), pH, X-ray diffraction, Scanning electron microscopy, Solutions, Kinetics, Reprints, *Dental tubules.

Calcium phosphate solutions at various concentrations and pH levels were used to obstruct the dental tubules. The effects were evaluated by measurements of permeability through dentin discs and by scanning electron microscopy. Precipitation kinetics were followed by pH changes in the solutions and products were determined by X-ray powder diffraction. The solutions were applied in two ways: (a) calcium and phosphate solutions were mixed before application and (b) one solution (calcium or phosphate) was applied first followed by the other solution.

00,158
PB95-151163 Not available NTIS
National Inst. of Standards and Technology (MSEL), Gaithersburg, MD. Polymers Div.
Modified Surface-Active Monomers for Adhesive Bonding to Dentin.
Final rept.
S. Venz, and B. Dickens. 1993, 5p.
Sponsored by American Dental Association Health Foundation, Chicago, IL.
Pub. in Jnl. of Dental Research 72, n3 p582-586 Mar 93.

Keywords: *Adhesive bonding, *Dentin, *Monomers, *Adhesives, Performance evaluation, Reliability, Curing, Synthesis(Chemistry), Surface properties, Reprints, *PMGDM, PMDM, Pyromellitic dianhydride, Glycerol dimethacrylate.

PMGDM, a PMDM-type adhesive monomer, was synthesized from pyromellitic dianhydride and glycerol dimethacrylate. Only the para isomer of PMDM, a solid, is used in dental adhesives. The adhesive monomer PMGDM is a liquid and consists of a mixture of para- and meta isomers. This study shows that PMGDM has several advantages over PMDM. The adhesive bonds were tested in both shear and tensile modes. PMDM was used as the control. The reliability of the bonds, as judged from the Weibull modulus and Weibull characteristic strength, was improved by (1) use of more concentrated solutions of PMGDM adhesive, (2) use of an adhesive thickness of about 25 micrometers and (3) modification of PMGDM with a diluent monomer which is expected to enhance the degree of cure and/or the dentin-wetting properties of the adhesive resin.

00,159
PB95-152831 Not available NTIS
National Inst. of Standards and Technology (MSEL), Gaithersburg, MD. Polymers Div.
Evaluation of Fracture Toughness and Residual Stress in Dental Porcelain by Indentation-Microfracture Method.
Final rept.
K. Asaoka, J. A. Tesk, and J. R. Kelly. 1994, 6p.
Pub. in Proceedings of International Conference on Residual Stresses (4th), Baltimore, MD., June 8-10, 1994, p854-859.

Keywords: *Dental materials, *Residual stress, *Porcelain, *Fracture strength, *Surfaces, Study estimates, Microstructure, Computerized simulation, Crack propagation, Reprints, *Indentation-microfracture method.

The indentation-microfracture (IM) method was applied to estimate both the fracture toughness, K(sub Ic) and residual stress in the surface of 2.0 x 10.0 mm disks of two dental porcelains (A and B) that were either slowly cooled or tempered by two different treatments. The shape parameter, m, for Weibull plots of the K(sub Ic)'s that were measured by IM method, was calculated to be within the range of 7.1 to 9.1 for the slowly cooled specimens. Tempering had no significant effect on the Weibull shape parameters. The surface residual stresses for porcelain A were estimated to be 26-28 and 64-88 MPa in compression for specimens cooled in ambient air and with forced air, respectively, as calculated from the median/radial crack length after indentation. The estimated residual stress were in good agreement with the results of computer simulations by Asaoka et al. It was concluded that the IM method can be applied for measurement of the fracture toughness and residual stress in the near surface region (100-400 micrometers deep) for dental metal-ceramic porcelains that have a micro structure that is unaffected by cooling rate.

00,160
PB95-153417 Not available NTIS
National Inst. of Standards and Technology (PL), Gaithersburg, MD. Quantum Metrology Div.

Noninvasive High-Voltage Measurement in Mammography by Crystal Diffraction Spectroscopy.
Final rept.
R. D. Deslattes, J. C. Levin, M. D. Walker, and A. Henins. 1994, 4p.
Pub. in Medical Physics 21, n1 p123-126 Jan 94.

Keywords: *Mammography, *X-ray spectrometers, *Radiology, High voltage, Medical equipment, Reprints.

Wavelength dispersive crystal diffraction spectrometry has been applied to the measurement of the accelerating voltage on an x-ray source in a prototype experiment in the mammographic source. The results indicate that this noninvasive approach can yield determinations of such voltages within 0.1 kV, a level of imprecision that appears adequate for high-level standardization of such potentials.

00,161
PB95-161972 Not available NTIS
National Inst. of Standards and Technology (MSEL), Gaithersburg, MD. Polymers Div.
Wear of Human Enamel against a Commercial Castable Ceramic Restorative Material.
Final rept.
D. S. Palmer, M. T. Barco, G. B. Pelleu, and J. E. McKinney. 1991, 4p.
Pub. in Jnl. of Prosthetic Dentistry 65, n2 p192-195 Feb 91.

Keywords: *Dental enamel, *Wear tests, *Ceramics, *Dental restoration, *Dental materials, Comparison, Casting, Porcelain, Reprints.

This study determined the effect of castable ceramic, with and without shading porcelain applied, on enamel wear. The wear produced by conventional dental porcelain was used as a control. Cusp tips from extracted human third molars were precision-machined into cones of enamel approximately 1 mm long. Three groups of nine cones each were abraded against rotating disks of (1) castable ceramic with shading porcelain, (2) castable ceramic without shading porcelain, and (3) conventional dental porcelain. Enamel wear was calculated from microscopic measurements of the enamel cones before and after abrading. Significant differences were found between castable ceramic with and without shading porcelain and between conventional dental porcelain and castable ceramic with shading porcelain ($p < 0.001$ ANOVA and 0.05 Scheffe's test). These findings suggest that castable ceramic with shading porcelain should not be used in regions that will function against opposing natural teeth.

00,162
PB95-162251 Not available NTIS
National Inst. of Standards and Technology (MSEL), Gaithersburg, MD. Polymers Div.
Ring-Opening Dental Resin Systems Based on Cyclic Acetals.
Final rept.
B. Reed, J. Stansbury, and J. Antonucci. 1994, 7p.
Pub. in Polymers of Biological and Biomedical Significance, Chapter 15, p184-190 1994.

Keywords: *Dental materials, *Polymerization, *Monomers, *Cyclic compounds, *Acetals, Free radicals, Mechanical properties, Resin matrix composites, Molecular structure, Reprints.

For monomers of comparable size, ring-opening polymerization results in less shrinkage than that which accompanies 1,2-vinyl addition polymerization. Two monomer types were synthesized, nonvinyl (NVCA) and vinyl (VCA) cyclic acetals. The goals of this study were to assess the potential for reduced shrinkage through free radical ring-opening polymerization of NVCA and VCA type monomers, and to test the mechanical strength of dental resin composites formulated with these novel monomers. Homo- and copolymerizations were conducted with several NVCAs and VCAs to evaluate their potential as comonomers in dental polymeric composites. Composite specimens were formulated with PBMD, a VCA derived from terephthaldehyde, and EBPADM, an ethoxylated bisphenol A dimethacrylate, and tested for their mechanical strength.

00,163
PB95-163507 Not available NTIS
National Inst. of Standards and Technology (MSEL), Gaithersburg, MD. Polymers Div.
Effect of Ethanol on the Solubility of Dicalcium Phosphate Dihydrate in the System Ca(OH)2-H3PO4-H2O at 37C.
Final rept.
M. S. Tung, and T. J. O'Farrell. 1993, 7p.
Sponsored by American Dental Association Health Foundation, Chicago, IL.
Pub. in Jnl. of Molecular Liquids 56, p237-243 1993.

Keywords: *Dental materials, *Calcium phosphates, *Solubility, *Ethanol, Mixtures, Dielectric properties, Born approximation, Reprints, *Dicalcium phosphate dihydrate.

Solubility values of dicalcium phosphate dilhydrate were determined in 0, 7.86, 16.04, 24.53, and 33.38% by weight ethanol-water mixtures at 37 C. The decreased solubility of DCPD, expressed as solubility product (K(sub sp)), from pK(sub sp) = 6.69 at 0% ethanol to 8.91 at 33.38% ethanol, was mainly due to the decrease in the dielectric constant. The data were fitted to the simple Born equation as follows: pK(sub sp) - 6.69 = 575.2(1/epsilon - 0.0135).

00,164
PB95-164661 Not available NTIS
National Inst. of Standards and Technology (MSEL), Gaithersburg, MD. Polymers Div.
Evaluation of Methylene Lactone Monomers in Dental Resins.
Final rept.
J. W. Stansbury, and J. M. Antonucci. 1992, 4p.
Sponsored by National Inst. of Dental Research, Bethesda, MD.
Pub. in Dental Materials 8, p270-273 Jul 92.

Keywords: *Dental materials, *Monomers, *Polymerization, Mechanical properties, Free radicals, Synthesis(Chemistry), Cyclic compounds, Curing, Chemical bonds, Methacrylates, Reprints, *Methylene lactones, Methylene butyrolactone.

alpha-Methylene-gamma-butyrolactone (MBL), which can be described as the cyclic analog of methyl methacrylate, exhibits greater reactivity in free radical polymerizations than conventional methacrylate monomers. Unfilled resin formulations composed of Bis-GMA/MBL or Bis-GMA/TEGDMA/MBL were light-cured. The effect of the more reactive methylene lactone monomer on mechanical properties and the degree of conversion of the polymers was examined. The infrared absorption bands for the carbon-carbon double bonds of MBL and the methacrylate monomers are well resolved and allow the conversion of each component to be calculated individually. The synthesis and polymerization of several substituted methylene lactones was also studied.

00,165
PB95-168712 Not available NTIS
National Inst. of Standards and Technology (MSEL), Gaithersburg, MD. Polymers Div.
Behavior of a Calcium Phosphate Cement in Simulated Blood Plasma In vitro.
Final rept.
K. Ishikawa, S. Takagi, L. C. Chow, K. Asaoka, Y. Ishikawa, and E. D. Eanes. 1994, 7p.
Sponsored by American Dental Association Health Foundation, Chicago, IL.
Pub. in Dental Materials 10, p26-32 1994.

Keywords: *Calcium phosphate, *Dental cements, *Biocompatibility, In vitro analysis, Dental materials, Hardness, Physical properties, Blood plasma, Synthetic materials, Biochemistry, Performance evaluation, Reprints, Hydroxyapatite.

The purpose of the study was to gain a better understanding of the integration of calcium phosphate cement (CPC) implants in biological tissue. An invitro continuous flow system was employed to examine the protracted behavior of disc-shaped specimens of this bioactive material under sustained physiological-like solution conditions. The results suggest that under in vivo conditions, CPC implants would not dissolve in phyisological fluids. Carbonate hydroxyapatite (OHAp) coatings may form on the implants, which may enhance bonding of implants to bone by mechanically strengthening the interface between them.

00,166
PB95-168894 Not available NTIS
National Inst. of Standards and Technology (MSEL), Gaithersburg, MD. Polymers Div.
Octacalcium Phosphate Carboxylates. 5. Incorporation of Excess Succinate and Ammonium Ions in the Octacalcium Phosphate Succinate Structure.
Final rept.
M. Markovic, B. O. Fowler, and W. E. Brown. 1993, 6p.
Sponsored by American Dental Association Health Foundation, Chicago, IL.
Pub. in Proceedings of Materials Research Society Symposium, Hydroxyapatite and Related Compounds, San Francisco, CA., April 13-15, 1993, p139-144 1994.

Keywords: *Dental materials, *Ions, *Crystal structure, X ray diffraction, Hydration, Chemical analysis, Infrared spectroscopy, Reprints, *Octacalcium phosphate succinate, Octacalcium phosphate, Octacalcium phosphate carboxylates.

Octacalcium phosphate succinate, Ca8(HPO4)1.07(succ)0.93(PO4)4-6H2O (OCP-SUCC), has an approx 50% larger hydrated layer volume than that of its parent compound, octacalcium phosphate, Ca8(HPO4)2(PO4)4-5H2O (OCP). The incorporation of structurally excess ions in OCP-SUCC was established by chemical analysis, X-ray powder diffraction, and infrared spectroscopy. Both excess succinate and counter ammonium ions were found to incorporate in the hydrated layer of the OCP-SUCC structure; this incorporation caused a slight expansion in the alpha-axis of up to 3%. Removal of these excess ions resulted in contraction of the alpha-axis to near that of OCP-SUCC. OCP-SUCC and particularly other OCP-carboxylates (OCPCs) that have larger hydrated layer volumes have a potential to incorporate various molecules and ions; these OCPCs could serve as vehicles to facilitate slow release of these additives into aqueous solutions.

00,167
PB95-168928 Not available NTIS
National Inst. of Standards and Technology (MSEL), Gaithersburg, MD. Polymers Div.
Crystal Structure of Calcium Succinate Monohydrate.
Final rept.
M. Mathew, S. Takagi, B. O. Fowler, and M. Markovic. 1994, 4p.
Sponsored by American Dental Association Health Foundation, Chicago, IL.
Pub. in Jnl. of Chemical Crystallography 24, n7 p437-440 1994.

Keywords: *Dental materials, *Crystal structure, Calcium compounds, X ray diffraction, Hydrates, Chemical bonds, Monocrystals, Polymers, Reprints, *Calcium succinate monohydrate, Calcium adipate monohydrate.

The crystal structure of calcium succinate monohydrate, Ca(C4H4O4)-H2O, has been determined by single crystal X-ray diffraction. The crystals are monoclinic. The structure was refined by full-matrix least-squares techniques to R = 0.027, R(sub w) = 0.040, for 829 reflections with I > or = 3 sigma(I). Ca is coordinated to seven oxygen atoms, and the coordination polyhedron is best described as a pentagonal bipyramid. One carboxylate group in the succinate ion is bonded to three different Ca ions, forming a four-membered chelate ring with one Ca ion and unidentate bridge bonds to two other Ca ions. The other carboxylate group is bonded to two Ca ions through unidentate bonds. The structure is highly polymeric. The general structural features are nearly identical to those of calcium adipate monohydrate.

00,168
PB95-169074 Not available NTIS
National Inst. of Standards and Technology (MSEL), Gaithersburg, MD. Metallurgy Div.
Ambient Temperature Synthesis of Bulk Intermetallics.
Final rept.
M. Ratzker, D. S. Lashmore, and M. P. Dariel. 1994, 6p.
Sponsored by American Dental Association Health Foundation, Chicago, IL.
Pub. in Materials Research Society Symposia Proceedings, v350 p41-46 1994.

Keywords: *Intermetallic compounds, *Dental materials, *Ambient temperature, *Synthesis(Chemistry), Interfaces, Thin films, Binary systems(Materials), Melting points, Diffusion, Indium alloys, Silver alloys, Tin alloys, Reprints.

Room-temperature intermetallic compound formation occurs when one of the component metals has a very

low melting point or when two metals in close contact interdiffuse very rapidly. Compound formation at room temperature at the interface of superposed thin films has been observed in several instances, often in systems relating to electronic materials. The overall amount of compound produced in such configurations, however, is limited, due to the intrinsic limitations involved in the thin layer geometry. Bulk quantities of intermetallic can be produced at ambient temperature in solids by increasing the interface area between the components that interdiffuse rapidly. This condition can be achieved by having small size powder particles of one component coated with a layer of the second component. The very large interface area leads to rapid formation of bulk quantities of compounds even at ambient temperature. By appropriate control of the initial constituents and the coating parameters, it is possible to custom-prepare various intermetallic compounds present in binary systems such as silver-tin, gold-tin and silver-indium in which fast interdiffusion takes place.

00,169
PB95-169231 Not available NTIS
National Inst. of Standards and Technology (MSEL), Gaithersburg, MD. Polymers Div.
Effect of Ethanol on the Solubility of Hydroxyapatite in the System Ca(OH)2-H3PO4-H2O at 25C and 33C.
Final rept.
M. S. Tung, C. Lin, T. H. Chow, and P. Sung. 1993, 7p.
Sponsored by American Dental Association Health Foundation, Chicago, IL.
Pub. in Proceedings of Materials Research Society Meeting: Hydroxyapatite and Related Materials, San Francisco, CA., April 13-15, 1993, p145-151 1994.

Keywords: *Ethanol, *Dental materials, *Solubility, Physicochemical properties, Aqueous solutions, Calcium phosphates, Reprints, *Apatite/hydroxy.

Hydroxyapatite (HA), Ca5(PO4)3OH, is the prototype of the inorganic constituent found in tooth and bone. Its physico-chemical properties have wide biological and industrial importance. Hence, its solubility in aqueous solutions has been extensively studied. Although ethanol has been known to increase the association constants of ionic compounds and decrease their solubilities, the effect of ethanol on the solubility of HA has not been studied. Recently, ethanol has been reported to affect the precipitation of HA and other calcium phosphates. This effect of ethanol may be due to the increase in precipitation rate or the effect on the solubility of HA or both. Therefore, the purpose of this study is to investigate the effect of ethanol on the solubility of HA.

00,170
PB95-175261 Not available NTIS
National Inst. of Standards and Technology (MSEL), Gaithersburg, MD. Polymers Div.
Formation of Hydroxyapatite in Cement Systems.
Final rept.
L. C. Chow, S. Takagi, and K. Ishikawa. 1994, 11p.
Contract NIH-DE05030
Sponsored by American Dental Association Health Foundation, Chicago, IL.
Pub. in Proceedings of Conference on Hydroxyapatite and Related Materials, San Francisco, CA., April 13-15, 1993, p127-137 1994.

Keywords: *Dental cements, *Sealing compounds, *Physicochemical properties, Calcium phosphates, Acid bonded reaction cements, Biocompatible materials, Sealants, Surface chemistry, Hardness, Physical properties, Dental materials, Reprints, *Hydroxyapatite, *Cement systems, Self setting.

Among the self-setting calcium phosphate cement systems, those cements that consist of tetracalcium phosphate (TTCP) and dicalcium phosphate anhydrous (DCPA) or dicalcium phosphate dihydrate (DCPD) form OHAp as the only reaction product. The paper reports the effects of the TTCP/DCA ratio and the phosphate concentration in the cement liquid on the formation of OHAp in the TTCP+DCPA system. Also reported is the formation of OHAp in new cement compositions comprising TTCP and alpha-tricalcium phosphate (alpha-TCP), octacalcium phosphate (OCP), amorphous calcium phosphate (ACP), or monocalcium phosphate monohydrate (MCPM).

00,171
PB95-180212 Not available NTIS
National Inst. of Standards and Technology (MSEL), Gaithersburg, MD. Polymers Div.
Physical and Chemical Properties of Resin-Reinforced Calcium Phosphate Cements.
Final rept.
S. Dickens-Venz, S. Takagi, L. C. Chow, B. Dickens, R. L. Bowen, and A. D. Johnston. 1994, 7p.
Sponsored by American Dental Association Health Foundation, Chicago, IL.
Pub. in Dental Materials 10, p100-106 Mar 94.

Keywords: *Dental materials, *Calcium phosphates, *Dental cements, *Physical properties, *Chemical properties, Dental pulp capping, Dental pulp cavity, Dental cavity lining, Hydroxyapatites, Chemical reactions, Monomers, Hydrophylic polymers, Reprints, *Self-setting, Apatite/hydroxy, Cement polymer composites.

The purpose of this study was to improve the handling and physical properties of a self-setting, water-based calcium phosphate cement by combining it with polymerizable resins and to study the setting reactions involved. Dual-cured composite cements were prepared from a calcium phosphate cement powder and dental monomers that contain carboxylated hydrophilic resins or resin/water mixtures. The hydrophilic acidic resins allows mixing with water and/or allow rapid diffusion of water into the resinous cement so that the dissolution and reprecipitation processes required for the conversion of the calcium phosphate components to hydroxyapatite can occur. The characteristics of the resulting composite cements suggest that the materials may be useful in pulp capping and/or cavity lining.

00,172
PB95-180626 Not available NTIS
National Inst. of Standards and Technology (MSEL), Gaithersburg, MD. Polymers Div.
Diagnosis and Treatment of an Oral Base-Metal Contact Lesion Following Negative Dermatologic Patch Tests.
Final rept.
W. A. Lyzak, C. M. Flaitz, R. S. McGuckin, F. Eichmiller, and R. S. Brown. 1994, 5p.
Sponsored by American Dental Association Health Foundation, Chicago, IL.
Pub. in Annals of Allergy 73, p161-165 Aug 94.

Keywords: *Dental materials, *Immunologic diseases, *Allergic diseases, *Nickel alloys, Base metal, Reprints.

We report a confirmed case of intraoral contact mucositis secondary to nickel dental alloy hypersensitivity. The lesion resolved after removal of the offending prosthesis. The patient responded nagatively to dermatologic patch tests, but a positive intraoral rechallenge confirmed the mucositis diagnosis. A nonreactive, gold alloy prosthesis was inserted for a successful result.

00,173
PB95-180642 Not available NTIS
National Inst. of Standards and Technology (MSEL), Gaithersburg, MD. Polymers Div.
Formation of Hydroxyapatite in a Polymeric Calcium Phosphate Cement.
Final rept.
Y. Matsuya, S. Matsuya, J. M. Antonucci, S. Takagi, and L. C. Chow. 1994, 2p.
See also PB95-175261. Sponsored by American Dental Association Health Foundation, Chicago, IL.
Pub. in Proceedings of International Conference on Composites Engineering, New Orleans, LA., August 28-31, 1994, p861-862.

Keywords: *Dental cements, *Calcium phosphates, *Polymers, *Hydroxyapatites, X ray diffraction, Chemical reactions, Reprints, Apatite/hydroxy, Poly(maleic acid-ether/methyl vinyl), Tetracalcium phosphate, Dicalcium phosphate anhydrous.

Recently it was shown that the reaction of aqueous solutions of poly(alkenoic acids) with mixtures of tetracalcium phosphate (TTCP) and dicalcium phosphate anhydrous (DCPA) formed strong polymeric calcium phosphate cements. Surprisingly, x-ray diffraction (XRD) analysis of these cements, even after prolonged storage in water, failed to reveal the presence of hydroxyapatite (OHAp). In this study poly(methyl vinyl ether-maleic acid), (PMVE-Ma) was reacted with only TTCP to form polymeric calcium phosphate cements. TTCP samples ground for different lengths of time were used as the base powder. Grinding enhanced the reactivity of TTCP with PMVE-Ma and yielded cements with higher diametral tensile strengths than similar cements formulated with unground TTCP. XRD analysis of the ground TTCP/PMVE-Ma cements also showed the presence of significant amounts of OHAp.

00,174
PB96-102405 Not available NTIS
National Inst. of Standards and Technology (MSEL), Gaithersburg, MD. Polymers Div.
Reduction of Marginal Gaps in Composite Restorations by Use of Glass-Ceramic Inserts.
Final rept.
L. A. George, N. D. Richards, and F. C. Eichmiller. 1995, 4p.
Sponsored by American Dental Association Health Foundation, Chicago, IL.
Pub. in Operative Dentistry 20, p151-154 1995.

Keywords: *Dental materials, *Inserts, *Composite materials, *Shrinkage, Glass, Ceramics, Polymerization, Monomers, Gaps, Teeth, Reprints.

The objective of this study was to evaluate the effects of glass-ceramic inserts on reducing the marginal gaps caused by polymerization shrinkage in composite restorations. A light microscope was used to measure the largest gap at margins around restorations made in glass cylinders and tooth cavities with and without adhesion promoters. Where the cylinder was not silanated, the average gap was less in samples containing an insert than in those without. Two preparations were made in the dentin of 20 human molars. In each molar one cavity was restored with a dentin bonding agent and composite and the other with a dentin bonding agent and an inserted seated in the composite. The average maximum gap width of restorations containing inserts was statistically less than for those with only composite (paired t-test, $P < 0.0001$). When considering the volume of composite displaced by the insert, these results indicate that the use of a glass-ceramic insert decreased the marginal gaps resulting from polymerization shrinkage.

00,175
PB96-122536 Not available NTIS
National Inst. of Standards and Technology (MSEL), Gaithersburg, MD. Polymers Div.
Failure of All-Ceramic Fixed Partial Dentures 'In vitro' and 'In vivo': Analysis and Modeling.
Final rept.
J. R. Kelly, J. A. Tesk, and J. A. Sorensen. 1995, 6p.
Pub. in Jnl. of Dental Research, v74 n6 p1253-1258 1995.

Keywords: *Dental materials, *Failure analysis, In vitro analysis, Reprints, Prosthodontics.

Hertzian cone cracks visible at the loading site of 20 all-ceramic fixed partial dentures (FPDs), tested in vitro, led to the hypotheses that failure was due to the propagation of localized contact damage crack systems (Hertizian stress state) and that such damage was an unlikely clinical failure mode. Fractographic analysis of the 20 laboratory-failed and nine clinically-failed all-ceramic FPDs allowed for definitive testing of these hypotheses and a comparison between in vitro and in vivo failure behavior. In all cases, failure occurred in the FPD connectors (none from contact damage), with approximately 70 to 78% orginating from the interface between the core and veener ceramics. The coincidence between failure origins provides strong evidence that the in vitro test modeled aspects of structural behavior having clinical importance. The fractographic observations, coupled with the in vitro failure load data, furnished very specfic boundary conditions which were applied to constrain mathematical models of FPD connector failure. Finite element analysis (FEA) of the laboratory PPDs found that maximum principal tensile stresses would occur at locations consistent with the fractographic observations only if (1) there were appropriate elastic moduli differences between the ceramics; and (2) a small amount of abutment rotation was allowed. Weibull failure probability (Pf) calculations, incorporating FEA stress profiles, very closely replicate the veneer interface was much lower than that for the free veneer surface (i.e, the interface is of lower quality with regard to defects).

00,176
PB96-122635 Not available NTIS
National Inst. of Standards and Technology (EEEL), Gaithersburg, MD. Electricity Div.
Overview of Bioelectrical Impedance Analyzers.
Final rept.
N. M. Oldham. 1994, 3p.
Pub. in Proceedings of the Technology Assessment Conference on Bioelectrical Impedance Analysis in

Body Composition Measurement, NIH, Bethesda, MD., December 12, 1994, p1-3.

Keywords: *Bioinstrumentation, *Electrical impedance, *Body composition, Humans, Algorithms, Lipids, Bodywater, Height, Body weight, Age, Physical fitness, Electrical measuring instruments, Reprints, *Bioelectrical impedance analyzers, BIAs, Body fat.

The class of instruments referred to as bioelectrical impedance analyzers (BIAs) are designed to measure human body impedance-a parameter that has been used to estimate body composition based on algorithms that also include height, weight, gender, age, and level of physical activity. The algorithms have been described in the literature, as have evaluations of commercial BIAs on human subjects. This paper describes a project to investigate the properties of these instruments as electrical impedance meters.

00,177
PB96-122940 Not available NTIS
National Inst. of Standards and Technology (MSEL), Gaithersburg, MD. Polymers Div.
Dental Applications of Ceramics.
Final rept.
L. A. George, and F. C. Eichmiller. 1995, 16p.
Pub. in Proceedings of American Ceramic Society, Bioceramics: Materials and Applications, Indianapolis, IN., April 24-28, 1994, v48 p157-172.

Keywords: *Dental materials, *Biocompatible materials, *Reconstruction, Ceramics, Porcelain, Glasses, Dental cements, Temporary dental restoration, Permanent dental restoration, Teeth, Reprints.

Properties of ceramics that make them appropriate for use in dental applications include compressive strength, durability, radiopacity, and inertness towards the oral environment. The principle dental use of ceramics is in the aesthetic restoration of missing teeth or tooth structure. Aesthetic dental ceramics are primarily manufactured from two classes of materials, beneficiated feldspathic minerals, and glass-ceramics. Processing restorations with feldspathic materials generally involves stacking powder-water slurries upon a metal framework and subsequent sintering. Glass-ceramics used in restorative parts involves the casting or forming of complex shapes that are then cerammed.

00,178
PB96-123229 Not available NTIS
National Inst. of Standards and Technology (MSEL), Gaithersburg, MD. Polymers Div.
Properties and Mechanisms of Fast-Setting Calcium Phosphate Cements.
Final rept.
K. Ishikawa, S. Takagi, L. C. Chow, and Y. Ishikawa. 1995, 6p.
Pub. in Jnl. of Materials Science: Materials in Medicine, v6 p528-533 1995.

Keywords: *Dental cements, *Calcium phosphates, Phosphate additive, Tetracalcium phosphate, Reprints, Dicalcium phosphate, Fast setting cement, Hydroxyapatite.

The setting time of a calcium phosphate cement consisting of tetracalcium phosphate (TTCP) and dicalcium phosphate anhydrous (DCPA) was reduced from 30 to 5 min by use of a cement liquid that contained a phosphate concentration of 0.25 mol/l or higher. The diametral tensile strength and conversion of the cement ingredients to hydroxyapatite (OHAp) during the first 3 h were also significantly increased by the phosphate. However, the phosphate produced no significant effects on the properties of the 24-h cement samples. Results from additional experiments in a slurry system verified that the high phosphate concentration in the solution accelerated the formation of OHAp in the TTCP-DCPA system, and this reaction could explain the fast-setting properties of the cements.

00,179
PB96-158001 Not available NTIS
National Inst. of Standards and Technology (MSEL), Gaithersburg, MD. Polymers Div.
Reinforcement of Cancellous Bone Screws with Calcium Phosphate Cement.
Final rept.
L. E. Mermelstein, L. C. Chow, C. Friedman, and J. J. Crisco. 1996, 6p.
Pub. in Jnl. of Orthopaedic Trauma, v10 n1 p15-20 1996.

Keywords: *Cancellous bone, *Biomaterials, Reprints, *Calcium phosphate cement, *Screw fixation.

The ability of calcium phosphate cement (CPC) to reinforce cancellous screws placed in previously stripped holes was studied in vitro. The distal end of canine femurs were harvested. A total of fifteen screws were placed in six femurs. The pullout strength (failure force), failure displacement, stiffness and energy absorbed were determined for the screws in the intact cancellous bone. Next, these stripped screw holes were packed with CPC. The pullout test was repeated, and the results were compared using a paired, Student's t test. We found that the CPC was able to reinforce the previously stripped holes and significantly increase the pullout strength (1159 plus or minus 278 N vs. 678 plus or minus 297 N) and the stiffness (1,900 plus or minus 569 N/mm vs. 1,519 plus or minus 609 N/mm) of the constructs, as well as the energy absorbed by the constructs until failure (467 plus or minus 180 N/mm vs. 278 plus or minus 140 N mm). There was no difference in the failure displacement (0.94 plus or minus 0.23 vs. 0.85 plus or minus 0.51 mm). This study documents the ability of CPC to acutely reinforce cancellous bone screws in a region with no or poor quality cancellous bone.

00,180
PB96-164264 Not available NTIS
National Inst. of Standards and Technology (MSEL), Gaithersburg, MD. Polymers Div.
Polymeric Calcium Phosphate Cements Derived from Poly(methyl vinyl ether-maleic acid).
Final rept.
Y. Matsuya, J. M. Antonucci, S. Matsuya, S. Takagi, and L. C. Chow. 1996, 6p.
Pub. in Dental Materials, v12 p2-7 Jan 96.

Keywords: *Dental materials, *Acid bonded reaction cements, *Polybasic organic acids, *Calcium phosphates, Cements, Reprints.

The purpose of this study was to assess the feasibility of forming polymeric calcium phosphate cements from a mixed powder of dicalcium phosphate/tetracalcium phosphate or only tetracalcium phosphate and poly(methyl vinyl ether-maleic acid) (PMVE-Ma), and to study their setting reaction. The setting reaction process of the polymeric cements was evaluated by mechanical strength tests, infrared spectroscopy and x-ray diffraction analysis and compared with that of a water-setting calcium phosphate cement. The machanical strength data were analyzed using ANOVA and Scheffe's multiple comparisons test.

00,181
PB97-118780 Not available NTIS
National Inst. of Standards and Technology (EEEL), Gaithersburg, MD. Electricity Div.
Overview of Bioelectrical Impedance Analyzers.
Final rept.
N. M. Oldham. 1996, 8p.
See also PB96-122635.
Pub. in American Jnl. of Clinical Nutrition, v64 n3 p405S-412S Sep 96.

Keywords: *Bioinstrumentation, *Electrical impedance, *Body composition, Humans, Algorithms, Liquids, Bodywater, Physical fitness, Electrical measuring instruments, Reprints, *Bioelectrical impedance analyzers, Body fat.

Six commercial bioelectrical impedance analyzers were evaluated to determine their accuracy as impedance meters, their sensitivity to contact impedance, and other operating parameters such as maximum current amplitude and test waveform. Over a range of impedances that simulate human body impedance, analyzer errors varied from less than 1% to nearly 20%. Larger errors were observed when the contact impedance was at the limits of the operating range of the analyzer. Body models, sources of error, and several simple tests that the user can perform are also discussed.

Bionics & Artificial Intelligence

00,182
PB94-172277 Not available NTIS
National Inst. of Standards and Technology (CSL), Gaithersburg, MD. Advanced Systems Div.
Analysis of a Biologically Motivated Neural Network for Character Recognition.
Final rept.
M. D. Garris, R. A. Wilkinson, and C. L. Wilson. 1991, 16p.
Pub. in Conference of Analysis of Neural Network Applications, ANNA-91, Fairfax, VA., May 29-31, 1991, p160-175.

Keywords: *Character recognition, *Neural nets, Image processing, Feature extraction, Pattern recognition, Fonts, Accuracy, Reprints, Back propagation, Gabor functions.

A neural network architecture for size and local shape invariant digit recognition has been developed. The network is based on known biological data on the structure of vertebrate vision but is implemented using more conventional numerical methods for image feature extraction and pattern classification. The input receptor field structure of the network uses Gabor function feature selection. The classification section of the network uses back propagation. Using these features as neurode input, an implementation of back propagation on a serial machine achieved 100% accuracy when trained and tested on a single font size and style while classifying at a rate of 2ms per character.

00,183
PB95-220505 PC A03/MF A01
National Inst. of Standards and Technology (MEL), Gaithersburg, MD. Intelligent Systems Div.
Texture-Independent Vision-Based Closed-Loop Fuzzy Controllers for Navigation Tasks.
S. R. Kundur, and D. Raviv. Apr 95, 40p, NISTIR-5637.
Grant NSF-IRI-9115939
Prepared in cooperation with Florida Atlantic Univ., Boca Raton. Sponsored by National Science Foundation, Arlington, VA. Div. of Information, Robotics and Intelligent Systems.

Keywords: *Fuzzy logic, *Computer vision, *Controllers, *Autonomous navigation, Computerized simulation, Cameras, Image processing, Visual perception, Real time operations.

The paper deals with vision-based closed-loop control schemes for collision avoidance as well as maintenance of clearance in a-priori unknown textured environments. These control schemes are base on fuzzy logic and employ a visual motion cue, they call the Visual Threat Cue (VTC) that provides some measure for a relative change in range as well as clearance between 3D surface and a fixated observer in motion. It is a collective measure obtained directly from the raw data of gray level images, is independent of the 3D surface texture and needsno optical flow information, 3D reconstruction, segmentation, feature tracking or preprocessing. This motion cue is scale-independent, rotation independent and is measure in (time-1) units. Design of a closed-loop conventional controller for vision based navigation tasks pose a problem as the system is complex and ill-defined. On the other hand fuzzy control which is closer in spirit to human thinking and can implement linguistically expressed heuristic contrl policies directly without any knowledge about the dynamics of the complex process. The fuzzy controllers were tested in real time using a 486-based Personal Computer and a camera capable of undergoing 6-DOF motion. Results are highly encouraging.

Prosthetics & Mechanical Organs

00,184
PB94-172863 Not available NTIS
National Inst. of Standards and Technology (MSEL), Gaithersburg, MD. Polymers Div.
Physicochemical Properties of Calcific Deposits Isolated from Porcine Bioprosthetic Heart Valves Removed from Patients Following 2-13 Years Function.
Final rept.
B. B. Tomazic, W. E. Brown, and F. J. Schoen. 1994, 13p.
Pub. in Jnl. of Biomedical Materials Research 28, p35-47 1994. Sponsored by American Dental Association Health Foundation, Chicago, IL.

Keywords: *Calcium phosphates, *Heart valve prosthesis, *Prosthesis failure, *Chemical properties, *Physical properties, Humans, Mineralization, Fourier

transform infrared spectroscopy, Scanning electron microscopy, X-ray diffraction, Chemical analysis, Swine, Reprints.

The purpose of the study was to characterize the physicochemical properties of calcific deposits that cause the failure of tissue-derived heart valve bioprosthese. This was done in an effort to understand the mechanism of pathologic biomineralization in the cardiovascular system and potentially prevent deterioration of bioprosthese. Calcific deposits taken from 10 failed bioprosthetic valves that had been implanted in patients for 2-13 years were characterized by chemical analysis, x-ray diffraction, FTIR spectroscopy, scanning electron microscopy, polarized light microscopy, and solubility measurements. The combined results identified the biomineral as an apatitic calcium phosphate salt with substantial incorporation of sodium, magnesium and carbonate. The average Ca/PO4 ratio for this young pathologic biomineral was approximately 1.3, considerably lower than approximately 1.7 found in mature atherosclerotic plaque biomineral and mature skeletal biomineral, both of which approximate hydroxyapatite in composition. Deproteinated calcific deposits from bioprosthese had thermodynamic solubilities comparable to those of both atherosclerotic plaque, typical pathologic biomineral and hydrolyzed octacalcium phosphate, a proposed precursor phase to biomineral apatite. This suggests an approach toward prevention of bioprosthetic tissue calcification through control of the formation of the kinetically favored OCP precursor and/or its transformation into bioapatite.

00,185
PB94-185238 Not available NTIS
National Inst. of Standards and Technology (MSEL), Gaithersburg, MD. Polymers Div.
Tapered Cross-Pin Attachments for Fixed Bridges.
Final rept.
F. C. Eichmiller, and E. E. Parry. 1994, 4p.
Pub. in Operative Dentistry 19, p7-10 1994. Sponsored by American Dental Association Health Foundation, Chicago, IL.

Keywords: *Dental prosthesis design, Dental cements, Partial denture, Alignment, Pins, Reprints.

The design and fabrication of multi-unit fixed prostheses where abutment teeth are misaligned have been difficult technical challenges for dentists and dental technicians. There have been a number of methods developed to attain a common path of insertion, including modified preparation designs, telescopic copings placed on abutments to correct alignment, adhesively retained bridge frameworks, and mechanical precision attachments between sections of a segmented prosthesis. This paper describes a method of fabricating a precision attachment on a segmented prosthesis that can be rigidly fixed after cementation. The technique involves the use of a cast tapered pin to permanently attach the prosthesis segments together. All parts can be fabricated by conventional lost-wax techniques with a minimum of instrumentation. The technique has the added advantage of being reversible should the prosthesis ever need to be separated for repair or recementation.

00,186
PB95-150959 Not available NTIS
National Inst. of Standards and Technology (MSEL), Gaithersburg, MD. Polymers Div.
Critical Evaluation of the Purification of Biominerals by Hypochlorite Treatment.
Final rept.
B. B. Tomazic, W. E. Brown, and E. D. Eanes. 1993, 9p.
Sponsored by American Dental Association Health Foundation, Chicago, IL.
Pub. in Jnl. of Biomedical Materials Research 27, p217-225 1993.

Keywords: *Heart valve prosthesis, *Purification, *Mineralization, Extraction, X-ray diffraction, Crystallization, Calcification, Performance evaluation, Comparison, Reprints, *Hypochlorite treatment, *Deproteination, *Hydrazine treatment.

The quantitative deproteination of calcific deposits from surgically explanted heart valve bioprostheses was carried out by both hypochlorite and hydrazine extraction to establish which is better procedure for preparing purified mineral suitable for detailed chemical and structural characterization. Hypochlorite treatment resulted in a material with a higher Ca/PO4 ratio than that of the untreated deposits. The hydrazine treatment did not produce such an effect. A systematic comparison of x-ray diffraction patterns of calcific deposits showed an increase in crystallinity of hypochlorite-treated versus native material, while the crystallinity of hydrazine-treated materials did not change. The deproteination is preferable to hypochlorite extraction in isolating pathologic mineral deposits from bioprosthetic materials for further study.

00,187
PB96-156039 Not available NTIS
National Inst. of Standards and Technology (MSEL), Gaithersburg, MD. Polymers Div.
Physicochemical Characterization of Natural and Bioprosthetic Heart Valve Calcific Deposits: Implications for Prevention.
Final rept.
B. B. Tomazic, W. E. Edwards, and F. J. Schoen. 1995, 6p.
See also PB94-172863. Sponsored by American Dental Association Health Foundation, Chicago, IL.
Pub. in Proceedings of the International Symposium Cardiac Bioprostheses (6th), Vancouver, Canada, July 29-31, 1994, The Annals of Thoracic Surgery, v60 pS322-S327 1995.

Keywords: *Heart valve prothesis, *Prothesis, Cardiovascular system, Precursors, Solubility, Reprints, *Foreign technology, Bioapatities, Calcific deposits, Octacalcium phosphate hydrolyzate.

This investigation was performed to provide a comprehensive physicochemical characterization of clacific deposits (CDs) that form on human heart valves under various pathological conditions. The authors examined and characterized CDs associated with aortic stenosis on congenitally bicuspid valves (n = 10), degenerative aortic stenosis on valves with previously normal anatomy (n = 10), an Rheumatic aortic (n = 10) and mitral (n = 10) stenosis. Native and deproteinated CDs underwent chemical analysis and structural characterization, whereas deproteinated CDs were measured for thermodynamic solubility. The CDs in valvular heart disease were microcrystalline apatitic products containing substantial amounts of sodium, magnesium, carbonate, fluoride, and organic fraction.

00,188
PB97-113120 Not available NTIS
National Inst. of Standards and Technology (MSEL), Gaithersburg, MD.
International Standards and Reference Materials.
Final rept.
J. A. Tesk. 1996, 4p.
See also PB90-217894.
Pub. in Proceedings, Conference on Implant Retrieval and Analysis, Buffalo, NY., June 2-3, 1996, p1-4.

Keywords: *Standards, Biocompatible materials, Certification, Interlaboratory comparisons, Chemical analysis, Reprints, *Standard reference materials, *Medical implants, Implant retrieval.

International organization for Standardization Definitions of reference materials and NIST definitions are given and compared. The question of needs for special reference materials for retrieved implant analysis is raised for discussion.

Protective Equipment

00,189
PB95-151171 Not available NTIS
National Inst. of Standards and Technology (MSEL), Gaithersburg, MD. Polymers Div.
NIR-Spectroscopic Investigation of Water Sorption Characteristics of Dental Resins and Composites.
Final rept.
S. Venz, and B. Dickens. 1991, 18p.
Sponsored by American Dental Association Health Foundation, Chicago, IL.
Pub. in Jnl. of Biomedical Materials Research 25, p1231-1248 1991.

Keywords: *Dental materials, *Composite materials, *Water, *Absorption, Moisture content, Sorption, Hydrogen bonds, Reprints, *Near infrared spectroscopy.

A near infrared (NIR) method using the 5200/cm absorption of water has been employed to examine water absorbed in photopolymerized dental resins and composites in the form of 0.01 cm- to 0.15 cm-thick specimens. Water sorption was determined gravimetrically and correlated to the absorbance in the NIR spectrum. The NIR absorptivity, epsilon, of water absorbed in a polymeric medium was found to be inversely related to the degree of hydrophilicity and hydrogen bonding capability of the polymer. The presence of water clusters in a polyethylene oxide methacrylate polymer was inferred from convex-up curvature in the plot of epsilon vs. water content.

00,190
PB96-190301 Not available NTIS
National Inst. of Standards and Technology (EEEL), Boulder, CO. Optoelectronics Div.
Optical Density Measurements of Laser Eye Protection Materials.
Final rept.
T. R. Scott, R. J. Rockwell, and P. Batra. 1993, 10p.
Pub. in Proceedings of the International Laser Safety Conference, Cincinnati, OH., December 1-4, 1992, p8-7-8-16 1993.

Keywords: *Laser hazards, *Eye safety, *Optical density, Laser beams, Laser safety, Protective equipment, Optical filters, Optical properties, Vision, Configurations, Wavelengths, Reprints, *Protective eyewear, Eye protectors.

Various types of protective eyewear are available for use in shielding the user's eyes from the harmful effects of intense laser radiation. Proper protective eyewear is chosen by selecting materials whose inherent transmission characteristics are appropriate for the expected laser operating conditions (e.g. wavelength, power level, etc). For convenience, the transmittance values of protective eyewear are typically expressed in terms of optical density (i.e. the logarithm to the base 20 of the reciprocal of the transmittance) for specific laser wavelengths. These density values are usually stamped or printed on the eyewear assemblies. The paper describes the measurement methods and results of the optical density measurements performed on designated protective eyewear samples at several specific laser wavelengths. The measurement configurations and associated measurement error sources will also be reviewed.

BUILDING INDUSTRY TECHNOLOGY

General

00,191
PB94-145976 PC A04/MF A01
National Inst. of Standards and Technology (BFRL), Gaithersburg, MD.
Use of Computer Models to Predict Temperature and Smoke Movement in High Bay Spaces.
K. A. Notarianni, and W. D. Davis. Dec 93, 64p, NISTIR-5304.
Sponsored by National Aeronautics and Space Administration, Greenbelt, MD. Goddard Space Flight Center. and Public Buildings Service, Washington, DC.

Keywords: *Bays(Structural units), *Fire tests, *Computerized simulation, Warehouses, Smoke, Industrial buildings, Plumes, Hangars.

Large spaces, such as those found in warehouses, historical buildings, atriums, and aircraft hangars, represent some of the most difficult fire protection challenges since they are frequently of historical significance, contain large quantities of fuel, have unique geometries, and/or present special life safety problems. Accurate detector activation predictions are important in these large spaces, as timely detection of a fire is more difficult due to the distance heat and products of combustion must travel to reach sprinklers and detectors. The Building and Fire Research Laboratory (BFRL) was given the opportunity to make measurements during fire calibration tests of the heat detection system in an aircraft hangar with a nominal 30.4 m (100 ft) ceiling height near Dallas, TX. Three closed-door tests were conducted.

00,192
PB94-164191 PC A03/MF A01
National Inst. of Standards and Technology (BFRL), Gaithersburg, MD.
BFRL Fire Publications, 1993.
N. H. Jason. Apr 94, 38p, NISTIR-5397.
See also PB94-121050.

Keywords: *Fire tests, *Bibliographies, Combustion, Smoke, Soot, Fire hazards, Fire protection, Technology transfer, Carbon monoxide, Models, *Building fires.

The document contains references to the publications prepared by the members of the Building and Fire Research Laboratory (BFRL) fire research staff, by other National Institute of Standards and Technology (NIST) personnel for BFRL, or by external laboratories under contract or grant from the BFRL during the calendar year 1993.

00,193
PB94-199270 Not available NTIS
National Inst. of Standards and Technology (BFRL), Gaithersburg, MD. Fire Safety Engineering Div.
Analysis of the Happyland Social Club Fire with HAZARD I.
Final rept.
R. W. Bukowski, and R. C. Spetzler. 1992, 14p.
Pub. in Jnl. Fire Prot. Engr. 4, n4 p117-130 1992.

Keywords: *Fire hazards, *Buildings, Fires, Fire safety, Egress, Fire protection, Safety engineering, Sprinklers, Finishes, Reprints, *Happyland Social Club Fire, HAZARD I model, Fire analysis.

The paper presents the reconstruction of the Happyland Social Club fire using the HAZARD I fire hazard assessment method along with an examination of four potential mitigation strategies: automatic sprinklers, a door at the base of the stairway to the second floor, a second means of egress from the second floor, or a noncombustible interior finish. The paper concludes that the traditional second means of egress might have not eliminated the observed fatalities, and that the noncombustible interior finish or sprinkler options would, with the former being the more cost effective approach.

00,194
PB94-205952 PC A03/MF A01
National Inst. of Standards and Technology (BFRL), Gaithersburg, MD.
Fire Growth Analysis of the Fire of March 20, 1990, Pulaski Building, 20 Massachusetts Avenue, N.W., Washington, DC.
H. E. Nelson. Jun 94, 42p, NISTIR-4489.
See also PB92-132984. Sponsored by Corps of Engineers, Washington, DC.

Keywords: *Office buildings, *Fires, Smoke, District of Columbia, Flames, Flashover, *Building fires, Pulaski building.

An analysis of an office building fire was made using fire modeling techniques. The data to conduct the analysis was obtained through on-site inspection and interviews. The analysis describes a rapid fire developing in easily ignited boxing materials that flashed over in about six minutes from flame initiation, causing failure of the ceiling system, venting of fire products in the plenum system above the ceiling, and rapid filling of the entire flow area with smoke. The report suggests a likely source of ignition and provides analysis of the impact that several fire protection systems would have had were they present at the time of the fire.

00,195
PB94-206356 PC A04/MF A01
National Inst. of Standards and Technology (BFRL), Gaithersburg, MD. Fire Safety Engineering Div.
Evaluating Small Board and Care Homes: Sprinklered vs. Nonsprinklered Fire Protection.
S. Deal. Nov 93, 63p, NISTIR-5302.
Sponsored by Fire Administration, Emmitsburg, MD.

Keywords: *Fire safety, *Nursing homes, Evacuating(Transportation), Computerized simulation, Sprinklers, Egress, Fire hazards.

This report studied the effectiveness of sprinklered and nonsprinklered fire protection options in small Board and Care homes. The tools used to compare the effectiveness of these fire protection options were mathematical fire models, experimental data and documented fire incidents. The mathematical models estimated fire protection effectiveness through a margin of safety analysis. The margin of safety is defined in this report as the excess time an evacuee has to reach a point of safety before that evacuee's exit path becomes untenable. The margin of safety calculations considered fire growth, detection/alarm activation, evacuee egress movement and smoke tenability analysis. Two egress movement plans were simulated; one plan reflected necessary movement in a one-exit home, the second plan reflected movement in a two-exit home. Two fast-growing, large flashover fires (with high and low CO production rates) and a small, smoldering fire were modeled. Two sets of full-scale spinklered and post-flashover fire experiments, as well as 61 documented fire incidents were included in the study of fire protection system effectiveness.

00,196
PB94-501988 Diskette $250.00
National Inst. of Standards and Technology, Gaithersburg, MD.
HAZARD I Fire Hazard Assessment Method (Version 1.2) (for Microcomputers).
Software.
Jun 94, 3 diskettes, NIST/SW/DK-94/001.
System: IBM PC or compatible; MS DOS 3.0+ operating system. Language: FORTRAN and Assembly. Hardware requirements: 386 processor or later with 3 megabytes of RAM. Supersedes PB92-500420.
The software is available on three 3 1/2 inch diskettes, 1.44M high density.

Keywords: *Software, *Fire hazards, *Buildings, Fire damage, Fire losses, Injuries, Casualties, Fire safety, Fires, Evacuation, Building materials, Furniture, Diskettes, *Hazard assessment, HAZARD I computer program, Fire models.

A method for quantifying the hazards to occupants of buildings from fires, and the relative contribution of specific products (e.g., furniture, wire insulation) to those hazards is presented. The method, called HAZARD I, combines expert judgement and calculations to estimate the consequences of a specified fire. These procedures involve four steps: (1) defining the content, (2) defining the scenario, (3) calculating the hazard, and (4) evaluating the consequences. Steps 1, 2, and 4 are largely judgemental and depend on the expertise of the user. Step 3, which involves use of the extensive computer software, requires considerable expertise in fire safety practice. The heart of HAZARD I is a sequence of computer software procedures which calculate the development of hazardous conditions over time, calculate the time needed by building occupants to escape under those conditions, and estimate the resulting loss of life based on assumed occupant behavior and tenability criteria.

00,197
PB94-501996 CP D99
National Inst. of Standards and Technology, Gaithersburg, MD.
HAZARD I Fire Hazard Assessment Method, Version 1.2 (Upgrade Package) (for Microcomputers).
Software.
Jun 94, 3 diskettes, NIST/SW/DK-94/002.
System: MS DOS 3.0+ operating system, 640K. Language: FORTRAN, Assembly. Hardware requirements: 386 processor or later with 3 megabytes of RAM. Available to previous buyers of PB92-500438 only. One copy per registered buyer. Supersedes PB92-500438. See also PB94-501988.
The software is on three 3 1/2 inch DOS diskettes, 1.44M high density.

Keywords: *Software, *Fire hazards, *Buildings, Fire damage, Fire losses, Injuries, Casualties, Fire safety, Fires, Evacuation, Building materials, Furniture, Diskettes, *Hazard assessment, HAZARD I computer program, Fire models.

A method for quantifying the hazards to occupants of buildings from fires, and the relative contribution of specific products (e.g., furniture, wire insulation) to those hazards is presented. The method, called HAZARD I, combines expert judgement and calculations to estimate the consequences of a specified fire. These procedures involve four steps: (1) defining the content, (2) defining the scenario, (3) calculating the hazard, and (4) evaluating the consequences. Steps 1, 2, and 4 are largely judgmental and depend on the expertise of the user. Step 3, which involves use of the extensive computer software, requires considerable expertise in fire safety practice. The heart of HAZARD I is a sequence of computer software procedures which calculate the development of hazardous conditions over time, calculate the time needed by building occupants to escape under those conditions, and estimate the resulting loss of life based on assumed occupant behavior and tenability criteria.

00,198
PB95-161188 Not available NTIS
National Inst. of Standards and Technology (BFRL), Gaithersburg, MD. Fire Safety Engineering Div.
Locating Fire Engineering Information.
Final rept.
N. H. Jason. 1993, 4p.
Pub. in Society of Fire Protection Engineers Bulletin, p5-8 Sep/Oct 93.

Keywords: *Fire research, *Information systems, *Databases, Fire protection, Fire hazards, Fire safety, Fire prevention, Fire damage, Fire fighting, Safety engineering, Fires, Online systems, Information retrieval, Information dissemination, Reprints.

Various information resources are discussed. FIREDOC, the online bibliographic database of the Building and Fire Research Laboratory's literature collection, is discussed in depth and its role for the fire protection engineer.

00,199
PB95-164588 Not available NTIS
National Inst. of Standards and Technology (NEL), Gaithersburg, MD. Center for Fire Research.
Quantitative Evaluation of Building Fire Safety: New Tools for Assessing Fire and Building Code Provisions.
Final rept.
J. E. Snell. 1989, 12p.
Pub. in Proceedings of Pacific Rim Conference on Building Officials, Honolulu, HI., April 9-13, 1989, p1-12.

Keywords: *Fire hazards, *Building codes, *Risk assessment, Fire safety, Safety engineering, Fire prevention, Fire damage, Fire losses, Buildings, Computerized simulation, Reprints, HAZARD I computer program, Hazard assessment.

The National Institute of Standards and Technology has developed a quantitative method for evaluation of fire hazard, HAZARD I, built around a computer software package designed for use on a personal computer. This system permits the user to simulate the consequences, in terms of loss of life, injury, or ultimately property damage of a specified fire in a prescribed building. The paper outlines HAZARD I and recent improvements to it, and reports the results of trial uses of this new tool. The steps envisioned for the effective transfer of this new technology within the fire safety community are examined and the implications of it for fire and building code officials are drawn.

00,200
PB95-175220 Not available NTIS
National Inst. of Standards and Technology (BFRL), Gaithersburg, MD. Fire Safety Engineering Div.
Developing Rational Performance-Based Fire Safety Requirements in Model Building Codes.
Final rept.
R. W. Bukowski, and V. Babrauskas. 1994, 19p.
Pub. in Fire and Materials 18, p173-191 1994.

Keywords: *Building codes, *Fire safety, *Performance standards, Fire protection, Risk analysis, Design standards, Buildings, Performance tests, Fire tests, Japan, United States, Reprints.

The technical and philosophical basis for performance-based assessment of building fire performance is reviewed. A strategy for the evolutin of a performance code is described. Current efforts toward the development of performance codes in the USA and Japan are reviewed. Recommendations for critical steps necessary to advance the development and acceptance of performance codes are presented. The table of contents of the Japanese risk methodology for assessing 'Article 38 equivalencies' is included in an appendix.

00,201
PB95-175238 Not available NTIS
National Inst. of Standards and Technology (BFRL), Gaithersburg, MD. Fire Safety Engineering Div.
Earthquake and Fire in Japan: When the Threat Became a Reality.
Final rept.
R. W. Bukowski, and C. Scawthorn. 1994, 6p.
Pub. in NFPA Jnl. 88, n3 p89-92, 94, 96, May/Jun 94.

General

Keywords: *Earthquakes, *Fires, *Emergency preparedness, *Risk analysis, *Japan, *United States, Fire hazards, Fire safety, Fire departments, Emergency plans, Fire protection, Warning systems, Disasters, Seismic effects, Earthquake engineering, Buildings, Reprints.

San Francisco Fire Department released a report that identified problem areas encountered following the quake. Despite all of the problems, the fire department of 1989 was better prepared for a disaster than the department of 1906. The department and the city learned from the destruction and made many needed changes.

00,202
PB95-175808 Not available NTIS
National Inst. of Standards and Technology (BFRL), Gaithersburg, MD. Fire Safety Engineering Div.
Fire and Smoke Control: An Historical Perspective.
Final rept.
J. H. Klote. 1994, 5p.
Pub. in American Society of Heating, Refrigeration and Air-Conditioning Engineers Jnl. 36, n7 p46-50 Jul 94.

Keywords: *Fire prevention, *Air flow, *Ventilation, *Historical aspects, Smoke abatement, Fire safety, Fire protection, Safety engineering, Buildings, Reprints, *Smoke control.

In commemoration of the ASHRAE Centennial, the paper is a brief history of ASHRAE's activities in fire and smoke control. The first ASHRAE fire related symposium marked the start of a period of ASHRAE fire related activity that is ongoing. This was followed by formation of a Technical Committee 5.6 on Fire and Smoke Control. In those early years, the committee also found time to develop a chapter for the ASHRAE handbook and to play a vital role in member education. In later years, the committee became well focused and highly efficient at most every aspect of technical committee effort.

00,203
PB95-217162 PC A04/MF A01
Virginia Polytechnic Inst. and State Univ., Blacksburg. Dept. of Mechanical Engineering.
Compartment Fire Combustion Dynamics. Annual Report, September 1, 1993-September 1, 1994.
U. Vandsburger, B. Y. Lattimer, and R. J. Roby. Dec 94, 57p, NIST/GCR-95/666.
Grant NIST-60NANB1D1176
See also PB92-156744. Prepared in cooperation with Hughes Associates, Inc., Columbia, MD. Sponsored by National Inst. of Standards and Technology, Gaithersburg, MD.

Keywords: *Fires, *Combustion products, *Buildings, Carbon monoxide, Soot, Toxicity, Gases, Tests.

The overall scope of this research is to investigate the phenomena that control the generation and oxidation of compartment fire exhaust gases, specifically carbon monoxide (CO), total unburned hydrocarbons (THC) and soot, which are transported down an adjacent corridor. The first year of the investigation concentrated on the formation of exhaust gases, mainly CO, within the compartment. In the second year, a hallway was attached to the compartment in such a manner that the gases from the compartment entered at the ceiling of the corridor. The oxidation of the exhaust gases down the hallway was studied for a corridor having no soffits at either end. During the past year, three additional hallway soffit combinations were added to see the results of varying the fluid mechanics of the exhaust gases within the hallway.

00,204
PB95-269817 PC A03/MF A01
Civil Engineering Research Foundation, Washington, DC.
National Construction Sector Goals: Industry Strategies for Implementation.
Jul 95, 44p, NISTIR/GCR-95/680.
Contract NIST-50SBNB56C8506
Sponsored by National Inst. of Standards and Technology (BFRL), Gaithersburg, MD.

Keywords: *Residential buildings, *Public works, *Construction industry, Goals, Objectives, Cost engineering, Strategic analysis, Research and development, Technology transfer.

The strategy outlined in this report is an important first step towards the success of this bold national construction goals initiative for public works infrastructure. The process has begun with this initial strategy; it will be continued through the monthy (or more often) meetings of the public works oversight group, commencing in July with the first meeting of the four organizations who have stepped forward to provide the initial leadership for this vital national initiative.

00,205
PB96-102108 Not available NTIS
National Inst. of Standards and Technology (BFRL), Gaithersburg, MD. Fire Safety Engineering Div.
Fire Codes for Global Practice.
Final rept.
R. W. Bukowski. 1995, 3p.
Pub. in Progressive Architecture, p117-119 Jun 95.

Keywords: *Fire safety, *Building codes, *Design standards, Fire codes, Safety design, Safety engineering, Fire research, Fire hazards, Buildings, Design analysis, Design criteria, Risk management, Compliance, Global, Reprints.

Architecture in a world economy, with multinational clients and a global range of building materials and systems, demands fire codes based on performance. The International Council for Building Research is now working on methods to verify compliance under performance-based fire codes. Performance codes will have several advantages: code objectives clearly stated and understood by all parties, and analytical methods, data, and assumptions formallized in a single code of practice.

00,206
PB96-102116 Not available NTIS
National Inst. of Standards and Technology (BFRL), Gaithersburg, MD. Fire Safety Engineering Div.
How to Evaluate Alternative Designs Based on Fire Modeling.
Final rept.
R. W. Bukowski. 1995, 6p.
Pub. in NFPA Jnl., v89 n2 p68-70, 72-74 Mar/Apr 95.

Keywords: *Buildings, *Design analysis, *Fire safety, Fire research, Fire hazards, Safety design, Design standards, Safety engineering, Building codes, Fire codes, Alternatives, Regulations, Reprints, Fire models.

Fire models and other predictive methods are becoming common means of supporting the design and arrangement of building fire safety features to code officials where strict compliance with prescriptive requirements is not possible. This paper provides code officials faced with such analyses guidance on the key elements which should be addressed to ensure credibility. Guidelines are presented covering the selection of appropriate models and methods, design fires, evacuation calculations, sensitivity and uncertainty, and documentation. Some comments on establishing an independent review process for alternative design analyses and on certification of appropriate methods are included.

00,207
PB96-102934 Not available NTIS
National Inst. of Standards and Technology (BFRL), Gaithersburg, MD. Fire Safety Engineering Div.
Santa Ana Fire Department Experiment at 1315 South Bristol, July 14, 1994. (Reprint).
Final rept.
A. D. Putorti, W. D. Walton, W. H. Twilley, S. Deal, and J. C. Albers. 1995, 3p.
See also PB95-188868.
Pub. in Fire Technology, v31 n1 p62-67 1995.

Keywords: *Residential buildings, *Fire tests, Fire protection, Fire detectors, Sprinklers, Flammability, Construction materials, Temperature measurement, Fire safety, Smoke, Reprints, *Santa Ana(California).

This report of test addresses a fire experiment conducted on July 14, 1994 in a vacant single family dwelling at 1315 South Bristol Street in Santa Ana, California. Fire phenomena measured included: temperatures within various rooms, the velocity and temperature of outflowing cases, smoke detector activation times, and time to full room involvement.

00,208
PB96-102967 Not available NTIS
National Inst. of Standards and Technology (CAML), Gaithersburg, MD.
Pressure Equations in Zone-Fire Modeling.
Final rept.
R. G. Rehm, and G. P. Forney. 1994, 13p.
See also PB92-238617.
Pub. in Fire Science and Technology, v14 n1-2 p61-73 1994.

Keywords: *Fire tests, *Pressure dependence, *Ordinary differential equations, Compartment analysis, Heat transfer, Exothermic reactions, Combustion, Pressure gradients, Mathematical models, Numerical analysis, Phase plane analysis, Thermodynamics, Reprints, Fire models, Zone fires, Singular perturbation analysis.

The nonadiabatic nature of low-speed combustion and fire, in which strongly exothermic reactions produce large temperture variations but only mild pressure variations, can cause difficulty when integrating zone models of enclosure fires. Examples of simple zone fire models are examined to illustrate the analytical nature of the problems encountered. These difficulties arise in the solution of the equations for the pressure in general enclosures because the pressure equilibrates much more rapidly than other dynamical variables. Singular perturbation methods and phase plane analyses, together with numerical integration of the nondimensionalized equations, are employed to study the stiff nature of the equations. We conclude that many of the difficulties associated with numerical integration of zone fire models may be circumvented by appropriate analysis of the zone fire model equations.

00,209
PB96-117916 PC A04/MF A01
National Inst. of Standards and Technology (BFRL), Gaithersburg, MD.
Post-Earthquake Fire and Lifelines Workshop. Held in Long Beach, California on January 30-31, 1995. Proceedings.
Special pub.
R. M. Chung, N. H. Jason, B. Mohraz, F. W. Mowrer, and W. D. Walton. Aug 95, 56p, NIST/SP-889.

Keywords: *Earthquake damage, *Fire hazards, *Emergency planning, *Meetings, Earthquakes, Fires, Damage assessment, Pipelines, Highways, Water supply, Public utilities, Natural gas, Electric power, Telecommunication, Transportation sector, Liquid fuels, Sprinkler systems, Fire damage, Fire alarm systems, Fire protection, Fire fighting, Fire suppression, Fire research, Seismic design.

A postearthquake fire and lifeline workshop sponsored by the Building and Fire Research Laboratory, National Institute of Standards and Technology, was held January 30-31, 1995, in Long Beach, California. The objective of the workshop was to identify technology development and research needs that will be used in developing recommendations to reduce the number and severity of postearthquake fires. The workshop participants included leaders in the fire service, fire protection engineering, codes and standards, insurance, transportation systems, and water, gas, power distribution, and telecommunication utilities systems with experience in dealing with consequences of earthquakes. The workshop participants developed a list of priority project areas where further research, technology development, or information collection and dissemination would serve as a vital step in the future reduction of the losses from postearthquake fires.

00,210
PB96-146790 Not available NTIS
National Inst. of Standards and Technology (BFRL), Gaithersburg, MD. Fire Science Div.
Global Equivalence Ratio Concept and the Formation Mechanisms of Carbon Monoxide in Enclosure Fires.
Final rept.
W. M. Pitts. 1995, 41p.
See also PB94-207511.
Pub. in Progress in Energy and Combustion Science, v21 p197-237 1995.

Keywords: *Crabon monoxide, *Fire hazards, *Combustion products, Compartment fires, Enclosures, Flame propagation, Combustion kinetics, Chemical reaction kinetics, Polymers, High temperature, Mathematical models, Reprints, *Global Equivalence Ratio.

This report summarizes a large number of investigations designed to characterize the formation of carbon monoxide (CO) in enclosure fires--the most important factor in fire deaths. It includes a review analysis of the studies which form the basis for the global equivalence ratio (GER) concept. Based on the findings, two completely new mechanisms for the formation of CO, in addition to the quenching of a fire plume by a rich

upper layer, which is described by the GER concept, are identified.

00,211
PB96-148119 Not available NTIS
National Inst. of Standards and Technology (BFRL), Gaithersburg, MD. Fire Safety Engineering Div.
Information Resources for the Fire Community.
Final rept.
N. H. Jason. 1995, 6p.
Pub. in Proceedings of the International Conference of Fire Research and Engineering, Orlando, FL., September 10-15, 1995, p469-474.

Keywords: *Fire research, *Information retrieval, *Data bases, Information systems, Fire protection, Fire safety, Safety engineering, Information dissemination, Fire prevention, Reprints.

As information technology expands, information has become more readily available but the sources of this information have become more diverse. Within the field of fire research and engineering, it has become more challenging to find critical information because traditional sources of information have been augmented by a variety of electronic sources. Looking for specific information used to be performed by brute force, i.e., checking the library card catalog. With the explosion in computer communication, information retrieval has become an art form. The fire scientists or engineer must develop a familiarity with a wide range of old and new methods for acquiring information as well as staying abreast of latest developments. Success in the new world order of information science will go to the well informed user. An overview of print and electronic resources that are described in this paper can provide a starting point for responding to any information request.

00,212
PB96-148192 Not available NTIS
National Inst. of Standards and Technology (BFRL), Gaithersburg, MD. Fire Safety Engineering Div.
Heights of Wall-Fire Flames.
Final rept.
H. E. Mitler. 1995, 5p.
Pub. in Proceedings of the International Conference on Fire Research and Engineering, Orlando, FL., September 10-15, 1995.

Keywords: *Fire research, *Walls, *Flames, Height, Fires, Pyrolysis, Reprints, Line fire, Wall fires.

A correlation between the visible height of a flame and the power output of the flame is useful for a number of reasons. Thus, observation of a fire can permit one to estimate the rate of heat release and therefore the fuel flow rate. Again, an expression for the flame height is needed in order to calculate the upward flame spread rate on walls. It is therefore important that such an expression be reliable. The heights of flames from line burners adjacent to walls have been correlated by a number of workers.

00,213
PB96-151394 Not available NTIS
National Inst. of Standards and Technology (BFRL), Gaithersburg, MD. Building and Fire Research Lab.
Fire Safety Engineering Research in the United States.
Final rept.
J. E. Snell. 1992, 9p.
Pub. in International Fire Safety Engineering Conference: The Concepts and the Tools, Kings, Cross, Sydney, NSW, Australia, October 18-20, 1992, Session 3, p1-9.

Keywords: *Fire research, *Fire safety, *Safety engineering, Fire prevention, Fire codes, Fire losses, Research programs, Technology innovation, United States, Reprints, US NIST.

The paper describes fire research in the United States and particularly the fire research program at the National Institute of Standards and Technology. First, it comments on the background to this program, and then describes the context in which it functions, i.e., the building regulatory and product approval systems and other fire research activities in the USA. Next, it outlines the rationale for NIST fire research and notes some of the research products and their impacts.

00,214
PB96-151402 Not available NTIS
National Inst. of Standards and Technology (BFRL), Gaithersburg, MD. Building and Fire Research Lab.
Elements of a Framework for Fire Safety Engineering.
Final rept.
J. E. Snell. 1993, 10p.
Pub. in International Fire Conference (6th), Interflam '93, Oxford, England, March 30-April 1, 1993, p447-456.

Keywords: *Fire safety, *Safety engineering, *Design criteria, Fire prevention, Fire codes, Fire research, Risk analysis, Decision making, Standards, Reprints.

The paper lays out a framework for fire safety engineering based on scientific tools for fire safety design and decision-making. These tools include computer-based models for fire safety hazard and risk prediction, measurement methods to provide data for such methods, databases and expert systems to provide access to them, and the ultimate integration of these tools with other elements of computer-aided design, construction and conformity assessment. The paper suggests needs, roles and actions required to bring fire safety engineering to the level of sophistication enjoyed in most other areas of engineering practice. The need for international cooperation and public-private collaboration is stressed.

00,215
PB96-154968 PC A03/MF A01
Clemson Univ., SC.
Sensitivity Analysis for Mathematical Modeling of Fires in Residential Buildings.
Final rept. Oct 94-Sep 95.
M. M. Kostreva. Feb 96, 15p, NIST/GCR-95/683.
Grant NIST-NANB4D1649
Sponsored by National Inst. of Standards and Technology (BFRL), Gaithersburg, MD.

Keywords: *Fires, *Residential buildings, *Mathematical models, *Sensitivity analysis, Rooms, Gases, Smoke, Parameters, Heat flux, Flame propagation, Differential equations, Fires safety.

The Building and Fire Research Laboratory engages in research and development of mathematical models of fires in residential buildings together with human egress of the building occupants. The research here analyzes the existing approach of HAZARD I, together with the likely modifications incorporated into HAZARD II (CONRAD2) and establishes a prototype sensitivity analysis equipped fire model computer program, thereby evaluating and demonstrating recently obtained results on the mathematical foundations of fire models.

00,216
PB96-155767 Not available NTIS
National Inst. of Standards and Technology (BFRL), Gaithersburg, MD. Structures Div.
Spectrum of the Stochastically Forced Duffing-Holmes Oscillator.
Final rept.
E. Simiu, and M. Frey. 1993, 4p.
Pub. in Physics Letters A, v177 p199-202 1993.

Keywords: *Noise, *Chaos, Building technology, Dynamics, Stochastic processes, Structural dynamics, Reprints, *Foreign technology.

The Brudsen-Holmes method of power spectrum estimation for the Duffing-Holmes oscillator is applied to the case of weak quasiperiodic excitation and then extended to weak colored noise excitation with any specified spectral density. A novel model of near-Gaussian noise is introduced to achieve this extension. The results obtained by this approach coincide with and extend those obtained by Stone and Holmes' application of the Fokker-Planck equation. In particular, our results confirm Stone's conjecture that the expression for the mean time between successive maxima in the case of colored noise similar to that for white noise.

00,217
PB96-156120 Not available NTIS
National Inst. of Standards and Technology (BFRL), Gaithersburg, MD. Structures Div.
Noise-Induced Transitions to Chaos.
Final rept.
M. Frey, and E. Simiu. 1995, 16p.
Contract ONR-N-00014-93-F-0028
Sponsored by Office of Naval Research, Arlington, VA.
Pub. in Proceedings of the NATO Advanced Research Workshop on Spatio-Temporal Patterns in Non-Equilibrium Complex Systems, p529-544 1995.

Keywords: *Noise, *Chaos, Building technology, Dynamical systems, Reprints, Melnidov transforms, Multistable systems, Phase space flux, Stochastic equations.

Additive noise is shown to induce chaotic motion with sensitive dependence on initial conditions in multistable dynamical systems. This establishes a fundamental connection between two fields hitherto viewed as distinct: deterministic chaos and stochastic differential equations modeling the dynamics of multistable systems. Our results for additive noise are then generalized to multiplicative noise. Using a newly introduced model of shot noise, these results for multiplicative noise are applied to the Duffing oscillator with shot noise-like dissipation.

00,218
PB96-156138 Not available NTIS
National Inst. of Standards and Technology (BFRL), Gaithersburg, MD. Structures Div.
Deterministic and Stochastic Chaos.
Final rept.
M. Frey, and E. Simiu. 1993, 22p.
Pub. in Computational Stochastic Mechanics, Chapter 9, p195-216 1993.

Keywords: *Chaos, *Noise, Dynamical systems, Reprints, *Foreign technology, Nonlinear systems, Shot noise, Stochastic systems.

Stochastic differential equations and classical technique related to the Fokker-Planck equation are standard bases for the analysis of nonlinear systems perturbed by noise. An alternative, complementary approach applicable to systems featuring heteroclinic or homoclinic orbits uses phases space flux as a measure of noise-induced chaotic dynamics. We continue our development of this method, extending our previous treatment additive noise to the more general case of multiplicative noise. This extension is used with a new model of shot noise to treat the Duffing oscillator with shot noise-like dissipation.

00,219
PB96-156146 Not available NTIS
National Inst. of Standards and Technology (BFRL), Gaithersburg, MD. Structures Div.
Experimental and Numerical Chaos in Continuous Systems: Two Case Studies.
Final rept.
G. R. Cook, and E. Simiu. 1991, 4p.
Pub. in Proceedings of the ASCE Engineering Mechanics Specialty Conference, Columbus, OH., May 20-22, 1991, p786-789.

Keywords: *Chaos, *Buckled columns, Structural engineering, Reprints, Fluid elasticity, Galloping oscillators.

Motivated by recent numerical investigations according to which certain types of deep-water compliant offshore structures may experience undesirable chaotic motions, two types of experimental structural systems capable of exhibiting chaotic or apparently chaotic behavior were studied. The first type of system is a harmonically forced buckled column with a concentrated mass at midspan and with pretensioned continuous springs. For this system a model with pretensioned continuous springs. For this system a model with acceptable predictive capabilities can be constructed if the continuous springs are represented by a sufficient number of lumped masses with discrete stiffnesses. The second type of system consists either of a galloping square bar or of a pair of parallel, elastically coupled galloping square bars. Our results suggest that the behavior of this type of system, including apparently chaotic behavior, can be described at least to a first approximation by conventional fluidelastic models. However, the predictive capabilities of such models are poor, i.e., in the present state of the art the existence of certain types of hydroelastic behavior may be altogether missed at the design stage. The incorporation of stochastic excitations in the models to account for small flow irregularities may result in improved prediction capabilities.

00,220
PB96-156153 Not available NTIS
National Inst. of Standards and Technology (BFRL), Gaithersburg, MD. Building and Fire Research Lab.
Internationalization of Fire Safety Engineering Research and Strategy.
Final rept.
J. E. Snell. 1992, 12p.
Pub. in Proceedings of the International Fire Safety Engineering Conference: The Concept of Tools, Kings Cross, Sydney, NSW, Australia, October 18-20, 1992, Session 1, p1-12 .

Keywords: *Fire safety, *Safety engineering, *Research programs, Fire research, Fire hazards, Fire protection, Fire suppression, Fire provention, International cooperation, Reprints.

This paper address this new era of fire safety engineering, the trends and other factors driving it, what it means to how we provide fire safety in our societies, and why an international strategy for its further development is i our mutual interest. The role of the Forum for International Cooperation on Fire Research is discussed and actions are suggested.

00,221
PB96-156179 Not available NTIS
National Inst. of Standards and Technology (BFRL), Gaithersburg, MD. Fire Safety Engineering Div.
Fire Protection Engineering Tools. Simple Tools: The Equations.
Final rept.
R. W. Bukowski. 1992, 6p.
See also PB92-132984.
Pub. in Proceedings of International Fire Safety Engineering Conference, 'The Concept and the Tools', Sydney, NSW, Australia, October 18-20, 1992, Session 4, p1-6 Oct 92.

Keywords: *Fire safety, *Software tools, *Computer programs, Fire protection, Fire hazards, Fire tests, Risk analysis, Mathematical models, Reprints, Fire models.

The paper reviews the development and current state of calculational tools for fire safety engineering, particularly algebraic equations and simple models, in relation to the more complex zone and field models also being used in practice. Examples of some of the more common relations are presented along with a discussion of their important limitations. Some comments on accuracy and precision are included.

00,222
PB96-156195 Not available NTIS
National Inst. of Standards and Technology (BFRL), Gaithersburg, MD. Fire Safety Engineering Div.
Review of Internatioanl Fire Risk Predictions Methods.
Final rept.
R. W. Bukowski. 1992, 9p.
Pub. in Proceedings of International Fire Safety Engineering Conference 'The Concept and the Tools', Sydney, NSW, Australia, October 18-20, 1992, Session 7, p1-9.

Keywords: *Flame propagation, *Risk assessment, *Fire hazards, Fire damage, Fire safety, Fire research, Performance evaluation, Fire codes, Computer programs, Fire tests, Reprints, Fire models, Fire growth.

In the 1980's, computer models and other predictive methods were increasingly applied to a broad range of practical problems in fire safety. Incertainties in the models' predictions were no greater than those associated with the traditional, but much more expensive full-scale experimental studies. Seperate, multi-year research projects in Japan and the United States resulted in the publication of prototype fire hazard analysis systems which demonstrated the ability to account for the complex interaction of the fire, building, active protection systems, occupant actions, and detailed outcomes including damage estimates and fatality counts.

00,223
PB96-159660 Not available NTIS
National Inst. of Standards and Technology (BFRL), Gaithersburg, MD. Fire Safety Engineering Div.
International Organization for Standardization: Current Activities in Fire Safety Engineering.
Final rept.
A. J. Fowell. 1993, 3p.
Pub. in NFPA/SFPE Annual Meeting, Orlando, FL., May 20-28, 1993, 3p.

Keywords: *Fire safety, *Safety engineering, *Standards, Buildings, Fire tests, Risk assessment, Fire hazards, Fire protection, Fire codes, International cooperation, ISO, Reprints.

The International Organization for Standardization's Technical Committee on Fire Tests on Building Components and Structures (ISO TC92) has performed a new Subcommittee, SC4 - Fire Safety and Engineering to extend the scope of the Technical Committee to include calculation methods in addition to standardized testing. This paper outlines the scope, organization, direction, and current progress on each of these efforts. The UK Code of Practice on the Application of Fire Engineering Principles to Fire Safety of Buildings, currently under development, is being offered as a strawman for a logical way to consider the many parameters and interactions involved in fire risk assessment.

00,224
PB96-175708 Not available NTIS
National Inst. of Standards and Technology (BFRL), Gaithersburg, MD. Fire Science Div.
Scaling Compartment Fires: Reduced- and Full-Scale Enclosure Burns.
Final rept.
N. P. Bryner, E. L. Johnsson, and W. M. Pitts. 1995, 6p.
Pub. in International Conference on Fire Research and Engineering, Orlando, FL., September 10-15, 1995, p9-14.

Keywords: *Fire tests, *Combustion chemistry, *Combustion products, *Scale models, Carbon monoxide, Toxic agents, Flashover, Air flow, Ventilation, Concentration(Composition), Temperature, Fuel-air ratio, Mathematical models, Reprints, *Compartment fires, Room fires.

This work extends the earlier reduced-scale enclosure (SRE) study to a full-scale enclosure (FSE) and focuses on comparing the gas concentrations and temperatures of the upper layers and the ventilation behaviors of the two compartments. The study is part of a larger research effort which is designed to develop a better understanding and a predictive capability for the generation of carbon monoxide, the major toxicant in fires. The findings will be incorporated into realistic fire models and used in the development of strategies for reducing the number of deaths attributed to carbon monoxide.

00,225
PB96-177373 PC A13/MF A03
National Inst. of Standards and Technology (BFRL), Gaithersburg, MD. Fire Science Div.
Innovation in the Japanese Construction Industry: A 1995 Appraisal.
Special pub.
R. G. Gann. Mar 96, 262p, NIST/SP-898.
Also available from Supt. of Docs. as SN003-003-03401-1.

Keywords: *Japan, *Construction industry, *Research and development, Technology innovation, Construction materials, Safety engineering, Construction management.

The objective of the project is to provide an evaluation of the state-of-the-art of the various aspects of the Japanese building and construction industry, featuring comparison with the U.S. counterparts. To accomplish this task, a team of experts was assembled in the technical areas to be included in the assessment. The experts were selected from the industry, academia, and research laboratories.

00,226
PB96-183074 PC A08/MF A02
National Inst. of Standards and Technology (BFRL), Gaithersburg, MD. Fire Safety Engineering Div.
Publications 1995: NIST Building and Fire Research Laboratory.
Special pub.
N. H. Jason. Apr 96, 140p, NIST/SP-838/9.
Also available from Supt. of Docs. as SN003-003-003-03408-8. See also PB95-270047.

Keywords: *Research laboratories, *US NIST, *Bibliographies, Research programs, Buildings, Fire safety, Standards, Documents, Hazards.

Building and Fire Research Laboratory Publications, 1995 contains references to the publications prepared by the members of the Building and Fire Research Laboratory (BFRL) staff, by other National Institute of Standards and Technology (NIST) personnel for BFRL, or by external laboratories under contract or grant from the BFRL during the calendar year 1995.

00,227
PB96-190137 Not available NTIS
National Inst. of Standards and Technology (BFRL), Gaithersburg, MD. Fire Safety Engineering Div.
Locating Fire Information.
Final rept.
N. H. Jason. 1996, 8p.
See also PB95-161188.
Pub. in INTERFLAM '96, International Interflam Conference (7th), Cambridge, England, March 26-28, 1996, p691-698.

Keywords: *Fire research, *Computer systems programs, *Databases, Information retrieval, Information systems, Bibliographies, Fire protection, Fire safety, Fires, Fire hazards, Online systems, Information dissemination, Reprints, Electronic resources.

Locating the best reference or answer to a specific question in fire science may be difficult. There are standard reference books and journals that may be used. New sources continue to become available, in particular, electronic tools that are available internationally. This discussion will center on developing an information tool kit identifying resources from the print media, multitopic bibliographic databases, fire databases, and the World Wide Web, to enable one to find the answer from either the traditional print media or an electronic resource.

00,228
PB96-193743 PC A05/MF A01
Washington State Univ., Pullman. Dept. of Mechanical and Materials Engineering.
Development of an Economical Video Based Fire Detection and Location System.
O. A. Plumb, and R. F. Richards. Jul 96, 73p, NIST/GCR-96/695.
Grant NIST-60NANB2D1290
Sponsored by National Inst. of Standards and Technology, Gaithersburg, MD.

Keywords: *Fire detection systems, *Video recording, Smoke detectors, Position(Location), Computerized simulation.

In the report we present the results of work directed toward the development of a working prototype of a system that can automatically detect, locate, and size an accidential fire. The fire detection system uses a video camera to gather temperature data from an array of temperature-sensitive, color-changing sensors distributed around a compartment, and a personal computer based inverse problem solution algorithm to determine the fire's location and heat release rate using the gathered temperature data. Such a system offers great promise for use in industrial facilities such as warehouses and factor floors which combine significant fire risks with minimal human monitoring for extended periods.

00,229
PB96-195508 PC A06/MF A01
Virginia Polytechnic Inst. and State Univ., Blacksburg. Dept. of Mechanical Engineering.
Dynamics, Transport and Chemical Kinetics of Compartment Fire Exhaust Gases.
Annual rept. Sep 94-Sep 95.
U. Vandsburger, and R. J. Roby. Jun 96, 77p, NIST/GCR-96/688.
Grant NANB1D1176
See also PB95-231700. Prepared in cooperation with Hughes Associates, Inc., Baltimore, MD. Sponsored by National Inst. of Standards and Technology, Gaithersburg, MD.

Keywords: *Combustion kinetics, *Thermodynamics, *Flame propagation, Gases, Smoke, Fires, Combustion products, Burning rate, Thermochemistry, Air flow, Fire chemistry, Fire research, *Compartment fires, Hallways.

The investigation focuses on the transport of carbon monoxide (CO) away from a burning compartment and the conditions necessary for the existence of fatally high concentrations of CO at remote locations. During the past year, the research has concentrated on the transport of CO away from a reduced-scale burning compartment located on the side of the end of a hallway. High levels of CO were transported to remote locations by limiting the air entrainment into the plume of compartment fire gases entering the hallway. The non-uniform transport of combustion gases down the hallway explains the locations of fatalities in previously reported fires.

00,230
PB96-202221 PC A07/MF A02
National Inst. of Standards and Technology (BFRL), Gaithersburg, MD. Office of Applied Economics.

Benefits and Costs of Research: Two Case Studies in Building Technology.
R. E. Chapman, and S. K. Fuller. Jul 96, 117p, NISTIR-5840.

Keywords: *Buildings, *Research management, Cost benefit analysis, Case studies, Economic analysis, Construction management, Energy conservation, Life cycle costs.

This report is the outgrowth of a series of microstudies prepared by NIST's Building and Fire Research Laboratory (BFRL). This report has four major purposes. First, it examines five standardized methods for evaluating existing and past research projects. Second, it establishes a framework for identifying, classifying, quantifying, and analyzing the benefits and costs of a research project, of a research program, or of a new technology. Third, it presents a generic format and a set of guidelines for summarizing the economic impacts of alternative research investments. Fourth, it illustrates--by way of two case studies--how the framework and standardized methods would be applied in practice.

00,231
PB96-202247 PC A04/MF A01
National Fire Protection Association, Quincy, MA. Fire Analysis and Research Div.
Enhancement of EXIT89 and Analysis of World Trade Center Data.
Final rept.
R. F. Fahy. Jun 96, 48p, NIST/GCR-95/684.
Grant NIST-NANB4D1584
Sponsored by National Inst. of Standards and Technology (BFRL), Gaithersburg, MD.

Keywords: *Evacuation, *Fire safety, *Human behavior, Fire hazards, Smoke, Escape(Abandonment), Exits, Egress, Decision making, Office buildings, Surveys, Computerized simulation, *EXIT89 computer model, Emergency escape, World Trade Center, New York City(New York).

The features of an enhanced model for egress from fires in non-residential occupancies is presented along with a users manual describing the use of the model. The enhancements to the model include analysis of locations of safety, smoke blockages, disabled occupants, and delays in egress. Comparisons with some available field measurements is presented. Further analysis of human behavior during a fire in the World Trade Center is presented. While previous human behavior studies have shown that people will move through smoke, this incident demonstrated that people will not only move through smoke, but also through worsening conditions. Implications for evacuation and training are discussed.

00,232
PB96-202288 PC A06/MF A01
National Inst. of Standards and Technology (BFRL), Gaithersburg, MD. Office of Applied Economics.
Benefits and Costs of Research: A Case Study of the Fire Safety Evaluation System.
Final rept.
R. E. Chapman, and S. F. Weber. Jul 96, 93p, NISTIR-5863.
See also PB96-202221.

Keywords: *Fire safety, *Research management, Benefit cost analysis, Case studies, Investments, Buildings, Life cycle costs, Hospitals, Nursing homes.

This report focuses on a critical analysis of the economic impacts from past BFRL research efforts leading to the development and introduction of the performance-based Fire Safety Evaluation System (FSES) for hospital and nursing home occupancies. The FSES was developed as an alternative to prescriptive compliance to the Life Safety Code for hospitals and nursing homes participating in the Medicare and Medicaid programs. The case study estimates the cost saving from using FSES-based modifications to promote fire safety in existing hospitals and nursing homes over the period from 1975 through 1995.

00,233
PB97-114235 PC A04/MF A01
Maryland Univ., College Park. Dept. of Fire Protection Engineering.
Survey of Fuel Loads in Contemporary Office Buildings.
T. C. Caro, and J. A. Milke. Sep 96, 35p, NIST/GCR-96/697.
Grant NIST-60NANB4D1625
Sponsored by National Inst. of Standards and Technology (BFRL), Gaithersburg, MD.

Keywords: *Office buildings, *Fire safety, Federal buildings, Combustion, Flammability, Surveys, Furniture, Books, Papers.

The method, used in the latest study performed in 1975, for surveying offices to determine fuel load estimates is presented. The frequency distribution for the estimates of the fuel load found in the study are presented. Two methods for determining movable fuel load are utilized in this study. Movable fuel load is considered to be the furniture, equipment, and other items brought in for the service of the occupants after construction of the building. Direct weighing techniques are utilized in both methods. In one method, the office contents are taken from their operational location and weighed. The second method, weighs the office contents when packaged for either relocation or remodeling purposes. Surveys were conducted in buildings at the University of Maryland College Park and at the General Services Administration (GSA) Headquarters Building in Washington, D.C.

00,234
PB97-114250 PC A04/MF A01
National Inst. of Standards and Technology (BFRL), Gaithersburg, MD.
Summary of Federal Construction and Building R and D in 1994.
S. McGaraghan. Sep 96, 38p, NISTIR-5849.
Prepared in cooperation with Department of Energy, Washington, DC.

Keywords: *Federal building, *Construction, *Research and development, Tables(Data), Contracts, Databases, US DOA, US DOC, US DOD, US DOE, US EPA, US DOT, US HHS, NSF(National Science Foundation).

In 1994, the federal government supported approximately $70 billion of research and development (R&D) in many different areas through a wide variety of government agencies and contractors. Because the work is spread among so many different entities, it can be difficult to develop a clear picture of the work being done in any one area. In response to this, a new database has been developed which tracks funding from the appropriation down to the project award level, allowing for comprehensive searches. The study, found that approximately $566 million was spent on R&D for construction and building in 1994. Two agencies, the Department of Defense and the Department of Energy, together account for nearly 75% of the total. In all, 12 agencies were found to have supported R&D in this area.

00,235
PB97-114482 PC A07/MF A02
National Inst. of Standards and Technology (BFRL), Gaithersburg, MD. Fire Safety Engineering Div.
Fire Safety Engineering in the Pursuit of Performance-Based Codes: Collected Papers.
R. W. Bukowski. Oct 96, 109p, NISTIR-5878.

Keywords: *Fire safety, *Building codes, *Research and development, Safety engineering, Smoke, Fire hazards, Risk, Performance standards.

This is a collection of papers on the application of modern fire safety engineering concepts to the evaluation of building performance in the context of performance-based codes.

00,236
PB97-116081 PC A04/MF A01
Maryland Univ., College Park. Dept. of Fire Protection Engineering.
Full-Scale Room Fire Experiments Conducted at the University of Maryland.
Test rept.
J. A. Milke, and S. M. Hill. 25 Jun 96, 34p, NIST/GCR-96/703.
Sponsored by National Inst. of Standards and Technology (BFRL), Gaithersburg, MD.

Keywords: *Fire tests, *Residential buildings, Furniture, Chairs, Desks, Tables, Bedding equipment, Mattresses, Flashover.

Two full size furnished bedrooms were burned, June 5 and June 6, at the University of Maryland Fire and Rescue Institute Facilities. These burns were performed for two cooperating agencies; The Alcohol, Tobacco and Firearms Agency of the Treasury Department, who used them as part of their Certified Fire Investigator training, and the Building and Fire Research Laboratory of NIST, who used them for forensic research. It was intended that these two burns be identical, to see if close analysis of the results would find differences. There were differences, possibly due to small differences in the inflow of ventilation air. In both cases, ignition was caused by burning newspaper on an upholstered chair. This report describes the test arrangement and instrumented results.

00,237
PB97-116131 PC A10/MF A02
Maryland Univ., College Park. Dept. of Mechanical Engineering.
Fire Protection Foam Behavior in a Radiative Environment.
Final rept. Sep 95-Sep 96.
C. F. Boyd, and M. di Marzo. Oct 96, 184p, NIST/GCR-96/702.
Grant NIST-60NANB5D0136
Sponsored by National Inst. of Standards and Technology (BFRL), Gaithersburg, MD.

Keywords: *Fire protection, *Foam, FORTAN, Numerical analysis, Mathematical models, Thermal radiation.

The overall objective of the current research program is to identify the parameters associated with the performance of fire-fighting foams used to protect structures from heat and fire damage. Specifically, the current research focuses on the destruction of a fire-fighting foam subjected to heat radiation. A numerical model which predicts the foam's properties during the destruction process is sought. The model is developed using experimental measurements and observations as a guide. Experimental results and the numerical model are used to identify the role of the various parameters which govern the foam's behavior.

00,238
PB97-116222 PC A03/MF A01
Maryland Univ., College Park. Dept. of Fire Protection Engineering.
Evaluation of Survey Procedures for Determining Occupant Load Factors in Contemporary Office Buildings.
J. A. Milke, and T. Caro. Jun 96, 25p, NIST/GCR-96/698.
Grant NIST-60NANB4D1625
Sponsored by National Inst. of Standards and Technology (BFRL), Gaithersburg, MD.

Keywords: *Office buildings, *Fires, Furniture, Fuels, Surveys, Flammability, Federal buildings.

The development of survey methods for determining the occupant load in office buildings (business occupancies) is described. Considerations involved in formulating the survey methods are presented. The type of data to be collected and data collection techniques are discussed. The two survey methods utilized to collect the population counts within contemporary office building are a building walk-through and a telephone survey. Occupant load data obtained from the survey methods applied in 23 office buildings located in the Washington, DC area are presented. Data are presented on the magnitude and distribution of the loads. The building data is sorted according to the following groups: open plan office designs versus well-compartmented office designs, and government (federal and county) versus privater sector tenants. Statistical summaries of the data are presented.

Architectural Design & Environmental Engineering

00,239
PB94-145653 PC A07/MF A02
National Inst. of Standards and Technology (BFRL), Gaithersburg, MD. Building and Fire Research Lab. Office.
Manual for Ventilation Assessment in Mechanically Ventilated Commercial Buildings.
A. K. Persily. Jan 94, 128p, NISTIR-5329.
See also PB92-145374 and PB93-113595. Sponsored by Environmental Protection Agency, Washington, DC. Office of Air and Radiation, and Bonneville Power Administration, Portland, OR.

Keywords: *Office buildings, *Air quality, *Ventilation, Space HVAC systems, Indoor air pollution, Air flow, Ducts, Comfort.

The manual describes procedures for assessing ventilation system performance and other aspects of build-

ing ventilation in mechanically ventilated commercial buildings. These procedures are intended to provide basic information on building ventilation for comparing ventilation performance to standards, guidelines and building design values and for investigating indoor air quality problems. The procedures in the manual are based on established measurement techniques and available instrumentation and provide practical means for obtaining reliable information on ventilation performance.

00,240
PB94-165982 PC A04/MF A01
National Inst. of Standards and Technology (CAML), Gaithersburg, MD. Office of Applied Economics.
Least-Cost Energy Decisions for Buildings: Part 2. Uncertainty and Risk Video Training Workbook.
H. E. Marshall. Apr 93, 53p, NISTIR-5178.
See also PB89-129522 and PB90-232810. Sponsored by Federal Energy Management Program, Washington, DC.

Keywords: *Buildings, *Investments, *Economic analysis, *Energy conservation, *Risk, Training films, Decision making, Cost analysis, Financing.

This workbook accompanies the video training film 'Uncertainty and Risk: Least-Cost Energy Decisions for Buildings'. The workbook and its companion video are the second in a series of training video-workbook packages designed to assist you in using economic analysis to improve the long-run economy of your buildings. The workbook supports the video in providing some of the fundamentals for measuring, describing, and interpreting uncertainty and risk in economic evaluations of energy conservation and other projects.

00,241
PB94-172160 Not available NTIS
National Inst. of Standards and Technology (BFRL), Gaithersburg, MD. Building Environment Div.
Psychological Aspects of Lighting: A Review of the Work of CIE TC 3.16.
Final rept.
B. L. Collins. 1990, 10p.
Pub. in Proceedings of Psychological Aspects of Architectural Lighting Symposium, University Park, PA., October 26-28, 1990, p1-10.

Keywords: *Lighting systems, *Psychological effects, *Buildings, *Human factors engineering, Illuminance, Emotions, Glare, Architecture, Color, Brightness, Disorientation, Reprints.

The work of Commission Internationale de l'Eclairage (CIE) TC 3.16 on 'Psychological Response to Lighting' is described. The committee is charged with reviewing the literature on the psychological response to lighting and preparing a report for CIE. The committee has identified about 260 research documents, developed a framework for review, prepared an outline, abstracted about 60% of the documents and developed an initial draft. Tentative output from the draft is described in the area of preferred task illuminance, glare, adaptation level, luminance distributions, light source position and extent, light source characteristics such as color temperature, color rendering and daylight, and dynamic temporal effects such as flicker, variation, and photobiology. A list of references is included.

00,242
PB94-173077 Not available NTIS
National Inst. of Standards and Technology (NEL), Gaithersburg, MD. Center for Fire Research.
Fire Hazard and Risk: Evaluating Alternative Technologies.
Final rept.
J. E. Snell. 1990, 20p.
Pub. in Proceedings of Symposium Sprinklers in Residential and Commercial Buildings, Charleston, SC., August 19-20, 1990, 20p.

Keywords: *Fire hazards, *Risk assessment, *Buildings, Fire protection, Sprinklers, Fire safety, Fire detectors, Fire resistance, Design, Reprints.

Fire safety decisions typically involve difficult choices between safety, cost and functionality. Obviously, buildings could be made completely fire safe by making sure they, and their contents simply do not burn, or by providing technologies that would clearly overpower any possible fire threat. Unfortunately, few would like, could afford or would be comfortable in such surroundings. Typically, the cost and functionality aspects of designs and products are well understood and effectively communicated. However, until recently means have not been available to quantify the fire hazard or risk people face, or to measure the effectiveness of fire protection technologies in specific real world situations. The paper reviews the status and potential of new tools for evaluating fire hazard and risk, cites examples of recent applications, and offers observations relevant to the current debate on the best means to provide fire safety in residential and commercial buildings.

00,243
PB94-185766 Not available NTIS
National Inst. of Standards and Technology (BFRL), Gaithersburg, MD. Building Environment Div.
Air Change Effectiveness Measurements in Two Modern Office Buildings.
Final rept.
A. K. Persily, W. S. Dols, and S. J. Nabinger. 1994, 16p.
Pub. in Indoor Air 4, p40-55 1994. Sponsored by Department of Energy, Washington, DC. Office of Buildings Energy R and D.

Keywords: *Office buildings, *Indoor air quality, *Tracer techniques, *Ventilation, Flow measurement, Air circulation, Air flow, Indoor air pollution, Pollution monitoring, HVAC systems, Test methods, Reprints, *Air change effectiveness.

Local age of air and air change effectiveness were determined in two office buildings using tracer gas techniques to study the applicability of the associated measurement procedures in the mechanically ventilated office buildings. Measurement issues examined include the establishment of a uniform tracer gas concentration at the start of the test and the relationship of ventilation system configuration and system operation to the test procedure. Air change effectiveness was determined at locations in the occupied space based on the local age of air at that location and the age of air in the corresponding ventilation system return duct. These tests provide data on air change effectiveness to supplement the limited database on mechanically ventilated office buildings in the U.S. In addition, the experience obtained with the measurement procedures will assist in the development of a standardized approach to measuring air change effectiveness in the field.

00,244
PB94-200383 Not available NTIS
National Inst. of Standards and Technology (NEL), Gaithersburg, MD. Building Environment Div.
Papers Presentations Shine.
Final rept.
B. L. Collins. 1990, 3p.
Pub. in Lighting Design and Application, p21-23 Oct 90.

Keywords: *Lighting systems, *Luminaires, *Energy conservation, *Energy efficiency, *Daylighting, Illuminating, Light sources, Computer graphics, Visibility, Lighting equipment, Highway lighting, Reprints.

The technical highlights from the recent IESNA Conference in Baltimore, MD are summarized in some detail. At the session 48 papers on lighting research, technology, design and application were presented. Topics discussed included light sources and conservation issues for displays; efficiency standards for lamps; daylight measurement and modeling; lamp performance including fluorescent, incandescent, metal halide, high pressure sodium, and special sources; tunnel and roadway lighting; measurement and controls; modeling and lighting geometry; calculations; visibility and visual performance; computer graphics; and VDT's. Issues relating to energy conservation, such as efficiency standards, daylighting, and new lamp technology generated considerable attention, as did papers on lighting and conservation as well as computer graphics as a design tool.

00,245
PB94-212735 Not available NTIS
National Inst. of Standards and Technology (NEL), Gaithersburg, MD. Building Environment Div.
Using Emulator/Testers for Commissioning EMCS Software, Operator Training, Algorithm Development, and Tuning Local Control Loops.
Final rept.
G. E. Kelly, C. Park, and J. P. Barnett. 1991, 10p.
Sponsored by Department of Energy, Washington, DC.
Pub. in American Society of Heating, Refrigerating and Air-Conditioning Engineers Transactions, pt1 p669-678 1991.

Keywords: *Buildings, *Energy management, *Control systems, Simulation, Simulators, Real time, Computer graphics, Man computer interface, Heating, Air conditioning, Algorithms, Reprints, EMCS(Energy Management and Control System), US NIST, HVACSIM+ computer program.

A Building Emulator/EMCS Tester emulates a building and its mechanical system in real time. The Emulator/Tester is connected to the Energy Management and Control System (EMCS) in place of the regular sensors and actuators. The EMCS then controls the simulated building as it would a real building, while the Emulator/Tester evaluates the EMCS performance. An Emulator/Tester has been developed by the National Institute of Standards and Technology (NIST). Two studies were performed. The first involved a model of a building operated in the heating mode, while the second consisted of the building air handling system supplying conditioned air to a single building zone during summer operation. Both studies showed good agreement between the simulation and emulation results. An exercise using the Emulator/Tester to facilitate the tuning of local control loops was performed. Two different tuning methods were explored. Information is also presented on how the Emulator/Tester can be used for training, commissioning EMCS software, and developing new control algorithms.

00,246
PB94-219367 (Order as PB94-219326, PC A05/MF A02)
National Inst. of Standards and Technology, Gaithersburg, MD.
Improved Automated Current Control for Standard Lamps.
J. H. Walker, and A. Thompson. 1994, 7p.
Included in Jnl. of Research of the National Institute of Standards and Technology, v99 n3 p255-261 May/Jun 94.

Keywords: *Lamps, *Standards, *Radiance, Irradiance, Radiometry.

As radiometric lamp standards improve, the need to set lamp current to specific values becomes more important. Commercially available power supplies typically provide 12 bit internal digital-to-analog logic which permits current control with a relative expanded uncertainty of about 1 part in 4096, corresponding to an expanded uncertainty of the current of about 2 mA at 8 A (in this paper, expanded uncertainties are given as 2 standard deviations). For the FEL-type standard spectral irradiance lamp, this corresponds to a spectral irradiance difference of 0.12% at 655 nm. The authors have developed a technique using 16 bit digital-to-analog conversion which permits current control with a relative expanded uncertainty of about 1 part in 65536, corresponding to an expanded uncertainty of the current of about 0.1 mA at 8 A.

00,247
PB95-108833 Not available NTIS
National Inst. of Standards and Technology (NEL), Gaithersburg, MD. Building Environment Div.
Field Measurements of Ventilation and Ventilation Effectiveness in an Office/Library Building.
Final rept.
A. K. Persily, and W. S. Dols. 1990, 21p.
Sponsored by Department of Energy, Washington, DC.
Pub. in Proceedings of the AIVC Conference on Ventilation System Performance (11th), Belgirate, Italy, September 18-21, 1990, p294-313.

Keywords: *Ventilation, *Office buildings, *Indoor air pollution, *Air flow, *Libraries, *Thermal comfort, Field tests, District of Columbia, Tracer techniques, Spatial distribution, Performance evaluation, Environmental engineering, Reprints.

Mechanical ventilation system performance involves the provision of adequate amounts of outdoor air, uniform distribution of ventilation air within the occupied space, and the maintenance of thermal comfort. Standardized measurement techniques exist to evaluate thermal comfort and air exchange rates in mechanically ventilated buildings; field techniques to evaluate air distribution or ventilation effectiveness are still being developed. The paper presents field measurements of air exchange rates and ventilation effectiveness in an office/library building in Washington D.C. The tracer gas decay technique was used to measure whole building air exchange rates. Ventilation effectiveness was investigated at several locations within the building through the measurement of local tracer gas decay rate and mean local age of air. The ventila-

tion effectiveness measurements serve as an investigation of the applicability of the measurement procedures employed, providing insight into the measurement issue of establishing initial conditions, the spatial variation in tests results within a building, and the repeatability between tests.

00,248
PB95-125951 Not available NTIS
National Inst. of Standards and Technology (TS), Gaithersburg, MD. Lab. Accreditation Program.
Water Efficient Plumbing Fixtures through Standards and Test Methods.
Final rept.
L. S. Galowin, and J. A. Swaffield. 1990, 5p.
Pub. in Proceedings of CONSERV 90 - National Conference and Exposition Offering Water Supply Solutions for the 1990s, Phoenix, AZ., August 12-16, 1990, p179-183.

Keywords: *Standards, *Test methods, *Waste consumption, *Sewage, *Building codes, *Piping systems, Drainage, Waste disposal, Buildings, Water flow, Conservation, Reprints, *Low flow plumbing fixtures.

Concern exists for low volume fixture flows from water conserving plumbing fixtures and devices discharged into the drainage system to perform the functions for waste removal, transport and clearing the drains. Reduced flow rates and volumetric limits on water consumption for plumbing fixtures and appliances for the water saving plumbing products are proposed in national legislation introduced in the U.S. Congress. Research, experiments and test measurements in both laboratories and actual field installments are reviewed. Conditions included measured solid waste transport from water closet discharges into drainlines and loading conditions for a variety of laboratory type simulants applicable for test methods in standards. Data shows that sweeping of wastes through the drainage piping with low flows can be accomplished. The application of selected research results in the preparation of test method procedures for plumbing standards is discussed, e.g., drainline waste transport test of low flush water closets. Computer modeling calculations and data show the 'carry out' of the waste solids from the building to the sewer, or septic system, may occur in a series of successive carries and not necessarily from a single discharge of a fixture.

00,249
PB95-135596 PC A06/MF A02
National Inst. of Standards and Technology (BFRL), Gaithersburg, MD. Building and Fire Research Lab. Office.
Indoor Air Quality Impacts of Residential HVAC Systems, Phase 1 Report: Computer Simulation Plan.
S. J. Emmerich, and A. K. Persily. Feb 94, 123p, NISTIR-5346.
Sponsored by Consumer Product Safety Commission, Washington, DC. Directorate of Engineering Science.

Keywords: *Indoor air pollution, *Residential buildings, *Computerized simulation, Design criteria, HVAC systems, Air flow, Combustion products, Air quality, Air pollution control, Ventilation, Contaminants.

NIST has completed the first phase of a project to study the impact of HVAC systems on residential indoor air quality and to assess the potential for using residential forced-air systems to control indoor pollutant levels. This project will use computer simulations to assess the ability of modifications to central forced-air heating and cooling systems to control the concentrations of selected pollutants in single-family residential buildings. The first phase consisted of three major efforts: conducting a literature review, developing a plan for computer analysis, and holding an expert workshop to discuss the plan. The second phase of the project will involve performing the computer simulations and analyzing the results. This report details the results of the Phase I efforts. The objective of the literature review was to obtain information for planning computer simulations that will be performed in Phase II of the project.

00,250
PB95-150991 Not available NTIS
National Inst. of Standards and Technology (BFRL), Gaithersburg, MD. Building Environment Div.
Lighting and HVAC.
Final rept.
S. J. Treado. 1991, 6p.
Pub. in Lighting Design and Application, p18-23 Jul 91.

Keywords: *Lighting systems, *Space HVAC systems, *Energy consumption, *Commercial buildings, *Cost analysis, Interior lighting, Fluorescent lamps, Lighting loads, Heat transfer, Thermal analysis, Energy use, Performance evaluation, Reprints.

Lighting in commercial buildings is the single largest user of electric energy, typically ranging from 25 to 50 percent of total building electrical energy requirements. The performance of the dominant commercial light source, the fluorescent lamp, is strongly dependent on thermal conditions: Both lamp light output and power consumption vary with minimum lamp wall temperature, as much as 20 percent under typical conditions. Proper control of room thermal conditions can ensure that the lamps are operating at thier most efficient level.

00,251
PB95-151007 Not available NTIS
National Inst. of Standards and Technology (BFRL), Gaithersburg, MD. Building Environment Div.
NIST Lighting and HVAC Interaction Test Facility.
Final rept.
S. J. Treado. 1991, 3p.
Pub. in American Society of Heating, Refrigeration and Air-Conditioning Engineers Jnl., p47-48, 50, Apr 91.

Keywords: *Test facilities, *Lighting systems, *Space HVAC systems, *Research programs, Commercial buildings, Interior lighting, Fluorescent lamps, Lighting loads, Energy consumption, Energy efficiency, Thermal analysis, Heat transfer, Cost analysis, Reprints.

Lighting in commercial buildings is the single largest user of electric energy, typically ranging from 25 to 50 percent of total building electrical energy requirements. The performance of the dominant commercial light source, the fluorescent lamp, is strongly dependent on thermal conditions. Both lamp light output and power consumption vary with minimum lamp wall temperature by as much as 20 percent under typically encountered conditions. Proper control of room thermal conditions can ensure that the lamps are operating at their most efficient level.

00,252
PB95-151783 Not available NTIS
National Inst. of Standards and Technology (NEL), Gaithersburg, MD. Building Environment Div.
Lighting Quality and Light Source Size.
Final rept.
J. A. Worthey. 1990, 7p.
Pub. in Jnl. of the Illuminating Engineering Society 19, n2 p142-148 1990.

Keywords: *Daylight, *Light sources, *Optical properties, *Size(Dimensions), Lighting equipment, Color, Luminance, Sunlight, Reflection, Reprints.

The sun covers only about 10(exp -5) of the sky dome, while a luminous ceiling in effect presents an entire bright sky. Through its effects on veiling reflections and highlights, source size affects the range of colors and luminances in a scene. Some new calculations of these phenomena are presented.

00,253
PB95-151791 Not available NTIS
National Inst. of Standards and Technology (EEEL), Gaithersburg, MD. Electronics and Electrical Engineering Lab. Office.
Lighting Research and Theory Can Create Business Prospects.
Final rept.
J. A. Worthey. 1991, 4p.
Pub. in Lighting Design and Application 21, n9 p14-17 Sep 91.

Keywords: *Lighting systems, *Theories, *Research projects, *Technology transfer, Illumination, Luminance, Light sources, Design, Economic analysis, Reprints.

The topics of the article are: What can theory really do for the business of lighting; and What benefits can come from a more theoretical approach to lighting research and design. The answer proposed will be this: Better theory can give better lighting system designs and, in particular, new and better luminaires.

00,254
PB95-153276 Not available NTIS
National Inst. of Standards and Technology (NEL), Gaithersburg, MD. Building Environment Div.
Psychological Aspects of Lighting: A Review of the Work of CIE TC 3.16.
Final rept.
B. L. Collins. 1990, 10p.
Pub. in Proceedings of Psychological Aspects of Architectural Lighting Symposium, University Park, PA., October 26-28, 1990, p1-10.

Keywords: *Lighting equipment, *Psychological effects, *Workplace layout, Glare, Illuminance, Color, Luminance, Visibility, Workloads(Psychophysiology), Human reactions, Stress(Psychology), Emotions, Comfort, Reprints.

The work of Commission Internationale de l'Eclairage (CIE) TC 3.16 on 'Psychological Response to Lighting' is described. The committee is charged with reviewing the literature on the psychological response to lighting and preparing a report for the CIE. The committee has identified about 260 research documents, developed a framework for review, prepared an outline, abstracted about 60% of the documents and developed an initial draft. Tentative output from the draft is described in the area of preferred task illuminance, glare, adaptation level, luminance distributions, light source position and extent, light source characteristics such as color temperature, color rendering and daylight, and dynamic temporal effects such as flicker, variation, and photobiology. A list of references is included.

00,255
PB95-162079 Not available NTIS
National Inst. of Standards and Technology (BFRL), Gaithersburg, MD. Building Environment Div.
Assessing Ventilation Effectiveness in Mechanically Ventilated Office Buildings.
Final rept.
A. K. Persily. 1993, 12p.
Sponsored by Department of Energy, Washington, DC.
Pub. in Proceedings of International Symposium on Room Air Convection and Ventilation Effectiveness, Tokyo, Japan, July 22-24, 1992, p201-212 1993.

Keywords: *Office buildings, *Ventilation systems, *Air circulation, *Indoor air quality, Air infiltration, Air flow, Air intakes, Intake systems, Vents, Space HVAC systems, Test and evaluation, Reprints.

Mechanical ventilation systems are designed and operated to bring outdoor air into buildings, distribute ventilation air within the occupied space, remove internally generated contaminants, and maintain thermal comfort. The paper presents a general discussion of ventilation effectiveness in mechanically ventilated office buildings as the ability of the ventilation system to provide ventilation air in a manner consistent with the design goals of the system. The design and performance of air distribution systems are discussed on a range of scales, from the air handler to the individual workspace, as are the means for assessing ventilation effectiveness on each of these scales. Various approaches to the assessment of mixing within ventilated spaces, the most common conception of ventilation effectiveness, are presented and discussed in relation to their use in mechanically ventilated office buildings.

00,256
PB95-162087 Not available NTIS
National Inst. of Standards and Technology (BFRL), Gaithersburg, MD. Building Environment Div.
Modeling Radon Transport in Multistory Residential Buildings.
Final rept.
A. K. Persily. 1993, 17p.
Pub. in Modeling of Indoor Air Quality and Exposure, ASTM STP 1205, p226-242 1993.

Keywords: *Residential buildings, *Radon, *Radionuclide migration, *Flow models, Air flow, Air circulation, Spatial distribution, Air infiltration, Leakage, Radioecological concentration, Indoor air pollution, Air pollution monitoring, Computerized simulation, Reprints.

Radon concentrations have been studied extensively in single-family residential buildings, but relatively little work has been done in large buildings, including multistory residential buildings. The paper presents the results of a computer simulation of airflow and radon transport in a twelve-story residential building. Interzone airflow rates and radon concentrations were predicted using the multizone airflow and contaminant dispersal program CONTAM88. Limited simulations were conducted to study the influence of two different radon source terms, indoor-outdoor temperature difference and exterior wall leakage values on radon transport and radon concentration distributions.

00,257
PB95-175006 PC A11/MF A03
National Inst. of Standards and Technology (CAML), Gaithersburg, MD. Office of Applied Economics.
Life-Cycle Costing Workshop for Energy Conservation in Buildings: Student Manual.
Final rept.
S. K. Fuller, and S. R. Petersen. Oct 94, 236p, NISTIR-5165.
Supersedes PB93-198984. See also PB93-208460. Sponsored by Federal Energy Management Program, Washington, DC.

Keywords: *Federal buildings, *Energy conservation, *Life cycle costs, *Training, Space HVAC systems, Facilities management, Operation and maintenance, Operating costs, Cost analysis, Energy efficiency, Computer applications, Education, *BLCC computer program, BLCC(Building Life-Cycle Cost).

The Student Manual for the Life-cycle Costing Workshop for Energy Conservation in Buildings is a workbook for a two-day course on life-cycle cost (LCC) analysis. The purpose of the workshop is to provide professionals concerned with energy conservation in federal buildings with the knowledge and skills they need to perform economic analyses quickly and correctly. The Student Manual presents the criteria and methods that govern LCC analysis for energy conservation in federal buildings; treats basic economic concepts; gives step-by-step instructions for performing LCC analyses; and introduces computer software and hands-on exercises for performing LCC analyses both manually and on PCs.

00,258
PB95-175329 Not available NTIS
National Inst. of Standards and Technology (TS), Gaithersburg, MD. Office of Standards Services.
Performance of Compact Fluorescent Lamps at Different Ambient Temperatures.
Final rept.
B. L. Collins, S. J. Treado, and M. J. Ouellette. 1994, 14p.
Pub. in Jnl. of the Illuminating Engineering Society 23, n2 p72-85 1994.

Keywords: *Fluorescent lamps, *Temperature effects, *Performance evaluation, *Luminous intensity, Light sources, Power factor, Energy efficiency, Energy conservation, Reprints.

Compact fluorescent lamps are used to replace incandescent lamps to aid in energy conservation in commercial and domestic lighting applications. In conjunction with the Institute for Research in Construction (IRC) at the National Research Council, Canada (NRCC), the Lighting Group at the National Institute of Standards and Technology (NIST) conducted an experimental evaluation of twelve sets of different types of compact fluorescent lamps at six different ambient temperature conditions. An additional set of incandescent lamps was also evaluated for comparison. A total of three lamps were tested for each of the thirteen lamp types, both compact fluorescent and incandescent.

00,259
PB95-175774 Not available NTIS
National Inst. of Standards and Technology (BFRL), Gaithersburg, MD. Building Environment Div.
Using Emulators to Evaluate the Performance of Building Energy Management Systems.
Final rept.
G. E. Kelly, W. B. May, J. Y. Kao, and C. Park. 1994, 12p.
Sponsored by Department of Energy, Washington, DC. Building Systems and Materials Div.
Pub. in American Society of Heating, Refrigerating and Air-Conditioning Engineers Transactions 100, pt1 p1482-1493 1994.

Keywords: *Space HVAC systems, *Computerized simulation, *Performance tests, Control systems, Heating systems, Ventilation, Air conditioning, Energy consumption, Comfort, Performance evaluation, Reprints, *Building Energy Management Systems, Emulators.

The performance of a building energy management system (BEMS) is directly related to the amount of energy consumed in a building and the comfort of the building's occupants. The paper describes using emulators to evaluate a BEMS. Major topics include setting up a BEMS and an emulator, evaluating system/command and DDC software, and methodologies for testing BEMS application algorithms. Considerations are presented for evaluating the programming capabilities of a BEMS, DDC control loop performance, and rating different aspects of BEMS performance. A brief discussion of BEMS software is also included.

00,260
PB95-175980 Not available NTIS
National Inst. of Standards and Technology (BFRL), Gaithersburg, MD. Building Environment Div.
Reproducibility of Tests on Energy Management and Control Systems Using Building Emulators.
Final rept.
H. C. Peitsman, S. Wang, S. Karki, C. Park, and P. Haves. 1994, 10p.
Sponsored by Department of Energy, Washington, DC. Office of Conservation and Renewable Energy.
Pub. in American Society of Heating, Refrigerating and Air-Conditioning Engineers Transactions 100, pt1 p1455-1464 1994.

Keywords: *Energy management systems, *Control systems, *Performance tests, *Computerized simulation, *Space HVAC systems, Ventilation, Air conditioning, Heating systems, Comfort, Real time, Performance evaluation, Energy consumption, Predictions, Test methods, Reprints.

An emulator consists of a real-time simulation of a building and its HVAC system and a hardware interface that allows the simulation to be connected to a real control system. As part of a research project, an experiment involving four different emulators with two different (EMCS) was performed to study the reproducibility of the emulation method. The paper presents the results of this experiment in the form of a comparison of the predictions of energy consumption, thermal comfort, and control activity obtained from tests of the EMCS using emulators based on different design and different simulation programs.

00,261
PB95-182259 PC A04/MF A01
National Inst. of Standards and Technology (BFRL), Gaithersburg, MD.
Algorithm to Describe the Spread of a Wall Fire under a Ceiling.
H. E. Mitler. Nov 94, 62p, NISTIR-5547.

Keywords: *Algorithms, *Ceilings(Architecture), *Buildings, *Flame propagation, Thermal radiation, Convection(Heat transfer), Plumes, Ignition, Mathematical models, Combustion, Flames, Burning rate, *Wall fires, SPREAD computer program.

After some discussion of wall fires, the effects that a ceiling has on a wall fire are analyzed and discussed qualitatively. There are two kinds of effects: first, when the upper sill of the ventilating opening lies below the ceiling (as is usual), a layer of hot gas is trapped, which heats the walls by convection and radiation; the heated ceiling also radiates to the walls. A calculation which uses the wall-fire computer model SPREAD is carried out to demonstrate how these effects can be calculated now. Second, when the flame impinges on the ceiling, it bifurcates and spreads horizontally, rather than vertically. A simple algorithm is presented which calculates the spread rate of these horizontal flame extensions, as well as the modified pyrolysis rate, due to the modified radiation feedbacks.

00,262
PB95-182309 PC A04/MF A01
National Inst. of Standards and Technology (BFRL), Gaithersburg, MD.
Indoor Air Quality Commissioning of a New Office Building.
W. S. Dols, A. K. Persily, and S. J. Nabinger. Jan 95, 60p, NISTIR-5586.
See also PB90-164484. Sponsored by Nuclear Regulatory Commission, Washington, DC.

Keywords: *Office buildings, *Indoor air quality, *Ventilation systems, *Test and evaluation, Space HVAC systems, Indoor air pollution, Air quality standards, Specifications, Cooling and ventilating equipment, Building materials, Air flow, Air infiltration, Comfort.

Commissioning does not always include the verification of an 'acceptable' indoor environment for the building occupants, including factors related to indoor air quality (IAQ). In light of growing concern about indoor air quality, IAQ commissioning could become an important part of building commissioning programs. The program described in this report consisted of three tasks: (1) evaluate the mechanical ventilation system design from an IAQ perspective; (2) develop a set of environmental performance parameters and associated reference values that will be used to evaluate IAQ in the building; and, (3) measure these environmental parameters in the building and compare them with the reference values developed in Task 2.

00,263
PB95-190682 PC A06/MF A02
National Inst. of Standards and Technology (BFRL), Gaithersburg, MD.
BLCC: The NIST 'Building Life-Cycle Cost' Program, Version 4.21. User's Guide and Reference Manual.
S. R. Petersen. Jan 95, 103p, NISTIR-5185-2.
Sponsored by Federal Energy Management Program, Washington, DC.

Keywords: *Buildings, *Energy efficiency, *Life cycle costs, User manuals, Investments, Computer applications, Energy conservation, Operating costs, Economic analysis, Benefit cost analysis.

The NIST Building Life-Cycle Cost (BLCC) computer program provides economic analysis of proposed capital investments that are expected to reduce long-term operating costs of buildings or building systems/components. It is especially useful for evaluating the costs and benefits of energy conservation projects in buildings. Two or more alternative designs can be evaluated to determine which has the lowest life-cycle cost and therefore is most economical in the long run. Economic measures, including net savings, savings-to-investment ratio, adjusted internal rate of return, and years to payback can be calculated for any design alternative relative to the designated base case. BLCC can be used for evaluating federal (including Department of Defense), state, and local government projects as well as projects in the private sector. It complies with ASTM standards related to building economics as well as FEMP and OMB Circular A-94 guidelines for economic analysis of federal building projects. BLCC has new capabilities for using demand charges and block rate calculations for computing annual electricity costs. While BLCC is primarily intended for the economic evaluation of building systems, it can be applied to a wide range of project investments which are intended primarily to reduce future operating-related costs.

00,264
PB95-210944 PC A04/MF A01
National Inst. of Standards and Technology (BFRL), Gaithersburg, MD. Building Environment Div.
Measurements of Outdoor Air Distribution in an Office Building.
W. S. Dols, and A. K. Persily. Jun 94, 58p, NISTIR-5320.
Sponsored by Bonneville Power Administration, Portland, OR.

Keywords: *Office buildings, *Air circulation, *Ventilation, *Indoor air quality, Air infiltration, Air flow rates, Flow measurement, Air sampling, Tracer techniques, Environmental surveys, Outdoor air.

The National Institute of Standards and Technology (NIST) has performed a study of methods to measure the local outdoor air delivery rates in an office building. This is a follow-up study of one which was performed in the same building to measure outdoor airflow rates to the building as a whole. This study focuses on the delivery of outdoor air to smaller sections of the building. Airflow rates were measured to various zones of the building which range in size from that served by an entire air handler to individual workstations served by a single supply air diffuser. Comparisons were made between the use of different procedures used to measure airflow rates to the same zones in terms of relative accuracies and levels of effort involved in performing the measurements. The use of tracer gas techniques to measure local ages of air was also demonstrated. The local ages of air were then used to determine air change effectiveness of the ventilation system at the measurement locations. Air change effectiveness provides a measure of the uniformity of outdoor air delivery and mixing in a space.

00,265
PB95-253597 PC A04/MF A01
National Inst. of Standards and Technology (BFRL), Gaithersburg, MD.

Least-Cost Energy Decisions for Buildings. Part 3. Choosing Economic Evaluation Methods. Video Training Workbook.
H. E. Marshall. May 95, 56p, NISTIR-5604.
See also PB94-165982. Sponsored by Federal Energy Management Program, Washington, DC.

Keywords: *Buildings, *Energy efficiency, *Cost benefit analysis, Environmental engineering, Value engineering, Facilities management, Operation and maintenance, Energy conservation, Life cycle costs, Operating costs, Return on investment, Cost analysis, Economic analysis, Alternatives, Workbooks, Savings-to-investment ratio.

The workbook and its companion video are the third in a series of training video-workbook modules designed to assist you in using economic analysis to improve the long-run economy of your buildings. This module describes the types of investment decisions that you will have to deal with when you evaluate energy conservation projects--decisions to accept or reject a project, what design to choose, and what priority to assign candidate projects. Then it tells you how to match the different types of investment decisions with the appropriate economic methods. The workbook supports the video with expanded descriptions of technical material shown in the video; figures and tables presented in the video; formulas for computing economic measures used in the video; exercises to give you practice; and a glossary of technical terms used by the video instructors.

00,266
PB95-501953 CP D02
National Inst. of Standards and Technology, Gaithersburg, MD.
Building Life Cycle Cost Computer Program (BLCC), Version 4.2-95 (for Microcomputers).
Software.
1995, diskette, NIST/SW/DK-94/003.
System: MS DOS operating system. Open READ.ME file for installation instructions. Supersedes PB94-500055. See also PB94-500097 (ERATES).
The software is on one 3 1/2 inch DOS diskette, 1.44M high density. File format: ASCII text. Documentation included; may be ordered separately as PB93-208460 and PB91-167288.

Keywords: *Software, *Buildings, *Life cycle costs, *Energy conservation, Economic analysis, Long range(Time), Operating costs, Return on investment, Savings, Prices, Benefit cost analysis, Diskettes.

Product provides economic analysis of proposed capital investments that are expected to reduce long-term operating costs of buildings or building systems/components. It is especially useful for evaluating the costs and benefits of energy conservation projects in buildings. Two or more alternative designs can be evaluated to determine which has the lowest life-cycle cost and therefore is most economical in the long run. Economic measures, including net savings, savings-to-investment ratio, adjusted internal rate of return, and years to payback can be calculated for any design alternative relative to the designated base case. BLCC can be used for evaluating federal (including Department of Defense), state, and local government projects as well as projects in the private sector. It complies with ASTM standards related to building economics as well as FEMP and OMB Circular A-94 guidelines for economic analysis of federal building projects. It has new capabilities for using demand charges and block rate calculations for computing annual electricity costs. While it is primarily intended for the economic evaluation of building systems, it can be applied to a wide range of project investments which are intended primarily to reduce future operating-related costs.

00,267
PB95-502779 CP D02
National Bureau of Standards, Gaithersburg, MD.
Building Life Cycle Cost Computer Program (BLCC) Version 4.21-95 (for Microcomputers).
Software.
1995, diskette, NIST/SW/DK-95/002.
MS DOS operating system. Open READ.ME file for installation instructions. Supersedes PB95-501953. See also PB94-500097 (ERATES).
The software is on one 1.44M, 3 1/2 inch disc. File format: ASCII text. Documentaion included; may be ordered separately as PB95-169652.

Keywords: *Software, *Buildings, *Life cycle costs, *Energy conservation, Economic analysis, Benefit cost analysis, Operating costs, Long range(Time), Return on investment, Savings, Prices, Project management, National government, State government, Local government, Standards, Diskettes.

The product provides economic analysis of proposed capital investments that are expected to reduce long-term operating costs of buildings or building systems/components. It is especially useful for evaluating the costs and benefits of energy conservation projects in buildings. Two or more alternative designs can be evaluated to determine which has the lowest life-cycle cost and therefore is most economical in the long run. Economic measures, including net savings, savings-to-investment ratio, adjusted internal rate of return, and years to payback can be calculated for any design alternative relative to the designated base case. Building Life Cycle Cost (BLCC) can be used for evaluating federal (including Department of Defense), state, and local government projects, as well as projects in the private sector. It complies with ASTM standards related to building economics as well as FEMP and OMB Circular A-94 guidelines for economic analysis of federal building projects. It has new capabilities for using demand charges and block rate calculations for computing annual electricity costs. While it is primarily intended for the economic evaluation of building systems, it can be applied to a wide range of project investments which are intended primarily to reduce future operating-related costs.

00,268
PB95-503397 CP D02
National Inst. of Standards and Technology, Gaithersburg, MD.
Building Life Cycle Cost Computer Program (BLCC) Version 4.22-95 (for Microcomputers).
Software.
1995, 1 diskette, NIST/SW/DK-95/002.
MS DOS operating system. Open READ.ME file for installation instructions. Supersedes PB95-502779. See also PB94-500097 (ERATES).
The software is on one 3 1/2 inch DOS diskette, 1.44M high density. File format: ASCII text. Documentation included; may be ordered separately as PB95-169652.

Keywords: *Software, *Buildings, *Life cycle costs, *Energy conservation, *Benefit-cost analysis, Operating costs, Economic analysis, Return on investment, Savings, Prices, Project management, National government, State governments, Local governments, Standards, Diskettes, Documentation.

Product provides economic analysis of proposed capital investments that are expected to reduce long-term operating costs of buildings or building systems/components. It is especially useful for evaluating the costs and benefits of energy conservation projects in buildings. Two or more alternative designs can be evaluated to determine which has the lowest life-cycle cost and therefore is most economical in the long run. Economic measures, including net savings, savings-to-investment ratio, adjusted internal rate of return, and years to payback can be calculated for any design alternative relative to the designated base case. BLCC can be used for evaluating federal (including Department of Defense), state, and local government projects as well as projects in the private sector. It complies with ASTM standards related to building economics as well as FEMP and OMB Circular A-94 guidelines for economic analysis of federal building projects. It has new capabilities for using demand charges and block rate calculations for computing annual electricity costs. While it is primarily intended for the economic evaluation of building systems, it can be applied to a wide range of project investments which are intended primarily to reduce future operating-related costs.

00,269
PB96-111901 Not available NTIS
National Inst. of Standards and Technology (BFRL), Gaithersburg, MD. Building Environment Div.
Use of Building Emulators to Evaluate the Performance of Building Energy Management Systems.
Final rept.
H. Vaezi-Nejad, E. Hutter, P. Haves, P. Nusgens, S. Wang, A. L. Dexter, and G. Kelly. 1994, 6p.
See also PB95-175774. Sponsored by Department of Energy, Washington, DC.
Pub. in Proceedings of Building Simulation Conference, Nice, France, August 20-22, 1991, p1-6.

Keywords: *Space HVAC systems, *Computerized simulation, *Performance tests, Control systems, Heating systems, Ventilation, Air conditioning, Energy consumption, Comfort, Performance evaluation, Reprints, *Building Energy Management Systems, Emulators.

Three complementary approaches may be used in the performance of building control systems-simulation, emulation and field testing. In emulation a real-time simulation of the building and HVAC plant is connected to a real building energy management system (BEMS) via a hardware interface. Emulation has the advantage of allowing controlled, repeatable experiments whilst testing real devices that may contain proprietary algorithms. Building emulators have been developed by the authors in the context of IEA Annex 17, which is concerned with the use of simulation to evaluate the performances of BEMS. The paper discusses different approaches to the design of building emulators and describes the different architectures, hardware and software used by the authors. The problem of evaluating the overall performance of BEMS is discussed and results are presented that illustrate the use of emulators to investigate the influence of the tuning of local loop controls on building performance.

00,270
PB96-122932 Not available NTIS
National Inst. of Standards and Technology (TS), Gaithersburg, MD. Lab. Accreditation Program.
Laboratory Accreditation for Testing Energy Efficient Lighting.
Final rept.
L. Galowin, W. Rossiter, R. Runkles, and R. Brown. 1994, 12p.
Pub. in Proceedings: Technology Research, Development and Evaluation, Asilomar Conference Center, Monterey, CA., August 28-September 3, 1994, v3 p3.77-3.88 1994.

Keywords: *Lighting equipment, *Energy efficiency, *Accreditation, *Laboratories, Lamps, Energy conservation, Procedures, Requirements, Comparative evaluations, Standards, Tests, Reprints.

NEMA requested establishment of the accreditation program for laboratory testing of lamps and luminaires from concensus standards prior to enactment of EPACT. NVLAP conducts regulatory and voluntary accreditation programs. Impacts cited by NEMA for NVLAP were; third-party objective accreditation programs for establishment of credible testing data, avoidance of duplicated efforts by different Federal government agencies, avoidance of confusion in the marketplace, improving product quality, and assistance to utilities/conservation planners. Following public comment by interested organizations, NVLAP developed the Energy Efficient Lighting Program for laboratories conducting standard test methods for electrical, photometric, and color measurements. Industry recommendations at FTC hearings supported NVLAP accredited laboratory data for labeling.

00,271
PB96-138508 Not available NTIS
National Inst. of Standards and Technology (BFRL), Gaithersburg, MD. Building Environment Div.
Improving the Evaluation of Building Ventilation.
Final rept.
A. K. Persily. 1995, 15p.
Pub. in Annual Meeting of the Air and Waste Management Association (88th), San Antonio, TX., June 18-23, 1995, p1-15.

Keywords: *Commercial buildings, *Ventilation systems, *Air circulation, Performance evaluation, Test and evaluation, Standardization, Air flow, Air infiltration, Research projects, Reprints, Mechanical ventilation.

A project is being conducted at the National Institute of Standards and Technology (NIST) to identify approaches to improve these evaluations, to develop selected ventilation assessment protocols, and to identify research needed to make further advances in the field. This project has included a characterization of the applications of ventilation assessment in buildings, an identification of the objectives addressed by different approaches to ventilation assessment, and a review of existing protocols. This paper discusses the characterization of ventilation evaluation that was performed as part of this project and is organized into the following sections: Uses of Ventilation Evaluation; Specific Evaluation Objectives; Existing Evaluation Protocols; and Current Inadequacies: Problems, Reasons and Solutions.

00,272
PB96-141353 Not available NTIS
National Inst. of Standards and Technology (BFRL), Gaithersburg, MD. Building Environment Div.

Optimal Control of Building and HVAC Systems.
Final rept.
J. M. House, and T. F. Smith. 1995, 5p.
Pub. in Proceedings of the American Control Conference, Seattle, WA., June 21-23, 1995, p4326-4330.

Keywords: *Space HVAC systems, *Optimal control, *Buildings, Comfort, Energy efficiency, Energy consumption, Control systems, Reprints.

An optimal control strategy is compared with a conventional strategy to demonstrate the capability of optimal control to maintain comfort while reducing the utility cost for a two-zone building and HVAC system. The optimal control strategy yields a reduction in the utility cost of 11 percent for the conditions considered. A new-optimal control strategy that requires less implementation effort is also discussed.

00,273
PB96-154463 PC A04/MF A01
National Inst. of Standards and Technology (BFRL), Gaithersburg, MD.
Workplan to Analyze the Energy Impacts of Envelope Airtightness in Office Buildings.
S. J. Emmerich, A. K. Persily, and D. A. VanBronkhorst. Dec 95, 34p, NISTIR-5758.
See also PB93-183770. Sponsored by Department of Energy, Washington, DC.

Keywords: *Office buildings, *Space HVAC systems, *Ventilation systems, Air flow, Air infiltration, Thermal insulation, Energy efficiency, Energy consumption, Commercial buildings, Temperature control, Heating systems, Air conditioning, Standards, Computerized simulation, Mathematical models, *Air tightness.

This report describes the impact of building airflows on energy consumption in multi-zone buildings and the analysis approaches that can be used to account for the energy associated with these airflows. Plans to link a multi-zone network airflow analysis program with a building energy analysis program are disussed. An initial estimate of the energy associated with infiltration in U.S. office buildings, based on a simplified analysis approach, is presented.

00,274
PB96-155593 Not available NTIS
National Inst. of Standards and Technology (BFRL), Gaithersburg, MD. Building Environment Div.
Study of Ventilation Measurement in an Office Building.
Final rept.
W. Stuart Dols, and A. K. Persily. 1995, 24p.
See also PB93-113595.
Pub. in Airflow Performance of Building Envelopes, Components, and Systems, ASTM STP 1255, p23-46 1995.

Keywords: *Office buildings, *Air flow, *Ventilation, Commercial buildings, Air infiltration, Air circulation, Flow measurement, Monitoring, Indoor air pollution, Tracer techniques, Reprints, Air exchange rates.

The National Institute of Standards and Technology has conducted a study of ventilation and ventilation measurement techniques in the Bonneville Power Administration (BPA) Building in Portland, Oregon. The project involved in the use of the following outdoor air ventilation measurement techniques: tracer gas decay measurements of whole-building air change rates, the determination of air change rates based on peak carbon dioxide (CO2) concentrations, the determination of percent outdoor air intake using tracer gas (Sulfur hexafluoride and occupant-generated CO2), and direct airflow rate measurements with in the air handling system. In addition, air change rate measurements made approximately three years apart with an automated tracer gas decay system were compared.

00,275
PB96-155601 Not available NTIS
National Inst. of Standards and Technology (BFRL), Gaithersburg, MD. Building Environment Div.
Development and Application of an Indoor Air Quality Commissioning Program in a New Office Building.
Final rept.
W. Stuart Dols, A. K. Persily, and S. J. Nabinger. 1994, 11p.
Pub. in Indoor Air Quality Engineering Indoor Environments, p33-43 1994.

Keywords: *Office buildings, *Indoor air quality, *Environmental surveys, Ventilation systems, Building materials, Air flow, Air circulation, Air infiltration, Air intakes, Baseline measurements, Monitoring, Air sampling, Flow measurement, Design analysis, Reprints.

An indoor air quality commissioning program has been developed and is being implemented in a new office building in Rockville, Maryland. New buildings can have an increased potential for indoor air quality (IAQ) problems due to new building materials and deficiencies in mechanical ventilation system operation during construction and initial occupancy. This IAQ commissioning effort is being implemented to reduce the potential for such problems in this building. This commissioning program consists of three tasks: (1) evaluate the mechanical ventilation system design, (2) develop a set of environmental parameters and associated reference values that will be used to evaluate IAQ in the building, and (3) measure various environmental parameters for comparison with the reference values developed in task 2.

00,276
PB96-164181 Not available NTIS
National Inst. of Standards and Technology (BFRL), Gaithersburg, MD. Building Environment Div.
Distributed Architecture for Standards Processing.
Final rept.
H. Kiliccote, J. H. Garrett, B. Choi, and K. A. Reed. 1995, 8p.
Sponsored by Carnegie-Mellon Univ., Pittsburgh, PA.
Pub. in Proceedings of the International Conference on Computing in Civil and Building Engineering (6th), Berlin, Germany, July 12-15, 1995, p343-350.

Keywords: *Computer-aided design, *Design criteria, Architecture, Design analysis, Building codes, Requirements, Standards compliance, Reprints, *Building design, Standards processing.

An approach to providing computer-aided support for using design standards in design system is presented. The standards processing system we developed is composed of five major components that interact with each other using the Internet: standards processing servers which evaluate a given design to check whether it satisfies the requirements of a specific design standard; the standards processor broker which is used by the designer to identify applicable design standards; the data server which acts as a front-end between the database of the design system and the standards processing activities, multiple standards can be dealt with by the design system and the design system is insulated from changes in standards.

00,277
PB96-502794 CP D02
National Inst. of Standards and Technology, Gaithersburg, MD.
Building Life Cycle Cost Computer Program (BLCC) Version 4.22-95 (for Micrcomputers).
Model-Simulation.
1995, 2 diskettes.
MS DOS operating system. Supersedes PB95-502779 and PB95-503397.
The software is on two 3 1/2 inch DOS diskettes, 1.44M high density. Documentaion included; may be ordered separately as PB96-199229.

Keywords: *Software, *Buildings, *Life cycle costs, *Energy conservation, Economic analysis, Cost benefit analysis, Operating costs, Return on investment, Savings, Prices, Project management, Long range(Time), Federal government, State government, Standards, Diskettes.

The software provides economic analysis of proposed capital investments that are expected to reduce long-term operating costs of buildings or building systems/components. It is especially useful for evaluating the costs and benefits of energy conservation projects in buildings. Two or more alternative designs can be evaluated to determine which has the lowest life-cycle cost and therefore is most economical in the long run. Economic measures, including net savings, savings-to-investment ratio, adjusted internal rate of return, and years to payback can be calculated for any design alternative relative to the designated base case. BLCC can be used for evaluating federal (including Department of Defense), state, and local government projects as well as projects in the private sector. It complies with ASTM standards related to building economics as well as FEMP and OMB Circular A-94 guidelines for economic analysis of federal building projects. It has new capabilities for using demand charges and block rate calculations for computing annual electricity costs. While it is primarily intended for the economic evaluation of building systems, it can be applied to a wide range of project investments which are intended primarly to reduce future operating-related costs.

00,278
PB97-106843 PC A05/MF A01
National Inst. of Standards and Technology (BFRL), Gaithersburg, MD.
Mathematical Analysis of Practices to Control Moisture in the Roof Cavities of Manufactured Houses.
D. M. Burch, G. A. Tsongas, and G. N. Walton. Sep 96, 63p, NISTIR-5880.
Prepared in cooperation with Portland State Univ., OR. Dept. of Mechanical Engineering.

Keywords: *Moisture, *Roofs, *Prefabricated buildings, Mathematical models, Vents, Cavities, Venting, Mobile homes.

This report presents a mathematical model to simulate the performance of a double-wide manufactured house constructed in compliance with HUD Standards. An interior vapor retarder was installed in the ceiling construction and ventilation openings were installed in the roof cavity consistent with HUD's 1/300 Rule. The effect of passive and mechanical ventilation, as well as a wide range of other factors on the roof sheathing moisture content was investigated as a function of time. The weekly average moisture content of the lower surface of the plywood sheathing was analyzed in several cold climates, while the relative humidity at the lower surface of the ceiling insulation was analyzed in a hot and humid climate.

00,279
PB97-110142 Not available NTIS
National Inst. of Standards and Technology (BFRL), Gaithersburg, MD. Building Environment Div.
Indoor Air Quality Commissioning of a New Office Building.
Final rept.
W. S. Dols, A. K. Persily, and S. J. Nabinger. 1995, 13p.
See also PB95-182309 and PB96-155601.
Pub. in Indoor Air Quality (IAQ) '95: Practical Engineering of IAQ, Denver, CO., October 22-24, 1995, p29-41 Dec 95.

Keywords: *Office buildings, *Indoor air quality, *Environmental surveys, Ventilation systems, Building materials, Air circulation, Monitoring, Air sampling, Design analysis, Reprints.

New buildings can have an increase potential for indoor air quality problems due to new building materials and deficiencies in mechanical ventilation system performance during construction and initial occupany. In order to decrease the potential for such problems, an indoor air quality commissioning program was developed and implemented in a new office building for the U.S. Nuclear Regulatory Commission (NRC). The indoor air quality commissioning effort consisted of three tasks: (1) evaluation of the mechanical ventilation system design, (2) development of a set of environmental parameters and associated reference values to be used in evaluating the building indoor air quality, and (3) measurement of these environmental parameters in this building and comparison of them with the reference values developed in task 2. The evaluation of the mechanical ventilation system design was based on the recommendations of the 1987 BOCA mechanical code and ASHRAE Standard 62-1989. The design evaluation showed that the system ventilation rates were consistent with the recommendations of both documents. The environmental parameters identified in task 2 address ventilation system performance, indoor pollutant levels, and thermal comfort. The reference values for these parameters were based on available standards and guidelines as well as on the results of previous indoor air quality research. In task 3, these environmental parameters were measured in three phases of building construction: after completion of interior buildout, after the installation of the systems furniture, and roughly one month after occupancy. The measured values were within the project reference values with only a few exceptions, and these exceptions were usually attributed to a correctable circumstance.

00,280
PB97-111298 Not available NTIS
National Inst. of Standards and Technology (BFRL), Gaithersburg, MD. Building Environment Div.

Post-Occupancy Evaluation of the Forrestal Building.
Final rept.
P. A. Sanders, and B. L. Collins. 1996, 15p.
Pub. in Jnl. of the Illuminating Engineering Society, p89-103, Summer 1996.

Keywords: *Office buildings, *Work environments, *Surveys, Workplace layout, Comfort, Human reactions, Reprints.

Post-occupancy evaluation techniques provide a means for evaluating occupant responses to changes in an environment and linking this response to physical measures of that environment. Post-occupancy evaluations use a battery of tests to assess environmental conditions in the facility, including questionnaire surveys of the occupants, physical measures, personal observations, and individual interviews. The post-occupancy evaluation technique is designed to provide information about the occupants' reaction to their work spaces and document the physical conditions to which they are responding, usually on a pre- and post-retrofit basis.

00,281
PB97-112221 Not available NTIS
National Inst. of Standards and Technology (MEL), Gaithersburg, MD. Manufacturing Systems Integration Div.
HVAC CAD Layout Tools: A Case Study of University/Industry Collaboration.
Final rept.
J. Cagan, R. Clark, P. Dastidar, S. Szykman, and P. Weisser. 1996, 10p.
Pub. in Proceedings of the American Society of Mechanical Engineers Design Engineering Technical Conference and Computers in Engineering Conference, Irvine, CA., August 18-22, 1996, p1-10.

Keywords: *Space HVAC systems, *Computer-aided design, *Heat pumps, Tubes, Energy efficiency, On-line control systems, Heat transfer, Computer tools, Computerized simulation, Reprints.

An effective partnership between industry and the university resulted in the system of design tools for the layout of HVAC systems presented in the paper and illustrated with the design of a heat pump. The system provides tools to assist in the placement of components and routing of tubes between the components. The paper provides insight on both the collaborative research interaction and the resulting set of tools.

00,282
PB97-112544 Not available NTIS
National Inst. of Standards and Technology (PL), Gaithersburg, MD. Radiometric Physics Div.
Characterization of Modified FEL Quartz-Halogen Lamps for Photometric Standards.
Final rept.
Y. Ohno, and J. K. Jackson. 1996, 4p.
Pub. in Metrologia, v32 p693-696 1995/96.

Keywords: *Photometry, *Standards, Luminous intensity, Illuminance, Lumens, Light sources, Luminous flux, Flux density, Color, Spectrum analysis, Optical measurement, Reprints, *Halogen lamps, *Incandescent lamps.

The stability of luminous intensity and color temperature of modified FEL-type, 1000 W quartz-halogen lamps has been tested at various color temperatures to investigate the suitability of these lamps for use as photometric transfer standards. Characteristics of the lamps have also been investigated for operation at 2000 K to 3100 K, for reversed polarity, and for long-term storage.

00,283
PB97-121321 Not available NTIS
National Inst. of Standards and Technology (BFRL), Gaithersburg, MD. Building Environment Div.
Fault Diagnosis of an Air-Handling Unit Using Artificial Neural Networks.
Final rept.
W. Y. Lee, and C. Park. 1996, 10p.
Pub. in American Society of Heating, Refrigerating and Air-Conditioning Engineers Transactions: Symposia, v102 pt1 p540-549 Jun 96.

Keywords: *Neural nets, *Fault detection, *Space HVAC systems, Air conditioning, Heating systems, Ventilation systems, Control systems, Error analysis, Error detection codes, Reprints, Air handling systems.

The objective of the study is to describe the application of artificial neural networks to the problem of fault diagnosis in an air-handling unit. Initially, residuals of system variables that can be used to quantify the dominant symptoms of fault modes of operation are selected. Idealized steady-state patterns of the residuals are then defined for each fault mode of operation. The study-state relationship between the dominant symptoms and the faults is learned by an artificial neural network using the backpropagation algorithm. The trained neural network is applied to experimental data for various faults and successfully identifies each fault.

00,284
PB97-500342 CP D02
National Inst. of Standards and Technology, Gaithersburg, MD.
Building Life Cycle Cost Computer Program (BLCC) Version 4.4-97 (for Microcomputers).
Model-Simulation.
Sep 96, 2 diskettes.
MS DOS operating system. Documentation is in Word Perfect 5.1. Supersedes PB95-502779, PB95-503397 and PB96-5002794.
The software is on two 3 1/2 inch DOS diskettes, 1.44M high density. File format: ASCII text.

Keywords: *Software, *Buildings, *Life cycle costs, *Energy conservation, *Benefit-cost analysis, Operating costs, Economic analysis, Return on investment, Savings, Prices, Project management, National government, State government, Local government, Standards, Diskettes, Documentation.

The software provides economic analysis of proposed capital investments that are expected to reduce long-term operating costs of buildings or building systems/components. It is especially useful for evaluating the costs and benefits of energy conservation projects in buildings. Two or more alternative designs can be evaluated to determine which has the lowest life-cycle cost and therefore is most economical in the long run. Economic measures, including net savings, savings-to-investment ratio, adjusted internal rate of return, and years to payback can be calculated for any design alternative relative to the designated base case. BLCC can be used for evaluating federal (including Department of Defense), state, and local government projects as well as projects in the private sector. It complies with ASTM standards related to building economics as well as FEMP and OMB Circular A-94 guidelines for economic analysis of federal building projects. It has new capabilities for using demand charges and block rate calculations for computing annual electricity costs. While it is primarily intended for the economic evaluation of building systems, it can be applied to a wide range of project investments which are intended primarily to reduce future operating-related costs.

Building Equipment, Furnishings, & Maintenance

00,285
PB94-139193 PC A03/MF A01
National Inst. of Standards and Technology (BFRL), Gaithersburg, MD.
Some Factors Affecting Design of a Furniture Calorimeter Hood and Exhaust.
L. Y. Cooper. Dec 93, 26p, NISTIR-5298.

Keywords: *Calorimeters, *Fire tests, *Furniture, Exhaust systems, Plumes, Hoods, Flames, Flow rate, Mathematical models, Design criteria.

This work considers factors affecting the design of an effective and versatile furniture calorimeter hood and exhaust system. The purpose of the furniture calorimeter, design functions, and inherent limitations of a particular design are discussed. The interactions between the hood structure and the fire and its plume are analyzed in the context of avoiding: flame impingement on the hood; enhanced combustion of a test article, over and above that of a free-burn; loss of combustion product plume gases due to 'spill-over' below the hood; unacceptable dilution of plume gases in the measurement section of the exhaust duct. The concept of the ideally designed hood is introduced, where, throughout the course of the burn of a test article the hood is always immediately above the flame tip and the exhaust rate always exactly matches the hood-ceiling-elevation plume-flow rate. Methods to partially or completely achieve the ideal design are presented. These include the combined features of adjustable hood evaluation and adjustable hood exhaust rate. The ideas and results of analyses developed are applied in examples relevant to the existing furniture calorimeter hood and exhaust system of the NIST Fire Research Laboratory Building 205. Recommendations for improvements to this facility are presented.

00,286
PB94-160876 PC A10/MF A03
National Inst. of Standards and Technology (NEL), Gaithersburg, MD. Center for Fire Research.
Summaries of Center for Fire Research In-House Projects and Grants: 1990.
S. M. Cherry. Oct 90, 224p, NISTIR-4440.
See also report for 1989, PB90-127101.

Keywords: *Combustion, *Furniture, Flammability, Carbon monoxide, Grants, Research projects, Toxicity, Ignition, Soot, Fire hazards, Fire safety.

This report describes the research projects performed in the Center for Fire Research (CFR) and under its grants program during FY 1990. Topics considered include the following: Turbulent Combustion; Soot Formation; CO Prediction; Polymer Gasification; Flame Spread; Toxic Potency; Furniture Flammability; Building Fire Modeling and Smoke Transfer; Fire Hazard Assessment; Engineering Analysis System and Fire Reconstruction; Suppression; Cone Calorimeter Development; Fire/Modeling Interactions; and Fire Protection Technology.

00,287
PB94-163441 PC A07/MF A02
National Inst. of Standards and Technology (BFRL), Gaithersburg, MD.
Feasibility and Design Considerations of Emergency Evacuation by Elevators.
J. H. Klote, D. M. Alvord, B. M. Levin, and N. E. Groner. Sep 92, 127p, NISTIR-4870.
See also PB92-164771 and PB92-238641. Prepared in cooperation with George Mason Univ., Fairfax, VA. Sponsored by Public Buildings Service, Washington, DC. Office of Real Property Management and Safety.

Keywords: *Elevators(Lifts), *Evacuating(Transportation), Design criteria, Handicapped workers, Feasibility, Human factors engineering, Fire safety, Emergencies, Computerized simulation, Smoke, Egress.

Throughout most of the world, warning signs next to elevators indicate they should not be used in fire situations, and today's elevators have not been designed for fire evacuation and should not be used for fire evacuation. However, the idea of using elevators to speed up fire evacuation and to evacuate persons with disabilities has gained considerable attention. The potential of elevator evacuation is so significant that the U.S. General Services Administration (GSA) has sponsored a research project at NIST to develop techniques for occupant use of elevators during building evacuations. This paper is the final report of that project, and it addresses fundamental system considerations, engineering design considerations, design analysis, and human behavior. This paper shows that use of elevators in addition to stairs during a fire emergency allows occupants and firefighters an additional system of vertical transportation.

00,288
PB94-194339 PC A03/MF A01
National Inst. of Standards and Technology (BFRL), Gaithersburg, MD. Fire Science Div.
Performance Parameters of Fire Detection Systems.
R. L. Smith. Jun 94, 20p, NISTIR-5439.

Keywords: *Fire detectors, *Buildings, Fire prevention, Parameters, Fire extinguishers, Warning systems, Probability theory, Smoke detectors, Mathematical models, Fires.

This report is a formal, functional analysis of fire detection systems' requirements. The performance parameters of fire detection systems are given as conditional probabilities. These parameters are identified by the objective analysis of the functions of a fire detection system. It is demonstrated that using the false alarm rate to specify the malfunctioning of a threshold detection system is inadequate. The principal function of fire detection systems is identified as the notification of anti-fire agents of the probability of an unwanted fire. The evaluation of the information provided by a detector system is central to its worth.

00,289
PB94-198454 Not available NTIS
National Inst. of Standards and Technology (BFRL), Gaithersburg, MD. Fire Safety Engineering Div.
Toxicity, Fire Hazard and Upholstered Furniture.
Final rept.
V. Babrauskas. 1992, 9p.
Pub. in Proceedings of European Conference on Furniture Flammability (3rd), Brussels, London, November 24-25, 1992, p125-133.

Keywords: *Fire hazards, *Toxicity, *Furniture, Fires, Combustion products, Burning rate, Fire safety, Safety engineering, Reprints, *Upholstery.

Fire fatalities associated with upholstered furniture fires commonly involve the toxic effects of fire gases. Extensive results, however, both from experiments and from modeling, are presented in this paper that demonstrate that occupant life safety can only be ensured by assuring that furniture fires do not reach a high heat release rate. Differences among commercial products associated with toxicity effects are not significant. A very remote possibility exists that someone could produce furniture having combustion products' toxicity significantly greater than exists in the present marketplace. A combustion toxicity test does exist which would allow the accurate screening out of such products. Any usable combustion toxicity test method requires the use of test animals; no non-animal-based test is possible which can successfully identify products of unusual or extreme toxicity.

00,290
PB94-199262 Not available NTIS
National Inst. of Standards and Technology (BFRL), Gaithersburg, MD. Fire Safety Engineering Div.
Studies Assess Performance of Residential Detectors.
Final rept.
R. W. Bukowski. 1993, 7p.
Pub. in National Fire Protection Association Jnl. 87, n1 p48-54 Jan/Feb 93.

Keywords: *Residential buildings, *Fire detectors, *Fire safety, Performance, Fire protection, Smoke detectors, Warning systems, Literature surveys, Reprints, *Building fires, *Heat detectors.

Current thinking on the performance of residential heat detectors compared to smoke detectors has recently been challenged. The paper was prepared to assemble a comprehensive picture from the literature of what is known about the relative performance of these two detector types in residential fires. The paper reviews 10 independent studies, conducted over two decades, in four countries, involving 206 tests in houses and apartments, typically burning actual items (furniture, mattresses, boxes of trash, clothing, etc.) and using real heat and smoke detectors representative of devices being sold at the time. In each case, the study is summarized and the conclusions relative to heat and smoke detector performance are quoted. All of the studies reach essentially identical conclusions, that: (1) either the ionization or photoelectric smoke detectors when located outside bedrooms and on each level of a house provides adequate warning to allow occupants to evacuate through their normal egress routes for most residential fire scenarios; and (2) heat detectors, even when located in the room of fire origin (effectively requiring locating a heat detector in every room) do not provide adequate warning in most fire scenarios.

00,291
PB94-212883 Not available NTIS
National Inst. of Standards and Technology (NEL), Gaithersburg, MD. Fire Science and Engineering Div.
Smoke Control Systems for Elevator Fire Evacuation.
Final rept.
J. H. Klote, and G. T. Tamura. 1991, 12p.
Pub. in Proceedings of American Society of Mechanical Engineers Symposium on Elevators and Fire, Baltimore, MD., February 19-20, 1991, p83-94.

Keywords: *Elevators(Lifts), *Evacuation, *Smoke, *Fire safety, Buildings, Handicapped persons, Emergencies, Pressurizing, Ventilation, Fire tests, Stairways, Reprints, *Smoke control, *Elevator fires, Piston effect.

Some people cannot use stairwells because of physical disabilities, and for these people fire evacuation is a serious problem. A potential solution of this problem is the use of elevators for fire evacuation. A joint project of the U.S. National Institute of Standards and Technology (NIST) and the National Research Council of Canada (NRCC) was formed to evaluate the feasibility of using elevators for the evacuation of the handicapped during a fire. This project consisted of conceptual studies, full scale fire experiments, and theoretical analysis. This paper summarizes the findings of the joint project that are relevant to the design of smoke control systems for elevators. A method of dealing with elevator piston effect is discussed. All other things being equal, piston effect is considerably greater for single car hoistways than for multiple car hoistways. Different approaches to deal with the pressure fluctuations due to opening and closing of building doors are presented. A method of design analysis is presented with an example analysis. Results indicate that there are many types of elevator smoke control systems which can be designed to provide acceptable levels of pressurization even under severe conditions of doors opening and closing.

00,292
PB94-213717 PC A07/MF A02
National Inst. of Standards and Technology (BFRL), Gaithersburg, MD.
Measurement of Room Conditions and Response of Sprinklers and Smoke Detectors during a Simulated Two-Bed Hospital Patient Room Fire.
K. A. Notarianni. Jul 93, 142p, NISTIR-5240.
See also PB88-164223. Sponsored by National Institutes of Health, Bethesda, MD. Div. of Engineering Services.

Keywords: *Sprinklers, *Smoke detectors, *Fire protection, *Beds, Fire safety, Heat flux, Temperature, Safety equipment, Furniture, Time dependence, *Hospital fires.

A series of experiments are reported in which a wood crib was burned within a simulated two bed hospital patient room in order to measure the activation times of various types of quick and standard response sprinklers and ionization and photoelectric smoke detectors at several locations in the room simulating multiple options for protection of the space. Gas and surface temperatures, heat flux, carbon dioxide, carbon monoxide, and oxygen concentrations were continuously measured in order to access the tenability of the room. Of the parameters measured, temperature was the best indicator of the tenability of the space. Temperature at time of activation of the quickl response sprinklers was at or below 77 deg C (171 deg F) at the five foot level and at or below 48 deg C (118 deg F) at the three foot level between the patient beds, in all tests with the exception of the shielded fire scenario where temperatures at the five and three foot levels reached 111 deg C (232 deg F), and 78 deg C (172 deg F) respectively. An initial detector activation was received between 232-377 seconds prior to activation of the first sprinkler, and 552-722 seconds prior to activation of the QR-EC sidewall sprinkler.

00,293
PB94-216181 Not available NTIS
National Inst. of Standards and Technology (BFRL), Gaithersburg, MD. Fire Science Div.
Sprinkler Fire Suppression Algorithm.
Final rept.
D. Madrzykowski, and R. L. Vettori. 1992, 14p.
Pub. in Jnl. of Fire Prot. Engr. 4, n4 p151-164 1992.

Keywords: *Sprinklers, *Fire suppression, *Algorithms, *Furniture, *Buildings, Fire protection, Fire hazards, Models, Activation, Burning rate, Time dependence, Reprints, *Building fires.

A study was conducted to develop a sprinkler fire suppression algorithm for use with sprinkler activation time models. Large-scale experiments were performed to determine the heat release rate (HRR) of selected office fuel packages with and without sprinklers operating. Eight different fuel packages were evaluated. The results from these experiments were used to develop a time dependent HRR reduction factor. The sprinkler fire suppression algorithm consists of multiplying the HRR reduction factor by the HRR at the time of sprinkler activation, yielding an expected upper bound to the HRR at a given time after sprinkler activation for office furnishing fires that are not heavily shielded. This sprinkler fire suppression algorithm can be thought of as a 'zeroth order' fire suppression model for 'light hazard' occupancies with a sprinkler spray density of 0.07 mm/s (0.1 gpm/sq ft) or greater.

00,294
PB95-126330 Not available NTIS
National Inst. of Standards and Technology (BFRL), Gaithersburg, MD. Fire Science Div.
Assessment of Technologies for Advanced Fire Detection.
Final rept.
W. Grosshandler. 1992, 10p.
Pub. in Proceedings of a Conference on Heat and Mass Transfer in Fire and Combustion Systems, Anaheim, CA., November 8-13, 1992, p1-10.

Keywords: *Fire alarm systems, *Fire detectors, *Technology assessment, *Buildings, Fire safety, Microelectronics, Fire protection, False alarms, Flame propagation, Infrared detectors, Ignition, Reprints.

The majority of fires are sensed either by the heat or the smoke they produce at a set location in space, with an alarm signal being issued when a threshold temperature or particulate level is exceeded. Many of these sensors are inexpensive and perfectly suitable for certain applications, but issues such as false alarms and increased performance can necessitate alternative sensing techniques. Advances in sensor technology, in microelectronics, and in our understanding of ignition and flame spread provide an opportunity to greatly enhance the performance of fire detection systems in traditional applications. Technological advances have also led to new situations with unique protection requirements at a time when environmental considerations have eliminated our most effective suppressants (halons), making the early detection of a fire even more critical. This article describes some of these developments, suggests possible applications, and indicates limitations to the technologies which need to be overcome before exploitation is feasible.

00,295
PB95-155560 PC A04/MF A01
National Inst. of Standards and Technology (TS), Gaithersburg, MD. National Voluntary Lab. Accreditation Program.
National Voluntary Laboratory Accreditation Program: Carpet and Carpet Cushion.
Handbook.
L. S. Galowin, W. J. Rossiter, W. A. Hall, and L. I. Knab. Oct 94, 74p, NIST/HB-150/6.
Also available from Supt. of Docs as SN003-003-03300-6. See also PB95-155552.

Keywords: *Carpets, *Laboratories, *Certification, Materials testing, Procedures, Requirements, Calibration standards, Standardization, Licensure, Methodology, Accuracy, Performance evaluation, Carpet cushion, Carpet pads, National Voluntary Laboratory Accreditation Program, US NIST.

NIST Handbook 150-6 presents the technical requirements of the National Voluntary Laboratory Accreditation Program (NVLAP) for Carpet and Carpet Cushion (formerly called the Carpet Testing program). It is intended for information and use by staff of accredited laboratories, those laboratories seeking accreditation, other laboratory accreditation systems, users of laboratory services, and others needing information on the requirements for accreditation under the Carpet and Carpet Cushion program. This publication supplements NIST Handbook 150 (PB94-178225) 'NVLAP Procedures and General Requirements', which contains Part 285 of Title 15 of the U.S. Code of Federal Regulations (CFR) plus all general NVLAP procedures, criteria, and policies. Handbook 150-6 contains information that is specific to the Carpet and Carpet Cushion program and does not duplicate information contained in the Procedures and General Requirements. It is organized to cross-reference with Handbook 150.

00,296
PB95-164810 Not available NTIS
National Inst. of Standards and Technology (BFRL), Gaithersburg, MD. Fire Science Div.
Acoustic Emission of Structural Materials Exposed to Open Flames.
Final rept.
W. Grosshandler, and M. Jackson. 1994, 20p.
See also PB93-138980.
Pub. in Fire Safety Jnl. 22, p209-228 1994.

Keywords: *Fire tests, *Acoustic emission, *Construction materials, *Fire detectors, Heat flux, Signal processing, Fires, Plywood, Wallboard, Flames, Fire safety, Transducers, Reprints.

The use of acoustic emission (AE) as an early indicator of structural materials exposed to a flame has been investigated and found to be possible. Piezoelectric

transducers have been mounted directly on 0.5 m long, simply supported beams of aluminum, gypsum board, wood and plastic, and have been used to record ultrasonic events resulting from a small flame placed under the beam. The number of AE events in a minute and the cumulative energy released during the heating cycle provide a good measure of the overheated state of some of these materials even before a temperature increase is indicated. The measured signals varied in energy and number with the type of material, the thickness of the specimen and heat flux. Wood was particularly susceptible to acoustic emission, producing more than 1000 events/min in a solid fir board and 30/min in 13 mm thick plywood when the flame exceeded 1 kW. Some critical issues which remain to be investigated before this technique can be adapted to practical fire detection are mentioned.

00,297
PB95-180162 Not available NTIS
National Inst. of Standards and Technology (BFRL), Gaithersburg, MD. Fire Science Div.
Influence of Ignition Source on the Flaming Fire Hazard of Upholstered Furniture. (NIST Reprint).
Final rept.
T. G. Cleary, T. J. Ohlemiller, and K. Villa. 1994, 24p.
See also PB92-205384.
Pub. in Fire Safety Jnl. 23, p79-102 1994.

Keywords: *Fire hazards, *Ignition, *Upholstery, Fires, Combustion, Furniture, Calorimeters, Residential buildings, Fabrics, Chairs, Reprints, *Home fires.

A set of upholstered chairs constructed from five different fabric/foam combinations was subjected to a variety of ignition sources suggested by fire statistics. The sources included a cigarette, a small match-like flame, an incandescent lamp, a space heater, and a large flame source (TB 133 ignition source). The tests were performed in a furniture calorimeter where heat release rate and species production rates were obtained. For any chair type, the time to the peak heat release rate depended on the ignition sequence, but the magnitude of the peak did not, within the scatter of the data for any given chair. HAZARD 1, the fire hazard assessment method developed at the National Institute of Standards and Technology (NIST), was used to quantify the hazard posed by the different ignition scenarios.

00,298
PB95-180311 Not available NTIS
National Inst. of Standards and Technology (BFRL), Gaithersburg, MD. Fire Science Div.
Early Detection of Room Fires Through Acoustic Emission. (NIST Reprint).
Final rept.
W. Grosshandler, and E. Braun. 1994, 12p.
See also PB94-112257.
Pub. in Proceedings of International Symposium on Fire Safety Science (4th), Ottawa Ontario, Canada, June 13-17, 1994, p773-784.

Keywords: *Fire detectors, *Acoustic emissions, Warning systems, Signal processing, Fire alarm systems, Acoustic detectors, Fire safety, Transducers, Acoustic signals, Reprints.

Acoustic emission (AE) has been shown to be a viable concept for the early indication of an open flame impinging on various structural materials. To assess its effectiveness in a more realistic environment, experiments have been performed in a 2.4 m cubical room constructed of gypsum board and wood. AE transducers were mounted on top of a ceiling joist and on a wall stud. The threats examined were a natural gas fire producing a thermal load up to 125 kW, and a charring condition achieved by attaching a 550 W electrical heater to a wall stud. A signal discernable above the background was recorded from at least one AE sensor in six of nine situations. The conclusion is that AE emission appears to be sufficiently sensitive to detect two particular threats, and that an overheated condition in a wall or ceiling can be detected if it is not more than 3 m from the transducer.

00,299
PB95-182267 PC A03/MF A01
National Inst. of Standards and Technology (BFRL), Gaithersburg, MD.
Comparison of Fire Sprinkler Piping Materials: Steel, Copper, Chlorinated Polyvinyl Chloride and Polybutylene, in Residential and Light Hazard Installations.
K. A. Notarianni, and M. A. Jackson. Jun 94, 48p, NISTIR-5339.
Sponsored by Fire Administration, Emmitsburg, MD.

Keywords: *Sprinklers, *Vinyl plastics, *Piping systems, *Steels, *Buildings, *Mechanical properties, *Copper, Design criteria, Corrosion, Pipes, Polyvinyl chloride, Bending, Fire protection, Specifications, Degradations, Thermal expansion, *Chlorinated polyvinyl chloride, *Polybutylene.

A literature based study was conducted at the Building and Fire Research Laboratory of the National Institute of Standards and Technology to compare characteristics and usage of steel, copper, chlorinated polyvinyl chloride and polybutylene fire sprinkler pipe primarily related to residential and light hazard installations. This report addresses key variables, such as material properties, usage criteria and limitations, design and installation requirements, economics and maintenance. This study was sponsored by the United States Fire Administration, and presents information useful for the selection of a sprinkler pipe material.

00,300
PB95-189452 PC A03/MF A01
National Inst. of Standards and Technology (BFRL), Gaithersburg, MD. Fire Science Div.
Review of Measurements and Candidate Signatures for Early Fire Detection.
W. L. Grosshandler. Jan 95, 44p, NISTIR-5555.

Keywords: *Fire detectors, *Infrared signatures, *Fire protection, Combustion, Smoke, Fires, Acoustic measurement, Transport properties, Flames, Carbon monoxide, Test methods.

The physical and chemical transformations associated with a burgeoning fire are discussed and the results of past experimental measurements of these transformations are summarized. Standard test methods for the current generation of fire detectors and recent developments in detection technologies for which existing standards may not be suitable are described. The literature has been reviewed to determine the extent to which fires have been characterized in their early phase. One finds dramatic variations in the measured magnitude and rate of growth of CO concentration in a variety of standard fires. The variation is also large between repeat runs of the same tests. When scaled by estimated mass consumed of fuel, the different standard fires group a bit more systematically. Additional measurements of species, temperature and velocity just above the flame are suggested to get a more complete footprint of each fire type. Similar measurements of non-fire nuisance sources are required in order to discriminate between a fire and non-threatening situation with a high degree of certainty. The concept of a universal fire emulator/detector evaluator (FE/DE) is introduced. The objective is to have a facility that will eliminate the unavoidable run-to-run variations associated with full-scale tests, and to allow more well controlled environments. Computational fluid dynamics could then be used to insert the fire source into the space being protected to guide detector placement and to predict system performance, as well as to compare alternative systems and new concepts on a level, realistic playing field.

00,301
PB95-231585 PC A05/MF A01
National Inst. of Standards and Technology (BFRL), Gaithersburg, MD. Fire Science Div.
Behavior of Mock-Ups in the California Technical Bulletin 133 Test Protocol: Fabric and Barrier Effects.
T. J. Ohlemiller, and J. R. Shields. May 95, 80p, NISTIR-5653.

Keywords: *Furniture, *Flammability testing, *Heat transmission, Upholstery, Fabrics, Buring rate, Heat flux, Ignition, Heat transmission, Flame propagation, Heat transfer, Calorimeters, Fire tests, *California Technical Bulletin 133.

Twenty-seven material combinations (seven fabrics, four barriers and two polyurethane foams) were tested in four cushion mock-up form in accord with California Technical Bulletin 133 using a furniture calorimeter. Both mock-up and Cone sample behavior were recorded on video to facilitate behavioral comparisons of the samples; distinct differences were noted for thermoplastics fabrics. The mock-up behavior always comprised at least a heat release peak during the 80 second gas burner exposure; it often included a later and larger peak as well. A statistical fit of the available data to these more complex types of correlations appears to work best for charring fabrics; it helps improve the correlation for all types of fabrics but at least two material combinations were outliers.

00,302
PB96-102181 Not available NTIS
National Inst. of Standards and Technology (BFRL), Gaithersburg, MD. Fire Safety Engineering Div.
Some Factors Affecting the Design of a Calorimeter Hood and Exhaust.
Final rept.
L. Y. Cooper. 1994, 14p.
See also PB94-139193.
Pub. in Jnl. of Fire Protection Engineering, v6 n3 p99-112 1994.

Keywords: *Plumes, *Calorimeters, *Fire tests, *Furniture, Exhaust systems, Hoods, Flames, Walls, Flow rate, Design criteria, Mathematical models, Combustion, Reprints.

This paper considers factors affecting the design of an effective and versatile calorimeter hood and exhaust system. The purpose of the calorimeter, design functions, and inherent limitations of a particular design are discussed. The interactions between the hood structure and the fire and its plume are analyzed in the context of avoiding: flame impingement on the hood; enhanced combustion of a test article, over and above that of a free-burn; loss of combustion product plume gases due to 'spill-over' below the hood; and unacceptable dilution of plume gases in the measurement section of the exhaust duct. Methods to partially or completely achieve the ideal design are presented. These include the combined features of adjustable hood elevation and adjustable hood exhaust rate.

00,303
PB96-128095 PC A06/MF A02
National Inst. of Standards and Technology (BFRL), Gaithersburg, MD. Fire Science Div.
Study of Technology for Detecting Pre-Ignition Conditions of Cooking-Related Fires Associated with Electric and Gas Ranges and Cooktops, Phase 1 Report.
E. L. Johnsson. Oct 95, 117p, NISTIR-5729.
Contract CPSC-IAG-95-1145
Sponsored by Consumer Product Safety Commission, Bethesda, MD.

Keywords: *Fires, *Cooking devices, *Ignition, Residential buildings, Kitchens, Reviews, Technlogy innovation.

A significant portion of residential fires stem from kitchen cooking fires. Existing fire data indicate that cooking fires primarily are unattended and most often involve oil or grease. The purpose of this investigation was to ascertain the existence of one or more common features or characteristics of the pre-ignition environment that could be used as input to a sensor in a pre-fire detection device. The ultimate goal of this continuing study is to evaluate the feasibility of incorporating such a device into the range that would react to a pre-fire condition and reduce the occurrence of unwanted kitchen fires.

00,304
PB96-141056 Not available NTIS
National Inst. of Standards and Technology (BFRL), Gaithersburg, MD. Fire Safety Engineering Div.
Evaluation of Sprinkler Activation Prediction Methods.
Final rept.
D. Madrzykowski. 1995, 8p.
Pub. in International Conference on Fire Science and Engineering (1st), ASIAFLAM '95, Kowloon, Hong Kong, March 15-16, 1995, p211-218.

Keywords: *Sprinklers, *Activation, *Time lapse, Fire suppression, Flame propagation, Fire detectors, Gas burners, Fire tests, Computer models, Reprints, Compartment fires, Heat release rate, Thermal detectors.

The objective of this study was to evaluate the ability of sprinkler activation models to predict activation time. Large scale compartment fire tests were used to obtain activation times for four different types of sprinklers. The tests were conducted in an 18.9 m by 2.35 m high compartment using floor based, gas burner fires with constant heat release rates of 115, 155, 215, 290, and

520 kW. Non-dimensional sprinkler radial positions, r/H, of 0.67 and 1.3 were evaluated. In addition to sprinkler activation times, ceiling jet temperature, velocity, and radiation measurements were made. The study included: (1) a review of public domain, personal-computer based, single-compartment thermal-detector activation models; (2) an analysis of predicted vs. experimental sprinkler activation times; and (3) a method to determine the applicability of current sprinkler activation models.

00,305
PB96-154810 PC A11/MF A03
National Inst. of Standards and Technology (BFRL), Gaithersburg, MD.
Santa Ana Fire Department Experiments at South Bristol Street.
W. D. Walton, A. D. Putorti, W. H. Twilley, and J. C. Albers. Feb 96, 220p, NISTIR-5776.
See also PB95-188868 and PB96-102934. Prepared in cooperation with Santa Ana City Fire Dept., CA. Fire Safety Div.

Keywords: *Residential buildings, *Fire tests, Furniture, Flammability, Rooms, Smoke detectors, Sprinklers, Temperature measurement, Velocity measurement, Flame propagation, Heat flux, Santa Ana(California), Fuel loads, Mass loss.

A series of fire experiments were conducted in vacant single family dwelling on South Bristol Street in Santa Ana, California. Fire experiments were conducted in bedrooms and living rooms. Fuel consisted of either home furnishings or a propane burner. Fire phenomena measured included: temperatures within various rooms, wall jet velocity, fuel mass dring burning, heat flux smoke detector activation time, sprinkler activation time, oxygen concentration, and time to full room involvement.

00,306
PB96-155411 Not available NTIS
National Inst. of Standards and Technology (BFRL), Gaithersburg, MD. Fire Science Div.
Quantifying the Ignition Propensity of Cigarettes.
Final rept.
T. J. Ohlemiller, K. M. Villa, E. Braun, J. R. Lawson, R. G. Gann, K. R. Eberhardt, and R. H. Harris. 1995, 15p.
Pub. in Fire and Materials, v19 p155-169 1995.

Keywords: *Ignition, *Flammability testing, *Fire hazards, Upholstery, Fabrics, Furniture, Combustion, Tobacco products, Fire tests, Test products, Statistical analysis, Reprints, *Cigarettes.

Research funded under the Fire Safe Cigarette Act of 1990 (United States Public Law 101-352) has led to the development of two test methods for measuring the ignition propensity of cigarettes. The Mock-Up Ignition Test Method uses substrates physically similar to upholstered furniture and mattresses: a layer of fabric over padding. The measure of cigarette performance is ignition or non-ignition of the substrate. The Cigarette Extinction Test Method replaces the fabric/padding assembly with multiple layers of common filter paper. The measure of performance is full-length burning or self-extinguishment of the cigarette. Routine measurement of the relative ignition propensity of cigarettes is feasible using either of the two methods. Using the two methods, some current commercial cigarettes are shown to have reduced ignition propensities relative to the current best-selling cigarettes.

00,307
PB96-156187 Not available NTIS
National Inst. of Standards and Technology (BFRL), Gaithersburg, MD. Fire Safety Engineering Div.
Protecting Your Family from Fire.
Final rept.
R. W. Bukowski. 1993, 19p.
Sponsored by Fire Administration, Emmitsburg, MD.
Pub. in U.S. Fire Administration Public Fire Safety Educational Booklet, p1-19 Feb 93.

Keywords: *Fire safety, *Residential buildings, *Fire protection, Smoke detectors, Fire detectors, Fire detection systems, Warning systems, Fire alarm systems, Sprinklers, Reprints, Heat detectors.

This fire safety educational booklet provides information on residential fires, especially involving children and older persons. The proper use of smoke detectors, heat detectors, fire alarm systems, and residential sprinklers is presented. Guidelines on the preparation of a home escape plan is included.

00,308
PB96-193800 PC A06/MF A01
National Inst. of Standards and Technology (BFRL), Gaithersburg, MD. Structures Div.
State of the Art Report on Seismic Design Requirements for Nonstructural Building Components.
L. T. Phan, and A. W. Taylor. Jun 96, 78p, NISTIR-5857.

Keywords: *Earthquake engineering, *Building codes, *Lighting equipment, *Ceilings, *Sprinkler systems, Seismic design, United States, New Zealand, Japan, Seismic effect, Earthquake damage, Damage assessment, Dynamic response, Loads(Forces), Displacement, Requirements, Nonstructural components.

Seismic design requirements for nonstructural building components of five major building codes, including the 1994 Uniform Building Code, the 1994 Standard Building Code, the 1994 NEHRP Recommended Provisions for Seismic Regulations for New Buildings, the New Zealand Building Code, and the Japanese Building Code, were reviewed in this study. Comparisons of codes reveal wide variation in seismic force and displacement requirements, both in terms of levels of stringency and levels of details. The study also found a lack of focused investigations, dedicated to mitigating seismic damage to nonstructural building components, even though widespread damage to nonstructural building components continues to be observed in recent earthquakes. Based on the findings of this review, areas of needed research were identified.

00,309
PB97-111546 Not available NTIS
National Inst. of Standards and Technology (BFRL), Gaithersburg, MD. Building Environment Div.
Experimental Verification of a Moisture and Heat Transfer Model in the Hygroscopic Regime.
Final rept.
D. M. Burch, R. R. Zarr, and A. H. Fanney. 1995, 10p.
Pub. in 'Thermal VI' Thermal Performance of the Exterior Envelopes of Buildings VI, Clearwater Beach, FL., December 4-8, 1996, p273-282 1995.

Keywords: *Moisture, *Heat transfer, Building envelopes, Calibrated hot box, Manufactured housing, Analysis, Transfer, Reprints, MOIST.

The National Institute of Standards and Technology (NIST) has developed a personal computer model, called NOIST, for predicting the transient moisture and heat transfer within building envelopes. The paper summarizes selected results from a comprehensive laboratory experiment conducted to verify the accuracy of the computer model in the hygroscopic regime. The paper discusses three different multilayer wall specimens installed in a calibrated hot box. The exterior surfaces of the wall specimens were first exposed to both steady and time-dependent winter conditions, while their interior surfaces were maintained at 21 degrees C (70 degrees F) and 50% relative humidity.

00,310
PB97-111553 Not available NTIS
National Inst. of Standards and Technology (BFRL), Gaithersburg, MD. Building Environment Div.
Testing Conformance and Interoperability of BACnet (Trade Name) Building Automation Products.
Final rept.
S. T. Bushby. 1996, 7p.
See also PB92-181221. Sponsored by General Services Administration, Washington, DC. and Department of Energy, Washington, DC.
Pub. in CIBSE/ASHRAE Joint National Conference, Harrogate, United Kingdom, September 29-October 1, 1996, p1-7.

Keywords: *Buildings, *Automation, *Control systems design, Automatic control, Computer communications, Communication networks, Protocol(Computers), Energy management systems, Space HVAC systems, Digital systems, Conformance, Interoperability, Reprints.

The BACnet standard defines classes of conformance and other collections of protocol functionality. The paper describes BACnet conformance classification issues and the work of the NIST consortium in developing testing tools and applying them to test products made by member companies.

00,311
PB97-112312 Not available NTIS
National Inst. of Standards and Technology (BFRL), Gaithersburg, MD. Building Environment Div.
Factors Affecting the Energy Consumption of Two Refrigerator-Freezers.
Final rept.
J. Y. Kao, and G. E. Kelly. 1996, 11p.
Sponsored by Department of Energy, Washington, DC. Office of Codes and Standards.
Pub. in American Society of Heating, Refrigerating and Air-Conditioning Engineers Transaction Annual Meeting, San Antonio, TX., June 23-26, 1996, v102 pt2 p1-11.

Keywords: *Refrigerators, *Freezers, *Energy consumption, *Performance evaluation, Temperature measurement, Room temperature, Humidity, Doors, Performance tests, Reprints.

Two refrigerator-freezers, one with a top-freezer and one with side-by-side doors, were tested in the laboratory to determine the sensitivity of their energy consumption to various operational factors. Room temperature, room humidity, door openings, and the setting of the anti-sweat heater switch were the factors examined. The results indicated that the room temperature and door openings had a significantly greater effect on energy consumption than the other two factors. More detailed tests were then performed under different room temperature and door opening combinations. The relationship of door openings and the equivalent test room temperature were established. Finally, the effect on energy of different temperature settings were studied. Test results are presented and discussed.

Building Standards & Codes

00,312
PB94-185196 Not available NTIS
National Inst. of Standards and Technology (BFRL), Gaithersburg, MD.
Standards Development in North America for Performance of Whole Buildings and Facilities.
Final rept.
G. Davis, and J. G. Gross. May 93, 6p.
Pub. in Some Examples of the Application of the Performance Concept in Building, CIB Report 157, p61-66 May 93.

Keywords: *Standards, *Building codes, Residential buildings, Office buildings, School buildings, Energy consumption, Quality, Maintenance, Performance(Engineering), Reprints, *Building operation and maintenance, Building performance, ASTM E06.

This paper reviews the activities of ASTM Committee E06 on Performance of Buildings and the Subcommittee E06.25 on Whole Buildings and Facilities. Planned standards activities are outlined for 14 task groups. Under development are standards related to objective rating of quality and functionality of office facilities, area measurements, scales for comparing the operation and maintenance of facilities, rating scales for comparing the functionality and quality of educational facilities, behavioral measures, measurement of serviceability, rating buildings for their overall energy performance and monitoring and comparing end-use electrical consumption of commercial buildings and monitoring the energy use of residential buildings. An overview of the full ASTM Committee E06 on Performance of Buildings is provided.

00,313
PB94-207511 PC A08/MF A02
National Inst. of Standards and Technology (BFRL), Gaithersburg, MD.
Global Equivalence Ratio Concept and the Prediction of Carbon Monoxide Formation in Enclosure Fires.
W. M. Pitts. Jun 94, 172p, NIST/MONO-179.
Also available from Supt. of Docs. as SN003-003-03271-9. See also PB89-200091 and PB90-209602.

Keywords: *Carbon monoxide, *Fire hazards, *Buildings, Mortality, Combustion products, Global, Standards, Natural gas, Rooms, Exhaust gases, Enclosures, Safety engineering, Reaction kinetics, Pyrolysis, Ventilation, Polymers, Plywood, Mathematical models, Flow distribution, Reduced scale enclosure, Oxygenated polymers.

This report summarizes investigations of the formation of carbon monoxide (CO) in enclosure fires--the most

important factor in fire deaths. It contains the first complete review and analysis of the literature available on the global equivalence ratio (GER) concept. The results of a number of recent investigations (including work during the past fiscal year) which were either supported by the BFRL Grants Program or carried out in-house are then discussed. Based on the findings, two completely new mechanisms for the formation of CO, in addition to the quenching of a fire plume by a rich upper layer covered by the GER concept, are identified. The first involves reaction of rich flame gases with air which is entrained directly into the high-temperature upper layer of an enclosure fire. The second results from the pyrolysis of oxygenated polymers (such as wood) which are located in a rich, high-temperature upper layer. The findings of these studies form the basis of an analysis which yields the conditions for which use of the GER concept is appropriate for predicting CO formation in enclosure fires.

00,314
PB95-126306 Not available NTIS
National Inst. of Standards and Technology (BFRL), Gaithersburg, MD. Building and Fire Research Lab. Office.
Growing Significance of CIB.
Final rept.
J. G. Gross. 1992, 1p.
Pub. in CIB Newsletter 'Information', p1 Nov/Dec 92.

Keywords: *Building codes, *Research, Buildings, Standards, Standardization, Construction materials, Fire safety, Reprints, *Building technology, International Council for Building Research Studies and Documentation.

This editorial addresses the need for worldwide cooperation in building research. Activities and opportunities are cited where the International Council for Building Research, Studies and Documentation (CIB) can provide a forum for facilitating cooperative activities.

00,315
PB95-231858 PC A05/MF A02
Green (Melvyn) and Associates, Inc., Torrance, CA.
Comparison of the Seismic Provisions of Model Building Codes and Standards to the 1991 NEHRP Recommended Provisions.
May 95, 98p, NIST/GCR-95/674.
Sponsored by National Inst. of Standards and Technology (BFRL), Gaithersburg, MD. and Federal Emergency Management Agency, Washington, DC. Mitigation Directorate.

Keywords: *Building codes, *Earthquake resistant structures, Federal building, Structural design, Seismic waves, Design standards, Earthquake engineering, Standards, Design criteria, Regulations, Tables(Data).

The intent of this study is to review the seismic provisions of the current editions the BOCA National, SBCCI Standard and the ICBO Uniform Codes to determine whether the codes provide an equivalent level of safety to that contained in the 1991 Edition of the NEHRP Provisions. In addition the provision of the CABO One and Two Family Dwelling Code and ASCE 7-93 are reviewed.

00,316
PB96-141239 Not available NTIS
National Inst. of Standards and Technology (BFRL), Gaithersburg, MD. Fire Safety Engineering Div.
Predicting the Fire Performance of Buildings: Establishing Appropriate Calculation Methods for Regulatory Applications.
Final rept.
R. W. Bukowski. 1995, 10p.
Pub. in Proceedings of the International Conference on Fire Science and Engineering (1st), ASIAFLAM '95, Kowloon, Hong Kong, March 15-16, 1995, p9-18.

Keywords: *Fire safety, *Design standards, *Safety factors, Fire codes, Building codes, Regulations, Risk analysis, Fire protection, Performance standards, Fire hazards, Models, Reprints.

This paper explores questions from the perspective of the fire scientist, the practicing engineer, and the regulatory official. The fir scientist needs to be explicit about the impact of assumptions on the applicability of the results. The engineer needs to utilize methods and assumptions which are justified by the application and to assess the sensitivity and uncertainty implications. The regulatory officials are insisting on appropriate and properly documented methods. There is a need for models and calculations incorporated into codes of practice, handbooks, or the codes themselves to be reviewed, verified, documented, and approved for use in specific manners and by qualified persons. There are international efforts to define levels of risk acceptable to society in specific occupancies.

Construction Management & Techniques

00,317
PB94-185998 Not available NTIS
National Inst. of Standards and Technology (BFRL), Gaithersburg, MD. Building and Fire Research Lab. Office.
Infratechnologies: Tools for Innovation.
Final rept.
R. N. Wright. 1993, 2p.
Pub. in Civil Engineering 63, n11 p68-69 Nov 93.

Keywords: *Construction, *Technology innovation, *Quality assurance, Building codes, Standards, Computer aided design, Technology assessment, Technology utilization, Reprints.

The quest for innovation and quality assurance in construction makes it important to recognize the need for technologies far beyond those in use today. Although we now check for conformance to codes and standards, gather and document product information, use computer-aided design (CAD) and engineering, and apply the principles that help ensure quality, there will be better ways to do these tasks in the future. We call them infratechnologies.

00,318
PB94-186004 Not available NTIS
National Inst. of Standards and Technology (BFRL), Gaithersburg, MD. Building and Fire Research Lab. Office.
Status of Construction and Construction Technologies.
Final rept.
R. N. Wright. 1993, 9p.
Pub. in Proceedings Symposium on Advanced Building Technologies, Troy, NY., April 10, 1992, p10-18 1993.

Keywords: *Construction industry, *Competition, *North America, Automation, Productivity, Buildings, Design, Construction materials, Maintainability, Market research, Reprints, *Building technology, Intelligent buildings, Constructability.

Trends in building technology for North America will be dominated by advances in building process technologies: advanced computation and automation. These will facilitate effective responses to demands for increasing the international competitiveness of North American commerce and industry, supporting new industries, commerce and life styles, improving safety and health, and conserving energy and the environment. Advanced information technologies will affect organization of the building process to allow better attention to design to issues such as constructability, maintainability, and productivity of constructed facilities. Automation will advance in design, construction and operation (intelligent buildings) of constructed facilities.

00,319
PB94-193646 PC A03/MF A01
National Inst. of Standards and Technology, Gaithersburg, MD.
Program of the Subcommittee on Construction and Building.
R. N. Wright, A. H. Rosenfeld, and A. J. Fowell. Jun 94, 50p, NISTIR-5443.
Prepared in cooperation with Department of Energy, Washington, DC. Assistant Secretary for Energy Efficiency and Renewable Energy.

Keywords: *Construction, *Competitiveness, *Technology innovation, Health, Automation, Construction materials, Buildings, Energy efficiency, Productivity, Research, Safety, *Building technology.

The National Science and Technology Council (NSTC), a cabinet-level group charged with setting Federal technology policy, has established the Committee on Civilian Industrial Technology (CCIT), to enhance the international competitiveness of U.S. industry. The Subcommittee on Construction and Building (C&B) of CCIT deals with Federal technology policies and programs related to the industries that conduct R&D, and produce, operate and maintain constructed facilities including buildings and infrastructure. The report provides some background on the construction industry, describes the role, the goals, and milestones of the program, and lists the Federal agencies participating in the Subcommittee. The goals of better buildings and improved health and safety of construction workers have been strongly endorsed in a white paper developed and published by the Civil Engineering Research Foundation. The white paper is included as an appendix.

00,320
PB94-216405 Not available NTIS
National Inst. of Standards and Technology (CAML), Gaithersburg, MD.
Standards in Building Economics: Why We Need Them and How to Write Them.
Final rept.
H. E. Marshall. 1992, 7p.
Pub. in Proceedings of 1992 American Association of Cost Engineers Transactions, Orlando, FL., June 28-July 1, 1992, pL.5.1-L.5.7.

Keywords: *Buildings, *Economic analysis, *Standards, Construction management, Budgeting, Life cycle costs, Profits, Benefit cost analysis, Reprints.

Standard methods, guides, and classifications are available for use in the economic evaluation of buildings and building components. Standards help owners, consultants, designers, and managers to reduce project costs and enhance profits by providing a consistent basis for comparing the economic worth of building alternatives. This applies to government and private projects undertaken domestically and abroad. The paper explains how sometimes conflicting vested interests can work as a team in the standards process to create consensus standards. It surveys and explains the application of specific ASTM standard methods, such as life-cycle costing and the savings-to-investment ratio methods. It explains the role that business, government agencies, and professional societies such as the American Association of Cost Engineers (AACE) play in the promulgation of standards. The paper concludes that organizations need to participate in or at least be abreast of the latest developments in standard methods to reduce expenditures, keep competitive, and maximize profits.

00,321
PB95-122537 PC A03/MF A01
National Inst. of Standards and Technology, Gaithersburg, MD.
Program of the Subcommittee on Construction and Building (July 1994).
R. N. Wright, A. H. Rosenfeld, and A. J. Fowell. Jul 94, 48p, NISTIR-5443-A.
Supersedes PB94-193646. Prepared in cooperation with Department of Energy, Washington, DC. Assistant Secretary for Energy Efficiency and Renewable Energy.

Keywords: *Construction, *Competitiveness, *Technology innovation, Health, Buildings, Construction materials, Safety, Automation, Research and development, Productivity, Energy efficiency.

The President has established the National Science and Technology Council (NSTC), a cabinet-level group charged with setting Federal science and technology policy, to coordinate and prioritize R&D and deployment strategies across a broad cross-section of public and private interests. It has established nine research and development committees, including the Committee on Civilian Industrial Technology (CCIT) to collaborate with the private sector in developing a comprehensive national technology policy. The purpose of CCIT is to enhance the international competitiveness of U.S. industry through Federal technology policies and programs. The Subcommittee on Construction and Building coordinates and defines priorities for Federal research, development and deployment related to the industries that produce, operate and maintain constructed facilities, including buildings and infrastructure. The Subcommittee on Construction and Building has studied research priorities including those expressed by the construction industry and defined two priority thrusts; better constructed facilities and health and safety of the construction workforce.

00,322
PB95-154704 PC A07/MF A02

National Inst. of Standards and Technology (BFRL), Gaithersburg, MD.
Rationale and Preliminary Plan for Federal Research for Construction and Building.
R. N. Wright, A. H. Rosenfeld, and A. J. Fowell. Nov 94, 140p, NISTIR-5536.
Also available from Supt. of Docs. Sponsored by Department of Energy, Washington, DC. Assistant Secretary for Energy Efficiency and Renewable Energy.

Keywords: *Research, *Buildings, *Construction, *Technology assessment, Construction materials, Government/industry relations, Technology transfer, Competitiveness, Project management, Occupational safety, Civil engineering.

The National Science and Technology Council (NSTC), a cabinet-level group charged with setting federal technology policy, coordinates R&D strategies across a broad cross-section of public and private interests. It has established nine research and development committees, including the Committee on Civilian Industrial Technology (CCIT), to collaborate with the private sector in developing a comprehensive national technology policy. The purpose of CCIT is to enhance the international competitiveness of U.S. industry through federal technology policies and programs. The Subcommittee on Construction and Building (C&B) of CCIT coordinates and defines priorities for Federal research, development and deployment related to the industries that produce, operate and maintain constructed facilities, including buildings and infrastructure.

00,323
PB96-122593 Not available NTIS
National Inst. of Standards and Technology (CAML), Gaithersburg, MD.
Economic Methods and Risk Analysis Techniques for Evaluating Building Investments: A Survey.
Final rept.
H. E. Marshall. 1991, 55p.
See also PB90-241589.
Pub. in CIB Report, Published by the International Council for Building Research, Studies and Documentation, n136 55p 1991.

Keywords: *Buildings, *Construction management, *Life cycle costs, *Cost benefit analysis, Cost engineering, Investments, Budgeting, Interest rate of return, Return on investment, Cost estimation, Economic analysis, Project administration, Risk management, Decision making, Reprints.

Traditional economic methods--life cycle costing, benefit-to-cost ratio, net benefits analysis, adjusted internal rate of return, and discounted payback--are described for evaluating building decisions about accepting or rejecting a given building, and the economically efficient combination of projects competing for a limited budget. Appropriate applications for each economic method are described. Technically correct formulas for the methods are presented. Techniques are described that to some extent account for uncertainty in input variables and in some cases risk exposure and risk attitude. The techniques are conservative benefit and cost estimating, sensitivity analysis, the risk-adjusted discount rate, mean-variance criterion, coefficient of variation, decision analysis, simulation, mathematical/analytical technique, and portfolio analysis. Advantages and disadvantages of each are described. Guidance is provided for selecting the appropriate technique for any given investment problem.

00,324
PB96-137104 PC A06/MF A02
National Inst. of Standards and Technology (BFRL), Gaithersburg, MD.
National Planning for Construction and Building R and D.
R. N. Wright, A. H. Rosenfeld, and A. J. Fowell. Dec 95, 105p, NISTIR-5759.
Prepared in cooperation with National Science and Technology Council, Washington, DC. Subcommittee on Construction and Building. Sponsored by Department of Energy, Washington, DC. Assistant Secretary for Energy Efficiency and Renewable Energy,.

Keywords: *Construction industry, *Building materials, *Research and development, *Government/industry relations, Construction materials, Research projects, Cooperation, Coordination, Research management, Competitiveness, Technology innovation, Goals, Human factors engineering, Automation, Information systems, Regulations, Private sector.

This planning report is a resource document designed to provide the private sector with a straw man on a direction and strategy for construction and building research, development, and demonstration to achieve the National Construction Goals, and the products likely to be produced by that effort. The report also will provide federal agencies with information on each other's R&D programs to facilitate coordination of effort. The Federal and private sector plans will be coordinated to form an industry-led National Plan to meet the National Construction Goals. This report provides background on each of the goals, the measures by which progress can be gauged, and research needed. The industry perspective on relative importance of the different goals by the various sectors of the construction industry is reported, and the intitial strategy proposed by some of those sectors to provide a platform for the National Plan is outlined.

00,325
PB96-158670 PC A06/MF A01
National Inst. of Standards and Technology (BFRL), Gaithersburg, MD. Office of Applied Economics.
Multiattribute Decision Analysis Method for Evaluating Buildings and Building Systems.
Final rept.
G. A. Norris, and H. E. Marshall. Sep 95, 90p, NISTIR-5663.
See also PB93-146017.

Keywords: *Buildings, *Life cycle costs, *Cost benefit analysis, Building materials, Construction, Fabrication, Architecture, Space HVAC systems, Energy management systems, Ranking, Project administration, Operating costs, Cost engineering, Investments, Return on investment, Economic analysis, Alternatives, Decision making, MADA(Multiattribute Decision Analysis).

Multiattribute decision analysis (MADA) methods consider non-financial attributes (qualitative and quantitative) in addition to common financial worth measures when evaluating project alternatives. The report reviews 14 classes of methods for performing MADA. It summarizes their usefulness for screening, ranking, and choosing among projects; their data input requirements; and how each method scores project alternatives. Two methods--the analytical hierarchy process (AHP) and non-traditional capital investment criteria (NCIC)--are described in detail. Assumptions, procedures, strengths, and limitations are described for each.

Construction Materials, Components, & Equipment

00,326
AD-A310 426/2 PC A03/MF A01
National Bureau of Standards, Gaithersburg, MD.
Polyvinyl Chloride (PVC) Plastic Drain, Waste, and Vent Pipe and Fittings.
Apr 65, 28p.
Availability: Document partially illegible.

Keywords: *Pipes, *Drainage, *Plastics, *Vents, *Polyvinyl chloride, Requirements, Quality assurance, Wastes, Fittings.

The purpose of this Commercial Standard is to establish, on a national basis, standard dimensions and significant quality requirements for polyvinyl chloride (PVC) plastic drain, waste, and vent (DWV) pipe and fittings. It is also intended to inform producers, distributors, engineers, code officials, and users of the significant qualities of this product to assist buyers and vendors in obtaining and vending quality merchandize for the benefit of the user, and to promote understanding among all these groups concerning commercially available PVC plastic DWV pipe and fittings.

00,327
AD-A310 724/0 PC A03/MF A01
National Bureau of Standards, Gaithersburg, MD.
Acrylonitrile-Butadiene-Styrene (ABS) Plastic Drain, Waste, and Vent Pipe and Fittings.
Commercial standard.
Apr 65, 27p, CS270-65.
Availability: Document partially illegible.

Keywords: *Styrenes, *Acrylonitrile polymers, *Pipes, *Drainage, *Wastes, *Butadienes, *Vents, *Fittings, Organic compounds, Standards, Quality assurance, Plastics, Abs(Acrylonitrile- butadiene-styrene), Dvw(Drain-vent-waste).

The purpose of this Commercial Standard is to establish, on a national basis, standard dimensions and significant quality requirements for acrylonitrile-butadiene-styrene (ABS) plastic drain, waste, and vent (DWV) pipe and fittings. It is also intended to inform producers, distributors, engineers, code officials, and users of the significant qualities of this product, to assist buyers and vendor in obtaining and vending quality merchandise for the benefit of the user, and to promote understanding among all these groups concerning commercially available ABS plastic DWV pipe and fittings.

00,328
PB94-139722 PC A03/MF A01
California Univ., Berkeley. Dept. of Mechanical Engineering.
Fire Induced Thermal Fields in Window Glass I: Theory.
Rept. for 31 Aug 91-31 Aug 92.
A. A. Joshi, and P. J. Pagni. Nov 93, 35p, NIST-GCR-93-634.
Grant 60NANB1D1168
Sponsored by National Inst. of Standards and Technology (BFRL), Gaithersburg, MD.

Keywords: *Glass, *Windows, *Fires, *Thermal analysis, Heat transfer, Buildings, Heat flux, Mathematical models, Construction materials, Temperature distribution.

Window glass breaking plays an important role in compartment fire dynamics as the window acts as a wall before breaking and as a vent after breaking. Previous work suggested a model for the time to breakage of a window glass exposed to a particular fire. In this paper, the glass thermal fields obtained using that model are examined in detail. The temperature field dependence on heat transfer coefficients, radiative decay length and flame radiation is explored. The results show that the glass surface temperature increases with a decrease in the decay length and increases with an increase in flame radiation heat flux. Early in the fire, the glass temperature may be higher than the hot layer temperature due to direct impingement of flame radiation. Later the glass temperature lags the hot layer temperature. The variation of the time to breakage as a function of the shading width and decay length is also presented and the results indicate that the breaking time decreases with an increase in the shading width and decreases with a decrease in decay length. Heat flux maps for typical conditions indicate that most of the heat influx is stored in the glass, increasing its temperature.

00,329
PB94-160751 PC A03/MF A01
National Inst. of Standards and Technology (BFRL), Gaithersburg, MD.
Performance Approach to the Development of Criteria for Low-Sloped Roof Membranes.
W. J. Rossiter, G. J. C. Frohnsdorff, L. W. Masters, and J. W. Martin. Jul 91, 35p, NISTIR-4638.

Keywords: *Roofs, *Membranes, *Waterproofing, *Industrial buildings, *Commercial buildings, Composite materials, Polymers, Bitumens, Thermoplastic resins, Insulation boards, Barrier coatings, Vapor deposition, Requirements, Diagrams, Test methods, Performance evaluation, United States, Low-sloped roof system, Structural deck.

Waterproofing of roofs of commercial and industrial buildings in the United States is primarily accomplished using low-sloped membrane roofing systems. Estimates indicate that approximately 300 million square meters (3 billion square feet) of membrane roofing is installed annually. The three main types of membranes are built-up bituminous, single-ply elastomeric and thermoplastic, and polymer-modified bitumens. In addition to the membrane, the other main components are insulation boards and the structural deck, with elements such as vapor retarders and membrane surfacings used in some systems.

00,330
PB94-160777 PC A03/MF A01
National Inst. of Standards and Technology (BFRL), Gaithersburg, MD.

Microstructural Features of Some Low Water/Solids, Silica Fume Mortars Cured at Different Temperatures.
P. E. Stutzman, and J. R. Clifton. Apr 92, 20p, NISTIR-4790.

Keywords: *Mortars(Materials), *Microstructure, Silicon dioxide, Portland cements, Plasticizers, Concretes, *HPC(High Performance Concrete).

The microstructure of mortars with water/solids ratios (w/s) of 0.36 and 0.29, cured under water at 7, 23, and 40 C, were studied by scanning electron microscopy and X-ray powder diffractometry. The mortars contained silica fume and a superplasticizer. The degree of hydration and extent of pozzolanic reaction was estimated after quantifying the residual unhydrated cement by image analysis and the mass percent calcium hydroxide by X-ray powder diffraction. Their microstructures were fairly homogeneous in both the bulk paste and at the past-aggregate transition zone. In all mortars, the outer 250 micrometers was hydrated to about 85 percent and highly microcracked. The degree of hydration decreased rapidly beyond the outer zone to about 69 percent and less microcracking was observed. A temperature effect on the reactivity of silica fume was found.

00,331
PB94-164407 PC A03/MF A01
National Inst. of Standards and Technology (MSEL), Gaithersburg, MD. Metallurgy Div.
Analysis of Failed Dry Pipe Fire Suppression System Couplings from the Filene Center at Wolf Trap Farm Park for the Performing Arts.
M. R. Stoudt, J. L. Fink, and R. E. Ricker. Mar 94, 16p, NISTIR-5389.
Sponsored by Wolf Trap Farm Park for the Performing Arts, Vienna, VA.

Keywords: *Pipe joints, *Sprinkler systems, *Brittle fracturing, Pipe bends, Cast iron, Metallurgical analysis, Freezing, Wolf Trap Farm Park(Virginia).

A detailed metallurgical analysis was performed on a number of gray cast iron couplings taken from a dry pipe fire suppression system at the Filene Center to verify the source of failure. The results of the analysis indicated that all of the specimens failed in a brittle manner due to the stresses induced by the expansion of freezing water. The available background information indicated that the ambient air temperature on the night of the failures was low enough to induce freezing in a relatively short time period.

00,332
PB94-172418 Not available NTIS
National Inst. of Standards and Technology (BFRL), Gaithersburg, MD. Fire Safety Engineering Div.
Improvement in Predicting Smoke Movement in Compartmented Structures.
Final rept.
W. W. Jones, and G. P. Forney. 1993, 29p.
Pub. in Fire Safety Jnl. 21, p269-297 1993.

Keywords: *Fires, *Flow models, *Buildings, Fire safety, Radiative transfer, Ventilation, Smoke, Transport properties, Buoyancy, Reprints, *Smoke propagation, *Compartment fires, CFAST Model.

This paper describes improvements which have been made in the CFAST model of fire growth and smoke transport for compartmented structures. In particular, we are interested in the ability to model the movement of toxic gases from the room of origin of a fire to a distant compartment. The newest phenomena in the model are vertical flow and mechanical ventilation. Finally, we have improved the radiation transport scheme which affects energy distribution, and therefore the buoyancy forces. These are very important in actual situations relevant to fire growth and smoke propagation, as is demonstrated.

00,333
PB94-173051 Not available NTIS
National Inst. of Standards and Technology (BFRL), Gaithersburg, MD. Building Materials Div.
Quantitative Phase Abundance Analysis of Three Cement Clinker Reference Materials by Scanning Electron Microscopy.
Final rept.
P. E. Stutzman. 1990, 12p.
Pub. in Proceedings of Conference on Advances in Cementitious Materials, Gaithersburg, MD., July 22-26, 1990, p199-210 1991.

Keywords: *Cements, *Scanning electron microscopy, *Image analysis, Test methods, X rays, Backscattering, Microstructure, Grain size, Brightness, Construction materials, Reprints, *Portland cement clinker, *Reference materials.

Three portland cement clinker reference materials are available from the Standard Reference Materials Program at the National Institute of Standards and Technology. They are the first clinker reference materials for phase abundance analyses and were selected as representative of North American clinker production with respect to the range of phase abundance, grain size, and distribution. They are intended for use in the development and testing of methods for quantitative phase abundance analyses of portland cement clinker. Portland cement clinker microstructures were characterized by backscattering electron imaging in the scanning electron microscope. Clinker phases were identified on the basis of their brightness, grain morphology, occurrence within the clinker, and composition. Quantitative phase abundance analyses by point counting, and by image analysis of backscattered electron images and, for periclase, of X-ray maps, generally agreed with the reference material values. With its capability to clearly image polished clinker sections at a wide range of magnifications, the scanning electron microscope with X-ray analysis and with image analysis capabilities is a powerful tool for quantitative cement clinker microscopy.

00,334
PB94-185774 Not available NTIS
National Inst. of Standards and Technology, Gaithersburg, MD.
Proficiency Testing as a Component of Quality Assurance in Construction Materials Laboratories.
Final rept.
J. H. Pielert. 1990, 11p.
Pub. in Proceedings of International Symposium Test Quality and Quality Assurance in Testing Laboratories for Construction Materials and Structures, Saint-Remy-les-Chevreuse, France, October 15-17, 1990, p60-70. Sponsored by American Society for Testing and Materials, Philadelphia, PA.

Keywords: *Laboratories, *Construction materials, *Quality assurance, *Interlaboratory comparisons, Standards, Test facilities, Quality control, Standardization, Sampling, Concretes, Accuracy, Precision, Reprints, *Proficiency testing, Construction Materials Reference Laboratories.

Proficiency testing is a procedure for using results generated in interlaboratory test comparisons for the purpose of assessing the technical competence of participating testing laboratories. This gives users of laboratory services confidence that a testing laboratory is capable of obtaining reliable results. Interlaboratory testing involves the organization, performance and evaluation of tests on the same or similar materials by two or more different laboratories in accordance with predetermined conditions. Interlaboratory testing may also be used for checking the individual performance of laboratory staff, evaluating the effectiveness of a test method, and determining characteristics of a material or product. Programs in the United States which use proficiency testing to evaluate laboratory performance are discussed along with international programs which have been identified by RILEM Technical Committee 91-Cement Reference Laboratories. The U.S. Construction Materials Reference Laboratories which distributes over 6,000 samples of 13 different construction materials is highlighted, along with ASTM standardization activities related to proficiency and interlaboratory testing.

00,335
PB94-187283 PC A04/MF A01
National Inst. of Standards and Technology (BFRL), Gaithersburg, MD.
Calculating Flame Spread on Horizontal and Vertical Surfaces.
G. N. Ahmed, M. A. Dietenberger, and W. W. Jones. Apr 94, 58p, NISTIR-5392.
Prepared in cooperation with Portland Cement Association, Skokie, IL. and Forest Products Lab., Madison, WI.

Keywords: *Algorithms, *Flame propagation, Fires, Buildings, Heat flux, Pyrolysis, Geometry, Ignition, Mathematical models, Soot, *Compartment fires, *Fire models.

The flame spread model described in this paper is a new algorithm which provides the capability to calculate a self-consistent fire based substantially on bench scale fire data. The flame spread model simulates object fire growth and burnout of a slab in a room and produces acceptable predictions of the spread of fire, smoke and production of both toxic and nontoxic gases. The purpose of the flame spread model is to allow a fire to grow realistically, possibly making a hole in the material surface. This is one mechanism for barrier penetration. The algorithm is based on empirical data, gathered from standard test apparatus, including the Cone Calorimeter and the LIFT (lateral ignition flame spread test method). The objective of including the flame spread model is to predict the accelerative growth of a fire from ignition to a peak value and then the gradual termination normally seen in a fire. The intent of the project was to develop an algorithm which could be utilized in a complete model of a fire in a building. The three-dimensional aspects of the flame spread model include: first, panels made of combustible materials with different thicknesses and at various orientations; second, flames of two basic types, pool fire and purely wall fire; third, a radiation heat exchange between objects, flames, and gases. The pool fire has a flame spreading polygon on a horizontal panel and the wall fire is used either for inclined or vertical panels.

00,336
PB94-193620 PC A03/MF A01
Factory Mutual Research Corp., Norwood, MA.
Prediction of Fire Dynamics.
Quarterly rept. 28 Jun-28 Aug 92 (Final).
R. L. Alpert, and J. de Ris. Sep 92, 39p, NIST/GCR-94/642.
Grant NIST-60NANB1D1177
Sponsored by National Inst. of Standards and Technology (BFRL), Gaithersburg, MD.

Keywords: *Combustion physics, *Buildings, Fires, Heat flux, Radiative heat transfer, Accuracy, Flame propagation, Building codes, Mathematical models, Algorithms, *Ceiling jets, *Fire dynamics, Fire codes.

The report summarizes accomplishments of a Factory Mutual Research Corporation (FMRC) project on the Prediction of Fire Dynamics for the NIST grant period August 1991 through August 1992. Work performed under a subcontract by Professor H.W. Emmons on Ceiling-Jet Dynamics and on Development of Strategies for Performance Fire Codes is first described under Task 1. The accomplishment of three tasks performed at FMRC are then presented in summaries of Tasks 2-4. All of this work is aimed at the development of subroutines or algorithms that can be used in NIST/BFRL comprehensive computer models. During the past year, there has been further progress in the development of predictive models for flame radiant heat flux and in the development of a practical laboratory test method for measuring the smoke point of solid noncharring or charring materials. This progress should allow continuing improvements in the accuracy and applicability of fire propagation theories.

00,337
PB94-193778 PC A05/MF A02
Clemson Univ., SC. Dept. of Mathematical Sciences.
Mathematical Modeling of Human Egress from Fires in Residential Buildings.
Final technical rept.
M. M. Kostreva. Jun 94, 100p, NIST/GCR-94/643.
Grant NIST-60NANB0D1023
See also PB-273 166. Sponsored by National Inst. of Standards and Technology (BFRL), Gaithersburg, MD.

Keywords: *Residential buildings, *Mathematical models, *Egress, *Human behavior, *Fires, *Fire safety, Algorithms, Reprints, Human reactions, Decision making, Injury prevention, Escape(Abandonment), HAZARD I Computer program.

The Building and Fire Research Laboratory has been developing mathematical models for predicting the environmental conditions which occur as a fire develops and spreads. These models form a significant part of the computer program entitled HAZARD I. Human egress modeling has been implemented in HAZARD I by means of simulation of actual human movement, invoking psychological theories and heuristic methodologies to create paths which the humans in the residential building under consideration would likely have taken. The research supported by this grant has been rather successful at finding mathematical models, appropriate solution techniques, coding the techniques, and making sample applications. In seven different research papers the results of the research have been documented. Six of these papers have appeared in print, while the seventh is submitted for publication. The full copies of the papers are included as appendices of this report, while summaries are presented

here for the reader's convenience. The research performed has advanced the state of the art in fire egress analysis, which forms an important part of fire hazard analysis and modeling as embodied in HAZARD I. In doing so, some new mathematical ideas, algorithms and theories have also been advanced. It is particularly satisfying to have new mathematics derived in support of such an important national priority as fire safety, and, as the mathematical knowledge is general, it may be of service to others in the future.

00,338
PB94-199320 Not available NTIS
National Inst. of Standards and Technology (BFRL), Gaithersburg, MD. Building Environment Div.
Analysis of Moisture Accumulation in a Wood-Frame Wall Subjected to Winter Climate.
Final rept.
D. M. Burch, and W. C. Thomas. 1992, 13p.
Pub. in Proceedings of Conference on Thermal Performance of the Exterior Envelopes of Buildings V, Clearwater Beach, FL., December 7-10, 1992, p467-479. See also PB92-116334. Sponsored by Department of Energy, Washington, DC.

Keywords: *Wood products, *Moisture content, *Walls, *Mathematical models, *Environmental effects, Winter, Performance evaluation, Construction materials, Moisture resistance, Capillary flow, Diffusion, Heat transfer, Water vapor, Finite difference method, Framed structures, Permeability, Humidity, Reprints.

A transient, one-dimensional, finite-difference model is presented that predicts that coupled transfer of heat and moisture in a multilayer wall under nonisothermal conditions. The model can predict moisture transfer in the diffusion through the capillary flow regimes. It has a provision to account for convective moisture transfer by including embedded cavities that may be coupled to indoor and outdoor air. The model is subsequently used to predict the time-varying average moisture content in the sheathing and siding of a wood-frame wall as a function of time of year. The effect of several construction parameters on the winter moisture accumulation is investigated. The parameters include the interior vapor retarder permeance, sheathing permeance, exterior paint permeance, indoor air leakage, and the amount of insulation.

00,339
PB94-206091 PC A03/MF A01
Maryland Univ., College Park. Dept. of Fire Protection Engineering.
Development of the Fire Data Management System.
Final rept.
F. W. Mowrer. Aug 93, 37p, NIST/GCR-94/639.
Grant NIST-60NANB1D1164
See also PB94-198462. Sponsored by National Inst. of Standards and Technology (BFRL), Gaithersburg, MD.

Keywords: *Data base management systems, *Information systems, *Fire tests, *Buildings, Construction materials, Furniture, Data bases, Fire safety, Flammability, Ignition, Burning rate, *Fire Data Management System.

The Fire Data Management System (FDMS) is being developed under international collaboration to provide uniform means for storing fire test data. The purpose of the present work has been to aid the development of the FDMS for practical use by fire safety design professionals. To be of practical use by fire safety design professionals, the FDMS must contain relevant data and these data must be readily accessible. Currently, the data fields in the FDMS are too general and too restricted to be of practical design use. Additional data fields are needed in the FDMS to assist the design professional find flammability test data relevant to the design of different combustible objects in buildings. To help identify the types of additional data fields that are needed, a series of morphological charts have been developed to describe the types, elements and attributes of combustible objects in buildings. These morphological charts represent a first effort to describe a common syntax for identifying appropriate objects and their attributes for flammability analyses. Further refinement of the charts is needed.

00,340
PB94-206299 PC A03/MF A01
Kentucky Univ., Lexington. Dept. of Mechanical Engineering.
Upward Flame Spread along the Vertical Corner Walls (October 1993).
Final rept.
C. Qian, H. Ishida, and K. Saito. Oct 93, 46p, NIST/GCR-94/648.
Grant NIST-NANB2D1295
See also PB89-214787. Sponsored by National Inst. of Standards and Technology (BFRL), Gaithersburg, MD.

Keywords: *Walls, *Pyrolysis, *Flame propagation, Burning rate, Fire safety, Fires, Heat flux, Mathematical models, Temperature measuring instruments.

Flame spread behavior and the pyrolysis region spread characteristics along vertical corner walls were studied in detail with an automated infrared imaging temperature measurement technique (IR technique). The technique was recently developed for the measurement of transient pyrolysis temperature on both charring and non-charring materials. Temporal isotherms on PMMA samples were successfully obtained, from which the progress rate of the pyrolysis front was automatically deduced. It was found that the pyrolysis front shape was always M-shaped, i.e., no spread along the corner, and the maximum spread is in a few centimeters away from the corner. Understanding of the mechanism of the M-shape formation is important in developing a prediction model of the spread rate. Four possible mechanisms were identified and flame displacement effects are found to be the principal mechanism. Transient total heat flux distributions above the M-shape pyrolysis peak for a spreading fire were measured. Using these values, it was shown that the upward spread rate is predictable from a simple, one-dimensional, thermal model.

00,341
PB94-207388 PC A05/MF A01
Pennsylvania State Univ., University Park. Dept. of Mechanical Engineering.
Turbulent Upward Flame Spread on a Vertical Wall under External Radiation.
Annual rept. 30 Sep 91-15 Jan 93.
A. K. Kulkarni, E. Brehob, S. Manohar, and R. Nair.
Feb 94, 93p, NIST/GCR-94/638.
Grant NIST-NANB8D0849
See also PB92-112531. Sponsored by National Inst. of Standards and Technology (BFRL), Gaithersburg, MD.

Keywords: *Walls, *Turbulent flow, *Flame propagation, Heat flux, Burning rate, Data bases, Radiant flux density, Mathematical models.

Progress made on NIST grant number 60NANB8D0849 for the period September 30, 1991 to January 15, 1993 is reported. The overall objective is to understand the upward flame spread phenomenon under simulated surrounding fire conditions by establishing a data base for upward flame spread under external radiation, developing a mathematical model, measuring the relevant basic material properties needed, and checking the validity of the model by comparing its results with data. Emphasis is placed on studying and predicting the behavior of practical wall materials used in building and vehicle interiors, and textiles. In the past year, the authors measured flame spread on several different materials under a range of external radiant fluxes of up to 15 kW/sq m. A model for describing the upward flame spread process was developed and numerical results were compared with data. The model needed input of certain properties, such as the burning rate characteristics and surface radiation properties. A series of supporting studies were undertaken which provided the needed input properties to the model and other useful material property data.

00,342
PB94-207404 PC A03/MF A01
National Inst. of Standards and Technology (BFRL), Gaithersburg, MD.
Comparison of Wall-Fire Behavior With and Without a Ceiling.
H. E. Mitler, and K. D. Steckler. Nov 93, 34p, NISTIR-5380.
See also PB85-133973.

Keywords: *Burning rate, *Walls, *Ceilings, *Flame propagation, Heat flux, Fire tests, Mathematical models, Fires, FIRST room fire model, SPREAD wall fire model.

This paper demonstrates that the effects of the ceiling on the progress of a wall fire are quite significant, and that a project to quantify and model the effects of a ceiling on the progress of a wall fire is indeed justified. Experimental results from the open literature are used for this purpose, as well as previously unpublished experimental results obtained at NIST. The wall-fire SPREAD and the room-fire model FIRST are used seriatim to show that part of this effect can be calculated now.

00,343
PB94-207495 PC A08/MF A02
National Inst. of Standards and Technology (BFRL), Gaithersburg, MD.
Project Summaries 1994: NIST Building and Fire Research Laboratory.
Special pub.
N. J. Raufaste. Jun 94, 161p, NIST/SP-838/5.
Also available from Supt. of Docs. as SN003-003-03273-5. See also PB94-113420.

Keywords: *Buildings, *Fires, *Research management, *Testing laboratories, Building codes, Fire safety, Flammability testing, Standards, Construction materials.

The report summarizes the Building and Fire Research Laboratory's research for 1994. The report is arranged by its research programs, structural engineering, materials engineering, mechanical and environmental systems, fire science and engineering, and fire measurement and research. Each summary lists the project title, point of contact, sponsor, research, and results. BFRL's mission is to increase the usefulness, safety, and economy of constructural facilities, and reduce the human and economic costs of unwanted fires in buildings.

00,344
PB94-210077 PC A03/MF A01
National Inst. of Standards and Technology (BFRL), Gaithersburg, MD.
Combined Buoyancy- and Pressure-Driven Flow Through a Shallow, Horizontal, Circular Vent.
L. Y. Cooper. Apr 94, 50p, NISTIR-5384.
See also PB94-103694.

Keywords: *Vents, *Air flow, *Buoyancy, *Flame propagation, Fire protection, Buildings, Boundary value problems, Boundary conditions, Mathematical models, Flow rate, *Compartment fires, *Fire models.

Combined buoyancy- and pressure-driven (i.e., forced) flow through a horizontal vent is considered where the vent-connected spaces near the elevation of the vent are filled with fluids of different density in an unstable configuration, with the density of the top space larger than that of the bottom space. With zero-to-moderate cross-vent pressure difference, delta p, the instability leads to a bi-directional exchange flow between the two spaces. For relatively large delta p, the flow through the vent is unidirectional, from the high- to the low-pressure space. Previously published experimental data and results of an analysis of the relevant boundary value problems are used to develop a flow model which takes all of these effects into account. The result is a uniformly valid algorithm to calculate flow through shallow (small depth-to-span ratio), horizontal, circular vents under high-Grashof number conditions. This is suitable for general use in zone-type compartment fire models (e.g., an ambient temperature environment above the vent and a hot smoky environment below). The algorithm is used in example applications where steady rate-of-burning in a ceiling-vented room is estimated as a function of room temperature, vent area, and oxygen concentration. Results of the analysis are seen to be consistent with previously published data involving ceiling-vented fire scenarios.

00,345
PB94-210127 PC A04/MF A01
National Inst. of Standards and Technology (BFRL), Gaithersburg, MD. Fire Safety Engineering Div.
VENTCF2: An Algorithm and Associated FORTRAN 77 Subroutine for Calculating Flow through a Horizontal Ceiling/Floor Vent in a Zone-Type Compartment Fire Model.
L. Y. Cooper. Aug 94, 71p, NISTIR-5470.

Keywords: *Fire protection, *Vents, *Algorithms, *Subroutines, *Flame propagation, Air flow, Fire safety, Enthalpy, Mass flow, Mathematical models, Buildings, *Compartment fires, *VENTCF2 computer program, *Fire models.

An algorithm and associated FORTRAN 77 subroutine, called VENTCF2, is presented for calculating the effects on two-layer compartment fire environments of

the quasi-steady flow through a circular, shallow (i.e., small ratio of depth to diameter), horizontal vent connecting two spaces. The two spaces can be either two inside rooms of a multi-room facility or one inside room and the outside ambient environment local to the vent. The description of the flow through the vent is determined by combining considerations of the uni-directional-type of flow driven by a cross-vent pressure difference and, when appropriate, the combined pressure- and buoyancy-driven flows which occur when the density configuration across the vent is unstable, i.e., a relatively cool, dense gas in the upper space overlays a less dense gas in the lower space. In the algorithm, calculation of the rates of flow exchange between the two spaces is based on previously reported model equations. Characteristics of the geometry and the instantaneous environments of the two spaces are assumed to be known and specified as inputs. The outputs calculated by the algorithm/subroutine are the rates and the properties of the vent flow at the elevation of the vent as it enters the top space from the bottom space and/or as it enters the bottom space from the top space. Rates of mass, enthalpy, and products of combustion extracted by the vent flows from upper and lower layers of inside room environments and from outside ambient spaces are determined explicitly.

00,346
PB94-211372 Not available NTIS
National Inst. of Standards and Technology (BFRL), Gaithersburg, MD. Fire Science Div.
Suppression Research: Strategies.
Final rept.
D. D. Evans. 1992, 15p.
Pub. in Proceedings of International Conference on Fire Suppression Research (1st), Stockholm, Sweden, May 5-8, 1992, p21-35.

Keywords: *Fire extinguishers, *Fire tests, Burning rate, Fire fighting, Fires, Diffusion, Sprinklers, Mathematical models, Furniture, Reprints, *Extinction time.

Millions of unwanted fires occur each year. More effective fire suppression is a means to minimizing property damage and life loss due to fire. The Damkohler number, which is the ratio of the characteristic time for flow or diffusion of reactants to the time required for reaction, is the basis for a fire extinction criterion that may provide insight for many fire suppression situations. A correlation of wood crib fire extinction data is used to show the predictive capabilities that can be developed from experimental results alone, even without complete and general understanding of the fire suppression phenomena. The use of computer field modeling techniques is discussed as a means to generate insight into the complex physical interactions that occur during fire suppression in an enclosure.

00,347
PB94-212859 Not available NTIS
National Inst. of Standards and Technology (NEL), Gaithersburg, MD. Fire Science and Engineering Div.
Full Scale Smoke Control Tests at the Plaza Hotel Building.
Final rept.
J. H. Klote. 1989, 3p.
Pub. in Jnl. of American Society of Heating, Refrigeration and Air-Conditioning Engineers 31, n4 p28-30 Apr 89.

Keywords: *Fire tests, *Buildings, Ventilation, Fire safety, Smoke, Pressurization, Air flow, Pressure gradients, Stairways, Reprints, *Smoke control, *Hotel fires.

No zoned smoke control system has been tested under real fire conditions. This paper presents a general overview of a project of full scale fire experiments to be conducted at the Plaza Hotel Building in Washington, DC. The objectives of these experiments are to evaluate the current approach concerning minimum pressure difference and to achieve smoke control for zoned smoke control systems with and without stairwell pressurization. Also, the interaction between smoke control and the fire will be studied. Air will be exhausted at six changes per hour from the fire floor to evaluate the effect of this common exhaust rate on the fire energy release rate.

00,348
PB94-212867 Not available NTIS
National Inst. of Standards and Technology (BFRL), Gaithersburg, MD. Fire Science and Engineering Div.
Overview of Smoke Control Technology.
Final rept.
J. H. Klote. 1988, 11p.
Pub. in American Society of Heating, Refrigerating and Air-Conditioning Engineers Transactions 94, pt1 p1211-1221 1988.

Keywords: *Buildings, *Fire safety, *Smoke, Evacuation, Stairways, Elevators(Lifts), Leakage, Fire protection, Ventilation, Reprints, *Smoke control, *Building fires.

Considerable advances in smoke control technology have occurred in the last few decades. However, smoke control is just beginning to take its proper place as a fire protection tool. This paper provides an overview of this technology, including discussions of the fundamental principles, stairwell pressurization, zoned smoke control, elevator smoke control, system activation and acceptance testing. In addition the problems of smoke purging are addressed.

00,349
PB94-212875 Not available NTIS
National Inst. of Standards and Technology (BFRL), Gaithersburg, MD. Fire Safety Engineering Div.
Preview of ASHRAE's Revised Smoke Control Manual.
Final rept.
J. H. Klote. 1992, 4p.
Pub. in American Society of Heating, Refrigeration and Air-Conditioning Engineers Jnl., p34-37 Nov 92.

Keywords: *Buildings, *Fire safety, *Smoke, Manuals, Elevators(Lifts), Stairways, Pressurization, Air flow, Ventilation, Toxicity, Reliability, Reprints, *Smoke control, *Building fires, ASHRAE(American Society of Heating Refrigerating and Air Conditioning Engineers).

The American Society of Heating, Refrigerating, and Air-Conditioning Engineers (ASHRAE) smoke control manual has been extensively revised and expanded. This manual consolidates and systematically presents data and calculational procedures for use by smoke management system designers. Fundamental issues of smoke management include reliability, activation, smoke obscuration, toxicity, and the driving forces of smoke movement. The mechanisms of compartmentation, dilution, air flow, pressurization, and buoyancy are used by themselves or in combination to manage smoke conditions in fire situations. The new manual presents systems for stairwell pressurization, elevator smoke control, zoned smoke control, and atrium smoke management.

00,350
PB94-213253 Not available NTIS
National Inst. of Standards and Technology (BFRL), Gaithersburg, MD. Building and Fire Research Lab. Office.
Development of a New Small-Scale Smoke Toxicity Test Method and Its Comparison with Real-Scale Fire Tests.
Final rept.
B. C. Levin. 1992, 8p.
Pub. in Toxicology Letters 64/65, p257-264 1992.

Keywords: *Smoke, *Toxicity, *Test methods, Computerized simulation, Fire hazards, Fire safety, Heat flux, Combustion products, Buildings, Reprints, *Building fires.

A comprehensive methodology has been developed for obtaining and using smoke toxicity data for fire hazard analysis. This bench-scale method can simulate diverse fire conditions and identify extremely toxic smoke under both pre- and post-flashover conditions. However, incidence data show that most of the fire deaths in the U.S. occur outside the room of fire origin from smoke and toxic gases that are generated from a fire under post-flashover conditions. Therefore, the most relevant real-scale combustion conditions to simulate in the bench-scale apparatus would be the post-flashover conditions which are achieved by using radiant heat, a high heat flux, and correcting the bench-scale carbon monoxide (CO) results to agree with CO yields observed in real-scale post-flashover fires. The number of test animals (Fischer 344 male rats) is minimized by using the N-Gas Model to estimate the LC50 value from the chemical analysis of the smoke. The prediction is checked with a small number of animal tests and an approximate LC50 value is determined. The bench-scale results have been validated with full-scale room wall burns of a limited number of materials of widely differing characteristics chosen to challenge the system. The toxic potency values are assessed to determine if the smoke from a material or product is unusually or extremely toxic and can then be used in computations of fire hazard.

00,351
PB94-213261 Not available NTIS
National Inst. of Standards and Technology (NEL), Gaithersburg, MD. Fire Science and Engineering Div.
EXITT: A Simulation Model of Occupant Decisions and Actions in Residential Fires.
Final rept.
B. M. Levin. 1989, 10p.
Pub. in Proceedings of International Symposium on Fire Safety Science (2nd), Tokyo, Japan, June 13-17, 1988, p561-570 1989.

Keywords: *Residential buildings, *Computerized simulation, *Evacuation, *Decision making, Fire hazards, Smoke, Fire safety, Emergencies, Human behavior, Reprints, *Residential building fires, EXITT computer program, Escape time.

EXITT is a discrete event simulation of occupant decisions and actions in a postulated fire. To run the model the physical descriptions of a residence, a specific fire in that residence, and the assumed occupants of the residence are entered into the computer. Based on a large set of decision rules, the occupants make decisions which are a function of the smoke conditions in the building, the characteristics and status of the occupants (including their capabilities), and the available travel routes. The occupants investigate the fire, alert and assist others, and evacuate the building. The simulation ends when all the occupants are either out of the building or are trapped by the smoke.

00,352
PB94-217486 PC A14/MF A03
National Inst. of Standards and Technology (BFRL), Gaithersburg, MD. Structures Div.
Hollow Clay Tile Prism Tests for Martin Marietta Energy Systems: Task 2 Testing.
C. W. C. Yancey. 1993, 324p, NISTIR-5328.
Color illustrations reproduced in black and white.

Keywords: *Compressive strength, *Modulus of elasticity, *Clays, *Tiles, *Poisson ratio, Masonry, Construction materials, Mechanical properties, Loads(Forces), Displacement, *Hollow clay tile prisms.

Forty-one Hollow Clay Tile prisms were tested in monotonic, uniaxial compression to failure as the second task in a two-task prism test program for the Department of Energy (DOE). Twenty prisms were nominally 330 mm (13 in) thick and twenty-one were nominally 200 mm (8 in) thick. Twenty-one prisms were tested with the compressive load applied normal to the axis of the hollow cores and the other twenty were subjected to compressive load acting parallel to the axis of the cores. The objectives of the Task 2 test series were to: (1) obtain the compressive strength, (2) determine the modulus of elasticity in compression, (3) determine Poisson's ratio for the prisms, (4) study and understand the behavior of this type of masonry prism, (5) determine whether workmanship during construction of the prisms significantly affects the strength and (6) compare the results of using load control versus displacement control while loading the prisms. Test results are presented in tabular form to report the gross and net area compressive strengths, and Secant Modulus of Elasticity on the gross and net areas. Load-displacement plots are presented to graphically report on the output from vertical and horizontal Linear Variable Differential Transformers attached to the prism faces.

00,353
PB94-218583 PC A03/MF A01
National Inst. of Standards and Technology (BFRL), Gaithersburg, MD. Building Materials Div.
Survey of Recent Cementitious Materials Research in Western Europe.
D. P. Bentz. Aug 94, 35p, NISTIR-5480.

Keywords: *Cements, *Concretes, *Hydration, *Research management, Microstructure, Shrinkage, Cracking(Fracturing), Concrete durability.

The report summarizes recent research on cementitious materials in western Europe, based on a perspective gained during a six month stay at the Centre Scientifique et Technique du Batiment in Grenoble, France. During this time period, the author visited sixteen laboratories in seven different European countries. Numerous publications, all included in the reference list of this report, were obtained during these visits. Research is grouped into topical areas with a

brief description of separate activities at each institution. Emphasis has been placed on those research topics of interest to the Building Materials Division of NIST. A list of researchers working on cementitious materials in western Europe is also provided for those readers wishing to obtain further information on specific topics.

00,354
PB94-219052 PC A06/MF A02
National Inst. of Standards and Technology (BFRL), Gaithersburg, MD. Structures Div.
NIST Research Program on the Seismic Resistance of Partially-Grouted Masonry Shear Walls.
A. E. Shultz. Jun 94, 112p, NISTIR-5481.
See also PB92-116342.

Keywords: *Masonry, *Walls, Shear stress, Cyclic loads, Tests, Seismic design, Earthquake engineering, Buildings.

A review of the current status of research on masonry structures at the Building and Fire Research Laboratory of the National Institute of Standards and Technology (NIST) is presented, and an ongoing project on partially-grouted masonry shear walls is summarized. The report draws from previous work conducted at NIST including a comprehensive literature review, simulated seismic load tests of unreinforced and reinforced masonry walls, and numerical analyses employing empirical formulations and finite element models. The previous NIST research culminates with a preliminary draft outlining a research program on partially-grouted masonry walls and numerical analyses.

00,355
PB95-105136 PC A03/MF A01
National Inst. of Standards and Technology (BFRL), Gaithersburg, MD.
Controlling Moisture in the Walls of Manufactured Housing.
Technical note.
D. M. Burch, and A. TenWolde. Dec 92, 42p, NISTIR-4981, HUD-0006080.
See also AD-A139 637. Sponsored by Department of Housing and Urban Development, Washington, DC. Office of Policy Development and Research and Forest Products Lab., Madison, WI.

Keywords: *Walls, *Moisture, *Permeability, *Construction materials, *Housing(Dwellings), Humidity, Boundary conditions, Diffusion, Condensation, Wallboard, Ventilation, *Manufactured housing.

This report contains the results of a detailed computer analysis to investigate the effectiveness of three alternative practices for controlling moisture accumulation in the walls of manufactured housing during the winter. The three practices included: (1) providing a vapor retarder, (2) using permeable sheathing and siding, and (3) providing an outdoor ventilated cavity. The current Manufactured Home Construction and Safety Standards do not require a vapor retarder for practices 2 and 3. The analysis was carried out for a cold winter climate (Madison, WI), an intermediate winter climate (Boston, MA), a mild winter climate (Atlanta, GA), and a Pacific northwest climate (Portland, OR). The practice of providing a vapor retarder was found to be effective in all four climates. The moisture content of the siding was always considerably below fiber saturation. On the other hand, the practice of using permeable sheathing and siding and the practice of providing an outdoor ventilated cavity were not always effective in colder climates.

00,356
PB95-107397 Not available NTIS
National Inst. of Standards and Technology (BFRL), Gaithersburg, MD. Building Environment Div.
Measurements of Moisture Diffusivity for Porous Building Materials.
Final rept.
R. F. Richards. 1992, 11p.
Sponsored by Department of Energy, Washington, DC. Pub. in Proceedings of Conference on Thermal Performance of the Exterior Envelopes of Buildings V, Clearwater Beach, FL., December 7-10, 1992, p501-511.

Keywords: *Construction materials, *Porous materials, *Diffusivity, *Moisture, Mass transfer, Flux(Rate), Pressure, Steady state, Moisture content, Reprints.

Moisture diffusivities of several common porous building materials were determined experimentally. Both wood-based and inorganic materials were included in the study. A steady-flux method was used that involved determining the one-dimensional moisture content profile produced in a sample through which a known constant flux of water is flowing. The transient mass fluxes through samples upon exposure to water, steady-state mass fluxes, one-dimensional moisture content profiles, and capillary pressure curves for low suction pressures, as well as the moisture diffusivities for a range of moisture contents, are presented for each material. Results of the study are compared to previously published measurements for similar materials.

00,357
PB95-108718 Not available NTIS
National Inst. of Standards and Technology (BFRL), Gaithersburg, MD. Fire Science Div.
Verification of a Model of Fire and Smoke Transport.
Final rept.
R. D. Peacock, W. W. Jones, and R. W. Bukowski. 1993, 41p.
Pub. in Fire Safety Jnl. 21, p89-129 1993.

Keywords: *Fires, *Smoke, Flame propagation, Fire tests, Computer programs, Combustion products, Mathematical models, Algorithms, Reprints, *Fire models, *Smoke transport, *Room fires.

A set of comparisons between a comprehensive room fire model and a range of real-scale fire experiments is presented. For these comparisons, a zone-based model, CFAST ('consolidated fire and smoke transport' model) is used. The model predicts the evolution of a fire in a room and the subsequent transport of the smoke and toxic gases which result from this fire. These comparisons serve two purposes: to determine, within limits, the accuracy of the predictions for those quantities of interest to the users of the models (usually those extensive variables related to hazard), and to highlight the strengths and weaknesses of the underlying algorithms in the models to guide future improvements in this and other models. The predicted variables selected for comparison deal with both of these purposes. Although differences between the model and the experiments were clear, they can be explained by limitations of the model and of the experiments.

00,358
PB95-125795 Not available NTIS
National Inst. of Standards and Technology (NEL), Gaithersburg, MD. Building Materials Div.
Suggestions for a Logically-Consistent Structure for Service Life Prediction Standards.
Final rept.
G. Frohnsdorff, and L. Masters. 1990, 14p.
Pub. in Proceedings of International Conference on Durability of Building Materials and Components (5th), Brighton, UK., November 7-9, 1990, p113-126.

Keywords: *Service life, *Construction materials, *Aging(Materials), *Standards, Degradation, Life(Durability), Buildings, Prediction analysis techniques, Reprints, *Environmental characterization.

Ability to predict the service life of building materials, components, and systems is needed to improve the selection process. Evaluation of durability using existing standards does not give adequate service life information. Because service life prediction is more complex than current durability evaluations, its standardization will require a new body of standards to be put in place. The standards must define a general methodology, and essential components of the methodology. These are environmental characterization, characterization of the item whose service life is to be predicted, identification of the mechanisms and kinetics of the degradation processes, development of mathematical models of degradation, application of the models in service life prediction, and reporting of the results. It is proposed that the needed standards must comprise a hierarchy with the highest level being the general methodology, the second level defining the essential components of the methodology, and the third and lower levels describing the application of the generic standards to specific materials, components, or systems.

00,359
PB95-125845 Not available NTIS
National Inst. of Standards and Technology (NEL), Gaithersburg, MD. Building Materials Div.
Application of Thermal Analysis Techniques to the Characterization of EPDM Roofing Membrane Materials.
Final rept.
G. D. Gaddy, W. J. Rossiter, and R. K. Eby. 1990, 16p.
Sponsored by National Roofing Contractors Association, Rosemont, IL. and Johns Hopkins Univ., Baltimore, MD.
Pub. in Proceedings of a Symposium on Roofing Research and Standards Development, ASTM STP 1088, San Francisco, CA., June 17, 1990, v2 p37-52.

Keywords: *Thermal analysis, *Membranes, *Roofs, *Test methods, Construction materials, Elongation, Calorimetry, Thermogravimetric analysis, Heat measurement, Reprints, *EPDM rubber roofing, ASTM D 4637, Dynamic mechanical analysis.

This study was conducted to provide data on the feasibility of using thermal analysis (TA) methods for the characterization of roofing membrane materials. TA methods have never been widely applied to such materials. The TA methods used were thermogravimetry (TG), differential scanning calorimetry (DSC), and dynamic mechanical analysis (DMA). Three black (carbon black filled), two white (titanium dioxide pigmented), and one white on black laminate ethylene propylene diene terpolymer (EPDM) membrane materials were analyzed before and after exposure to the heat, ozone and UV conditions given in ASTM D 4637, and also to outdoor exposure. Load-elongation tests were conducted to compare the results with those of the TA methods. The results indicated that: (1) TA techniques can be used to analyze EPDM membrane materials; (2) both the black and white membrane materials showed only slight property changes under exposure, as determined using the TA methods; and (3) in contrast to the TA results, the load elongation values displayed relatively large changes.

00,360
PB95-125852 Not available NTIS
National Inst. of Standards and Technology (NEL), Gaithersburg, MD. Building Materials Div.
Use of Thermal Mechanical Analysis to Characterize Ethylene-Propylene-Diene Terpolymer (EPDM) Roofing Membrane Materials.
Final rept.
G. D. Gaddy, W. J. Rossiter, and R. K. Eby. 1991, 8p.
Sponsored by National Roofing Contractors Association, Rosemont. IL. and Johns Hopkins Univ., Baltimore, MD.
Pub. in Proceedings of a Conference on Materials Characterization by Thermomechanical Analysis, ASTM STP 1136, Philadelphia, PA., March 19-20, 1990, p168-175 1991.

Keywords: *Roofs, *Membranes, *Test methods, Thermal analysis, Construction materials, Elongation, Heat measurement, Reprints, *EPDM rubber roofing, *Thermal mechanical analysis, ASTM D 4637.

This study was conducted to provide baseline data on the applicability of thermal mechanical analysis (TMA) for characterizing EPDM roofing membrane materials. TMA has not been used extensively for the analysis of such materials. Three black and three white membrane materials were analyzed before and after exposure to the heat, ozone, and UV conditions described in ASTM D 4637, as well as to outdoor exposure. Load-elongation was conducted as a comparison to the TMA results. The results indicated that: (1) TMA can be applied to the characterization of EPDM membrane materials showing the differences in glass transition temperature between various brand name products; (2) changes in glass transition temperatures induced by the exposure conditions were relatively low and covered the same range for both the black and white membrane materials; and (3) in contrast to the TMA testing, the percent elongation values displayed relatively large changes.

00,361
PB95-125977 Not available NTIS
National Bureau of Standards (NEL), Gaithersburg, MD. Fire Measurement and Research Div.
Relating Bench-Scale and Full-Scale Toxicity Data.
Final rept.
R. G. Gann, E. Braun, and B. C. Levin. 1988, 4p.
Pub. in Proceedings of Joint Panel Meeting UJNR Panel on Fire Research and Safety (10th), Tsukuba, Japan, June 9-10, 1988, p50-53.

Keywords: *Fires, *Toxicity, *Test methods, *Buildings, Exposure(Physiology), Fire tests, Fire hazards,

Smoke, Combustion products, Construction materials, Reprints.

This work proposes criteria for comparing the toxic potency of fire smokes as measured by bench-scale toxicity tests with that measured in real-scale fire tests. A first set of experiments finds that this protocol is practicable, and that the NBS toxicity test method shows only partial correlation.

00,362
PB95-125985 Not available NTIS
National Inst. of Standards and Technology (NEL), Gaithersburg, MD. Building Materials Div.
Computer Simulation of the Diffusivity of Cement-Based Materials.
Final rept.
E. J. Garboczi, and D. P. Bentz. 1992, 10p.
Sponsored by Northwestern Univ., Evanston, IL. Center for Advanced Cement-Based Materials.
Pub. in Jnl. of Materials Science 27, n8 p2083-2092 1992.

Keywords: *Portland cement, *Microstructure, *Computerized simulation, *Diffusivity, *Chlorides, Hydration, Durability, Construction materials, Transport properties, Image analysis, Porosity, Reprints.

A digital-image-based model of the microstructure of cement paste, coupled with exact transport algorithms, is used to study the diffusivity of portland cement paste. The principal preparation and material variables are water:cement ratio, degree of cement hydration, and capillary porosity. Computational methods are described in some detail, and diffusivity results are presented and found to agree within experimental error with the available experimental measurements. Model cement pastes prepared with different water:cement ratios, and having different degrees of cement hydration, are found to have diffusivities that lie on a single master curve when plotted as a function of capillary porosity. Using percolation ideas, the diffusivity of cement paste is mapped out as a function of capillary porosity for any water:cement ratio cement paste.

00,363
PB95-125993 Not available NTIS
National Inst. of Standards and Technology (NEL), Gaithersburg, MD. Building Materials Div.
Digital Simulation of the Aggregate-Cement Paste Interfacial Zone in Concrete.
Final rept.
E. J. Garboczi, and D. P. Bentz. 1991, 6p.
Sponsored by Northwestern Univ., Evanston, IL. Dept. of Civil Engineering.
Pub. in Jnl. of Materials Research 6, n1 p196-201 1991.

Keywords: *Concretes, *Interfaces, *Aggregates, *Computerized simulation, Hydration, Curing, Portland cement, Image analysis, Porosity, Diffusion, Construction materials, Scanning electron microscopy, Reprints, *Interfacial zone.

Back-scattered scanning electron microscopy, along with quantitative image analysis techniques, have clearly demonstrated the existence of a highly porous interfacial region between the aggregate and the hardened cement paste matrix in ordinary Portland cement concrete. This paper presents the results of a digital-image-based simulation model of this interfacial zone. A dissolution-diffusion-reaction cycle of hydrating cement particles is directly simulated using cement particles packed around a simple non-reactive aggregate particle. The model is two-dimensional, as we are comparing to experimental results obtained on images of polished sections. The qualitative features seen in the experiment, such as large amounts of porosity and calcium hydroxide in the interfacial zone, are faithfully reproduced. The new mechanism of one-sided growth is proposed, along with the usual particle-packing ideas, as an explanation of the origin of the characteristic features of the interfacial zone.

00,364
PB95-126009 Not available NTIS
National Inst. of Standards and Technology (NEL), Gaithersburg, MD. Building Materials Div.
Fundamental Computer Simulation Models for Cement-Based Materials.
Final rept.
E. J. Garboczi, and D. P. Bentz. 1991, 29p.
Pub. in Mater. Sci. Concr., v2 p249-277 1991.

Keywords: *Cements, *Microstructure, *Construction materials, *Mechanical properties, *Computerized simulation, Hydration, Admixtures, Curing, Durability, Literature surveys, Mathematical models, Reprints.

The report is a critical review of fundamental computer-simulation models that have been applied to cement-based materials, to relate microstructure to properties. The report also contains a significant literature survey.

00,365
PB95-126264 Not available NTIS
National Inst. of Standards and Technology (BFRL), Gaithersburg, MD. Building Environment Div.
Comparison of Heat-Flow-Meter Tests from Four Laboratories.
Final rept.
R. S. Graves, D. L. McElroy, R. G. Miller, D. W. Yarbrough, and R. R. Zarr. 1992, 4p.
Pub. in Jnl. of Thermal Insulation 15, p354-357 Apr 92.

Keywords: *Thermal conductivity, *Heat measurement, *Test methods, *Laboratories, *Thermal insulation, Heat transmission, Transport properties, Calibration, Heat transfer, Reprints, *Heat flowmeters, ASTM C 518.

A recent comparison of apparent thermal conductivities measured at the Oak Ridge National Laboratory (ORNL), Jim Walter Research Corp (JWRC), Tennessee Technological University (TTU), and the National Institute of Standards and Technology (NIST) has been discussed in an ORNL Report. The four laboratories used equipment built and operated in accordance with ASTM C 518, and used different calibration materials and procedures. These tests are discussed in this paper.

00,366
PB95-130845 PC A10/MF A03
National Inst. of Standards and Technology (BFRL), Gaithersburg, MD. Fire Safety Engineering Div.
Summaries of BFRL Fire Research In-House Projects and Grants, 1994.
N. H. Jason. Oct 94, 213p, NISTIR-5504.
See also report for 1993, PB94-121050.

Keywords: *Fire safety, *Fire resistant materials, *Standards, *Fires, *Fire suppression, *Furniture, *Buildings, *Industrial plants, Flames, Flame propagation, Combustion, Models, Turbulent flow, Combustion products, Fire extinguishing agents, Smoke, Fire alarm systems, Fire protection, Construction materials, Fire hazards.

This report describes the fire research projects performed in the Building and Fire Research Laboratory (BFRL) and under its extramural grants program during Fiscal Year 1993. Included are research performed both with funds appropriated to the BFRL Fire Research Program and under contract to outside organizations. The BFRL Fire Research Program has directed its efforts under four program thrusts. The in-house priority projects, extramural grants, and externally-funded efforts thus form an integrated, focussed ensemble. This publication is organized along those lines: (1) Performance-based Fire Standards; (2) Fire Safe Materials and Products; (3) Advanced Fire Sensing and Suppression; (4) Large/Industrial Fires. For the convenience of the reader, an alphabetical listing of all grants is contained in the Part 2.0.

00,367
PB95-140885 Not available NTIS
National Inst. of Standards and Technology (NEL), Gaithersburg, MD. Fire Science and Engineering Div.
FPETOOL: Fire Protection Tools for Hazard Estimation. An Overview of Features.
Final rept.
H. E. Nelson. 1990, 8p.
See also PB92-132984.
Pub. in Proceedings of the International Fire Conference Interflam '90 (5th), Canterbury, England, September 3-6, 1990, p85-92.

Keywords: *Fire hazards, *Buildings, *Fire protection, *Fire safety, Computer programs, Fires, Computerized simulation, Fire detectors, Heat transfer, Risk assessment, Flame propagation, Sprinklers, Reprints, *FPETOOL computer program.

FPETOOL is a computerized package of relatively simple engineering equations and models. It contains engineering tools useful in estimating potential fire hazard and the response of the space and fire protection systems to the developing hazard. The computations use established engineering relationships, which are discussed in this paper for the benefit of engineers and others interested in using the tools in the package.

00,368
PB95-143152 PC A03/MF A01
National Inst. of Standards and Technology (BFRL), Gaithersburg, MD. Fire Safety Engineering Div.
Simulating Smoke Movement through Long Vertical Shafts in Zone-Type Compartment Fire Models.
L. Y. Cooper. Nov 94, 40p, NISTIR-5526.

Keywords: *Smoke, *Air flow, *Buoyancy, *Two phase flow, Turbulence, Vents, Plumes, Diffusion, Elevators(Lifts), Density, Mathematical models, *Zone-type compartment fire models, *Building fires.

A limitation of traditional zone-type compartment fire modeling concepts identify; namely, the inadequacy of two-layer quasi-steady-buoyant-plume analyses to simulate the fire-generated environment in room configurations with large height-to-span ratios, e.g., elevator shafts and long, vertical, ventilation shafts and ducts. A possible means of removing this limitation is developed. This involves a method of analysis and associated model equations that can be implemented and used to advance zone-type models. The model equations simulate time-dependent flows in a long, ventilated, vertical shaft/duct with an arbitrary vertical density distribution, including one or more intervals along the shaft/duct length where the vertical distribution of the average cross-section density may be unstably stratified, i.e., density increasing with increasing elevation. The model equations are partially verified by favorable comparisons between solutions and previously published data from unsteady experiments in long vertical tubes involving initially unstable configurations: salt-water over fresh-water and heavy-gas over light-gas. Additional verification of the proposed equation set with cold-air over hot-air systems and with fire-driven smoke flows, both of which involve gas-to-surface heat transfer, is required before this model can be used with confidence in professional practice.

00,369
PB95-143202 PC A06/MF A02
National Inst. of Standards and Technology (BFRL), Gaithersburg, MD. Fire Safety Engineering Div.
Building and Fire Research Laboratory Publications, 1993.
Special pub.
N. H. Jason. Sep 94, 113p, NIST/SP-838/6.
Also available from Supt. of Docs. as SN003-003-03295-6. See also report for 1992, PB93-188845.

Keywords: *Buildings, *Fires, *Bibliographies, *Research, Combustion, Fire protection, Abstracts, Flammability, Construction materials, Heat transfer, Building codes, Fire resistance, Ignition.

Building and Fire Research Laboratory Publications, 1993 contains references to the publications prepared by the members of the Building and Fire Research Laboratory (BFRL) staff, by other National Institute of Standards and Technology (NIST) personnel for BFRL, or by external laboratories under contract or grant from the BFRL during the calendar year 1993.

00,370
PB95-150439 Not available NTIS
National Inst. of Standards and Technology (BFRL), Gaithersburg, MD. Building Materials Div.
Percolation and Pore Structure in Mortars and Concrete.
Final rept.
D. Winslow, M. Cohen, D. Bentz, K. Snyder, and E. Garboczi. 1994, 13p.
Sponsored by Center for Advanced Cement-Based Materials, Evanston, IL.
Pub. in Cement and Concrete Research 24, n1 p25-37 1994.

Keywords: *Building materials, *Concretes, *Motars, *Pore structure, *Percolation, Computerized simulation, Microstructure, Interfaces, Durability, Transport properties, Reprints, Mercury intrusion porosimetry, Silica fume.

The cement paste in concrete and mortar has been shown to have a pore size distribution different than that of plain paste hydrated without aggregate. For mortar and concrete, additional porosity occurs in pore sizes larger than the plain paste's threshold diameter as measured by mercury intrusion. Based on the assumption that these larger pores are essentially present only in the interfacial zones surrounding each aggregate, an experimental program was designed in which the volume fraction of sand in a mortar was varied in a systematic fashion and the resultant pore sys-

tem probed using mercury intrusion porosimetry. The intrusion characteristics were observed to change drastically at a critical sand content. Similar results are observed for a series of mortar specimens in which the cement paste contains 10% silica fume. To better interpret the experimental results, a hard core/soft shell computer model has been developed to examine the percolation characteristics of these interfacial zone pores. Using the model, interfacial zone percolation in concretes is also examined. Finally, the implications of interfacial zone percolation for transport properties and durability of mortar and concrete are discussed.

00,371
PB95-150462 Not available NTIS
National Inst. of Standards and Technology (BFRL), Gaithersburg, MD. Building Environment Div.
Effects of Humidity and Elevated Temperature on the Density and Thermal Conductivity of a Rigid Polyisocyanurate Foam Co-Blown with CCl3F and CO2.
Final rept.
R. R. Zarr, and T. Nguyen. 1994, 21p.
Pub. in Jnl. of Thermal Insul. and Bldg. Envs. 17, p330-350 Apr 94.

Keywords: *High temperature tests, *Humidity, *Thermal conductivity, *Density(Mass/volume), *Foams, *Thermal insulation, Thermal resistance, Heat measurement, Thermodynamic properties, Laminates, Thermophysical properties, Temperature dependence, Test facilities, Reprints, *Rigid polyisocyanurate foam.

Measurements of density and apparent thermal conductivity are presented for specimens cut from rigid polyisocyanurate foam co-blown with trichlorofluoromethane and carbon dioxide. Eight specimens, nominally 580 by 580 by 27 mm, were prepared from two boards (1.2 by 2.4 m by 50mm) of foam laminated with permeable facers. Four specimens were placed in an ambient condition of 22 C and 40% relative humidity (RH). The other four specimens were each placed in one of the following environments: (1) 60 C and less than 10% RH; (2) 60 C and 40% RH; (3) 60 C and 60% RH; and (4) 60 C and 75% RH. Measurements of apparent thermal conductivity at 24 C were conducted over a period of 372 days at approximately 50-day intervals. Curves of specimen mass, volume, density, and thermal conductivity versus time are presented, and the implications of changes in these properties are discussed.

00,372
PB95-151338 Not available NTIS
National Inst. of Standards and Technology (NEL), Gaithersburg, MD. Building Materials Div.
Effects of Adhesive Thickness, Open Time, and Surface Cleanness on the Peel Strength of Adhesive-Bonded Seams of EPDM Rubber Roofing Membrane.
Final rept.
H. Watanabe, and W. J. Rossiter. 1990, 16p.
Pub. in Roofing Research and Standards Development: ASTM STP 1088, v2 p21-36 1990.

Keywords: *Roofing, *Adhesion, *Peel strength, *Seams(Joints), Adhesive bonding, Surface properties, Construction materials, Roofs, Contamination, Failure modes, Rubber, Membranes, Curing, Strength(Mechanics), Cleanliness, Reprints, *EPDM Rubber Roofing Membrane, Open time.

A laboratory study was undertaken to examine the effects of adhesive thickness, open time, and surface cleanness on T-peel strength of EPDM rubber seam specimens. Seam specimens bonded with butyl-based contact adhesive were tested after a 2-week cure time. The peel strength generally showed a positive dependency on the adhesive thickness except that it tended towards a plateau value for thick adhesive layers. The leveling of peel strength at large thickness might result from the presence of small voids in the adhesive layer. The peel strength was not dependent on the open times used in this study. Increased levels of surface contamination lowered the peel strength and changed the failure mode from cohesive to interfacial.

00,373
PB95-152021 Not available NTIS
National Inst. of Standards and Technology (BFRL), Gaithersburg, MD. Building Environment Div.
Effects of Humidity and Elevated Temperature on the Density and Thermal Conductivity of a Rigid Polyisocyanurate Foam.
Final rept.
R. R. Zarr, and T. Nguyen. 1992, 9p.
Pub. in Proceedings of Society of the Plastics Industry Annual Technical/Marketing Conference (34th) Polyurethanes 92, New Orleans, LA., October 21-24, 1992, p422-430.

Keywords: *Humidity, *High temperature tests, *Density(Mass/volume), *Thermal conductivity, *Thermal insulation, Test methods, Heat measurement, Temperature dependence, Thermal resistance, Thermodynamic properties, Thermophysical properties, Test facilities, Reprints, *Rigid polyisocyanurate foam.

Measurements of apparent thermal conductivity are presented for specimens of rigid polyisocyanurate (PIR) foam cut from a commercial insulation product and aged in air 60 C and different humidities. Eight specimens, nominally 600 by 600 mm, were prepared from two boards (1.2 by 2.4 by 0.05 m) of rigid PIR foam blown with trichlorofluoromethane and having permeable organic-inorganic facers. Facers and excess foam were removed by sanding the specimens to a thickness of 27.9 + or - 0.1 mm. Four specimens were placed in ambient conditions of 22 C and 40% relative humidity (RH). Measurements of apparent thermal conductivity were conducted at 24 C and a temperature difference of 22 C using a heat-flow-meter apparatus conforming to ASTM Test Method C 518. Measurements were conducted for a period of 357 days at approximately 50-day intervals. Aging curves of specimen mass, volume, density, and thermal conductivity for rigid PIR foam are presented and implications of changes in these properties are discussed in the paper.

00,374
PB95-152039 Not available NTIS
National Inst. of Standards and Technology (NEL), Gaithersburg, MD. Building Environment Div.
Room Temperature Thermal Conductivity of Fumed-Silica Insulation for a Standard Reference Material.
Final rept.
R. R. Zarr, T. A. Somers, and D. F. Ebberts. 1991, 23p.
Pub. in Improved Thermal Insulation Problems and Perspectives, Chapter 5, p97-119 1991.

Keywords: *Thermal conductivity, *Thermal insulation, *Silicon dioxide, Conductive heat transfer, Thermal resistance, Heat measurement, Thermodynamic properties, Test facilities, Reprints, *Standard reference materials.

Thermal conductivity of fumed-silica insulation board was measured using the National Institute of Standards and Technology 1-meter Guarded Hot Plate. Measurements were conducted for the following range of parameters: bulk density, 304.5 to 325.4 kg/cu m, mean temperature, 283.1 to 311.0 K; and barometric pressure, 97.51 to 103.43 KPa. The effect of moisture content on room-temperature measurements was minimized by prior conditioning of the specimen at 100 C for 24 hours. Seventy-five samples (600 by 600 by 25.4 mm) were transferred to the Office of Standard Reference Materials in Gaithersburg, Maryland, USA. The material is offered as a Standard Reference Material having a low thermal conductivity at room temperature.

00,375
PB95-152864 Not available NTIS
National Inst. of Standards and Technology (BFRL), Gaithersburg, MD. Fire Science Div.
Effects of Specimen Edge Conditions on Heat Release Rate.
Final rept.
V. Babrauskas, W. H. Twilley, and W. J. Parker. 1993, 13p.
Pub. in Fire and Materials 17, n2 p51-63 1993.

Keywords: *Calorimeters, *Fire tests, *Edges, *Construction materials, *Heat flux, Burning rate, Heat transmission, Flammability, Plastics, Wood, Heat measurement, Reprints, *Reaction-to-fire tests.

When bench-scale specimens are tested for heat release rate, it is generally of interest that the behavior of the specimen simulate, as much as is possible, that of a real-scale product performing in a real fire. A number of issues have been raised recently by workers trying to understand the optimal conditions of specimen preparation and mounting. In the present study a large number of materials were explored in the Cone Calorimeter to determine the effect of edge conditions and edge frames. It was found that by the use of an insulated edge frame, heat release rate values can be obtained which are slightly closer to expected true values. The testing procedure, however, is significantly more complicated. This makes the insulated edge frame useful for collecting specialized data for fire modeling, but not for conducting routine reactions-to-fire tests. For routine testing use, it is recommended: (1) that no edge frame needs to be used unless the test specimen presents special difficulties, such as due to intumescence; (2) that in those cases where the use of the steel edge frame is found necessary, the results should be reported on the basis of an effective exposure area of 0.0081 sq m. When reported on such a basis, the heat release rate results do not show a systematic bias, compared to results with no edge frame.

00,376
PB95-154746 PC A05/MF A01
National Inst. of Standards and Technology (BFRL), Gaithersburg, MD. Fire Safety Engineering Div.
Method of Predicting Smoke Movement in Atria with Application to Smoke Management.
J. H. Klote. Oct 94, 96p, NISTIR-5516.
Also available from Supt. of Docs.

Keywords: *Smoke, *Air flow, *Fires, *Buildings, *Atria, Unsteady flow, Fire tests, Temperature distribution, Mathematical models, Architecture, Building codes, Mass flow, Steady flow, *Smoke management, *Fire models, ASMET computer program, ASMET (Atria Smoke Management Engineering Tools).

The paper presents information that can be used for predicting smoke movement for design of atrium smoke management systems. NFPA 92B (1991) and the smoke control design book by Klote and Milke (1992) define smoke as the airborne solid and liquid particulates and gases evolved when a material undergoes pyrolysis or combustion, together with the quantity of air that is entrained or otherwise mixed into the mass. In recent years, approaches to smoke management in atria have been introduced into codes and engineering guides (BOCA; UBC 1993; NFPA 92B 1991; Klote and Milke 1992; Hansel and Morgan 1994). While these basic approaches differ in many respects, they all have the zone fire model concept as a common foundation and consist of a collection of algebraic equations intended for design calculation. For simplicity, discussion of the basic approaches is limited to those of NFPA 92B. However, much of this applies to the other approaches as well. The paper explains the physical concepts behind NFPA 92B including system limitations. The conservative nature of this approach is investigated, and the unique design challenge of atrium smoke detection is discussed. The application of zone computer fire models to atrium design is addressed. This paper also presents a computer program entitled Atria Smoke Management Engineering Tools (ASMET) that consists of a set of equations that may be of help for conventional applications. Appendices C and D describe ASMET including brief user instructions.

00,377
PB95-162491 Not available NTIS
National Inst. of Standards and Technology (NEL), Gaithersburg, MD. Building Materials Div.
Characteristics of Adhesive-Bonded Seams Sampled from EPDM Roof Membranes.
Final rept.
W. Rossiter, J. Seiler, W. Spencer, J. Lechner, and P. Stutzman. 1991, 13p.
Pub. in Proceedings of International Symposium on Roofing Technology (3rd), Montreal, Canada, April 17-19, 1991, p167-179.

Keywords: *Failure analysis, *Seams(Joints), *Adhesive bonding, *Roofing, *Characterization, Rubber, Membranes, Construction materials, Adhesives, Scanning electron microscopy, Sampling, Nondestructive tests, Mechanical properties, Defects, Reprints, *EPDM roof membranes.

This study reports on the characterization of seam samples cut from EPDM roof systems. The availability of data on seam characteristics and failure analysis is beneficial to furthering the understanding of seam performance and to developing performance criteria for seams. Forty-eight samples were cut from EPDM roofs whose seams were rated as having provided satisfactory or unsatisfactory performance. The samples were

subjected to laboratory tests which included identification of the adhesive, measurement of adhesive thickness, and determination of the strength and mode of failure in peel. Comparisons were made between the test results and performance ratings. It was found that the majority of the unsatisfactorily performing seams contained neoprene-based adhesives and were exposed on roofs for 45 months or more when sampled. Of the samples subjected to SEM analysis, the majority showed evidence of release agent on the rubber and adhesive surfaces analyzed. This finding provided evidence that a field method to judge rubber surface cleanness before application of the adhesive is needed.

00,378
PB95-163150 Not available NTIS
National Inst. of Standards and Technology (NEL), Gaithersburg, MD. Building Materials Div.
Rheology of Fresh Cement Paste.
Final rept.
L. J. Struble. 1991, 23p.
Sponsored by National Science Foundation, Washington, DC. and Northwestern Univ., Evanston, IL. Center for Advanced Cement-Based Materials.
Pub. in Ceram. Trans. 16, p7-29 1991.

Keywords: *Cements, *Rheology, *Microstructure, Construction materials, Binders(Materials), Curing, Particulates, Dispersions, Flow theory, Reprints.

Rheology provides considerable information about the microstructure of dense particulate suspensions, and an important reason for studying the flow behavior of fresh cement paste is to infer the extent to which particles are flocculated, how densely they are picked, and how their microstructure is modified by hydration reactions prior to set. These aspects of the fresh paste microstructure influence both the initial flow behavior and the ultimate performance of concrete. The rheology of fresh cement paste and other dense particulate suspensions is reviewed. There has been much progress in formulating relationships between flow behavior and microstructure of disperse suspensions, and recent advances in dense, flocculated suspensions have been assisted in part by new experimental techniques. This recent understanding offers encouragement as well as promising research directions in developing direct relationships between flow behavior and microstructure for flocculated cement particles in fresh paste.

00,379
PB95-163168 Not available NTIS
National Inst. of Standards and Technology (NEL), Gaithersburg, MD. Building Materials Div.
Cement and Concrete Characterization by Scanning Electron Microscopy.
Final rept.
P. E. Stutzman. 1991, 5p.
Pub. in Proceedings of American Society of Civil Engineers Engineering Mechanics Specialty Conference, Columbus, OH., May 20-22, 1991, p1087-1091.

Keywords: *Concrete, *Portland cement, *Characterization, *Scanning electron microscopy, Microstructure, Image analysis, X-ray analysis, Petrography, Nondestructive tests, Microanalysis, Inspection, Reprints.

The scanning electron microscope (SEM) is a powerful tool for the microstructural and chemical characterization of cement and concrete. Imaging techniques such as secondary electron, backscattered electron, and X-ray imaging provide information about surface texture, microstructure, aggregates, and the air void system. X-ray microanalysis is useful for qualitative and quantitative chemical analysis and X-ray mapping of element distribution. Image processing and analysis is used for quantification of microstructural features. The linking of these operations will provide automated, quantitative, and consistent analysis of portland cement and concrete.

00,380
PB95-163481 Not available NTIS
National Inst. of Standards and Technology (NEL), Gaithersburg, MD. Fire Science and Engineering Div.
Wall Flame Heights with External Radiation.
Final rept.
K. M. Tu, and J. G. Quintiere. 1991, 9p.
Pub. in Fire Technology 27, n3 p195-203 Aug 91.

Keywords: *Walls, *Burning rate, *Fire tests, *Fiberboard, Heat flux, Wallboard, Heat transfer, Construction materials, Fire safety, Wood particle boards, PMMA, Reprints, *Upward flame spread.

This work was an experimental study of upward flame spread of vertically oriented wall material with external radiation. Its inherent potentials of high fire growth rate and spreading to surrounding materials makes this study a very challenged task. An existing flame heat transfer fire testing apparatus was used to study the upward flame spread potential of two kinds of wall materials: (1) the PMMA (Polymethylmethacrylate) and (2) the Douglas Fir Particle Board. PMMA is non-charring whereas Douglas Fir Particle Board is a charring material. Various levels of external radiant heat flux ranging from 1.8 W/sq cm to 3.4 W/sq cm were imposed on to the wall samples for carrying out the series of fire tests. Relevant parameters measured were fuel mass burning rate, wall fire flame height, external radiant heat flux level and flame heat transfer, etc. Observations and data measurements of these experimental results were employed to evaluate flammability characteristics of wall materials as well as validating the application of ignition and flame spread theory on predicting material performance.

00,381
PB95-163804 Not available NTIS
National Inst. of Standards and Technology (NEL), Gaithersburg, MD. Building Materials Div.
Pulse-Echo Ultrasonic Evaluation of the Integrity of Seams of Single-Ply Roof Membranes.
Final rept.
H. Watanabe, and W. J. Rossiter. 1991, 12p.
Pub. in Proceedings of 1991 International Symposium on Roofing Technology, p72-83.

Keywords: *Roofing, *Ultrasonic tests, *Seams(Joints), *Adhesive bonding, Membranes, Defects, Voids, Nondestructive tests, Construction materials, Reprints, *Single-ply roof membranes, *Pulse-echo ultrasonic evaluation.

This paper summarizes results of a study to develop an ultrasonic pulse-echo method for evaluating the integrity of seams of single-ply roofing membranes. A prototype pulse-echo apparatus (the field scanner), which was designed to scan across seams of roofs while maintaining acoustic coupling to the seam surface, was developed. Results of initial laboratory investigations showed that voids in seams could be distinguished from well-bonded sections using the intensity of the echo from the adhesive layer. This echo was relatively weak for well-bonded seams, and relatively strong for voids. Seams of existing EPDM single-ply membranes were examined by roof-top scanning to evaluate the performance of the field scanner in practice. The findings indicated that the field scanner was sensitive to detecting micro-cavities that could be created in the adhesive layer at the time of seam fabrication, thus resulting in false positive readings. It was concluded that, at least in its present form, the field scanner had limited applicability to resolving micro-cavities from voids and delaminations in solvent-adhesive seams.

00,382
PB95-164711 Not available NTIS
National Inst. of Standards and Technology (BFRL), Gaithersburg, MD. Fire Safety Engineering Div.
Fire-Plume-Generated Ceiling Jet Characteristics and Convective Heat Transfer to Ceiling and Wall Surfaces in a Two-Layer Fire Environment: Uniform Temperature Ceiling and Walls.
Final rept.
L. Y. Cooper. 1993, 17p.
See also PB92-123074. Sponsored by Nuclear Regulatory Commission, Washington, DC.
Pub. in Fire Science and Technology 13, n1-2 p1-17 1993.

Keywords: *Fires, *Plumes, *Convective heat transfer, *Ceilings(Architecture), *Walls, Jet flow, Heat flux, Temperature distribution, Algorithms, Velocity distribution, Subroutines, Mathematical models, Reprints, CEILHT subroutine.

This work presents a model to predict the instantaneous rate of convective heat transfer form fire plume gases to the overhead ceiling surface in a room of fire origin. The room is assumed to be a rectangular parallelopiped and, at times of interest, ceiling temperatures are simulated as being uniform. Also presented is an estimate of the convective heat transfer, due to ceiling-jet-driven wall flows, to both the upper and lower portions of the walls. The effect on the heat transfer of the location of the fire within the room is taken into account. Finally presented is a model of the velocity and temperature distributions in the ceiling jet. The model equations were used to develop an algorithm and associated modular computer subroutine to carry out the indicated heat transfer calculations. The subroutine is written in FORTRAN 77 and called CEILHT. The algorithm and subroutine are suitable for use in two-layer zone-type compartment fire model computer codes. The subroutine was tested for a variety of fire environments involving a 10(exp 7) W fire in a 8m x 8m x 4m high enclosure. While the calculated results were plausible, it is important to point out that CEILHT simulations have not been experimentally validated.

00,383
PB95-178885 PC A03/MF A01
National Inst. of Standards and Technology (BFRL), Gaithersburg, MD.
Manufactured Housing Walls That Provide Satisfactory Moisture Performance in All Climates.
D. M. Burch, C. A. Saunders, and A. TenWolde. Jan 95, 36p, NISTIR-5558.
See also PB95-105136. Prepared in cooperation with Forest Products Lab., Madison, WI. Sponsored by Department of Housing and Urban Development, Washington, DC. Office of Policy Development and Research.

Keywords: *Construction materials, *Walls, *Moistureproofing, *Prefabricated buildings, Moisture, Diffusion, Plywood, Wallboard, Cold regions, Mathematical models, Humidity, Thermal insulation, Permeability, Hot regions, *Moisture transfer.

We used the MOIST Computer Model to conduct a detailed analysis of the moisture performance of one wall typical of current construction practice in manufactured housing, and two new alternative wall designs with potential for better moisture performance in a wider variety of climates. The analysis showed that the current-practice wall with an interior vapor retarder performed acceptably in a cold climate (Madison, WI), but poorly in a hot and humid climate (Miami, FL). The alternative wall designs both exhibited satisfactory moisture performance in the cold climate and the hot and humid climate, even with moderately severe indoor conditions. The alternative wall designs also performed satisfactorily in a mixed climate (Little Rock, AR). These alternative wall designs should be of interest to the manufactured housing industry, which distributes homes to all climatic regions of the United States.

00,384
PB95-180063 Not available NTIS
National Inst. of Standards and Technology (BFRL), Gaithersburg, MD. Fire Science and Engineering Div.
Mathematical Modeling and Computer Simulation of Fire Phenomena.
Final rept.
H. R. Baum, K. B. McGrattan, and R. G. Rehm. 1994, 9p.
Pub. in Proceedings of International Symposium on Fire Safety Science (4th), Ottawa, Ontario, Canada, June 13-17, 1994, p185-193.

Keywords: *Transport properties, *Convective flow, *Computational fluid dynamics, Computerized simulation, Mathematical models, Finite difference theory, Combustion, High Reynolds number, Fires, Buoyancy, Navier-Stokes equations, Reprints, *Enclosure fires.

A method of studying the large scale transport of smoke and hot gases induced by fires in enclosures is described. The approach is based on solving the governing equations directly (if approximately) by decomposing the fire-driven flow field into large scale convective and small scale combustion components. In this work, results involving large scale convective transport generated by flow fields associated with typical fire scenarios are presented. The large scale flow is studied using finite difference techniques to solve large eddy simulations of the Navier-Stokes equations at high Reynolds numbers.

00,385
PB95-180139 Not available NTIS
National Inst. of Standards and Technology (BFRL), Gaithersburg, MD. Structures Div.
Nondestructive Testing of Concrete: History and Challenges.
Final rept.
N. J. Carino. 1994, 56p.
Pub. in Proceedings of V. Mohan Malhotra Symposium on Concrete Technology: Past, Present, and Future, San Francisco, CA., March 21-23, 1994, p623-678.

Keywords: *Concretes, *Nondestructive tests, Ultrasonic tests, Statistical analysis, Test methods, Durability, Mechanical properties, Infrared spectroscopy, Thermography, Reprints.

A brief history of nondestructive testing of hardened concrete over the past 50 years is presented. The contributions of V.M. Malhotra towards the development and promotion of nondestructive testing are emphasized. The underlying principles and inherent limitations of the methods are reviewed, and historical highlights of their development are presented. Test methods are grouped into those which assess in-place strength and those which evaluate non-strength characteristics, such as flaws and deterioration. The paper concludes with a discussion of the challenges for the 21st century in the area of nondestructive testing.

00,386
PB95-181194 Not available NTIS
National Inst. of Standards and Technology (BFRL), Gaithersburg, MD. Building Environment Div.
Control Stability of a Heat-Flow-Meter Appartus.
Final rept.
R. R. Zarr. 1994, 12p.
Pub. in Jnl. Thermal Insul. and Bldg. Envs. 18, p116-127 Oct 94.

Keywords: *Thermal insulation, *Heat meters, *Calibration, Heat transmission, Errors, Steady state, Precision, Measuring instruments, Reprints.

Calibration measurements of a commercial heat-flow-meter apparatus are presented. The apparatus has been calibrated using the same speciment of high-density fibrous-glass board over a period of four years, from 1989 to 1993. Seventy-three tests have been conducted, generally at ambient conditions of 24 C with a moderate temperature difference of either 15, 22, or 27 C across the specimen. Variations within a set of data for each test have been examined to verify underlying assumptions of randomness, normal frequency distribution of errors, repeatability, and stability of the data. Variations between test data indicate a small drift, on the order of one percent over four years, in the calibration factor of the apparatus. A model has been developed to describe the small drift with time. The analysis of variations between test data has also identified intermittent shifts in the precision of the calibration factor of the apparatus.

00,387
PB95-181202 Not available NTIS
National Inst. of Standards and Technology (BFRL), Gaithersburg, MD. Building Environment Div.
Intra-Laboratory Comparison of a Line-Heat-Source Guarded Hot Plate and Heat-Flow-Meter Apparatus.
Final rept.
R. R. Zarr. 1991, 18p.
Sponsored by Department of Energy, Washington, DC. and Oak Ridge National Lab., TN.
Pub. in Insulation Materials: Testing and Applications, ASTM STP 1116, p502-519 1991.

Keywords: *Heat meters, *Thermal insulation, *Thermal conductivity, Heat transmission, Heat flux, Measuring instruments, Calibration, Standards, Thickness, Comparison, Transducers, Test methods, Test facilities, Reprints, *Line heat sources, *Guarded hot plate, Standard reference materials, Fibrous-glass board.

The apparent thermal conductivity and thermal resistance of several building insulations were determined at the National Institute of Standards and Technology (NIST) using three apparatus. Reference values were determined with NIST's 1-meter Line-Heat-Source Guarded Hot Plate (GHP). The other two apparatus were heat-flow-meter (HFM) apparatus calibrated with a Standard Reference Material of fibrous-glass board. Deviations from reference values of the GHP were calculated for the HFM apparatus. The apparatus, test procedure, and analysis of the deviations are described in the paper.

00,388
PB95-181210 Not available NTIS
National Inst. of Standards and Technology (BFRL), Gaithersburg, MD. Building Environment Div.
Effect of Environmentally Exposures on the Properties of Polyisocyanurate Foam Insulation: Thermal Conductivity Measurements.
Final rept.
R. R. Zarr, and T. Nguyen. 1991, 15p.
Pub. in Proceedings of International Workshop on the Long-Term Thermal Performance of Cellular Plastics (2nd), Ontario, Canada, June 5-7, 1991, 15p.

Keywords: *Thermal conductivity, *Thermal insulation, *Aging(Materials), *Test methods, Heat meters, Thermophysical properties, Heat transmission, Humidity, Foams, Measuring instruments, Expanded plastics, Reprints, *Polyisocyanurate, ASTM C 518.

Measurements of apparent thermal conductivity are presented for specimens of rigid polyisocyanurate (PIR) foam conditioned in one of four environments. Measurements were conducted at 24 C and a temperature difference of 22 C at monthly intervals for six months using a heat-flow-meter apparatus (ASTM Test Method C 518). Four specimens (nominally 610 by 610 mm) were prepared from one commercial board (nominally 1.2 by 2.4 m) of rigid PIR foam blown, with R11 and having permeable organic/inorganic facers. For the six-month period, the increase in apparent thermal conductivity for the four specimens ranged from 11.5 to 14.2%. Aging curves of thermal conductivity for each specimen are described in the paper.

00,389
PB95-188868 PC A03/MF A01
National Inst. of Standards and Technology (BFRL), Gaithersburg, MD. Fire Safety Engineering Div.
Santa Ana Fire Department Experiment at 1315 South Bristol, July 14, 1994.
A. D. Putorti, W. D. Walton, W. H. Twilley, S. Deal, and J. C. Albers. 31 Aug 94, 23p, FR-3995.
Prepared in cooperation with Santa Ana City Fire Dept., CA. Fire Safety Div.

Keywords: *Residential buildings, *Fire tests, *Fire protection, *Fire detectors, Sprinklers, Flammability, Construction materials, Temperature measurement, Fire safety, Smoke, *Santa Ana(California).

The Santa Ana Fire Department of Santa Ana, California conducted a series of fire experiments in residences on South Bristol Street in the City of Santa Ana in July, 1994. The National Institute of Standards and Technology (NIST) provided technical support, consisting of measurements of fire phenomena, to the fire department during these experiments. The experiment addressed in this report occurred on July 14, 1994, at 1315 South Bristol Street. The measurements included: temperatures within various rooms, the velocity and temperature of outflowing gases, smoke detector activation time, sprinkler activation times, and time to full room involvement. Data were recorded every 5 seconds with a computerized acquisition system.

00,390
PB95-188918 PC A04/MF A01
National Inst. of Standards and Technology (BFRL), Gaithersburg, MD. Fire Safety Engineering Div.
Fire Performance of an Interstitial Space Construction System.
J. R. Lawson, E. Braun, L. DeLauter, and G. Roadarmel. Feb 95, 67p, NISTIR-5560.
See also PB86-106002. Sponsored by Office of the Chief of Engineers (Army), Washington, DC. Medical Facilities Office.

Keywords: *Floors, *Fire tests, *Steel structures, Fire resistance, Test methods, Surface temperature, Construction materials, Structural members, Fire protection, Fire safety, *Interstitial space construction systems.

An interstitial space building construction assembly, consisting of a walk-on deck suspended from above by structural steel which also supported a functional floor, reproduce a design planned for use in a new hospital complex at Elmendorf Air Force Base, Alaska. This interstitial space assembly was built in the multistory steel test structure at the National Institute of Standards and Technology. The construction assembly was tested by the same protocol used to evaluate the Veteran's Administration interstitial space construction assembly, tested in 1984. This protocol followed the National Fire Protection Association's NFPA 251 Fire Tests of Building Construction and Materials Standards, 1990 edition. Fire testing of the interstitial space system was carried out during the summer of 1994. This construction assembly met the requirements for a 2 hour fire endurance rating. The maximum surface temperature on the unexposed functional floor above the interstitial space reached 33 C (91 F) at the end of the two hour period. The maximum structural steel temperature inside of the interstitial space was 123 C (253 F). The structural assembly was evaluated for a total of 2 hours and 30 minutes before the test was terminated.

00,391
PB95-200655 PC A05/MF A01
National Inst. of Standards and Technology (BFRL), Gaithersburg, MD. Building Environment Div.
Heat and Moisture Transfer in Wood-Based Wall Construction: Measured versus Predicted.
Building science series.
R. R. Zarr, D. M. Burch, and A. H. Fanney. Feb 95, 92p, NIST/BSS-173.
Also available from Supt. of Docs. as SN003-003-03325-1.

Keywords: *Walls, *Heat transfer, *Moisture content, *Wood, Construction materials, Buildings, Wall temperature, Humidity, Heat flux, Thermal insulation, Wooden structures, Steady state, Thermodynamic properties, MOIST computer program.

This report describes a comprehensive laboratory study to verify the accuracy of MOIST for 12 different wall specimens. The rate of heat transfer through each of the 12 wall specimens was measured. The moisture content of the exterior construction materials was measured for eight of the twelve wall specimens. For the remaining four walls, the relative humidity level was measured at the interior side of the exterior sheathing. The measured heat transfer rates, moisture content levels and relative humidities were compared to the predictions of MOIST. In general, the agreement between MOIST and the experimental measurements was good. The moisture content predicted by MOIST was within one percent of the measured values for seven of the eight walls that contained moisture content sensors. The measured relative humidities for two of the remaining four walls agreed well with the MOIST predictions. The relative humidity measurements from the other two walls could not be compared to MOIST since the walls were constructed with vapor retarder defects that introduced two-dimensional effects. The heat flux predicted by MOIST was within ten percent of the values measured under steady-state conditions.

00,392
PB95-208757 PC A09/MF A02
National Inst. of Standards and Technology (BFRL), Gaithersburg, MD.
Optical Performance of Commercial Windows.
S. J. Treado, and J. W. Bean. Jan 92, 184p, NISTIR-4711.

Keywords: *Windows, *Absorptance, *Privacy, Contrast, Window glazing, Visibility, Performance.

The role of window system characteristics on privacy-related issues was examined. The optical characteristics of various window materials were measured and compared to determine the best candidates for enhancing building occupant privacy. Strategies for inducing privacy are discussed, along with related performance characteristics of window systems.

00,393
PB95-216990 PC A07/MF A02
Maryland Univ., College Park.
Burning Rate and Flame Heat Flux For PMMA in the Cone Calorimeter.
Master's thesis.
B. T. Rhodes. Dec 94, 130p, NIST/GCR-95/664.
Grant NIST-60NA2D1266
Sponsored by National Inst. of Standards and Technology (BFRL), Gaithersburg, MD. Fire Science Div.

Keywords: *Calorimeters, *Burning rate, *Flames, *Heat flux, Ignition temperature, Ignition time, Models, Thermoplastic resins, Polymethyl methacrylate, Fire tests, Theses, Black Polycast PMMA, Cone calorimeter.

Ignition and burning rate data are developed for thick (25 mm.) black Polycast PMMA in a Cone Calorimeter heating assembly. The objective is to establish a testing protocol that will lead to the prediction of ignition and burning rate from Cone data. This is done for a thermoplastic like PMMA. For black PMMA, ignition temperatures of 250 to 350 deg C and vaporization temperatures of approximately 325 to 380 deg C were measured over irradiance levels of 15 to 65 kW/sq m. The incident flame heat flux, for irradiation levels of 0

to 75 kW/sq m, is found to be approximately 37 kW/sq m for black PMMA. Its constancy is shown due to the geometry of the Cone flame.

00,394
PB95-217147 PC A08/MF A02
Maryland Univ., College Park. Dept. of Mechanical Engineering.
Water Droplet Evaporation from Radiantly Heated Solids.
Final rept. Sep 92-May 94.
S. Tinker, and M. di Marzo. Dec 94, 157p, NIST/GCR-95/665.
Contract NIST-70NANB1H1173
Sponsored by National Inst. of Standards and Technology (BFRL), Gaithersburg, MD. Fire Safety Engineering Div.

Keywords: *Drops(Liquids), *Evaporative cooling, *Radiant heating, *Solids, Evaporation, Heat transfer, Models, Sprinkler systems, Water sprays, Dissolved gases, Computer programs, Surface temperature, Thermal conductivity, Vaporizing, Contact angle.

A model describing the configuration of a water droplet evaporating on the surface of a radiantly heated semi-infinite solid is developed. A shape factor and the solid-liquid-vapor contact angle described the transient droplet shape, though the initial value of the latter parameter is found to have a negligible effect on the droplet's evaporation. The droplet shape model and a modified radiation heat term are incorporated into a previously-developed computer model to predict the evaporation of a single droplet on a semi-infinite solid subjected to radiant heat input. The code predicts transient temperature profiles that agree well with experiment.

00,395
PB95-220455 PC A03/MF A01
National Inst. of Standards and Technology (BFRL), Gaithersburg, MD. Building Materials Div.
Testing of Selected Self-Leveling Compounds for Floors.
C. F. Ferraris. Jan 95, 36p, NISTIR-5633.
Contract GSA-862-2500
Sponsored by General Services Administration, Washington, DC.

Keywords: *Lightweight concretes, *Construction materials, *Floors, Bonding, Office buildings, Technology utilization, Tests, Concretes, Shrinkage, Adhesives, Properties, Substitutes, Self-leveling compounds.

During the past year, a severe odor has developed in some floors of the Silver Spring Metro Center I building. The odor has been attributed to interactions among a self-leveling compound, carpet adhesive, and the carpet. The owner of the building, General Services Administration (GSA), wants to ascertain if by removing the existing self-leveling compound and replacing it with a compound of a different composition will elminate the odor. The National Institute of Standards and Technology (NIST) was asked to evaluate the properties of selected self-leveling compounds for use at the Silver Spring Metro Center I building. Lightweight concrete was also to be tested for possible use as a substrate for the self-leveling compounds. The report gives the test results obtained on the self-leveling compounds alone or in combination with regular concrete or lightweight concrete. It also gives the results obtained on lightweight concrete alone.

00,396
PB95-220489 PC A04/MF A01
National Inst. of Standards and Technology (BFRL), Gaithersburg, MD. Building Materials Div.
Survey of Concrete Transport Properties and Their Measurement.
N. S. Martys. Feb 95, 52p, NISTIR-5592.

Keywords: *Concretes, *Transport properties, *Service life, *Standards, Permeability, Microstructure, Test methods, Chlorides, Porosity, Tomography, X ray analysis.

In this report we present a survey of the current knowledge of the transport properties of concrete. The basic theory and measurement methods are discussed. Emphasis is placed on transport properties, such as diffusion, permeability, and capillary flow, that may play a large role in degradation processes in high performance concrete. It is concluded that standard test methods used to predict the service life of concrete via measurement of transport properties, especially in high performance concrete, are in general, inadequate or need further development.

00,397
PB95-220497 PC A03/MF A01
National Inst. of Standards and Technology (BFRL), Gaithersburg, MD.
Compositional Analysis of Beneficiated Fly Ashes.
P. E. Stutzman, and L. Centeno. May 95, 28p, NISTIR-5598.

Keywords: *Fly ash, *Concretes, *Physical properties, Admixtures, Particle size.

The study is part of a study of the material properties of fly ashes and other mineral admixtures to identify factors that control the performance of mineral admixtures in concrete. The study includes the determination of the kinetics of reactions, development of microstructure, and simulation modelling. The development of microstructure, and simulation modelling. The overall goal is understanding of how the material properties of fly ash affect the properties and durability of concrete. The report examines the composition of a set of fly ashes segregated by particle size, and comments on the effects of compositional and physical attributes on the performance of concrete.

00,398
PB95-226684 PC A07/MF A02
National Inst. of Standards and Technology (BFRL), Gaithersburg, MD. Fire Safety Engineering Div.
Building and Fire Research Laboratory Publications, 1994.
Special pub.
N. H. Jason. May 95, 132p, NIST/SP-838/7.
Also available from Supt. of Docs. See also report for 1993, PB95-143202.

Keywords: *Buildings, *Fires, *Bibliographies, *Research, Combustion, Fire protection, Abstracts, Flammability, Construction materials, Heat transfer.

Building and Fire Research Laboratory Publications, 1994 contains references to the publications prepared by the members of the Building and Fire Research (BFRL) staff, by other National Institute of Standards and Technology (NIST) personnel for BFRL, or by external laboratories under contract or grant from the BFRL during the calendar year 1994.

00,399
PB95-251617 PC A03/MF A01
National Inst. of Standards and Technology (BFRL), Gaithersburg, MD. Building Environment Div.
Water-Vapor Measurements of Low-Slope Roofing Materials.
D. M. Burch, and A. O. Desjarlais. 1995, 34p, NISTIR-5681.
Sponsored by Oak Ridge National Lab., TN.

Keywords: *Moisture, *Isotherms, *Roofing, *Permeability, Water vapor, Moisture content, Humidity, Construction materials, Test methods.

New measurement methods recently developed at the National Institute of Standards and Technology were used to measure the sorption isotherm and permeability of several low-slope roofing materials at a mean temperture of 24 deg C (75 F). The materials included: fireboard, perlite board, exterior-grade plywood, polyisocyanurate board insulation with glass-matt facers, and glass-fiber insulation with a facer. For the sorption isotherm measurements, the materials were placed in various ambient relative humidities ranging from a dry to a saturated state. The equilibrium moisture content plotted versus ambient relative humidity at 24 deg C (75 F) gave the sorption isotherm. Separate sorption isotherms were obtained for specimens initially dry (adsorption isotherm) and specimens initially saturated (desorption isotherm). For the permeability measurements, a series of cup measurements was performed, and the permeability was plotted as a function of the mean relative humidity across the specimen.

00,400
PB95-270047 PC A10/MF A03
National Inst. of Standards and Technology (BFRL), Gaithersburg, MD.
Project Summaries 1995: NIST Building and Fire Research Laboratory.
Special pub.
N. J. Raufaste. Aug 95, 218p, NIST/SP-838/8.
Also available from Supt. of Docs. as SN003-003-03350-2. See also report for 1994, PB94-207495.

Keywords: *Building, *Fires, *Research management, *Testing laboratories, Building codes, Fire safety, Flammability testing, Standards, Construction materials.

NIST's Building and Fire Research Laboratory (BFRL), one of NIST's eight Laboratories, enhances the competitiveness of U.S. industry and public safety through performances prediction and measurement technologies and technical advances that improve the life cycle quality of constructed facilities. BFRL's efforts are closely coordinated with complementary activities of industry, professional and trade organizations, academe, and other agencies of government. This report summarizes BFRL's research for 1995. The report is arranged by its research programs; structural engineering, materials engineering, mechanical and environmental systems, fire safety and engineering, fire science, and applied economics. Each summary lists the project title, the BFRL point of contact, sponsor, research, and recent results.

00,401
PB96-109541 PC A04/MF A01
National Inst. of Standards and Technology (BFRL), Gaithersburg, MD. Fire Safety Engineering Div.
CFAST Output Comparison Method and Its Use in Comparing Different CFAST Versions.
D. M. Alvord. Aug 95, 52p, NISTIR-5705.
See also PB93-174902.

Keywords: *Computer models, *Fires, *Flame propagation, *Building, Smoke, Plums, Fire test, Combustion products, Transport properties, Algorithms, Variables, Computerized simulation, Comparison, CFAST computer model.

A multiple step method was developed to compare the output of CFAST simulations, produced either by the same version of CFAST, or by different versions of the model. Scenarios to be compared are run with CFAST before the method is used, producing files containing a history of the model results. The first step of the comparision method produces a text file of important output variables from each of these history files, corresponding to significant fire phenomena occuring during the course of each fire simulation. The next step of the method is used to compare two such text files, and store their differences. Finally, the last step summarizes the difference information found in one or more files from the previous step. The comparison method can be used to find differences between CFAST runs, and track changes in the CFAST model and detect if they perform as anticipated.

00,402
PB96-122130 (Order as PB96-117767, PC A08/MF A02)
National Inst. of Standards and Technology, Gaithersburg, MD.
Study on the Reuse of Plastic Concrete Using Extended Set-Retarding Admixtures.
C. Lobo, W. F. Guthrie, and R. Kacker. 1995, 15p.
Prepared in cooperation with National Ready Mixed Concrete Association, Silver Spring, MD.
Included in Jnl. of Research of the National Institute of Standards and Technology, v100 n5 p575-589 Sep/Oct 95.

Keywords: *Plastic concrete, *Admixtures, Recycling, Shrinkage, Process variables, Stabilizers(Agents), Environmental issues, Strength, Reprints, NIST(National Institute of Standards and Technology).

The disposal of ready mixed concrete truck wash water and returned plastic concrete is a growing concern of the ready mixed concrete industry. Recently, extended set-retarding admixtures, or stabilizers, which slow or stop the hydration of portland cement have been introduced to the market. In a statistically designed experiment, the properties of blended concrete containing stabilized plastic concrete were evaluated. The variables in the study included (1) concrete age when stabilized, (2) stabilizer dosage, (3) holding period of the treated (stabilized) concrete prior to blending with fresh ingredients, and (4) amount of treated concrete in the blended batch. The setting time, strength, and drying shrinkage of the blended concretes were evaluated.

00,403
PB96-123419 Not available NTIS
National Inst. of Standards and Technology (BFRL), Gaithersburg, MD. Building Materials Div.
Hydraulic Radius and Transport in Reconstructed Model Three-Dimensional Porous Media.
Final rept.
D. P. Bentz, and N. S. Martys. 1994, 18p.
Pub. in Transportation in Porous Media, v17 p221-238 1995.

Keywords: *Building technology, *Porous media, *Hydraulic radius, Conductivity, Critical diameter, Permeability, Reconstruction, Reprints, *Foreign technology.

Methods for reconstructing three-dimensional porous media from two-dimensional cross sections are evaluated in terms of the transport properties of the reconstructed systems. Two-dimensional slices are selected at random from model three-dimensional microstructures, based on penetrable spheres, and processed to create a reconstructed representation of the original system. Permeability, conductivity, and a critial pore diameter are computed for the original and reconstructed microstructures to assess the validity of the reconstruction technique. A surface curvature algorithm is utilized to further modify the reconstructed systems by matching the hydraulic radius of the reconstructed three-dimensional system to that of the two-dimensional slice. While having only minor effects on conductivity, this modification significantly improves the agreement between permeabilities and critical diameters of the original and reconstructed systems for porosities in the range of 25-40%. For lower porosities, critical pore diameter is unaffected by the curvature modification so that little improvement between original and reconstructed permeabilities is obtained by matching hydraulic radii.

00,404
PB96-147111 Not available NTIS
National Inst. of Standards and Technology (BFRL), Gaithersburg, MD. Fire Safety Engineering Div.
Computing the Effect of Sprinkler Sprays on Fire Induced Gas Flow.
Final rept.
G. P. Forney, and K. B. McGrattan. 1995, 6p.
Pub. in Proceedings of the International Conference of Fire Research and Engineering, Orlando, FL., September 10-14, 1995, p59-64.

Keywords: *Sprinklers, *Time lapse, *Fire suppression, Fire protection, Gas flow, Fluid flow, Fire tests, Simulation, Walls, Flame propagation, Smoke detectors, Fire fighting, Reprints.

Over the past twenty years there has been much debate concering the interaction of sprinklers and draft curtains in large storage facilities. At issue is whether or not the two fire protection systems are mutually beneficial. Draft curtains inhibit the spread of hot gases near the ceiling. In some cases this may accelerate the activation of sprinklers and in others it could delay the activation of sprinklers needed to suppress the fire. The intent is not necessarily to simulate in detail the two phase interaction of droplets and air from a single sprinkler, nor to predict the suppression of the fire itself, but rather to study the effect of dozens of sprinklers on a fire-driven flow field in enclosures up to 60 meters on a side and 10 meters high. The sprinkler spray serves to cool the upper layer hot gases by mechanical mixing with cooler gases below and absorption of heat by the droplets.

00,405
PB96-154836 PC A06/MF A01
National Inst. of Standards and Technology (BFRL), Gaithersburg, MD. Structures Div.
Simplified Design Procedure for Hybrid Precast Concrete Connections.
G. S. Cheok, W. C. Stone, and S. D. Nakaki. Feb 96, 91p, NISTIR-5765.
Sponsored by Concrete Research Council, Detroit, MI.

Keywords: *Earthquake resistant structures, *Precast concrete, *Construction joints, *Beams(Supports), Design criteria, Buildings, Dynamic response.

A design procedure is presented to compute the maximum (plastic) moment, and the story drift capacities of a hybrid precast moment-resisting beam-to-column connection. The hybrid connections consist of mild steel which is used to dissipate energy by yielding and high strength prestressing steel which is used to provide the shear resistance through friction developed at the beam-column interface by the post-tensioning force. The design procedure is based on three 1/3-scale hybrid precast beam-to-column connections tested at the National Institute of Standards and Technology (NIST). The simplified procedure relies on the stess-strain behavior of mild steel up to its ultimate strength and is based on equilibrium equations at the beam-column joint. The appendices include a proposed evaluation criteria for this hybrid connection, sample calculations using the design procedure, and other calculations used to develop the design criteria.

00,406
PB96-156161 Not available NTIS
National Inst. of Standards and Technology (BFRL), Gaithersburg, MD. Building Materials Div.
Application of Digital-Image-Based Models to Microstructure, Transport Properties, and Degradation of Cement-Based Materials.
Final rept.
D. P. Bentz, E. J. Garboczi, and N. S. Martys. 1996, 19p.
Pub. in Modelling Microstructure and Its Potential for Studying Transport Properties and Durability, p167-185 1996.

Keywords: *Cements, *Construction materials, Percolation, Transport properties, Microstructure, Durability, Reprints, *Foreign technology.

As multi-phase composites, cement-based materials have physical properties that are strongly influenced by the volume fractions and topologies of the individual phases. Because of their inherent random nature, these materials often defy a simple geometrical description. The use of digital-image-based models allows one to realistically represent this class of materials, as resultant microstructures can be quickly quantified with respect to the volume fraction and interconnectivity or percolation of each phase or any combination of phases. In addition, physical properties such as diffusivity and permeability can be conveniently computed using finite-difference or finite-element techniques. These computer modelling techniques will be demonstrated for microstructural models of these materials at two scales: hydrated cement past at the micrometer level and calcium silicate hydrate gel at the nanometer level. The properties computed for the gel at the nanometer level can be used as input for the micrometer-level model.

00,407
PB96-159652 Not available NTIS
National Inst. of Standards and Technology (BFRL), Gaithersburg, MD. Fire Safety Engineering Div.
Fire Hazard Model Developments and Research Efforts at NIST.
Final rept.
A. J. Fowell. 1993, 7p.
Pub. in Fire Retardant Chemicals Association Meeting Proceedings on Fire Safety, New Orleans, LA., March 21-24, 1993, 7p.

Keywords: *Fire hazards, *Computerized simulation, Fire tests, Fire research, Fire safety, Combustion, Ventilation, Flammability testing, Burning rate, Materials tests, Standards, Reprints, *US NIST, *Fire Models.

Exposure conditions such as location, orientation, ventilation, and proximity to other materials can influence the fire performance of the material, so these parameters must be addressed by the models and/or the flammability characteristics measurements. Before the combination of fire models and bench scale measurement methods become universally accepted as tools for assessing the fire safety suitability of materials for specific aplication, the models must be shown to be valid, some of the shortcomings in the measurement methods need to be addressed and a usable data base needs to be assembled.

00,408
PB96-164066 Not available NTIS
National Inst. of Standards and Technology (BFRL), Gaithersburg, MD. Fire Science Div.
Heat Transfer in an Intumescent Material Using a Three-Dimensional Lagrangian Model.
Final rept.
K. M. Butler, H. R. Baum, and T. Kashiwagi. 1996, 6p.
Pub. in International Conference on Fire Research and Engineering, Orlando, FL., September 10-15, 1995, p261-266.

Keywords: *Bubbles, *Intumescence, Mathematical models, Numerical analysis, Thermoplastics, Reprints.

Intumescence is a property of an important class of fire-resistant materials. In the presence of fire, a succession of chemical reactions results in melting, the generation of multiple tiny bubbles causing the material to swell, and solidification into a thick multicellular char layer. An intumescent coating protects the underlying substrate from the fire through two mechanisms: heat is absorbed by the endothermic chemical reactions that produce the bubbles, and the low thermal conductivity of the bubbles provides an insulating layer. The chemical mechanism causes a plateau in the plot of substrate temperature vs. time, and the decreased effective thermal conductivity slows the temperature increase with time for the final char layer.

00,409
PB96-164108 Not available NTIS
National Inst. of Standards and Technology (BFRL), Gaithersburg, MD. Fire Safety Engineering Div.
Calculating Combined Buoyancy- and Pressure-Driven Flow Through a Shallow, Horizontal, Circular Vent; Application to Problem of Steady Burning in a Ceiling-Vented Enclosure.
Final rept.
L. Y. Cooper. 1995, 6p.
See also PB96-164116.
Pub. in International Conference on Fire Research and Engineering Proceedings, Orlando, FL., September 10-15, 1995, p321-326.

Keywords: *Vents, *Air flow, *Buoyancy, *Flame propagation, Fire protection, Buildings, Mathematical models, Flow rate, Reprints.

A model was developed previously for calculating combined buoyancy- and pressure-driven (i.e., forced) flow through a shallow, circular, horizontal vent where the vent-connected spaces are filled with fluids of different density in an unstable configuration (density of the top fluid is larger than that of the bottom). In this paper the model equations are summarized and then applied to the problem of steady burning in a ceiling-vented enclosure where normal atmospheric conditions characterize the upper space environment. Such fire scenarios are seen to involve a zero-to-relatively-moderate cross-vent pressure difference and bi-directional exchange flow between the enclosure and the upper space. A general solution to the problem is obtained. This relates the rate of energy release of the fire to the area of the vent and to the temperature and oxygen concentration of the upper portion of the enclosure environment. The solution is seen to be consistent with previously-published data involving ceiling-vented fire scenarios.

00,410
PB96-164116 Not available NTIS
National Inst. of Standards and Technology (BFRL), Gaithersburg, MD. Fire Safety Engineering Div.
Combined Buoyancy and Pressure-Driven Flow Through a Shallow, Horizontal, Circular Vent.
Final rept.
L. Y. Cooper. 1995, 9p.
See also PB96-164108 and PB94-210077.
Pub. in American Society of Mechanical Engineers International Mechanical Engineering Congress and Exhibition, Chicago, IL., November 6-11, 1994, Jnl. of Heat Transfer, v117 p659-667 Aug 95.

Keywords: *Vents, *Air flow, *Buoyancy, *Flame propagation, Boundary conditions, Reprints, Fire protection, Buildings, Mathematical models, Flow rate, Boundary value problems.

Combined buoyancy and pressure-driven (i.e., forced) flow through a horizontal vent is considered where the vent-connected spaces are filled with fluids of different density in an unstable configuration (density of the top is larger than that of the bottom). With zero-to-moderate cross-vent pressure difference, delta p, the instability leads to bidirectional exchange flow between the two spaces, e.g., as in the emptying from the bottom of a liquid-filled can with a single vent opening. For relatively large delta p, the flow through the vent is unidirectional, from the high to the low-pressure space, e.g., as is the case when the can has a large enough second vent at the top. Problems of a commonly used unidirectional orifice vent flow model, with Bernoulli's equation and a constant flow coefficient, Cd, are discussed.

00,411
PB96-193651 PC A03/MF A01
National Inst. of Standards and Technology (BFRL), Gaithersburg, MD. Building Materials Div.
Warping of Terrace Pavers at the U.S. Capitol Building.
C. F. Ferraris, P. Stutzman, and J. Clifton. May 96, 26p, NISTIR-5847.

Keywords: Construction materials, Aggregates, Cements, Concretes, Alkali aggregate reactions, Concrete durability, Chemical reactivity, Composition, Silicon dioxide, Environmental effects, Expansion, Shrinkage, Overlays, Substrates, Washington DC, *Pavers,

*United States Capitol, *Warping, Alkali-silica reactions.

The terraces of the U.S. Capitol are covered with cement-based pavers designed to emulate the granite pavers used elsewhere on the Capitol grounds. These pavers are composed of two layers; an upper, decorative white-cement-based mortar with crushed micaceous quartz aggregate supported by a base of conventional concrete. Field inspection and laboratory testing indicates that warping is probably due to the high cement content, environmental exposure conditions, and possibly differences in hydraulic length changes of two layers comprising the pavers. Alkali-silica reactivity (ASR) tests indicate that the base layer aggregate is marginally reactive and the upper layer aggregate is non-reactive.

00,412
PB96-193693 PC A04/MF A01
National Inst. of Standards and Technology (BFRL), Gaithersburg, MD. Building Environment Div.
Room-Temperature Thermal Conductivity of Expanded Polystyrene Board for a Standard Reference Material.
R. R. Zarr, M. W. Davis, and E. H. Anderson. May 96, 45p, NISTIR-5838.

Keywords: *Thermal insulation, *Standards, *Polystyrene, Building materials, Tests, SRM(Standard Reference Material).

Thermal conductivity measurements at room temperature are presented as the basis for certified values of SRM 1453, expanded polystyrene board. The measurements have been conducted in accordance with a randomized full factorial experimental design with two variables, bulk density and temperature, using NIST's one-meter line-heat-source guarded hot plate apparatus. Uncertainties of the measurements, consistent with current ISO guidelines, have been prepared. The thermal conductivity measurements were conducted over a range of bulk density of 37.4 to 45.8 km/cu m and mean temperature of 281 to 313 K. Statistical analyses of the physical properties of the SRM are presented and include variations between boards, as well as within boards. Measurements of the foam's compressive properties and microstructure are presented.

00,413
PB96-202239 PC A09/MF A02
National Inst. of Standards and Technology (BFRL), Gaithersburg, MD.
NIST Construction Automation Program Report No. 2. Proceedings of the NIST Construction Automation Workshop. Held in Gaithersburg, Maryland on March 30-31, 1995.
W. C. Stone. May 96, 159p, NISTIR-5856.

Keywords: *Meetings, *Buildings, *Automation, *Robotics, *Construction, Excavation, Data exchange, Laser metrology, Global positioning system, Telemetry, Virtual reality, Display systems, Wireless communications, Optical detectors, Standards, *Helmet mounted displays.

A two-day workshop on Construction Automation was hosted at NIST from March 30-31, 1995. Research programs actively underway at NIST in this area include the development of sensing systems, hardware, and software algorithms for advanced real-time construction site metrology; wide band telemetry and data acquisition (the ability to track many sensors at once through wireless communications); virtual site simulation and object representation standards (development of robust virtual reality models for construction site objects and machines); person-in-loop systems including head-up displays, virtual simulators, tele-operations workstations, and portable database interrogators which provide information-on-demand to construction site personnel; and semi-autonomous machine operations. These topics, and the need for database and machine interfacing standards, were discussed by workshop participants representing industry, government, and academe. Specific invited presentations included laser distancing, non-line-of-sight and kinematic GPS metrology, automated data exchange standards, real-time kinematic modeling, military helmet-mounted displays, virtual reality displays, construction robotics, automated excavation, virtual site representation, and automated building construction.

00,414
PB96-202338 PC A04/MF A01
National Inst. of Standards and Technology (BFRL), Gaithersburg, MD. Building Materials Div.
Measurement of Rheological Properties of High Performance Concrete: State of the Art Report.
C. F. Ferraris. Jul 96, 41p, NISTIR-5869.

Keywords: *Concretes, *Rheological properties, Test methods, Viscosity, Cements, Slumping, Workability.

The rheology or flow properties of concrete in general and of high performance concrete (HPC) in particular, is important, because many factors such as ease of placement, consolidation, durability, and strength depend on the flow properties. This report gives an overview of the flow properties of a fluid or a suspension, followed by a critical review of the most often used tests for concrete rheology. Particular attention is given to tests that could be used for HPC. Tentative definitions of terms such as workability, consistency, and rheological parameters are provided. An overview of the most promising tests and models for cement paste is given.

00,415
PB97-111892 Not available NTIS
National Inst. of Standards and Technology (BFRL), Gaithersburg, MD. Building Environment Div.
Test Procedures for Advanced Insulation Panels.
Final rept.
A. H. Fanney, C. A. Saunders, and S. D. Hill. 1995, 13p.
Pub. in Superinsulations and the Building Envelope, Washington, DC., November 14, 1995, p149-161.

Keywords: *Panels, *Thermal insulation, *Heat transfer, *Test methods, Wallboard, Calorimeters, Flowmeters, Moisture proofing, Humidity, Procedures, Reprints.

The National Institute of Standards and Technology (NIST) has undertaken a research program to develop thermal measurement techniques appropriate for advanced insulation panels. The paper describes the design of a calorimetric apparatus, compares the calorimetric results to measurements made using a heat flow meter apparatus for homogenous materials, and describes the procedure used to determine the thermal resistance of an advanced insulation panel. Finite-element modeling results are presented which show the effect of various physical parameters on the overall thermal resistance of a metal-clad powder-filled vacuum insulation system.

00,416
PB97-111991 Not available NTIS
National Inst. of Standards and Technology (BFRL), Gaithersburg, MD. Building Environment Div.
Empirical Validation of a Transient Computer Model for Combined Heat and Moisture Transfer.
Final rept.
C. Rode, and D. M. Burch. 1995, 13p.
Pub. in 'Thermal VI' Thermal Performance of the Exterior Envelopes of Buildings VI, Clearwater Beach, FL., December 4-8, 1996, p283-295 1995.

Keywords: *Wallboards, *Heat transfer, *Moisture content, *Computer models, Panels, Building materials, Water vapor, Condensation, Diffusion, Transient response, Transfer functions, Reprints.

A computer program for transient modeling of combined heat and moisture transfer in building constructions is introduced. The model's predictions are compared against moisture content and heat flux data obtained for six typical North American lightweight wall constructions that have been exposed to climatic conditions in a calibrated hot box. The experiment, and thus the validation, was restricted to diffusive transport mechanisms taking place in the hygroscopic region.

00,417
PB97-118996 Not available NTIS
National Inst. of Standards and Technology (BFRL), Gaithersburg, MD. Building Environment Div.
Line-Heat-Source Guarded-Hot-Plate Apparatus.
Final rept.
R. R. Zarr, and M. H. Hahn. 1995, 32p.
See also PB95-181202.
Pub. in Line-Heat-Source Guarded-Hot-Plate Apparatus, ASTM C 1043, 32p Dec 95.

Keywords: *Design, *Construction, Heat meters, Thermal insulation, Thermal conductivity, Heat transmission, Thermodynamic properties, Thermal measurement, Reprints, *Line heat sources, *Guarded hot plate.

The adjunct describes the line-heat-source guarded-hot-plate apparatus fabricated by the National Institute of Standards and Technology. It is intended as a guide in the design and construction of a guarded hot plate having circular line heat sources. The essential requirements for steady-state testing of heat insulators are described in ASTM Test Method C 177 and the essential requirements for the design of guarded hot plates having circular line-heat sources are covered in ASTM Practice C 1043.

00,418
PB97-121339 Not available NTIS
National Inst. of Standards and Technology (BFRL), Gaithersburg, MD. Building Materials Div.
Computer Simulations of Binder Removal from 2-D and 3-D Model Particulate Bodies.
Final rept.
J. A. Lewis, M. A. Galler, and D. P. Bentz. 1996, 12p.
Pub. in Jnl. of the American Ceramic Society, v79 n5 p1377-1388 1996.

Keywords: *Binders, *Thermoplastic resins, *Particulates, *Removal, Plasticizers, Microstructure, Liquid phases, Porosity, Transport properties, Isothermal processes, Two dimensional models, Three dimensional models, Computerized simulation, Reprints.

A series of computer simulations were developed to investigate the removal of multicomponent, thermoplastic binders from two- and three-dimensional model particulate bodies. Monosized particles with varying diameters were randomly placed in such systems, and all unoccupied pixels were assigned to the binder phase at ratios of 1:9, 1:2, or 1:1 plasticizer (volatile) to polymeric (nonvolatile) species. Simulations were carried out under isothermal conditions to study the influence of liquid-phase transport processes, i.e., plasticizer diffusion in the binder-filled pore network and capillary-driven redistribution of the binder phase, on plasticizer removal rates. Plasticizer diffusion was modeled by a random-walk algorithm, and nonplanar pore development arising from capillary-driven binder redistribution was modeled by an invasion percolation algorithm. For comparison, simulations were also carried out on systems in which binder redistribution was not permitted.

00,419
PB97-122535 Not available NTIS
National Inst. of Standards and Technology (BFRL), Gaithersburg, MD. Building Environment Div.
Parametric Study of Wall Moisture Contents Using a Revised Variable Indoor Relative Humidity Version of the 'Moist' Transient Heat and Moisture Transfer Model.
Final rept.
G. Tsongas, D. Burch, C. Roos, and M. Cunningham. 1995, 13p.
Pub. in 'Thermal VI' Thermal Performance of the Exterior Envelopes of Buildings VI, Clearwater Beach, FL., December 4-8, 1996, p307-319 1995.

Keywords: *Relative humidity, *Moisture content, *Walls, Water vapor, Wallboards, Panels, Condensation, Diffusion, Heat transfer, Building materials, Winter, Computer models, Computerized simulation, Reprints, *Indoor environments, Moisture transfer, MOIST computer model.

The authors modified the model to calculate the hourly indoor relative humidity during the heating season as a function of outdoor weather conditions, indoor air temperature, building size and airtightness, and indoor moisture generation rate. This enhanced version of MOIST was subsequently used to investigate moisture accumulation in a 5-cm by 15-cm (2-in. by 6-in.) wood-framed wall exposed to a number of different winter climates. Predictions with a constant indoor relative humidity were compared to those with a 'floating' or variable indoor relative humidity. In addition, the variable indoor relative humidity program was used to analyze the effect of building airtightness, the indoor moisture generation rate, and the existence of exfiltration. The need for an interior vapor retarder in walls exposed to cold climates also was examined. Moreover, the effects of exterior insulating sheathing and an exterior vapor retarder were modeled. Results and findings are presented along with pertinent conclusions regarding appropriate building construction techniques in winter heating climates.

Structural Analyses

00,420
PB94-159779 PC A04/MF A01
National Inst. of Standards and Technology (BFRL), Gaithersburg, MD. Center for Building Technology.
Seismic Instrumentation of Existing Buildings.
Final rept.
L. T. Phan. Oct 90, 62p, NISTIR-4419.
Contract GSA/PBS-87-03
Sponsored by Public Buildings Service, Washington, DC. Office of Real Property Development.

Keywords: *Federal buildings, *Earthquake engineering, US GSA, Seismic design, Dynamic structural analysis, Instruments, Computerized simulation, Portland(Oregon), Long Beach(California).

Two existing GSA buildings, one in Long Beach, California, and one in Portland, Oregon, were subjected to low-level vibration tests to determine their dynamic properties and response frequencies. The measured dynamic properties of the buildings were incorporated into the computer models of the buildings and time-history analyses using these models were performed. The purpose of the analyses is to reveal building response under these realistic earthquake excitations, so that logical seismic instrumentation schemes can be developed for these buildings. The results of the analyses suggest that the response of the Portland building is influenced more by torsional and rocking motions, while the response of the Long Beach building is influenced mainly by translational modes. From the observed behavior of the buildings, a seismic instrumentation scheme is developed for each building, and a general guideline for seismic instrumentation in existing building is recommended.

00,421
PB94-161114 PC A09/MF A02
National Inst. of Standards and Technology (BFRL), Gaithersburg, MD. Structures Div.
Northridge Earthquake, 1994. Performance of Structures, Lifelines and Fire Protection Systems.
D. Todd, N. Carino, R. M. Chung, W. D. Walton, H. S. Lew, and A. W. Taylor. Mar 94, 176p, NISTIR-5396.

Keywords: *Earthquakes, *Damage assessment, *California, Buildings, Bridges(Structures), Office buildings, Freeways, Apartment buildings, Los Angeles(California), Northridge(California).

A magnitude 6.8 (MS) earthquake centered under the community of Northridge in the San Fernando Valley shook the entire Los Angeles metropolitan area at 4:31 a.m. local time Monday, January 17, 1994. Moderate damage to the built environment was widespread; severe damage included collapsed buildings and highway overpasses. A total of 58 deaths were attributed to the earthquake by the Los Angeles Coroner. About 1,500 people were admitted to hospitals with major injuries; another 16,000 or so were treated and released. Estimates indicated that this will be the United States' most costly natural disaster ever. A multi-agency team, organized under the auspices of the Interagency Committee on Seismic Safety in Construction and headed by the National Institute of Standards and Technology, arrived at the earthquake site within days of the event to document the effects of the earthquake. The team focused on the effects to the built environment, with the goal of capturing perishable data and quickly identifying situations deserving in-depth study. The report includes a summary of the team's observations. While most structural damage occurred in buildings and bridges of construction type and vintage known to be vulnerable to earthquake shaking, there were some unexpected failures. Notable among these were the collapses of relatively modern parking structures and a bridge that appeared to be adequate by today's standards. Recommendations are made for further studies of the Northridge earthquake that can lead to improved mitigation of earthquake effects.

00,422
PB94-161734 PC A03/MF A01
National Inst. of Standards and Technology (BFRL), Gaithersburg, MD. Structures Div.
Draft Guidelines for Quality Control Testing of Elastomeric Seismic Isolation Systems.
H. W. Shenton. Feb 94, 33p, NISTIR-5345.
See also PB92-139732.

Keywords: *Vibration isolators, *Buildings, *Earthquake engineering, Seismic design, Quality control, Design criteria, Tests, Lateral forces.

Seismic isolation systems designed according to the 1991 Uniform Building Code, or the 1991 AASHTO Guide Specification for Seismic Isolation Design are required to undergo a series of prototype and quality control tests before being installed in the structure. At the present time standards do not exist for conducting these tests and results are subject to unknown variability. The document represents the initiation of the process to develop standards for quality control testing of seismic isolation systems built in the U.S. The guidelines are devoted specifically to quality control testing of elastomeric systems. The guidelines address material and component tests to be conducted during production, and tests on completed isolation units.

00,423
PB94-172947 Not available NTIS
National Inst. of Standards and Technology (BFRL), Gaithersburg, MD. Structures Div.
Draft Guideline for Testing and Evaluation of Seismic Isolation Systems.
Final rept.
H. W. Shenton. 1993, 6p.
Pub. in Proceedings of a Seminar on Seismic Isolation, Passive Energy Dissipation, and Active Control, San Francisco, CA., March 11-12, 1993, p349-354.

Keywords: *Vibration isolators, *Earthquake resistant structures, *Building codes, *Test methods, Standards, Structural vibration, Earthquake engineering, Damping, Energy dissipation, Reprints, *Seismic isolation systems.

The Building and Fire Research Laboratory of the National Institute of Standards and Technology is developing a draft guideline for testing and evaluation of seismic base isolation systems. This is a multi-year effort with the goal being the adoption of the guidelines by model code organizations and the Interagency Committee on Seismic Safety in Construction (ICSSC). A five member Oversight Committee has been formed to guide NIST in the development of the guidelines. The committee includes individuals from the research and private sectors with expertise in the design, fabrication and testing of seismic isolation components and hardware, and in the design of structures which incorporate seismic isolation. The draft guideline is intended to be general and comprehensive; it will be applicable to an isolation system regardless of the superstructure; it will be applicable to all viable systems, whether they be elastomeric, sliding or hybrid; and will be applicable to systems which consist of multiple isolator units, or incorporate different components that are distributed throughout the isolation interface. It will cover all pertinent structural evaluation tests of the isolation device. The objective and scope of the effort are described, along with a preliminary multi-year schedule. Progress to date is summarized.

00,424
PB94-176278 PC A08/MF A02
National Inst. of Standards and Technology (BFRL), Gaithersburg, MD.
Evaluation and Strengthening Guidelines for Federal Buildings: Identification of Current Federal Agency Programs.
Final rept.
C. D. Poland, W. T. Holmes, J. O. Malley, D. Provencher, and J. Soulages. Mar 94, 153p, NIST/GCR-94/649.
Prepared in cooperation with Interagency Committee on Seismic Safety in Construction. and Degenkolb (H.J.) Associates, San Francisco, CA. Sponsored by Federal Emergency Management Agency, Washington, DC.

Keywords: *Federal buildings, *Earthquake engineering, Seismic design, Standards, Building codes.

The National Institute of Standards and Technology (NIST), by order of the President, is developing seismic evaluation and strengthening guidelines (Guidelines for Federal Buildings) for federally owned and leased buildings. The project is overseen by the Interagency Committee on Seismic Safety in Construction (ICSSC) and funded by the Federal Emergency Management Agency (FEMA). The report develops Task 1, the identification of seismic mitigation programs. The report includes a detailed work plan and schedule for the entire project, a list of ICSSC member contacts, the results of telephone conversations with all ICSSC committee members to identify existing seismic strengthening programs, the results of detailed meetings with seven federal agencies and four private sector organizations selected for in-depth study, and summaries of the performance objectives for all agencies and organizations.

00,425
PB94-181856 PC A08/MF A02
National Inst. of Standards and Technology (BFRL), Gaithersburg, MD.
Evaluation and Strengthening Guidelines for Federal Buildings: Assessment of Current Federal Agency Evaluation Programs and Rehabilitation Criteria and Development of Typical Costs for Seismic Rehabilitation.
Final rept.
C. D. Poland, W. T. Holmes, J. R. Soulages, and D. L. Provencher. Mar 94, 162p, NIST/GCR-94/650.
Prepared in cooperation with Degenkolb (H.J.) Associates, San Francisco, CA. Sponsored by Federal Emergency Management Agency, Washington, DC.

Keywords: *Federal buildings, *Earthquake engineering, *Design standards, Seismic design, Public Law 101-614.

The National Institute of Standards and Technology (NIST), in accordance with Public Law 101-614, is developing seismic evaluation and strengthening guidelines (Guidelines for Federal Buildings) for federally-owned and leased buildings. The project is overseen by the Interagency Committee on Seismic Safety in Construction (ICSSC) and funded by the Federal Emergency Management Agency (FEMA). The report develops Task 2, (see Appendix A for complete scope of work) assessment of current federal agency evaluation programs and rehabilitation criteria and Task 3, development of typical costs for seismic rehabilitation. Part I of the Task 2 report includes a qualitative and quantitative comparison of six federal agency programs to the most recent versions of the NEHRP Evaluation Handbook and the NEHRP Techniques Handbook.

00,426
PB94-187648 PC A03/MF A01
National Inst. of Standards and Technology (BFRL), Gaithersburg, MD.
Strengthening Methodology for Lightly Reinforced Concrete Frames-II. Recommended Calculation Techniques for the Design of Infill Walls.
L. T. Phan, D. R. Todd, and H. S. Lew. May 94, 46p, NISTIR-5421.
See also PB94-161354.

Keywords: *Reinforced concrete, *Reinforcement(Structures), *Dynamic structural analysis, *Frames, Concrete structures, Loads(Forces), Shear strength, Earthquake engineering, Displacement, Dynamic response, Infilled walls.

Empirical equations were developed for estimations of ultimate lateral shear strength, story drift ratio at ultimate load, and ductility factor of existing lightly reinforced concrete frames (bare frames), existing monolithic shear walls, and reinforced concrete frames strengthened either by cast-in-place infilled walls or by single or multiple precast concrete panels. These equations were derived based on experimental results of many independently conducted test programs. Estimations of the ultimate shear stress, ultimate story drift ratio (story drift at ultimate load divided by story height), and ductility factor using the empirical equations compared favorably with the experimental results. The estimations confirm many observations made independently in individual test programs. The empirical expressions also provide benchmark values or ranges for these important parameters and thus provide a useful means for quick estimations of seismic capacity of bare, monolithic, and strengthened lightly reinforced concrete frames.

00,427
PB94-199981 Not available NTIS
National Inst. of Standards and Technology (BFRL), Gaithersburg, MD. Structures Div.
Dynamic Characteristics of Five Tall Buildings during Strong and Low-Amplitude Motions.
Final rept.
M. Celebi, L. T. Phan, and R. D. Marshall. 1993, 15p.
Pub. in Structural Design of Tall Buildings 2, p1-15 1993.

Keywords: *Structural vibration, *Buildings, *Dynamic response, *Seismic effects, *Soil-structure interactions, Earthquake damage, Earthquake engineering, Dynamic structural analysis, Data acquisition, Accelerometers, Earth movements, Reprints.

The objectives of the paper are to present (1) a comparison of dynamic characteristics of five buildings de-

termined from recorded strong-motion response data and from low-amplitude (ambient vibration) tests, and (2) a description of the low-amplitude ambient testing and PC-based data-acquisition approach that is integrated with the permanent strong-motion instrumentation in the five buildings. All five buildings are within the San Francisco Bay area and the strong-motion dynamic characteristics are extracted from the October 17, 1989 Loma Prieta earthquake response records. Ambient vibration tests on the same five buildings were conducted in September 1990. Analyses of strong-motion response and low-amplitude test data have been performed by many investigators. The present study differs from numerous previous investigations because (1) in the study, accelerometers in the five permanently-instrumented buildings were used during the low-amplitude testing, and (2) rapid screening of the strong-motion response data was achieved with a concerted use of system identification software. The results show for all cases that the fundamental periods and corresponding percentages of critical damping determined from low-amplitude tests are appreciably lower than those determined from strong-motion response records.

00,428
PB94-206125 PC A06/MF A02
National Inst. of Standards and Technology (BFRL), Gaithersburg, MD.
Wind Load Provisions of the Manufactured Home Construction and Safety Standards: A Review and Recommendations for Improvement.
R. D. Marshall. May 93, 107p, NISTIR-5189.
See also PB-297 463. Sponsored by Department of Housing and Urban Development, Washington, DC.

Keywords: *Wind loads, *Prefabricated buildings, Hurricanes, Florida, Damage assessment, Building codes, Computerized simulation, *Mobile homes, Hurricane Andrew, Dade County(Florida).

Limited wind speed measurements obtained during landfall of Hurricane Andrew in south Florida and wind speed estimates obtained from a computer-based model and from analyses are summarized and compared with code-specified design speeds for the affected area. Published reports of wind damage to manufactured homes and to conventional wood-framed dwellings are reviewed to identify modes of failure and intensity of damage. In general, manufactured homes which were built subsequent to issuance of the Manufactured Home Construction and Safety Standards (MHCSS) suffered less damage than did units built prior to issuance of the MHCSS.

00,429
PB94-216421 Not available NTIS
National Inst. of Standards and Technology (NEL), Gaithersburg, MD. Structures Div.
Lessons Learned by a Wing Engineer.
Final rept.
R. D. Marshall. 1991, 10p.
Pub. in Proceedings of Symposium and Public Forum on Hurricane Hugo One Year Later, Charleston, SC., September 13-15, 1990, p160-169 1991.

Keywords: *Wind pressure, *Building codes, *Damage assessment, Hurricanes, Wind effects, Structural analysis, Gust loads, Dynamic loads, Wind measurement, Wind velocity, Reprints, Hurricane Hugo.

Surface wind speeds during the passage of Hurricane Hugo through the U.S. Virgin Islands and Puerto Rico are described. Although damage to the affected areas was extensive, an assessment of relevant data indicates that the actual wind speeds were far lower than those reported by the news media. The consequences of overstating the wind speeds are examined and actions to improve the accuracy of measuring and reporting wind speeds are outlined.

00,430
PB95-108841 Not available NTIS
National Inst. of Standards and Technology (BFRL), Gaithersburg, MD. Structures Div.
Seismic Strengthening of Reinforced Concrete Frame Buildings.
Final rept.
L. T. Phan, D. R. Todd, and H. S. Lew. 1993, 10p.
Pub. in Proceedings of the National Earthquake Conference, Memphis, TN., May 2-5, 1993, v2 p235-244.

Keywords: *Reinforced concrete, *Reinforcement(Structures), *Earthquake resistant structures, *Structural response, Earthquake engineering, Structural analysis, Concrete structures, Seismic effects, Dynamic response, Frames, Reprints.

Most reinforced concrete (RC) frame structures in the mid-western and eastern regions of the United States are built mainly for gravity loads without proper seismic design, and thus are vulnerable to severe damage in the event of a major earthquake in these regions. While the need to retrofit these RC frame structures is recognized and different strengthening techniques have been laboratory-tested and applied in practice worldwide, ability to assess the relative merits of different strengthening schemes or to predict the improved performance of a strengthened structure is still lacking. The paper describes the development of experimental-based hysteresis models of unstrengthened and strengthened concrete frames by using the system identification method. The analytical models are validated by comparing the analytical results with results of experiments on strengthened RC frames.

00,431
PB95-130209 PC A06/MF A02
National Inst. of Standards and Technology (BFRL), Gaithersburg, MD. Structures Div.
Standards of Seismic Safety for Existing Federally Owned or Leased Buildings and Commentary.
D. R. Todd. Feb 94, 110p, NISTIR-5382.
See also PB92-205343. Prepared in cooperation with Interagency Committee on Seismic Safety in Construction. Sponsored by Federal Emergency Management Agency, Washington, DC. Mitigation Directorate.

Keywords: *Federal buildings, *Seismic design, Earthquake engineering, Building codes, Design standards, Safety engineering, Retrofitting.

These seismic evaluation and mitigation standards, Standards of Seismic Safety for Existing Federally Owned or Leased Buildings and Commentary, were developed for use by the Federal government by the Interagency Committee on Seismic Safety in Construction (ICSSC) in conjunction with the National Institute of Standards and Technology (NIST). The project was funded by the Federal Emergency Management Agency (FEMA). The intent of this document is to provide Federal agencies with minimum standards for the evaluation and mitigation of seismic hazards in their building inventories.

00,432
PB95-143129 PC A04/MF A01
National Inst. of Standards and Technology (BFRL), Gaithersburg, MD. Structures Div.
Manufactured Homes: Probability of Failure and the Need for Better Windstorm Protection through Improved Anchoring Systems.
Final rept.
R. D. Marshall. Nov 94, 64p, NISTIR-5370.
Contract DU100I93000037
See also PB94-206125. Sponsored by Department of Housing and Urban Development, Washington, DC.

Keywords: *Wind loads, *Prefabricated buildings, *Mobile homes, Hurricanes, Florida, Damage assessment, Building codes, Computerized simulation, Dade County(Florida).

The report describes a continuation of earlier studies carried out by the National Institute of Standards and Technology (NIST) at the request of the Department of Housing and Urban Development (HUD) following the devastation caused by Hurricane Andrew in south Florida on August 24, 1992. In the earlier work, damage to manufactured homes was examined in light of the probable maximum wind speeds in the affected area, and the wind load provisions of selected codes and standards used for structural design in hurricane-prone regions were compared. On the basis of that work, it was recommended that ASCE 7-88 (Minimum Design Loads for Buildings and Other Structures) should be the primary resource document for updating and improving the wind load provisions of the Manufactured Home Construction and Safety Standards (MHCSS).

00,433
PB95-147385 PC A99/MF A06
National Inst. of Standards and Technology (BFRL), Gaithersburg, MD.
Wind and Seismic Effects. Proceedings of the U.S.-Japan Cooperative Program in Natural Resources Panel on Wind and Seismic Effects (26th). Held in Gaithersburg, Maryland on May 17-20, 1994.
Special pub. (Final).
N. J. Raufaste. Sep 94, 732p, NIST/SP-871.
Also available from Supt. of Docs. as SN003-003-03297-2. See also PB93-120152.

Keywords: *Seismic effects, *Wind effects, *Structural engineering, *Dynamic structural analysis, *Meetings, Earthquake engineering, Design standards, Design criteria, Research programs, Dynamic loads, Structural vibration, Wind pressure, Wind loads, Earthquakes, Tsunamis, Storm surges, Foundations(Structures), Highway engineering, Bridges, Dams, Retrofitting, Earthquake resistant structures, Wind engineering.

The publication is the Proceedings of the 26th Joint Meeting of the U.S.-Japan Panel on Wind and Seismic Effects. The Proceedings include the program, list of members, panel resolutions, task committee reports, and 45 technical papers. The papers were presented under five themes: (1) Wind Engineering, (2) Earthquake Engineering, (3) Storm Surge and Tsunamis, (4) Joint Cooperative Research Program, and (5) Northridge Southern California and Hokkaido Nansei-Oki Earthquakes.

00,434
PB95-150918 Not available NTIS
National Inst. of Standards and Technology (BFRL), Gaithersburg, MD. Structures Div.
Evaluation and Retrofit Standards for Existing Federally Owned and Leased Buildings.
Final rept.
D. Todd. 1993, 5p.
Pub. in Proceedings of National Earthquake Conference, Memphis, TN., May 2-5, 1993, v2 p25-29.

Keywords: *Federal buildings, *Reinforcement(Structural), *Earthquake engineering, *Building codes, *Design standards, Earthquake resistant structures, Retrofitting, Seismic design, Reinforcing materials, Safety engineering, Design criteria, Dynamic structural analysis, Reprints, *Seismic safety.

Public Law 101-614 requires the Interagency Committee on Seismic Safety in Construction to develop 'standards for assessing and enhancing the seismic safety of existing buildings constructed for or leased by the Federal Government.' The paper describes the process that is being used to develop the standards; presents the results of an Issues Workshop held for potentially affected Federal agencies, at which philosophical and administrative concerns were addressed; and describes the anticipated content of the standard.

00,435
PB95-150926 Not available NTIS
National Inst. of Standards and Technology (BFRL), Gaithersburg, MD. Structures Div.
Some Basics on Who's Who and What's What in Seismic Safety.
Final rept.
D. Todd. 1992, 11p.
Pub. in Federal Construction Council Technical Report 120. Seismic Safety Technology and Regulations: A Look At the Near Future, p1-11 1992.

Keywords: *Earthquake engineering, *Safety engineering, *Acronyms, Seismic design, Earthquake resistance, Design criteria, Building codes, Design standards, Seismic effects, Dynamic structural analysis, Reprints, *Seismic safety, NEHRP(National Earthquake Hazards Reduction Program).

The tendency of both governments and engineers to form acronyms seems to reach an apex in the U.S. earthquake engineering community. The paper defines organization acronyms and presents short idiomatic and official titles of earthquake-related documents. The text uses a description of the Federal earthquake program, the world of building codes, and the history of the NEHRP Recommended Provisions to illustrate how many of these organizations and documents are related.

00,436
PB95-151809 Not available NTIS
National Inst. of Standards and Technology (BFRL), Gaithersburg, MD. Building and Fire Research Lab. Office.

Structural Analyses

Implementation of Executive Order 12699: Seismic Safety of Federal and Federally Assisted or Regulated New Building Construction.
Final rept.
R. N. Wright. 1992, 3p.
Pub. in Phenomenal News 3, n2 p12-14 Jan 92.

Keywords: *Federal buildings, *Public buildings, *Earthquake engineering, *Seismic design, *Safety engineering, Earthquake resistant structures, Federal aid, Building codes, Design standards, Design criteria, Structural response, Reprints, Seismic safety.

Losses of property approaches $10 billion, losses of 62 lives, and severe disruption of human activities from the October 17, 1989, Loma Prieta, California, earthquake reminded the United States of the severe threats posed by great earthquakes. Unless enhanced efforts are made to reduce earthquake hazards, a large earthquake close to a major metropolitan area can kill tens of thousands of people, cause tens of billions of dollars of direct property losses, and, through consequent losses, severely disrupt economic activity for the whole nation. 46 of the 50 states are vulnerable to strong earthquakes. In the eastern half of the country, the area that would be affected by an earthquake could be 10 times as large as for a similar earthquake in California.

00,437
PB95-151817 Not available NTIS
National Inst. of Standards and Technology (BFRL), Gaithersburg, MD. Building and Fire Research Lab. Office.
Structural Analysis in Context.
Final rept.
R. N. Wright. 1993, 6p.
Pub. in Proceedings of Structures Congress 93, Structural Engineering in Natural Hazards Mitigation, Irvine, CA., April 19-21, 1993, v2 p1657-1662.

Keywords: *Structural analysis, *Education, Structural engineering, Structural design, Design analysis, Students, Engineers, Reprints.

The issues of what students should learn about structural analysis and how it should be taught are explored considering the purposes of structural analysis in engineering practice and the motivation of structural engineering students. Structural analysis is considered to be the process by which the structure and its environment are modeled to predict structural response. Structural analysis is addressed as a process linked integrally to professional responsibilities such as design, review for safety and serviceability, construction, condition assessment of existing structures, performance investigations, modification and renovation.

00,438
PB95-153094 Not available NTIS
National Inst. of Standards and Technology (BFRL), Gaithersburg, MD. Structures Div.
Model Precast Concrete Beam-to-Column Connections Subject to Cyclic Loading.
Final rept.
G. S. Cheok, and H. S. Lew. 1993, 13p.
Pub. in PCI Jnl. 38, n4 p80-92 Jul/Aug 93.

Keywords: *Cyclic loads, *Precast concrete, *Columns(Supports), *Beams(Structural), *Structural analysis, *Joints(Junctions), *Model tests, Earthquake resistant structures, Dynamic loads, Concrete structures, Structural components, Energy dissipation, Structural design, Strands, Ductility, Displacement, Structural failure, Dynamic response, Reprints, *Beam-column joints.

Experimental results of eight 1/3-scale model precast concrete beam-to-column connections are presented. The test specimens consisted of interior connections designed in accordance with the 1985 Uniform Building Code provisions for Seismic Zones 2 and 4. These tests constitute the second and third phases of a multi-year test program being conducted at the National Institute of Standards and Technology. The objective of the test program is to develop guidelines for an economical precast beam-to-column connection for regions of high seismicity. Variables considered in the research program include location of the post-tensioning steel, the use of post-tensioning bars vs. prestressing strands and fully bonded vs. partially bonded strands. Specimens were subjected to reversed cyclic loading according to a prescribed displacement history. Comparison of results with the monolithic test specimens indicates that the post-tensioned precast concrete specimens had comparable connection strengths, higher ultimate displacement ductilities and total energy dissipation to failure, but lower energy dissipation per cycle.

00,439
PB95-153102 Not available NTIS
National Inst. of Standards and Technology (BFRL), Gaithersburg, MD. Structures Div.
Partially Prestressed and Debonded Precast Concrete Beam-Column Joints.
Final rept.
G. S. Cheok, W. C. Stone, and H. S. Lew. 1992, 9p.
Sponsored by Concrete Research Council, Detroit, MI.
Pub. in Proceedings of Meeting of the U.S.-Japan Joint Technical Coordinating Committee (3rd) on Precast Seismic Structural Systems, La Jolla, CA., November 18-20, 1993, p1-9.

Keywords: *Precast concrete, *Prestressing, *Beams(Structural), *Columns(Supports), *Model tests, *Structural analysis, *Cyclic loads, *Joints(Junctions), Concrete structures, Reinforcing materials, Structural components, Structural failure, Structural design, Strands, Earthquake resistant structures, Dynamic response, Energy dissipation, Ductility, Dynamic loads, Reprints, *Beam-column joints.

The experimental test results from three 1/3-scale model precast concrete beam-to-column connections is summarized. These tests are part of a multi-phased test program being conducted at the National Institute of Standards and Technology. The objective of the test program is to develop guidelines for an economical precast beam-to-column connection for regions of high seismicity. The test specimens were interior connections designed using the Uniform Building Code (ICBO, 1985 and 1988) criteria for seismic Zones 2 and 4 as design guidelines. Partially debonded strands were employed in two of the specimens and while the third combined low strength steel with post-tensioning steel. Specimens were subjected to reversed cyclic loading according to a prescribed displacement history. Comparisons are made between the behavior of these precast specimens with previous precast and monolithic specimens which were tested earlier. The comparisons were based on connection strength, connection ductility, and energy absorption characteristics.

00,440
PB95-153110 Not available NTIS
National Inst. of Standards and Technology (BFRL), Gaithersburg, MD. Structures Div.
Seismic Performance Behavior of Precast Concrete Beam-Column Joints.
Final rept.
G. S. Cheok, W. C. Stone, and H. S. Lew. 1993, 6p.
Pub. in Proceedings of American Society of Civil Engineers Structures Congress '93, Irvine, CA., April 19-21, 1993, v1 p83-88.

Keywords: *Precast concrete, *Prestressing, *Beams(Structural), *Columns(Supports), *Model tests, *Structural analysis, *Cyclic loads, *Joints(Junctions), Concrete structures, Reinforcing materials, Structural components, Structural failure, Structural design, Strands, Earthquake resistant structures, Dynamic response, Energy dissipation, Ductility, Dynamic loads, Reprints, *Beam-column joints.

The experimental test program being conducted at the National Institute of Standards and Technology on 1/3-scale model precast concrete beam-to-column connections is summarized. The objective of the test program is to develop guidelines for an economical precast beam-to-column connection for regions of high seismicity. The test specimens were interior connections designed using the Uniform Building Code (ICBO, 1985 and 1988) criteria for seismic Zones 2 and 4 as guidelines. To date, fifteen specimens have been tested. Variables in the study include location of the post-tensioning steel, the use of post-tensioning bars versus prestressing strands, fully bonded versus partially bonded strands, and the combination of low strength steel and post-tensioning. Specimens were subjected to reversed cyclic loading according to a prescribed displacement history. Comparisons are made between the behavior of these precast specimens with previous precast and monolithic specimens. The comparisons were based on connection strength, connection ductility, and energy absorption characteristics.

00,441
PB95-161360 Not available NTIS
National Inst. of Standards and Technology (CAML), Gaithersburg, MD. Statistical Engineering Div.
Assessment of 'Peaks Over Threshold' Methods for Estimating Extreme Value Distribution Tails.
Final rept.
J. A. Lechner, E. Simiu, and N. A. Heckert. 1993, 10p.
Pub. in Structural Safety 12, p305-314 1993.

Keywords: *Structural analysis, *Wind effects, *Extreme-value problems, Statistical analysis, Methodology, Comparison, Monte Carlo method, Simulation, Reprints, Peaks over threshold methods, CME(Conditional Mean Exceedance) methods.

In the past twenty years a vast new body of extreme value theory was developed, referred to as 'peaks over threshold modeling.' This theory allows the use in the analysis of all data exceeding a sufficiently high threshold, a feature that may result in improved extreme value estimates. The application of the theory depends upon the performance of methods for estimating the distribution parameters corresponding to any given set of extreme data. We present a comparative assessment of the performance of three such methods. The assessment is based on Monte Carlo simulations from populations with four distributions: Gumbel, Weibull, generalized Pareto, and normal. The simulation results showed that the de Haan and the Conditional Mean Exceedance (CME) methods performed consistently better than the Pickands method (NIST implementation). For the distributions, parameter values, and mean recurrence intervals assumed in this work, the CME method outperformed the de Haan method only when the percent estimation errors were about one percent or smaller, a case unlikely to be encountered in wind engineering practice.

00,442
PB95-164091 Not available NTIS
National Inst. of Standards and Technology (BFRL), Gaithersburg, MD. Building and Fire Research Lab. Office.
Lessons from the Loma Prieta Earthquake.
Final rept.
R. N. Wright. 1993, 18p.
Pub. in Proceedings of Joint Meeting UJNR Wind and Seismic Effects (25th), Japan, May 17-20, 1993, p769-786.

Keywords: *Earthquake engineering, *Structural engineering, *Design standards, Seismic design, Structural design, Safety engineering, Dynamic structural analysis, Earthquake resistance, Building codes, Public policy, Reprints, *Seismic safety, Loma Prieta Earthquake.

The Loma Prieta, California earthquake (LPE) of October 17, 1989, has had profound influence on both policies and practices for earthquake hazards reduction in the United States. The paper describes lessons in public policy as well as those in earth, engineering and soil sciences and practices resulting from the earthquake.

00,443
PB95-174488 PC A04/MF A01
National Inst. of Standards and Technology (BFRL), Gaithersburg, MD. Structures Div.
Performance of HUD-Affiliated Properties during the January 17, 1994 Northridge Earthquake.
D. Todd, E. Anderson, N. Carino, J. Gross, L. Phan, A. E. Schultz, H. W. Shenton, A. Taylor, C. W. C. Yancey, G. Cheok, and R. Chung. Aug 94, 70p, NISTIR-5488.
Contract DU100I940000027
Portions of this document are not fully legible. Sponsored by Department of Housing and Urban Development, Washington, DC.

Keywords: *Residential buildings, *US HUD, *Earthquake damage, *Damage assessment, Seismic effects, Dynamic structural analysis, Soil structure interactions, Dynamic response, Structural vibration, Multifamily housing, Performance evaluation, California, *Northridge Earthquake, Southern Region(California), Structural damage, Nonstructural damage.

The magnitude 6.8 January 17, 1994 Northridge Earthquake was centered under the densely populated San Fernando Valley northeast of Los Angeles, California. At the request of the Department of Housing and Urban Development (HUD), the Building and Fire Research Laboratory (BFRL) of the National Institute of Standards and Technology (NIST) conducted field observations of multi-family residences three stories or more in height in the affected area for the purposes of identifying common damage states in residential construc-

tion. Sixty-nine HUD-affiliated sites, totalling 425 buildings and over 10,000 living units, were visually examined from the exterior and interior. By collecting information primarily on damaged buildings, it was possible to identify typical types and degrees of damage to residential buildings.

00,444
PB95-179024 PC A04/MF A01
National Inst. of Standards and Technology (BFRL), Gaithersburg, MD.
Performance of 1/3-Scale Model Precast Concrete Beam-Column Connections Subjected to Cyclic Inelastic Loads. Report No. 4.
G. S. Cheok, and W. C. Stone. Jun 94, 72p, NISTIR-5436.
Errata sheet inserted. See also PB93-227502 and PB94-101813.

Keywords: *Earthquake resistant structures, *Construction joints, *Precast concrete, *Cyclic loads, *Beams(Supports), Model tests, Concrete structures, Earthquake engineering, Structural analysis, Structural failure, Stress analysis, Failure modes, Compressive strength.

Test results of four hybrid post-tensioned concrete beam-to-column connections are presented. The objective of the test program is to develop guidelines for the design of moment resistant precast connections in regions of high seismicity. The hybrid connections consist of mild steel used as energy dissipators and post-tensioning steel used to provide the required shear resistance. Variables examined were different amounts and type of mild steel. The amount of post-tensioning steel was kept constant. The specimens were subjected to reversed cyclic loading in accordance with a prescribed displacement history. The performances of the connections were evaluated based on comparisons of energy dissipation capacity, connection strength, and drift capacity with previous NIST tests. The results show that a hybrid precast connection can be designed so that it matches the performance of a monolithic connection in terms of energy dissipation, strength, and drift capacity.

00,445
PB95-179040 PC A07/MF A02
National Inst. of Standards and Technology, Gaithersburg, MD.
Effects of Testing Variables on the Measured Compressive Strength of High-Strength (90 MPa) Concrete.
N. J. Carino, and W. F. Guthrie. Oct 94, 147p, NISTIR-5405.
Sponsored by Federal Highway Administration, McLean, VA. Office of Advanced Research.

Keywords: *Compressive strength, *Test methods, Loads(Forces), Stress strain relations, Test facilities, Aggregates, Construction materials, Experimental design, Statistical analysis, Standards, Mechanical properties, *High strength concrete, ASTM C 39, AASHTO T 22.

A review is presented on the factors affecting the measured compressive strength of concrete specimens, with particular emphasis on the testing of high-strength concrete. A full factorial experiment was designed to examine the effects of cylinder size, end preparation, stress rate and type of testing machine on the measured compressive strength. Two concrete mixtures (45 MPa and 90 MPa) were used to determine whether there were interactions between strength level and the other factors. In addition, a 65-MPa mixture was required to allow testing four combinations of specimen size and testing machine. The cylinder sizes were 100 x 200 mm and 150 x 300 mm. The ends of the cylinders were either capped with sulfur mortar or ground flat. The stress rate was either 0.14 MPa/s or 0.34 MPa/s, which are limits currently specified in ASTM C 39 (AASHTO T 22). Besides the main test series, supplementary tests were done to investigate the effects of a defective spherically-seated bearing block. The defective bearing block had a concave depression within the central 100 mm. The maximum value of the depression was more than 0.2 mm, compared with the value of 0.025 mm currently allowed by ASTM C 39 (AASHTO T 22). Comparative tests with 68-MPa concrete showed no difference in mean strength due to the defective bearing block. Analysis of dispersion showed that the 100-mm cylinders had higher within-test variability, but the differences were not statistically significant. Recommendations for modifications to testing standards and future research are provided.

00,446
PB95-180469 Not available NTIS
National Inst. of Standards and Technology (BFRL), Gaithersburg, MD. Structures Div.
Gust Factors Applied to Hurricane Winds.
Final rept.
W. R. Krayer, and R. D. Marshall. 1992, 7p.
Pub. in Bulletin of the American Meteorological Society 73, n5 p613-617 May 92.

Keywords: *Wind loads, *Hurricanes, *Structural analysis, *Buildings, *Gust loads, Structural engineering, Stress analysis, Dynamic response, Wind pressure, Statistical analysis, Wind velocity, Reprints, *Gust factors.

An important consideration in the design of structures is their response to extreme winds. This is especially true in regions affected by hurricanes. In this research, gust factors derived from hurricane wind-speed records are compared with those derived by Durst and others from open-scale records obtained in well-developed, extratropical storms. Based on records obtained from four hurricanes and 11 different recording stations, it is concluded that an upward adjustment of the Durst gust factors for the estimation of hurricane gust speeds may be in order. Anomalously high gust factors observed for hurricane winds in inland areas suggest the need for additional study. Also, it is concluded that a reexamination of the statistics of gust factors obtained from extratropical storm data would be useful in clearly identifying the appropriate probability distribution function.

00,447
PB95-182291 PC A03/MF A01
National Inst. of Standards and Technology (BFRL), Gaithersburg, MD. Structures Div.
Seismic Safety of Federal Buildings. Initial Program: How Much Will It Cost.
D. R. Todd. Apr 94, 40p, NISTIR-5419.
See also PB94-176278, PB94-181856, and PB95-130209. Sponsored by Federal Emergency Management Agency, Washington, DC. Mitigation Directorate.

Keywords: *Federal buildings, *Earthquake engineering, *Reinforcement(Structures), *Cost estimates, Seismic design, Design standards, Design criteria, Structural design, Earthquake resistant structures, Retrofitting, Building codes, Cost analysis, *Seismic safety.

A proposed Executive order titled 'Seismic Safety of Existing Federally Owned or Leased Buildings' sets forth an initial program aimed at laying the foundation of achieving the long-term goal of seismic safety in all Federal buildings. This paper identifies direct costs associated with adoption of the proposed Executive Order and develops an estimate of those costs. It does not consider the value of the benefits associated with adopting the proposed order. The estimated costs represent the aggregate impact on the Federal budget. Note that the estimate of that is presented in this paper does not include the costs of continuing already-existing seismic rehabilitation programs, but considers only costs that would be newly imposed on the Federal budget.

00,448
PB95-189528 PC A05/MF A01
National Inst. of Standards and Technology (BFRL), Gaithersburg, MD. Structures Div.
Proceedings: Workshop on Research Needs in Wind Engineering. Held in Gaithersburg, Maryland on September 12-13, 1994.
R. D. Marshall. Feb 95, 78p, NISTIR-5597.

Keywords: *Meetings, *Wind effects, *Wind pressure, *Structural failure, Loads(Forces), Wind(Meteorology), Wind tunnel tests, Storms(Meteorology), Buildings, Damage.

This report presents findings and recommendations developed at a workshop on research needs in wind engineering. Representatives from universities, the private sector, and Federal agencies presented program overviews and participated in working group sessions addressing various aspects of wind engineering research and wind disaster mitigation. Research needs and topics for technology transfer were identified and prioritized. It was concluded that current funding of wind engineering research in the United States falls far short of what is needed to effectively address the problem of spiraling losses due to wind damage. There is, however, considerable wind engineering knowledge now available for implementation by the model building codes and by the building industry in general.

00,449
PB95-203428 Not available NTIS
National Inst. of Standards and Technology (BFRL), Gaithersburg, MD. Structures Div.
World of Building Codes.
Final rept.
D. Todd. 1992, 3p.
Pub. in Phonomenal News 3, n3 p1-3 Apr 92.

Keywords: *Building codes, *Design standards, *Earthquake resistant structures, Earthquake engineering, Structural engineering, Design criteria, Structural design, Reprints, *Seismic design.

Improvements to the seismic provisions of the legally enforceable building codes implemented by states, counties, and localities derive from improvements to the three major model building codes. The model codes draw from national standards and resource documents for improvements. The NEHRP Recommended Provisions and the SEAOC Blue Book are the two major resource documents for seismic design and construction in this country. Both documents are periodically updated to include new research and investigation results.

00,450
PB95-210928 PC A07/MF A02
California Univ., Davis. Dept. of Civil and Environmental Engineering.
Assessment of Site Response Analysis Procedures.
I. M. Idriss. Jul 93, 148p, NIST/GCR-95/667.
Sponsored by National Inst. of Standards and Technology (BFRL), Gaithersburg, MD.

Keywords: *Site characterization, *Soil-structure interactions, *Ground motion, *Seismic waves, Seismic velocity, Seismic effects, Soil dynamics, Soil mechanics, Shear waves, Shear strain, Shear stress, Seismographs, Accelerometers, Seismological station, Spectrum analysis, Subsurface investigations, Yerba Buena Island, California, *San Francisco Airport, *Treasure Island Naval Station, *Loma Prieta Earthquake, San Francisco(California), Seismic response.

The Loma Prieta earthquake occured on October 17, 1989 at 5:04 pm Pacific daylight time along a 45-km long segment of the San Andreas fault in the Santa Cruz Mountains. The earthquake triggered by far the largest number of instruments ever triggered by an earthquake and recordings were obtained at well over 200 locations, including free-field stations, small buildings, high rise structures and dams. The records obtained from the free-field stations are summarized in Appendix A of this report. These include 31 stations at rock sites, nine stations at soft soil sites and 48 stations at other soils sites. The results of subsurface investigations at Treasure Island site and at the San Francisco Airport site were used in the study to calculate the horizontal components of site reponse at these two sites and to assess the procedures used for conducting such response calculations.

00,451
PB95-211918 PC A09/MF A02
National Inst. of Standards and Technology (BFRL), Gaithersburg, MD. Structures Div.
Survey of Steel Moment-Resisting Frame Buildings Affected by the 1994 Northridge Earthquake.
N. F. G. Youssef, D. Bonowitz, and J. L. Gross. Apr 95, 176p, NISTIR-5625.
Prepared in cooperation with Nabih Youssef and Associates, Los Angeles, CA.

Keywords: *Buildings, *Steel structures, *Frame structures, *Earthquake damage, Damage assessment, Seismic effects, Structural members, Dynamic response, Dynamic structural analysis, Construction joints, Cracking(Fracturing), Moments, Surveys, *Northridge Earthquake, Los Angeles(California).

The January 1994 Northridge earthquake caused unexpected widespread damage to steel moment-resisting frame (MRF) buildings throughout greater Los Angles. The report presents results of a survey of MRF's inspected for connection damage since the earthquake. The survey is intended to provide an overall view of the greater Los Angeles steel frame population, as well as a single-source building-specific record of observed conditions. A computerized database was developed to track submittals, compile basic survey data, and generate summary tables. Principal conclu-

sions from the survey data support the observation that MRF connection damage is not well correlated to any single structural characteristic. On the contrary, the survey data show that connection performance may be best understood in probabilistic, not deterministic, terms with emphasis on construction and inspection quality.

00,452
PB95-231601 PC A05/MF A01
University of Central Florida, Orlando.
Enhancements to Program IDARC: Modeling Inelastic Behavior of Welded Connections in Steel Moment-Resisting Frames.
S. K. Kunnath. May 95, 80p, NIST/GCR-95/673.
See also PB93-227502. Sponsored by National Inst. of Standards and Technology (BFRL), Gaithersburg, MD.

Keywords: *Earthquake engineering, *Reinforced concrete, *Farmed structures, *Computerized simulation, Steels, Damage analysis, Walls, Retrofitting, Computer programs, Hysteresis, IDARC computer program.

An existing computer code, IDARC, is enhanced to permit the modeling of steel moment-resisting frames (SMRFs) with the potential for weld failures at beam-to-column connections. The steel member model is derived from flexibility formulations in order to allow complex degrading hysteresis behavior to be incorporated. A panel zone element is developed to account for inelastic shear deformations in the beam-to-column connection region. Finally, a new conceptual hysteresis model is developed to represent the force-deformation characteristics at a welded connection, before and after weld failure. The results of the study indicate that the enhanced program, referred to as IDASS, is capable of adequately reproducing observed behavior of SMRFs and can be used as an effective tool to investigate the effects of weld failure in steel structures under earthquake loading.

00,453
PB95-231775 PC A03/MF A01
National Inst. of Standards and Technology (BFRL), Gaithersburg, MD. Structures Div.
Performance of Federal Buildings in the January 17, 1994 Northridge Earthquake.
D. Todd, and A. Bieniawski. Jan 95, 28p, NISTIR-5574.

Keywords: *Federal buildings, *Earthquake damage, *Seismic effects, Damage assessment, Dynamic structural analysis, Structural response, Structural vibration, US DOC, US DOD, NASA, US DOA, US DOE, US DOI, US GSA, US DOJ, US Postal Service, *Northridge Earthquake, Southern Region(California), Structural damage, Federal Bureau of Prisons, Department of Veterans Affairs.

On January 17, 1994, a magnitude 6.8 earthquake struck Northridge, California, in the northeast suburbs of Los Angeles. This report summarizes information collected by the Interagency Committee on Seismic Safety in Construction (ICSSC) on the performance of federally-owned buildings in the Northridge earthquake. Ten agencies reported that they owned buildings in the affected area. Collectively, over 4000 federally-owned buildings were shaken; approximately 100 were damaged by the quake. Only two sites suffered major damage; most damage was minor.

00,454
PB95-260725 PC A04/MF A01
National Inst. of Standards and Technology (BFRL), Gaithersburg, MD. Structures Div.
Strengthening Methodology for Lightly Reinforced Concrete Frames: Recommended Design Guidelines for Strengthening with Infill Walls.
L. T. Phan, G. S. Cheok, and D. R. Todd. May 95, 66p, NISTIR-5682.
See also PB94-187648.

Keywords: *Reinforced concrete, *Reinforcement(Structures), *Structural design, *Frames, Concrete structures, Design analysis, Structural analysis, Earthquake engineering, Displacement, Dynamic response, Design criteria, Structural failure, Shear strength, Loads(Forces), *Infilled walls.

A study of the sensitivity of the behavior of lightly reinforced concrete frames strengthened using the infill wall method to certain variables was conducted. These variables include the infill wall type (cast-in-place and precast), wall thickness, and the amount of anchor area and anchor type. The hysteretic behavior of the frames were predicted using three parameters and equations proposed in previous NIST work. Both quasi-static and transient dynamic analyses were performed using the program IDARC. General design guidelines are proposed based on these analyses and on observations gathered from existing experimental tests.

00,455
PB96-106901 PC A09/MF A02
Cladding Research Inst., Emeryville, CA.
Literature Review on Seismic Performance of Building Cladding Systems.
Feb 95, 181p, NIST/GCR-95/681.
Sponsored by National Inst. of Standards and Technology (BFRL), Gaithersburg, MD.

Keywords: *Cladding, *Construction, *Buildings, *Earthquake resistance, *Literature surveys, Precast concrete, Reinforced concrete, Steels, Seismic design, Structural members, Structural analysis, Structural response, Seismic effects, Ground motion, Building codes, Earthquake engineering, Seismic isolation, Soil-structure interactions.

Chapter 1 is an introduction that includes definitions, cladding panel configurations, details of architectural precast concrete cladding systems in the U.S.A., New Zealand, Japan, and Canada. Chapter 2 describes the current practice for seismically isolated precast concrete cladding panels and connections, including U.S. codes and their interpretation and foreign codes. Chapter 3 offers information on the structural utilization of precast concrete cladding panels and connections, including a historical overview, levels of contribution in seismic response, architectural implications for structural cladding, conditions for effective structural cladding, and issues of responsibility. Chapter 4 contains abstracts and informational highlights from research on the structural utilization of precast concrete cladding panels and connections, including eleven sets of research projects from the U.S.A., one project from Canada, and one project from Japan. Chapter 5 outlines other cladding materials for heavy panels, including prefabricated panel systems, GFRC panels, new types of reinforcement, a new type of RC sandwich panels, and steel and steel alloy panels.

00,456
PB96-112198 Not available NTIS
National Inst. of Standards and Technology (BFRL), Gaithersburg, MD. Structures Div.
Effects of Testing Variables on the Strength of High-Strength (90 Mpa) Concrete Cylinders.
Final rept.
N. J. Carino, W. F. Guthrie, E. S. Lagergren, and G. M. Mullings. 1994, 44p.
Pub. in Proceedings of the American Concrete Institute International Conference on High-Performance Concrete, Sinapore, November 15-18, 1994, p589-632.

Keywords: *Compressive strength, *Test methods, Reprints, Meetings, Loads(Forces), Stress strain relations, Test facilities, Aggregates, Construction materials, Statistical analysis, Test equipment, *High strength concrete.

A full factorial experimental design was used to investigate the effects of the following variables on cylinder strength: end preparation (sulfur capping versus grinding), cylinder size (100 versus 150 mm diameter), type of testing machine (1.33-MN capacity versus a 4.45-MN capacity), and nominal stress rate (0.14 versus 0.34 Mpa/s). Two levels of strength were used (45 and 90 Mpa), and three replicates were tested for each run. Specific gravities were measured to check on the consistency of cylinder fabrication. Statistical analyses indicated that all the factors had significant effects on the measured compressive strength. There were significant interactions among the factors, so that the effects were greater than the average values for particular factor settings. For example, the effect of end preparation depended on the strength level. Recommendations for modifications to testing standards are provided.

00,457
PB96-119607 Not available NTIS
National Inst. of Standards and Technology (BFRL), Gaithersburg, MD. Structures Div.
Response of Buildings to Ambient Vibration and the Loma Prieta Earthquake: A Comparison.
Final rept.
L. T. Phan, R. D. Marshall, and M. Celebi. 1992, 4p.
Pub. in Structures Congress '92, San Antonio, TX., April 13-15, 1992, p583-586.

Keywords: *Structural vibration, *Seismic waves, *Dynamic response, Structural dynamics, Seismic effects, Structural response, Buildings, Ground motion, Earthquakes, San Francisco(CA), Vibration damping, Seismic waves, Spectrum analysis, Soil-structure interactions, Reprints, Loma Prieta Earthquakes, Seismic spectra.

Structural response characteristics of five existing buildings in the San Francisco bay area, obtained from ambient vibration testing conducted after the Loma Prieta earthquake (LPE), are compared with the response characteristics observed during the LPE. The purpose is to provide an assessment of the applicability of ambient vibration testing as a means to obtain dynamic properties for use in earthquake design. The comparisons show that, for all five buildings, the response frequencies measured from ambient vibration testing are higher than those obtained from the LPE, and damping estimates computed from ambient vibration response records are smaller than those from the LPE response records.

00,458
PB96-122601 Not available NTIS
National Inst. of Standards and Technology (BFRL), Gaithersburg, MD. Structures Div.
Some Notable Hurricanes Revisited.
Final rept.
R. Marshall. 1992, 4p.
Pub. in Structures Congress '92, San Antonio, TX., April 13-15, 1992, p250-253.

Keywords: *Wind velocity, *Hurricanes, *Damage assessment, Tropical storms, Storm damage, Gust loads, Wind loads, Buildings, Dynamic response, Structural analysis, Structural engineering, Reprints.

Recorded hurricane wind speeds, uncorrected for instrument height, averaging time or local wind exposure, can be very misleading. This is particularly true when such records are used to assess the performance of structures exposed to extreme winds. Only when proper corrections are applied can the true distribution of surface wind speeds in a hurricane be ascertained. Recent improvements to adjustment procedures and resulting corrections to wind speed records from some notable hurricanes are described.

00,459
PB96-128103 PC A03/MF A01
National Inst. of Standards and Technology (BFRL), Gaithersburg, MD. Structures Div.
ICSSC Guidance on Implementing Executive Order 12941 on Seismic Safety of Existing Federally Owned or Leased Buildings.
D. Todd, and A. Bieniawski. Oct 95, 27p, NISTIR-5734.
Prepared in cooperation with Interagency Committee on Seismic Safety in Construction. Sponsored by Federal Emergency Management Agency, Washington, DC. Mitigation Directorate.

Keywords: *Federal buildings, *Seismic design, *Design standards, *Earthquake resistant structures, Retrofitting, Reinforcement(Structural), Structural stability, Seismic waves, Earthquake engineering, Vulnerability, Building codes, Cost estimates, Government policies, Federal government.

In this guidance document, the Interagency Committee on Seismic Safety in Construction (ICSSC) recommends appropriate approaches for Federal departments and agencies to use in implementing the inventorying and cost estimating requirements of Executive Order 12941. The ICSSC recommends that all Federally-owned buildings be included in an electronic inventory database of specified format. Buildings are to be identified as either exempt or non-exempt from the seismic standards adopted by the order. All exceptionally high risk buildings are to be seismically evaluated, and estimates of the cost of their rehabilitation developed. Additionally, agencies are to perform seismic evaluations on a representative sample of their non-high-risk, non-exempt buildings, and use this information to estimated the vulnerability of that population and the cost of achieving adequate seismic safety.

00,460
PB96-128285 PC A05/MF A01
National Inst. of Standards and Technology (BFRL), Gaithersburg, MD. Structures Div.

Recommended Performance-Based Criteria for the Design of Manufactured Home Foundation Systems to Resist Wind and Seismic Loads.
R. D. Marshall, and F. Y. Yokel. Aug 95, 77p, NISTIR-5664.
Contract DU100I93000037
Sponsored by Department of Housing and Urban Development, Washington, DC. Office of Research Evaluation and Monitoring.

Keywords: *Wind effects, *Seismic effects, *Prefabricated buildings, *Building codes, *Design criteria, Earthquake engineering, Wind loads, Hurricanes, Structural vibrations, Dynamic structural analysis, Soil structure interactions, Foundations(Structures), Anchors(Structural), Soils, Performance evaluation, Wind engineering.

This report addresses the issue of tornado wind speeds as a basis for the design of manufactured homes and compares base shears due to earthquake excitation with base shears due to wind loading for various seismic and wind zones. In view of the accepted probabilities of attaining or exceeding design limit states for ordinary buildings, it is concluded that tornadoes should not be a part of the wind load design criteria for manufactured homes. Also, it is concluded that base shears due to wind loading will always govern the design of anchor and tiedown systems in the direction normal to the axis for a manufactured home, regardless of seismic zone. There are several alternative systems on the market or under development that show considerable promise for providing the required resistance to wind and earthquake loads. Finally, a set of performance-based criteria for anchoring manufactured homes against wind and earthquake loads is proposed.

00,461
PB96-131552 PC A10/MF A03
National Inst. of Standards and Technology (BFRL), Gaithersburg, MD.
How-To Suggestions for Implementing Executive Order 12941 on Seismic Safety of Existing Federal Buildings, A Handbook.
A. Bieniawski, and D. Todd. Nov 95, 210p, NISTIR-5770.
Also pub. as Interagency Committee on Seismic Safety in Construction rept. no. ICSSC/TR-17. See also PB95-130209. Prepared in cooperation with Interagency Committee on Seismic Safety in Construction. Sponsored by Federal Emergency Management Agency, Washington, DC. Office of Mitigation and Research.

Keywords: *Federal buildings, *Retrofitting, *Earthquake engineering, Reinforcement(Structures), Earthquake resistance, Seismic design, Structural design, Building codes, Safety engineering, Cost estimates, Cost analysis, Design standards, Inventories, Regulatory guides.

This document supplements 'ICSSC guidance on Implementing Executive Order 12941 on Seismic Safety of Existing Federally Owned or Leased Buildings' (RP5). This Handbook offers two additional levels of guidance beyound that presented in RP5: (1) detailed methodologies for fulfilling the RP5 recommendations for inventorying and cost estimating, which can be followed as default procedures by agencies which do not have agency-specific programs in place and which do not wish to develop agency-specific programs, and (2) detailed specifications for preparing and submitting the cost estimate and supporting documentation called for in the Executive Order. While the first type of guidance, presented in Sections 1-4 of this Handbook, is optional, the second type, presented in Section 5, is to be considered mandatory in order to ensure uniform reporting.

00,462
PB96-141148 Not available NTIS
National Inst. of Standards and Technology (BFRL), Gaithersburg, MD. Structures Div.
De Facto Microzonation through the Use of Soils Factors in Design Triggers.
Final rept.
D. Todd, and J. R. Harris. 1995, 8p.
Pub. in Proceedings of the International Conference on Seismic Zonation (5th), Nice, France, October 17-19, 1995, p510-517.

Keywords: *Soil-structure interactions, *Seismic design, Soil mechanics, Soil profiles, Seismic events, Earthquake resistant structures, Design criteria, Design standards, Dynamic structural analysis, Earthquake engineering, Reprints, *Microzonation, Soil factors.

The 1994 edition of the National Earthquake Hazard Reduction Program (NEHRP) Recommended Provisions for the Development of Seismic Regulations for New Buildings takes a step toward becoming a microzonation-based design guideline by including soils factors in its design control factors (triggers). This paper discusses the effect of the changes adopted in the 1994 edition of the NEHRP Recommended Provisions, and examines the impact of full conversion to soils-factor-based control factors.

00,463
PB96-154901 PC A04/MF A01
National Inst. of Standards and Technology (BFRL), Gaithersburg, MD.
Summary and Results of the NIST Workshop on Proposed Guidelines for Testing and Evaluation of Seismic Isolation Systems. Held in San Francisco, California on July 25, 1994.
H. W. Shenton. Jan 96, 44p, NISTIR-5785.
See also PB94-161734, PB94-161940 and PB94-161957.

Keywords: *Vibration isolators, *Earthquake resistant structures, *Building codes, *Test methods, *Meetings, Seismic design, Quality control, Earthquake engineering, Design criteria, Standards, Structural vibration, Prototypes, Dynamic response, Damping, Model tests, Guidelines, Compression tests, Aging, *Seismic isolation systems.

The Building and Fire Research Laboratory (BFRL) of the National Institute of Standards and Technology (NIST) has published comprehensive draft guidelines for testing and evaluating seismic isolation systems. The procedures outlined in the guidelines encompass all the required tests of the isolation systems, from the early stages of development to final production tests. The principal mechanism for soliciting feedback on the draft guidelines was a workshop held on July 25, 1994 in San Francisco. The purpose of the workshop was to provide a forum for review and discussion of the draft guidelines. This report is a summary of the workshop discussions. Topics which received the most attention in the discussions were scale model testing, performance criteria, quality control testing, factors of safety, aging of isolation systems, and the sustained compression test for elastomeric systems. Recommendations were made regarding third party inspection of the test procedure, a test to evaluate the re-centering capability of the isolation system, a direct shear test for elastomeric systems, and fire rating.

00,464
PB96-155783 Not available NTIS
National Inst. of Standards and Technology (BFRL), Gaithersburg, MD. Structures Div.
Development of Computer-Based Models of Standards and Attendant Knowledge-Base and Procedural Systems.
Final rept.
E. Simiu, J. H. Garrett, and K. A. Reed. 1993, 6p.
Pub. in Proceedings of the Structures Congress, Irvine, CA., April 19-21, 1993, p841-846.

Keywords: *Knowledge-based systems, *Standards, *Extreme-value problems, Building codes, Wind loads, Wind velocity, Wind effects, Data bases, Object-orieted programming, Expert systems, Reprints.

We propose the development of computer-based models of standards, and of knowledge-based and procedural systems to be incorporated in or used in conjunction with such models. Pilot projects should demonstrate the significant potential for inprovement in design and construction productivity inherent in such a new generation of standards. Wind loading examples are used for illustration.

00,465
PB96-156021 Not available NTIS
National Inst. of Standards and Technology (BFRL), Gaithersburg, MD. Structures Div.
Executive Order 12941. Seismic Safety of Existing Federally Owned or Leased Buildings: It's History, Content and Objectives.
Final rept.
D. Todd. 1995, 4p.
See also PB96-128103 and PB96-131552.
Pub. in EERI Technical Seminar, 'The Kobe Earthquake: Impact on the Executive Order for Existing Buildings', Alexandria, VA., December 5, 1995, 4p.

Keywords: *Federal buildings, *Seismic design, *Earthquake engineering, Earthquake resistance, Retrofitting, Reinforcement(Structural), Structural stability, Vulnerability, Safety engineering, Inventories, Cost estimates, Reprints.

Work by the Interagency Committee on Seismic Safety in Construction (ICSSC) is expected to lead to the eventual development of a systematic program of seismic upgrading for Federally owned buildings. Steps that have been taken to date include (1) the development of seismic evaluation and rehabilitation standards, (2) the drafting of an Executive Order which adopts the technical standards and calls for a seismic inventory and cost estimate, and (3) the issuance of guidance on how to efficiently and consistently inventory Federally owned buildings and how to estimate the costs of mitigating unacceptable seismic risks.

00,466
PB96-158050 Not available NTIS
National Inst. of Standards and Technology (BFRL), Gaithersburg, MD. Structures Div.
Strengthening Methodology for Lightly Reinforced Concrete Frames.
Final rept.
L. T. Phan, D. R. Todd, and H. S. Lew. 1993, 8p.
See also PB95-260725.
Pub. in Wind and Seismic Effect: Proceedings of the Joint Meeting (25th), UJNR, Japan, May 1993, p265-272.

Keywords: *Reinforcement(Structures), *Dynamic structural analysis, *Buildings, *Frames, Concrete structures, Reinforced concrete, Load bearing capacity, Shear strength, Earthquakes, Design criteria, Hysteresis, Computerized simulation, Mathematical models, Reprints, Infilled walls.

An analytical method for evaluating the inelastic dynamic structural response of lightly reinforced concrete (RC) frames strengthened by infilled shear walls was developed. This method involved the development of hysteresis failure models for existing and strengthened RC frames and the incorporation of the models into the computer program IDARC for analysis. The hysteresis models were developed in terms of the stiffness degradation parameter, the strength degradation parameter, and the pinching parameter. The results of the analyses showed that (1) hysteresis models developed using one-story, one-bay frames can be incorporated into IDARC for the analysis of frames with more than one-story height, and (2) reasonable predictions of structural behavior, both in terms of ultimate load capacity and in absorbed energy on a per cycle basis, can be determined using the hysteresis models.

00,467
PB96-159645 Not available NTIS
National Inst. of Standards and Technology (BFRL), Gaithersburg, MD. Structures Div.
Comparison of Responses of a Select Number of Buildings to the 10/17/1989 Loma Prieta (California) Earthquake and Low-Level Amplitude Test Results.
Final rept.
M. Celebi, L. T. Phan, and R. D. Marshall. 1991, 25p.
Pub. in Proceedings, UJNR Joint Meeting (23rd), US-Japan Panel on Wind and Seismic Effects, Tokyo, Japan, May 12-25, 1991, p475-499.

Keywords: *Earthquake damage, *Damage assessment, *Buildings, *Dynamic response, Dynamic structural analysis, Ground motion, Structural vibration, Seismic discrimination, Amplitudes, Seismic effects, Damping, Reprints.

This paper summarizes dynamic characteristics of five buildings within the San Francisco Bay area. The dynamic characteristics are extracted from the October 17, 1989 Loma Prieta earthquake response records and from ambient tests conducted in November 1990. Dynamic characteristics determined for two of the five buildings prior to the Loma Prieta earthquake are also included for comparison. The preliminary results show, in some cases, that low-level test are useful and, in other cases, they show considerable differences with those determined from strong-motion response records.

00,468
PB96-159686 Not available NTIS
National Inst. of Standards and Technology (BFRL), Gaithersburg, MD. Structures Div.

Extreme Winds Estimation by 'Peaks Over Threshold' and Epochal Methods.
Final rept.
J. L. Gross, N. A. Heckert, J. A. Lechner, and E. Simiu. 1994, 6p.
See also PB96-159694.
Pub. in Structures Congress XII, Atlanta, GA., April 24-28, 1994, v2 p1472-1477.

Keywords: *Wind loads, *Extreme-value problems, *Estimation, Wind effects, Wind velocity, Wind pressure, Wind profiles, Data analysis, Statistical analysis, Mathematical models, Monte Carlo method, Reprints, Peaks over threshold method, Extreme winds, Wind engineering.

With a view to applying the 'peaks over threshold' method to the estimation of extreme wind speed data, we perform Monte Carlo simulations for which the parameters of the population distributions were estimated from sets of actual extreme wind speed data. We summarize results concerning (1) the relative efficiency of several estimation procedures used in such methods, (2) the optimal threshold for any given set of data, and (3) estimates based on the 'peaks over threshold' method as compared to estimates based on the epochal approach.

00,469
PB96-159694 Not available NTIS
National Inst. of Standards and Technology (BFRL), Gaithersburg, MD. Structures Div.
Modeling of Extreme Loading by 'Peaks Over Threshold' Methods.
Final rept.
J. L. Gross, N. A. Heckert, J. A. Lechner, and E. Simiu. 1993, 8p.
See also PB96-159686.
Pub. in Dynamic Response and Progressive Failure of Special Structures, Charlottesville, VA., June 6-9, 1993, p135-147.

Keywords: *Wind loads, *Extreme-value problems, *Statistical analysis, Wind effects, Wind velocity, Wind profiles, Wind pressure, Gumbel distribution, Weibull distribution, Estimation, Monte Carlo method, Mathematical models, Reprints, Peaks over threshold methods, Extreme winds, Load factors.

In this work, we seek to apply the 'peaks over threshold' theory to the estimation of extreme wind speeds. The studies presented are based on Monte Carlo simulations for which the parameters of the population distributions were estimated from sets of actual extreme wind speed data. Results are presented concerning (1) the relative efficiency of several estimation procedures used in such methods, (2) the optimal threshold for any given set of data, and (3) estimates based on the 'peaks over threshold' method as compared to estimates based on the epochal approach using largest yearly wind speeds.

00,470
PB96-159702 Not available NTIS
National Inst. of Standards and Technology (BFRL), Gaithersburg, MD. Structures Div.
Workgroup Summary Report: Plastic Hinge-Based Techniques for Advanced Analysis.
Final rept.
J. L. Gross. 1993, 3p.
Pub. in Plastic Hinge-Based Methods for Advanced Analysis and Design of Steel Frames, Pittsburgh, PA., April 5, 1992, p175-177 Mar 93.

Keywords: *Construction joints, *Steel structures, *Structural analysis, Framed structures, Structural members, Buckling, Loads(Forces), Moments, Plasticity, Mechanical properties, Dynamic response, Reprints.

The purpose of this workgroup was to demonstrate, clarify, and discuss the current capabilities and limitations of contemporary plastic hinge-based methods for advanced analysis and design of steel frames. The approach taken was to discuss and comment on whether capabilities of current methods are essential to advanced analysis, beneficial (and under what circumstances), or whether there is insufficient information for immediate application of the capability. Some capabilities were assumed to be beyond the present scope and were not addressed.

00,471
PB96-162540 PC A04/MF A01
National Inst. of Standards and Technology, Gaithersburg, MD.
Estimates of Hurricane Wind Speeds by the 'Peaks Over Threshold' Method.
Technical note.
E. Simiu, N. A. Heckert, and T. Whalen. Feb 96, 49p, NIST/TN-1416.
Grant NSF-CMS-9411642
Also available from Supt. of Docs. as SN003-003-03396. See also PB95-219416. Prepared in cooperation with Johns Hopkins Univ., Baltimore, MD. Dept. of Civil Engineering. Sponsored by National Science Foundation, Arlington, VA. and North Atlantic Treaty Organization, Brussels (Belgium).

Keywords: *Hurricanes, *Wind velocity, *Estimation, Wind effects, Wind loads, Wind pressure, Dynamic loads, Structural reliability, Structural engineering, Design standards, Building codes, Extreme valve problems, Weibull distribution, Graphs(Charts), *Peaks over threshold method, Load factors.

We report results that lend support to the hypothesis that extreme hurricane wind speeds are described predominantly by reverse Weibull distributions, which have limited upper tails. The results are based on the analysis of hurricane wind speed data obtained in an earlier project and used for the development of the ASCE 7-83 and ASCE 7-93 Standard wind speed map. According to our results, wind load factors should be larger in hurricane-prone regions than the load factor specified in current standard provisions. However, the requisite increases are smaller than would be the case in the distributions were assumed to have infinite upper tails, as has been done so far in all principal studies of hurricane winds in the United States.

00,472
PB96-165949 PC A04/MF A01
National Inst. of Standards and Technology (BFRL), Gaithersburg, MD. Structures Div.
Modified Optimal Algorithm for Active Structural Control.
F. Sadek, and B. Mohraz. Jan 96, 36p, NISTIR-5782.
Sponsored by Southern Methodist Univ., Dallas, TX. School of Engineering and Applied Science.

Keywords: *Optimal control, *Active control, *Algorithms, Structural dynamics, Seismic isolation, Vibration isolators, Control systems, Buildings, Degrees of freedom, Structureal response, Seismic waves, Dynamic response, Excitation, *Base isolation, Gain matrices, Seismic loads.

This study presents a modification to two linear optimal control algorithms, namely classical and instantaneous, to achieve a greater reduction in structural displacements and control forces. The modification consists of building a library of gain matrices and selecting the gain matrix that would result in the maximum control force without exceeding the control system capacity. The modification was used to compute the response of several single-degree-of-freedom (MDOF) system, and a base isolated structure. The study shows that the external excitation influences the selection of the control system parameters such as controller capacity and gain matrices. These parameters, therefore, should be determined according to the seismic excitation intensity expected at the site.

00,473
PB96-167820 PC A04/MF A01
Southern Methodist Univ., Dallas, TX.
Method of Estimating the Parameters of Tuned Mass Dampers for Seismic Applications.
F. Sadek, B. Mohraz, A. W. Taylor, and R. M. Chung. Apr 96, 36p, NISTIR-5806.
Sponsored by National Inst. of Standards and Technology (BFRL), Gaithersburg, MD. Structures Div.

Keywords: *Dampers, *Vibration damping, *Structural vibration, Passive systems, Energy dissipation, Buildings, Structural response, Dynamic response, Seismic waves, Seismic effects, Loads(Forces), Tuning, Degrees of freedom, Earthquake engineering, *Passive control, Seismic loads.

The optimum parameters of tuned mass dampers (TMD) that result in considerable reduction in the response of structures to seismic loading are presented. The criterion used to obtain the optimum parameters is to select, for given mass ratio, the frequency (tuning) and damping ratios that would result in equal and larger modal damping in the first two modes of vibration. The parameters are used to compute the response of several single and multi-degree-of-freedom structures with TMDs to different earthquake excitations. The results indicate that the use of the proposed parameters reduces the displacement and acceleration responses significantly. It is shown that as a result of selecting the parameters as proposed in this paper, significant reduction in the response of tall buildings can be achieved.

00,474
PB96-183223 PC A04/MF A01
National Inst. of Standards and Technology (BFRL), Gaithersburg, MD. Structures Div.
Probabilistic Estimates of Design Load Factors for Wind-Sensitive Structures Using the 'Peaks Over Threshold' Approach.
Technical note.
T. M. Whalen. Apr 96, 34p, NIST/TN-1418.
Also available from Supt. of Docs. as SN003-003-03407-0. See also PB96-162540.

Keywords: *Hurricanes, *Wind velocity, *Probabilistic estimation, Wind effects, Wind loads, Wind pressure, Dynamic loads, Structural reliability, Structural engineering, Design standards, Building codes, Extreme value problems, Weibull distribution, *Peaks over threshold method, Load factors.

The 'peaks over threshold' method is used to estimate ratios of wind-induced loads with various long mean recurrence intervals to loads with a 50-year mean recurrence interval. The results support the conclusion that the load factor value of 1.3 specified in the ASCE Standards 7-93 and 7-95 is adequate for extratropical storm regions. However, for hurricane-prone regions, the results imply that the standard value of the load factor (even after being augmented by an importance factor specified in the standards) leads to nominal ultimate wind loads with considerably shorter mean recurrence intervals than is the case for extratropical regions. This suggests that the 1.3 load factor value specified in the ASCE Standards 7-93 and 7-95 is inadequate for wind-sensitive structures in hurricane-prone regions.

00,475
PB97-104160 PC A99/MF A06
National Inst. of Standards and Technology (BFRL), Gaithersburg, MD.
January 17, 1995 Hyogoken-Nanbu (Kobe) Earthquake. Performance of Structures, Lifelines and Fire Protection Systems. Executive Summary and Paper.
Special pub.
R. Chung. Jul 96, 578p, NIST/SP-901.
Also available from Supt. of Docs. as SN003-053-03412-6. Also pub. as Interagency Committee on Seismic Safety in Construction rept. no. ICSSC/TR-18.

Keywords: *Earthquake damage, *Damage assessment, *Seismic effects, *Soil-structure interactions, *Dynamic structural analysis, Hokkaido Island, Earthquake engineering, Airports, Bridges, Highways, Buildings, Public utilities, Gas utilities, Pipelines, Subways, Transportation sector, Harbors, Electric power, Sewer systems, Water treatment plants, Sewage treatment plants, Steel structures, Reinforced concrete, Fires, Liquefaction, *Hyogoken-Nanbu Earthquake, Kobe(Japan), Communication links, Lifelines, Wood structures.

The National Institute of Standards and Technology's Building and Fire Research Laboratory (BFRL) dispatched an advance team of three BFRL members, followed by a larger team of 18 members made up of individuals from a number of federal agencies and others affiliated with national earthquake engineering research centers. The teams were to observe, document, and summarize important lessons from this earthquake.

00,476
PB97-104376 PC A99/MF A06
National Inst. of Standards and Technology (BFRL), Gaithersburg, MD.
Wind and Seismic Effects: Proceedings of the Joint Meeting of the U.S.-Japan Cooperative Program in Natural Resources Panel on Wind and Seismic Effects (28th). Held in Gaithersburg, Maryland on May 14-17, 1996.
Special pub.
N. J. Raufaste. Aug 96, 648p, NIST/SP-904.
Also available from Supt. of Docs. as SN003-003-03424-0. See also PB95-147385.

Keywords: *Seismic effects, *Wind effects, *Structural engineering, *Dynamic structural analysis, *Meetings, Earthquake engineering, Geotechnical engineering,

Design standards, Design criteria, Research programs, Dynamic loads, Structural vibration, Wind pressure, Wind loads, Earthquakes, Tsunamis, Storm surges, Risk assessment, Foundations(Structures), Highway engineering, Bridges, Dams, Repairing, Retrofitting, Earthquake resistant structures, Wind engineering, Lifelines.

This publication is the Proceedings of the 28th Joint Meeting of the U.S.-Japan Panel on Wind and Seismic Effects. The Proceedings include the program, list of members, panel resolutions, task committee reports, and the 46 technical papers written for this joint meeting. The papers were presented within five themes: (1) Storm Surge and Tsunamis, (2) Earthquake Engineering, (3) Joint Cooperative Research Program, (4) Wind Engineering, and (5) Summaries of Task Committee Workshop Reports (oral presentations only).

00,477
PB97-113245 Not available NTIS
National Inst. of Standards and Technology (BFRL), Gaithersburg, MD. Structures Div.
Dynamics of Multi-DOF Stochastic Nonlinear Systems.
Final rept.
T. M. Whalen. 1996, 4p.
Pub. in Proceedings of the Specialty Conference on Probabilistic Mechanics and Structural Reliability, Worchester, MA., August 7-9, 1996, p82-85.

Keywords: *Column buckling, *Multidimensional systems, Building technology, Chaos, Feedback control, Gaussian noise, Reprints, *Melnikov's method.

Melnikov's method for finding necessary conditions for homoclinic chaos is extended to stochastically forced multi degree of freedom nonlinear systems. The stochastic forcing induces a stochastic Melnikov process, from which information can be obtained on probabilities of escape and mean exit rates from regions of phase space as well as parameter bounds for nonchaotic motion. Applications are presented to the dyhnamics of a feedback controlled buckled column.

BUSINESS & ECONOMICS

General

00,478
PB94-173002 Not available NTIS
National Inst. of Standards and Technology, Gaithersburg, MD. Program Office.
Functions of Technology Infrastructure in a Competitive Economy.
Final rept.
G. Tassey. 1991, 17p.
Pub. in Research Policy 20, p345-361 1991.

Keywords: *Economic models, *Technology innovation, Economic growth, Economy, Competition, Research and development, Laboratories, Government policies, Standards, US NIST, Reprints, *Infrastructure.

Governments of industrialized nations play varied but important roles in providing the diverse technology infrastructure that supports a modern, competitive economy. The required technology infrastructure policy model is derived from a microeconomic model of the typical technology-based industry. Existing national strategies have demonstrated the importance of efficiency at the production and market development stages as well as at the R&D stage, but the trend is towards promoting simultaneous efficiency at all these stages. That is, the model and the derived infrastructure functions must cover all stages and interfaces in the technology and related product life cycles.

00,479
PB94-210150 PC A04/MF A01
National Inst. of Standards and Technology (TS), Gaithersburg, MD. Office of Standards Services.
Survey on the Implementation of ISO/IEC Guide 25 by National Laboratory Accreditation Programs.
Final rept.
M. Breitenberg. Jul 94, 51p, NISTIR-5473.

Keywords: International organizations, Laboratories, Test methods, Calibration, Standards, Meetings, Surveys, *ISO/IEC guide 25, *Laboratory accreditation, *Accreditation, NVLAP Program.

The International Organization for Standardization/ International Electrotechnical Commission (ISO/IEC) Guide 25, 'General requirements for the competence of calibration and testing laboratories,' has been used by many laboratory accreditation programs worldwide to establish accreditation requirements designed to promote confidence in the calibrations and testing results of laboratories which conform to the guide's requirements. National delegations to the International Laboratory Accreditation Conference (ILAC), an international conference of national organizations interested in laboratory accreditation, were surveyed to collect information on the implementation and supplementation of the requirements of ISO/IEC Guide 25 within the context of their countries' laboratory accreditation programs. This report summarizes the results of that survey. The report also includes a bibliographic list of publications concerned with ISO/IEC Guide 25 implementation compiled from the information submitted by the national delegations.

00,480
PB94-219102 PC A03/MF A01
National Inst. of Standards and Technology (NCSL), Gaithersburg, MD. Systems and Network Architecture Div.
Analyzing Electronic Commerce.
Special pub.
L. Gebase, and S. Trus. Jun 94, 43p, NIST/SP-500/218.
Also available from Supt. of Docs. as SN003-003-03270-1.

Keywords: *Commerce, *Telecommunication, *Data management, Electronic mail, Data processing security, Models, Computer networks, Man machine systems, Data base management systems, Distributed computer systems, *Electronic commerce, EDI(Electronic Data Interchange).

This report begins, after citing some important technological advances, by defining electronic commerce and identifying the scope of issues to be addressed within this paper. It then proceeds to examine some ways in which electronic commerce is presently being conducted, most notably with Electronic Data Interchange (EDI). An architectural model for supporting services necessary to conduct electronic commerce is then defined. The chapters that follow provide further detail on the model's components. The final chapter draws some conclusions about the benefits of deploying electronic commerce.

00,481
PB96-189444 PC A07/MF A02
National Research Council, Washington, DC. Commission on Engineering and Technical Systems.
Financing Tomorrow's Infrastructure: Challenges and Issues. Proceedings of a Colloquium. Held in Washington, DC. on October 20, 1995.
c1996, 115p, ISBN-0-309-05543-1.
Grant NSF-CMS-9505733
Library of Congress catalog card no. 96-69107. Sponsored by Economic Development Administration, Washington, DC., National Science Foundation, Arlington, VA. and National Inst. of Standards and Technology, Gaithersburg, MD.

Keywords: *Meetings, *Finance, Financing, Investments, Economic development, United States, *Infrastructure.

The colloquium was an attempt to explore these issues in a social, political, and fincancial context, to examine models for successfully financing infrastructure projects, and to discuss new and innovative ways of dealing with contemporary realities.

Consumer Affairs

00,482
PB94-178969 PC A08/MF A02
National Inst. of Standards and Technology (TS), Gaithersburg, MD. National Voluntary Lab. Accreditation Program.
National Voluntary Laboratory Accreditation Program 1994 Directory.
Special pub.
V. R. White. Mar 94, 161p, NIST/SP-810-ED-1994.
Supersedes PB93-156644. Also available from Supt. of Docs. as SN003-003-03259-0.

Keywords: *Laboratories, *Directories, Acoustic measurement, Computer applications, Construction materials, Electromagnetic compatibility, Thermal insulation, Lighting equipment, Seals(Stoppers), Asbestos, Carpets, Dosimetry, Paints, Paper, Plastics, Plumbing, Sealers, Telecommunication, States(United States), Tests, *National Voluntary Laboratory Accreditation Program, NVLAP program, Product testing.

The Directory is published annually and provides a listing of laboratories accredited by the National Institute of Standards and Technology, National Voluntary Laboratory Accreditation Program (NVLAP). Approximately 700 laboratories in 20 fields of accreditation are included in the 1994 edition. The Directory lists the name, address, contact person, phone number, accreditation renewal data and scope of accreditation for each accredited laboratory. A brief description of the NVLAP program, a summary of laboratory participation, and user instructions are provided. The Directory consists of four indexes which are cross-referenced by NVLAP Lab Code: Index A, Listing by Laboratory Name; Index B, Listing by Field of Accreditation; Index C, Listing by State/Country; and Index D, Listing by NVLAP Lab Code. A listing of the test methods (Scope of Accreditation) is provided for each laboratory in Index D.

00,483
PB95-174454 PC A08/MF A02
National Inst. of Standards and Technology (TS), Gaithersburg, MD. National Voluntary Lab. Accreditation Program.
National Voluntary Laboratory Accreditation Program 1995 Directory.
Special pub.
V. R. White, and C. L. Monti. Jan 95, 165p, NIST/SP-810-ED-1995.
Supersedes PB94-178969. Also available from Supt. of Docs. as SN003-003-03315-4.

Keywords: *Laboratories, *Directories, Asbestos, Calibrating, Computer applications, Dosimetry, Electromagnetic compatibility, Standards, Tests, States(United States), *National Voluntary Accreditation Program, *National Institute of Standards and Technology, NVLAP Program, Product testing.

The Directory is published annually and provides a listing of laboratories accredited by the National Institute of Standards and Technology, National Voluntary Laboratory Accreditation Program (NVLAP). Over 700 laboratories in 17 fields of accreditation are included in the 1995 edition. The Directory lists the name, address, contact person, phone number, accreditation renewal date and scope of accreditation for each accredited laboratory. A brief description of the NVLAP program, a summary of laboratory participation, and user instructions are provided. The Directory consists of four indexes which are cross-referenced by NVLAP Lab Code: Index A, Listing by Laboratory Name; Index B, Listing by Field of Accreditation; Index C, Listing by State/Country; and Index D, Listing by NVLAP Lab Code. A listing of the test methods (Scope of Accreditation) is provided for each laboratory in Index D.

00,484
PB95-182226 PC A04/MF A01
National Inst. of Standards and Technology (TS), Gaithersburg, MD. Weights and Measures Program.
Checking the Net Contents of Packaged Goods as Adopted by the 79th National Conference on Weights and Measures, 1994, Third Edition, Supplement 4.
Handbook.
C. S. Brickenkamp, K. Butcher, and T. Coleman. Oct 94, 64p, NIST/HB-133-ED-3-SUP-4, ISBN-0-16-045384-4.
Also available from Supt. of Docs. as SN003-003-03299-9. See also PB93-124956.

Keywords: *Packaging, *Commodities, *Labels, Handbooks, Revisions, Requirements, Sampling, Tests, Procedures, Changes, US NIST, Handbook 133.

Only minor additions and revisions to the National Institute of Standards and Technology (NIST) Handbook

133, Third Edition, 'Checking the Net Contents of Packaged Goods,' were adopted by the 79th National Conference on Weights and Measures in 1994. A few editorial changes have also been made. This document consists of change pages to be added to Handbook 133, Third Edition, as amended by the 1993 Supplement.

00,485
PB96-162714 PC A10/MF A03
National Inst. of Standards and Technology (TS), Gaithersburg, MD. National Voluntary Lab. Accreditation Program.
National Voluntary Laboratory Accreditation Program 1996 Directory.
Special pub.
V. R. White. Jan 96, 193p, NIST/SP-810-ED-1996.
Supersedes PB95-174454. Also available from Supt. of Docs. as SN003-003-03388-0.

Keywords: *Laboratories, *Directories, Asbestos, Calibrating, Computer applications, Dosimetry, Electromagnetic compatibility, Standards, Tests, United States, Acoustic measurement, *National Voluntary Laboratory Accredition Program(NVLAP), *NVLAP(National Voluntary Laboratory Accredition Program), *National Institute of Standards and Technology Product Testing.

The Directory is published annually and provides a listing of laboratories accredited by the National Institute of Standards and Technology, National Voluntary Laboratory Accreditation Program (NVLAP). Approximately 700 laboratories in 19 fields of accreditation are included in the 1996 edition. The Directory lists the name, address, contact person, phone and fax numbers, accreditation renewal date, and scope of accreditation of each accredited laboratory. The Directory contains a description of the NVLAP program, a summary of laboratory participation, and user instructions, followed by five laboratory indexes which are cross-referenced by NVLAP Lab Code: Index A. Listing by Laboratory Name; Index B, Listing by Field of Accreditation; Index C, Listing by State/ Country; Index D. Listing of Testing Laboratories by NVLAP Lab Code; Index E, Listing of Calibration Laboratories by NVLAP Lab Code. The Scopes of Accreditation are provided for testing and calibration laboratories in Indexes D and E, respectively. Current accreditation statuses of participating laboratories may be verified by calling or writing NVLAP.

00,486
PB97-110183 Not available NTIS
National Inst. of Standards and Technology (TS), Gaithersburg, MD.
Evaluation and Accreditation of State Calibration Laboratories.
Final rept.
G. L. Harris. 1993, 16p.
Pub. in National Conference of Standards Laboratories Managing Quality to Improve Profitability Workshop and Symposium, Albuquerque, NM., July 25-29 1993, p395-410.

Keywords: *Calibration, *Laboratory accreditation, Measurement control, Metrology training, Interlaboratory testing, Accreditation, Assessments, Reprints.

The primary function of any accreditation process should be the evaluation of laboratory competency. Can the laboratory do what it claims. However, the assessment process should also evaluate the degree of proficiency (skill) that the laboratory demonstrates. Assessment of laboratory facilities is usually straighforward when using documented criteia and checklists. Since accuracy of measurements is an important attribute of any laboratory, how do we evaluate measurement accuracy. We often use the phrase, 'traceable to NIST standards' to convey accuracy relative to national standards, but how do we verify measurement traceability.

Domestic Commerce, Marketing, & Economics

00,487
PB94-168390 PC A19/MF A04
National Inst. of Standards and Technology (CSL), Gaithersburg, MD. Advanced Systems Div.
Design and Development of an Information Retrieval System for the EAMATE Data. Volume 2 of 2. Appendices.
N. Willman, and L. L. Downey. Apr 94, 448p, NISTIR-5394.
Sponsored by Social Security Administration, Baltimore, MD.

Keywords: *Information retrieval, *Wages, *Optical disks, Records management, Automation, Systems engineering, Man machine systems, Prototypes, Computer programs, *EAMATE system.

The Social Security Administration maintains records of wages earned by every person who has a social security number. Currently, all reports are converted to and maintained on microfilm. When a person's wage record must be verified, the process is cumbersome as the film is difficult to read and employees are listed in no particular order. The EAMATE system automates this manual process through the use of cost effective optical disk technology. The volume contains the appendices to the report on the information retrieval system for EAMATE. It includes user instructions, installation and configuration, system error messages, listing of the code, scout comments from EAMATE testing, and preliminary employer report statistics.

00,488
PB95-111514 PC A05/MF A01
National Inst. of Standards and Technology, Gaithersburg, MD.
NIST Industrial Impacts: A Sampling of Successful Partnerships.
Special pub.
Sep 94, 77p, NIST/SP-872.
Also available from Supt. of Docs. as SN003-003-03293-0.

Keywords: *Industries, *Technical assistance, *Government/industry relations, Organizational structure, Technology innovation, Manufacturing, Laboratories, Corporations, Businesses, *US NIST, Malcolm Baldrige National Quality Awards.

The National Institute of Standards and Technology (NIST) has a mission to work in partnership with industry toward the shared goal of strengthening the nation's technological and economic bases. This booklet briefly chronicles recent cases in which U.S. companies and NIST have crossed paths to their mutual benefit. It includes: Organizational Contacts, Advanced Technology Program Impacts, Manufacturing Extension Partnership Impacts, Laboratory Impacts, Malcolm Baldrige National Quality Award Impacts, Index of Companies, and Index of Applications.

00,489
PB95-209193 PC A05/MF A01
National Inst. of Standards and Technology, Gaithersburg, MD.
NIST Industrial Impacts: A Sampling of Successful Partnerships (Revision, March 1995).
Special pub.
Mar 95, 89p, NIST/SP-872-REV-1-95.
See also PB95-111514.

Keywords: *Industries, *Technical assistance, *Government/industry relations, Organizational structure, Technology innovation, Manufacturing, Laboratories, Corporations, Businesses, *US NIST, Malcolm Baldridge National Quality Awards.

The National Institute of Standards and Technology (NIST) has a mission to work in partnership with industry toward the shared goal of strengthening the nation's technological and economic bases. It includes: Organizational Contacts; Advanced Technology Program Impacts; Manufacturing Extension Partnership Impacts; Laboratory Impacts; Baldrige National Quality Program Impacts; Index of Companies.

00,490
PB95-219325 PC A08/MF A02
New Jersey Inst. of Tech., Newark. Center for Manufacturing Systems.
Network Brokers Handbook: An Entrepreneurial Guide to Cooperative Strategies for Manufacturing Competitiveness.
C. R. Hatch. Jan 95, 164p, NIST/GCR-94/663.
Grant NIST-70NANBIH1146
Sponsored by National Inst. of Standards and Technology, Gaithersburg, MD. Manufacturing Extension Partnership.

Keywords: *Manufacturers, *Networks, *Small businesses, *Manufacturing, Technical assistance, Economic development, Industries, Productivity, *Entrepreneurship.

Contents:
Five Ways to Launch Manufacturing Networks;
Introduction;
Section One:
Broker Skills;
Section Two:
Targeting Firms;
Section Three:
Network Focus Groups;
Section Four:
Resource Access;
Section Five:
Pilot Network Projects;
Section Six:
Building a Strong Network Culture;
and Appendices.

00,491
PB96-190046 Not available NTIS
National Inst. of Standards and Technology (TS), Gaithersburg, MD. Office of Standards Services.
Helping to Reduce Technical Barriers to Trade.
Final rept.
B. L. Collins. 1995, 6p.
Pub. in Bringing Standards Together: An International Framework Conference, Washington, DC., July 18, 1995, p48-53.

Keywords: *Trade, *Barriers, *Standards, Consumer products, Marketing, International trade, Regulations, Conformity, Reprints, *Technical barriers, World trade organization, TBTs(Technical barriers to trade).

Dramatic changes are occurring in the international markets that form the background for U.S. standards and conformity assessment activities. Last year the United States exported about $700 billion worth of goods and services. These goods and services were sold into an increasingly competitive global market containing many barriers to trade. Having a large domestic market, good quality and reasonable prices are not longer guarantees of market access for a product. Technical barriers to trade (TBTs) almost always must be overcome or dealt with constructively to gain access to a market before any product can be traded. Trade experts have indicated that additional exports worth $20 to $40 billion could be produced right now if we could overcome all technical barriers to trade.

Foreign Industry Economic Development

00,492
PB94-212461 Not available NTIS
National Inst. of Standards and Technology (NML), Gaithersburg, MD.
Aid for Smaller Businesses.
Final rept.
D. R. Johnson. 1990, 2p.
Pub. in Issues in Science and Technology VI, n4 p7-8 1990.

Keywords: *Economic development, *Regional development, *Europe, Industries, Competition, Manufacturing, Productivity, United States, Small businesses, Reprints, US NIST.

This letter comments on the article, 'Regional Development, European Style.' It expresses agreement that the U.S. can learn from European programs and experiences in technically oriented economic development and describes several new activities at the National Institute of Standards and Technology.

00,493
PB97-110126 Not available NTIS
National Inst. of Standards and Technology (TS), Gaithersburg, MD. Office of Standards Services.
Stacking the Cards in Europe: One Company's Story.
Final rept.
H. D. Delaney. 1996, 4p.
Pub in American Society for Testing and Materials Standardization News, v24 n8 p34-37 Aug 96.

Keywords: *Barriers, Europe, Directives, Performance, Standards, Trade, Reprints, *Conformity assessments.

A U.S. manufacturer of connector hoses for gas appliances has encountered a series of difficulties in re-

maining in European markets as a consequence of shifting interpretations of an EU Directive and the applicability of the standards and conformity assessment requirements of individual European nations. Critical issues include the European use of design, rather than performance, standards and lack of access to the European technical committees and working groups. The staff of the U.S. Mission to the European Union, including the NIST standards expert, are assisting American manufacturers and exporters to resolve standards-related trade barriers.

International Commerce, Marketing, & Economics

00,494
PB94-185832 Not available NTIS
National Inst. of Standards and Technology (CSL), Gaithersburg, MD.
Planning the Infrastructure for Global Electronic Commerce.
Final rept.
R. G. Saltman. 1993, 5p.
Pub. in EDI Forum: Jnl. of Electronic Data Interchange 6, n3 p52, 59-62 1993.

Keywords: *International trade, *Telecommunication, Commerce, Data transmission, Computer networks, Government/industry relations, Standards, Reprints, *Electronic commerce, *Infrastructure.

The components of global electronic commerce and the matrix of concepts underlying its feasibility are elucidated. Some of the issues and choices facing decision-makers on the direction of its development are discussed. Electronic commerce has implications for the way business is conducted, and may in the long run affect the ability of nations to compete effectively in international trade. It is proposed that government-private sector coordination may help provide a sound basis for U.S. representation in forums deciding the future of global electronic commerce. Many of these forums are multi-governmental; they concern technical standards and the administration of international trade. An aim of such representation would be to maximize the probability of outcomes at such forums favorable for U.S. competitiveness.

00,495
PB95-103461 PC A03/MF A01
National Inst. of Standards and Technology, Gaithersburg, MD. Office of Standards Code and Information.
Questions and Answers on Quality, the ISO 9000 Standard Series, Quality System Registration, and Related Issues. More Questions and Answers on the ISO 9000 Standard Series and Related Issues.
M. Breitenberg. Apr 93, 40p, NISTIR-4721, NISTIR-5122.
Supersedes PB93-152080 and PB93-140689.

Keywords: *International trade, *Quality assurance, *Standards, Quality control, Test facilities, Assessments, Reliability, Inspection, Specifications, *ISO(International Organization for Standardization), *International Organization for Standardization, ISO 9000, US NIST, Registration.

The report provides information on the development, content and application of the ISO 9000 standards to readers who are unfamiliar with these aspects of the standards. It attempts to answer some of the most commonly asked questions on quality; quality systems; the content, application and revision of the ISO 9000 standards; quality system approval/registration; European Community requirements for quality system approval/registration; and sources for additional help.

00,496
PB95-255881 PC A11/MF A03
National Inst. of Standards and Technology (TS), Gaithersburg, MD. Office of Standards Services.
Proceedings of the Meeting of the Intergovernmental U.S.-Russian Business Development Committee's Standard Working Group (4th). Held in New York City, New York on March 27-29, 1995 and in Northbrook, Illinois on March 30-31, 1995.
Internal rept.
E. E. Zulfugarzade. Jul 95, 247p, NISTIR-5688.
See also PB93-179968.

Keywords: *Russian Federation, *Standards, Proceedings, Metrology, Standardization, International trade, Automobile industry, Commerce, Intergovernmental relations, Commercial development, Certification, ASME(American Society of Mechanical Engineers), Gosstandart, Harmonization.

The fourth meeting of the U.S.-Russia Business Development Committee's Standards Working Group took place on March 27-29, 1995 in New York City, New York hosted by the American Society of Mechanical Engineers International (ASME), and on March 30-31, 1995 in Northbrook, Illinois hosted by Underwriters Laboratories, Inc. (UL). The Russian delegation consisted of representatives of the Committee of the Russian Federation for Standardization, Metrology and Certification (GOSSTANDART). The U.S. delegation included representatives from government agencies and the private sector, including testing and certification bodies, individual companies, and trade associations. The meeting resulted in an exchange of information regarding standards and conformity assessment programs and practices in areas of mutual interest, such as Boilers and Pressure Vessels, occupational and food and drug safety, automotive and telecommunications standards, and electrical and fire safety of consumer and industrial products. Of particular significance was the signing of a Joint Statement on Conformity Assessment between GOSSTANDART and ASME International, a Joint Statement of Information Exchange between GOSSTANDART and FDA, and a working statement between GOSSTANDART and UL.

00,497
PB96-106935 PC A03/MF A01
National Inst. of Standards and Technology (TS), Gaithersburg, MD. Office of Standards Services.
GATT Standards Code Activities of the National Institute of Standards and Technology 1994.
J. R. Overman. Aug 95, 39p, NISTIR-5697.
See also report for 1991, PB92-187095.

Keywords: *International trade, *Multilateral agreements, *Standards, Governments, Regulations, Foreign government, U.S. Government, Certification, Experts, Technical assistance, GATT(General Agreement on Tariffs and Trade).

This report describes the General Agreement on Tariffs and Trade (GATT) Standards Code activities conducted by the National Institute of Standards and Technology (NIST), for calendar year 1994. NIST received and processed 508 notifications of proposed technical regulations; reported 67 proposed U.S. technical regulations to the GATT Secretariat; respond to 409 inquiries for GATT notification information; participated in various bilateral and multilateral standards-related trade discussions; and responded to inquiries on the existence, source and availability of standards-related trade discussions; and responded to inquiries on the existence, source and availability of standards and standards-related information.

00,498
PB96-160361 Not available NTIS
National Inst. of Standards and Technology (TS), Gaithersburg, MD. Office of Standards Services.
International Challenges in Defining the Public and Private Interest in Standards.
Final rept.
S. I. Warshaw, and M. H. Saunders. 1995, 8p.
Pub. in SPRU-OECD International Workshop on Standards, Innovation, Competitiveness and Policy, Brighton, England, November 10-12, 1993, p67-74 1995.

Keywords: *Standards, *Regulations, *International agreements, Conformity, Competition, Global, Market analysis, ISO, European Communities, Reprints, Competitiveness, IEC(International Electrotechnical Commission), GATT(General Agreement on Tariffs and Trade).

Increasing global trade and technological integration raise important issues concerning: (1) existing infrastructures and their efficacy for developing internationally accepted standards; (2) the interaction of conformity assessment activities and systems among market-led economies; and (3) the changing prerogatives of governments. As a basis for world trade, manufactures and processors are demanding single globally acceptable technical standards and conformance tests. However, national governments must accommodate domestic health, safety and environmental goals that often differ dramatically between countries and regions.

00,499
PB97-104178 PC A04/MF A01
National Inst. of Standards and Technology (TS), Gaithersburg, MD. Office of Standards Services.
TBT Agreement Activities of the National Institute of Standards and Technology, 1995.
Annual rept.
J. R. Overman. Sep 96, 35p, NISTIR-5898.
See also PB96-190046.

Keywords: *International trade, *Barriers, *Standards, *Multilateral agreements, Conformity, Consumer products, Regulations, United States, Marketing, Notifications, Foreign government, Federal government, Certifications, *TBT(Technical barriers to trade), *Technical barriers to trade(TBT), World trade organization.

This report describes the World Trade Organization (WTO) Agreement on Technical Barriers to Trade (TBT Agreement) activities conducted by the National Institute of Standards and Technology (NIST), for calendar year 1995. NIST received and processed 378 notifications of proposed technical regulations; reported 20 proposed U.S. technical regulations to the WTO Secretariat; responded to 329 inquiries for notification information; participated in various bilateral and multilateral standards-related trade discussions; and responded to inquiries on the existence, source and availability of standards and standards-related information. In 1995, NIST also served as the U.S. inquiry point under the Agreement on the Application of Sanitary and Phytosanitary Measures (SPS Agreement).

CHEMISTRY

General

00,500
AD-A278 140/9 PC A03/MF A01
National Bureau of Standards, Boulder, CO.
Standard Materials. A Descriptive List with Prices.
12 Mar 62, 39p, NBS-MR-241.

Keywords: *Standardization, *Chemical composition, *Metals, *Ceramic materials, *Chemicals, *Hydrocarbons, Procurement, Composite materials, Measurement, Accuracy, Tables(Data), *National Bureau of Standards, Descriptive listing, Fees, Certification.

No abstract available.

00,501
PB94-185535 Not available NTIS
National Inst. of Standards and Technology (CAML), Gaithersburg, MD. Statistical Engineering Div.
Experimental Optimization of Peak Shape with Application to Aerosol Generation.
Final rept.
W. S. Liggett, and K. Ehara. 1993, 9p.
Pub. in Proceedings of the Society of Physical and Engineering Science, Rochester, NY., October 1993, p174-182.

Keywords: *Aerosol generators, *Particle size distribution, Hermite polynomials, Laser applications, Optimization, Measurement, Polystyrene, Spheres, Reprints, Chemometrics, Nebulizers.

Consider measuring instruments that respond to a single-component experimental material with a function having a single peak. In the experimental optimization of such instruments, one task is the minimization of peak width. This paper presents an approach to this task based on Hermite function approximation of the peaks observed under various instrument configurations. The approach requires at least two experimental materials with different peak locations and at least two different strengths (concentrations) of each material so that both the horizontal and vertical scale of the instrument response can be adjusted in the comparison of instrument configurations. The approach is applied to the optimization of an aerosol generator that nebulizes polystyrene latex spheres with nearly identical sizes.

In the experiment, the size distribution of the particles in the resulting aerosol is measured with a laser particle counter. The results show that the size distribution in the aerosol changes with time and that various nebulizer adjustments have an important effect on the peak width observed after the nebulizer has run for some period.

00,502
PB94-199213 Not available NTIS
National Inst. of Standards and Technology (NML), Boulder, CO. Thermophysics Div.
Summary of the Patent Literature of Supercritical Fluid Technology.
Final rept.
T. J. Bruno. 1991, 50p.
Pub. in Supercritical Fluid Technology: Reviews in Modern Theory and Applications, p525-574 1991.

Keywords: *Supercritical fluids, Technology utilization, Literature surveys, Inventions, Abstracts, Uses, Reprints, Patenting.

The major patents issued in the field of supercritical fluid technology between 1982 and 1989 are summarized. In each case, the title, the names of the inventors, the critical dates and the assignee are provided. The abstract of each patent is also supplied.

00,503
PB94-200664 Not available NTIS
National Inst. of Standards and Technology (NEL), Gaithersburg, MD. Precision Engineering Div.
Report of Density Intercomparisons Undertaken by the Working Group on Density of the CCM.
Final rept.
R. S. Davis. 1990, 6p.
Pub. in Metrologia 27, n3 p139-144 1990.

Keywords: *Density measurement, Interlaboratory comparisons, International cooperation, Stainless steels, Metrology, Silicon, Reprints, Intercomparison.

The results of international comparisons of density measurements are reported. Participants include national laboratories of Australia, the Federal Republic of Germany, Italy, Japan, the United Kingdom, and the United States, as well as the Bureau International des Poids et Mesures. The comparisons involved hydrostatic density determinations of samples made of single-crystal silicon and samples made of stainless steel. Agreement among laboratories is generally better for samples of silicon than for samples of stainless steel. Overall discrepancies do not, however, appear to be serious with respect to scientific and metrological needs.

00,504
PB94-200672 Not available NTIS
National Inst. of Standards and Technology (MEL), Gaithersburg, MD. Automated Production Technology Div.
Mass and Density Determinations.
Final rept.
R. S. Davis, and W. F. Koch. 1992, 99p.
Pub. in Physical Methods of Chemistry, Chapter 1, v6 p1-99 1992.

Keywords: *Density measurement, Weight measurement, Densitometers, Dilatometers, Pycnometers, Balances, Buoyancy, Accuracy, Surveys, Reprints, *Mass measurement.

Basic concepts of mass and density measurements are presented as well as a survey of practical techniques. Ample references are provided for the interested reader to find the basic work in a given area and a sampling of recent uses of the techniques discussed. Emphasis is placed on the suitability of each method for specific problems, the major experimental difficulties, and the accuracy which can be obtained. The presentation is aimed at advanced undergraduates and graduate students in chemistry and related sciences.

00,505
PB95-125654 Not available NTIS
National Inst. of Standards and Technology (NCSL), Gaithersburg, MD. Information Systems Engineering Div.
Application of Expert System to Select Data Sources from Chemical Information Databases.
Final rept.
E. N. Fong, and C. E. Dabrowski. 1988, 11p.
Pub. in Proceedings of American Society of Mechanical Engineers International Computers in Engineering Conference and Exhibition, San Francisco, CA., July 31-August 4, 1988, p107-117.

Keywords: *Chemical engineering, *Information systems, *Data base management systems, *Expert systems, Data acquisition, Knowledge bases(Artificial intelligence), Knowledge representation, Data bases, Vapor pressure, Reprints.

This paper describes a research project of building a prototype expert system called 'Automated Advisor.' This expert system conducts dialog with the engineers and recommends a list of data sources from chemical information databases.

00,506
PB95-170387 PC A07/MF A02
National Inst. of Standards and Technology (MEL), Gaithersburg, MD. Precision Engineering Div.
Workshop Summary Report: Industrial Applications of Scanned Probe Microscopy. A Workshop Co-sponsored by NIST, SEMATECH, ASTM, E42.14, and the American Vacuum Society. Held in Gaithersburg, Maryland on March 24-25, 1994.
Conference proceedings.
J. A. Dagata, A. C. Diebold, C. K. Shih, and R. J. Colton. Dec 94, 131p, NISTIR-5550.
See also AD-A245 300. Prepared in cooperation with SEMATECH, Austin, TX. and Texas Univ. at Austin.

Keywords: *Microscopy, *Industries, *Technology utilization, *Meetings, Research and development, Manufacturing, Metrology, Standards, Calibrating, Test methods, Scanning, Probes, Measuring instruments, US NBS, Critical dimension metrology, Electrical characterization, Microroughness, National Institute of Standards and Technology.

This report is a summary outcome statement for the Industrial Applications of Scanned Probe Microscopy (SPM) workshop which was held at National Institute of Standards and Technology (NIST) Gaithersburg on March 24-25, 1994. The meeting, co-sponsored by NIST, SEMATECH, ASTM E42.14, and the American Vacuum Society, was attended by over one hundred SPM users, suppliers, researchers and program managers from industry, government, and academia. The focus of the workshop was on fostering a common understanding of the roles of each of these groups in evolution of applied SPM, to achieve a consensus view on standard practices of SPM-based measurements, and to establish the basic features required of future generations of commercially available SPMs required for quantitative measurement. This report assesses the effectiveness of the workshop format and concludes with specific recommendations for a second, follow-up workshop.

00,507
PB95-210225 PC A08/MF A02
National Inst. of Standards and Technology (CSTL), Gaithersburg, MD. Process Measurements Div.
NIST Workshop on Gas Sensors: Strategies for Future Technologies. Proceedings of a Workshop. Held in Gaithersburg, Maryland on September 8-9, 1993.
Special pub.
S. Semancik. Dec 94, 172p, NIST/SP-865.
Also available from Supt. of Docs. as SN003-003-03327-8.

Keywords: *Gas detectors, *Air pollution monitoring, *Safety, *Meetings, Technology innovation, Commercial development, Indoor air pollution, Process control, Manufacturing, Occupational safety and health, Research and development, Performance, Transductance.

This Proceedings issue describes a Workshop on gas sensing held in Gaithersburg, MD, September, 8-9, 1993. Future gas sensors with improved response characteristics, higher reliability, and lower cost can be expected to have increased application in diverse areas, including environmental monitoring, process control, and personal safety. This Workshop brought together gas sensor manufacturers, present and potential users, and researchers to explore ways to incorporate research discoveries and emerging technologies more efficiently into new, high-performance sensors. The Proceedings includes publications on invited and contributed presentation, reports on discussions of Emerging Technologies and Commercialization and Standards issues, and reports summarizing breakout sessions.

00,508
PB95-232518 PC A03/MF A01
National Inst. of Standards and Technology (TS), Gaithersburg, MD. Standard Reference Materials Program.
NIST Standard Reference Materials (Trade Name) Catalog 1995-1996.
Special pub.
N. M. Trahey. Jan 95, 40p, NIST/SP-260.
Also available from Supt. of Docs. as SN003-003-03326-0. See also PB92-181163.

Keywords: *Catalogs(Publications), *Standards, Chemical analysis, Chemical composition, Quality assurance, Quality control, Callibrating, Concentration(Composition), Standardization, Measurement, *Standard reference materials, *Reference materials, Certified reference materials.

The document contains the description of NIST SRM Program and comprehensive listing of all 1300+ Standard Reference Materials (SRMs) and Reference Materials (RMs) developed, certified and distributed by NIST.

00,509
PB96-131602 PC A07/MF A02
National Inst. of Standards and Technology (MEL), Gaithersburg, MD.
Summary Report: Workshop on Industrial Applications of Scanned Probe Microscopy (2nd). A Workshop Co-Sponsored by NIST, SEMATECH, ASTM E42.14, and the American Vacuum Society. Held in Gaithersburg, Maryland on May 2-3, 1995.
J. A. Dagata, A. C. Diebold, C. K. Shih, and R. J. Colton. Nov 95, 140p, NISTIR-5752.
See also PB95-170387. Prepared in cooperation with SEMATECH, Austin, TX., Texas Univ. at Austin. Dept. of Physics. and Naval Research Lab., Washington, DC.

Keywords: *Microscopy, *Industries, *Technology utilization, *Meetings, Magnetic recording, Polymers, Coatings, Semiconductor devices, Tools, Standards, Calibrating, Tests, Surface properties, Metrology, *Scanned probe microscopy, National Institute of Standards and Technology.

The Second Workship on Industrial Applications of Scanned Probe Microscopy (IASPM) was held at the National Institute of Standards and Technology (NIST) Gaithersburg, MD on May 2-3, 1995. The meeting, cosponsored by NIST, SEMATECH, the American Society for Testing and Materials (ASTM) E.42.14 Subcommittee, and the Manufacturing Science and Technology Group of the American Vacuum Society, was attended by approximately one hundred scanned probe microscopy (SPM) users, suppliers, and researchers from industry, government, and academia. This Summary Report presents an overview of industrial applications of SPM in the areas of magnetic recording technology, polymers and coatings, and semiconductors, and reviews recent progress on SPM standardization and tool development.

00,510
PB96-161773 Not available NTIS
National Inst. of Standards and Technology (CSTL), Gaithersburg, MD. Biotechnology Div.
Conformational Alterations of Bovine Insulin Adsorbed on a Silver Electrode.
Final rept.
V. Reipa, A. Gaigalas, and S. Abramowitz. 1993, 16p.
Pub. in Jnl. of Electroanalytical Chemistry, v348 p413-428 1993.

Keywords: *Insulin, *Electrodes, *Silver electrodes, Bovines, Reprints, Disulfide reduction, Protein adsorption, SERS.

Surface enhanced Raman spectra of bovine insulin, adsorbed on the silver electrode from aqueous solutions of micromolar concentrations, are presented for the potential range -0.2 to -1.2 V/AgCl. The data suggest that insulin is bound to silver through ionized tyrosine residues and carboxy terminal groupings. Disulfide linkages are reduced sequentially upon increasing negative potential: A7-B7 at -0.3 to -0.5 V, and A20-B19 at -0.5 to -0.6 V. Rupture of disulfide bonds increased the portion of beta/disordered conformation at the expense of the alpha helix.

00,511
PB96-163654 Not available NTIS
National Inst. of Standards and Technology (CSTL), Gaithersburg, MD. Biotechnology Div.

Feasibility of Fluorescence Detection of Tetracycline in Media Mixtures Employing a Fiber Optic Probe.
Final rept.
S. A. Glazier, and J. J. Horvath. 1995, 18p.
Pub. in Analytical Letters, v28 n15 p2607-2624 1995.

Keywords: *Fiber optics, *Fluorescence, *Tetracycline, *Fermentation, Media, Reprints.

The work assesses the feasbility of fluorescence detection of tetracycline in very optically dense mixtures of highly fluorescent media ingredients used in tetracycline production by fermentation. The fluorescence measurements are accomplished with a fiber optic probe. Seven difference mixtures were examined in this study. Each one contained a nonfluorescent based on nutrients and salts along with one of the following media ingredients at 5 g/100 mL: cottonseed flour, corn gluten meal, soybean flour, distiller's grains and solubles, corn steep liquor, brewer's yeast, and molasses. The concentration of tetracycline was varied in each mixture and flourescence measurements were made at every concentration step. Excitation light of 390 nm was used to probe the samples, and emission spectra were obtained over the wavelength range from 400 to 600 nm. In most of the samples studied, the fluorescence intensity in the wavelength range corresponding to background media fluorescence (420-480 nm) decreased as the tetracycline concentration increased. The decreases in the short wavelength range might be explained by the absorption by tetracycline of 390 nm excitation light (in competition with absorption by the media) and/or by absorption of background media fluorescence by tetracycline. Frequently, the maximum emission of the mixtures shifted to longer wavelengths. The maximum approached that of tetracycline (approximately 520 nm). Plots of integrated fluorescence intensity, in the emission wavelength regions of 420-480 nm and 500-560 nm, versus tetracycline hydrochloride concentration reflect these shifts. The authors have found that the changes in fluorescence intensity in these two wavelength regions during tetracycline addition depend on the indentity of the media component in the mixture.

00,512
PB96-163662 Not available NTIS
National Inst. of Standards and Technology (CSTL), Gaithersburg, MD. Biotechnology Div.
Novel Amperometric Immunosensor for Procainamide Employing Light Activated Labels.
Final rept.
S. A. Glazier, and H. H. Weetall. 1994, 1p.
Pub. in Third World Congress on Biosensors, New Orleans, LA., June 1-3, 1994, 1p.

Keywords: *Immunoassays, *Amperometric, Reprints, *Electrochemical immunoassays, *Background currents, Anthraquinone, Procainamide.

Electrochemical immunoassays are often complicated by the presence of electroactive interferences which cause high current backgrounds. The authors are studying a method to correct for background currents in homogeneous immunoassays. The assays are conducted with an immunosensor employing 9,10-anthraquinone derivatives as electroactive labels for the model analyte, procainamide. Anthraquinones have the ability to be photochemically reduced by light to their hydroquinone analogues. In the assay, background correction may possibly be achieved by subtracting the oxidation current of a sample containing the anthraquinone-procainamide conjugate from the current obtained after photoreduction. This scheme relies of preferential reduction of the anthraquinone by proper wavelength selection, and the greater electroactivity of the hydroquinone form at oxidative potentials relative to the parent anthrquinone.

00,513
PB96-163712 Not available NTIS
National Inst. of Standards and Technology (BFRL), Gaithersburg, MD. Fire Science Div.
Inhibition of Premixed Methane-Air Flames by Iron Pentacarbonyl.
Final rept.
G. T. Linteris, and G. Gmurczyk. 1995, 5p.
Sponsored by Department of the Air Force, Wright-Patterson AFB, OH.
Pub. in International Colloquium on the Dynamics of Explosions and Reactive Systems, Boulder, CO., July 30-August 4, 1995, 5p.

Keywords: *Chemical inhibition, *Flame chemistry, Reprints, Flame models, Retardants, Flame speed.

Brominated fire suppressants are effective and widely used. Due to their destruction of stratospheric ozone, however, the production of these chemicals was halted in January 1994. Although testing and development of possible substitutes is occurring, a replacement with all of the desirable properties of CF3Br (the most common fire suppressant) has yet to be identified. Consequently, the Fire Science Division at the National Institute of Standards and Technology (NIST) is conducting research to identify new chemical inhibitors, understand the mechanisms of inhibition of known or widely used agents, and evaluate the performance of proposed agents.

00,514
PB96-163720 Not available NTIS
National Inst. of Standards and Technology (BFRL), Gaithersburg, MD. Fire Science Div.
Parametric Study of Hydrogen Fluoride Formation in Suppressed Fires.
Final rept.
G. Linteris, and G. Gmurczyk. 1995, 12p.
Pub. in Halon Options Technical Working Conference, Albuquerque, NM., May 9-11, 1995, 12p.

Keywords: *Chemical inhibition, *Fire research, *Flame chemistry, Reprints, Flame models, Retardants, Halon alternatives.

Some of the proposed replacements for CF3Br, the fluorinated hydrocarbons, are required in higher concentrations to extinguish fires and contain more halogen atoms per molecule. Since they decompose in the flame, they produce correspondingly more hydrogen fluoride than CF3Br when suppressing a fire. Recent laboratory experiments with burners using heptane, propane, and methane have indicated that the amount of HF formed in steady state can be estimated within about a factor of two for diffusion flames and within 10% for premixed flames based on equilibrium thermodynamics. In this model for HF formation, the inhibitor molecule is transported to the reaction zone by convection and diffusion and is consumed in the flame sheet to form the most stable products (usually HF, CO2, and COF2). In the present work, the equilibrium model is used to estimate the upper limit of HF formation in suppressed fires. The effects of fuel and agent type, fuel consumption rate, and agent injection rate are included in the model, as are room volume, humidity, and concentration of inhibitor necessary to extinguish the fire.

00,515
PB96-163738 Not available NTIS
National Inst. of Standards and Technology (CSTL), Boulder, CO. Thermophysics Div.
Molar Heat Capacity at Constant Volume for Air from 67 to 300 K at Pressures to 35 MPa.
Final rept.
J. W. Magee. 1994, 13p.
Pub. in International Jnl. of Thermophysics, v15 n5 p849-861 Sep 94.

Keywords: *Air, *Calorimeters, *Heat capacity, Reprints, High pressure, Isochoric.

Measurements of the molar heat capacity at constant volume Cv for air were conducted with an adiabatic calorimeter. Temperatures ranged from 67 to 300 K, and pressures ranged up to 35 MPa. Measurements were conducted at 17 densities which ranged from gas to highly compressed liquid states. In total, 227 Cv values were obtained. The air sample was prepared gravimetrically from research purity gases resulting in a mole fraction composition of 0.78112 N2 + 0.20966 O2 + 0.00922 Ar. The primary sources of uncertainty are the estimated temperature rise and the estimated quantity of substance in the calorimeter. Overall, the uncertainty of the Cv values is estimated to be less than plus or minus 2% for the gas and plus or minus 5% for the liquid.

00,516
PB97-109052 (Order as PB97-109011, PC A11/MF A03)
Cambridge Crystallographic Data Centre (England).
Cambridge Structural Database (CSD): Current Activities and Future Plans.
D. G. Watson. 1996, 3p.
Included in Jnl. of Research of the National Institute of Standards and Technology, v101 n3 p227-229 May/Jun 96.

Keywords: *Crystallography, *Organic compounds, *Organometallic compounds, *Information systems, Crystal structures, Polymers, Searching, Information retrieval, Data analysis, Chemical structure, Computer graphics, Chemical composition, Numeric data.

This paper reviews the search and analysis software packages QUEST3D and VISTA, also the database-building program Pre Quest. The relationship between the CSD and the Protein Data Bank is discussed and development plans are outlined.

00,517
PB97-109060 (Order as PB97-109011, PC A11/MF A03)
Brookhaven National Lab., Upton, NY.
Protein Data Bank: Current Status and Future Challenges.
E. E. Abola, N. O. Manning, J. Prilusky, D. R. Stampf, and J. L. Sussman. 1996, 11p.
Prepared in cooperation with Weizmann Inst. of Science, Rehovoth (Israel).
Included in Jnl. of Research of the National Institute of Standards and Technology, v101 n3 p231-141 May/Jun 96.

Keywords: *Crystallography, *Proteins, *Information systems, Crystal structure, Three dimensional, Software tools, Data base management.

The Protein Data Bank (PDB) is an archive of experimentally determined three-dimensional structures of proteins, nucleic acids, and other biological macromolecules with a 25 year history of service to a global community. PDB is being replaced by 3DB, the Three-Dimensional Database of Biomolecular Structures that will continue to operate from Brookhaven National Laboratory. 3DB will be a highly sophisticated knowledege-based system for archiving and accessing structural information that combines the advantages of object oriented and relational database systems.

00,518
PB97-109078 (Order as PB97-109011, PC A11/MF A03)
Rutgers - The State Univ., Piscataway, NJ. Dept. of Chemistry.
Nucleic Acid Database: Present and Future.
H. M. Berman, A. Gelbin, L. Clowney, J. Westbrook, S. H. Hsieh, and C. Zardecki. 1996, 15p.
Included in Jnl. of Research of the National Institute of Standards and Technology, v101 n3 p243-257 May/Jun 96.

Keywords: *Crystallography, *Nucleic acids, *Information systems, Chemical structure, Crystal structure, Three dimensional, Information retrieval, DNA, RNA, Data base management.

The Nucleic Acid Database is a relational database containing information about three-dimensional nucleic acid structures. The methods used for data processing, structure validation, database management and information retrieval, as well as the various services available via the World Wide Web, are described. Plans for the future include greater reliance on the Macromolecular Crystallographic Information File for both data processing and data management.

00,519
PB97-109144 (Order as PB97-109011, PC A11/MF A03)
Kentucky Univ., Lexington. Dept. of Chemistry.
Investigations of the Systematics of Crystal Packing Using the Cambridge Structural Database.
C. P. Brock. 1996, 5p.
Included in Jnl. of Research of the National Institute of Standards and Technology, v101 n3 p321-325 May/Jun 96.

Keywords: *Crystallography, *Molecular structure, *Information systems, Crystal packing.

Several studies that used the Cambridge Structural Database to elucidate principles of packing in molecular crystals are described. Some possible sources of bias in the statistical distributions are discussed.

00,520
PB97-110225 Not available NTIS
National Inst. of Standards and Technology (CSTL), Gaithersburg, MD. Process Measurements Div.
Thin-Film Ruthenium Oxide - Iridium Oxide Thermocouples.
Final rept.
K. G. Kreider. 1991, 8p.
Pub. in Proceedings of the Materials Research Society Symposium, Anaheim, CA., April 29-May 3, 1991, v234 p205-212.

General

Keywords: *Iridium oxide, *Ruthenium oxide, *Thin films, Sputtering, Temperature measurement, Thermocouples, Reprints.

Ruthenium oxide and iridium oxide have outstanding resistance to corrosion. These oxides are also excellent electrical conductors and have been used as biochemical charge injection electrodes. Their unique electrical and electrochemical properties have also led to their consideration as high temperature pH electrodes. Thin films are the most useful form for these applications as they permit the miniaturization of fast response sensors and electrodes. The study was used to characterize the thermoelectric and electrical conductance parameters of ruthenium and iridium oxide sputtered thin films. The electric and thermoelectric properties of the thin films were found to be sensitive to the annealing temperature of the sputtered oxides. The properties of the film are related to the microstructure, stoichiometry and crystal structure as determined by x-ray diffraction. Heat treatments were used to stabilize the thermoelectric response and the thermal coefficient of resistivity.

00,521
PB97-112460 Not available NTIS
National Inst. of Standards and Technology (CSTL), Gaithersburg, MD. Chemical Kinetics and Thermodynamics Div.
Ferric Ion Assisted Photooxidation of Halocetates.
Final rept.
P. Maruthamuthu, and R. E. Huie. 1995, 9p.
Pub. in Chemosphere, v30 n11 p2199-2207 1995.

Keywords: *Haloacetates, *Photooxidation, Photodecarboxylation, Hydroxyl radical, Hydrofluorocarbons, Hydrochlorofluorocarbons, Reprints, *Foreign technology.

Aqueous solutions containing ferric ions and chloro- or fluoroacetates were photolyzed by light with wavelengths greater than 300 nm. Significant variation in the extent of reaction was observed, with the totally halogenated acetates degraded very little in the course of the experiments. The relative rates of degradation were found to correlate very well with the relative rates of reaction of the haloacetate with the hydroxyl radical.

Analytical Chemistry

00,522
DE94018563 PC A02/MF A01
National Inst. of Standards and Technology, Gaithersburg, MD.
Improvement of Ultrasensitive Techniques Isotopic Biasing in the RIS Process Ionization Efficiencies and Selectivities.
Progress rept.
1989, 10p, DOE/ER/60447-T3.
Contract AI05-86ER60447
Sponsored by Department of Energy, Washington, DC.

Keywords: *Resonance Ionization Mass Spectroscopy, Isotope Ratio, Progress Report, Sensitivity, Trace Amounts, EDB/400102.

Work in improvement of ultrasensitive (RIMS) techniques, RIS schemes and atomic data, and development of isotopic ratio standards and standards for ultratrace analysis is reported.

00,523
DE94018565 PC A02/MF A01
National Inst. of Standards and Technology, Gaithersburg, MD.
I: Improvement of Resonance Ionization Spectroscopy (RIS) Techniques; II: Atomic Data for RIS; III: Standards for Ultratrace Analysis. Progress Report.
1991, 6p, DOE/ER/60447-T5.
Contract AI05-86ER60447
Sponsored by Department of Energy, Washington, DC.

Keywords: *Resonance Ionization Mass Spectroscopy, Isotope Ratio, Progress Report, Trace Amounts, EDB/400102.

I: Work focused on converting the VG SIMS system into a dual purpose instrument for analysis in SIMS or SIRIS mode, and on a glow discharge source for the NIST magnetic sector mass spectrometer. Ionization efficiencies and selectivities are being studied. II: The first two groups of 10 elements each have been published; draft data sheets have been completed for a third group of 5 elements; the data base of published and unpublished RIS work has been expanded. III: Dilution checks are being performed on the (sup 36)Cl standard.

00,524
PB94-140563 (Order as PB94-140555, PC A06/MF A02)
National Inst. of Standards and Technology, Gaithersburg, MD.
36Cl/Cl Accelerator-Mass-Spectrometry Standards: Verification of Their Serial-Dilution-Solution Preparations by Radioactivity Measurements.
R. Colle, and J. W. L. Thomas. 1993, 25p.
Included in Jnl. of Research of the National Institute of Standards and Technology, v98 n6 p653-677 Nov/Dec 93.

Keywords: *Mass spectrometry, *Chlorine 36, *Standards, Proportional counters, Liquid scintillators, Beta decay, Gravimetric analysis, Isotope dilution, Isotope ratio, Radioactivity, Radioisotopes, Metrology, Solutions, *Accelerator mass spectroscopy, Dilution factors.

A consortium of accelerator-mass-spectrometry (AMS) laboratories recently prepared a series of (36)Cl/Cl isotopic ratio AMS standards by an eight-step serial gravimetric dilution scheme. Of the resulting nine solutions, only the latter six could be assayed by AMS to confirm the gravimetric dilution factors. The paper provides the results of relative radioactivity measurements on the first four solutions to verify the first three dilution factors. The fourth solution was the only dilution capable of being directly measured by both AMS and radionuclidic metrology of (36)Cl, and therefore its assay by radioactivity counting was deemed of considerable importance.

00,525
PB94-163003 PC A02/MF A01
National Inst. of Standards and Technology (CSTL), Gaithersburg, MD. Surface and Microanalysis Science Div.
Airborne Asbestos Method: Standard Test Method for High Precision Counting of Asbestos Collected on Filters. Version 1.0.
S. Turner, and E. B. Steel. Mar 94, 10p, NISTIR-5350.

Keywords: *Asbestos, *Counting techniques, *Particles, *Chemical analysis, Transmission electron microscopy, Standards, Regulations, Air pollution detection, Water pollution detection, Filters, Procedures.

The analysis of asbestos by transmission electron microscopy (TEM) is important for the determination of the cleanliness of air or water and for research purposes. Counting rules are used to determine the amount of asbestos observed by TEM. This method describes a high precision set of counting rules. For this method, all qualifying particles are counted as one structure; the number of asbestos fibrils within a particle does not affect the number of structures assigned to the particle.

00,526
PB94-163045 PC A03/MF A01
National Inst. of Standards and Technology (CSTL), Gaithersburg, MD. Surface and Microanalysis Science Div.
Airborne Asbestos Method: Standard Test Method for Verified Analysis of Asbestos by Transmission Electron Microscopy. Version 2.0.
S. Turner, and E. B. Steel. Mar 94, 26p, NISTIR-5351.
See also PB94-113578.

Keywords: *Asbestos, *Chemical analysis, Air pollution detection, Transmission electron microscopy, Quality assurance, Water pollution detection, Standard, Procedures, *Verified analysis.

The analysis of asbestos by transmission electron microscopy is important for determination of the cleanliness of air or water and for research purposes. Verified analysis provides a method for determining the quality of the analyses. Verified analysis is a procedure in which a grid opening is independently analyzed for asbestos by two or more transmission electron microscope (TEM) operators and in which a comparison and evaluation of the correctness of the analyses are made by a verifying analyst. Detailed information - including absolute or relative location, a sketch, orientation, sized (length, width), morphology, analytical information and structure identification - is recorded for each observed asbestos structure. Comparisons of the analyses are made on a structure-by-structure basis and the percentage of true positives, false positives and false negatives are determined for each TEM operator. Verified analyses can be used as part of a quality assurance program for asbestos analyses and as a training procedure. This report describes a method for conducting a verified analysis. The method is reported in ASTM format. This version contains a revised procedure, examples and flow charts.

00,527
PB94-172095 Not available NTIS
National Inst. of Standards and Technology (CSTL), Gaithersburg, MD. Inorganic Analytical Research Div.
Local Area Networks in NAA: Advantages and Pitfalls.
Final rept.
M. Blaauw, and R. M. Lindstrom. 1993, 10p.
Pub. in Jnl. of Radioanalytical and Nuclear Chemistry 169, n2 p443-452 1993.

Keywords: *Gamma ray spectroscopy, *Activation analysis, *Local area networks, *Computer networks, Data acquisition, Workstations, Reprints.

Both at IRI and at NIST, Local Area Networks (LANs) are being used to acquire and process data from multiple gamma-ray spectrometers. In this paper, differences and similarities between three systems are discussed, resulting in recommendations for new systems to be set up.

00,528
PB94-185063 Not available NTIS
National Inst. of Standards and Technology (CSTL), Gaithersburg, MD. Inorganic Analytical Research Div.
Classical Analysis: A Look at the Past, Present, and Future.
Final rept.
C. M. Beck. 1994, 14p.
Pub. in Analytical Chemistry 66, n4 p224A-239A, 15 Feb 94.

Keywords: *Analytical techniques, *Chemical analysis, Measuring instruments, Comparison, Performance evaluation, Laboratories, Testing procedures, Reprints, *Classical analysis.

Despite the fact that instrumental analysis has rightfully assumed an overwhelmingly major role in the analytical laboratory, there remains a limited, although important, need for classical analysis. Instrumental analysis is most useful for elemental determinations at minor and trace levels (about 1% all the way down to 1 atom), and in this range classical analysis performs either poorly or not at all. However, instrumental analysis generally does not give high precision and accuracy at major levels (about 1% up to 100%), and in this range classical analysis does perform well. Moreover, instrumental and classical analysis complement each other and can be used in tandem to the analyst's advantage.

00,529
PB94-185071 Not available NTIS
National Inst. of Standards and Technology (CSTL), Gaithersburg, MD. Inorganic Analytical Research Div.
Preparation and Certification of a Rhodium Standard Reference Material Solution.
Final rept.
C. M. Beck, M. L. Salit, R. L. Watters, T. A. Butler, and L. J. Wood. 1993, 4p.
Pub. in Analytical Chemistry 65, n20 p2899-2902, 15 Oct 93.

Keywords: *Rhodium, *Standards, *Chemical analysis, Solutions, Comparison, Certification, Sample preparation, Gravimetric analysis, Spectrum analysis, Solubility, Inorganic salts, Quality assurance, Reprints, *Standard Reference Materials, SRM 3144.

A dual-path approach has been developed for the production of an accurate rhodium solution standard. First, a water-soluble rhodium salt was assayed for rhodium by gravimetry. Second, a different water-soluble rhodium salt was synthesized from a known mass of high-purity rhodium metal. The agreement between both rhodium solution standards, each based on gravimetry, and subject to different random and systematic errors, confirmed the accuracy of their rhodium concentrations. Based on this work an accurate rhodium solution standard (NIST Standard Reference Material (SRM) 3144) was prepared by dissolving in water a weighed

portion of an accurately assayed, homogeneous, water-soluble rhodium salt, which had been dried to constant weight.

00,530
PB94-185253 Not available NTIS
National Inst. of Standards and Technology (CSTL), Gaithersburg, MD. Organic Analytical Research Div.
Liquid Chromatography: Laser-Enhanced Ionization Spectrometry for the Speciation of Organolead Compounds.
Final rept.
K. S. Epler, T. C. O'Haver, and G. C. Turk. 1994, 4p.
Pub. in Jnl. of Analytical Atomic Spectrometry 9, p79-82 Feb 94.

Keywords: *Liquid chromatography, *Chromatographic analysis, *Organometallic compounds, *Lead compounds, Chemical analysis, Ion spectroscopy, Trace amounts, Reprints, Laser enhanced ionization, Standard reference materials.

Liquid chromatography (LC) and laser-enhanced ionization spectrometry (LEI) have been combined to provide a very sensitive method for the measurement of organolead species. Measurement is possible in environmental and biological matrices, which often contain high levels of easily ionized elements that normally interfere with LEI measurements. However, LC is able to resolve the interferents from the analytes, and LEI is sensitive enough to counterbalance the increase in detection limits that results from the use of LC. The method has been applied to the determination of organolead compounds in National Institute of Standards and Technology Standard Reference Material 1566a, Oyster Tissue. Trace levels of trimethyllead were observed in the Oyster Tissue, but concentrations were variable among the samples tested.

00,531
PB94-185261 Not available NTIS
National Inst. of Standards and Technology (CSTL), Gaithersburg, MD. Inorganic Analytical Research Div.
Comparative Strategies for Correction of Interferences in Isotope Dilution Mass Spectrometric Determination of Vanadium.
Final rept.
J. D. Fassett, E. S. Beary, X. Xiong, and L. J. Moore. 1994, 5p.
Pub. in Analytical Chemistry 66, n7 p1027-1031, 1 Apr 94.

Keywords: *Resonance ionization mass spectroscopy, *Mass spectroscopy, *Vanadium, Quantitative chemical analysis, Interference, Chromium, Titanium, Reprints, *Thermal ionization mass spectroscopy, *Isotope dilution mass spectroscopy, Standard reference materials.

Vanadium has been determined in SRM 1573a, Tomato Leaves, by isotope dilution mass spectrometry using thermal ionization (TIMS) and resonance ionization (RIMS). The capabilities of the two techniques to compensate for interferences from chromium and titanium are compared. Results are discussed.

00,532
PB94-185337 Not available NTIS
National Inst. of Standards and Technology (CSTL), Gaithersburg, MD. Inorganic Analytical Research Div.
Frozen Human Serum Reference Material for Standardization of Sodium and Potassium Measurements in Serum or Plasma by Ion-Selective Electrode Analyzers.
Final rept.
P. Gunaratna, W. Koch, R. Paule, N. Greenberg, K. O'Connell, A. Malenfant, A. Okorodudu, R. Miller, D. Kus, G. Bowers, A. Cormier, and P. D'Orazio. 1992, 7p.
Pub. in Clinical Chemistry 38, n8 p1459-1465 1992.

Keywords: *Sodium, *Potassium, *Blood analysis, Blood serum, Standards, Medical laboratories, Interlaboratory comparisons, Ion selective electrode analysis, Atomic spectroscopy, Emission spectroscopy, Reprints, *Standard reference materials.

Three interlaboratory round-robin studies (RR1, RR2, and RR3) were conducted to identify a serum-based reference material that would aid in the standardization of direct ion-selective electrode (ISE) measurements of sodium and potassium. Ultrafiltered frozen serum reference materials requiring no reconstitution reduced between-laboratory variability (the largest source of imprecision) more than did other reference materials. ISE values for RR3 were normalized by the use of two points at the extremes of the clinical range for sodium (i.e., 120 and 160 mmol/L), with values assigned by the flame atomic emission spectrometry (FAES) Reference Method.

00,533
PB94-185980 Not available NTIS
National Inst. of Standards and Technology (CSTL), Gaithersburg, MD. Inorganic Analytical Research Div.
Fourier Transform Atomic Emission Studies Using a Glow Discharge as the Emission Source.
Final rept.
M. R. Winchester, J. C. Travis, and M. L. Salit. 1993, 13p.
Pub. in Spectrochimica Acta 48B, n11 p1325-1337 1993.

Keywords: *Glow discharges, *Emission spectroscopy, Measurement, Precision, Reprints, Fourier transform atomic emission spectroscopy, Photon noise.

The glow discharge (GD) is investigated as a possible atomic emission source for Fourier transform atomic emission spectroscopy (FT-AES). Noise power spectra are presented to demonstrate that GD emission is primarily characterized by photon noise, although a drift noise component exists at extremely low frequencies. The photon noise character is important, as photon noise limited sources are expected to outperform source flicker noise limited sources in terms of measurement precision. The implementation of bandpass restriction and dual channel subtractive noise cancellation as possible means of improving measurement precision are also presented. In both cases, the improvements were found to be minimal, a fact attributed to the probable suitability of the GD for FT-AES.

00,534
PB94-187564 PC A03/MF A01
National Inst. of Standards and Technology, Gaithersburg, MD.
Application of the Electronic Balance in High Precision Pycnometry.
R. M. Schoonover, M. S. Hwang, and W. E. Crupe. May 94, 18p, NISTIR-5422.

Keywords: *Pycnometers, *Electronic equipment, *Weight indicators, Laboratory equipment, Calibrating, Standardization, Density(Mass/Volume), Measuring instruments, Glassware, Liquids, Volume, Precision, Mass, Electronic balance, Liquid density.

Pycnometers are used to measure the density of fluids. Usually pycnometer volume is determined by measuring the mass and temperature of contained water and thereafter is used to determine the density of contained fluid by further weighing. The calibration and use of the pycnometer can be achieved on a modern electronic balance without the use of the usual set of mass standards. This paper explores the electronic balance application to pycnometry, presents supporting data with analysis and discusses a pycnometer design.

00,535
PB94-188836 PC A07/MF A02
National Inst. of Standards and Technology (CSTL), Gaithersburg, MD. Surface and Microanalysis Science Div.
Proficiency Tests for the NIST Airborne Asbestos Program, 1990.
S. Turner, S. S. Doorn, E. B. Steel, K. K. Starner, J. M. Phelps, and E. S. Windsor. May 94, 146p, NISTIR-5431.
Prepared in cooperation with Research Triangle Inst., Research Triangle Park, NC. Center for Environmental Systems.

Keywords: *Asbestos, *Air pollution detection, *Chemical analysis, *Standards, Transmission electron microscopy, Performance evaluation, Laboratories, Sampling, Personnel development, Quality assurance, Quality control, *National Voluntary Accreditation Program, *Proficiency tests.

The National Voluntary Accreditation Program (NVLAP) at the National Institute of Standards and Technology (NIST) has since 1990 had a program to accredit those laboratories involved in the analysis of airborne asbestos by transmission electron microscopy. As a part of that program, laboratories are sent proficiency tests twice yearly to evaluate their ability to correctly analyze samples and to test the general knowledge of laboratory personnel. The results of the tests are sent to the participating laboratories in the form of a summary report. This NIST Internal Report (NISTIR) contains the instructions and summary reports issued for the proficiency tests in 1990 (PT90-1, PT90-2).

00,536
PB94-188844 PC A10/MF A03
National Inst. of Standards and Technology (TS), Gaithersburg, MD. Office of Measurement Services.
Standard Reference Materials: Glass Filters as a Standard Reference Material for Spectrophotometry - Selection, Preparation, Certification, and Use of SRM 930 and SRM 1930.
Special pub. (Final).
R. Mavrodineanu, R. W. Burke, J. R. Baldwin, J. C. Travis, J. C. Colbert, M. V. Smith, and J. D. Messman. Mar 94, 207p, NIST/SP-260/116.
Also available from Supt. of Docs. as SN003-003-03256-5. See also PB-246 437.

Keywords: *Spectrophotometers, *References(Standards), *Optical filters, Performance evaluation, Procedures, Certification, Accuracy, Precision, Calibrating, Electromagnetic absorption, Transmittance, Reproducibility, Wavelengths, *Standard reference materials, SRM 930, SRM 1930.

This publication describes the various factors that can affect the proper functioning of a spectrophotometer and suggests procedures to assess and control these factors. Particular consideration is given to the long- and short-term stability of a spectrophotometer, wavelength accuracy, spectral bandpass, stray radiation, and the accuracy of the transmittance or absorbance scale. A description is given of the Standard Reference Materials (SRMs) that can be used to control these factors. The methods for the preparation, certification, and use of two such materials (SRM 930 and SRM 1930) are also presented. The results obtained in the actual use of the SRMs are examined in some detail. An Appendix contains the reproduction of several publications and Certificates relevant to the subject discussed in this publication.

00,537
PB94-193828 PC A04/MF A01
National Inst. of Standards and Technology (CSTL), Gaithersburg, MD. Surface and Microanalysis Science Div.
Proficiency Tests for the NIST Airborne Asbestos Program - 1991.
S. Turner, E. B. Steel, S. S. Doom, and S. B. Burris. May 94, 52p, NISTIR-5432.
See also PB94-188836. Prepared in cooperation with Research Triangle Inst., Research Triangle Park, NC. Center for Environmental Measurements and Quality Assurance.

Keywords: *Asbestos, *Air pollution detection, *Chemical analysis, *Transmission electron microscopy, Performance evaluation, Sampling, Quality control, Quality assurance, Comparison, *Proficiency tests, National Voluntary Accreditation Program.

The National Voluntary Accreditation Program (NVLAP) at the National Institute of Standards and Technology (NIST) has since 1990 had a program to accredit those laboratories involved in the analysis of airborne asbestos by transmission electron microscopy. As a part of that program, laboratories are sent proficiency tests twice yearly to evaluate their ability to correctly analyze samples and to test the general knowledge of laboratory personnel. The results of the tests are sent to the participating laboratories in the form of a summary report. This NIST Internal Report (NISTIR) contains the instructions and summary reports issued for the proficiency tests in 1991 (PT91-1, PT91-2).

00,538
PB94-193885 PC A03/MF A01
National Inst. of Standards and Technology (MSEL), Gaithersburg, MD. Polymers Div.
Preparation and Monitoring of Lead Acetate Containing Drinking Water Solutions for Toxicity Studies.
Final rept.
W. R. Blair, K. L. Jewett, F. W. Wang, and S. B. Schiller. May 94, 28p, NISTIR-5388.
See also PB86-189875 and PB92-126499. Sponsored by Maryland Univ. at Baltimore.

Keywords: *Drinking water, *Lead inorganic compounds, *Animal husbandry, Water pollution monitoring, Concentration(Composition), Exposure, Toxicity, Absorption spectra, Atomic spectroscopy, Chemical analysis, US NBS, Dosage, *Lead acetate,

FAAS(Flame Atomic Absorption Spectrophotometry), Lead nephropathy, NIST(National Institute of Standards and Technology).

The protocols developed and implemented to provide lead acetate containing drinking water solutions for animal toxicity studies are described in detail. The procedure involved preparation of 20 liter batches of high concentration lead acetate solution (20,000 ppm) at National Institute of Standards and Technology (NIST). Conventional flame atomic absorption spectrophotometry (FAAS) was employed to confirm that the lead concentration of the solution was within five percent of the target value. This solution was then dispensed into containers of appropriate volume such that upon dilution at the animal research facility, drinking water solutions containing lead concentrations of 50, 250 and 1000 ppm were produced. Samples of these diluted solutions and samples taken from animal cage water bottles were returned to NIST for follow-up FAAS determination of lead concentration to insure that animal exposure to lead was meeting experimental goals.

00,539
PB94-194362 PC A03/MF A01
National Inst. of Standards and Technology (CSTL), Gaithersburg, MD. Surface and Microanalysis Science Div.
Proficiency Tests for the NIST Airborne Asbestos Program - 1992.
S. Turner, E. B. Steel, S. S. Doorn, and S. B. Burris. May 94, 48p, NISTIR-5433.
Prepared in cooperation with Research Triangle Inst., Research Triangle Park, NC. Center for Environmental Measurements and Quality Assurance.

Keywords: *Asbestos, *Air pollution detection, *Chemical analysis, *Transmission electron microscopy, Performance evaluation, Sampling, Quality control, Quality assurance, Comparison, *Proficiency tests, National Voluntary Accreditation Program.

The National Voluntary Accreditation Program (NVLAP) at the National Institute of Standards and Technology (NIST) has since 1990 had a program to accredit those laboratories involved in the analysis of airborne asbestos by transmission electron microscopy. As a part of that program, laboratories are sent proficiency tests twice yearly to evaluate their ability to correctly analyze samples and to test the general knowledge of laboratory personnel. The results of the tests are sent to the participating laboratories in the form of a summary report. This NIST Internal Report (NISTIR) contains the instructions and summary reports issued for the proficiency tests in 1992 (PT92-1, PT92-2).

00,540
PB94-198710 Not available NTIS
National Inst. of Standards and Technology (NML), Gaithersburg, MD. Inorganic Analytical Research Div.
Laser Ablation of Thin Films as a Free Atom Source for Pulsed RIMS.
Final rept.
L. Bengtsson, J. Travis, T. B. Lucatorto, K. Kreider, and L. Brown. 1989, 4p.
Contract DEAIO586ER60446
Pub. in Proceedings of the International Symposium on Resonance Ionization Spectroscopy and Its Applications (4th), Gaithersburg, MD., April 10-15, 1988, p167-170 1989. Sponsored by Department of Energy, Washington, DC.

Keywords: *Resonance ionization mass spectroscopy, Chemical analysis, Laser ablation, Pulsed lasers, Trace elements, Thin films, Reproducibility, Sampling, Reprints, Atom sources.

The efficient application of pulsed-laser resonance ionization mass spectrometry (RIMS) to ultrasensitive analysis requires conservation of samples during the analysis dead time. Laser ablation of solids has been shown to provide vapor plumes of appropriate spatial and temporal properties, but free atom fractions suffer from particle formation due to thermal stress fracturing. The authors report here preliminary studies with semitransparent thin (about 50 A) films, intended to improve the reproducibility and atom yield of laser ablation sampling.

00,541
PB94-198736 Not available NTIS
National Inst. of Standards and Technology (NML), Gaithersburg, MD. Gas and Particulate Science Div.
Relative Sensitivity Factors and Useful Yields for a Microfocused Gallium Ion Beam and Time-of-Flight Secondary Ion Mass Spectrometer.
Final rept.
J. Bennett, and D. Simons. 1991, 6p.
Pub. in Jnl. of Vacuum Science and Technology A 9, n3 p1379-1384 1991.

Keywords: *Ion sources, *Gallium ions, Secondary ion mass spectroscopy, Time-of-flight method, Mass spectrometers, Liquid metals, Thin films, Sensitivity, Yield, Magnesium, Calcium, Glass, Reprints.

Relative sensitivity factors for several elements in micrometer size glass particles, bulk glasses and glass thin films have been determined for a Ga(1+) liquid metal ion gun combined with a time-of-flight secondary ion mass spectrometer. The reproducibility of the values within and among glasses of various compositions is better than 20%. Reproducibility is improved by sputter-cleaning the sample prior to data collection. Relative sensitivity factors have also been obtained from bulk glasses using pulsed, low-energy electrons to neutralize charge build-up on the sample. Useful yields for Mg and Ca in a thin glass film were calculated to be a 3.4 x 10(sup -4) and 8.0 x 10(sup -4), respectively.

00,542
PB94-199114 Not available NTIS
National Inst. of Standards and Technology (NML), Gaithersburg, MD. Gas and Particulate Science Div.
Concentration Histogram Imaging: A Scatter Diagram Technique for Viewing Two or Three Related Images.
Final rept.
D. S. Bright, and D. E. Newbury. 1991, 7p.
Pub. in Analytical Chemistry 63, n4 p243A-244A, p246A-250A, 15 Feb 91.

Keywords: *Image processing, *Histograms, *Concentration(Composition), *Microanalysis, Reprints, Scatter diagrams, Quantitative analysis, Chemical analysis, X-ray analysis, *Concentration histogram imaging, X-ray maps.

Quantitative compositional mapping involves the production of images, which directly depict the concentrations of the elemental constituents present in a specimen. A problem is encountered when numerical concentration information is to be presented in the form of an image--the authors wish to simultaneously present both spatial position information and numerical concentration data for two or more constituents. The authors have developed the Concentration Histogram Image (CHI) which is a modified scatter diagram, where compositional maps are transformed from real space to concentration space. Unlike the scatter diagram, the CHI is displayed by encoding the frequency information with a thermal color scale. The authors have implemented the CHI on various computers to view the CHI for selected areas of the sample and show the correspondence between features (clumps or bands of points) in the CHI with specific areas in the original maps. The CHI is a useful diagnostical tool for detecting inhomogeneities in materials, checking quantitative corrections of x-ray maps, evaluating sampling and measurements statistics, and selecting features of interest for further analysis.

00,543
PB94-199155 Not available NTIS
National Inst. of Standards and Technology, Gaithersburg, MD. Occupational Health and Safety Div.
Germanium Detector Optimization of MDA for Efficiency vs. Low Intrinsic Background.
Final rept.
D. R. Brown, and L. A. Slaback. 1988, 7p.
Pub. in Proceedings of Health Physics Society Midyear Topical Meeting on Instrumentation (22nd), San Antonio, TX., December 4-8, 1988, p46-52.

Keywords: *Detectors, *Germanium, Samples, Spectrum analysis, Standards, Performance evaluation, Reprints, *Minimum detectable activity.

The paper will discuss research performed in selecting a high purity germanium detector of between 20 and 45 percent relative efficiency. The primary goal will be to optimize the minimum detectable activity (MDA) of the detector. Several factors will be evaluated that contribute to MDA; such as, relative background nuclides in the detector structural material, relative detector efficiency, and shield design. Results to be presented include efficiencies for various sample geometries, MDA for several detector/sample configurations, and gamma spectrum analysis of detector background counts.

00,544
PB94-199171 Not available NTIS
National Inst. of Standards and Technology (CSTL), Boulder, CO. Thermophysics Div.
Applications of the Vortex Tube in Chemical Analysis.
Final rept.
T. J. Bruno. 1992, 13p.
Pub. in Process Control and Quality 3, p195-207 1992. Sponsored by Gas Research Inst., Chicago, IL.

Keywords: *Hilsch tubes, Heat transfer, Laboratory equipment, Chemical analysis, Reprints, *Vortex tubes.

The vortex tube is a unique heating and cooling device that has no moving parts, but operates only with a stream of compressed air. Although first described nearly six decades ago, it has only recently been 'discovered' by scientists and engineers outside of the heat transfer fraternity. The vortex tube can provide air streams at temperatures as low as -40 C, and as high as 190 C. It is especially useful for heating and cooling the small, irregularly shaped instrument components and devices that are so common in chemical analysis. In this paper, the operational essentials of the vortex tube are presented, and several applications in chemical analysis are discussed.

00,545
PB94-199197 Not available NTIS
National Inst. of Standards and Technology (CSTL), Boulder, CO. Thermophysics Div.
Simple and Efficient Low-Temperature Sample Cell for Infrared Spectrophotometry.
Final rept.
T. J. Bruno. 1992, 2p.
Pub. in Review of Scientific Instruments 63, n10 p4459-4460 Oct 92. Sponsored by Gas Research Inst., Chicago, IL.

Keywords: *Optical equipment, *Infrared spectrophotometers, Hilsch tubes, Solvents, Refrigerants, Design, Reprints, *Low temperature cell, Vortex tubes.

It is often helpful in infrared spectrophotometry to contain a liquid sample in a cell that is maintained at a subambient or nearly cryogenic temperature. Volatile samples and solvents being studied can vaporize and form bubbles in conventional liquid sample cells, especially under the influence of the infrared radiation from the source in a continuous-wave instrument. This will result in the formation of spikes on the spectra. In addition, some analytes are thermally labile and must be protected from warming while the spectrum is recorded. An easily constructed cell cooled with a vortex tube can solve many of these problems, and is in many ways an improvement over commercial devices. In this note, such a cell is described and its application to volatile alternative refrigerants is discussed.

00,546
PB94-199205 Not available NTIS
National Inst. of Standards and Technology (CSTL), Boulder, CO. Thermophysics Div.
Simple, Inexpensive Apparatus for Sample Concentration.
Final rept.
T. J. Bruno. 1992, 2p.
Pub. in Jnl. of Chemical Education 69, n10 p837-838 Oct 92. Sponsored by Gas Research Inst., Chicago, IL.

Keywords: *Concentrating, *Laboratory equipment, *Design, Reprints, *Sample concentrators, Vortex heating and cooling.

In many synthetic and analytical procedures, it is often necessary to concentrate samples by controlled evaporation of the solvent. Several glass concentrators are available (such as the micro or Kuderna Danish type), consisting of a solution vessel with a collection cold finger directly below, and a reflux tube above. In conventional practice, the solution vessel section is electrically heated in an aluminum block, while the cold finger is kept in ambient air at a lower temperature. An alternative to this technique that provides several important advantages is to use a Ranque-Hilsch vortex tube to both heat the solution vessel and cool the cold finger. In this note, the construction and application of such an apparatus is described.

00,547
PB94-199460 Not available NTIS
National Inst. of Standards and Technology (NML), Gaithersburg, MD. Surface Science Div.
Performance of a Reflectron Energy Compensating Mirror.
Final rept.
P. P. Camus, and A. J. Melmed. 1991, 5p.
Pub. in Surface Science 246, n1-3 p415-419 1991.

Keywords: Surface analysis, Performance, Resolution, Mirrors, Reprints, *Atom probes, Einzel lenses, Reflectrons.

This paper describes the performance characteristics of a first order reflectron energy compensating lens system on a voltage-pulsed atom probe. The performance of the instrument using the electrostatic mirror is compared to that obtained using the same electronics and a linear flight path, and the effect of an einzel lens on the performance is presented.

00,548
PB94-199726 Not available NTIS
National Inst. of Standards and Technology (NML), Gaithersburg, MD. Inorganic Analytical Research Div.
Establishing Quality Measurements for Inorganic Analysis of Biomaterials.
Final rept.
J. R. DeVoe. 1991, 6p.
Pub. in American Chemical Society Symposium Series - Biol. Trace Elem. Res., v445 p101-106 1991.

Keywords: *Biocompatible materials, *Chemical analysis, *Inorganic compounds, *Trace elements, Diseases, Quality assurance, Interlaboratory comparisons, Reprints.

While there have been a number of excellent studies showing the effects of trace element concentrations in biomaterials in a number of diseases and other health-related processes, the inconsistencies of quantitative analytical data still limit progress. It is suggested that a well integrated system of laboratories that is dedicated to analytical chemistry quality assurance can provide an interlaboratory structure that will improve the quality of the measurements. Quantitative measurement of the elemental-bound compound appears to be greatly needed, and significant effort needs to be expended in this most difficult area. Progress can be greatly enhanced by including the analytical chemist in the biomedical research team.

00,549
PB94-200516 Not available NTIS
National Inst. of Standards and Technology (CSTL), Gaithersburg, MD. Organic Analytical Research Div.
Carotenoid Reversed-Phase High-Performance Liquid Chromatography Methods: Reference Compendium.
Final rept.
N. E. Craft. 1992, 21p.
Pub. in Methods in Enzymology, Chapter 17, v213 p185-205 1992. Sponsored by National Cancer Inst., Bethesda, MD.

Keywords: *Carotenoids, *Chemical analysis, High pressure liquid chromatography, Solvents, Temperature, Test methods, Reprints.

A survey of reversed-phase liquid chromatography (LC) methods for the separation of carotenoids is tabulated. The tables include carotenoid sources, individual carotenoids separated, LC stationary phase, LC mobile phase, flow rate, and column temperature. The influence of various stationary (pore diameter, carbon load, mode of synthesis, end-capping) and mobile phase (modifiers, buffers) parameters on the separation and recovery of carotenoid compounds are discussed and illustrated. Both isocratic and gradient reversed-phase LC methods developed at NIST for the separation of carotenoids are presented.

00,550
PB94-200599 Not available NTIS
National Inst. of Standards and Technology (NML), Gaithersburg, MD. Gas and Particulate Science Div.
Importance of Chemometrics in Biomedical Measurements.
Final rept.
L. A. Currie. 1991, 27p.
Pub. in American Chemical Society Symposium Series 445, p74-100 1991.

Keywords: *Biomedical measurements, Trace elements, Multivariate analysis, Quality control, Mathematics, Statistics, Environmental pollutants, Diet, Reprints, *Chemometrics.

Chemometrics as a discipline blends modern mathematical and statistical techniques with chemical knowledge for the design, control, and evaluation of chemical measurements. For complex systems, such as those involving biomedical trace element research the multi-disciplinary efforts toward problem formulation and measurement process design and evaluation can be substantially aided by exploratory chemometric approaches. Following a brief overview of potential chemometrics contributions, primary attention is to be given to exploratory multivariable data analysis techniques, which can capture the essence of a complex data set in a few, visualizable dimensions. Such techniques are appropriate because nuclear-related measurements, quality control samples and data, global dietary intakes, and biological compositions all comprise multiple chemical species, frequently exhibiting correlated behavior. Applications of some of the more powerful techniques, such as principal component factor analysis, are illustrated by multivariable interlaboratory quality control, assessment of pollutant origins, and exploration of daily dietary intake data.

00,551
PB94-200607 Not available NTIS
National Inst. of Standards and Technology (NML), Gaithersburg, MD. Gas and Particulate Science Div.
Metrological Measurement Accuracy: Discussion of 'Measurement Error Models' by Leon Jay Gleser.
Final rept.
L. A. Currie. 1991, 9p.
Pub. in Chemom. Intell. Lab. Syst. 10, n1-2 p59-67 1991.

Keywords: *Metrology, Multivariate analysis, Factor analysis, Error analysis, Accuracy, Matrices, Reprints, *Chemometrics.

The paper represents a contribution to the chemist - statistician colloquy on multivariate measurement and model error. Specifically, it is a discussion of 'measurement error models' by Leon Jay Gleser (Dept. of Mathematics and Statistics, Univ. of Pittsburgh). Basic topics addressed include the 'errors in x(-) and y(-)', extended to the multivariable domain, as realized in factor analysis and errors in variables regression. The distinction between structural and functional models for statistical relationships is considered, as well as their asymptotic character. Most importantly, approaches are suggested for complementing the important advances in mathematical statistics (as reviewed by Gleser) with chemical knowledge and insight. These take three forms: chemical limitations imposed on the several statistical assumptions of the measurement error models (especially those involving the diagonal and off-diagonal elements of the variance covariance matrix); chemically feasible approaches to measurement refinement, such as tracer and unique variable techniques for reducing multi-collinearity; and linear and non-linear model refinement, based on scientific knowledge of the system under investigation.

00,552
PB94-210168 PC A03/MF A03
National Inst. of Standards and Technology (CSTL), Gaithersburg, MD. Surface and Microanalysis Science Div.
Airborne Asbestos Method: Standard Practice for Recording Transmission Electron Microscopy Data for the Analysis of Asbestos Collected onto Filters. Version 1.0.
E. S. Windsor, S. Turner, and E. B. Steel. Feb 94, 14p, NISTIR-5358.

Keywords: *Asbestos, *Test methods, *Chemical analysis, Air pollution detection, Quality assurance, Water pollution detection, Electron microscopy, Standard, Procedures, US NBS, *TEM(Transmission electron microscopy), Transmission electron microscopy, Verified analysis, National Institute of Standards and Technology.

This is a standard practice that describes the procedure for recording information obtained during a Transmission Electron Microscope (TEM) analyses of asbestos. Included in this practice is a TEM analysis form that serves as a record and work sheet for the analyst. Forms completed according to this practice allow for the verification of asbestos structures determined by two or more analysts. The practice is designed to give a uniform recording format so that analytical data may be compared among laboratories.

00,553
PB94-211620 Not available NTIS
National Inst. of Standards and Technology (CSTL), Gaithersburg, MD. Biotechnology Div.
L-threo-beta-Hydroxyhistidine, an Unprecedented Iron(III) Ion-Binding Amino Acid in a Pyoverdine-type Siderophore from Pseudomonas fluorescens 244.
Final rept.
D. K. Hancock, B. Coxon, S. Y. Wang, J. M. Bellama, V. E. White, and D. J. Reeder. 1993, 3p.
Pub. in Jnl. of Chem. Soc., Chemical Communications 5, p468-470 1993.

Keywords: *Nuclear magnetic resonance, *Mass spectrometry, *Amino acids, *Pseudomonas fluorescens, Ions, Binding sites, Reprints, *L-threo-beta-hydroxyhistidine, Pyoverdine.

Nuclear magnetic resonance spectroscopy and mass spectrometric analysis of a unique pyoverdine-type siderophore isolated from the culture filtrate of Pseudomonas fluorescens 244 reveals a new natural amino acid, L-threo-beta-hydroxyhistidine, that functions as an iron(III) bidentate ligand.

00,554
PB94-212289 Not available NTIS
National Inst. of Standards and Technology (NML), Gaithersburg, MD. Inorganic Analytical Research Div.
Determination of Boron and Lithium in Diverse Biological Matrices Using Neutron Activation - Mass Spectrometry (NA-MS).
Final rept.
G. V. Iyengar, W. B. Clarke, and R. G. Downing. 1990, 5p.
Pub. in Fresenius Jnl. of Analytical Chemistry 338, n4 p562-566 1990.

Keywords: *Neutron activation analysis, *Mass spectrometry, *Boron, *Lithium, *Chemical analysis, Trace elements, Food, Tissues(Biology), Reprints.

Essential features of the Neutron Activation-Mass Spectrometry (Na-MS) technique are described. Applicability of this technique for the simultaneous determination of boron and lithium is demonstrated for a diverse group of biomaterials. This is a non-destructive type of analytical technique, and dynamic in nature since its coverage extends to a broad range of concentration levels. At the post-irradiation stage, extraneous contamination by natural lithium or boron is nonexistent, since only the radioactive products are the analytes assayed. Coupling the nuclear activation phenomenon which generates (4)He and (3)He (from (10)B and (6)Li, respectively), with the high accuracy potential of mass spectrometry forms the principle of this technique. Under ideal conditions the detection limit is extendable to pg/g concentration ranges and therefore, it is extremely well suited to investigate the natural concentration levels of boron and lithium in biomaterials. The potential of this method for the determination of lithium in biomedical trace element research investigations is of special significance since determination of sub-ppb levels of lithium faces serious analytic difficulties by other analytical techniques due to mainly contamination control and in some cases also to detection limit problems.

00,555
PB94-213386 Not available NTIS
National Inst. of Standards and Technology (NML), Gaithersburg, MD. Inorganic Analytical Research Div.
High-Sensitivity Determination of Iodine Isotopic Ratios by Thermal and Fast Neutron Activation.
Final rept.
R. M. Lindstrom, G. J. Lutz, and B. R. Norman. 1991, 12p.
Pub. in Jnl. of Trace Microprobe Technology 9, n1 p21-32 1991.

Keywords: *Neutron activation analysis, *Activation analysis, *Iodine 129, *Iodine 127, Radioactive contaminants, High sensitivity, Neutron irradiation, Fission products, Isotope ratio, Thermal neutrons, Fast neutrons, Reprints.

In order to study the transformations of radioiodine in the environment, the analytical method used for the determination of iodine-129 concentrations and of (129)I/(127)I ratios must be capable of measuring concentrations down to the present-day background level, of order 100 million atoms/gram, with acceptable precision and low blank. A neutron activation procedure has been developed to perform reliable concentration

measurements at this level in a few grams of sample. (129)I/(127)I ratios as low as 6 X 10(sup -10) have been measured. The procedure described uses oxygen combustion both before and after irradiation to separate iodine from other elements. Irradiation is performed with optimized fluxes of both thermal and fast neutron. Bromine-82 and other interferences are removed by a gas-solid reaction with Hydrated Manganese Dioxide. High-resolution gamma-ray assay permits small amounts of induced (130)I to be measured simultaneously with (126)I produced from stable iodine by the (n,2n) reaction.

00,556
PB94-213394 Not available NTIS
National Inst. of Standards and Technology (CSTL), Gaithersburg, MD. Inorganic Analytical Research Div.
Neutron Capture Prompt Gamma-Ray Activation Analysis at the NIST Cold Neutron Research Facility.
Final rept.
R. M. Lindstrom, R. Zeisler, D. H. Vincent, E. A. Mackey, D. L. Anderson, D. D. Clark, R. R. Greenberg, and C. A. Stone. 1993, 6p.
Pub. in Jnl. of Radioanalytical and Nuclear Chemistry 167, n1 p121-126 1993.

Keywords: *Activation analysis, Radiation measuring instruments, Neutron capture gamma rays, Prompt gamma radiation, Chemical analysis, Cold neutrons, NBSR reactor, Radiation shielding, Reprints, CNRF facility, US NIST.

An instrument for neutron capture prompt gamma-ray activation analysis (PGAA) has been constructed as part of the Cold Neutron Research Facility at the 20 MW National Institute of Standards and Technology Research Reactor. The neutron fluence rate (thermal equivalent) is 1.5 X 10(sup 8)n/sq cm/s with negligible fast neutrons and gamma-rays. With compact geometry and hydrogen-free construction, the sensitivity is sevenfold better than an existing thermal instrument. Hydrogen background is thirtyfold lower.

00,557
PB94-216140 Not available NTIS
National Inst. of Standards and Technology (CSTL), Gaithersburg, MD. Inorganic Analytical Research Div.
Scattering and Absorption Effects in Neutron Beam Activation Analysis Experiments.
Final rept.
E. A. Mackey, and J. R. D. Copley. 1993, 6p.
Pub. in Jnl. of Radioanalytical and Nuclear Chemistry 167, n1 p127-132 1993.

Keywords: *Neutron activation analysis, *Activation analysis, Monte Carlo method, Prompt gamma radiation, Neutron absorption, Neutron scattering, Sensitivity, Simulation, Corrections, Reprints.

We have investigated the effects of scattering and absorption in neutron beam activation analysis experiments, both by direct measurement and by Monte Carlo simulation. Significant sensitivity enhancements occur for thin disks placed at 45 deg to the beam but very much smaller effects occur for spheres. The agreement between measurement and calculation is generally good.

00,558
PB94-216157 Not available NTIS
National Inst. of Standards and Technology (NML), Gaithersburg, MD. Inorganic Analytical Research Div.
Effects of Target Shape and Neutron Scattering on Element Sensitivities for Neutron-Capture Prompt Gamma-ray Activation Analysis.
Final rept.
E. A. Mackey, G. E. Gordon, R. M. Lindstrom, and D. L. Anderson. 1991, 5p.
Pub. in Analytical Chemistry 63, n3 p288-292 1991.

Keywords: *Activation analysis, Neutron capture gamma rays, Neutron scattering, Sensitivity, Hydrogen, Reprints, Target shape.

A study of the effects of neutron scattering by hydrogen on elemental sensitivities of in-beam neutron capture prompt gamma-ray activation analysis (PGAA) is presented. Elemental sensitivities (counts/s/mg) for H, B, Na, Cl, K, Mn, Br, Ag, Cd, I, Sm, and Gd, increase linearly with H density (g/mL). Nine of the twelve elements studied undergo 1.69 + or - 0.18% enhancement per percent increase in H density. The enhancement of the sensitivity for H itself varies with matrix composition. In a scattering matrix, elemental sensitivity is also a function of target shape. For several series of disk-shaped hydrogenous targets, elemental sensitivities increase with decreasing target thickness until, at some limiting thickness the probability for multiple interactions begins to decrease and this trend is reversed. Consistent with theory, sensitivities measured for spherical hydrogenous targets show no enhancement.

00,559
PB94-216348 Not available NTIS
National Inst. of Standards and Technology (NML), Gaithersburg, MD. Gas and Particulate Science Div.
Study of Diffusion Zones with Electron Microprobe Compositional Mapping.
Final rept.
R. B. Marinenko, D. S. Bright, C. A. Handwerker, and J. J. Mecholsky. 1990, 3p.
Pub. in Microbeam Analysis 25, p190-192 1990.

Keywords: *Electron microprobe analysis, X-ray analysis, Reprints, *Diffusion zones, *Compositional mapping, Metal-metal interfaces, Glass-metal interfaces, X-ray mapping.

Electron microprobe x-ray compositional mapping has been used to study diffusion zones between metal-metal and glass-metal interfaces. Image analysis techniques including gray-level enhancement, product and quotient images, and concentration-histogram images have proven to be extremely useful in visualizing the extent of diffusion. The qualitative and quantitative information provided by these digital acquisition and display techniques far exceeds what conventional line scan and x-ray dot maps could provide.

00,560
PB94-219250 (Order as PB94-219219, PC A06/MF A02)
National Inst. of Standards and Technology, Gaithersburg, MD.
Measurement and Uncertainty of a Calibration Standard for the Scanning Electron Microscope.
J. Fu, M. C. Croarkin, and T. V. Vorburger. 1994, 9p.
Included in Jnl. of Research of the National Institute of Standards and Technology, v99 n2 p191-199 Mar/Apr 94.

Keywords: *Scanning electron microscopy, *Calibration standards, Precision, Data covariances, Interferometers, Measuring instruments, Random error, Standard error, Uncertainty, SRM(Standard reference material), SRM-484, National Institute of Standards and Technology.

Standard Reference Material 484 is an artifact for calibrating the magnification scale of a Scanning Electron Microscope (SEM) within the range of 1000 x to 20000 x. Seven issues, SRM-484, and SRM-484a to SRM-484f, have been certified between 1977 and 1992. This publication documents the instrumentation, measurement procedures and determination of uncertainty for SRM-484 and illustrates with data from issues 484e and 484f.

00,561
PB94-219383 (Order as PB94-219326, PC A05/MF A02)
Mississippi State Univ., Mississippi State.
Theoretical Analysis of the Coherence-Induced Spectral Shift Experiments of Kandpal, Vaishya, and Joshi.
J. T. Foley, and M. Wang. 1994, 14p.
Included in Jnl. of Research of the National Institute of Standards and Technology, v99 n3 p267-280 May/Jun 94.

Keywords: *Spectroscopy, *Radiometry, *Spectral shift, Optus, Coherence, Wolf shifts.

The optical system used by Kandpal, Vaishya, and Joshi in their experiments on coherence-induced spectral shifts is analyzed theoretically. An approximate form for the cross-spectral density in the secondary source plane is obtained, and it is shown that, contrary to the assertions of Kandpal, Vaishya, and Joshi, the corresponding complex degree of spectral coherence in this plane is wavelength dependent. After making some assumptions about the behavior of the interference filter used in the system, an approximate form for the spectrum of the light on-axis in the observation plane is obtained. It is shown that the peak wavelengths of this spectrum do not agree with those reported by Kandpal, Vaishya, and Joshi. Possible reasons for this disagreement are discussed.

00,562
PB95-107165 Not available NTIS
National Inst. of Standards and Technology (NML), Gaithersburg, MD. Gas and Particulate Science Div.
Electron Probe X-Ray Microanalysis.
Final rept.
D. E. Newbury. 1992, 17p.
Pub. in Encyclopedia of Materials Characterization: Surfaces, Interfaces, Thin Films, Chapter 3.5, p175-191 1992.

Keywords: *Electron probes, *Microanalysis, *X-ray anlaysis, Electron scanning, Electron microscopy, Spatial resolution, Digital systems, Quantitative analysis, Qualitative analysis, Reprints, Elemental analysis, Scanning electron microscopy, Compositional maps.

Electron probe x-ray microanalysis (EPMA) is an elemental analysis technique based upon bombarding a specimen with a focussed beam of energetic electrons (beam energy from 5 - 30 keV) to induce emission of characteristic x-rays (energy range from 0.1 - 15 keV). The energy (wavelength) of the x-rays identifies the elements present in the specimen (qualitative analysis), and the x-ray intensity can be related to the quantity present (quantitative analysis). Elemental coverage extends from beryllium to the actinides. Detection limits are approximately 100 parts per million for elements with atomic numbers greater than 10. Spatial distributions of elemental constituents can be visualized qualitatively by x-ray area scans (dot maps) and quantitatively by digital compositional maps.

00,563
PB95-107173 Not available NTIS
National Inst. of Standards and Technology (NML), Gaithersburg, MD. Gas and Particulate Science Div.
Microanalysis to Nanoanalysis: Measuring Composition at High Spatial Resolution.
Final rept.
D. E. Newbury. 1990, 28p.
Pub. in Nanotechnology 1, n2 p103-130 Oct 90.

Keywords: *Spectrochemistry analysis, *Microanalysis, *Measuring instruments, *Spatial resolution, Mass spectrometers, Electron probes, X-ray analysis, Auger electron spectroscopy, Electron scanning, Electron microscopy, High resolution, Reprints, *Nanoanalysis, Laser microbe mass spectrometry, Secondary ion mass spectrometry, Field ion microscopy, Composition.

Spatially-resolved analysis of elemental, isotopic, and molecular constituents is possible with microanalysis and nanoanalysis techniques. At the micrometer scale of spatial resolution, electron probe x-ray microanalysis provides elemental coverage from Be to the actinides with detection limits in the range from 100-1000 parts per million (ppm). Secondary ion mass spectrometry and laser microprobe mass spectrometry detect all elements and isotopes with sensitivity from parts per billion to parts per million, and molecular signals can also be detected. Molecular microanalysis is also performed with photon detection techniques, including infrared, fluorescence, and Raman spectroscopies. Analytical electron microscopy and time-of-flight secondary ion mass spectrometry extend spatial resolution to the 100-nm spatial level.

00,564
PB95-107181 Not available NTIS
National Inst. of Standards and Technology (CSTL), Gaithersburg, MD. Surface and Microanalysis Science Div.
Design of a Protocol for an Electron Probe Microanalyzer k-Value Round Robin.
Final rept.
D. E. Newbury, and R. B. Marinenko. 1989, 3p.
Pub. in Microbeam Analysis 24, p257-259 1989.

Keywords: *X-ray analysis, *X-ray spectroscopy, Microanalysis, Matrices, Correction, Quantitative analysis, Reprints, *Electron probe microanalysis, *k-value.

The basic measurement in quantitative electron probe microanalysis is the determination of the 'k-value', which is the ratio of the characteristic x-ray intensity measured for an unknown to that measured for a standard. Models for quantitative matrix corrections are tested on suites of k-value measurememts which are not standardized. A k-value round robin is planned which will attempt to establish a new base of measurements with sufficient accuracy and precision to permit adequate testing of the models. A proposal for the measurement protocol for the k-value round robin is described. This protocol is critical if adequate measurements are to be obtained.

00,565
PB95-107199 Not available NTIS
National Inst. of Standards and Technology (NML), Gaithersburg, MD. Gas and Particulate Science Div.
Compositional Mapping of the Microstructure of Materials.
Final rept.
D. E. Newbury, R. B. Marinenko, R. L. Myklebust, and D. S. Bright. 1991, 19p.
Pub. in Images of Materials, Chapter 10, p290-308 1991.

Keywords: *Microstructure, *Mass spectrometers, *Image processing, Reprints, Microanalysis, Electron probes, Mapping, Chemical analysis, Digital systems, Compositional mapping, Secondary ion mass spectrometry, Microbeam analysis.

Recent developments in electron probe microanalysis and secondary ion mass spectrometry techniques enable the analyst to prepare compositional maps of the microstructure of materials. The technique of compositional mapping involves performing a complete quantitative analysis at each beam location in the imaged field of view on the specimen. The images directly convey the sense of the spatial distribution and compositional interrelationships of the elemental constituents in the microstructure. The images are supported at every picture element by numerical values of the concentrations, as well as data on the statistical precision of the measurement. The combination of images and conventional numerical concentration data provides a powerful tool for microstructural analysis.

00,566
PB95-107249 Not available NTIS
National Inst. of Standards and Technology (NML), Gaithersburg, MD. Organic Analytical Research Div.
Separation and Identification of Organic Gunshot and Explosive Constituents by Micellar Electrokinetic Capillary Electrophoresis.
Final rept.
D. M. Northrop, D. E. Martire, and W. A. MacCrehan. 1991, 5p.
Pub. in Analytical Chemistry 63, n10 p1038-1042 1991.

Keywords: *Electrophoresis, *Forensic science, *Chemical explosives, Capillaries, Micellar systems, Sodium sulfates, Parameters, Chromatography, Reprints, *MECC(Micellar electrokinetic capillary chromatography), *Micellar electrokinetic capillary chromatography, Gunshot residue, Sodium dodecylsulfate, Capillary zone electrophoresis.

Micellar electrokinetic capillary chromatography (MECC) was used to effect a rapid and efficient separation of some common constituents of gunshot and explosive residues. A separation of 26 constituents of interest was accomplished in under 10 minutes with efficiencies typically between 200,000 and 400,000. The effects of various experimental parameters were studied. Sodium dodecylsulfate (SDS) concentration, pH, addition of a tetraalkylammonium salt, capillary diameter, and injection times were all examined in order to optimize the system. It was found that capillary diameter and injection time played an important role in improving detection limits and efficiencies. This method was applied to extracts from swabbings of a .38 caliber and a .45 caliber shell casing demonstrating the presence of gunshot residues.

00,567
PB95-107272 Not available NTIS
National Inst. of Standards and Technology (TS), Gaithersburg, MD. Office of Measurement Services.
Certification, Development and Use of Standard Reference Materials.
Final rept.
S. D. Rasberry, and T. E. Gills. 1991, 6p.
Pub. in Spectrochimica Acta B 46, n12 p1577-1582 1991.

Keywords: *Chemical analysis, *Quality assurance, *Standards, Accuracy, Certification, Concentration(Composition), Procedures, Environmental tests, Industries, Clinical medicine, Nutrition, Construction materials, Reprints, *Standard reference materials.

Analytical measurements are increasingly important to industrial quality assurance (QA) and to critical decision making in such fields as clinical, nutritional, and environmental chemistry. Several factors are important to attaining analyses that are reliably accurate. Some of these include well-designed methods, trained staff, adequate instrumentation, reliable reference materials, laboratory QA procedures, and periodic proficiency testing. The paper will focus on the role of reference materials in accurate chemical analysis. Fundamental attributes of reference materials will be described together with details on how limits of uncertainty are established for certified values. Examples will be drawn from materials recently certified at NIST. Besides industrial examples, such as new alloys and construction materials such as cement and glass, recent clinical, nutritional, and environmental certifications will be cited. Matrices for these types of materials are very wide-ranging and includes human serum (for vitamins in serum, in whole egg powder, and in diet material), lead in reference fuel, organics in cod liver oil, and several others.

00,568
PB95-108536 Not available NTIS
National Inst. of Standards and Technology (CSTL), Gaithersburg, MD. Surface and Microanalysis Science Div.
Formation of Technical Committee 201 on Surface Chemical Analysis by the International Organization for Standardization.
Final rept.
C. J. Powell, and R. Shimizu. 1993, 4p.
Pub. in Surface and Interface Analysis 20, p322-325 1993.

Keywords: *Chemical analysis, *Surface analysis, Standards, Reprints, International Organization for Standardization, Technical Committee 201.

The International Organization of Standardization (ISO) recently created a new Technical Committee (ISO/TC 201) on Surface Chemical Analysis in response to a proposal from Japan. As of February 1993, ten national standards bodies had indicated willingness to become participating members of ISO/TC 201 (Austria, China, Germany, Italy, Japan, Russia, Sweden, Turkey, the United Kingdom and the United States of America) and fifteen national standards bodies had indicated willingness to become observer members (Australia, Belgium, Egypt, Finland, France, India, Ireland, Korea, Norway, Philippines, Poland, Romania, Singapore, South Africa and Switzerland). The following subcommittees are planned: Terminology; General Procedures; Data Management and Treatment; Depth Profiling; Auger Electron Spectroscopy; Secondary Ion Mass Spectrometry and X-ray Photoelectron Spectroscopy. ISO/TC 201 will develop international standards and will consider standards and documents prepared by other groups as potential international standards. Information is given in this article on the purpose, structure and planned work of ISO/TC 201.

00,569
PB95-108742 Not available NTIS
National Inst. of Standards and Technology (NML), Gaithersburg, MD. Gas and Particulate Science Div.
Addition of M and L-Series Lines to NIST Algorithm for Calculation of X-Ray Tube Output Spectral Distributions.
Final rept.
P. A. Pella, L. Feng, and J. A. Small. 1991, 2p.
Pub. in X-ray Spectrometry 20, n3 p109-110 1991.

Keywords: *X-ray fluorescence analysis, *X-ray tubes, Spectral energy distribution, Computation, Tungsten, Gold, Reprints, M lines, L lines, NIST algorithm.

Characteristic M x-ray tube target lines and some minor L-series lines have been added to a previously developed National Institute of Standards and Technology (NIST) algorithm for calculation of the output spectral distributions from x-ray tubes. This algorithm is used in first principle calculations for correction of interelement effects in quantitative x-ray fluorescence analysis. The M lines from x-ray tube targets such as W and Au can be important for excitation of low atomic number elements in some applications. Also, minor L-series lines have been added to give a more complete description of the L-series in the calculated output spectral distribution.

00,570
PB95-126108 Not available NTIS
National Inst. of Standards and Technology (NML), Gaithersburg, MD. Gas and Particulate Science Div.
Use of Kinetic Energy Distributions to Determine the Relative Contributions of Gas Phase and Surface Fragmentation in KeV Ion Sputtering of a Quaternary Ammonium Salt.
Final rept.
G. Gillen. 1991, 10p.
Pub. in International Jnl. of Mass Spectrometry and Ion Processes 105, n3 p215-224 1991.

Keywords: *Ammonium compounds, *Mass spectroscopy, *Secondary ion mass spectroscopy, *Quaternary ammonium salts, Organic nitrogen compounds, Kinetic energy, KeV range, Fragmentation, Sputtering, Reprints.

Kinetic energy distributions have been used to evaluate the extent to which gas phase decompositions contribute to the production of fragment ions in organic secondary ion mass spectra. Molecular kinetic energy distributions demonstrate that many fragment ions have a prominent gas phase component which may account for as much as 50% of the observed fragment ion signal obtained in a double focussing mass spectrometer.

00,571
PB95-126124 Not available NTIS
National Inst. of Standards and Technology (NML), Gaithersburg, MD. Gas and Particulate Science Div.
Molecular Ion Imaging and Dynamic Secondary Ion Mass Spectrometry of Organic Compounds.
Final rept.
G. Gillen, D. S. Simons, and P. Williams. 1990, 9p.
Pub. in Analytical Chemistry 62, n19 p2122-2130 1990.

Keywords: *Secondary ion mass spectroscopy, *Mass spectroscopy, *Imaging techniques, Quaternary ammonium salts, Aromatic hydrocarbons, Amino acids, Molecular ions, Radiation damage, Fragmentation, Reprints, *Ion imaging.

An ion microscope equipped with a resistive anode encoder imaging system has been used to acquire molecular secondary ion images, with lateral resolutions on the order of 1 micrometer, from several quaternary ammonium salts, an amino acid, and a polynuclear aromatic hydrocarbon, which were deposited onto copper transmission electron microscope grids. All images were generated using the secondary ion signal of the parent molecular species. The primary ion dose dependence of parent and fragment molecular ion signal decays indicate that, for many bulk organic compounds, bombardment-induced fragmentation of parent molecules reaches a saturation at primary ion doses of 1-8 x 10(sup 14) ions/sq cm. Subsequent ion impacts do not significantly contribute to further accumulation of damage in the sample, resulting in desorption of intact parent molecular ions even after prolonged ion bombardment. This saturation process allows molecular images to be obtained at high primary ion doses and allows depth profiles to be obtained from simple molecular/metal test structures.

00,572
PB95-140141 Not available NTIS
National Inst. of Standards and Technology (NEL), Gaithersburg, MD. Statistical Engineering Div.
Combining Data from Independent Chemical Analysis Methods.
Final rept.
S. Schiller, and K. R. Eberhardt. 1991, 7p.
Pub. in Spectrochimica Acta B 46, n12 p1607-1613 1991.

Keywords: *Chemical analysis, Statistical analysis, Data analysis, Inhomogeneity, Certification, Uncertainty, Reprints, Standard reference materials, Systematic errors, Weighted mean.

Often, data from several different chemical analysis methods must be combined to form an overall mean value and uncertainty. However, the data from these different methods frequently do not agree when a statistical comparison is done, so taking a simple average of all of the individual observations is inappropriate. Computation of a weighted mean and corresponding uncertainty that take into consideration the random measurement error within each method as well as the disagreement between methods will be described. Examples of this approach, applied to the certification of NIST's Standard Reference Materials, will be given.

00,573
PB95-140604 Not available NTIS
National Inst. of Standards and Technology (NML), Gaithersburg, MD. Organic Analytical Research Div.

Device for Subambient Temperature Control in Liquid Chromatography.
Final rept.
L. C. Sander, and N. E. Craft. 1990, 3p.
Pub. in Analytical Chemistry 62, n14 p1545-1547 1990.

Keywords: *Liquid column chromatography, *Temperature control, *Cooling systems, *Thermoelectric coolers, Temperature measurement, Heat exchangers, Selectivity, Design, Performance evaluation, Reprints, *Subambient temperature control.

The construction of a device for regulating column temperature in liquid chromatography (LC) is described. The device is based on the thermoelectric cooling principle, and utilizes four thermoelectric heat exchangers placed in contact with an aluminum block. This block is machined to accept commercial LC columns. In the cooling mode, temperatures in the range .25 to 17 C are possible using 'tap water' (17 C) at a flow rate of 1.25 L/min. Although the main purpose of this device is cool LC columns, elevated temperatures are possible (maximum temperature, 99 C) by reversing the polarity of the power supply output. The column cooling device provides an economical, compact and portable means of controlling column temperature. The design allows for maximum flexibility in use and permits the device to be moved between instruments with little effort, as the need arises.

00,574
PB95-140976 Not available NTIS
National Inst. of Standards and Technology (NML), Gaithersburg, MD. Organic Analytical Research Div.
Comparison of the Liquid Chromatographic Behavior of Selected Steroid Isomers Using Different Reversed-Phase Materials and Mobile Phase Compositions.
Final rept.
M. Olsson, L. Sander, and S. Wise. 1991, 11p.
Pub. in Jnl. of Chromatography 537, n1-2 p73-83 1991.

Keywords: *Liquid column chromatography, *Chromatographic analysis, *Isomers, Comparison, Stereochemistry, Temperature dependence, Liquid crystals, Phase change materials, Polymers, Aromatic polycyclic hydrocarbons, Separation, Reprints, *Mobile phase compositions, *Selection rules, *Retention.

Reversed-phase liquid chromatographic selectivity for steroid isomers was found to change as a function of both temperature and mobile-phase composition. The influence of the stationary phase was studied by investigating retention and selectivity on a number of different monomeric and polymeric C18 stationary phase materials, as well as beta-cyclodextrin based phases. Three steroid isomers, i.e., equilin, 17 alpha- and 17 beta-estradiol, were chosen as probe solutes to illustrate the dramatic effect of changes in mobile-phase composition. Selectivity of androstane standards on a polymeric C18 phase was compared to selectivity on liquid crystalline phase in supercritical fluid chromatography (SFC). Although liquid crystalline and polymeric C18 phases have similar shape-selectivity for certain classes of solutes, such as polycyclic aromatic hydrocarbons (PAHs), different trends were observed for androstane isomers.

00,575
PB95-150199 Not available NTIS
National Inst. of Standards and Technology (CSTL), Gaithersburg, MD. Inorganic Analytical Research Div.
Automated, High-Precision Coulometric Titrimetry. Part 1. Engineering and Implementation.
Final rept.
K. W. Pratt. 1994, 10p.
See also Part 2, PB95-150207.
Pub. in Analytica Chimica Acta 289, p125-134 1994.

Keywords: *Coulometers, *Chemical analysis, *Primary standards, *Automatic control, Standard deviation, Statistical analysis, Error analysis, Electrochemistry, Benzoic acids, Chromates, Reprints.

Automated constant-current coulometry, based on Faraday's Laws, achieves uncertainties (relative standard deviation) of less than 1 part in 20,000 without chemical standardization. It is applicable to acid-base, redox, and precipitation titrations of high-purity compounds and solutions. Automation of the technique permits unsupervised operation and reduces operator-dependent errors. Initial setup and sample introduction are the sole manual steps. Each assay consists of a main titration at high, constant current, bracketed by the initial and final endpoint routines, each at a lower current. The coulometric assay is analogous to a conventional titration in which two different concentrations of the titrant are used to attain optimum accuracy. The initial endpoint determination corresponds to the blank determination in a classical titration. Each titration includes a statistical analysis of the random and systematic uncertainties associated with the analysis. Individual steps in the procedure are performed by a hierarchical series of subroutines to reduce program complexity. Results are presented for K2Cr2O7, benzoic acid, and solutions of strong acids.

00,576
PB95-150207 Not available NTIS
National Inst. of Standards and Technology (CSTL), Gaithersburg, MD. Inorganic Analytical Research Div.
Automated, High Precision Coulometric Titrimetry. Part 2. Strong and Weak Acids and Bases.
Final rept.
K. W. Pratt. 1994, 8p.
See also Part 1, PB95-150199.
Pub. in Analytical Chimica Acta 289, p135-142 1994.

Keywords: *Coulometers, *Chemical analysis, *Benzoic acids, *Sodium carbonates, *Hydrochloric acid, *Automatic control, Standard deviation, Precision, Titration, Reprints.

Automated constant-current coulometric acidimetry, based on Faraday's Laws, is uncertain to less than 1 part in 20,000 (relative standard deviation) and requires no chemical standardization. It is applicable to strong and weak acids and bases, with bases back-titrated after addition of excess strong acid. Initial setup and sample introduction are the sole manual steps. Assays of HCl, benzoic acid, Na2CO3, and tris(hydroxymethyl)aminomethane are presented. In the endpoint determination procedure, a generalized titration equation yields the theoretical charge remaining to the endpoint before each charge addition. The ratio of the experimental to the theoretical charge for the preceding aliquot corrects for experimental deviations.

00,577
PB95-150231 Not available NTIS
National Inst. of Standards and Technology (CSTL), Gaithersburg, MD. Inorganic Analytical Research Div.
Integrating Automated Systems with Modular Architecture.
Final rept.
M. L. Salit, F. R. Guenther, G. W. Kramer, and J. M. Griesmeyer. 1994, 7p.
Pub. in Analytical Chemistry 66, n6 p361 A-367 A, 15 Mar 94.

Keywords: *Chemical analysis, *Modules, *Automatic control, Chemical laboratories, Interfaces, Design, Reprints, *Chemistry workcell, *Laboratory automation, System integration.

An architecture has been developed to facilitate the creation of automated chemical analysis systems. This architecture is based upon the functionality of the traditional analytical chemistry organization, with automated entities specified to anthropomorphically fill the roles of the client for the chemical information, the expert analyst, the laboratory manager and the bench chemist. Standard interfaces between these entities are in the process of being designed. These interfaces, when coupled with standard entity behaviors, will allow for a modular 'plug-and-play' systems integration environment. This paper describes the architecture as it is currently understood and outlines the plan for its further evolution.

00,578
PB95-150249 Not available NTIS
National Inst. of Standards and Technology (CSTL), Gaithersburg, MD. Organic Analytical Research Div.
Development of Engineered Stationary Phases for the Separation of Carotenoid Isomers.
Final rept.
L. Sander, K. Sharpless, N. Craft, and S. Wise. 1994, 8p.
Pub. in Analytical Chemistry 66, n10 p1667-1674, 15 May 94.

Keywords: *Carotene, *Isomerization, *Separation processes, *Distillation equipment, Ligands, Substrates, Carotenoids, Standards, Phase separation(Materials), Retaining, Aromatic polycyclic hydrocarbons, Nutrients, Reprints.

A variety of bonded phase parameters (endcapping, phase chemistry, ligand length, and substrate parameters) were studied for their effect on column retention and selectivity toward carotenoids. Decisions were made on how each of these variables should be optimized based on the separation of carotenoid and polycyclic aromatic hydrocarbon test probes. A column was designed with the following properties: high absolute retention, enhanced shape recognition of structured solutes, and moderate silanol activity. The effectiveness of this 'carotenoid phase' was demonstrated for the separation of a mixture of structurally similar carotenoid standards, an extract of a food matrix Standard Reference Material, and a beta-carotene dietary supplement under consideration as an agent for cancer intervention/prevention.

00,579
PB95-150256 Not available NTIS
National Inst. of Standards and Technology (CSTL), Gaithersburg, MD. Organic Analytical Research Div.
Shape Selectivity Assessment of Stationary Phases in Gas Chromatography.
Final rept.
L. C. Sander, M. Schneider, S. A. Wise, and C. Woolley. 1994, 11p.
Pub. in Jnl. of Microcol. Sep. 6, p115-125 1994.

Keywords: *Gas chromatography, *Separation processes, *Distillation equipment, Solutes, Aromatic polycyclic hydrocarbons, Liquid crystals, Phase stability(Materials), Reprints, *Shape selectivity, Methyl polysiloxane.

Column selectivity is examined for a series of smectic liquid crystalline columns and is compared with methyl and C18 polysiloxane columns for the separation of polycyclic aromatic hydrocarbon (PAH) isomers. A set of extended and condensed solute probes is described that provides a sensitive indication of variations in column shape selectivity. Examples of shape selectivity differences are presented for smectic liquid crystalline columns and 5% phenyl polysiloxane columns using various PAH isomer sets. Variations in selectivity have been observed among different smectic liquid crystalline columns, and this problem appears more significant than for methyl polysiloxane columns. The selectivity ratio for tetraphenylmethane and p-terphenyl provides a sensitive indication of column shape selectivity, with a change in elution order occurring between ordered (smectic liquid crystalline) columns and non-ordered (methyl polysiloxane) columns. Shape selectivity differences indicated by this test mixture are apparent for more complex PAH isomer mixtures. Despite stationary phase selectivity variability, smectic liquid crystalline columns offer considerable potential for solving difficult separation problems involving structured solutes.

00,580
PB95-150603 Not available NTIS
National Inst. of Standards and Technology (EEEL), Gaithersburg, MD. Semiconductor Electronics Div.
Tin Oxide Gas Sensor Fabricated Using CMOS Micro-Hotplates and In-situ Processing.
Final rept.
J. S. Suehle, R. E. Cavicchi, M. Gaitan, and S. Semancik. 1993, 3p.
Pub. in Institute of Electrical and Electronics Engineers Electron Device Letters 14, n3 p118-120 Mar 93.

Keywords: *Gas detectors, *Tin oxides, Monolithic structures(Electronics), Micromachining, Fabrication, Hydrogen, Oxygen, Substrates, Silicon, Arrays, Films, CMOS, Reprints, Microhotplates.

We report the first monolithic tin oxide (SnO2) gas sensor realized by commercial CMOS foundry fabrication (MO-SIS) and post-fabrication processing techniques. The device is composed of a sensing film that is sputter-deposited on a silicon micromachined hotplate. The fabrication technique requires no masking and utilizes in-situ process control and monitoring of film resistivity during film growth. Gas sensor responses of pure SnO2 films to H2 and O2 with an operating temperature of 350 C are reported. The fabrication methodology allows integration of an array of gas sensors of various films with separate temperature control for each element in the array, and circuits for a low-cost CMOS-based gas sensor system.

00,581
PB95-150835 Not available NTIS
National Inst. of Standards and Technology (NML), Gaithersburg, MD. Radiometric Physics Div.

Standards for Corrected Fluorescence Spectra.
Final rept.
A. Thompson, and K. Eckerle. 1989, 6p.
Pub. in Proceedings of Society of Photo-Optical Instrumentation Engineers: Fluoresc. Detect. 3, v1054 p20-25 1992.

Keywords: *Spectral emission, *Standards, *Fluorescence spectroscopy, Interlaboratory comparisons, Near infrared radiation, Visible radiation, Phosphors, Mixtures, Fluorimeters, Fluorometers, Reprints, *Fluorescence standards, *Standard reference materials, Polytetrafluorethylene, Spectrofluorimeters, Spectrofluorometers.

A set of four fluorescent standards has been produced and calibrated at the National Institute of Standards and Technology (NIST) for corrected relative spectral emission over the wavelength range from 400 to 740 nm. This new Standard Reference Material (SRM) 1931 has been produced in the form of sintered mixtures of inorganic phosphors and polytetrafluorethylene (PTEE) powder for spectral response calibration of spectrofluorimeters used in biology, medicine and studies of molecular structure. They provide a means for correcting spectrofluorimeter errors due to wavelength dependencies of optics, monochromators, and detectors, thus permitting meaningful intercomparison of results obtained in different laboratories.

00,582
PB95-150876 Not available NTIS
National Inst. of Standards and Technology (CSTL), Gaithersburg, MD. Thermophysics Div.
Characteristics of Partial Pressure Analyzers.
Final rept.
C. R. Tilford. 1992, 11p.
Pub. in Proceedings of Society of Photo-Optical Instrumentation Engineers: Damage to Space Optics and Properties and Characteristics of Optical Glass, San Diego, CA., July 20, 22-23, 1992, v1761 p119-129.

Keywords: *Gas analysis, *Partial pressure, *Mass spectrometers, Calibration, Sensitivity, Vacuum apparatus, Measuring instruments, Pressure measurement, Reprints, *Partial pressure analyzers, Residual gas analyzers.

Partial pressure or residual gas analyzers are often invaluable for materials and contamination studies. However, some instrument design features and combination of operating parameters can cause performance features quite different from what many users expect. These unexpected performance characteristics can include pressure-dependent sensitivities, the sensitivity for one gas depending on the pressures of other gases, and time-dependent sensitivities after operation with gases such as oxygen or water. These characteristics can greatly complicate instrument calibration and can cause errors as large as two orders of magnitude. This paper discusses measured performance characteristics for different partial pressure analyzers that illustrate a wide range of performances from the different instruments, as well as several features that seem to be common to most instruments.

00,583
PB95-151130 Not available NTIS
National Inst. of Standards and Technology (CSTL), Gaithersburg, MD. Organic Analytical Research Div.
High-Performance Liquid Chromatography of Phytoplankton Pigments Using a Polymeric Reversed-Phase C18 Column.
Final rept.
L. Van Heukelem, A. J. Lewitus, T. M. Kana, and N. E. Craft. 1992, 6p.
Pub. in Jnl. of Phycology 28, p867-872 1992.

Keywords: *Phytoplankton, *Pigments, *Purification, High pressure liquid chromatography, Molecular structure, Chlorophyll, Carotenoids, Solvents, Reprints, Lutein, Zeaxanthin, Neoxanthin, 19'-hexanoyloxyfucoxanthin, HPLC columns.

A high-performance liquid chromatographic (HPLC) method is described that allows improved resolution of several chemotaxonomically significant phytoplankton pigments. The protocol, which employs two pumps and a modified Mantoura and Llewellyn (1983) solvent system, can be easily adapted for many HPLC systems currently in use. The most unique aspect of the method is the use of a polymeric C18 reversed-phase HPLC column (VYDAC 201TP). In comparison to the monomeric C18 columns typically used in the characterization of phytoplankton pigments, polymeric C18 columns offer superior selectivity for structurally similar compounds. The protocol was evaluated for the ability to resolve most of the phytoplankton pigments of diagnostic importance using algal cultures from nine classes. Pigment pairs that were resolved by the method include (1) lutein and zeaxanthin, (2) neoxanthin and 19'-hexanoyloxyfucoxanthin, and (3) alpha-carotene and beta-carotene, and partial resolution of chlorophyll C1 and chlorophyll C2.

00,584
PB95-151197 Not available NTIS
National Inst. of Standards and Technology (CSTL), Gaithersburg, MD. Surface and Microanalysis Science Div.
Factorial Design Techniques Applied to Optimization of AMS Graphite Target Preparation.
Final rept.
R. M. Verkouteren, and G. A. Klouda. 1992, 9p.
Pub. in Radiocarbon 34, n3 p335-343 1992.

Keywords: *Mass spectroscopy, *Carbon 14, *Particle accelerator targets, *Factor analysis, Graphite, Error analysis, Methane, Experimental design, Reduction(Chemistry), Monte Carlo method, Carbon dioxide, Reprints, *Accelerator mass spectrometry.

Many factors influence the preparation and quality of graphite targets for (14)C accelerator mass spectrometry (AMS). We identified four factors (sample size, H2 pressure, catalyst temperature and pretreatment time) as potentially critical, and investigated their effects on two particular characteristics: the integrated rates of CO2 reduction (to graphite) and methane production. We used a 2-level fractional factorial experimental design and determined chemical reduction yield rates through manometry and partial pressure monitoring of residual gases by mass spectrometry. Chemical reduction yield rates ranged from 0.2% to 6.2% per hour. With respect to their influence on percent yield rate, the factors we studied were ordered as: sample size > level of hydrogen > pretreatment of the catalyst. The temperature of the catalyst, and the sample size x hydrogen (2-factor) interaction, were only marginally influential. We estimated uncertainty in the order of influence and magnitudes of the effects by the Monte Carlo method of error propagation. We observed significant methane production in only one experiment, which suggests that methane originates from indigenous carbon in untreated iron catalyst only in the presence of hydrogen and only at thermodynamically favorable temperatures. This exploratory investigation indicates that factorial design techniques are a useful means to investigate multivariate effects on the preparation and quality of AMS graphite targets.

00,585
PB95-151650 Not available NTIS
National Inst. of Standards and Technology (CSTL), Gaithersburg, MD. Organic Analytical Research Div.
Determination of Polycyclic Aromatic Hydrocarbons by Liquid Chromatography.
Final rept.
S. A. Wise, L. C. Sander, and W. E. May. 1993, 21p.
Pub. in Jnl. of Chromatography 642, p329-349 1993.

Keywords: *Liquid column chromatography, *Polycyclic aromatic hydrocarbons, *Quantitative chemical analysis, Extraction columns, Fluorescence spectroscopy, Chromatographic analysis, Pollution sampling, Measurement, Reference standards, Reprints, *Environmental samples, Standard reference materials.

Reversed-phase liquid chromatography (LC) using fluorescence detection is a powerful analytical technique for the measurement of polycyclic aromatic hydrocarbons (PAHs) in environmental samples. The NIST experience in the use of LC for the determination of PAHs in environmental samples is summarized in the paper including: selection of the appropriate column, approaches to analyzing complex PAH mixtures, and the accurate quantitation of PAHs in environmental samples.

00,586
PB95-151668 Not available NTIS
National Inst. of Standards and Technology (CSTL), Gaithersburg, MD. Organic Analytical Research Div.
Standard Reference Materials for the Determination of Polycyclic Aromatic Hydrocarbons in Environmental Samples - Current Activities.
Final rept.
S. A. Wise, M. M. Schantz, B. A. Benner, L. C. Sander, B. J. Koster, S. N. Chesler, W. E. May, R. M. Parris, and R. E. Rebbert. 1993, 5p.
Pub. in Fresenius Jnl. of Analytical Chemistry 345, p325-329 1993.

Keywords: *Polycyclic aromatic hydrocarbons, *Pollution sampling, *Chemical analysis, Water pollution, Marine environments, Sediments, Animal tissues, Mussels, Bioassay, Air pollution, Calibration standards, Reference standards, Reprints, *Environmental samples, *Standard reference materials, Mutagenicity.

Recent activities at the National Institute of Standards and Technology (NIST) related to the development of standard reference materials (SRMs) for the determination of polycyclic aromatic hydrocarbons (PAHs) are described. These activities include: (1) the development of four new calibration solution SRMs, a marine sediment SRM, and a frozen mussel tissue SRM; (2) noncertified measurements of PAHs for two additional sediment SRMs; and (3) the establishment of reference Ames bioassay mutagenicity values on three existing SRMs. Activities in progress include the recertification of the existing air particulate and diesel particulate SRMs and the preparation of a new diesel particulate extract SRM.

00,587
PB95-151676 Not available NTIS
National Inst. of Standards and Technology (CSTL), Gaithersburg, MD. Organic Analytical Research Div.
Development of Frozen Whale Blubber and Liver Reference Materials for the Measurement of Organic and Inorganic Contaminants.
Final rept.
S. Wise, M. Schantz, B. Koster, R. Greenberg, M. Burow, P. Ostapczuk, T. Lillestolen, R. Demiralp, and E. Mackey. 1993, 8p.
Sponsored by National Oceanic and Atmospheric Administration, Washington, DC.
Pub. in Fresenius Jnl. of Analytical Chemistry 345, p270-277 1993.

Keywords: *Water pollution effects(Animals), *Whales, *Biological Accumulation, *Animal tissues, Bioassay, Trace elements, Polycyclic aromatic hydrocarbons, Pesticides, Liver, Neutron activation analysis, Voltammetry, Atomic spectroscopy, Bioaccumulation, Environmental monitoring, Reference standards, Reprints, *Standard reference materials, Blubber.

Fresh frozen homogenates of pilot whale blubber and liver tissue were prepared for use as control materials for the determination of organic and inorganic contaminants in marine mammal tissue analyses. The blubber material was analyzed to determine 30 polychlorinated biphenyl congeners and 16 chlorinated pesticides using gas chromatography with electron capture detection and gas chromatography-mass spectrometry. A total of 39 trace elements and methyl-mercury were determined in the liver homogenate using instrumental neutron activation analysis, voltammetry, and cold vapor atomic absorption spectroscopy. The preparation and analysis of these two tissue materials are part of the development of marine mammal tissue reference materials.

00,588
PB95-151924 Not available NTIS
National Inst. of Standards and Technology (NML), Gaithersburg, MD. Ionizing Radiation Div.
Pattern-Recognition Analysis of Low-Resolution X-Ray Fluorescence Spectra.
Final rept.
L. I. Yin, and S. M. Seltzer. 1990, 7p.
Pub. in Nuclear Instruments and Methods in Physics Research A299, p571-577 1990.

Keywords: *X-ray fluorescence analysis, *Pattern recognition, Proportional counters, Correlation coefficients, X-ray spectra, Spectrum analysis, Chemical composition, Reprints, Geological samples.

Using a high-resolution Si(Li) spectrometer to perform X-ray fluorescence (XRF) analysis of various geological, alloy, and paint samples, we have demonstrated that in situations where quantitative information is not the primary concern, a pattern-recognition approach may be used to obtain qualitative results very quickly and efficiently. Specifically, the pattern-recognition technique uses a single parameter, the normalized cor-

relation coefficient, to identify and select samples with similar chemical compositions from their raw XRF spectra. The algorithm can be easily implemented on a personal computer; typically it takes only a few seconds to perform the pairwise comparison of 9 or 10 spectra. We report here the results of our attempt to extend the pattern-recognition technique to the analysis of low-resolution XRF spectra from a proportional counter where the spectral information is considerably poorer than that of the Si(Li) detector. Analyzing the XRF spectra obtained from a set of geological samples both in air and in vacuum, we find that even with a proportional counter the pattern-recognition technique can nevertheless satisfactorily identify samples with similar chemical compositions.

00,589
PB95-152047 Not available NTIS
National Inst. of Standards and Technology (CSTL), Gaithersburg, MD. Inorganic Analytical Research Div.
Determination of Inorganic Constituents in Marine Mammal Tissues.
Final rept.
R. Zeisler, R. Demiralp, B. J. Koster, P. Ostapczuk, S. A. Wise, P. R. Becker, and M. Burow. 1993, 22p.
Pub. in Science of the Total Environment 139/140, p365-386 1993.

Keywords: *Marine mammals, *Animal tissues, *Inorganic compounds, *Water pollution effects(Animals), *Bioaccumulation, Tissue banks, Liver, Kidney, Muscles, Seals(Mammals), Whales, Methyl mercury, Trace elements, Biological accumulation, Bioassay, Neutron activation analysis, Environmental monitoring, Reference standards, Reprints.

Analyses of selected tissues from the Alaska Marine Mammal Tissue Archival Project (AMMTAP) have provided comprehensive information related to levels of 36 trace elements and methyl-mercury in marine mammal tissues. Liver, kidney and muscle tissues from two northern fur seals, four ringed seals and six belukha whales were analyzed. The bulk of the investigated tissues and additional tissues from a total of 65 marine mammals are banked in the AMMTAP. The results are compared to literature values for trace element concentrations in marine mammal tissues and their relevance to environmental studies is discussed.

00,590
PB95-152799 Not available NTIS
National Inst. of Standards and Technology (CSTL), Gaithersburg, MD. Biotechnology Div.
Resolution of DNA in the Presence of Mobility Modifying Polar and Nonpolar Compounds by Discontinuous Electrophoresis on Rehydratable Polyacrylamide Gels.
Final rept.
R. Allen, B. Budowle, and D. Reeder. 1993, 9p.
Pub. in Applied and Theoretical Electrophoresis 3, p173-181 1993.

Keywords: *Deoxyribonucleic acid, *Polyacrylamide gel electrophoresis, *Hydration, Monosaccharides, Alanine, Buffers, Serine, Disaccharides, Alcohols, Glycerol, Reprints.

Ultrathin-layer rehydratable gels were surface loaded and run in the horizontal position to study effects of mobility modification of DNA. Mobility modification of DNA fragments was achieved by the addition of nonpolar monosaccharides and their corresponding sugar alcohols as well as glycerol and ethylene glycol in the leading ion buffer. These compounds show little effect when included in the trailing ion buffer. Disaccharides show no mobility modification. Trailing ions such as serine and members of the Good buffer series reduced also the R(sub F) of double- or single-stranded DNA. While beta-alanine had no effect, serine and members of the Good buffer series, particularly MOPSO, showed a marked ability to decrease the R(sub F), presumably due to changing the unstacking limits. Rapid separation of sequencing gels with high resolution was achieved with discontinuous buffer systems. The potential methodology for high-resolution scanning of gels as DNA zones unstack from moving boundary is suggested.

00,591
PB95-152815 Not available NTIS
National Inst. of Standards and Technology (PL), Boulder, CO. Quantum Physics Div.
Single-Photon Ionization and Detection of Ga, In, and As(sub n) Species in GaAs Growth.
Final rept.
A. L. Alstrin, P. G. Strupp, L. Cook, and S. R. Leone. 1993, 11p.
Contract AFOSR90-0166
Pub. in Proceedings of Society of Photo-Optical Instrumentation Engineers: Laser Techniques for State-Selected and State-to-State Chemistry, Los Angeles, CA., January 21-23, 1993, v1858 p367-377. Sponsored by Air Force Office of Scientific Research, Bolling AFB, DC.

Keywords: *Molecular beam epitaxy, *Gallium arsenides, *Indium, *Gallium, *Arsenic, *Mass spectroscopy, Time-of-flight method, Far ultraviolet radiation, Real time operations, Monitoring, Ionization, Laser radiation, Desorption, Silicon, Reprints.

Single photon ionization time-of-flight mass spectroscopy (SPI-TOFMS) is used to monitor chemical fluxes of In, Ga, and As(n), relevant in molecular beam epitaxy of GaAs. With single photon ionization at 118 nm (10.5 eV), the photon energy is large enough to ionize the species, but not sufficient to ionize and fragment. The lack of molecular dissociation of species such as As2 and As4 greatly simplifies the interpretation of mass spectra. SPI-TOFMS provides the ability to measure densities, and hence fluxes, of multiple chemical species above a substrate noninvasively and in real time during conventional molecular beam epitaxy. The relative ionization efficiencies of Ga and the As(n) species at 118 nm are determined. Additionally, this laser probing technique is used to study the isothermal and temperature programmed desorption of arsenic from Si(100). The catalytic cracking of As4 on Si is also examined and discussed. This technique promises to be a valuable in-situ optical diagnostic for III-V and II-VI molecular beam epitaxy.

00,592
PB95-153383 Not available NTIS
National Inst. of Standards and Technology (TS), Gaithersburg, MD. Standard Reference Materials Program.
Reference Materials by Isotope Dilution Mass Spectrometry.
Final rept.
P. DeBievre, J. R. DeLaeter, H. S. Peiser, and W. P. Reed. 1993, 30p.
Pub. in Mass Spectrometry Review 12, p143-172 1993.

Keywords: *Mass spectroscopy, Geochronology, Geology, Metrology, Precision, Accuracy, Reprints, *Reference materials, Isotope dilution mass spectroscopy, Measurement evaluation program.

This is a review of the role of inorganic mass spectrometers in Chemical Metrology. It discusses measurements by isotope dilution mass spectrometry, and how it contributes to precision and accuracy in Chemical Metrology and the Certification of Reference Material. It also reviews reference materials available for geology and geochronology.

00,593
PB95-153599 Not available NTIS
National Inst. of Standards and Technology (CSTL), Gaithersburg, MD. Organic Analytical Research Div.
Liquid Chromatographic Method for the Determination of Carotenoids, Retinoids, and Tocopherols in Human Serum and in Food.
Final rept.
K. S. Epler, R. G. Ziegler, and N. E. Craft. 1993, 12p.
Pub. in Jnl. of Chromatography 619, p37-48 1993.

Keywords: *Liquid chromatography, *Carotenoids, *Retinoids, *Tocopherol, *Chemical analysis, *Food analysis, Ultraviolet spectroscopy, Solvents, Methodology, Reprints.

A liquid chromatographic (LC) has been developed for the quantitative measurement of the six major carotenoids in human serum (lutein, zeaxanthin, beta-cryptoxanthin, lycopene, alpha-carotene, and beta-carotene) as well as retinol, retinyl palmitate, alpha-tocopherol, gamma-tocopherol, and delta-tocopherol. Several polar carotenoids, 2',3'-anhydrolutein, alpha-cryptoxanthin, and geometric isomers of lycopene and beta-carotene are also separated. Retinoids and carotenoids are monitored using a programmable ultraviolet-visible detector, while tocopherols are monitored using a fluorescence detector. The method uses a gradient containing acetonitrile, methanol, and ethyl acetate. Ammonium acetate is introduced with the methanol to minimize carotenoid losses on the LC column aggravated by the use of acetonitrile and ethyl acetate. The method is also applicable to the analysis of foods.

00,594
PB95-161162 Not available NTIS
National Inst. of Standards and Technology (NML), Boulder, CO. Chemical Engineering Science Div.
Enzyme and Protein Mass Transfer Coefficient in Aqueous Two Phase Systems. 1. Spray Extraction Columns.
Final rept.
K. R. Jafarabad, S. B. Sawant, J. B. Joshi, and S. K. Sikdar. 1992, 12p.
Pub. in Chemical Engineering Science 47, n1 p57-68 1992.

Keywords: *Proteins, *Enzymes, *Mass transfer, Purification, Bovine serum albumin, Salts, Polyethylene glycol, Reprints, *Spray extraction columns, Amyloglucosidase.

Fractional dispersed phase hold-up and dispersed side mass transfer coefficients for bovine serum albumin (BSA) and amyloglucosidase were measured in 22, 34, 50, 56, 70 and 95 mm i.d. spray columns using salt-polyethylene glycol (potassium phosphate-PEG and sodium sulphate-PEG) systems. The effect of distributor design and column height was investigated. The effect of phase compositions of the aqueous phase system was also studied. Empirical and semiempirical correlations have been developed for fractional dispersed phase hold-up and dispersed side mass transfer coefficients.

00,595
PB95-162228 Not available NTIS
National Inst. of Standards and Technology (NML), Boulder, CO. Chemical Engineering Science Div.
Protein Extraction in a Spray Column Using a Polyethylene Glycol Maltodextrin Two-Phase Polymer System.
Final rept.
K. S. M. S. Raghav Rao, D. S. Szlag, S. K. Sikdar, J. B. Joshi, and S. B. Sawant. 1991, 7p.
Pub. in Chemical Engineering Jnl. 46, n3 pB75-B81 1991.

Keywords: *Proteins, *Polyethylene glycol, *Purification, Bovine serum albumin, Mass transfer, Water, Reprints, *Maltodextrin.

Recovery of a model protein, bovine serum albumin (BSA), was demonstrated in a spray column contractor using immiscible aqueous phases, composed of polyethylene glycol (PEG) and maltodextrin (MDX). Dispersed phase (PEG) hold-up and protein transfer coefficients were measured in a 22 mm and a 32 mm i.d. spray columns using several designs of spargers. Protein transfer coefficients were greater in the PEG/maltodextrin system than those encountered in PEG/dextran systems. Empirical correlations have been proposed for mass transfer coefficients and PEG-hold-ups.

00,596
PB95-162608 Not available NTIS
National Inst. of Standards and Technology (CSTL), Gaithersburg, MD. Organic Analytical Research Div.
Shape Selectivity in Reversed-Phase Liquid Chromatography for the Separation of Planar and Non-Planar Solutes.
Final rept.
L. C. Sander, and S. A. Wise. 1993, 17p.
Pub. in Jnl. of Chromatography A 656, p335-351 1993.

Keywords: *Liquid column chromatography, *Liquid chromatography, *Aromatic polycyclic hydrocarbons, *Solutes, Separation, Mixtures, Isomers, Reviews, Reprints, Shape selectivity, Solute retention.

Solute retention in reversed-phase liquid chromatography is the result of a variety of complex interactions between solute, mobile phase and stationary phase species. An understanding of the parameters that influence retention is useful in the development of separation methods with existing columns. Such knowledge is even more important for the design of new bonded stationary phases with engineered chromatographic properties. This review will examine some of the factors that affect retention and selectivity with alkyl-modified sorbents, particularly for the separation of solutes with well defined, rigid structure (e.g., polycyclic aromatic hydrocarbons). The chromatographic discrimination of compounds on the

basis of molecular structure, namely 'shape selectivity', will be studied in terms of contributions from bonded phase morphology, and in terms of operational conditions. An emphasis is placed on practical choices that are available to control selectivity and optimize separations for isomers and related mixtures.

00,597
PB95-163101 Not available NTIS
National Inst. of Standards and Technology (NML), Gaithersburg, MD. Inorganic Analytical Research Div.
Trace Elements Associated with Proteins. Neutron Activation Analysis Combined with Biological Isolation Techniques.
Final rept.
S. F. Stone, R. Zeisler, G. E. Gordon, R. P. Viscidi, and E. H. Cerny. 1991, 13p.
Pub. in American Chemical Society Symposium Series Biol. Trace Elem. Res. 445, p265-277 1991.

Keywords: *Neutron activation analysis, *Phosphoproteins, *Trace elements, Polyacrylamide gel electrophoresis, Antigen-antibody reactions, Casein, Milk, Eggs, Immunoassay, Gold colloid, Reprints, Phosvitin.

Combinations of biological techniques with neutron activation analysis (NAA) can be employed for protein quantification in biological samples. A protein of interest can be isolated physically with a high resolution separation technique such as polyacrylamide gel electrophoresis (PAGE) or by immunochemical properties, such as with a specific antibody-antigen reaction. NAA is then used for quantification of the isolated protein by determining either an element that is structurally intrinsic, or one that has been introduced as a label. An example of the former method is the determination of phosphoproteins by PAGE/NAA. This method is discussed and results for two phosphoproteins, alpha-casein and phosvitin, are presented for several materials, including an alpha-casein concentration of 26 mg/mL in low-fat milk, and a phosvitin concentration of 4.7 mg/mL in whole egg powder (lyophilized). The second method presented is an immunoassay combining a colloidal gold tag with detection by NAA.

00,598
PB95-163424 Not available NTIS
National Inst. of Standards and Technology (NML), Gaithersburg, MD. Inorganic Analytical Research Div.
Trace Detection in Conducting Solids Using Laser-Induced Fluorescence in a Cathodic Sputtering Cell.
Final rept.
J. C. Travis, G. C. Turk, R. L. Watters, L. J. Yu, and J. L. Blue. 1991, 11p.
Pub. in Jnl. of Analytical Atomic Spectrometry 6, n4 p261-271 1991.

Keywords: *Laser induced fluorescence, *Atomic spectroscopy, *Chemical analysis, Glow discharges, Trace amounts, Background noise, Background radiation, Sensitivity, Samplers, Brasses, Iron, Reprints, Cathodic sputtering.

A cathodic sputtering atom reservoir designed for atomic absorption spectroscopy of conducting solid samples is examined as a potential sampling device for trace and ultra-trace detection using laser-induced fluorescence (LIF) spectrometry. The analytical results are promising, with sub-(micro)g/g sensitivity for the model analyte (Fe) in brass samples, and with reasonable precision and accuracy (+ or - 15%) for the pulsed laser system used, but with far less sensitivity than might be predicted. Noise studies clearly indicate that laser-induced background fluorescence is the principal limiting noise source. Fundamental material transport studies indicate that diffusional loss of atomic number density to the walls is of much less importance than the background fluorescence in determining the sensitivity of the system. Extrapolations based on cell/experiment design to maximize number density and minimize background emission and fluorescence promise ng/g sensitivities for future implementations.

00,599
PB95-164653 Not available NTIS
National Inst. of Standards and Technology (CSTL), Gaithersburg, MD. Biotechnology Div.
Enhanced Detection of PCR Products Through Use of TOTO and YOYO Intercalating Dyes with Laser Induced Fluorescence - Capillary Electrophoresis.
Final rept.
K. Srinivasan, S. C. Morris, J. E. Girard, M. C. Kline, and D. J. Reeder. 1993, 5p.
Pub. in Applied and Theoretical Electrophoresis 3, p235-239 1993.

Keywords: *Polymerase chain reaction, *Fluorescence spectroscopy, *Dyes, *Intercalating agents, *Chemical analysis, Reprints, *Capillary electrophoresis, *Thiazole orange, *Oxazole orange.

Recent developments in the chemical synthesis of DNA-binding dyes have enhanced detection of polymerase chain reaction (PCR) products by capillary electrophoresis. These dyes are dimers of thiazole orange (TOTO) or oxazole orange (YOYO) and have a very high binding affinity for DNA. These dyes show enhanced fluorescence signals when they bind to double-stranded DNA and their fluorescence in the unbound state is almost zero, making them extremely useful in detecting minute (fg) quantities of DNA. We report here the utility of these dyes in DNA typing applications using a laser-induced fluorescence detector in conjunction with a capillary electrophoresis system.

00,600
PB95-175485 Not available NTIS
National Inst. of Standards and Technology (PL), Boulder, CO. Time and Frequency Div.
Diode Laser as a Spectroscopic Tool.
Final rept.
R. W. Fox, C. S. Weimer, L. Hollberg, and G. C. Turk. 1993, 9p.
Sponsored by National Aeronautics and Space Administration, Washington, DC. and Air Force Office of Scientific Research, Bolling AFB, DC.
Pub. in Spectrochimica Acta Rev. 15, n5 p291-299 1993.

Keywords: *Laser spectroscopy, *Semiconductor lasers, *Spectroscopic analysis, Near infrared radiation, Aluminum gallium arsenides, Laser cavities, Tunable lasers, Nonlinear optics, Visible radiation, Red(Color), Line width, Reprints.

The properties of diode lasers that make them attractive as spectroscopic sources are discussed, along with the use of extended cavities to enhance their tuning range and reduce their linewidths. Semiconductors can now provide efficient, tunable, narrow linewidth laser light over much of the red and near infrared region of the spectrum. The progress in using nonlinear optics to extend the useful wavelength range of diodes lasers is also considered. Our recent analytical work with diode laser spectroscopy provides examples of their application.

00,601
PB95-175709 Not available NTIS
National Inst. of Standards and Technology (CSTL), Gaithersburg, MD. Biotechnology Div.
Fluorescence Measurements of Tetracycline in High Cell Mass for Fermentation Monitoring.
Final rept.
J. J. Horvath, and S. A. Glazier. 1993, 2p.
Pub. in American Biotechnology Laboratory 11, n7 2p Jun 93.

Keywords: *Tetracycline, *Chemical analysis, *Cells(Biology), *Fluorescence spectroscopy, Fermentation, Streptomyces aureofaciens, Fiber optics, Soybeans, Reprints.

This work describes a new spectroscopic optical fiber/rod sensor for in situ real time measurement of product concentrations in bioreactors. The variable excitation/emission wavelength capability of this sensor allows for species selective measurement during fermentations. Product concentrations (tetracycline) have been measured in high cell mass fermentation media of Streptomyces aureofaciens with 5% (w/v) soybean meal. By using multiple excitation wavelengths (390 and 413 nm) the linear measurement range was extended to 8160 microgram/ml at cell densities of greater than 50 g/l dry weight. The sensor is robust, able to undergo many cycles of in situ steam sterilization without degradation, and its fluorescence signal is linear with concentration for all species studied in this work.

00,602
PB95-175964 Not available NTIS
National Inst. of Standards and Technology (CSTL), Gaithersburg, MD. Inorganic Analytical Research Div.
Cold Neutron Prompt Gamma Activation Analysis at NIST: A Progress Report.
Final rept.
R. L. Paul, R. M. Lindstrom, and D. H. Vincent. 1994, 7p.
Pub. in Jnl. of Radioanalytical and Nuclear Chemistry 180, n2 p263-269 1994.

Keywords: *Activation analysis, Neutron capture gamma rays, Allende meteorite, Cold neutrons, Progress report, Sensitivity, Reprints, CNRF facility, US NIST.

An instrument for prompt gamma-ray activation analysis is now in operation at the NIST Cold Neutron Research Facility (CNRF). The cold neutron beam is relatively free of contamination by fast neutrons and reactor gamma rays, and the neutron fluence rate is 1.5 (center dot) 10(exp 8)/sq cm (center dot) s (thermal equivalent). As a result of a compact target-detector geometry, the sensitivity is better by a factor of as much as seven than that obtained with an existing thermal instrument, and hydrogen background is a factor of 50 lower. We have applied this instrument to multielement analysis of the Allende meteorite and other materials.

00,603
PB95-175972 Not available NTIS
National Inst. of Standards and Technology (CSTL), Gaithersburg, MD. Inorganic Analytical Research Div.
Neutron Scattering by Hydrogen in Cold Neutron Prompt Gamma-Activation Analysis.
Final rept.
R. L. Paul, and E. A. Mackey. 1994, 13p.
Pub. in Jnl. of Radioanalytical and Nuclear Chemistry 181, n2 p321-333 1994.

Keywords: *Activation analysis, *Neutron scattering, *Hydrogen, Neutron capture gamma rays, Cold neutrons, Sensitivity, Reprints.

The effects of neutron scattering by hydrogen within targets for cold neutron prompt gamma-ray activation analysis (CNPGAA) have been characterized. For most targets studied, the probability for neutron absorption, and hence CNPGAA sensitivities (counts (center dot) 1/s (center dot) 1/mg), decrease with increasing H content and with target thickness. Comparisons with results from thermal neutron PGAA indicate that the effects of cold neutron scattering differ from those of thermal neutron scattering. CNPGAA sensitivities for '1/nu' nuclides show similar sensitivity decreases, while Sm sensitivities show smaller decreases.

00,604
PB95-180113 Not available NTIS
National Inst. of Standards and Technology (CSTL), Boulder, CO. Thermophysics Div.
Chromatographic Cryofocusing and Cryotrapping with the Vortex Tube.
Final rept.
T. J. Bruno. 1994, 4p.
Contract GRI-5088-260-1700
Sponsored by Gas Research Inst., Chicago, IL.
Pub. in Jnl. of Chromatographic Science 32, p112-115 1994.

Keywords: *Chromatographic analysis, *Cryotrapping, *Cryogenic cooling, *Hilsch tubes, Vortices, Solutes, Injections, Desorption, Gas chromatography, Reprints, *Cryofocusing.

Cryofocusing and cryotrapping techniques are the analytical-scale preconcentration or collection of solutes using low temperature, with subsequent solute removal and analysis. Although these methods have been used with many analytical procedures including spectroscopic techniques, the major applications have been in chromatographic methods that involved a wide variety of sample mixtures. We describe a simple, entirely pneumatic approach to chromatographic sample cryofocusing--cryotrapping. The two airstreams from a vortex tube (cold and hot, respectively) are used to both chill the cryofocus region of the injector and then to thermally desorb the collected solutes for injection.

00,605
PB95-180246 Not available NTIS
National Inst. of Standards and Technology (CSTL), Gaithersburg, MD. Inorganic Analytical Research Div.
Traceability to the Mole: A New Initiative by CIPM.
Final rept.
J. D. Fassett, and R. L. Watters. 1994, 7p.
Pub. in Reviews on Analytical Chemistry: Euroanalysis VIII, p13-19 1994.

Keywords: *Chemical analysis, Interlaboratory comparisons, Primary standards, Metrology, Reprints, Isotope dilution mass spectroscopy, Traceability.

The CIPM has established a Working Group on Metrology in Chemistry to address the specific problem of traceability of chemical measurements. One of the terms of reference of the Working Group is to draw up an exploratory program of cooperative work among leading national chemical metrology laboratories. This program is designed to test the hypothesis that coordinated analysis of a few key reference materials, using one or two reference methods of wide application, will provide such laboratories with a base from which to extend international comparability to a wider range of methods and reference materials. NIST is coordinating the details of the first interlaboratory exercise. Isotope dilution mass spectrometry (IDMS) has been chosen as the reference method for the initial comparison. The design and status of the interlaboratory exercise is summarized.

00,606
PB95-180758 Not available NTIS
National Inst. of Standards and Technology (CSTL), Gaithersburg, MD. Organic Analytical Research Div.
Instrument for Evaluating Phase Behavior of Mixtures for Supercritical Fluid Experiments.
Final rept.
S. H. Page, J. F. Morrison, R. G. Christensen, and S. J. Choquette. 1994, 5p.
Pub. in Analytical Chemistry 66, n21 p3553-3557, 1 Nov 94.

Keywords: *Supercritical fluids, *Phase studies, *Instrumentation, Supercritical fluid chromatography, Light scattering, Binary mixtures, Carbon dioxide, Methanol, Water, Reprints.

Fluid phase behavior has a profound impact on supercritical fluid chromatography performance. The effect of fluid phase behavior on supercritical fluid extraction performance has not been studied. Generally, methods available to generate phase diagrams of fluid mixtures are time-consuming. This paper describes relatively easily constructed instrumentation for the rapid screening of fluid mixtures to determine whether or not they are single phase. Either scattered or transmitted light can be used to probe the phase behavior of the fluids. Examples using CO2/methanol and CO2/water are presented. The phase behavior of multicomponent mixtures of CO2 or Freon (R22, chlorodifluoromethane) with methanol/triethylamine/water was determined.

00,607
PB95-180824 Not available NTIS
National Inst. of Standards and Technology (CSTL), Gaithersburg, MD. Surface and Microanalysis Science Div.
Activities of ISO Technical Committee 201 on Surface Chemical Analysis.
Final rept.
C. J. Powell, and R. Shimizu. 1994, 400p.
Pub. in Surface and Interface Analysis 21, p615-620 1994.

Keywords: *Chemical analysis, *Surface chemistry, Standards, ISO, Reprints.

A status report is given on activities of ISO Technical Committee 201 (ISO/TC 201) on Surface Chemical Analysis. The committee has seven subcommittees which met for the first time in 1993. Information is given on the working groups that have been established for specific purposes. We show national participation in ISO/TC 201 and its subcommittees, and we identify the chairmen and secretariats of the subcommittees and the conveners of the working groups.

00,608
PB95-242319 PC A16/MF A03
National Inst. of Standards and Technology (CSTL), Gaithersburg, MD.
CSTL Technical Activities, 1994.
H. G. Semerjian. 1994, 374p, NISTIR-5584.
Presented to the Board on Assessment of NIST Programs, National Research Council, March 22-23, 1995. See also report for 1993, PB95-160602, report for 1992, PB93-173482 and report for 1991, PB94-160769.

Keywords: *Chemistry, *Research and development, Chemical engineering, Biotechnology, Measurements, Metrology, Models, Measurement traceability, Process technology, Reference data.

This report summarizes the scientific and engineering activities of the Chemical Science and Technology Laboratory (CSTL) for fiscal year 1994. Activity reports are grouped into Divisions of CSTL Biotechnology, Chemical Kinetics and Thermodynamics, Inorganic Analytical Research, Organic Analytical Research, Process Measurements, Surface and Microanalysis Science, and Thermophysics. In addition to the technical reports, outputs and interactions are listed for reach Division, which include publications, talks, CRADAs, patents, SRMs, SRDs, calibrations, committee assignments, editorships, seminars, conferences, and workshops. The overall program is summarized and yearly highlights are given.

00,609
PB96-102488 Not available NTIS
National Inst. of Standards and Technology (MSEL), Gaithersburg, MD. Ceramics Div.
Standard Reference Material for the Measurement of Particle Mobility by Electrophoretic Light Scattering.
Final rept.
V. A. Hackley, R. S. Premachandran, S. G. Malghan, and S. B. Schiller. 1995, 16p.
Pub. in Colloids and Surfaces A 98, p209-224 1995.

Keywords: *Electrophoresis, *Light scattering, *Calibration standards, Particle motion, Goethite, Phosphates, Statistical quality control, Interlaboratory comparisons, Reprints.

A standard reference material (SRM) was developed for the calibration and evaluation of light scattering equipment used to measure electrophoretic mobility. SRM 1980 is a positive mobility standard containing 500 mg/cubic dm microcrystalline goethite (alpha-FeOOH) and 100 micromol/g phosphate in 0.05 mol/cubic dm sodium perchlorate electrolyte solution at pH 2.5. The suspension is diluted prior to use. A certified mobility value (2.53 + or - 0.12 micrometer cm/v/s) was determined from a statistical analysis of round robin data from five laboratories according to NIST guidelines. This paper documents the development, characterization and evaluation of this material. Also discussed are the various contributions to measurement uncertainty and inconsistency, and appropriate protocols for dealing with these problems.

00,610
PB96-106463 PC A03/MF A01
National Inst. of Standards and Technology (CSTL), Gaithersburg, MD. Surface and Microanalysis Science Div.
Proficiency Tests for the NIST Airborne Asbestos Program, 1993.
S. Turner, E. B. Steel, O. S. Crankshaw, S. Silberstein, and H. M. Richmond. Jun 95, 45p, NISTIR-5680.
See also report for 1992, PB94-194362. Prepared in cooperation with Research Triangle Inst., Research Triangle Park, NC. Center for Environmental Measurements and Quality Assurance.

Keywords: *Asbestos, *Materials testing, *Laboratories, Requirements, Certification, Air pollution detection, Calibration standards, Standardization, Test methods, Procedures, Transmission electron microscopy, Chrysotile, Amosite, Crocidolite, Amphiboles, Performance evaluation, Forms(Paper), *Proficiency tests, National Voluntary Laboratory Accreditation Program, Anthophyllite, Actinolite, Tremolite.

NIST has published proficiency test instructions and summary reports for the airborne asbestos program since 1990. The reports provide a historical record of proficiency testing materials sent to the laboratories so that they can be referenced in other publications and background material can be given to those laboratories entering the accreditation program. This report contains the instructions and summary reports issued for 1993 proficiency tests.

00,611
PB96-111653 Not available NTIS
National Inst. of Standards and Technology (CSTL), Gaithersburg, MD. Biotechnology Div.
Overview of Reference Materials Prepared for Standardization of DNA Typing Procedures.
Final rept.
D. J. Reeder, M. C. Kline, and K. L. Richie. 1995, 4p.
Pub. in Fresenius Jnl. of Analytical Chemistry, v352 p246-249 1995.

Keywords: *Calibrating standards, *Quality assurance, *DNA, Standardization, Test methods, Analytical chemistry, Laboratories, Reprints, DNA typing, SRM(Standard Reference Material), NIST(National Institute of Standards and Technology).

Although DNA typing is an accurate, precise, and robust procedure, quality assurance is enhanced by availability of a suitable reference material. The National Institute of Standards and Technology (NIST) recently released a Standard Reference Material (SRM) that meets the calibration and quality assurance needs of laboratories that perform DNA typing. Each step of the analytical process of DNA typing maybe verified by one or more of twenty different components of the SRM. As newer, more sensitive methods for DNA typing have been introduced into the human identification laboratory repertoire, new SRMs will be required for quality assurance.

00,612
PB96-111877 Not available NTIS
National Inst. of Standards and Technology (CSTL), Gaithersburg, MD. Inorganic Analytical Research Div.
Measuring Hydrogen by Cold-Neutron Prompt-Gamma Activation Analysis.
Final rept.
R. M. Lindstrom, R. L. Paul, D. H. Vincent, and R. R. Greenberg. 1994, 5p.
Pub. in Jnl. of Radioanalytical and Nuclear Chemistry, v180 n2 p271-275 1994.

Keywords: *Activation analysis, *Hydrogen, Long wavelength, Prompt gamma radiation, Chemical analysis, Reprints, Cold neutrons, *Foreign technology.

By irradiating with cold neutrons and avoiding hydrogenous materials of construction, we have developed a PGAA instrument at the Cold Neutron Research Facility at NIST with hydrogen detection limits in the microgram range in many materials. Quantities of 5-10 micrograms H/g are presently measureable in gram-sized samples of silicon or quartz, and of order 0.01 wt % can be quantitatively measured in complex silicate rocks.

00,613
PB96-111968 Not available NTIS
National Inst. of Standards and Technology (CSTL), Gaithersburg, MD. Organic Analytical Research Div.
Stability of Compressed Gas Mixtures Containing Low Level Volatile Organic Compounds in Aluminum Cylinders.
Final rept.
W. R. Miller, and G. C. Rhoderick. 1995, 9p.
Pub. in Fresenius Jnl. of Analytical Chemistry, v351 p221-229 1995.

Keywords: *Gas cylinders, *Compressed gas, Stability, Reprints, Gases, Mixtures, *Foreign technology, *Volatile organic compounds.

Compressed gas mixtures containing up to twenty-six volatile organic compounds (VOCs) in a balance of nitrogen have been prepared and analyzed at the National Institute of Standards and Technology (NIST). The mixtures are contained in aluminum cylinders and the hydrocarbons included are aromatic or aliphatic, both saturated and unsaturated and some containing a halogen, oxygen or nitrogen atom. The individual compounds are present at concentrations ranging from 0.1-3000 nmol/mol and the relative standard uncertainty in the concentration of each is between plus or equal to 2-5%. The stability of the mixtures over various time intervals is discussed.

00,614
PB96-112099 Not available NTIS
National Inst. of Standards and Technology (CSTL), Gaithersburg, MD. Analytical Chemistry Div.
Spectral Interference in the Determination of Arsenic in High-Purity Lead and Lead-Base Alloys Using Electrothermal Atomic Absorption Spectrometry and Zeeman-Effect Background Correction.
Final rept.
M. S. Epstein, G. C. Turk, and L. J. Yu. 1994, 8p.
Pub. in Spectrochimica Acta, v49B, n12-14 p1681-1688 1994.

Keywords: *Spectrometry, *Lead(Metal), *Absorption spectrometry, Metals, Reprints, Arsenic, Lead alloys, *Spectral interference, Zeeman effect background correction.

Arsenic, antimony, and tellurium are determined at part-per-million concentration levels in bullet lead, lead-base alloy, and high purity lead using

electrothermal atomization atomic absorption spectrometry (ETAAS) with Zeeman-effect background correction. A spectral interface by lead absorption lines resulting from excited state transitions is observed on both primary arsenic lines, at 193.696 nm and 197.197 nm. Analytical bias caused by the interference at 197.197 nm is eliminated by using temperature programming and temporal resolution.

00,615
PB96-112107 Not available NTIS
National Inst. of Standards and Technology (CSTL), Boulder, CO. Thermophysics Div.
Applications of the Vortex Tube in Chemical Analysis. Part 2. Applications.
Final rept.
T. J. Bruno. 1993, 9p.
See also PB94-199171.
Pub. in American Laboratory, v25 n14 p16-24 1993.

Keywords: *Hilsch tubes, Reprints, Heat transfer, Laboratory equipment, Chemical analysis, *Vortex tubes.

Many applications of the vortex tube in chromatographic analysis have been devised in recent years mainly because of the usefulness of low-temperature chromatographic techniques. One of the most important is GC column temperature control, especially in subambient ranges. The operation of a GC column at low temperatures began in the mid-1950's, but has received renewed attention for the trace analysis of priority pollutants in air and in the analysis of alternative refrigerant fluids. Subambient temperature GC generally refers to procedures in which the column temperature is between -100 and 0 degrees C, but many separations are greatly enhanced at temperatures no lower than -40 degrees C.

00,616
PB96-112131 Not available NTIS
National Inst. of Standards and Technology (CSTL), Gaithersburg, MD. Inorganic Analytical Research Div.
Effects of Target Temperature on Analytical Sensitivities of Cold-Neutron Capture Prompt gamma-ray Activation Analysis.
Final rept.
E. A. Mackey. 1994, 6p.
Pub. in Biological Trace Element Research, p103-108 1994.

Keywords: *Activation analysis, *Neutron scattering, Reprints, Neutron capture gamma rays, Cold neutrons, Sensitivity, *Foreign technology.

Cold-neutron prompt gamma-ray activation analysis sensitivities are often decreased because of an increase in the average neutron energy on scattering within room temperature targets. Experiments were performed to determine whether target cooling would alleviate these effects. Cooling the targets to 77 K increased hydrogen sensitivity by as much as 25%. Target cooling decreases those effects of neutron scattering on CNPGAA sensitivities that are the result of an increased average neutron energy. However, cold-neutron scattering may also change the average path length traveled, and this effect on sensitivity is not alleviated by controlling temperature.

00,617
PB96-112149 Not available NTIS
National Inst. of Standards and Technology (CSTL), Gaithersburg, MD. Inorganic Analytical Research Div.
SUM and MEAN: Standard Programs for Activation Analysis.
Final rept.
R. M. Lindstrom. 1994, 7p.
Pub. in Biological Trace Element Research, p597-603 1994.

Keywords: *Activation analysis, *Computer programs, Reprints, Emission spectra, Weighted means, Peak integration, Gamma ray spectrometry.

Two computer programs in use for over a decade in the Nuclear Methods Group at NIST illustrate the utility of standard software: programs widely available and widely used, in which (ideally) well-tested public algorithms produce results that are well understood, and thereby capable of comparison, within the community of users. SUM interactively computes the position, net area, and uncertainty of the area of spectral peaks, and can give better results than automatic peak search programs when peaks are very small, very large, or unusually shaped. MEAN combines unequal measurements of a single quantity, tests for consistency, and obtains the weighted mean and six measures of its uncertainty.

00,618
PB96-119458 Not available NTIS
National Inst. of Standards and Technology (CSTL), Gaithersburg, MD. Analytical Chemistry Div.
Comparison of Selectivities for PCBs in Gas Chromatography for a Series of Cyanobiphenyl Stationary Phases.
Final rept.
B. R. Hillery, J. E. Girard, M. M. Schantz, M. L. Lee, S. A. Wise, and A. Malik. 1995, 10p.
Pub. in Jnl. of Microcolumn Separations, v7 n3 p221-230 1995.

Keywords: *Chlorinated aromatic hydrocarbons, *Gas chromatography, Columns(Process engineering), Phase, Planar structures, Selectivity, Shapes, Reprints, *Cyanobiphenyl phases, Stationary phases.

Selectivity for polychlorinated biphenyl (PCB) congeners was examined for a series of cyanobiphenyl stationary phases, and the results were compared to a nonpolar 5% phenyl methylpolysiloxane phase and a shape-selective smectic liquid crystalline phase. For all of the columns studied, the degree of ortho substitution of the congener was found to be a significant factor controlling chromatographic retention of PCBs. The retention pattern on six different cyanobiphenyl phases followed the same general pattern as on the liquid crystalline column, though the trends were more exaggerated on the liquid crystalline phase. While the general retention pattern was similar for all of the cyanobiphenyl phases studied, subtle differences were observed, resulting in significant selectivity differences.

00,619
PB96-123435 Not available NTIS
National Inst. of Standards and Technology (CSTL), Gaithersburg, MD. Chemical Kinetics and Thermodynamics Div.
All-Metal Collection System for Preparative-Scale Gas Chromatography: Purification of Low-Boiling-Point Compounds.
Final rept.
T. J. Buckley, and K. A. Gillis. 1995, 8p.
Pub. in Jnl. of Chromatography A, v702 p243-250 1995.

Keywords: *Gas chromatography, *Collection systems, *Purification, Low boiling point, Reprints, Preparative scale gas chromatography.

We describe a purification system based on a commercial preparative-scale chromatograph with a custom-design condenser, collector, and fraction handling system. In our fraction collector design, all the wetted surfaces were either 316 stainless-steel or nickel. The collectors and the integrated gas-handling manifold were designed to be used down to liquid nitrogen temperature and up to 7 MPa of pressure to accommodate low-boiling-point compounds, such as refrigerants. The design, operation, and performance of this apparatus are presented.

00,620
PB96-123443 Not available NTIS
National Inst. of Standards and Technology (CSTL), Gaithersburg, MD. Surface and Microanalysis Science Div.
Ultrafast Time-Resolved Infrared Probing of Energy Transfer at Surfaces.
Final rept.
R. R. Cavanagh, T. A. Germer, and J. C. Stephenson. 1995, 7p.
Pub. in Vibrational Spectroscopy, v9 p77-83 1995.

Keywords: *Infrared spectrometry, *Energy transfer, *Absorbates, Surfaces, Carbonyl groups, Reprints, *Foreign technology.

Picosecond and femtosecond infrared techniques are used to characterize vibrational energy transfer rates and provide novel insights into the relaxation of non-equilibrium energy distributions. For absorbates on metal surfaces, it is essential to determine the absolute coupling strengths between different degress of freedom, i.e., vibrational modes and low-lying electronic states. In the present work, the spectral shift of the CO stretch has been used to follow the temporal evolution of the adlayer response as a consequence of ultrashort infrared, visible and ultraviolet excitation of the underlying metal. Results from CO/Pt(111) and CO/Cu(100) will be presented, Their differences will be discussed, and comparison will be made to current theoretical models of the damping rates.

00,621
PB96-123682 Not available NTIS
National Inst. of Standards and Technology (CSTL), Gaithersburg, MD. Organic Analytical Research Div.
Influence of Stationary Phase Chemistry on Shape Recognition in Liquid Chromatography.
Final rept.
L. C. Sander, and S. A. Wise. 1995, 9p.
Pub. in Analytical Chemistry, v67 n18 p3284-3292 1995.

Keywords: *Bonded phase, *Liquid chromatography, Selectivity, Reprints, Polymeric stationary phase, Retention mechanism, Self-assembled monolayer.

Molecular shape recognition is examined for a series of C18 columns prepared using a variety of synthetic approaches. Mono-, di-, and trifunctional silanes are used to prepare stationary phases through monomeric and poly meric surface modification procedures, including an approach employing self-assembled monolayer technology. Shape discrimination properties of the columns were investigated with various nonplanar, planar, and linear polycyclic aromatic hydrocarbon solute probes. Chromatographic retention behavior is examined in the context of recently proposed statistical mechanical 'interphase' retention models.

00,622
PB96-138581 Not available NTIS
National Inst. of Standards and Technology (CSTL), Gaithersburg, MD. Analytical Chemistry Div.
Selectivity Trends in Packed Column Supercritical Fluid Chromatography with C18 Stationary Phases.
Final rept.
K. L. Williams, L. C. Sander, S. H. Page, and S. A. Wise. 1995, 6p.
Pub. in Jnl. of High Resolution Chromatography, v18 p477-482 1995.

Keywords: *Chromatography, Polycyclic aromatic hydrocarbons, Isomers, Reprints, *Shape selectivity, Coupled columns, Coal tar.

The retention behavior of polycyclic aromatic hydrocarbons (PAHs) in packed-column supercritical fluid chromatography (SFC) is studied for monomeric and polymeric C18 columns. Molecular shape discrimination (shape selectivity) is assessed through the use of Standard Reference Materials (SRMs), and changes in selectivity are studied as a function of temperature, pressure, and mobile phase composition. Examples of separations of complex PAH isomer mixtures are presented, and guidelines are provided for modification and optimization of shape selectivity in SFC.

00,623
PB96-146766 Not available NTIS
National Inst. of Standards and Technology (CSTL), Gaithersburg, MD. Analytical Chemistry Div.
Amperometric Measurement of Moisture in Transformer Oil Using Karl Fischer Reagents.
Final rept.
S. A. Margolis. 1995, 8p.
Pub. in Analytical Chemistry, v67 n23 p4239-4246 Dec 95.

Keywords: *Moisture content, *Electrical measurement, Calibration standards, Coulometers, Mineral oil, Insulating oil, Volumetric analysis, Reprints, Karl Fisher reagents, RMs(Reference Materials).

Moisture was measured in two oil Reference Materials (RMs), transformer oil (RM 8506) and mineral oil (RM 8507), by the volumetric and coulometric Karl Fisher methods. A variety of analysis conditions were used, including the solvent composition of the titration vessel. The maximum amount of moisture was obtained when the chloroform content of the titration vessel was above 65 percent after the solvent had been titrated to dryness. The highest moisture titers were measured by the volumetric method using either the Hydranal or Pyridine-based Karl Fisher reagents or by the coulometric method using Hydranal AG-H reagent. Other coulometric reagents measured lower amounts of moisture even after the addition of organic solvents.

00,624
PB96-155536 Not available NTIS
National Inst. of Standards and Technology (CSTL), Gaithersburg, MD. Organic Analytical Research Div.
Population Distributions and Intralaboratory Reproducibility for Fat-Soluble Vitamin-Related Compounds in Human Serum.
Final rept.
K. S. Sharpless, and D. L. Duewer. 1995, 7p.
Pub. in Analytical Chemistry, v67 n23 p4416-4422 Dec 95.

Keywords: *Carotenoids, *Vitamins, Histograms, Liquid chromatography, Statistics, Reprints, *Bivariate distributions.

Concentrations of alpha and beta-carotene, lycopene, beta-cryptoxanthim, zeaxanthin, lutein, alpha-, gamma-, and delta-tocopherol, retinol, and retinyl palmitate have been determined in over 1400 human sera from two epidemiologial studies. Complete adult population distributions for these analytes, and for a chromatographically defined 'total carotenids' component, are detailed as data-defined histograms. The distributions for retinol and alpha-tocopherol concentrations are much narrower than those for the other analytes. Information provided by analysis of control samples facilitated intercomparison of the two studies and provided univariate and bivariate and bivariate estimates of the intralaboratory measurement reproducibility.

00,625
PB96-158068 Not available NTIS
National Inst. of Standards and Technology (PL), Gaithersburg, MD. Electron and Optical Physics Div.
Resonance Ionization Spectroscopy/Resonance Ionization Mass Spectrometry Data Service. V-Data Sheets for Ga, Mn, Sc, and Tl.
Final rept.
E. B. Saloman. 1994, 31p.
Pub. in Spectrochimica Acta, v49B n3 p251-281 1994.

Keywords: *Analytical chemistry, *Atomic data, *Data service, Elemental analysis, Spectroscopy, Reprints, *Foreign technology, Resonance ionization, Mass spectrometry.

A data service has been established at the National Institute of Standards and Technology to provide the necessary information to apply to the techniques of resonance ionization spectrocopy (RIS) and resonance ionization mass spectrometry (RIMS) to routine use in analytical chemistry. This service collects and calculates the relevant atomic data, chooses appropriate resonance ionization schemes, and indicates pertinent operating details of successful RIMS studies. The first group of data sheets was published previously covering the elements As, B, Cd, C, Ge, Au, Fe, Pb, Si and Zn. The second group published covered the elements Al, Ca, Cs, Cr, Co, Cu, Kr, Mg, Hg and Ni. The third group published covered the elements Sb, Bi, P, Na and Sn. The fourth group published covered the elements Be, In, Li, K, Rb, Ag, Ti and V. The fifth group of data sheets is presented here. It covered the elements Ga, Mn, Sc and Tl.

00,626
PB96-160833 Not available NTIS
National Inst. of Standards and Technology (CSTL), Gaithersburg, MD. Process Measurements Div.
Development of the NIST Transient Pressure and Temperature Calibration Facility.
Final rept.
V. E. Bean, G. J. Rosasco, W. S. Hurst, and W. J. Bowers. 1991, 5p.
Pub. in Proceedings of the Conference of the National Conference of Standards Laboratories, Albuquerque, NM., August 18-22, 1991, p197-201.

Keywords: *Calibration, *Raman spectroscopy, Shock tube, Transducers, Standards, Pressure, Temperature, Reprints, *Foreign technology.

NIST is developing the capability transient-pressure transducers and transient-temperature transducers. The source for both of these calibrations is a chock tube capable of generating reflected shock pressures up to 20 MPa and temperatures in the range of 1200 K with submicrosecond rise times. The shock tube will be calibrated to avoid the assumptions and uncertainties involved in calculating the pressure and temperature from shock tube theory. The primary standard for the calibration of the shock tube is a sample of diatomic gas. Diatomic gas molecules have a fundamental vibrational motion whose frequency is affected by pressure in a simple way. These molecules also have well defined rotational energy levels whose populations provide a reliable measure of temperature. The vibrational frequencies and the populations of the rotational energy levels can be determined by laser spectroscopy. As the time required for the spectroscopic measurements can be reduced to nanoseconds, spectra can be obtained under shock conditions and these spectra can be evaluated in terms of spectra obtained under known static pressure and temperature conditions.

00,627
PB96-160916 Not available NTIS
National Inst. of Standards and Technology (CSTL), Gaithersburg, MD. Process Measurements Div.
ITS-90 Calibration Facility.
Final rept.
R. S. Kaeser, and G. F. Strouse. 1992, 10p.
Pub. in National Conference of Standards Laboratories, Washington, DC., June 18, 1992, 10p.

Keywords: *Bridge, *Furnace, *Thermometers, Computers, Laboratory, Resistance, Standards, Calibration, Reprints, International Temperature Scale of 1990, SPRT.

A platinum resistance thermometer calibration laboratory is described that provides ten of the defining fixed points of the New International Temperature Scale of 1990 (ITS-90)1, from the argon triple point up to the gold freezing point. Data are taken by computer using the IEEE-488 bus to access resistance bridges, digital multimeters, and scanners for thermometer selection and measurement. Details include laboratory layout, furnace controls and performance, measuring instruments, and a description of the software.

00,628
PB96-161286 Not available NTIS
National Inst. of Standards and Technology (CSTL), Gaithersburg, MD. Process Measurements Div.
Direct Comparison of Three PTB Silver Fixed-Point Cells with the NIST Silver Fixed-Point Cell.
Final rept.
G. F. Strouse, B. W. Mangum, H. G. Nubbemeyer, and H. J. Jung. 1993, 9p.
Pub. in Comite Consultatif de Thermometrie (CCT), 18, Paris, France, September 1993, 9p.

Keywords: *Silver, *Freezing point, *Thermometers, Reprints, *Foreign technology, International Temperature Scale of 1990, ITS-90, HISPRT.

An accurate realization of the International Temperature Scale of 1990 (ITS-90) requires a measurement assurance program for the thermometric fixed-point cells of the defining fixed points. A previous comparison in 1991 of the scales realized at PTB and NIST, through the use of a high-temperature standard platinum resistance thermometer (HTSPRT) calibrated in fixed-point cells in the range between 0 degrees C and 961.78 degrees C at NIST and at PTB, indicated that the differences between the freezing-point temperatures, as realized on the plateaus of the freezing curves, of Sn, Zn and Al fixed-point cells of NIST and PTB were all approximately 1 m degrees C. For silver, however, the maximum temperature difference between the freezing plateaus of the PTB and NIST silver cells appeared to be approximately 18 m degrees C. This extremely large difference was estimated from independent calibrations of the same HTSPRT at PTB and at NIST. In order to determine more accurate values of the temperature differences at the silver point, cell to cell comparisons were carried out recently at NIST.

00,629
PB96-161294 Not available NTIS
National Inst. of Standards and Technology (CSTL), Gaithersburg, MD. Process Measurements Div.
Investigation of High-Temperature Platinum Resistance Thermometers at Temperatures Up to 962C, and, in Some Cases, 1064C.
Final rept.
G. F. Strouse, B. W. Mangum, A. I. Pokhodun, and N. P. Moiseeva. 1992, 6p.
Pub. in Temperature: Its Measurement and Control in Science and Industry, v6 pt1 p389-394 1992.

Keywords: *Thermometers, Stability, Annealing, Reprints, *High temperature thermometry, International Temperature Scale of 1990.

The stability of high temperature standard platinum resistance thermometers, having nominal resistances of 0.25 to 2.5 ohms, and their use in the realization of the International Temperature Scale of 1990 over the range of 0 degrees C to 961 degrees C were investigated. Special procedures were employed for their use above 500 degrees C. These techniques involved annealing and protection against contamination. A sodium heat-pipe furnace was used to realize the freezing points of aluminum, silver, and gold. The results to be presented yielded information on non-uniqueness, subrange inconsistencies and the effects of heating above 600 degrees C.

00,630
PB96-161302 Not available NTIS
National Inst. of Standards and Technology (CSTL), Gaithersburg, MD. Process Measurements Div.
Investigation of the ITS-90 Subrange Inconsistencies for 25.5 Omega SPRTs.
Final rept.
G. F. Strouse. 1992, 4p.
Pub. in Temperature: Its Measurement and Control in Science and Industry, v6 pt1 p165-168 1992.

Keywords: *Thermometry, Reprints, *Foreign technology, *Water triple point cells, International Temperature Scale of 1990, Platinum resistance.

Large variations in observations over extended time were recently reported on water triple point (WTP) cells prepared by using liquid nitrogen (LN) cooled rods to freeze the ice mantle. Experiments were conducted to test the results by using the same technique for preparing the WTP cell ice mantle and by using, for comparison, two other techniques -- solid-CO2 and immersion-cooler methods. Because of the strains that are introduced in preparing the ice mantle by the three methods, results that have been obtained at the National Institute of Standards and Technology (NIST) thus far indicate some variations in the observations during the first few days. The LN-cooled-rod technique caused the ice mantle to crack and the observations on WTP cells prepared by this technique indicate more variations than were observed in cells with mantles prepared by other techniques.

00,631
PB96-161310 Not available NTIS
National Inst. of Standards and Technology (CSTL), Gaithersburg, MD. Process Measurements Div.
NIST Assessment of ITS-90 Non-Uniqueness for 25.5 Ohm SPRTs at Gallium, Indium and Cadmium Fixed Points.
Final rept.
G. F. Strouse. 1992, 4p.
Pub. in Temperature: Its Measurement and Control in Science and Industry, v6 pt1 p175-178 1992.

Keywords: *Thermometry, *Fixed points, Temperature, Reprints, International Temperature Scale of 1990, Platinum resistance.

The use of temperature subranges in the definition of the International Temperature Scale of 1990 (ITS-90) permits standard platinum resistance thermometers (SPRTs) to be measured at defining fixed points of a particular subrange as well as at fixed points not utilized in that subrange. These redundant fixed points allow analysis of the non-uniqueness of the scale. Specifically, with 25.5 ohm SPRTs at gallium, indum, and cadmium fixed points have been made and examined to determine the non-uniqueness at these points. The results of this investigation indicate that the levels of non-uniqueness of the ITS-90 at the three redundant fixed points does not contribute significantly to the total error associated with the calibration of an SPRT.

00,632
PB96-161328 Not available NTIS
National Inst. of Standards and Technology (CSTL), Gaithersburg, MD. Process Measurements Div.
NIST Implementation and Realization of the ITS-90 Over the Range 83 K to 1235 K: Reproducibility, Stability, and Uncertainties.
Final rept.
G. F. Strouse. 1992, 6p.
Pub. in Temperature: Its Measurement and Control in Science and Industry, v6 pt1 p169-174 1992.

Keywords: *Thermometry, *Fixed points, Temperature, Reprints, International Temperature Scale of 1990, Platinum resistance.

The National Institute of Standards and Technology is using thermometric fixed points to realize the International Temperature Scale of 1990 (ITS-90) and disseminate the temperature scale through the calibrations of standard platinum resistance thermometers over the range of 83.8058 K to 1234.93 K. This work involved the optimization of experimental techniques and measurement procedures to reduce uncertainty in the data. The realization of the scale allows for an in-depth investigation of reproducibility and stability of the fixed points used to define the various temperature subranges of the ITS-90. Additionally, propagation of errors associated with the ITS-90 is discussed.

00,633
PB96-161336 Not available NTIS
National Inst. of Standards and Technology (CSTL), Gaithersburg, MD. Process Measurements Div.

NIST Measurement Assurance of SPRT Calibrations on the ITS-90: A Quantitative Approach.
Final rept.
G. F. Strouse, and B. W. Mangum. 1993, 17p.
Pub. in Measurement Science Conference, Anaheim, CA., January 21-22, 1993, 17p.

Keywords: *Thermometry, *Fixed points, High temperature, Reprints, HTSPRT, International Temperature Scale of 1990, Platinum resistance.

The National Institute of Standards and Technology (NIST) is responsible for realizing, maintaining and disseminating the International Temperature Scale of 1990 (ITS-90) for the United States of America. One of the methods used for the dissemination of the scale is the calibration of standard platinum resistance thermometers (SPRTs) and high-temperature SPRTs (HTSPRTs), using thermometric fixed points. At NIST, the calibration of these thermometers as defining, interpolating devices for the ITS-90 includes various internal quality control checks in order to minimize the uncertainty associated with a calibration. The internal measurement assurance program incorporated at NIST includes the use of check (HT)SPRTs, control charts, redundant fixed points, and statistical process control. This program, as well as some results showing fixed-point reproducibility and calibration uncertainties, will be discussed.

00,634
PB96-161344 Not available NTIS
National Inst. of Standards and Technology (CSTL), Gaithersburg, MD. Process Measurements Div.
Preliminary Results of a Comparison of Water Triple-Point Cells Prepared by Different Methods.
Final rept.
G. F. Strouse, G. T. Furukawa, and B. W. Mangum. 1993, 23p.
Pub. in Comite Consultatif de Thermometrie (CCT), 18, Paris, France, September 1993, 23p.

Keywords: *Thermometry, *Fixed points, Temperatures, Reprints, International Temperature Scale of 1990, Platinum resistance.

The International Temperature Scale of 1990 provides greater flexibility than the International Practice Temperature Scale of 1968, Amended Edition 1975, through the use of more fixed points and more temperature subranges. The present investigation examined the ranges of 83.8058 K to 273.16 K and 273.15 K to 933.473 K for 25.5 omega standard platinum resistance thermometers. These two ranges have multiple subranges that partly overlap, creating inconsistencies. The magnitude of the inconsistencies in the interpolation between the appropriate defining fixed points in the temperature overlap regions were investigated. The results show that in all 16 possible combinations of subranges, there were no significant differences between manufacturer/models and that the inconsistencies in most cases are within estimated measurement uncertainties.

00,635
PB96-164041 Not available NTIS
National Inst. of Standards and Technology (CSTL), Boulder, CO. Thermophysics Div.
Simple and Efficient Methane-Marker Devices for Chromatographic Samples.
Final rept.
T. J. Bruno. 1996, 8p.
Pub. in Jnl. of Chromatography A, v721 p157-164 1996.

Keywords: *Chromatography, Reprints, *Hold-up times, *Methane-marker devices, Retention times.

Calculation of the most useful gas chromatographic retention parameters, such as net and specific retention volumes, relative retentions, and retention indices, requires that raw retention data be corrected for gas hold-up time or volume (sometimes called dead time or volume) of the chromatographic system. When a flame-ionization detector is used, a common technique (where it is physically appropriate) is to introduce methane into the sample as a marker to approximate unretained species to correct for hold-up. This is often done by bubbling methane (or natural gas) through the sample just before injection. In this paper, we describe two easily constructed devices that provide continuous release of methane into liquid samples, sustainable for several weeks or even months. This long-term feature makes the techniques especialy suitable to extensive retention studies done at multiple temperatures as several stationary phases. Moreover, one of the devices described is applicable to commercially available automatic sampler vials. After a detailed description of the construction of the devices is provided, some applications are discussed.

00,636
PB96-164272 Not available NTIS
National Inst. of Standards and Technology (CSTL), Gaithersburg, MD. Inorganic Analytical Research Div.
Certifying the Chemical Composition of a Biological Material: A Case Study.
Final rept.
R. Zeisler, D. A. Becker, and T. E. Gills. 1995, 5p.
Pub. in Fresenius Jnl. of Analytical Chemistry, n352 p111-115 1995.

Keywords: *Chemical compositions, *Biological materials, *Trace elements, Comparative evaluations, Reprints, Food, *Foreign technology, Analytical Quality Control Services.

A worldwide laboratory intercomparison was organized by the International Atomic Energy Agency's Analytical Quality Control Services (AQCS) involving the determination of trace elements in plant materials used for human consumption. The National Institute of Standards and Technology (NIST) Standard Reference Materials Program donated 5 kg of spinach designated for the production of the future Standard Reference Material SRM 1570a to this intercomparison: the AQCS provided a similar amount of cabbage. For the study, 150 units of each material were distributed and 114 laboratories reported results on both materials to AQCS. The results for the spinach, encompassing more than forty elements, have been compiled and evaluated; estimates of the elemental concentrations were made based on statistical evaluations, principles of analytical procedures and the laboratory performance indicated by the results on the cabbage material. Satisfactory estimates were obtained for 27 elements. Comparison with IAEA laboratory and NIST reference data did not reveal any significant bias that might have been introduced by the intercomparison approach or its evaluation.

00,637
PB96-167168 Not available NTIS
National Inst. of Standards and Technology (CSTL), Gaithersburg, MD. Analytical Chemistry Div.
Supercritical Fluid Extraction-Immunoassay for the Rapid Screening of Cocaine in Hair.
Final rept.
J. F. Morrison, S. N. Chesler, and J. L. Reins. 1996, 9p.
Pub. in Jnl. of Microcolumn Separations, v8 n1 p37-45 1996.

Keywords: *Cocaine, *Hair, *Radioimmunoassay, Reprints, Supercritical fluid extraction.

Supercritical fluid extraction-radioimmunoassay (SFE-RIA) was evaluated as a rapid screening tool for the detecion of cocaine residues in human hair. SFE was performed using carbon dioxide modified with triethylamine (TEA) and water, with off-line collection of extracted cocaine in methanol. Extracts were analyzed for the presence of cocaine using a commercially available solid-phase RIA kit. In order to develop a suitable RIA calibration method for reliable measurement of cocaine in SF extracts, calibration data was compared for methanolic standards both with and without the presence of the SF modifier. Methanol had only a minor impact on immunoassay performance, producing an 11% decrease in maximum binding counts. In contrast, the presence of TEA/H2O profoundly degraded assay performance, producing a 60% suppression in assay counts. To preserve RIA sensitivity, SF extracts were evaporated under nitrogen to remove the modifier and reconstituted in menthanol for RIA analysis. Incorporation of the evaporation step permitted the use of modifier-free cocaine calibrators in memthanol. Calibration data was fit to a four-parameter logistic model. SFE-RIA analysis of a series of drug-free hair samples established an RA cut-off value for distinguishing between a negative and presumptive positive cocaine sample at an SF extract concentration of 1.2 ng/mL, or a hair concentration of 0.07 ng/mg. The robustness of the SFE-RIA method was demonstrated by the analysis of a variety of hair samples from both users and non-users. The quantitative SFE-RIA findings correlated well with the values obtained by an acid incubation/GC-MS method.

00,638
PB96-167283 Not available NTIS
National Inst. of Standards and Technology (CSTL), Gaithersburg, MD. Inorganic Analytical Research Div.
Resolution of Discrepant Analytical Data in the Certification of Platinum in Two Automobile Catalyst SRMs.
Final rept.
D. A. Becker. 1995, 3p.
Pub. in Fresenius Jnl. of Analytical Chemistry, v352 p224-226 1995.

Keywords: *Automobile catalyst, Analytical interference, Accuracy, Reprints, Quality assurance, *Instrumental neutron activation analysis, *Foreign technology, Standard reference materials, Plantinum determination.

The National Institute of Standards and Technology (NIST) recently developed two recycled automobile catalyst materials as standard reference materials (SRMs), in response to a request from the International Precious Metals Institute. Results of analyses for platinum by two different analytical techniques did not agree well, with the mean differing up to 6%. The palladium results for these same two techniques in the same materials showed much better agreement. Finally, it was determined that on technique (instrumental neutron activation analysis - INAA) had a small, random interference due to a tantalum impurity in/on the acid washed polyethylene bag used to hold the finely powered sample. This Ta was not present in any of the empty bags used to evaluate the bag blank. Once this problem was identified, the unique characteristics of the INAA technique allowed the magnitude of the interference to be accurately determined for each sample, data recalculated, and a final result obtained which agreed well with the second technique.

00,639
PB96-167291 Not available NTIS
National Inst. of Standards and Technology (CSTL), Boulder, CO. Thermophysics Div.
Permeation Tube Approach to Long-Term Use of Automatic Sampler Retention Index Standards.
Final rept.
T. J. Bruno. 1995, 6p.
Pub. in Jnl. of Chromatography A, v704 p157-162 1995.

Keywords: *Alternative refrigerants, *Chromatographic analysis, Reprints, Hydrocarbons, Permeation tubes, Chromatographic samples.

A permeation tube that is sealed internally in a commercially-available automatic sampler vial provides a simple and convenient method of preparing, using, and storing standard retention index samples for long periods of time. The approach is especially suited to the handling of volatile organic compounds that are very important in fuels research, alternative refrigerant research and in many environmental analyses. It also provides the very desirable feature of dispensing sample that is at very low concentration or even at infinite dilution, since no commercial automatic sampler is currently capable of doing this for the analyst. The device is very simple, and can be constructed and prepared with a liquid sample in a few minutes. It requires the use of minimal quantities of sample, and substantially descreases the hazards associated with handling volatile organics in the laboratory.

00,640
PB96-190061 Not available NTIS
National Inst. of Standards and Technology (CSTL), Gaithersburg, MD. Analytical Chemistry Div.
Isolation and Structural Elucidation of the Predominant Geometrical Isomers of alpha-Carotene.
Final rept.
C. Emenhiser, G. Englert, L. C. Sander, B. Ludwig, and S. J. Schwartz. 1996, 11p.
Pub. in Jnl. of Chromatography A, v719 p333-343 May 96.

Keywords: *Carotene, *Isomers, *Stereochemistry, Isomerization, Chromatographic analysis, Carotenoids, Polymers, Carbon 30, Spectroscopic analysis, Reprints, Liquid chromatography, Geometrical isomers, Shape selectivity.

The recent development and application of a polymeric C30 stationary phase have given unique separations of cis-trans carotenoid isomers in reversed-phase (RP) liquid chromatography (LC) owing to the expectional shape selectivity of this stationary phase. In the present research, several geometrical isomers of alpha-carotene were at least partially resolved from a photo-isomerized mixture when chromatographed on

a 3-micro m polymeric C30 column. Confirmation of the structures of geometrical alpha-carotene isomers will aid further studies on the possible physiological roles of these compounds in biological tissues.

00,641
PB96-190277 Not available NTIS
National Inst. of Standards and Technology (CSTL), Gaithersburg, MD. Analytical Chemistry Div.
Embossable Grating Couplers for Planar Waveguide Optical Sensors.
Final rept.
B. L. Ramos, S. J. Choquette, and N. F. Fell. 1996, 5p.
Pub. in Analytical Chemistry, v68 n7 p1245-1249 1996.

Keywords: *Grating coupling, *Optical sensors, *Embossable grating, Reprints, Planar waveguide.

Planar optical waveguides are an attractive tool for use in analytical chemistry and spectroscopy. Although similar to fiber optics, planar waveguides have been slow to be commercially accepted due to the difficulty of coupling light into the guide. Generally, prism coupling is the method of choice in the laboratory, as efficiencies approaching 80% can be reached. However, prisms are impractical for routine use for several reasons: expensive positioning equipment is required, coupled power is sensitive to environmental fluctuations, and prism coupling prohibits the fabrication of a truly planar device. The use of thin gratings on the surface of the waveguide allows for a two-dimensional structure to be maintained, while providing enough efficiency to be useful as a sensor. The research efforts focus on developing a technique to make inexpensive, reproducible gratings that are easy to fabricate. By chemically modifying the surface of a commercial grating with a suitable release agent, it is possible to emboss replica gratings onto a variety of waveguide types. The fabrication of embossed gratings will be described, and their performance on glass, ion-diffused, polymer, and semiconductor waveguides will be presented.

00,642
PB96-200951 Not available NTIS
National Inst. of Standards and Technology (CSTL), Gaithersburg, MD. Analytical Chemistry Div.
Flow Immunoassay Using Solid-Phase Entrapment.
Final rept.
L. Locascio-Brown, L. Martynova, R. G. Christensen, and G. Horvai. 1996, 6p.
Pub. in Analytical Chemistry, v68 n9 p1665-1670 May 96.

Keywords: *Flow injection, *Immunoassay, Sorbents, Separation, Assays, Reprints, *Solid-phase entrapment.

A flow injection immunoassay was performed using a column packed with reversed-phase sorbents to effect separation of the immunoreacted species by entrapping free analyte and allowing antibody-conjugated analyte to pass unretained. Fluorescein-labeled analyte was measured in a competitive assay for the anticonvulsant drug phenytoin. The simplicity of the assay was the greatest advantage of the technique, which allowed for measurement of phenytoin in a 2-min assay time. The reliable detection limit for the assay was 5 nmol L to the minus 1 power of phenytoin in serum. The columns were regenerated with periodic injections of ethanol solutions to remove the entrapped analyte and prepare the column for subsequent analyses.

00,643
PB96-201041 Not available NTIS
National Inst. of Standards and Technology (CSTL), Gaithersburg, MD. Chemical Kinetics and Thermodynamics Div.
UV Absorption Cross Sections of Methylchloroform: Temperature-Dependent Gas and Liquid Phase Measurements.
Final rept.
A. K. Nayak, M. J. Kurylo, and A. Fahr. 1995, 5p.
Pub. in Jnl. of Geophysical Research, v100 nD6 p11,185-11,189 Jun 95.

Keywords: *Tungsten silicide, *Formation enthalpy, *Calorimetry, Analytical chemistry, Reprints, *Foreign technology, Methylchloroform.

The absorption cross sections for methylchloroform (CH_3CCl_3) have been measured in the gas phase (from 160 to approximately 240 nm) and in the liquid phase (from approximately 235 to 260 nm) over the temperature range 220-330 K. The liquid phase results were converted into effective gas phase cross sections using a wavelength shift procedure described and verified in earlier work. The results are compared with other available data in the wavelength region 185-240 nm. The multiplicity of measurements in different laboratories lends increased confidence in the quantification of uncertainties in the atmospheric (photolysis and kinetic) lifetime calculations for this important chemical species.

00,644
PB96-210786 PC A04/MF A01
National Inst. of Standards and Technology (CSTL), Gaithersburg, MD. Analytical Chemistry Div.
NIST Traceable Reference Material Program for Gas Standards: Standard Reference Materials.
Special pub.
F. R. Guenther, W. D. Dorko, W. R. Miller, and G. C. Rhoderick. Jul 96, 44p, NIST-SP-260-126.
Also available from Supt. of Docs. as SN003-003-03419-3.

Keywords: *Gas analysis, *Calibration standards, *Tracer techniques, Gas mixtures, Samples, Concentration(Composition), Certification, Validation, Maintenance, Interlaboratory comparisons, Data quality, Quality assurance, *Standard Reference Materials.

A program is described by which the concentration of commerically produced gas mixtures may be related to gaseous primary standards maintained by the National Institute of Standards and Technology (NIST). The responsibilities of the producer and NIST are detailed along with recommended procedures the producer should follow during production and analysis of the mixtures. Procedures also are included for the maintenance of NTRM batches. Appendices are included for the preparation of NTRMs related to various Standard Reference Materials.

00,645
PB96-210877 PC A05/MF A01
National Inst. of Standards and Technology (CAML), Gaithersburg, MD. Statistical Engineering Div.
Statistical Aspects of the Certification of Chemical Batch SRMs. Standard Reference Materials.
Special pub.
S. B. Schiller. Jul 96, 52p, NIST-SP-260-125.
Also available from Supt. of Docs. as SN003-003-03416-9. See also PB95-143087.

Keywords: *Chemical analysis, *Calibration standards, *Certification, *Statistical analysis, Analytical methods, Sampling, Chemical composition, Homogeneity, Uncertainty, Confidence level, Accuracy, Precision, Quality control, Quality assurance, *Standard reference materials.

The accurate determination of chemical analytes in batches of material is the principal requirement in chemical Standard Reference Material (SRM) certification. Many measurement made for chemical constituent batch SRMs are destructive, and batches are usually large, so selecting a random but representative sample from the batch is vital to inference about the material. Homogeneity assessment must be done to verify the materials suitability for sale, and to determine what type of statistical interval will make an appropriate summary for the certificate. Finally, results from more than one independent chemical method often must be combined in a statistically meaningful way to arrive at a realistic estimate of the uncertainty of the results achieved. This paper provide guidelines for addressing these statistical issues. The motivations behind those guidelines are also explained to facilitate understanding of them.

00,646
PB96-214614 PC A04/MF A01
National Inst. of Standards and Technology (CSTL), Gaithersburg, MD. Surface and Microanalysis Science Div.
Airborne Asbestos Method: Bootstrap Method for Determining the Uncertainty of Asbestos Concentration. Version 1.0.
S. Turner, R. L. Myklebust, B. B. Thorne, S. D. Leigh, and E. B. Steel. Aug 96, 36p, NISTIR-5723.
Sponsored by Environmental Protection Agency, Washington, DC.

Keywords: *Asbestos, *Test methods, *Chemical analysis, *Statistical analysis, *Standards, Electron microscopy, Air pollution detection, Quality assurance, Air filters, Air sampling, *Transmission electron microscopy.

The determination of the uncertainty of the analytical value for the concentration of asbestos in air is of practical use for: (1) comparison of analyses obtained by different operators or laboratories on the same sampling area and (2) providing an indication of how an analytical value compares with values set by government regulations. This test method describes a procedure for determining the component of uncertainty that is due to variation in sampling of a population of values (corresponding to the Type A evaluation of uncertainty described in NIST Technical Note 1297). The test method describes use of a bootstrapping procedure for determination of a 95% confidence interval for the concentration of asbestos deposited onto filters.

00,647
PB96-214630 PC A10/MF A03
National Inst. of Standards and Technology (CSTL), Gaithersburg, MD.
CSTL Technical Activities, 1995.
H. G. Semerjian, and W. F. Koch. 1995, 200p, NISTIR-5828.
See also report for 1994, PB95-242319.

Keywords: *Chemistry, *Research and development, Chemical engineering, Biotechnology, Measurements, Metrology, Models, Measurement traceability, Process technology, Reference data.

This report summarizes the research and services provided by the Chemical Science and Technology Laboratory of the National Institute of Standards and Technology for Fiscal Year 1995. The report includes: a general overview of the laboratory's activities, a summary of the technical accomplishments in the six CSTL divisions - Biotechnology, Chemical Kinetics and Thermodynamics, Process Measurements, Surface and Microanalysis, Thermophysics and Analytical Chemistry, and a description of 130 selected technical projects.

00,648
PB97-109037 (Order as PB97-109011, PC A11/MF A03)
Gmelin Inst. for Inorganic Chemistry of the Max Plank Society, Frantfurt (Germany).
Inorganic Crystal Structure Database (ICSD) and Standardized Data and Crystal Chemical Characterization of Inorganic Structure Types (TYPIX): Two Tools for Inorganic Chemists and Crystallographers.
E. Fluck. 1996, 4p.
Included in Jnl. of Research of the National Institute of Standards and Technology, v101 n3 p217-220 May/Jun 96.

Keywords: *Crystallography, *Inorganic compounds, *Information systems, *Chemical composition, Data base management.

The two databases ICSD and TYPIX are described, ICSD is a comprehensive compilation of crystal structure data of inorganic compounds (about 39,000 entries). TYPIX contains 3600 critically evaluated data sets representative of structure types formed by inorganic compounds.

00,649
PB97-109045 (Order as PB97-109011, PC A11/MF A03)
Bonn Univ. (Germany, F.R.). Inst. for Inorganic Chemistry.
Evaluation of Crystallographic Data with the Program DIAMOND.
G. Bergerhoff, M. Berndt, and K. Brandenburg. 1996, 5p.
Included in Jnl. of Research of the National Institue of Standards and Technology, v101 n3 p221-225 May/Jun 96.

Keywords: *Crystallography, *Chemical composition, *Information systems, *Inorganic compounds, Information retrieval, Crystal structure, Computer graphics, Database management.

The new crystal structure information system DIAMOND is presented. It handles all kinds of crystallographic databases on PCs including SHELX files and Chemical Information Files (CIF's). DIAMOND, because of its graphics capability, is a powerful tool for establishing structural relationships and for evaluating crystallographic data.

00,650
PB97-110019 Not available NTIS

National Inst. of Standards and Technology (CSTL), Gaithersburg, MD. Analytical Chemistry Div.
Role of Certified Reference Materials in Trace Analysis Quality Assurance.
Final rept.
D. A. Becker. 1995, 4p.
Pub. in Proceedings of Polish Conference on Analytical Chemistry (5th), Gdansk, Poland, September 3-8, 1995, p39-42.

Keywords: *Standards, Chemical analysis, Reprints, *Foreign technology, *Certified reference materials, *Standards reference materials.

The quest for accuracy in trace element chemical analysis requires a constant effort by the analyst in the location, elucidation, determination and elimination of error in any of its many forms. At NIST, the authors obviously have a high degree of interest in obtaining the highest accuracy and precision practicable, for certification of elemental content in NIST Standard Reference materials (SRM). The paper will discuss the author's concept of the role of Certified Reference Materials (CRM) in trace analysis quality assurance, with specific illustrations from the author's work in neutron activation analysis (NAA).

00,651
PB97-111975 Not available NTIS
National Inst. of Standards and Technology (CSTL), Gaithersburg, MD. Chemical Kinetics and Thermodynamics Div.
Oxidation of Caffeic Acid and Related Hydroxycinnamic Acids.
Final rept.
P. Hapiot, A. Neudeck, J. Pinson, C. Rolando, H. Fulcrand, and P. Neta. 1996, 8p.
Pub. in Jnl. of Electroanalytical Chemistry, v405 p169-176 1996.

Keywords: *Oxidation, *Caffeic acid, Electrooxidation, Ferulic acid, Pulse radiolysis, Reprints, 4-coumaric acid.

Oxidation of caffeic acid (3,4-dihydroxycinnamic acid) 1H3 has been studied by electrochemical methods and by pulse radiolysis in aqueous and organic solvents. The results have been compared with the behavior of 4-coumaric acid 2H2 and ferulic acid 3H2. The first oxidative intermediates have been characterized by their UV spectra and oxidation potentials. In case of 2H2 and 3H2, the initial radicals decay by a second order process indicating a radical-radical coupling mechanism. On the contrary, for caffeic acid the oxidation leads to the formatuion of the corresponding o-quinone through disproportionation of the initial semiquinone radical.

00,652
PB97-112437 Not available NTIS
National Inst. of Standards and Technology (CSTL), Gaithersburg, MD. Analytical Chemistry Div.
Use of Neutron Beams for Chemical Analysis at NIST.
Final rept.
E. A. Mackey, D. L. Anderson, H. Chen-Mayer, G. P. Lamaze, R. M. Lindstrom, D. F. R. Mildner, R. L. Paul, R. G. Downing, and R. R. Greenberg. 1996, 15p.
Pub. in Jnl. of Radioanalytical and Nuclear Chemistry, Articles, v203 n2 p413-427 1996.

Keywords: *Quantitative chemical analysis, *Neutron capture gamma rays, Cold neutrons, Neutron activation analysis, Neutron scattering, Reprints, Neutron focusing, Neutron depth profiling, Target irradiation.

At the National Institute of Standards and Technology, there are two techniques for chemical analysis that use neutron beams from the reactor for target irradiation: neutron depth profiling (NDP) and prompt gamma-ray activation analysis (PGAA). The paper includes a brief description of the facilities, the measurement capabilities of each, some recent applications of NDP and PGAA, and neutron focusing as applied to these techniques.

00,653
PB97-113260 Not available NTIS
National Inst. of Standards and Technology (CSTL), Gaithersburg, MD. Analytical Chemistry Div.
Use of a Naphthylethylcarbamoylated- beta-Cyclodextrin Chiral Stationary Phase for the Separation of Drug Enantiomers and Related Compounds by Sub- and Supercritical Fluid Chromatography.
Final rept.
K. L. Williams, L. C. Sander, and S. A. Wise. 1996, 7p.
Pub. in Chirality, v8 p325-331 Sep 96.

Keywords: *Enantiomeric separation, *Chrial recognition, Derivatized cyclodextrin, Chromatography, Drug analysis, Reprints.

Enantiomeric separation of a variety of drugs and related compounds was achieved on an (S)-naphthylethylcarbamoy lated-beta-cyclodextrin (S-NEC-CD) chiral stationary phase (CSP) using sub- and subcritical fluid chromatography (SFC). Compounds previously resolved on native or derivatized cyclodextrin CSPs in liquid chromatography (LC) using reversed phase or polar organic mobile phase modes could be resolved in SFC using a simple carbon dioxide/methanol eluent. Resolution of cromakalim, which is not possible on the S-NEC-CD column in LC, was readily accomplished in SFC. The importance of modifier, temperature, and pressure was assessed in relation to retention, selectivity, and resolution. The nature of the modifier and the modifier concentration were found to be crucial parameters.

00,654
PB97-119002 Not available NTIS
National Inst. of Standards and Technology (MSEL), Gaithersburg, MD.
Segmental Concentration Profiles of End-Tethered Polymers with Excluded-Volume and Surface Interactions.
Final rept.
M. Adamuti-Trache, W. E. McMullen, and J. F. Douglas. 1996, 14p.
Pub. in Jnl. of Chemical Physics, v105 n11 p4798-4811 Sep 96.

Keywords: *Grafted polymer layer, *Excluded volume, *Surface interaction, Concentration profiles, Reprints, End-tethered polymers.

The segmental concentration profile p of end-tethered flexible polymer chains is calculated for comparison with recent measurements on polymer layers having a low surface grafting density omega. Moments of p are also calculated as these quantities, rather than the full concentration profiles, are usually measured experimentally. Exact calculations of p are summarized for ideal flexible chains with an arbitrary short-range polymer-surface interaction. Though technical difficulties restrict the renormalization group (RG) calculations for swollen chains to limiting values of the polymer-surface interaction, the analysis indicates that the relatively simple, closed-form, Gaussian-chain expression for p provides a good approximation to the RG results if the average size of the Gaussian chain is replaced by its swollen-chain analog. This approximate concentration profile for chains with excluded volume and variable polymer-surface interaction should prove useful when interpretating experimental results for low-grafting-density polymer layers formed in good solvents.

00,655
PB97-119242 Not available NTIS
National Inst. of Standards and Technology (CSTL), Gaithersburg, MD. Process Measurements Div.
Comparisons of Some NIST Fixed-Point Cells with Similar Cells of Other Standards Laboratories.
Final rept.
B. W. Mangum, E. R. Pfeiffer, G. F. Strouse, T. I. Yeh, P. Marcarino, R. Dematteis, Y. Liu, Q. Zhao, A. T. Ince, F. Cakiroglu, H. G. Nubbemeyer, H. J. Jung, J. Valencia-Rodriguez, and J. H. Lin. 1996, 11p.
Pub. in Metrologia, v33 n3 p215-255 1996.

Keywords: *Fixed points, *Temperature measurement, *Interlaboratory comparisons, Gallium, Water, Tin, Indium, Zinc, Aluminum, Silver, Thermometry, Calibration standards, Uncertainty, Reprints, International Temperature Scale of 1990.

In the paper, the authors present results of international comparisons of fixed-point cells of some of the defining fixed-point materials of the International Temperature Scale of 1990. These comparisons involved cells from seven national laboratories, although in some cases only one type of fixed-point material from the various laboratories was to within 1 mK.

Basic & Synthetic Chemistry

00,656
AD-A286 620/0 PC A03/MF A01
National Bureau of Standards, Gaithersburg, MD.
Fuzed-Quartz Fibers. A Survey of Properties, Applications and Production Methods.
25 Jan 56, 30p, NBS-569.

Keywords: *Fused silica, *Fibers, *Quartz, Fabrication, Hardness, Silica glass, Thermal expansion, Viscosity, Elastic properties, Surveys.

Fused-silica fibers have an important function in many measuring instruments used in scientific research. Much of the information on the production and fabrication methods and on the properties of the fibers is widely scattered throughout the technical literature. This Circular is a survey of this literature and a summary findings. A bibliography of pertinent references on the subject is included to provide the sources of more complete and detailed information necessary for specific applications. (Author).

00,657
AD-A297 265/1 PC A03/MF A01
National Bureau of Standards, Gaithersburg, MD.
Physical Properties of Some Purified Aliphatic Hydrocarbons.
Research paper.
D. B. Brooks, F. L. Howard, and H. C. Crafton. Jan 40, 13p.
Pub. in Jnl. of Research of the National Bureau of Standards, v24.

Keywords: *Physical properties, *Refractive index, *Aliphatic hydrocarbons, Density, Temperature, High rate, Methyl radicals, Efficiency, Alkanes, Purification, Freezing, Pressure, Aviation fuels, Butenes, Ethyl radicals, Butanes, Distillation, Pentanes, Olefin polymers, Fractionation, Heptanes, Reprints, *Paraffin hydrocarbons, *Oiling point, Dimethylbutene, Dimethylbutane, Ethylpentane, Heptane.

In an investigation of the suitability of various paraffin hydrocarbon constituents of aviation fuel, which is being conducted for the National Advisory committee for Aeronautics, the Navy Bureau of Aeronautics, and the Army Air Corps, four olefin and seven paraffin hydrocarbons have been obtained in a state of high purity. Eight of these materials were synthesized, one was isolated from a commercial synthetic crude, and two were obtained from commercial sources. All were purified by distillation in automatically controlled fractionating columns of high efficiency. The measured physical properties of these materials included freezing point, oiling point and its variation with pressure, refractive index and density and their variations with temperature. jg p.1.

00,658
PB94-211208 Not available NTIS
National Inst. of Standards and Technology (MSEL), Gaithersburg, MD. Polymers Div.
Proteoglycan Inhibition of Calcium Phosphate Precipitation in Liposomal Suspensions.
Final rept.
E. D. Eanes, A. W. Hailer, R. J. Midura, and V. C. Hascall. 1992, 8p.
Sponsored by National Inst. of Dental Research, Bethesda, MD.
Pub. in Glycobiology 2, n6 p571-578 1992.

Keywords: *Proteoglycans, *Liposomes, *Calcium phosphates, Precipitation, Cartilage, Calcification, Chondroitin sulfate, Calcium, Reprints, Aggrecan.

The major proteoglycan in cartilage (aggrecan) is a complex macromolecule with numerous chondroitin sulphate, keratan sulphate, and oligosaccharide substituents. It has been proposed that this macromolecule has an important role in regulating mineralization in this tissue, a process which is initiated by the deposition of apatite in matrix vesicles. We have used a liposome-centered endogenous precipitation method as a model for matrix vesicle mineralization to study the effect of the rat chondrosarcoma aggrecan and its chondroitin sulphate and core protein components on apatite formation from solution. Aggrecan (0.5%) in the suspending medium had no effect on intraliposomal precipitation, but severely reduced (approximately 70% reduction at 24 h) its subsequent spread into the medium. The chondroitin sulphate and core protein were similarly inhibitory. The degree to which aggrecan and its constituent parts inhibited pre-

cipitation correlated with their capacity to bind Ca(2+) ions. These findings suggest that functional groups in aggrecan blocked apatite growth by linking via Ca(2+) bridges to growth sites on the crystal surfaces. Similar Ca-mediated interactions may well have a critical regulatory role in cartilage mineralization.

00,659
PB95-151981 Not available NTIS
National Inst. of Standards and Technology (NML), Gaithersburg, MD. Chemical Process Metrology Div.
Flame Synthesis of High Tc Superconductors.
Final rept.
M. R. Zachariah, and S. Huzarewicz. 1991, 4p.
Pub. in Combustion and Flame 87, n1 p100-103 1991.

Keywords: *High temperature superconductors, *High-TC superconductors, *YBCO superconductors, Diffusion flames, Particle size distribution, Reprints, *Flame synthesis, *Yttrium barium cuprates.

High temperature superconducting particles of the 1:2:3 Yttrium-Barium-Copper oxide system have been synthesized in an inverted configuration coannular diffusion flame. The particles were produced from a spray pyrolysis technique, employing aerosolized nitrate salts of Y, Ba and Cu. Particles produced showed a transition temperature of 92 K as determined by magnetic susceptibility measurements. The particles were shown to have a wide particle size distribution, ranging from 10 to 1000 nm. It was also observed that due to the effects of water vapor reactions at high temperatures, only a diffusion flame successfully produced the correct phase.

00,660
PB95-161535 Not available NTIS
National Inst. of Standards and Technology (MSEL), Gaithersburg, MD. Polymers Div.
Octacalcium Phosphate Carboxylates. 1. Preparation and Identification.
Final rept.
M. Markovic, B. O. Fowler, and W. E. Brown. 1993, 5p.
See also Part 2, PB95-161543. Sponsored by American Dental Association Health Foundation, Chicago, IL.
Pub. in Chem. Mater. 5, n10 p1401-1405 1993.

Keywords: *Chemical preparation, *Chemical analysis, Dentistry, Calcium phosphates, X-ray diffraction, Infrared spectroscopy, Raman spectroscopy, Ions, Molecular structure, Precipitation(Chemistry), Minerals, Calcification, Reprints, *Octacalcium phosphate carboxylates.

The formation of octacalcium phosphate carboxylates, Ca8(HPO4)m(carboxylate)n(PO4)4-yH2O, by conversion of alpha-Ca3(PO4)2 in solutions of 19 ammonium carboxylates (monocarboxylates; saturated, unsaturated, hydroxy, keto, and amino dicarboxylates; and tricarboxylates) was investigated. The various solid phases formed, depending on initial pH's and conversion times, were determined by X-ray diffraction and infrared and Raman spectroscopy. Octacalcium phosphate carboxylates containing structurally incorporated malonate, succinate, adipate, suberate, sebacate, fumarate, malate, and citrate ions were formed and identified. Octacalcium phosphate carboxylates were also formed from pyruvate and alpha-ketoglutarate solutions but with uncertain carboxylate ion structures. All of these identified compounds are structurally similar to octacalcium phosphates, Ca8(HPO4)2(PO4)4-5H2O, but have expanded a-axis unit-cell dimensions that generally increased with increasing number of carbon atoms in the carboxylate ion. Among these compounds, of special importance are those containing carboxylates that are present as intermediates in the Krebs cycle. The possible precipitation of these octacalcium phosphate carboxylates in mitochondria and their possible role as precursors in calcified tissue formation are discussed.

00,661
PB95-163317 Not available NTIS
National Inst. of Standards and Technology (CSTL), Gaithersburg, MD. Biotechnology Div.
Equilibrium and Calorimetric Investigation of the Hydrolysis of L-Tryptophan to (Indole + Pyruvate + Ammonia).
Final rept.
Y. B. Tewari, and R. N. Goldberg. 1994, 18p.
Pub. in Jnl. of Solution Chemistry 23, n2 p167-184 1994.

Keywords: *Calorimetry, *Hydrolysis, *Tryptophan, *Indoles, *Ammonia, *Pyruvates, *Chemical reactions, *Equilibrium, High pressure liquid chromatography, pH, Temperature, Enthalpy, Catalysis, Reprints.

Apparent equilibrium constants and calorimetric enthalpies of reaction have been measured for the reaction L-tryptophan(aq) + H2O(l) = indole(aq) + pyruvate(aq) + ammonia(aq) which is catalyzed by L-tryptophanase. High-pressure liquid-chromatography and microcalorimetery were used to perform these measurements. The equilibrium measurements were performed as a function of pH, temperature, and ionic strength. The results have been interpreted with a chemical equilibrium model to obtain thermodynamic quantities for the reference reaction: L-tryptophan(aq) + H2O(l) = indole(aq) + pyruvate(-)(aq) + NH4(+)(aq). At T = 25 C and I(sub m) = 0 the results for this reaction are: K(sup o) = (1.05 + or - 0.13) times ten to the minus fourth power, Delta(sub r)G(sup o) = (22.71 + or - 0.33) kJ/mol, Delta(sup r)H(sup o) = (62.0 + or - 2.3) kJ/mol, and Delta(sub r)S(sup o) = (132 + or - 8) J/K/mol. These results have been used together with thermodynamic results from the literature to calculate standard Gibbs energies of formation, standard enthalpies of formation, standard molar entropies, standard molar heat capacities, and standard transformed formation properties for the substances participating in this reaction.

00,662
PB96-167333 Not available NTIS
National Inst. of Standards and Technology (CSTL), Boulder, CO. Thermophysics Div.
Structure and Rheology of Hard-Sphere Systems.
Final rept.
S. M. Clarke, J. Melrose, A. R. Rennie, P. J. Mitchell, H. J. M. Hanley, G. C. Straty, R. H. Ottewill, and D. Heyes. 1994, 5p.
Pub. in Jnl. Phys. Condens. Matter, v6 pA333-A337 1994.

Keywords: *Colloidal dispersion, *Shear thinning, *Rheology, Computerized simulation, Reprints, *Foreign technology, *Small angle neutron scattering.

There is need to understand the structure of hard-sphere dispersions under flow in order to develop models for colloid rheology since changes in structure are related to non-Newtonian behavior. Small-angle neutron scattering (SANS) data for polymer lattices, behaving as nearly hard spheres, at shear rates through the region of the shear thinning are presented. Intensity distributions from these new and detailed low-angle scattering experiments are compared with the intensities calculated directly from computer simulations employing a Rouse model.

00,663
PB96-167374 Not available NTIS
National Inst. of Standards and Technology (CSTL), Gaithersburg, MD. Thermophysics Div.
Small Angle Neutron Scattering Study of a Clay Suspension Under Shear.
Final rept.
H. J. M. Hanley, G. C. Straty, and F. Tsvetkov. 1994, 3p.
Pub. in Langmuir, v10 p3362-3364 1994.

Keywords: *Clay, Shear, Suspension, Disks, Reprints, *Small angle neutron scattering.

The most useful expression for the orientational probability of cylinders on a suspension subjected to a shear field is that of Hayter and Penfold, reported in 1984. Here an alternative equation is proposed to account for the shear induced orientation of disks. Our equation is then used to interpret SANS (small angle neutron scattering) intensity data from dilute aqueous suspensions of Na-montmorillonite. Parenthetically we note that SANS studies on dilute clay suspensions in equilibrium are well-known but that investigations of clay suspensions under shear are not in the literature.

00,664
PB96-200225 Not available NTIS
National Inst. of Standards and Technology (MSEL), Boulder, CO. Materials Reliability Div.
Accurate Modeling of Size and Strain Broadening in the Rietveld Refinement: The 'Double-Voigt' Approach.
Final rept.
D. Balzar, and H. Ledbetter. 1995, 8p.
Pub. in Advances in X-ray Analysis, v38 p397-404 1995.

Keywords: *Lattice strain, *X ray diffraction, Peak profile, Peak broadening, Reprints, *Rietveld refinement, *Voight function.

In the 'double-Voight' approach, an exact Voigt function describes both size- and strain-broadened profiles. The lattice strain is defined in terms of physically credible mean-square strain averaged over a distance in the diffracting domains. Analysis of Fourier coefficients in a harmonic approximation for strain coefficients leads to the Warren-Averbach method for the separation of size and strain contributions to diffraction line broadening. The model is introduced in the Rietveld refinement program in the following way: Line widths are modeled with only four parameters in the isotropic case. Varied parameters are both surface- and volume-weighted domain sizes and root-mean-square strains averaged over two distances. Refined parameters determine the physically broadened Voigt line profile. Instrumental Voigt line profile parameters are added to obtain the observed (Voigt) line profile. To speed computation, the corresponding pseudo-Voigt function is calculated and used as a fitting function in refinement. The approach allows for both fast computer code and accurate modeling in terms of physically identifiable parameters.

00,665
PB96-200613 Not available NTIS
National Inst. of Standards and Technology (PL), Boulder, CO. Quantum Physics Div.
Kinetic-Energy-Enhanced Neutral Etching.
Final rept.
S. R. Leone. 1995, 10p.
Contract DAAL03-91G-0191, Grant NSF-PHY90-12244
Sponsored by Army Research Office, Research Triangle Park, NC. and National Science Foundation, Arlington, VA.
Pub. in Japan Jnl. of Applied Physics, v34 pt1 n4B p2073-2082 Apr 95.

Keywords: *Silicon, *Etching, *Dry processes, Kinetics, Chlorine, Energy, Reprints, *Foreign technology.

A review is presented of the emerging field of neutral-species kinetic-energy-enhanced etching of silicon. As the gate oxide thickness of metal oxide semiconductor field-effect transistors (MOSFET) is decreased to dimensions of 50 Angstroms or less, the potentially damaging effects of high-kinetic-energy ions in plasma processing become important. New methods are required to remove material in a more refined, selective manner. In this review, the motivations of studies of neutral-species enhanced-kinetic-energy etching are described. Currently available sources of neutral reactive species with enhanced kinetic energies of 1-10 eV are discussed, and published experimental and theoretical investigations of enhanced-kinetic-energy neutral etching are reviewed. Problems associated with neutral species etching are also considered, and some possible future developments in the field are summarized.

00,666
PB97-122568 Not available NTIS
National Inst. of Standards and Technology (MSEL), Gaithersburg, MD. Reactor Radiation Div.
Determination of Anomalous Superexchange in MnCl2 and Its Graphite Intercalation Compound.
Final rept.
D. G. Wiesler, M. Suzuki, I. S. Suzuki, and N. Rosov. 1995, 4p.
Pub. in Physical Review Letters, v75 n5 p842-945 Jul 95.

Keywords: *Intercalation compound, *Neutron diffractions, Molecular structure, Synthesis, Chemical properties, Reprints, *Graphite, Manganese chloride.

The low-temperature magnetic structure of MnCl2 graphite intercalation compound has been studied by neutron diffraction. Magnetic peaks occur at wave vectors incommensurate with the MnCl2 and graphene sublattices. The in-plane spin configuration is explained by an exchange Hamiltonian that includes three shells of nearest neighbors in the plane. The nearest-neighbor exchange is ferromagnetic but anamalously weak, and the magnetic behavior is dominated instead by the antiferromagnetic third-neighbor interaction. The exchange parameters are used to explain the spin configuration of bulk MnCl2 after adding an interplanar coupling.

Industrial Chemistry & Chemical Process Engineering

00,667
DE95013079 PC A03/MF A01
National Inst. of Standards and Technology (CSTL), Boulder, CO.
Distributed measurements of tracer response on packed bed flows using a fiberoptic probe array. Final report.
PROGRESS REPT.
M. C. Jones, R. Nassimbene, J. Wolfe, and N. Frederick. 28 Oct 94, 28p, DOE/ER/13770-T3.
Contract AI05-87ER13770
Sponsored by Department of Energy, Washington, DC.

Keywords: *Extraction, *Packed Beds, Chromatography, Columns(Process engineering), Column packings, Dyes, Experimental Data, Fiber Optics, Flow Models, Flow Visualization, Fluid Flow, Fluorescence, Mass Transfer, Progress Report, Tracer Techniques, Tables(Data), EDB/400105.

Scale-up of packed bed processes, particularly those involving chromatographic separations, is made difficult by a seemingly inevitable increase in dispersion due to packing nonuniformity. To provide a suitable characterization, the authors measured the spatial distribution of dispersion and mixing in packed beds of uniform impervious spherical glass particles by a tracer impulse technique. The key feature in this work is the use of a fiberoptic array at the exit plane to obtain a time-resolved spatially distributed response. All experiments were in the creeping flow regime. The authors used a fluorescent dye with laser excitation through the fiber terminations in the bed. The fluoresced radiation was collected through the same fibers. They analyzed the data by the use of indices of the extent of micromixing based on Danckwerts's original degree of segregation and an additional index of structural uniformity. The computations involve a moment analysis of the individual and average probe responses. A simple model gives expressions for the indices in terms of the Peclet number and is shown to provide a useful limiting case. The computed indices are also shown to be very sensitive to adsorption of dye on the surface of the glass. However, for some of the experiments with the largest spheres using Pyrex glass, the effects of adsorption are indiscernible. This technique successfully separates the contribution of micromixed fluid to overall bed dispersion from the contribution due to the transverse variation of the flow residence time.

00,668
PB94-199221 Not available NTIS
National Inst. of Standards and Technology (NML), Boulder, CO. Thermophysics Div.
Thermophysical Property Data for Supercritical Fluid Extraction Design.
Final rept.
T. J. Bruno. 1991, 32p.
Pub. in Supercritical Fluid Technology: Reviews in Modern Theory and Applications, Chapter 7, p293-324 1991.

Keywords: *Thermophysical properties, *Supercritical state, *Extraction, Reprints, Vapor pressure, Solubility, Stability, Equations of state, Diffusivity, *Supercritical fluid extraction, Chemical stability.

The design of any industrial-scale separation process requires some degree of knowledge about the thermophysical and chemical properties of the materials to be separated. This knowledge can take the form of experimentally measured data, particular for that system, or predictions obtained from a suitable mathematical model such as an equation of state or empirical data correlation. It is generally considered better to use predicted properties, since calculations are far more economical to perform than are experimental studies. Unfortunately, there are relatively few reliable predictive methods currently available that have sufficient accuracy to be used in the design of supercritical fluid extraction (SFE) processes. This is because such processes usually involve high pressures and large, often polar, solutes. In addition, SFE processes often require operation near solvent critical points, where even good models of well-studied systems become marginal. This lack of data is slowly improving as more experimental and applied theoretical studies are completed. In the chapter, the more important thermophysical properties needed for supercritical fluid extraction design are discussed from the experimental point of view. Both the solvent and solute are discussed in terms of equilibrium and transport properties.

00,669
PB94-211745 Not available NTIS
National Inst. of Standards and Technology (MSEL), Gaithersburg, MD. Metallurgy Div.
Vapor Transport in Materials and Process Chemistry.
Final rept.
J. W. Hastie, and J. P. Hager. 1990, 24p.
Pub. in Proceedings of Elliott Symposium on Chemical Process Metallurgy, Cambridge, MA., June 10-13, 1990, p301-324.

Keywords: *Extractive metallurgy, *Metal vapors, *Materials recovery, Thermochemistry, Halides, Oxides, Sulfides, High temperature, Reprints, *Vapor transport, *Materials chemistry.

As was effectively illustrated by H. H. Kellogg in his 1966 Extractive Metallurgy Lecture to AIME, vaporization chemistry can play a very significant role in extractive metallurgy as well as in other materials processes. The field of high temperature chemistry, with its emphasis on vapor phase material transport, has continued its rapid growth over the almost twenty five year period since Kellogg's milestone lecture. This presentation reviews the results and implications of this growth, and makes recommendations concerning future directions in the research and application of vapor transport to process metallurgy. Particular emphasis is given to advances in measurement and diagnostic techniques and to the development of process models. Representative examples, taken primarily from the authors' respective laboratories, are given for the metallurgically important halide, oxide and sulfide systems.

00,670
PB95-151031 Not available NTIS
National Inst. of Standards and Technology (NML), Gaithersburg, MD. Chemical Kinetics Div.
Resonance Enhanced Multiphoton Ionization Spectroscopy of 2-Butene-1-yl (C4H7) between 455-485 nm.
Final rept.
B. P. Tsai, R. D. Johnson, and J. W. Hudgens. 1989, 4p.
Pub. in Proceedings of International Symposium on Resonance Ionization Spectroscopy and Its Applications (4th), Gaithersburg, MD., April 10-15, 1988, p129-132 1989.

Keywords: *Free radicals, *Butenes, *Electronic spectra, *Spectrum analysis, Barriers, Potential energy, Energy levels, Molecular spectroscopy, Chemical reactions, Reprints, Resonance enhanced multiphoton ionization spectroscopy.

Resonance enhanced multiphoton ionization (REMPI) studies of 2-butene-1-yl (1-methylallyl) radicals from two geometric isomers of C4H8 precursors yield two distinct REMPI spectra. Analysis of these spectra reveal: (1) that geometric structure is preserved in this chemical reaction due to the existence of a rotational barrier between the cis- and trans-1-methylallyl radicals; (2) a Rydberg-like 3p doublet B(sub 1) intermediate state in each of the isomeric radicals through which REMPI occurs; and (3) an upper limit to the adiabatic ionization potential for the cis-1-methylallyl radical.

00,671
PB95-151965 Not available NTIS
National Inst. of Standards and Technology (NML), Gaithersburg, MD. Chemical Process Metrology Div.
Modeling Ceramic Sub-Micron Particle Formation from the Vapor Using Detailed Chemical Kinetics: Comparison with In-situ Laser Diagnostics.
Final rept.
M. R. Zachariah. 1990, 8p.
Pub. in Chemical Engineering Science 45, n8 p2551-2558 1990.

Keywords: *Silicon dioxide, *Particle production, *Particle size distribution, *Ceramics, *Chemical reactors, *Chemical vapor deposition, *Reaction kinetics, Mathematical models, Ionization, Spectrum analysis, Silicon, Hydroxyl radicals, Nucleation, Reprints, *Laser diagnostics, Multiphoton ionization spectroscopy.

In this paper we review the in-situ measurements and modeling of an aerosol flame reactor producing submicron silica aerosols as a generic ceramic. Silica powders are produced in a hydrogen-oxygen counter flow diffusion flame reactor and interrogated with light scattering methods for determination of the time-temperature history of particle growth. In addition laser-induced fluorescence and multi-photon ionization have shown to be applicable as diagnostics in a heavily particle laden flow. These diagnostics have been used to measure the OH radical and silicon atoms. These experimental results have been used in conjunction with detailed chemical kinetics and aerosol dynamic models for particle growth. The results show the effects of multi-component nucleation can alter the chemical purity of the resulting solids.

00,672
PB95-151973 Not available NTIS
National Inst. of Standards and Technology (NML), Gaithersburg, MD. Chemical Process Metrology Div.
Controlled Nucleation in Aerosol Reactors for Supression of Agglomerate Formation.
Final rept.
M. R. Zachariah, and P. Dimitriou. 1990, 13p.
Pub. in Aerosol Science and Technology 13, n4 p413-425 1990.

Keywords: *Aerosols, *Nucleation, *Retarding, *Agglomeration, *Sintering, Particle size, Monomers, Reprints, *Controlled nucleation.

The formation of agglomerated particles can be a detriment to the production of highly sinterable materials. It has been seen experimentally that agglomerates are almost exclusively constructed from 10-30 nm primary particles. This paper develops criteria for the avoidance of these small primary particles through control of the nucleation rate. The relationship between particle size and number density can be used to obtain regions of stable and unstable particle growth. It is seen that the critical source rate for the prevention of runaway nucleation can be scaled without knowledge of the monomer number density.

00,673
PB95-152005 Not available NTIS
National Inst. of Standards and Technology (NML), Gaithersburg, MD. Chemical Process Metrology Div.
Experimental and Numerical Studies of Refractory Particle Formation in Flames: Application to Silica Growth.
Final rept.
M. R. Zachariah, and H. G. Semerjian. 1989, 13p.
Pub. in High Temperature Science 28, p113-125 1989.

Keywords: *Particle production, *Silicon dioxide, *Diffusion flames, Mathematical models, Vapor phases, Nucleation, Density(Number/volume), Temperature gradients, Light scattering, Optical measurement, Silanes, Particle size distribution, Ceramics, Computerized simulation, Reprints.

Recent interest in high temperature materials have focused attention on the processing requirements as well as the fundamentals of submicron particle formation and growth. In this study, silica particle growth in flames was followed by in-situ light scattering dissymmetry methods for the measurement of particle size and number density. In addition, temperature profiles for the flames were obtained by thermocouple thermometry. The majority of the experiments conducted have used silane as the source of silicon, although a limited number of experiments using organo-silicon compounds have been tried. The results have shown that the silicon source concentration and the temperature are the two dominant variables controlling particle growth and morphology. Two particle growth models have been applied, which account for the consumption of the gas precursor, nucleation, and subsequent growth by surface condensation and coalescence. Comparison with experiment have shown good agreement. Finally, numerical simulations of the gas phase chemistry of silicon have shown the presence of multicomponent nucleation under some conditions, evidence for which has been observed by laser extinction measurements.

00,674
PB95-152013 Not available NTIS
National Inst. of Standards and Technology (NML), Gaithersburg, MD. Chemical Process Metrology Div.
Simulation of Ceramic Particle Formation: Comparison with In-situ Measurements.
Final rept.
M. R. Zachariah, and H. G. Semerjian. 1989, 10p.
Pub. in American Institute of Chemical Engineers Jnl. 35, n12 p2003-2012 Dec 89.

Keywords: *Particle production, *Silicon dioxide, *Ceramics, *Vapor phases, *Computerized simulation, Particle size, Particle size distribution, Density(Number/volume), Diffusion flames, Light scat-

tering, Chemical reactors, Chemical vapor deposition, Mathematical models, Reprints.

Ceramic particle formation processes have been studied using SiO2 as a model compound. Silica particles have been synthesized in a counterpropagating diffusion flame reactor, in which in-situ measurements of particle size and number density have been made. In addition, the time-temperature history of the particle field has been calculated from a flame simulation. Numerical simulations using moment and sectional methods for particle formation have been applied and compared to the experimental measurements. The simulations for the particle formation assume a kinetically-constrained approach, allowing a simple representation of nucleation, surface growth and coagulation. The results suggest that, if the source rates are known well enough, particle formation of low vapor pressure species can be predicted. Both models do well in predicting the gross features of particle formation (number density and mean particle size), although the moment solution does a poor job of predicting the polydispersity effects during periods of high monomer generation rates.

00,675
PB95-161212 Not available NTIS
National Inst. of Standards and Technology (NML), Boulder, CO. Chemical Engineering Science Div.
Continuous Counter-Current Two Phase Aqueous Extraction.
Final rept.
J. B. Joshi, S. B. Sawant, K. S. M. S. Raghava Rao, S. K. Sikdar, T. A. Patil, and K. M. Rostami. 1990, 14p.
Pub. in Bioseparation 1, n3-4 p311-324 1990.

Keywords: *Proteins, *Extraction columns, *Columns(Process engineering), Purification, Separation, Polymers, Reprints, *Two phase aqueous extraction systems, Packed columns, Spray columns, York Scheibel columns.

Continuous counter-current column operation has been shown to provide operating convenience for contacting two-phase aqueous partitioning systems for protein extraction. The authors discuss in detail the important parameters for designing spray, packed, plate and York-Scheibel columns for protein recovery using both polymer-polymer and polymer-salt two-phase aqueous systems. The authors compare the various contactors for their operating and extraction efficiency. The work also provides a step-by-step design procedure, and specific recommendations for future data needs.

00,676
PB95-161998 Not available NTIS
National Inst. of Standards and Technology (NEL), Boulder, CO. Chemical Engineering Science Div.
Two Phase Aqueous Extraction: Rheological Properties of Dextran, Polyethylene Glycol, Bovine Serum Albumin and Their Mixtures.
Final rept.
A. Pandit, S. B. Sawant, J. B. Joshi, R. A. Perkins, and S. K. Sikdar. 1989, 6p.
Pub. in Biotechnology Techniques 3, n2 p125-130 1989.

Keywords: *Polyoxyethylene, *Serum albumin, *Dextran, *Viscosity, *Aqueous solutions, Mixtures, Viscometers, Temperature dependence, Rheological properties, Shear properties, Reprints, *Polyethylene glycol.

Rheological properties have been measured for aqueous solutions of dextran, polyethylene glycol and bovine serum albumin. Mixtures of these materials have also been studied. A rotating concentric cylinder viscometer was used to study the rheological properties of these materials over the temperature range 10 to 40 C. Over the range of concentrations, molecular weights, temperature and shear rates covered in this work, all aqueous solutions exhibited Newtonian behavior. Correlations have been reported for viscosities of dextran, polyethylene glycol, and bovine serum albumin. The viscosity of mixtures of these materials is not linear with respect to concentration.

00,677
PB96-201199 Not available NTIS
National Inst. of Standards and Technology (CSTL), Gaithersburg, MD. Thermophysics Div.
Vapor Pressure of Pentafluorodimethyl Ether.
Final rept.
L. A. Weber, and D. R. Defibaugh. 1996, 4p.
Pub. in Jnl. of Chemical and Engineering Data, v41 n3 p382-385 1996.

Keywords: *Pentafluorodimethyl ether, *Vapor pressure, Thermophysical properties, Vaporization, Reprints, Ebulliometry.

Vapor pressures of pentafluorodimethyl ether (E125) have been measured from (228 to 331) K using two ebulliometers. Experimental pressures ranged from (65 to 2024) kPa. Thermodynamic calculations were used to estimate pressures down to 140 K (16.5 Pa), and a vapor pressure curve is given which is valid from 140 K to the critical point (354.49 K). The normal boiling temperature was determined to be 238.06 K. The enthalpy of vaporization has been calculated from (140 to 300) K.

00,678
PB96-204029 Not available NTIS
National Inst. of Standards and Technology (CSTL), Gaithersburg, MD. Chemical Kinetics and Thermodynamics Div.
Enthalpy Increment Measurements from 4.5 to 350 K and the Thermodynamic Properties of Titanium Disilicide(cr) to 1700 K.
Final rept.
D. G. Archer, M. S. Sabella, S. E. Stillman, and E. J. Cotts. 1995, 5p.
Pub. in Jnl. of Chemical and Engineering Data, v40 p1237-1241 1995.

Keywords: *Thermodynamic properties, Reprints, Enthalpy, Temperature scales, Measurements, *Titanium disilicide.

Enthalpy increments for titanium disilicide were measured from 4.5 to 350 K with an adiabatic calorimeter. The enthalpy increments were combined with previous differential scanning calorimetry values to 500 K. Kopp's rule estimates for 500-800 K, and previous enthalpy increment measurements for temperatures to 1700 K in order to give the thermodynamic properties of titanium disilicide to 1700 K. Values of the Dibye temperature, theta(D), and the coefficient for the heat capacity of the conduction electrons, lambda(ei), were determined from the model. Thermodynamic properties for formation from the elements at 298.15 K were also given.

00,679
PB96-204037 Not available NTIS
National Inst. of Standards and Technology (CSTL), Gaithersburg, MD. Chemical Kinetics and Thermodynamics Div.
Enthalpy Increment Measurements from 4.5 K to 350 K and the Thermodynamic Properties of the Titanium Silicide Ti5Si3(cr).
Final rept.
D. G. Archer, D. Filor, E. Oakley, and E. J. Cotts. 1996, 5p.
Pub. in Jnl. of Chemical and Engineering Data, v41 n3 p571-575 1996.

Keywords: *Thermodynamic properties, Reprints, Enthalpy, Temperature scales, Measurements, *Titanium silicides.

Enthalpy increments for Ti(5)Si(3)(cr) were measured from 4.5K to 350K with an adiabatic calorimeter. From a representation of these measurements the enthalpy relative to 0 k, the entropy, and the heat capacity of Ti(5)Si(3)(cr) to 350 K were calculated. Values of the Debye temperature, O sub D, and the coefficient for the heat capacity of the conduction electrons, gamma(ei), were determined from the model. Thermodynamic properties for formation from the elements at 298.15 K were also given. Our previous value of O sub D for TiSi(2) was revised due to improvement in the method of representation.

00,680
PB97-111447 Not available NTIS
National Inst. of Standards and Technology (CSTL), Gaithersburg, MD. Chemical Kinetics and Thermodynamics Div.
Thermodynamic Properties of Synthetic Otavite, CdCO3(cr): Enthalpy Increment Measurements from 4.5 K to 350 K.
Final rept.
D. G. Archer. 1996, 7p.
Pub. in Jnl. of Chemical and Engineering Data, v41 p852-858 1996.

Keywords: *Otavite, *Thermodynamics, *Enthalpy, Entropy, Heat capacity, Reprints.

Enthalpy increments for cadmium carbonate were measured for temperatures from 4.5 K to 350 K with an adiabatic calorimeter. These measurements were used to compute the entropy, enthalpy relative to 0 K, and the heat capacity of cadmium carbonate. A small anomaly was observed for the sample in the temperature region from approximately 175 K to 265 K. Comparison of the calculated entropy for 298.15 K, 103.88 J.K-1.mol-1, is made with other previously published reference values to arrive at a more precise and consistent set of thermodynamic properties for otavite.

00,681
PB97-113047 Not available NTIS
National Inst. of Standards and Technology (CSTL), Gaithersburg, MD. Process Measurements Div.
In-situ Studies of a Novel Sodium Flame Process for Synthesis of Fine Particles.
Final rept.
K. L. Steffens, M. R. Zachariah, D. P. Dufaux, and R. L. Axelbaum. 1996, 6p.
Pub. in Proceedings of the Materials Research Society Symposium, Boston, MA., November 27-30, 1995, v400 p71-76 Jul 96.

Keywords: *Flames, *Particles, *Sodium, Synthesis, Boron, Nanoparticles, Titanium, Fluorescence, Reprints.

The study focuses on the optical characterization of a novel method of forming nanoscale titanium and boron particles, which can be used to form ceramic precursors such as TiB2. TiCl4 or BCl3 reacts with heated Na vapor in a counterflow diffusion flame reactor. After Na strips the Ti or B of its Cl atoms, nanosize Ti or B particles form and become encased in NaCl, which helps to prevent agglomeration and oxidation. The two-dimensional spatial distribution of the Na dimer has been optically interrogated using planar laser-induced fluorescence (PLIF) to clarify the influence of the concentration distributions and transport on particle formation rates.

00,682
PB97-113054 Not available NTIS
National Inst. of Standards and Technology (CSTL), Gaithersburg, MD. Process Measurements Div.
Optical and Modeling Studies of Sodium/Halide Reactions for the Formation of Titanium and Boron Nanoparticles.
Final rept.
K. L. Steffens, M. R. Zachariah, D. P. DuFaux, and R. L. Axelbaum. 1996, 10p.
Pub. in Chemistry of Materials, v8 n8 p1871-1880 1996.

Keywords: *Titanium, *Boron, *Sodium, Nanostructural materials, Fluorescence, Reprints.

The study focuses on the optical characterization of a method for the formation of nanoscale titanium and boron particles. The versatile method can also be used to form a variety of metals as well as ceramic powders such as TiB2. The gas-phase chemical process, given by (mn)Na + (n)MClm -> (M)n + (mn)NaCl, should be generic to many metal chlorides or mixtures of metal chlorides. In the study, either TiCl4 or BCl3 is reacted with Na vapor in a counterflow diffusion flame reactor. After the Cl is stripped from the metal chloride by the Na vapor, nanosize Ti or B particles form and, under certain thermodynamic circumstances, become encased in NaCl, which helps to prevent agglomeration and postflame oxidation. The two-dimensional spatial distribution of Na2 has been optically interrogated using planar laser-induced fluorescence under various conditions to clarify the influence of concentration and transport on particle formation. Reactant concentration and time available for reaction were found to dramatically influence the reactive flow.

00,683
PB97-113153 Not available NTIS
National Inst. of Standards and Technology (CSTL), Gaithersburg, MD. Thermophysics Div.
Critical Evaluation of Thermal Mass Flow Meters.
Final rept.
S. A. Tison. 1996, 10p.
Pub. in Jnl. of Vacuum Science and Technology A, v14 n4 p2582-2591 Jul/Aug 96.

Keywords: *Flow meters, *Thermal mass flow meters, Gas admission, Correction factors, Reprints.

Many semiconductor processes require that stable and known flows of gas be delivered to the processing

chamber. The thermal mass flow meter (TMFM) is used almost exclusively in the semiconductor industry for the admission of process gases. While TMFM's have been used in the semiconductor industry for over twenty years, much still remains to be understood about their behavior. The abundance of TMFM manufacturers that make instruments which are supposedly interchangeable complicates the use of TMFM's because the instruments generally have different designs and performance. While some attempt has been made via written standards to address the specifications of the instruments, these standards do not address all performance issues and cannot eliminate the systematic errors in the original manufacturers calibration of the TMFM's. Further, the TMFM's used to measure the process gases are generally calibrated with nitrogen and 'corrected' for other gases, but the correction factors are not well understood and are of questionable reliability. It is also important to understand how the TMFM's perform under conditions that differ from the laboratory conditions where they were calibrated and the measurement errors that are introduced as a result of these different operating conditions. This article presents data on the performance of five low-flow TMFM's, from different manufacturers, with full scale ranges of 1.5x10(-6)-3.7x10(-6) mol/s (2-5 sccm). The manufacturers' calibration of the TMFM's with nitrogen as compared to the National Institute of Standards and Technology (NIST) measured values differed by up to 17%. Three of the five tested TMFM's were within the manufacturers' stated tolerance of + or - 1% of full scale. While some of the instruments' initial calibration was poor, all of the TMFM's were stable to within + or - 1% of full scale over the test interval of nine months.

00,684
PB97-113237 Not available NTIS
National Inst. of Standards and Technology (CSTL), Gaithersburg, MD. Thermophysics Div.
Vapor Pressure of 1,1,1,2,2-Pentafluoropropane.
Final rept.
L. A. Weber, and D. E. Defibaugh. 1996, 3p.
Pub. in Jnl. of Chemical and Engineering Data, v41 n4 p762-764 1996.

Keywords: *Vapor pressure, *Pentafluoropropane, Ebulliometry, Refrigerants, Reprints.

The authors have used a comparative ebulliometer to measure the vapor pressure of 1,1,1,2,2-pentafluoropropane (HFC245cb) in the temperature range (248 to 326) K. Pressures ranged from (74 to 995) kPa. The data were adjusted for impurities in the sample. The temperature of the normal boiling point was found to be (255.11 plus or minus 0.10)K, and the Pitzer acentric factor was calculated to be 0.297. An estimate for the critical pressure is given, Pc=(3148 plus or minus 15) kPa.

Photochemistry and Radiation Chemistry

00,685
PB94-185170 Not available NTIS
National Inst. of Standards and Technology (PL), Gaithersburg, MD. Ionizing Radiation Div.
Long-Term Stability of Carrier-Free Polonium Solution Standards.
Final rept.
R. Colle. 1993, 11p.
Pub. in Radioactivity and Radiochemistry 4, n2 p20-35 1993.

Keywords: *Polonium 208, *Solutions, *Stability, *Trace elements, Radiochemistry, Hydrochloric acid, Concentration(Composition), Scintillation counters, Reprints.

The long-term solution stability of trace quantities of polonium in dilute hydrochloric acid has been investigated. Polonium solutions at trace concentrations, under various alkaline, neutral, or weakly acidic conditions are known to be unstable: being readily hydrolyzed, chemically deposited, or volatilized; exhibiting 'radiocollodial' behavior; and undergoing 'plate-out' or adsorption onto glass surfaces. Although stored polonium solutions are generally considered to be stable in the acid range of 0.1 to 1.0 normality (N), scant data exist on any possible long-term effects, particularly for very dilute, aged solutions. In this study, previously standardized carrier-free solutions of (208)Po activity concentration, ranging in age from 1.2 to nearly 9 years, and with acid concentrations from about 0.1 to 2.0 N HCl were re-assayed to determine the remaining soluble fraction of polonium. The results indicate that at acid concentrations of a few tenths of 1 N, the solutions are clearly unstable. In the range of 0.3 to 0.5 N, the results are somewhat equivocal. Only in the range at or above 1 N do the solutions appear to be stable over many years, approaching a decade. All measurements were performed by 4 pi-alpha liquid scintillation counting of gravimetrically-determined aliquots of the standardized, aged solution samples.

00,686
PB94-185733 Not available NTIS
National Inst. of Standards and Technology (CSTL), Gaithersburg, MD. Biotechnology Div.
Application of Photochemical Reaction in Electrochemical Detection of DNA Intercalation.
Final rept.
P. C. Pandey, and H. H. Weetall. 1994, 6p.
Pub. in Analytical Chemistry 66, n8 p1236-1241, 15 Apr 94.

Keywords: *Electrochemistry, *DNA damage, *Intercalating agents, *Photochemistry, Anthraquinones, Flow injection analysis, Oxidation, Deoxyribonucleic acids, Reduction(Chemistry), Reprints.

A flow injection analysis (FIA) system for the detection of the compounds that intercalate within DNA is reported. A derivative of 9,10-anthraquinone has been used as the reference compound for photoelectrochemical detection. The sodium salts of 9,10-anthraquinone-2,6-disulfonic acid and 9,10-anthraquinone-2 sulfonic acid are photochemically activated and then reduced in the presence of an electron donor (glucose). The electrochemical signal is based on the measurement of the anodic current resulting from the oxidation of the reduced form of 9,10-anthraquinone. The reduced form of the 9,10-anthraquinone is oxidized through a mediated mechanism at the surface of a tetracyanoquinodimethane-(TCNQ)-modified graphite paste electrode covered by a Nucleopore membrane. TCNQ acts as an efficient mediator for the oxidation of reduced 9,10-anthraquinone. Cyclic voltammetry, photocyclic voltammetry, and the photoelectrochemical FIA response of 9,10-anthraquinone are reported. Experimental results show that these anthraquinones can be intercalated within the helix of double-stranded calf thymus DNA.

00,687
PB94-199288 Not available NTIS
National Inst. of Standards and Technology (CSTL), Gaithersburg, MD. Surface and Microanalysis Science Div.
Photodecomposition Dynamics of Mo(CO)6/Si(111) 7x7: CO Internal State and Translational Energy Distributions.
Final rept.
S. A. Buntin, R. R. Cavanagh, and L. J. Richter. 1993, 4p.
Pub. in Jnl. of Chemical Physics 98, n9 p7651-7654, 1 May 93. Sponsored by Department of Energy, Washington, DC.

Keywords: *Carbon monoxide, Reprints, Rotational states, Metal carbonyls, Photodecomposition, Absorption, Photolysis, Silicon, Hexacarbonylmolybdenum, Photodesorption, Translations.

The rotational state and translational energy distributions of CO photodesorption products resulting from the 266 nm photolysis of Mo(CO)6 absorbed on Si(111) 7X7 with coverages in the multilayer regime are reported. State-resolved measurements show two desorption components with highly disparate energy dispositions. Results for different surface temperatures indicate that the energy content in one component reaches quasi-equilibration with the surface temperature, which is attributed to collisional relaxation of nascent photodecomposition products within the adlayer. The other component exhibits disparate rotational and translational 'temperatures' that are significantly greater than, and independent of, the surface temperature. These nascent photodecomposition products are influenced by both energy quenching effects and dynamical constraints imposed by the existence of the adlayer.

00,688
PB94-199965 Not available NTIS
National Inst. of Standards and Technology (CSTL), Gaithersburg, MD. Surface and Microanalysis Science Div.
Dynamics of Nonthermal Reactions: Femtosecond Surface Chemistry.
Final rept.
R. R. Cavanagh, D. S. King, J. C. Stephenson, and T. F. Heinz. 1993, 13p.
Pub. in the Jnl. of Physical Chemistry 97, n4 p786-798 1993. Sponsored by Department of Energy, Washington, DC.

Keywords: *Surface reactions, Laser radiation, Light pulses, Energy transfer, Reviews, Reprints, Femtosecond pulses.

Optically driven surface reactions are attracting an increasing level of attention in the physical chemistry community. Not only have there been recent advances in establishing the viability of laser driven surface reactions, but there has also been an increased awareness of the need to understand the underlying reaction mechanisms. The necessity of accounting for energy-transfer processes that occur on the femtosecond time scale is now apparent. In this review the experimental and theoretical basis of our current understanding is surveyed, and prospective areas of advancement are considered.

00,689
PB94-212255 Not available NTIS
National Inst. of Standards and Technology (PL), Gaithersburg, MD. Ionizing Radiation Div.
Role of the Office of Radiation Measurement in Quality Assurance.
Final rept.
K. G. W. Inn, B. M. Coursey, E. Eisenhower, H. T. Heaton, K. C. Duvall, M. D. Walker, and J. C. Humphreys. 1993, 11p.
Pub. in Science of the Total Environment 130/131, p497-507 1993.

Keywords: *Quality assurance, *Ionizing radiation, *Calibrating, Radiation dosage, Laboratories, Dosimetry, Radiation protection, Radiation measuring instruments, Environmental monitoring, Standards, Radon, Health physics, Bioassay, Radiochemistry, Reprints.

Over the past ten years the National Institute of Standards and Technology has, through its Office of Radiation Measurement, developed several national Secondary Laboratories systems in the field of ionizing radiation. These Secondary Laboratories systems provide the necessary calibrations and quality assurance testing to support and affirm the caliber of the measurements in special areas of ionizing radiation. The areas that are supported by the program include State Radiation Protection, Personnel Dosimetry, Survey Instrument Calibration, High-level Dosimetry, Radiation Therapy, Bioassay, Survey Instrument Testing, Ionizing Radiation, Environmental Radioactivity, Radioactivity Standards, and Radon.

00,690
PB95-108726 Not available NTIS
National Inst. of Standards and Technology (PL), Boulder, CO. Quantum Physics Div.
Laboratory Studies of Low-Temperature Reactions of C2H with C2H2 and Implications for Atmospheric Models of Titan.
Final rept.
J. O. P. Pedersen, B. J. Opansky, and S. R. Leone. 1993, 8p.
Contract NAGW-2438
Sponsored by National Aeronautics and Space Administration, Washington, DC.
Pub. in Jnl. of Physical Chemistry 97, n26 p6822-6829 1993.

Keywords: *Satellite atmospheres, *Acetylene, *Titan, Temperature range 0065-0273-K, Temperature range 0273-0400 K, Temperature dependence, Photochemical reactions, Chemical radicals, Laboratory tests, Reprints, Acetylene radicals.

Rate coefficients for the reaction C2H + C2H2 -> C4H2 + H are measured over the temperature range 170-350 K. The reactions are carried out in a temperature variable flow cell. C2H radicals are produced by pulsed laser photolysis of C2H2, and a tunable infrared color-center laser is used to probe the transient removal of C2H in absorption to derive the rate coefficients. The results show that the rate coefficient is independent of temperature over the range 170-350 K and equal to (1.1 + or - 0.2) x 10(sup -10) exp((28 + or - 20)/T) cc/molecule/s. The reaction studied is of central impor-

tance for models of the photochemistry of the atmospheres of the outer planets, in particular for the satellite Titan, and the implications of the present results for these models are discussed.

00,691
PB95-125720 Not available NTIS
National Inst. of Standards and Technology (NML), Gaithersburg, MD. Molecular Physics Div.
Vibrational Predissociation Dynamics of Overtone-Excited HN3.
Final rept.
B. R. Foy, M. P. Casassa, J. C. Stephenson, and D. S. King. 1989, 3p.
Pub. in American Institute of Physics Conference Proceedings on Advances in Laser Science-IV, Atlanta, GA., October 2-7, 1988, n191 p612-614 1989.

Keywords: *Photodissociation, Photochemical reactions, Molecular spectroscopy, Rotational spectra, Vibrational states, Visible spectra, Predissociation, Reprints, *Hydroazoic acid, Intramolecular dynamics.

Vibrational overtone photodissociation is used to examine rotationally resolved spectra of HN3 at E(vib) = 15120/cm and 17670/cm. The spectra exhibit extensive coupling of the NH stretching overtones to background vibrational states. Lifetimes for vibrational predissociation, HN3(X tilde) --> HN(X) + N2(X), are found to be 210 nsec and 0.95 nsec for the levels v(NH) = 5 and 6, respectively.

00,692
PB95-151643 Not available NTIS
National Inst. of Standards and Technology (NML), Gaithersburg, MD. Ionizing Radiation Div.
Unusual Spin-Trap Chemistry for the Reaction of Hydroxyl Radical with the Carcinogen N-Nitrosodimethylamine.
Final rept.
D. A. Wink, and M. F. Desrosiers. 1991, 6p.
Pub. in Radiation Physics and Chemistry 38, n5 p467-472 1991.

Keywords: *Hydroxyl radicals, *Radiolysis, Radiochemistry, Carcinogens, Reprints, *Chemical reaction mechanisms, *Amine/N-nitrosodimethyl, *Spin trap, Benzene sulfonate/dibromo-nitroso, EPR(Electron Paramagnetic Resonance).

The reaction of the potent carcinogen N-nitrosodimethylamine (NDMA) with hydroxyl radical generated via radiolysis was studied using EPR techniques. Attempts to spin trap NDMA radical intermediates with 3,5-dibromo-4-nitrosobenzene sulfonate (DBNBS) produced only unusual DBNBS radicals. One of these radicals was shown to be generated by both reaction of DBNBS with nitric oxide, and direct oxidation of DBNBS with an organic oxidant (Br2(-)). Another DBNBS radical was identified as a sulfite spin adduct resulting from the degradation of DBNBS by a NDMA reactive intermediate. In the absence of DBNBS, hydroxyl radical reaction with NDMA gave the dimethylnitroxide radical. Unexpectedly, addition of DBNBS to a solution containing dimethylnitroxide produced an EPR spectrum nearly identical to that of NDMA solutions with DBNBS added before radiolysis. A proposed mechanism accounting for these observations is presented.

00,693
PB95-175790 Not available NTIS
National Inst. of Standards and Technology (CSTL), Gaithersburg, MD. Surface and Microanalysis Science Div.
Comparative Study of Fe-C Bead and Graphite Target Performance with the National Ocean Sciences AMS (NOSAMS) Facility Recombinator Ion Source.
Final rept.
D. B. Klinedinst, A. P. McNichol, L. A. Currie, K. F. vonReden, R. M. Verkouteren, G. A. Jones, R. J. Schneider, and G. A. Klouda. 1994, 6p.
Pub. in Nuclear Instruments and Methods in Physics Research B 92, p166-171 1994.

Keywords: *Carbon 14 target, Concentration(Composition), Sampling, Environmental materials, Performance evaluation, Poisson equation, Reprints, *Accelerator mass spectrometry.

An accelerator mass spectrometry (AMS) experiment was designed to investigate (14)C target performance for two target types over a range of isotopic concentrations and sample sizes, with a special focus on the ability to measure (14)C in environmental samples having only microgram amounts of carbon. The findings were positive, showing that precision, accuracy, and stability were adequate to determine (14)C to 1% or better in samples containing as little as 25 micrograms carbons. Satisfactory Poisson uncertainty and target stability were demonstrated down to a level of 7 micrograms carbon, but experimental data showed that accurate measurements at that level require detailed knowledge of blank variability and mass dependence of the modern carbon calibration factor.

00,694
PB96-146899 Not available NTIS
National Inst. of Standards and Technology (CSTL), Gaithersburg, MD. Chemical Kinetics and Thermodynamics Div.
Experimental Determination of the Ionization Energy of IO(X(sup 2)II(sub 3/2)) and Estimations of Delta(sub f)H(sup deg)(sub 0)(IO(sup -)) and PA(IO).
Final rept.
Z. Zhang, P. S. Monks, L. J. Stief, S. C. Kuo, R. B. Klemm, J. F. Liebman, and R. E. Huie. 1996, 6p.
Pub. in Jnl. of Physical Chemistry, v100 n1 p63-68 1996.

Keywords: *Photoionization, *Iodine oxide, Mass spectrometers, Reprints, *Ionization energy.

Photoionization efficiency (PIE) spectra of IO(X2Ili) were measured over the wavelength range lambda = 115.0 - 130.0 nm and in the ionization threshold region lambda = 126.0 - 130.0 nm, using a discharge flow-photoionization mass spectrometer apparatus coupled to a synchrotron radiation source. Iodine oxide was generated by the reactions of O(3P) atoms with I2 and CF3I. The PIE spectra displayed step-function behavior.

00,695
PB96-160346 Not available NTIS
National Inst. of Standards and Technology (PL), Gaithersburg, MD. Ionizing Radiation Div.
New and Revised Half-Life Measurement Results.
Final rept.
M. P. Unterweger, D. D. Hoppes, and F. J. Schima. 1992, 4p.
Pub. in Nuclear Instruments and Methods in Physics Research, Section A, nA312 p349-352 1992.

Keywords: *Radioisotopes, *Half-life, *Measurement, Counting techniques, Comparisons, Cobalt 60, Krypton 85, Cesium 137, Sodium 22, Barium 133, Bismuth 207, Europium 152, Europium 154, Europium 155, Antimony 125, Reprints.

The results of these measurements for many long-lived radionuclides such as Co-60, Cs-137, Kr-85, Na-22, Ba-133, Bi-207, Eu-152, Eu-154, Eu-155, and Sb-125 have been recently revised. The results for the half-lives of the many radionuclides measured over the last three decades are tabulated. Comparisons with recommended values from the International Atomic Energy Agency Coordinated Research Program (IAEA-CRP) are given for the long-lived radionuclides.

00,696
PB96-164157 Not available NTIS
National Inst. of Standards and Technology (CSTL), Gaithersburg, MD. Analytical Chemistry Div.
Isotopic and Nuclear Analytical Techniques in Biological Systems: A Critical Study. 10. Elemental Isotopic Dilution Analysis with Radioactive and Stable Isotopes (Technical Report).
Final rept.
J. D. Fassett. 1995, 7p.
Pub. in Pure and Applied Chemistry, v67 n11 p1943-1949 1995.

Keywords: *Isotope dilution, *Chemical analysis, *Biological systems, Reprints, Accuracy, *Foreign technology, Nuclear analytical techniques.

Isotope dilution is a method of chemical analysis based on the mixing (or dilution) of a radioisotope or a separated stable isotope with its natural isotope(s) in the sample. The activity or isotopic ratio of the mixture defines the concentration of the analyte, which is a tremendous advantange for measurement since quantitative separation of the analyte is not required. The technique has a multitude of variations and has been combined with many classical and instrumental procedures used in analytical chemistry. The technique is noted for its accuracy. This review focuses on the application of the technique in the determination of elemental concentrations in biological systems.

00,697
PB96-167101 Not available NTIS
National Inst. of Standards and Technology (CSTL), Gaithersburg, MD. Inorganic Analytical Research Div.
Dead Time, Pileup, and Accurate Gamma-Ray Spectrometry.
Final rept.
R. M. Lindstrom, and R. F. Fleming. 1995, 7p.
Pub. in Radioactivity and Radiochemistry, v6 n2 p20-27 1995.

Keywords: *Gamma ray spectrometry, *Pulse pileup, Dead times, Reprints, Radioactive decay, *Foreign technology, Random summing.

The accuracy of gamma-ray spectrometric measurements is ultimately limited by the precision of Poisson counting statistics. With careful attention to detail, all other sources of error in the ratio of activities of two sources of a radionuclide in small samples can be made insignificant, even when the statistical limit is well below one percent. An important source of error comes from the dinite time required by the counting electronics to detect and process pulses. Dead-time losses (mostly in the analog-digital converter) are usually compensated very well by the pulse-height analyzer, but pileup losses (mostly in the amplifier) may not be. Errors of 10% or more may result. Several methods are available for detecting and correcting rate-related losses. These methods are sufficiently reliable and well understood that a decaying source can be measured with acceptably small errors even at count rates as high as tens of thousands per second.

00,698
PB96-167242 Not available NTIS
National Inst. of Standards and Technology (CSTL), Gaithersburg, MD. Inorganic Analytical Research Div.
Determination of 21 Elements by INAA for Certification of SRM 1570a, Spinach.
Final rept.
D. A. Becker. 1995, 8p.
Pub. in Jnl. of Radioanalytical and Nuclear Chemistry, Articles, v193 n1 p25-32 1995.

Keywords: *Neutron activation analysis, *Spinach, Elemental analysis, Reprints, Accuracy, *Foreign technology, *Botanical reference material, Standard reference materials.

Analysis for certification have been made by instrumental neutron activation analysis (INAA) for the determination of 21 elements in the Natiaonl Institute of Standards and Technology (NIST) Spinach renewal reference material, SRM 1570a. Elements determined included ones with short halflife products (Al,V, Ca, Mg), intermediate halflife products (Mn, Na, K, La) and long halflife products (Ba, Co, Cr, Cs, Eu, Fe, Rb, Sb, Sc, Se, Sr, Th, and Zn). For the first time a new robotic samplechanger was used in the counting of long halflife indicator isotopes for certification of an SRM. Uncertainties obtained averaged plus or minus 1.80% for the four major and minor constituents (Ca, K, Mg, Na); plus or minus 3.14% for elements with concentrations from 1 to 400 mg/kg (Al, Ba, Cr, Fe, Mn, Rb, Sr, and Zn); and plus or minus 8.31% for the ultra trace elements (less than mg/kg) (Co, Cs, Eu, La, Sb, Sc, Se, Th, and V).

00,699
PB96-200811 Not available NTIS
National Inst. of Standards and Technology (CSTL), Gaithersburg, MD. Process Measurements Div.
Unique Quality Assurance Aspects of INAA for Reference Material Homogeneity and Certification.
Final rept.
D. A. Becker. 1993, 4p.
Pub. in Fresenius Jnl. of Analytical Chemistry, v345 p298-301 1993.

Keywords: *Neutron activation analysis, *Radiation detection, *Quality assurance, Neutron detection, Radiochemistry, Incident radiation, Excitation, Measurement, Certification, Trace elements, Analytical methods, Reprints, *Standard reference materials, Emitted radiation.

Instrumental neutron activation analysis (INAA) has become one of the primary analytical techniques for certification of elemental content in biological Standard Reference Materials (SRMs) at the National Institute of Standards and Technology (NIST). One important reason why INAA has become so widely used and valuable in the certification of NIST SRMs is that INAA has unique inherent quality assurance (QA) character-

istics which provide the capability for accurate analysis and which often allow the analytical values obtained to be internally evaluated and cross checked. While the NAA technique has the general characteristics of most spectroscopic techniques, the specific characteristics include uniform activation, long and well-documented excited states, highly penetrating emitted radiation, and an excited state decay process which is statistically random in nature.

00,700
PB97-111603 Not available NTIS
National Inst. of Standards and Technology (PL), Gaithersburg, MD. Ionizing Radiation Div.
63Ni Half-Life: A New Experimental Determination and Critical Review.
Final rept.
R. Colle, and B. E. Zimmerman. 1996, 15p.
Pub. in Applied Radiation and Isotopes, v47 n7 p677-691 1996.

Keywords: *Nickel 63, *Standardization, *Calibration standards, *Half life, Liquid scintillators, Calorimetry, Gravimetric analysis, Radiation measurement, Tritium, Reprints.

The Ni-63 half-life has been determined to be 101.06 + or - 1.97 years based on three independent measurements, conducted over the past 27 years, of the massic activity of gravimetrically-related Ni-63 sources. The present result is the first and only determination of the Ni-63 half-life which is based on actually following the radioactive decay of Ni-63. Based on a critical evaluation of the extant data set, a Ni-63 half-life value of T = 101.1 + or - 1.4 years is recommended.

00,701
PB97-111819 Not available NTIS
National Inst. of Standards and Technology (PL), Gaithersburg, MD. Ionizing Radiation Div.
Nickel-63 Standardization: 1968-1995.
Final rept.
R. Colle, and B. E. Zimmerman. 1996, 16p.
See also PB92-236553.
Pub. in Radioactivity and Radiochemistry, v7 n2 p12-27 Aug 96.

Keywords: *Nickel 63, *Calibration standards, *Standardization, Radiation measurement, Liquid scintillators, Spectroscopy, Calorimetry, Tritium, Beta decay, Beta particles, Emanation, Reprints, Efficiency tracing.

The radionuclide Ni-63 is widely employed as a relatively long-lived, low-energy beta-particle-emitting calibration standard. Between 1968 and 1995, the National Institute of Standards and Technology (NIST), formerly the National Bureau of Standards (NBS), actively engaged in the preparation and calibration of Ni-63 solution standards. The chronicle summarizes these NIST/NBS standardization activities and highlights the remarkably consistent measurement results obtained on the standards over the past 27 years.

00,702
PB97-119119 Not available NTIS
National Inst. of Standards and Technology (CSTL), Gaithersburg, MD. Chemical Kinetics and Thermodynamics Div.
Resonance Enhanced Multiphoton Ionization Spectroscopy of the PF Radical.
Final rept.
J. Howe, M. N. R. Ashfold, C. M. Western, and J. W. Hudgens. 1996, 3p.
Pub. in Jnl. of Chemical Physics, v104 n8 p2789-2800 1996.

Keywords: *Spectroscopy, *Ionization spectroscopy, *Multiphoton, Resonance, Reprints, *PF radicals.

PF radicals in both their ground and metastable electronic states have been produced by the gas phase reaction of F atoms with phosphine in a discharge flow reactor and detected by mass selective resonance enhanced multiphoton ionization (REMPI) spectroscopy in the wavelength range 410-225 nm. Analysis of the longer wavelength end of this spectrum has enabled identification and spectroscopic characterization of five hitherto unknown Rydberg states of this radical.

00,703
PB97-119291 Not available NTIS
National Inst. of Standards and Technology (PL), Gaithersburg, MD. Ionizing Radiation Div.
Calibration and Performance of GafChromic DM-100 Radiochromic Dosemeters.
Final rept.
B. J. Mincher, M. K. Zaidi, R. E. Arbon, W. L. McLaughlin, and G. L. Schwendiman. 1996, 4p.
Pub. in Solid State Dosimetry, Budapest, Hungary, July 10-14, 1995, Radiation Protection Dosimetry, v66 n1-4 p233-236 1996.

Keywords: *Dosemeters, *Radiochromic films, Gamma radiation, Organic chemistry, Radiation chemistry, Calibration, Reprints, *Foreign technology.

GafChromic DM-100 dosemeters were used to measure absorbed doses in liquid samples exposed to a 137Cs gamma ray source. The initial calibration of the commercially available film was performed using 60Co gamma rays. A comparison of simultaneously irradiated bare dosemeters mocked to simulate the liquid samples shows the importance of iraddiation of dosemeters under conditions as nearly identical to that of the actual sampels as possible. In addition, the dosemeter response to absorbed dose for two different batches of GafChromic film, to different temperatures at the time of irradiation and to delay before readout, was examined. the reproducibility of the GafChromic dosemeter is also discussed.

Physical & Theoretical Chemistry

00,704
AD-A234 043/8 PC A03/MF A01
National Inst. of Standards and Technology (NML), Gaithersburg, MD. Molecular Spectroscopy Div.
Production and Spectroscopy of Small Polyatomic Molecular Ions Isolated in Solid Neon. (Reannouncement with New Availability Information).
M. E. Jacox, and W. E. Thompson. 1990, 11p, ARO-25664.2-CH.
Contract ARO-MIPR-120-90
Pub. in High Temperature Science, v28 p225-234 1990.

Keywords: *Molecular ions, Absorption, Spectroscopy, Neon, Infrared spectra, Reprints, *Matrix isolation, Molecular clusters, Cluster ions, Solidified gases.

No abstract available.

00,705
AD-A238 415/4 PC A02/MF A01
National Inst. of Standards and Technology, Gaithersburg, MD.
Vibrational Spectra of Molecular Ions Isolated in Solid Neon. 6. CO4(-). (Reannouncement with New Availability Information).
M. E. Jacox, and W. E. Thompson. 4 Apr 91, 8p, ARO-25664.9-CH.
Contract ARO-MIPR-120-90
Pub. in Jnl. of Physical Chemistry, v95 n7 p2781-2787, 4 Apr 91.

Keywords: *Molecular vibration, Molecular spectroscopy, Carbonates, Carbon dioxide, Oxygen, Nitrogen, Reprints, *Neon matrices, *Vibrational spectra, *Molecular ions.

No abstract available.

00,706
AD-A239 729/7 PC A03/MF A01
National Inst. of Standards and Technology (NML), Gaithersburg, MD. Molecular Physics Div.
Vibrational Spectra of Molecular Ions Isolated in Solid Neon. 7. CO(+), C2O2(+), and C2O2(-). (Reannouncement with New Availability Information).
W. E. Thompson, and M. E. Jacox. 15 Jul 91, 11p, ARO-25664.10-CH.
Pub. in Jnl. of Chemical Physics, v95 n2 p735-745, 15 Jul 91.

Keywords: *Neon, *Carbon monoxide, *Ion molecule interactions, *Infrared spectra, *Molecular ions, *Vibrational spectra, Photoionization, Ionized gases, Vapor deposition, Absorption, Atomic beams, Electron capture, Reprints, Solids, Penning ionization, Low temperature research.

No abstract available.

00,707
AD-A253 551/6 PC A03/MF A01
National Inst. of Standards and Technology, Gaithersburg, MD.
Vibrational Spectra of Molecular Ions Isolated in Solid Neon: HCCH+ and HCC-. (Reannouncement with New Availability Information).
D. Forney, M. E. Jacox, and W. E. Thompson. 1992, 13p, ARO-25664.12-CH.
Contract ARO-MIPR-120-90
Pub. in Jnl. of Molecular Spectroscopy, v153 p680-691 1992.

Keywords: *Neon, *Solids, *Molecular ions, *Vibrational spectra, *Acetylenes, Reprints, Cations, Excitation, Carbon, Ground state, Argon, Chemical bonds, Microwave discharges, Polarizability, Stretching.

When a Ne:C2H2 sample is codeposited at approximately 5 K with a beam of neon atoms that has been excited in a microwave discharge, a sharp, prominent absorption assigned to Upsilon(3) of HCCH(+) appears at 3137.6 cm(-1), very close to the previously reported gas-phase band center. Experiments on carbon-13 and deuterium substituted samples support this assignment and permit the identification of all of the infrared-active CH- and CD-stretching fundamentals of the isotopically substituted acetylene cations, as well as the determination of the stretching and stretching-interaction force constants. The absorptions of the carbon-13 substituted acetylene cations have also been identified in the analogous argon-matrix experiments, but exhibit a matrix shift of approximately 30 cm(-1), possibly because of the larger polarizability of argon.

00,708
AD-A275 828/2 Not available NTIS
National Inst. of Standards and Technology (NML), Gaithersburg, MD. Molecular Physics Div.
Vibrational Spectra of Molecular Ions Isolated in Solid Neon. 11. NO2(+), NO2(-), and NO3(-).
D. Forney, W. E. Thompson, and M. E. Jacox. 15 Nov 93, 12p, ARO-30094.3-CH.
Availability: Pub. in Jnl. of Chemical Physics, v99 n10 p7393-7403, 15 Nov 93.

Keywords: *Infrared spectra, *Cations, *Vibration, *Solids, *Molecular ions, *Neon, *Anions, Electron capture, Ionization, High energy, Nitrites, Deposition, Reprints, *Vibrational spectra, Photodetachment.

When a NE:NO2 or a Ne:NO:O2 sample is codeposited at approximately 5 K with a beam of neon atoms that have been excited in a microwave discharge, infrared absorptions of NO2+, NO2-, and NO3- appear. Detailed isotopic substitution studies support the assignment of prominent absorptions to v3 of NO2+ and NO2- and of weak to moderately intense absorptions to the v1 + v3 combination band of each of these species. When the contribution of anharmonicity is considered, the positions of the NO2+ absorptions are in satisfactory agreement with the values for the stretching fundamentals obtained in a recent gas-phase study of that species. When the sample is exposed to 240-420 nm mercury-arc radiation, the initially present absorptions of NO3- trapped in sites with a small residual cation interaction diminish in intensity, and the unsplit v3 (e') absorption of isolated NO3- grows. The mechanism responsible for this growth in the absorption of isolated NO3- is considered. Electron capture, Infrared spectrum, Ionization, Neon matrix, NO2+, NO2-, NO3-, Photodetachment.

00,709
AD-A278 131/8 PC A03/MF A01
National Bureau of Standards, Boulder, CO.
Ultraviolet Multiplet Table. Finding List for Spectra of the Elements Molybdenum to Lanthanum (Z = 42 to 57); Hafnium to Radium (Z = 72 to 88).
C. E. Moore. 6 Apr 62, 37p.

Keywords: *Ultraviolet spectra, *Transition metals, Tables(Data), Chemical elements, *Multiplet table, *Finding list, *Molybdenum to lanthanum, *Hafnium to radium, N-2309.

No abstract available.

00,710
AD-A278 446/0 PC A08/MF A02
National Bureau of Standards, Gaithersburg, MD.
Ultraviolet Multiplet Table.
C. E. Moore. 28 Apr 50, 169p.

Keywords: *Ultraviolet spectra, Chemical elements, Hydrogen, Helium, Lithium, Beryllium, Boron, Carbon, Nitrogen, Oxygen, Fluorine, Neon, Sodium, Magne-

sium, Aluminum, Silicon, Phosphorus, Sulfur, Chlorine, Argon, Potassium, Calcium, Scandium, Titanium, Vanadium, *Finding list, *Multiplet table, Tables(Data).

No abstract available.

00,711
AD-A278 517/8 PC A03/MF A01
National Bureau of Standards, Gaithersburg, MD.
Density of Solids and Liquids.
P. Hidnert, and E. L. Peffer. 15 Mar 50, 34p, NBS-CIRC-487.

Keywords: *Liquids, *Solids, *Density, Thermal expansion.

No abstract available.

00,712
AD-A278 956/8 PC A04/MF A01
National Bureau of Standards, Gaithersburg, MD.
Table of Dielectric Constants of Pure Liquids.
A. A. Maryott, and E. R. Smith. 10 Aug 51, 51p, NBS-514.

Keywords: *Liquids, *Dielectric properties, Tables(Data), Low frequencies, Temperature control, Constants, Methanols, Nitrobenzenes, Water, Liquid hydrogen, Inorganic compounds, Organic compounds.

No abstract available.

00,713
AD-A279 951/8 PC A05/MF A01
National Bureau of Standards, Boulder, CO.
Tabulation of the Thermodynamic Properties of Normal Hydrogen from Low Temperatures to 300K and from 1 to 100 Atmospheres.
Technical note no. 12.
J. W. Dean. Nov 61, 76p.

Keywords: *Enthalpy, *Entropy, *Hydrogen, *Thermodynamic properties, Temperature, Barometric pressure, Specific volume, Hydrogen gas.

Pressure, volume, temperature, internal energy, enthalpy, and entropy of normal hydrogen gas have been tabulated along isobars in 1 deg K temperature steps. The range covered is from the saturation temperature to 300 deg K and from a pressure of 1 to 100 atmospheres. The source of data is the Research Paper 1932 of the National Bureau of Standards Journal of Research. The method is described by which the data presented in Research Paper 1932 is reduced to properties directly useful for engineering calculations. A method is also described for estimating the effect of ortho-para compositions upon the tabulated properties. Tabular values are presented in the dimensional units of the metric system. The tabulations are also available in the dimensional units of the British system as Technical Note No. 120, Supplement A.

00,714
AD-A280 279/1 PC A13/MF A03
National Bureau of Standards, Gaithersburg, MD.
Atomic Energy Levels. As Derived From the Analyses of Optical Spectra. Volume 3.
C. E. Moore. 1 May 58, 284p.

Keywords: *Atomic energy levels, *Optics, *Spectra, *Atomic spectra, Standards, Molybdenum, Lanthanum, *Molybdenum-lanthanum.

No abstract available.

00,715
AD-A280 293/2 PC A20/MF A04
National Bureau of Standards, Gaithersburg, MD.
Tables of Chemical Kinetics Homogeneous Reactions.
15 Sep 61, 464p, NBS-34.

Keywords: *Chemical reactions, *Tables(Data), *Reaction kinetics.

No abstract available.

00,716
AD-A286 603/6 PC A05/MF A01
National Bureau of Standards, Boulder, CO.
Compilation of the Physical Equilibria and Related Properties of the Hydrogen-Carbon Monoxide System.
Technical note.
D. E. Drayer, and T. M. Flynn. May 61, 96p.

Keywords: *Hydrogen, *Carbon monoxide, *Chemical equilibrium, Physical properties, Solid phases, Vapor phases, Liquid phases, K Factor.

Literature data have been used to calculate K-factors for the hydrogen-carbon monoxide system over the range of 68.2 to 122.2 deg K and 10 to 225 atmospheres. K-factors are presented graphically for eight isotherms over this range. Published data on the solid-vapor region are presented separately as composition versus pressure at constant temperature. A bibliography of approximately 450 references is also presented on related properties for this system and for the pure components.

00,717
AD-A286 648/1 PC A03/MF A01
National Bureau of Standards, Gaithersburg, MD.
High Temperature Reactions of Uranium Dioxide with Various Metal Oxides.
S. M. Lang, F. P. Knudsen, C. L. Fillmore, and R. S. Roth. 20 Feb 56, 30p, NBS-CIRC-568.

Keywords: *Metals, *Oxides, Uranium, Dioxides, Oxides, Chemical reactions, Phase diagrams, Chemical equilibrium, Cations, Valence, Oxygen, *Uranium oxides.

No abstract available.

00,718
AD-A295 411/3 PC A03/MF A01
National Bureau of Standards, Gaithersburg, MD.
Arc Spectra of Gallium, Indium, and Thallium.
W. F. Meggers, and R. J. Murphy. 4 Apr 52, 11p.
Pub. in Jnl. of Research of the National Bureau of Standards, v48 n4 p334-344 Apr 52.

Keywords: *Gallium, *Indium, *Infrared spectra, *Thallium, Reprints, Optical properties, Spectra, Visible spectra, Atomic energy levels, *Arc spectra.

This research was inspired by the compilation of Atomic energy levels as derived from the analyses of optical spectra. While compiling the data on gallium spectra, C. E. Moore noted that the first spectrum of gallium (Ga I) was very incompletely investigated. In particular, no Ga I lines had been observed with wavelengths greater than 6414 A in the red, although two infrared lines (11904 and 12096 A) were predicted in 1914 from spectral-series formulas. These predicted infrared lines have now been recorded photographically, and, in addition, 37 new Ga I lines have been discovered. These observations have led to revision and extension of the known atomic-energy levels is derived from the analysis of the Ga I spectrum. jg p.1.

00,719
AD-A296 377/5 PC A03/MF A01
National Inst. of Standards and Technology, Gaithersburg, MD.
Microwave Spectrum and Structure of CH3NO2-H20.
F. J. Lovas, N. Zobov, G. T. Fraser, and R. D. Suenram. 1995, 12p, ARO-29596.1-CH.
Contract ARO-MIPR-126-94
Pub. in Jnl. of Molecular Spectroscopy, v171 p189-199 1995.

Keywords: *Structural properties, *Microwaves, *Spectra, *Nitromethane, Fourier transformation, Mirrors, Reprints, Water, Mass, Quadrupole moment, Fabry perot interferometers, Separation, Molecular structure, Rotation, Fourier spectrometers, Moment of inertia, Dipole moments, Nuclear electric moments, Pulsed beams.

The microwave spectrum of the nitromethane-water complex (CH3NO2-H2O) has been studied with a pulsed-beam Fourier-transform Fabry-Perot-cavity spectrometer. Both a-type and b-type transitions were observed for the A state of the complex with the b-type transition being more intense by a factor of 2. Critical to the rotational assignments were well resolved (14)N nuclear electric quadrupole transitions, and the incorporation of the pulsed nozzle in one of the mirrors which provided a beam coaxial with the cavity axis to attain linewidths of about 2 kHz (full-width at half maximum-FWHM). To provide additional structural information, the spectra of the HDO, D2O, and Cd3NO2 substituents were assigned. The molecular structure derived from the moments of inertia has a center of mass separation of 3.506(7) A. The moments of inertia can not distinguish between two possible forms of the complex, one with the dipole moment vectors aligned and the other with them antialigned. jg p.2.

00,720
AD-A296 498/9 PC A03/MF A01
National Bureau of Standards, Gaithersburg, MD.
Molecular Microwave Spectra Tables.
P. Kisliuk, and C. H. Townes. Jun 50, 31p, NBS-RP-2107.
Pub. in Jnl. of Research of the National Bureau of Standards, v44 p611-641, Jun 50. Available only to DTIJ users. No copies furnished by NTIS.

Keywords: *Microwaves, *Spectra, *Molecular properties, Coupling(Interaction), Frequency, Reprints, Vibration, Molecules, Quantum theory, Intensity, Eigenvalues, Cavities, Quadrupole moment, Measuring instruments, Tables(Data), Absorption, Rotation, Moment of inertia, Dipole moments, Wavemeters.

This paper presents a group of tables that give the frequencies, assignment of quantum numbers, and intensities of over 700 microwave absorption lines. The best available values of other pertinent molecular data, such as moments of inertia, dipole moments, quadrupole coupling constants, and rotation-vibration constants are also included. The frequencies are listed once for each molecule and again in consecutive ascending order of frequency. References are given for all data included. Frequencies listed to the nearest megacycle were generally measured with a cavity wave meter and may be in error by as much as 10 megacycles, whereas those given to a fraction of megacycle are generally known to an accuracy of about 0.1 megacycle. jg p.1.

00,721
AD-A297 943/3 PC A03/MF A01
National Inst. of Standards and Technology, Gaithersburg, MD.
Crystal Diffraction Spectrometry for Accurate, Non-Invasive kV/Spectral Measurement for Improvement of Mammographic Image Quality.
Annual rept. 18 Apr 94-31 Mar 95.
R. D. Deslattes, and L. Hudson. 30 Apr 95, 23p.
Contract MIPR-94MM4539
Document partially illegible.

Keywords: *Spectrometry, *Image registration, Breast cancer, Setting(Adjusting), Detection, Clinical medicine, Prototypes, Crystals, X rays, Radiography, Diffraction, Quantum efficiency, Spectrometers, Solid state electronics, Pharmacology, Mammography, Retrofitting, Abrasives, Image tubes, Dental equipment.

Phase one of this contract has been devoted to the development and demonstration of the MST prototype crystal spectrometer which was designed to provide accurate measurement of x-ray source voltage and full spectral characterization of the radiation emitted from mammographic x-ray sources. A major advance has been the movement from film to solid state image registration. Our current systems take advantage of recently introduced large area digital radiography sensors which are now being used in place of dental film. Initial clinical trials indicated the need for improved detection quantum efficiency. This has been overcome primarily by increasing the crystal bandpass with an air abrasive treatment of the surface and retrofitting the sensor with a thicker scintillating material. The significance of these advances is that we now have an instrument which: measures kVp to an accuracy in excess of clinical requirements, is easily adaptable to the clinical setting, records the entire spectral profile, including the effects of both inherent and added filtration, and is sensitive enough to obtain these data within the time of a typical mammographic exposure. Not only will this contribute to the quality control of mammography but potentially to refinements in technique.

00,722
DE94017816 PC A02/MF A01
National Inst. of Standards and Technology, Boulder, CO.
Measurement of the Thermal Properties of Electrically Conducting Fluids Using Coated Transient Hot Wires.
R. A. Perkins. 1994, 9p, CONF-9404137-6.
Contract AI05-89ER13992
Symposium on Energy Engineering Sciences (12th), Argonne, IL (United States), 27-29 Apr 1994. Sponsored by Department of Energy, Washington, DC.

Keywords: *Argon, *Fluorinated Aliphatic Hydrocarbons, *Probes, *Thermal conductivity, Design, Electrical Insulation, Experimental Data, Performance, Protective Coatings, Refrigerants, Supercritical State, Tantalum Oxides, Tables(data), EDB/360606, EDB/440500.

Measurements of fluid thermal properties using the transient hot-wire technique are described. When bare

hot wires are used in electrically conducting fluids there are additional measurement uncertainties due to the formation of electric double layers on the surfaces of the wires and the cell wall. If the electrical conductivity of the fluid is large enough there is also significant power generation in the fluid. These measurement uncertainties can be eliminated by electrically insulating the hot wires with a thin film. The use of tantalum hot wires with an anodized layer of tantalum pentoxide is demonstrated with measurements on nonpolar argon and polar 1,1,1,2 tetrafluorethane (R134a). Although coated tantalum hot wires have been used previously in a transient mode to measure the thermal conductivity of liquids, this work is the first demonstration of the use of coated wires to measure thermal conductivity in the liquid, vapor, and supercritical gas phases.

00,723
DE94018562 PC A02/MF A01
National Bureau of Standards, Gaithersburg, MD.
Atom-counting standards and Doppler-free resonance ionization mass spectroscopy. (Progress report).
J. M. R. Hutchinson, and K. G. W. Inn. 1988, 9p, DOE/ER/60447-T2.
Contract AI05-86ER60447
Sponsored by Department of Energy, Washington, DC.

Keywords: *Resonance Ionization Mass Spectroscopy, Beryllium Isotopes, Molybdenum Isotopes, Progress Report, Trace Amounts, Uranium, EDB/400102.

This program has two components: quantification and improvement of ultrasensitive techniques, and development of isotopic ratio standards in the ultrasensitive range of 10(sup (minus)10) and lower. Data sheets were developed.

00,724
N95-15839/0 (Order as N95-15827/5, PC A07/MF A02)
National Inst. of Standards and Technology, Boulder, CO.
Investigating the 3.3 Micron Infrared Fluorescence from Naphthalene Following Ultraviolet Excitation.
R. M. Williams, and S. R. Leone. May 94, 6p.
In NASA Ames Research Center, the Diffuse Interstellar Bands: Contributed Papers p 59-64.

Keywords: *Infrared spectra, *Naphthalene, Absorption spectra, Fluorescence, Molecular excitation, Vapor phases, Excimer lasers, Fourier transformation, Polycyclic aromatic hydrocarbons, Spectrometers, Ultraviolet lasers, Intermediate infrared radiation.

Polycyclic aromatic hydrocarbon (PAH) type molecules are proposed as the carriers of the unidentified infrared (UIR) bands. Detailed studies of the 3.3 micrometer infrared emission features from naphthalene, the simplest PAH, following ultraviolet laser excitation are used in the interpretation of the 3.29 micrometer (3040 cm(sup -1)) UIR band. A time-resolved Fourier transform spectrometer is used to record the infrared emission spectrum of gas-phase naphthalene subsequent to ultraviolet excitation facilitated by an excimer laser operated at either 193 nm or 248 nm. The emission spectra differ significantly from the absorption spectrum in the same spectral region. Following 193 nm excitation the maximum in the emission profile is red-shifted 45 cm(sup -1) relative to the absorption maximum; a 25 cm(sup -1) red-shift is observed after 248 nm excitation. The red-shifting of the emission spectrum is reduced as collisional and radiative relaxation removes energy from the highly vibrationally excited molecules. Coupling between the various vibrational modes is thought to account for the differences between absorption and emission spectra. Strong visible emission is also observed following ultraviolet excitation. Visible emission may play an important role in the rate of radiative relaxation, which according to the interstellar PAH hypothesis occurs only by the slow emission of infrared photons. Studying the visible emission properties of PAH type molecules may be useful in the interpretation of the DIB's observed in absorption.

00,725
PB94-112695 PC A15/MF A03
National Inst. of Standards and Technology (MSEL), Gaithersburg, MD. Ceramics Div.
Electroacoustics for Characterization of Particulates and Suspensions. Proceedings of a Workshop. Held in Gaithersburg, Maryland on February 3-4, 1993.
Special pub.
S. G. Malghan. Sep 93, 343p, NIST/SP-856.
Also available from Supt. of Docs. as SN003-003-03237-9.

Keywords: *Meetings, *Electroacoustics, *Laboratory equipment, *Particulates, *Colloids, Ceramics, Electrokinetics, Suspensions, Measuring instruments, Zeta potential, Performance evaluation, Aqueous solutions, Surface chemistry, Coatings, Polarity.

The electroacoustic technique, based on physical affects described by Debye, is relatively new and the laboratory instrumentation has become available only in the last decade. This new instrumentation by Matec Applied Sciences and Pen Kem Inc. is based on the application of either electrical fields or ultrasound as external fields to the particles and measurement of the resulting electrical or ultrasonic response. These instruments, while addressing the primary drawbacks of electrophoresis instruments, allow the determination of signals that are related to the electrokinetic zeta potential for colloidal suspensions in polar and nonpolar media. In recent years, the electroacoustic technique has been extensively utilized for the characterization of a variety of particulates in dense suspensions of polar and nonpolar liquids with great success. As a result of this surge in activity, a number of technical issues have surfaced. In order to discuss these issues and develop a common understanding of the fundamentals of electroacoustics, a workshop was organized at the suggestion of the user community. The volume contains all but two papers presented at the workshop.

00,726
PB94-140571 (Order as PB94-140555, PC A06/MF A02)
Los Alamos National Lab., NM.
Pressure-Volume-Temperature Relations in Liquid and Solid Tritium.
E. R. Grilly. 1993, 12p.
Included in Jnl. of Research of the National Institute of Standards and Technology, v98 n6, p679-690 Nov/Dec 93.

Keywords: *Tritium, *Thermodynamic properties, Temperature range 0013-0065 K, Temperature dependence, Pressure dependence, Solidified gases, Liquefied gases, Deuterium, Hydrogen.

PVT relations in liquid and solid T2 near the melting curve were measured over 20.5 K-22.1 K and 0 MPa-7 MPa (0 bar-70 bar) with a cell that used diaphragms for pressure and volume variation and measurement. Because of ortho-para self conversion, the melting pressure P(m) and the liquid molar volume V(lm) increased with time. Measurements of the volume change on melting and the thermal expansion and compressibility for liquid T2 were consistent with those for H2 and D2. Impurities such as H2, HT, DT, and (3)He were removed by a technique using an adsorption column of cold activated alumina. Corrections for (3)He growth during an experiment were adequate except near the triple point.

00,727
PB94-151842 PC A06/MF A02
National Inst. of Standards and Technology, Gaithersburg, MD.
NIST Standard Reference Data Products Catalog, 1994.
Special pub.
M. W. Chase, and J. C. Sauerwein. Jan 94, 117p, NIST/SP-782-1994ED.
Supersedes PB93-173409. Also available from Supt. of Docs. as SN003-003-03247-6.

Keywords: *Catalogs(Publications), *Data bases, Chemical analysis, Atomic physics, Biotechnology, Reaction kinetics, Molecular structure, Molcular spectroscopy, Thermophysical properties, Thermochemistry, Thermodynamics, Numerical data, Software tools, Fluids.

The National Institute of Standards and Technology's (NIST) Standard Reference Data Program provides reliable, well-documented data to scientists and engineers for use in technical problem-solving, research, and development. This catalog lists published data compilations and current databases in the Standard Reference Database Series. The activities concentrate in the following disciplines: Analytical Chemistry; Atomic and Molecular Physics; Biotechnology; Chemical Kinetics; Materials Properties; Process Design; Thermodynamics and Thermochemistry; and Thermophysical Properties of Fluids.

00,728
PB94-160769 PC A16/MF A03
National Inst. of Standards and Technology (CSTL), Gaithersburg, MD.
CSTL Technical Activities 1991.
H. S. Hertz, and B. I. Diamondstone. Feb 92, 353p.
See also report for 1992, PB93-173482. Presented to the Board on Assessment of NIST Programs, National Research Council, February 11-12, 1992.

Keywords: *Research and development, *Chemistry, Biochemistry, Biotechnology, Chemical engineering, Analytical chemistry, Reaction kinetics, Metrology, Thermodynamics, Inorganic compounds, Particulates, Organic compounds, Technology transfer, Surface chemistry, Measurement, Thermophysics, Processing, Microanalysis, Quality assurance, US NIST, *Chemical Science and Technology Library.

The report summarizes the technical activities of the Chemical Science and Technology Laboratory at the National Institute of Standards and Technology. It emphasizes activities over the Fiscal Year 1991 in the Biotechnology Division, the Chemical Engineering Division, the Chemical Kinetics and Thermodynamics Division, the Inorganic Analytical Research Division, the Organic Analytical Research Division, the Process Measurements Division, the Surface and Microanalysis Division and the Thermophysics Division.

00,729
PB94-160975 Not available NTIS
American Chemical Society, Washington, DC.
Journal of Physical and Chemical Reference Data, Volume 22, No. 1, January/February 1993.
Bimonthly rept.
J. W. Gallagher. c1993, 289p.
See also PB94-160983 through PB94-161007 and PB93-149136. Prepared in cooperation with American Inst. of Physics, New York. Sponsored by National Inst. of Standards and Technology, Gaithersburg, MD.
Available from American Chemical Society, 1155 Sixteenth St., NW, Washington, DC. 20036-9976.

Keywords: *Physical properties, *Chemical properties, *Physical chemistry, Alkaline earth metals, Thermodynamics, Oxygen, Reaction kinetics, Liquid phases, Tables(Data), Spectroscopy, Periodicals, *Reference materials.

Table of Contents:
Thermodynamic Properties of the Group IIA Elements;
Spectroscopy and Structure of the Lithium Hydride Diatomic Molecules and Ions;
Quantum Yields for the Photosensitized Formation of the Lowest Electronically Excited Singlet State of Molecular Oxygen in Solution;
Cumulative Listing of Reprints;
Cumulative Listing of Supplements, Monographs, and Special Issues.

00,730
PB94-160983 Not available NTIS
Notre Dame Univ., IN. Center for Sensor Materials.
Thermodynamic Properties of the Group IIA Elements.
C. B. Alcock, M. W. Chase, and V. Itkin. c1993, 85p.
Prepared in cooperation with National Inst. of Standards and Technology (NML), Gaithersburg, MD. Standard Reference Data. and Toronto Univ. (Ontario). Dept. of Metallurgy and Materials Science.
Included in Jnl. of Physical and Chemical Reference Data, v22 n1 p1-85 Jan/Feb 93. Available from American Chemical Society, 1155 Sixteenth St., NW, Washington, DC. 20036-9976.

Keywords: *Research, *Physical chemistry, Alkaline earth metals, Thermodynamics, Gibbs free energy, Specific heat, Enthalpy, Phase transformations, Chemical equilibrium, Heat of fusion, Heat of transformation.

The thermodynamic properties of the alkaline earth metals in the condensed state have been critically reassessed, and recommended values for all of the relevant thermodynamic properties are given. These values are compared with those published in recent reviews by the staff at the Institute for High Temperatures (Moscow) and the National Institute of Standards and

Technology (Washington, DC), and the reasons for any differences are discussed in detail. A direct result of this review is a set of recommendations for experimental studies which should enhance the reliability of the thermodynamic results.

00,731
PB94-160991 Not available NTIS
Iowa Univ., Iowa City.
Spectroscopy and Structure of the Lithium Hydride Diatomic Molecules and Ions.
W. C. Stwalley, and W. T. Zemke. c1993, 26p.
Prepared in cooperation with Wartburg Coll., Waverley, IA. Dept. of Chemistry.
Included in Jnl. of Physical and Chemical Reference Data, v22 n1 p87-112 Jan/Feb 93. Available from American Chemical Society, 1155 Sixteenth St., NW, Washington, DC. 20036-9976.

Keywords: *Research, *Physical chemistry, Lithium hydride, Hydrides, Reaction kinetics, Dissociation energy, Molecular spectroscopy, Molecular structure, Isotope effect, Potential energy, Born-Oppenheimer approximation.

All significant experimental measurements and many theoretical calculations of the spectroscopy and structure of the isotopic lithium hydrides ((6)LiH, (7)LiH, (6)LiD, (7)LiD) are identified and reviewed. Published molecular constant determinations from conventional and laser spectroscopy are evaluated; recommended spectroscopic constants for the X(1)sigma(+1), A(1)sigma(+1) and B(1)II states are tabulated. Potential energy curves (RKR, IPA and hybrid) for the X(1)sigma(+1), A(1)sigma(+1) and B(1)II states are evaluated and recommended curves are tabulated. Adiabatic corrections to the Born-Oppenheimer approximation are also reviewed. Calculations on LiH(+1) and LiH(-1) are also listed and described briefly.

00,732
PB94-161007 Not available NTIS
Loughborough Univ. of Technology (England). Dept. of Chemistry.
Quantum Yields for the Photosensitized Formation of the Lowest Electronically Excited Singlet State of Molecular Oxygen in Solution.
F. Wilkinson, W. P. Helman, and A. B. Ross. c1993, 150p.
Prepared in cooperation with Notre Dame Univ., IN. Radiation Lab.
Included in Jnl. of Physical and Chemical Reference Data, v22 n1 p113-262, Jan/Feb 93. Available from American Chemical Society, 1155 Sixteenth St., NW, Washington, DC. 20036-9976.

Keywords: *Research, *Physical chemistry, Data processing, Energy transfer, Oxygen, Quantum efficiency, Quantum chemistry, Photosensitivity, Atomic energy levels, Solutions, Decay.

Quenching of excited singlet and triplet states of many substances by ground state molecular oxygen produces singlet oxygen, the lowest electronically excited singlet state of molecular oxygen, O2(1 delta sub g). The fractions of singlet and triplet states quenched which produce singlet oxygen and the quantum yields of formation of singlet oxygen in fluid solutions have been critically compiled. Methods for determining yield parameters have been reviewed. Data have been compiled from the literature through 1991. Photosensitizers are included in Table 1. Porphyrins and phthalocyanines are included in Table 2. Other materials which have been investigated for singlet oxygen production, such as dyes and drugs, are collected in Table 3 along with heterogeneous systems such as polymer-bound photosensitizers.

00,733
PB94-162211 Not available NTIS
American Chemical Society, Washington, DC.
Journal of Physical and Chemical Reference Data, Volume 22, No. 2, March/April 1993.
Bimonthly rept.
J. W. Gallagher. c1993, 322p.
See also PB94-162229 through PB94-162252 and PB94-160975. Prepared in cooperation with American Inst. of Physics, New York. Sponsored by National Inst. of Standards and Technology, Gaithersburg, MD.
Available from American Chemical Society, 1155 Sixteenth St., NW, Washington, DC. 20036-9976.

Keywords: *Physical properties, *Chemical properties, *Physical chemistry, Chemical reactions, Wavelengths, Thermodynamics, Reaction kinetics, Vapor phases, Table(Data), Periodicals, *Reference materials.

Table of Contents:
- Wavelengths and Energy Level Classifications for the Spectra of Sulfur (S I through S XVI);
- Thermodynamic Properties of Alkenes (Mono-Olefins Larger Than C(4));
- The Thermodynamic Behavior of the CO2-H2O System from 400 to 1000 K, up to 100 MPa and 30% Mole Fraction of CO2;
- Thermodynamics of Enzyme-Catalyzed Reactions:
- Part 1. Oxidoreductases;
- Cumulative Listing of Reprints;
- Cumulative Listing of Supplements, Monographs, and Special Issues.

00,734
PB94-162229 Not available NTIS
National Inst. of Standards and Technology, Gaithersburg, MD.
Wavelengths and Energy Level Classifications for the Spectra of Sulfur (S I through S XVI).
V. Kaufman, and W. C. Martin. c1993, 96p.
Included in Jnl. of Physical and Chemical Reference Data, v22 n2 p279-375, Mar/Apr 93. Available from American Chemical Society, 1155 Sixteenth St., NW, Washington, DC. 20036-9976.

Keywords: *Research, *Physical chemistry, Atomic energy levels, Ions, Spectra, Wavelengths, Frequencies, Sulfur, Infrared radiation, Ultraviolet radiation, Tables(Data).

Wavelengths and their classifications have been compiled for the spectra of the atom and all positive ions of sulfur (Z = 16). The selections of data are based on the compilations of energy levels by Martin, Zalubas, and Musgrove in 1990, with some updating from the more recent literature. Wavelengths (or wavenumbers) calculated from the differences of the energy levels are given along with the observed values for all classified lines; these calculated wavelengths should in general be more accurate than the observed values wherever the two values differ significantly. No limitation has been imposed on the wavelength range of the classified lines, except for the omission of x-ray transitions in the neutral atom. Two finding lists are also included, one for S I through S III and the other for S IV through S XVI.

00,735
PB94-162237 Not available NTIS
National Inst. for Petroleum and Energy Research, Bartlesville, OK.
Thermodynamic Properties of Alkenes (Mono-Olefins Larger Than C4).
W. V. Steele, and R. D. Chirico. c1993, 53p.
Included in Jnl. of Physical and Chemical Reference Data, v22 n2 p377-430, Mar/Apr 93. Available from American Chemical Society, 1155 Sixteenth St., NW, Washington, DC. 20036-9976.

Keywords: *Research, *Physical chemistry, Alkene compounds, Thermodynamic properties, Entropy, Gibbs free energy, Specific heat, Vapor pressure, Heat of vaporization, Heat of formation, Ideal gas, Density(Mass/Volume).

The thermodynamic properties of the mono-olefins with carbon numbers greater than C4 were reviewed. Properties included critical properties, vapor pressures, densities, second virial coefficients, enthalpies of vaporization, heat capacities, and enthalpies of combustion. Enthalpies of formation for the liquid, gas, and ideal-gas state at 298.15 K were calculated for 47 compounds based on the experimental values. Gaps in the available data were identified and recommendations for additional experiments are made. Evidence for errors in several of the original experimental results is presented, and revised values are suggested.

00,736
PB94-162245 Not available NTIS
National Inst. of Standards and Technology (CSTL), Gaithersburg, MD. Thermophysics Div.
Thermodynamic Behavior of the CO2-H2O System from 400 to 1000 K, up to 100 MPa and 30% Mole Fraction of CO2.
J. S. Gallagher, R. Crovetto, and J. M. H. L. Sengers. c1993, 82p.
Included in Jnl. of Physical and Chemical Reference Data, v22 n2 p431-513, Mar/Apr 93. Available from American Chemical Society, 1155 Sixteenth St., NW, Washington, DC. 20036-9976.

Keywords: *Research, *Physical chemistry, Thermodynamic properties, Carbon dioxide, Water, Enthalpy, Equations of state, Volume, Fugacity, Henrys law, Mixtures, Steam, Critical point, FORTRAN, Phases, Boundaries, Computer programs.

A model is presented for the thermodynamic properties of the aqueous mixture of carbon dioxide, up to 30 mol% composition, in a large range of temperatures (400-1000 K) and pressures (0-100 MPa) around the critical point of water. The model for the Helmholtz free energy of the mixture is based on the principle of generalized corresponding states, with the NBS/NRC Steam Tables as the reference state for pure water. Input to the model are data for the critical line of the mixture, apparent molar volume and pVTx data in supercritical water, phase boundaries, excess enthalpies and mixture second virial coefficient data. Comparisons are presented with those data, with Henry's constants and with other formulations available for this system. The Fortran codes for generating these properties are listed in Appendix B.

00,737
PB94-162252 Not available NTIS
National Inst. of Standards and Technology (CSTL), Gaithersburg, MD. Biotechnology Div.
Thermodynamics of Enzyme-Catalyzed Reactions: Part 1. Oxidoreductases.
R. N. Goldberg, Y. B. Tewari, D. Bell, K. Fazio, and E. Anderson. c1993, 68p.
Prepared in cooperation with Food and Drug Administration, Rockville, MD.
Included in Jnl. of Physical and Chemical Reference Data, v22 n2 p515-582, Mar/Apr 93. Available from American Chemical Society, 1155 Sixteenth St., NW, Washington, DC. 20036-9976.

Keywords: *Research, *Physical chemistry, Thermodynamics, Enthalpy, Enzymes, Chemical reactions, Catalysts, Oxidoreductases, Heat of reaction, Chemical equilibrium.

Equilibrium constants and enthalpy changes for reactions catalyzed by oxidoreductases have been compiled. For each reaction the following information is given: the reference for the data; the reaction studied; the name of the enzyme used and its Enzyme Commission number; the method of measurement; the conditions of measurement (temperature, pH, ionic strength, and the buffer(s) and cofactor(s) used); the data and an evaluation of it; and, sometimes, commentary on the data and on any corrections which have been applied to it. The data from 205 references have been examined and evaluated. Chemical Abstract Service Registry Numbers have been assigned to the substances involved in these various reactions. There is a cross reference between the substances and the Enzyme Commission numbers of the enzymes used to catalyze the reactions in which the substances participated.

00,738
PB94-162260 Not available NTIS
American Chemical Society, Washington, DC.
Journal of Physical and Chemical Reference Data, Volume 22, No. 3, May/June 1993.
Bimonthly rept.
J. W. Gallagher. c1993, 216p.
See also PB94-162278 through PB94-162302 and PB94-162211. Prepared in cooperation with American Inst. of Physics, New York. Sponsored by National Inst. of Standards and Technology, Gaithersburg, MD.
Available from American Chemical Society, 1155 Sixteenth St., NW, Washington, DC. 20036-9976.

Keywords: *Physical properties, *Chemical properties, *Physical chemistry, Thermodynamics, Nitrogen organic compounds, Temperature, Reaction kinetics, Vapor phases, Tables(Data), *Reference materials.

Table of Contents:
- Estimation of the Heat Capacities of Organic Liquids as a Function of Temperature Using Group Additivity. I. Hydrocarbon Compounds;
- Estimation of the Heat Capacities of Organic Liquids as a Function of Temperature Using Group Additivity. II. Compounds of Carbon, Hydrogen, Halogens, Nitrogen, Oxygen, and Sulfur;
- Thermodynamic and Thermophysical Properties of Organic Nitrogen Compounds. Part II. 1- and 2- Butanamine, 2-Methyl-1-Propanamine, 2-Methyl-2-Propanamine, Pyrrole, 1-, 2-, and 3-Methylpyrrole, Pyridine, 2-, 3-, and 4-Methylpyridine, Pyrrolidine, Piperidine, Indole,

Quinoline, Isoquinoline, Acridine, Carbazole, Phenanthridine, 1- and 2- Naphthalenamine, and 9-Methylcarbazole;
International Equations for the Saturation Properties of Ordinary Water Substance. Revised According to the International Temperature Scale of 1990. Addendum to Journal of Physical and Chemical Reference Data 16, 893 (1987);
Cumulative Listing of Reprints;
Cumulative Listing of Supplements, Monographs, and Special Issues.

00,739
PB94-162278 Not available NTIS
National Inst. of Standards and Technology (CSTL), Gaithersburg, MD. Chemical Kinetics and Thermodynamics Div.
Estimation of the Heat Capacities of Organic Liquids as a Function of Temperature Using Group Additivity. I. Hydrocarbon Compounds.
V. Ruzicka, and E. S. Domalski. c1993, 22p.
Included in Jnl. of Physical and Chemical Reference Data, v22 n3 p597-618, May/Jun 93. Available from American Chemical Society, 1155 Sixteenth St., NW, Washington, DC. 20036-9976.

Keywords: *Research, *Physical chemistry, Specific heat, Estimating, Liquid phases, Hydrocarbons, Temperature dependence, Least squares method, Organic compounds, Group additivity, Organic liquids.

A second-order group additivity method has been developed for the estimation of the heat capacity of liquid hydrocarbons as a function of temperature in the range from the melting temperature to the normal boiling temperature. The temperature dependence of group contributions and structural corrections has been represented by a polynomial expression. Recommended heat capacities from a large compilation of critically evaluated data that contains over 1300 organic liquids served as a database both for the development and testing of the method.

00,740
PB94-162286 Not available NTIS
National Inst. of Standards and Technology (CSTL), Gaithersburg, MD. Chemical Kinetics and Thermodynamics Div.
Estimation of the Heat Capacities of Organic Liquids as a Function of Temperature Using Group Additivity. II. Compounds of Carbon, Hydrogen, Halogens, Nitrogen, Oxygen, and Sulfur.
V. Ruzicka, and E. S. Domalski. c1993, 39p.
Included in Jnl. of Physical and Chemical Reference Data, v22 n3 p619-657, May/Jun 93. Available from American Chemical Society, 1155 Sixteenth St., NW, Washington, DC. 20036-9976.

Keywords: *Research, *Physical chemistry, Specific heat, Estimating, Liquid phases, Hydrocarbons, Temperature dependence, Least squares method, Organic compounds, Nitrogen organic compounds, Oxygen organic compounds, Sulfur organic compounds, Halogen organic compounds, Group additivity, Organic liquids.

A second-order group additivity method has been developed for the estimation of the heat capacity of liquid organic compounds containing carbon, hydrogen, halogens, nitrogen, oxygen, and sulfur. The method permits the estimation of the heat capacity as a function of temperature in the range from the melting temperature to the normal boiling temperature. Group contributions and structural corrections have been made temperature dependent by the use of a polynomial expression. The work has drawn information for both the development and testing of the method from a large compilation of critically evaluated heat capacity data for over 1300 organic liquids.

00,741
PB94-162294 Not available NTIS
Texas A and M Univ., College Station. Thermodynamics Research Center.
Thermodynamic and Thermophysical Properties of Organic Nitrogen Compounds. Part II. 1- and 2-Butanamine, 2-Methyl-1-Propanamine, 2-Methyl-2-Propanamine, Pyrrole, 1-, 2-, and 3-Methylpyrrole, Pyridine, 2-, 3-, and 4-Methylpyridine, Pyrrolidine, Piperidine, Indole, Quinoline, Isoquinoline, Acridine, Carbazole, Phenanthridine, 1- and 2-Naphthalenamine, and 9-Methylcarbazole.
A. Das, M. Frenkel, N. A. M. Gadalla, A. S. Rodgers, R. C. Wilhoit, S. Kudchadker, and K. N. Marsh. c1993, 124p.
See also PB91-192542.
Included in Jnl. of Physical and Chemical Reference Data, v22 n3 p659-782, May/Jun 93. Available from American Chemical Society, 1155 Sixteenth St., NW, Washington, DC. 20036-9976.

Keywords: *Research, *Physical chemistry, Thermodynamic properties, Nitrogen organic compounds, Enthalpy, Heat of vaporization, Heat of combustion, Specific heat, Ideal gas, Thermochemistry, Vapor pressure, Condensed phase.

The thermodynamic and thermophysical properties of 1- and 2-butanamine, 2-methyl-1-propanamine, 2-methyl-2-propanamine, pyrrole, 1-, 2- and 3-methylpyrrole, pyridine, 2-, 3-, and 4-methylpyridine, pyrrolidine, piperidine, indole, quinoline, isoquinoline, acridine, carbazole, phenanthridine, 1- and 2-naphthalenamine, and 9-methylcarbazole have been evaluated. Recommended values are given for the following properties: normal boiling, freezing and triple point temperatures, critical constants, thermodynamic properties in the solid and liquid phases, vapor pressure, enthalpy of vaporization, density, second virial coefficients, and enthalpy of combustion. Ideal gas thermodynamic properties have been calculated by statistical mechanical methods.

00,742
PB94-162302 Not available NTIS
Ruhr Univ., Bochum (Germany, F.R.). Inst. fuer Thermo- und Fluiddynamik.
International Equations for the Saturation Properties of Ordinary Water Substance. Revised According to the International Temperature Scale of 1990. Addendum to Journal of Physical and Chemical Reference Data 16, 893 (1987).
W. Wagner, and A. Pruss. c1993, 5p.
Included in Jnl. of Physical and Chemical Reference Data, v22 n3 p783-787, May/Jun 93. Available from American Chemical Society, 1155 Sixteenth St., NW, Washington, DC. 20036-9976.

Keywords: *Research, *Physical chemistry, Enthalpy, Entropy, Water saturation, Density(Mass/Volume), Temperature, Vapor pressure, Correlation, IAPWS(International Association for the Properties of Water and Steam), Saturated liquid density, Saturated vapor density.

In 1987, consistent with the latest experimental data and the internationally recommended values for the critical parameters, the authors published compact and accurate correlation equations for properties on the saturation line of ordinary (light) water substance. (A. Saul and W. Wagner, J. Phys. Chem. Ref. Data 16, 893 (1987)). As an addendum to this 1987 paper the present paper brings all temperature values and adjusted coefficients in all correlation equations given in the 1987 paper into agreement with the International Temperature Scale of 1990 (ITS-90). The new equations form the basis of the 'Revised Supplementary Release on Saturation Properties of Ordinary Water Substance' issued by the International Association for the Properties of Water and Steam (IAPWS). This revised release which contains all equations and coefficients adjusted with regard to the ITS-90 is the main part of this paper.

00,743
PB94-162310 Not available NTIS
American Chemical Society, Washington, DC.
Journal of Physical and Chemical Reference Data, Volume 22, No. 4, July/August 1993.
Bimonthly rept.
J. W. Gallagher. c1993, 380p.
See also PB94-162328 and PB94-162260. Prepared in cooperation with American Inst. of Physics, New York. Sponsored by National Inst. of Standards and Technology, Gaithersburg, MD.
Available from American Chemical Society, 1155 Sixteenth St., NW, Washington, DC. 20036-9976.

Keywords: *Physical properties, *Chemical properties, *Physical chemistry, Thermodynamic properties, Solid phases, Liquid phases, Vapor phases, Tables(Data), *Reference materials.

Table of Contents:
Estimation of the Thermodynamic Properties of C-H-N-O-S-Halogen Compounds at 298.15 K;
Cumulative Listing of Reprints;
Cumulative Listing of Supplements, Monographs, and Special Issues.

00,744
PB94-162328 Not available NTIS
National Inst. of Standards and Technology (CSTL), Gaithersburg, MD. Chemical Kinetics and Thermodynamics Div.
Estimation of the Thermodynamic Properties of C-H-N-O-S-Halogen Compounds at 298.15 K.
E. S. Domalski, and E. D. Hearing. c1993, 354p.
Included in Jnl. of Physical and Chemical Reference Data, v22 n4 p805-1159, Jul/Aug 93. Available from American Chemical Society, 1155 Sixteenth St., NW, Washington, DC. 20036-9976.

Keywords: *Research, *Physical chemistry, Specific heat, Entropy, Enthalpy, Thermodynamic properties, Organic compounds, Hydrocarbons, Halogen organic compounds, Nitrogen organic compounds, Oxygen organic compounds, Sulfur organic compounds, Solid phases, Liquid phases, Vapor phases, Estimating.

An estimation method, which was developed by S. W. Benson and coworkers for calculating the thermodynamic properties of organic compounds in the gas phase, has been extended to the liquid and solid phases for organic compounds at 298.15 K and 101,325 Pa. As with a previous paper dealing with hydrocarbon compounds, comparisons of estimated enthalpies of formation, heat capacities, and entropies with literature values show that extension of the Benson's group additivity approach to the condensed phase is easy to apply and gives satisfactory agreement. This work covers 1512 compounds containing the elements: carbon, hydrogen, oxygen, nitrogen, sulfur, and halogens in the gas, liquid, and solid phases. About 1000 references are provided for the literature values which are cited.

00,745
PB94-162336 Not available NTIS
American Chemical Society, Washington, DC.
Journal of Physical and Chemical Reference Data, Volume 22, No. 5, September/October 1993.
Bimonthly rept.
J. W. Gallagher. c1993, 266p.
See also PB94-162344 through PB94-162369 and PB94-162310. Prepared in cooperation with American Inst. of Physics, New York. Sponsored by National Inst. of Standards and Technology, Gaithersburg, MD.
Available from American Chemical Society, 1155 Sixteenth St., NW, Washington, DC. 20036-9976.

Keywords: *Physical properties, *Chemical properties, *Physical chemistry, Atomic properties, Oxygen, Germanium, Chromium, Spectrum analysis, Tables(Data), Atomic energy levels, Periodicals, *Reference materials.

Table of Contents:
A Compilation of Energy Levels and Wavelengths for the Spectrum of Singly-Ionized Oxygen (O II);
Energy Levels of Germanium, Ge I through Ge XXXII;
Spectral Data and Grotrian Diagrams for Highly Ionized Chromium, Cr V through Cr XXIV;
Cumulative Listing of Reprints;
Cumulative Listing of Supplements, Monographs, and Special Issues.

00,746
PB94-162344 Not available NTIS
National Inst. of Standards and Technology (PL), Gaithersburg, MD. Physics Lab. Office.
Compilation of Energy Levels and Wavelengths for the Spectrum of Singly-Ionized Oxygen (O II).
W. C. Martin, V. Kaufman, and A. Musgrove. c1993, 33p.
Included in Jnl. of Physical and Chemical Reference Data, v22 n5 p1179-1212, Sep/Oct 93. Available from American Chemical Society, 1155 Sixteenth St., NW, Washington, DC. 20036-9976.

Keywords: *Research, *Physical chemistry, Atomic energy levels, Oxygen, Wavelengths, Frequencies, Ionization potentials, Atomic structure, Atomic spectra.

The authors have assembled a complete list of the most accurately measured wavelengths for all classified lines of singly-ionized oxygen (O II). The data are based mainly on recent extensions of the observations and analysis of this spectrum carried out at the University of Lund, Sweden. They derived new optimal values for the energy levels using a computer code and the observed wavelengths for all classified lines. Relevant astrophysical wavelength measurements, appropriately weighted, were included in the level-optimization calculation.

00,747
PB94-162351 Not available NTIS

National Inst. of Standards and Technology (PL), Gaithersburg, MD. Atomic Physics Div.
Energy Levels of Germanium, Ge I through Ge XXXII.
J. Sugar, and A. Musgrove. c1993, 65p.
Included in Jnl. of Physical and Chemical Reference Data, v22 n5 p1213-1278, Sep/Oct 93. Available from American Chemical Society, 1155 Sixteenth St., NW, Washington, DC. 20036-9976.

Keywords: *Research, *Physical chemistry, *Germanium, *Atomic energy levels, *Ions, *Spectra, *Tables(Data).

Atomic energy levels of germanium have been compiled for all stages of ionization for which experimental data are available. No data have yet been published for Ge VIII through Ge XIII and Ge XXXII. Very accurate calculated values are compiled for Ge XXXI and XXXII. Experimental g-factors and leading percentages from calculated eigenvectors of levels are given. A value for the ionzation energy, either experimental when available or theoretical, is included for the neutral atom and each ion.

00,748
PB94-162369 Not available NTIS
Japan Atomic Energy Research Inst., Tokai.
Spectral Data and Grotrian Diagrams for Highly Ionized Chromium, Cr V through Cr XXIV.
T. Shirai, Y. Nakai, T. Nakagaki, J. Sugar, and W. L. Wiese. c1993, 144p.
Prepared in cooperation with National Inst. of Standards and Technology, Gaithersburg, MD.
Included in Jnl. of Physical and Chemical Reference Data, v22 n5 p1279-1423, Sep/Oct 93. Also available from American Chemical Society, 1155 Sixteenth St., NW, Washington, DC. 20036-9976.

Keywords: *Research, *Physical chemistry, Chromium, Spectrum analysis, Wavelengths, Spectral lines, Atomic energy levels, Ions, Diagrams.

Wavelengths, energy levels, ionization energies, line classifications, oscillator strengths, and atomic transition probabilities for Cr V to Cr XXIV are tabulated. A short review of the line identifications and wavelength measurements is given for each stage of ionization. Grotrian diagrams are given to provide graphical overviews. The literature has been surveyed through December 1991.

00,749
PB94-168556 Not available NTIS
American Chemical Society, Washington, DC.
Journal of Physical and Chemical Reference Data, Volume 22, No. 6, November/December 1993.
Bimonthly rept.
J. W. Gallagher. c1993, 178p.
See also PB94-168564 through PB94-168606 and PB94-162336. Prepared in cooperation with American Inst. of Physics, New York. Sponsored by National Inst. of Standards and Technology, Gaithersburg, MD.
Available from American Chemical Society, 1155 Sixteenth St., NW, Washington, DC. 20036-9976.

Keywords: *Physical properties, *Chemical properties, *Physical chemistry, Atomic properties, Chemical reactions, Thermodynamics, Reaction kinetics, Vapor phases, Tables(Data), *Reference materials.

Contents:
- Thermodynamic Properties of Synthetic Sapphire (alpha-Al2O3), Standard Reference Material 720 and the Effect of Temperature-Scale Differences on Thermodynamic Properties;
- Thermodynamic Properties of Gaseous Silicon Monotelluride and the Bond Dissociation Enthalpy DM(SiTe) at T -> 0;
- The Disilicides of Tungsten, Molybdenum, Tantalum, Titanium, Cobalt, and Nickel, and Platinum Monosilicide:
- A Survey of Their Thermodynamic Properties;
- Evaluated Bimolecular Ion-Molecule Gas Phase Kinetics of Positive Ions for Use in Modeling Planetary Atmospheres, Cometary Comae, and Interstellar Clouds;
- Atomic Weights of the Elements 1991;
- Index of Properties and Classes of Materials - Volumes 21-22 (1992-1993);
- Author Index - Volumes 21-22 (1992-1993) Cumulative Listing of Reprints;
- Cumulative Listing of Supplements, Monographs, and Special Issues.

00,750
PB94-168564 Not available NTIS
National Inst. of Standards and Technology (CSTL), Gaithersburg, MD. Chemical Kinetics and Thermodynamics Div.
Thermodynamic Properties of Synthetic Sapphire (alpha-Al2O3), Standard Reference Material 720 and the Effect of Temperature-Scale Differences on Thermodynamic Properties.
D. G. Archer. c1993, 12p.
Included in Jnl. of Physical and Chemical Reference Data, v22 n6 p1441-1453, Nov/Dec 93. Available from American Chemical Society, 1155 Sixteenth St., NW, Washington, DC. 20036-9976.

Keywords: *Research, *Physical chemistry, Thermodynamic properties, Aluminum oxide, Specific heat, Enthalpy, Temperature scales, Calibration standards, SRM720(Standard Reference Material 720), Synthetic sapphire.

Comparison of the National Institute of Standards and Technology's Standard Reference Material 720 certificate values for heat capacity with those obtained from recent experimental determinations indicated the possibilty of a systematic error in the certificate values. Selected experimental determinations of enthalpy increments and heat capacities were fitted in order to obtain a representation of the thermodynamic properties of alpha-Al2O3, a sample of which is the standard reference material (SRM720) for calibration of some types of calorimeters. The fitted equation and calculated values of the heat capacity, the relative enthalpy, and the entropy are given. The new values are more accurate and result from a better representation of the experimental values than did the 1982 SRM720 certificate values.

00,751
PB94-168572 Not available NTIS
National Inst. of Standards and Technology (CSTL), Gaithersburg, MD. Chemical Kinetics and Thermodynamics Div.
Thermodynamic Properties of Gaseous Silicon Monotelluride and the Bond Dissociation Enthalpy D(sub m)(SiTe) at T approaches 0.
P. A. G. O'Hare. c1993, 4p.
Included in Jnl. of Physical and Chemical Reference Data, v22 n6 p1455-1458, Nov/Dec 93. Available from American Chemical Society, 1155 Sixteenth St., NW, Washington, DC. 20036-9976.

Keywords: *Research, *Physical chemistry, Statistical analysis, Thermodynamic properties, Silicon compounds, Enthalpy, Entropy, Gibbs free energy, Silicon monotelluride, Dissociation enthalpy, Enthalpy of formation.

Statistical-thermodynamic calculations have been combined with the results of high-temperature Knudsen-effusion studies of the vaporization of Si2Te3 to calculate the thermodynamic properties of SiTe(g) from T -> 0 to T = 2000 K. The dissociation enthalpy D(sub m)(SiTe, T -> 0) is (448 + or - 8) kJ/mol; its value is discussed vis-a-vis the other silicon monochalcogenides.

00,752
PB94-168580 Not available NTIS
Houston Advanced Research Center, The Woodlands, TX. Materials Science Research Center.
Disilicides of Tungsten, Molybdenum, Tantalum, Titanium, Cobalt, and Nickel, and Platinum Monosilicide: A Survey of Their Thermodynamic Properties.
M. S. Chandrasekharaiah, J. L. Margrave, and P. A. G. O'Hare. c1993, 10p.
Prepared in cooperation with National Inst. of Standards and Technology (CSTL), Gaithersburg, MD. Chemical Kinetics and Thermodynamics Div.
Included in Jnl. of Physical and Chemical Reference Data, v22 n6 p1459-1468, Nov/Dec 93. Available from American Chemical Society, 1155 Sixteenth St., NW, Washington, DC. 20036-9976.

Keywords: *Research, *Physical chemistry, Thermodynamics, Enthalpy, Gibbs free energy, Molybdenum silicides, Tungsten silicides, Titanium silicides, Tantalum silicides, Platinum silicides, Cobalt silicides, Nickel silicides, Evaluated properties.

A critical evaluation is presented of the thermodynamic properties of six disilicides and one monosilicide that are important in the manufacture of very large scale integrated circuits. Values of the standard molar enthalpies of formation HM at T = 298.15 K and p = 0.1 MPa are recommended as follows: WSi2, -(79 + or - 5) kJ/mol, MoSi2, -(137 + or - 4) kJ/mol, TiSi2, -(171 + or - 11) kJ/mol, CoSi2, -(103 + or - 15) kJ/mol, NiSi2, -(88 + or - 12) kJ/mol, TaSi2, -(120 + or - 20) kJ/mol, and PtSi, -(119 + or - 7) kJ/mol. Equations are given for the molar enthalpy increments of some of the silicides along with a few evaluated standard Gibbs free energies of formation. Brief descriptions of methods of synthesis and limited structural information have also been included.

00,753
PB94-168598 Not available NTIS
Jet Propulsion Lab., Pasadena, CA.
Evaluated Bimolecular Ion-Molecule Gas Phase Kinetics of Positive Ions for Use in Modeling Planetary Atmospheres, Cometary Comae, and Interstellar Clouds.
V. G. Anicich. c1993, 100p.
Included in Jnl. of Physical and Chemical Reference Data, v22 n6 p1469-1569, Nov/Dec 93. Available from American Chemical Society, 1155 Sixteenth St., NW, Washington, DC. 20036-9976.

Keywords: *Research, *Physical chemistry, Planetary atmospheres, Comets, Cosmic gas dynamics, Interstellar matter, Reaction kinetics, Cations, Chemical composition, Tables(Data), Evaluated results, Product distributions, Ion-molecule reactions.

Recommendations of reaction rate coefficients and product distributions for bimolecular positive ion-molecule reactions of importance in planetary atmospheres, cometary comae, and interstellar clouds are presented. Two publications Anicich and Huntress, Astrophys. J. Suppl. Ser. 62, 553 (1986) and Anicich, Astrophys. J. Suppl. Ser. 84, 215 (1993) served as the basis for this evaluation, which covers the literature from 1965 through 1991 with some additional citations missed in the original surveys.

00,754
PB94-168606 Not available NTIS
Commission on Atomic Weights and Isotopic Abundances, Reston, VA.
Atomic Weights of the Elements 1991.
c1992, 14p.
Included in Jnl. of Physical and Chemical Reference Data, v22 n6 p1571-1584, Nov/Dec 93. Available from American Chemical Society, 1155 Sixteenth St., NW, Washington, DC. 20036-9976.

Keywords: *Research, *Physical chemistry, Isotope ratio, Atomic mass, Atomic properties, Radioactive isotopes, Elements, Periodic system, Abundance, IUPAC(International Union of Pure and Applied Chemistry).

The biennial review of atomic weight, Ar(E), determinations and other cognate data has resulted in changes for the standard atomic weight of indium from 114.82 + or - 0.01 to 114.818 + or - 0.003, for tungsten from 183.85 + or - 0.03 to 183.84 + or - 0.01 and for osmium from 190.2 + or - 0.1 to 190.23 + or - 0.03 due to new high precision measurements. Recent investigations on silicon and antimony confirmed the presently accepted Ar values. The footnote 'g' was added for carbon and potassium because it has come to the notice of the Commission that isotope abundance variations have been found in geological specimens in which these elements have an isotopic composition outside the limits for normal material. Because many elements have a different isotopic composition in non-terrestrial materials, recent data on non-terrestrial material are included in this report for the information of the interested scientific community.

00,755
PB94-172178 Not available NTIS
National Inst. of Standards and Technology (MSEL), Gaithersburg, MD. Reactor Radiation Div.
Rotational Dynamics of Solid C70: A Neutron-Scattering Study.
Final rept.
C. Christides, T. J. S. Dennis, K. Prassides, J. R. D. Copley, R. L. Cappelletti, and D. A. Neumann. 1994, 7p.
Pub. in Physical Review B 49, n4 p2897-2903, 15 Jan 94.

Keywords: *Fullerenes, Neutron diffraction, Neutron scattering, Inelastic scattering, Temperature dependence, Reprints, Rotational dynamics.

The authors report the results of neutron-diffraction and low-energy neutron-inelastic-scattering experiments on high-purity solid C70 between 10 and 640 K. Thermal hysteresis effects are found to accompany

structural changes both on cooling and on heating. The observed diffuse scattering intensity does not change with temperature. At 10 K broad librational peaks are observed at 1.82(16)meV (full width at half maximum = 1.8(5)meV). The peaks soften and broaden further with increasing temperature. At and above room temperature, they collapse into a single quasielastic line. At 300 K, the diffusive reorientational motion appears to be somewhat anisotropic, becoming less so with increasing temperature. An isotropic rotational diffusion model, in which the motions of adjacent molecules are uncorrelated, describes well the results at 525 K. The temperature dependence of the rotational diffusion constants is consistent with a thermally activated process having an activation energy of 32(7)meV.

00,756
PB94-172244 Not available NTIS
National Inst. of Standards and Technology (MSEL), Gaithersburg, MD. Polymers Div.
Octacalcium Phosphate. 3. Infrared and Raman Vibrational Spectra.
Final rept.
B. O. Fowler, M. Markovic, and W. E. Brown. 1993, 7p.
Pub. in Chem. Mater. 5, n10 p1417-1423 1993. See also PB89-131288. Sponsored by American Dental Association Health Foundation, Chicago, IL.

Keywords: *Raman spectra, *Vibrational spectra, Water, Binding sites, Dentistry, Reprints, *Octacalcium phosphate.

Infrared and Raman band assignments are given for powdered samples of the biologically important compound, octacalcium phosphate, in the 4,000-300-cm(sup -1) range. Specific assignments were made for bands of the two crystallographically independent acidic phosphate groups. The numbers of observed bands were markedly less than those predicted by factor group analysis; additional unresolved bands are probably present. Infrared spectra indicate that two polymorphs of octacalcium phosphate may exist whose structures differ mainly in acidic phosphate and water bonding and in possibly different contents of water. Polymorphic forms of octacalcium phosphate are structurally plausible because of possible differences in bonding of its acidic phosphate groups and water molecules and in number of water molecules. The wavenumber positions of Raman bands, especially acidic phosphate bands, were sensitive to laser excitation power.

00,757
PB94-172269 Not available NTIS
National Inst. of Standards and Technology (NML), Gaithersburg, MD. Gas and Particulate Science Div.
Complementary Molecular Information on Phthalocyanine Compounds Derived from Laser Microprobe Mass Spectrometry and Micro-Raman Spectroscopy.
Final rept.
R. A. Fletcher, E. S. Etz, and S. Hoeft. 1990, 4p.
Pub. in Proceedings on Annual Conference of the Microbeam Analysis Society (25th), Seattle, WA., August 12-18, 1990, p89-92.

Keywords: *Phthalocyanines, *Molecular structure, *Spectrum analysis, Raman spectroscopy, Mass spectroscopy, Vibrational spectra, Reprints, Laser microprobe mass spectrometry.

The purpose of this work is to show the complementary information about molecular structural characteristics of metal phthalocyanine compounds provided by laser microprobe mass spectrometry (LAMMS) and micro-Raman spectroscopy. The vibrational frequencies found in micro-Raman spectroscopy indicate molecular structure, and mass spectrometry indicates the mass (m/z value) of the molecule, as well as certain structural features. The characteristic fragment peaks that result during the ionization process contain additional information about the molecular species being analyzed.

00,758
PB94-172285 Not available NTIS
National Inst. of Standards and Technology (CSTL), Gaithersburg, MD. Surface and Microanalysis Science Div.
Hot Carrier Excitation of Adlayers: Time-Resolved Measurement of Adsorbate-Lattice Coupling.
Final rept.
T. A. Germer, J. C. Stephenson, E. J. Heilweil, and R. R. Cavanagh. 1993, 4p.
Pub. in Physical Review Letters 71, n20 p3327-3330, 15 Nov 93.

Keywords: *Carbon monoxide, Infrared absorption, Picosecond pulses, Laser pumping, Adsorbates, Excitation, Phonons, Copper, Reprints, Hot carriers.

Picosecond time-resolved infrared absorption measurements of CO/Cu(100) following visible and ultraviolet laser pumping allow a determination of the time scales for photoexcited carriers and lattice phonons to couple to the CO frustrated translation vibrational mode.

00,759
PB94-172343 Not available NTIS
National Inst. of Standards and Technology (MSEL), Gaithersburg, MD. Metallurgy Div.
Recent Experimental and Modeling Developments in High Temperature Thermochemistry.
Final rept.
J. W. Hastie, and D. W. Bonnell. 1989, 15p.
Pub. in Proceedings of Symposium on Thermochemistry and Chemical Processing, Kalpakkam, India, p179-193 1989.

Keywords: *High temperature tests, *Thermochemistry, Vapor phases, Mass spectroscopy, Thermodynamics, Experimental design, Mathematical models, Slags, Glass, Dolomite, Reprints.

The application of thermochemical principles to high temperature processes requires advanced measurement and modeling techniques. Recent work in this area, primarily from the authors' laboratory, is reviewed. Emphasis is on the vapor phase, present in equilibrium with complex liquid and solid process-media such as salts, slags, glasses, minerals, etc. Examples of the thermochemical characterization of several practical systems are given, including silicate glasses, a nuclear waste borosilicate glass, a coal-derived slag and the mineral dolomite. The experimental techniques described include, a modified Knudsen effusion mass spectrometric method and the relatively novel methods of transpiration mass spectrometry and laser vaporization mass spectrometry. The modeling approach considered involves the multicomponent equilibrium calculation of phase compositions and activities using an ideal mixing of complex components, or liquid associate model.

00,760
PB94-172517 Not available NTIS
National Inst. of Standards and Technology (MSEL), Gaithersburg, MD. Metallurgy Div.
Electrodeposition.
Final rept.
D. S. Lashmore. 1990, 3p.
Pub. in Electrochemistry and Solid State Science in the Electrochemical Society, p12-14 1990.

Keywords: *Electrodeposition, *Metal ions, Metals, Electrochemistry, Amorphous state, Electroforming, Metal matrix composites, Substrates, Alloys, Coatings, Catalysis, Reprints.

Electrodeposition involves reducing metal ions electrochemically from aqueous, inorganic and fused salt electrolytes to form coherent metals and alloys on various substrates. These coatings may be removed from the substrate to constitute free standing parts using a process called electroforming. The reduction of the ions to metal is usually a result of an external electrolytic process; however, autocatalytic processes exist, in which the reducing agent is incorporated into the electrolyte. One of these processes, the autocatalytic nickel phosphorus process, is now in wide commercial use.

00,761
PB94-172525 Not available NTIS
National Inst. of Standards and Technology (NEL), Boulder, CO. Electromagnetic Technology Div.
Use of Ion Scattering Spectroscopy to Monitor the Nb Target Nitridation during Reactive Sputtering.
Final rept.
D. J. Lichtenwalner, A. C. Anderson, and D. A. Rudman. 1991, 6p.
Pub. in Proceedings of Surface Chemistry and Beam-Solid Interactions Symposium, Boston, MA., November 26-29, 1990, p613-618 1991.

Keywords: *Niobium nitrides, Surface reactions, Surface chemistry, Thin films, Monitoring, Nitrogen, Targets, Reprints, Ion beam reactive sputtering, Ion scattering spectroscopy.

Ion scattering spectroscopy (ISS) has been used to directly monitor the nitrogen coverage of a niobium target during ion-beam reactive sputtering. The measurement shows that the fully reacted target is nearly completely covered with nitrogen, revealing a major difference in the target surface state when reactive sputtering versus the sputtering of a compound target. The functional dependence of the nitrogen coverage on the nitrogen pressure has also been obtained. Taking the fractional target coverage to be a steady-state equilibrium between nitrogen sputter removal and thermal N2 arrival, the measured target coverage has been accurately modeled. The results indicate that the nitridation reaction is controlled by the thermal N2 molecules, which stick to the target with a high probability. This firmly establishes the fact that the molecular N2 flux can control the target reaction. The target coverage model has also been applied to fit the measured deposition rate as a function of the nitrogen pressure, and shows that the deposition rate does not accurately reflect the target coverage.

00,762
PB94-172574 Not available NTIS
National Inst. of Standards and Technology (NML), Gaithersburg, MD. Surface Science Div.
Role of Adsorbed Alkalis in Desorption Induced by Electronic Transitions.
Final rept.
T. E. Madey, S. A. Joyce, and C. Benndorf. 1989, 10p.
Pub. in Physics and Chemistry of Alkali Metal Adsorption, p185-194 1989. Sponsored by Department of Energy, Washington, DC.

Keywords: *Surface chemistry, *Alkali metals, Adsorption, Desorption, Ions, Reprints, Electron stimulated desorption ion angular distribution.

DIET processes (desorption induced by electronic transitions) involving atoms and molecules on metal surfaces are strongly influenced by coadsorption with alkali metal atoms. Angular distributions and yields of positive ions, negative ions and electronically excited neutrals from adsorbed species are affected by alkali coadsorption, due to a combination of molecular reorientation and electronic effects.

00,763
PB94-172673 Not available NTIS
National Inst. of Standards and Technology (MSEL), Gaithersburg, MD. Reactor Radiation Div.
Inelastic Neutron Scattering Studies of Rotational Excitations and the Orientational Potential in C60 and A3C60 Compounds.
Final rept.
D. A. Neumann, J. R. D. Copley, D. Reznik, R. L. Paul, R. M. Lindstrom, W. A. Kamitakahara, and J. J. Rush. 1993, 14p.
Pub. in Jnl. of Physics and Chemistry of Solids 54, n12 p1699-1712 1993.

Keywords: *Fullerenes, Alkali metal compounds, Rotational states, Neutron scattering, Inelastic scattering, Excitation, Reprints, *Buckminsterfullerene, Orientational potentials, Interatomic potentials.

The authors describe neutron scattering studies of rotational excitations of the C(60) molecule in pure C(60) and in A3C(60) (A = alkali metal) compounds. Well-defined peaks due to librations are observed below the orientational ordering transition temperature in C(60) itself, and at all temperatures at which measurements were made (up to 675 K in K3C(60)) in the compounds. The energies of these excitations have been used to extract information about orientational potentials and reorientation mechanisms. For the systems studied so far, the authors find that the size of the ion occupying the tetrahedral site correlates with the librational energy, demonstrating that the repulsive part of the A-C interaction makes a significant contribution to the interatomic potential.

00,764
PB94-172699 Not available NTIS
National Inst. of Standards and Technology (CSTL), Gaithersburg, MD. Surface and Microanalysis Science Div.
Inelastic Interactions of Electrons with Surfaces: Application to Auger-Electron Spectroscopy and X-ray Photoelectron Spectroscopy.
Final rept.
C. J. Powell. 1994, 15p.
Pub. in Surface Science 299/300, p34-48 1994.

Keywords: *X ray photoelectron spectroscopy, *Auger electron spectroscopy, *Electron scattering, *Surface

analysis, Mean free path, Inelastic scattering, Reprints, Surface composition.

Electron-based probes of surface properties are used frequently in surface science since strong inelastic scattering for electron energies between about 50 and 2000 eV ensures high surface sensitivity. An overview is given of developments in the understanding of inelastic electron scattering in solids with emphasis on important surface properties. Auger-electron spectroscopy (AES) and X-ray photoelectron spectroscopy (XPS) are the two techniques most commonly used for measurements of surface composition. The authors give a brief description of the development of AES and XPS and then proceed to describe the role of inelastic electron scattering in AES and XPS. Attention is given to the measurement of electron attenuation lengths, to the calculation of electron inelastic mean free paths, and to intensity measurements for quantitative AES and XPS.

00,765
PB94-172798 Not available NTIS
National Inst. of Standards and Technology (NML), Gaithersburg, MD. Inorganic Analytical Research Div.
Absolute Determination of Electrolytic Conductivity for Primary Standard KC1 Solutions from 0 to 50C.
Final rept.
Y. C. Wu, and W. F. Koch. 1991, 11p.
Pub. in Jnl. of Solution Chemistry 20, n4 p391-401 1991.

Keywords: *Potassium chloride, *Conductivity, *Aqueous electrolytes, *Primary standards, Electrical resistivity, Temperature dependence, Reprints.

An absolute determination of aqueous electrolytic conductivity has been made for primary standards 0.01 demal (D) and 0.1 D potassium chloride solutions over the temperature range of 0 to 50 C in 5 degree intervals. A cell with a removable center section of accurately known length and area was used for measurements. Values were adjusted to be in conformity with the ITS-90 temperature scale. The overall uncertainty over the entire temperature range is estimated to be 0.03%. Values at 25 C for 0.01 D and 0.1 D are 0.00140841 S/cm and 0.0128506 S/cm, respectively.

00,766
PB94-172822 Not available NTIS
National Inst. of Standards and Technology (CSTL), Gaithersburg, MD. Surface and Microanalysis Science Div.
Environmental Scanning Electron Microscope Imaging Examples Related to Particle Analysis.
Final rept.
S. A. Wight, and C. J. Zeissler. 1993, 5p.
Pub. in Microscopy Research and Technique 25, p393-397 1993.

Keywords: *Scanning electron microscopy, *Particles, *Environmental monitoring, Air pollution sampling, Particulates, Image processing, Filters, Surface energy, Reprints.

The work provides examples of some of the imaging capabilities of environmental scanning electron microscopy applied to easily charged samples relevant to particle analysis. Environmental SEM (also referred to as high pressure or low vacuum SEM) can address uncoated samples that are known to be difficult to image. Most of these specimens are difficult to image by conventional SEM even when coated with a conductive layer. Another area where environmental SEM is particularly applicable is for specimens not compatible with high vaccum, such as volatile specimens. Samples from which images were obtained that otherwise may not have been possible by conventional methods included fly ash particles on an oiled plastic membrane impactor substrate, a one micrometer diameter fiber mounted on the end of a wire, uranium oxide particles embedded in oil-bearing cellulose nitrate, teflon and polycarbonate filter materials with collected air particulate matter, polystyrene latex spheres on cellulosic filter paper, polystyrene latex spheres 'loosely' sitting on a glass slide, and subsurface tracks in an etched nuclear track-etch detector. Surface charging problems experienced in high vacuum SEMs are virtually eliminated in the low vacuum SEM, extending imaging capabilities to samples previously difficult to use or imcompatible with conventional methods.

00,767
PB94-173036 Not available NTIS
National Inst. of Standards and Technology (CSTL), Gaithersburg, MD. Chemical Kinetics and Thermodynamics Div.
Thermal Decomposition of Hydroxy- and Methoxy-Substituted Anisoles.
Final rept.
M. M. Suryan, S. A. Kafafi, and S. E. Stein. 1989, 7p.
Pub. in Jnl. of American Chemical Society 111, n4 p1423-1429 1989.

Keywords: *Anisole, *Aryl ethers, *Reaction kinetics, *Pyrolysis, *Binding energy, Chemical bonds, Organic oxygen compounds, Isomers, Reprints, *Hydroxyanisoles, *Methoxyanisoles, Bond homolysis.

Rates of decomposition of anisole and the three isomeric hydroxyanisoles and methoxyanisoles were determined in a very low pressure pyrolysis apparatus. The predominant reaction was O-methyl bond homolysis. Therefore, relative rates provide a quantitative measure of the effects of hydroxy and methoxy substituents on bond strengths in anisoles. The o-hydroxy effect is unusually large (7j kcal/mol bond strength weakening). Rate ratios of ethyoxybenzene (phenetole) and o-hydroxyphenetole were similar to the anisole/o-hydroxyanisole pair, confirming the large o-hydroxy effect. The p-hydroxy group, however, only weakened the anisole O-methyl bond by 2.5 kcal/mol and meta substitution had little effect. Both o- and p-methoxy groups weakened the O-methyl bond by 4 kcal/mol and m-methoxy weakened this bond by 1 kcal/mol. Rates of these reactions, extrapolated to lower temperatures, were similar to rates of condensed phase thermolysis reactions, indicating that homolysis is a key step in the liquid phase reactions.

00,768
PB94-185014 Not available NTIS
National Inst. of Standards and Technology (PL), Boulder, CO. Quantum Physics Div.
Can Quantum Mechanical Description of Electron-Sodium Collisions Be Considered Complete. Present Status and Future Prospects for 3s <-> 3p Transitions.
Final rept.
N. Andersen, and K. Bartschat. 1993, 32p.
Pub. in Comments on Atomic and Molecular Physics 29, n3 p157-188 1993. Sponsored by National Science Foundation, Washington, DC.

Keywords: *Electron-atom collisions, *Sodium, Electron scattering, Electron transitions, Quantum mechanics, Polarization(Spin polarization), Reprints, Electron spin polarization.

In the spirit of Bederson's 'Perfect Scattering Experiment,' we generalize the existing description of collision induced atomic S <--> P transitions by spin-polarized electrons on spin-polarized target atoms. Analysis of existing experimental and theoretical data on the 3s <--> 3p transitions in Na determines to what extent the 'perfect scattering experiment' has been achieved to date. Using theoretical data, we demonstrate to what extent additional missing parameters can be extracted from present experiments. Finally, new experimental arrangements are suggested to remove remaining ambiguities.

00,769
PB94-185030 Not available NTIS
National Inst. of Standards and Technology (PL), Boulder, CO. Quantum Physics Div.
Low-Energy Electron Scattering from Caesium Atoms: Comparison of a Semirelativistic Breit-Pauli and a Full Relativistic Direc Treatment.
Final rept.
K. Bartschat. 1993, 15p.
Grant NSF-PHY-9014103
Pub. in Jnl. of Phys. B: At. Mol. Opt. Phys. 26, p3595-3609 1993. Sponsored by National Science Foundation, Washington, DC.

Keywords: *Electron-atom collisions, *Cesium, Electron scattering, Differential cross sections, Total cross sections, Relativistic effects, Hamiltonians, R matrix, Comparison, Reprints, Electron spin polarization.

The discrepancies between a previous Breit-Pauli R-matrix calculation by Scott et al and a recent calculation using the Dirac Hamiltonian by Thumm and Norcross are further analyzed and partially resolved. When comparable methods are applied to obtain the best possible target description in both approaches, a reduced Breit-Pauli formulation, with only the one-body spin-orbit operator included to account for relativistic effects explicitly, seems sufficient for an accurate description of most of the low-energy collision processes in this system. There remain, however, some interesting differences between the Breit-Pauli and the Dirac results for spin polarization and asymmetry functions, as well as for very sensitive resonance parameters. To shed more light on the possible origin of these differences, the effect of including additional close-coupling channels on the results is investigated.

00,770
PB94-185089 Not available NTIS
National Inst. of Standards and Technology (PL), Boulder, CO. Quantum Physics Div.
Electron-Impact Ionization of In(+) and Xe(+).
Final rept.
E. W. Bell, N. Djuric, and G. H. Dunn. Dec 93, 6p.
Contract DE-A105-86ER53237
Pub. in Physical Review A 48, n6 p4286-4291 Dec 93.
Sponsored by Department of Energy, Washington, DC.

Keywords: *Electron-ion collisions, *Indium ions, *Xenon ions, Ionization cross sections, EV range 100-1, 000, Colliding beams, Reprints.

Absolute ionization cross sections for In(1+) and Xe(1+) by electron impact have been measured from below threshold to 200 eV using the crossed-beams technique. The cross sections for In(1+) were possibly enhanced by indirect ionization processes. The excitation of the ion from the 4d(10)5s(2) ground state to the 4d(9)5s(2)5P state followed by autoionization has been postulated. Experimental measurements are compared to configuration-averaged distorted-wave calculations (M. S. Pindzola et al, J. Phys. B 16, L355 (1983)), the semiempirical formula of Lotz (Z. Phys. 216, 241 (1968)), and, in the case of Xe(1+), previous experimental results (C. Achenbach et al, J. Phys. B 17, 1405 (1984)). Also presented are ionization-rate coefficients and fitting parameters for both ions for temperatures in the range 10,000 K = or < T = or < 10 million K.

00,771
PB94-185097 Not available NTIS
National Inst. of Standards and Technology (PL), Boulder, CO. Time and Frequency Div.
Measurement of the J=2 less than 1 Fine-Structure Interval for (28)Si and (29)Si in the Ground (3)P State.
Final rept.
J. M. Brown, L. R. Zink, and K. M. Evenson. 1994, 8p.
Contract NASA-W15-047
Pub. in Astrophysical Jnl. 423, pL151-L154, 10 Mar 94.
Sponsored by National Aeronautics and Space Administration, Washington, DC.

Keywords: *Infrared spectra, *Silicon 28, *Silicon 29, Far infrared radiation, Interstellar matter, Ground state, Fine structure, Reprints, Laser magnetic resonance.

We report the first observation of the far-infrared laser magnetic resonance spectrum associated with the J = 2 <-- 1 fine-structure interval of (28)Si and (29)Si in the triplet P ground state. In (28)Si this separation is 4378.3280(2) GHz, and for (29)Si it is 4378.3306(6) GHz. The magnetic hyperfine parameter A2 has also been determined for (29)Si, apparently for the first time. Zero-field transition frequencies for the hyperfine components of the J = 2 <-- 1 transition in (29)Si are determined and will aid in their identification in interstellar sources.

00,772
PB94-185204 Not available NTIS
National Inst. of Standards and Technology (CSTL), Gaithersburg, MD. Thermophysics Div.
Thermodynamic Properties of Difluoromethane.
Final rept.
D. R. Defibaugh, G. Morrison, and L. A. Weber. Apr 94, 8p.
Contract DE-FG02-91CE23810
Pub. in Jnl. of Chemical and Engineering Data 39, n2 p333-340 Apr 94. Sponsored by Department of Energy, Washington, DC.

Keywords: *Fluorohydrocarbons, *Thermodynamic properties, Pressure, Volume, Refrigerants, Density(Mass/volume), Temperature, Equations of state, Liquid phases, Vapor phases, Saturation, Reprints, *Methane/difluoro, R32, Burnett apparatus.

The pressure-volume-temperature (PVT) behavior of difluoromethane (R32) has been measured using a vibrating tube densimeter apparatus and a Burnett/isochoric apparatus. Liquid PVT data from the vibrating

tube densimeter ranged in temperature from 242 to 348 K with a pressure range of 2,000-6,500 kPa. Data from the Burnett apparatus consisted of 11 isochores for the gas and supercritical fluid, along with vapor pressure measurements. The temperature ranged from 268 to 373 K. The gas-phase data are correlated with a virial equation of state. The compressed liquid data are fit with an abbreviated form of the modified Benedict-Webb-Rubin (mBWR) equation. A table of thermodynamic properties is presented for the saturated liquid and vapor states.

00,773
PB94-185303 Not available NTIS
National Inst. of Standards and Technology (PL), Boulder, CO. Quantum Physics Div.
Quantum Dynamics of Renner-Teller Vibronic Coupling: The Predissociation HCO.
Final rept.
E. M. Goldfield, S. K. Gray, and L. B. Harding. 1993, 16p.
Pub. in Jnl. of Chemical Physics 99, n8 p5812-5827, 15 Oct 93.

Keywords: Reprints, Wave packets, Quantum theory, Predissociation, Hamiltonians, *Formyl radicals, Renner-Teller coupling, Potential energy surfaces, Ab initio calculations.

A Hamiltonian model and parity-adapted wave packet representation are developed to describe a rotating triatomic system with two Renner-Teller coupled potential surfaces, and HCO predissociation is studied. New configuration interaction calculations on HCO are performed to determine its excited (A bar) ((sup 2)A(double prime)) potential surface, and Bowman, Bittman, and Harding ground potential surface is employed. The properties of many resonances, correlating with stretch/bend excitations on the A(double prime) surface, are determined.

00,774
PB94-185444 Not available NTIS
National Inst. of Standards and Technology (PL), Boulder, CO. Quantum Physics Div.
Selected Ion Flow Tube-Laser Induced Fluorescence Instrument for Vibrationally State-Specific Ion-Molecule Reactions.
Final rept.
S. Kato, M. J. Frost, V. M. Bierbaum, and S. R. Leone. 1993, 13p.
Contract FA9620-92-J-0072
Pub. in Review of Scientific Instruments 64, n10 p2808-2820 Oct 93. Sponsored by Air Force Office of Scientific Research, Washington, DC.

Keywords: *Ion molecule interactions, *Nitrogen ions, Laser induced fluorescence, Vibrational states, Rotational states, Molecular ions, Charge transfer, Oxygen, Argon, Reprints, Ion flow tubes.

A selected ion flow tube apparatus is coupled with laser induced fluorescence (LIF) detection for the selective monitoring of ion vibrational states and their reactions. Mass selected ions are injected into a flow tube with a venturi inlet using He carrier gas. A 200 Hz dye laser system provides sensitive LIF detection of the injected ions at densities as low as 100,000/cc for N2(1+). The rotational temperatures of the N2(1+) ions are estimated to be about 300 K using the LIF detection, while the vibrational temperatures can be high and may be varied by the injection potentials. Vibrationally state-selected ion-molecule reactions of N2(1+)(nu = 0, 1, and 2) are studied with N2, Ar, and O2 at thermal kinetic energies (E(lab) < 0.1 eV), where translation-to-vibration energy transfer is negligible. Isotopically specific charge-transfer reactions of (15)N2(1+)(nu) with (14)N2 are also studied. The ability to mass select ions and characterize their vibrational states and those of their reaction products allows novel studies of state-to-state ion chemistry.

00,775
PB94-185584 Not available NTIS
National Inst. of Standards and Technology (PL), Boulder, CO. Quantum Physics Div.
Charge Transfer and Collision-Induced Dissociation Reactions of CF(2+) and CF2(2+) with the Rare Gases at a Laboratory Collision Energy of 49 eV.
Final rept.
M. Manning, S. D. Price, and S. R. Leone. 1993, 10p.
Contract AFOSR-F49620-92-J-0071
Pub. in Jnl. of Chemical Physics 99, n11 p8695-8704, 1 Dec 93. Sponsored by Air Force Office of Scientific Research, Bolling AFB, DC.

Keywords: *Ion-atom collisions, *Carbon fluorides, *Rare gases, *Charge transfer, Molecular ions, EV range 10-100, Chemical radicals, Cross sections, Dissociation, Reprints, Dications.

Multiple product channels are observed for the reactions of CF(2+) and CF2(2+) with the rare gases at a laboratory collision energy of 49 + or - 1 eV. A dication beam is produced in an electron impact ion source and mass selected using a quadrupole mass spectrometer. The ion beam is focused into a collision region and a time-of-flight mass spectrometer is used to monitor the reaction products. Reactions of CF(2+) produce CF(1+), C(1+), and F(1+) ions and reactions of CF2(2+) result in CF(2+), CF(1+), C(1+), and F(1+) ion formation accompanied by the corresponding rare gas ions when charge transfer occurs. The relative yields of these products are measured directly. For reactions of both dications, there is a substantial increase in the total reaction cross section as the rare gas collision partner changes from He to Xe. The trends in charge transfer reactivity are successfully modeled using Landau-Zener theory.

00,776
PB94-185600 Not available NTIS
National Inst. of Standards and Technology (MSEL), Gaithersburg, MD. Polymers Div.
Octacalcium Phosphate Carboxylates IV. Kinetics of Formation and Solubility of Octacalcium Phosphate Succinate.
Final rept.
M. Markovic, B. O. Fowler, and W. E. Brown. 1994, 6p.
Pub. in Jnl. of Crystal Growth 135, p533-538 1994. Sponsored by American Dental Association Health Foundation, Chicago, IL.

Keywords: *Reaction kinetics, *Thermodynamics, *Solubility, pH, Chemical analysis, X-ray diffraction, Infrared spectroscopy, Phase transformations, Reprints, *Octacalcium phosphate succinate, Octacalcium phosphate carboxylates.

Kinetic and thermodynamic studies of octacalcium phosphate succinate (OCP-SUCC), Ca8(HPO4)(2-x)(succ)x(PO4)4'yH2O, where 0.8 < x < 1.0 and 5.5 < y < 6.5, broaden the present knowledge in the chemistry of octacalcium phosphate carboxylates. The kinetics of formation of OCP-SUCC by conversion of alpha-tricalcium phosphate (alpha-TCP), alpha-Ca3(PO4)2, in ammonium succinate solutions was followed at varied initial pH, 37 C. The changes in the liquid phase were monitored by pH measurements. Solid phases were characterized by means of chemical analyses, X-ray diffraction and infrared spectroscopy. The rate of conversion decreased with increasing initial pH. In the solubility experiments the concentrations of calcium, phosphate, succinate, ammonium and pH were determined in solutions equilibrated with OCP-SUCC (6.1 < pH < 7.4).

00,777
PB94-185691 Not available NTIS
National Inst. of Standards and Technology (PL), Boulder, CO. Quantum Physics Div.
High Resolution IR Studies of Polymolecular Clusters: Micromatrices and Unimolecular Ring Opening.
Final rept.
D. J. Nesbitt. 1994, 15p.
Contracts NSF-CHE90-00641, NSF-PHY90-12244
Pub. in Reaction Dynamics in Clusters and Condensed Phases, p137-151 1994. Sponsored by National Science Foundation, Arlington, VA.

Keywords: Van der Waals forces, Intermolecular forces, Infrared spectroscopy, High resolution, Matrix isolation, Hydrogen bonds, Argon complexes, Reprints, *Molecular clusters, Hydrogen fluoride complexes.

A long standing goal in the field of cluster research has been to elucidate the transition between the properties of isolated monomer species in the gas phase and the corresponding properties in the condensed phase. One of the most exacting probes of small clusters in this transition region has recently been offered by high resolution spectroscopies, particularly in the microwave and IR region of the spectrum. Such high resolution studies at rotational resolution can provide detailed information on the distribution of the masses in the cluster, as well as clearly distinguish between various low lying isomeric structures of the same molecular composition. High resolution spectroscopy in the IR also provides the opportunity to study dynamical phenomena such as predissociation, isomerization, and IVR channels that can be accessed by quantum state selected vibrational excitation of the clusters.

00,778
PB94-185725 Not available NTIS
National Inst. of Standards and Technology (PL), Boulder, CO. Quantum Physics Div.
Angular Distributions for Near-Threshold (e,2e) Processes for Li and Mg.
Final rept.
C. Pan, and A. F. Starace. Mar 93, 4p.
Contract NSF-PHY-9108002
Pub. in Physical Review A 47, n3 p2389-2392 Mar 93. Sponsored by National Science Foundation, Arlington, VA.

Keywords: *Electron-atom collisions, *Lithium, *Magnesium, Differential cross sections, Angular distribution, Electron impact, Ionization, Reprints.

Distorted-wave calculations of the triply differential cross sections for electron-impact ionization of Li and Mg are presented for the coplanar, theta (12) = pi geometry in which the final-state electrons share 2 eV of excess energy equally. Our theoretical approach, described in detail elsewhere (C. Pan and A. F. Starace, Phys Rev A 45, 4588 (1992)), employs a partial-wave expansion of initial- and final-state wave functions, treats direct and exchange interactions of initial- and final-state electrons with the target core, and treats the final-state interaction between the two continuum electrons by a screening potential. Li and Mg targets are found to have more complex (e, 2e) angular distributions than either H or He targets, stemming in large part from significant p-wave and higher one-electron phase shifts in the former elements.

00,779
PB94-185790 Not available NTIS
National Inst. of Standards and Technology (CSTL), Gaithersburg, MD. Surface and Microanalysis Science Div.
Compositional Analyses of Surfaces and Thin Films by Electron and Ion Spectroscopies.
Final rept.
C. J. Powell. 1993, 19p.
Pub. in Critical Reviews in Surface Chemistry 2, n1-2 p17-35 1993.

Keywords: *Surface analysis, *Electron spectroscopy, *Ion spectroscopy, Secondary ion mass spectroscopy, Auger electron spectroscopy, Ion scattering analysis, Rutherford scattering, X-ray photoelectron spectroscopy, Chemical composition, Thin films, Limitations, Reviews, Reprints, Sputtered neutral mass spectroscopy.

An overview is given of the current capabilities, advantages, and limitations of the six techniques in common use for compositional analyses of surfaces and thin films: Auger electron spectroscopy (AES), X-ray photoelectron spectroscopy (XPS), secondary ion mass spectrometry (SIMS), sputtered-neutral mass spectrometry (SNMS), ion-scattering spectroscopy (ISS), and Rutherford backscattering spectroscopy (RBS). Information is also given on efforts to improve these techniques and on the potential of other methods for determining surface compositions during processing.

00,780
PB94-185808 Not available NTIS
National Inst. of Standards and Technology (PL), Boulder, CO. Quantum Physics Div.
Collision-Induced Neutral Loss Reactions of Molecular Dications.
Final rept.
S. D. Price, M. Manning, and S. R. Leone. 1993, 6p.
Contract AFOSR-F49620-92-J-0249
Pub. in Chemical Physics Letters 214, n6 p553-558, 19 Nov 93. Sponsored by Air Force Office of Scientific Research, Bolling AFB, DC.

Keywords: *Ion-atom collisions, *Carbon fluorides, *Sulfur fluorides, *Rare gases, Molecular ions, EV range 10-100, Chemical radicals, Reprints, Neutral loss reactions, Dications.

Collision-induced neutral loss reactions are observed to be a major product channel for reactions of CF3(2+), SF4(2+), SF3(2+) and SF2(2+) with the rare gases at 49 eV laboratory collision energy. This reactivity, which involves the formation of doubly charged molecular daughter ions, differs markedly from that observed for other molecular dications. The doubly charged product

ion yield is largest for systems in which charge transfer does not compete effectively with the collision-induced process.

00,781
PB94-185816 Not available NTIS
National Inst. of Standards and Technology (CSTL), Gaithersburg, MD. Biotechnology Div.
Thermodynamic and NMR Study of the Interactions of Cyclodextrins with Cyclohexane Derivatives.
Final rept.
M. V. Rekharsky, F. P. Schwarz, Y. B. Tewari, Y. Yamashoji, R. N. Goldberg, and M. Tanaka. 1994, 6p.
Pub. in Jnl. of Physical Chemistry 98, n15 p4098-4103 1994.

Keywords: *Cyclodextrins, *Cyclohexanols, *Heat of reaction, *Equilibrium, Specific heat, Temperature dependence, Calorimetry, Thermodynamic properties, Nuclear magnetic resonance, Spectrum analysis, Entropy, Reprints.

Equilibrium constants and standard molar enthalpies of reaction have been determined for a series of cyclohexanols and other cyclohexane derivatives with alpha-cyclodextrin (a-cyclodextrin) and beta-cyclodextrin (b-cyclodextrin) by titration calorimetry. For reactions involving cyclohexanol, standard molar heat capacity changes as a function of temperature were also determined. The equilibrium constants for the reactions of the compounds were always larger with b-cyclodextrin than with a-cyclodextrin. The standard molar enthalpies of reaction were similar for both cyclodextrins; however, the standard molar entropies of reaction with b-cyclodextrin were substantially more positive than for the reactions with a-cyclodextrin. The hydrophilic nature of the groups on the cyclohexane ring as well as steric effects were found to influence the thermodynamics of these reactions. NMR spectral analysis indicated that while the proximity of these cyclohexane derivatives to the walls of the two cyclodextrins were comparable, the cyclohexane derivatives penetrate deeper into the larger b-cyclodextrin cavity than into the smaller a-cyclodextrin cavity.

00,782
PB94-185972 Not available NTIS
National Inst. of Standards and Technology (MSEL), Gaithersburg, MD. Reactor Radiation Div.
X-Ray Diffraction from Anodic TiO2 Films: In situ and Ex situ Comparison of the Ti(0001) Face.
Final rept.
D. G. Wiesler, M. F. Toney, O. R. Melroy, C. S. McMillan, and W. H. Smyrl. 1994, 9p.
Pub. in Surface Science 302, p341-349 1994.

Keywords: *Titanium dioxide, X-ray diffraction, Synchrotron radiation, Single crystals, Thin films, Crystal structure, Epitaxy, Anodizing, Anatase, Reprints.

X-ray diffraction with synchrotron radiation is used to study the structure and epitaxy of a thin (about 250 A) anodic film grown slowly on the basal plane of single-crystal Ti. Anatase crystallites, roughly 130 A in diameter, are observed, with no indication of other forms of TiO2 or films with lower oxidation state. The oxide is more orientationally disordered than films grown on the (11-20) and (10-10) faces of Ti, but it exhibits weak six- and twelve-fold texturing by the metal sublayer. In situ and ex situ measurements are qualitatively similar, suggesting that the oxide does not change appreciably upon emersion.

00,783
PB94-198280 PC A02
National Inst. of Standards and Technology (NML), Gaithersburg, MD. Chemical Kinetics Div.
Temperature Dependence of the Rate Constants for Reaction of Inorganic Radicals with Organic Reductants.
Final rept.
Z. B. Alfassi, R. E. Huie, P. Neta, and L. C. T. Shoute. 1990, 6p.
Pub. in Jnl. of Physical Chemistry 94, n25 p8800-8805 1990.

Keywords: *Chemical radicals, *Phenols, *Ascorbic acid, *Reaction kinetics, *Temperature dependence, Reprints, Activation energy, Chemical reactions, Molecular ions, Halogens.

Rate constants for the reactions of several inorganic radicals with several organic reductants in aqueous solutions have been measured by pulse radiolysis as a function of temperature, generally between 5 and 75 deg C. The reactions studies were those of the radicals N3, NO2, Br2(-), I2(-), (SCN)2(-) reacting with several phenols and ascorbate. Rate constants were also measured for the reactions of Cl2(-) with phenol and of ClO2 with p-methoxyphenolate. The rate constants measured were in the range of 100,000 to nearly 10 to the 10th power and the calculated Arrhenius activation energies ranged from 7 to 41 kJ/mol. The pre-exponential factors also varied considerably, with log A ranging from 9.2 to 13.9. The temperature dependence of these reactions do not seem to relate to their exothermicities. Variations in rate constants appear to be more strongly dependent on changes in preexponential factors rather than on changes in activation energy.

00,784
PB94-198314 Not available NTIS
National Inst. of Standards and Technology (PL), Boulder, CO. Quantum Physics Div.
Vibrational Distributions of As2 in the Cracking of As4 on Si(100) and Si(111).
Final rept.
A. L. Alstrin, R. V. Smilgys, P. G. Strupp, and S. R. Leone. 1992, 7p.
Contract AFOSR90-0166
Pub. in Jnl. of Chemical Physics 97, n9 p6864-6870, 1 Nov 92. Sponsored by Air Force Office of Scientific Research, Bolling AFB, DC.

Keywords: *Silicon, *Arsenic, *Desorption, Reprints, Laser induced fluorescence, Vibrational states, Surface temperature, Temperature dependence, Chemisorption, Dimers.

The desorption dynamics of arsenic from Si(100) and Si(111) are studied by measuring the vibrational population distributions of desorbed As2 using laser-induced fluorescence. In these measurements, a steady state flux of desorbing As2 is produced by continuously dosing a heated Si surface with a beam of As4 from a conventional molecular beam epitaxy oven. Measurements of the fluxes of As2 as a function of surface temperature suggest that the As2 may be kinetically formed in two distinct steps: The As4 first chemisorbs to form atoms on the surface which then recombine to desorb as dimers. However, there may also be direct dissociation of As4 at the hot surface. The vibrational populations of As2 desorbed from Si(100) are Boltzmann and indicate a vibrational temperature that is nearly 350 K lower than the surface temperature. The vibrational populations of As2 desorbed from Si(111) are not Boltzmann, but also have an effective vibrational temperature 400 K colder than the surface temperature. The observed lack of accommodation in the desorption from both surfaces is discussed in terms of the possible mechanisms.

00,785
PB94-198371 Not available NTIS
National Inst. of Standards and Technology (NML), Gaithersburg, MD. Chemical Kinetics Div.
Oxidation of 10-Methylacridan, a Synthetic Analogue of NADH and Deprotonation of Its Cation Radical. Convergent Application of Laser Flash Photolysis and Direct and Redox Catalyzed Electrochemistry to the Kinetics of Deprotonation of the Cation Radical.
Final rept.
A. Anne, P. Hapiot, J. Moiroux, P. Neta, and J. M. Saveant. 1991, 8p.
Pub. in Jnl. of Physical Chemistry 95, n6 p2370-2377 1991.

Keywords: *Nitrogen heterocyclic compounds, *Oxidation, *Decomposition reactions, *Reaction kinetics, *Chemical radicals, Radiolysis, Chemical reactions, Electrochemistry, Photolysis, Reprints, *10-Methylacridan, Cation radicals, Deprotonation.

Photolysis of 10-methylacridan (AH) in acetonitrile solutions containing CCl4 led to quantitative oxidation of AH to A(+). Laser flash photolysis of the solution with 248 or 308 nm light yielded the cation radical AH(sup dot,+) which decays by deprotonation to give the neutral radical A(sup dot). There is a good agreement between the values determined for k(sub H) here and, previously, by direct electrochemistry using ultramicroelectrodes. The vast majority of the data points in a plot of logk(sub H) vs the pKa of the bases, covering 18 pKa units and rate constants up to the diffusion limit, fall on the same Bronsted line in spite of the fact that they involve bases of quite different structure: pyridines, aliphatic nitrogen bases and carboxylates. Pulse radiolysis experiments in acidic aqueous solutions showed that AH is oxidized by Cl2(sup dot,-) to give AH(sub dot,+), which decays with a first order rate constant of 900/s. Reduction of A(+) gave A(sup dot) which did not undergo protonation even at 2 M HClO4, but reaction of A(+) with H atoms resulted in partial addition of H to the 9 position to give AH(sup dot,+).

00,786
PB94-198504 Not available NTIS
National Inst. of Standards and Technology (CSTL), Gaithersburg, MD. Surface and Microanalysis Science Div.
Energy Dependence of Collision Characteristics in Molecule-Surface Collisions.
Final rept.
V. Balasubramanian, A. Bahel, I. P. Dubey, N. Sathyamurthy, and J. W. Gadzuk. 1992, 4p.
Pub. in Jnl. of Physical Chemistry 96, n20 p7870-7873 1992.

Keywords: *Molecule collisions, Surface reactions, Diatomic molecules, Chemisorption, Fractals, Chaos, Reprints, Surface dynamics, Translations.

For a model diatomic molecule-surface collision, we show that the extent of chaoticity, as evidenced in action-angle and lifetime plots, decreases dramatically with an increase in the translational energy of the molecule. In addition to the existence of a threshold for the dissociative chemisorption, there is also an antithreshold at higher energies. The implications for the existence (or lack thereof) of chaos/fractals in molecule-surface collisions are also discussed, particularly as related to translational-vibrational energy redistribution.

00,787
PB94-198546 Not available NTIS
National Inst. of Standards and Technology (NML), Gaithersburg, MD. Molecular Physics Div.
Density Matrix Calculation of Population Transfer between Vibrational Levels of Na2 by Stimulated Raman Scattering with Temporally Shifted Laser Beams.
Final rept.
Y. B. Band, and P. S. Julienne. 1991, 8p.
Pub. in Jnl. of Chemical Physics 94, n8 p5291-5298 1991.

Keywords: *Sodium, Reprints, Vibrational states, Electron transitions, Density matrix, Raman spectra, Bloch equations, Laser radiation.

We compare the results of full density matrix calculations with recently reported experimental results describing the population transfer in Na2 using Raman scattering with the fundamental laser beam temporally shifted relative to the Stokes laser beam. Our calculations confirm the conclusion that almost total transfer of the population into the terminal level of the Raman transition can be achieved when the laser frequencies are tuned to resonance and the fundamental laser beam is temporally delayed relative to the Stokes shifted laser beam but still partially overlapping it. We analyze our results when the frequencies of the lasers are tuned off resonance as a function of the Rabi frequencies and the detuning, and compare with experimental and theoretical results. The alignment of the terminal level as a function of time displacement of the Stokes and pump beams is predicted.

00,788
PB94-198595 Not available NTIS
National Inst. of Standards and Technology (NML), Gaithersburg, MD. Quantum Metrology Div.
Strong Hydrogen Bond in the Formic Acid-Formate Anion System.
Final rept.
H. Basch, and W. J. Stevens. 1991, 7p.
Pub. in Jnl. of the American Chemical Society 113, n1 p95-101 1991. Sponsored by Bar-Ilan Univ., Ramat Gan (Israel).

Keywords: *Hydrogen bonds, *Formic acid, *Molecular orbitals, Mathematical models, Dimerization, Formates, Bonding strength, Quantum chemistry, Reprints, Formate anion.

Hydrogen bond energies and geometric structures of several symmetric and asymmetric formic acid-formate anion dimer complexes have been determined. Ab initio gradient optimization at the self-consistent field (SCF) level in a double zeta + polarization + diffuse Gaussian function basis set was followed by a series of second order Moller Plesset (MP2) single point cal-

culations for the lowest energy structures. The equilibrium asymmetric dimer with the (anti)formic-(syn)formate conformation has the highest binding energy both on the SCF and MP2 levels at 28.8 and 33.0 kcal/mole, respectively. Experimentally, a gas phase heat of dimerization value of 36.8 kcal/mole has been reported for the biformate anion. The calculated stability of this anti dimer includes a C-H-O interaction which is estimated to contribute approximately 2.4 (SCF) or approximately 1.8 (MP2) kcal/mole to the dimer binding energy. The corresponding proton-transferred (syn)formic-(anti)formate complex is calculated less stable by 5.6 (SCF) or 3.7 (MP2) kcal/mole, even though in the isolated monomer syn formic acid is the lower energy conformer by 5.8 (SCF) or 5.4 (MP2) kcal/mole in the same basis set. The greater stability of the anti dimer can be attributed both to less interfragment exchange repulsion and to more coulomb attraction compared with the syn dimer conformation.

00,789
PB94-198603 Not available NTIS
National Inst. of Standards and Technology (NML), Gaithersburg, MD. Chemical Thermodynamics Div.
Structure of Glycine-Water H-Bonded Complexes.
Final rept.
H. Basch, and W. J. Stevens. 1990, 6p.
Pub. in Chemical Physics Letters 169, n4 p275-280 1990.

Keywords: *Glycine, *Hydrogen bonds, *Water, *Molecular structure, Reprints, Molecular orbitals, Quantum chemistry, Amino acids, *Glycine-water complex, Moller-Plesset perturbation theory, Self consistent field optimization.

Ab initio calculations have been carried out on several cyclic hydrogen-bonded structures of glycine with water. Single configurations self-consistent-field energy-gradient optimization methods were used to obtain the structures using double-zeta plus polarization basis sets. Second-order Moller-Plesset perturbation theory was used to determine the effect of correlation on the hydrogen-bonded distances. The most stable structure is a double hydrogen-bonded structure with the water accepting a proton from the O-H of the carboxyl groups while donating a proton to the carbonyl group. This structure is bound by 8.6 kcal/mol and should be observable experimentally.

00,790
PB94-198611 Not available NTIS
National Inst. of Standards and Technology (PL), Boulder, CO. Quantum Physics Div.
Femtosecond Time-Resolved Wave Packet Motion in Molecular Multiphoton Ionization and Fragmentation.
Final rept.
T. Baumert, B. Buhler, M. Grosser, E. Wiedenmann, G. Gerber, R. Thalweiser, and V. Weiss. 1991, 8p.
Pub. in Jnl. of Physical Chemistry 95, n21 p8103-8110 1991.

Keywords: *Molecular dynamics, *Sodium, Reprints, Multi-photon processes, Molecular beams, Molecular ions, Time dependence, Laser radiation, Diatomic molecules, Photoelectron spectroscopy, Mass spectroscopy, Dye lasers, Photoionization, Fragmentation, Sodium ions, Wave packets, *Multiphoton ionization, Femtosecond pulses.

The dynamics of molecular multiphoton ionization and fragmentation of a diatomic molecule (Na2) have been studied in molecular beam experiments. Femtosecond laser pulses from an amplified colliding-pulse modelocked (CPM) ring dye laser are employed to induce and probe the molecular transitions. The final continuum states are analyzed by photoelectron spectroscopy, by ion mass spectrometry, and by measuring the kinetic energy of the formed ionic fragments. Pump-probe spectra employing 70-fs laser pulses have been measured to study the time dependence of molecular multiphoton ionization and fragmentation. The oscillatory structure of the transient spectra showing the dynamics on the femtosecond time scale can best be understood in terms of the motion packets in bound molecular potentials. The transient Na2(1+) ionization and the transient Na(1+) fragmentation spectra show that contributions from direct photoionization of singly excited electronic state and from excitation and autoionization of a bound doubly excited molecular state determine the time evolution of molecular multiphoton ionization.

00,791
PB94-198629 Not available NTIS
National Inst. of Standards and Technology (MSEL), Gaithersburg, MD. Reactor Radiation Div.
Neutron Powder Diffraction Study of a Na, Cs-Rho Zeolite.
Final rept.
W. H. Baur, A. Bieniok, R. D. Shannon, and E. Prince. 1989, 14p.
Pub. in Zeitschrift fur Kristallographie 187, p253-266 1989.

Keywords: *Zeolites, *Crystal structure, Reprints, Neutron diffraction, Deuterium compounds, Hydrates, Powder(Particles), Temperature range 0273-0400 K, Sodium cesium aluminum silicates, Rho zeolites, Rietveld method.

The crystal structure of a Na, Cs-Rho zeolite was studied at 373 K (Na(8.4)Cs(3.2)Si(36.4)Al(11.6)O96. 5D2O) by neutron powder diffraction and Rietveld profile analysis. It crystallizes in the noncentrosymmetric space group I(bar 4)3m and has a unit cell constant a = 14.6566(4) A. The final residuals are R(I) = 9.65% and R(wp) = 8.01%. The distortion of the (Al,Si)O2-framework of this zeolite fits into the pattern established for other noncentrosymmetric Rho zeolites. Particularly, the ellipticity of the eight-ring and the pore size are strictly a function of the cell constant of the zeolite. The mean distance (Al,Si)-O is observed to be 1.636 A, in excellent agreement with the mean (Al,Si)-O distance of 1.638 A calculated for the Si and Al content of our sample.

00,792
PB94-198637 Not available NTIS
National Inst. of Standards and Technology (NML), Boulder, CO. Time and Frequency Div.
Rotational Spectrum of Copper Hydride Using Tunable Far Infrared Radiation.
Final rept.
S. P. Beaton, and K. M. Evenson. 1990, 4p.
Pub. in Jnl. of Molecular Spectroscopy 142, n2 p336-339 1990.

Keywords: *Copper hydrides, *Rotational spectra, Far infrared radiation, Molecular spectra, Electron transitions, Interstellar matter, Copper 63, Reprints.

We have detected and measured five low-J rotational transitions of (63)CuH between 40 and 125/cm using coherent tunable far infrared radiation. A least squares fit to the data yields two orders of magnitude improvement in the values for the rotational molecular constants. The 1<-0 transition of astronomical interest is predicted to be 468 652.2 (2) MHz.

00,793
PB94-198678 Not available NTIS
National Inst. of Standards and Technology (NML), Gaithersburg, MD. Molecular Physics Div.
Tunneling-Rotation Spectrum of the Hydrogen Fluoride Dimer.
Final rept.
S. P. Belov, E. N. Karyakin, I. N. Kozin, M. Y. Tretyakov, N. F. Zobov, R. D. Suenram, W. J. Lafferty, A. F. Krupnov, and O. L. Polyansky. 1990, 19p.
Pub. in Jnl. of Molecular Spectroscopy 141, n2 p204-222 1990.

Keywords: *Hydrogen fluoride, *Microwave spectra, Far infrared radiation, Submillimeter waves, Millimeter waves, Rotational spectra, Electron transitions, Ground state, Dimers, Reprints.

The tunneling-rotation spectrum of the ground state of the hydrogen fluoride dimer, HF---HF, has been extended to the submillimeter wavelength region with the RAD-3 submillimeter spectrometer at Gorky in the frequency range 180-380 GHz at 210 K and pressure from 0.5 to 1.5 Torr. The spectrum has been reinvestigated at lower frequencies with a conventional Stark spectrometer at pressures between 0.1 to 0.2 Torr at NIST. Lines of the a-type K=3 subband have been observed for the first time. The tunneling frequency for the K=3 state is 114306.35(53) MHz. An atlas of all a- and b-type far infrared and microwave ground state tunneling-rotation transitions for K up to 3 giving frequency, uncertainty, and relative intensity has been prepared.

00,794
PB94-198892 Not available NTIS
National Inst. of Standards and Technology (PL), Gaithersburg, MD. Molecular Physics Div.
Infrared and Microwave Spectroscopy of the Argon - Propyne Dimer.
Final rept.
T. A. Blake, D. F. Eggers, S. H. Tseng, R. Beck, R. O. Watts, F. J. Lovas, M. Lewerenz, and R. P. Swift. 1993, 13p.
Grants NSF-CHE-8703766, NSF-CHE-9015765
Pub. in Jnl. of Chemical Physics 98, n8 p6031-6043, 15 Apr 93. Sponsored by National Science Foundation, Arlington, VA. and Petroleum Research Fund, Washington, DC.

Keywords: *Argon complexes, Reprints, Van der Waals forces, Infrared spectroscopy, Microwave spectroscopy, Molecular structure, Dipole moments, Hamiltonians, Dimers, *Propyne complexes.

Microwave and infrared measurements are reported for the van der Waals complex ArCH3CCH and its isotopomers. The structure is T shaped with equilibrium center-of-mass separation of 3.73 A and an angle of 82 deg. between the molecule symmetry axis and the van der Waals bond. The infrared and microwave spectra are complex due to the effects of a slightly hindered internal rotor. Analysis of the spectral data shows that the dipole moment is almost parallel to the dimer b axis. A modified vibration/rotation Hamiltonian that includes an internal rotor potential is used to show that the barrier to internal rotation is near 10.8/cm.

00,795
PB94-199189 Not available NTIS
National Inst. of Standards and Technology (CSTL), Boulder, CO. Thermophysics Div.
Measurement of Diffusion in Supercritical Fluid Systems: A Review.
Final rept.
T. J. Bruno. 1993, 7p.
Pub. in Proceedings of Aerospace Sciences Meeting and Exhibit (31st), Reno, NV., January 11-14, 1993, p1-7.

Keywords: *Supercritical state, *Diffusion coefficient, *Aviation fuels, *Chromatographic analysis, Reprints, Diffusion, Thermophysical properties, Chemical analysis, *Supercritical fluid solutions.

In the paper, the experimental procedures that are applicable to the measurement of diffusion in supercritical fluid solutions will be reviewed. This topic is of great importance to the proper design of advanced aircraft and the turbine fuels these aircraft will use. The main reason for this is that the fuels on these high performance aircraft may sometimes operate under supercritical fluid conditions when they are used as a heat sink, for the cooling of friction-heated surfaces. These conditions may produce unfavorable chemical reactions in the fuel. The decomposition products so produced will therefore be a major cause of heat exchanger fouling, and this must be addressed in the early stages of fuel and component design. Since transport properties are needed for these designs, the authors will consider measurements of one of the most critical: the binary interaction diffusion coefficient. After a brief introduction to the concept of diffusion, the authors will discuss in detail the use of chromatographic methods, and then briefly treat light scattering, nuclear magnetic resonance spectra, and physical methods.

00,796
PB94-199452 Not available NTIS
National Inst. of Standards and Technology (PL), Gaithersburg, MD. Molecular Physics Div.
Experimental Studies of Line Shapes from a Balle-Flygare Spectrometer.
Final rept.
E. J. Campbell, and F. J. Lovas. 1993, 6p.
Pub. in Review of Scientific Instruments 64, n8 p2173-2178 Aug 93.

Keywords: *Microwave spectrometers, *Line shape, Fourier transformation, Carbon oxysulfide, Molecular beams, Reprints, *Balle-Flygare spectrometers, Carbonyl sulfides.

The line shape problem for the Balle-Flygare-type microwave spectrometer is reexamined experimentally using the method of sine and cosine Fourier transforms with a phase correction.

00,797
PB94-199544 Not available NTIS
National Inst. of Standards and Technology (NML), Gaithersburg, MD. Chemical Kinetics Div.

New Rydberg States of Aluminum Monofluoride Observed by Resonance-Enhanced Multiphoton Ionization Spectroscopy.
Final rept.
D. V. Dearden, R. D. Johnson, and J. W. Hudgens. 1991, 6p.
Pub. in Jnl. of Physical Chemistry 95, n11 p4291-4296 1991.

Keywords: *Aluminum fluorides, *Rydberg states, *Electronic spectra, *Vibrational spectra, *Chemical reactions, Metastable state, Aluminum, Spectrum analysis, Ionization potentials, Reprints, *Aluminum monofluoride, Resonance enhanced multiphoton ionization spectroscopy.

AlF has been generated in the gas phase by high temperature reduction of AlF3 by Al, and detected and characterized using resonance-enhanced multiphoton ionization. Five Rydberg series comprised of thirteen new Rydberg states have been identified for the first time. Least-squares fitting of the Rydberg series to the Rydberg equation yields the adiabatic ionization potential of AlF, IP(sub a) = 9.729 + or - 0.001 Ev. Vibrational intervals for all of the new Rydberg states are about 20% greater than those of AlF (X(sup 1)Sigma(sup +)), with most lying between 930-980/cm. The vibrational frequencies are in agreement with an ionic bonding model for AlF.

00,798
PB94-199569 Not available NTIS
National Inst. of Standards and Technology (CSTL), Gaithersburg, MD. Thermophysics Div.
Thermodynamic Properties of CHF2-O-CHF2,Bis(difluoromethyl) Ether.
Final rept.
D. R. Defibaugh, K. A. Gillis, M. R. Moldover, G. Morrison, and J. W. Schmidt. 1992, 21p.
Contract N0002490MP33493
Pub. in Fluid Phase Equilibria 81, p285-305 1992. Sponsored by Department of the Navy, Washington, DC.

Keywords: *Fluorine organic compounds, *Ethers, *Refrigerants, *Thermodynamic properties, Reprints, Substitutes, Equations of state, Interfacial tension, Specific heat, Critical temperature, Boiling points, *bis(Difluoromethyl)ether, *E134, Speed of sound.

The authors have measured the thermodynamic properties of bis(difluoromethyl) ether, a candidate alternative refrigerant that is also known as E134. From the data the authors obtained the coefficients of a Carnahan-Starling-DeSantis equation of state and a polynomial representation of the ideal-gas heat capacity. This representation of the thermodynamic properties of E134 is consistent with the computer package REFPROP distributed by the National Institute of Standards and Technology to represent the properties of many candidate refrigerants. The representation is based on measurements of the refractive index of the saturated liquid and vapor, and the speed of sound of the dilute vapor. These measurements provide the boiling point, critical parameters, and the ideal-gas heat capacity of E134. Measurements on less pure samples were used to estimate the density of saturated liquid E134 and compressed liquid E134, and the interfacial tension. The pure samples appeared to be stable during the measurements; under similar conditions impure samples were not. Azeotropy in mixtures of E134 with CHF2CH2F (also known as R143) was discovered.

00,799
PB94-199577 Not available NTIS
National Inst. of Standards and Technology (PL), Gaithersburg, MD. Radiometric Physics Div.
Vibrational Autoionization in H2: Vibrational Branching Ratios and Photoelectron Angular Distributions Near the v(+)=3 Threshold.
Final rept.
J. L. Dehmer, P. M. Dehmer, J. B. West, A. C. Parr, M. A. Hayes, and M. R. F. Siggel. 1992, 7p.
Pub. in Jnl. of Chemical Physics 97, n11 p7911-7917, 1 Dec 92. Sponsored by Department of Energy, Washington, DC.

Keywords: *Hydrogen, *Photoionization, Reprints, Vibrational states, Branching ratio, Angular distribution, Autoionization, Photoelectrons, Asymmetry.

Vibrational branching ratios and photoelectron angular distributions are reported for photoionization of normal (the equilibrium ortho/para mixture) hydrogen in the region just above the nu(+) = 3 ionization limit. This region contains a number of vibrationally autoionizing Rydberg states, and the goal of the work was to observe experimentally the characteristic behavior associated with the decay of these states that was predicted by Raoult and Jungen (J. Chem. Phys. 74,3388 (1981)) on the basis of an MQDT (multichannel quantum defect theory) calculation on para-H2 (J double prime = 0). We have indeed observed that vibrational autoionization strongly favors the ionization channel representing the minimum change in the vibrational state of the ion core, as predicted. We also observed a sharp reduction in the photoelectron asymmetry of the nu(+) = 3 (and, to a lesser extent, the nu(+) = 2) ionization channel for resonant photoionization. Hence, qualitative agreement with theory is observed; however, a quantitative comparison now requires an extended calculation that includes the additional rotational levels that were populated under the present experimental conditions.

00,800
PB94-199619 Not available NTIS
National Inst. of Standards and Technology (MSEL), Gaithersburg, MD. Reactor Radiation Div.
Maximum Entropy as a Tool for the Determination of the C-Axis Profile of Layered Compounds.
Final rept.
P. Depondt, D. A. Neumann, and S. F. Trevino. 1993, 6p.
Pub. in Acta Crystallographica B49, p153-158 1993.

Keywords: *Organometallic compounds, Reprints, Molybdenum compounds, Maximum entropy method, Room temperature, Neutron scattering, Structure factors, Deuterium compounds, Intercalation, Graphite, *Layered compounds.

A simple procedure for the determination of the structure normal to the basal plane of layered compounds based on the now ubiquitous maximum-entropy method is presented. It is illustrated by the analysis of room-temperature (00l) elastic neutron-scattering experiments performed on two graphite intercalation compounds, stage 3 C(44.6)MoCl(5) and stage 1 KC24(ND3)4.3. The former example is quite simple, requiring only a crude heuristic model to determine the structure-factor phases. The latter shows good sensitivity to the orientation of the ND3 threefold axis with respect to the basal plane, thus providing its first direct determination.

00,801
PB94-199817 Not available NTIS
National Inst. of Standards and Technology (NML), Gaithersburg, MD. Chemical Thermodynamics Div.
Calibration Standards for Differential Scanning Calorimetry. 1. Zinc Absolute Calorimetric Measurement of Enthalpy of Fusion and Temperature of Fusion HM.
Final rept.
D. A. Ditmars. 1993, 13p.
Pub. in Jnl. of Chemical Thermodynamics 22, n7 p639-651 1990.

Keywords: *Zinc, *Heat of fusion, *Fusion(Melting), *Enthalpy, Reprints, Specific heat, Transition temperature, Calorimetry, Measurement, Standard reference materials, Method of mixtures.

The temperature and enthalpy of fusion of a pure zinc specimen chosen from NIST SRM 2221a have been measured for the first time simultaneously in a high-precision, method-of-mixtures, isothermal, phase-change calorimeter. The measured temperature of fusion (692.745 + or - 0.010) K was obtained with a new partial-fusion technique described herein. This result agrees well with the IPTS-68 temperature for the freezing point of pure zinc. The measured enthalpy of fusion (7026 + or - 40) J/mol differs substantially from previous values in the evaluated literature. Detailed examination of the original zinc literature data and of the several published attempts to derive from them the enthalpy of fusion has reinforced the author's conclusion that the present result for the enthalpy of fusion of zinc is of higher accuracy than any value currently given in evaluated data compilations.

00,802
PB94-199908 Not available NTIS
National Inst. of Standards and Technology (NML), Gaithersburg, MD. Molecular Physics Div.
Fragment Energy and Vector Correlations in the Overtone-Pumped Dissociation of HN3X(1)A'.
Final rept.
M. P. Casassa, B. R. Foy, J. C. Stephenson, and D. S. King. 1993, 12p.
Pub. in Jnl. of Chemical Physics 94, n1 p250-261 1991.

Keywords: *Hydrazoic acid, *Dissociation, *Photochemical reactions, Vibration, Energy levels, Molecular structure, Reprints, Vibrational predissociation.

NH stretching overtone and combination states in the HN3 singlet XA' state were excited by IR-visible double resonance pumping and by direct overtone pumping in the range 17670/cm to 20070/cm. NH fragments in the singlet a-delta and triplet X sigma(sup-1) states were detected by laser induced fluorescence with sub-Doppler resolution to determine branching ratios, correlated fragment rotational state and kinetic energy distributions, and fragment vector correlations. The spin-forbidden triplet channel was accessible to all states excited, while the threshold for the singlet channel was determined to lie in the range 18190 to 18755/cm. Vector correlations and lambda-doublet propensities show that nonplanar dissociation processes influence the NH rotations, but become less important for higher NH rotational states.

00,803
PB94-199957 Not available NTIS
National Inst. of Standards and Technology (CSTL), Gaithersburg, MD. Surface and Microanalysis Science Div.
Time-Resolved Probes of Surface Dynamics.
Final rept.
R. R. Cavanagh, E. J. Heilweil, and J. C. Stephenson. 1993, 7p.
Pub. in Surface Science 283, p226-232 1993.

Keywords: *Carbon monoxide, Reprints, Vibrational spectra, Density matrix, Transient response, Excited states, Line shape, Infrared radiation, Absorption, Surfaces, Platinum, Femtosecond pulses.

The excited vibrational state dynamics of CO absorbed on Pt(111) are explored using subpicosecond infrared pump-probe techniques. The response for a CO(nu = 1) adlayer for coverages of 0.1, 0.3, and 0.5 monolayers is measured as a function of time delay and probe wavelength. The observed transient CO vibrational spectra reveal a shift to lower frequency of the CO internal stretch mode as the degree of excitation of the adlayer is increased. These spectra are discussed in terms of density matrix models which address the coherence time of the adlayer (nu = 1) excitation and the excited state spectral characteristics of strongly-coupled anharmonic oscillators. The two-to-three picosecond recovery time of the transient response is consistent with relaxation through electron-hole pair creation. The relationship of the measured T(1) decay to the observed lineshape is addressed.

00,804
PB94-199973 Not available NTIS
National Inst. of Standards and Technology (CSTL), Gaithersburg, MD. Process Measurements Div.
Reactivity of Pd and Sn Adsorbates on Plasma and Thermally Oxidized SnO2(110).
Final rept.
R. Cavicchi, and S. Semancik. 1991, 9p.
Pub. in Surface Science 257, p70-78 1991.

Keywords: *Tin oxides, *Surface analysis, Reprints, Surface reactions, Metal films, Semiconductors, Chemisorption, Absorbates, Interfaces, Palladium.

The surface accumulation layer that forms as a result of oxygen vacancies near the surface of an oxide semiconductor can be used as an extremely sensitive probe of phenomena occurring at the surface. By incorporating a UHV-compatible, four-point conductance measurement in our surface analysis apparatus, we have investigated the formation of metal-semiconductor interfaces on SnO2(110) with varying oxygen stoichiometry. For only a 0.1 monolayer equivalent (ML) coverage of Sn deposited onto a high-oxygen-content surface prepared by oxygen plasma treatment, we observe a 500-fold increase in conductance. Our results suggest that at this coverage, Sn reacts with the excess chemisorbed oxygen and also creates point defects by abstracting oxygen from the lattice. In contrast, Pd reacts only with chemisorbed species, as indicated by a smaller conductance change and by differences in the size-effect shifted core levels observed at the

same coverage for thermal and plasma oxidized surfaces. Oxygen plasma treatment of an 8 ML Pd film is shown to be an effective room temperature oxidation procedure and is used as a basis of comparison for studies of the reaction of submonolayer coverages of Pd on plasma and thermally oxidized surfaces.

00,805
PB94-200037 Not available NTIS
National Inst. of Standards and Technology (CSTL), Gaithersburg, MD. Surface and Microanalysis Science Div.
Pure Element Sputtering Yield Data: Appendix 4.
Final rept.
G. P. Chambers, and J. Fine. 1992, 16p.
Pub. in Practical Surface Analysis, v2 p705-720 1992.

Keywords: *Surface analysis, *Sputtering, Ion bombardment, Argon ions, Xenon ions, EV range 100-1000, KeV range 01-10, KeV range 10-100, Yield, Reprints, Depth profiles.

An evaluated compilation of absolute sputtering yield data has been prepared for those parameters specific to surface analysis and depth profiling. This compilation was done for elemental targets bombarded with ion species of Ar and Xe at energies from O.5 to 20 keV. Data evaluation was based on the target surface cleanliness during measurement and on the total ion dose. Calculated yields were fitted to the evaluated data to obtain evaluated sputtering yields. We have shown this approach to be consistent and reliable.

00,806
PB94-200219 Not available NTIS
National Inst. of Standards and Technology (MSEL), Gaithersburg, MD. Reactor Radiation Div.
Neutron-Scattering Study of C60(n-) (n=3,6) Librations in Alkali-Metal Fullerides.
Final rept.
C. Christides, D. A. Neumann, K. Prassides, M. J. Rosseinsky, D. W. Murphy, R. C. Haddon, J. R. D. Copley, and J. J. Rush. 1992, 4p.
Pub. in Physical Review B 46, n18 p12 088-12 091, 1 Nov 92.

Keywords: *Superconductors, Rubidium compounds, Potassium compounds, Room temperature, Neutron scattering, Inelastic scattering, Doped materials, Librations, Fullerenes, Reprints, *Fullerides.

We have measured the low-energy inelastic neutron scattering spectra of superconducting K3C60 and insulating Rb6C60. Well-defined peaks are observed at room temperature at 3.59(4) meV (full width at half maximum (FWHM) = 1.11(15) meV) and 5.49(38) meV (FWHM = 3.41(44) meV), respectively. They harden with decreasing temperature and the dependence of their intensities on the scattering vector shows that they are due to small-amplitude librational motion. No anomalous behavior of the librational peak was observed on cooling through the superconducting transition temperature, indicating that electron-librational coupling is weak. The energy barrier for reorientation is estimated to be at least twice as large in K3C60 as in C60. Substantial disorder persists for K3C60 in the superconducting state.

00,807
PB94-200318 Not available NTIS
National Inst. of Standards and Technology (MSEL), Gaithersburg, MD. Ceramics Div.
Introduction of a NIST Instrument Sensitivity Standard Reference Material for X-Ray Powder Diffraction.
Final rept.
J. P. Cline, S. B. Schiller, and R. Jenkins. 1992, 12p.
Pub. in Advances in X-Ray Analysis, v35 p341-352 1992.

Keywords: *Sample preparation, *X-ray diffraction, *Diffractometers, *Powder(Particles), Interlaboratory comparisons, Aluminum oxide, Chemical analysis, Performance evaluation, Design criteria, Error analysis, Certification, Sensitivity, Reprints, *Standard reference materials, NIST(National Institute of Standards and Technology), SRM 1976.

Improvements in sample preparation methods have resulted in increased accuracy in x-ray powder diffraction intensity measurements. This improvement has focused scrutiny on the instrument as a potential source of error. NIST Standard Reference Material, SRM 1976 consists of a sintered alpha alumina, corundum, plate certified with respect to 12 relative intensity values from 25 to 145 degrees 2 theta. Its function is to allow for standardization of powder diffraction intensity as a function of 2 theta angle (instrument sensitivity). An increase in the accuracy of interlaboratory comparisons of diffraction intensity and related determinations will result. Utilization of the SRM requires the user to collect intensity data from the test instrument in a manner which conforms to that used in the certification. Graphical interpretation of the ratio of these data to those on the certificate will allow for appropriate judgment as to the condition of the test instrument.

00,808
PB94-200466 Not available NTIS
National Inst. of Standards and Technology (NML), Gaithersburg, MD. Molecular Spectroscopy Div.
2-Tunneling Path Internal-Axis-Method-Like Treatment of the Microwave Spectrum of Divinyl Ether.
Final rept.
L. H. Coudert. 1988, 22p.
Pub. in Jnl. of Molecular Spectroscopy 132, n1 p13-34 1988.

Keywords: *Ethers, *Spectrum analysis, *Microwave spectra, Molecular structure, Rotational spectra, Isomers, Stereochemistry, Reprints, *Divinyl ether.

The microwave spectrum of the cis-trans conformer of divinyl ether, previously measured by Hirose and coworkers, has been fit using a multidimensional Internal Axis Method-like (IAM-like) treatment which accounts for the 27 MHz tunneling splitting displayed by this molecule. This multidimensional IAM-like treatment begins by first determining the various feasible tunneling path(s) connecting the two frameworks of the molecules. For the tunneling process corresponding to an antigeared rotation of each vinyl unit about axes coinciding with the respective CO bonds, two limiting cases are considered: if the molecule goes through a planar configuration during the tunneling, only one tunneling path arises; if the intermediate configuration is not planar, two equivalent tunneling paths occur. The consequences for the J and K dependence of the splitting area are examined, and using this formalism the microwave data are fitted with an RMS deviation of 0.17 MHz. The parameters to the J and K dependence of the splitting are also determined and their values are interpreted in favor of a two tunneling path system. A comparison with the values obtained theoretically for those parameters is also carried out.

00,809
PB94-200508 Not available NTIS
National Inst. of Standards and Technology (NML), Gaithersburg, MD. Organic Analytical Research Div.
Two-Dimensional POMMIE Carbon-Proton Chemical Shift Correlated (13)C NMR Spectrum Editing.
Final rept.
B. Coxon. 1990, 6p.
Pub. in Canadian Jnl. of Chemistry 68, n7 p1145-1150 1990.

Keywords: *Triacetyloleandomycin, *Nuclear magnetic resonance, *Carbon 13, *Spectrum analysis, Reprints, Molecular structure, Computer programs, Protons, Chemical shift.

Two pulse sequences are described for acquisition of two-dimensional carbon-proton chemical shift correlated, (13)C NMR spectra by the 'phase oscillations to maximize editing technique'. One of these sequences provides two-dimensional, carbon-proton chemical shift correlated spectra in which the (1)H-(1)H coupling constants are present in the (1)H chemical shift dimension, whereas the other sequence includes a bilinear rotation decoupling unit that removes the vicinal (1)H-(1)H couplings in this dimension. Extensions of these techniques to generation of two-dimensional, carbon-proton chemical shift correlated CH, CH2, and CH3, (13)C NMR subspectra from linear combinations of three, two-dimensional data sets are described. Decreased residual signals in the edited 2D subspectra have been achieved by Pascal programs that include six floating point coefficients, and a method for their calibration is discussed. Results are reported for troleandomycin (1).

00,810
PB94-200581 Not available NTIS
National Inst. of Standards and Technology (NML), Gaithersburg, MD. Chemical Kinetics Div.
Rate Constants for Hydrogem Atom Attack on Some Chlorinated Benzenes at High Temperature.
Final rept.
J. P. Cui, Y. Z. He, and W. Tsang. 1989, 4p.
Pub. in Jnl. of Physical Chemistry 93, n2 p724-727 1989.

Keywords: *Reaction kinetics, *Chlorobenzenes, *High temperature, *Hydrogen, *Displacement reactions, Reprints, Temperature dependence, Pressure dependence, Dissociation, Shock tubes, *Hydrogen atoms.

Hydrogen atoms from the decomposition of hexamethylethane were reacted with chlorobenzene, o-dichlorobenzene, p-dichlorobenzene and 1,2,3 trichlorobenzene in the presence of toluene or 1,3,5 trimethylbenzene in single pulse shock tube experiments. Rate laws for the reactions were written using the rate expression for the displacement of the methyl group from the methylated aromatics as standards for temperatures of 1050-1150 K and pressures between 2.5 to 3.2 atm. In this temperature range the relative rate constants on a per chlorine basis for the reactions are 1:1.15:1.05:1.8:2.4.

00,811
PB94-200680 Not available NTIS
National Inst. of Standards and Technology (PL), Boulder, CO. Time and Frequency Div.
Extension of Heterodyne Frequency Measurements on OCS to 87 THz (2900 cm(-1)).
Final rept.
A. Dax, M. Murtz, J. S. Wells, W. Urban, M. Schneider, and E. Bachem. 1992, 6p.
Pub. in Jnl. of Molecular Spectroscopy 156, p98-103 1992.

Keywords: *Carbon oxysulfide, *Frequency measurement, Reprints, Transition radiation, Carbon monoxide lasers, Infrared radiation, Calibration, Frequencies, Tables(Data), *Carbonyl sulfide.

Heterodyne frequency measurements have been extended to 87 THz by using the CO overtone laser as a transfer oscillator. Measurements were made on the 11(sup 1)1-01(sup 1)0 band of OCS at 2900/cm. Frequency differences were measured between a tunable diode laser (TDL) which was locked to OCS absorption lines and a stabilized overtone laser which was referenced to stabilized CO2 lasers. These measurements have been combined with earlier Fourier transform (FT) measurements and a comprehensive set of data from frequency and FT measurements on lower lying transitions in OCS. This permits obtaining accurate values of transition frequencies for calibration of spectra in the 3.4-micrometer region.

00,812
PB94-211125 Not available NTIS
National Inst. of Standards and Technology (NML), Gaithersburg, MD. Molecular Physics Div.
Multichannel Quantum Defect Half Collision Analysis of K2 Photodissociation Through the B1Pi(sub u) State.
Final rept.
R. L. Dubs, and P. S. Julienne. 1991, 11p.
Pub. in Jnl. of Chemical Physics 95, n6 p4177-4187 1991.

Keywords: *Photodissociation, *Potassium, Polarization(Waves), Fluorescence, Alignment, Reprints, Multichannel quantum defect theory, Half collision analysis.

Recent experiments by Zafiropulos et al (Phys. Rev. Lett. 61, 1485 (1988)) indicate that K2 photodissociation through the B singlet Pi(u) state results in fluorescence polarization which is strongly dependent on excitation wavelength. To understand these results, we have studied the K2 system quantum mechanically using a half collision analysis derived from the generalized form of multichannel quantum defect theory. An approximation called the Adiabatic (a->c) / Recoil(c->e) approximation is developed for the half collision matrix which reproduces quantitatively the exact half collision results projected for the close-coupled wavefunction. The quantum mechanical expression for the polarization as a function of J(0) and total energy E is found to be extremely simple in this approximation, depending only on J(0) and the single-channel P, Q and R phase shifts for the adiabatic reference states corresponding to the B singlet Pi(u) state at short distance.

00,813
PB94-211133 Not available NTIS
National Inst. of Standards and Technology (NML), Gaithersburg, MD. Molecular Physics Div.

Intersystem Crossing in Collisions of Aligned Ca(4s5p (1)P) + He: A Half Collision Analysis Using Multichannel Quantum Defect Theory.
Final rept.
R. L. Dubs, P. S. Julienne, and F. H. Mies. 1990, 9p.
Pub. in Jnl. of Chemical Physics 93, n12 p8784-8792 1990.

Keywords: *Atom-atom collisions, *Atomic collisions, Factorization, Scattering, Alignment, Calcium, Helium, Reprints, Intersystem crossings, Multichannel quantum defect theory, Half collision analysis.

A half collision analysis of alignment effects on intersystem crossing in the collisions of Ca (4s5p singlet P) with He has been performed using generalized Multichannel Quantum Defect Theory (MCQDT). The theory provides a rigorous analytical representation of the numerically exact close-coupled scattering wavefunctions. The half collision analysis results in a factorization of the full quantum collision problem into a number of simpler quantum mechanical problems which reflect different regions of development during the collision. A WKB-assisted, frame transformation approximation to the incoming half collision matrix is tested numerically and is found to be useful in projecting out information on the 'locking results' concept.

00,814
PB94-211331 Not available NTIS
National Inst. of Standards and Technology (MSEL), Gaithersburg, MD. Polymers Div.
Total Surface Areas of Group IVA Organometallic Compounds: Predictors of Toxicity to Algae and Bacteria.
Final rept.
G. Eng, E. J. Tierney, G. J. Olson, F. E. Brinckman, and J. M. Bellama. 1991, 5p.
Pub. in Appl. Organomet. Chem. 5, n1 p33-37 1991.

Keywords: *Toxicity, *Organometallic compounds, *Surface area, *Algae, *Bacteria, Structure-activity relationships, Group 4A compounds, Metals, Solubility, Organotin compounds, Organosilicon compounds, Reprints, Organogermanium compounds, Organolead compounds.

There exists a high correlation between molecular surface area (TSA) of triorganotin and triorganolead compounds and their toxicity towards an algae (E. coli) and a bacterium (S. capricornutum). Parallel attempts to correlate other Group IVA organometals incorporating silicon or germanium were unsuccessful. It was further demonstrated, however, that a high correlation was obtainable between certain series of compounds with the same organic substituent but different metal centers involving all Group IVA elements. In both instances, the inability to obtain a quantitative structure-activity relationship (QSAR) for all systems studied appears to be a function of the solubility of the compounds. While organotin TSA values have been found to correlate well with their toxicities toward various organisms, this study clearly suggests that this type of QSAR can be readily extended to include other organometal systems, provided that there is no solubility problem and the toxicity is a function of the hydrophobicity of the organometal compounds.

00,815
PB94-211398 Not available NTIS
National Inst. of Standards and Technology (NML), Gaithersburg, MD. Chemical Kinetics Div.
Reaction Rate Determinations of Vinyl Radical Reactions with Vinyl, Methyl, and Hydrogen Atoms.
Final rept.
A. Fahr, A. Laufer, R. Klein, and W. Braun. 1991, 7p.
Pub. in Jnl. of Physical Chemistry 95, n8 p3218-3224 1991.

Keywords: *Reaction kinetics, *Free radicals, Photolysis, Atoms, Hydrogen, Reprints, *Vinyl radicals, Kinetic spectroscopy.

Laser photolysis-kinetic spectroscopy, end-product analysis, and detailed modeling were used to investigate three reaction systems in detail. Included were vinyl-vinyl, vinyl-methyl, and vinyl-methyl-hydrogen atoms. Product ratios, as a function of the rate constants, could be approximated using simple expressions. This greatly simplified the precise numerical modeling of these complex systems and also permitted a realistic error analysis. Reactions and rate constants at 25 C are summarized.

00,816
PB94-211448 Not available NTIS
National Inst. of Standards and Technology (PL), Boulder, CO. Quantum Physics Div.
High-Resolution Infrared Overtone Spectroscopy of ArHF via Nd:YAG/Dye Laser Difference Frequency Generation.
Final rept.
J. T. Farrell, O. Sneh, A. McIlroy, A. E. W. Knight, and D. J. Nesbitt. 1992, 12p.
Contracts NSF-PHY90-12244, NSF-CHE90-00641
Sponsored by National Science Foundation, Washington, DC.
Pub. in Jnl. of Chemical Physics 97, n11 p7967-7978, 1 Dec 92.

Keywords: *Argon complexes, *Infrared spectroscopy, Van der Waale forces, Near infrared radiation, Infrared absorption, High resolution, Difference frequency, Neodymium lasers, Reprints, *Hydrogen fluoride complexes, Potential energy surfaces, Overtone spectroscopy, Supersonic expansion.

The first high-resolution spectra of ArHF excited to the nu(HF)=2 <- 0 manifold near 7,800/cm are recorded via direct infrared absorption in a slit supersonic expansion. The tunable difference frequency light is generated via nonlinear subtraction of a cw Nd:YAG laser from a tunable cw ring dye laser in temperature phase matched LiNbO3, and permits continuous single-mode access to the 1-2 micrometer near-IR region. In conjunction with previous results from the nu(HF)=1 and nu(HF)=0 vibrational levels, these studies provide the necessary data for fitting an atom + diatom potential energy surface as a function of all intermolecular and intramolecular internal degrees of freedom.

00,817
PB94-211463 Not available NTIS
National Inst. of Standards and Technology (NML), Gaithersburg, MD. Molecular Physics Div.
P-Type Doubling in the Infrared Spectrum of NO-HF.
Final rept.
W. M. Fawzy, G. T. Fraser, J. T. Hougen, and A. S. Pine. 1990, 13p.
Pub. in Jnl. of Chemical Physics 93, n5 p2992-3004 1990.

Keywords: *Hydrogen bonds, *Nitrogen oxides, *Hydrogen fluoride, *Infrared spectra, Spectrum analysis, Rotational states, Vibrational spectra, Reprints, *Van der Waals complex.

The HF stretching band of the NO-HF open-shell complex has been recorded using a molecular-beam optothermal spectrometer. The spectrum exhibits P-type doubling indicative of an unpaired electron spin coupled to the rotational angular momentum of a bent complex with substantially quenched electron orbital angular momentum. From B' = 0.111316(28)/cm, the zero-point center-of-mass separation is estimated to be 3.439(3) A. The HF frequency shift of 84/cm indicates that the complex is hydrogen bonded, and the spectral intensities imply that the HF axis is aligned closely to the center-of-mass axis and the NO is off axis by 30 + or - 15 deg. The Renner-Teller-like orbital quenching parameter is somewhat larger than the spin-orbit constant in the free NO molecule and increases substantially upon vibrational excitation. The transitions in this band exhibit vibrational predissociation broadening of 200 + or - 40 MHz (FWHM), similar to that observed for a number of closed-shell hydrogen-bonded HF complexes.

00,818
PB94-211661 Not available NTIS
National Inst. of Standards and Technology (NML), Gaithersburg, MD. Chemical Kinetics Div.
Radiation Chemistry of Cyanine Dyes: Oxidation and Reduction of Merocyanine 540.
Final rept.
A. Harriman, and P. Neta. 1991, 6p.
Pub. in Jnl. of Physical Chemistry 95, n6 p2415-2420 1991.

Keywords: *Reaction kinetics, *Oxidation reduction reactions, *Antiviral agents, *Radiolysis, *Cyanine dyes, Decomposition reactions, Free radicals, Leukemias, Reprints, *Merocyanine 540.

Merocyanine 540 (MC) shows promise as a treatment for certain types of leukemia. It is shown that MC readily undergoes one-electron reduction under pulse radiolytic conditions. The pi-radical anion, produced by reduction with hydrated electrons and 2-hydroxypropyl radicals, disproportionates rapidly under anaerobic conditions but reduces O2 to superoxide ions in aerated solution. The dye reacts with trichloromethylperoxyl radicals to form several products, one of which is believed to be an adduct formed by addition of CCl3OO(dot) to the bridgehead carbon-atom of the benzoxazole subunit. This species decays via first-order kinetics under pulse radiolytic conditions to form cleavage products. A second primary product is believed to arise from addition of CCl3O2(dot) to the polymethine chain to form an alpha-amino carbon-centered radical capable of reducing O2 to superoxide ions. Preliminary studies indicate that the breakdown products are cytotoxic and could be important intermediates for the known antiviral activity of MC.

00,819
PB94-211703 Not available NTIS
National Inst. of Standards and Technology (NML), Gaithersburg, MD. Thermophysics Div.
Supercritical Solubility of Solids from Near-Critical Dilute-Mixture Theory.
Final rept.
A. H. Harvey. 1990, 4p.
Pub. in Jnl. of Physical Chemistry 94, n22 p8403-8406 1990.

Keywords: *Critical point, *Solubility, *Supercritical fluids, *Phase diagrams, *Solids, Henrys law, Phase transformations, Thermodynamics, Reprints, *Near-critical Dilute Mixture Theory.

A recently derived asymptotic theory for Henry's Law constants near the critical point of a solvent is adapted to the description of the solubility of solids in supercritical fluids. When solubility data for several systems are examined in the manner suggested by the theory, all the experimental isotherms for a given system (with the exception of a few near-critical points where we attribute the deviations to finite-concentration effects) collapse onto a single curve which is linear over a substantial range of solvent densities. This work provides a theoretical justification for some often-noted empirical relationships between solubilities and enhancement factors and the density of the supercritical solvent.

00,820
PB94-211810 Not available NTIS
National Inst. of Standards and Technology (NML), Gaithersburg, MD. Molecular Spectroscopy Div.
Vibrational Relaxation Measurements of Carbon Monoxide on Metal Clusters.
Final rept.
E. J. Heilweil, R. R. Cavanagh, and J. C. Stephenson. 1988, 3p.
Pub. in Ultrafast Phenomena VI, Springer Series in Chemical Physics, v48 p447-449 1988.

Keywords: *Carbon monoxide, *Solid clusters, *Adsorbates, Picosecond pulses, Light pulses, Infrared radiation, Tunable lasers, Transition metals, Metal carbonyls, Energy transfer, Measurement, Reprints, Vibrational relaxation.

Measurements using tunable picosecond infrared pulses of CO(v=1) vibrational population relaxation for carbon monoxide bound to transition metal cluster compounds and supported metal particles give the first time-resolved evidence for vibrational-to-electronic energy damping of adsorbates on metals.

00,821
PB94-211828 Not available NTIS
National Inst. of Standards and Technology (MSEL), Gaithersburg, MD. Reactor Radiation Div.
Discontinuous Volume Change at the Orientational-Ordering Transition in Solid C60.
Final rept.
P. A. Heiney, G. B. M. Vaughan, J. E. Fischer, J. R. D. Copley, D. A. Neumann, W. A. Kamitakahara, K. M. Creegan, D. M. Cox, J. P. McCauley, A. B. Smith, N. Coustel, and D. E. Cox. 1992, 4p.
Pub. in Physical Review B 45, n8 p4544-4547, 15 Feb 92.

Keywords: *Buckminsterfullerene, *Fullerenes, Crystal-phase transformations, X-ray diffraction, Neutron diffraction, Lattice parameters, Volume, Reprints.

X-ray and neutron-diffraction measurements have been used to study the evaluation of the lattice parameter of solid C(60) through the orientational-ordering transition. The lattice parameter jumps by +0.044 + or - 0.004 A on heating, indicating a strongly first-order transition. The average isobaric volume thermal-expansion coefficient both above and below the transition is 6.2 + or - 0.2 X 10(sup -5)/K. We observe phase

coexistence over a 5-K range, but little if any hysteresis.

00,822
PB94-211901 Not available NTIS
National Inst. of Standards and Technology (NML), Gaithersburg, MD. Chemical Kinetics Div.
International Conference on Chemical Kinetics (2nd). Held in Gaithersburg, Maryland on July 24-27, 1989.
Final rept.
J. T. Herron, S. E. Stein, W. Tsang, and D. M. Golden. 1990, 2p.
Pub. in Jnl. of Physical Chemistry 94, n8 p3229-3230 1990.

Keywords: *Reaction kinetics, *Meetings, Physical chemistry, Reprints.

This is a brief report on 'The Second International Conference on Chemical Kinetics', held July 24-27, 1989, at NIST, Gaithersburg, MD.

00,823
PB94-212032 Not available NTIS
National Inst. of Standards and Technology (NML), Gaithersburg, MD. Molecular Physics Div.
Use of Extended Permutation-Inversion Groups in Constructing Hyperfine Hamiltonians for Symmetrical-Top Internal Rotor Molecules Like H3C-SiH3.
Final rept.
J. T. Hougen, W. L. Meerts, and I. Ozier. 1991, 41p.
Pub. in Jnl. of Molecular Spectroscopy 146, n1 p8-48 1991.

Keywords: *Molecular beams, Selection rules, Hamiltonians, Silicon compounds, Reprints, Permutation groups.

The m-fold extended group G(sub 18, sup m), corresponding to the permutation-inversion group G(sub 18) for molecules like H3C-SiH3, has been obtained. In this group, m is the smallest integer for which m(rho) is also an 'integer,' where rho is the usual ratio of the moment of inertia of the top about A axis to the moment of inertia of the molecule about the A axis. The extended group has 18m elements, divided into (9m+3)/2 or (9m+6)/2 classes, for odd and even values of m, respectively. It is possible to rationalize the pattern of observed and unobserved avoided-crossing signals in recent molecular beam studies of symmetric top internal rotor molecules. With the understanding, it also proved possible to detect for the first time one of the 'missing' avoided-crossing signals in CH3SiH3.

00,824
PB94-212115 Not available NTIS
National Inst. of Standards and Technology (NML), Gaithersburg, MD. Chemical Kinetics Div.
Kinetics of the Reaction of CCl3-Br-2 and the Thermochemistry of CCl3 Radical and Cation.
Final rept.
J. W. Hudgens, R. D. Johnson, R. S. Timonen, J. A. Seetula, and D. Gutman. 1991, 6p.
Pub. in Jnl. of Physical Chemistry 95, n11 p4400-4405 1991.

Keywords: *Reaction kinetics, *Free radicals, *Temperature dependence, *Thermodynamic properties, Entropy, Specific heat, Heat of formation, Chemical equilibrium, Thermochemistry, Reprints, *Trichloromethyl radicals.

The rate constant of the CCl3 + Br2 -> CCl3Br + Br reaction was determined as a function of temperature between 300 and 532 K and fit to an Arrhenius expression. The reaction was studied in a tubular flow reactor using laser photolysis to produce the CCl3 reactant and photoionization mass spectrometry to monitor CCl3 in time resolved experiments. Previously published kinetic data were evaluated to calculate k(sub-1), the rate constant for the reverse reaction, and recent spectroscopic data were used to calculate accurate entropies and heat capacities. The rate constants were used in a Third Law thermodynamic calculation to obtain values for the standard enthalpies of formation of CCl3 and CCl3(1+), 17.7 and 205.9 kcal/mol, respectively.

00,825
PB94-212123 Not available NTIS
National Inst. of Standards and Technology (CSTL), Gaithersburg, MD. Chemical Kinetics and Thermodynamics Div.
Resonance Enhanced Multiphoton Ionization Detection of GeF and GeCl Radicals.
Final rept.
J. W. Hudgens, R. D. Johnson, and B. Tsai. 1989, 4p.
Pub. in Inst. Phys. Conf. Ser. Reson. Ioniz. Spectrosc. 94, p125-128 1989.

Keywords: *Electron transitions, *Rydberg states, *Germanium, *Electronic spectra, Energy levels, Excited states, Chemical radicals, Laser spectroscopy, Spectrum analysis, Reprints, *Germanium fluoride radicals, *Germanium chloride radicals, Multiphoton ionization.

Resonance enhanced multiphoton ionization (REMPI) spectra of GeF and GeCl radicals were observed between 400-500 nm. Numerous vibrational bands of several electronic states were observed through 2+1, 1+2, and 1+1+1 REMPI excitation mechanisms. The use of REMPI spectroscopy enabled observation of several 'one photon forbidden' transitions.

00,826
PB94-212131 Not available NTIS
National Inst. of Standards and Technology (NML), Gaithersburg, MD. Chemical Kinetics Div.
Experimental and Abinitio Studies of Electronic Structures of the CCl3 Radical and Cation.
Final rept.
J. W. Hudgens, R. D. Johnson, B. P. Tsai, and S. A. Kafafi. 1990, 10p.
Pub. in Jnl. of the American Chemical Society 112, n15 p5763-5772 1990.

Keywords: *Electron transitions, *Rydberg states, *Electronic spectra, *Free radicals, Energy levels, Spectrum analysis, Molecular orbitals, Optical spectra, Molecular structure, Reprints, *Trichloromethyl radicals, Multiphoton ionization.

The structures and optical spectroscopy of the CCl3 radical and cation were studied by ab initio molecular orbital calculations and by experiment. The structures of the X singlet A'(sub 1) state of the CCl3 cation and the X doublet A(sub 1) and X doublet A(sub 2)(sup double prime) structures of the CCl3 radical were optimized by ab initio calculations using the 6-31G(star) basis set. The ground state of the CCl3 radical is of X doublet A(sub 1) symmetry with r(sub e) (C-Cl)= 1.7142 A and Cl-C-Cl bond angle = 117.10 deg. Vibrational frequencies for each CCl3 species were computed. In experiments the electronic spectrum of (35)C Cl3 radicals was observed between 336-440 nm using mass resolved resonance enhanced multiphoton ionization (REMPI) spectroscopy. The spectrum arose from two-photon resonances with planar Rydberg states.

00,827
PB94-212164 Not available NTIS
National Inst. of Standards and Technology (CSTL), Gaithersburg, MD. Chemical Kinetics and Thermodynamics Div.
Kinetics of the Self-Reaction of Hydroxymethylperoxyl Radicals.
Final rept.
R. E. Huie, and C. L. Clifton. 1993, 5p.
Pub. in Chemical Physics Letters 205, n2,3 p163-167, 9 Apr 93.

Keywords: *Reaction kinetics, *Peroxy radicals, Temperature dependence, Chemical reactions, Methanol, Reprints, *Hydroxymethyl peroxy radicals, *Methanol peroxy radical, Sulfate radicals.

The rate constant for the self-reaction of the peroxyl radical derived from methanol, HOCH2OO(dot), has been measured over the temperature range 5-53 C. The radical has a maximum absorptivity of 970 l/mol/cm at 240 nm and an absorptivity of about 510 l/mol/cm at 280 nm. From a modified Arrhenius fit to the data, the rate constant at 25 C was calculated to be K298K = ((7.4 + or - 0.1) X 10 to the 8th power) l/mol/s and the temperature dependence of the reaction to be E/R = 1395 + or - 66 K. As part of this study, the rate constant for the recombination of the sulfate radical, SO4(1-), was found to be ((4.4 + or - 0.4) X 10 to the 8th power) l/mol/s, independent of temperature over the range 12 to 53 C.

00,828
PB94-212172 Not available NTIS
National Inst. of Standards and Technology (NML), Gaithersburg, MD. Chemical Kinetics Div.
Temperature Dependence of the Rate Constants for Reactions of the Sulfate Radical, SO4-, with Anions.
Final rept.
R. E. Huie, and C. L. Clifton. 1990, 7p.
Pub. in Jnl. of Physical Chemistry 94, n23 p8561-8567 1990.

Keywords: *Reaction kinetics, *Sulfates, *Chemical radicals, *Anions, Activation energy, Temperature dependence, Electron transfer, Chemical reactions, Reprints, *Sulfate radicals.

Rate constants have been measured as a function of temperature over the range 10 to 60 C for the reactions of the sulfate radical, SO4(1-) with azide, chloride, cyanate, cyanide, acetate, and carbonate anions. Room temperature rate constants ranged from about 5,000,000 to 5 times 10 to the 11th power/M/s. The variation of the rate constant with substrate depended mainly on the Arrhenius pre-exponential factor and less on the activation energy. For the reaction of SO4(1-) with Cl(1-), the dependence of the rate constant on ionic strength was determined to be in agreement with the theoretical prediction.

00,829
PB94-212180 Not available NTIS
National Inst. of Standards and Technology (NML), Gaithersburg, MD. Chemical Kinetics Div.
Electron Transfer Reaction Rates and Equilibria of the Carbonate and Sulfate Radical Anions.
Final rept.
R. E. Huie, C. L. Clifton, and P. Neta. 1991, 5p.
Pub. in Radiation Physics and Chemistry 38, n5 p477-481 1991.

Keywords: *Electron transfer, *Oxidation reduction reactions, *Free radicals, *Reaction kinetics, *Chemical equilibrium, Radiolysis, Anions, Electric potential, Electrodes, Reprints, *Carbonate radicals, *Sulfate radicals, Reduction potentials.

Electron transfer reactions of the carbonate radical anion with azide, bromide, and hypochlorite ions have been studied by pulse radiolysis. From the equilibrium Br2(1-)(dot) + CO3(2-) = 2Br(1-) + CO3(-)(dot) and the known redox potential for the Br2(1-)(dot)/2Br(1-) half reaction, the redox potential for the ClO(dot)/ClO(1-) half reaction was derived. The equilibrium reaction SO4(1-)(dot) + Cl(1-) = SO4(2-) + Cl(dot) was studied by laser photolysis using 284 nm excitation of S208(2-) to produce SO4(1-)(dot) by examining the rate of reaction of this radical with Cl(1-) in the presence of varying concentrations of SO4(2-). By modeling the reactions occurring in this system, the rate constant and equilibrium constant for the reaction of Cl(dot) with SO4(2-) were derived.

00,830
PB94-212198 Not available NTIS
National Inst. of Standards and Technology (CSTL), Gaithersburg, MD. Chemical Kinetics and Thermodynamics Div.
Reaction of NO with Superoxide.
Final rept.
R. E. Huie, and S. Padmaja. 1993, 5p.
Sponsored by Department of Energy, Washington, DC.
Pub. in Free Rad. Res. Comms. 18, n4 p195-199 1993.

Keywords: *Reaction kinetics, *Nitric oxide, *Superoxide radicals, Free radicals, Catalysts, Formates, Reprints, *Peroxynitrite radicals.

The rate constant for the reaction of NO with the superoxide anion was determined to be ((6.7 + or - 0.9) X 10 to the 9th power)l/mol/s, considerably higher than previously reported. Rate measurements were made from pH 5.6 to 12.5 both by monitoring the loss of the superoxide anion and the formation of the product peroxynitrite radical. The decay rate of the peroxynitrite radical, in the presence of 0.1 mol/l formate, ranges from 1.2/s at pH 5 to about 0.2/s in strong base, the latter value probably reflecting catalysis by formate.

00,831
PB94-212206 Not available NTIS
National Inst. of Standards and Technology (NML), Gaithersburg, MD. Chemical Kinetics Div.
Temperature Dependence of the Rate Constants for Reactions of the Carbonate Radical with Organic and Inorganic Reductants.
Final rept.
R. E. Huie, L. C. T. Shoute, and P. Neta. 1991, 12p.
Pub. in International Jnl. of Chemical Kinetics 23, n6 p541-552 1991.

Keywords: *Reaction kinetics, *Chemical radicals, *Carbonates, *Anions, *Temperature dependence, *Organic ions, Activation energy, Oxidation reduction reactions, Radiolysis, Reprints, *Carbonate radicals.

Rate constants have been measured by pulse radiolysis for the reactions of the carbonate radical with a number of organic and inorganic reactants as a function of temperature, generally over the range 5 to 80 C. The reactants include the substitution-inert cyano complexes of Fe(II), Mo(IV), and W(IV), the simple inorganic anions (SO3)(2-), (ClO2)(1-), (NO2)(1-), I(1-), SCN(1-), several phenolates, ascorbate, tryptophane, cysteine, cystine, methionine, triethylamine, and allyl alcohol. The measured rate constants ranged from less than 100,000 to (3 X 10 to the 9th power)/M/s and the activation energies ranged from -11.4 to 18.8 kJ/mol. The activation energies for the metal complexes and inorganic anions generally decrease with increasing driving force for the reaction, as expected for an outer sphere electron transfer. For highly exothermic reactions, however, the activation energy appears to increase, probably reflecting the temperature dependence of diffusion. For many of the organic reactants, the activation energies were low and independent of driving force, suggesting that the oxidation is via an inner sphere mechanism.

00,832
PB94-212297 Not available NTIS
National Inst. of Standards and Technology (CSTL), Gaithersburg, MD. Surface and Microanalysis Science Div.
Formalism and Parameters for Quantitative Surface Analysis by Auger Electron Spectroscopy and X-Ray Photoelectron Spectroscopy.
Final rept.
A. Jablonski, and C. J. Powell. 1993, 16p.
Pub. in Surface and Interface Analysis 20, p771-786 1993.

Keywords: *Surface analysis, X-ray photoelectron spectroscopy, Auger electron spectroscopy, Elastic scattering, Electron scattering, Electron transport, Quantitative analysis, Reprints.

It has been realized during the last 5 years that quantitative surface analyses by Auger electron spectroscopy (AES) and x-ray photoelectron spectroscopy (XPS) can be greatly complicated by the effects of elastic electron scattering. These effects had previously been largely ignored. We review here the effects of elastic scattering in the formalism of quantitative surface analysis by AES and XPS and discuss the various definitions of terms (inelastic mean free path, attenuation length and escape depth) that have been used to describe inelastic scattering and the surface sensitivities of various electron spectroscopies. We show how a realistic theoretical model of electron transport that includes elastic electron scattering can be related, for some analytical situations, to the common simple formalism of AES and XPS in which elastic scattering is neglected. We consider specifically measurements of overlayer thickness, determination of surface composition for a homogeneous surface region and estimation of the average depth of analysis and we indicate which parameter describing inelastic scattering can be used in the simple formalism for these applications.

00,833
PB94-212305 Not available NTIS
National Inst. of Standards and Technology (MSEL), Gaithersburg, MD. Polymers Div.
Glass Transition of Organic Liquids Confined to Small Pores.
Final rept.
C. L. Jackson, and G. B. McKenna. 1991, 4p.
Pub. in Jnl. of Non-Crystalline Solids 131, p221-224 1991.

Keywords: *Organic compounds, *Porous materials, *Glass, *Glass transition temperature, Phase transformations, Benzyl alcohols, Calorimetry, Reprints, *Organic liquids, o-Terphenyl.

The glass transition temperatures, Tg, of organic liquids confined to small pores were studied by differential scanning calorimetry (DSC). The Tg was measured as a function of pore size in controlled pore glasses having pore diameters in the range of 40-730 A. The surface of the glass was treated with hexamethyldisilazane to promote wetting by the organic liquids studied (o-terphenyl and benzyl alcohol). Glasses formed in the pores had a lower Tg than in the bulk and the reduction in Tg increased as the pore size decreased. For example, the depression of the glass transition temperature, delta Tg, of benzyl alcohol in 40 A and 85 A pores was 7.2 K and 3.1 K, respectively. The magnitude of delta Tg also depends on the material, e.g. for o-terphenyl in the 85 A pores delta Tg was 8.8K versus 3.1K for benzyl alcohol. In general, it was noted that delta Tg was considerably less than for the depression of the crystalline melting point delta Tm, studied in related work. For example, for benzyl alcohol in the 85 A pores, delta Tm was approximately 25 K and delta Tg was approximately 3 K.

00,834
PB94-212313 Not available NTIS
National Inst. of Standards and Technology (MSEL), Gaithersburg, MD. Polymers Div.
Melting Behavior of Organic Materials Confined in Porous Solids.
Final rept.
C. L. Jackson, and G. B. McKenna. 1990, 10p.
Pub. in Jnl. of Chemical Physics 93, n12 p9002-9011 1990.

Keywords: *Melting points, *Organic compounds, *Porous materials, *Glass, Phase transformations, Heat of fusion, Cyclohexane, Benzene, Naphthalene, Heptanes, Chlorobenzenes, Reprints, *Melting point depression, *Organic liquids, Crystal size.

The solid-liquid phase transition temperatures and heats of fusion (HOF), of non-polar organic solids confined in the pores of controlled pore glasses were measured by differential scanning calorimetry. The pore diameters, d, were in the range of 40-730A and the organics studied were cis-decalin, trans-decalin, cyclohexane, benzene, chlorobenzene, naphthalene and heptane. In accordance with previous reports on studies of inorganic materials, the melting point of the pore solid, T(d), decreased with decreasing pore diameter. In addition, a large reduction in the bulk HOF of the pore solid was measured, which has not been studied in detail by other workers. A linear correlation was found between the melting point depression and the reciprocal diameter, in accordance with the Gibbs-Thomson equation. The calculated values of the solid-liquid interfacial energy, using a modification of the Gibbs-Thomson equation were in good agreement with values reported in the literature based on other methods of measurement.

00,835
PB94-212487 Not available NTIS
National Inst. of Standards and Technology (NML), Gaithersburg, MD. Chemical Kinetics Div.
Multiphoton Ionization of SiH3 and SiD3 Radicals. 2. Three Photon Resonance-Enhanced Spectra Observed between 460 and 610 nm.
Final rept.
R. D. Johnson, and J. W. Hudgens. 1991, 10p.
Pub. in Jnl. of Chemical Physics 94, n8 p5331-5340 1991.

Keywords: *Electron transitions, *Rydberg states, *Electronic spectra, *Free radicals, Energy levels, Vibrational spectra, Isotope effect, Spectrum analysis, Reprints, *Silyl radicals, Multiphoton ionization.

The electronic spectra of silyl radicals, SiH3 and SiD3, were observed between 460-610 nm (49,200-65,200/cm) by resonance enhanced multiphoton ionization (REMPI) mass spectroscopy. The spectra were produced through a 3+1 REMPI mechanism. Spectra of four new planar Rydberg states were observed and assigned. In SiH3 the observed states and spectroscopic constants are D doublet A'(sub 1) (3d): To = 49787(30), omega(sub 2) = 808(31)/cm; I' (4d): To = 56253(30), omega(sub 2) = 814(25)/cm; J' (4d): To = 57726(30), omega(sub 2) = 835(26)/cm; and K' (5d): To = 59615(30)/cm, omega(sub 2) = 835(26)/cm. In SiD3, the observed states and spectroscopic constants are D doublet A'(sub 1) (3d): To = 49787(30), omega(sub 2) = 604(28)/cm; I' (4d): To = 56253(30), omega(sub 2) = 604(17)/cm; and J' (4d): To = 57726(30), omega(sub 2) = 599(20)/cm.

00,836
PB94-212495 Not available NTIS
National Inst. of Standards and Technology (NML), Gaithersburg, MD. Chemical Kinetics Div.
New Electronic States of NH and ND Observed from 258 to 288 nm by Resonance Enhanced Multiphoton Ionization Spectroscopy.
Final rept.
R. D. Johnson, and J. W. Hudgens. 1990, 6p.
Pub. in Jnl. of Chemical Physics 92, n11 p6420-6425 1990.

Keywords: *Electron transitions, *Rydberg states, *Electronic spectra, *Free radicals, Energy levels, Excited states, Rotational spectra, Vibration, Photolysis, Hydrazoic acid, Spectrum analysis, Reprints, *Imidogen radicals, Multiphoton ionization.

Four new electronic states of NH and ND have been observed and analyzed by REMPI (Resonance Enhanced Multiphoton Ionization) Spectroscopy in the region of 258 through 288 nm. The NH (ND) was produced by the photolysis of HN3 (DN3) (hydrazoic acid) in the same wavelength region. The observed two-photon transitions are from the a singlet delta state to 3s and 3p Rydberg states. The new state assignments are : e singlet Pi (3s sigma) at 82857/cm, f singlet Pi (3p sigma) at 86378/cm, g singlet delta (3p pi) at 88141/cm, and h singlet Sigma (3p pi) at 89151/cm. Rotational constants (B and D) and, where possible, vibrational spacings for the twelve observed bands are also determined.

00,837
PB94-212503 Not available NTIS
National Inst. of Standards and Technology (NML), Gaithersburg, MD. Chemical Kinetics Div.
Multiphoton Ionization of SiH3 and SiD3 Radicals: Electronic Spectra, Vibrational Analyses of the Ground and Rydberg States, and Ionization Potential.
Final rept.
R. D. Johnson, B. P. Tsai, and J. W. Hudgens. 1989, 20p.
Pub. in Jnl. of Chemical Physics 91, n6 p3340-3359, 15 Sep 89.

Keywords: *Electron transitions, *Rydberg states, *Electronic spectra, *Free radicals, Energy levels, Spectrum analysis, Reprints, *Silyl radicals.

The electronic spectra of silyl radicals, SiH3 and SiD3, were observed between 310 and 430 nm (46,000-64,000/cm) by resonance enhanced multiphoton ionization (REMPI) mass spectroscopy. The spectra were generated through a 2 + 1 REMPI mechanism. Two Rydberg series originating from planar, D(sub 3h) point group states were observed. One series, of quantum defect delta = 1.45(2), is comprised of the E doublet A(sub 2)(sup double prime) (4p), J doublet A(sub 2)(sup double prime) (5p), and M doublet A(sub 2)(sup double prime) (6p) Rydberg states which have origins at nu(sub o-o) = 48,438, 56,929, and 60,341/cm in SiH3 and at nu(sub o-o) = 48,391, 56,874, and 60,267/cm in SiD3. In SiD3, the P doublet A(sub 2)(sup double prime) (7p) Rydberg origin was observed at nu(sub o-o) = 62,002/cm. The H, K, and N states observed in the SiD3 spectrum comprise the second Rydberg series, delta = 2.09, and were tentatively assigned as ns doublet A'(sub 1) Rydberg states (n = 5, 6, 7).

00,838
PB94-212792 Not available NTIS
National Inst. of Standards and Technology (PL), Gaithersburg, MD. Molecular Physics Div.
Product Kinetic Energies, Correlations, and Scattering Anisotropy in the Bimolecular Reactor O((1)D)+H2O yields 2OH.
Final rept.
D. S. King, D. G. Sauder, and M. P. Casassa. 1992, 4p.
Sponsored by Air Force Office of Scientific Research, Bolling AFB, DC.
Pub. in Jnl. of Chemical Physics 97, n8 p5919-5922, 15 Oct 92.

Keywords: *Hydroxyl radicals, Chemical reactions, Internal energy, Kinetic energy, Oxygen 16, Oxygen 18, Anisotropy, Correlations, Ozone, Water, Reprints, Doppler spectroscopy.

Doppler spectroscopy of the (16)OH and (18)OH products of the (16)O(singlet D) + H2(18)O reaction reveals scattering anisotropy: (16)OH scatters in the hemisphere containing the (16)O-atom velocity vector. Internal energies of geminate OH fragments are correlated: fragments of high internal energy form with cofragments of low internal energy.

00,839
PB94-212826 Not available NTIS
National Inst. of Standards and Technology (NML), Gaithersburg, MD. Center for Atomic, Molecular and Optical Physics.

Molecular-Beam Optothermal Spectrum of the OH Stretching Band of Methanol.
Final rept.
I. Kleiner, G. T. Fraser, J. T. Hougen, and A. S. Pine. 1991, 18p.
Pub. in Jnl. of Molecular Spectroscopy 147, n1 p155-172 1991.

Keywords: *Methanol, Molecular spectroscopy, Molecular beams, Perturbation, Line width, Reprints, Vibrational relaxation.

The OH stretching fundamental band, nu(1), of CH3OH has been recorded with sub-Doppler resolution using a molecular-beam optothermal spectrometer. The low effective temperature (about 6 K) of the molecular beam greatly reduces the spectral congestion from hot torsional vibrations and high rotational levels seen at room temperature, permitting a reasonably complete assignment, a fit to a global hindered internal rotor Hamiltonian, and identification of several perturbations and their likely perturbers. The observed linewidths are about 15 MHz, yielding an upper limit to any intramolecular vibrational relaxation rate.

00,840
PB94-212834 Not available NTIS
National Inst. of Standards and Technology (NML), Gaithersburg, MD. Molecular Physics Div.
Fundamental Torsion Band in Acetaldehyde.
Final rept.
I. Kleiner, M. Godefroid, M. Herman, and A. R. W. McKellar. 1990, 16p.
Pub. in Jnl. of Molecular Spectroscopy 142, n2 p238-253 1990.

Keywords: *Acetaldehyde, Far infrared radiation, Infrared spectra, Band spectra, Rotational states, High resolution, Microwave spectra, Reprints, Fourier transform spectroscopy.

High resolution and low temperature experimental conditions allowed us to carry out the rotational analysis of the nu(15) fundamental band of acetaldehyde, observed around 150/cm. Some 1,000 lines of A and E types have been assigned to the main band and some 90 A-type lines have been identified in the first overtone of the torsion mode. A simultaneous fit, using the non rigid internal axis method, of a very severely selected set of unblended FIR data, together with microwave data published in the literature, allowed us to obtain accurate molecular parameters describing internal and overall rotation in acetaldehyde. In particular, the Fourier coefficients V(3) and V(6) of the barrier for internal rotation as well as the rotationless origins of the nu(15) fundamental band and its first overtone were determined with improved accuracy, compared to the data previously available in the literature. Some difficulties in treating v(t)=1 microwave data lead us to suspect problems in the theoretical model adopted or in the present v(t)=1 microwave data set.

00,841
PB94-212891 Not available NTIS
National Inst. of Standards and Technology (CSTL), Gaithersburg, MD. Thermophysics Div.
Determination of Osmotic Pressure and Fouling Resistances and Their Effects on Performance of Ultrafiltration Membranes.
Final rept.
M. K. Ko, and J. J. Pellegrino. 1992, 17p.
Pub. in Jnl. of Membrane Science 74, p141-157 1992.

Keywords: *Osmotic pressure, *Ultrafiltration, *Artificial membranes, *Proteins, Adsorption, Bovine serum albumin, Lactoglobins, pH, Sodium chloride, Polarization, Reprints, *Fouling resistance.

A study was made of the effects of material and geometric properties of ultrafiltration (UF) membranes on flux decline due to concentration-polarization (osmotic pressure) and adsorption (fouling) resistances. UF experiments with solutions of beta-lactoglobulin and bovine serum albumin on commercial membranes of poly(vinylpyrrolidone)-coated polycarbonate (PC) and regenerated cellulose (RC) were carried out. A three-stage experimental strategy based on an osmotic pressure-adsorption model was used to separately determine the effective hydraulic membrane resistance, osmotic pressure, and fouling resistance. By a normalization procedure, the performance of membranes with varying material and geometric characteristics could be compared and evaluated in terms of the extent of flux reduction individually due to concentration-polarization and fouling. Under all the conditions studied, the total flux reduction for the PC membrane was mainly controlled by the fouling resistance and for the RC membrane by the osmotic pressure build-up due to concentration-polarization. The effect of bulk protein concentration, transmembrane pressure, crossflow velocity, pH, and NaCl concentration on the individual, relative contributions to flux reduction by osmotic pressure and fouling were found to depend on membrane material properties.

00,842
PB94-212909 Not available NTIS
National Inst. of Standards and Technology (CSTL), Gaithersburg, MD. Thermophysics Div.
Characterization of the Adsorption-Fouling Layer Using Globular Proteins on Ultrafiltration Membranes.
Final rept.
M. K. Ko, J. J. Pellegrino, R. D. Nassimbene, and P. Marko. 1993, 20p.
Pub. in Jnl. of Membrane Science 76, p101-120 1993.

Keywords: *Adsorption, *Ultrafiltration, *Proteins, *Artificial membranes, Lactoglobins, Bovine serum albumin, Osmotic pressure, Reprints, *Fouling resistance.

The mechanisms of membrane fouling and the effects of properties and structure of the adsorbed-protein layer on membrane fouling were studied using bovine serum albumin (BSA) and beta-lactoglobulin (beta-LG) as test proteins, and poly(vinylpyrrolidone)-coated polycarbonate (PC) and regenerated cellulose (RC) as membranes. Ultrafiltration (UF) experiments were modeled with a 3-parameter resistance model to separately determine resistances due to osmotic pressure and adsorption. An analytical method was also developed to determine protein loadings under UF and static conditions. The dynamic behavior of osmotic pressure or interfacial concentration is discussed on the basis of the material balance around the interface. Derjaguin-Landau and Verwey-Overbeek (DLVO) theory and the concept of a rate-limiting step are applied to phenomena that occur at the interface during protein adsorption. A steric hindrance repulsion due to PVP tails on the PC membrane has a pronounced effect on protein loading. The hydrophilic matrix of RC may act as a water reservoir that maintains continuous hydration of the adsorbed layer, which can be dehydrated during protein adsorption. We believe that hydration results in a lower fouling resistance. Additionally, the size of the pores relative to the protein molecule has a pronounced effect on the properties and structure of the adsorbed layer and its fouling resistance.

00,843
PB94-212974 Not available NTIS
National Inst. of Standards and Technology (NML), Gaithersburg, MD. Molecular Physics Div.
Active Site Ionicity and the Mechanism of Carbonic Anhydrase.
Final rept.
M. Krauss, and D. Garmer. 1991, 10p.
Pub. in Jnl. of the American Chemical Society 113, n17 p6426-6435 1991.

Keywords: *Carbonic anhydrase, *Surface properties, Ligands, Protons, Hydrolysis, Bicarbonates, Mathematical models, Bonding strength, Reprints, *Active site ionicity, *Cluster models.

We report ab initio calculations on a cluster model for the active site of the enzyme carbonic anhydrase which also considers the effect of the ionicity of the site on the energetics of ligand binding and reaction behavior. Hydrolysis occurs by a direct attachment of the Zn-bound hydroxyl oxygen on the carbon atom of CO2 with a small activation energy. The final product state in the cluster model has bicarbonate bound by one short and one long metal to oxygen bond. Detailed mechanisms for the initial attachment of OH(1-) on CO2 and proton movement out to the free oxygen atom were studied by locating intermediates and transition states. Two mechanisms for rearrangement of bound bicarbonate to its most stable form are found to have low barriers. The first involves rocking of the bicarbonate from the initial intermediate. The second accomplishes this shift by a cycle exchange of protons with a hydrogen-bound water or Thr-119. Both pathways with a small barrier may be required to explain (18)O exchange experiments.

00,844
PB94-212982 Not available NTIS
National Inst. of Standards and Technology (NML), Gaithersburg, MD. Molecular Physics Div.
Dipole Moments in Rare Gas Interactions.
Final rept.
M. Krauss, and B. Guillot. 1989, 3p.
Pub. in Chemical Physics Letters 158, n1-2 p142-144 1989.

Keywords: *Rare gases, *Dipole moments, Self-consistent field, Atomic interactions, Perturbation theory, Dimers, Trimers, Neon, Argon, Krypton, Xenon, Reprints.

A hybrid model is used to calculate the dipole moments of rare gas dimers and trimers. The exchange and polarization interactions are obtained with a single-configuration self-consistent-field (SCF) calculation and the dispersion contribution to the dipole obtained by perturbation theory. The SCF dipoles for the trimers are found to compare well with values modeled by an exchange quadrupole induced dipole mechanism. The dispersion dipole for the ArKr dimer is found to be significant compared to the exchange contribution even to the region of the equilibrium separation. Values of the B hyperpolarizability are evaluated for Ne, Ar, Kr, and Xe which allow the perturbation calculation of the dispersion dipole for any pairs of rare gas atoms.

00,845
PB94-212990 Not available NTIS
National Inst. of Standards and Technology (NML), Gaithersburg, MD. Molecular Physics Div.
Analysis of Protein Metal Binding Selectivity in a Cluster Model.
Final rept.
M. Krauss, and W. J. Stevens. 1990, 7p.
Pub. in Jnl. of the American Chemical Society 112, n4 p1460-1466 1990.

Keywords: *Calcium ions, *Molecular orbitals, *Subtilisins, Clusters, Water, Formamides, Formates, Proteins, Ligands, Hydrations, Cations, Reprints, *Metal-ligand binding, Binding sites.

Ab initio molecular orbital calculations of the binding energy of metal cations to octahedral clusters of water, formamide, and formate ligands are used to analyze Ca binding sites in proteins. The intrinsic energetics of the first coordination shall provide a basis for evaluating the conformation behavior and the selectivity of cation binding. The enthalpies of binding are modeled by estimating the environmental polarization energy relative to the model cluster of the first shell. Cluster reaction enthalpies are calculated for transferring Mg, Ca, and Na cations from a water cluster to the protein model cluster as a function of cluster size which is found to strongly affect cation binding selectivity between cations of the same and different charges. The selectivity is a function of both steric and electrostatic interactions. As is well known, selectivity between cations of the same charge is dependent on steric factors but there is also an electrostatic component independent of steric influences which is selective between cations of different charge. The data is applied to an analysis of the binding sites in the protein, Subtilisin BPN'.

00,846
PB94-213006 Not available NTIS
National Inst. of Standards and Technology (NML), Gaithersburg, MD. Molecular Physics Div.
Cs Cluster Binding to a GaAs Surface.
Final rept.
M. Krauss, and W. J. Stevens. 1990, 10p.
Pub. in Jnl. of Chemical Physics 93, n12 p8915-8924 1990.

Keywords: *Solid clusters, *Gallium arsenides, *Cesium, Van der Waals forces, Polarization characteristics, Charge transfer, Surface reactions, Reprints.

The binding of Cs atoms to cluster models of the (110) surface of GaAs is examined for the polarization, charge transfer, and dispersion interactions. Single-configuration self-consistent-field binding energies to GaAs per Cs atom for two or three Cs atom clusters are calculated to be less than 0.1 eV. Orbital and total charge density plots exhibit a polarized alkali valence charge weakly bound between the alkali atoms and to the Ga atom. A London analysis of the correlation energy between the Cs and GaAs clusters or van der Waals interaction energy finds it is large compared to the difference in binding energies between gas-phase or polyhedral clusters and the quasi-linear clusters that are experimentally observed on the GaAs surface. The large VDW energy is due to the large polarizabilities for quasi-linear chains of Cs atoms those longitudinal component increases approximately with the square of the chain length.

00,847
PB94-213071 Not available NTIS
National Inst. of Standards and Technology (NML), Gaithersburg, MD. Molecular Physics Div.
Spectroscopic Constants for the 2.5 and 3.0 micrometer Bands of Acetylene.
Final rept.
W. J. Lafferty, and A. S. Pine. 1990, 8p.
Pub. in Jnl. of Molecular Spectroscopy 141, n2 p223-230 1990.

Keywords: *Acetylene, Near infrared radiation, Laser spectroscopy, Infrared spectroscopy, Band spectra, Rotational states, Vibrational states, Reprints, Fourier transform spectroscopy.

Fourier-transform interferometer and difference-frequency laser spectra of acetylene have been recorded in the 2.5 and 3.0 micrometer regions, yielding improved rotation-vibration constants for the nu2+nu4+nu5, for their associated hot bands originating in the nu4 and nu5 bends, and for the C-H stretch-bend combination bands. An analysis of the Fermi resonance gives more reliable estimates for the deperturbed constants and the anharmonic coupling.

00,848
PB94-213139 Not available NTIS
National Inst. of Standards and Technology (PL), Boulder, CO. Quantum Physics Div.
Laser-Induced Fluorescence Measurements of Rotationally Resolved Velocity Distributions for CO(+) Drifted in He.
Final rept.
C. P. Lauenstein, M. J. Bastian, V. M. Bierbaum, S. M. Penn, and S. R. Leone. 1991, 9p.
Contract AFOSR89-0073
Sponsored by Air Force Office of Scientific Research, Bolling AFB, DC. and National Science Foundation, Washington, DC.
Pub. in Jnl. of Chemical Physics 94, n12 p7810-7818, 15 Jun 91.

Keywords: *Carbon monoxide, Laser induced fluorescence, Rotational states, Molecular ions, Ionic mobility, Electric fields, Velocity, Helium, Doppler effect, Reprints.

Measurements of ion-velocity distributions of CO(1+) in a He buffer gas are presented as a function of an applied electric field. The distributions are obtained by single frequency, laser-induced fluorescence from various initial rotational states with the laser beam propagating parallel and perpendicular to the drift velocity vector. All distributions are well represented by a Maxwellian for the observed E/N range of 0-13 Td. From the width of the Doppler profiles, translational 'temperatures' are calculated, which are compared to simple attractive and repulsive Maxwell models as a function of the field. The measured values disagree with the predictions, which are well established for atomic ion systems. The differences are discussed in terms of rotationally inelastic energy transfer in the collisions, which is predicted by kinetic theory models.

00,849
PB94-213295 Not available NTIS
National Inst. of Standards and Technology (NML), Gaithersburg, MD. Electron and Optical Physics Div.
RIS Studies of Autoionization in Calcium.
Final rept.
Q. Li, T. J. McIlrath, E. B. Saloman, and T. B. Lucatorto. 1991, 4p.
Pub. in Institute of Physics, Conference Series on Resonance Ionization Spectroscopy, v114 p55-58 1991.

Keywords: *Autoionization, *Calcium, Resonance ionization mass spectroscopy, Time-of-flight spectrometers, Laser isotope separation, Atomic energy levels, Photoionization, Reprints, Two photon processes.

Autoionization levels belonging to configurations of 3p(6) 3dnl are being studied as part of an effort to find efficient ionization pathways applicable to ultrasensitive isotopic analysis and laser isotope separation. The studies are performed in a RIMS (Resonance Ionization Mass Spectroscopy) apparatus with a time-of-flight mass spectrometer and simple thermal filament atomization source. Estimates of two-photon transition rates and excited state photoionization cross sections show that the 4s(2) singlet S(0)-->-->3d5x singlet D(2)-->3d7p singlet P(1) (autoionizing) ionization pathway might be efficient enough to allow effective isoptically selective ionization with cw Ti:sapphire lasers.

00,850
PB94-216058 Not available NTIS
National Inst. of Standards and Technology (PL), Boulder, CO. Quantum Physics Div.
Spectroscopic Puzzle in ArHF Solved: The Test of a New Potential.
Final rept.
C. M. Lovejoy, J. M. Hutson, and D. J. Nesbitt. 1992, 10p.
Pub. in Jnl. of Chemical Physics 97, n11 p8009-8018, 1 Dec 92.

Keywords: *Argon complexes, Van der Waals forces, Infrared spectroscopy, Intermolecular forces, High resolution, Predissociation, Reprints, *Hydrogen fluoride complexes, Supersonic expansion, Potential energy surfaces.

The perturbed (nu,b,k,n)=(1210),(1113)<-(0000) band of ArHF is observed in a tunable laser/slit supersonic expansion spectrometer. The (1210) level correlates with j=2 rotation of the HF within the complex and therefore provides a test of high-order terms in a Legendre expansion of the intermolecular potential. Transitions to (1113) are observed due to intensity sharing with (1210), induced by a strong homogeneous (J-independent) perturbation that is analyzed quantitatively. The (1113) level has three quanta of Van der Waals stretch and thus probes the radial dependence of the potential close to the dissociation limit. The vibrational and rotational assignment is made possible by predictions based on the new H6(4,3,2) intermolecular potential of Hutson (J. Chem. Phys. 96, 6752 (1992)), which agree nearly quantitatively with experiment.

00,851
PB94-216108 Not available NTIS
National Inst. of Standards and Technology (CSTL), Boulder, CO. Thermophysics Div.
Modified Leung-Griffiths Model of Vapor-Liquid Equilibrium: Extended Scaling and Binary Mixtures of Dissimilar Fluids.
Final rept.
J. J. Lynch, and J. C. Rainwater. 1992, 15p.
Pub. in Fluid Phase Equilibria 75, p23-37 1992. Sponsored by Department of Energy, Washington, DC.

Keywords: *Liquid-vapor equilibrium, *Carbon dioxide, *Butanes, Binary mixtures, Simplex method, Critical point, Reprints, Leung-Griffiths model, Wegner correction.

Extended scaling or the Wegner correction has been added to a model of vapor-liquid equilibrium (VLE) designed for the extended critical region. The model, that of Leung and Griffiths as modified by Moldover, Rainwater and co-workers, has heretofore incorporated only simple scaling. The revised formalism has been applied to the abundant data on carbon dioxide + n-butane, where versions of the model with and without extended scaling have been optimized by the simplex method. With extended scaling, the average thermodynamic 'distance' between a measured and calculated dew or bubble point decreases by approximately 30 percent.

00,852
PB94-216165 Not available NTIS
National Inst. of Standards and Technology (CSTL), Gaithersburg, MD. Surface and Microanalysis Science Div.
Structure of Molecules on Surfaces as Determined Using Electron-Stimulated Desorption.
Final rept.
T. E. Madey, S. A. Joyce, and A. L. Johnson. 1990, 18p.
Pub. in Interaction of Atoms and Molecules with Solid Surfaces, Chapter 14, p459-476 1990.

Keywords: *Surface chemistry, *Molecular structure, Reprints, Electron stimulated desorption.

The structure of molecules on surfaces is an area of great importance in surface science, and a variety of surface-sensitive methods have been applied to structural problems. Many of these techniques (including Angle Resolved Ultraviolet Photoemission Spectroscopy (ARUPS), X-ray absorption near-edge structure (XANES), surface extended X-ray absorption fine structure (EXAFS), high-resolution electron energy loss spectroscopy (HREELS), and photoelectron diffraction (PD)) are discussed in other chapters in this volume.

00,853
PB94-216173 Not available NTIS
National Inst. of Standards and Technology (NML), Gaithersburg, MD. Surface Science Div.
Desorption Induced by Electronic Transitions.
Final rept.
T. E. Madey, S. A. Joyce, and J. A. Yarmoff. 1990, 14p.
Pub. in Springer Ser. Surf. Sci. Chem. Phys. Solid Surf. 8, v22 p55-68 1990.

Keywords: *Surfaces, *Desorption, Electron transitions, Electron beams, Radiation damage, Reprints, Electron stimulated desorption, Photon stimulated desorption.

We summarize the principles and mechanisms of DIET (desorption induced by electronic transitions) with emphasis on ESD (electron stimulated desorption) and PSD (photon stimulated desorption). We describe applications of ESDIAD (electron stimulated desorption ion angular distributions) to surface structure, and provide examples of electron beam damage at surfaces.

00,854
PB94-216199 Not available NTIS
National Inst. of Standards and Technology (NML), Boulder, CO. Thermophysics Div.
Thermophysical Properties of CO2 and CO2-Rich Mixtures.
Final rept.
J. W. Magee. 1991, 9p.
Pub. in Supercritical Fluid Technology: Reviews in Modern Theory and Applications, Chapter 8, p326-334 1991.

Keywords: *Carbon dioxide, *Thermophysical properties, Thermal conductivity, Supercritical fluids, Density(Mass/volume), Transport properties, Specific heat, Viscosity, Mixtures, Bibliographies, Reviews, Reprints.

Thermophysical properties data, including thermodynamic and transport properties, are fundamental to the clear understanding of supercritical fluid processes and technology. Benchmark experimental measurements provide the best check of theoretically-based predictive models for the thermophysical properties of supercritical fluids, including CO2 and CO2-rich mixtures. For this reason, a review of published data will be given herein. Only highly accurate thermophysical property data, capable of testing predictive models, has been considered in this context.

00,855
PB94-216223 Not available NTIS
National Inst. of Standards and Technology (NML), Gaithersburg, MD. Molecular Physics Div.
High-Resolution Measurements of the nu2 and 2nu2-nu2 Bands of (34)S(16)O2.
Final rept.
A. G. Maki, and Y. A. Kuritsyn. 1990, 2p.
Pub. in Jnl. of Molecular Spectroscopy 144, n1 p242-243 1990.

Keywords: *Sulfur dioxide, Infrared spectroscopy, Molecular spectroscopy, Band spectra, Air pollution, Acid rain, Sulfur 34, Oxygen 16, Reprints.

Infrared measurements have been made on (34)SO2 between 450 and 600/cm with a resolution of 0.004/cm. The B-type bands due to the bending transitions 010-000 and 020-010 have been assigned and analyzed. Revibrational constants are given that fit the current measurements and the pure rotational transitions reported in the literature.

00,856
PB94-216231 Not available NTIS
National Inst. of Standards and Technology (NML), Gaithersburg, MD. Molecular Physics Div.
FTS Infrared Measurements of the Rotational and Vibrational Spectrum of LiH and LiD.
Final rept.
A. G. Maki, W. B. Olson, and G. Thompson. 1990, 12p.
Pub. in Jnl. of Molecular Spectroscopy 144, n2 p257-268 1990.

Keywords: *Lithium deuterides, *Lithium hydrides, Vibrational spectra, Rotational spectra, Vapor phases, High resolution, Measurement, Reprints, Fourier transform spectroscopy, Dunham constants.

Fourier transform spectra have been measured for the rotational (Delta v = 0) and vibrational (Delta v = 1) spectrum of lithium hydride and lithium deuteride in the gas phase. Dunham potential constants and

rovibrational constants are given for LiH and LiD. Difficulties were encountered in attempts to fit all four isotopic species to a single modified Dunham potential function. Even data for a single isotopic species could not be fit to a Dunham potential function without significant systematic deviations. These problems are attributed to break down in the Born-Oppenheimer approximation.

00,857
PB94-216371 Not available NTIS
National Inst. of Standards and Technology (PL), Gaithersburg, MD. Molecular Physics Div.
Self Broadening in the nu1 Band of NH3.
Final rept.
V. N. Markov, A. S. Pine, G. Buffa, and O. Tarrini. 1993, 12p.
Sponsored by National Aeronautics and Space Administration, Washington, DC. Upper Atmospheric Research Program.
Pub. in Jnl. of Quantitative Spectroscopy and Radiative Transfer 50, n2 p167-178 1993.

Keywords: *Ammonia, Band spectra, Laser spectrometers, Pressure dependence, Reprints, Self broadening, Pressure shifts, Dicke narrowing.

Self-broadening coefficients, pressure shifts and integrated intensities have been measured for Q- and R-branch transitions in the nu(1) fundamental band of ammonia using a difference-frequency laser spectrometer. A strong, systematic J and K dependence of the broadening coefficients, reminiscent of the ground-state inversion transitions, is observed and compared with semiclassical line broadening calculations. Dicke narrowing is evident at intermediate pressures for the sharpest lines, primarily the R(J, O) transitions. Incipient line mixing is apparent in the Q branch at pressures above about 0.1 bar.

00,858
PB94-216454 Not available NTIS
National Inst. of Standards and Technology (NML), Gaithersburg, MD. Chemical Kinetics Div.
Precision and Accuracy in Tandem Mass Spectrometry Measurements: A Kinetics-Based Protocol for Instrument-Independent Measurements of Collision-Activated Dissociation in RF-Only Quadrupoles.
Final rept.
R. I. Martinez. 1990, 2p.
Pub. in Jnl. of the American Society for Mass Spectroscopy 1, n3 p272-273 1990.

Keywords: *Mass spectroscopy, Reaction kinetics, Measurement, Precision, Accuracy, Protocols, Quadrupoles, Particle collisions, Reprints, Collisionally induced dissociation.

This is a news item to announce NIST protocol for MS/MS measurements.

00,859
PB94-216462 Not available NTIS
National Inst. of Standards and Technology (NML), Gaithersburg, MD. Chemical Kinetics Div.
Kinetics and Mechanism of the Collision-Activated Dissociation of the Acetone Cation.
Final rept.
R. I. Martinez, and B. Ganguli. 1992, 18p.
Pub. in Jnl. of the American Society for Mass Spectrometry 3, n4 p427-444 1992.

Keywords: Branching ratio, Reprints, *Acetone cations, Acetyl cations, Methyl cations, Collisionally induced dissociation, Tandem mass spectrometers.

For center-of-mass collision energies E(cm) = 1-60 eV, the major fragment ions for the collision-activated dissociation (CAD) of the acetone cation are the acetyl cation (m/z 43; absolute branching ratios of 0.96-0.60) and the methyl cation (m/z 15; absolute branching ratios of 0.02-0.26); the absolute total cross-sections were 24-35 A(sup 2). The breakdown curves (viz, plots of the absolute branching ratios versus E(cm)) show complex, complementary energy dependences for production of MeCO(1+) and Me(1+), indicating apparent closure of the Me(1+) channel for E(cm) > 30 eV. Our observations are consistent with a competition between three fast, primary (direct) reactions, each of which opens sequentially at its respective threshold energy.

00,860
PB94-216595 Not available NTIS
National Inst. of Standards and Technology (NML), Gaithersburg, MD. Chemical Kinetics Div.
Carbon Acidities of Aromatic Compounds. 1. Effects of In-Ring Aza and External Electron-Withdrawing Groups.
Final rept.
M. Mautner, and S. A. Kafafi. 1988, 7p.
Pub. in Jnl. of the American Chemical Society 110, n19 p6297-6303 1988.

Keywords: *Acidity, *Carbon, *Diazines, *Benzene, *Structural chemical analysis, Aromatic compounds, Heterocyclic compounds, Chemical reactivity, Anions, Hydrogen ions, Reprints, *Electron withdrawing groups, *Carbon acidity, Topological charge distribution, Gas phase acidity.

We report experimental intrinsic carbon acidities and theoretical AM1 results on benzene derivatives and nitrogen heterocyclics. When benzene and pyridine are compared, in-ring aza substitution increases the acidity, i.e. decreases the acid dissociation energy by 9.7 kcal/mol. Further aza substitution in 1,2- and 1,3-diazine increases the acidity by an additional 8.6 and 5.8 kcal/mol, respectively. However, in 1,4-diazine, where the deprotonated carbon must be adjacent to nitrogen, lone-pair repulsion decreases the acidity below pyridine. The in-ring aza-substitution effects are qualitatively similar in those observed in azoles by Taft et al., but their parameters for one-pair repulsion and electronegative substituents do not reproduce the effects quantitatively. The electron-withdrawing substituents, F, CF3, CN, and NO2 also increase the acidity of benzene by 13.5, 13.6, 17.5, and 46.5 kcal/mol, and CHCH2 increases it by 9.7 kcal/mol. The effects of F and CHCH2 demonstrate that the ring acidity is affected by the sigma rather than pi donating or withdrawing ability of substituents. Ab initio calculations at the MP2=FC/6-31G(star)/ /RHF/6-31G level were performed on pyridine and diazines. The computed ab initio DPEs were consistently higher than the experimental values by about 22 kcal/mol. Semiempirical computations using Dewar's AM1 method for 1,4-diazine suggest that a correction of 11 kcal/mol is needed for adjacent lone-pair repulsion. With this correction, AM1 predicts qualitatively sensible deprotonation sites for diazines and F-, CN-, CF3-, and CHCH2-substituted benzenes and reproduces the deprotonation energies within 6 kcal/mol.

00,861
PB94-216603 Not available NTIS
National Inst. of Standards and Technology (NML), Gaithersburg, MD. Chemical Kinetics Div.
Proton Affinity Ladders from Variable-Temperature Equilibrium Measurements. 1. A Re-Evaluation of the Upper Proton Affinity Range.
Final rept.
M. Meot-Ner, and L. W. Sieck. 1991, 13p.
Pub. in Jnl. of the American Chemical Society 113, n12 p4448-4460 1991.

Keywords: *Proton transport, *Thermodynamic equilibrium, Thermochemistry, Temperature dependence, Reaction kinetics, Reprints, *Proton affinity, Ionic equilibria.

An interlocking ladder of relative proton affinities (PA) of 43 compounds, over a range of 55 kcal/mol, was obtained from the temperature dependence of proton transfer equilibria. From C3H6 (PA=179.5 kcal/mol) to i-C4H8 (PA-195.9 kcal/mol) the results agree well with tabulated values, but for the upper PA range the present values are increased significantly. For example, the present vs. literature PA values are: NH3, 208.3 + or - 1 vs. 204.0; CH3NH2; 219.6 vs. 214.1; t-C4H9NH2, 229.2 vs. 220.8 kcal/mol (all relative values + or - 1 kcal/mol, related to PA(i-C4H8) = 195.9 kcal/mol). The new value for the latter is also confirmed by the association thermochemistry of t-C4H9(1+) with NH3.

00,862
PB94-216751 Not available NTIS
National Inst. of Standards and Technology (PL), Boulder, CO. Quantum Physics Div.
High-Resolution IR Laser-Driven Vibrational Dynamics in Supersonic Jets: Weakly Bound Complexes and Intramolecular Energy Flow.
Final rept.
A. McIlroy, and D. J. Nesbitt. 1991, 29p.
Grants NSF-PHY86-04504, NSF-CHE86-05970
Sponsored by National Science Foundation, Washington, DC.
Pub. in Advances in Molecular Vibrations and Collision Dynamics, v1A p109-137 1991.

Keywords: *Molecular vibration, *Complexes, Van der Waals forces, Infrared spectroscopy, Infrared absorption, Molecular dynamics, Line broadening, Excited states, High resolution, Predissociation, Reprints, Intermolecular potentials, Supersonic expansion.

The combination of low temperatures from supersonic jet expansions and high-resolution laser IR absorption methods provides a nearly ideal probe of quantum state resolved unimolecular dynamics in vibrationally excited molecules under collision-free conditions. In this paper we present three classes of examples of such studies from our laboratory. (1) First, we discuss how precise (< 10(sup -4)/cm) rotation-vibration spectroscopy can be used to obtain intermolecular potentials for weakly bound complexes. (2) Next we analyze data on van der Waals systems where the internal vibrational energy in the complex is sufficient to photofragment the weak bond and thereby lead to predissociative line broadening in the spectra. (3) Finally, we consider vibrational dynamics in the limit of chemically bound, stable molecules such as terminal acetylenes, where excess fine structure in a high-resolution spectrum can be used to infer rates of intramolecular energy flow.

00,863
PB94-219268 (Order as PB94-219219, PC A06/MF A02)
Commission of the European Communities, Geel (Belgium). Inst. for Reference Materials and Measurements.
New Values for Silicon Reference Materials, Certified for Isotope Abundance Ratios. Letter to the Editor.
P. De Bievre, S. Valkiers, and H. S. Peiser. 1994, 2p.
Prepared in cooperation with National Inst. of Standards and Technology, Gaithersburg, MD.
Included in Jnl. of Research of the National Institute of Standards and Technology, v99 n2 p201-202 Mar/Apr 94.

Keywords: *Silicon, *Isotope ratios, *Atomic mass, Abundance, Cyclotron frequency, Silicon tetrafluoride, Penning effect, Penning trap, Reference materials, National Institute of Standards and Technology.

New isotope abundance and relative atomic mass (atomic weight) values-with low, hitherto unattained uncertainty-are reported for two previously described silicon reference materials using a well-known method with an improved isotope-ratio mass spectrometer. These new values are directly traceable to the SI, more specifically to the unit for amount of substance, the mole, and independent of the SI unit of mass and of the Avogadro constant. Besides, the residual mass-spectrometric uncertainties, these new values depend in effect only on a recently published direct comparison of the cyclotron frequency in a Penning trap of (28)Si(+1) with that of (12)C(1+).

00,864
PB95-107017 Not available NTIS
National Inst. of Standards and Technology (NML), Gaithersburg, MD. Chemical Kinetics Div.
Changes in the Redox State of Iridium Oxide Clusters and Their Relation to Catalytic Water Oxidation: Radiolytic and Electrochemical Studies.
Final rept.
G. S. Nahor, P. Hapiot, P. Neta, and P. Harriman. 1991, 6p.
Pub. in Jnl. of Physical Chemistry 95, n2 p616-621 1991.

Keywords: *Iridium oxides, *Catalysts, *Water, *Photochemical reactions, *Oxidation, Reaction kinetics, Oxidation reduction reactions, Electrochemistry, Radiolysis, Optical properties, Reprints.

Radiolytically prepared iridium oxide (IrOx.nH2O) clusters have been shown to catalyze the photochemical oxidation of water. These catalysts have been oxidized by radiolytic or electrochemical methods and the changes in their optical absorption and redox state have been studied. The clusters contain 4-5 Ir atoms in a mixture of Ir(III) and Ir(IV) states, formally described as Ir(3.2+). Time-resolved pulse radiolytic studies revealed three processes in the sub-second time-scale. The same species were observed in gamma-radiolysis and in spectroelectrochemical experiments. Further oxidation of the cluster leads to oxidation of water to O2. The kinetics of all the above processes are pH dependent and involve acid-base equilibria in the various oxidation states.

00,865
PB95-107058 Not available NTIS

National Inst. of Standards and Technology (NML), Gaithersburg, MD. Chemical Kinetics Div.
One-Electron Oxidation of Nickel Porphyrins. Effect of Structure and Medium on Formation of Nickel(III) Porphyrin or Nickel(II) Porphyrin pi-Radical Cation.
Final rept.
G. S. Nahor, P. Neta, P. Hambright, and L. R. Robinson. 1991, 4p.
Pub. in Jnl. of Physical Chemistry 95, n11 p4415-4418 1991.

Keywords: *Nickel compounds, *Porphyrins, *Oxidation, Photochemical reactions, Spectrum analysis, Cations, Radicals, Transition element compounds, Reprints, One-electron oxidation, Pi-radical cations.

The oxidation of several nickel(II) porphyrins by various radicals has been studied by pulse radiolysis in different media. Photochemical oxidation was also examined in some cases. The absorption spectrum of the oxidation product was monitored within several microseconds after the pulse. Two types of differential spectra were observed, a broad absorption at 640-700 nm ascribed to the pi-radical cation, or a sharp absorption at 560-580 nm ascribed to nickel(III) porphyrin. Ni(II)TPP (tetraphenylporphyrin) in several organic solvents, protic and aprotic, was oxidized to Ni(III)TPP.

00,866
PB95-107066 Not available NTIS
National Inst. of Standards and Technology (NML), Gaithersburg, MD. Chemical Kinetics Div.
Site of One-Electron Reduction of Ni(II) Porphyrins. Formation of Ni(I) Porphyrin of Ni(II) Porphyrin pi-Radical Anion.
Final rept.
G. S. Nahor, P. Neta, P. Hambright, L. R. Robinson, and A. Harriman. 1990, 5p.
Pub. in Jnl. of Physical Chemistry 94, n17 p6659-6663 1990.

Keywords: *Radiolysis, *Reduction(Chemistry), *Nickel compounds, *Porphyrins, Spectroscopic analysis, Reaction kinetics, Radicals, Anions, Electrochemistry, Reprints, One-electron reduction, Pi-radical anions.

The products (Ni(II)P) have been examined by radiolytic reduction in protic media to determine whether (Ni(I)P) or the pi-radical anion Ni(II)P(1-) is formed. Kinetic spectrophotometric detection was utilized to record absorption spectra of products immediately after one-electron reduction and gamma-radiolysis was used for recording the spectra of the stable reduction products. The initial reduction product was dependent on the nature of substituents on the porphyrin but not on the redox potential; a meso-4-pyridyl group seems to direct the reduction toward the porphyrin ring whereas, in most other cases, reduction occurred on the metal. On longer time-scales (minutes) all porphyrins produced the two-electron reduced products, chlorin or phlorin anion.

00,867
PB95-107074 Not available NTIS
National Inst. of Standards and Technology (NML), Gaithersburg, MD. Chemical Kinetics Div.
Reduction of Dinitrogen to Ammonia in Aqueous Solution Mediated by Colloidal Metals.
Final rept.
G. S. Nahor, L. C. T. Shoute, P. Neta, and A. Harriman. 1990, 6p.
Pub. in Jnl. of the Chemical Society 86, n23 p3927-3933 1990.

Keywords: *Reduction(Chemistry), *Nitrogen, *Colloids, Reprints, Metals, Radicals, Radiolysis, Photolysis, Ammonia, Rubidium, Rhenium, Platinum, PVA(Polyvinyl alcohol), PB(Polybrene), PSS(Polystyrene sulfonate).

Reduction of N2 to NH3 was investigated by radiolysis and photolysis in N2-saturated aqueous solutions containing colloidal dispersions of Ru, Pt, or Rh stabilized either by neutral (poly(vinyl alcohol), PVA) or charged (polybrene, PB, or polystyrene sulfonate, PSS) polymers. The yield depends on the irradiation time, colloid concentration, type of reducing radical, and pH. At longer irradiations the concentration of NH3 increased at a much slower rate until the reaction stopped. The results suggest fast and efficient reduction of any N2 that is pre-absorbed at highly reactive, possibly metal oxide, sites on the surface of the colloid.

00,868
PB95-107082 Not available NTIS
National Inst. of Standards and Technology (NML), Gaithersburg, MD. Chemical Kinetics Div.
Metalloporphyrin Sensitized Photooxidation of Water to Oxygen on the Surface of Colloidal Iridium Oxides - Photochemical and Pulse Radiolytic Studies.
Final rept.
G. S. Nahor, A. N. Thompson, P. Neta, P. Hambright, and A. Harriman. 1989, 7p.
Pub. in Jnl. of Physical Chemistry 93, n16 p6181-6187 1989.

Keywords: *Porphyrins, *Photolysis, *Water, *Oxidation, Colloids, Radicals, Cations, Photochemical reactions, Reaction kinetics, Radiolysis, Transition metals, Iridium, Reprints, Iridium oxide.

Derviatives of TSPP (tetrakis(4-sulfonatophenyl)porphyrin) were prepared and tested as photosensitizers for oxidation of water to oxygen on the surface of colloidal iridium oxide. Triplet quantum yields, energies, and lifetimes were measured by laser flash photolysis. Rate constants for quenching the porphyrin triplet state with 02 and with persulfate ions were also determined. The rate of interaction between the porphyrin radical cations and colliodal Ir02 particles were measured by pulse radiolysis for several of the compounds. Illumination of a porphyrin in the presence of sodium perfulfate and an Ir02 colloid resulted in generation of 02 in a process that was strongly dependent upon pH and upon the nature of the photosensitizer in the same manner as the kinetics determined by pulse radiolysis. The rate of 02 production under any conditions could be explained on the basis of thermodynamic criteria relating to either of the individual quenching or water oxidation steps.

00,869
PB95-107116 Not available NTIS
National Inst. of Standards and Technology (NML), Gaithersburg, MD. Time and Frequency Div.
Determination of the Molecular Parameters of NiH in Its (2)Delta Ground State by Laser Magnetic Resonance.
Final rept.
T. Nelis, S. P. Beaton, K. M. Evenson, and J. M. Brown. 1991, 17p.
Pub. in Jnl. of Molecular Spectroscopy 148, n2 p462-478 1991.

Keywords: *Molecular structure, *Nickel hydrides, Laser spectroscopy, Magnetic resonance, Rotational states, Far infrared radiation, Radicals, Transition metals, Ground state, Infrared spectra, Zeeman effect, Reprints, *LMR(Laser magnetic resonance), *Laser magnetic resonance.

The rotational spectrum of the NiH radical in the nu=0 level of its X(2)Delta state has been studied by laser magnetic resonance (LMR) at far-infrared wavelengths. Transitions have been detected for all 5 isotopes of nickel and within both the lower ((sup2)Delta 5/2) and upper ((sup 2)Delta 3/2) spin components. Nuclear hyperfine splittings for both the proton and (61)Ni (I=3/2) are observed. The effective Zeeman Hamiltonian for a molecule in a (2s+1)Delta state is developed and used to fit all the data together with the similar magnetic resonance observations of the (1,0) vibration-rotation band. There are several indications that this exercise is only just possible in the case of NiH in its X(2)Delta state.

00,870
PB95-107124 Not available NTIS
National Inst. of Standards and Technology (MSEL), Gaithersburg, MD. Reactor Radiation Div.
Crystal Structure of a New Sodium Zinc Arsenate Phase Solved by 'Simulated Annealing'.
Final rept.
T. M. Nenoff, W. T. A. Harrison, G. D. Stucky, J. M. Nicol, and J. M. Newsam. 1993, 5p.
Sponsored by National Science Foundation, Arlington, VA.
Pub. in Zeolites 13, p506-510 Sep/Oct 93.

Keywords: *Crystal structure, *Powder metals, *Phase studies, Simulation, Annealing, Crystallography, Neutron diffraction, X-ray diffraction, Sodium compounds, Zinc compounds, Reprints, *Sodium zinc arsenate, Simulated annealing, Sodalite analogs, Rietvelt profile refinement.

The framework structure of a new sodium zinc arsenate, produced by dehydration of the Na6(ZnAsO4)6 8 H2O sodalite analog, has been solved by a simulated annealing method. This method utilizes typical tetrahedral-atom bonding schemes with possible space group and unit cell dimensions to randomly generate possible continuous frameworks and their calculated energies. The Rietveld refinement of the Na6(ZnAsO4)6 solution phase was initially performed on room temperature X-ray data and then continued on low-temperature constant wavelength neutron data. The sodium zinc phosphate is a hexagonal polycrystalline material. The tridymite structural analog undergoes a room-temperature transformation to the open-framework sodalite structure.

00,871
PB95-107132 Not available NTIS
National Inst. of Standards and Technology (PL), Boulder, CO. Quantum Physics Div.
Mode Specific Vibrational Predissociation Dynamics in Fragile Molecules.
Final rept.
D. J. Nesbitt. 1991, 14p.
Grant NSF-CHE86-05970
Sponsored by National Science Foundation, Washington, DC.
Pub. in Mode Selective Chemistry, p113-126 1991.

Keywords: *Infrared spectroscopy, *High resolution, *Hydrogen bonds, Energy transfer, Van der Waals forces, Quantum chemistry, Frequencies, Slits, Supersonic jet flow, Reprints, Mode specific, Predissociation, Sub-Doppler.

State resolved vibrational dynamics in weakly bound complexes is investigated via high resolution IR absorption spectroscopy in a slit supersonic jet expansion. The tunable frequency near IR source can readily excite the high frequency intramolecular vibrations of the subunits, as well as the low frequency, intermolecular vibrations via combination band excitations built on the high frequency modes. These upper state energies lie far above the van der Waals binding energy limit, and yet predissociate typically on the nsec time scale or longer (i.e. many millions of vibrational periods). This exceptional metastability in such small systems is highly non-statistical, and proves to be a rich arena of vibrational mode mixing and mode-specific predissociation behavior. The authors select recent examples from their group effort to illustrate these concepts.

00,872
PB95-107140 Not available NTIS
National Inst. of Standards and Technology (PL), Boulder, CO. Quantum Physics Div.
Vibration, Rotation, and Parity Specific Predissociation Dynamics in Asymmetric OH Stretch Excited ArH2O: A Half Collision Study of Resonant V-V Energy Transfer in a Weakly Bound Complex.
Final rept.
D. J. Nesbitt, and R. Lascola. 1992, 15p.
Grant NSF-PHY90-12244
Sponsored by National Science Foundation, Washington, DC.
Pub. in Jnl. of Chemical Physics 97, n11 p8096-8110, 1 Dec 92.

Keywords: *Infrared spectroscopy, *Water, *Argon, *High resolution, Quantum chemistry, Energy transfer, Van der Waals forces, Spectrum analysis, Frequencies, Supersonic jet flow, Kinetics, Collisions, Reprints, Local mode, Vibrational predissociation.

Para ArH2O complexes are detected in the near IR via slit jet direct absorption spectroscopy using cw difference frequency generation of high resolution tunable infrared radiation (IR) in the 3780 cm(-1)V3=10 asymmetric OH stretch region. Frequency shifts in the f parity levels (Q branch), and both frequency shifts and predissociation broadened linewidths in the e parity levels (P/R branch) are evidenced in the spectrum, unambiguously characteristic of an avoided crossing in the vicinity of J'=6 with a second, near resonant vibration-internal rotation state in ArH2O. The data establish a clear upper limit on the dissociation bond strength for para ArH2O, and place spectroscopic constraints on the promoting internal rotor state in ArH2O (v1=1). A simple local mode theory of half-collision induced mixing between symmetric and asymmetric stretch excitation in H2O is presented.

00,873
PB95-107157 Not available NTIS
National Inst. of Standards and Technology (NML), Gaithersburg, MD. Chemical Kinetics Div.

Solvent Effects in the Reactions of Peroxyl Radicals with Organic Reductants. Evidence for Proton Transfer Mediated Electron Transfer.
Final rept.
P. Neta, P. Maruthamuthu, S. Steenken, and R. E. Huie. 1989, 6p.
Pub. in Jnl. of Physical Chemistry 93, n22 p7654-7659 1989.

Keywords: *Electron transfer, *Radiolysis, *Radicals, *Solvents, Protons, Reduction(Chemistry), Reaction kinetics, Solvent properties, Reprints, *Peroxyl radicals, Proton transfer.

Absolute rate constants for the reactions of substituted methylperoxyl radicals with ascorbate, urate, trolox (6-hydroxy-2,5,7,8-tetramethylchromane-2-carboxylic acid), and TMPD (N,N,N',N'-tetramethyl-p-phenylenediamine) have been determined by pulse radiolysis in different solvents. In water-alcohol or water-dioxane solutions the rate constants for trihalomethylperoxyl radicals generally increase with increasing water content. The rate constants were found to correlate well with a two-parameter equation which includes the dielectric constant of the solvent and the coordinate covalency parameter, a measure of the proton-transfer basicity of the solvent.

00,874
PB95-107223 Not available NTIS
National Inst. of Standards and Technology (IMSE), Gaithersburg, MD. Reactor Radiation Div.
Inelastic Neutron Scattering Studies of Nonlinear Optical Materials: p-Nitroaniline Adsorbed in ALPO-5.
Final rept.
J. Nicol, T. J. Udovic, J. J. Rush, S. D. Cox, and G. D. Stucky. 1990, 6p.
Pub. in Materials Research Society Symposia Proceedings Neutron Scattering Materials Science, v166 p367-372 1990.

Keywords: *Vibrational spectra, *Analines, Reprints, Optical materials, Nonlinear optics, Nitro compounds, Molecular sieves, Hydrogen bonds, Neutron scattering, Inelastic scattering, Adsorption, *Nitroanilines.

Inelastic neutron scattering has been used to characterize the vibrational spectroscopy below 220 meV of para-nitroaniline adsorbed in the molecular sieve ALPO-5. Samples at loadings of both 3 and 13 weight %, which represent the onset of and the maximum in the nonlinear optical properties respectively, were studied. The torsional vibration of the amino (NH2) group has been identified at ca. 50 meV. The splitting and structure of this mode is sensitive to the loading level. This can be related to differences in the nature of the hydrogen bonding in these materials.

00,875
PB95-107264 Not available NTIS
National Inst. of Standards and Technology (NML), Gaithersburg, MD. Thermophysics Div.
Fluctuation Dominated Recombination Kinetics with Traps.
Final rept.
J. C. Rasaiah, J. Zhu, J. B. Hubbard, and R. J. Rubin. 1990, 7p.
Pub. in Jnl. of Chemical Physics 93, n8 p5768-5774, 15 Oct 90.

Keywords: *Recombination reactions, *Fluctuations, Annihilation reactions, Computerized simulation, Kinetics, Diffusion, Trapping, Exponential functions, Reprints, Donsker-Varadhan Model, Lattices.

Theoretical and computer simulation studies of annihilation reactions with traps on two and in three dimensional lattice systems are discussed. Several remarkable features of these reactions, some predicted by theory and others observed in computer simulations, are pointed out. The stretched exponential behavior of the Donsker-Varadhan formula A(t) approximately equal to e raised to the -t(supd/(d + 2)) power, where d is the dimensionality, already found for the reactant decay in A-A annihilation reactions with traps on a square lattice (Rasaiah et al. - J. Phys. Chem., in press), was tested for universality by studying triangular and hexagonal lattices in two dimensions (2d) and a cubic lattice in three dimensions (3d). The same behavior is also observed when the free particle annihilation is turned off.

00,876
PB95-108445 Not available NTIS
National Inst. of Standards and Technology (PL), Gaithersburg, MD. Molecular Physics Div.
Self-, N2- and Ar-Broadening and Line Mixing in HCN and C2H2.
Final rept.
A. S. Pine. 1993, 18p.
Sponsored by National Aeronautics and Space Administration, Washington, DC.
Pub. in Jnl. of Quantitative Spectroscopy and Radiative Transfer 50, n2 p149-166 1993.

Keywords: *Hydrogen cyanide, *Acetylene, Intermediate infrared radiation, Pressure broadening, Band spectra, Tunable lasers, Nitrogen, Argon, Reprints, Collisional energy transfer, Q branches, Self broadening.

Self-, N2- and Ar-broadening coefficients have been measured for the stretch-bend infrared combination bands nu(sub 1) + nu(sub 2, sup 1) (4004/cm) of HCN and nu(sub 1) + nu(sub 5, sup 1) (4091/cm) of C2H2 using a tunable difference-frequency laser. At atmospheric pressures, the Q branches of these bands exhibit significant rotational narrowing or line mixing. The broadening coefficients have been fit with empirical rotationally inelastic collision rate laws, which are then used to model the line mixing in the overlapped Q-branch profiles. Simple energy gap fitting laws appear to be suitable for the shorter-range intermolecular quadrupole-quadrupole and induction forces, whereas an energy-corrected-sudden scaling law works better for the longer-range dipole-dipole and dipole-quadrupole collision partners. In all cases, the line-coupling coefficients are substantially reduced from the rotationally inelastic rates fit to the broadening coefficients, indicating that 35-70% of the broadening may be due to other collisional mechanisms such as cross-relaxation to the degenerate (Pi) state vibrational level.

00,877
PB95-108452 Not available NTIS
National Inst. of Standards and Technology (PL), Gaithersburg, MD. Molecular Physics Div.
Decoupling in the Line Mixing of Acetylene Infrared Q Branches.
Final rept.
A. S. Pine, and J. P. Looney. 1990, 12p.
Pub. in Jnl. of Chemical Physics 93, n10 p6942-6953 1990.

Keywords: *Acetylene, Near infrared radiation, Infrared spectroscopy, Pressure broadening, Line shape, Reprints, Q branches.

The Q-branch profiles of the nu(1) + nu(5), nu(3) + nu(4) and nu(2) + 2nu(4) + nu(5) II(u) - Sigma(g) combination bands in the 2.5 micrometer C-H stretch-bend region of acetylene have been recorded with a difference-frequency laser spectrometer at pressures from 1 to 500 Torr (0.13 to 66.7 kPa). The broadening coefficients, obtained from the nu(1) + nu(5) band at pressures low enough to avoid significant spectral overlap, can be well fit with empirical rotationally-inelastic energy-gas scaling laws or satisfactorily modeled with semiclassical line broadening theory using known intermolecular potential parameters.

00,878
PB95-108460 Not available NTIS
National Inst. of Standards and Technology (CSTL), Gaithersburg, MD. Biotechnology Div.
Self-Assembled Phospholipid/Alkanethiol Biomimetic Bilayers on Gold.
Final rept.
A. L. Plant. 1993, 4p.
Pub. in Lagmuir 9, n11 p2764-2767 Nov 93.

Keywords: *Phospholipids, *Lipid bilayers, *Gold, *Electrochemistry, Melittin, Substrate specificity, Solvents, Artificial membranes, Reprints, *Alkanethiols.

Alkanethiols can act as hydrophobic monolayer substrates for the formation of phospholipid-containing bilayers. Phospholipid vesicles were allowed to fuse to alkanethiol monolayers, resulting in stable, solvent-free lipid bilayers on gold electrodes. The capacitance of these belayers has been determined by impedance measurements, and the effect of the pore-forming peptide melittin on the bilayer has been determined by the measurement of faradaic current. These supported self-assembling phospholipid/alkanethiol bilayers demonstrate properties consistent with those of fluid membranes, and provide a useful way to study the electrical characteristics of membranes in the absence of solvent.

00,879
PB95-108478 Not available NTIS
National Inst. of Standards and Technology (CSTL), Gaithersburg, MD. Biotechnology Div.
Fokker-Planck Description of Multivalent Interactions.
Final rept.
A. L. Plant, M. Gray, and J. B. Hubbard. 1993, 15p.
Pub. in Biophysical Chemistry 48, p75-89 1993.

Keywords: *Binding sites, *Kinetics, *Chemical models, Liposomes, Reprints, *Fokker-Planck descriptions.

A dynamic model is presented which uses a mean first passage time to characterize multivalent binding as the continuum limit of a one-step stochastic process. The use of a stochastic model instead of a model based on rate equations permits consideration of fluctuations in the number of bonds formed. The importance of fluctuations to the problem of multivalent interactions, especially low affinity interactions, is discussed. Assumptions for the theory are based on data in which liposomes were used as a model system for multivalency. The data suggest a linear sequential process of bond rupture, and thus a high degree of cooperativity in the microscopic events associated with multivalent liposomal binding.

00,880
PB95-108494 Not available NTIS
National Inst. of Standards and Technology (PL), Boulder, CO. Quantum Physics Div.
Photoelectron Spectroscopy of Negatively Charged Bismuth Clusters: Bi(-)2, Bi(-)3, and Bi(-)4.
Final rept.
M. L. Polak, J. Ho, G. Gerber, and W. C. Lineberger. 1991, 11p.
Grant NSF-CHE88-19444
Sponsored by National Science Foundation, Washington, DC.
Pub. in Jnl. of Chemical Physics 95, n5, p3053-3063, 1 Sep 91.

Keywords: *Photoelectron spectroscopy, *Atomic clusters, Negative ions, Electron affinity, Excited states, Ground state, Reprints, *Bismuth clusters.

The authors have recorded the 351 nm photoelectron spectra of Bi(-)2, Bi(-)3, and Bi(-)4. The spectrum of Bi(-)2 shows transitions to at least seven electronic states of Bi2 neutral, four of which are observed with vibrational resolution. Term energies, bond lengths, and vibrational frequencies are obtained for the anion ground state and for the first three excited states of Bi2. These results are compared to previous spectroscopic measurements and to the ab initio calculations presented in the accompanying paper. The photoelectron spectrum of Bi(-)3 reveals some of the electronic structure of Bi3 and the results are discussed in comparison to recent theoretical work. Adiabatic electron affinities are obtained for Bi2 (1.271(8) eV) and for Bi3 (1.60(3) eV). The electron affinity of Bi4 is estimated from the onset of photodetachment to be 1.05(10) eV.

00,881
PB95-108528 Not available NTIS
National Inst. of Standards and Technology (CSTL), Gaithersburg, MD. Surface and Microanalysis Science Div.
Activities of the ASTM Committee E-42 on Surface Analysis.
Final rept.
C. J. Powell. 1992, 4p.
Pub. in Surface and Interface Analysis 19, p237-240 1992.

Keywords: *Surface analysis, *Standards, Surface chemistry, Reprints, ASTM committees, Reference materials.

The ASTM Committee E-42 on Surface Analysis was formed in 1976 to advance the field of surface analysis and the quality of surface analyses through the development of appropriate standards (reference procedures, reference materials and reference data), round robins, symposia, workshops and publications. A major function of the Committee is the development of documentary standards or reference procedures. This article contains a brief summary of Committee activities, with emphasis on the reference procedures that have been published and those that are under development.

00,882
PB95-108593 Not available NTIS
National Inst. of Standards and Technology (MSEL), Gaithersburg, MD. Reactor Radiation Div.

Construction of Maximum-Entropy Density Maps, and Their Use in Phase Determination and Extension.
Final rept.
E. Prince. 1993, 5p.
Pub. in Acta Cryst. D49, p61-65 1993.

Keywords: *Electron density(Concentration), *Molecular structure, Fourier analysis, Macromolecules, Reprints, Phase determination, Maximum entropy.

Methods for constructing everywhere-positive electron-density maps with Fourier amplitudes matching those for arbitrarily large sets of observed data, using dual-function methods for maximization of entropy, are described. Possible strategies for using these maps for the determination and extension of phases in macromolecular structure determination are suggested, and problems are discussed.

00,883
PB95-108619 Not available NTIS
National Inst. of Standards and Technology (PL), Boulder, CO. Quantum Physics Div.
Vibrational Energy Transfer in S1 p-Difluorobenzene. A Comparison of Low and Room Temperature Collisions.
Final rept.
C. J. Pursell, and C. S. Parmenter. 1993, 7p.
Pub. in Jnl. of Physical Chemistry 97, n8 p1615-1621 1993.

Keywords: *Atom-molecule collisions, Temperature range 0013-0065 K, Room temperature, Vibrational states, Energy transfer, Difluoro compounds, Helium, Argon, Reprints, *Difluorobenzene.

Vibrational energy transfer in S(1) p-difluorobenzene has been studied at low temperature within a supersonic free jet. Quantitative relative cross sections for the state-to-state vibrational energy transfer channels (i.e. flow patterns) from the 8(sup 2) vibrational level (epsilon(vib) = 346/cm) were obtained for low energy collisions (T approx = 20-35 K) with He and Ar. They are qualitatively similar to analogous flow patterns obtained earlier from the 0(sup 0) level from room temperature (300 K) collisions with He and Ar. Both the 300 K and the low temperature flow patterns show that the vibrational energy transfer is selective among the possible channels and that the competition among vibrational channels is distinctive for each collisional partner. The low and room temperature flow patterns differ, however, in quantitative detail. A treatment of the standard SSH-T vibrational energy transfer model describes semiquantitatively the flow patterns at both low and room temperature and for collisions with He and Ar. The success of a single model suggests that vibrational energy transfer in S(1) p-difluorobenzene is governed by the same mechanism over the entire span of collision energies associated with temperatures from about 20 to 300 K.

00,884
PB95-108627 Not available NTIS
National Inst. of Standards and Technology (NML), Gaithersburg, MD. Chemical Process Metrology Div.
Measurement of the Self Broadening of the H2Q(0-5) Raman Transitions from 295 to 1000 K.
Final rept.
L. A. Rahn, R. L. Farrow, and G. J. Rosasco. 1991, 14p.
Pub. in Physical Review A 43, n11 p6075-6088 1991.

Keywords: *Raman spectroscopy, *Hydrogen, Temperature range 0273-0400 K, Temperature range 0400-1000 K, Temperature dependence, Pressure dependence, Vibrational states, Line broadening, High resolution, Reprints, Self broadening, Q branches.

High-resolution inverse Raman spectroscopy (IRS) has been used to measure the self-broadening coefficients of the Raman Q-branch transitions in pure (natural) hydrogen. Measurements of six lines (Q(0)-Q(5)) were made at pressures from 2 to 50 atmospheres and from 295 to 1000 K. The dependence of the derived broadening coefficients on temperature and rotational quantum number is analyzed using the energy-corrected-sudden scaling law (A. E. DePristo, J. Chem. Phys. 73, 2145 (1980)). The authors discuss three models for the J-dependence of the pure-vibrational dephasing and find that models with little or no J-dependence in the pure-vibrational dephasing are preferred.

00,885
PB95-108635 Not available NTIS
National Inst. of Standards and Technology (CSTL), Boulder, CO. Thermophysics Div.
Calculation of Enthalpy and Entropy Differences of Near-Critical Binary Mixtures with the Modified Leung-Griffiths Model.
Final rept.
J. C. Rainwater, and D. G. Friend. 1993, 10p.
Pub. in Jnl. of Chemical Physics 98, n3 p2298-2307, 1 Feb 93.

Keywords: *Liquid vapor equilibrium, *Binary mixtures, *Benzene, *Alkanes, *Entropy, *Enthalpy, Thermodynamic properties, Phase transformations, Fugacity, Free energy, Mathematical models, Reprints, *Clapeyron equation, *Leung-Griffiths Model.

In previous applications of the Leung-Griffiths model as modified by Moldover and Rainwater, many near-critical vapor-liquid equilibrium surfaces have been described successfully in the space of pressure, temperature, density, and composition, but calorimetric properties such as entropy and enthalpy have not been examined. Such calculations are difficult in general because of the need to determine a parameter that is usually unknown in the definition of an independent field variable (the fugacity fraction). However, a generalization for mixtures of the Clapeyron equation is available which allows for the calculation of differences in entropy, enthalpy, and free energies between a pair of (noncoexisting) dew and bubble points at the same temperature and composition. A calculation of entropy differences from a correlation of carbon dioxide + propylene agrees well with results inferred indirectly from experimental data. As a more direct check, calculation of enthalpy differences from a correlation of n-pentane + benzene agrees with an interpolation of enthalpy data provided by calorimetric measurements of Lenoir and Hipkin. The generalized Clapeyron equation appears to be singular at the maxcondentherm point, but it is shown that the singular terms cancel one another and that the leading-order finite term is consistent with a thermodynamic Maxwell relation.

00,886
PB95-108817 Not available NTIS
National Inst. of Standards and Technology (CSTL), Boulder, CO. Thermophysics Div.
Polarized Transient Hot Wire Thermal Conductivity Measurements.
Final rept.
R. A. Perkins, A. Laesecke, and C. A. Nieto de Castro. 1992, 12p.
Sponsored by Department of Energy, Washington, DC.
Pub. in Fluid Phase Equilibria 80, p275-286 1992.

Keywords: *Thermal conductivity, *Fluorohydrocarbons, Liquids, Refrigerants, Substitutes, Reprints, *1, *1-chloro-1, *R134a, *R142b, 1, 1, 2-Tetrafluoroethane, 1-difluoroethane, Transient hot wire instruments.

Additional experimental uncertainty is introduced in thermal conductivity data obtained with the transient hot-wire technique when bare hot wires are used in polar liquids. The use of a dc polarization voltage applied between the hot wires and the cell wall greatly reduces this uncertainty for polar liquids. Differences between polarized and nonpolarized experiments are described for the alternative refrigerants 1,1,1,2-tetrafluoroethane (R134a) and 1-chloro-1,1-difluoroethane (R142b). Comparisons are made between data from the polarized transient hot-wire technique and other experimental techniques for R142b. The polarization technique enables existing transient hot-wire instruments with bare wires to study the thermal conductivity of moderately polar liquids with confidence.

00,887
PB95-125621 Not available NTIS
National Inst. of Standards and Technology (PL), Gaithersburg, MD. Molecular Physics Div.
Reanalysis of the (010), (020), (100), and (001) Rotational Levels of (32)S(16)O2.
Final rept.
J. M. Flaud, A. Perrin, L. M. Salah, W. J. Lafferty, and G. Guelachvili. 1993, 7p.
Sponsored by National Aeronautics and Space Administration, Washington, DC.
Pub. in Jnl. of Molecular Spectroscopy 160, p272-278 1993.

Keywords: *Sulfur dioxide, *Rotational states, Infrared spectra, Band spectra, High resolution, Oxygen 16, Sulfur 32, Reprints, Molecular constants.

Using high-resolution infrared spectra, a reanalysis of the nu(sub 2), 2nu(sub 2)-nu(sub 2), nu(sub 1), and nu(sub 3) bands of (32)S(16)O2 has been performed. These infrared data, combined with the available heterodyne and microwave data, were fitted within their respective experimental accuracies. For the (010) levels it was sufficient to use a Watson-type Hamiltonian, whereas it proved necessary to consider explicitly interaction terms for the (020)(100)(001) states. More precisely, a (Delta)K = 2 quadratic distortion-correction to the Fermi interaction term was used to treat the interactions between (020) and (100) and a (Delta)K = 3 Coriolis-type term to treat the interactions between (100) and (001).

00,888
PB95-125662 Not available NTIS
National Inst. of Standards and Technology (PL), Gaithersburg, MD. Molecular Physics Div.
Mid- and Near-Infrared Spectra of Water and Water Dimer Isolated in Solid Neon.
Final rept.
D. Forney, M. E. Jacox, and W. E. Thompson. 1993, 5p.
Sponsored by Army Research Office, Research Triangle Park, NC.
Pub. in Jnl. of Molecular Spectroscopy 157, p479-493 1993.

Keywords: *Water, *Infrared spectra, Temperature range 0000-0013 K, Intermediate infrared radiation, Near infrared radiation, Deuterium compounds, Matrix isolation, Oxygen 16, Oxygen 18, Dimers, Reprints, Solid neon.

Spectra have been obtained between 700 and 8000/cm for H2(16)O, and between 700 and 5000/cm for deuterium and/or oxygen-18-enriched water, trapped in solid neon at approximately 5 K. Samples with Ne:water mole ratios between 400 and 6400 were studied. As in the heavier rare-gas solids, isolated water molecules can undergo relatively free rotation in solid neon, and nuclear spin equilibration is slow. The observed spectra can be explained by postulating excitation from the two lowest rotational levels of the water molecule. Absorptions of nonrotating water are also present in the spectrum. The matrix shifts for water isolated in a neon matrix are much smaller than those reported for water in matrices of the heavier rare gases. Absorptions contributed by the H- or D-donor moiety of (H2O)2, (HDO)2, and (D2O)2 have also been identified and assigned.

00,889
PB95-125670 Not available NTIS
National Inst. of Standards and Technology (PL), Gaithersburg, MD. Molecular Physics Div.
Vibrational Spectra of Molecular Ions Isolated in Solid Neon. X. H2O(+), HDO(+), and D2O(+).
Final rept.
D. Forney, M. E. Jacox, and W. E. Thompson. 1993, 9p.
Sponsored by Army Research Office, Research Triangle Park, NC.
Pub. in Jnl. of Chemical Physics 98, n2 p841-849, 15 Jan 93.

Keywords: *Molecular ions, *Vibrational spectra, *Water, Temperature range 0000-0013 K, Infrared absorption, Infrared spectra, Deuterium compounds, Matrix isolation, Photodetachment, Reprints, Solid neon.

When a Ne:H2O = or > 200 sample is codeposited at approximately 5 K with a beam of neon atoms that have been excited in a microwave discharge, new infrared absorptions appear close to the gas-phase band centers of the three vibrational fundamentals of H2O(1+). Detailed isotopic substitution studies confirm this assignment and provide assignments for all of the vibrational fundamentals of HDO(1+) and D2O(1+). When ions are present in the neon matrix, rotation of a significant fraction of the water molecules is inhibited. Electrons produced by the photodetachment of anions, which must be present to maintain overall charge neutrality of the deposit, accelerate nuclear spin equilibration of water in the matrix. As the concentration of H2O(1+) is decreased by capture of the photodetached electrons, the absorptions assigned to nonrotating water are also reduced in intensity. The nature of the other ionic species which may be present in the sample is considered.

00,890
PB95-125688 Not available NTIS
National Inst. of Standards and Technology (PL), Gaithersburg, MD. Molecular Physics Div.

Vibrational Spectra of Molecular Ions Isolated in Solid Neon. XI. NO2(+), NO2(-), and NO3(-).
Final rept.
D. Forney, W. E. Thompson, and M. E. Jacox. 1993, 11p.
Sponsored by Army Research Office, Research Triangle Park, NC.
Pub. in Jnl. of Chemical Physics 99, n10 p7393-7403, 15 Nov 93.

Keywords: *Molecular ions, *Nitrogen dioxide, *Vibrational spectra, Temperature range 0000-0013 K, Infrared absorption, Infrared spectra, Electron capture, Matrix isolation, Reprints, *Solid neon, *Nitrite ions, *Nitrate ions.

When a Ne:NO2 or a Ne:NO:O2 sample is codeposited at approximately 5 K with a beam of neon atoms that have been excited in a microwave discharge, infrared absorptions of NO2(1+), NO2(1-), and NO3(1-) appear. Detailed isotopic substitution studies support the assignment of prominent absorptions to nu(sub 3) of NO2(1+) and NO2(1-) and of weak to moderately intense absorptions to the nu(sub 1) + nu(sub 3) combination band of each of these species. When the contribution of anharmonicity is considered, the positions of the NO2(1+) absorptions are in satisfactory agreement with the values for the stretching fundamentals obtained in a recent gas-phase study of that species. When the sample is exposed to 240-420 nm mercury-arc radiation, the initially present absorptions of NO3(1-) trapped in sites with a small residual cation interaction diminish in intensity, and the unsplit nu(sub 3)(e') absorption of isolated NO3(1-) grows. The mechanism responsible for this growth in the absorption of isolated NO3(1-) is considered.

00,891
PB95-125779 Not available NTIS
National Inst. of Standards and Technology (CSTL), Boulder, CO. Thermophysics Div.
Thermodynamic Properties of the Methane-Ethane System.
Final rept.
D. G. Friend, and J. F. Ely. 1992, 12p.
Sponsored by Department of Energy, Washington, DC. and Gas Research Inst., Chicago, IL.
Pub. in Fluid Phase Equilibria 79, p77-88 1992.

Keywords: *Thermophysical properties, *Methane, *Ethane, *Binary mixtures, Thermodynamic properties, Liquid phases, Equations of state, Critical point, Specific heat, Phase stability(Materials), Pressure, Volume, Temperature, Acoustic velocity, Reprints, *Extended corresponding states.

Our recently completed wide-ranging correlations for the thermophysical properties of methane and ethane fluids have enabled us to improve the extended corresponding states calculations for the properties of the binary mixtures. The pure fluid equations are based on the analytic Schmidt-Wagner equation of state and give improved results in the general region of the critical point. We use these pure fluid equations (and a reference fluid for which an equivalent equation is known) to calculate properties and compare with experimental PVT data, isochoric heat capacities, and sound speeds of binary mixtures of methane and ethane. We also examine the properties at the vapor-liquid boundary and compare the representation from the classical extended corresponding states calculations with quantities derived from a scaling theory model. The shape of the binary mixture phase boundary is improved with this model, however our new representation of the single phase properties provides only a slight improvement over models based on modified Benedict-Webb-Rubin pure fluid equations of state.

00,892
PB95-125803 Not available NTIS
National Inst. of Standards and Technology (NML), Gaithersburg, MD. Chemical Process Metrology Div.
Conductance Response of Pd/SnO2(110) Model Gas Sensors to H2 and O2.
Final rept.
T. B. Fryberger, and S. Semancik. 1990, 5p.
Pub. in Sensors and Actuators B 2, n4 p305-309 1990.

Keywords: *Gas detectors, *Tin oxides, *Palladium, *Hydrogen, *Oxygen, Metal oxide semiconductors, Electrical conductivity, Gas analysis, Surface analysis, Adsorption, Reprints.

Gases can influence the conductance of tin oxide sensors by a variety of mechanisms. In general, it is difficult to distinguish between different sensing mechanisms because so little is known about the sensor surface during operation. We have used surface analytical techniques together with in situ gas conductance response measurements to study gas sensing mechanisms on well-characterized Pd/SnO2(110) model sensor surfaces. In this letter, we report results for H2 and O2 adsorption and coadsorption: hydrogen was chosen because of its importance both as a gas to be monitored and as an adsorption product of hydrocarbons and alcohols, and oxygen because it is nearly always abundant in the sensor ambient (often, air).

00,893
PB95-125860 Not available NTIS
National Inst. of Standards and Technology (CSTL), Gaithersburg, MD. Surface and Microanalysis Science Div.
Single-Atom Point Source for Electrons: Field-Emission Resonance Tunneling in Scanning Tunneling Microscopy.
Final rept.
J. W. Gadzuk. 1993, 8p.
Pub. in Physical Review B 47, n19 p12 832-12 839, 15 May 93.

Keywords: *Scanning tunneling microscopy, *Resonant tunneling, Field emission, Atomic clusters, Point sources, Electron sources, Atoms, Reprints, Tunneling spectroscopy.

Many years ago spectroscopic evidence based on a single-electron process, namely, field-emission resonance tunneling, was reported showing the electronic structure of single atoms adsorbed on metal surfaces. Huge enhancements in the highly collimated tunneling current through the virtual states of the adparticle made the single-atom spectroscopy feasible when the field-emission spectrometer was operated in the 'probe-hole mode.' A related effect is currently popular in today's scanning tunneling microscopy and also in nanometer-cluster spectroscopy. The phenomenology and theory of the effect is presented, and the current activity is considered in light of what has been uncovered in the field-emission work.

00,894
PB95-125878 Not available NTIS
National Inst. of Standards and Technology (CSTL), Gaithersburg, MD. Biotechnology Div.
Aggregation Kinetics of Colloidal Particles Destabilized by Enzymes.
Final rept.
A. K. Gaigalas, and H. H. Weetall. 1993, 7p.
Pub. in Analytical Biochemistry 213, p329-335 1993.

Keywords: *Colloids, *Kinetics, *Enzymes, Radiation scattering, Light, Diffusion, Particle density(Concentration), Chemical models, Agglomeration, Proteins, Carbohydrates, Photons, Reprints.

Dynamic light scattering was used to measure enzymatic activity by monitoring the rate of destabilization of colloidal particles coated with proteins or carbohydrates. The photon autocorrelation spectrum was analyzed using a cumulant expansion or direct inversion. In all cases, the measured average diffusion coefficient and the standard deviation of the diffusion coefficient decreased with time. A kinetic model with a bimodal particle distribution function was used to represent the time dependence of the cumulants. The cumulants are very sensitive to the details of the particle distribution.

00,895
PB95-126041 Not available NTIS
National Inst. of Standards and Technology (CSTL), Gaithersburg, MD. Surface and Microanalysis Science Div.
Picosecond Measurement of Substrate-to-Adsorbate Energy Transfer: The Frustrated Translation of CO/Pt(111).
Final rept.
T. A. Germer, J. C. Stephenson, E. J. Heilweil, and R. R. Cavanagh. 1993, 9p.
Pub. in Jnl. of Chemical Physics 98, n12 p9986-9994, 15 Jun 93.

Keywords: *Carbon monoxide, *Adsorbates, Vibrational states, Temperature dependence, Picosecond pulses, Infrared radiation, Energy transfer, Excitation, Substrates, Platinum, Phonons, Reprints, Translations.

The transient infrared response of CO/Pt(111) following picosecond visible excitation is reported. A spectrally broad decrease in reflectivity correlates with heating of the Pt lattice, and an observed shift in the CO(nu = 0 --> 1) transition is interpreted as heating of the 60/cm in-plane frustrated translational mode. A phenomenological three temperature model that assumes the adsorbate vibrational temperature exclusively couples to either the electronic temperature (with a time constant tau(e)) or to the lattice temperature (with a time constant tau(lat)) describes the temporal response of the adsorbate vibrations. The lattice phonon temperature and measured temperature dependence of the optical constants predict the observed spectrally broad reflectivity change. Density matrix methods model the infrared response of the transiently heated molecule. Limits of tau(e) = 2 plus or minus 1 ps or tau(lat) < 1 ps are established by comparison of predicted spectra and the data.

00,896
PB95-126140 Not available NTIS
National Inst. of Standards and Technology (PL), Gaithersburg, MD. Molecular Physics Div.
Rotational Spectrum and Structure of a Weakly Bound Complex of Ketene and Acetylene.
Final rept.
C. W. Gillies, J. Z. Gillies, F. J. Lovas, and R. D. Suenram. 1993, 10p.
Pub. in Jnl. of the American Chemical Society 115, n20 p9253-9262 1993.

Keywords: Van der Waals forces, Microwave spectroscopy, Rotational spectra, Deuterium compounds, Electric moments, Dipole moments, Hamiltonians, Reprints, *Acetylene complexes, *Ketene complexes, Fourier transform spectroscopy.

Rotational spectra of CH2CO-C2H2, CD2CO-C2H2, CH2CO-C2HD, and CH2CO-C2D2 were observed with a pulsed-beam Fabry-Perot cavity Fourier-transform microwave spectrometer. The b-type transitions were split into four states for CH2CO-C2H2 and CD2CO-C2H2, while two states were assigned for CH2CO-C2HD and CH2CO-C2D2. All states were fit individually to a quartic Watson Hamiltonian. The electric dipole moment of CH2CO-C2H2 was measured.

00,897
PB95-126157 Not available NTIS
National Inst. of Standards and Technology (NML), Gaithersburg, MD. Chemical Thermodynamics Div.
Biological Macromolecular Crystallization Database: A Tool for Developing Crystallization Strategies.
Final rept.
G. L. Gilliland, and D. Bickham. 1990, 6p.
Pub. in Methods 1, n1 p6-11 1990.

Keywords: *Crystallization, *Data bases, X-ray diffraction, Reprints, *Biological macromolecules.

The Biological Macromolecule Crystallization Database (BMCD) contains the crystallization conditions and crystal data for crystal forms of all classes of biological macromolecules which have had the unit cell dimensions and space group determined by single-crystal x-ray diffraction analysis. The BMCD provides a menu driven interface which allows searching the data for a value or a range of values for any of nineteen different parameters, individually or in any combination. The results of a search may be displayed or printed in a variety of different formats. Besides providing the information necessary to crystallize a particular macromolecule, the BMCD may be utilized to design strategies for the crystallization of molecules which have not previously been crystallized. Strategies for the crystallization of modified (or mutant) biological macromolecules, biological macromolecules which are homologous to previously crystallized macromolecules, and unique biological macromolecules which have not been previously crystallized are discussed.

00,898
PB95-126181 Not available NTIS
National Inst. of Standards and Technology (MSEL), Gaithersburg, MD. Reactor Radiation Div.
Characterization of Chemically Modified Pore Surfaces by Small Angle Neutron Scattering.
Final rept.
C. J. Glinka, L. C. Sander, S. A. Wise, and N. F. Berk. 1990, 6p.
Pub. in Materials Research Society Symposia Proceedings, v166 p415-420 1990.

Keywords: *Surface chemistry, *Silicon dioxide, *Porous media, *Small angle scattering, *Molecular

structure, *Particles, Neutron scattering, Adsorbates, Hydrocarbons, Grafted polymerization, Chemical bonds, Liquid column chromatography, Reprints.

Small angle neutron scattering has been used to characterize the structure of linear hydrocarbon chains chemically grafted to the internal pore surfaces of microporous silica particles. The aim of this work has been to relate the structure of the bonded adsorbate layers in these particles to their performance in, for example, reverse-phase liquid chromatography. By filling the pore space in the modified silica with a solution that matches the scattering density of the silica framework, the scattering from the adsorbate layers is enhanced and provides a sensitive probe of the effective thickness, uniformity and degree of solvent penetration in the layers. Results are presented for both monomeric and polymeric phases of alkyl chains ranging from C8 to C30 bonded to silica particles with a mean pore size of 100 nm.

00,899
PB95-126231 Not available NTIS
National Inst. of Standards and Technology (CSTL), Gaithersburg, MD. Thermophysics Div.
Vapor Pressure of 1,1-dichloro-2,2,2-trifluoroethane (R123).
Final rept.
A. R. H. Goodwin, D. R. Defibaugh, G. Morrison, and L. A. Weber. 1992, 11p.
Pub. in International Jnl. of Thermophysics 13, n6 p999-1009 Nov 92.

Keywords: *Vapor pressure, *Refrigerants, Fluorohydrocarbons, Freons, Thermodynamic properties, Ebulliometry, Static tests, Reprints, *Ethane/dichloro-trifluoro, Freon 123.

The vapor pressure of 1,1-dichloro-2,2,2-trifluoroethane (R123) has been measured at temperatures between 256.4 and 453.8 K by ebulliometric and static techniques. These results have been combined to obtain a correlation for the vapor pressure from 256.4 K to the critical temperature.

00,900
PB95-140133 Not available NTIS
National Inst. of Standards and Technology (NML), Gaithersburg, MD. Thermophysics Div.
Formulation of the Refractive Index of Water and Steam.
Final rept.
P. Schiebener, J. Straub, J. M. H. Levelt Sengers, and J. S. Gallagher. 1990, 8p.
Pub. in Properties of Water and Steam, p103-110 1990.

Keywords: *Water vapor, *Water, *Steam, *Refractive index, Equations of state, Temperature dependence, Infrared radiation, Visible radiation, Ultraviolet radiation, Supercooling, Reprints, Density dependence.

A new formulation is presented of the refractive index of water and steam over large ranges of temperature and density, and in the visible, infared and ultraviolet up to the first resonances. The formulation makes use of the fact that the molar refractivity of water and steam, at constant wavelength, varies no more than a few percent, so that temperature and density dependence require very few adjustable parameters. The NBS/NRC equation is used to convert experimental pressures to temperatures. It is demonstrated that the formulation, in conjunction with the best refractive index data, can be used to discriminate between various highly accurate equations of state for water.

00,901
PB95-140166 Not available NTIS
National Inst. of Standards and Technology (NML), Gaithersburg, MD. Thermophysics Div.
Near Critical Fluid Interfaces: A Comparison of Theory and Experiment.
Final rept.
J. W. Schmidt. 1991, 13p.
Pub. in Physica A 172, n1-2 p40-52 1991.

Keywords: *Interfaces, *Liquids, *Reflectivity, *Elliptical configuration, Capillary waves, Temperature dependence, Density(Mass/Volume), Phase transformations, Reprints, Consolute points.

Measurements of the ellipticity and reflectivity of liquid-liquid interfaces in mixtures near their consolute points are compared with theories of the interface. Both sets of measurements yield the same interfacial thickness within experimental error when scaled appropriately by theories that combine both the density-profile and capillary-wave aspects of the interface. The theories correctly predict the temperature dependence of the thickness, but systematically overestimate the thickness itself. When the few comparable data for pure fluids are scaled to the same theories, they show an unexpected temperature dependence of the thickness which is not consistent with the mixture results.

00,902
PB95-140174 Not available NTIS
National Inst. of Standards and Technology (CSTL), Gaithersburg, MD. Thermophysics Div.
Structure of the Vapor-Liquid Interface Near the Critical Point.
Final rept.
J. W. Schmidt, and M. R. Moldover. 1993, 8p.
Pub. in Jnl. of Chemical Physics 99, n1 p582-589, 1 Jul 93.

Keywords: *Liquid-vapor interfaces, *Ellipsometry, *Critical point, Carbon dioxide, Sulfur hexafluoride, Fluroalkanes, Phase diagrams, Refractivity, Reprints, Trifluoromethane.

We measured the thicknesses of the vapor-liquid interfaces near the critical points of carbon dioxide (CO_2), sulfur hexafluoride (SF_6), and trifluoromethane (CHF_3), using ellipsometry. The data (when scaled by the refractive index difference and the correlation length) are in agreement with other ellipticity data for binary and pseudobinary mixtures at low pressures. Fully constrained theories of the interface correctly predict the temperature dependence and scaling of the thickness but systematically overestimate the thickness itself by 15%-20%. The theory can be brought into agreement with experiment when an intrinsic interfacial stiffness is added to the theory. A novel feature of the present measurements is that the effects from pressure-induced window strain were measured and mitigated by using a cylindrically-symmetric pressure cell with floating seals.

00,903
PB95-140182 Not available NTIS
National Inst. of Standards and Technology (CSTL), Gaithersburg, MD. Thermophysics Div.
Operational Mode and Gas Species Effects on Rotational Drag in Pneumatic Dead Weight Pressure Gages.
Final rept.
J. W. Schmidt, B. E. Welch, and C. D. Ehrlich. 1993, 9p.
Pub. in Meas. Sci. Technol. 4, p26-34 1993.

Keywords: *Relaxation(Mechanics), *Rotation, *Pressure gages, *Gas dynamics, *Helium, *Hydrogen, *Nitrogen, *Sulfur hexafluoride, Pistons, Mathematical models, Low pressure, Spin, Annuli, Reprints, *Rotational drag, Spin time.

Rotational dissipation in a low-pressure pneumatic dead weight piston gauge has been measured for four gases: He, H_2, N_2 and SF_6. Significant differences in the rotational dissipation were observed between the four gas species. Even larger differences were observed between two operational modes (gauge and absolute). The measured results are interpreted by a model for the rotational dissipation due to the gas in the annular region between the piston and cylinder. Good agreement was found between the measured and modeled results for all four gas species with essentially no adjustable parameters.

00,904
PB95-140414 Not available NTIS
National Inst. of Standards and Technology (NEL), Gaithersburg, MD. Precision Engineering Div.
Scanning Tunneling Microscopy and Fabrication of Nanometer Scale Structures at the Liquid-Gold Interface.
Final rept.
J. Schneir, H. H. Harary, J. A. Dagata, P. K. Hansma, and R. Sonnenfeld. 1989, 6p.
Pub. in Scanning Microscopy 3, n3 p719-724 1989.

Keywords: *Liquid-solid interfaces, *Scanning tunneling microscopy, *Metal surfaces, *Gold, Atomic force microscopy, Imaging techniques, Electrochemistry, Electroplating, Fabrication, Lithography, Reprints, Nanostructures.

The Scanning Tunneling Microscope (STM) can image gold surfaces covered with a variety of liquids. This paper reviews the results obtained using the STM to image gold surfaces covered with liquid. These results include the creation of 10 nm structures, images of the electrochemical process of electroplating, and the production of atomically flat Au (111) surfaces. We conclude that in the future STM will find further application in the area of nanostructure fabrication and electrochemistry. The trend in the field is toward greater control of the electrochemical environment.

00,905
PB95-140463 Not available NTIS
National Inst. of Standards and Technology (CSTL), Gaithersburg, MD. Thermophysics Div.
Flow of Microemulsions through Microscopic Pores.
Final rept.
D. Ripple, and R. F. Berg. 1992, 5p.
Pub. in Jnl. of Chemical Physics 97, n10 p7761-7765, 15 Nov 92.

Keywords: *Viscosity, *Microemulsions, Drops(Liquids), Volume, Water, Decanes, Porosity, Reprints, Dioctylsulfosuccinate, AOT, Ternary systems.

The flow of the microemulsion dioctylsulfosuccinate (AOT)/decane/water through 0.1 and 1.0 micrometer diameter pores was studied for water droplet volume fractions ranging from 0 to 0.5. The viscosity of these microemulsions, as measured in a capillary viscometer with a bore of approximately 1 mm diameter, exceeds by as much as a factor of 4 theoretical predictions of the viscosity of suspensions of hard or liquid spheres. If droplet clustering causes this viscosity enhancement, then flow of the microemulsions through pores with diameter small compared to the characteristic cluster size should display a large finite-size effect. The apparent viscosity of the microemulsions in pores differed from the viscosity measured in the capillary viscometer by less than 40% for 0.1 micrometer diameter pores and by less than 8% for 1.0 micrometer diameter pores. These differences are of the same scale as estimates of two effects: adsorption of droplets on the pore wall and the enhanced flow of suspensions near a wall. The absence of larger finite-size effects implies that clustering of droplets on length scales of 0.1 micrometer or larger does not contribute substantially to the microemulsion viscosity.

00,906
PB95-140489 Not available NTIS
National Inst. of Standards and Technology (NML), Gaithersburg, MD. Chemical Process Metrology Div.
Michaelis-Menten Equation for an Enzyme in an Oscillating Electric Field.
Final rept.
B. Robertson, and R. D. Astumian. 1990, 6p.
Pub. in Biophysical Jnl. 58, p969-974 Oct 90.

Keywords: *Enzymes, *Electric fields, Oscillations, Protein conformation, Catalysis, Thermodynamics, Reprints, *Michaelis-Menten equation.

The electric charges on an enzyme may move concomitantly with a conformational change. Such an enzyme will absorb energy from an oscillating electric field. If, in addition, the enzyme has a larger association constant for substrate than for product, as is often true, it can use this energy to drive the catalyzed reaction away from equilibrium. Approximate analytical expressions are given for the field-driven flux, electrical power absorbed, free-energy produced per unit time, thermodynamic efficiency, and zero-flux concentrations. The field-driven flux is written as a generalized Michaelis-Menten equation.

00,907
PB95-140992 Not available NTIS
National Inst. of Standards and Technology (EEEL), Gaithersburg, MD. Electricity Div.
Associative Electron Attachment to S2F10, S2OF10, and S2O2F10.
Final rept.
J. K. Olthoff, K. L. Stricklett, R. J. Van Brunt, I. Sauers, J. H. Moore, and J. A. Tossell. 1993, 6p.
Sponsored by Department of Energy, Washington, DC. Office of Electrical Systems.
Pub. in Jnl. of Chemical Physics 98, n12 p9466-9471, 15 Jun 93.

Keywords: *Electron-molecule collisions, *Sulfur fluorides, *Electron attachment, *Gas dissociation, Milli eV Range, EV range 01-10, Fluorine ions, Negative ions, Cross sections, Resonance, Reprints, *Sulfur oxofluorides.

The absolute cross sections for dissociative electron attachment to the molecules S2F10S2OF10, and

S2O2F10 were measured in an electron transmission experiment. The corresponding negative-ion fragments were identified in a separate mass spectrometric measurement. For S2F10, the attachment of thermal electrons (energy less than 0.1 eV) appears to result primarily in the formation of F(-) and SF5(-) with possibly a small fraction of SF4(-) and SF6(-). The ions F(-) and SF5(-) are also produced from two attachment resonances at electron energies of about 4.5 and 9.5 eV. Both S2OF10 and S2O2F10 have unusually large dissociative attachment cross sections at energies near 0.1 eV. Electron attachment to S2OF10 yields primarily SOF5(-), while S2O2F10 yields both SF5(-) and SOF5(-) with possible minor fractions of F(-) and SOF3(-).

00,908
PB95-141032 Not available NTIS
National Inst. of Standards and Technology (PL), Gaithersburg, MD. Molecular Physics Div.
Infrared Spectrum of OClO in the 2000/cm(-1) Region: The 2(nu sub 1) and (nu sub 1 + nu sub 3) Bands.
Final rept.
J. Ortigoso, R. Escribano, J. B. Burkholder, and W. J. Lafferty. 1993, 10p.
Sponsored by National Aeronautics and Space Administration, Washington, DC. Upper Atmospheric Research Program.
Pub. in Jnl. of Molecular Spectroscopy 158, p347-356 1993.

Keywords: *Chlorine oxides, *Infrared spectra, Atmospheric composition, High resolution, Infrared spectroscopy, Band spectra, Dioxides, Chlorine 35, Chlorine 37, Reprints, Molecular constants.

Fourier Transform Infrared (FTIR) spectra of the 2nu(sub 1) and nu(sub 1) + nu(sub 3) of ClO2 (OClO) have been recorded in the 2000/cm region, with an instrumental resolution of about 0.004/cm. The spectra have been analyzed using a Hamiltonian which includes spin-rotation terms to provide the first high-resolution analysis of these bands. Around 1900 transitions of (35)ClO2 (plus about 600 of (37)ClO2) have been assigned in 2nu(sub 1), and 1100 transitions of (35)ClO2 (plus about 450 of (37)ClO2) have been identified in nu(sub 1) + nu(sub 3). By making use of all available data, accurate band centers, rotational constants, spin rotational constants, and a number of the chi(sub rs) anharmonicity constants as well as alpha and gamma parameters have been obtained.

00,909
PB95-141040 Not available NTIS
National Inst. of Standards and Technology (PL), Gaithersburg, MD. Molecular Physics Div.
Intensities and Dipole Moment Derivatives of the Fundamental Bands of (35)ClO2 and an Intensity Analysis of the nu1 Band.
Final rept.
J. Ortigoso, R. Escribano, J. B. Burkholder, and W. J. Lafferty. 1992, 9p.
Pub. in Jnl. of Molecular Spectroscopy 156, p89-97 1992.

Keywords: *Chlorine oxides, *Infrared spectra, Dipole moments, Band spectra, Luminous intensity, Brightness, Chlorine 35, Dioxides, Reprints, Herman-Wallis factors.

Integrated band intensities of all the fundamental bands of OClO as well as the 2nu(sub 1) overtone and the nu(sub 1) + nu(sub 3) combination band have been measured. Dipole moment derivatives with respect to the normal coordinates have been derived for these bands. For the nu(sub 1) band (35)ClO2 individual relative lines intensities have been obtained for many high K(sub alpha) (sup r)R branch lines, and a systematic deviation from intensities calculated from a zero order model, in which rotation-vibration interactions are not included, has been found. The deviation can be explained with the use of a transformed dipole moment operator. We have compared these results with those obtained using an expression derived by Watson for symmetric tops.

00,910
PB95-141107 Not available NTIS
National Inst. of Standards and Technology (CSTL), Gaithersburg, MD. Chemical Kinetics and Thermodynamics Div.
Reaction of Nitric Oxide with Organic Peroxyl Radicals.
Final rept.
S. Padmaja, and R. E. Huie. 1993, 6p.
Pub. in Biochemical and Biophysical Research Communications 195, n2 p539-544 1993.

Keywords: *Peroxyl radicals, *Nitric oxide, *Reaction kinetics, Free .radicals, Aqueous solutions, Biochemistry, Reprints, Alcoholic solutions.

Nitric oxide and organic peroxyl radicals are key reactive radicals implicated in a wide range of biological processes. We have measured rate constants for the reactions of several organic peroxyl radicals with nitric oxide in aqueous solution and found that they are all fast, with k = 1-3 X 10(exp 9) L/mol/s. The reactions lead to the formation of an intermediate, identified as the organic peroxynitrite, which decayed with a rate constant of k = 0.1-0.3/s. Possible products of this decay include the more reactive alkoxyl and nitrogen dioxide free radicals, or the less reactive organic nitrate. In alcoholic solutions, the rate constants of the initial reactions were similar, but the product decay rates were about 200 times faster. Because of the ubiquity of both nitric oxide and organic peroxyl radicals, their interaction could make a significant contribution to many physiological processes.

00,911
PB95-141131 Not available NTIS
National Inst. of Standards and Technology (MSEL), Gaithersburg, MD. Ceramics Div.
Ca4Bi6O13: A Compound Containing an Unusually Low Bismuth Coordination Number and Short Bi Bi Contacts.
Final rept.
J. B. Parise, C. C. Torardi, M. H. Whangbo, B. P. Burton, C. J. Rawn, and R. S. Roth. 1990, 5p.
Pub. in Chemistry of Materials 2, n4 p454-458 1990.

Keywords: *Crystal structure, Second harmonic generation, Orthorhombic lattices, Molecular orbitals, Bismuth oxides, Calcium oxides, Reprints, *Calcium bismuthates, *Calcium bismuth oxides.

Single crystals and powder samples of Ca4Bi6O13 have been synthesized and studied by x-ray diffraction. This compound crystallizes in the orthorhombic space group C2mm, with a= 5.9368(7), b= 17.356(4), c= 7.206(4)A. The absence of a center of symmetry was confirmed by the presence of a second harmonic signal some 60 times that observed for quartz. A weak superstructure exists along c due to alternation of oxygen and vacancies along the c-axial direction. The structure consists of ribbons of edge-linked BiO5 square pyramids running parallel with the c-axis. These chains are linked via a 3-coordinate Bi atom to form semicylinders stacked along the a-axial direction.

00,912
PB95-141180 Not available NTIS
National Inst. of Standards and Technology (CSTL), Gaithersburg, MD. Thermophysics Div.
Interatomic Potential of Argon.
Final rept.
S. J. Boyes. 1994, 6p.
Pub. in Chemical Physics Letters 221, p467-472 1994.

Keywords: *Argon, Virial coefficients, Predictions, Acoustics, Reprints, *Interatomic potentials.

The recent literature abounds with proposed interatomic potential functions for argon. Of these the Hartree-Fock dispersion (HFD) type functions have been very successful and are considered to be among the best characterizations of the argon interaction to date. It is the purpose of this Letter, however, to show that of the proposed HFD-type potentials, none predict the recent acoustic virial coefficients measured by Moldover et al. In view of this, an alternative interatomic potential has been constructed for argon. The potential is of the Hartree-Fock dispersion individually damped (HFD-ID) type and represents a subtle but significant improvement for the interaction.

00,913
PB95-141198 Not available NTIS
National Inst. of Standards and Technology (CSTL), Gaithersburg, MD. Surface and Microanalysis Science Div.
Time-Resolved Measurements of Energy Transfer at Surfaces.
Final rept.
R. R. Cavanagh, E. J. Heilweil, and J. C. Stephenson. 1994, 13p.
Pub. in Surface Science 299/300, p643-655 1994.

Keywords: *Surfaces, *Adsorbates, Solid surfaces, Liquid surfaces, Metal surfaces, Energy transfer, Excited states, Picosecond pulses, Semiconductors, Dielectrics, Electronic states, Measurement, Reprints, Femtosecond pulses.

Developments in time-resolved measurements of energy transfer at surfaces are reviewed. Picosecond and femtosecond measurements of vibrational and electronic relaxation at surfaces are highlighted. Experimental results for vibrational relaxation of simple adsorbates on metals, semiconductors, and insulators are reviewed, and relaxation mechanisms such as electron-hole pair formation, multiphonon relaxation and image dipole damping are considered. Energy transfer involving excited electronic states of molecules on liquid and solid dielectric surfaces and the relaxation of surface electronic states on semiconductors and of image states on metal surfaces are discussed.

00,914
PB95-150090 Not available NTIS
National Inst. of Standards and Technology (MSEL), Gaithersburg, MD. Reactor Radiation Div.
Phase Transitions in Solid C70: Supercooling, Metastable Phases, and Impurity Effect.
Final rept.
A. R. McGhie, J. E. Fischer, P. A. Heiney, D. A. Neumann, W. H. Mueller, H. Mohn, H. U. ter Meer, P. W. Stephens, and R. L. Cappelletti. 1994, 5p.
Contract DEFG-0291-ER45231, Grant NSF-DMR91-20668
Sponsored by National Science Foundation, Arlington, VA. and Department of Energy, Washington, DC.
Pub. in Physical Review B 49, n18 p12 614-12 618, 1 May 94.

Keywords: *Fullerenes, *Phase transformations, Orientation(Direction), Metastable state, Supercooling, Impurities, Reprints, Differential scanning calorimetry.

Modulated differential scanning calorimetry of sublimed C(70) shows clear evidence for four first-order transitions, two strong and two weak, which we associate with the two different molecular rotational degrees of freedom in majority (equilibrium) and minority (metastable) phases. The latter correspond to the two different stacking sequences of close-packed layers, and their relative contributions of the thermal data correlate well with high-temperature x-ray powder-diffraction results. The upper of the thermal data correlate well with high-temperature x-ray powder-diffraction results. The upper (long axis tumbling) transition in the majority phase exhibits 50 K supercooling when scanned at 2 K/min. C(60) impurities at the few % level depress the transition temperatures substantially.

00,915
PB95-150124 Not available NTIS
National Inst. of Standards and Technology (CSTL), Gaithersburg, MD. Thermophysics Div.
Simulations of Glass Forming Liquids: What Has Been Learned.
Final rept.
R. D. Mountain. 1994, 3p.
Pub. in International Jnl. of Modern Physics C 5, n2 p247-249 1994.

Keywords: Computerized simulation, Molecular dynamics, Amorphous state, Thermodynamic properties, Supercooling, Glass, Reprints, *Supercooled liquids.

Molecular dynamics simulations of supercooled fluid mixtures of soft-spheres and of Lennard-Jones particles have revealed the existence of a kinetic transition that occurs above the glass transition temperature. This transition appears to be thermodynamic in origin. It is associated with a change in the local mobility of the particles. The basis of these conclusions is discussed.

00,916
PB95-150355 Not available NTIS
National Inst. of Standards and Technology (CSTL), Gaithersburg, MD. Surface and Microanalysis Science Div.
Calculations of Electron Inelastic Mean Free Paths. 5. Data for 14 Organic Compounds over the 50-2000 eV Range.
Final rept.
S. Tanuma, C. J. Powell, and D. R. Penn. 1993, 12p.
Pub. in Surface and Interface Analysis 21, p165-176 1993.

Keywords: *Mean free path, *Electron scattering, *Electron collisions, EV range 10-100, EV range 100-

1000, KeV range 1-10, Inelastic scattering, Paraffins, Adenines, Carotene, Albumins, Diphenyl compounds, Guanines, Polyacetylene, Polyethylene, Polymethyl methacrylate, Polystyrene, DNA, Surface analysis, Electron spectroscopy, Reprints, Kapton(Trademark).

We report calculations of electron inelastic mean free paths (IMFPs) of 50-2000 eV electrons for a group of 14 organic compounds: 26-n-paraffin, adenine, beta-carotene, bovine plasma albumin, deoxyribonucleic acid, diphenyl-hexatriene, guanine, kapton, polyacetylene, poly(butene-1-sulfone), polyethylene, polymethylmethacrylate, polystyrene and poly(2-vinylpyridine). The computed IMFPs for these compounds showed greater similarities in magnitude and in the dependences on electron energy than was found in our previous calculations for groups of elements and inorganic compounds (Papers II and III in this series). Comparison of the IMFPs for the organic compounds with values obtained from our predictive IMFP formula TPP-2 showed systematic differences of approx 40%. These differences are due to the extrapolation of TPP-2 from the regime of mainly high-density elements (from which it had been developed and tested) to the low-density materials such as the organic compounds. We analyzed the IMFP data for the groups of elements and organic compounds together and derived a modified empirical expression for one of the parameters in our predictive IMFP equation. The modified equation, denoted TPP-2M, is believed to be satisfactory for estimating IMFPs in elements, inorganic compounds and organic compounds.

00,917
PB95-150421 Not available NTIS
National Inst. of Standards and Technology (MSEL), Gaithersburg, MD. Reactor Radiation Div.
Neutron Reflectometry Studies of Surface Oxidation.
Final rept.
D. G. Wiesler, and C. F. Majkrzak. 1994, 6p.
Pub. in Physica B 198, p181-186 1994.

Keywords: *Titanium oxides, *Oxide films, *Oxidation, Anodic coatings, Film thickness, Aqueous electrolytes, Surface chemistry, Corrosion resistance, Reprints, Neutron reflectometry, Film density, Hydrogen loading.

We have employed neutron reflectometry to study the thickness and density of thin oxide films of Ti in contact with electrolyte. Such films play an important role in corrosion resistance and surface chemistry in aqueous environments. We compare the structures of such oxides formed by either ramping the potential or by step polarization. The effect of subsequent cathodic bias on the films is explored, and the time evolution of the hydrogen content in the oxide and metal is investigated.

00,918
PB95-150561 Not available NTIS
National Inst. of Standards and Technology (CSTL), Gaithersburg, MD. Thermophysics Div.
Contrast Matched Studies of a Sheared Binary Colloidal Suspension.
Final rept.
G. C. Straty, J. Pieper, and H. J. M. Hanley. 1991, 6p.
Sponsored by Department of Energy, Washington, DC.
Pub. in Molecular Physics 72, n1 p241-246 1991.

Keywords: *Suspensions, *Dispersions, Small angle scattering, Neutron scattering, Shear stress, Structure factors, Couette flow, Polystyrene, Colloids, Mixtures, Silica, Latex, Heavy water, Reprints, *Colloidal suspensions.

A method is proposed to measure by neutron scattering the partial scattered intensities from a suspension mixture in an H2O/D2O solvent that will match out one of the components. Total and partial neutron-scattered intensities from an aqueous colloidal suspension mixture (volume fraction phi = 0.15) of 91 nm polystyrene latex and 54 nm silica particles in water are reported. Results are given for the mixture at rest and under shear. We comment on the standard assumption that structure factors of components in a mixture should scale with the particle radii.

00,919
PB95-150611 Not available NTIS
National Inst. of Standards and Technology (NML), Gaithersburg, MD. Molecular Physics Div.
Microwave Spectra of van der Waals Complexes of Importance in Planetary Atmospheres.
Final rept.
R. D. Suenram, and F. J. Lovas. 1989, 7p.
Pub. in Proceedings of International Conference on Laboratory Research for Planetary Atmospheres (1st), Bowie, MD., October 25-27, 1989, p78-84.

Keywords: *Microwave spectra, *Planetary atmospheres, *Complexes, Van der Waals forces, Hydrogen bonds, Nitrogen complexes, Oxygen complexes, Rotational spectra, Trimers, Reprints, *Water dimers, Carbon dioxide complexes, Carbon monoxide complexes, Hydrogen sulfide complexes, Sulfur dioxide complexes, Water complexes, Ozone complexes.

The Fourier-transform Fabry-Perot pulsed-molecular-beam microwave spectrometer at NIST has been used to study the microwave spectra of a number of molecular dimers and trimers that may be present in planetary atmospheres. The weak van der Waals bonds associated with these species usually give rise to rotational-tunneling splittings in the microwave spectra. We have used the microwave spectrum of the water dimer species to illustrate the complications that can arise in the study of the rotational spectra of these loosely bound species. In addition to the water dimer species, the microwave spectra of the following hydrogen-bonded and van der Waals complexes have been studied: (CO2)2 H20, CO2 (H2O)2, CO2 H2S, N2 H2O, CO H2O, SO2 H2O, and O3 H2O.

00,920
PB95-150678 Not available NTIS
National Inst. of Standards and Technology (PL), Boulder, CO. Quantum Physics Div.
High-Resolution Infrared Spectroscopy of DF Trimer: A Cyclic Ground State Structure and DF Stretch Induced Intramolecular Vibrational Coupling.
Final rept.
M. A. Suhm, J. T. Farrell, S. Ashworth, and D. J. Nesbitt. 1993, 5p.
Pub. in Jnl. of Chemical Physics 98, n7 p5985-5989, 1 Apr 93.

Keywords: *Deuterium fluorides, *Hydrogen fluoride, *Molecular clusters, *Infrared spectroscopy, Molecular vibration, Absorption spectra, Hydrogen bonds, High resolution, Deuterium compounds, Fine structure, Ground state, Trimers, Reprints, Supersonic expansion.

We present high resolution, infrared laser absorption spectra of (DF)3 in a slit supersonic jet expansion. In contrast to previous structureless near IR spectra of (HF)3, the (DF)3 data reveal clear rotational structure characteristic of a cyclic, 6-membered 'ring,' and therefore provide the first accurate experimental evidence for the equilibrium geometry of any hydrogen fluoride oligomer beyond the well-studied dimer. Furthermore, the spectra display homogeneous rotational fine structure 2-3 orders of magnitude in excess of what could be anticipated from a single vibrational band. Analysis of this fine structure elucidates a novel IVR mechanism which involves single hydrogen bond cleavage, and consequent opening of the (DF)3 ring on the 40 ps time scale.

00,921
PB95-150694 Not available NTIS
National Inst. of Standards and Technology (PL), Boulder, CO. Quantum Physics Div.
Laser Double Resonance Measurements of the Quenching Rates of Br((2)P1/2) with H20, D20, HDO, and O2.
Final rept.
C. A. Taatjes, C. M. Lovejoy, B. J. Opansky, and S. R. Leone. 1991, 6p.
Grants NSF-WLK-1-043, NSF-CHE87-13646
Sponsored by National Science Foundation, Washington, DC.
Pub. in Chemical Physics Letters 182, n1 p39-44, 19 Jul 91.

Keywords: Laser applications, Room temperature, Excited states, Heavy water, Quenching, Oxygen, Reprints, *Bromine atoms, Rate constants.

Quenching rate constants for spin-orbit excited Br* atoms (doublet P(1/2)) with H2O, D2O, HDO, and O2 are measured at 300 K using a two-laser pump-probe technique. The rate constants and error bars for the water species are given. The relative rates for the water species are in qualitative agreement with models for electronic-to-vibrational energy transfer based upon dipole-quadrupole coupling. Quenching of Br* by oxygen is found to be extremely inefficient, which is in disagreement with previously reported results by four orders of magnitude.

00,922
PB95-150728 Not available NTIS
National Inst. of Standards and Technology (CSTL), Gaithersburg, MD. Surface and Microanalysis Science Div.
Calculations of Electron Inelastic Mean Free Paths (IMFPs). 4. Evaluation of Calculated IMFPs and of the Predictive IMFP Formula TPP-2 for Electron Energies between 50 and 2000 eV.
Final rept.
S. Tanuma, C. J. Powell, and D. R. Penn. 1993, 13p.
Pub. in Surface and Interface Analysis 20, p77-89 1993.

Keywords: *Mean free path, *Electron scattering, *Electron collisions, EV range 10-100, EV range 100-1000, KeV range 1-10, Inelastic scattering, Aluminum oxides, Gallium arsenides, Uncertainty, Reprints.

We have made additional evaluations of the electron inelastic mean free paths (IMFPs) and of the predictive IMFP formula TPP-2 presented in papers II and III of this series. Comparisons have been made with other formulae for the IMFPs and electron attenuation lengths (ALs). We find substantial differences between our IMFP results for 27 elements and 15 inorganic compounds and the AL formulae of Seah and Dench; these differences include different dependences on electron energy and on material parameters. We present IMFP calculations for Al2O3 and GaAs from TPP-2 in which each parameter of the formula is varied in some physically reasonable range about the true value for each compound; these results show the sensitivity of the computed IMFPs to the choices of parameter values. Finally, we give a summary of sources of uncertainty in the IMFP algorithm, in the experimental optical data from which IMFPs are calculated, and of the TPP-2 formula. We conclude that TPP-2 is robust and useful for predicting IMFPs for electron energies and material parameter values in ranges for which the formula was developed and tested.

00,923
PB95-150744 Not available NTIS
National Inst. of Standards and Technology (CSTL), Gaithersburg, MD. Process Measurements Div.
Silver Metalization of Octadecanethiol Monolayers Self-Assembled on Gold.
Final rept.
M. J. Tarlov. 1992, 10p.
Pub. in Langmuir 8, n1 p80-89 1992.

Keywords: *Thiols, *Monomolecular films, *Silver, *Gold, *Surface chemistry, *Vapor deposition, Atomic energy levels, Temperature dependence, X-ray analysis, Ultraviolet spectroscopy, Reprints, *Octadecanethiol, *Self assembled monolayers, *Silver deposition.

The interaction between evaporated silver and self-assembled monolayers of octadecanethiol (ODT) on gold was studied at temperatures of 300 and 90 K using X-ray photoelectron spectroscopy (XPS), ultraviolet photoelectron spectroscopy (UPS), and ion scattering spectroscopy (ISS). Equivalent Ag coverages ranging from submonolayers to multilayers were examined. Ag deposited at 300 K penetrates the ODT monolayer and resides at the ODT/gold interface. The attenuation behavior of the XPS C 1s and Au 4f signals reveals that Ag nucleates as clusters underneath the ODT monolayer. UPS and ISS data are in accord with XPS results and, furthermore, indicate that the deposited Ag does not significantly alter the ODT monolayer film structure. In contrast to the behavior observed at 300 K, results from Ag deposition at 90 K indicate that Ag forms clusters on the ODT monolayer surface. In this case the Ag 3d core level exhibits a shift to higher binding energy relative to that of metallic silver that is attributable to a final state Coulombic effect characteristic of metal clusters on relatively poorly conducting substrates. There is apparently little chemical interaction between Ag and the hydrocarbon chains at both 90 and 300 K, although at 300 K Ag 3d XPS data suggest that Ag bonds to sulfur head groups. The low-temperature Ag/ODT/Au structure is apparently a metastable phase because warming of the sample to room temperature results in the migration of the Ag to the ODT/Au interface and possibly further clustering.

00,924
PB95-150751 Not available NTIS

National Inst. of Standards and Technology (CSTL), Gaithersburg, MD. Process Measurements Div.
UV-Photopatterning of Alkylthiolate Monolayers Self-Assembled on Gold and Silver.
Final rept.
M. J. Tarlov, D. R. F. Burgess, and J. G. Gillen.
1993, 2p.
Pub. in Jnl. of the American Chemcial Society 115, n12 p5305-5306, 16 Jun 93.

Keywords: *Thiols, *Monomolecular films, *Gold, *Silver, *Ultraviolet radiation, *Coating processes, Surface properties, X-ray analysis, Mass spectroscopy, Surface chemistry, Reprints, *Alkylthiolates, *Self assembled monolayers, *Photopatterning.

A method of photopatterning alkylthiolate self-assembled monolayers (SAMs) on gold and silver is described. A pattern of alkylsulfonates is first formed on the alkylthiolate SAMs by ultraviolet (UV) irradiation through a mask. The sample is then immersed in a dilute solution of a different alkylthiol and the alkylsulfonates in the exposed areas are displaced resulting in the incorporation of the second alkylthiol. X-ray photoelectron spectroscopy (XPS) and secondary ion mass spectrometry (SIMS) imaging were used to characterize the UV-irradiated and exchanged monolayers. XPS spectra of the S 2p region indicate the formation of sulfonate species upon UV irradiation and their displacement by thiolates following immersion. SIMS images of photopatterned and thiol-exchanged SAMs confirm the existence of two molecularly distinct assemblies with faithful reproduction of the mask pattern and resolution of features as small as 15 micrometers.

00,925
PB95-150819 Not available NTIS
National Inst. of Standards and Technology (CSTL), Gaithersburg, MD. Thermophysics Div.
Activated Dynamics, Loss of Ergodicity, and Transport in Supercooled Liquids.
Final rept.
D. Thirumalai, and R. D. Mountain. 1993, 11p.
Sponsored by National Science Foundation, Washington, DC.
Pub. in Physical Review E 47, n1 p479-489 Jan 93.

Keywords: Ergodic processes, Molecular dynamics, Self-diffusion, Computerized simulation, Temperature dependence, Shear properties, Supercooling, Viscosity, Mixtures, Glass, Reprints, *Supercooled liquids.

The dynamics of the transition from supercooled liquid to glass is examined in terms of several probes: ergodic measures, self-diffusion coefficients, the Van Hove self-correlation functions, and the shear viscosity. Constant-pressure molecular-dynamics calculations at several temperatures are performed for a Lennard-Jones mixture and binary mixtures of soft spheres. The temperature dependence of the ergodicity diffusion parameters for both systems follow the Vogel-Fulcher law. On the other hand, the self-diffusion coefficients exhibit Arrhenius behavior for the soft-sphere system, but Vogel-Fulcher behavior for the Lennard-Jones system. These observations suggest that loss of effective ergodicity may be the universal feature of glass-forming substances. Various probes of the dynamics of the mixtures studied here suggest that the mechanism for mass transport dramatically changes from a simple diffusive process to one that involves activated transitions.

00,926
PB95-151015 Not available NTIS
National Inst. of Standards and Technology (MSEL), Gaithersburg, MD. Reactor Radiation Div.
Methyl Torsional Levels of Solid Acetonitrile (CH3CN): A Neutron Scattering Study.
Final rept.
S. F. Trevino, C. S. Choi, and D. A. Neumann. 1993, 5p.
Pub. in Jnl. of Chemical Physics 98, n1 p78-82, 1 Jan 93.

Keywords: *Acetonitrile, Neutron scattering, Neutron diffraction, Crystal structure, Deuterium compounds, Rotational states, Activation energy, Methyl radicals, Reprints.

Neutron powder diffraction has been used to obtain the thermal parameters for the deuterium atoms and to confirm the crystal structure of acetonitrile-d(3) at 4 K. Inelastic neutron scattering from both isotopic species is used to determine the energies of the first and second rotational levels of the methyl group. These four levels are reasonably reproduced by a threefold potential with V(3) = 125 meV. The activation energy derived from this potential is in agreement with that previously obtained from the temperature dependence of T(1) in proton magnetic resonance measurements.

00,927
PB95-151023 Not available NTIS
National Inst. of Standards and Technology (NML), Gaithersburg, MD. Chemical Kinetics Div.
Electronic Spectra of CF2Cl and CFCl2 Radicals Observed by Resonance Enhanced Multiphoton Ionization.
Final rept.
B. P. Tsai, J. W. Hudgens, and R. D. Johnson. 1989, 3p.
Pub. in Jnl. of Physical Chemistry 93, n14 p5334-5336 1989.

Keywords: *Rydberg States, *Fluoroalkanes, *Free radicals, *Vibrational states, *Electronic spectra, Spectrum analysis, Energy levels, Reprints, *Multiphoton ionization.

CFCl2 and CF2Cl radicals were observed between 365-410 nm using resonance enhanced multiphoton ionization spectroscopy. Both spectra were generated by two-photon resonances with planar 3p Rydberg states. A third laser photon ionized the radicals. The CF2Cl spectrum displayed a vibrational progression assigned to the out-of-plane bending nu'(sub 4) b(sub 1) (OPLA) mode (omega'(sub 4) = 745/cm) and a origin at 406.2 nm (nu(sub 0-0) = 49,230/cm). Assignments for the CFCl2 radical included the nu'(sub 4) b(sub 1) OPLA (omega'(sub 4) = 590/cm) and the nu'(sub 2) a(sub 1) CCl symmetric stretch (omega'(sub 2) = 870(30)/cm) modes. An observed origin was assigned to lie at 49,260/cm.

00,928
PB95-151049 Not available NTIS
National Inst. of Standards and Technology (NML), Gaithersburg, MD. Chemical Kinetics Div.
Homogeneous Gas Phase Decyclization of Tetralin and Benzocyclobutene.
Final rept.
W. Tsang, and J. P. Cui. 1990, 7p.
Pub. in Jnl. of the American Chemical Society 112, n5 p1665-1671 1990.

Keywords: *Tetralin, *Cyclobutene compounds, *Reaction kinetics, *Vapor phases, Temperature dependence, Shock tubes, Chemical reactions, Aromatic hydrocarbons, Styrene, Lasers, Pyrolysis, Reprints, *Benzocyclobutene, *Decyclization, Unimolecular reactions.

Tetralin has been decomposed in single pulse shock tube experiments in the temperature range of 1,000-1,400 K. The initial unimolecular decomposition channels are the formation of benzocyclobutene and o-allytoluene. Benzocyclobutene decomposes to form styrene. The main products from the hydrogen atom induced decomposition of tetralin are dihydronaphthalenes, styrene, indene and napthalene. Rate constant expressions for these reactions were determined. Comparisons are made with published results from the laser powered pyrolysis and shock tube studies, and it is concluded that in both cases the initial unimolecular channels are accessed. The temperatures in the laser experiments are at least as high as in the shock tube studies. The rate expressions for tetralin decomposition are compatible with a biradical mechanism and follow the general patterns for related cyclic compounds.

00,929
PB95-151064 Not available NTIS
National Inst. of Standards and Technology (CSTL), Gaithersburg, MD. Chemical Kinetics and Thermodynamics Div.
Mechanism and Rate Constants for the Reactions of Hydrogen Atoms with Isobutene at High Temperatures.
Final rept.
W. Tsang, and J. A. Walker. 1989, 8p.
Pub. in Proceedings of Conference International Symposium on Combustion (22nd), National Institute of Standards and Technology, p1015-1022 1989.

Keywords: *Butenes, *Hydrogen, *Reaction kinetics, *Decomposition reactions, *2-Methylpropene, Shock tubes, Temperature dependence, High temperature, Pyrolysis, Reprints, *Hydrogen atoms, *Isobutene, Hydrogen abstraction.

Hydrogen atoms from the thermal decomposition of 2,3,3 trimethylbutanol-2 have been used to induce the decomposition of isobutene in single pulse shock tube experiments. We have been able to observe products arising from all of the high temperature reaction channels for hydrogen attack on isobutene. The following rate expressions have been determined: k(H + isobutene -> propylene + CH3) = 1.72 x 10(exp 10) Exp(-1808/T) l/mol-s and k(H + isobutene -> 2-methyl-2-allyl + H2) = 1.72 x 10(exp 11) Exp(-4024/T) l/mol-s in the temperature range of 1,000-1,180 K and at 2.5-3 atmospheres of pressure. The rate constants for the abstraction of vinylic hydrogens are not more than 8% of that for abstraction of the allylic hydrogens. Comparisons are made with rate constants of similar processes involving branched aromatics and lower temperature results on isobutene. Interesting correlations are observed and lead to the possibility of estimating rate expressions for reactions involving other olefins.

00,930
PB95-151148 Not available NTIS
National Inst. of Standards and Technology (CSTL), Boulder, CO. Thermophysics Div.
Experimental Method for Obtaining Critical Densities of Binary Mixtures: Application to Ethane + n-Butane.
Final rept.
L. J. Van Poolen, V. G. Niesen, and J. C. Rainwater. 1991, 25p.
Pub. in Fluid Phase Equilibria 66, p161-185 1991.

Keywords: *Binary mixtures, *Ethane, *Butanes, *Density(Mass/volume), Phase transformations, Vapor phases, Liquid phases, Thermophysical properties, Reprints, *Critical density, *Rectilinear diameter, Van Poolen-Rainwater procedure, Leung-Griffiths theory.

According to the experimental and analytical procedure proposed by Van Poolen and Rainwater, rectilinear diameters based on measured vapor-liquid coexistence densities along a path of constant overall density and composition have been determined and used to obtain critical densities of the binary mixture ethane + n-butane. Seven experimental runs for the mixture were made at compositions ranging from 21.65 to 80.75 mol% ethane. The procedure has been explored as a new way to determine critical densities of mixtures. Results are compared with densities generated from a modified Leung-Griffiths correlation of the extensive vapor-liquid equilibrium data of Kay. The critical densities obtained are in agreement with the correlation within the overall uncertainty of the method, thereby verifying the proposed technique.

00,931
PB95-151361 Not available NTIS
National Inst. of Standards and Technology (CSTL), Gaithersburg, MD. Thermophysics Div.
Ebulliometric Measurement of the Vapor Pressure of Difluoromethane.
Final rept.
L. A. Weber, and A. R. H. Goodwin. 1993, 3p.
Sponsored by Department of Energy, Washington, DC. and Environmental Protection Agency, Washington, DC.
Pub. in Jnl. of Chemical and Engineering Data 38, n2 p254-256 Apr 93.

Keywords: *Vapor pressure, *Fluorohydrocarbons, *Refrigerants, Ebulliometry, Temperature dependence, Mathematical models, Boiling points, Reprints, *R32, *Difluoromethane, Antoine equation.

We have used a comparative ebulliometer to make accurate measurements of the vapor pressure of difluoromethane (R32) in the range 49-214 kPa, which corresponds to temperatures on ITS-90 between 208 and 237 K. The results are represented with an Antoine equation and are compared with literature values. We have combined our results with literature values, and we present an interpolating equation for the vapor pressure at temperatures between 190 K and the critical temperature (351.36 K). We also tabulate thermodynamic properties for R32 on the saturation boundary between 200 and 250 K.

00,932
PB95-151387 Not available NTIS
National Inst. of Standards and Technology (PL), Boulder, CO. Quantum Physics Div.

Van der Waals Bond Lengths and Electronic Spectral Shifts of the Benzene-Kr and Benzene-Xe Complexes.
Final rept.
T. Weber, E. Riedle, H. J. Neusser, and E. W. Schlag. 1991, 7p.
Pub. in Chemical Physics Letters 183, n1-2 p77-83, 23 Aug 91.

Keywords: *Krypton complexes, *Xenon complexes, *Chemical bonds, *Spectral shift, Van der Waals forces, Electronic spectra, Ultraviolet spectra, Ground states, Excited states, Reprints, *Benzene complexes.

Rotationally resolved UV-spectra are presented for the 6(sub 0, sup 1) bands of benzene-Kr and benzene-Xe complexes yielding precise rotational constants and van der Waals bond lengths for the ground and excited vibronic state, and electronic band shifts. These values complement the previously published data for the other rare gases and the various quantities have now been determined for all the benzene-rare gas complexes. Measured values of the bond length were used to calculate the band shifts from recent theoretical predictions. They are compared with the experimental values of this work.

00,933
PB95-151395 Not available NTIS
National Inst. of Standards and Technology (PL), Boulder, CO. Quantum Physics Div.
N2(a'(sup 1)Sigma(sub g)(sup +)) Metastable Collisional Destruction and Rotational Excitation Transfer by N2.
Final rept.
A. B. Wedding, J. Borysow, and A. V. Phelps. 1993, 8p.
Contract USAF-FY1455-84-N0641
Sponsored by Phillips Lab., Kirtland AFB, NM.
Pub. in Jnl. of Chemical Physics 98, n8 p6227-6234, 15 Apr 93.

Keywords: *Molecular collisions, *Nitrogen, Molecular energy levels, Molecular excitation, Metastable state, Rotational states, Electric discharges, Optical pumping, Time dependence, Laser applications, Reprints, Rate coefficients.

Quenching and rotational coupling rate coefficients have been measured for the J = 4-10, nu = O levels of the a(double prime) singlet Sigma(g)(1+) metastable state of N2 in collisions with ground state N2. Laser absorption is used to monitor the population of rotational levels of the a(double prime) singlet Sigma(g)(1+) state following depletion of the population of one or more levels by optical pumping to other states. The observed time dependence of the recovery of population of the perturbed level and the collision induced growth and decay of the populations of adjacent levels are interpreted in terms of quenching to other electronic levels and excitation exchange among adjacent rotational levels.

00,934
PB95-151437 Not available NTIS
National Inst. of Standards and Technology (NML), Boulder, CO. Quantum Physics Div.
Nonadiabatic Effects in the Photoassociation of H2S.
Final rept.
K. Weide, V. Staemmler, and R. Schinke. 1990, 2p.
Pub. in Jnl. of Chemical Physics 93, n1 p861-862, 1 Jul 90.

Keywords: *Hydrogen sulfide, *Photodissociation, Nonadiabatic conditions, Vibrational states, Excited states, Reprints, *Photoassociation.

The photodissociation of H2S in the 195 nm band has been extensively investigated in the last decade. Although the major part of the experimental data indicates an overall dissociation dynamics similar to H2O, pronounced differences have been noted. The central question is whether H2S dissociates via a single electronic state, like H2O, or if two states are involved. This question concerns also the origin of the very diffuse vibrational structure. Using the CEPA method we calculated the potential energies of the two lowest excited singlet states for a fixed bond angle of 92 deg. In C(2nu) symmetry these states are singlet B(1) and singlet A(2).

00,935
PB95-151601 Not available NTIS
National Inst. of Standards and Technology (EEEL), Boulder, CO. Electromagnetic Technology Div.
Studies of the Higher Order Smectic Phase of the Large Electroclinic Effect Material W317.
Final rept.
P. A. Williams, L. Komitov, A. G. Rappaport, D. M. Walba, G. W. Day, B. N. Thomas, and N. A. Clark. 1993, 11p.
Pub. in Liquid Crystals 14, n4 p1095-1105 1993.

Keywords: *Liquid crystals, Temperature dependence, Electric fields, Reprints, *Electroclinic effect, *W317 liquid crystal, Smectic phases.

We present studies of the large electroclinic effect material W317. We found via X-ray scattering, calorimetry and optical observation that quenching from the smectic A phase results in several higher order phases including an orthogonal (hexatic) smectic with short range in-layer translational order and no interlayer order. We characterize the electroclinic response in the quenched phase, and determine its magnitude and response time as a function of electric field amplitude and temperature.

00,936
PB95-151759 Not available NTIS
National Inst. of Standards and Technology (MSEL), Gaithersburg, MD. Ceramics Div.
Crystal Chemistry and Phase Equilibria Studies of the BaO(BaCO3)-R2O3-CuO Systems. 4. Crystal Chemistry and Subsolidus Phase Relationship Studies of the CuO-Rich Region of the Ternary Diagrams, R=Lanthanides.
Final rept.
W. Wong-Ng, B. Paretzkin, and E. R. Fuller. 1990, 16p.
See also PB95-151742, Part 2, PB95-151734 and Part 5, PB95-151718.
Pub. in Jnl. of Solid State Chemistry 85, n1 p117-132 1990.

Keywords: *Barium oxides, *Yttrium oxides, *Copper oxides, *Rare earth compounds, *Phase diagrams, *Crystal chemistry, High temperature superconductors, YBCO superconductors, Solid solutions, Ternary systems, Crystal phase transformations, Reprints, Yttrium barium cuprates, Phase equilibrium.

A general trend of phase formation, solid solution formation and phase relationship is found to be correlated with the size of R in the BaO-1/2R2O3-CuO systems, where R=lanthanides and yttrium. There is a progressive change in the phase relationship and appearance of these ternary diagrams in the CuO rich region, from the La through the Nd, Sm, Eu, Gd, Y to the Er system, with samples prepared in air at 950 C. Firstly, the La system has the greatest number of ternary compounds. Secondly, the superconductor materials, Ba2RCu3O(6+x), of the first half of the f-block elements, e.g. R=La, Nd, Sm, Eu and Gd, which are relatively larger in size, exhibit solid solution of Ba(2-z)R(1+z)Cu3O(6+x) with range of formation according to the size of R. These solutions terminate at Gd, after which the superconductor phase presumably assumes a point stoichiometry. Thirdly, a trend regarding the tieline connection between the phases Ba(2-x)R(1+x)Cu3O(6+x), CuO, BaR2CuO5 and binary phase R2CuO4/R2Cu2O5 is observed.

00,937
PB95-151775 Not available NTIS
National Inst. of Standards and Technology (PL), Boulder, CO. Quantum Physics Div.
Photodissociation of Ammonia at 193.3nm: Rovibrational State Distribution of the NH2(A(2)A1) Fragment.
Final rept.
E. L. Woodbridge, M. N. R. Ashfold, and S. R. Leone. 1991, 10p.
Contract DE-FG02-883ER-13860, Grant NSF-PHY86-04504
Sponsored by Department of Energy, Washington, DC. Office of Energy Research. and National Science Foundation, Washington, DC.
Pub. in Jnl. of Chemical Physics 94, n6 p4195-4204, 15 Mar 91.

Keywords: *Ammonia, *Photodissociation, Far ultraviolet radiation, Rotational states, Vibrational states, Infrared spectroscopy, Emission spectroscopy, Room temperature, Reprints, *Ammonia radicals, Fourier transform spectroscopy.

The rovibrational state distribution of the nascent NH2(A(tilde) doublet A(1)) fragments generated by 193.3 nm photodissociation of a room temperature sample of NH3 is determined through an analysis of a major portion (6000-13000/cm) of the NH2(A(tilde) doublet A(1) --> X(tilde) doublet B(1)) near infrared emission spectrum obtained by time-resolved Fourier transform infrared emission spectroscopy. The essential features are entirely consistent with a direct carry over, into the fragment, of the out-of-plane bending vibrational motion introduced in the parent molecule by the photoexcitation process.

00,938
PB95-152112 Not available NTIS
National Inst. of Standards and Technology (CSTL), Gaithersburg, MD. Thermophysics Div.
Susceptibility Critical Exponent for a Nonaqueous Ionic Binary Mixture Near a Consolute Point.
Final rept.
K. C. Zhang, M. E. Briggs, R. W. Gammon, and J. M. H. Levelt Sengers. 1992, 6p.
Contract NASA-NAS3-25370
Sponsored by National Aeronautics and Space Administration, Washington, DC.
Pub. in Jnl. of Chemical Physics 97, n11 p8692-8697 Dec 92.

Keywords: *Nonaqueous electrolytes, Temperature dependence, Phenyl ether, Binary mixtures, Ammonium compounds, Reprints, Phase separation(Materials), Critical exponents, Consolute points.

We report turbidity measurements of a nonaqueous ionic solution of triethyl n-hexylammonium triethyl n-hexylboride in diphenyl ether. A classical susceptibility critical exponent gamma = 1.01 + or - 0.01 is obtained over the reduced temperature range 10(exp -4) = or < t = or < 10(exp -1). The best fits of the sample transmission had a standard deviation of 0.39% over this range. Ising and spherical model critical exponents are firmly excluded. The correlation length amplitude zeta(0) from fitting is 1.0 + or - 0.2 nm which is much larger than values found in neutral fluids and some aqueous binary mixtures.

00,939
PB95-152146 Not available NTIS
National Inst. of Standards and Technology (NML), Gaithersburg, MD. Chemical Kinetics Div.
Gas Phase Reactivity Study of OH Radicals with 1,1-Dichloroethene and cis-1,1-Dichloroethene and Trans-1,2-Dichloroethene over the Temperature Range 240-400 K.
Final rept.
Z. Zhang, R. Liu, R. E. Huie, and M. J. Kurylo. 1991, 3p.
Pub. in Jnl. of Physical Chemistry 95, n1 p194-196 1991.

Keywords: *Vapor phases, *Reaction kinetics, *Hydroxyl radicals, *Chlorohydrocarbons, Temperature, Fluorescence, Reprints, *Ethylene/dichloro.

Rate constants have been measured for the reactions of hydroxyl radicals with the three dichloroethenes over the temperature range 240 to 400 K using the flash photolysis resonance fluorescence technique. The Arrhenius equations derived from the data are given. There was no apparent effect of pressure on the rate constant for the reaction of OH with trans-1,2-dichloroethene over the range 5 to 50 torr (with Ar).

00,940
PB95-152153 Not available NTIS
National Inst. of Standards and Technology (NML), Gaithersburg, MD. Chemical Kinetics Div.
Rate Constants for the Gas Phase Reactions of the OH Radical with CF3CF2CHCl2 (HCFC-225ca) and CF2ClCF2CHClF (HCFC-225cb).
Final rept.
Z. Zhang, R. Liu, R. E. Huie, and M. J. Kurylo. 1991, 3p.
Pub. in Geophysical Research Letters 18, n1 p5-7 1991.

Keywords: *Reaction kinetics, *Hydroxyl radicals, *Vapor phases, Temperature, Reprints, *Hydrochlorofluorocarbons.

Rate constants have been measured for the gas phase reactions of the hydroxyl radical (OH) with the hydrochlorofluorocarbons CF3CF2CHCl2 (HCFC-225ca) over the temperature range 270 to 400 K and CF2ClCF2CHClF (HCFC-225cb) over the temperature range 298 to 400 K.

00,941
PB95-152187 Not available NTIS

National Inst. of Standards and Technology (NML), Gaithersburg, MD. Time and Frequency Div.
Rotational Far Infrared Spectrum of (13)CO.
Final rept.
L. R. Zink, P. De Natale, F. S. Pavone, M. Inguscio, M. Prevedelli, and K. M. Evenson. 1990, 7p.
Pub. in Jnl. of Molecular Spectroscopy 143, n2 p304-310 1990.

Keywords: *Carbon monoxide, *Rotational spectra, *Infrared spectra, Far infrared radiation, Carbon 13, Reprints, Fourier transform spectroscopy.

The pure rotational spectrum of (13)CO between 0.66 and 3.3 THz has been measured with a tunable far infrared spectrometer. Revised values for B(o), D(o), and H(o) have been obtained with a 50 kHz 1 sigma standard deviation of the fit. Additional measurements were performed with a Fourier transform spectrometer, and a 1 MHz (3.3 x 10(exp -5)/cm) measurement accuracy is demonstrated with this device. The rotational spectrum from J double prime = O to J double prime = 30 is calculated and gives the frequencies with an accuracy (one sigma) of better than 120 kHz.

00,942
PB95-152211 Not available NTIS
National Inst. of Standards and Technology (NML), Gaithersburg, MD. Molecular Physics Div.
Microwave and Submillimeter Spectroscopy of Ar-NH3 States Correlating with Ar+NH3(j=1, k=1).
Final rept.
E. Zwart, H. Linnartz, W. L. Meerts, W. Klemperer, G. T. Fraser, and D. D. Nelson. 1991, 11p.
Pub. in Jnl. of Chemical Physics 95, n2 p793-803 1991.

Keywords: *Argon complexes, *Microwave spectroscopy, Van der Waals forces, Submillimeter waves, Microwave spectra, Hamiltonians, Anisotropy, Reprints, *Ammonia complexes, Intermolecular potentials.

Microwave and submillimeter transitions for Ar-NH3 have been observed and assigned for the two Sigma and two Pi states correlating asymptotically with Ar + NH3 (j=1, k=1). The Sigma states are found to lie below the Pi states and are separated by approximately the inversion splitting of free NH3. For the Pi states the NH3 inversion tunneling is nearly quenched, being only weakly allowed through Coriolis interactions with the nearby Sigma states. The observed microwave and submillimeter spectra also allow the determination of (14)N quadrupole coupling constants and relative submillimeter absorption intensities. All the above results are interpreted using a model internal-rotation inversion Hamiltonian, leading to detailed information about the anisotropy of the intermolecular potential.

00,943
PB95-152823 Not available NTIS
National Inst. of Standards and Technology (NML), Gaithersburg, MD. Center for Chemical Technology.
Crystal Packing Interactions of Two Different Crystal Forms of Bovine Ribonuclease A.
Final rept.
L. A. Svensson, J. Dill, L. Sjolin, D. Bacon, J. Moult, B. Veerapandian, G. L. Gilliand, A. Wlodawer, and M. Toner. 1991, 12p.
Pub. in Jnl. of Crystal Growth 110, n1-2 p119-130 1991.

Keywords: *Pancreatic ribonuclease, *Crystals, pH, Hydrogen bonding, Electrostatics, Van der Waals forces, Binding sites, Solvents, Cattle, Reprints.

The crystal packing interactions of two crystal forms of bovine ribonuclease A are compared. An analysis of the crystal packing interactions, including solvent bridging, indicates that the high-alcohol crystal form of ribonuclease A has a balance of hydrogen bonding, electrostatic and van der Waals interactions. In contrast, the high-salt crystal packing forces are dominated by van der Waals interactions, but at the dimer interface of the molecules in this crystal form the interactions have a large electrostatic component. The electrostatic interactions of the dimer may be due to a rearrangement in the charge-charge interactions at the active site, a direct result of the presence of the inhibitor, deoxythymidine, covalently bound to His 12.

00,944
PB95-152930 Not available NTIS
National Inst. of Standards and Technology (MSEL), Gaithersburg, MD. Office of Intelligent Processing of Materials.
Memory Function Approach to the Shape of Pressure Broadened Molecular Bands.
Final rept.
G. Birnbaum. 1994, 14p.
Pub. in Molecular Physics 81, n3 p519-532 1994.

Keywords: *Molecular absorption, *Absorption spectra, *Pressure broadening, Molecular collisions, Quantum mechanics, Spectral bands, Line spectra, Spectroscopy, Reprints, *Memory function, Far wings, Line interference.

A unified treatment of the shape of pressure-broadened molecular absorption bands from near resonance to the far wings is achieved by an approach using memory functions. Empirical models for these functions are employed that interpolate between known short and long time behavior. This treatment includes the following band shaping mechanisms: line interference, finite duration of collision, molecular torques, and detailed balance. Line interference can produce a very sharp decrease in absorption in the periphery of a band, e.g., as in the nu(sub 3) band of carbon dioxide. Absorption in the far wings, which in this band exhibits a much less rapid decrease with increasing frequency, is attributed to the effect of molecular torques acting during collisions. By using a model memory function, a simple analytical expression is obtained for the far wing absorption. The parameters in this model are related to known molecular quantities. The computed and measured far wing absorption of the nu(sub 3) band of carbon dioxide broadened by argon at 296 K and 613 K are compared.

00,945
PB95-152989 Not available NTIS
National Inst. of Standards and Technology (PL), Gaithersburg, MD. Radiometric Physics Div.
Interatomic Potential of Argon.
Final rept.
S. J. Boyes. 1994, 6p.
Pub. in Chemical Physics Letters 221, p467-472 1994.

Keywords: *Argon, Virial coefficients, Interatomic forces, Reprints, *Interatomic potentials.

The recent literature abounds with proposed interatomic potential functions for argon. Of these at Hartree-Fock dispersion (HFD) type functions have been very successful and are considered to be among the best characterizations of the argon interaction to date. It is the purpose of this Letter, however, to show that of the proposed HFD-type potentials, none predict the recent acoustic virial coefficients measured by Moldover et al. In view of this, an alternative interatomic potential has been constructed for argon. The potential is of the Hartree-Fock dispersion individually damped (HFD-ID) type and represents a subtle but significant improvement for the interaction.

00,946
PB95-153011 Not available NTIS
National Inst. of Standards and Technology (PL), Gaithersburg, MD. Molecular Physics Div.
Product State Correlations in the Reaction of O((1)D) and H2O in Bimolecular Collisions and in O3.H2O Clusters.
Final rept.
M. P. Casassa, D. G. Sauder, and D. S. King. 1993, 7p.
Sponsored by Air Force Office of Scientific Research, Bolling AFB, DC.
Pub. in Proceedings of Society of Photo-Optical Instrumentation Engineers: Laser Techniques for State-Selected and State-to-State Chemistry, Los Angeles, CA., January 21-23, 1993, v1858 p256-262.

Keywords: *Molecular collisions, *Molecular clusters, *Oxygen, *Ozone, *Water, Hydroxyl radicals, Chemical reactions, Oxygen 16, Oxygen 18, Reprints, Translations.

Measurements of the translational energy and internal state distributions of OH products produced in the bimolecular reaction (16)O(singlet D) + H2(18)O --> (16)OH + (18)OH are reviewed. These detailed measurements reveal relationships between the states of geminate fragments produced in individual reaction events. Preliminary measurements on the same reaction initiated in O3 (dot) H2O clusters formed in free jet expansions are reported. The dynamics of the cluster reaction are dramatically different than those of the bimolecular reaction. The results indicate that the third body present in the cluster (O2), carries a significant amount of the energy released in the reaction.

00,947
PB95-153037 Not available NTIS
National Inst. of Standards and Technology (CSTL), Gaithersburg, MD. Surface and Microanalysis Science Div.
Time-Resolved Measurements of Energy Transfer at Surfaces.
Final rept.
R. R. Cavanagh, E. J. Heilweil, and J. C. Stephenson. 1994, 13p.
Pub. in Surface Science 299/300, p643-655 1994.

Keywords: *Surface chemistry, *Adsorbates, Molecular relaxation, Picosecond pulses, Time dependence, Excited states, Energy transfer, Semiconductors, Dielectrics, Metals, Reprints, Femtosecond pulses, Vibrational relaxation.

Developments in time-resolved measurements of energy transfer at surfaces are reviewed. Picosecond and femtosecond measurements of vibrational and electronic relaxation at surfaces are highlighted. Experimental results for vibrational relaxation of simple adsorbates on metals, semiconductors, and insulators are reviewed, and relaxation mechanisms such as electron-hole pair formation, multiphonon relaxation and image dipole damping are considered. Energy transfer involving excited electronic states of molecules on liquid and solid dielectric surfaces and the relaxation of surface electronic states on semiconductors and of image states on metal surfaces are discussed.

00,948
PB95-153201 Not available NTIS
National Inst. of Standards and Technology (MSEL), Gaithersburg, MD. Reactor Radiation Div.
Rotational Dynamics of C60 in Na2RbC60.
Final rept.
C. Christides, K. Prassides, D. A. Neumann, K. Tanigak, I. Hirosawa, T. W. Ebbesen, J. R. D. Copley, and J. Mizuki. 1993, 6p.
Pub. in Europhysics Letters 24, n9 p755-760 1993.

Keywords: *Buckminsterfullerene, *Fullerenes, Temperature range 0013-0065 K, Temperature range 0065-0273 K, Temperature dependence, Order-disorder transformations, Rubidium compounds, Sodium compounds, Neutron scattering, Inelastic scattering, Superconductors, Reprints, *Sodium rubidium fullerides, Rotational dynamics.

We have measured the low-energy neutron inelastic-scattering (NIS) spectra of superconducting Na2RbC(60) in the temperature range 50-350 K. Well-defined librational peaks are observed at 50 K at 2.83(17) meV (FWHM = 1.7(5) meV). They soften and broaden with increasing temperature. Their behavior mimics that found in solid C(60) and differs markedly from K3C(60). The rotational barrier for C(60) reorientations in Na2RbC(60) is somewhat higher than in pristine C(60) and approximately half as large as in K3C(60). An order-disorder transition is anticipated at a temperature higher than that found in C(60).

00,949
PB95-153219 Not available NTIS
National Inst. of Standards and Technology (MSEL), Gaithersburg, MD. Reactor Radiation Div.
Rotational Dynamics of Solid C70: A Neutron-Scattering Study.
Final rept.
C. Christides, T. J. S. Dennis, K. Prassides, J. R. D. Copley, R. L. Cappelletti, and D. A. Neumann. 1994, 7p.
Pub. in Physical Review B 49, n4 p2897-2903, 15 Jan 94.

Keywords: *Fullerenes, Temperature range 0000-0013 K, Temperature range 0013-0065 K, Temperature range 0065-0273 K, Temperature range 0273-0400 K, Temperature range 0400-1000 K, Temperature dependence, Neutron diffraction, Neutron scattering, Inelastic scattering, Low energy, Reprints, Rotational dynamics.

We report the results of neutron-diffraction and low-energy neutron-inelastic-scattering experiments on high-purity solid C(70) between 10 and 640 K. Thermal hysteresis effects are found to accompany structural changes both on cooling and on heating. The observed diffuse scattering intensity does not change with temperature. At 10 K broad librational peaks are observed at 1.82(16) meV (full width at half maximum = 1.8(5) meV). The peaks soften and broaden further with in-

creasing temperature. At and above room temperature, they collapse into a single quasielastic line. At 300 K, the diffusive reorientational motion appears to be somewhat anisotropic, becoming less so with increasing temperature. An isotropic rotational diffusion model, in which the motions of adjacent molecules are uncorrelated, describes well the results at 525 K. The temperature dependence of the rotational diffusion constants is consistent with a thermally activated process having an activation energy of 32(7) meV.

00,950
PB95-153292 Not available NTIS
National Inst. of Standards and Technology (MSEL), Gaithersburg, MD. Reactor Radiation Div.
Structure and Dynamics of Buckyballs.
Final rept.
J. R. D. Copley, W. I. F. David, and D. A. Neumann. 1993, 9p.
Pub. in Neutron News 4, n4 p20-28 1993.

Keywords: *Buckminsterfullerene, *Fullerenes, Molecular structure, X-ray diffraction, Neutron scattering, Inelastic scattering, Molecular dynamics, Reviews, Reprints, US NIST.

C(60) (buckminsterfullerene) is the most well-known, the most stable, the most readily available, and in many respects the most interesting member of a recently discovered class of pure carbon molecules known as the fullerenes. A method of making macroscopic quantities of fullerene mixtures was described in late 1990, and since that time many scientists have been investigating the properties of C(60), the higher fullerenes, and their various compounds and derivatives. To date most of the neutron scattering research on these materials has been carried out either at the 20 MW research reactor of the National Institute of Standards and Technology (NIST), or at the ISIS spallation source, Rutherford-Appleton Laboratory. In this article we shall describe the research that has interested and occupied us the most, namely diffraction and low energy inelastic scattering studies of solid C(60). Much of the work that we omit is discussed in two recently published reviews.

00,951
PB95-153300 Not available NTIS
National Inst. of Standards and Technology (MSEL), Gaithersburg, MD. Reactor Radiation Div.
Neutron and X-Ray Scattering Cross Sections of Orientationally Disordered Soild C60.
Final rept.
J. R. D. Copley, and K. H. Michel. 1993, 18p.
Pub. in Jnl. of Phys: Condens. Mater. 5, p4353-4370 1993.

Keywords: *Buckminsterfullerene, *Fullerenes, Differential cross sections, Scattering cross sections, X-ray scattering, Neutron scattering, Orientation(Direction), Single crystals, Powder(Particles), Distribution functions, Crystal fields, Reprints.

Differential cross sections for neutron and x-ray scattering have been derived for the orientationally disordered phase of solid C(60). Interaction centers are placed at nuclei and at the centers of interatomic bonds. Bragg and diffuse scattering cross sections, for single crystals and for powders, are formulated using symmetry-adapted rotator functions. Thermal averages are calculated taking account of crystal field effects. Thermally averaged orientational distribution functions have also been calculated.

00,952
PB95-153730 Not available NTIS
West Coast Information System, Walnut Creek, CA.
Dielectric Studies of Fluids with Reentrant Resonators.
Final rept.
A. R. H. Goodwin, and M. R. Moldover. 1993, 10p.
Contract DE-AI05-88ER13823
Sponsored by Department of Energy, Washington, DC.
Pub. in Proceedings of Symposium on Energy Engineering Sciences (11th), Argonne, IL., May 3-5, 1993, p139-148.

Keywords: *Fluorohydrocarbons, *Refrigerants, *Dielectric properties, *Cavity resonators, Radio waves, Dipole moments, Binary mixtures, Ethane, Carbon dioxide, Argon, Calibration, Helium, Mathematical models, Reprints, *1,1,1,2,3,3-hexafluoropropane, *R236ea, Phase boundaries, Clausius-Mossotti equation.

We have used a reentrant radio-frequency (rf) cavity as a resonator operating near 375 MHz to measure changes in the dielectric constant of fluids within it. The utility of these measurements was demonstrated by determining the dipole moment of 1,1,1,2,3,3-hexafluoropropane, a candidate replacement refrigerant (denoted R236ea) and by detecting the phase boundaries in the mixture ((1-x)C2H6 + xCO2), for the mole fraction x = 0.492. The densities of the coexisting phases of the mixture were determined using the Clausius-Mossotti relation which has errors on the order of 0.5% in this application. To test the accuracy of the present techniques, the rf resonator was calibrated with helium and then used to redetermine the molar polarizability A(sub e) of argon. The results were in excellent agreement with published values. Our design of the reentrant resonator makes it suitable for use with corrosive fluids at temperatures up to 400 C.

00,953
PB95-160602 PC A17/MF A04
National Inst. of Standards and Technology (CSTL), Gaithersburg, MD.
CSTL Technical Activities, 1993.
Feb 94, 385p, NISTIR-5303.
Presented to the Board on Assessment of NIST Programs, National Research Council, February 1-2, 1994. See also report for 1992, PB93-173482 and report for 1991, PB94-160769.

Keywords: *Research and development, *Chemistry, Biochemistry, Biotechnology, Chemical engineering, Reaction kinetics, Thermodynamics, Inorganic compounds, Technology transfer, Standards, Thermophysics, Organic compounds, Surface chemistry, Microanalysis, Measurement, Quality assurance, Processing, *Chemical Science and Technology Library, Standard reference materials, US NIST, National Institute of Standards and Technology.

The expanded responsibilities the authors were given nearly six years ago in becoming the National Institute of Standards and Technology have provided us with a significant challenge. In response to this challenge, the authors have expanded their interactions with U.S. industry to meet their needs and help improve their global competitiveness, while continuing to provide the national system of chemical and physical measurements, the fundamental research base for tomorrow's chemical science and technology, and a national reference laboratory to address critical problems related to public health and safety. With these goals in mind, the report contains research from the following divisions: Biotechnology, Chemical Engineering, Chemical Kinetics and Thermodynamics, Inorganic Analytical Research, Organic Analytical Research, Process Measurements, Surface and Microanalysis Science, and Thermophysics.

00,954
PB95-161097 Not available NTIS
National Inst. of Standards and Technology (MSEL), Gaithersburg, MD. Reactor Radiation Div.
Neutron Powder Diffraction Study of the Nuclear and Magnetic Structures of the Oxygen-Deficient Perovskite YBaCuCoO5.
Final rept.
Q. Huang, P. Karen, V. L. Karen, A. D. Mighell, I. N. Sora, N. Rosov, A. Santoro, A. Kjekshus, and J. W. Lynn. 1994, 7p.
Pub. in Jnl. of Solid State Chemistry 108, p80-86 1994.

Keywords: *Crystal structure, Barium oxides, Cobalt oxides, Copper oxides, Yttrium oxides, Perovskites, Room temperature, Tetragonal lattices, Lattice parameters, Neutron diffraction, Magnetic moments, Reprints, *Yttrium barium cuprate cobaltates, *Magnetic ordering.

The nuclear and magnetic structures of the oxygen-deficient perovskite YBaCuCoO5 have been determined by neutron powder diffraction at room temperature. The nuclear structure has the symmetry of space group P4/mmm and lattice parameters a = 3.8679(1), c = 7.5674(2) A. Copper and cobalt atoms are completely disordered in this compound and the oxygen vacancies are located on the layer of the yttrium atoms. As a consequence of this configuration, the Co/Cu atoms have fivefold, pyramidal coordination. The magnetic structure is based on a unit cell related to that of the nuclear structure by an axis transformation of matrix (1, -1, 0/1, 1, 0/0, 0, 2). The magnetic origin of the extra reflections observed experimentally was established by polarized neutron diffraction measurements. If we assume that the magnetic structure has tetragonal symmetry, then the magnetic moments have to assume an orientation parallel to the c axis of the unit cell.

00,955
PB95-161543 Not available NTIS
National Inst. of Standards and Technology (MSEL), Gaithersburg, MD. Polymers Div.
Octacalcium Phosphate Carboxylates. 2. Characterization and Structural Consideration.
Final rept.
M. Markovic, B. O. Fowler, and W. E. Brown. 1993, 11p.
See also Part 1, PB95-161535. Sponsored by American Dental Association Health Foundation, Chicago, IL.
Pub. in Chem. Mater. 5, n10 p1406-1416 1993.

Keywords: *Molecular structure, *Physicochemical properties, Calcium phosphates, Ions, Dentistry, X-ray diffraction, Infrared spectroscopy, Raman spectroscopy, Crystallography, Crystal lattices, Reprints, *Octacalcium phosphate carboxylates.

Detailed physicochemical characterization of octacalcium phosphate carboxylates (OCPCs) with structurally incorporated succinate, adipate, suberate, sebacate, fumarate, and citrate ions is reported. Compositional formulas of the OCPCs were derived from Ca, P, C, H, and H2O analyses. X-ray diffraction patterns of OCPCs show structural similarity with the parent compound octacalcium phosphate (OCP); the b and c axes of the unit cells were nearly the same as those of OCP but the a axes were progressively expanded concomitant with carbon chain length. Infrared and Raman assignments were made for nearly all bands of these six OCPCs; an OCP-succinate containing the deuterated succinate ion was prepared to facilitate band assignments. Spectra of the OCPCs, as compared to that of OCP, showed the presence of carboxylate groups, changes in water bonding, only slight changes in PO4 environments, and preferential reduction in HPO4(5) content. OCP has two crystallographically nonequivalent HPO4 groups (designated 5 and 6); the preferential replacement of HPO4(5) by the dicarboxylate ion is plausible considering lattice geometry. By utilizing combined data from the different methods, the possible positions of carboxylate ions in the OCPC structures are discussed.

00,956
PB95-161873 Not available NTIS
National Inst. of Standards and Technology (PL), Boulder, CO. Quantum Physics Div.
Slit Jet Infrared Spectroscopy of Hydrogen Bonded N2HF Isotopomers: Rotational Rydberg-Klein-Rees Analysis and H/D Dependent Vibrational Predissociation Rates.
Final rept.
D. J. Nesbitt, T. G. Lindeman, J. T. Farrell, and C. M. Lovejoy. 1994, 11p.
Grant NSF-PHY90-12244
Sponsored by National Science Foundation, Arlington, VA.
Pub. in Jnl. of Chemical Physics 100, n2 p775-785, 15 Jan 94.

Keywords: *Nitrogen complexes, *Infrared spectroscopy, Vibrational states, Rotational states, Absorption spectra, High resolution, Hydrogen bonds, Infrared lasers, Nitrogen 14, Nitrogen 15, Isomers, Reprints, *Hydrogen fluoride complexes, *Deuterium fluoride complexes, *Isotopomers, Vibrational predissociation, Supersonic expansion, Potential energy surfaces.

High resolution IR laser direct absorption spectra in a slit jet are presented and analyzed for nitrogen ((15)N(14)N-HF, (14)N(15)N-HF, (15)N(15)N-HF, and deuterium ((14)N(14)N-DF) substituted N2HF isotopomers. Both (14)N(15)N-HF and (15)N(14)N-HF isomers are observed, indicating a sufficiently deep minimum in the hydrogen bonding potential energy surface to quench internal rotation of the N2. The vibrationally averaged stretching potentials for each substituted species are recovered from rotational Rydberg-Klein-Rees (RKR) analysis. Features of the one-dimensional (1D) potential surface such as hydrogen bond length, harmonic force constant, and well depth are then tested for isotopic invariance by direct comparison of the different isotopomers. Agreement among the various N substituted species for HF based complexes for either nu(HF)=0 or 1 is excellent, and provides effective 1D potentials for the stretching coordinate between 3.39 and 3.75 A.

00,957
PB95-162152 Not available NTIS
National Inst. of Standards and Technology (EEEL), Boulder, CO. Electromagnetic Fields Div.
Diffusion of Copper into Gold Plating.
Final rept.
S. P. Pucic. 1993, 4p.
Pub. in Proceedings of Institute of Electrical and Electronics Engineers Instrumentation and Measurement Technology Conference, Irvine, CA., May 18-20, 1993, p114-117.

Keywords: *Copper alloys, *Gold alloys, *Diffusion coefficient, *Electroplating, *Electrical resistivity, *Microwaves, *Interfaces, Electromagnetic radiation, Copper oxides, Surface properties, Electrical engineering, Nickel, Skin effects, Ambient temperature, Reprints.

The value of the room temperature copper - gold interdiffusion coefficient derived by extrapolating from high temperature measurements is an underestimate by several orders of magnitude. Once the full thickness of the gold film is penetrated, copper accumulates on the surface, and a layer of high concentration of copper exists immediately below the gold/air interface. Electrical resistivity of an alloy is much higher than the resistivity of either component. This high resistivity layer may be localized within the skin depth of propagating electromagnetic waves; in cases where copper has reached the surface, it is permanently within the skin depth at any frequency. A nickel 'diffusion barrier,' commonly applied between copper and gold, is unsuitable in many microwave and millimeter-wave applications because of ferromagnetism of nickel at room temperature. The compound that forms on the surface of untreated copper at room temperature in a reasonably clean atmosphere is cuprous oxide. Its properties make it a better alternative to gold in microwave and millimeter-wave engineering.

00,958
PB95-162269 Not available NTIS
National Inst. of Standards and Technology (MSEL), Gaithersburg, MD. Reactor Radiation Div.
Neutron-Scattering Study of Librations and Intramolecular Phonons in Rb2.6K0.4C60.
Final rept.
D. Reznik, W. A. Kamitakahara, D. A. Neumann, R. M. Strongin, M. A. Cichy, A. B. Smith, J. R. D. Copley, and J. E. Fischer. 1994, 6p.
Pub. in Physical Review B 49, n2 p1005-1010, 1 Jan 94.

Keywords: *Fullerenes, Neutron scattering, Inelastic scattering, Temperature dependence, MeV range 1-10, Superconductors, Librations, Potentials, Phonons, Reprints, *Rubidium potassium fullerides, Density of states.

We report the results of inelastic neutron-scattering measurements on Rb(2.6)K(0.4)C(60). Librational modes were observed as broad peaks with maxima between 4.1 and 4.7 meV, as the temperature is lowered from 300 to 12 K. As in K3C(60), no change in the width or position of the librational peak was observed when the sample was cooled through the superconducting transition. Thus any coupling of the librations to electronic states is small. The magnitude of the orientational potential barrier was estimated from the librational peak frequency. A flat background observed in the low-energy inelastic-scattering spectra is ascribed to two-phonon scattering. The density of states of intramolecular modes is similar to that of previously studied M3C(60) compounds; modes at 53 and 66 meV in pure C(60) are not observed in Rb(2.6)K(0.4)C(60).

00,959
PB95-162319 Not available NTIS
National Inst. of Standards and Technology (CSTL), Gaithersburg, MD. Surface and Microanalysis Science Div.
Laser-Induced Desorption of NO from Si(111): Effects of Coverage on NO Vibrational Populations.
Final rept.
L. J. Richter, S. A. Buntin, D. S. King, and R. R. Cavanagh. 1990, 10p.
Contract DE-AI05-84ER13150
Sponsored by Department of Energy, Washington, DC.
Pub. in Jnl. of Electron Spectroscopy and Related Phenomena 54/55, p181-190 1990.

Keywords: *Nitric oxide, *Desorption, Near infrared radiation, Visible radiation, Vibrational states, Surface chemistry, Substrates, Silicon, Reprints, *Laser induced desorption.

Laser-induced desorption of NO from Si(111) has been investigated using state-specific detection techniques. The observed energy partitioning in the desorbed NO varies significantly with the NO coverage. Characterization of energy partitioning with desorption-laser wavelengths in the range 355-1907 nm indicates that different substrate electronic excitations are responsible for the desorption at low NO coverage vs saturation coverage. The relationship between the substrate electronic excitation and observed vibrational-state-population distributions is explored.

00,960
PB95-162368 Not available NTIS
National Inst. of Standards and Technology (CSTL), Gaithersburg, MD. Thermophysics Div.
Viscosity of the Saturated Liquid Phase of Six Halogenated Compounds and Three Mixtures.
Final rept.
D. Ripple, and O. Matar. 1993, 5p.
Pub. in Jnl. of Chemical and Engineering Data 38, n4 p560-564 1993.

Keywords: *Kinematic viscosity, *Fluorohydrocarbons, *Binary mixtures, Viscometers, Temperature dependence, Refrigerants, Reprints, *1,1,1,2-Tetrafluoroethane, *Bis(difluoromethyl) ether, *2-Difluoromethoxy-1,1,1-trifluoroethane, *Pentafluoroethane, *1-Chloro-1,2,2,2-tetrafluoroethane, *Difluoromethane, *R134a, *RE134, *RE245, *R125, *R124, *R32.

Data are reported for the viscosity of six saturated liquids and three mixtures of these liquids over a temperature range from 250 to 330 K. The liquids studied are the halogenated compounds, 1,1,1,2-tetrafluoroethane (R134a), bis(difluoromethyl) ether (RE134), 2-(difluoromethoxy)-1,1,1-trifluoroethane (RE245), pentafluoroethane (R125), 1-chloro-1,2,2,2-tetrafluoroethane (R124), and difluoromethane (R32). The mixtures studied are R125 + R134a, R32 + R134a, and R32 + R124, all at approximately 50% mole fraction. A capillary viscometer constructed of stainless steel and sapphire was used to obtain the data. The measurements are accurate to 3-5% of the kinematic viscosity. A free volume model of viscosity was used to correlate the data.

00,961
PB95-162459 Not available NTIS
National Inst. of Standards and Technology (NML), Gaithersburg, MD. Chemical Process Metrology Div.
Simultaneous Forward-Backward Raman Scattering Studies of D2 Broadened by D2, He, and Ar.
Final rept.
G. J. Rosasco, W. J. Bowers, W. S. Hurst, A. D. May, J. P. Looney, and K. C. Smyth. 1991, 9p.
Pub. in Jnl. of Chemical Physics 94, n12 p7625-7633, 15 Jun 91.

Keywords: *Raman spectra, *Deuterium, *Hydrogen, Atom-molecule collisions, Atom-atom collisions, Line broadening, Line shape, Colliding beams, Helium, Argon, Reprints.

Beam crossings within a spherical-mirror, multipass-cell provide the opportunity to measure, simultaneously, the Raman spectrum for both the forward and backward scattering geometries. The analyses necessary to quantitatively account for such forward-backward spectra are summarized. These simultaneous forward-backward spectra enable unique experimental tests of lineshape functions used for the description of the Raman Q-branch spectrum under conditions where Doppler contributions and Dicke narrowing are significant. Results for the D2:D2 and D2:He systems support the well-known Galatry, or soft collision, lineshape function. For the case of D2:Ar, evidence is advanced for the need to employ the more general complex soft collision function. In addition, these studies have provided data on linear-with-density line broadening (previously published) and line shifting coefficients (reported here) for these molecular systems.

00,962
PB95-162509 Not available NTIS
National Inst. of Standards and Technology (NML), Gaithersburg, MD. Radiometric Physics Div.
Vibronic Coupling and Other Many-Body Effects in the 4sigmag(-1) Photoionization Channel of CO2.
Final rept.
P. Roy, R. J. Bartlett, W. J. Trela, S. H. Southworth, J. E. Hardis, V. Schmidt, J. L. Dehmer, T. A. Ferrett, and A. C. Parr. 1991, 8p.
Pub. in Jnl. of Chemical Physics 94, n2 p949-956 1991.

Keywords: *Carbon dioxide, *Photoionization, EV range 10-100, Photoelectron spectroscopy, Branching ratio, Vibrational states, Angular distribution, Forbidden transitions, Autoionization, Reprints.

Vibrational branching ratios and photoelectron angular distributions were measured for 4(sigma)g photoionization of CO2 in the energy range 20-28 eV. Of particular interest are three vibrational components of the resulting CO2(1+) C(tilde) doublet Sigma(sub g, sup +) state--the allowed (000) and (100) bands and the forbidden (101) band. The wavelength dependence of the beta parameter for the forbidden band deviated significantly from that of the two allowed bands, showing instead a strong resemblance to that of the B(tilde) doublet Sigma(sub u, sup +) state. This behavior suggests that vibronic coupling to the B(tilde) doublet Sigma(sub u, sup +) state is responsible for the appearance of the forbidden (101) band in the C(tilde) doublet Sigma(sub g, sup +) state photoelectron spectrum. We also observe evidence for other many-body effects--shape-resonance-induced continuum-continuum coupling and doubly-excited autoionizing resonances--in the present data.

00,963
PB95-162731 Not available NTIS
National Inst. of Standards and Technology (NML), Gaithersburg, MD. Chemical Process Metrology Div.
Fundamental Studies of Gas Sensor Response Mechanisms: Palladium on SnO2(110).
Final rept.
S. Semancik, and T. Fryberger. 1990, 4p.
Pub. in Proceedings of International Meeting on Chemical Sensors (3rd), Cleveland, OH., September 24-26, 1990, p23-26.

Keywords: *Surface chemistry, *Gas detectors, *Palladium, Adsorption, Oxygen, Hydrogen, Planar devices, Electrical properties, Tin oxides, Surface properties, Reprints, Coadsorption.

Surface analytical techniques and in situ conductance measurements have been used to study the sensing action of low coverage Pd dispersed on a SnO2(110) crystal. The Pd coverage dependence and the temperature dependence for H2 detection are discussed for this system. The authors also examine the role of coadsorbate reactions between hydrogen and oxygen at the Pd/SnO2 surfaces in controlling interfacial electrical properties. Results from this model study are being used to guide the fabrication of prototype conductance sensors consisting of thin (epitaxial) oxide films with metal layers.

00,964
PB95-162756 Not available NTIS
National Inst. of Standards and Technology (NML), Gaithersburg, MD. Chemical Kinetics Div.
Temperature Dependence of the Rate Constants for Reaction of Dihalide and Azide Radicals with Inorganic Reductants.
Final rept.
L. C. T. Shoute, Z. B. Alfassi, P. Neta, and R. E. Huie. 1991, 5p.
Pub. in Jnl. of Physical Chemistry 95, n8 p3238-3242 1991.

Keywords: *Radiolysis, *Radicals, *Temperature, *Reaction kinetics, Inorganic azides, Chemical reactions, Inorganic compounds, Reduction(Chemistry), Radiation chemistry, Activation energy, Reprints, Rate constants.

Rate constants for several reactions of inorganic radicals with inorganic reductants in aqueous solutions have been measured by pulse radiolysis as a function of temperature, generally between 5 and 75 deg C. The temperature dependence of the reaction rate constant is correlated to the reaction exothermicity for the metal complexes, which apparently react by outersphere electron transfer. The simple anions, however, have lower activation energies, which do not correlate well with the exothermicities, suggesting that these anions probably react by an inner-sphere mechanism.

00,965
PB95-162764 Not available NTIS
National Inst. of Standards and Technology (NML), Gaithersburg, MD. Chemical Kinetics Div.
Iodine Atoms and Iodomethane Radical Cations: Their Formation in the Pulse Radiolysis of Iodomethane in Organic Solvents, Their Complexes, and Their Reactivity with Organic Reductants.
Final rept.
L. C. T. Shoute, and P. Neta. 1991, 4p.
Pub. in Jnl. of Physical Chemistry 95, n11 p4411-4414 1991.

Keywords: *Radiolysis, *Iodine, *Iodine organic compounds, *Reaction kinetics, Atoms, Cations, Chemical reactions, Organic solvents, Radicals, Radiation chemistry, Chemical reactivity, Reprints, Pulse radiolysis.

Pulse radiolysis of iodomethane in various organic solvents leads to formation of iodine atoms or iodomethane radical cations, which in turn form complexes with iodomethane or with the solvent. Radiolysis in cyclohexane gives CH3I.I, which exhibits an absorption peak at 390 nm, whereas radiolysis in benzene forms the solvent complex, C6H6.I, which exhibits an intense broad absorption centered at 490 nm. Replacing the methyl group of iodomethane radical cation with ethyl or isopropyl decreases the reactivity, whereas trifluoromethyl increases the reactivity. These oxidation reactions proceed via an intermediate complex between the iodine species and the organic reductant.

00,966
PB95-162814 Not available NTIS
National Inst. of Standards and Technology (NML), Gaithersburg, MD. Chemical Kinetics Div.
Ionization Energy of Sulfur Pentafluoride and the Sulfur Pentafluoride-Fluorine Atom Bond Dissociation Energy.
Final rept.
L. W. Sieck, and P. J. Ausloos. 1990, 5p.
Pub. in Jnl. of Chemical Physics 93, n11 p8374-8378 1990.

Keywords: *Thermochemistry, *Mass spectroscopy, *Ionization potentials, Thermodynamic properties, Atomic properties, Chemical reactions, Chemical equilibrium, Sulfur hexafluoride, Fluorides, Reprints, Ion-molecule reactions.

The techniques of Fourier Transform Spectroscopy and High Pressure Mass Spectrometry have been used to investigate the ionization potential (I.P.) of SF5 via electron exchange reactions. An I.P. of 9.60 + or - 0.05 eV has been derived from this data, which is in disagreement with estimates from flowing afterflow measurements (I.P. > or - 10.15 eV). In addition, no evidence has been found for a fluoride transfer equilibrium involving CF3(1+) and SF6, which was thought to interrelate the heats of formation of CF3(1+) and SF5(1+).

00,967
PB95-163051 Not available NTIS
National Inst. of Standards and Technology (NML), Gaithersburg, MD. Chemical Kinetics Div.
Diamond and Graphite Precursors: Comments.
Final rept.
S. E. Stein. 1990, 1p.
Pub. in Nature 346, n6284 p517 1990.

Keywords: *Diamonds, *Graphite, *Precursors, Thermodynamics, Nucleation, Stability, Reprints, Nanostructures.

The letter 'Nanometre-Sized Diamonds are More Stable Than Graphite' by Badziag et al. (BVEG) attempts to provide a basis for the increasingly common observation that diamond is a product in carbon-forming reaction systems. In a plot of bonding energy versus H/C ratio they find diamond precursors to be of lower energy than graphite precursors. They suggest that this implies that diamond precursors are more 'stable' than graphite precursors, hence, from a thermodynamic standpoint, homogeneous diamond nucleation is no more difficult than graphite nucleation.

00,968
PB95-163465 Not available NTIS
National Inst. of Standards and Technology (NML), Gaithersburg, MD. Chemical Kinetics Div.
Shock Tube Techniques in Chemical Kinetics.
Final rept.
W. Tsang, and A. Lifshitz. 1990, 41p.
Pub. in Annual Review of Physical Chemistry 41, p559-599 1990.

Keywords: *Shock tubes, *Reaction kinetics, *Reviews, High temperature, Chemical reactions, Ignition, Reprints.

The review is concerned with the use of shock tubes to study the kinetics of high temperature gas phase chemical processes. It will emphasize reports on investigations published during the past ten years. The last Annual Review article on this subject was published in 1969 by Belford and Strehlow. A book 'Shock Waves in Chemistry', published in 1981, covers much of the literature during the intervening years. There are many reasons for interest in high temperature chemical kinetics. Increasing the temperature opens new reaction channels and thus expands the range of phenomena that can be studied. In conjunction with lower temperature results, the nature of the chemical reaction can be more properly defined. Many important industrial processes occur at high temperatures. With the increasing role of computer simulations for the understanding of such complex processes, there is a great need for fundamental quantitative kinetic information which are the necessary inputs for such programs. The shock tube provides a unique means of generating controlled and chemically well defined high temperature environments.

00,969
PB95-163473 Not available NTIS
National Inst. of Standards and Technology (NML), Gaithersburg, MD. Chemical Kinetics Div.
Hydrogen Atom Attack on Perchloroethylene.
Final rept.
W. Tsang, and J. A. Walker. 1991, 7p.
Pub. in Proceedings of International Symposium on Combustion, v23 p139-145 1991.

Keywords: *Tetrachloroethylene, *Hydrogen, *Reaction kinetics, *Combustion kinetics, Shock tubes, High temperature, Temperature dependence, Chemical reactions, Reprints, *Hydrogen atoms, *Perchloroethylene.

Hydrogen atoms have been reacted with perchloroethylene under the high temperature conditions of a single pulse shock tube. Rate expressions over the temperature range 950-1100 K and at pressures near 2.5 atm were determined. Comparisons are made with results from other olefinic, aromatic and related systems and the effects on hydrogen reactivity with olefins upon chlorine substitution are deduced.

00,970
PB95-163523 Not available NTIS
National Inst. of Standards and Technology (MSEL), Gaithersburg, MD. Reactor Radiation Div.
Neutron Spectroscopic Comparison of Rare-Earth/Hydrogen alpha-Phase Systems.
Final rept.
T. J. Udovic, J. J. Rush, N. F. Berk, P. Vajda, O. Blaschko, I. S. Anderson, and J. N. Daou. 1993, 9p.
Pub. in Zeitschrift fuer Physikalische Chemie 179, p349-357 1993.

Keywords: *Lutetium hydrides, *Scandium hydrides, *Yttrium hydrides, *Vibrational spectra, Neutron spectroscopy, Neutron scattering, Solid solutions, Deuterides, Reprints.

Incoherent inelastic neutron scattering was used to study the vibrational spectroscopy of hydrogen (and deuterium) in alpha-phase solid solution with Sc, Lu, and Y. Low-resolution spectra of the tetrahedrally-bound H (and D) in the three rare-earth metals exhibit similar behavior: a soft c-axis-polarized vibration about 25-30% lower in energy than the doubly-degenerate vibrations polarized along the basal plane. Previous diffuse elastic neutron scattering studies of these systems indicate the existence of short-range ordering of metal-atom-bridged hydrogen pairs into c-axis directed chains. High-resolution spectra of the broad c-axis vibrations reveal a temperature- and H-concentration-dependent splitting believed to represent local 'optic' and 'acoustic' bands associated with the dynamical coupling of these hydrogen pairs.

00,971
PB95-163531 Not available NTIS
National Inst. of Standards and Technology (PL), Gaithersburg, MD. Radiometric Physics Div.
Photoelectron Study of Electronic Autoionization in Rotationally Cooled N2: The n=6 Member of the Hopfield Series.
Final rept.
K. Ueda, J. B. West, M. A. Hayes, J. L. Dehmer, M. R. F. Siggel, and A. C. Parr. 1993, 6p.
Contract W-31-109-ENG-38
Sponsored by Department of Energy, Washington, DC. and Science and Engineering Research Council, Swindon (England).
Pub. in Jnl. of Physics B: Atomic and Molecular Optical Physics 26, pL601-L606 1993.

Keywords: *Nitrogen, *Autoionization, Molecular energy levels, Rotational states, Angular distribution, Synchrotron radiation, Electron spectroscopy, Cross sections, Photoionization, Photoelectrons, Asymmetry, Reprints, Ab initio calculations.

We report preliminary results of a study of the Hopfield series in rotationally cooled molecular nitrogen. By using angle resolved electron spectroscopy in combination with synchrotron radiation, partial cross sections and asymmetry parameters for formation of the vibrationally resolved X and A states of N2(1+) were measured in the region of the n = 6 member of the Hopfield bands. The results are compared with earlier ab initio MQDT calculations and reflect qualitative agreement for the X doublet Sigma(sub g, sup +) decay channel, but sharp disagreement for the A doublet Pi(sub mu) decay channel.

00,972
PB95-163812 Not available NTIS
National Inst. of Standards and Technology (CSTL), Gaithersburg, MD. Thermophysics Div.
Criteria for Establishing Accurate Vapor Pressure Curves.
Final rept.
L. A. Weber. 1994, 6p.
Sponsored by Department of Energy, Washington, DC.
Pub. in Rev. Int. Froid 17, n2 p117-122 1994.

Keywords: *Vapor pressure, *Fluorohydrocarbons, *Refrigerants, Specific heat, Thermodynamic properties, Reprints, *R123, *R134a.

The authors used standard thermodynamic relationships to demonstrate the accuracy of new vapor pressure measurements by using them in the calculation of liquid-phase heat capacities and comparing the results with recently published experimental values. The results for new alternative refrigerants R134a and R123 are used as examples.

00,973
PB95-164059 Not available NTIS
National Inst. of Standards and Technology (MSEL), Gaithersburg, MD. Ceramics Div.
Molecular Orbital Calculations of Bond Rupture in Brittle Solids.
Final rept.
W. Wong-Ng, G. S. White, and S. W. Freiman. 1990, 3p.
Pub. in Proceedings of Conference on Frontiers of Chemistry (2nd), Columbus, OH., November 11-14, 1990, v2 p21-23.

Keywords: *Molecular orbitals, *Chemical bonds, *Solids, *Brittleness, *Environmental effects, Silicon dioxide, Numerical analysis, Crack propagation, Covalent bonds, Self consistent field, Strains, Reprints.

Based on crack growth rate data, it is known that most brittle solids, ranging from completely ionic (MgF2) to mixed ionic/covalent (SiO2, Al2O3), undergo environmentally enhanced bond rupture. In order to further our understanding of the bond rupture mechanism, we have carried out molecular orbital calculations (MO) using the ab initio self-consistent field technique. The work to date has involved investigations of the effects of strain on the atomic charges, bond overlap population and ionic character of the Si-O bond at the crack tip of silica. Silica was chosen as the model material because of the extensive experimental data available on it.

00,974
PB95-164281 Not available NTIS
National Inst. of Standards and Technology (PL), Boulder, CO. Quantum Physics Div.
Laser Flash Photolysis/Time-Resolved FTIR Emission Study of a New Channel in the Reaction of CH3+O: Production of CO(v).
Final rept.
P. W. Seakins, and S. R. Leone. 1992, 8p.
Sponsored by Department of Energy, Washington, DC. Office of Energy Research.

Pub. in Jnl. of Physical Chemistry 96, n11 p4478-4485 1992.

Keywords: *Methyl radicals, *Oxygen atoms, *Carbon monoxide, Vibrational spectra, Chemical reactions, Photolysis, Reprints, Fourier transform infrared spectroscopy.

The reaction of CH3 radicals and O atoms is studied using laser flash photolysis/time-resolved Fourier transform infrared emission spectroscopy. In addition to observing formaldehyde vibrational CH emission, molecular CO vibrational emission is also detected. Experiments are performed to confirm that CO is a primary product from the title reaction. The observed CO vibrational distribution (nu = 1-8) can be fit with a vibrational temperature of 12700 + or - 1400 K, and the fraction of the reaction exothermicity released into CO vibration is 0.22. The branching fraction to CO is estimated to be 0.40 + or - 0.10.

00,975
PB95-164307 Not available NTIS
National Inst. of Standards and Technology (CSTL), Gaithersburg, MD.
Brownian Diffusion of Hard Spheres at Finite Concentrations.
Final rept.
M. S. Selim, M. A. Al-Naafa, and M. C. Jones. 1993, 14p.
Pub. in American Institute of Chemical Engineers Jnl. 39, n1 p3-16 Jan 93.

Keywords: *Viscosity, *Spheres, *Brownian movement, *Diffusion coefficient, Dispersions, Silica, Concentration(Composition), Colloids, Reprints, Concentration dependence.

The authors investigated the effect of concentration on the Brownian diffusion of uncharged rigid spheres. Monosize silica spheres were prepared according to the method of Stober (1968). The particles were sterically stabilized by chemisorption of stearic alcohol at their surface by the method developed by van Helden (1981). Particle radius was 14.5 nm from electron micrographs of the coated particles. Osmotic pressure measurements of the sterically stabilized particles dispersed in cyclohexane showed that the particles behaved as hard spheres. The measurements agreed well with predictions from the Carnahan-Starling equation over the concentration range 0.0458 < phi < 0.37 where phi is the volume fraction of the particles in the suspension. Viscosity measurements of silica dispersions were made over the concentration range 0 < phi < 0.25. The Brownian diffusion coefficient of the particles dispersed in cyclohexane was measured over the concentration range 0.0055 < phi < 0.248 using Taylor's hydrodynamic stability method.

00,976
PB95-164315 Not available NTIS
National Inst. of Standards and Technology (PL), Boulder, CO. Quantum Physics Div.
Bonding in Doubly Charged Diatomics.
Final rept.
J. Senekowitsch, S. ONeil, and W. Meyer. 1992, 9p.
Contracts AFOSR-NSFG0, AFOSR890074
Sponsored by Air Force Office of Scientific Research, Bolling AFB, DC.
Pub. in Theoretica Chimica Acta 84, p85-93 1992.

Keywords: *Chemical bonds, *Atomic ions, Potential energy, Wave functions, Reprints, Dication potentials.

The potential energy of interacting atomic ions A(+) + B(+) often shows a shallow local minimum separated by a broad potential barrier from the dissociation products at much lower energy. Early interpretations of dication potential shapes were based on the similarity of the electronic structure between isoelectronic neutral and ionic species and led to a picture of a chemical bond superimposed on a repulsive Coulomb potential. More recently, barriers in dication potentials have commonly been interpreted as avoided curve crossings involving covalent and ionic structures. In this paper, we demonstrate that the former model is the appropriate one except in cases with very small asymptotic ionic/covalent energy splittings. By deriving dication wavefunctions from their neutral isoelectronic counterparts, we obtain upper bound dication potential curves which show all the characteristic features. By further modeling induction effects, we arrive at an almost quantitative fit of accurate ab initio dication potentials.

00,977
PB95-164323 Not available NTIS
National Inst. of Standards and Technology (CSTL), Gaithersburg, MD. Thermophysics Div.
Application of the Taylor Dispersion Method in Supercritical Fluids.
Final rept.
J. M. H. L. Sengers, U. K. Deiters, U. Klask, P. Swidersky, and G. M. Schneider. 1993, 30p.
Pub. in International Jnl. of Thermophysics 14, n4 p893-922 Jul 93.

Keywords: *Supercritical fluids, Diffusion coefficient, Light scattering, Critical point, Carbon dioxide, Benzene, Toluene, Diffusivity, Reprints, Taylor dispersion.

This paper describes some of the experimental and theoretical problems encountered when the Taylor dispersion method is applied to the measurement of diffusion coefficients near gas-liquid critical points. We have used our own measurements of diffusion of benzene and toluene in supercritical carbon dioxide, along with measurements from several other sources, to illustrate some of the experimental challenges. Special attention is given to the peak shape. The intercomparisons are greatly simplified by comparing the experimental data as functions of density, rather than pressure. We find large and unexplained discrepancies between the various experimental sources. We discuss the theoretical predictions for the relationships between the diffusion coefficients and diffusivities obtained from Taylor dispersion and dynamic light scattering in fluids near critical points. We conclude that there is no strong reason to press for Taylor dispersion measurements near the gas-liquid critical point of the carrier gas.

00,978
PB95-164331 Not available NTIS
National Inst. of Standards and Technology (CSTL), Gaithersburg, MD. Thermophysics Div.
Critical Behavior of Ionic Fluids.
Final rept.
J. M. H. L. Sengers, and J. A. Given. 1993, 15p.
Pub. in Molecular Physics 80, n4 p899-913 1993.

Keywords: *Electrolytes, Thermodynamic properties, Critical point, Reviews, Reprints, Ionic fluids, Phase separation.

The past 25 years have seen detailed experimental confirmation, in many fluids, of concepts from the theory of critical phenomena. It has been demonstrated that fluids belong to the universality class of the 3D Ising model, with critical exponents as given by renormalization group calculations. Nevertheless, there is an important class of fluid systems, those with ionic components, for which it is not clear that the notions of critical behavior developed for uncharged systems apply. We will review the available experimental evidence, and assess the state of theoretical knowledge.

00,979
PB95-164349 Not available NTIS
National Inst. of Standards and Technology (CSTL), Gaithersburg, MD. Thermophysics Div.
Standard States, Reference States and Finite-Concentration Effects in Near-Critical Mixtures with Applications to Aqueous Solutions.
Final rept.
J. M. H. L. Sengers, A. H. Harvey, R. Crovetto, and J. S. Gallagher. 1992, 23p.
Pub. in Fluid Phase Equilibria 81, p85-107 1992.

Keywords: *Aqueous solutions, *Critical point, Critical experiments, Liquid-gas mixtures, Debye-Huckel theory, Supercritical fluids, Helmholtz free energy, Concentration(Composition), Activity coefficients, Carbon dioxide, Dilution, Reprints.

The excess Gibbs free energy reference states of both solvent and solute, as commonly used for aqueous solutions, behave anomalously near the critical point of water. This leads to a concentration-dependence of the partial and apparent molar properties that is stronger than usually assumed for nonelectrolyte as well as for electrolyte solutions, and affects a large range of pressure-temperature space where water is highly compressible. As a consequence, extrapolation techniques developed for extracting infinite-dilution properties from data at finite concentration will fail. Examples from various experimental sources, including recent volume measurements in supercritical dilute aqueous CO2, will be used to make this point. The anomalous initial concentration dependence of apparent molar properties interferes with the determination of the Debye-Huckel limiting law description, conventionally incorporated in the excess Gibbs free energy, fails when the compressibility of the solvent changes rapidly. A more appropriate frame of reference will be proposed.

00,980
PB95-164414 Not available NTIS
National Inst. of Standards and Technology (NML), Gaithersburg, MD. Electron and Optical Physics Div.
Surface Geometry of BaO on W(100): A Surface-Extended X-Ray-Absorption Fine-Structure Study.
Final rept.
A. Shih, C. Hor, W. Elam, J. Kirkland, and D. Mueller. 1991, 9p.
Pub. in Physical Review B 44, n11 p5818-5826, 15 Sep 91.

Keywords: *Barium oxides, *Monomolecular films, Surface analysis, Substrates, Single crystals, Adsorption, Tungsten, Reprints, X-ray absorption fine structure.

A surface-extended x-ray-absorption fine-structure study of ordered monolayers of coadsorbed barium and oxygen on a single-crystal W(100) surface is described. A (square root of 2) X (square root of 2) R45(degrees) structure with a stoichiometric barium-to-oxygen ratio, and a (2(square root of 2)) X (square root of 2) R45(degrees) structure with a nearly 1:2 barium-to-oxygen atomic ratio both form on W(100). The surface-extended x-ray absorption fine-structure results indicate that all of the barium and oxygen atoms are nearly coplanar in the (square root of 2) X (square root of 2) R45(degrees) overlayer. The Ba-to-O distance in this overlayer is 3.20 + or - 0.05 A and beta = 82 deg + or - 5 deg, where beta is the angle between the Ba-O internuclear axis and the surface normal. For the (2(square root of 2)) X (square root of 2) R45(degrees) overlayer, there are two types of oxygen sites. Oxygen atoms, nearly coplanar with the barium atoms are also present in these films.

00,981
PB95-164422 Not available NTIS
National Inst. of Standards and Technology (CSTL), Gaithersburg, MD. Surface and Microanalysis Science Div.
Observation of a Stable Methoxy Intermediate on Cr(110).
Final rept.
N. D. Shinn. 1992, 9p.
Sponsored by Department of Energy, Washington, DC.
Pub. in Surface Science 278, p157-165 1992.

Keywords: *Surface chemistry, Photoelectron spectroscopy, Ultraviolet spectroscopy, Chemical dissociation, Temperature range 0065-0273 K, Temperature range 0273-0400 K, Stability, Work functions, Photoemission, Methanol, Chromium, Reprints, *Methoxy radicals.

Ultraviolet photoelectron spectroscopy (UPS) and work function changes are used to identify a stable methoxy intermediate, CH3O(ads), on Cr(110) at 90 K following low exposures of methanol, CH3OH(g). Higher methanol exposures at 90 K add subsequent layers of physisorbed methanol which desorb above 120 K. Methoxy dissociation into atomic fragments occurs between 250 and 400 K. The absence of a stable CO(ads) dissociation intermediate indicates that methyl group dehydrogenation is rate limiting on Cr(110). As was previously found on Fe(100) and Mo(100), the stability of CH3O(ads) over CO(ads) on Cr(110) is opposite of that proposed by Sexton based upon relative heats of adsorption. Consideration of the CH3O:metal and CO:metal bonding mechanisms leads to the proposition that substrate electronic properties, rather than steric or substrate morphological factors, are responsible for the anomalous methoxy stability on these surfaces.

00,982
PB95-164430 Not available NTIS
National Inst. of Standards and Technology (PL), Gaithersburg, MD. Molecular Physics Div.
Fragment State Correlations in the Dissociation of NO.HF(v=1).
Final rept.
J. H. Shorter, M. P. Casassa, and D. S. King. 1992, 8p.
Pub. in Jnl. of Chemical Physics 97, n3 p1824-1831, 1 Aug 92.

Keywords: *Chemical dissociation, Chemical bonds, Excited states, Vibrational states, Rotational states, Fragments, Dimers, Reprints, *Nitric oxide complexes, *Hydrogen fluoride complexes, *Vibrational predissociation.

The NO(nu,J)-fragment population distributions and recoil energies were measured for the vibrational predissociation of NO (dot) HF following excitation of the H-F stretch. Most of the available energy appears in NO vibration and/or HF rotation. There is little recoil momentum. The data support two possibilities for the NO (dot) HF dimer bond energy: (1) D(0) = 448 + or - 5/cm with coincident pairs of fragments NO(nu = 0) + HF(J = 12) and NO(nu = 1) + HF(J = 8); (2) D(0) = 1769 + or - 10/cm with J(HF) = 9 and 2, respectively.

00,983
PB95-164471 Not available NTIS
National Inst. of Standards and Technology (PL), Gaithersburg, MD. Radiometric Physics Div.
Shape-Resonance-Enhanced Continuum-Continuum Coupling in Photoionization of CO2.
Final rept.
M. R. F. Siggel, J. B. West, M. A. Hayes, I. Iga, A. C. Parr, and J. L. Dehmer. 1993, 8p.
Pub. in Jnl. of Chemical Physics 99, n3 p1556-1563, 1 Aug 93.

Keywords: *Carbon monoxide, *Photoionization, EV range 10-100, Angular distribution, Branching ratio, Electronic states, Photoelectrons, Asymmetry, Reprints.

We have measured photoionization branching ratios and photoelectron asymmetry parameters for photoionization of CO2 leading to the first four electronic states of CO2(1+) over the photon energy range from 20 to 50 eV. The motivation for this work was the prediction by Lucchese (J. Chem. Phys. 92, 4203 (1990)) that the sigma(sub mu) shape resonance in the (4 sigma(sub g))(sup -1) C(tilde) doublet Sigma(sub g, sup +) ionization channel would influence the photoionization dynamics in the other valence-shell continua through continuum-continuum channel interaction, with the main effect occurring in the (3 sigma(sub mu))(sup -1) B(tilde) doublet Sigma(sub mu, sup +) channel. Indeed, clear evidence for this phenomenon is observed in this channel, the most prominent indication being a broad, shallow minimum in the asymmetry parameter at approx 40 eV. Comparisons of the present results with theory and other measurements reflect good overall agreement and provide some guidance regarding the effectiveness of alternative approximations used in the theoretical calculations.

00,984
PB95-164489 Not available NTIS
National Inst. of Standards and Technology (CSTL), Gaithersburg, MD. Thermophysics Div.
Ebulliometric Measurement of the Vapor Pressure of 1-Chloro-1,1-Difluoroethane and 1,1-Difluoroethane.
Final rept.
A. M. Silva, and L. A. Weber. 1993, 3p.
Pub. in Jnl. of Chemical and Engineering Data 38, n4 p644-646 1993.

Keywords: *Vapor pressure, *Fluorohydrocarbons, *Refrigerants, Ebulliometry, Temperature dependence, Boiling points, Reprints, 1-Chloro-1,1-difluoroethane, R142b, 1,1-Difluoroethane, R152a.

The vapor pressures of 1-chloro-1,1-difluoroethane (R142b) and 1,1-difluoroethane (R152a) have been measured at temperatures between 224.8 and 284.7 K for R142b and between 219.9 and 273.1 K for R152a by a comparative ebulliometric technique. Our results have been combined with selected published results to provide a smoothing equation for the vapor pressure. For R142b, our equation is valid from 200 to 300 K while for R152a the temperature range goes from 215 K to the critical temperature, near 386 K.

00,985
PB95-164513 Not available NTIS
National Inst. of Standards and Technology (PL), Gaithersburg, MD. Molecular Physics Div.
2nu9 Band of Propyne-d3.
Final rept.
K. Singh, G. Rajappan, V. A. Job, W. B. Olson, V. B. Kartha, and A. Weber. 1993, 12p.
Pub. in Jnl. of Molecular Spectroscopy 157, p467-478 1993.

Keywords: *Propyne, *Infrared spectra, Molecular spectra, Vibrational spectra, Rotational spectra, Band spectra, Temperature range 0065-0273 K, Room temperature, Deuterium compounds, High resolution, Reprints, Fourier transform spectroscopy.

High-resolution Fourier transform spectra of CD3CCH at room temperature and at 195 K have been recorded in the region of the 2nu(sub 9) band (1225-1285/cm) at an apodized resolution of 0.004/cm. Approximately 1000 vibration-rotation transitions in the P and R branches of 2nu(sub 9) (A(sub 1)) have been fitted with a standard deviation of 0.00035/cm. Two vibration-rotation interactions have been identified and analyzed. The parameters of the 2nu(sub 9) (A(sub 1)) state and some of the those of the interacting states have been determined.

00,986
PB95-164596 Not available NTIS
National Inst. of Standards and Technology (CSTL), Boulder, CO. Chemical Engineering Div.
Phase Composition, Viscosities, and Densities for Aqueous Two-Phase Systems Composed of Polyethylene Glycol and Various Salts at 25C.
Final rept.
S. M. Snyder, K. D. Cole, and D. C. Szlag. 1992, 7p.
Pub. in Jnl. of Chemical and Engineering Data 37, n2 p268-274 Apr 92.

Keywords: *Polyoxyethylene, *Inorganic salts, *Phase diagrams, Density(Mass/volume), Viscosity, Sodium carbonates, Sodium sulfates, Magnesium sulfates, Potassium phosphates, Ammonium sulfate, Phase transformations, Reprints, *Polyethylene glycol.

Phase diagrams of aqueous two-phase systems composed of polyethylene glycol and various salt solutions were measured. The densities and viscosities of these phase systems were also measured. Polyethylene glycol was used with three average molecular masses of 1000, 3350, and 8000. The salts used were magnesium sulfate, sodium sulfate, sodium carbonate, ammonium sulfate, and potassium phosphate. Phase diagram data, as well as the densities and viscosities of the phases, were measured at 25 C.

00,987
PB95-164638 Not available NTIS
National Inst. of Standards and Technology (CSTL), Gaithersburg, MD. Process Measurements Div.
Characterization of Cytochrome c/Alkanethiolate Structures Prepared by Self-Assembly on Gold.
Final rept.
S. Song, R. A. Clark, E. F. Bowden, and M. J. Tarlov. 1993, 9p.
Pub. in Jnl. of Physical Chemistry 97, n24 p6564-6572 1993.

Keywords: *Cytochrome c, *Monomolecular films, *Gold, *Adsorption, Electron transfer, Electrodes, Spectrum analysis, Kinetics, Surface properties, Biochemistry, Reprints, *Alkane thiolates.

Composite monolayer structures comprised of cytochrome c strongly adsorbed to alkanethiolate self-assembled (SA) monolayers on sputter-deposited gold film electrodes, i.e., cyt c/HOOC(CH2)nS/Au(n = 5, 10, 15), were examined using cyclic voltammetry (CV), electrochemical impedance spectroscopy (EIS), and X-ray photoelectron spectroscopy (XPS). Monolayer coverage of cytochrome c in a stable, functional, electroactive state was obtained in neutral phosphate buffer of low ionic strength for the thickest film (n = 15). Somewhat lower electroactive coverages were generally observed with the thinner SA monolayers (n = 5, 10). The surface formal potential of cytochrome c, +215 mV vs NHE, is nearly identical to values previously reported for cytochrome c bound to physiological membranes. The potential usefulness of these composite monolayers for investigating biological electron transfer is highlighted.

00,988
PB95-168704 Not available NTIS
National Inst. of Standards and Technology (CSTL), Boulder, CO. Thermophysics Div.
Thermodynamic Properties of R134a(1,1,1,2-Tetrafluoroethane).
Final rept.
M. L. Huber, and M. O. McLinden. 1992, 10p.
Pub. in Proceedings of International Refrigeration Conference, Purdue University, July 14-17, 1992, 10p.

Keywords: *Fluorohydrocarbons, *Thermodynamic properties, *Refrigerants, Temperature dependence, Pressure dependence, Specific heat, Density(Mass/volume), Vapor pressure, Acoustic velocity, Vapor phases, Liquid phases, Phase transformation, Equations of state, Volume, Reprints, *R134a, *1,1,1,2-Tetrafluoroethane, Benedict-Webb-Rubin equation.

The thermodynamic surface of R134a is expressed in terms of a 32-term modified Benedict-Webb-Rubin (MBWR) equation of state. Coefficients for this equation and for the ancillary equations representing the saturated liquid and vapor densities and the vapor pressure are presented. Temperatures are given on the new International Temperature Scale of 1990 (ITS 90). The MBWR coefficients were obtained using a multi-property fit that used experimental data for PVT properties, isochoric heat capacity, second-virial coefficients, speed of sound, and coexistence properties, including new measurements not used in previous formulations. The formulation is applicable to both the liquid and vapor phases at pressures up to 70 MPa, and for a temperature range from the triple point to 450 K. The accuracy of the equation of state is estimated to be + and - 0.2 % in density, + and - 1.0 % in constant-volume heat capacities, and + and - 0.6 % in the sound velocity, except in the critical region, based on comparisons with experimental data. In addition, a comprehensive bibliography of experimental data for R134a is presented.

00,989
PB95-168860 Not available NTIS
National Inst. of Standards and Technology (CSTL), Boulder, CO. Thermophysics Div.
High-Temperature Adiabatic Calorimeter for Constant-Volume Heat Capacity Measurements of Compressed Gases and Liquids.
Final rept.
J. W. Magee. 1991, 5p.
Sponsored by Department of Energy, Washington, DC.
Pub. in Proceedings of Symposium on Energy Engineering Sciences (9th), Argonne, IL., May 13-15, 1991, 5p.

Keywords: *Specific heat, *Calorimeters, Calorimetry, Compressed gases, High pressure, High temperature, Reprints, *Constant volume heat capacity, *Adiabatic calorimeters.

A high-temperature adiabatic calorimeter has been developed to measure constant-volume molar heat capacity. The chief design feature is its nearly identical twin cells which allow accurate measurement of energy differences without large corrections for energy losses due to thermal radiation fluxes. Operating conditions for the calorimeter are temperatures from 300 to 700 K at pressures from 0 to 20 MPa. The calorimeter is designed to measure heat capacities of both gases and liquids, especially fluids of interest to emerging energy technologies.

00,990
PB95-169249 Not available NTIS
National Inst. of Standards and Technology (CSTL), Gaithersburg, MD. Thermophysics Div.
Critical Scaling Laws and a Classical Equation of State.
Final rept.
A. van Pelt, G. X. Jin, and J. V. Sengers. 1994, 11p.
Contract DE-FG05-883413902
Sponsored by Department of Energy, Washington, DC.
Pub. in International Jnl. of Thermophysics 15, n4 p687-697 Jul 94.

Keywords: *Equations of state, *Critical point, *Scaling laws, Mathematical models, Thermodynamic properties, Thermophysical properties, Ideal gas law, Reprints, Carnahan-Starling-DeSantis equation of state.

In this paper we present a method which modifies a classical equation of state by incorporating the nonclassical critical behavior. As an example we have applied our procedure to the Carnahan-Starling-DeSantis (CSD) equation of state. The resulting equation reproduces the universal scaling behavior near the critical point and reduces to the universal ideal-gas behavior at low densities. We show that the renormalized CSD equation yields an improved and consistent representation of both mechanical and caloric thermodynamic properties. In addition, the suppression of the critical temperature due to the critical fluctuations is clearly demonstrated.

00,991
PB95-171948 PC A03/MF A01
National Inst. of Standards and Technology (CSTL), Gaithersburg, MD. Thermophysics Div.
Neighbor Tables for Molecular Dynamics Simulations.
R. D. Mountain. Dec 94, 15p, NISTIR-5545.

Keywords: *Condensed matter physics, *Molecular dynamics, *Computerized simulation, Monte Carlo meth-

od, Thermodynamic properties, Transport properties, Computer programs, Particle interactions, Sorting, Liquids, Solids, *Neighbor tables, Fortran 77 programming language, Cell index method, Method of shadows, Particle simulations.

Two methods for constructing a neighbor table for use in Molecular Dynamics simulations are discussed. A linked-list based method is shown to require time for generation of the table that is roughly proportional to the number of particles, N, in the system when the range of forces is small compared to the volume of the system. An alternative method that requires O (N(sup 2)) operations is also discussed and problems where it may be preferable to the linked-list method are mentioned. Source code listing both methods is included in appendices.

00,992
PB95-175048 Not available NTIS
National Inst. of Standards and Technology (PL), Boulder, CO. Time and Frequency Div.
Rotational Spectroscopy of the CoH Radical in Its Ground (3)Phi State by Far-Infrared Laser Magnetic Resonance: Determination of Molecular Parameters.
Final rept.
S. P. Beaton, K. M. Evenson, and J. M. Brown. 1994, 21p.
Contract NASA-W15-047
Sponsored by National Aeronautics and Space Administration, Washington, DC.
Pub. in Jnl. of Molecular Spectroscopy 164, p395-415 1994.

Keywords: *Rotational spectra, Far infrared radiation, Hyperfine structure, Chemical radicals, Chemical bonds, Ground states, M1-transitions, E2-transitions, Reprints, *Cobalt hydrides, Laser magnetic resonance.

Five rotational transitions of CoH in its ground triplet Phi state have been detected by far-infrared laser magnetic resonance, three in the lowest Omega = 4 component and two in the Omega = 3 component. All of the Zeeman transitions show an octet hyperfine pattern due to the (59)Co nucleus (I = 7/2). The much smaller proton doubling was also resolved for most transitions. The data have been fitted to experimental accuracy by an effective Hamiltonian for a molecule in an isolated triplet Phi state. The electron orbital and spin g factors determined by the data confirm conclusively that the ground state of CoH is a triplet Phi state. The accurate measurement of the rotational constant allows the equilibrium bond length to be determined. The cobalt hyperfine splittings have been fitted to determine magnetic dipole and electric quadrupole parameters.

00,993
PB95-175162 Not available NTIS
National Inst. of Standards and Technology (PL), Boulder, CO. Time and Frequency Div.
Fine-Structure Intervals of (14)N(+) By Far-Infrared Laser Magnetic Resonance.
Final rept.
J. M. Brown, and A. L. Cooksy. 1994, 4p.
Pub. in Astrophysical Jnl. 428, pL37-L40, 10 Jun 94.

Keywords: *Nitrogen ions, Far infrared radiation, Laser spectroscopy, Hyperfine structure, Fine structure, Ground states, Nitrogen 14, Reprints, Laser magnetic resonance.

The far-infrared laser magnetic resonance spectra associated with both fine-structure transitions in (14)N(1+) in its ground triplet P state have been recorded. This is the first laboratory observation of the J = 1 <-- 0 transition and its frequency has been determined two orders of magnitude more accurately than previously. The measurement of the J = 2 <-- 1 spectrum revealed a small error in the previous laboratory measurements. The fine-structure splittings (free of hyperfine interactions) determined in this work are (Delta)E(10) = 1461.13190 (61) GHz, (Delta)E(21) = 2459.38006 (37) GHz. Zero-field transition frequencies which include the effects of hyperfine structure have also been calculated. Refined values for the hyperfine constants and the g(J) factors have been obtained.

00,994
PB95-175170 Not available NTIS
National Inst. of Standards and Technology (PL), Boulder, CO. Time and Frequency Div.
Laser Magnetic-Resonance Measurement of the (3)P1 - (3)P2 Fine-Structure Splittings in (17)O and (18)O.
Final rept.
J. M. Brown, K. M. Evenson, and L. R. Zink. 1993, 3p.
Pub. in Physical Review A 48, n5 p3761-3763 Nov 93.

Keywords: *Oxygen atoms, *Oxygen 17, *Oxygen 18, *Isotope effects, Far infrared radiation, Laser spectroscopy, Fine structure, Reprints, Laser magnetic resonance.

The triplet P(1) - triplet P(2) fine-structure splittings of (17)O and (18)O have been measured by far-infrared laser magnetic-resonance spectroscopy. The signals for (17)O were detected with a sample in its natural abundance (0.038%). The isotopic shifts from the corresponding interval in (16)O are + 13.0 MHz for (17)O and + 23.5 MHz for (18)O, in accord with theoretical expectations.

00,995
PB95-175287 Not available NTIS
National Inst. of Standards and Technology (CSTL), Boulder, CO. Thermophysics Div.
Vapor-Liquid Equilibria of Mixtures of Propane and Isomeric Hexanes.
Final rept.
S. W. Chun, W. B. Kay, and J. C. Rainwater. 1993, 8p.
Sponsored by Department of Energy, Washington, DC.
Pub. in Jnl. of Chemical and Engineering Data 38, n4 p494-501 1993.

Keywords: *Liquid-vapor equilibrium, *Hexanes, *Propanes, *Phase diagrams, Phase transformations, Temperature, Critical pressure, Pressure dependence, Concentration(Composition), Density(Mass/volume), Thermodynamic properties, Reprints, *Dew bubble curves, *Leung-Griffiths theory, *Ternary mixtures.

Vapor-liquid equilibrium data extending to critical pressures are reported for mixtures of propane with each of the hexane isomers, n-hexane, 2-methylpentane, 3-methylpentane, 2,2-dimethylbutane, and 2,3-dimethylbutane. Dew-bubble curves for five different compositions are tabulated for each of the five mixtures. The data in pressure, temperature, and density are successfully correlated by the Leung-Griffiths model as modified by Moldover, Rainwater, and coworkers. The coexistence surfaces are all quite similar with only subtle differences due to the different shapes of the isomeric hexane molecules.

00,996
PB95-175618 Not available NTIS
National Inst. of Standards and Technology (CSTL), Boulder, CO. Thermophysics Div.
Partial Scattered Intensities from a Binary Suspension of Polystyrene and Silica.
Final rept.
H. J. M. Hanley, G. C. Straty, and P. Lindner. 1994, 8p.
Sponsored by Department of Energy, Washington, DC.
Pub. in LANGMUIR 10, n1 p72-79 1994.

Keywords: *Neutron scattering, *Suspensions, *Binary systems(Materials), *Silicon dioxide, *Polystyrene, Small angle scattering, Latex, Particles, Mixtures, Water, Structure factors, Reprints, *Colloidal suspensions.

The paper reports SANS (small angle neutron scattering) experiments on aqueous binary suspension mixtures of charged polystyrene latex and silica particles, characterized by the size ratio, gamma= sigma(sub si)/sigma(sub pa) approximately 0.72, with a nominal polystyrene diameter, sigma(sub pa) = 91 nm. The scattered intensities are reported over the wave vector (Q) range 0.025 < Q/nm(sup -1) < 0.4. Partial scattered intensities were obtained by contrast matching the constituents with an appropriate D2O/H2O solvent. Results are presented. The partial scattered intensity of polystyrene differs significantly from that of silica at a given value of n, and the partial scattered intensity of a component in a mixture suspension can differ markedly from the equivalent scattered intensity of the component in a pure suspension. The variation of the intensity with Q for silica in a 1/1 mixture suggests long range silica order at low Q. There is some evidence that the larger component, polystyrene, may form a polycrystalline fcc phase, in agreement with the density functional theory. The effect of multiple scattering on the data is discussed.

00,997
PB95-175626 Not available NTIS
National Inst. of Standards and Technology (CSTL), Boulder, CO. Thermophysics Div.
Solubility Measurement by Direct Injection of Supercritical-Fluid Solutions into a HPLC System.
Final rept.
B. N. Hansen, and T. J. Bruno. 1993, 4p.
Pub. in Jnl. of Supercritical Fluids 6, p229-232 1993.

Keywords: *Solubility, *Supercritical fluids, *Chromatography, *Solutes, Naphthalene, Thermophysical properties, Carbon dioxide, Test facilities, Measuring instruments, Reprints.

A new apparatus has been built for measuring solubility of solutes in supercritical fluids by direct injection of saturated supercritical-fluid solutions into a high-performance liquid chromatograph. To test the system, we measured the solubility of solid naphthalene in supercritical carbon dioxide at 55 C for pressures between 6.58 and 10.23 MPa. The system was designed to operate at pressures and temperatures up to 34 MPa and 140 C.

00,998
PB95-175634 Not available NTIS
National Inst. of Standards and Technology (CSTL), Boulder, CO. Thermophysics Div.
High-Pressure Equilibrium Cell for Solubility Measurements in Supercritical Fluids.
Final rept.
B. N. Hansen, A. F. Lagalante, R. E. Sievers, and T. J. Bruno. 1994, 3p.
Pub. in Review of Scientific Instruments 65, n6 p2112-2114 Jun 94.

Keywords: *Supercritical fluids, *Solubility, *Ferrocenes, *Measuring instruments, Carbon dioxide, Thermophysical properties, Solutes, Test facilities, Concentration(Composition), Reprints, *High pressure cells.

This paper describes the design, construction, and operation of an ultraviolet-visible light-transmission cell for high-pressure fluids. The cell can be operated at pressures as high as 70 MPa and at temperatures up to 100 C. This instrument was specifically designed to measure the solubility of solutes in supercritical fluids. The cell has an internal saturator and fluid circulator that are easy to remove and clean. The solubility of ferrocene in supercritical carbon dioxide was measured in the high-pressure cell described here. At 40 C, the mole fraction of ferrocene in carbon dioxide increased from 0.00005 to 0.0015 as the solvent density was increased from 5 to 17 mol/L.

00,999
PB95-175683 Not available NTIS
National Inst. of Standards and Technology (CSTL), Boulder, CO. Thermophysics Div.
Critical Properties and Vapor-Liquid Equilibria of the Binary System Propane + Neopentane.
Final rept.
D. W. Hissong, W. B. Kay, and J. C. Rainwater. 1993, 8p.
Pub. in Jnl. of Chemical and Engineering Data 38, n4 p486-493 1993.

Keywords: *Propane, *Pentanes, *Liquid-vapor equilibrium, *Binary mixtures, *Phase diagrams, Phase transformations, Temperature, Critical pressure, Pressure dependence, Density(Mass/volume), Thermodynamic properties, Reprints, *Leung-Griffiths theory, Dew bubble curves.

Vapor-liquid equilibrium data extending to critical pressures are reported for five mixtures of propane with neopentane. The data in pressure, temperature, and density are correlated to high accuracy by the Leung-Griffiths model as modified by Moldover, Rainwater, and co-workers. In addition, a complete bibliography of similar experiments on binary mixtures from the laboratory of W.B.K. is presented.

01,000
PB95-175758 Not available NTIS
National Inst. of Standards and Technology (CSTL), Gaithersburg, MD. Surface and Microanalysis Science Div.
Elastic-Electron-Scattering Effects on Angular Distributions in X-ray Photoelectron Spectroscopy.
Final rept.
A. Jablonski, and C. J. Powell. 1994, 10p.
Pub. in Physical Review B 50, n7 p4739-4748, 15 Aug 94.

Keywords: *X ray photoelectron spectroscopy, *Electron scattering, Monte Carlo method, Angular distribution, Surface analysis, Elastic scattering, Photoionization, Photoemission, Simulation, Gold, Reprints.

Electron trajectories in x-ray photoemission from solids are partially randomized by elastic collisions, and thus the angular distribution of photoelectrons leaving the surface is different from that for isolated atoms. This problem is approached in the present work by extensive Monte Carlo simulations of electron trajectories resulting from photoionization of the gold 4s, 4p(3/2), 4d(5/2), and 4f(7/2) subshells by Mg characteristic x rays. Calculations were made for the full range of angles of x-ray incidence and for all possible positions of the electron energy analyzer. In comparisons with intensities predicted from the common formalism in which elastic scattering is neglected, it was found that the elastic-scattering effects can be accounted for with two correction factors. These factors are, to a large extent, independent of experimental geometry for certain ranges of angles.

01,001
PB95-175766 Not available NTIS
National Inst. of Standards and Technology (CSTL), Gaithersburg, MD. Surface and Microanalysis Science Div.
Grazing Incidence X-ray Photoemission and Its Implementation on Synchrotron Light Source X-ray Beamlines.
Final rept.
T. Jach, M. J. Chester, and S. M. Thurgate. 1994, 3p.
Pub. in Nuclear Instruments and Methods in Physics Research A 347, p507-509 1994.

Keywords: *X ray photoelectron spectroscopy, Synchrotron radiation sources, X ray sources, Grazing incidence, KeV range 1-10, Chemical composition, Oxide films, Surface layers, Photoemission, Germanium, Reprints, Surface composition.

Grazing incidence X-ray photoemission spectroscopy provides a method of obtaining information about surface chemical composition as well as the variation of composition with depth. Photoemission spectra are taken as X-rays are directed onto a surface over a range of incidence angles near the critical angle for total external reflection. The technique is particularly suited to the study of surface layers in the thickness range 10-40 A, using X-rays in the energy range of 1-2 keV. We have implemented the technique in a geometry that minimizes distortion of the spectral lineshape by keeping a fixed relationship between the sample and the electron spectrometer. We present data taken in the laboratory that illustrate its application to the study of oxide films on Ge. The counting time for a spectrum would be shortened considerably by implementing the method on a soft X-ray beamline at a synchrotron light source. We present a method for doing so that retains the advantages of a fixed geometry between the sample and the electron spectrometer.

01,002
PB95-175816 Not available NTIS
National Inst. of Standards and Technology (CSTL), Boulder, CO. Thermophysics Div.
Correlation of the Ideal Gas Properties of Five Aromatic Hydrocarbons.
Final rept.
A. Laesecke. 1993, 3p.
Pub. in Ind. Eng. Chem. Res. 32, p759-761 1993.

Keywords: *Benzene, *Toluene, *Xylenes, *Ideal gas, *Specific heat, *Enthalpy, *Entropy, *Empirical equations, Thermodynamic properties, Temperature dependence, Mathematical models, Statistical mechanics, Reprints, *Temperature functions.

The ideal gas thermodynamic properties specific heat capacity, specific entropy, and specific enthalpy have been correlated for benzene, toluene, o-xylene, m-xylene, and p-xylene by a uniform, semiempirical function of temperature. The correlation is based on literature values calculated from statistical mechanics for temperatures up to 1500 K for benzene and up to 3000 K for the other molecules. The temperature function chosen is more accurate than that used for previous correlations, and can be used in a wider temperature range.

01,003
PB95-176038 Not available NTIS
National Inst. of Standards and Technology (CSTL), Boulder, CO. Thermophysics Div.
Composition Dependence of a Field Variable Along the Binary Fluid Mixture Critical Locus.
Final rept.
J. C. Rainwater, and D. G. Friend. 1994, 7p.
Sponsored by Department of Energy, Washington, DC.
Pub. in Physics Letters A 191, p431-437 1994.

Keywords: Binary mixtures, Liquid-vapor equilibrium, Critical point, Concentration(Composition), Temperature, Phase transformations, Phase diagrams, Thermodynamic properties, Fluids, Reprints, *Field variables, Critical line.

There are several classes of field variables used to extend the principle of critical-point universality to binary fluid mixtures. In particular, one can construct a field variable with sufficient flexibility to allow linearity in composition along the critical locus for the large class of binary systems with a critical line which is monotonic in temperature. This choice of hidden field variable has been used extensively in studies of vapor-liquid equilibrium, but a recent study of an alternative class of field variables suggests that linearity in composition along the critical locus cannot, in principle, be imposed exactly. It is demonstrated that several arguments presented by proponents of this proposition do not, in fact, apply to the field variable constructed in our studies.

01,004
PB95-176046 Not available NTIS
National Inst. of Standards and Technology (CSTL), Boulder, CO. Thermophysics Div.
Equilibrium Pair Distribution Function of a Gas: Aspects Associated with the Presence of Bound States.
Final rept.
J. C. Rainwater, and R. F. Snider. 1993, 11p.
Sponsored by Department of Energy, Washington, DC.
Pub. in Jnl. of Chemical Physics 99, n11 p9111-9121, 1 Dec 93.

Keywords: *Distribution functions, *Potential energy, *Dimers, *Gases, Momentum, Chemical equilibrium, Thermodynamic equilibrium, Moments, Mathematical models, Atoms, Reprints, *Potential functions.

At thermal equilibrium the momentum distribution of atoms in a gas is usually assumed to be Maxwellian, whether classically or quantally. However, if an atom is bound in a diatomic molecule, the atom's momentum distribution is non-Maxwellian. This paper explores the consequent singlet and pair particle distribution functions in a gas having both unbound atoms and bound pairs of atoms. Comment is made on the range of behavior associated with whether the chemical equilibrium constant for diatom formation is small or large. Calculations of distribution functions and their moments for atoms which are members of dimers are presented for some specific model potentials.

01,005
PB95-176194 Not available NTIS
National Inst. of Standards and Technology (PL), Boulder, CO. Time and Frequency Div.
Pure Rotational Spectra of CuH and CuD in Their Ground States Measured by Tunable Far-Infrared Spectroscopy.
Final rept.
T. D. Varberg, and K. M. Evenson. 1994, 5p.
Pub. in Jnl. of Molecular Spectroscopy 164, p531-535 1994.

Keywords: *Copper hydrides, *Rotational spectra, *Infrared spectra, Molecular spectroscopy, Far infrared radiation, Ground states, Copper 63, Copper 65, Reprints, *Copper deuterides.

Pure rotational transitions of CuH and CuD within the Chi singlet Sigma(+) (upsilon = 0) state were measured over the ranges J(double prime) = 1 to 10 for CuH and J(double prime) = 2 to 18 for CuD, including both the (63)Cu and (65)Cu isotopes. The rotational parameters B(0), D(0), H(0), and L(0) were separately determined for each of the four isotopomers by least-squares fitting to the observed transitions. For (65)CuH, (63)CuD and (65)CuD, these parameters are about two orders of magnitude more accurate than those determined by previous workers. Accurate calculated frequencies of all four isotopomers which will be useful in astronomical studies of CuH and CuD are given.

01,006
PB95-176202 Not available NTIS
National Inst. of Standards and Technology (PL), Boulder, CO. Time and Frequency Div.
Rotational Spectrum of OH in the v=0-3 Levels of Its Ground State.
Final rept.
T. D. Varberg, and K. M. Evenson. 1993, 13p.
Sponsored by National Aeronautics and Space Administration, Washington, DC.
Pub. in Jnl. of Molecular Spectroscopy 157, p55-67 1993.

Keywords: *Hydroxyl radicals, *Hydroxyl emission, *Rotational spectra, *Infrared spectra, Far infrared radiation, Frequency shift, Spectral shift, Fine structure, Ground states, Pressure dependence, Helium, Reprints.

Rotational and fine structure transitions have been observed between low rotational levels in the upsilon = 0-3 levels of the OH Chi doublet Pi state by tunable far-infrared spectroscopy. The rotational and fine structure constants of the ground state have been refined by least-squares fitting to the observed data in combination with far-infrared and microwave measurements by other authors. Pressure-induced frequency shifts with helium as a buffer gas are also reported for some of the upsilon = 0 transitions.

01,007
PB95-180105 Not available NTIS
National Inst. of Standards and Technology (PL), Boulder, CO. Time and Frequency Div.
Atomic Sulfur: Frequency Measurement of the J=0 inversely maps 1 Fine-Structure Transition at 56.3 Microns by Laser Magnetic Resonance.
Final rept.
J. M. Brown, K. M. Evenson, and L. R. Zink. 1994, 3p.
Pub. in Astrophysical Jnl. 431, pL147-L149, 20 Aug 94.

Keywords: *Infrared spectra, Far infrared radiation, Electron transitions, Fine structure, Ground state, Reprints, *Sulfur atoms, Laser magnetic resonance.

The J = 0 <-- 1 fine-structure transition in atomic sulfur (S I) in its ground triplet P state has been detected in the laboratory by far-infrared laser magnetic resonance. The fine-structure interval has been measured accurately as 5,322,492.9 + or - 2.8 MHz which corresponds to a wavelength of 56.325572 + or - 0.000030 micrometers.

01,008
PB95-180121 Not available NTIS
National Inst. of Standards and Technology (MSEL), Gaithersburg, MD. Polymers Div.
Cyclic Polyamine Ionophore for Use in a Dibasic Phosphate-Selective Electrode.
Final rept.
C. M. Carey, and W. B. Riggan. 1994, 5p.
Sponsored by American Dental Association Health Foundation, Chicago, IL.
Pub. in Analytical Chemistry 66, n21 p3587-3591, 1 Nov 94.

Keywords: *Polyamines, *Phosphates, Electrodes, Anions, Cyclic compounds, Reprints, *Selective electrodes, Cyclodecane-dione/decyl-triaza, Ionophore.

A cyclic polyamine, 3-decyl-1,5,8-triazacyclodecane-2,4-dione (N3-cyclic amine), was used as the ionophore for a dibasic phosphate-selective electrode. This electrode exhibited a linear response between 1.0 micromol/L and 0.1 mol/L dibasic phosphate activity with a near-Nernstian slope of approximately -29 mV per activity decade. The electrode selectivity for dibasic phosphate over other commonly occurring anions was evaluated. A mechanism for the selectivity of the electrode toward HPO4(-2) ions is postulated to be a function of the size and charge of the N3- cyclic amine ionophore relative to the size and charge of HPO4(-2) ions. The electrode's superior selectivity and sensitivity make possible the direct measurement of phosphate activity in a wide variety of applications.

01,009
PB95-180154 Not available NTIS
National Inst. of Standards and Technology (CSTL), Gaithersburg, MD. Surface and Microanalysis Science Div.
Photodecomposition of Mo(CO)6/Si(111) 7x7: CO State-Resolved Evidence for Excited State Relaxation and Quenching.
Final rept.
P. M. Chu, S. A. Buntin, L. J. Richter, and R. R. Cavanagh. 1994, 11p.
Contract DE-AI02-93ER14330
Sponsored by National Science Foundation, Arlington, VA. and Department of Energy, Washington, DC.

Pub. in Jnl. of Chemical Physics 101, n4 p2929-2939, 15 Aug 94.

Keywords: *Metal carbonyls, *Photodecomposition, Temperature range 0065-0273 K, Photochemical reactions, Surface chemistry, Ultraviolet radiation, Excited states, Silicon, Reprints, *Hexacarbonylmolybdenum, Laser induced desorption.

State-resolved detection techniques have been used to characterize the ultraviolet photodecomposition dynamics of Mo(CO)6 on Si(111) 7 X 7 at 100 K. Details of the excitation/fragmentation mechanism including adsorbate energy transfer were examined by measuring the cross sections and the internal and translational energies of the photoejected CO from submonolayer through multilayer coverage regimes. The CO energy distributions are found to be independent of Mo(CO)6 coverage, and can be characterized by two components with markedly different mean energies. In contrast to the coverage independence of the measured energy disposal, the cross section was found to decrease by a factor of 3 from multilayer coverages to submonolayer coverages.

01,010
PB95-180667 Not available NTIS
National Inst. of Standards and Technology (CAML), Gaithersburg, MD. Applied and Computational Mathematics Div.
Rayleigh Instability for a Cylindrical Crystal-Melt Interface.
Final rept.
G. B. McFadden, S. R. Coriell, and B. T. Murray. 1993, 11p.
Sponsored by National Aeronautics and Space Administration, Washington, DC. and Defense Advanced Research Projects Agency, Arlington, VA.
Pub. in Variational and Free Boundary Problems, p159-169 1993.

Keywords: Binary systems(Materials), Temperature gradients, Temperature effects, Rayleigh Taylor instability, Cylindrical configuration, Capillarity, Metals, Reprints, *Crystal-melt interface, Two phase systems.

The temperature of a crystal-melt interface at equilibrium is given by the Gibbs-Thomson equation, which relates the interface temperature to the mean curvature of the interface. As isothermal cylindrical crystal-melt interface is subject to capillary instabilities of the type originally studied by Rayleigh. The dependence of this instability on the materials properties of the system is described for a two-phase, single-component system with isotropic surface energy. The effect of radial temperature gradients on the instability is also given. For metallic systems, the instability can be important at micrometer-sized length scales, but become insignificant at macroscopic (millimeter-sized) length scales. Heating the liquid causes stabilization, and the instability is completely suppressed for large enough temperature gradients in the liquid.

01,011
PB95-180691 Not available NTIS
National Inst. of Standards and Technology (CSTL), Gaithersburg, MD. Thermophysics Div.
Quantitative Measure of Efficiency of Monte Carlo Simulations.
Final rept.
R. D. Mountain, and D. Thirumalai. 1994, 8p.
Contract AFOSR-F496209410106
Sponsored by Air Force Office of Scientific Research, Bolling AFB, DC.
Pub. in Physica A 210, p453-460 1994.

Keywords: *Monte Carlo method, Lennard-Jones potential, Computerized simulation, Triple point, Efficiency, Sampling, Liquids, Algorithms, Reprints.

An easily applied, physically motivated algorithm for determining the efficiency of Monte Carlo simulations is introduced. The theoretical basis for the algorithm is developed. As an illustration, I apply the method to the Lennard-Jones liquid near the triple point. We show that an acceptance ratio of 0.2 is twice as efficient for the purpose of generating a satisfactory sample as is an acceptance ratio of 0.5. There is a strong correlation between the efficiency measure and the diffusion rate of liquid particles during the simulation. We argue that the optimal value of the acceptance ratio is calculable from short Monte Carlo simulations. The method is very general and is applicable to Monte Carlo simulations involving arbitrary potentials.

01,012
PB95-180733 Not available NTIS
National Inst. of Standards and Technology (MSEL), Gaithersburg, MD. Reactor Radiation Div.
Structural and Chemical Investigations of Na3(ABO4)3.4H2O-Type Sodalite Phases.
Final rept.
T. M. Nenoff, W. T. A. Harrison, T. E. Gier, V. I. Srdanov, J. M. Nicol, G. D. Stucky, N. L. Keder, and C. M. Zaremba. 1994, 9p.
Grant NSF-DMR91-20007
Sponsored by Office of Naval Research, Arlington, VA. and National Science Foundation, Arlington, VA.
Pub. in Inorganic Chemistry 33, p2472-2480 1994.

Keywords: *Crystal structure, Synthesis(Chemistry), Neutron diffraction, X ray diffraction, Cubic lattices, Precursor, Hydrates, Sodalite, Reprints, Sodium aluminum silicates, Sodium gallium silicates, Sodium aluminum germanates, Sodium gallium germanates, Sodium zinc arsenates.

The sodalite cage containing only an electron as a nonframework 'anion' is well adapted for the study of solvated 'electride' Wigner lattices and quantitative mapping of the intra- and intercage electronic potential surfaces. In this paper we report the direct synthesis of anion free cage structures of the form Na3( )(ABO4)3(center dot)nH2O (A: B = Al.Ga:Si.Ge) as possible precursors for sodalite electride synthesis. A novel, low-temperature sodalite dehydroxylation method is presented for the preparation of Na3( )(AlSiO4)3(center dot)4H2O from Na4(OH)(AlSiO4)3(center dot)1.72H2O. Results from a neutron diffraction study of Na3(ZnAsO4)3(center dot)4H2O give evidence of hydrogen bonding between the framework oxygen atoms and the Beta-cage substructure and aid in explanation of analog unit cell trends. All of the investigated sodalites have an ordered array of their framework tetrahedral cations and crystallize in the cubic space group P(bar 4)3n, Z = 2.

01,013
PB95-180741 Not available NTIS
National Inst. of Standards and Technology (MSEL), Gaithersburg, MD. Reactor Radiation Div.
Characterization of the Interaction of Hydrogen with Iridium Clusters in Zeolites by Inelastic Neutron Scattering Spectroscopy.
Final rept.
J. M. Nicol, T. J. Udovic, R. R. Cavanagh, T. Mure, B. C. Gates, Z. Xu, and S. Kawi. 1994, 6p.
Pub. in Matierals Research Society Symposia Proceedings, v351 p189-194 1994.

Keywords: *Metal clusters, *Iridium, *Hydrogen, Atomic clusters, Neutron scattering, Inelastic scattering, Catalysis, Zeolites, Chemical bonds, Interactions, Hydrides, Reprints.

Incoherent inelastic neutron scattering (IINS) measurements of hydrogen bound to Ir6 clusters in the nanoscale pores of zeolite NaY and similar clusters in KL zeolite are reported. On the basis of hydrogen uptake measurements and the observation of peaks in the IINS spectra, we infer that hydrogen is bound to the metal nanoclusters in the zeolite pores. The IINS data for both zeolites are similar and consistent with the presence of IrH2 species.

01,014
PB95-180766 Not available NTIS
National Inst. of Standards and Technology (MSEL), Gaithersburg, MD. Reactor Radiation Div.
Inelastic-Neutron-Scattering Studies of Poly(p-phenylene vinylene).
Final rept.
P. Papanek, J. E. Fischer, J. L. Sauvajol, M. J. Winokur, F. A. Karasz, A. J. Dianoux, and G. Mao. 1994, 10p.
Grant NSF-DMR91-20668
Sponsored by National Science Foundation, Arlington, VA.
Pub. in Physical Review B 50, n21 p15 668-15 677, 1 Dec 94.

Keywords: Time-of-flight spectrometers, Polarization characteristics, Vibrational states, Deuterium compounds, Neutron scattering, Inelastic scattering, Films, Reprints, *Poly(p-phenylene vinylene), Density of states, Lattice modes.

Mode polarization and energy spectra for the lattice modes of poly(p-phenylene vinylene) are obtained by inelastic-incoherent-neutron-scattering methods. Experiments were performed on stretch-oriented, highly crystalline films with time-of-flight and filter-analyzer spectrometers. By measuring all-hydrogen and vinylene-deuterated samples, we show that almost all of the observed modes can be attributed to phenylene motions. The low-energy features in the vibrational density of states consist of a longitudinal 2.5-meV mode assigned to a damped translational motion along the chain axis, a 7-meV phenyl ring in-phase librational mode (transverse with respect to the chain axis), and strong bands at 15 and 25 meV showing mixed polarization, the latter also displaying negative frequency shift with increasing temperature. Higher-frequency modes are in excellent agreement with published infrared and Raman studies, as well as with the results of our vibrational analysis based on the semiempirical AM1 method.

01,015
PB95-180865 Not available NTIS
National Inst. of Standards and Technology (MSEL), Gaithersburg, MD. Reactor Radiation Div.
Powder Neutron Diffraction Investigation of Structure and Cation Ordering in Ba2+xBi2-xO6-y.
Final rept.
K. P. Reis, A. J. Jacobson, and J. M. Nicol. 1993, 16p.
Pub. in Jnl. of Solid State Chemistry 107, p428-443 1993.

Keywords: *Crystal structure, Time-of-flight method, Ambient temperature, Neutron diffraction, Monoclinic lattices, Cubic lattices, Cations, Reprints, *Barium bismuthates, *Barium bismuth oxides.

The structures and cation ordering of several barium bismuth oxide phases, Ba(2+x)Bi(2-x)O(6-y) (x = 0.22, 0.28, 0.40, 0.67), have been determined at ambient temperature from constant wavelength and time-of-flight neutron powder diffraction data. The end member of the series, Ba2Bi(III)Bi(V)O6, has a monoclinic distortion of the simple cubic perovskite structure with an ordered arrangement of the Bi(3+) and Bi(5+) cations on the B sites. When additional barium atoms are introduced into the structure, substitution of Ba for Bi(III) occurs to give phases with the composition Ba2((Bi(1-x)Ba(x))Bi)O6 when x < 0.6. The monoclinic structure at x = 0 changes first to a rhombohedral structure and then to cubic as x is increased. At x = 0.67, the structure remains cubic but the cation distribution changes to give an unusual arrangement, with Bi(3+) cations on the perovskite A sites and complete Ba(2+)/Bi(5+) ordering on the B sites.

01,016
PB95-180873 Not available NTIS
National Inst. of Standards and Technology (CSTL), Boulder, CO. Biotechnology Div.
Thermodynamic Study of the Reactions of Cyclodextrins with Primary and Secondary Aliphatic Alcohols, with D- and L-Phenylalanine, and with L-Phenylalanineamide.
Final rept.
M. V. Rekharsky, F. P. Schwarz, Y. B. Tewari, and R. N. Goldberg. 1994, 7p.
Pub. in Jnl. of Physical Chemistry 98, n40 p10282-10288, 6 Oct 94.

Keywords: *Thermodynamic properties, *Cyclodextrins, *Alcohols, *Chemical reactions, Heat of reaction, Equilibrium, Specific heat, Entropy, Calorimetry, Volumetric analysis, Gibbs free energy, Aliphatic compounds, Reprints.

Equilibrium constants and standard molar enthalpies of reaction have been determined by titration calorimetry for the reactions of 1-propanol, 2-propanol, 1-butanol, (R)-(+)-2-butanol, (S)-(-)-2-butanol, (+ or -)-butanol, (R)-(+)-2-pentanol, (S)-(-)-2-pentanol, (R)-(+)-2-hexanol, (S)-(-)-2-hexanol, (R)-(+)-2-heptanol, (S)-(-)-2-heptanol, D-phenylalanine, L-phenylalanine, and L-phenylalanineamide with alpha-cyclodextrin and Beta-cyclodextrin. The standard molar Gibbs energies, standard molar enthalpies, and standard molar entropies for these reactions correlate well with respect to the number of carbon atoms in the chemical formula of the alcohol and form a series of distinct curves for the different types of alcohols. The results are also discussed in relation to hydrophobic, steric, and charge effects and the exchange reaction for a ligand from alpha-cyclodextrin to Beta-cyclodextrin. With the exception of the results for the standard molar enthalpies of reaction of the 2-butanols with alpha-cyclodextrin, the results obtained in this study show that, within the indicated uncertainties, there are no differences in any of the thermodynamic quantities for the reactions of these ligands with either alpha- or Beta-cyclodextrin due to the change in the location of a hydrogen atom on an optically active carbon atom.

01,017
PB95-181012 Not available NTIS
National Inst. of Standards and Technology (MSEL), Gaithersburg, MD. Reactor Radiation Div.
Local-Mode Dynamics in YH2 and YD2 by Isotope-Dilution Neutron Spectroscopy.
Final rept.
T. J. Udovic, J. J. Rush, and I. S. Anderson. 1994, 5p.
Pub. in Physical Review B 50, n21 p15 739-15 743, 1 Dec 94.

Keywords: *Yttrium hydrides, Neutron scattering, Inelastic scattering, Vibrational spectra, Phonons, Dynamics, Reprints, *Yttrium deuterides, Isotope dilution neutron spectroscopy, Density of states.

Isotope-dilution neutron spectroscopy was used to investigate the dynamics of the H and D optic vibrations in YH2 and YD2, respectively. The broad, complex, densities of states of the tetrahedrally coordinated H and D atoms in the isotopically pure materials collapse to single, sharp, triply degenerate features when the H and D atoms are sufficiently diluted with their companion isotopes. This demonstrates that the vibrational dispersion for the pure materials is due to the presence of significant H-H and D-D dynamic-coupling interactions. Moreover, a spectral doublet (with 5-meV splitting) superimposed on the sharp D-defect-mode feature for Y(H(0.9)D(0.1))2 is suggestive of localized acoustic and optic branches of dynamically coupled, near-neighbor D-D pairs isolated in the predominantly hydrided material. The magnitude of the splitting implies a D-D/Y-D force-constant ratio of about 6%. The dynamics of both light (H) and heavy (D) mass defects are in general agreement with simple mass-defect theory.

01,018
PB95-181020 Not available NTIS
National Inst. of Standards and Technology (MSEL), Gaithersburg, MD. Reactor Radiation Div.
Neutron Spectroscopic Evidence of Concentration-Dependent Hydrogen Ordering in the Octahedral Sublattice of beta-TbH2+x.
Final rept.
T. J. Udovic, J. J. Rush, and I. S. Anderson. 1994, 3p.
Pub. in Physical Review B 50, n10 p7144-7146, 1 Sep 94.

Keywords: *Terbium hydrides, Concentration(Composition), Quantity ratio, Neutron scattering, Inelastic scattering, Reprints, *Hydrogen ordering, Density of states.

The octahedrally coordinated hydrogen (H(o)) of the superstoichiometric rare-earth dihydrides beta-TbH(2 + x)(0.03 < x < 0.25) has been probed by incoherent inelastic neutron scattering. The H(o) sublattice arrangements and associated optical vibrations are sensitive to the value of x. For x = 0.03 at low temperature, the majority of the low-concentration o-site hydrogens are isolated in a local cubic environment and exhibit a relatively sharp vibrational density of states at 80.8 meV, in accord with the presence of triply degenerate normal modes. In contrast, for x = 0.25, a broad bimodal band peaking at about 76.7 and 83.1 meV is evident, consistent with the type of long-range order that is known to occur in the H(o) sublattice at this higher concentration. Increasing the temperature above the long-range ordering transition leads to a more disordered H(o) sublattice and a density of states similar to that at low values of x but broadened, most likely by the persistence of some short-range order.

01,019
PB95-181038 Not available NTIS
National Inst. of Standards and Technology (MSEL), Gaithersburg, MD. Reactor Radiation Div.
Vibrations of Hydrogen and Deuterium in Solid Solution with Lutetium.
Final rept.
T. J. Udovic, J. J. Rush, I. S. Anderson, J. N. Vajda, and O. Blaschko. 1994, 6p.
Pub. in Physical Review B 50, n6 p3696-3701, 1 Aug 94.

Keywords: *Vibrational spectra, *Hydrogen, *Deuterium, *Lutetium, Solid solutions, Neutron scattering, Inelastic scattering, Temperature dependence, Reprints.

The vibrational spectroscopy of hydrogen isotopes in alpha-phase solid solution with Lu was probed by incoherent-inelastic-neutron-scattering methods. Low-resolution spectra of H and D located at tetrahedral interstices are qualitatively similar to those of other rare-earth/hydrogen alpha phases, indicating a vibrational mode along the c direction that is about 30% softer and significantly broader than the doubly degenerate vibrational modes in the basal plane. High-resolution spectra of these broad c-axis vibrations reveal a temperature- and concentration-dependent line shape believed to consist of local acoustic and optic bands associated with the dynamical coupling of hydrogen atoms paired on either side of a metal atom along the c direction. Previous diffuse-elastic-neutron-scattering studies indicate the existence of short-range ordering of these hydrogen pairs into c-axis-oriented chains possessing interchain correlations. The shape and width of these bands at low temperature near the alpha/Beta-phase boundary compared to those of the analogous Sc and Y alpha-phase systems suggest that the extent of ordering in alpha-LuH(x) is intermediate with respect to that in the (less ordered) alpha-ScH(x) and (more ordered) alpha-YH(x) solid solutions.

01,020
PB95-181053 Not available NTIS
National Inst. of Standards and Technology (EEEL), Gaithersburg, MD. Electricity Div.
Plasma Chemical Model for Decomposition of SF6 in a Negative Glow Corona Discharge.
Final rept.
R. J. Van Brunt, and J. T. Herron. 1994, 21p.
Sponsored by Electric Power Research Inst., Palo Alto, CA. and Department of Energy, Washington, DC.
Pub. in Physica Scripta T53, p9-29 1994.

Keywords: *Sulfur hexafluoride, *Corona discharges, *Glow discharges, *Plasma chemistry, Decomposition reactions, Gas mixtures, Electron impact, Oxygen fluorides, Oxidation, Reprints.

A zonal plasma chemical model is proposed to account for the observed oxidation and decomposition of sulfur hexafluoride (SF6) by a negative, point-to-plane glow-type corona discharge in pressurized SF6/O2/H2O gas mixtures. The model yields dependencies of stable neutral oxidation by-products such as SOF2, SO2F2, SOF4, S2F(10), and SO2 on time, discharge current, and O2 and H2O concentrations which are consistent with measured results. Electron-impact-induced dissociation of SF6 in the glow region of the discharge is the decomposition rate-controlling process. The relative roles played by different reactions involving neutral free radicals and ions in different zones of the discharge are examined, and in some cases, reaction rate coefficients have been adjusted within reasonable limits to give best fits to observed production rates of various by-products.

01,021
PB95-181087 Not available NTIS
National Inst. of Standards and Technology (PL), Boulder, CO. Time and Frequency Div.
Detection of OH+ in Its a(1)Delta State by Far Infrared Laser Magnetic Resonance.
Final rept.
T. D. Varberg, K. M. Evenson, and J. M. Brown. 1994, 5p.
Pub. in Jnl. of Chemical Physics 100, n4 p2487-2491, 15 Feb 94.

Keywords: *Hydroxyl radicals, Far infrared radiation, Laser spectroscopy, Electronic structure, Metastable state, Rotational spectra, Infrared spectra, Positive ions, Reprints, Laser magnetic resonance.

The spectrum associated with the J = 3 <-- 2 transition of OH(1+) in the alpha singlet Delta (nu = 0) state has been observed by far infrared laser magnetic resonance spectroscopy. A new microwave discharge source enabled the detection of this spectrum, which is the first observation of the rotational spectrum of an ion in a metastable state. Assignment and least-squares fitting of the observed transitions have determined the following molecular constants: B(0) = 494.420 388 (22) GHz, the proton hyperfine parameter alpha = 74.84 (32) MHz, g'(L) = 1.000 915 (15), and g(r) = - 0.001 815 (18), with the 1(sigma) uncertainties of the last digits in parentheses. The relationship of these parameters to the geometric and electronic structure of OH(1+) is discussed.

01,022
PB95-181178 Not available NTIS
National Inst. of Standards and Technology (MSEL), Gaithersburg, MD. Polymers Div.
Water Adsorption at Polymer/Silicon Wafer Interfaces.
Final rept.
W. L. Wu. 1994, 5p.
Contract N00014-92-F-0036
Sponsored by Office of Naval Research, Arlington, VA.
Pub. in Materials Research Society Symposia Proceedings, v338 p565-569 1994.

Keywords: *Interfaces, *Water, *Adsorption, *Neutron scattering, *Wafers, Monocrystals, Reflectivity, Polymers, Silicon, Polyimides, Epoxy resins, Reprints.

Neutron reflectivity (NR) was applied to measure the concentration of water at the buried interfaces between polymer and silicon single crystal wafers. In the polyimide samples excess water was discovered within 30 A of the silicon/polymer interface, where the water concentration reached 17% (by volume) for the samples without a coupling agent and 12% for the ones with a coupling agent. Beyond the interface, the water concentration was measured at 2-3%, which is typical of bulk polyimide. Excess water was also found at the silicon/epoxy interface; more than 30% water was found within 150 A of the interface in the samples with their interface precoated with a coupling agent. The equilibrium moisture content in bulk epoxy used in this study is about 6%. The above results demonstrate conclusively the unique power of NR in determining water concentration near a buried interface, and provide the first quantitative evidence for a water concentration profile which peaks in the interface region.

01,023
PB95-202222 Not available NTIS
National Inst. of Standards and Technology (PL), Boulder, CO. Quantum Physics Div.
In-situ Monitoring of Molecular Beam Epitaxial Growth Using Single Photon Ionization.
Final rept.
A. L. Alstrin, A. K. Kunz, and S. R. Leone. 1994, 9p.
Contract ACS-PRF-15190-AC6, Grant NSF-PHY90-12244
Sponsored by National Science Foundation, Arlington, VA. and Petroleum Research Fund, Washington, DC.
Pub. in Proceedings of Society of Photo-Optical Instrumentation Engineers: Laser Techniques for Surface Science, Los Angeles, CA., January 27-29, 1994, v2125 p42-50.

Keywords: *Molecular beam epitaxy, *Gallium arsenides, *Crystal growth, *Gallium, *Arsenic, Real time operations, Semiconducting films, Laser radiation, Desorption, Reprints, Time-of-flight mass spectroscopy, Reflection high energy electron diffraction, In situ monitoring, Optical probes.

Single photon laser ionization time-of-flight mass spectroscopy (SPI-TOFMS) is used to monitor the gaseous fluxes of Ga, As2, and As4, which are relevant in molecular beam epitaxy (MBE) of GaAs. This noninvasive and real-time technique measures densities, and hence fluxes, of multiple chemical species impinging on or scattered from a substrate during conventional MBE. With single photon ionization at 118 nm (10.5 eV), the energy is sufficient to ionize the species, but insufficient to ionize and fragment. The lack of molecular fragmentation greatly simplifies the interpretation of mass spectra. Additionally, the probe geometry permits simultaneous film growth monitoring using RHEED. Results will be presented on the probing of scattering and desorption of III-V MBE species during GaAs growth. This technique promises to be a valuable in-situ diagnostic for III-V and II-VI MBE.

01,024
PB95-202230 Not available NTIS
National Inst. of Standards and Technology (PL), Boulder, CO. Quantum Physics Div.
Direct Detection of Atomic Arsenic Desorption from Si(100).
Final rept.
A. L. Alstrin, P. G. Strupp, and S. R. Leone. 1993, 3p.
Contract AFOSR90-0166
Sponsored by Air Force Office of Scientific Research, Bolling AFB, DC.
Pub. in Applied Physics Letters 63, n6 p815-817, 9 Aug 93.

Keywords: *Arsenic, *Silicon, *Desorption, Molecular beam epitaxy, Far ultraviolet radiation, Gallium arsenides, Photoionization, Laser radiation, Reprints, Time-of-flight mass spectroscopy.

Application of the 118 nm single photon laser ionization technique to a molecular beam epitaxy machine is

used for the first time to demonstrate direct desorption of As atoms from Si(100). Both As2 and As are the desorbing species from 1 ML of arsenic on silicon above 1,000 K. This is in contrast to previously reported models that considered only dimer desorption. With a continuous flux of As4, the scattered and desorbing arsenic species from Si(100) are examined as a function of surface temperature (650-1200 K). Atomic desorption is large, 75% + or - 19%, above 1,000 K, and complete conversion of As4 to As2 and As occurs at 1,200 K. The species selectivity of laser ionization time-of-flight mass spectroscopy has broader implications for GaAs growth.

01,025
PB95-202313 Not available NTIS
National Inst. of Standards and Technology (PL), Boulder, CO. Quantum Physics Div.
Location of a (1)A(sub g) State in Bithiophene.
Final rept.
D. Birnbaum, and B. E. Kohler. 1992, 4p.
Pub. in Jnl. of Chemical Physics 96, n4 p2492-2495, 15 Feb 92.

Keywords: *Thiophenes, Temperature range 0065-0273 K, Molecular excitation, Fluorescence spectroscopy, Oligomers, Hexanes, Reprints, *Bithiophenes, Polythiophenes, Two photon processes, Dilute solutions.

The 0-0 excitation energy of a singlet A(g) state of 2,2'-bithiophene has been determined by measuring the two-photon fluorescence excitation spectrum of a dilute solution of this molecule in crystalline n-hexane at 77 K. Because the 0-0 energy is what would have been predicted by extrapolating previously measured alpha, omega-dithienylpolyene 2 singlet A(g) 0-0 energies to zero polyene chain length, it is assigned to the 2 singlet A(g) state. The 0-0 band is centered at 36,173/cm, approximately 6,570/cm above the 0-0 of the 1 singlet A(g) to 1 singlet B(u) transition. This order of bithiophene excited singlet states is opposite to that of the linear polyene with the same number of double bonds but may reverse for chains longer than six repeat units.

01,026
PB95-202339 Not available NTIS
National Inst. of Standards and Technology (PL), Boulder, CO. Quantum Physics Div.
Lowest Excited Singlet State of Isolated 1-phenyl-1,3-butadiene and 1-phenyl-1,3,5-hexatriene.
Final rept.
W. J. Buma, B. E. Kohler, J. M. Nuss, T. A. Shaler, and K. Song. 1992, 9p.
Sponsored by National Science Foundation, Washington, DC. and National Institutes of Health, Bethesda, MD.
Pub. in Jnl. of Chemical Physics 96, n7 p4860-4868, 1 Apr 92.

Keywords: *Polyenes, Molecular spectra, Excited states, Multi-photon processes, Supersonic jet flow, Reprints, *Phenylbutadiene, *Phenylhexatriene, Supersonic expansion, Multiphoton ionization, Singlets.

We report vibrationally resolved S(0) --> S(1) excitation spectra and vibronic level decay times for the phenyl-substituted polyenes 1-phenylbutadiene and 1-phenylhexatriene seeded in supersonic He expansions. This information was obtained using one- and two-color resonance-enhanced multiphoton ionization techniques. The shift in the excitation energy of the lowest excited singlet state upon deuteration of the phenyl ring demonstrates that in 1-phenylbutadiene S(1) is mainly an excitation of the benzene ring while in 1-phenylhexatriene S(1) is mainly the 2 singlet A(g) state of hexatriene. Analysis of the excitation spectrum of 1-phenylhexatriene shows that the spectrum contains contributions from two species, the trans,trans and the trans,cis isomers, whose 2 singlet A(g) state excitation energies differ by about 155/cm.

01,027
PB95-202537 Not available NTIS
National Inst. of Standards and Technology (PL), Boulder, CO. Quantum Physics Div.
Plasma Chemistry in Silane/Germane and Disilane/Germane Mixtures.
Final rept.
J. R. Doyle, D. A. Doughty, and A. Gallagher. 1992, 12p.
Contract SERI-XG-1-1216
See also PB90-187659. Sponsored by Solar Energy Research Inst., Golden, CO.
Pub. in Jnl. of Applied Physics 71, n10 p4727-4738, 15 May 92.

Keywords: *Glow discharges, *Plasma chemistry, *Germanes, *Silanes, Silicon solar cells, Photovoltaic cells, Amorphous silicon, Gas mixtures, Reprints, Disilanes.

A detailed kinetic study of silane-germane glow discharges is presented. Stable gas decomposition and production rates have been measured using mass spectrometry and a kinetic model for the plasma chemistry is developed. It is found that germane depletes about four times faster than silane, nearly independently of their relative fractions. Germane is found to be much more reactive than silane with silylene, germalyn, and atomic hydrogen, and the silylene-germane reaction leads in large part to film, rather than stable gases. The spatial characteristics of the discharge are studied, using optical emission and fiber deposition profiles. From these it is deduced that the present, low-power discharge operates in a 'hybrid' alpha-gamma regime, and that ion effects are important near the electrodes.

01,028
PB95-202586 Not available NTIS
National Inst. of Standards and Technology (PL), Boulder, CO. Quantum Physics Div.
Vibrations of S1((1)B2u) p-Difluorobenzene - d4. S1-S0 Fluorescence Spectroscopy and ab Initio Calculations.
Final rept.
H. J. Elston, E. R. Davidson, F. G. Todd, and C. S. Parmenter. 1993, 13p.
Sponsored by National Science Foundation, Washington, DC.
Pub. in Jnl. of Physical Chemistry 97, n21 p5506-5518 1993.

Keywords: *Vibrational spectra, Fluorescence spectroscopy, Molecular spectroscopy, Molecular vibration, Fermi resonance, Supersonic jet flow, Reprints, *Difluorobenzene, Ab initio calculations.

The S(1)(singlet B(2u))-S(0)(singlet A(g)) spectroscopy of p-difluorobenzene-d(4) (C6D4F2,pDFB-d(4)) cooled in a supersonic free jet expansion has been characterized by fluorescence excitation (FE) and dispersed fluorescence. The 0(sub 0, sup 0) band lies at 36,987 + or - 1.0/cm (vacuum). The FE band assignments have provided the values of 11 S(1) fundamentals. The pattern of Franck-Condon allowed vibrational activity and of vibronically induced transitions is similar to that of pDFB-h(4). An exception concerns the a(g) mode nu(4) that is a prominent source of progressions in d(4) on account of harmonic mode scrambling but inactive in h(4). Bands involving an out-of-phase mode (nu(8)) that undergoes large frequency change in many aromatics upon formation of rare gas van der Waals complexes have anomalously large intensity when S(1) overtones are excited but normal Franck-Condon intensity for S(0) overtones. This singular behavior occurs in both h(4) and d(4). Four Fermi resonances have been detected.

01,029
PB95-202685 Not available NTIS
National Inst. of Standards and Technology (PL), Boulder, CO. Quantum Physics Div.
Vibrational Dependence of the Anisotropic Intermolecular Potential of Ar-HCl.
Final rept.
J. M. Hutson. 1992, 11p.
See also PB95-202693.
Pub. in Jnl. of Physical Chemistry 96, n11 p4237-4247 1992.

Keywords: *Argon complexes, Van der Waals forces, Intermolecular forces, Infrared spectroscopy, High resolution, Microwave spectroscopy, Anisotropy, Reprints, *Hydrogen chloride complexes, *Deuterium chloride complexes, *Intermolecular potentials, Potential energy surfaces, Vibrational dependence.

A new intermolecular potential for Ar-HCl is obtained by fitting to results from high-resolution microwave, far-infrared, and infrared spectroscopy. The new potential is substantially more accurate than any previous Ar-HCl potential and is the first to include the dependence of the potential on the HCl monomer vibration: it is a function of the diatom mass-reduced vibrational quantum number, as well as the intermolecular distance and angle. The functional form used has 19 adjustable parameters, which are determined from the spectroscopic data. The resulting potential, designated H6(4,3,0), reproduces all of the available spectroscopic data for levels of Ar-HCl and Ar-DCl correlating with HCl nu = 0 and 1 and DCl nu = 0 and 1. The trends in intermolecular potentials for the series Ar-HF, Ar-HCl, and Ar-HBr are discussed.

01,030
PB95-202693 Not available NTIS
National Inst. of Standards and Technology (PL), Boulder, CO. Quantum Physics Div.
Vibrational Dependence of the Anisotropic Intermolecular Potential of Ar-HF.
Final rept.
J. M. Hutson. 1992, 16p.
See also PB95-202685.
Pub. in Jnl. of Chemical Physics 96, n9 p6752-6767, 1 May 92.

Keywords: *Argon complexes, Van der Waals forces, Intermolecular forces, Microwave spectroscopy, Infrared spectroscopy, High resolution, Anisotropy, Reprints, *Hydrogen fluoride complexes, *Deuterium fluoride complexes, *Intermolecular potentials, Potential energy surfaces, Vibrational dependence.

A new intermolecular potential for Ar-HF is obtained by fitting to results from high-resolution microwave, far-infrared, and infrared spectroscopy. The new potential, designated H6(4,3,2) is a function of the diatom mass-reduced vibrational quantum number, as well as the intermolecular distance R and angle theta, and has 22 adjustable parameters. It reproduces all of the available spectroscopic data for levels of Ar-HF correlating with HF, nu = 0, 1, and 2, and DF, nu = 0 and 1. The H6(4,3,2) potential is qualitatively similar to previous potentials, with a linear Ar-H-F equilibrium geometry and a secondary minimum at the linear Ar-F-H geometry. Predictions of additional spectroscopic properties that would test the new potential are given, including far-infrared and overtone spectra of Ar-DF and dipole moments of excited states of Ar-HF and Ar-DF.

01,031
PB95-202743 Not available NTIS
National Inst. of Standards and Technology (MSEL), Gaithersburg, MD. Polymers Div.
Generalized Stokes-Einstein Equation for Spherical Particle Suspensions.
Final rept.
A. Kholodenko, and J. Douglas. 1995, 10p.
Pub. in Physical Review E 51, n2 p1081-1090 Feb 95.

Keywords: *Suspensions, Diffusion coefficient, Coupled modes, Sum rules, Polymers, Droplets, Spheres, Reprints, Stokes-Einstein equations.

The cooperative diffusion coefficient D(c) for spherical particle suspensions is calculated using a 'mode-coupling' method which extends previous calculations of D(c) for critical fluids and semidilute polymer solutions. The renormalization of the viscosity in the velocity-velocity correlation function from the solvent to the suspension viscosity leads to a generalized Stokes-Einstein (SE) equation in which the suspension viscosity eta replaces the solvent viscosity eta(0) and the correlation length xi (related to the osmotic compressibility) replaces the sphere radius R at nonvanishing suspension concentrations. Insertion of the leading order hard sphere virial expansions for eta and the osmotic compressibility into our generalized SE equation gives a virial expansion for D(c) which is consistent with theoretical estimates obtained by alternative methods. These leading order virial expansions are also consistent with experiments on model ('hard sphere') suspensions. Results are given for the virial expansion of spherical liquid droplets interacting via a contact attractive interaction. Further experiments are required to test the generalized SE equation at higher suspension concentrations.

01,032
PB95-202776 Not available NTIS
National Inst. of Standards and Technology (PL), Boulder, CO. Quantum Physics Div.
Single Photon Ionization, Laser Optical Probe Technique for Semiconductor Growth.
Final rept.
A. K. Kunz, A. L. Alstrin, S. M. Casey, and S. R. Leone. 1994, 8p.
Sponsored by National Science Foundation, Arlington, VA. and Petroleum Research Fund, Washington, DC.
Pub. in Proceedings of Society of Photo-Optical Instrumentation Engineers: Optical Characterization Techniques for High-Performance Microelectronic Device Manufacturing, Austin, TX., October 20, 1994, v2337 p20-27.

Keywords: *Molecular beam epitaxy, *Surface reactions, *Gallium arsenides, *Crystal growth, Real time operations, Semiconducting films, Laser radiation, Monitoring, Desorption, Arsenic, Silicon, Substrates, Reprints, Time-of-flight mass spectroscopy, Reflection high energy electron diffraction, Optical probes.

Single Photon Ionization Time-of-Flight Mass Spectroscopy (SPI-TOFMS) is used as an in situ optical characterization technique to monitor chemical reactions occurring at semiconductor surfaces during molecular beam epitaxial (MBE) growth by detecting gaseous species. In this approach, 118 nm (10.5 eV) laser photons are generated and passed in front of a semiconductor substrate in the ultra-high vacuum (UHV) chamber. Here, the photons ionize the gaseous scattered and desorbed growth species which are detected by time-of-flight mass spectroscopy. SPI-TOFMS has been used to study As(n)/Si(100) desorption kinetics and, more recently, MBE growth of GaAs. Results are presented on the real-time monitoring of GA(n) and As(n) growth species. Simultaneous monitoring of growth with Reflection High-Energy Electron Diffraction (RHEED) is also discussed. Future work includes SPI-TOFMS studies of Si delta-doping in GaAs and surfactant-enhanced epitaxy of Ge on Si. SPI-TOFMS is an in situ UHV optical probe used to study the growth chemistry of semiconductor surfaces. This non-intrusive, species-specific real-time monitor of growth can be applied to increase the quality of device manufacturing.

01,033
PB95-202792 Not available NTIS
National Inst. of Standards and Technology (PL), Boulder, CO. Quantum Physics Div.
Slit-Jet Near-Infrared Spectroscopy and Internal Rotor Dynamics of the ArH2O van der Waals Complex: An Angular Potential-Energy Surface for Internal H2O Rotation.
Final rept.
R. Lascola, and D. J. Nesbitt. 1991, 16p.
Grants NSF-CHE90-00641, NSF-DJNB1
Sponsored by National Science Foundation, Washington, DC.
Pub. in Jnl. of Chemical Physics 95, n11 p7917-7932, 1 Dec 91.

Keywords: *Argon complexes, Van der Waals forces, Supersonic jet flow, Near infrared radiation, Infrared spectroscopy, High resolution, Rotational states, Reprints, *Water complexes, Potential energy surfaces.

Near-infrared vibration-rotation spectra of jet-cooled Ar-H2O complexes are detected for the first time via direct absorption of tunable difference frequency infrared radiation in a slit supersonic expansion source. Transitions from both the lowest para and ortho complexes are observed which correlate to 0(sub 00) and 1(sub 01) rotational levels of free H2O, respectively, and permit spectroscopic characterization of the complex in both the ground (nu(3) = 0) and asymmetric stretch excited (nu(3) = 1) levels. Information obtained in the study permits determination of a two-dimensional (2D) angular potential-energy surface of the complex as a function of the H2O orientation.

01,034
PB95-202800 Not available NTIS
National Inst. of Standards and Technology (PL), Boulder, CO. Quantum Physics Div.
Orbital Stereochemistry: Discovering the Symmetries of Collision Processes.
Final rept.
S. R. Leone. 1992, 6p.
Grants NSF-PHY90-12244, NSF-CHE84-08403
Sponsored by National Science Foundation, Washington, DC.
Pub. in Accounts of Chemical Research 25, n2 p71-76 Feb 92.

Keywords: *Stereochemistry, Molecular orbitals, Directional control, Energy transfer, Laser radiation, Polarization, Alignment, Symmetry, Collisions, Reprints.

One of the most exciting recent aspects of laser chemistry is the ability to prepare highly aligned, or directional, reagents using the polarization of lasers. It is now possible to investigate chemical processes with directional control in a variety of new measurements. The results provide a means of visualizing the important symmetries of the chemical process with unprecedented detail. Many mechanistic interpretations of chemical transformations are built upon compelling pictures of orbital directionality, electron overlap and transfer, and symmetry arguments. Chemists can exploit the methods of directional control to verify these pictures and to broaden our understanding of chemical stereospecificity.

01,035
PB95-202875 Not available NTIS
National Inst. of Standards and Technology (PL), Boulder, CO. Quantum Physics Div.
Preferential In-Plane Rotational Excitation of H2O (001) by Translational-to-Vibrational Transfer from 2.2 eV H Atoms.
Final rept.
C. M. Lovejoy, L. Goldfarb, and S. R. Leone. 1992, 3p.
Contract DE-FG02-883413860, Grant NSF-CHE87-13646
Sponsored by National Science Foundation, Washington, DC. and Department of Energy, Washington, DC. Office of Energy Research.
Pub. in Jnl. of Chemical Physics 96, n9 p7180-7182, 1 May 92.

Keywords: *Atom-molecule collisions, Water, EV range 1-10, Rotational states, Energy transfer, Excitation, Reprints, Fourier transform infrared spectroscopy, Hydrogen atoms.

The translational-to-vibrational and rotational (T-V,R) excitation of H2O with 2.2 eV hydrogen atoms is studied by time-resolved Fourier-transform infrared spectroscopy. Up to 2900/cm of rotational excitation is observed in (001), with a strong preference for in-plane rather than out-of-plane rotation for J = or > 7, which implies a unique collision process leading to rotational alignment.

01,036
PB95-202933 Not available NTIS
National Inst. of Standards and Technology (PL), Boulder, CO. Quantum Physics Div.
Large Amplitude Skeletal Isomerization as a Promoter of Intramolecular Vibrational Relaxation in CH Stretch Excited Hydrocarbons.
Final rept.
A. McIlroy, and D. J. Nesbitt. 1994, 15p.
Grants NSF-PHY90-12244, NSF-CHE90-00641
Sponsored by National Science Foundation, Arlington, VA.
Pub. in Jnl. of Chemical Physics 100, n5 p3421-3435, 1 Sep 94.

Keywords: *Butenes, Supersonic jet flow, Molecular vibration, Vibrational states, Infrared spectra, High resolution, Isomerization, Reprints.

The high resolution, slit jet cooled infrared nu = 1 <- - 0 methyl asymmetric stretch spectra of trans-2-butene and 1-butene are reported. Both of these molecules are singly unsaturated butene chains, have 30 vibrational degrees of freedom, and yield nearly equivalent vibrational state densities at CH stretch levels of excitation. The key difference between these two molecules is the presence of a large amplitude C-C-C skeletal torsional coordinate in 1-butene corresponding to a low barrier, internal isomerization pathway which is completely absent in trans-2-butene. The trans-2-butene asymmetric CH stretch (nu 16) spectrum is fully discrete at 0.002/cm resolution, and the coarse structure readily assigned to zero order rovibrational transitions in an asymmetric top. Fragmentation of these zero order transitions into spectral 'clumps' of fine structure provides direct evidence for coupling of the CH stretch to vibrational bath states.

01,037
PB95-202941 Not available NTIS
National Inst. of Standards and Technology (PL), Boulder, CO. Quantum Physics Div.
Sub-Doppler, Infrared Laser Spectroscopy of the Propyne 2nu1 Band: Evidence of z-Axis Coriolis Dominated Intramolecular State Mixing in the Acetylenic CH Stretch Overtone.
Final rept.
A. McIlroy, D. J. Nesbitt, E. Kerstel, G. Scoles, B. H. Pate, and K. K. Lehmann. 1994, 16p.
Grant NSF-PHY90-12244
Sponsored by National Science Foundation, Arlington, VA.
Pub. in Jnl. of Chemical Physics 100, n4 p2596-2611, 15 Feb 94.

Keywords: *Propyne, Infrared spectroscopy, Laser spectroscopy, Molecular relaxation, Vibrational states, Absorption spectra, Reprints.

The eigenstate-resolved 2nu(1) (acetylenic CH stretch) absorption spectrum of propyne has been observed for J' = 0-11 and K = 0-3 in a skimmed supersonic molecular beam using optothermal detection. Radiation near 1.5 micrometers was generated by a color center laser allowing spectra to be obtained with a full-width at half-maximum resolution of 6 X 10(exp 4)/cm (18 MHz). Three distinct characteristics are observed for the perturbations suffered by the optically active (bright) acetylenic CH stretch vibrational state due to vibrational coupling to the nonoptically active (dark) vibrational bath states.

01,038
PB95-202966 Not available NTIS
National Inst. of Standards and Technology (MSEL), Gaithersburg, MD. Reactor Radiation Div.
Determination of Complex Structures from Powder Diffraction Data: The Crystal Structure of La3Ti5Al15O37.
Final rept.
R. E. Morris, J. J. Owen, J. K. Stalick, and A. K. Cheetham. 1994, 6p.
Grant NSF-DMR-9123048
Sponsored by National Science Foundation, Arlington, VA.
Pub. in Jnl. of Solid State Chemistry 111, p52-57 1994.

Keywords: *Crystal structure, Synchrotron radiation, Neutron diffraction, X ray diffraction, Complex systems, Reprints, *Lanthanum titanium aluminates, Rietveld method, Powder diffraction.

The applicability of powder diffraction techniques to structure determination has improved substantially in recent times, but it has only been successfully utilized in the solution of relatively simple structures of up to 29 atoms in the asymmetric unit. The structure La3Ti5Al15O37, which has 60 atoms in the asymmetric unit, has been solved using a combination of synchrotron X-ray and neutron powder diffraction. This represents a considerable advance in the size of structure that has been solved using powder diffraction techniques. The structure of La3Ti5Al15O37 consists of small regions of simpler structure types in the La/Ti/Al/O system, interleaved to form a complex 3D network.

01,039
PB95-202982 Not available NTIS
National Inst. of Standards and Technology (PL), Boulder, CO. Quantum Physics Div.
Acceleration of Intramolecular Vibrational Redistribution by methyl Internal Rotation. A Chemical Timing Study of p-fluorotoluene and p-fluorotoluene-d3.
Final rept.
D. B. Moss, and C. S. Parmenter. 1993, 9p.
Pub. in Jnl. of Chemical Physics 98, n9 p6897-6905, 1 May 93.

Keywords: *Molecular vibration, Vibrational spectra, Vibrational states, Rotational states, Fluorescence spectroscopy, Chemical bonds, Deuteration, Reprints, *Fluorotoluenes, Methyl groups.

Time-integrated, frequency-resolved fluorescence spectroscopy has been used to determine rates of intramolecular vibrational energy redistribution (IVR) from the vibrational levels 3(sup l) (epsilon (vib) approx = 1,200/cm) and 3(sup l)5(sup l) (epsilon (vib) approx = 2,000/cm) in both p-fluorotoluene and p-fluorotoluene-d(3) for comparison with each other and with comparable levels in p-difluorobenzene. Methyl substitution increases the rate of IVR by roughly two orders of magnitude, while deuteration of the methyl rotor produces at most a small (two- to fourfold) further increase in the rate of IVR. It is argued that the IVR response to methyl substitution is a consequence of the methyl internal rotation without significant influence from the methyl vibrations.

01,040
PB95-203006 Not available NTIS
National Inst. of Standards and Technology (PL), Boulder, CO. Quantum Physics Div.
High-Resolution, Direct Infrared Laser Absorption Spectroscopy in Slit Supersonic Jets: Intermolecular Forces and Unimolecular Vibrational Dynamics in Clusters.
Final rept.
D. J. Nesbitt. 1994, 33p.
Grant NSF-PHY90-12244
Sponsored by National Science Foundation, Arlington, VA.
Pub. in Annual Review of Physical Chemistry 45, p367-399 1994.

Keywords: *Infrared spectroscopy, Absorption spectroscopy, Laser spectroscopy, Near infrared radiation, Supersonic jet flow, Van der Waals forces, Intermolecular forces, Hydrogen bonds, Argon complexes, High resolution, Predissociation, Reviews, Reprints, Potential energy surfaces, Hydrogen fluoride complexes, Deuterium fluoride complexes.

The organization of this review will be as follows: In Sections 2 and 3, some basic experimental considerations are presented to highlight the specific advantages of direct absorption near IR laser methods, as well as the role of pulsed 'slit' jet expansions in obtaining the requisite path lengths and sensitivities. In Section 4, an overview of van der Waals spectroscopy of rare gas hydrogen halides is presented, illustrating the transition between a nearly 'rigid' to a nearly 'free' internal rotor dynamics. In Section 5, we discuss the role of large amplitude motion and intermolecular orientation on energy flow and bond breaking dynamics, focusing on internal rotor predissociation and V-V transfer between the monomer subunits. In Sections 6 and 7, we look to two ongoing areas of investigation of larger clusters. Section 6 presents experimental and theoretical results on the series of Ar(n)-HF and Ar(n)-DF clusters (n = 1, 2, 3 and 4), addressing the n-dependent vibrational red shifts, multibody effects, and intermolecular vibrational modes supported by these 'micromatrices.' Section 7 describes recent explorations into the spectroscopy and dynamics of (DF)3, which provides direct evidence for a cyclic ring 'structure,' and elucidates the hydrogen bond breaking dynamics that lead to ring opening on the 40 psec time scale.

01,041
PB95-203014 Not available NTIS
National Inst. of Standards and Technology (PL), Boulder, CO. Quantum Physics Div.
Rotational-RKR Inversion of Intermolecular Stretching Potentials: Extension to Linear Hydrogen Bonded Complexes.
Final rept.
D. J. Nesbitt, and M. S. Child. 1993, 9p.
Grant NSF-PHY90-12244
Sponsored by National Science Foundation, Washington, DC.
Pub. in Jnl. of Chemical Physics 98, n1 p478-486, 1 Jan 93.

Keywords: *Nitrogen complexes, Near infrared radiation, Infrared spectroscopy, Rotational spectra, Van der Waals forces, High resolution, Hydrogen bonds, Reprints, *Hydrogen fluoride complexes, Interatomic potentials, RKR method.

A Rydberg-Klein-Rees (RKR)-based method is described which determines effective 1D intermolecular stretching potentials for polyatomic linear complexes from high precision rotational data alone. This extends the 'rotational RKR' inversion method from pseudodiatomic van der Waals clusters with only two nonhydrogenic atoms to much larger complexes with several heavy atoms. Sample inversion of rotational eigenvalues generated from a model 1D potential reproduces the model potential to approx = or < 0.13/cm accuracy and correctly predicts harmonic frequencies, force constants, and dissociation energies to approx = or < 0.1%. In contrast, the commonly used 'pseudodiatomic' approximation lead to quite significant (10%-20%) errors, even for exact model potentials for which these approximations were developed. The method is further tested on high resolution near IR spectroscopic data of (14)N(14)N-HF, which determines the vibrationally averaged hydrogen bond stretching potential from 3.39 approx = or < R(cm) approx = or < 3.85 A. The RKR data yield a hydrogen bond length of R(N-H) = 2.106 A (2.079 A) and predict a van der Waals stretching frequency of 86.9/cm (90.7/cm) for nu(HF) = 0 (nu(HF) = 1).

01,042
PB95-203022 Not available NTIS
National Inst. of Standards and Technology (PL), Boulder, CO. Quantum Physics Div.
Rigid Bender Analysis of van der Waals Complexes: The Intermolecular Bending Potential of a Hydrogen Bond.
Final rept.
D. J. Nesbitt, and C. M. Lovejoy. 1992, 14p.
Grants NSF-DJNB1, NSF-DJNC1
Sponsored by National Science Foundation, Washington, DC.
Pub. in Jnl. of Chemical Physics 96, n8 p5712-5725, 15 Apr 92.

Keywords: *Hydrogen bonds, Van der Waals forces, Supersonic jet flow, Intermolecular forces, Rotational spectra, Vibrational spectra, High resolution, Predissociation, Reprints, *Hydrogen fluoride complexes, Intermolecular potentials, Potential energy surfaces.

High resolution IR data on weakly bound OCOHF complexes formed in a slit supersonic expansion reveal a progression of extremely low frequency vibrational levels associated with the bending of the OCO-HF hydrogen bond. In a previous paper (J Chem Phys 93, 7716 (1990)), we presented a spectroscopic analysis of the fundamental, combination and hot bands observed, corresponding to transitions between nu(bend)(sup l) = 0(sup 0), 1(sup 1), 2(sup 0), 2(sup 2), and 3(sup 1), where nu(bend)(sup l) denotes quanta of OCOHF skeletal bend excitation with l units of vibrational angular momentum. In this paper, we analyze the rotationally resolved data in terms of the rigid bender formalism of Hougen, Bunker and Johns to determine an explicit angular potential, V(theta), for the OCOHF complex in both the HF ground (nu(HF) = 0) and vibrationally excited (nu(HF) = 1) state.

01,043
PB95-203055 Not available NTIS
National Inst. of Standards and Technology (PL), Boulder, CO. Quantum Physics Div.
Kinetics of the Reaction C2H + O2 from 193 to 350 K Using Laser Flash Kinetic Infrared Absorption Spectroscopy.
Final rept.
B. J. Opansky, P. W. Seakins, J. O. P. Pedersen, and S. R. Leone. 1993, 7p.
Contract NASA-NAGW-2438
Sponsored by NASA Scientific and Technical Information Facility, Baltimore, MD.
Pub. in Jnl. of Physical Chemistry 97, n33 p8583-8589 1993.

Keywords: *Reaction kinetics, *Oxidation, Temperature range 0065-0273 K, Temperature range 0273-0400 K, Temperature dependence, Absorption spectroscopy, Infrared spectroscopy, Photolysis, Oxygen, Reprints, *Acetylene radicals, Color center lasers, Rate coefficients, Ethynyl radicals.

Rate coefficients for the reaction C2H + O2 are measured from 193 to 350 K by using transient absorption spectroscopy with an infrared color center laser. Ethynyl radicals are produced by pulsed laser photolysis of C2H2 in a temperature variable flow cell and a tunable color center laser probes the transient removal of C2H in absorption. The rate coefficient has a slight negative temperature dependence over the range 193-350 K, and an expression is obtained. The lack of a pressure dependence under our experimental conditions strongly suggests that the HCCOO* complex is short lived with respect to encountering a collision and rapidly dissociates to products without competition from collisional stabilization to HCCOO or collisionally induced dissociation to reactants.

01,044
PB95-203121 Not available NTIS
National Inst. of Standards and Technology (PL), Boulder, CO. Quantum Physics Div.
Photodissociation Dynamics in Quantum State-Selected Clusters: A Test of the One-Atom Cage Effect in Ar-H2O.
Final rept.
D. Plusquellic, O. Votava, and D. J. Nesbitt. 1994, 3p.
Sponsored by National Science Foundation, Arlington, VA.
Pub. in Jnl. of Chemical Physics 101, n7 p6356-6358, 1 Oct 94.

Keywords: *Argon complexes, Van der Waals forces, Supersonic jet flow, High resolution, Excimer lasers, Parametric oscillators, Photodissociation, Photolysis, Reprints, *Water complexes.

High resolution IR overtone pumping with an injection seeded optical parametric oscillator (OPO) is used in conjunction with excimer laser photolysis to investigate the state-resolved dynamics of quantum state-selected van der Waals clusters in a slit supersonic expansion. The narrow band IR light source (160 MHz, 5 mJ) preselects a specific upper state via the internal rotor band of Ar-H2O which correlates to a transition in H2O monomer. At fixed UV photolysis and probe wavelength, scanning the high resolution OPO yields the overtone action spectrum of Ar-H2O complexes.

01,045
PB95-203139 Not available NTIS
National Inst. of Standards and Technology (PL), Boulder, CO. Quantum Physics Div.
Photoelectron Spectroscopy of Small Antimony Cluster Anions: Sb(-), Sb2(-), Sb3(-), and Sb4(-).
Final rept.
M. L. Polak, G. Gerber, J. Ho, and W. C. Lineberger. 1992, 11p.
Grants NSF-PHY90-12244, NSF-CHE88-19444
Sponsored by National Science Foundation, Washington, DC.
Pub. in Jnl. of Chemical Physics 97, n12 p8990-9000, 15 Dec 92.

Keywords: *Photoelectron spectroscopy, *Atomic clusters, Near ultraviolet radiation, Ultraviolet spectra, Electronic structure, Electron affinity, Excited states, Negative ions, Reprints, *Antimony clusters.

We report the 351 nm photoelectron spectra of Sb(1-), Sb2(1-), Sb3(1-), and Sb4(1-). The electron affinity of atomic Sb is measured to be 1.046(5) eV. The Sb2(1-) photoelectron spectrum displays rich vibrational and electronic structure. For the photoelectron spectra of Sb3(1-) and Sb4(1-), the observed electronic structure is explained in terms of recently reported ab initio calculations. We report photoelectron angular distributions for all of the observed spectra, and find that the autodetaching resonance causes unusual angular distributions for Sb2(1-) photodetachment. Finally, electron affinity trends for group V atoms, dimers, and small clusters are discussed in light of the present study.

01,046
PB95-203196 Not available NTIS
National Inst. of Standards and Technology (PL), Boulder, CO. Quantum Physics Div.
High Resolution, Jet-Cooled Infrared Spectroscopy of (HCl)2: Analysis of nu1 and nu2 HCl Stretching Fundamentals, Interconversion Tunneling, and Mode-Specific Predissociation Lifetimes.
Final rept.
M. D. Schuder, C. M. Lovejoy, R. Lascola, and D. J. Nesbitt. 1993, 17p.
Grants NSF-PHY90-12244, NSF-CHE90-00641
Sponsored by National Science Foundation, Washington, DC.
Pub. in Jnl. of Chemical Physics 99, n6 p4346-4362, 15 Sep 93.

Keywords: Supersonic jet flow, Near infrared radiation, Temperature range 0000-0013 K, Absorption spectra, Infrared spectroscopy, High resolution, Reprints, *Hydrogen chloride dimers, Vibrational predissociation.

An extensive series of near-infrared absorption spectra are recorded for jet-cooled (6-14 K) hydrogen chloride dimer (HCl)2. Both Delta K(alpha) = 0 and Delta K(alpha) = + or - 1 bands are observed for both the free (nu(1)) and bonded (nu(2)) HCl stretches; all three chlorine isotopomers (H(35)Cl-H(35)Cl,H(35)Cl-H(37)Cl, and H(37)Cl-H(37)Cl) are observed and analyzed for K(alpha)(double prime) = or < 2. The slit jet spectrum extends significantly the previous cooled cell infrared study of this complex and provides a measure of tunneling splittings for K(alpha) = 0 and 1 for each of the HCl ground (nu = 0) and excited (nu = 1) states. Mode specific vibrational predissociation is observed via analysis of the absorption line shapes, with Lorentzian contributions to the line profiles of Delta nu(1) approx = or < 1.6 MHz and Delta nu(2) = 5.1 + or - 1.2 (2 sigma) MHz full width at half-maximum for nu(1) and nu(2) excitation, respectively.

01,047
PB95-203204 Not available NTIS
National Inst. of Standards and Technology (PL), Boulder, CO. Quantum Physics Div.
Slit-Jet Near-Infrared Diode Laser Spectroscopy of (DCl)2: nu1, nu2 DCl Stretching Fundamentals, Tunneling Dynamics, and the Influence of Large Amplitude 'Geared' Intermolecular Rotation.
Final rept.
M. D. Schuder, D. D. Nelson, and D. J. Nesbitt. 1993, 16p.
Grants NSF-PHY90-12244, NSF-CHE90-00641
Sponsored by National Science Foundation, Washington, DC.
Pub. in Jnl. of Chemical Physics 99, n7 p5045-5060, 1 Oct 93.

Keywords: *Hydrogen chloride, Supersonic jet flow, Near infrared radiation, Infrared spectroscopy, Laser

spectroscopy, High resolution, Hydrogen bonds, Vibrational spectra, Chlorine 35, Chlorine 37, Reprints, *Deuterium chloride dimers, Vibrational predissociation.

The first high resolution spectra of (DCl)2 are reported using direct IR laser absorption spectroscopy in a slit supersonic expansion. The spectral data are analyzed to obtain vibrational frequencies, rotational constants, and tunneling (interconversion) level splittings for isotopically symmetric (D(35)Cl)2 and (D(37)Cl)2, and mixed D(35)Cl-D(37)Cl dimers. Six dimer absorption bands are observed and analyzed for both (D(35)Cl)2 and D(35)Cl-D(37)Cl.

01,048
PB95-203212 Not available NTIS
National Inst. of Standards and Technology (PL), Boulder, CO. Quantum Physics Div.
High Resolution Near Infrared Spectroscopy of HCl-DCl and DCl-HCl: Relative Binding Energies, Isomer Interconversion Rates, and Mode Specific Vibrational Predissociation.
Final rept.
M. D. Schuder, and D. J. Nesbitt. 1994, 18p.
Grants NSF-PHY90-12244, NSF-CHE80-00641
Sponsored by National Science Foundation, Arlington, VA.
Pub. in Jnl. of Chemical Physics 100, n10 p7250-7267, 15 May 94.

Keywords: Supersonic jet flow, Near infrared radiation, Infrared spectroscopy, Laser spectroscopy, Binding energy, Hydrogen bonds, Energy transfer, High resolution, Isomers, Dimers, Reprints, *Hydrogen chloride complexes, *Deuterium chloride complexes, Vibrational predissociation.

Both D- and H-bonded isomers of the mixed dimers formed between HCl and DCl are investigated via high resolution infrared difference frequency and diode laser spectroscopy in the 2,885 and 2,064/cm regions. From an analysis of the relative integrated absorption intensities, the D-bonded complex (i.e., HCl-DCl) is determined to be more stable by 16 + or - 4/cm than the H-bonded (i.e., DCl-HCl) species. All four chlorine isotopic combinations of the lower energy (HCl-DCl) complex are probed via excitation of both HCl and DCl stretches. Additionally, two chlorine isotopomers of the higher energy (DCl-HCl) complex are investigated through HCl excitation. Compared to the facile tunneling observed in both (HCl)2 or (DCl)2 complexes, these mixed dimers exhibit more rigid behavior characteristic of two distinct isomeric species. However, the relatively small energy difference (16 + or - 4/cm) between the two isomers still allows the wave functions for both species to sample both the HCl-DCl and DCl-HCl local minima on the potential surface.

01,049
PB95-203238 Not available NTIS
National Inst. of Standards and Technology (PL), Boulder, CO. Quantum Physics Div.
Laser Flash Photolysis, Time-Resolved Fourier Transform Infrared Emission Study of the Reaction Cl + C2H5 yields HCl(v) + C2H4.
Final rept.
P. W. Seakins, E. L. Woodbridge, and S. R. Leone. 1993, 10p.
Contract DE-FG02-883413860
See also PB95-164281. Sponsored by Department of Energy, Washington, DC.
Pub. in Jnl. of Physical Chemistry 97, n21 p5633-5642 1993.

Keywords: *Chlorine, Chemical reactions, Hydrogen chloride, Ethylene, Emission spectroscopy, Infrared spectroscopy, Vibrational states, Chemiluminescence, Photolysis, Reprints, *Atom radical reactions, *Ethyl radicals.

The atom-radical reaction Cl + C2H5 --> HCl(nu) + C2H4 is studied using laser flash photolysis, time-resolved Fourier transform infrared emission spectroscopy and broad band infrared chemiluminescence. The Cl atoms and ethyl radicals are produced from a number of different precursors using one or two lasers. The initial HCl vibrational distribution is determined. The vibrational distribution is characteristic of an addition-elimination mechanism and can be reproduced using modified statistical theories of energy partitioning within the (C2H5Cl) intermediate. The time evolution of the HCl(nu = 4) emission is used to estimate a rate coefficient for this reaction of (3.0 + or - 1.0) X 10(exp -10) cc/molecule/s.

01,050
PB95-203311 Not available NTIS
National Inst. of Standards and Technology (PL), Boulder, CO. Quantum Physics Div.
Laser-Induced Desorption of In and Ga from Si(100) and Adsorbate Enhanced Surface Damage.
Final rept.
P. G. Strupp, A. L. Alstrin, B. J. Korte, and S. R. Leone. 1992, 6p.
Contract AFOSR90-0166
Sponsored by Air Force Office of Scientific Research, Bolling AFB, DC.
Pub. in Materials Research Society Symposia Proceedings, v236 p27-32 1992.

Keywords: *Indium, *Gallium, Laser induced fluorescence, Neodymium lasers, YAG lasers, Pulsed lasers, Laser radiation, Radiation damage, Surface reactions, Ultrahigh vacuum, Adsorbates, Silicon, Reprints, *Laser induced desorption, Surface damage.

Laser-induced desorption (LID) of In and Ga from Si(100) under ultra-high vacuum conditions is investigated. The frequency doubled 532 nm, 2-6 ns output of a Nd:YAG laser is focussed to 0.14 + or - 0.03 J/sq cm on the Si surface to induce desorption. Desorbed In or Ga atoms are detected by laser-induced fluorescence initiated by a pulsed dye laser propagating in front of the surface. Adsorbate-enhanced laser-induced surface damage is also observed; only 0.2 monolayer of In reduces the number of laser pulses required to observe damage by greater than a factor of 30.

01,051
PB95-203329 Not available NTIS
National Inst. of Standards and Technology (PL), Boulder, CO. Quantum Physics Div.
Pulsed Laser Irradiation at 532 nm of In and Ga Adsorbed on Si(100): Desorption, Incorporation, and Damage.
Final rept.
P. G. Strupp, A. L. Alstrin, B. J. Korte, and S. R. Leone. 1992, 7p.
Contract AFOSR90-0166
Sponsored by Air Force Office of Scientific Research, Bolling AFB, DC.
Pub. in Jnl. of Vacuum Science and Technology A 10, n3 p508-514 May/Jun 92.

Keywords: *Indium, *Gallium, Laser induced fluorescence, Radiation damage, Surface reactions, Ultrahigh vacuum, Neodymium lasers, YAG lasers, Pulsed lasers, Laser radiation, Silicon, Adsorbates, Reprints, *Laser induced desorption, Surface damage.

Laser-induced desorption (LID) of In and Ga from Si(100) under ultrahigh vacuum conditions is investigated. The frequency-doubled 532 nm, 2-6 ns output of Nd:YAG laser is focused to 0.14 + or - 0.03 J/sq cm on the Si surface to induce desorption. Desorbed In or Ga atoms are detected by laser-induced fluorescence initiated by a second pulsed laser propagating in front of the surface. LID occurs by thermal desorption with approximate desorption energies and preexponential factors in agreement with the literature values obtained previously by isothermal desorption measurements. Experiments at higher coverages suggest that desorption occurs predominantly from the two-dimensional (2D) adlayer with little desorption occurring from the adsorbate islands directly into the vacuum. The 2D layer is resupplied by either diffusion out of adsorbate islands or by diffusion of incorporated adsorbate out of the bulk. Adsorbate-enhanced laser-induced surface damage is also observed; only 0.2 monolayer of In reduces the number of laser pulses required to observe damage by greater than a factor of 30.

01,052
PB95-203337 Not available NTIS
National Inst. of Standards and Technology (PL), Boulder, CO. Quantum Physics Div.
Single-Photon Laser Ionization Time-of-Flight Mass Spectroscopy Detection in Molecular-Beam Epitaxy: Application to As4, As2, and Ga.
Final rept.
P. G. Strupp, A. L. Alstrin, R. V. Smilgys, and S. R. Leone. 1993, 5p.
Contract AFOSR90-0166
Sponsored by Air Force Office of Scientific Research, Bolling AFB, DC.
Pub. in Applied Optics 32, n6 p842-846, 20 Feb 93.

Keywords: *Molecular beam epitaxy, *Gallium arsenides, *Gallium, *Arsenic, Real time operations, Semiconducting films, Gas ionization, Far ultraviolet radiation, Laser radiation, Neodymium lasers, YAG lasers, Reprints, Time-of-flight mass spectroscopy.

Single-photon laser ionization time-of-flight mass spectroscopy (TOF-MS) is used to monitor fluxes of As4, As2, and Ga, species that are important in molecular-beam epitaxy of GaAs. With this technique, fluxes of multiple chemical species above a substrate can be measured noninvasively and in real time during conventional molecular-beam epitaxy. Additionally, the geometry of the single-photon ionization TOF-MS permits simultaneous film-growth monitoring by using techniques such as reflection high-energy electron diffraction (RHEED). Here gas-phase arsenic and gallium beams are ionized by a single 118-nm (10.5-eV) photon and detected with a TOF-MS. The 118-nm photons are produced by frequency tripling 355-nm light from a pulsed Nd:YAG laser in Xe. With single-photon ionization, less than 0.4% of the As4(1+) signal fragments to As2(1+). Neither As4(1+) nor As2(1+) fragments to As(1+) at 118 nm. The relative ionization probability of As4/As2 at 118 nm is approximately 4:1. This technique promises to be a powerful tool for analyzing most III-V and II-VI molecular-beam epitaxy growth species.

01,053
PB95-203386 Not available NTIS
National Inst. of Standards and Technology (CSTL), Gaithersburg, MD. Biotechnology Div.
Thermodynamics of the Hydrolysis of N-Acetyl-L-phenylalanine Ethyl Ester in Water and in Organic Solvents.
Final rept.
Y. B. Tewari, M. M. Schantz, P. C. Pandey, M. V. Rekharsky, and R. N. Goldberg. 1995, 8p.
Pub. in Jnl. of Physical Chemistry 99, n5 p1594-1601, 2 Feb 95.

Keywords: *Thermodynamics, *Hydrolysis, Water, Organic solvents, Equilibrium, Gibbs free energy, Entropy, Enthalpy, Reprints, *Phenylalanine/N-acetyl-(ethyl-ester).

Equilibrium measurements have been performed on the alpha-chymotrypsin-catalyzed hydrolysis reaction of N-acetyl-L-phenylalanine ethyl ester to (N-acetyl-L-phenylalanine + ethanol) with carbon tetrachloride, dichloromethane, toluene, and aqueous phosphate buffer as solvents for the reactants and products. Apparent equilibrium constants were measured as a function of temperature for this reaction in all four solvents. Calorimetric measurements were also performed for this reaction in aqueous phosphate buffer. The rather limited range of values that was found for the equilibrium constants is significant. The very limited amount of information available from the literature is also suggestive of the rule that equilibrium constants for hydrolysis reactions in different solvents are comparable if the reaction refers to neutral species and the concentration of water is included in the formulation of the equilibrium constant. Also, the standard molar enthalpy of reaction was found to be a linear function (slope = 313 K) of the standard molar entropy of reaction. This is indicative of an enthalpy-entropy compensation effect.

01,054
PB95-203485 Not available NTIS
National Inst. of Standards and Technology (PL), Boulder, CO. Quantum Physics Div.
Signatures of Large Amplitude Motion in a Weakly Bound Complex: High-Resolution IR Spectroscopy and Quantum Calculations for HeCO2.
Final rept.
M. J. Weida, J. M. Sperhac, D. J. Nesbitt, and J. M. Hutson. 1994, 13p.
Sponsored by National Science Foundation, Arlington, VA.
Pub. in Jnl. of Chemical Physics 101, n10 p8351-8363, 15 Nov 94.

Keywords: *Helium complexes, Molecular dynamics, Infrared spectroscopy, High resolution, Van der Waals forces, Supersonic jet flow, Reprints, *Carbon dioxide complexes, Potential energy surfaces.

The infrared spectrum of the HeCO2 van der Waals molecule is recorded in the region of the CO2 nu(3) asymmetric stretch via direct absorption of a tunable Pb-salt diode laser. HeCO2 is formed in a slit jet supersonic expansion; the slit valve and the stagnation gas must be precooled to -35 C before substantial formation of the complex is observed. Sixty-six rovibrational transitions are recorded by exciting the nu(3) asymmetric stretch of the CO2 monomer within the complex.

Forty-three of these transitions can be assigned using internally consistent combination differences as a b-type band of a T-shaped asymmetric rotor. There are several indications that large amplitude motion is significant to HeCO2, including the poor quality of the fit to an asymmetric rotor model and the large positive inertial defects of Delta = 8.54 and 10.98 u(Angstrom squared) in the ground and excited states, respectively. However, a hindered rotor analysis based on these inertial defects demonstrates that the CO2 motion within the complex is far from the free rotor limit. No evidence of predissociation broadening is observed, indicating a lifetime for the complex of tau > 6 ns.

01,055
PB95-251732 PC A03/MF A01
National Inst. of Standards and Technology (CSTL), Gaithersburg, MD. Process Measurements Div.
Standard Reference Material 1744: Aluminum Freezing-Point Standard.
Special pub.
G. F. Strouse. May 95, 41p, NIST/SP-260-124.
Also available from Supt. of Docs. as SN003-003-03342-1.

Keywords: *Aluminum, *Melting points, *Calibration standards, Temperature, Phase transformations, Scale(Ratio), Standardization, Interlaboratory comparisons, *Standard Reference Material 1744, SRM 1744, International Temperature Scale of 1990, ITS-90, Fixed-point cell.

The freezing point of aluminum (660.323 deg. C) is a defining fixed point of the International Temperature Scale of 1990 (ITS-90). Realization of this freezing point is performed using a fixed-point cell containing high purity (greater than or equal to 99.9999% pure) aluminum. The aluminum constituting Standard Reference Material 1744 (SRM 1744) has been evaluated, and certified as suitable for use in the realization of the freezing-point temperature of aluminum for the ITS-90. Based on results obtained with three fixed-point cells containing random samples of SRM 1744, the plateau temperature of a freezing curve of the SRm 1744 aluminum is expected to differ by not more than 1 m deg C from the ITS-90 assigned temperature. In the document, the methods used for the construction of the aluminum freezing-point cells and for the evaluation of SRM 1744 are described.

01,056
PB95-260618 PC A09/MF A02
National Inst. of Standards and Technology (CSTL), Boulder, CO. Process Measurements Div.
Thermochemical and Chemical Kinetic Data for Fluorinated Hydrocarbons.
Technical note.
D. R. F. Burgess, M. R. Zachariah, W. Tsang, and P. R. Westmoreland. Jul 95, 184p, NIST/TN-1412.
Also available from Supt. of Docs. as SN003-003-03343-0. Prepared in cooperation with Massachusetts Univ., Amherst. Dept. of Chemical Engineering.

Keywords: *Halohydrocarbons, *Fluorination, *Thermochemistry, *Reaction kinetics, Molecular orbitals, Molecular theory, Transport properties, Models, Environmental chemical substitutes, Chemical extinguishers.

A comprehensive, detailed chemical kinetic mechanism was developed for fluorinated hydrocarbon destruction and flame suppression. Existing fluorinated hydrocarbon thermochemistry and kinetics were compiled and evaluated. For species where no or incomplete thermochemistry was available, these data were calculated through application of ab initio molecular orbital theory. Group additivity values were determined consistent with experimental and ab initio data. For reactions where no or limited kinetics was available, these data were estimated by analogy to hydrocarbon reactions, by using empirical relationships from other fluorinated hydrocarbon reactions, by ab initio transition state calculations, and by application of RRKM and QRRK methods. This report provides the thermochemical and chemical kinetic data used in this work.

01,057
PB95-260808 PC A03/MF A01
National Inst. of Standards and Technology (TS), Gaithersburg, MD. Standard Reference Data Program.
NIST Standard Reference Data Products Catalog, 1995-96. Achieve with Standard Reference Data.
Special pub.
J. C. Sauerwein. Jul 95, 45p, NIST/SP-782.
Supersedes PB94-151842. Also available from Supt. of Docs. as SN003-003-03346-4.

Keywords: *Catalogs(Publications), *Data bases, Chemistry, Chemical analysis, Atomic physics, Biotechnology, Reaction kinetics, Numeric data, Physics, Fluids, Thermochemistry, Molecular structure, Molecular spectroscopy, Software tools, Compilations, Character recognition, Evaluated data, Materials.

The National Institute of Standards and Technology's (NIST) Standard Reference Data Program provides reliable, well-documented data to scientists and engineers for use in technical problem-solving, research, and development. This catalog lists published current databases and published data in the National Standard Reference Database Series. This edition of the catalog contains many new databases and updates current ones. These data compilations have been subdivided into ten categories. Prices and ordering information are located at the back of the document.

01,058
PB95-261962 (Order as PB95-261897, PC A07/MF A02)
National Inst. of Standards and Technology, Gaithersburg, MD.
New IUPAC Guidelines for the Reporting of Stable Hydrogen, Carbon, and Oxygen Isotope-Ratio Data. Letter to the Editor.
T. B. Coplen. 1995, 1p.
Included in Jnl. of Research of the National Institute of Standards and Technology, v100 n3 p285 May/Jun 95.

Keywords: *Isotope ratio, *Abundance, *Hydrogen isotopes, *Carbon isotopes, *Oxygen isotopes, Chemical elements, Atomic mass, Sea water, Standards, IUPAC guideliness.

To eliminate possible confusion in the reporting of isotopic abundances on noncorresponding scales, the Commission on Atomic Weights and Isotopic Abundances of the Internationl Union of Pure and Allied Chemistry (IOPAC) recommended at the IUPAC 37th General Assembly in August 1993 at Libson, Portugal, that (1) 2H/1H relative ratios of all substances be expressed relative to VSMOW (Vienna Standard Mean Ocean Water) on a scale such that 2H/1H of SLAP (Standard Light Antarctic Precipitation) is 0.572 times that of VOSMOW; (2) 13C/12C relative ratios of all substances be expressed relative to VPDB (Vienna Peedee belemnite) on a scale such that 13C/12C of NBS-lime-stone (RM 8544) is 1.00195 times that of VPDB; and (3) 18O/16O ratios of all substances be expressed relative to either VSMOW or VPDB an scales such that 18O/16O of SLAP is 0.9445 times that of VSMOW.

01,059
PB96-102025 Not available NTIS
National Inst. of Standards and Technology (PL), Boulder, CO. Quantum Physics Div.
Single Photon Laser Ionization as an In-situ Diagnostic for MBE growth.
Final rept.
A. L. Alstrin, A. K. Kunz, P. G. Strupp, and S. R. Leone. 1994, 6p.
Contract ACS-PRF-27135-AC6
Sponsored by Petroleum Research Fund, Washington, DC.
Pub. in Materials Research Society Symposia Proceedings, v324 p359-364 1994.

Keywords: *Molecular beam epitaxy, *Gallium arsenides, *Flux(Rate), Time-of-flight mass spectrometers, YAG lasers, Photons, Neodymium lasers, Diagnostic techniques, Scattering, Desorption, Laser radiation, Ionization, Reprints.

Single photon laser ionization time-of-flight mass spectroscopy (SPI-TOFMS) is used to monitor the gaseous fluxes of Ga and Asn, during molecular beam epitaxy of GaAs. This noninvasive and real-time probe measures densities, and hence fluxes, of multiple chemical species impinging on or scattered from a substrate during conventional MBE. With single photon ionization at 118 nm (10.5 eV, ninth harmonic of Nd: YAG laser), the photon energy is large enough to ionize the species, but insufficient to both ionize and fragment. Results will be presented on the probing of scattering and desorption of III-V MBE species during GaAs growth. This technique promises to be a valuable in-situ diagnostic for III-V and II-VI MBE.

01,060
PB96-102041 Not available NTIS
National Inst. of Standards and Technology (CSTL), Gaithersburg, MD. Thermophysics Div.
Ab initio Calculations for Helium: A Standard for Transport Property Measurements.
Final rept.
R. A. Aziz, A. R. Janzen, and M. R. Moldover. 1995, 4p.
Pub. in Physical Review Letters 74, n9 p1586-1589, 27 Feb 95.

Keywords: *Helium, *Transport properties, *Standards, Thermal conductivity, Virial equation, Coefficients, Viscosity, Potentials, Thermodynamics, Reprints, *Ab initio calculation.

For helium, the accuracy of calculated transport properties and virial coefficients based on accurate ab initio potential now exceeds that of the best measurements. The ab initio results should be used to calibrate measuring apparatus.

01,061
PB96-102298 Not available NTIS
National Inst. of Standards and Technology (PL), Boulder, CO. Quantum Physics Div.
High-Resolution Infrared Overtone Spectroscopy of N2-HF: Vibrational Red Shifts and Predissociation Rate as a Function of HF Stretching Quanta.
Final rept.
J. T. Farrell, O. Sneh, and D. J. Nesbitt. 1994, 7p.
Sponsored by National Science Foundation, Arlington, VA.
Pub. in Jnl. of Physical Chemistry 98, n24 p6068-6074 1994.

Keywords: *Nitrogen compounds, *Hydrofluoric acid, *Infrared spectroscopy, Van der Waals forces, Infrared absorption, High resolution, Potentials, Difference frequency, Electrostatics, Red shift, Reprints.

The high-resolution infrared spectrum of the nu(sub HF) = 2 inversely maps to 0 stretch in N2-HF has been recorded using direct absorption of tunable infrared light in a slit jet spectrometer. The ban origin is located at 7657.4057 1/cm red-shifted 93.39 1/cm from the nu(sub HF) = 2 inversely maps to 0 origin of the HF monomer. The changes in vibrational red shift with HF stretching quanta provide explicit information on the coupling between the high-frequency (i.e., intramolecular) and low-frequency (i.e., intermolecular) degrees of freedom, which can be understood with a simple electrostatic model. Additional evidence for coupling between the low- and high-frequency modes is provided through an analysis of the rotational constants.

01,062
PB96-102355 Not available NTIS
National Inst. of Standards and Technology (CSTL), Gaithersburg, MD. Biotechnology Div.
Non-Perturbative Relation between the Mutual Diffusion Coefficient, Suspension Viscosity, and Osmotic Compressibility: Application to Concentrated Protein Solutions.
Final rept.
A. K. Gaigalas, V. Reipa, J. Hubbard, J. Edwards, and J. Douglas. 1995, 8p.
Pub. in Chemical Engineering Science, v50 n7 p1107-1114 1995.

Keywords: *Proteins, *Diffusion coefficient, *Viscosity, *Osmosis, Concentration(Composition), Mixtures, Suspensions, Aqueous solutions, Compressibility, Reprints.

The authors test a proposed relation between mutual diffusion coefficient and viscosity in suspensions which is essentially identical to a dynamic mode-coupling theory of diffusion in binary fluid mixtures near a critical mixing point. In contrast to conventional treatments of suspension hydrodynamics, this relation is non-perturbative in the sense that is not necessary to assume that the volume fraction of suspended particles is a small parameter. The mutual diffusion coefficient was then related to the viscosity and osmotic compressibility of the concentrated suspension relative to the infinite dilution limit. The authors conclude that this non-perturbative relation provides a convenient estimate of protein diffusion coefficients as a function of protein concentration.

01,063
PB96-102371 Not available NTIS
National Inst. of Standards and Technology (CSTL), Gaithersburg, MD. Thermophysics Div.
Critical Lines for Type-III Aqueous Mixtures by Generalized Corresponding-States Models.
Final rept.
J. S. Gallagher, D. G. Friend, J. A. Given, and J. M. H. L. Sengers. 1994, 8p.
Sponsored by Department of Energy, Washington, DC.
Pub. in International Jnl. of Thermophysics 15, n6 p1271-1278 1994.

Keywords: *Aqueous solutions, *Binary mixtures, *Carbon dioxide, *Phase diagrams, Algorithms, Gases, Nitrogen, Chemical composition, Chemical equilibrium, Critical point, Pressure, Reprints, *Critical lines, *Type-III mixtures, Gas-gas equilibrium, ECS(Extended corresponding states).

An algorithm has been developed for calculating the gas-gas critical line of type-III binary fluid mixtures for extended corresponding-states (ECS) models. The algorithm searches for an extremum in pressure on the spinodal curve of an isothermal pressure-composition phase diagram of a binary mixture. The method has been applied to solutions of carbon dioxide and of nitrogen in water, starting at the water critical point. Two variants of ECS have been tested for their ability to represent reliable PVTx data in the nitrogen-water mixture. It is demonstrated that in the latter system both ECS variants produce an artifact in the gas-gas critical line in the range of 0-0.2 mole fraction of nitrogen.

01,064
PB96-102769 Not available NTIS
National Inst. of Standards and Technology (PL), Gaithersburg, MD. Ionizing Radiation Div.
NBS/NIST Peltier-Effect Microcalorimeter: A Four-Decade Review.
Final rept.
W. B. Mann, and M. P. Unterweger. 1995, 6p.
Pub. in Applied Radiation and Isotopes 46, n3 p185-190 1995.

Keywords: *Calorimeters, *Radioactivity, *Peltier effects, Radioactive isotopes, Ionizing radiation, Nickel 63, Radium 226, Theromophysical properties, US NBS, Reprints.

Radioactivity measurements made with the National Bureau of Standards/National Institute of Standards and Technology (NBS/NIST) Peltier-effect microcalorimeter since January 1954 are reviewed.

01,065
PB96-102801 Not available NTIS
National Inst. of Standards and Technology (CSTL), Gaithersburg, MD. Thermophysics Div.
Length Scales for Fragile Glass-Forming Liquids.
Final rept.
R. D. Mountain. 1995, 3p.
Pub. in Jnl. of Chemical Physics 102, n3 p5408-5410, 1 Apr 95.

Keywords: *Glass, *Supercooling, *Liquids, *Computerized simulation, Molecular flow, Phase transformations, Secondary waves, Wavelengths, Clumps, Transverse waves, Mixtures, Reprints, Soft-sphere mixture, Molecular dynamic.

Molecular dynamics simulation results are used to demonstrate the existence of a growing length in supercooled, fragile glass-forming liquids. This length is the longest wavelength, propagating shear wave the fluid can support. Explicit results are reported for an equimolar soft-sphere mixture. A possible connection between this length and the size of locally rigid clusters is discussed.

01,066
PB96-102835 Not available NTIS
National Inst. of Standards and Technology (PL), Boulder, CO. Quantum Physics Div.
Probing Potential-Energy Surfaces via High-Resolution IR Laser Spectroscopy.
Final rept.
D. J. Nesbitt. 1994, 18p.
Grants NSF-PHY90-12244, NSF-CHE90-00641
Sponsored by National Science Foundation, Arlington, VA. and Air Force Office of Scientific Research, Bolling AFB, DC.
Pub. in Faraday Discussions 97, p1-18 1994.

Keywords: *IR laser spectroscopy, Foreign technology, Infrared spectroscopy, Van der Waals, High resolution, Supersonic expansion, Energy transfer, Reprints.

The use of high-resolution IR lasers for spectroscopic detection and characterization of trace, weakly bound cluster species in low-density, jet-cooled environments has led to enormous program in the study of collision dynamics, intermolecular forces and intramolecular energy flow. As a particular focus of this talk, direct absorption methods in combination with slit supersonic expansions and crossed molecular beams offer an extremely general tool for probing unimolecular and biomolecular dynamics with full quantum-state resolution.

01,067
PB96-102884 Not available NTIS
National Inst. of Standards and Technology (PL), Gaithersburg, MD. Ionizing Radiation Div.
Total-Dielectric-Function Approach to Electron and Phonon Response in Solids.
Final rept.
D. R. Penn, S. P. Lewis, and M. L. Cohen. 1995, 15p.
Sponsored by National Science Foundation, Arlington, VA. and Department of Energy, Washington, DC.
Pub. in Physical Review B 51, n10 p6500-6514, 1 Mar 95.

Keywords: *Electron scattering, *Phonon response, *Solids, Reprints, Superconductivity, Total dielectric function.

The interaction between two test charges, the response of a solid to an external field, and the normal modes of the solid can be determined from a total dielectric function that includes both electronic and lattice polarizabilities as well as local-field effects. In this paper we examine the relationship between superconductivity and the stability of a solid and derive sum rules for the electronic part of the dielectric function. It is also shown that there are negative eigenvalues of the total static dielectric function, implying the possibility of an attractive interaction between test charges. An attractive interaction is required for superconductivity.

01,068
PB96-102892 Not available NTIS
National Inst. of Standards and Technology (CSTL), Gaithersburg, MD. Thermophysics Div.
Principle of Congruence and Its Application to Compressible States.
Final rept.
C. J. Peters, L. J. Florusse, J. L. de Roos, J. de Swaan Arons, and J. M. H. Sengers. 1995, 27p.
Pub. in Fluid Phase Equilibria, v105 p193-219 1995.

Keywords: *Congruence, *Chain molecules, Reprints, Corresponding states, Bubble points, Thermodynamic properties, Mixtures, Dew points.

The principle of congruence claims that certain thermodynamic and transport properties of a mixture of n-alkanes are the same as those of the pure n-alkane of the mole-fraction-averaged carbon number. We discuss the origin of the principle, and attempts at theoretical justification and validation with respect to experimental data. We demonstrate that the principle applies even in cases where no fundamental justification exists. Whenever the principle applies, prediction of thermodynamic behavior of a mixture of n-alkanes in inherently simpler and usually more accurate than that based on empirical equations of state, molecular interaction parameters, and mixing and combining rules. Our experimental verification serves to pinpoint those properties that can be safely and accurately predicted on the basis of the principle of congruence. The solubility of hydrogen in mixtures of long-chain n-alkanes is used as a prime example.

01,069
PB96-103171 Not available NTIS
National Inst. of Standards and Technology (PL), Boulder, CO. Quantum Physics Div.
Collisional Alignment of CO2 Rotational Angular Momentum States in a Supersonic Expansion.
Final rept.
M. J. Weida, and D. J. Nesbitt. 1994, 14p.
Contract AFOSR-90-0055, Grant NSF-PHY90-12244
Sponsored by National Science Foundation, Arlington, VA. and Air Force Office of Scientific Research, Bolling AFB, DC.
Pub. in Jnl. of Chemical Physics 100, n9 p6372-6385, 1 May 94.

Keywords: *Alignment, *Carbon dioxide, *Molecular collisions, *Angular momentum, Anisotropy, Infrared lasers, Polarization(Spin alignment), Supersonics, Expansion, Molecular rotation, Reprints.

The rotational alignment of CO2 seeded in a supersonic expansion is measured using a general, direct absorption method based on fast (75 kHz) polarization modulation and phase sensitive detection with of a narrow band tunable IR laser. The anisotropic distribution of bar M(sub j)bar states is created by a directed velocity slip between the carrier gas and a nonspherical seed gas. Strong alignment signals are observed in a pinhole expansion that depend systematically on the carrier gas, stagnation pressure, and J state. In a slit expansion, however, no alignment is detected for comparable conditions. The observed effects are quite significant and occur at rather modest expansion conditions (e.g., 2.5% CO2 in He at 1000 Torr).

01,070
PB96-103197 Not available NTIS
National Inst. of Standards and Technology (MSEL), Gaithersburg, MD. Polymers Div.
Water Adsorption at a Polyimide/Silicon Wafer Interface.
Final rept.
W. L. Wu, W. J. Orts, C. J. Majkrzak, and D. L. Hunston. 1995, 5p.
Contract N00014-92-F-0036
Sponsored by Office of Naval Research, Arlington, VA.
Pub. in Polymer Engineering and Science, v35 n12 p1000-1004 Jun 95.

Keywords: *Interfaces, *Moisture, *Wafers, *Polyimides, Concentration(Composition), Adsorption, Water, Neutron scattering, Reflectivity, Polymers, Silicon, Reprints.

Neutron reflectivity (NR) was applied to measure the concentration of water at the buried interfaces between an amorphous polyimide and silicon single crystal wafers. Excess water was discovered within 30 Angstroms of the metal/polymer interface, where the water concentration reached 17% (by volume) for the samples without a coupling agent and 12% for the one with coupling agent. The above results demonstrate conclusively the unique power of NR in determining water concentration near a buried interface, and provide the first quantitative evidence for a water concentration profile which peaks in the interface region.

01,071
PB96-103205 Not available NTIS
National Inst. of Standards and Technology (PL), Boulder, CO. Quantum Physics Div.
Phase Shifts and Intensity Dependence in Frequency-Modulation Spectroscopy.
Final rept.
H. R. Xia, J. I. Cirac, S. Swartz, J. L. Hall, P. Zoller, B. Kohler, and D. S. Elliott. 1994, 10p.
Contract N00014-89-J-1227, Grant NSF-PHY90-12244
Sponsored by Office of Naval Research, Arlington, VA., Air Force Office of Scientific Research, Bolling AFB, DC. and National Science Foundation, Arlington, VA.
Pub. in Jnl. of the Optical Society of America B 11, n4 p721-730 May 94.

Keywords: *Phase shift, *Spectroscopy, *Intensity, Frequency modulation, Spectrum analysis, Optical heterodyning, Line spectra, Shape, Reprints, RF signal, Optical Block equations.

The authors discuss experimental observations of an induced phase shift of the rf signal produced in frequency-modulated saturated-absorption measurements under the conditions of large probe-beam intensities. This phase shift can be understood in terms of the phase difference between the phase modulation of the optical driving field and the steady-state macroscopic polarization of the medium. The authors also present theoretically calculated spectra that are based on the optical Bloch equations and that are in excellent agreement with the experimental results.

01,072
PB96-111620 Not available NTIS
National Inst. of Standards and Technology (CSTL), Gaithersburg, MD. Thermophysics Div.
Comparison of a Fixed-Charge and a Polarizable Water Model.
Final rept.
R. D. Mountain. 1995, 7p.
Pub. in Jnl. of Chemical Physics, v103 n8 p3084-3090, 22 Aug 95.

Keywords: *Hydrogen bonds, *Water, *Mathematical models, *Molecular structure, Chemical bonds, Pairing interactions, Distribution functions, Lifetime, Density, Temperature, Polarization, Reprints, *Molecular dynamics.

Molecular dynamics simulations are used to examine two models for water. The first model is the fixed-charge model introduced by Stillinger and Rahman and the second model is the polarizable model developed by Dang. The site-site, intermolecular pair distribution functions and the hydrogen bond lifetimes are determined for three fluid states for which neutron-diffraction determined pair function exist. The trends in the pair functions and the bond lifetimes with decreasing density and increasing temperature for both models are similar, with the fixed-charge model pair functions changing more slowly, and the bond lifetimes more rapidly than those for the polarizable model.

01,073
PB96-111760 Not available NTIS
National Inst. of Standards and Technology (MSEL), Gaithersburg, MD. Ceramics Div.
Surface Chemistry of Silicon Nitride Powder in the Presence of Dissolved Ions.
Final rept.
V. A. Hackley, and S. G. Malghan. 1994, 11p.
Pub. in Jnl. of Materials Science, v29 p4420-4430 1994.

Keywords: *Silicon nitrides, *Surface chemistry, *Powders(Particles), Chemical reactions, Interfaces, Colloids, Electrolytes, Impurities, Additives, Contaminants, Adsorption, Ceramics, Reprints.

Colloidal processing of silicon nitride (Si3N4) powders depends largely on the control of reactions at the solid-solution interface. The role of dissolved ions in the surface chemistry of impurities, contaminants and additives in processing are discussed. The interaction of ions at the solid-solution interface was characterized by particle electrokinetic behavior determined for electroacoustic measurements in moderately concentrated suspensions. Ions were classified according to chemical similarity and surface specificity. Specific adsorption was inferred from the movement of the isoelectric point relative to the endemic native value.

01,074
PB96-111893 Not available NTIS
National Inst. of Standards and Technology (MSEL), Gaithersburg, MD. Polymers Div.
Crystal Structure of Calcium Glutarate Monohydrate.
Final rept.
M. Mathew, and S. Takagi. 1995, 3p.
Sponsored by American Dental Association Health Foundation, Chicago, IL.
Pub. in Zeitschrift fuer Kristallographie, v210 p199-201 1995.

Keywords: *Crystal structure, Reprints, Monocrystals, X ray diffraction, Hydrates, Chemical bonds, *Foreign technology, *Calcium glutarate monohydrate.

The crystal structure of calcium glutarate monohydrate, Ca(C5H6O4).H2O, has been determined by single crystal X-ray diffraction. The crystals are orthorhombic with a = 6.805(1) Angstrom, b = 18.486(2) Angstrom, c = 5.884(1) Angstrom, space group P2(sub 1)2(sub 1)2(sub 2), Z = 4, V = 740.1(2) Angstrom(3), dm = 1.69, and dc = 1.688 mg/cubic m. The structure was refined by the full-matrix least-squares techniques to R = 0.019, Rw = 0.026, for 1198 reflections with I greater than or equal to 3 sigma (I). The absolute configuration was determined. Ca is coordinated to seven oxygen atoms and the coordination polyhedron is best described as pentagonal bipyramid. One carboxylate group of the glutarate ion is bonded to three different Ca ions, forming a four-membered chelate ring with one Ca ion and unidentate bridge bonds to two other Ca ions. The other axis, with the hydrocarbon chains sandwich between the polar regions consisting of the Ca and carboxylate ions and water molecules.

01,075
PB96-112057 Not available NTIS
National Inst. of Standards and Technology (CSTL), Boulder, CO. Thermophysics Div.
Shear-Induced Melting of Two-Dimensional Solids.
Final rept.
T. Weider, M. A. Glaser, H. J. M. Hanley, and N. A. Clark. 1993, 7p.
Pub. in Physical Review B, v47 n10 p5622-5628, 1 Mar 93.

Keywords: *Melting, *Solids, Reprints, Two dimensions, Shear, Molecular dynamics, Voroni construction.

We have carried out detailed nonequilibrium molecular-dynamics simulation studies of the shear-induced melting transition of a model two-dimensional solid. We find that the shear melting of the two-dimensional soft-disk solid at temperture T=1 and density p=1.03 occurs in two stages: (1) a transition from elastic to plastic behavior takes place as soon as any finite shear rate is applied; (2) qualitativechanges in structural and dynamic behavior occur near a shear rate of gamma = 0.07. For y equal to or less than 0.07, the system possesses very long-range bond-orientational correlations, and the instantaneous static structure factor exhibits pronounced sixfold anisotropy, with a sixfold pattern that rotates uniformly with time in response to the applied shear. For y equal to or greater than 0.07, the system behaves like an ordinary two-dimensional liquid under shear in that the ranges of translational and bond-orientational correlations are comparable and the instances static structure factor does not exhibit persistent sixfold anisotropy. We discuss our results in terms of the two competingpossibilities of a Kosterlitz-Thouless- Halperin-Nelson-Young two-stage melting scenario or a single first-order melting transition.

01,076
PB96-112172 Not available NTIS
National Inst. of Standards and Technology (PL), Boulder, CO. Quantum Physics Div.
Laser Gas Ionization Technique Monitors MEB Crystal Growth.
Final rept.
S. R. Leone, A. L. Alstrin, P. G. Strupp, and R. V. Smilgys. 1993, 4p.
Pub. in Laser Focus World, 4p Jul 93.

Keywords: *Molecular beam epitaxy, *Crystal growth, Reprints, Laser radiation, Real time operations, Ionization.

Single-photon ionization technique simultaneously detects complete gaseous species to provide real-time feedback and control during molecular-beam-epitaxial crystal growth.

01,077
PB96-112255 Not available NTIS
National Inst. of Standards and Technology (MSEL), Gaithersburg, MD. Reactor Radiation Div.
Structure of a Triglyceride Microemulsion: A Small Angle Neutron Scattering Study.
Final rept.
S. F. Trevino, R. Joubran, N. Parris, and N. F. Berk. 1994, 6p.
Pub. in Langmuir, v10 n8 p2547-2552 Aug 94.

Keywords: *Microemulsions, *Triglycerides, Reprints, Concentration(Composition), Temperature, Soybean oil, *Neutron scattering.

The microscopic structure of a microemulsion of soybean oil, water-ethanol (80/20 wt %), and polyoxyethylene(40) sorbitol hexaoleats has been studied with small angle neutron scattering. The concentrations of the three components are varied such that the oil-surfactant ratio is constant and stable microemulsions are obtained in regions of the phase diagram corresponding to bicontinuous and L2 phases. Small angle neutron scattering is measured as a function of concentration and temperature in order to describe the structure of the microemulsions. The results are consistent with a biocontinuous phase in the cases of largest aqueous content. In the low aqueous concentration samples, a substantial correlation is found in the spatial distribution of this minority phase.

01,078
PB96-119375 Not available NTIS
National Inst. of Standards and Technology (CSTL), Gaithersburg, MD. Thermophysics Div.
Measurements of the Relative Permittivity of Liquid Water at Frequencies in the Range of 0.1 to 10 kHz and at Temperatures between 273.1 and 373.2 K at Ambient Pressure.
Final rept.
D. P. Fernandez, A. R. H. Goodwin, and J. M. H. Levelt Sengers. 1995, 25p.
Pub. in International Jnl. of Thermophysics, v16 n4 p929-955 1995.

Keywords: *Water, *Dielectric properties, Electrical resistivity, Audio frequencies, Acoustic measurement, Capacitors, Electrodes, Polarization, Correction, Reprints.

The static relative permittivity (dielectric constant) of water has been determined from capacitance measurements at frequencies between 0.1 and 10 kHz, in the temperature range from 273.2 to 373.2 K at ambient pressure. The capacitor used for these measurements was formed from sapphire-insulated concentric cylinders. The specific conductance of the water used was maintained within 20% of the lowest value ever observed, which is better than in all previous experiments in this range. The new data shed some light on a discrepancy between sets of literature data in liquid water between the triple and boiling points.

01,079
PB96-119425 Not available NTIS
National Inst. of Standards and Technology (MSEL), Gaithersburg, MD. Ceramics Div.
Electroacoustic Characterization of Particle Size and Zeta Potential in Moderately Concentrated Suspensions.
Final rept.
V. A. Hackley, and S. G. Malghan. 1995, 8p.
Pub. in Ceramics Transactions, v56 p283-290 1995.

Keywords: *Ceramics, *Powders(Particles), *Electroacoustic waves, Electrophoresis, Particle size, Size determination, Measuring instruments, Silicon dioxide, Suspensions, Zeta potential, Performance evaluation, Reprints.

A novel electroacoustic technique for the measurement of particle size and charge in opaque suspensions is reviewed, and a new commercial instrument based on this method is evaluated for applications to ceramic powder processing.

01,080
PB96-119730 Not available NTIS
National Inst. of Standards and Technology (EEEL), Gaithersburg, MD. Electricity Div.
Appearance Potentials of Ions Produced by Electron-Impact Induced Dissociative Ionization of SF6, SF4, SF5Cl, S2F10, SO2, SO2F2, SOF2, and SOF4.
Final rept.
K. L. Stricklett, J. M. Kassoff, J. K. Olthoff, and R. J. Van Brunt. 1995, 8p.
Pub. in International Symposium on Gaseous Dielectrics (7th), Knoxville, TN., April 24-28, 1994, p257-264.

Keywords: *Appearance potential, Reprints, Sulfur fluorides, *Dissociative ionization, Sulfur oxyfluorides.

Appearance potential for ion produced by electron-impact induced dissociative ionization are measured. Appearance potentials are reported for SF5, SF4, SF5Cl, S2F10, SO2, SO2F2, SOF2, SOF4.

01,081
PB96-122098 (Order as PB96-117767, PC A08/MF A02)
National Inst. of Standards and Technology, Gaithersburg, MD.
Low Electrolytic Conductivity Standards.
Y. C. Wu, and P. A. Berezansky. 1995, 7p.
Included in Jnl. of Research of the National Institute of Standards and Technology, v100 n5 p521-527 Sep/Oct 95.

Keywords: *Conductivity, *Electrolytes, *Calibration standards, Reprints, Electric power plants, Water quality, Quality assurance, Benzoic acids, Dielectric properties, Potassium chloride, NIST(National Institute of Standards and Technology).

Standards of low electrolytic conductivity were developed to satisfy the demands of the U.S. Navy and American industry for the measurement of high quality water. The criteria for the selection of appropriate solvent and solutes, based on the principles of equivalent conductivity and Onsager's limiting law, are described. Dilute solutions of potassium chloride and benzoic acid in 30% n-propanol-water have been chosen as standards. The electrolytic conductivity of both sets of these solutions as a function of molality was determined.

01,082
PB96-122429 Not available NTIS
National Inst. of Standards and Technology (CSTL), Gaithersburg, MD. Thermophysics Div.
Hydrodynamic Similarity in an Oscillating-Body Viscometer.
Final rept.
R. F. Berg. 1995, 10p.
Pub. in International Jnl. of Thermophysics, v16 n5 p1257-1266 Sep 95.

Keywords: *Viscometers, *Hydrodynamics, Calibration, Reprints, Oscillating bodies.

Hydrodynamic similarity can be used to calibrate simply and accurately an oscillating-body viscometer of arbitrarily complicated geometry. Usually, an explicit hydrodynamic model based on a simple geometry is required to deduce viscosity from the transfer function of an oscillating body such as a vibrating wire or a quartz torsion crystal. However, at low Reynolds numbers the transfer function of any immersed oscillator depends on the fluid's viscosity only through the viscous penetration depth. This hydrodynamic similarity can be exploited if the oscillator is over damped and thus is sensitive to viscosity in a broad frequency range. Even an osillator of poorly known geometry can be characterized over a range of penetration depths by measurements in a fluid of known n and p over the corresponding range of frequencies.

01,083
PB96-122551 Not available NTIS
National Inst. of Standards and Technology (CSTL), Gaithersburg, MD. Thermophysics Div.
Physical Limit to the Stability of Superheated and Stretched Water.
Final rept.
S. B. Kiselev, J. M. H. Levelt Sengers, and Q. Zheng. 1995, 8p.
Pub. in Proceedings of the International Conference on the Properties of Water and Steam (12th), Orlando, FL., September 9-16, 1994, p378-385.

Keywords: *Steam, *Spinodal, Molecular structure, Stability, Reprints, *Water structure, Equations of state.

Several highly accurate formulations of the thermodynamic properties of water and stream are investigated in the regions of supercooled, superheated and stretched liquid water. It is shown that they give considerably different locations for the spinodal, which diminishes the physical relevance of this curve. It is argued that nucleation theories based on local equilibrium fail long before the spinodal is reached. We calculate the physical limit of metastability for superheated and stretched water based on the theory of relaxation of metastable states of Patashinskii and Shumilo. For this application a crossover formalism is used to enable calculation of the critical radius of the nucleus for both positive and negative pressures. The calculated physical limit of metastability agrees with the extrema of superheat, realized in homogeneous states by Skripov et al., and of negative pressure, realized in homogeneous states by Zheng et al.

01,084
PB96-122619 Not available NTIS
National Inst. of Standards and Technology (EEEL), Gaithersburg, MD. Electricity Div.
Decomposition of SF6 and Production of S2F10 in Power Arcs.
Final rept.
H. D. Morrison, F. Y. Chu, M. Eygenraam, I. Sauers, and R. J. Van Brunt. 1995, 7p.
Pub. in International Symposium on Gaseous Dielectrics (7th), Knoxville, TN., April 24-28, 1994, p475-481 1995.

Keywords: *Sulfur hexafluoride, *Decomposition, *Arc discharges, *Electric arcs, Toxic substances, Dielectrics, Electrical insulation, Kinetics, Gas chromatography, Infrared spectroscopy, Gases, Reprints, SF6, S2F10.

Decomposition of SF6 in electrical discharges produces many toxic solids and gases. S2F10 is the most toxic of the gaseous byproducts and has been found in arcs, sparks and corona. We have conducted a series of tests of a power arc discharge contained completely within a bus duct configuration. Among the many other gaseous byproducts, we have detected S2F10 at or below the part per million (ppm) by volume level, providing that S2F10 can be formed directly by a power arc within SF6-insulated equipment. The relative production rate of S2F10 with respect to that of SOF2 and SF4, however, implies that S2F10 is not a significant contributor to the hazard of exposure to decomposed SF6.

01,085
PB96-122627 Not available NTIS
National Inst. of Standards and Technology (CSTL), Gaithersburg, MD. Thermophysics Div.
Simulation Studies of Supercooled and Glass Forming Liquids.
Final rept.
R. D. Mountain. 1995, 15p.
Pub. in Proceedings of the Winter Meeting on Statistical Physics (23rd), Cuernava, Mexico, January 9-12, 1994, p1-15 1995.

Keywords: *Computerized simulation, *Supercooling, *Glass, *Liquids, Molecular structure, Ergodic process, Convergence, Models, Time, Length, Relaxation time, Reprints, *Supercooled liquids, Molecular dynamics.

A brief review of the results of a number of molecular dynamics simulations of glass forming model systems is presented. A method for determining the ergodic convergence time is described. The results indicate that relaxation of dynamical correlations occurs over many time scales. The characterization of relevant length scales is not well understood. Some suggestions for further studies are presented.

01,086
PB96-122734 Not available NTIS
National Inst. of Standards and Technology (EEEL), Gaithersburg, MD. Electricity Div.
Modification of Cast Epoxy Resin Surfaces during Exposure to Partial Discharges.
Final rept.
H. Slowikowska, T. Las, J. Slowikowski, and R. J. Van Brunt. 1995, 8p.
Pub. in International Symposium on Gaseous Dielectrics (7th), Knoxville, TN., April 24-28, 1994, p635-642 1995.

Keywords: *Dielectrics, *Electrical insulation, *Gas discharges, *Epoxy resins, Electrical resistivity, Surface roughness, Morphology, Sulfur hexafluoride, Nitrogen, Oxygen, Gas mixtures, Reprints, PD(Partial discharges).

Cast epoxy resin materials are commonly used in insulating spacers of gas-insulated high-voltage power systems. It has been showed, that the discharge-induced decrease in surface resisitivity is responsible for dramatic changes in the stochastic behavior of the electrical discharge. In the present work, the nature of partial-discharge (PD) induced damage to cast epoxy resin surfaces has been investigated in more detail using various techniques to examine surface roughness and morphology, as well as resistivity. The effect of generating PD in gases other than air, such as SF6, N2, and N2/O2 mixtures, was also examined.

01,087
PB96-122809 Not available NTIS
National Inst. of Standards and Technology (EEEL), Gaithersburg, MD. Electricity Div.
Electron Attachment to Excited Molecules(1).
Final rept.
L. G. Christophorou. 1995, 1p.
See also DE94019124.
Pub. in International Symposium on Electron- and Photon-Molecule Collisions and Swarms, Berkley, CA., July 22-25, 1995, pE-1.

Keywords: *Electron attachment, *Molecular excitation, Molecular energy levels, Internal energy, Vibration, Rotation, Photodissociation, Cross sections, Lasers, Irradiation, Reprints, *Slow electrons.

The interactions of slow electrons with molecules-especially the processes of electron attachment-depend rather strongly on the internal energy content of the molecules themselves. As a rule, excited molecules interact with slow electrons with substantially larger cross section than do ground-state molecules. 1-5 Studies of electron attachment to vabrationally/rotationally excited, 'hot', molecules 1,3,5-18 and especially to electronically excited molecules 1,3,4,19-24 are rather recent, in contrast to the extensive studies on electron attachment to ground-state molecules which cover many decades 6,25,26.

01,088
PB96-123252 Not available NTIS
National Inst. of Standards and Technology (CSTL), Gaithersburg, MD. Thermophysics Div.
Significant Contributions of IAPWS to the Power Industry, Science and Technology.
Final rept.
J. M. H. Levelt Sengers. 1995, 12p.
Pub. in Proceedings of the International Conference on the Properties of Water and Steam (12th), Orlando, FL., September 9-16, 1994, p1-12 1995.

Keywords: *Aqueous solutions, History, Steam tables, Water, Reprints, IAPWS(International Association for the Properties of Water and Steam), Supercritical states, Thermodynamic properties, Transport properties.

The lines are traced from the early international cooperational necessary for efficient design of, and global trade in turbines, boilers and heat exchangers for power generation, to the past and current forms this cooperation assumes in the International Association for the Properties of Water and Steam (IAPWS). The mutually enriching interaction of IAPSW and the scientific world will be illustrated by several examples, taken from the fields of critical phenomena, molecular simulation, and supercritical fluids. The acceptance of IAPWS formulations of steam and water properties of de facto world standards for many other applications besides power generation is a consequence of IAPW's firm commitment to excellence. IAPWS's branching out to impure water and steam, necessitated by the threat impurities pose to the components of power plants, has led to fruitful interactions with aqueous physical chemistry and geochemistry, and may help reach a new synthesis in the science and engineering of reactive supercritical fluid mixtures.

01,089
PB96-123450 Not available NTIS
National Inst. of Standards and Technology (EEEL), Gaithersburg, MD. Electricity Div.
Fundamental Processes in Gas Discharges.
Final rept.
L. G. Christophorou, R. J. Van Brunt, and J. K. Olthoff. 1995, 13p.
Pub. in Proceedings of the International Conference on Gas Discharges and Their Applications (11th), v1 pl-536-I-548.

Keywords: *Gas discharges, *Discharges, Dissociation, Electron, Excited atoms, Ionization, Negative ions, Reprints, *Foreign technology.

Recent aspects of fundamental processes in gas discharges are discussed. These include the effect of internal energy of excitation of atoms and molecules on their interactions with slow electrons, the effect of tempearture on electron attachment and detachment processes, photodissociation of molecules and photodetachment of anoins, and interactions involved in discharge byproduct formation and discharge diagnostics. Referecne is also made to fundamental processes in gas discharge materials used in plasma processing.

01,090
PB96-123559 Not available NTIS
National Inst. of Standards and Technology (CSTL), Gaithersburg, MD. Thermophysics Div.
Static Dielectric Constant of Water and Steam.
Final rept.
D. P. Fernandez, A. R. H. Goodwin, R. C. Williams, S. G. Penoncello, Y. Mulev, and J. M. H. Levelt Sengers. 1995, 8p.
Pub. in Proceedings of the International Conference on the Properties of Water and Steam (12th), Orlando, FL., September 9-16, 1994, p109-116 1995.

Keywords: *Dielectric properties, *Steam, *Water, Experimental data, Data correlation, Data bases, Reprints, Relative permittivity.

All relevant static dielectric constant data for water and steam have been collected and evaluated, and will be made available in print and in computerized form. A new formulation of the static dielectric constant or relative permittivity of water and stream has been developed. It is based on the ITS-90 temperature scale, and uses a new fundamental equation for water and steam, likewise based on this scale. It also includes our recently obtained dielectric constant data in liquid water and in saturated steam. The new formulation ranges from -45 to + 600 degrees C in temperature, and from 0.1 to 1189 MPa in pressure. It is based on the dipole correlation or g-factor of Alder and Harris, and formulates this factor with 10 adjustable coefficients and associated powers of reduced density and inverse reduced temperature.

01,091
PB96-123724 Not available NTIS
National Inst. of Standards and Technology (MSEL), Gaithersburg, MD. Reactor Radiation Div.

Characterization of the Vibrational Dynamics in the Octahedral Sublattices of LaD2.25 and LaH2.25.
Final rept.
T. J. Udovic, J. J. Rush, and I. S. Anderson. 1995, 10p.
Pub. in Jnl. of Physics: Condensed Matter, v7 p7005-7014 1995.

Keywords: *Vibrational spectroscopy, *Denterides, Dynamics, Hybride, Reprints, Lanthanum, Neutron scattering, Octahedral site, *Tetrahedral site vibrations.

Incoherent inelastic neutron scattering spectroscopy was used to characterize the optic-vibrational density of states (DOS) of the octahedrally coordinated deuterium (Do) and hydrogen (Ho) atoms in LaD2.25, LaH2.25, and LaH2.03. The DOS exhibits a temperature- and concentration-dependent behavior consistent with that oserved previously for the analogous beta-TbH2+x system. At low temperature, the Ho DOS for LaH2.03 is fairly sharp with minor spectral sidebands, indicating that the Ho atoms are predominantly isolated, with some atoms residing in short-range-order domains. Increasing the Ho (or Do) concentration to LaH2.25 (or LaD2.25) yields a dispersion-broadened bimodal DOS characteristic of the Ho (or Do) I4/mmm long-range order that develops in the octahedral sublattice at low temperatures and these higher Ho (or Do) concentrations. For LaH2.25 at higher temperature (340 K), a broad, somewhat asymmetric DOS is suggestive of an Ho sublattice that is now largely disordered yet still possesses some degree of short-range order.

01,092
PB96-123732 Not available NTIS
National Inst. of Standards and Technology (EEEL), Gaithersburg, MD. Electricity Div.
Kinetic-Energy Distributions of Ions Sampled from Radio-Frequency Discharges in Helium, Nitrogen, and Oxygen.
Final rept.
R. J. Van Brunt, J. K. Olthoff, and S. B. Randovanov. 1995, 4p.
Pub. in Proceedings of the International Conference on Gas Discharges and Their Applications (11th), Tokyo, Japan, September 11-15, 1995, v1 pI-486-I-489.

Keywords: *Gas discharges, *Helium, Nitrogen, Oxygen, Reprints, *Foreign technology, Ion kinetic energies, Radio-frequency plasma.

Mass-resolved ion kinetic energy distributions are measured for radio-frequency (rf) discharges sustained in helium, nitrogen, and oxygen in a parallel-plate plasma reactor. The dominate ions for each of the gases are observed to be the parent ions He+, N2+, and O2+, respectively over a wide range of pressures (1.3 to 67 Pa) with an applied rf voltage of 200 V. Ion kinetic-energy distributions at the grounded electrode were measured for these ions, as well as for less abundant ions, such as He2+, N+, N2H+, N3+, N4+, O+, and 3+.

01,093
PB96-123740 Not available NTIS
National Inst. of Standards and Technology (EEEL), Gaithersburg, MD. Electricity Div.
Measurement of S2OF10, and S2O2F10 Production Rates from Spark and Negative Glow Corona Discharge in SF6/O2 Gas Mixtures.
Final rept.
R. J. Van Brunt, J. K. Olthoff, S. L. Firebaugh, and I. Sauers. 1995, 4p.
Sponsored by Electric Power Research Inst., Palo Alto, CA. and Department of Energy, Washington, DC.
Pub. in Proceedings of the International Conference on Gas Discharges and Their Applications (11th), Tokyo, Japan, September 11-15, 1995, v1 pI-316-I-319.

Keywords: *Corona discharge, *Oxygen, Production rates, Spark discharge, Sulfur hexafluoride, Reprints, *Foreign technology, Disulfur decafluoride.

The rates for production of the compounds S2F10, and S2OF10, and S2O2F10 have been measured both in spark and continuous, constant-current (40 micro A) negative glow corona discharges generated using point-to-plane electrode gaps in 'pure' SF6 and SF6/O2 gas mixtures containing different relative amounts of oxygen, up to 10 percent. The measurements were performed for the total gas pressures in the range of 100 to 200 kPa, and the SF6 discharge byproduct concentrations were mesured using a gas chromatograph-mass spectrometric technique and a cryogenic enrichment chromatographic technique, respectively, for the corona and spark experiments. When O2 is added to the gas, there is a dramatic drop in the S2F10 yield from the corna discharge. The results can be explained within the framework of a plasma-chemical model from considerations of the competition among reactions of SF, radicals produced by dissociation of SF6 in the discharge with SF5 itself as well as with O2 and O, and the relative degree of O2 dissociation in the two types of discharges.

01,094
PB96-123765 Not available NTIS
National Inst. of Standards and Technology (MSEL), Gaithersburg, MD. Polymers Div.
Zimm Plot and Its Analogs as Indicators of Vesicle and Micelle Size Polydispersity.
Final rept.
J. H. van Zanten. 1995, 8p.
Pub. in Jnl. of Chemical Physics, v102 n22 p9121-9128 Jun 95.

Keywords: *Light scattering, *Liposomes, *Vesicles, Size distributions, Reprints.

The utility of using the Zimm plot and its analogs, the Debye and Berry plots, as a sensitive means of determining the degree of polydispersity present in solutions of surfactant aggregates such as vesicles or micelles is conclusively demonstrated. These methods of interpreting the excess scattered light intensity due to the surfactant aggregates lead to the determination of the weight-average molecular weight (Mw) and z-average mean square radius ((r2 sub g) z), or radius of gyration, of the surfactant aggregates. These two parameters are very sensitive to any polydispersity which is present in the aggregate solution, since these two experimentally determined quantities represent different moments of the aggregate size distribution. For a given geometric model, apparent surfactant aggregate structural parameters, such as the radius and wall thickness in the case of surfactant vesicles, can be calculated under the assumption of monodisperse aggregates from (r2 sub g)z and Mw determined from a Zimm or Debye analysis of static light scattering spectra.

01,095
PB96-135314 Not available NTIS
National Inst. of Standards and Technology (EEEL), Gaithersburg, MD. Electricity Div.
Decomposition of Sulfur Hexafluoride by X-rays.
Final rept.
J. K. Olthoff, and R. J. Van Brunt. 1995, 6p.
Pub. in International Symposium on Gaseous Dielectrics (7th), Knoxville, TN., April 24-28, 1994, p417-422.

Keywords: *Sulfur hexafluoride, *Physical radiation effects, *Decomposition reactions, *X-rays, Radiation doses, Chemical reaction kinetics, Electric discharges, Corona discharges, Byproducts, Electrical insulation, Gas pressure, Reprints.

In the paper, the authors present results of by-product formation in gaseous SF6 exposed to high-energy X-rays. The identity and concentration of the decomposition by-products are determined by gas chromotography/mass spectrometry techniques that were developed to investigate the decomposition of SF6 exposed to corona discharges. The production curves of SOF2 and S2F10 are determined for a range of SF6 gas pressures, X-ray energies, and X-ray fluxes. Evidence for the presence of other by-products, such as SOF4, SO2F2, and S2O2F10 is also presented. The decomposition data for the SF6 exposed to X-rays are compared with previously published data for SF6 exposed to corona discharges.

01,096
PB96-138516 Not available NTIS
National Inst. of Standards and Technology (MSEL), Gaithersburg, MD. Reactor Radiation Div.
q Dependence of Self-Energy Effects of the Plane Oxygen Vibration in YBa2Cu3O7.
Final rept.
D. Reznik, B. Keimer, F. Dogan, and I. A. Aksay. 1995, 4p.
Pub. in Physical Review Letters, v75 n12 p2396-2399 Sep 95.

Keywords: *Vibrations, Reprints, *YBCO, *Plane oxygen vibration, Brillouin, q-dependence, Temperature dependence.

The authors have measured the temperature dependence of the peak position and linewidth of the 42.5 meV phonon branch in a twinned single crystal of BYa2Cu2O- as a function of wave vector q. In the (100)/(010) direction in the Brillouin zone, considerable softening and broadening occur below the superconducting transition temperature Tc at some values of q. The authors observe an order of magnitude smaller softening and no linewidth broadening for q in the (110)/(110) direction. Possible implications of these findings for the symmetry of the superconducting order parameter are discussed.

01,097
PB96-138565 Not available NTIS
National Inst. of Standards and Technology (CSTL), Gaithersburg, MD. Surface and Microanalysis Science Div.
Silicon Surface Chemistry by IR Spectroscopy in the Mid- to Far-IR Region: H2O and Ethanol on Si(100).
Final rept.
L. M. Struck, B. E. Bent, Y. J. Chabal, S. Christman, E. E. Chaban, K. Raghavachari, G. W. Flynn, K. Radermacher, S. Mantl, G. P. Williams, and A. E. White. 1995, 6p.
Pub. in Material Research Society Symposium Proceedings, v386 p395-400 1995.

Keywords: *Infrared spectroscopy, *Silicon, *Surface chemistry, Water, Ethanol, Reprints.

The technique of external reflection infrared (IR) spectroscopy is used to study silicon surface chemistry. External reflection is enhanced by implanting a buried cobalt silicide layer in silicon to act as an infrared reflector. The preparation of clean well-ordered surfaces from the ion implanted substrates is demonstrated. The reactions of water and ethanol with Si(100) are investigated.

01,098
PB96-140397 Not available NTIS
National Inst. of Standards and Technology (EEEL), Boulder, CO. Optoelectronics Div.
Dielectric Spectroscopic Determination of Temperature Behavior of Electroclinic Parameters in the Liquid Crystal W317.
Final rept.
P. A. Williams, and N. A. Clark. 1995, 5p.
Pub. in Jnl. of Applied Physics, v78 n1 p413-417 Jul 95.

Keywords: *Liquid crystals, Electric fields, Spectroscopy, Free energy, Reprints, *Electroclinic effect, W317 liquid crystal.

We report measurements of the temperature behavior of the electroclinic coupling coefficient c(T) and the inverse tilt suscepitbility A(T), the principal phenomenological parameters determining the magnitude of the electroclinic effect in the chiral smectic A phase of the liquid crystal W317, a material which exhibits an anomalously large electroclinic effect with unusual thermal behavior. We find that c(T) decreases by approximately 30 percent in response to a 40 degrees C increase in temperature. A(T) exhibits a mean field behavior at high temperature, increasing by a factor of 3 as temperature is increased over the range 40 degrees C less than T less than 65 degrees C. However, below approximately 40 degrees C, A(T) becomes nearly independent of temperature over a approximately 10 degrees C range around temperature. This A(T) behavior has not been previously found in electroclinic materials.

01,099
PB96-141064 Not available NTIS
National Inst. of Standards and Technology (MSEL), Gaithersburg, MD. Polymers Div.
Crystal Structure of Decacalcium Tetrapotassium Hexakis (Pyrophosphate) Nonahydrate.
Final rept.
M. Mathew, and H. L. Ammon. 1995, 4p.
Pub. in Jnl. of Chemical Crystallography, v25 n5 p219-222 1995.

Keywords: *Crystal structure, *Calcium phosphates, *Pyrophosphates, Potassium phosphates, Layers, Reprints.

The crystal structure of Ca10K4(P2O7)6.9H2O has been determined by single crystal X-ray diffraction. Crystal are hexagonal, space group P6(sub 3)cm with a = 11.76(1), c = 9.7701(1) Angstroms, and Z = 1. The structure was refined to R = 0.028 and Rw = 0.037 for 468 reflections with I greater than or equal to 3 sigma(I). The structure consists of a compact assembly of Ca and P2O7 ions arranged in layers per-

pendicular to the c-axis in a hexagonal array large open channels along the c-axis. The K ions and the water molecules are located in these open channels and are disordered.

01,100
PB96-141080 Not available NTIS
National Inst. of Standards and Technology (EEEL), Boulder, CO. Electromagnetic Technology Div.
X-ray Observation of Electroclinic Layer Constriction and Rearrangement in a Chiral Smectic-A Liquid Crystal.
Final rept.
A. G. Rappaport, P. A. Williams, B. N. Thomas, D. M. Walba, N. A. Clark, and M. Blanca Ros. 1995, 3p.
Pub. in Applied Physics Letters, v67 n3 p362-364 Jul 95.

Keywords: *Liquid crystals, X ray, Reprints, *Electroclinic effect, *Layer constriction, Smectic.

An x-ray scattering study of electroclinic layer constriction verifies the interpretation of the electroclinic effect as field-induced molecular tilt. The tilt angles deduced from the layer spacing changes are in close agreement with those from optical measurements. Layer buckling, a consequence of the layer constriction, is also observed and may be the cause of the loss of optical contrast observed in electroclinic devices.

01,101
PB96-145560 Not available NTIS
American Chemical Society, Washington, DC.
Journal of Physical and Chemical Reference Data, Volume 24, No. 1, January/February 1995.
Bimonthly rept.
J. W. Gallagher. c1995, 669p.
See also PB96-145578 through PB96-145594, PB94-168556 and PB96-145818. Prepared in cooperation with American Inst. of Physics, New York. Sponsored by National Inst. of Standards and Technology, Gaithersburg, MD.
Available from American Chemical Society, 1155 Sixteenth St., NW, Washington, DC. 20036-9976.

Keywords: *Physical properties, *Chemical properties, Physical chemistry, Atomic properties, Chemical reactions, Thermodynamics, Reaction kinetics, Vapor phases, Tables(Data), Reprints, *Reference materials.

Contents:
- The Millimeter- and Submillimeter-Wave Spectrum of trans-Ethyl Alcohol;
- A Database for the Static Dielectric Constant of Water and Steam;
- Theoretical Form Factor, Attenuation and Scattering Tabulation of Z = 1-92 from E = 1-10 eV to E = 0.4-1.0 MeV.

01,102
PB96-145578 Not available NTIS
Ohio State Univ., Columbus. Dept. of Physics.
Millimeter- and Submillimeter-Wave Spectrum of trans-Ethyl Alcohol.
J. C. Pearson, K. V. L. N. Sastry, M. Winnewisser, E. Herbst, and F. C. De Lucia. c1995, 32p.
Prepared in cooperation with New Brunswick Univ., Fredericton. Dept. of Physics. and Giessen Univ. (Germany, F.R.). Physikalisch-Chemisches Inst.
Included in Jnl. of Physical and Chemical Reference Data, v24 n1 p1-32 Jan/Feb 95. Availabale from American Chemical Society, 1155 Sixteenth St., NW, Washington, DC. 20036-9976.

Keywords: *Ethanol, *Wave spectrums, Intensities, Microwave spectra, Molecular constants, Radio astronomy, Reprints, Interstellar molecules, Rotational spectrum, Internal rotation.

The rotational-torsional spectrum of the trans rotational isomer of ethyl alcohol was investigated in the 65-350 GHz frequency region. A total of 481 ground state transitions over a range of J and Ka values up to 33 and 10, respectively, were measured and assigned. Doublets or triplets arising from the A and E torsional states of the v=0 torsional level of the three-fold-symmetric methyl internal rotation have been resolved in 168 of these transitions. Internal rotation theory predicts a significant number of c-type E-state transitions normally forbidden, but allowed when the rotational symmetry operators mix E-state rotational-torsional levels. Over 40 of these transitions have been observed. The newly measured transitions, along with the results of many previous measurements, have been analyzed using an IAM internal rotation Hamiltonia and a Watson A-reduced Hamiltonias to determine the rotational, centrifugal distortion, and torsional constants. (Copyright (c) 1995 American Institute of Physics and American Chemical Society.)

01,103
PB96-145586 Not available NTIS
National Inst. of Standards and Technology (CSTL), Gaithersburg, MD. Thermophysics Div.
Database for the Static Dielectric Constant of Water and Steam.
D. P. Fernandez, Y. Mulev, A. R. H. Goodwin, and J. M. H. Levelt Sengers. c1995, 36p.
Included in Jnl. of Physical and Chemical Reference Data, v24 n1 p33-69 Jan/Feb 95. Available from American Chemical Society, 1155 Sixteenth St., NW, Washington, DC. 20036-9976.

Keywords: *Databases, *Steam, *Water, Data, Compilation, Reprints, *Capacitance bridges, *Static dielectric constants, Electrode polarization, ITS-90, Resonant circuits.

All reliable sources of data for the static dielectric constant or relative permittivity of water and steam, many of them unpublished or inaccessible, have been collected, evaluated, corrected when required, and converted to the ITS-90 temperature scale. The data extend over a temperature range from 238 to 873 K and over a pressure range from 0.1 MPa up to 1189 MPa. The evaluative part of this work includes a review of the different types of measurement techniques, and the corrections for frequency dependence due to the impedance of circuit components, and to electrode polarization. It also includes a detailed assessment of the uncertainty of each particular data source, as compared to other sources in the same range of pressure and temperature. Both the raw and the corrected data have been tabulated, and are also available on diskette. A comprehensive list of references to the literature is included. (Copyright (c) 1995 American Institute of Physics and American Chemical Society.)

01,104
PB96-145594 Not available NTIS
Melbourne Univ., Parkville (Australia). School of Physics.
Theoretical Form Factor, Attenuation and Scattering Tabulation for Z=1-92 from E=1-10 eV to E=0.4-1.0 MeV.
C. T. Chantler. c1995, 572p.
Included in Jnl. of Physical and Chemical Reference Data, v24 n1 p71-643 Jan/Feb 95. Available from American Chemical Society, 1155 Sixteenth St., NW., Washington, DC. 20036-9976.

Keywords: *Anomalous dispersions, *Attenuation, Form factors, Reprints, Photoabsorption tabulation, Scattering cross-sections.

In the present study, the primary interactions of x-rays with isolated atoms from Z = 1 (hydrogen) to Z = 92 (uranium) are described and computed within a self-consistent Dirac-Hartree-Fock framework. This has general application across the range of energy from 1-10 eV to 400-1000 keV, with limitations (described below) as the low- and high-energy extremes are approached. Tabulations are provided for the f1 and f2 components of the form factors, together with the photoelectric attenuation coefficient for the atom, micro, and the value for the K-shell, microk, as functions of energy and wavelength. Also provided are estimated correction factors as described in the text, conversion factors, and a simple estimate for the sum of the scattering contributions (from an isolated atom). The method used herein is primarily theoretical and considers intermediate assumptions which limit the precision and applicability of previous theoretical tabulations. Particular concern involves the application of the dispersion relation to derive Re(f) from photoelectric absorption cross-sections.

01,105
PB96-145818 Not available NTIS
American Chemical Society, Washington, DC.
Journal of Physical and Chemical Reference Data, Volume 24, No. 2, March/April 1995.
Bimonthly rept.
J. W. Gallagher. c1995, 394p.
See also PB96-145826, PB96-145834, Volume 24, No. 1, PB96-145560, and Volume 24, No. 3, PB96-145842. Prepared in cooperation with American Inst. of Physics, New York. Sponsored by National Inst. of Standards and Technology, Gaithersburg, MD.
Available from American Chemical Society, 1155 Sixteenth St., NW, Washington, DC. 20036-9976.

Keywords: *Physical properties, *Chemical properties, Physical chemistry, Atomic properties, Chemical reactions, Thermodynamics, Reaction kinetics, Vapor phases, Tables(Data), Reprints, *Reference materials.

Contents:
- Rate Constants for the Decay and Reactions of the Lowest Electronically Excited Singlet State of Molecular Oxygen in Solution. An Expanded and Revised Compilation;
- Thermodynamic Properties of the Aqueous Ba2+ Ion and the Key Compounds of Barium.

01,106
PB96-145826 Not available NTIS
Loughborough Univ. of Technology (England). Dept. of Chemistry.
Rate Constants for the Decay and Reactions of the Lowest Electronically Excited Singlet State of Molecular Oxygen in Solution. An Expanded and Revised Compilation.
F. Wilkinson, W. P. Helman, and A. B. Ross. c1995, 358p.
Prepared in cooperation with Notre Dame Univ., IN. Radiation Chemistry Data Center.
Included in Jnl. of Physical and Chemical Reference Data, v24, n2 p663-1021 Mar/Apr 95. Available from American Chemical Society, 1155 Sixteenth St., NW, Washington, DC. 20036-9976.

Keywords: *Chemical kinetics, *Rate constants, Data compilation, Decay, Oxidation, Photochemistry, Photosensitization, Quenching, Reprints.

An expanded and revised compilation on the reactivity of singlet oxygen, the lowest electronically excited singlet state of molecular oxygen, 1O(star)2(1deltag), in fluid solution is presented, which supersedes the publication of Wilkinson and Brummer, J. Phys. Chem. Ref. Data 10, 809 (1981). Rate constants for the chemical reaction and physical deactivation of singlet oxygen available through 1993 have been critically compiled. Solvent deactivation rates (kd) are tabulated for 145 solvents or solvent mixtures and second-order rate constants for interaction of singlet oxygen with 1915 compounds are reports. (Copyright (c) 1995 American Institute of Physics and American Chemical Society.)

01,107
PB96-145834 Not available NTIS
National Inst. of Standards and Technology (CSTL), Gaithersburg, MD. Chemical Kinetics and Thermodynamics Div.
Thermodynamic Properties of the Aqueous Ba(sup 2+) Ion and the Key Compounds of Barium.
V. B. Parker. c1995, 31p.
Included in Jnl. of Physical and Chemical Reference Data, v24 n2 p1023-1054 Mar/Apr 95. Available from American Chemical Society, 1155 Sixteenth St., NW, Washington, DC. 20036-9976.

Keywords: *Barium ions, Data evaluation, Enthalpy, Entropy, Key compounds, Reprints, CODATA, Gibbs energy, Thermochemical measurements.

Recommended thermochemical property values, delta(f)H(deg), delta(f)G(deg) and S(deg) for the aqueous ion of barium, Ba2+, are given at 298.15 K in SI units. The values are: delta(f)H(deg) = -534.64 plus or minus 1.80 kJ.mol(-1), delta(f)G(deg) = -557.60 plus or minus 1.81 kJ.mol(-1) and S(deg) = 8.80 plus or minus 0.50 J-K(-1) mol(-1). They are consistent with the CODATA Key Values for Thermodynamics. The evaluation involves the analysis of the enthalpy changes, Gibbs energy changes, and the entropy measurements for all key substances in the key network. A consistent set of thermochemical property values is given for BaO(cr), BaH2(cr), BaCl2(cr), BaCl2.2H2O(cr), Ba(NO3)2(cr), and BaCO3(cr, witherite), as well as reconstituted recommended process values with uncertainties for reactions involving these substances. (Copyright (c) 1995 American Institute of Physics and American Chemical Society.)

01,108
PB96-145842 Not available NTIS
American Chemical Society, Washington, DC.
Journal of Physical and Chemical Reference Data, Volume 24, No. 3, May/June 1995.
Bimonthly rept.
J. W. Gallagher. c1995, 347p.
See also PB96-145859 through PB96-145875, Volume 24, No. 2, PB96-145818 and Volume 24, No. 4, PB96-145883. Prepared in cooperation with American Inst. of Physics, New York. Sponsored by National Inst. of Standards and Technology, Gaithersburg, MD.

Available from American Chemical Society, 1155 Sixteenth St., NW, Washington, DC. 20036-9976.

Keywords: *Physical properties, *Chemical properties, Physical chemistry, Atomic properties, Chemical reactions, Thermodynamics, Reaction kinetics, Vapor phases, Tables(Data), Reprints.

Contents:
- Critical Review of Rate Constants for Reactions of Transients from Metal Ions and Metal Complexes in Aqueous Solution;
- Ideal Gas Thermodynamic Properties of Sulphur Heterocyclic Compounds;
- Standard Reference Data for the Thermal Conductivity of Water.

01,109
PB96-145859 Not available NTIS
Cookridge Radiation Research Centre, Leeds (England).
Critical Review of Rate Constants for Reactions of Transients from Metal Ions and Metal Complexes in Aqueous Solution.
G. V. Buxton, Q. G. Mulazzani, and A. B. Ross. c1995, 294p.
Prepared in cooperation with Consiglio Nazionale delle Ricerche, Bologna (Italy). Ist. di Fotochimica e Radiazioni d'Alta Energia. and Notre Dame Univ., IN. Radiation Chemistry Data Center.
Included in Jnl. of Physical and Chemical Reference Data, v24 n3 p1055-1349 May/Jun 95. Available from American Chemical Society, 1155 Sixteenth St., NW, Washington, DC. 20036-9976.

Keywords: *Aqueous solutions, *Chemical kinetics, Critical review, Data compilation, Pulse radiolysis, Rate constants, Transients, Reprints, Flash photolysis, Metal ions.

Kinetic data for transient metal species in aqueous solution have been critically reviewed. The compilation covers over 2000 measurements of rate constants involving 660 metal ions and metal complexes from Groups 4-15; lanthanides and actinides are not included. Most of the data have been obtained by the methods of pulse radiolysis or flash photolysis. Data have been collected from 500 publications through 1993. (Copyright (c) 1995 American Institute of Physics and American Chemical Society.)

01,110
PB96-145867 Not available NTIS
Akademiya Nauk SSSR, Moscow. Inst. Vysokikh Temperatur.
Ideal Gas Thermodynamic Properties of Sulphur Heterocyclic Compounds.
O. V. Dorofeeva, and L. V. Gurvich. c1995, 25p.
Included in Jnl. of Physical and Chemical Reference Data, v24 n3 p1351-1376 May/Jun 95. Available from American Chemical Society, 1155 Sixteenth St., NW, Washington, DC. 20036-9976.

Keywords: *Thermodynamic properties, Molecular structure, Reprints, *Sulphur heterocyclic compounds, Vibrational frequencies.

The available structural parameters, fundamental frequencies and enthalpies of formation for thiirane, thiirene, thietane, 2H-thiete, 1,2-dithiete, tetrahydrothiophene, 2,3-dihydrothiophene, 2,5-dihydrothiophene, thiophene, 1,2-dithiolane, 1,3-dithiolane, 1,2,4-trithiolane, tetrahydro-2H-thiopyran, 5,6-dihydro-2H-thiopyran, 2,4-dithiane, 1,4-dithiane, 1,4-dithiin, 1,3,5-trithiane, thiepane and 1,3,5,7-tetrathiocane were critically evaluated and recommended values were selected. Molecular constants and enthalpies of formation for some of the molecules were estimated, as experimental values for these compounds are not available.

01,111
PB96-145875 Not available NTIS
Lisbon Univ. (Portugal). Dept. de Quimica.
Standard Reference Data for the Thermal Conductivity of Water.
M. L. V. Ramires, C. A. Nieto de Castro, Y. Nagasaka, W. A. Wakeham, A. Nagashima, and M. J. Assael. c1995, 5p.
Prepared in cooperation with Keio Univ., Yokohama (Japan). Dept. of Mechanical Engineering., Imperial Coll. of Science, Technology and Medicine, London (England). Dept. of Chemical Engineering. and Thessaloniki Univ., Salonika (Greece). Dept. of Chemical Engineering.
Included in Jnl. of Physical and Chemical Reference Data, v24 n3 p1377-1381 May/Jun 95. Available from American Chemical Society, 1155 Sixteenth St., NW, Washington, DC, 20036-9976.

Keywords: *Water, *Thermal conductivity, Liquids, Reprints, Reference materials, Standard reference data.

New experimental data on the thermal conductivity of liquid water along the saturation line have been obtained recently, using the bare and coated transient hot wire technique, with high accuracy. The quality of the data is such that new standard reference values can be proposed with confidence limits of 0.7% at a 95% confidence level. These data and the correlation herein presented revise a previous correlation endorsed by IUPAC. (Copyright (c) 1995 American Institute of Physics and American Chemical Society.)

01,112
PB96-145883 Not available NTIS
American Chemical Society, Washington, DC.
Journal of Physical and Chemical Reference Data, Volume 24, No. 4, July/August 1995.
Bimonthly rept.
J. W. Gallagher. c1995, 249p.
See also PB96-145891 through PB96-145917, Volume 24, No. 3, PB96-145842 and Volume 24, No. 5, PB96-145925. Errata sheets inserted. Prepared in cooperation with American Inst. of Physics, New York. Sponsored by National Inst. of Standards and Technology, Gaithersburg, MD.
Available from American Chemical Society, 1155 Sixteenth St., NW, Washington, DC. 20036-9976.

Keywords: *Physical properties, *Chemical properties, Physical chemistry, Atomic properties, Chemical reactions, Thermodynamics, Reaction kinetics, Vapor phases, Tables(Data), Reprints, *Reference materials.

Contents:
- Summary of the Apparent Standard Partial Molal Gibbs Free Energies of Formation of Aqueous Species, Minerals, and Gases at Pressure 1 to 5000 Bars and Temperatures 25 to 1000 degees C;
- Atomic Weights of the Elements 1993;
- Spectral Data for Highly Ionized Krypton, Kr V through Kr XXXVI.

01,113
PB96-145891 Not available NTIS
Centre National de la Recherche Scientifique, Toulouse (France).
Summary of the Apparent Standard Partial Molal Gibbs Free Energies of Formation of Aqueous Species, Minerals, and Gases at Pressures 1 to 5000 Bars and Temperatures 25 to 1000C.
E. H. Oelkers, H. C. Helgeson, E. L. Shock, V. A. Pokrovskii, D. A. Sverjensky, and J. W. Johnson. c1995, 159p.
Prepared in cooperation with California Univ., Berkeley. Dept. of Geology and Geophysics., Washington Univ., St. Louis, MO. Dept. of Earth and Planetary Sciences., Johns Hopkins Univ., Baltimore, MD. Dept. of Earth and Planetary Sciences. and Lawrence Livermore National Lab., CA. Earth Sciences Dept.
Included in Jnl. of Physical and Chemical Reference Data, v24 n4 p1401-1560 Jul/Aug 95. Available from American Chemical Society, 1155 Sixteenth St., NW, Washington, DC. 20036-9976.

Keywords: *Aqeous species, *Electrolyte solutions, Gases, Water, Reprints, Water mineral interaction, Gibbs free energies of formation.

Accurate values of the apparent standard partial molal Gibbs free energies of formation (delta G deg) of aqueous species, minerals, and gases at high temperatures and pressures are a requisite for characterizing a variety of industrial and natural processes including corrosion of metals, solvent extraction, crystal growth, metamorphism, and the formation of hydrothermal ore deposits. Revision of the HKF equations of state for aqueous species other than H2O (Helgeson, Kirkham and Flowers, 1981) by Tanger and Helgeson (1988) and Shock et al. (1992) permits calculation of delta G deg for these species at temperatures to 1000 deg C and pressures to 5000 bars.

01,114
PB96-145909 Not available NTIS
Commission on Atomic Weights and Isotopic Abundances, Reston, VA.
Atomic Weights of the Elements, 1993.
c1995, 15p.
Included in Jnl. of Physical and Chemical Reference Data, v24 n4 p1561-1576 Jul/Aug 95. Available from American Chemical Society, 1155 Sixteenth St., NW, Washington, DC 20036-9976.

Keywords: *Atomic weights, Critical evaluation, Elements, Reprints, *Isotopic compositions, *IUPAC Commission on Atomic Weights.

The biennial review of atomic weight, Ar(E), determinations and other cognate data has resulted in changes for the standard atomic weight of titanium from 47.88 plus or minues 0.03 to 47.867 plus or minus 0.001, of iron from 55.847 plus or minus 0.003 to 55.845 plus or minus 0.002, of antimony from 121.757 plus or minus 0.003 to 121.760 plus or minus 0.001, and of iridium from 192.22 plus or minus 0.03 to 192.217 plus or minus 0.003. Recent investigations on chlorine and bromine confirmed the presently accepted values of Ar(Cl) and Ar(Br). To emphasize the fact that the atomic weight of lithium commonly available in laboratory reagents can vary significantly, the value of lithium, Ar(Li), was enclosed in brackets and a footnote was added. As a result of several changes, the Table of Standard Atomic Weights Abridged to Five Significant Figures has been updated. Because relative isotoperatio data for stable hydrogen, carbon, and oxygen are commonly being expressed on non-corresponding scales, the Commission recommends that such isotopic data be expreseed only relative to the references VSMOW and VPDB. (Copyright (c) 1995 American Institute of Physics and American Chemical Society.)

01,115
PB96-145917 Not available NTIS
Japan Atomic Energy Research Inst., Ibaraki.
Spectral Data for Highly Ionized Krypton, Kr V through Kr XXXVI.
T. Shirai, K. Okazaki, and J. Sugar. c1995, 31p.
Prepared in cooperation with Institute of Physical and Chemical Research, Wako (Japan). and National Inst. of Standards and Technology, Gaithersburg, MD.
Included in Jnl. of Physical and Chemical Reference Data, v24 n4 p1577-1608 Jul/Aug 95. Available from American Chemical Society, 1155 Sixteenth St., NW, Washington, DC. 20036-9976.

Keywords: *Atomic data, *Krypton, Energy levels, Ions, Spectra, Wavelengths, Reprints, Grotrian diagrams, Transition probabilities.

Wavelengths, energy levels, ionization energies, line classifications, intensities and transition probabilities for Kr V through Kr XXXVI, with the exception of Kr XI through Kr XVII, are tabulated. No data have been published for Kr XI through Kr XXVII. These data are based on the energy levels compilation of Sugar and Musgrove (13). Transition probabilities for selected M1 lines have been reported and are quoted here. A short review of the line identifications and wavelength measurements is given for each stage of ionization. The literature has been surveyed through February 1995. (Copyright (c) 1995 American Institute of Physics and American Chemical Society.)

01,116
PB96-145925 Not available NTIS
American Chemical Society, Washington, DC.
Journal of Physical and Chemical Reference Data, Volume 24, No. 5, September/October 1995.
Bimonthly rept.
J. W. Gallagher. c1995, 117p.
See also PB96-145933 through PB96-145958, Volume 24, No. 4, PB96-145883 and Volume 24, No. 6, PB96-145966. Prepared in cooperation with American Inst. of Physics, New York. Sponsored by National Inst. of Standards and Technology, Gaithersburg, MD.
Available from American Chemical Society, 1155 Sixteenth St., NW, Washington, DC. 20036-9976.

Keywords: *Physical properties, *Chemical properties, Physical chemistry, Atomic properties, Chemical reactions, Thermodynamics, Reaction kinetics, Vapor phases, Tables(Data), Reprints, *Reference materials.

Contents:
- The Viscosity of Ammonia;
- Thermodynamics of Enzyme-Catalyzed Reactions:
- Part 4. Lyases;
- Thermodynamic Properties of the Aqueous Ions (2+ and 3+) of Iron and the Key Compounds of Iron.

01,117
PB96-145933 Not available NTIS
Imperial Coll. of Science and Technology, London (England).

Viscosity of Ammonia.
A. Fenghour, W. A. Wakeham, V. Vesovic, E. Vogel, J. T. R. Watson, and J. Millat. c1995, 18p.
Prepared in cooperation with Rostock Univ. (German D.R.). Fachbereich Chemie., National Engineering Lab. Executive Agency, Glasgow (Scotland). and Nordum Inst. fuer Umwelt und Analytik G.m.b.H., Rostock (Germany). Gewerbepark am Weidenbruch.
Included in Jnl. of Physical and Chemical Reference Data, v24 n5 p1649-1667 Sep/Oct 95. Available from American Chemical Society, 1155 Sixteenth St., NW, Washington, DC. 20036-9976.

Keywords: *Ammonia, *Viscosity, Correlation, Critical assessment, Liquids, Representation, Vapors, Reprints.

A new representation of the viscosity of ammonia is presented. The representative equations are based on a set of experimental data selected as a result of a critical assessment of the available information. The validity of the representation extends from 196 K to the critical temperature for both liquid and vapor phases. In the supercritical region the temperature range extends to 680 K for pressures at or below ambient and to 600 K for pressure up to 50 MPa. The accuracy of the representation varies from 0.5% for the viscosity of the dilute gas phase at moderate temperatures to about 5% for the viscosity at high pressures and temperatures. Tables of the viscosity generated by the correlating equation at selected temperatures and pressures and along the saturation line are presented to provide easy reference as well as for the validation of computer codes. (Copyright (c) 1995 American Institute of Physics and American Chemical Society.)

01,118
PB96-145941 Not available NTIS
National Inst. of Standards and Technology (CSTL), Gaithersburg, MD. Biotechnology Div.
Thermodynamics of Enzyme-Catalyzed Reactions. Part 4. Lyases.
R. N. Goldberg, and Y. B. Tewari. c1995, 29p.
Included in Jnl. of Physical and Chemical Reference Data, v24 n5 p1669-1698 Sep/Oct 95. Available from American Chemical Society, 1155 Sixteenth St., NW, Washington, DC. 20036-9976.

Keywords: *Thermodynamic properties, *Lyases, *Enzyme-catalyzed reactions, Data evaluation, Reprints, Apparent equilibrium constants, Reaction enthalpies.

Equilibrium constants and enthalpy changes for reactions catalyzed by the lyase class of enzymes have been compiled. For each reaction the following information is given: the reference for the data; the reaction studied; the name of the enzyme used and its Enzyme Commission number; the method of measurement; the conditions of measurement (temperature, pH, ionic strength, and the buffer(s) and cofactor(s) used); the data and an evaluation of it; and, sometimes, commentary on the data and on any corrections which have been applied to it or any calculations for which the data have been used. The data from 106 references have been examined and evaluated. Chemical Abstract Service registry numbers are given for the substances involved in these various reactions. There is a cross reference between the substances and the Enzyme Commission numbers of the enzymes used to catalyze the reactions in which the substances participate. (Copyright (c) 1995 American Institute of Physics and American Chemical Society.)

01,119
PB96-145958 Not available NTIS
National Inst. of Standards and Technology (CSTL), Gaithersburg, MD. Chemical Kinetics and Thermodynamics Div.
Thermodynamic Properties of the Aqueous Ions (2+ and 3+) of Iron and the Key Compounds of Iron.
V. B. Parker, and I. L. Khodakovskii. c1995, 46p.
Prepared in cooperation with Akademiya Nauk SSSR, Moscow. Inst. Geokhimii i Analiticheskoi Khimii.
Included in Jnl. of Physical and Chemical Reference Data, v24 n5 p1699-1745 Sep/Oct 95. Available from American Chemical Society, 1155 Sixteenth St., NW, Washington, DC. 20036-9976.

Keywords: *Thermodynamic properties, *Aqueous iron, *Iron compounds, Data evaluation, Enthalpy, Entropy, Key values, Reprints, CODATA, Gibbs energy, Reaction catalogs.

The evaluation involves the analysis of the enthalpy changes, Gibbs energy changes, and the entropy measurements for all key substances in the key network. A consistent set of thermochemical property values is given for FeOOH(cr, Goethite), FeCl2(cr), FeCl3(cr), FeBr2(cr), FeBr3(cr) FeI2(cr), and FeSO4.7H2O(cr), as well as 'reconstituted' recommended process values with uncertainties involving these substances. All recommnded values are also given for a standard state of P(deg)=1 atm. A computer based reaction catalog of measurements accompanies the text analysis.

01,120
PB96-145966 Not available NTIS
American Chemical Society, Washington, DC.
Journal of Physical and Chemical Reference Data, Volume 24, No. 6, November/December 1995.
Bimonthly rept.
J. W. Gallagher. c1995, 143p.
See also PB96-145974, PB96-145982 and Volume 24, No. 5, PB96-145925. Prepared in cooperation with American Inst. of Physics, New York. Sponsored by National Inst. of Standards and Technology, Gaithersburg, MD.
Available from American Chemical Society, 1155 Sixteenth St., NW, Washington, DC. 20036-9976.

Keywords: *Physical properties, *Chemical properties, Physical chemistry, Atomic properties, Chemical reactions, Thermodynamics, Reaction kinetics, Vapor phases, Tables(Data), Reprints, *Reference materials.

Contents:
Thermodynamics of Enzyme-Catalyzed Reactions:
Part 5. Isomerases and Ligases;
Energy Levels of Zinc, Zn I through Zn XXX.

01,121
PB96-145974 Not available NTIS
National Inst. of Standards and Technology (CSTL), Gaithersburg, MD. Biotechnology Div.
Thermodynamics of Enzyme-Catalyzed Reactions. Part 5. Isomerases and Ligases.
R. N. Goldberg, and Y. B. Tewari. c1995, 36p.
Included in Jnl. of Physical and Chemical Reference Data, v24, n6 p1765-1801 Nov/Dec 95. Available from American Chemical Society, 1155 Sixteenth St., NW, Washington, DC. 20036-9976.

Keywords: *Isomerases, *Ligases, Data, Reprints, Equilibrium constants, Reaction enthalpies, Enzyme-catalyzed reactions, Thermodynamic properties.

Equilibrium constants and enthalpy changes for reactions catalyzed by the isomerase and ligase classes of enzymes have been compiled. For each reaction the following information is given: the reference for the data; the reaction studies; the name of the enzyme used and its Enzyme Commission number; the method of measurement; the conditions of measurement (temperature, pH, ionic strength, and the buffer(s) and cofactor(s) used); the data and an evaluation of it; and, sometimes, commentary on the data and on any corrections which have been applied to it or any calculations for which the data have been used. The data from 176 references have been examined and evaluated. Chemical Abstract Service registry numbers are given for the substances involved in these various reactions. There is a cross reference between the substances and the Enzyne Commission numbers of the enzymes used to catalyze the reactions in which the substances participate. (Copyright (c) 1995 American Institute of Physics and American Chemical Society.)

01,122
PB96-145982 Not available NTIS
National Inst. of Standards and Technology (PL), Gaithersburg, MD. Atomic Physics Div.
Energy Levels of Zinc, Zn I through Zn XXX.
J. Sugar, and A. Musgrove. c1995, 69p.
Included in Jnl. of Physical and Chemical Reference Data, v24 n6 p1803-1872 Nov/Dec 95. Available from American Chemical Society, 1155 Sixteenth St., NW, Washington, DC. 20036-9976.

Keywords: *Zinc, *Energy levels, Atomic, Ions, Spectra, Reprints.

Atomic energy levels of zinc have been compiled for all stages of ionization for which experimental data are available. No data have yet been published for Zn IX, Zn X, Zn XXVI, and ZN XXVIII, and only several resonance lines of Zn XXIX and ZN XXX. Very accurate calculated values are compiled for Zn XXIX and ZN XXX. Experimental g-factors and leading percentages from calculated eigenvectors are given. A value for the ionization energy, either experimental when available or theoretical, is included for the neutral atom and each ion. A review of the published literature is given. (Copyright (c) 1995 American Institute of Physics and American Chemical Society.)

01,123
PB96-146618 Not available NTIS
National Inst. of Standards and Technology (CSTL), Gaithersburg, MD. Thermophysics Div.
High-Temperature High-Pressure Oscillating Tube Densimeter.
Final rept.
R. F. Chang, and M. R. Moldover. 1996, 6p.
Pub. in Review of Scientific Instruments, v67 n1 p251-256 Jan 96.

Keywords: *Densitometers, *Oscillations, Density, High pressure, High temperature, Tubes, Calibrating, Toluene, Thermophysical properties, Reprints.

We describe an oscillating tube densimeter for use at temperatures up to at least 575 K and at pressures up to 20 MPa. After the densimeter was calibrated under vaccum and filled with water, it was used to measure the density of toluene from 298 to 575 k at 13.8 MPa. The results agree (0.1 percent rms deviation) with those obtained using other techniques. In the present densimeter, an alternating current is passed through the tube containing the sample to force the tube to oscillate in the field of a permanent magnet. This design avoids the use of electromagnets (with their attendant polymer or ceramic insolations) and does not require attachment of appendages to the oscillating tube.

01,124
PB96-146733 Not available NTIS
National Inst. of Standards and Technology (PL), Gaithersburg, MD. Ionizing Radiation Div.
Radiation-Chemical Reaction of 2,3,5-Triphenyl-Tetrazolium Chloride in Liquid and Solid State.
Final rept.
A. Kovac, L. Wojnarovits, W. L. McLaughlin, S. E. Ebrahim Eid, and A. Miller. 1996, 4p.
Pub. in Radiation Physics and Chemistry, v47 n3 p483-486 1996.

Keywords: *Radiolysis, *Reaction kinetics, *Pulses, Dosimetry, Oxidation, Reduction(Chemistry), Dosage, Liquids, Solids, Chemical reactions, Radiation chemistry, Reprints, TTC(Triphenyl-tetrazolium chloride), TTC films.

In pulse radiation of 2,3,5-triphenyl-tetrazolium chloride (TTC) at around 360 nm fast formation of intermediate tetrazolium radical was observed under both oxidizing and reducing conditions. In the latter case biomolecular formation of formazan, absorbing at around 480 nm, was observed. This reaction is accompanied by combination to the diformazan dimer, absorbing over the spectral range 500-550 nm. A polyvinyl-alcohol-based TTC film was produced and tested for dosimetry purposes: it gave a measureable response in the 1-100kGy dose range by evaluating the 50 micrometers thick TTC films at the absorption maximum of 493 nm.

01,125
PB96-147079 Not available NTIS
National Inst. of Standards and Technology (EEEL), Boulder, CO. Electromagnetic Technology Div.
Pinch Effect in Commensurate Vortex-Pin Lattices.
Final rept.
L. D. Cooley, and A. M. Grishin. 1995, 4p.
Pub. in Physical Review Letters, v74 n14 p2788-2791 Apr 95.

Keywords: *Commensurate lattices, *Critical state, Magnetization, Superconductors, Reprints, Flux pinning.

The critical state in a superconductor with periodic pins has properties similar to the pinch effect, known in plasma physics. It forms a terrace structure around the average flux density gradient, causing stratification of the transport current into the terrace edges where the flux density gradient is large. Regions of extremely high current thus interlace with regions of near zero current. The appearance of each new terrace inside the superconductor causes the magnetization jump, a new quantum effect in superconductors, corresponds to the addition of one flux quantum threading the pin lattice unit cell.

01,126
PB96-147152 Not available NTIS

National Inst. of Standards and Technology (MSEL), Gaithersburg, MD. Reactor Radiation Div.
Neutron Scattering Study of the Lattice Modes of Solid Cubane.
Final rept.
P. M. Gehring, D. A. Neuman, W. A. Kamitakahara, D. P. VanMeurs, J. J. Rush, and P. E. Eaton. 1995, 6p.
Pub. in Jnl. of Physical Chemistry, v99 p4429-4434 1995.

Keywords: *Molecular structure, *Chemical bonds, *Neutron scattering, Lattices, Reprints, *Cubanes.

The authors use neutron time-of-flight scattering techniques to measure the low-frequency vibrational density of states of solid cubane at 100 and 300 K. Debye-like behavior is observed up to approximately 60 cm(-1) at both temperatures. At 100 K, the density of states exhibits three distinct peaks at 78, 94, and 114 cm(-1) before cropping to zero around 150 cm(-1). The authors identify the 114 cm(-1) peak with the Eg librational mode of cubane based on the marked temperature dependence of its frequency and a comparison to Raman measurements. In similar fashion they identify the 94 cm(-1) peak with the Ag librational mode. At 300 K, the librational modes have softened to the extent that the density of states exhibits a plateau-like feature between 60 and 100 cm(-1).

01,127
PB96-147889 PC A03/MF A01
National Inst. of Standards and Technology (CSTL), Gaithersburg, MD. Thermophysics Div.
Collection of Results for the SPC/E Water Model.
R. D. Mountain, and A. Wallqvist. Jan 96, 15p, NISTIR-5778.
Prepared in cooperation with National Cancer Inst., Frederick, MD. Frederick Cancer Research and Development Center. and Science Applications International Corp., Frederick, MD.

Keywords: *Water, *Molecular properties, *Simulation, Constants, Dielectric constant, Diffusion, Potential energy, Sample cubic lattices, Tables(Data), SPC/E(Simple Point Charge Extended), Simple point charge.

The report contains a compilation of molecular dynamics computer simulation results for the simple point charge extended model (SPC/E) for water. In addition to published results, this compilation contains unpublished results developed by the author. The properties included are the static dielectric constant, the self-diffusion coefficient, the internal energy, and the pressure. The simulation values of the dielectric constant are compared with a new correlation based on available experimental values.

01,128
PB96-156054 Not available NTIS
National Inst. of Standards and Technology (CSTL), Gaithersburg, MD. Thermophysics Div.
Virial Coefficients of Five Binary Mixtures of Fluorinated Methanes and Ethanes.
Final rept.
L. A. Weber, and D. R. Defibaugh. 1994, 18p.
Pub. in Internaitonal Jnl. of Thermophysics, v15 n5 p863-880 1994.

Keywords: *Hydroflurorocarbons, Refrigerants, Viral coefficients, Reprints, *Pressure vapor temperature, *Polar gases.

The authors have made new measurements of the gas-phase PVT surface of five binary mixtures of hydrofluorocarbons (HFCs) in a Burnett/isochoric apparatus. The components chosen all have moderate to large reduced dipole moments. The authors present PVT data, derived mixture virial coefficients, cross second virial coefficients, and binary interaction parameters for these systems, and the authors compare the results with a recently published model for calculating second and third viral coefficients of polar gases and their mixtures. That model accounts for the polar nature of the molecules with a term containing the reduced dipole moment and it contains mixing rules for the substance-specific parameters needed to calculate the second and third cross virial coefficients. The model and data are in satisfactory agreement, and the model can be used to greatly extend the useful range of the limited set of data.

01,129
PB96-160510 Not available NTIS
National Inst. of Standards and Technology (MSEL), Gaithersburg, MD. Reactor Radiation Div.
Tetrahedral-Framework Lithium Zinc Phosphate Phases: Location of Light-Atom Positions in LiZnPO4 H2O by Powder Neutron Diffraction and Structure Determination of LiZnPO4 by ab Initio Methods.
Final rept.
W. T. A. Harrison, T. E. Gier, J. M. Nicol, and G. D. Stucky. 1995, 9p.
Pub. in Jnl. of Solid State Chemistry, v114 p249-257 1995.

Keywords: *Ion exchange resins, *Cations, *Crystal structure, Powder(Particles), Neutron diffraction, Synthesis(Chemistry), Phase transformations, Lithium inorganic compounds, Zinc phosphates, Reprints, Powder neutron diffraction, Zeolite A phases.

The syntheses, crystal structures, and certain properties of two lithium zinc phosphate phases, LiZnPO4.H2O and LiZnPO4, are reported. LiZnPO4.H2O is an isostructure of the Li-A-type zeolite LiAlSiO4.H2o and consists of a fully ordered three-dimensional network of vertex-sharing ZnO4 and PO4 tetrahedral units surrounding 8-, 6-, and 4-ring windows. The extraframework lithium cation and water molecular are located in this cavity system. The structure of LiZnPO4 was solved ab initio using synchrontron X-ray powder data and consists of a new semicondensed tetrahedral-framework structure, incorporating the guest lithium cations in squashed 6-ring channels.

01,130
PB96-160528 Not available NTIS
National Inst. of Standards and Technology (MSEL), Gaithersburg, MD. Reactor Radiation Div.
Characterization of the Structure of TbD2.25 at 70 K by Neutron Powder Diffraction.
Final rept.
Q. Huang, T. J. Udovic, J. J. Rush, J. Schefer, and I. S. Anderson. 1995, 4p.
Pub. in Jnl. of Alloys and Compounds, v231 p95-98 1995.

Keywords: *Terbium compounds, *Crystal structure, Powder(Particles), Neutron diffraction, Lattice parameters, Rare earth compounds, Chemical bonds, Reprints, Terbium deuteride, Long-range order, Octahedral site occupation.

A neutron-powder-diffraction pattern of the superstoichiometric rare-earth dideuteride TbD2.25 was measured at 70 K. Profile refinements indicated that the TbD2.25 structure possesses I4/mmm symmetry with deuterium fully occupying the tetrahedral (t) interstices of the nominally fcc Tb lattice and the excess deuterium occupying one-fourth of the octahedral (o) interstices with long-range order. Ideal order corresponds to the occupation of only those o sites within every fourth (042)cubic plane, in agreement with the results of a previous TbD2+x study.

01,131
PB96-160585 Not available NTIS
National Inst. of Standards and Technology (MEL), Gaithersburg, MD. Precision Engineering Div.
Fabrication Issues for the Prototype National Institute of Standards and Technology SRM 2090A Scanning Electron Microscope Magnification Calibration Standard.
Final rept.
B. L. Newell, M. T. Postek, and J. P. van der Ziel. 1995, 5p.
Pub. in Jnl. of Vacuum Science and Technology, Chapter 2671, vB 13 n6 p2671-2675 Nov/Dec 95.

Keywords: *Electron microscopes, *Scanning, *Calibration standards, Prototypes, Lithography, Electron beams, Fabrication, Design, Reprints.

A new National Institute of Standards and Technology scanning electron microscope magnification calibration standard has been fabricated and distributed in production prototype form. The SRM 2090A samples contain structures ranging in pitch from 3000 to 0.2 microm and are useful at both high- and low-accelerating voltages. The design and fabrication of the samples has incorporated many of the improvements suggested through two previous prototype series. This article discusses optimization of the lithographic techniques in the fabrication process. We used electron beam lithography for fabrication because of the 0.1 microm features required on the samples.

01,132
PB96-160643 Not available NTIS
National Inst. of Standards and Technology (CSTL), Gaithersburg, MD. Process Measurements Div.
Q Branch Lineshape Functions for CARS Thermometry.
Final rept.
G. J. Rosasco, and W. S. Hurst. 1992, 6p.
Pub. in Temperature, Its Measurements and Control in Science and Industry, v6 pt2 p655-660 Feb 92.

Keywords: *Raman spectroscopy, *Temperature measurement, Line spectra, Spectra analysis, Temperature dependence, Pressure, Collision parameters, Reprints, CARS(Coherent Anti-Stokes Raman Spectroscopy), Collisional narrowing, Dicke narrowing.

Knowledge of the pressure and temperature dependence of the spectra distribution is required to allow determination of the temperature from a coherent anti-Stokes Raman spectroscopy (CARS) spectrum. We review our understanding of the physics of line formation for the Raman vibrational Q-branch of diatomic molecules. While we can demonstrate that the role of velocity, phase, and state changing collisions in line formation is reasonably well understood, there are relatively few first principle calculations which allow prediction of the molecular parameters which determine the spectra distribution. We show how quasi-empirical models, which are consistent with our physical understanding, can provide a reliable basis for prediction.

01,133
PB96-160734 Not available NTIS
National Inst. of Standards and Technology (MSEL), Gaithersburg, MD. Reactor Radiation Div.
Low-Energy Vibrations and Octahedral Site Occupation in Nb95V5H(D)y.
Final rept.
T. J. Udovic, J. J. Rush, R. Hempelmann, and D. Richter. 1995, 3p.
Pub. in Jnl. of Alloys and Compounds, v231 p144-146 1995.

Keywords: *Niobium compounds, *Neutron scattering, *Microstructure, Inelastic scattering, Alloys, Spectroscopic analysis, Vibration spectra, Lattice parameters, Hydrides, Reprints, Octahedral site occupation, Metal hydrides.

Nb(100-x)VxHy is a random b.c.c. alloy system with an H sublattice disordered with respect to site energies. Previous incoherent inelastic neutron scattering (IINS) studies ascertained both octahedral (o) and tetrahedral (t) site occupation by H for x = 5, 10 and 50. On the basis of spectroscopic and statistical arguments, the low-temperature H vibrational peaks in the Nb-rich, low-H-concentration Nb95V5H1 alloy were assigned to Nb4V2 o sites and NbV3 t sites. To probe the regime of lower H concentration and the effects of D substitution, further IINS spectra were measured for Nb95 V5Hy (y=0.5 and 0.8) and Nb95V5D2.7.

01,134
PB96-160742 Not available NTIS
National Inst. of Standards and Technology (MSEL), Gaithersburg, MD. Reactor Radiation Div.
Neutron Spectroscopic Comparison of beta-Phase Rare Earth Hydrides.
Final rept.
T. J. Udovic, J. J. Rush, and I. S. Anderson. 1995, 6p.
Pub. in Jnl. of Alloys and Compounds, v231 p138-143 1995.

Keywords: *Rare earth elements, *Hydrides, *Neutron scattering, *Microstructure, Inelastic scattering, Spectroscopic analysis, Vibrational spectra, Lattice parameters, Phase transformations, Reprints.

The Beta-phase hydrides Beta-RH2+x of a variety of rare metals (R = Tb, Y, La, Ce and Dy) were investigated by incoherent inelastic neutron scattering spectroscopy. The broad, complex vibrational density of states (DOS) of the tetrahedrally coordinated (t-site) Hydrogen (Ht) typically found for these systems is a manifestation of the dynamic coupling within the Ht sublattice due to significant Ht-Ht interactions. A breakdown of this dynamic coupling via isotopic dilution of the Ht atoms with larger mass deuterium atoms is observed spectroscopically by a collapse of the complex DOS into a single sharp feature.

01,135
PB96-160999 Not available NTIS
National Inst. of Standards and Technology (CSTL), Gaithersburg, MD. Process Measurements Div.

Effects of Pipe Elbows and Tube Bundles on Selected Types of Flowmeters.
Final rept.
G. E. Mattingly, and T. T. Yeh. 1991, 10p.
Pub. in Flow Measurement and Instrumentation Jnl., v2 p4-13 Jan 91.

Keywords: *Pipe elbows, *Measurement accuracy, *Flowmeters, Swirl, Reprints, *Foreign technology, Tube bundles.

The paper presents experimental results for the decay of pipe elbow-produced swirl in pipeflows and its effects on flowmeter measurement accuracy. Experiments include the decay of swirl produced by single and double elbow configurations for pipe diameter Reynolds number of 10 to the 4th power to 10 to the 5th power using water in a 50 mm diameter facility at NIST in Gaithersburg, MD. Results show that different types of swirl are produced by the different piping configurations. The swirl decay is found to be dependent on the type of swirl and the pipe Reynolds number. A high Reynolds number very long lengths of straight, constant diameter pipe are required to dissipate the single eddy type swirl that is produced by the two elbows out-of-plane configuration. Without flow conditioning, it is concluded that the specifications of upstream pipe lengths in the current flowmetering standards may not be sifficient to achieve the desired flow metering accuracy. Experimental results are also presented for the effects produced by tube bundle-type flow conditioners. These results show shifts in orifice meter discharge coefficients that are both positive and negative depending upon pertinent conditions. A range of orifice geometries, Reynolds numbers and meter locations are studied and explanations are put forth to explain these shifts.

01,136
PB96-161005 Not available NTIS
National Inst. of Standards and Technology (CSTL), Gaithersburg, MD. Process Measurements Div.
Pressure Measurements with the Mercury Melting Line Referred to ITS-90.
Final rept.
G. F. Molinar, V. E. Bean, J. Houck, and B. Welch. 1991, 2p.
Pub. in Metrologia, v28 p353-354 Feb 91.

Keywords: *Melting line, *Mercury, Pressure, Standards, Reprints, *Foreign technology.

In this letter the authors recalculate the mercury melting line, for use as an accurate pressure transfer standard up to 1,200 MPa, with a reference to the new International Temperature Scale of 1990 (ITS-90). In previous work the authors obtained fifty-two experimental temperature and absolute pressure points, each point representing a melting point of mercury under specified temperature and pressure conditions. The temperatures were referenced to the International Practical Temperature Scale of 1968 (IPTS-68).

01,137
PB96-161625 Not available NTIS
National Inst. of Standards and Technology (CSTL), Gaithersburg, MD. Biotechnology Div.
Imposed Oscillations of Kinetic Barriers Can Cause an Enzyme to Drive a Chemical Reaction Away from Equilibrium.
Final rept.
R. D. Astumian, and B. Robertson. 1993, 6p.
Pub. in Jnl. of the American Chemical Society, v115 n24 p11063-11068 Dec 93.

Keywords: *Chemical affinity, *Enzyme kinetics, Reprints, Thermodynamics, *Free energy transduction.

The overall Gibbs free energy change (delta G) of a chemical reaction is often termed the driving force of the reaction. The sign of delta G defines the direction of spontaneous reaction, and the condition delta G = 0 defines the point of chemical equilibrium. This is strictly true for elementary reactions--reactions that pass through only one local maximum (the transition state) along the reaction coordinate connecting reactant and product states. However, under many circumstances it is also true for reactions that involve one or more intermediates, particularly if the steady state intermediate concentrations are very small. Here the authors show that externally imposed oscillations or fluctuations can drive a net chemical reaction away from equilibrium so long as the rate constants of at least one elementary step of the overall reaction depend on the fluctuating parameter. This is true even if the overall delta G is independent of the perturbation and it is also true even if the concentrations of the intermediate states are very, very small (i.e., experimental undetectable).

01,138
PB96-161633 Not available NTIS
National Inst. of Standards and Technology (CSTL), Gaithersburg, MD. Biotechnology Div.
Quadratic Response of a Chemical Reaction to External Oscillations.
Final rept.
R. D. Astumian, B. Robertson, R. S. Li, and J. Ross. 1992, 7p.
Pub. in Jnl. of Chemical Physics, v96 n9 p6536-6542 May 92.

Keywords: *Chemical reactions, *Oscillations, Reprints, *Quadratic response, External periodic perturbations.

The authors develop a second-order response theory to investigate the effects of external periodic perturbations on a chemical reaction at a stable steady state in an open reactor. The authors apply the theory to the quadratic Schlogl model, a single-variable nonlinear reaction. In the presence of oscillating reactant or product concentrations or oscillating rate coefficients, the average intermediate concentration, the fluxes, and the dissipation are each a Lorentzian function of frequency with midpoint at the inverse relaxation time of the system. Thus even very short relaxation times can be determined by measuring average rates as a function of frequency of the perturbation. The amplitude of the Lorentzian depends on the chemical mechanism of the reaction and is proportional to the square of the amplitude of the applied perturbation. The authors also show that energy from the perturbation can be used to drive the reaction in a direction opposite of that predicted by the Gibb's free energy difference of the reactants and products, even under circumstances where the overall affinity is independent of the perturbation.

01,139
PB96-161856 Not available NTIS
National Inst. of Standards and Technology (CSTL), Gaithersburg, MD. Thermophysics Div.
Vapor-Liquid Equilibria of Ternary Mixtures in the Critical Region on Paths of Constant Temperature and Overall Composition.
Final rept.
L. J. Van Poolen, and J. C. Rainwater. 1995, 9p.
Pub. in International Jnl. of Thermophysics, v16 n2 p473-481 Mar 95.

Keywords: *Critical region, *Ethane, Reprints, Ternary mixtures, Phase rule, *Vapor liquid equilibrium, Leung Griffiths model, N-butane, N-pentain.

High-pressure vapor-liquid equilibrium (VLE) data for the ternary mixture ethane + n-butane + n-pentane due to Thodos and co-workers have been correlated by a ternary version of the modified Leung-Griffiths model. Data were taken along paths of constant temperature and approximately constant overall composition, and a separate test was made for such constancy. Seventeen different specified overall compositions at four different temperatures were correlated. In general, agreement between the correlation and data is very good, particularly for those curves that satisfy the test for constant overall composition. The ternary model has been constructed from correlations of each of the three constituent binaries without any further adjustable parameters.

01,140
PB96-161898 Not available NTIS
National Inst. of Standards and Technology (CSTL), Boulder, CO. Thermophysics Div.
Density Dependence of Fluid Properties and Non-Newtonian Flows: The Weisenberg Effect.
Final rept.
J. C. Rainwater, H. J. M. Hanley, and A. Narayan. 1995, 17p.
Pub. in Jnl. of Rheology, v39 n6 p1343-1359 Nov/Dec 95.

Keywords: *Rotating cylinders, Compressibility, Couette flow, Reprints, *Weissenberg effect, *Non-Newtonian fluids, Rivlin-Ericksen tensors, Shear dilatancy.

Two approaches which describe the Weissenberg effect (height profile of a non-Newtonian fluid between rotating vertical concentric cylinders) are discussed. The first is based on an earlier calculation with rheological properties of a simple liquid from nonequilibrium molecular dynamics (NEMD). The calculation is redone here using new results on the density dependence of the normal pressure differences. The NEMD calculations are restricted to Couette flow, but describe specifically, in a consistent manner, the effects of finite compressibility. The pressure, viscosity, and normal pressure differences are all found from NEMD to be sensitive functions of density, which requires that the equations of motion be solved iteratively and self-consistently, and a sample calculation is presented for the soft sphere fluid. The second approach is that of Joseph and Fosdick. Their assumptions and techniques are examined and compared with the NEMD calculations.

01,141
PB96-161906 Not available NTIS
National Inst. of Standards and Technology (CSTL), Boulder, CO. Thermophysics Div.
Nonlinear Correlation of High-Pressure Vapor-Liquid Equilibrium Data for Ethylene + n-Butane Showing Inconsistencies in Experimental Compositions.
Final rept.
J. C. Rainwater, and J. J. Lynch. 1994, 9p.
Pub. in International Jnl. of Thermophysics, v15 n6 p1231-1239 Nov 94.

Keywords: *Critical region, *Ethylene, High pressure, Reprints, *Mole fraction errors, N-butane, Simplex optimization, Vapor-liquid equilibrium.

The modified Leung-Griffiths model is applied to the previously unpublished data, tabulated here, of Williams for high-pressure vapor-liquid equilibria of ethylene + n-butane. It is not possible to obtain a hihgly accurate correlation with the experimentally stated compositions, but evidence is given that those composition measurements may be suspect, although pressure, temperature, and density data are accurate. A simplex optimization method was used for the parameters of the model, and the compositions were also treated as adjustible parameters. With this method a much more accurate correlation is obtained, but the optimized compositions differ in two of four cases by more than 3% from the stated compositions.

01,142
PB96-161914 Not available NTIS
National Inst. of Standards and Technology (CSTL), Gaithersburg, MD. Thermophysics Div.
Quantum Collisional Transfer Contributions to the Density Dependence of Gaseous Viscosity.
Final rept.
J. C. Rainwater. 1995, 7p.
Pub. in Proceedings of the Conference on Rarefied Gas Dynamics (19th), Oxford, England, July 25-29, 1994, p114-120 1995.

Keywords: *Boltzmann equation, *Classical limit, *Density correction, Reprints, Kinetic theory, Quantum theory, Viscosity, Weyl transform.

The linearly extended Waldmann-Snider equation of Thomas and Snider is solved by a Chapman-Enskog method to derive the quantum collisional transfer contributions to the viscosity of a gas. These contributions, which are linear in density, are then reduced by Weyl correspondence methods to their classical limits, and are shown to agree with the known classical results.

01,143
PB96-161930 Not available NTIS
National Inst. of Standards and Technology (CSTL), Boulder, CO. Process Measurements Div.
Cryogenic Flow Calibration in NIST.
Final rept.
J. L. Scott, and M. A. Lewis. 1995, 5p.
Pub. in International Jnl. of Metrology, v2 n5 p12-16 Sep/Oct 95.

Keywords: *Cryogenics, *Flow calibration, Data acquisition, Load cell, Reprints, *Mass flow measurement.

A unique flow calibration facility for cryogenic liquids is located at the National Institute of Standards and Technology (NIST) in Boulder, Colorado. A dynamic weighing system is used to measure totalized mass flow and, with the use of NIST thermodynamic property data for density, volumetric flow. Calibrations are typically performed with liquid nitrogen in a flow of 0.95 to 9.5 kg/s, pressure range of 0.4 to 0.76 Mpa, and temperature range of 80 to 90 k.

01,144
PB96-163670 Not available NTIS

National Inst. of Standards and Technology (CSTL), Gaithersburg, MD. Process Measurements Div.
Effect of Finite Beam Width on Elastic Light Scattering from Droplets.
Final rept.
J. T. Hodges, and C. Presser. 1993, 5p.
Pub. in Annual Conference on Liquid Atomization and Spray Systems (6th), Worcester, MA., May 17-19, 1993, Volume of Extended Abstracts, p152-156.

Keywords: *Droplets, *Elastic scattering, *Gaussian beam, Reprints, Lorenz-Mie.

A number of experimental techniques based on elastic light scattering are used to measure the size of micron-sized spherical particles and droplets. Some examples include, phase Doppler anemometry, laser diffraction methods, light intensity deconvolution as well as ensemble scattering measurements from axi-symmetric Gaussian and Gaussian sheet beams. In the interpretation of these measurements, the classical Lorenz-Mie theory (LMT) of elastic light scattering or principles of diffraction and ray optics are invoked to predict the phase, amplitude and intensity of the scattered radiation as a function of particle size, refractive index and scattering angle. The reliability and accuracy of these measurements, thus depend on the degree to which the invoked theory predicts the observed features of the scattered field. In this context, it is therefore important to consider realistic situations for which departures from the LMT are significant enough to warrant the use of more exact theories of light scattering.

01,145
PB96-163803 Not available NTIS
National Inst. of Standards and Technology (CSTL), Boulder, CO. Thermophysics Div.
CO2/CH4 Transport in Polyperfluorosulfonate Ionomers: Effects of Polar Solvents on Permeation and Solubility.
Final rept.
J. Pellegrino, and Y. S. Kang. 1995, 12p.
Pub. in Jnl. of Membrane Science, v99 p163-174 1995.

Keywords: *Permeation, *Solubility, Membranes, Reprints, Modeling, Alcohols, *Polyperfluorosulfonate ionomer, PFSI.

The authors measured CO2 and CH4 gas permeation through polyperfluorosulfonate ionomer (PFSI) that was solvated with water, methanol, ethanol, or 1-propanol. These measurements were compared with predictions based on a two-phase, effective-media, membrane model that considered a number of possible geometries for the distributed phase (the ionic clusters). The transport parameters (solubility and diffusivity) for each of the phases and the volume fraction of dispersed phase were either measured independently or estimated from prior literature data. The authors were unable to match all the experimental observations with this two-phase model. The authors conclude that different polar solvents an incorporate themselves into the fluorocarbon 'continuous phase' in ways that will alter the effective diffusion coefficient of that phase to gas permeation.

01,146
PB96-164199 Not available NTIS
National Inst. of Standards and Technology (EEEL), Gaithersburg, MD. Semiconductor Electronics Div.
Electrical Characterization of Narrow Gap n-Type Bulk HgCdTe Single Crystals by Variable-Magnetic-Field Hall Measurements and Reduced-Conductivity-Tensor Analyses.
Final rept.
J. S. Kim, D. G. Seiler, R. A. Lancaster, and M. B. Reine. 1996, 2p.
Pub. in Extended Abstracts of the 1995 U.S. Workshop on the Physics and Chemistry of Mercury Cadmium Telluride and Other IR Materials, Baltimore, MD., October 10-12, 1995, p31-32 1996.

Keywords: *Hall effect, *Resistance, *Supercondictivity, Reprints, Electron mobility, Electron transport, Gapless state, HgCdTe, Magnetotransport, MCT, Narrow gap.

We have investigated, for the first time, magnetotransport properties of very narrow gap HgCdTe single crystals in the light of the reduced-conductivity-tensor (RCT) scheme to determine the variations of the carrier density and mobility as a function of temperature in the semiconductor-to-semimetal transition region. In this paper, we report the results of variable-magnetic-field and variable-temperature Hall measurements (0 to 1.5 T and 10 K to 300 K) on three n-type bulk HgCdTe single crystals, labeled MCT-1 (x=0.190), MCT-2 (x=0.175), and MCT-3 (x=0.160). The experimental data are analyzed in the context of the RCT scheme of multicarrier characterization, which we have previously used to electrically characterize liquid-phase-epitaxially (LPE) grown HgCdTe films. The latter work deals with type classification if LPE samples according to the degree of anomalous electrical behavior present, from normal to severely anomalous.

01,147
PB96-164215 Not available NTIS
National Inst. of Standards and Technology (CSTL), Boulder, CO. Thermophysics Div.
Solubilities of Copper(II) and Chromium(III) beta-Diketonates in Supercritical Carbon Dioxide.
Final rept.
A. F. Lagalante, B. N. Hansen, T. J. Bruno, and R. E. Sievers. 1995, 5p.
Pub. in Inorganic Chemistry, v34 p5781-5785 1995.

Keywords: *Carbon dioxide, *Copper, *Solubility, Parameter, Reprints, Beta-diketonates, Supercritical fluids.

The mole fraction solubilities of ten copper(II) and five chromium(III) beta-diketonates were measured in supercritical carbon dioxide with a spectroscopic technique and found to vary over 4 orders of magnitude. Observed trends indicate that the solubility on supercritical carbon dioxide is strongly dictated by the character of the hydrocarbon or fluorocarbon shell surrounding the central metal atom. A group-contribution approach was used to calculate the solubility parameter of the anion of the uncomplexed beta-diketone that was correlated to the experimentally measured solubility. A regular solutions approach was used for Cr(acac)3 to quantitatively attempt to predict the solubility in supercritical carbon dioxide. Solubility data, solubility parameter trends, and limitations of regular solutions theory applied to supercritical fluids are discussed.

01,148
PB96-167135 Not available NTIS
National Inst. of Standards and Technology (CSTL), Boulder, CO. Thermophysics Div.
Molar Heat Capacity at Constant Volume for (xCO2 + (1-x)C2H6) from 220 to 340 K at Pressures to 35 MPa.
Final rept.
J. W. Magee. 1995, 5p.
Pub. in Jnl. of Chemical and Engineering Data, v40 n2 p438-442 1995.

Keywords: *Heat capacity, *Calorimeters, *High pressure, Ethane, Carbon dioxide, Reprints, Isochoric, Measurement, Mixtures.

Measurements of the molar heat capacity at constant volume (Cv) for (xCO2+(1-x)C2H6), x= 0.25, 0.49, 0.74, were conducted. Tempertures ranged from about 220 to 340 K, and pressures were as high as 35 MPA. Meaurements were conducted on samples in compressed gas and liquid states. The primary sources of uncertainty are the estimated temperature rise and the estimated quantity of substance in the calorimeter. Overall, the uncertainty of the Cv values is estimated to be less than plus or minus 2.0% for vapor and plus or minus 0.5% for liquid.

01,149
PB96-167150 Not available NTIS
National Inst. of Standards and Technology (CSTL), Boulder, CO. Thermophysics Div.
REFPROP Refrigerant Properties Database: Capabilities, Limitations, and Future Directions.
Final rept.
M. O. McLinden, J. G. Gallagher, M. L. Huber, and G. Morrison. 1993, 13p.
Pub. in ASHRAE/NIST Refrigerants Conference, Gaithersburg, MD., August 19-20, 1993, p59-71.

Keywords: *Refrigerants, *Chlorofluorocarbons, Databases, Mixtures, Reprints, Equation of state, Hydrochlorofluorocarbons, Hydrofluorocarbons.

The REFPROP computer database has been developed to meet the needs of the refrigeration industry in their evaluation of alternative refrigerants. In this paper, we highlight the capabilities and discuss the limitations of the database through examples of several representative pure refrigerants and refrigerant blends. The database employs the Carnahan-Starling-Desantis (CSD), modified Bennedict-Webb-Rubin (MBWR), and Haar-Gallagher equations of state for thermodynamic properties, and an extended corresponding states (ECS) model for thermodynamic and transport properties; the most appropriate model for specific applications is recommended.

01,150
PB96-167176 Not available NTIS
National Inst. of Standards and Technology (CSTL), Boulder, CO. Thermophysics Div.
Simulation and SANS Studies of Gelation Under Shear.
Final rept.
C. D. Muzny, D. Hansen, G. C. Straty, D. J. Evans, and H. J. M. Hanley. 1995, 10p.
Pub. in International Jnl. of Thermophysics, v16 n2 p337-346 Mar 95.

Keywords: *Gelation, *Shear, Reprints, *Foreign technology, *Small angle neutron scattering, *Nonequilibrium molecular dynamics, Colloidal silica, Lennard Jones fluid, Spinodal decomposition.

Computer simulations of a two-dimensional Lennard-Jones fluid undergoing spinodal decomposition are reported for the system subjected to planar Couette flow. Key results are the images of the atomic structure and plots of the corresponding pair correlation functions. A companion small-angle neutron scattering (SANS) study of shear-influenced gelation on colloidal silica suspensions at volume fractions phi = 0.1, 0.12, 0.18, and 0.24 is discussed. It is found that the scattered intensity-wave vector curves from the unsheared gels obey a power law for phi less than 0.24. At higher volume fractions, the power law does not seem to be followed. Shear, however, induces an apparent fractal structure in the gel at phi = 0.24. Results from the computer and the SANS experiments indicate that the spinodal decomposition process and the gelation mechanism have features in common.

01,151
PB96-167184 Not available NTIS
National Inst. of Standards and Technology (CSTL), Boulder, CO. Thermophysics Div.
Small-Angle Neutron-Scattering Study of Dense Sheared Silica Gels.
Final rept.
C. D. Muzny, G. C. Straty, and H. J. M. Hanley. 1994, 4p.
Pub. in Physical Review E, v50 n2 pR675-R678 Aug 94.

Keywords: *Gels, *Shear, Fractal, Reprints, *Small angle neutron scattering, Colloidal silica.

Small-angle neutron-scattering (SANS) shearing experiments on dense colloidal silica suspensions in a H2O-D2O medium are reported for the wave vector range 0.03 less than Q (nm to the minus 1 power) less than 0.8, at volume fractions phi = 0.1, 0.12, 0.18, 0.24, and 0.3. For the unsheared gels, apparent fractal structures were observed at the lower volume fractions, and a small maximum at a Q corresponding to a contact particle morphology was apparent at all volume fractions. A fractional dimension d - 1.60 plus or minus 0.05 was estimated for phi = 0.10 and 0.12 by fitting the power law behavior of the structure factor. Shear induces an apparent fractal domain into the dense gels and enhances the contact particle structure.

01,152
PB96-167218 Not available NTIS
National Inst. of Standards and Technology (CSTL), Boulder, CO. Thermophysics Div.
Status of the Round Robin on the Transport Properties of R134a.
Final rept.
M. J. Assael, Y. Nagasaka, C. A. Nieto de Castro, E. Vogel, W. A. Wakeham, R. A. Perkins, and K. Strom. 1995, 16p.
Pub. in International Jnl. of Thermophysics, v16 n1 Jan 95.

Keywords: *Refrigerants, *Thermal conductivity, Saturation properties, Transport properties, Viscosity, Reprints, R134a, Dilute gas.

The paper contains a status report on an international project coordinated by the Subcommittee on Transport Properties of commission 1.2 of the International Union of Pure and Applied Chemistry. The project has been conducted to investigate the large discrepancies between the results reported by various authors for the transport properties of R134a. The project has involved the remeasurement of the transport properties of a sin-

gle sample of R134a in nine laboratories throughout the world in order to test the hypothesis that at least part of the discrepancy could be attributed to the purity of the sample. This paper provides an intercomparison of the new experimental results obtained to data in this project for the viscosity and the thermal conductivity in both gaseous and liquid phases. The agreement between the viscosity data from the laboratories contributing to the project was improved with several techniques, now producing consistent results. This suggests that the purity of the samples of R134a used in previous work was at least partly responsible for the discrepancies observed. For the thermal conductivity in the liquid phase the results of the measurements are also more consistant than before, although not for all experimental techniques. Not all of the previous measurements suffered from significant sample impurities, so the present measurements on a consistent high-purity sample can be used to detect data sets which are outliners, possibly because of impurities. Identification of laboratories and techniques with systematic differences may require the examination of data for several fluids. The implications for future measurements of the transport properties of other refrigerants are significant.

01,153
PB96-167358 Not available NTIS
National Inst. of Standards and Technology (CSTL), Boulder, CO. Thermophysics Div.
Thermophysical Property Standard Reference Data from NIST.
Final rept.
D. G. Friend, and M. L. Huber. 1994, 10p.
Pub. in International Jnl. of Thermophysics, v15 n6 p1279-1288 Nov 94.

Keywords: *Thermodynamic properties, *Refrigerants, Databases, Mixtures, Predictive models, Standards, Reprints, *Foreign technology, *Transport properties.

The National Institute of Standards and Technology (NIST) has a primary function to develop and disseminate standard reference data for the thermophysical properties of fluids and fluid mixtures of interest to the industrial and scientific communities. In this paper we discuss five computerized databases distributed by the Standard Reference Data (SRD) Program of NIST. The databases provide national standards for the properties of pure fluids, an accurate evaluated mixture program focusing on the properties of natural gas mixtures, a predictive package emphasizing hydrocarbon systems up to C20, a database for refrigerant and prospective alternative refrigerant fluids, and the current scientifc thermophysical property surfaces for the pure water and steam.

01,154
PB96-167390 Not available NTIS
National Inst. of Standards and Technology (CSTL), Boulder, CO. Thermophysics Div.
Isochoric (p-p-T) Measurements on Liquid and Gaseous Air from 67 to 400 K at Pressures to 35 MPa.
Final rept.
J. B. Howley, J. W. Magee, and W. M. Haynes. 1994, 12p.
Pub. in International Jnl. of Thermophysics, v15 n5 p881-902 Sep 94.

Keywords: *Isochoric, *High pressure, Air, Density, Reprints, Mixtures, Vapor.

Comprehensive isochronic p-p-T measurements have been carried out on liquid and gaseous air along 16 isochores at densities ranging from 2 to 32 mol-dm to the minus 3rd power. The air mixture has a nominal composition of 0.7812 N2 + 0.2096 O2 + 0.0092 Ar. The p-p-T data cover a temperature range from 67 to 400 K at pressures up to 35 MPa. Comparisions with experimental results from independent sources are presented using a fundamental equation of state based, in part, on the p-p-T data from this study.

01,155
PB96-176508 Not available NTIS
National Inst. of Standards and Technology (PL), Boulder, CO. Time and Frequency Div.
Potential Surfaces and Dynamics of Weakly Bound Trimers: Perspectives from High Resolution IR Spectroscopy.
Final rept.
M. A. Suhm, and D. J. Nesbitt. 1995, 10p.
Sponsored by National Science Foundation, Arlington, VA.
Pub. in Chemical Society Reviews, p45-54 1995.

Keywords: *Clusters, *Trimers, Reprints, *High resolution, IVR, Hydrogen bonding, Predissociation, Potential energy surfaces, Three-body forces.

If we want to understand the properties of condensed molecular matter in detail, we have to study the interactions between molecules, which are often summarized under the name 'van der Waals interactions.' These intermolecular interactions are of a profoundly subtle, multidimensional, long-range, and coupled nature. This is in contrast to intramolecular interactions, where the concepts of chemical bond and harmonic force-field usually form a reasonably localized zero-order reference point at sufficiently low excitation levels. Infrared spectroscopy provides a powerful general tool to study both inter- and intramolecular interactions, since it can cover the full frequency range of fundamental and few-quantum excitation of the associated degrees of freedom. It is in the 'floppy molecule', intermolecular regime where the inversion of high resolution spectroscopic data to interaction potentials is particularly difficult, and thus the demand for interaction between theory and experiment is particularly intense. As one consequence is this difficulty, initial spectroscopic research efforts have concentrated on pairs of molecules, the obvious prototypes of any interaction study. These binary complexes or dimers have revealed an unprecedented richness of structural properties and dynamical behavior, when viewed through the eyes of high resolution microwave, far- and near-IR spectroscopy, 2-5 and modern theoretical tools. Indeed, the astonishing range of challenges and insights provided by dimer spectroscopy deflected the original thrust of a spectroscopy-based understanding of bulk matter toward an extensive, albeit very fruitful, series of diversions.

01,156
PB96-176524 Not available NTIS
National Inst. of Standards and Technology (MSEL), Gaithersburg, MD. Ceramics Div.
Magnetic Dielectric Oxides: Subsolidus Phase Relations in the BaO: Fe2O3: TiO2 System.
Final rept.
T. A. Vanderah, J. M. Loezos, and R. S. Roth. 1996, 13p.
Pub. in Jnl. of Solid State Chemistry, Article No. 0006, v121 p38-50 1996.

Keywords: *Phase diagrams, *Solid solutions, *Barium oxides, Reprints, BaO, Fe2O3, TiO2.

The BaO-Fe2O3-TiO2 ternary phase diagram has been investigated at 1250-1270 degrees C in air. X-ray diffraction studies of approximately 150 polycrystalline specimens at room temperature confirmed the existence of sixteen ternary compounds. Two of these compounds, BaFe4Ti2O11 and Ba12Fe28Ti15O84, were previously reported, four were found to be isostructural with known chemically similar compounds, and ten apparently adopt new structure-types. The crystal structures of five of the new ternary phases are briefly described. The oxidation state of iron found in this study is similar to that reported for a study of the BaO-Fe2O3-SnO2 system in air at 1200 degrees C.

01,157
PB96-176607 Not available NTIS
National Inst. of Standards and Technology (PL), Boulder, CO. Quantum Physics Div.
State-Resolved Rotational Energy Transfer in Open Shell Collisions: Cl((2)P3/2)+HCl.
Final rept.
Z. Q. Zhao, W. B. Chapman, and D. J. Nesbitt. 1995, 13p.
Contract AFOSR93-NC-231
Sponsored by Air Force Office of Scientific Research, Bolling AFB, DC.
Pub. in Jnl. of Chemical Physics, v102 n18 p7046-7058 May 95.

Keywords: *Hydrogen bonds, *Energy transfer, *Rotation, *Collisions, *Chlorine, Preparation, Photochemical reactions, Chemical dissociation, Interactions, Chemicals, Dynamics, Quantum theory, Elastic properties, Reactivities, Reprints, Open shells.

Time- and frequency-resolved infrared (IR) laser absorption methods are used to probe hot atom energy transfer in open shell interactions of Cl(2P3/2) + HCl(J) in the single collision regime. The Cl(2P3/2) atoms are prepared by 308 nm laser photolysis of Cl2, and suffer collisions at E rel approx. 3500 cm to the minus one power with a room temperature HCl distribution in a fast flow cell. Selective collisional excitation of final HCl(Jf) states is monitored by transient IR absorption on R(J equal to or greater than 4) branch lines in the HCl(v=1 greater than 0) band, while depletion of the initial HCl(Ji) states is monitored by transient bleaching of the room temperature Doppler profiles. Analysis of the J dependent Doppler profiles permits extraction of rotational loss cross sections, as a function of initial and final J states, respectively. Absolute transient concentrations of the HCl(Ji) and HCl(Jf) are measured directly from absorbances via Beer's Law, and used to extract absolute collisional cross sections.

01,158
PB96-176771 Not available NTIS
National Inst. of Standards and Technology (CSTL), Gaithersburg, MD. Process Measurements Div.
Surface Plasmon Microscopy of Biotin-Streptavidin Binding Reactions on UV-Photopatterned Alkanethiol Self-Assembled Monolayers.
Final rept.
D. Piscevic, W. Knoll, and M. J. Tarlov. 1995, 8p.
Pub. in Supermolecular Science, v2 p99-106 1995.

Keywords: *Surface plasmon resonance, Alkanethiols, Reprints, *Foreign technology, *Self assembled monolayers, Photopatterning, Biotin streptavidin.

The authors report surface plasmon imaging of streptavidin binding to photopatterned biotinylated alkanethiol self-assembled monolayers (SMAs) on gold. Micrometer-scale patterns of a mixed biotin- and hydroxyl-terminated monolayer were formed in an inert, hydroxy-terminated alkanethiol monolayer using a UV-photopatterning procedure. Using surface plasmon microscopy, contrast is readily observed between the mixed biotin- and hydroxy-terminated SAM region after specific binding of streptavidin has occurred and the pure hydroxy-terminated region where nonspecific binding of streptavidin is negligible. Surface plasmon microscopy was also to monitor in situ and in real time the binding of streptavidin to the patterned SAMs. The ability of surface plasmon microscopy to detect and spatially resolve 2-dimensional monolayer binding events may prove useful in diagnostic applications involving the parallel interrogation at surface biomolecular arrays.

01,159
PB96-180161 Not available NTIS
National Inst. of Standards and Technology (MSEL), Gaithersburg, MD. Polymers Div.
Adsorption of Potassium N-phenylglycinate on Hydroxyapatite: Role of Solvents and Ionic Charge.
Final rept.
D. N. Misra. 1996, 9p.
Pub. in Colloids and Surfaces, A: Physiocochemical and Engineering Aspects, v108 p277-285 1996.

Keywords: *Adsorption, *Hydroxyapatite, Ionic charge, Reprints, Solvent role, *Foreign technology, Potassium salts, N-phenylglycinate.

The adsorption of the potassium salt of N-phenylglycine (KNPG) on synthetic hydroxyapatite from aqueous and ethanol solutions was studied at 22 degrees C. The adsorption isotherm of KNPG from aqueous solutions is Langmuirian in shape, and the analysis showed that one glycinate ion was adsorbed per about two (100) faces of the unit cell of hydroxyapatite. For each glycinate ion adsorbed, 3.5 phosphate ions were released to the aqueous solution while the calcium concentration decreased slightly. The adsorption from ethanol (99.8%) was total and irreversible from dilute solutions up to a threshold concentration, and reversible and Langmuirian thereafter from concentrated solutions, while the amounts of phosphate and calcium ions in solution are negligible. At maximum coverage from ethanol solution, the surface is fully occupied by reversibly adsorbed molecules which are perched on a one-to-one basis on the top of irreversibly adsorbed molecules totally covering the substrate. The amount of irreversibly adsorbed solute is thus equal to the reversibly adsorbed solute and about twice the maximum amount adsorbed from aqueous solutions.

01,160
PB96-186143 Not available NTIS
National Inst. of Standards and Technology (CSTL), Boulder, CO. Biotechnology Div.

Thermodynamics of the Hydrolysis of 3,4,5-Trihydroxybenzoic Acid Propyl Ester (n-Propylgallate) to 3,4,5-Trihydroxybenzoic Acid (Gallic Acid) and Propan-I-ol in Aqueous Media and in Toluene.
Final rept.
Y. B. Tewari, M. M. Schantz, M. V. Rekharsky, and R. N. Goldberg. 1996, 15p.
Pub. in Jnl. of Chemical Thermodynamics, v28 p171-185 May 96.

Keywords: *Calorimetry, *Enthalpy, *Equilibrium constants, Gallic acid, Reprints, High performance liquid chromatography, 2-(N-morpholino) ethanesulfonic acid.

Equilibrium measurements at several temperatures between 293 K and 309 K have been performed on the tannase catalyzed reaction; 3,4,5-trihydroxybenzoic acid propyl ester(sin) + H2O(sin) = 2,4,5-trihydroxybenzoic acid(sin) + propan-1-o1(sin), where sin = aqueous phosphate buffer, aqueous acetate buffer, and toluene. The change in binding of the hydrogen ion delta(r)N(H+) for this biochemical reaction in aqueous solution was calculated both from an equilibrium model for the biochemical reaction and from the dependence of the apparent equilibrium constant on pH. Calorimetric measurements were also performed for this biochemical reaction in aqueous phosphate and 2-(N-morpholino)ethanesulfonic acid (MES) buffers. Standard transformed thermodynamic quantities for the overall biochemical reaction as well as standard thermodynamic quantities for chemical reference reactions that involve specific chemical species have been calculated from the experimental results.

01,161
PB96-186150 Not available NTIS
National Inst. of Standards and Technology (MSEL), Gaithersburg, MD. Reactor Radiation Div.
Characterization of the Structure of YD3 by Neutron Powder Diffraction.
Final rept.
T. J. Udovic, Q. Huang, and J. J. Rush. 1996, 13p.
Pub. in Jnl. of Physics and Chem Solids, v57 n4 p423-435 1996.

Keywords: *Alloys, *Inorganic compounds, *Metals, Neutron scattering, Crystal structure, Reprints, *Foreign technology.

Neutron-powder-diffraction (NPD) measurements of the hexagonal rare-earth trideuteride gamma-YD3 were undertaken between 10 and 400 K. Rietveld refinements indicated that the YD3 structure possesses P3cl(D(sup 4)(sub 3d)) symmetry, in agreement with previous NPD studies of YD3 and HoD3. The unit cell is a (sq. root of 3 x sq. root of 3) R30 degrees expansion of the conventional hcp unit cell in the ab plane. To accomodate the D atoms, the c axis for YD3 is elongated by approx 15%(co/ao = 1.8019(1), ao = 3.6627(1) Angstrom, at 295K) compared with that for Y. The D atoms occupy unusual interstitial positions of a slightly distored, hcp metal lattice, instead of the ideal octahedral (o) and tetrahedral (t) sites. In particular, the hypothetical o-site D atoms are displaced vertically toward the Y-defined basal planes, with correlated placements at either near-plane or in-plane threefold metal (m) sites. The t-site D(Dt) atoms are displaced horizontally, also in a correlated fashion, with respect to the m-site D(Dm) atoms.

01,162
PB96-186176 Not available NTIS
National Inst. of Standards and Technology (MSEL), Gaithersburg, MD. Ceramics Div.
Preparation, Crystal Structure, Dielectric Properties, and Magnetic Behavior of Ba2Fe2Ti4O13.
Final rept.
T. A. Vanderah, Q. Huang, W. Wong-Ng, R. G. Geyer, J. Baker-Jarvis, R. S. Roth, A. Santoro, B. C. Chakoumakos, and R. B. Goldfarb. 1995, 7p.
Pub. in Jnl. of Solid State Chemistry, v120 p121-127 1995.

Keywords: *Magnetic properties, *Dielectric constant, *Barium iron titanate, Neutron diffraction, Reprints, Single crystal structure determination.

The preparation, crystal structure, dielectric properties, and magnetic behavior of the new compound Ba2Fe2Ti4O13 are reported. Structural studies carried out by single-crystal X-ray diffraction and neutron powder diffraction show that this phase is isostructural with K2Ti6O13 and Ba2ZnTi5O13 (C2/m(No. 12); a = 15.216(1), b = 3.8979(3), c = 9.1350(6) Angstrom, Beta = 98.460(7) degrees; V = 535.90(8) Angstrom; Z = 2). The cations Fe(sup 3+) and Ti(sup 4+) are partially ordered among distorted octahedral sites with Ba(sup 2+) occupying eleven-coordinated polyhedra. Ba2Fe2Ti4O13 exhibits TE0 resonance near 10 GHz with a dielectric constant of approx. 28 and a dielectric loss tangent of 2 x 10 to the minus 3. The compound displays complex paramagnetic behavior with marked field dependence; the magnetization at 80 kA/m is several orders of magnitude smaller than that of most ferrites.

01,163
PB96-200274 Not available NTIS
National Inst. of Standards and Technology (PL), Boulder, CO. Quantum Physics Div.
Excitation Transfer in Barium by Collisions with Noble Gases.
Final rept.
J. Brust, and A. C. Gallagher. 1995, 12p.
Grant NSF-PHY90-12244
Sponsored by National Science Foundation, Arlington, VA.
Pub. in Physical Review A, v52 p2120-2131 Sep 95.

Keywords: *Barium, *Energy transfer, *Noble gases, Reprints, *Molecule-molecule collisions, Transition probabilities.

We present a time-resolved study of excitation transfer processes between the low-lying excited states of barium induced by collisions with noble gases. The transient excited-state populations have been measured by means of fluorescence and absorption spectroscopy. Cross sections for spin-changing collisions from 3P1 to 1D2 and from 1D2 to 3D3 as well as for fine-structure mixing within the 3D multiplet were obtained by fitting the numerical solution of a seven-state system of rate equations including diffusion to the experimental data. We compare our results to experimental findings for other alkaline earth metals and report an improved value of the lifetime of the 6s6p3P1 state of barium.

01,164
PB96-201082 Not available NTIS
National Inst. of Standards and Technology (MEL), Gaithersburg, MD. Precision Engineering Div.
Scanning Electron Microscope Magnification Calibration Interlaboratory Study.
Final rept.
M. T. Postek, A. E. Vladar, S. N. Jones, and W. J. Keery. 1993, 2p.
Pub. in Proceedings of the Annual Meeting of the Microscopy Society of America (51st), p1-2 1993.

Keywords: *Electron microscopes, *Scanning, *Calibration standards, Prototypes, Lithography, Electron beams, Fabrication, Design, Reprints.

The National Institute of Standards and Technology (NIST) is in the process of developing a new scanning electron microscope (SEM) magnification calibration reference standard useful at both high and low accelerating voltages. The standard will be useful for all applications to which the SEM is currently being used, but it has been specifically tailored to meet many of the particular needs of the semiconductor industry. A small number of test samples with the pattern were prepared on silicon substrates using electron beam lithography at the National Nanofabrication Facility at Cornell University. The structures were patterned in titanium/palladium with maximum nominal pitch of approximately 3000 micro m scaling down to structures with minimum nominal pitch of 0.4 micro m. Several of these samples were sent out to a number of university, research, semiconductor and their industrial laboratories in an interlaboratory study. The purpose of the study was to test the SEM instrumentation and to review the suitability of the sample design.

01,165
PB96-201181 Not available NTIS
National Inst. of Standards and Technology (MSEL), Gaithersburg, MD. Ceramics Div.
NMR Characterization of Injection-Moulded Alumina Green Compacts. Part 2. T2-Weighted Proton Imaging.
Final rept.
P. S. Wang, S. G. Malghan, S. J. Dapkunas, K. F. Hens, and R. Raman. 1995, 6p.
Pub. in Jnl. of Materials Science, v30 p1069-1074 1995.

Keywords: *Nuclear magnetic resonance, *Ceramic slurries, *Proton imaging, Injection moulding, Alumina, Reprints, *Water distribution.

Injection-moulded alumina green compacts containing polypropylene, max, and stearic acid were studied for binder distribution by proton nuclear magnetic resonance (1H NMR) imaging. The solid imaging technique of nuclear spin-spin relaxation time, T2, weighted imaging at 400 MHz was used. This imaging technique utilizes a multiple pulse sequence of D0-(phi/2)plus or minus x-tau-D10-D7-(phi)x-D7-D10-AQ-D0 for echo detection and phase encoding. Two- and three-dimensional images were constructed from the intensities of these nuclear echo signals. Spatially resolved two-dimensional images obtained by the application of this technique indicated that the green compacts fabricated from the same nominal binder composition did not contain the same amounts of binder. This observation agrees well with our previous conclusion drawn from nuclear spin echo studies by Hahn's pulse sequence. A 64x64x64 three-dimensional imaging revealed that the inhomogeneity of binder distribution and internal inperfection do exist at certain locations of the samples. A binder-rich folder line was also detected in one of these green compacts.

01,166
PB96-204011 Not available NTIS
National Inst. of Standards and Technology (CSTL), Gaithersburg, MD. Chemical Kinetics and Thermodynamics Div.
Enthalpy Increment Measurements from 4.5 to 318 K for Bismuth(cr). Thermodynamic Properties from 0 K to the Melting Point.
Final rept.
D. G. Archer. 1995, 10p.
Pub. in Jnl. of Chemical and Engineering Data, v40 p1015-1024 1995.

Keywords: *Bismuth, *Thermodynamic properties, Reprints, Enthalpy, Temperature scales, Measurements.

Enthalpy increments for bismuth(cr) were measured from 4.5 to 318 K with an adiabatic calorimeter. The calorimeter's performance was demonstrated through comparison of measured enthalpy increments for copper and aluminum oxide to literature values. The effect that different temperature scales had on these comparisons for copper at low temperatures was discussed. The new enthalpy increments for bismuth(cr) were combined with previously measured thermodynamic properties for temperatures below 4 K and about 300 K in order to generate the thermodynamic properties of bismuth(cr) from 0 K to the melting point.

01,167
PB96-204151 Not available NTIS
National Inst. of Standards and Technology (CSTL), Gaithersburg, MD. Chemical Kinetics and Thermodynamics Div.
Deuterium Isotope Effect in Vinyl Radical Combination/Disproportionation Reactions.
Final rept.
A. Fahr, and A. H. Laufer. 1995, 3p.
Pub. in Jnl. of Physical Chemistry, v99 p262-264 1995.

Keywords: *Isotope effect, *Vinyl radical, Reprints, Combination reactions, Disproportionation reactions.

The deuterium isotope effect for the vinyl radical combination and disproportionation reactions have been investigated. Protonated or deuterated vinyl and methyl radicals are produced from the 193 nm photolysis of protonated or perdeuterated methyl vinyl ketone. On the basis of product yield measurements, no isotope effect for the combination reactions of either vinyl-vinyl or vinyl-methyl has been observed. From the relative yields of ethylene, an isotope effect of kh/kd=1.20 is determined for the vinyl-vinyl disproportionation reaction.

01,168
PB96-204169 Not available NTIS
National Inst. of Standards and Technology (CSTL), Gaithersburg, MD. Chemical Kinetics and Thermodynamics Div.
Temperature Dependence of the Ultraviolet Absorption Cross Section of CF3I.
Final rept.
A. Fahr, A. K. Nayak, and R. E. Huie. 1995, 10p.
Pub. in Chemical Physics, v199 p275-284 1995.

Keywords: *Ultraviolet spectra, *Temperature dependence, Reprints, Temperatures, Absorption, Cross sections, *CF3I.

The ultraviolet absorption cross section of CF3I has been measured in the gas phase over the wavelength range 160-240 nm for temperatures 240, 295, 355 K

and over the wavelength range 240-350 nm for temperatures ranging from 218 to 333 K. Two intense and sharp absorption bands centered at about 160 and 171 nm and a broad and relatively strong band centered at about 267.5 nm were observed. The absorption band centered at 171 nm shows significant vibrational structure. The cross sections, at absorption peaks, between 160 and 175 nm, increased by increasing temperature. At the near-UV maximum of 267.5 nm, the absorption increased with decreasing temperature, but decreased at the lowest temperature. At wavelengths greater than about 280 nm, the absorption cross section decreased with decreasing temperature. The absorption cross sections were found to all fit a triple Gaussian expression for lambda greater than 250 nm.

01,169
PB96-204177 Not available NTIS
National Inst. of Standards and Technology (CSTL), Gaithersburg, MD. Chemical Kinetics and Thermodynamics Div.
Temperature Dependent Ultraviolet Absorption Cross Sections of Propylene, Methylacetylene and Vinylacetylene.
Final rept.
A. Fahr, and A. Nayak. 1996, 8p.
Pub. in Chemical Physics, v203 p351-358 1996.

Keywords: *Temperature dependence, *Ultraviolet, *Absorption cross sections, Reprints, Propylene, Methylacetylene, Vinylacetylene, Planetary atmosphere.

The temperature dependence of the UV absorption cross sections of propylene (CH3CH=CH2) and the methylacetylene (CH3C identical with CH) from 160 to 200 nm and vinylacetylene (CH2 = CHC identical with CH) from 160 to 240 nm have been measured in the gas phase, for temperatures ranging from about 220 to 330 K. The propylene spectrum, exhibits a broad absorption band with a maximum at 172.0 nm with some structure to the short wavelength side of the broad band. At the absorption peaks a small increase (about 5%) in the cross sections has been observed with decreasing temperature from 333 to 233 K. At the long wavelength tail of the absorptionn band the cross sections are found to decrease with decreasing temperature. The absorption spectrum of methylacetylene in the region of 160 to 200 nm consists of a broad continuum with a maximum at 172.4 nm. The cross section values, for methylacetylene, near the absorption peak are found to remain nearly independent of temperture. However, at the long wavelength side of the absorption band the cross sections increase with increasing temperature. The spectrum of vinylacetylene consists of a very strong and structured absorption in the 160 to 170 nm region and strong diffuse bands between around 190 and 230 nm. The cross section values at the absorption peaks, determined at low temperatures, are significantly higher than those at higher temperatures.

01,170
PB96-210711 PC A04/MF A01
National Inst. of Standards and Technology (CAML), Gaithersburg, MD. Applied and Computational Mathematics Div.
Diffuse-Interface Description of Fluid Systems.
D. M. Anderson, and G. B. McFadden. Aug 96, 37p, NISTIR-5887.
Figures in this document may not be legible in microfiche.

Keywords: *Critical point, *Diffuse interface, Hydrodynamics, Surface tension, Internal waves, Models, Fluid-fluid systems.

The authors consider a diffuse-interface model for fluid-fluid systems. In classical models, an iterface between two fluids is treated as infinitely thin, or sharp, and is endowed with properties such as surface tension. Diffuse-interface theories replace this sharp interface with continuous variation of an order parameter such as density in a way consistent with microscopic theories of the interface. Surface tension effects, for example, are incorporated into the model through a modified stress tensor in the classical Navier-Stokes equations. The authors relate the diffuse-interface model to classical, sharp interface models by deriving asymptotically the governing equations and the associated boundary conditions used in the sharp-interface formulation. The authors illustrate the diffuse-interface approach by modeling internal gravity waves, which have been observed experimentally be Berg et al. in xenon near its critical point. The authors obtain static density profiles, compute internal wave frequencies and compare with their experimental data and theoretical (classical) results both above and below the critical temperature. The results reveal a singularity in the diffuse-interface model in the limit of incompressible perturbations.

01,171
PB97-109116 (Order as PB97-109011, PC A11/MF A03)
National Inst. of Standards and Technology, Gaithersburg, MD.
Biological Macromolecule Crystallization Database and NASA Protein Crystal Growth Archive.
G. L. Gilliland, M. Tung, and J. Ladner. 1996, 12p.
Prepared in cooperation with Maryland Univ., Rockville. Center for Advanced Research in Biotechnology.
Included in Jnl. of Research of the National Institute of Standards and Technology, v101 n3 p309-320 May/Jun 96.

Keywords: *Crystallography, *X ray diffraction, Data bases, Information systems, Crystal structure, Three dimensional models, Microgravity, Nucleic acids, Pesticides, Proteins, *Biological macromolecules.

The NIST/CARB Biological Macromolecule Crystallization Datbase (BMCD), NIST Standard Reference Database 21, contains crystal data and crystallization conditions for biological macromolecules. The database entries include data abstracted from published crystallographic reports. Each entry consists of information describing the biological macromolecule crystallization conditions for each crystal form. The BMCD serves as the NASA Protein Crystal Growth Archive in that it conains protocols and results of crystallization experiments undertaken in microgravity (space). These database entries report the results, whether successful or not, from NASA-sponsored protein crystal growth experiments in microgravity and from microgravity crystallization studies sponsored by other international organizations. The BMCD was designed as a tool to assist x-ray crystallographers in the development of protocols to crystallize biological macromolecules, those that have previously been crystallized, and those that have not been crystallized.

01,172
PB97-109151 (Order as PB97-109011, PC A11/MF A03)
Du Pont de Nemours (E.I.) and Co., Wilmington, DE. Central Research and Development Dept.
Troublesome Crystal Structures: Prevention, Detection, and Resolution.
R. L. Harlow. 1996, 13p.
Included in Jnl. of Research of the National Institute of Standards and Technology, v101 n3 p327-339 May/Jun 96.

Keywords: *Crystallography, *Error analysis, *Information systems, Data bases, Performance evaluation, Crystal structure.

A large number of incorrect crystal structures is being published today. These structures are proving to be a particular problem to those of us who are interested in comparing structural moieties found in the databases in order to develop structure-property relationships. Problems can reside in the input data, e.g., wrong unit cell or low quality intensity data, or in the structural model, e.g., wrong space group or atom types. Many of the common mistakes are, however, relatively easy to detect and thus should be preventable; at the very least, suspicious structures can be flagged, it not by the authors then by the references and, ultimately, the crystallographic databases. This article describes some of the more common mistakes and their effects on the resulting structures, lists a series of tests that can be used to detect incorrect structures, and makes a strong plea for the publication of higher quality structures.

01,173
PB97-110118 Not available NTIS
National Inst. of Standards and Technology (CSTL), Gaithersburg, MD. Physical and Chemical Properties Div.
Compressed Liquid Densities, Saturated Liquid Densities, and Vapor Pressures of 1,1-Difluoroethane.
Final rept.
D. R. Defibaugh, and G. Morrison. 1996, 6p.
Pub. in Jnl. of Chemical and Engineering Data, v41 n3 p376-381 1996.

Keywords: *Vapor pressures, *Liquid densities, Compression, Saturation, Measurements, Correlations, Comparisons, Reprints, *Difluoroethane.

The compressed liquid densities and vapor pressures of 1,1,-difluoroethane (HFC-152a) have been measured, correlated, and compared with other data. The liquid densities were measured with a combined standard uncertainty of plus or minus 0.05% using a vibrating tube densimeter over a temperature range of 243 K to 371 K and at pressures from near the saturated vapor pressure to 6500 kPa; thus the data extend nearly to the critical point (Tc=386.41 K and Pc=4514.7 kPa). The vapor pressures were measured with a combined standard uncertainty of plus or minus 0.02% using a stainless steel ebulliometer in the temperature range from 280 K to 335 K. Saturated liquid densities were calculated by extrapolating the compressed liquid isotherms to the saturation pressure.

01,174
PB97-110241 Not available NTIS
National Inst. of Standards and Technology (CSTL), Gaithersburg, MD. Biotechnology Div.
Electrolytes Constrained on Fractal Structures: Debye-Huckel Theory.
Final rept.
S. H. Lee, and J. B. Hubbard. 1993, 5p.
Pub. in Jnl. of Chemical Physics, v98 n2 p1504-1508 Jan 93.

Keywords: *Debye-Huckel theory, *Fractal structures, *Electrolytes, Ionic screening, Thermodynamic properties, Reprints.

The authors calculate, via the Debye-Huckel theory, the effect of ionic screening on the thermodynamic properties of an electrolyte confined topologically to an isotropic random fractal structure embedded in three dimensions. It is found that screening effects are generally important, even for low fractal dimensions. In many instances crossover effects occur, whereby with increasing ionic strength, a low dimension fractal is more stabilized by screening than a fractal of higher dimension.

01,175
PB97-110365 Not available NTIS
National Inst. of Standards and Technology (CSTL), Gaithersburg, MD. Chemical Kinetics and Thermodynamics Div.
Isopiestic Investigation of the Osmotic and Activity Coefficients of Aqueous NaBr and the Solubility of NaBr2H2O(cr) at 298.15 K: Thermodynamic Properties of the NaBr + H2O System over Wide Ranges of Temperature and Pressure.
Final rept.
J. A. Rard, and D. G. Archer. 1995, 16p.
Pub. in Jnl. of Chemical and Engineering Data, n40 p170-185 1995.

Keywords: *Sodium bromide, *Thermodynamics, Isopiestic, Activity, Solubility, Reprints, CODATA key values.

Isopiestic vapor-pressure measurements have been performed for aqueous solutions of well-characterized high-purity NaBr from 1.9551 to 9.4778 mol-kg(-1) at 298.15 K; the highest five molalities correspond to supersaturated concentrations. Solubilities have also been determined by the methods. A few equilibrations were made between solutions of NaCl and H2SO4 to refine the osmotic coefficients of H2So4 at high molalities. These isopiestic results for NaBr have been combined with other experimental thermodynamic quantities (vapor pressures, activity coefficients, solubilities, freezing temperatures, and volumetric and calorimetric measurements) to yield revised parameters for an extended form a Pitzer's equation applicable over wide ranges of molality, temperature, and pressure. It was not possible to obtain a complete consistency between the experimental results for either the NaBr + H2O system or the NaCl + H2O system with entropies from the CODATA Key Values for Thermodynamics.

01,176
PB97-111223 Not available NTIS
National Inst. of Standards and Technology (CSTL), Gaithersburg, MD. Chemical Kinetics and Thermodynamics Div.
Resonance Enhanced Multiphoton Ionization Spectroscopy of the SnF Radical.
Final rept.
J. Pearson, R. N. Dixon, J. W. Hudgens, and R. D. Johnson. 1996, 5p.
See also PB90-170028.
Pub. in Jnl. of Chemical Physics, v104 n12 p4406-4410 1996.

Keywords: *Chemical radicals, *Tin monofluoride, Visible spectrum, Vibrational spectra, Reprints, *Multiphoton ionization, *Multi-photon processes, Rydberg states.

The resonance enhanced multiphoton ionization spectrum of the free radical SnF has been recorded using excitation wavelengths in the range 540 to 360 nm. The previously documented C2(delta), D, E(2)II, and F(2)sigma states and two hitherto unidentified excited states, the H and I(2)phi states, were all observed as two-photon resonances. Band contour simulations yielded spectroscopic constants for the E, F, and I states.

01,177
PB97-111314 Not available NTIS
National Inst. of Standards and Technology (CSTL), Gaithersburg, MD. Chemical Kinetics and Thermodynamics Div.
Fluoride Elimination Upon Reaction of Pentafluoroaniline with e (sub eq')(sup -), H, and OH Radicals in Aqueous Solution.
Final rept.
L. C. T. Shoute, J. P. Mittal, and P. Neta. 1996, 5p.
Pub. in Jnl. of Physical Chemistry, v100 n27 p11355-11359 1996.

Keywords: *Pentafluoroaniline, *Pulse radiolysis, Absorption spectra, Reduction, Oxidation, Reprints.

Reduction of pentafluoroaniline (PFA) leads to rapid fluoride elimination to form the aminotetrafluorophenyl radical. This radical undergoes rapid intramolecular electron transfer from the amino group to the phenyl radical site and protonates at the latter site to form the tetrafluoroaniline radical cation or its deprotonated form (pKa = 2.3). Oxidizing radicals such as SO4-, N3, and Cl2- oxidize PFA to the pentafluoroaniline radical cation. The pKa = 1.9 of the pentafluoroaniline radical cation is 3.6 units lower than that expected from the substituent effects of fluorine atoms. Addition of OH to PFA is followed by rapid HF elimination to yield the aminotetrafluorophenoxyl radical. In acidic solution, however, the reaction of OH leads to formation of the pentafluoroaniline radical cation. Fluoride elimination upon reduction and upon OH addition to PFA was confirmed by determination of fluoride ion yield.

01,178
PB97-111538 Not available NTIS
National Inst. of Standards and Technology (CSTL), Gaithersburg, MD. Chemical Kinetics and Thermodynamics Div.
Ionization Energies, Appearance Energies and Thermochemistry of CF2O and FCO.
Final rept.
T. J. Buckley, R. D. Johnson, R. E. Huie, R. B. Klemm, Z. Zhang, and S. C. Kuo. 1995, 7p.
Pub. in Jnl. of Physical Chemistry, v99 n14 p4879-4885 1995.

Keywords: *Ionization energy, *Photoionization, Discharge flow, Mass spectrometry, Formation heat, Bond strength, Appearance energy, Reprints.

With the discharge flow-photoionization mass spectrometer (DF-PIMS) coupled to the U-11 beamline at the National Synchrotron Light Source, the authors have measured the ionization energies of C2F4, CF4, and CF2O and appearance energy of FCO+ from CF2O. The PIMS results corroborate those determined by other techniques. With high-level ab initio calculations that utilize a large basis set and isogyric corrections, they have determined an ionization energy of 9.3 plus or minus 0.1 eV for FCO. At 298 K, the heats of formation of FCO (-152 plus or minus 12 kJ/mol) and FCO+ (745.3 plus or minus 9.6 kJ/mol) (relative to (delta)fH 298 (CF2O)= -607.9 plus or minus 7.1 kJ/mol) were determined and agree to within the uncertainties of other measurements but with much higher precision. The authors have evaluated the bond strengths D 298(F-CFO) and D 298(F-CO) to be 535 plus or minus 12 and 121 plus or minus 12 kJ/mol, respectively.

01,179
PB97-111967 Not available NTIS
National Inst. of Standards and Technology (CSTL), Gaithersburg, MD. Chemical Kinetics and Thermodynamics Div.
One-Electron Oxidation of Metalloporphycenes as Studied by Radiolytic Methods.
Final rept.
D. M. Guldi, J. Field, J. Grodkowski, P. Neta, and E. Vogel. 1996, 6p.
Pub. in Jnl. of Physical Chemistry, v100 n32 p13609-13614 1996.

Keywords: *Metalloporphycenes, *Radiolysis, Oxidation, Porphycenes, Pulse radiolysis, Absorption spectra, Reprints.

One-electron and two-electron oxidation of 2,7,12,17-tetrapropylporphycene (H2TPrPc) and its Fe, Co, Ni, Cu, and Sn complexes in Ch2Cl2, CCl4, and 2-PrOH solutions have been studied by radiolytic techniques. Formation and decay of intermediates formed upon one-electron oxidation have been followed by kinetic spectrophotometric pulse radiolysis, and the absorption spectra of stable oxidation products have been recorded following gamma-radiolysis. H2TPrPc is oxidized to the pi-radical cation and then to the dication, which is stable in aprotic solvents but is transformed to a different product in 2-PrOH. Similar oxidation to the pi-radical cation and then to the dication was observed for the CuII, SnIV, CoIII, and FeIII porphycenes. CoII and NiII porphycenes underwent radiolytic oxidation to form stable CoIII and NiIII products. The stability of the latter is in contrast with previous electrochemical observations, the difference is ascribed tc the effect of the axial ligand.

01,180
PB97-112361 Not available NTIS
National Inst. of Standards and Technology (CSTL), Gaithersburg, MD. Chemical Kinetics and Thermodynamics Div.
Absorption Cross Sections, Kinetics of Formation, and Self-Reaction of the IO Radical Produced via the Laser Photolysis of N2O/I2/N2 Mixtures.
Final rept.
1995, 7p.
Sponsored by Department of the Air Force, Washington, DC. and Department of the Army, Washington, DC.
Pub. in Jnl. of Physical Chemistry, v99 p11701-11707 1995.

Keywords: *Iodine monoxide, *Laser photolysis, Atmosphere chemistry, Kinetics, Ozone, Spectra, Reprints.

The laser photolytic production of the IO radical from N2O/I2/N2 mixtures was used to measure the radical absorption spectrum from 340 to 450 nm. Two new absorption peaks at 403 and 411 nm were observed along with an underlying continuum starting at about 420 nm and extended to about 350 nm. An absorption cross section (2.8 plus or minus 0.5) x 10(-17) cm(2), in good agreement with previous measurements, was determiend for the (4-0) band head at 427.2 nm. From the rate of formation of IO and the rate of loss of I2, rate constants for the reactions O = I2 -> IO + I and O + OI -> O2 + I of (1.4 plus or minus 0.4) x 10(-10) and (1.2 plus or minus 0.5) x 10 to the minus 10 power cm(3)s(-1), respectively, were derived. Finally, from the rate of decay of IO, a rate constant for the reaction IO + IO -> products of (8.0 plus or minus 1.8) x 10(-11) cm(3)s(-1) was obtained. All of the uncertainties expressed are 2 standard deviations derived from the statistical analysis and do not include estimates for possible systematic errors.

01,181
PB97-112528 Not available NTIS
National Inst. of Standards and Technology (CSTL), Gaithersburg, MD. Chemical Kinetics and Thermodynamics Div.
Thermochemical Studies of Inorganic Chalocogenides by Fluorine-Combustion Calorimetry: Binary Compounds of Germanium and Silicon with Sulfur, Selenium and Tellurium.
Final rept.
P. A. G. O'Hare. 1995, 13p.
Pub. in Thermochimica Acta, v267 p1-13 1995.

Keywords: *Chalcogenides, *Thermochemistry, *Enthalpy, Dissociation, Germanium silicides, Germanium selenides, Silicon compounds, Tellurides, Selenium, Reprints, *Fluorine-combustion calorimetry.

A general outline is given of the technique of fluorine-bomb calorimetry, including equipment, experimental procedures, sample purity requirements, post-combustion analyses, and interpretation of the results. Some recent measurements are described on Si2Te3, SiSe2, GeS, and GeS2. How the thermochemistry-based results for the dissociation enthalpies D(sup o)(sub m) of the gaseous diatomic molecules SiTe, SiSe, GeS, and GeSe correlate with the D(sup o)(sub m) derived from spectroscopy is also discussed.

01,182
PB97-112536 Not available NTIS
National Inst. of Standards and Technology (CSTL), Gaithersburg, MD. Chemical Kinetics and Thermodynamics Div.
Thermodynamics of (Germanium + Selenium): A Review and Critical Assessment.
Final rept.
P. A. G. O'Hare, A. Zywocinski, and L. A. Curtiss. 1996, 22p.
Pub. in Jnl. of Chemical Thermodynamics, v28 p459-480 1996.

Keywords: *Thermodynamic properties, *Germanium, *Selenium, Thermochemistry, Molecular structure, Heat capacity, Combustion kinetics, Heat of formation, Enthalpy, Dissociation, Gibbs free energy, Wavenumbers, Reprints, Bond energy.

The review deals with the critical assessment of the thermodynamic properties of several germanium selenides: GeSe(cr), GeSe(g), GeSe2(cr), GeSe2(g), and Ge2Se2(g). In the absence of experimental information, the structures, internuclear distances, and vibrational wavenumbers were calculated for GeSe2(g) and Ge2Se2(g) by molecular orbital methods.

01,183
PB97-113112 Not available NTIS
National Inst. of Standards and Technology (MSEL), Gaithersburg, MD. Reactor Radiation Div.
Molecular Dynamics Investigation of the Surface/Bulk Equilibrium in an Ethanol-Water Solution.
Final rept.
M. Tarek, D. J. Tobias, and M. L. Klein. 1996, 5p.
Pub. in Jnl. of the Chemical Society, Faraday Trans., v92 n4 p559-563 1996.

Keywords: *Ethanol water solution, *Molecular dynamics, *Surface tension, Surface excess, Hydrogen bonding, Density profiles, Air liquid interface, Reprints, *Foreign technology.

Molecular dynamics simulations of the vapor/solution interface, initiated from an ethanol-water mixture at a mole fraction of ethanol, Xc = 0.1, have been performed. Rapid redistribution of ethanol molecules to the free surface was observed during simulations of two different sized systems. Inspection of the calculated surface structure reveals that after redistributing the ethanol molecules are preferentially oriented such that the alkyl group points out the solution. A 'depletion layer' of enhanced water density beneath the ethanol surface excess was revealed by the simulation. Analysis of the structure involving molecules close to the surface shows that water molecules are arranged to maximize the hydrogen bonding between the oriented ethanol and the adjacent water molecules. The enhanced water density beneath the interface results from this optimization. The surface tension calculated from the simulation is ca. 50% higher than the results of macroscopic experimental measurements. This overestimation is attributed to shortcomings to both the potential function and the simulation methodology. The number of density profiles of the ethanol surface excess were compared with results from neutron reflectivity measurements. The calculated profiles agree better with the experimental measurements at the calculated surface tension (i.e. Xc = 0.022) than those reported for Xc = 0.1 mixtures.

01,184
PB97-118343 Not available NTIS
National Inst. of Standards and Technology (PL), Gaithersburg, MD. Molecular Physics Div.
Excitons in Complex Quantum Nanostructures.
Final rept.
G. W. Bryant, P. S. Julienne, and Y. B. Band. 1996, 4p.
Pub. in Surface Science, n361/362 p801-804 Oct 96.

Keywords: *Excitons, *Quantum wells, Reprints, *Nanostructures, Semiconductor-semiconductor heterostructures, Semi-empirical models, Model calculations.

A theory for excitons in complex quantum nanostructures with complicated geometries and strong coupling between nanostructures is presented. Effective mass models with screened Coulomb interaction give reasonable ground-state energies for excitons in T-shaped quantum wires, coupled T-quantum wires and quantum dot quantum wells, provided the effects of complex geometry are included. A sizable shift between exciton states in quantum wells and T-shaped wires occurs due to a 40% enhancement in binding energy, confirnment in the wire, and significant interwire coupling.

01,185
PB97-118350 Not available NTIS
National Inst. of Standards and Technology (PL), Gaithersburg, MD. Atomic Physics Div.
Quantum Dots in Quantum Well Structures.
Final rept.
G. W. Bryant. 1996, 12p.
Pub. in Jnl. of Luminescence, v70 p108-119 Nov 96.

Keywords: *Quantum dots, *Energy levels, Quantum wells, Strain, Reprints.

Recent progress toward fabricating and characterizing quantum dots in III-V quantum well structures is reviewed. Quantum dots made by use of lithography and etching, including deep-etched, barrier-modulated, strain-induced and interdiffused quantum dots, are described. Quantum dots fabricated by growth, including natural quantum dots, dots on patterned substrates, and self-assembled dots, are discussed. Dot sizes and uniformity, energy-level splittings, and luminescence efficiencies that are now being achieved are discussed. The status of key issues, such as the energy relaxation in quantum dots, is mentioned.

01,186
PB97-119127 Not available NTIS
National Inst. of Standards and Technology (CSTL), Gaithersburg, MD. Chemical Kinetics and Thermodynamics Div.
Kinetics of the Reaction of the Sulfate Radical with the Oxalate Anion.
Final rept.
R. E. Huie, and C. L. Clifton. 1996, 5p.
Pub. in International Jnl. of Chemical Kinetics, v28 p195-199 1996.

Keywords: *Atmospheric chemistry, *Chemical kinetics, *Sulfate radicals, Oxalate anions, Reprints.

The kinetics of the reaction of the sulfate radical, SO4, with the oxalate anion, C2O4(2-), was studied in aqueous solution and second-order rate constants, corrected for the effects of ionic strength, derived. Measurements were carried out over the temperature range 24 - 60 degrees C resulting in the expression k(0) = 2.10 plus or minus 0.96 x 10 to the 8th power exp(-1080 plus or minus 140/T) L mol to the minus 1 power s to the minus 1 power.

01,187
PB97-119143 Not available NTIS
National Inst. of Standards and Technology (PL), Gaithersburg, MD. Molecular Physics Div.
Matrix Isolation Study of the Interaction of Excited Neon Atoms with BCl3: Infrared Spectra of BCl(sub 3, sup +), BCl(sub 2, sup +), and BCl(sub 3, sup -).
Final rept.
M. E. Jacox, K. K. Irikura, and W. E. Thompson. 1996, 8p.
See also PB97-112403.
Pub. in Jnl. of Chemical Physics, v104 n22 p8871-8878 Jun 96.

Keywords: *Neon, *Molecular ions, *Vibrational spectra, Boron chlorides, Interactions, Infrared spectra, Reprints, *Matrix isolation.

When a Ne:BCl3 sample is codeposited at approximately 5 K with a beam of neon atoms that have been excited in a microwave discharge, the infrared spectrum of the resulting solid deposit shows a weak to moderately intense absorption of BCl2 and more prominent absorptions which are assigned to the v3 fundamentals of BCl3 (D3h) and of linear, centrosymmetric BCl2. The boron- and chlorine-isotopic structure of the spectrum is consistent with both of these assignments. Ab initio calculations support the BCl2 assignment. An absorption is also tentatively assigned to V3(e) of BCl3. Ab initio calculations for BCl3 are consistent with that assignment. The processes which occur when the solid deposit is exposed to visible and ultraviolet radiation are considered.

01,188
PB97-119234 Not available NTIS
National Inst. of Standards and Technology (PL), Gaithersburg, MD. Optical Technology Div.
Vibrational Spectra of Molecular Ions Isolated in Solid Neon. 13. Ions Derived from HBr and HI.
Final rept.
C. L. Lugez, M. E. Jacox, and W. E. Thompson. 1996, 10p.
See also PB95-125688.
Pub. in Jnl. of Chemical Physics, v105 n10 p3901-3910 1996.

Keywords: *Molecular ions, *Vibrational spectra, Infrared absorption, Infrared spectra, Electron capture, Matrix isolation, Reprints, *Solid neon.

When a Ne:HBr or a Ne:HI sample is codeposited at approximately 5 K with discharge-excited neon atoms, the infrared spectrum of the resulting solid includes not only the absorptions of the HX molecule and its multimers but also a prominent absorption of HBr+ or HI+. The absorption of each of the two cations lies close to its gas-phase band center. The vibrational fundamentals of DBr+ and DI+ are also identified in experiments on deuterium-enriched samples. Other infrared absorptions are assigned to normal and deuterium-substituted (HBr)2+ and (HI)2+, as well as to BrHBr-, and IHI-. Studies of changes in the absorption spectrum which result from exposure of the deposit to filtered visible and near ultraviolet radiation support these assignments and provide further information on photodissociation and photodetachment processes which occur in these systems.

01,189
PB97-119341 Not available NTIS
National Inst. of Standards and Technology (PL), Gaithersburg, MD. Optical Technology Div.
Self-Consistent 'GW' and Higher-Order Calculations of Electron States in Metals.
Final rept.
E. L. Shirley. 1996, 7p.
Pub. in Physical Review B, v54 n11 p7758-7764 Sep 96.

Keywords: *Electron states, *Metals, Self-consistent, Vertex correction, Bandwidths, Reprints.

Past work, treating simple metals in the GW approximation, has largely neglected effects of self-consistency and higher-order vertex corrections on occupied bandwidths. The work presents self-consistent GW results, plus nearly self-consistent higher-order results, for jellium, illustrating that both effects are large, yet largely canceling (e.g., 0.65-eV effects on the sodium bandwidth, but a combined effect of only 0.13 eV). This supports findings that many-body effects substantially reduce such bandwidths.

01,190
PB97-119358 Not available NTIS
National Inst. of Standards and Technology (CSTL), Gaithersburg, MD. Chemical Kinetics and Thermodynamics Div.
Thermodynamic Properties of Silicides. 5. Standard Molar Enthalpy of Formation at the Temperature 298.15 K of Trimolybdenum Monosilicide Mo3Si Determined by Fluorine-Combustion Calorimetry.
Final rept.
I. Tomaszkiewicz, G. A. Hope, C. M. Beck, and P. A. G. O'Hare. 1996, 14p.
Pub. in Jnl. of Chemical Thermodynamics, v28 p29-42 1996.

Keywords: *Thermochemistry, *Heat capacities, *Enthalpy increments, Silicides, Temperatures, Calorimetry, Reprints, Trimolybdenum monosilicide.

The massic (formerly called specific) energies of combustion in fluorine of two different specimens of trimolybdenum monosilicide have been measured in a bomb calorimeter and the standard molar enthalpy of formation delta(f)H(m)(Mo3Si,cr,298.15 K) determined to be -(125.2 plus or minus 5.8) kJ-mol to the minus one power. A critical evaluation of the thermodynamic properties of Mo3Si is also presented, and recommended values for the standard molar enthalpy increments, standard molar heat capacities, standard molar enthalpies of formation, and standard molar Gibbs free energeis of formation have been tabulated to T = 2300 K.

01,191
PB97-122402 Not available NTIS
National Inst. of Standards and Technology (CSTL), Gaithersburg, MD.
Oxidation of Ferrous and Ferrocyanide Ions by Peroxyl Radicals.
Final rept.
G. I. Khaikin, Z. B. Alfassi, R. E. Huie, and P. Neta. 1996, 6p.
Pub. in Jnl. of Physical Chemistry, v100 n17 p7072-7077 1996.

Keywords: *Oxidation, *Iron ions, *Peroxyl radicals, Ferrous ions, Ferrocyanide ions, Reprints.

Alkylperoxyl and arylperoxyl radicals were produced by pulse radiolysis in aqueous solutions, and their reactions with ferrous and ferrocyanide ions were studied by kinetic spectrophotometry. Oxidation of Fe(CN)6(4-) took place with rate constants that varied from less than 1 x 10 to the 5th power to 5 x 10 to the 7th power L mol(-1)s(-1), depending on the electron-withdrawing effects of the substituents on the peroxyl radical and presumably reflecting variations in reduction potential of the peroxyl radical, as expected for outer-sphere electron transfer. Oxidation of Fe(aq)(2+), on the other hand, took place by an inner-sphere mechanism controlled by the rate of dissociative interchange of the water ligand. The rate constants were nearly the same for all the peroxyl radicals examined (k=(0.5 - 1.1) x 10 to the 6th power L mol(-1)s(-1)) and involved the formation of a transient intermediate, RO2(-)Fe(3+), which later decomposed to yield Fe(aq)(3+). The decomposition was accelerated by H(+) and by Fe(2+). The proposed mechanism is a modification of a previously suggested reaction scheme.

01,192
PB97-122451 Not available NTIS
National Inst. of Standards and Technology (PL), Gaithersburg, MD. Molecular Physics Div.
Perpendicular C-H Stretching Band nu9/nu13 and the Torsional Potential of Dimethylacetylene.
Final rept.
J. Pliva, A. S. Pine, and S. Civis. 1996, 11p.
Pub. in Jnl. of Molecular Spectroscopy, Article No. 0220, v180 p15-25 1996.

Keywords: *Free rotors, *Infrared spectrums, Internal rotation, Torsional potential, Tunable laser, Reprints, *Dimethylacetylene.

The perpendicular band of the fourfold degenerate C-H stretching vibration of dimethylacetylene (2-butyne) occurring in the region 2955-3065 cm(-1) has been measured with Doppler-limited resolution at a temperature of approximately 195 K on a difference-frequency laser spectrometer, and on a high-resolution Fourier transform instrument at room temperature as well as in a molecular jet at approximately 20 K. From a detailed rotational analysis of this complex band, based on an extension of the mode of the rotational-torsional interactions described by P. R. Bunker and C. di Lauro (Chem. Phys. 190, 159-169, 1995), accurate spectroscopic constants were determined for the upper CH stretching state, along with values for the first three components of the Fourier expansion for the torsional potential in the ground state, and for six components of this potential in the upper state. Over 700 lines assigned to 37 well-resolved subbands plus 25 additional unresolved line-like Q-branches were fitted with an overall standard deviation of 0.0024 cm(-1). the results yield a value of 6.316 plus or minus 0.034 cm(-1) for the barrier to internal rotation in the ground state, and 6.643 plus or minus 0.006 cm(-1) for the C-H stretching state. This value for the ground state barrier is somewhat higher than that recently determined from an analysis of the CH3 rocking band by P. R. Bunker et al.

01,193
PB97-122493 Not available NTIS
National Inst. of Standards and Technology (PL), Gaithersburg, MD. Radiometric Physics Div.
Measuring Nondipolar Asymmetries of Photoelectron Angular Distributions.
Final rept.
P. S. Shaw, U. Arp, and S. H. Southworth. 1996, 10p.
Pub. in Physical Review A, v54 n2 p1463-1472 Aug 96.

Keywords: *Angular distributions, *X rays, *Photoelectrons, Non-dipolar effects, Synchrotrons, Reprints.

In theories of photoelectron angular distributions at soft x-ray energies from 1keV to 10 keV, first-order corrections to the dipole approximation give rise to two non-dipolar asymmetry parameters in addition to the well-known dipolar asymmetry parameter, beta. The non-dipolar parameters characterize the forward/backward asymmetry with respect to the propagation vector of the photon beam. Experimentally, the measurement of the non-dipolar effect has been hampered because of the complications resulting from the three-parameter angular distribution. In the paper, the authors suggest various experimental approaches to the measurement of the three asymmetry parameters using partially linearly polarized x-rays, corresponding to measurements on synchrotron radiation beamlines. They

decribe methods to extract the asymmetry parameters using such approaches.

01,194
PB97-122543 Not available NTIS
National Inst. of Standards and Technology (CSTL), Gaithersburg, MD. Physical and Chemical Properties Div.
Absence of Quantum-Mechanical Effects on the Mobility of Argon Ions in Helium Gas at 4.35 K.
Final rept.
L. A. Viehland, and J. J. Hurly. 1996, 4p.
Pub. in Jnl. of Chemical Physics, v105 n24 p1-4 1996.

Keywords: *Transport cross sections, *Argon, *Helium, Mobilities, Potential, Spectroscopy, Reprints.

Quantum-mechanical transport cross sections are accurately computed from recent spectroscopic potentials for the three lowest energy levels of the molecular ion HeAr+. Statistical and ground state combinations of the cross sections are used to compute the transport coefficients describing the motion of Ar+ ions through He gas at 4.35 K. The calculated mobilities do not show the rapid decrease of the experimental values as the ratio of the electric field strength to the gas number density becomes very small. The experimental observations therefore are not due to the effects of orbiting resonance.

Polymer Chemistry

01,195
PB94-172293 Not available NTIS
National Inst. of Standards and Technology (MSEL), Gaithersburg, MD. Polymers Div.
Thermal Pulse Study of the Polarization Distributions Produced in Polyvinylidene Fluoride by Corona Poling at Constant Current.
Final rept.
J. A. Giacometti, and A. S. DeReggi. 1 Sep 93, 9p.
Pub. in Jnl. of Applied Physics 74, n5 p3357-3365, 1 Sep 93.

Keywords: *Vinyl resins, *Polarization, *Profiles, Electric corona, Pulse heating, Reprints, *Polyvinylidene fluoride, *Polarization profiles, Corona poling.

A thermal pulse study of the polarization profiles in samples of 12-micrometer-thick, biaxially oriented polyvinylidene fluoride after corona poling under approximately constant-current conditions, using a modified corona triode in atmospheric air, is reported. An electrical characterization of the corona triode is also reported to show how it may be operated in the constant-current mode. Samples poled without electrode on the corona-exposed surface show polarization distributions sensitive to the corona polarity, with polarization depletion on the corona side of the samples when the corona is positive. Polarization-reversal experiments show switching inhomogeneities with a pronounced dependence on the initial corona polarity. The above observations are consistent with a simple model in which positive charges from the positive corona partially penetrate the sample during poling and cause an inhomogeneous reduction of the poling field.

01,196
PB94-172392 Not available NTIS
National Inst. of Standards and Technology (MSEL), Gaithersburg, MD. Polymers Div.
Shear-Excited Morphological States in a Triblock Copolymer.
Final rept.
C. L. Jackson, M. Muthukumar, K. A. Barnes, A. I. Nakatani, C. C. Han, F. A. Morrison, and J. W. Mays. 1994, 2p.
Pub. in Polymer Preprints 35, p624-625 1994.

Keywords: *Shear rate, *Block copolymers, *Morphology, *Polystyrene, *Polybutadiene, Molecular structure, Small angle scattering, Transmission electron microscopy, Excitation, Neutron scattering, Reprints, Molecular configuration.

The effect of shear on the morphology of a triblock copolymer of polystyrene-d8/polybutadiene/polystyrene-d8 (SBS) (23 wt. % styrene-d8, cylindrical morphology) was studied by small angle neutron scattering (SANS) and transmission electron microscopy (TEM). The copolymer was sheared (0.585/s at 100 C) in a cone-and-plate rheometer and quenched to room temperature. The morphology consisted of two distinct structures, including a primary cylindrical spacing of 22 nm, as expected for the equilibrium state, and a secondary spacing of 12 nm, which is hypothesized to be a shear-excited state for this material. A mechanism for producing such a unique morphology is proposed to be the conversion of a bridging configuration between cylinders to a looping configuration.

01,197
PB94-172624 Not available NTIS
National Inst. of Standards and Technology (MSEL), Gaithersburg, MD. Polymers Div.
Neutron Scattering Study of Shear Induced Turbidity in Polystyrene/Dioctyl Phthalate Solutions at High Shear Rates.
Final rept.
A. I. Nakatani, J. F. Douglas, Y. B. Ban, and C. C. Han. 1993, 2p.
Pub. in Jnl. of American Chemical Society Polymer Preprints 34, p554-555 1993.

Keywords: *Polystyrene, *Neutron scattering, *Turbidity, *Solutions, *Mixing, Small angle scattering, Shear rate, Polymers, Binary systems(Materials), Non-Newtonian systems, Reprints, *Phthalic acid/(dioctyl-ester), Polymer blends.

The phenomenon of shear induced 'mixing' and 'demixing' in polymer solutions has attracted theoretical and experimental attention since the 1950's. Helfand and Fredrickson (HF) developed a theory which is appropriate for describing the distorted scattering in polymer solutions at low shear rates, but the HF theory is not applicable to fluids in the non-Newtonian flow regime. The range of shear rates where PS/DOP solutions becomes turbid to the eye is typically > 100/s in our experiments where the HF theory is not applicable. We have conducted small angle neutron scattering (SANS) investigations of these PS/DOP solutions at high shear rates in order to examine the scattering in this 'strong shear' regime.

01,198
PB94-172632 Not available NTIS
National Inst. of Standards and Technology (MSEL), Gaithersburg, MD. Polymers Div.
Time Dependent Small Angle Neutron Scattering Behavior in Triblock Copolymers Under Steady Shear.
Final rept.
A. I. Nakatani, F. A. Morrison, J. W. Mays, M. Muthukumar, and C. C. Han. 1993, 2p.
Pub. in American Chemical Society Polymer Preprints 34, p630-631 1993.

Keywords: *Neutron scattering, *Block copolymers, *Temperature dependence, *Polystyrene, *Polybutadiene, Shear rate, Small angle scattering, Shear flow, Isotropy, Anisotropy, Reprints.

We examine a styrene-butadiene-styrene triblock copolymer (23 wt. % styrene, cylindrical morphology, M(sub w) = 8,000/54,000/8,000) in two ways: (a) the shear rate and temperature dependence of the steady shear small angle neutron scattering (SANS) patterns; (b) the transient SANS behavior during steady shear as a function of temperature and shear rate. At low shear rates, above and below the triplet optical density (ODT), an isotropic scattering pattern is observed. Below the quiescent ODT, at somewhat higher shear rates, the sample orients in the flow direction and the scattering becomes anisotropic. Below ODT, at even higher shear rates, a second pair of diffraction spots are observed at higher q. In the third regime, the intensity of the low q peak passes through two distinct maxima and a minimum. The intensity of the higher q peak appears to pass through a maximum at the same time the low q peak is at a minimum.

01,199
PB94-172756 Not available NTIS
National Inst. of Standards and Technology (IMSE), Gaithersburg, MD. Reactor Radiation Div.
Temperature Dependence of the Morphology of Thin Diblock Copolymer Films as Revealed by Neutron Reflectivity.
Final rept.
T. P. Russell, S. H. Anastasiadis, S. K. Satija, and C. F. Majkrzak. 1990, 6p.
Pub. in Proceedings on Neutron Scattering for Materials Science Symposium, Boston, MA., November 27-30, 1989, p145-150 1990. See also PB92-170620.

Keywords: *Temperature dependence, *Morphology, *Block copolymers, *Thin films, *Surface properties, Neutron radiography, Reflectivity, Phase transformations, Annealing, Transition temperature, Interfaces, Reprints.

In the report neutron reflectivity studies on the temperature dependence of the morphology of diblock copolymers in the vicinity of the microphase separation transition temperature (MST) is discussed. At temperatures below the MST the ordered multilayered lamellar morphology is found to penetrate through the entire specimen. At temperatures above the MST the periodic variation in the composition of the components is maintained but a clear dissipation of the order is found with increasing distance from either the air copolymer or copolymer/substrate interfaces. An exponentially damped squared cosine function from both interfaces is found to well describe the reflectivity results. The characteristic decay length is found to decrease with increasing temperature in accordance with mean field arguments. Results from two different copolymers with two different molecular weights and, consequently, two different MSTs are found to be identical on a reduced temperature scale.

01,200
PB94-185055 Not available NTIS
National Inst. of Standards and Technology (MSEL), Gaithersburg, MD. Polymers Div.
Grafted Interpenetrating Polymer Networks.
Final rept.
B. J. Bauer, R. M. Briber, and B. Dickens. 1994, 17p.
Pub. in Interpenetrating Polymer Networks, Chapter 7, p179-195 1994.

Keywords: *Graft polymerization, *Polymethyl methacrylate, Thermal analysis, Neutron scattering, X-ray diffraction, Phase transformation, Reprints, *Interpenetrating polymer networks.

A new class of interpenetrating polymer network (IPN) has been studied in which grafting reactions between the two components are varied. Small-angle neutron scattering of grafted and nongrafted IPNs shows that grafting greatly enhances the miscibility of the components. Five nonfunctionalized poly(methyl methacrylates) (PMMAs) with alkacrylate, methacrylate, acrylate, and alpha-methylstyrene end groups were dissolved in styrene-divinylbenzene and polymerized. Small-angle X-ray scattering was used to characterize the extent of phase separation. The uniformity of the IPNs is strongly dependent on the grafting efficiency. Grafted and nongrafted IPNs were also made from the PMMAs and polyethylene glycol diacrylates. Thermal studies showed one transition in the grafted samples and two distinct transitions in a nongrafted sample.

01,201
PB94-185105 Not available NTIS
National Inst. of Standards and Technology (MSEL), Gaithersburg, MD. Polymers Div.
In-Line Optical Monitoring of Injection Molding.
Final rept.
A. J. Bur, F. W. Wang, C. L. Thomas, and J. L. Rose. Apr 94, 9p.
Pub. in Polymer Engineering and Science 34, n8 p671-679 Apr 94.

Keywords: *Solidification, *Injection molding, *Sensors, *Polymers, Fiber optics, Polyethylene, Polystyrene, Crystallization, Fluorescence, In-situ processing, Monitoring, Plastics processing, Reprints.

An optical sensor, consisting of optical fibers to transmit light to and from the mold cavity, was constructed for the purpose of measuring the onset of polymer solidification during injection molding. The sensor was used to detect characteristic fluorescence radiation from a dye which had been doped into the resin at very low concentration. By measuring changes in fluorescence intensity, it was possible to detect whether the state of the resin was liquid or solid. We observed that, as the resin cooled in the mold, the onset of solidification was indicated by highly characteristic and distinct changes in the fluorescence intensity/time profile. Application of the method involved the use of a calibration relationship between the fluorescence intensity and temperature of the doped polymer in order to determine the distinct features which characterize the onset of solidification. Injection molding of a glass forming polymer (polystyrene) and a crystallizable polymer (polyethylene) was monitored by this technique.

01,202
PB94-185188 Not available NTIS

National Inst. of Standards and Technology (MSEL), Gaithersburg, MD. Polymers Div.
Phase Behavior of a Hydrogen Bonding Molecular Composite.
Final rept.
M. D. Dadmun, and C. C. Han. 1993, 6p.
Pub. in Materials Research Society Symposium Proceedings, v305 p171-176 1993.

Keywords: *Composite materials, *Phase transformations, *Hydrogen bonds, Microscopy, Glass transition temperature, Polypeptides, Liquid crystals, Copolymers, Reprints, *Molecular composites, *Liquid crystalline polymers, Poly(hydroxypropyl-L-glutamine).

The phase behavior of a blend containing poly(hydroxypropyl-L-glutamine), a rod-like polypeptide, and a coil-like random copolymer with 1.5% hydrogen bonding monomer is studied using light scattering, DSC, and optical microscopy. The results show that this system has an LCST. The phase behavior of this binary system is complicated by a glass transition and an ordering transition. Evidence is also observed of a possible change in phase demixing process, from nucleation and growth to spinodal decomposition, for a 50/50 blend with a change in temperature.

01,203
PB94-185469 Not available NTIS
National Inst. of Standards and Technology (MSEL), Gaithersburg, MD. Polymers Div.
Influence of Surface Interaction and Chain Stiffness on Polymer-Induced Entropic Forces and the Dimensions of Confined Polymers.
Final rept.
A. L. Kholodenko, D. W. Bearden, and J. F. Douglas. 1994, 19p.
Pub. in Physical Review E 49, n3 p2206-2224 Mar 94.

Keywords: *Polymers, *Entropy, *Stiffness, *Surfaces, Mathematical models, Critical temperature, Reprints, *Confined semiflexible polymers, *Entropic Casimin forces.

The theories of Dolan and Edwards and Eisenriegler et al. for Gaussian chains confined between parallel plates and to a half-space are generalized to chains having arbitrary stiffness. The generalized theory exploits a recently discovered relation between semiflexible polymers and Euclidean-type Dirac fermions in which 'flexible' and 'stiff' polymers correspond to the nonrelativistic (massive) and relativistic (massless) limits of the Dirac propagator, respectively. We show that half-space and parallel-plate problems are interrelated and this allows for a simplified and unified treatment of confined semiflexible polymers. The properties of confined semiflexible chains exhibit a complicated dependence on the polymer-surface interaction and chain stiffness. Results for polymer dimensions and entropic Casimir-like forces between plates are consistent with those obtained previously for flexible chains and corresponding results are obtained for semiflexible polymers. The new results for the forces between plates, having a semiflexible polymer in the gap, exhibit qualitative agreement with experimental data on confined chains at nonvanishing concentrations.

01,204
PB94-185543 Not available NTIS
National Inst. of Standards and Technology (MSEL), Gaithersburg, MD. Polymers Div.
Fluorescence Monitoring of Polarity Change and Gelation during Epoxy Cure.
Final rept.
K. F. Lin, and F. W. Wang. 1994, 5p.
Pub. in Polymer 35, n4 p687-691 1994.

Keywords: *Curing, *Fluorescence, *Polymerization, *Epoxy resins, Temperature, Gelation, Polarity, Monitoring, Molecular structure, Reprints, Hexatriene/(dimethylaminophenyl)-phenyl, Ether/diglycidyl, Bisphenol A, Diethylene triamine.

The fluorescence spectrum of 1-(4-dimethylaminophenyl)-6-phenyl-1,3,5-hexatriene (DMA-DPH) dissolved in a stoichiometric mixture of diglycidyl ether of bisphenol A and diethylene triamine was measured as a function of cure time at various cure temperatures. The frequency of the fluorescence maximum for DMA-DPH increased during the curing reactions because of the change in the polarity of the epoxy resin. In an isothermal cure, the fluorescence frequency increased linearly with the cure time until the gelation occurred. The total change in fluorescence frequency that occurred from the beginning of the isothermal cure to the gelation time was 1,000/cm and was independent of the cure temperature, implying that the chemical structure of the infinite network at the gelation time was independent of the cure temperature. The rate constant, K(sub T), for the polarity change during an isothermal cure of the epoxy resin, defined as the rate constant for the linear increase in fluorescence frequency, was determined. The activation energy of K(sub T) was estimated to be 60 kJ/mol.

01,205
PB94-185550 Not available NTIS
National Inst. of Standards and Technology (MSEL), Gaithersburg, MD. Polymers Div.
Electron Beam Crosslinking of Poly(vinylmethyl ether).
Final rept.
X. Liu, R. M. Briber, and B. J. Bauer. 1994, 5p.
Pub. in Jnl. of Polymer Science B 32, p811-815 1994.

Keywords: *Vinyl ether resins, *Crosslinking, Molecular structure, Electron beams, Solutions, Alcohols, Solvation, Chromatographic analysis, Reprints.

The electron beam induced branching of poly(vinylmethyl ether) (PVME) in bulk and in isopropanol solutions has been studied by gel permeation chromatography. The branching probability of bulk PVME induced by high-energy electrons can be characterized by gel permeation chromatography and a simple probability constant obtained. In isopropanol solutions this branching probability is not constant as a function of dose and is found to decrease with decreasing concentration. These results indicate the importance of solvent effects on the crosslinking of PVME in isopropanol solution by electron beam radiation.

01,206
PB94-185758 Not available NTIS
National Inst. of Standards and Technology (MSEL), Gaithersburg, MD. Reactor Radiation Div.
Neutron Reflectivity of End-Grafted Polymers: Concentration and Solvent Quality Dependence in Equilibrium Conditions.
Final rept.
D. Perahia, D. G. Wiesler, S. K. Satija, S. T. Milner, L. J. Fetters, and S. K. Sinha. 1994, 4p.
Pub. in Physical Review Letters 72, n1 p100-103, 3 Jan 94.

Keywords: *Polymers, *Density(Mass/volume), *Monomers, Concentration(Composition), Neutron scattering, Polystyrene, Temperature dependence, Reprints, *End grafted polymers, Neutron reflectivity.

Neutron reflectometry is used to obtain a direct measurement of the monomer distribution of a weakly bound end-grafted polystyrene layer in equilibrium with bulk solution, as a function of the polymer concentration and temperature. We report for the first time two new regions in the density profile of the polymers, an excess polymer near the surface and a wetting layer on top of the brush. The physical properties of the polymer layer are strongly affected by the equilibrium between the bound and free polymer molecules.

01,207
PB94-198389 Not available NTIS
National Inst. of Standards and Technology (MSEL), Gaithersburg, MD. Polymers Div.
Facile Synthesis of Novel Fluorinated Multifunctional Acrylates.
Final rept.
J. M. Antonucci, J. W. Stansbury, and G. W. Cheng. 1990, 1p.
Pub. in Abstracts of Papers of the American Chemical Society 199, p111 Apr 90.

Keywords: *Acrylates, *Fluorine organic compounds, *Chemical reactions, Reprints, Chemical preparation, Chemical analysis, Dienes, *Fluorinated acrylates, Oligomers.

Previously it was shown that the bulk reaction alkyl acrylates with paraformaldehyde catalyzed by triethylenediamine yields bis(acrylate) monomers having a 1,6 diene structure which favors free radical cyclopolymerization via 6-membered ring formation. In this study the feasibility of extending this reaction to convert fluoro-acrylates and -diacrylates to difunctional and oligomeric fluorinated monomers was explored. The reaction of 2,2,3,3,4,4,4-heptafluorobutyl acrylate (7FBA) under the usual ambient, bulk conditions yielded only trace amounts of products. Elevated temperature (80C) and the use of dimethyl sulfoxide resulted in an improved yield of two types of bis products, a 1,4-diene as well as the expected 1,6 diene (proton NMR). The analogous reaction with 2,2,3,3,4,4-hexafluoropentane-1,5-diacrylate yields a soluble, highly fluorinated, multifunctional oligomer. This type of aldehyde insertion reaction offers an attractive means of preparing otherwise not readily available highly fluorinated multifunctional monomers.

01,208
PB94-198496 Not available NTIS
National Inst. of Standards and Technology (MSEL), Gaithersburg, MD. Polymers Div.
Thermodynamic Interactions in Model Polyolefin Blends Obtained by Small-Angle Neutron Scattering.
Final rept.
N. P. Balsara, L. J. Fetters, N. Hadjichristidis, W. W. Graessley, R. Krishnamoorti, D. J. Lohse, and C. C. Han. 1992, 11p.
Pub. in Macromolecules 25, n23 p6137-6147 1992.

Keywords: *Polymer blends, *Polyolefins, Small angle scattering, Random phase approximation, Amorphous materials, Neutron scattering, Temperature dependence, Phase studies, Deuterium compounds, Polybutadiene, Reprints, Polyolefin blends.

The dependence of Flory-Huggins interaction parameter chi on temperature, composition, and chain length was investigated for binary blends of amorphous model polyolefins, materials which are structurally analogous to copolymers of ethylene and butene-1. The components were prepared by saturating the double bonds of nearly monodisperse polybutadienes (78%, 88%, and 97% vinyl content) with H2 and D2, the latter to provide contrast for small-angle neutron scattering (SANS) experiments. Values of chi were extracted from SANS data in the single-phase region for two series of blends, H97/D88 and H88/D78, using the random phase approximation and the Flory-Huggins expression for free energy of mixing. These values were found to be insensitive to chain length (one test only) and to the component volume fractions for phi = 0.25, 0.50, and 0.75. Their temperature dependence (27-170 C) obeys the form chi(T) = A/T + B with coefficients that connote upper critical solution behavior.

01,209
PB94-199296 Not available NTIS
National Inst. of Standards and Technology (MSEL), Gaithersburg, MD. Polymers Div.
Fluorescence Anisotropy Measurements on a Polymer Melt as a Function of Applied Shear Stress.
Final rept.
A. J. Bur, R. E. Lowry, S. C. Roth, C. L. Thomas, and F. W. Wang. 1992, 8p.
Pub. in Macromolecules 25, p3503-3510 1992.

Keywords: *Polymer chemistry, *Shear stress, *Molecular structure, *Orientation, *Melts(Crystal growth), *Anistropy, Reprints, Polybutadiene, Anthracene, Marking, Tracer techniques, Probes, Crosslinking, Relaxation time, Extensions, Crystal structure.

Polybutadiene tagged with anthracene was synthesized and used as a fluorescent molecular probe to study shear-induced orientation in a matrix polymer melt. With the tagged polybutadiene doped into a polybutadiene matrix at 0.1% concentration, steady-state fluorescence anisotropy measurements were carried out under zero shear and under finite shear conditions using an optically instrumented cone and plate rheometer. Measurements were made over a shear rate range for which the specimen displayed non-Newtonian behavior, .00264 to 5.3/S. Anisotropy was observed to decrease with increasing applied shear stress. The magnitude of the effect is small and is attributed to shear-induced orientation of the probe molecule which is engaged in the entanglement network of the host polymer. Diluting the entanglement network using plasticizer produced a smaller effect. For polybutadiene plasticized with 50% cetane, the authors observed that anisotropy was independent of the applied shear stress, indicating that the probe molecule was not participating in the orientation of the matrix entanglement network. A relationship between anisotropy, chromophore relaxation time, and orientation factors was derived and used to deduce an orientation distribution of fluorescent absorption dipoles and to illustrate the difference between shear and extension stress observations. Extension experiments, carried out using a cross-linked polybutadiene specimen, showed that anisotropy increased as a function of applied extensional stress.

01,210
PB94-199304 Not available NTIS
National Inst. of Standards and Technology (MSEL), Gaithersburg, MD. Polymers Div.
Observations of Shear Induced Molecular Orientation in a Polymer Melt Using Fluorescence Anisotropy Measurements.
Final rept.
A. J. Bur, R. E. Lowry, S. C. Roth, C. L. Thomas, and F. W. Wang. 1991, 3p.
Pub. in Macromolecules 24, n12 p3715-3717 1991.

Keywords: *Polymer chemistry, *Shear stress, *Molecular structure, *Orientation, *Melts(Crystal growth), Polybutadiene, Crystal structure, Anisotropy, Molecular weight, Fluorescence, Marking, Tracer techniques, Anthracene, Reprints.

Polybutadiene tagged with anthracene was synthesized and used as a fluorescent molecular probe to study shear induced orientation in a matrix polymer melt. With the tagged polybutadiene doped into a polybutadiene matrix at 0.1% concentration, steady state fluorescence anisotropy measurements were carried out under zero shear and under finite shear conditions using an optically instrumented cone and plate rheometer. For polybutadiene plasticized with 50% cetane, we observed that anisotropy of the tagged polybutadiene was independent of the applied shear stress indicating that the probe molecule was not participating in the orientation of the matrix entanglement network.

01,211
PB94-199312 Not available NTIS
National Inst. of Standards and Technology (MSEL), Gaithersburg, MD. Polymers Div.
Observations of Shear Stress and Molecular Orientation Using Fluorescence Anisotropy Measurements.
Final rept.
A. J. Bur, R. E. Lowry, S. C. Roth, C. L. Thomas, and F. W. Wang. 1991, 4p.
Pub. in Proceedings of Annual Technical Conference (49th), Montreal, Quebec, Canada, May 5-9, 1991, p842-845.

Keywords: *Polymer chemistry, *Shear stress, *Molecular structure, *Orientation, *Melts(Crystal growth), Polybutadiene, Crystal structure, Anisotropy, Molecular weight, Fluorescence, Marking, Tracer techniques, Anthracene, Reprints.

Polybutadiene tagged with anthracene was synthesized and used as a fluorescent molecular probe to study shear induced orientation in a matrix polymer melt. With the tagged polybutadiene doped into a polybutadiene matrix at 0.1% concentration, steady state fluorescence anisotropy measurements were carried out under zero shear and under finite shear conditions using an optically instrumented cone and plate rheometer. For polybutadiene plasticized with 50% cetane, we observed that anisotropy of the tagged polybutadiene was independent of the applied shear stress indicating that the probe molecule was not participating in the orientation of the matrix entanglement network.

01,212
PB94-199387 Not available NTIS
National Inst. of Standards and Technology (NML), Boulder, CO. Chemical Engineering Science Div.
Statistical Thermodynamics of Phase Separation and Ion Partitioning in Aqueous Two-Phase Systems.
Final rept.
H. Cabezas, M. Kabiri-Badr, and D. C. Szlag. 1990, 7p.
Pub. in Bioseparation 1, n3/4 p227-233 1990.

Keywords: *Binary system(Materials), *Polymer blends, *Phase diagrams, *Thermodynamics, *Mathematical models, Aqueous solutions, Statistical mechanics, Separation, Molecular weight, Dextran, Polyoxyethylene, Reprints.

A general model for the phase behavior of polymer-polymer aqueous two-phase systems containing small amounts of added inorganic salts has been developed from statistical thermodynamics. The model is based on the solution theory of Hill and new electrolyte model based on Fluctuation Solution Theory. It includes the effect of polymer molecular weight with scaling expressions from the Renormalization Group theory of polymer solutions. The model has been used to calculate the phase diagram and the partitioning of salt for an aqueous two-phase system containing polyethylene glycol (MW=8000) and dextran (MW=28700) with Na2SO4. The calculations have been compared to experiment with good agreement.

01,213
PB94-199809 Not available NTIS
National Inst. of Standards and Technology (MSEL), Gaithersburg, MD. Polymers Div.
Peeling a Polymer from a Surface or from a Line.
Final rept.
E. A. DiMarzio, and C. M. Guttman. 1991, 9p.
Pub. in Jnl. of Chemical Physics 95, n2 p1189-1197 1991.

Keywords: *Polymers, *Adhesion, *Surface chemistry, Equations of state, Rubbers, Elasticity, Molecular structure, Chemical bonds, Gels, Crosslinking, Reprints, Polymeric chains, Zippering.

The authors calculate the force on a long linear polymer molecule whose one end is zippered down onto a surface or onto a line and whose other end is at a perpendicular distance R from the surface of line. Random coil statistics are used for the unattached portion of the chain. The method is extended to the case when the bonds within the zippered portion are breaking and reforming. They also consider the case where the attached portion is in the form of loops and trains. Applications are discussed briefly. They include (1) Self-healing systems of gels and rubbers where the crosslinks may be hydrogen bonds, (2) Adhesion, (3) The degree of crystallinity in crystal-amorphous lamellar system, (4) The packing of DNA into the head of a bacteriophage virus, and pulling apart of double stranded DNA, (5) An insight into the theory of rubber elasticity, (6) Understanding the critical force for flow in thixotropic systems.

01,214
PB94-200052 Not available NTIS
National Inst. of Standards and Technology (MSEL), Gaithersburg, MD. Polymers Div.
Effect of Curing History on Ultimate Glass Transition Temperature and Network Structure of Crosslinking Polymers.
Final rept.
S. S. Chang. 1992, 11p.
Pub. in Polymer 33, n22 p4768-4778 1992.

Keywords: *Glass transition temperature, *Curing, *Polymerization, *Crosslinking, Differential thermal analysis, Phase transformations, Reprints, *Glycidyl ethers, *Bisphenol-A, *Crosslinking network.

For a particular crosslinking polymer, it is often considered that the final state of crosslinking may be reached by post-curing at temperatures above its ultimate glass transition temperature, T(sub g,u) regardless of previous curing histories. Although this appears to be true over a certain range of variation in curing history, the T(sub g,u) and the network structure depend strongly on the curing history over a wide range of conditions for the homopolymerization of diglycidyl ether of bisphenol-A (DGEBA) catalyzed by 2-ethyl-4-methyl imidazole. As degrees of cure and crosslink increase, the glass transition temperature, T(sub g), of a sample may increase from the monomeric DGEBA value of -22 C to the highest value near 180 C. Depending on the curing thermal history, some samples may only attain a T(sub g,u) of approximately 100 C, even after post-curing at 200 C for 16 h. Although the influence of thermal history on T(sub g) may rank second after the influence of the degree of cure, it is the most important factor on T(sub g,u) for a fixed resin and catalyst composition. The reversible physical aging process appears to be the least influential on T(sub g). As all crosslinking reactions involve competing reactions with different kinetic parameters, we believe that these phenomena are universally observable to a greater or lesser degree in all crosslinking reactions.

01,215
PB94-211026 Not available NTIS
National Inst. of Standards and Technology (MSEL), Gaithersburg, MD. Polymers Div.
Hypercubic Lattice SAW Exponents nu and gamma : 3.99 Dimensions Revisited.
Final rept.
J. F. Douglas, T. Ishinabe, A. Nemirovsky, and K. F. Freed. 1993, 11p.
Pub. in Jnl. of Physics A: Mathematical and General 26, p1835-1845 1993.

Keywords: *Polymers, Partition functions, Computation, Exponents, Reprints, Self-avoiding walks, Spatial dimensions, Lattice models.

The self-avoiding walk (SAW) exponents nu and gamma are computed over a range of dimensions (1 = or < d < infinity) from exact expressions for the mean-square end-to-end distance < R(sub n, sup 2) > and the partition function Q(sub n) of SAWs having a limited number of steps, n = or < 11. SAW exponents (nu, gamma) for arbitrary dimension d are estimated by applying standard extrapolation techniques to our direct enumeration data which has been analytically continued to variable dimension. Exponent estimates obtained from continuum theories of self-avoiding paths are compared with the SAW calculations.

01,216
PB94-211034 Not available NTIS
National Inst. of Standards and Technology (MSEL), Gaithersburg, MD. Polymers Div.
Effect of Swelling on the Elasticity of Rubber: Localization Model Description.
Final rept.
J. F. Douglas, and G. B. McKenna. 1993, 7p.
Pub. in Macromolecules 26, n13 p3282-3288 1993.

Keywords: *Elastomers, *Spatial distribution, *Mathematical models, Elastic properties, Crosslinking, Swelling, Polymers, Reprints, *Localization model, *Mooney-Rivlin equation.

The success of the localization model in describing the elasticity of unswollen natural rubber is reviewed and the model is extended to describe the elasticity of swollen networks. In contrast to the Frenkel-Flory-Rehner modeling of network elasticity, the localization model predicts that the mechanical response of swollen rubbers changes qualitatively in going from low to high cross-link densities. The implications of these predictions are discussed.

01,217
PB94-211141 Not available NTIS
National Inst. of Standards and Technology (MSEL), Gaithersburg, MD. Polymers Div.
How Far Is Far from Critical Point in Polymer Blends. Lattice Cluster Theory Computations for Structured Monomer, Compressible Systems.
Final rept.
J. Dudowicz, M. Lifschitz, K. Freed, and J. Douglas. 1993, 17p.
Pub. in Jnl. of Chemical Physics 99, n6 p4804-4820, 15 Sep 93.

Keywords: *Polymer blends, Critical point, Compressibility, Renormalization, Monomers, Computation, Reprints, Lattice cluster theory.

Although the lattice cluster theory (LCT) incorporates many features which are essential in describing real polymer blends, such as compressibility, monomer structures, local correlations, chain connectivity, and polymer-polymer interactions, it still remains a mean field theory and is therefore not applicable in the vicinity of the critical point where critical fluctuations become large. The LCT, however, permits formulating the Ginzburg criterion, which roughly specifies the temperature range in which mean field applies. The present treatment abandons the conventional assumptions of incompressibility and of composition and the molecular weight independent effective interaction parameter upon which all prior analyses of the Ginzburg criterion are based. Blend compressibility, monomer structure, and local correlations are found to exert profound influences on the blend phase diagram and other critical properties and, thus, exhibit a significant impact on the estimate of the size of the nonclassical region.

01,218
PB94-211422 Not available NTIS
National Inst. of Standards and Technology (MSEL), Gaithersburg, MD. Polymers Div.
Monitoring Polymer Cure by Fluorescence Recovery After Photobleaching.
Final rept.
B. M. Fanconi. 1991, 8p.
Pub. in Rev. Prog. Quant. Nondestr. Eval. 10A, p1127-1134 1991.

Keywords: *Curing, *Polymers, *Monitors, *Tracer techniques, Fiber optics, Fluorescence, Diffusion coefficient, Dyes, Laser applications, Reprints, *Fluorescence Recovery After Photobleaching technique.

Fluorescence recovery after photobleaching (FRAP) is a technique to measure the translational diffusion coef-

ficient of dye molecules in polymer matrices. The sensitivity of the diffusion coefficient to the degree of cure of the polymer matrix provides a means to monitor cure. The aim of the present work is to examine the potential of optic fibers as a means probing the interior of thick specimens by FRAP. The temporal response of the fluorescence intensity has been calculated for an evanescent wave type fiber optic probe. With this probe, the evanescent wave of the photobleaching laser creates a region near the fiber surface devoid of fluorescent molecules. The diffusion coefficient of the dye molecule is determined from the temporal response of the fluorescence. With fiber optics it should be possible to measure translational diffusion coefficients an order of magnitude smaller than those detected by the conventional microscope-based method.

01,219
PB94-211547 Not available NTIS
National Inst. of Standards and Technology (MSEL), Gaithersburg, MD. Polymers Div.
Neutron Scattering by Multiblock Copolymers of Structure (A-B)N-A.
Final rept.
G. Hadziioannou, H. Benoit, W. Tang, K. Shull, and C. C. Han. 1992, 5p.
Pub. in Polymer 33, n22 p4677-4681 1992.

Keywords: *Block copolymers, *Neutron scattering, *Small angle scattering, *Molecular structure, Styrene resins, Polymerization, Deuterium compounds, Monomers, Reprints.

Multiblock copolymers were prepared by anionic copolymerization of deuterated and classical styrene monomers. The use of bifunctional initiators gives copolymers with an odd number of sequences. Neutron scattering experiments were performed on these samples in order to check the existing theories which are extended in the first part to multiblock copolymers with an odd number of blocks. The agreement between theory and experiment is excellent and, surprisingly, the height of the maximum of the curves:scattered intensity versus scattering angle, does not depend on the number of blocks.

01,220
PB94-211612 Not available NTIS
National Inst. of Standards and Technology (MSEL), Gaithersburg, MD. Polymers Div.
Shear Dependence of Critical Fluctuations in Binary Polymer Mixtures by Small Angle Neutron Scattering.
Final rept.
C. C. Han, and A. I. Nakatani. 1990, 1p.
Pub. in Abstracts of Papers of the American Chemical Society 200, p105 Aug 90.

Keywords: *Binary systems(Materials), *Shear rate, *Small angle scattering, *Polystyrene, *Concentration(Composition), Polybutadiene, Neutron scattering, Thermoplastic resins, Deuterium compounds, Polymer blends, Vinyl ether resins, Labeled substances, Temperature dependence, Phase diagrams, Reprints, Poly(ether/vinylmethyl).

Small angle neutron scattering (SANS) has been used to study the concentration fluctuations of binary polymer mixtures under shear. Two different polymer systems: deuterated polystyrene/poly(vinylmethylether) and deuterated polystyrene/polybutadiene have been studied as a function of temperature and shear rate.

01,221
PB94-211729 Not available NTIS
National Inst. of Standards and Technology (MSEL), Gaithersburg, MD. Polymers Div.
Small-Angle X-Ray and Neutron Scattering Study of Block Copolymer/Homopolymer Mixtures.
Final rept.
H. Hasegawa, H. Tanaka, T. Hashimoto, and C. C. Han. 1990, 1p.
Pub. in Abstracts of Papers of the American Chemical Society 200, p279 Aug 90.

Keywords: *Small angle scattering, *X-ray scattering, *Neutron scattering, *Block copolymers, *Binary systems(Materials), *Polystyrene, Polymer blends, Molecular weight, Thermoplastic resins, Polybutadiene, Deformation, Molecular chains, Reprints, Molecular conformations.

We investigated lateral and vertical one-dimensional components of radius of gyration for a single block copolymer chain (Study I) and those of a single homopolymer chain (Study II) in a microdomain space formed by a mixture of diblock copolymers and homopolymers by means of small-angle neutron and X-ray scattering techniques. The molecular weights of the homopolymers were much smaller than those of the corresponding block copolymer chains. The results imply that both the block copolymer and the homopolymer chains in the microdomain space are compressed in the direction parallel to the interface and stretched in the direction perpendicular to the interface. The block copolymer chains undergo an isochoric affine deformation on addition of the homopolymers.

01,222
PB94-211976 Not available NTIS
National Inst. of Standards and Technology (MSEL), Gaithersburg, MD. Polymers Div.
Crossover to Strong Shear in a Low-Molecular-Weight Critical Polymer Blend.
Final rept.
E. K. Hobbie, D. W. Hair, A. I. Nakatani, and C. C. Han. 1992, 4p.
Pub. in Physical Review Letters 69, n13 p1951-1954, 28 Sep 92.

Keywords: *Small angle scattering, *Neutron scattering, *Polymer blends, *Shear flow, Molecular weight, Critical point, Light scattering, Reprints.

Small-angle neutron scattering has been used to measure the influence of shear flow on a low-molecular-weight polymer blend near the critical point. When combined with light scattering measurements of the equilibrium (gamma=0) critical dynamics, these measurements reveal that the long-range critical fluctuations begin to break apart when the shear rate becomes comparable to the characteristic relaxation rate 1/tau(sub c), where tau(sub c) is the equilibrium lifetime of the critical fluctuations. This effect is directly related to the decrease in the critical temperature caused by the flow, and the data are found to be in very good agreement with the theoretical predictions of Onuki and Kawasaki.

01,223
PB94-212321 Not available NTIS
National Inst. of Standards and Technology (MSEL), Gaithersburg, MD. Polymers Div.
Anomalous Freezing and Melting of Solvent Crystals in Swollen Gels of Natural Rubber.
Final rept.
C. L. Jackson, and G. B. McKenna. 1991, 9p.
Pub. in Rubber Chemistry and Technology 64, n5 p760-768 1991.

Keywords: *Elastomers, *Freezing, *Cryoscopy, Gels, Polymers, Crosslinking, Calorimetry, Solvents, Swelling, Reprints, *Freezing point depression.

The anomalously large solvent freezing point depression (fpd), observed in crosslinked rubbers swollen in solvent has been a subject of study for over thirty years without clear resolution. While a sizeable fpd is accounted for by the lowering of the thermodynamic potential of solvent molecules in a polymer solution described by Flory-Huggins theory, the additional fpd observed for crosslinked rubbers has been attributed to various physical effects such as restriction of solvent crystals to small size by the network mesh or difficulty in nucleation of the solvent crystals. In this paper, we identify two points of misunderstanding in the literature on this problem, and attempt to clarify the analysis of fpd for solvent swollen rubbers. The first point relates to the use of Flory-Huggins theory for solvent freezing, where nucleation is a concern, rather than for solvent melting, for which it was intended. We present new experimental calorimetric data on both the freezing and melting of solvent crystals in crosslinked and uncrosslinked natural rubber swollen in benzene to illustrate this point. The second point relates to a reconsideration of the hypothesis of Kuhn, et al., that the anomalous fpd can be accounted for by small crystallite size.

01,224
PB94-212339 Not available NTIS
National Inst. of Standards and Technology (MSEL), Gaithersburg, MD. Polymers Div.
Polymer Liquid Crystalline Materials.
Final rept.
C. L. Jackson, and M. T. Shaw. 1991, 22p.
Pub. in International Materials Reviews 36, n5 p165-186 1991.

Keywords: *Liquid crystals, *Polymers, Molecular structure, Physical properties, Liquid phases, Molecular chains, Rheology, Melts, Solutions, Reprints.

A review of the chemical structures, physical properties and current and potential applications of liquid crystalline polymers (LCPs) is presented. Comparisons are made between LCPs, low molecular weight liquid crystals (LCs) and conventional polymers for readers unfamiliar with the field. The ordered liquid phases are classified and molecular requirements for the formation of LC phases in both LCP melts (thermotropics) and LCP solutions (lyotropics) are discussed. The theoretical predictions of the formation of ordered phases given by Flory and Onsager are compared to experimental data, and other aspects of the phase behavior of LCPs in solution are considered, including physical gelation and crystal-solvate complexes. A wide variety of polymer structures which exhibit LC behavior are presented. These include main-chain (rigid-rod), semiflexible, main-chain with flexible spacers, side-chain LCPs and various new combinations which have been recently devised. An emphasis is placed on the relationship between chemical and physical structure of LCPs, rather than on the details of the synthesis.

01,225
PB94-212438 Not available NTIS
National Inst. of Standards and Technology (MSEL), Gaithersburg, MD. Polymers Div.
Effect of Cross-Links on the Miscibility of a Deuterated Polybutadiene and Protonated Polybutadiene Blend.
Final rept.
H. Jinnai, H. Hasegawa, T. Hashimoto, R. Birber, and C. C. Han. 1993, 7p.
Pub. in Macromolecules 26, n1 p182-188 1993.

Keywords: *Polymer blends, *Polybutadiene, *Crosslinking, Elastomers, Deuterium compounds, Hydrogen, Labeled substances, Small angle scattering, Neutron scattering, Binary systems(Materials), Temperature, Phase separation(Materials), Reprints.

The effect of peroxide crosslinking on the phase diagram and the scattering function for a critical mixture of perdeuterated polybutadiene (DPB) and protonated polybutadiene (HPB) has been examined by small-angle neutron scattering as a function of temperature. The scattering curves for the cross-linked blends were essentially temperature independent. A comparison of the scattering for the cross-linked blend with that of the linear blend at the cross-linking temperature (150 C) showed a suppression in the scattering due to the presence of the crosslinks. However, it was experimentally found that the concentration fluctuations present at the temperature of crosslinking dominate the scattering, which made it rather difficult to verify the prediction on the scattering function made by de Gennes.

01,226
PB94-212446 Not available NTIS
National Inst. of Standards and Technology (MSEL), Gaithersburg, MD. Polymers Div.
Inversion of the Phase Diagram from UCST to LCST in Deuterated Polybutadiene and Protonated Polybutadiene Blends.
Final rept.
H. Jinnai, H. Hasegawa, T. Hashimoto, and C. C. Han. 1992, 3p.
Pub. in Macromolecules 25, n22 p6078-6080 1992.

Keywords: *Phase diagrams, *Polymer blends, *Polybutadiene, Microstructure, Elastomers, Hydrogen, Labeled substances, Deuterium compounds, Temperature dependence, Small angle scattering, Neutron scattering, Reprints.

Miscibility of elastomer blends with various microstructures have been extensively studied in recent years. The separation of the isotope labeling effect from the microstructure effect has been successfully carried out by Sakurai et al. by using mean-field approximation. One of the important predictions is the possibility of phase diagram inversion from UCST to LCST or vice versa for these random copolymer blends. In this study, such phenomena have been found for a deuterated polybutadiene and hydrogenated polybutadiene pair by studies from small angle neutron scattering (SANS) experiments.

01,227
PB94-212479 Not available NTIS
National Inst. of Standards and Technology (MSEL), Gaithersburg, MD. Polymers Div.

Topological Influences on Polymer Adsorption and Desorption Dynamics.
Final rept.
H. E. Johnson, J. F. Douglas, and S. Granick. 1993, 4p.
Pub. in Physical Review Letters 70, n21 p3267-3270, 24 May 93.

Keywords: *Polymers, *Adsorption, *Desorption, Comparison, Molecular weight, Surface chemistry, Transport properties, Reprints.

The desorption of polymer chains through an overlayer of strongly adsorbed chains was studied to determine the influence of topological constraints on the polymer desorption process. The desorption time of linear chains fits a power law, M(sup a), where M is molecular weight and a = 2.3 + or - 0.2. A comparison of linear and star-branched chains shows that desorption of star-branched chains was greatly suppressed. These findings are reminiscent of entanglement effects in bulk systems. They suggest a unifying perspective from which to analyze polymer mobility at surfaces.

01,228
PB94-212610 Not available NTIS
National Inst. of Standards and Technology (NEL), Gaithersburg, MD. Fire Science and Engineering Div.
Effects of Molecular Weight and Thermal Stability on Polymer Gasification.
Final rept.
T. Kashiwagi, and A. Omori. 1988, 4p.
Pub. in Chem. Phys. Processes Combust., p68/1-68/4 1988.

Keywords: *Polymers, *Gasification, *Molecular weight, *Thermal stability, Polystyrene, Polymethyl methacrylate, Plastics, Heat rate, Heat of vaporization, Reprints.

Effects of initial molecular weight and thermal stability on the gasification process of polymeric materials were studied by determining differences in gasification rate, global heat of vaporization and rate of heat release rate between two polystyrene (PS) samples and two polymethylmethacrylate (PMMA) samples.

01,229
PB94-212941 Not available NTIS
National Inst. of Standards and Technology (MSEL), Gaithersburg, MD. Polymers Div.
Effects of Variable Excluded Volume on the Dimensions of Off-Lattice Polymer Chains.
Final rept.
D. E. Kranbuehl, and P. H. Verdier. 1993, 6p.
Pub. in Macromolecules 26, n15 p3986-3991 1993.

Keywords: *Molecular models, *Polymers, *Monte Carlo method, Statistical mechanics, Mathematical models, Volume, Reprints, *Off lattice polymer chains, *Bend stick models, Excluded model.

The expansion of bead-stick models of polymer chains by excluded volume has been obtained by Monte Carlo methods for chains with ratios d of hard-sphere bead diameter to stick length between zero (no excluded volume) and unity (connected beads touching) for chains of from 9 to 99 beads. We report values of mean square end-to-end length (l(sup 2)) and apparent power law exponents 2 nu = d(ln(l sup 2))/d(ln(N-1)) for chains of N beads, for eight values of d from 0.30 to 0.93. For the range of chain lengths reported here, the apparent power-law exponent is not independent of d but rather shows a smooth, gradual transition from the well-known result for d = 0 to the previously reported value for d = 1. The variation of 2 nu with bead size is remarkably similar to its variation with short-range attractive energy in other models. The results reported here are compared with those obtained by other workers on and off lattices, for hard-sphere and Lennard-Jones potentials, and with predictions of two-parameter and scaling theories.

01,230
PB94-217031 PC A03/MF A01
National Inst. of Standards and Technology (MSEL), Gaithersburg, MD. Polymers Div.
Determination of the Weight Average Molecular Weight of Two Poly(Ethylene Oxides), SRM 1923 and SRM 1924.
C. M. Guttman, and J. R. Maurey. Feb 94, 48p, NISTIR-5286.

Keywords: *Polyoxyethylene, *Molecular weight, *Calibration standards, US NBS, Organic polymers, Chemical analysis, Quality assurance, Measurement, Uncertainty, Precision, Accuracy, Chromatographic analysis, Size determination, *Standard reference materials, Statistical control, National Institute of Standards and Technology, Size exclusion chromatography, SRM 1923, SRM 1924.

The characterization of two narrow molecular weight distribution poly(ethylene oxide) standard reference materials, SRM 1923 and SRM 1924, is described. The weight-average molecular weight of SRM 1923 by light scattering was determined to be 26.9 x 1000 g/mole with a sample standard deviation of 0.87 x 1000 g/mole, based on 3 degrees of freedom. A combined expanded uncertainty of 2 x 1000 g/mole is estimated for this determination. The weight-average molecular weight of SRM 1924 by light scattering was determined to be 120.9 x 1000 g/mole with a sample standard deviation of 1.0 x 1000 g/mole, based on 3 degrees of freedom. A combined expanded uncertainty of 9.0 x 1000 g/mole is estimated for this determination.

01,231
PB95-107090 Not available NTIS
National Inst. of Standards and Technology (MSEL), Gaithersburg, MD. Polymers Div.
SANS and LS Studies of Polymer Mixtures Under Shear Flow.
Final rept.
A. I. Nakatani. 1993, 4p.
Pub. in Polymer Preprints, Japan 42, n1 p134-137 1993.

Keywords: *Polymers, *Mixtures, *Light scattering, *Shear flow, Neutron scattering, Phase transformations, Shear rate, Kinetics, Rheology. Reprints, SANS(Small angle neutron scattering), LS(Light scattering), Polymer blends.

Small angle neutron scattering (SANS) and light scattering (LS) techniques have been used recently for in situ observations of the behavior of polymer mixtures under the influence of an applied shear field. Many prior studies examine the phase behavior of polymer mixtures under shear by turbidimetric or light scattering methods. The smaller size scales accessible with SANS make a combination of LS and SANS desirable. A couette geometry shear cell for SANS and a cone and plate geometry cell for LS have been constructed at the National Institute of Standards and Technology. Details of the two instruments will be described. Various examples of the results from the two instruments will be presented.

01,232
PB95-107389 Not available NTIS
National Inst. of Standards and Technology (MSEL), Gaithersburg, MD. Polymers Div.
Polyethylene Crystallized from an Entangled Solution Observed by Scanning Tunneling Microscopy.
Final rept.
D. H. Reneker, J. Schneir, B. Howell, and H. Harary. 1990, 3p.
Pub. in Polymer Communications 31, n5 p167-169 1990.

Keywords: *Polyethylene, *Crystallization, *Surfaces, Molecular weight, Scanning electron microscopy, Reprints, *Scanning tunneling microscopy.

Rapid cooling of a thin layer of an entangled solution of ultra-high molecular weight polyethylene on a mica sheet resulted in a structure composed of elongated patches of polymer a few nanometers thick, aligned over distances of several micrometers. Some rows of side-by-side patches were thicker and formed a structure with a moss-like appearance at lower magnification. The scanning tunneling microscope was shown to be useful for the examination, at high magnification, of polymer surfaces. The top surface of a thin, conducting layer of evaporated platinum and carbon on a polymer reveals much the same information as could be obtained by removing the platinum and carbon layer and examining it with a transmission electron microscope. The often troublesome step of removing the platinum/carbon replica is not needed for the scanning tunneling microscope.

01,233
PB95-108668 Not available NTIS
National Inst. of Standards and Technology (MSEL), Gaithersburg, MD. Polymers Div.
Response of a Terminally Anchored Polymer Chain to Simple Shear Flow.
Final rept.
R. S. Parnas, and Y. Cohen. 1991, 11p.
Pub. in Macromolecules 24, n16 p4646-4656 1991.

Keywords: *Polymers, *Shear flow, *Dynamic response, Plastic flow, Molecular structure, Brownian movement, Fluid dynamics, Hydrodynamics, Reprints.

The dynamic behavior of a terminally anchored freely-jointed bead rod chain, subjected to uniform solvent shear flow, was investigated via Brownian dynamics simulations. Computed segment density distributions and other statistical expressions of the chain conformation demonstrate a strong effect of shear rate on chain behavior. Values of the effective hydrodynamic thickness computed from the numerical similations were also found to be a strong function of the shear rate. Stationary statistical results obtained for the chain extension show two regimes in the configuration space of the model chain, a Brownian regime at low shear rates and a hydrodynamic regime at high shear rates.

01,234
PB95-140075 Not available NTIS
National Inst. of Standards and Technology (MSEL), Gaithersburg, MD. Reactor Radiation Div.
Morphology of Symmetric Diblock Copolymers as Revealed by Neutron Reflectivity.
Final rept.
S. K. Satija, C. F. Majkrzak, S. H. Anastasiadis, and T. P. Russell. 1990, 6p.
Pub. in Materials Research Society Symposia Proceedings 166, p139-144 1990.

Keywords: *Block copolymers, *Morphology, *Thin films, *Polystyrene, *Polymethyl methacrylate, Surface properties, Substrates, Neutron radiography, Reflectivity, Annealing, Interfaces, Laminates, Phase transformations, Reprints.

Recently, it has been shown that symmetric diblock copolymers of polystyrene (PS), and polymethylmethacrylate (PMMA), when prepared as thin films (5000A or less) on silicon substrates, exhibit a strong orientation of the lamellar microdomains parallel to the surface of the substrate. This orientation occurs when the copolymer films are annealed at temperatures above the glass transition temperatures of the PS and PMMA blocks and results from the interactions of the two blocks with the air and substrate interfaces. PMMA, the more polar species, preferentially resides at the silicon (silicon oxide)/copolymer interfaces, whereas PS, the lower surface energy component, preferentially segregates to the air/copolymer interface. These interactions, coupled with the chemical connectivity of the PS and PMMA blocks, result in the observed multilayered structure.

01,235
PB95-140125 Not available NTIS
National Inst. of Standards and Technology (MSEL), Gaithersburg, MD. Polymers Div.
Novel Polydiacetylenes Derived from Liquid Crystalline Monomers.
Final rept.
M. A. Schen. 1988, 10p.
Pub. in Proceedings of International Conference on Electrical, Optical and Acoustic Properties of Polymers (1st), Canterbury, UK., September 5-7, 1988, p12/1-12/10.

Keywords: *Liquid crystals, *Acetylene, Small angle scattering, X-ray scattering, Reaction kinetics, Polymerization, Monomers, Reprints, *Polydiacetylenes.

The liquid crystal phase polymerization of a liquid crystalline diacetylene monomer, 1,6 bis-(4-oxybenzylidene 4'-n-octylaniline) 2,4-hexadiyne is reported and characterized. Within the crystal and liquid crystal phases, first-order disappearance of monomer is seen by differential scanning calorimetry with a thermal activation energy of 155 kJ/mol. The lamellar structure characteristic of the monomer smectic phase is conserved with polymerization as shown by X-ray scattering. The topochemical polymerization of diacetylenes is therefore extended to include polymerization in the liquid crystal phase.

01,236
PB95-140190 Not available NTIS
National Inst. of Standards and Technology (MSEL), Gaithersburg, MD. Polymers Div.
Glass Temperature of Polymer Blends: Comparison of Both the Free Volume and the Entropy Predictions with Data.
Final rept.
H. A. Schneider, and E. A. Di Marzio. 1992, 9p.
Pub. in Polymer 33, n16 p3453-3461 1992.

Keywords: *Blends, *Polymers, *Glass transition temperature, *Volume, *Entropy, Mathematical models,

Phase transformations, Monomers, Experimental data, Reprints, *Polymer blends.

An equation derived from the hypothesis that the glass temperature is determined by entropy considerations, and an equation derived from the hypothesis that the glass temperature is determined from free volume considerations are each compared to 17 polymer blend systems. The curves mimic experiment in about half (the same half) of the cases. The (roughly) equivalent predictions of the two equations suggests that the glass temperature of an infinite molecular weight polymer is proportional to the mass of a monomer unit divided by the number of flexible bonds of a monomer unit. A slightly modified treatment suggests proportionality to monomer volume per flexible bond. It is pointed out each of the two equations are zeroth order treatments and that they can each be improved. The improvement arising from the entropy theory requires no parameters.

01,237
PB95-141156 Not available NTIS
National Inst. of Standards and Technology (MSEL), Gaithersburg, MD. Polymers Div.
Effect of Hydrodynamic Interactions on a Terminally Anchored Bead-Rod Model Chain.
Final rept.
R. S. Parnas, and Y. Cohen. 1993, 5p.
Pub. in Proceedings of Symposium on Dynamics in Small Confining Systems, Boston, MA., November 30-December 4, 1990, 5p 1993.

Keywords: *Hydrodynamics, *Polymers, *Chains, Brownian movement, Simulation, Shear flow, Molecular structure, Statistical distributions, Radius of gyration, Reprints, *Hydrodynamic interactions, *Bead-rod model.

Brownian dynamics simulations of a terminally anchored, freely-jointed bead-rod chain were used to reveal the effects of Yamakawa hydrodynamic interactions on the statistical properties of the chain. Properties such as the RMS and effective hydrodynamic thicknesses were computed with and without hydrodynamic interactions. Although hydrodynamic interactions significantly influenced the magnitude of the statistical properties of the terminally anchored bead-rod chain, the general trends seen in such properties were not altered. Additionally, the results obtained with the freely-jointed bead-rod model are in better agreement with experimental results than those obtained with bead-spring models, for surface bound polymer layers.

01,238
PB95-150033 Not available NTIS
National Inst. of Standards and Technology (MSEL), Gaithersburg, MD. Reactor Radiation Div.
Observed Frustration in Confined Block Copolymers.
Final rept.
P. Lambooy, T. P. Russell, G. J. Kellog, S. K. Satija, A. M. Mayes, and P. D. Gallagher. 1994, 4p.
Contract DE-FG03-88ER45375
Sponsored by Department of Energy, Washington, DC.
Pub. in Physical Review Letters 72, n18 p2899-2902, 2 May 94.

Keywords: *Block copolymers, *Solids, *Surface properties, Neutron radiography, Reflectivity, Interfaces, Films, Separation, Reprints.

Symmetric, diblock copolymers confined between two solid surfaces were studied by neutron reflectivity. A multilayered morphology with an integral number of layers oriented parallel to the solid interfaces was found in all cases. The period of the confined multilayers deviated from the bulk period in a cyclic manner as a function of the confined film thickness. A first-order transition occurred between the expanded and contracted states of the copolymer chains. The data suggest that the deviation of the period from the bulk value decreases with increasing separation distance.

01,239
PB95-150454 Not available NTIS
National Inst. of Standards and Technology (MSEL), Gaithersburg, MD. Polymers Div.
Structural Stabilization of Phase Separating PC/Polyester Blends through Interfacial Modification by Transesterification Reaction.
Final rept.
H. Yoon, Y. Feng, Y. Qiu, and C. C. Han. 1994, 8p.
Pub. in Jnl. of Polymer Science: Part B. Polymer Physics 32, p1485-1492 1994.

Keywords: *Molecular structure, *Phase separation(Materials), *Polymer blends, *Interfaces, *Esterification, Copolymers, Polycarbonate resins, Time dependence, Temperature dependence, Small angle scattering, Neutron scattering, Melting, Heat measurement, Reprints, Differential scanning calorimetry.

Competition between phase separation and transesterification in immiscible polymer blends of polycarbonate (PC) and a copolyester (PET) is studied as a function of time and temperature by differential scanning calorimetry (DSC) and small-angle neutron scattering (SANS). We found that (1) Global structure coarsens at T greater than or equal to 200 C due to the dominance of phase separation over transesterification and melts at T greater than or equal to 200 C due to the dominance of transesterification at the domain interface. However, transesterification is slow but still significant even at T greater than or equal to 200 C. (2) An intricate balance of transesterification and phase separation rates controls global and interfacial structures. (3) Interfacial structures become measureable under certain conditions, and the interfacial thickness between PC or PET and the copolymers generated by transesterification increases with time. (4) DSC results are consistent with results obtained by SANS, but the latter is more sensitive than the former and differentiates the structural change at different length scales caused by phase separation and transesterification.

01,240
PB95-151072 Not available NTIS
National Inst. of Standards and Technology (MSEL), Gaithersburg, MD. Polymers Div.
Thermal Stability of Internal Electric Field and Polarization Distribution in Blend of Polyvinylidene Fluoride and Polymethylmethacrylate.
Final rept.
N. Tsutsumi, Y. Ueda, T. Kiyotsukuri, A. S. DeReggi, and G. T. Davis. 1993, 7p.
Pub. in Jnl. of Applied Physics 74, n5 p3366-3372, 1 Sep 93.

Keywords: *Thermal stability, *Polymer blends, *PMMA, *Polarization(Charge separation), Polyvinylidenes, Ferroelectric materials, Dyes, Electric fields, Reprints, *Polyvinylidene fluorides, *Internal electric fields.

It is confirmed that a melt-quenched and annealed blend of 80 wt % polyvinylidene fluoride and 20 wt % polymethylmethacrylate has the beta-crystal form of PVDF with optical clarity and other properties that are desirable for a host material in a guest-host system where the guest is an optically nonlinear dye that is orientationally stabilized by the strong internal electric field of a poled ferroelectric. Combined measurements, in such a blend, of the internal electric field E(sub i), the pyroelectric coefficient C(sub pyro), and the polarization distribution after electrically poling and subsequently thermally aging for 2 h intervals at temperatures up to 120 C are reported.

01,241
PB95-151247 Not available NTIS
National Inst. of Standards and Technology (MSEL), Gaithersburg, MD. Polymers Div.
Anisotropic Phase Separation Kinetics in a Polymer Blend Solution Following Cessation of Shear Studied by Light Scattering.
Final rept.
D. A. Waldow, A. I. Nakatani, and C. C. Han. 1992, 4p.
Pub. in Polymer 33, n21 p4635-4638 1992.

Keywords: *Polymer blends, *Phase separation(Materials), *Kinetics, *Anisotropy, *Laboratory equipment, *Shear flow, Light scattering, Solutions, Polystyrene, Polybutadiene, Monitoring, Reprints.

A light scattering instrument capable of monitoring the scattering from samples under the influence of a simple shear field has been constructed. The apparatus consists of transparent cone-and-plate fixtures and a two-dimensional charge coupled device array detector. The detector unit is also capable of measuring the scattering patterns as a function of time. The phase separation kinetics of an 8% solution of a polystyrene/polybutadiene (50:50) blend in dioctyl phthalate following cessation of a steady shear is monitored with this instrument. The sample is two-phase in the quiescent state and the applied shear is sufficient to suppress all scattering observed from the quiescent sample (shear-induced mixing). The evolution of the scattering profiles following cessation of shear is quite different parallel and perpendicular to the original flow direction. In the normal direction, a spinodal growth and coarsening mechanism similar to that observed in temperature quench experiments is observed. In the parallel direction, a different mechanism is followed. We believe this is the first report of this type of anisotropic behavior in the phase separation kinetics of a polymer blend.

01,242
PB95-151841 Not available NTIS
National Inst. of Standards and Technology (MSEL), Gaithersburg, MD. Polymers Div.
SANS Study of the Plastic Deformation Mechanism in Polyethylene.
Final rept.
W. Wu, G. D. Wignall, and L. Mandelkern. 1993, 4p.
Pub. in Polymer 33, n19 p4137-4140 1992.

Keywords: *Polyethylene, *Neutron scattering, *Polymer blends, *Plastic deformation, Small angle scattering, Thermoplastic resins, Deuterium compounds, Protons, Separation, Melting, Reprints, SANS(Small Angle Neutron Scattering).

Small angle neutron scattering was used to investigate the role of partial melting and recrystallization in the solid state deformation of polyethylene. Blends containing 4 vol% deuteropolyethylene in protonated polyethylene were deformed in a pure shear mode. The scattering cross section of the undeformed blends was well in excess of that expected for randomly (statistically) dispersed molecules, due to isotopic segregation effects between the deuterated and the protonated species. A significant reduction in the excess scattering was observed as the blends were deformed beyond the yield point. Upon further deformation the cross section underwent a further modest decrease. Such a reduction is known to occur on melting. The neutron scattering results, hence, support the notion of local melting during the yielding and the subsequent deformation processes.

01,243
PB95-151866 Not available NTIS
National Inst. of Standards and Technology (MSEL), Gaithersburg, MD. Polymers Div.
Structural Heterogeneity in Epoxies.
Final rept.
W. L. Wu, J. T. Hu, and D. L. Hunston. 1990, 6p.
Pub. in Polymer Engineering and Science 30, n14 p835-840 1990.

Keywords: *Molecular structure, *Curing, *Epoxy resins, *Heterogeneity, Small angle scattering, X-ray scattering, Mechanical properties, Fracture properties, Toughness, Modulus of elasticity, Impact strength, Glass transition temperature, Reprints.

The effects of different cure procedures on the structure and properties of epoxy samples made from diglycidyl ether of bisphenol A (DGEBA) and mixtures of two linear aliphatic diamines were studied. The elastic modulus, fracture toughness, impact resistance and glass transition temperature were determined for various cure schemes. The morphologies of the cured resins were characterized with small angle x-ray scattering. The results show that samples with the same average morphology (molecular network structure) have similar elastic moduli and glass transition temperatures. If some heterogeneity is introduced in the molecular network structure without changing the average structure, however, the experiments indicate that the toughness can be increased without significantly sacrificing other properties.

01,244
PB95-151882 Not available NTIS
National Inst. of Standards and Technology (MSEL), Gaithersburg, MD. Polymers Div.
Characterization of Polyquinoline Block Copolymer Using Small Angle Scattering.
Final rept.
W. L. Wu, J. K. Stille, J. W. Tsang, and A. J. Parker. 1989, 4p.
Pub. in Materials Research Society Symposia Proceedings, v134 p493-496 1989.

Keywords: *Block copolymers, *Small angle scattering, Neutron scattering, X-ray scattering, Deuterium compounds, Separation, Rigidity, Flexibility, Reprints, *Polyquinolines.

To determine the compatibility between the rigid rod and the flexible chain polyquinolines, both small angle

x-ray and neutron scattering measurements were conducted on a sample containing deuterated flexible components. The scattering intensities from both x-ray and neutron were reduced to the absolute scale in order to remove the scattering contribution from microvoids which tended to overshadow the signal from the molecular origin. Quantitative information regarding the extent of segregation of this rigid rod containing blends can be obtained from the scattering data free of microvoid contribution.

01,245
PB95-151890 Not available NTIS
National Inst. of Standards and Technology (MSEL), Gaithersburg, MD. Polymers Div.
Dynamic Light-Scattering Study of a Diluted Polymer Blend Near Its Critical Point.
Final rept.
H. Yajima, D. Hair, A. Nakatani, J. Douglas, and C. Han. 1993, 4p.
Pub. in Physical Review B 47, n18 p12 268-12 271, 1 May 93.

Keywords: *Polymer blends, *Light scattering, *Critical point, *Dynamics, *Polystyrene, *Polybutadiene, Experimental design, Reprints, Phthalate/dioctyl.

The critical dynamics of a moderately-high-molecular-weight polymer blend of polystyrene and polybutadiene diluted in dioctyl phthalate is studied near the consolute point by dynamic light scattering. Fast and slow modes are observed as in previous experiments on a low-molecular-weight binary-polymer-blend melt. The light-scattering data are consistent with a Fisher renormalization of the correlation-length exponent.

01,246
PB95-152237 Not available NTIS
National Inst. of Standards and Technology (MSEL), Gaithersburg, MD. Polymers Div.
Thermal Behaviour of Methyl Methacrylate and N-Phenyl Maleimide Copolymers.
Final rept.
L. Choudhary, D. S. Varma, I. K. Varma, and F. W. Wang. 1993, 10p.
Pub. in Jnl. of Thermal Analysis 39, p633-642 1993.

Keywords: *Copolymers, *Methyl methacrylate, *Synthesis(Chemistry), *Thermal stability, PMMA, Reprints, *Maleimide/N-phenyl.

The paper describes the synthesis and characterization of six copolymers of methyl methacrylate (MMA) and N-phenyl maleimide (NPM). Thermal stability of PMMA was markedly improved by incorporation of even a very low mole fraction of NPM in the backbone. An increase in mole fraction of NPM from 0.0979 to 0.4766 only marginally affected thermal stability.

01,247
PB95-152872 Not available NTIS
National Inst. of Standards and Technology (MSEL), Gaithersburg, MD. Polymers Div.
Thermodynamic Interactions and Correlations in Mixtures of Two Homopolymers and a Block Copolymers by Small Angle Neutron Scattering.
Final rept.
N. P. Balsara, S. V. Jonnalagadda, C. C. Lin, C. C. Han, and R. Krishnamoorti. 1993, 10p.
Pub. in Jnl. of Chemical Physics 99, n12 p10011-10020, 15 Dec 93.

Keywords: *Polymer blends, *Thermodynamics, *Copolymers, *Neutron scattering, *Polyolefins, Small angle scattering, Random phase approximation, Hydrogen, Deuterium, Synthesis(Chemistry), Phase studies, Reprints.

Thermodynamic interactions in mixtures of two homopolymers and a block copolymer were obtained from small-angle neutron scattering (SANS) measurements. Experimental SANS profiles from homogeneous, ternary mixtures of model polyolefins--poly(ethyl butylene)/poly(methyl butylene)/poly(methyl butylene)-b-poly(ethyl butylene)--were compared with theoretical predictions based on the multicomponent random phase approximation (RPA). The polymers were nearly monodisperse and were synthesized by saturating the double bonds in anionically synthesized polydienes with H2 and D2, thus yielding polyolefins with neutron scattering contrast.

01,248
PB95-153144 Not available NTIS
National Inst. of Standards and Technology (MSEL), Gaithersburg, MD. Polymers Div.
Copolymerization of N-Phenyl Maleimide and gamma-Methacryloxypropyl Trimethoxysilane.
Final rept.
L. Choudhary, D. S. Varma, F. W. Wang, V. Choudhary, and I. K. Varma. 1993, 5p.
Pub. in Jnl. of Applied Polymer Science 49, p91-95 1993.

Keywords: *Copolymerization, Reaction kinetics, Decomposition reactions, Endothermic reactions, Reprints, *Maleimide/N-phenyl, *Silane/methacryloxyprophyl trimethoxy.

Copolymerization of N-phenyl maleimide (NPM) and gamma-methacryloxypropyl trimethoxysilane (MTS) in dioxan solution using benzoyl peroxide as an initiator is described. The rate of copolymerization depended on the mole fraction of NPM in the initial feed and decreased with an increase in NPM content. Copolymers having a mole fraction of NPM varying from 0.29 to 0.55 exhibited similar thermal behavior in terms of initial decomposition temperature of maximum rate of weight loss. However, char yield at 600 C depended on NPM content, showing a tendency to increase with the increase in NPM content.

01,249
PB95-153151 Not available NTIS
National Inst. of Standards and Technology (MSEL), Gaithersburg, MD. Polymers Div.
Thermal Behavior of 4-Maleimidophenyl Glycidyl Ether Resins.
Final rept.
L. Choudhary, D. S. Varma, F. W. Wang, V. Choudhary, and I. K. Varma. 1993, 10p.
Pub. in Thermochimica Acta 220, p261-270 1993.

Keywords: *Thermodynamic properties, *Polymerization, *Thermochemistry, Infrared spectroscopy, Nuclear magnetic resonance, Curing, Heat of reaction, Molecular structure, Epoxy resins, Reprints, *Ether/maleimidophenyl glycidyl.

A novel epoxy-maleimide resin, 4-maleimidophenyl glycidyl ether (MGE), was prepared from 4-aminophenol. Characterization was carried out by estimation of the epoxy equivalent and by IR and (1)H-NMR spectroscopy. The MGE resin was cured by heating above 250 C. A decrease in the curing temperature was observed after the addition of a stoichiometric or non-stoichiometric amount of an aromatic diamine. The values of the curing temperature and the heat of the polymerization reaction (Delta H) were independent of diamine concentration but depended on the structure of the diamine. The char yield of cured resins at 800 C in a nitrogen atmosphere ranged from 25% to 40%, which is much higher than the values reported for epoxy resins.

01,250
PB95-153367 Not available NTIS
National Inst. of Standards and Technology (MSEL), Gaithersburg, MD. Polymers Div.
Piezoelectric and Pyroelectric Polymers.
Final rept.
G. T. Davis. 1993, 31p.
Pub. in Polymers for Electronic and Photonic Applications, p435-465 1993.

Keywords: *Vinyl copolymers, *Piezoelectricity, *Pyroelectricity, *Polarization(Charge separation), Nylon fibers, Ferromagnetic materials, Hysteresis, Thermal stresses, Reprints.

Piezoelectric and pyroelectric response from polymers arises from changes in polarization resulting from stress or temperature-induced changes in volume. Factors which determine the polarization that can be induced by poling are outlined for amorphous polymers and for semicrystalline polymers. Definitions of piezoelectric and pyroelectric coefficients and the conventions of nomenclature are presented. Typical coefficients for polymers are compared with those for other organic or inorganic materials which exhibit such properties. A brief description of the properties of specific polymers is presented with frequent reference to more detailed review articles.

01,251
PB95-153789 Not available NTIS
National Inst. of Standards and Technology (MSEL), Gaithersburg, MD. Polymers Div.
SANS Studies of Space-Time Organization of Structure in Polymer Blends.
Final rept.
T. Hashimoto, H. Jinnai, H. Hasegawa, and C. C. Han. 1993, 11p.
Pub. in Proceedings of International Symposium on Advanced Nuclear Energy Research (5th) - Neutrons as Microscopic Probes, Ibaraki, Japan, March 10-12, 1993, p73-83.

Keywords: *Molecular structure, *Polymer blends, *Neutron scattering, *Polybutadiene, *Polyisoprene, Small angle scattering, Light scattering, Deuterium compounds, Synthetic elastomers, Spinodal decomposition, Time resolution, Protons, Reprints, SANS(Small Angle Neutron Scattering).

Self-organization of structure in polymer blends via spinodal decomposition (SD) was studied over a wide spatial-scale and time-scale (both being covered over 4 orders of magnitude) by using a combined time-resolved small-angle neutron scattering and light scattering method. The system studied was a binary critical fluid of deuterated polybutadiene and proton polyisoprene having a narrow molecular weight distribution in a weak segregation limit. The scattering analyses made it possible to study space-time organization of various elements of the structures: (1) global structure, (2) interfacial structure such as mean curvature of the tangled interface, interfacial area density, and interfacial thickness, (3) 'interphase', i.e., interfacial region with characteristic thermal concentration fluctuations, and (4) the local structure characterized by the thermal concentration fluctuations within each domain. In the late stage SD, the form factor from the 'interphase' was found to be time-independent, having the q-dependence of q(sup -2.5).

01,252
PB95-161196 Not available NTIS
National Inst. of Standards and Technology (MSEL), Gaithersburg, MD. Polymers Div.
Time-Resolved Small-Angle Neutron Scattering Study of Spinodal Decomposition in Deuterated and Protonated Polybutadiene Blends. 1. Effect of Initial Thermal Fluctuations.
Final rept.
H. Jinnai, H. Hasegawa, T. Hashimoto, and C. C. Han. 1993, 327p.
Pub. in Jnl. of Chemical Physics 99, n6 p4845-4854, 15 Sep 93.

Keywords: *Polymer blends, *Spinodal decomposition, *Polybutadiene, *Neutron scattering, Synthetic elastomers, Small angle scattering, Deuterium compounds, Protons, Time resolution, Temperature effects, Binary systems(Materials), Phase diagrams, Reprints.

Time-resolved small-angle neutron scattering (SANS) experiments have been performed on the self-assembling process of a binary mixture of deuterated polybutadiene and protonated polybutadiene at the critical composition. This mixture has an upper critical solution temperature type of phase diagram with the spinodal temperature at 99.2 C. Specimens held in the single-phase state at an initial temperature (T(sub i)) were quenched to a point inside the spinodal phase boundary at a final temperature (T(sub f)) to induce phase separation via spinodal decomposition (SD). In order to examine the effect that thermal concentration fluctuations have on SD, three different initial temperatures, T(sub i) = 102.3 C, 123.9 C, and 171.6 C, were chosen while T(sub f) was fixed at -7.5 C. A critical test of the linearized Cahn-Hilliard-Cook theory led to the conclusion that this theory can describe satisfactorily the early stage SD in the deep-quench region.

01,253
PB95-161592 Not available NTIS
National Inst. of Standards and Technology (MSEL), Gaithersburg, MD. Polymers Div.
Localization of a Homopolymer Dissolved in a Lamellar Structure of a Block Copolymer Studied by Small-Angle Neutron Scattering.
Final rept.
Y. Matsushita, N. Torikai, Y. Mogi, I. Noda, and C. C. Han. 1993, 4p.
Pub. in Macromolecules 26, n24 p6346-6349 1993.

Keywords: *Block copolymers, *Neutron scattering, *Molecular structure, *Polymers, Small angle scattering, Lamellar structure, Deuterium compounds, Molecular chains, Phase separation(Materials), Reprints.

The localization of deuterated styrene homopolymer dissolved in a lamellar structure of a styrene-2-

vinylpyridine diblock copolymer was studied in comparison with that of the end part of the block copolymer by observing diffraction from the styrene and 2-vinylpyridine microdomains of deuterated styrene homopolymer/styrene-2-vinylpyridine diblock copolymer blends by small-angle neutron scattering (SANS). Even when the average scattering lengths of both domains were equal, that is, 'phase contrast matching' was theoretically achieved, diffraction was definitely observed. From the diffraction profiles in SANS and the dependence of domain spacing on the volume fraction of the styrene homopolymer, it was found that the homopolymers are isolated in the middle of the polystyrene domain, although they are concentrated less than the end parts of the block chains.

01,254
PB95-161691 Not available NTIS
National Inst. of Standards and Technology (MSEL), Gaithersburg, MD. Polymers Div.
Molecular Weight Dependence of the Lamellar Domain Spacing of ABC Triblock Copolymers and Their Chain Conformation in Lamellar Domains.
Final rept.
Y. Mogi, K. Mori, H. Kotsuji, C. Han, Y. Matsushita, and I. Noda. 1993, 5p.
Pub. in Macromolecules 26, n19 p5169-5173 1993.

Keywords: *Molecular weight, *Block copolymers, *Molecular chains, *X-ray scattering, Lamellar structure, Small angle scattering, Phase separation(Materials), Reprints, *Molecular conformation, Styrene vinylpyridine.

The molecular weight dependence of the lamellar domain spacing of isopren-styrene-2-vinylpyridine triblock copolymers in bulk was studied over the molecular weight range from 40K to 280K by using a small-angle X-ray scattering (SAXS) method. It was found that the lamellar domain spacings of the triblock copolymers are larger than those of styrene-2-vinylpyridine diblock copolymers with the same molecular volumes. This result can be interpreted by theories of microphase separation at the strong segregation limit, taking into account the fact that the number of boundaries in the repeating structure of triblock copolymers is twice as large as that of diblock copolymers. Moreover, small-angle neutron scattering (SANS) studies imply that the middle block chain of triblock copolymers is contracted along the direction parallel to lamellae in almost the same manner as the block chain of the diblock copolymers.

01,255
PB95-161816 Not available NTIS
National Inst. of Standards and Technology (MSEL), Gaithersburg, MD. Polymers Div.
Elastic Scattering of Polymer Networks.
Final rept.
W. L. Wu. 1991, 4p.
Pub. in Macromolecules 24, n5 p1145-1148 1991.

Keywords: *Neutron scattering, *Crosslinking, *Molecular structure, *Spatial distribution, *Polymers, Random phase approximation, Reprints.

The theoretical aspect of the scattering of crosslinked polymers was investigated with emphasis on the fact that the number of spatial neighbors for any given network is finite. A random phase approximation scheme was used; however, the interaction terms was truncated to account for this finiteness. The result indicates that the expression based on infinite neighbors hold true in all the cases.

01,256
PB95-161865 Not available NTIS
National Inst. of Standards and Technology (MSEL), Gaithersburg, MD. Polymers Div.
Neutron Scattering Study of Shear Induced Turbidity in Polystyrene Dissolved in Dioctyl Phthalate.
Final rept.
A. I. Nakatani, J. F. Douglas, Y. B. Ban, and C. C. Han. 1994, 9p.
Pub. in Jnl. of Chemical Physics 100, n4 p3224-3232, 15 Feb 94.

Keywords: *Neutron scattering, *Polystyrene, *Turbidity, *Solutions, Shear rate, Small angle scattering, Deuterium compounds, Hydrogenation, Temperature dependence, Specific heat, Critical temperature, Reprints, Phthalate/dioctyl.

The influence of shear on the small angle neutron scattering from a semidilute solution of polystyrene (PS) dissolved in dioctyl phthalate (DOP) is examined in the limit of strong shear (gamma greater than or = to 100/s). These experiments are restricted to room temperature, which is close to the theta point of PS/DOP. The fraction of deuterated PS chains is varied, while the total polymer weight fraction is fixed at 3%. This is near the critical composition of hydrogenated PS in DOP. The increased scattering at high shear rates ('shear induced turbidity') is interpreted in terms of a critical temperature shift. Scattering along the flow direction is distorted and the scattering data normal to flow is uninfluenced by shear above a wave vector cutoff q*, which is independent of shear rate. This cutoff is found to correspond to the Debye length, characterizing the average intermolecular potential range.

01,257
PB95-163044 Not available NTIS
National Inst. of Standards and Technology (MSEL), Gaithersburg, MD. Polymers Div.
Synthesis and Polymerization of Difunctional and Multifunctional Monomers Capable of Cyclopolymerization.
Final rept.
J. W. Stansbury. 1990, 2p.
Pub. in Polymer Preprints 31, n1 p503-504 1990.

Keywords: *Synthesis(Chemistry), *Polymerization, *Monomers, *Cyclic compounds, Esters, Crosslinking, Vitreous state, Ethers, Intramolecular forces, Reprints.

The reaction of an acrylate ester with paraformaldehyde in the presence of DABCO has given access to a novel class of ether-fused pseudodimethacrylate monomers. The 1,6-diene unit incorporated in the monomers can be polymerized through an inter-intramolecular cyclopolymerization process which yields a soluble, ester-substituted, cyclic ether polymer structure. A series of monomers was prepared to evaluate the effect of the substituents on the synthesis and cyclopolymerization. A method was developed which efficiently provided even monomers with very bulky ester groups. Solution polymerization studies indicated that both monomer concentration and ester structure exert significant influence on the mode of polymerization. Apparently, the more hindered monomers are more effective at cyclopolymerization. The bulk polymerization of these monomers resulted in crosslinked, glassy polymers with little or no residual unsaturation. Multifunctional oligomers based on this same chemistry were also prepared and polymerized in this study.

01,258
PB95-163770 Not available NTIS
National Inst. of Standards and Technology (MSEL), Gaithersburg, MD. Polymers Div.
Applications of Fluorescence Spectroscopy in Polymer Science and Technology.
Final rept.
F. W. Wang. 1991, 6p.
Pub. in Polymer Science 2, p546-551 1991.

Keywords: *Polymers, *Epoxy resins, *Curing, *Spectrum analysis, Marking, Labeled substances, Viscosity, Diffusion coefficient, Polystyrene, Bleaching, Photochemical reactions, Transport properties, Reprints, *Fluorescent dyes.

Two approaches using fluorescent dyes dissolved in epoxy resins were used to determine the viscosity changes during the curing process. First, we used a dye whose fluorescence intensity increases with the increase in the local viscosity, and a second dye whose fluorescence intensity is insensitive to the local viscosity. The ratio of the fluorescence intensities of the two dyes was measured to monitor the cure of epoxy resins. In another approach, we measured the diffusion coefficient of a fluorescent dye dissolved in epoxy resins by fluorescence recovery after photobleaching to monitor the cure of epoxy resins. Finally, self-diffusion in concentrated polystyrene solutions was measured by the method of fluorescence recovery after photobleaching.

01,259
PB95-164109 Not available NTIS
National Inst. of Standards and Technology (MSEL), Gaithersburg, MD. Polymers Div.
Characterization of Molecular Network of Thermosets Using Neutron Scattering.
Final rept.
W. L. Wu. 1990, 4p.
Pub. in Materials Research Society Symposia Proceedings, v166 p475-478 1990.

Keywords: *Molecular structure, *Epoxy resins, *Thermosetting resins, *Neutron scattering, Curing, Polymerization, Reprints.

Neutron scattering measurements were conducted to investigate the conformation of the molecular networks in epoxies. Emphasis was placed on the changes in the scattering intensity resulting from curing. Experimental results on homopolymerized epoxy as well as a theoretical interpretation of the results are presented.

01,260
PB95-164117 Not available NTIS
National Inst. of Standards and Technology (MSEL), Gaithersburg, MD. Polymers Div.
Small-Angle Neutron Scattering of Poly(vinyl alcohol) Gels.
Final rept.
W. Wu, H. Kurokawa, S. Roy, and R. S. Stein. 1991, 6p.
Pub. in Macromolecules 24, n15 p4328-4333 1991.

Keywords: *Neutron scattering, *Gels, *Polyvinyl alcohol, *Molecular structure, Small angle scattering, Temperature, Transition temperature, Sols, Reprints.

The structure of aqueous poly(vinyl alcohol) (PVA) gels with and without borate ions, hereafter referred to as alkaline gels and hydrogels, respectively, was investigated using small-angle neutron scattering (SANS). The correlation length Xi, a measure of the wavelength of concentration fluctuation, was estimated from the SANS results. The value of Xi showed a modest decrease with increasing temperature. Even at the highest temperature of observation, 95 C, Xi was still a few times greater than the radius of gyration of individual PVA molecules, indicating the presence of PVA clusters in the sol state. The scattered intensities for both the hydrogels and the alkaline gels over a wide temperature range could be superimposed onto one master curve by employing the reduced variables I(q)/Xi(exp 3) and (Xi)(q), where q is the magnitude of the scattering vector. This indicates that the concentration fluctuation can be described adequately by a single characteristic length over a wide temperature range embracing the sol-gel transition temperature.

01,261
PB95-164125 Not available NTIS
National Inst. of Standards and Technology (MSEL), Gaithersburg, MD. Polymers Div.
Characterization of Polyquinoline Blends Using Small Angle Scattering.
Final rept.
W. L. Wu, J. K. Stille, J. W. Tsang, and A. J. Parker. 1990, 5p.
Sponsored by Defense Advanced Research Projects Agency, Arlington, VA. and Air Force Office of Scientific Research, Bolling AFB, DC.
Pub. in Materials Research Society Symposia Proceedings, v171 p189-193 1990.

Keywords: *Polymer blends, *Neutron scattering, *X-ray scattering, Small angle scattering, Molecular chains, Deuterium compounds, Reprints, *Polyquinolines, Rigid rod polymers, Flexible chain polymers.

To determine the compatibility between the rigid rod and the flexible chain polyquinolines, both small angle x-ray and neutron scattering measurements were conducted on blends containing deuterated flexible chains. The scattering intensities from both x-ray and neutron were reduced to their absolute scales in order to remove the scattering contribution from microvoids which tended to overshadow the signal of molecular origin. Quantitative information regarding the molecular dispersion in a 50/50 rigid rod and flexible chain blend was obtained. The result indicated that this material was partially segregated but not to the point of single component phases.

01,262
PB95-164372 Not available NTIS
National Inst. of Standards and Technology (MSEL), Gaithersburg, MD. Polymers Div.
Small Angle Neutron Scattering Studies on Chain Asymmetry of Coextruded Poly(Vinyl Alcohol) Film.
Final rept.
M. Shibayama, H. Kurokawa, S. Nomura, W. L. Wu, S. Roy, and R. S. Stein. 1990, 6p.
Pub. in Macromolecules 23, n5 p1438-1443 1990.

Keywords: *Neutron scattering, *Polyvinyl alcohol, *Molecular chains, *Coextruding, Small angle scatter-

ing, Deformation, Birefringence, Least squares method, Regression analysis, Radius of gyration, Reprints, *Molecular conformation.

Chain asymmetry of solid state co-extruded poly(vinyl alcohol) film was studied using small-angle neutron scattering. The radius of gyration R(sub g) was estimated by a nonlinear least square regression analysis with a theoretical scattered intensity function which is based on a model of deformed Gaussian chains. The R(sub g) values for deformed PVA indicate that the poly(vinyl alcohol) chains are deformed affinely at least up to the extension draw ratio of ca. 5, which is in good accordance with the results of birefringence measurement.

01,263
PB95-164380 Not available NTIS
National Inst. of Standards and Technology (MSEL), Gaithersburg, MD. Polymers Div.
Small Angle Neutron Scattering Study on Poly(N-Isopropyl Acrylamide) Gels Near Their Volume-Phase Transition Temperature.
Final rept.
M. Shibayama, T. Tanaka, and C. C. Han. 1992, 13p.
Pub. in Jnl. of Chemical Physics 97, n9 p6829-2841, 1 Nov 92.

Keywords: *Neutron scattering, *Polymers, *Gels, *Phase transformations, *Temperature dependence, Small angle scattering, Heavy water, Solutions, Lorentz transformations, Gauss equation, Ising model, Reprints, *Poly(amide/N-propylacryl).

The small angle neutron scattering experiments were conducted on N-isopropyl acrylamide (NIPA) gels in D2O and on the corresponding NIPA solutions. The NIPA gels underwent a sharp, but a continuous volume phase transition at 34.6 C from a swollen state to a shrunken state with increasing temperature. In the case of the gels, an excess scattering due to the presence of crosslinks was observed at low q region (q < 0.02/A), where q is the magnitude of the scattering vector. The scattered intensity function for the gel was well described with a combination of Gauss and Lorentz-type functions. The Gaussian part results from solidlike inhomogeneity, having a characteristic size of Xi, which is due to the introduction of crosslinks into the system. The Lorentzian part is originated from the liquid nature of the local concentration fluctuations of the gel characterized with a thermal blob of dimension Xi. The critical exponents for the gels support that the volume-phase transition of gels is classified to the three dimensional Ising model reported by Li and Tanaka.

01,264
PB95-164398 Not available NTIS
National Inst. of Standards and Technology (MSEL), Gaithersburg, MD. Polymers Div.
Small-Angle Neutron Scattering Study on Weakly Charged Temperature Sensitive Polymer Gels.
Final rept.
M. Shibayama, T. Tanaka, and C. C. Han. 1992, 13p.
Pub. in Jnl. of Chemical Physics 97, n9 p6842-6854, 1 Nov 92.

Keywords: *Neutron scattering, *Temperature dependence, *Polymers, *Gels, *Statics, Small angle scattering, Electrolytes, Phase transformations, Scattering coefficients, Phase separation(Materials), Heavy water, Reprints, *Poly(amide/N-propylacryl), *Polyacrylic acid.

The static structure factor for poly(N-isopropylacrylamide-co-acrylic acid) (NIPA/AAc) gels was investigated in terms of small-angle neutron scattering (SANS). The NIPA/AAc gels underwent a discrete volume phase transition at 50.8 C from swollen to shrunken states as temperature increased. The static structure factors for NIPA/AAc gels were well described by a Lorentz-type scattered intensity function at temperatures below 34 C which was near the so-called Theta temperature of NIPA in D2O. At higher temperatures, the static structure factor had a distinct scattering maximum although the gel was still in the highly swollen state. The static structure factors were analyzed quantitatively with the theory of Borue and Erukhimovich for polyelectrolyte solutions in a poor solvent. It is found that the concentration fluctuations lead to a microphase separation between polymer rich and poor domains before the system undergoes the volume-phase transition.

01,265
PB95-175402 Not available NTIS
National Inst. of Standards and Technology (MSEL), Gaithersburg, MD. Polymers Div.
Competition between Hydrodynamic Screening ('Draining') and Excluded Volume Interactions in an Isolated Polymer Chain.
Final rept.
J. F. Douglas, and K. F. Freed. 1994, 12p.
Pub. in Macromolecules 27, n21 p6088-6099 1994.

Keywords: *Polymers, *Molecular structure, *Hydrodynamics, *Solutions, Solvents, Dynamics, Coefficient of friction, Intermolecular forces, Configuration interaction, Reprints, Excluded volume, Preaveraging approximation.

A remaining challenge in the theory of polymer solution dynamics is associated with establishing a relation between the macroscopic hydrodynamic properties of polymer solutions and the molecular structure of the polymer and solvent. This problem is unsolved even for the simplest case of polymer solutions at 'infinite dilution'. Recent studies have focused on technical problems such as the 'preaveraging' approximation, epsilon-expansion truncation errors, and the influence of ternary excluded volume interactions which limit the accuracy of analytic calculations. The present paper examines the role of polymer excluded volume in altering intramolecular hydrodynamic interactions and the possible significance of dynamic chain flexibility on hydrodynamic polymer solution properties. This investigation is aided by analysis of our previous renormalization group (RG) computations and simple exactly solvable models. We also examine experimental trends for the variation of the polymer hydrodynamic interaction with solvent and the variation of the translational friction of small molecules with molecular size.

01,266
PB95-175733 Not available NTIS
National Inst. of Standards and Technology (MSEL), Gaithersburg, MD. Polymers Div.
Examination of the l/d Expansion Method from Exact Enumeration for a Self-Interacting Self-Avoiding Walk.
Final rept.
T. Ishinabe, J. F. Douglas, A. M. Nemirovsky, and K. F. Freed. 1994, 11p.
Pub. in Jnl. of Physics A: Mathematical and General 27, p1099-1109 1994.

Keywords: *Polymers, *Series expansion, *Enumeration, Comparison, Thermodynamics, Molecular structure, Reprints, *Self-avoiding walks.

The 1/d expansion method of polymer chains is examined by comparing these expansions for several thermodynamic and structural quantities with the results of standard series analysis of exact enumeration data. The comparisons cover a wide range of spatial dimensions d, including non-integer ones, and are performed for particular values of interaction energy. Good agreement is generally found for d > 4, whereas discrepancies become conspicuous as d decreases to d = 2. Reasonable values are obtained for the exponents nu and gamma in d = 2 - 4 by applying the coherent-anomaly method of Suzuki to our 1/d expansions through fifth order in 1/d.

01,267
PB95-175998 Not available NTIS
National Inst. of Standards and Technology (CSTL), Boulder, CO. Thermophysics Div.
Gas Transport Properties of Solution-Cast Perfluorosulfonic Acid Ionomer Films Containing Ionic Surfactants.
Final rept.
J. Pellegrino, D. Wang, R. Rabago, R. Noble, and C. Koval. 1993, 9p.
Pub. in Jnl. of Membrane Science 84, p161-169 1993.

Keywords: *Polymeric films, *Gas transport, *Membranes, Casting, Ions, Separation, Carbon dioxide, Methane, Permeability, Diffusion, Fluorine organic compounds, Surfactants, Reprints, *Poly(sulfonic acid/tetrafluoro).

We have made solution-cast films of perfluorosulfonic acid ionomer (PFSA) that included ionic surfactants in the casting solution. Gas transport measurements were made, using mixtures of CO2 and CH4, through both solution-cast and commercial PFSA films that contained either Na(+) or HEDA(+) (monoprotonated ethylenediamine) counterions. The HEDA(+) provides facilitated transport of CO2 at low partial pressures. For all the films with the Na(+) counterion the difference in permeability was greater at lower feed total pressures than at the higher pressures (approximately 11 MPa). We interpret this result as a mechanical pressure effect on the free volume around the ionic clusters. Additional observations include a 'hindering' effect of the HEDA(+) counterion on both CO2 and CH4 permeation rates but more so for the CO2. We discuss these results in the context of separate factors that are economically attractive at all the pressures studied. However, the permeability of the membranes was below economic targets by a factor of 100 considering the fact that they were 30 micrometers thick.

01,268
PB95-176145 Not available NTIS
National Inst. of Standards and Technology (MSEL), Gaithersburg, MD. Polymers Div.
Ring-Opening Polymerication of a 2-Methylene Spiro Orthocarbonate Bearing a Pendant Methacrylate Group.
Final rept.
J. W. Stansbury. 1994, 13p.
Sponsored by National Inst. of Dental Research, Bethesda, MD.
Pub. in Polymers of Biological and Biomedical Significance, Chapter 14, p171-183 1994.

Keywords: *Monomers, *Synthesis(Chemistry), *Polymerization, *Methacrylates, Dental materials, Molecular structure, Medical supplies, Composite materials, Adhesives, Coatings, Chemical bonds, Crosslinking, Polycarbonate resins, Methylene radicals, Reprints, Chemical reaction mechanisms.

A methacrylate-substituted spiro orthocarbonate monomer was synthesized and evaluated in polymerizations using radical and/or cationic initiators. The monomer contains an exocyclic double bond on the spiro group for radical addition and ring opening independent of the remote methacrylate functionality. Crosslinked polymers were obtained by all modes of initiation with mixed radical and cationic giving optimum conversions and ring opening. The incorporation of the pendant methacrylate group minimizes concerns of leachable products generated by polymerization mechanisms involving single ring opening with elimination of a cyclic carbonate. The spiro vinyl ether-type double bond appears to activate the monomer toward cationic polymerization. The ring-opening polymerization of spiro orthocarbonate monomers can yield expansion in volume and may improve a variety of dental and medical materials such as composites, adhesives, and coatings.

01,269
PB95-180014 Not available NTIS
National Inst. of Standards and Technology (PL), Gaithersburg, MD. Ionizing Radiation Div.
Polymerization Initiation by N-p-Tolylglycine: Free-Radical Reactions Studied by Pulse and Steady-State Radiolysis.
Final rept.
M. Al-Sheikhly, M. Farahani, and R. L. Bowen. 1994, 10p.
Sponsored by American Dental Association Health Foundation, Chicago, IL.
Pub. in Jnl. of Applied Polymer Science 54, p1049-1058 1994.

Keywords: *Polymerization, *Free radicals, *Adhesive bonding, Hydroxyl radicals, Oxidation, Reduction(Chemistry), Cations, Anions, Reprints, *Chemical reaction mechanisms, Peroxyl radicals, Glycine/N-tolyl.

The extensive use of N-p-tolylglycine (NTG) and analogous compounds in adhesive bonding technologies requires a better understanding of their role in initiating free-radical polymerization. The fast oxidation and reduction reactions of NTG proceed via the formation of various free radicals and radical cation and anion intermediates. These intermediates were identified and their reactivity with oxygen, to produce the corresponding peroxyl radicals, was measured. Hydroxyl radicals (OH) were used to initiate oxidation reactions of NTG, while the reduction reactions were initiated with hydrated electrons (e(sub aq)(sup -)).

01,270
PB95-180196 Not available NTIS
National Inst. of Standards and Technology (MSEL), Gaithersburg, MD. Polymers Div.
Neutron Scattering Study of the Orientation of a Liquid Crystalline Polymer by Shear Flow.
Final rept.
M. D. Dadmun, and C. C. Han. 1994, 11p.
Pub. in Macromolecules 27, n26 p7522-7532 1994.

Keywords: *Neutron scattering, *Shear flow, *Polymers, *Orientation, Solutions, Shear rate, Dynamics, Rheology, Anistropy, Reprints, *Liquid crystalline polymers, Poly(glutamate/benzyl).

The orientational response of a liquid crystalline polymer (LCP) solution, specifically poly-(benzyl L-glutamate) (PBLG) in deuterated benzyl alcohol, to the application of a shear field has been determined by in-situ neutron scattering. By analyzing the anisotropic two-dimensional scattering pattern, the orientation of the LCP at different shear rates (dot-gamma) in the flow-vorticity plane was determined. It was found that the LCP response has three regimes. At low shear rates, dot-gamma < dot-gamma 1, the orientation of the LCP molecule increases with dot-gamma; at intermediate flow rates, dot-gamma 1 < dot-gamma < dot-gamma 2, there is not much change in the orientation of the PBLG molecule with dot-gamma; and at high dot-gamma, dot-gamma > dot-gamma 2, there is again an increase in the orientation of the LCP with shear rate. The crossover shear rates, dot-gamma 1, and dot-gamma 2, have been shown to correlate well to the first two relaxation times of a rodlike polymer in concentrated solution. The results are also compared and contrasted to some recent studies of the rheology of LCP in solution.

01,271
PB95-180683 Not available NTIS
National Inst. of Standards and Technology (PL), Gaithersburg, MD. Ionizing Radiation Div.
Radiochromic Solid-State Polymerization Reaction.
Final rept.
W. L. McLaughlin, M. Al-Sheikhly, D. F. Lewis, A. Kovacs, and L. Wojnarovits. 1994, 2p.
Pub. in Polymer Preprints 35, n2 p920-921 Aug 94.

Keywords: *Polymerization, Reaction kinetics, Electron beams, Dispersions, Dosimetry, Radiolysis, Uses, Reprints, *Radiochromic films.

The GafChromic radiochromic film is a colorless microcrystalline dispersion of an active monomer in a gel binder. It has been developed for direct radiographic imaging and dosimetry (no chemical, optical, or thermal development). This relatively sensitive sensor may be used as a thin-coating on a transparent or reflecting substrate for broad-range dosimetry (5-10(exp 4) Gy) and for registering permanent, high-resolution, high-contrast blue images. Pulse radiolysis studies show that the primary radiation-initiated image formation (lambda(max) = 675 nm) and propagation of the polymerization are terminated within 2 ms with a first-order rate constant of 900/s. Subsequently, there is a much slower exponential hypsochromic shift of the absorption maximum from 675 nm to 665 nm. The devices are currently finding application in clinical radiography, stereotactic radiosurgery, food irradiation, blood irradiation, insect population control, and industrial radiation processing (including medical sterilization qualification and quality control).

01,272
PB95-181061 Not available NTIS
National Inst. of Standards and Technology (MSEL), Gaithersburg, MD. Polymers Div.
Terminally Anchored Chain Interphases: Their Chromatographic Properties.
Final rept.
J. H. van Zanten. 1994, 11p.
See also PB95-181079.
Pub. in Macromolecules 27, n23 p6797-6807, 7 Nov 94.

Keywords: *Polymers, *Chromatographic analysis, *Interfaces, *Solvents, Dispersions, Molecular structure, Phase studies, Block copolymers, Graft polymerization, Solutes, Thermodynamics, Separation processes, Reprints, *Polymer brushes.

A previously developed Flory-type mean-field analysis of the mixing of a multicomponent, polydisperse solvent with an interphase of terminally anchored chains of finite extensibility is utilized in the determination of the chromatographic properties of the interphase. These interphases could be surface-grafted polymer layers or block copolymers at interfaces. The partitioning and retention of solute molecules in the interphase depend on the chain configurations, the entropy of mixing, and the contact interactions among the species present. The theory allows for the calculation of average or global properties such as the polymer, solvent, and solute volume fractions in the interphase, the interphase thickness, and solute partition coefficients and retention factors. Size exclusion and enhancement, affinity, and gradient chromatography are considered.

01,273
PB95-181079 Not available NTIS
National Inst. of Standards and Technology (MSEL), Gaithersburg, MD. Polymers Div.
Terminally Anchored Chain Interphases: The Effect of Multicomponent, Polydisperse Solvents on Their Equilibrium Properties.
Final rept.
J. H. van Zanten. 1994, 8p.
See also PB95-181061.
Pub. in Macromolecules 27, n18 p5052-5059, 29 Aug 94.

Keywords: *Polymers, *Interfaces, *Solvents, *Equilibrium, Qualitative analysis, Thermodynamics, Molecular structure, Numerical analysis, Surface properties, Dispersions, Phase studies, Reprints, *Polymer brushes.

A theoretical description of terminally anchored chain interphases is presented for the case of an interphase in contact with a multicomponent solvent composed of species of varying quality and size. This work is an extension of a model proposed by Lai and Halperin to calculate the global properties of a terminally anchored chain interphase, or polymer brush, in contact with a binary solvent in which each component is of monomeric size. Here it is shown that the solvent size, in addition to the solvent quality and chain surface density, has a profound influence on the equilibrium properties of the terminally anchored chain interphase. The approach outlined here yields a simple calculational procedure for qualitatively examining the various global properties of these interphases which are inherent to each potential application as a function of chain surface density and solvent quality and size.

01,274
PB95-202735 Not available NTIS
National Inst. of Standards and Technology (MSEL), Gaithersburg, MD. Reactor Radiation Div.
Neutron Reflectivity Study of the Density Profile of a Model End-Grafted Polymer Brush: Influence of Solvent Quality.
Final rept.
A. Karim, S. K. Satija, J. F. Douglas, J. F. Ankner, and L. J. Fetters. 1994, 4p.
Pub. in Physical Review Letters 73, n25 p3407-3410, 19 Dec 94.

Keywords: *Density(Mass/volume), Polymers, Neutron scattering, Temperature dependence, Solvents, Reprints, *End grafted polymers, *Neutron reflectivity, *Polymer brush.

Neutron reflectivity measurements are made on a chemically end-grafted polymer brush swollen over a range of temperatures above and below the theta point. Good agreement between the brush profiles and recent self-consistent field calculations and numerical simulations is obtained for temperatures in the vicinity of the theta point and in a good solvent. The expansion of the main body of the brush resembles a swelling gel, while the brush tail expands similarly to a polymer in solution.

01,275
PB95-209896 PC A07/MF A02
National Inst. of Standards and Technology (MSEL), Gaithersburg, MD. Polymers Div.
Polymers Technical Activities 1994. NAC-NRC Assessment Panel, April 6-7, 1995.
L. E. Smith, and B. M. Fanconi. 1995, 142p, NISTIR-5581.
See also PB92-116284.

Keywords: *Polymers, *Composite materials, *Medical supplies, *Dental materials, Organic polymers, Standards, Technology transfer, Viscoelasticity, Rheological properties, Computerized simulation, Transport properties, Mechanical properties, Durability, Models, Ceramics, *Polymer blends, Annual report.

The annual report of the Polymers Division, Materials Science and Engineering Laboratory, describes technical activities for the fiscal 1994 year and summarizes technical publications, industrial interactions, patents, and invited talks.

01,276
PB96-102231 Not available NTIS
National Inst. of Standards and Technology (MSEL), Gaithersburg, MD. Polymers Div.
Self-Avoiding-Walk Contacts and Random-Walk Self-Intersections in Variable Dimensionality.
Final rept.
J. F. Douglas, and T. Ishinabe. 1995, 27p.
Pub. in Physical Review E 51, n3 p1791-1817 Mar 95.

Keywords: *Polymers, *Series expansion, *Enumeration, Lattices, Molecular structure, Critical temperature, Percolation, Integral equations, Exponents, Interactions, Probability theory, Reprints, *Self-avoiding walks, *Random walks, NN(Nearest-neighbor), Hamilton walks, Wiener sausage.

The average number of nearest-neighbor (NN) contacts (m) of self-avoiding walks (SAW's) on a hypercubic lattice is calculated using direct enumeration and 1/d expansion methods, where d is the spatial dimension. These calculations are compared with exact analytic determinations for the asymptotic number of random-walk (RW) self-intersections in the limit of long chains n maps to infinity. the number of RW (binary, ternary, etc.) self-intersections is a function of the probability Cd that a RW escapes from the origin to infinity and an accurate tabulation of Cd is given in the dimension range 2 < d < 10.

01,277
PB96-119508 Not available NTIS
National Inst. of Standards and Technology (MSEL), Gaithersburg, MD. Polymers Div.
Shear-Induced Martensitic-Like Transformation in a Block Copolymer Melt.
Final rept.
C. L. Jackson, K. A. Barnes, F. A. Morrison, C. C. Han, J. W. Mays, and A. I. Nakatani. 1995, 10p.
Pub. in Macromolecules, n28 p713-722 1995.

Keywords: *Martensitic transformations, *Shear, *Copolymers, *Melts(Crystal growth), Microstructure, Styrenes, Polystyrene, Electron microscopy, Neutron scattering, Deformation, Reprints, SBS block copolymer, Polybutadiene.

The coexistence of two cylindrical microstructures of different symmetries has been observed in a sheared and quenched poly(styrene-d8)/polybut adiene/poly(styrene-d8) (SBS) block copolymer (23 wt % styrene-d8) by small-angle neutron scattering and transmission electron microscopy. Near the order-disorder transition (ODT) temperature, the equilibrium cylindrical microstructure with d(100) = 21plus or minus 2 nm and cylinder diameter of about 12nm orients in the shear field as expected based on previous reports. Above a critical shear rate and at an appropriate strain, a new shear-induced cylindricalmicrostructure forms.

01,278
PB96-122478 Not available NTIS
National Inst. of Standards and Technology (CAML), Gaithersburg, MD. Applied and Computational Mathematics Div.
Nonlinear Dynamics of Stiff Polymers.
Final rept.
R. E. Goldstein, and S. A. Langer. 1995, 4p.
Pub. in Physical Review Letters, v75 n6 p1094-1097 Aug 95.

Keywords: *Polymers, *Curve motion, *Nonlinear dynamics, Models, Formalism, Reprints.

A formalism is presented for the nonlinear dynamics of inextensible stiff polymers within the model of local viscous dissipation. By casting the internal elastic forces in an intrinsic representation enforcing the constraint of local inextensibility through a Lagrange multiplier function and utilizing techniques from the differential geometry of curve motion, the dynamics of configurations of arbitrary complexity is reduced to a scalar partical differential equation amenable to analytical and efficient numerical study. As an example, the formalism is applied to the 'folding' dynamics of stiff polymers with pairwise self-interactions and intrinsic curvature.

01,279
PB96-123245 Not available NTIS
National Inst. of Standards and Technology (BFRL), Gaithersburg, MD. Fire Science Div.
Polymer Combustion and Flammability: Role of the Condensed Phase.
Final rept.
T. Kashiwagi. 1994, 15p.
Pub. in International Symposium on Combustion (25th), Irvine, CA., July 31-August 5, 1994, p1423-1437.

Keywords: *Polymers, *Combustion, *Flammability, Combustion products, Reprints, *Condensed phase.

The combustion process of polymers is a complex coupling of energy feedback from a flame to the polymer surface with gasification of the polymer surface with gasification of the polymer to generate combustible degradation products. Although there are extensive studies of the effects of wind velocity, gas phase oxygen concentration, external thermal radiation, and gravity on the combustion of polymers, the effects of polymer characteristics on combustion and flammability are not nearly as well understood as those in the gas phase. At present, detailed governing equations for continuity, momentum, energy, and chemical species concentration in the gas phase can readily be written with appropriate boundary conditions, and their solutions can be derived for various cases. However, even those governing equations cannot be derived for the condensed phase without understanding of the governing chemical and physical processes that control the gasification of polymers. This paper concentrates on describing various observed phenomena in polymers (which have been often ignored or neglected) during their combustion, some or all of which might have significant effects on the burning rate and flammability properties. Because of a lack of understanding of the basic combustion mechanisms of polymers, theoretical models able to predict combustion phenomena and flammability properties are not available.

01,280
PB96-123526 Not available NTIS
National Inst. of Standards and Technology (MSEL), Gaithersburg, MD. Polymers Div.
Book Review: Statistical Physics of Macromolecules.
Final rept.
J. Douglas. 1995, 2p.
Pub. in American Scientist, v83 p479-480 1995.

Keywords: *Polymer physics, *Macromolecules, *Statistical analysis, Polymers, Reviews, Reprints.

A review of 'Statistical Physics of Macromolecules' is given. Basically, this text is well written and provides a good introduction to polymer science.

01,281
PB96-123591 Not available NTIS
National Inst. of Standards and Technology (MSEL), Gaithersburg, MD. Polymers Div.
Slow Dynamics of Segregation in Hydrogen-Bonded Polymer Blends.
Final rept.
E. K. Hobbie, G. Merkle, B. J. Bauer, and C. C. Han. 1995, 4p.
Pub. in Physical Review E, v52 n3 p3256-3259 Sep 95.

Keywords: *Molecular structure, *Neutron scattering, *Polymer blends, Phase separation, Hydrogen bonding, Reprints, Spinodal decomposition, Fractal dimensions.

Time-resolved small-angle neutron scattering has been used to study the dynamics of phase separation in hydrogen-bonded polymer blends under a variety of shallow-quench conditions. Above a well defined cutoff wave vector qc(star), the structure factor S(q,t) is described by an exponential or a stretched exponential decay. The early-stage growth rate R(q) appears to change sign precipitously at the cutoff, however, which is not consistent with a linear theory. Below the cutoff, S(q,t) exhibits nonlinear growth with a characteristic time scale tm(q), and scales as q(-D)f(t/t sup m) with a scaling exponent D that is often different from the universal value d=3.

01,282
PB96-128251 PC A03/MF A01
National Inst. of Standards and Technology (MSEL), Gaithersburg, MD. Polymers Div.
Certification of the Standard Reference Material 1473a, a Low Density Polyethylene Resin.
J. R. Maurey, W. R. Blair, and C. M. Guttman. Oct 95, 24p, NISTIR-5639.

Keywords: *Certification, *Calibration standards, *Polyethlenes, Temperature, US NBS, Thermoplastic resins, Quality assurance, Organic polymers, Error analysis, Viscosisty, Test methods, *Standard reference material 1473a, NIST(National Institute of Standards and Technology), Plastometer, Melt viscosity.

The melt flow rate of Standard Reference Material (SRM) 1473a, a polyethylene resin, was determined to be 1.17 g/10 min at 190 deg C under the load of 2.16 kg using the ASTM Method D 1238-90b. The average results from 66 determinations on samples with a standard deviation of a single measurement of 0.015 g/10 min. A small but measureable drift from the first timed extrudate to the third timed extrudate was observed.

01,283
PB96-146667 Not available NTIS
National Inst. of Standards and Technology (MSEL), Gaithersburg, MD. Polymers Div.
Response to 'Draining in Dilute Polymer Solutions and Renormalization'.
Final rept.
K. F. Freed, and J. F. Douglas. 1995, 2p.
Pub. in Macromolecules, n28 p8460-8461 1995.

Keywords: *Polymers, *Hydrodynamics, *Mathematical models, Solutions, Fluid dynamics, Normality, Reprints, Renormalization group.

This paper discusses a dispute regarding the correct method of modeling the hydrodynamics of polymer solutions and the correct mathematical procedure for performing renormalization group calculations for polymer solution hydrodynamic properties.

01,284
PB96-146808 Not available NTIS
National Inst. of Standards and Technology (MSEL), Gaithersburg, MD. Polymers Div.
Thermodynamic Properties of Dilute and Semidilute Solutions of Regular Star Polymers.
Final rept.
J. Roovers, P. M. Toporowski, and J. Douglas. 1995, 7p.
Pub. in Macromolecules, p7064-7070 Oct 95.

Keywords: *Virial coefficients, *Polymers, *Thermodynamic properties, Solutions, Polybutadiene, Light scattering, Osmosis, Reprints, *Star ploymers, Dilute solutions, Semidilute solutions, Osmotic modulus.

The osmotic modulus of solutions of polybutadiene stars with f=32, 64, and 128 arms have been measured from the dilute to the semidilute regime in the good solvent cyclohexane by static light scattering. Some complementry results on low molecular weight stars have been obtained using SANS. Values of the dimensionless viral ratio g A3/A2(exp2)M is approximately 0.62 for these many-arm stars accord well with the hard-sphere value (5/8). The concentration dependence of the osmotic modulus near the polymer coil overlap concentration, A2Mc is approximately 1, is characterized by a steep increase. In the semidilute regime the osmotic modulus becomes identical with that of a homogeneous linear polymer solution. A linear polybutadiene sample was also considered for comparison with the star polybutadiene measurements.

01,285
PB96-146840 Not available NTIS
National Inst. of Standards and Technology (MSEL), Gaithersburg, MD. Polymers Div.
Preparation and Characterization of Cyclopolymerizable Resin Formulations.
Final rept.
J. W. Stansbury, B. Dickens, and D. W. Liu. 1995, 6p.
See also PB90-242181.
Pub. in Jnl. of Dental Research, v74 n5 p1110-1115 1995.

Keywords: *Acrylic resins, *Dental materials, *Polymers, Polymerization, Chemical reactions, Viscosity, Molecualr weight, Acrylates, Formaldehyde, Reprints.

An amine-catalyzed reaction between acrylates and formaldehyde has been used to convert monoacrylates to difunctional monomers and di-acrylates to multifunctional oligomers by linking the acrylic double bonds together in 1,6-diene pairs. In this study, a convenient single-step process was used with mixtures of mono- and di-acrylate starting materials to produce a series of resins with potential for effective cyclopolymerization. Incremental changes in the ethyl acrylate (EA) to ethoxylated bisphenol A diacrylate (EBPAD) ratio directly supplied cyclopolymerizable resins with a broad range of viscosities and product distributions. Those resins produced from reaction mixtures rich in EA have low viscosities because of high diluent monomer contents and limited oligomerization of EBPAD due to end-cap formation. Resin viscosity and average molecular weight of the oligometric component of the resin were inversely related to the amount of EA used in the reaction. Through the choice of reactants and their ratio, this simple technique has the potential to provide cyclopolymerzable resins for use in a variety of dental polymer applications.

01,286
PB96-146865 Not available NTIS
National Inst. of Standards and Technology (MSEL), Gaithersburg, MD. Polymers Div.
Light-Scattering Studies on Phase Separation in a Binary Blend with Addition of Diblock Copolymers.
Final rept.
L. Sung, and C. C. Han. 1995, 8p.
Pub. in Jnl. of Polymer Science. Part B: Polymer Physics, v33 p2405-2412 1995.

Keywords: *Polymer blends, *Copolymers, *Phase separation, Critical temperature, Diblock, Kinetics, Light scattering, Reprints, Spinodal decomposition.

Time-resolved light-scattering measurements have been conducted to investigate the influence of a diblock copolymer additive on the phase boundaries and the kinetics of the phase separation of a polymer blend. The blend studied was a polystyrene-d8/polybutadiene (PSD/PB) mixture with a diblock copolymer composed of the same homopolymers. It was observed that the critical temperature of the blend, which has an upper critical solution temperature (UCST), decreased with increasing copolymer content and the kinetics of the phase separation via a spinodal decomposition mechanism slowed down in the presence of the copolymer. The features of the spinodal peak position and intensity as a function of time with and without copolymer additive were analyzed for near and off-critical compositions in various temperature jumps. The intermediate and late-stage growth rates do not follow a universal scaling function with the addition of diblock copolymers.

01,287
PB96-148085 Not available NTIS
National Inst. of Standards and Technology (MSEL), Gaithersburg, MD. Polymers Div.
Shear-Induced Mixing in Polymer Blends.
Final rept.
E. K. Hobbie, A. I. Nakatani, and C. C. Han. 1994, 19p.
Pub. in Modern Physics Letters B, v8 n19 p1143-1161 1994.

Keywords: *Polymers, *Shear flow, Neutron scattering, Critical temperature, Phases, Separation, Molecular weight, Stratified flow, Reprints, Critical polymer blends, SANS(Small angle neutron scattering).

The effect of shear flow on phase separation in critical polymer blends is reviewed. For a low-molecular-weight blend, the response is in good agreement with the theoretical predictions of Onuki and Kawasaki. The break-up of large-scale critical fluctuations by the flow leads to a drop in the temperature Tc at which phase separation begins. For a high-molecular-weight blend, the data suggest that the mode-coupling contribution to the decay rate of composition fluctuations is significant in both the miscible and immiscible phases.

01,288
PB96-163753 Not available NTIS
National Inst. of Standards and Technology (MSEL), Gaithersburg, MD. Polymers Div.
Influence of Shear on the Ordering Temperature of a Triblock Copolymer Melt.
Final rept.
A. I. Nakatani, F. A. Morrison, J. F. Douglas, M. Muthukumar, C. C. Han, J. W. Mays, and C. L. Jackson. 1996, 11p.
Pub. in Jnl. of Chemical Physics, v104 n4 p1589-1599 Jan 96.

Keywords: *Block copolymers, *Melts, *Neutron scattering, Copolymers, Reprints, Temperature, Shear, Polystyrene polybutadiene polystyrene.

The effect of shear on the ordering temperature of a triblock copolymer melt of polystyrene-polybut adient-polystyrene (SBS) is examined by in situ small angle neutron scattering (SANS). Results obtained by SANS arecompared to the rheologically determining order-disorder transition temperature, TRODT == 115 plus or minus C. The SANS measurements from a Couette geometry shear cell are then used to construct a 'dy-

namical phase diagram' based on characteristic changes in the scattering with temperature and shear rate, gamma. A shear rate dependent ordering temperature, T ord(gamma), is identified as the system is sheared isothermally from the disordered state. The scattering behavior is shownto be highly strain dependent. The authors compare their findings on theshear rate dependence of the ordering transition in triblock materials with previous observations on diblock copolymer materials and theoretical expectations for the shear rate dependence of the order-disorder transition temperature. A simple scaling argument leads to a good description of the shear rate dependence of T ord(gamma) in both diblock and triblock copolymer measurements over the range of shearrates examined.

01,289
PB96-176532 Not available NTIS
National Inst. of Standards and Technology (MSEL), Gaithersburg, MD. Polymers Div.
Solid State (13)C NMR and Raman Studies of Cellulose Triacetate: Oligomers, Polymorphism, and Inferences about Chain Polarity.
Final rept.
D. L. VanderHart, J. A. Hyatt, R. H. Atalla, and V. C. Tirumalai. 1996, 10p.
Pub. in Macromolecules, v29 p730-739 1996.

Keywords: *Cellulose triacetate, *Oligomers, Crystal structure, Polymorphy, Reprints, *Chain polarity, Raman.

13 C CPMAS NMR and Raman spectra have been taken to oligomers (DP = 2 - 9) and several preparations of cellulose triacetate (CTA). CTA exhibits polymorphism and the NMR spectra of the CTA(I) and CTA(II) allomorphs along with the spectrum of noncrystalline CTA have been isolated. Magnetic inequivalence within the unit cell of CTA(II) is greater than for CTA(I), indicating a lower symmetry in the CTA(II) unit cell. An attempt is made to correlate some of the NMR resonances with proposed X-ray crystal structures for each of these allomorphs. From both the Raman and the NMR spectra of the oligomers, in comparison with the different CTA preparations, it is determined that the pentamer and higher oligomers crystallize into the CTA(I) lattice. On the basis of the Raman spectra, it is argued that CTA(I) and CTA(II) are distinguished by backbone conformational differences. In a single attempt to explore the role of the solvent in determining the crystal habit of the oligomers, the pentamer persisted in the CTA(I) lattice even when crystallization took place in dibenzyl ether, the solvent out of which the CTA polymer forms CTA(II) crystallites. Based on these findings, an approach of obtaining a definitive crystal structure of CTA(I) would be to grow and perform a structural determination on a single crystal of an oligomer of DP greater than 4.

01,290
PB96-180146 Not available NTIS
National Inst. of Standards and Technology (PL), Gaithersburg, MD. Ionizing Radiation Div.
Radiochromic Solid-State Polymerization Reaction.
Final rept.
W. L. McLaughlin, M. Al-Sheikhly, D. F. Lewis, A. Kovacs, and L. Wojnarovits. 1996, 15p.
See also PB95-180683.
Pub. in Irradiation of Polymers: Fundamental and Technological Applications, American Chemical Society Symposium Series 620, Chapter 11, p152-166 1996.

Keywords: *Diacetylenes, *Film dosimeters, Dosimetry, Reprints, GafChromic films, Polydiacetylenes, Pulse radiolysis, Radiation processing, Radiographic imaging.

Radiochromic films (GafChromic DM 1260 and MD55), consisting of thin, colorless transparent coatings of a polycrystalline, substituted-diacetylene sensor layer on a clear polyester base, are studied by pulse radiolysis and flash photolysis, in terms of the kinetics of their response to ionizing radiation and ultraviolet light. These films have recently been established for broad applications in radiographic imaging, nuclear medicine, and dosimetry for radiotherapy, blood irradiation, insect population control, food irradiation, and industrial radiation processing. The radiochromic reaction is a solid-state polymerization, whereby the films turn deep blue proportionately to radiation dose, due to progressive 1,4-trans additions as polyconjugations along the ladder-like polymer chains. The pulsed-electron-induced propagation of polymerization has an observed first-order rate constant of the order of 10 to the 3rd power s to the minus 1 power, depending on the irradiation temperature. The UV-induced polymerization is faster by about one order of magnitude. In the case of the electron beam effect, the radiation-induced absorption spectrum exhibits a much slower blue-sift of the primary absorption band on the 10 to the minus 3 power - 10 to the minus 1 power second time scale. This effect is attributed to crystalline strain rearrangements of the stacked polymer strand units.

01,291
PB96-193719 PC A10/MF A02
National Inst. of Standards and Technology (MSEL), Gaithersburg, MD. Polymers Div.
Polymers Technical Activities, 1995.
L. E. Smith, and B. M. Fanconi. 1995, 177p, NISTIR-5749.
See also PB95-209896.

Keywords: *Polymers, *Composite materials, *Medical supplies, *Dental materials, Organic polymers, Standards, Technology transfer, Viscoelasticity, Electronic packaging, Rheological properties, Transport properties, Computerized simulation, Mechanical properties, Durability, Models, Ceramics, Polymer blends, Annual report.

Technical activities of the Polymers Division, 854, for the 1995 fiscal year are described. The report is organized by programs: Electronic Packaging and Interconnections, Polymer Blends, Polymer Matrix Composites, Viscoelastic Behavior of Polymers, Polymer Characterization, Dental and Medical Materials, Theory and Modeling and Other. The objectives, accomplishments and outputs of each project included in the Programs are given, as well as summaries of publications, patents, industrial and academic interactions, invited talks and participation by Division staff in technical and professional committees.

01,292
PB96-200753 Not available NTIS
National Inst. of Standards and Technology (MSEL), Boulder, CO. Materials Reliability Div.
Thermal Conductivity of Polypyromellitimide Film with Alumina Filler Particles from 4.2 to 300 K.
Final rept.
D. L. Rule, D. R. Smith, and L. L. Sparks. 1996, 8p.
Pub. in Cryogenics, v36 n4 p283-290 1996.

Keywords: *Polymeric films, *Thermal conductivity, *Contact resistance, Alumina, Reprints, *Foreign technology, Polypyromellitimide film, Kapton.

The thermal conductivities of several types of a commercial polyimide (namely polypyromellitimide, PPMI) film were measured over a range of temperatures from 4.2 to 300 K with an unguarded steady state parallel-plate apparatus. Specimens were made by stacking multiple layers of film together. Conductive grease was used between the layers of film to reduce thermal contact resistance. Two specimens were made from two different types of neat film with a thickness of 76 micro m, and three specimens were made from films that contained two different amounts of alumina filler and had thicknesses of 25 or 76 micro m. The conductivity of PPMI film increases with the amount of alumina filler present. The thermal conductivity of specimens made from film of the same type but of different thickness is independent of film thickness, within the limits of experimental uncertainty. The conductivity of a specimen subjected to a simulated curing process by being held at a temperature of 150 degrees C for 90 minutes was indistinguishable from that of a similar, control specimen not subjected to such treatment.

01,293
PB96-204078 Not available NTIS
National Inst. of Standards and Technology (BFRL), Gaithersburg, MD. Fire Science Div.
Gas Phase Oxygen Effect on Chain Scission and Monomer Content in Bulk Poly(methyl methacrylate) Degraded by External Thermal Radiation.
Final rept.
J. E. Brown, and T. Kashiwagi. 1996, 10p.
Pub. in Polymer Degradation and Stability, v52 p1-10 1996.

Keywords: *Chain scission, *Polymers, *Thermal degradation, Reprints, Decomposition, Fire research, Gasification, Molecular weight, Chromatography, *Foreign technology, Poly(methyl methacrylate).

The effect of atmospheric oxygen on the thermal decomposition of poly(methyl methacrylate), PMMA, in a slab-like configuration was investigated. Blackbody irradiation of 12 mm thick PMMA slabs on one side was used to simulate the thermal decomposition and gasification of the polymer in a fire environment. Results are reported for chain scission number obtained from molecular weight measurements and for residual monomer content at various levels below the slab surfaces irradiated at 17 and 30k W/sq. m. in atmospheres containint 0, 10, 21 and 41% oxygen in nitrogen. The scission number and polydispersity of surface layers, about 0.1 mm thick, were found to increase linearly with the mole fraction of oxygen in nitrogen. Over this range (0 to 41% O2) the scission number increased from 1.5 to 5.0 and the polydispersity increased from 3.6 yo 11.3 when the PMMA was degraded at the lower flux, while at the higher flux.

01,294
PB96-204482 Not available NTIS
National Inst. of Standards and Technology (MSEL), Gaithersburg, MD. Polymers Div.
Phase Separation in Thin Film Polymer Blends With and Without Block Copolymer Additives.
Final rept.
L. Sung, A. Karim, J. F. Douglas, and C. C. Han. 1996, 2p.
Pub. in Proceedings of the American Chemical Society Division of Polymeric Materials: Science and Engineering, New Orleans, LA., Spring Meeting 1996, v74 p106-107.

Keywords: *Meetings, *Polymer blends, *Thin films, Reprints, *Phase separation kinetics, Symmetric diblock copolymer, Surface pattern formation, Optical microscopy.

Studies of finite size effects on the equilibrium properties and kinetic processes of materials confined to thin films provide important insight into thin film coating applications. Many recent experimental and theoretical investigations have focused on the influence of film thickness on phase stability. Modification of surface interactions near the boundaries of confined materials can lead to essentially new phenomena which should provide the basis for technological applications. Surfactant materials, such as block copolymers, are known to be effective in modifying interfacial properties so that these additives are expected to have a large effect in thin films.

01,295
PB97-111900 Not available NTIS
National Inst. of Standards and Technology (MSEL), Gaithersburg, MD. Polymers Div.
Compatibilization of Polymer Blends by Complexation. 2. Kinetics of Interfacial Mixing.
Final rept.
Y. Feng, R. A. Weiss, A. Karim, D. G. Peiffer, C. C. Han, and J. F. Ankner. 1996, 7p.
Pub. in Macromolecules, v29 n11 p3918-3924 1996.

Keywords: *Neutron reflectivity, *Polymer interface, Complexation, Ionomer, Diffusion, Reprints.

The interfacial composition and kinetics of interfacial mixing of two polymers that exhibit strong exothermic interactions, poly(N,N'-dimethyle thylenesebacamide) (mPA) and the lithium salt of a lightly sulfonated polystyrene ionomer containing 7.4 mol% sulfonate groups (Li-SPS), were characterized by neutron reflectivity measurements. Blends of Li-SPS and mPA are miscible below ca. 150 degrees C as a result of the formation of an ion-dipole complex between the Li+-sulfonate and amide groups. Neutron reflectivity measurements were carried out on spun-coated bilayer films of the polyamide and a deuterated sample of the ionomer. The films were annealed at 96 degrees C, which is above the melting temperature of the mPA(Tm=75 degrees C) but below the glass transition temperature of the ionomer (Tg=120 degrees C). The interface between the two films exhibited an asymmetric concentration profile due to the large viscosity mismatch between the two polymer, and the interfacial mixing followed neither Fickian nor Case II diffusion. A kinetic model that combined Fickian diffusion with a suppression of mobility due to intermolecular crosslinking adequatelyrepresented the experimental data.

01,296
PB97-113146 Not available NTIS
National Inst. of Standards and Technology (MSEL), Gaithersburg, MD. Polymers Div.
Microstructure Effect on the Phase Behavior of Blends of Deuterated Polybutadiene and Protonated Polyisopene.
Final rept.
R. N. Thudium, and C. C. Han. 1996, 7p.
Pub. in Macromolecules, v29 n6 p2143-2149 1996.

Keywords: *Elastomer blends, *Interaction parameters, *Microstructure effects, Phase behavior, Neutron scattering, Reprints.

Small-angle neutron scattering (SANS) was used to measure the miscibility of blends of protonated polyisoprene (HPI) with 3,4 microstructure in the range of 7-44%, and of deuterated polybutadiene (DPB) with 1,2 microstructure in the range of 9-70%. These data suggest that, for deuterated polybutadiene/protonated polyisoprene blends, overall miscibility is controlled by the 3,4 content of the polyisoprene. This isomeric group is strongly immiscible with the 1,4 -butadiene group and the immiscibility decreases with temperature, while the 3,4 group is weakly miscible with the 1,4 isoprene group and miscibility increases with temperature. Conversely, the 3,4 group is strongly miscible with the 1,2 butadiene group and miscibility decreases with increasing temperature. The differing trends of the interaction parameter with temperature suggest that shifts in the LCST phase diagram can be controlled by judicious changes in microstructure. These theoretical predications were confirmed with experimental small-angle light scattering (SALS) results on all protonated blends. The statistical segment length, b, appears to be independent of temperature, but is dependent on total vinyl level. For the blends used in the study, b has a minimum value at approximately 30-35% total vinyl isomeric groups.

01,297
PB97-119135 Not available NTIS
National Inst. of Standards and Technology (MSEL), Gaithersburg, MD. Polymers Div.
Morphology and Phase Separation Kinetics of a Compatibilized Blend.
Final rept.
C. L. Jackson, L. Sung, and C. C. Han. 1996, 4p.
Pub. in Society of Plastics Engineers Annual Technical Meeting, Indianapolis, IN., May 5-9, 1996, p1599-1602.

Keywords: *Polymer blends, *Block copolymers, *Microscopy, Light scattering, Reprints.

The phase diagram for a low molecular weight blend of deuterated polystyrene (PSD, M(W) = 1000 g/mol) and polybutadiene (PB, M = 5100 g/mol) was determined by light scattering measurements. The critical temperature of the blend was 51 degrees C and the critical composition was approximately 0.75 g/g polysytrene (75% PSD by weight). Upon addition of the PSD-PB diblock copolymer (total M(W) = 10,600 g/mol) linearly to a lower temperature and the rate of phase separation was greatly retarded. The size scale of the phase separated microstructure was also greatly reduced as block copolymer was added, indicating compatibilization of the blend.

CIVIL ENGINEERING

General

01,298
PB95-151825 Not available NTIS
National Inst. of Standards and Technology (BFRL), Gaithersburg, MD. Building and Fire Research Lab. Office.
Think Metric.
Final rept.
R. N. Wright. 1992, 2p.
Pub. in Jnl. of Structural Engineering 118, n12 p3253-3254 Dec 92.

Keywords: *Metric system, *Structural engineering, *Standardization, Structural design, Metrication, SI units, Metrology, International system of units, Standards, Conversion, Reprints.

The modern metric, International System (SI) of measurement is coming to structural engineering practice. For instance, Federal agencies are required by law to implement SI procurements, specifications, grants, etc., by September 30, 1992. Perhaps the most important challenge this brings to structural engineers is to learn to think quantitatively and exert good engineering judgment in metric dimensions.

01,299
PB95-216891 PC A08/MF A02
National Inst. of Standards and Technology (BFRL), Gaithersburg, MD.
White Papers Prepared for the White House: Construction Industry Workshop on National Construction Goals. Held on December 14-16, 1994.
A. J. Fowell. 6 Mar 95, 155p, NISTIR-5610.

Keywords: *Construction industry, *Goals, *National interests, Research management, Competition, Meetings, Proceedings, Commercial buildings, Government buildings.

The report contains seven white papers prepared for a December 1994 White House--Construction Industry Workshop organized by the Civil Engineering Research Foundation on behalf of the National Science and Technology Council's Subcommittee on Construction and Building.

Civil Engineering

01,300
PB94-217163 PC A03/MF A01
George Mason Univ., Fairfax, VA.
Human Factors Considerations for the Potential Use of Elevators for Fire Evacuation of FAA Air Traffic Control Towers.
B. M. Levin, and N. E. Groner. Aug 94, 25p, NIST/GCR-94/656.
Contract NIST-50SBNBIC6678
See also PB92-187129 and PB92-238641. Sponsored by National Inst. of Standards and Technology (BFRL), Gaithersburg, MD.

Keywords: *Fire safety, *Elevators(Lifts), *Evacuation, *Airport towers, *Human factors, Fire protection, Emergencies, Escape systems, Fires, Human factors engineering, Air traffic control.

The Federal Aviation Administration (FAA) is interested in the possibility of using elevators for evacuation of air traffic control towers during fire emergencies. Assuming that the FAA could design, install, and maintain elevators that could safely be used by tower occupants during fire evacuations, it would be important to study a number of human factor considerations. This report, which is partly based on interviews of occupants in thirteen FAA towers, discusses these issues. Given the fact that there has been a 20-year campaign to discourage elevator use during fire emergencies, most interviewees indicated a willingness to use such elevators as a backup mode of escape with some reluctance. The controls in the elevator would not need any major modification but a special communication system would be needed. Fire emergency plans and training are important to assure proper use of the proposed system and confidence in the safety it provides.

01,301
PB96-167978 PC A04/MF A01
Virginia Transportation Research Council, Charlottesville.
Application of Electromagnetic-Acoustic Transducers for Nondestructive Evaluation of Stresses in Steel Bridge Structures.
Final rept.
M. G. Lozev, A. V. Clark, and P. A. Fuchs. cApr 96, 43p, VTRC-96-R30.
Prepared in cooperation with National Inst. of Standards and Technology, Boulder, CO. and West Virginia Univ., Morgantown. Constructed Facilities Center. Sponsored by Virginia Dept. of Transportation, Richmond.

Keywords: *Bridges(Structures), *Nondestructive tests, Bridge foundations, Steel structures, Transducers, Electromagnetic testing, Virginia, Ultrasonic tests, Dynamic loads.

The report presents the results of a study to (1) assess the applicability of electromagnetic-acoustic transducers for nondestructive evaluation of stresses in bridge structures and (2) evaluate the new ultrasonic instruments as an effective technique for stress surveys in bridge structures. Field tests were performed on two bridges, one a simply supported design and the other an integral backwall bridge. Residual stress measurements were made on a vertical scanline in the web at midspan of a simply-supported bridge. Live load measurements were made by determining the normalized change in arrival times of surface waves propagating between two tranducers mounted on the bottom flange. Good agreement between strain gage and ultrasonic data was obtained, both for the time-history of strain and also for the equivalent stress range.

01,302
PB97-115794 PC A16/MF A03
National Inst. of Standards and Technology (BFRL), Gaithersburg, MD.
Proceedings of a Workshop on Developing and Adopting Seismic Design and Construction Standards for Lifelines. Held in Denver, Colorado on September 25-27, 1991.
Rept. for 1991-92.
R. D. Dikkers, R. M. Chung, B. Mohraz, H. S. Lew, and R. N. Wright. Oct 96, 346p, NISTIR-5907.
Sponsored by Federal Emergency Management Agency, Washington, DC.

Keywords: *Earthquake resistance, *Seismic design, *Meetings, Earthquake engineering, Construction, Design standards, Vulnerability, Public utilities, Electric power, Natural gas distribution systems, Liquid fuels, Telecommunication, Transportation sector, Water systems, Sewer systems, Government agencies, Federal government, Soil-structure interactions, Government policies, Economic analysis, Regulations, Guidelines, *Lifelines.

These recommendations for developing and adopting seismic design and construction standards for lifelines describe the properties intended for lifeline systems, equipment, and materials. They provide both the mechanism for communication between buyers and sellers of lifeline products and services and the basis for regulations protecting the public health, safety and welfare.

Construction Equipment, Materials, & Supplies

01,303
PB94-145661 PC A08/MF A02
National Inst. of Standards and Technology (BFRL), Gaithersburg, MD.
System for Calibration of the Marshall Compaction Hammer.
H. W. Shenton, M. M. Cassidy, P. A. Spellerberg, and D. A. Savage. Jan 94, 152p, NISTIR-5338, FHWA/RD-94/002.
See also PB92-134683. Prepared in cooperation with American Association of State Highway and Transportation Officials, Gaithersburg, MD. Materials Reference Lab. Sponsored by Federal Highway Administration, Washington, DC.

Keywords: *Marshall method, *Hot mix paving mixtures, *Flexible pavements, Test methods, Bituminous concretes, Road materials, Specifications, Asphalts, Calibration, Compacting.

The Marshall method is used by many state and local highway agencies for the design of hot-mix asphalt pavement. Although the procedure is specified by several industry standards, round-robin programs have confirmed wide variability in Marshall test results. Much of the scatter in the data is attributed to compaction hammer variables, such as: variation in drop weight, drop height, friction, hammer alignment, pedestal support and foundation. With the objective of reducing the variability of Marshall test results, a robust, easy to use and relatively inexpensive test apparatus, described in the report, has been developed for calibration of mechanical Marshall compaction hammers.

01,304
PB94-172236 Not available NTIS
National Inst. of Standards and Technology (BFRL), Gaithersburg, MD. Building Materials Div.
Digitized Simulation of Mercury Intrusion Porosimetry.
Final rept.
E. Garboczi, and D. Bentz. 1990, 16p.
Pub. in Proceedings of a Conference on Advances in Cementitious Materials, Gaithersburg, MD., July 22-26, 1990, p365-380.

Keywords: *Cements, *Porous materials, *Microstructure, *Computerized simulation,

Porosimeters, Mercury, Pore structure, Permeability, Porosity, Percolation, Reprints, *Mercury intrusion porosimetry.

Mercury intrusion porosimetry is a widely used method for measuring the pore-size distribution of porous materials. The paper describes an algorithm that has been developed that simulates mercury intrusion into a two-dimensional porous material. The simulation can be implemented on model structures or on micrographs of real porous materials. Using a burning algorithm, the critical pore diameter for mercury connectivity can be directly computed and studied as a function of microstructure. The point at which the intruding mercury becomes continuous is found to occur at the inflection point of the cumulative intrusion curve, in agreement with recent experimental results.

01,305
PB94-172640 Not available NTIS
National Inst. of Standards and Technology (NEL), Gaithersburg, MD. Building Materials Div.
Serial Sectioning of Hardened Cement Paste for Scanning Electron Microscopy.
Final rept.
P. E. Stutzman. 1990, 13p.
Pub. in Proceedings of Conference on Advances in Cementitious Materials, Gaithersburg, MD., July 22-26, 1990, p237-249 1991.

Keywords: *Cements, Scanning electron microscopy, Sequential sampling, Surface preparation, Microstructure, Polishing, Procedures, Indentation hardness tests, Reprints, *Cement pastes, *Serial sectioning.

Serial sectioning is a technique of making and examining thin sections of material to obtain information on three-dimensional structures from a series of two-dimensional images. Procedures were developed to make serial sections of hardened cement paste by the removal of thin layers by polishing. Backscattered electron imaging of the remaining paste block was used to record the paste microstructure after each section was removed. Procedures developed cover the polishing practice, the removal of thin layers by polishing, the estimation of layer thickness, and the location and alignment of specific regions for imaging.

01,306
PB94-185121 Not available NTIS
National Inst. of Standards and Technology (NEL), Gaithersburg, MD. Structures Div.
Detection of Voids in Grouted Ducts Using the Impact-Echo Method.
Final rept.
N. J. Carino, and M. Sansalone. 1990, 15p.
Pub. in Proceedings of RILEM Workshop on Testing during Concrete Construction, Mainz, Germany, March 5-7, 1990, p369-383.

Keywords: *Nondestructive tests, *Voids, *Concrete structures, Stress waves, Ducts, Grout, Wave propagation, Spectrum analysis, Structural members, Defects, Reprints, *Impact-echo method.

The impact-echo method was used to detect simulated voids in grouted post-tensioning tendon ducts cast in a 1-m thick concrete wall specimen. The study was part of a program to evaluate nondestructive test methods based on stress wave propagation. The locations of the voids in the ducts were not known by the authors until after their results had been reported to the principal investigator of the project. The impact-echo method was successful in locating the voids. However, the study showed that additional research is needed to gain a complete understanding of the interaction of stress waves with voids in cylindrical ducts.

01,307
PB94-185618 Not available NTIS
National Inst. of Standards and Technology (BFRL), Gaithersburg, MD. Building Materials Div.
Corrosion Resistant Epoxy-Coated Reinforcing Steel.
Final rept.
R. G. Mathey, and J. R. Clifton. 1994, 7p.
Pub. in Proceedings of the ASCE Structures Congress (12th), Atlanta, GA., April 24-28, 1994, v1 p109-115.

Keywords: *Epoxy coatings, *Corrosion resistance, *Reinforced concrete, *Bridge decks, Concrete structures, Steel structures, Case studies, Structural engineering, Construction materials, Corrosion inhibition, Reprints, *Reinforcing steels.

Research conducted in the 1970s to evaluate and develop criteria for nonmetallic coatings to protect steel reinforcing bars embedded in concrete bridge decks from the corrosive action of chlorides is reviewed to provide a case study for successes and disappointments in structural research. The objectives of the research, the technical challenges faced, the conduct of the research, and how the results were implemented for improvement of structural engineering practice are discussed. Also, reasons for the successful transition from research to field application are explored.

01,308
PB94-196557 PC A06/MF A02
National Inst. of Standards and Technology (BFRL), Gaithersburg, MD. Building Materials Div.
Graphical Analysis of the CCRL Portland Cement Proficiency Sample Database (Samples 1-72). (Part 1. Univariant Analysis of Portland Cement).
C. B. Spring, J. H. Pielert, S. Leigh, and N. A. Heckert. Mar 94, 121p, NISTIR-5387.
Prepared in cooperation with American Society for Testing and Materials, Philadelphia, PA.

Keywords: *Portland cements, *Construction materials, *Concrete construction, *Standards, *Test methods, Production, Statistical analysis, Graphic methods, Histograms, Physical properties, Chemical properties, Compression tests, Sampling, Turbidimeters, Fineness, Performance evaluation, Air entrainment, Tables(Data), *Building technology, *National Institute of Standards and Technology, CCRL(Cement and Concrete Reference Laboratory).

A large database of Portland Cement and Portland Cement Concrete interlaboratory test results has been generated at the Cement and Concrete Reference Laboratory (CCRL) since 1965. The database represents a rich resource inasmuch as the cements tested were produced by many different production facilities, from raw materials obtained from different geological areas, and over a long period of time. Participation varies from 120 to over 200 laboratories, located throughout the United States and in several other countries. Computer and statistical techniques are used to present the data from the first 72 samples in graphical forms to better understand cement and cement testing. Data for each of 10 physical test properties and 11 chemical 'compounds' of Portland cement are represented graphically through use of box plots. For each property and compound, the box plots of data from multiple samples are plotted sequentially as distributed by CCRL and also sorted on median values. In several instances, box plots for one test property are ordered by the median values of another property to analyze possible relationships. Also, the characteristics of each of 72 cements are profiled (graphically) in relation to the population of results of other cements.

01,309
PB94-198777 Not available NTIS
National Inst. of Standards and Technology (NEL), Gaithersburg, MD. Building Materials Div.
Digitized Direct Simulation Model of the Microstructural Development of Cement Paste.
Final rept.
D. P. Bentz, and E. J. Garboczi. 1990, 8p.
Pub. in Mater. Res. Soc. Symp. Proc. Phys. Phenom. Granular Mater., v195 p523-530 1990. Sponsored by Northwestern Univ., Evanston, IL. Center for Advanced Cement-Based Materials.

Keywords: *Cements, *Curing, *Computerized simulation, *Hydration, Diffusivity, Algorithms, Percolation, Transport properties, Microstructure, Models, Reprints.

The complex microstructure of hardened cement paste is produced by hydration reactions between cement particles and the water in which they are suspended. In recent years, algorithms like the diffusion-limited aggregation (DLA) and Eden models have demonstrated that simple growth rules can result in complex aggregated structures. The model described in the paper simulates, via simplified growth rules, the microstructural development of hydrating cement paste. The model has simularities to DLA, but with the additional novel features of dissolution of solid particles, and a free-space nucleation probability. The percolation aspects and transport properties of the model's pore space are computed and discussed.

01,310
PB94-198785 Not available NTIS
National Inst. of Standards and Technology (NEL), Gaithersburg, MD. Building Materials Div.
Digitized Simulation Model for Microstructural Development.
Final rept.
D. P. Bentz, and E. J. Garboczi. 1991, 16p.
Pub. in Ceram. Trans. Adv. Cem. Mater., v16 p211-226 1991.

Keywords: *Cements, *Curing, *Computerized simulation, *Hydration, Diffusivity, Algorithms, Porosity, Transport properties, Microstructure, Models, Reprints.

Characterization of the microstructure of hydrating cement is difficult due to its complexity. Models of the hydration process provide one means of characterization as they attempt to duplicate features of real microstructures. This paper presents a simple model for hydration consisting of random dissolution, diffusion, nucleation, and surface reaction. The model has been developed in a digitized format. Space is represented as an array of pixels, each of which is classified as a given material: reactant, dissolved species, hydrate, or pore. Having the model in digitized format allows for the visualization of the hydration as it occurs and for rapid subsequent quantification of the resultant microstructure. In addition, real images or cement particles can be digitized and used as the starting material for model execution. Algorithms for, and results of, the model are presented.

01,311
PB94-198793 Not available NTIS
National Inst. of Standards and Technology (BFRL), Gaithersburg, MD. Building Materials Div.
Modelling the Leaching of Calcium Hydroxide from Cement Paste: Effects on Pore Space Percolation and Diffusivity.
Final rept.
D. P. Bentz, and E. J. Garboczi. 1992, 11p.
Pub. in Materials and Structures 25, p523-533 1992. Sponsored by National Science Foundation, Arlington, VA.

Keywords: *Cements, *Leaching, *Hydration, *Models, Porosity, Percolation, Microstructure, Diffusivity, Calcium hydrides, Durability, Reprints.

As concrete is exposed to the elements, its underlying microstructure can be attacked by a variety of aggressive agents. For example, rainwater and groundwater can degrade the concrete by dissolving soluble constituents such as calcium hydroxide. Using computer simulation, the paper examines the effects of calcium hydroxide dissolution on two material properties: the percolation properties or connectivity of the capillary pore space, and the relative ionic diffusivity. A microstructural model for cement paste is used to produce a hydrated specimen which is subsequently subjected to the leaching process. Pore space percolation characteristics and relative ionic diffusivity are computed throughout the leaching process as a function of total capillary porosity. Material variables examined are water:solids ratio and silica fume content. Percolation theory is used to develop the concept of a critical volume fraction of calcium hydroxide plus capillary pore space. It is shown that this critical combined volume fraction determines the magnitude of the effect of leaching on relative ionic diffusivity.

01,312
PB94-198801 Not available NTIS
National Inst. of Standards and Technology (NEL), Gaithersburg, MD. Building Materials Div.
Diffusion Studies in a Digital-Image-Based Cement Paste Microstructural Model.
Final rept.
D. P. Bentz, E. J. Garboczi, D. Gingold, C. J. Lobb, and H. M. Jennings. 1991, 9p.
Pub. in Ceram. Trans. Adv. Cem. Mater., v16 p227-235 1991. Sponsored by Northwestern Univ., Evanston, IL. Center for Advanced Cement-Based Materials.

Keywords: *Cements, *Curing, *Computerized simulation, *Hydration, Diffusivity, Algorithms, Percolation, Transport properties, Microstructure, Models, Reprints.

A digital-image-based microstructural model of cement paste, along with a new, fast algorithm for computing and conductance of random conductor lattices, are used to study the diffusivity of cement paste as a function of degree of hydration and water:cement ratio. The computational methods and some preliminary data are presented, and comparison with experimental results is discussed.

01,313
PB94-199494 Not available NTIS

National Inst. of Standards and Technology (NEL), Gaithersburg, MD. Structures Div.
Maturity Method.
Final rept.
N. J. Carino. 1991, 46p.
Pub. in CRC Handbook on Nondestructive Testing of Concrete, Chapter 5, p101-146 1991.

Keywords: *Concretes, *Curing, *Compressive strength, Temperature effects, Mechanical properties, Activation energy, Arrhenius equation, Standards, Aging(Materials), Concrete durability, Reprints, *Maturity method, ASTM standards.

The chapter reviews the history and technical basis of the maturity method, a technique for estimating the strength gain of concrete based upon the measured temperature history during curing. The combined effects of time and temperature on strength gain are quantified by means of a maturity function. The widely used maturity functions are reviewed critically. It is shown that the traditional maturity function is inadequate compared with the function based upon the Arrhenius equation. The concept of equivalent age, which is the most convenient measure of maturity, is explained. The strength gain of a specific concrete mixture is estimated using the measured maturity and the strength vs. maturity relationship for that mixture. Various proposed strength-maturity relationships are reviewed. It is also explained why the maturity method can only be used reliably to estimate relative strength. Examples are presented to illustrate how this technique can be used in combination with other in-place tests of concrete strength. The ASTM standard dealing with the method is also summarized.

01,314
PB94-199502 Not available NTIS
National Inst. of Standards and Technology (BFRL), Gaithersburg, MD. Structures Div.
Maturity Functions for Concrete Made with Various Cements and Admixtures.
Final rept.
N. J. Carino, and R. C. Tank. 1991, 15p.
Pub. in Proceedings of International Workshop on Testing during Concrete Construction (RILEM), Mainz, Germany, March 5-7, 1990, p192-206 1991.

Keywords: *Concretes, *Curing, *Compressive strength, Temperature effects, Mechanical properties, Arrhenius equation, Aging(Materials), Cements, Models, Concrete durability, Reprints, *Maturity functions.

A model is proposed for estimating relative strength gain of concrete under isothermal curing conditions. The key feature of the model is the relationship between curing temperature and the rate constant for relative strength development. The strength gain of seven concrete and mortar mixtures under three curing temperatures was studied. It was found that a simple exponential function may be used to describe the observed variations of the rate constant with curing temperature. It is shown that the relative strength development of concrete can be estimated from its temperature history using parameters determined experimentally from tests of isothermally-cured mortar specimens.

01,315
PB94-199759 Not available NTIS
National Inst. of Standards and Technology (NEL), Gaithersburg, MD. Building Materials Div.
Interaction between Naphthalene Sulfonate and Silica Fume in Portland Cement Pastes.
Final rept.
S. Diamond, and L. Struble. 1988, 10p.
Contract AFOSR-155A86-0057
Pub. in Materials Research Society Symposia Proceedings, v114 p117-126 1988. Sponsored by Air Force Office of Scientific Research, Bolling AFB, DC.

Keywords: *Portland cement, *Admixtures, *Curing, Hardening(Materials), Concentration(Composition), Superplasticity, Compressive strength, Reprints, Silica fume, Naphthalene sulfonate, Superplasticizers.

Portland cement pastes were mixed with predissolved naphthalene sulfonate superplasticizer at normal water:cement ratios. Solutions were separated from the fresh pastes at intervals and the residual concentration of the superplasticizer determined by UV spectrophotometry. At low dosage levels essentially all of the superplasticizer was found to be removed from solution within a few minutes; at high dosage levels a substantial concentration was maintained in solution at least to approximately the time of set. In pastes in which silica fume replaced 10% by weight of the cement, it was found that the incorporation of silica fume significantly increased the uptake of superplasticizer. In separate trials it was found that the silica fume by itself absorbed little superplasticizer, even from high pH solution simulating that of cement paste.

01,316
PB94-215670 PC A08/MF A02
National Inst. of Standards and Technology (BFRL), Gaithersburg, MD.
Highway Concrete (HWYCON) Expert System User Reference and Enhancement Guide.
L. J. Kaetzel, J. R. Clifton, P. Klieger, and K. Snyder. May 93, 170p, NISTIR-5184.
See also PB93-198885 and PB94-182995.

Keywords: *Concretes, *Expert systems, *Highway maintenance, *Information systems, Concrete durability, Road materials, Pavement condition, Bridge decks, Maintenance management, Concrete pavements, Pavement damage.

The report discusses the expert system HWYCON (Highway Concrete). HWYCON is designed to assist state highway departments in three areas: (1) diagnosing distresses in highway pavements and structures; (2) selecting materials for construction and reconstruction; and (3) obtaining recommendations on materials and procedures for repair and rehabilitation methods. HWYCON is an operational system and will be distributed to state DOT's through SHRP. This document is intended to provide a reference for users of the system who need information that is not covered in the overview and installation document provided with the system.

01,317
PB95-143079 PC A03/MF A01
National Inst. of Standards and Technology (BFRL), Gaithersburg, MD.
Quantitative X-Ray Powder Diffraction Methods for Clinker and Cement.
P. E. Stutzman. May 94, 26p, NISTIR-5403.
See also PB92-183664.

Keywords: *Portland cements, *Clinker, X-ray diffraction, Quantitative analysis, Particle size distribution, Chemical composition, Construction materials, *Reference materials, Phase abundance, Sample preparation.

Performance of concrete is influenced by the portland cement phase composition. Phase abundance determination has traditionally been accomplished using two different methods; optical microscopy, and a Bogue calculation based on a chemical analysis. X-ray powder diffraction is a direct, bulk analytical method for phase analysis of fine-grained materials including clinker and cements. Each phase produces a unique diffraction independently of the others with each pattern intensity being proportional to phase concentration. Difficulties in X-ray powder diffraction analysis include correction for sample absorption, selection of reference standards, and determination of individual pattern intensity. These problems are minimized by use of an internal standard, profile fitting, and careful reference standard selection.

01,318
PB95-143095 PC A03/MF A01
National Inst. of Standards and Technology (BFRL), Gaithersburg, MD. Building Materials Div.
Diagnosis of Causes of Concrete Deterioration in the MLP-7A Parking Garage.
P. E. Stutzman, and J. R. Clifton. Jun 94, 26p, NISTIR-5492.

Keywords: *Parking garages, *Concrete durability, *Deterioration, Alkali aggregate reactions, Cracking(Fracturing), Efflorescence, Petrography, Water repellants.

Parking garage MLP-7A at the National Institutes of Health (NIH) is a four-level, cast-in-place concrete structure, approximately seventeen years of age which is exhibiting expansion and cracking of the parapet walls. An accelerated expansion test of aggregate extracted from the structure indicates that the aggregate is reactive and that there is a potential for further expansion. The performance of water repellant treatments were evaluated in field studies on the garage structure. Each repellant treatment reduced water infiltration relative to an untreated test region however, some treatments performed better in regions with visible, fine surface cracks.

01,319
PB95-155552 PC A05/MF A01
National Inst. of Standards and Technology (TS), Gaithersburg, MD. National Voluntary Lab. Accreditation Program.
National Voluntary Laboratory Accreditation Program: Construction Materials Testing.
Handbook.
P. R. Martin. Sep 94, 79p, NIST/HB-150/5.
Also available from Supt. of Docs as SN003-003-03301-4. See also PB94-178225 and PB95-128658.

Keywords: *Highway construction, *Construction materials, *Laboratories, *Certification, Admixtures, Concretes, Aggregates, Cements, Rocks, Soils, Road materials, Stainless steels, Geotechnical fabrics, Geotextiles, Procedures, Requirements, Calibration standards, Standardization, Licensure, Methodology, Accuracy, Performance evaluation, National Voluntary Laboratory Accreditation Program, US NIST.

NIST Handbook 150-5 presents the technical requirements of the National Voluntary Laboratory Accreditation Program (NVLAP) for the Construction Materials Testing program. It is intended for information and use by staff of accredited laboratories, those laboratories seeking accreditation, other laboratory accreditation systems, users of laboratory services, and others needing information on the requirements for accreditation under the Construction Materials Testing program. This publication supplements NIST Handbook 150 (PB94-178225), NVLAP Procedures and General Requirements, which contains Part 285 of Title 15 of the U.S. Code of Federal Regulations (CFR) plus all general NVLAP procedures, criteria, and policies. Handbook 150-5 contains information that is specific to the Construction Materials Testing program and does not duplicate information contained in the Procedures and General Requirements. It is organized to cross-reference with Handbook 150.

01,320
PB95-175055 Not available NTIS
National Inst. of Standards and Technology (BFRL), Gaithersburg, MD. Building Materials Div.
Cellular Automaton Simulations of Cement Hydration and Microstructure Development.
Final rept.
D. P. Bentz, P. V. Coveney, E. J. Garboczi, M. F. Kleyn, and P. E. Stutzman. 1994, 26p.
Sponsored by Northwestern Univ., Evanston, IL.
Pub. in Modelling and Simulation in Materials Science and Engineering 2, p783-808 1994.

Keywords: *Hydration, *Cement, *Microstructure, *Simulation, Models, Slurries, Percolation, Image analysis, Algorithms, Reprints.

Cellular automation algorithms, which operate on a starting digital image of a water-cement suspension, are described. The algorithms simulate the microstructure development process due to hydration reactions that occur between cement and water. This paper describes the evolution of the cement model from a simple model, which treated the cement particles as a single-phase materials, with a greatly simplified hydration chemistry, into a model which has many more chemical species and includes numerous reactions which eventually convert the viscous water-cement suspension into a rigid porous solid. Methods are presented for generating two- and three-dimensional images representing suspension initial conditions; these are derived from both micrographs of real cements and computer-based algorithms. A convenient measure of the point at which the initial paste turns into a solid material is the percolation threshold of the solids. Consideration of these models has already led to the prediction and subsequent experimental observation of a sharply defined onset of shear wave propagation, from ultrasonic measurements through hydrating cement slurries. The amount of hydration needed to reach the percolation threshold can be determined in the present simulations, and our results are compared with time of shear wave onset in actual cement slurries.

01,321
PB95-175063 Not available NTIS
National Inst. of Standards and Technology (BFRL), Gaithersburg, MD. Building Materials Div.
Evolution of Porosity and Calcium Hydroxide in Laboratory Concretes Containing Silica Fume.
Final rept.
D. P. Bentz, and P. E. Stutzman. 1994, 7p.
Pub. in Cement and Concrete Research 24, n6 p1044-1050 1994.

Keywords: *Durability, *Concrete, *Calcium hydroxides, Image analysis, Scanning electron microscopy, Interfaces, Microstructure, Hydration, Construction materials, Aggregates, Reprints, *Silica fume.

Laboratory concretes containing only coarse aggregates and 0, 10, or 20% silica fume as a cement replacement were prepared at a constant water-to-solids ratio and sampled at 1, 7, and 28 days. Scanning electron microscopy was utilized to monitor the progress of the hydration reactions both in the bulk paste and in regions near an aggregate surface. Phase volume fractions were determined by quantitative image analysis of the backscattered electron images. In addition, the size of 'individual' two-dimensional cross sections of calcium hydroxide crystals and capillary pores were assessed. Silica fume additions are seen to affect both the amount and size of these microstructural features. Differences are observed between interfacial zone and bulk areas which support previous mercury intrusion measurements of mortar specimens. This analysis lends support to the hypothesis that when silica fume is present, calcium hydroxide crystals form and then dissolve away, contributing to a connected pathway of capillary porosity in the interfacial zone regions.

01,322
PB95-180147 Not available NTIS
National Inst. of Standards and Technology (BFRL), Gaithersburg, MD. Structures Div.
High-Performance Concrete: Research Needs to Enhance Its Use.
Final rept.
N. J. Carino, and J. R. Clifton. 1991, 7p.
Pub. in Concrete International 13, n9 p70-76 Sep 91.

Keywords: *Concretes, Research, Durability, Mechanical properties, Construction materials, Workshops, Reprints, *High-performance concretes.

The National Institute of Standard and Technology and the American Concrete Institute cosponsored a workshop on high-performance concrete (HPC). The objectives were to identify technical and institutional barriers which impede the widespread use of HPC and to recommend actions to overcome these barriers. The recommended research, summarized in this paper, is proposed as the basis for developing a national program to exploit the potential of HPC and assure U.S. competence in concrete technology.

01,323
PB95-190674 PC A05/MF A01
National Inst. of Standards and Technology (BFRL), Gaithersburg, MD. American Association of State Highway and Transportation Officials, Gaithersburg, MD. Materials Reference Lab.
Field Evaluation of the System for Calibration of the Marshall Compaction Hammer.
H. W. Shenton, and M. M. Cassidy. Feb 95, 80p, NISTIR-5553, FHWA/RD-95/063.
Prepared in cooperation with American Association of State Highway and Transportation Officials, Gaithersburg, MD. Materials Reference Lab. Sponsored by Federal Highway Administration, Washington, DC.

Keywords: *Calibrating, *Compactors, *Hot mix paving mixtures, Bituminous materials, Asphalts, Road materials, Test methods, Highway construction, Mechanical properties, *Marshall compaction hammer.

A system for calibrating the Marshall compaction hammer has recently been developed at the National Institute of Standards and Technology, in collaboration with the American Association of State Highway Transportation Officials (AASHTO), Materials Reference Laboratory (AMRL). The calibration system consists of a spring-mass device with an integral force transducer and a high-speed data acquisition system. The proposed calibration procedure is based on adjusting the number of hammer blows delivered to a specimen, such that a standard compactive effort is supplied during the compaction process, regardless of slight variations in the Marshall hammer. In an earlier laboratory evaluation program, the calibration system and procedure proved to be effective in reducing the variability of Marshall test results. Presented in the report is a summary of a field evaluation program of the calibration system and procedure. In this study, Marshall specimens were prepared in bituminous laboratories using production Marshall hammers: twelve laboratories, or field sites, participated in the study. Sixteen Marshall specimens were prepared at each site.

01,324
PB96-112180 Not available NTIS
National Inst. of Standards and Technology (BFRL), Gaithersburg, MD. Structures Div.
Prediction of Potential Concrete Strength at Later Ages.
Final rept.
N. J. Carino. 1994, 13p.
Pub. in Significance of Tests and Properties of Concrete and Concrete-Making Materials, ASTM STP 169C, Chapter 15, p140-152 1994.

Keywords: *Concrete, *Reinforced concrete, *Compressive strength, Reprints, Strength(Mechanics), Construction materials, Failure(Mechanics), Curing, Standards.

This chapter deals with methods for estimating the potential, later-age strength of a concrete mixture based upon the compressive strength measured on cylindrical specimens at early ages. The results of the cooperative research program leading to the development of ASTM Test Method for Making, Accelerated Curing, and Testing Concrete Compression Test Specimens (C 684) are reviewed. This review is based on Chapter 13 of ASTM STP 169B, which was written by M.H. Wills, Jr., and was titled 'Accelerated Strength Tests.' The earlier text has been augmented by the addition of information on the high-temperature and pressure accelerated test method that was added to ASTM C 684 in 1989. In addition, the chapter has been expanded by including the basis of ASTM Test Method for Developing Early-Age Compression Test Values and Projecting Later-Age Strengths (C 918).

01,325
PB96-122445 Not available NTIS
National Inst. of Standards and Technology (BFRL), Gaithersburg, MD. Structures Div.
Recent Development in Nondestructive Testing of Concrete.
Final rept.
N. J. Carino. 1992, 57p.
Pub. in Advances in Concrete Technology, International Symposium on Advances in Concrete Technology, Athens, Greece, May 11-13, 1992, p281-337.

Keywords: *Concrete, *Nondestructive testing, Flaw detection, Impulse response, Reprints, Break-off test, Impact-echo, Torgue test.

Advances in nondestructive testing of concrete are summarized. Test methods are classified into those used to assess in-place strength and those used to locate hidden defects. In the first category, recent developments are presented on the pullout test, the break-off test, the torque test, a review is presented of infrared thermography, ground penetrating radar, and several methods based upon stress wave propagation. The principles of the methods, their advantages and their inherent limitations are discussed. Where appropriate, requirements of relevant ASTM standards are discussed. Future directions for research in the area of nondestructive testing of concrete are presented.

01,326
PB96-146816 Not available NTIS
National Inst. of Standards and Technology (BFRL), Gaithersburg, MD. Building Materials Div.
Interfacial Transport in Porous Media: Application to dc Electrical Conductivity of Mortars.
Final rept.
L. M. Schwartz, E. J. Garboczi, and D. P. Bentz. 1995, 11p.
Pub. in Jnl. of Applied Physics, v78 n10 p5898-5908 Nov 95.

Keywords: *Electrical resistivity, *Direct current, *Mortars(Materials), Concretes, Transport properties, Percolation, Durability, Construction materials, Reprints.

A mortar is a composite of inert sand grains surrounded by a porous cement paste matrix. We investigate the electrical conductivity of model mortars that include enhanced electrical conduction in the matrix-sand grain interfacial region. The electrical conductivity is evaluated by a combination of finite element, finite difference, and random walk methods for periodic and disorderd models of motar. Since the effective conductivity within the interfacial zone is often much higher than the bulk matrix conductivity, the qualitative features of transport in these systems is often controlled by the connectivity if the interfacial zone. Special attention is thus given to the geometrical percolation of this zone.

01,327
PB96-165394 PC A04/MF A01
National Inst. of Standards and Technology (BFRL), Gaithersburg, MD. Building Materials Div.
Guide to a Format for Data on Chemical Admixtures in a Materials Property Database.
C. F. Ferraris. Apr 96, 31p, NISTIR-5796.

Keywords: *Admixtures, *Properties, *Data bases, *Format, Concretes, Construction materials, Standards, NIST(National Institute of Standards and Technology).

This guide is the second in a series of related documents that present recommended formats for use in computerization of concrete materials property data. It addresses the problem of distinguishing one chemical admixture from another by providing a logical scheme for systematically organizing and subdividing material characteristics and parameter to create a unique chemical admixture material identifier. The organization and structure presented in this guide provide a framework for cross-referencing chemical admixture properties, data, and other information which is consistent with reporting recommendations contained in the other ACI Committee 126 guides. ACI Committee 126 guides are consistent with the principles laid down in the standard guides that have been prepared by ASTM Committee E-49. This guide is intended for use by those responsible for entering data into a concrete materials property database or preparing tables of concrete properties and information for use by others.

01,328
PB96-186192 PC A04/MF A01
National Inst. of Standards and Technology (BFRL), Gaithersburg, MD. Building Materials Div.
Guide to a Format for Data on Chemical Admixtures in a Materials Property Database. (Reannouncement with new abstract).
C. F. Ferraris. Apr 96, 31p, NISTIR-5796.
Supersedes PB96-165394. Reannouncement with new abstract.

Keywords: *Admixtures, *Properties, *Data bases, *Format, Concretes, Construction materials, Standards, NIST(National Institute of Standards and Technology).

The formats for data on chemical admixtures that are described in the report are intended to aid the creation of a coherent system of concrete materials property databases. The preliminary document is a guide that presents a recommended format for use in computerization of concrete materials property data. It addresses the problem of distinguishing one chemical admixture from another by providing a logical scheme for organizing and subdividing material characteristics and parameters to create a unique chemical admixture material identifier. The organization and structure presented in the guide provide a framework for cross-referencing chemical admixture properties, data, and other information which is consistent with the principles laid down in the standard guides that have been prepared by ASTM Committee E-49 and which are due to be adopted by American Concrete Institute (ACI) Committee 126. The preliminary working document is intended to assist the work of ACI committee 126 by providing a draft for use by committee members and others who may wish to offer suggestions for its development. The preliminary document will be superseded by an official ACI document in the series on concrete materials property database formats that is being prepared by ACI 126.

01,329
PB96-202296 PC A09/MF A02
National Inst. of Standards and Technology (BFRL), Gaithersburg, MD. Office of Applied Economics.
Development of a Method for Measuring Water-Stripping Resistance of Asphalt/Siliceous Aggregate Mixtures.
T. Nguyen, E. Byrd, D. Bentz, and J. Seiler. Jul 96, 152p, NISTIR-5865.
See also PB96-197249. Sponsored by National Research Council, Washington, DC. Transport Research Board.

Keywords: *Asphalt pavements, *Water effects, *Nondestructive tests, Bonding, Aggregates, Spectroscopic analysis, Interfacial tension, Test methods.

The main objective of this study was to develop a sensitive, spectroscopic technique to nondestructively evaluate the water stripping resistance at the molecular level of an asphalt on a siliceous aggregate. This study consisted of three phases. Phase 1 involved the

development of a nondestructive, spectroscopic technique to measure the amount and thickness of the water layer at the interface between an asphalt and a siliceous aggregate. Phase 2 was to develop a technique to measure the adhesion loss of the asphalt/aggregate mixture exposed to water. And Phase 3 aimed to relate the quantity of the interfacial water layer obtained in Phase 1 with the adhesion loss data generated in Phase 2.

01,330
PB96-214713 PC A11/MF A03
National Inst. of Standards and Technology (BFRL), Gaithersburg, MD. Structures Div.
Shear Design of High-Strength Concrete Beams: A Review of the State-of-the-Art.
D. Duthinh, and N. J. Carino. Aug 96, 205p, NISTIR-5870.

Keywords: *Concrete structures, *Beams(Supports), Reinforced concrete, Shear strength, State of the art.

This state-of-the-art review of the shear design of high-strength concrete beams consists of four parts. In the first part, various analysis methods are presented: (1) The plastic solution assumes that both steel reinforcement and concrete, modeled as a modified Mohr-Coulomb material, are at yield. Under shear loading, the concrete web develops an inclined compression field which satisfies both upper and lower bound theorems. A plastic solution of shear friction is also discussed. (2) Both the compression field theory and the modified compression field theory (MCFT) are exact theories in the sense that they satisfy equilibrium, compatibility of displacements and stress-strain relationships. The MCFT accounts for the contribution of the tensile strength of concrete to shear resistance. (3) Other exact solutions are also discussed, that do not assume that the principal stress and principal strain directions are aligned with the shear cracks in the web. (4) The 45 deg truss, the variable angle truss (VAT) and strut-and-tie models (STM) belong to a class of solutions that only satisfy equilibrium.

Highway Engineering

01,331
PB94-161940 PC A06/MF A01
National Inst. of Standards and Technology (BFRL), Gaithersburg, MD. Structures Div.
Draft Guidelines for Pre-Qualification and Prototype Testing of Seismic Isolation Systems.
H. W. Shenton. Mar 94, 104p, NISTIR-5359.

Keywords: *Vibration isolators, *Bridges(Structures), *Prototypes, *Test methods, *Earthquake resistant structures, Building codes, Displacement, Structural vibration, Dynamic structural analysis, Earthquake engineering, Dynamic response, Standards, Stiffness, Vibration damping, Loads(Forces), Test facilities.

At the present time, at least in the United States, seismic isolation systems are custom designed and built on a per project basis. As a result, testing has become an essential element in the design and construction of isolated structures. Prototype and quality control tests are required by the 1991 Uniform Building Code and the American Association of State Highway and Transportation Officials, 1991 Guide Specifications for Seismic Isolation Design. Currently, however, standards do not exist for conducting these tests. The Building and Fire Research Laboratory of the National Institute of Standards and Technology has developed draft guidelines for testing and evaluation of seismic isolation systems. Presented in the report are guidelines for conducting pre-qualification and prototype tests. Pre-qualification tests are currently not required by the codes but are generally conducted during development of a new system and are aimed at evaluating fundamental properties and characteristics of the isolation system. The guidelines include general requirements of the test facility, instrumentation, calibration, data acquisition, data analysis and reporting of result. A total of twenty three tests are included in the guidelines. Performance criteria have been established for all tests, systems that do not meet or exceed these criteria may not function adequately in service. The guidelines are to serve as a resource document for voluntary standard/specification writing organizations, and for practitioners and researchers involved in the design, manufacture and testing of seismic isolation systems.

01,332
PB94-161957 PC A03/MF A01
National Inst. of Standards and Technology (BFRL), Gaithersburg, MD. Structures Div.
Draft Guidelines for Quality Control Testing of Sliding Seismic Isolation Systems.
H. W. Shenton. Mar 94, 36p, NISTIR-5371.

Keywords: *Vibration isolators, *Bridges(Structures), *Quality control, *Test methods, *Earthquake resistant structures, Standards, Earthquake engineering, Displacement, Building codes, Vibration damping, Energy dissipation, Structural vibration, Dynamic response, Dynamic structural analysis.

Seismic isolation systems designed according to the 1991 Uniform Building Code, or the 1991 AASHTO Guide Specification for Seismic Isolation Design are required to undergo a series of prototype and quality control tests before being installed in the structure. At the present time, however, standards do not exist for conducting these tests, consequently, results are subject to unknown variability. The document represents the initiation of the process to develop standards for quality control testing of seismic isolation systems built in the U.S. The guidelines are devoted specifically to quality control testing of sliding systems (another report is devoted to quality control testing of elastomeric isolation systems). The guidelines address component part and material tests to be conducted during production, and tests on completed isolation units or components. Production tests are outlined in broad terms for a generic pure sliding device. Two completed isolation unit tests are outlined: sustained compression, and effective stiffness and energy dissipation. Complete details of the test set-up, test procedure, data acquisition, analysis and reporting of results are given in the guidelines. Performance criteria are established for all tests; systems that do not meet these criteria may not perform satisfactorily in service and should be set aside for disposition by the engineer of record.

01,333
PB94-182995 PC A13/MF A03
Construction Technology Labs., Skokie, IL.
Optimization of Highway Concrete Technology.
Final rept.
D. Whiting, M. Nagi, P. Okamoto, K. Smith, M. Darter, J. Clifton, L. Kaetzel, T. Yu, and D. Peshkin.
cJan 94, 291p, SHRP-C-373, ISBN-0-309-05751-5.
Contract SHRP-C-206
See also PB88-244330, PB90-113440 and PB91-100537. Prepared in cooperation with ERES Consultants, Inc., Savoy, IL. and National Inst. of Standards and Technology, Gaithersburg, MD. Sponsored by Strategic Highway Research Program, Washington, DC.

Keywords: *Concrete pavements, *Portland cements, *Bridge maintenance, Pavement damage, Permeability, Temperature effects, Density, Pavement overlays, Highway maintenance, Compressive strength, Aggregates, Mechanical properties, Admixtures.

The report provides (1) state-of-the-art information on new developments in portland cement concrete materials and applications to users in the highway agencies, especially young engineers just beginning their careers in the field; and (2) new materials and testing methodologies for a variety of important highway and bridge rehabilitation applications. The report includes a condensation of the state-of-the-art synthesis of concrete highway technology prepared as part of this research project. Descriptions of evaluations of test methods for in-place concrete density with the use of nuclear methods and determination of water content of fresh concrete using microwave drying are also incorporated in the report. The report gives summaries of guidelines for avoiding thermal effects in concrete pavement slab placements and packing-based aggregate proportioning for concrete mixtures. The report contains a detailed description of field evaluations of a variety of concrete mixes used for early opening of full depth concrete pavement repairs and bridge deck overlays. Opening times ranged from 2 to 24 hours. Brief descriptions of the methodology and content of the HWYCON expert system, available from SHRP, are also included. Finally, a description of the contents of audiovisual implementation packages for highway personnel dealing with materials testing and pavement and bridge rehabilitation is included. (Copyright (c) 1994 National Academy of Sciences.)

01,334
PB94-193471 PC A08/MF A02
Montana State Univ., Bozeman. Dept. of Chemistry.
Binder Characterization and Evaluation by Nuclear Magnetic Resonance Spectroscopy.
Final rept.
P. W. Jennings, J. A. Pribanic, B. Franconi, and D. L. VanderHart. cMay 93, 155p, ISBN-0-309-05252-1, SHRP-A-335.
Contract SHRP-A-002C
Prepared in cooperation with National Inst. of Standards and Technology, Gaithersburg, MD. Sponsored by Strategic Highway Research Program, Washington, DC.

Keywords: *Binders, *Nuclear magnetic resonance, *Magnetic spectroscopy, *Bituminous concretes, *Highways, Asphalt, Molecular diffusion, Chemical properties, Molecular structure, Aggregates, Road materials.

Nuclear magnetic resonance (NMR) spectroscopy was used in solution-state and solid-state experiments on eight asphalt cements. Using a variety of chemical and solution-state NMR spectroscopic techniques, data were obtained about the amounts of aromatic carbon in an average molecule of the asphalt sample, how that carbon is arranged in terms of the size of the average aromatic system and the extent of substitution. The arrangement of the aliphatic portion has also been described in terms of the average number of alicyclic rings, of aliphatic chain length and extent of branching. Concentrations of carboxylic acids and phenols were measured both before and after laboratory oxidative aging. All these data show both surprising similarities and significant differences among the asphalts studied. By using solid-state NMR spectroscopic techniques, the structure of asphaltic cements was probed on a small-distance scale of a few angstroms to 30 micrometers. Differences in molecular mobility were found among the asphalts studied. Changes in molecular mobility after laboratory oxidative aging were found to be small. The implications of these data with regard to the micellar model of asphalt are discussed. The research results' potential impact on understanding asphalt cement properties is explored. (Copyright (c) 1993 National Academy of Sciences.)

01,335
PB95-163259 Not available NTIS
National Inst. of Standards and Technology (BFRL), Gaithersburg, MD. Structures Div.
Evaluating the Seismic Performance of Lightly-Reinforced Circular Concrete Bridge Columns.
Final rept.
A. W. Taylor, and W. C. Stone. 1993, 10p.
Sponsored by Federal Highway Administration, McLean, VA. Office of Research, Development, and Technology.
Pub. in Proceedings of National Earthquake Conference, Memphis, TN., May 2-5, 1993, p543-552.

Keywords: *Failure modes, *Concrete structures, *Bridges(Structures), *Columns(Supports), *Earthquake damage, *Cyclic loads, Dynamic response, Earthquake engineering, Reinforced concrete, Loads(Forces), Displacement, Hysteresis, Bridge design, Structural analysis, Earthquake engineering, Structural failure, Reprints, *Spirally-reinforced bridge columns, *Hysteretic failure model.

The ability to analytically predict the inelastic dynamic behavior of reinforced concrete bridge structures during earthquakes is dependent on the availability of appropriate hysteretic failure models. To date, several such models have been implemented in research computer codes. However, little information is available concerning the selection of appropriate parameters for the solution of specific types of reinforced concrete structures. As part of an effort to develop an integrated seismic design procedure (ISDP) for reinforced concrete bridge piers, the National Institute of Standards and Technology (NIST) is conducting extensive studies of hysteretic failure models and laboratory data from tests of bridge columns subjected to cyclic lateral loading. A digital database of load-displacement histories has been established for circular, spirally-reinforced bridge columns. A system identification analysis was performed to determine optimal values of three hysteretic failure model parameters for each test specimen. Subsequent regression analyses were conducted to develop equations correlating the hysteretic failure model parameters to the material and geometric properties of the specimens.

01,336
PB95-163267 Not available NTIS
National Inst. of Standards and Technology (BFRL), Gaithersburg, MD. Structures Div.

Jacket Thickness Requirements for Seismic Retrofitting of Circular Bridge Columns.
Final rept.
A. W. Taylor, and W. C. Stone. 1993, 10p.
Pub. in Proceedings of Symposium on Practical Solutions for Bridge Strengthening and Rehabilitation, Des Moines, IA., April 5-6, 1993, p249-258.

Keywords: *Earthquake resistant structures, *Bridges(Structures), *Reinforcement(Structures), *Thickness, Bridge design, Design criteria, Reinforcing materials, Reinforced concrete, Earthquake engineering, Hysteresis, Failure modes, Earthquake damage, Structural failure, Columns(Supports), Reprints, *Steel jacketing, *Circular bridge columns, *Seismic retrofitting, Cumulative damage model.

Steel jacketing is a common seismic retrofit strategy for circular, spirally-reinforced concrete bridge piers. Although jacketing is recognized as an effective and relatively inexpensive method for improving column ductility, little guidance is available for determining the required thickness of the jacket. In this study jacket thickness requirements were investigated using a time-step inelastic analysis algorithm which incorporates a hysteretic failure rule and a cumulative damage model. A variety of column designs were subjected to a range of real earthquake acceleration histories, and the resulting damage levels, or damage indices were calculated. These same columns were then re-analyzed with steel jackets of varying thicknesses. It was determined that a relatively thin steel jacket--on the order of a few millimeters in thickness--can dramatically improve the seismic performance of a column. Guidelines are presented for calculating required jacket thicknesses, and practical considerations regarding the installation and performance of jackets are discussed.

01,337
PB95-170551 PC A06/MF A02
National Inst. of Standards and Technology, Gaithersburg, MD.
Robotics Application to Highway Transportation. Volume 2. Literature Search.
Final rept. Sep 92-Nov 93.
E. W. Kent, and R. Finkelstein. Jan 95, 114p, FHWA/RD-94/054.
Contract DTFH61-92-Y-00160
See also PB95-171633. Prepared in cooperation with Robotic Technology, Inc., Potomac, MD. Sponsored by Federal Highway Administration, McLean, VA. Office of Advanced Research.

Keywords: *Robotics, *Highway transportation, *Literature surveys, *Exoskeleton, *Technology assessment, Human factors engineering, Highway design, Highway construction, Highway maintenance, Man machine systems, Robots, Manipulators, Data bases, Bibliographies, Automation.

The National Institute of Standards and Technology, at the request of the Federal Highway Administration, has conducted a study of potential applications of automation and robotics technology in construction, maintenance, and operation of highway systems. The study included a workshop exploring industry perceptions of needs and barriers to adoption, a workshop and a literature search to assess current state of the art practices and trends, and site visits by automation experts to typical highway worksites. Potential technology opportunities were highlighted for short, medium, and long-term efforts in a matrix of intersections between common highway jobs and areas of current technological thrust. From among the opportunities identified, six potential research areas were developed as specific proposals, and subjected to life-cycle cost-benefits analysis. Four were projected to return significant savings by comparison with current practice. Of these, two were identified as also likely to return benefits of significant impact on total highway expenditures and the national economy due to their ability to leverage savings across large numbers of jobs or their effect on a large percentage of highway traffic. This is Volume II of IV.

01,338
PB95-171633 PC A20/MF A04
National Inst. of Standards and Technology, Gaithersburg, MD.
Robotics Application to Highway Transportation. Volume 3. Proposed Research Topics and Cost/Benefit Evaluations by CERF.
Final rept. Sep 92-Nov 93.
E. W. Kent. Jan 95, 468p, FHWA/RD-94/094.
Contract DTFH61-92-Y-00160
See also Volume 2, PB95-170551. Prepared in cooperation with Civil Engineering Research Foundation, Washington, DC. Sponsored by Federal Highway Administration, McLean, VA. Office of Advanced Research.

Keywords: *Robotics, *Cost benefit analysis, *Highway transportation, *Technology assessment, Highway design, Highway maintenance, Highway construction, Bridge inspection, Man machine systems, Automation, Surveys, Research programs, Nondestructive tests, Trenching.

The National Institute of Standards and Technology, at the request of the Federal Highway Administration, has conducted a study of potential applications of automation and robotics technology in construction, maintenance, and operation of highway systems. The study included a workshop exploring industry perceptions of needs and barriers to adoption, a workshop and a literature search to assess current state of the art practices and trends, and site visits by automation experts to typical highway worksites. Potential technology opportunities were highlighted for short, medium, and long-term efforts in a matrix of intersections between common highway jobs and areas of current technological thrust. From among the opportunities identified, six potential research areas were developed as specific proposals, and subjected to life-cycle cost-benefits analysis. Four were projected to return significant savings by comparison with current practice. Of these, two were identified as also likely to return benefits of significant impact on total highway expenditures and the national economy due to their ability to leverage savings across large numbers of jobs or their effect on a large percentage of highway traffic. This is Volume III of IV.

01,339
PB95-193173 PC A07/MF A02
National Inst. of Standards and Technology, Gaithersburg, MD.
Robotics Application to Highway Transportation. Volume 4. Proposals for Potential Research.
Final rept. Sep 92-Nov 93.
E. W. Kent. Jan 95, 132p, FHWA/RD-94/095.
Contract DTFH61-92-Y-00160
See also PB95-171633. Sponsored by Federal Highway Administration, McLean, VA. Office of Advanced Research.

Keywords: *Robotics, *Highway construction, *Highway maintenance, *Highway management, *Technology assessment, Telemetry, Life cycle costs, Cost benefit analysis, Robots, Automation, Bridge inspection, Real time.

The National Institute of Standards and Technology, at the request of the Federal Highway Administration, has conducted a study of potential applications of automation and robotics technology in construction, maintenance, and operation of highway systems. The study included a workshop exploring industry perceptions of needs and barriers to adoption, a workshop and a literature search to assess current state of the art practices and trends, and site visits by automation experts to typical highway worksites. Potential technology opportunities were highlighted for short, medium, and long-term efforts in a matrix of intersections between common highway jobs and areas of current technological thrust. From among the opportunities identified, six potential research areas were developed as specific proposals, and subjected to life-cycle cost-benefits analysis. Four were projected to return significant savings by comparison with current practice.

01,340
PB95-251641 PC A06/MF A02
National Inst. of Standards and Technology (MEL), Gaithersburg, MD. Intelligent Systems Div.
Study of Potential Applications of Automation and Robotics Technology in Construction, Maintenance and Operation of Highway Systems: A Final Report. Volume 4.
E. W. Kent. Jun 95, 118p, NISTIR-5667-V4.
See also PB95-251690. Sponsored by Federal Highway Administration, McLean, VA.

Keywords: *Highway construction, *Highway maintenance, *Robotics, *Automation, Research and development, Proposals, Computer aided design, Sites, System integration, Pavements, Image analysis, Cracking(Fracturing).

The National Institute of Standards and Technology (NIST) at the request of the Federal Highway Administration, has conducted a study of potential applications of automation and robotics technology in construction, maintenance, and operation of highway systems. The study included a workshop exploring industry perceptions of needs and barriers to adoption, a workshop and a literature search to assess current state of the art practices and trends, and site visits by automation experts to typical highway worksites. The final volume contains the set of final research proposals setting out specific studies with proposed deliverables, support levels, and timetables.

01,341
PB95-251682 PC A06/MF A02
National Inst. of Standards and Technology (MEL), Gaithersburg, MD. Intelligent Systems Div.
Study of Potential Applications of Automation and Robotics Technology in Construction, Maintenance and Operation of Highway Systems: A Final Report. Volume 1.
E. Kent. Jun 95, 105p, NISTIR-5667-V1.
See also Volume 3, PB95-251690. Sponsored by Federal Highway Administration, McLean, VA.

Keywords: *Highway construction, *Highway maintenance, *Robotics, *Automation, Highway bridges, Technology assessment, Computer applications, Systems integration, Bridge inspection, Bibliographies.

The National Institute of Standards and Technology (NIST) at the request of the Federal Highway Administration, has conducted a study of potential applications of automation and robotics technology in construction, maintenance, and operation of highway systems. The study included a workshop exploring industry perceptions of needs and barriers to adoption, a workshop and a literature search to assess current state of the art practices and trends, and site visits by automation experts to typical highway worksites. The first volume of the report contains an overview of the study and the methods employed, a summary of the principal results, several white papers examining selected topics of interest, and a bibliographic study.

01,342
PB95-251690 PC A15/MF A03
National Inst. of Standards and Technology (MEL), Gaithersburg, MD. Intelligent Systems Div.
Study of Potential Applications of Automation and Robotics Technology in Construction, Maintenance and Operation of Highway Systems: A Final Report. Volume 3.
E. Kent. Jun 95, 336p, NISTIR-5667-V3.
See also PB95-251682. Sponsored by Federal Highway Administration, McLean, VA.

Keywords: *Highway construction, *Highway maintenance, *Robotics, *Automation, *Meetings, Technology innovation, Technology assessment, Requirements, Control systems, Highway design, Teleoperators, Man machine systems, Robot sensors, Inspection.

The National Institute of Standards and Technology (NIST) at the request of the Federal Highway Administration, has conducted a study of potential applications of automation and robotics technology in construction, maintenance, and operation of highway systems. The study included a workshop exploring industry perceptions of needs and barriers to adoption, a workshop and a literature search to assess current state of the art practices and trends, and site visits by automation experts to typical highway worksites. The third volume contains proceedings of workshops organized to educate the study panel with respect to the highway industry, and with respect to current state of the art.

01,343
PB95-255865 PC A19/MF A04
National Inst. of Standards and Technology (MEL), Gaithersburg, MD. Intelligent Systems Div.
Study of Potential Applications of Automation and Robotics Technology in Construction, Maintenance and Operation of Highway Systems: A Final Report. Volume 2.
E. Kent. Jun 95, 428p, NISTIR-5667-V2.
See also Volume 1, PB95-251682, Volume 3 PB95-251690 and Volume 4, PB95-251641. Sponsored by Federal Highway Administration, McLean, VA.

Keywords: *Highway construction, *Highway maintenance, *Robotics, *Automation, Research and development, Proposals, Benefit cost analysis, Life cycle costs, Technology innovation, Sites, Systems integration, Highway bridges, Inspection, Pavements, Trenching.

The National Institute of Standards and Technology (NIST), at the request of the Federal Highway Adminis-

tration, has conducted a study of potential applications of automation and robotics technology in construction, maintenance, and operation of highway systems. The study included a workshop exploring industry perceptions of needs and barriers to adoption, a workshop and a literature search to assess current state of the art practices and trends, and site visits by automation experts to typical highway worksites. The second volume presents proposals for particular research possibilities developed by the study panel, and a life-cycle cost-benefit analysis of the proposed research under the assumption the expected technological goals could be achieved.

01,344
PB96-101050 PC A03/MF A01
National Inst. of Standards and Technology (BFRL), Gaithersburg, MD. Building Materials Div.
Degradation of Powder Epoxy Coated Panels Immersed in a Saturated Calcium Hydroxide Solution Containing Sodium Chloride.
Final rept. Aug 92-Jul 94.
J. W. Martin, T. Nguyen, D. Alsheh, E. Byrd, J. Seiler, J. A. Lechner, and E. Embree. Oct 95, 46p, FHWA/RD-94/174.
Contract DTFH61-92-Y-30115
Sponsored by Federal Highway Administration, McLean, VA. Office of Engineering and Highway Operations Research and Development.

Keywords: *Reinforcing steels, *Bars, *Epoxy coatings, *Immersion test(Corrosion), *Corrosion, Marine environments, Chemical attack, Degradation, Protective coatings, Peeling, Exfoliation corrosion, Blistering, Calcium hydroxides, Sodium chloride, Thermography, Anodic blisters, Cathodic disbondment, Wet adhesion, Infrared thermography.

Blasted-steel panels were coated with two commercial powder epoxy coatings. Approximately half (80) of the coated panels were scribed; while the other half remained defect-free. All of the panels were immersed in a saturated calcium hydroxide solution containing 3.5 percent sodium chloride maintained at either 35 or 50 deg. C. None of the unscribed panels degraded after 3074 h of immersion at 35 deg C; whereas, all of the scribed panels degraded within 24 h after immersion, regardless of the immersion solution temperature. Scribed panels degraded in three ways: (1) anodic corrosion, (2) Cathodic disbondment, and (3) wet-adhesion loss.

01,345
PB96-131537 PC A03/MF A01
National Inst. of Standards and Technology (BFRL), Gaithersburg, MD. Building Materials Div.
Alkali-Silica Reaction and High Performance Concrete.
C. F. Ferraris. Aug 95, 20p, NISTIR-5742.
Sponsored by Nuclear Regulatory Commission, Washington, DC.

Keywords: *Alkali aggregate reactions, *Silicon dioxide, *Concretes, Air, Cement aggregate reactions, Concrete durability, Standards, Tests, Chemical reactions, Performance, Construction materials, ASR(Alkali-silica reaction), HPC(High performance concrete), National Institute of Standards and Technology.

Damage due to alkali-silica reaction (ASR) in concrete is a phenomenon that was first recognized in the U.S. since 1940 and has since been observed in many countries. Despite numerous studies published, the machanism is not yet clearly understood. Nevertheless, the three major factors in concrete have been identified, i.e., the alkalies contained in the pore solution, reactive amorphous or poorly crystallized silica present in certain aggregates, and water. In this study, we attempted to address the question of whether high-performance concrete (HPC) is susceptible to ASR. It was found that air content is the most important variable (other than the three majors factors cited above) that increase expansion of concretes affected by ASR. This study seems to indicate that even HPC is susceptible to ASR if reactive aggregates are used.

01,346
PB96-146352 PC A07/MF A02
National Inst. of Standards and Technology (BFRL), Gaithersburg, MD. Building and Fire Research Lab.
Seismic Performance of Circular Bridge Columns Designed in Accordance with AASHTO/CALTRANS Standards.
Building science series (Final).
W. C. Stone, and A. W. Taylor. Feb 93, 132p, NIST/BSS-170.
Also available from Supt. of Docs. as SN003-003-03195-0. Sponsored by Federal Highway Administration, McLean, VA.

Keywords: *Bridges(Structures), *Earthquake resistant structures, *Dynamic structural analysis, Seismic design, Bridge design, Columns(Supports), Earthquake damage, Failure modes, Cyclic loads, Dynamic loads, Lateral pressure, Hysteresis, Reinforcement(Structures), Reinforced concrete, Earthquake engineering, Standards, Circular bridge columns, Spiral reinforcement.

Limitations of present procedures for the design of bridge columns to withstand seismic loads are discussed. Techniques for achieving the earthquake resistant capabilities are described and new design criteria, based on acceptable damage indices as functions of earthquake magnitude, distance, and structural importance, are proposed. Using the proposed procedure and criteria the performance of 72 representative bridge columns designed in accordance with 1992 CALTRANS specifications is analyzed. Analysis parameters included earthquake magnitude, distance from epicenter, subsurface soil characteristics, column aspect ratio, and normalized column axial load. Design charts, based on allowable damage index versus earthquake magnitude, are developed and retrofit strategies are discussed for those designs which do not meet the proposed design criteria.

01,347
PB96-193685 PC A08/MF A02
National Inst. of Standards and Technology (BFRL), Gaithersburg, MD.
Guidelines for Pre-Qualification, Prototype and Quality Control Testing of Seismic Isolation Systems.
Final rept.
H. W. Shenton. Jan 96, 137p, NISTIR-5800.
See also PB94-161940.

Keywords: *Vibration isolators, *Test methods, *Earthquake resistant structures, Building codes, Displacement, Structural vibration, Dynamic structural analysis, Earthquake engineering, Dynamic response, Vibration dampling, Sliding, Hybrid systems, Prototypes, Loads(Forces), Bridges(Structures), Standards, Requirements, Quality control, Elastomeric systems, Qualification.

The Building and Fire Research laboratory of the National Institute of Standards and Technology has developed guidelines for testing and evaluation of seismic isolation systems. Included in the report are comprehensive guidelines for conducting pre-qualification, prototype and quality control tests of the isolation system. The guidelines are independent of the type of isolation system and application. Thus, they can be used to test elastomeric, sliding or hybrid isolation systems, for applications that involve buildings, bridges, facilities and other special structures. The guidelines include general requirements of the test facilities and other special structures. The guidelines include general requirements of the test facility, instrumentation, calibration, data acquisition, data analysis and reporting of results. All tests are presented in a standard format that includes test designation, purpose, sequence, procedure, performance criteria, special requirements and exceptions.

01,348
PB96-197249 PC A04/MF A01
Transportation Research Board, Washington, DC. IDEA Program.
Development of a Method for Measuring Water-Stripping Resistance of Asphalt/Siliceous Aggregate Mixtures.
Rept. of investigation (Final) Apr 93-May 96.
T. Nguyen, E. Byrd, D. Bentz, and J. Seiler. 6 May 96, 37p, TRB/NCHRP-ID002.
Prepared in cooperation with National Inst. of Standards and Technology, Gaithersburg, MD. Sponsored by Federal Highway Administration, Washington, DC. and American Association of State Highway and Transportation Officials, Washington, DC.

Keywords: *Bituminous concretes, *Flexible pavements, *Water resistance, *Nondestructive tests, Aggregates, Mechanical proerties, Infrared spectroscopy, Adhesion, Concrete durability, Pavement bases, Stripping.

The objective of the study was to develop a nondestructive spectroscopic method for measuring water stripping resistance of asphalt/siliceous aggregates exposed to water. Phase 1 of the study developed a technique based on Fourier transform infrared spectroscopy/multiple reflection mode to quantify water layer at the asphalt-siliceous aggregate interface. In Phase 2, a technique to measure adhesion loss of the asphalt-aggregate system exposed to water environment was developed. Phase 3 correlated the quantity of interfacial water layer with the adhesion loss data. In addition, results on the use of spectroscopic technique to evaluate the effectiveness of asphalt antistripping agents are presented. Based on interfacial water inforamtion, mechanisms of stripping asphalt from siliceous aggregates and of transport of water from the environment to asphalt-aggregate interface are presented.

01,349
PB96-202353 PC A06/MF A01
National Inst. of Standards and Technology (BFRL), Gaithersburg, MD. Office of Applied Economics.
Economics of New-Technology Materials: A Case Study of FRP Bridge Decking.
Final rept.
M. A. Ehlen, and H. E. Marshall. Jul 96, 76p, NISTIR-5864.

Keywords: *Bridge decks, *Cost analysis, *Composite materials, Life cycle costs, Highway bridges, Economic analysis, Technology innovation, Construction materials, Advanced materials, FRP(Fiber reinforced polymers).

The purpose of this report is to provide a general method for evaluating the life-cycle cost effectiveness of new-technology materials in relation to conventional materials. The methods provides users with a tool that helps them choose that material among competing alternative materials that performs the required function at minimum life-cycle cost. To illustrate an application of the economic method, the authors prepare a case study of highway bridge decks. The authors evaluate the use of FRP (Fiber reinforced polymers) materials as an alternative to conventionally used concrete. The rapidly increasing research on FRPs suggest that it will be a major construction material in the future. The authors choose sbridge decks for two reasons: first, this application of FRPs appears technically promising, and second, there is a large number of bridges in the United States that will need to be replaced in the next 10-15 years, suggesting that there will be considerable interest in a case study of this application.

Soil & Rock Mechanics

01,350
PB96-128111 PC A05/MF A01
National Inst. of Standards and Technology (BFRL), Gaithersburg, MD. Structures Div.
Ground Improvement Techniques for Liquefaction Remediation Near Existing Lifelines.
R. D. Andrus, and R. M. Chung. Oct 95, 89p, NISTIR-5714.

Keywords: *Liquefaction, *Soil stabilization, *Earthquake resistance, Grouting, Soil dynamics, Mixing, Drainage, Conduits, Pipelines, Buildings, Storage tanks, Bridges(Structures), Dams, Soil structure interactions, Deformation, Earth movements, Ground motion, Displacement, Ground subsidence, Seismic effects, Soil mechanics, Earthquake engineering, Cost estimates, *Lifeline systems.

This report reviews five low vibration ground improvement techniques suitable for remedial work near existing structures. The five techniques are: compaction grouting, permeation grouting, jet grouting, in situ soil mixing, and drain pile. The factors which can influence the effectiveness of each technique are identified. Cost estimates are given for each technique, except the drain pile technique which is not yet available in the United States. Nineteen case studies of liquefaction remediation and remedial work near existing lifelines are reviewed. Advantages and constraints of the five techniques are compared. A combination of techniques may provide the most cost-effective ground improvement solution for preventing damage to existing life-

lines resulting from liquefaction-induced horizontal ground displacement, subsidence, and uplift.

01,351
PB96-214697 PC A10/MF A03
Colorado School of Mines, Golden. Div. of Engineering.
Estimation of System Damping at the Lotung Site by Application of System Identification.
S. D. Glaser, and A. L. Leeds. Aug 96, 197p, NIST/GCR-96/700.
Contract NIST-60NANB5D0074
See also PB96-165972. Sponsored by National Inst. of Standards and Technology (BFRL), Gaithersburg, MD. and National Science Foundation, Arlington, VA.

Keywords: *Nuclear power plants, *Soil mechanics, *Excitation, *Seismic waves, Soil structure interactions, Earthquake resistant structures, Liquefaction, Displacement, Structure response, Vibration damping, Stiffness, Earthquake magnitude, Seismic effects, Earthquakes, Ground motion, Soil profiles, Site characterization, Nonlinearity, Earthquake engineering, Graphs(Charts), Lotung(Taiwan), System identification.

This report presents detailed system identification (SI) analyses of the full suite of seismic events at the Lotung site. Estimates of resonant frequencies and damping, and the dependence of these quantities on earthquake intensity is presented. The Lotung site is introduced in Chapter 2 through geological, seismological, and geotechnical descriptions. The SI precedures are discussed in detail in Chapter 3. Chapter 4 presents results of the system identification of the Lotung site data, with a discussion and conclusions given in Chapter 5. Appendix A describes the signal processing used on the raw data, with the integration procedure given in Appendix B. The pore water pressure time histories are shown in Appendix C. A literature review of damping values measured by other researchers is compiled in Appendix D. Finally, comparisons of actual interval outputs and modeled outputs for all events and intervals is given in Appendix E.

COMBUSTION, ENGINES, & PROPELLANTS

General

01,352
PB97-112270 Not available NTIS
National Inst. of Standards and Technology (CSTL), Gaithersburg, MD. Process Measurements Div.
Analysis of Droplet Arrival Statistics in a Pressure-Atomized Spray Flame.
Final rept.
J. T. Hodges, C. Presser, A. K. Gupta, and C. T. Avedisian. 1994, 9p.
Pub. in International Symposium on Combustion (25th), Irvine, CA., July 31-August 5, 1994, p353-361.

Keywords: *Combustion, *Fuel sprays, *Drops, Flow visualization, Image analysis, Flames, Kerosene, Reprints.

The statistical behavior of droplets in a kerosene pressure-atomized spray was investigated under swirling and burning conditions. This case was studied in order to better understand individual droplet transport processes downstream of the fuel spray flame. A two-component phase-Doppler particle sizing system was employed to provide information on the droplet size and velocity distributions as well as interarrival-time statistics. Time-resolved information is presented on the instantaneous values of diameter, and the respective axial and radial velocity components. The results provide some evidence of nonsteady interarrival-time statistics (associated with droplet clustering) immediately downstream of the fuel nozzle and at radial coordinates near the center of the spray. The unsteady statistical behavior was most prominent within the shear layer formed near the inner spray boundary. Decomposition of the results into size classes indicated that clustering (attributed to entrainment by recirculating gases) occurred only for the smallest droplets, 0-20 micrometers in diameter. For larger droplets, analysis on the random nature of the spray process revealed that droplet transport generally follows steady Poisson statistics. Furthermore, the information provided here shows that size-class decomposition is important in the analysis of spray behavior.

Combustion & Ignition

01,353
AD-A274 609/7 PC A03/MF A01
National Inst. of Standards and Technology, Gaithersburg, MD.
Gordon Research Conference on the Physics and Chemistry of Laser Diagnostics in Combustion Held in Plymouth, New Hampshire on 12-16 July 1993.
Final rept.
K. C. Smyth. 16 Jul 93, 24p.

Keywords: *Combustion, Diagnostic equipment, Laser applications, Symposia, Quantitative analysis, Phase studies, Multiphase flow, Flow fields, Laser diagnostics, In situ analysis, Spectroscopy.

The 1993 Gordon Research Conference on the Physics and Chemistry of Laser Diagnostics in Combustion was held at Plymouth State College (South) in Plymouth, New Hampshire, July 12-16, 1993. This conference is primarily concerned with the fundamental physics and chemistry underlying the wide variety of laser-based optical spectroscopic diagnostic techniques which are used for studying combustion processes. The focus is on in-situ and nonperturbing optical methods for one-, two-, and three-dimensional measurements of species concentrations, temperature, and velocity. The development of such quantitative methods using linear and nonlinear optical interactions encompasses a broad scope of interdisciplinary research including basic and applied physics and chemistry.

01,354
N96-15569/2 (Order as N96-15552, PC A20/MF A04)
National Inst. of Standards and Technology, Gaithersburg, MD.
Combustion of a Polymer (PMMA) Sphere in Microgravity.
J. C. Yang, and A. Hamins. Aug 95, 6p.
In NASA. Lewis Research Center, the 3RD International Microgravity Combustion Workshop p 115-120.

Keywords: *Aerospace vehicles, *Combustion, *Liquid fuels, *Reduced gravity, *Polymers, *Polymethyl methacrylate, *Propulsion, Aerospace safety, Burning rate, Chemical reactions, Flammability, Gravitational effects, *Microgravity.

Polymer combustion is a highly complicated process where chemical reactions may occur not only in the gas phase, but also in the condensed phase as well as at the solid-gas interphase. The chemistry depends strongly on the coupling between the condensed phase and gas phase phenomena. For some polymers, additional complications arise due to the formation of char layers. For others, the behavior of the condensed phase involves swelling, bubbling, melting, sputtering, and multi-stage combustion. Some of these features bear resemblance to the phenomena observed in coal particle combustion. In addition to its relevance to spacecraft fire safety, the combustion of polymeric materials is related to many applications including solid and hybrid rocket propulsion, and of recent interest, waste incineration . The burning rate is one of the most important parameters used to characterize the combustion of polymers. It has been used to rank the polymer flammability under the same experimental conditions and to evaluate various modes of inhibiting polymer flammability. The main objective of this work is to measure the burning rates of a polymeric material in low gravity. Because of inherent logistical difficulties involved in microgravity experiments, it is impossible to examine a wide spectrum of polymeric materials. It is desirable to investigate a polymer whose combustion is less complicated, and yet will lead to a better understanding of the burning characteristics of other more complicated materials. Therefore, a typical non-charring polymer is selected for use in this experimental study. PMMA (polymethylmethacrylate) has been chosen because its thermo-physical properties are well characterized. Although the combustion of PMMA has been extensively studied in 1G experiments, only a limited amount of work has been conducted in low gravity. A spherical sample geometry is chosen in this study because it is the simplest configuration in terms of the microgravity hardware design requirements. Furthermore, a burning PMMA sphere in microgravity represents a one-dimensional flame with overall combustion characteristics expected to be analogous to the combustion of a liquid fuel droplet, a field with many well-developed theories and models. However, differences can also be expected such as the flame-front standoff ratios and the condensed phase processes occurring during combustion.

01,355
PB94-142973 PC A04/MF A01
National Inst. of Standards and Technology (BFRL), Gaithersburg, MD.
In situ Burning of Oil Spills: Mesoscale Experiments.
W. D. Walton. Nov 93, 63p, NISTIR-5266.
See also PB94-101839. Sponsored by Minerals Management Service, Herndon, VA. Technology Assessment and Research Branch.

Keywords: *Oil spills, *In-situ combustion, *Fire tests, Crude oil, Burning rate, Plumes, Smoke, Particulates, Water pollution control, Mitigation, Oil-water interfaces, Mesoscale tests.

In 1991 a series of 14 mesoscale fire experiments were performed to measure the burning characteristics of crude oil on salt water. These oil burns in a pan ranged in size from 6 m square to 15 m square. Results of the measurements for burning rate, oil temperature, water temperature, smoke particle size distribution, smoke plume trajectory, and smoke particulate yield are provided. The burning rate as indicated by the regression rate of the oil surface was found to be 0.055 (+ or -) 0.005 mm/s and smoke particulate yields were found to be approximately 0.13 of the oil burned on a mass basis.

01,356
PB94-156866 PC A08/MF A02
California Univ., Berkeley. Dept. of Mechanical Engineering.
Concurrent Flow Flame Spread Study.
H. T. Loh. Mar 92, 161p, NIST/GCR-92/603.
Grant NIST-NANB7D737
See also N93-24946. Sponsored by National Inst. of Standards and Technology (BFRL), Gaithersburg, MD.

Keywords: *Flame propagation, *Gas flow, Combustion, Temperature distribution, Reaction kinetics, Pyrolysis, Mathematical models, Boundary layer, Computer programs, Diffusion flames, Computational fluid dynamics.

An experimental study has been performed of the spread of flames over the surface of thick PMMA and thin filter paper sheets in a forced gaseous flow of varied oxygen concentration moving in the direction of flame spread. It is found that the rate of spread of the PMMA pyrolysis front is time independent, linearly dependent on the gas flow velocity and approximately square power dependent on the oxygen concentration of the gas. The experimental data with thin filter paper sheets shows that the flame spread rate is independent of the flow velocity for forced flow conditions and linearly dependent on the oxygen concentration of the flow. In both experiments, it was found that the flame spread rate data can be correlated in terms of parameters deduced from heat transfer considerations only. This indicates that heat transfer from the flame to the condensed fuel is the primary mechanism controlling the spread of flame. Finite rate chemical kinetic effects have apparently a small influence on the flame spread process itself. Analytical and numerical methods were also employed to study theoretically the flame spread process over thermally thick fuel and in the influence on the flow field behavior in the presence of a flame.

01,357
PB94-156965 PC A04/MF A01
Clemson Univ., SC. Dept. of Mathematical Sciences.

Numerical Analysis Support for Compartment Fire Modeling and Incorporation of Heat Conduction into a Zone Fire Model.
Final rept. 15 Aug 88-31 Mar 91.
W. F. Moss. Mar 92, 51p, NIST/GCR-92/605.
Grant NANB-8D0857
See also PB90-250192 and PB92-172790. Sponsored by National Inst. of Standards and Technology (BFRL), Gaithersburg, MD.

Keywords: *Mathematical models, *Conduction, *Heat transmission, *Fires, Numerical analysis, Prototypes, Temperatures, Fortran, Floors, Walls, Ceilings, Differential equations, Zone fire model.

The research goal for the first year of the grant was to determine the best available numerical technology for use in zone fire modeling. The goal for the second year was to incorporate heat conduction into a zone fire model in a numerically robust and efficient manner. Three prototype zone fire models named MCCFM, CONRAD1 and CONRAD2 were constructed to test the numerical technology used to realize these goals. These zone fire models and their implementations as Fortran codes are presented. The code MCCFM, developed during the first year of the grant, demonstrates the advantages of using mass as a solution variable instead of density. CONRAD1 and CONRAD2 examine two strategies for coupling the heat conduction equation (a one dimensional partial differential equation) with the zone fire modeling ordinary differential equations. CONRAD2 reduces the heat conduction problem to a set of implicitly defined functional equations, a strategy never before used in zone fire modeling.

01,358
PB94-164019 PC A05/MF A01
National Inst. of Standards and Technology (BFRL), Gaithersburg, MD.
Fire Data Management System, FDMS 2.0, Technical Documentation.
Technical note.
R. W. Portier. Feb 94, 86p, NIST/TN-1407.
Also available from Supt. of Docs.as SN003-003-03251-4. See also PB93-182038.

Keywords: *Data bases, *User manuals, *Management information systems, *Fire tests, Information retrieval, Information systems, Data management, Systems engineering, Data storage systems, Data processing, *FDMS Computer data base, *Fire Data Management System.

Fire Data Management System, FDMS, is a computer database specifically designed to store and retrieve fire test results. A version, FDMS 1.0, of the database is currently available. This guide provides detailed descriptions of the physical file implementations planned for the next generation of the database, FDMS 2.0.

01,359
PB94-165941 PC A12/MF A03
California Inst. of Tech., Pasadena.
Experimental and Numerical Studies on Two-Dimensional Gravity Currents in a Horizontal Channel.
W. R. Chan, E. E. Zukoski, and T. Kubota. Jul 93, 264p, NIST/GCR-93/630.
Grant NIST-NANB9D0958
Sponsored by National Inst. of Standards and Technology (NEL), Gaithersburg, MD. Center for Fire Research.

Keywords: *Fire tests, *Computational fluid dynamics, Smoke, Channel flow, Currents.

The objective of this investigation is to examine the behavior of two-dimensional gravity currents, especially as applied to the spreading of smoke, generated from a room fire, along a long corridor. Both experimental and numerical techniques were used to provide a model that can adequately explain and predict the behavior of a gravity current under certain boundary conditions. A series of experiments was carried out to study the effects of Reynolds number on gravity currents in a horizontal water channel. Measurements of the time varying front position, velocity profile of the following current, and the depth of a gravity current were made using either dyed liquids or hydrogen bubble technique. Quantitative results were shown to agree with previously published results.

01,360
PB94-165974 PC A04/MF A01
Michigan Univ., Ann Arbor.
Radiation and Mixing Properties of Buoyant Turbulent Diffusion Flames.
U. U. Koylu, Z. Dai, L. K. Tseng, and G. M. Faeth. Jul 93, 61p, NIST/GCR-93/631.
Grant NANB1D1175
See also PB84-155829. Sponsored by National Inst. of Standards and Technology, Gaithersburg, MD.

Keywords: *Fires, *Flame propagation, Diffusion flames, Plumes, Optical properties, Raleigh scattering, Soot, Turbulent flow.

Two aspects of unwanted fires were considered: (1) the optical properties of soot in the fuel-lean region of buoyant turbulent diffusion flames, and (2) the structure and mixing properties of buoyant turbulent plumes. The scattering, absorption and extinction properties of soot were measured for conditions where soot structure was known from earlier transmission electron microscopy measurements. The plume study involved laser-induced iodine fluorescence measurements of mean and fluctuating mixture fractions. The results indicated that past measurements of plume properties represent transitional plumes and that self-preserving turbulent plumes are somewhat narrower, with higher levels of mean and fluctuating mixture fractions near the axis.

01,361
PB94-172988 Not available NTIS
National Inst. of Standards and Technology (BFRL), Gaithersburg, MD. Fire Science Div.
Greatly Enhanced Soot Scattering in Flickering Ch4/Air Diffusion Flames.
Final rept.
K. C. Smyth, J. E. Harrington, E. L. Johnsson, and W. M. Pitts. 1993, 11p.
Pub. in Combustion and Flame 95, p229-239 1993.

Keywords: *Soot, *Laser induced fluorescence, *Diffusion flames, *Optical images, Combustion, Hydroxyl radicals, Scattering, Strain rate, Particles, Methane, Sampling, Reprints.

Planar images of laser-induced fluorescence from OH radicals and elastic scattering from soot particles are presented in time-varying, laminar CH4/air diffusion flames burning in a co-flowing, axisymmetric configuration at atmospheric pressure. Acoustic forcing is used to phase lock the periodic flame flicker to the pulsed laser system operating at 10.13 Hz. For conditions where the tip of the flame is clipped, the intensity of the light scattered by the soot particles increases dramatically (by more than a factor of 7 for the maximum signals at a point) compared to a steady-state, laminar flame with the same mean fuel flow velocity. Comparison of the scattering signals integrated along the flame radius is carried out in the steady-state and time-varying flames as a function of height above the burner. Time-varying flames exhibit a larger range of combustion conditions than observed in corresponding steady-state flames, including different residence times, temperature histories, local stoichiometries, and strain and scalar dissipation rates. Thus, their investigation promises to yield new insights into a wide variety of chemistry-flowfield interactions which are prominent in turbulent combustion.

01,362
PB94-185113 Not available NTIS
National Inst. of Standards and Technology (CSTL), Gaithersburg, MD. Process Measurements Div.
Fluorinated Hydrocarbon Flame Suppression Chemistry.
Final rept.
D. Burgess, W. Tsang, M. R. Zachariah, and P. R. Westmoreland. 1994, 6p.
Preprints of papers presented at the American Chemical Society National Meeting (207th), San Diego, CA., March 13-17, 1994, p141-146.

Keywords: *Combustion kinetics, *Thermochemistry, *Fluorohydrocarbons, *Fire suppression, *Flames, Combustion chemistry, Fuels, Transport properties, Combustion efficiency, Inhibitors, Reprints, *Chemical reaction mechanisms, Ab initio molecular orbital theory.

A comprehensive, detailed chemical kinetic mechanism was developed for fluorinated hydrocarbon destruction and flame suppression. Existing fluorinated hydrocarbon thermochemistry and kinetics were compiled and evaluated. For species where no or incomplete thermochemistry was available, these data were calculated through application of ab initio molecular orbital theory. Group additivity values were determined consistent with experimental and ab initio data. For reactions where no or limited kinetics was available, these data were estimated by analogy to hydrocarbon reactions, by using empirical relationships from other fluorinated hydrocarbon reactions, by ab initio transition state calculations, and by application of RRKM and QRRK methods. The chemistry was modeled considering different transport conditions (plug flow, premixed flame, opposed flow diffusion flame) and using different fuels (methane, ethylene), equivalence ratios, agents (fluoromethanes, fluoroethanes) and agent concentrations. An overview of this work is presented.

01,363
PB94-185287 Not available NTIS
National Inst. of Standards and Technology (BFRL), Gaithersburg, MD. Fire Science Div.
Flame Retardants - Overview.
Final rept.
R. G. Gann. 1994, 7p.
Pub. in Kirk-Othmer Encyclopedia of Chemical Technology, v10 p930-936 1994.

Keywords: *Flame retardants, Fire tests, Fire resistant coatings, Fire prevention, Polymers, Marketing, Performance evaluation, Reprints.

This article provides an introduction to succeeding chapters on fire retardants in the 'Encyclopedia of Chemical Technology.' The text describes why fire retardants are useful, general mechanisms for their effectiveness, how the performance of polymer/retardant composites is measured, a snapshot of the market for these chemicals, and forces that might change that market.

01,364
PB94-185352 Not available NTIS
National Inst. of Standards and Technology (BFRL), Gaithersburg, MD. Fire Science Div.
Laser Imaging of Chemistry-Flowfield Interactions: Enhanced Soot Formation in Time-Varying Diffusion Flames.
Final rept.
J. E. Harrington, C. R. Shaddix, and K. C. Smyth. 1994, 14p.
Pub. in Proceedings of the Society of Photo-Optical Instrumentation Engineers Laser Techniques for State-Selected and State-to-State Chemistry II, Los Angeles, CA., January 27-29, 1994, v2124 14p.

Keywords: *Diffusion flames, *Soot, *Laser induced fluorescence, *Flow fields, Reprints, Light scattering, Luminosity, Methane, Combustion products, Image processing, Unsteady flow.

Models of detailed flame chemistry and soot formation are based upon experimental results obtained in steady, laminar flames. For successful application of these descriptions to turbulent combustion, it is instructive to test predictions against measurements in time-varying flowfields. This paper reports the use of optical methods to examine soot production and oxidation processes in a co-flowing, axisymmetric CH4/air diffusion flame in which the fuel flow rate is acoustically forced to create a time-varying flowfield. For a particular forcing condition in which tip clipping occurs (0.75 V loudspeaker excitation), elastic scattering of vertically polarized light from the soot particles increases by nearly an order of magnitude with respect to that observed for a steady flame with the same mean fuel flow rate. The visible flame luminosity and laser-induced fluorescence attributed to polycyclic aromatic hydrocarbons (PAH) are also enhanced. Peak soot volume fractions, as measured by time-resolved laser extinction/tomography at 632.8 and 454.5 nm and calibrated laser-induced incandescence (LII), show a factor of 4-5 enhancement in this flickering flame. The LII method is found to track the soot volume fraction closely and to give better signal-to-noise than the extinction measurements in both the steady and time-varying flowfields. A Mie analysis suggests that most of the enhanced soot production results from the formation of larger particles in the time-varying flowfield.

01,365
PB94-193844 PC A04/MF A01
California Univ., Berkeley. Dept. of Mechanical Engineering.
Fire Propagation in Concurrent Flows.
Final progress rept. 1 Sep 92-31 Aug 93.
A. C. Fernandez-Pello. Jun 94, 68p, NIST/GCR-94/644.
Grant NIST-60NANB1D1174
See also PB91-157206. Sponsored by National Inst. of Standards and Technology (BFRL), Gaithersburg, MD.

Keywords: *Flame propagation, *Turbulence, *Fire tests, Velocity distribution, Buoyancy, Soot, Burning rate, Test facilities, Heat flux, Combustion products, Mathematical models, Heat transfer, *Concurrent flow.

A research program is being conducted to study the mechanisms controlling the spread of flames in an oxidizing gas flow moving in the direction of flame propagation. During this reporting period research has been conducted to study the effect of the oxidizer flow characteristics on the concurrent flame spread over thick PMMA sheets. The parameters varied in the experiments are the oxidizer flow velocity, turbulence intensity and oxygen concentration, and the geometrical orientation (floor and ceiling). Their effect on the flame spread process is studied by measuring the rate of flame spread, flame length, surface heat flux, products of combustion and soot. The results of the experiments show that the combined effect of flow velocity, turbulence intensity, and oxygen concentration has a complex influence on the flame spread process. At low flow velocity, the flame spread rate increases monotonically with turbulence intensity. At high flow velocity, however, the flame spread rate increases with flow turbulence at low turbulence intensities, but it decreases at high turbulence intensity values. The effect is more pronounced at high oxygen concentration. These trends appear to be due to a strong influence of the turbulence intensity on the flame temperature and length, and on that heat flux from the flame to the solid fuel. Turbulence enhances mixing, which increases the flame temperature and then the heat flux.

01,366
PB94-193927 PC A11/MF A03
California Univ., Berkeley.
Backdraft Phenomena.
Doctoral thesis 1990-92 (Final).
C. M. Fleischmann. cJun 94, 237p, NIST/GCR-94/646.
Grant NIST-60NANB0D1042
Sponsored by National Inst. of Standards and Technology (BFRL), Gaithersburg, MD.

Keywords: *Flame propagation, *Flow velocity, Combustion physics, Fires, Mixing layers(Fluids), Compartments, Ignition, Theses, Mathematical models, Froude number, Convective flow, Flow visualization, *Backdraft phenomena, *Compartment fires.

The purpose of this project was to develop a fundamental physical understanding of backdraft phenomena. The research was divided into three phases: exploratory simulations, gravity current modeling, and quantitative backdraft experiments. The primary goal of the first phase was to safely simulate a backdraft in the laboratory. A half-residential-scale compartment was built to conduct exploratory experiments. The initial experiments concluded with a scenario describing the fundamental physics of backdrafts. The importance of the gravity current which enters the compartment after opening was identified. In the second phase, the gravity current speed and the extent of its mixed region was investigated in a series of scaled salt water experiments. The scaled compartment (0.3m x 0.15m x 0.15m) was fitted with a variety of end openings; full, slot, door, and window. Video and photo data indicate that the mixing layer which rides on the gravity current in the full opening case, expands to occupy nearly the entire current in the partial opening cases. The Froude number and nondimensional head height are independent of beta and are in good agreement with numerical simulations and special limits from the literature. In the final phase, 28 backdraft experiments were conducted in a 1.2m by 1.2m by 2.4m compartment. (Copyright (c) 1993 Charles Martin Fleischmann.)

01,367
PB94-195856 PC A03/MF A01
Maryland Univ., College Park. Dept. of Fire Protection Engineering.
Fire Growth Models for Materials.
Final rept. Jun 92-Dec 93.
J. G. Quintiere, and B. Rhodes. Jun 94, 49p, NIST/GCR-94/647.
Grant NIST-60NANB2D1266
Sponsored by National Inst. of Standards and Technology (BFRL), Gaithersburg, MD.

Keywords: *Burning rate, *Materials, *PMMA, Fire hazards, Calorimeters, Flame propagation, Heat flux, Ignition, Mathematical models, Test facilities, Combustion, *Fire models.

Ignition and burning rate data have been developed for thick (25 mm.) black Polycast PMMA in a Cone Calorimeter heating assembly. The objective was to establish a testing protocol that would lead to the prediction of ignition and burning rate from Cone data. This has been done for a thermoplastic like PMMA. For black PMMA we measured ignition temperatures of 250 to 350 C and vaporization temperatures of approximately 325 to 380 C over irradiance levels of 15 to 60 kW/sq m. The incident flame heat flux, for irradiation levels of 0 to 75 kW/sq m, was found to be approximately 37 kW/sq m for black PMMA. Its constancy has been shown due to the geometry of the Cone flame. Also, this flame can be shown to be nearly transparent for Cone irradiance (greater than 90 percent). The heat of gasification of the black PMMA used was found to be approximately 2.8 kJ/g; higher than other values reported for PMMA. This is believed to be due to differences in molecular structure or pigmentation effects and the types of PMMA tested. A burning rate model was demonstrated to yield good accuracy (greater than 80 percent) in comparison to measured transient values.

01,368
PB94-196045 PC A99/MF A06
Brown Univ., Providence, RI. Div. of Engineering.
Behavior of Charring Materials in Simulated Fire Environments.
Final rept. 1990-92.
E. M. Suuberg, I. Milosavljevic, and W. D. Lilly. Jun 94, 625p, NIST/GCR-94/645.
Grant NIST-60NANB0D1042
Sponsored by National Inst. of Standards and Technology (BFRL), Gaithersburg, MD.

Keywords: *Fire models, *Pyrolysis, *Cellulose, *Charring, Fire chemistry, Reaction kinetics, Polymers, Heat transfer, Laboratories, Thermodynamics, Combustion products, Fire research, Solids, Flammable gases, US NBS, Carbon monoxide, Char, Char depth, NIST(National Institute of Standards and Technology).

The focus of this study was the behavior of thick charring solids in fire situations. Clearly one of the most important parameters governing the fire phenomenon is the rate of release of combustible volatiles into the gas phase, in which they actually burn. Over the years, fire researchers have learned how to model the processes in the gas phase, so that the rate of heat feedback to the solid surface can be reasonably well predicted. Likewise, there exists the ability to model the heat transfer processes at the solid surface and within the solid itself. This study was concerned with the possibility that the inability to come to complete closure on the charring polymer fire problem might derive from difficulties in applying laboratory scale kinetics to actual fire conditions. Specifically, we were concerned about how well small scale laboratory experiments used to derive the kinetics of pyrolysis could be used to predict the behavior of charring solids in fire situations.

01,369
PB94-198439 Not available NTIS
National Inst. of Standards and Technology (BFRL), Gaithersburg, MD. Fire Measurement and Research Div.
Effective Measurement Techniques for Heat, Smoke, and Toxic Fire Gases.
Final rept.
V. Babrauskas. 1991, 14p.
Pub. in Fire Safety Jnl. 17, p13-26 1991.

Keywords: *Fires, *Smoke, *Heat, *Toxicity, *Test methods, Combustion products, Measuring instruments, Bench tests, Test facilities, Measurement, Reprints, *Fire gases.

The latest techniques which have been developed for the measurement of heat, smoke, and toxic gas emissions from fires are reviewed. The current objective of minimizing apparatus dependence of the data is emphasized. Forms of data and their units are outlined. Differences between data obtained in large-scale and in bench-scale tests are discussed, and areas where further research is needed are indicated.

01,370
PB94-198447 Not available NTIS
National Inst. of Standards and Technology (NEL), Gaithersburg, MD. Fire Measurement and Research Div.
Modern Test Methods for Flammability.
Final rept.
V. Babrauskas. 1990, 20p.
Pub. in Proceedings of a Conference on Recent Adv. Flame Retard. Polym. Mater., Stanford, CT., May 1990, p50-69.

Keywords: *Flammability, *Test methods, *Bench tests, *Fire hazards, Burning rate, Combustion, Toxicity, Smoke, Ignition, Test facilities, Reprints.

During the last decade, significant improvements have become available in flammability testing. Rationally-based new methods, derived from fundamental engineering principles, are replacing the previously used empirical tests. The major emphasis in this development work has been to provide a basic set of bench-scale methods which can be used to predict full-scale product performance. Reference methods for conducting full-scale tests will continue to be needed to handle products or situations where the bench-scale methods are not applicable. The bulk of the testing needs, however, can now be fulfilled by use of bench-scale tests which are not only simple to run, but are known to accurately predict the full-scale performance.

01,371
PB94-198462 Not available NTIS
National Inst. of Standards and Technology (NEL), Gaithersburg, MD. Fire Measurement and Research Div.
Standardization of Formats and Presentation of Fire Data - The FDMS.
Final rept.
V. Babrauskas, R. D. Peacock, and M. Janssens. 1991, 8p.
Pub. in Fire and Materials 15, n2 p85-92 Apr-Jun 91.

Keywords: *Standardization, *Fires, *Data transfer(Computers), *Data base management systems, Test methods, Data processing, Standards, Computer programs, Data integration, Reprints, *Fire test data, *Fire Data Management System.

Effective exchange of fire test data, even within a single laboratory, has been difficult due to the multiple incompatible data formats and hardware. This issue has been addressed by a careful study of user needs, leading to the development of a series of standard formats whereby fire test data could easily be exchanged among laboratories and design professionals. Both scalar and vector data are included. These formats have been made practical by the development of a computer program, the Fire Data Management System (FDMS), and pertinent hardware standards. The system includes the most commonly used of modern day fire test methods, but also has provisions for future extension to other tests of interest.

01,372
PB94-200292 Not available NTIS
National Inst. of Standards and Technology (NEL), Gaithersburg, MD. Fire Science and Engineering Div.
Generation and Characterization of Acetylene Smokes.
Final rept.
T. G. Cleary, R. A. Fletcher, G. W. Mulholland, L. K. Ives, and J. W. Gentry. 1990, 4p.
Pub. in Chemical Physics Processes Combustion, p128-1-128-4 1990.

Keywords: *Particles, *Diffusion flames, *Smoke generators, Acetylene, Combustion products, Mass spectroscopy, Aerosol generators, Soot, Particle size, Laminar flow, Reprints.

Acetylene smokes from a laminar diffusion flame are characterized. The smoke generator is capable of producing mono-sized 7 nm particles and soot agglomerates containing 20-30 nm in diameter primary particles. Size distributions and structural information were obtained by electron and optical microscopy. Laser microprobe mass spectroscopy was used to measure the chemical composition of the smokes.

01,373
PB94-200300 Not available NTIS
National Inst. of Standards and Technology (NEL), Gaithersburg, MD. Fire Science and Engineering Div.
Ultrafine Combustion Aerosol Generator.
Final rept.
T. G. Cleary, G. W. Mulholland, L. K. Ives, R. A. Fletcher, and J. W. Gentry. 1992, 5p.
Pub. in Aerosol Science and Technology 16, n3 p166-170 1992.

Keywords: *Diffusion flames, *Aerosol generators, *Smoke, Smoke generators, Particles, Combustion products, Particle size, Laminar flow, Soot, Reprints.

A laminar diffusion flame system capable of producing a narrowly distributed ultrafine aerosol is described. Diffusion battery and transmission electron microscopy

indicate a mean particle diameter on the order of 10 to 7 nm respectively. Laser microprobe mass analysis indicates that the particles are composed of phosphates and sulfates in addition to carbonaceous material.

01,374
PB94-211679 Not available NTIS
National Inst. of Standards and Technology (BFRL), Gaithersburg, MD. Fire Science Div.
Laser-Induced Fluorescence Measurements of Formaldehyde in a Methane/Air Diffusion Flame.
Final rept.
J. E. Harrington, and D. C. Smyth. 1993, 7p.
Pub. in Chemical Physics Letters 202, n3,4 p196-202, 22 Jan 93.

Keywords: *Diffusion flames, *Laser induced fluorescence, *Formaldehyde, Combustion, Test methods, Methane, Excitation, Extinction, Burning rate, Reprints.

Laser-induced fluorescence has been observed from the formaldehyde electronic transition in a well-characterized, laminar methane/air diffusion flame burning at atmospheric pressure. This represents the first optical measurement in flames of naturally occurring formaldehyde, an important intermediate in the oxidation of hydrocarbons. Both 355 nm and tunable dye laser excitation of fluorescence are demonstrated. The observed fluorescence signals are corrected for partition function effects and for estimated collisional quenching rates to obtain relative concentration profiles.

01,375
PB94-212693 Not available NTIS
National Inst. of Standards and Technology (NEL), Gaithersburg, MD. Fire Science and Engineering Div.
Application of Boundary Element Methods to a Transient Axis-Symmetric Heat Conduction Problem.
Final rept.
F. Kavoosi, M. di Marzo, H. R. Baum, and D. D. Evans. 1989, 7p.
Pub. in Proceedings of National Heat Transfer Conference, Philadelphia, PA., August 6-9, 1989, p79-85.

Keywords: *Conductive heat transfer, *Sprinklers, *Boundary element method, Heat transfer coefficients, Cooling, Drops(Liquids), Evaporation, Fire fighting, Heat flux, Reprints.

A long term study of the phenomena controlling the extinguishment of solid fuel fires is based on the modeling of the interactions of sprinkler generated droplets impinging hot solid surfaces. The thermal interactions during the evaporation of a liquid droplet deposited on a low conductivity semi-infinite solid are complex because the evaporative process is coupled to intense local cooling of the solid. Sharp temperature gradients in the proximity of the droplet edge cause instabilities in finite difference solutions using reasonable time steps due to the explicit coupling of the liquid-solid region. A boundary element method is proposed in order to overcome these difficulties. The methodology and its application to this specific problem are described in detail. Formal solutions are obtained in the form of surface integrals over the solid and the droplet surfaces. These surface integrals are discretized into summations, which lead to matrix equations for the discretized surface temperatures and heat fluxes. Results for some preliminary tests are discussed to provide an insight on the various aspects of this solution procedure

01,376
PB95-104964 PC A09/MF A02
National Inst. of Standards and Technology (BFRL), Gaithersburg, MD. Fire Science Div.
Annual Conference on Fire Research: Book of Abstracts, October 17-20, 1994.
S. B. Smith. Oct 94, 181p, NISTIR-5499.
See also report for 1993, PB94-121324.

Keywords: *Fire suppression, *Meetings, *Fire hazards, *Flame propagation, *Abstracts, Fires, Research, Fire extinguishing agents, Combustion, Soot, Smoke, Flow distribution, Plumes, Pool fires.

Contents: Suppression Using Halocarbons - Laboratory Studies; Fire Hazard, Risk, and Data; Suppression Using Halocarbons - Large-Scale Studies; Suppression Using Water; Pool Fires; Fire-Induced Flows; Chemistry and Physics of Material and Product Combustion; Soot; Fire Signatures; Flame Spread; Fire Plumes.

01,377
PB95-107405 Not available NTIS
National Inst. of Standards and Technology (MSEL), Gaithersburg, MD. Metallurgy Div.
Optimization of Inert Gas Atomization.
Final rept.
S. D. Ridder, F. I. Espina, and F. S. Biancaniello. 1989, 11p.
Pub. in Proceedings of International Symposium on Physical Chemistry of Powder Metals Production and Processing, St. Marys, PA., October 16-18, 1989, p163-173.

Keywords: *Atomization, *Rare gases, Particle size distribution, Powder metallurgy, Size determination, Powder metals, Expert systems, Feedback control, Hypersonic flow, Reprints.

Inert gas atomization via close-coupled hypersonic jets (Mach number > 7) has promise in providing metal powder with mean size < 30 micrometers in large quantities for even difficult materials such as 304 SS. Recent studies at the National Institute of Standards and Technology (formerly NBS) have been focused on the implementation of an in-situ particle size measurement sensor for feed-back control of powder size during atomization. This work involves a detailed analysis of the compressible supersonic jets, liquid disruption studies using high-speed cinematography (10,000 fps) and holography (25 ns exposure time), development of the particle sizing sensor, and incorporation of this data into an intelligent process control system.

01,378
PB95-128674 PC A03/MF A01
National Inst. of Standards and Technology (BFRL), Gaithersburg, MD. Fire Safety Engineering Div.
FIREDOC Users Manual, 3rd Edition.
N. H. Jason. Dec 93, 50p, NISTIR-5305.
Errata sheet inserted. See also 2nd edition, PB91-178830.

Keywords: *User manuals(Computer programs), *Information systems, *Fire safety, *Information retrieval, Information transfer, Online systems, US NIST, Bibliographies, Data bases, *FIREDOC computer program, *Fire Research Information Services.

FIREDOC is the on-line bibliographic database which reflects the holdings (published reports, journal articles, conference proceedings, books, and audiovisual items) of the Fire Research Information Services (FRIS) at the Building and Fire Research Laboratory (BFRL), National Institute of Standards and Technology (NIST). This manual provides step-by-step procedures for entering and exiting the database via telecommunication lines, as well as a number of techniques for searching the database and processing the results of the searches. This Third Edition is necessitated by the change to a UNIX platform. The new computer allows for faster response time if searching via a modem and, in addition, offers internet accessibility. FIREDOC may be used with personal computers, using DOS or Windows, or with Macintosh computers and workstations. A new section on how to access Internet is included, and one on how to obtain the references of interest to you. Appendix F: Quick Guide to Getting Started will be useful to both modem and Internet users.

01,379
PB95-140919 Not available NTIS
National Inst. of Standards and Technology (BFRL), Gaithersburg, MD. Fire Science Div.
Comparison of Experimental and Computed Species Concentration and Temperature Profiles in Laminar, Two-Dimensional Methane/Air Diffusion Flames.
Final rept.
T. S. Norton, K. C. Smyth, J. H. Miller, and M. D. Smooke. 1993, 34p.
Pub. in Combustion Science and Technology 90, p1-34 1993.

Keywords: *Diffusion flames, *Concentration(Composition), *Temperature distribution, Methane, Laminar flow, Scalars, Radicals, Dissipation, Combustion, Reprints.

Experimental concentration measurements of the major stable species and five radical species (OH, H atom, O atom, CH, and CH3) obtained on a rectangular Wolfhard-Parker slot burner are compared with a detailed computation of the chemical structure of an axisymmetric laminar, CH4/air diffusion flame burning at atmospheric pressure. In order to examine these CH4/air flames with different geometries and different sizes, the species profiles are plotted as functions of the local mixture fraction, and the scalar dissipation rate has been matched in a region around the stoichiometric surface. The overall agreement in the absolute concentrations, the shape of the profiles, and their location in terms of the local mixture fraction is good to excellent for the stable species (except for O2) and for the most abundant radicals OH, H atom, and O atom. For example, the calculated OH maximum concentration is in much better agreement with the experimental results than are full equilibrium and partial equilibrium estimates. Less satisfactory agreement is found for the CH and CH3 radicals. In addition, significant discrepancies are observed in the temperature field and in the degree of O2 penetration into rich flame regions.

01,380
PB95-143160 PC A08/MF A02
Pennsylvania State Univ., University Park. Dept. of Mechanical Engineering.
Fundamental Mechanisms for CO and Soot Formation.
Final rept.
R. J. Santoro. Nov 94, 174p, NIST/GCR-94/661.
Grant NIST-60NANBOD1035
See also PB88-173976 and AD-A192 733. Sponsored by National Inst. of Standards and Technology (BFRL), Gaithersburg, MD.

Keywords: *Diffusion flames, *Carbon monoxide, *Soot, Combustion products, Laminar flow, Concentration(Composition), Measuring instruments, Mathematical models.

Studies investigating the oxidation of soot and carbon monoxide (CO) have been conducted in a series of laminar diffusion flames. Both overventilated and underventilated conditions have been examined. For the overventilated studies, the production and destruction of CO has been found to be influenced by the amount of soot present in the flame. Measurements of the hydroxyl radical OH(-) have demonstrated that soot can compete for OH(-) when undergoing oxidation and, thus, impede the oxidation of CO to CO2. Absolute concentration measurements for OH(-) have shown that superequilibrium values of OH(-) are achieved in the upper region of these diffusion flames. The results clearly demonstrate that soot particles are far from passive species in flames and can directly affect the chemical pathways involved in the oxidation process through radiative effects on temperature and soot particle reactivity effects on radical concentrations. The chemical makeup and structure of the smoke produced at high equivalence ratio is qualitatively different from smoke produced under overventilated conditions; the smoke is mainly organic rather than graphitic and it has an agglutinated structure rather than an agglomerate structure with distinct primary spheres usually observed in overventilated burning.

01,381
PB95-150041 Not available NTIS
National Inst. of Standards and Technology (BFRL), Gaithersburg, MD. Fire Science Div.
Airborne Smoke Sampling Package for Field Measurements of Fires.
Final rept.
J. R. Lawson, G. W. Mulholland, and H. Koseki. 1994, 18p.
Pub. in Fire Technology 30, n1 p155-172 1994.

Keywords: *Airborne equipment, *Measuring instruments, *Combustion products, *Plumes, Crude oil, Petroleum products, Polycyclic aromatic hydrocarbons, Particulates, Sampling, Field tests, Reprints, *Smoke yield, Pool fires.

A unique airborne smoke sample package (ASSP) for determining the smoke yield of large fires has been developed. The ASSP, which weighs less than 4 kg, is light enough to be flown suspended below a tethered helium-filled balloon or attached to a small radio-controlled aircraft. Measurements are made by flying the sampling equipment into a fire's smoke plume. Additional smoke plume measurements that can be made with the ASSP include particle size distribution using a cascade impactor, smoke agglomerate structure using transmission electron microscope (TEM) grids, and polycyclic aromatic hydrocarbons (PAHs) analysis using various sorbent tubes. The application of the ASSP in measuring laboratory and large outdoors petroleum pool fires is discussed.

01,382
PB95-150215 Not available NTIS
National Inst. of Standards and Technology (BFRL), Gaithersburg, MD. Fire Science Div.

Oxidation of Soot and Carbon Monoxide in Hydrocarbon Diffusion Flames.
Final rept.
R. Puri, R. J. Santoro, and K. C. Smyth. 1994, 20p.
Pub. in Combustion and Flame 97, p125-144 1994.

Keywords: *Diffusion flames, *Oxidation, *Soot, *Carbon monoxide, Hydrocarbons, Combustion products, Laser induced fluorescence, Hydroxyl radicals, Methane, Collision rates, Concentration(Composition), Reprints.

Quantitative OH(-) concentrations and primary soot particle sizes have been determined in the soot oxidation regions of axisymmetric diffusion flames burning methane, methane/butane, and methane/1-butene in air at atmospheric pressure. The total carbon flow rate was held constant in these flames while the maximum amount of soot varied by a factor of seven along the centerline. Laser-induced fluorescence measurements of OH(-) were placed on an absolute basis by calibration against earlier absorption results. The primary size measurements of the soot particles were made using thermophoretic sampling and transmission electron microscopy. OH(-) concentrations are greatly reduced in the presence of soot particles. Whereas large superequilibrium ratios are observed in the high-temperature reaction zones in the absence of soot, the OH(-) concentrations approach equilibrium values when the soot loading is high. The diminished OH(-) concentrations are found to arise from reactions with the soot particles and only to a minor degree from lower temperatures due to soot radiation losses. Analysis of the soot oxidation rates computed from the primary particle size profiles as a function of time along the flame centerlines shows that OH(-) is the dominant oxidizer of soot, with O2 making only a small contribution. Higher collision efficiencies of OH(-) reactions with soot particles are found for the flames containing larger soot concentrations at lower temperatures. A comparison of the soot and CO oxidation rates shows that although CO is inherently more reactive than soot, the soot successfully competes with CO for OH(-) and hence suppresses CO oxidation for large soot concentrations.

01,383
PB95-150264 Not available NTIS
National Inst. of Standards and Technology (BFRL), Gaithersburg, MD. Fire Safety Engineering Div.
Fire Service and Fire Sciences: A Winning Combination.
Final rept.
R. E. Sanders, and D. Madrzykowski. 1994, 6p.
Pub. in NFPA Jnl. 88, n2 p55-60 Mar/Apr 94.

Keywords: *Fire fighting, *Risk assessment, *Fire hazards, Fire tests, Fire safety, Fire departments, Fire suppression, Sprinklers, Fire damage, Computerized simulation, Public relations, Reprints, Louisville(Kentucky).

The NIST study provided the information that was needed to predict conditions firefighters would face on the fire floor, elevator lobby, and floor above, without placing firefighters at extraordinary risk, providing for a meaningful and safe training exercise for high rise fire fighting. Also by using the test data and HAZARD I to transfer fire science technology to the media, legislators, and the public in an understandable context, this exercise provided the catalyst that was needed to pass the sprinkler retrofit ordinance in Louisville, Kentucky.

01,384
PB95-151056 Not available NTIS
National Inst. of Standards and Technology (NML), Gaithersburg, MD. Chemical Kinetics Div.
Progress in the Development of a Chemical Kinetic Database for Combustion Chemistry.
Final rept.
W. Tsang, G. Mallard, and J. T. Herron. 1988, 5p.
Pub. in Scientific and Technical Data in a New Era, p167-171 1988.

Keywords: *Combustion chemistry, *Chemical reaction kinetics, *Thermodynamic properties, *Databases, Combustion products, Combustion kinetics, Thermochemistry, Hydrocarbons, Alkanes, Combustion properties, Free radicals, Data compilation, Information storage, Information systems, Reprints.

A data base of chemical kinetic information for use in the modeling of the combustion of organic fuels has been developed at the National Institute of Standards and Technology. The authors have now extended the data base to cover light alkanes with up to four carbon atoms and are now carrying out work involving C3 and C4 unsaturates. They have also carried out extensive compilations of chemical kinetic data pertinent to combustion. They begin with a brief description of the rationale for the effort and their approach to the problem. This will be followed by a summary of their most recent work. They will conclude with a discussion of their approach to solving a number of the special problems that have been encountered.

01,385
PB95-153748 Not available NTIS
National Inst. of Standards and Technology (BFRL), Gaithersburg, MD. Fire Science Div.
Turbulent Spray Burner for Assessing Halon Alternative Fire Suppressants.
Final rept.
W. Grosshandler, D. Lowe, W. Rinkinen, and C. Presser. 1993, 8p.
Sponsored by Department of the Air Force, Wright-Patterson AFB, OH.
Pub. in Proceedings of American Society of Mechanical Engineers Winter Annual Meeting, New Orleans, LA., November 28-December 3, 1993, p1-8.

Keywords: *Sprays, *Atomization, *Fire suppression, *Aircraft fires, Flame propagation, Turbulent flow, Liquid fuels, Aircraft fuels, Combustion kinetics, Combustion properties, Thermodynamic properties, Halon alternatives, Nozzles, Fire research, Reprints.

A research program to characterize candidate compounds for replacing halon 1301 for in-flight aircraft fire protection is described in the paper. The thermodynamical, fluid mechanical, and flame extinction properties are examined, and a number of fuels and flame arrangements are investigated in an attempt to develop a general test protocol which will reliably predict the relative fire suppression efficiency of new agents being considered for a variety of applications. A coaxial turbulent spray burner was built to evaluate the relative effectiveness of agents for suppressing high intensity fuel fires such as one might encounter in a jet engine nacelle. A key element of the facility is the agent delivery system, which is designed to inject the desired amount of material into the air upstream of the fuel nozzle. The influence of air velocity, fuel flow, and injection period on the amount of a N(sub 2) required to extinguish the turbulent spray flame is discussed, and the effectiveness of twelve gaseous agents is compared.

01,386
PB95-161790 Not available NTIS
National Inst. of Standards and Technology (BFRL), Gaithersburg, MD. Fire Science Div.
Reactivity of Product Gases Generated in Idealized Enclosure Fire Environments.
Final rept.
W. M. Pitts. 1992, 10p.
Pub. in Proceedings of International Symposium on Combustion (24th), Sydney, Australia, July 5-10, 1992, p1737-1746.

Keywords: *Combustion products, *Reactivity, High temperature gases, Combustion chemistry, Carbon monoxide, Chemical reactions, Flue gases, Reaction products, Reprints, *Combustion gases, *Enclosure fires.

Previous experiments have demonstrated that the mole fractions of major product gases trapped in a hood located above a fire can be correlated in terms of the global equivalence ratio. Full-kinetic calculations are employed to characterize the reactivity and reaction behavior for the product gases observed in a hood experiment burning natural gas as fuel. A range of temperatures (700-1300 K) typical of enclosure fires is considered. Mixing is assumed to be infinitely fast (perfectly-stirred reactor) or infinitely slow (plug-flow reactor). Both isothermal and adiabatic cases are treated. Calculations are reported for a range of residence times (0-20 s) and global equivalence ratios (0.5-2.83). The dominant variable for reaction behavior is found to be temperature. Effects due to mixing and heat transfer assumptions are less important. The results indicate that the hood product gases are reactive for temperatures greater than 800 K. For rich mixtures, reaction generates primarily carbon monoxide as opposed to carbon dioxide. At higher temperatures the formation of hydrogen is favored over water while water is favored in the 800-1000 K range. In the lower temperature range HO2 is the dominant free radical. Uncertainties in rates for reactions involving this species introduce considerable uncertainty into the calculated behaviors. At high temperatures (1100-1300 K) the important free radicals are H atom and OH. The findings suggest that the results of the hood experiments cannot be used directly for the modeling of species production in enclosure fires.

01,387
PB95-162160 Not available NTIS
National Inst. of Standards and Technology (BFRL), Gaithersburg, MD. Fire Science Div.
Laser-Induced Fluorescence Measurements of OH. Concentrations in the Oxidation Region of Laminar, Hydrocarbon Diffusion Flames.
Final rept.
R. Puri, M. Moser, R. J. Santoro, and K. C. Smyth. 1992, 8p.
Pub. in Proceedings of International Symposium on Combustion (24th), Sydney, Australia, July 1992, p1015-1022.

Keywords: *Diffusion flames, *Concentration(Composition), *Laser induced fluorescence, *Soot, *Oxidation, Combustion, Laminar flow, Hydroxyl radicals, Ethene, Methane, Flow rate, Combustion products, Reprints.

Quantitative OH(-) concentrations have been measured in four coannular diffusion flames, burning methane at a single fuel flow rate and ethene at fuel flow rates which produce non-smoking, incipient smoking conditions. Laser-induced fluorescence has been used to make point profile, line image, and two-dimensional image measurements. These data have been placed on an absolute basis by reference to earlier absorption results. Particular emphasis has been placed on the investigation of the soot oxidation region in these laminar flames, since current soot models must utilize either assumed or estimated OH(-) concentrations. As the soot concentration increases, both the OH(-) concentration and the flame temperature are found to decrease. Estimates of the superequilibrium levels of OH(-) increase as the measured concentrations decrease, which makes accurate a priori prediction of OH(-) concentrations problematic in diffusion flames containing significant soot concentrations.

01,388
PB95-163457 Not available NTIS
National Inst. of Standards and Technology (NML), Gaithersburg, MD. Chemical Kinetics Div.
Incinerability of Perchloroethylene and Chlorobenzene.
Final rept.
W. Tsang, and D. Burgess. 1992, 17p.
Pub. in Combustion Science and Technology 82, n1-6 p31-47 1992.

Keywords: *Chlorobenzenes, *Tetrachloroethylene, *Incinerators, *Computerized simulation, Combustion kinetics, Hydroxyl radicals, Methane, Data bases, Reprints, *Perchloroethylene.

The paper reports on the results of computer simulations of the destruction of trace quantities of perchloroethylene and chlorobenzene in organic combustion systems. These results are derived from a data base dealing with methane combustion kinetics, recent measurements on hydrogen atom attack on the chlorinated compounds, and estimates based on literature values of the rate constants for a variety of destruction processes. The roles of OH-radicals and H-atoms as the key agents for destruction are demonstrated. At higher temperatures, unimolecular decompositions begin to become important. The juxtaposition of the various processes makes difficult the construction of a simple algorithm that will readily define the relative ease of destruction of any two compounds. Additional complications arise from the dependence on fuel composition and at higher hazardous waste concentrations. The advantages of using computer simulations in conjunction with laboratory and field results and in deriving a better understanding of incinerator behavior are discussed.

01,389
PB95-176020 Not available NTIS
National Inst. of Standards and Technology (CSTL), Gaithersburg, MD. Process Measurements Div.
Effect of Dodecanol Content on the Combustion of Methanol Spray Flames.
Final rept.
C. Presser, A. K. Gupta, C. T. Avedisian, and H. G. Semerjian. 1994, 16p.
Sponsored by Department of Energy, Washington, DC.
Pub. in Atomization and Sprays 4, p207-222 1994.

Keywords: *Methyl alcohol, *Combustion, Droplets, Sprays, Flames, Binary mixtures, Reprints, *Dodecanol, *Dodecanoic acid, Lauric acid.

The structure of a swirl-stabilized spray flame, fueled by a 75/25 mixture (by volume) of methanol and dodecanol has been examined. Spatially resolved information on droplet size and velocity distributions was obtained under burning conditions using a phase Doppler interferometry system. The effect of system gain (i.e., voltage setting of the photomultiplier tube detectors and laser power) on interpretation of the results was also assessed. The relatively large volatility difference between methanol and dodecanol provided an opportunity to examine the occurrence of microexplosions within spray flames. Evidence of microexploded droplets was revealed by a sudden decrease in droplet size and velocity, and an increase in number density at different spatial positions within the flame. On this basis, results were obtained that indicated the occurrence of microexplosions in the 75/25 mixture flame, but at a reduced extent as compared to prior results reported for methanol flames containing a larger fraction of dodecanol.

01,390
PB95-180576 Not available NTIS
National Inst. of Standards and Technology (BFRL), Gaithersburg, MD. Fire Science Div.
Acid Gas Production in Inhibited Diffusion Flames.
Final rept.
G. Linteris, M. D. King, A. Liu, C. Womeldorf, and Y. E. Hsin. 1994, 15p.
Sponsored by Department of the Air Force, Wright-Patterson AFB, OH.
Pub. in Proceedings of Halon Options Technical Working Conference, Albuquerque, NM., May 3-5, 1994, p177-191.

Keywords: *Diffusion flames, *Combustion products, *Fire extinguishing agents. Fire suppression, Inhibitors, Combustion, Transport properties, Fluorinated hydrocarbons, Acids, Concentration(Composition), Production rate, Hydrogen fluoride, Hydrogen chloride, Reprints, *Acid gas production.

The proposed replacements to halon 1301, mainly fluorinated and chlorinated hydrocarbons, are expected to be required in significantly higher concentrations than CF3Br to extinguish fires. At these higher concentrations the by-products of the inhibited flames may include correspondingly higher portions of corrosive gases, including HF and HCl. To examine the chemical and transport-releated mechanisms important in producing these acid gases, a series of inhibited flame tests have been performed with several types of laboratory-scale burners, varying agent type and concentration, and fuel type. Production rates were measured for co-flow laminar and turbulent diffusion flames. Systematic selection of the agent concentrations, burner type, and air flow rates allowed an assessment of the relative importance of agent transport and chemical kinetics on the acid gas production rates. These experimental results were then compared to a model which estimates the maximum HF and HCl production rates based on stoichiometric reaction to the most stable products. The results demonstrate the relative significance of F, Cl, and H in the inhibitor and fuel, as well as the effect of different burner configurations.

01,391
PB95-180584 Not available NTIS
National Inst. of Standards and Technology (BFRL), Gaithersburg, MD. Fire Science Div.
Burning Rate of Premixed Methane-Air Flames Inhibited by Fluorinated Hydrocarbons.
Final rept.
G. T. Linteris, and L. Truett. 1994, 12p.
See also PB95-180592. Sponsored by Department of the Air Force, Wright-Patterson AFB, OH.
Pub. in Proceedings of Halon Options Technical Working Conference, Albuquerque, NM., May 3-5, 1994, 12p.

Keywords: *Burning rate, *Diffusion flames, *Fire extinguishing agents, *Fluorinated hydrocarbons, Fire suppression, Fire protection, Combustion, Oxidation, Flame propagation, Inhibitors, Concentration(Composition), Reprints.

This paper presents the first measurements of the burning rate of premixed flames inhibited by three fluorinated hydrocarbons that have oxidation chemistry which is similar to agents which may be used as replacements for CF3Br. The burning rate of premixed methane-air flames stabilized on a Mache-Hebra nozzle burner was determined using the total area method from schlieren images of the flame. The inhibitors were tested over a range of concentrations and fuel-air equivalence ratios. The measured burning rate reductions are compared with those predicted by numerical solution of the species and energy conservation equations employing a detailed chemical kinetic mechanism recently developed at the National Institute of Standards and Technology (NIST). This paper presents initial efforts at testing and validation of the mechanism using burning rate data. The mode of inhibition of these chemicals is inferred through interpretation of the numerical results.

01,392
PB95-180592 Not available NTIS
National Inst. of Standards and Technology (BFRL), Gaithersburg, MD. Fire Science Div.
Experimental and Numerical Burning Rates of Premixed Methane-Air Inhibited by Fluoromethanes.
Final rept.
G. T. Linteris, and L. Truett. 1994, 4p.
See also PB95-180584. Sponsored by Department of the Air Force, Wright-Patterson AFB, OH.
Pub. in Proceedings of Combustion Institute/Eastern State Section Meeting, Clearwater Beach, FL., December 5-7, 1994, 4p.

Keywords: *Burning rate, *Fire extinguishing agents, *Diffusion flames, Fire suppression, Flame propagation, Combustion, Methane, Fire protection, Inhibitors, Mass transfer, Heat transfer, Concentration(Composition), Reprints, *Fluoromethanes.

The agents which are currently being considered as a replacements for fire suppressant agent CF3Br are mostly fluorinated hydrocarbons and perfluorinated alkanes. This abstract describes measurements of the reduction in burning rate of premixed methane-air flames by the single carbon inhibitors CF4, CF3H, and CF2H2. Early studies of the inhibitory effects of halogenated hydrocarbons on flames were conducted in premixed systems. The premixed laminar burning rate is a fundamental parameter describing the overall reaction rate, heat release, and heat and mass transport in a flame. In addition, the reduction in the premixed flame burning rate is useful for understanding the mechanism of chemical inhibition of fires since diffusion flames often have a stabilization region which is premixed, and good correlation has been found between the reduction in burning rate and the concentration of inhibitors found to extinguish diffusion flames. The present burning rate measurements allow an early assessment of the performance of the National Institute of Standards and Technology fluorinated species chemical kinetic mechanism in premixed flames and are considered to be an initial step in the validation and refinement of the mechanism.

01,393
PB95-203246 Not available NTIS
National Inst. of Standards and Technology (BFRL), Gaithersburg, MD. Fire Science Div.
Quantitative Measurements of Enhanced Soot Production in a Flickering Methane/Air Diffusion Flame.
Final rept.
C. R. Shaddix, J. E. Harrington, and K. C. Smyth. 1994, 10p.
Pub. in Combustion and Flame 99, p723-732 1994.

Keywords: *Diffusion flames, *Soot, Flow fields, Oxidation, Methane, Flicker, Air, Reprints, Laser induced incandescence, Time varying systems.

Integrated models of soot production and oxidation are based upon experimental results obtained in steady, laminar flames. For successful application of these descriptions to turbulent combustion, it is instructive to test predictions of soot concentrations against experimental measurements obtained in time-varying flowfields. This paper reports quantitative measurements of the local soot volume fraction in a co-flowing, flickering CH4/air diffusion flame burning at atmospheric pressure. Acoustic forcing of the fuel flow rate is used to phase lock the periodic flame flicker close to the natural flicker frequency. Our measurements show that soot production is four times greater for a forcing condition in which flame tip clipping occurs, compared with a steady flame burning with the same mean fuel flow velocity. The soot field in the flickering flame has been characterized using tomographic reconstruction of extinction data obtained at 632.8 nm, laser-induced incandescence (LII) images calibrated against steady CH4/air extinction results, and vertically polarized scattering data.

01,394
PB95-231700 PC A10/MF A03
National Inst. of Standards and Technology (BFRL), Gaithersburg, MD. Fire Science Div.
Carbon Monoxide Production in Compartment Fires: Reduced-Scale Enclosure Test Facility.
N. P. Bryner, E. L. Johnsson, and W. M. Pitts. Nov 94, 218p, NISTIR-5568.
See also PB93-146702.

Keywords: *Fire research, *Carbon monoxide, *Fire tests, *Combustion products, Solid fuels, Reaction kinetics, Flashover, Fire chemistry, Prototypes, Oxidation, *Compartment fires, Fuel/air ratio, Scale models.

Carbon monoxide production during room fires has been investigated using natural-gas fires within a reduced-scale enclosure (RSE), an 0.98 m x 0.98 m x 1.46 m(w x h x d) room with a single door opening centered in the front wall. This series of 125 fires with heat release rates (HRR) from 7 to 650 kW and global equivalence ratio phi sub g from 0.2 to 4.2, respectively, has demonstrated that the upper layer is nonuniform in temperature and gas species, and that upper-layer oxygen is depleted for underventilated fires with high-temperature upper layers. For fires having HRR exceeding 400 kW (phi sub g > 2), carbon monoxide concentrations of up to 3.5 percent have been observed in the front portion of the upper layer. Carbon monoxide concentrations in the rear were consistently lower being on the order of 2.0 percent for phi sub g > 2.

01,395
PB95-231817 PC A04/MF A01
National Inst. of Standards and Technology (BFRL), Gaithersburg, MD.
Suppression of High Speed Turbulent Flames in a Detonation/Deflagration Tube.
G. Gmurczyk, and W. L. Grosshandler. Jan 95, 62p, NISTIR-5642.
Sponsored by Wright Lab., Wright-Patterson AFB, OH. and Naval Air Systems Command, Washington, DC.

Keywords: *Fire extinguishing agents, *Aviation safety, Aircraft fires, Fire fighting, Fire tests, Performance evaluation, Chemical properties, Detonation, Military air facilities, Halon 1301.

Live-fire, full-scale testing has been conducted at Wright-Patterson Air Force Base to identify an agent to replace CF3Br (halon 1301) for suppressing fires in military aircraft dry bays. The three chemicals being considered (C2HF5, HFC-125; C3F8, FC-218; and CF3I, halon 13001) had been evaluated in a previous laboratory study, in which unique properties of each chemical were identified in small-scale experiments. The FC-218 provided the most consistent performance in this new series of experiments which examined lean, stoichiometric and rich initial conditions. Large pressure build ups were not observed during suppression of the propane/air mixtures under the current set of conditions. None of the agents could be ruled out for dry bay applications based upon the results of this study.

01,396
PB95-242327 PC A05/MF A02
Michigan Univ., Ann Arbor. Dept. of Aerospace Engineering.
Mixing and Radiation Properties of Buoyant Turbulent Diffusion Flames.
Z. Dai, L. K. Tseng, U. O. Koeylue, and G. M. Faeth. Jun 95, 100p, NIST/GCR-95/671.
Contract NIST-60NANB1D1175
Also pub. as Michigan Univ., Ann Arbor. Gas Dynamics Labs. rept. no. GDL/GMF-94-01. See also PB94-165974. Sponsored by National Inst. of Standards and Technology (BFRL), Gaithersburg, MD.

Keywords: *Turbulence, *Diffusion flames, Models, Mixing, Plumes, Soot, Optical properties, Velocity, Combustion products, Fuels.

An investigation of the mixing and radiation properties of buoyant turbulent diffusion flames is described. The study was divided into two phases: (1) the structure and mixing properties of turbulent plumes, which must be understood in order to resolve effects of turbulence/radiation interactions and to benchmark models of buoyant turbulent flows; and (2) the fractal and structure properties of soot aggregates, which must be understood in order to develop nonintrusive methods for measuring soot properties of soot in flame environments. Measurements of the turbulent mixing prop-

erties of buoyant turbulent plumes involved laser induced fluorescence (LIF), laser velocimetry (LV) and combined LIF/LV to find mixture fraction and velocity statistics in buoyant turbulent plumes.

01,397
PB96-102132 Not available NTIS
National Inst. of Standards and Technology (BFRL), Gaithersburg, MD. Fire Science Div.
Simultaneous Optical Measurement of Soot Volume Fraction, Temperature, and CO2 in Heptane Pool Fire.
Final rept.
M. Choi, A. Hamins, H. Rushmeier, and T. Kashiwagi. 1994, 10p.
Pub. in Proceedings of the International Symposium on Combustion (25th), Irvine, CA., July 31-August 5, 1994, p1471-1480.

Keywords: *Optical properties, *Soot, *Fires, *Heptane, Carbon dioxide, Concentration(Composition), Heat transfer, Temperature, Surfaces, Heat flux, Reprints, Soot volume fraction, Pool fires.

Detailed measurements of the temperature, soot volume fraction and CO2 concentrations have been performed for a 10 cm diameter heptane fire. In addition, the concentrations of H2O and CO were inferred from generalized state relationships. The heat feedback to the surface was calculated by using a reverse Monte Carlo method in conjunction with RADCAL. The use of average and instantaneous values of the temperature and species concentrations results in a 21% difference in the heat flux to the surface. Simultaneous optical measurements using two probes were used to investigate the importance of temperal correlations on the heat transfer calculations. Measurements made throughout the fire indicate that non-simultaneous data sets can be used to accurately predict the heat transfer to the surface.

01,398
PB96-102173 Not available NTIS
National Inst. of Standards and Technology (BFRL), Gaithersburg, MD. Fire Safety Engineering Div.
Generation Rate and Distribution of Products of Combustion in Two-Layer Fire Environments: A Model and Applications.
Final rept.
L. Y. Cooper. 1994, 26p.
See also PB91-107151.
Pub. in Fire Safety Jnl., v23 p245-270 1994.

Keywords: *Two phase flow, *Flame propagation, *Thermodynamics, Combustion products, Fires, Compartment analysis, Time dependence, Stoichiometry, Methane, Algorithms, Mathematical models, Reprints, *Fire models, GGERM(Generalized Global Equivalence Ratio Model).

A model is developed for predicting the generation rates of oxygen, fuel, and other products of combustion in rooms containing fires and time-dependent fire environments. The model is called the Generalized Global Equivalence Ratio Model (GGERM). It extends the steady state global equivalence ratio model established previously from data of several steady state experimental studies. After describing the GGERM, a concise algorithm is outlined for implementing it in two-layer zone-type compartment fire models. With the algorithm in place, such models could be used to simulate the distribution of combustion products in single or multi-room fire environments under conditions of arbitrary ventilation.

01,399
PB96-102306 Not available NTIS
National Inst. of Standards and Technology (BFRL), Gaithersburg, MD. Fire Safety Engineering Div.
Computing Radiative Heat Transfer Occurring in a Zone Fire Model.
Final rept.
G. P. Forney. 1994, 16p.
See also PB92-156777.
Pub. in Fire Science and Technology, v14 n1-2 p31-47 1994.

Keywords: *Radiative heat transfer, *Compartment analysis, *Algorithms, Fires, Smoke, Gases, Walls, Heat transmission, Conduction, Convection, Numerical analysis, Computerized simulation, Mathematical models, Reprints, *Fire models, Zone models.

This paper presents algorithms for efficiency computing the radiative heat exchange between four wall surfaces, several fire, and two interior gases. A two-wall and a ten-wall radiation model is also discussed. The structure of this radiation model is exploited to show that only a few configuration factors need to be calculated directly (two rather than 16 for the four-wall model and eight rather than 100 for the ten-wall model) and matrices needed to solve for the net radiative flux striking each surface are shown, after the appropriate transformation is taken, to be diagonally dominant. Iterative methods may then be used to solve the linear equations more efficiently than direct methods such as Gussian elimination.

01,400
PB96-102314 Not available NTIS
National Inst. of Standards and Technology (BFRL), Gaithersburg, MD. Fire Safety Engineering Div.
Analyzing and Exploiting Numerical Characteristics of Zone Fire Models.
Final rept.
G. P. Forney, and W. F. Moss. 1994, 12p.
See also PB92-172790.
Pub. in Fire Science and Technology, v14 n1-2 p49-60 1994.

Keywords: *Algorithms, *Compartment analysis, Mathematical models, Computerized simulation, Fires, Conduction, Pressure dependence, Differential equations, Numerical analysis, Reprints, *Fire models.

In order to design robust and stable zone fire modeling algorithms, the numerical properties of the fire modeling differential equations must be understood. This paper examines some of these properties. Many sets of differential equations for zone fire modeling can be derived using the conservation of mass and energy. A comparison between various possible formulations is made in terms of numerical properties. One property that many formulations possess is the presence of multiple time scales. Pressures equilibrate much faster than other quantities, such as density and temperature. Numerically, this property is known as stiffness. Stiffness, in the context of fire modeling, and numerical methods for handling it are discussed.

01,401
PB96-102454 Not available NTIS
National Inst. of Standards and Technology (BFRL), Gaithersburg, MD. Fire Science Div.
Assessing Halon Alternatives for Aircraft Engine Nacelle Fire Suppression.
Final rept.
W. Grosshandler, C. Presser, D. Lowe, and W. Rinkinen. 1995, 6p.
Pub. in Jnl. of Heat Transfer, v117 p489-494 May 95.

Keywords: *Fire extinguishing agents, *Aircraft fires, *Environmental chemical substitutes, Nacelles, Fire suppression, Thermodynamic properties, Effectiveness, Performance evaluation, Fire fighting, Alternatives, Fluorocarbons, Halohydrocarbons, Fuel sprays, Jet engine fuels, Reprints, Hydrofluorocarbons, Hydrochlorofluorocarbons.

A coaxial turbulent spray burner was built to evaluate the relative effectiveness of different chemicals for suppressing fires in a jet engine nacelle. An agent delivery system was designed to inject the desired amount of material into the air upstream of a fuel nozzle and to control the agent injection rate through variation of the storage pressure and the duration of time that a solenoid valve remains open. The influence of air velocity, fuel flow, and injection period on the amount of nitrogen required to extinguish a jet fuel spray flame is discussed. The effectiveness of eleven different fluorocarbons, hydrofluorocarbons, and hydrochlorofluorocarbons is compared to that of halon 1301.

01,402
PB96-109574 PC A03/MF A01
National Inst. of Standards and Technology (BFRL), Gaithersburg, MD. Fire Science Div.
Effect of Suppressants on Metal Fires.
T. J. Ohlemiller, and J. R. Shields. Aug 95, 28p, NISTIR-5710.

Keywords: *Fire suppressants, *Titanium, *Magnesium, *Combustion kinetics, Fire extinguishing agents, Halons, Environmental chemical substitutes, Alternatives, Burning rate, Heat transmission, Reaction kinetics, Vapors, Air flow, Fire tests.

The present study is limited to examining the effect of the vapors of various halogen-containing suppressants on the burning of pure magnesium and titanium rods in a slow flow of oxygen-containing gas. The test configuration was instrumented to allow quantitation of the effect of the vapors on the rate of burning. The agents examined in the presence of burning magnesium included halon 1301 (the reference case), HFC-125, HFC-227ea, FC-218 and CF3I. For titanium, time limitations narrowed the study to halon 1301, HFC-227ea(sup 2) and HFC-125.

01,403
PB96-114764 PC A08/MF A02
Kentucky Univ., Lexington. Dept. of Mechanical Engineering.
Turbulent Flame Spread on Vertical Corner Walls.
Doctoral thesis.
C. Qian. Apr 95, 163p, NIST/GCR-95/669.
Grant NIST-60NANB3D1443
Sponsored by National Inst. of Standards and Technology (BFRL), Gaithersburg, MD.

Keywords: *Walls, *Burning rate, Flame propagation, Turbulent flow, Heat flux, Pyrolysis, Thermodynamics, Combustion kinetics, Heat trasnfer, Infared imagery, Fire tests, Fire research, Theses, *Turbulent flames, *Flame spreading.

In this study, attention is given to the corner fire spread mechanism and the flame spread behavior. Infrared (IR) radiometry and image analysis techniques have been developed in this study to measure flame spread rate on large areas with high resolution and frequency. In addition to the flame spread measurement, the fire-induced flow was studied by flow visualization, and the total incident heat flux to the wall surface from the flame was measured by Gardon-type heat flux meters. Based on these experimental studies, a thermal model for corner fire spread has been successfully developed.

01,404
PB96-119342 Not available NTIS
National Inst. of Standards and Technology (BFRL), Gaithersburg, MD. Fire Safety Engineering Div.
Flame Heights and Heat Release Rates of 1991 Kuwait Oil Field Fires.
Final rept.
D. D. Evans, D. Madrzykowski, and G. A. Haynes. 1994, 11p.
Pub. in Fire Safety Science Proceedings of the International Symposium (4th), Ottawa, Ontario, Canada, June 13-17, 1994, p1279-1289.

Keywords: *Oil wells, *Flame propagation, *Radiative heat transfer, *Fires, Kuwait, Burning rate, Heat flux, Heat of combustion, Diffusion flames, Heat release rate, Dissipation, Smoke, Turbulent diffusion, Jet flow, Reprints, Flame height.

A series of measurements were made in the Al Mawqa/Al Ahmadi oil field region of Kuwait to explore the feasibility of assessing the heat release rate of individual well fires through flame height and thermal radiation measurements. The heat release rate of the crude oil well fires was correlated with the flame height. The 12 Kuwait oil field fires measured ranged in calculated heat relaese rate from 90 MW to 2 GW which correspond to flow rates of 0.003 cu m/s (1500 bbls/day) to 0.059cu m/s (30000 bbls/day) which is only 20 percent greater than published National Oceanic and Atmospheric Administration (NOAA) estimates based on information from the Kuwait Oil Company.

01,405
PB96-122676 Not available NTIS
National Inst. of Standards and Technology (BFRL), Gaithersburg, MD. Fire Science Div.
Experimental Study of the Stabilization Region of Lifted Turbulent-Jet Diffusion Flames.
Final rept.
C. D. Richards, and W. M. Pitts. 1991, 4p.
See also PB92-117191.
Pub. in Combustion Institute/Eastern States Section Fall Technical Meeting (24th), Ithaca, NY., October 14-16, 1991, p1-4.

Keywords: *Diffusion flames, *Turbulent flow, *Lift, *Jet flow, Fuel combustion, Flame stability, Rayleigh scattering, Image analysis, Concentrations(Composition), Spatial resolution, Light scattering, Reprints, Fuel jets, Temporal resolution.

The stabilization mechanism of a lifted turbulent-jet diffusion flame remains an active area of research despite numerous studies. The early work of Vanquickenbourne and Van Tiggelen provided experimental documentation of lift-off heights for a variety of

fuels. Although this time-averaged view provides a means of predicting lift-off height, more physical insight is required to develop a model of stabilization which includes current knowledge on the structure of turbulent jets and mixing. The present study is in many ways an update of the Vanquickenborne and Van Tiggelen experiments. The anchoring position of a lifted flame is obtained through image analysis of video images and concentration profiles are independently acquired in the corresponding isothermal fuel jets with Rayleigh light scattering (RLS). These diagnostics provide both temporal and spatial resolution.

01,406
PB96-122866 Not available NTIS
National Inst. of Standards and Technology (BFRL), Gaithersburg, MD. Fire Safety Engineering Div.
Field Modeling: Simulating the Effect of Sloped Beamed Ceilings on Detector and Sprinkler Response.
Final rept.
W. D. Davis, G. P. Forney, and R. W. Bukowski. 1994, 42p.
Pub. in National Fire Protection Research Foundation, Batterymarch Park, Quincy, MA., 42p.

Keywords: *Fire detectors, *Sprinkler systems, *Ceilings, *Mathematical models, Smoke detectors, Fire suppression systems, Fire detection systems, Beams, Ventilation, Fire safety, Reprints.

The report describes the results of the second year of the project. During the second year, numerical simulations of smoke movement in response to sloped, beam ceilings were studied. Slopes of 10, 25 and 50 degrees were studied with beams running along or across the slope. It was found that channeling of smoke flow was more prevalent as ceiling slope increased for parallel beam cases. For beams perpendicular to the slope, increasing the ceiling slope decreased the effectiveness of the beams in preventing smoke flow up the ceiling. Based on the predicted smoke movement, recommendations on sensor selection and placement are made for the slope beamed ceilings.

01,407
PB96-122890 Not available NTIS
National Inst. of Standards and Technology (BFRL), Gaithersburg, MD. Fire Science Div.
Smoke Emission from Burning Crude Oil.
Final rept.
D. Evans, W. Walton, H. Baum, H. Koseki, A. Ghoniem, G. Mulholland, and J. Lawson. 1991, 29p.
Pub. in Proceedings of the Arctic and Marine Oil Spill Conference (14th), Vancouver, B.C., June 12-14, 1991, p421-449.

Keywords: *Oil spills, *In situ combustion, *Burning rate, *Combustion kinetics, Crude oil, Plumes, Smoke, Soot, Combustion products, Combustion properties, Fir tests, Oil-water interfaces, Reprints.

Research has shown that burning can be an effective means to remove oil from the surface of the water after a spill. The paper describes instrument packages developed to determine the amount of various combustion products emitted from large (15 m x 15 m) crude oil pool fires. The increase in burning rate and smoke production with increasing fire size is discussed. Progress is reported on new calculation methods for smoke dispersion and downwind deposition of particulate. Results of example calculations are presented.

01,408
PB96-122965 Not available NTIS
National Inst. of Standards and Technology (BFRL), Gaithersburg, MD. Fire Science Div.
Development of Hazard Assessment and Suppression Technology for Oil and Gas Well Blowout and Diverter Fires.
Final rept.
J. P. Gore, and D. D. Evans. 1991, 6p.
Pub. in OCS Study MMS 91-0057 (ALSO) Biennial Report of the Technology Assessment and Research Program (7th), Reston, VA., p27-32 1991.

Keywords: *Blowouts, *Oil wells, *Natural gas wells, *Fire suppression, Fires, Flame propagation, Radiative heat transfer, Jet flow, Burning rate, Diffusion flames, Fire fighting, Fire extinguishing agents, Reprints.

The report summarizes progress during the past two years on understanding the radiation production from both vertical and horizontal jet-flames. These two cases represent two forms of blowout fire events on offshore platforms. The laminar flamelet representation of a turbulent flame is used successfully to predict radiation from vertical methane jet-flames in the range of 1 to 7 MW. Peak temperature in the vertical methane jet-flame with water addition were over predicted by about 20% using the model. The trajectory of horizontal jet-flames, which turn under the influence of buoyancy are predicted using a parabolic finite difference scheme developed in this research program. References are given to other technical reports and publications for details of the work summarized in this paper.

01,409
PB96-123120 Not available NTIS
National Inst. of Standards and Technology (BFRL), Gaithersburg, MD. Fire Science Div.
Laser-Induced Fluorescence Measurements of OH in Laminar Diffusion Flames in the Presence of Soot Particles.
Final rept.
R. Puri, M. Moser, R. J. Santoro, and K. C. Smyth. 1991, 4p.
Pub. in Eastern States Section the Combustion Institute (24th) Fall Technical Meeting, Ithaca, NY, October 14-16, 1991, p34-1-34-4.

Keywords: *Diffusion flames, *Soot, Combustion products, Laminar flow, Reprints, *Hydroxyl radicals.

Combustion in a simple view is the process of oxidation to form stable products, usually CO2 and H2O, accompanied by the release of energy. Although we often view this as a simple case of oxygen reacting with a fuel to exothermically form product species, it is well known that radicals such as OH, H and O have a significant role in the reaction chemistry. It is the specifics of these reactions which determine the rates at which they proceed and the routes by which minor products such as NO, soot and CO result. The radical species participate in numerous reactions, and there exists a competition among several chemical steps for each reactive species. Important to determining the dominant set of reactions are the local conditions involving temperature, pressure and species concentrations. As these conditions vary, the dominant reactive pathways will also change. It is this dynamic situation which challenges researchers as they attempt to understand the variety of processes which characterize combustion. In the present study, measurements of hydroxyl radicals obtained in laminar diffusion flames containing soot particles are described.

01,410
PB96-123385 Not available NTIS
National Inst. of Standards and Technology (BFRL), Gaithersburg, MD. Fire Science Div.
Chemical Stability of Upper-Layer Fire Gases.
Final rept.
W. M. Pitts. 1991, 4p.
Pub. in Fall Technical Meeting of the Eastern Section (24th): Combustion Institute, Cornell University, Ithaca, NY., October 14-16, 1991, 4p.

Keywords: *Carvon monoxide, *Fire gases, Kinetics, Reaction models, Toxic products, Reprints.

The chemical stability of upper-layer fire gases generated during burning in an enclosure is investigated by the use of a full-kinetic model. Initial concentrations of flame gases are those observed in experiments where fire gases are trapped in a hood. Calculations are preformed as a fucntion of layer temperature (700-1300), global equivalence ratio (0.5-2.8), mixing model (perfectly stirred and plug-flow reactors), and heat loss conditions (adiabatic or isothermal). The calculations indicate the flame gases become reactive for temperatures above 800 K.

01,411
PB96-123625 Not available NTIS
National Inst. of Standards and Technology (BFRL), Gaithersburg, MD. Fire Science Div.
New Approach for Reducing the Toxicity of the Combustion Products from Flexible Polyurethane Foam.
Final rept.
B. C. Levin, M. Paabo, E. Braun, and R. H. Harris. 1991, 6p.
Pub. in Annual Conference on Flame Retardancy of Polymeric Materials, Applications, Industry Developments, Markets, Stamford, CT., May 14-16, 1991, p1-6.

Keywords: *Polyurethane foam, *Hydrogen cyanide, *Combustion chemistry, *Thermodynamic properties, Combustion products, Copper compounds, Flammability, Ignition, Burning rate, Toxicity, Inhalation, Fire hazards, Fire tests, Reprints.

Hydrogen cyanide (HCN) is one of the gases which is produced during the thermal decomposition of flexible polyurethane foams and which (in combination with carbon monoxide and other fire gases) contributes to the toxicity of the smoke. Flexible polyurethane foams treated with copper or various copper compounds produced significantly less HCN when thermally decomposed that the identical but untreated control foams. The decreased atmospheric concentrations of HCN resulted in the reduction of the acute inhalation toxicity (as measured by lethality in Fischer 344 rats) produced from exposure to this smoke. This reduction of HCN and toxicity occurred regardless of whether the copper or copper compound was added to the foam during its formulation (prior to the foaming process) or as a post-treatment (after formulation).

01,412
PB96-131479 PC A11/MF A03
National Inst. of Standards and Technology (BFRL), Gaithersburg, MD.
Solid Propellant Gas Generators: Proceedings of the 1995 Workshop. Held in Gaithersburg, Maryland on June 28-29, 1995.
J. C. Yang, and W. L. Grosshandler. Nov 95, 226p, NISTIR-5766.

Keywords: *Solid propellant combustion, *Gas generators, *Fire extinguishing agents, *Meetings, Fire suppression, Fire fighting, Halons, Aircraft fires, Aircraft safety, Solid propellants, Nacelles, Test methods, Certification, Effectiveness, Performance evaluation, Halon 1301, Fire protection systems.

The intent of the workshop was to bring together gas generator manufacturers, researchers, and potential users to discuss various critical issues related to the evaluation and performance of the gas generators as a fire fighting tool and the search for new propellants. The specific objectives of the workshop, which reflected the need for such an apparatus, were: Identification of certification procedure(s) for gas generators in fire suppression applications; determination of critical parameters for evaluating the fire suppression efficiency of various gas generators; development of a standard methodology to facilitate testing of gas generators; identification of possible applications other than protection of engine nacelles and dry bays; and identification of a new generation of propellants.

01,413
PB96-135322 Not available NTIS
National Inst. of Standards and Technology (BFRL), Gaithersburg, MD. Fire Science Div.
Application of Thermodynamic and Detailed Chemical Kinetic Modeling to Understanding Combustion Product Generation in Enclosure Fires.
Final rept.
W. M. Pitts. 1994, 33p.
Pub. in Fire Safety Jnl., v23 n3 p271-303 1994.

Keywords: *Combustion products, *Thermodynamics, *Rooms, *Fire tests, Combustion chemistry, Gases, Enclosures, Carbon monoxide, Chemical reaction kinetics, Chemical equilibrium, Models, Reprints.

Experiments in idealized two-layer fire environments have demonstrated that concentrations of carbon monoxide and other gaseous combustion products can be correlated in terms of the global equivalence ratio. In this paper, the results of detailed chemical kinetic modeling and equilibrium calculations are used to gain insight into the chemical stability of the gases observed within the upper layers of such fires. It is demonstrated that the production of upper-layers gases is kinetically controlled and that for rich conditions concentrations of the upper-layer gas components are far from those expected for thermo-dynamic equilibrium at the layer temperatures. Criteria are provided for determining whether or not the correlations can be employed to predict the generation of combustion products in enclosure fires.

01,414
PB96-146741 Not available NTIS
National Inst. of Standards and Technology (BFRL), Gaithersburg, MD. Fire Science Div.

Inhibition of Premixed Methane-Air Flames by Halon Alternatives.
Final rept.
G. T. Linteris, and L. Truett. 1995, 6p.
Pub. in Proceedings of the International Conference of Fire Research and Engineering, Orlando, FL., September 10-15, 1995, p153-158.

Keywords: *Fire extinguishing agents, *Alternatives, *Combustion kinetics, Inhibitors, Fire suppression, Fire fighting, Burning rate, Fluorinated hydrocarbons, Methane, Chemical reaction kinetics, Flame propagation, Energy transfer, Heat transfer, Mass transfer, Environmental chemical substitutes, Halons, Reprints.

This article describes the first measurements of the reduction in burning rate of premixed methane-air flames inhibited by the two-carbon fluorinated species C2F6, C2HF5, C2H2F4 and the three-carbon species C3F8 and C3HF7 all of which are being considered as replacements to CF3Br. The burning rate of premixed methane-air flames stabilized on a Mache-Hebra nozzle burner is determined using the total area method from a schlieren image of the flame. The inhibitors are tested over a range of concentration and fuel-air equivalence ratio. The measured burning rate reduction caused by addition of the inhibitor is compared (for the two-carbon species) with that predicted by numerical solution of the mass, species, and energy conservation equations employing a detailed chemical kinetic mechanism recently developed at the National Institute of Standards and Technology (NIST).

01,415
PB96-147046 Not available NTIS
National Inst. of Standards and Technology (BFRL), Gaithersburg, MD. Fire Safety Engineering Div.
Gravity-Current Transport in Building Fires.
Final rept.
H. R. Baum, K. W. Cassel, K. B. McGrattan, and R. G. Rehm. 1995, 6p.
Pub. in Proceedings of the International Conference on Fire Research and Engineering, Orlando, FL., September 10-15, 1995, p27-32 1995.

Keywords: *Fires, *Numerical simulation, Smoke, Gas flow, Convective flow, Dispersion, Heat transfer coefficients, Buildings, Buoyancy, Navier-Stokes equations, Reprints, *Gravity currents.

Gravity currents (GC) are also of interest in the movement of gases in buildings. A GC produced by a fire can transport smoke, toxic material and hot gases, and when the building has long corridors, the current often is one of the most important mechanisms for large-scale mass and energy transport. It is now possible to compute the structure of GCs in detail and to compare features of GCs with available experimental and analytical results. In the next section, the authors describe GCs by solving the Navier-Stokes equations in two dimensions. The authors make comparisons between results from salt-water, fresh-water experiments carried out by Zukoski and coworkers, and the results obtained from the authors' computational simulations.

01,416
PB96-147897 PC A04/MF A01
California Inst. of Tech., Pasadena. Dept. of Mechanical Engineering.
Review of Flows Driven By Natural Convection in Adiabatic Shafts.
E. E. Zukoski. Oct 95, 48p, NIST/GCR-95/679.
Grant NIST-60NANB6D1444
Sponsored by National Inst. of Standards and Technology (BFRL), Gaithersburg, MD.

Keywords: *Adiabatic conditions, *Natural convection, *Fire tests, *Turbulent flow, Shafts, Vertical orientation, Hot gases, Air flow, Convective heat transfer, Turbulent mixing, Buoyancy, Burning rate, Combustion, Flame propagation, Computational fluid dynamics, Gas dynamics, Mathematical models, Stack effect.

An experimental study of the motion of hot gas through vertical shafts and passages under the influence of buoyancy forces is being made with the support of the Building and Fire Research Laboratory of the Natioanl Institute of Science and Technology, the Department of Commerce. The aim of this work is to derive the information required for the preparation of models which can be used to describe these flows in computer-based models of fire spread through structures.

01,417
PB96-148200 Not available NTIS
National Inst. of Standards and Technology (BFRL), Gaithersburg, MD. Fire Science Div.
Examination of the Correlation between Cone Calorimeter Data and Full-Scale Furniture Mock-Up Fires.
Final rept.
T. J. Ohlemiller. 1995, 6p.
Sponsored by Society of Fire Protection Engineers, Boston, MA.
Pub. in Proceedings of the International Conference of Fire Research and Engineering, Orlando, FL., September 10-15, 1995, p217-222 1995.

Keywords: *Calorimeters, *Furniture, *Fires, Heat transfer, Barriers, Rates(Per time), Fire research, Fire tests, Reprints, *Cone calorimeters, California Technical Bulletin 133, Heat release rate.

As part of an on-going study of the factors which affect heat release rate performance of furniture in the California Technical Bulletin 133, the authors have focused most recently on the role played by interliners or barriers. A barrier in this context is a layer of very low flammability material placed between the fabric and the polyurethane foam to minimize the participation of the latter in a fire. In CB 133 that fire is initiated on the seating area of an upholstered furniture item by an 18 kW gas burner that sprays flames on the seat, seatback and inner arm surfaces. The response of the chair is required to be at most an 80 kW peak in heat release rate. The test applies to furniture in public occupancies; it has been adopted in four states and is under consideration in several others.

01,418
PB96-154794 PC A10/MF A03
Maryland Univ., College Park. Dept. of Fire Protection Engineering.
Predicting the Ignition Time and Burning Rate of Thermoplastics in the Cone Calorimeter.
Master's thesis.
D. Hopkins. Sep 95, 193p, NIST/GCR-95/677.
Grant NIST-60NANB2D1266
Sponsored by National Inst. of Standards and Technology (BFRL), Gaithersburg, MD.

Keywords: *Thermoplastic resins, *Ignition time, *Burning rate, *Flammability testing, Polyethylene, Polypropylene, Nylon 66, Fire tests, Ignition temperature, Flame propagation, Heat flux, Heat measurement, Calorimetry, Theses, Cone calorimeter, Mass loss.

Ignition and burning rate data are developed for Nylon 6/6, Polyethylene, and Polypropylene in a Cone Calorimeter heating assembly. The objective is to examine a testing protocol that leads to the prediction of ignition and burning rate for thermoplastics from Cone data. The flame heat flux is not measured, but is inferred from Cone data. The flame heat flux is not measured, but is inferred from Cone data. The constancy of the flame heat flux for thermoplastics in the Cone calorimeter is due to the geometry of the flame. The burning rate model is shown to yield good accuracy in comparison to measured transient values. Ignition and burning rate data are developed for Redwood and Red Oak in a Cone Calorimeter heating assembly. Measements of the flame plus external heat flux are presented. The data is intended to be used for future work to develop a testing protocol and burning rate model for charring materials.

01,419
PB96-160593 Not available NTIS
National Inst. of Standards and Technology (BFRL), Gaithersburg, MD. Fire Science Div.
New Generation of Fire Resistant Polymers. Part 1. Computer-Aided Molecular Design.
Final rept.
M. R. Nyden, and J. E. Brown. 1993, 7p.
Pub. in UJNR on Fire Research, Tsukuba, Japan, October 1992, p257-263.

Keywords: *Computer-aided design, *Fire resistant materials, *Molecular structure, Nonflammable materials, Flammability, Thermal degradation, Charring, Combustion products, Mathematical models, Polymers, Reprints.

Molecular dynamics modeling and experimental measurements are used to identify factors which reduce flammability by promoting the formation of heat resistant chars during the thermal degradation of polymers. Computer movies of the calculated trajectories reveal that cross-linked model polymers tend to undergo further cross-linking when burned. The presence of strong potential energy interactions with a surface or filler further facilities the formaton of high molecular weight, thermally stable chars.

01,420
PB96-161831 Not available NTIS
National Inst. of Standards and Technology (BFRL), Gaithersburg, MD. Fire Science Div.
Effect of CF3H and CF3Br on Laminar Diffusion Flames in Normal and Microgravity.
Final rept.
B. A. VanDerWege, M. T. Bush, S. Hochgreb, and G. T. Linteris. 1995, 6p.
See also N96-15609 and PB96-161849.
Pub. in International Microgravity Combustion Conference (3rd), Cleveland, OH., April 11-13, 1995, 6p.

Keywords: *Chemical inhibition, *Flame chemistry, Reprints, Flame models, Flame retardants, Diffusion flame.

Chemical inhibition of diffusion flames through addition of halogenated inhibitors is a problem of significant practical and scientific interested. Extension studies on diffusion flames in microgravity have shown that these flames have significantly different characteristics than those under normal gravity (1,2). However, the mechanisms through which inhibitors reach the reactions zone to suppress combustion in diffusion flames and the effectiveness of these compounds under reduced gravity have yet to be investigated. This study reports preliminary results of investigations on the behavior of laminar jet diffusion flames upon the addition of bromotrifluoromethane (CF3Br) and trifluoromethane (CF3H) to the surroundings under normal and microgravity conditions. The results show that the flame structure in microgravity is significantly different from that under normal gravity conditions, and more importantly, that conditions for flame stability are less stringent under microgravity.

01,421
PB96-161849 Not available NTIS
National Inst. of Standards and Technology (BFRL), Gaithersburg, MD. Fire Science Div.
Effect of CF3H and CF3Br on Laminar Diffusion Flames in Normal and Microgravity.
Final rept.
B. A. VanDerWege, M. T. Bush, S. Hochgreb, and G. T. Linteris. 1995, 4p.
See also PB96-161831.
Pub. in Eastern States Section Meeting/The Combustion Institute, Worcester, MA., October 16-18, 1995, p443-446.

Keywords: *Chemical inhibition, *Flame chemistry, Reprints, Flame models, Flame retardants, Diffusion flame.

Due to the ban on production of bromotrifluoromethane (CF2Br) because of its high ozone destruction potential, there has been recent interest in finding a replacement for it for fire extinguishing applications. While a variety of potential replacement are being considered, halogenated hydrocarbons may be a viable alternative for some applications. Consequently, an improved understanding of their action in flames will aid in their effective use. In addition, CF3Br is used as a fire suppressant on the space shuttle, and its action in microgravity has not been tested in diffusion flames. The present study investigates the effects of CF3Br and trifluoromethane (CF3H), the simplest compound representative of the fluorocarbons, in laminar diffusion flames. The primary experiments are laminar gas-jet diffusion flames burning in a quiescent environment containing the inhibitor in normal and microgravity. Experiments were conducted with CF2Br mole fractions in the oxidizer gas of 0.5% to 3%, CF3H mole fractions of 4% to 12%, oxygen mole fractions from 18% to 30%, and ambient pressures of 101 kPa and 25 kPa. Additional opposed-jet counterflow diffusion flame experiments were used to investigate flame structures observed in the microgravity flames.

01,422
PB96-164256 Not available NTIS
National Inst. of Standards and Technology (BFRL), Gaithersburg, MD. Fire Science Div.
Asymptotic and Numerical Analysis of a Premixed Laminar Nitrogen Dioxide-Hydrogen Flame.
Final rept.
G. T. Linteris, and F. A. Williams. 1995, 13p.
Pub. in Combustion Science and Technology, v105 p165-182 1995.

Keywords: *Nitrogen dioxide, *Hydrogen, *Combustion chemistry, Laminar flames, Premixed flames, Combustion kinetics, Reduction(Chemistry), Burning rate, Thermodynamics, Thermochemistry, Stoichiometry, Numerical analysis, Reprints.

A kinetic mechanism of eight-some reactions for flames in mixtures of hydrogen and nitrogen dioxide is systematically reduced to twenty-four-, eleven-, seven-, two-, and one-step mechanisms. The numerically predicted burning rates for the full mechanism describing a near-stocichiometric burner-stablized flame at a pressure of 25 torr, and final temperature of 2000 K are compared with the results using the reduced mechanisms, and the sources of inaccuracies are identified.

01,423
PB96-183108 PC A04/MF A01
National Inst. of Standards and Technology (BFRL), Gaithersburg, MD.
NASA Fire Detector Study.
W. D. Davis, and K. A. Notarianni. Mar 96, 40p, NISTIR-5798.
Color illustrations reproduced in black and white.

Keywords: *Fire detectors, *Air flow, *Ventilation, Fire detection systems, Clean rooms, Hangars, Ceilings, Size, Warning systems, Smoke detectors, Radiation detection, Infrared detectors, Ultraviolet detectors, Activation, Mathematical models, Fire protection, NASA, Computational fluid dynamics, Heat detectors, Fire models.

A study of fire detection methods for use by NASA in protecting their high bay structures is presented. A high bay structure is defined in this study as a structure having a ceiling height in excess of 18 m (60 ft). The analysis conducted in this study dealt with prediction of the expected performance of heat, smoke, and radiation detection systems for simulated fires of the type expected in NASA high bay facilities. The expected performance of smoke, heat, and radiation detectors in simulated fires is calculated using computer modeling. The results of this analysis will aid the development of fire detection strategies for high bay spaces.

01,424
PB96-183132 PC A03/MF A01
National Inst. of Standards and Technology (BFRL), Gaithersburg, MD. Fire Safety Engineering Div.
Numerical Simulation of Rapid Combustion in an Underground Enclosure.
K. B. McGrattan, H. R. Baum, and S. P. Deal. Apr 96, 19p, NISTIR-5809.
See also PB93-174902.

Keywords: *Underground space, *Combustion, *Thermodynamic properties, Ignition, Mass transport, Energy transport, Convective flow, Thermal absorption, Accelerating agents, Energy dissipation, Momentum, Equations of motion, Mach number, Equations of state, High temperature, Conservation equations, Conservation laws, Mathematical models, Computational fluid dynamics, *Fire models, Zone models, Field models.

The scenario of interest is a 2-second firing of a rocket in an underground enclosure intended to mimic the effect of burning a high temperature accelerant (HTA). Because of the unusual nature of the problem, at least in the context of typical fire scenarios, two types of numerical models have been applied to the problem. The first, a zone model, divides each room in the enclosure into one or two control volumes, and the transport of mass and energy from the burn room is estimated from the basic conservation laws. The second model, a field model designed for relatively low Mach number flows, solves the conservation equations of mass, momentum and energy discretized over hundreds of thousands of cells.

01,425
PB96-183181 PC A05/MF A01
National Inst. of Standards and Technology (BFRL), Gaithersburg, MD. Fire Science Div.
Minimum Mass Flux Requirements to Suppress Burning Surfaces with Water Sprays.
J. C. Yang, C. I. Boyer, and W. L. Grosshandler. Apr 96, 52p, NISTIR-5795.
Sponsored by Fire Administration, Emmitsburg, MD.

Keywords: *Solid fuels, *Burning rate, *Fire estinguishing agents, Wood, Methylmethacrylates, Polystyrene, Flames, Flow rates, Heat flux, Flow velocity, Water flow, Drop size, Spraying, Mist, Nozzles, Atomization, Low pressure, Mass flow, Fire fighting, Fire suppression, Piezoelectric gages, Requirements, Micronozzles.

Experimental measurements of extinghishment times of burning solid fuels using water were conducted using a prototype micronozzle array and a piezoelectric droplet generator. Solid fuels considered included solid white pine, polymethyl methacrylate, and polystyrene foam. External heat flux was applied to the sample surface during burning. The effects of drop size, sample orientation with respect the the nozzle, and nozzle distance from the sample surface on extinguishment time were examined. The extinguishment time was found to decrease with increasing water flow rate. For a given water flow rate, significant reduction in extinguishment time decreased when the nozzle was positioned further from the sample surface. At high flow rates, the extinghishment was independent of the nozzle-to-sample distance.

01,426
PB96-190012 Not available NTIS
National Inst. of Standards and Technology (BFRL), Gaithersburg, MD. Fire Safety Engineering Div.
Large Eddy Simulations of Smoke Movement in Three Dimensions.
Final rept.
H. R. Baum, K. B. McGrattan, and R. G. Rehm. 1996, 10p.
Pub. in INTERFLAM: Proceedings of the International Interflam Conference (7th), Cambridge, England, March 26-28, 1996, p189-198.

Keywords: *Smoke, *Convection, *Transport, *Computerized simulation, Fire, Gases, Mathematical models, Computation, Navier-stokes equations, Fluid flow, Reprints.

This paper describes a methdology for simulating the transport of smoke and hot gases in enclosures. The approach is based on the use of efficient CFD techniques and high performance computers to solve a form of the Navier Stokes equations specialized to the smoke movement problem. The fire is prescribed in a manner consistent with a mixture fraction based approach to combustion, but the combustion phenomena themselves are not simulated. The mixing and transport of smoke and hot gases is calculated directly from an approximate for of the Navier Stokes equations. The next two sections give a brief description of the mathematical and computational aspects of the model, while the final section illustrates its capability with sample results and a comparison with experiment.

01,427
PB96-190079 Not available NTIS
National Inst. of Standards and Technology (BFRL), Gaithersburg, MD. Fire Safety Engineering Div.
Large Fire Experiments for Fire Model Evaluations.
Final rept.
D. D. Evans. 1996, 6p.
Pub. in Proceedings of the International Interflam Conference (7th), Cambridge, England, March 26-28, 1996, p329-334.

Keywords: *Fire research, *Hydrocarbons, *Fuels, Oilspills, Smoke, Yield, Models, Fire safety, Building codes, Reprints.

Recent movement towards performance based evaluation of building safety has placed a premium on demonstrating the accuracy of engineering methods and increased the demand for fire performance data from large scale experiments. Data from large scale experiments are generally the basis for development and evaluation of fire models. Verification of engineering methods for prediction of fire related performance of structures, contents, and fire protection systems has become a priority need to support the development of performance based codes and standards. Generally a great impediment to model verification is the lack of means to quantify the degree of agreement between experiments and predictions or repeated experiments. The results have shown that modeling of building fire flows at a resolution of several centimeters is feasible. The advent of high resolution calculations for use in fire safety analysis has increased the demand for high resolution measurements of fire.

01,428
PB96-190178 Not available NTIS
National Inst. of Standards and Technology (BFRL), Gaithersburg, MD. Fire Safety Engineering Div.
Office Work Station Heat Release Rate Study: Full Scale versus Bench Scale.
Final rept.
D. Madrzykowski. 1996, 9p.
Pub. in INTERFLAM '96, Proceedings of the International Interflam Conference (7th), March 26-28, 1996, Cambridge, England, p47-55 1996.

Keywords: *Fire research, *Calorimeters, *Office equipment, Furniture, Fire tests, Heat flux, Reprints, Cone calorimeter, Radiation heat flux.

The National Institute of Standards and Technology (NIST) has conducted a study with office work stations to examine their heat release rates and to determine if the peak heat release rate for a work station can be predicted accurately from cone calorimeter results. Fifteen full scale fire experiments were conducted. Three types of work station panel construction and three work station configurations were examined. Preliminary results for the most common panel construction, fabric over fiberglass batting with a 6 mm thick hardboard core, are presented here. A method utilizing the peak heat release rate from the cone calorimeter experiments has been used successfully to predict peak heat release rates for the most common construction work station.

01,429
PB96-190210 Not available NTIS
National Inst. of Standards and Technology (BFRL), Gaithersburg, MD. Fire Science Div.
Analysis of High Bay Hangar Facilities for Detector Sensitivity and Placement.
Final rept.
K. A. Notarianni, W. Davis, D. Lowe, S. Laramee, and J. E. Gott. 1996, 10p.
Pub. in INTERFLAM '96: Proceedings of the International Interflam Conference, Cambridge, England, March 26-28, 1996, p487-496.

Keywords: *Hangars, *Sprinkler systems, *Fire suppression, *Smoke detectors, Fire protection, Fire detectors, Activation, Ventilation, Air flow, Ceilings, Thermodynamic properties, Burning rate, Combustion kinetics, Heat flux, Flame propagation, Fire detection systems, Bays(Structural units), Reprints.

The study was conducted to investigate the response of various fire detectors and automatic sprinklers in high bay aircraft hangars. Laboratory and full-scale experiments as well as computer modeling were conducted to better understand the movement of heat and products of combustion in high bay spaces. Temperature distribution across the ceiling was measured along with the response of various types of fire protection devices as a function of fire size, fuel type, and ventilation conditions. Key findings are presented relating to detector spacing, threshold fire sizes, sprinkler type and temperature ratings, burn rates, heat release rates, and the effect of draft curtains.

01,430
PB96-193701 PC A04/MF A01
Kansas State Univ., Manhattan. Dept. of Physics.
Post-Flame Soot.
Final rept. Sep 94-Dec 95.
C. M. Sorensen. Jun 96, 36p, NIST/GCR-96/694.
Grant NIST-NANB4H1652
Sponsored by National Inst. of Standards and Technology (BFRL), Gaithersburg, MD.

Keywords: *Soot, *Combustion products, Diffusion flames, Acetylene, Agglomerates, Light scattering, Standards.

The smoke agglomerates produced by a co-annular diffusion flame with acetylene fuel were characterized by sampling/microscopy and by light scattering measurements. Particles were sampled at various heights above the flame using both thermophoretic sampling and impaction. Transmission electron microscopy was used for the smaller agglomerates obtained by thermophoretic sampling and optical microscopy was used for analysis of particles as large as .4 mm in diameter collected by impaction. The number of primary spheres was estimated from the projected area of the agglomerate and the primary sphere size. The fractal analysis extended over four orders of magnitude in the radius of gyration - the widest range studied for smokes.

01,431
PB96-195532 PC A04/MF A01
California Univ., San Diego, La Jolla. Dept. of Applied Mechanics and Engineering Sciences.
Chemical Inhibition of Methane-Air Diffusion Flame.
Final rept. 15 Sep 93-15 Sep 95.
K. Seshadri. Jun 96, 43p, NIST/GCR-95/685.
Grant NANB3D1435
Sponsored by National Inst. of Standards and Technology, Gaithersburg, MD.

Keywords: *Halons, *Diffusion flames, *Methane, *Combustion kinetics, *Thermochemistry, Fire extinguishing agents, Oxygen, Burning rate, Flame propagation, Inhibition, Asymptotic series, Numerical analysis, Reprints, Halon 1301.

The principal objective of the research is to clarify the mechanisms of chemical inhibition of methane-air diffusion flames by CF3Br and CF3H. An experimental, numerical, and analytical study is conducted. An asymptotic analysis is performed to characterize the structure and critical conditions of extinction of uninhibited methane-air diffusion flames. This analyses is extended to methane-air diffusion flames inhibited with CF3Br. Critical conditions of extinction of the flame are measured over a wide range with agents added to the air stream and to the fuel stream. Numerical calculations with detailed chemistry are performed to calculate the structure and critical conditions of flame extinction. The numerical results are compared with the measurements.

01,432
PB96-202254 PC A06/MF A01
Michigan Univ., Ann Arbor. Dept. of Aerospace Engineering.
Mixing and Radiation Properties of Buoyant Luminous Flame Environments.
Z. Dai, S. K. Krishnan, R. Sangras, J. S. Wu, and G. M. Faeth. Jun 96, 91p, GDL/GMF-95-02, NIST/GCR-96/691.
Grant NIST-60NANB4D1696
See also PB95-242327. Sponsored by National Inst. of Standards and Technology (BFRL), Gaithersburg, MD.

Keywords: *Diffusion flames, *Fire tests, *Optical properties, Soot, Combustion products, Acetylene, Propylene, Ethylene, Propane, Standards, Turbulent flow.

An investigation of the radiation and mixing properties of buoyant turbulent diffusion flames is described. The study was divided into two phases: (1) the optical and radiative properties of soot, which must be understood in order to develop nonintrusive methods for measuring soot properties and to estimate the continuum radiation properties of soot in flame environments, and (2) the structure and mixing properties of buoyant turbulent plumes, which must be understood in order to resolve effects of turbulence/radiation interactions and to benchmark computationally tractable models of buoyant turbulent flows.

01,433
PB96-202304 PC A13/MF A03
Maryland Univ., College Park. Dept. of Mechanical Engineering.
Sparse Water Sprays in Fire Protection.
M. di Marzo. Jun 96, 254p, NIST/GCR-96/687.
Grant NIST-NANB5D0136
Sponsored by National Inst. of Standards and Technology (BFRL), Gaithersburg, MD.

Keywords: *Fire tests, *Evaporative cooling, Heat flux, Spraying, Fire protection, Water.

Selected reports: Dropwise Evaporative Cooling; Infrared Thermography of Dropwise Evaporative Cooling; Evaporative Cooling Due to a Gently Deposited Droplet; Infrared Thermography of Dropwise Evaporative Cooling of a Semi-Infinite Solid Subjected to Radiant Heat Input; Modeling of Dropwise Evaporative Cooling on a Semi-Infinite Solid Subjected to Radiant Heat Input; Multi-Droplet Evaporative Cooling: Experimental Results; Effect of Liquid-Solid Contact Angle on Droplet Evaporation; Effect of Dissolved Gasses on Spray Evaporative Cooling With Water; and Flooding Criterion for Evaporative Cooling on Horizontal Semi-Infinite Solids.

01,434
PB96-204433 Not available NTIS
National Inst. of Standards and Technology (CSTL), Gaithersburg, MD. Process Measurements Div.
Role of Combustion on Droplet Transport in Pressure-Atomized Spray Flames.
Final rept.
A. K. Gupta, C. Presser, J. T. Hodges, and C. T. Avedisian. 1996, 11p.
Pub. in Jnl. of Propulsion and Power, v12 n3 p543-553 Jun 96.

Keywords: *Spray combustion, *Flames, Reprints, Droplets, Kerosene, Velocity.

The transport of droplets in a pressure-atomized kerosene spray flame was examined using a two-component phase Doppler system to measure the droplet size and velocity distributions at several locations within the spray. The effect of combustion on droplet transport was examined by comparing the results to a nonburning spray under similar flow conditions. Directions of motion of droplets are calculated from the measured droplet velocity components to provide information on trajectories and dispersion of droplets. Results show that combustion reduces the strength of gas recirculation as evience by significantly fewer droplets being transported upstream toward the nozzle along the centerline for the burning spray as compared to the nonburning spray. Combustion enhances droplet vaporization and results in reduced number density and larger droplet mean diameters and velocities when compared to the nonburning spray. At the spray centerline there is a wide range of droplet trajectories that are associated with recirculated droplets and those originating from the nozzle There is some correlation between droplet velocity and diameter. Some larger size droplets are also found to be entrained into the recirculation pattern. At the spray boundary, few droplets deviate from the mean direation. Also, droplet velocity is well correlated with increasing diameter but appears to approach an asymptotic value in which droplet velocity becomes insensitive to diameter.

01,435
PB97-110050 Not available NTIS
National Inst. of Standards and Technology (BFRL), Gaithersburg, MD. Fire Safety Engineering Div.
Flammability Characterization with the Lift Apparatus and the Cone Calorimeter.
Final rept.
T. G. Cleary. 1992, 17p.
Pub. in Proceedings of the Fire Retardant Chemicals Association Spring Conference, Orlando, FL., March 29-April 1, 1992, 17p.

Keywords: *Flammability, *Calorimeters, Heat measurement, Characterization, Ignitability, Flame spread, Reprints, *Life apparatus, *Cone calorimeters.

Two small-scale test apparatuses, the LIFT apparatus and the Cone Calorimeter provide ignitability, flame spread, and heat release rate data for combustible solid materials. Data gathered with these apparatuses can be reduced to a limited number of key flammability or fire properties for a particular material. These key properties, in conjunction with the appropriate modelling equations, characterize the time to ignition, flame spread rate, and heat release rate over the range of applicable heating conditions and surface temperatures likely in full-scale fires. These key properties may be used as input parameters in a fire model that predicts flame spread and heat release rates for certain full-scale fire scenarios.

01,436
PB97-110068 Not available NTIS
National Inst. of Standards and Technology (BFRL), Gaithersburg, MD. Fire Science Div.
Letter Report on Flame Spread Testing of a Composite Material.
Final rept.
T. G. Cleary. 1993, 16p.
Sponsored by Naval Surface Warfare Center Carderock Div., Annapolis, MD.
Pub. in a Letter Report on Flame Spread Testing of a Composite Material, p1-16 Feb 93.

Keywords: *Composites, *Flame spread, Ignition, Reprints, LIFT apparatus, ASTM E 1321.

Ignition delay time, lateral flame spread and upward flame spread data were gathered on a composite material (glass fiber/organic resin type). These tests were performed at the request of the Naval Surface Warfare Center. The Navy desires some assessment of the flame spread characteristics of the selected composite; the data gathered here are part of that flame spread characterization. The ignition delay time and lateral spread results were obtained with the LIFT apparatus in accordance with ASTM E 1321. The upward flame spread tests were performed using an experimental electrical radiant panel apparatus.

01,437
PB97-110076 Not available NTIS
National Inst. of Standards and Technology (BFRL), Gaithersburg, MD. Fire Safety Engineering Div.
Interaction of an Isolated Sprinkler Spray and a Two-Layer Compartment Fire Environment. Phenomena and Model Simulations.
Final rept.
L. Y. Cooper. 1995, 19p.
See also PB91-216804.
Pub. in Fire Safety Jnl., v25 n2 p89-107 Sep 95.

Keywords: *Fire tests, *Sprinkler systems, Spraying, Mathematical models, Nozzles, Computerized simulation, Water, Combustion, Buildings, Reprints, *Foreign technology.

A general description of the interaction of sprinklers and compartment-fire-generated smoke layers is presented. Various possible aspects of the interaction phenomena (upper-layer smoke entrainment into the sprinkler spray, momentum and mass exchange between droplets and entrained gas, gas cooling by evaporation, buoyancy effects, and others) are discussed in the context of a two-layer-type description of the fire environment. The inputs and outputs for a mathematical submodel which simulates the phenomena are discussed. The submodel is suitable for general use in any two-layer, zone-type compartment fire model. Results from exercising the submodel are presented. These example calculations simulate the interaction between the spray of a real sprinkler device and a range of two-layer fire environments. The calculations reveal an important generic interaction phenomenon, namely, an abrupt and large change in the growth rate of the upper layer that would accompany an increase in upper-layer thickness beyond a critical thickness (for a given upper-layer temperature) or an increase in upper-layer temperature beyond a critical temperature (for a given upper-layer thickness). Exceeding these critical values would lead to a very large rate of growh of upper layer thickness, a growth that could lead to rapid and complete smoke filling of even the largest compartments of fire origin.

01,438
PB97-110357 Not available NTIS
National Inst. of Standards and Technology (BFRL), Gaithersburg, MD. Fire Safety Engineering Div.
Heat Flux from Flames to Vertical Surfaces.
Final rept.
J. G. Quintiere, and T. G. Cleary. 1992, 10p.
Pub. in American Society of Mechanical Engineers Winter Annual Meeting, Anaheim, CA., November 1992, 10p.

Keywords: *Heat flux, *Flames, *Vertical surfaces, Walls, Corners, Dimensional analysis, Reprints.

Dimensional analysis is used to examine heat transfer from flames to vertical surfaces. Configurations include a line fire against a wall, a square burner flame against a wall and in a corner, and window flames impinging on a wall. Dimensionless parameters that affect flame heat flux include x/l(f), y/D, l(f)/D, and kD where x is vertical distance, y is horizontal distance, l(f) if flame length, D is burner dimension, and k is the flame absorption coefficient. Only the effect of these variables is shown; no general correlation is developed, and more data are needed.

01,439
PB97-118632 Not available NTIS
National Inst. of Standards and Technology (BFRL), Gaithersburg, MD. Fire Science Div.
NIST Research on Less-Flammable Materials.
Final rept.
R. G. Gann. 1996, 5p.
Pub. in Society for the Advancement of Material and Process Engineers Jnl., v32 n3 p16-20 May/Jun 96.

Keywords: *Building materials, *Furniture, *Flammability, *Fire tests, Polymers, Composite materials, Service life, Fire safety, Fire research, Research programs, Reprints, US NIST.

A principal objective of the NIST Fire Research Program is supporting the development by U.S. manufacturers of a new generation of buiding and furnishing materials and products that contribute less to a fire, maintain their fire safety performance over the product life, and are environmentally friendly. The paper describes the NIST roles in fire safety science and engineering, as well as research projects currently underway on less fire-prone materials and products.

01,440
PB97-119218 Not available NTIS
National Inst. of Standards and Technology (BFRL), Gaithersburg, MD. Fire Science Div.
Computations of Enhanced Soot Production in Time-Varying CH4/Air Diffusion Flames.
Final rept.
C. R. Kaplan, C. R. Shaddix, and K. C. Smyth. 1996, 11p.
See also PB95-203246.

Pub. in Combustion and Flame, v106 n4 p392-405 Sep 96.

Keywords: *Soot, *Diffusion flames, *Methane, Turbulent flow, Heat transmission, Flicker, Instability, Temporal variations, Navier-Stokes equation, Computations, Two dimensional models, Mathematical models, Reprints.

The paper presents time-dependent numerical simulations of both steady and time-varying CH4/air diffusion flames to examine the differences in combustion conditions which lead to the observed enhancement in soot production in the flickering flames. The numerical model solves the two-dimensional, time-dependent reactive-flow Navier-Stokes equations coupled with submodels for soot formation and radiation transport.

01,441
PB97-119325 Not available NTIS
National Inst. of Standards and Technology (CAML), Gaithersburg, MD.
Transport by Gravity Currents in Building Fires.
Final rept.
R. G. Rehm, K. B. McGrattan, H. R. Baum, and K. W. Cassel. 1996, 12p.
Pub. in Proceedings of the International Symposium on Fire Safety Science (5th), Melbourne, Australia, 12p 1996.

Keywords: *Fires, *Computational fluid dynamics, *Boundary conditions, Buildings, Walls, Convection, Smoke, Gas flow, Heat transfer, Buoyancy, Convective flow, Eddies(Fluid mechanics), Navier-Stokes equation, Two-dimensional models, Three-dimensional models, Computerized simulation, Reprints, *Gravity currents.

Gravity currents (GC) are important physical phenomena which transport smoke and hot gases in corridors of buildings. In the paper, they are studied using large eddy simulations (LES). The transient Navier-Stokes (N-S) equations are numerically integrated with very high resolution, in two dimensions and with high resolution in three dimensions. The LES computations require no adjustable parameters, and are found to agree well with available experimental results in the absence of heat transfer.

01,442
PB97-122311 Not available NTIS
National Inst. of Standards and Technology (BFRL), Gaithersburg, MD. Fire Science Div.
Materials and Fire Threat.
Final rept.
R. G. Gann, R. Lyon, U. Sorathia, and L. Gritzo. 1996, 8p.
Pub. in Society for the Advancement of Material and Process Engineers Jnl., v32 n3 p8-15 May/Jun 96.

Keywords: *Aircraft fire, *Ship fires, *Fire resistant materials, *Polymers, Fiber reinforced composites, Composite materials, Materials replacement, Flammability, Military applications, Naval vessels, Ship structural components, Barriers, Fire protection, Fire research, Fire safety, Reprints.

Fiber-reinforced polymer composites offer the U.S. military the potential for significant reductions in weight and signatures. Current seaborne applications of composite materials in the U.S. Navy include sonar bow domes and windows, and coastal minehunter MHC-51 hulls. The U.S. navy is also evaluating composite materials of both primary and secondary load-bearing structures such as foundations, deckhouses, and hulls; machinery components such as composite piping, valves, centrifugal pumps, and heat exchangers; and auxiliary or support items such as gratings, stanchions, ventilation ducts, and screens. This new interest in composite materials is due to increased need for a corrosion-free, lightweight, and affordable low-cost alternative to metallic components. The U.S. Army is evaluating composite combat vehicles and the U.S. Air Force has taken the lead in transitioning composite technology to military advantage as evidenced by superior performance of the Stealth Fighter.

01,443
PB97-122519 Not available NTIS
National Inst. of Standards and Technology (BFRL), Gaithersburg, MD. Fire Science Div.
NO Production and Destruction in a Methane/Air Diffusion Flame.
Final rept.
K. C. Smyth. 1995, 35p.
Pub. in Combustion Science and Technology, v115 p151-176 1996.

Keywords: *Diffusion flames, *Methane, *Nitrogen oxides, *Combustion chemistry, Combustion products, Laminar flow, Thermodynamic properties, Laser induced fluorescence, Boltz mann equation, Reprints, Collisional quenching.

Concentration profiles have been measured for naturally occurring NO in a laminar CH4/air diffusion flame burning on a rectilinear Wolfhard-Parker slot burner at atmospheric pressure. The observed fluorescence signals have been corrected for (1) the Boltzmann population in the R(sub 1) rotational level of the ground vibronic state and (2) collisional quenching rates as a function of the local temperature and collider concentrations. A reaction path analysis and determination of NO fluxes strongly indicate that prompt NO production outweights the thermal route, but uncertainties in determining the relative contributions to instantaneous NO production are large.

Fuel & Propellant Tanks

01,444
PB97-110043 Not available NTIS
National Inst. of Standards and Technology (BFRL), Gaithersburg, MD. Fire Science Div.
Effect of Fuel Tank Rupture Mode on the Ignitability of Expelled Fuel.
Final rept.
T. G. Cleary, and R. G. Gann. 1993, 7p.
Sponsored by National Highway Traffic Safety Administration, Washington, DC.
Pub. in Effect of Fuel Tank Rupture Mode on the Ignitability of Expelled Fuel, p1-7 Mar 93.

Keywords: *Fuel tanks, *Crash tests, Fuel work rupture, Trucks, Automotive fuels, Reprints.

At the request of the Office of Defects Investigation (ODI) of the National Highway Traffic Safety Administration (NHTSA), the Building and Fire Research Laboratory (BFRL) of the National Institute of Standards and Technology (NIST) analyzed data from vehicle collision tests and tank crush tests to provide an assessment of the effect of tank rupture mode on the ignitability of expelled fuel for two different ignition scenarios: compression of a tank, resulting in increased internal pressure and rapid, violent expulsion of the gasoline as a result of a puncture or rupture; and simple puncture of a vehicle fuel tank, resulting in gasoline drainage. For the work, ODI/NHTSA provided NIST with: video tapes of the tank crush tests and video tapes and high-speed film of two high speed vehicle collision tests (one of the latter resulted in violent expulsion of fluid; the other in fuel tank puncture and fluid drainage); estimates of the fuel dispersion from the tank crush tests and the vehicle collision tests; and a list of potential ignition sources and their locations on the vehicle of interest.

Jet & Gas Turbine Engines

01,445
AD-A278 138/3 PC A04/MF A01
National Bureau of Standards, Boulder, CO.
Bibliography of Books and Published Reports on Gas Turbines, Jet Propulsion, and Rocket Power Plants.
E. F. Fiock, and C. Halpern. 1 Jun 51, 68p, NBS-CIRCULAR-509.

Keywords: *Jet engines, *Gas turbines, *Bibliographies, Jet propulsion, Rockets, Auxiliary power plants, Reports, *Rocket engines, N-10173.

No abstract available.

01,446
AD-A278 213/4 PC A06/MF A02
National Bureau of Standards, Gaithersburg, MD.
Bibliography of Books and Published Reports on Gas Turbines, Jet Propulsion, and Rocket Power Plants, January 1950 through December 1953.
E. F. Fiock, and C. Halpern. Dec 53, 115p, NBS-CIRC-509-SUPPL.

Keywords: *Gas turbines, *Bibliographies, Jet propulsion, Rockets, Reports, *Rocket engines, *Jet engines.

No abstract available.

01,447
N95-26123/6 (Order as N95-26119, PC A03/MF A01)
National Inst. of Standards and Technology, Gaithersburg, MD.
Measurement Methods and Standards for Processing and Application of Thermal Barrier Coatings.
Abstract Only.
S. J. Dapkunas. Mar 95, 1p.
In NASA. Lewis Research Center, Thermal Barrier Coating Workshop p 9.

Keywords: *Spraying, *Thermal control coatings, *Vapor deposition, Aircraft engines, Diesel engines, Gas turbine engines, Stationary engines.

Application of thermal barrier coatings deposited by thermal spray, physical vapor and possibly other methods is expected to be extended from aircraft gas turbines to industrial and utility gas turbines as well as diesel engines. This increased usage implies the participation of greater numbers of processors and users, making the availability of standards for process control and property measurement more important. Available standards for processing and evaluation of thermal barrier coatings are identified as well as those needed in the future but currently unavailable.

01,448
PB95-175956 Not available NTIS
National Inst. of Standards and Technology (CSTL), Gaithersburg, MD. Inorganic Analytical Research Div.
Determination of Hydrogen in Titanium Alloy Jet Engine Compressor Blades by Cold Neutron Capture Prompt Gamma-ray Activation Analysis.
Final rept.
R. L. Paul, and R. M. Lindstrom. 1994, 6p.
Pub. in Review of Progress in Quantitative Nondestructive Evaluation, v13 p1619-1624 1994.

Keywords: *Jet engines, *Titanium alloys, *Hydrogen embrittlement, *Concentration(Composition), *Compressor blades, *Nondestructive tests, Test methods, Structural failure, Hydrogen, Gamma ray scattering, Compressors, Defect analysis, Reprints, *Cold neutron capture prompt gamma-ray activation analysis.

Titanium, an important structural metal, readily absorbs hydrogen. Since the presence of trace amounts of hydrogen causes embrittlement in metals, a reliable nondestructive method of measuring hydrogen in titanium is much needed. We have found cold neutron capture prompt gamma-ray activation analysis (CNPGAA) to be ideal for the measurement of trace amounts of hydrogen. The technique is nondestructive, gives bulk analyses, the results are independent of the chemical form of the element being measured, and the hydrogen peak is interference free. The detection limit for hydrogen in titanium and its alloys is near 100 mg/kg. We have used CNPGAA to measure hydrogen in two titanium alloy jet engine compressor blades from an engine in which a blade had failed during service. While H concentrations in one blade were nearly uniform (approximately 200 mg/kg Ti) at all points measured, H concentrations in the second blade ranged from 140 to 750 mg/kg Ti, with greater H concentrations toward the edges of the blade than in the interior. Analysis of three cross sections, cut from different regions of another blade, showed a similar concentration gradient.

Reciprocation & Rotating Combustion Engines

01,449
PB94-172103 Not available NTIS
National Inst. of Standards and Technology (NEL), Gaithersburg, MD. Chemical Process Metrology Div.
Thin Film Thermocouples for Measurement of Wall Temperatures in Internal Combustion Engines.
Final rept.
D. Burgess, M. Yust, and K. Kreider. 1990, 6p.
Pub. in Proceedings of American Institute of Aeronautics and Astronautics/American Society of Mechanical Engineers Thermophysics and Heat Transfer Conference, Seattle, WA., June 18-20, 1990, p43-48.

Keywords: *Thermocouples, *Thermal conductions, *Internal combustion engines, Ceramics, Heat flux,

Thin films, Lasers, Temperature measuring instruments, Zirconium oxides, Aluminum oxide, Thermal diffusion, Reprints, Zirconia, Alumina.

The transient temperature response of thin film thermocouples (TFTC) was measured using a pulsed laser heating technique. Pt/Pt-10% Rh, Pt/Au, and In2O3/In2O3-SnO2 (ITO) TFTC's with thicknesses ranging from 0.4 to 28 microns were fabricated by sputter deposition on alumina, plasma-sprayed zirconia, and Min-K 2000 substrates. The zirconia TFTC's are used in plugs for determination of the wall heat flux in internal combustion engines. The thermocouple output of the TFTC's was measured as a function of time following irradiation-heating of the thermocouple junction by a 12 ns laser pulse. The magnitude of the temperature jump (thermocouple output) and the temporal response of the TFTCs were found to be consistent with those predicted from a solution to the heat conduction equation. This model assumes that the heat flow is one-dimensional and that the film is thick compared to the thermal diffusion length during the laser heating pulse. For example, it was found that TFTCs with nominal 4 micron thick junctions has temperature decay times of about 5 microseconds, 60 microseconds, and 20 ms for alumina, zirconia, and Min-K 2000 substrates, respectively. These results are related to similar work using thin film resistance sensors and to measurements of the frequency response of TFTCs using an intensity modulated laser heating method. The fabrication of the TFTCs and the utility of heat flux sensors in internal combustion engines are discussed.

01,450
PB95-104915 PC A04/MF A01
National Inst. of Standards and Technology (MSEL), Gaithersburg, MD. Ceramics Div.
Abrasive Wear by Diesel Engine Coal-Fuel and Related Particles.
L. K. Ives. Sep 94, 66p, NISTIR-5461, ORNL/SUB/83-21322/03.
Contracts DE-A105-83OR21322, DE-AC05-84OR21400
See also DE93000834 and DE87008697. Sponsored by Oak Ridge National Lab., TN. and Department of Energy, Washington, DC.

Keywords: *Diesel engines, *Abrasion, *Coal, *Wear tests, Piston rings, Fuel slurries, Fuel substitution, Pulverized fuels, Scanning electron microscopy, Engine cylinders, Wear resistance.

The purpose of the work summarized in this report was to obtain a basic understanding of the factors which are responsible for wear of the piston ring and cylinder wall surfaces in diesel engines utilizing coal-fuel. The approach included analytical studies using scanning electron microscopy and energy dispersive x-ray analyses to characterize coal-fuel and various combustion particles, and two different wear tests. The wear tests were a modified pin-on-disk test and a block-on-ring test capable of either unidirectional or reciprocating-rotational sliding. The wear tests in general were conducted with mixtures of the particles and lubricating oil. The particles studied included coal-fuel, particles resulting from the combustion of coal fuel, mineral matter extracted during the processing of coal, and several other common abrasive particle types among which quartz was the most extensively examined. The variables studied included those associated with the particles, such as particle type, size, and hardness; variables related to contact conditions and the surrounding environment; and variables related to the type and properties of the test specimen materials.

01,451
PB95-152120 Not available NTIS
National Inst. of Standards and Technology (MSEL), Gaithersburg, MD. Ceramics Div.
New Method to Evaluate Deposit Forming Tendencies of Liquid Lubricants by Differential Scanning Calorimetry.
Final rept.
Y. Zhang, P. Pei, J. M. Perez, and S. M. Hsu. 1992, 7p.
Sponsored by Department of Energy, Washington, DC. Energy Conversion and Utilization Technologies Program.
Pub. in Lubrication Engineering 48, n3 p189-195 1992.

Keywords: *Lubricating oils, *Deposits, *Engine tests, Lubricants, Calorimeters, Lubrication, Contamination, Test methods, Oxidation, Reprints, *Two-peak method, Pressurized differential scanning calorimetry.

A new laboratory bench test, using the technique of pressurized differential scanning calorimetry (PDSC), has been developed to evaluate deposit forming tendency for liquid lubricants. This method, called 'PDSC two-peak method', attempts to simulate deposit formation mechanism in an engine by heating thin films of oil on steel discs in an oxidative atmosphere. In this paper, the development and optimization of the two-peak test procedure are described. The test was evaluated by characterizing the deposit forming tendencies of five liquid lubricants. The deposit performance ranking for the five oils obtained from this new test method was consistent with engine test ranking.

01,452
PB95-152138 Not available NTIS
National Inst. of Standards and Technology (IMSE), Gaithersburg, MD. Ceramics Div.
Deposit Forming Tendencies of Diesel Engine Oils-Correlation between the Two-Peak Method and Engine Tests.
Final rept.
Y. Zhang, J. M. Perez, P. Pei, and S. M. Hsu. 1992, 6p.
Sponsored by Department of Energy, Washington, DC. Energy Conversion and Utilization Technologies Program.
Pub. in Lubrication Engineering 48, n3 p221-226 1992.

Keywords: *Diesel engines, *Lubricating oils, *Deposits, *Engine tests, Lubricants, Colorimeters, Sampling, Contamination, Test methods, Lubrication, Reprints, *Two-peak method, Pressurized differential scanning calorimetry.

The ability to determine the deposit forming tendencies of lubricants utilizing a newly developed laboratory bench method was established using three individual sets of lubricants. The 'Two-Peak Method' was developed at NIST using a pressurized differential scanning calorimeter and a unique sample pan. The method is described and repeatability between operators is demonstrated. The oils used in the study were evaluated in engine oil performance tests, or field tests, by the cooperating laboratories. For each set of oils highly correlatable results between the two-peak method and the engine performance tests were obtained. Several reference oils were included in each set of samples to show agreement between the three sets of samples. The method can be used to predict top land deposits that result increased oil consumption in different types of diesel engines.

Rocket Engines & Motors

01,453
PB95-169215 Not available NTIS
National Inst. of Standards and Technology (CSTL), Boulder, CO. Process Measurements Div.
Vortex Shedding Flowmeters for SSME Ducts.
Final rept.
J. D. Siegwarth, and M. A. Lewis. 1992, 9p.
Pub. in Proceedings of Advanced Earth-to-Orbit Propulsion Technology Conference, Huntsville, AL., May 19-21, 1992, NASA Conference Publication 3174, v1 p217-225 1992.

Keywords: *Space shuttle main engine, *Liquid oxygen, *Ducted rocket engines, Vortex shedding, Flow meters, Gas flow, Flow measurement, Ducted flow, Reprints, *Vortex shedding flowmeters.

Previous work has shown that vortex shedding flowmeters can measure flow in the Space Shuttle Main Engines (SSME) liquid oxygen ducts under the extreme conditions found there and without any upstream flow conditioning. Though measurement of liquid flow in the 28 mm (1.1 in.) duct is more difficult, recent tests have shown vortex shedders can make this measurement also. An encapsulated sensor design is presented and vortex shedding flowmeters for selected fuel ducts are discussed. A hydrogen gas test facility is needed to complete development of gas meters because of the high velocities found in the fuel ducts.

Rocket Propellants

01,454
AD-A280 398/9 PC A05/MF A01
National Bureau of Standards, Boulder, CO.
Cryogenic Research and Development (Quarterly Report Number 2 for Period Ending December 31, 1960).
Quarterly rept. no. 2 for period ending 31 Dec 60.
31 Dec 61, 88p, NBS-6736.

Keywords: *Cryogenics, *Liquid hydrogen, Temperature control, Thermodynamics, Vapor pressure, Electric batteries, Thermophysical properties.

No abstract available.

01,455
AD-A280 399/7 PC A04/MF A01
National Bureau of Standards, Boulder, CO.
Cryogenic Research and Development (Progress Report Number 4 for Period Ending December 31, 1961).
Progress rept. no. 4 for period ending 31 Dec 61.
31 Dec 61, 74p, NBS-7219.

Keywords: *Cryogenics, *Liquid hydrogen, Thermodynamic properties, Gravity(Artificial), Density, Specific heat.

No abstract available.

01,456
AD-A280 401/1 PC A04/MF A01
National Bureau of Standards, Boulder, CO.
Cryogenic Research and Development (Quarterly Report Number 1 for Period Ending September 30, 1960).
Quarterly rept. no. 1 for period ending 30 Sep 60.
30 Sep 60, 71p, NBS-6728.

Keywords: *Cryogenics, *Cryogenic propellants, Liquid hydrogen, Thermal properties, Thermal conductivity, Gravity, Densitometers, Gravity(Artificial), Gas dynamics, Pressure transducers, Zero gravity, Compressibility.

No abstract available.

01,457
AD-A280 679/2 PC A04/MF A01
National Bureau of Standards, Gaithersburg, MD.
Cryogenic Research and Development (June 30, 1961).
30 Jun 61, 73p, NBS-6785.

Keywords: *Cryogenics, Thermophysical properties, Isotherms, Flanges, Rings, Temperature, Pressure, Densitometers, Ball bearings, Hydrogen, *Cryogenic propellants, Liquid hydrogen.

No abstract available.

01,458
AD-A286 612/7 PC A05/MF A01
National Bureau of Standards, Gaithersburg, MD.
Progress Report to National Aeronautics and Space Administration on Cryogenic Research and Development.
Progress rept. no. 4, for period ending 31 Dec 61.
31 Dec 61, 77p, NBS-7219.

Keywords: *Cryogenics, *Liquid hydrogen, Instrumentation, Hydrogen, Physical properties, Specific heat, Fluids, Saturation, Density, Vapor pressure, Heat of vaporization, Thermal conductivity, Dielectrics, Temperature, Detectors, Pressure transducers, Vibration, Thermodynamics.

No abstract available.

COMMUNICATION

Common Carrier & Satellite

01,459
AD-A286 619/2 PC A10/MF A03
National Bureau of Standards, Gaithersburg, MD.
Ionospheric Radio Propagation.
25 Jun 48, 214p, NBS-462.

Keywords: *Ionospheric propagation, *Radio waves, Signal to noise ratio, Solar disturbances, Field inten-

sity, Wave propagation, Noise(Radio), High frequency, Magnetic fields, Radio transmission, Antenna radiation patterns, Sky waves, Range(Distance).

No abstract available.

01,460
FIPS PUB 182 PC E03
National Inst. of Standards and Technology (CSL), Gaithersburg, MD.
Integrated Services Digital Network (ISDN); Category: Telecommunications Standard; Subcategory: Integrated Services Digital Network.
5 Oct 93, 35p.
Three ring vinyl binder also available; North American Continent price $7.00; all others write for quote.

Keywords: *Communication networks, *Digital communications, Communications management, Data transmission, Protocols, Data links, Packet switching, Interoperability, Signal transmission, Telecommunication, *Integrated services digital network, Telecommunications standards, Primary rate interface, Basic rate interface.

The publication defines the generic protocols necessary to establish transparent Integrated Services Digital Network (ISDN) connections among government networks and between government and conformant common carrier networks. This FIPS provides a minimal set of bearer services, and is based on national standards, international standards, and implementation agreements developed by the North American ISDN Users' Forum (NIUF). Future versions of this FIPS will provide protocols for additional services, teleservices and applications. This standard supports a range of integrated services including voice, data, image, and video services.

01,461
FIPS PUB 187 PC A02/MF A01
National Inst. of Standards and Technology (CSL), Gaithersburg, MD.
Administration Standard for the Telecommunications Infrastructure of Federal Buildings. Category: Telecommunications Standard; Subcategory: Telecommunications Administration.
11 Aug 94, 9p.
Prepared in cooperation with National Communications System, Arlington, VA.
Three ring vinyl binder also available; North American Continent price $7.00; all others write for quote.

Keywords: *Telecommunication, *Public buildings, *Federal information processing standards, Passageways, Communication cables, Electrical grounding, Communication equipment, Wire, Administration, National government, Specifications.

This standard, by adoption of ANSI/TIA/EIA-606-1993, Administration Standard for the Telecommunications Infrastructure of Commercial Buildings, specifies the administrative requirements of the telecommunications infrastructure within a new, existing, or renovated office building or campus. Telecommunications infrastructure can be thought of as the collection of those components (telecommunications equipment spaces, cable pathways, grounding, wiring, and termination hardware) that provide the basic support for the distribution of all information within a building or campus. Administration of telecommunications includes documentation (record-keeping, drawings, labeling, etc.) of telecommunications outlet boxes, connectors, cables, termination hardware, patching and cross-connect facilities, conduits, other cable pathways, telecommunications closets, and other spaces.

01,462
PB94-123080 PC A03/MF A01
National Inst. of Standards and Technology (CSL), Gaithersburg, MD.
Technology Trends in Telecommunications: An Overview.
Oct 93, 36p, NISTIR-5282.

Keywords: *Telecommunication, *Trends, *Technological innovations, Economic surveys, Computer networks, User requirements, Data transmission, Wireless communication, Signal processing, Global aspects, Competition, Economic impact, Computer information security, Local area networks, Fiber optics, Information systems, *Diversification.

The article describes the technology trends for telecommunications and their impact on the services provided to the user. The impact of divestiture, together with the advancement of some enabling technologies, is leading to a rapid diversification of the telecommunication industry. The diversification is the subject of the study that summarizes trends in a historic perspective.

01,463
PB94-139045 PC A04/MF A01
National Inst. of Standards and Technology (CSL), Gaithersburg, MD.
Good Security Practices for Electronic Commerce, Including Electronic Data Interchange.
Special pub. (Final).
R. G. Saltman. Dec 93, 68p, NIST/SP-800/9.
Also available from Supt. of Docs. as SN003-003-03243-3. See also PB90-147489 and PB90-148784. Sponsored by Farmers Home Administration, Washington, DC.

Keywords: *Electronic mail, *Data processing security, Computer security, Computer communications, Commerce, Risk assessment, Documents, Data management, Access control, Cryptography, Authentication, Computer privacy, EC(Electronic Commerce), EDI(Electronic Data Interchange).

Electronic commerce (EC) is the use of documents in electronic form, rather than paper, for carrying out functions of business or government that require interchange of information, obligations, or monetary value between organizations. Electronic data interchange (EDI) is the computer-to-computer transmission of strictly formatted messages that can represent documents; EDI is an essential component of EC. With EC, human participation in routine transaction processing is limited or non-existent. Transactions are processed and decisions are made more rapidly, leaving much less time to detect and correct errors. This report presents security procedures and techniques (which encompass internal controls and checks) that constitute good practice in the design, development, testing and operation of EC systems. Principles of risk management and definition of parameters for quantitative risk assessments are provided. The content of the trading partner agreement is discussed, and the components of EC, including the network(s) connecting the partners, are described. Some security techniques considered include audit trails, contingency planning, use of acknowledgments, electronic document management, activities of supporting networks, user access controls to systems and networks, and cryptographic techniques for authentication and confidentiality.

01,464
PB94-142494 PC A03/MF A01
National Inst. of Standards and Technology, Gaithersburg, MD.
Introduction to Traffic Management for Broadband ISDN.
Y. Chang, D. Su, and S. Wakid. Dec 93, 25p, NISTIR-5214.
See also PB93-149433.

Keywords: *Communications networks, *Traffic management, Communications management, Computer networks, Traffic control, Telecommunication, Standards, Protocols, Congestion, *Broadband Integrated Services Digital Network, *Integrated Services Digital Network, Asynchronous transfer mode.

This paper presents an overview of issues related to the traffic management for the Broadband Integrated Services Digital Networks (B-ISDN). B-ISDN is an emerging high bandwidth telecommunications infrastructure with transmission speeds in the range of mega-bit to giga-bits per second. This paper first analyzes traffic profiles in a B-ISDN environment and their impact on traffic management. It then presents an overview of traffic management for existing communications protocols, and discusses, in depth, how it can be applied to the B-ISDN environment. Finally, the paper gives a brief review of the current work on B-ISDN traffic management by the National Accredited Standards Committee T1 and the International Telegraph and Telephone Consultative Committee (CCITT).

01,465
PB94-142528 PC A05/MF A01
National Inst. of Standards and Technology (CSL), Gaithersburg, MD.
Context Analysis of the Network Management Domain. Conducted as Part of the Domain Analysis Case Study.
C. Dabrowski, and S. B. Katz. Dec 93, 84p, NISTIR-5309.

Keywords: *Communication networks, *Network control, Software engineering, Protocols, Fault detection, *Software reuse, *Domain analysis, Context analysis, FODA(Feature Oriented Domain Analysis), Network management.

A key to increasing software producibility in the development of large, reliable software applications is the systematic reuse of existing software products. Domain analysis is a pivotal technique for developing reusable products that can be used to engineer software systems. The Domain Analysis Case Study was created to investigate domain analysis methods. This report is a product of the Domain Analysis Case Study. This report describes the application of the first phase of a domain analysis effort to the domain of network management systems--software systems that manage communications networks. The first phase of the domain analysis process is called the context analysis phase.

01,466
PB94-162559 PC A16/MF A03
National Inst. of Standards and Technology (CSL), Gaithersburg, MD. Advanced Systems Div.
North American ISDN Users' Forum Agreements on Integrated Services Digital Network.
Special pub. (Final).
D. P. Stokesberry, and T. A. Antonishek. Mar 94, 354p, NIST/SP-823/5.
Also available from Supt. of Docs. as SN003-003-03248-4. See also PB93-173091.

Keywords: Communication networks, Digital communications, Telephone systems, Computer networks, North America, Workstations, Agreements, *Integrated Services Digital Network, Basic rate interface, Primary rate interface, Application profiles, Conformance tests, NIUF forum, Voice mail.

This document compiles the existing North American Integrated Services Digital Network (ISDN) Users' Forum (NIUF) agreements for an ISDN developed and approved in the NIUF as of October 1992. New agreements superseded or added during 1992 cover Layer 1 BRI at the U, and S/T reference points. In addition, this document references the Conformance tests which have been completed by the NIUF. These include: Layer 3 BRI, Layer 2 BRI, PRI at the U reference point, and PRI at the U/S/T reference points. Finally, this document contains the Application Profiles for: Secure Voice Mail; Data Conferencing--Multi-Point; ISDN Telephone Workstation Integration; Engineering Workstation Interface; and the Remote Agent Application Profile.

01,467
PB94-164035 PC A06/MF A02
National Inst. of Standards and Technology, Gaithersburg, MD.
Supplement to Stable Implementation Agreements for Open Systems Interconnection Protocols. Version 3, September 1990. Change Page Index, Version 3, June 1990 (Stable) Change Pages Issued December 1990; Output from September 1990 OSI Workshop (NIST Special Publication 500-177).
Dec 90, 108p.
See also PB90-269556.

Keywords: *Computer networks, *Communication networks, Standards, Agreements, Implementation, Protocols, *Open systems interconnections.

This document records, in replacement page format, all changes to stable material current (according to Version and Edition number) as of the end of the June Workshop. In this case, that would be NIST SP 500-177, Version 3, Edition 1 with previous Change Pages incorporated. By following the instructions and replacing or inserting the indicated pages, text will be created which reflects the current status of relevant stable material as of September 14, 1990.

01,468
PB94-166006 PC A99/MF A06
North American ISDN Users' Forum, Gaithersburg, MD.
Catalog of National ISDN Solutions for Selected NIUF Applications.
Feb 94, 679p.
Supersedes PB93-162881.

Keywords: *Telecommunication, *Technology utilization, Decision making, Telephone systems, Work stations, Local area networks, Supercomputers, Facsimile communication, Voice communication, Screens(Displays), Computer networks, Computer software, Data transmission, Bibliographies, Dictionaries, Real property, Computer files, *ISDN(Integrated Services Digital Network), LAN(Local area networks), Videoconferencing systems, Teleconferencing, Telecommuting.

The NIUF is pleased to present the Second Edition of its ISDN Solutions Catalog. The purpose of the Second Edition remains the same as the first, to make it easier for vendors to develop and support ISDN applications and for users to understand and install them. In February of 1993, the NIUF authorized work on this Second Edition. It provides a more robust set of solutions in Section 3, and adds Section 2 for the 'decision maker', who must decide whether to use ISDN. Many other refinements were made. The scope is essentially the same as the First Edition, with additional coverage of National ISDN-2. New solutions in the Catalog cover National ISDN-2, especially Primary Rate. Of course, changes in products and services are tracked through an updated chapter of product information.

01,469
PB94-214756 PC A08/MF A02
National Inst. of Standards and Technology, Gaithersburg, MD. Office of the Director.
Information Infrastructure: Reaching Society's Goals. Report of the Information Infrastructure Task Force Committee on Applications and Technology.
Special pub.
Sep 94, 160p, NIST/SP-868.
Also available from Supt. of Docs. as SN003-003-03283-2.

Keywords: *Sectoral analysis, *Computer networks, *Information services, Information systems, National interests, Information dissemination, Delivery systems, Citizen participation, Transportation sector, Electric power industry, Social services, Handicapped persons, Emergency preparedness, Public safety, Arts, Humanities, Telecommunications, *NII(National Information Infrastructure), *National Information Infrastructure, Government services, Information superhighways, Information networks, Telecommuting, Intelligent Vehicle Highway System.

Table of Contents:
Introduction;
NII:
An Investment in People with Disabilities;
Supply and Demand of Electric Power and the NII;
Improving Transportation:
The NII and Intelligent Transportation Systems;
Promoting Telecommuting:
An Application of the NII;
The Effect of the NII on Local, State, and Federal Emergency Management;
Public Empowerment with Environmental Information;
Arts, Humanities, and Culture on the NII;
and Public Safety and the NII:
Supporting Law Enforcement and Criminal Justice.

01,470
PB94-217023 PC A04/MF A01
National Inst. of Standards and Technology (CSL), Gaithersburg, MD.
Videoconferencing Procurement and Usage Guide.
Rept. for Oct 93-Jul 94.
M. A. Wallace, and D. E. Rorrer. Aug 94, 54p, NISTIR-5485.
Sponsored by Internal Revenue Service, Washington, DC.

Keywords: *Teleconferencing, *Video communication, *Procurement, Interactive systems, Systems analysis, Integrated systems, Requirements, Personnel development, Training, Sites, Videoconferencing.

A brief history and technical discussion of videoconferencing is presented along with the processes that are required in order to evaluate the need for a videoconferencing system. Guidance is provided for the evaluation, selection, purchase, installation, and use of various options and system types. Communication and physical requirements are discussed with respect to each of the most common systems that are currently available. Personnel training and site preparation requirements are also developed.

01,471
PB94-219094 PC A03/MF A01
National Inst. of Standards and Technology (CSL), Gaithersburg, MD. Advanced Systems Div.
ISDN Conformance Testing Guidelines: Guidelines for Implementors of ISDN Customer Premises Equipment to Conform to Both National ISDN-1 and North American ISDN Users' Forum Layer 3 Basic Rate Interface Basic Call Control Abstract Test Suites.
Special pub.
L. A. Collica, and D. M. Hoffman. Jul 94, 29p, NIST/SP-823/6.
Also available from Supt. of Docs as SN003-003-03278-6.

Keywords: *Tests, *Protocols, *Telecommunication, Interfaces, Guidelines, Communication networks, Communications management, Communication equipment, *ISDN(Integrated Services Digital Network), *Integrated Services Digital Network.

The document is intended to provide information, as a supplement to the abstract test suites, to allow conformance to both the Bellcore National ISDN-1 (NI-1) and North American ISDN Users' Forum (NIUF) NIU.301 specifications for the ISDN Layer 3 Basic Rate Interface for Basic Call Control (user-side). It was developed to guide implementors in the design of customer premises equipment in a manner which would allow them to pass both the NI-1 and NIUF conformance tests. It may also be useful to vendors of test equipment, government procurement agents, and testing laboratories.

01,472
PB95-103677 PC A09/MF A03
National Inst. of Standards and Technology (EEEL), Gaithersburg, MD. Electricity Div.
Report on the Workshop on Advanced Digital Video in the National Information Infrastructure. Held in Washington, D.C. on May 10-11, 1994.
C. Fenimore, B. Field, H. Frank, G. Reitmeier, W. Stackhouse, C. Van Degrift, E. Georg, and M. Papillo. Jul 94, 195p, NISTIR-5457.

Keywords: *Meetings, *Information systems, *Digital data, *Video data, Communication networks, Information services, Television systems, Telecommunication, Telemedicine, High definition television, Video compression, Standards, Interactive systems, *NII(National Information Infrastructure), *National Information Infrastructure, *ADV(Advanced Digital Video), *Advanced Digital Video, ATM(Asynchronous Transfer Mode), ATV(Advanced Television System).

Contents:
Summary Report by the Program Committee;
Workshop Agenda;
Breakout Group Reports;
Visions and Services of the National Information Infrastructure;
Production and Distribution of Entertainment in the NII;
Medical Applications;
Putting Advanced Digital Video on the Technology Curve;
National Information Infrastructure:
An Administration Perspective;
Interoperability Aspects of the Grand Alliance HDTV System;
Video Compression Technology;
Advanced Digital Video over ATM Networks;
Digital Video in the Internet:
Status, Technology, and Issues;
Standards Panel:
Old Game, New Rules;
Advancing the National Interactive Communications Systems;
The National Information Infrastructure and the Grand Alliance ATV System:
A Commentary on Some Aspects of Interoperation;
A Commentary on Requirements for the Interoperation of Advanced Television with the National Information Infrastructure;
Arguments in Support of Embedded Multiresolution Signaling Strategies for HD Video Transmission.

01,473
PB95-105383 PC A13/MF A03
National Inst. of Standards and Technology (CSL), Gaithersburg, MD.
Security in Open Systems.
Special pub.
R. Bagwill, J. Barkley, L. Carnahan, P. Markovitz, A. Nakassis, K. Olsen, M. Ransom, J. Wack, S. Chang, and R. Kuhn. Jul 94, 290p, NIST/SP-800/7.
Also available from Supt. of Docs. as SN003-003-03276-0. Sponsored by National Communications System, Arlington, VA.

Keywords: *Telecommunication, *Applications programs(Computers), *Computer security, Standards, Software engineering, Operating systems(Computers), UNIX(Operating system), Specifications, Cryptography, Man computer interface, Computer networks, Open systems, US NIST, PSN(Public Switched Network), POSIX(Portable Operating System Interface).

The report is intended to provide information for the practicing programmer involved in development of telecommunications application software. It provides information on building security into software based on open system platforms. It is not intended to be tutorial in nature and assumes some knowledge of open systems and UNIX. It covers the following topics: Portable Operating System Interface (POSIX) Open System Environment; Functional Requirements Specifications for Computer Security; POSIX Security Interfaces and Mechanisms; Standard Cryptographic Service Calls; Human/Computer Interaction Services Security; the X Window System; SQL; Network Security Threats; Improving Security in a Network Environment; X.400 Message Handling Services; X.500 Directory Services.

01,474
PB95-143145 PC A03/MF A01
National Inst. of Standards and Technology (CSL), Gaithersburg, MD. Systems and Software Technology Div.
Information Technology Engineering and Measurement Model: Adding Lane Markings to the Information Superhighway.
M. Zelkowitz, and B. Cuthill. Nov 94, 46p, NISTIR-5522.
See also PB94-163383. Prepared in cooperation with Maryland Univ., College Park. Dept. of Computer Science.

Keywords: *Information systems, *Systems engineering, *Software engineering, *Computer systems design, Distributed data processing, Database management, Information flow, Information dissemination, Computer networks, Information services, Information technology, Telecommunications, *National Information Infrastructure, Information superhighways, Information networks, ITEM(Information Technology Engineering and Measurement).

Development of the National Information Infrastructure (NII) will depend upon building vast networks on the interconnected computers communicating over high-speed digital lines. This paper describes the growth of the NII concept and proposes a model-the Information Technology Engineering and Measurement (ITEM) model-that may be useful in describing the set of services an operational NII may contain.

01,475
PB95-143178 PC A03/MF A01
National Inst. of Standards and Technology (CSL), Gaithersburg, MD. Advanced Systems Div.
Channel Coding for Code Excited Linear Prediction (CELP) Encoded Speech in Mobile Radio Applications.
E. Bracha, N. Farvardin, and Y. Yesha. Aug 94, 40p, NISTIR-5503.
See also PB93-173938.

Keywords: *Mobile communication systems, *Channels(Data transmission), *Coding, Radio communication, Error correction codes, Computerized simulation, Algorithms, *CELP(Code Excited Linear Prediction), *Code Excited Linear Prediction.

The National Wireless Performance Benchmarking Program seeks to provide tools, performance metrics, methodologies and testbed facilities to the wireless industry and users, so as to allow consistent and impartial performance measurement of wireless communication systems. As a part of this program, a research program is currently being undertaken, in which the mobile radio channel effects on Code Excited Linear Prediction (CELP) encodes speech data are studied. This research uses software simulations to test the various algorithms and evaluate their performance. This report provides a detailed description of the tests performed

in this study, including bit error and bit protection sensitivity tests as well as various error correction code tests. It also evaluates different error correction codes for use for channel coding of wireless communication systems.

01,476
PB95-151270 Not available NTIS
National Inst. of Standards and Technology (PL), Boulder, CO. Quantum Physics Div.
Slant Path Atmospheric Refraction Calibrator: An Instrument to Measure the Microwave Propagation Delays Induced by Atmospheric Water Vapor.
Final rept.
S. Walter, and P. Bender. 1992, 10p.
Pub. in Institute of Electrical and Electronics Engineers Transactions on Geoscience and Remote Sensing 30, n3 p462-471 May 92.

Keywords: *Microwave transmission, *Water vapor, Tropospheric propagation, Light transmission, Radio transmission, Atmospheric composition, Atmospheric refraction, Microwave radiometers, Performance evaluation, Remote sensing, Travel time, Time delay, Measuring instruments, Reprints, *SPARC calibrator, Atmospheric transmissivity.

The Slant Path Atmospheric Refraction Calibrator, SPARC, has been developed to measure the water vapor induced propagation delay experienced by a radio signal traversing the atmosphere. SPARC measures the difference in the travel times between an optical and a microwave signal propagating along the same atmospheric path. Since the refractivity of dry air is similar for both the microwave and optical signals, the difference in arrival times is a sensitive measure of the water vapor induced microwave delay. The instrument is capable of measuring the difference in the optical and microwave travel times with an accuracy of 15 ps or better. SPARC was developed to provide an accurate, independent method for evaluating other techniques used to determine the atmospheric water vapor induced delay. The theoretical and experimental issues involved in making measurements of the delay induced by water vapor are discussed. Measurements along a 13.35-km ground-based path are presented, which will illustrate the instrument's stability, precision, and accuracy.

01,477
PB95-154696 PC A03/MF A01
National Inst. of Standards and Technology (CSL), Gaithersburg, MD.
ISDN LAN Bridging.
T. Boland. Nov 94, 26p, NISTIR-5532.
Also available from Supt. of Docs. Sponsored by Internal Revenue Service, Washington, DC.

Keywords: *Local area networks, Computer networks, Communication networks, Routing, Narrowband, Multimedia, Procurement, Personal computer, Protocols, Data processing security, Data integrity, *ISDN(Integrated Services Digital Network), *Integrated Services Digital Network, *Bridging.

This paper describes the interconnection of a user to a local area network (LAN) across a wide area using an Integrated Services Digital Network (ISDN). This interconnection enables users to access remote applications and services as though they were local to the user.

01,478
PB95-163176 Not available NTIS
National Inst. of Standards and Technology (ICST), Gaithersburg, MD. Advanced Systems Div.
ISDN Conformance Testing.
Final rept.
D. H. Su, and L. A. Collica. 1991, 9p.
Pub. in Proceedings of the Institute of Electrical and Electronics Engineers 79, n2 p190-198 1991.

Keywords: Protocols, Telecommunications, Communication networks, Digital communications, Interoperability, Interfaces, Tests, Standards, Reprints, *ISDN(Integrated Services Digital Networks), *Integrated Services Digital Networks, *Conformance testing.

Advances in communication networks have increased the complexity of communications protocols and interfaces significantly, and correct interpretation of standards has become a critical issue in ensuring interoperability of equipments from different vendors. The challenge to the telephony industry in providing high quality Integrated Services Digital Network (ISDN) service and interoperable ISDN products is unprecedented, as the ISDN protocols and interfaces are very complex and more open in terms of how services are to be provided. Conformance testing is a fundamental task in meeting this challenge.

01,479
PB95-163689 Not available NTIS
National Inst. of Standards and Technology (ICST), Gaithersburg, MD. Advanced Systems Div.
Application Profile for ISDN.
Final rept.
S. Wakid, and K. Roberts. 1991, 6p.
Pub. in Proceedings of the Institute of Electrical and Electronics Engineers 79, n2 p199-204 Feb 91.

Keywords: *Data processing, Standards, File management systems, Data transfer(Computers), Facsimile communication, Information retrieval, Electronic mail, Reprints, *ISDN(Integrated Services Digital Network), *Integrated Services Digital Network, EDI(Electronic Data Interchange).

This paper emphasizes some key data processing applications to be used in conjunction with the voice and facsimile services as a platform for deploying Integrated Services Digital Network (ISDN) in North America. Special emphasis is placed on the emerging standards of both ANSI T1 and X3 in an attempt to harmonize the computer and telecommunication industries towards providing the user with an integrated platform that is vendor transparent and ubiquitous. This generic platform, which spans a large sector of businesses, is only presented as a base context for defining user specific needs and incubating the applications that directly relate to businesses. Distributed Transaction Processing, Electronic Data Interchange, Information Retrieval, Electronic Mail, and File Transfer together with seven supplementary services for voice and G4 facsimile are proposed for ISDN deployment in the marketplace. This paper, therefore, describes how the relevant standards may be exercised via the various ISDN channels and emphasizes the value of the North American ISDN Users' Forum for commercializing this platform.

01,480
PB95-168563 Not available NTIS
National Inst. of Standards and Technology (EEEL), Boulder, CO. Electromagnetic Technology Div.
Lightwave Standards Development at NIST.
Final rept.
D. L. Franzen. 1994, 310p.
Pub. in Proceedings of Department of Defense Fiber Optics '94 'Optical Networks in the Concept of a Global Grid', McLean, VA., March 22-24, 1994, p443-445.

Keywords: *Optical communication, *Optical fibers, *Optical detectors, *Standards, Infrared detectors, Wave dispersion, Frequency response, Fiber optics, Wavelengths, Reprints, Optical power, US NIST.

Standards being developed at the National Institute of Standards and Technology support the following parameters of interest to lightwave communications: optical fiber geometry, optical fiber chromatic dispersion, absolute optical power, high speed detector frequency response, and wavelength.

01,481
PB95-174967 PC A03/MF A01
National Inst. of Standards and Technology (CSL), Gaithersburg, MD.
Asynchronous Transfer Mode Procurement and Usage Guide.
T. Boland. Dec 94, 43p, NISTIR-5561.
Sponsored by Internal Revenue Service, Washington, DC.

Keywords: *Procurement, *Utilization, Telecommunication, Data transfer(Computers), Computer networks, Data transmission, Access control, Data processing security, Local area networks, Management, *ATM(Asynchronous Transfer Mode), *Asynchronous Transfer Mode, B-ISDN(Broadband Integrated Services Digital Network).

This paper gives complete procurement and usage guidance to acquisition of asynchronous transfer mode (ATM) technology. ATM uses a high-speed cell switching technology to move data rapidly between distinct end points.

01,482
PB95-178604 PC$9.00
National Inst. of Standards and Technology (NML), Gaithersburg, MD. National Telecommunications and Information Administration, Washington, DC. Office of Management and Budget, Washington, DC.
Global Information Infrastructure: Agenda for Cooperation.
Feb 95, 57p.
Also available from Supt. of Docs. See also PB93-231272. Prepared in cooperation with National Telecommunications and Information Administration, Washington, DC. and Office of Management and Budget, Washington, DC. Office of Information and Regulatory Affairs.

Keywords: *Information systems, *Access to information, *Online systems, Information dissemination, Information retrieval, Information technology, Information services, Computer networks, Benefits, Investments, Policies, International cooperation, Global aspects, *GII(Global Information Infrastructure), *Global Information Infrastructure, Information networks, Information superhighways.

Table of Contents:
Introduction;
Building a Foundation for the Global Information Infrastructure (GII)-- Five Basic Principles;
Encouraging The Use of the GII;
Implementing The GII;
Conclusion;
Appendix A - Summary of Recommendations;
Appendix B - GII Hearing Testimony;
Appendix C - GII Key Contacts.

01,483
PB95-189445 PC A03/MF A01
National Inst. of Standards and Technology (CSL), Gaithersburg, MD.
Impact of the FCC's Open Network Architecture on NS/NP Telecommunications Security.
Special pub.
K. Olsen, and J. Tebbutt. Feb 95, 50p, NIST/SP-800/11.
Also available from Supt. of Docs. as SN003-003-03318-9. See also PB95-105383.

Keywords: *National security, *Emergency preparedness, *Telecommunication, *Security, Access control, Data processing security, Threats, Vulnerability, Computer networks, Communication networks, FCC(Federal Communications Commission), ONA(Open Network Architecture), PSN(Public Switched Network), NS/EP(National Security/Emergency Preparedness).

The Public Switched Network (PSN) provides National Security and Emergency Preparedness (NS/EP) telecommunications. Service vendors, equipment manufacturers, and the federal government are concerned that vulnerabilities in the PSN could be exploited and result in disruptions or degradation of service. The National Institute of Standards and Technology (NIST) is investigating the vulnerabilities and related security issues that result from use of the Federal Communications Commission's (FCC's) Open Network Architecture (ONA). This report provides an overview of ONA, describes NS/EP telecommunications security concerns, and describes NS/EP telecommunications security concerns that the FCC's ONA requirement introduces into the PSN.

01,484
PB95-210936 PC A03/MF A01
National Inst. of Standards and Technology (CSL), Gaithersburg, MD. Systems and Software Technology Div.
Electronic Implementors' Workshop.
A. T. Landberg, R. H. Bagwill, and B. J. Gray. Mar 95, 19p, NISTIR-5623.
Presented at the RWS-CC Meeting (13th), Osaka, Japan, March 7-8, 1995.

Keywords: *Telecommunication, *Interoperability, *Information technology, Computer networks, Digital communications, Communication networks, Systems integration, Data access, User needs, Information dissemination, Standards, Protocols, *Electronic workshops, Internet.

The report has been prepared for the 13th RWS-CC Meeting held in Osaka, Japan, March 7-8, 1995. It describes the various elements of an electronic workshop and provides a list of capabilities needed to operate one. The primary elements of an electronic workshop include use of the Internet for basic communications such as electronic mail and public forums and publica-

tion and distribution of publications using computer based media such as Info Servers and CD ROM technology. The necessary prerequisites for establishing an electronic workshop are discussed along with policy and procedures that must be put into plane. Going electronic in the operation of the OSE Implementors Workshop has meant substantial cost savings while improving the timeliness and accessibility of information to the public and members.

01,485
PB95-231882 PC A20/MF A04
National Inst. of Standards and Technology (CSL), Gaithersburg, MD.
Standards Policy and Information Infrastructure.
May 95, 454p, NIST/GCR-95/670.

Keywords: *Standards, *Policy making, *Intellectual property, Telecommunication, Government policies, Federal government, Communication networks, Information systems, Information technology, Information flow, Information dissemination, Standarization, Interoperability, *National Information Infrastructure, Open systems.

The purpose of this book is not to think about how formal de jure standards might best be developed, but to consider how standards work as a dynamic, living process--a dialog about technology and how limited common implementations of technology may be useful to enable interoperability and spur market development. The test lies in the market response to the standards process and its expressions--reference models, architectures, draft specifications, or standards--and in the further response of the standards process to the market.

01,486
PB95-267993 PC A06/MF A02
National Inst. of Standards and Technology (TS), Gaithersburg, MD. National Voluntary Lab. Accreditation Program.
National Voluntary Laboratory Accreditation Program. GOSIP: Government Open Systems Interconnection Profile.
Handbook.
J. Horlick, S. Nightingale, and J. P. Favreau. Feb 95, 120p, NIST/HB-150/12.
Also available from Supt. of Docs. as SN003-003-03353-7. See also FIPS PUB 146-1.

Keywords: *Computer networks, *Communication networks, *Message processing, Protocols, File management systems, Data transmission systems, Computer architecture, Requirements, Certification, Procedures, Calibration standards, Standardization, Equipment, Management, Auditing, Test methods, Personnel, *GOSIP(Government Open Systems Interconnection Profile), *Government Open Systems Interconnection Profile, NVLAP(National Voluntary Laboratory Accreditation Program).

NIST Handbook 150-12 presents the technical requirements of the National Voluntary Laboratory Accreditation Program (NVLAP) for the GOSIP - Government Open Systems Interconnection Profile program. It is intended for information and use by staff of accredited laboratories, those laboratories seeking accreditation, other laboratory accreditation systems, of laboratory services, and others needing information on the requirements for accreditation under the GOSIP program.

01,487
PB96-106851 PC A04/MF A01
National Inst. of Standards and Technology (CSL), Gaithersburg, MD. Advanced Systems Div.
NIST ATM Network Simulator: Operation and Programming, Version 1.0.
N. Golmie, A. Koenig, and D. Su. Aug 95, 63p, NISTIR-5703.

Keywords: *Communication networks, *Systems simulation, *Data transmission systems, *Manuals, Telecommunication, Computer graphics, Technology assessment, Models, Information systems, *ATM(Asynchronous Transfer Mode), *Asynchronous Transfer Mode, Graphical user interface, Network topology.

An Asynchronous Transfer Mode (ATM) network simulator has been developed to provide a means for researchers and network planners to analyze the behavior of ATM networks without the expense of building a real network. The simulator is a tool that gives the user an interactive modeling environment with a graphical user interface. With this tool, the user may create different network topologies, control computer parameters, measure network activity, and log data from simulation runs. Part 1 of this document is the user's manual for the simulator; it includes instructions for creating network configurations, specifying component parameters, manipulating the display, logging and saving measurements, and post-processing of data. Part 2 has been prepared as a guide for the user who wishes to modify the simulator software to accommodate network components not previously defined or to change the behavior of components already defined.

01,488
PB96-119367 Not available NTIS
National Inst. of Standards and Technology (EEEL), Gaithersburg, MD. Electricity Div.
National Information Infrastructure and Advanced Digital Video.
Final rept.
C. Fenimore. 1994, 17p.
See also PB95-103677.
Pub. in International Symposium of Digital Imagery '94 'Digital Image and Interactive Services', Tokyo, Japan, October 17-24, 1994, p1-17.

Keywords: *Digital data, *Video data, *Information services, *Image processing, Video compression, Television systems, Telecommunication, Interactive systems, Communication networks, Information systems, Standards, Reprints, National Information Infrastructure.

The U.S. Administration regards the development of a National Information Infrastructure (NII) as a way of putting vast amounts of information at the fingertips of users in America and around the world. Digital video services are likely to be the most technically demanding NII service. Recognizing this, the National Institute of Standards and Technology (NIST), the Technology Policy Working Group of the Administration's Information Infrastructure Task Force and several industrial organizations sponsored a recent Workshop to: (1) define a vision of the role of digital video in the NII; (2) identify the architectural, scaling, and performance issues in realizing this vision; and (3) recommend the research, experiments, and other steps to taken to resolve these issues.

01,489
PB96-119433 Not available NTIS
National Inst. of Standards and Technology (EEEL), Gaithersburg, MD. Electricity Div.
Perception of Clamp Noise in Television Receivers.
Final rept.
S. Herman, B. F. Field, P. Boynton, and G. de Haan. 1994, 4p.
Pub. in International Display Research Conference, Monterey, CA., October 10-13, 1994, p317-320.

Keywords: *Television systems, *Clamping circuits, *Signal-to-noise ratio, Clamps, Signal processing, Video signals, Scintillation, Time constants, Reprints.

Clamp circuits in television systems adjust the black level of each scan line to a reference voltage derived from the 'back porch' of the T.V signal. If the TV signal is noisy, then the derived black level can vary from scan line, resulting in a displayed streaking effect called 'clamp noise.' This paper reports on clamp noise research performed on a video processing supercomputer at the National Institute of Standards and Technology (NIST). This research measured the average input video signal-to-noise ratio (SNR) at which human observers can just begin to perceive clamp noise against a background of moving color pictures. This threshold was measured as a function of two parameters: two-dimensional scintillation noise due to broadband video noise, and the time constant of the clamp circuitry. These results may give TV system designers guidance in choosing tradeoffs between scintillation noise processing and clamp noise reduction.

01,490
PB96-122411 Not available NTIS
National Inst. of Standards and Technology (EEEL), Gaithersburg, MD. Electronics and Electrical Engineering Lab. Office.
Making Displays Deliver a Full Measure.
Final rept.
H. S. Bennett, C. Fenimore, B. F. Field, and E. F. Kelley. 1995, 8p.
Pub. in Official Monthly Publication of the Society for Information Display, 'Information Display', v11 n1 p20-27 Jan 95.

Keywords: *Display devices, *High resolution, *Standards, Video data, Information systems, Image processing, Measurement, Performance evaluation, Technology innovation, Reprints.

High-Resolution Displays are essential for market acceptance of advanced video systems and for sophisticated exploitation of 'the information age'. Developing and manufacturing such displays will require advanced measurement capabilities. This is a subject that interests us greatly at the National Institute of Standards and Technology (NIST), where the development of measurement standards and their application to industrial competitiveness have long been a central part of the authors' mission.

01,491
PB96-122452 Not available NTIS
National Inst. of Standards and Technology (CSL), Gaithersburg, MD. Advanced Systems Div.
Error Protecting Characteristics of CDMA and Impacts on Speech.
Final rept.
D. Cypher, S. Wakid, J. Bose, and D. Vaman. 1995, 6p.
Pub. in Institute of Electrical and Electronics Engineers Workshop (3rd) on the Architecture and Implementation of High Performance Communication Subsystems (HPCS '95), Mystic, CT., August 23-25, 1995, p141-146.

Keywords: *Code division multiple access, *Mobile communication systems, *Satellite communication, *Speech, Synchronism, Feedback control, Automatic control, Errors, Reprints.

A Code Division Multiple Access (CDMA) wireless network is simulated to analyze errors, determine impact on services, and provide an upper bound on the number of active channels. The simulation emphasizes the encoder, decoder/correlator, and a threshold detector; but assumes a resultant Gaussian Function for the 'air interface' noise. Since the characteristics of a wireless enviroment vary significantly, we examine, as a whole, the errors on the received signal without accounting for specific error contributions from power, fading, propagation, interference from other users, and other factors in such environment. The CDMA encoder uses the 64 Walsh codes that are specified in the draft Wideband CDMA Air Interface Compatibility Standard for 1.85 to 1.99 GHz PCS Applications (1). We use a digitized actual speech database to test for the intelligibility of the voice service over such a CDMA air interface. Therefore, we are able to learn about the nature of the errors inherent in such a frequency spreading technique and also determine an upper bound on the Simultaneous active channels that would preserve the quality of service (QOS).

01,492
PB96-131487 PC A03/MF A01
National Inst. of Standards and Technology, Gaithersburg, MD.
Application Software Interface: ISDN Services for an Open Systems Environment.
D. P. Stokesberry. Feb 95, 36p, NISTIR-5595.

Keywords: *Communication networks, *Specifications, Integrated systems, Digital communications, Computer program portability, Interoperability, Computer networks, Telecommunication, Information technology, Criteria, Evaluation, Standards, Interfaces, *ISDN(Integrated Services Digital Network), *Integrated Services Digital Network, Open System Environment, ATM(Asynchronous Transfer Mode), APP(Application Portability Profile), ASI(Application Software Interface), National Information Infrastructure.

This report provides the specific information required to evaluate the Application Software Interface (ASI) as one component of an Open System Environment (OSE) which might include POSIX, GOSIP, and other specifications to provide the functionality necessary to address a broad range of federal information technology requirements.

01,493
PB96-131511 PC A03/MF A01
National Inst. of Standards and Technology (CSL), Gaithersburg, MD. Distributed Systems Engineering.
Sharing Information via the Internet: An Infoserver Case Study.
R. H. Bagwill. Nov 95, 28p, NISTIR-5757.

Keywords: *Information dissemination, *Data access, Computer networks, On-line systems, Computer com-

munications, Application programs(Computers), Electronic mail, Specifications, Standards, Requirements, Case studies, *Internet, World wide web, Gopher, Data formats, Software protocols.

A variety of proprietary systems are available from commercial vendors, but the most rapid deployment of electronic document distribution has been by systems on the Internet using software based on open standards. This report describes some of the experiences of the Distributed Systems Engineering Group has had employing this software.

01,494
PB96-131578 PC A03/MF A01
National Inst. of Standards and Technology (CSL), Gaithersburg, MD. Information Access and User Interface Div.
Electronic Access to Standards on the Information Highway.
S. J. Laskowski, and V. V. Ramayya. Aug 95, 18p, NISTIR-5708.
See also PB95-103719. Prepared in cooperation with National Standards Systems Network Project, Arlington, VA.

Keywords: *Accessibility, *On-line systems, *Standards, Information systems, Computer networks, Technical assistance, User needs, Information needs, Information retrieval, Information technology, Telecommunication, *National Information Infrastructure, *Information highways, NSSN(National Standards Systems Network), Internet, World wide web, Virtual libraries, System architecture.

We discuss how the information highay can be used to support electronic access standards and standards information. We then show how a network of collections of standards and standards information based on an Internet architecture can be viewed as a 'virtual library of standards' by the users, while allowing standards providers to control and maintain the ownership of these collections on a set of heterogeneous databases. Next, we focus on how the needs of users and developers can be supported through search for standards via a common user interface. We conclude with some thoughts on support for standards development on the information highway and other related issues.

01,495
PB96-138607 Not available NTIS
National Inst. of Standards and Technology (PL), Boulder, CO. Time and Frequency Div.
High Resolution Time Interval Counter.
Final rept.
V. S. Zhang, D. D. Davis, and M. A. Lombardi. 1994, 10p.
See also DE95009972, and N95-32331 (available as N95-32319).
Pub. in Annual Precise Time and Time Interval (PTTI) Applications and Planning Meeting (26th), Reston, VA., December 6-8, 1995, p191-200 1994.

Keywords: *Time interval analyzers, *Modems, Time log, Frequency measurement, Frequency analysis, High resolution, Counters, Reprints.

In recent years, we have developed two types or high resolution, multi-channel time interval counters. In the NIST two-way time transfer MODEM application, the counter is designed for operating primarily in the interrupt-driven mode, with 3 start channels and 3 stop channels. The intended start and stop signals are 1 PPS, although other frequencies can also be applied to start and stop the count. The time interval counters used in the NIST Frequency Measurement and Analysis System are implemented with 7 start channels and 7 stop channels. Four of the 7 start channels are devoted to the frequencies of 1 MHz, 5 MHz or 10 MHz, while triggering signals to all other start and stop channels can arrange from 1 PPS to 100 kHz. Time interval interpolation plays a key role in achieving the high resolution time interval measurements for both counters.

01,496
PB96-139415 PC A03/MF A01
National Inst. of Standards and Technology (NCSL), Gaithersburg, MD. Systems and Network Architecture Div.
Telecommunications Security Guidelines for Telecommunications Management Network. Computer Security.
Special pub.
J. Kimmins, C. Dinkel, and D. Walters. Oct 95, 46p, NIST/SP-800/13.
Also available from Supt. of Docs. as SN003-003-03376-6. See also PB95-189445.

Keywords: *Secure communications, *Voice communications, *Guidelines, Communication networks, Threats, Access control, Confidentiality, Vulnerability, Life cycles, Operation and maintenance, Integrity, Requirements, Telecommunication, *PSN(Public Switched Network), *Public Switched Network, Open systems architecture.

The Public Switched Network (PSN) provides critical commercial telecommunications services and National Security and Emergency Preparedness (NSEP). Telecommunication Service providers, equipment manufacturers, users, and the Federal Government are concerned that vulnerabilities in the PSN could be exploited and result in disruptions or degradation of service. This guideline focuses on two specific components of a Telecommunications Management Network (TMN) - Network Elements (NEs) and Mediation Devices (MDs) - with emphasis on the security features needed to protect the Operations, Administration, Maintenance, and Provisioning (OAM&P) of these components. This document is intended to provide a security baseline for NEs and MDs that is based on commercial security needs. In addition, some National Security and Emergency Preparedness (NS/EP) security requirements will be integrated into the baseline to address specific network security needs. The guideline should assist telecommunications vendors in developing systems and service providers in implementing systems with appropriate security for integration into the PSN.

01,497
PB96-141320 Not available NTIS
National Inst. of Standards and Technology (EEEL), Gaithersburg, MD. Electricity Div.
Summary Report on the Workshop on Advanced Digital Video in the National Information Infrastructure.
Final rept.
C. Fenimore, B. Field, H. Frank, G. Reitmeier, W. Stackhouse, C. Van Degrift, E. Georg, and M. Papillo. 1995, 5p.
See also PB95-103677 and PB96-119367.
Pub. in Society of Motion Picture and Television Engineers, Inc., v104 n3 p148-152 Mar 95.

Keywords: *Digital data, *Video data, *Standards, *Telecommunication, Communication systems, High definition, Television systems, Image processing, Video compression, Interactive systems, Information services, Reprints, National Information Infrastructure.

The development of a National Information Infrastructure (NII) is a way of putting vast amounts of information at the fingertips of users in America and around the world. Digital video is likely to be the most technically demanding NII service. Recognizing this, several industrial and governmental organizations sponsored a recent workshop to define a vision of the role of digital video in the NII; identify the architectural, scaling, and performance issues in realizing this vision; and recommend the research, experiments, and other steps to be taken to resolve these issues. It was the sense of the participant in the workshop that the Grand Alliance proposal for HDTV is the best available alternative for terrestrial broadcast of HDTV in the U.S.

01,498
PB96-160452 Not available NTIS
National Inst. of Standards and Technology (CSL), Gaithersburg, MD. Computer Security Div.
Comparison of FDDI Asynchronous Mode and DQDB Queue Arbitrated Mode Data Transmission for Metropolitan Area Network Applications.
Final rept.
W. E. Burr, S. Wakid, D. Vaman, and X. Qian. 1994, 12p.
Pub. in Institute of Electrical and Electronics Engineers Workshop on Metropolitan Area Networks (5th), Taormina, Italy, May 12, 1992, 12p Apr 94.

Keywords: *Wide area networks, *Computer networks, *Data transmission, Packet transmission, Network analysis, Communication traffic, Computer performance evaluation, Communication networks, Protocols, Mathematical models, Reprints, DQDB(Distributed Queve Dual Bus), FDDI(Fiber Distributed Data Interface).

The performance of the FDDI token ring and IEEE 802.6 DQDB protocols are compared using discrete event simulation models. A Metropolitan Aera Network (MAN) of 100 km and with 50 stations was moldeled. A 100 Mbps channel is used for both networks, with a traffic model with large (1 kbyte) low priority packets and smaller (100 byte) high priority packets. The delay and fairness characteristics of both networks are analyzed. The simulations show that FDDI has advantages in fairness and maximum capacity, while DQDB offers lower delay at all except very heavy loads and has a stronger priority mechanism.

01,499
PB96-160460 Not available NTIS
National Inst. of Standards and Technology (CSL), Gaithersburg, MD. Advanced Systems Div.
Standardization for ATM and Related B-ISDN Technologies.
Final rept.
D. Cypher, and S. Wakid. 1993, 14p.
Pub. in Association for Computing Machinery (ACM) Standard Review, p1-14 Sep 93.

Keywords: *Computer networks, *Interfaces, *Standards, Communication networks, Protocols, User needs, Wide area networks, Local area networks, Operation and maintenance, Compatibility, Telecommunication, Reprints, ATM(Asychronous Trasfer Mode), B-ISDN(Broad Integrated Services Digital Network), Interconnections.

The Computer and Telecommunication industries are finally converging towards one single communication technology that permits transparency between the Local and Wide Area networks. This Asynchronous Transfer Mode (ATM) enables the remote interconnection of Local Area Networks (LANs) with compatibly switched telecommunication services rather than expensive private lines. ATM provides scalable high bandwidths, therefore promoting applications in imagery, visualization, video, and others; however, its key value is in shielding the dependency of protocols on media thus providing a seamless shell for interfacing and upgrading current communication gear. In, addition, users are able to dynamically allocate bandwidth on demand, use one unified addressing scheme, and obtain a spectrum of integrated services.

01,500
PB96-160551 Not available NTIS
National Inst. of Standards and Technology (CSL), Gaithersburg, MD. Advanced Systems Div.
Hardware Measurement Techniques for High-Speed Networks.
Final rept.
A. Mink, Y. Fouquet, and S. Wakid. 1994, 21p.
Pub. in Institute of Electrical and Electronics Engineers Summer Topical Meeting, Santa Barbara, CA., July 28-30, 1993, Jnl. of High-Speed Networks, v3 p187-207 1994.

Keywords: *Computer performance evaluation, *Very large scale integration, *Data flow analysis, *Network analysis, Computer networks, Computer systems hardware, Computer architecture, High speed, Applications programs(Computers), Bandwidth, Standardization, Protocols, Kernel functions, Reprints, Ethernet.

The utilization of the inherent bandwidth in high-speed networks is often obstructed by implementation of the protocols. NIST and ARPA developed VLSI measurement components that permit researchers and product developers to better understand computing and communication bottlenecks by accurate measurement techniques. To illustrate and promote the use of such public domain components, this paper uses image transfer as an example application via a commercial UNIX (BSD 4.3.1 variant) implementation of the TCP/IP protocol over an Ethernet (10 Mbits/s), and a HIPPI (800 Mbits/s) medium. The only modification done to this commercially available kernel was to add the simple probe code necessary to interface to the NIST MultiKron measurement chip. The accurate data obtained for the various aspects of this protocol implementation clearly illustrate the major bottlenecks, provide insight with regard to scaling, and determine upper bounds on performance.

01,501
PB96-160635 Not available NTIS
National Inst. of Standards and Technology (CSL), Gaithersburg, MD. Advanced Systems Div.

Provision of Isochronous Service on IEEE 802.6.
Final rept.
X. Qian, S. Kumar, D. Vaman, S. Wakid, and D. Cypher. 1994, 7p.
Pub. in Institute of Electrical and Electronics Engineers Transactions on Communications, 7p Apr 94.

Keywords: *Circuit interconnections, *Communication networks, *Data links, Data transmission, Message processing, Channel capacity, Communications traffic, Signal transmission, Packet switching, Bandwidth, Reprints, Integrated Services Digital Network.

Ths paper concentrates on the provision of isochronous services to users via the existing IEEE 802.6 framework using q.931 as the signalling protocol for providing call control functions. We present possible scenarios of isochronous service provisioning via the IEEE 802.6 network. Real time performance for call setup procedures is simulated and analyzed with different priority schemes for transferring signalling messages. Call setup delays are determined using both Poisson-type and bursty type data traffic models.

01,502
PB96-160767 Not available NTIS
National Inst. of Standards and Technology (CSL), Gaithersburg, MD. Advanced Systems Div.
ISDN in North America.
Final rept.
S. Wakid, and D. Stokesberry. 1993, 13p.
Pub. in Institute of Electrical and Electronic Engineers Communications Magazine, 13p May 93.

Keywords: *Communication networks, *Standards, Digital communications, Agreements, Telecommunication, North America, Reprints, *ISDN(Integrated Services Digital Network), *Integrated Services Digital Network, FIPS(Federal Processing Standards).

This paper is an overview of the progression of Integrated Services Digital Networks (ISDN) in North America with a focus on the activities of the North American ISDN Users' Forum (NIUF), a consortium of users, service providers, network equipment manufacturers, customer premises equipment manufacturer, and applications software developers. This article discusses the role of the NIUF in the product development cycle, provides an overview of its activities and briefly discusses other important and complementary ISDN work. It outlines the beginning deployment of a natioanl ISDN and a major demonstration of ISDN capability within North America. Finally, it offers the perspective of ISDN as an enabling technology and not as a network that meets all communications requirements for all users.

01,503
PB96-160775 Not available NTIS
National Inst. of Standards and Technology (CSL), Gaithersburg, MD. Advanced Systems Div.
North American Agreements on ISDN.
Final rept.
S. A. Wakid, and K. Roberts. 1992, 6p.
See also PB94-162559 and PB96-160767.
Pub. in Institute of Electrical and Electronics Engineers Communications Magazine, Special Issue, p42-47 Aug 92.

Keywords: *Communication networks, *Standards, Digital communications, Agreements, Telecommunication, North America, Reprints, *ISDN(Integrated Services Digital Network), *Integrated Services Digital Network, FIPS(Federal Processing Standards).

This article presents the work of the NIUF and discusses its relationship to the Accredited Standards Committee T1 and other standrards bodies. The important role of the NIUF within the ISDN arena is evident when considering the Federal Information Processing Standard (FIPS) for ISDN and the Transcontinental ISDN Project (TRIP), both of which are briefly described. Brief statements on the relationship of the ISDN FIPS to the Government Open System Interconnection Profile (GOSIP) and the military standrad on ISDN are included.

01,504
PB96-161229 Not available NTIS
National Inst. of Standards and Technology (CSL), Gaithersburg, MD.
GOSIP Testing Program.
Final rept.
S. M. Radack. 1991, 4p.
See also PB94-211455 and PB96-119359.
Pub. in Computer Systems Laboratory Bulletin, p-4 May 91.

Keywords: *Computer communications, *Standards, *Testing, Communication networks, Conformance, Interoperability, Protocols, Specifications, Reprints, *GOSIP(Government Open Systems Interconnection Profile), *Government Open Systems Interconnection Profile, OSI(Open Systems Interconnection), Federal Information Processing Standards.

This bulletin discusses the testing program recently established by the Computer Systems Laboratory for Federal Information Processing Standard (FIPS) 146, Government Open Systems Interconnection Profile (GOSIP).

01,505
PB96-161245 Not available NTIS
National Inst. of Standards and Technology (CSL), Gaithersburg, MD.
Industry/Government Open Systems Specification: The Development of GOSIP Version 3.
Final rept.
S. M. Radack. 1993, 2p.
See also PB94-219110.
Pub. in Federation of Facts, Quarterly Publication, p3,6 1993.

Keywords: *Specifications, *Government/industry relations, Computer networks, Communication networks, Data transmission, Interoperability, Standards, Protocols, Testing, Reprints, *GOSIP(Government Open Systems Interconnection Profile), *Government Open Systems Interconnection Profile, OSI(Open Systems Interconnection), IGOSS(Industry/Government Open Systems Specification).

Open Systems Interconnection (OSI) standards describe in a general way how data communications should take place in an open network, and include many options and undefined conditions. The development of products that implement OSI standards has been slow. It has been necessary to define the options, subsets, parameters and other conditions that are precisely specified in the standards, and to get agreements among the implementors to implement in a compatible way. Conformance and interoperability testing are needed to assure that different implementations work together, Different profiles, or groupings, of the OSI standards have been developed by different organizations to carry out similar functions. This condition also may be slowing down the development of OSI-compliant products.

01,506
PB96-172325 PC A05/MF A01
National Inst. of Standards and Technology (NCSL), Gaithersburg, MD. Systems and Network Architecture Div.
Guidelines for the Evaluation of Electronic Data Interchange Products.
Special pub.
J. J. Garguilo, and P. Markovitz. Feb 96, 63p, NIST/SP-500/231.
Also available from Supt. of Docs. as SN003-003-03382-1.

Keywords: *Information systems, *Telecommunication, *Commerce, Standards, Procurement, Computer networks, Information exchange, Performance evaluation, Industries, *EDI(Electronic Data Interchange), *Electronic Data Exchange, Electronic commerce.

Electronic Data Interchange (EDI) is defined as the computer-to-computer exchange of standardized business information. As with most software products, EDI products can differ greatly. The host of options potentially present in an EDI product can make purchasing the 'right' one a difficult task. This document assists the reader in determining which EDI product, among many candidate products, best meets the reader's requirements. Specifically, this document addresses: (1) EDI product fuctionality, (2) EDI product performance, and (3) the integration of EDI products into the business process.

01,507
PB96-176672 Not available NTIS
National Inst. of Standards and Technology (CSL), Gaithersburg, MD. Advanced Network Technologies Div.
Strategy to Support Multipoint Communication Service Over Native ATM Service.
Final rept.
S. Y. Kim. 1996, 4p.
Pub. in Institute of Electrical and Electronics Engineers Southeastcon '96, Tampa, FL., April 11-14, 1996, p1-4.

Keywords: *Protocols, Communication networks, Telecommunication, Standards, Reprints, *Multipoint communication, *ATM(Asynchronous Transfer Mode), *Asynchronous Transfer Mode, Adaptation layer, Functionality.

This paper presents the simplified Multipoint Communication Service Protocol on the adaptation layer with multicast functionality over ATM. This protocol structure makes the adaptation layer take over the domain management function of the MCS protocol as the adaptation layer can do this function without difficulty by its own multicast functionality to support multimedia teleconferencing. As both the multicast functionality and the domain management function of the MCS layer combine into the adaptation layer over ATM, the authors can get more efficient multipoint communication without duplication of functions.

01,508
PB96-183165 PC A05/MF A01
National Inst. of Standards and Technology (CSL), Gaithersburg, MD.
Distributed Communication Methods and Role-Based Access Control for Use in Health Care Applications.
J. Poole, J. Barkley, K. Brady, A. Cincotta, and W. Salamon. Apr 96, 66p, NISTIR-5820.

Keywords: *Software tools, *Access control, *Health care, Distributed, Security, CORBA, OLE, RBAC, Role-based.

The use of software in the health care industry is becoming of increasing importance. One of the major roadblocks to efficient health care is the fact that important information is distributed across many sites. These sites can be located across a significant area. The problem is to provide a uniform mechanism to integrate this information. This paper documents the results of an investigation into the suitability of several different distributed access mechanisms. Five methods were examined; the Common Object Request Broker (CORBA), Object Linking and Embedding (OLE), remote procedure call (RPC), remote database access (SQL/RDA) and Protocol Independent Interfaces (PII, the authors specifically examined sockets). These mechanisms were compared with regard for use in health care applications. In particular, the following capabilities were compared: Ease of use by the developer, Class of applications for which the technology is particularly effective in developing, Security capabilities.

01,509
PB96-190111 Not available NTIS
National Inst. of Standards and Technology (PL), Boulder, CO. Time and Frequency Div.
Wavelet Variance, Allan Variance, and Leakage.
Final rept.
D. A. Howe, and D. B. Percival. 1995, 4p.
Pub. in Proceedings of the Institute of Electrical and Electronics Engineers Transactions on Instrumentation, v44 n2 p94-97 Apr 95.

Keywords: *Clock, *Waves, *Time series analysis, Synchronism, Time measurement, Frequencies, Standards, Phase meters, Variance(Statistics), Reprints, Wavelet transform.

Wavelets have recently been a subject of great interest in geophysics, mathematics and signal processing. The discrete wavelet transform can be used to decompose a time series with respect to a set of basis functions, each one which is associated with a particular scale. The properties of a time series at different scales can then be summarized by the wavelet variance, which decomposes the variance corresponding to some of the recently discovered wavelets can provide a more accurate conversion between the time and frequency domains than can be accomplished using the Allan variance. This increase in accuracy is due to the fact that these wavelet variances give better protection against leakage than does the Allan variance.

01,510
PB96-190202 Not available NTIS
National Inst. of Standards and Technology (PL), Boulder, CO. Time and Frequency Div.
New 5 and 10 MHz High Isolation Distribution Amplifier.
Final rept.
C. W. Nelson, F. L. Walls, M. Sicarrdi, and A. De Marchi. 1994, 5p.
Pub. in Proceedings of the Institute of Electrical and Electronics Engineers International Frequency Control Symposium, Boston, MA., June 1-3, 1994, p567-571.

Keywords: *Distributed amplifiers, *Amplifier design, Noise, Phase control, Frequency control, Temperature, Coefficients, Reprints, *Isolation amplifiers, Phase noise.

Increasing performance demands made by precision timing have made NIST's present 5 MHz distribution amplifier system obsolete. A new design providing improved phase stability with temperature, harmonic purity, and phase noise is presented. By building on previous designs, a modified cascode amplifier was created with performance increases of more than 10 fold in phase noise, temperature coefficient and isolation.

01,511
PB96-201124 Not available NTIS
National Inst. of Standards and Technology (EEEL), Boulder, CO. Optoelectronics Div.
Precise Laser-Based Measurements of Zero-Dispersion Wavelength in Single-Mode Fibers.
Final rept.
J. B. Schlager, S. E. Mechels, and D. L. Franzen. 1996, 2p.
Pub. in Conference on Optical Fiber Communication (OFC '96), San Jose, CA., February 25-March 1, 1996, Technical Digest Series, v2 p293-294.

Keywords: *Optical communication, *Optical fibers, *Optical detectors, *Standards, Infrared detectors, Wave dispersion, Frequency response, Fiber optics, Wavelengths, Tunable lasers, Reprints.

The transmission performance of ultralong-distance optical communication systems critically depends on fiber chromatic dispersion. To achieve desired performance, system designers require knowledge of the zero-dispersion wavelength, lambda sub 0 to within 0.1 nm. The authors have developed two laser-based systems to measure lambda sub 0 of long optical fibers. Both systems are based on tunable narrow-line laser sources with output wavelengths that can be accurately measured with an interferometric wavemeter. The first system uses the phase-shift method to measure group delay in the fiber sample as a function of wavelength. The second system directly measures the wavelength-averaged differential group delay or fiber chromatic dispersion by dithering the laser wavelength in a new implementation of the differential phase-shift technique. Both systems give lambda sub zero with a precision (repeatability) of 0.022 nm or less at the 99% confidence level.

01,512
PB97-110498 Not available NTIS
National Inst. of Standards and Technology (CSL), Gaithersburg, MD.
Introduction to Secure Telephone Terminals.
Final rept.
D. Branstad. 1992, 6p.
Pub. in CSL Bulletin, p1-6 Mar 92.

Keywords: *Telephone systems, *Data encryption, *Secure communications, Telecommunications, Computer security, Cryptography, Data processing security, Standards, Reprints.

The bulletin addresses several frequently asked questions about secure telephone terminals, discusses practical security issues from a federal user's viewpoint, and provides sources for additional information. A secure telephone terminal is a device that connects to a telephone line or a cellular telephone system and provides a variety of security services to the conversation of information being transmitted.

01,513
PB97-112395 Not available NTIS
National Inst. of Standards and Technology (CSL), Gaithersburg, MD.
Using Technology to Manage and Protect Intellectual Property.
Final rept.
R. J. Linn. 1996, 17p.
Pub. in Proceedings of the IMA/Copyright Office Forum on Technology-Based Intellectual Property Management, Reston, VA., March 7, 1996, p1-17.

Keywords: *Intellectual property, *Property rights, *Protection, Computer networks, Inforamtion technology, Internet, Digital systems, Information services, Encryption, Access control, Authentication, Copyrights, Systems management, Legal aspects, Reprints, Information infrastructure, Digital libraries, Digital signature.

Digital libraries and related information technologies are the fruits of recent research and development and are enabling the management, dissemination, and protection of intellectual property by means of a network-based information infrastructure. Presented is a discussion of several technologies whose convergence enables new applications which can serve as the foundations for a digital information infrastructure and enable new modes of electronic commerce. The goal of the report is to help those unfamiliar with information technologies better understand the potential of technology to manage, disseminate, and protect information and intellectual property in a new, networked world.

01,514
PB97-122287 Not available NTIS
National Inst. of Standards and Technology (CSL), Gaithersburg, MD. Information Access and User Interface Div.
Usability Engineering: Industry-Government Collaboration for System Effectiveness and Efficiency.
Final rept.
L. L. Downey, S. J. Laskowski, E. A. Buie, and H. R. Hartson. 1996, 2p.
Pub. in SIGCHI Bulletin, v28 n4 p66-67 Oct 96.

Keywords: *Systems engineering, *System effectiveness, *Efficiency, *Usability, Information systems, Computer networks, User needs, User requirements, Government/industry relations, Reprints.

The report summarizes the activities of Usability Engineering: Industry-Government Collaboration for System Effectiveness and Efficiency, a symposium held February 26, 1996, at the National Institute of Standards and Technology (NIST) in Gaithersburg, Maryland.

Communication & Information Theory

01,515
PB95-125753 Not available NTIS
National Inst. of Standards and Technology (NEL), Gaithersburg, MD. Statistical Engineering Div.
Capacity of the Lp Norm-Constrained Poisson Channel.
Final rept.
M. R. Frey. 1992, 6p.
Pub. in Institute of Electrical and Electronics Engineers Transactions on Information Theory 38, n2 p445-450 Mar 92.

Keywords: *Information capacity, *Channel capacity, Norms, Reprints, *Communication channels, Poisson channels, Coding capacity, Channels(Data transmission).

The information and coding capacities of the Poisson channel are derived with a constraint imposed on the L(sub p) norm (Norm chi (sub i))(sub p) of the encoder intensity chi; that is, we fix 1 = or < p = or < infinity and suppose (Norm chi (sub i))(sub p) = or < Q for all t (a member of) (in brackets:0,T) and some Q = or > 0. Formulae are given for the capacity which establish previously known results for p = 1, p = 2, and p = infinity to be part of a system of capacity problems with common form and solution. These formulae apply with or without causal feedback and whether or not the encoder intensity is OOK-constrained.

Graphics

01,516
FIPS PUB 148 PC E99
Electronic Industries Association, Washington, DC. Engineering Dept.
Procedures for Document Facsimile Transmission Issued by General Services Administration, April 14, 1982. Federal Standard 1063.
14 Apr 82, 30p, EIA-RS-466.
Sponsored by General Services Administration, Washington, DC.

Keywords: *Facsimile transmission, *Signals, *Interoperability, Facsimile communications, Data transmission, Signal processing, Pitch, Audio tones, Binary codes, Interfaces, Connectors, Terminals, Procedures, Documents, Federal Information Processing Standards, Calls.

This Standard is concerned with the procedures which are necessary for document transmission between two facsimile stations operating on voice band analog circuits. These procedures essentially comprise: call establishment and call release; compatibility checking, status and control command; checking and supervision of line conditions; control function and facsimile operator recall; and both recognized optional functions as well as other (non-standard) options. In this Standard two separate signalling systems are described; first a simple tonal system using single frequency tones, and second a binary-coded system offering a much wider range of signals for more complex procedures.

Policies, Regulations, & Studies

01,517
AD-A297 905/2 PC A02/MF A01
National Inst. of Standards and Technology (NML) Washington, DC. Central Radio Propagation Lab.
Standard of Attenuation for Microwave Measurements.
R. E. Grantham, and J. J. Freeman. 4 Oct 48, 8p, CRPL-9-8.
Pub. in Transactions of the American Institute of Electrical Engineers, V67 p1-7 1948.

Keywords: *Microwave equipment, *Standards, Reprints, Measurement, Specifications, Accuracy, Electrical properties, Consistency, Radiation attenuation, Calibration, Direct current, Attenuators.

In line with the program of the National Bureau of Standards for extending the standards of electrical quantities up through microwaves, the establishment of a standard of attenuation was undertaken. For such a standard to be useful, it must be readily adaptable to the calibration of commercial attenuators over the entire frequency range. Also, for self consistency, such a standard must be capable of being checked by d-c measurements, thus relating the radiofrequency (r-f) standard to the more accurate primary standards. A standard of any physical quantity consists not merely in the unique specification of that particular quantity but equally important, in the specification of the operations, or procedures, through which an unknown quantity is measured in terms of it. The purpose of this paper is to describe such a standard, and the preliminary experiments employed in its evaluation and development.

01,518
AD-P009 114/0 PC A03/MF A01
National Inst. of Standards and Technology (NML), Boulder, CO. Time and Frequency Div.
Comparison of GPS Broadcast and DMA Precise Ephemerides.
M. A. Weiss, G. Petit, and S. Shattil. 2 Dec 93, 14p.
This article is from 'Proceedings of the Annual Precise Time and Time Interval (PTTI) Applications and Planning Meeting (25th) Held in Marina Del Rey, California on 29 November - 2 December 1993', AD-A280 955, p293-306.

Keywords: *Ephemerides, Estimates, Perturbations, Phase modulation, Residuals, Time, Global positioning system, Navigation satellites, Kalman filtering, Component Reports, Satellite orbits.

We compare the broadcast ephemerides from Global Positioning Satellites (GPS) to the postprocessed ephemerides from the Defense Mapping Agency (DMA). We find significant energy in the spectrum of the residuals at 1 cycle/day and higher multiples. We estimate the time variance of the residuals and show that the short term residuals, from 15 min, exhibit power law processes with greater low frequency perturbations than white phase modulation. We discuss the significance of these results for the performance of the GPS Kalman filter which estimates the broadcast orbits.

01,519
AD-P009 132/2 PC A02/MF A01
National Inst. of Standards and Technology, Boulder, CO.
NIST Internet Time Service.
J. Levine. 2 Dec 93, 7p.
This article is from 'Proceedings of the Annual Precise Time and Time Interval (PTTI) Applications and Plan-

ning Meeting (25th) Held in Marina Del Rey, California on 29 November - 2 December 1993', AD-A280 955, p505-511.

Keywords: *Time standards, Calibration, Clocks, Daylight, Formats, Communications networks, Uncertainty, Radio links, Synchronism, Component Reports, Internet, US NIST.

We will-describe the NIST Network Time Service which provides time and frequency information over the internet. Our first time server is located in Boulder, Colorado, a second backup server is under construction there, and we plan to install a third server on the East Coast later this year. The servers are synchronized to UTC(Universal Coordinated Time)(NIST) with an uncertainty of about 0.8 ms RMS and they will respond to time requests from any client on the internet in several different formats including the DAYTIME, TIME and NTP protocols. The DAYTIME and TIME protocols are the easiest to use and are suitable for providing time to PCs and other small computers. In addition to UTC(NIST), the DAYTIME message provides advance notice of leap seconds and of the transitions to and from Daylight Saving Time. The Daylight Saving Time notice is based on the US transition dates of the first Sunday in April and the last one in October. The NTP is a more complex protocol that is suitable for larger machines; it is normally run as a demon process in the background and can keep the time of the client to within a few milliseconds of UTC (NIST). We will describe the operating principles of various kinds of client software ranging from a simple program that queries the server once and sets the local clock to more complex 'demon processes (such as NTP) that continuously correct the time of the local clock based on periodic calibrations.

01,520
AD-P009 138/9 PC A02/MF A01
National Inst. of Standards and Technology, Boulder, CO.
Future of Time and Frequency Dissemination.
J. Levine. 2 Dec 93, 6p.
This article is from 'Proceedings of the Annual Precise Time and Time Interval (PTTI) Applications and Planning Meeting (25th) Held in Marina Del Rey, California on 29 November - 2 December 1993', AD-A280 955, p573-578.

Keywords: *Frequency standards, *Time standards, Bandwidth, Computer networks, Technology forecasting, Communications traffic, *Time transfer, Component Reports.

I will try to extrapolate the changes in the dissemination of time and frequency information that have taken place during the last 25 years to predict the future developments both in the methods of disseminating time and frequency and in the kinds of customers we will be asked to serve. Two important developments are likely to play pivotal roles in driving the evolution of dissemination. The first is the commercial availability of very high quality clocks - devices whose performance may eventually rival that of the current generation of primary frequency standards. The widespread use of these devices may blur the traditional distinction between client and server, and may replace it with a more symmetrical interchange of data among peers. The second is the increasing demand for digital time and frequency information driven by the increasing sophistication of everything from traffic lights to electric power meters. The needs of these individual users may not tax the state of the art of primary frequency standards in principle, but their large numbers and wide geographical distribution present a technological challenge that is difficult to meet at a reasonable price using existing methods. Some of these problems may be solved (or at least addressed) using developments in communications and consumer electronics such as the increasing use of fiber-optic telephone circuits and the increasing bandwidth and sophistication of the cable network used to transmit television pictures. To be useful, these advances in hardware must stimulate parallel advances in software algorithms and methods. These advances are more difficult to predict with great confidence, but the developments of the last few years will be examined to provide some indications of the future.

01,521
N19960042622 (Order as N19960042616, PC A20/MF A04)
National Inst. of Standards and Technology, Boulder, CO.
Utc Dissemination to the Real-Time User.
J. Levine. 1 May 96, 10p.
In National Inst. Of Standards and Technology, 27TH Annual Precise Time and Time Interval (Ptti) Applications and Planning Meeting p 103-112.

Keywords: *Accuracy, *Atomic clocks, *Frequency standards, *International cooperation, *Real time operation, *Statistical analysis, *Time measurement, *Time signals, *Transit time, *Universal time, Annual variations, Cesium, Hyperfine structure, Synchronism.

The current definition of Coordinated Universal Time (UTC) dates from 1972. The duration of a UTC second is defined in terms of the frequency of a hyperfine transition in the ground state of cesium. This standard frequency is realized in a number of different laboratories using ensembles of commercial cesium clocks and a few primary frequency standards. The data from all of these devices are transmitted periodically to the Bureau International des Poids et Mesures (BIPM) in Sevres, France, where they are combined in a statistical procedure to produce International Atomic Time (TAI). The time of this scale is adjusted as needed ('coordinated') by adding or dropping integer seconds so as to keep it within plus or minus 0.9 s of UT1, a time scale based on the observation of the transit times of stars and corrected for the predicted seasonal variations in these observations. When the leap seconds are included into TAI, the result is called UTC. The difference between TAI and UTC is therefore an exact integer number of seconds. This difference is currently 29 s and will become 30 s at 0 UTC on 1 January 1996.

01,522
N94-30641/2 (Order as N94-30639/6, PC A25/MF A06)
National Inst. of Standards and Technology, Boulder, CO.
Time and Frequency Technology at NIST.
D. B. Sullivan. May 94, 6p.
In NASA. Goddard Space Flight Center, the 25TH Annual Precise Time and Time Interval (Ptti) Applications and Planning Meeting p 33-38.

Keywords: *Clocks, *Frequency standards, *Standards, *Time measurement, *Timing devices, Laser pumping, Oscillators, Semiconductor lasers, Temporal distribution, Computer networks, Digital systems, Standardization, Telephones, Cesium frequency standards, Rubidium frequency standards, Time transfer.

The state of development of advanced timing systems at NIST is described. The work on cesium and rubidium frequency standards, stored-ion frequency standards, diode lasers used to pump such standards, time transfer, and methods for characterizing clocks, oscillators, and time distribution systems is presented. The emphasis is on NIST-developed technology rather than the general state of the art in this field.

01,523
N94-30660/2 (Order as N94-30639/6, PC A25/MF A06)
National Inst. of Standards and Technology, Boulder, CO.
Comparison of GPS Broadcast and DMA Precise Ephemerides.
M. A. Weiss, G. Petit, and S. Shattil. May 94, 14p.
In NASA. Goddard Space Flight Center, the 25TH Annual Precise Time and Time Interval (Ptti) Applications and Planning Meeting p 293-306.

Keywords: *Ephemerides, *Global positioning system, *Kalman filters, *Satellite tracking, Autonomous spacecraft clocks, Ground stations, Position (Location), Tracking stations.

We compare the broadcast ephemerides from Global Positioning Satellites (GPS) to the postprocessed ephemerides from the Defense Mapping Agency (DMA). We find significant energy in the spectrum of the residuals at 1 cycle/day and higher multiples. We estimate the time variance of the residuals and show that the short term residuals, from 15 min, exhibit power law processes with greater low frequency perturbations than white phase modulation. We discuss the significance of these results for the performance of the GPS Kalman filter which estimates the broadcast orbits.

01,524
N94-30684/2 (Order as N94-30639/6, PC A25/MF A06)
National Inst. of Standards and Technology, Boulder, CO.
Future of Time and Frequency Dissemination.
J. Levine. May 94, 6p.
In NASA. Goddard Space Flight Center, the 25TH Annual Precise Time and Time Interval (Ptti) Applications and Planning Meeting p 573-578.

Keywords: *Clocks, *Frequency standards, *Time measurement, Technology assessment, Accuracy, Computer networks, Information dissemination, Telecommunication, Trends.

I will try to extrapolate the changes in the dissemination of time and frequency information that have taken place during the last 25 years to predict the future developments both in the methods of disseminating time and frequency and in the kinds of customers we will be asked to serve. Two important developments are likely to play pivotal roles in driving the evolution of dissemination. The first is the commercial availability of very high quality clocks -- devices whose performance may eventually rival that of the current generation of primary frequency standards. The widespread use of these devices may blur the traditional distinction between client and server, and may replace it with a more symmetrical interchange of data among peers. The second is the increasing demand for digital time and frequency information driven by the increasing sophistication of everything from traffic lights to electric power meters. The needs of these individual users may not tax the state of the art of primary frequency standards in principle, but their large numbers and wide geographical distribution present a technological challenge that is difficult to meet at a reasonable price using existing methods. Some of these problems may be solved (or at least addressed) using developments in communications and consumer electronics such as the increasing use of fiber-optic telephone circuits and the increasing bandwidth and sophistication of the cable network used to transmit television pictures. To be useful, these advances in hardware must stimulate parallel advances in software algorithms and methods. These advances are more difficult to predict with great confidence, but the developments of the last few years will be examined to provide some indications of the future.

01,525
PB94-172772 Not available NTIS
National Inst. of Standards and Technology (NML), Boulder, CO. Time and Frequency Div.
Time Scale Algorithm for Post-Processing: AT1 Plus Frequency Variance.
Final rept.
M. A. Weiss, and T. Weissert. 1990, 1p.
Pub. in Proceedings of Conference on Precision Electromagnetic Measurements, Ottawa, Canada, June 11-14, 1990, p11. See also PB93-151926.

Keywords: *Time measurement, Kalman filters, Reprints, Frequency step detection, Time scale algorithms, Postprocessing.

There are some applications where the output of a time scale is not needed in real time. Such applications can make use of a post-processed time scale for improving long term performance. A post-processed scale can take advantage of improved characterizations of clocks in the scale and improved capability of frequency step detection. The authors study a particular time scale algorithm run in post-processed mode being studied at the National Institute of Standards and Technology. Results are reported based on both simulation and real data.

01,526
PB94-216017 Not available NTIS
National Inst. of Standards and Technology (PL), Boulder, CO. Time and Frequency Div.
Using LORAN-C Broadcasts for Automated Frequency Calibrations.
Final rept.
M. Lombardi. 1992, 13p.
Pub. in Proceedings of National Conference of Standards Laboratories Workshop and Symposium Managing Worldwide Measurements, Washington, DC., August 2-6, 1992, p361-373.

Keywords: *Frequency measurement, *LORAN C, *Calibration, Ground wave propagation, Oscillators, Accuracy, Reprints, Path noise.

The LORAN-C (LOng RAnge Navigation) system is a radio navigation system maintained by the United States Coast Guard. LORAN-C signals are widely used as a navigation aid. Since the signals are extremely stable, they can also serve as an excellent reference for frequency calibrations. Any quartz, rubid-

ium, or cesium oscillator can be calibrated with LORAN-C. This paper tells how to use LORAN-C signals for frequency calibrations. It describes the LORAN-C system, lists the equipment that you need, shows the data you can obtain, and discusses the accuracy you can expect. It also discusses the NIST Frequency Measurement System, an automated calibration system that uses LORAN-C signals.

01,527
PB94-216066 Not available NTIS
National Inst. of Standards and Technology (PL), Boulder, CO. Time and Frequency Div.
Ultra-High Stability Synthesizer for Diode Laser Pumped Rubidium.
Final rept.
J. Lowe, F. L. Walls, and R. E. Drullinger. 1992, 5p.
Pub. in Proceedings of Institute of Electrical and Electronics Engineers Frequency Control Symposium, Hershey, PA., May 27-29, 1992, p183-187.

Keywords: *Rubidium frequency standards, *Frequency standards, *Local oscillators, Frequency stability, Optical pumping, Room temperature, Design, Reprints, Laser diodes.

We describe the design of a synthesized local oscillator for a rubidium (Rb) passive frequency standard pumped by radiation from a diode laser. The design goals for this new oscillator are: (1) To operate at room temperature, (2) To have the ability to step quickly to different frequencies for measuring parameters such as magnetic fields, (3) To contribute less than 2 X 10(sup -14)/tau(sup 1/2) to the frequency stability of the Rb standard for measurement times between 30 and 200 seconds. Potential limits for obtaining these goals, as well as solutions to such problems, are discussed.

01,528
PB95-108585 Not available NTIS
National Inst. of Standards and Technology (NML), Gaithersburg, MD. Time and Frequency Div.
High-Order Harmonic Mixing with GaAs Schottky Diodes.
Final rept.
M. Prevedelli, F. L. Walls, and S. P. Beaton. 1990, 4p.
Pub. in Proceedings of the Annual Symposium on Frenquency Control (44th), Baltimore, MD., May 23-25, 1990, p555-558.

Keywords: *Frequency multipliers, Frequency synthesizers, Frequency control, Laser radiation, Schottky diodes, Planar structures, Extremely high frequency, Far infrared radiation, Gallium arsenides, Klystrons, Reprints, *Harmonic mixing.

In many areas of precision frequency metrology, it is useful to use a single nonlinear element to both multiply a source frequency and mix this harmonic with a higher frequency source. This process is commonly referred to as harmonic mixing. When the frequency span is great, it is advantageous to use large harmonic numbers to reduce the complexity, the number of local oscillators, and ultimately the cost. Planar GaAs Schottky diodes are good candidates for high order harmonic mixing because of their high cut-off frequency. Their robust construction should lead to excellent lifetime, reliability, and reproducibility. The authors have investigated the performance of one type of fast planar Schottky diode for harmonic mixing with harmonic numbers from 8 to 201. Their measurements indicate that, with optimum biasing and power, harmonic mixing with harmonic numbers of up to approximately 80 can be achieved with good signal-to-noise ratios. Detectable signals have been observed for harmonic numbers of 201. From the nonlinear characteristics of the diode and the signal-to-noise ratio obtained at lower frequencies, it looks as though we can multiply from 70 GHz to about 4.5 THz in one step.

01,529
PB95-151098 Not available NTIS
National Inst. of Standards and Technology (PL), Boulder, CO. Time and Frequency Div.
Preliminary Comparison of Time Transfers via LASSO, GPS and Two-Way Satellite.
Final rept.
P. Uhrich, R. Tourde, M. Granveaud, C. Veillet, D. Feraudy, J. M. Torre, J. F. Mangin, J. Gaignebet, J. L. Hatat, W. Hanson, A. Clements, J. Jespersen, M. Lombardi, P. Grudler, and F. Baumont. 1991, 9p.
Pub. in Proceedings of European Frequency and Time Forum (5th), Besancon, France, March 12-14, 1992, p96-104.

Keywords: *Global positioning system, *Navigation satellites, *Laser range finders, *Signal transmission, *Time signals, Position indicators, Satellite ground support, Time measuring instruments, Timing devices, Rangefinding, Ground stations, Calibration, Accuracy, Synchronism, Precision, Reprints, *Time transfer.

Presently, the three primary techniques for achieving nanosecond time transfer are Common-View GPS. Two-Way Satellite Time Transfer and the Laser Ranging Technique of the LASSO Experiment. Through the cooperative efforts of several international laboratories, all the three methods were implemented at two stations within Europe, CERGA and TUG. At each of these two stations, a common reference clock to all three systems allows the direct intercomparison of these three state-of-the-art techniques. The paper will discuss the operations at these two stations, present the available data and an intercomparison of it.

01,530
PB95-151445 Not available NTIS
National Inst. of Standards and Technology (PL), Boulder, CO. Time and Frequency Div.
Smart Clock: A New Time.
Final rept.
M. A. Weiss, D. W. Allan, D. D. Davis, and J. Levine. 1992, 4p.
Pub. in Institute of Electrical and Electronics Engineers Transactions on Instrumentation and Measurement 41, n6 p915-918 Dec 92.

Keywords: *Clocks, *Synchronism, *Calibration, Time measuring instruments, Reference standards, Time standards, Time signals, Random walk, Frequency stability, Accuracy, Reprints, *Smart Clock, *Time transfer.

The Smart Clock, opens up the possibility for any clock to be automatically synchronized to an external standard with a minimum of measurements. The Smart Clock enhances the accuracy or stability of a clock or oscillator by characterizing it against an external standard. The Smart Clock algorithm uses optimal estimation and prediction to apply a correction to the output of the oscillator, maintaining any combination of time or frequency accuracy or stability within specified limits. The algorithm decides when external measurements are necessary to maintain the desired accuracy or stability. The authors present here a tutorial description of the Smart Clock system and an example of how it could be used to maintain a simple clock to 1 s using measurements over the telephone lines.

01,531
PB95-151452 Not available NTIS
National Inst. of Standards and Technology (PL), Boulder, CO. Time and Frequency Div.
Calibration of GPS Equipment in Japan.
Final rept.
M. A. Weiss, and D. D. Davis. 1988, 9p.
Pub. in Proceedings of Annual Precise Time and Time Interval (PTTI) Applications and Planning Meeting (20th), Tysons Corner/Vienna, VA., November 29-December 1, 1988, p101-109.

Keywords: *Japan, *Global positioning system, *Calibration, *Time measuring instruments, Ground stations, Satellite tracking, Tracking stations, Interlaboratory comparisons, Time standards, Standardization, Time measurement, Precision, Clocks, Diurnal variations, Reprints, *Time transfer.

With the development of common view time comparisons using GPS satellites the Japanese time and frequency standards laboratories have been able to contribute with more weight to the international unification of time under the coordination of the Bureau of International de Poids et Measures (BIPM). During the period from June 1 through June 11, 1988, the differential delays of time transfer receivers of the global Poisitioning System (GPS) were calibrated at three different laboratories in Japan, linking them for absolute time transfer with previously calibrated labs of Europe and North America. The authors report here the results of the calibration trip, along with some interesting problems that developed concerning this technique.

01,532
PB95-151460 Not available NTIS
National Inst. of Standards and Technology (PL), Boulder, CO. Time and Frequency Div.
Confidence on the Second Difference Estimation of Frequency Drift.
Final rept.
M. A. Weiss, D. W. Allan, and D. Howe. 1992, 6p.
Pub. in Proceedings of Institute of Electrical and Electronics Engineers Frequency Control Symposium, May 27-29, 1992, p300-305.

Keywords: *Frequency standards, *Frequency stability, Rubidium frequency standards, Frequency modulation, White noise, Simulation, Estimates, Reprints, Frequency drift.

We use simulation to compare the confidence in estimating frequency drift in the presence of stochastic noise between two different estimators: (1) a mean second difference using neighboring data, and (2) a single second difference over the entire data set. In each case we simulate 100 s data sampling and 10,000 samples (11 and 1/2 days of data). The two estimators show a similar confidence when the noise is purely random walk frequency modulation, but when there is also white frequency modulation, as is common in oscillators, method (2) is more efficient. An advantage of (1) is that it provides an internal confidence to an estimate on a single data set. As a practical example, when we simulate a typical rubidium gas cell frequency standard, the confidence of the drift estimate was ten times better for method (2) over method (1).

01,533
PB95-151478 Not available NTIS
National Inst. of Standards and Technology (PL), Boulder, CO. Time and Frequency Div.
Promise into Practice: Implementing TA2 on Real Clocks at NIST.
Final rept.
M. A. Weiss, and T. Weissert. 1991, 7p.
Pub. in Proceedings of European Frequency and Time Forum (5th), March 12-14, 1991, p442-448.

Keywords: Global positioning system, Kalman filters, Random walk, Stability, Clocks, Reprints, *Time scale algorithms, *TA2 algorithm, Postprocessors, US NIST.

TA2 is a time scale algorithm designed to run as a post-processor by smoothing, i.e. combining estimates from runs in both forward and backward temporal directions. It has been tested using the time-scale data at NIST from 1989 through the first half of 1990. We review the characterization parameters for clocks with white FM, and random-walk FM, and the dependence of these estimates on integration time. We also discuss the transformation of these parameters from their use as time deviations to frequency variances. We compare the scale generated by TA2 over 541 d starting at the beginning of 1989, with the two other scales at NIST, AT1 and TA.

01,534
PB95-153458 Not available NTIS
National Inst. of Standards and Technology (PL), Boulder, CO. Time and Frequency Div.
NIST-7, the New US Primary Frequency Standard.
Final rept.
R. E. Drullinger, J. P. Lowe, D. J. Glaze, and J. Shirley. 1993, 3p.
Pub. in Proceedings of European Frequency and Time Forum (7th), Neuchatel, Switzerland, March 16-18, 1993, p549-551 and Proceedings of the Institute for Electrical and Electronics Engineers International Frequency Control Symposium, Salt Lake City, UT., June 2-4, 1993 p71-74.

Keywords: *Cesium frequency standards, *Frequency standards, *Primary standards, Optical pumping, Frequency stability, Reprints, *NIST-7 standard.

NIST-7, an optically pumped, cesium-beam frequency standard has replaced NBS-6 as the official US primary frequency standard. The present short-term stability of the standard, measured with respect to an active hydrogen maser, is characterized by sigma(sub y)(tau) approx = 8 x 10(exp -13) tau(sup -1/2). Our first evaluation has resulted in an uncertainty of 4 x 10(exp -14). An improved servo-electronic system is being developed and this should improve stability and allow for more precise evaluation of the various systematic errors.

01,535
PB95-153482 Not available NTIS
National Inst. of Standards and Technology (PL), Boulder, CO. Time and Frequency Div.

Error Analysis of the NIST Optically Pumped Primary Frequency Standard.
Final rept.
R. E. Drullinger, J. H. Shirley, J. L. Lowe, and D. J. Glaze. 1992, 2p.
Pub. in Proceedings of Conference on Precision Electromagnetic Measurements, Paris, France, June 9-12, 1992, p198-199.

Keywords: *Frequency standards, *Primary standards, Optical pumping, Error analysis, Reprints, US NIST.

An error analysis of the NIST optically pumped, primary frequency standard is presented. Where possible, direct, in-situ measurements have been made. Alternatively, electrical measurements have been made on subassemblies during construction. Where measurements are not yet available, model calculations have been applied to the design. The analysis indicates that in the present configuration of the servo, the error budget is dominated by microwave power instability entering through the second-order Doppler shift at the level of a few parts in 10(exp 14).

01,536
PB95-161089 Not available NTIS
National Inst. of Standards and Technology (PL), Boulder, CO. Time and Frequency Div.
Satellite Two-Way Time Transfer: Fundamentals and Recent Progress.
Final rept.
D. A. Howe, D. W. Hanson, J. L. Jespersen, and M. A. Lombardi. 1988, 12p.
Pub. in Proceedings of Precise Time and Time Interval Conference, Redondo Beach, CA., November 28-30, 1988, p117-128.

Keywords: *Synchronous satellites, *Ground stations, *Calibration, *Signal processing, Synchronism, Signal reception, Signal transmission, Time signals, Synchronous platforms, Time measurement, Time standards, Accuracy, Reprints, *Time transfer.

The authors discuss fundamental aspects of two-way timing and show an implementation of a satellite two-way time transfer system which has been used for two-years between USNO, Washington, D.C. and NIST, Boulder, CO. The raw data collection procedure will be discussed. The authors also outline the rationale for the choice of satellite uplink/downlink frequencies, signal structure, and reduction of data. Short-term noise in the time transfer limits the precision to about 300 ps in a 300 s average. Uncertainty in accuracy is due to uncertainty in the non-reciprocity of the two-way signal path. Accuracy limits due to the atmosphere, earth-satellite rotating system (Sagnac effect), and the equipment are discussed. The goal is to achieve an accuracy level of 1 ns after a suitable calibration of earth-station (differential) equipment delays.

01,537
PB95-161410 Not available NTIS
National Inst. of Standards and Technology (PL), Boulder, CO. Time and Frequency Div.
Keeping Time on Your PC.
Final rept.
M. A. Lombardi. 1993, 4p.
Pub. in Byte Magazine, p57-62 Oct 93.

Keywords: *Clocks, *Personal computers, *Calibration, Time signals, Time measurement, Timing devices, Synchronism, Accuracy, ACTS, GOES satellites, Computer networks, Reprints, Smart Clock, World Wide Web.

A summary of the differential methods that can be used to set computer clocks on time. It describes how the clock inside a PC works, how computer clocks can be set by modem or through the Internet, and discusses the NIST Smart Clock Technology. It also discusses how computer time can be obtained by radio or through the use of an add-on clock board.

01,538
PB95-163218 Not available NTIS
National Inst. of Standards and Technology (PL), Boulder, CO. Time and Frequency Div.
Diode-Laser Pumped, Rubidium Cell Frequency Standards.
Final rept.
C. Szekely, R. E. Drullinger, F. L. Walls, J. P. Lowe, and A. Novick. 1993, 5p.
Pub. in Proceedings of European Frequency and Time Forum (7th), Neuchatel, Switzerland, March 16-18, 1993, p593-597.

Keywords: *Rubidium frequency standards, *Frequency standards, Semiconductor lasers, Frequency stability, Optical pumping, Reprints, Phase noise.

We report on our project to experimentally investigate the limits to the short-term stability achievable in optically pumped, rubidium cell frequency standards. Theory indicates that the atomic limited stability is several orders of magnitude better than what has actually been achieved. The difference is related to the complex spectral output of the lamps used in conventional standards as well as phase noise in the interrogating microwave radiation. Using a novel filter technique, we have built a microwave synthesis chain with phase noise capable of supporting a standard with (sigma(sub y))(tau) = or < 4 X 10(exp -14) tau(sup -1/2). With extended-cavity, diode lasers we have demonstrated measured line Q and signal-to-noise ratios commensurate with (sigma(sub y))(tau) = 4 X 10(exp -13) tau(sup -1/2) in a commercial, buffer gas type standard and (sigma(sub y))(tau) = 2 X 10(exp -13) tau(sup -1/2) in an evacuated, wall-coated cell. Both of these numbers can be improved significantly in a fully engineered and optimized standard.

01,539
PB95-163838 Not available NTIS
National Inst. of Standards and Technology (PL), Boulder, CO. Time and Frequency Div.
Confidence on the Three-Point Estimator of Frequency Drift.
Final rept.
M. A. Weiss, and C. Hackman. 1993, 8p.
Pub. in Proceedings of Annual Precise Time and Time Interval (PTTI) Applications and Planning Meeting (24th), McLean, VA., December 1-3, 1992, p451-458 1993.

Keywords: *Frequency standards, *Atomic clocks, Estimators, Uncertainty, Reprints, *Frequency drift, Allan variance.

It has been shown that a three-point second difference estimator is nearly optimal for estimating frequency drift in many common atomic oscillators. We derive a formula for the uncertainty of this estimate as a function of the integration time and of the Allan variance associated with this integration time.

01,540
PB95-163853 Not available NTIS
National Inst. of Standards and Technology (NML), Gaithersburg, MD. Time and Frequency Div.
Use of Ionospheric Data in GPS Time Transfer.
Final rept.
M. Weiss, T. Weissert, C. Thomas, M. Imae, and K. Davies. 1990, 7p.
Pub. in Proceedings of European Frequency and Time Forum (4th), Neuchatel, March 13-15, 1990, p327-333.

Keywords: *Ionospherics, *Global positioning system, *Error analysis, *Delay time, Synchronism, Data smoothing, Periodic variations, Electromagnetic noise, Time standards, Frequency standards, Time measuring instruments, Interlaboratory comparisons, Calibrating, Accuracy, Reprints, *Time transfer, Ionospheric delay.

With solar activity near maximum, the largest error in the use of the Global Positioning System (GPS) for common-view time transfer can be the correction for ionospheric delay. The paper describes the use of data from two different codeless ionospheric measurement systems to correct common-view time transfer measurements. The authors compare the measured ionospheric values with those from the ionospheric values with those from the ionspheric model parameters broadcast from the GPS satellites, computer time transfer values among three time standards laboratories: Observatoir de Paris, Paris, France; National Institute of Standards and Technology, Boulder, Colorado, USA; and Communications Research Laboratory, Tokyo, Japan. Combining these time transfers the authors can obtain closure around the world. The authors make another comparison between these results and ionospheric measurements using a Faraday rotation system.

01,541
PB95-180501 Not available NTIS
National Inst. of Standards and Technology (PL), Boulder, CO. Time and Frequency Div.

Microwave Leakage as a Source of Frequency Error and Long-Term Instability in Cesium Atomic-Beam Frequency Standards.
Final rept.
W. D. Lee, J. P. Lowe, J. H. Shirley, and R. E. Drullinger. 1994, 4p.
Pub. in Proceedings of European Frequency and Time Forum (8th), Weihenstephan, Germany, March 9-11, 1994, p513-516.

Keywords: *Cesium frequency standards, *Frequency standards, Frequency stability, Microwave radiation, Instability, Reprints, Microwave leakage, Systematic errors.

We identify leakage from the microwave electronics in cesium atomic-beam frequency standards as a potential source of frequency error and instability in these standards. The problem arises when radiation that is phase coherent with the interrogating radiation finds its way to the atoms in regions outside the Ramsey cavity. We discuss techniques for evaluating and reducing the problem.

01,542
PB95-180519 Not available NTIS
National Inst. of Standards and Technology (PL), Boulder, CO. Time and Frequency Div.
Velocity Distribution of Atomic Beams by Gated Optical Pumping.
Final rept.
W. D. Lee, J. H. Shirley, and R. E. Drullinger. 1994, 4p.
Pub. in Proceedings of Institute of Electrical and Electronics Engineers International Frequency Control Symposium, Boston, MA., June 1-3, 1994, p658-661.

Keywords: *Cesium frequency standards, *Frequency standards, *Atomic beams, *Velocity distribution, Velocity measurement, Optical pumping, Doppler effect, Accuracy, Reprints, *NIST-7 frequency standard, US NIST.

In evaluating the accuracy of a cesium-beam frequency standard, accurate measurement of the atomic velocity distribution is important. In frequency standards which employ atoms with thermal velocities, the measured atomic resonance frequency differs from the true resonance by several parts in 10(exp 13) due to the second-order Doppler shift. To achieve the frequency accuracy goal for NIST-7 of 1 . 10(exp -14), an upper bound on the uncertainty of the mean-square atomic velocity of about 1 percent is needed. We present the results of experiments designed to measure the velocity distribution of NIST-7 using two independent techniques: gated optical pumping, and Ramsey fringe inversion. We show that these techniques yield velocity distributions and corresponding second-order Doppler shifts that agree within the stated tolerances.

01,543
PB95-180535 Not available NTIS
National Inst. of Standards and Technology (PL), Boulder, CO. Time and Frequency Div.
Cross-Correlation Analysis Improves Time Domain Measurements.
Final rept.
A. Lepek, and F. L. Walls. 1993, 9p.
Pub. in Proceedings of Institute of Electrical and Electronics Engineers International Frequency Control Symposium, Salt Lake City, UT., June 2-4, 1993, p312-320.

Keywords: Frequency stability, Cross correlation, Time domain, Reprints, *Allan variance.

We introduce cross correlation-based variances to estimate the Allan variance, the modified Allan variance, and the time variance in the presence of the measurement system noise. These variances substantially lower the short-term measurement noise floor; however, they require significantly more data. The cross correlation based variances are also used as a tool to analyze and improve the measurement system noise. The cross correlation based variances bear a precise relation to the 3-cornered-hat sigma. We have reduced the short-term noise floor for sigma(sub y) (1 s) by factor of 100 relative to our initial hardware and software configuration.

01,544
PB95-180618 Not available NTIS
National Inst. of Standards and Technology (PL), Boulder, CO. Time and Frequency Div.

Hybrid Digital/Analog Servo for the NIST-7 Frequency Standard.
Final rept.
J. P. Lowe, W. D. Lee, F. L. Walls, and R. E. Drullinger. 1994, 4p.
Pub. in Proceedings of Institute of Electrical and Electronics Engineers International Frequency Control Symposium, Boston, MA., June 1-3, 1994, p662-665.

Keywords: *Cesium frequency standards, *Frequency standards, Hybrid systems, Servomechanisms, Digital systems, Analog systems, Design, Stability, Reprints, *NIST-7 frequency standard, US NIST.

This paper describes a hybrid (analog/digital) approach to the servo electronics for the NIST-7 cesium-beam, frequency standard. A digital servo system has been added to the existing analog system to enhance the capabilities of both servos. The analog servo allows a 5 MHz oscillator to be frequency locked directly to the atomic transition frequency. The digital servo reduces the frequency perturbations due to changes in the ambient magnetic field. Also, the existence of separate servo systems allows independent measurements of systematic errors. Design specifications are given and stability measurement results are presented.

01,545
PB95-180972 Not available NTIS
National Inst. of Standards and Technology (PL), Boulder, CO. Time and Frequency Div.
Reducing the Effect of Local Oscillator Phase Noise on the Frequency Stability of Passive Frequency Standards.
Final rept.
C. Szekely, F. L. Walls, J. P. Lowe, R. E. Drullinger, and A. Novick. 1993, 6p.
Pub. in Proceedings of Institute of Electrical and Electronics Engineers International Frequency Control Symposium, Salt Lake City, UT., June 2-4, 1993, p81-86.

Keywords: *Frequency standards, *Frequency stability, Rubidium, Frequency standards, Notch filters, Local oscillators, Performance tests, Reduction, Reprints, Phase noise.

We report on the experimental test of a new concept for reducing limitation on short-term frequency stability of passive frequency standards due to local oscillator phase noise. Systems that use sinewave modulation to interrogate a stable resonance are limited in short-term frequency stability by phase noise at the second harmonic of the modulation, f(m). This effect limits the fractional frequency stability. This new concept uses notch filters at + or - 2f(m) from the carrier to reduce this effect. Tests on a modified passive rubidium standard demonstrate an improvement of approximately 18 in fractional frequency stability. The dual notch filters proved to be feasible and were obtained commercially.

01,546
PB95-181129 Not available NTIS
National Inst. of Standards and Technology (PL), Boulder, CO. Time and Frequency Div.
Practical Standards for PM and AM Noise at 5, 10 and 100 MHz.
Final rept.
F. L. Walls. 1993, 10p.
Pub. in Proceedings of European Frequency and Time Forum (7th), Neuchatel, Switzerland, March 16-18, 1993, p189-198.

Keywords: *Amplitude modulation, *Phase modulation, *Standards, Very high frequency, High frequency, Carrier frequencies, Reprints, *Noise standards.

This paper describes a practical implementation of secondary standards for phase modulation noise (PM) and amplitude modulation noise (AM) at carrier frequencies of 5 MHz, and 100 MHz. In each case the standard simultaneously produces output signals at approximately + 15 + 17 dBm. The PM and AM noise between the two signals can be set to a calibrated level, which is constant to better than 0.2 dB for Fourier frequency offsets from nearly dc to 5% of the carrier, or set ot a minimum value. The calibrated level of PM and AM noise is used to evaluate the accuracy versus Fourier frequency.

01,547
PB95-181137 Not available NTIS
National Inst. of Standards and Technology (PL), Boulder, CO. Time and Frequency Div.

Sifting Through Nine Years of NIST Clock Data with TA2.
Final rept.
M. A. Weiss, and T. P. Weissert. 1993, 12p.
Pub. in Proceedings of the European Frequency and Time Forum (7th), Neuchatel, Switzerland, March 16-19, 1993, p199-210.

Keywords: *Clocks, Optimization, Anomalies, Reprints, TA2 algorithm, Time scales, Stochastic noise, US NIST.

We have extended the new TA2 post-process time scale at NIST beyond our previous reports to include all of the period from January of 1984 to the present. Derived from the ensemble of clocks at NIST, this time scale includes the benefits of several recent refinements to the algorithm. By iteratively running the algorithm on the ensemble clock data and characterizing anomalous behavior in the dominant individual clocks of the ensemble between iterations, we obtain an optimized scale which benefits from the informed anticipation of that anomalous behavior and demonstrates an overall decrease in scale disruption. Herein we discuss: changes to the TA2 algorithm that we made while processing the eight-year run, our method of characterizing anomalous behavior in individual clocks, the way unanticipated anomalous behavior is dealt with by the algorithm, and our resulting nine-year time scale.

01,548
PB95-220463 PC A06/MF A02
National Inst. of Standards and Technology (PL), Boulder, CO. Time and Frequency Div.
Time and Frequency: Bibliography of NIST Publications, March 1995.
G. E. Bennett, and D. B. Sullivan. Mar 95, 110p, NISTIR-5035.

Keywords: *Atomic clocks, *Time standards, *Frequency standards, Lasers, Time, Ion storage, Time measurement, Frequency measurement, Time transfer, US NIST.

This bibliography includes most NIST publications in this field dating from the development of the first atomic clock. The publications are sorted into 23 categories. While the majority cover topics that are central to time and frequency measurements and standards, the bibliography does include other publications of the Time and Frequency Division that are only peripherally related to the field.

01,549
PB96-102652 Not available NTIS
National Inst. of Standards and Technology (PL), Boulder, CO. Time and Frequency Div.
Measurement Methods and Algorithms for Comparison of Local and Remote Clocks.
Final rept.
J. Levine. 1993, 9p.
Pub. in Proceedings of Annual Precise Time and Time Interval Applications and Planning Meeting (PTTI) (24th), McLean, VA., December 1-3, 1992, p277-285 1993.

Keywords: *Time measuring instruments, *Synchronism, *Algorithms, Time measurements, Calibration, Comparison, Clocks, Time standards, Time domain, Frequency domain, Computers, Global positioning system, Accuracy, Reprints, Time transfer.

We will discuss several methods for characterizing the performance of clocks with special emphasis on using calibration information that is acquired via an unreliable of noisy channel. We will discuss time-domain variance estimators and frequency-domain techniques such as cross-spectral analysis. Each of these methods has advantages and limitations that we will illustrate using data obtained via GPS, ACTS and, other methods. We will also discuss the inverse problem of communicating frequency and time corrections to a real-time steered clock.

01,550
PB96-103049 Not available NTIS
National Inst. of Standards and Technology (PL), Boulder, CO. Time and Frequency Div.
Time Generation and Distribution.
Final rept.
D. B. Sullivan, and J. Levine. 1991, 9p.
Pub. in Proceedings of the Institute of Electrical and Electronics Engineers, v79 p906-914 Jul 91.

Keywords: *Time standards, *Frequency standards, *Synchronism, Atomic clocks, Time signals, Frequency measurements, Calibration, Reprints.

This paper presents a broad overview of time and frequency technology, particularly those trends relating to the generation and distribution of time and frequency signals. The characterization of components and systems is also addressed.

01,551
PB96-112230 Not available NTIS
National Inst. of Standards and Technology (PL), Boulder, CO. Time and Frequency Div.
Local Oscillator Requirements and Strategies for the Next Generation of High-Stability Frequency Standards.
Final rept.
F. L. Walls. 1992, 4p.
Pub. in Proceedings of the Institute of Electrical and Electronics Engineers Frequency Control Symposium, Hershey, PA., May 27-29, 1992, p2-5.

Keywords: *Oscillators, *Frequency stability, *Standards, Reprints, Meetings, Requirements, Strategies, *Foreign technology, Frequency synthesis.

This paper provides a brief introduction to the special session on high-stability frequency synthesis from rf to the visible. The special session is motivated by a number of proposals that have been made for developing frequency standards with frequency stabilities in the 10 to the minus 16th power to 10 to the minus 18th power range. Currently available local oscillators, frequency synthesis techniques, and the measurement methods are not, however, sufficient to support this level of stability. Some general approaches to solve these problems, such as the effect of interrogation type on local oscillator induced white frequency noise, are briefly introduced. The details are to be found in the individual presentations.

01,552
PB96-119482 Not available NTIS
National Inst. of Standards and Technology (PL), Boulder, CO. Time and Frequency Div.
Accurate Measurement of Time.
Final rept.
W. M. Itano, and N. F. Ramsey. 1993, 10p.
Pub. in Scientific American, v269 n1 p56-65 Jul 93.

Keywords: *Atomic clocks, *Time measurements, *Frequency measurements, Time standards, Trapped particles, Ion storage, Hydrogen masers, Cesium frequency standards, Rubidium frequency standards, Atomic beams, Reprints, Atomic fountains.

The current status of atomic frequency standards and clocks is reviewed. The operating principles of frequency standards based on cesium atomic beams, hydrogen masers, rubidium cells, trapped ions, and atomic fountains are discussed. Applications of such frequency standards are discussed.

01,553
PB96-119490 Not available NTIS
National Inst. of Standards and Technology (PL), Boulder, CO. Time and Frequency Div.
Atomic Clock.
Final rept.
W. M. Itano. 1992, 3p.
Pub. in McGraw-Hill Encyclopedia of Science and Technology, 7th Edition, p240-242 1992.

Keywords: *Atomic clocks, *Time measurements, *Frequency measurement, Time standards, Atomic beams, Rubidium frequency standards, Gas cells, Cesium frequency standards, Hydrogen masers, Reprints.

Atomic clocks measure the passage of time using an internal resonance frequency of an atom. The most commonly used types of atomic clocks are the cesium atomic beam, the hydrogen maser, and the rubidium gas cell. In addition, there are many other kinds of atomic clocks under development which may prove to have even greater accuracy and stability. Atomic clocks are used in international timekeeping, navigation, communications, radio astronomy, space exploration, and fundamental science.

01,554
PB96-123187 Not available NTIS
National Inst. of Standards and Technology (PL), Boulder, CO. Time and Frequency Div.

Secondary Standard for PM and AM Noise at 5, 10, and 100 MHz.
Final rept.
F. L. Walls. 1992, 10p.
Pub. in Special Issue of the Institute of Electrical and Electronics Engineers Instrumentation and Measurement Transactions of CPEM '92, p290-299.

Keywords: *Amplitude modulation, *Phase modulation, *Standards, *Electromagnetic noise, Frequency domain, Time domain, High frequency, Electrical measurement, Reprints, Phase noise.

This paper describes a practical implementation of a portable secondary standard for phase modulation (PM) and amplitude modulation (AM) noise at 5, 10, and 100 MHz. The accuracy of the standard for both PM and AM noise is + or - 0.14 dB, and the temperature coefficient is less than 0.02 dB/K. The noise floor of the standard for PM noise measurements, is less than -190 dBC, rel, to 1 sq rad/Hz at 5, 10, and 100 MHz. The noise floor for AM measurements depends on the configuration. A calibrated level of PM and AM noise of approximately -130 + or - 0.2 dB rel to 1 square rad/Hz (for Fourier frequencies from approximately 1 Hz to 10% of the carrier frequency) is used to evaluate the accuracy versus Fourier frequency. Similar PM/AM measurements. Some types of time-domain measurement equipment can also be calibrated.

01,555
PB96-176581 Not available NTIS
National Inst. of Standards and Technology (PL), Boulder, CO. Time and Frequency Div.
Implementation of a Standard Format for GPS Common View Data.
Final rept.
M. A. Weiss, and C. Thomas. 1995, 10p.
Also available as N95-32323; order as N95-32319.
Pub. in Annual Precise Time and Time Interval (PTTI) Applications and Planning Meeting (26th), Reston, VA., December 6-8, 1994, p75-84 1995.

Keywords: *Global positioning system, *Standardization, Calibration, Time signals, Precision, Implementation, Data processing, Ionospherics, Synchonism, Reprints, *Time transfer, Selective availability.

A new format for standardizing common view time transfer data, recommended by the Consultative Committee for the Definition of the Second, is being implemented in receivers commonly used for contributing data for the generation of International Atomic Time. We discuss three aspects of this new format that potentially improve GPS common-view time transfer: (1) the standard specifies the method for treating short term data, (2) it presents data in consistent formats including needed terms not previously available, and (3) the standard includes a header of parameters important for the GPS common-view process.

01,556
PB96-190319 Not available NTIS
National Inst. of Standards and Technology (PL), Boulder, CO. Time and Frequency Div.
Time and Frequency Metrology.
Final rept.
D. B. Sullivan, and J. Levine. 1996, 10p.
Pub. in Advances in Metrology and Its Role in Quality Improvement and Global Trade, New Delhi, India, February 20-23, 1996, p287-296.

Keywords: *Time standards, *Frequency standards, *Calibration, Time signals, Time measurement, Frequency measurement, Atomic clocks, Oscillators, Ion storage, Hydrogen masers, Cesium frequency standards, Rubidium frequency standards, Reprints, Time transfer.

The paper presents an overview of some of the trends which are shaping the directions of development in time and frequency metrology. The paper focuses on the characteristics of frequency sources, methods for comparing separated clocks/oscillators, and techniques for distributing time and frequency signals.

01,557
PB96-190376 Not available NTIS
National Inst. of Standards and Technology (PL), Boulder, CO. Time and Frequency Div.
Confidence on the Modified Allan Variance and the Time Variance.
Final rept.
M. A. Weiss, F. L. Walls, C. A. Greenhall, and T. Walter. 1995, 14p.
Pub. in Proceedings of the European Frequency and Time Forum, Besancon, France, March 8-10, 1995, 14p.

Keywords: *Degrees of freedom, *Confidence limits, Time domain, Overlap, White noise, Electromagnetic noise, Signal to poise ratio, Frequency stability, Time stability, Reprints, *Allan variance, Chi square distribution, Time variance.

The paper presents tabulated factors for calculating confidence intervals for the square root of the Modified Allan Variance and the related time Variance when the analysis uses full overlapping of the data. Confidence intervals are determined by multiplying factors from the appropriate table times sample deviations. These factors have been calculated from the equivalent degrees of freedom (EDF) for the five common power law noise types. Closed form expressions for calculating the EDF for these variances and noise types have only recently become available for fully overlapped data analysis. We compute the EDF using two different closed form expressions as well as simulations to ensure correctness of the results. We also show the relative advantage of using the modified Allan variance instead of the Allan variance to evaluate frequency or time stability in the presence of white phase modulated noise.

01,558
PB96-200381 Not available NTIS
National Inst. of Standards and Technology (PL), Boulder, CO. Time and Frequency Div.
Wavelet Analysis for Synchronization and Timekeeping.
Final rept.
D. A. Howe, and D. B. Percival. 1994, 5p.
Pub. in Institute of Electrical and Electronics Engineers International Frequency Control Symposium, Boston, MA., June 1-3, 1994, p567-571.

Keywords: *Wavelet analysis, *Synchronism, Frequency standards, Time functions, Frequency synchronization, Time measurement, Phase meters, Frequencies, Reprints, *Timekeeping, Wavelet transform, Wavelet variance.

We discuss the concept of the wavelet variance as a generalized formalism for representing variations in a time series on a scale by scale basis. In particular, we note that the wavelet variance corresponding to some of the recently discovered wavelets can provide a more accurate conversion between the time and frequency domains that can be accomplished using the Allan variance. The increase in accuracy is due to the fact that these wavelet variances give better protection against leakage than does the Allan variance.

01,559
PB96-200647 Not available NTIS
National Inst. of Standards and Technology (PL), Boulder, CO. Time and Frequency Div.
How to Get NIST-Traceable Time on Your Computer.
Final rept.
M. A. Lombardi. 1994, 15p.
Pub. in Proceedings of the Workshop and Symposium of the Role of Metrology in a Changing World, Chicago, IL., July 31-August 4, 1994, p299-313.

Keywords: *Computers, *Time signals, *Calibration standards, Computer networks, Time measurement, Time standards, Accuracy, Synchronism, ACTS, GOES satellites, Global positioning system, Reprints, *Time keeping, Smart clock.

The paper describes a number of different ways that you can use to get accurate time that is traceable to NIST on your computer system. This includes receiving time signals by radio, by telephone, or through the Internet. The cost and performance of each technique is also described.

01,560
PB96-200654 Not available NTIS
National Inst. of Standards and Technology (PL), Boulder, CO. Time and Frequency Div.
Introduction to Frequency Calibration. Part 1.
Final rept.
M. Lombardi. 1996, 12p.
Pub. in Cal Lab: The International Jnl. of Metrology, v3 n1 p17-28 Feb 96.

Keywords: *Frequency measurement, *Calibration standards, Frequency synchronization, Frequency stability, Phase modulation, Oscillators, Specifications, Reprints, Traceability, Transfer standards.

The article is part I of a two-part series on frequency calibrations. Part I introduces the topic of frequency calibrations, discusses the specifications involved, and describes the different types of oscillators.

01,561
PB96-200662 Not available NTIS
National Inst. of Standards and Technology (PL), Boulder, CO. Time and Frequency Div.
NIST Frequency Measurement Service.
Final rept.
M. A. Lombardi. 1995, 7p.
See also PB92-165851.
Pub. in Cal Lab: The International Jnl. of Metrology, v2 n3 p11-17 Jun 95.

Keywords: *Frequency measurement, *Calibration, *Accuracy, Frequency stability, Frequency synchronization, Interlaboratory comparisons, Validation, Accreditation, Reprints, *US NIST, Traceability.

The NIST Frequency Measurement Service (FMS) began operation in 1984 to assist users who needed to make high-level frequency calibrations traceable to NIST. The FMS provides a complete solution to all frequency calibration problems by providing a frequency measurement system that can be installed in the customer's lab. The system includes all hardware, software, and documentation needed to automate the frequency measurement process. NIST provides training and phone support and validates customer data through a modem hookup. Each lab receives a monthly report that certifies traceability to NIST.

01,562
PB96-200688 Not available NTIS
National Inst. of Standards and Technology (EEEL), Boulder, CO. Electromagnetic Fields Div.
General Order 'N' Analytic Correction of Probe-Position Errors in Planar Near-Field Measurements.
Final rept.
L. A. Muth. 1995, 10p.
Pub. in Annual Meeting and Symposium of 1995 Antenna Measurement Techniques Association (17th), Williamsburg, VA., November 13-17, 1995, p331-340.

Keywords: *Probes(Electromagnetic), *Antennas, Near field, Extremely high frequency, Reprints, Error correction.

An analytic technique recently developed at NIST (1)(2) to correct for probe position errors in planar near-field measurements has been implemented to arbitrary accuracy. The nth-order correction scheme is composed of an mth-order ordered expansion and an n - m higher-order approximation, where both n and m are arbitrary. The technique successfully removes very large probe position errors in the near-field, so the residual near-field probe position errors are substantially below levels that can be measured on a near-field range. Only the error-contaminated near-field measurements and an accurate probe position errors are substantially below levels that can be measured on a near-field range. Only the error-contaminated near-field measurements and an accurate probe position error function are needed for implementation of the correction technique. The method also requires the ability to obtain derivatives of the error-contaminated near field defined on an error-free regular grid with respect to the coordinates. In planar geometry the derivatives are obtained using FFTs (1), giving an approximate operation count of (3.2(m-1) -1+(n - m))N log N, where N is the number of data points. Efficient computer codes have been developed to demonstrate the technique. The results of simulations are more accurate than those obtained using the well-known k correction (3), which can correct for position errors in some direction in k space, but further contaminates the sidelobe levels.

01,563
PB96-200779 Not available NTIS
National Inst. of Standards and Technology (PL), Boulder, CO. Time and Frequency Div.
Effect of Harmonic Distortion on Phase Errors in Frequency Distribution and Synthesis.
Final rept.
F. L. Walls, and F. G. Ascarrunz. 1995, 8p.
Pub. in Proceedings of the European Frequency and Time Forum (9th), Besancon, France, March 8-10, 1995, 8p.

Keywords: *Phase error, *Frequency distribution, *Frequency synthesizers, Frequency measurement, Frequency stability, Phase detectors, Radio frequencies, Roots of equations, Harmonics, Reprints, *Harmonic distortion, Timing errors.

The paper explores the effect of harmonic distortion on phase errors in frequency distribution and synthesis. Harmonic distortion gives rise to large timing errors in phase or zero crossing detectors. These large timing errors may cause unacceptable sensitivity to environmental conditions or signal fluctuations. Two types of phase detectors are considered in the paper. The timing errors in an ideal zero crossing detector is calculated as a function of harmonic number and the phase of the harmonic relative to the fundamental. Experimental data from several mixers at 5 MHz and different drive levels show that this model is a first-order approximation to real devices. The low sensitivity to the second harmonic is an important advantage over true zero-crossing detectors because it is difficult to significantly reduce the second harmonic without introducing large phase shifts due to filtering networks.

Radio & Television Equipment

01,564
PB94-172020 Not available NTIS
National Inst. of Standards and Technology (EEEL), Boulder, CO. Electromagnetic Fields Div.
Electric-Field Strengths Measured Near Personal Transceivers.
Final rept.
J. Adams. 1993, 4p.
Pub. in Proceedings of International Symposium on Electromagnetic Compatibility, Dallas, TX., August 9-13, 1993, p42-45.

Keywords: *Transmitter receivers, *Electric fields, *Electrical measurement, Very high frequencies, Ultrahigh frequencies, Portable equipment, Walkie talkies, Exposure, Standards, Reprints.

Electric-field strengths were measured at a number of points near 5-W personal transceivers. The points were located on cylinders of revolution with radii of 7 and 12 cm around the antenna. The transceivers operated on four authorized frequencies of 40.27, 162.475, 464, and 823 MHz, and radiated powers of 5, 5, 5, and 3 W, respectively. In some cases, these measured values exceeded the exposure limits suggested in ANSI Standard C95.1-1982.

01,565
PB96-147202 Not available NTIS
National Inst. of Standards and Technology (EEEL), Boulder, CO. Electromagnetic Technology Div.
Heterodyne Mixing and Direct Detection in High Temperature Josephson Junctions.
Final rept.
E. N. Grossman, and L. R. Vale. 1994, 20p.
Pub. in International Symposium on Space Terahertz Technology (5th), Ann Arbor, MI., May 10-12, 1994, p244-263.

Keywords: *Lasers, *Heterodyne detection, Reprints, *Josephson junctions, Microwave noise temperature.

The authors have examined various properties of high characteristic frequency YBCO superconductor- normal-superconductor (SNS) Josephson junctions that are important to their performance as low-noise THz frequency mixers. Without far-infrared laser illumination, the microwavefrequency noise temperature to our lowest noise device shows good agreement with the predictions of the resistivity shunted Josephson model in applicable regions of bias. It has a maximum noise temperature of 36 plus or minus K at a physical temperature of 4 K. When illuminatedwith a 404 GHz far-IR laser local oscillator (LO) and a chopped 77 K blackbody signal, strong modulation of the 1 GHz IF noise power is observed. However, certain features of the modulated IF power signal strongly suggest that a larger fraction of it is not true heterodyne detection. The spurious component is probably due to direct detection ofthe broadband hot load/cold load signal. The authors believe that reliable measurement of heterodyne performance will require narrowband signal sources.

Verbal

01,566
PB94-211539 Not available NTIS
National Inst. of Standards and Technology (NCSL), Gaithersburg, MD. Advanced Systems Div.
Benchmarks for the Evaluation of Speech Recognizers.
Final rept.
W. M. Fisher. 1991, 2p.
Pub. in Digital Signal Processing 1, n2 p64-65 Apr 91.

Keywords: *Speech recognition, *Computer applications, *Technology assessment, CD-ROM, Data bases, Computer software, Evaluation, Reprints, US NIST.

Materials produced by the National Institute of Standards and Technology (NIST) for the standardized evaluation of computer speech recognition systems are described.

COMPUTERS, CONTROL & INFORMATION THEORY

General

01,567
FIPS PUB 140-1 PC E05
National Inst. of Standards and Technology (CSL), Gaithersburg, MD.
Security Requirements for Cryptographic Modules; Category: Computer Security; Subcategory: Cryptography.
11 Jan 94, 44p.
Supersedes FIPS PUB 140.
Three ring vinyl binder also available; North American Continent price $7.00; all others write for quote.

Keywords: *Computer security, *Cryptography, *Federal information processing standards, Telecommunication, Data processing security, Algorithms, Software engineering, Requirements.

The selective application of technological and related procedural safeguards is an important responsibility of every Federal organization in providing adequate security in its computer and telecommunications systems. The publication provides a standard to be used by Federal organizations when these organizations specify that cryptographic-based security systems are to be used to provide protection for sensitive or valuable data. Protection of accryptographic module within a security system is necessary to maintain the confidentiality and integrity of the information protected by the module. This standard specifies the security requirements that are to be satisfied by a cryptographic module. The standard provides four increasing, qualitative levels of security intended to cover a wide range of potential applications and environments. The security requirements cover areas related to the secure design and implementation of a cryptographic module. These areas include basic design and documentation, module interfaces, authorized roles and services, physical security, software security, operating system security, key management, cryptographic algorithms, electromagnetic interference/electromagnetic compatibility (EMI/EMC), and self-testing. This revision supersedes FIPS 140 in its entirety.

01,568
FIPS PUB 180-1 PC E04
National Inst. of Standards and Technology (CSL), Gaithersburg, MD.
Secure Hash Standard. Category: Computer Security.
17 Apr 95, 25p.
Supersedes FIPS PUB 180.
Three ring vinyl binder available; North American Continent price $7.00; all others write for quote.

Keywords: *Computer security, *Federal Information Processing Standards, *Algorithms, Message processing, Data processing, Cryptology, Data encryption, *FIPS PUB 180, *Hash algorithm, Digital signatures.

This standard specifies a Secure Hash Algorithm (SHA-1) which can be used to generate a condensed representation of a message called a message digest. The SHA-1 is required for use with the Digital Signature Algorithm (DSA) as specified in the Digital Signature Standard (DSS) and whenever a secure hash algorithm is required for Federal applications. The SHA-1 is used by both the transmitter and intended receiver of a message in computing and verifying a digital signature.

01,569
FIPS PUB 185 PC E03
National Inst. of Standards and Technology (CSL), Gaithersburg, MD.
Escrowed Encryption Standard (EES); Category: Computer Security; Subcategory: Cryptography.
9 Feb 94, 11p.
Three ring vinyl binder also available; North American Continent price $7.00; all others write for quote.

Keywords: *Data encryption, *Federal information processing standards, Cryptography, Computer security, Telecommunication, Algorithms, Data processing security, LEAF(Law Enforcement Access Field).

The standard specifies an encryption/decryption algorithm and a Law Enforcement Access Field (LEAF) creation method which may be implemented in electronic devices and used for protecting government telecommunications when such protection is desired. The algorithm and the LEAF creation method are classified and are referenced, but not specified, in the standard. Electronic devices implementing the standard may be designed into cryptographic modules which are integrated into data security products and systems for use in data security applications. The LEAF is used in a key escrow system that provides for decryption of telecommunications when access to the telecommunications is lawfully authorized.

01,570
FIPS PUB 186 PC E04
National Inst. of Standards and Technology (NCSL), Gaithersburg, MD.
Digital Signature Standard (DSS). Category: Computer Security; Subcategory: Cryptography.
19 May 94, 24p.
Three ring vinyl binder also available; North American price $7.00; all others write for quote.

Keywords: *Cryptography, *Computer security, Algorithms, Access control, Data processing security, Data integrity, Data encryption, Message processing, Information security, Random number generators, Authentication, Verification, *Digital signatures, Federal Information Processing Standard, ADP(Automated Data Processing).

This standard specifies a Digital Signature Algorithm (DSA) which can be used to generate a digital signature. Digital signatures are used to detect unauthorized modifications to data and to authenticate the identity of the signatory. In addition, the recipient of signed data can use a digital signature in proving to a third party that the signature was in fact generated by the signatory. This is known as nonrepudiation since the signatory cannot, at a later time, repudiate the signature.

01,571
FIPS PUB 188 PC E04
National Inst. of Standards and Technology (CSL), Gaithersburg, MD.
Standard Security Label for Information Transfer; Category: Computer Security; Subcategory: Security Labels.
6 Sep 94, 28p.
Also available from Supt. of Docs.
Three ring vinyl binder also available; North American Continent price $7.00; all others write for quote.

Keywords: *Computer information security, *Federal information processing standards, Computer security, Access control, Protocols, Computer communications, Syntax, Computer networks, Data processing security, *Security labels.

Information Transfer security labels convey information used by protocol entities to determine how to handle data communicated between open systems. Information on a security label can be used to control access, specify protective measures, and determine handling

restrictions required by a communications security policy. This standard defines a security label syntax for information exchanged over data networks and provides encodings of that syntax for use at the Application and Network Layers.

01,572
FIPS PUB 46-2 PC E04
National Inst. of Standards and Technology (CSL), Gaithersburg, MD.
Data Encryption Standard (DES); Category: Computer Security; Subcategory: Cryptography.
30 Dec 93, 23p.
Supersedes FIPS PUB 46-1.
Three ring vinyl binder available; North American Continent price $7.00; all others write for quote.

Keywords: *Data encryption, *Federal information processing standards, Computer security, Algorithms, Cryptography, Data integrity, Data processing security.

The selective application of technological and related procedural safeguards is an important responsibility of every Federal organization in providing adequate security to its electronic data systems. The publication specifies a crypotographic algorithm which may be used by Federal organizations to protect sensitive data. Protection of data during transmission or while in storage may be necessary to maintain the confidentiality and integrity of the information represented by the data. The algorithm uniquely defines the mathematical steps required to transform data into a crypotographic cipher and also to transform the cipher back to the original form. The Data Encryption Standard is being made available for use by Federal agencies within the context of a total security program consisting of physical security procedures, good information management practices, and computer system/network access controls. The revision supersedes FIPS 46-1 in its entirety.

01,573
PB94-134897 PC A03/MF A01
National Inst. of Standards and Technology (CSL), Gaithersburg, MD.
General Procedures for Registering Computer Security Objects.
N. A. Nazario. Dec 93, 23p, NISTIR-5308.

Keywords: *Computer security, *Standards, Services, Fees, Requirements, Labels, *CSOR(Computer Security Objects Register), Registration.

The document defines a Computer Security Objects Register (CSOR). It outlines the information required for the assignment of unique identifiers to the specifications of Computer Security Objects (CSOs). A CSO can be defined as a resource, tool, or mechanism used to maintain a condition of security in computerized environments. This broad definition covers many elements that are referred to in standards but that are either selected or defined by separate user communities (e.g., network security labels, cryptographic algorithm operation modes, authentication techniques). The CSOR services organizations and individuals seeking to further interoperability by using a common set of tools and techniques in the area of computer security.

01,574
PB94-135001 PC A09/MF A02
National Inst. of Standards and Technology (CSL), Gaithersburg, MD.
Report of the NIST Workshop on Digital Signature Certificate Management. Held on December 10-11, 1992.
D. K. Branstad. Oct 93, 187p, NISTIR-5234.

Keywords: *Computer security, *Cryptography, *Meetings, Certification, Standards, Data processing security, *Digital signatures, National Institute of Standards and Technology.

This report summarizes the major topics of discussion held during a Workshop on Ditigal Signature Certificate Management held at the National Institute of Standards and Technology (NIST) on December 10-11, 1992. The purpose of the workshop was to review existing and required technologies for digital signature certification authorities and to develop recommendations for certificate contents, formats, generation, distribution and storage. The results of the workshop have been provided as input to a federally sponsored study of support infrastructures of a set of international and national signature certification authorities. A summary of the major issues discussed and the recommendations on several of them are presented.

01,575
PB94-162583 PC A04/MF A01
National Inst. of Standards and Technology (CSL), Gaithersburg, MD. Computer Security Div.
Proceedings of the Workshop on the Federal Criteria for Information Technology Security. Held in Ellicot City, Maryland on June 2-3, 1993.
J. A. Cugini, P. Toth, G. Troy, T. Mayfield, M. Abrams, L. Fraime, V. Gligor, L. M. Ambuel, and F. Mayer. Mar 94, 74p, NISTIR-5386.
Prepared in cooperation with National Security Agency/Central Security Service, Fort George G. Meade, MD.

Keywords: *Meetings, *Computer security, Access control, Data processing security, Computer privacy, Standards, North America, Europe, *Federal Criteria, National Institute of Standards and Technology, National Security Agency, Common Criteria Editorial Board, ISO(International Standards Organization).

The first draft of the Federal Criteria was made public in January 1993. Several thousand copies of the Federal Criteria were distributed and comments on this first draft were received. The purpose of the Federal Criteria Workshop was to address these comments. The purpose of these proceedings is to inform the Federal Criteria commentators and the workshop attendees of the outcome of the workshop. Also, these proceedings will be used as a blueprint for updating the Federal Criteria. These proceedings, and the revised portions of the draft Federal Criteria contents, will be the two principal National Institute of Standards and Technology (NIST)/National Security Agency (NSA) inputs to the Common Criteria Editorial Board (CCEB). Preliminary plans for dealing with the Federal Criteria comments are included in this document, and all revisions will be performed under the direction of NIST and the NSA.

01,576
PB94-164373 PC A03/MF A01
National Inst. of Standards and Technology (CSL), Gaithersburg, MD.
Conformance Assessment of Transport Layer Security Implementations.
W. A. Jansen. Dec 93, 23p, NISTIR-5325.
See also AD-A207 905 and AD-A255 422.

Keywords: *Computer networks, *Protocols, *Computer security, Tests, Data integrity, Computer information security, Authentication, Access control, OSI(Open System Interconnection), TLSP(Transport Layer Security Protocol), SP4(Security Protocol at layer 4), SDNS(Secure Data Network System).

The paper presents a framework for evaluating conformance of a protocol implementation to the Security Protocol at layer 4 (SP4) standard. SP4 is one element of the Secure Data Network System (SDNS) architecture, used to provide security services at the Transport layer of the Open System Interconnection (OSI) reference model. SP4 also forms the basis of the International Organization for Standardization (ISO) standard for the OSI Transport Layer Security Protocol (TLSP). Therefore, with few exceptions, the findings of the paper are applicable to TLSP. The paper explores the relationship between conformance assessment, interoperability assessment, and security evaluation of security protocols. The OSI conformance testing methodology and framework is reviewed, and a strategy is given for applying this methodology to SP4 implementations.

01,577
PB94-185402 Not available NTIS
National Inst. of Standards and Technology (CSL), Gaithersburg, MD. Computer Security Div.
Conformance Testing of a Lower Layer Security Protocol.
Final rept.
W. A. Jansen. 1993, 13p.
Pub. in Proceedings of Symposium on Military Communications Network, The Hague, The Netherlands, June 8-11, 1993, p843-855.

Keywords: *Computer networks, *Computer security, *Protocols, *Conformity, Tests, Communication networks, Reprints, Conformance testing, OSI(Open System Interconnection), SDNS(Secure Data Network System), ISO(International Organization for Standardization), TLSP(Transport Layer Security Protocol).

This paper presents a framework for evaluating conformance of a protocol implementation to the Security Protocol at layer 4 (SP4) standard. SP4 is one element of the Secure Data Network System (SDNS) architecture, used to provide security services at the transport layer of the Open System Interconnection (OSI) reference model. SP4 also forms the basis of the recently completed ISO standard for the Transport Layer Security Protocol (TLSP). The paper explores the relationship between conformance testing and security evaluations of security protocols in general, and SP4 in particular. The OSI conformance testing methodology is reviewed, and a strategy is given for applying the methodology to SP4 implementations.

01,578
PB94-191202 PC A21/MF A04
Independent Monitoring, Cambridge, MA.
Federal Certification Authority Liability and Policy: Law and Policy of Certificate-Based Public Key and Digital Signatures.
M. S. Baum. Jun 94, 485p, NIST/GCR-94/654.
Sponsored by National Inst. of Standards and Technology, Gaithersburg, MD.

Keywords: *Computer security, *Cryptography, *Law(Jurisprudence), Computer information security, Government policies, Legal aspects, Data processing security, Electronic mail, Recommendations, Digital signatures, EDI(Electronic Data Interchange), National Institute of Standards and Technology, FCA(Federal Certification Authority), Infrastructure, PEM(Privacy Enhanced Mail).

The report identifies diverse technical, legal and policy issues affecting a certificate-based public key cryptographic infrastructure utilizing digital signatures supported by 'trusted entities.' It examines potential legal implications, surveys existing legal paradigms and the structures and roles of relevant governmental agencies and presents various institutional approaches to controlling liability. It considers the underpinnings of a legal and policy framework which might serve as a foundation for security policies and their implementation and concludes with a series of recommendations, both general and specific.

01,579
PB94-193653 PC A07/MF A02
National Inst. of Standards and Technology (CSL), Gaithersburg, MD. Computer Security Div.
Study of Federal Agency Needs for Information Technology Security.
Rept. for Feb-Aug 92.
D. M. Gilbert. May 94, 126p, NISTIR-5424.
See also PB93-138956.

Keywords: *Data processing security, *Federal agencies, Requirements, Standards, Computer security, Computer information security, Surveys, Tables(Data), *IT(Information Technology), *Information Technology, *National Institute of Standards and Technology.

The report presents the results of a National Institute of Standards and Technology (NIST) study to determine and document what federal agencies need to meet their information technology (IT) security requirements. A meeting of the NIST IT Security Needs Study Working Group was held at NIST in September 1992 to review and comment on the study results. This report reflects the working group input. The results of the study contribute to a sound basis for planning future NIST IT security standards, guidance, and related activities.

01,580
PB94-198256 Not available NTIS
National Inst. of Standards and Technology (NEL), Gaithersburg, MD. Robot Systems Div.
Hierarchical Interaction between Sensory Processing and World Modeling in Intelligent Systems.
Final rept.
J. S. Albus. 1990, 7p.
Pub. in Proceedings of the Institute of Electrical and Electronics Engineers International Symposium on Intelligent Control (5th), Philadelphia, PA., September 5-7, 1990, v1 p53-59.

Keywords: *Artificial intelligence, *Machine vision, Learning machines, Robotics, Sensory perception, Models, Image processing, Pattern recognition, Reprints.

The role of the sensory processing system is to transform sensory maps into world model maps and to extract entity attributes and states. The role of the world modeling system is to store best estimates of the extracted values, and to generate from them, predicted inputs. There is a tight coupling between sensory proc-

essing and world modeling. The world model generates predicted sensory input from stored state estimates. The sensory processing system compares predictions with observations, and returns the difference signals to the world model for updating state estimators. The sensory processing system also performs spatial and temporal integration on various combinations of observed and predicted data, and compares the resulting correlation function against thresholds of recognition and detection.

01,581
PB94-198264 Not available NTIS
National Inst. of Standards and Technology (NEL), Gaithersburg, MD. Robot Systems Div.
Role of World Modeling and Value Judgment in Perception.
Final rept.
J. S. Albus. 1990, 10p.
Pub. in Proceedings of the Institute of Electrical and Electronics Engineers International Symposium on Intelligent Control (5th), Philadelphia, PA., September 5-7, 1990, v1 p154-163.

Keywords: *Artificial intelligence, *Models, Machine learning, Knowledge representation, Robotics, Task planning(Robotics), Sensory perception, Interfaces, Reprints, *World models.

The world model is the intelligent system's best estimate of the external world. It provides an interface between sensory processing and task decomposition. A world model architecture is proposed that represents knowledge in terms of maps, entity frames, and state variables. The structure is hierarchically organized so as to provide multiple levels of resolution in space and time. Three types of map coordinates are important: egospheres, object coordinates, and world coordinates. Value judgments provided an evaluation of hypothesized plans, and perceived objects, events, and situations. Evaluations produce value state-variables that indicate cost, benefit, risk, priority, desirability, attractiveness, and uncertainty.

01,582
PB94-198272 PC A02
National Inst. of Standards and Technology (NEL), Gaithersburg, MD. Robot Systems Div.
Theory of Intelligent Systems.
Final rept.
J. S. Albus. 1990, 10p.
Pub. in Proceedings of the Institute of Electrical and Electronics Engineers International Symposium on Intelligent Control (5th), Philadelphia, PA., September 5-7, 1990, p866-875.

Keywords: *Artificial intelligence, Robotics, Learning machines, Machine vision, Feedback control, Models, Theories, Reprints.

A theoretical model is proposed consisting of seven basic elements: actuators, sensors, sensory processing, world modeling, task decomposition, value judgment, and global memory/communications. These elements are integrated into a hierarchical system architecture wherein: (1) control bandwidth decreases about an order of magnitude at each higher level, (2) perceptual resolution of spatial and temporal patterns contracts about an order-of-magnitude at each higher level, (3) goals expand in scope and planning horizons expand in space and time about an order-of-magnitude at each higher level, and (4) models of the world and memories of events expand in space and time by about an order-of-magnitude at each higher level. At each level, tightly coupled functional modules perform task decomposition, world modeling, sensory processing, and value judgments. Feedback control loops are closed at every level.

01,583
PB94-199247 Not available NTIS
National Inst. of Standards and Technology (NCSL), Gaithersburg, MD. Systems and Network Architecture Div.
Integrated Network Management.
Final rept.
P. Brusil, and D. P. Stokesberry. 1989, 7p.
Pub. in Proceedings of International Federation for Information Processing TC 6/WG 6.6 Symposium on Integrated Network Management, Boston, MA., May 16-17, 1989, p3-9.

Keywords: *Computer networks, *Integrated systems, Reprints, Communication networks, Vendors, *Network management, OSI(Open Systems Interconnection).

The document contains the introductory remarks to the First International Symposium on Integrated Network Management.

01,584
PB94-209459 PC A08/MF A02
Iowa State Univ., Ames. Dept. of Computer Science.
Report of the NIST Workshop on Key Escrow Encryption. Held in Gaithersburg, Maryland on June 8-10, 1994.
A. E. Oldehoeft, and D. K. Branstad. Jun 94, 164p, NISTIR-5468.
See also FIPS PUB 185. Sponsored by National Inst. of Standards and Technology (CSL), Gaithersburg, MD. Computer Security Div.

Keywords: *Data encryption, *Data processing security, Federal information processing standards, Algorithms, Computer software, Computer program integrity, Requirements, Industries, Computer security, *Key escrow encryption, EES(Escrowed Encryption Standard), US NIST.

The purpose of this workshop was to initiate a dialogue among representatives from industry, government and academia regarding issues of key escrow encryption. Workshop presentations and discussions included current progress in the planned usage of CAPSTONE/CLIPPER chips, the alternative of software key escrowing, multipurpose key escrowing methods, private key escrow management, integrity requirements of application systems, and international implications. The proposed plan of action, arising from this workshop, is to establish a joint industry/government working group to critically evaluate all known key escrowing proposals; examine the adequacy of existing (and possibly suggesting new) vehicles for collaborative industry/government research and development; identify and evaluate suitable algorithms for use in conjunction with key escrow along with criteria for determining acceptability; identify and address the issues of intellectual property which are inherent in any public royalty-free usage of algorithms, key escrow methodology, and supporting infrastructure; and create a key escrowing task force to manage and expedite the search for key escrow alternatives.

01,585
PB94-213030 Not available NTIS
National Inst. of Standards and Technology (NCSL), Gaithersburg, MD. Systems and Software Technology Div.
Formal Specification and Verification of Control Software for Cryptographic Equipment.
Final rept.
D. R. Kuhn, and J. F. Dray. 1990, 11p.
Pub. in Proceedings of Annual Computer Security Applications Conference (6th), Tucson, AZ., December 3-7, 1990, p32-43.

Keywords: *Cryptography, *Computer program verification, *Specifications, Access control, Software engineering, Computer security, Microprocessors, Workstations, Reprints, Smart cards, Formal methods, VDM(Vienna Development Method).

This paper describes the application of formal specification and verification methods to two microprocessor-based devices: a 'smart-token' system that controls access to a network of workstations, and a message authentication device implementing the ANSI X9.9 message authentication standard. A state-based specification for the smart token system was prepared and verified using the Unisys Formal Development Methodology. The message authentication device specification used the Vienna Development Method, which is based on denotational semantics. Formal specification and verification were found to be practical, cost-effective tools for detecting potential security weaknesses. The security of the access control system was strengthened as a result of the analysis. An unexpected result was the discovery of ambiguities in a published standard.

01,586
PB94-215746 PC A05/MF A01
National Inst. of Standards and Technology (NCSL), Gaithersburg, MD. Computer Security Div.
Head Start on Assurance: Proceedings of an Invitational Workshop on Information Technology (IT) Assurance and Trustworthiness. Held in Williamsburg, Virginia on March 21-23, 1994.
Special pub.
M. D. Abrams, and P. R. Toth. Aug 94, 92p, NISTIR-5472.
See also PB91-235978. Sponsored by Aerospace Computer Security Associates, Silver Spring, MD.

Keywords: *Meetings, *Computer security, Data processing security, Computer privacy, Computer information security, Data integrity, Government policies, Distributed computer systems, Operating systems(Computers).

The purpose of the Invitational Workshop on Information Technology (IT) Assurance and Trustworthiness was to identify crucial issues on assurance in IT systems and to provide input into the development of policy guidance on determining the type and level of assurance appropriate in a given environment. The readers of these proceedings include those who handle sensitive information involving national security, privacy, commercial value, integrity, and availability. Existing IT security policy guidance is based on computer and communications architectures of the early 1980s. Technological changes since that time mandate a review and revision of policy guidance on assurance and trustworthiness, especially since the changes encompass such technologies as distributed systems, local area networks, the worldwide Internet, policy-enforcing applications, and public key cryptography.

01,587
PB94-216710 Not available NTIS
National Inst. of Standards and Technology (CSL), Gaithersburg, MD. Computer Security Div.
Bibliography of Computer Security Glossaries.
Final rept.
S. P. McCrea. 1990, 2p.
Pub. in National Computer Systems Laboratory Bulletin, p1-2 Sep 90.

Keywords: *Computer security, *Dictionaries, *Bibliographies, Federal agencies, Data processing security, Reprints, NCSL(National Computer Systems Laboratory), US NIST, ANSI(American National Standards Institute).

The National Computer Systems Laboratory (NCSL) developed a bibliography that identifies eight glossaries that contain computer security terms and definitions. These glossaries were developed by Federal Government agencies, the American National Standards Institute (ANSI) Accredited Standards Committee X3K5, and private sector organizations. The purpose of the bibliography is to provide a guide to computer security glossaries that can be used by Federal Government agencies to promote common understanding of computer security terms, concepts, and procedures.

01,588
PB94-218575 PC A03/MF A01
National Inst. of Standards and Technology (MEL), Gaithersburg, MD. Intelligent Systems Div.
Adaptive, Predictive 2-D Feature Tracking Algorithm for Finding the Focus of Expansion.
S. Krishnan, and D. Raviv. Jun 94, 30p, NISTIR-5460.
Grant NSF-IRI-9115939
Prepared in cooperation with Florida Atlantic Univ., Boca Raton. Robotics Center. Sponsored by National Science Foundation, Arlington, VA.

Keywords: *Motion, *Optical tracking, *Computer vision, *Two dimensional flow, Feature extraction, Pattern recognition, Image processing, Algorithms, Pixels, FOE(Focus of Expansion).

This paper describes a robust, pixel-based adaptive algorithm to track image features, both spatially and temporally, over a sequence of monocular images. The algorithm assumes no a priori knowledge about the features to be tracked, or the motion of the camera or the objects, in the 3-D scene. The features to be tracked are selected by the algorithm and these correspond to the peaks of a 'matching surface' constructed from the first image of the sequence to be analyzed. Any kind of motion can be tolerated keeping in mind the pixels-per-frame motion limitations. In our experiments, we have used the algorithm for tracking up to 3 pixels motion between frames with absolutely no subpixel calculations being necessary. Taking into account constraints of temporal continuity, the algorithm uses simple and efficient predictive tracking over multiple

frames. The algorithm accepts a slow, continuous change of brightness D.C. level in the pixels of the feature. Trajectories of features on multiple objects can be computed. As an application of the algorithm we show how the algorithm can be used to find the Focus of Expansion (FOE) using a sequence of real images.

01,589
PB95-130985 PC A09/MF A02
National Inst. of Standards and Technology (CSL), Gaithersburg, MD.
Computer Security Training and Awareness Course Compendium.
K. Everhart. Sep 94, 192p, NISTIR-5495.
See also PB92-205442 and PB90-780172.

Keywords: *Computer security, *Training, *Curricula, Directories, Government employees, Government agencies, Personnel development, Vendors, Auditing, Computer viruses, Local area networks, Data processing security, Computer information security, Information systems, Telecommunication.

The training and awareness courses in this compendium correspond to the matrix in NIST Special Publication 500-172, Computer Security Training Guidelines (PB90-780172). Special Publication 500-172 is used as reference under the OPM regulation that implements Public Law 100-235, the Computer Security Act of 1987, which requires training for all employees responsible for the management and use of federal computer systems that process sensitive information. Under the regulation, agencies will be responsible for identifying the employee to be trained and providing appropriate training. In addition to the table of contents, which lists the courses, there are four appendices: (1) lists the course by training areas within audience categories as defined in NIST Special Publication 500-172; (2) lists the vendors that participated in this effort; (3) lists the specific products for which training is available; and (4) lists the product specific courses.

01,590
PB95-150983 Not available NTIS
National Inst. of Standards and Technology (NEL), Gaithersburg, MD. Electricity Div.
Compensation of Markov Estimator Errors in Time-Jittered Sampling of Nonmonotonic Signals.
Final rept.
G. Tong, and T. M. Souders. 1993, 5p.
Pub. in Institute of Electrical and Electronics Engineers Transactions on Instrumentation and Measurement 42, n5 p931-935 Oct 93.

Keywords: Probability density functions, Sampling, Errors, Reprints, *Signal estimation, *Markov estimators, Sampling voltage trackers, Bias compensation, Time jitter.

The so-called Markov estimator is sometimes used to estimate signals from their time-jittered samples. The estimates are unbiased for monotonic signals, but exhibit errors in regions of nonmonotonicity. A method of compensation is presented to reduce this error. It requires a knowledge of the probability density functions (PDF) of the time jitter, and a proposed method for determining the PDF based on the generalized Markov estimator has been verified through simulations. The performance of the compensation approach is presented for four different nonmonotonic waveforms.

01,591
PB95-161030 Not available NTIS
National Inst. of Standards and Technology (MEL), Gaithersburg, MD. Robot Systems Div.
Visual Road Following without 3-D Reconstruction.
Final rept.
M. Herman, D. Raviv, H. Schneiderman, and M. Nashman. 1993, 11p.
Pub. in Proceedings of Society of Photo-Optical Instrumentation Engineers Applied Imagery Pattern Recognition Workshop (22nd), Washington, DC., October 1993, v2103 p1-11.

Keywords: *Robots, *Autonomous navigation, *Computer vision, Robotics, Robot dynamics, Ground vehicles, Two dimensional models, Optical flow(Image analysis), Cues, Algorithms, Real time, Reprints, *Road following.

The paper discusses an alternative approach to visual road following in which a minimal road model is generated. The model contains only task-relevant information and a minimum of vision processing is performed to extract this information. This approach leads to rapid and continuous update of the road model from the visual data. Road following is achieved by servoing on the visual cues in the 2-D model. In this paper, two specific examples of road following that use this approach are presented. In the first example, we show that road following commands can be generated from visual cues consisting of the projection into the image of the tangent point on the edge of the road, along with the optical flow of this point. Using this cue, the resulting servo loop is very simple and fast. In the second example, we show that lane markings can be robustly tracked in real time while confining all processing to the 2-D image plane. Neither knowledge of vehicle motion nor a calibrated camera is required.

01,592
PB95-161170 Not available NTIS
National Inst. of Standards and Technology (CSL), Gaithersburg, MD. Computer Security Div.
SDNS Security Management.
Final rept.
W. A. Jansen. 1992, 10p.
Pub. in Proceedings of National Computer Security Conference (15th), Baltimore, MD., October 13-16, 1992, p574-583.

Keywords: *Computer networks, *Computer security, Standards, Protocols, Access control, Systems management, Reprints, *SDNS(Secure Data Network System), *Secure Data Network System, OSI(Open Systems Interconnection).

The Secure Data Network System (SDNS) program has developed a security architecture based on the International Organization for Standardization (ISO) Basic Reference Model for Open Systems Interconnection (OSI). The SDNS standards include lower layer security protocols, a key management protocol, and a framework for access control. This paper provides an overview of SDNS security management and its relationship to OSI systems management. A conceptual data model of SDNS security management information is presented. The overview also includes the naming hierarchy for the object classes defined for SDNS management and the registration scheme proposed for identifying elements of SDNS management information.

01,593
PB95-162236 Not available NTIS
National Inst. of Standards and Technology (NEL), Gaithersburg, MD. Robot Systems Div.
Reconstruction during Camera Fixation.
Final rept.
D. Raviv. 1991, 8p.
Pub. in Proceedings of Society of Photo-Optical Instrumentation Engineers: Intelligent Robots and Computer Vision IX: Neural, Biological and 3-D Methods, Boston, MA., November 7-9, 1990, v1382 p312-319 1991.

Keywords: *Autonomous navigation, *Robots, *Computer vision, Robot dynamics, Optical flow(Image analysis), Cameras, Reprints, *Camera fixation.

A fixation point is a point in 3-D space that projects to zero optical flow in an image over some period of time while the camera is moving. This paper deals with quantitative aspects of camera fixation for a static scene. In general, when the camera undergoes translation and rotation, there is an infinite number of points that produce equal optical flow for any instantaneous point in time. Using a camera-centered spherical coordinate system, it is shown how to find these points in space. If the elevation component of the optical flow is set to zero, then these points form a circle (called the Equal Flow Circle (EFC)) and a line. A special case of the EFCs is the Zero Flow Circle (ZFC) where both components of the optical flow are equal to zero. In a set of experiments using simulated as well as real data, we show how the concept of the EFC and ZFC can be used to explain the optical flow produced by points near the fixation point, and to explicitly map the space while fixating. It is also shown experimentally that points near the fixation point may change the sign of their optical flow as the camera moves.

01,594
PB95-162244 Not available NTIS
National Inst. of Standards and Technology (MEL), Gaithersburg, MD. Robot Systems Div.
Unified Approach to Camera Fixation and Vision-Based Road Following.
Final rept.
D. Raviv, and M. Herman. 1994, 53p.
Pub. in Institute of Electrical and Electronics Engineers Transactions on Systems, Man, and Cybernetics 24, n8 53p Aug 94.

Keywords: *Autonomous navigation, *Robotics, *Computer vision, Robots, Robot dynamics, Optical flow(Image analysis), Cameras, Reprints, *Camera fixation, *Road following.

Both camera fixation and vision-based road following are problems that involve tracking or fixating on 3-D points and features. These problems also require an analysis of depth and motion. We present a theoretical approach to analyzing optical flow and show the application of this unified approach to both problems. In general, when a camera undergoes translation and rotation, there is an infinite number of points in 3-D space that produce equal optical flow for any point in time. Using a camera-centered spherical coordinate system, we show how to find these points in space. If the elevation component of the optical flow is set to zero, then these points form a circle (called the Equal Flow Circle (EFC)) and a line. A special case of the EFCs is the Zero Flow Circle (ZFC) where both components of the optical flow are equal to zero. The fixation point is the intersection of all the ZFCs. Points inside and outside of the ZFC can be quantitatively mapped using the EFCs. Using the ZFCs approach, we suggest a new, quantitative, vision-based approach to road following. We show that motion commands can be generated from a visual feature, or cue, consisting of the projection into the image of the tangent point on the edge of the road, along with the optical flow of this point. Using this cue, we suggest a vision-based control approach.

01,595
PB95-162376 Not available NTIS
National Inst. of Standards and Technology (NCSL), Gaithersburg, MD.
Data Encryption Standard.
Final rept.
E. Roback. 1990, 6p.
Pub. in National Computer Systems Laboratory Bulletin, p1-6 Jun 90.

Keywords: *Data encryption, *Cryptology, *Secure communications, Cryptography, Coding, Message processing, Information security, Data integrity, Computer security, Electronic security, Reprints, Data security.

This NCSL Bulletin provides an overview of the most frequently asked questions regarding Federal Information Processing Standard 46-1 (FIPS PUB 46-1), Data Encryption Standard (DES), and associated topics including: its background, technical overview, applicability, waivers and procedures, DES crytographic keys, endorsement of DES devices, exportability issues, and validation of DES implementations. The document does not establish new policy. The Bulletin also provides a list of reference documents regarding the DES.

01,596
PB95-163432 Not available NTIS
National Inst. of Standards and Technology (NCSL), Gaithersburg, MD. Computer Security Div.
Computer Security Management and Planning in the U.S. Federal Government.
Final rept.
E. F. Troy. 1990, 519p.
Pub. in Proceedings of Comsec International 1990, London, United Kingdom, October 10-12, 1990, 519p.

Keywords: *Federal government, *Computer information security, *Selective dissemination of information, *Data base administrators, *Access control, Data processing security, Electronic security, Classified information, Classified materials, Vulnerability, Privacy, Confidentiality, Risk assessment, Computer networks, Operating systems(Computers), Computer program integrity, Data management systems, Policies, Reprints, Computer security management, Computer security planning, Trusted systems, Computer Security Act.

The paper describes a number of activities sponsored by NIST to improve computer security management in the U.S. Federal government. The paper presents the results of the computer Security Act-mandated security plan review process and describes a number of procedural initiatives NIST has taken to help Federal computer security managers meet their computer security responsibilities. The paper also discusses new NIST technical initiatives in applying trusted systems technology concepts to sensitive systems, as a powerful new aid to assure better security protection. The paper asserts that a balanced combination of technical and non-technical security controls is needed to provide adequate computer security for Federal systems.

01,597
PB95-163440 Not available NTIS
National Inst. of Standards and Technology (NCSL), Gaithersburg, MD. Computer Security Div.
Guidance to Federal Agencies on the Use of Trusted Systems.
Final rept.
E. F. Troy, and E. E. Flahavin. 1990, 4p.
Pub. in National Computer Systems Laboratory Bulletin, p1-4 Jul 90.

Keywords: *Federal agencies, *Computer information security, *Selective dissemination of information, *Access control, Data processing security, Electronic security, Privacy, Confidentiality, Computer networks, Data management systems, Operating systems(Computers), Policies, Standards, Guidelines, Reprints, *Trusted systems, *Unclassified sensitive information, Computer security management.

The document provides initial guidance to Federal departments and agencies on the use of trusted systems technology in computer systems which handle unclassified sensitive information.

01,598
PB95-163895 Not available NTIS
National Inst. of Standards and Technology (NEL), Gaithersburg, MD. Robot Systems Div.
Configuration and Performance Evaluation of a Real-Time Robot Control System: A Skeleton Approach.
Final rept.
T. Wheatley, and J. Michaloski. 1990, 4p.
Pub. in Proceedings of Institute of Electrical and Electronics Engineers International Conference on Systems Engineering, Pittsburgh, PA., August 9-11, 1990, p268-271.

Keywords: *Robot control, *Systems analysis, *Performance evaluation, Real time, Computer system hardware, Operating systems(Computers), Multiprocessors, Concurrent processing, Hierarchies, Control systems, Reprints, Skeleton systems.

The use of a skeleton system to model a multi-processor robot control architecture offers the system designer a powerful tool to configure and evaluate system parameters. This paper describes the skeleton approach as applied to the NASREM robot control architecture. The skeleton approach creates the shell of a functioning real-time control system utilizing the actual hardware and operating system code without using actual application code. This is done by replacing the processing part of the application code with time delays. Parameterization of time delays, communication paths, message buffer lengths, and process allocation provides for rapid prototyping of alternative system architectures. Actual system performance is measured to provide realistic data on computation and communication loads. The skeleton reporting facility provides quantitative assessments of system activity. To illustrate the use of this technique, the servo level of the NASREM hierarchy will be modeled using a 5.0 msec cycle time on a multiprocessor system, and compared with the actual system.

01,599
PB95-169108 Not available NTIS
National Inst. of Standards and Technology (CSL), Gaithersburg, MD. Systems and Software Technology Div.
Approaches Using Virtual Environments with Mosaic.
Final rept.
S. Ressler. 1994, 8p.
Pub. in Proceedings of International WWW Conference '94 Mosaic and the Web (2nd), Chicago, IL., October 17-20, 1994, p853-860.

Keywords: *Virtual reality, *Environment simulation, *Interactive graphics, Computer graphics, Interactive control, Computerized simulation, Man computer interfaces, Data transmission, Information technology, Reprints, *Mosaic, *Computer generated environments, User interfaces, World Wide Web, National Information Infrastructure.

The paper describes several ways to use a computer generated environment with Mosaic. The first is to allow the user to interact with an environment displayed as part of the Mosaic document, an in-line image. The second is to create an independent process with which the user can have high bandwidth interaction, i.e. real time manipulations, which can drive Mosaic remotely. These techniques demonstrate that the use and interaction with spatially oriented information spaces are practical. Both techniques have advantages and disadvantages which are discussed.

01,600
PB95-171435 PC A03/MF A01
Florida Atlantic Univ., Boca Raton. Robotics Center.
New Method to Calculate Looming for Autonomous Obstacle Avoidance.
K. Joarder, and D. Raviv. Nov 94, 32p, NISTIR-5512.
Grant NSF-IRI-9115939
Sponsored by National Inst. of Standards and Technology (MEL), Gaithersburg, MD. Intelligent Systems Div. and National Science Foundation, Arlington, VA. Div. of Information, Robotics and Intelligent Systems.

Keywords: *Autonomous navigation, *Obstacle avoidance, Computer vision, Cameras, Ocular fixation, Textures, Motion, Image processing, *Visual looming.

The idea of visual looming, i.e., the expansion of an object's size on the retina due to its decreasing distance from the observer, can be used as a powerful visual cue for autonomous obstacle avoidance. In this paper we describe a method of measuring looming quantitatively by fixating a camera at a point on the surface of an object and studying the texture near this point. A reduced distance of the camera from the surface results in a decline in the density of the texture primitives in the image. We show analytically how looming can be calculated from the relative change in this density and from the local orientation of the surface. The method is applicable for both stationary and moving obstacles and does not require calculation of range. Results of looming are presented for various textural surfaces, in different orientations.

01,601
PB95-171955 PC A05/MF A01
National Inst. of Standards and Technology (CSL), Gaithersburg, MD. Computer Security Div.
Multi-Agency Certification and Accreditation (C and A) Process: A Worked Example.
E. Flahavin, A. Lee, and D. Wolcott. Dec 94, 86p, NISTIR-5540.
Contract DEA-50SBNB1C6732
Sponsored by Drug Enforcement Administration, Washington, DC.

Keywords: *Federal agencies, *Computer security, Data processing security, Systems engineering, Federal information processing standards, Risk assessment, DEA(Drug Enforcement Administration), C&A(Certification and Accreditation), Mountain Pass project.

This document describes a worked example of a multi-agency certification and accreditation (C&A) process implemented by several Federal agencies. The objective of the document is to provide a practical example of how to perform multi-agency C&A. The example is based on a project implemented for the Drug Enforcement Administration (DEA), called Mountain Pass. The project was implemented to improve the El Paso Intelligence Center (EPIC) information system and related communications to satisfy EPIC's current and anticipated system needs.

01,602
PB95-180386 Not available NTIS
National Inst. of Standards and Technology (CSL), Gaithersburg, MD.
Taxonomy for Security Standards.
Final rept.
W. A. Jansen. 1994, 10p.
Pub. in Proceedings of National Computer Security Conference (17th), Baltimore, MD., October 11-14, 1994, p165-174.

Keywords: *Computer security, *Standards, *Taxonomy, US DoD, Standardization, Classifications, Reprints.

This paper presents a taxonomy of security standards developed to ensure a systematic review of security standardization areas appropriate to the Department of Defense (DoD) Goal Security Architecture. The taxonomy relies on a simple paradigm based on the notions of uniformity and quality. This approach attempts to provide full coverage of all relevant security standards, yet be simple to understand and apply. The taxonomy is also open to further refinements and adjustments. Because of the flexibility and simplicity of the taxonomy, other initiatives involving the classification of standards may benefit from its use.

01,603
PB95-203089 Not available NTIS
National Inst. of Standards and Technology (EEEL), Gaithersburg, MD. Electricity Div.
Casual Regularizing Deconvolution Filter for Optimal Waveform Reconstruction.
Final rept.
N. G. Paulter. 1994, 8p.
Pub. in Institute of Electrical and Electronics Engineers Transactions on Instrumentation and Measurement 43, n5 p740-747 Oct 94.

Keywords: Iterative methods, Optimization, Convergence, Reprints, *Signal reconstruction, *Waveform reconstruction, Deconvolution filters.

A causal regularizing filter is described for selecting an optimal reconstruction of a signal from a deconvolution of its measured data and the measurement instrument's impulse response. Measurement noise and uncertainties in the instrument's response can cause the deconvolution (or inverse problem) to be ill-posed, thereby precluding accurate signal restoration. Nevertheless, close approximations to the signal may be obtained by using reconstruction techniques that alter the problem so that it becomes numerically solvable. A regularizing reconstruction technique is implemented that automatically selects the optimal reconstruction via an adjustable parameter and a specific stopping criterion, which is also described. Waveforms reconstructed using this filter do not exhibit large oscillations near transients as observed in other regularized reconstructions. Furthermore, convergence to the optimal solution is rapid.

01,604
PB95-210522 PC A03/MF A01
National Inst. of Standards and Technology (MEL), Gaithersburg, MD. Intelligent Systems Div.
Calculating Time-to-Contact Using Real-Time Quantized Optical Flow.
T. A. Camus. Mar 95, 18p, NISTIR-5609.

Keywords: *Computer vision, *Optical flow(Image analysis), Robotics, Autonomous navigation, Collision avoidance, Real time, Algorithms, Correlation, Measurement, *Time-to-contact, Time-to-collision.

Recently it has been demonstrated that robust, real-time optical flow is possible using standard computing hardware. One limitation of this correlation-based algorithm is that it does not give truly real-valued image velocity measurements. Therefore, it is not obvious that it can be used for a wide range of robotic vision tasks. One particular application for optical flow is time-to-contact: based on the equations for the expansion of the optical flow field it is possible to compute the number of frames remaining before contact with an observed object. Although the individual motion measurements of this algorithm are of limited precision, they can be combined to produce remarkably accurate time-to-contact measurements, which can be produced in real-time on standard computing hardware.

01,605
PB96-122833 Not available NTIS
National Inst. of Standards and Technology (CSL), Gaithersburg, MD. Computer Security Div.
EDI and EFT Security Standards.
Final rept.
E. Barker. 1994, 17p.
Pub. in Handbook of Information Security Management, 1994-95 Yearbook, Chapter IV-9, pS-397-S-413 1994.

Keywords: *Electronic security, *Data encryption, *Cryptography, *Standards, Electronic funds transfer, Data processing security, Computer security, Risk management, Authentication, Confidentiality, Specifications, Reprints, Electronic data interchange.

The use of electronic rather than paper-based transactions has reduced costs and improved efficiency for many organizations. However, the use of this technology also exposes the business community and its customers to potential/severe risks from the accidental or deliberate alteration of data. In response to this increased risk, several standards-setting bodies have developed or are developing standards to protect information transferred electronically. This chapter discusses two computer-based technologies--electronic funds transfer (EFT) and electronic data interchange (EDI)--and several of the standards that have been developed specifically for them including message authentication, encryption, and key management.

General

01,606
PB96-123484 Not available NTIS
National Inst. of Standards and Technology (CSL), Gaithersburg, MD. Computer Security Div.
Common Criteria: On the Road to International Harmonization.
Final rept.
J. Cugini. 1995, 6p.
Pub. in Computer Standards and Interfaces, v17 n4 p315-320 Sep 95.

Keywords: *Information technology, *Data processing security, *Systems management, Information systems, Information security, Computer security, Electronic security, Access control, Safeguards, Computer networks, Operating systems(Computers), Reprints, Common criteria.

The Common Criteria is an effort of the United States, Europe, and Canada to align their existing Information Technology (IT) security criteria into one Common Criteria. The goals of the Common Criteria are to enhance existing IT product security development and evaluation criteria, to protect previous investments in IT product security, and to facilitate international harmonization of IT product security development and evaluation criteria. The Common Criteria has both functional and assurance requirements. These requirements can be combined to form Protection Profiles and Security Targets.

01,607
PB96-123492 Not available NTIS
National Inst. of Standards and Technology (CSL), Gaithersburg, MD. Computer Security Div.
Functional Security Criteria for Distributed Systems.
Final rept.
J. Cugini, R. Dobry, V. Gligor, and T. Mayfield. 1995, 12p.
Pub. in National Information Systems Security Conference (18th), Baltimore, MD., October 10-13, 1995, p310-321.

Keywords: *Information technology, *Data processing security, *Systems management, *Access control, Reprints, Computer security, Computer privacy, Data encryption, Cryptography, Data integrity, Authentication, Auditing, Distributed systems, Information systems, Computer networks, Requirements, Common Criteria.

The National Security Agency (NSA) with the cooperation of the National Institute of Standards and Technology (NIST) formed a technical group to create security requirements for distributed systems. These include requirements for data confidentiality, data integrity, cryptography, distributed identification and authentication, as well as for access control, auditing, system management, trusted path, and trusted recovery for distributed systems. These requirements are being reviewed for incorporation within the Common Criteria, which is a joint effort of the United States (NSA and NIST), Canada, France, Great Britain, and Germany to come up with a single criteria for security requirements.

01,608
PB96-131610 PC A13/MF A03
National Inst. of Standards and Technology (NCSL), Gaithersburg, MD. Computer Security Div.
Computer Security: An Introduction to Computer Security. The NIST Handbook.
Special pub.
B. Guttman, and E. A. Roback. Oct 95, 290p, NIST/SP-800/12.
Also available from Supt. of Docs. as SN003-003-03374-0.

Keywords: *Computer security, *Electronic security, *Handbooks, Data processing security, Data integrity, Computer information security, Cryptography, Secure communications, Authentication, Computer networks, Access control, Risk management, Contingency planning, Disasters, Program management, Training, Guidelines, Management controls, Operational controls, Technical controls, Life cycle analysis.

The Handbook provides a broad overview of computer security to help readers understand their computer security needs and develop a sound approach to the selection of appropriate security controls. The Handbook includes chapters on each of the major types of computer security controls and an example of how they could be applied within a hypothetical organization. The Handbook contains references to more detailed how-to books and articles.

01,609
PB96-141304 Not available NTIS
National Inst. of Standards and Technology (EEEL), Gaithersburg, MD. Electricity Div.
Bounds on Least-Squares Four-Parameter Sine-Fit Errors Due to Harmonic Distortion and Noise.
Final rept.
J. P. Deyst, T. M. Souders, and O. M. Solomon. 1995, 6p.
See also DE94007859.
Pub. in Institute of Electrical and Electronics Engineers Transactions on Instrumentation and Measurement, v44 n3 p637-642 Jun 95.

Keywords: *Least square fit, *Signal conditioning, Algorithms, Reprints, Errors, Harmonics, Noise.

Least-squares sine-fit algorithms are used extensively in signal-processing applications. The parameter estimates produced by such algorithms are subject to both random and systematic errors when the record of input samples consists of a fundamental sine wave corrupted by harmonic distortion or noise. The errors occur because, in general, such sine-fits will incorporate a portion of the harmonic distortion or noise into their estimate of the fundamental. Bounds are developed for these errors for least-squares four-parameter (amplitude, frequently, phase, and offset) sine-fit algorithms. The errors are functions of the number of periods in the records, the number of samples in the record, the number of samples in the record, the harmonic order, and fundamental and harmonic amplitudes and phases. The bound do not apply to cases in which harmonic components become aliased.

01,610
PB96-156112 Not available NTIS
National Inst. of Standards and Technology (CSL), Gaithersburg, MD. Computer Security Div.
Security Program Management.
Final rept.
B. Guttman, and E. Roback. 1993, 5p.
Pub. in CSL Bulletin, p1-5 Aug 93.

Keywords: *Computer security, *Information systems, *Federal agencies, Information resources, Information management, Electronic security, Access control, Computer networks, Policies, Systems analysis, Reprints.

This bulletin discusses the establishment and operation of a security program as a management function and describes some of the features and issues common to most organizations.

01,611
PB96-160577 Not available NTIS
National Inst. of Standards and Technology (CSL), Gaithersburg, MD. Computer Security Div.
Addressing U.S. Government Security Requirements for OSI.
Final rept.
N. A. Nazario. 1992, 4p.
Pub. in Panel Session Overview for the National Computer Security Conference (15th), Baltimore, MD., October 13-16, 1992, p740-743.

Keywords: *Computer information security, *Data transmission, *Requirements, *Federal government, Computer networks, Data processing security, Electronic security, Secure communications, Protocols, Standards, Reprints, OSI(Open Systems Interconnection), GOSIP(Government Open Systems Interconnection Profile), Security labels.

This session focuses on security requirements that need to be addressed within the U.S. Government Open Systems Interconnection Profile (FIPS 146-1) and current efforts to meet them. The session examines Government requirements, discusses emerging security protocols, and describes a labeling infrastructure necessary to support security services and protocols.

01,612
PB96-160817 Not available NTIS
National Inst. of Standards and Technology (CSL), Gaithersburg, MD. Systems and Software Technology Div.
Point Probe Decision Trees for Geometric Concept Classes.
Final rept.
E. M. Arkin, M. T. Goodrich, J. S. B. Mitchell, S. S. Skiena, D. Mount, and C. D. Piatko. 1993, 12p.
Pub. in Workshop on Algorithms and Data Structures (WADS '93) (3rd), Montreal, Canada, Spring 1993, v709 p95-106.

Keywords: *Computer vision, *Decision tree analysis, Image resolution, Geometric accuracy, Computational geometry, Reprints, Probing.

A fundamental problem in model-based computer vision is that of identifying to which of a given set of concept classes of geometric models an observed model belongs. Considering a 'probe' to be an oracle that tells whether or not the observed model present at a given point in an image, we study the problem of computing efficient strategies ('decision trees') for probing an image, with the goal to minimize the number of probes necessary (in the worst case) to determine in which class the observed model belongs. We prove a hardness result and give strategies that obtain decision trees whose height is within a log factor of optimal.

01,613
PB96-160825 Not available NTIS
National Inst. of Standards and Technology (CSL), Gaithersburg, MD. Computer Security Div.
Precise Identification of Computer Viruses.
Final rept.
L. E. Bassham, and W. T. Polk. 1992, 9p.
Pub. in National Computer Security Conference Proceedings (15th), p1-9 1992.

Keywords: *Computer viruses, *Personal computers, *Identification, Debugging(Computers), Data integrity, Data encryption, Error detection codes, Computer security, Electronic security, Vulnerability, Reprints.

The number of personal computer viruses continues to grow at an alarming rate. Many of these viruses are variants (i.e., close relatives) of 'old' viruses. This often results in less than accurate identification of viruses. A public domain technique for precise identification of viruses if needed, This paper explores various alternatives.

01,614
PB96-160882 Not available NTIS
National Inst. of Standards and Technology (CSL), Gaithersburg, MD. Computer Security Div.
Concept Paper: An Overview of the Proposed Trust Technology Assessment Program.
Final rept.
E. E. Flahavin, and P. R. Toth. 1992, 9p.
Pub. in National Computer Security Conference Proceedings (15th), 9p 1992.

Keywords: *Computer information security, *Information technology, Electronic security, Data processing security, Classified information, Systems engineering, Performance tests, Assessments, Evaluation, Quality assurance, Reprints, *Trusted systems, National Voluntary Laboratory Accreditation Program.

This paper provides an overview of the philosophy, objectives, amd methodology of a proposed new program for the evaluation of trusted information technology products. The program will focus on products with the features and assurances characterized by the TCSEC (Trusted Computer System Evaluaton Criteria, or Orange Book) B1 and lower levels. The program is intended to be fully compatible with the Federal Criteria Version I. The program will continue to emphasize the credibility and fairness of the evaluation process. The program will allow a sealless transition from the current process in which National Security Agency (NSA) alone evaluates products and populates the Evaluated Products List (EPL). The new program is to be called the Trust Technology Assesment Program (TTAP).

01,615
PB96-161815 Not available NTIS
National Inst. of Standards and Technology (CSL), Gaithersburg, MD. Computer Security Div.
Response to Comments on the NIST Proposed Digital Signature Standard.
Final rept.
M. E. Smid, and D. K. Branstad. 1992, 14p.
See also PB94-135001.
Pub. in Proceedings of Crypto '92, Santa Barbara, CA., August 16-20, 1992, p1-14.

Keywords: *Computer security, *Cryptography, *Meetings, Reprints, Certification, Standards, Data

processing security, *Digital signatures, National Institute of Standards and Technology.

NIST received comments from 109 separate government agencies, companies, and private individuals concerning the proposed Digital Signature Standard. Both positive and negative comments were received. However, the number of negative comments was significantly larger than normally received for a proposed Federal Information Processing Standard (FIPS). This paper summarizes the major comments, both positive and negative and provides responses where appropriate. The paper highlights the anticipated significant modifications to the proposed standard and concludes by discussing the future milestones that need to be accomplished before the proposed DSS becomes a FIPS.

01,616
PB96-166004 PC A08/MF A02
National Inst. of Standards and Technology (CSL), Gaithersburg, MD. Computer Security Div.
Public Key Infrastructure Invitational Workshop. Held in McLean, Virginia on September 28, 1995.
W. E. Burr. Nov 95, 146p, NISTIR-5788.
Sponsored by MITRE Corp., McLean, VA. Program Management Office.

Keywords: *Computer security, *Meetings, Computer networks, Cryptography, Data encryption, Access control, Data integrity, Authentication, Verification, Confidentiality, Data processing security, Electronic security, Infrastructure, Costs, *Public key certificates, *Digital signatures.

The document is the report of the Invitational Workshop on Public Key Infrastructure. A public key infrastructure provides a means for issuing and managing public key certificates, which may be used to provide security services, such as authentication, integrity, confidentiality and non-repudiation, between strangers who have no previous knowledge of each other. Papers were presented on the current state of technology and standards for a Public Key Infrastructure, management and technical issues, escrowing keys used for confidentiality exchanges, and cost models.

01,617
PB96-179155 (Order as PB96-177381, PC A07/MF A02)
Cray Research, Inc., Calverton, MD.
MasPar MP-1 as a Computer Arithmetic Laboratory.
M. A. Anuta, D. W. Lozier, and P. R. Turner. 1996, 10p.
Prepared in cooperation with National Inst. of Standards and Technology, Gaithersburg, MD. and Naval Academy, Annapolis, MD.
Included in Jnl. of Research of the National Institute of Standards and Technology, v101 n2 p165-174 Mar/Apr 96.

Keywords: *Computer arithmetics, Fixed-point, Floating-point, Logarithmic, Level-index, Reprints, Residue number system, Serial simulation, Parallel simulation.

The paper is a blueprint for the use of a massively parallel SIMD computer architecture for the simulation of various forms of computer arithmetic. The particular system used is a DEC/MasPar MP-1 with 4096 processors in a square array. This architecture has many advantages for such simulations due largely to the simplicity of the individual processors. Arithmetic operations can be spread across the processor array to simulate a hardware chip. Alternatively they may be performed on individual processors to allow simulation of a massively parallel implementation of the arithmetic.

01,618
PB96-195318 PC A03/MF A01
National Inst. of Standards and Technology (CSL), Gaithersburg, MD. Computer Security Div.
TMACH Experiment Phase 1. Preliminary Developmental Evaluation.
E. C. Flahavin. Jun 96, 14p, NISTIR-5810.
Sponsored by Defense Advanced Research Projects Agency, Arlington, VA.

Keywords: *Federal agencies, *Computer security, *Access control, *European communities, Data processing security, Electronic security, Privacy, Confidentiality, Computer networks, Data management systems, Operating systems(Computers), Policies, Standards, Performance evaluation, Criteria, *Trusted systems, Commercial Licensed Evaluation Facilities.

In November 1990, James Burrows, then Director of the Computer Systems Laboratory of the National Institute of Standards and Technology (NIST), met with European officials and Steve Walker of Trusted Information Systems to discuss initiating a preliminary developmental evaluation of the trusted Mach (Tmach) system against the European developed Inforamtion Security Evaluation Criteria (ITSEC). As a result, NIST finalized an agreement with the Advanced Research Projects Agency (ARPA) to coordinate and oversee the TMach evaluation work to be done by Germany and the United Kingdom. The document describes the multi-national evaluation experiment of the Trusted Mach system. The report focuses on Phase I - The Development Evaluation Phase. The objective is to provide a historical journal discussing the experiment, and providing insight into what has been learned and accomplished thus far. Discussed are the objectives of the effort, the participants, how the evaluation has proceeded, and the benefit. It is in the interest of the U.S. Government to understand how these two criteria differ in practice and how evaluations done under each may be compared.

01,619
PB97-110811 PC A05/MF A01
National Inst. of Standards and Technology (CSL), Gaithersburg, MD.
Computer Security: Generally Accepted Principles and Practices for Securing Information Technology Systems.
Special pub.
M. Swanson, and B. Guttman. Sep 96, 63p, NIST/SP-800/14.

Keywords: *Computer security, Information systems, Federal agencies, Local area networks, Risk, Computer viruses, Computer prevacy, Data integrity, Management, Personal computers, Principles, Computer networks, Data encryption, *Generally Accepted Principles and Practices.

As more organizations share information electronically, a common understanding of what is needed and expected in securing information technology (IT) resources is required. This document provides a baseline that organizations can use to establish and review their IT security programs. The document gives foundation that organizations can reference when conducting multi-organizational business as well as internal business. Management, internal auditors, users, system developers and security practioners can use the guideline to gain an understanding of the basic security requirements most IT systems should contain. The foundation begins with generally accepted system security principles and continues with common practices that are used in securing IT systems.

Computer Hardware

01,620
N95-24130/3 (Order as N95-24108, PC A17/MF A04)
National Inst. of Standards and Technology, Gaithersburg, MD.
Optical Storage Media Data Integrity Studies.
F. L. Podio. Mar 94, 12p.
In NASA. Goddard Space Flight Center, Fourth NASA Goddard Conference on Mass Storage Systems and Technologies p 265-276.

Keywords: *Data storage, *Error correcting codes, *Optical disks, *Optical memory (Data storage), *Quality control, Degradation, Error analysis, Information systems, On-line systems.

Optical disk-based information systems are being used in private industry and many Federal Government agencies for on-line and long-term storage of large quantities of data. The storage devices that are part of these systems are designed with powerful, but not unlimited, media error correction capacities. The integrity of data stored on optical disks does not only depend on the life expectancy specifications for the medium. Different factors, including handling and storage conditions, may result in an increase of medium errors in size and frequency. Monitoring the potential data degradation is crucial, especially for long term applications. Efforts are being made by the Association for Information and Image Management Technical Committee C21, Storage Devices and Applications, to specify methods for monitoring and reporting to the user medium errors detected by the storage device while writing, reading or verifying the data stored in that medium. The Computer Systems Laboratory (CSL) of the National Institute of Standard and Technology (NIST) has a leadership role in the development of these standard techniques. In addition, CSL is researching other data integrity issues, including the investigation of error-resilient compression algorithms. NIST has conducted care and handling experiments on optical disk media with the objective of identifying possible causes of degradation. NIST work in data integrity and related standards activities is described.

01,621
PB94-135761 PC A06/MF A02
National Inst. of Standards and Technology (CSL), Gaithersburg, MD.
Planning for the Fiber Distributed Data Interface (FDDI).
W. E. Burr. Oct 93, 110p, NIST/SP-500/212.
Also available from Supt. of Docs. as SN003-003-03239-5. Sponsored by Internal Revenue Service, Washington, DC.

Keywords: *Local area networks, *Standards, Fiber optics, Workstations, Protocols, Wiring, *FDDI, *Fiber Distributed Data Interface, GOSIP(Government Open Systems Interconnection Profile), Token rings.

The Fiber Distributed Data Interface (FDDI) is an emerging Standard fiber optic Local Area Network (LAN) technology suitable for backbone and high performance workstation applications. FDDI will be widely used by federal agencies in the 1990's. This report describes FDDI standards and the media that FDDI uses, and provides information about writing for FDDI LANs and about effectively configuring FDDI LANs. It also describes the relationship of FDDI to the Government Open Systems Interconnection Profile (GOSIP) and discusses connecting FDDI to other networks.

01,622
PB94-162518 PC A05/MF A02
National Inst. of Standards and Technology (CSL), Gaithersburg, MD.
Computer Systems Laboratory Annual Report, 1993.
E. B. Lennon, S. M. Radack, and R. K. Roach. Feb 94, 100p, NISTIR-5342.
See also PB93-181873.

Keywords: *Computers, *Computer software, Organizational structure, Information systems, Systems engineering, Computer security, Telecommunication, Federal information processing standards, Computer networks, Computer architecture, Technology transfer, *Computer Systems Laboratory, National Institute of Standards and Technology.

The Computer Systems Laboratory (CSL) Annual Report - 1993 describes the annual computer and related telecommunications activities and accomplishments of the laboratory. Following the Director's Foreword, a CSL overview is presented, followed by overviews of the five technical divisions. The Technology Transfer section describes the vehicles used by CSL to disseminate research and technical information to the public. A list of Federal Information Processing Standards (FIPS) and FIPS order information conclude the annual report.

01,623
PB94-216470 Not available NTIS
National Inst. of Standards and Technology (NEL), Gaithersburg, MD. Electricity Div.
Guarding Against Transients.
Final rept.
F. D. Martzloff. 1990, 1p.
Pub. in Institute of Electrical and Electronics Engineers Spectrum, p16 Dec 90.

Keywords: *Computers, *Surges, *Circuit protection, Reliability, Data processing, Electromagnetic interference, Quality, Overvoltage, Overcurrent, Reprints.

This article is a response to a reader's comment on the IEEE Spectrum article (April 1990) by Martzloff entitled Protecting Computer Systems Against Power Transients.

01,624
PB95-108486 Not available NTIS
National Inst. of Standards and Technology (NCSL), Gaithersburg, MD. Advanced Systems Div.

Computer Hardware

Standardization of Testing Methods for Optical Disk Media Characteristics and Related Activities at NIST.
Final rept.
F. L. Podio, R. Onyshczak, and E. S. Villagran. 1990, 5p.
Pub. in Optical Information Systems 10, n4 p174-178 Jul/Aug 90.

Keywords: *Optical disks, *Tests, *Standardization, Media, Standards, Optical storage materials, Service life, Reprints, US NIST.

Standard testing methods for measuring the characteristics of optical disks are needed to verify conformance to the related industry media interchange standards. Technical Committee (TC) X3B11 is addressing the standardization of those testing methods. Through its optical disk computer storage media research program, the National Institute of Standards and Technology, National Computer Systems Laboratory (NIST/NCSL) is involved in the research of testing methods for media characteristics and is participating in the development of optical media standards in TC X3B11 and other standard committees. Standard testing methods for predicting the life expectancy of the media are also needed. NIST is designed a methodology for predicting life expectancy of optical media and is also contributing to those standardization efforts and data permanence studies.

01,625
PB95-136388 PC A11/MF A03
National Inst. of Standards and Technology (CSL), Gaithersburg, MD. Advanced Systems Div.
NIST Workshop on the Computer Interface to Flat Panel Displays. Held in San Jose, California on January 13-14, 1994.
Special pub.
M. P. Williamson, W. E. Burr, and J. W. Roberts. Aug 94, 231p, NIST/SP-500/219.
Also available from Supt. of Docs. as SN003-003-03289-1.

Keywords: *Display devices, *Standards, *Meetings, Liquid crystal display systems, Cathode ray tubes, Electric connectors, Personal computers, Flat surfaces, Workstations, *Flat panel displays, *Computer interface, Interface standards, US NIST.

On January 13 and 14, 1994, the NIST Workshop on the Computer Interface to Flat Panel Displays was held at the San Jose Hilton and Towers in San Jose, California. The meeting was attended by representatives from computer, flat panel display, and graphics controller companies. The objectives of this workshop were: to determine the need for a standard or a series of standards for the computer interface to flat panel displays; to identify what types of standards are needed; to identify approaches for developing flat panel display interface standards; and to obtain a consensus on a coordinated plan for standards development. The workshop attendees agreed that a standard flat panel display interface for integrated devices is needed. A special interest group was formed under the Video Electronics Standards Association (VESA) to undertake the development of a standard or a series of standards for the interface between a flat panel display and its controller. This interface standard will address both active and passive flat panel displays in integrated devices. It will cover both the electrical and the mechanical (connector) specifications. The interface for remote flat panel displays requires additional technical discussions before a standard can be written. Additional workshops on display interfaces and/or technical sessions at the SID (Society for Information Display) Symposium should be explored. In addition, the VESA Monitor Committee invited interested parties to participate in their committee which will be considering interfaces and connectors to desktop and remote flat panel displays in addition to their CRT interface work.

01,626
PB95-169496 PC A08/MF A02
National Inst. of Standards and Technology (CSL), Gaithersburg, MD. Systems and Software Technology Div.
Guide on Open System Environment (OSE) Procurements.
Special pub.
G. E. Fisher. Oct 94, 161p, NIST/SP-500/220.
Also available from Supt. of Docs. as SN-003-003-03302-2. See also PB95-166260.

Keywords: *Government procurement, Requirements, Guidelines, Specifications, Operating systems(Computers), Man computer interface, Software engineering, Data management, Data transfer(Computers), Computer graphics, Computer networks, Management, Computer systems hardware, *OSE(Open System Environment), *Open System Environment, RFPs(Requests for proposals).

The guide provides program managers and senior system engineers with much-needed information for developing plans and requirements to establish an Open System Environment (OSE). U.S. Government procurements that have already taken place have provided numerous lessons-learned which have been incorporated in this report. A decision model is defined in the introductory material to provide a mechansim for making choices concerning the applicability of standards. Side-bars in the text provide associated information about the use of specific standards in order to more clearly describe the effects of relationships among different standards. Additional information includes text that can be included in requests for proposals (RFPs), a sample statement of work based on the guidance contained in the report, a glossary, and methods for evaluating individual proposals made in response to OSE requirements.

01,627
PB95-189437 PC A03/MF A01
National Inst. of Standards and Technology (CAML), Gaithersburg, MD. Applied and Computational Mathematics Div.
MasPar MP-1 as a Computer Arithmetic Laboratory.
M. A. Anuta, D. W. Lozier, and P. R. Turner. Jan 95, 24p, NISTIR-5569.
Prepared in cooperation with Cray Research, Inc., Calverton, MD. and Naval Academy, Annapolis, MD. Dept. of Mathematics.

Keywords: *Arithmetic units, *SIMD(Computers), Algorithms, Computer architecture, Computer systems hardware, Massively parallel processors, Very large scale integration, Computer software, Array processors, *DEC/MasPar MP-1 computer systems, LI(Level-index) arithmetic, SLI(Symmetric level-index) arithmetic.

This paper describes the use of a massively parallel SIMD computer architecture for the simulation of various forms of computer arithmetic. The particular system used is a DEC/MasPar MP-1 with 4096 processors in a square array. This architecture has many advantages for such simulations due largely to the simplicity of the individual processors. Arithmetic operations can be spread across the processor array to simulate a hardware chip. Alternatively, they may be performed on individual processors to allow simulation of a massively parallel implementation of the arithmetic. Compromises between these extremes permit speed-area trade-offs to be examined. The paper includes a description of the architecture and its features. It then summarizes some of the arithmetic systems which have been, or are to be implemented. The implementation of the level-index (LI) and symmetric level-index (SLI) systems is described in some detail. An extensive bibliography is included.

01,628
PB95-189486 PC A03/MF A01
National Inst. of Standards and Technology (CSL), Gaithersburg, MD. Advanced Systems Div.
Operating Principles of MultiKron II Performance Instrumentation for MIMD Computers.
A. Mink. Dec 94, 32p, NISTIR-5571.
See also PB92-181072. Sponsored by Advanced Research Projects Agency, Arlington, VA.

Keywords: *MIMD(Computers), *Very large scale integration, Chips(Electronics), Multiprocessors, Computer performance evaluation, Parallel processors, *MultiKron II.

The MultiKron II design is an enhanced version of our earlier MultiKron performance instrumentation chip. They are both 179 pin chips, and although pin compatibility is close they are not 100% compatible. The MultiKron II has a longer TRACE sample, 20 bytes vs 16, to allow a larger user data and Timestamp fields. The 16 counters for resource utilization measurements are now writable, to allow for 'virtual' use, and their programming interface has changed to allow more options. Although designed for a 64-bit processor bus interface, an internal holding register provides for 32-bit mode operation.

01,629
PB95-209920 PC A07/MF A02
National Inst. of Standards and Technology (CSL), Gaithersburg, MD.
Computer Systems Laboratory Annual Report 1994.
E. B. Lennon, S. M. Radack, and R. K. Roach. 26 Mar 92, 126p, NISTIR-5576.
See also PB94-162518.

Keywords: *Computers, *Information technology, *Information systems, Systems engineering, Computer security, Organizational structures, Computer software, Telecommunication, Federal Information Processing Standards, Computer networks, Computer architectures, Technology transfer, US NIST, *Computer Systems Laboratory.

The annual report describes the annual computer and related telecommunications activities and accomplishment of the Laboratory. Following the Director's Foreword, an overview of the Laboratory is presented, including a current CSL Organization Chart. Overviews of CSL's major technical units are featured next, followed by a section on Interactions and Accomplishments which details the vehicles CSL uses to disseminate research and inforamtion to the public and technical communities. A list of Federal Information Processing Standards (FIPS) concludes the annual report.

01,630
PB95-231783 PC A03/MF A01
National Inst. of Standards and Technology (CSL), Gaithersburg, MD.
Operating Principles of the SBus MultiKron Interface Board.
A. Mink, G. G. Nacht, and J. K. Antonishek. May 95, 14p, NISTIR-5652.
See also PB92-181072, PB93-234730 and PB95-189486. Sponsored by Defense Advanced Research Projects Agency, Arlington, VA.

Keywords: *Computer systems hardware, *Circuit boards, *Very large scale integration, Printed circuits, MIMD(Computers), Multiprocessors, Computer architecture, Data acquisition, SIB(SBus MultiKron Interface Board), US NIST.

The MultiKron Experimenter's Toolkit contains an SBus MultiKron interface board (SIB) or alternatively a VME MultiKron interface board (MIB), installation software, data logging software, and analysis software; all of the software supplied is written in C. The Toolkit allows users to take advantage of the National Institute of Standards and Technology (NIST) MultiKron performance measurement chip in systems that do not already have a MultiKron designed into them. The SIB is applicable to both multiprocessor systems and single-processor systems. The Experimenter's Toolkit allows researchers to obtain hands-on experience with the MultiKron performance measurement chip, without the engineering effort required to design and build a hardware interface between the MultiKron and their computer. Over 800,000 Trace Samples can be collected during an experiment to the SIB on-board memory; a practically-unlimited number of Samples can be collected if an optional external data-collection computer is used.

01,631
PB96-102686 Not available NTIS
National Inst. of Standards and Technology (CSL), Gaithersburg, MD.
Conformance Testing for OSI Protocols.
Final rept.
R. J. Linn. 1990, 17p.
Pub. in Computer Networks and ISDN Systems 18, p203-219 1989/90.

Keywords: *Computer communications, *ISO, *Protocols, Computer architecture, Communication networks, Conformity, Tests, Test methods, Specifications, Standards, Reprints, *OSI(Open Systems Interconnection), *Open Systems Interconnection, Test systems, ANC1(Abstract Syntax Notation 1), TICN(Tree and Tabular Combined Notation), Estelle.

In the early 1980's, research and development was initiated on methods to test the developing International Standards Organinzation's Open Systems Interconnection (ISO/OSI) communications protocols. A tutorial overview of the test methods and test notation named TTCN which were developed within ISO are presented. Issues regarding multilayer test methods are still not completely resolved. These issues are identified and alternatives to ISO's methods are explored. Application of the formal description techniques named ASN.1 and Estelle to multi-layer test systems

is illustrated. Concluding remarks summarize the status of current practice in conformance testing and status of evolving OSI testing standards.

01,632
PB96-131529 PC A03/MF A01
National Inst. of Standards and Technology (CSL), Gaithersburg, MD. Advanced Systems Div.
Operating Principles of MultiKron Virtual Counter Performance Instrumentation for MIMD Computers.
A. Mink. Nov 95, 24p, NISTIR-5743.
See also PB93-234730, PB95-189486 and PB95-231783. Sponsored by Defense Advanced Research Projects Agency, Arlington, VA.

Keywords: *Computer systems hardware, *Multiprocessors, *Circuit boards, Very large scale integration, MIMD(Computers), Printed circuits, Computer architecture, Performance tests, Multikron Performance Instrumentation.

The MultiKron* and MultiKron II performance instrumentation provided both Trace sampling and Resource Counters, but required a separate measurement data collection facility for collecting sample data. Although providing a large amount of measurement detail, trace sampling has the disadvantage of requiring additional investment in logic, wires and space to provide for the collection facilities. An alternative measurement approach that would eliminate the need for a collection facility, and its associated cost, is to eliminate Trace sampling and only provide for a very large number of Resource Counters, at the cost of some loss of measurement detail. The MultiKron virtual counter (MultiKron vc) performance instrumentation chip provides such a feature. Similar in concept to virtual memory, thousands of virtual counters are available but only a small number are real counters that can be active at any one time. Unlike virtual memory, where swapping is transparent to the programmer, due to extra hardware and kernel software support, swapping of counter blocks must currently be handled by the programmer.

01,633
PB96-160304 Not available NTIS
National Inst. of Standards and Technology (CSL), Gaithersburg, MD. Advanced Systems Div.
Research on Methods for Determining Optical Disk Media Life Expectancy Estimates.
Final rept.
F. L. Podio. 1992, 9p.
Pub. in Society of Photo-Optical Instrumentation Engineers, v1663 p447-455 Feb 92.

Keywords: *Optical data storage materials, *Life(Durability), *Aging tests(Materials), Optical disks, Service life, Stress testing, Test methods, Error analysis, Quality control, Standards, Reprints, Arrhenius model, Byte error rate.

Methodologies for determining extrapolated life expectancy values for optical disk media were investigated at the National Institute of Standards and Technology (NIST). These investigations showed that the life expectancy values of optical disk media vary greatly due to several factors, including the method used to derive the value of the quality parameter (the byte error rate), the areas measured in the disks, the written patterns used, and the criteria for data analysis. Vendor's life expectancy claims can be properly assessed by prospective users if standard methods for calculating and reporting extrapolated life expectancy values are implemented.

01,634
PB96-160619 Not available NTIS
National Inst. of Standards and Technology (CSL), Gaithersburg, MD. Advanced Systems Div.
Status of Emerging Standards for Removable Computer Storage Media and Related Contributions of NIST.
Final rept.
F. L. Podio. 1991, 25p.
Also available as N93-14778 (Order as N93-14771).
Pub. in National Space Science Data Center Conference on Mass Storage Systems and Technologies for Space and Earth Science Applications, Greenbelt, MD., July 23-25, 1991, NASA Conference Publication 3165, v3 p163-187.

Keywords: *Computer storage devices, *Data storage, *Digital data, Magnetic tapes, Optical disks, Optical memory(Data storage), Optical data (Storage materials), Interchangeability, Error detection codes, Life (Durability), Service life, Error analysis, Standards, Reprints, Standard reference materials.

Standards for removable computer storage media are needed so that users may reliably interchange data both within and among various computer installations. Industry standards for digital magnetic tapes require the use of Standard Reference Materials (SRMs) developed and maintained by NIST. In addition, NIST has been studying Care and handling procedures for optical digital data disks and is involved in a program to investigate error reporting capabilities of optical disk drives. NIST has developed a methodology for determining the life expectancy of optical disks. NIST is developing care and handling procedures for optical digital data disks and is involved in a program to investigate error reporting capabilities of optical disk drives.

01,635
PB96-160627 Not available NTIS
National Inst. of Standards and Technology (CSL), Gaithersburg, MD. Advanced Systems Div.
NIST Program for Investigating Error Reporting Capabilities of Optical Disk Drives.
Final rept.
F. L. Podio. 1991, 8p.
Pub. in Proceedings of a Workshop held in Colorado Springs, CO., August 5, 1991, p1-8.

Keywords: *Error detection codes, *Optical disks, *Research programs, Computer storage devices, Optical data storage materials, Optical memory(Data storage), Quality control, Error correcting codes, Life(Durability), Service life, Error analysis, Reprints.

Optical disk drives are designed with strong but unlimited error corrections capabilities. If the level of errors overcome the error detection and corrections mechanisms implemented in the optical disk drive controllers, incorrectable errors may occur. Federal Government data managers are interested in being able to monitor error rate activity in optical disk drive systems. This could be achieved through the interface, if the drives would provide information on correctable error rate activity, such as maximum number of correctable errors, maximum number of errors per interleave, and the location of those errors. Reports on errors encountered while reading header information is also necessary. This information would provide data managers with a better understanding of the status of their data and would allow them to design more efficient recopying policies to copy the data to similar or different media in a timely and economic fashion.

01,636
PB96-161252 Not available NTIS
National Inst. of Standards and Technology (CSL), Gaithersburg, MD.
Information Technology Standards in Federal Acquisitions.
Final rept.
S. M. Radack. 1992, 8p.
See also PB96-161260.
Pub. in Federal Data Center Issues 1992: A View to the Future Council of Federal Data Center Directors, p1-8.

Keywords: *Information technology, *Government procurement, *Electronic security, *Standards, Federal agencies, Acquisition, Information resources, Computer program portability, Interoperability, Computer information security, Reprints, GOSIP(Government Open Systems Interconnection Profile), POSIX(Portable Operating Sytems Interface for Computer Environments), Conformance testing.

Information technology (IT) standards are an important part of Federal Government strategies for managing information resources. Standards help to promote the interoperability of different manufactures' systems, the portability of applications, and the sharing of ideas, data, and training. But while the abstract concept of standards is acceptable and easily understood, it is not always easy for managers and users to put standards to work for their organizations. This paper discusses some of the activities of the National Institute of Standards and Technology (NIST) that support the implementation of standards in products that organizations can buy.

01,637
PB96-161260 Not available NTIS
National Inst. of Standards and Technology (CSL), Gaithersburg, MD.
Using Information Technology Standards in Federal Acquisitions.
Final rept.
S. M. Radack. 1992, 6p.
See also PB96-161252.
Pub. in Computer Systems Laboratory Bulletin, p1-6 Dec 92.

Keywords: *Information technology, *Government procurement, *Electronic security, *Standards, Federal agencies, Acquisition, Information resources, Computer program portability, Interoperability, Computer information security, Reprints, GOSIP(Government Open Systems Interconnection Profile), POSIX(Portable Operating Sytems Interface for Computer Environments), Conformance testing.

Information technology (IT) standards are an important part of federal government strategies for managing information resources. Standards help to promote the interoperability of different manufactures' systems, the portability of applications, and the sharing of ideas, data, and training.

01,638
PB96-193768 PC A05/MF A01
National Inst. of Standards and Technology (CSL), Gaithersburg, MD. Software Diagnostics and Conformance Testing Div.
Computer Systems Laboratory Computing and Applied Mathematics Laboratory Technical Accomplishments, October 1994-March 1996.
E. B. Lennon. Jun 96, 67p, NISTIR-5854.

Keywords: *Computers, *Information technology, *Information systems, *Applied mathematics, Systems engineering, Computer security, Organizational structures, Computer software, Telecommunications, Computer networks, Computer architecture, Technology transfer, Research programs, *Computer Systems Laboratory, National Institute of Standards and Technology.

The document describes the technical accomplishments and activities of National Institute of Standards and Technology (NIST's) Computer Systems Laboratory/Computing and Applied Mathematics Laboratory during the period October 1994 through March 1996.

Computer Software

01,639
AD-A274 872/1 PC A04/MF A01
National Inst. of Standards and Technology, Gaithersburg, MD.
Ada Compiler Validation Summary Report: Certificate Number: 931029S1.11330, Digital Equipment Corporation, DEC Ada for DEC OSF/1 AXP Systems, Version 3.1, DEC 3000 Model 400 AXP Workstation, DEC 3000 Model 400 AXP Workstation.
26 Oct 93, 70p.

Keywords: *Compilers, *Ada programming language, Standards, Test and evaluation, *Validation summary reports.

The Ada implementation described above was tested according to the Ada Validation Procedures (Pro92) against the Ada Standard (Ada83) using the current Ada Compiler Validation Capability (ACVC). This Validation Summary Report (VSR) gives an account of the testing of this Ada implementation.

01,640
AD-A275 977/7 PC A03/MF A01
National Inst. of Standards and Technology, Gaithersburg, MD.
Ada Compiler Validation Summary Report: Certificate Number: 931217S1.11336 Control Data Systems, Inc. NOS/VE Ada, Version 1.4 Cyber 180-930-31 => Cyber 180-930-31.
17 Dec 93, 48p.

Keywords: *Compilers, *Ada programming language, Validation, Data processing, Standards, *Validation summary reports, Computer program verification.

This Validation Summary Report describes the extent to which a specific Ada compiler conforms to the Ada Standard, ANSI/MIL-STD-1815A. This report explains all technical terms used within it and thoroughly reports

the results of testing this compiler using the Ada Compiler Validation Capability. An Ada compiler must be implemented according to the Ada Standard, and any implementation-dependent features must conform to the requirements of the Ada Standard. The Ada Standard must be implemented in its entirety, and nothing can be implemented that is not in the Standard. Even though all validated Ada compilers conform to the Ada Standard, it must be understood that some differences do exist between implementations. The Ada Standard permits some implementation dependencies--for example, the maximum length of identifiers or the maximum values of integer types. Other differences between compilers result from the characteristics of particular operating systems, hardware, or implementation strategies. All the dependencies observed during the process of testing this compiler are given in this report. The information in this report is derived from the test results produced during validation testing. The validation process includes submitting a suite of standardized tests, the ACVC, as inputs to an Ada compiler and evaluating the results.

01,641
AD-A276 181/5 PC A04/MF A01
National Inst. of Standards and Technology, Gaithersburg, MD.
Ada Compiler Validation Summary Report. Certificate Number: 931119S1.11332, DDC-I, Inc. DACS MIPS R3000 Bare Ada Cross Compiler System, Version 4.7.1 Sun SPARCstation IPX => DACS Sun SPARC/SunOS to MIPS R3000 Bare Instruction Set Architecture Simulator, Version 4.7.1.
10 Dec 93, 55p, NIST92DDI510-5-1.11.

Keywords: *Compilers, *Ada programming language, Test and evaluation, Standards, *Validation summary reports, Computer program verification.

This Validation Summary Report describes the extent to which a specific Ada compiler conforms to the Ada Standard, ANSI/MIL-STD-1815A. This report explains all technical terms used within it and thoroughly reports the results of testing this compiler using the Ada Compiler Validation Capability. An Ada compiler must be implemented according to the Ada Standard, and any implementation-dependent features must conform to the requirements of the Ada Standard. The Ada Standard must be implemented in its entirety, and nothing can be implemented that is not in the Standard. Even though all validated Ada compilers conform to the Ada Standard, it must be understood that some differences do exist between implementations. The Ada Standard permits some implementation dependencies--for example, the maximum length of identifiers or the maximum values of integer types. Other differences between compilers, result from the characteristics of particular operating systems, hardware, or implementation strategies. All the dependencies observed during the process of testing this compiler are given in this report. The information in this report is derived from the test results produced during validation testing. The validation process includes submitting a suite of standardized tests, the ACVC, as inputs to an Ada compiler and evaluating the results.

01,642
AD-A276 283/9 PC A08/MF A02
National Inst. of Standards and Technology, Gaithersburg, MD.
Ada Compiler Validation Summary Report: Certificate Number: 931119S1.11331 DDC-I, Inc. DACS Sun SPARC/SunOS to 80386 PM Bare Ada Cross Compiler System, Version 4.6.4 Sun Sparcstation 1+ => Bare Board iSBC 386/116.
19 Nov 93, 158p.

Keywords: *Compilers, *Ada programming language, Standards, *Validation summary reports, Computer program verification, Runtime.

This Validation Summary Report describes the extent to which a specific Ada compiler conforms to the Ada Standard, ANSI/MIL-STD-1815A. This report explains all technical terms used within it and thoroughly reports the results of testing this compiler using the Ada Compiler Validation Capability. An Ada compiler must be implemented according to the Ada Standard, and any implementation-dependent features must conform to the requirements of the Ada Standard. The Ada Standard must be implemented in its entirety, and nothing can be implemented that is not in the Standard. Even though all validated Ada compilers conform to the Ada Standard, it must be understood that some differences do exist between implementations. The Ada Standard permits some implementation dependencies--for example, the maximum length of identifiers or maximum values of integer types. Other differences between compilers result from the characteristics of particular operating systems, hardware, or implementation strategies. All the dependencies observed during the process of testing this compiler are given in this report. The information in this report is derived from the test results produced during validation testing. The validation process includes submitting a suite of standardized tests, the ACVC, as inputs to an Ada compiler and evaluating the results.

01,643
AD-A277 981/7 PC A03/MF A01
National Inst. of Standards and Technology (NCSL), Gaithersburg, MD. Software Standards Validation Group.
Ada Compiler Validation Summary Report. Certificate Number: 930927S1.11328 Green Hills Software C Ada, Version 1.1 ZENY 386 => ZENY 386.
30 Sep 93, 324p.

Keywords: *Compilers, *Ada programming language, Standards, *Validation summary reports, Computer program verification.

The Ada implementation described was tested according to the Ada Validation Procedures (Pro92) against the Ada Standard (Ada83) using the current Ada Compiler Validation Capability (ACVC). This Validation Summary Report (VSR) gives an account of the testing of this Ada implementation.

01,644
AD-A279 642/3 PC A06/MF A02
National Inst. of Standards and Technology, Gaithersburg, MD.
Ada Compiler Validation Summary Report: Certificate Number: 940325S1.11348 DDC-I, DACS Sun SPARC/Solaris to 80386 PM Bare Ada Cross Compiler System, Version 4.6.4 Sun SPARCclassic => Intel iSBC 386/116 (Bare Machine).
25 Mar 94, 118p.

Keywords: *Compilers, *Ada programming language, Standards, Validation.

This Validation Summary Report describes the extent to which a specific Ada compiler conforms to the Ada Standard, ANSI/MIL-STD-1815A. This report explains all technical terms used within it and thoroughly reports the results of testing this compiler using the Ada Compiler Validation Capability. An Ada compiler must be implemented according to the Ada Standard, and any implementation-dependent features must conform to the requirements of the Ada Standard. The Ada Standard must be implemented in its entirety, and nothing can be implemented that is not in the Standard. Even though all validated Ada compilers conform to the Ada Standard, it must be understood that some differences do exist between implementations. The Ada Standard permits some implementation dependencies--for example, the maximum length of identifiers or maximum values of integer types. Other differences between compilers result from the characteristics of particular operating systems, hardware, or implementation strategies. All the dependencies observed during the process of testing this compiler are given in this report. The information in this report is derived from the test results produced during validation testing. The validation process includes submitting a suite of standardized tests, the ACVC, as inputs to an Ada compiler and evaluating the results.

01,645
AD-A279 643/1 PC A06/MF A02
National Inst. of Standards and Technology, Gaithersburg, MD.
Ada Compiler Validation Summary Report: Certificate Number: 940325S1.11341 DDC-I, DACS Sun SPARC/SunOS to 80186 Bare Ada Cross Compiler System, Version 4.6.4 Sun SPARCstation IPX => Intel iSBC 186/100 (Bare Machine).
25 Mar 94, 118p.

Keywords: *Compilers, *Ada programming language, Standards, *Validation summary reports, Computer program verification.

This Validation Summary Report describes the extent to which a specific Ada compiler conforms to the Ada Standard, ANSI/MIL-STD-1815A. This report explains all technical terms used within it and thoroughly reports the results of testing this compiler using the Ada Compiler Validation Capability. An Ada compiler must be implemented according to the Ada Standard, and any implementation-dependent features must conform to the requirements of the Ada Standard. The Ada Standard must be implemented in its entirety, and nothing can be implemented that is not in the Standard. Even though all validated Ada compilers conform to the Ada Standard, it must be understood that some differences do exist between implementations. The Ada Standard permits some implementation dependencies--for example, the maximum length of identifiers or maximum values of integer types. Other differences between compilers result from the characteristics of particular operating systems, hardware, or implementation strategies. All the dependencies observed during the process of testing this compiler are given in this report. The information in this report is derived from the test results produced during validation testing. The validation process includes submitting a suite of standardized tests, the ACVC, as inputs to an Ada compiler and evaluating the results.

01,646
AD-A279 644/9 PC A06/MF A02
National Inst. of Standards and Technology, Gaithersburg, MD.
Ada Compiler Validation Summary Report: Certificate Number: 940325S1.11349 DDC-I, DACS Sun SPARC/Solaris to 80386 PM Bare Ada Cross Compiler System with Rate Monotonic Scheduling, Version 4.6.4 Sun SPARCclassic => Intel iSBC 386/116 (Bare Machine).
25 Mar 94, 119p.

Keywords: *Compilers, *Ada programming language, Standards, *Validation summary reports, Computer program verification.

This Validation Summary Report describes the extent to which a specific Ada compiler conforms to the Ada Standard, ANSI/MIL-STD-1815A. This report explains all technical terms used within it and thoroughly reports the results of testing this compiler using the Ada Compiler Validation Capability. An Ada compiler must be implemented according to the Ada Standard, and any implementation-dependent features must conform to the requirements of the Ada Standard. The Ada Standard must be implemented in its entirety, and nothing can be implemented that is not in the Standard. Even though all validated Ada compilers conform to the Ada Standard, it must be understood that some differences do exist between implementations. The Ada Standard permits some implementation dependencies--for example, the maximum length of identifiers or maximum values of integer types. Other differences between compilers result from the characteristics of particular operating systems, hardware, or implementation strategies. All the dependencies observed during the process of testing this compiler are given in this report. The information in this report is derived from the test results produced during validation testing. The validation process includes submitting a suite of standardized tests, the ACVC, as inputs to an Ada compiler and evaluating the results.

01,647
AD-A279 645/6 PC A04/MF A01
National Inst. of Standards and Technology, Gaithersburg, MD.
Ada Compiler Validation Summary Report: Certificate Number: 940325S1.11354 DDC-I, DACS Sun SPARC/Solaris Native Ada Compiler System, Version 4.6.2 Sun SPARCclassic => Sun SPARCclassic.
25 Mar 94, 57p.

Keywords: *Compilers, *Ada programming language, Standards, *Validation summary reports, Computer program verification.

This Validation Summary Report describes the extent to which a specific Ada compiler conforms to the Ada Standard, ANSI/MIL-STD-1815A. This report explains all technical terms used within it and thoroughly reports the results of testing this compiler using the Ada Compiler Validation Capability. An Ada compiler must be implemented according to the Ada Standard, and any implementation-dependent features must conform to the requirements of the Ada Standard. The Ada Standard must be implemented in its entirety, and nothing can be implemented that is not in the Standard. Even though all validated Ada compilers conform to the Ada Standard, it must be understood that some differences do exist between implementations. The Ada Standard permits some implementation dependencies--for example, the maximum length of identifiers or maximum values of integer types. Other differences between compilers result from the characteristics of particular

operating systems, hardware, or implementation strategies. All the dependencies observed during the process of testing this compiler are given in this report. The information in this report is derived from the test results produced during validation testing. The validation process includes submitting a suite of standardized tests, the ACVC, as inputs to an Ada compiler and evaluating the results.

01,648
AD-A279 646/4 PC A05/MF A02
National Inst. of Standards and Technology, Gaithersburg, MD.
Ada Compiler Validation Summary Report: Certificate Number: 940325S1.11346 DDC-I, DACS Sun SPARC/SunOS to 680x0 Bare Ada Cross Compiler System (BASIC MODE), Version 4.6.9 Sun SPARCstation IPX => Lynwood j435TU (68030) (Bare Machine).
25 Mar 94, 100p.

Keywords: *Compilers, *Ada programming language, Standards, *Validation summary reports, Computer program verification.

This Validation Summary Report describes the extent to which a specific Ada compiler conforms to the Ada Standard, ANSI/MIL-STD-1815A. This report explains all technical terms used within it and thoroughly reports the results of testing this compiler using the Ada Compiler Validation Capability. An Ada compiler must be implemented according to the Ada Standard, and any implementation-dependent features must conform to the requirements of the Ada Standard. The Ada Standard must be implemented in its entirety, and nothing can be implemented that is not in the Standard. Even though all validated Ada compilers conform to the Ada Standard, it must be understood that some differences do exist between implementations. The Ada Standard permits some implementation dependencies--for example, the maximum length of identifiers or maximum values of integer types. Other differences between compilers result from the characteristics of particular operating systems, hardware, or implementation strategies. All the dependencies observed during the process of testing this compiler are given in this report. The information in this report is derived from the test results produced during validation testing. The validation process includes submitting a suite of standardized tests, the ACVC, as inputs to an Ada compiler and evaluating the results.

01,649
AD-A279 757/9 PC A06/MF A02
National Inst. of Standards and Technology, Gaithersburg, MD.
Ada Compiler Validation Summary Report: Certificate Number: 940325S1.11343 DDC-I, DACS Sun SPARC/Solaris to 80186 Bare Ada Cross Compiler System, Version 4.6.4 Sun SPARCclassic => Intel iSBC 186/100 (Bare Machine).
25 Mar 94, 118p.

Keywords: *Compilers, *Ada programming language, Standards, Validation, *Validation summary reports, Computer program verification.

This Validation Summary Report describes the extent to which a specific Ada compiler conforms to the Ada Standard, ANSI/MIL-STD-1815A. This report explains all technical terms used within it and thoroughly reports the results of testing this compiler using the Ada Compiler Validation Capability. An Ada compiler must be implemented according to the Ada Standard, and any implementation-dependent features must conform to the requirements of the Ada Standard. The Ada Standard must be implemented in its entirety, and nothing can be implemented that is not in the Standard. Even though all validated Ada compilers conform to the Ada Standard, it must be understood that some differences do exist between implementations. The Ada Standard permits some implementation dependencies--for example, the maximum length of identifiers or maximum values of integer types. Other differences between compilers result from the characteristics of particular operating systems, hardware, or implementation strategies. All the dependencies observed during the process of testing this compiler are given in this report. The information in this report is derived from the test results produced during validation testing. The validation process includes submitting a suite of standardized tests, the ACVC, as inputs to an Ada compiler and evaluating the results.

01,650
AD-A279 758/7 PC A06/MF A02
National Inst. of Standards and Technology, Gaithersburg, MD.
Ada Compiler Validation Summary Report: Certificate Number: 940325S1.11344 DDC-I, DACS Sun SPARC/Solaris to 80186 Bare Ada Cross Compiler System with Rate Monotonic Scheduling, Version 4.6.4 Sun SPARCclassic => Intel iSBC 186/100 (Bare Machine).
25 Mar 94, 117p.

Keywords: *Compilers, *Ada programming language, Standards, *Validation summary reports, Computer program verification.

This Validation Summary Report describes the extent to which a specific Ada compiler conforms to the Ada Standard, ANSI/MIL-STD-1815A. This report explains all technical terms used within it and thoroughly reports the results of testing this compiler using the Ada Compiler Validation Capability. An Ada compiler must be implemented according to the Ada Standard, and any implementation-dependent features must conform to the requirements of the Ada Standard. The Ada Standard must be implemented in its entirety, and nothing can be implemented that is not in the Standard. Even though all validated Ada compilers conform to the Ada Standard, it must be understood that some differences do exist between implementations. The Ada Standard permits some implementation dependencies--for example, the maximum length of identifiers or maximum values of integer types. Other differences between compilers result from the characteristics of particular operating systems, hardware, or implementation strategies. All the dependencies observed during the process of testing this compiler are given in this report. The information in this report is derived from the test results produced during validation testing. The validation process includes submitting a suite of standardized tests, the ACVC, as inputs to an Ada compiler and evaluating the results.

01,651
AD-A279 778/5 PC A06/MF A02
National Inst. of Standards and Technology, Gaithersburg, MD.
Ada Compiler Validation Summary Report: Certificate Number: 940325S1.11347 DDC-I, DACS Sun SPARC/SunOS to 680x0 Bare Ada Cross Compiler System (SECURE MODE), Version 4.6.9 Sun SPARCstation IPX => Lynwood j435TU (68030) (Bare Machine).
25 Mar 94, 101p.

Keywords: *Compilers, *Ada programming language, Standards, *Validation summary reports, Computer program verification.

This Validation Summary Report describes the extent to which a specific Ada compiler conforms to the Ada Standard, ANSI/MIL-STD-1815A. This report explains all technical terms used within it and thoroughly reports the results of testing this compiler using the Ada Compiler Validation Capability. An Ada compiler must be implemented according to the Ada Standard, and any implementation-dependent features must conform to the requirements of the Ada Standard. The Ada Standard must be implemented in its entirety, and nothing can be implemented that is not in the Standard. Even though all validated Ada compilers conform to the Ada Standard, it must be understood that some differences do exist between implementations. The Ada Standard permits some implementation dependencies--for example, the maximum length of identifiers or maximum values of integer types. Other differences between compilers result from the characteristics of particular operating systems, hardware, or implementation strategies. All the dependencies observed during the process of testing this compiler are given in this report. The information in this report is derived from the test results produced during validation testing. The validation process includes submitting a suite of standardized tests, the ACVC, as inputs to an Ada compiler and evaluating the results.

01,652
AD-A279 779/3 PC A06/MF A02
National Inst. of Standards and Technology, Gaithersburg, MD.
Ada Compiler Validation Summary Report: Certificate Number: 940325S1.11342 DDC-I, DACS Sun SPARC/SunOS to 80186 Bare Ada Cross Compiler System with Rate Monotonic Scheduling Version 4.6.4 Sun SPARCstation IPX => Intel iSBC 186/100 (Bare Machine).
25 Mar 94, 117p.

Keywords: *Compilers, *Ada programming language, Standards, *Validation summary reports, Computer program verification.

This Validation Summary Report describes the extent to which a specific Ada compiler conforms to the Ada Standard, ANSI/MIL-STD-1815A. This report explains all technical terms used within it and thoroughly reports the results of testing this compiler using the Ada Compiler Validation Capability. An Ada compiler must be implemented according to the Ada Standard, and any implementation-dependent features must conform to the requirements of the Ada Standard. The Ada Standard must be implemented in its entirety, and nothing can be implemented that is not in the Standard. Even though all validated Ada compilers conform to the Ada Standard, it must be understood that some differences do exist between implementations. The Ada Standard permits some implementation dependencies--for example, the maximum length of identifiers or maximum values of integer types. Other differences between compilers result from the characteristics of particular operating systems, hardware, or implementation strategies. All the dependencies observed during the process of testing this compiler are given in this report. The information in this report is derived from the test results produced during validation testing. The validation process includes submitting a suite of standardized tests, the ACVC, as inputs to an Ada compiler and evaluating the results.

01,653
AD-A279 804/9 PC A06/MF A02
National Inst. of Standards and Technology, Gaithersburg, MD.
Ada Compiler Validation Summary Report: Certificate Number: 940325S1.11351 DDC-I, DACS Sun SPARC/SunOS to Pentium PM Bare Ada Cross Compiler System with Rate Monotonic Scheduling, Version 4.6.4 Sun SPARCstation IPX => Intel Pentium (operated as Bare Machine) based in Xpress Desktop (Intel product number: XBASE6E4F-B).
11 Apr 94, 118p.

Keywords: *Compilers, *Ada programming language, Standards, Validation, *Validation summary reports, Computer program verification.

This Validation Summary Report describes the extent to which a specific Ada compiler conforms to the Ada Standard, ANSI/MIL-STD-1815A. This report explains all technical terms used within it and thoroughly reports the results of testing this compiler using the Ada Compiler Validation Capability. An Ada compiler must be implemented according to the Ada Standard, and any implementation-dependent features must conform to the requirements of the Ada Standard. The Ada Standard must be implemented in its entirety, and nothing can be implemented that is not in the standard. Even though all validated Ada compilers conform to the Ada Standard, it must be understood that some differences do exist between implementations. The Ada Standard permits some implementation dependencies--for example, the maximum length of identifiers or the maximum values of integer types. Other differences between compilers result from the characteristics of particular operating systems, hardware, or implementation strategies. All the dependencies observed during the process of testing this compiler are given in this report. The information in this report is derived from the test results produced during validation testing. The validation process includes submitting a suite of standardized tests, the ACVC, as inputs to an Ada compiler and evaluating the results.

01,654
AD-A279 805/6 PC A06/MF A02
National Inst. of Standards and Technology, Gaithersburg, MD.

Ada Compiler Validation Summary Report: Certificate Number: 940325S1.11353 DDC-I, DACS Sun SPARC/Solaris to Pentium PM Bare Ada Cross Compiler System with Rate Monotonic Scheduling, Version 4.6.4 Sun SPARCclassic => Intel Pentium (operated as Bare Machine) based in Xpress Desktop (Intel product number: XBASE6E4F-B).
11 Apr 94, 123p.

Keywords: *Compilers, *Ada programming language, Standards, Validation.

This Validation Summary Report describes the extent to which a specific Ada compiler conforms to the Ada Standard, ANSI/MIL-STD-1815A. This report explains all technical terms used within it and thoroughly reports the results of testing this compiler using the Ada Compiler Validation Capability. An Ada compiler must be implemented according to the Ada Standard, and any implementation-dependent features must conform to the requirements of the Ada Standard. The Ada Standard must be implemented in its entirety, and nothing can be implemented that is not in the Standard. Even though all validated Ada compilers conform to the Ada Standard, it must be understood that some differences do exist between implementations. The Ada Standard permits some implementation dependencies--for example, the maximum length of identifiers or the maximum values of integer types. Other differences between compilers, result from the characteristics of particular operating systems, hardware, or implementation strategies. All the dependencies observed during the process of testing this compiler are given in this report. The information in this report is derived from the test results produced during validation testing. The validation process includes submitting a suite of standardized tests, the ACVC, as inputs to an Ada compiler and evaluating the results.

01,655
AD-A279 864/3 PC A06/MF A02
National Inst. of Standards and Technology, Gaithersburg, MD.
Ada Compiler Validation Summary Report: Certificate Number: 940325S1.11350 DDC-I, DACS Sun SPARC/SunOS to Pentium PM Bare Ada Cross Compiler System, Version 4.6.4 Sun SPARCstation IPX => Intel Pentium (Operated as Bare Machine) Based in Xpress Desktop (Intel Product Number: XBASE6E4F-B).
11 Apr 94, 118p.

Keywords: *Compilers, *Ada programming language, Standards, *Validation summary reports, Computer program verification.

This Validation Summary Report describes the extent to which a specific Ada compiler conforms to the Ada Standard, ANSI/MIL-STD-1815A. This reports explains all technical terms used within it and thoroughly reports the results of testing this compiler using the Ada Compiler Validation Capability. An Ada compiler must be implemented according to the Ada Standard, and any implementation-dependent features must conform to the requirements of the Ada Standard. The Ada Standard must be implemented in its entirety, and nothing can be implemented that is not in the Standard. Even though all validated Ada compilers conform to the Ada Standard, it must be understood that some differences do exist between implementations. The Ada Standard permits some implementation dependencies--for example, the maximum length of identifiers or the maximum values of integer types. Other differences between compilers, result from the characteristics of particular operating systems, hardware, or implementation strategies. All the dependencies observed during the process of testing this compiler are given in this report. The information in this report is derived from the test results produced during validation testing. The validation process includes submitting a suite of standardized tests, the ACVC, as inputs to an Ada compiler and evaluating the results.

01,656
AD-A280 145/4 PC A05/MF A02
National Inst. of Standards and Technology, Gaithersburg, MD.
Ada Compiler Validation Summary Report: Certificate Number 940325S1.11345 DDC-I. DACS Sun SPARC/SunOS to 680x0 Bare Ada Cross Compiler System, Version 4.6.9 Sun SPARCstation IPX => Motorola MVME143 68030/68882 (Bare Machine).
11 Apr 94, 100p.

Keywords: *Ada programming language, *Compilers, Computer program verification, Functional analysis, Optimization, Software engineering, Test and evaluation, Standards, *Validation summary reports, ACVC(Ada Compiler Validation Capability).

No abstract available.

01,657
AD-A280 295/7 PC A06/MF A02
National Inst. of Standards and Technology, Gaithersburg, MD.
Ada Compiler Validation Summary Report: Certificate Number: 940325S1.11352 DDC-I DACS Sun SPARC/Solaries to Pentium PM Bare Ada Cross Compiler System, Version 4.6.4 Sun SPARCclassic => Intel Pentium (Operated as Bare Machine) Based in Xpress Desktop (Intel Product Number: XBASE6E4F-B).
25 Mar 94, 117p.

Keywords: *Ada programming language, *Compilers, Operating systems(Computers), Software engineering, *Validation summary reports, Standards, Computer program verification.

The ADA implementation described above was tested according to the Ada Validation Procedures Pro92 against the Ada Standard Ada83 using the current Ada Compiler Validation Capability (ACVC). This Validation Summary Report (VSR) gives an account of the testing of this ADA implementation. For any technical terms used in this report, the reader is referred to Pro92. A detailed description of the ACVC may be found in the current ACVC User's Guide UG89.

01,658
AD-A288 571/3 PC A03/MF A01
National Inst. of Standards and Technology, Gaithersburg, MD.
Ada Compiler Validation Summary Report: Certificate Number 940902S1.11377 UNISYS Corporation. IntegrAda for Windows NT, Version 1.0. Intel Deskside Server with Intel 80486DX266 => Intel Deskside Server with Intel 80486DX266.
D. K. Jefferson, L. A. Johnson, and D. J. Peifer. 14 Sep 94, 36p.

Keywords: *Validation, *Compilers, *Ada programming language, Standards.

The Ada implementation described above was tested according to the Ada Validation Procedures Pro92 against the Ada Standard Ada83 using the current Ada Compiler Validation Capability (ACVC). This Validation Summary Report (VSR) gives an account of the testing of this Ada implementation. For any technical terms used in this report, the reader is referred to Pro92.

01,659
AD-A288 572/1 PC A03/MF A01
National Inst. of Standards and Technology, Gaithersburg, MD.
Ada Compiler Validation Summary Report: Certificate Number 940902S1.11376. UNISYS Corporation IntegrAda for Windows NT, Version 1.0. Intel Deskside Server for Intel Pentium 60 MHz =>. Intel Deskside Server with Intel Pentium 60 MHz.
D. K. Jefferson, L. A. Johnson, and D. J. Reifer. 14 Sep 94, 36p.

Keywords: *Validation, *Compilers, *Ada programming language, Standards.

The Ada implementation described above was tested according to the Ada Validation Procedures Pro92 against the Ada Standard Ada83 using the current Ada Compiler Validation Capability (ACVC). This Validation Summary Report (VSR) gives an account of the testing of this Ada implementation. For any technical terms used in this report, the reader is referred to Pro92.

01,660
AD-A288 573/9 PC A03/MF A01
National Inst. of Standards and Technology, Gaithersburg, MD.
Ada Compiler Validation Summary Report: Certificate Number 94101251.11379 TISOFT, Inc. Green Hills Optimizing Ada Compileer, Version 1.8.7 with PATCK ID 1 COMPAQ ProLiiant 2000 Model 55/66 => COMPAQ ProLiant 2000 Model 5/66.
Oct 94, 34p.

Keywords: *Validation, *Compilers, *Ada programming language, Standards.

The Ada implementation described above was tested according to the Ada Validation Procedures Pro92 against the Ada Standard Ada83 using the current Ada Compiler Validation Capability (ACVC). This Validation Summary Report (VSR) gives an account of the testing of this Ada implementation. For any technical terms used in this report, the reader is referred to Pro92.

01,661
AD-A288 574/7 PC A05/MF A01
National Inst. of Standards and Technology, Gaithersburg, MD.
Ada Complier Validation Summary Report: Certificate Number: 940929S1.11378. Digital Equipment Corporation DEC Ada for DEC OSF/1 AXP Systems, Version 3.2; DEC 3000 Model 400 AXP Workstation => DEC 3000 Model 400 AXP Workstation.
4 Oct 94, 77p.

Keywords: *Validation, *Compilers, *Ada programming language, Facilities, Standards.

The Ada implementation described above was tested according to the Ada Validation Procedures Pro92 against the Ada Standard Ada83 using the current Ada Compiler Validation Capability (ACVC). This Validation Summary Report (VSR) gives an account of the testing of this Ada implementation. For any technical terms used in this report, the reader is referred to Pro92.

01,662
AD-A289 895/5 PC A05/MF A01
National Inst. of Standards and Technology (NCSL), Gaithersburg, MD. Software Standards Validation Group.
Ada Compiler Validation Summary Report. Certificate Number 941117S1.11380. Electronic Data Systems Corp. Compiler: OC Systems Legacy Ada/370, Release 1.4.1 (without optimization).
2 Dec 94, 94p.

Keywords: *Compilers, *Ada programming language, Optimization, Information systems, Validation, Electronic equipment, Spn-19950119011.

The following Ada implementation was tested and determined to pass ACVC I.ll.: Compiler Name and Version - OC Systems Legacy Ada/370, Release 1.4.1, Host Computer System - AMDAHL 5990 under VM/ESA, Release 2.1, and Target Computer System - AMDAHL 5990 under VM/ESA, Release 2.1. This Validation Summary Report (VSR) gives an account of the testing of this Ada implementation. For any technical terms used in this report, the reader is referred to (Pro92). A detailed description of the Ada Compiler Validation Capability (ACVC) may be found in the current ACVC User's Guide (UG89).

01,663
AD-A293 709/2 PC A05/MF A01
National Inst. of Standards and Technology, Gaithersburg, MD.
ADA Compiler Validation Summary Report, VC Number 950303S1.11381. Digital Equipment Corporation - Compiler Name: DEC Ada for OpenVMS Alpha Systems, Version 3.2.
28 Mar 95, 78p.

Keywords: *Validation, *Compilers, *Ada programming language, Test and evaluation, Digital systems, Host computers, Standards, Work stations, Implementation(Computers).

This Ada implementation was tested and determined to pass ACVC 1.11. Testing was completed on March 3, 1995. Host Computer System: DEC 3000 Model 400 AXP Workstation under OpenVMS Alpha Operating System, Version 6.1 Target Computer System: DEC 3000 Model 400 AXP Workstation under OpenVMS Alpha Operating System, Version 6.1.

01,664
AD-A296 794/1 PC A05/MF A01
National Inst. of Standards and Technology, Gaithersburg, MD.
Ada Compiler Validation Summary Report, VC No. 950609S1.11390 Digital Equipment Corporation - Compiler Name: DEC Ada Version 3.2 for OpenVMS VAX Systems.
Final rept.
12 Jun 95, 80p.

Keywords: *Compilers, *Ada programming language, Validation, Standards, Computer program verification.

This Ada implementation was tested and determined to pass ACVC I.II. Testing was completed on 9 June

1995. Host Computer System: VAXstation 3100 Model 76 under OpenVMS VAX Operating System, Version 6.2 Target Computer System: VAXstation 3100 Model 76 under OpenVMS VAX Operating System, Version 6.2 (KAR) P. 1.

01,665
DE94014586 PC A03/MF A01
National Inst. of Standards and Technology (NEL), Gaithersburg, MD. Center for Computing and Applied Mathematics.
Measuring Performance of Parallel Computers. Final Report.
F. Sullivan. 1994, 23p, DOE/ER/25046-T1.
Contract AI05-87ER25046
Sponsored by Department of Energy, Washington, DC.

Keywords: *Parallel Processing, Algorithms, Benchmarks, Performance Testing, EDB/990200.

Performance Measurement - the authors have developed a taxonomy of parallel algorithms based on data motion and example applications have been coded for each class of the taxonomy. Computational benchmark kernels have been extracted for several applications, and detailed measurements have been performed. Algorithms for Massively Parallel SIMD machines - measurement results and computational experiences indicate that top performance will be achieved by 'iteration' type algorithms running on massively parallel SIMD machines. Reformulation as iteration may entail unorthodox approaches based on probabilistic methods. The authors have developed such methods for some applications. Here they discuss their approach to performance measurement, describe the taxonomy and measurements which have been made, and report on some general conclusions which can be drawn from the results of the measurements.

01,666
DE94014587 PC A03/MF A01
National Inst. of Standards and Technology (NEL), Gaithersburg, MD. Center for Computing and Applied Mathematics.
Measuring Performance of Parallel Computers. Progress Report, 1989.
F. Sullivan. 1994, 23p, DOE/ER/25046-T2.
Contract AI05-87ER25046
Sponsored by Department of Energy, Washington, DC.

Keywords: *Parallel Processing, Algorithms, Benchmarks, Performance Testing, Progress Report, EDB/990200.

Performance Measurement - the authors have developed a taxonomy of parallel algorithms based on data motion and example applications have been coded for each class of the taxonomy. Computational benchmark kernels have been extracted for several applications, and detailed measurements have been performed. Algorithms for Massively Parallel SIMD machines - measurement results and computational experiences indicate that top performance will be achieved by 'iteration' type algorithms running on massively parallel SIMD machines. Reformulation as iteration may entail unorthodox approaches based on probabilistic methods. The authors have developed such methods for some applications. Here they discuss their approach to performance measurement, describe the taxonomy and measurements which have been made, and report on some general conclusions which can be drawn from the results of the measurements.

01,667
FIPS PUB 119-1 PC$278.00
National Inst. of Standards and Technology (CSL), Gaithersburg, MD.
ADA; Category: Software Standard; Subcategory: Programming Language.
13 Mar 95, 546p, ANSI/ISO/IEC-8652-1995.
Supersedes FIPS PUB 119. Prepared in cooperation with American National Standards Inst., New York.
Three ring binder also available. North American Continent price $6.25; all others write for quote.

Keywords: *Ada programming language, *Standards, *Data processing, Computer program portability, Compilers, Decoding, Semantics, Syntax, High level languages, Conformance, Software standards, Programming languages, Federal Information Processing Standards.

The purpose of the standard is to promote portability of Ada programs for use on a variety of data processing systems. The standard is for use by implementors as the reference authority in developing compilers, interpreters, or other forms of high level language processors; and by other computer professionals who need to now the precise syntactic and semantic rules of the standard.

01,668
FIPS PUB 153-1 PC E99
National Inst. of Standards and Technology (CSL), Gaithersburg, MD.
Programmer's Hierarchical Interactive Graphics System (PHIGS). Category: Software Standard; Subcategory: Graphics.
27 Jan 95, 199p.
Supersedes FIPS PUB 153.
Three ring vinyl binder available; North American Continent price $7.00; all others write for quote.

Keywords: *Interactive graphics, *Computer software, *Federal information processing standards, Computer program portability, Computer graphics, Computer animation, Computer aided design, Data structures, Specifications, PHIGS(Programmers Hierarchical Interactive Graphics Systems), PLUS(Plus Lumiere and Surfaces).

The publication is a revision of FIPS PUB 153 and supersedes that document in its entirety. This revision provides a substantial, upward-compatible enhancement of the basic Programmer's Hierarchical Interactive Graphics System (PHIGS) functionality known as Plus Lumiere and Surfaces, (PHIGS PLUS) (ANSI/ISO 9592.1a,2a,3a,4:1992). PHIGS PLUS adds facilities for the specification of curved lines, curved and facetted surfaces, lighting and shading, and adds a mechanism for color specification to allow non-indexed color specification. Amendments to each part of the PHIGS specification details revisions required by PHIGS PLUS. Also, each language binding of PHIGS has been amended as a result of PHIGS PLUS. The specifications and amendments that comprise the complete PHIGS standard as a result of this revision are detailed in the Specification section of this document.

01,669
FIPS PUB 194 PC E04
National Inst. of Standards and Technology (CSL), Gaithersburg, MD.
Open Document Architecture (ODA) Raster Document Application Profile (DAP). Category: Software Standard; Subcategory: Graphics.
13 Mar 95, 54p.
Three ring vinyl binder available; North American Continent price $7.00; all others write for quote.

Keywords: *Federal information processing standards, *Computer graphics, *Documents, Raster scanning, Format, Data transfer(Computers), Image processing, Text processing, DAP(Documents Application Profile), ISP(International Standardized Profile), ODA(Open Document Architecture).

This Federal Information Processing Standard (FIPS) adopts the International Organization for Standardization (ISO)/International Electrotechnical Commission (IEC) 12064-1 International Standard Profile (ISP) FOD112, which specifies the use of subset of the Open Document Architecture (ODA) standard. It facilitates the interchange of raster documents among different raster graphics applications by specifying the constraints on document structure and content according to the rules of the ODA standard. The documents supported by this standard are based on a paradigm of an electronic engineering drawing, illustration, or other electronic image. The FIPS PUB specifies the structure and parameters for describing and interchanging bi-level untiled compressed images as well as tiled raster images.

01,670
FIPS PUB 21-4 PC E99
National Inst. of Standards and Technology (CSL), Gaithersburg, MD.
COBOL. Category: Software Standard; Subcategory: Programming Language. Includes ANSI'S X3.23-1985, X3.23A-1989 and X3.23B-1993.
23 Jan 95, 975p.
Supersedes FIPS PUB 21-3. Also available from Supt. of Docs. Also pub. as American National Standards Committee, New York rept no. ANSI-X3.23-1985, ANSI-X3.23A-1989 and ANSI-X3.23B-1993. Prepared in cooperation with American National Standards Committee, New York.
Three ring vinyl binder also available; North American Continent price $7.00, all others write for quote.

Keywords: *COBOL, *Standards, *Programming languages, Memory(Computers), ANSI(American National Standards Institute).

This standard is a revision of American National Standard for Programming Language COBOL, ANSI X3.23-1974. The language specifications contained in this standard were drawn from both ANSI X3.23-1974 and the CODASYL COBOL Journal of Development. Like its prodecessors, this document provides specifications for both the form and interpretation of programs expressed in COBOL. It is intended to provide a high degree of machine independence in such programs in order to permit their use on a variety of automatic data processing systems.

01,671
FIPS PUB 21-4A PC E99
National Inst. of Standards and Technology (CSL), Gaithersburg, MD.
COBOL. Category: Software Standard; Subcategory: Programming Language. Part A.
23 Jan 95, 94p.
Supersedes FIPS PUB 21-3A. Also available from Supt. of Docs. Also pub. as American National Standards Committee, New York rept no. ANSI-X3.23A-1989. Prepared in cooperation with American National Standards Committee, New York.
Three ring vinyl binder also available; North American Continent price $7.00, all others write for quote.

Keywords: *COBOL, *Standards, *Programming languages, Memory(Computers), ANSI(American National Standards Institute).

This supplement, the first to the document entitled 'American National Standard for Information Systems - Programming Language - COBOL, ANSI X3.23-1985, ISO 1989-1985,' presents a new COBOL module, the Intrinsic Function module. This module provides the capability of referencing a data item whose value is derived automatically during the execution of a program.

01,672
FIPS PUB 21-4B PC E99
National Inst. of Standards and Technology (CSL), Gaithersburg, MD.
COBOL. Category: Software Standard; Subcategory: Programming Language. Part B.
23 Jan 95, 80p.
Supersedes FIPS PUB 21-3. Also available from Supt. of Docs. Also pub. as American National Standards Committee, New York rept. no. ANSI-X3.23B-1993. Prepared in cooperation with American National Standards Committee, New York.
Three ring vinyl binder also available; North American Continent price $7.00, all others write for quote.

Keywords: *COBOL, *Standards, *Programming languages, Memory(Computers), ANSI(American National Standards Institute).

This amendment, the second to the document entitled American National Standard for Information Systems - Programming Language - COBOL, ANSI X3.23-1985, ISO 1989:1985, presents correction of errors and clarification of ambiguities in Programming Language COBOL.

01,673
FIPSPUB184 PC E10
National Inst. of Standards and Technology (CSL), Gaithersburg, MD.
Integration Definition for Information Modeling (IDEF1X); Category: Software Standard; Subcategory: Modeling Techniques.
21 Dec 93, 163p.
Also available from Supt. of Docs. See also AD-A266 176.
Three ring vinyl binder also available; North American Continent price $7.00; all others write for quote.

Keywords: *Data models, *Systems engineering, Data base management systems, Information systems, Data management, Semantics, Syntax, Computer models, *IDEF1X(Information Definition for Information Modeling), Software standards, Modeling techniques, Graphical languages, Data definition.

This standard is based on the Integration Information Support System (IISS), Volume V - Common Data Model Subsystem, Part 4 - Information Modeling Manual - IDEF1 Extended, 1 (IDEF1X) November 1985 (AD-A181 952). This standard describes the IDEF1X modeling language (semantics and syntax) and associated rules and techniques, for developing a logical

model of data. IDEF1X is used to produce a graphical information model which represents the structure and semantics of information within an environment or system. Use of this standard permits the construction of semantic data models which may serve to support the management of data as a resource, the integration of information systems, and the building of computer databases.

01,674
N94-36857/8 (Order as N94-36853/7, PC A10/MF A03)
National Inst. of Standards and Technology, Gaithersburg, MD.
Open System Environments.
F. Schulz. Aug 94, 31p.
In National Aeronautics and Space Administration, NASA Sti Program Coordinating Council Twelfth Meeting: Standards p 85-115.

Keywords: *Distributed processing, *Information systems, *Standards, *Applications programs (Computers), Computer networks, Internets, Protocol (Computers), Systems compatibility, Systems engineering, User requirements.

An open system is defined as a system that implements open specifications for interfaces, services, and supporting formats to enable properly engineered applications software to be ported with minimal changes across a wide range of systems; and to interact with users in a style which facilitates user portability. Based on that definition, a reference model for an open system environment is presented.

01,675
PB94-139623 PC A03/MF A01
National Inst. of Standards and Technology (CSL), Gaithersburg, MD.
Computing Effects and Error for Large Synthetic Perturbation Screenings.
N. Drouin, R. Kacker, and G. Lyon. Dec 93, 15p, NISTIR-5296.
See also PB93-161339, PB93-178572 and PB93-189835. Sponsored by Defense Advanced Research Projects Agency, Arlington, VA.

Keywords: *Parallel programming, *Statistical analysis, Analysis of variance, Standard error, Experimental design, Computation, *Synthetic Perturbation Screening, Hadamard matrices.

Synthetic Perturbation Screening (SPS) is a powerful, statistically-based method of performance improvement for parallel computer programs. SPS uses statistically designed experiments to identify segments of code that consume significant computing resources or otherwise impede a parallel application. Analysis typically starts with a preliminary screening of a large number of code segments; SPS does this via fractional factorial designs based upon Hadamard matrices. Since Hadamard matrix designs are not commonly discussed in introductory texts, there is a need to survey briefly the calculation of their effects and especially, their standard error. The result is a practical, supplementary sketch that should help users of SPS automatic tools understand how investigations and analyses are being performed.

01,676
PB94-140167 PC A04/MF A01
National Inst. of Standards and Technology, Gaithersburg, MD.
Guide to Software Engineering Environment Assessment and Evaluation.
B. B. Cuthill. Nov 93, 69p, NISTIR-5295.
Sponsored by Defense Information Systems Agency, Arlington, VA.

Keywords: *Software engineering, *Evaluation, Software tools, Methodology, Requirements, User needs, *SEE(Software Engineering Environment), CASE(Computer Aided Software Engineering).

This guide outlines general approaches to software engineering environment (SEE) assessment and evaluation. This guide defines SEE assessment as the process of accurately describing the capabilities of a software engineering environment to support and integrate a range of computer aided software engineering (CASE) tools. The guide defines SEE evaluation as the process of determining how well a SEE matches the customer's requirements. The assessment and evaluation approaches presented here focus on accurately defining the integration and functional capabilities of candidate SEEs and the requirements of the customer.

01,677
PB94-143401 PC A06/MF A02
National Inst. of Standards and Technology (CSL), Gaithersburg, MD.
Next Generation Computer Resources: Reference Model for Project Support Environments (Version 2.0).
Special pub.
A. Brown, D. Carney, P. Oberndorf, and M. Zelkowitz. Nov 93, 123p, NIST/SP-500/213.
Also available from Supt. of Docs. as SN003-003-03244-1. Also pub. as Carnegie-Mellon Univ., Pittsburgh, PA. Software Engineering Inst. rept. no. CMU/SEI/93-TR-23. See also AD-A255 575. Prepared in cooperation with Carnegie-Mellon Univ., Pittsburgh, PA. Software Engineering Inst. Sponsored by Space and Naval Warfare Systems Command, Washington, DC.

Keywords: *Software engineering, Systems engineering, User needs, Support services, Software tools, Computer software management, Project management, *Reference models, *PSEs(Project Support Environments), Frameworks.

Software engineering environments (SEEs) are typically built on hardware and operating system platforms. Current SEE architectures distinguish between a set of relatively fixed number of services called the framework, and application-specific tools called end-user services. This report extends the concept of SEE frameworks with appropriate end-user services for defining project support environments.

01,678
PB94-150919 PC A03/MF A01
National Inst. of Standards and Technology, Gaithersburg, MD.
Guide to Configuration Management and the Revision Control System for Testbed Users.
S. Bodarky. Aug 91, 25p, NISTIR-4646.
See also PB91-107615. Sponsored by Assistant Secretary of Defense (Production and Logistics), Washington, DC. Computer-aided Acquisition and Logistic Support Program.

Keywords: *Configuration management, *Computer software, Software tools, Standards, File management systems, Documents, Software engineering, Systems analysis, *RCS(Revision Control System), *PDES(Product Data Exchange using STEP), STEP(Standard for the Exchange of Product Model Data).

Product Data Exchange using STEP (PDES) refers to the United States organizational activities in support of the development of the Standard for the Exchange of Product Model Data (STEP). These activities have resulted in the creation of large amounts of information and software, which reside in the PDES File System on the computer systems at the National Institute of Standards and Technology. The PDES software, documents, and data have been placed under configuration management using the Revision Control System (RCS), in order to ensure that change to these items occurs in a controlled manner, and that any services provided by them are done so as reliably as possible. This document provides instructions for anyone needing to access this material.

01,679
PB94-160793 PC A03/MF A01
National Inst. of Standards and Technology (CAML), Gaithersburg, MD. Applied and Computational Mathematics Div.
Review of Mathematical Function Library for Microsoft-FORTRAN, John Wiley and Sons, 1989.
Final rept.
D. W. Lozier, and F. W. J. Olver. Dec 90, 16p, NISTIR-4490.
Prepared in cooperation with Maryland Univ., College Park. Inst. for Physical Science and Technology.

Keywords: *FORTRAN, *Subroutine libraries, Computer programming, Software, Algorithms, US NIST, Calculators, Tables(Data), Mathematical tables, Manuals.

The loose-leaf manual and accompanying diskettes under review, which we shall refer to as the 'UL Library', may be regarded as an attempt to replace the numerical tables of the higher transcendental functions supplied in the NBS Handbook by a comprehensive software package. The functions treated include Bessel and related functions, hypergeometric and confluent hypergeometric functions, elliptic functions and integrals, exponential integral and related functions, error function and related functions, Gamma and incomplete Gamma functions, orthogonal polynomials, probability functions and random number generators.

01,680
PB94-163086 PC A03/MF A01
National Inst. of Standards and Technology (NCSL), Gaithersburg, MD. Systems and Software Technology Div.
Distributed Supercomputing Software: Experiences with the Parallel Virtual Machine - PVM.
R. D. Schneeman. Mar 94, 25p, NISTIR-5381.
See also DE91014961.

Keywords: *Supercomputers, *Distributed computer systems, *Parallel processing, *Computer software, Computer program portability, Requirements, Parallel programming, Graphic methods, Man computer interface, Models, Heterogeneity, US NIST, Graphical user interface.

The Parallel Virtual Machine (PVM) is a general purpose distributed system developed by researchers at the Oak Ridge National Laboratory and Emory University. The PVM system consists of a portable suite of software specifically designed for use by parallel and supercomputing application engineers. The National Institute of Standards and Technology (NIST) researchers are studying PVM to assist them in defining the system service requirements needed to support parallel programming and supercomputing activities in the general purpose distributed setting. The report focuses on defining the profile requirements culminating from our PVM assessment; therefore, the document will also provide reference material for those involved in evaluating distributed system software for the supercomputing domain.

01,681
PB94-164399 PC A03/MF A01
National Inst. of Standards and Technology (CSL), Gaithersburg, MD.
Time-Perturbation Tuning of MIMD Programs.
G. Lyon, R. Snelick, and R. Kacker. Jun 82, 22p, NISTIR-4859.
See also PB93-161339. Sponsored by Defense Advanced Research Projects Agency, Arlington, VA.

Keywords: *Parallel programming, Experimental design, Distributed computer systems, Optimization, Performance evaluation, Response time(Computers), *Time-perturbation tuning, *MIMD, *Multiple-instruction Multiple-data, Code perturbation, DEX(Design experiments).

Time-perturbation tuning (TPT) is a novel technique for assaying and improving the performance of programs on Multiple-instruction Multiple-data (MIMD) systems. Small, synthetic program delays are combined with statistically designed experiments (DEX). Claims for TPT are two: (1) Conceptually, it brings the powerful, mathematical perspective of experiment design to interdependent, sometimes refractory aspects of MIMD program tuning; (2) Practically, it provides a needed speedup mechanism, synthetic time delays for what otherwise would be ad-hoc, hand tailored program setups for DEX. Overall, the technique identifies bottlenecks in programs directly, as quantitative effects upon response time. TPT works on programs for both shared and distributed-memory, and it scales well with increasing system size.

01,682
PB94-165206 PC A08/MF A02
National Inst. of Standards and Technology (CSL), Gaithersburg, MD. Information Systems Engineering Div.
User's Guide for the PHIGS Validation Tests (Version 2.1).
K. G. Brady, J. V. Cugini, and Q. Wang. Apr 94, 174p, NISTIR-5398.
Supersedes PB93-126365 and PB93-228617. See also PB90-269580.

Keywords: *Interactive graphics, *Standards, *Computer program verification, Computer graphics, Hierarchies, Tests, Data structures, Specifications, Subroutine libraries, Computer software, PHIGS(Programmers Hierarchical Interactive Graphics System), PVT(PHIGS Validation Tests), NIST(National Institute of Standards and Technology).

The Programmers Hierarchical Interactive Graphics System (PHIGS) Validation Tests (PVT), developed by the National Institute of Standards and Technology

(NIST), consist of a large set of Fortran and C programs which may be used to test how well implementations of PHIGS conform to the standard. The tests are organized into a hierarchical structure of modules which corresponds to the conceptual overview of the standard. The tests are associated with the standard via a set of semantic requirements which are derived directly from the standard. Cross-reference tables allow the user to find tests relating to specific PHIGS functions and data structures. Directions for installation and operation of the tests are included.

01,683
PB94-172301 Not available NTIS
National Inst. of Standards and Technology (NCSL), Gaithersburg, MD. Systems and Network Architecture Div.
RDI-SIM ECMA Inter-Domain Routing Protocol Simulation Tool.
Final rept.
K. R. Glenn. 1990, 5p.
Pub. in Proceedings of Institute of Electrical and Electronics Engineers Global Telecommunications Conference and Exhibition, San Diego, CA., December 2-5, 1990, p579-583.

Keywords: *Routing, *Protocols, *Computerized simulation, *Software tools, Performance evaluation, Reprints, ECMA(European Computer Manufacturers Association), OSI(Open Systems Interconnection), IS-IS(Intermediate System to Intermediate System), Interdomain.

Three classes of Open Systems Interconnection (OSI) routing protocols have been defined by the International Organization for Standardization (ISO): End System to Intermediate System (ES-IS), intra-domain Intermediate System to Intermediate System (IS-IS), and inter-domain IS-IS. The paper addresses a simulation tool developed at the National Institute of Standards and Technology (NIST) to aid in the design and performance evaluation of the European Computer Manufacturers Association (ECMA) inter-domain IS-IS protocol proposal. The paper discusses the inner-workings of the simulation tool and how it models the ECMA protocol. Finally, a set of experiments are defined that test the performance of the routing algorithm defined by ECMA.

01,684
PB94-172566 Not available NTIS
National Inst. of Standards and Technology (CSL), Gaithersburg, MD. Advanced Systems Div.
Time-Perturbation Tuning of MIMD Programs.
Final rept.
G. Lyon, R. Snelick, and R. Kacker. 1992, 14p.
Pub. in Proceedings of International Conference on Modelling Techniques and Tools for Computer Performance Evaluation (6th), Edinburgh, Scotland, September 16-18, 1992, p211-224. Sponsored by Defense Advanced Research Projects Agency, Arlington, VA.

Keywords: *Software engineering, Response time(Computers), Computer systems performance, Multiprocessors, Reprints, *TPT, *Time Perturbation Tuning, *MIMD, *Multiple Instruction Multiple Data, DEX(Designed experiments).

Time-perturbation tuning (TPT) is a novel technique for assaying and improving the performance of programs on Multiple Instruction Multiple Data (MIMD) systems. Conceptually, TPT brings the powerful, mathematical perspective of statistically designed experiments (DEX) to the interdependent, sometimes refractory aspects of MIMD program tuning. Practically, TPT provides a needed speedup mechanism of synthetic time delays for what otherwise would be ad hoc, hand-tailored program setups for DEX. Overall, the technique identifies bottlenecks in programs directly as quantitative effects upon response time. TPT works on programs for both shared and distributed-memory, and it scales well with increasing system size.

01,685
PB94-172657 Not available NTIS
National Inst. of Standards and Technology (CSL), Gaithersburg, MD. Advanced Systems Div.
Using Synthetic-Perturbation Techniques for Tuning Shared Memory Programs (Extended Abstract).
Final rept.
R. Snelick, J. JaJa, R. Kacker, and G. Lyon. 1993, 9p.
Pub. in Proceedings of 1993 Int. Conf. on Parallel Processing, St. Charles, IL, Aug. 16-20, 1993, pII-2-II-10. Sponsored by Defense Advanced Research Projects Agency, Arlington, VA.

Keywords: *Parallel programming, Software engineering, Computer program portability, Memory(Computers), Multiprocessors, Case studies, Image processing, Sorting routines, Parallel processing, Reprints, *SPI, *Synthetic Perturbation Tuning, *MIMD, *Multiple Instruction Multiple Data.

The Synthetic-Perturbation Tuning (SPT) methodology is based on an empirical approach that introduces artificial delays into the Multiple Instruction Multiple Data (MIMD) program and captures the effects of such delays by using the modern branch of statistics called design of experiments. SPT provides the basis of a powerful tool for tuning MIMD programs that is portable across machines and architectures. The purpose of this paper is to explain the general approach and to extend it to address specific features that are the main source of poor performance on the shared memory programming model. These include performance degradation due to load imbalance and insufficient parallelism, overhead introduced by synchronizations and by accessing shared data structures, and compute time bottlenecks. The authors illustrate the practicality of SPT by demonstrating its use on two very different case studies: a large image processing benchmark and a parallel quicksort.

01,686
PB94-178407 PC A21/MF A04
National Inst. of Standards and Technology (CSL), Gaithersburg, MD. Advanced Systems Div.
Second Text REtrieval Conference (TREC-2). Held in Gaithersburg, Maryland on August 31-September 2, 1993.
Special pub.
D. K. Harman. Mar 94, 497p, NIST/SP-500-215.
Also available from Supt. of Docs. as SN003-003-03255-7. See also PB93-191641.

Keywords: *Meetings, *Information retrieval, *Text processing, Thesauri, Automation, Natural language processing, Pattern recognition, Routing, Probability theory, Documents, Approximation, Search structuring, Knowledge bases(Artificial intelligence), Machine learning, Algorithms, Semantics, Vector processing.

The second Text REtrieval Conference (TREC-2) was held in August 1993 and was attended by about 150 people involved in the 31 participating groups. The goal of the Conference was to bring research groups together to discuss their work on a new large test collection. There was a large variation of retrieval techniques reported on, including methods using automatic thesauri, sophisticated term weighting, natural language techniques, relevance feedback, and advanced pattern matching. As results had been run through a common evaluation package, groups were able to compare the effectiveness of different techniques, and discuss how differences between the systems affected performance.

01,687
PB94-185568 Not available NTIS
National Inst. of Standards and Technology (CSL), Gaithersburg, MD. Advanced Systems Div.
Synthetic-Perturbation Tuning of MIMD Programs.
Final rept.
G. Lyon, R. Snelick, and R. Kacker. 1994, 24p.
Pub. in Jnl. of Supercomputing 8, p5-28 1994.

Keywords: *Parallel programming, Computer program verification, Distributed computer systems, Performance evaluation, Response time(Computers), Concurrent processing, Reprints, *SPT(Synthetic perturbation tuning), *Synthetic perturbation tuning, *MIMD(Multiple instruction Multiple data), *Multiple instruction Multiple data, DEX(Designed experiments).

Synthetic-perturbation tuning (SPT) is a novel technique for assaying and improving the performance of programs on the Multiple instruction Multiple data (MIMD) systems. Conceptually, SPT brings the powerful, mathematical perspective of statistically designed experiments to the interdependent, sometimes refractory aspects of MIMD program tuning. Practically, synthetic perturbations provide a much needed quick-change mechanism for what otherwise would be ad hoc, hand-configured experiment setups. Overall, the technique identifies bottlenecks in programs directly as quantitative effects upon a measured response. SPT works on programs for both shared and distributed memory, and it scales well with increasing system size.

01,688
PB94-193638 PC A03/MF A01
National Inst. of Standards and Technology (CSL), Gaithersburg, MD. Advanced Systems Div.
Simple Scalability Test for MIMD Code.
G. Lyon, and R. Kacker. Jun 94, 21p, NISTIR-5417.
Sponsored by Defense Advanced Research Projects Agency, Arlington, VA.

Keywords: *Parallel programming, *Scaling, *Computer program portability, Parallel processors, Computer performance evaluation, Tests, Computer program verification, Coding, Taylors series, *MIMD(Multiple Instruction Multiple Data), Code scalability, DEX(Designed experiments).

Code scalability, crucial on any parallel system, determines how well parallel code avoids becoming a bottleneck as its host computer is made larger. Scalability of computer code can be estimated by statistically designed experiments that empirically approximate a multivariate Taylor expansion of the code's execution response function. Each suspected code bottleneck corresponds to a first-order term in the expansion, the coefficient for that term indicating how sensitive execution is to changes in the suspect location. However, it is the coefficients for second-order interactions between code segments and the number of processors that are fundamental in discovering which program elements limit parallel speedup. Extending an earlier formulation, a new unified view via these second-order terms yields an informal scaling test of high utility in code development.

01,689
PB94-198967 Not available NTIS
National Inst. of Standards and Technology (CAML), Gaithersburg, MD. Applied and Computational Mathematics Div.
Software Libraries, Numerical and Statistical.
Final rept.
R. F. Boisvert. 1993, 4p.
Pub. in Encyclopedia of Computer Science, p1229-1232 1993.

Keywords: *Subroutine libraries, Computer software, Software reuse, Computation, Computer calculations, Reprints, *Mathematical software, Statistical software.

A program library is a collection of computer programs for a particular application. This article surveys program libraries for general-purpose numerical computation and statistical analysis.

01,690
PB94-198975 Not available NTIS
National Inst. of Standards and Technology (CAML), Gaithersburg, MD. Applied and Computational Mathematics Div.
Portable Vectorized Software for Bessel Function Evaluation.
Final rept.
R. F. Boisvert, and B. V. Saunders. 1992, 14p.
Pub. in Association for Computing Machinery Transactions on Mathematical Software 18, n4 p456-469 Dec 92. See also PB91-216598.

Keywords: *Bessel functions, *Computation, *Computer software, Computer calculations, Hyperbolic functions, Hypergeometric functions, Vector processing, Computer program portability, Reprints, *Mathematical software.

A suite of computer programs for the evaluation of Bessel functions and modified Bessel functions of orders zero and one for a vector of real arguments is described. Distinguishing characteristics of these programs are that (a) they are portable across a wide range of machines, and (b) they are vectorized in the case when multiple function evaluations are to be performed. The performance of the new programs are compared with software from the FNLIB collection of Fullerton on which the new software is based.

01,691
PB94-198983 Not available NTIS
National Inst. of Standards and Technology (CAML), Gaithersburg, MD. Applied and Computational Mathematics Div.
Virtual Software Repository System.
Final rept.
R. F. Boisvert, J. L. Springmann, and M. L. Strawbridge. 1992, 5p.
Pub. in Proceedings of Semi-Annual Cray User Group Meeting (13th), Washington, DC., September 14-18, 1992, p68-72.

Keywords: *Computer software, Software reuse, Computation, Computer calculations, Distributed computer

systems, Computer networks, Catalogs, On-line systems, Reprints, *Mathematical software, Statistical software, GAMS(Guide to Available Mathematical Software).

Much reusable software is available for solving routine mathematical and statistical problems. Unfortunately, locating this software is often quite difficult for the average user in current distributed computing environments. The Guide to Available Mathematical Software (GAMS) virtual software repository seeks to remedy this situation by providing users with convenient access to some 8000 software modules from more than 50 packages physically distributed among several Internet repositories, including netlib. In this paper we illustrate the use of GAMS and outline its implementation.

01,692
PB94-200573 Not available NTIS
National Inst. of Standards and Technology (NCSL), Gaithersburg, MD. Information Systems Engineering Div.
Graphical Conceptual Navigation as a Presentation Technique for a Graphics Standard.
Final rept.
J. V. Cugini. 1989, 10p.
Pub. in Proceedings of Annual Conference and Exposition Dedicated to Computer Graphics (10th), Philadelphia, PA., April 17-20, 1989, v1 p87-96.

Keywords: *Computer graphics, *Standards, Knowledge representation, Knowledge bases(Artificial intelligence), Object-oriented programming, Reprints, *Conceptual navigation, COOL(COncept Oriented Language), Prolog programming language, Conceptual networks.

Conceptual navigation can serve as a powerful tool to help users understand and explore a given domain. COOL (COncept Oriented Language) is a system, implemented with Prolog and GKS, which gives the knowledge engineer a high level language in which to express the conceptual relations among objects within a domain. The facilities for inspecting the Knowledge base (KB) support the metaphore of a complex graph of related concepts. Thus, a close conceptual relationship among objects is expressed as spatial proximity. Although not mandatory, the system is set up to allow the conceptual graph to be grounded in some authoritative reference text explaining or defining the domain. The system also has the ability to express relations among the concepts of the domain intensionally, as well as extensionally. The GKS standard is a suitable domain for the COOL system.

01,693
PB94-203437 PC A03/MF A01
National Inst. of Standards and Technology (CSL), Gaithersburg, MD. Systems and Software Technology Div.
Quality Characteristics and Metrics for Reusable Software (Preliminary Report).
Rept. for Oct 92-Jun 94.
W. J. Salamon, and D. R. Wallace. May 94, 43p, NISTIR-5459.
Contracts BMDO-92-A-012, BMDO-OA-005
Sponsored by Ballistic Missile Defense Organization, Washington, DC.

Keywords: *Software reuse, *Software reliability, Quality, Characteristics, Computer program reliability, Computer software, Software metrics.

This report identifies a set of quality characteristics of software and provides a summary of software metrics that are useful in measuring these quality characteristics for software products. The metrics are useful in assessing the reusability of software products.

01,694
PB94-212016 Not available NTIS
National Inst. of Standards and Technology (NCSL), Gaithersburg, MD. Advanced Systems Div.
Associated Object Model for Distributed Systems.
Final rept.
Z. Hong, and W. McCoy. 1990, 18p.
Pub. in Operating Systems Review 24, n4 p34-51 Oct 90.

Keywords: *Distributed computer systems, *Applications programs(Computers), *Object programs, Models, Distributed processing, Operating systems(Computers), Reprints.

A model for supporting distributed applications, called the Associated Object Model, is described. In this model, multi-objects (different distributed application objects) can join in an association, making it possible for application objects to cooperate in wider degree than possible under other models. A mechanism supporting associations is introduced in this paper. By the mechanism, many associations between cooperating application objects can be established and maintained. The paper also includes some discussions about the description and implementation of the model and the mechanism.

01,695
PB94-213303 Not available NTIS
National Inst. of Standards and Technology (MEL), Gaithersburg, MD. Factory Automation Systems Div.
Debugger for Tcl Applications.
Final rept.
D. Libes. 1993, 16p.
Pub. in Proceedings of Tcl/Tk Workshop, Berkeley, CA., June 10-11, 1993, p3-18.

Keywords: *Debugging(Computers), Applications programs(Computers), Interpreters, Software tools, Reprints, *Tcl(Tool Command Language) programming language, *Tool Command Language, *Tcl programming language, C programming language.

This paper describes an implementation of a debugger for Tcl applications. The debugger has a typical front-end but with some extremely unusual commands, in part because of the features and limitations of Tcl. The debugger is modeless, allowing users to issue Tcl and application commands along with debugger commands. Each type of command may invoke the other, allowing debugging to be programmed, dynamically or in advance. The debugger is written in C and is very fast. When linked in but not used, it does not slow applications at all. The debugger requires no modifications to the Tcl core, and can be plugged into applications with little effort.

01,696
PB94-213311 Not available NTIS
National Inst. of Standards and Technology (MEL), Gaithersburg, MD. Factory Automation Systems Div.
Kibitz-Connecting Multiple Interactive Programs Together.
Final rept.
D. Libes. 1993, 11p.
Pub. in Software-Practice and Experience 23, n5 p465-475 May 93.

Keywords: *Interactive systems, *Computer software, *Interprocessor communication, Automation, Software reuse, Computer program portability, Debugging(Computers), Reprints, *Expert programming language, Kibitz.

Expect is a programming language for automating interactive programs. Recently, people have begun using Expect to connect multiple interactive programs together, allowing for new classes of applications. With some basic building blocks and a little scripting, it is possible to build such applications quickly. This paper discusses the general technique, while focusing on a particular example: Kibitz. Kibitz connects multiple sessions and applications together, providing a means for consulting, group editing, or other cooperative tasks. Kibitz in turn, can be used as a module in building additional programs of this type. Using Kibitz, we demonstrate how to enable cron or background processes to call upon and interact with users, e.g. for guidance or debugging. Owing to program reuse, our approach avoids many portability issues already addressed and solved by existing programs. Kibitz has no special coding for byte swapping, structure encoding, or job control, and requires neither kernel modifications nor setuid or other permissions even though it runs over a network and deals with multiple users, job control, and sophisticated programs such as shells and full screen editors.

01,697
PB94-213329 Not available NTIS
National Inst. of Standards and Technology (NEL), Gaithersburg, MD. Factory Automation Systems Div.
Using Expect to Automate System Administration Tasks.
Final rept.
D. Libes. 1990, 8p.
Pub. in Proceedings of Large Installation System Administrator's Conference (4th), Colorado Springs, CO., October 17-19, 1990, p107-114.

Keywords: *UNIX(Operating system), *Computer systems programs, *Systems management, Interactive systems, Interprocessor communication, Computer software management, Automation, Reprints, Systems administration.

UNIX system administration often involves programs designed only for interactive use. 'Expect' is a program which can 'talk' to interactive programs. A script is used to guide the dialogue. Scripts are written in a high-level language and provide flexibility for arbitrarily complex dialogues. By writing an 'Expect' script, one can run interactive programs non-interactively. Shell scripts are incapable of managing these system administration tasks, but 'Expect' scripts can control them and many others. 'Expect' is similar in style to the shell, and can easily be mastered by any system administrator who can program in the shell already. This paper presents real examples of using 'Expect' to automate system administration tasks such as passwd and fsck. Also discussed are a number of other systems administration tasks that can be automated.

01,698
PB94-500691 CP T99
National Inst. of Standards and Technology (CSL), Gaithersburg, MD. Software Standards Validation Group.
FORTRAN Compiler Validation System, Version 2.1.
Software.
1 Jan 94, mag tape, NIST/SW/MT-93/008.
Language: FORTRAN. Supersedes PB85-226736.
Available in 9-track, ASCII character set tape, 1600 bpi, 6250 bpi, or 3480 cartridge. Documentation included; may be ordered separately as PB94-114055.

Keywords: *Software, *Compilers, *Computer program verification, Federal information processing standards, Error detection codes, Validation, Magnetic tapes, *Fortran programming language, Conformance testing.

This Version of the Fortran Compiler Validation System (FCVS) has been revised to include all of the Temporary Program Files (TPFs) that were used with Version 2.0. The tests are progressively complex exercises of statement combinations representing typical language usage. They can be used to evaluate compiler usability and conformance to the 1978 FORTRAN Standard, and can aid in precise identification of compiler flaws. The test case outputs are tailored to each of the tests involved in order to aid in the specific diagnosis of instances of non-conformance or of compiler errors. For each test, the output indicates whether the test passes; if a test fails, the correct results and the compiler produced results are displayed on the output report. The test cases are so designed that the user can quickly and easily locate the source code which caused the failure for further analysis. The FCVS architecture supports thorough quality testing of the compiler; at the same time, with no loss of efficiency or increase in complexity, the system also provides for the auditability of the testing operation. The system was produced to be used in support of the procurement of 1978 FORTRAN Standard compilers, but it is also designed for the general user.

01,699
PB94-502077 Diskette $250.00
National Inst. of Standards and Technology, Gaithersburg, MD.
M (also known as MUMPS) Validation Test Suite, Version 8.3 (for Microcomputers).
Software.
c1 Jul 94, diskette.
System: MS DOS 3.0 or higher operating system. Language: MUMPS. Supersedes PB91-507699, PB91-507707, PB91-507715, PB91-507723.
The software is on one 3 1/2 inch DOS diskette, 1.4M high density. The diskette is in ASCII format. Documentation included; may be ordered separately as PB94-180486.

Keywords: *Software, *Compilers, *Tests, Federal information processing standards, Precompilers, Validation summary reports, Interpreters, Computer systems programs, Computer program verification, Microcomputers, Diskettes, *M programming language, *MUMPS programming language.

The M (also known as MUMPS) Validation Test Suite, Version 8.3 was developed to assess conformance to the FIPS PUB 125-1. This test suite contains 3,592 tests and incorporates features such as (1) pass/fail conditions for individual tests, (2) imbedded instructions and warnings, and (3) fully automated tabulation of the test results. This test suite can be used by Federal Agencies, M programming language developers,

physicians, hospital administrators, large group medical practices, and other industries which have requirements for M to assess the technical correctness of one or more M programming language processors. This test suite is approximately 99% self driven.

01,700
PB94-937300 Contact NTIS for subscription information and price.
National Inst. of Standards and Technology, Gaithersburg, MD.
Validated Products List (Cobol, Fortran, ADA, Pascal, MUMPS, SQL).
1994, 1p.
Supersedes PB93-937300.
Paper copy available on Standing Order, deposit account required (U.S., Canada, and Mexico $100; all others $200). Single copies also available in paper copy only.

Keywords: *Cobol programming language, *Fortran programming language, Language programming, *Federal Information Processing Standards, *Validation summary reports, *Pascal programming language, *Ada programming language, SQL programming language.

The Validated Processor List identifies those COBOL, Fortran, Ada and Pascal programming language processors that have a current validation certificate and those SQL language processors that have a registered test report, referencing the applicable Federal Information processing Standard (FIPS) as of the date of the publication. The list also includes GOSIP Conformance Testing Registers. The testing of language processors to determine the degree to which they conform to the Federal Standards is required by Government agencies in accordance with Federal Information Resources Management regulation (FIRMR) Parts 201.13 and 201.39, and the associated Federal ADP and Telecommunications Standards Index. The list is updated and published quarterly.

01,701
PB95-105037 PC A03/MF A01
National Inst. of Standards and Technology (CSL), Gaithersburg, MD. Systems and Software Technology Div.
Making Sense of Software Engineering Environment Framework Standards.
B. Cuthill. May 94, 35p, NISTIR-5487.
Sponsored by Assistant Secretary of Defense, Washington, DC. Director of Defense Information.

Keywords: *Softwear engineering, *Standards, Specifications, Operating systems(Computers), Software tools, Data base management systems, Man computer interface, *SEEs(Software Engineering Environments), *Software Engineering Environments, POSIX(Portable Operating System Interface), PCTE(Portable Common Tool Environment), CORBA(Common Object Request Broker Architecture), ODBMS(Object Database Management Standard), CDIF(Computer Aided Software Engineering (CASE) Data Interchange Format), X3H6 Draft Messaging Standard, X Windows, Motif.

The purpose of software environment framework standards and specifications is to enhance tool portability, interoperability, and integration by creating public interfaces to functionality incorporated into the framework. If tools can access framework services in predictable ways, tool vendors can take advantage of these services to avoid duplicating services and concentrate on the unique functionality of the tool. This describes the functionality and integration support supplied by a selected set of software environment framework standards and specifications with respect to common models.

01,702
PB95-105045 PC A03/MF A01
National Inst. of Standards and Technology (CAML), Gaithersburg, MD. Applied and Computational Mathematics Div.
Software Needs in Special Functions.
D. W. Lozier. Aug 94, 19p, NISTIR-5490.

Keywords: *Computer software, *Computation, Algorithms, Subroutine libraries, Interactive systems, Requirements, Tests, Computer applications, Computer program verification, *Special functions.

Currently available software for special functions exhibits gaps and defects in comparison to the needs of modern high-performance scientific computing and also, surprisingly, in comparison to what could be constructed from current algorithms. In this paper, we expose some of these deficiencies and identify the related need for user-oriented testing software.

01,703
PB95-125894 Not available NTIS
National Inst. of Standards and Technology (CSL), Gaithersburg, MD. Systems and Software Technology Div.
Software Safety and Program Slicing.
Final rept.
K. B. Gallagher, and J. R. Lyle. 1993, 10p.
Pub. in Proceedings of the Annual Conference on Computer Assurance (8th), COMPASS '93, Gaithersburg, MD., June 14-17, 1993, p71-80.

Keywords: *Computer program reliability, *Safety, *Quality assurance, Software engineering, Computer program verification, Functional integration, Prototypes, Reprints, *Program slicing, US NIST.

Software quality assurance auditors are faced with a myriad of difficulties. One particular problem is the localization of safety critical code that may be interleaved throughout the entire system. Moreover, once this code is located, its effects throughout the system are difficult to ascertain. We present a method that uses program slicing to mitigate these difficulties in two ways. First, we show how program slicing can be used to locate all code that contributes to the value of variables that might be part of a safety critical component. Second, we show how slicing-based techniques can be used to validate functional diversity, i.e., that there are no interactions of one critical component with another critical component and that there are no interactions of non critical components with the safety critical components.

01,704
PB95-125902 Not available NTIS
National Inst. of Standards and Technology (CSL), Gaithersburg, MD. Information Systems Engineering Div.
Object SQL: Language Extensions for Object Data Management.
Final rept.
L. J. Gallagher. 1992, 10p.
Pub. in Proceedings of ISMM International Conference on Information and Knowledge Management, Baltimore, MD., November 8-11, 1992, p17-26.

Keywords: *Query languages, *Object-oriented programming, *Data management, Data bases, Data base management systems, Standards, Specifications, Standardization, Reprints, *SQL database language, ISO(International Organization for Standardization), RDA(Remote Database Access).

Database Language SQL is enjoying success as an effective International Standard for the definition and management of relationally structured data. National and international SQL standardization committees are now focusing on development of future extensions for meeting the stated requirements of managing complex objects in engineering and multimedia environments. These extensions include object identifiers, abstract data types, inheritance hierarchies, and all of the other features normally associated with object data management. This paper presents the object management features contained in the draft specification for the next SQL standard, discusses problems and alternatives, and addresses planned future standardization activities.

01,705
PB95-136339 PC A10/MF A03
National Inst. of Standards and Technology (CSL), Gaithersburg, MD. Information Systems Engineering Div.
Domain Analysis of the Alarm Surveillance Domain. Version 1.0. Conducted as Part of the Domain Analysis Case Study Project.
C. Dabrowski, and J. Watkins. Sep 94, 210p, NISTIR-5494.

Keywords: *Software reuse, *Communications networks, *Management, Fault detection, Information systems, Models, Domain analysis, Alarm surveillance, FODA(Feature Oriented Domain Analysis).

The Domain Analysis Case Study was created to examine the potential use of domain analysis methods in supporting software reuse. To this end, the Domain Analysis Case Study has investigated the use of a particular domain analysis method, called the Feature Oriented Domain Analysis (FODA) method. This report describes the results of the application of the second phase of the FODA method--the domain modeling phase--to the alarm surveillance domain. During this phase, a domain model of alarm surveillance systems was created. This model captured commonalities and variabilities of the alarm surveillance domain with respect to the features of systems in the domain, the functions system perform, and the underlying structure of data used by systems. The domain model is intended to be reused to derive functional requirements for new software systems in this domain.

01,706
PB95-136370 PC A03/MF A01
National Inst. of Standards and Technology (CAML), Gaithersburg, MD. Applied and Computational Mathematics Div.
Faster BKL Monte Carlo Simulations.
J. L. Blue, I. Beichl, and F. Sullivan. 20 Sep 94, 11p, NISTIR-5489.

Keywords: *Computerized simulation, *Monte Carlo method, *Run time(Computers), Algorithms, Crystal growth.

For Monte Carlo simulations of systems of size M that use the method of Bortz, Kalos, and Liebowitz (BKL), the best computer time per event has been O(M to the 1/2 power). We present two new methods whose computer time per event is O(M to the 1/K power) or O(log M). In practice, for typical simulation sizes, K = 4 or K = 5 is fastest, requiring even less computer time than the O(log M) method. For typical simulation sizes, we are able to achieve speedup factors of 5 to 7.

01,707
PB95-136610 PC A03/MF A01
National Inst. of Standards and Technology (CSL), Gaithersburg, MD. Systems and Software Technology Div.
Report on the Advanced Software Technology Workshop. Held on February 1, 1994.
D. R. Wallace, D. R. Kuhn, and T. R. Rhodes. 25 Aug 94, 15p, NISTIR-5500.

Keywords: *Computer software, *Software engineering, *Technology assessment, Computer program reliability, Software reuse, Computer security, Standards, Businesses, Computer program portability, Computer applications, Requirements, US NIST.

On February 1, 1994, the Director of the Computer Systems Laboratory of the National Institute of Standards and Technology (NIST) convened an invitational workshop attended by eleven executives for whom software is critical to business. The purpose of the workshop was to identify advanced software technology requirements for U.S. business and to identify opportunities that NIST might pursue in the area of advanced software technology. This report summarizes the deliberations of the workshop.

01,708
PB95-151262 Not available NTIS
National Inst. of Standards and Technology (CSL), Gaithersburg, MD. Systems and Software Technology Div.
Analysis of Selected Software Safety Standards.
Final rept.
D. R. Wallace, D. R. Kuhn, and L. M. Ippolito. 1992, 14p.
Pub. in Proceedings of COMPASS '92 Conference, Gaithersburg, MD., June 15-18, 1992, p1-14.

Keywords: *Computer software, *Software reliability, *Data processing security, *Standards, Computer program integrity, Software engineering, Computer security, Quality assurance, Requirements, Guidelines, Reprints, Software safety.

The study examines standards, draft standards, and guidelines that provide requirements for the assurance of high integrity software. The study focuses on identifying the attributes necessary in a document for providing reasonable assurance for high integrity software, and on identifying the relative strengths and weaknesses of the documents. The documents vary widely in their requirements and the precision with which the requirements are expressed. Overall there is little relationship between the degree of risk and the rigor of applicable standards. Recommendations are provided for a base standard for the assurance of high integrity software.

01,709
PB95-152062 Not available NTIS

National Inst. of Standards and Technology (CSL), Gaithersburg, MD. Systems and Software Technology Div.
Use of an Environment Classification Model.
Final rept.
M. V. Zelkowitz. 1993, 10p.
Pub. in Proceedings of International Conference on Software Engineering (15th), Baltimore, MD., May 17-21, 1993, p348-357.

Keywords: *Software engineering, *Environments, Environment models, Integrated systems, Mapping, Reprints.

Various reference models have been proposed for the classification of features present in an integrated software engineering environment. In this paper, two such models are studied and a target is mapped to the set of services present in these models. The results of this mapping and comments on the effectiveness of the models are given.

01,710
PB95-153029 Not available NTIS
National Inst. of Standards and Technology (NCSL), Gaithersburg, MD. Systems and Network Architecture Div.
Formal Methods in Conformance Testing: Result and Perspectives.
Final rept.
A. R. Cavalli, J. P. Favreau, and M. Phalippou. 1993, 16p.
Pub. in Proceedings of the International Workshop on Protocol Test Systems (6th), Pau, France, September 1993, p1-16.

Keywords: Tests, Standardization, Protocols, Reprints, *Conformance testing, *Formal methods.

The application of formal methods to conformance testing becomes a more and more active research area. This paper presents the results and perspectives of the application of these languages for tests and test generation methods.

01,711
PB95-154670 PC A06/MF A02
National Inst. of Standards and Technology (CSL), Gaithersburg, MD. Information Systems Engineering Div.
Mapping Integration Definition for Information Modeling (IDEF1X) Model into CASE Data Interchange Format (CDIF) Transfer File.
I. Simakhodskiy. Nov 94, 103p, NISTIR-5530.
Also available from Supt. of Docs. See also FIPS PUB 184.

Keywords: *Data transfer(Computers), *Standards, Models, Software tools, *IDEF1X(Integration Definition for Information Modeling), *Integration Definition for Information Modeling, *CDIF(CASE Data Interchange Format), *CASE Data Interchange Format, Meta data.

This document describes a mapping of an Integration Definition for Information Modeling (IDEF1X) model into a CASE Data Interchange Format (CDIF) transfer file. This work will demonstrate that it is possible to use the CDIF standard exchange for moving information between different IDEF tools. It will also show how CDIF can provide a common definition of model data for communicating between different CASE tools.

01,712
PB95-161444 Not available NTIS
National Inst. of Standards and Technology (CAML), Gaithersburg, MD. Applied and Computational Mathematics Div.
Underflow-Induced Graphics Failure Solved by SLI Arithmetic.
Final rept.
D. W. Lozier. 1993, 8p.
Pub. in Proceedings of the Institute of Electrical and Electronics Engineers Symposium on Computer Arithmetic (11th), Windsor, Ontario, Canada, June 29-July 2, 1993, p10-17.

Keywords: *Computer graphics, *Floating point arithmetic, Computation, Algorithms, Errors, Scaling, Accuracy, Reprints, SLI(Symmetric level-index) arithmetic.

Floating-point underflow is often regarded as either harmless or as an indication that the computational algorithm is in need of scaling. A counter example to this view is given of a function for which contour plotting is difficult due to floating-point underflow. The function arose as an asymptotic solution to a model problem in turbulent combustion in which two chemical species (fuel and oxidizer) mix and react in a vortex field. Scaling is not a viable option because of extreme sensitivity to a small physical parameter. Standard graphics software packages produce erroneous contours without any indication of difficulty. This example provides support for considering symmetric level-index (SLI) arithmetic, a new form of computer arithmetic which is immune to underflow and overflow.

01,713
PB95-161881 Not available NTIS
National Inst. of Standards and Technology (CSL), Gaithersburg, MD. Information Systems Engineering Div.
Standards and Linkages: What Data Sharing Needs.
Final rept.
J. J. Newton, and D. C. Wahl. 1994, 5p.
Pub. in Data Base Newsletter 22, n1 p3-7 Jan/Feb 94.

Keywords: *Data structures, *Information transfer, *Linkages, Data links, Data integration, Data management, Information processing, Data elements, Standardization, Information systems, Reprints, *Data sharing, Legacy systems, Data administration, Data representation.

Legacy systems data must be integrated into newly-developed standardized system data in order to achieve fully interchangeable information. Standards for data element representation and legacy data linkages are two components of a successful program for fully-realized data sharing. A data hierarchy reference model provides a framework for integration of data standards. Chained, coupled, and multi-purpose linkages supply characteristic associations to existing elements.

01,714
PB95-163309 Not available NTIS
National Inst. of Standards and Technology (CAML), Gaithersburg, MD. Applied and Computational Mathematics Div.
Data-Parallel Algorithm for Three-Dimensional Delaunay Triangulation and Its Implementation.
Final rept.
Y. A. Teng, F. Sullivan, I. Beichl, and E. Puppo. 1993, 10p.
Pub. in Proceedings of Supercomputing '93, Portland, OR., November 15-19, 1993, p112-121.

Keywords: *Triangulation, *Computational geometry, *Three dimensional models, Parallel processing, Algorithms, Run time(Computers), Computer program reliability, Connection machine, Reprints.

In this paper, we present a parallel algorithm for constructing the Delaunay triangulation of a set of vertices in three-dimensional space. The algorithm achieves a high degree of parallelism by starting the construction from every vertex and expanding over all open faces thereafter. In the expansion of open faces, the search is made faster by using a bucketing technique. The algorithm is designed under a data-parallel paradigm. It uses segmented list structures and virtual processing for load-balancing. As a result, the algorithm achieves a fast running time and good scalability over a wide range of problem sizes and machine sizes. We also incorporate a topological check to eliminate inconsistencies due to degeneracies and numerical errors. The algorithm is implemented on Connection Machines CM-2 and CM-5, and experimental results are presented.

01,715
PB95-163655 Not available NTIS
National Inst. of Standards and Technology (NCSL), Gaithersburg, MD. Computer Security Div.
Computer Virus Attacks.
Final rept.
J. P. Wack, and S. A. Kurzban. 1990, 4p.
Pub. in National Computer Systems Laboratory Bulletin, p1-4 Aug 90.

Keywords: *Computer viruses, *Electronic security, *Threat evaluation, *Risk analysis, Computer program integrity, Vulnerability, Computer information security, Data processing security, Personal computers, Reprints, Worms(Computers), Logic bombs, Time bombs(Computers), Trojan horses.

The popular media contain many stories about computer viruses and similar phenomena. There are many things users and organizations can do to protect themselves from the damage that viruses can do, but some protective measures remain to be fully developed. The solution to the virus problem involves a broad range of issues, and requires us to regard viruses and computer crime in a more serious light.

01,716
PB95-173084 PC A05/MF A01
National Inst. of Standards and Technology (CSL), Gaithersburg, MD. Systems and Software Technology Div.
Framework for the Development and Assurance of High Integrity Software.
Special pub.
D. R. Wallace, and L. M. Ippolito. Dec 94, 92p, NIST/SP-500/223.
Also available from Supt. of Docs. as SN003-003-03312-0. See also PB90-111691.

Keywords: *Software engineering, *Project management, Computer software management, Computer program reliability, Computer program verification, Configuration management, Quality assurance, Software tools, Fault tolerant computing, Error detection codes.

The purpose of this document is to recommend a framework for the development and assurance of high integrity software. The framework addresses the fact that these processes must take into account properties and requirements of a high integrity system and the processes and standards used in developing other system components. This framework provides guidance to developers, assurers, and buyers of software, researchers for high integrity software systems, and vendors of Computer Aided Software Engineering tools and integrated environments.

01,717
PB95-174959 PC A03/MF A01
National Inst. of Standards and Technology (CSL), Gaithersburg, MD. Systems and Software Technology Div.
SGML Parser Validation Procedures.
R. B. Wilson. Jan 95, 33p, NISTIR-5538.
Sponsored by Assistant Secretary of Defense (Production and Logistics), Falls Church, VA. Computer-aided Acquisition and Logistic Support Program.

Keywords: *Parsers, *Computer program verification, Federal information processing standards, Tests, *SGML(Standard Generalized Markup Language), *Standard Generalized Markup Language, Conformance testing, US NIST.

This document establishes operating policy and procedures for the Computer Systems Laboratory's (CSL) validation program for Federal Information Processing Standards (FIPS) 152, Standard Generalized Markup Language (SGML), parsers. The testing methodology is based on ANSI X3.190-1992, Text and Office Systems - Conformance Testing for Standard Generalized Markup Language Systems.

01,718
PB95-175550 Not available NTIS
National Inst. of Standards and Technology (CSL), Gaithersburg, MD. Systems and Software Technology Div.
Testers Open Dialogue at Inaugural NIST Workshop.
Final rept.
M. M. Gray, and K. Liburdy. 1994, 2p.
Pub. in Institute of Electrical and Electronics Engineers Software 11, n5 p120-121 Sep 94.

Keywords: *Computer program verification, *Tests, *Automation, Standards, Computer software, Technology assessment, Costs, Reprints, Conformance testing.

This paper is a summary report of a recent invitational workshop on automated testing. One of the goals of the workshop was to propose an agenda to support and accelerate efforts in automated testing. Attendees were urged to identify 'areas of synergy' and a common focus that could lead to increased participation and funding for automated testing and reduce the 'exorbitant' cost of building test suites. Participants also reviewed existing and emerging technologies and explored the relationship between automated testing and standards development.

01,719
PB95-175741 Not available NTIS
National Inst. of Standards and Technology (PL), Boulder, CO. Time and Frequency Div.

Obtaining and Installing a Public Domain TEX.
Final rept.
W. Itano. 1991, 2p.
Pub. in Optics and Photonics News 2, n10 p41, 61, Oct 91.

Keywords: *Text processing, *Computer software, Microcomputers, Reprints, *Public domain, TEX computer program, Typesetting.

Instructions are given for obtaining a public-domain version of the TEX computer program for MS-DOS computers. The installation and operation procedures are outlined.

01,720
PB95-178992 PC A03/MF A01
National Inst. of Standards and Technology (CSL), Gaithersburg, MD. Information Systems Engineering Div.
Glossary of Software Reuse Terms.
S. Katz, C. Dabrowski, K. Miles, and M. Law. Dec 94, 37p, NIST/SP-500/222.
Also available from Supt. of Docs.

Keywords: *Software reuse, *Dictionaries, Software engineering, Computer programming, Software tools.

One method proposed for increasing the efficiency of software production in the development of large, reliable software applications is the systematic reuse of existing software products. Effective software reuse will require new techniques to supplement traditional software engineering practices. Preliminary research has already produced new methods and reports. As a result, new terminology has emerged. This report provides a baseline set of recommended definitions for terms commonly used in the software reuse community. The glossary will be expanded as further research results become available and are evaluated for use in software reuse programs.

01,721
PB95-180360 Not available NTIS
National Inst. of Standards and Technology (PL), Boulder, CO. Time and Frequency Div.
Getting Started on Mosaic.
Final rept.
W. M. Itano. 1994, 2p.
Pub. in Optics and Photonics News 5, n6 p48-49 Jun 94.

Keywords: *Computer software, Super computers, Information retrieval, Operating systems(Computers), Applications programs(Computers), Reprints, *Mosaic computer program, World Wide Web, Internet.

Mosaic, a free computer program developed by the National Center for Supercomputing Applications, is described. Mosaic works with the World Wide Web, and Internet-based information retrieval system. Information on obtaining, installing, and using the software is given. Mosaic operates on computers running the X Window, Microsoft Windows, and Macintosh operating systems.

01,722
PB95-180550 Not available NTIS
National Inst. of Standards and Technology (MEL), Gaithersburg, MD. Factory Automation Systems Div.
Handling Passwords with Security and Reliability in Background Processes.
Final rept.
D. Libes. 1994, 8p.
Pub. in Proceedings of Systems Administration Conference (8th), (LISA VIII), San Diego, CA., September 19-23, 1994, 8p.

Keywords: *Interactive systems, *Computer security, Data processing security, Computer program reliability, Automation, Access control, Reprints, Passwords, Expect computer program, Background processes.

Traditionally, background automation of interactive processes meant giving up security and reliability. With the advent of software such as Expect for controlling interactive processes, it has become possible to improve reliability and security with relative ease. This paper reviews the reliability aspects but focuses primarily on the security aspects, presenting several non-obvious techniques for dealing with passwords and other sensitive information in background processes. These techniques require no changes to existing programs and no new security systems are necessary. With the appropriate tools and examples, these techniques can be applied with surprisingly little effort to a wide variety of problems.

01,723
PB95-180832 Not available NTIS
National Inst. of Standards and Technology (CAML), Gaithersburg, MD. Applied and Computational Mathematics Div.
Performance Characteristics of Fast Elliptic Solvers on Parallel Platforms.
Final rept.
R. Pozo. 1994, 5p.
Pub. in Proceedings of the European Parallel Virtual Machine Users Group Meeting (1st), Rome, Italy, October 9-11, 1994, p1-5.

Keywords: *Elliptic differential equations, *Computation, Connection machine, Computer calculations, Computer software, Computer networks, Partial differential equations, Interprocessor communication, Run time(Computers), Performance evaluation, Reprints, *PVM(Parallel Virtual Machine), *Parallel Virtual Machine, OSC(Orthogonal spline collocation).

We present performance analyses of a fast three-dimensional elliptic orthogonal spline collocation (OSC) method on the Connection Machine CM-5, and various network clusters using the Parallel Virtual Machine (PVM) software package. While the OSC method is an efficient approach for solving Poisson, Helmholtz, and other separable partial differential equation (PDE) problems, it poses serious challenges for parallel architectures because of its high communication to computation ratio: O(N cubed) data movement to O(N cubed log N) computation. Furthermore, the communication pattern is one of the most expensive: personalized all-to-all. Results show that communication time occupies roughly 5% of total execution time in native message-passing systems (such as NX and CMMD), 10% with PVM layer on MPP's and roughly 50% for Ethernet networks.

01,724
PB95-194205 PC A03/MF A01
National Inst. of Standards and Technology (CSL), Gaithersburg, MD. Systems and Software Technology Div.
Comparing Remote Procedure Calls: Open Network Computing, Distributed Computing Environment and International Organization for Standardization.
J. F. Barkley. Oct 93, 23p, NISTIR-5277.
Sponsored by Defense Information Systems Agency, Arlington, VA. and Department of the Army, Fort Belvoir, VA. Sustaining Base Information Services.

Keywords: *Computer networks, *Computer communications, *Protocols, Applications programs(Computers), Compilers, Semantics, Programming languages, Computer program portability, Run time(Computers), *RPC(Remote procedure calls), *Remote procedure calls, ONC(Open Network Computing), DCE(Distributed Computing Environment), ISO(International Organization for Standardization).

Almost all computer systems are connected to a network supporting data communications. As a result, many techniques have evolved to support the development of applications which require processes on different systems to communicate and coordinate their activities. One such technique is remote procedure call (RPC). RPC is a mature method with several specifications and implementations. Among these are: Open Network Computing (ONC) RPC, Distributed Computing Environment (DCE) RPC, and the RPC specification from the International Organization for Standardization (ISO). This report describes the RPC concept, how this concept is commonly implemented, and compares the features and capabilities of these three RPCs. The RPC language, semantics, and protocol of ONC RPC, DCE RPC, and ISO RPC are compared. Since ONC RPC and DCE RPC have implementations, the output of their RPC language compiler and the support provided by their runtime libraries are also compared.

01,725
PB95-198727 PC A04/MF A01
National Inst. of Standards and Technology (CSL), Gaithersburg, MD. Systems and Software Technology Div.
Study on Hazard Analysis in High Integrity Software Standards and Guidelines.
L. M. Ippolito, and D. R. Wallace. Jan 95, 65p, NISTIR-5589.
See also PB92-112267.

Keywords: *Computer software, *Hazards, *Computer program integrity, Standards, Guidelines, Safety, Quality assurance, Software engineering, Computer program reliability, Systems analysis.

This report presents the results of a study on hazard analysis, especially software hazard analysis, in high integrity software standards and guidelines. It describes types of system hazard analysis (that influence software), types of software hazard analysis, techniques for conducting hazard analysis (along with some of their advantages and disadvantages), and other practices and processes that should be employed in order to ensure the safety of software.

01,726
PB95-199329 PC A03/MF A01
National Inst. of Standards and Technology (CSL), Gaithersburg, MD. Systems and Software Technology Div.
Object-Oriented Technology Research Areas.
W. J. Salamon, and D. R. Wallace. 21 Feb 95, 29p, NISTIR-5600.

Keywords: *Object-oriented programming, *Technology assessment, Distributed computer systems, Distributed processing, Software engineering, Computer program verification, Technology innovation, Research projects, *Object-oriented technology, US NIST.

This paper discusses some of the issues surrounding object technology. The topics which are discussed are object-oriented (OO) development methodologies, measuring the quality of OO software, testing, the use of OO technology in high-integrity systems, and distributed object computing. The purpose of this report is to identify research topics in OO technology for the National Institute of Standards and Technology (NIST) Computer Systems Laboratory. A bibliography is included to assist the reader in selecting material for further reading.

01,727
PB95-203253 Not available NTIS
National Inst. of Standards and Technology (NCSL), Gaithersburg, MD. Systems and Network Architecture Div.
PET and DINGO Tools for Deriving Distributed Implementations from Estelle.
Final rept.
R. Sijelmassi, and B. Strausser. 1993, 18p.
Pub. in Computer Networks and ISDN Systems 25, p841-851 1993.

Keywords: *Software tools, *Distributed computer systems, Operating systems(Computers), Compilers, Finite state machines, Specifications, Translators, Computer networks, Reprints, *Estelle translator, OSI(Open systems interconnection).

The combination of the Portable Estelle Translator (PET) and the Distributed ImplementatioN GeneratOr (DINGO) tools produces distributed implementations from Estelle specifications. The resulting implementations run as one or more operating system processes distributed over several sites of a target distributed system. In addition, the tools generate elements of an X-Window interface which allows centralized or distributed monitoring of some or all of the running modules.

01,728
PB95-216883 PC A25/MF A06
National Inst. of Standards and Technology (CSL), Gaithersburg, MD. Advanced Systems Div.
Overview of the Text REtrieval Conference (3rd) (TREC-3). Held in Gaithersburg, Maryland on November 2-4, 1994.
Special pub.
D. K. Harman. Apr 95, 595p, NIST/SP-500/225.
Also available from Supt. of Docs. as SN003-003-03328-6. Sponsored by Advanced Research Projects Agency, Arlington, VA.

Keywords: *Meetings, *Information retrieval, *Text processing, Thesauri, Automation, Natural language processing, Pattern recognition, Routing, Probability theory, Documents, Search structuring, Knowledge bases(Artificial intelligence), Vector processing, Semantics, Evaluation.

The third Text REtrieval Conference (TREC-3) was held in Gaithersburg, Maryland, November 2-4, 1994 and was attended by 150 people involved in the 33 participating groups. The goal of the Conference was to bring research groups together to discuss their work on a new large text collection. There was a large variation of retrieval techniques reported on, including

methods using automatic thesauri, sophisticated term weighting, natural language techniques, relevance feedback, and advanced pattern matching. As results were run through a common evaluation package, groups were able to compare the effectiveness of different techniques, and discuss how differences between the systems affected performance.

01,729
PB95-220554 PC A03/MF A01
National Inst. of Standards and Technology (NCSL), Gaithersburg, MD. Systems and Network Architecture Div.
Analysis of ANSI ASC X12 and UN/EDIFACT Electronic Data Interchange (EDI) Standards.
R. Aronoff, and K. Hsing. Apr 95, 35p, NISTIR-5631.

Keywords: *Information systems, *Message processing, *Software engineering, *Standards, Data processing, Electronic commerce, Health insurance, EDI(Electronic Data Interchange), EDI, American National Standards Institute ASC X12, UN/EDIFACT(United Nations Electronic Data Exchange for Information), UN/EDIFACT.

The report discusses the two Electronic Data Interchange (EDI) standards that are being developed by the ANSI ASC X12 and the UN/EDIFACT committees, respectively. Discussion is focused on the basic EDI data structures, syntax rules, and functionality. In order to illustrate the concepts and issues involved, a particular application, health care claim submission, is examined. An example scenario is presented which demonstrates how EDI can be used to support this traditional business process. An analysis is then presented which compares these two standards in detail. This analysis look at functionality, efficiency, and existing levels of standards development. To investigate issues of relative efficiency, a comparison is made of record lengths for the basic control/service elements for both standards.

01,730
PB95-220588 PC A05/MF A01
National Inst. of Standards and Technology (CSL), Gaithersburg, MD. Information Systems Engineering Div.
Persistent Object Base System Testing and Evaluation.
E. N. Fong. Apr 95, 84p, NISTIR-5636.
Sponsored by Defense Advanced Research Projects Agency, Arlington, VA.

Keywords: *Software engineering, *Object database management, Database management systems, Performance evaluation, Performance tests, *POB(Persistent Object Based Systems), *POB.

The report summarizes the role of the Computer Systems Laboratory (CSL) of the National Institute of Standards and Technology (NIST) in support of the Advanced Research Projects Agency (ARPA) in the testing and evaluation of persistent object base (POB) systems. The actual evaluation consists of designing a testing suite for exercising the POB system for the features supported. The goal of actual testing is to reveal how well each feature is being supported. The testing methodology, the abstract test suite, and the actual test results on the ARPA funded prototype POB system called Open OODB developed by Texas Instruments are described.

01,731
PB95-231726 PC A03/MF A01
National Inst. of Standards and Technology (CSL), Gaithersburg, MD. Systems and Software Technology Div.
Introduction to the P1003.1g and CPI-C Network Application Programming Interfaces.
K. Olsen. 25 May 95, 50p, NISTIR-5657.

Keywords: *Computer networks, *Computer programming, *Distributed processing, *Programming environments, Applications programs(Computers), Interprocessor communication, Protocols, Data transfer(Computers), Specifications, APIs(Application programming Interfaces).

Numerous network application programming interfaces (APIs) have been developed to assist programmers in developing distributed applications. Both IEEE P1003.1g and Common Programming Interface for Communications (CPI-C) are examples of network APIs. The report provides an overview of the P1003.1g and CPI-C calls is given, along with a simple programming example for each API. The report does not contain sufficient detail needed to develop distributed applications using these network APIs, however, a list of references is provided.

01,732
PB95-242335 PC A03/MF A01
National Inst. of Standards and Technology (CAML), Gaithersburg, MD. Applied and Computational Mathematics Div.
Parallel and Serial Implementations of SLI Arithmetic.
D. W. Lozier, and P. R. Turner. Jun 95, 28p, NISTIR-5660.
See also PB93-153476 and PB95-161444.

Keywords: *Floating point arithmetic, Computation, Parallel processing, Vector processing, Algorithms, Accuracy, Reprints, *Foreign technology, SLI(Symmetric Level Index).

The paper describes the various algorithms and software implementations of the Level-Index LI and Symmetric Level-Index SLI arithmetic schemes. After a brief introduction to the number representations and the arithmetic algorithms, the authors describe the original precompiler for including LI and SLI variables and their arithmetic in a Fortran 77 program.

01,733
PB95-242418 PC A05/MF A01
Reliable Software Technology Corp., Reston, VA.
Testability of Object-Oriented Systems.
Final rept. on Phase 1.
Jun 95, 83p, NIST/GCR-95/675.
Contract NIST-50DKNA-Y-00119
Sponsored by National Inst. of Standards and Technology (CSL), Gaithersburg, MD.

Keywords: *Object-oriented programming, *Tests, *Improvements, Software reuse, Fault tolerant computing, Computer software.

We have studied the feasibility of building an object-oriented software testability improvement tool that can be sued in conjuction with RST Corporation's C++ Softwre Testability Analysis (TM) or as a standalone assertion injection tool. We have also produced a set of recommended validation and design techniques that will improve testability, and as a side benefit, the testing of OO systems. If awarded a Phase II effort, RST will provide NIST with a means of improving the testability of C++ systems; to do so within the Phase II cost limit, RST will leverage knowledge gained from building next-generation software assessment tools. Here, RST will rely on experience gained during the building of RST's C and Fortran-77 testability tools, as well as the experimental results from the Phase I effect (which required our building a prototype C++ front-end for PiSCES Software Analysis Toolkit(TM)). Such a Phase II innovation can also be used by NIST or other US Government agencies to empirically research the fault masking ability provided between procedural and object-oriented languages.

01,734
PB95-251674 PC A03/MF A01
National Inst. of Standards and Technology (CSL), Gaithersburg, MD. Systems and Software Technology Div.
Center for High Integrity Software System Assurance: Initial Goals and Activities.
D. R. Wallace, and M. Zelkowitz. Jun 95, 28p, NISTIR-5677.

Keywords: *Computer program reliability, Quality assurance, Technology transfer, Industries, National government, Universities, Software engineering, Measurement, Goals, Software tools, Prototypes, *Center for High Integrity Software System Assurance, *CHISSA(Center for High Integrity Software System Assurance), US NIST, Formal methods.

To enable the U.S. software industry to build high integrity software and to provide U.S. industries and government confidence in the software systems on which they are dependent, the National Institute of Standards and Technology (NIST) created the Center for High Integrity Software System Assurance (CHISSA) to establish measurements and software methods for software assurance for use by those who build these systems. The measurements and associated methods will be embodied in a software development and assurance framework that will enable CHISSA to guide research in development, analysis, and testing techniques, to promote research in measurement and experimentation in the software engineering domain to be able to measure the impact of new high-integrity techniques, to accelerate use of effective technology into industry, and to develop standards and guidelines in cooperation with industry, other Federal agencies, and the research community.

01,735
PB95-267829 PC A03/MF A01
National Inst. of Standards and Technology (CAML), Gaithersburg, MD. Applied and Computational Mathematics Div.
Expression Formatter for MACSYMA.
B. R. Miller. Jul 95, 26p, NISTIR-5618.

Keywords: *Format, Computer software, Formulas(Mathematics), Coefficients, Semantics, *CAS(Computer Algebra System), *Computer Algebra System, MACSYM computer program.

A package for formatting algebraic expressions in MACSYMA is described. It provides facilities for user-directed heirarchical structuring of expressions, as well as for directing simplifications to selected subexpressions. It emphasizes a semantic rather than syntactic description of the desired form. The package also provides utilities for obtaining efficiently the coefficients of polynomials, trigonometric sums and power series.

01,736
PB95-267886 PC A05/MF A01
National Inst. of Standards and Technology (CSL), Gaithersburg, MD. Systems and Software Technology Div.
Unravel: A CASE Tool to Assist Evaluation of High Integrity Software. Volume 1. Requirements and Design.
J. R. Lyle, D. R. Wallace, J. R. Graham, D. W. Binkley, K. B. Gallagher, and J. P. Poole. Aug 95, 94p, NISTIR-5691-V1.
See also Volume 2, PB95-267894.

Keywords: *Software engineering, *Computer program reliability, *Software tools, Computer program verification, Computer software maintenance, Debugging(Computers), Safety, Algorithms, Requirements, *Program slicing, CASE(Computer Aided Software Engineering), ANSI C programming language.

This report describes a Computer Aided Software Engineering (CASE) tool, unravel, that can assist evaluation of high integrity software by using program slices to extract computations for examinations. The tool can currently be used to evaluate software written ANSI C and is designed such that other languages can be added. Program slicing is a static analysis technique that extracts all statements relevant to the computation of a given variable. Program slicing is useful in program debugging, software maintenance and program understanding. Application of program slicing is evaluation high integrity software reduces the effort in examining software by allowing a software reviewer to focus attention on one computation at a time. Once a software reviewer has identified a variable for further investigation, the reviewer directs unravel to compute a program slice on the variable. Instead of examining the entire program, only the statements in the slice need to be examined by the reviewer. By speeding up the process of locating relevant code for examination by the reviewer, a larger sample of the software can be inspected with greater confidence that some relevant section of source code has not been missed. Volume 1 of this report describes the requirements, design and evaluation of unravel.

01,737
PB95-267894 PC A04/MF A01
National Inst. of Standards and Technology (CSL), Gaithersburg, MD. Systems and Software Technology Div.
Unravel: A CASE Tool to Assist Evaluation of High Integrity Software. Volume 2. User Manual.
J. R. Lyle, D. R. Wallace, J. R. Graham, D. W. Binkley, K. B. Gallagher, and J. P. Poole. Aug 95, 56p, NISTIR-5691-V2.
See also Volume 1, PB95-267886.

Keywords: *Software engineering, *Computer program reliability, *Software tools, Computer program verification, Computer software maintenance, Debugging(Computers), Safety, User manuals(Computer programs), *Program slicing, CASE(Computer Aided Software Engineering), ANSI C programming language.

This is the second volume of a two volume report on unravel, a Computer Aided Software Engineering

(CASE) tool for software written in ANSI C, that assist evaluation of high integrity software by using program slices to extract computations for examination. In this volume, we provide a user manual for unravel. This manual is intended to provide the user with enough information to use unravel without any other reference. To this end, a brief simplified description of program slicing is provided in additon to a tutorial example and a detailed description of unravel operation. This user manual also discusses limitations of unravel and how to deal with code containing extensions to ANSI C that would inhibit the correct operation of unravel.

01,738
PB95-937300 Contact NTIS for subscription information and price.
National Inst. of Standards and Technology, Gaithersburg, MD.
Validated Products List (Cobol, Fortran, ADA, Pascal, MUMPS, SQL).
1995, 1p.
Supersedes PB94-937300.
Paper copy available on Standing Order, deposit account required (U.S., Canada, and Mexico $100; all others $200). Single copies also available in paper copy only.

Keywords: *Cobol programming language, *Fortran programming language, Language programming, Language programming, *Federal Information Processing Standards, *Validation summary reports, *Pascal programming language, *Ada programming language, SQL programming language.

The Validated Processor List identifies those COBOL, Fortran, Ada and Pascal programming language processors that have a current validation certificate and those SQL language processors that have a registered test report, referencing the applicable Federal Information processing Standard (FIPS) as of the date of the publication. The list also includes GOSIP Conformance Testing Registers. The testing of language processors to determine the degree to which they conform to the Federal Standards is required by Government agencies in accordance with Federal Information Resources Management regulation (FIRMR) Parts 201.13 and 201.39, and the associated Federal ADP and Telecommunications Standards Index. The list is updated and published quarterly.

01,739
PB96-102678 Not available NTIS
National Inst. of Standards and Technology (MEL), Gaithersburg, MD. Manufacturing Systems Integration Div.
Ouch Those Programs are Painful.
Final rept.
D. Libes. 1995, 3p.
Pub. in O'Reilly and Associates, Inc., p9-11 1994.

Keywords: *Interactive systems, *Computer communications, Interprocessor communication, Applications programs(Computers), UNIX(Operating system), Systems management, Software tools, Reprints, *Expect computer program, Shells(Computers), TCL computer language, Programmed dialogue.

UNIX programs used to be designed so that they could be connected with pipes created by a shell. This paradigm is insufficient when dealing with many modern interactive problems. Expect is a program designed to control interactive programs. Expect reads a script that resembles the dialogue itself but which may include multiple paths through it. The scripting language used by Expect is usually Tcl but may be other languages. In addition, Expect may be compiled into C, C++, or other complied languages.

01,740
PB96-103031 Not available NTIS
National Inst. of Standards and Technology (CSL), Gaithersburg, MD. Advanced Systems Div.
Using Synthetic Perturbations and Statistical Screening to Assay Shared-Memory Programs.
Final rept.
R. Snelick, J. JaJa, R. Kacker, and G. Lyon. 1995, 7p.
Pub. in Information Processing Letters, v54 p147-153 1995.

Keywords: *Parallel processing, MIMD(Computers), Response time(Computers), Computer performance evaluation, Computer systems performance, Distributed computer systems, Statistical analysis, Reprints, *Shared memory programs, *Synthetic perturbation screening.

Synthetic-perturbation screening (SPS, hereafter, for brevity) is a diagnostic technique employing artifical code-in discussion to follow, delays-placed within segments of an MIMD program. These insertions simulate code changes in suspected program bottlenecks. Screening techniques based upon statistical experimental design then flag those program segments that are most sensitive to perturbation (delay). A subset of program segments so flagged can be candidates for improvement. The results are sensitivity analyses of specimen programs in terms of their questionable sections of code.

01,741
PB96-109533 PC A07/MF A02
National Inst. of Standards and Technology (CSL), Gaithersburg, MD. Information Systems Engineering Div.
Mapping Integration Definition for Function Modeling (IDEFO) Model into CASE Data Interchange Format (CDIF) Transfer File.
I. V. Simakhodskiy. Sep 95, 128p, NISTIR-5719.
See also PB95-154670.

Keywords: *Data transfer(Computers), *Standards, *Models, Software tools, *IDEFO(Integration Definition for Function Modeling), *Integration Definition for Function Modeling, *CDIF(Case Data Interchange Format), *Case Data Interchange Format, CASE(Computer Aided Software Engineering), Computer Aided Software Engineering.

The Integration Definition for Function Modeling (IDEFO) is a standard modeling technique used in the logical definition of an organization's data resources. One serious limitation to the standard is the lack of a formal standard mechanism for transferring information between different IDEF tools and between IDEF tools and other tools supporting different modeling techniques. This leaves the users of IDEF tools at a great disadvantage. A user is restricted to using a particular tool provided by a particular vendor thus seriously hindering the reusability of the information represented in a model. One solution is the use of a standard method to exchange data between tools. The CASE Data Interchange Format (CDIF) Family of Standards is primarily designed to be used as a description of a mechanism for transferring information between CASE tools. This document will describe a conceptual mapping of an IDEF0 model into the CDIF transfer file. The document will cover both syntax and semantics of the model. This work will demonstrate that it is possible to use the standard exchange for moving information between different tools.

01,742
PB96-109582 PC A02/MF A01
National Inst. of Standards and Technology (CAML), Gaithersburg, MD. Applied and Computational Mathematics Div.
Error-Bounding in Level-Index Computer Arithmetic.
D. W. Lozier, and P. R. Turner. Oct 95, 10p, NISTIR-5724.
Presented at the International IMACS-GAMM Symposium on Numerical Methods and Error-Bounds, Oldenburg, Germany, July 9-12, 1995. Prepared in cooperation with Naval Academy, Annapolis, MD. Dept. of Mathematics.

Keywords: *Computer programs, *Computation, *Accuracy, Algorithms, Computer systems performance, Level Index, SLI(Symmetric Level Index).

This paper proposes the use of level-index (LI) and symmetric level-index (SLI) computer arithmetric for practical computation with error bounds. Comparisons are made with floating-point and several advantages are identified.

01,743
PB96-111844 Not available NTIS
National Inst. of Standards and Technology (CSL), Gaithersburg, MD. Systems and Software Technology Div.
SQA Standards and Total Quality Management.
Final rept.
C. E. Wardle, D. R. Wallace, R. Khorramshahgol, E. G. McGuire, and B. Kaplan. 1991, 19p.
Pub. in Annual Pacific Northwest Software Quality Conference (9th), Portland, OR., October 7-8, 1991, v9 p1-19.

Keywords: *Total quality management, *Computer program integrity, Computer software, Software engineering, Software reliability, Program verification(Computers), Computer architecture, Quality control, Reprints, *SQA(Software Quality Assurance), *Software Quality Assurance, Software standards, Process improvement.

Total Quality Management (TQM) programs, which focus on continuous process improvement, are becoming increasingly popular in corporations today and may, in fact, be superceding quality assurance activities. Quality assurance has been used by corporations to ensure the quality of released products. What we are finding now is the thrust of management attention is on process improvement rather than on quality assurance. This paper examines some major standards and programs in SQA and TQM. Because few companies are using SQA standards, the difficulties in implementing SQA standards are addressed. Results from an on-going research project studying SQA standards and the interrelationships between TQM and SQA are presented.

01,744
PB96-112214 Not available NTIS
National Inst. of Standards and Technology (CSL), Gaithersburg, MD. Systems and Software Technology Div.
High Integrity Software Standards Activities at NIST.
Final rept.
D. R. Kuhn, D. R. Wallace, and J. C. Cherniavsky. 1991, 15p.
Pub. in Annual Pacific Northwest Software Quality Conference (9th), Portland, OR., October 7-8, 1991, v9 p47-61.

Keywords: *Computer software, *Standards, *Software reliability, Computer program integrity, Computer program performance, Standardization, Quality assurance, Software engineering, Research and development, Technology transfer, Guidelines, Research programs, Reprints, *High integrity.

This paper provides information about the National Institute of Standards and Technology (NIST) effort to produce a comprehensive set of standards and guidelines for the assurance of high integrity software. In particular, the paper presents the results of a Workshop on the Assurance of High Integrity Software held at NIST on January 22-23, 1991 and activities at NIST in support of assuring high integrity software.

01,745
PB96-122122 (Order as PB96-117767, PC A08/MF A02)
National Inst. of Standards and Technology, Gaithersburg, MD.
Performance Measures for Geometric Fitting in the NIST Algorithm Testing and Evaluation Program for Coordinate Measurement Systems.
T. H. Hopp, and M. S. Levenson. 1995, 12p.
Included in Jnl. of Research of the National Institute of Standards and Technology, v100 n5 p563-574 Sep/Oct 95.

Keywords: *Algorithms, *Computer software, *Calibration standards, Reprints, Metrology, Geometry, Performance tests, Orthogonal functions, Quality control.

The Algorithm Testing and Evaluation Program for Coordinate Measurement Systems (ATEP-CMS) is a Special Test Service offered under the NIST Calibration Program. ATEP-CMS evaluates the performance of geometric fitting software used in coordinate measurement systems. It is a Special Test because it is a new type of NIST service, experimental in nature and unsupported by historical data. This report documents and explains the rationale of the performance measures used in ATEP-CMS and analyzes the uncertainties of those measures.

01,746
PB96-128202 PC A03/MF A01
National Inst. of Standards and Technology (CSL), Gaithersburg, MD. Distributed Systems Engineering.
Distributed Systems: Survey of Open Management Approaches.
J. Hungate, and G. Fernandes. 21 Sep 95, 34p, NISTIR-5735.

Keywords: *Distributed computer systems, *Management, System engineering, Computer networks, Computer communications, Integrated systems, Interoperability, Models.

Networks and distributed systems are becoming critical for the working of many enterprises. Traditionally,

tools necessary to perform effective system management were inherent to proprietary operating systems and dealt with user and resource allocation and administration. With the introduction of local area networks (LANs), distributed computing environments started to develop. System management tools were enhanced with network management facilities, but rarely in an integrated fashion. Management services, providing mechanisms to monitor and control a great diversity of components and user interactions with these components, and an integrated approach to assure consistency are just now being addressed by standard development organizations and user consortia. The report gives an overview of some existing approaches proposed by differnet organizations: IEEE POSIX Working Group P1003.0, X/Open, ISO/IEC, and the Network Management Forum (NMF).

01,747
PB96-131503 PC A03/MF A01
National Inst. of Standards and Technology (CSL), Gaithersburg, MD. Systems and Software Technology Div.
Method to Determine a Basis Set of Paths to Perform Program Testing.
J. Poole. Nov 95, 18p, NISTIR-5737.

Keywords: *Computer program verification, *Software tools, Algorithms, Computer software, *Debugging(Computers), *Flowgraphs, Software testing.

A major problem in unit testing of programs is to determine which test cases to use. One technique that is in widespread use is to take the control flowgraph from each of the program functions and calculate a basis set of test paths. A basis set is a set of paths through the functions that are linearly independent and the paths in the basis set can be used to construct any path through the program flowgraph. Path construction is defined as adding or subtracting the number of times each edge is traversed. While this is not a total solution for test case generation, it does provide a good starting set of test cases. This paper gives an algorithm for taking a function's flowgraph and determining a basis set of paths. Proofs that the algorithm generates a set of paths that fulfill the above requirements are provided. A prototype tool, STest, is also discussed. Some general ideas for further improvement are also provided.

01,748
PB96-141296 Not available NTIS
National Inst. of Standards and Technology (CAML), Gaithersburg, MD. Scientific Computing Environments Div.
Experience with MPI: 'Converting Pvmmake to Mpimake under LAM' and 'MPI and Parallel Genetic Programming'.
Final rept.
J. E. Devaney. 1995, 13p.
Pub. in MPI Developers Conference, Notre Dame, IN., June 22-23, 1995.

Keywords: *Parallel processing, *Computer codes, Personal computers, Computer programming, Utility routines, Software engineering, Systems approach, Algorithms, Reprints, *MPI(Message-Passing Interface), *Message-Passing Interface, PVM(Parallel Virtual Machine).

The paper looks at issues which arose in porting the pvmmake utility from PVM to MPI. Pvmmake application which allows a user to send files, execute commands, and receive results from a single machine on any machine in the virtual machine. Its actions are controlled by the contents of a configuraton file. A utility with the same features, mpimake, was coded up to run under LAM. The implementation under MPI requires the transfer of dynamic data structures such as lists and trees. This paper discusses the match between the requirements of this algorithm and the datatype feature on MPI.

01,749
PB96-146758 Not available NTIS
National Inst. of Standards and Technology (CSL), Gaithersburg, MD. Advanced Systems Div.
Scalability Test for Parallel Code.
Final rept.
G. Lyon, R. Kacker, and A. Linz. 1995, 17p.
See also PB94-193638.
Pub. in Institute of Electrical and Electronics Engineers International Software Metrics Symposium (2nd), Lond, United Kingdom, October 24-26, 1994, Software: Practice and Experience, v25 n12 p1299-1314 Dec 95.

Keywords: *Parallel processing(Computers), *MIMD(Computers), *Response time(Computers), Computer performance evaluation, Computer systems performance, Computer program verification, Coding, Distributed computer systems, Sensitivity analysis, Optimization, Experimental design, Reprints, *Code scalability.

Code scalability, crucial on any parallel system, determines how well parallel code avoids becoming a bottleneck as its host computer is made larger. Each suspected code bottleneck corresponds to a first-order term in the expansion, the coefficient for that term indicating how sensitive execution is to changes in the suspect location. However, it is the expansion coefficients for second-order interactions between code segments and the number of processors that are fundamental to discovering which program elements impede parallel speedup. A new, unified view of these second-order coefficients yields an informal relative scalability test of high utility in code development. Discussion proceeds through actual examples, including a straightforward illustration of the test applied to SLALOM, a complex, multiphase benchmark.

01,750
PB96-154588 PC A04/MF A01
National Inst. of Standards and Technology (CSL), Gaithersburg, MD. Systems and Software Technology Div.
C++ in Safety Critical Systems.
D. W. Binkley. Nov 95, 34p, NISTIR-5769.

Keywords: *Systems engineering, *Safety engineering, Reliability, Computer programs, Verification, Validation, Classification, Guidelines, Software, Nuclear reactor safety, Fault tolerant systems, Aviation, Motor vehicle transportation, *High integrity software, *C++(Programming language).

The safety of software is influenced by the choice of implementation language and the choice of programming idioms. The C++ language is gaining popularity as the implementation of choice for large software projects because of its promise to reduce the complexity and cost of their construction. But is C++ an appropriate choice for such systems. An assessment of how well C++ fits into recent software guidelines for safety critical systems is presented along with a collection of techniques and idioms for constructing safer C++ code.

01,751
PB96-154992 PC A03/MF A01
National Inst. of Standards and Technology (CSL), Gaithersburg, MD. Systems and Software Technology Div.
Standard Generalized Markup Language Test Suite Evaluation Report.
C. S. Russell. Nov 95, 28p, NISTIR-5762.

Keywords: *Parsers, *Computer program verification, Federal information processing standards, Tests, Documents, Publishing, Automation, *SGML(Standard Generalized Markup Language), Standard Generalized Markup Language, Conformance Testing, CALS(Computer Acquisition and Life Cycle Support).

NIST has been tasked by the CALS Project Office to organize an SGML Conformance Testing Service. The first step in producing a conformance testing service was to produce a thorough test suite. The goal of this project was to evaluate existing test suites for use as the basis within an SGML conformance testing service. This document describes the methodology used in analyzing Exoterica Corporation's SGML Test Suite and the different types of tests run with the various SGML products at NIST's disposal.

01,752
PB96-155791 Not available NTIS
National Inst. of Standards and Technology (CSL), Gaithersburg, MD. Advanced Systems Div.
Findings and Recommendations from a Software Reengineering Case Study.
Final rept.
M. K. Ruhl. 1991, 5p.
Pub. in Proceedings of Annual Systems Reengineering Workshop (2nd), Silver Spring, MD., March 25-27, 1991, p1-5.

Keywords: *Software engineering, *Computer software maintenance, *Data base management, Relational data bases, Feasibility studies, Cost effectiveness, US IRS, Case studies, Reprints, CASE(Computer-Aided Software Engineering), Open system environment, Network data bases, US NIST.

Our objective was to examine the effort needed and issues by attempting to reengineer the system for use on a more open environment and convert the network database to a relational database.

01,753
PB96-158712 PC A07/MF A02
National Inst. of Standards and Technology (CSL), Gaithersburg, MD. Systems and Software Technology Div.
Application Portability Profile (APP): The U.S. Government's Open System Environment Profile Version 3.0.
Special pub.
G. E. Fisher. Feb 96, 112p, NIST/SP-500/230.
Supersedes PB93-216943. Also available from Supt. of Docs. as SN003-003-03389-8.

Keywords: *Computer program portability, *Interoperability, *Distributed processing, Computer program transferability, Federal agencies, Computer networks, Computer communications, Software engineering, Operating systems(Computers), Applications programs(Computers), Network analysis, Data transfer(Computers), Data flow, Data management, Computer graphics, Graphical user interface, Human-computer interface, Standardization, Specifications, Recommendations, *Open System Environment, *Application Portability Profile, Federal Information Processing Standards.

The report is designed to provide recommendations on a variety of specifications that will generally fit the requirements of U.S. government information systems. As the U.S. Government's Open System Environment (OSE) profile, the guidance is provided to assist Federal agencies in making informed choices regarding the selection and use of OSE specifications, and in the development of more selective application profiles based on the APP. It is directed toward managers and project leaders who have the responsibilities of acquiring, developing, and maintaining information systems supported by heterogeneous application platform environments.

01,754
PB96-160791 Not available NTIS
National Inst. of Standards and Technology (CSL), Gaithersburg, MD. Systems and Software Technology Div.
SQA and TQM in Software Quality Improvement.
Final rept.
C. E. Wardle, and D. Wallace. 1993, 2p.
Pub. in Software Engineering Research Forum (SERF '93), Orlando, FL., November 1993, 2p.

Keywords: *Total quality management, Software engineering, Software reliability, Computer program integrity, Program verification(Computers), Debugging(Computers), Quality control, Computer program reliability, Research and development, Reprints, *SQA(Software Quality Assurance), *Software quality assurance, Software development, Process improvement.

Software Quality Assurance (SQA) has traditionally been used to ensure the quality of released software products. The authors suggest that a combination of techniques drawn from both SQA and TQM will be more effective in producing the desired level of software quality, than will either SQA or TQM separately.

01,755
PB96-160858 Not available NTIS
National Inst. of Standards and Technology (CSL), Gaithersburg, MD. Systems and Software Technology Div.
Slicing in the Presence of Parameter Aliasing.
Final rept.
D. Binkley. 1993, 8p.
Pub. in Proceedings of the Software Engineering Research Forum (3rd), Orlando, FL., November 1993, p261-268.

Keywords: *Software engineering, *Computer program integrity, Algorithms, Debugging(Computers), Computer software maintenance, Software reliability, Computer programming, Parameterization, Functional integration, Reprints, *Program slicing, Aliasing, Data dependence, Program dependence graph.

The notion of a program slice, originally introduced by Mark Weiser, is useful in program debugging, automatic parallelization, program integration, and software maintenance. A slice of a program is taken with respect to a point p and a variable x; the slice consists of all

statements of the program that might affect the value of x at point p. This paper presents an algorithm for interprocedural slicing in the presence of parameter aliases: two formal parameters that refer to the same memory location. The algorithm is parameterized by a set of parameter aliasing information.

01,756
PB96-160908 Not available NTIS
National Inst. of Standards and Technology (CSL), Gaithersburg, MD. Information Systems Engineering Div.
Impact of Computer-Aided Acquisition and Logistic Support (CALS) in the Application of Standards.
Final rept.
D. K. Jefferson. 1992, 11p.
Pub. in International Conference on the Application of Standards for Open Systems (7th), Paris, France, November 4, 1992, p1-11.

Keywords: *Concurrent engineering, *Standards, Information systems, Weapon systems, Logistics management, Systems engineering, Distributed processing, Application program(Computers), Protocols, Reprints, *CALS(Computer-aided Acquisition and Logistic Support), *Computer-aided Acquisition and Logistic Support, Conformance testing, CALS(Continuous Acquisition and Life-cycle Support), Open systems.

Computer-aided Acquisition and Logistic Support (CALS) is a major initiative by the U.S. Department of Defense to enable the use of shared digital technical information in support of weapon systems. CALS is reducing the use of paper-based technical information, improving the information systems supporting weapon systems, and improving work processes. CALS is based on broad support nationally and internationally, particularly from the CALS/Concurrent Engineering Industry Steering Group and the Natioanl Institute of Standards and Technology within the U.S. Department of Commerce. CALS is based on Open Systems and has actively supported the development of standards, Application Protocols/Profiles, and conformance tests and test services.

01,757
PB96-160924 Not available NTIS
National Inst. of Standards and Technology (CSL), Gaithersburg, MD. Systems and Software Technology Div.
IEEE's POSIX: Making Progress.
Final rept.
D. R. Kuhn. 1991, 4p.
Pub. in Institute of Electrical and Electronics Engineers Spectrum, p36-39 Dec 91.

Keywords: *Software development, *Computer program verification, Operating systems(Computers), Computer program portability, Object-oriented programming, Interfaces, Interoperability, Computer-aided design, UNIX(Operating system), C++(Programming language), Standards, Reprints, *POSIX(Portable Operating Systems Interface for Computer Environments), *Portable Operating Systems Interface for Computer Environments.

As the circuit design drew near, the pace became more frantic by the hour, elevating the project leader's anxiety level and his blood pressure. And for good reason - all the users of DEC workstations, where the computer-aided design software resided, were out at a seminar. To be sure, IBM, Sun, and other workstations were available that would have allowed other engineers to complete the job on time. Only a DEC version was obtainable in house; in no way could it be ported to the IBM or Sun on time to beat the deadline - even though the project leader had received assurances from the software vendor that such versions 'were forthcoming.'

01,758
PB96-160932 Not available NTIS
National Inst. of Standards and Technology (CSL), Gaithersburg, MD. Systems and Software Technology Div.
Open Systems Software Standards in Concurrent Engineering.
Final rept.
D. R. Kuhn, W. J. Majurski, W. McCoy, and F. Schulz. 1994, 30p.
Pub. in Concurrent Engineering Techniques and Applications, Control and Dynamics Systems, v62 p59-88 Feb 94.

Keywords: *Operating systems(Computers), *Computer program portability, *Concurrent engineering, Software development, Software tools, Platforms, Interoperability, Interfaces, Application programs(Computers), Standards, Reprints, POSIX(Portable Operating Systems Interface for Computer Environments), OST(Open Systems Interconnection).

The movement toward concurrent engineering comes at a time when the computer industry is undergoing a fundamental change in the way computers and software are developed and used. Products based on 'open systems' standards - particularly the ISO Open System Interconnection (OSI), and IEEE POSIX - are beginning to replace reliance on proprietary computing platforms. Engineers who develop products that incorporate embedded computer and software are thus faced with the challenge of understanding two technological developments that will change the way they do their jobs: concurrent engineering and open systems.

01,759
PB96-160940 Not available NTIS
National Inst. of Standards and Technology (CSL), Gaithersburg, MD. Systems and Software Technology Div.
Predicate Differences and the Analysis of Dependencies in Formal Specifications.
Final rept.
D. R. Kuhn. 1991, 10p.
Pub. in National Computer Security Conference (14th), Washington, DC., October 1-4, 1991, Information Systems Security: Requirements and Practices, v2 p436-445.

Keywords: *Predicate logic, *Computer software, *Specifications, *Electronic security, Mathematical logic, Boolean functions, Software engineering, Software reliability, Computer program integrity, Computer program verification, Standards, Computer information security, Reprints.

This paper defines the notion of predicate differences in predicate calculus. The paper shows how predicate differences may be used to analyze the effect of changes to formal specifications; to investigate the conditions under which invalid assumptions will render a system non-secure; and in some cases may help to simplify re-verification of a modified formal specification.

01,760
PB96-160957 Not available NTIS
National Inst. of Standards and Technology (CSL), Gaithersburg, MD. Systems and Software Technology Div.
Technique for Analyzing the Effects of Changes in Formal Specifications.
Final rept.
D. R. Kuhn. 1992, 5p.
Pub. in the Computer Jnl., v35 n6 p574-578 1992.

Keywords: *Predicate logic, *Computer software, *Specifications, *Electronic security, Mathematical logic, Boolean functions, Software engineering, Software reliability, Computer program integrity, Computer program verification, Standards, Computer information security, Reprints.

This paper defines the notion of predicate differences and shows how predicate differences may be used to analyze the effects of changes in formal specifications. Predicate differences have both theoretical and practical applications. As a theoretical tool, predicate differences may be used to define a meaning for the 'size' of a change to a formal specification. Practical applications include analyzing the effect of design changes on a previously verified design; defining an affinity function for reusable software components; computing slices of formal specifications, similar to program slices; investigating the conditions under which invalid assumptions will render a system non-secure; and formalizing the database inference problem.

01,761
PB96-160981 Not available NTIS
National Inst. of Standards and Technology (CSL), Gaithersburg, MD. Systems and Software Technology Div.
Program Slicing.
Final rept.
J. R. Lyle. 1994, 6p.
See also PB95-125894.
Pub. in Encyclopedia of Software Engineering, v2 p873-878 Feb 94.

Keywords: *Debugging(Computers), *Software engineering, *Computer software maintenance, Computer programming, Computer program vertification, Computer program reliability, Computer program integrity, Software reliability, Mathematical calculations, Algorithms, Functional integration, Reprints, *Program slicing.

Program slicing is a family of program decomposition techniques based on extracting statements relevant to a computation in a program. This is advantageous because the slice can collect an algorithm for a given calculation that may be scattered throughout a program excluding irrelevant statements. It should be easier for a programmer interested in a subset of the program's behavior to understand the corresponding slice than to deal with the entire program. The utility and power of program slicing comes from the potential automation of tedious and error-prone tasks. Program slicing has applications in program debugging, program testing, program integration, parallel program execution, and software maintenance. Several variations on this theme have been developed, including program dicing, dynamic slicing, and decomposition slicing.

01,762
PB96-161211 Not available NTIS
National Inst. of Standards and Technology (CSL), Gaithersburg, MD.
Conference Report: International Conference on the Application of Standards for Open Systems (6th).
Final rept.
S. M. Radack. 1991, 3p.
Pub. in International Conference on the Application of Standards for Open Systems (6th), Gaithersburg, MD., October 2-4, 1990, Jnl. of Research of the National Institute of Standards and Technology, v96 n6 p767-769 Nov/Dec 91.

Keywords: *Standards, Application programs(Computers), Computer program portability, Distributed processing, Interoperability, Interfaces, Policy making, International cooperation, Computer security, Reprints, *Open systems, OSI(Open Systems Interconnection), Conformance testing.

Worldwide interest in advancing open computing systems was highlighted at the Sixth International Conference on the application of Standards for Open Systems. The conference featured papers and discussion on key issues affecting the implementation of open systems including policy development, international collaboration, trade issue, implementation, conformance, and security.

01,763
PB96-161377 Not available NTIS
National Inst. of Standards and Technology (CSL), Gaithersburg, MD. Systems and Software Technology Div.
Report of a Workshop on the Assurance of High Integrity Software.
Final rept.
D. R. Wallace, D. R. Kuhn, and J. C. Cherniavsky. 1991, 5p.
Pub. in Proceedings of the Annual Conference on Computer Assurance (COMPASS '91) (6th), Gaithersburg, MD., June 24-27, 1991, p151-155.

Keywords: *Software reliability, *Computer performance evaluation, *Standards, Software engineering, Computer program integrity, Electronic security, Computer information security, Quality assurance, Specifications, Reprints, *High integrity, Critical systems.

This paper provides information about the National Institute of Standards and Technology (NIST) effort to produce a comprehensive set of standards and guidelines for the assurance of high integrity software. In particular, the paper presents the results of a Workshop on the Assurance of High Integrity Software held at NIST on January 22-23, 1991.

01,764
PB96-161385 Not available NTIS
National Inst. of Standards and Technology (CSL), Gaithersburg, MD. Systems and Software Technology Div.
Standards for High Integrity Software.
Final rept.
D. R. Wallace, and L. Beltracchi. 1992, 2p.
Pub. in Transactions of the Water Reactor Safety Information Meeting (20th), Bethesda, MD., October 21-23, 1992, p9-3 - 9-4.

Keywords: *Software reliability, *Computer performance evaluation, *Standards, Software engineering,

Computer program integrity, Electronic security, Computer information security, Quality assurance, Specifications, Reprints, *High integrity, Critical systems.

High integrity software is software that must be trusted to work dependably in some critical function, and whose failure to do so may have catastrophic results, such as serious injury, loss of life or property, business failure or breach of security. Examples include software used in safety systems of nuclear power plants, medical devices, electronic baking, air traffic control, automated manufacturing, and military systems.

01,765
PB96-161393 Not available NTIS
National Inst. of Standards and Technology (CSL), Gaithersburg, MD. Systems and Software Technology Div.
Verification and Validation.
Final rept.
D. R. Wallace. 1994, 24p.
See also PB90-111691 and PB96-161401.
Pub. in Encyclopedia of Software Engineering, p1409-1434 Feb 94.

Keywords: *Software engineering, *Computer program verification, *Validation, Software development, Software reliability, Computer program integrity, Computer performance evaluation, Error detection codes, Project management, Quality assurance, Standards, Reprints.

This chapter describes how the software verification and validation (V&V) methodology and software provide a strong framework for developing quality software. First, the chapter describes software V&V, its objectives, recommended tasks, and guidance for selecting V&V techniques to perform V&V. An analysis of two studies of V&V's cost-effectiveness concludes that cost benefits of V&V early error detection outweigh the cost of performing V&V. The chapter describes several software engineering standards for V&V, project management, and quality assurance. The chapter describes each V&V standard according to its V&V requirements and techniques. The chapter provides insights on how to use management, quality, and V&V techniques to structure a quality software development.

01,766
PB96-161401 Not available NTIS
National Inst. of Standards and Technology (CSL), Gaithersburg, MD. Systems and Software Technology Div.
Verification and Validation of Reengineered Software.
Final rept.
D. R. Wallace. 1993, 1p.
See also PB96-161393.
Pub. in Business Reengineering: The Competitive Edge Proceedings of the Annual DAMA-NCR Symposium (6th), Gaithersburg, MD., May 11-12, 1993, p80.

Keywords: *Computer program verification, *Validation, Software engineering, Software reuse, Software reliability, Computer program integrity, Quality assurance, Federal agencies, Reprints, *Software reengineering.

Many Federal agencies are currently examining their inventories of software systems to identify those which are suitable for reuse. Reuse of software may range from conversion of code from one language to another, adaption of the system for another platform, or the use of an existing system in a new system with additional requirements. To accomplish these and other forms of reuse, the agencies are finding that reengineeringing is often necessary.

01,767
PB96-165964 PC A05/MF A01
National Inst. of Standards and Technology (CSL), Gaithersburg, MD. Advanced Systems Div.
Using S-Check, Alpha Release 1.0.
R. D. Snelick, N. V. Drouin, and J. K. Antonishek.
Feb 96, 54p, NISTIR-5789.
Sponsored by Defense Advanced Research Projects Agency, Arlington, VA.

Keywords: *Parallel processing, *Computer performance evaluation, *Debugging(Computers), Multiprocessers, Software tools, Distributed computer systems, Sensitivity analysis, Users guide, Synthetic Perturbation Screening.

S-Check is a tool for detecting performance bottlenecks in programs on computer systems with multiple processors. S-Check automates the techniques of Synthetic Perturbation Screnning. Synthetic Perturbation Screening systematically perturbs selected program code segments and determines performance sensitivities of these selected segments by using the statistical techniques of Design of Experiments. The resulting sensitivity analysis serves as a basis for performance evaluations. This document serves as a user's guide for S-Check.

01,768
PB96-167838 PC A03/MF A01
National Inst. of Standards and Technology (CSL), Gaithersburg, MD. Information Systems Architecture Div.
Application of the Pointer State Subgraph to Static Program Slicing.
D. W. Binkley, and J. R. Lyle. Mar 96, 22p, NISTIR-5799.
Contract DISA-DNR046115
Sponsored by Defense Information Systems Agency, Arlington, VA.

Keywords: *Static analysis, *Computer programs, Software engineering, Data flow analysis, Interface slicing, Pointers.

A new technique for performing static analysis of programs that contain unconstrained pointers is presented. The technique is based on the pointer state subgraph: a reduced control flow graph that takes advantage of the fact that in any program there exists a smaller program that computes only the values of pointer variables. The pointer state subgraph is useful in building static analysis tools. As an example the application of the pointer state subgraph to program slicing is considered. Finally, some experimental results, obtained using the ANSI-C slicer Unravel, are reported. These results show a clear reduction in the time taken to compute data-flow information from programs that contain pointers. They also show a substantial reduction in the space needed to store this information.

01,769
PB96-169099 PC E99
Massachusetts Inst. of Tech., Cambridge.
X Window System, Version 11, Release 5.
R. W. Scheifler. c1988, 897p.

Keywords: *Protocols, *Computer programming, *X Window System, Programming languages, Software tools, Operating systems(Computers), Personal computers, Computer networks, Computer graphics, Computer systems programs, Format, C programming language, User interfaces.

Table of Contents:
Acknowledgments;
Protocol Formats;
Syntactic Conventions;
Common Types;
Errors;
Keyboards;
Pointers;
Predefined Atoms;
Connection Setup;
Requests;
Connection Close;
Events;
Flow Control and Concurrency;
Appendix A - KEYSYM Encoding;
and Appendix B - Protocol Encoding.

01,770
PB96-179411 Not available NTIS
National Inst. of Standards and Technology (CAML), Gaithersburg, MD. Applied and Computational Mathematics Div.
Tree-Lookup for Partial Sums Or: How Can I Find This Stuff Quickly.
Final rept.
I. Beichl, and F. Sullivan. 1996, 3p.
Pub. in Institute of Electrical and Electronics Engineers Computational Science and Engineering, v3 n1 p13-15 Spring 96.

Keywords: *Parallel processing, *Searching, *Monte Carlo method, *Data structures, Trees(Mathematics), Data processing, Data storage, Data management, Structured programming, Computer systems performance, Run time(Computers), Simulation, Reprints.

Suppose that you need to maintain a large list of data that is to be searched and modified frequently in the course of a computation. Although there are several elegant ways to do this, the authors present one, a simple tree that doesn't require a lot of thinking to implement. It can speed up execution tremendously because instead of searching through a list item after item for each update, possibly examining 'n' items per operation.

01,771
PB96-180187 Not available NTIS
National Inst. of Standards and Technology (CSL), Gaithersburg, MD. Information Systems Architecture Div.
Application of Metadata Standards.
Final rept.
J. Newton. 1996, 14p.
Pub. in Institute of Electrical and Electronics Engineers Metadata Conference Proceedings (1st), Silver Spring, MD., April 16-18, 1996, p1-14.

Keywords: *Standards, Data transfer(Computers), Data management, Interoperability, Formats, Data bases, Standardization, Specifications, Procedures, Reprints, *Metadata, *Data elements, Attributes.

Application of metadata standards in the development of data elements assures a consistent, sharable set of data described and named in a predictable way. National and international efforts are underway to produce this metadata standardization. Classification of the components of data elements into a taxonomic structure facilitates the selection of appropriate components for particular elements. In this way, sets of complete and discrete data elements can be developed in to coherent descriptions of subject areas. A set of standardized attributes, some with sample values, prescribe the base set of information to be recorded about each data element. Finally, procedures for registration of standard data elements provide a facility for sharing the benefits of standardization among organizations.

01,772
PB96-183140 PC A04/MF A01
National Inst. of Standards and Technology (CSL), Gaithersburg, MD. Information Systems Architecture Div.
Interoperability Experiments with CORBA and Persistent Object Base Systems.
E. Fong, and D. Yang. Apr 96, 38p, NISTIR-5824.
See also PB95-220588.

Keywords: *Software engineering, *Object database management, *Computer programming, Distributed data processing, Models, Standards, Operating systems(Computers), Software tools, *POB(Persistent Object Based Systems), *Platform interoperability, Persistent Object Based Systems, CORBA(Common Object Request Broker Architecture), Common Object Request Broker Architecture.

This report describes the design and development of interoperability experiments using the common Object Request Broker Architecture (CORBA) products. The experiments will focus on establishing practical experiences for how to do 'plug and play' using CORBA products with Persistent Object Base (POB) systems such as Texas instruments' Open OODB and commercially available object database systems (ODBMS) such as MATISSE. The experiments will also investigate methodologies for integration of new or legacy distributed applications through the CORBA middleware infrastructure.

01,773
PB96-188164 PC A06/MF A01
National Inst. of Standards and Technology (CSL), Gaithersburg, MD. Information Systems Architecture Div.
Reference Information for the Software Verification and Validation Process.
Special pub.
D. R. Wallace, L. M. Ippolito, and B. B. Cuthill. Apr 96, 96p, NIST/SP-500-234.
Also available from Supt. of Docs. as SN003-003-03410-0.

Keywords: *Computer program verification, *Software engineering, *Computer program management, Standards, Guidelines, Computer software maintenance, Knowledge based systems, Performance evaluation, Tests, Health care, Software validation.

Computing systems may be employed in the health care environment in efforts to increase reliability of care and reduce costs. Software verification and validation (V&V) is an aid in determining that the software requirements are implemented correctly and com-

pletely and are traceable to system requirements. It helps to ensure that those system functions controlled by software are secure, reliable, and maintainable. Software V&V is conducted throughout the planning, development and maintenance of software systems, including knowledge-based systems, and may assist in assuring appropriate reuse of software.

01,774
PB96-190053 Not available NTIS
National Inst. of Standards and Technology (MEL), Gaithersburg, MD. Manufacturing Systems Integration Div.
Dynamic Objects and Meta-Level Programming of an EXPRESS Language Environment.
Final rept.
P. Denno. 1996, 6p.
Pub. in Dynamic Objects Workshop, Object World, 1996, p1-6.

Keywords: *Programming languages, LISP programming languages, Object programs, Reprints, *EXPRESS language environment.

This paper describes design and programming techniques employed in the development of a language environment for the EXPRESS information modeling language. A fundamental concern in the development of language environments for object flavored languages is the degree to which the object model of the implementation language matches that of the language being modeled. This paper describes how object model mismatch was eliminated and a responsive, incremental EXPRESS language environment is being developed using the Common Lisp Object System (CLOS) metaobject protocol (MOP) and dynamic object techniques.

01,775
PB96-193636 PC A03/MF A01
National Inst. of Standards and Technology (CAML), Gaithersburg, MD. Applied and Computational Mathematics Div.
SparseLib++ v. 1.5 Sparse Matrix Class Library. Reference Guide.
R. Pozo, K. A. Remington, and A. Lumsdaine. Jun 96, 25p, NISTIR-5861.
Prepared in cooperation with Notre Dame Univ., IN.

Keywords: *Linear systems, *Matrices(Mathematics), Algebra, Distributed data processing, Array processors, Parallel processing, Computer architecture, Object oriented programming, Computer codes, Subroutine libraries, Data storage systems, Computatuion, Iterations, Sparse matrix, SparseLib plus plus, C plus plus programming language, Kernel functions.

SparseLib++ is a C++ class library for efficient sparse matrix computations across various computational platforms. The software package consists of matrix objects representing several sparse storage format currently in use (in the release: compressed row, compressed column and coordinate formats), providing basic functionality for managing sparse matrices, together with efficient kernel mathematical operations (e.g. sparse matrix-vector multiply). The Sparse BLAS Toolkit(1) is used to enhance portability and performance across a wide range of computer architectures. Included in the package are various preconditioners commonly used in iterative solvers for linear systems of equations. The focus here is on computational support for iterative methods (see IML++(5)), but the sparse matrix objects presented here can be used in their own right.

01,776
PB96-195219 PC A04/MF A01
National Inst. of Standards and Technology (CAML), Gaithersburg, MD. Applied and Computational Mathematics Div.
IML++ v.1.2 Iterative Methods Library Reference Guide.
J. Dongarra, A. Lumsdaine, R. Pozo, and K. A. Remington. Jun 96, 43p, NISTIR-5860.
Prepared in cooperation with Notre Dame Univ., IN. and Oak Ridge National Lab., TN.

Keywords: *Algorithms, *Computer program documentation, Iterative methods, Object oriented computing, Linear algebra, Matrices(Mathematics), Vector fields.

The Iterative Methods Library, IML++, is a collection of algorithms implemented in C++ for solving both symmetric and nonsymmetric linear systems of equations by using iterative techniques. The goal of the package is to provide working code which separates the numerical algorithm from the details of the matrix/vector implementation. The separation allows the same algorithm to be used without modification, regardless of the specific data representation.

01,777
PB96-195326 PC A03/MF A01
National Inst. of Standards and Technology (CAML), Gaithersburg, MD. Applied and Computational Mathematics Div.
MV++ v. 1.5a Matrix/Vector Class Reference Guide.
R. Pozo. 27 Jun 96, 18p, NISTIR-5859.
See also DE95017458.

Keywords: *Matrix algebra, *Vector fields, *User guide, Algorithms, Compute program documentation, MV++ v 1.5a computer program.

MV++ is a small, efficient set of concrete vector and matrix classes specifically designed for high performance numerical computing. The MV++ package includes interfaces to the computational kernels found in the Basic Linear Algebra Subprograms (BLAS), such as scalar updates, vector sums, and dot products. The idea behind MV++ is to leverage vendor-supplied or optimized BLAS routines that are fine-tuned for particular plantforms. The various MV++ classes form the building blocks of larger user-level libraries such as SparseLib++(2) and LAPACK++(1). The MV++ library was built to supply simple, concrete, numerical vector and column oriented dense matrix classes.

01,778
PB96-200977 Not available NTIS
National Inst. of Standards and Technology (CAML), Gaithersburg, MD. Applied and Computational Mathematics Div.
Software Needs in Special Functions.
Final rept.
D. W. Lozier. 1995, 17p.
See also PB95-105045.
Pub. in Jnl. of Computational and Applied Mathematics 66, p344-360 Jun 96.

Keywords: *Special functions(Mathematics), *Computer software, *Faults, *Error analysis, Computer programming, Computations, Algorithms, Diagnosis, User needs, User requirements, Reprints, Functional testing.

Currently available software for special functions exhibits gaps and defects in comparison to the needs of modern high-performance scientific computing and also, surprisingly, in comparison to what could be constructed from current algorithms. In the paper we expose some of these deficiencies and identify the related need for user-oriented testing software.

01,779
PB96-201009 Not available NTIS
National Inst. of Standards and Technology (NCSL), Gaithersburg, MD. Systems and Network Architecture Div.
Experimental Evaluation of Specification Techniques for Improving Functional Testing.
Final rept.
K. L. Mills. 1996, 13p.
Pub. in Jnl. of Software and Systems Engineering, n32 p83-95 Jan 96.

Keywords: *Computer programming, *Specifications, *Man-computer interface, Computer software, Natural language(Computers), Performance tests, Graphical user interface, Real time, Reprints, *Functional testing, Structured analysis, Program execution.

The article reports results from one experiment to compare the effectiveness of functional testing given three different sets of software specifications. Three groups of experienced programmers independently developed functional test cases for the same automated cruise control software. One group worked solely from a natural language description, one was given a graphical real-time structured analysis (RTSA) specification to augment the natural langauge description, and a third was given, in addition to the English language description and the RTSA specification, an executable specification. Two measures of performance were evaluated: the degree of statement coverage achieved by the test cases created by each group, and the amount of time taken to create the test cases. No significant difference in performance was found among any of the groups for either of the measures.

01,780
PB97-112502 Not available NTIS
National Inst. of Standards and Technology (CSL), Gaithersburg, MD. Advanced Network Technologies Div.
Knowledge-Based Approach for Automating a Design Method for Concurrent and Real-Time Systems.
Final rept.
K. L. Mills, and H. Gomaa. 1996, 8p.
Pub. in International Conference on Software Engineering and Knowledge Engineering, SEKE '96 (8th), Lake Tahoe, NV., June 10-12, 1996, p529-536.

Keywords: *Concurrent engineering, *Real time operation, *Computer-aided design, Knowledge bases(Artificial intelligence), Design analysis, Software engineering, Automation, Software tools, Specifications, Semantics, Reprints.

The paper describes a knowledge-based approach to automate CODARTS, a software design method for concurrent and real-time systems. The approach uses multiple paradigms to represent knowledge embedded within CODARTS. Semantic data modeling provides the means to model specifications and related designs. Production rules form the basis for modeling a set of heuristics that can generate concurrent designs based upon semantic concepts from the specification and design meta-models. Together, the semantic data models and production rules, encoded using an expert-system shell, compose CODA, an automated designer's assistant.

01,781
PB97-113138 Not available NTIS
National Inst. of Standards and Technology (CSL), Gaithersburg, MD. Information Systems Architecture Div.
Measurement of Process Complexity.
Final rept.
R. Tesoriero, and M. V. Zelkowitz. 1996, 12p.
Pub. in Proceedings of the European Control and Metrics Conference (7th), Wilmslow, United Kingdom, May 15-17, 1996, p304-315.

Keywords: *Software engineering, *Technology transfer, *Complexity, Computer program reliability, Computer programming, Design analysis, Scheduling, Specifications, Measurement, Requirements, Reprints, Process models.

The ability to quantitatively assess a given project has meant one of two different approaches: (1) a study of the complexity of the software being produced, (2) or a study of the process being used to develop that software. In the apper, the authors try to indicate that neither approach is sufficient. They are developing a model that evolved from an earlier study on software engineering technology transfer. In it, the authors look at the evolving nature of the software development to develop a process model that keeps up with these changes. The paper presents an initial overview of the process model.

01,782
PB97-113799 PC A03/MF A01
National Inst. of Standards and Technology (MEL), Gaithersburg, MD. Manufacturing Systems Integration Div.
Representation of Axes for Geometric Fitting.
T. H. Hopp. Sep 96, 18p, NISTIR-5897.

Keywords: *Dimensional measurement, *Algorithms, Metrology, Geometry, Estimates, *Geometric fitting software, Coordinates measuring systems.

The authors review methods for representing geometric axes in three dimensions and discuss why these methods have undesirable properties for geometric fitting applications. The authors then describe a new representation that seems better suited for use in problems of fitting geometric elements to data points. This representation was developed in the course of the authors' work on testing of data analysis software in coordinate measurement systems. The new representation has allowed us to lower significantly the estimated uncertainty of the authors' test results. Details and properties of the representation are discussed.

01,783
PB97-113906 PC A04/MF A01
National Inst. of Standards and Technology (CSL), Gaithersburg, MD.
Experimental Models for Software Diagnosis.
M. V. Zelkowitz, and D. R. Wallace. Aug 96, 39p, NISTIR-5889.
Prepared in cooperation with Maryland Univ., College Park. Dept. of Computer Science.

Computer Software

Keywords: *Software engineering, *Information systems, *Computer program validation, Computer systems design, Distributed data processing, Data collection, Experimental data, Models.

Experimentation and data collection are becoming accepted practices within the software engineering community to determine the effectiveness of various software development practices. However, there is wide disagreement as to exactly what the term 'experimentation' means in this domain. It is important that we be able to understand this concept and identify how we can best collect data needed to validate software methods that seem to be effective. This understanding will provide a basis for improved technical exchange of information between scientists and engineers within the software community.

01,784
PB97-114169 PC A07/MF A02
National Inst. of Standards and Technology (CSL), Gaithersburg, MD. Software Diagnostics and Conformance Testing Div.
Structured Testing: A Testing Methodology Using the Cyclomatic Complexity Metric.
Special pub.
D. R. Wallace, A. H. Watson, and T. J. McCabe. Aug 96, 124p, NIST/SP-500/235.
Portions of this document are not fully legible. Also available from Supt. of Docs. as SN003-003-03426-6.

Keywords: *Computer programs, *Test methods, Integration, Object oriented programs, Life cycles, Quality assurance, Measurement, Software engineering, Cyclomatic complexity.

The purpose of this document is to describe the structured testing methodology for software testing, also known as basis path testing. Based on the cyclomatic measure of McCabe, structured testing uses the control flow structure of software to establish path coverage criteria. The resultant test sets provide more through testing than statement and branch coverage. Extensions of the fundamental structured testing techniques for integration testing and object-oriented systems are also presented. Several related software complexity metrics are described. Summaries of technical papers, case studies, and empirical results are presented in the appendices.

01,785
PB97-119044 Not available NTIS
National Inst. of Standards and Technology (CAML), Gaithersburg, MD. Applied and Computational Mathematics Div.
Making Connections.
Final rept.
I. Beichl, and F. Sullivan. 1996, 4p.
Pub. in Institute of Electrical and Electronics Engineers Computational Science and Engineering, v3 n3 p9-12 Fall 96.

Keywords: *Data structures, *Connection machine, *Parallel processing, Algorithms, Sequences(Mathematics), Computations, Computational geometry, Reprints, Depth first search.

The paper is part of a series of expository articles on scientific computing with non-numeric methods. The depth first search method of graph traversal is used to find connectivity information.

01,786
PB97-121636 PC A99/MF E08
National Inst. of Standards and Technology (CSL), Gaithersburg, MD. Information Access and User Interface Div.
Text REtrieval Conference (4th) (TREC-4). Held in Gaithersburg, Maryland on November 1-3, 1995.
Special pub.
D. K. Harman. Oct 96, 776p, NIST/SP-500-236.
Also available from Supt. of Docs. as SN003-003-03430-4.

Keywords: *Meetings, *Information retrieval, *Text processing, Thesauri, Automation, Natural language processing, Pattern recognition, Routing, Probability theory, Documents, Search structuring, Knowledge bases(Artificial intellegience), Vector processing, Semantics, Evaluation.

This report constitutes the proceedings of the fourth Text REtrival Conference (TREC-4) held in Gaithersburg, Maryland, November 1-3, 1995. The conference was co-sponsored by the National Institute of Standards and Technology (NIST) and the Defense Advanced Research Agency (DARPA), and was attached by 140 people involved in the 36 participating groups. The goal of the conference was to bring research groups together to discuss their work on a large test collection. There was a wide variation of retrieval techniques reported on, including methods using automatic thesaurii, sophisticated term weighting, natural language techniques, relevance feedback, and advanced pattern matching. As results had been run through a common evaluation package, groups were able to compare the effectiveness of different techniques, and discuss how differences between the systems affected performance. In addition to the main evaluation, 5 more focussed evaluations, called 'tracks' were run. The conference included paper sessions and discussion groups. This proceeding includes papers from most of the participants (several poster groups did not submit papers), tables of the system results, and brief system descriptions including timing and storage information.

01,787
PB97-122303 Not available NTIS
National Inst. of Standards and Technology (CSL), Gaithersburg, MD. Information Systems Architecture Div.
CSL View of Applications Portability, Scalability, and Interoperability.
Final rept.
G. E. Fisher. 1996, 1p.
Pub. in ACM StandardView, v4 n2 p1 Jun 96.

Keywords: *Computer program portability, *Interoperability, *Software engineering, Distributed processing, Computer program transferability, Applications programs(Computers), Integrated systems, Computer networks, Standardization, Specifications, Standards, Recommendations, Reprints, Application Portability Profile, Scalability, US NIS, Computer Systems Laboratory.

The document presents an overview summary of the Computer Systems Laboratory position on portability, scalability, and interoperability in the computer software arena.

Control Systems & Control Theory

01,788
PB95-107108 Not available NTIS
National Inst. of Standards and Technology (NEL), Gaithersburg, MD. Robot Systems Div.
Three Dimensional Position Determination from Motion.
Final rept.
M. Nashman, and K. Chaconas. 1991, 10p.
Pub. in Proceedings of Society of Photo-Optical Instrumentation Engineers - Sensor Fusion III: 3-D Perception and Recognition, Boston, MA., November 5-8, 1990, v1383 p166-175 1991.

Keywords: *Manipulators, *Control systems, *Position finding, *Motion, Algorithms, Image processing, Three dimensional motion, Real time, Sensory feedback, Trajectory planning, Reprints.

The analysis of sequences of images over time provides a means of extracting meaningful information which is used to compute and track the three-dimensional position of a moving object. This paper describes an application in which sensory feedback based on time-varying camera images is used to provide position information to a manipulator control system. The system operates in a real-time environment and provides updated information at a rate which permits intelligent trajectory planning by the control system.

01,789
PB95-143137 PC A03/MF A01
National Inst. of Standards and Technology (MEL), Gaithersburg, MD. Robot Systems Div.
Reference Model Architecture for Intelligent Systems Design.
J. S. Albus. Sep 94, 48p, NISTIR-5502.

Keywords: *Control systems design, *Real time systems, *Artificial intelligence, Autonomy, Self adaptive control systems, Hierarchies, Task planning(Robotics), Canonical forms, Data bases, Robots, Manufacturing, Workstations, Models, RCS(Real-time Control System).

A reference model architecture based on the Real-time Control System (RCS) is proposed for real-time intelligent control systems. RCS partitions the control problem into four basic elements: behavior generation (or task decomposition), world modeling, sensory processing, and value judgment. It clusters these elements into computational nodes that have responsibility for specific subsystems, and arranges these nodes in hierarchical layers such that each layer has characteristic functionality and timing. The RCS reference model architecture has a systematic regularity, and recursive structure that suggests a canonical form. Control systems based on the RCS have been built for a number of applications. Examples of a control system architecture and a world model database for an intelligent robot in a manufacturing work-station are described. Each level of the control architecture performs real-time planning and sensory interactive execution. Each level of the world model knowledge database contains state variables, system parameters, entity frames, and maps.

01,790
PB95-198859 PC A03/MF A01
National Inst. of Standards and Technology (MEL), Gaithersburg, MD. Factory Automation Systems Div.
Expert Control System Shell Version 1.0 User's Guide.
S. A. Osella. Feb 95, 44p, NISTIR-5601.

Keywords: *Control systems design, *Expert systems, *Software tools, Prototypes, Systems engineering, Real time systems, Controllers, Graphical user interface, Control equipment, Software engineering, User manuals(Computer programs).

The Expert Control System Shell (ECSS) is a software tool for rapidly prototyping and deploying control systems of arbitrary complexity. With the ECSS, a control system designer creates a controller which consists of a graphical user interface (called the operator front panel) and, optionally, a collection of expert system rule-based programs. A controller can be operated in manual mode where an operator interacts directly with the system to be controlled without using the expert system, in automatic mode where the expert system is used to perform most, if not all, system interactions, or in a combination of the two modes. The User's Guide is discussed in the following order: (1) a tutorial on how to create a controller, (2) creating controllers, (3) creating and importing device interface functions, (4) creating rule-based programs, (5) importing expert system functions, and (6) operating controllers.

Information Processing Standards

01,791
DE94015308 PC A03/MF A01
National Inst. of Standards and Technology, Gaithersburg, MD.
NIST Cooperative Laboratory for OSI Routing Technology.
D. Montgomery. 23 May 94, 40p, DOE/ER/25114-1.
Contract AI05-92ER25114, Grant NCR-9120054
Sponsored by Department of Energy, Washington, DC.

Keywords: *Computer Networks, *Equipment Interfaces, *Standards, Data Transmission, Information Dissemination, On-Line Systems, Performance Testing, EDB/990300.

This document is one of two reports on the Integrated ISIS protocol. Required by the IAB/IESG in order for an Internet routing protocol to advance to Draft Standard Status. Integrated ISIS is an Interior Gateway Protocol and is designed to carry both IP and ISO CLNP routing information. Integrated ISIS is currently designated as a Proposed Standard. The protocol was first published in RFC 1195. Internet Draft was published subsequently to RFC 1195 and documents the current version of the protocol. This report documents experience with Integrated ISIS. This includes reports on interoperability testing, field experience and the current state of Integrated ISIS implementations. It also presents a summary of the Integrated ISIS Management Information Base (MIB), and a summary of the Integrated ISIS authentication mechanism.

01,792
FIPS PUB 120-1C PC A06/MF A02
National Inst. of Standards and Technology (CSL), Gaithersburg, MD.

Graphical Kernel System (GKS). Category: Software Standard. Subcategory: Graphics. International Standard: Information Technology; Computer Graphics; Graphical Kernel System (GKS) Language Bindings. Part 4: C.
8 Jan 91, 113p.
Also available from Supt. of Docs. Also pub. as American National Standards Inst., New York rept. no. ISO/IEC-8651-4.1991E. Supersedes FIPS PUB 120. Prepared in cooperation with American National Standards Inst., New York.

Keywords: *Federal information processing standards, *Computer graphics, *Computer software, Applications programs(Computers), Computer program portability, GKS(Graphical Kernel System), ANSI(American National Standard Institute), ISO(International Organization for Standardization), C programming language.

This revision supersedes Federal Information Processing Standard (FIPS) PUB 120 and modifies the standard by adding a requirement for validation of GKS implementations that are acquired by Federal agencies. FIPS 120-1 adopts American National Standard Graphical Kernel System (ANS GKS), ANSI X3.124-1985, Functional Description, which consists of four parts (X3.124.1-1985 FORTRAN Binding, X3.124.2-1988 Pascal Binding, X3.124.3-1989 Ada Binding), as a FIPS.ANS GKS specifies a library (or toolbox package) of subroutines for an application programmer to incorporate within a program in order to produce and manipulate two-dimensional pictures. The purpose of the standard is to promote portability of graphics application programs between different installations. The standard is for use by implementors as the reference authority in developing graphics software systems; and by other computer professionals who need to know the precise syntactic and semantic rules of the standard.

01,793
FIPS PUB 158-1 PC E01
National Inst. of Standards and Technology (NCSL), Gaithersburg, MD.
User Interface Component of the Applications Portability Profile Category: Software Standard; Subcategory: Application Program Interface.
Federal information processing standards.
c8 Oct 93, 5p.
Supersedes FIPS PUB 158. Also available from Supt. of Docs.
Three ring binder also available. North American Continent price $7.00; all other write for quote.

Keywords: *Standards, *Windowing, Interfaces, Computer graphics, *Federal information processing standards, *Man computer interface, *Application programs(Computers), *Software engineering, Portable Operating System Interface (POSIX), Computer program portability, Application program interface, Open systems interconnections.

This publication announces the adoption of the X Protocol, Xlib Interface, Xt Intrinsics and Bitmap Distribution Format specifications of the X Window System, Version 11, Release 5 (X Window System is a trademark of the Massachusetts Institute of Technology (MIT) as a Federal Information Processing Standard). This FIPS is identical to FIPS PUB 158, except that the specification is updated from Release 3 to Release 5 of the X Window System, Version 11. The standard is for use by computing professionals involved in system and application software development and implementation. The standard is part of a series of specifications needed for application portability. The standard covers the Data Stream Encoding, Data Stream Interface, and Subroutine Foundation layers of the reference model. It is the intention of NIST to provide standards for other layers of the reference model as consensus develops within industry. This standard addresses the user interface functional area of the Applications Portability Profile (NIST SP 500-87).

01,794
FIPS PUB 173-1 PC A04/MF A01
National Inst. of Standards and Technology (CSL), Gaithersburg, MD.
Spatial Data Transfer Standard (SDTS): Category: Software Standard; Subcategory: Information Interchange.
10 Jun 94, 51p.
Supersedes FIPS PUB 173.

Keywords: *Data transfer(Computers), *Federal information processing standards, Digital data, Mapping, Data structures, Geographic information systems, Topology, Specifications, Requirements, Data dictionaries, TVP(Topological Vector Profile).

This standard provides specifications (developed through the U.S. Department of the Interior (DOI), United States Geological Survey (USGS), National Mapping Division) for the organization and structure of digital spatial data transfer, definition of spatial features and attributes, and data transfer encoding. The purpose of the standard is to promote and facilitate the transfer of digital spatial data between dissimilar computer systems. This revision adds Part 4, Topological Vector Profile (TVP), to the specifications adopted by the Spatial Data Transfer Standard (SDTS) and makes minor changes and clarifications to the Parts 1 and 3 of the SDTS.

01,795
FIPS PUB 173-1A PC$44.50
National Inst. of Standards and Technology (CSL), Gaithersburg, MD.
Spatial Data Transfer Standard (SDTS). Category: Software Standard; Subcategory: Information Interchange. (FIPS PUB 173-1A).
10 Jun 94, 348p.
Supersedes FIPS PUB 173.
Three ring vinyl binder also available; North American Continent price $7.00; all other write for quote.

Keywords: *Data transfer(Computers), *Federal information processing standards, *Position(Location), Mapping, Data structures, Format, Data integrity, Geographic information systems, Topology, Rasters.

This standard provides specifications (developed through the Department of the Interior) for the organization and structure of digital spatial data transfer, definition of spatial features and attributes, and data transfer encoding. The purpose of the standard is to promote and facilitate the transfer of digital spatial data between dissimilar computer systems.

01,796
FIPS PUB 173-1B PC E99
National Inst. of Standards and Technology (CSL), Gaithersburg, MD.
Spatial Data Transfer Standard (SDTS). Category: Software Standard; Subcategory: Information Interchange. (FIPS PUB 173-1B).
10 Jun 94, 54p.
Supersedes FIPS PUB 173.
Three ring vinyl binder also available; North American Continent price $7.00; all other write for quote.

Keywords: *Data transfer(Computers), *Federal information processing standards, *Position(Location), Mapping, Data structures, Format, Data integrity, Geographic information systems, Topology, Rasters.

This standard provides specifications (developed through the Department of the Interior) for the organization and structure of digital spatial data transfer, definition of spatial features and attributes, and data transfer encoding. The purpose of the standard is to promote and facilitate the transfer of digital spatial data between dissimilar computer systems.

01,797
FIPS PUB 189 PC A03/MF A01
National Inst. of Standards and Technology (CSL), Gaithersburg, MD.
Portable Operating System Interface (POSIX). Part 2. Shell and Utilities. Category: Software Standard; Subcategory: Operating Systems.
11 Oct 94, 12p.
Also available from Supt. of Docs.
Three ring vinyl binder also available; North American Continent price $7.00; all others write for quote.

Keywords: *Federal information processing standards, *Operating systems(Computers), Data processing, Application programs(Computers), Computer program portability, Utility routines, Computer software, Software engineering, Specifications, Open systems.

This publication announces the adoption of International Standard ISO/IEC 9945-2:1993, Information Technology--Portable Operating System Interface (POSIX)--Part 2: Shell and Utilities as a Federal Information Processing Standard (FIPS). ISO/IEC 9945-2:1993 defines a command language interpreter (shell) and a set of utility programs. This standard is for use by computing professionals involved in system and application software development and implementation and is part of a series of specifications needed for application portability. This standard addresses the Applications Portability Profile functional area that deals with methods by which a person interacts with the operating system.

01,798
FIPS PUB 190 PC A04/MF A01
National Inst. of Standards and Technology (CSL), Gaithersburg, MD.
Guideline for the Use of Advanced Authentication Technology Alternatives. Category: Computer Security. Subcategory: Access Control.
Final rept.
J. F. Dray. 28 Sep 94, 66p.
Also available from Supt. of Docs.
Three ring vinyl binder also available; North American Continent price $7.00; all others write for quote.

Keywords: *Computer security, *Authentication, *Federal information processing standards; Cryptography, Telecommunication, Data processing security, Data encryption, Biometrics, Access control, Passwords.

This Guideline describes the primary alternative methods for verifying the identities of computer system users, and provides recommendations to Federal agencies and departments for the acquisition and use of technology which supports these methods. Although the traditional approach to authentication relies primarily on passwords, it is clear that password-only authentication often fails to provide an adequate level of protection. Stronger authentication techniques become increasingly more important as information processing evolves toward an open systems environment. Modern technology has produced authentication tokens and biometric devices which are reliable, practical, and cost-effective. Passwords, tokens, and biometrics can be used in various combinations to provide far greater assurance in the authentication process than can be attained with password alone.

01,799
FIPS PUB 191 PC A04/MF A01
National Inst. of Standards and Technology (CSL), Gaithersburg, MD.
Guideline for the Analysis of Local Area Network Security. Category: Computer Security; Subcategory: Risk Analysis and Contingency Planning.
Final rept.
L. J. Carnahan. 9 Nov 94, 62p.
Also available from Supt. of Docs.
Three ring vinyl binder also available; North American Continent price $7.00; all others write for quote.

Keywords: *Local area networks, *Computer security, *Federal information processing standards, Risk assessment, Vulnerability, Distributed computer systems, Data processing security, Protocols, Message processing, Access control, Authentication, Data integrity, Personal computers, Training.

Local area networks (LANs) that are used to store, process or transmit sensitive information must provide appropriate protection to prevent undesirable events such as compromise of information or denial of service. This document can be used as a tool to help improve the security of a local area network. A LAN security architecture is described that discusses threats and vulnerabilities that should be examined, as well as security services and mechanisms that should be explored. A five step process is defined that helps the reader to determine LAN assets, environment-specific threats and vulnerabilities, the risk of those threats to the LAN, and possible security services and mechanisms that can be used to help reduce the risk to the LAN. A discussion concerning LAN security policy, contingency planning, and training issues is also included.

01,800
FIPS PUB 192 PC A03/MF A01
National Inst. of Standards and Technology (CSL), Gaithersburg, MD.
Application Profile for the Government Information Locator Service (GILS). Category: Software Standard; Subcategory: Information Interchange.
7 Dec 94, 34p.
Three ring vinyl binder also available; North American Continent price $7.00; all others write for quote.

Keywords: *Federal information processing standards, Information retrieval, Government, Specifications, Information systems, Internets, Protocols, Records, Services, *GILS(Government Information Locator Service), *Government Information Locator Service.

This standard describes an application profile for the Government Information Locator Service (GILS). This

application profile is based primarily on the American National Standard for Information Retrieval Application Service Definition and Protocol Specification for Open Systems Interconnection (ANSI/NISO Z39.50-1992), developed by the National Information Standards Organization (NISO). The Government Information Locator Service (GILS) is a decentralized collection of servers and associated information services that will be used by the public either directly or through intermediaries to find public information throughout the Federal government.

01,801
FIPS PUB 193 PC A04/MF A01
National Inst. of Standards and Technology (CSL), Gaithersburg, MD.
SQL Environments. Category: Software Standard; Subcategory: Database.
3 Feb 95, 72p.
Also available from Supt. of Docs.
Three ring vinyl binder also available; North American Continent price $7.00; all others write for quote.

Keywords: *Federal information processing standards, *Programming environments, *Data processing, Data bases, Multimedia, Integrated systems, Tests, Procurement, Specifications, *SQL(Structured Query Language), *Structured Query Language, Internet, ERI(External repository interface), CLI(Call Level Interface).

AN SQL environment is an integrated data processing environment in which heterogeneous products, all supporting some aspect of the FIPS SQL standard (FIPS PUB 127), are able to communicate with one another and provide shared access to data and data operations and methods under appropriate security, integrity, and access control mechanisms. This Federal Information Processing Standards Publication (FIPS PUB) is the beginning of a continuing effort to define appropriate conformance profiles that can be used by both vendors and users to specify exact requirements for how various products fit into an SQL environment. The emphasis in this first publication is to specify general purpose, SQL external repository interface (SQL/ERI) server profiles for non-SQL data repositories. Two major SQL/ERI Server Profiles are specified: read-only and read-write. To make it easier to specify integration among heterogeneous, non-SQL data models, this specification defines a new minimal level of the SQL language that can be supported by various non-SQL implementations.

01,802
FIPS PUB 195 PC E18
National Inst. of Standards and Technology (CSL), Gaithersburg, MD.
Federal Building Grounding and Bonding Requirements for Telecommunications. Category: Telecommunications Standard; Subcategory: Grounding and Bonding.
15 Aug 95, 46p.
Also pub. as Telecommunications Industry Association, Washington, DC. Standards and Technology Dept. rept. no. ANSI/TIA/EIA-607-1994. Prepared in cooperation with Telecommunications Industry Association, Washington, DC. Standards and Technology Dept.
Three ring vinyl binder also available; North American Continent price $7.00, all others write for quote.

Keywords: *Telecommunication, *Public buildings, Communication cables, Electrical grounding, Wires, Communication equipment, National government, Passageways, Electrical circuits, Safety engineering, Fire prevention, *Federal information processing standards.

This standard, by adoption of ANSI/TIA/EIA-607-1994, Commercial Building Grounding and Bonding Requirements for Telecommunications, specifies the requirements for a uniform telecommunications grounding and bonding infrastructure for Federal buildings where telecommunications equipment is installed. The standard provides the requirements for a ground reference for telecommunications systems within the telecommunications entrance facility, the telecommunications closet, and equipment room; it also provides the requirements for bonding and connecting pathways, cable shields, conductors, and hardware at telecommunications closets, equipment rooms, and entrance facilities. The grounding and bonding approach described in this standard is consistent with the cabling topology specified in FIPS PUB 174, Federal Building Telecommunications Wiring Standard (ANSI/EIA/TIA-568-1991), and installed in accordance with FIPS PUB 175, Federal Building Standard for Telecommunications Pathways and Spaces (ANSI/EIA/TIA-569-1990).

01,803
PB94-142536 PC A07/MF A02
National Inst. of Standards and Technology (CSL), Gaithersburg, MD.
Report on Application Integration Architectures (AIA) Workshop. Held in Dallas, Texas on February 8-12, 1993.
R. Hodges, C. Thompson, and E. Fong. Jan 94, 138p, NISTIR-5326.
Also available from Supt. of Docs. Prepared in cooperation with Texas Instruments, Inc., Dallas.

Keywords: *Meetings, *Standards, Interoperability, Computer software, Information management, *IT(Information technology), *Information technology, Open systems.

This report provides a proceedings of the workshop on Application Integration Architectures (AIA) held on February 8-12, 1993, in Dallas, Texas. The workshop addressed various means of coordinating and improving information technology (IT) standards to achieve open systems interoperability. The purpose of this workshop was to provide a forum where individuals active in one or more standards efforts or industrial consortia in the information technologies software area could meet to discuss how their efforts relate and work to formulate a roadmap to insure convergence of de jure or de facto standards in software information technology.

01,804
PB94-161809 PC A03/MF A01
National Inst. of Standards and Technology (CSL), Gaithersburg, MD. Information Systems Engineering Div.
Computer Graphics Metafile (CGM): Procedures for NIST CGM Validation Test Service.
L. S. Rosenthal, and J. A. Schneider. Feb 94, 29p, NISTIR-5372.
See also FIPS PUB 128-1E and PB93-198273.

Keywords: *Computer graphics, *Standards, Federal information processing standards, Conformity, Tests, Verifying, Interpreters, *Computer Graphics Metafile, *CALS, Continuous Acquisition and Life-Cycle Support, Computer-aided Acquisition and Logistics Support, Application Protocols, National Institute of Standards and Technology.

This document provides general procedures for the National Institute of Standards and Technology's (NIST) Computer Graphics Metafile (CGM) Validation Test Service. The NIST CGM Validation Test Service provides a way of determining the degree to which an implementation conforms to the CGM standard (Federal Information Processing Standard 128-1, Computer Graphics Metafile, and the Continuous Acquisition and Life-Cycle Support Application Profile, MIL-D-28003A). The goal of the NIST Test Service is to maximize the probability of successful interchange of CGMs between conforming systems. The document is divided into three testing programs: metafile testing, generator testing, and interpreter testing. In order to take into account the differences among the three testing programs, many procedures have been tailored to the specific testing program. The policies and procedures presented in this document are organized into five sections: an introduction, general procedures, and specific procedures for each of the three testing programs.

01,805
PB94-163474 PC A06/MF A02
National Inst. of Standards and Technology (CSL), Gaithersburg, MD.
Compatibility Analysis of the ANSI and ISO IRDS Services Interfaces.
J. Berube, and A. Goldfine. Sep 92, 104p, NISTIR-4904.
See also PB88-163779.

Keywords: *Data management, *Dictionaries, *Standards, Compatibility, IRDS(Information Resource Dictionary System), ANSI(American National Standards Institute), ISO(International Organization for Standardization).

The primary purpose of the report is to compare: the ANSI IRDS standards (ANSI 1992), (IRDS 1988); and the ISO IRDS standards (FRAMEWORK 1990), (ISO 1992). The following are also part of the context of the report and will be surveyed: the IBM Repository Manager Interface (RM 1990); the ATIS IRDS proposal (ATIS 1990); and the PCTE standard (PCTE 1988). The principal objective of the report is to establish the level of compatibility and interoperability possible between an ANSI IRDS environment and an ISO IRDS environment. This is done by attempting to establish if these environments can be reconciled: in definition. That is, can they share data. in operation. That is, could a single product offer the two types of services.

01,806
PB94-207453 PC A07/MF A02
National Inst. of Standards and Technology (NCSL), Gaithersburg, MD. Systems and Network Architecture Div.
IGOSS-Industry/Government Open Systems Specification.
Special pub.
G. Mulvenna. May 94, 131p, NIST/SP-500/217.
Also available from Supt. of Docs as SN003-003-03269-7. See also FIPS PUB-107, FIPS PUB 100-1 and PB93-166809.

Keywords: *Computer networks, *Standards, Protocols, Government/industry relations, Computer architecture, File management systems, Message processing, Communication networks, *OSI(Open Systems Interconnection), *Open Systems Interconnection, GOSIP(Government Open Systems Interconnection Profile), IGOSS(Industry/Government Open Systems Specification).

The IGOSS is a standard reference to use when acquiring and operating computer networking products and services intended to conform to the Open Systems Interconnection (OSI) protocols. The IGOSS is jointly authored by the U.S. Government, the Canadian Government, Manufacturing Automation Protocol (MAP) group, the Technical and Office Protocol (TOP) group, and the electric power group. Each of these organizations has previously issued their own procurement profiles and are now consolidating their procurement requirements into a single domain.

01,807
PB94-211455 Not available NTIS
National Inst. of Standards and Technology (NCSL), Gaithersburg, MD. Systems and Network Architecture Div.
U.S. GOSIP Testing Program.
Final rept.
J. P. Favreau, K. L. Mills, and J. S. Nightingale. 1990, 5p.
Pub. in Proceedings of International Conference on the Applications of Standards for Open Systems (6th), Falls Church, VA., October 2-4, 1990, p125-129.

Keywords: *Tests, Protocols, Federal information processing standards, Federal agencies, Government procurement, Reprints, *GOSIP(Government Open Systems Interconnection Profile), *Government Open Systems Interconnection Profile, OSI(Open Systems Interconnection).

This paper discusses progress to date in the development and deployment of a Testing Policy for U.S. Government Open Systems Interconnection Profile (GOSIP) protocol implementations. The policy itself is fully discussed in the Federal Information Processing Standards (FIPS): 'GOSIP Conformance and Interoperation Testing and Registration.' Realization of the policy has included solicitation and assessment of abstract test suites, means of testing, conformance test laboratories and interoperability test suites and facilities. Public registers of all of these items are compiled and published so that Federal Agencies may make informed procurement decisions for GOSIP products.

01,808
PB94-216645 Not available NTIS
National Inst. of Standards and Technology (CSL), Gaithersburg, MD. Advanced Systems Div.
NIST-Coordinated Standard for Fingerprint Data Interchange.
Final rept.
R. M. McCabe. 1993, 5p.
Pub. in Jnl. of Forensic Identification 43, n4 p344-348 1993.

Keywords: *Data transfer(Computers), *Standards, Image processing, Data compression, Format, Quality assurance, Reprints, *US NIST, *Fingerprints, ANSI(American National Standards Institute).

This editorial is a clarification of the National Institute of Standards and Technology's (NIST's) role in the de-

velopment of the American National Standards Institute (ANSI) standard ANSI/NIST-CSL 1-1993 entitled 'Data Format for the Interchange of Fingerprint Information.' Several misrepresentations of the NIST role appeared in an editorial published in the May/June 1993 issue of the Journal of Forensic Identification.

01,809
PB94-219110 PC A06/MF A02
National Inst. of Standards and Technology (CSL), Gaithersburg, MD.
Industry/Government Open Systems Specification Testing Framework. Version 1.0.
J. P. Favreau. Jun 94, 124p, NISTIR-5438.
Supersedes PB92-110105.

Keywords: *Tests, Quality control, Data transmission, Data transfer(Computers), Protocols, Computer networks, Message processing, Commodities, Procurement, Government/industry relations, Standards, *IGOSS(Industry/Government Open Systems Specification), *Industry/Government Open Systems Specification, US NIST, OSI(Open Systems Interconnection).

The development of National Institute of Standards and Technology (NIST) Special Publication 500-217 which specifies the Industry/Government Open Systems Specification (IGOSS), resulted in the need to establish policy and procedures aimed at ensuring that the IGOSS Partners' data communications products adhere to the technical documents referenced by IGOSS and that they interoperate. The goal of this document is to aid an Industry/Government Acquisition Authority in procurement of IGOSS products by employing publicly accessible registers verifying supplier claims of conformance and documenting instances of interoperability of IGOSS CONFORMANT PRODUCTS. This document supersedes NISTIR 4594.

01,810
PB95-126207 Not available NTIS
National Inst. of Standards and Technology (NCSL), Gaithersburg, MD. Information Systems Engineering Div.
Information Resource Dictionary System (IRDS): A Status Report.
Final rept.
A. Goldfine. 1990, 2p.
Pub. in AFFIRMation 12, n8 p1-2 Oct 90.

Keywords: *Data dictionaries, *Standards, Federal information processing standards, Standardization, Information systems, Systems engineering, Reprints, *IRDS(Information Resource Dictionary System), *Information Resource Dictionary System, ANSI(American National Standards Institute).

This article discusses the status of the Information Resource Dictionary System (IRDS). It provides brief background information, reviews the current standardization situation, and discusses extensions to the IRDS that are under development.

01,811
PB95-171377 PC A03/MF A01
National Inst. of Standards and Technology (CSL), Gaithersburg, MD.
Perspective on Software Engineering Standards.
D. R. Wallace, and R. J. Martin. Dec 94, 12p, NISTIR-5546.
See also PB95-136610 and NUREG/CP-0136.

Keywords: *Software engineering, *Standards, Federal information processing standards, Computer software, Organizations, Industries, US NIST.

This paper provides information about the National Institute of Standards and Technology's (NIST) Federal Information Processing Standards (FIPS) and other standards organizations and presents a perspective on software engineering standards.

01,812
PB95-180840 Not available NTIS
National Inst. of Standards and Technology (CSL), Gaithersburg, MD.
Federal Government and Information Technology Standards: Building the National Information Infrastructure.
Final rept.
S. M. Radack. 1994, 13p.
Pub. in Government Information Quarterly 11, n4 p373-385 1994.

Keywords: *Standards, *Information processing, Government policies, National government, Federal information processing standards, Computers, Information systems, Telecommunication, Reprints, NII(National Information Infrastructure), NPR(National Performance Review), US NIST.

For many years, standards have been important considerations in the Federal government's policies for the use of information technology. The Computer Systems Laboratory (CSL) at the National Institute of Standards and Technology develops and issues technical standards that are used by the Federal government in its information technology systems. The new Federal initiative for the National Information Infrastructure (NII) and the National Performance Review (NPR) make information technology an agent for change and emphasize standards as a means for achieving connectivity of computer and telecommunications technologies and for easy access to information. The Federal government will be challenged to address the technical, organizational and policy issues that affect the development of the standards needed for future information systems.

01,813
PB96-111190 PC A03/MF A01
National Inst. of Standards and Technology (CSL), Gaithersburg, MD.
Federal Implementation Guideline for Electronic Data Interchange: ASC X12 003040 Transaction Set 838 Trading Partner Profile (Confirmation of Vendor Registration). Implementation Convention.
J. P. Favreau. Aug 95, 25p, NIST/SP-881/2.
Also available from Supt. of Docs. as SN003-003-03364-2. See also PB96-112651.

Keywords: *Computer programs, *Information exchange, *Logistics management, Procurement, Standards, Acquisition, Databases, Telecommunication, Businesses, Corporations, Purchasing, Vendors, Electronic Data Interchange ASC X12 003040 Transaction Set 838.

The ASC X12 003040 Transaction Set 838, Trading Partner Profile (Confirmation of Vendor Registration), Implementation Convention defines the Federal Government interpretation of the use of ASC X12 003040 standards. This implementation convention provides the information necessary for the user to be able to develop an interface program between the computer application and the ASC X12 translator.

01,814
PB96-114913 PC A11/MF A03
National Inst. of Standards and Technology (NCSL), Gaithersburg, MD. Systems and Network Architecture Div.
Federal Implementation Guideline for Electronic Data Interchange. ASC X12 003050 Transaction Set 850 Award Instrument. Implementation Convention.
Special pub.
J. P. Favreau. Aug 95, 228p, NIST/SP-881/3.
Also available from Supt. of Docs as SN003-003-03365-1. See also PB96-114921.

Keywords: *Information systems, *Standards, *Procurement, Commerce, Computer networks, Information exchange, Computer software, United States government, Contract administration, Data processing, *Electronic Data Interchange, *EDI(Electronic Data Interchange), Standard ASC 12 003050 Transaction Set 860, Draft standard.

The ASC X12 003050 Transaction Set 850, Award Instrument, Implementation Convention defines the Federal Government interpretation of the use of ASC X12 003050 standards. This implementation convention provides the information necessary for the user to be able to develop an interface program between the computer application and the ASC X12 translator.

01,815
PB96-114921 PC A11/MF A03
National Inst. of Standards and Technology (NCSL), Gaithersburg, MD. Systems and Network Architecture Div.
Federal Implementation Guideline for Electronic Data Interchange. ASC X12 003050 Transaction Set 860 Modifications to Award Instrument. Implementation Convention.
Special pub.
J. P. Favreau. Aug 95, 230p, NIST/SP-881-4.
Also available from Supt. of Docs as SN003-003-03366-9. See also PB96-114913.

Keywords: *Information systems, *Standards, *Procurement, Commerce, Computer networks, Information exchange, Computer software, United States government, Contract administration, Data processing, *Electronic Data Interchange, *EDI(Electronic Data Interchange), Standard ASC X12 003050 Transaction Set 860, Draft standards.

This Draft Standard for Trial Use contains the format and establishes the data contents of the Purchase Order Change Request - Buyer Initiated Transaction Set (860) for use within the context of an Electronic Data Interchange (EDI) environment. The transaction set can be used to provide the information required for the customary and established business and industry practice relative to a purchase order charge. This transaction can be used: (1) by a buyer to request a change to a previously submitted purchase order or (2) by a a buyer to confirm acceptance of a purchase order change initiated by the seller or by mutual agreement of the two parties.

01,816
PB96-114939 PC A07/MF A02
National Inst. of Standards and Technology (CSL), Gaithersburg, MD.
Z39.50 Implementation Experiences.
Special pub.
P. Over, W. E. Moen, R. Denenberg, and L. Stovel.
Sep 95, 129p, NIST/SP-500/229.
Also available from Supt. of Docs. Prepared in cooperation with University of North Texas, Denton. School of Library and Information Sciences., Library of Congress, Washington, DC. and Research Libraries Group, Inc., Mountain View, CA.

Keywords: *Computer networks, *Computer software, *Information retrieval, Implementation, Z39.50 ANSIINISO protocol, Open systems interconnections.

Contents:
- Z39.50 for Full-Text Search and Retrieval;
- Basic Z39.50 Server Concepts and Creation;
- Building a Z39.50 Client;
- Implementing Explain;
- Implementing Z39.50 in a multi-national and multilingual environment;
- Use of Z39.50 for Search and Retrieval of Scientific and Technical Information;
- Structural Components of the Isite Information System;
- Z39.50 - implications and implementation at the AT&T library network;
- The Implementation of Z39.50 in the National Library of Canada's AMICUS System;
- Developing a Multi-Platform Z39.50 Service;
- and Use of Z39.50 for the Delivery of Current Awareness Products.

01,817
PB96-119359 Not available NTIS
National Inst. of Standards and Technology (NCSL), Gaithersburg, MD. Systems and Network Architecture Div.
Lessons from the Establishment of the U.S. GOSIP Testing Program.
Final rept.
J. P. Favreau, and J. S. Nightingale. 1991, 16p.
See also PB94-211455.
Pub. in Proceedings of the International Workshop on Protocol Test Systems (4th), Leidschendam, The Netherlands, October 15-17, 1991, 16p.

Keywords: *Computer communications, *Protocols, Computer networks, Communication networks, Interfaces, Interoperability, Message processing, Computer architecture, Systems engineering, Standardization, Specifications, Requirements, Reprints, *OSI(Open Systems Interconnection), *Open Systems Interconnection, *GOSIP(Government Open Systems Interconnection Profile), *Government Open Systems Interconnection Profile, Conformance.

Currently, the U.S. Government mandates use of Open Systems Interconnection (OSI) protocols in procurement of new networks and major upgrades to existing networks. Vendors strive to meet the challenge of making OSI products available. Users are confused by this new technology. In order to respond to this problem the National Institute of Standards and Technology has set up a comprehensive testing program. An overview of the U.S. GOSIP Testing Program is presented with some of the issues in OSI protocol conformance and interoperability testing raised during its design and implementation.

01,818
PB96-122908 Not available NTIS

National Inst. of Standards and Technology (NCSL), Gaithersburg, MD. Systems and Network Architecture Div.
Open Issues in OSI Protocol Development and Conformance Testing.
Final rept.
J. P. Favreau, G. V. Bochmann, and P. Mondain-Monval. 1991, 19p.
Pub. in Computer Networks '91, Wroclaw, Poland, 19p 1991.

Keywords: *Protocols, *Conformance, *Interoperability, Standards, Testing, Computer networks, Computer software, Computer equipment, Procurement, Communications, Reprints, *OSI(Open Systems Interconnection), *Open Systems Interconnection.

As of August 15, 1990 the U.S. Government mandated use of Open Systems Interconnection (OSI) in procurement of new networks and major upgrades to existing networks. The goal of OSI is to allow interworking of separately developed pieces of software and equipment. However, it is not easy to allow interworking of separately developed pieces of software and equipment. However, it is not easy to insure that OSI products provided by different vendors will properly interoperate. This paper presents some unresolved issues in OSI protocol development and conformance testing, and proposes an approach for the protocol development and testing cycle that would alleviate some of the present problems.

01,819
PB96-122924 Not available NTIS
National Inst. of Standards and Technology (CSL), Gaithersburg, MD. Information Systems Engineering Div.
Database Management Standards: Status and Applicability.
Final rept.
L. Gallagher. 1991, 11p.
Pub. in Computers and Standards, 11p, 18 Nov 91.

Keywords: *Data base management, *Standards, Computer languages, Query languages, Conformance, Applicability, Reprints, ISO(International Organization for Standards), RDA(Remote Database Access), NDL computer language, SQL computer language.

This article presents the current status of existing and emerging ISO, ANSI, and FIPS standards for database management, specifically Database Languages NDL and SQL and Remote Database Access (RDA). It describes the general content of each standard and discusses its applicability, availability, completeness, maturity, stability, existing usage, and known limitations. Where appropriate, it also addresses the availability of conformance test suites and future plans for enhancements and follow-on standardization efforts.

01,820
PB96-131495 PC A03/MF A01
National Inst. of Standards and Technology (CSL), Gaithersburg, MD. Distributed Systems Engineering.
Comparison of POSIX Open System Environment (OSE) and Open Distributed Processing (ODP) Reference Models.
G. Fernandes, and J. Hungate. 13 Nov 95, 26p, NISTIR-5736.

Keywords: *Models, *Standardization, Computer program portability, Interfaces, Distributed processing, Interoperability, Data flow analysis, Computer networks, Information systems, Information centers, Informaton services, Operating systems(Computers), Information dissemination, Systems management, Specifications, *POSIX(Portable Operating System Interface for Computing Environments), *Portable Operating System Interface for Computing Environments, *OSE(Open System Environment), *Open System Environment, *ODP(Open Distributed Processing), *Open Distributed Processing, Distributed systems.

This report presents two existing reference models for describing distributed systems. These models are the Open Distributed Processing reference model and the POSIX OSE reference model. They both address distributed open systems, but from different perspectives, with different objectives and methodology. After a brief description of the two models, a comparison is made referring in particular to the extent distributed systems management is accommodated in both models.

01,821
PB96-160973 Not available NTIS
National Inst. of Standards and Technology (CSL), Gaithersburg, MD.
NIST POSIX Testing Program.
Final rept.
E. Lennon. 1991, 4p.
Pub. in Computer Systems Laboratory Bulletin, p1-4 Oct 91.

Keywords: *Operating systems(Computers), *Computer program portability, *Interfaces, Computer program verification, Application programs(Computers), Computer systems programs, Interoperability, Distributed processing, Reprints, *POSIX(Portable Operating Systems Interface for Computer Environments), *Conformance testing, *Portable Operating Systems Interface for Computer Environments.

This CSL Bulletin describes NIST's program to test POSIX products for conformance to Federal Information Processing Standard (FIPS) 151-1, Portable Operating System Interface for Computer Environments (POSIX). The bulletin discusses the NIST POSIX Conformance Test Suite, POSIX testing procedures, accredited POSIX testing laboratories, POSIX validated products, and the availability of POSIX information.

01,822
PB96-168984 PC A09/MF A02
National Inst. of Standards and Technology (CSL), Gaithersburg, MD. Electronic Commerce Acquisition Program.
Federal Implementation Guideline for Electronic Data Interchange. ASC X12 003050 Transaction Set 843 Response to Request for Quotation. Implementation Convention.
Special pub.
J. P. Favreau. 1996, 154p, NIST/SP-881-7.

Keywords: *Information systems, *Standards, *Procurement, Commerce, Computer networks, Telecommunication, Information exchange, Computer software, United States Government, Contract administration, Data processing, Purchasing, *EDI(Electronic Data Interchange), *Electronic Data Interchange, Standard ASC X12 003050 Transaction Set 843, Draft Standard, Electronic commerce.

This Draft Standard for Tidal Use contains the format and establishes the data contents of the Response to Request for Quotation Trasaction Set (843) for use within the context of an Electronic Data Interchange (EDI) environment. The transaction set can be used to provide potential buyers with price, delivery schedule, and other terms from potential sellers of goods and services, in response to a request for such information.

01,823
PB96-172374 PC A04/MF A01
National Inst. of Standards and Technology (NCSL), Gaithersburg, MD. Systems and Network Architecture Div.
Federal Implementation Guideline for Electronic Data Interchange. ASC X12 003050 Transaction Set 855 Purchase Order Acknowledgment: Implementation Convention.
Special pub.
J. P. Favreau. Feb 96, 41p, NIST/SP-881/6.
Also available from Supt. of Docs. as SN003-003-03398-7. See also PB96-114921.

Keywords: *Information systems, *Standards, *Procurement, Commerce, Computer networks, Telecommunication, Information exchange, Computer software, United States Government, Contract administration, Data processing, Purchasing, *EDI(Electronic Data Interchange), *Electronic Data Interchange, Standard ASC X12 003050 Transaction Set 855, Draft standard, Electronic commerce.

This Draft Standard for Tidal Use contains the format and establishes the data contents of the Purchase Order Acknowledgement Transaction Set (855) for use within the context of an Electronic Data Interchange (EDI) environment. The transaction set can be used to provide for customary and established business and industry practice relative to a seller's acknowledgment of a buyer's purchase order. This transaction set can also be used as notification of a vendor generated order. The usage advises a buyer that a vendor has or will ship merchandise as prearranged in their partnership.

01,824
PB96-172531 PC A10/MF A03
National Inst. of Standards and Technology (NCSL), Gaithersburg, MD. Systems and Network Architecture Div.
Federal Implementation Guideline for Electronic Data Interchange. ASC X12 003050 Transaction Set 840 Request for Quotation. Implementation Convention.
Special pub.
J. P. Favreau. Feb 96, 196p, NIST/SP-881-8.
Also available from Supt. of Docs. as SN003-003-03402-9.

Keywords: *Data processing, *Computer networks, *Standards, Information systems, Government procurement, Information exchange, Contract administration, Computer software, *Electronic data interchange, ASC X12 003050 Transaction Set 840.

This Draft Standard for Tidal Use contains the format and establishes the data contents of the Request for Quotation Transaction Set (840) for use within the context of an Electronic Data Interchange (EDI) environment. The transaction set can be used to provide buyers with the ability to solict price, delivery schedule, and other items from potential sellers of goods and services.

01,825
PB96-172549 PC A09/MF A02
National Inst. of Standards and Technology (NCSL), Gaithersburg, MD. Systems and Network Architecture Div.
Federal Implementaion Guideline for Eletronic Data Interchange. ASC X12 003050 Transaction Set 865 Purchase Order Change Acknowledgement/ Request - Seller Initiated. Implementation Convention.
Special pub.
J. P. Favreau. Feb 96, 162p, NIST/SP-881-5.
Also available from Supt. of Docs. as SN003-003-03397-9. See also PB96-114921.

Keywords: *Information systems, *Standards, *Computer networks, *Procurement, Commerce, Information exchange, Computer software, United States Government, Contract administration, Purchasing, Telecommunications, Data processing, *EDI(Electronic Data Interchange), Electronic Data Interchange, Standard ASC X 12 003050 Transaction Set 865, Implementation Convention, Electric Commerce, Draft standard.

The ASC X12 003050 Transaction Set 865, Purchase Order Change Acknowledgement/Request - Sell Initiated Implementation Convention defines the Federal Government interpretation of the use of ASC X12 003050 standards. This implementation convention provides the information necessary for the user to be able to develop an interface program between the computer application and the ASC X12 translator.

01,826
PB96-175716 Not available NTIS
National Inst. of Standards and Technology (NCSL), Gaithersburg, MD. Systems and Network Architecture Div.
Five Q's (Cues) of the U.S. GOSIP Testing Program.
Final rept.
J. P. Favreau. 1992, 14p.
Pub. in Government Open Systems Interconnection Profile Procurement Symposium, Gaithersburg, MD., December 7, 1992, p1-14.

Keywords: *Computer networks, *Interoperability, Conformance, Systems engineering, File management systems, Data transmission systems, Product development, Procedures, Requirements, Specifications, Standards, Testing, Procurement, Quality assurance, Computer communications, Reprints, *GOSIP(Government Open Systems Interconnection Profile), *Government Open Systems Interconnection Profile.

The National Institute of Standards and Technology (NIST) has developed a comprehensive test policy and procedures that must demonstrate technical credibility, acceptability to both vendors and users, assurance of interoperability and provide a basis for international recognition of national testing. The U.S. GOSIP Testing Program includes the identification of abstract test suites, the development of method to assess means of testing, the setting up a test laboratory accreditation program, a definition for the role of interoperability testing and the creation of publicly available registers.

01,827
PB96-178892 PC A04/MF A01

National Inst. of Standards and Technology (NCSL), Gaithersburg, MD. Systems and Network Architecture Div.
Federal Implementation Guideline for Electronic Data Interchange: ASC X12 003050 Transaction Set 836 Procurement Notices. Implementation Convention.
Special pub.
J. P. Favreau. Feb 96, 43p, NIST/SP-881/9.
Also available from Supt. of Docs. as SN003-003-03400-2. See also PB96-172374.

Keywords: *Telecommunication, *Contract management, *Government procurement, *Federal government, Standards, Computer networks, Information systems, Data processing systems, Purchasing, Acquisition, Contract administration, Implementation, Computer communications, *Electronic Data Interchange, Electric commerce, Standard ASC X12 003050 Transaction Set 836.

This implementation convention provides the information necessary for the user to be able to develop an interface program between the computer application and the ASC X12 translator.

01,828
PB96-180047 Not available NTIS
National Inst. of Standards and Technology (CSL), Gaithersburg, MD. Information Systems Architecture Div.
Open System Environment Implementors Workshop (OIW); Standardization Role Defined.
Final rept.
J. Hungate. 1996, 2p.
Pub. in Open Systems Standards Tracking Report, v5 n2 p2-3, 2 May 96.

Keywords: *Computer networks, *Interoperability, *Standardization, Distributed computer systems, Systems management, Integrated systems, Systems engineering, Interfaces, Specifications, Data flow analysis, Reprints, *Open Systems Environment.

The Open System Environment Implementors' Workshop (OIW), cosponsored by NIST and the IEEE, offers a neutral, inexpensive, public-consensus forum that is recognized by national and international standards organizations. The output of this technical work is primarily information technology (IT) profiles, also known as implementors' agreements or functional standards.

Pattern Recognition & Image Processing

01,829
PB94-145620 PC A03/MF A01
National Inst. of Standards and Technology (MEL), Gaithersburg, MD. Robot Systems Div.
Reliable Optical Flow Algorithm Using 3-D Hermite Polynomials.
H. Liu, T. H. Hong, M. Herman, and R. Chellappa.
Dec 93, 35p, NISTIR-5333.
Prepared in cooperation with Maryland Univ. Coll., College Park.

Keywords: *Image analysis, Image reconstruction, Scene analysis, Computer vision, Hermite polynomials, Three dimensional, Matrices, Algorithms, Theorems, *Optical flow.

Algorithms that attempt to accurately compute optical flow must cope with occlusion, brightness changes, irregular motion, and the aperture problem. Most optical flow algorithms have tried to overcome one or more of the problems mentioned above. Yet, claims about the reliability of computed flow are still based on ad hoc evaluation schemes. While a perfect algorithm that is free of all the problems is not yet available, we present a reliable algorithm, which despite all the difficulties, generates the output flow field wherever possible, and associates with the output evaluation metrics that reflect the reliability of the output. The evaluation metrics are complete in the sense that they are theoretically related to the physical phenomena that cause the inherent problems noted above. Our approach to computing optical flow expands the spatio-temporal image in terms of Hermite polynomials and then derives multiple Gaussian smoothed gradient constraint equations, which constitute an overdetermined linear system that can be solved for image flow with a least square method.

01,830
PB94-168044 PC A06/MF A02
National Inst. of Standards and Technology (NCSL), Gaithersburg, MD. Advanced Systems Div.
Evaluating Form Designs for Optical Character Recognition.
M. D. Garris, and D. L. Dimmick. Feb 94, 117p, NISTIR-5364.

Keywords: *Optical character recognition, *Human factors engineering, *Forms(Paper), *Taxes, Errors, Performance evaluation, Data bases, NIST(National Institute of Standards and Technology), IRS(Internal Revenue Service).

The National Institute of Standards and Technology (NIST), under the sponsorship of the Internal Revenue Service, has conducted an extensive study of three different redesigned tax forms. The NIST Model Recognition System was used in conjunction with the NIST Scoring Package to generate performance measures at the form, field, and character levels. The analyses of these measures conclude that factors introduced onto forms by the writer are the primary cause of segmentation errors, which are the major source of errors within the recognition system. Analysis shows that 97% of these segmentation errors can be attributed to factors introduced by the writer. The paper cites three ways in which these types of human factors can be handled so as to increase recognition performance. First, the algorithms and techniques deployed within the system can be improved. Second, the instances of human factors leading to system errors can be detected. Third, writers can be influenced by the design of the form including the layout and structure of the fields. By applying a combination of these three approaches, human factors can be dealt with, and the errors made by a form processing system can be effectively reduced to classification errors.

01,831
PB94-168051 PC A03/MF A01
National Inst. of Standards and Technology (CSL), Gaithersburg, MD. Advanced Systems Div.
Unconstrained Handprint Recognition Using a Limited Lexicon.
M. D. Garris. Dec 93, 15p, NISTIR-5310.
See also PB94-118213.

Keywords: *Word recognition, *Handwriting, Character recognition, Pattern recognition, Neural nets, Automation, Classification, Lexicography, NIST(National Institute of Standards and Technology).

A word recognition system has been developed at the National Institute of Standards and Technology (NIST) to read free-formatted text paragraphs containing handprinted characters. The system has been developed and tested using samples of handprint from NIST Special Database 1. This database of binary images contains 2,100 different writers' printings of the Preamble to the U.S. Constitution. Each writer was asked to print these sentences in an empty 70mm by 175mm box. The Constitution box contains no guidelines for the placement and spacing of the handprinted text, nor are there guidelines to instruct the writer where to stop printing one line and to begin the next. This paper discusses the word recognition system in detail.

01,832
PB94-188711 PC A12/MF A03
National Inst. of Standards and Technology (CSL), Gaithersburg, MD. Advanced Systems Div.
Second Census Optical Character Recognition Systems Conference.
Final rept. 1993-94.
J. Geist, R. A. Wilkinson, S. Janet, N. W. Larsen, R. M. Klear, M. J. Matsko, C. J. C. Burges, R. Creecy, J. J. Hull, T. P. Vogl, C. L. Wilson, P. J. Grother, and B. Hammond. May 94, 266p, NISTIR-5452.
See also PB92-238542.

Keywords: *Meetings, *Optical character recognition, *Handwriting, Character recognition, Image processing, Dictionaries, Scoring, Voting, Tests, US Bureau of the Census, NIST(National Institute of Standards and Technology).

The results of the Second Census Optical Character Recognition (OCR) Systems Conference are described. There were two conference tests, one scanned from microfilm, the other from paper. Each test consisted of three thousand miniforms with three answer fields per form. The answers consisted of phases associated with the respondant's occupation. Twenty-five organizations participated in the conference, but only ten submitted results for scoring by the National Institute of Standards and Technology (NIST). The results from one organization were good enough to suggest that OCR may now be sufficiently well developed to be used in a future Census.

01,833
PB94-199106 Not available NTIS
National Inst. of Standards and Technology (NML), Gaithersburg, MD. Gas and Particulate Science Div.
Object Finder for Digital Images Based on Multiple Thresholds, Connectivity, and Internal Structures.
Final rept.
D. S. Bright. 1989, 120p.
Pub. in Jnl. of Computer Assisted Microscopy 1, n4 p307-329 Dec 89.

Keywords: *Image processing, Transmission electron microscopy, Ion microscopy, Electron diffraction, Reprints, *Feature extraction, Blob Splitting Algorithm, Image segmentation, Digital images.

The Blob Splitting Algorithm (BSA), developed for segmenting digital images (Bright 1987a), finds simple objects in micrographs that have troublesome backgrounds. Locating objects can be difficult when they have a wide range of sizes or shapes, when they have fuzzy edges, when they are not clearly separated, or when they do not stand out well from the background. The algorithm works without any preprocessing, filtering, or transforming of the images. It is not sensitive to object width or even to object size or shape, but rather to intensities relative to a local surround. Although computationally expensive, it is robust and is used routinely in our laboratory for locating particles in TEM and ion microscope images, locating spots in electron diffraction patterns, and finding regions of interest in complex particles.

01,834
PB94-200029 Not available NTIS
National Inst. of Standards and Technology (NCSL), Gaithersburg, MD. Advanced Systems Div.
VLSI Architectures for Template Matching and Block Matching.
Final rept.
C. Chakrabarti, and J. JaJa. 1991, 24p.
Grants NSF-DCR-86-00378, NSF-OIR-85-00108
Pub. in Parallel Architectures and Algorithms for Image Understanding, p3-26 1991. Sponsored by National Science Foundation, Arlington, VA.

Keywords: *Image processing, *Templates, *Blocks, *Computer architecture, Pattern recognition, Parallel processing, Very large scale integration, Systolic arrays, Chips (Electronics), Input output processing, Reprints.

Image template matching and block matching are representative of many window based tasks in image processing. While the existing architectures for template matching and block matching consist of a systolic array of processors, most of them either ignore the I/O issues or employ schemes involving frequent off-chip memory accesses. We propose a systolic architecture consisting of a linear array of processors which handles the I/O bandwidth problem efficiently.

01,835
PB94-203510 PC A03/MF A01
National Inst. of Standards and Technology (MEL), Gaithersburg, MD. Robot Systems Div.
Certainty Grid to Object Boundary Algorithm.
J. A. Horst, H. M. Huang, and T. M. Tsai. Jun 94, 16p, NISTIR-5447.

Keywords: *Image processing, *Robotics, Algorithms, Edge detection, Curve fitting, Approximation, Mapping, *CGOB(Certainty grid to object boundary), *Certainty grid to object boundary.

An edge linking algorithm is modified for a mobile robot map representation application. Certainty grid 'images' are transformed to an appropriate set of object boundary curves. The latter are expressed as oriented piecewise linear segments. Image processing techniques, such as edge detection, thinning, curve tracing, and linear approximation are employed with various modifications. The most significant modification is a new method for linear curve approximation that is simple, accurate, and efficient. The method monitors chord and arc length, and its excellent performance is demonstrated against similar algorithms. The certainty grid to object boundary algorithm is tested against simulated noisy certainty grid maps.

01,836
PB94-206281 PC A03/MF A01
National Inst. of Standards and Technology (MEL), Gaithersburg, MD. Robot Systems Div.
Visual-Motion Fixation Invariant.
D. Raviv, and N. Ozery. Jun 94, 11p, NISTIR-5442.
Grant NSF-IRI-9115939
See also PB92-133016. Prepared in cooperation with Florida Atlantic Univ., Boca Raton. Sponsored by National Science Foundation, Washington, DC. Directorate for Engineering.

Keywords: *Computer vision, *Three dimensional motion, *Optical flow(Image analysis), Invariance, Three dimensional bodies, Cameras, Rotation, Fixation.

The paper deals with a visual-motion fixation invariant. The authors show that during fixation there is a measurable nonlinear function of optical flow that produces the same value for all points of a stationary environment regardless of the 3-D shape of the environment. During fixated camera motion relative to a rigid object, e.g., a stationary environment, the projection of the fixated point remains (by definition) at the same location in the image, and all other points located on the 3-D rigid object can only rotate relative to the 3-D fixation point. This rotation rate of the points is invariant for all points that lie on the particular environment, and it is measurable from a sequence of images. This new invariant is obtained from a set of monocular images, and is expressed explicitly as a closed form solution. In the paper the authors show how to extract this invariant analytically from a sequence of images using optical flow information, and they present results obtained from real data experiments.

01,837
PB94-207768 PC A05/MF A01
National Inst. of Standards and Technology (CSL), Gaithersburg, MD. Advanced Systems Div.
Face Recognition Technology for Law Enforcement Applications.
C. L. Wilson, C. S. Barnes, R. Chellappa, and S. A. Sirohey. Jul 94, 77p, NISTIR-5465.

Keywords: *Face(Anatomy), *Law enforcement, *Pattern recognition, Neural networks, Character recognition, Image processing, Computer aided analysis, Psychophysics, Photographic images, Feature extraction, Segmented elements, Eigenvectors, Technology transfer, *Forensic sciences, *Face recognition, National Institute of Standards and Technology.

The goal of the report is to relate existing face recognition technology to law enforcement applications. These applications range from static matching of controlled photographs as in mugshot matching to surveillance video images and have different constraints in terms of complexity of processing requirements and thus present a wide range of different technical challenges. The ongoing research activities have been given a renewed emphasis over the last five years. The existing techniques and systems have been tested on different sets of images of varying complexities. Also, very little synergism exists between studies in psychophysics and the engineering literature. Most importantly, there exist no evaluation or benchmarking studies using large databases with the image quality that arises in law enforcement applications.

01,838
PB94-217106 PC A04/MF A01
National Inst. of Standards and Technology (CSL), Gaithersburg, MD. Advanced Systems Div.
NIST Form-Based Handprint Recognition System.
M. D. Garris, J. L. Blue, G. T. Candela, P. J. Grother, S. A. Janet, C. L. Wilson, D. L. Dimmick, and J. Geist. Jul 94, 72p, NISTIR-5469.
See also PB94-168044 and PB94-188711.

Keywords: *Optical character recognition, *Handwriting, Data structures, Utility routines, Computer software, Feature extraction, UNIX(Operating system), *Handprint, US NIST, CD-ROM, C programming language.

The National Institute of Standards and Technology (NIST) has developed a standard reference form-based handprint recognition system for evaluating optical character recognition. NIST is making this recognition system freely available to the general public on CD-ROM. This is a source code distribution written primarily in C with two additional utilities having FORTRAN components. Library utilities are provided with the recognition system for conducting form registration, form removal, field isolation, field segmentation, character normalization, feature extraction, character classification, and dictionary-based postprocessing. A host of data structures and low-level utilities are also provided. The recognition system has been successfully compiled and tested on a host of UNIX workstations. This report documents the system in terms of its installation, organization, and functionality.

01,839
PB95-108650 Not available NTIS
National Inst. of Standards and Technology (NEL), Gaithersburg, MD. Robot Systems Div.
Real-Time Implementation of a Differential Range Finder.
Final rept.
R. Rangachar, T. Hong, M. Herman, and J. Lupo. 1990, 12p.
Pub. in Proceedings of Society of Photo-Optical Instrumentation Engineers - Real Time Image Processing II, Orlando, FL., April 16-18, 1990, v1295 p211-222.

Keywords: *Optical range finders, *Optical flow(Image analysis), *Real time, Edge detection, Spatial distribution, Temporal distribution, Algorithms, Gradients, Cameras, Motion, Reprints, *Differential range, PIPE(Pipelined Image Processing Engine).

A scheme to estimate differential range using optical flow along a known direction is described. The factors affecting the accuracy of results, and various spatial and temporal smoothing algorithms used to increase the accuracy of the method are described. The effect of using edge detectors and a prior knowledge of the environment is considered next. While the former reduces the noise, the latter improves the range discriminability of the method. The authors have implemented the method on a real time, high speed, Pipelined Image Processing Engine (PIPE), which processes sixty frames per second. For the PIPE implementation, a horizontally moving camera is used, which produces optical flow along a scan line.

01,840
PB95-136362 PC A03/MF A01
National Inst. of Standards and Technology (CSL), Gaithersburg, MD. Advanced Systems Div.
Comparison of FFT Fingerprint Filtering Methods for Neural Network Classification.
C. I. Watson, G. T. Candela, and P. J. Grother. Sep 94, 38p, NISTIR-5493.
See also PB92-213339 and PB93-184273. Sponsored by Federal Bureau of Investigation, Washington, DC.

Keywords: *Fast Fourier transformations, *Neural nets, Data bases, Image enhancement, Pattern recognition, Karhunen-Loeve expansion, Errors, Feature extraction, *Fingerprint classification.

Two types of Fourier Transform based filters are presented and used to enhance fingerprint images for use with a neural network fingerprint classification system developed at the National Institute of Standards and Technology (NIST). With image enhancement the system is capable of achieving classification error rates of 8.65% with 10% rejects, a 2 percentage point improvement in error rate versus using no fingerprint enhancement. Speed of the filters range from 2 to 9 seconds. Classification tests were performed using ridge-valley based feature extraction, Karhunen Loeve transform, and a Probabilistic Neural Network (PNN) classifier. The testing method used differs from past reports because no rolling of the same print is allowed to appear in both the training and testing set used by the Neural Network classifier.

01,841
PB95-143285 PC A03/MF A01
National Inst. of Standards and Technology (MEL), Gaithersburg, MD. Intelligent Systems Div.
Visual Pursuit Systems.
J. C. Fiala, and A. J. Wavering. Oct 94, 21p, NISTIR-5513.
Also available from Supt. of Docs. Prepared in cooperation with Boston Univ., MA. Dept. of Cognitive and Neural Systems.

Keywords: *Computer vision, *Optical tracking, Systems analysis, Predictions, Bandwidth, Image processing, Algorithms, Kinematics, *Visual pursuit systems, TRICLOPS system.

Visual pursuit systems are reviewed using a generalized form with the principal delay in the visual feedback pathway. The performance of several different control methods are compared through analysis of the tracking error. A high-performance active vision system, called TRICLOPS, is used to obtain experimental data on the tracking performance of the various methods, some of which had previously only been tested through simulation. Image processing delay is shown to be the primary limiting factor in performing high-speed tracking. Prediction is necessary to achieve high performance tracking, and the effectiveness of prediction depends on several factors, including the coordinate system used for motion modeling and the noise content of the target motion signal. It is demonstrated that, using relatively simple tracking algorithms which incorporate prediction with an advanced robotic device like TRICLOPS, it is now possible to outperform humans in the domain of visual pursuit of simple targets.

01,842
PB95-151932 Not available NTIS
National Inst. of Standards and Technology (NML), Gaithersburg, MD. Ionizing Radiation Div.
Tomographic Decoding Algorithm for a Nonoverlapping Redundant Array.
Final rept.
L. I. Yin, and S. M. Seltzer. 1993, 10p.
Sponsored by Department of Energy, Washington, DC.
Pub. in Applied Optics 32, n20 p3726-3735, 10 Jul 93.

Keywords: *Image reconstruction, *Tomography, X-ray imagery, Computerized simulation, Pinhole cameras, Three dimensional, Algorithms, Reprints, *Image decoding.

A tomographic reconstruction algorithm is developed for the nonoverlapping redundant array x-ray imaging system whereby the background contributions from out-of-focus planes can be eliminated. The algorithm makes use of two constraints derived from the physical characteristics of the nonoverlapping redundant array system in tandem with the correlation decoding process. It is simple, direct, and noniterative. Tomographic images of computer-generated planar and three-dimensional objects are provided to illustrate the effectiveness of the algorithm.

01,843
PB95-153003 Not available NTIS
National Inst. of Standards and Technology (CAML), Gaithersburg, MD. Applied and Computational Mathematics Div.
Image Restoration and Diffusion Processes.
Final rept.
A. S. Carasso. 1993, 12p.
Pub. in Proceedings of Society of Photo-Optical Instrumentation Engineers: Mathematical Methods in Medical Imaging, San Diego, CA., July 15-16, 1993, v2035 p255-266.

Keywords: *Image restoration, *Image reconstruction, Noise reduction, Diffusion theory, Reprints, Tikhonov-Miller restoration, SEB restoration, Ill posed problems, Image deblurring.

A new supplementary a priori constraint, the slow evolution from the boundary constraint, (SEB) sharply reduces noise contamination in a large class of space-invariant image deblurring problems that occur in medical, industrial, surveillance, environmental, and astronomical applications. The noise suppressing properties of SEB restoration can be proved mathematically, on the basis of rigorous error bounds for the reconstruction, as a function of the noise level in the blurred image data. This analysis proceeds by reformulating the image deblurring problem into an equivalent ill-posed problem for a time-reversed diffusion equation. The SEB constraint does not require smoothness of the image. An effective, fast, non-iterative procedure, based on FFT algorithms, may be used to compute SEB restorations. For a 512 X 512 image, the procedure requires about 45 seconds of cpu time on a Sun/sparc2. A documented deblurring experiment, on an image with significant high frequency content, illustrates the computational significance of the SEB constraint by comparing SEB and Tikhonov-Miller reconstructions using optimal values of the regularization parameters.

01,844
PB95-161808 Not available NTIS
National Inst. of Standards and Technology (NEL), Gaithersburg, MD. Robot Systems Div.

Real Time Differential Range Estimation Based on Time-Space Imagery Using PIPE.
Final rept.
R. Rangachar, T. H. Hong, M. Herman, R. Luck, and J. Lupo. 1990, 10p.
Pub. in Proceedings of Society of Photo-Optical Instrumentation Engineers: Real-Time Image Processing II, Orlando, FL., April 16-18, 1990, v1295 p247-256.

Keywords: *Optical flow(Image analysis), *Image processing, Spatial resolution, Temporal resolution, Pipelining(Computers), Edge detection, Gradients, Reprints, PIPE(Pipelined Image Processing Engine).

The paper examines spatio-temporal methods of image flow and shows how differential range can be estimated from time-space imagery. We consider one scan line of the image obtained from a camera moving in the horizontal direction. At the next instant of time, we shift the previous line up by one pixel, and obtain another line from the image. We continue the procedure to obtain a time-space image, where each horizontal line represents the spatial relationship of the pixels, and each vertical line the temporal relationship. Each feature along the horizontal scan line will generate an edge in the time-space image, the slope of which depends upon the distance of the feature from the camera. We apply two mutually perpendicular edge operators to the time-space image, and determine the slope of each edge. We show that this corresponds to optical flow. We use the result to obtain the differential range, and show how this can be implemented on the Pipelined Image Processing Engine (PIPE). We discuss several kinds of edge operators, show how using the zero crossings reduces the noise, and demonstrate how better discrimination can be achieved by knowing the range we are interested in.

01,845
PB95-163994 Not available NTIS
National Bureau of Standards (ICST), Gaithersburg, MD. Advanced Systems Div.
Self-Organizing Neural Network Character Recognition on a Massively Parallel Computer.
Final rept.
C. L. Wilson, R. A. Wilkinson, and M. D. Garris. 1990, 5p.
Pub. in Proceedings of International Joint Conference on Neural Networks, San Diego, CA., June 17-21, 1990, p325-329.

Keywords: *Neural nets, *Character recognition, *Massively parallel processors, Array processors, Image processing, Self organizing systems, Algorithms, Accuracy, Reprints.

Two neural network based methods are combined to develop font independent character recognition on a distributed array processor. Feature localization and noise reduction are achieved using least squares optimized Gabor filtering. The filtered images are then presented to an ART-1 based learning algorithm which produces self-organizing sets of neural network weights used for character recognition. Implementation of these algorithms on a highly parallel computer with 1,024 processors allows high speed character recognition to be achieved in 8ms/image with greater than 99% accuracy on machine print and 80% accuracy on unconstrained hand printed characters.

01,846
PB95-164075 Not available NTIS
National Inst. of Standards and Technology (EEEL), Gaithersburg, MD. Electronics and Electrical Engineering Lab. Office.
Physics-Based Vision: Principles and Practice, Shape Recovery (Book Review).
Final rept.
J. A. Worthey. 1993, 3p.
Pub. in Color Research and Application 18, n3 p221-223 Jun 93.

Keywords: *Computer vision, Stereoscopic vision, Multisensor fusion, Specular reflection, Photometry, Shapes, Reprints, *Shape recovery, *Machine vision.

Shape Recovery is a useful compilation of recent papers in the machine vision specialty of 'shape from shading'.

01,847
PB95-171096 PC A03/MF A01
National Inst. of Standards and Technology (MEL), Gaithersburg, MD. Intelligent Systems Div.
General Motion Model and Spatio-Temporal Filters for Computing Optical Flow.
H. Liu, T. H. Hong, M. Herman, and R. Chellappa. Nov 94, 50p, NISTIR-5539.
Prepared in cooperation with Maryland Univ., College Park.

Keywords: Image motion compensation, Image filters, Image analysis, Mathematical models, Three dimensional, Hermite polynomials, Matrices, Algorithms, *Image motion analysis, *Optical flow.

Traditional optical flow algorithms assume local image translational motion and apply simple image filtering. Recent studies have taken two separate approaches toward improving the accuracy of computed flow: the application of spatio-temporal filtering schemes and the use of generalized motion models such as the affine model. Each has achieved some improvement over traditional algorithms in specialized situations. In this paper, we analyze the interdependency between them and propose a unifed approach. The general motion model we adopt characterizes arbitrary 3-D steady motion. Under perspective projection, we derive an image motion equation that describes the spatio-temporal relation of gray-scale intensity in an image sequence, thus making the utilization of 3-D filtering possible. However, to accommodate this complex motion, we need to extend the filter design to derive additional motion constraint equations. Using Hermite polynominals, we design differentiation filters, whose orthogonality and Gaussian derivative properties insure numerical stability. The resulting algorithm produces accurate optical flow and other useful motion parameters. It is evaluated quantitatively using the scheme established by Barron, et al. and qualitatively with real images.

01,848
PB95-171971 PC A03/MF A01
National Inst. of Standards and Technology (CSL), Gaithersburg, MD. Advanced Systems Div.
Binary Decision Clustering for Neural Network Based Optical Character Recognition.
C. L. Wilson, P. J. Grother, and C. S. Barnes. Dec 94, 23p, NISTIR-5542.
See also PB92-238542 and PB94-217106.

Keywords: *Optical character recognition, *Neural nets, *Handwriting, Pattern recognition, Dynamical systems, Image processing, Karhunen-Loeve expansion, Errors, BDMs(Binary Decision Machines).

A multiple neural network system for handprinted character recognition is presented. It consists of a set of input networks which discriminate between all two class pairs, and an output network which takes the signals from the input networks and yields a digit recognition decision. For a ten digit classification problem this requires forty-five binary decision machines in the input network. The output stage is typically a single trained network. The neural network paradigms adopted in these input and output networks are the multi-layer perceptron, the radial basis function network, and the probabilistic neural network. A simple majority vote rule was also tested in place of the output network.

01,849
PB95-189502 PC A03/MF A01
National Inst. of Standards and Technology (MEL), Gaithersburg, MD. Intelligent Systems Div.
Motion-Model-Based Boundary Extraction.
H. Liu, T. H. Hong, M. Herman, and R. Chellappa. Jan 95, 29p, NISTIR-5587.
Presented at International Conference on Computer Vision, Cambridge, MA., June 20-23, 1995. Prepared in cooperation with Maryland Univ., College Park.

Keywords: *Computer vision, *Motion, *Edge detection, Algorithms, Flow, Iteration, Mathematical models, Pattern recognition, Three dimensional models, Segmentation.

Motion boundary extraction and optical flow computation are two subproblems of the motion recovery problem that cannot be solved independently of each other. They represent the most common dilemma in motion research. A popular approach uses an iterative scheme that consists of motion boundary extraction and optical flow computation components and refines each result through iteration. This approach is typically time-consuming and sometimes does not converge. We present a local, noniterative algorithm that extracts motion boundaries and computes optical flow simultaneously. This is achieved by modeling a 3-D image intensity block with a general motion model that presumes locally coherent motion. Local motion coherence, which is measured by the fitness of the motion model, is the criterion we use to determine whether motion should be estimated, or otherwise motion boundaries should be located. The motion boundary extraction algorithm is evaluated quantitatively and qualitatively against other existing algorithms in a scheme originally developed for edge detection. The results show that our algorithm is accurate in locating boundaries.

01,850
PB95-251724 PC A03/MF A01
National Inst. of Standards and Technology (CSL), Gaithersburg, MD. Advanced Systems Div.
Method and Evaluation of Character Stroke Preservation on Handprint Recognition.
M. D. Garris. Jul 95, 32p, NISTIR-5687.

Keywords: *Optical character recognition, *Handwriting, Artificial intelligence, Image processing, Performance evaluation, Statistical analysis, Algorithms, Edge detection, Automation, Matrices(Mathematics), *Form removal.

A new technique for intelligent form removal has been developed along with a new method for evaluating its impact on optical character recognition (OCR). The form removal technique automatically detects the dominant lines in an image and erases them while preserving as much of the overlapping character strokes as possible. This method of form removal relaxes the recognition systems dependence on rigid form design, printing, and reproduction by automatically detecting and removing some of the physical structures (lines) on the form. The line detection and removal technique operates on loosely defined zones in which no image deskewing is performed. The technique was tested on a large number of randomly-ordered handprinted lowercase alphabet fields, as these letters (especially those with descenders) frequently touch and extend through the line along which they are written. It is shown that intelligent form removal can improve lowercase recognition by as much as 3%, but this net increase in performance is insufficient to understand the inpact on the recognition. There is expected to be trade-offs with the introduction of any new technique into a complex recognition system. A new statistical analysis was designed to evaluate the impact of intelligent line removal on OCR. The evaluation method compares the statistical distributions of individual confusion pairs between two systems and automatically determines the significant improvements and the significant losses in performance. In order for system developers to continue to reduce error rates, sophisticated analyses like this become necessary to understand the real impact a modification has on recognition performance. The statistical analysis presented in the paper was used to evaluate the new line removal technique, and the results are reported.

01,851
PB95-267803 PC A03/MF A01
National Inst. of Standards and Technology (CSL), Gaithersburg, MD. Advanced Systems Div.
Improving Neural Network Performance for Character and Fingerprint Classification by Altering Network Dynamics.
C. L. Wilson, J. L. Blue, and O. M. Omidvar. Aug 95, 12p, NISTIR-5695.
See also PB95-171971.

Keywords: *Optical character recognition, *Neural nets, Self organizing systems, Optimization, Conjugate gradient method, Iteration, Handwriting, Performance evaluation, Machine learning, Image processing, Pattern recognition, Reprints, *Fingerprint classification, PNN(Probabilistic Neural Network), MLPs(Multilayer Perceptrons).

The paper shows that performance equal to or better than the Probabilistic Neural Network (PNN) can be achieved with a single three-layer Multilayer Perceptron (MLP) by making fundamental changes in the network optimization strategy. These changes are: (1) Neuron activation functions are used which reduce the probability of singular Jacobians; (2) Successive regularization is used to constrain volume of the weight space being minimized; (3) Boltzmann pruning is used to constrain the dimension of the weight space; and (4) Prior class probabilities are used to normalize all error calculations so that statistically significant samples of rare but important classes can be included without distortion of the error surface. All four of these changes are made in the inner loop of a conjugate gradient optimization iteration and are intended to simplify

the training dynamics of the optimization. On handprinted digits and fingerprint classification problems these modifications improve error-reject performance by factors between 2 and 4 and reduce network size by 40% to 60%.

01,852
PB95-267845 PC A03/MF A01
National Inst. of Standards and Technology (CSL), Gaithersburg, MD. Advanced Systems Div.
Effect of Training Dynamics on Neural Network Performance.
C. L. Wilson, J. L. Blue, and O. M. Omidvar. Aug 95, 32p, NISTIR-5696.
Prepared in cooperation with District of Columbia Univ., Washington. Dept. of Computer Science.

Keywords: *Neural nets, *Machine learning, *Optical character recognition, Self organizing systems, Optimization, Dynamical systems, Conjugate gradient method, Iteration, Handwriting, Pattern recognition, Image processing, Mathematical models, Fingerprint classification, MLP(Multilayer Perceptrons), PNN(Probabilistic Neural Network).

In this paper, analysis of a simple model of recurrent network dynamics is used to gain qualitative insights into the training dynamics of multilayer perceptrons (MLPs). These insights allow the training methods used by MLPs to be modified to significantly improve network performance. We will show that performance equal to or better than the Probabilistic Neural Network (PNN) can be achieved with a single three-layer MPL by making fundamental changes in the network optimization strategy. These changes are: (1) Neuron activation functions are used which reduce the probability of singular Jacobians; (2) Successive regularization is used to constrain the volume of the minimized weight space; (3) Boltzmann pruning is used to constrain the dimension of the weight space; and (4) Prior class probabilities are used to normalize all error calculations so that statistically significant samples of rare but important classes can be included without distorting the error surface. All four of these changes are made in the inner loop of a conjugate gradient optimization iteration and are intended to simplify the training dynamics of the optimization. On handprinted digits and fingerprint classification problems, these modifications improve error-reject performace by factors between 2 and 4 and reduce network size by 40% to 60%.

01,853
PB95-267936 PC A03/MF A01
National Inst. of Standards and Technology (CSL), Gaithersburg, MD. Advanced Systems Div.
PCASYS: A Pattern-Level Classification Automation System for Fingerprints.
G. T. Candela, P. J. Grother, C. I. Watson, R. A. Wilkinson, and C. L. Wilson. Aug 95, 46p, NISTIR-5647.

Keywords: *Pattern recognition, *Automation, Image processing, Data base management, Image classification, Image enhancement, Feature extraction, Neural nets, Algorithms, Machine learning, Accuracy, *Fingerprint classification, PNN(Probabilistic Neutral Network), AFIS(Automated Fingerprint Identification System).

This report describes a system we have developed that automatically classifies images of fingerprints into six pattern-level classes. Our program takes gray-level images of fingerprints as input, and for each fingerprint it produces a hypothesized classification as arch, left loop, right loop, scar, tented arch, or whorl, as well as a number indicating how much confidence should be assigned to its classification decision. The system performs these processing steps: image segmentation; image enhancement; feature extraction; registration; application of a linear transform that both applies a pattern of regional weights and reduces dimensionality; running of a main classifier, which is a Probabilistic Neural Net, and of an auxiliary whorl-detecting classifier that traces and analyzes pseudoridges (approximate trajectories through the ridge flow); and finally, the combining of the outputs of the main and auxiliary classifiers so as to decide on a hypothesized class and a confidence level.

01,854
PB96-111687 Not available NTIS
National Inst. of Standards and Technology (CSL), Gaithersburg, MD. Advanced Systems Div.
Human and Machine Recognition of Faces: A Survey.
Final rept.
R. Chellappa, C. L. Wilson, and S. Sirohey. 1995, 36p.
Pub. in Proceedings of Institute of Electrical and Electronics Engineers, v83 n5 p705-740 May 95.

Keywords: *Computer vision, *Visual perception, *Humans, *Pattern recognition, *Photographic images, Face(Anatomy), Optical images, Feature extraction, Image processing, Computer aided analysis, Identification systems, Psychophysics, Reprints.

The goal of this paper is to present a critical survey of existing literature on human and machine recognition of faces. Machine recognition of faces has several applications, ranging from static matching of controlled photographs, as in mug shots matching and credit card verification to surveillance video images. Over the last 20 years researchers in psychophysics, neural sciences and engineering, image processing, analysis and computer vision have investigated a number of issues related to face recognition by humans and machines. Ongoing research activities hvae been given a renewed emphasis over the last five years. Existing techniques and systems have been tested on different sets of images of varing complexities.

01,855
PB96-119797 Not available NTIS
National Inst. of Standards and Technology (CSL), Gaithersburg, MD. Advanced Systems Div.
Self-Organizing Neural Network Character Recognition Using Adaptive Filtering and Feature Extraction.
Final rept.
C. L. Wilson, R. A. Wilkinson, and M. D. Garris. 1995, 24p.
Pub. in Progress in Neural Networks, Chapter 10, v3 p295-318 1995.

Keywords: *Feature extraction, *Character recognition, *Neural networks, Image processing, Pattern recognition, Adaptive features, Machine learning, Computer architecture, Massively parallel processors, Optical filters, Data management, Algorithms, Accuracy, Reprints.

Neural network methods show great promise for providing highly accurate, noise resistant, parallel algorithms, and data organization of image recognition. One specific area of image recognition, the conversion of images of hand written and machine print characters to computer representation, has been studied in detail in the past. Both special purpose hardware and software approaches have been used on the character recognition problem with promising results. The present work addresses the problem of using a specific class of computer architecture, an array of 1024 processors arranged in a 32 x 32 grid and operated in a parallel mode, as a neural network character recognition device.

01,856
PB96-123195 Not available NTIS
National Inst. of Standards and Technology (CSL), Gaithersburg, MD. Advanced Systems Div.
Improving Neural Network Performance for Character and Fingerprint Classification by Altering Network Dynamics.
Final rept.
C. L. Wilson, J. L. Blue, and O. M. Omidvar. 1995, 8p.
See also PB95-267803.
Pub. in World Congress on Neural Networks Proceedings II, Washington, DC., July 20, 1995, p151-158.

Keywords: *Optical character recognition, *Neural nets, Self organizing systems, Optimization, Conjugate gradient method, Heration, Handwriting, Performance evaluation, Machine learning, Image processing, Pattern recognition, Reprints, *Fingerprint classification, PNN(Probabilistic Neural Network), MLPs(Multilayer Perceptions).

In this paper, the authors will show that performance equal to or better than PNN can be achieved with a single three-layer MLP by making fundamental changes in the network optimization strategy. These changes are: (1) Neuron activation functions are used which reduce the probability of singular Jacobians; (2) Successive regularization is used to constrain volume of the weight space being minimized; (3) Boltzmann pruning is used (4) to constrain the dimension of the weight space; and (4) Prior class probabilities are used to normalize all error calculations so that statistically significant samples of rare but important classes can be included without distortion of the error surface. All four of these changes are made in the inner loop of a conjugate gradient optimization iteration (5) and are intended to simplify the training dynamics of the optimization.

01,857
PB96-186184 Not available NTIS
National Inst. of Standards and Technology (CSL), Gaithersburg, MD. Advanced Systems Div.
Binary Decision Clustering for Neural-Network-Based Optical Character Recognition.
Final rept.
C. L. Wilson, P. J. Grother, and C. S. Barnes. 1995, 13p.
See also PB95-171971.
Pub. in Pattern Recognition, v29 n3 p425-437 Jul 96.

Keywords: *Optical character recognition, *Neural nets, *Handwriting, Pattern recognition, Dynamical systems, Image processing, Karhunen-Loeve expansion, Errors, Reprints, BDMs(Binary Decision Machines).

A multiple neural network system for handprinted character recognition is presented. It consists of a set of input networks which discriminate between all-two-class pairs, for example '1' from '7' and an output network which takes the signals from the input networks and yields a digit recognition decision. For a ten-digit classification problem this requires 45 binary decision machines in the input network. The output stage is typically a single trained network. The neural network paradigms adopted in these input and output networks are the multi-layer perceptron, the radial-bias function network and the probabilistic neural network. A simple majority vote rule was also tested in place of the output network. The various resulting digit classifiers were trained on 7480 isolated images and tested on a disjoint set of size 32140. The Karhunen-Loeve transforms of the images of each pair of two classes formed the training set for each BDM. Several different combinations of neural network input and output structures gave similar classification performance. The minimum error rate achieved was 2.5% with no rejection obtained by comining a PNN input array with an RBF output stage. This combined network has an error rate of 0.7% with 10% rejection.

01,858
PB96-191374 PC A03/MF A01
National Inst. of Standards and Technology (CSL), Gaithersburg, MD. Advanced Systems Div.
Generalized Form Registration Using Structure-Based Techniques.
M. D. Garris, and P. J. Grother. Apr 96, 16p, NISTIR-5726.
See also PB94-217106.

Keywords: *Forms(Paper), *Optical character recognition, *Handwriting, Data structures, Utility routines, Computer software, Databases, Image processing, Automation, Registration, Feature extraction, US NIST.

A new method for registering forms has been developed at the National Institute of Standards and Technology. This method automatically estimates the amount of rotation and translation in the image without any detailed knowledge of the form. This is accomplished through the automatic detection of dominant vertical and horizontal structures (lines) commonly found in forms. A general method for rotation estimation and a robust method for translation estimation are presented. Results demonstrate that this technique is extremely tolerant to spurious annotations on the form and scanner noise in the image, and the computational requirements of the utility can be tuned by optionally choosing to process and analyze downsampled versions of the image. All 3,669 Handwriting Sample Forms distributed with NIST Special Database 19 were successfully registered with the new technique, and using the same code, 255 uniformly laid out IRS tax forms and 500 Census miniforms were also tested and registered. Every type of form contained in the numerous NIST (public) form databases can be registered using this technique. These results also demonstrate how easy it is to set up the computer to register new types of forms, introducing a set-up interface that is much more automated and less tedious than what is currently required to specify new forms for the NIST public domain Form-Based Handprint Recognition System.

01,859
PB96-193669 PC A03/MF A01
National Inst. of Standards and Technology (CSL), Gaithersburg, MD. Information Access and User Interface Div.
Component-Based Handprint Segmentation Using Adaptive Writing Style Model.
M. D. Garris. Jun 96, 29p, NISTIR-5843.

Keywords: *Optical character recognition, *Handwriting, *Data structures, Feature extraction, Image processing, Forms(Paper), Statistical analysis, Classifying, Databases, Expert systems, *Handprint, Character segmentation.

Building upon the utility of connected components, NIST has designed a new character segmentor based on statistically modeling the style of a person's handwriting. Simple spatial features (the thickness of the pen stroke and the height of the handwriting) capture the characteristics of a particular writer's style of handprint, enabling the new method to maintain a traditional character-level segmentation philosophy without the integration of recognition or the use of oversegmentation and linguistic postprocessing. Estimates for stroke width and character height are used to compute aspect ratio and standard stroke count features that adapt to the writer's style at the field level. The new method has been developed with a predetermined set of fuzzy rules making the segmentor much less fragile and much more adaptive, and the new method successfully reconstructs fragmented characters as well as splits touching characters. The new segmentor was integrated into the NIST public domain Form-Based Handprint Recognition System and then tested on a set of 490 Handwriting Sample Forms found in NIST Special Database 19. When compared to a simple component-based segmentor, the new adaptable method improved the overall recognition of handprinted digits by 3.4% and field level recognition by 6.9%, while effectively reducing deletion errors by 82%. The same program code and set of parameters successfully segments sequences of uppercase and lowercase characters without any context-based tuning. While not as dramatic as digits, the recognition of uppercase and lowercase characters improved by 1.7% and 1.3% respectively. The segmentor maintains a relatively straightforward and logical process flow avoiding convolutions of encoded exceptions as is common in expert systems. As a result, the new segmentor operates very efficiently, and throughout as high as 362 characters per second can be achieved. Letters and numbers are constructed from a predetermined configuration of a relatively small number of strokes. Results in the paper show that capitalizing on this knowledge through the use of simple adaptable features can significantly improve segmentation, whereas recognition-based and oversegmentation methods fail to take advantage of these intrinsic quality of handprinted characters.

01,860
PB96-195524 PC A04/MF A01
National Inst. of Standards and Technology (EEEL), Gaithersburg, MD.
Specification for Interoperability between Ballistic Imaging Systems. Part 1. Cartridge Cases.
B. F. Field, E. F. Kelley, and R. M. McCabe. Jun 96, 44p, NISTIR-5855.

Keywords: *Cartridges(Explosives), *Guns, *Identification, *Image processing, Ammunition, Crimes, Pattern recognition, Computer equipment, Interoperability, Databases, Specifications, Optical equipment, *Forensics.

To facilitate interoperability between existing ballistic imaging systems, the Office of National Drug Control Policy (ONDCP), the Federal Bureau of Investigation (FBI), and the Bureau of Alcohol, Tobacco, and Firearms (ATF) executed a Memorandum of Understanding that recognized, in part, that it is imperative that the Drugfire and IBIS Ballistic Imaging Systems are interoperable. Further, the National Institute of Standards and Technology (NIST) was asked to provide technical assistance in this effort. This document is the first of a series of planned documents that will specify the hardware and software requirements to permit interoperability between the Drugfire and IBIS systems as specified in the MOU. This specific document provides a complete specification of hardware requirements for capture of cartridge image and ancillary data for each system, and the data exchange formats required for transmitting and processing information requests.

01,861
PB96-210703 PC A07/MF A02
Maryland Univ., College Park. Dept. of Electrical Engineering.
General Motion Model and Spatio-Temporal Filters for 3-D Motion Interpretations.
H. Liu. Nov 95, 122p, NISTIR-5763.
Sponsored by National Inst. of Standards and Technology (MEL), Gaithersburg, MD. Intelligent Systems Div.

Keywords: *Image motion compensation, Image filters, Image analysis, Algorithms, Three dimensional, Hermite polynomials, Mathematical models, Matrices(Mathematics), Theorems, *Image motion analysis, *Optical flow.

Motion cues are a rich source of visual information. Object boundaries due to motion parallax, perception of collision, and transparency provide crucial information to any mobile vision system, biological or robotic. This report presents the formulation, design, evaluation and implementation of a motion algorithm which accurately and efficiently interprets the above motion cues.

DETECTION & COUNTERMEASURES

Magnetic Detection

01,862
PB95-175667 Not available NTIS
National Inst. of Standards and Technology (EEEL), Boulder, CO. Electromagnetic Fields Div.
Gradiometer Antennas for Detection of Long Subsurface Conductors.
Final rept.
D. A. Hill. 1994, 12p.
Sponsored by Army Belvoir Research Development and Engineering Center, Fort Belvoir, VA.
Pub. in Jnl. of Electromagnetic Waves and Applications 8, n2 p237-248 1994.

Keywords: *Gradiometers, *Magnetic detection, *Electromagnetic measurement, Electrical impedance, Antennas, Boreholes, Magnetic dipoles, Magnetic fields, Tunnels, Electromagnetic wave transmission, Reprints, *Subsurface conductors.

The use of gradiometer antennas for detection of long conductors in tunnels is analyzed. For reception in vertical boreholes, the gradiometer consists of two vertical magnetic dipoles with a vertical separation. The source is a vertical magnetic dipole located in an adjacent vertical borehole. Both sum and difference responses are useful, but the difference response has the potential advantage of suppressing the primary field and making the scattered field easier to detect. The difference response is most effective in suppressing the primary field for a parallel scan where the transmitting antenna and receiving gradiometer are always at the same height.

Optical Detection

01,863
PB96-177381 PC A07/MF A02
National Inst. of Standards and Technology, Gaithersburg, MD.
Journal of Research of the National Institute of Standards and Technology, March/April 1996. Volume 101, Number 2.
1996, 105p.
See also PB96-179114 through PB96-179163 and PB96-175666. Also available form Supt. of Docs. as SN703-027-00069-5.

Keywords: *Calibration, *Cryogenic radiometers, *Quartz-halogen lamps, *Gravimetry, *Computer arithmetic, *Quantized dissipation, Absolute spectral response, Color temperature, Lamp orientation, Human serum, Definitive method, Candela, Breakdown, Reprints.

Contents:
- The NIST Detector-Based Luminous Intensity Scale;
- The NIST High Accuracy Scale for Absolute Spectral Response from 406 nm to 920 nm;
- Irradiance of Horizontal Quartz-Halogen Standard Lamps;
- Development of the Ion Exchange-Gravimetric Method for Sodium in Serum as a Definitive Method;
- The MasPar MP-1 as a Computer Arithmetic Laboratory;
- Evidence That Voltage Rather Than Resistance is Quantized in Breakdown of the Quantum Hall Effect.

01,864
PB96-179114 (Order as PB96-177381, PC A07/MF A02)
National Inst. of Standards and Technology, Gaithersburg, MD.
NIST Detector-Based Luminous Intensity Scale.
C. L. Cromer, G. Eppeldauer, J. E. Hardis, A. C. Parr, T. C. Larason, and Y. Ohno. 1996, 24p.
Included in Jnl. of Research of the National Institute of Standards and Technology, v101 n2 p109-132 Mar/Apr 96.

Keywords: *Calibration, *Candela, Illuminance, Lumen, Luminous intensity, Lux, Measurement, Photometers, Scale, Standards, Units, Reprints.

The Systeme International des Unites (SI) base unit for photometry, the candela, has been realized by using absolute detectors rather than absolute sources. This change in method permits luminous intensity calibrations of standard lamps to be carried out with a relative expanded uncertainty (coverage factor k=2, and thus a 2 standard deviation estimate) of 0.46%, almost a factor-of-two improvement. A group of eight reference photometers has been constructed with silicon photodiodes, matched with filters to mimic the spectral luminous efficiency function for photopic vision. The wide dynamic range of the photometers aid in their calibration. The components of the photometers were carefully measured and selected to reduce the sources of error and to provide baseline data for aging studies. Periodic remeasurement of the photometers indicate that a yearly recalibration is required. The design, characterization, calibration, evaluation, and application of the photometers are discussed.

01,865
PB96-179122 (Order as PB96-177381, PC A07/MF A02)
National Inst. of Standards and Technology, Gaithersburg, MD.
NIST High Accuracy Scale for Absolute Spectral Response from 406 nm to 920 nm.
T. C. Larason, S. S. Bruce, and C. L. Cromer. 1996, 8p.
Included in Jnl. of Research of the National Institute of Standards and Technology, v101 n2 p133-140 Mar/Apr 96.

Keywords: *Absolute spectral response, *Cryogenic radiometers, Light-trapping detectors, Measurements, Optical power, Scale, Silicon photodiode, Quantum efficiency, Quality system, Reprints.

The authors describe how the National Institute of Standards and Technology obtains a scale of absolute spectral response from 406 nm to 920 nm. This scale of absolute spectral response is based solely on detector measurements traceable to the NIST High Accuracy Cryogenic Radiometer (HACR). Silicon photodiode light-trapping detectors are used to transfer optical power measurements from the HACR to a monochromator-based facility where routine measurements are performed. The transfer also involves modeling the quantum efficiency (QE) of the silicon photodiode light-trapping detectors. The authors describe their planned quality system for these measurements that follows ANSI/NCSL Z540-1-1994. A summary of current NIST capabilities based on these measurements is also given.

01,866
PB96-179130 (Order as PB96-177381, PC A07/MF A02)
National Inst. of Standards and Technology, Gaithersburg, MD.

Optical Detection

Irradiance of Horizontal Quartz-Halogen Standard Lamps.
E. A. Early, and A. Thompson. 1996, 13p.
Included in Jnl. of Research of the National Institute of Standards and Technology, v101 n2 p141-153 Mar/Apr 96.

Keywords: *Color temperature, *Lamp orientation, *Quartz-halogen lamps, Spectral irradiance, Standard lamps, Ultraviolet, Reprints.

Spectral irradiance calibration often require that irradiance standard lamps be oriented differently than the normal calibration orientation used at the National Institute of Standards and Technology and at other standards laboratories. For example, in solar measurements the instruments are generally upward viewing, requiring horizontal working standards for minimization of irradiance calibration uncertainties. To develop a working standard for use in a solar ultraviolet intercomparison. NIST determined the irradiance of quartz-halogen lamps operating in the horizontal position, rather than in the customary vertical position. An experimental technique was developed which relied upon equivalent lamps with independent mounts for each orientation and a spectroradiometer with an integrating sphere whose entrance port could be rotated 90 degrees to view either lamp position.

01,867
PB96-179148 (Order as PB96-177381, PC A07/MF A02)
National Inst. of Standards and Technology, Gaithersburg, MD.
Development of the Ion Exchange-Gravimetric Method for Sodium in Serum as a Definitive Method.
J. R. Moody, and T. W. Vetter. 1996, 10p.
Included in Jnl. of Research of the National Institute of Standards and Technology, v101 n2 p155-164 Mar/Apr 96.

Keywords: *Human serum, *Gravimetry, *Definitive method, Accuracy, Instrumental determination, Ion-exchange, Repeatability, Sodium, Uncertainty, Reprints.

An ion exchange-gravimetric method, previously developed as a National Committee for Clinical Laboratory Committee for Clinical Laboratory Standards (NCCLS) reference method for the determination of sodium in human serum, has been re-evaluated and improved. Sources of analytical error in this method have been examined more critically and the overall uncertainties decreased. Additionally, greater accuracy and repeatability have been achieved by the application of this definitive method to a sodium chloride reference material.

01,868
PB96-179163 (Order as PB96-177381, PC A07/MF A02)
National Inst. of Standards and Technology, Gaithersburg, MD.
Evidence That Voltage Rather Than Resistance is Quantized in Breakdown of the Quantum Hall Effect.
M. E. Cage. 1996, 6p.
Included in Jnl. of Research of the National Institute of Standards and Technology, v101 n2 p175-180 Mar/Apr 96.

Keywords: *Breakdown, *Quantized dissipation, Resistance states, Voltage states, Hall effect, Level scattering, Electron gas, Reprints.

Quantized longitudinal voltage drops are observed along a length of a GaAs/AlGaAs heterostructure quantum Hall effect device at applied currents large enough for the device to be in the breakdown regime. The range of currents is extensive enough to demonstrate that it is the longitudinal voltage that is quantized, rather than the longitudinal resistance. A black-box and a quasi-elastic inter-Landau level scattering (QUILLS) model are then employed to calculate the fraction of electrons making transitions into higher Landau levels, the transition rates, and the maximum electric field across the device.

01,869
PB96-202122 PC A05/MF A01
National Inst. of Standards and Technology (PL), Gaithersburg, MD. Optical Technology Div.
Developing Quality System Documentation Based on ANSI/NCSL Z540-1-1994: The Optical Technology Division's Effort.
S. S. Bruce, and T. C. Larason. Aug 96, 58p, NISTIR-5866.
See also PB95-103461.

Keywords: *Quality assurance, *Absolute spectral response, *Calibration, Optical measuring instruments, Photometers, Spectroradiometers, Optical detectors, Optical properties, Radiance, Test facilities, ISO(International Standards Organization), International Standards Organization 4000, ANSI/NCSL Z540-1-1994.

The Optical Technology Division, formerly known as the Radiometric Physics Division, at the National Institute of Standards and Technology (NIST) began a project in 1993 to develop a quality system that is based on the American National Standard for Calibration - Calibration Laboratories and Measuring and Test Equipment, ANSI/NCSL Z540-1-1994. This document is intended to complement the NCSL 'Handbook for the Interpretation and Application of ANSI/NCSL Z540-1-1994' and to provide guidance to other calibration services at NIST, particularly those starting to develop their quality systems. The appendix of this publication contains a reprint of a paper entitled, 'Building a Quality System Based on ANSI/NCSL Z540-1-1994 An Effort by the Radiometric Physics Division at NIST'.

Radiofrequency Detection

01,870
PB94-218591 PC A03/MF A01
National Inst. of Standards and Technology (EEEL), Boulder, CO. Electromagnetic Fields Div.
RangeCAD and the NIST RCS Uncertainty Analysis.
R. L. Lewis, L. A. Muth, and R. C. Wittmann. Aug 94, 18p, NISTIR-5022.

Keywords: *Uncertainty, *Error analysis, *Radar cross sections, Calibration, Radar signals, Noise(Radar), Amplitude, Estimation, Mathematical models, Range CAD computer program.

We discuss the salient features of a computer program, RangeCAD, and then translate the program's output into a catalogue of radar cross section (RCS) uncertainties. This specific catalogue was developed by the National Institute of Standards and Technology (NIST) to standardize RCS uncertainty computations at the various RCS measurement sites. We check uncertainty estimates generated by RangeCAD against alternative formulations that approximate equivalent uncertainty specifications. Based on this comparison, we conclude that the uncertainty estimates generated by RangeCAD provide realistic values for the NIST RCS uncertainty analysis.

01,871
PB95-203568 Not available NTIS
National Inst. of Standards and Technology (EEEL), Boulder, CO. Electromagnetic Fields Div.
Proposed Analysis of RCS Measurement Uncertainty.
Final rept.
R. C. Wittmann, M. H. Francis, L. A. Muth, and R. L. Lewis. 1994, 7p.
Pub. in Proceedings of the Antenna Measurement Techniques Association Symposium, Long Beach, CA., October 3-7, 1994, p51-57.

Keywords: *Radar cross sections, Measurement, Uncertainty, Errors, Reprints.

From a study of several radar cross section (RCS) measurement facilities, we identify significant sources of uncertainty and develop methods for estimating their effect. Our goal is to provide a 'reasonable' and uniform formalism for evaluating RCS measurements which can be used on a variety of test ranges to produce comparable estimates of uncertainty.

01,872
PB95-216925 PC A03/MF A01
National Inst. of Standards and Technology (EEEL), Boulder, CO. Electromagnetic Fields Div.
Polarimetric Calibration of Reciprocal-Antenna Radars.
R. L. Lewis, L. A. Muth, and R. C. Wittmann. Mar 95, 24p, NISTIR-5033.

Keywords: *Radar cross sections, Radar antennas, Radar targets, Error analysis, Depolarization, Calibration, *Radar polarimetry, Measurement uncertainty, Reciprocity.

We discussed how radar target depolarization enhances a radar's cross polarization contamination, and we dramatize the effect by presenting a graphical study of radar cross section (RCS) measurement error due to depolarization by an inclined dihedral reflector. Since error mitigation requires full polarimetric RCS measurements, we recommend upgrading singly polarized radars to full polarimetric capability. We present a novel polarimetric calibration technique that is applicable to reciprocal antenna radars, saves calibration time by requiring a single calibration target, uses simple mathematical expressions, and smoothes measured calibration data to reduce clutter.

ELECTROTECHNOLOGY

General

01,873
PB94-126901 PC A09/MF A02
National Inst. of Standards and Technology (EEEL), Gaithersburg, MD.
Electronics and Electrical Engineering Laboratory 1994 Program Plan: Supporting Technology for U.S. Competitiveness in Electronics.
J. M. Surette. Dec 93, 184p, NISTIR-5337.
See also PB93-228625 and PB94-161320.

Keywords: *Electrical measurement, *Electronics industry, Semiconductor devices, Electric equipment, Optoelectronic devices, Microwave equipment, Optical fibers, Electromagnetic compatibility, Superconductors, Metrology, Competitiveness, US NIST.

The Electronics and Electrical Engineering Laboratory (EEEL), working in concert with other NIST Laboratories, is providing measurement and other generic technology critical to the competitiveness of the U.S. electronics industry and the U.S. electrical-equipment industry. This 1994 Program Plan describes the projected metrological support that EEEL intends to provide to U.S. industry.

01,874
PB94-161320 PC A04/MF A01
National Inst. of Standards and Technology (EEEL), Gaithersburg, MD.
Electronics and Electrical Engineering Laboratory: 1994 Strategic Plan. Supporting Technology for U.S. Competitiveness in Electronics.
R. M. Powell. Apr 94, 70p, NISTIR-5409.
See also PB92-123082.

Keywords: *Electrical measurement, Electronics industry, Optical communication, Semiconductor devices, Microwave equipment, Video equipment, Optical processing, Signal processing, Optical storage, Magnetic storage, Electric power, Integrated optics, Optical fibers, Electromagnetic compatibility, Metrology, Standards, Superconductors, Electronics and Electrical Engineering Laboratory, Competitiveness, US NIST, Fiber optic sensors.

The U.S. electronics and electrical-equipment industries are outstripping available measurement capability with adverse effects on their international competitiveness. Improved measurement support is an essential part of any successful strategy for improving their competitiveness. Among U.S. manufacturing industries, the electronics industry is the largest employer with 1.8 million employees and is virtually tied with the chemical industry for largest shipments of nearly $300 billion (1992). The electrical-equipment industry is also quite large, with shipments of nearly $50 billion (1990). U.S. competitiveness in many fields of electronic and elec-

trical products has been declining. Improved competitiveness will require outstanding performance from manufacturers in every step required to realize a competitive product in the marketplace: research and development, manufacturing, marketplace exchange, and after-sales support. All of these steps are highly measurement intensive. The Electronics and Electrical Engineering Laboratory (EEEL), within the National Institute of Standards and Technology, has identified the principal needs for improved measurement capability and other supporting technology in several important fields: semiconductors, magnetics, superconductors, low frequency, microwaves, lightwaves, power, video, electromagnetic compatibility, electronic data exchange, and national electrical standards. The document describes EEEL's strategic plan for a response to these needs. The plan was developed in consultation with U.S. industry and other NIST Laboratories.

01,875
PB94-165990 PC A06/MF A02
National Inst. of Standards and Technology (EEEL), Boulder, CO. Electromagnetic Fields Div.
Bibliography of the NIST Electromagnetic Fields Division Publications.
R. M. Lyons, and K. A. Gibson. Aug 92, 108p, NISTIR-3993.
Supersedes PB94-112547.

Keywords: *Electromagnetic fields, *Bibliographies, *US NIST, Electrical measurement, Dielectric properties, Electromagnetic interference, Electromagnetic noise, Remote sensing, Time domain, Radiation, Impedance, Attenuation, Radiation hazards, Antennas, Near fields, Metrology, Waveforms, Microwaves, Standards, *Nonionizing radiation.

The bibliography lists the publications by the staff of the Electromagnetic Fields Division of the National Institute of Standards and Technology for the period January 1970 through July 1992. It supersedes NISTIR 3973 which listed the publications of the Electromagnetic Fields Division from January 1970 through July 1991. Selected earlier publications from the Division's predecessor organizations are included.

01,876
PB94-172186 Not available NTIS
National Inst. of Standards and Technology (IMSE), Gaithersburg, MD. Ceramics Div.
Dielectric Properties Measurements and Data.
Final rept.
J. A. Carpenter. 1991, 11p.
Pub. in Materials Research Society Symposia Proceedings, v189 p477-487 1991.

Keywords: Dielectric properties, Minerals, Polymers, Solids, Ceramics, Microwave frequencies, Reprints, *Dielectric measurements.

This paper reviews measurement techniques and sources of data for the dielectric constant and loss factor of solid materials. Accurate values of such properties are basic to intelligent design of materials processing schemes using electromagnetic energy. Emphasis is on techniques and data for these properties in the 'microwave' range of frequencies of roughly 10(sup 8) to 10(sup 11) Hz and at elevated temperatures.

01,877
PB94-185410 Not available NTIS
National Inst. of Standards and Technology (EEEL), Boulder, CO. Electromagnetic Fields Div.
Time-Domain Measurements of the Electromagnetic Backscatter of Pyramidal Absorbers and Metallic Plates.
Final rept.
R. T. Johnk, A. Ondrejka, S. Tofani, and M. Kanda. 1993, 5p.
Pub. in Institute of Electrical and Electronics Engineers Transactions on Electromagnetic Compatibility 35, n4 p429-433 Nov 93.

Keywords: *Electromagnetic scattering, Electromagnetic measurement, Very high frequency, Ultrahigh frequency, MHz range 01-100, MHz range 100-1, 000, Absorbers(Materials), Time domain, Metal plates, Backscattering, Microwave scattering, Broadband, Pyramids, Reprints.

A wideband time-domain measurement system has been developed for the evaluation of the backscatter performance of dissipative macrostructures. Backscatter measurements have been performed in an ordinary room environment on metal plates as well as samples of pyramidal absorbing material. The backscattering performance of pyramidal absorbers is evaluated in the 50- to 1,000 MHz frequency range with a varying incident field angle of incidence. In the case of rectangular metal plates, numerically generated results are compared with measured data in order to gauge the accuracy of the system.

01,878
PB94-185634 Not available NTIS
National Inst. of Standards and Technology (EEEL), Gaithersburg, MD. Electricity Div.
Approach to Setting Performance Requirements for Automated Evaluation of the Parameters of High-Voltage Impulses.
Final rept.
T. R. McComb, C. Cherbaucich, L. Coffen, E. Hanique, K. Lehmann, J. McBride, J. J. Ribot, G. Rizzi, P. Vaessen, W. Zaengl, M. F. Deschamps, and G. J. FitzPatrick. 1993, 4p.
Pub. in Proceedings of the International Symposium on High Voltage Engineering (8th), Yokohama, Japan, August 23-27, 1993, p309-312.

Keywords: *High voltage, *Waveforms, *Signal processing, Wave analyzers, Pulse analyzers, Automation, Performance evaluation, Computer applications, Data bases, Reprints.

This paper reports the present status of an ongoing study of digital signal processing applied to various impulse waveforms. In a round-robin study, twelve laboratories are using their own software to evaluate the parameters of impulse waveforms in a data base of thirty-one waveforms with the objective of establishing minimum performance requirements. This paper presents the results obtained for smooth full impulses and some examples of results on more complex waveforms.

01,879
PB94-185931 Not available NTIS
National Inst. of Standards and Technology (EEEL), Gaithersburg, MD. Semiconductor Electronics Div.
Reproducibility of JEDEC Standard Current and Voltage Ramp Test Procedures for Thin-Dielectric Breakdown Characterization.
Final rept.
J. S. Suehle. 1993, 13p.
Pub. in Proceedings of the International Integrated Reliability Workshop, Lake Tahoe, CA., October 24-27, 1993, p22-34.

Keywords: *Dielectric breakdown, *Electrical measurement, Interlaboratory comparisons, Integrated circuits, Electric fields, Charge density, Reproducibility, Test methods, Reprints, JEDEC.

Six laboratories and a reference laboratory participated in an interlaboratory experiment that was conducted to determine the reproducibility of breakdown electric field, E(BR), and breakdown charge density, q(bd), measurements using the JEDEC standard voltage and current ramp dielectric test procedures. The results indicate that the measurement of E(BR) is much more reproducible than q(bd). Much of the variability in the q(bd) measurements was found to be due to an allowed range of values that could be chosen for a parameter in the current ramp procedure. When this source of variability is accounted for, the results indicate that the standard test procedures can be implemented to obtain critical dielectric integrity parameters with good reproducibility for a large variety of test equipment.

01,880
PB94-193786 PC A04/MF A01
National Inst. of Standards and Technology (EEEL), Boulder, CO. Electromagnetic Fields Div.
Coaxial Reference Standard for Microwave Power.
Technical note.
F. R. Clague, and P. G. Voris. Apr 93, 54p, NIST/TN-1357.
Also available from Supt. of Docs. as SN003-003-03213-1.

Keywords: *Power measurement, *Microwaves, *Standards, Coaxial cables, Calibration, Performance, Design, *Reference standards, *Bolometer mounts, *Thermistor mounts.

Design and construction details are given for the bolometer (thermistor) mounts used by NIST as working reference standards for microwave power calibrations in coaxial transmission line. The effective efficiency of these reference standards can be measured directly in the NIST coaxial microcalorimeters. The standards are then used to calibrate other microwave power sensors. Two versions are described: one with a Type N connector and one with an APC-7 connector. The operating frequency range is 0.05 to 18 GHz with either connector. Detailed drawings and performance measurements are included.

01,881
PB94-193984 PC A04/MF A01
National Inst. of Standards and Technology (EEEL), Gaithersburg, MD. Semiconductor Electronics Div.
Realizing Suspended Structures on Chips Fabricated by CMOS Foundry Processes Through the MOSIS Service.
J. Marshall, M. Gaitan, M. Zaghloul, J. I. Pi, C. Pina, W. Hansford, D. Novotny, and V. Tyree. Jun 94, 60p, NISTIR-5402.
Prepared in cooperation with George Washington Univ., Washington, DC. School of Engineering and Applied Science. and University of Southern California, Marina del Rey. Information Sciences Inst.

Keywords: Chips(Electronics), Etching, Wafers, Tiles, Design, Silicon, CMOS, Hazards, *Micromachining, Microelectromechanics, MOSIS.

Chips can be inexpensively fabricated at Complementary Metal-Oxide Semiconductor (CMOS) foundries through the MOSIS (MOSIS is an acronym for 'MOS Implementation System') Service at the University of Southern California's Information Sciences Institute. MOSIS now supports CMOS-compatible micromachining to realize microelectromechanical systems (MEMS) and devices such as suspended corners, cantilevers, and pixels. The MEMS designs are fabricated through MOSIS on a multi-project wafer, and the user performs a post-processing maskless anisotropic etch. Two new design tiles called 'open' and 'pstop' have been added to support these designs.

01,882
PB94-200409 Not available NTIS
National Inst. of Standards and Technology (EEEL), Gaithersburg, MD. Electricity Div.
President's Column for Dielectrics and Electrical Insulation Society Newsletter.
Final rept.
A. H. Cookson. 1993, 1p.
Pub. in EE Electrical Insulation Magazine 9, n3 and 5, May/Jun 93.

Keywords: Planning, Reprints, *Dielectrics and Electrical Insulation Society.

A summary of plans for the coming year, for the Dielectrics and Electrical Insulation Society, is given.

01,883
PB94-213774 PC A03/MF A01
National Inst. of Standards and Technology (EEEL), Gaithersburg, MD. Semiconductor Electronics Div.
Electronics and Electrical Engineering Laboratory Technical Publication Announcements Covering Laboratory Programs, January to March 1994 with 1994/1995 EEEL Events Calendar.
J. M. Rohrbaugh. Aug 94, 33p, NISTIR-5471.
See also PB94-193752.

Keywords: *Microelectronics, *Metrology, *Bibliographies, Electrical measurement, Integrated circuits, Millimeter waves, Microwaves, Optical fibers, Integrated optics, Semiconductor devices, Electric power, High temperature superconductors, Electromagnetic interference, Magnetic measurement, Abstracts.

This is the fortieth issue of a quarterly publication providing information on the technical work of the National Institute of Standards and Technology Electronics and Electrical Engineering Laboratory (EEEL). This issue of the EEEL Technical Publication Announcements covers the first quarter of calendar year 1994. This issue contains citations and abstracts for Laboratory publications published in the quarter. Main topic areas include: Fundamental Electrical Measurements; Semiconductor Microelectronics; Signal Acquisition, Processing, and Transmission; Electrical Systems; Electromagnetic Interference; Additional Information.

01,884
PB94-219334 (Order as PB94-219326, PC A05/MF A02)
National Inst. of Standards and Technology, Gaithersburg, MD.

General

Sources of Uncertainty in a DVM-Based Measurement System for a Quantized Hall Resistance Standard.
K. C. Lee, M. E. Cage, and P. S. Rowe. 1994, 14p.
Included in Jnl. of Research of the National Institute of Standards and Technology, v99 n3 p227-240 May/Jun 94.

Keywords: *Resistors, *Standards, *Calibrating, Voltmeters, Electrical resistance meters, Hall effect, Drift(Instrumentation).

The paper describes a simple automated measurement system that uses a single, high accuracy, commercially available digital voltmeter (DVM) to compare the voltages developed across a 10 kilohm standard resistor and a quantized Hall resistor when the same current is passed through the two devices. From these measurements, the value of the 10 kilohm standard resistor is determined. The sources of uncertainty in this system are analyzed in detail and it is shown that it is possible to perform calibrations with relative combined standard uncertainties less than 0.1 ppm.

01,885
PB94-219359 (Order as PB94-219326, PC A05/MF A02)
National Inst. of Standards and Technology, Gaithersburg, MD.
Three-Axis Coil Probe Dimensions and Uncertainties during Measurement of Magnetic Fields from Appliances.
M. Misakian, and C. Fenimore. 1994, 7p.
Included in Jnl. of Research of the National Institute of Standards and Technology, v99 n3 p247-253 May/Jun 94.

Keywords: *Electric appliances, *Magnetic fields, *Probability theory, Coils, Computation.

Comparisons are made between the average magnetic flux density for a three-axis circular coil probe and the flux density at the center of the probe. The results, which are determined assuming a dipole magnetic field, provide information on the uncertainty associated with measurements of magnetic fields from some electrical appliances and other electrical equipment. The present investigation extends an earlier treatment of the problem, which did not consider all orientations of the probe. A more comprehensive examination of the problem leaves unchanged the conclusions reached previously.

01,886
PB95-135562 PC A06/MF A02
National Inst. of Standards and Technology (EEEL), Boulder, CO. Electromagnetic Fields Div.
Bibliography of the NIST Electromagnetic Fields Division Publications.
R. M. Lyons, and K. A. Gibson. Sep 94, 120p, NISTIR-5028.
Supersedes PB94-165990.

Keywords: *Electromagnetic fields, *Bibliographies, Electrical measurement, Dielectric properties, Electromagnetic interference, Electromagnetic noise, Radiation hazards, Remote sensing, Time domain, Near field, Microwaves, Metrology, Attenuation, Waveforms, Standards, Impedance, Antennas, Nonionizing radiation, US NIST.

This bibliography lists the publications by the staff of the Electromagnetic Fields Division of the National Institute of Standards and Technology for the period January 1970 through July 1994. It supersedes NISTIR 5009 which listed the publications of the Electromagnetic Fields Division from January 1970 through July 1993. Selected earlier publications from the Division's predecessor organizations are included.

01,887
PB95-144309 PC A06/MF A02
National Inst. of Standards and Technology (EEEL), Gaithersburg, MD.
Electronics and Electrical Engineering Laboratory 1994 Technical Accomplishments Supporting Technology for U.S. Competitiveness in Electronics.
Special pub.
Dec 94, 102p, NISTIR-5551.
See also PB94-136777.

Keywords: *Electronics industry, *Metrology, Technology innovation, Competition, United States, Measurement, Semiconductor devices, Technology transfer, Research projects, Commercial development, Organizational structure, US NIST, EEEL(Electronics and Electrical Engineering Laboratory).

The Electronics and Electrical Engineering Laboratory (EEEL), working in concert with other National Institute of Standards and Technology (NIST) Laboratories, is providing measurements capability and other generic technology critical to the competitiveness of the U.S. electronics industry and the U.S. electrical-equipment industry. This report summarizes selected technical accomplishments and describes activities conducted by the Laboratory in Fiscal Year 1994. Also included is a profile of EEEL's organization, its customers, and the Laboratory's long-term goals.

01,888
PB95-150389 Not available NTIS
National Inst. of Standards and Technology (EEEL), Gaithersburg, MD. Electricity Div.
Performance Evaluation of a New Digital Partial Discharge Recording and Analysis System.
Final rept.
P. von Glahn, and R. J. VanBrunt. 1994, 5p.
Pub. in Proceedings of Conference Record of the 1994 Institute of Electrical and Electronics Engineers International Symposium on Electrical Insulation, Pittsburgh, PA., June 5-8, 1994, p12-16.

Keywords: *Digital recording systems, *Electrical insulation, Epoxy matrix composites, Performance evaluation, Personal computers, Stochastic processes, Real time, Digitizers, Reprints, *Partial discharges.

We describe the design and performance evaluation of a new digital partial discharge (PD) recording system capable of real-time recording of PD pulse trains for later off-line computerized stochastic analysis. By way of illustration, measurements were made of the time-varying stochastic behavior of ac-generated PDs in point-to-dielectric gaps in air where the insulation material was cast epoxy with aluminum oxide filler, extending the work reported previously. Sample analysis results are presented, demonstrating that the new system provides analysis results comparable with the results achieved by the existing NIST analog PD stochastic analysis system. Sample stochastic analysis results are presented demonstrating the additional insights possible with the new system.

01,889
PB95-150579 Not available NTIS
National Inst. of Standards and Technology (EEEL), Gaithersburg, MD. Electricity Div.
Electrical Breakdown in Transformer Oil in Large Gaps.
Final rept.
K. L. Stricklett, D. M. Weidenheimer, N. R. Pereira, and D. C. Judy. 1992, 7p.
Sponsored by Defense Nuclear Agency, Washington, DC. and Department of Energy, Washington, DC.
Pub. in Proceedings of Annual Report Conference on Electrical Insulation and Dielectric Phenomena, Victoria, British Columbia, Canada, October 18-21, 1992, p248-254.

Keywords: *Electric discharges, *Dielectric breakdown, *Pulse transformers, *Spark gaps, Shadowgraph photography, Electric fields, High speed photography, Pulses, Switches, Reprints.

The Aurora accelerator uses four parallel Blumlein pulse-forming lines to provide an intense flash x-ray pulse. Proper timing of the pulses generated by each Blumlein is important to the quality of the radiation. The pulse on each Blumlein, and the synchronization between the Blumleins are affected by the closure of high-voltage triggered oil switches in each line. The triggered oil switch utilizes a uniform field geometry with a gap spacing between 40 and 50 cm, a unique environment for observation of arc development in transformer oil. High-speed photography of switch closure shows timing to be influenced by the initiation and spatial development of prebreakdown streamers.

01,890
PB95-150777 Not available NTIS
National Inst. of Standards and Technology (NML), Gaithersburg, MD. Center for Atomic, Molecular and Optical Physics.
New International Representations of the Volt and Ohm Effective January 1, 1990.
Final rept.
B. N. Taylor. 1990, 4p.
Pub. in Institute of Electrical and Electronics Engineers Transactions on Instrumentation and Measurement 39, n1, 2-5, 1990.

Keywords: *Standards, International agreements, Josephson effect, Reprints, *Resistance standards, *Voltage standards, *Volt, *Ohm, Consultative Committee on Electricity, Quantum Hall effect.

Starting on January 1, 1990, new representations of the volt and ohm based on the Josephson and quantum Hall effects, respectively, are to come into effect worldwide. Implementation of the new representations in the U.S. requires that on this date, the value of the present national representation of the volt maintained at the National Institute of Standards and Technology (NIST) be increased by 9.264 parts per million (ppm) and that the value of the national representation of the ohm maintained at NIST be increased by 1.69 ppm. The resulting increases in the U.S. representations of the ampere and watt will be about 7.57 ppm and 16.84 ppm, respectively.

01,891
PB95-150934 Not available NTIS
National Inst. of Standards and Technology (EEEL), Boulder, CO. Electromagnetic Fields Div.
Bistatic Scattering of Absorbing Materials from 30 to 1000 MHz.
Final rept.
S. Tofani, A. R. Ondrejka, M. Kanda, and D. A. Hill. 1992, 4p.
Pub. in Institute of Electrical and Electronics Engineers Transactions of Electromagnetic Compatibility 34, n3 p304-307 Aug 92.

Keywords: *Absorbers(Materials), Electromagnetic scattering, Electromagnetic measurement, Very high frequency, Ultrahigh frequency, Scattering coefficients, MHz range 01-100, MHz range 100-1000, Anechoic chambers, Specular reflection, Time domain, Broadband, Reprints, *Microwave absorbers, *Bistatic scattering.

A wide-band time-domain reflectometer has been used to evaluate the bistatic performance of the scattering coefficient of rf/microwave absorbers. The scattering coefficient has been measured inside an anechoic chamber in the 30-1000 MHz frequency range in the case of specular reflection. The scattering coefficient increases with incidence angle, and the measurement accuracy is + or - 2 dB.

01,892
PB95-153227 Not available NTIS
National Inst. of Standards and Technology (EEEL), Boulder, CO. Electromagnetic Fields Div.
New Coaxial Microwave Microcalorimeter Evaluation Technique.
Final rept.
F. R. Clague. 1992, 2p.
Pub. in Proceedings of Conference on Precision Electromagnetic Measurements, Paris, France, June 9-12, 1992, p387-388.

Keywords: *Power measurement, *Calorimeters, *Standards, Coaxial cables, Microcalorimetry, Corrections, Reprints, *Microwave power standards, *Microcalorimeters.

A technique for improving the evaluation of the microcalorimeter portion of a coaxial microwave power standard is described. The evaluation results in a factor that corrects for varying thermal paths and losses. This technique allows major components of the correction factor to be determined by direct measurement, rather than estimated indirectly.

01,893
PB95-154662 PC A03/MF A01
National Inst. of Standards and Technology (EEEL), Boulder, CO. Electromagnetic Fields Div.
Effective Medium Theory for Ferrite-Loaded Materials.
Technical note.
R. G. Geyer, J. Mantese, and J. Baker-Jarvis. Oct 94, 26p, NIST/TN-1371.
Also available from Supt. of Docs. as SN003-003-03304-9. See also PB92-205376. Prepared in cooperation with General Motors Research Labs., Warren, MI.

Keywords: *Electromagnetic theory, Binary systems(Materials), Composite materials, Barium titanates, Very high frequency, Ultrahigh frequency, Dielectric properties, Magnetic properties, Permeability, Permittivity, Inclusions, Integral equations, Spheres, Maxwell-Garnett formulae, Magnesium copper zinc ferrites, Two phase systems.

A ferrite-loaded composite medium is modeled by spherical inclusions spaced equally on a cubic lattice

within a host matrix. Both the inclusions and host matrix may be magnetically permeable and possess dielectric and magnetic loss. The ferrite-loaded medium may be considered to consist of excited Hertzian electric and magnetic dipole sources. Effective medium rules of a modified Maxwell-Garnett form can be derived by analysis of plane-wave propagation through the composite. These rules do not yield symmetric characterization of two-phase media. They are compared with other effective medium theories (Lorentz-Lorenz, Maxwell-Garnett, and Bruggeman) and broadband coaxial transmission line data measured on ferrite-loaded titanates of known composition. The modified Maxwell-Garnett rules give both lower and upper bounds for the effective permittivities and permeabilities of the composite and yield accurate estimates of bulk electric and magnetic properties for low volumetric inclusion loading. The Bruggeman formalism yields the best predicitive permittivity and permeability values when volumetric percentages of the inclusions and host matrix are approximately equal. Generally, maximal magnetic loss factors occur at a frequency where the static initial permeability decreases by a factor of one-half, and the relaxation fequency for ferrite composites increases with decreasing static initial permeability.

01,894
PB95-159885 PC A09/MF A03
National Inst. of Standards and Technology (EEEL), Gaithersburg, MD.
Electronics and Electrical Engineering Laboratory 1995 Program Plan. Supporting Technology for U.S. Competitiveness in Electronics.
Jan 95, 200p, NISTIR-5563.

Keywords: *Electronics industry, *Electrical measurement, *Metrology, *Technology transfer, Electric equipment, International trade, Competition, Microelectronics, Law enforcement, Standards, Electric utilities, Electric power generation, Semiconductor devices, Electromagnetic compatibility, Electromagnetic fields, Optoelectronic devices, US NIST.

The Electronics and Electrical Engineering Laboratory (EEEL), working in concert with other National Institute of Standards and Technology (NIST) laboratories, is providing measurement and other generic technology critical to the competitiveness of the U.S. electronics industry and the U.S. electrical-equipment industry. This 1995 Program Plan describes the projected metrological support that EEEL intends to provide to U.S. industry.

01,895
PB95-161253 Not available NTIS
National Inst. of Standards and Technology (EEEL), Gaithersburg, MD. Electricity Div.
Frequency Extension of the NIST AC-DC Difference Calibration Service for Current.
Final rept.
J. R. Kinard, T. E. Lipe, and C. B. Childers. 1993, 12p.
Pub. in Proceedings of the National Computer Systems Laboratory Workshop and Symposium, Albuquerque, NM., July 25-29, 1993, 12p.

Keywords: *Electrical measurement, *Electric current, *Standards, Frequencies, Reprints, Thermal converters, US NIST.

This paper describes the NIST standards of the ac-dc difference for current and the results of a study underway to extend the frequency range down to 10 Hz and up to 100 kHz.

01,896
PB95-161287 Not available NTIS
National Inst. of Standards and Technology (EEEL), Gaithersburg, MD. Electricity Div.
Modeling and Test Point Selection for a Thermal Transfer Standard.
Final rept.
A. D. Koffman, and H. L. Stott. 1993, 12p.
Pub. in Proceedings of National Computer Systems Laboratory Workshop and Symposium, Albuquerque, NM., July 25-29, 1993, p299-310.

Keywords: Case studies, Calibration, Selection, Frequency, Voltage, Reprints, *Thermal transfer standards, *Multirange instruments, Test points.

Full calibration support for multirange instruments can be costly and time consuming. This paper presents a case study in which a new empirical-model-based approach was used to substantially reduce the number of tests required to fully characterize an instrument. The Fluke 792A Thermal Transfer Standard was the subject instrument for the study. Test results showed that measurements made at 50 test points were sufficient to allow accurate predictions of the instrument's performance at all 255 test points specified by the manufacturer. An accurate model relating ac/dc difference to voltage and frequency for the instrument was formulated using complete test data for many devices collected by the manufacturer over several production runs. An empirical test point selection procedure was used to select an optimal set of test points and subsequently to predict the ac/dc differences of other 792As based on the limited set of measurements taken at the selected test points.

01,897
PB95-161485 Not available NTIS
National Inst. of Standards and Technology (EEEL), Boulder, CO. Electromagnetic Fields Div.
Characterization of Unknown Linear Systems Based on Measured CW Amplitude.
Final rept.
M. T. Ma, and J. W. Adams. 1993, 5p.
Pub. in Proceedings of International Symposium on Electromagnetic Compatibility, Dallas, TX., August 9-13, 1993, p78-82.

Keywords: *Linear systems, Electromagnetic compatibility, Continuous radiation, Laplace transformation, Transfer functions, Approximation, Characteristics, Reprints, Impulse response.

An approximate squared-magnitude function is derived from a given measured cw amplitude response to characterize an unknown linear system. Various possible system transfer functions (both amplitude and phase) and the corresponding impulse responses are then deduced. These transfer functions may or may not be minimum phase. The first impulse maximum and accumulated energy content are the greatest when the transfer function is at minimum phase.

01,898
PB95-161568 Not available NTIS
National Inst. of Standards and Technology (EEEL), Boulder, CO. Electromagnetic Fields Div.
Comments on 'Protecting EFIE-Based Scattering Computations from Effects of Internal Resonances'.
Final rept.
R. B. Marks. 1993, 3p.
Pub. in Institute of Electrical and Electronics Engineers Transactions on Antennas and Propagation 41, n3 p387-389 Mar 93.

Keywords: *Electromagnetic scattering, Electric fields, Magnetic fields, Integral equations, Computation, Reprints.

This letter discusses a recently-published paper which presents an approach to the problem of internal resonances of the electric field integral equation. This method, which requires the determination of the smallest singular value of the associated integral operator, may fail due to the accumulation of singular values at the origin. In contrast, another method, already in the literature, applies the magnetic field integral equation, which does not suffer from this problem.

01,899
PB95-162210 Not available NTIS
National Inst. of Standards and Technology (EEEL), Boulder, CO. Electromagnetic Fields Div.
Condensed Catalogue of Electromagnetic Environment Measurements, 30 - 300 Hz.
Final rept.
J. Randa, D. Gilliland, W. Gjertson, W. Lauber, and M. McInerney. 1993, 6p.
Pub. in Proceedings of International Symposium on Electromagnetic Compatibility, Dallas, TX., August 9-13, 1993, p126-131.

Keywords: *Electromagnetic environments, *Extremely low frequency, *Catalogs(Publications), Electromagnetic measurement, Bibliographies, Reprints.

The IEEE Electromagnetic Compatibility Society's Technical Committee on Electromagnetic Environments (TC-3) has undertaken a long-term project to compile an inventory or catalog of published measurements of electromagnetic environments. The frequency spectrum has been divided into tractable bands which will be considered one at a time. We have now completed the 30-300 Hz band. We present here an abridged version of the resulting bibliography, along with a brief summary of what has been measured.

01,900
PB95-163127 Not available NTIS
National Inst. of Standards and Technology (EEEL), Gaithersburg, MD. Electricity Div.
Observations of Partial Discharges in Hexane Under High Magnification.
Final rept.
K. L. Stricklett, E. F. Kelley, H. Yamashita, T. V. Blalock, A. L. Wintenburg, I. Alexeff, C. Fenimore, and M. O. Pace. 1990, 6p.
Proceedings of International Conference on Conduction and Breakdown in Dielectric Liquids (10th), Grenoble, France, September 10-14, 1990, p381-386.

Keywords: *Electric discharges, *Dielectric breakdown, *Hexanes, Shadowgraph photography, Photographic techniques, Direct current, Liquids, Reprints, *Partial discharges, Streamer initiation, Point cathodes.

Partial discharges are observed in n-hexane by shadow photography under the application of dc voltages. A non-uniform field geometry is employed and the growth of low-density streamers at a point cathode is recorded. Photographs of the partial discharge streamers are obtained at 200x magnification. The use of an image-preserving optical delay allows a record of the conditions which exist in the liquid prior to the initiation of low density streamer to be obtained.

01,901
PB95-163572 Not available NTIS
National Inst. of Standards and Technology (EEEL), Gaithersburg, MD. Electricity Div.
Importance of Unraveling Memory Propagation Effects in Interpreting Data on Partial Discharge Statistics.
Final rept.
R. J. Van Brunt, E. W. Cernyar, and P. von Glahn. 1993, 12p.
Sponsored by Department of Energy, Washington, DC. Office of Energy Storage and Distribution.
Pub. in Institute of Electrical and Electronics Engineers Transactions on Electrical Insulation 28, n6 p905-916 Dec 93.

Keywords: *Electric discharges, *Electrical insulation, Monte Carlo method, Static electricity, Pulse amplitude, Stochastic processes, Pattern recognition, Dielectrics, Simulation, Reprints, *Partial discharges.

The significance of memory propagation in controlling the stochastic behavior of partial-discharge phenomena is demonstrated by determination of various conditional amplitude and phase-of-occurrence distributions for both measured and simulated discharge pulses. A system that can be used to measure directly a set of both conditional and unconditional pulse amplitude and phase distributions needed to reveal memory effects and quantify the phase-resolved stochastic properties of partial-discharge pulses, is briefly described. It is argued that not only is an unraveling of memory effects essential in any attempt to understand the physical basis for the observed stochastic behavior of partial-discharge phenomena, but also that the data on conditional distributions provide additional statistical information that may be needed to optimize the reliability of partial-discharge pattern recognition schemes now being considered for use in insulation testing.

01,902
PB95-163580 Not available NTIS
National Inst. of Standards and Technology (EEEL), Gaithersburg, MD. Electricity Div.
Nonstationary Behavior of Partial Discharge during Insulation Aging.
Final rept.
R. J. Van Brunt, P. von Glahn, and T. Las. 1993, 2p.
See also PB95-163598. Sponsored by Nuclear Regulatory Commission, Washington, DC. Div. of Engineering.
Pub. in Proceedings of the International Conference on Partial Discharges, Canterbury, United Kingdom, September 28-30, 1993, p29-30.

Keywords: *Electrical insulation, *Aging(Materials), *Electric discharges, Surface resistivity, Alternating current, Aluminum oxides, Epoxy resins, Stochastic processes, Dielectrics, Fillers, Reprints, *Partial discharges.

The statistical properties of pulsating partial discharges (PD) generated by applying an alternating voltage to a point-dielectric gap were measured with a stochastic analyzer under conditions where the PD induced changes in the dielectric surface conductivity. The

epoxy materials with and without Al203 filler were considered in this investigation. In the case of epoxy with filler, dramatic changes in the statistical behavior of the PD were observed to be correlated with changes in surface conductivity. These results illustrate the difficulties to be encountered in defining meaningful PD pulse patterns that can be used for reliable defect site identification. An analysis of the positive and negative integrated-charge distribution also reveal problems of relating PD pulse-height data to average current measured by standard techniques.

01,903
PB95-163598 Not available NTIS
National Inst. of Standards and Technology (EEEL), Gaithersburg, MD. Electricity Div.
Partial Discharge: Induced Aging of Cast Epoxies and Related Nonstationary Behavior of the Discharge Statistics.
Final rept.
R. J. Van Brunt, P. von Glahn, and T. Las. 1993, 7p.
See also PB95-163580. Sponsored by Nuclear Regulatory Commission, Washington, DC. Div. of Engineering.
Pub. in 1993 Annual Report, Conference on Electrical Insulation and Electric Phenomena, Pocono Manor, PA., October 17-20, 1993, p455-461.

Keywords: *Electric discharges, *Electrical insulation, *Epoxy resins, *Aging(Materials), Time dependence, Alternating current, Stochastic processes, Monte Carlo method, Electrical measurement, Aluminum oxides, Dielectrics, Simulation, Surface resistivity, Fillers, Reprints, *Partial discharges.

Measurements were made of the time dependences of positive and negative integrated-charge distributions for ac-generated pulsating partial discharge (PD) in point-to-dielectric gaps where the dielectric material was cast epoxy either with or without an aluminum oxide filler. Other statistical characteristics of the PD were measured such as pulse-phase distributions. The dielectric surface resistivity was measured before and after exposure to PD. For epoxy with filler, the PD statistical characteristics changed significantly during times when there was a corresponding decrease in local surface resistivity. For example, the positive PD pulses were observed to cease after a time that is inversely proportional to the frequency of the applied voltage. Partial discharge from epoxy without filler exhibited a much more stationary behavior. The connection between changes in surface resistivity and changes in stochastic behavior are explained using a Monte Carlo simulation.

01,904
PB95-163960 Not available NTIS
National Inst. of Standards and Technology (EEEL), Boulder, CO. Electromagnetic Fields Div.
Verification of Scattering Parameter Measurements.
Final rept.
D. F. Williams, and R. B. Marks. 1992, 2p.
Pub. in Proceedings of Conference on Precision Electromagnetic Measurements, Paris, France, June 9-12, 1992, p371-372.

Keywords: *Electrical measurement, *Calibration, Electrical impedance, Verification, Comparison, Accuracy, Reprints, *Scattering parameters, Automatic network analyzers, On wafer calibration.

A powerful new technique enables the verification of the measurement accuracy of scattering parameter calibrations. This technique determines the relative reference impedance, the reference plane offset, and the worst-case measurement deviations of any calibration in comparison to a standard calibration. Experimental results for on-wafer measurements are presented.

01,905
PB95-164612 Not available NTIS
National Inst. of Standards and Technology (CSTL), Gaithersburg, MD. Process Measurements Div.
Electrical Characterization of Radio-Frequency Discharges in the Gaseous Electronics Conference Reference Call.
Final rept.
M. A. Sobolewski. 1993, 13p.
Pub. in Jnl. of Vacuum Science and Technology A 10, n6 p3550-3562 Nov/Dec 92.

Keywords: *Radio frequency discharge, *Gas discharges, *Glow discharges, *Argon plasma, Electrical measurement, Electrical impedance, Error analysis, Reprints, Reference cells, Plasma processing.

Measurements of the electrical characteristics of radio-frequency (rf) discharges can be subject to large errors due to limitations in the measurement instruments and the stray impedance of the discharge cell. This study reports electrical measurements of argon discharges in the GEC Reference Cell in which special care has been taken to identify and minimize these sources of error. These techniques should improve the utility of electrical measurements for gauging the reproducibility of plasma conditions among rf discharge cells, for testing theoretical results, and for monitoring plasma processing.

01,906
PB95-164695 Not available NTIS
National Inst. of Standards and Technology (EEEL), Gaithersburg, MD. Electricity Div.
Voltage Ratio Measurements of a Zener Reference Using a Digital Voltmeter.
Final rept.
R. L. Steiner, E. A. Early, and C. Kiser. 1992, 2p.
Pub. in Conference Record for Conference on Precision Electromagnetic Measurements, Paris, France, June 9-12, 1992, p300-301.

Keywords: *Electrical measurement, Calibration, Voltmeters, Accuracy, Reprints, *Voltage measurement, Voltage ratio, Voltage standards, Josephson arrays.

A high precision digital voltmeter can be used to measure the ratio of 1 V to 10 V very accurately. Preliminary tests of calibrating 10-V Zener references from a 1-V Josephson array standard indicate that an accuracy with an uncertainty of several parts in 10(exp 8) is possible.

01,907
PB95-168761 Not available NTIS
National Inst. of Standards and Technology (EEEL), Boulder, CO. Electromagnetic Fields Div.
Revised Uncertainty Analysis for the NIST 30-MHz Attenuation Calibration System.
Final rept.
J. A. Jargon. 1994, 6p.
Pub. in Proceedings of Measurement Science Conference Symposium and Workshop, Pasadena, CA., January 27-28, 1994, 6p.

Keywords: Very high frequency, Electrical measurement, Phase shift, Modification, Revisions, Attenuators, Uncertainty, Reprints, *Attenuation Calibration System, US NIST.

Although the 30-MHz Attenuation Calibration System has been in operation for many years at the National Institute of Standards and Technology, several modifications have been made to the system since the last published uncertainty analysis. The linear displacement of the standard attenuator's receiving coil is now measured with a laser interferometer instead of a steel ruled scale and optical projector, and a new comparison receiver has been installed in the system. The expanded uncertainty is on the order of + or - 0.003 dB per 10 dB step. Type A uncertainties depend upon the repeatability and resettability of the system and the device under test. Type B uncertainties are due to the standard waveguide below-cutoff (WBCO) attenuator, the resolution of the comparison receiver, the change in level of the precision phase shift standard, the level set attenuator, rf leakage, and mismatch uncertainty.

01,908
PB95-180329 Not available NTIS
National Inst. of Standards and Technology (EEEL), Boulder, CO. Electromagnetic Fields Div.
Electronic Mode Stirring for Reverberation Chambers.
Final rept.
D. A. Hill. 1994, 6p.
Pub. in Institute of Electrical and Electronics Engineers Transactions on Electromagnetic Compatibility 36, n4 p294-199 Nov 94.

Keywords: *Reverberation chambers, Electromagnetic theory, Rectangular configuration, Two dimensional, Superhigh frequency, Modal response, Numerical solution, Bandwidth, Reprints.

A modal analysis and a uniform-field approximation are presented for the fields in an idealized two-dimensional, rectangular cavity excited by an electric line source. The model is used to evaluate the effectiveness of frequency stirring, an alternative to mechanical stirring in reverberation chamber immunity measurements. Numerical results indicate that good field uniformity (standard deviation less than 1 dB) can be obtained with a bandwidth of 10 MHz at a center frequency of 4 GHz. The bandwidth requirement is determined primarily by the number of modes excited, and higher frequencies can achieve the same field uniformity with a smaller bandwidth because of the higher mode density. Cavity excitation by two single-frequency sources is also analyzed.

01,909
PB95-180444 Not available NTIS
National Inst. of Standards and Technology (EEEL), Gaithersburg, MD. Electricity Div.
NIST Strategies for Reducing Testing Requirements.
Final rept.
A. D. Koffman, T. M. Souders, and G. N. Stenbakken. 1994, 7p.
Pub. in Proceedings of Conference Test and Calibration Symposium, Arlington, VA., November 30-December 2, 1994, p267-273.

Keywords: *Electronic equipment, *Test methods, Mathematical models, Standard deviation, Analog systems, Calibration, Optimation, Reduction, Strategy, Reprints, Singular value decomposition, US NIST.

For the past several years, research has been carried out in the Electricity Division at the National Institute of Standards and Technology (NIST) to reduce the testing requirements for analog and mixed-signal devices. The most significant testing technique to result has been a model-based approach to the testing and calibration of such devices. The model is developed from empirical data, physical information, a priori information, or a combination of the three. Algebraic operations are performed on these data to create a model. The model approximately spans the vector space within which the device behavior can be described. With this model, the device can be characterized using significantly fewer measurements than is possible with traditional methods. A brief description of the techniques will be presented, along with a summary of the results achieved in testing analog and mixed-signal devices.

01,910
PB95-181046 Not available NTIS
National Inst. of Standards and Technology (EEEL), Gaithersburg, MD. Electricity Div.
Physics and Chemistry of Partial Discharge and Corona: Recent Advances and Future Challenges.
Final rept.
R. J. Van Brunt. 1994, 24p.
Sponsored by Nuclear Regulatory Commission, Washington, DC. Div. of Engineering.
Pub. in Institute of Electrical and Electronics Engineers Transactions on Dielectrics and Electrical Insulation 1, n5 p761-784 Oct 94.

Keywords: *Electric discharges, Electrical insulation, Dielectric breakdown, Electric corona, Aging(Materials), Stochastic processes, Reprints, *Partial discharges.

Results of recent research on physical and chemical processes in partial discharge (PD) phenomena are reviewed. The terminology used to specify different types or modes of PD are discussed in light of a general theory of electrical discharges. The limitations and assumptions inherent to present theoretical models are examined. The influence of memory propagation effects in controlling the stochastic behavior of PD is shown. Examples of experimental results are presented that demonstrate the nonstationary characteristics of PD which can be related to permanent or quasi-permanent discharge-induced modifications (aging) of the site where the PD occur. Recommendations for future research are proposed.

01,911
PB95-198917 PC A03/MF A01
National Inst. of Standards and Technology (EEEL), Boulder, CO. Electromagnetic Fields Div.
Electromagnetic Shielding Characterization of Gaskets.
D. A. Hill. Feb 95, 29p, NISTIR-5032.

Keywords: *Electromagnetic shielding, *Gaskets, Two dimensional models, Mathematical models, Reverberation chambers, Transfer impedance, Time domain, Slots, Shielding effectiveness, Coaxial fixtures.

Numerous measurement methods are used for determining the shielding performance of rf gaskets, but different methods give significantly different results for

the same gasket. Various measurement methods and the reasons for the discrepancies are reviewed. Simple models and theories are used to explain the meaning of transfer impedance and shielding effectiveness for gaskets and to determine the frequency range of validity. Transfer impedance should be a valid characterization at low frequencies, and shielding effectiveness is more appropriate at high frequencies. The precise frequency limitations of these characterizations and current measurement methods are not well known, but a time-domain method is proposed for determining gasket properties over a broad frequency range.

01,912
PB95-198925 PC A03/MF A01
National Inst. of Standards and Technology (EEEL), Gaithersburg, MD. Semiconductor Electronics Div.
Electronics and Electrical Engineering Laboratory Technical Publication Announcements Covering Laboratory Programs, July to September 1994 with 1995 EEEL Events Calendar.
J. M. Rohrbaugh. Mar 95, 25p, NISTIR-5607.
See also PB94-213774.

Keywords: *Microelectronics, *Metrology, *Bibliographies, Electrical measurement, Integrated circuits, Integrated optics, High temperature superconductors, Superconducting films, YBCO superconductors, Superconducting devices, Electromagnetic interference, Magnetic measurement, Microwave equipment, Video equipment, Electric power, Antennas, Silicon, Abstracts, SOI(Semiconductors), Partial discharges, SIMOX.

This is the forty-second issue of a quarterly publication providing information on the technical work of the National Institute of Standards and Technology, Electronics and Electrical Engineering Laboratory (EEEL). The issue of the EEEL Technical Publication Announcements covers the third quarter of calendar year 1994. Abstracts are provided by technical areas for papers published. Main topic areas include: Fundamental Electrical Measurements; Semiconductor Microelectronics; Signal Acquisition, Processing, and Transmission; Electrical Systems; Electromagnetic Interference; Product Data Systems (includes net information tools); Video Technology; Additional Information.

01,913
PB95-202404 Not available NTIS
National Inst. of Standards and Technology (EEEL), Boulder, CO. Electromagnetic Fields Div.
Method to Determine the Calorimetric Equivalence Correction for a Coaxial Microwave Microcalorimeter.
Final rept.
F. R. Clague. 1994, 5p.
Pub. in Institute of Electrical and Electronics Engineers Transactions on Instrumentation and Measurement 43, n3 p421-425 Jun 94.

Keywords: *Power measurement, *Calorimeters, *Standards, Coaxial cables, Microcalorimetry, Reprints, *Microwave power standards, *Microcalorimeters, Reference standards, Thermistor mounts.

A way is presented to obtain the microcalorimeter correction factor by direct measurement rather than by an indirect estimate or modeling. The microcalorimeter is used to measure the effective efficiency of a reference standard thermistor mount. The correction factor accounts for the different thermal paths and losses in the microcalorimeter reference standard combination. The uncertainty in the measurement depends primarily on an accurate determination of the correction factor. This has been an especially difficult problem in the coaxial case because of the center conductor. The method requires the fabrication of components that duplicate the thermal and RF loss in the microcalorimeter and reference standard. Using the technique with the new National Institute of Standards and Technology (NIST) type N coaxial microcalorimeter has substantially reduced the systematic uncertainty. The total uncertainty is about one-half the uncertainty of the prior NIST standard at frequencies above 1 GHz.

01,914
PB95-202412 Not available NTIS
National Inst. of Standards and Technology (EEEL), Boulder, CO. Electromagnetic Fields Div.
Developing a NIST Coaxial Microwave Power Standard at 1 mW.
Final rept.
F. R. Clague, and J. D. Splett. 1994, 8p.
Pub. in Proceedings of National Conference of Standards Laboratories 1994 Workshop and Symposium, Chicago, IL., July 31-August 4, 1994, p291-298.

Keywords: *Power measurement, *Standards, Coaxial configurations, Calibration, Thermistors, Uncertainty, Error analysis, Reprints, *Microwave power standards, Reference standards, Thermistor mounts, US NIST.

Some customers of the NIST microwave power calibration service report that they are using their calibrated reference standard at a power of about 1 mW, rather than 10 mW where the NIST measurement is made. Since the coaxial reference standards accepted by NIST for calibration are dual-element thermistor mounts, they are subject to a dual-element substitution error if not used at the calibration power level. The error differs for each mount. The error is not easily measured, nor is it possible to readily estimate an additional uncertainty for using the mount at a different power. Initial measurements indicate the error can be up to 50 percent of the quoted calibration uncertainty. If the calibration uncertainty does not increase too much, a reasonable solution is to extend the NIST calibration service to powers under 10 mW. This paper briefly describes the present standard and the approach being taken to add the 1 mW capability. Preliminary uncertainty estimates are included.

01,915
PB95-203519 Not available NTIS
National Inst. of Standards and Technology (EEEL), Boulder, CO. Electromagnetic Fields Div.
Compensation for Substrate Permittivity in Probe-Tip Calibration.
Final rept.
D. F. Williams, and R. B. Marks. 1994, 11p.
Pub. in Proceedings of Automatic Radio Frequency Techniques Group Conference Digest (44th), Boulder, CO., December 1-2, 1994, p20-30.

Keywords: Capacitance, Compensation, Permittivity, Substrates, Reprints, *Probe tip calibration, Multiline TRL method, On wafer measurement, Coplanar waveguides, Scattering parameters.

We demonstrate a method of compensation for the effect of substrate permittivity on coplanar waveguide probe-tip scattering parameter calibrations, modeling the effect as a capacitance at the probe tip. Comparison to on-wafer multiline TRL (through-reflect-line) calibration verifies its accuracy. The method allows calibration to the probe tip using generic off-wafer standards with accuracy comparable to that of on-wafer calibration.

01,916
PB95-209821 PC A03/MF A01
National Inst. of Standards and Technology (EEEL), Gaithersburg, MD. Semiconductor Electronics Div.
Electronics and Electrical Engineering Laboratory Technical Progress Bulletin Covering Laboratory Programs, April to June 1991, with 1992 EEEL Events Calendar.
Oct 91, 24p, NISTIR-4670.
See also PB92-164672 and PB94-145968.

Keywords: *Microelectronics, *US NIST, *Metrology, Standards, Research projects, Electrical engineering, Semiconductor devices, Signal processing, Electrooptics.

Contents includes research summaries on Fundamental Electrical Measurements; Semiconductor Microelectronics; Signal Acquisition, Processing and Transmission; Electrical Systems; and Electromagnetic Interference.

01,917
PB95-210480 PC A03/MF A01
National Inst. of Standards and Technology (EEEL), Gaithersburg, MD. Semiconductor Electronics Div.
Electronics and Electrical Engineering Laboratory Technical Progress Bulletin Covering Laboratory Programs, January to March 1992, with 1992/1993 EEEL Events Calendar.
Rept. for Jan-Mar 92.
J. A. Gonzalez. Sep 92, 34p, NISTIR-4901.
See also PB92-164672 and PB94-165958.

Keywords: *Electrical engineering, *Electronics, *Metrology, *US NIST, Semiconductor devices, Signal processing, Detectors, Electrical measurement, Electrooptics, Research projects.

Contents includes research summaries of: Semiconductor Microelectronics; Signal Acquisition, Processing, and Transmission; Electrical Systems; and Electromagnetic Interference.

01,918
PB95-231841 PC A03/MF A01
National Inst. of Standards and Technology (EEEL), Gaithersburg, MD. Semiconductor Electronics Div.
Electronics and Electrical Engineering Laboratory Technical Publication Announcements Covering Laboratory Programs, October to December 1994 with 1995 EEEL Events Calendar.
J. M. Rohrbaugh. May 95, 34p, NISTIR-5649.
See also PB95-198925.

Keywords: *Semiconductors, *Electrical engineering, *Signals, *Electrical systems, Electronics, Optical fibers, Microwaves, Semiconductors, Magnet measurement, *Electromagnetic interference.

This is the forty-third issue of a quarterly publication providing information on the technical work of the National Institute of Standards and Technology, Electronics and Electrical Engineering Laboratory. This issue of the EEEL Technical Publication Announcements covers the fourth quarter of calendar year 1994. Abstracts are provided by technical areas for papers published.

01,919
PB95-261954 (Order as PB95-261897, PC A07/MF A02)
National Inst. of Standards and Technology, Gaithersburg, MD.
High Accuracy Measurement of Aperture Area Relative to a Standard Known Aperture.
J. B. Fowler, and G. Dezsi. 1995, 7p.
Prepared in cooperation with National Office of Measures, Budapest (Hungary).
Included in Jnl. of Research of the National Institute of Standards and Technology, v100 n3 p277-283 May/Jun 95.

Keywords: *Apertures, *Area, *Metrology, Accuracy, Calibration standards, Precision, Radiometers, Uncertainty, National Institute of Standards and Technology.

Precise knowledge of the area of apertures used in high precision radiometry is extremely important. A method is presented here for the determination of the area of round and irregularly shaped apertures by comparison to a standard aperture which has been measured by other means to high accuracy. The method presented here is quick and has no physical contact with the fragile edge of the aperture opening.

01,920
PB96-102496 Not available NTIS
National Inst. of Standards and Technology (EEEL), Boulder, CO. Electromagnetic Technology Div.
Voltage-Standard Devices.
Final rept.
C. A. Hamilton. 1992, 4p.
Pub. in Concise Encyclopedia of Magnetic and Superconducting Materials, p621-624 1992.

Keywords: *Electrical measurement, *Standards, Measuring instruments, Volt-ampere characteristics, Electric current, Ohms Law, Electric equipment, Reprints.

The International Systems of Units, abbreviated SI, has been developed to meet the need for a uniform and consistent set of units. One of the most important and widely used of these units is the volt. The SI definition of the volt is that electromotive force between two points on a conductor carrying a constant current of 1 A when the power dissipated between the two points is 1 W. The realization of the SI volt, therefore depends on experiment that relate the primary electrical units to mechanical units of length, force and power. Precise modern instrumentation requires voltage measurements with a reproducibility exceeding the accuracy with which the SI volt can be realized. To meet this need, realizations of the volt that are stable and reproducible at a level near 0.01 ppm have been developed even though their value relative to the SI volt is uncertain within about 0.4 ppm.

01,921
PB96-102637 Not available NTIS

National Inst. of Standards and Technology (EEEL), Gaithersburg, MD. Electricity Div.
Bonding Wires to Quantized Hall Resistors.
Final rept.
K. C. Lee. 1995, 4p.
Pub. in Institute of Electrical and Electronics Engineers Transactions on Instrumentation and Measurement, v44 n2 p249-252 Apr 95.

Keywords: *Resistors, *Wire bonding, Resistance meters, Quality, Reprints, *Bonding.

Three different techniques for attaching wires on quantized Hall resistors with gold-germanium-nickel (AuGe/Ni) alloyed contacts were evaluated. The best quality and most robust samples were made by evaporating bonding pads that overlapped the alloyed contacts and the substrate, so that bonds could be made over the substrate rather than over the heterostructure.

01,922
PB96-103114 Not available NTIS
National Inst. of Standards and Technology (EEEL), Gaithersburg, MD. Electricity Div.
Nonstationary Behaviour of Partial Discharge during Discharge Induced Ageing of Dielectrics.
Final rept.
R. J. Van Brunt, P. Von Glahn, and T. Las. 1995, 9p.
Sponsored by Nuclear Regulatory Commission, Washington, DC. Div. of Engineering.
Pub. in Institute of Electrical and Electronics Engineers Proceedings: Science, Measurement and Technology, v142 n1 p37-45 Jan 95.

Keywords: *Dielectric materials, *Electric discharges, *Aging(Materials), Monte Carlo method, Simulation, Pattern recognition, Stochastic processes, Surface properties, Electric conductivity, Reprints, Nonstationary behavior, Partial discharges, Point-dielectric gaps.

Changes in the stochastic behavior of pulsating partial discharge with time have been observed when an alternative voltage is applied to point-dielectric gaps in which the dielectric is a cast epoxy resin either with, or without, Al2O3 filler. The changes in discharge behavior are shown, with the help of a Monte-Carlo simulation, to be consistent with discharge induced increases in the surface conductivity of the epoxy. This 'ageing' effect is shown to be accelerated as the frequency of applied voltage is increased from 50 to 800 Hz. The implications of the results on accelerated aging tests and definition of partial discharge 'signatures' for possible pattern recognition are discussed.

01,923
PB96-106455 PC A03/MF A01
National Inst. of Standards and Technology (EEEL), Gaithersburg, MD. Semiconductor Electronics Div.
Electronics and Electrical Engineering Laboratory Technical Progress Bulletin Covering Laboratory Programs, April to June 1995 with 1995 EEEL Events Calendar.
J. M. Rohrbaugh. Sep 95, 36p, NISTIR-5709.
See also PB95-143186.

Keywords: *Electrical engineering, *Research projects, Semiconductor devices, Metrology, Laboratories, Abstracts, US NIST, Antennas, Lasers, Optical fibers, Superconductors.

This is the fifty-first issue of a quarterly publication providing information on the technical work of the National Institute of Standards and Technology, Electronics and Electrical Engineering Laboratory. This issue of the EEEL Technical Progress Bulletin covers the second quarter of calendar year 1995. Abstracts are provided by technical area for both published papers and papers approved by NIST for publication.

01,924
PB96-111851 Not available NTIS
National Inst. of Standards and Technology (EEEL), Boulder, CO. Electromagnetic Fields Div.
Relative Accuracy of Isolated and Unisolated Noise Comparison Radiometers.
Final rept.
D. F. Wait. 1994, 2p.
Pub. in Conference on Precision Electromagnetic Measurements Digest, Boulder, CO., June 27-July 1, 1994, p256-257.

Keywords: *Radiometers, *Noise measurement, Accuracy, Isolators, Noise reduction, Comparison, Estimates, Radiometric correction, Equations, Reprints.

A rigorous radiometer equation is derived and used to develop better corrections and uncertainty estimates. Isolated and well corrected unisolated radiometers have similar accuracies for low reflection coefficient sources. To ignore corrections for the finite isolation of a radiometer, about 38 dB isolation is needed.

01,925
PB96-112156 Not available NTIS
National Inst. of Standards and Technology (EEEL), Gaithersburg, MD. Electricity Div.
Continuous Recording and Stochastic Analysis of PD.
Final rept.
P. von Glahn, and R. J. Van Brunt. 1995, 12p.
Pub. in Institute of Electrical and Electronics Engineers Transactions on Dielectrics and Electrical Insulation, v2 n4 p590-601 Aug 95.

Keywords: *Digital recording systems, *Stochastic analysis, Reprints, Design, Personal computers, Digitizers, Real time, *Partial discharges.

We describe the design and use of a digital partial discharge (PD) data recording system capable of continuous real-time recording of PD pulse trains. The recording system consists of a custom two-channel PD digitizer coupled to a personal computer via a 16-bit parallel interface. The digitizer is under software control with the resulting data being stored in binary files on the computer's hard disk. The stored data subsequently are subjected to stochastic analysis using appropriate computer software. Because all data are retained and the computer provides the desired stochastic analysis of data files, the new system is well suited to investigate non-stationary PD behavior such as encountered in aging studies. The results confirm and extend previous measurements made with an analog stochastic analyzer. With these sample results, we demonstrate how the system allows detailed stochastic analyzes not possible with data obtained from existing conventional PD measurement systems.

01,926
PB96-113568 (Order as PB96-113535, PC A05/MF A01)
National Institute of Standards and Technology, Boulder, CO.
Screened-Room Measurements on the NIST Spherical-Dipole Standard Radiator.
G. Koepke, and J. Randa. 1994, 13p.
Sponsored by Naval Air Systems Command, Washington, DC.
Included in Jnl. of Research of the National Institute of Standards and Technology, v99 n6 p737-749 Nov/Dec 94.

Keywords: *Radiators, *Electromagnetic interference, *Standards, Interlaboratory comparisons, Electromagnetic compatibility, Test chambers, Radiation sources, Field strength, Spherical configuration, Dipoles, Graphs(Charts), *Standard radiators, Screened-rooms, NIST(National Institute of Standards and Technology).

We report the results of a study of measurements of radiated emissions from the NIST spherical-dipole standard radiator in several screened rooms. The study serves as a demonstration of possible applications of the standard radiator as well as an investigation of radiated-emissions measurements in screened rooms. The screened-room measurements were performed in accordance with MIL-STD 462 (1967). Large differences occurred in the field intensity measured at different days at the same laboratory. There was a systematic difference at low frequencies between the screened-room results obtain in a transverse electromagnetic (TEM) cell, open-area test site (OATS), and anechoic chamber.

01,927
PB96-117767 PC A08/MF A02
National Inst. of Standards and Technology, Gaithersburg, MD.
Journal of Research of the National Institute of Standards and Technology, September/October 1995. Volume 100, Number 5.
1995, 160p.
See also PB96-122098 through PB96-122148 and PB96-113311. Also available from Supt. of Docs. as SN703-027-00066-1.

Keywords: *Research and development, *Calibration standards, *Metrology, Reprints, Conductivity, Electric measuring instruments, Rockwell hardness, Diamond pyramid hardness tests, Performance tests, Plastic concrete, Blackbody radiation, NIST(National Institute of Standards and Technology).

Table of Contents:
Articles:
Low Electrolytic Conductivity Standards;
Potential and Current Distributions Calculated Across a Quantum Hall Effect Sample at Low and High Currents;
Microform Calibration Uncertainties of Rockwell Diamond Indenters;
Performance Measures for Geometric Fitting in the NIST Algorithm Testing and Evaluation Program for Coordinate Measurement Systems;
A Study on the Reuse of Plastic Concrete Using Extended Set-Retarding Admixtures;
A Third Generation Water Bath Based Blackbody Source.

01,928
PB96-118039 PC A19/MF A04
National Inst. of Standards and Technology, Gaithersburg, MD.
Opportunities for Innovation: Optoelectronics.
D. E. Edgerly. May 95, 426p, NIST/GCR-95/672.

Keywords: *Electrooptics, *Technology utilization, *Fiber optics, Communication networks, Telecommunications, Technology innovation, Local area networks, Cable television, Phased array antennas, Sensors, Holography, Automotive industry, Air pollution monitors, Optical equipment, Transmitters, Receivers, Electronics industry, *Optoelectronics.

Contents:
Preface;
Optoelectronic Technology Applications in Data Processing and Data Communications Networks;
Optoelectronic Technologies for Advanced Optical Telecommunications Networks;
The Evolving Cable Television Architecture;
Intra-machine Optoelectronic Interconnection;
Optoelectronics for Phased Array Antennas;
Fiber Optic Sensors;
Optoelectronic Technology for Optical Information Processing;
Opportunities for Optoelectronics in Holographic Data Storage Systems and Neural Networks;
Automotive Industry Applications of Optoelectronics;
and Electro-optical Instrumentation for Pollution Monitoring.

01,929
PB96-119235 Not available NTIS
National Inst. of Standards and Technology (TS), Gaithersburg, MD. Standards Code and Information Program.
Electrical Product Requirements (Especially Quality Requirements) in the United States.
Final rept.
M. Breitenberg. 1995, 10p.
Pub. in Proceedings of Seminar in Microelectronics and It's Applications, Campinas, Brazil, June 20-23, 1995, p1-10.

Keywords: *Electrical equipment, *Quality assurance, *Standards, *Certification, *United States, Testing, Quality control, Requirements, Specifications, Inspection, Assessments, Reliability, Reprints.

The U.S. standardization, testing, certification, and quality system registration system is an intricate one, based on principles of openness and transparency. Responsibility for the saftey of elecctrical products is shared between the public and private sectors, with opportunity for consumers, government agencies at all levels, retailers, manufactors, and third party testing and inspection bodies to participate in the decisions that affect them. This paper attempts to answer some frequently raised questions on the U.S. system.

01,930
PB96-122486 Not available NTIS
National Inst. of Standards and Technology (EEEL), Gaithersburg, MD. Electricity Div.
Standardised Computer Data File Format for Storage, Transport, and Off-Line Processing of Partial Discharge Data.
Final rept.
T. Hucker, P. von Glahn, H. G. Kranz, and T. Okamoto. 1995, 4p.
Pub. in International Symposium on High Voltage Engineering (9th). Subject 5: Dielectrics Diagnostics and Expert Systems, Graz, Austria, August 28-September 1, 1995, p5613-1-5613-4.

Keywords: *Data files, *Data storage, *Formats, Electrical discharges, Data exchange, Data retrieval, Data processing, Data analysis, Reprints, *Partial discharges.

The authors present an overview of a proposed data file format for digitized partial discharge (PD) data. The proposed format will permit investigators at different institutions to exchange PD data and collaborate on the analysis and understanding of the PD phenomenon. The authors include an example in which investigators at all three institutions evaluated the same data record and report their analysis results.

01,931
PB96-122767 Not available NTIS
National Inst. of Standards and Technology (EEEL), Gaithersburg, MD. Electricity Div.
Influence of Surface Charge on the Stochastic Behavior of Partial Discharge in Dielectrics.
Final rept.
R. J. van Brunt, P. von Glahn, and T. Las. 1995, 8p.
Pub. in Proceedings of the International Conference on Space Charge in Solid Dielectrics (2nd), Antibes - Juan-las-Pins, France, April 2-7, 1995, p439-446.

Keywords: *Surface properties, *Charge distribution, *Dielectrics, *Stochastic processes, Pulse duration, Electrical pulses, Aluminum oxides, Impurities, Statistical analysis, Electric discharges, Reprints, PD(Partial discharge), Surface charge.

Experimental techniques have been developed in recent years that enable a complete stochastic characterization of pulsating partial-discharge (PD) phenomena in terms of a set of conditional and unconditional discharge pulse phase (or time), amplitude, and integrated-charge distributions and related correlation coefficients. Investigations using these techniques have shown the importance of pulse-to-pulse memory propagation on the statistical behavior of PD. It has been shown that the observed stochastic behavior of PD can be simulated using a theoretical model that invokes surface Charging and considers the effect of surface charge on the probability of discharge pulse initiation.

01,932
PB96-122775 Not available NTIS
National Inst. of Standards and Technology (EEEL), Gaithersburg, MD. Electricity Div.
Comment and Discussion on Digital Processing of PD Pulses.
Final rept.
P. von Glahn. 1995, 15p.
Pub. in Institute of Electrical and Electronics Engineers Transactions on Dielectrics and Electrical Insulation, v2 n4 p685-699 Aug 95.

Keywords: *Digital systems, *Signal processing, *Pulses, Dielectrics, Pulse amplitude, Pattern recognition, Errors, Identification, Reprints, PD(Partial discharge), PD pulses.

Some of the more salient aspects of the digital processing technology of PD signals are examined. Most of the efforts in this field are concentrated on the application of digital analyzers for pulse height analysis, pattern recognition and identification of the physical phenomena. It is demonstrated that errors in the signal processing unit can lead to dominant mistakes in the interpretation of the test results.

01,933
PB96-122791 Not available NTIS
National Inst. of Standards and Technology (EEEL), Boulder, CO. Electromagnetic Fields Div.
Electromagnetic Properties of Materials: The NIST Metrology Program.
Final rept.
C. M. Weil. 1993, 8p.
Pub. in Proceedings of the DOD Electromagnetic Windows Symposium (5th), Boulder, CO., October 19-21, 1993, v1 p175-182.

Keywords: *Electromagnetic properties, *Metrology, *Standards, Magnetic materials, Dielectrics, Electrical measurement, Microwave frequencies, Research programs, Reprints, US NIST.

The Electromagnetic Properties of Materials program at the National Institute of Standards and Technology (NIST) is described, including an outline of the current goals of the project and details of measurement techniques being used at NIST for characterizing dielectric and magnetic materials at RF and microwave frequencies.

01,934
PB96-123153 Not available NTIS
National Inst. of Standards and Technology (EEEL), Gaithersburg, MD. Electricity Div.
Methods for Aligning the NIST Watt-Balance.
Final rept.
G. N. Stenbakken, R. Steiner, P. T. Olsen, and E. R. Williams. 1995, 5p.
Pub. in Proceedings of Instrumentation and Measurement Technology Conference, Waltham, MA., April 24-26, 1995, p247-251.

Keywords: *Magnetic forces, Electrical measurement, Simulation, Reprints, *Watt measurement, Induced voltage, Mass stability.

The NIST watt-balance has been developed to explore the possibility of monitoring the stability of the mass standard by means of electrical quantum standards. The mass standard is the last basic standard that is kept as an artifact. The watt-balance uses a movable coil in a radial magnetic field to compare the mechanical energy required to lift a kilogram mass in earth's gravity with the electrical energy required to move the coil the same distance in a magnetic field. The electrical energy is monitored in terms of quantized Hall resistance and Josephson's junction voltage standards. The accuracy of this experiment depends on a large number of factors. Among them are the ability to align the apparatus so that the movable coil and magnet are coaxial and aligned to the local vertical. Misalignment of the coil and magnet results in forces and torques on the coil. The coil is suspended like a pendulum, so responds easily to these torques and horizontal forces. This paper describes a computer program that was written to calculate the shape of the magnetic field and the torques and forces on the movable coil that result from any misalignments. This information is being used to develop an alignment procedures that minimizes misalignments and the errors they cause. This program has enhanced our understanding of the cause of torques about the vertical axis on the coil and the dependence of this torques on the magnetic field gradient.

01,935
PB96-123179 Not available NTIS
National Inst. of Standards and Technology (EEEL), Gaithersburg, MD. Electricity Div.
Influence of Electrode Material on Measured Ion Kinetic-Energy Distributions in Radio-Frequency Discharges.
Final rept.
R. J. Van Brunt, J. K. Olthoff, and S. B. Radovanov. 1995, 2p.
Pub. in Proceedings of the International Conference on Phenomena in Ionized Gases (22nd), Hoboken, NJ., July 31-August 4, 1995.

Keywords: *Gas discharges, *Radio frequency discharges, Mass spectrometry, Plasma, Surface charging, Reprints, Ion kinetic energy, Ion sampling.

Evidence is presented for a significant influence of electrode surface material and condition on the measurement of the kinetic energies of ions samples from discharges through an orifice in the electrode. Significant differences in ion energy shifts and/or discrimination of low-energy ions are found using aluminum and stainless-steel electrodes in a radio-frequency (rf) discharge cell. It is argued that the observed differences in energy shifts may be attributable in part to differences in charging of oxide layers on the electrode surface around the sampling orifice.

01,936
PB96-123757 Not available NTIS
National Inst. of Standards and Technology (EEEL), Gaithersburg, MD. Electricity Div.
Physics and Chemistry of Partial Discharge and Corona - Recent Advances and Future Challenges.
Final rept.
R. J. Van Brunt. 1995, 42p.
Pub. in 1994 Annual Report - Conference on Electrical Insulation and Dielectric Phenomena, Arlington, TX., October 23-26, 1994, p29-70 1995.

Keywords: *Electric discharges, Electrical insulation, Dielectric breakdown, Electric corona, Aging(Materials), Stochastic processes, Reprints, *Partial discharges.

Results of recent research on physical and chemical processes on partial-discharge (PD) phenomena are reviewed. The terminology used to specify different types of modes of PD are discussed in the light of the general theory of discharges. The limitations and assumptions inherent to present theoretical models of PD are examined. The influence of memory propagation effects in controlling the stochastic behavior of PD is shown. Examples of experimental results are presented which demonstrate the nonstationary characteristics of PD which can be related to PD-induced aging of insulating materials. Recommendations for future research are proposed.

01,937
PB96-123781 Not available NTIS
National Inst. of Standards and Technology (EEEL), Gaithersburg, MD. Electricity Div.
Behavior of Surface Partial Discharge on Aluminum Oxide Dielectrics.
Final rept.
P. von Glahn, and R. J. Van Brunt. 1995, 7p.
Pub. in 1995 Annual Report: Conference on Electrical Insulation and Dielectric Phenomena, Virginia Beach, VA., October 22-25, 1995, p365-371.

Keywords: *Dielectrics, *Partial discharge, Aluminum oxide, Data recording, Behavior, Phase distributions, Purity effect, Statistical parameters, Reprints.

Partial discharge (PD) was generated with alternating voltage applied to a point electrode touching the surfaces of aluminum oxide (Al2O3) dielectrics of different purity in air. The amplitudes and phases of all pulsating PD events that occured during voltage application periods up to 35 minutes were recorded and the results were analyzed to reveal details of the characteristics of PD exhibit rapid changes with time that depend significantly on voltage and the purity of the Al2O3 sample. Example are shown of statistical data for individual positive and negative pulses in a voltage cycle that are much more refined than data that can be obtained from conventional Pd measurment systems. The results presented here illustrate the advantages of using continuous data records in the investigation and characterization of pulsating PD phenomena.

01,938
PB96-128269 PC A05/MF A01
National Inst. of Standards and Technology (EEEL), Boulder, CO. Electromagnetic Technology Div.
Metrology for Electromagnetic Technology: A Bibliography of NIST Publications, September 1995.
A. G. Bradford. Sep 95, 81p, NISTIR-5040.
See also PB95-135588 and PB96-128210.

Keywords: *Metrology, *Bibliographies, Superconductor devices, Magnetic measurements, Cryogenics, Josephson junctions, High temperature superconductors, US NIST, Cryoelectronics, Electromagnetic metrology.

This bibliography lists the publications of the personnel of the Electromagnetic Technology Division of NIST during the period from January 1970 through the publication of this report. A few earlier references that are directly related to the present work of the Division are also included. This edition of the bibliography is the first since the Electromagnetic Technology Division split into two Divisions, and it includes publications in cryoelectronic metrology and superconductor and magnetic measurements. The optical electronic metrology section found in earlier editions is now being produced seperately by the new Optoelectronics Division of NIST. That companion bibliography to this publication is NISTIR 5041.

01,939
PB96-128277 PC A08/MF A02
National Inst. of Standards and Technology (PL), Gaithersburg, MD. Radiometric Physics Div.
Metrology Issues in Terahertz Physics and Technology.
R. U. Datla, E. Grossman, and M. K. Hobish. 13 Dec 94, 164p, NISTIR-5701.
Proceedings of a workshop held in Gaithersburg, MD. on December 13, 1994.

Keywords: *Metrology, *Physics, *Meetings, Technology utilization, Infrared radiation, Research and development, Radiation measuring instruments, Accuracy, Calibrating, Standards, Infrared equipment, *Terahertz physics, THz technology.

Tremendous progress has been made in recent years in the development of new sources, detectors, antennas, and materials for the terahertz (THz) spectral region, i.e., from 100 GHz (3 mm wavelength) to 10 THz (30 micro m wavelength). However, very little attention

has been paid to questions of accurate measurement techniques, calibration, and standards at THz frequencies. In order to discuss metrology issues and the role NIST might play in the rapidly advancing field of THz technology, the staff in various divisions of NIST's Physics Laboratory, in collaboration with the staff in the Electronics and Electrical Engineering Laboratory (EEEL), convened a Workshop on Metrology Issues in THz Physics and Technology. The workshop was held at NIST on December 13, 1994, and was attended by 50 representatives from industry, academia, and federal agencies.

01,940
PB96-135116 Not available NTIS
National Inst. of Standards and Technology (EEEL), Boulder, CO. Electromagnetic Fields Div.
Analysis of an Open-Ended Coaxial Probe with Lift-Off for Nondestructive Testing.
Final rept.
J. Baker-Jarvis, M. D. Janezic, P. D. Domich, and R. G. Geyer. 1994, 8p.
Pub. in Institute of Electrical and Electronics Engineers Transactions on Instrumentation and Measurement, v43 n5 p711-718 Oct 94.

Keywords: *Calibration, *Dielectric constants, Reprints, Loss factor, Microwaves, Nondestructive, Permeability, Measurement, *Coaxial probes, Open ended probe.

The open-ended coaxial probe with lift-off is studied using a full-wave analysis, and an uncertainty analysis is presented. The field equations for the following terminations are worked out: (1) the sample extends to infinity in the positive axial direction, (2) the sample is backed by a well-characterized material, and (3) the sample is backed by a short-circuit termination. The equations are valid for both dielectric and magnetic materials. The model allows the study of the open-ended coaxial probe as a nondestructive testing tool. The analysis allows a study of the effects of air gaps on the probe measurements. The reflection coefficient and phase are studied as a function of lift-off, coaxial line size, permittivity, permeability, and frequency. Numerical results indicate the probe is very sensitive to lift-off. For medium to high permittivity values and electrically small probes, gaps on the order of fractions of a millimeter strongly influence the reflection coefficient.

01,941
PB96-137187 PC A03/MF A01
National Inst. of Standards and Technology (EEEL), Gaithersburg, MD. Semiconductor Electronics Div.
Electronics and Electrical Engineering Laboratory Technical Publication Announcements Covering Laboratory Programs, April to June 1995 with 1995 EEEL Events Calendar.
J. M. Rohrbaugh. Dec 95, 23p, NISTIR-5773.
See also PB95-242277.

Keywords: *Electrical engineering, *Electronics, *Research management, *Electrical measurement, Semiconductor devices, Metrology, Signal processing, Electromagnetism, Fiber optics, Abstracts, Catalogs(Publications), Bibliographies, Superconductors, Antennas, Electric power, Lasers, *National Institute of Standards and Technology.

This is the forty-fifth issue of quarterly publication providing information on the technical work of the National Institute of Standards and Technology, Electronics and Electrical Engineering Laboratory. This issue of the EEEL Technical Publication Announcements covers the second quarter of calendar year 1995. Abstracts are provided by technical areas for papers published.

01,942
PB96-147905 PC A04/MF A01
National Inst. of Standards and Technology (EEEL), Gaithersburg, MD. Semiconductor Electronics Div.
Electronics and Electrical Engineering Laboratory Technical Progress Bulletin Covering Laboratory Programs, July to September 1995 with 1996 EEEL Events Calendar.
J. M. Rohrbaugh. Jan 96, 37p, NISTIR-5774.
See also PB96-106455.

Keywords: *Electrical engineering, *Research projects, Semiconductors, Electromagnetic interference, Signals, Electrical systems, Metrology, Abstracts.

Contents:
Introduction;
Fundamental Electrical Measurements;
Semiconductor Microelectronics;
Signal Acquisition, Processing, and Transmission;
Electrical Systems;
Electromagnetic Interference;
Additional Information.

01,943
PB96-155452 Not available NTIS
National Inst. of Standards and Technology (EEEL), Boulder, CO. Electromagnetic Fields Div.
Catalogue of Electromagnetic Environment Measurements, 30-300 Hz.
Final rept.
J. Randa, D. Gilliland, W. Gjertson, W. Lauber, and W. McInerney. 1995, 8p.
See also PB95-162210.
Pub. in Institute of Electrical and Electronics Engineers Transactions on Electromagnetic Compatability, v37 n1 p26-33 Feb 95.

Keywords: *Electromagnetic environments, *Extremely low frequency, *Bibliographies, Electromagnetic fields, Electromagnetic measurements, Bandwidth, Reprints.

The IEEE Electromagnetic Compatibility Society's Technical Committee on Electromagnetic Environments (TC-3) has undertaken a long-term project to compile an inventory or catalogue of published measurements of electromagnetic envionments. The authors have now completed the 30-300 Hz band. The paper presents the resulting bibliography, along with a brief overview of what has been measured.

01,944
PB96-156062 Not available NTIS
National Inst. of Standards and Technology (EEEL), Boulder, CO. Electromagnetic Fields Div.
NIST Metrology Program on Electromagnetic Characterization of Materials.
Final rept.
C. M. Weil. 1994, 14p.
See also PB96-122791.
Pub. in Proceedings of the Symposium on Materials and Processes for Wireless Communication, Boston, MA., November 15-16, 1994, p35-48.

Keywords: *Electromagnetic properties, *Ceramics, *Polymers, *Microwave communities, Dielectric materials, Magnetic materials, Electrical measurement, Wireless communications, Substrates, Metrology, Research programs, Reference standards, Reprints.

The Electromagnetic Properties of Materials (EPM) Program at the National Institute of Standards and Technology (NIST) is described, including an outline of the current goals of the project and details of measurement techniques being used at NIST for characterizing dielectric and magnetic materials of importance on wireless communications in the RF spectrum of interest.

01,945
PB96-157854 Not available NTIS
National Inst. of Standards and Technology (EEEL), Boulder, CO. Electromagnetic Fields Div.
Applicability of Effective Medium Theory to Ferroelectric/Ferrimagnetic Composites with Composition and Frequency-Dependent Complex Permittivities and Permeabilities.
Final rept.
R. G. Geyer, J. V. Mantese, A. L. Micheli, J. Grosvenor, D. F. Dungan, and J. Baker-Jarvis. 1996, 6p.
Pub. in Jnl. of Applied Physics, v79 n3 p1655-1660 Feb 96.

Keywords: *Composites, *Ferrites, Microwaves, Permeability, Permittivity, Reprints, Effective medium, Mixing rules.

High-frequency (1 MHz-1 GHz) transmission line measurements were used to determine the composition and frequency-dependent complex permitivities and complex permeabilities of ferroelectric/ferrimagnetic (barium titanate and a magnesium-copper-zinc ferrite) composites. The effective medium rules of Maxwell-Garnett give both lower and upper bounds for the effective permittivities and permeabilities and yield accurate estimates of the bulk electric and magnetic properties at low volume fill fraction of either component provided the proper host matrix is chosen. Bruggeman theory yielded the best predictive values for the permittivity and permeability over the entire composition range. In all cases these complex quantities were shown to be constrained by Bergman-Milton bounds.

01,946
PB96-157862 Not available NTIS
National Inst. of Standards and Technology (EEEL), Boulder, CO. Electromagnetic Fields Div.
Influence of Films' Thickness and Air Gaps in Surface Impedance Measurements of High Temperature Superconductors Using the Dielectric Resonator Technique.
Final rept.
R. G. Geyer, J. Ceremuga, J. Krupka, and J. Modelski. 1995, 5p.
Pub. in Institute of Electronics, Information and Communications Engineers Transactions on Electronics, Japan, vE78-C n8 p1106-1110 Aug 95.

Keywords: *Dielectric resonators, *Surface resistance, Reprints, *Foreign technology, *High temperature superconductors.

The dielectric resonator technique is commonly used for microwave surface resistance measurements of High Temperature superconducting (HTS) films. Thickness of superconductors and its impact on measurement results has not been taken into consideration so far. A theoretical mode-match solution analysis of a TE011 10 GHz sapphire resonator was performed. The results of this analysis demonstrate that the thickness of the films under test can significantly affect the resonant frequencies (Fres) and quality factor Q of the resonant system, particularly when the thickness is less than three times the penetration depth lambda of the films at the operating temperature.

01,947
PB96-157888 Not available NTIS
National Inst. of Standards and Technology (EEEL), Boulder, CO. Electromagnetic Fields Div.
Two-Tier Multiline TRL for Calibration of Low-Cost Network Analyzers.
Final rept.
J. A. Jargon, and R. B. Marks. 1995, 8p.
Pub. in Automatic RF Techniques Group Meeting (ARFTG), Scottsdale, AZ., November 30-December 1, 1995, p1-8.

Keywords: *Network analyzers, *Scattering parameters, Wireless, Calibration, Measurement, Multiline, Reprints, TRL, Two-tier.

We compare calibrations for use on three-sampler vector network analyzers (VNAs) which do not allow the direct application of some advanced error-correction schemes such as TRL (thru-reflect-line). Here we compare various alternatives, including an approximate version of TRL that has been introduced commercially and two-tier multiline TRL using external software. We consider both coaxial and coplanar open-short-load-thru (OSLT) calibrations for the first tier, showing that the latter can lead to inaccuracies. Finally, we investigate the stability of the load reflection terms to show that the first tier calibration need not be frequently repeated.

01,948
PB96-158688 PC A06/MF A01
National Inst. of Standards and Technology (MSEL), Gaithersburg, MD. Ceramics Div.
Conference Proceedings: International Workshop on Instrumented Indentation. Held in San Diego, California on April 22-23, 1995.
Special pub.
D. T. Smith. Feb 96, 78p, NIST/SP-896.
Also available from Supt. of Docs. as SN003-003-03386-3.

Keywords: *Instruments, *Indentation hardness tests, *Meetings, Calibration standards, Thin films, Metal coatings, Mechanical properties, Nanoindentation, NIST(National Institute of Standards and Technology).

An international workshop was held on April 22-23, 1995, at the Town and Country Hotel in Sand Diego, to discuss the scientific and standardization issues associated with instrumented identation, also known as dynamic hardness testing or depth-sensing, ultra-low-load, or nano indentation. The workshop was sponsored jointly by the NIST Standard Reference Materials Program and the Institute for Mechanics and Materials in San Diego, with additional support for student travel from Nano Instruments, Inc., Oak Ridge, TN, and Instron Corporation, Canton, MA, and was part of the program of the 1995 International Conference on Metallurgical Coatings and Thin Films (ICMCTF95).

01,949
PB96-159215 PC A08/MF A02

National Inst. of Standards and Technology, Gaithersburg, MD.
Journal of Research of the National Institute of Standards and Technology, November/December 1995. Volume 100, Number 6.
1995, 144p.
See also PB96-159223 through PB96-159264 and PB96-117767. Also available from Supt. of Docs. as SN-703-027-00067-9.

Keywords: *Research and development, *Calibration standards, *Metrology, Performance tests, NIST(National Institute of Standards and Technology).

Contents:
- Calibration of Electret-Based Integral Radon Monitors Using NIST Polyethylene-Encapsulated 226Ra/222Rn Emanation (PERE) Standards;
- Microstructural Characterization of Cobalt-Tungsten Coated Graphite Fibers;
- On Using Collocation in Three Dimensions and Solving a Model Semiconductor Problem;
- Precision Tests of a Quantum Hall Effect Device DC Equivalent Circuit Using Double-Series and Triple-Series Connections;
- Analysis of the (5d2 + 5d6s) - 5d6p Transition Arrays of Os VII and Ir VIII, and the 6s 2S-6p2P Transitions of Ir IX.

01,950
PB96-159223 (Order as PB96-159215, PC A07/MF A02)
National Inst. of Standards and Technology, Gaithersburg, MD.
Calibration of Electret-Based Integral Radon Monitors Using NIST Polyethylene-Encapsulated (226)Ra/(222)Rn Emanation (PERE) Standards.
R. Colle, P. Kotrappa, and J. M. R. Hutchinson. 1995, 10p.
Prepared in cooperation with Rad Elec Inc., Frederick, MD.
Included in Jnl. of Research of the National Institute of Standards and Technology, v100 n6 p629-639 Nov/Dec 95.

Keywords: *Calibration standards, *Metrology, *Electret, Emanation, Environment, Ionization chamber, Measurement, Radium-226, Radon-222.

The recently developed 222Rn emanation standards that are based on polythylene-encapsulated 226Ra solutions were employed for a first field-measurement application test to demonstrate their efficacy in calibrating passive integral radon monitors. The performance of the capsules was evaluated with respect to the calibration needs of electret ionization chambers (E-PERM, Rad Elec Inc.). The encapsulated standards emanate well-characterized and known quanties of 222Rn, and were used in two different-sized, relatively-small, accumulation vessels (about 3.6 L and 10 L) which also contained the deployed electret monitors under test.

01,951
PB96-159231 (Order as PB96-159215, PC A07/MF A02)
National Inst. of Standards and Technology, Gaithersburg, MD.
Microstructural Characterization of Cobalt-Tungsten Coated Graphite Fibers.
N. S. Wheeler. 1995, 18p.
Prepared in cooperation with Virginia Univ., Charlottesville. Dept. of Materials Science and Engineering.
Included in Jnl. of Research of the National Institute of Standards and Technology, v100 n6 p641-659 Nov/Dec 95.

Keywords: *Carbon, *Cobalt, *Tungsten, Composite, Graphite, TEM, XRD.

The research concerns an electrodeposited cobalt-tungsten alloy coating on graphite fibers. Annealed and unannealed coated fibers were analyzed by scanning electron microscopy/energy dispersive x-ray spectroscopy (SEM/EDS), x-ray diffraction (XRD), and transmission electron microscopy (TEM). The mole fraction of tungsten in the as-deposited cobalt-tungsten coating was found to be (7.10 plus or minus 0.82) %, and the crystalline lattice was determined to be hexagonal closepacked. Note: The uncertainties reported here are expanded uncertainties (i.e., 2 standard deviation estimates).

01,952
PB96-159249 (Order as PB96-159215, PC A07/MF A02)
National Inst. of Standards and Technology, Gaithersburg, MD.
Using Collocation in Three Dimensions and Solving a Model Semiconductor Problem.
J. F. Marchiando. 1995, 15p.
Included in Jnl. of Research of the National Institute of Standards and Technology, v100 n6 p661-676 Nov/Dec 95.

Keywords: *Boundary, *Collocation, *Semiconductors, Poisson's equation, Three dimensional.

A research code has been written to solve an elliptic system if coupled nonlinear partial differential equations of conservation form on a rectangulary shaped three-dimensional domain. The code uses the method of collation of Gauss points with tricubic Hermite piecewise continuous polynomial basis functions. The system of equations is solved by iteration. The system of nonlinear equations is linearized, and the sysem of linear equations is solved by iterative methods.

01,953
PB96-159256 (Order as PB96-159215, PC A07/MF A02)
National Inst. of Standards and Technology, Gaithersburg, MD.
Precision Tests of a Quantum Hall Effect Device DC Equivalent Circuit Using Double-Series and Triple-Series Connections.
A. Jeffery, R. E. Elmquist, and M. E. Cage. 1995, 8p.
Included in Jnl. of Research of the National Institute of Standards and Technology, v100 n6 p677-685 Nov/Dec 95.

Keywords: *Electrical circuits, *Circuits, *Quantum Hall effect, Cryogenic current comparator, Two dimensional electron gas.

Precision tests verify the dc equivalent circuit used by Ricketts and Kemeny to describe a quantum Hall effect device in terms of electrical circuit elements. The terms employ the use of cryogenic current comparators and the double-series and triple-series connection techniques of Delahaye. Verification of the dc equivalent circuit in double-series and triple-series connections is a necessary step in developing the acquantum Hall effect as an intrinsic standard of resistance.

01,954
PB96-159264 (Order as PB96-159215, PC A07/MF A02)
National Inst. of Standards and Technology, Gaithersburg, MD.
Analysis of the (5d(2)+5d6s)-5d6p Transition Arrays of Os VII and Ir VIII, and the 6s (2)S-6p (2)P Transitions of Ir IX.
G. J. van het Hof, Y. N. Joshi, J. F. Wyart, and J. Sugar. 1995, 10p.
Prepared in cooperation with Centre National de la Recherche Scientifique, Orsay (France). Lab. Aime Coton. and Saint Francis Xavier Univ., Antigonish (Nova Scotia). Dept. Physics.
Included in Jnl. of Research of the National Institute of Standards and Technology, v100 n6 p687-697 Nov/Dec 95.

Keywords: *Energy levels, *Iridium, *Osmium, Spectra.

The spectra of osmium and iridium were photographed in the 300 Angstroms to 1600 Angstroms region on a 3 m normal incidence spectrograph using a triggered spark source. The (5d2 + 5d6s)-5d6p transition arrays of Os VII and Ir VIII were analyzed. All levels of these configurations in both spectra have been established. There are 77 lines in Os VII and 71 lines in Ir VIII classified. The parametric least squares fitting calculations are used to interpret both spectra. The 6s2S1/2-6p2P1/2,3/2 transitions in Ir IX have also been identified.

01,955
PB96-159793 Not available NTIS
National Inst. of Standards and Technology (CSTL), Gaithersburg, MD. Inorganic Analytical Research Div.
Faraday Constant.
Final rept.
W. F. Koch. 1991, 6p.
Pub. in Units and Fundamental Constants, Subvolume b: Fundamental Constants, Chapter 3.2.13, p3-213-3-218.

Keywords: *Faraday constant, *Electrochemistry, Coulomb, Reprints, Coulometry, Electricity, Silver, *Foreign technology, Fundamental physical constant.

The discovery of the quantitative relationship among electric current, time, and the amount of chemical change effected by the electric current was the first announced by Michael Faraday in the 1830's (1839 F). Because of religious convictions, Faraday, himself, never derived a mathematical expression for these laws of nature. However, these laws may be simply expressed in summary as: mole = (1/F)fIdt, where mole is the amount of substance, I is the current in amperes, and t is the time in seconds. The proportionality factor F has been appropriately named the Faraday constant (or just Faraday), and has units of coulombs per mole of univalent substance, C/mol. (A mole of univalent substance is synonymous with the term 'equivalent'.)

01,956
PB96-160320 Not available NTIS
National Inst. of Standards and Technology (EEEL), Gaithersburg, MD. Semiconductor Electronics Div.
Electron and Hole Trapping in Irradiated SIMOX, ZMR and BESOI Buried Oxides.
Final rept.
R. E. Stahlbush, G. J. Campisi, J. B. McKitterick, G. A. Brown, W. P. Maszara, and P. Roitman. 1992, 12p.
Pub. in Institute of Electrical and Electronics Engineers Transactions on Nuclear Science, v39 n6 p2086-2097 Dec 92.

Keywords: *Buried oxides, *Electron traps, Reprints, *RESOI, Silicon on insulator, SIMOX, ZMR.

Shallow electron and deep hole trapping in the buried oxides of SIMOX, ZMR and BESOI material are examined. By irradiating the oxides with x-rays at cryogenic temperatures, 40 - 50 K, hole motion is frozen and electrons are trapped. The oxide charge is determined by C-V measurements. Following the cryogenic irradiation, the electrons are detrapped by field stressing (tunneling) or by annealing (thermal excitation). Hole trapping is examined by annealing after the trapped electrons are removed by field stressing. Substantial shallow electron and deep hole trapping distributed uniformly through the oxide is observed for all buried oxides that are processed above about 1100 degrees C. A comparison to thermal oxides grown at 850 degress C and annealed at 1300 degress C with and without a polysilicon capping layer shows that the top silicon layer significantly increases trap formation.

01,957
PB96-160353 Not available NTIS
National Inst. of Standards and Technology (EEEL), Gaithersburg, MD. Semiconductor Electronics Div.
Effect of Single versus Multiple Implant Processing on Defect Types and Densities in SIMOX.
Final rept.
D. Venables, S. J. Krause, J. C. Park, J. D. Lee, and P. Roitman. 1993, 2p.
Pub. in Proceedings of the Institute of Electrical and Electronics Engineers SOI Conference, Palm Springs, CA., October 1993, p48-49.

Keywords: *Silicon, Defects, Reprints, *SIMOX, TEM, Silicon on insulator, Stacking faults.

Silicon-on-insulator material fabricated by high-dose oxygen implantation (SIMOX) has applications for high speed, radiation hard and low power devices. However, a continuing problem has been crystalline defects in the top silicon layer. SIMOX is fabricated by two distinct methods: a single oxygen implant to a dose of 1.8x10 to the 18th power cm to the minus 2 power followed by a high-temperature anneal (equal to or greater than 1300 degress C, 4-6 hr) or by multiple lower dose implants (approx. 6x10 to the 17th power cm to the minus 2 power) with high-temperature anneals after each implant. To data, there has been no systematic comparison of the defect structures produced by these two fabrication methods. Therefore, we have compared the defect structure and densities on multiple vs. single implant wafers produced on a high current implanter. In this paper we describe the origin and characteristics of the defect structures in contemporary SIMOX and show how their densities are controlled by the processing method and conditions.

01,958
PB96-162722 PC A07/MF A02
National Inst. of Standards and Technology (EEEL), Boulder, CO. Electromagnetic Fields Div.
Calibration Service for Coaxial Reference Standards for Microwave Power.
Technical note.
F. R. Clague. May 95, 116p, NIST/TN-1374.
Also available from Supt. of Docs. as SN003-003-03348-1.

Keywords: *Microwaves, *Power measurement, *Coaxial configurations, *Calibration standards, Calorimeters, Thermistors, Error analysis, Uncertainty, Frequencies, NIST(National Institute of Standards and Technology), Microwave power standards, Thermistor mounts.

A calibration service at the National Institute of Standards and Technology (NIST) for coaxial microwave power reference standards is described. The service provides measurements of the reference standard effective efficiency from 50 MHz to 18 GHz at a power level of 10 mW. In the Report of Calibration, the effective efficiency is reported in percent. The NIST microwave power standards consist of both a microcalorimeter and an associated reference standard. The reference standard is a bolometric type power detector (a thermistor mount). The only thermistor mounts accepted for measurement are those constructed to NIST specifications which are compatible with the coaxial microcalorimeter. These thermistor mounts and the automated microcalorimeter are described. A detailed error analysis with an estimate of the calibration uncertainties and their sources is included.

01,959
PB96-164520 PC A05/MF A01
National Inst. of Standards and Technology (EEEL), Gaithersburg, MD.
Electronics and Electrical Engineering Laboratory 1995 Technical Accomplishments: Advancing Metrology for Electrotechnology to Support the U.S. Economy.
J. Surette. Dec 95, 72p, NISTIR-5818.
See also PB96-147905.

Keywords: *Electrical engineering, *Research and development, *Metrology, Standards, US NIST, Semiconductor devices, Superconductors, Magnetic properties, Microwaves, Display devices, Electromagnetic compatibility, Research management.

Table of Contents:
Laboratory Director's Message;
EEEL and its Customer Interactions;
Fiscal Year 1995 Activities;
Selected FY 1995 Technical Accomplishments;
Programs Matrix-Managed by EEEL;
EEEL Awards and Recognition;
FY 1995 CRADAs;
and EEEL Organization.

01,960
PB96-165410 PC A07/MF A02
National Inst. of Standards and Technology (EEEL), Boulder, CO. Electromagnetic Fields Div.
Band-Limited, White Gaussian Noise Excitation for Reverberation Chambers and Applications to Radiated Susceptibility Testing.
Technical note.
M. L. Crawford, T. A. Loughry, M. O. Hatfield, and G. J. Freyer. Jan 96, 112p, NIST/TN-1375.
Also available from Supt. of Docs. as SN003-003-03392-8.

Keywords: *Reverberation chambers, *Electromagnetic shielding, *Electromagnetic susceptibility, Bandwidth, Shielding effectiveness, Mode stirred chambers, Frequency stirring.

The report gives the results of demonstration tests conducted to (1) evaluate the electromagnetic environment (EME) produced by band-limited, white gaussian noise (BLWGN) excitation of a reverberation chamber and to verify its applications to susceptibility and shielding effectiveness (SE) testing. Data were collected to compare the EME produced in a reverberation chamber by CW and swept frequency excitation using both mechanical stirring and BLWGN to excite the cavity mode structure. The feasibility of using the BLWGN technique for radiated susceptibility testing was evaluated by comparison with mechanical stirring in a reverberation chamber and with anechoic chamber results. Within normal measurement uncertainties, the response of both types of systems were the same for mechanical stirring and for BLWGN excitation and were consistent with the results obtained in the anechoic chamber.

01,961
PB96-165998 PC A05/MF A01
National Inst. of Standards and Technology (MSEL), Gaithersburg, MD. Polymers Div.
Beyond the Technology Roadmaps: An Assessment of Electronic Materials Research and Development.
M. A. Schen, T. J. Russell, R. F. Leheny, G. Borsuk, A. Yang, H. Simon, and V. Hess. Mar 96, 60p, NISTIR-5777.
Prepared in cooperation with Defense Advanced Research Projects Agency, Arlington, VA., Department of Commerce, Washington, DC. Technology Administration., National Science Foundation, Arlington, VA. and Naval Research Lab., Washington, DC.

Keywords: *Electronic equipment, *Microelectronics, *Materials, Photonics, Research management, Microwaves, Radiofrequency, Electronic industry, Modules(Electronics), Mass storage.

This report, produced by the National Science and Technology Council, Electronic Materials Working Group, captures the findings of the December 6-7, 1994 industry-government-university Workshop on Electronic Materials held in Dallas, TX. It provides summary of the dominant electronics materials issues facing U.S. industry and contains recommendations critical to the advancement and competitiveness of the U.S. electronics and materials industries. The technologies encompassed within this report are microelectronics, radio frequency and microwave electronics, photonics, mass storage, and module interconnection. In addition, materials characterization and materials research, two areas essential to the understanding, discovery and utilization of materials, are included.

01,962
PB96-175237 PC A10/MF A03
National Inst. of Standards and Technology (EEEL), Gaithersburg, MD.
Electronics and Electrical Engineering Laboratory: 1996 Program Plan. Supporting Technology for U.S. Competitiveness in Electronics.
L. L. Sacchet. 1996, 198p, NISTIR-5832.
See also PB95-159885.

Keywords: *Electronic industry, *Electrical measurement, *Metrology, *Technology transfer, *Electronics, Electric equipment, International trade, Competition, Microelectronics, Law enforcement, Standards, Electric utilities, Semiconductor devices, Electromagnetic compatibility, Electromagnetic fields, Optoelectronics devices, Commercialization, Abstracts, Research projects.

The Electronics and Electrical Engineering Laboratory (EEEL), working in concert with other NIST Laboratories, is providing measurement capability and other generic technology critical to the competitiveness of the U.S. electronics industry and the U.S. electrical-equipment industry. This 1996 Program Plan describes the technical projects that EEEL plans to conduct in fiscal year 1996 to provide metrological support to U.S. industry.

01,963
PB96-176573 Not available NTIS
National Inst. of Standards and Technology (MSEL), Gaithersburg, MD. Ceramics Div.
Electromagnetic Coupling Character of (001) Twist Boundaries in Sintered Bi2Sr2CaCu2O8+x Bicrystals.
Final rept.
J. L. Wang, X. Y. Cai, R. J. Kelley, D. C. Larbalestier, M. D. Vaudin, and S. E. Babcock. 1994, 10p.
Pub. in Physica C, v230 p189-198 1994.

Keywords: *Bicrystals, *Electromagnetic coupling, Reprints, *Critical current density, Grain boundaries, Weak coupling, Weak links.

The electromagnetic characteristics of (001) twist grain boundaries in Bi2Sr2CaCu2O8+x (BSCCO-2212) have been deduced from measurements of the resistive transitions, voltage-current (V-I) characteristics, and field-dependent transport critical current densities (Jct(H)) of single- and bicrystalline samples. The bicrystals were prepared by solid-state sintering of (001) faces of freshly-cleaved, bulk-scale single crystals placed at a pre-determined misorientation angle, O. A low-angle 2 degrees bicrystal was strongly coupled with V-I and Jct(H) characteristics that were indistinguishable from those of the single crystals, indicating that the sintering process itself does not produce weak coupling. 30 degrees and 36 degrees (001) bicrystals were weakly coupled. 23 degrees and 88 degrees twist bicrystals were strongly coupled, even though their boundary Tc values were reduced. This behavior contrast starkly with that of (001) tilt boundaries in YBa2Cu3O7-, where a reduced boundary Tc is always associated with weak coupling.

01,964
PB96-180070 Not available NTIS
National Inst. of Standards and Technology (EEEL), Gaithersburg, MD. Semiconductor Electronics Div.
Scanning Capacitance Microscopy Measurements and Modeling: Progress Towards Dopant Profiling of Silicon.
Final rept.
J. J. Kopanski, J. F. Marchiando, and J. R. Lowney. 1996, 6p.
See also PB96-148150 and PB96-164207.
Pub. in Jnl. of Vacuum Science and Technology B, v14 n1 p242-247 Jan/Feb 96.

Keywords: *Capacitance imaging, Modeling, Collocation, Reprints, *Scanning capacitance microscopy, *Poisson's equation.

A scanning capacitance microscope (SCM) has been implemented by interfacing a commercial contact-mode atomic force microscope with a high-sensitivity capacitance sensor. The SCM has promise as a next-generation dopant-profiling technique because the measurement in inherently two dimensional, has a potential spatial resolution limited by tip diameter of at least 20 nm, and requires no current carrying metal-semiconductor contact. Differential capacitance images have been made with the SCM of a variety of bulk-doped samples and in the vicinity of pn junctions and homojunctions. Also, a computer code has been written that can numerically solve Poisson's equation for a model SCM geometry by using the method of collocation of Gaussian points. Measured data and model output for similar structures are presented. How data and model output can be combined to achieve an experimental determination of dopant profile is discussed.

01,965
PB96-183066 PC A03/MF A01
National Inst. of Standards and Technology (EEEL), Gaithersburg, MD. Semiconductor Electronics Div.
Electronics and Electrical Engineering Laboratory Technical Publication Announcements Covering Laboratory Programs, July to September 1995 with 1996 EEEL Events Calendar.
J. M. Rohrbaugh. Apr 96, 26p, NISTIR-5816.
See also PB96-137187.

Keywords: *Electrical engineering, *Research projects, Semiconductor devices, Metrology, Laboratories, Abstracts, Electromagnetic interference, Optical fibers, Lasers, Antennas, Electrical measurement.

This is the forty-sixth issue of a quarterly publication providing information on the technical work of the National Institute of Standards and Technology, Electronics and Electrical Engineering Laboratory. This issue of the EEEL Technical Publication Announcements covers the third quarter of calendar year 1995. Abstracts are provided by technical areas for papers published.

01,966
PB96-183116 PC A04/MF A01
National Inst. of Standards and Technology (EEEL), Gaithersburg, MD. Semiconductor Electronics Div.
Electronics and Electrical Engineering Laboratory Technical Progress Bulletin Covering Laboratory Programs, October to December 1995 with 1996 EEEL Events Calendar.
J. M. Rohrbaugh. Apr 96, 40p, NISTIR-5815.
See also PB96-147905.

Keywords: *Electrical engineering, *Research projects, Semiconductor devices, Metrology, Microelectronics, Laboratories, Abstracts, Signal processing, Optical fibers, Electromagnetic interference, Standards, US NIST, Dielectrics, Superconductors, Electrical measurement, Antennas, Lasers, Electronics, Electrical insulation, Microwave equipment.

This is the fifty-third issue of a quarterly publication providing information on the technical work of the National Instititute of Standards and Technology, Electronics and Electrical Engineering Laboratory. This issue of the EEEL Technical Progress Bulletin covers the fourth quarter of calendar year 1995. Abstracts are provided by technical area for both published papers and papers approved by NIST for publication.

01,967
PB96-186010 Not available NTIS
National Inst. of Standards and Technology (PL), Boulder, CO. Time and Frequency Div.
Surface Transverse Wave Oscillators with Extremely Low Thermal Noise Floors.
Final rept.
I. D. Avramov, F. L. Walls, T. E. Parker, and G. K. Montress. 1994, 16p.
Pub. in Proceedings of the Institute of Electrical and Electronics Engineers International Frequency Control Symposium, Boston, MA., June 1-3, 1994, p379-394.

Keywords: *Phase noise, *Power oscillator, Reprints, *Surface transverse wave resonators, Line discriminator, A-B class power amplifier.

This paper presents state-of-the-art results on 1 Ghz surface transverse wave (STW) power oscillators running at extremely high loop power levels. High-Q single-mode STW resonators used in these designs have an insertion loss of 3.6 dB, an unloaded Q of 8000, a residual phase noise of -142 dBc/Hz at 1 Hz intercept and operate at an incident power of up to 31 dBm in the loop. Other low-Q STW resonators and coupled resonator filters (CRF) with an insertion loss in the 5-9 dB range can conveniently handle power level in escess of 2 W. These devices were implemented in voltage controlled oscillators (VCO's) running from a 9.6 V source at an output power of 23 dBm and a RF/dc efficiency of 28%. Their tuning range was 750 kHz and the noise floor - 180 dBc/Hz. The oscillators, stabilized with the high-Q devices, use specially designed AB-class power amplifiers, deliver an output power of 29 dBm and demonstrate a noise floor of -184 dBc/Hz and a 1 Hz intercept of -17 dBc/Hz. The 1 Hz intercept was improved to -33 dBc/Hz using the UTO-1023 as a loop amplifier. In this case the output power was 22 dBm. In all cases the loop amplifier was the limiting factor for the close-to-carrier oscillator phase noise performance.

01,968
PB96-190228 Not available NTIS
National Inst. of Standards and Technology (EEEL), Boulder, CO. Electromagnetic Technology Div.
Models of Granualr Giant Magnetoresistance Multilayer Thin Films.
Final rept.
J. O. Oti, S. E. Russek, S. C. Sanders, and R. W. Cross. 1996, 9p.
Pub. in Institute of Electrical and Electronics Engineers Transactions on Magnetics, v32 n2 p590-598 Mar 96.

Keywords: *Thin films, *Magnetoresistance, Models, Anisotropy, Exchange, Multilayers, Spin-valves, Micromagnetic, Reprints.

Phenomenological micromagnetic and large-scale magnetization-dependent models of resistivity that produce giant magnetoresistance in granular multilayer magnetic thin films are described. Included in the models are intralayer and interlayer scattering components formulated explicitly in terms of the microstructural properties and characteristic transport lengths of the medium. The micromagnetic model provides insight into the influence of the magnetization distribution on the giant magnetoresistance response of the medium. The large-scale model which is derived from the micromagnetic model, is useful for obtaining media transport parameters from experimental data. Both models are used to study a set of annealed NiFe/Ag multilayer films.

01,969
PB96-191390 PC A04/MF A01
National Inst. of Standards and Technology (EEEL), Gaithersburg, MD. Semiconductor Electronics Div.
Electronics and Electrical Engineering Laboratory Technical Progress Bulletin Covering Laboratory Programs, January to March 1996, with 1996 EEEL Events Calendar.
J. M. Rohrbaugh. Jun 96, 40p, NISTIR-5853.
See also PB96-183116.

Keywords: *Electrical engineering, *Research projects, Semiconductor devices, Metrology, Laboratories, Abstracts, US NIST, Antennas, Lasers, Optical fibers, Superconductors, Electronics, Microwaves, Electrical measurement, Microelectronics.

This is the fifty-fourth issue of a quarterly publication providing information on the technical work of the National Institute of Standards and Technology, Electronics and Electrical Engineering Laboratory. This issue of the EEEL Technical Progress Bulletin covers the first quarter of calendar year 1996. Abstracts are provided by technical area for both published papers and papers approved by NIST for publication.

01,970
PB96-200282 Not available NTIS
National Inst. of Standards and Technology (EEEL), Boulder, CO. Electromagnetic Fields Div.
Data Evaluation of a Linear System by a Second-Order Transfer Function.
Final rept.
D. G. Camell, and M. T. Ma. 1995, 5p.
See also PB95-182390.
Pub. in Institute of Electrical and Electronics Engineers EMC Symposium Conference Record, August 14-18, 1995, p511-515.

Keywords: *Electromagnetic interference, *Convolution integrals, Electromagnetic pulses, Transfer functions, Continuous radiation, Resonant frequency, Linear systems, Magnitude, Reprints, Impulse response.

A recently developed technique for predicting the response of a linear system to an electromagnetic pulse, based only on the measured sontinuous-wave magnitude, is applied to a particular system as a case study. The measured magnitude representing the system's transfer function is deduced first from the measured response to a known cw source. The authors next derive an analytic expression for the magnitude square of the transfer function to approximate the measured data and obtain a system transfer function in terms of the complex frequency. Finally, the authors predict the system's cw phase characteristics and its multiple solutions due to a given impulse source.

01,971
PB96-200332 Not available NTIS
National Inst. of Standards and Technology (EEEL), Boulder, CO. Electromagnetic Technology Div.
Observation of the Transverse Second Harmonic Magneto-Optic Kerr Effect from Ni81Fe19 Thin Film Structures.
Final rept.
T. M. Crawford, C. T. Rogers, T. J. Silva, and Y. K. Kim. 1996, 3p.
Pub. in Applied Physics Letters, v68 n11 p1573-1575 Mar 96.

Keywords: *Thin films, *Multiple reflection theory, Magnetic interfaces, Second harmonics, Reprints, *Kerr effect, MOKE, Non-linear optics, Second order susceptibility, SH conversion efficiency.

We report second-harmonic magneto-optic Kerr measurements on air-exposed, polycrystalline Ni81Fe19 thin films, ranging in thickness from 1 nm to 2 micro m, on Al2O3 coated Si (001). For samples thicker than 20 nm, in the tranverse Kerr geometry, we observe a factor of 4 change in second-harmonic intensity upon magnetization reversal. For thin samples, we observe interference between second-harmonic fields from the various interfaces and deterioration of ferromagnetism in the 1 and 2 nm films. Modeling suggests that the Ni81Fe19/Al2O3 interface has a larger second-order susceptibility than the air/Ni81Fe19 surface.

01,972
PB96-200407 Not available NTIS
National Inst. of Standards and Technology (EEEL), Boulder, CO. Electromagnetic Fields Div.
30 MHz Comparison Receiver.
Final rept.
J. A. Jargon. 1995, 3p.
Pub. in Asia-Pacific Microwave Conference Proceedings, Taejon, Korea, October 10-13, 1995, v1 p94-96.

Keywords: *Electrical measurements, *Microwave circuits, Phase shift, Reprints, *Attenuation Calibration System.

The National Institute of Standards and Technology has developed a highly sensitive 30 MHz comparison receiver for detecting low-level rf signals in the nanvolt region. The purpose of this instrument is to detect a null between two signals that can be adjusted in phase and magnitude. This paper contains a description of the receiver, specifications, and theory of operation.

01,973
PB96-200837 Not available NTIS
National Inst. of Standards and Technology (MSEL), Gaithersburg, MD. Ceramics Div.
Measurements of Properties of Materials in Electronic Packaging.
Final rept.
J. A. Carpenter. 1991, 13p.
Pub. in Proceedings of a Symposium Metal-Ceramic Joining, Detroit, MI., October 8-9, 1990, p205-217 1991.

Keywords: *Electronic packaging, *Measurement, *Reliability analysis, Manufacturing, Performance, Physical properties, Mechanical properties, Electrical properties, Thermal properties, Costs, Reprints.

Designers require reliable values of properties of the materials in electronic packaging in order to accurately predict the performance of their products. This chapter looks at techniques for measuring the important electrical, thermal, mechanical, and physical properties of electronic packaging, and three other properties which assess the ease, efficiency, degree of success, or costs of processing the materials' manufacturability properties.

01,974
PB96-200852 Not available NTIS
National Inst. of Standards and Technology (EEEL), Boulder, CO. Electromagnetic Technology Div.
Self-Reciprocal Fourier Functions.
Final rept.
M. W. Coffey. 1994, 3p.
Pub. in Jnl. of Optical Society of America A, v11 n9 p2453-2455 Sep 94.

Keywords: *Fourier transformation, *Self reciprocal function, Optical applications, Diffraction theory, Inverse transform, Reprints, Mellin transform, Laplace transform.

By definition, a self-reciprocal (SR) function is its own Fourier or Hankel transform. Areas of application of SR functions, including fourier optics, are noted. Integral representations for SR functions are obtained and are illustrated with the exponential Fourier transformation on the half-line. It is pointed out that there are a large number of classes of SR functions, and examples of these functions are given.

01,975
PB96-200878 Not available NTIS
National Inst. of Standards and Technology (EEEL), Boulder, CO. Electromagnetic Technology Div.
Wideband Current and Magnetic Field Sensors Based on Iron Garnets.
Final rept.
M. N. Deeter, K. B. Rochford, A. H. Rose, and G. W. Day. 1993, 6p.
Pub. in Proceedings of the Annual Defense Advanced Research Projects Agency Symposium on Photonics Systems for Antenna Applications (3rd), Monterey, CA., January 20-22, 1993, p92-97.

Keywords: *Magnetic field sensors, *Iron garnets, Faraday effect, Flux concentration, Waveguides, Magneto-optics, Reprints, Electric current sensors, Radiation-induced darkening.

Sensors based on the Faraday effect can be configured to measure either magnetic fields or electric currents. Such sensors can be constructed without introducing conducting materials which are often undesirable. Presently, the most sensitive Faraday effect sensors employ ferrimagnetic iron garnets as the sensing elements. With these materials, we have demonstrated minimum detectable fields as low as 1 pT/Hz1/2 and currents as low as 200 nA/Hz1/2. The paper reviews these and other recent research results obtained at NIST and considers prospects for still further improvements in sensitivity and frequency response.

01,976
PB96-200902 Not available NTIS
National Inst. of Standards and Technology (EEEL), Boulder, CO. Electromagnetic Technology Div.
Performance of the Electron Pump with Stray Capacitances.
Final rept.
H. D. Jensen, and J. M. Martinis. 1994, 2p.
Pub. in Physica B, v194-196 p1255-1256 1994.

Keywords: *Electron pumps, *Coulomn blockage, *Metrology, Reprints, Single electron tunneling.

We calculate the effect of stray capacitance on the performance of the electron pump for a simplified and experimentally appropriate circuit model. We show that to first order the effect of the stray capacitances can

be accounted for by replacing the junction capacitance C with C + A C(stray), where a equals 1 and C(stray) is the average total stray capacitance of the metal islands between the junctions.

01,977
PB96-201025 Not available NTIS
National Inst. of Standards and Technology (EEEL), Boulder, CO. Electromagnetic Technology Div.
Novel Hot-Electron Microbolometer.
Final rept.
M. Nahum, and J. M. Martinis. 1994, 2p.
See also DE93002542.
Pub. in Physica B, v194-196 p109-110 1994.

Keywords: *Infrared detectors, *Bolometers, *Antennas, Superconducting junctions, Electron tunneling, Microbolometers, Hot electrons.

The authors present measurements of a novel power detector which can be used as an ultra-sensitive detector of millimeter and sub-millimeter radiation. The absorbing element consists of a thin film resistor with submicrometer dimensions, which is connected to superconducting electrodes. This device exploits the Andreev reflection of electrons, and the weak interaction between electrons and phonons at low temperatures, in order to produce a large temperature rise for a small input power (approximately 10 mK/fW). The temperature rise of the electrons is measured from the temperature dependence of the current-voltage characteristic of a superconductor-insulator-normal metal tunnel junction, where part of the resistor strip forms the normal electrode. The authors have measured a voltage responsitivity approximately 10 to the ninth power V/W, and an amplifier-limited electrical NEP approximately 3x 10 to the minus 18th power WHz to the minus one half power at an operating temperature of 100 mK. If infrared radiation were coupled to the absorbing element by using superconducting planar anntennas, then the sensitivity of this detector would be at least a factor of 10 higher than the best available direct detectors and thus may become the detector of choice for important astrophysics investigations.

01,978
PB96-202346 PC A04/MF A01
National Inst. of Standards and Technology (EEEL), Gaithersburg, MD. Semiconductor Electronics Div.
Electronics and Electrical Engineering Laboratory Technical Publication Announcements Covering Laboratory Programs, October to December 1995, with 1996 EEEL Events Calendar.
J. M. Rohrbaugh. Jul 96, 31p, NISTIR-5872.
See also PB96-183066.

Keywords: *Electrical engineering, *Research projects, Electrical measurement, Semiconductor devices, Metrology, Abstracts, Electromagnetic interference, Laboratories, Optical fibers, Signals.

This is the forty-seventh issue of a quarterly publication providing information on the technical work of the National Institute of Standards and Technology, Electronics and Electrical Engineering Laboratory. This issue of the EEEL Technical Publication Announcements covers the fourth quarter of calendar year 1995. Abstracts are provided by technical areas for papers published.

01,979
PB96-210026 PC A04/MF A01
National Inst. of Standards and Technology (EEEL), Boulder, CO. Electromagnetic Fields Div.
Rapid Evaluation of Mode-Stirred Chambers Using Impulsive Waveforms.
Technical note.
J. M. Ladbury, R. T. Johnk, and A. R. Ondrejka. Jun 96, 39p, NIST/TN-1381.
Also available from Supt. of Docs. as SN003-003-03417-7.

Keywords: *Reverberation, *Electromagnetic compatibility, Electromagnetic fields, Electromagnetic noise.

In this paper, the authors present an experimental technique for the rapid evaluation of mode-stirred (or reverberation) chambers. The measurement provides an estimate of the average chamber quality factor (Q) by measuring the chamber impulse response and observing the decay of the spectral components of the response. The results show good agreement with those obtained using conventional CW techniques. The measurement is well suited for low-frequency analysis of a chamber, where costly and time consuming mode-tuned approaches are generally employed. Since this technique does not use paddle stirring, the time savings can be considered.

01,980
PB96-210778 PC A08/MF A02
National Inst. of Standards and Technology (EEEL), Boulder, CO. Electromagnetic Fields Div.
Bibliography of the NIST Electromagnetic Fields Division Publications.
R. M. Lyons. Aug 96, 134p, NISTIR-5050.
See also PB95-135562.

Keywords: *Electromagnetic fields, *Bibliographies, Antennas, Dielectric properties, Electrical measurement, Electromagnetic interference, Microwaves, Metrology, Electromagnetic noise, Remote sensing, Time domain, Waveforms, Attenuation, Electrical impedance, Impedance measurement, Near fields, Antenna radiation patterns, Radiation hazards, Standards, *US NIST, Nonionizing radiation.

This bibliography lists the publications by the staff of the Electromagnetic Fields Division of the National Institute of Standards and Technology for the period January 1970 through July 1996. It supersedes NISTIR 5039, which listed the publications of the Electromagnetic Fields Division from January 1970 through July 1995. Selected earlier publications from the division's predecessor organizations are included.

01,981
PB96-214622 PC A03/MF A01
National Inst. of Standards and Technology (EEEL), Gaithersburg, MD. Semiconductor Electronics Div.
Electronics and Electrical Engineering Laboratory Technical Publication Announcements Covering Laboratory Programs, January to March 1996, with 1996 EEEL Events Calendar.
J. M. Rohrbaugh. Aug 96, 25p, NISTIR-5892.
See also PB96-202346.

Keywords: *Electrical engineering, *Research projects, Semiconductor devices, Metrology, Laboratories, Abstracts, US NIST, Antennas, Electromagnetic interference, Optical fibers, Lasers, Microelectronics, Electrical measurements, Standards, Electronics, Microwaves.

This is the forty-eight issue of a quarterly publication providing information on the technical work of the National Institute of Standards and Technology. Electronics and Electrical Engineering Laboratory. This issue of the EEL Technical Publication Announcements covers the first quarter of calendar year 1996. Abstracts are provided by technical areas for both published papers and papers approved by NIST for publication.

01,982
PB97-111454 Not available NTIS
National Inst. of Standards and Technology (EEEL), Gaithersburg, MD. Electricity Div.
Proposed Tests to Evaluate the Frequency-Dependent Capacitor Ratio for Single Electron Tunneling Experiment.
Final rept.
S. Avramov-Zamurovic, N. M. Zimmerman, A. F. Clark, and A. Jeffery. 1996, 2p.
Pub. in Conference on Precision Electromagnetic Measurements, Braunschweig, Germany, June 17-20, 1996, p265-266.

Keywords: *Capacitor ratio, *Single electron tunneling, Voltage divider, Frequency dependence, Capacitance, Reprints, *Foreign technology.

A precise measurement of the ratio of two cryogenic capacitors is needed for a capacitor charging experiment using Single Electron Tunneling (SET) phenomena. To support the capacitor charging metrology a frequency characterization of the capacitors is required. To cover the frequency range from 1 Hz to 1 kHz, resistive and inductive voltage divider bridges are proposed. Preliminary tests suggest that the uncertainty with which the capacitor ratio can be evaluated is less than one part per 10 to the sixth power.

01,983
PB97-111512 Not available NTIS
National Inst. of Standards and Technology (EEEL), Gaithersburg, MD. Electricity Div.
Transient Errors in a Precision Resistive Divider.
Final rept.
S. A. Boggs, G. J. FitzPatrick, and J. Kuang. 1996, 4p.
Pub. in Proceedings of the Institute of Electrical and Electronics Engineers International Symposium on Electrical Insulation, Montreal, Quebec, Canada, June 16-19, 1996, p482-485.

Keywords: *Resistive dividers, *Transient errors, Heating effects, High voltage, Impulse measurements, Reprints.

Resistive dividers have the advantages of dc response and stability. However unlike capacitive dividers, they inevitably involve power dissipation and also generally involve an appreciable inductance. These aspects of a resistive divider result in transient errors, i.e., errors which are a function of the applied waveform. The paper discusses transient measurement errors of precision high voltage resistive dividers such as the one recently developed by NIST.

01,984
PB97-111843 Not available NTIS
National Inst. of Standards and Technology (EEEL), Gaithersburg, MD. Electricity Div.
Uncertainties of Frequency Response Estimates Derived from Responses to Uncertain Step-Like Inputs.
Final rept.
J. P. Deyst, T. M. Souders, and J. J. Blair. 1996, 4p.
Pub. in Institute of Electrical and Electronics Engineers Instrumentation and Measurement Technology Conference, Brussels, Belgium, June 4-6, 1996, p151-154.

Keywords: *Frequency response, *Step response, Electrical measurement, Signal conditioning, Algorithms, Errors, Test methods, Mathematical models, Estimates, Reprints.

The frequency response of a linear time-invariant system can be estimated from the measurement of its response to an ideal step input. However, an ideal step is unrealizable, and various other error sources affect the accuracy of such estimates. The paper investigates the effect of using an uncertain (inexactly known), step-like test signal. An approach is developed here for determining the systematic uncertainties of the frequency response estimate of a device under test (DUT), when it is estimated from the response, are converted to the frequency domain and processed, resulting in uncertainties for the frequency response of the DUT. Also, a mathematical proof is provided for the 'envelope-modulation' method of calculating the systematic uncertainties of a frequency response estimate of a device, as derived from the uncertain response of the device to an ideal step.

01,985
PB97-111918 Not available NTIS
National Inst. of Standards and Technology (EEEL), Gaithersburg, MD. Electricity Div.
Optical and Mass Spectrometric Investigations of Ions and Neutral Species in SF6 Radio-Frequency Discharges.
Final rept.
R. Foest, J. K. Olthoff, R. J. Van Brunt, E. C. Benck, and J. R. Roberts. 1996, 12p.
Pub. in Physical Review E, v54 n2 p1876-1887 Aug 96.

Keywords: *Radio frequency discharges, *Electrode surface effects, Ion kinetic energy, Laser induced fluorescence, Electric characteristics, Degree of dissociation, Reprints.

Radio-frequency (rf) discharges at 13.56 MHz were generated in pure SF6 using a capacitively coupled, parallel-plate GEC reference cell for gas pressures in the range of 4-33.3 Pa (30-250 mTorr) and for peak-to-peak applied rf voltages in the range of 100-300 V. The following measurements were made during operation of the discharge: (1) electrical characteristics which included power dissipation, voltage-current phase angle, and the dc self-bias; (2) time-averaged vertical and horizontal profiles of the optical emissions from neutral atomic fluorine for the 2p(4)3p' 2F(0)7/2 -> 2p(4)3s' 2D5/2 and 2p(4)3p(2)p(0)3.2 -> 2p(4)3s(2)P3/2 transitions; (3) spatially resolved, laser-induced fluorescence (LIF) utilizing the 2p(4)3s(4)p5/2 metastable level of atomic fluorine; (4) mass spectra of neutral species in the plasma; and (5) kinetic-energy distributions and relative fluxes of mass-selected positive ions extracted from the plasma through a 0.1 mm diameter orifice in the grounded electrode. The dependence of the electrical characteristics on gas pressure confirms previous observations and model predictions which indicate, for example, that the plasma becomes more resistive as pressure increases.

01,986
PB97-111926 Not available NTIS

National Inst. of Standards and Technology (EEEL), Gaithersburg, MD.
New Refractometer by Combining a Variable Length Vacuum Cell and a Double-Pass Michelson Interferometer.
Final rept.
K. Fujii, E. R. Williams, and R. L. Steiner. 1996, 2p.
Pub. in Conference on Precision Electromagnetic Measurements, Braunschweig, Germany, June 17-20, 1996, p128-129.

Keywords: *Interferometers, *Refractometers, *Polarized interferometer, Air index, Watt determination, Reprints, *Foreign technology, *Michelson interferometers, Variable length vacuum.

A new refractometer with a variable length vacuum cell has been developed, where the refractive index of air is determined by measuring the changes in the optical path difference between the air of interest and a vacuum as a function of the changes in the cell length. An accuracy of 4 x 10 to the minus 9th power has been achieved.

01,987
PB97-111959 Not available NTIS
National Inst. of Standards and Technology (EEEL), Gaithersburg, MD. Electricity Div.
Measurement and Reduction of Alignment Errors of the NIST Watt Experiment.
Final rept.
A. Gillespie, K. Fujii, D. Newell, R. Steiner, G. Stenbakken, E. Williams, P. T. Olsen, and A. Picard. 1996, 2p.
Pub. in Conference on Precision Electromagnetic Measurements, Braunschweig, Germany, June 17-20, 1996, p614-615.

Keywords: *Magnetic fields, *Electrical measurement, Monitoring, Standards, Fundamental constants, Superconducting magnets, Reprints, *Watt balance method, Induced voltage, Mass stability, Kilogram.

The effects of uncertainties in the alignment of the NIST watt balance with local gravity and the magnetic field of the balance have been analyzed, and techniques for measuring all misalignment parameters have been developed. The systematic uncertainty in the watt measurement due to alignment has been reduced to 0.04 micrometers W/W.

01,988
PB97-112007 Not available NTIS
National Inst. of Standards and Technology (EEEL), Boulder, CO. Electromagnetic Technology Div.
Observation of Hot-Electron Shot Noise in a Metallic Resistor.
Final rept.
A. H. Steinbach, J. M. Martinis, and M. H. Devoret. 1996, 4p.
Pub. in Physical Review Letters, v76 n20 p3806-3809 May 96.

Keywords: *Mesoscopics, *Noise, *Shot noise, *Resistors, Reprints.

The authors have measured the current noise of silver thin-film resistors as a function of current and temperature and for resistor lengths of 7000, 100, 30 and 1 micrometers. As the resistor becomes shorter than the electron-phonon interaction length, the current noise of large current increases from a nearly current independent value to the interacting hot-electron value (square root 3/4)2el. However, further reduction in length below the electron-electron interaction length decreases the noise to a value approaching the independent hot-electron value (1/3)2el first predicted for mesoscopic resistors.

01,989
PB97-112379 Not available NTIS
National Inst. of Standards and Technology (EEEL), Gaithersburg, MD. Electricity Div.
High-Current Thin Film Multijunction Thermal Converters and Multi-Converter Modules.
Final rept.
J. R. Kinard, T. E. Lipe, C. B. Childers, and D. B. Novotny. 1996, 2p.
Pub. in Conference on Precision Electromagnetic Measurements, Braunschweig, Germany, June 17-20, 1996, p594-595.

Keywords: *Current converters, *Thin films, *Thermal converters, Thermal sensors, Multilayers, Ac-dc difference, Multijunctions, Reprints, *Foreign technology.

High-current, thin-film multijunction thermal converters (HCFMJTCs) have been fabricated at NIST with heater ranges from a new milliamperes to 1 A. Multi-converter modules containing HCFMJTCs have also been constructed to measure currents up to several amperes.

01,990
PB97-113039 Not available NTIS
National Inst. of Standards and Technology (EEEL), Gaithersburg, MD. Electricity Div.
Wideband Sampling Voltmeter.
Final rept.
T. M. Souders, B. C. Waltrip, O. B. Laug, and J. P. Deyst. 1996, 6p.
Pub. in Institute of Electrical and Electronics Engineers Instrumentation and Measurement Technology Conference, Brussels, Belgium, June 4-6, 1996, p1139-1144 Jun 96.

Keywords: *Sampling, *Wideband, *Voltmeters, Error sources, RMS voltage, Time-base, Reprints, *Foreign technology, Quasi-equivalent-time.

A high accuracy sampling voltmeter, designed to span the frequency range of 10 Hz to 200 MHz is described. The instrument operates autonomously, at a measurement update rate of at least one per second. A novel quasi-equivalent time sampling process is sued, with a custom strobed comparator as the sampling device and decision element. The architecture and control are presented, along with the time-base design principles. Major error sources associated with the time-base are also discussed.

01,991
PB97-113062 Not available NTIS
National Inst. of Standards and Technology (EEEL), Gaithersburg, MD. Electricity Div.
NIST Watt Balance: Progress Toward Monitoring the Kilogram.
Final rept.
R. Steiner, A. Gillespie, K. Fujii, A. Picard, G. Stenbakken, P. T. Olsen, E. Williams, and D. Newell. 1996, 2p.
See also PB96-123153.
Pub. in Conference on Precision Electromagnetic Measurements, Braunschweig, Germany, June 17-20, 1996, p6-7.

Keywords: *Magnetic forces, Electrical measurement, Simulation, Reprints, *Watt measurement, *Foreign technology, Induced voltage, Mass stability.

Random uncertainty of 0.08 microW/W in the NIST watt balance has been achieved by inmprovements in a velocity measurement using three laser interferometers and by the elimination of filter delays and electrical noise. The latest results of this experiment are presented.

01,992
PB97-113211 Not available NTIS
National Inst. of Standards and Technology (EEEL), Gaithersburg, MD. Electricity Div.
DC-MHz Wattmeter Based on RMS Voltage Measurements.
Final rept.
B. C. Waltrip, and N. M. Oldham. 1996, 2p.
Pub. in Institute of Electrical and Electronics Engineers Instrumentation and Measurement Technology Conference, Brussels, Belgium, June 4-6, 1996, p214-215.

Keywords: *Wattmeters, *Power, Buffer, RMS voltage, Reprints, *Foreign technology, 3 DVM method.

A wideband wattmeter for measuring active power over a frequency range of dc to 1 MHz is described. The wattmeter is based on the three voltmeter method in which three rms voltage measurements are used to calculate power.

01,993
PB97-113252 Not available NTIS
National Inst. of Standards and Technology (EEEL), Gaithersburg, MD. Electricity Div.
Magnetometer Calibration Services.
Final rept.
E. R. Williams, and D. W. Matson. 1995, 5p.
Pub. in Proceedings of the National Conference on Standards Laboratories, The Impact of Metrology on Global Trade, July 16-20, 1995, Dallas, TX., p495-499.

Keywords: *Magnetometers, *Calibrations, Gauss meters, Magnetic standards, Reprints, Hall effect meters, Nuclear magnetic resonance.

A new facility to calibrate magnetometers in San Diego has recently been completed as a cooperative effort between the Naval Primary Standards Laboratory and the National Institute of Standards and Technology. All measurements are NIST traceable through a nuclear magnetic resonance-based measurement. Magnetic fields from the 0.1 microT to 1.4 T can be calibrated by comparisons with fields generated by a series of coils or an electromagnet.

01,994
PB97-113880 PC A04/MF A01
National Inst. of Standards and Technology (EEEL), Gaithersburg, MD. Semiconductor Electronics Div.
Electronics and Electrical Engineering Laboratory Technical Progress Bulletin Covering Laboratory Programs, April to June 1996 with 1996-1998 EEEL Events Calendar.
J. M. Rohrbaugh. Oct 96, 37p, NISTIR-5895.
See also report dated Sep 95, PB96-106455.

Keywords: *Electrical engineering, *Research projects, Semiconductor devices, Metrology, Laboratories, Abstracts, US NIST, Antennas, Superconductors, Electronics, Microwaves, Electromagnetic interference, Microelectronics, Optical fibers, Electrical measurement, Lasers, Lightwave technology.

This is the fifty-fifth issue of a quarterly publication providing information on the technical work of the National Institute of Standards and Technology, Electronics and Electrical Engineering Laboratory. This issue of the EEEL Technical Progress Bulletin covers the second quarter of calendar year 1996. Abstracts are provided by technical area for both published papers and papers approved by NIST for publication.

01,995
PB97-118616 Not available NTIS
National Inst. of Standards and Technology (MSEL), Gaithersburg, MD. Ceramics Div.
Effect of Beam Voltage on the Properties of Aluminum Nitride Prepared by Ion Beam Assisted Deposition.
Final rept.
J. H. Edgar, C. A. Carosella, C. R. Eddy, and D. T. Smith. 1996, 7p.
Pub. in Jnl. of Materials Science: Materials in Electronics, v7 p247-253 1996.

Keywords: *Aluminum nitride, *Beam voltage, Mechanical properties, Reprints, *Ion beam assisted deposition.

The effects of nitrogen-beam voltage on the structure, stress, energy band gap and hardness of AlN thin films deposited on Si(111), Si(100) and sapphire (0001) by ion beam assisted deposition (IBAD) are reported. As the nitrogen-bean voltage was increased from 50 to 200 V, the stress and disorder in the AlN films increased as determined by X-ray diffraction, FTIR and Raman spectroscopy. The preferred orientation of the film's c-axis changed from completely normal to the film at 100 V, to a mixture of normal and in the plane of the film at 200 V. For AlN films deposited under the same conditions, the films were more highly oriented on sapphire (0001) than in SI(111). The hardness of the films increased from 18.2 to 23.7 GPa with the nitrogen-beam voltage, and possible reasons for this change in hardness are considered.

01,996
PB97-122253 Not available NTIS
National Inst. of Standards and Technology (EEEL), Gaithersburg, MD. Electricity Div.
Dependence of the Thermal Electron Attachment Rate Constant in Gases and Liquids on the Energy Position of the Electron Attaching State.
Final rept.
L. G. Christophorou. 1996, 21p.
Pub. in Zeitschrift fur Physikalische Chemie, Bd., v95 S p195-215 1995.

Keywords: *Electron attachment, *Thermal electrons, *Energy positions, Gases, Liquids, Constants, Reprints, *Foreign technology.

Thermal electron attachment rate constants for halocarbons in the gaseous phase, (ka)th, and thermal electron attachment rate constants for a number of molecules in liquid cyclohexane, (ka)L, are summarized in an effort to discern the dependence of the thermal electron attachment rate constant for molecules embedded in gases and in liquids on the energy position, E(NIS), of the electron attaching state. For these molecules the (ka)th varies only slightly with E(NIS) as long as E(NIS) is less than 0.0 eV (i.e., as long as the electron affinity of the molecule is positive), but it de-

General

creases precipitously with increasing E(NIS) when E(NIS) greater than 0.0 eV (i.e., when the electron affinity of the molecule becomes negative). The (ka)L exhibits a similar behavior except that it remains virtually constant well above 0.0 eV, up to E(NIS) approximately 0.9 eV, and thereafter decreases precipitously. This energy shift between the gaseous and the liquid phase correlations is consistent with the magnitude of the polarization energy of the anions in liquid cyclohexane and its effect on E(NIS).

01,997
PB97-122329 Not available NTIS
National Inst. of Standards and Technology (EEEL), Gaithersburg, MD. Electricity Div.
NIST Watt Experiment: Monitoring the Kilogram.
Final rept.
A. Gillespie. 1996, 1p.
See also PB97-111959.
Pub. in Bulletin/Conference Abstract Program of the 1996 March Meeting, St. Louis, MI., March 18-22, 1996, v41 n1 p506.

Keywords: *Calibration standards, *Magnetic field, *Voltage, *Mass, Interlaboratory comparisons, Electrical measurement, Weight measurement, Fundamental constants, Mechanical measurement, Metrology, Precision, Monitoring, Reprints, *Kilograms, Current loops.

An apparatus has been constructed which measures both the force on a current loop in a magnetic field and the voltage induced around that loop when it moves at some velocity through that same magnetic field. By comparing the force times the velocity to the current times the voltage, mechanical power is compared to electrical power, and a value for the watt which is consistent in both electrical mechanical units can be derived. The kilogram is defined in terms of a physical artifact, and intercomparisons among various kilogram masses suggest that the kilogram mass standard changes over time. Present research on the watt experiment aims to improve the precision of the measurement so that a defined value of the watt can be used to monitor the drift of the kilogram mass standard in terms of fundamental natural constant.

Antennas

01,998
PB94-172491 Not available NTIS
National Inst. of Standards and Technology (EEEL), Boulder, CO. Electromagnetic Fields Div.
Planar Near-Field Alignment.
Final rept.
D. Kremer, A. Newell, A. Repjar, M. Pinkasi, C. Rose, and A. Trabelsi. 1993, 7p.
Pub. in Proceedings of the Annual Meeting and Symposium of Antenna Measurement Techniques Association (15th), Dallas, TX., October 4-8, 1993, p198-204.

Keywords: Alignment, Reprints, *Antenna measurements, Planar near field technique.

This paper discusses one method of characterizing the scan plane for planar near-field measurements. The method uses a theodolite autocollimator, a laser interferometer, an electronic level and an optical square. The data obtained using these techniques are first used to make alignment corrections to the scan plane; then new data are used to determine the best fit for the realigned scan plane. The normal to this plane is referenced using a permanently placed mirror. In addition, the final data obtained can be used in probe position-correction techniques, developed for planar near-field measurements.

01,999
PB94-185436 Not available NTIS
National Inst. of Standards and Technology (EEEL), Boulder, CO. Electromagnetic Fields Div.
Standard Probes for Electromagnetic Field Measurements.
Final rept.
M. Kanda. 1993, 16p.
Pub. in Institute of Electrical and Electronics Engineers Transactions on Antennas and Propagation 41, n10 p1349-1364 Oct 93.

Keywords: *Probes(Electromagnetic), *Electric probes, *Antennas, Electrical measurement, Electric fields, Magnetic fields, Radio frequencies, Near field, Sensors, Reprints.

This tutorial paper discusses various standard antennas for measuring radio-frequency electric and magnetic fields. A theoretical analysis of each antenna's receiving characteristics is summarized and referenced. The standard probes described are an electrically short dipole, a resistively-loaded dipole, a half-wave dipole, an electrically small loop, and a resistively-loaded loop. A single-turn loop designed for simultaneous measurement of the electric and magnetic components of near-fields and other complex electromagnetic environments is also described. Each type of antenna demonstrates a different compromise between broadband frequency response and sensitivity.

02,000
PB94-219219 PC A06/MF A02
National Inst. of Standards and Technology, Gaithersburg, MD.
Journal of Research of the National Institute of Standards and Technology. March/April 1994. Volume 99, Number 2.
B. N. Taylor, and D. R. Harris. 1994, 118p.
See also PB94-219227 through PB94-219268, PB94-169737 and PB94-219326. Also available from Supt. of Docs. as SN703-027-00057-1.

Keywords: *Calorimeters, *Radiation doses, *Water, Dissolved gases, Calorimetric dosemeters, Measuring instruments, Temperature effects, Thermistors, Exothermic reactions, Endothermic reactions, Heat defect, Convective barrier, National Institute of Standards and Technology.

Contents:
- Articles--A Sealed Water Calorimeter for Measuring Absorbed Dose;
- Planar Near-Field Measurements of Low-Sidelobe Antennas;
- On the Physics Required for Prediction of Long Term Performance of Polymers and Their Composites;
- The Measurement and Uncertainty of a Calibration Standard for the Scanning Electron Microscope;
- New Values for Silicon Reference Materials, Certified for Isotope Abundance Ratios;
- News Briefs.

02,001
PB94-219235 (Order as PB94-219219, PC A06/MF A02)
National Inst. of Standards and Technology, Gaithersburg, MD.
Planar Near-Field Measurements of Low-Sidelobe Antennas.
M. H. Francis, A. C. Newell, K. R. Grimm, J. Hoffman, and H. E. Schrank. 1994, 25p.
Prepared in cooperation with Nichols Research Corp., Vienna, VA. and System Engineering Corp., Columbia, MD.
Included in Jnl. of Research of the National Institute of Standards and Technology, v99 n2 p143-167 Mar/Apr 94.

Keywords: *Antennas, *Microwaves power transmission, *Sidelobes, Microwave probes, Waveguides, Antenna radiation patterns, Near fields, Far field, Antenna arrays, Measuring instruments, Uncertainty, Planar near field, National Institute of Standards and Technology.

The planar near-field measurement technique is a proven technology for measuring ordinary antennas operating in the microwave region. The development of very low-sidelobe antennas raises the question whether this technique can be used to accurately measure these antennas. The authors show that data taken with an open-end waveguide probe and processed with the planar near-field methodology, including probe correction, can be used to accurately measure the sidelobes of very low-side-lobe antennas to levels of -55 dB to -60 dB relative to the main beam peak. A special probe with a null in the direction of the main beam was also used for some of these measurements. This special probe reduced some of the measurement uncertainties but increased the uncertainties due to probe-antenna interactions. The authors discuss the major sources of uncertainty and show that the probe-antenna interaction is one of the limiting factors in making accurate measurements. The test antenna for this study was a slotted-waveguide array whose low sidelobes were known.

02,002
PB95-108643 Not available NTIS
National Inst. of Standards and Technology (EEEL), Boulder, CO. Electromagnetic Fields Div.
Correction Factor for Nonplanar Incident Field in Monopole Calibrations.
Final rept.
J. Randa. 1993, 3p.
Pub. in Institute of Electrical and Electronics Engineers Transactions on Electromagnetic Compatibility 35, n1 p94-96, 1 Feb 93.

Keywords: *Antenna radiation patterns, *Calibration, *Monopole antennas, Antenna design, Electromagnetic properties, Monopoles, Incidence, Electromagnetic fields, Electromagnetic compatibility, Reprints.

In calibrating monopole antennas, the length of the antenna can be comparable to the separation distance. In that case, there is a significant variation in both the magnitude and the phase of the incident field along the length of the antenna under test. This paper presents an expression for a correction factor to account for this effect. We evaluate the correction factor for some representative cases and present some guidelines for when this factor should be taken into account. The effect can exceed 1 dB in some practical cases.

02,003
PB95-152781 Not available NTIS
National Inst. of Standards and Technology (EEEL), Boulder, CO. Electromagnetic Fields Div.
Time-Domain Antenna Characterizations.
Final rept.
O. E. Allen, D. A. Hill, and A. R. Ondrejka. 1993, 8p.
Pub. in Institute of Electrical and Electronics Engineers Transactions on Electromagnetic Compatibility 35, n3 p339-346 Aug 93.

Keywords: *Broadband antennas, Horn antennas, Time domain, Frequency domain, Characteristics, Directivity, Comparison, Reprints.

A set of time-domain characterizations that can efficiently describe wide bank antennas is proposed in this paper. The experimentally measured responses of transverse electromagnetic horn antennas are used to evaluate the utility of these characterizations. Comparisons are made between the antennas' frequency-domain response and their time-domain characterizations. The comparisons show that the time-domain characterizations can provide significant insight into an antenna's behavior as well as providing a means to accurately compare two or more different antennas.

02,004
PB95-153755 Not available NTIS
National Inst. of Standards and Technology (EEEL), Boulder, CO. Electromagnetic Fields Div.
New Extrapolation/Spherical/Cylindrical Measurement Facility at the National Institute of Standards and Technology.
Final rept.
J. R. Guerrieri, D. P. Kremer, and T. Rusyn. 1993, 10p.
Pub. in Proceedings of Annual Meeting and Symposium on Antenna Measurement Techniques Association (15th), Dallas, TX., October 4-8, 1993, p343-352.

Keywords: *Test facilities, Antenna radiation patterns, Polarization(Waves), Cylindrical configuration, Spherical configuration, Probes(Electromagnetic), Near field, Extrapolation, Gain, Reprints, *Antenna measurements, US NIST.

A new multi-purpose antenna measurement facility was put into operation at the National Institute of Standards and Technology (NIST) in 1993. This facility is currently used to perform gain, pattern, and polarization measurements on probes and standard gain horns. The facility can also provide spherical and cylindrical near-field measurements. The frequency range is typically from 1 to 75 GHz. This paper discusses the capabilities of this new facility in detail.

02,005
PB95-161915 Not available NTIS
National Inst. of Standards and Technology (EEEL), Boulder, CO. Electromagnetic Fields Div.

Optically Linked Three-Loop Antenna System for Determining the Radiation Characteristics of an Electrically Small Source.
Final rept.
D. R. Novotny, K. D. Materson, and M. Kanda. 1993, 5p.
Pub. in Proceedings of International Symposium on Electromagnetic Compatibility, Dallas, TX., August 9-13, 1993, p300-304.

Keywords: *Antenna arrays, *Radio emission, Electromagnetic compatibility, Poynting theorem, Loop antennas, Near field, Dipole moments, Electric moments, Magnetic moments, Reprints, *Electromagnetic emissions, *Photonic probes.

This paper presents the experimental results of an antenna system for determining the radiation characteristics of an electrically small source. Three orthogonal loop antennas, each terminated at diametrically opposite points with identical loads, encircle the source and characterize its equivalent electric and magnetic dipole moments. The total radiated power can be determined from this near-field measurement of the device under test. The test system operates from 3 kHz to over 100 MHz with up to 90 dB of dynamic range.

02,006
PB95-180378 Not available NTIS
National Inst. of Standards and Technology (EEEL), Boulder, CO. Electromagnetic Fields Div.
Dual Frequency mm-Wave Radiometer Antenna for Airborne Remote Sensing of Atmosphere and Ocean.
Final rept.
M. D. Jacobson, L. S. Fedor, D. A. Hazen, D. P. Kremer, W. B. Madsen, and M. H. Francis. 1994, 8p.
Contract NIPR-N93051
Sponsored by Department of Defense, Washington, DC.
Pub. in Microwave Jnl. 27, n9 p24-38 Sep 94.

Keywords: *Radiometers, *Antennas, Extremely high frequency, Superhigh frequency, Millimeter waves, Remote sensors, Remote sensing, Airborne equipment, Atmospheres, Oceans, Reprints.

Accurate multiwavelength radiometric remote sensing of the ocean and the atmosphere from an aircraft requires antennas with the same beamwidth at the various frequencies of operation. An offset antenna was designed with a pressure-compensating corrugated feed horn to meet this criterion. A specially designed fairing was incorporated into the antenna to optimize the aerodynamics and minimize the liquid build up on the antenna surfaces. The antenna has two positions, the zenith (up) position and the nadir (down) position. The far-field pattern results show that the antenna beamwidths at 23.87 and 31.65 GHz agree well with design criterion. This antenna was recently used in an ocean remote-sensing experiment and performed according to expectations.

02,007
PB96-102561 Not available NTIS
National Inst. of Standards and Technology (EEEL), Boulder, CO. Electromagnetic Fields Div.
Standard Antennas for Electromagnetic Interference Measurements and Methods to Calibrate Them.
Final rept.
M. Kanda. 1994, 13p.
Pub. in Institute of Electrical and Electronics Engineers Transactions on Electromagnetic Compatibility, v36 n4 p261-273 Nov 94.

Keywords: *Antennas, *Electromagnetic interference, Radiofrequency interference, Electric fields, Magnetic fields, Calibrating, Radio reception, Reprints.

This tutorial paper discusses various standard antennas for measuring radio-frequency electric and magnetic fields. A theoretical analysis of each antenna's receiving characteristics is summarized and referenced. The antennas described are an electrically short dipole, a resistively loaded short dipole and half-wave dipole, an electrically small loop, a resistively loaded loop, photonic probes, and a single-turn loop designed for simultaneous measurement of the electric and magnetic components of near-fields and other complex electromagnetic (EM) environments. Each type demonstrates a different compromise between broadband responses and sensitivity. This paper also discusses the calibration techniques for these probes using standard EM fields established in transmission electron microscopy (TEM) cells, waveguide cells, anechoic chambers, and open-field sites.

02,008
PB96-111166 PC A08/MF A02
National Inst. of Standards and Technology (EEEL), Boulder, CO. Electromagnetic Fields Div.
Spherical-Wave Source-Scattering Matrix Analysis of Antennas and Antenna-Antenna Interactions.
Technical note.
R. L. Lewis. Jul 95, 159p, NIST/TN-1373.
Also available from Supt. of Docs. as SN003-003-03358-8.

Keywords: *Autennas, *Near field, Spherical waves, Algorithms, Antenna coupling, Antenna measurements, Probes(Electromagnetic).

Expressions are presented for describing incoming and outgoing fields about an antenna in terms of a series of exciting and emergent vector spherical-wave functions. The exciting and emergent fields around the antenna's exterior are related to the field in the antenna feed via a source-scattering matrix representation. A series of so called spherical-wave source-scattering matrix coefficients are then related to more conventional parameters such as antenna gain and receiving cross section. An overview of rotation and translation theorems for transforming vector spherical-wave functions between two distinct coordinate systems is given, followed by a general solution to the problem of expressing the coupling between two coupled antennas in terms of each antenna's spherical-wave source-scattering matrix representation. The authors go on to consider special results to substantiate their formulation, such as showing equivalence between the coupling equations for transmission in opposite directions when the antennas are reciprocal, showing uniform convergence of some series representations for antenna coupling and simultaneously obtaining a coordinate-system translation theorem for the dyadic Green's function, and lastly showing that the authors' two-antenna coupling equations reduce to expressions for the incident and emergent fields about a single antenna when the other antenna is an elementary dipole. Efficient probe-corrected spherical and hemispherical scanning algorithms are then developed for processing measured near-field data to obtain antenna's far-field pattern. Finally, the authors describe a number of self-consistency tests and theoretical-data simulations that were developed to validate their spherical-scanning algorithm, and they describe an independent experimental verification.

02,009
PB96-112289 Not available NTIS
National Inst. of Standards and Technology (EEEL), Boulder, CO. Electromagnetic Fields Div.
Dual-Frequency Millimeter-Wave Radiometer Antenna for Airborne Remote Sensing of Atmosphere and Ocean.
Final rept.
M. H. Francis, D. P. Kremer, M. D. Jacobson, W. B. Madsen, L. S. Fedor, and D. A. Hazen. 1995, 7p.
Pub. in Proceedings of the Antenna Measurement Techniques Association Symposium, Long Beach, CA., October 3-7, 1994, p3-9.

Keywords: *Antennas, *Radiometers, *Millimeter wave equipment, *Airborne equipment, *Remote sensors, Extremely high frequencies, Remote sensing, Design criteria, Far fields, Oceans, Earth atmosphere, Reprints, Planar near field.

Accurate multiwavelength radiometric remote sensing of the ocean and the atmosphere from an aircraft requires antennas with the same beamwidth at the various frequencies of operation. Scientists at the National Oceanic and Atmospheric Administration designed an offset antenna with a pressure-compensating corrugated feed horn to meet this criterion. A specially designed fairing was incorporated into the antenna to optimize the aerodynamics and minimize the liquid build-up on the antenna surfaces. The antenna has two positions: the zenith (up) position and the nadir (down) position. The planar near-field facility at the National Institute of Standards and Technology was used to determine the far-field pattern of the antenna. The results show that the antenna beamwidths at 23.87 and 31.65 Ghz are nearly the same as expected from the design criterion. This antenna was recently used in an ocean remote-sensing experiment and performed according to expectations.

02,010
PB96-135082 Not available NTIS
National Inst. of Standards and Technology (EEEL), Boulder, CO. Electromagnetic Fields Div.
Development of Near-Field Test Procedures for Communication Satellite Antennas.
Final rept.
C. F. Stubenrauch. 1994, 19p.
See also PB86-164357 and PB89-156152.
Pub. in Antenna Measurement Techniques Association Workshop on Communication Satellite Antenna Measurements, Ann Arbor, MI., July 2, 1993, p1-19.

Keywords: *Satellite antennas, *Tests, *Specifications, *Near fields, Antenna design, Multibeam antennas, Communication satellites, Simulation, Procedures, Reprints.

The presentation defines and discusses the capabilities of near-field antenna test techniques, specifically for the requirements associated with the development and verification testing of reconfigurable, multibeam frequency reuse, commercial satellite antennas. This discussion focuses on the planar near-field measurement method and covers the determination of sampling criteria and scan limits, development of diagnostic and design assist methods, development of beam alignment technqiues, and specification of hardware requirements for the measurement system.

02,011
PB96-141361 Not available NTIS
National Inst. of Standards and Technology (EEEL), Boulder, CO. Electromagnetic Fields Div.
Alternative Contour Technique for the Efficient Computation of the Effective Length of an Antenna.
Final rept.
R. T. Johnk, and M. Kanda. 1994, 3p.
Pub. in Institute of Electrical and Electronics Engineers Transactions on Antennas and Propagation, v42 n5 p747-749 May 94.

Keywords: *Dipole antennas, *Length, *Galerkin method, Convergence, Current density, Electric potential, Open circuit density, Charge density, Scattering, Electrostatics, Reprints.

The scattering of a plane wave broadside incident to a dipole antenna with a symmetrically placed, open-circuited gap is treated. The induced currents on the antenna are found by solving the electric-field integral equation by means of a Galerkin moment method. The resulting current distribution is then used to compute line integrals of the scattered electric field along appropriate paths. The line integral is first evaluated directly across the dipole gap in order to compute the effective length, but severe convergence problems are encountered. This problem is due to the presence of charge singularities at the gap edges. Instead of incorporating the singular charge behavior into the basis functions, a line integral is evaluated along a path that alleviates the convergence difficulties. This remedy is developed first for an electrostatic case and then for the dynamic scattering problem.

02,012
PB96-147137 Not available NTIS
National Inst. of Standards and Technology (EEEL), Boulder, CO. Electromagnetic Fields Div.
Comparison of k-Correction and Taylor-Series Correction for Probe-Position Errors in Planar Near-Field Scanning.
Final rept.
M. H. Francis. 1995, 7p.
Pub. in Annual Meeting and Symposium Antenna Measurement Techniques 1995 Assoc. (17th), Williamsburg, VA., November 13-17, 1995, p341-347.

Keywords: *Antennas, *Extremely high frequencies, Antenna arrays, Phased arrays, Near fields, Far fields, Planar structures, Antenna radiation patterns, Response functions, Error analysis, Taylor series, Reprints, *Probe-position errors.

The authors investigated two methods of probe-position error correction to determine how well the corrected results compare to the uncorrupted far field: the k-correction method and the Taylor-series method. For this investigation, the authors measured a 1.2 m dish at 4 GHz and a 1.2 m by 0.9 m phased array at 2.2 GHz. Measurements were made first without position errors and then with deliberate z-position errors. The authors performed probe-position error correction using both methods and compared the results to the error-free far field.

02,013
PB96-183157 PC A04/MF A01
National Inst. of Standards and Technology (EEEL), Boulder, CO. Electromagnetic Fields Div.

Antennas

Standard Source Method for Reducing Antenna Factor Errors in Shielded Room Measurements.
Technical note.
D. Camell, G. Koepke, R. Smith, and B. Rakoski.
Mar 96, 43p, NIST/TN-1382.
Also available from Supt. of Docs. as SN003-003-03405-3.

Keywords: *Antennas, *Electromagnetic fields, *Calibration, *Shields, Test facilities, Errors.

In this report the authors will examine the use of a well characterized standard source of electromagnetic radiation as a means to calibrate the effects of the shielded room on a receiving antenna used for MILSTD 461/462 RE102 emissions measurement. The goal was to compensate for the shielded room environment so that radiated emissions measurements can be more accurately compared from one room to another. This was accomplished by using a characterized spherical dipole source to calibrate an antenna's response in the location that it was used. An interlaboratory comparison was made of the detected emissions from a simulated equipment-under-test at three sites to see how this in-situ calibration of the receive antenna helped the shielded room test repeatability.

02,014
PB96-200126 Not available NTIS
National Inst. of Standards and Technology (EEEL), Boulder, CO. Electromagnetic Fields Div.
Methodology for Electromagnetic Interference Measurements.
Final rept.
M. Kanda. 1995, 27p.
See also PB96-102561.
Pub. in Handbook of Electromagnetic Compatibility, Chapter 15, p599-625 1995.

Keywords: *Electromagnetic interference, *Antennas, *Measurement, Standards, Radio frequency interference, Radio reception, Electric fields, Magnetic fields, Radio receptor, Reprints.

Establishing standards for electromagnetic (EM) field measurements is a multifacted endeavor which requires measurements made (1) in anechoic chambers, (2) at open sites, and (3) within guided-wave structures and the means of transferring these measurements from one situation to another. The underlying principles of these standard measurements and transfer standards fall into one of two categories: measurements and theoretical modeling. That is, either a parameter or a set of parameters is measured, or a parameter is calculated by established physical and mathematical principles. In the following, the three measurement topics and field transfer standards will be discussed, with the guided-wave structures restricted to the transverse electromagnetic (TEM) cell and the waveguide chamber. Throughout the discussion the interplay between measured quantitites and predicted (modeled) quantities will be seen. The frequencies considered here range from 10 kHz to 40 Ghz (and upward) and are determined by our ability to made an actual measurement and the restrictions imposed by rigorous theoretical analysis of a given model.

02,015
PB96-200373 Not available NTIS
National Inst. of Standards and Technology (EEEL), Boulder, CO. Electromagnetic Fields Div.
Comparison of Ultralow-Sidelobe-Antenna Far-Field Patterns Using the Planar-Near-Field Method and the Far-Field Method.
Final rept.
M. H. Francis, A. C. Newell, K. R. Grimm, J. Hoffman, and H. E. Schrank. 1995, 9p.
Pub. in Institute of Electrical and Electronics Engineers Antennas and Propagation Magazine, v37 n6 p7-15 Dec 95.

Keywords: *Antennas, *Sidelobes, *Measurement, Far fields, Near fields, Measuring instruments, Reprints, Planar near field.

The development of very-low-sidelobe antennas raises the question of whether or not the planar-near-field method can be used to accurately measure these antennas. Recently, scientists at several organizations showed that data taken and processed with the planar-near-field methodology, including probe correction, can be used to accurately measure the sidelobes of ver-low-sidelobe antennas. This can be done to levels of -55 dB to -60 dB, relative to the mainbeam peak (1). This paper highlights these results, including a comparison of the far field, from the planar-near-field method, with the far field, found on a far-field range. The test antenna for this study was slotted-waveguide array, the low sidelobes for which were known. The near-field measurements were conducted on the NIST planar-near-field facility.

02,016
PB96-200696 Not available NTIS
National Inst. of Standards and Technology (EEEL), Boulder, CO. Electromagnetic Fields Div.
Polarimetric Calibration of Reciprocal-Antenna Radars.
Final rept.
L. A. Muth, R. L. Lewis, and R. C. Wittmann. 1995, 6p.
See also PB95-216925.
Pub. in Annual Meeting and Symposium of the 1995 Antenna Measurement Techniques Association (17th), Williamsburg, VA., November 13-17, 1995, p3-8.

Keywords: *Radar cross sections, *Depolarization, *Polarimetry, Radar antennas, Radar targets, Cross polarization, Error analysis, Calibration standards, Reprints, Reciprocal antenna radars.

We discuss how RCS targer depolarization enhances cross-polarization contamination, and we present a graphical study of measurement error due to depolarization by an inclined dihedral reflector. Error correction requires complete polarimetric RCS measurements. We present a simple polarimetric calibration scheme that is applicable to reciprocal antenna radars. This method uses a dihedral calibration target mounted on a rotator. Because the calibration standard can be rotated, there is no need to mount and align multiple separate standards, and clutter and noise may be rejected by averaging over rotation angle.

02,017
PB97-110555 Not available NTIS
National Inst. of Standards and Technology (MEL), Gaithersburg, MD. Precision Engineering Div.
Numerical Evaluation of Hypersingular Integrals for Scattering by a Dielectric Wedge.
Final rept.
E. Marx. 1993, 4p.
Pub. in Institute of Electrical and Electronics Engineers Antennas and Propagation Society of International Symposium, Ann Arbor, MI., June 28-July 2, 1993, 1993 Digest, v2 p906-909.

Keywords: *Dielectric wedges, *Electromagnetic scattering, Hypersingular integral, Numerical integration, Reprints, Neighboring-patch contributions.

Some components of the electromagnetic field near the edge of a dielectric wedge diverge. The computation of the fields scattered by the wedge can be done by solving a singular integral equation (SIE) or a hypersingular integral equation (HIE) (2) - (4). The unknown boundary function diverges near the edge for the SIE and tends to a constant for the HIE. Thus, the method using the HIE does not require the computation of the boundary function closer to the edge that the closest field point, since this function can be approximated by a constant and the remainder of the integral can be evaluated numerically. Nevertheless, the integrand varies rapidly, like I/R2, over the patch and a number of special precautions have to be taken. The authors need to verify the expected behavior of fields near sharp edges because the theory is not rigorous. If the unknown function is constant near the edge of the wedge, the behavior of the fields is determined by the remainder of the integrand. The neighboring-patch contributions were previously examined under the assumption taht the small-argument approximation of the Hankel functions could be used. Here the authors relax this assumption. Similar corrections are required in the computation of the field components when the distance between the field point and the patch is small compared to the wavelength. Although the field integrals are finite, the behavior of the integrand is the same as that for the neighboring-patch contributions.

Circuits

02,018
PB94-135803 PC A03/MF A01
National Inst. of Standards and Technology (EEEL), Boulder, CO. Electromagnetic Fields Div.
NIST Model PM2 Power Measurement System for 1 mW at 1 GHz.
F. R. Clague. Dec 93, 46p, NISTIR-5016.

Keywords: *Microwave equipment, *Power measurement, Computerized control systems, Electric power meters, GHz range 01-100, Ultrahigh frequency, Computer programs, Automation, Uncertainty.

The design and operation of an automated measurement system designed to measure power accurately at the level of 1 mW and at the frequency of 1 GHz are described. The system consists of commercial IEEE Std-488 bus-controlled instruments, a computer controller, and software. The results of a series of measurements are output to the computer display and, optionally, to a printer. The results are the mean of the measurement series and an estimate of the Type A (here random) and Type B (here systematic) uncertainty. The estimated total expanded uncertainty for the average of six consecutive measurements of a nominal 1 mW, 1 GHz source is typically less than 1 percent. The system can measure any power for 0.1 to 10 mW at any microwave frequency by making appropriate changes to the software and, possibly, the hardware.

02,019
PB94-169737 PC A07/MF A02
National Inst. of Standards and Technology, Gaithersburg, MD.
Journal of Research of the National Institute of Standards and Technology. January/February 1994. Volume 99, Number 1.
1994, 131p.
See also PB94-169745 through PB94-169802 and PB94-140555. Also available from Supt. of Docs. as SN703-027-00056-3.

Keywords: Lattice parameters, X-ray diffraction, Blackbody radiation, Electric measuring instruments, Dimensional measurement, Thermal noise, Silicon, Length, Calibration, *Noise calibration system, *NCS1 system.

Contents:
- Precision Comparison of the Lattice Parameters of Silicon Monocrystals;
- The NIST 30 MHz Linear Measurement System;
- Uncertainties in Dimensional Measurements Made at Nonstandard Temperatures;
- A Null-Balanced Total-Power Radiometer System NCS1;
- Derivation of the System Equation for Null-Balanced Total-Power Radiometer System NCS1;
- Evaluation of Uncertainties of the Null-Balanced Total-Power Radiometer System NCS1;
- Cryogenic Blackbody Calibrations at the National Institute of Standards and Technology Low Background Infrared Calibration Facility.

02,020
PB94-169752 Not available NTIS
National Inst. of Standards and Technology, Boulder, CO.
NIST 30 MHz Linear Measurement System.
J. A. Jargon, R. A. Ginley, and D. D. Sutton. 1994, 12p.
Included in Jnl. of Research of the National Institute of Standards and Technology, v99 n1 p19-30 Jan/Feb 94.

Keywords: *Electric measuring instruments, Power measurement, High frequency, Linear systems, Nonlinearity, Automation, Calibration, Thermistors, Attenuators, Uncertainty, Reprints, Reference standards, US NIST.

There has been a recent interest in and demand for a calibration service at NIST to support rf attenuators and voltage doublers that operate specifically at 30 MHz. The first step required to offer such a service is to develop a reference standard. For the best possible accuracy, a tuned single-element thermistor mount was chosen. A linear measurement system was designed and constructed at NIST to calibrate the nonlinearity of this mount. The paper contains a description of the LMS, an explanation of the measurement scheme, calibration results, and an uncertainty analysis.

02,021
PB94-169778 Not available NTIS
National Inst. of Standards and Technology, Boulder, CO.

Null-Balanced Total-Power Radiometer System NCS1.
S. P. Pucic. 1994, 9p.
Included in Jnl. of Research of the National Institute of Standards and Technology, v99 n1 p45-53 Jan/Feb 94.

Keywords: *Thermal noise, *Calibration, Noise temperature, GHz range 01-100, Cryogenic temperature, Radiometers, Reprints, *Noise calibration system, *NCS1 system, Noise standards.

A recently developed radiometer system NCS1 is used to calibrate thermal noise temperature at any frequency between 1.0 GHz and 12.0 GHz. Any cryogenic noise source can be measured; the upper limit of noise temperatures measured without a loss of accuracy is estimated to be about 100,000 K. For a typical hot noise source with the noise temperature of 8400 K and a reflection coefficient magnitude of 0.1, the expanded uncertainty is about 1.8%, and the system sensitivity about 2 K. Implemented in Type N connector, it can be easily modified to calibrate noise sources with other coaxial connectors or waveguide flanges.

02,022
PB94-169786 Not available NTIS
National Inst. of Standards and Technology, Boulder, CO.
Derivation of the System Equation for Null-Balanced Total-Power Radiometer System NCS1.
S. P. Pucic. 1994, 9p.
Included in Jnl. of Research of the National Institute of Standards and Technology, v99 n1 p55-63 Jan/Feb 94.

Keywords: Noise temperature, Mathematical models, Calibration, Broadband, Radiometers, Reprints, *Noise calibration system, *NCS1 system.

A system equation of a recently developed null-balanced, total-power radiometer system is rigorously derived. Delivered noise power and temperature is related to available power (temperature) through an extension of the mismatch factor to broadband systems. The available power ratio, the available gain, and the delivered power ratio (efficiency) are defined. Properties of idealized, but in principal realizable components such as an infinitely directive isolator and a lossless matched waveguide-below-cutoff attenuator are used. A cascading technique is repeatedly applied to the fundamental noise equation. Mathematically modeling the experimental procedure of sequentially attaching the two noise standards and the unknown source to the system input, the authors obtain the system of three equations that can be solved for the noise temperature of the unknown noise source.

02,023
PB94-169794 Not available NTIS
National Inst. of Standards and Technology, Boulder, CO.
Evaluation of Uncertainties of the Null-Balanced Total-Power Radiometer System NCS1.
S. P. Pucic. 1994, 11p.
Included in Jnl. of Research of the National Institute of Standards and Technology, v99 n1 p65-75 Jan/Feb 94.

Keywords: Noise temperature, GHz range 01-100, Thermal noise, Radiometers, Uncertainty, Calibration, Reprints, *Noise calibration system, *NCS1 system, Noise standards.

Standard uncertainties are evaluated for the null-balanced, total-power, heterodyned radiometer system with a switched input that was recently developed at NIST to calibrate thermal noise sources. Eight significant sources of uncertainty due to systematic effects are identified, two, attributable to the two noise standards, and one each to connectors, the input mismatch, the input switch asymmetry, the isolator, the broadband mismatch and the attenuator. The combined standard uncertainty of a typical coaxial noise source calibration at the representative frequency of 2 GHz is about 1%. A strategy for reducing uncertainties is discussed.

02,024
PB94-172228 Not available NTIS
National Inst. of Standards and Technology (EEEL), Gaithersburg, MD. Electricity Div.
Leakage Current Detection in Cryogenic Current Comparator Bridges.
Final rept.
R. E. Elmquist. 1993, 3p.
Pub. in Institute of Electrical and Electronics Engineers Transactions on Instrumentation and Measurement 42, n2 p167-169 Apr 93.

Keywords: *Resistance bridges, *Comparator circuits, *Leakage current, Electrical measurement, Error analysis, Cryogenic equipment, Ratios, Tests, Reprints, Cryogenic current comparators, Quantum Hall effect.

Several tests have been developed to locate leakage currents in cryogenic current comparator (CCC) resistance ratio bridges used at NIST to measure ratios of 1,000 ohms/100 ohms, 6,453.2 ohms/100 ohms, and 10 k(ohms)/100 ohms. The major advantage of the tests is that they can be performed in situ using the sensitivity of the CCC bridge. These test procedures have been used to reduce the leakage error uncertainty of CCC ratio measurements linking working standards to the quantized Hall resistance (QHR) and to the NIST calculable capacitor experiment. CCC bridges require that the current which passes through a standard resistor must equal the current through the appropriate CCC winding to very high precision. This can be difficult to verify at or below 1 pA because a large number of possible leakage paths exist. Errors due to six important leakage current paths are given.

02,025
PB94-172384 Not available NTIS
National Inst. of Standards and Technology (EEEL), Gaithersburg, MD. Electricity Div.
Investigation of the Effects of Aging on the Calibration of a Kerr-Cell Measuring System for High Voltage Impulses.
Final rept.
G. J. FitzPatrick, and T. R. McComb. 1993, 4p.
Pub. in Proceedings of International Symposium on High Voltage Engineering (8th), Yokohama, Japan, August 23-27, 1993, p387-390.

Keywords: *High voltage, *Kerr cells, *Calibration, Aging(Materials), Electrical measurement, Electric pulses, Precision, Impulses, Reprints, Reference standards, Transfer standards.

Kerr-cell measuring systems can be used for high-voltage measurements from direct voltage up to impulses with a few nanoseconds risetime. In principle, this allows a measuring system for impulses to be calibrated at high-voltage using direct or alternating voltage which can be measured with a smaller uncertainty than is needed for impulse measurements. Unfortunately, the liquid normally used in such systems, nitrobenzene, degrades with time. This paper reports on an investigation into methods of calibrating an aged Kerr-cell so that a measuring system based on a Kerr-cell could be used as a Reference Measuring System. The repeatability of measurements using a fixed geometry to determine the voltage scale factor was also investigated.

02,026
PB94-172442 Not available NTIS
National Inst. of Standards and Technology (EEEL), Gaithersburg, MD. Electricity Div.
Intercomparison of NIST, NPL, PTB, and VSL Thermal Voltage Converters from 100 kHz to 1 MHz.
Final rept.
J. R. Kinard, R. B. D. Knight, P. Martin, J. Dessens, M. Klonz, and J. P. M. de Vreede. 1993, 3p.
Pub. in Institute of Electrical and Electronics Engineers Transactions on Instrumentation and Measurement 42 n2 p615-617 Apr 93. See also PB93-129328, PB93-151181 and PB94-172459.

Keywords: Electrical measurement, kHz range 100-1000, Interlaboratory comparisons, Reprints, *Thermal voltage converters, *Thermal converters, Intercomparison.

Coaxial, thermal voltage converters were hand-carried among NIST, NPL, PTB, and VSL for intercomparison of ac-dc difference from 100 kHz to 1 MHz. This paper briefly describes the highly varied methods and underlying principles on which ac-dc difference determinations are based in each laboratory, the transport standards used, and the results of the intercomparisons. The ac-dc differences reported by the participating laboratories are in very good agreement. It has been concluded that representative values of ac-dc difference in the 100 kHz to 1 MHz frequency range have been established with 2(Sigma) uncertainties of 4-8 ppm.

02,027
PB94-172459 Not available NTIS
National Inst. of Standards and Technology (EEEL), Gaithersburg, MD. Electricity Div.
Intercomparison of Thermal Converters at NIM, NIST, PTB, SIRI and VSL from 10 to 100 MHz.
Final rept.
J. R. Kinard, Z. Zhen, D. Huang, J. de Vreede, G. Rebuldela, and D. Janik. 1993, 4p.
Pub. in Institute of Electrical and Electronics Engineers Transactions on Instrumentation and Measurement 42, n2 p618-621 Apr 93.

Keywords: Electrical measurement, MHz range 01-100, Interlaboratory comparisons, Reprints, *Thermal voltage converters, *Thermal converters, Intercomparison.

Coaxial thermal voltage converters have been intercompared among NIM, NIST, PTB, SIRI, and VSL in the frequency range from 10 MHz to 100 MHz. The intercomparisons were made from 1988 through 1990. This paper briefly describes the highly varied methods and underlying principles on which RF-dc difference determinations are based in each laboratory, the transport standards used, and the results of the intercomparisons. The results from the participating laboratories are in very good agreement; therefore, we believe that the determinations of RF-dc difference in this frequency range are very well established.

02,028
PB94-172582 Not available NTIS
National Inst. of Standards and Technology (EEEL), Gaithersburg, MD. Electricity Div.
Comparative Measurements of High-Voltage Impulses Using a Kerr Cell and a Resistor Divider.
Final rept.
T. R. McComb, and G. J. FitzPatrick. 1993, 4p.
Pub. in Proceedings of International Symposium on High Voltage Engineering (8th), Yokohama, Japan, August 23-27, 1993, p383-386.

Keywords: *High voltage, *Electric pulses, Electrical measurement, Comparative evaluations, Kerr cells, Voltage dividers, Lightning, Impulses, Tests, Reprints, Reference standards, Transfer standards.

Recent proposals in committee drafts of IEC TC42 have placed greater emphasis on the use of comparative measurements as a method of qualifying impulse measuring systems. This paper describes some further investigations of comparative measurements where a Kerr-cell system is compared against a system based on a resistor divider. The paper describes the experimental techniques used to make comparative measurements, and the results of tests on the linearity of the systems are presented. Finally, recommendations are made for the use of comparative measurements in qualifying impulse measuring systems.

02,029
PB94-172954 Not available NTIS
National Inst. of Standards and Technology (MSEL), Boulder, CO. Materials Reliability Div.
Evaluation and Qualification Standards for an X-Ray Laminography System.
Final rept.
T. A. Siewert, M. W. Austin, G. Lucey, and M. Plott. Sep 92, 9p.
Pub. in Materials Evaluation, p1027-1035 Sep 92. Sponsored by Harry Diamond Labs., Adelphi, MD.

Keywords: *Circuit boards, *X-ray inspection, Calibration standards, Qualifications, Resolution, Reprints, *X-ray laminography, *Laminography, Image quality.

X-ray laminography, a tomographic technique that can examine individual planes of focus within a three-dimensional structure, promises to be an excellent method of inspecting complicated circuit boards. The system has accuracy and reproducibility that are appropriate for circuit board inspection, however its application has been limited by a lack of physical standards to verify machine performance. The report describes the development of devices to measure the resolution of a laminography system and reports the system resolution measured with these devices. The system which the authors evaluated uses a scanned beam technique to select a plane of focus (slice) within a three-dimensional structure. The scanned beam technique provides very good z-dimension resolution. It is able to minimize the contribution from out-of-plane objects to the image. However, the authors noted one example of an incorrect height (measurement artifact due to ge-

ometry), when used with a hollow sphere image quality indicator design (not representative of solder joint shapes).

02,030
PB94-185451 Not available NTIS
National Inst. of Standards and Technology (NEL), Boulder, CO. Electromagnetic Technology Div.
Design and Operation of Series-Array Josephson Voltage Standards.
Final rept.
R. L. Kautz. 1992, 38p.
Pub. in Proceedings of Int. School of Physics Enrico Fermi, Villa Marigola, Italy, June 27-July 7, 1989, p259-296 1992.

Keywords: *Standards, Phase locked systems, Josephson junctions, Josephson effect, Operation, Arrays, Design, Chaos, Electrochemical cells, Calibration, Reprints, *Voltage standards.

Series arrays typically including 1,500 Josephson junctions driven at 90 GHz have been used to generate quantized reference voltages in excess of 10 V. Such standards simplify the procedure and reduce the measurement uncertainties in the calibration of electrochemical cells.

02,031
PB94-198306 PC A03
National Inst. of Standards and Technology (PL), Boulder, CO. Time and Frequency Div.
Precision Oscillators: Dependence of Frequency on Temperature, Humidity and Pressure.
Final rept.
D. W. Allan, J. Barnes, F. Cordara, R. Kinsman, J. Kusters, R. Smythe, F. L. Walls, M. Garvey, and W. Hanson. 1992, 12p.

Keywords: *Oscillators, *Frequency stability, Temperature dependence, Pressure dependence, Test methods, Specifications, Guidelines, Precision, Humidity, Reprints.

The purpose of the research is to arrive at tractable (non-burdensome) guidelines, standards, and precautions for test methods used in determining the dependence of the output frequency of precision oscillators on temperature, humidity, and pressure. Over specification, under specification, or the lack of proper specification will miscommunicate. We offer a perspective for the manufacturer and the designer, as well as the user so that clear understanding and communication can occur. The guidelines, standards and precautions encourage consistency and repeatability for measurement and specification of environmental sensitivities. We believe very large cost savings will be appreciated if these guidelines, standards and precautions are followed.

02,032
PB94-198413 Not available NTIS
National Inst. of Standards and Technology (EEEL), Gaithersburg, MD. Electricity Div.
Automatic Inductive Voltage Divider Bridge Operates from 10 Hz to 100 kHz.
Final rept.
S. Avramov, N. M. Oldham, D. G. Jarrett, and B. C. Waltrip. 1993, 5p.
Pub. in Institute of Electrical and Electronics Engineers Transactions on Instrumentation and Measurement 42, n2 p131-135 Apr 93. See also PB93-135572.

Keywords: *Voltage dividers, *Impedance bridges, Calibrating, Instrument compensation, Automation, Computer applications, Alternating current, Inductance, Reprints, IVD(Inductive voltage dividers).

A bridge to calibrate programmable and manual inductive voltage dividers is described. The bridge is based on a programmable 30 b binary inductive voltage divider with terminal linearity of + or - 0.1 ppm in phase and + or - 2 ppm quadrature at 400 Hz. Measurements of programmable test dividers can be automated using software developed to align the bridge components and perform an automatic balance.

02,033
PB94-211588 Not available NTIS
National Inst. of Standards and Technology (NEL), Boulder, CO. Electromagnetic Technology Div.
24 GHz Josephson Array Voltage Standard.
Final rept.
C. A. Hamilton, R. L. Kautz, M. Stieg, M. B. Simmonds, K. Chieh, and W. F. Avrin. 1991, 4p.
Pub. in Institute of Electrical and Electronics Engineers Transactions on Instrumentation and Measurement 40, n2 p301-304 1991.

Keywords: *Standards, Superhigh frequency, Reprints, *Voltage standards, Josephson arrays.

A Josephson array voltage standard that operates at 24 GHz has been designed and fabricated. Optimum selection of junction parameters makes possible step stability times of 20 minutes, which is more than adequate for calibrations at the 1-V level. Designs using both probe and finline microwave couplers were tested. The probe coupler was about 3 dB more efficient and allowed a smaller chip and a less expensive mount. The reduced operating frequency allows substantial advantages in cost and reliability over more conventional devices that operate at 70-100 GHz.

02,034
PB94-212669 Not available NTIS
National Inst. of Standards and Technology (EEEL), Boulder, CO. Electromagnetic Technology Div.
Proposed High-Accuracy Superconducting Power Meter for Millimeter Waves.
Final rept.
R. L. Kautz, D. G. McDonald, D. K. Walker, and D. Williams. 1993, 4p.
Contract N66001-92MP00017
Sponsored by Naval Ocean Systems Center, San Diego, CA.
Pub. in Institute of Electrical and Electronics Engineers Transactions on Applied Superconductivity 3, n1 p2152-2155 Mar 93.

Keywords: *Power meters, *Millimeter waves, Extremely high frequency, Superconducting devices, Microwave equipment, Bolometers, Niobium, Reprints.

The accuracy of conventional microwave power meters is limited by the fact that some of the power dissipated in the meter is not sensed by the bolometric detector. In a proposed power meter, superconducting materials are used to virtually eliminate this source of error. Our goal is to measure a power of 10mW at frequencies in the WR-22 band (33 to 50 GHz) with an accuracy of 0.02%.

02,035
PB94-216702 Not available NTIS
National Inst. of Standards and Technology (EEEL), Gaithersburg, MD. Electricity Div.
Digital Techniques in HV Tests - Summary of 1989 Panel Session.
Final rept.
T. R. McComb, C. Fenimore, E. Gockenbach, K. Schon, L. Van der Sluis, B. Ward, Y. X. Zhang, J. Kuffel, and R. Malewski. 1992, 5p.
Pub. in Institute of Electrical and Electronics Engineers Transactions on Power Delivery 7, n4 p1800-1804 Oct 92.

Keywords: *Digital techniques, *High voltage, *Tests, Signal processing, Analog to digital converters, Industries, Reprints.

A panel session on digital techniques in high voltage (HV) tests was held at the IEEE PES Summer Meeting in Long Beach, CA (July 1989). This panel addressed the question of how signal processing can be used to enhance HV tests and extract more information from them. Part 1 dealt with the evaluation of digitizers and records, and Part 2 dealt with the application of digitizers to industrial testing. This paper presents an outline of the Panel Session and lists pertinent reference material.

02,036
PB95-126371 Not available NTIS
National Inst. of Standards and Technology (NEL), Gaithersburg, MD. Electricity Div.
Wide Band Active Current Transformer and Shunt.
Final rept.
T. Guang-qiu, and X. Xiu-ye. 1991, 5p.
Pub. in Institute of Electrical and Electronics Engineers Transactions on Instrumentation and Measurement 40, n6 p908-912 1991.

Keywords: *Bypasses, *Circuits, *Transformers, Voltage converters(AC to AC), Alternating current, Inductance, Frequency ranges, Audio frequencies, Resistors, Transducers, Electromagnetic measurement, Reprints.

An active inductive shunt with high accuracy and wide frequency range is introduced in this paper. The new shunt can be used in the audio frequency band. It has a wide current ratio (0.01 - 1) and good loading capacity. If the external burden of the inductive shunt is an ac standard resistor, it will become an ac current to voltage transducer that can be used in many electromagnetic measurements. The relative uncertainty in the current ratio of the new shunt is (1+j1) ppm to (8+j8) ppm over the frequency range from 40 Hz to 10 kHz.

02,037
PB95-150520 Not available NTIS
National Inst. of Standards and Technology (EEEL), Gaithersburg, MD. Electricity Div.
Developing Linear Error Models for Analog Devices.
Final rept.
G. N. Stenbakken, and T. M. Souders. 1993, 6p.
Pub. in Proceedings of Instrumentation and Measurement Technology Conference '93, Irvine, CA., May 18-20, 1993, p280-285.

Keywords: *Analog to digital converters, *Analog circuits, *Tests, Mathematical models, Error analysis, Simulation, Optimization, Reprints.

Techniques are presented for developing linear error models for analog and mixed-signal devices. A simulation program developed to understand the modeling process is described and results of simulations are presented. Methods for optimizing the size of empirical error models based on simulated error analyses are included. Once established, the models can be used in a comprehensive approach for optimizing the testing of the subject devices. Models are developed using data from a group of 13-bit A/D converters and compared with the simulation results.

02,038
PB95-150538 Not available NTIS
National Inst. of Standards and Technology (EEEL), Gaithersburg, MD. Electricity Div.
Diakoptic and Large Change Sensitivity Analysis.
Final rept.
G. N. Stenbakken, and J. A. Starzyk. 1992, 5p.
Pub. in IEE Proceedings-G 139, n1 p114-118 Feb 92.

Keywords: *Electrical networks, *Analog circuits, *Circuit analysis, Sensitivity analysis, Nonlinear systems, Reprints.

An approach to the analysis of large circuits based on the use of the large change sensitivity technique applied to decomposed networks is presented. As a result of this approach, a simple, compact notation for the solution vector is derived. The method is applicable to nonlinear analogue networks with hierarchical decomposition simulated by inserted ideal switches. A simple illustrative example is given.

02,039
PB95-150785 Not available NTIS
National Inst. of Standards and Technology (EEEL), Gaithersburg, MD. Electricity Div.
Flux-Locked Current Source Reference.
Final rept.
W. L. Tew, and E. R. Williams. 1993, 5p.
Pub. in Institute of Electrical and Electronics Engineers Transactions on Instrumentation and Measurement 42, n2 p186-190 Apr 93.

Keywords: Temperature range 0000-0013 K, SQUID devices, Quantization, Stability, Reprints, *Current sources, Flux transformers, Voltage references.

The quantization of flux in a closed superconducting circuit is used to provide a stable reference current. A 10 mA current source is coupled through a toroidal transformer to a dc SQUID input, and the resulting signal is fed back as an error current. The result is a net flux linkage that exhibits short-term stability of 1 part in 10(exp 9)/h. The net current is quantized with a step size of 59.4 nA, and it will exhibit the same stability as the flux provided the mutual inductance of the transformer remains constant. This current is passed through a precise 100 ohm resistor and compared against Zener diode references. The observed temperature coefficient for the flux transformer is 28.5 + or - 3 ppm/K at 4.2 K. Possible sources for the temperature dependence are discussed.

02,040
PB95-152310 Not available NTIS

National Inst. of Standards and Technology (EEEL), Gaithersburg, MD. Electricity Div.
Cryogenic Precision Capacitance Bridge Using a Single Electron Tunneling Electrometer.
Final rept.
R. N. Ghosh, E. R. Williams, A. F. Clark, and R. J. Soulen. 1994, 2p.
Pub. in Physica B 194-196, p1007-1008 1994.

Keywords: *Capacitance bridges, Cryogenic temperature, Cryogenic equipment, Electrometers, Precision, Reprints, Single electron tunneling, Electron charge, Dilution refrigerators.

The electronic charge can be determined by placing a known number of electrons on a calibrated capacitor and measuring the resulting voltage. Single electron tunneling (SET) electrometers with sufficient sensitivity for this application have been fabricated. We report on the design and preliminary results of a capacitance bridge experiment using an SET electrometer to measure two capacitors in a dilution refrigerator. This includes discussion of issues such as the leakage rate of a capacitor at cryogenic temperatures and the optimum coupling of the electrometer to the bridge circuit.

02,041
PB95-152849 Not available NTIS
National Inst. of Standards and Technology (EEEL), Gaithersburg, MD. Electricity Div.
Automatic Calibration of Inductive Voltage Dividers for the NASA Zeno Experiment.
Final rept.
S. Avramov, and N. M. Oldham. 1993, 3p.
Pub. in Review of Scientific Instruments 64, n9 p2676-2678 Sep 93.

Keywords: *Voltage dividers, *Calibration, Temperature control, Temperature measurement, Automation, Linearity, Hz range, Reprints, Inductive voltage dividers, Zeno experiment.

Two inductive voltage dividers (IVDs) used for temperature measurements in NASA's Zeno experiment were tested. In order to obtain the required resolution of 10 parts-per-billion, a 30-bit binary inductive voltage divider developed at the National Institute of Standards and Technology was used to measure the differential linearity of the Zeno IVDs. Automatic measurements were performed on the dividers in the Zeno engineering model at frequencies of 266 and 351 Hz over a ratio range of 0.55-0.56. The measured differential linearity limits of temperature resolution of 5 microK.

02,042
PB95-152856 Not available NTIS
National Inst. of Standards and Technology (EEEL), Gaithersburg, MD. Electricity Div.
Inductive Voltage Divider Calibration for the NASA Flight Experiment.
Final rept.
S. Avramov, N. M. Oldham, and R. W. Gammon. 1993, 8p.
Contract NASA-NAS-3-25370
Sponsored by National Aeronautics and Space Administration, Washington, DC.
Pub. in Proceedings of National Computer Systems Laboratory Workshop and Symposium, Albuquerque, NM., July 25-29, 1993, p225-232.

Keywords: *Voltage dividers, *Calibration, Temperature control, Thermostats, Automation, Impedance bridges, Hz range, Linearity, Tests, Reprints, Inductive voltage dividers, Zeno experiment.

The inductive voltage dividers (IVDs) used in the thermostat of NASA's Zeno experiment were tested using an automatic IVD bridge developed at the National Institute of Standards and Technology (NIST). To achieve + or -10 microK temperature control, the thermostat must be able to measure resistance ratios with a differential linearity of + or -0.1 parts-per-million (ppm). The test results show that within a ratio range of O.5 to 0.6 at frequencies between 200 Hz and 400 Hz, the thermostat IVDs were linear to + or -0.07 ppm.

02,043
PB95-153573 Not available NTIS
National Inst. of Standards and Technology (EEEL), Boulder, CO. Electromagnetic Fields Div.
Terminal Invariant Description of Amplifier Noise.
Final rept.
G. F. Engen, and D. F. Wait. 1992, 2p.
Pub. in Proceedings of Conference on Precision Electromagnetic Measurements, Paris, France, June 9-12, 1992 p250-251.

Keywords: *Electromagnetic noise, *Electric terminals, Models, Electric connectors, Electrical impedance, Reprints, *Amplifier noise.

An alternative treatment of amplifier noise which, in contrast to some of the earlier treatments, is 'terminal invariant' at the output as well as input terminals is presented. As a practical consequence, the model provides a reduced sensitivity to connector imperfections, and the problems in defining characteristic impedance.

02,044
PB95-162061 Not available NTIS
National Inst. of Standards and Technology (EEEL), Boulder, CO. Electromagnetic Fields Div.
Broadband Mismatch Error in Noise Measurement Systems.
Final rept.
S. Perera. 1992, 2p.
Pub. in Proceedings of Conference on Precision Electromagnetic Measurements, Paris, France, June 9-12, 1992, p256-257.

Keywords: *Electromagnetic noise measurement, Microwave radiometers, Radiofrequency filters, Thermal noise, Error analysis, Heterodyning, Reprints, Mismatch(Electrical).

Microwave noise measurement systems of a double-sideband heterodyne design, with a wide bandwidth and an electrically long transmission line at the input, may suffer from a large error; systems with a high IF are especially vulnerable. An IF filter may be employed to reduce the error to a negligible level.

02,045
PB95-163713 Not available NTIS
National Inst. of Standards and Technology (NML), Boulder, CO. Time and Frequency Div.
High Spectral Purity X-Band Source.
Final rept.
F. L. Walls, and C. M. Felton. 1990, 7p.
Pub. in Proceedings of the Annual Symposium on Frequency Control (44th), Baltimore, MD., May 23-25, 1990, p542-548.

Keywords: *Frequency synthesizers, *X band, Frequency discriminators, Microwave oscillators, Superhigh frequency, Sources, Reprints, Phase noise.

We have developed a X-band frequency source that has very high spectral purity and is suitable for frequency synthesis and many kinds of high-resolution spectroscopy. A commercial dielectric resonator oscillator (DRO) is frequency locked to a high-Q cavity used as a frequency discriminator. Many systems have been developed in the past for locking a source to a reference cavity. The distinguishing features of our approach are given. We describe the design of the discriminator cavity, the phase compensated frequency-locked loop, and the phase and amplitude noise performance. We also discuss vibration sensitivity, techniques for automatically locking to the low frequency reference, and the reduction of 60 Hz sidebands.

02,046
PB95-163861 Not available NTIS
National Inst. of Standards and Technology (NEL), Boulder, CO. Electromagnetic Technology Div.
Series Array of DC SQUIDs.
Final rept.
R. P. Welty, and J. M. Martinis. 1991, 3p.
Pub. in Institute of Electrical and Electronic Engineers Transactions on Magnetics 27, n2 p2924-2926 Mar 91.

Keywords: *SQUID devices, Direct current, Amplifiers, Arrays, Aluminum oxides, Niobium, Reprints, SIS(Superconductors), Multilayers.

We have fabricated series arrays of 100 dc SQUIDs using a Nb-AlO(x)-Nb trilayer junction process. The SQUIDs are modulated with a common flux bias line, and produce an output voltage swing of several millivolts across the array. The large output voltage allows direct connection to room temperature electronics without the transformer coupling and resulting frequency limitations commonly associated with dc SQUID amplifiers. We have measured a bandwidth of dc to at least 175 MHz for a 100-SQUID array.

02,047
PB95-164687 Not available NTIS
National Inst. of Standards and Technology (EEEL), Gaithersburg, MD. Electricity Div.
Accuracy Comparisons of Josephson Array Systems.
Final rept.
R. L. Steiner, A. F. Clark, C. Kiser, T. J. Witt, and D. Reymann. 1993, 4p.
Pub. in Institute of Electrical and Electronics Engineers Transactions on Applied Superconductivity 3, n1 p1874-1877 Mar 93.

Keywords: *Electrical measurement, *Standards, Comparative evaluations, Josephson junctions, Accuracy, Reprints, *Josephson arrays, *Voltage standards.

Five Josephson-array voltage standard systems were compared using several different methods. All of the tests were performed on site at a 1.018-V level, either by direct connection or through successive measurements of independent voltage sources. The resulting agreement between different systems measuring the same source were generally better than 10.0 parts in 10(exp -9), limited by source noise and detector resolution. Direct array-to-array comparisons for independent systems achieved agreement to within random uncertainties of 0.2 parts in 10(exp -9).

02,048
PB95-168423 Not available NTIS
National Inst. of Standards and Technology (EEEL), Boulder, CO. Electromagnetic Technology Div.
Tunable High Temperature Superconductor Microstrip Resonators.
Final rept.
J. A. Beall, R. H. Ono, D. Galt, and J. C. Price. 1993, 3p.
Sponsored by Office of Naval Research, Arlington, VA.
Pub. in Institute of Electrical and Electronics Engineers MTT-S International Microwave Symposium Digest, Atlanta, GA., June 14-18, 1993, p1421-1423.

Keywords: *Resonators, High temperature superconductors, Ferroelectric materials, Superconducting devices, Microstrip devices, Tuning devices, Microwave equipment, YBCO superconductors, Strontium titanates, Thin films, Reprints, Yttrium barium cuprates.

We have fabricated and characterized electrically tunable high temperature superconductor microstrip resonators incorporating YBa2Cu3O(7-x) superconductor and SrTiO3 ferroelectric films. Early versions of these and similar devices were described previously. The resonators consist of two co-linear microstrip line-sections separated by a 5 micrometer gap. The capacitance of the gap influences the frequencies of the odd-order coupled resonances. Inductively choked dc bias lines are attached to each line section so that a bias voltage can be applied to the gap. When the gap is filled with a ferroelectric material, the odd resonances can be tuned. Frequency shifts of 300 MHz have been observed with a bias voltage of 50 V for resonances at 5.6 GHz and 11.6 GHz. The tunability is independent of temperature from 4 K to 80 K.

02,049
PB95-168530 Not available NTIS
National Inst. of Standards and Technology (EEEL), Boulder, CO. Electromagnetic Fields Div.
Multi-State Two-Port: An Alternative Transfer Standard.
Final rept.
G. F. Eugen, R. M. Judish, and J. Juroshek. 1994, 8p.
Pub. in Proceedings of Automatic Radio Frequency Techniques Group Conference Digest (43rd), San Diego, CA., May 27, 1994, p11-18.

Keywords: *Network analyzers, Solid state devices, Electric connectors, Performance evaluation, Reproducibility, Calibration, Automation, Tests, Reprints, *Transfer standards, *Impedance generators.

In a companion paper, the proposed use of a 'stable solid programmable impedance generator' as a calibration transfer and verification standard for vector network analyzers (VNA) has been suggested. An obvious requirement is that the multistate device provide a high degree of stability and repeatability. This paper describes a series of preliminary tests, using the NIST six-port systems, to evaluate the parameters of interest. The application of this device in connector evaluation is also reported.

02,050
PB95-168811 Not available NTIS
National Inst. of Standards and Technology (EEEL), Boulder, CO. Electromagnetic Technology Div.

Observation of Vortex Dynamics in Two-Dimensional Josephson-Junction Arrays.
Final rept.
S. G. Lachenmann, T. Doderer, D. Hoffmann, S. P. Benz, R. P. Huebener, and P. A. A. Booi. 1994, 7p.
Pub. in Physical Review B 50, n5 p3158-3164, 1 Aug 94.

Keywords: *Josephson junctions, Scanning electron microscopy, Two dimensional, Aluminum oxides, Niobium, Reprints, Josephson arrays, Vortex dynamics.

Spatially resolved images of the dynamic states of current-biased two-dimensional arrays of Nb/AlO(x)/Nb Josephson junctions were obtained using low-temperature scanning electron microscopy. The arrays were square or rectangular and the maximum size was 20 junctions X 20 junctions. In overdamped arrays, our images at zero or small applied perpendicular magnetic field, together with model calculations, confirm the nucleation of a vortex at one sample edge (or an antivortex at the opposite edge) and its subsequent motion into the array interior. Vortex annihilation due to vortex-antivortex collision was observed to take place in the middle of the array or at the edge opposite to the nucleation edge. These dynamics and the underlying model considerations are similar to that for Abrikosov vortices in the current-induced resistive state of thin film type-II superconductors. The phenomenon of 'row switching' is directly confirmed in images of underdamped arrays. The specific rows experiencing this process change randomly when the same bias point on the current-voltage characteristic is established many times, starting each time from zero current.

02,051
PB95-169165 Not available NTIS
National Inst. of Standards and Technology (EEEL), Boulder, CO. Electromagnetic Technology Div.
Optimization of ECR-Based PECVD Oxide Films for Superconducting Integrated Circuit Fabrication.
Final rept.
J. E. Sauvageau, C. J. Burroughts, M. W. Cromar, and J. A. Koch. 1994, 6p.
Pub. in Proceedings of Annual Technical Conference of Society of Vacuum Coaters (37th), Boston, MA., May 8-13, 1994, 6p.

Keywords: *Chemical vapor deposition, *Chemical reactors, *Oxide films, *Silicon dioxide, Electron cyclotron resonance, Dielectric films, Superconducting devices, Integrated circuits, Microwave equipment, Optimization, Reprints, Plasma deposition.

A commercial microwave electron cyclotron resonance (ECR) reactor has been optimized for plasma enhanced chemical vapor deposition of silicon dioxide films at deposition temperatures lower than 150 C. A spool piece was added to the system resulting in improved deposition uniformity and lower deposition temperatures. Response surface methodology was used in the ECR system optimization before and after the modification. The response variables were deposition rate, uniformity, index of refraction, film stress, and wet-etch rate. As a result of the studies, several oxide deposition processes have been developed at ambient temperatures. These processes are presently being used in the superconducting-integrated-circuit fabrication facility at NIST. The optimization process and results are discussed.

02,052
PB95-169314 Not available NTIS
National Inst. of Standards and Technology (EEEL), Boulder, CO. Electromagnetic Technology Div.
Phase-Locked Oscillator Optimization for Arrays of Josephson Junctions.
Final rept.
K. Wiesenfeld, S. P. Benz, and P. A. A. Booi. 1994, 12p.
Sponsored by Office of Naval Research, Arlington, VA.
Pub. in Jnl. of Applied Physics 76, n6 p3835-3846, 15 Sep 94.

Keywords: *Josephson junctions, Phase locked systems, Two dimensional, Frequency standards, Design criteria, Stability, Reprints, *Josephson oscillators, Josephson arrays.

An overview of phase locking in two-dimensional (2D) arrays of identical Josephson junctions is presented. General design criteria are discussed for optimization of power and linewidth. A harmonic balance technique is used to derive an analytic expression for the fundamental power as a function of bias voltage for a single shunted tunnel junction with an external shunt resistor having parasitic inductance. A linear stability analysis is performed on the in-phase state of 2D arrays in the absence of any external load. Most excitation modes in the 2D array are damped, leading to stable phase locking between parallel junctions within each row; however, within the theoretical model, no mechanisms intrinsic to the array were found to induce phase locking between rows of junctions. The results of these calculations and their impact on and relevance to the design of phase-locked Josephson oscillators are discussed.

02,053
PB95-175071 Not available NTIS
National Inst. of Standards and Technology (EEEL), Boulder, CO. Electromagnetic Technology Div.
Experimental Results on Single Flux Quantum Logic.
Final rept.
S. P. Benz, C. J. Burroughs, and C. A. Hamilton. 1993, 4p.
Sponsored by Defense Advanced Research Projects Agency, Arlington, VA.
Pub. in Institute of Electrical and Electronics Engineers Transactions on Applied Superconductivity 3, n1 p2582-2585 Mar 93.

Keywords: *Superconducting devices, *Logic devices, Josephson junctions, SQUID devices, Design, Reprints, Single flux quantum.

We have optimized the design and calculated the margins for a number of single flux quantum (SFQ) logic elements including AND, OR, XOR, Splitter, DC-to-SFQ converter, and SFQ-to-DC converter. These are the fundamental building blocks necessary to construct more complex logic functions such as the half adder, and full adder. Experimental tests of the primary gates, the AND, OR, XOR, and splitter, were made by imbedding each test gate between DC-to-SFQ converters at the inputs and SFQ-to-DC converters at the outputs. Automated testing of each circuit was used to determine functionality, optimum bias levels, and margins. The experimental bias current margins for each gate are consistent with the simulations. This is the first experimental functional confirmation of these SFQ logic gates.

02,054
PB95-175121 Not available NTIS
National Inst. of Standards and Technology (EEEL), Boulder, CO. Electromagnetic Technology Div.
Characterization of the Emission from 2D Array Josephson Oscillators.
Final rept.
P. A. A. Booi, and S. P. Benz. 1994, 10p.
Pub. in Proceedings of International Symposium on Space Terahertz Technology (5th), Ann Arbor, MI., May 10-12, 1994, p234-243.

Keywords: *Josephson junctions, Phase locked systems, Experimental data, Two dimensional, Noise temperature, Line width, Emission, Reprints, *Josephson oscillators, Josephson arrays.

We present experimental results on the emission from phase-locked two-dimensional arrays of Josephson junctions. We have coupled the emission from 10 x 10 arrays to a room-temperature mixer through a fin-line antenna and WR-12 waveguide. A single voltage-tunable peak was detected up to 230 GHz. A stripline resonance in the antenna reduced the array's dynamic resistance and thereby the emission linewidth to as low as 10 kHz. We extract an effective noise temperature of 14 K from the linewidth data. When the array's emission was coupled to an on-chip detector junction through a dc blocking capacitor, we detected voltage-tunable emission from 75 GHz up to 300 GHz, and in some circuits emission above 400 GHz. The coherent power spectrum depends primarily on internal resonances.

02,055
PB95-175139 Not available NTIS
National Inst. of Standards and Technology (EEEL), Boulder, CO. Electromagnetic Technology Div.
Emission Linewidth Measurements of Two-Dimensional Array Josephson Oscillators.
Final rept.
P. A. A. Booi, and S. P. Benz. 1994, 3p.
Pub. in Applied Physics Letters 64, n16 p2163-2165, 18 Apr 94.

Keywords: *Josephson junctions, Noise temperature, Two dimensional, Line width, Emission, Reprints, *Josephson oscillators, Josephson arrays.

We have coupled emission from 10 X 10 arrays of Josephson junctions at 4 K to a room-temperature mixer through a fin-line antenna and a WR-12 waveguide. A single voltage-tunable peak was detected in the frequency range from 53 to 230 GHz. A stripline resonance in the antenna reduced the array's dynamic resistance and thereby the emission linewidth to as low as 10 kHz. We extract an effective noise temperature of 14 K from the linewidth data.

02,056
PB95-175147 Not available NTIS
National Inst. of Standards and Technology (EEEL), Boulder, CO. Electromagnetic Technology Div.
Frequency Dependence of the Emission from 2D Array Josephson Oscillators.
Final rept.
P. A. A. Booi, S. P. Benz, T. Doderer, S. Lachenmann, R. P. Huebener, D. Hoffmann, and J. Schmidt. 1993, 3p.
Contract ONR-N00014-92-F-00040
Sponsored by Office of Naval Research, Arlington, VA.
Pub. in Institute of Electrical and Electronics Engineers Transactions on Applied Superconductivity 3, n1 p2493-2495 Mar 93.

Keywords: *Josephson junctions, Phase locked systems, Frequency dependence, Two dimensional, Coherent radiation, Standing waves, Emission, Reprints, *Josephson oscillators, Josephson arrays.

Coherent emission from two-dimensional arrays of Josephson junctions, coupled to a detector junction through a dc blocking stripline capacitor, was detected over a frequency range from 50 to 210 GHz. A power of 0.26 (micro)W which is larger than the 0.1 (micro)W expected from the RSJ model was detected in a range from 140 to 150 GHz. Frequencies where no emission was detected correspond to standing waves in the capacitor when multiples of the half-wavelength match the capacitor length. Low temperature scanning electron microscopy confirmed the presence of standing waves at these frequencies, but also revealed standing waves at other frequencies indicating an impedance mismatch and a possible extension of the standing waves into the array.

02,057
PB95-175246 Not available NTIS
National Inst. of Standards and Technology (EEEL), Boulder, CO. Electromagnetic Technology Div.
Automated Josephson Integrated Circuit Test System.
Final rept.
C. J. Burroughs, and C. A. Hamilton. 1993, 3p.
Pub. in Institute of Electrical and Electronics Engineers Transactions on Appl. Supercond. 3, p2687-2689 Mar 93.

Keywords: *Circuit testers, *Integrated circuits, Test equipment, Josephson junctions, Automation, Reprints, *Superconducting networks.

We have developed an automated test system for complex superconductive integrated circuits. Its low speed capability consists of 96 identical I/O channels which are controlled by a PC-486 computer. Each channel is capable of driving currents and reading voltages at frequencies up to 40 kHz. Integrating this low speed I/O capability with high speed test equipment controlled over the IEEE 488 bus allows measurements at frequencies up to the limits of the test equipment. The system can automatically set biases, display I-V curves, measure parameter margins, plot threshold curves, extract experimental circuit values, and collect statistical data on parameter spreads and error rates. Issues of noise suppression, ground loop handling, and auto-calibration are discussed.

02,058
PB95-175600 Not available NTIS
National Inst. of Standards and Technology (EEEL), Boulder, CO. Electromagnetic Technology Div.
Josephson Voltage Standard Based on Single-Flux-Quantum Voltage Multipliers.
Final rept.
C. A. Hamilton. 1992, 4p.
Pub. in Institute of Electrical and Electronics Engineers Transactions on Applied Superconductivity 2, n3 p139-142 Sep 92.

Keywords: *Josephson junctions, Frequency multipliers, Design, Reprints, *Voltage standards, Single flux quantum.

A Josephson single-flux-quantum voltage/frequency multiplier circuit is proposed as the basic building block

for a new generation of voltage standards. The circuit uses magnetic coupling to synchronize a series array of independent junction oscillators to the flux flow in a Josephson transmission line. A cascade of these circuits can multiply an arbitrarily low input frequency up to the frequency limit of the circuit (approx. 250 GHz) and then add the voltages across approximately 30,000 oscillators to generate precise voltages up to 10 V. Because the oscillators can be switched on and off with a bias current, the output voltage is rapidly programmable. A complete design for a voltage standard programmable in 1.2 (micro)V increments to a maximum of 10 V is proposed. Using existing fabrication technology, the circuit would cover a substrate area of about 1 sq cm and use 67,210 junctions.

02,059
PB95-175857 Not available NTIS
National Inst. of Standards and Technology (EEEL), Boulder, CO. Electromagnetic Technology Div.
Fabrication Issues in Optimizing YBa2Cu3O7-x Flux Transformers for Low l/f Noise.
Final rept.
F. Ludwig, E. Dantsker, D. T. Nemeth, J. Clarke, S. Knappe, H. Koch, R. E. Thomson, D. Koelle, and A. H. Miklich. 1994, 4p.
Contract DE-AC03-76SF00098
Sponsored by Department of Energy, Washington, DC.
Pub. in Superconducting Science and Technology 7, p273-276 1994.

Keywords: *Transformers, Superconducting devices, High temperature superconductors, YBCO superconductors, Strontium titanates, Magnetometers, Fabrication, Reprints, *Flux transformers, Yttrium barium cuprates, Multilayers.

We describe an improved interconnect technology for the fabrication of multiturn flux transformers from YBa2Cu3O(7-x)-SrTiO3-YBa2Cu3O(7-x) multilayers. The essential improvements are reductions in the thicknesses of the trilayer films, typically to 100 nm, 250 nm, and 250 nm respectively, and in the deposition rate, to 0.07 nm/laser pulse. This process yields crossovers in which the critical current density in the upper YBa2Cu3O(7-x) film at 77 K is (2-3) x 10(sup 6) A/sq cm. In situ trilayers exhibited 1/f flux noise levels at 1 Hz below the measurement sensitivity of 15 (mu)(Phi)(sub 0) Hz(sup -1/2), where Phi(sub 0) is the flux quantum. However, the flux noise of trilayers in which each layer had been patterned was significantly higher. The best flip-chip magnetometer had a white noise of 40 fT Hz(sup -1/2), increasing to 340 fT Hz(sup -1/2) at 1 Hz; the corresponding flux noise levels were 9 (mu)(Phi)(sub 0) Hz(sup -1/2) and 75 (mu)(Phi)(sub 0) Hz(sup -1/2).

02,060
PB95-176053 Not available NTIS
National Inst. of Standards and Technology (EEEL), Boulder, CO. Electromagnetic Technology Div.
Phase Locking in Two-Junction Systems of High-Temperature Superconductor-Normal Metal-Superconductor Junctions.
Final rept.
C. D. Reintsema, R. H. Ono, T. E. Harvey, N. Missen, and L. R. Vale. 1994, 3p.
Pub. in Applied Physics Letters 64, n5 p637-639, 31 Jan 94.

Keywords: *Phase locked systems, *Josephson junctions, High temperature superconductors, Temperature range 0000-0013 K, Temperature range 0013-0065 K, Temperature dependence, YBCO superconductors, Planar structures, Reprints, Yttrium barium cuprates, Josephson arrays, Multilayers.

Mutual phase locking between two high-temperature step-edge superconducting-normal metal-superconducting junctions has been investigated using a two-junction circuit with a nonsuperconducting feedback path. The strength of the phase-locked state has been characterized as a function of locking frequency and temperature. Results are presented for a planar circuit as well as for a multilayer circuit incorporating a superconducting ground plane. The observed behavior was significantly enhanced for the circuit over a ground plane. Characterization of the phase locked state at 4 K yielded locking strengths as large as (absolute value of I(sub L))/(I bar)(sub c) = 9%, and maximum locking frequencies to 1.06 THz. The magnitude of the locking strength decreased rapidly with increasing temperature with complete loss of coherence occurring at temperatures greater than 35 K.

02,061
PB95-176277 Not available NTIS
National Inst. of Standards and Technology (EEEL), Boulder, CO. Electromagnetic Technology Div.
Two-Stage Integrated SQUID Amplifier with Series Array Output.
Final rept.
R. P. Welty, and J. M. Martinis. 1993, 4p.
Contract ONR-N00014-92-F-0003
Sponsored by Office of Naval Research, Arlington, VA.
Pub. in Institute of Electrical and Electronics Engineers Transactions on Applied Superconductivity 3, n1 p2605-2608 Mar 93.

Keywords: *SQUID devices, Integrated circuits, Low noise, Reprints, *SQUID amplifiers, SQUID arrays.

We have fabricated a 2-stage integrated dc SQUID amplifier which uses a compact series array of 100 dc SQUIDs as the readout device for a low-noise single SQUID. The results suggest the general utility of series SQUID arrays as readout devices for SQUIDs.

02,062
PB95-180022 Not available NTIS
National Inst. of Standards and Technology (PL), Boulder, CO. Time and Frequency Div.
Investigations of AM and PM Noise in X-Band Devices.
Final rept.
F. G. Ascarunz, E. S. Ferre, and F. L. Walls. 1993, 9p.
Pub. in Proceedings of Institute of Electrical and Electronics Engineers International Frequency Control Symposium, Salt Lake City, UT., June 2-4, 1993, p303-311.

Keywords: *Microwave amplifiers, *Microwave oscillators, *Mixers(Electronics), *Electromagnetic noise, *Amplitude modulation, *Phase modulation, Electrical measurement, Superhigh frequency, X band, White noise, Reprints.

In this paper we report on measurements of phase modulation (PM) and amplitude modulation (AM) noise in a variety of amplifiers, dielectric resonator oscillator (DRO) sources and mixers at 10.6 GHz. There is little information on AM noise and only limited information on PM noise in microwave devices. Two channel measurement systems and cross-correlation analysis were used in these noise measurements. In amplifiers there are at least two random noise processes that generate equal levels of PM and AM noise when the amplifier is in the linear operating range. The noise processes correspond to a flicker noise process and a white noise process. In the DRO sources we show that these noise mechanisms are present in the active components and determine the AM and PM characteristics of the oscillator. We report on noise residuals in mixers from three different companies.

02,063
PB95-198685 PC A04/MF A01
National Inst. of Standards and Technology (EEEL), Gaithersburg, MD. Electricity Div.
10 kV DC Resistive Divider Calibration.
R. S. Turgel. Jan 95, 57p, NISTIR-5566.

Keywords: *Voltage dividers, *Calibration, Electrical networks, Direct current, Temperature control, High voltage, Computer programs, Voltmeters, Resistors, Kilovolts.

A calibration method for a 10 kV dc ratio divider was developed. The method uses a high-precision digital voltmeter, at the 10 V level, to establish a 10:1 voltage ratio for each decade of the resistive divider and combines these results to obtain an overall voltage ratio of 10,000:1. The linearity of the voltmeter was checked using a Josephson-array voltage standard. The overall ratio agreed with measurements made at 10 kV using a Park-type divider to within the uncertainty limits.

02,064
PB95-202644 Not available NTIS
National Inst. of Standards and Technology (EEEL), Boulder, CO. Electromagnetic Fields Div.
Accuracy and Repeatability in Time Domain Network Analysis.
Final rept.
L. A. Hayden, R. B. Marks, and J. B. Rettig. 1994, 8p.
Pub. in Proceedings of Automatic Radio Frequency Techniques Group Conference Digest, Boulder, CO., December 1-2, 1994, p39-46.

Keywords: *Network analysis, *Electrical measurement, Electrical networks, Electromagnetic noise, Time domain, Reproducibility, Reflectometers, Attenuation, Accuracy, Reprints.

This paper examines the importance of measurement repeatability in time domain network analysis and includes an analysis of the limitations imposed on theoretical accuracy by measurement noise. A closed-loop correction algorithm implemented in a fast, equivalent-time sampling, time domain reflectometer improves source timing accuracy, the dominant cause of nonrepeatability. An example measurement of attenuation in a 3.5 mm coaxial air-line demonstrates performance approaching this theoretical noise limit and the limits imposed by connector repeatability.

02,065
PB95-202925 Not available NTIS
National Inst. of Standards and Technology (EEEL), Boulder, CO. Electromagnetic Fields Div.
Time Domain Network Analysis Using the Multiline TRL Calibration.
Final rept.
R. B. Marks, L. A. Hayden, J. A. Jargon, and F. Williams. 1994, 9p.
Pub. in Proceedings of Automatic Radio Frequency Techniques Group Conference Digest (44th), Boulder, CO., December 1-2, 1994, p47-55.

Keywords: *Network analyzers, *Calibration, Time domain, Reprints, Multiline TRL method, On wafer measurement, Scattering parameters.

We apply the multiline TRL (through-reflect-line) method to the calibration of a time domain network analyzer (TDNA). The calibration removes the effects of cables and connectors, nonideal source and sampler responses, source and sampler mismatch, and frequency-dependent characteristic impedance of the transmission lines. Multiline TRL is especially well suited to TDNA and provides not only a complete calibration but also a full characterization of the transmission lines, information useful in the study of interconnections.

02,066
PB96-102082 Not available NTIS
National Inst. of Standards and Technology (EEEL), Boulder, CO. Electromagnetic Technology Div.
Resonances in Two-Dimensional Array Oscillator Circuits.
Final rept.
P. A. A. Booi, and S. P. Benz. 1995, 4p.
Sponsored by Office of Naval Research, Arlington, VA.
Pub. in Institute of Electrical and Electronics Engineers Transactions on Applied Superconductivity, v5 n2 p2899-2902 Jun 95.

Keywords: *Josephson junctions, *Resonance, *Emission, Antennas, Waveguides, Resonance lines, Spectra line width, Oscillators, Circuits, Reprints.

The authors present experimental results on the emission from phase-locked two-dimensional arrays of Josephson junctions. The authors have coupled the emission from 10 x 10 arrays to a room-temperature mixer through a fin-line antenna and WR-12 waveguide. A single voltage-tunable peak was detected up to 230 GHz. A stripline resonance in the antenna reduced the array's dynamic resistance and thereby the emission linewidth to as low as 10 kHz. The authors extract an effective noise temperature of 14 K from the linewidth data.

02,067
PB96-102223 Not available NTIS
National Inst. of Standards and Technology (EEEL), Boulder, CO. Electromagnetic Technology Div.
Direct Observation of Vortex Dynamics in Two-Dimensional Josephson-Junction Arrays.
Final rept.
T. Doderer, S. G. Lachenmann, R. P. Huebener, P. A. A. Booi, and S. P. Benz. 1995, 4p.
Pub. in Institute of Electrical and Electronics Engineers Transactions on Applied Superconductivity, v5 n2 p2723-2726 Jun 95.

Keywords: *Josephson junctions, *Arrays, *Vortices, Absolute zero, Magnetic fields, Electric current, Nucleation, Bias, Reprints, Two dimensional array, SEM(Scanning electron microscopy), Vortex dynamics, LTSEM.

Spatially resolved images of the dynamic states of current-biased overdamped two-dimensional arrays of

Nb/AlOx/Nb Josephson junctions were obtained using low-temperature scanning electron microscopy. The authors present two-dimensional imaging results describing various vortex dynamic regimes in zero applied magnetic field. The nucleation of current-induced vortices at the array boundaries and their subsequent motion into the array interior are observed for bias currents slightly above the array critical current. With increasing bias current, vortex-vortex interaction becomes important. Discussions on the coherent microwave radiation emission are presented.

02,068
PB96-102629 Not available NTIS
National Inst. of Standards and Technology (EEEL), Gaithersburg, MD. Electricity Div.
100 Ampere, 100 kHZ Transconductance Amplifier.
Final rept.
O. B. Laug. 1995, 6p.
Pub. in Institute of Electrical and Electronics Engineers Instrumentation and Measurement Technology Conference (IMTC), Waltham, MA., April 24-26, 1995, p506-511 1995.

Keywords: *Power amplifiers, *Voltage amplifiers, Reprints, Transconductance, Electric power meters.

A high-current, wide-band transconductance amplifier is described that provides an unprecedented level of output current at high frequencies with exceptional stability. It is capable of converting a signal voltage applied to its input into a ground-referenced output current up to 100 amperes rms over a frequency range from dc to 100 kHz with a useable frequency extending to 1 MHz. The amplifier has a 1000 watt output capability, + or - 10 volts of compliance, and can deliver up to 400 amperes peak-to-peak of pulsed current. The amplifier design is based on the principle of paralleling a number of precision bipolar voltage-to-current converters. The design incorporates a unique ranging system controlled by opto-isolated switches, which permit a full-scale range from 5 to 100 amperes. The design considerations for maintaining wide bandwidth, high output impedance, and unconditional stability for all loads are discussed.

02,069
PB96-102785 Not available NTIS
National Inst. of Standards and Technology (EEEL), Boulder, CO. Electromagnetic Fields Div.
Comments on 'Conversions between S, Z, Y, h, ABCD, and T Parameters Which Are Valid for Complex Source and Load Impedances'.
Final rept.
R. B. Marks, and D. F. Williams. 1995, 2p.
Pub. in Institute of Electrical and Electronics Engineers Transactions on Microwave Theory and Techniques, v43 n4 p914-914 Apr 95.

Keywords: *Characteristic impedance, *Electric converters, *Microwave circuits, Electrical impedance, Electric networks, Matrices(Circuits), Wave scattering, Travelling waves, Transmission circuits, Reprints, *Scattering parameters.

A recently published paper presents formulas for converting between various network parameters. However, these parameters are defined using an unconventional definition of the waves and therefore yield unexpected results.

02,070
PB96-111984 Not available NTIS
National Inst. of Standards and Technology (EEEL), Boulder, CO. Electromagnetic Fields Div.
Uncertainties of the NIST Coaxial Noise Calibration System.
Final rept.
S. P. Pucic. 1994, 2p.
Pub. in Proceedings of Conference on Precision Electromagnetic Measurements Digest, Boulder, CO., June 27-July 1, 1994, p254-255.

Keywords: *Calibration, Radiometers, Broadband, Cryogenic temperature, Standards, Reprints, *Noise calibration systems, National Institutes of Standards and Technology.

Uncertainties of the NIST broadband coaxial calibration system are analyzed. The expanded relative uncertainty for a source with the ENR of approximately 15 dB is typically 1.6%.

02,071
PB96-112263 Not available NTIS
National Inst. of Standards and Technology (EEEL), Gaithersburg, MD. Electricity Div.
Binary versus Decade Inductive Voltage Divider Comparison and Error Decomposition.
Final rept.
S. Avramov-Zamurovic, G. N. Stenbakken, A. D. Koffman, N. M. Oldham, and R. W. Gammon. 1995, 5p.
Pub. in Institute of Electrical and Electronics Transactions on Instrumentation and Measurement, v44 n4 p904-908, 28 Aug 95.

Keywords: *Voltage dividers, Reprints, Electrical networks, Linearity, Structural models, Inductive voltage dividers.

An automatic Inductive Voltage Divider (IVD) characterization method that can measure linearity by comparing IVD's with different structures is suggested. Structural models are employed to decompose an error vector into components that represent each divider. Initial tests at 400 Hz show that it is possible to assign independent errors due to the binary and decade structures with a 2-sigma uncertainty of 0.05 parts per million (ppm) at the measured ratio values.

02,072
PB96-112271 Not available NTIS
National Inst. of Standards and Technology (EEEL), Gaithersburg, MD. Electricity Div.
Cryogenic Precision Capacitance Bridge Using a Single Electron Tunneling Electrometer.
Final rept.
R. N. Ghosh, A. F. Clark, B. A. Sanborn, and E. R. Williams. 1994, 6p.
See also PB95-126074 and PB95-152310.
Pub. in Coulomb and Interference Effects in Small Electronic Structures, p311-316 1994.

Keywords: *Capacitance bridges, *Electrometers, Reprints, Cryogenic temperature, Cryogenic equipment, Precision, Single electron tunneling, Electron charge.

The value of the electronic charge can be determined by placing a known number of electrons on a calibrated capacitor and measuring the resulting voltage, which can lead to a measure of the fine structure constant, alpha. Single electron tunneling (SET) electrometers with sufficient sensitivity for this application have been fabricated. We report on the design and preliminary results of a capacitance bridge experiment using an SET electrometer as a detector to measure two capacitors in a dilution refrigerator. AC measurements of the capacitance ratio have a precision of one part in 10 to the 4th power and DC measurements provide information on the leakage rate of the standard capacitors.

02,073
PB96-112362 Not available NTIS
National Inst. of Standards and Technology (MSEL), Gaithersburg, MD. Reactor Radiation Div.
Vortex Dynamics and Melting in Niobium.
Final rept.
J. W. Lynn, N. Rosov, and T. E. Grigereit. 1995, 2p.
Pub. in Jnl. of Magnetism and Magnetic Materials, v140-144 p2067-2068 1995.

Keywords: *Niobium, *Neutron scattering, Reprints, Melting, *Foreign technology, Vortex dynamics.

Small angle neutron scattering has been used to investigate the vortex scattering in a single of crystal niobium. Below the irreversibility line resolution-limited Bragg peaks are observed, indicating that a crystalline vortex lattice with long range order exists. Above the irreversibility line intrinsic transverse widths develop, while close to Hc2 intrinsic radial widths also develop. Nevertheless the basic six-fold dymmetry of scattering is observed throughout the vortex phase, indicating that a correlated flux fluid exists in the reversible regime.

02,074
PB96-119334 Not available NTIS
National Inst. of Standards and Technology (EEEL), Gaithersburg, MD. Electricity Div.
High-Temperature Superconductor Cryogenic Current Comparator.
Final rept.
R. E. Elmquist, and R. F. Dziuba. 1995, 3p.
Pub. in Institute of Electrical and Electronics Engineers Transactions on Instrumentation and Measurement, v44 n2 p262-264 Apr 95.

Keywords: *Computer circuits, *High temperature, *Superconductors, *Cryogenics, Magnetic shielding, Diamagnetism, Superconductivity, Resistance, SOVID detectors, Reprints, *Cryogenic current comparators, HTS(High temperature superconductor).

The National Institute of Standards and Technology (NIST) is developing a cryogenic current comparator (CCC) to operate at 77K, using high-temperature superconductor (HTS) ceramic shielding material and an HTS-based superconducting quantum interference device (SQUID) detector. The shielding properties of at least two polycrystalline oxide HTS materials appear sufficient for use in a high-accuracy CCC. A measurement of current-linkage error, a figure of merit for CCC devices, is made for one type of HTS CCC. The design of a second HTS CCC which uses improved magnetic shielding is described.

02,075
PB96-119771 Not available NTIS
National Inst. of Standards and Technology (PL), Boulder, CO. Time and Frequency Div.
Reducing Errors, Complexity, and Measurement Time of PM Noise Measurements.
Final rept.
F. L. Walls. 1993, 9p.
Pub. in Proceedings of the Institute of Electrical and Electronics Engineers International Frequency Control Symposium, Salt Lake City, UT., June 2-4, 1993, p289-297.

Keywords: *Signal generators, *Frequency synthesizers, *Oscillators, Reprints, Standards, *Phase noise.

This paper shows that a new measurement technique based on the two-oscillator technique and the addition of a noise source in series with the reference oscillator can significantly reduce calibration time for accurate PM measurements in oscillators and other components as compared to the traditional two-oscillator technique. This technique also significantly reduces the measurement time and improves the accuracy of 3-corner-hat measurements. Measurement complexity is greatly reduced. The noise source is used to generate a known level of PM noise (PMCAL) for calibrating the product of mixer sensitivity and amplifier gain with Fourier frequency. This can be used to correct for PLL effects whem PMCAL is larger than the residual phase noise in the oscillator under test. PMCAL is typically constant to equal to or greater than 0.1 dB for Fourier frequencies from 0 to 5% of the carrier (maximum width typically less than 500 MHz). When the PMCAL is off, the noise added to the reference signal is typically less than -150 dBc/Hz at 1 Hz and -190 dBc/Hz at 10 kHz for carrier frequencies of 5 to 100 MHz. A similar system also works in the microwave range.

02,076
PB96-122502 Not available NTIS
National Inst. of Standards and Technology (EEEL), Boulder, CO. Electromagnetic Technology Div.
Optical Sampling Using Nondegenerate Four-Wave Mixing in a Semiconductor Laser Amplifier.
Final rept.
M. Jinno, J. B. Schlager, and D. L. Franzen. 1994, 3p.
Pub. in Tech. Digest, OSA, Optical Amplifers and Their Applications, Topical Meeting, Breckenridge, CO., August 3-5, 1994, v4 p147-149 1994.

Keywords: *Laser amplifiers, *Optical sampling, Semiconductors, Reprints, Four wave mixing, Fiber laser.

Picosecond optical sampling using nondegenerate four-wave mixing in a semiconductor amplifier (SLA) is demonstrated for the first time. High-peak-power probe pulses and electrical gating of the SLA produce an optical sampling signal with high signal-to-noise ratio.

02,077
PB96-122585 Not available NTIS
National Inst. of Standards and Technology (EEEL), Boulder, CO. Electromagnetic Fields Div.
Microwave Characterization of Printed Circuit Transmission Lines.
Final rept.
R. B. Marks, and D. F. Williams. 1994, 8p.
Pub. in National Electronics Packaging and Production Conference (NEPCON) East '94, Proceedings of the Technical Program, Boston, MA., June 13-16, 1994, p520-527.

Keywords: *Microwaves, *Printed circuit boards, Electrical characterization, Reprints, Electronic packaging, Impedance.

This paper reviews basic methodology for the microwave characterization of printed circuit transmission

lines in terms of scattering parameters, impedances, and frequency-dependent transmission lines parameters. The focus is on a suite of methods developed at the National Institute of Standards and Technology for the characterization of high-performance electronic packaging and interconnections as well as monolithic microwave integrated circuits.

02,078
PB96-122825 Not available NTIS
National Inst. of Standards and Technology (EEEL), Boulder, CO. Electromagnetic Fields Div.
Open-Ended Coaxial Probes for Nondestructive Testing of Substrates and Circuit Boards.
Final rept.
J. R. Baker-Jarvis, and M. D. Janezic. 1994, 6p.
Pub. in Proceedings of Materials Research Society, April 4-8, 1994, San Francisco, CA., v347 p215-220.

Keywords: *Circuit boards, *Coaxial cables, *Nondestructive tests, Substrates, Probes, Dielectrics, Wave equations, Mathematical models, Numerical analysis, Sensitivity, Low frequencies, Reprints, *Open-ended probes.

The results of the full-wave model theory for the open-ended coaxial probe with lift-off are presented and are applied to mesurements of thin materials. The model allows the study of the open-ended coaxial prode as a nondestructive testing tool. The equations presented are valid for both dielectric and magnetic materials. The analysis yields insight into the effects of air gaps on probe measurements. Numerical results indicate that the probe is very sensitive to lift-off at low frequencies. This sensitivity decreases somewhat as frequency increases.

02,079
PB96-123583 Not available NTIS
National Inst. of Standards and Technology (EEEL), Gaithersburg, MD. Semiconductor Electronics Div.
Wire Bonding to Multichip Modules and Other Soft Substrates.
Final rept.
G. G. Harman. 1995, 10p.
Pub. in Proceedings of the International Conference on Multichip Modules, Denver, CO., April 19-21, 1995, p292-301.

Keywords: *Multichip modules, *Microwave substrates, *Material modules, Skin(Anatomy), Reprints, *Wire bonding, Soft substrates.

Several classes of 'soft substrates' can be difficult to wire bond. These include MCM-Ds, MCM-Ls, flex substrates, some complex IC chips with multilevel polymer-insulated metallization, and microwave hybrids made on PTFE substrates. The bonding solutions include: increasing the bond-pad metal thickness and area and applying a hard metal under-layer, a hard metal top-layer, or some combination of these, -capped with a highly-bondable metal. A summary is given of the bond-pad metallurgy and bonding machine parameters that have produced successful wire bonding to a wide variety of MCMs and other 'soft substrates.' Wire-bonding yield is also generally correlated to the elastic modulus and Tg of the polymer or laminate, and to the yield strength of the metal pads. Thus, the choice of material properties for the substrate and bond pads is at least as important as the actual bonding machine setup in achieving high-yield wire bonding. Other considerations, such as the possible use of high-frequency ultrasonic bonding and high-clock-rate skin-effect losses on the multilayer bond pads, are discussed.

02,080
PB96-135157 Not available NTIS
National Inst. of Standards and Technology (EEEL), Boulder, CO. Electromagnetic Technology Div.
High-Frequency Oscillators Using Phase-Locked Arrays of Josephson Junctions.
Final rept.
S. P. Benz, and P. A. A. Booi. 1994, 4p.
Pub. in Proceedings of the Institute of Electrical and Electronics Engineers International Frequency Control Symposium, Boston, MA., June 1-3, 1994, p666-669.

Keywords: *Josephson junctions, Phase locked systems, Emission, Linewidths, Reprints, Power, *2D arrays.

The authors present a basic description of Josephson junctions and discuss their use as GHz and THz oscillators. The resistively shunted junction model is used to calculate the available power, linewidth and operating frequency of the oscillators. The authors discuss how phase-locked arrays of junctions are used to achieve higher power and narrower linewidth. Two experimental examples of phase-locked emission are shown: one from on-chip detection circuits at 150 GHz and one detected off-chip showing a 13 kHz linewidth at 88.8 GHz.

02,081
PB96-135165 Not available NTIS
National Inst. of Standards and Technology (EEEL), Boulder, CO. Electromagnetic Technology Div.
Noise Reduction in Low-Frequency SQUID Measurements with Laser-Driven Switching.
Final rept.
C. E. Cunningham, G. S. Park, B. Cabrera, and M. E. Huber. 1993, 3p.
See also AD-A253 821.
Pub. in Applied Physics Letters, v63 n8 p1152-1154 Aug 93.

Keywords: *SQUID devices, *Noise reduction, *Low frequency, *Switches, Optical switching, Niobium, Laser radiation, Superconducting devices, Circuits, Modulation, Frequency dependence, Reprints, SQUID(Superconducting Quantum Interference Device), Microbridges.

The authors have developed a technique to modulate the input to a superconducting quantum interference device (SQUID) using a very low noise double-pole, double-throw switching network. This network is composed of four niobium microbridges that are driven normal in pairs by pulses of laser light. An input signal is modulated at a frequency above the 1/frequency noise regime, amplified by the SQUID, and subsequently demodulated to obtain an output in which the excess low-frequency SQUID noise has been removed. With this technique, the authors have reduced the low-frequency noise by an order of magnitude in energy over measurements made without this technique.

02,082
PB96-135207 Not available NTIS
National Inst. of Standards and Technology (EEEL), Gaithersburg, MD. Semiconductor Electronics Div.
Wire Bonding to Multichip Modules and Other Soft Substrates.
Final rept.
G. G. Harman. 1995, 9p.
See also PB96-123583.
Pub. in Proceedings of the International Conference and Exhibition on Multichip Modules Compendium of Papers 1992-1995, Denver, CO., April 19-21, 1995, p629-637.

Keywords: *Multichip modules, *Microwave substrates, *Material modules, Skin(Anatomy), Reprints, *Wire bonding, Soft substrates.

Several classes of 'soft substrates' can be difficult to wire bond. These include MCM-Ds, MCM-Ls, flex substrates, some complex IC chips with multilevel polymer-insulated metallization, and microwave hybrids made on PTFE substrates. The bonding solutions include: increasing the bond-pad metal thickness and area and applying a hard metal under-layer, a hard metal top-layer, or some combination of these, capped with a highly-bondable metal. A summary is given of the bond-pad metallurgy and bonding machine parameters that have produced successful wire bonding to a wide variety of MCMs and other 'soft substrates.' Wire-bonding yield is also generally correlated to the elastic modulus and Tg of the polymer or laminate, and to the yield strength of the metal pads. Thus, the choice of material properties for the substrate and bond pads is at least as important as the actual bonding machine setup in achieving high-yield wire bonding. Other considerations, such as the possible use of high-frequency ultrasonic bonding and high-clock-rate skin-effect losses on the multilayer bond pads, are discussed.

02,083
PB96-148093 Not available NTIS
National Inst. of Standards and Technology (EEEL), Gaithersburg, MD. Electricity Div.
AC-DC Difference Characteristics of High-Voltage Thermal Converters.
Final rept.
D. X. Huang, T. E. Lipe, J. R. Kinard, and C. B. Childers. 1995, 4p.
Pub. in Institute of Electrical and Electronics Engineers Transactions on Instrumentation and Measurement, vIM-44 n2 p387-390 Apr 95.

Keywords: *Alternating current, *Direct current, *Converters, Dielectric loss, Measurement, Electric potential, Coefficients, Resistors, Reprints, Thermal voltage converters, Voltage coefficients, HVTCs(High Voltage Thermal Converters).

This paper describes a study of high-voltage thermal converters (HVTC's) at voltages above 100 V at frequencies up to 100 kHz. Techniques for the construction of HVTC's are described, and the effects of aging and dielectric loss on the resistor, changes in the timing sequence of ac-dc difference tests, relay deadtimes, warmup times, and voltage level dependence are given.

02,084
PB96-148135 Not available NTIS
National Inst. of Standards and Technology (EEEL), Gaithersburg, MD. Electricity Div.
Performance of Multilayer Thin-Film Multijunction Thermal Converters.
Final rept.
J. R. Kinard, D. X. Huang, and D. B. Novotny. 1995, 4p.
See also PB95-196143.
Pub. in Institute of Electrical and Electronics Engineers Transactions on Instrumentation and Measurement, v44 n2 p383-386 Apr 95.

Keywords: *Thin films, *Converters, Fabrication, Alternating current, Direct current, Performance, Thermodynamic properties, Physical properties, Silicon, Machining, Microminiaturization, Reprints, MJTCs(Multijunction thermal converters), Multilayer TVCs, Multijunction TVCs, Micromachining.

New multilayer, thin-film multijunction thermal converters (MJTC's) suitable as high performance ac-dc transfer standards have been fabricated and studied at National Institute of Standards and Technology (NIST). This paper describes their thermal and physical features and the materials chosen to improve performance. Performance data are given over a wide range of frequencies and conditions.

02,085
PB96-157821 Not available NTIS
National Inst. of Standards and Technology (EEEL), Boulder, CO. Electromagnetic Fields Div.
Optimizing Time-Domain Network Analysis.
Final rept.
D. C. DeGroot, and R. B. Marks. 1995, 10p.
Pub. in Automatic RF Techniques Group Meeting (ARFTG), Scottsdale, AZ., November 30-December 1, 1995, p19-28.

Keywords: Automation, Calibration, Reprints, *Time domain network analysis, *Instrument settings.

In this work, we demonstrate how changes in sample density, time-window size, and waveform averaging affect the accuracy and acquisition time of calibrated time-domain network analysis. One of the key results from this study is that accuracy can be enhanced by eliminating the incident step-edge signal from the time-domain reflection waveform before maximizing the instrument's vertical scale. This study identifies the trade offs between accuracy and measurement speed and examines other trands to provide general guidance in establishing reliable and efficient time-domain network analysis measurements for a variety of rf and microwave applications.

02,086
PB96-158654 PC A03/MF A01
National Inst. of Standards and Technology (EEEL), Boulder, CO. Electromagnetic Fields Div.
Direct Comparison Transfer of Microwave Power Sensor Calibrations.
Technical note.
M. P. Weidman. Jan 96, 20p, NIST/TN-1379.
Also available from Supt. of Docs. as SN003-003-03385-5.

Keywords: *Power measurement, *Microwave equipment, *Calibration, Electrical measurement, *Microwave power standards.

This report describes a basic, but potentially accurate, transfer technique for comparing microwave power sensors. The technique is not new, but the specific applications are. This report is written to supplement the existing literature. The method transfer the effective efficiency of a standard power sensor to an unknown (uncalibrated) power sensor. The power sensors may be bolometric (thermistor mounts), thermoelectric, or

diode types, and each type will have inherent limitations. The technique can be implemented with a variety of commercial coaxial and rectangular waveguide components. Measurement uncertainty is discussed in this report so that a potential user can quantify transfer uncertainties.

02,087
PB96-164017 Not available NTIS
National Inst. of Standards and Technology (EEEL), Gaithersburg, MD. Semiconductor Electronics Div.
Natural Convection from an Array of Electronic Packages Mounted on a Horizontal Board in a Narrow Aspect Ratio Enclosure.
Final rept.
V. H. Adams, Y. Joshi, and D. L. Blackburn. 1995, 7p.
Pub. in Proceedings of the National Heat and Mass Transfer Conference, Surathkal, India, December 28-30, 1995, p911-917.

Keywords: *Electronic packaging, *Natural convection, *Heat transfer, Chips(Electronics), Circuit boards, Computational fluid dynamics, Temperature distribution, Temperature measurement, Air cooling, Space(Room), Reprints, Electronic cooling.

Three-dimensional natural convection flow and heat transfer were numerically studied for a 3 by 3 array of discretely heated electronic packages mounted on a horizontal circuit board in an air-filled, narrow aspect ratio rectangular enclosure with length, width, and height ration of 6:6:1. It was found that conduction-only analysis under-predicts heat transfer from the top surfaces of the electronic packages by a factor of 1.5 to 4.4, with a resultant over-prediction of the maximum chip to ambient temperature difference of up to 235%.

02,088
PB96-176441 Not available NTIS
National Inst. of Standards and Technology (EEEL), Boulder, CO. Electromagnetic Fields Div.
Single-Port Technique for Adaptor Efficiency Evaluation.
Final rept.
S. P. Pucic, and W. C. Daywitt. 1995, 6p.
Pub. in Proceedings of the Automatic Radio Frequency Techniques Group Conference (45th), Orlando, FL., May 19, 1995, p113-118.

Keywords: *Adapters, *Electrical measurement, *Radiometers, Electric connectors, Broadband, Reflectance, Efficiency, Dissipation, Insertion loss, Losses, Reprints, Swept frequency measurements.

The single-port adaptor efficiency evaluation' (SPAEE) technique uses swept-frequency measurements to evaluate broadband efficiency of low-loss, reciprocal 2-ports, including noninsertable devices such as adaptors. The 2-port is terminated in two reflective terminations, a shielded open and a short. The frequency range is limited only by the availability of the two reflective terminations. The major advantages of the SPAEE technique are its simplicity, speed, and accuracy.

02,089
PB96-200134 Not available NTIS
National Inst. of Standards and Technology (EEEL), Boulder, CO. Electromagnetic Technology Div.
Metallic-Barrier Junctions for Programmable Josephson Voltage Standards.
Final rept.
R. L. Kautz, and S. P. Benz. 1995, 4p.
Pub. in Applied Superconductivity Conference, Edinburgh, Scotland, July 3-6, 1995, p1407-1410.

Keywords: *Josephson junctions, *Niobium, *Superconductors, Voltage standards, Arrays, Palladium, Gold, Reprints, SNS junctions.

The current amplitudes of Shapiro steps are studied in large-area metallic-barrier Josephson junctions by simulation and experiment. In the absence of a ground plane, simulations show tht junctions larger than about 4 times the Josephson penetration depth are of limited utility because the microwave power required to induce Shapiro steps increases rapidly with junction size. Experimentally, step amplitudes as large as 7 mA are observed in Nb-PdAu-Nb sandwich junctions.

02,090
PB96-200142 Not available NTIS
National Inst. of Standards and Technology (EEEL), Boulder, CO. Electromagnetic Technology Div.
Shapiro Steps in Large-Area Metallic-Barrier Josephson Junctions.
Final rept.
R. L. Kautz. 1995, 9p.
Pub. in Jnl. of Applied Physics, v78 n9 p5811-5819 Nov 95.

Keywords: *Josephson junctions, *Superconductivity, Phase locking, Voltage standards, Reprints, Josephson effect, Shapiro steps.

The current amplitudes of Shapiro steps in large-area metallic-barrier Josephson junctions, both with and without a ground plane, are investigated with the goal of optimizing junction parameters for programmable voltage standards. Using the resistively shunted junction model without capacitance, the authors calculate maximum step amplitudes as a function of reduced frequency and junction dimension for both one- and two-dimensional junctions. For junctions without a ground plane, the authors conclude that step amplitudes of order 10 mA are practical, but significantly larger amplitudes require excessive microwave power.

02,091
PB96-200167 Not available NTIS
National Inst. of Standards and Technology (EEEL), Boulder, CO. Electromagnetic Technology Div.
Novel Vortex Dynamics in Two-Dimensional Josephson Arrays.
Final rept.
S. G. Lachenmann, T. Doderer, R. P. Huebener, P. A. A. Booi, and S. P. Benz. 1994, 8p.
Pub. in Proceedings of the International Conference on Nonlinear Superconducting Devices and High-Tc Materials, Capri, Italy, October 8-13, 1994, p365-372.

Keywords: *Josephson junctions, *Arrays, *Vortices, Superconductivity, Reprints, Two dimensional array, Vortex dynamics.

The authors present spatially resolved studies of vortex dynamics in two-dimensional Josephson-junction arrays. For bias currents smaller than the array critical current, a small local thermal perturbation at the array boundaries lowers the vortex entry barrier and the array switches to the resistive state. For bias currents slightly above the array critical current vortices and antivortices are nucleated at opposite edges of the array. An alternating crossing vortex motion (ACVM) is observed experimentally.

02,092
PB96-200233 Not available NTIS
National Inst. of Standards and Technology (EEEL), Boulder, CO. Electromagnetic Technology Div.
Superconductor- Normal-Superconductor Junctions for Digital/Analog Converters.
Final rept.
S. P. Benz. 1995, 3p.
Pub. in International Superconductive Electronics Conference (5th), Nagoya, Japan, September 18-21, 1995, p216-218.

Keywords: *Josephson junctions, *Niobium, *Superconductors, Palladium, Gold, Arrays, Optical wave guides, Analog to digital converters, Optical circuits, Voltage standards, Reprints, SNS junctions.

Series arrays of Nb-PdAu-Nb Josephson junctions have been fabricated with characteristics ideally suited for application in programmable voltage standards and digital/analog convertors. Large arrays of junction with applied microwave power showed constant voltage steps with current amplitudes as large as 7 mA. A novel coplanar waveguide design has enabled uniform microwave power coupling to a 5-segment array of 8192 total junctions so that each array segment has constant voltage steps over the same bias current range. The 8192-junction device generated 1.1 mA steps at 186 mV with 11 GHz power and a maximum constant voltage step of 260 mV at 15.34 GHz.

02,093
PB96-200241 Not available NTIS
National Inst. of Standards and Technology (EEEL), Boulder, CO. Electromagnetic Technology Div.
Superconductor- Normal-Superconductor Junctions for Programmable Voltage Standards.
Final rept.
S. P. Benz. 1995, 3p.
Pub. in Applied Physics Letters, v67 n18 p2714-2716 Oct 95.

Keywords: *Josephson junctions, *Niobium, *Arrays, Palladium, Gold, Optical waveguides, Analog to digital converters, Optical circuits, Voltage standards, Reprints, SNS junction.

Series arrays of Nb-PdAu-Nb Josephson junctions were fabricated with characteristics ideally suited for application in programmable voltage standards and D/A converters with fundamental accuracy. Large arrays of junctions with applied microwave power showed constant voltage steps with current amplitudes as large as 7 mA. A novel coplanar waveguide design enabled uniform microwave power coupling to a five-segment array of 8192 junctions, so each segment had constant voltage steps over the same bias range. The 8192-junction device generated 1.1 mA steps at 186 mV with 11 GHz power and a maximum constant voltage step of 260 mV at 15.34 GHz.

02,094
PB96-200258 Not available NTIS
National Inst. of Standards and Technology (EEEL), Boulder, CO. Electromagnetic Technology Div.
Design of High-Frequency, High-Power Oscillators Using Josephson-Junction Arrays.
Final rept.
P. A. A. Booi, and S. P. Benz. 1995, 4p.
See also PB96-200266.
Pub. in Proceedings of the Applied Superconductivity Conference, Edinburgh, Scotland, July 3-6, 1995, Inst. Phys. Conf. Series No. 148, p1479-1482.

Keywords: *Josephson junctions, *Arrays, Niobium, Aluminum oxide, Frequency standards, Performance tests, Aluminum, Reprints, *Josephson oscillators.

The authors analyze the limitations imposed by junction capacitance and the parasitic inductance associated with shunt resistors on the performance of Nb/Al-AlOx/Nb-junction-array oscillators. The authors use wide junctions that are in situ deposited on top of PdAu resistor films (to minimize inductance) and are situated about Nb ground planes to ensure uniform current injection. From the measured parasitics, the authors infer that maximum power and frequency that can be obtained for critical-current densities Jc less than or equal to 100 kA/cm squared. The authors illustrate these findings with experimental results of a 1.968 junction array have Jc=10 Ka/cm squarted that was found to couple 0.1 - 0.8 mW to a 56-ohm load in the range 100-300 GHz.

02,095
PB96-200266 Not available NTIS
National Inst. of Standards and Technology (EEEL), Boulder, CO. Electromagnetic Technology Div.
High-Power, High-Frequency Oscillators Using Distributed Josephson-Junction Arrays.
Final rept.
P. A. A. Booi, and S. P. Benz. 1995, 3p.
See also PB96-200258.
Pub. in International Superconductive Electronics Conference (5th) (ISEC '95), September 18-21, 1995, Nagoya, Japan, p513-515.

Keywords: *Josephson junctions, *Arrays, Phase locked systems, Reprints, *Josephson oscillators.

The authors present experimental results showing emission that is coupled from distributed series arrays of wide, resistively shunted tunnel junctions to on-chip 50 ohm loads. The authors have detected poweer output of 0.85 mW at 240 GHz and power greater than 100 microW at most frequencies in the range of 100-300 GHz.

02,096
PB96-200787 Not available NTIS
National Inst. of Standards and Technology (PL), Boulder, CO. Time and Frequency Div.
Origin of l/f PM and AM Noise in Bipolar Junction Transistor Amplifiers.
Final rept.
F. L. Walls, E. S. Ferre-Pikal, and S. R. Jefferts. 1995, 11p.
Pub. in Proceedings of the International Institute of Electrical and Electronics Engineers Frequency Control Symposium, San Francisco, CA., May 31-June 2, 1995, p294-304.

Keywords: *Microwave amplifiers, *Amplitude modulation, *Phase modulation, *Electromagnetic noise, Frequency domain, Standards, Electrical measurement, Very high frequency, High frequency, Reprints.

In the paper, the authors report the results of extensive research on phase modulation (PM) and amplitude modulation (AM) noise in linear bipolar junction transis-

tor (BJT) amplifiers. BJT amplifiers exhibit 1/f PM and AM noise about a carrier signal that is much larger than the amplifier's thermal noise at those frequencies in the absence of the carrier signal. The authors work whows that the 1/f PM noise of a BJT based amplifier is accompanied by 1/f AM nose which can be higher, lower, or nearly equal depending on the circuit implementation. The 1/fAM and PM noise in BJT's is primarily the result of the 1/f fluctuations in transistor, current, transistor capacitance, circuit supply voltages, circuit impedances, and circuit configuration. The author discuss the theory and present experimental data in reference to common emitter emplifiers, but the analysis can be applied to other configurations as well. The study provides the functional dependence of 1/f AM and PM noise on transistor parameters, circuit parameters, and signal frequency, thereby laying the groundwork for a comprehensive theory of 1/f AM and PM noise in BJT amplifiers. The authors show that in many cases the 1/f PM and AM noise can be reduced below the thermal noise of the amplifier.

02,097
PB96-200795 Not available NTIS
National Inst. of Standards and Technology (PL), Boulder, CO. Time and Frequency Div.
Quest to Understand and Reduce l/f Noise in Amplifiers and Baw Quartz Oscillators.
Final rept.
F. L. Walls. 1995, 18p.
Pub. in Proceedings of the European Frequency and Time Forum (9th), Besancon, France, March 8-10, 1995, p227-244.

Keywords: *Microwave amplifiers, *Microwave oscillators, *Quartz resonators, Amplitude modulation, Phase modulation, Electromagnetic noise, Frequency measurement, Reprints, Phase noise.

The paper attempts to trace the highlights in the development of precision oscillators from a historical point of view and speculates on further improvements in their 1/f performance. Using Leeson's model the closed loop phase modulation (PM) noise and frequency stability can be estimated from the stability of the quartz resonator, the resonator quality factor, and the noise of the sustaining amplifier coupled with the stability of the oven and various environmental parameters. The inherent frequency stability of the oscillator is primarily limited by the 1/f PM noise of the BAW quartz resonator and the sustaining amplifier. The paper, therefore, focuses on describing the quest to characterize, understand, and reduce the 1/f PM noise of amplifiers and BAW resonators.

02,098
PB96-200936 Not available NTIS
National Inst. of Standards and Technology (EEEL), Gaithersburg, MD. Electricity Div.
100 A, 100 kHz Transconductance Amplifier.
Final rept.
O. B. Laug. 1996, 5p.
See also PB96-102629.
Pub. in Institute of Electrical and Electronics Engineers Transacations on Instrumentation and Measurement, v45 n3 p440-444 Jun 96.

Keywords: *Power amplifiers, *Voltage amplifiers, Transconductance, Electric power meters, Reprints.

A high-current, wide-band transconductance amplifier is described that provides an unprecedented level of output current at high frequencies with exceptional stability. It is capable of converting a signal voltage applied to its input into a ground-referenced output rms current up to 100 A over a frequency range from dc to 100 kHz with a useable frquency extending to 1 MHz. The amplifier has a 1000-W output capability plus or minus 10 V of compliance, and can deliver up to 400 A of pulsed peak-to-peak current. The amplifier design is based on the principle of paralleling a number of precision bipolar voltage-to-current converters. The design incorporates a unique ranging system controlled by optoisolated switches, which permit a full-scale range from 5 A to 100 A. The design considerations for maintaining wide bandwidth, high output inpedance, and unconditional stability for all loads are discussed.

02,099
PB97-111520 Not available NTIS
National Inst. of Standards and Technology (EEEL), Boulder, CO. Electromagnetic Technology Div.
High Power Generation with Distributed Josephson-Junction Arrays.
Final rept.
A. A. P. Booi, and S. P. Benz. 1996, 3p.
See also PB96-200266.
Pub. in Applied Physics Letters, v68 n26 p3799-3801 Jun 96.

Keywords: *Josephson junctions, *Arrays, Phase locked systems, Current, Power, Reprints, *Josephson oscillators.

The authors have experimentally coupled emission from a distributed series array of 1968 wide Josephson junctions to an on-chip 10.8 omega load and detected 0.16 mW at 240 HGz. The result is achieved by reducing the parasitic inductance associated with shunt resistors so that functions with critical currents of 23 mA are effectively shunted at the operating frequency. The power is less than the 1.3 mW expected from theory due to the presence of a large impedance mismatch. Optimization of the load design will allow the detection of mW power.

02,100
PB97-112569 Not available NTIS
National Inst. of Standards and Technology (EEEL), Gaithersburg, MD. Electricity Div.
Low Voltage Standards in the 10 Hz to 1 MHz Range.
Final rept.
N. M. Oldham, M. E. Parker, B. C. Waltrip, and S. Avramov-Zamurovic. 1996, 2p.
Pub. in Conference on Precision Electromagnetic Measurements, CPEM '96 Conference Digest, Braunschweig, Germany, June 17-20, 1996, p570-571.

Keywords: *Electrical measurement, Standards, Potentiometers(Resistors), Reprints, *Voltage standards, *Thermal voltage converters, Thermal converters, Low voltage.

A step down procedure is described for establishing voltage standards in the 1 mV to 100 mV range at frequencies between 10 Hz and 1 MHz. The step down employs low-voltage thermal voltage converters and micropotentiometers. Techniques are given for measuring input inpedance and calculating loading errors.

02,101
PB97-113187 Not available NTIS
National Inst. of Standards and Technology (PL), Boulder, CO. Time and Frequency Div.
Frequency Synthesis and Metrology at 10(-17) and Beyond.
Final rept.
F. L. Walls, F. Ascarrunz, C. W. Nelson, and L. M. Nelson. 1996, 3p.
Pub. in Proceedings of the Symposium on Frequency Standards and Metrology (5th), Woods Hole, MA., October 15-19, 1995, p468-470 1996.

Keywords: *Frequency synthesizers, *Mixers(Electronics), *Amplifiers, Spectrum analysis, Stability, Signal generators, Superhigh frequency, Phase modulation, Amplitude modulation, Electromagnetic noise, Transmission lines, Reprints, *Timing errors.

The paper investigates the systematic timing errors due to variations in temperature and signal amplitude in distribution amplifiers, cables, mixers, frequency dividers and multipliers. The effect of harmonic distortion in the reference signals on timing errors in phase detectors is also considered. The authors outline the basic configurations necessary to synthesize and distribute the reference frequencies and measure the performance of potential new clocks having a frequency stability of approximately 3 x 10 to the -15th power tau(sup 1/2) and 10 to the -17th power in the long term.

02,102
PB97-113195 Not available NTIS
National Inst. of Standards and Technology (PL), Boulder, CO. Time and Frequency Div.
Reducing the 1/f AM and PM Noise in Electronics for Precision Frequency Metrology.
Final rept.
F. L. Walls, E. S. Ferre-Pikal, and S. R. Jefferts. 1996, 2p.
Pub. in Proceedings of the Symposium on Frequency Standards and Metrology (5th), Woods Hole, MA., October 15-19, 1995, p480-481 1996.

Keywords: *Phase modulation, *Amplitude modulation, *Electromagnetic noise, *Frequency synthesizers, Electrical measurement, Amplifiers, Mixers(Electronics), Signal generators, Transfer functions, Reprints.

The authors report on a fundamental breakthrough in understanding how l/f PM and amplitude modulation (AM) noise is generated. They show how one can analyze the transfer function of a two port device to calculate the dependence of added AM and PM noise on circuit and active element parameters. Using this new approach, the authors have developed sample silicon BJT amplifiers with exceptionally low l/f AM and PM noise.

02,103
PB97-119176 Not available NTIS
National Inst. of Standards and Technology (EEEL), Gaithersburg, MD. Electricity Div.
Conversion of a 2-Terminal-Pair Bridge to a 4-Terminal-Pair Bridge for Increased Range and Precision in Impedance Measurements.
Final rept.
A. Jeffery, J. Q. Shields, and L. H. Lee. 1996, 2p.
Pub. in Conference on Precision Electromagnetic Measurements, Braunschweig, Germany, June 17-20, 1996, p358-359.

Keywords: *Bridges, *Electrical measurements, Ratio transformers, Measurements, Impedance bridges, Alternating current, Precision measurements, Reprints, *Foreign technology, Four-terminal-pair.

A new 4-terminal-pair bridge, capable of a relative uncertainty of 1 in 10 to the 9th power, has been constructed at NIST by converting a 2-terminal pair bridge. The conversion requirees only addition of components which are easily removed if 2-pair measurements are to be made. The design and testing of this bridge will be described.

02,104
PB97-119317 Not available NTIS
National Inst. of Standards and Technology (EEEL), Gaithersburg, MD. Electricity Div.
Active High Voltage Divider with 20-PPM Uncertainty.
Final rept.
O. Petersons, E. Simmon, and G. J. FitzPatrick. 1996, 2p.
Pub. in Conference on Precision Electromagnetic Measurement Digest (CPEM '96), Braunschweig, Germany, June 17-20, 1996, p486-487.

Keywords: *Voltage dividers, Electrical networks, Capacitors, Circuitry, Feedback amplifiers, Reprints.

A voltage divider has been designed which consists of a group of solid dielectric capacitors maintained in a temperature-controlled environment, an external compressed-gas capacitor, and special electronic circuitry. The prototype divider has been constructed and preliminary results obtained to validate the operating principle and accuracy target. The principal innovative part is a feedback amplifier, complemented with an 'open-loop' voltage source controlled from the high voltage. This enables achievement of a voltage ratio that is equal to the reciprocal of the capacitance ratio to well within one ppm without encountering dynamic instability problems.

Electromechanical Devices

02,105
PB95-150488 Not available NTIS
National Inst. of Standards and Technology (EEEL), Gaithersburg, MD. Semiconductor Electronics Div.
Test Structures for Determining Design Rules for Microelectromechanical-Based Sensors and Actuators.
Final rept.
C. Zincke, M. Gaitan, M. E. Zaghloul, and L. W. Linholm. 1994, 7p.
Pub. in Proceedings of Institute of Electrical and Electronics Engineers International Conference on Microelectronic Test Structures, San Diego, CA., March 22-24, 1994, v7 p44-50.

Keywords: *Electromechanical devices, Microminiaturization, Design criteria, Etching, Actuators, Sensors, CMOS, Reprints, *Microactuators, *Microsensors, *Test structures, Wafer alignment, MOSIS service.

Electromechanical Devices

We present two test structures for establishing design rules for minimum spacing of a new class of microelectromechanical-based sensors and actuators fabricated through commercial complementary metal-oxide-semiconductor (CMOS) foundries. The microelectromechanical devices are suspended membranes of passivation glass that encapsulates polysilicon and aluminum layers in the CMOS process. The membranes are suspended by anisotropically etching the silicon substrate through openings in the passivation glass. These test structures measure the lateral undercutting and the rotational misalignment of openings in passivation oxide that are used to make the microelectromechanical devices, and give information for the layout, and proximity to circuits of the microelectromechanical devices. Two test structures are discussed, one optical and one electrical, and results for a 2 micrometer n- and p-well CMOS process run are presented.

02,106
PB95-153797 Not available NTIS
National Inst. of Standards and Technology (EEEL), Gaithersburg, MD. Electronics and Electrical Engineering Lab. Office.
Directions in MEMS Research Application Development.
Final rept.
R. E. Hebner. 1993, 19p.
Pub. in Proceedings of Microsensors and Micromachines Conference, Washington, DC., December 6-7, 1993, p1-19.

Keywords: *Microminiaturization, Materials science, Thin films, Metrology, Uses, Reprints, *Microelectromechanics, *MEMS systems, Microheating elements, Thermal converters.

NIST's laboratory-based metrology programs are planned and implemented in cooperation with industry and focus on measurements, standards, evaluated data, and test methods. It is as part of this program that NIST is developing microelectromechanical systems (MEMS). The NIST program has three primary thrusts: the development of MEMS-based devices for metrology applications; materials characterization, and standards.

02,107
PB96-111174 PC A05/MF A01
National Inst. of Standards and Technology (TS), Gaithersburg, MD. National Voluntary Lab. Accreditation Program.
Efficiency of Electric Motors. National Voluntary Lab. Accreditation Program (NVLAP).
Handbook.
L. S. Galowin, W. J. Rossiter, and W. A. Hall. Aug 95, 85p, NIST/HB-150/10.
Also available from Supt. of Docs. as SN003-003-03356-1.

Keywords: *Electric motors, *Testing laboratories, *Standards, US NIST, Calibrating, Tests, Accreditation.

NIST Handbook 150-10 presents the technical requirements of the National Voluntary Laboratory Accreditation Program (NVLAP) for the Efficiency of Electric Motors (EEM) field of accreditation. The same document is published for use by the Standards Council of Canada (SCC); selected differences may be specified for implementation in both countries. This handbook is intended for information and use by staff of accredited laboratories, those laboratories seeking accreditation, other laboratory accreditation systems, users of laboratory services, and others needing information on the requirements for accreditation under the EEM program.

02,108
PB96-122544 Not available NTIS
National Inst. of Standards and Technology (EEEL), Gaithersburg, MD. Electricity Div.
Programmable Guarded Coaxial Connector Panel.
Final rept.
L. L. Kile. 1995, 5p.
Pub. in National Conference of Standards Laboratories, Dallas, TX., July 16-20, 1995, p285-289.

Keywords: *Coaxial cables, *Connectors, *Automated systems, Programmable switch, Resistance measurements, Reprints.

A programmable guarded connector panel using coaxial connectors has been specifically designed for an automated measurement system for the comparison of four-terminal resistors. A computer controlled XYZ positioning system is used to move a 4-connector Z arm over a panel of 72 coaxial connectors mounted in the XY plane. This provides for 30 four-terminal channels. The outer shields of the connectors are electrically isolated from one another to allow the shields to be driven at guard voltages to supress errors caused by leakage currents. The resistance repeatability of the plug-socket connections including resistance variations of 12 m of AWG 12 connecting cable is typically 10 microohms. Variations of thermoelectric voltages over a 10-minute measurement period of the plug-socket connections are typically less than 10 nV. This automatic switching system may be useful for other types of precision measurements where guarding, contact resistances, and thermoelectric voltages are critical factors.

02,109
PB96-146709 Not available NTIS
National Inst. of Standards and Technology (EEEL), Gaithersburg, MD. Electricity Div.
Integrated Thin-Film Micropotentiometers.
Final rept.
J. R. Kinard, D. X. Huang, and D. B. Novotny. 1995, 3p.
Pub. in Institute of Electrical and Electronics Engineers Transactions on Instrumentation and Measurement, vIM-44 n2 p374-376 Apr 95.

Keywords: *Potentiometers, *Thin films, *Microinstrumentation, Machining, Silicon, Microminiaturization, Alternating current, Frequencies, Reprints, Thermal converters, Microvolts, Millivolts.

Integrated micropotentiometers, new devices fabricated with thin-film technology and the micromachining of silicon, have been developed for the accurate determination of ac voltage from 1 to 100 mV at frequencies from audio to 1 MHz and with the potential for higher frequencies.

02,110
PB96-180153 Not available NTIS
National Inst. of Standards and Technology (EEEL), Gaithersburg, MD. Electricity Div.
Distributions of Measurement Error for Three-Axis Magnetic Field Meters during Measurements Near Appliances.
Final rept.
M. Misakian, and C. Fenimore. 1996, 6p.
Pub. in Institute of Electrical and Electronics Engineers Transactions on Instrumentation and Measurement, v45 n1 p244-249 Feb 96.

Keywords: *Electric appliances, *Magnetic fields, *Magnetic measurement, *Residential buildings, Coils, Magnetic dipoles, Magnetic flux, Magnetic probes, Frequency measurement, Measuring methods, Error analysis, Uncertainty, Probability distribution functions, Reprints, Power frequency.

Comparisons are made between the average magnetic flux density as would be measured with a three-axis coil probe and the flux density at the center of the probe. Probability distributions of the differences between the two quantities are calculated assuming a dipole magnetic field and are found to be asymmetric. The distributions allow estimates of uncertainty for resultant magnetic field measurements made near some electrical appliances and other electrical equipment.

Electron Tubes

02,111
AD-A285 495/8 PC A06/MF A02
National Bureau of Standards, Gaithersburg, MD.
Tabulation of Data on Receiving Tubes. Handbook 68.
1960, 111p.

Keywords: *Tabulation processes, *Data acquisition, Transmit receive tubes, Electrodes, Handbooks, *Receiving tubes.

A tabulation of Receiving-Type Electron Tubes with some characteristics of each type has been prepared in the form of two major listings, a Numerical Listing in which the tubes are arranged by type number, and a Characteristic Listing in which the tubes are arranged by tube type and further ordered on the basis of one or two important parameters. The tabulation is accompanied by a listing of similar tube types and basing diagrams for the listed tubes.

02,112
PB96-103064 Not available NTIS
National Inst. of Standards and Technology (PL), Gaithersburg, MD. Quantum Metrology Div.
Planar Lenses for Field-Emitter Arrays.
Final rept.
C. M. Tang, T. A. Swyden, and A. C. Ting. 1995, 5p.
Pub. in Jnl. of Vacuum Science and Technology B, v13 n2 p571-575 Mar/Apr 95.

Keywords: *Electron beams, *Field emission, *Planar structures, *Lenses, Collimation, Focusing, Electrodes, Gates(Circuits), Experimental data, Cathodes, Reprints, *Field emitter arrays, *Spindt cathodes.

Experimental data is analyzed for a method of collimating and focusing electron beams emitted from field-emitter arrays (FEAs) where the focusing electrode is co-planar of nearly co-planar or nearly co-planar with the gate electrode. The focusing mechanism is provided by the fringe field formed along the edge of the gate electrode due to the potential difference between grid and the substrate or the gate and another lens electrode. The concept is verified by EGUN2 simulations. Experiments performed to verify the theory and focusing of electron beams emitted from FEAs were observed. Elongated emission patterns were consistently observed, indicative of one-dimensional focusing.

Optoelectronic Devices & Systems

02,113
PB94-145968 PC A03/MF A01
National Inst. of Standards and Technology (EEEL), Gaithersburg, MD. Semiconductor Electronics Div.
Electronics and Electrical Engineering Laboratory Technical Progress Bulletin Covering Laboratory Programs, January to March 1991, with 1991 EEEL Events Calendar.
J. A. Gonzalez. Jul 91, 31p, NISTIR-4621.
See also PB92-112309.

Keywords: *Microelectronics, *Metrology, Electrical measurement, Semiconductors, Bipolar transistors, Signal processing, High temperature superconductors, Laser radiation, Optical waveguides, Microwaves, Silicon, Photodiodes, Antennas, Magnetic materials, Electromagnetic interference, Millimeter waves, Progress report, Abstracts, Fiber optic sensors, Erbium lasers.

This is the thirty-fourth issue of a quarterly publication providing information on the technical work of the National Institute of Standards and Technology, Electronics and Electrical Engineering Laboratory. This issue of the EEEL Technical Progress Bulletin covers the first quarter of calendar year 1991. Abstracts are provided by technical area for both published papers and papers approved by NIST for publication. Topics covered include the following: Fundamental Electrical Measurements; Semiconductor Microelectronics; Signal Acquisition, Processing, and Transmission; Electrical Systems; Electromagnetic Interference.

02,114
PB94-152733 PC A05/MF A01
National Inst. of Standards and Technology (MSEL), Gaithersburg, MD. Ceramics Div.
Photonic Materials: A Report on the Results of a Workshop. Held in Gaithersburg, Maryland on August 26-27, 1992, Volume 1.
Internal rept.
J. A. Carpenter, and S. W. Freiman. Feb 94, 94p, NISTIR-5299.

Keywords: *Optoelectronic devices, *Phonetics, *Meetings, Light emitting diodes, Semiconductor lasers, Silicon solar cells, Infrared detectors, Display devices, Optical disks, Holography, Lithium niobates, Aluminum gallium arsenides, Optical fibers, Optical storage, Packaging, Flat panel displays.

This is a report on the results of a workshop held August 26-27, 1992, on the title subject. Sponsored by NIST and the Optoelectronics Industry Development Association (OIDA), the major objectives were to identify and set priorities on R&D needed to advance photonic materials in commercial products appearing in the market place in the next 3-15 years. Working

group sessions were held in six areas: sources and detectors, display, storage, active devices (other than the four previously listed), packaging, and passive devices (other than packaging).

02,115
PB94-154341 PC A03/MF A01
National Inst. of Standards and Technology (NEL), Gaithersburg, MD. Center for Electronics and Electrical Engineering.
Electronics and Electrical Engineering Laboratory Technical Progress Bulletin Covering Programs, October to December 1993, with 1994/1995 EEEL Events Calendar.
J. M. Rohrbaugh. Feb 94, 37p, NISTIR-5357.
See also PB93-120723.

Keywords: *Optoelectronic devices, *Microelectronics, *Metrology, Integrated circuits, Dimensional measurement, Electromagnetic interference, Signal processing, Optical fibers, Magnetic materials, Millimeter waves, Photodetectors, Microwave equipment, Integrated optics, High temperature superconductors, Semiconductors, Progress report, Abstracts, Fiber optic sensors.

This is the forty-fifth issue of a quarterly publication providing information on the technical work of the National Institute of Standards and Technology, Electronics and Electrical Engineering Laboratory. This issue of EEEL Technical Progress Bulletin covers the fourth quarter of calendar year 1993. Abstracts are provided by technical area for both published papers and papers approved by NIST for publication. Major subject headings include the following: Fundamental Electrical Measurements; Semiconductor Microelectronics; Signal Acquisition, Processing, and Transmission; Electrical Systems; Electromagnetic Interference; Law Enforcement Standards; Video Technology.

02,116
PB94-159761 PC A04/MF A01
National Inst. of Standards and Technology (EEEL), Boulder, CO. Electromagnetic Technology Div.
Metrology for Electromagnetic Technology: A Bibliography of NIST Publications.
M. E. DeWeese, and S. Moynihan. Sep 92, 73p, NISTIR-3994.

Keywords: *Metrology, *Bibliographies, Optical communication, Optical fibers, Fiber optics, Optoelectronic devices, Solid state lasers, Superconducting devices, High temperature superconductors, Josephson junctions, Electrooptics, Magnetic measurement, Cryogenics, *Electromagnetic metrology, Cryoelectronics, SQUID devices, US NIST.

This bibliography lists the publications of the personnel of the Electromagnetic Technology Division of NIST during the period from January 1970 through publication of this report. A few earlier references that are directly related to the present work of the Division are also included.

02,117
PB94-169802 Not available NTIS
National Inst. of Standards and Technology, Gaithersburg, MD.
Cryogenic Blackbody Calibrations at the National Institute of Standards and Technology Low Background Infrared Calibration Facility.
R. U. Datla, M. C. Croarkin, and A. C. Parr. 1994, 43p.
Included in Jnl. of Research of the National Institute of Standards and Technology, v99 n1 p77-119 Jan/Feb 94.

Keywords: *Blackbody radiation, *Calibration, Intermediate infrared radiation, Near infrared radiation, Infrared radiometers, Cryogenic equipment, Light sources, Measurement, Uncertainty, Sensors, Reprints, Low Background Infrared Calibration Facility, LBIR facility, US NIST.

The Low Background Infrared Calibration Facility (LBIR) at the National Institute of Standards and Technology has been in operation for calibration measurements of the radiant power emitted from infrared radiation (IR) sources, such as cryogenic blackbodies, for more than 2 years. The IR sources are sent to NIST by customers from industry, government, and university laboratories. An absolute cryogenic radiometer is used as the standard detector to measure the total radiant power at its aperture. The low background is provided by a closed cycle helium refrigeration system that maintains the inner parts of the calibration chamber at 20 K. The radiance temperature of the blackbody is deduced from the measured power and compared with the blackbody temperature sensor data. The calibration procedures and data analysis are illustrated using the measurements of a typical blackbody.

02,118
PB94-185154 Not available NTIS
National Inst. of Standards and Technology (EEEL), Gaithersburg, MD. Semiconductor Electronics Div.
Interface Roughness-Induced Changes in the Near-E(sub 0) Spectroscopic Behavior of Short-Period AlAs/GaAs Superlattices.
Final rept.
D. Chandler-Horowitz, J. G. Pellegrino, N. V. Nguyen, and S. B. Qadri. 1994, 5p.
Pub. in Materials Research Society Symposium Proceedings, v326 p145-149 1994.

Keywords: *Superlattices, Aluminum gallium arsenides, Aluminum arsenides, Optical properties, Perturbations, Ellipsometry, Reprints, *Interface roughness, Photoreflectance.

The perturbations on the optical properties introduced by increased interface roughness in 3x3 short-period AlAs/GaAs superlattices (SLs) were investigated through an examination of the position and line shape of the E(o) (direct gap) feature in photoreflectance (PR) and spectroscopic ellipsometry (SE). The degree of interface roughness in the SLs was controlled by a choice of the growth conditions and the buffer layer thickness. The structural behavior was characterized by X-ray diffraction. The measured spectra from PR and SE were compared to those from an Al(x)Ga(1-x)As (x=0.5) alloy reference specimen grown under nearly identical conditions.

02,119
PB94-185485 Not available NTIS
National Inst. of Standards and Technology (PL), Gaithersburg, MD. Electron and Optical Physics Div.
One Gigarad Passivating Nitrided Oxides for 100% Internal Quantum Efficiency Silicon Photodiodes.
Final rept.
R. Korde, J. S. Cable, and L. R. Canfield. 1993, 5p.
Pub. in Institute of Electrical and Electronics Engineers Transactions on Nuclear Science 40, n6 p1655-1659 Dec 93.

Keywords: *Ultraviolet detectors, *Silicon diodes, *Photodiodes, Vacuum ultraviolet radiation, Radiation resistance, Quantum efficiency, Silicon dioxide, Reprints.

100% internal quantum efficiency silicon photodiodes with 4 to 8 nm passivating silicon dioxide have been fabricated by rapid thermal nitridation in nitrous oxide and ammonia ambients with the aim of increasing their radiation hardness. The fabricated diodes were exposed to 10.2 eV photons using a hydrogen plasma light source and a normal incidence monochromator. The measured quantum efficiency degradation indicates that the interface trap area density increases sublinearly with dose up to a measured dose of one Gigarad. No noticeable change in quantum efficiency over the range of 50 to 250 nm was observed after exposure to 100% relative humidity. This suggests that the nitrided SiSiO2 interface is practically insensitive to moisture.

02,120
PB94-185824 Not available NTIS
National Inst. of Standards and Technology (EEEL), Boulder, CO. Electromagnetic Technology Div.
Modified Airy Function Method for the Analysis of Tunneling Problems in Optical Waveguides and Quantum Well Structures.
Final rept.
R. Sukhdev, A. K. Ghatak, I. C. Goyal, and R. L. Gallawa. 1993, 6p.
Pub. in Institute of Electrical and Electronics Engineers Jnl. of Quantum Electronics 29, n2 p340-345 Feb 93.

Keywords: *Optical waveguides, *Quantum wells, *Electron tunneling, One dimensional, Airy function, WKB approximation, Potentials, Reprints.

We present a simple method for the analysis of tunneling through an arbitrary one-dimensional potential barrier, based on the modified Airy function approach. We have considered truncated step-linear, step-exponential, parabolic, and quartic potential barriers. The results have been compared with those obtained by the conventional WKBJ, modified WKBJ, and the matrix method. The effect of the truncation level on the tunneling coefficient has also been investigated. The tunneling coefficient is sensitive to the truncation level. For the step-linear potential, the tunneling coefficient is a monotonically decreasing function of the truncation level, while for the parabolic potential, it oscillates before saturating to a constant value.

02,121
PB94-185907 Not available NTIS
National Inst. of Standards and Technology (EEEL), Gaithersburg, MD. Electricity Div.
Optical Current Transducer for Calibration Studies.
Final rept.
E. D. Simmon, A. H. Rose, and G. J. Fitzpatrick. 1993, 4p.
Pub. in Proceedings of International Symposium on High Voltage Engineering (8th), Yokohama, Japan, August 23-27, 1993, p399-402.

Keywords: *Electric current, *Electrical measurement, Faraday effect, High voltage, Electric power, Magnetooptics, Error analysis, Operation, Design, Tests, Reprints, *Optical current transducers, *Current sensors.

Optical current transducers (OCTs) are well-suited for current measurements in high voltage applications because they offer advantages over conventional oil-filled current transformers such as greater immunity from electromagnetic interference (EMI), intrinsic safety, and wide dynamic range. This paper describes an OCT designed and built at the National Institute of Standards and Technology (NIST) for in the development of calibration methods for OCTs for power system applications. The design and operating characteristics of the NIST OCT are described, and the results of tests for sensitivity, linearity, and dynamic range are reported. Some of the sources of measurement error are discussed.

02,122
PB94-188810 PC A09/MF A02
National Inst. of Standards and Technology (EEEL), Gaithersburg, MD. Semiconductor Electronics Div.
Semiconductor Measurement Technology: Improved Characterization and Evaluation Measurements for HgCdTe Detector Materials, Processes, and Devices Used on the GOES and TIROS Satellites.
Special pub.
D. G. Seiler, J. R. Lowney, W. R. Thurber, J. J. Kopanski, and G. G. Harman. Apr 94, 188p, NIST/SP-400-94.
Also available from Supt. of Docs as SN003-003-03263-8. See also PB92-112382.

Keywords: *Satellite instruments, *Infrared detectors, *TIROS satellites, *GOES satellites, Mercury cadmium tellurides, Intermediate infrared radiation, Shubnikov-de Haas effect, Meteorological satellites, Photoconductive cells, Magnetoresistivity, Metallizing, Packaging, Bonding, Calibration, Scanning capacitance microscopy, Test structures.

An extensive study was carried out to improve the characterization and evaluation methods used for HgCdTe (mercury cadmium telluride) photoconductive infrared detectors used in GOES and TIROS satellites. High-field magnetotransport techniques were used to determine the electrical properties of the detector accumulation layers, which partially control their detectivities. Assessments were made of the quality of the bonding and packaging used in detector fabrication, and a list of recommended practices was produced. The applicability of scanning capacitance microscopy and test structures to detector-array evaluation is discussed, and finally recommendations are made for standardized detector calibration. The results of this work have provided new and more refined measurement methods that can be adapted by the detector manufacturers to improve performance and yield.

02,123
PB94-198223 Not available NTIS
National Inst. of Standards and Technology (NEL), Gaithersburg, MD. Chemical Process Metrology Div.
Electro-Optical Sensor for Surface Displacement Measurements of Compliant Coatings.
Final rept.
D. Adair, W. M. Madigosky, and N. E. Mease. 1991, 2p.
Pub. in Review of Scientific Instruments 62, n6 p1652-1653 1991. Sponsored by Admiralty Research Establishment, Portland (England). and Naval Research Lab., Washington, DC.

Keywords: *Displacement measurement, *Vibration measurement, Light emitting diodes, Phototransistors, Hydroelasticity, Hydrodynamics, Gallium arsenides, Silicon, Sensors, Reprints, Compliant coatings.

A method has been developed primarily to quantify the characteristics of hydroelastic instability waves on an elastic surface but which may also be applied to vibration measurements in general. The instability waves to be investigated result from the reaction of a compliant coating to the hydrodynamic forces of the boundary layer flowing over it. The present displacement sensor comprises a gallium arsenide infrared emitting diode in conjunction with a spectrally matched silicon phototransistor. It was found that this conbination could be designed to give an analog linear response in the region 4.5mm < d < 6.5mm, where is the distance from the reflecting surface to the phototransistor. Variation in voltage to change in d was found to be approximately 1.5mV/m when using polished aluminum as the reflecting surface and 0.5mV/(mu)m when using silicon gel impregnated with calcium carbonate.

02,124
PB94-199478 Not available NTIS
National Inst. of Standards and Technology (NML), Gaithersburg, MD. Electron and Optical Physics Div.
Silicon Photodiodes Optimized for EUV and Soft X-Ray Regions.
Final rept.
L. R. Canfield, J. Kerner, and R. Korde. 1990, 6p.
Pub. in Proceedings of Society of Photo-Optical Instrumentation Engineers - Extreme Ultraviolet, X-ray, and Gamma-ray Instrumentation for Astronomy, San Diego, CA., July 11-13, 1990, v1344 p372-377.

Keywords: *X-ray detection, *Ultraviolet detectors, *Silicon diodes, *Photodiodes, Extreme ultraviolet radiation, Soft x rays, Radiometry, Reprints.

Silicon photodiode detectors are now being routinely fabricated with almost no internal loss mechanisms. Such detectors have also been optimized in a windowless configuration for use in the extreme ultraviolet/soft X-ray region. These photodiodes have stable efficiencies (electrons per incident photon) which are essentially linear with photon energy (in this region), and which exceed 1 electron per incident photon for photon energies of about 10eV and beyond. In addition to reporting the most recent performance parameters of devices with active areas of 1 sq cm and 3 sq cm, the temporal stability of devices with measurements spanning more than a year will be shown to be quite acceptable for photon energies > 25eV. Silicon photodiodes of this type have numerous applications in the extreme ultraviolet and soft X-ray regions where their relative ease of use, low cost, stability, extremely high efficiency, and ability to operate in the presence of gases can be profitably exploited. Although silicon detectors are by nature very wide band detectors, narrow bandpass characteristics may be easily developed by directly overcoating the silicon dioxide outer surface of the basic photodiode with one or more thin films of appropriate materials. Examples of photodiodes whose responses have been thus tailored for use in the extreme ultraviolet are presented.

02,125
PB94-199551 Not available NTIS
National Inst. of Standards and Technology (EEEL), Boulder, CO. Electromagnetic Technology Div.
Magneto-Optic Magnetic Field Sensor with 1.4pT/ square root of 1(Hz) Minimum Detectable Field at 1 kHz.
Final rept.
M. N. Deeter, G. W. Day, T. J. Beahn, and M. Manheimer. 1993, 2p.
Pub. in Electronics Letters 29, n11 p993-994, 27 May 93. Sponsored by Laboratory for Physical Sciences, College Park, MD.

Keywords: Yttrium iron garnets, Faraday effect, Magnetooptics, Substitutes, Sensitivity, Cylinders, Gallium, Reprints, *Magnetic field sensors, Fiber optic sensors, Nickel zinc ferrites.

The Letter demonstrates that the sensitivity of magneto-optic magnetic field sensors employing iron garnets can be increased by approximately two orders of magnitude by applying flux concentration. A minimum detectable field of 1.4pT/(Hz)(sup 1/2) was measured when a cylindrical gallium-substituted yttrium iron garnet crystal was combined with two conically tapered nickel-zinc ferrite cylinders.

02,126
PB94-200193 Not available NTIS
National Inst. of Standards and Technology (EEEL), Boulder, CO. Electromagnetic Technology Div.
Characterization of Vertical-Cavity Semiconductor Structures.
Final rept.
D. H. Christensen, J. G. Pellegrino, R. K. Hickernell, R. S. Rai, S. M. Crochiere, and C. A. Parsons. 1992, 8p.
Pub. in Jnl. of Applied Physics 72, n12 p5982-5989, 15 Dec 92.

Keywords: *Surface emitting lasers, Electron microscopy, Photoluminescence, Gallium arsenides, Metrology, Wafers, Reprints, Double crystal x-ray diffractometry, Photoreflectance.

Several analytical tools are applied to characterize vertical-cavity surface-emitting laser structures grown on GaAs wafers. These epitaxial structures are amenable to x-ray, electron-beam, and optical metrologies. Cross-sectional scanning electron microscopy and transmission electron microscopy were used to measure layer thicknesses and uniformity. Photoluminescence wafer mapping was used to determine alloy composition uniformity across the wafer. Photoreflectance was also used to determine alloy composition. Cross-sectional microphotoluminescence was used to measure average alloy compositions in the top and bottom mirrors. Reflectance spectroscopy was used to characterize the cavity resonances and mirror layers. Double-crystal x-ray diffractometry (DCXRD) was used to characterize mirror layer dimensions, uniformity, and average alloy composition. Excellent agreement was found among these measurement techniques and between simulations and measurements. The results demonstrate the accuracy of the device simulation tools and the applicability of DCXRD in analyzing these structures.

02,127
PB94-200698 Not available NTIS
National Inst. of Standards and Technology (EEEL), Boulder, CO. Electromagnetic Technology Div.
Faraday Effect Current Sensors.
Final rept.
G. W. Day, M. N. Deeter, and A. H. Rose. 1992, 8p.
Pub. in Proceedings of Australian Conference on Optical Fibre Technology (17th), Hobart, Tasmania, Australia, November 29-December 2, 1992, p20-27.

Keywords: *Electric current, Faraday effect, Optical fibers, Thermal stability, Sagnac effect, Birefringence, Reviews, Reprints, *Fiber optic sensors, *Current sensors, Sagnac interferometers.

This paper contains a review of Faraday effect current sensors, including both those based on bulk materials and on single mode optical fiber. Among the topics discussed are new materials for bulkbased sensors leading to the best reported sensitivities, methods of dealing with fiber birefringence, temperature stability, speed limitations, and new configurations, including the Sagnac Interferometer.

02,128
PB94-200706 Not available NTIS
National Inst. of Standards and Technology (EEEL), Boulder, CO. Electromagnetic Technology Div.
Faraday Effect Sensors: A Review of Recent Progress.
Final rept.
G. W. Day, M. N. Deeter, and A. H. Rose. 1991, 16p.
Pub. in Proceedings of International Conference on Optical Fiber Sensors, Wuhan, China, October 9-11, 1991, p11-26.

Keywords: *Electric current, *Magnetic fields, *Magnetometers, Reprints, Magnetic measurement, Faraday effect, Thermal stability, Optical fibers, Birefringence, Reviews, *Fiber optic sensors, *Current sensors.

The last few years have seen dramatic progress in the development of Faraday effect sensors for measuring both magnetic fields and electric current. In the case of magnetic field sensors, the most significant advances have resulted from an investigation of new materials, especially the ferrimagnetic iron garnets. Minimum detectable magnetic fields have been reduced by several orders of magnitude to about 100 pT/Hz(sup 1/2) at 500 Hz and bandwidths of hundreds of megahertz have been obtained. In the case of electric current sensors, new methods of avoiding the effects of linear birefringence in optical fiber have resulted in much smaller and more stable sensors. One of those approaches, annealing of the fiber to reduce birefringence, has yielded sensors with temperature stabilities near that of the material limit, < 10(sup -4)/ K. These topics and other developments that have occurred since a previous summary (Proc. SPIE 985 138-150 (1988)) are discussed in the review.

02,129
PB94-200714 Not available NTIS
National Inst. of Standards and Technology (IMSE), Gaithersburg, MD. Ceramics Div.
Correlation of HgCdTe Epilayer Defects with Underlying Substrate Defects by Synchrotron X-Ray Topography.
Final rept.
B. E. Dean, C. J. Johnson, S. C. McDevitt, R. C. Dobbyn, M. Kuriyama, J. Ellsworth, H. R. Vydyanath, J. J. Kennedy, G. T. Neugebauer, and J. L. Sepich. 1991, 7p.
Pub. in Jnl. of Vacuum Science and Technology B 9, n3 p1840-1846 May/Jun 91.

Keywords: *Mercury cadmium tellurides, *Crystal defects, Focal plane devices, Infrared detectors, Synchrotron radiation, X-ray sources, Substrates, Reprints, Diffraction imaging, Epilayers.

Synchrotron X-ray topography studies have been conducted at the National Synchrotron Light Source (NSLS) at Brookhaven National Laboratories to correlate defects in HgCdTe epilayers with those in underlying CdTe family substrates. IR detectors are being fabricated on these epilayers to investigate the performance impact of specific defects. This paper describes synchrotron X-ray facilities and methods. Images of substrates and epilayers are discussed and mapping of epilayer/substrate defects, such as microtwins, subgrain boundaries and slip lines, is demonstrated. Efforts to map detector array performance to epilayer and substrate topographs are described.

02,130
PB94-212594 Not available NTIS
National Inst. of Standards and Technology (NEL), Boulder, CO. Electromagnetic Fields Div.
Optically Sensed EM-Field Probes for Pulsed Fields.
Final rept.
M. Kanda, and K. D. Masterson. 1992, 7p.
Pub. in Proceedings of the Institute of Electrical and Electronics Engineers 80, n1 p209-215 Jan 92.

Keywords: *Probes(Electromagnetic), *Photonics, Electromagnetic fields, Electromagnetic pulses, Transfer functions, Electrooptics, Modulators, Reprints.

We discuss the characteristics of photonic probes that give them the potential to measure pulsed electromagnetic fields more accurately than has been possible in the past. An overview of system design is presented with particular emphasis placed on the transfer functions of appropriate antennas and electro-optic modulators. Noise sources which limit the sensitivity to low level signals are discussed and used to determine the noise equivalent field (NEF). The characteristics of some sensors developed by NIST are presented, and their performances relative to estimated practical limits for the NEF are indicated. Optical guided wave technology appears to hold considerable promise for fabricating modulators with a wide variety of operating parameters that can improve probe performance and extend their applications to a wider region of the electromagnetic spectrum.

02,131
PB94-212917 Not available NTIS
National Inst. of Standards and Technology (EEEL), Gaithersburg, MD. Semiconductor Electronics Div.
High-Spatial-Resolution Resistivity Mapping Applied to Mercury Cadmium Telluride.
Final rept.
J. J. Kopanski, J. R. Lowney, D. B. Novotny, J. Ramsey, D. G. Seiler, and A. Simmons. 1992, 7p.
Sponsored by Night Vision and Electro-Optics Lab., Fort Belvoir, VA. and Defense Advanced Research Projects Agency, Arlington, VA.
Pub. in Jnl. of Vacuum Science and Technology B 10, n4 p1553-1559, Jul/Aug 92.

Keywords: *Mercury cadmium tellurides, *Electrical resistivity, Liquid phase epitaxy, High resolution, Bulk semiconductors, Room temperature, Electric contacts, Recrystallization, Thin films, Reprints, *Resistivity mapping, Contact resistivity.

The fine-scale resistivity variations of slices of bulk, n-type Hg(1-x)Cd(x)Te (HgCdTe) grown by the solid-

state recrystallization (SSR) process and thin-film epitaxial layers of HgCdTe grown by liquid phase epitaxy (LPE) on SSR substrates were mapped at room temperature (297 K). An automatic probe station was used to make four-probe resistance measurements, spaced 80 micrometers apart, on lithographically defined metal-to-HgCdTe contacts. Most slices of SSR HgCdTe were found to have resistivities that increased from the center to the outside edge, and some SSR material also showed small inclusions with resistivity either higher or lower than the surrounding material. LPE material was found to have a more random variation in resistivity than SSR HgCdTe material. Also, the metal-semiconductor contact resistivity of In/Pb/In/Ni contacts to n-type HgCdTe was measured to be in the range of 0.3 to 20 X 10(-5) ohm cm for HgCdTe resistivities varying from 0.0l to 0.1 ohm cm.

02,132
PB94-212925 Not available NTIS
National Inst. of Standards and Technology (EEEL), Gaithersburg, MD. Semiconductor Electronics Div.
Review of Semiconductor Microelectronic Test Structures with Applications to Infrared Detector Materials and Processes.
Final rept.
J. J. Kopanski, and C. E. Schuster. 1993, 23p.
Pub. in Semicond. Sci. Technol. 8, p888-910 1993.

Keywords: *Mercury cadmium tellurides, *Infrared detectors, Integrated circuits, Process control, Gallium arsenides, Microelectronics, Silicon, Reviews, Reprints, *Test structures.

The impact of microelectronic test structures, as they have been applied to silicon integrated circuits (ICS) and gallium arsenide monolithic microwave integrated circuits (MMICS), is reviewed. General principles for the use of test structures with possible applications to infrared (IR) detector technology based on HgCdTe and other materials are emphasized. The uses of test structures for Si and GaAs, test chip design methodology and some examples of how test structures have been applied for process control and to increase yield are discussed. Specific test structures and techniques that have been applied to IR detectors are also reviewed. The basic design considerations and measurements possible with each class of test structure are discussed. The important experience of the Si and GaAs industries, applicable to IR detectors, is that significant yield improvement is possible with improved process control using test structures. Increased research efforts to expand the applications of test structures to IR detector manufacture are indicated.

02,133
PB94-213485 Not available NTIS
National Inst. of Standards and Technology (EEEL), Gaithersburg, MD. Semiconductor Electronics Div.
Investigation of Mercury Interstitials in Hg(1-x)CdxTe Alloys Using Resonant Impact-Ionization Spectroscopy.
Final rept.
C. L. Littler, E. Maldonado, X. N. Song, D. G. Seiler, J. R. Lowney, Z. Yu, and J. L. Elkind. 1992, 5p.
Pub. in Jnl. of Vacuum Science and Technology B 10, n4 p1466-1470 Jul/Aug 92.

Keywords: *Mercury cadmium tellurides, Activation energy, Electron traps, Hole traps, Interstitials, Impurities, Reprints, Resonance ionization spectroscopy.

A technique for studying low concentrations of trap levels in narrow-gap Hg(1-x)Cd(x)Te has been combined with the deliberate introduction of defects to determine the activation energies of these impurities in this ternary material. In this investigation, mercury (Hg) interstitials, believed to be responsible for dark current in metal-insulator-semiconductor devices, were deliberately introduced into samples with x approx = 0.22 and x approx = 0.24. Each sample was divided into two parts with the second part of each slice used as a control. The results from these samples provide direct evidence that Hg interstitials create trap levels near 45 and 60 meV above the valence-band edge for these x-value samples.

02,134
PB94-216074 Not available NTIS
National Inst. of Standards and Technology (EEEL), Gaithersburg, MD. Semiconductor Electronics Div.
Heavily Accumulated Surfaces of Mercury Cadmium Telluride Detectors: Theory and Experiment.
Final rept.
J. R. Lowney, D. G. Seiler, W. R. Thurber, C. L. Littler, Z. Yu, and X. N. Song. 1993, 7p.
Pub. in Jnl. of Electronic Materials 22, n8 p985-991 1993.

Keywords: *Mercury cadmium tellurides, *Infrared detectors, *Passivation, Shubnikov-de Haas effect, Photoconductive cells, Two dimensional, Electron gas, Surfaces, Reprints.

Some processes used to passivate n-type mercury cadmium telluride photoconductive infrared detectors produce electron accumulation layers at the surfaces, which result in 2D electron gases. The dispersion relations for the electric subbands that occur in these layers have been calculated from first principles. Poisson's equation for the built-in potential and Schroedinger's equation for the eigenstates have been solved self-consistently. The cyclotron effective masses and Fermi energies have been computed for each subband density for 12 total densities between 0.1 to 5.0 X 10(sup 12)/sq cm. Results are discussed. These results provide a basis for characterizing the passivation processes, which greatly affect device performance.

02,135
PB94-216280 Not available NTIS
National Inst. of Standards and Technology (EEEL), Boulder, CO. Electromagnetic Technology Div.
Integrated Optic Laser Emitting at 906, 1057, and 1358 nm.
Final rept.
K. J. Malone, N. A. Sanford, and J. S. Hayden. 1993, 3p.
Pub. in Electronics Letters 29, n8 p691-693, 15 Apr 93.

Keywords: *Neodymium lasers, *Glass lasers, Infrared lasers, Near infrared radiation, Integrated optics, Phosphate glass, Doped materials, Optical waveguides, Reprints.

Laser oscillation at 906, 1057, and 1358 nm has been achieved in the same neodymium-doped-glass integrated optic laser. This is believed to be the first report of a 906 nm integrated optic laser. High slope efficiency and high output power were observed at 1057 nm. The laser was fabricated by silver ion exchange in a phosphate glass.

02,136
PB94-216298 Not available NTIS
National Inst. of Standards and Technology (EEEL), Boulder, CO. Electromagnetic Technology Div.
Integrated Optic Laser Emitting at 905, 1057, 1356 nm.
Final rept.
K. J. Malone, N. A. Sanford, J. S. Hayden, and D. L. Sapak. 1993, 3p.
Pub. in Advanced Solid-State Lasers, New Orleans, LA., February 1-3, 1993, 3p.

Keywords: *Neodymium lasers, *Glass lasers, Infrared lasers, Near infrared radiation, Integrated optics, Phosphate glass, Doped materials, Optical waveguides, Reprints.

We have achieved laser oscillation at 1057, 1356, and 905 nm in the same neodymium-doped-glass integrated optic device. We believe this is the first report of a 905 nm integrated optic laser. The laser was fabricated by solid silver ion exchange in a phosphate glass.

02,137
PB95-107215 Not available NTIS
National Inst. of Standards and Technology (EEEL), Gaithersburg, MD. Semiconductor Electronics Div.
Interface Roughness of Short-Period AlAs/GaAs Superlattices Studied by Spectroscopic Ellipsometry.
Final rept.
N. V. Nguyen, J. G. Pellegrino, P. M. Amirtharaj, D. G. Seiler, and S. B. Qadri. 1993, 8p.
Pub. in Jnl. of Applied Physics 73, n11 p7739-7746, 1 Jun 93.

Keywords: *Superlattices, *Interfaces, Molecular beam epitaxy, Gallium arsenides, Aluminum arsenides, Thin films, Optical properties, Ellipsometry, Roughness, Reprints.

Spectroscopic ellipsometry (SE) has been used to study the effects of interface roughness on the optical properties of ultrathin short-period 3x3 GaAs/AlAs superlattices grown by molecular-beam epitaxy (MBE). The complex dielectric function and thickness of the whole superlattice and the thickness of the native oxide overlayer were simultaneously determined by an inversion technique from data in the 1.5-5.0 eV region. The main optical critical points E(0), E(0) + Delta(0), E(1), E(1) + Delta(1), and E(2) were deduced by line-shape fitting of the second derivative of the complex dielectric function of the superlattice to the analytical line-shape expression. The interface roughness is found to shift the optical transitions, except E(2), to higher energy and broaden their line shapes. A simple interpretation of the shift and broadening is given. The interface roughness and layer thicknesses obtained by SE are found to be consistent with the results of x-ray diffraction and Raman scattering studies previously reported. The results in the study demonstrate the capability of the post-growth nondestructive characterization by SE to provide useful information about the interface quality of superlattice structures, and consequently to optimize the MBE growth conditions in order to achieve the desired structural parameters.

02,138
PB95-108775 Not available NTIS
National Inst. of Standards and Technology (EEEL), Gaithersburg, MD. Semiconductor Electronics Div.
Interface Sharpness in Low-Order III-V Superlattices.
Final rept.
J. Pellegrino, S. B. Qadri, P. M. Amirtharaj, N. V. Nguyen, and J. Comas. 1992, 8p.
Pub. in Thin Solid Films 220, p176-183 1992.

Keywords: *Superlattices, *Interfaces, Molecular beam epitaxy, Surface emitting lasers, Aluminum arsenides, Gallium arsenides, Thin films, X-ray diffraction, Roughness, Reprints, Edge emitting lasers.

Superlattices composed of aluminum, gallium and indium are currently employed in a variety of device-related applications. Among these are edge-emitting GRINSCH lasers and vertical cavity surface emitting laser diodes. As the individual layer thickness is reduced, the role of interface sharpness becomes more critical in ensuring good two-dimensional growth. This work addresses the relationship between interface roughness and superlattice crystallinity for short-period AlAs/GaAs superlattices. Thin short-period superlattices with active layer thicknesses of 30 nm or less were also investigated to help determine the interface sharpness in the initial stages of growth. X-ray diffraction was used to assess interface roughness and to calculate superlattice periodicity. These results are compared with those obtained by reflection high energy electron diffraction (RHEED), Raman spectroscopy, and spectroscopic ellipsometry. The results indicate that interface roughness is promoted by a reduced arsenic flux growth condition at normal growth temperatures for short-period superlattices. The results also suggest that, for thin superlattices, a 10 nm buffer layer enhances interface roughness in the initial stages of growth and compromises the subsequent epilayer crystallinity. An analysis of these results in the light of structural, dynamical, and optical data is presented.

02,139
PB95-108783 Not available NTIS
National Inst. of Standards and Technology (EEEL), Gaithersburg, MD. Semiconductor Electronics Div.
Interface Sharpness during the Initial Stages of Growth of Thin, Short-Period III-V Superlattices.
Final rept.
J. G. Pellegrino, S. B. Qadri, C. M. Cotell, J. Comas, P. M. Amirtharaj, and N. V. Nguyen. 1993, 6p.
Pub. in Jnl. of Vacuum Science and Technology A 11, n4 p917-922, Jul/Aug 93.

Keywords: *Superlattices, *Interfaces, Molecular beam epitaxy, X-ray diffraction, Gallium arsenides, Roughness, Thin films, Reprints, Heterostructures.

Superlattices composed of III-V heterostructures have established applications in high-speed electronic and optoelectronic devices. As layer thicknesses are reduced, the role of heterostructure interface sharpness becomes more critical to ensuring high quality two-dimensional growth. In this work, short-period (less than 1 nm) superlattices with active layer thicknesses of 31 nm were investigated to assess interface roughness in the initial stages of growth. X-ray diffraction was used to evaluate interface roughness and to calculate superlattice periodicity. Results suggest that surface roughening by islanding may be promoted by GaAs buffer layers that are 10-100 nm thick. Smoother inter-

faces were obtained in samples with buffer layers 250 nm and greater.

02,140
PB95-125928 Not available NTIS
National Inst. of Standards and Technology (EEEL), Boulder, CO. Electromagnetic Technology Div.
International Intercomparison of Detector Responsivity at 1300 and 1550 nm.
Final rept.
R. L. Gallawa, J. L. Gardener, D. H. Nettleton, and K. D. Stock. 1992, 2p.
Pub. in Proceedings of a Conference on Precision Electromagnetic Measurements, Paris, France, June 9-12, 1992, p268-269.

Keywords: *Ge semiconductor detectors, *Infrared detectors, Near infrared radiation, Interlaboratory comparisons, International cooperation, Optical communication, Spectral response, Optical measurement, Power meters, Calibration, Standards, Reprints, Intercomparison.

An international intercomparison of spectral responsivity measurements at wavelengths of interest to optical communications was recently completed. Thirteen countries participated in the test, which was conducted in the course of a year. Agreement is within about 1%.

02,141
PB95-126017 Not available NTIS
National Inst. of Standards and Technology (EEEL), Boulder, CO. Electromagnetic Technology Div.
International Intercomparison of Detector Responsivity at 1300 and 1550 nm.
Final rept.
J. L. Gardener, R. L. Gallawa, K. D. Stock, and D. H. Nettleton. 1992, 6p.
Pub. in Applied Optics 31, n34 p7226-7231, 1 Dec 92.

Keywords: *Ge semiconductor detectors, *Infrared detectors, *Photodiodes, Interlaboratory comparisons, Near infrared radiation, Optical communication, Radiometry, Reprints, Intercomparison.

An intercomparison of spectral responsivity measurements has been carried out among the national laboratories of 13 countries. Measurements were made at wavelengths of 1300 and 1550 nm, which are important in optical communication systems. Three germanium photodiodes were circulated in each of three separate paths, beginning and ending at the National Institute of Standards and Technology as the coordinating laboratory. The results show agreement within 1%.

02,142
PB95-126348 Not available NTIS
National Inst. of Standards and Technology (NEL), Boulder, CO. Electromagnetic Technology Div.
Far-Infrared Kinetic Inductance Detector.
Final rept.
E. N. Grossman, D. G. McDonald, and J. E. Sauvageau. 1991, 4p.
Sponsored by Strategic Defense Initiative Organization, Washington, DC. Innovative Science and Technology.
Pub. in Institute of Electrical and Electronics Engineers Transactions on Magnetics 27, n2 p2677-2680 Mar 91.

Keywords: *Superconducting devices, *Infrared bolometers, *Infrared detectors, Superconducting films, Far infrared radiation, SQUID devices, Mixers(Electronics), Temperature range 0000-0013 K, Thin films, Inductance, Inductors, Heterodyning, Reprints, Niobium titanium, Photoinductors.

Extremely sensitive far-infrared detectors suitable for both direct detection and heterodyne applications are possible, based on micrometer-sized thin films with thickness less than a superconducting penetration depth. The penetration depth of such a film, and therefore its inductance, varies with temperature and with quasiparticle population (described by an effective temperature T*), resulting in both bolometric and nonequilibrium 'photoinductive' responses. Common magnet alloys such as NbTi are the natural choice for liquid-He temperature operation. A detailed analysis predicts a (phonon-limited) NEP of about 4 x 10 (exp -17) W/Hz(sup 1/2) for a bolometer with an iridium kinetic inductor operated at 0.1 K. A heterodyne noise temperature of 2250 K (SSB) at 3 THz, with 200 MHz bandwidth is predicted for a NbTi mixer operated at 4 K.

02,143
PB95-135588 PC A05/MF A01
National Inst. of Standards and Technology (EEEL), Boulder, CO. Electromagnetic Technology Div.
Metrology for Electromagnetic Technology: A Bibliography of NIST Publications.
A. J. Smith. Sep 94, 93p, NISTIR-5029.
Supersedes PB94-108776.

Keywords: *Optoelectronic devices, *Superconductor devices, *Magnetic measurement, *Metrology, *Bibliographies, Optical communication, Optical fibers, Optical waveguides, Fiber optics, Solid state lasers, YBCO superconductors, High temperature superconductors, Josephson junctions, SQUID devices, Cryogenics, *Electromagnetic metrology, *Cryoelectronics, US NIST.

This bibliography lists the publications of the personnel of the Electromagnetic Technology Division of the National Institute of Standards and Technology (NIST) during the period from January 1970 through publication of this report. A few earlier references that are directly related to the present work of the Division are also included. Keywords include cryoelectronics, electromagnetic metrology, lasers, optical fibers, and superconducting materials. This bibliography is expected to be the last from the Electromagnetic Technology Division since the Division is in the process of being split into two Divisions. Each will produce its own bibliography in future editions.

02,144
PB95-140083 Not available NTIS
National Inst. of Standards and Technology (NEL), Boulder, CO. Electromagnetic Technology Div.
Superconducting Kinetic Inductance Radiometer.
Final rept.
J. E. Sauvageau, D. G. McDonald, and E. N. Grossman. 1991, 4p.
Pub. in Institute of Electrical and Electronics Engineers Transactions on Magnetics 27, n2 p2757-2760 1991.

Keywords: *Superconducting devices, *Infrared radiometers, *Infrared bolometers, Superconducting films, Impedance bridges, Integrated circuits, Temperature measurement, SQUID devices, Thermometers, Inductors, Prototypes, Silicon, Reprints, Inductance bridges, Photoinductors.

We are developing a bolometer based on a differential thermometer that senses temperature changes through changes in the kinetic inductance of a superconducting thin film. The composite bolometer is the sensor for a prototype radiometer that will provide an absolute measure IR power. The radiometer is intended to measure the spectrally dispersed power of a 300 K black body. This absolute radiometer is being developed for use at the Low Background Infrared (LBIR) Facility at NIST, Gaithersburg. The noise floor of the temperature transducer for the radiometer has been measured to be 0.75 pW for a 100 sec. integration time. This is 150 times lower noise level than that of the commercial absolute radiometer currently used at the LBIR Facility in Gaithersburg.

02,145
PB95-141115 Not available NTIS
National Inst. of Standards and Technology (EEEL), Boulder, CO. Electromagnetic Technology Div.
LP11-Mode Leakage Loss in Coated Depressed Clad Fibers.
Final rept.
B. P. Pal, R. L. Gallawa, and I. C. Goyal. 1992, 3p.
Pub. in Institute of Electrical and Electronics Engineers Photonics Technology Letters 4, n4 p376-378 Apr 92.

Keywords: *Optical fibers, *Fiber optics, *Transmission loss, Fiber optics transmission lines, Leakage, Reprints, Cutoff wavelength.

A quantitative investigation of the leakage loss spectrum of the LP(11)-mode in coated depressed index clad fibers is made using the matrix method. The study reveals oscillations similar to those seen in the measurement of cutoff wavelength. Our results do not agree with recently published results and a plausible explanation of the discrepancies is given.

02,146
PB95-150397 Not available NTIS
National Inst. of Standards and Technology (CSTL), Gaithersburg, MD. Biotechnology Div.
Retinal-Protein Complexes as Optoelectronic Components.
Final rept.
N. N. Vsevolodov, and T. V. Dyukova. 1994, 8p.
Pub. in Trends in Biotechnology 12, n3 p81-88 Mar 94.

Keywords: *Eye pigments, *Eye proteins, *Optical storage, *Rhodopsin, *Biosensors, Photosensitivity(Biological), Biotechnology, Complexes, Reprints, *Bacteriorhodopsin.

Naturally occurring retinal-protein complexes (RPCs) have recently received much attention with regard to their potential use as light-sensitive elements for optical recording. The best-known RPC is bacteriorhodopsin (BR), a photosensitive protein from the membrane of extreme halophilic bacteria, which has been studied in great detail. The remarkably robust nature of BR, coupled with its ability to reversibly change color upon illumination and its high cyclicity of ground-to-photoinduced state transitions, makes BR a promising material for optical information processing.

02,147
PB95-151114 Not available NTIS
National Inst. of Standards and Technology (EEEL), Gaithersburg, MD. Electricity Div.
Recent Developments at NIST on Optical Current Sensors and Partial Discharge Diagnostics.
Final rept.
R. J. Van Brunt. 1993, 15p.
Pub. in Proceedings of Workshop on Advanced Diagnostics for Substation Equipment, Palo Alto, CA., November 9-11, 1992, p6-159 - 6-173 1993.

Keywords: *Electric current meters, *Electric discharges, *Fault detection, Optical measurement, Pattern recognition, Faraday effect, Electric substations, Electrical insulation, Stochastic processes, Electric power, Diagnostic techniques, Reprints, *Fiber optic sensors, *Partial discharges, Optical fiber sensors, US NIST.

The purpose of this presentation is to draw attention to the NIST projects and discuss their relevance to the improvement of measurements applied to electric-power systems, especially those under the substations. The first activity discussed here is concerned with the use of optical fiber techniques to measure current. The second is concerned with a new approach to analyzing partial-discharge data that should prove useful in improving the reliability of pattern recognition schemes that are under development to identify the characteristics of defect sites in the insulation at which the discharges occur.

02,148
PB95-153177 Not available NTIS
National Inst. of Standards and Technology (EEEL), Boulder, CO. Electromagnetic Technology Div.
Vertical-Cavity Optoelectronic Structures: CAD, Growth, and Structural Characterization.
Final rept.
D. H. Christensen, S. M. Crochiere, J. G. Pellegrino, W. F. Tseng, R. K. Hickernell, R. S. Rai, and C. A. Parsons. 1993, 6p.
Pub. in Materials Research Society Symposia Proceedings, v281 p307-312 1993.

Keywords: *Semiconductor lasers, Scanning electron microscopy, Transmission electron microscopy, Computer aided design, Aluminum gallium arsenides, Molecular beam epitaxy, X-ray diffraction, Photoluminescence, Laser cavities, Superlattices, Reflectance, Mirrors, Reprints, Double crystal x-ray diffractometry, Heterostructures.

Simulations of reflectance spectra and electric field distributions for vertical-cavity structures were used in the computer aided design of epitaxial mirrors and lasers. The binary GaAs/AlAs superlattice alloys and Al(x)Ga(1-x)As random alloys that compose these structures were grown by molecular beam epitaxy. Photoluminescence, photoreflectance, reflectance spectroscopy, scanning electron microscopy, transmission electron microscopy, and double crystal x-ray diffractometry were applied to characterize cavity and Bragg mirror layer thicknesses and alloy composition.

02,149
PB95-153185 Not available NTIS
National Inst. of Standards and Technology (EEEL), Boulder, CO. Electromagnetic Technology Div.
Vertical-Cavity Semiconductor Structures: Materials Characterization.
Final rept.
D. H. Christensen, J. R. Hill, D. T. Schaafsma, W. F. Tseng, R. K. Hickernell, and J. G. Pellegrino. 1993, 2p.
Pub. in Proceedings of Conference on Lasers and Electro-Optics, Baltimore, MD., May 2-7, 1993, v11 p234-235.

Keywords: *Semiconductor lasers, *Laser materials, X-ray diffraction, Photoluminescence, Reflectance, Characteristics, Laser cavities, Reprints, Double crystal x-ray diffractometry, Microcavities, Microlasers.

Materials characterization of a variety of vertical-cavity semiconductor structures is reported. Double crystal x-ray diffractometry, reflectance spectroscopy, and photoluminescence measurements are correlated and used to determine cavity and Bragg mirror layer thicknesses.

02,150
PB95-153193 Not available NTIS
National Inst. of Standards and Technology (EEEL), Boulder, CO. Electromagnetic Technology Div.
Vertical-Cavity Semiconductor Lasers: Structural Characterization, CAD, and DFB Structures.
Final rept.
D. H. Christensen, C. A. Parsons, J. G. Pellegrino, S. M. Crochiere, R. K. Hickernell, D. T. Schaafsma, J. R. Hill, and R. S. Rai. 1993, 7p.
Pub. in Proceedings of Society of Photo-Optical Instrumentation Engineers: Laser Diode Technology and Applications V, Los Angeles, CA., January 18-20, 1993, v1850 p115-121.

Keywords: *Distributed feedback lasers, *Semiconductor lasers, *Computer aided design, Scanning electron microscopy, Transmission electron microscopy, Near infrared radiation, Laser materials, Materials tests, X-ray diffraction, Computerized simulation, Software tools, Laser arrays, Photoluminescence, Characteristics, Reflectance, Reprints, Nondestructive evaluation, Double crystal x-ray diffractometry.

One of the key technologies required for manufacturing vertical-cavity laser arrays at a production scale is rapid and nondestructive evaluation of the laser material. A brief review of methods for materials characterization of vertical-cavity semiconductor lasers is presented. Techniques based on reflectance spectroscopy, photoluminescence, photoreflectance, double crystal x-ray diffractometry, scanning electron microscopy, and transmission electron microscopy are used to determine alloy composition, cavity spacer thickness, and Bragg mirror layer thickness. Critical aspects of data gathering, analysis, interpretation, and simulation are highlighted. The optical simulation software used for computer aided device design and simulation of reflectance spectra is also briefly discussed. The usefulness of the software is demonstrated by applying it to the design of a novel distributed-feedback vertical-cavity laser with a vertically integrated pump reflector. The characterization techniques are applicable to all types of vertical-cavity devices: lasers, detectors, light emitting diodes, Bragg mirrors, modulators, micro-cavities, and vertically integrated devices.

02,151
PB95-153391 Not available NTIS
National Inst. of Standards and Technology (EEEL), Boulder, CO. Electromagnetic Technology Div.
High Speed, High Sensitivity Magnetic Field Sensors Based on the Faraday Effect in Iron Garnets.
Final rept.
M. N. Deeter. 1993, 6p.
Pub. in Proceedings of Optical Fiber Sensors Conference (9th), Firenze, Italy, May 4-6, 1993, p409-414.

Keywords: Faraday effect, Optical measurement, Magnetic measurement, Magnetic anisotropy, Yttrium iron garnets, Optical waveguides, High sensitivity, High speed, Reprints, *Magnetic field sensors, *Fiber optic sensors, Garnet films.

Recent research demonstrating greater performance of Faraday effect sensors based on iron garnet crystals is described. Bulk crystals are coupled to high-permeability flux concentrators, resulting in an increase in sensitivity of at least two orders of magnitude. Iron garnet films with perpendicular magnetic anisotropy and exploited in an optical waveguide geometry exhibit greater frequency response than bulk crystals. These films also exhibit larger values of saturation Faraday rotation and ideally should exhibit no hysteresis.

02,152
PB95-153409 Not available NTIS
National Inst. of Standards and Technology (EEEL), Boulder, CO. Electromagnetic Technology Div.
Magneto-Optic Magnetic Field Sensors Based on Uniaxial Iron Garnet Films in Optical Waveguide Geometry.
Final rept.
M. N. Deeter, G. W. Day, R. Wolfe, and V. Fratello. 1993, 1p.
Pub. in Digests of International Magnetics Conference INTERMAG'93, Stockholm, Sweden, April 13-16, 1993, pEF-09.

Keywords: Yttrium iron garnets, Magnetic anisotropy, Magnetic hysteresis, Magnetic measurement, Optical waveguides, Optical measurement, Magnetooptics, Barkhausen effect, Faraday effect, Ferrimagnetism, Reprints, *Magnetic field sensors, Uniaxial anisotropy, Garnet films.

The properties of iron garnet films exhibiting uniaxial (perpendicular) magnetic anisotropy are investigated as they relate to magneto-optic magnetic field sensors. When configured in an optical waveguide geometry, such films are expected to magnetize by the mechanism of domain rotation rather than domain wall motion. This distinction should result in magnetic field sensors which exhibit improved linearity and frequency response in comparison to garnet-based magneto-optic magnetic field sensors that rely on domain wall motion. We present data which show the predicted purely linear response function as well as data which exhibit hysteresis at higher driving fields.

02,153
PB95-153763 Not available NTIS
National Inst. of Standards and Technology (EEEL), Boulder, CO. Electromagnetic Technology Div.
Accurate Characterization of High Speed Photodectors.
Final rept.
P. D. Hale, and D. L. Franzen. 1993, 10p.
Pub. in Proceedings of Society of Photo-Optical Instrumentation Engineers: Photodetectors and Power Meters, San Diego, CA., July 15-16, 1993, v2022 p218-227.

Keywords: *Photodetectors, *Photodiodes, Frequency domain, Characteristics, Heterodyning, Metrology, Uncertainty, Reprints.

We designed a simple heterodyne system for frequency domain photodetector characterization which is intended to avoid many of the disadvantages of earlier characterization systems and to minimize errors due to intensity fluctuation, frequency calibration, and source impedance mismatch without using vector network analysis. A detailed uncertainty analysis for the system indicates 95% confidence intervals between + or - 0.25 and + or - 0.6 dB at 25 GHz, depending on the photodetector output impedance.

02,154
PB95-162426 Not available NTIS
National Inst. of Standards and Technology (EEEL), Boulder, CO. Electromagnetic Technology Div.
Polarization Dependence of Response Functions in 3x3 Sagnac Optical Fiber Current Sensors.
Final rept.
K. B. Rochford, G. W. Day, and P. R. Forman. 1993, 4p.
Sponsored by Los Alamos National Lab., NM.
Pub. in Proceedings of Optical Fiber Sensors Conference (9th), Firenze, Italy, May 4-6, 1993, 4p.

Keywords: Response functions, Optical coupling, Polarized light, Sagnac effect, Complexity, Reprints, *Electric current sensors, *Fiber optic sensors, *Optical fiber sensors, Polarization dependence, Optical couplers, Sagnac interferometers.

The response functions of an ideal Sagnac optical fiber current sensor, based on a 3x3 coupler, fundamentally depend on the polarization state of light entering the coupler, even for a zero birefringence system. The desired response functions, sinusoids separated by 120 deg phase shifts, are obtained only for circularly polarized light. The response functions for linearly polarized and depolarized inputs are sinusoids separated by 180 deg, and yield only zero-slope small-signal responses; in addition, two outputs are degenerate, so the response is similar to that observed in 2x2 systems. Thus, 3x3 couplers offer no advantage over 2x2 systems for linearly polarized light. This result increases system complexity in that polarization control optics are required to supply the proper polarization, even for an ideal, zero-birefringence system.

02,155
PB95-162467 Not available NTIS
National Inst. of Standards and Technology (EEEL), Boulder, CO. Electromagnetic Technology Div.
Submicroampere-Per-Root-Hertz Current Sensor Based on the Faraday Effect in Ga: YIG.
Final rept.
A. H. Rose, M. N. Deeter, and G. W. Day. 1993, 3p.
Pub. in Optics Letters 18, n17 p1471-1473, 1 Sep 93.

Keywords: *Yttrium iron garnets, *Faraday effect, Optical measurement, Materials replacement, Gallium additions, Sensitivity, Bandwidth, Substitutes, Reprints, *Electric current sensors.

We demonstrate an optical current sensor that is based on the Faraday effect in gallium-substituted yttrium iron garnet and has a measured sensitivity of about 3 deg/A, a noise-equivalent current of about 220 nA/Hz(sup 1/2) and a -3-dB bandwidth of about 2.6 MHz. The bandwidth-sensitivity product is a factor of about 10 greater than that of an all-silica-fiber current sensor with the same diameter.

02,156
PB95-164232 Not available NTIS
National Inst. of Standards and Technology (PL), Gaithersburg, MD. Radiometric Physics Div.
Thermal and Nonequilibrium Responses of Superconductors for Radiation Detectors.
Final rept.
Z. M. Zhang, and A. Frenkel. 1993, 14p.
Pub. in ASME Winter Annual Meeting, New Orleans, LA., November 28-December 3, 1993, p1-14.

Keywords: *Superconducting devices, *Radiation detectors, *Infrared detectors, *High temperature superconductors, *Bolometers, Optical properties, Thermal properties, Nonequilibrium conditions, High-Tc superconductors, Reprints.

This work summarizes the progress in the study of the superconductor response to optical radiation and in the development of infrared detectors. The recent advances in the design of high-temperature (high-T(c)) superconducting radiation detectors using silicon microfabrication technology are emphasized. Thermal and optical properties important for the detector performance are discussed. The mechanism of the nonequilibrium optical response and its potential use to build fast and sensitive radiation detectors are described. Future challenges and opportunities in the development of high-T(c) superconducting radiation detectors are highlighted.

02,157
PB95-164299 Not available NTIS
National Inst. of Standards and Technology (EEEL), Gaithersburg, MD. Semiconductor Electronics Div.
Hg1-xCdxTe Characterization Measurements: Current Practice and Future Needs.
Final rept.
D. G. Seiler, S. Mayo, and J. R. Lowney. 1993, 24p.
Pub. in Semicond. Sci. Technol. 8, p753-776 1993.

Keywords: *Mercury cadmium tellurides, *Infrared detectors, Semiconductor materials, Electrical measurement, Optical measurement, Characteristics, Reprints.

An extensive industrial survey of the importance and use of characterization measurements for HgCdTe materials, processes and devices has been completed. Seventy-two characterization/measurement techniques were considered and thirty-five responses were received. This information was sought for a study on materials characterization and measurement techniques of parameters and properties necessary to improve the manufacturing capabilities of HgCdTe infrared detectors. The nature of materials characterization is defined, and an overview is given of how it is related to improving IR detector manufacturing. Finally, we present a description of the characterization survey and a summary of the survey results.

02,158
PB95-168480 Not available NTIS
National Inst. of Standards and Technology (EEEL), Boulder, CO. Electromagnetic Technology Div.
Low-Coherence Interferometric Measurement of Group Transit Times in Precision Optical Fibre Delay Lines.
Final rept.
B. L. Danielson. 1993, 4p.
Pub. in Proceedings of Optical Fibre Measurement Conference (2nd), Torino, Italy, September 21-22, 1993, p159-162.

Keywords: *Optical fibers, *Delay lines, Optical measurement, Transit time, Interferometry, Calibration, Reprints, Optical time domain reflectometry, Group delay.

We describe a low-coherence interferometric method for measuring the transit time in optical fiber delay lines as long as 1.5 km. Group delays in 100 m standard reference fibers can be determined with an expanded uncertainty of about 4 ps (1 mm) and a resolution of 0.15 ps (0.03 mm). The principal limitations of this approach are identified and discussed.

02,159
PB95-168498 Not available NTIS
National Inst. of Standards and Technology (EEEL), Boulder, CO. Electromagnetic Technology Div.
Magneto-Optic Magnetic Field Sensors Based on Uniaxial Iron Garnet Films in Optical Waveguide Geometry.
Final rept.
M. N. Deeter, G. W. Day, R. Wolfe, and V. J. Fratello. 1993, 3p.
Pub. in Institute of Electrical and Electronics Engineers Transactions on Magnetics 29, n6 p3402-3404 Nov 93.

Keywords: *Ferrite garnets, Ferrimagnetic resonance, Magnetic hysteresis, Magnetic anisotropy, Magnetic films, Yttrium iron garnets, Domain walls, Optical waveguides, Faraday effect, Magnetooptics, Reprints, *Magnetic field sensors, Uniaxial anisotropy, Garnet films.

Iron garnet films which exhibit perpendicular uniaxial magnetic anisotropy are promising materials for magneto-optic magnetic field sensing. In an optical waveguide geometry, these materials exhibit large values of saturation Faraday rotation which in turn produce high sensitivity. The domain structure of these films favors magnetization rotation as the primary magnetization process. This process is significantly faster than domain wall motion, which is the primary magnetization process in bulk iron garnet crystals. We present data which confirm the high sensitivity and wideband frequency response to these materials. One film exhibits a virtually flat frequency response from dc to at least 1 GHz. Potential problems with waveguide sensors, such as birefringence and optical coupling efficiency appear to be soluble.

02,160
PB95-168647 Not available NTIS
National Inst. of Standards and Technology (EEEL), Boulder, CO. Electromagnetic Technology Div.
Terahertz Detectors Based on Superconducting Kinetic Inductance.
Final rept.
E. N. Grossman, D. G. McDonald, and J. E. Sauvageau. 1991, 16p.
Pub. in Proceedings of International Symposium on Space Terahertz Technology, Pasadena, CA., February 1991, p407-422.

Keywords: *Infrared radiometers, *Infrared detectors, *Bolometers, *Superconducting devices, Optical heterodyning, Antenna couplers, Far infrared radiation, Reprints, *Heterodyne mixers, SIS(Superconductors), Mixers(Optics), Kinetic inductance, Photoinductive detectors.

The inductance of a superconducting stripline varies with the concentration of Cooper pairs in the superconductor. This inductance variation may be used as the basis for highly sensitive radiometers, bolometers, and heterodyne mixers. We describe recent progress on three kinetic inductance devices: a large-area, absolute radiometer intended for use in the NIST Low-Background Infrared Calibration Facility, and small, antenna-coupled devices used either in a bolometric mode as direct detectors, or in a non-equilibrium, 'photoinductive' mode as heterodyne mixtures. The photoinductive mixers of a particular interest because their frequency coverage starts at approximately the energy gap, 2Delta, and extends upward. The impedance matching concerns which make extension of SIS mixers to high frequencies so difficult in practice are greatly relaxed for photoinductors because they lack the large parasitic capacitances inherent in a junction-like geometry.

02,161
PB95-168662 Not available NTIS
National Inst. of Standards and Technology (EEEL), Boulder, CO. Electromagnetic Technology Div.
Optical Performance of Photoinductive Mixers at Terahertz Frequencies.
Final rept.
E. N. Grossman, J. E. Sauvageau, and D. G. McDonald. 1993, 17p.
Pub. in Proceedings of International Symposium on Space Terahertz Technology (4th), Los Angeles, CA., February 1993, p588-604.

Keywords: *Infrared detectors, *Bolometers, *Superconducting devices, Superconducting films, Far infrared radiation, Temperature dependence, Electrical properties, Optical properties, SQUID devices, Niobium, Reprints, Kinetic inductance, Photoinductive detectors, Heterodyne mixers, Mixers(Optics).

We have investigated the electrical and optical properties of detectors based on the change in kinetic inductance of a superconducting film with incident terahertz-frequency radiation. Two different geometric configurations, stripline and slotline, of these photoinductive detectors have been explored. Both include a loop of thin niobium coupled to the incident radiation through a lithographic antenna; the loop inductance is read out via an integrated D.C. SQUID. The slotline geometry is substantially simpler to fabricate, but electrically, the two geometries have very similar properties. The loop inductance varies with temperature in good agreement with the 2-fluid model, while the critical current varies with temperature in agreement with Ginzburg-Landau theory.

02,162
PB95-168845 Not available NTIS
National Inst. of Standards and Technology (EEEL), Boulder, CO. Electromagnetic Technology Div.
Spatial Uniformity of Optical Detector Responsivity.
Final rept.
D. Livigni, and X. Li. 1994, 16p.
Pub. in Proceedings of National Computer Systems Laboratory Workshop and Symposium: The Role of Metrology in a Changing World, Chicago, IL., July 31-August 4, 1994, p337-352.

Keywords: *Optical detectors, *Infrared detectors, Optical measurement, Indium gallium arsenides, Spatial dependencies, Laser radiation, Coherent radiation, Ge semiconductor detectors, Si semiconductor detectors, Germanium, Silicon, Variability, Accuracy, Reprints.

A scanning system for measuring the spatial uniformity of the responsivity of optical detectors and methods of quantifying the degree of uniformity are described. Surface plots and contour maps of the measured responsivity are presented, along with a statistical treatment. Factors which can affect the accuracy of the uniformity measurement are described, including sampling theorem restrictions and interference artifacts produced when coherent light is used. Examples of these artifacts are presented, along with scans of actual Si, Ge, and InGaAs detectors.

02,163
PB95-168985 Not available NTIS
National Inst. of Standards and Technology (EEEL), Boulder, CO. Electromagnetic Technology Div.
Ultrasensitive-Hot-Electron Microbolometer.
Final rept.
M. Nahum, and J. M. Martinis. 1993, 3p.
Pub. in Applied Physics Letters 63, n22 p3075-3077, 29 Nov 93.

Keywords: *Infrared detectors, *Bolometers, *Superconducting devices, Submillimeter waves, Millimeter waves, Far infrared radiation, Electron-phonon coupling, Superconducting junctions, Tunnel junctions, Hot electrons, Reprints, *Microbolometers, Millikelvin temperature.

We present measurements on a novel power detector which can be used as an ultrasensitive detector of millimeter and submillimeter radiation. The absorbing element consists of a thin film resistor strip which is connected to superconducting electrodes. This device exploits the Andreev reflection of electrons and the weak electron-phonon coupling at low temperatures to produce a large temperature rise for a small input power (approx = 10 mK/fW). The temperature rise of the electrons is detected by a tunnel junction where part of the metal strip forms the normal electrode. We have measured a voltage responsivity of approximately 10(exp 9) V/W and an amplifier-limited electrical noise equivalent approx = 3 X 10(exp -18) W/sq root of Hz at an operating temperature of 100 mK. If infrared radiation were efficiently coupled to the absorbing element with an antenna or a waveguide, then the sensitivity of this detector would be at least a factor of 10 better than the best available direct detector operating at the same temperature.

02,164
PB95-169066 Not available NTIS
National Inst. of Standards and Technology (EEEL), Boulder, CO. Electromagnetic Technology Div.
Electrically Calibrated Pyroelectric Detector-Refinements for Improved Optical Power Measurements.
Final rept.
R. J. Phelan, J. H. Lehman, and D. R. Larson. 1993, 5p.
Pub. in Proceedings of Society of Photo-Optical Instrumentation Engineers: Photodetectors and Power Meters, San Diego, CA., July 15-16, 1993, v2022 p160-164.

Keywords: *Pyroelectric detectors, *Photodetectors, *Optical measurement, Power measurement, Variability, Accuracy, Reprints, *Optical power.

This paper describes the present efforts at NIST to improve the accuracy of the electrically calibrated pyroelectric detector for measuring optical power by an order of magnitude. The principal limitation, the uniformity of the responsivity over the receiving aperature, has been significantly improved.

02,165
PB95-169116 Not available NTIS
National Inst. of Standards and Technology (EEEL), Boulder, CO. Electromagnetic Technology Div.
Kinetic-Inductance Infrared Detector Based on an Antenna-Coupled High-Tc SQUID.
Final rept.
J. P. Rice. 1993, 2p.
Pub. in Proceedings of International Superconductive Electronics Conference (4th), Boulder, CO., August 11-14, 1993, p382-383.

Keywords: *Infrared detectors, *SQUID devices, Superconducting devices, High-Tc Superconductors, Antenna couplers, Performance, Design, Reprints, Kinetic inductance.

We describe the design and estimate the performance of a high-T(c) kinetic-inductance infrared detector.

02,166
PB95-169124 Not available NTIS
National Inst. of Standards and Technology (EEEL), Boulder, CO. Electromagnetic Technology Div.
High-Tc Superconducting Antenna-Coupled Microbolometer on Silicon.
Final rept.
J. P. Rice, Grossman, L. J. Borcherdt, and D. A. Rudman. 1994, 12p.
Pub. in Society of Photo-Optical Instrumentation Engineers 2159, p98-109 1994.

Keywords: *Bolometers, High temperature superconductors, Superconducting devices, Yttrium oxides, Zirconium oxides, YBCO superconductors, Silicon, Epitaxial growth, Micromachining, Fabrication, Substrates, Reprints, *Microbolometers, Yttrium barium cuprates.

A process is described for fabricating antenna-coupled resistive-edge microbolometers based on the high T(c) superconductor YBa2Cu3O7 (YBCO) on silicon. The YBCO and a buffer layer of yttria-stabilized zirconia (YSZ) were grown epitaxially on silicon to minimize excess electrical noise. A silicon-micromachined YBCO/YSZ air-bridge was incorporated to minimize the thermal conductance and the heat capacity. The thermal conductance of the air-bridge was measured to be 3 X 10(exp -6) W/K at a temperature of 100 K. At an operating temperature of 89 K, the detector is estimated to have a response time of 2 microseconds, a responsivity in the 1000 V/W range, and a noise-equivalent power (NEP) in the 10(exp -12) W/Hz(sup 1/2) range at 1000 Hz.

02,167
PB95-169132 Not available NTIS
National Inst. of Standards and Technology (EEEL), Boulder, CO. Electromagnetic Technology Div.
Effect of Semiconductor Laser Characteristics on Optical Fiber Sensor Performance.
Final rept.
K. B. Rochford, A. H. Rose, I. Clarke, and G. W. Day. 1994, 11p.
Pub. in Proceedings of Society of Photo-Optical Instrumentation Engineers: Laser Diode Technology and Applications VI, Los Angeles, CA., January 25-27, 1994, v2148 p269-279.

Keywords: *Semiconductor lasers, Frequency stability, Noise spectra, Error analysis, Calibration, Performance, Reprints, *Optical fiber sensors, *Fiber optic sensors.

Optical sensor systems have source requirements that can be significantly different from those of optical com-

munications and other technologies that have generally driven the development of semiconductor sources. In this paper, we examine basic interferometric, polarimetric, and other sensors. Relevant semiconductor source data is reviewed to illustrate the impact of source characteristics on sensor performance. The effect of low-frequency amplitude and frequency noise on sensor precision is described. Errors in sensor calibration due to amplitude and wavelength drifts are discussed. Examples of sensor performance using typical source data illustrate these issues.

02,168
PB95-169140 Not available NTIS
National Inst. of Standards and Technology (EEEL), Boulder, CO. Electromagnetic Technology Div.
Terahertz Shapiro Steps in High Temperature SNS Josephson Junctions.
Final rept.
P. A. Rosenthal, and E. N. Grossman. 1994, 8p.
Sponsored by National Aeronautics and Space Administration, Washington, DC.
Pub. in Institute of Electrical and Electronics Engineers Transactions on Microwave Theory and Techniques 42, n4 p707-714 Apr 94.

Keywords: *Josephson junctions, Far infrared radiation, High temperature superconductors, Temperature dependence, Laser radiation, Infrared lasers, Reprints, *Shapiro steps, Microfabrication, Microbridges, Josephson oscillators.

We have studied the far infrared behavior of high-T(c) superconductor-normal metal-superconductor (SNS) microbridges with T(c) > 85 K and critical current-resistance products (I(c)R(N)) as high as 10 mV at 4K. These are the highest I(c)R(N) products reported to date for microfabricated Josephson junctions of any material. The junctions were integrated at the feeds of planar log-periodic antennas made from Au thin films. The junctions had dc normal state resistances R(N) between 6 and 38 ohms, reasonably well matched to the antenna's estimated RF impedance of 53 ohms. Far infrared laser radiation at 404, 760, and 992 GHz induced distinct Shapiro steps (i.e. constant voltage steps at voltages n(hf/2e), n = 1, 2, ...) in the current voltage characteristics as well as modulation of the critical current. Steps were observed at voltages up to 17 mV and 6 mV, at temperatures of 9 K and 57 K, respectively. This corresponds to maximum Josephson oscillation frequencies of 8 and 3 THz at these temperatures.

02,169
PB95-169173 Not available NTIS
National Inst. of Standards and Technology (EEEL), Boulder, CO. Electromagnetic Technology Div.
Comparative Photoluminescence Measurement and Simulation of Vertical-Cavity Semiconductor Laser Structures.
Final rept.
D. T. Schaafsma, D. H. Christensen, R. K. Hickernell, and J. G. Pellegrino. 1994, 6p.
Pub. in Materials Research Society Symposia Proceedings, v326 p483-488 1994.

Keywords: *Quantum well lasers, *Surface emitting lasers, *Photoluminescence, Optical measurement, Dielectric properties, Epitaxy, Simulation, Comparison, Reprints, Distributed systems.

We present comparisons of photoluminescence (PL) data for various vertical-cavity surface-emitting laser (VCSEL) and distributed quantum well structures taken with the pump beam (and the collection path) in two different configurations: normal to the surface of the sample; and perpendicular to a cross-section of the epitaxial layers. We demonstrate that the cross-sectional PL (XPL) technique can resolve individual features in the structures, and that the surface-normal PL (NPL) spectra are perturbed by the multilayer mirrors in the VCSELs. We elucidate a potential method for transforming between the NPL spectra and the non-perturbed XPL spectra and evaluate the sensitivity of this method to various measurement as well as material parameters. This simulation technique is well-suited to wide parametric variations of the dispersion curves for the complex dielectric constant of the materials, the pump field distribution, and the depth profile of the gain medium.

02,170
PB95-169181 Not available NTIS
National Inst. of Standards and Technology (EEEL), Boulder, CO. Electromagnetic Technology Div.
Measurement and Simulation of Photoluminescence Spectra from Vertical-Cavity Quantum-Well Laser Structures.
Final rept.
D. T. Schaafsma, R. K. Hickernell, and D. H. Christensen. 1994, 11p.
Pub. in Proceedings of Society of Photo-Optical Instrumentation Engineers: Quantum Well and Superlattice Physics V, Los Angeles, CA., January 24-25, 1994, v2139 p92-102.

Keywords: *Quantum well lasers, *Surface emitting lasers, *Photoluminescence, Optical measurement, Dielectric properties, Spatial resolution, Quantum electrodynamics, Superlattices, Simulation, Epitaxy, Reprints, Distributed systems, Multilayers.

We compare photoluminescence data collected in either a surface-normal configuration (NPL) or with the pump and collection paths perpendicular to a cross-section of the epitaxial layers (XPL) for various vertical-cavity surface-emitting lasers and distributed quantum well structures. We report the spatial resolution of the XPL technique, particularly as it applies to distinguishing features in complex multilayer structures. We assess a potential simulation method for transforming the perturbed NPL spectra into the unperturbed XPL spectra, taking into account a number of experimental and material parameters which may influence the lineshape. These factors include the pump field distribution and its influence on the weighting of the emitters, the collection optics, and the changes in the dispersive complex dielectric constant of the quantum wells. This information is of import not only to optimizing device manufacture, but to basic physical and materials research as well. Thereas the XPL technique is a relatively simple but destructive characterization tool, a complete understanding of NPL emission could be made to yield the same information via rapid, non-destructive means.

02,171
PB95-169264 Not available NTIS
National Inst. of Standards and Technology (EEEL), Boulder, CO. Electromagnetic Technology Div.
Waveguide Polarizers Processed by Localized Plasma Etching.
Final rept.
D. L. Veasey, D. R. Larson, and I. Veigl. 1994, 3p.
Pub. in Applied Optics 33, n7 p1242-1244, 1 Mar 94.

Keywords: *Optical waveguides, *Plasma etching, *Polarizers, Chemical vapor deposition, Polarization(Waves), Amorphous silicon, Silicon films, Reprints, *Waveguide polarizers, In situ monitoring, Claddings.

We develop a downstream localized plasma-etching process that permits in situ monitoring of light throughput in a semiconductor-clad channel waveguide as the semiconductor thickness is trimmed. Hydrogenated amorphous silicon films are deposited on ion-exchanged channel waveguides by plasma-enhanced chemical vapor deposition. We then employ the localized plasma-etching process to maximize accurately the extinction ratio between TE and TM polarizations propagating in the clad waveguide. We achieve polarization extinction ratios of greater than 30 dB for both TE-pass and TM-pass polarizers.

02,172
PB95-169298 Not available NTIS
National Inst. of Standards and Technology (EEEL), Boulder, CO. Electromagnetic Technology Div.
Self-Calibrating Fiber Optic Sensors: Potential Design Methods.
Final rept.
H. K. Whitesel, G. W. Day, A. H. Rose, and C. A. Miller. 1993, 42p.
Pub. in Naval Surface Warfare Center Technical Report CARDIVNSWC-TR-80-92/15, 42p May 93.

Keywords: *Self tests, *Calibration, Self repairing devices, Redundant components, Temperature sensors, Military applications, Naval equipment, Reprints, *Optical fiber sensors, *Fiber optic sensors, *Self calibration.

Potential applications of optical fiber sensors in the Navy and elsewhere involve networks of hundreds of thousands of sensors. Routine maintenance and calibration of these sensor networks, if undertaken manually, would involve unacceptable commitments of ship personnel and time. This has led to the present investigation into methods that can be used to produce sensor systems that can be self testing and/or self calibrating. A self testing sensor is one in which one or more internal tests are used to verify the performance of the sensor. Self calibration extends the self testing concept to the point where when defects are identified, calibration corrections can be made automatically. Three design concepts can be considered for optical fiber sensors: substitution, redundancy, and internal diagnostics. Examples of how diagnostics of these types can be used to test and recalibrate various types of sensors are described in this report; a more detailed study of potential designs for a self calibration polarimetric temperature sensor is also included.

02,173
PB95-169306 Not available NTIS
National Inst. of Standards and Technology (EEEL), Boulder, CO. Electromagnetic Technology Div.
Self Calibrating Fiber Optic Sensors: Potential Design Methods.
Final rept.
H. K. Whitesel, C. A. Miller, G. W. Day, A. H. Rose, and W. F. Hamann. 1993, 18p.
Pub. in Proceedings of International Symposium on Spectral Sensing Research, Maui, HI., November 15-20, 1992, v1 p324-341 1993.

Keywords: *Self tests, *Calibration, Self repairing devices, Redundant components, Military applications, Naval equipment, Reprints, *Optical fiber sensors, *Fiber optic sensors, *Self calibration.

Potential applications of optical fiber sensor networks in the Navy include environmental and equipment monitoring and control. Such systems may involve hundreds if not thousands of sensors. Conventional methods of performing routine maintenance and calibration would require unacceptable amounts of manpower and time. This has led to the present investigation into methods that can be utilized to produce sensor systems that can be self-testing and/or self-calibrating. A self testing sensor is one in which internal tests are used to verify the performance of the sensor. Self calibration extends the self testing concept to a point where, when changes in system operational characteristics are measured, calibration corrections can be made automatically. Three general design concepts were considered: substitution, redundancy, and internal diagnostics. Substitution involves applying a measurand of known value to the sensor in a manner similar to most laboratory calibrations. Redundancy involves using multiple sensors in such a way that the failure of a single sensor can be detected: Correct values are then attributed to sensors giving consistent results. Internal diagnostics can take many forms, but involves the use of various optical tests to insure the proper performance of the sensor.

02,174
PB95-175279 Not available NTIS
National Inst. of Standards and Technology (EEEL), Boulder, CO. Electromagnetic Technology Div.
Correlation of Optical, X-ray, and Electron Microscopy Measurements of Semiconductor Multilayer Structures.
Final rept.
D. H. Christensen, R. K. Hickernell, D. T. Schaafsma, J. R. Hill, R. S. Rai, J. G. Pellegrino, and M. J. McCollum. 1994, 12p.
Pub. in Proceedings of Society of Photo-Optical Instrumentation Engineers: Spectroscopic Characterization Techniques for Semiconductor Technology V, Los Angeles, CA., January 25-26, 1994, v2141 p177-188.

Keywords: *Semiconductor devices, Electron microscopy, Optical microscopy, X ray microscopy, Aluminum gallium arsenides, Photoluminescence, Refractive index, Quantum wells, Reflectance, Correlation, Simulation, Epitaxy, Reprints, Bragg mirrors, Multilayers.

Techniques based on optical, X-ray, and electron microscopy measurements are applied to characterize a wide variety of semiconductor multilayer structures. Bragg mirrors serve as valuable test structures for evaluating the epitaxial uniformity of crystal growth systems. Careful characterization of half-wave spaced single quantum wells provides a method for determining their complex refractive indices using reflectance spectroscopy. Comparison of cross-sectional microphotoluminescence to surface-normal photoluminescence, combined with these characterization techniques, allows studies of spontaneous emission in microcavities and elucidates the difficulties with using surface-normal photoluminescence to determine the alloy composition of the mirror layers. The application of these characterization methods to visible-wavelength AlGaAs mirrors, 485-720nm, enables the

development of these mirrors for uses such as optically tailored substrates and visible surface-emitter or detector arrays.

02,175
PB95-175592 Not available NTIS
National Inst. of Standards and Technology (EEEL), Boulder, CO. Electromagnetic Technology Div.
Photodetector Frequency Response Measurements at NIST, US, and NPL, UK: Preliminary Results of a Standards Laboratory Comparison.
Final rept.
P. D. Hale, D. A. Humphreys, and A. Gifford. 1994, 12p.
Pub. in Proceedings of Society of Photo-Optical Instrumentation Engineers: Technologies for Optical Fiber Communications, Los Angeles, CA., January 25, 1994, v2149 p345-356.

Keywords: *Photodiodes, *Photodetectors, *Frequency response, Near infrared radiation, Frequency measurement, Interlaboratory comparisons, Infrared detectors, Heterodyning, Neodymium lasers, YAG lasers, Reprints, Mach-Zehnder modulators, Intercomparison.

We report the first comparison of high speed photodiode frequency response measurements up to 40 GHz between NIST and NPL in the 1.3 and 1.5 micrometer wavelength regions. This comparison is an important step in establishing international agreement on photodiode response measurements, with traceability to international microwave power and DC current standards. Measurements at NIST used a Nd:YAG heterodyne system. NPL used DFB heterodyne and integrated-optical modulator-based techniques. Measurements of a photodiode with nominally 20 GHz optical bandwidth show good agreement with average scatter of + or - 0.15 dB (2 sigma) below 20 GHz, and + or - 0.30 dB from 20 to 33 GHz. The results diverge systematically above 33 GHz, due to calibration of the RF power sensors. Scatter in the data is well represented by the combined uncertainties of the measurement systems up to 33 GHz.

02,176
PB95-175642 Not available NTIS
National Inst. of Standards and Technology (EEEL), Boulder, CO. Electromagnetic Technology Div.
Determination of the Complex Refractive Index of Individual Quantum Wells from Distributed Reflectance.
Final rept.
R. K. Hickernell, D. H. Christensen, J. G. Pellegrino, J. Wang, and J. P. Leburton. 1994, 4p.
Pub. in Applied Physics Letters 75, n6 p3056-3059, 15 Mar 94.

Keywords: *Quantum wells, *Refractive index, Aluminum gallium arsenides, Optical measurement, Reflectance, Absorption, Reprints, Bragg reflectors, Distributed systems.

We investigate the measurement of the complex refractive index of individual quantum wells by reflectance spectroscopy. Placing the wells at half-wavelength spacing to cause resonant feedback produces an order-of-magnitude increase in measurement sensitivity over that of nonresonant structures. Quantum well dispersive and absorptive effects on reflectance can be differentiated in certain spectral regions. Experimental data confirm a theoretical model of refractive index and absorption for quantum wells of GaAs in Al(0.2)Ga(0.8)As in the region of the well band gap.

02,177
PB95-175782 Not available NTIS
National Inst. of Standards and Technology (EEEL), Gaithersburg, MD. Semiconductor Electronics Div.
Electrical Characterization of Liquid-Phase Epitaxially Grown Single-Crystal Films of Mercury Cadmium Telluride by Variable-Magnetic-Field Hall Measurements.
Final rept.
J. S. Kim, D. G. Seiler, L. Colombo, and M. C. Chen. 1994, 10p.
Pub. in Semiconductor Science and Technology 9, p1696-1705 1994.

Keywords: *Mercury cadmium tellurides, Liquid phase epitaxy, Temperature dependence, Semiconducting films, Infrared detectors, Magnetic fields, Single crystals, Hall effect, Magnetoresistivity, Classification, Reprints.

We report a method for a new classification procedure for liquid-phase epitaxially grown mercury cadmium telluride single crystals. Variable-magnetic-field hall measurements are performed on nine liquid-phase epitaxially grown Hg(0.78)Cd(0.22)Te single-crystal films for magnetic fields from 0 to 1.4 T and in the temperature range from 10 K to 300 K. The data from these measurements are analyzed in the context of the reduced-conductivity-tensor scheme proposed by Kim and co-workers. Based on the degree of deviation from an ideal one-carrier behavior, these experimental samples are classified into several types to emphasize the transition in the behavior of the normal to anomalous n-type samples, finally leading to p-type samples. Our classification is also based on a general trend in the temperature dependence of the mobility and density of the majority carriers, which were extracted from the magnetoresistivity data. The classification provides a useful benchmark for materials characterization in the infrared detector industry.

02,178
PB95-202826 Not available NTIS
National Inst. of Standards and Technology (PL), Boulder, CO. Quantum Physics Div.
Low-Noise High-Speed Diode Laser Current Controller.
Final rept.
K. G. Libbrecht, and J. L. Hall. 1993, 3p.
Contract N00014-89-J-1227, Grant NSF-PHY90-12244
Sponsored by Office of Naval Research, Arlington, VA., Air Force Office of Scientific Research, Bolling AFB, DC. and National Science Foundation, Washington, DC.
Pub. in Review of Scientific Instruments 64, n8 p2133-2135 Aug 93.

Keywords: *Semiconductor lasers, Current regulations, Direct current, High speed, Low noise, Reprints, *Current controllers.

We describe a new diode laser current controller which features low current noise, excellent dc stability, and the capacity for high-speed modulation. While it is simple and inexpensive to construct, the controller compares favorably with the best presently available commercial diode laser current controllers.

02,179
PB95-202909 Not available NTIS
National Inst. of Standards and Technology (EEEL), Boulder, CO. Electromagnetic Technology Div.
Integrated-Optical Devices in Rare-Earth-Doped Glass.
Final rept.
K. J. Malone. 1994, 25p.
Pub. in Proceedings of Society of Photo-Optical Instrumentation Engineers: Glass Integrated Optics and Optical Fiber Devices, San Diego, CA., July 24-25, 1994, vCR53 p132-156.

Keywords: *Optoelectronic devices, *Integrated optics, Solid state lasers, Optical waveguides, Neodymium, Erbium additions, Doped materials, Fabrication, Glass, Reviews, Reprints.

A short overview is given of integrated-optical devices in rare-earth-doped glasses. Achievements in device performance are discussed. Fabrication of these components as well as analytical and diagnostic techniques that can improve performance are considered. The article concludes with a discussion of some current topics in this field.

02,180
PB95-203154 Not available NTIS
National Inst. of Standards and Technology (EEEL), Boulder, CO. Electromagnetic Technology Div.
Faraday Effect Current Sensor with Improved Sensitivity-Bandwidth Product.
Final rept.
K. B. Rochford, A. H. Rose, M. N. Deeter, and G. W. Day. 1994, 3p.
Contract DNA-IACRO-93-806
See also PB94-200698. Sponsored by Defense Nuclear Agency, Washington, DC.
Pub. in Optics Letters 19, n22 p1903-1905, 15 Nov 94.

Keywords: Yttrium iron garnets, Faraday effect, Sensitivity, Bandwidth, Design, Reprints, *Electric current sensors.

We report a new design for a Faraday effect current sensor based on yttrium iron garnet that has substantially greater bandwidth than previous designs and is much easier to fabricate. The measured sensitivity is 0.7 deg/A, with a -3-dB bandwidth of 500 MHz, which gives an improvement in sensitivity-bandwidth product of approximately 45. A noise-equivalent current of 840 nA/Hz(sup 1/2) was measured at 1.8 kHz by difference-over-sum processing. The use of turning prisms with phase-preserving coatings greatly simplifies construction, improves electrical isolation, and increases sensitivity through proximity effects.

02,181
PB95-203576 Not available NTIS
National Inst. of Standards and Technology (EEEL), Boulder, CO. Electromagnetic Technology Div.
Accurate Measurement of Optical Detector Nonlinearity.
Final rept.
S. Yang, I. Vayshenker, X. Li, and T. R. Scott. 1994, 10p.
Pub. in Proceedings of National Computer Systems Laboratory Workshop and Symposium 'Role of Metrology in a Changing World', Chicago, IL., July 31-August 4, 1994, p353-362.

Keywords: *Optical detectors, Optical measurement, Comparative evaluations, Computerized simulation, Nonlinearity, Accuracy, Reprints.

In this paper we describe the results of our efforts to analyze and compare by computer simulation three common methods of measuring detector nonlinearity: (1) superposition method, (2) attenuation method, and (3) differential or ac-dc method. We describe a definition and expressions which we used to intercompare the data analyses of these methods. Issues that are common to these methods or specific to one individual method and have an impact on the measurement accuracy were studied. We conclude that superposition and differential methods are better choices than the attenuation method. Suggestions about the choice of polynomial order of the fitting curve with regard to the data accuracy and detector nonlinearity are also given.

02,182
PB95-261921 (Order as PB95-261897, PC A07/MF A02)
National Inst. of Standards and Technology, Gaithersburg, MD.
Determination of the Transmittance Uniformity of Optical Filter Standard Reference Materials.
J. C. Travis, N. K. Winchester, and M. V. Smith. 1995, 16p.
Included in Jnl. of Research of the National Institute of Standards and Technology, v100 n3 p241-256 May/Jun 95.

Keywords: *Optical filters, *Calibration standards, *Transmittance, Spectrophotometry, Homogeneity, Certification, Charge coupled devices, Cameras, National Institute of Standards and Technology.

An instrument based on a scientific grade charge-coupled device (CCD) camera system is performance-qualified to evaluate the transmittance homogeneity of solid optical filter standard reference materials. Measurement results are presented for the new instrument, and compared, where appropriate, with an older, scanning instrument, for a variety of filters spanning transmittances down to 0.01. The new instrument is found to give comparable results with the older instrument, with reduced random uncertainty and improved information content.

02,183
PB96-102793 Not available NTIS
National Inst. of Standards and Technology (EEEL), Gaithersburg, MD. Semiconductor Electronics Div.
Scaling of the Nonlinear Optical Cross Sections of GaAs-AlGaAs Multiple Quantum-Well Hetero n-i-p-i's.
Final rept.
D. S. McCallum, A. N. Cartwright, A. L. Smirl, J. Comas, W. F. Tseng, and J. G. Pellegrino. 1994, 8p.
Pub. in Institute of Electrical and Electronics Engineers Jnl. of Quantum Electronics, v30 n12 p2790-2797 Dec 94.

Keywords: *Absorption cross sections, *Nonlinear optics, *Quantum wells, *Heterojunctions, Gallium arsenides, Aluminum gallium arsenides, Carrier density(Solid state), Semiconducters(Materials), Reprints.

The authors study the dependence of the Stark shift optical nonlinearity of GaAs-AlGaAs multiple quantum-well hetero n-i-p-i's on the number of quantum wells per intrinsic region in otherwise identical hetero n-i-p-i's. The authors determine that sigma (sub eh), the

nonlinear absorption cross section, is proportional to the number of quantum wells per intrinsic region. A study of the fluence dependence of sigma(sub eh) shows that the saturation carrier density is inversely proportional to the number of wells per intrinsic region. The authors find that the turn-on time of the nonlinear abosrption change in their samples is independent of the number of quantum wells per intrinsic region. All of these results are consistent with the absence of retrapping of photogenerated carriers.

02,184
PB96-111729 Not available NTIS
National Inst. of Standards and Technology (EEEL), Boulder, CO. Electromagnetic Technology Div.
Niobium Microbolometers for Far-Infrared Detection.
Final rept.
M. E. MacDonald, and E. N. Grossman. 1995, 4p.
Pub. in Institute of Electrical and Electronics Engineers Transactions on Microwave Theory and Techniques, v43 n4 p893-896 Apr 95.

Keywords: *Bolometers, *Far infrared radiation, *Niobium, Thin films, Temperature measurement, Room temperature, Bias, Noise, Detectors, Reprints, *Microbolometer.

Microbolometers have been fabricated using a thin niobium film as the detector element. These detectors operate at room temperature, are impedance matched to planar antennas, and are suitable for broadband use at far-infrared wavelengths. The authors have achieved responsitivities of up to 21 V/W at a bias of 6.4 mA, and electrical noise equivalent powers (NEP) of as low as 1.1 x 10(exp -10)W/(square root of H2) at 1 kHz at a bias of 3.6 mA. At this bias, the detectors are 1/f-noise limited below 1 kHz and are Johnson noise limited above 10 kHz. The 1/f noise in nV/(square root of Hz) increases approximately linearly with bias with a typical level of 0.39 I(MA)/(square root of f(kHz)). This level of 1/f noise is approximately a factor of 7 below the best reported for bismuth microbolometers.

02,185
PB96-111935 Not available NTIS
National Inst. of Standards and Technology (EEEL), Gaithersburg, MD. Electronics and Electrical Engineering Lab. Office.
Can Displays Deliver a Full Measure: Manufacturing.
Final rept.
H. S. Bennett, C. Fenimore, B. F. Field, and E. F. Kelley. 1994, 2p.
Pub. in Proceedings of the Annual Display Manufacturing Technology Conference (1st) 'Digest of Technical Papers', San Francisco, CA., January 11-13, 1994, p45-46.

Keywords: *Display devices, *Manufacturing, *Design criteria, *Standardization, High resolution, Research and development, Technology transfer, Standards, Measurement, Computation, Research programs, Reprints.

The National Institute of Standards and Technology (NIST) recently initiated a new program on measurements for displays. As part of this new program, NIST completed a preliminary assessment of the needs for measurements, standards, and computations to assist in the development of high-resolution displays. In this paper, we summarize the major results of this assessment and describe briefly NIST's ongoing intramural and extramural programs on displays.

02,186
PB96-119227 Not available NTIS
National Inst. of Standards and Technology (EEEL), Gaithersburg, MD. Electricity Div.
Display-Measurement Round-Robin.
Final rept.
D. J. Bechis, M. D. Grote, D. P. Bortfeld, E. F. Kelley, G. R. Jones, P. A. Boynton, L. H. Hammer, and M. J. Polak. 1995, 4p.
Pub. in Society for Information Display, International Symposium, Digest of Technical Papers, Orlando, FL., May 23-25, 1995, v26 p641-644, 15 May 95.

Keywords: *Cathode ray tube screens, *Display devices, Electronic equipment, Test and evaluation, Visual perception, Man-computer interface, Graphics, Performance evaluation, Standards, Procedures, Specifications, Reporting, Reprints, *Performance measurement.

Display measurement procedures intended for use by other laboratories and by industry for measuring, analyzing, and reporting the performance of display monitors are tested through the round-robin process in preparation for acceptance of the procedures as a standard. The National Information Display Laboratory (NIDL) and National Institute of Standards and Technololgy (NIST) results presented here show much quantitative agreement in support of the measurement procedures.

02,187
PB96-119276 Not available NTIS
National Inst. of Standards and Technology (EEEL), Boulder, CO. Optoelectronics Div.
Polarization Insensitive 3x3 Sagnac Current Sensor Using Polarizing Spun High-Birefringence Fiber.
Final rept.
I. G. Clarke, K. B. Rochford, A. H. Rose, and G. W. Day. 1994, 4p.
Pub. in International Conference on Optical Fibre Sensors (10th), Glasgow, Scotland, UK, October 11-13, 1994, Postdeadline paper, v2360 4p.

Keywords: *Electric current, *Sensors, *Birefringence, *Optical fibers, Fiber optics, Polarization(Waves), Response functions, Sensitivity analysis, Reprints, *Sagnac current sensor, Optical fiber sensor, Polarization dependence.

The response functions of previously reported 3x3 Sagnac current sensors are strongly dependent on input polarization, so systems require careful control of the input polarization state. In this paper, the authors describe a simple method for eliminating this polarization dependence so that stable response functions are obtained. The authors demonstrate the existence of a wavelength range over which spun high-birefringence fiber guides only one elliptically polarized mode, thus preserving a single polarization state. Using this effect, the authors show that 3x3 Sagnac current sensor response functions can exhibit current sensing without the need for polarization control.

02,188
PB96-122528 Not available NTIS
National Inst. of Standards and Technology (EEEL), Gaithersburg, MD. Electricity Div.
Survey of the Components of Display-Measurement Standards.
Final rept.
E. F. Kelley, G. R. Jones, P. A. Boynton, M. D. Grote, and D. J. Bechis. 1995, 4p.
Pub. in Society for Information Display International Symposium, Digest of Technical Papers, Orlando, FL., May 23-25, 1995, p637-640.

Keywords: *Display devices, *Standards, *Measurement, Cathod ray tubes, Liquid crystal display systems, Reprints, *Flat panel displays.

Several display standards are reviewed and distinctive elements are compared. With flat panel displays becoming more common and the CRT displays being so well established, the associated standards activities can be somewhat bewildering, even overwhelming. This paper attempts to identify complementary and inconsistent elements of related display standards.

02,189
PB96-122684 Not available NTIS
National Inst. of Standards and Technology (EEEL), Boulder, CO. Electromagnetic Technology Div.
Polarization Dependence of Response Functions in 3x3 Sagnac Optical Fiber Current Sensors.
Final rept.
K. B. Rochford, G. W. Day, and P. R. Forman. 1994, 6p.
See also PB95-162426.
Pub. in Jnl. of Lightwave Technology, v12 n8 p1504-1509 Aug 94.

Keywords: *Fiber optics, *Sagnac effect, *Functions(Mathematics), Interferometers, Birefringence, Electric current, Polarization(Waves), Phase shift, Optical coupling, Reprints, *Electric current sensors, *Optical fiber sensors, Sagnac interferometer.

We show theoretically that the response functions of a lossless Sagnac optical fiber current sensor based on a 3 x 3 coupler fundamentally depend on the polarization state of light entering the coupler, even for systems with no linear birefringence. Thus, 3 x 3 Sagnac systems offer no advantage over 2 x 2 systems for linearly polarized input light. The predicted polarization dependence of 3 x 3 Sagnac response functions is experimentally confirmed. This result establishes the need for increased system complexity in 3 x 3 Sagnac current sensors since polarization control optics are required to provide the proper input polarization.

02,190
PB96-122700 Not available NTIS
National Inst. of Standards and Technology (EEEL), Boulder, CO. Electromagnetic Technology Div.
Millimeter-Resolution Optical Time-Domain Reflectometry Using a Four-Wave Mixing Sampling Gate.
Final rept.
J. B. Schlager, M. Jinno, and D. L. Franzen. 1995, 3p.
Pub. in Institute of Electrical and Electronics Engineers Photonics Technology Letters, v7 n2 p206-208 Feb 95.

Keywords: *Semiconductor devices, *Laser mode locking, *Light amplifiers, Optical coupling, Switches, Spatial resolution, Waves, Mixing, Reprints, *Optical sampling, Optical reflectometry, Wave mixing.

We report on optical time-domain reflectometer that employs an ultrafast optical switch based on nondegenerate four-wave mixing in a semiconductor laser amplifier. Two-point spatial resolution on the order of 1 mm over 2 m is demonstrated; Fresnel reflections with optical return losses greater than 53 dB are detected. Submillimeter-resoluton optical time-domain reflectometery over a 100-m range should be possible with modifications to the pulse sources.

02,191
PB96-123021 Not available NTIS
National Inst. of Standards and Technology (EEEL), Gaithersburg, MD. Electricity Div.
Nonlinear Color Transformations in Real Time Using a Video Supercomputer.
Final rept.
E. F. Kelley, B. F. Field, and C. Fenimore. 1993, 4p.
Pub. in Proceedings of the Society for Imaging Science and Technology/Society for Information Display Color Imaging Conference: Transforms and Transportability of Color, Scottsdale, AZ., November 7-11, 1993, p122-125.

Keywords: *Color coding, *Video compression, *Supercomputers, *Visual discrimination, Nonlinear systems, Flat panel displays, Display devices, Colors, Electroluminescence, Video data, Image convertors, Computerized simulation, Reprints, Color image processing.

Investigations of the effects of color transformations used for video displays are often hampered by the inability to see the effects of these changes in real time for a variety of input signals. Using a video supercomputer, the Princeton Engine, the effects of a parametric nonlinear color transformation can be shown in real time.

02,192
PB96-123716 Not available NTIS
National Inst. of Standards and Technology (EEEL), Gaithersburg, MD. Electricity Div.
Refraction of Light by Graded Birefringent Media.
Final rept.
K. L. Stricklett, and C. Sununu. 1994, 5p.
Pub. in Conference of Electrical Insulation and Dielectric Phenomena, Pocono Manor, PA., October 17-20, 1993, Institute of Electrical and Electronics Engineers 1993 Annual Report, p444-448 1994.

Keywords: *Light refraction, *Birefringent media, Reprints, Kerr effect, Electric field mapping, Graded refractive index.

To date, proposals to use the Kerr effect to map divergent electric fields have not considered refraction of light in the graded potential. Spatial variation of the strength or direction of the field will produce non-uniform refractive indices, and significant refraction of light in regions of high divergence may disort the final image and introduce an error in the field measurement. Experimental evidence for this effect is presented and its implications to optical field mapping are discussed.

02,193
PB96-128210 PC A04/MF A01
National Inst. of Standards and Technology (EEEL), Boulder, CO. Optoelectronics Div.
Bibliography of the NIST Optoelectronics Division.
A. J. Smith, and L. S. Derr. Sep 95, 67p, NISTIR-5041.
See also PB96-128269.

Keywords: *Metrology, *Bibliographies, Optical communications, Optoelectronic devices, Optical fibers, Fiber optics, Electrooptics, Solid state lasers, US NIST.

The Optoelectronics Division was established in 1994 to provide the optoelectronics industry and its suppliers and customers with comprehensive and technically advanced measurement capabilities, standards, and traceability to those standards. The Division is organized into four groups: the Sources and Detectors Group, the Fiber and Integrated Optics Group, the Optical Components Group, and the Optoelectronic Manufacturing Group, with work in six project areas.

02,194
PB96-138490 Not available NTIS
National Inst. of Standards and Technology (EEEL), Gaithersburg, MD. Electricity Div.
Electro-Optic-Based RMS Voltage Measurement Technique.
Final rept.
N. G. Paulter. 1995, 8p.
Pub. in Review of Scientific Instruments, v66 n6 p3583-3690 Jun 95.

Keywords: *Electromagnetic fields, *Voltage measurement, Reprints, *Electro-optic crystals, *RMS voltage.

A new electro-optic-based technique for measuring the rms value of an applied voltage is presented. The technique incorporates a ratiometric method whereby the requirement for absolute laser power information is unnecessary. Description, analysis, and experimental results of the prototype measurement system are presented.

02,195
PB96-140363 Not available NTIS
National Inst. of Standards and Technology (EEEL), Boulder, CO. Electromagnetic Fields Div.
Radiometer Equation for Noise Comparison Radiometers.
Final rept.
D. F. Wait. 1995, 4p.
Pub. in Institute of Electrical and Electronics Engineers Transactions on Instrumentation and Measurement, v44 n2 p336-339 Apr 95.

Keywords: *Electromagnetic noise measurement, *Radiometers, *Calibrating, Accuracy, Error analysis, High temperature, Uncertainty, Reprints.

A complete radiometer equation is derived and used to develop better corrections and uncertainty estimates. We show that a corrected unisolated radiometer can have an accuracy similar to that of a well-isolated radiometer. The radiometer error is insignificant for radiometers with 40-dB isolation. However, for high-temperature applications (such as sources and standards above 3000 K), isolation is usually unnecessary.

02,196
PB96-156088 Not available NTIS
National Inst. of Standards and Technology (EEEL), Gaithersburg, MD. Semiconductor Electronics Div.
CMOS Circuit Design for Controlling Temperature in Micromachined Devices.
Final rept.
C. Zincke, M. Gaitan, and M. E. Zagloul. 1995, 4p.
Pub. in Proceedings of the Midwest Symposium on Circuits and Systems (37th), Lafayette, LA., August 3-5, 1995, p183-186.

Keywords: *Circuit design, *Temperature, Pixel, Reprints, *Constant power, CMOS, EDP etch, Micrmachining, MOSIS, Open area.

The authors present a CMOS circuit used for controlling the temperature of a CMOS compatible microheating element, known as a thermal pixel. The circuit uses nonlinear compensation to maintain constant power over large variation in the resistance. An external analog voltage controls the power delivered to the thermal pixel. This circuit was designed and fabricated through the MOSIS service foundry. Measurements are presented that verify the design and performance of the circuit.

02,197
PB96-157961 Not available NTIS
National Inst. of Standards and Technology (EEEL), Gaithersburg, MD. Semiconductor Electronics Div.
Characterization of LPE HgCdTe Film by Magnetoresistance.
Final rept.
J. S. Kim, D. G. Seiler, L. Colombo, and M. C. Chen. 1994, 2p.
Pub. in Extended Abstracts of the 1994 U.S. Workshop on the Physics and Chemistry of Mercury Cadmium Telluride and Other IR Materials, San Antonio, TX., October 4-6, 1994, p167-168.

Keywords: *Mercury cadmium tellurides, *Electrical resistivity, Liquid phase epitaxy, High resolution, Reprints, *Reduced conductivity tensor.

Magnetoresistance has been shown in the past to be a valuable tool for studying complex energy bands of semiconductors. In this paper, we demonstrate that magnetoresistance can be used as an extremely useful physical quantity to electrically characterize HgCdTe materials, structures, or devices which are of a multicarrier conduction nature. We take advantage of simple relationships between the magnetoresistance. The applied magnetic field, the lattice temperature, and relevant physical quantities in the reduced conductivity tensor (RCT) scheme. We have performed variable-magnetic-field and variable-temperature Hall measurements (0 to 1.5 T and 10 K 300 K) on LPE HgCdTe films and a GaAs-based HEMT structure. Magnetoresistance data obtained from these measurements are analyzed in the context of the RCT scheme.

02,198
PB96-158704 PC A03/MF A01
National Inst. of Standards and Technology (PL), Gaithersburg, MD. Radiometric Physics Div.
Liquid-Nitrogen-Cooled High Tc Electrical Substitution Radiometer as a Broadband IR Transfer Standard.
Technical note.
J. P. Rice, and Z. M. Zhang. Jan 96, 18p, NIST/TN-1414.
Also available from Supt. of Docs. as SN003-003-03375-8.

Keywords: *Infrared radiometers, *Calibration standards, Temperature control, Superconductors, High temperature, Infrared detectors, Electrical-substitution, NIST(National Institute of Standards and Technology).

A requirement exists for broadband radiometers that can be used to transfer NIST infrared radiometric scales to calibration laboratories elsewhere. The authors discuss the design of a liquid-nitrogen-cooled transfer standard radiometer that represents a practical tradeoff between room-temperature and liquid-helium-cooled radiometers. The detector utilizes high-Tc superconductors as temperature sensors for increased sensitivity. Such sensors have already been shown to enable temperature regulation of 100 microK peak-to-peak at 85 K, and have the potential for further improvements by three orders of magnitude. Electrical substitution is used to linearize the response over the dynamic range and to remove susceptibility to sensor aging effects.

02,199
PB96-165378 PC A04/MF A01
National Inst. of Standards and Technology (EEEL), Boulder, CO. Optoelectronics Div.
Optical Detector Nonlinearity: Simulation.
Technical note.
S. Yang, I. Vayshenker, X. Li, T. R. Scott, and M. Zander. May 95, 42p, NIST/TN-1376.
Also available from Supt. of Docs. as SN003-003-03338-3. See also PB95-169355 and PB95-203576.

Keywords: *Optical detectors, *Infrared detectors, *Power meters, Optical measurement, Mathematical models, Computerized simulation, Nonlinearity.

The authors developed a unified mathematical treatment for five commonly used measurement methods of optical detector nonlinearity and conducted computer simulation to compare these methods for different measurement conditions and data processing options. They found that the triplet and differential methods will give the overall best results, and third and fourth order polynomial representations of the measurement result will yield least total error for a common practical measurement system.

02,200
PB96-176649 Not available NTIS
National Inst. of Standards and Technology (MSEL), Gaithersburg, MD. Reactor Radiation Div.
Simulations of Neutron Focusing with Curved Mirrors.
Final rept.
J. R. D. Copley. 1996, 5p.
Pub. in Review of Scientific Instruments, v67 n1 p190-194 Jan 96.

Keywords: *Mirrors, *Neutron reflection, Gravitational effects, Ray tracing, Reprints, *Ellipsoidal mirror, Toroidal mirror.

The authors have developed a ray-tracing program to calculate the imaging properties of ellipsoidal and toroidal mirrors in glancing angle configurations. It has been proposed that such mirrors be used in small angle neutron scattering instruments, in order to achieve increased count rates without sacrificing angular resolution. The authors describe the method of calculation, including effects due to gravity, and they present a number of instructive examples of calculations for both types of mirrors. The authors also illustrate a practical method of reducing image degradation associated with gravitational effects.

02,201
PB96-200308 Not available NTIS
National Inst. of Standards and Technology (EEEL), Boulder, CO. Optoelectronics Div.
Fiber-Optic Faraday-Effect Magnetic-Field Sensor Based on Flux Concentrators.
Final rept.
M. N. Deeter. 1996, 4p.
Pub. in Applied Optics, v35 n1 p154-157 Jan 96.

Keywords: *Faraday effect, *Magneto optics, Magnetic field sensors, Optical fiber sensors, Yttrium iron garnets, Ferrimagnetism, Sensitivity, Reprints, Electric current sensors.

The principles and performance of a fiber-optic Faraday effect magnetic-field sensor designed around an yttrium-iron-granet (YIG) sensing element and two flux concentrations are described. The system design exploits the technique of polarization-rotated reflection in which a single polarization-maintaining optical fiber links the sensor head to the optical source and detection system. In the sensing head, ferrite flux concentrators are magnetically coupled to the YIG sensing element to achieve maximum sensitivity.

02,202
PB96-200860 Not available NTIS
National Inst. of Standards and Technology (EEEL), Boulder, CO. Optoelectronics Div.
Optoelectronics at NIST.
Final rept.
G. W. Day. 1995, 2p.
See also PB96-128210.
Pub. in Proceedings of the Annual Institute of Electrical and Electronics Engineers Laser and Electro-Optics Society Meeting (8th), San Francisco, CA., October 30-November 2, 1995, v2 p73-74.

Keywords: *Lasers, *Optoelectronic devices, *Research programs, Optical fibers, Wavelengths, Frequency stability, Frequency measurement, Calibration standards, Metrology, Reprints, *US NIST.

The Optics Division, one of the first divisions formed after NBS was established in 1901, was initially charged with work on radiometry, spectroscopy, and polarimetry. Over the next five or six decades optics remained a significant topic of research. Within a year of Maiman's first demonstration of the ruby laser in 1960, a similar laser was constructed at the NBS-Boulder Laboratories. Demands for assistance in measuring the power or energy produced by such lasers led to the establishment of laser calibration services beginning in 1967. Another early program was aimed at developing techniques for laser frequency stabilization and absolute frequency and wavelength measurements. That effort culminated in 1972 with the determination of a much improved value for the speed of light, which led ultimately to a redefinition of the meter.

02,203
PB96-204441 Not available NTIS
National Inst. of Standards and Technology (PL), Gaithersburg, MD. Radiometric Physics Div.
Improving Color Measurements of Displays.
Final rept.
J. E. Hardis. 1996, 10p.
Pub. in Color Imaging: Device-Independent Color, Color Hard Copy, and Graphic Arts, San Jose, CA., January 29-February 1, 1996, v2658 p182-191.

Keywords: *Calibration, *Cathode ray tubes, *Matrix transformation, Colorimeters, Reprints, Measurement, Standards, Tristimulus, Chromaticity.

It is generally believed that the most accurate means of measuring the CIE tristimulus values X, Y, Z or chromaticity coordinates x,y from a display is by using a spectroradiometer. Nevertheless, tristimulus colorimeters employing three or four colored filters find wide use because of their simplicity and lower cost. These devices cannot be calibrated to give accurate results in all situations because the spectral responsivities of their filtered detectors are not exactly the CIE color-matching functions. However, for a display that produces a linear superposition of three primary colored lights of fixed spectra, a tristimulus colorimeter can be correctly calibrated to measure all colors on that display. Signals from all of the filtered detectors are used to compute each of the X,Y,Z values. The calibration matrix is computed by data fitting to a reference colorimeter.. An improvement to the previously published method is reported, and a numerical example is shown. This technique is more tractable with today's digital instrumentation than it was when it was discovered, yet it remains underused. The American Society for Testing and Materials (ASTM), through its Committee on Color and Appearance, is revising its standard on display measurements using tristimulus colorimeters to encourage the adoption of the technique.

02,204
PB97-104186 PC A11/MF A03
National Inst. of Standards and Technology, Gaithersburg, MD. Advanced Technology Program.
Optoelectronics and Optomechanics Manufacturing: An ATP Focused Program Development. Workshop Proceedings. Held in Gaithersburg, Maryland on February 15, 1995.
T. Lettieri, V. R. McCrary, and J. C. Boudreaux. Feb 96, 210p, NISTIR-5715.

Keywords: *Electrooptics, *Computer aided manufacturing, *Research programs, Photonics, Economics, Product development, Display systems, Communication networks, Fiber otpics, Planning, Semiconductor devices, Packaging, Optical sensors, Modules(Electronics), Computer aided design, Chips(Electronics), Circuit interconnections, Industrial research, Workshops, Technology transfer, Precision engineering, *Optoelectronics, Optomechanics.

The ATP Workshop on Optoelectronics and Optomechanics Manufacturing was held at the National Institute of Standards and Technology in Gaithersburg, MD on February 15, 1995. The purpose of the Workshop was to respond to industry interest and provide an open forum for the exchange of ideas among interested members of the optics/photonics community concerning the strategic importance of optoelectronics (OE) and optomechanics (OM) technologies to U.S. economic growth. The Workshop brought together over 160 experts in OE/OM for the purpose of addressing the issues and requirements of U.S. industry in the area of OE/OM manufacturing. Input gained from the morning presentations and the breakout sessions will be used to help formulate the scope and range of a proposed ATP Focused Program in OE/OM manufacturing.

02,205
PB97-111835 Not available NTIS
National Inst. of Standards and Technology (EEEL), Boulder, CO. Optoelectronics Div.
Fundamentals and Problems of Fiber Current Sensors.
Final rept.
G. W. Day, K. B. Rochford, and A. H. Rose. 1996, 6p.
Pub. in Proceedings of the International Conference on Optical Fiber Sensors, Advanced Sensing Photonics (11th), Sapporo, Hokkaido, Japan, May 21-24, 1996, p124-129 May 96.

Keywords: *Detectors, *Faraday effect, Metrology, Reprints, *Electric current sensors, Fiber optic sensors, Optical fiber sensors.

The paper briefly reviews the history and present commercial status of optical fiber sensors, and then summarizes recent research aimed at improved performance, lower cost, and wider areas of applications.

02,206
PB97-113179 Not available NTIS
National Inst. of Standards and Technology (EEEL), Boulder, CO. Optoelectronics Div.
Integrated Optical Polarization-Discriminating Receiver in Glass.
Final rept.
D. L. Veasey, and D. R. Larson. 1995, 6p.
Pub. in Jnl. of Lightwave Technology, v13 n11 p2244-2249 Nov 95.

Keywords: *Receivers, *Glass, *Polarization, Waveguides, Cladding, Hybrid, Integrated, Optical, Polarizers, Semiconductors, Splitter, Reprints.

The authors have successfully demonstrated an integrated optical TE-TM mode discriminator using waveguide polarizers and guided-wave photodetectors for use in polarimetric optical sensor and positioning systems. The photonic integrated circuit consists of a Y-branch waveguide splitter formed by potassium-sodium ion exchange in silicate glass. Hydrogenated amorphous silicon claddings were deposited on each branch of the splitter to act as polarizers. One output cladding was trimmed to a thickness which attenuated the TE polarization, while the other cladding was trimmed to attenuate light having TM polarization. The thickness trimming is accomplished using a process of localized plasma etching which allows in situ extinction optimization by monitoring transmitted light. Optical extinction ratios of up to 27 dB were demonstrated on Y-branch waveguides for polarizers with claddings 1.2 mm in length. The integrated receiver was completed with the deposition of metal-semiconductor-metal photodetectors on each of the output waveguide branches following the polarizers. Amorphous silicon claddings were contacted with chrome-gold interdigitated Schottky contacts to form the waveguide detectors.

02,207
PB97-116040 PC A06/MF A01
National Inst. of Standards and Technology (EEEL), Boulder, CO. Optoelectronics Div.
Bibliography of the NIST Optoelectronics Division.
A. J. Smith. Sep 96, 78p, NISTIR-5052.
See also report for 1995, PB96-128210.

Keywords: *Electrical engineering, *Electrooptics, *Bibliographies, Research projects, Metrology, Optical communications, Optical fibers, Fiber optics, Optoelectronic devices, Laboratories, Electronics, Electrical measurement, Semiconductor devices, Superconductors, Lasers, *Optoelectronics.

This bibliography lists publications of the staff of the Optoelectronics Divison and its predescessor organizational units, from about 1970 through the data of this report.

02,208
PB97-119200 Not available NTIS
National Inst. of Standards and Technology (EEEL), Gaithersburg, MD. Electricity Div.
Specular and Diffuse Reflection Measurements of Electronic Displays.
Final rept.
G. R. Jones, E. F. Kelley, and T. A. Germer. 1996, 4p.
Pub. in International Symposium Digest of Technical Papers 1996, San Diego, CA., May 12-17, 1996, p203-206.

Keywords: *Display devices, *Specular reflection, *Diffuse reflection, *Measurement, Electronic equipment, Bidirectional reflection, Distribution functions, Coefficients, Electroluminescence, High resolution, Estimation, Reprints.

Display standards describe measurements of the diffuse and specular reflection coefficients. The adequacy of such procedures is compared with the bidirectional reflection distribution function (BRDF) measurements. Alternative methods are examined and their estimates of the specular and diffuse reflection coefficients are compared to the results of the BRDF measurement.

02,209
PB97-122394 Not available NTIS
National Inst. of Standards and Technology (EEEL), Gaithersburg, MD. Electricity Div.
Survey of the Components of Display-Measurement Standards.
Final rept.
E. F. Kelley, G. R. Jones, P. A. Boynton, M. D. Grote, and D. J. Bechis. 1996, 4p.
See also PB96-122528.
Pub. in Jnl. of the Society for Information Display, v3 n4 p219-222 Dec 95.

Keywords: *Display devices, *Measurement, *Performance evaluation, Flat panel displays, Liquid crystal display systems, Cathode ray tube screens, Electronic equipment, Logical elements, Visual perception, Components, Standards, Reprints.

Several display standards are reviewed and distinctive elements are compared. The paper attempts to identify complementary and inconsistent elements of related display standards.

Power & Signal Transmission Devices

02,210
PB94-135639 PC A03/MF A01
National Inst. of Standards and Technology (EEEL), Boulder, CO. Electromagnetic Fields Div.
Crosstalk between Microstrip Transmission Lines.
D. A. Hill, K. H. Cavcey, and R. T. Johnk. Dec 93, 38p, NISTIR-5015.

Keywords: *Microstrip transmission lines, *Crosstalk, Characteristic impedance, Mutual inductance, Scale models, Permittivity, Predictions, Mutual capacitance, Scalar potentials, Vector potentials.

Methods for prediction of crosstalk between microstrip transmission lines are reviewed and simplified for the weak coupling case. Classical coupled transmission line theory is used for uniform lines, and potential and induced EMF methods are used for crosstalk between nonuniform lines. It is shown that the potential method is equivalent to classical coupled transmission line theory for the case of uniform lines. An experiment was performed for uniform coupled microstrip lines for frequencies from 50 MHz to 5 GHz, and good agreement between theory and measurement was obtained for both near-end and far-end crosstalk.

02,211
PB94-165537 PC A06/MF A02
National Inst. of Standards and Technology (EEEL), Boulder, CO. Electromagnetic Fields Div.
Transmission/Reflection and Short-Circuit Line Methods for Measuring Permittivity and Permeability.
Technical note.
J. Baker-Jarvis, M. D. Janezic, J. H. Grosvenor, and R. G. Geyer. Dec 93, 121p, NIST/TN-1355-R.
Also available from Supt. of Docs. as SN003-003-03258-1. See also PB92-205376.

Keywords: *Transmission lines, *Magnetic permeability, *Permittivity, *Electrical measurement, Coaxial cables, Waveguides, Dielectric properties, Calibrating, Short circuits, Reflection, Algorithms, Optimization, Mathematical models, Frequency stability, Uncertainty analysis.

The transimission/reflection and short-circuit line methods for measuring complex permittivity and permeability of materials in waveguides and coaxial lines are examined. Equations for complex permittivity and permeability are developed from first principles. In addition, new formulations for the determination of complex permittivity and permeability independent of reference plane position are derived. For the one-sample transmission/reflection method and two-position short-circuit line measurements, the solutions are unstable at frequencies corresponding to integral multiples of one-half wavelength in the sample. For two-sample methods the solutions are unstable for frequencies where both samples resonate simultaneously. Criteria are given for sample lengths to maintain stability. An optimized solution is also presented for the scattering parameters. This solution is stable over all frequencies and is capable of reducing scattering parameter data on materials with higher dielectric constant. An uncertainty analysis for the various techniques is developed and the results are compared. The errors incurred due to the uncertainty in scattering parameters, length measurement, and reference plane position are used as inputs to the uncertainty models.

02,212
PB94-172350 Not available NTIS
National Inst. of Standards and Technology (MSEL), Gaithersburg, MD. Polymers Div.

Effect of DC Tests on Induced Space Charge.
Final rept.
N. Hozumi, J. Tanaka, A. DeReggi, B. Dickens, and N. Nagusrinivas. 1990, 3p.
Pub. in Proceedings Conference Record of the 1990 Institute of Electrical and Electronics Engineers International Symposium on Electrical Insulation, Toronto, Canada, June 3-6, 1990, p332-334.

Keywords: *Electric cables, *Space charge, Aging(Materials), Direct current, Polyethylenes, Tests, Reprints.

Poling-induced space charges in peeled samples of ac aged/dc tested cables were studied using the thermal pulse technique. Samples were poled at about 0.12 MV/cm for 3.5 hours at 70 C using the same polarity as that used for the dc tests. Previous work seemed to indicate that dc testing could have permanent effects which could be detected by the amount of poling-induced charge. An attempt was made to examine this by using three samples with about the same length of ac aging but with different amounts of dc testing. The sample with one dc test and the sample with 23 dc tests were appreciably oxidized whereas the sample with 11 dc tests was not oxidized. Other interesting observations were made.

02,213
PB94-172814 Not available NTIS
National Inst. of Standards and Technology (EEEL), Boulder, CO. Electromagnetic Fields Div.
Reciprocity Relations in Waveguide Junctions.
Final rept.
D. F. Williams, and R. B. Marks. 1993, 6p.
Pub. in Institute of Electrical and Electronics Engineers Transactions on Microwave Theory and Techniques 41, n6/7 p1105-1110 Jun/Jul 93.

Keywords: Characteristic impedance, Reprints, *Waveguide junctions, Microwave metrology, Reference impedance, Scattering parameters, Reciprocity.

The Lorentz reciprocity condition is applied to junctions composed of reciprocal media which connect uniform but otherwise arbitrary waveguides. An expression relating the forward and reverse transmission coefficients is derived and factored into two terms: the first involving the phase of the reference impedance in the guide, and the second a new reciprocity factor. The usual condition equating the forward and reverse transmission coefficients is shown not to hold in the general case. Experimental evidence supporting the theoretical results is presented.

02,214
PB94-199130 Not available NTIS
National Inst. of Standards and Technology (MSEL), Gaithersburg, MD. Polymers Div.
Spatial Dependence of Electrical Fields Due to Space Charges in Films of Organic Dielectrics Used for Insulation of Power Cables.
Final rept.
M. G. Broadhurst, A. S. DeReggi, B. Dickens, and R. M. Eichhorn. 1990, 5p.
Pub. in Conference of Record of the Institute of Electrical and Electronics Engineers International Symposium on Electrical Insulation, Toronto, Canada, June 3-6, 1990, p405-409.

Keywords: *Electrical insulation, *Dielectrics, *Electric wire, *Space charge, *Electric fields, Reprints, Polyethylenes, Electrical properties, Electric charge, Electrical measurement.

The authors measured the electric fields due to space charge within film samples of several commercial polyolefins used as medium voltage power cable insulation. They charged the films at 60 deg. C with DC voltages applied for several hours. For dry charged films, vacuum deposited gold or aluminum provided the electrodes. For wet charged films, one or both surfaces of the film were bare and in contact with an aqueous 0.05 molar solution of NaCl. They measured the fields using the thermal pulse (TP) method. To use this method with the wet charged films, they painted colloidal graphite electrodes onto the films after they were charged. The results show that thermoplastic polyethylene (PE) charges negatively for both wet and dry charging. Crosslinked polyethylene (XLPE) charges negatively when dry charged, but small amounts of either positive or negative charge were found after wet charging.

02,215
PB94-211943 Not available NTIS
National Inst. of Standards and Technology (EEEL), Boulder, CO. Electromagnetic Fields Div.
Currents Induced on Multiconductor Transmission Lines by Radiation and Injection.
Final rept.
D. A. Hill. 1992, 6p.
Pub. in Institute of Electrical and Electronics Engineers Transactions on Electromagnetic Compatibility 34, n4 p445-450 Nov 92.

Keywords: *Transmission lines, Excitation, Tests, Reprints, *Induced current, Wire assemblies.

Multiconductor transmission line theory is used to compare currents induced on individual wires within a bundle by injection and radiated excitation. Calculations show that the two types of excitation generally induce significantly different current distributions, but the differences are much smaller for electrically short lines. The results are relevant to the validity of using current injection testing to replace radiated immunity testing.

02,216
PB94-211968 Not available NTIS
National Inst. of Standards and Technology (EEEL), Boulder, CO. Electromagnetic Fields Div.
Aperture Coupling to a Coaxial Air Line: Theory and Experiment.
Final rept.
D. A. Hill, M. L. Crawford, M. Kanda, and D. I. Wu. 1993, 6p.
Pub. in Institute of Electrical and Electronics Engineers Transactions on Electromagnetic Compatibility 35, n1 p69-74, 1 Feb 93.

Keywords: *Electromagnetic shielding, Reverberation chambers, Polarization(Waves), Circular configuration, Dipole moments, Apertures, Reprints, *Coaxial air lines.

Coupling through a circular aperture in the shield of a coaxial air line is studied theoretically and experimentally. Polarizability theory is used to compute the effective dipole moments that excite the coaxial line in the internal region. Measurements of shielding effectiveness were made in a reverberation chamber over wide-frequency ranges. Agreement between theory and measurements is generally within + or - 10 dB. Recommendations for improvements in the measurements and theory are made for achieving closer agreement that would be desirable for an artifact standard for shielding effectiveness measurements.

02,217
PB94-216389 Not available NTIS
National Inst. of Standards and Technology (EEEL), Boulder, CO. Electromagnetic Fields Div.
Accurate Experimental Characterization of Interconnects: A Discussion of 'Experimental Electrical Characterization of Interconnects and Discontinuities in High-Speed Digital Systems'.
Final rept.
R. B. Marks, and D. F. Williams. 1992, 4p.
Pub. in Institute of Electrical and Electronics Engineers Transactions on Components, Hybrids, Manufacturing Technology 15, n4 p601-604 Aug 92.

Keywords: *Circuit interconnections, *Transmission lines, Characteristic impedance, Electrical measurement, Digital circuits, Permittivity, Capacitance, High speed, Accuracy, Reprints.

This paper discusses two issues concerning the accuracy of electrical characterizations of interconnect transmission lines, particularly in regard to a recently published paper. The error in the characteristic impedance may be reduced through an alternative approximation to the capacitance of the transmission line. Furthermore, measurements of both the propagation constant and characteristic impedance, which are the two primary parameters characterizing the line, may be improved by the use of a well conditioned algorithm.

02,218
PB94-216397 Not available NTIS
National Inst. of Standards and Technology (EEEL), Boulder, CO. Electromagnetic Fields Div.
Interconnection Transmission Line Parameter Characterization.
Final rept.
R. B. Marks, and D. F. Williams. 1992, 8p.
Pub. in Proceedings of the ARFTG Conference (40th), Orlando, FL., December 3-4, 1992, p88-95 1992.

Keywords: *Circuit interconnections, *Transmission lines, Characteristic impedance, Frequency dependence, Dielectric properties, Substrates, Silicon, Reprints, Coplanar waveguides.

This paper introduces a new method for the characterization of transmission lines fabricated on lossy or dispersive dielectrics. The method, which is more accurate than conventional techniques, is used to examine the resistance, inductance, capacitance, and conductance per unit length of coplanar waveguide transmission lines fabricated on lossy silicon substrates.

02,219
PB94-216504 Not available NTIS
National Inst. of Standards and Technology (EEEL), Gaithersburg, MD. Electricity Div.
Important Link in Entire-House Protection: Surge Reference Equalizers.
Final rept.
F. D. Martzloff, and M. Samotyj. 1993, 4p.
Pub. in Proceedings of Zurich EMC Symposium, Zurich, Switzerland, March 9-12, 1993, p395-398.

Keywords: *Electronic equipment, *Circuit protection, *Surges, Households, Residential buildings, Cable television, Telephones, Communication equipment, Voltage regulators, Reprints.

The increasing use of electronics in residential applications has been paralleled by a realization that surge protection may be necessary for this type of equipment. Installing a surge-protective device on the power-line port as well as on the communications-line port of a piece of equipment might appear sufficient to ensure this protection. However, the normal operation of one of the protective devices during a surge event can create differences in the voltages of the references of the two ports. This difference in voltages, applied across the equipment or across a communication link between two pieces of equipment, can result in permanent damage as well as upset. Equalizing these voltages can be achieved by proper routing of the two lines through a single device, called Surge Reference Equalizer, and thus avoid the risk of damage.

02,220
PB95-151593 Not available NTIS
National Inst. of Standards and Technology (EEEL), Boulder, CO. Electromagnetic Fields Div.
Accurate Transmission Line Characterization.
Final rept.
D. F. Williams, and R. B. Marks. 1993, 3p.
Pub. in Institute of Electrical and Electronics Engineers Microwave and Guided Microwave Letters 3, n8 p247-249 Aug 93.

Keywords: *Transmission lines, Characteristic impedance, Frequency dependence, Dielectric properties, Calibration, Substrates, Silicon, Reprints, Coplanar waveguides.

This letter introduces a new method for the characterization of transmission lines fabricated on lossy or dispersive dielectrics. The method, which is more accurate than conventional techniques, is used to examine the resistance, inductance, capacitance, and conductance per unit length of coplanar waveguide transmission lines fabricated on lossy silicon substrates.

02,221
PB95-168787 Not available NTIS
National Inst. of Standards and Technology (EEEL), Boulder, CO. Electromagnetic Fields Div.
Measurements of the Characteristic Impedance of Coaxial Air Line Standards.
Final rept.
J. R. Juroshek, and G. M. Free. 1994, 6p.
Pub. in Institute of Electrical and Electronics Engineers Transactions on Microwave Theory and Techniques 42, n2 p186-191 Feb 94.

Keywords: *Characteristic impedance, *Standards, *Impedance measurement, Electrical measurement, Network analyzers, Transmission lines, Capacitance, Electric connectors, Reprints, *Coaxial air lines, Scattering parameters.

A method for electrically measuring the characteristic impedance of coaxial air line standards is described. This method, called the gamma method, determines the characteristic impedance of a coaxial air line from measurements of its propagation constant and capacitance per unit length. The propagation constant is measured on a network analyzer, and the capacitance per unit length. The propagation constant is measured on a network analyzer, and the capacitance per unit length is measured on a capacitance bridge at 1 kHz.

The measurements of characteristic impedance with the gamma method are independent of any dimensional measurements. Measurements of the characteristic impedance using the gamma method are compared to theoretical predictions from dimensional measurements. Test results are shown for 14 mm, 7 mm, and 3.5 mm coaxial air lines.

02,222
PB95-169538 PC A05/MF A02
National Inst. of Standards and Technology (EEEL), Boulder, CO. Electromagnetic Technology Div.
Superconductor Critical Current Standards for Fusion Applications. Final Progress Report, October 1993-July 1994.
L. F. Goodrich, J. A. Wiejaczka, A. N. Srivastava, and T. C. Stauffer. Nov 94, 100p, NISTIR-5027.
Sponsored by Department of Energy, Washington, DC. Office of Fusion Energy. and Massachusetts Inst. of Tech., Cambridge. Plasma Fusion Center.

Keywords: *Thermonuclear reactor materials, *Superconducting wires, *Niobium stannides, *Critical current, *Electrical measurement, Interlaboratory comparisons, Fusion reactors, Homogeneity, Standards, Mandrels, Niobium intermetallics, Titanium intermetallics, ITER tokamak, Tables(Data), Graphs(Charts), Titanium alloy 6Al 4V, Reference materials, Reference wires, Intercomparison, Niobium titanides.

This report describes research conducted to help establish a standard critical current measurement technique for Nb3Sn wires that may be used in fusion applications. The main part of this report is a detailed presentation of results of the first ITER international interlaboratory comparison of Nb3Sn critical current measurements. A common procedure and a common reaction and measurement mandrel was used by US laboratories in this comparison, whereas there was no common procedure followed by other international laboratories. The largest difference in I(c) measurements of two laboratories that did not use a common procedure was 23%. The largest difference in I(c) measurements of two laboratories that did use a common procedure was 6.5%. There may still be room for improvement, but this indicates the strong need for a common detailed procedure. Results on the homogeneity of one of the Nb3Sn wires used in this study and a commentary on creating a Nb3Sn Reference Wire are also presented.

02,223
PB95-175535 Not available NTIS
National Inst. of Standards and Technology (EEEL), Boulder, CO. Electromagnetic Technology Div.
Reduction of Interfilament Contact Loss in Nb3Sn Superconductor Wires.
Final rept.
R. B. Goldfarb, and K. Itoh. 1994, 4p.
Sponsored by Department of Energy, Washington, DC.
Pub. in Jnl. of Applied Physics 75, n4 p2115-2118, 15 Feb 94.

Keywords: *Superconducting wires, *Niobium stannides, Proximity effect, Eddy currents, AC losses, Magnetization, Reduction, Reprints, Hysteresis losses, Twisted filaments, Length dependence.

Interfilament contact in Nb3Sn wires made by the internal-tin-diffusion process causes excess hysteresis loss beyond the intrinsic magnetic hysteresis loss of the filaments. In analogy with eddy-current and proximity-effect coupling losses, the excess contact loss can be reduced by decreasing the twist-pitch length of the filaments in the wire. One consequence of interfilament contact is that volume magnetization measurements are strongly dependent on sample length below about one twist pitch. We define a characteristic length whose reciprocal is equal to the sum of the reciprocals of the sample length and the twist pitch. Hysteresis loss is a universal function of characteristic length for different sample lengths and twist pitches. We discuss several experimental parameters for the magnetic determination of hysteresis loss.

02,224
PB95-176178 Not available NTIS
National Inst. of Standards and Technology (EEEL), Boulder, CO. Electromagnetic Technology Div.
Micromagnetic Scanning Microprobe System.
Final rept.
C. A. Thompson, R. W. Cross, and A. B. Kos. 1994, 7p.
Pub. in Review of Scientific Instrumentation 65, n2 p383-389 Feb 94.

Keywords: *Magnetoresistance, *Thin films, *Scanning electron microscopy, *Microanalysis, Magnetic tapes, Magnetic recordings, Instrumentation, Data acquisition, Domains, Apparatus, Barkhausen noise, Reprints, Read heads.

The authors describe the apparatus, instrumentation, and data acquisition techniques which make up the micromagnetic scanning microprobe system (MSMS). The system was developed to study magnetoresistive (MR) thin films used in magnetic recording read heads. It uses a dc, four-probe resistance measurement coupled with two pairs of orthogonal field sources. Results from magnetoresistance measurements of the dynamic response of a MR read head film are shown to demonstrate system operation and performance. Significant variations in MR responses were seen across the width of the device because of local domain formation. The MSMS is an effective tool for characterizing the effects of domain formation on the output of a MR read head.

02,225
PB95-180337 Not available NTIS
National Inst. of Standards and Technology (EEEL), Boulder, CO. Electromagnetic Fields Div.
Crosstalk between Microstrip Transmission Lines. (NIST Reprint).
Final rept.
D. A. Hill, K. H. Cavcey, and R. Johnk. 1994, 8p.
See also PB94-135639.
Pub. in Institute of Electrical and Electronics Engineers Transactions on Electromagnetic Compatibility 36, n4 p314-321 Nov 94.

Keywords: *Microstrip transmission lines, *Crosstalk, Characteristic impedance, Mutual inductance, Permittivity, Reprints, Mutual capacitance, Scalar potentials, Vector potentials.

Methods for prediction of crosstalk between microstrip transmission lines are reviewed and simplified for the weak-coupling case. Classical coupled transmission line theory is used for uniform lines, and potential and induced EMF methods are used for crosstalk between nonuniform lines. It is shown that the potential method is equivalent to classical coupled transmission line theory for the case of uniform lines. An experiment was performed for uniform coupled microstrip lines for frequencies from 50 MHz to 5 GHz, and good agreement between theory and measurement was obtained for both near- and far-end crosstalk.

02,226
PB95-202784 Not available NTIS
National Inst. of Standards and Technology (EEEL), Boulder, CO. Electromagnetic Technology Div.
Critical-Current Degradation in Nb3 Al Wires Due to Axial and Transverse Stress.
Final rept.
T. Kuroda, H. Wada, S. L. Bray, and J. W. Ekin. 1993, 5p.
See also PB93-153211.

Keywords: *Superconducting wires, *Critical current, *Stress analysis, Axial stress, Microstructure, Strains, Reprints, Transverse stress, Niobium aluminides, Multifilaments.

Effects of axial and transverse stress on the critical current of Nb-tube processed multifilamentary Nb3Al wires have been studied. The degradations of the critical current due to axial or transverse stress for these Nb3Al wires are much smaller than those for Nb3Sn wires. The microstructures and stress states of the Nb3Al wires have been investigated to understand the stress dependences of the critical current through the microscopic observations and the elastic theory. From an engineering standpoint, the importance of mechanical strength of the matrix material where superconducting filaments are embedded has been found especially for transverse stress effects.

02,227
PB96-119219 Not available NTIS
National Inst. of Standards and Technology (EEEL), Boulder, CO. Electromagnetic Technology Div.
Comparing the Accuracy of Critical-Current Measurements Using the Voltage-Current Simulator.
Final rept.
D. Aized, J. W. Haddad, C. H. Joshi, L. F. Goodrich, and A. N. Srivastava. 1994, 4p.
Pub. in Institute of Electrical and Electronics Engineers Transactions on Magnetics, v30 n4 p2014-2017 Jul 94.

Keywords: *Critical current, *Superconductors, Simulations, Reprints, Electric circuit, Data acquisition, Comparison, *Voltage current simulation.

A passive voltage-current simulator developed by the National Institute of Standards and Technology (NIST) is used to compare the accuracy of critical current measurements and the power-law behavior of high temperature superconductors (HTS). In this study, critical current measurements made from four data acquisition and analysis systems are compared with those carried out at NIST. This paper also discusses various measurement techniques, methods of calculating critical current, and n-values. The V-I simulator is believed to be an advancement towards defining the standards for critical current measurements and ensuring the traceability of results at different test facilities.

02,228
PB96-119268 Not available NTIS
National Inst. of Standards and Technology (EEEL), Gaithersburg, MD. Electricity Div.
Gaseous Dielectrics Research: Possible SF6 Substitutes.
Final rept.
L. G. Christophorou, and R. J. Van Brunt. 1995, 28p.
Pub. in Electrical Transmission and Distribution Systems, Sulfur Hexafluoride and Atmospheric Effects of Greenhouse Gas Emissions Conference, August 9-10, 1995, Washington, DC., p148-175.

Keywords: *Electrical insulation, *Environmental chemical substitutes, *Sulfur hexafluoride, Gases, Dielectrics, Mixtures, Greenhouse effect, Global air pollution, Nitrogen, Reprints.

Sulfur hexafluoride (SF6) is currently the most common insulating gas used in enclosed electrical systems. It is, however a potent greenhouse gas and, thus, its use could impart fears of environmental costs, regulations, and restrictions, in spite of its current low levels in the environment. An aspect of this potential problem, namely the search for alternative high-voltage insulants, such as high-pressure gaseous dielectrics (e.g., N2 and N2/SF6 mixtures), is addressed in this paper.

02,229
PB96-119409 Not available NTIS
National Inst. of Standards and Technology (EEEL), Boulder, CO. Electromagnetic Technology Div.
Simple and Repeatable Technique for Measuring the Critical Current of Nb3Sn Wires.
Final rept.
L. F. Goodrich, and A. N. Srivastava. 1994, 4p.
Pub. in Proceedings of the International Workshop on Critical Currents in Superconductors (7th), Alpbach, Austria, January 24-27, 1994, p609-612.

Keywords: *Critical current, *Niobium stannides, *Superconductors, *Wire, Interlaboratory comparisons, Mandrels, Strains, Titanium alloys, Variations, Reproducibility, Reprints.

We evaluated an alternative approach for measuring the critical current (Ic) of Nb3Sn wire which uses a standard mandrel geometry and apparatus interface. Preliminary data indicate that the tension in the conductor before reaction and measurement may affect the repeatability. We show preliminary summary statistics for measurements of conductors performed by five US laboratories. The reaction and measurement mandrel used was fabricated using a Ti-6 Al-4V alloy. This high temperature alloy was used to avoid transferring the specimen between mandrels, thus reducing the likelihood of inadvertent mechanical damage of the specimen. The U.S. International Thermonuclear Experimental Reactor (US ITER) Home Team adopted this approach in a recent test because it was expected to be easily implemented and yield consistent results.

02,230
PB96-123468 Not available NTIS
National Inst. of Standards and Technology (EEEL), Gaithersburg, MD. Electricity Div.
SF6/N2 Mixtures: Basic and High-Voltage-Insulation Properties.
Final rept.
L. G. Christophorou, and R. J. Van Brunt. 1995, 52p.
Pub. in Institute of Electrical and Electronics Engineers Transaction on Dielectrics and Electrical Insulation, Virginia Beach, VA., October 23-26, 1995, p952-1003.

Keywords: *Dielectrics, *Electrical insulation, Collision cross sections, Electron transport, Gas mixtures, Global warming, Reprints, High-voltage insulation.

The widespreed use of SF6 by the electric power and other industries has led to increased concentrations of SF6 in the atmosphere. This causes concern as to pos-

sible effects on global warming, because SF6 is a potent greenhouse gas. This paper first touches on this issue and then documents the behavior of high pressure gases such as N2 and SF6/N2 mixtures that can be realistically considered as acceptable intermediate or long-term replacements for pure SF6 in some HV applications. The possible use of dilute SF6/N2 mixtures as an alternative to pure SF6 for some of industry's insulation needs (albeit at higher pressure) is documented, and existing knowledge on these mixtures and on the individual components (N2 and SF6), both basic and applied, is compiled. A guide to existing literature is provided.

02,231
PB96-123633 Not available NTIS
National Inst. of Standards and Technology (EEEL), Gaithersburg, MD. Electricity Div.
Keeping Up with the Reality of Today's Surge Environment.
Final rept.
F. D. Martzloff. 1995, 7p.
Pub. in Proceedings of the Power Quality Solutions, Long Beach, CA., September 9-15, 1995, p246-252.

Keywords: *Surges, *Electric faults, *Overvoltage, Electrical equipment, Electric power distribution, Electric power failures, Overcurrent, Power measurement, Electromagnetic compatibility, Circuit protection, Voltage regulators, Reprints.

The paper proposes to establish a program for characterizing surge events by the capability of a surge event to deliver a surge current through the power system in end-user facilities. This characterization would complement or even supersede the conventional monitoring of surge voltages. Two approaches are suggested: (1) using a metal-oxide varistor with the lowest possible voltage to 'attract' surges away from other SPDs connected in the facility, and then recording the surge current waveform in the varitor; (2) gathering data on field failure attributable to surges or swells for all types of electrical appliances, then attempting to replicate the failure mode in the laboratory.

02,232
PB96-131586 PC A05/MF A01
National Inst. of Standards and Technology (EEEL), Gaithersburg, MD. Electricity Div.
Classified Bibliography: Insulation Condition Monitoring Methods, 1989-1995.
F. D. Martzloff. Nov 95, 96p, NISTIR-5760.
See also PB91-222687.

Keywords: *Bibliographies, *Electrical insulation, *Cables, *Nondestructive testing, *Defects, Aging, Monitoring, Test methods, Experimental data, Measurements, Polymers, Spectroscopy, Time domain, Nuclear power plants, Detection, Wire, Simulation, Data reduction, Dielectric properties, Electrical testing, Damage assessment, Partial discharges.

This Bibliography is a complement to the Annotated Bibliography that was initially compiled for identifying promising test methods to detect incipient defects due to aging of cables. That compilation led to the selection of two methods for a demonstration at the National Institute of Standards and Technology (NIST), Partial Discharge Analysis and Time-Domain Spectroscopy. The literature search covers the period 1989-1995, with emphasis on partial discharge measurements, data reduction and simulation, on measurement of dielectric properties, and to some degree, on insulation aging.

02,233
PB96-137781 Not available NTIS
National Inst. of Standards and Technology (EEEL), Boulder, CO. Electromagnetic Technology Div.
Anomalous Switching Phenomenon in Critical-Current Measurements When Using Conductive Mandrels.
Final rept.
L. F. Goodrich, J. A. Wiejaczka, and A. N. Srivastava. 1995, 3p.
Pub. in Institute of Electrical and Electronics Engineers Transactions on Applied Superconductivity, v5 n3 p3442-3444 Sep 95.

Keywords: *Critical current, *Superconducting wires, Switiching, Voltage-current, Reprints, Bypass current, Conductive mandrel, Multivalued, Nb-Ti.

NIST and other laboratories have observred an anomalous switching phenomenon that can occur in critical-current measurement of coiled Nb-Ti and Nb3Sn superconductors when mounted on an electrically-conductive measurement mandrel. During aquistion of the voltage-current (V-I) characteristic, large voltage discontinuities are observed. This switching phenomenon results in a multivalued V-I curve, and apparently multiple 'critical-current' values. An explanation of this phenomenon, some necessary conditions for switching to occur, as well as methods of detecting the phenomenon are given.

02,234
PB96-140389 Not available NTIS
National Inst. of Standards and Technology (EEEL), Boulder, CO. Optoelectronics Div.
Fiber Coating Diameter: Toward a Glass Artifact Standard.
Final rept.
D. H. Williams, M. Young, and L. A. Tietz. 1995, 3p.
Pub. in Proceedings of the Optical Fibre Measurement Conference (3rd), Liege, Belgium, September 25-26, 1995, 3p.

Keywords: *Fiber optics, *Calibration, Coatings, Reprints, Standards, Micrometers, *Foreign technology, *Optical fibers, Standard Reference Materials.

This paper proposes a glass fiber, 245 micrometers in diameter, with an appropriate index of refraction as a standard for the calibration of outer primary coating diameter measurements. Fibers will be manufactured by either a melt process or a draw process. The index of refraction will be measured by the Becke line method and the diameter with a contact micrometer.

02,235
PB96-141262 Not available NTIS
National Inst. of Standards and Technology (EEEL), Boulder, CO. Electromagnetic Technology Div.
Microwave Properties of Voltage-Tunable YBa2Cu3O7-delta/SrTiO3 Coplanar Waveguide Transmission Lines.
Final rept.
D. C. DeGroot, J. A. Beall, R. B. Marks, and D. A. Rudman. 1995, 4p.
Pub. in Institute of Electrical and Electronics Engineers Transactions on Applied Superconductivity, v5 n2 p2272-2275 Jun 95.

Keywords: *Waveguides, Integrated circuits, Reprints, Microwaves, Electromagnetic shielding, Superconductors, Ferroelectric, *Coplanar waveguides.

To explore the electrical characteristics of monolithic microwave circuits with integrated high-temperature superconductor and ferroelectric materials, the authors fabricated a series of coplanar waveguide transmission lines in laser-deposited YBa2Cu3O708 and SrTiO3 thin films. The authors characterized the voltage-tunable two-port microwave response of the transmission lines at cryogenic temperatures using a calibrated network analyzer system. Total phase shifts and phase tuning in these devices increased for increasing ferroelectric film thickness with only moderate increases in transmission loss.

02,236
PB96-147038 Not available NTIS
National Inst. of Standards and Technology (EEEL), Boulder, CO. Electromagnetic Fields Div.
Dielectric Measurements on Printed-Wiring and Circuit Boards, Thin Films, and Substrates: An Overview.
Final rept.
J. R. Baker-Jarvis, and C. A. Jones. 1995, 12p.
Pub. in Proceedings of the Material Research Society Symposium, San Francisco, CA., April 18, 1995, p153-164.

Keywords: *Calibration, *Coaxial cables, Dielectric constants, Loss factor, Microwaves, Permeability, Permittivity, Reflection method, Resonance, Resonator, Reprints, Open-ended probe.

A review of the most common methods of permittivity measurements on thin films, printed-wiring and circuit boards, and substrates is presented. Transmission-line techniques, coaxial apertures, open resonators, surface-wave modes, and dielectric resonators methods are examined. The frequency range of applicability and typical uncertainties associated with the methods are summarized.

02,237
PB96-155510 Not available NTIS
National Inst. of Standards and Technology (EEEL), Boulder, CO. Electromagnetic Technology Div.
Size Effects in Submicron NiFe/Ag GMR Devices.
Final rept.
S. E. Russek, R. W. Cross, S. C. Sanders, and J. O. Oti. 1995, 4p.
Pub. in Institute of Electrical and Electronics Engineers Transactions on Magnetics, v31 n6 p3939-3942 Nov 95.

Keywords: *Magnetoresistance, Barkhausen noise, Reprints, Submicrons, *GMR.

The authors measured the magnetoresistive response of submicron NIFe/Ag giant magnetoresistive (GMR) devices as a function of current density and field angle. In addition to magnetostatic broadening, the authors observe large jumps in the magnetoresistive response (Barkhausen jumps) due to domain switching. These effects lead to irregular device-specific magnetoresistive response curves. The large Barkhausen jumps are more pronounced at low current density while at high current densities the response is smoother due to self field stabilization. The detailed structure of the Barkhausen jumps is very sensitive to the angle of the applied magnetic field. These effects are general properties of wide class of GMR materials that rely on incoherent reversal of many small magnetic domains.

02,238
PB96-162649 PC A04/MF A01
National Inst. of Standards and Technology (EEEL), Boulder, CO. Electromagnetic Fields Div.
Radiated Emissions and Immunity of Microstrip Transmission Lines: Theory and Measurements.
Technical note.
D. A. Hill, D. G. Camell, K. H. Cavcey, and G. H. Koepke. Jul 95, 37p, NIST/TN-1377.
Also available from Supt. of Docs. as SN003-003-03360-0.

Keywords: *Microstrip transmission lines, *Irradiation, *Directivity, Emission, Immunity, Measurement, Power, Efficiency, Reverberation, Test chambers, NIST(National Institute of Standards and Technology), Mode stirring, Radiated power, Radia efficiency.

The authors analyze radiation from a microstrip transmission line and calculate total radiated power by numerical integration. Reverberation chamber methods for measuring radiated emissions and immunity are reviewed and applied to three microstrip configurations. Measurements from 200 to 2000 MHz are compared with theory, and excellent agreement is obtained for two configurations that minimize feed cable and finite ground plane effects. Emissions measurements are found to be more accurate than immunity measurements because the impedance mismatch of the receiving antenna cancels when the ratio of the microstrip and reference radiated power measurements is taken.

02,239
PB96-164090 Not available NTIS
National Inst. of Standards and Technology (EEEL), Gaithersburg, MD. Electronics and Electrical Engineering Lab. Office.
President's Column 'Editorial'.
Final rept.
A. H. Cookson. 1994, 1p.
Pub. in Institute of Electrical and Electronics Engineers Electrical Insulation Magazine, v10 n5 p3 Sep/Oct 94.

Keywords: *Dielectrics, *Electrical insulation, *Semiconductors, Reprints, Electronics, Medicine, IEEE.

As departing President of IEEE's Dielectrics and Electrical Insulation Society after two years, there are changes that have occured and highlights that have been noticed. The Society now has stronger conferences on a global scale with greater student representation. Membership size has grown and financially the Society is in sound condition. Work for the future will include broadening the scope of the Society to increase interest in the areas of semiconductors, electronic and medicine related to unique insulation and dielectrics challenges.

02,240
PB96-167143 Not available NTIS
National Inst. of Standards and Technology (EEEL), Boulder, CO. Electromagnetic Fields Div.
Accurate Electrical Characterization of High-Speed Interconnections.
Final rept.
R. B. Marks, and D. F. Williams. 1994, 6p.
See also PB94-216389.

Pub. in Proceedings of International Symposium on Microelectronics, Boston, MA., November 14-17, 1994, p96-101.

Keywords: *Circuit interconnections, *Transmission lines, Characteristic impedance, Electrical measurement, Digital circuits, Permittivity, Capacitance, High speed, Accuracy, Reprints.

A program at the National Institute of Standards and technology supports the electrical characterization of electronic packaging and interconnections in terms of scattering parameters, impedances, and transmission line. This paper reviews the basic methodology, including its orgins in the characterization of monolithic microwave integrated circuits, and describes the resulting calibration and measurement methods that have been developed.

02,241
PB96-176482 Not available NTIS
National Inst. of Standards and Technology (EEEL), Boulder, CO. Electromagnetic Fields Div.
Dimensional Characterization of Precision Coaxial Transmission Line Standards.
Final rept.
G. V. Sherwood. 1993, 10p.
Pub. in Proceedings of the Measurement Science Conference, Annaheim, CA., January 21-22, 1993, Session 5-B p1-10.

Keywords: *Coaxial cables, *Dimensional measurement, *Transmission lines, Waveguides, Standards, Calibration, Mechanical measurement, Pneumatic instruments, Surface roughness, Microwave equipment, Metrology, Reprints, Coordinate measuring machines, Air gauging, Gauging methods.

Precision, air-dielectric coaxial transmission line standards are commonly used with automatic network analyzers for impedance measurements. This report summarizes recent efforts at NIST to attain improved dimensional and geometric characterization of coaxial lines. The use of computer-sided methods that augment traditional air gaging, roundness testing, and coordinate measuring machine analysis will also be discussed.

02,242
PB96-176599 Not available NTIS
National Inst. of Standards and Technology (EEEL), Boulder, CO. Electromagnetic Fields Div.
Line-Reflect-Match Calibrations with Nonideal Microstrip Standards.
Final rept.
D. F. Williams, and J. B. Schappacher. 1995, 4p.
Pub. in Automatic RF Techniques Group Conference Digest (46th), Scottsdale, AZ., November 30-December 1, 1995, p35-38.

Keywords: *Microstrips, *Reference impedance, Reprints, *Line reflect match calibrations, *Scattering-parameter measurement, Thru-reflect-line calibration.

We apply a previously developed Line-Reflect-Match (LRM) calibration that compensates for the nonideal electrical behavior of the match standard to microstrip transmission lines and investigate impedance definitions, standard parasitics, and calibration accuracy.

02,243
PB96-180138 Not available NTIS
National Inst. of Standards and Technology (EEEL), Gaithersburg, MD. Electricity Div.
Surging the Upside-Down House: Measurements and Modeling Results.
Final rept.
F. D. Martzloff, A. Mansoor, K. O. Phipps, and W. M. Grady. 1996, 15p.
See also PB96-112313.
Pub. in PQA '95, International Conference on Power Quality (4th): Applications and Perspectives, New York, NY., May 9-11, 1995, 17p Aug 95.

Keywords: *Electrical equipment, *Residential buildings, *Surges, *Overcurrent, *Electromagnetic compatibility, Electromagnetic equipment, Circuit protection, Voltage regulation, Surge suppressors, Communication equipment, Wiring, Voltage regulators, Cascaded elements, Reprints.

To demonstrate real-world scenarios, a replica of the wiring system in a typical residence was installed in the laboratory. This paper reports selected results from many measurements, and presents the corresponding numerical modeling, thereby leading to mutual validation of the two processes. Two exposure scenarios for producing differences of voltages between the power and data ports of appliances are illustrated. Additional measurements and parametric variations are reported here to characterize the impedance of the various components of the wiring system and the source impendance of the resulting overvoltages appearing between the ports.

02,244
PB96-186119 Not available NTIS
National Inst. of Standards and Technology (EEEL), Gaithersburg, MD. Electricity Div.
Electrohydrodynamic Instability and Electrical Discharge Initiation in Hexane.
Final rept.
K. L. Stricklett, and R. A. C. Altafim. 1995, 4p.
Pub. in Annual Report, Conference on Electrical Insulation and Dielectric Phenomena, Virginia Beach, VA., October 22-25, 1995, p163-165.

Keywords: *Electrohydrodynamics, *Hexanes, Dielectric fluids, Surface instability, Reprints, *Laser triggered breakdown, Prebreakdown.

An experimental technique is described that tests the hydrodynamic stability of the fluid boundary in a fluid-insulated system: a quasi-uniform field configuration is used and a pulsed, Nd:YAG laser is employed to create a micro-bubble at the surface of one electrode. The gap is pulse-charged and the laser is synchronized with the time-of-application of the voltage pulse. Under appropriate experimental conditions of voltage and laser pulse energy, the bubble evolves to produce full electrical breakdown by the onset and propagation of instabilities in the bubble surface. Experimental data obtained in hexane are presented.

02,245
PB96-191382 PC A03/MF A01
National Inst. of Standards and Technology (EEEL), Boulder, CO. Electromagnetic Fields Div.
Dielectric and Magnetic Measurements from -50C to 200C and in the Frequency Band 50 MHz to 2 GHz.
J. Baker-Jarvis, and J. H. Grosvenor. Mar 96, 20p, NISTIR-5045.

Keywords: *Dielectric properties, *Magnetic properties, *Electrical measurement, *Transmission lines, Cavity resonators, Coaxial cables, Calibrating, Waveguides, High temperatures, Microwave measurements.

This is an overview of techniques for dielectric and magnetic measurements of low-loss through high-loss materials in the frequency range from 50 MHz to 2 GHz and over a temperature range of -50 deg C to 200 deg C. The authors conclude that a single fixture is not adequate to satisfy the measurement objectives. The necessary measurements can be met using a combination of reentrant cavity, coaxial line, and dielectric resonator fixtures. In order to minimize heat loss, the coaxial line fixture should be milled from stainless steel stock and then gold plated. The reentrant cavity and split post resonator fixtures should be fitted with high temperature coaxial cables and temperature control obtained from an environmental furnace.

02,246
PB96-200118 Not available NTIS
National Inst. of Standards and Technology (EEEL), Boulder, CO. Electromagnetic Fields Div.
Coaxial Line-Reflect-Match Calibration.
Final rept.
J. A. Jargon, R. B. Marks, and D. F. Williams. 1995, 4p.
Pub. in Asia-Pacific Microwave Conference Proceedings, Taejon, Korea, October 10-13, 1995, v1 p86-89.

Keywords: *Electrical measurements, *Coaxial cables, *Calibration standards, Transmission lines, Microwave equipment, Metrology, Reflection method, Test methods, Impedance matching, Reprints.

The authors describe a coaxial line-reflect-match calibration that corrects for imperfections in the load used as a match standard. The method provides a practical means of obtaining accurate, wideband calibrations with compact coaxial standard sets. When the load model is valid, the load may be characterized using an additional line of moderate length.

02,247
PB96-200324 Not available NTIS
National Inst. of Standards and Technology (EEEL), Boulder, CO. Electromagnetic Fields Div.
Alternative EMC Compliance Test Facilities.
Final rept.
M. L. Crawford. 1995, 30p.
Pub. in Handbook of Electromagnetic Compatibility, Chapter 18, p681-710 1995.

Keywords: *Electromagnetic capability, *Test facilities, Electrical measurement, Performance, Electromagnetic shielding, Transmission lines, Reprints, Mode stirred method.

Chapter 15 described conventional electromagnetic compatibility compliance test facilities which consist of open-field or shielded enclosures. Shielded enclosures have low residual noise levels and electrical isolation or shielding. Presumably, open-field sites provide both a reference and a perturbation-free environment in which actual operating conditions of the equipment can be simulated. However, open-field sites do not provide isolation from the environment and hence they can be used only under special circumstances.

02,248
PB96-204490 Not available NTIS
National Inst. of Standards and Technology (EEEL), Gaithersburg, MD. Electricity Div.
Correlations between Electrical and Acoustic Detection of Partial Discharge in Liquids and Implications for Continuous Data Recording.
Final rept.
P. von Glahn, K. L. Stricklett, R. J. Van Brunt, and L. A. V. Cheim. 1996, 6p.
Pub. in Conference Record of the Institute of Electrical and Electronics Engineers International Symposium on Electrical Insulation, Montreal, Quebec, Canada, June 16-19, 1996, v1 p67-74.

Keywords: *Acoustic detection, *Continuous recording, *Electrical detection, Reprints, Partial discharge, Signal analysis, Statistical properties, Correlation analysis.

Simultaneous measurements were made of electrical and acoustic signals from partial discharge (PD) produced by applying an alternative voltage at a frequency of 70 Hz to a point-plane electrode gap immersed in transformer oil. Both internally and externally mounted acoustic sensors were tested, and in all cases the intensity of the acoustic PD signal was found, on average, to increase with the amplitude of the electrical PD signal. The correlation between acoustic and electrical PD signal was found to be consistent with results reported from previous investigations. It is shown here that, because of this strong correlation, it is possible to extract statistical information from continuously recorded acoustic PD data, such as pulse phase (time) and amplitude distributions that are in agreement with those obtained from electrical data. It is demonstrated that by having continuous records of all PD events that occur during a test, it is possible to uncover new statistical information that is useful in attempts to understand the physical basis for the phenomenon.

Resistive, Capacitive, & Inductive Components

02,249
AD-A284 623/6 PC A03/MF A01
National Bureau of Standards, Gaithersburg, MD.
Precision Resistors and Their Measurement.
J. L. Thomas. 8 Oct 48, 35p, NBS-470.

Keywords: *Wirewound resistors, Precision, Calibration, Circular, Construction, Electrical resistance, Limitations, Measurement, Resistance, Test and evaluation.

This circular contains information on the construction and characteristics of wire-wound resistors of the precision type. There are also included descriptions of the methods used at this Bureau for the test of precision resistors and the calibration of precision resistance measuring apparatus. Although the presentation is nontechnical, there is a considerable amount of information on the characteristics and limitations of apparatus of this type that should be of interest to any one making accurate measurements of electrical resistance.

02,250
PB94-139672 PC A06/MF A02

National Inst. of Standards and Technology (EEEL), Boulder, CO. Electromagnetic Technology Div.
Electromechanical Properties of Superconductors for DOE Fusion Applications.
J. W. Ekin, S. L. Bray, C. L. Lutgen, and W. L. Bahn. Jan 94, 116p, NISTIR-5013.

Keywords: *Thermonuclear reactor materials, *Superconducting magnets, *Superconductors, *Niobium stannides, *Electromechanics, Superconducting wires, Stress analysis, Axial stress, Critical current, Fusion reactors, US DOE, Niobium aluminides, Vanadium gallides.

The electrical performance of many superconducting materials is strongly dependent on mechanical load. This report presents electromechanical data on a broad range of high-magnetic-field superconductors. The conductors that were studied fall into three general categories: candidate conductors, experimental conductors, and reference conductors. Research on candidate conductors for fusion applications provides screening data for superconductor selection as well as engineering data for magnet design and performance analysis. The effect of axial tensile strain on critical-current density was measured for several Nb3Sn candidate conductors including the US-DPC (United States Demonstration Poloidal Coil) cable strand and an ITER (International Thermonuclear Experimental Reactor) candidate conductor. Also, data are presented on promising experimental superconductors that have strong potential for fusion applications. Axial strain measurements were made on a V3Ga tape conductor that has good performance at magnetic fields up to 20 T. Axial strain data is also presented for three experimental Nb3Sn conductors that contain dispersion hardened copper reinforcement for increased tensile strength. Finally, electromechanical characteristics were measured for three different Nb3Sn reference conductors from the first and second VAMAS (Versailles Project on Advanced Materials and Standards) international Nb3Sn critical-current round robins. Published papers containing key results, including the first measurement of the transverse stress effect in Nb3Sn, the effect of stress concentration at cable-strand crossovers, and electromechanical characteristics of Nb3Al, are included throughout the report.

02,251
PB94-151776 PC A11/MF A03
National Inst. of Standards and Technology (EEEL), Boulder, CO. Electromagnetic Fields Div.
NIST 60-Millimeter Diameter Cylindrical Cavity Resonator: Performance Evaluation for Permittivity Measurements.
Technical note.
E. J. Vanzura, R. G. Geyer, and M. D. Janezic. Aug 93, 241p, NIST/TN-1354.
Also available from Supt. of Docs. as SN003-003-03226-3.

Keywords: *Cavity resonators, Cylindrical configuration, Dielectric materials, Performance evaluation, Computer programs, X band, Uncertainty, Superhigh frequency, *Permittivity measurements, Dielectric measurements, MEAS-RES computer program, CAVITYPROG computer program.

Uncertainty estimates are developed for dielectric permittivity calculations made using the NIST 60-mm diameter cylindrical resonator. A mode-filtering helical waveguide makes up the cavity's cylindrical wall, which permits the generation of high-purity TE(01p) resonant modes for high accuracy permittivity measurements. The cavity's length can be varied from 408 to 433 mm. Fixed-length and fixed-frequency measurements in the X-band frequency range are evaluated with particular emphasis on 10 GHz. Resonator theory and design, measurement tolerances, and software are included.

02,252
PB94-185501 Not available NTIS
National Inst. of Standards and Technology (CSTL), Gaithersburg, MD. Process Measurements Div.
High Temperature Silicide Thin-Film Thermocouples.
Final rept.
K. G. Kreider. 1994, 6p.
Pub. in Materials Research Society Symposia Proceedings, v322 p285-290 1994.

Keywords: *Thermocouples, Temperature measuring instruments, High temperature, Seebeck effect, Thin films, Molybdenum silicides, Rhenium silicides, Tantalum silicides, Titanium silicides, Tungsten silicides, Sputtering, Reprints.

High-temperature silicides have been used in mechanical structures, heating elements, and electronic, CMOS applications. Their stability in high temperature oxidizing environments and excellent electrical conductivity may also make them useful as high temperature thin-film sensors in harsh environments. We have investigated sputter deposited MoSi2, ReSi2, TaSi2, TiSi2, and WSi2 thin films and characterized their performance as thermoelements and stability up to 1200 C. A multilayer technique was developed to ensure constant silicide stoichiometry during oxidation thereby maintaining a constant Seebeck coefficient. In addition, techniques were developed to suppress the formation of metal oxides from the silicides. The results indicated excellent stability of Seebeck coefficient up to 1200 C. These results are compared with the problems of thin film instability in the Seebeck coefficient found in noble metal thermocouples. Potential applications for temperature and heat transfer measurements will be discussed.

02,253
PB94-185519 Not available NTIS
National Inst. of Standards and Technology (CSTL), Gaithersburg, MD. Process Measurements Div.
Thin Film Transparent Thermocouples.
Final rept.
K. G. Kreider. 1992, 5p.
Pub. in Sensors and Actuators A 34, p95-99 1992.

Keywords: *Thermocouples, Temperature measuring instruments, Antimony oxides, Indium oxides, Seebeck effect, Thin films, Sputtering, Transparence, Reprints, Antimony tin oxides, Indium tin oxides.

Transparent thin-film electrical conductors have been sputter deposited to form transparent thermocouples. Indium-tin oxide (ITO) and antimony-tin oxide (ATO) have demonstrated Seebeck coefficients of 7-77 micro V/C, depending on their conductivity and fabrication parameters. In addition to results for in-house-fabricated thermocouples, thermoelectric measurements are reported on commercial ATO, ITO, and fluorine-doped tin oxide transparent films.

02,254
PB94-200060 Not available NTIS
National Inst. of Standards and Technology (EEEL), Gaithersburg, MD. Electricity Div.
NIST Capacitance Measurement Assurance Program (MAP).
Final rept.
Y. M. Chang. 1993, 10p.
Pub. in Proceedings of Measurement Science Conference, Anaheim, CA., January 21-22, 1993, p1-10.

Keywords: *Capacitance, Calibration, Reprints, Measurement Assurance Program, MAP program, Reference standards, US NIST.

This paper describes the recently developed capacitance Measurement Assurance Program (MAP) service at the National Institute of Standards and Technology (NIST). Using a commercial digital capacitance meter as the transport standard, two separate pilot programs for the capacitance MAP have been carried out for standards at both the 1,000 pF and 100 pF levels. The first was carried out as a single transfer with a government standards laboratory, and the second was designed for round-robin measurements as a multiple transfer by three industrial standards laboratories. In contrast to the normal MAP, where the transport standards are measured by the client laboratory, the capacitance MAP involves measurements performed on 'dummy' standards by both the meter (transport standard) and the laboratory capacitance measuring systems. Results from these two pilot programs are presented. Also included are requirements and procedures for laboratories interested in participating in the capacitance MAP service.

02,255
PB94-211521 Not available NTIS
National Inst. of Standards and Technology (NEL), Boulder, CO. Electromagnetic Technology Div.
Roles of Copper in Applied Superconductivity.
Final rept.
F. R. Fickett. 1990, 8p.
Pub. in Proceedings of Conference on Copper '90: Refining, Fabrication, Markets, Vasteras Congress Centre, Sweden, October 1-3, 1990, p310-317.

Keywords: *Superconducting devices, *Superconductivity, *Copper alloys, *Copper, High temperature superconductors, Superconducting magnets, Historical aspects, Cryogenics, Cuprates, Uses, Reprints.

Copper plays many roles in applied superconductivity, but its contribution is seldom acknowledged. In this paper, we review the uses of copper in each of many categories, both historically and in the latest applications. A brief description of the desired properties of the copper used for each application will be given, along with some suggestions as to how to achieve these properties in commercial copper products.

02,256
PB95-151288 Not available NTIS
National Inst. of Standards and Technology (EEEL), Gaithersburg, MD. Electricity Div.
Electron Scattering and Dissociative Attachment by SF6 and Its Electrical-Discharge By-Products.
Final rept.
H. X. Wan, J. H. Moore, J. K. Olthoff, and R. J. Van Brunt. 1993, 16p.
Grant NSF-CHE91-20504
Sponsored by National Science Foundation, Washington, DC. and Department of Energy, Washington, DC.
Pub. in Plasma Chemistry and Plasma Processing 13, n1 p1-16 1993.

Keywords: *Electron-molecule collisions, *Electron scattering, *Sulfur fluorides, *Electric discharges, Scattering cross sections, Chemical dissociation, Electron attachment, Sulfur hexafluoride, Sulfur dioxide, Milli eV range, EV range 1-10, EV range 10-100, Plasma chemistry, Plasma etching, Negative ions, Reprints.

Discrete electron-molecule processes relevant to SF6 etching plasmas are examined. Absolute, total scattering cross sections for 0.2-12-eV electrons on SF6, SO2, SOF2, SO2F2, SOF4, and SF4, as well as cross sections for negative-ion formation by attachment of electrons, have been measured. These are used to calculate dissociative-attachment rate coefficients as a function of E/N for SF6 by-products in SF6.

02,257
PB95-153516 Not available NTIS
National Inst. of Standards and Technology (EEEL), Gaithersburg, MD. Electricity Div.
Pressure Dependencies of Standard Resistors.
Final rept.
R. F. Dziuba. 1993, 7p.
Pub. in Proceedings of National Computer Systems Laboratory Workshop and Symposium, Albuquerque, NM., July 25-29, 1993, p363-369.

Keywords: *Resistors, *Pressure, *Electrical resistance, Electrical measurement, Standards, Reprints.

The U.S. representation of the ohm is based on the quantized Hall resistance of 6453.20175 ohms with a combined standard uncertainty of 0.02 ppm. To maintain the ohm at this resistance or other resistances at this uncertainty level requires well characterized standard resistors. A sometimes overlooked parameter affecting standard resistors is pressure. A variety of standard resistors are examined for pressure dependencies over the range 250 hectopascals (hPa) above and below a standard atmosphere. Results indicate that the pressure coefficients of resistance for some standards are significant.

02,258
PB95-153557 Not available NTIS
National Inst. of Standards and Technology (EEEL), Boulder, CO. Electromagnetic Technology Div.
Preparation of Low Resistivity Contacts for High-Tc Superconductors.
Final rept.
J. W. Ekin. 1993, 37p.
Pub. in Processing and Properties of High-Tc Superconductors, Chapter 9, v1 p371-407 1993.

Keywords: *High temperature superconductors, *High-TC superconductors, *Electric contacts, YBCO superconductors, Soldering, Joining, Reprints, Yttrium barium cuprates.

Methods for preparing practical contacts to high-T(c) superconductors are described, including quick, easy techniques for attachment of voltage-taps, and detailed descriptions of how to fabricate high-quality contacts for current connections. Methods for soldering and lead attachment that preserve the low-resistivity of high-quality contacts are also presented.

02,259
PB95-161311 Not available NTIS

National Inst. of Standards and Technology (CSTL), Gaithersburg, MD. Process Measurements Div.
Sputtered High Temperature Thin Film Thermocouples.
Final rept.
K. G. Kreider. 1993, 5p.
Pub. in Jnl. of Vacuum Science and Technology A 11, n4 p1401-1405 Jul/Aug 93.

Keywords: *Thermocouples, Temperature measuring instruments, Temperature range 0400-1000 K, Rhodium containing alloys, Rhodium oxides, Platinum alloys, Thin films, Seebeck effect, Aluminum oxides, Annealing, Reprints.

Thin film thermocouples have the advantage of extremely fast response (< 1 ms), low cost, and very fine spatial resolution. These capabilities have permitted measurements never before possible, such as the instantaneous temperature measurements of the inside surfaces of a diesel engine cylinder during operation. Although these type S platinum plus platinum 10% rhodium thermocouples are stable at the 900-1100 C range, oxidation of rhodium can take place in the 600-800 C range in air which lessens the thermoelectric potential of the positive element. We evaluated the effect of air exposures to high temperature thin film thermocouples and attempted to find solutions to the problem. We found that after 50 h at 750 C the Seebeck coefficient of a platinum 10% rhodium element was reduced 50% compared to the as-sputtered condition. The reduction of Seeback coefficient at 700 and 800 C was also substantial. This reduction in Seeback coefficient could be recovered by annealing the thin film at 900 C. The degradation after 750 C could be suppressed using a 1 micrometer sputtered aluminum oxide coating. The reversible behavior suggests the formation of Rh2O3 at 700-800 C and its subsequent reduction at temperatures at which the free energy of formation is zero or positive. Microstructural evidence confirm these conclusions.

02,260
PB95-161386 Not available NTIS
National Inst. of Standards and Technology (EEEL), Gaithersburg, MD. Electricity Div.
Lithium-Drift Technique for Making Submicron Thick Silicon Membranes.
Final rept.
K. C. Lee. 1992, 8p.
Pub. in Proceedings of Symposium on Electrochemical Microfabrication, Phoenix, AZ., October 16, 1992, p1-8.

Keywords: *Electrochemistry, Pressure sensors, Cantilever beams, Room temperature, Wafers, Reprints, *Silicon membranes, Anodic etching, Lithium diffusion, Microfabrication.

An electrochemical method for preparing silicon membranes that relies on the use of room temperature lithium diffusion to create a compensated, high resistivity layer with very low etch rate near one surface of a p-type Si wafer is described. The bulk wafer can be dissolved away, leaving behind a membrane that can be between several tenths of a micrometer and several micrometers in thickness. The various parameters that affect the thickness of the membrane are described. As an example of this technique, the preparation of a 670 nm thick silicon membrane is described.

02,261
PB95-168852 Not available NTIS
National Inst. of Standards and Technology (PL), Boulder, CO. Time and Frequency Div.
Ultralinear Small-Angle Phase Modulator.
Final rept.
J. Lowe, and F. L. Walls. 1991, 4p.
Pub. in Proceedings of European Frequency and Time Forum, Besancon, France, March 12-14, 1991, p461-464.

Keywords: *Quartz resonators, Phase modulation, Frequency response, Electric fields, Direct current, Linear systems, Reprints, *Phase modulators, Polarizing effect.

A dc electric field applied to a quartz plate resonator causes changes in the elastic constants which can lead to a change in the frequency of the resonator. This effect, known as the polarizing effect, has been shown to be extremely linear. We have used this effect to build a phase modulator with 2nd-harmonic distortion that is at least 117 dB below the fundamental modulation and low added phase noise. A description of the modulator as well as methods of measurement are discussed.

02,262
PB95-169009 Not available NTIS
National Inst. of Standards and Technology (PL), Boulder, CO. Time and Frequency Div.
Relationship of AM to PM Noise in Selected RF Oscillators.
Final rept.
L. M. Nelson, C. W. Nelson, and F. L. Walls. 1994, 5p.
Pub. in Institute of Electrical and Electronics Engineers Transactions on Ultrasonics, Ferroelectrics, and Frequency Control 41, n5 p680-684 Sep 94.

Keywords: *Radiofrequency oscillators, *Quartz resonators, *Electromagnetic noise, Amplitude modulation, Phase modulation, Cross correlation, Very high frequency, High frequency, Reprints, Flicker noise, Phase noise.

We have studied the amplitude modulation (AM) and phase modulation (PM) noise in a number of 5 MHz and 100 MHz oscillators to provide a basis for developing models of the origin of AM noise. To adequately characterize the AM noise in high performance quartz oscillators, we found it necessary to use two-channel cross-correlation AM detection. In the quartz oscillators studied, the power spectral density (PSD) of the f(sup -1) and f(sup 0) regions of AM noise is closely related to that of the PM noise. The major difference between different oscillators of the same design depends on the flicker noise performance of the resonator. We therefore propose that the f(sup -1) and f(sup 0) regions of AM and PM noise arise from the same physical processes, probably originating in the sustaining amplifier.

02,263
PB95-171419 PC A03/MF A01
National Inst. of Standards and Technology (EEEL), Gaithersburg, MD. Electricity Div.
Design Challenges in a Commercial Quantum Hall Effect-Based Resistance Standard.
K. C. Lee, and M. E. Cage. Nov 94, 42p, NISTIR-5533.

Keywords: *Electrical resistance, *Primary standards, *Standards, Temperature range 0000-0013 K, Cryogenic temperature, Cryogenic cooling, Temperature dependence, Electrical measurement, Commercial equipment, Wire wound resistors, Calibration, Closed-cycle cooling systems, Design criteria, *Resistance standards, *Quantum Hall effect.

Of the electrical measurements that underpin the broad spectrum of modern industry, measurements of voltage, resistance, and impedance are among the most important. National Standards laboratories have developed intrinsic standards based on quantum effects, such as Josephson's Effect and the quantum Hall effect that can be used to realize standards of voltage and resistance. The equipment necessary to observe these phenomena is very complex and expensive, and these standards have not yet found wide application in industrial laboratories. This paper assesses the possibility of developing a commercially viable quantum Hall effect-based resistance standards system. The capabilities of resistance calibration systems currently in use are summarized, and specifications for a competitive quantum Hall effect-based system are described. The realization of such a system presents numerous challenges, from making suitable samples, to developing high accuracy, automated measurement systems, to developing low cost, reliable cryogenic systems. These technical challenges are discussed in detail, and several possible commercial systems are described.

02,264
PB95-175527 Not available NTIS
National Inst. of Standards and Technology (EEEL), Boulder, CO. Electromagnetic Technology Div.
Characterization of a Tunable Thin Film Microwave YBa2Cu3O7-x/SrTiO3 Coplanar Capacitor.
Final rept.
D. Galt, J. C. Price, J. A. Beall, and R. H. Ono. 1993, 3p.
Pub. in Applied Physics Letters 63, n22 p3078-3080 Nov 93.

Keywords: *Superconducting devices, *Resonators, High temperature superconductors, YBCO superconductors, Strontium titanates, Microwave equipment, Microstrip devices, Variable capacitors, Thin films, Coplanarity, Tuning, Reprints, Yttrium barium cuprates, Ferroelectric capacitors.

We have fabricated and characterized electrically tunable high temperature superconductor coplanar microstrip resonators incorporating tunable SrTiO3 ferroelectric thin films. The low frequency capacitance of the SrTiO3 capacitor is measured directly. High frequency capacitance and loss information are extracted from the observed resonances and compared with the low frequency data. Hysteresis loops display an onset of ferroelectricity at 160 K. The spontaneous charge and coercive voltage (at 10 kHz) as a function of temperature are extracted from these loops.

02,265
PB95-180451 Not available NTIS
National Inst. of Standards and Technology (EEEL), Boulder, CO. Electromagnetic Technology Div.
Improved Eddy-Current Decay Method for Resistivity Characterization.
Final rept.
A. B. Kos, and F. R. Fickett. 1994, 3p.
Sponsored by International Copper Research Association, Inc., New York.
Pub. in Institute of Electrical and Electronics Engineers Transactions on Magnetics 30, n6 p4560-4562 Nov 94.

Keywords: *Electrical resistivity, *Electrical measurement, *Eddy currents, Low temperature, Curve fitting, Metals, Copper, Reprints.

Eddy-current decay is a unique, nondestructive method for determining the low-temperature resistivity of large samples of pure metal. Furthermore, it is the only means available for measurement of the residual resistivity ratio (RRR), rho(273 K)/rho(4 K), of samples with shapes that do not lend themselves to conventional four-wire resistance measurement techniques. An improvement to an earlier implementation of the eddy-current decay method of resistivity characterization is presented. It involves modernizing the earlier apparatus by the use of a digitizing oscilloscope, commercial curve-fitting software, digital averaging techniques, and modern electronics. Data are shown for high-purity copper cylinders.

02,266
PB95-180477 Not available NTIS
National Inst. of Standards and Technology (EEEL), Boulder, CO. Electromagnetic Fields Div.
Dielectric Properties of Single Crystals of Al2O3, LaAlO3, SrTiO3, and MgO at Cryogenic Temperatures.
Final rept.
J. Krupka, R. G. Geyer, M. Kuhn, and J. H. Hinken. 1994, 190p.
Pub. in Institute of Electrical and Electronics Engineers Transactions on Microwave Theory and Techniques 42, n10 p1886-1890 Oct 94.

Keywords: *Aluminum oxide, *Strontium titanates, *Magnesium oxides, *Dielectric properties, Temperature range 0013-0065 K, Temperature range 0065-0273 K, Temperature range 0273-0400 K, Superconducting films, Microwave frequencies, Permittivity, Substrates, Reprints, *Lanthanum aluminates, *Neodymium gallates.

A dielectric resonator technique has been used for measurements of the permittivity and dielectric loss tangent of single-crystal dielectric substrates in the temperature range 20-300 K at microwave frequencies. Application of superconducting films made it possible to determine dielectric loss tangents of about 5 X 10(exp -7) at 20 K. Two permittivity tensor components for uniaxially anisotropic samples were measured. Generally, single-crystal samples made of the same material by different manufacturers or by different processes have significantly different losses, although they have essentially the same permittivities. The permittivity of one crystalline ferroelectric substrate, SrTiO3, strongly depends on temperature. This temperature dependence can affect the performance of ferroelectric thin-film microwave devices, such as electronically tunable phase shifters, mixers, delay lines and filters.

02,267
PB95-181160 Not available NTIS
National Inst. of Standards and Technology (EEEL), Boulder, CO. Electromagnetic Technology Div.
Dielectric Properties of Thin Film SrTiO3 Grown on LaAlO3 with YBa2Cu3O7-x Electodes.
Final rept.
H. Wu, F. Barnes, D. Galt, J. Price, and J. Beall. 1994, 10p.
Pub. in Proceedings of Society of Photo-Optical Instrumentation Engineers: High Tc Microwave Superconductors and Applications, Los Angeles, CA., January 25-27, 1994, v2156 p131-140.

Keywords: *Strontium titanates, *Dielectric properties, High-Tc superconductors, Temperature dependence, Microwave frequencies, Microstrip devices, YBCO superconductors, AC losses, Thin films, Capacitance, Capacitors, Substrates, Reprints, Yttrium barium cuprates, Lanthanum aluminates, Microstrip resonators.

We have fabricated and characterized YBCO (YBa2Cu3O(7-x)) microstrip resonators on LAO(LaAlO3) substrates that include thin film STO(SrTiO3) coplanar capacitors to study the dielectric properties of thin film STO. The low frequency capacitance of the STO/LAO capacitor is measured as a function of temperature and dc bias. We use the observed resonant frequencies to extract the microwave frequency capacitance of the structure and the Q's to determine the microwave losses. A conformal map is developed and used to transform the observed capacitances into dielectric constant values for the thin film STO.

02,268
PB95-202461 Not available NTIS
National Inst. of Standards and Technology (EEEL), Boulder, CO. Electromagnetic Technology Div.
Domain Effects in Faraday Effect Sensors Based on Iron Garnets.
Final rept.
M. N. Deeter. 1995, 4p.
See also PB92-197482.
Pub. in Applied Optics 34, n4 p655-658, 1 Feb 95.

Keywords: *Magnetic measurement, *Ferrite garnets, Yttrium iron garnets, Magnetic anisotropy, Magnetic domains, Magnetic films, Faraday effect, Thick films, Comparative evaluations, Magnetooptics, Diffraction, Reprints, *Magnetic field sensors.

Domain-induced diffraction effects produced by two iron garnet thick films and two bulk crystals are compared. The thick films, characterized by a serpentine magnetic domain structure, produced nonlinear response functions; this is in qualitative agreement with a one-dimensional diffraction model. Bulk iron garnet crystals, which exhibited a complex three-dimensional domain structure, produced qualitatively similar effects that diminished with increasing crystal length. Differential signal processing resulted in a linear signal for the thick films and a primarily sinusoidal response for the bulk crystals.

02,269
PB95-251625 PC A03/MF A01
National Inst. of Standards and Technology (EEEL), Gaithersburg, MD. Electricity Div.
SF6 Insulation: Possible Greenhouse Problems and Solutions.
L. G. Christophorou, and R. J. Van Brunt. Jul 95, 28p, NISTIR-5685.

Keywords: *Sulfur hexafluoride, *Electrical insulation, Dielectric materials, Gas-insulated substations, Gas-insulated cables, Gas-insulated transformers, Physical properties, Chemical properties, Dielectric properties, Recycling, Alternatives, Environmental chemical substitutes, Nitrogen, Mixtures, Greenhouse gases, Ozone depletion, Air pollution abatement, *Insulating gas.

Sulfur hexafluoride (SF6) is the most commonly used insulating gas in electrical systems to date. It is however, a potent greenhouse gas and, thus, its use entails fears of environmental costs, regulations, and restrictions, in spite of its current low levels in the environment. This potential problem and current efforts in the search for short-term and long-term solutions are briefly outlines and discussed in this report. Limiting the release of SF6 in the environment, recycling SF6, and using it where it is needed the most, are among the elements of an emerging consensus effort for the short run. A long-term solution may include the search for alternative high-voltage insulants such as high-pressure gaseous dielectrics (e.g., N2 and N2/SF6 mixtures).

02,270
PB96-102389 Not available NTIS
National Inst. of Standards and Technology (EEEL), Boulder, CO. Electromagnetic Technology Div.
Ferroelectric Thin Film Characterization Using Superconducting Microstrip Resonators.
Final rept.
D. Galt, J. C. Price, J. A. Beall, and T. E. Harvey. 1995, 4p.
Pub. in Institute of Electrical and Electronics Engineers Transactions on Applied Superconductivity, v5 n2 p2575-2578 Jun 95.

Keywords: *Ferroelectricity, *Thin films, *Resonators, *Microwave frequencies, Superconductors, Dielectric properties, Capacitors, Bias, Solid state devices, Reprints, YBCO film, Microstrip devices.

The authors describe a novel technique for characterizing the dielectric response of ferroelectric thin films at microwave frequencies. The method involves a microstrip resonator which incorporates a ferroelectric capacitor at its center. To demonstrate this method the authors have fabricated a superconducting microstrip resonator from a laser ablated Yba2Cu3O(7-delta) (YBCO) film on a LaAlO3(LAO) subsrate with a SrTiO3(STO) capacitor at its center. The authors report the observed dielectric behavior of the STO laser ablated film as a function of bias at liquid He and N2 temperatures and at high and low frequencies. It is observed that the electrically tunable dielectric constant of the STO film is roughly independent of frequency up to 20 GHz (especially at high bias). The loss tangent of the STO/LAO capacitor decreases with increasing bias and is apparently independent of frequency between 6 and 20 GHz.

02,271
PB96-103148 Not available NTIS
National Inst. of Standards and Technology (PL), Boulder, CO. Time and Frequency Div.
Environmental Sensitivities of Quartz Oscillators.
Final rept.
F. L. Walls, and J. J. Gagnepain. 1991, 9p.
See also N91-25797.
Pub. in Institute of Electrical and Electronics Engineers Transactions on Ultrasonics, Ferroelectrics, and Frequency Control, v39 n2 p241-249 Mar 92.

Keywords: *Oscillators, *Quartz, *Environmental effects, *Sensitivity, Frequency analysis, Amplitudes, Mechanical vibrations, Noise, Magnetic fields, Electric fields, Irradiation, Temperature, Humidity, Pressure, Acceleration, Reprints.

The frequency, amplitude, and noise of the output signal of a quartz oscillator are affected by a large number of environmental effects. The paper examines the physical bases for the sensitivity of precision oscillators to temperature, humidity, pressure, acceleration and vibration, magnetic field, electric field, load, and radiation. The sensitivity of quartz oscillators to radiaton is a very complex topic and poorly understood. Therefore only a few general results are mentioned. The senstivity to most external influences often varies significantly both from one oscillator type to another and from one unit of a given type to another. For a given unit, the sensitivity to one parameter often depends on the value of other parameters and on history.

02,272
PB96-103155 Not available NTIS
National Inst. of Standards and Technology (EEEL), Gaithersburg, MD. Electricity Div.
Digital Impedance Bridge.
Final rept.
B. C. Waltrip, and N. M. Oldham. 1995, 4p.
See also PB91-101196.
Pub. in Institute of Electrical and Electronics Engineers Transactions on Instrumentation and Measurement, v44 n2 p436-439 Apr 95.

Keywords: *Impedence measurement, *Digital systems, *Electric bridges, Electrical impedance, Circuits, Standards, Comparative evaluations, Inductance, Resistors, Reprints.

An impedance bridge that compares two-terminal standard inductors to characterized ac resistors in the frequency range of 10 Hz to 100 kHz is described. A dual-channel, digitally-synthesized source and sampling digital multimeter are used to generate and measure relevant bridge signals. A linear interpolation algorithm is used to autocalibrate the bridge to a 1 nF gas dielectric capacitor. An intercomparison of the new bridge with existing measurement standards conducted in the low audio frequency range shows agreement of 50 to 200 parts in 10(exp 6) for inductors for 1 mH to 10 H.

02,273
PB96-111869 Not available NTIS
National Inst. of Standards and Technology (EEEL), Boulder, CO. Electromagnetic Fields Div.
Measurements of Permittivity and the Dielectric Loss Tangent of Low Loss Dielectric Materials with a Dielectric Resonator Operating on the Higher Order Te(sub 0 gamma delta) Modes.
Final rept.
J. Krupka, R. G. Geyer, and D. Cros. 1994, 6p.
Pub. in International Microwave Conference (10th), MIKON - 94, Ksiaz Castle, Poland, May 30-June 2, 1994, v2 p567-572.

Keywords: *Resonators, *Dielectric resonators, Reprints, Microwaves, Permittivity, Metrology, Modes, *Foreign technology.

Dielectric resonator techniques are commonly used for permittivity and the dielectric loss tangent measurements of low-loss materials. Usually, the TE mode (1-2) or TE mode (3-5) is used. In this case, if dielectric characterization is required at various frequencies, more than one sample of the material under test must be provided. These samples must have differing physical dimensions. In order to perform dielectric measurements on a single sample at several contiguous frequency subbands, higher-order TE modes may be utilized. These higher-order modes are tuned by changing the distance between the conductor ground planes of the dielectric resonator. Identification of higher-order TE resonant modes in several cylindrical samples of the material under test allows properties to be determined over a broad frequency spectrum.

02,274
PB96-119326 Not available NTIS
National Inst. of Standards and Technology (EEEL), Gaithersburg, MD. Electricity Div.
Automated Resistance Measurements at NIST.
Final rept.
R. F. Dziuba. 1995, 7p.
Pub. in National Conference of Standards Laboratories (NCSL) Workshop and Symposium, Dallas, TX., July 16-20, 1995, p189-195.

Keywords: *Resistors, *Automation, *Calibration, *US NBS, Measurements, Quality assurance, Standards, Reprints, Standard resistors, NIST(National Institute of Standards and Technology).

The National Institute of Standards and Technology (NIST) provides a calibration service for dc standard resistors over 17 decades of resistance from 10(exp -4) Ohms to 10(exp 12) Ohms using seven independent measurement systems. Four measurement systems are completely automated for calibrating resistors from 1 Ohms to 1 M Ohms. A fifth system for high resistance measurements is semiautomated. Plans are underway to fully automate this system, along with the remaining two measurements is semiautomated. Plans are underway to fully automate this system, along with the remaining two measurement systems. The primary consideration to automate a measurement system is to improve the quality of measurements, and not simply to relieve the operator from tedious repetitive measurements. This paper describes the extent and future plans of resistance measurement automation at NIST.

02,275
PB96-122494 Not available NTIS
National Inst. of Standards and Technology (EEEL), Gaithersburg, MD. Electricity Div.
Constant Temperature and Humidity Chamber for Standard Resistors.
Final rept.
D. G. Jarrett. 1995, 5p.
Pub. in National Conference of Standards Laboratories, Dallas, TX., July 16-20, 1995, p501-505.

Keywords: *Test chambers, *Laboratory equipment, *Resistors, Environmental control, Calibration, Relative humidity, Air temperature, Heating systems, Air conditioning, Insulation, Reprints.

An environmental chamber has been developed for housing standard resistors under controlled temperature and humidity conditions during calibration in air. The design allows sufficient space for standard resistors to be housed in a volume of 0.25 cubic meters with sixteen pairs of coaxial connectors feeding through the chamber wall to the lab environment. The box is of double-walled construction with the inner box electrically and thermally insulated from the outer box. Improved insulation and control circuitry along with

added volume are some of the improvements this new air chamber has over other chambers previously used for calibrating standard resistors at NIST.

02,276
PB96-172333 PC A03/MF A01
National Inst. of Standards and Technology (EEEL), Gaithersburg, MD. Electricity Div.
NIST Measurement Assurance Program for Capacitance Standards at 1 kHz.
Technical note.
Y. M. Chang. Mar 96, 27p, NIST/TN-1417.
Also available from Supt. of Docs. as SN003-003-03393-6. See also PB94-200060.

Keywords: *Capacitance, *Calibration, Measuring instruments, *Measurement Assurance Program, MAP program, Reference Standards, US NIST.

The document describes the capacitance Measurement Assurance Program (MAP) service at the National Institute of Standards and Technology (NIST). This service, which uses a commercial digital capacitance meter as the transport standard, provides calibration for capacitance standards at both the 1000 pF and 100 pF levels, at a frequency of 1 kHz. In contrast to the normal MAP, where the transport standards are measured by the client laboratory, the capacitance MAP involves measurements performed on 'dummy' standards by both the Meter (transport standard) and the laboratory capacitance measuring system. Measurement procedures and requirements for client laboratories are included. Also presented are error analysis, assigned values, and equations to estimate the combined uncertainties of the assigned values.

02,277
PB96-176565 Not available NTIS
National Inst. of Standards and Technology (PL), Boulder, CO. Time and Frequency Div.
Fundamental Limits on the Frequency Stabilities of Crystal Oscillators.
Final rept.
F. L. Walls, and J. R. Vig. 1995, 14p.
Pub. in Institute of Electrical and Electronics Engineers Transactions on Ultrasonics, Ferroelectrics, and Frequency Control, v42 n4 p576-589, 13 Jul 95.

Keywords: *Frequency stability, *Crystal oscillators, Environmental effects, Quartz oscillators, Quartz resonators, Reprints, BAW resonators, Flicker FM.

The frequency instabilities of precision bulk acoustic wave (BAW) quartz crystal oscillators are reviewed. The fundamental limits on the achievable frequency stabilities, and the degree to which the fundamental limits have been approached to data are examined. Included are the instabilities as a function of time, temperature, acceleration, ionizing radiation, electromagnetic fields, humidity, atmospheric pressure, power supply, and load impedance. Most of the fundamental limits are zero or negligibly small, a few are finite. We speculate about progress which may be achievable in the future with respect to approaching the fundamental limits. Suggestions are provided about the paths that may lead to significant stability improvements.

02,278
PB96-180179 Not available NTIS
National Inst. of Standards and Technology (MEL), Gaithersburg, MD. Automated Production Technology Div.
Complicated Cases and Shielded Rooms: Audiometric Booths Shielded to Attenuate Electromagnetic Interference.
Final rept.
V. Nedzelnitsky. 1996, 2p.
Pub. in Jnl. of the Acoustical Society of America, v97 n5 pt2 p3321-3322 May 95.

Keywords: *Electromagnetic shielding, *Electroacoustics, *Test chambers, Electromagnetic interference, Radiofrequency, Hearing aids, Electromagnetic compatibility, Standards, Reprints, Audiometric equipment.

Electromagnetic compatibility (EMC) issues involving acoustical instruments, especially their susceptibility and immunity to electromagnetic interference (EMI), are increasing in importance. Of particular significance is the impact on commercial practice and international trade of two Councils of the European Communities directives regarding generic apparatus and medical devices. Directive 93/42/EED is being interpreted to include hearing aids and audiometric instruments. In the U.S.A., at least, existing standards for measuring such shielded-room performance were not specifically developed for audiometric booths. Methods in some of these standards have been adapted and applied to that purpose. Selected standards, methods, and some considerations regarding their application to measuring the shielding performance of audiometric booths in hospital/clinical environments are discussed.

02,279
PB96-186036 Not available NTIS
National Inst. of Standards and Technology (MSEL), Boulder, CO. Materials Reliability Div.
Determination of Sheet Steel Formability Using Wide Band Electromagnetic-Acoustic Transducers.
Final rept.
A. V. Clark, C. M. Fortunko, M. G. Lozev, S. R. Schaps, and M. C. Renken. 1992, 18p.
Pub. in Research in Nondestructive Evaluation, v4 n3 p165-182 1992.

Keywords: *Formability, *Acoustics, *Sheet metal, Resonance, Reprints, *Electromagnetic acoustic transducers, R-value.

An electromagnetic-acoustic transducer (EMAT) system was used in conjunction with a 'sample' CW signal-processing method to generate, receive, and process longitudinal and shear waves in thin steel sheets. Using the system, swept-frequency measurements were made up to 7.5 MHz., To relate the measurements to sheet steel formability, a dimensionless frequency ratio, K, was computed from the resonant frequencies. From theoretical considerations, K should be related to a measure of steel sheet formability, r. This parameter is traditionally measured by plastically deforming uniaxial tension specimens. Good correlation was found between K and r for a set of steel sheet represenative of those typically used to produce automobile body parts.

02,280
PB96-186044 Not available NTIS
National Inst. of Standards and Technology (MSEL), Boulder, CO. Materials Reliability Div.
Effect of Liftoff on Accuracu of Phase Velocity Measurements Made with Electromagnetic-Acoustic Transducers.
Final rept.
A. V. Clark, and Y. Berlinsky. 1992, 41p.
Pub. in Research in Nondestructive Evaluation, 41p 1992.

Keywords: *Acoustics, Liftoff, Reprints, *Electromagnetic acoustic transducers, *Phase velocity.

Electromagnetic-acoustic transducers (EMATs) work on transduction principles which allow them to operate with a clearance (liftoff) between them and a conducting specimen. They have the potential for on-line ultrasonic measurements of rapidly moving materials. Liftoff causes changes in the effective inductance and resistance of the EMAT. Consequently, it causes a phase shift in the output voltage of a receiving EMAT. This can cause errors when the EMAT is used for velocity measurements. In this paper, the authors develop a model for the effect of liftoff. The model gives good agreement with measured liftoff-induced arrival time changes. The model can be extended to the case of an EMAT used with a voltage stepup transformer. The maximum signal is obtained for EMATs operating at resonance; however, the maximum sensitivity to liftoff also occurs then. Thus, a tradeoff must be made between optimum signal and supressing liftoff artifacts. The authors' model, and experimental results, can be used to make these tradeoffs.

02,281
PB96-186051 Not available NTIS
National Inst. of Standards and Technology (MSEL), Boulder, CO. Materials Reliability Div.
Methods to Improve the Accuracy of On-Line Ultrasonic Measurement of Steel Sheet Formability.
Final rept.
A. V. Clark, Y. Berlinsky, N. Izworski, S. R. Schaps, Y. Cohen, and D. V. Mitrakovic. 1992, 36p.
Pub. in Jnl. of Nondestructive Evaluation, 36p 1992.

Keywords: *Formability, *Steel sheet, Nondestructive tests, Reprints, *Electromangetic acoustic transducers, Ultrasonic velocity, R value.

Ultrasonics offers a potential means to measure sheet steel formability nondestructively. The formability can be characterized by the plastic strain ratio, or r-value. To be practical, an ultrasonic system should resolve r-value accurately, on rapidly moving material. The authors report here on research which quantifies factors which could degrade this resolution. The authors also present means to suppress these artifacts. They have developed a moving sheet device (MSD) to be used as a test bed to demonstrate the feasibility of on-line measurement of r-value in a steel mill. The device can move specimens at speeds comparable to those in industrial practice. An automated velocity measurement system has also been developed and integrated with the MSD. This allows ultrasonic measurements to be made with an array of transducers. Measurements were made in both static and dynamic mode. Artifacts due to sheet motion were found to be small, and should not significantly degrade 4-value resolution.

02,282
PB96-190384 Not available NTIS
National Inst. of Standards and Technology (EEEL), Boulder, CO. Electromagnetic Technology Div.
High Frequency Magnetic Field Sensors Based on the Faraday Effect in Garnet Thick Films.
Final rept.
R. Wolfe, E. M. Gyorgy, R. A. Lieberman, M. N. Deeter, G. W. Day, V. J. Fratello, and S. J. Licht. 1992, 3p.
See also PB92-198167.
Pub. in Applied Physics Letters, v60 n17 p2048-2050 Apr 92.

Keywords: *Magnetic measurement, Magnetic anistropy, Magnetooptics, Faraday effect, Epitaxial films, Reprints, *Fiber optic sensors, *Magnetic field sensors, Stripe domains.

The Faraday effect in the thick epitaxial films of magnetic garnets of the type used in magnetooptic isolators can be used as the basis for a fiber-optic magnetic field sensor. These films have uniaxial anisotropy perpendicular to the surface and they contain bismuth to enhance the Faraday rotation. The typical magnetic domain pattern of meandering stripes changes in response to an applied field perpendicular to the film and this changes the polarization of infrared light propagating perpendicular to the film. Theory and experiment show that the speed of operation is limited by relaxation or resonance effects to upper frequencies between 10(6) and 10(9) Hz. Maximum sensitivity requires low magnetic moment and large thickness, in conflict with the requirements for high speed.

02,283
PB97-110233 Not available NTIS
National Inst. of Standards and Technology (CSTL), Gaithersburg, MD. Process Measurements Div.
Thin Film Thermocouple Research at NIST.
Final rept.
K. G. Kreider. 1991, 18p.
See also PB91-190116.
Pub. in ISA Conference Proceedings of the International Instrumentation Symposium (37th), Anaheim, CA., October 29-31, 1991, p13-30.

Keywords: *Thin films, *Thermocouples, *Indium oxides, *Tin oxides, Sputtering, Ceramics, Transparence, Platinum, Calibrating, Reprints.

Thin Film thermocouples have unique capabilities for measuring surface temperatures at high temperatures (above 800K) under harsh conditions. Their low mass, approximately 2 x ten to the minus 5 power g/mm permits very rapid response and very little disturbance of heat transfer to the surface being measured. This has led to applications inside gas turbine blades and vanes and ceramic liners in diesel cylinders. The most successful high temperature (up to 1300/K) thin film thermocouples are sputter deposited from platinum and platinum 10% rhodium targets although results using base metal alloys, gold, and platinel will also be presented. The paper reviews the fabrication techniques used to form the thermocouples, approaches used to solve the high temperature insulation and adherence problems, current applications, and test results using the thin film thermocouples. In addition, a discussion will be presented on the recent research on thin film transparent thermocouples.

02,284
PB97-111876 Not available NTIS
National Inst. of Standards and Technology (EEEL), Gaithersburg, MD. Electricity Div.

Resistors.
Final rept.
R. F. Dziuba. 1996, 13p.
Pub. in Encyclopedia of Applied Physics, v16 p423-435 Jul 96.

Keywords: *Resistors, *Automation, *Calibration, Measurements, Quality assurance, Standards, Hall effect, Reprints.

Resistors are inportant components in electrical and electronic circuits. The article begins with a brief historical account of the evolution of the different types of resistors starting with wirewounds and proceeding to carbon composition and the various film-type resistors. The concept of resistance is briefly described along with Ohm's Law and the unit of resistance. By international agreement, since, January 1, 1990, the unit of resistance has been expressed in terms of the quantum Hall effect which occurs in suitable semiconductors operating at high magnetic fields and low temperatures and is based on fundamental constants. The importance of resistors in the measurement of current, voltage ratios, temperature, and displacement is also discussed. The article describes, in more detail, resistor fabrication including the main constructural elements of base material, resistive element, terminations, and protective enclosure. Then separate categories of carbon composition, wirewound, metal foil, thin film, and thick film resistors are characterized. The article next discusses the key characteristics of the different types of resistors, including accuracy, stability, power rating, temperature coefficient, load coefficient, voltage coefficient, humidity effects, pressure effects, and freqency effects. Finally, the common classification of resistors, according to their intended use and inherent performence, is described. The classification includes standard resistors, resistors in electronic circuits, integrated circuit resistors, high current resistors, and high voltage resistors.

02,285
PB97-111884 Not available NTIS
National Inst. of Standards and Technology (EEEL), Gaithersburg, MD. Electricity Div.
Loading Effects in Resistance Scaling.
Final rept.
R. E. Elmquist, and R. F. Dziuba. 1996, 2p.
Pub. in Conference on Precision Electromagnetic Measurements 1996 Digest, (CPEM '96), Braunschweig, Germany, June 17-20, 1996, p334-335.

Keywords: *Electrical resistance, *Electrical measurement, Standards, Loading, Reprints.

Power loading effects in dc resistance references are not well understood even for the most commonly used high precision standards. The paper will examine loading effects and their contribution to the uncertainty of recent NIST comparisons of the quantum Hall effect and calculable capacitor.

02,286
PB97-112338 Not available NTIS
National Inst. of Standards and Technology (EEEL), Gaithersburg, MD. Electricity Div.
Development of Thin-Film Multijunction Thermal Converters at NIST.
Final rept.
J. R. Kinard, D. B. Novotny, T. E. Lipe, and D. X. Huang. 1996, 2p.
See also PB96-148135.
Pub. in Conference on Precision Electromagnetic Measurements 1996 Digest, (CPEM '96), Braunschweig, Germany, June 17-20, 1996, p493-494.

Keywords: *CMOS, *Thin films, Microinstrumentation, Machining, Alternating current, Direct current, Photolithography, Transfer characteristics, Standards, Reprints, *Multijunction thermal converters.

The paper gives an overview of the development of thin-film multijunction thermal converters (FMJTCs) at the National Institute of Standards and Technology (NIST). A historical perspective of film thermal converters is presented, followed by descriptions of the motivation, fabrication processes, physical characteristics and the electrical properties of the FMJTCs produced at NIST. Integrated micropotentiometers which incorporate FMJTCs and thermal converters, produced by an alternative fabrication technology using a CMOS foundry, are also described. The paper concludes with a report on the current status of the FMJTC project and future directions.

02,287
PB97-112353 Not available NTIS
National Inst. of Standards and Technology (EEEL), Gaithersburg, MD. Electricity Div.
Empirical Linear Prediction Applied to a NIST Calibration Service.
Final rept.
A. D. Koffman, T. M. Souders, G. N. Stenbakken, T. E. Lipe, and J. R. Kinard. 1996, 6p.
Pub. in Proceedings of the National Conference of Standards Laboratories Workshop and Symposium, Monterey, CA., August 25-29, 1996, p207-212.

Keywords: *Calibration, *Electronic equipment, Test methods, Mathematical models, Linear systems, Predictions, Reprints, Thermal transfer standards.

Empirical linear prediction, developed at NIST, has recently been applied to the NIST calibration of a commercial multi-range ac-dc thermal transfer standard. This approach reduced the number of required test points by 62 percent, resulting in significant cost savings. The calibration model was developed using extensive test data obtained from the instrument manufacturer. Calibration measurements for the instrument under test were made at the reduced set of test points enabling subsequent predictions of the response at all unmeasured points using the model. Uncertainties for the unmeasured points were developed by testing the goodness of fit of the calibration measurements to the model. These uncertainty intervals depend on the quality of the model as well as on the number of points actually measured. The ability of the model to characterize the instrument under test is key to achieving low uncertainties. A brief mathematical description of the modeling and prediction process is presented along with measurement results.

02,288
PB97-112452 Not available NTIS
National Inst. of Standards and Technology (EEEL), Gaithersburg, MD. Electricity Div.
Low Thermal Guarded Scanner for High Resistance Measurement Systems.
Final rept.
J. A. Marshall, T. A. Marshall, D. G. Jarrett, and R. F. Dziuba. 1996, 2p.
Pub. in Conference on Precision Electromagnetic Measurements, CPEM '96 Conference Digest, Braunschweig, Germany, June 17-20, 1996, p20-21.

Keywords: *Electrical resistance, *Electrical measurement, Resistance bridges, Standards, Test equipment, Reprints, Current comparators, Resistance standards.

The design and testing of a low thermal guarded scanner developed to provide completely guarded switching when used with guarded resisted bridge networks is described.

02,289
PB97-119150 Not available NTIS
National Inst. of Standards and Technology (EEEL), Gaithersburg, MD. Electricity Div.
Automated Guarded Bridge for Calibration of Multimegohm Standard Resistors.
Final rept.
D. G. Jarrett. 1996, 2p.
Pub. in Conference on Precision Electromagnetic Measurements, June 17-20, 1996, Braunschweig, Germany, p336-337, 1996.

Keywords: *Resistors, *Standard resistors, *Graphical user interface, *Automated bridge, Calibrators, Electrometers, High resistance, Multimegohm, Reprints, *Foreign technology, Wheatstone bridge.

The implementation of an automated guarded bridge for calibrating multimegohm standard resistors is described. A guarded Wheatstone bridge has been assembled with programmable dc calibrators in two of the arms allowing multiple ratios and test voltages to be remotely selected. Preliminary measurements will be reported along with the balancing algorithm.

02,290
PB97-119168 Not available NTIS
National Inst. of Standards and Technology (EEEL), Gaithersburg, MD. Electricity Div.
Resistance Measurements from 10 M Omega to 1 T Omega at NIST.
Final rept.
D. G. Jarrett. 1996, 8p.
Pub. in National Conference of Standards Laboratories, Monterey, CA., August 25-29, 1996, p291-298.

Keywords: *Resistance measurements, *Standard resistors, *Resistors, Temperature, Chambers, Environments, Humidity, Multimegohm, Reprints, National Institutes of Standards and Technology.

Described are the measurement systems and methods used for calibrating standard resistors from 10 M ohms to 1 T ohms at the National Institute of Standards and Technology (NIST). Presently four systems are used for the calibration of standard resistors at and above 10 M ohms. An automated guarded multimegohm bridge has recently been developed to augment a manual guarded Wheatstone bridge and a semiautomated teraohmmeter system. An automated resistance ratio bridge is used during the scaling process. Scaling from one decade to the next is done by using guarded Hamon boxes and the high resistance bridges.

02,291
PB97-119184 Not available NTIS
National Inst. of Standards and Technology (EEEL), Gaithersburg, MD. Electricity Div.
NIST Comparison of the Quantized Hall Resistance and the Realization of the SI Ohm Through the Calculable Capacitor.
Final rept.
A. Jeffery, R. E. Elmquist, L. H. Lee, J. Q. Shields, and R. F. Dziuba. 1996, 2p.
See also PB97-119192.
Pub. in Institute of Electrical and Electronics Engineers Transactions on Instrumentation and Measurement, p10-11 1996.

Keywords: *Calculable capacitors, *Comparators, Fundamental constants, Cryogenic currents, Fine structure constants, Reprints, *Four-terminal-pair-bridge, National Institutes of Standards and Technolology.

The latest NIST results from the comparison of the quantized Hall resistance (QHR), with the realization of the SI ohm obtained from the calculable capacitor measurement will be reported. Various systematic checks have been performed.

02,292
PB97-119192 Not available NTIS
National Inst. of Standards and Technology (EEEL), Gaithersburg, MD. Electricity Div.
NIST Comparison of the Quantized Hall Resistance and the Realization of the SI Ohm Through the Calculable Capacitor. Conference Proceedings, June 17-20, 1996.
Final rept.
A. Jeffery, R. E. Elmquist, L. H. Lee, J. Q. Shields, and R. F. Dziuba. 1996, 2p.
See also PB97-119184.
Pub. in Proceedings of the Conference Precision Electromagnetic Measurements, Braunschweig, Germany, June 17-20, 1996, CPEM '96 Conference Digest, p10-11, 1996.

Keywords: *Calculable capacitors, *Comparators, Fundamental constants, Cryogenic currents, Fine structure constants, Reprints, Four-terminal-pair-bridge, National Institutes of Standards and Technology.

The latest NIST results from the comparison of the quantized Hall resistance (QHR), with the realization of the SI ohm obtained from the calculable capacitor measurement will be reported. Various systematic checks have been performed.

02,293
PB97-122600 Not available NTIS
National Inst. of Standards and Technology (EEEL), Gaithersburg, MD. Electricity Div.
Capacitors with Very Low Loss: Cryogenic Vacuum-Gap Capacitors.
Final rept.
N. M. Zimmerman. 1996, 6p.
Pub. in Institute of Electrical and Electronics Engineers Transactions on Instrumentation and Measurement, v45 n5 p841-846 Oct 96.

Keywords: *Capacitors, Measurements, Resistance, Reprints, *Vacuum-gap capacitors, *Low-loss capacitors.

The authors report on measurements of capacitors with about 1 pF of capacitance, which have unmeasurably small leakage at very low frequencies, placing a lower bound of about 10 to the 19th power omega on the parallel resistance at an effective frequency of 1 mHz. These measurements are made possible by two themes: the use of vacuum-gap capacitors

(i.e., no dielectric material, operated in vacuum), and detection of leakage using single electron tunneling (SET) electrometers, which have very high input impedance. The authors also report on good achieved results in time stability and lack of frequency and voltage dependence.

Semiconductor Devices

02,294
DE95009287 PC A03/MF A01
National Renewable Energy Lab., Golden, CO.
Atomic-scale characterization of hydrogenated amorphous-silicon films and devices. Annual subcontract report, 14 February 1994--14 April 1995.
PROGRESS REPT.
A. Gallagher, D. Tanenbaum, A. Laracuente, and B. Jelenkovic. Aug 95, 18p, NREL/TP-411-8246.
Contract AC36-83CH10093
Sponsored by Department of Energy, Washington, DC.

Keywords: *Silicon Solar Cells, Amorphous State, Electrical Properties, Hydrogenation, Progress Report, Thin Films, EDB/140501.

Properties of the hydrogenated amorphous silicon (a-Si:H) films used in photovoltaic (PV) panels are reported. The atomic-scale topology of the surface of intrinsic a-Si:H films, measured by scanning tunneling microscopy (STM) as a function of film thickness, are reported and diagnosed. For 1-500-nm-thick films deposited under normal device-quality conditions from silane discharges, most portions of these surfaces are uniformly hilly without indications of void regions. However, the STM images indicate that 2-6-nm silicon particulates are continuously deposited into the growing film from the discharge and fill approximately 0.01% of the film volume. Although the STM data are not sensitive to the local electronic properties near these particulates, it is very likely that the void regions grow around them and have a deleterious effect on a-Si:H photovoltaics. Preliminary observations of particulates in the discharge, based on light scattering, confirm that particulates are present in the discharge and that many collect and agglomerate immediately downstream of the electrodes. Progress toward STM measurements of the electronic properties of cross-sectioned a-Si:H PV cells is also reported.

02,295
PB94-155579 PC A03/MF A01
National Inst. of Standards and Technology (EEEL), Gaithersburg, MD. Semiconductor Electronics Div.
Development and Characterization of Insulating Layers on Silicon Carbide: Annual Report for February 14, 1988 to February 14, 1989.
J. J. Kopanski, and D. B. Novotny. Sep 89, 48p, NISTIR-89-4157.
Contract NASA-C-30007-K
Sponsored by National Aeronautics and Space Administration, Cleveland, OH. Lewis Research Center.

Keywords: *Silicon carbides, *Capacitors, *Semiconductor devices, *Vapor deposition, Cubic lattices, Electrical properties, Semiconductor traps, MIS(Semiconductors), Capacitance-voltage characteristics, Metal oxide semiconductors, Multilayer insulation, Oxide coatings, Silicon inorganic compounds, *MIS capacitors, *MOS capacitors, *Compound semiconductors.

Processes to fabricate metal-insulator-semiconductor (MIS) capacitors on the cubic (3C) form of silicon carbide (SiC) were studied. The insulating layers were formed from either thermally grown oxide or chemical-vapor-deposited (CVD) silicon dioxide. The effects of wet or dry oxygen and of oxidation temperatures between 1050 and 1200 C on the electrical properties of devices with thermal oxides were determined. Electrical characterization techniques appropriate for these devices on SiC were developed and applied to the fabricated capacitors. The capacitors were characterized from multiple-frequency capacitance-voltage (C-V) measurements as a function of temperature from room temperature to 300 C. The apparent interface trap level densities were estimated from the high-frequency C-V curves.

02,296
PB94-159787 PC A03/MF A01
National Inst. of Standards and Technology (EEEL), Gaithersburg, MD. Semiconductor Electronics Div.
Center for Electronics and Electrical Engineering Technical Progress Bulletin Covering Center Programs, October to December, with 1991 CEEE Events Calendar.
J. A. Gonzalez. May 91, 45p, NISTIR-4548.
See also PB91-159749 and PB93-205524.

Keywords: *Electrical measurement, *Metrology, Semiconductor materials, Bipolar transistors, Signal processing, Josephson junctions, Electromagnetic interference, Millimeter waves, Optical fibers, High temperature superconductors, Microwaves, Photodiodes, MOSFET, Lasers, Antennas, Magnetic materials, Electric power, Progress report, Abstracts, Fiber optic sensors, US NIST, SIMOX.

This is the thirty-third issue of a quarterly publication providing information on the technical work of the National Institute of Standards and Technology (formerly the National Bureau of Standards) Center for Electronics and Electrical Engineering. This issue of the CEEE Technical Progress Bulletin covers the fourth quarter of calendar year 1990. Abstracts are provided by technical area for both published papers and papers approved by NIST for publication. Main headings from the Table of Contents include the following: Semiconductor Technology Program; Signals and Systems Metrology Program; Fast Signal Acquisition, Processing, and Transmission; Electrical Systems; Electromagnetic Interference; Additional Information: 1991 CEEE Calendar; Sponsor List; Key Contacts in Center, Center Organization.

02,297
PB94-163458 PC A05/MF A01
National Inst. of Standards and Technology (EEEL), Gaithersburg, MD. Semiconductor Electronics Div.
Design Guide for CMOS-On-SIMOX. Test Chips NIST3 and NIST4.
J. C. Marshall, M. W. Cresswell, C. H. Ellenwood, M. E. Zaghloul, L. W. Linholm, and P. Roitman. Jan 93, 93p, NISTIR-4889.
See also PB93-152106. Prepared in cooperation with George Washington Univ., Washington, DC. School of Engineering and Applied Science.

Keywords: *Very large scale integration, *Integrated circuits, *Computer aided design, Chips(Electronics), Computer programs, Gallium arsenides, Silicon, Transistors, Guidelines, Manuals, MOSFET, CMOS, Test structures, Test chips, SOI(Semiconductors), SIMOX.

The design guidelines for test chips NIST3 and NIST4 are specified in this manual. These chips were designed for process monitoring and device parameter extraction for a CMOS (Complementary Metal-Oxide-Semiconductor)-on-SOI (Silicon-On-Insulator) process. The chips contain structures which are common to a standard CMOS process as well as structures specifically designed for a SIMOX (Separation by the IMplantation of OXygen) process. In order to facilitate the CAD process, a unique 'technology file' was created for the Magic VLSI layout editor used on a Sun-3/280 system running Sun Version 3.5. This SIMOX technology file is very general and can be used to build CMOS as well as SIMOX chips. NIST3 is 6380 micrometers x 4780 micrometers and contains several large-geometry MOSFETs, resistors, and capacitors. NIST4 is 1 cm x 1 cm and contains approximately 300 small-geometry test structures. The SIMOX specific structures found on these chips include MOSFETs, capacitors, interconnects, and pads to be discussed in more detail. The test guide for the test structures on NIST3 and NIST4 is included in a separate manual (PB93-152106).

02,298
PB94-164316 PC A03/MF A01
National Inst. of Standards and Technology (EEEL), Gaithersburg, MD. Semiconductor Electronics Div.
Color Supplement to NIST Special Publication 400-93: Semiconductor Measurement Technology: Design and Testing Guides for the CMOS and Lateral Bipolar-on-SOI Test Library.
J. C. Marshall, and M. E. Zaghloul. Mar 94, 40p, NISTIR-5324.
Color illustrations reproduced in black and white. Prepared in cooperation with George Washington Univ., Washington, DC. School of Engineering and Applied Science.

Keywords: *Very large scale integration, *Integrated circuits, Computer aided design, Field effect transistors, Bipolar transistors, Chips(Electronics), Silicon, MOSFET, CMOS, Test chips, Test structures, SOI(Semiconductors), SIMOX.

This report is the supplement to the NIST Special Publication entitled, 'Semiconductor Measurement Technology: Design and Testing Guides for the CMOS and Lateral Bipolar-on-SOI Test Library.' This supplement contains the complete set of figures from the above mentioned document with the test structures provided in color for easier interpretation.

02,299
PB94-165958 PC A03/MF A01
National Inst. of Standards and Technology (EEEL), Gaithersburg, MD. Semiconductor Electronics Div.
Electronics and Electrical Engineering Laboratory Technical Progress Bulletin Covering Laboratory Programs, October to December 1992, with 1992/1993 EEEL Events Calendar.
J. M. Rohrbaugh. Mar 93, 31p, NISTIR-5145.
See also PB93-158632.

Keywords: *Electrical engineering, *Electronics, *Metrology, *US NIST, Semiconductors, Semiconductor devices, Electrical measurement, Microelectronics, Signal processing, Integrated circuits, Dimensional measurement, Electromagnetic interference, Lasers, Optical fibers, Magnetic materials, Microwaves, Antennas, Electric power, Superconductors, Abstracts.

This is the forty-first issue of a quarterly publication providing information on the technical work of the National Institute of Standards and Technology, Electronics and Electrical Engineering Laboratory. This issue of the EEEL Technical Progress Bulletin covers the fourth quarter of calendar year 1992. Abstracts are provided by technical area for both published papers and papers approved by NIST for publication.

02,300
PB94-172483 Not available NTIS
National Inst. of Standards and Technology (EEEL), Gaithersburg, MD. Semiconductor Electronics Div.
Efficient Method to Compute the Maximum Transient Drain Current Overshoot in Silicon on Insulator Devices.
Final rept.
C. Korman, I. Mayergoyz, M. Gaitan, and G. Tai. 1993, 6p.
Pub. in Jnl. of Applied Physics 73, n6 p2611-2626, 15 Mar 93.

Keywords: *Field effect transistors, Transport theory, Poisson equation, Computation, Silicon, MOSFET, Reprints, *SOI(Semiconductors), Drain current overshoot.

The authors present an efficient method to compute the maximum transient drain current overshoot in silicon-on-insulator metal-oxide-silicon field effect transistors. The method is based on the physical idea that the number of majority carriers remains unchanged immediately after a change in the applied gate bias. The maximum overshoot is computed by solving the Poisson and the stationary minority carrier transport equations under the constraint that the number of majority carriers is conserved. Hence, the novel aspect of the method is that it allows one to compute the maximum drain current overshoot without resorting to a computationally costly transient simulation. The accuracy of the method is verified by comparing the value of the drain current computed by the method with the maximum value of the drain current computed by transient simulations. The comparisons show that, with this method, the maximum transient drain current overshoot can be computed quite accurately for fast changes in the gate bias.

02,301
PB94-178019 PC A07/MF A02
National Inst. of Standards and Technology (EEEL), Gaithersburg, MD. Semiconductor Electronics Div.
Semiconductor Measurement Technology: Design and Testing Guides for the CMOS and Lateral Bipolar-on-SOI Test Library.
J. C. Marshall, and M. E. Zaghloul. Mar 94, 142p, NIST/SP-400-93.
Also available from Supt. of Docs. as SN003-003-03262-0. See also PB93-152106 and PB94-163458. Prepared in cooperation with George Washington Univ., Washington, DC. School of Engineering and Applied Science.

Keywords: *Very large scale integration, *Computer aided design, *Integrated circuits, Chips(Electronics), Bipolar transistors, Electronic modules, Computer programs, Wafers, MOSFET, CMOS, Tests, SOI(Semiconductors), Test structures, Test chips, SIMOX, NIST8, NIST9.

Design and testing guides have been developed for the test library from which test chip NIST8 and test wafer NIST9 were derived. They were designed for use in process monitoring and device parameter extraction to evaluate and compare CMOS (Complementary Metal-Oxide-Semiconductor) test structures, including devices and circuits, fabricated on both bulk silicon and SOI (Silicon-on-Insulator), specifically SIMOX (Separation by the IMplantation of OXygen), wafers. The test library consists of both CMOS-on-SOI and lateral bipolar-on-SOI modules. From it, 20 modules were assembled to create CMOS test chip NIST8 that was fabricated using a standard bulk CMOS foundry through the MOSIS service. SOI/SIMOX test wafer NIST9 contains approximately 1000 modules and was also assembled from modules in this test library. Fourteen processing masks are used to fabricate depletion-mode MOSFETs, lateral bipolar devices, and CMOS MOSFETs with source-to-channel ties. The SOI/SIMOX technology file used with the Magic VLSI layout editor was modified to include the layers necessary to generate these 14 processing masks. This modification is discussed, and unique test structure designs are presented.

02,302
PB94-181997 Not available NTIS
National Inst. of Standards and Technology (EEEL), Gaithersburg, MD. Semiconductor Electronics Div.
Application of the Modified Voltage-Dividing Potentiometer to Overlay Metrology in a CMOS/Bulk Process.
Final rept.
R. A. Allen, M. W. Cresswell, L. W. Linholm, T. A. Hill, J. D. Benecke, S. R. Volk, H. D. Stewart, J. C. Owen, and C. H. Ellenwood. Mar 94, 6p.
Contract DE-AC04-94AL85000
Pub. in Proceedings of the Institute of Electrical and Electronics Engineers International Conference on Microelectronic Test Structures, San Diego, CA., March 22-24, 1994, v7 p51-56. Sponsored by Department of Energy, Washington, DC.

Keywords: *Very large scale integration, *Integrated circuits, *Overlays, Positioning, Alignment, Metrology, Wafers, CMOS, Lithography, Reprints, Test structures, Registration.

The measurement of layer-to-layer feature overlay will, in the foreseeable future, continue to be a critical metrological requirement for the semiconductor industry. Meeting the image placement metrology demands of accuracy, precision, and measurement speed favors the use of electrical test structures. In this paper, a two-dimensional, modified voltage-dividing potentiometer is applied to a short-loop VLSI process to measure image placement. The contributions of feature placement on the reticle and registration on the wafer to the overall measurement are analyzed and separated. Additional sources of uncertainty are identified, and methods developed to monitor and reduce them are described.

02,303
PB94-185592 Not available NTIS
National Inst. of Standards and Technology (EEEL), Gaithersburg, MD. Semiconductor Electronics Div.
Electro-Thermal Simulation of an IGBT PWM Inverter.
Final rept.
H. A. Mantooth, and A. R. Hefner. 1993, 10p.
Pub. in Proceedings of the Power Electronics Specialists Conference, Seattle, WA., June 20-24, 1993, p75-84.

Keywords: *Inverters, Chips(Electronics), Computerized simulation, Thermal analysis, Silicon, Reprints, Insulated gate bipolar transistors, Circuit simulators.

A recently developed electro-thermal network simulation methodology is used to analyze the behavior of a full-bridge, pulse-width-modulated, voltage-source inverter which uses IGBTs (Insulated Gate Bipolar Transistors) as the switching devices. The electro-thermal simulations are performed using the Saber Circuit simulator and include the control logic circuitry, the IGBT gate drivers, the physics-based IGBT electro-thermal model, and the thermal network component models for the power device silicon chips, packages, and heat sinks. It is shown that the thermal response of the silicon chip determines the IGBT temperature rise during the device switching cycle. It is also shown that the full electro-thermal analysis is required to accurately describe the power losses and circuit efficiency.

02,304
PB94-185949 Not available NTIS
National Inst. of Standards and Technology (EEEL), Gaithersburg, MD. Semiconductor Electronics Div.
Experimental Investigation of the Validity of TDDB Voltage Acceleration Models.
Final rept.
J. S. Suehle, P. Chaparala, C. Messick, W. M. Miller, and K. C. Boyko. 1993, 9p.
Pub. in Proceedings of the International Integrated Reliability Workshop, Lake Tahoe, CA., October 24-27, 1993, p59-67.

Keywords: *Dielectric breakdown, *Silicon dioxide, Temperature dependence, High temperature, Integrated circuits, Electric fields, Reprints, Field acceleration models.

Time-Dependent Dielectric Breakdown (TDDB) data are presented for 15- and 22.5-nm oxides collected over a wide range of electric fields and temperatures. The results indicate that it is necessary to obtain data over this range to distinguish between the two field acceleration models and to quantify the electric field and temperature dependencies of the thermal activation energy and the field acceleration factor respectively. We also demonstrate the use of temperatures as high as 400 C to accelerate time-dependent dielectric breakdown.

02,305
PB94-185956 Not available NTIS
National Inst. of Standards and Technology (EEEL), Gaithersburg, MD. Semiconductor Electronics Div.
Field and Temperature Acceleration of Time-Dependent Dielectric Breakdown in Intrinsic Thin SiO2.
Final rept.
J. S. Suehle, P. Chaparala, C. Messick, W. M. Miller, and K. C. Boyko. 1994, 6p.
Pub. in Proceedings of the Institute of Electrical and Electronics Engineers International Reliability Physics Workshop, San Jose, CA., April 12-14, 1994, p120-125.

Keywords: *Dielectric breakdown, *Silicon dioxide, Temperature dependence, High temperature, Integrated circuits, Electric fields, Dielectric films, Thin films, Reprints, Field acceleration models.

Time-Dependent Dielectric Breakdown (TDDB) data are presented for 15- and 22.5-nm oxides collected over a wide range of electric fields and temperatures. The results indicate that it is necessary to obtain data over this range to distinguish between the two field acceleration models and to quantify the electric field and temperature dependencies of the thermal activation energy and the field acceleration factor, respectively. We also report on the TDDB characteristics of thin SiO2 films at temperatures as high as 400 C and demonstrate the use of these temperatures to accelerate TDDB.

02,306
PB94-185964 Not available NTIS
National Inst. of Standards and Technology (EEEL), Gaithersburg, MD. Semiconductor Electronics Div.
Junction Locations by Scanning Tunneling Microscopy: In-Air-Ambient Investigation of Passivated GaAs pn Junctions.
Final rept.
W. F. Tseng, J. A. Dagata, R. M. Silver, J. Fu, and J. R. Lowney. 1994, 5p.
Pub. in Jnl. of Vacuum Science and Technology B 12, n1 p373-377 Jan/Feb 94. Sponsored by Office of Naval Research, Arlington, VA.

Keywords: *Semiconductor junctions, *P-n junctions, *Gallium arsenides, Molecular beam epitaxy, Scanning tunneling microscopy, Aluminum arsenides, Passivation, Cleavage, Reprints, Atomic force microscopy.

Scanning tunneling microscopy (STM) and atomic force microscopy operating in air have been used to investigate locations of molecular-beam epitaxially grown GaAs multiple pn junctions cleaved and passivated with P2S5. Symmetrically and asymmetrically doped junctions were prepared within topographically delineated AlAs/GaAs marker regions for this in-air study of electronic junction contrast. Our results indicate that the STM-delineated junction locations do not coincide with the electrical junction locations, but rather shift into the p-type regions.

02,307
PB94-193752 PC A03/MF A01
National Inst. of Standards and Technology (EEEL), Gaithersburg, MD. Semiconductor Electronics Div.
Electronics and Electrical Engineering Laboratory Technical Publication Announcements Covering Laboratory Programs, October to December 1993 with 1994/1995 EEEL Events Calendar.
J. M. Rohrbaugh. Jun 94, 23p, NISTIR-5435.
See also PB94-118403 and PB94-154341.

Keywords: *Electrical measurement, *Microelectronics, *Metrology, *Bibliographies, Dimensional measurement, Integrated circuits, Integrated optics, High temperature superconductors, YBCO superconductors, Electromagnetic interference, Electric contacts, Electronic packaging, Photodetectors, Abstracts, Magnetic force microscopy.

This is the thirty-ninth issue of a quarterly publication providing information on the technical work of the National Institute of Standards and Technology, Electronics and Electrical Engineering Laboratory (EEEL). This issue of the 'EEEL Technical Publication Announcements' covers the fourth quarter of calendar year 1993. Abstracts are provided by technical areas for papers published. Major subject headings include the following: Semiconductor Microelectronics; Signal Acquisition, Processing, and Transmission; Electrical Systems; Electromagnetic Interference.

02,308
PB94-193810 PC A03/MF A01
National Inst. of Standards and Technology (EEEL), Gaithersburg, MD. Semiconductor Electronics Div.
Electronics and Electrical Engineering Laboratory Technical Progress Bulletin Covering Laboratory Programs, January to March 1994 with 1994/1995 EEEL Events Calendar.
J. M. Rohrbaugh. Jun 94, 50p, NISTIR-5434.
See also PB93-234698, PB94-118403 and PB94-154341.

Keywords: *Electrical measurement, *Microelectronics, *Metrology, *Bibliographies, Integrated circuits, Dimensional measurement, Dielectric breakdown, Josephson junctions, High temperature superconductors, Microwave equipment, Sulfur hexafluoride, Antennas, Integrated optics, Optical fibers, Photodetectors, Radiometers, Electric power, Electromagnetic interference, Abstracts, Fiber optic sensors, Test structures, Microfabrication, Magnetic force microscopy, Flat panel displays.

This is the forty-sixth issue of a quarterly publication providing information on the technical work of the National Institute of Standards and Technology, Electronics and Electrical Engineering Laboratory (EEEL). This issue of the 'EEEL Technical Progress Bulletin' covers the first quarter of calendar year 1994. Abstracts are provided by technical area for both published papers and papers approved by NIST for publication. Major subject headings include the following: Fundamental Electrical Measurements; Semiconductor Microelectronics; Signal Acquisition, Processing, and Transmission; Electrical Systems; Electromagnetic Interference; Video Technology.

02,309
PB94-194354 PC A03/MF A01
National Inst. of Standards and Technology (EEEL), Gaithersburg, MD. Semiconductor Electronics Div.
Electronics and Electrical Engineering Laboratory Technical Progress Bulletin Covering Laboratory Programs, July to September 1993 with 1994 EEEL Events Calendar.
J. M. Rohrbaugh. Nov 93, 49p, NISTIR-5288.

Keywords: *Electrical measurement, *Microelectronics, *Metrology, *Bibliographies, Josephson junctions, High temperature superconductors, Integrated circuits, Electromagnetic interference, Dimensional measurement, YBCO superconductors, Millimeter waves, Microwave equipment, Semiconductors, Magnetic materials, Optical fibers, Antennas, Abstracts, Quantum Hall effect, Microfabrication.

This is the forty-fourth issue of a quarterly publication providing information on the technical work of the National Institute of Standards and Technology, Electronics and Electrical Engineering Laboratory (EEEL). This issue of the 'EEEL Technical Progress Bulletin' covers the third quarter of calendar year 1993. Abstracts are provided by technical area for both published papers and papers approved by NIST for publication. Major subject headings include the following: Fundamental Electrical Measurements; Semiconductor Microelectronics; Signal Acquisition, Processing,

and Transmission; Electrical Systems; Electromagnetic Interference; Law Enforcement Standards; Product Data Systems; Video Technology.

02,310
PB94-198561 Not available NTIS
National Inst. of Standards and Technology (MSEL), Gaithersburg, MD. Metallurgy Div.
Numerical Simulation of Submicron Photolithographic Processing.
Final rept.
E. Barouch, J. W. Cahn, U. Hollerbach, and S. A. Orszag. Sep 91, 22p.
Pub. in Jnl. of Scientific Computing 6, n3 p229-250 Sep 91. Sponsored by Defense Advanced Research Projects Agency, Arlington, VA. Technology Reinvestment Project. and Air Force Office of Scientific Research, Bolling AFB, DC.

Keywords: *Photolithography, *MOSFET, Field effect transistors, Chips(Electronics), Computerized simulation, Photomasks, Reprints.

A complete numerical simulation package for submicron photolithography is described in depth. Four of the computational steps are analyzed: aerial image generation, exposure, postexposure bake, and dissolution. An application to bar printing over a MOSFET gate is described. In addition, the utility of phase-shift masks is described, and the effects of aberrations are explored.

02,311
PB94-198728 Not available NTIS
National Inst. of Standards and Technology (EEEL), Gaithersburg, MD.
Majority and Minority Mobilities in Heavily Doped Silicon for Device Simulations.
Final rept.
H. S. Bennett, and J. R. Lowney. 1992, 6p.
Pub. in Proceedings of International Workshop on Numerical Modeling of Processes and Devices for Integrated Circuits, Seattle, WA., May 31-June 1, 1992, p123-128.

Keywords: *Electron mobility, *Hole mobility, Carrier mobility, Doped materials, Simulation, Silicon, Reprints.

As silicon devices approach 0.2 micrometer in size, it will be essential to have accurate values for the majority and minority mobilities of electrons and holes. These mobilities have been calculated in silicon for donor and acceptor densities between 10(sup 17)/cc and 10(sup 20)/cc. All the important scattering mechanisms have been included. The ionized impurity scattering has been treated with a quantum-mechanical phase-shift analysis. The results are in good agreement with experiment. In addition, the ionized impurity scattering rates calculated from the quantum-mechanical phase shifts and those rates calculated from the Born approximation are shown to differ by more than factors of three. The commonly used Born approximation is not valid for low energy carriers near band extrema.

02,312
PB94-200391 Not available NTIS
National Inst. of Standards and Technology (EEEL), Gaithersburg, MD. Semiconductor Electronics Div.
Electron Traps, Structural Change, and Hydrogen Related SIMOX Defects.
Final rept.
J. F. Conley, P. M. Lenahan, and P. Roitman. 1992, 2p.
Contract DNA-IACRO-88-800
Pub. in Extended Abstract, Proceedings of Institute of Electrical and Electronics Engineers International SOI Conference, Ponte Vedra Beach, FL., October 6-8, 1992, p26-27. Sponsored by Office of Naval Research, Arlington, VA. and Defense Nuclear Agency, Washington, DC.

Keywords: Electron spin resonance, Vacuum ultraviolet radiation, Crystal defects, Electron traps, Hydrogen, Reprints, *SOI(Semiconductors), *SIMOX, Buried oxides.

Evidence for structural changes in SIMOX buried oxides is presented. We show that deep electron traps may be created in SIMOX buried oxides; these electron traps could compensate for some positively charged E' centers. In addition, we report observation of relatively high densities of hydrogen-related defects in VUV illuminated oxides. We suggest that this short range disorder may be responsible for the differences between the response of ordinary thermal oxide and SIMOX buried oxides.

02,313
PB94-200565 Not available NTIS
National Inst. of Standards and Technology (EEEL), Gaithersburg, MD. Semiconductor Electronics Div.
Test Structures for the In-Plane Locations of Projected Features with Nanometer-Level Accuracy Traceable to a Coordinate Measurement System.
Final rept.
M. W. Cresswell, R. A. Allen, L. W. Linholm, E. C. Teague, C. H. Ellenwood, and W. B. Penzes. 1993, 7p.
Pub. in Proceedings of Institute of Electrical and Electronics Engineers International Conference on Microelectronic Test Structures, Sitges, Barcelona, Spain, March 22-25, 1993, v6 p255-261.

Keywords: *Microelectronics, *Lithography, Metrology, Substrates, Masks, Reprints, Test structures, Coordinate measurement systems, Traceability.

A new test structure has been designed to measure the positions of the images of an array of fiducial marks projected from a mask into a resist film on a substrate. The resist film on the substrate covers a nominally matching array of partially formed versions of the test structure prepatterned in a conducting film. Instances of the finished structure are formed on the substrate by further selective removal of conducting material from the partially formed test structures where they are overlaid by images of the fiducial marks on the mask. At each array point, the feature of the completed test structure that is defined by the overlay of the image of the fiducial marks on the mask is called the pointer. The part of the partially formed test structure that is unaffected by the overlay of the images of the fiducial marks on the mask serves as a ruler. Electrical testing accurately provides the precise location of the pointer relative to the ruler within each test structure. The paper describes the test structure and provides examples of measurements that indicate precision to within less than 2 nm and accuracy of better than 7 nm.

02,314
PB94-211653 Not available NTIS
National Inst. of Standards and Technology (NEL), Gaithersburg, MD. Semiconductor Electronics Div.
Wire Bond Testing.
Final rept.
G. G. Harman. 1989, 48p.
Pub. in Reliability and Yield Problems of Wire Bonding in Microelectronics: The Application of Materials and Interface Science, Chapter 1, p1-48 1989.

Keywords: *Semiconductor devices, *Microelectronics, Fracture mechanics, Test methods, Gallium arsenides, Silicon, Reviews, Reprints, *Wire bonds.

The methods of testing wire bonds are reviewed. These include the bond pull test, the nondestructive bond pull test, and ball shear test, the 'pluck' test, and the thermal stress test. In the process of discussing the tests, their usage in production is emphasized and their reliability implications are discussed.

02,315
PB94-211711 Not available NTIS
National Inst. of Standards and Technology (EEEL), Boulder, CO. Electromagnetic Technology Div.
YBa2Cu3O7-x to Si Interconnection for Hybrid Superconductor/Semiconductor Integration.
Final rept.
T. E. Harvey, J. Moreland, B. Jeanneret, R. H. Ono, and D. A. Rudman. 1992, 3p.
Pub. in Applied Physics Letters 61, n18 p2225-2227, 2 Nov 92. Sponsored by Department of Energy, Washington, DC.

Keywords: *High temperature superconductors, *Superconducting films, *Integrated circuits, *Circuit interconnections, *Electric contacts, Metal oxide semiconductors, YBCO superconductors, Hybrid circuits, Laser ablation, Single crystals, Thin films, Substrates, Silicon, Silver, Gold, Reprints, Yttrium barium cuprates, Ohmic contacts.

We have successfully made low resistance contacts between high-quality films of YBa2Cu3O(7-x) (YBCO) and single-crystal Si substrates through Ag-Au interconnections. The YBCO films were deposited by laser ablation on an epitaxial yttria-stabilized zirconia buffer layer on Si and had zero-resistance critical temperatures of 83-85 K after patterning into lines. Specific contact resistivities (resistance-area products) of the YBCO to Si interconnection, limited by the Au to Si interface, of 10(sup -6) ohm (cm squared) were achieved on heavily doped Si after deposition and patterning of the YBCO film. This demonstrates the use of high-temperature superconductors as a wiring layer compatible with conventional Si metal-oxide semiconductor processing.

02,316
PB94-211794 Not available NTIS
National Inst. of Standards and Technology (EEEL), Gaithersburg, MD. Semiconductor Electronics Div.
Investigation of the Drive Circuit Requirements for the Power Insulated Gate Bipolar Transistor (IGBT).
Final rept.
A. R. Hefner. 1991, 12p.
Pub. in Institute of Electrical and Electronics Engineers Transactions on Power Electronics 6, n2 p208-219 Apr 91.

Keywords: *Bipolar transistors, Requirements, Reprints, *Insulated gate bipolar transistors, Drive circuits, Power transistors.

The drive circuit requirements of the insulated gate bipolar transistor (IGBT) are explained with the aid of an analytical model. It is shown that non-quasi-static effects limit the influence of the drive circuit on the time rate-of-change of anode voltage. Model results are compared with measured turn-on and turn-off waveforms for different drive, load, and feedback circuits and for different IGBT base lifetimes.

02,317
PB94-212776 Not available NTIS
National Inst. of Standards and Technology (EEEL), Gaithersburg, MD. Semiconductor Electronics Div.
Multicarrier Characterization Method for Extracting Mobilities and Carrier Densities of Semiconductors from Variable Magnetic Field Measurements.
Final rept.
J. S. Kim, D. G. Seiler, and W. F. Tseng. 1993, 12p.
Pub. in Jnl. of Applied Physics 73, n12 p8324-8335, 15 Jun 93.

Keywords: *High electron mobility transistors, *Carrier mobility, *Carrier density, Indium gallium arsenides, Electrical conductivity, Magnetic fields, Tensors, Reprints, Multilayers.

A simple, practical method is described to extract the carrier concentration and mobility of each component of a multicarrier semiconductor system (which may be either a homogeneous or multilayered structure) from variable magnetic field measurements. Advantages of the present method are mainly due to the inclusion of both the longitudinal and transverse components of the conductivity tensor and normalization of these quantities with respect to the zero-field longitudinal component of the conductivity tensor. This method also provides a simple, direct criterion by which one can easily determine whether the material under test is associated with a one-carrier or multicarrier conduction. The method is demonstrated for a simple one-carrier system (GaAs single-channel high-electron-mobility-transistor (HEMT) structure) and two multicarrier systems (an InGaAs-GaAs double-channel HEMT-structure and two types of carriers present in an InGaAs single-channel HEMT structure). The analysis of the experimental data obtained on these samples demonstrates the utility of the method presented here for extracting carrier concentrations and mobilities in advanced semiconductor structures.

02,318
PB94-212966 Not available NTIS
National Inst. of Standards and Technology (EEEL), Gaithersburg, MD. Semiconductor Electronics Div.
Defect of Thermal Ramping and Annealing Conditions on Defect Formation in Oxygen Implanted Silicon-On-Insulator Material.
Final rept.
S. J. Krause, J. C. Park, J. D. Lee, M. El-Ghor, and P. Roitman. 1992, 2p.
Sponsored by Defense Nuclear Agency, Washington, DC.
Pub. in Extended Abstract, Proceedings of Institute of Electrical and Electronics Engineers International SOI Conference, Ponte Vedra Beach, FL., October 6-8, 1992, p80-81.

Keywords: *Crystal defects, *CMOS, Integrated circuits, Ion implantation, Stacking faults, Annealing, Silicon, Oxides, Reprints, *SOI(Semiconductors), Thermal ramping, SIMOX.

SIMOX (Separation by IMplantation of OXygen) is a leading technology for providing SOI material for complementary metal-oxide-semiconductor (CMOS) circuits which have increased radiation hardness and higher operating speed. Defects in the top Si layer affect CMOS device yield, operation, and reliability. Defects in annealed SIMOX form from oxide precipitation and dissolution during thermal ramping and annealing. These defects include dislocations, stacking faults, stacking fault pairs, and stacking fault tetrahedra. Multiple cycles of implantation and annealing and higher temperature implantation, above 600 C, have been used to reduce the defect density. Thermal ramping rate and annealing ambient can significantly affect precipitation processes and defect formation during thermal ramping. In this work, the effect of thermal ramping conditions, including oxide capping, on defect formation was studied.

02,319
PB94-213105 Not available NTIS
National Inst. of Standards and Technology (MEL), Gaithersburg, MD. Precision Engineering Div.
Precision, Accuracy, Uncertainty and Traceability and Their Application to Submicrometer Dimensional Metrology.
Final rept.
R. D. Larrabee, and M. T. Postek. 1993, 12p.
Pub. in Solid-State Electronics 36, n5 p673-684 1993.

Keywords: *Dimensional measurement, *Semiconductor devices, *Integrated circuits, *Metrology, Reproducibility, Calibration, Precision, Uncertainty, Accuracy, Standards, Reprints, Traceability, Nanotechnology.

The terms in the title of this paper are often used to characterize the quality of any measurement result. However, these terms (particularly accuracy and traceability) are very often confused (and abused) in practice. They often do not have the same meaning to the seller, buyer, and user of metrology instruments. Each of these terms has a very specific meaning and definition and each should be fully understood and quantified properly before being used to convey metrological information for any purpose. This paper summarizes the generally-accepted generic metrological meaning and significance of these terms for the purpose of clarifying any misunderstanding that might otherwise arise between the metrologist and the user of metrological data. These meanings are illustrated by discussing their application to dimensional standards presently available to the semiconductor industry from NIST.

02,320
PB94-213147 Not available NTIS
National Inst. of Standards and Technology (EEEL), Gaithersburg, MD. Electricity Div.
Custom Integrated Circuit Comparator for High-Performance Sampling Applications.
Final rept.
O. B. Laug, T. M. Souders, and D. R. Flach. 1992, 5p.
Pub. in Proceedings of Institute of Electrical and Electronics Engineers Instrumentation and Measurement Technology Conference, Secaucus, NJ., May 12-14, 1992, p437-441.

Keywords: *Application specific integrated circuits, *Comparator circuits, Frequency domain, Time domain, Electrical measurement, Electric pulses, Voltage, Performance, Design, Silicon, Reprints, Waveform sampling.

This paper reports on the design and performance of an application specific integrated circuit (ASIC) comparator that has been optimized for equivalent-time waveform sampling applications. The comparator, which has been fabricated with an 8.5 GHz f(sub tau), bipolar silicon process, features a bandwidth of >2 GHz, a settling-time accuracy of 0.1% in 2 ns, and almost total elimination of 'thermal tails' in the settling response. Several novel design features that have been used to achieve this level of performance are presented. The comparator can be used in a sampling system for both frequency domain measurements, e.g. wideband rms voltage measurements, and high accuracy time domain pulse measurements.

02,321
PB94-216413 Not available NTIS
National Inst. of Standards and Technology (EEEL), Gaithersburg, MD. Semiconductor Electronics Div.
High-Level CAD Melds Micromachined Devices with Foundries.
Final rept.
J. C. Marshall, M. Parameswaran, M. Zaghloul, and M. Gaitan. 1992, 8p.
Sponsored by Navy Advance Test Equipment/Metrology Project, San Diego, CA. and Army Test Measurements and Diagnostic Equipment Activity, Redstone Arsenal, AL.
Pub. in Institute of Electrical and Electronics Engineers Circuits and Devices 8, n6 p10-17 Nov 92.

Keywords: *Computer aided design, *CMOS, Chips(Electronics), Etching, Silicon, Reprints, *Micromachining, MOSIS service.

The methodology for implementing the design of silicon micromachined devices in a standard CMOS foundry process is discussed, and a modified Magic technology file is introduced. The modified technology file is used to design silicon micromachined devices that are fabricated using a standard CMOS foundry through the MOSIS service. An additional maskless etch in EDP is required to realize the micromechanical structures once devices are delivered. The modified technology file implements a layer that we call 'open' that consists of a combination of vias and contact cuts. This open area exposes the silicon surface for an anisotropic etch procedure that creates suspended bridges of polysilicon or metal encapsulated in SiO2. Results from fabricated chips are included.

02,322
PB94-216629 Not available NTIS
National Inst. of Standards and Technology (EEEL), Gaithersburg, MD. Semiconductor Electronics Div.
Characterization of Interface Defects in Oxygen-Implanted Silicon Films.
Final rept.
S. Mayo, J. R. Lowney, and P. Roitman. 1993, 8p.
Pub. in Jnl. of Electronic Materials 22, n2 p207-214 1993.

Keywords: *Silicon films, *Film resistors, *Photoresistors, *Crystal defects, Ion implantation, Photoconductivity, Annealing, Interfaces, Oxygen, Wafers, Reprints, Photoinduced transient spectroscopy, SOI(Semiconductors), SIMOX.

Defects in ungated n- or p-type and gated p-type resistors have been characterized by photoinduced transient spectroscopy (PITS). These resistors were fabricated with p-type separation by implanted oxygen (SIMOX) wafers with a single-energy 200-keV oxygen implant to a total fluence of 1.8 X 10(sup 18)/sq cm. One wafer, used for gated resistor fabrication was implanted at 595 C and sequentially annealed at 1,325 C for 4 h in argon (plus 0.5% oxygen) followed by 4 h in nitrogen (plus 0.5% oxygen). Another wafer, used for ungated resistor fabrication, was implanted at 650 C and annealed at 1,275 C for 2 h in nitrogen (plus 0.5% oxygen). Our results indicate that more damage is present in the wafer annealed at 1,275 C than in the one annealed at 1,325 C. We estimate the average trap density at the back interface to be in the 10(sup 11)/sq cm range.

02,323
PB94-216637 Not available NTIS
National Inst. of Standards and Technology (EEEL), Gaithersburg, MD. Semiconductor Electronics Div.
Charge Trapping and Breakdown Mechanism in SIMOX.
Final rept.
S. Mayo, J. S. Suehle, and P. Roitman. 1992, 2p.
Contract DNA-IACRO-88-800
Sponsored by Defense Nuclear Agency, Washington, DC.
Pub. in Extended Abstract, Proceedings of 1992 Institute of Electrical and Electronics Engineers International SOI Conference, Ponte Vedra Beach, FL., October 6-8, 1992, p28-29.

Keywords: *Breakdown(Electronic threshold), *Dielectric breakdown, Electron traps, Hole traps, Capacitors, Reprints, *SIMOX, SIMOX(Separation by IMplanted OXygen), Buried oxides, SOI(Semiconductors).

We have studied the charge build-up mechanism in SIMOX (Separation by IMplanted OXygen) capacitors injected with electrons from the gate or substrate. The breakdown voltage corresponds to electric fields of 10(sup 7)V/cm for electron injection from the gate, or 7.5 X 10(sup 6)V/cm for electron injection from the substrate. These field values, comparable to breakdown fields in capacitors fabricated with thermally grown oxides, are reported here for the first time in SIMOX buried oxides. The breakdown voltage asymmetry in the SIMOX structure is determined by differences in interface morphology at the gate or substrate. Injection from the substrate yields higher current under equal bias and results in lower breakdown fields.

02,324
PB95-108510 Not available NTIS
National Inst. of Standards and Technology (NEL), Gaithersburg, MD. Precision Engineering Div.
Practical Photomask Linewidth Measurements.
Final rept.
J. Potzick. 1990, 9p.
Pub. in Proceedings of Society of Photo-Optical Instrumentation Engineers - Integrated Circuit Metrology, Inspection and Process Control IV, San Jose, CA., March 5-6, 1990, v1261, p114-122.

Keywords: *Dimensional measurement, *Integrated circuits, *Line width, *Photomasks, *Lithography, Process control, Comparison, Accuracy, Reprints, Microlithography, Micrometrology.

The measurement cycle for practical accurate photomask linewidth measurement is analyzed as a differential measurement--the linewidth to be measured is compared to a known linewidth on a standard photomask. The linewidth measuring instrument is thus a comparator. The conditions necessary for a valid measurement are discussed with regard to both the instrument and the comparison process. The principles discussed here apply to many other types of measurement as well.

02,325
PB95-111522 PC A03/MF A01
National Inst. of Standards and Technology (EEEL), Gaithersburg, MD. Semiconductor Electronics Div
User's Manual for the Program MONSEL-1: Monte Carlo Simulation of SEM Signals for Linewidth Metrology.
Special pub.
J. R. Lowney, and E. Marx. Aug 94, 46p, NIST/SP-400-95.
Also available from Supt. of Docs. as SN003-003-03282-4.

Keywords: *Integrated circuits, *Dimensional measurement, *Line width, Scanning electron microscopy, Monte Carlo method, Electron scattering, Computerized simulation, Programming manuals, Backscattering, Metrology, MONSEL-I computer code, Fortran 77 programming language, X-ray lithography, Silicon substrates, Multilayers.

This user's manual is a guide to the FORTRAN code MONSEL-I which is a Monte Carlo simulation of the transmitted and backscattered electron signals in a scanning electron microscope (SEM) associated with a line specimen with a trapezoidal cross section. The line is deposited on a multi-layer substrate. The primary purpose of the code is to determine the actual linewidth from measured SEM signals. However, it can be used for many other purposes such as transmission electron microscopy. Future extensions to model secondary electron signals and multiple lines are planned.

02,326
PB95-125076 PC A05/MF A01
National Inst. of Standards and Technology (EEEL), Gaithersburg, MD. Semiconductor Electronics Div.
Standard Reference Materials: Certification of a Standard Reference Material for the Determination of Interstitial Oxygen Concentration in Semiconductor Silicon by Infrared Spectrophotometry.
Special pub.
B. Rennex. Aug 94, 85p, NIST/SP-260/121.
Also available from Supt. of Docs. as SN003-003-03281-6.

Keywords: *Silicon, Concentration(Composition), Infrared spectrophotometers, Certification, Calibration, Interstitials, Semiconductors, Uncertainty, Tables(Data), Graphs(Charts), *Standard reference materials, *Oxygen concentration, Infrared spectrophotometry, Number fraction.

A Standard Reference Material, SRM-2551, has been prepared, measured, and certified for the determination of interstitial oxygen number fraction (commonly referred to as the oxygen concentration) in semiconductor silicon. This SRM is intended for calibration of infrared spectrophotometers used to measure the 1107/cm interstitial oxygen peak in silicon. Its purpose

is to enable its users to improve their measurement agreement. The expanded SRM uncertainty is 0.17% for the low-oxygen specimens, 0.13% for the medium-oxygen specimens, and 0.12% for the high-oxygen specimens. The certifying instrument was a Fourier-transform infrared spectrophotometer which measured the oxygen peak height. Specimens from an earlier international Grand Round Robin (GRR) were used to convert these infrared values to oxygen number fraction (concentration) values. A major source of uncertainty had been measurement drift; this was largely compensated using a control specimen. The remaining sources of uncertainty were instrument reproducibility, nonuniformity in oxygen concentration and thickness over the specimen area, and variation in residual oxygen in the SRM float-zone specimens, each of which float-zone specimens served as the zero-oxygen reference for a measurement. These sources were combined in quadrature to arrive at the above-quoted 2 sigma estimate of expanded SRM uncertainty.

02,327
PB95-141172 Not available NTIS
National Inst. of Standards and Technology (EEEL), Gaithersburg, MD. Semiconductor Electronics Div.
Physics for Device Simulations and Its Verification by Measurements.
Final rept.
H. S. Bennett, and J. R. Lowney. 1994, 41p.
Pub. in Semiconductors, v59 pt2 p33-73 1994.

Keywords: *Semiconductor devices, *Computerized simulation, Quantum mechanics, Carrier mobility, Bipolar transistors, Space charge, Doped materials, Band theory, Gallium arsenides, Silicon, Plasmons, Phonons, Reprints.

The motivations for using computers to simulate the electrical characteristics of transistors are discussed. Our work and that of others in the area of device physics and modeling are described. We compare conventional device physics with an alternative approach to device physics that is more directly traceable to quantum-mechanical concepts. We then apply this new approach to quasi-neutral regions, space-charge regions, and regions with high levels of carrier injection. Examples of applying quantum-mechanically-based device physics to energy band diagrams for bipolar transistors are given. The limits for using theoretical results from uniform media in numerical simulations of devices with large concentration gradients are discussed. We conclude with a discussion of the requirements for verifying and calibrating device simulators for the submicrometer domain.

02,328
PB95-143111 PC A05/MF A01
National Inst. of Standards and Technology (MSEL), Gaithersburg, MD. Polymers Div.
Metrology and Data for Microelectronic Packaging and Interconnection: Results of a Joint Workshop on Materials Metrology and Data for Commercial Electrical and Optical Packaging and Interconnection Technologies. Held in Gaithersburg, Maryland on May 5-6, 1994. Volume 1. Results.
M. A. Schen. Nov 94, 90p, NISTIR-5520.
See also PB94-152733. Sponsored by Optoelectronics Industry Development Association, Mountain View, CA. and Semiconductor Research Corp., Research Triangle Park, NC.

Keywords: *Circuit interconnections, *Electronic packaging, *Optoelectronic devices, *Metrology, *Microelectronics, *Meetings, Printed circuit boards, Integrated circuits, Chips(Electronics), Reliability(Electronics), Semiconductor devices, Measurement, Ceramics, Polymers, Metals, *Optical interconnections, Flat panel displays, US NIST.

This NISTIR documents the results of a joint Industry - University - Government workshop on 'Materials Metrology and Data for Commercial Electrical and Optical Packaging and Interconnection Technologies' conducted on May 5-6, 1994 at the Hilton Hotel in Gaithersburg, MD and was cosponsored by the National Institute of Standards and Technology, the Institute for Interconnecting and Packaging Electronic Circuits, the Optoelectronics Industry Development Association, and the Semiconductor Research Corporation. The workshop consisted of eight separate working groups. Four technology-focused working groups met to address the challenges and priorities in materials measurement and data to support the design, manufacture, and reliability assessment of critical electrical and optical packaging and interconnection materials, structures, and processes. Four performance-focused working groups also met to address the status, challenges, and gaps in metrology and data to describe the properties of materials utilized in the critical packaging and interconnection materials, structures, and processes identified earlier.

02,329
PB95-143186 PC A03/MF A01
National Inst. of Standards and Technology (EEEL), Gaithersburg, MD. Semiconductor Electronics Div.
Electronics and Electrical Engineering Laboratory Technical Progress Bulletin Covering Laboratory Programs, April to June 1994 with 1994/1995 EEEL Events Calendar.
J. M. Rohrbaugh. Sep 94, 44p, NISTIR-5483.
See also PB94-193810.

Keywords: *Electrical measurement, *Microelectronics, *Optoelectronic devices, *Metrology, *Bibliographies, Integrated circuits, Dimensional measurement, Dielectric breakdown, Josephson junctions, High temperature superconductors, Microwave equipment, Sulfur hexafluoride, Optical fibers, Electric power, YBCO superconductors, Antennas, Body armor, Abstracts, Fiber optic sensors, Test structures, Microfabrication, Cryoelectronics, Magnetic force microscopy, Scanning capacitance microscopy, US NIST.

This is the forty-seventh issue of a quarterly publication providing information on the technical work of the National Institute of Standards and Technology, Electronics and Electrical Engineering Laboratory (EEEL). This issue of the EEEL Technical Progress Bulletin covers the second quarter of calendar year 1994. Abstracts are provided by technical area for both published papers and papers approved by NIST for publication. Major subject headings include the following: Fundamental Electrical Measurements; Semiconductor Microelectronics; Signal Acquisition, Processing, and Transmission; Electrical Systems; Law-Enforcement Standards; Product Data Systems (includes net information tools); Video Technology.

02,330
PB95-143327 PC A08/MF A02
National Inst. of Standards and Technology, Gaithersburg, MD.
Metrology and Data for Microelectronic Packaging and Interconnection: Results of a Joint Workshop on Materials Metrology and Data for Commercial Electrical and Optical Packaging and Interconnection Technologies. Held in Gaithersburg, Maryland on May 5-6, 1994. Volume 2. Presentation Material.
M. A. Schen. Nov 94, 156p, NISTIR-5520-V2.
See also Volume 1, PB95-143111. Sponsored by Optoelectronics Industry Development Association, Mountain View, CA. and Semiconductor Research Corp., Research Triangle Park, NC.

Keywords: *Circuit interconnections, *Electronic packaging, *Optoelectronic devices, *Integrated circuits, *Meetings, Very large scale integration, Government policies, Chips(Electronics), Optical communication, Optical storage, Memory devices, Market surveys, Microelectronics, Metrology, Hardware, Optical interconnections.

This volume 2 consists of Appendix C, which contains presentations by representatives from Motorola, GTE Laboratories, Cornell University, SRC, IPC, ARPA, ITRI, and the National Institute of Standards and Technology (NIST).

02,331
PB95-150058 Not available NTIS
National Inst. of Standards and Technology (EEEL), Gaithersburg, MD. Semiconductor Electronics Div.
Monte Carlo Model for SEM Linewidth Metrology.
Final rept.
J. R. Lowney, M. T. Postek, and A. E. Vladar. 1994, 12p.
Pub. in Proceedings of Society of Photo-Optical Instrumentation Engineers: Integrated Circuit Metrology, Inspection, and Process Control VIII, San Jose, CA., February 28-March 2, 1994, v2196 p85-96.

Keywords: *Scanning electron microscopy, *Dimensional measurement, *Integrated circuits, *Line width, *Edge detection, Mathematical models, Monte Carlo method, Computerized simulation, Electron transport, Electron scattering, Backscattering, Metrology, Substrates, Silicon, Gold, Reprints, X-ray lithography, Microlithography.

A scanning electron microscope (SEM) can be used to measure the dimensions of the microlithographic features of integrated circuits. However, without a good model of the electron-beam/specimen interaction, accurate edge location cannot be obtained. A Monte Carlo code has been developed to model the interaction of an electron beam with a line lithographically produced on a multi-layer substrate. The purpose of the code is to enable one to extract the edge position of a line from SEM measurements. It is based on prior codes developed at NIST, but with a new formulation for the atomic scattering cross sections and the inclusion of a method to simulate edge roughness or rounding. The code is currently able to model the transmitted and backscattered electrons, and the results from the code have been applied to the analysis of electron transmission through a gold line on a thin silicon substrate, such as used in an X-ray lithographic mask. By comparing the predictions of the code with measured data, it is possible to obtain edge positions to the order of + or - 10 nm, which is needed for the advanced lithography projected for the year 2000. The uncertainty of this measurement is limited by the sample geometry and surface roughness and not by the measurement process.

02,332
PB95-150066 Not available NTIS
National Inst. of Standards and Technology (EEEL), Gaithersburg, MD. Semiconductor Electronics Div.
Transverse Magnetoresistance: A Novel Two-Terminal Method for Measuring the Carrier Density and Mobility of a Semiconductor Layer.
Final rept.
J. R. Lowney, W. R. Thurber, and D. G. Seiler. 1994, 3p.
Pub. in Applied Physics Letters 64, n22 p3015-3017, 30 May 94.

Keywords: *Carrier density, *Carrier mobility, *Magnetoresistance, Semiconductor devices, Semiconductors(Materials), Mercury cadmium tellurides, Infrared detectors, Electrical measurement, Cryogenic temperature, Reprints, Magnetic field dependence, Transverse magnetoresistance.

The magnetic-field dependence of the two-terminal magnetoresistance that occurs in rectangularly shaped samples can be used to determine both the free-carrier density and the mobility of a semiconductor layer. An approximate equation for the magnetoresistance was derived for variable length-to-width ratio. This technique was used to determine the electron density and mobility of accumulation layers in n-type Hg(0.8)Cd(0.2)Te photoconductive infrared detectors at 6 and 77 K. It should be applicable to a wide variety of fabricated devices and allow significant improvements in processing methods and quality control.

02,333
PB95-150348 Not available NTIS
National Inst. of Standards and Technology (EEEL), Gaithersburg, MD. Semiconductor Electronics Div.
High Temperature Reliability of Thin Film SiO2.
Final rept.
J. S. Suehle, P. Chaparala, and C. Messick. 1994, 9p.
Pub. in Proceedings of International High Temperature Electronics Conference (2nd), Charlotte, NC., June 5-10, 1994, pVIII 15-VIII 23.

Keywords: *Silicon dioxide, *Dielectric breakdown, Temperature range 0400-1000 K, Time dependence, Reliability(Electronics), High temperature, Dielectric films, Reprints.

We present Time-Dependent Dielectric Breakdown (TDDB) test results for thin SiO2 gate oxides at stress temperatures up to 400 C. The data were collected at the wafer level using a specially designed probe station that uses a water-cooled probe card and text fixture. It is demonstrated that these oxides exhibit extrapolated lifetimes in excess of 6.3 x 10(exp 10) s (2000 years) at 2.0 MV/cm for a stress temperature of 350 C under positive or negative bias. Our results indicate that the physical mechanism of TDDB does not change significantly up to stress temperatures of 400 C. It is necessary to obtain data over a wide range of electric fields and temperatures to distinguish between field acceleration models and to quantify the electric field and temperature dependencies of the thermal activation energy and the field acceleration factor, respectively.

02,334
PB95-150975 Not available NTIS
National Inst. of Standards and Technology (EEEL), Gaithersburg, MD. Semiconductor Electronics Div.

Effects of Heavy Doping on Numerical Simulations of Gallium Arsenide Bipolar Transistors.
Final rept.
M. Tomizawa, T. Ishibashi, H. S. Bennett, and J. R. Lowney. 1992, 10p.
Pub. in Solid-State Electronics 35, n6 p865-874 1992.

Keywords: *Bipolar transistors, Molecular beam epitaxy, Mathematical models, Numerical solution, Sensitivity analysis, Doped materials, Carrier mobility, Carrier density, Carrier lifetime, Gain, Reprints, *Gallium arsenide transistors.

Using the best available physical models is essential for predictive numerical simulations of advanced, high performance GaAs transistors. Among the many input parameters for numerical simulations, the effective intrinsic carrier concentrations, n(ie) minority carrier mobilities, mu, and recombination lifetimes, tau, are very critical parameters. The results from recent theoretical calculations for n(ie) were implemented into a two-dimensional, drift-diffusion simulator for GaAs transistors. In order to compare predicted and measured d.c. common emitter gains, NPN GaAs homojunction bipolar transistors with different but heavily doped bases and similarly doped emitters that have widths between 0.1 and 0.45 micrometer were fabricated by molecular beam epitaxy. The predicted gains of 8, 25, 46, 72 for these transistors agreed very well with their measured gains of 9, 22, 42 and 70 at high current, respectively. Without using the new theoretical data for n(ie) but setting n(ie) equal everywhere to the intrinsic carrier concentration, n(i), the predicted gains became 4, 14, 27 and 35, respectively. Sensitivity analyses on mobilities, lifetimes, and n(ie) showed that physically correct n(ie) values are quantitatively very important for predictive simulations of GaAs bipolar transistors.

02,335
PB95-151155 Not available NTIS
National Inst. of Standards and Technology (CSTL), Gaithersburg, MD. Thermophysics Div.
Effect of Electrode-Polymer Interfacial Layers on Polymer Conduction. Part 2. Device Summary.
Final rept.
A. van Roggen, and P. H. E. Meijer. 1988, 11p.
Pub. in Proceedings of International Symposium on Molecular Electronic Devices (3rd), Arlington, VA., October 6-8, 1986, p427-437 1988.

Keywords: *Electrodes, *Crystals, *Polymers, *Electric devices, Electron tunneling, Experimental design, Interfaces, Conductivity, Molecular electronics, Organic semiconductors, Reprints.

In this paper, chain-folded crystals are investigated as possible electronic devices. Active devices, showing negative resistance in the IV curve, have been demonstrated experimentally on single crystals of polymers. The operating principle of these devices is tunneling, which was confirmed by theory. The current paper describes the experimental evidence, the theoretical background with explicit calculations of the expected current-voltage profile, the model for such devices, and points to several possible device types and applications.

02,336
PB95-152278 Not available NTIS
National Inst. of Standards and Technology (EEEL), Gaithersburg, MD. Semiconductor Electronics Div.
Electrical Test Structure for Overlay Metrology Referenced to Absolute Length Standards.
Final rept.
M. W. Cresswell, W. B. Penzes, R. A. Allen, E. C. Teague, L. W. Linholm, and C. H. Ellenwood. 1994, 10p.
Pub. in Proceedings of Society of Photo-Optical Instrumentation Engineers: Integrated Circuit Metrology, Inspection, and Process Control VIII, San Jose, CA., February 28-March 2, 1994, p512-520.

Keywords: *Very large scale integration, *Integrated circuits, *Overlays, Potentiometers(Resistors), Microelectronics, Positioning, Alignment, Metrology, Lithography, Reprints, *Test structures, Coordinate measurement systems, Length standards, Traceability.

This test structure is based on the voltage-dividing potentiometer principle and was originally replicated in a single lithography cycle to evaluate feature placement by a primary pattern generator. A new test structure has now been developed from the single-cycle version and has been used for measuring the overlay of features defined by two different exposures with a stepping projection aligner. The as-measured overlay values are processed by an algorithm which minimizes the effects of nominal random pattern imperfections. The algorithm further partitions measurements of overlay into contributions which derive, respectively, from misregisteration of the image fields projected by the two masks and from the drawn misplacement of features on the masks. The numerical estimates of these contributions so obtained from the electrical measurements were compared with those extracted from the same features by the NIST Line Scale Interferometer, providing traceability to absolute length standards. The two sets of measurements were found to agree to within the several-nanometer uncertainty cited for the line scale interferometer's readings alone. The motivation for this work was to compare the nanometer-level distortions, produced by alternative chucking arrangements, of proximity X-ray masks having various support-ring architectures. However, the techniques may also be used to evaluate optical aligner tools and to determine image placement quality on optical reticles with traceability to the International Standard of length, the meter.

02,337
PB95-152773 Not available NTIS
National Inst. of Standards and Technology (EEEL), Gaithersburg, MD. Semiconductor Electronics Div.
Exact Solution of the Steady-State Surface Temperature for a General Multilayer Structure.
Final rept.
J. Albers. 1994, 9p.
Pub. in Proceedings of Annual Institute of Electrical and Electronics Engineers Semiconductor Thermal Measurement and Management Symposium (10th), San Jose, CA., February 1-3, 1994, p129-137.

Keywords: *Semiconductor devices, *Surface temperature, Thermal conductivity, Fourier analysis, Steady state, Heat flow, Microelectronics, Silicon, Reprints, SOI(Semiconductors), Multilayers, SIMOX.

A recursive technique is developed and is shown to provide the surface temperature of the multilayer steady-state heat flow equation. This recursive technique can be used with any number of layers while incurring only a small increase in computation time for each added layer. For the case of complete, uniform top surface coverage by a heat source, the technique gives rise to the generalized one-dimensional thermal resistance result. An example of the use of the new recursive method is provided by the preliminary calculations of the surface temperature of a buried oxide (SOI, SIMOX) structure containing several thicknesses of the surface silicon layers. This new technique should prove useful in the investigation and understanding of the steady-state thermal response of modern multilayer microelectronic structures.

02,338
PB95-152807 Not available NTIS
National Inst. of Standards and Technology (EEEL), Gaithersburg, MD. Semiconductor Electronics Div.
Comparisons of Measured Linewidths of Sub-Micrometer Lines Using Optical, Electrical, and SEM Metrologies.
Final rept.
R. A. Allen, P. Troccolo, J. C. Owen, J. Potzick, and L. W. Linholm. 1993, 10p.
Pub. in Proceeding of Society of Photo-Optical Instrumentation Engineers: Integrated Circuit Metrology, Inspection, and Process Control VII, San Jose, CA., March 2-4, 1993, v1926 p34-43.

Keywords: *Very large scale integration, *Integrated circuits, *Dimensional measurement, *Line width, Scanning electron microscopy, Optical microscopy, Comparative evaluations, Metal films, Lithography, Substrates, Metrology, Titanium, Quartz, Wafers, Reprints, Test structures.

An investigation is being carried out to determine the ability of three methods of linewidth metrology to measure the dimensions of features to less than 0.5 micrometer. The three methods are transmitted-light optical microscopy, electrical test structure, and scanning electron microscopy (SEM). Electrical, SEM, and reflected-light microscopy techniques are widely used for linewidth metrology in VLSI fabrication. However, none of these widely-used techniques currently permits traceability to international standards of length. Transmitted-light optical microscopy allows traceability; however, this technique is applicable only to transparent substrates. To permit the inclusion of transmitted-light optical microscopy in this investigation, 100-nm thick Ti films were patterned using normal VLSI processing techniques on a 150-mm diameter quartz wafer. The cross-bridge resistor test structure was used as this structure has been widely used in industry and it allows the results from all three metrological techniques to be compared. The design bridge widths of the test structures range from 0.4 micrometer to 1.0 micrometer. The results of these measurements show systematic and uniform offsets between the different techniques. In this paper we discuss the different techniques and describe the observed results.

02,339
PB95-152914 Not available NTIS
National Inst. of Standards and Technology (EEEL), Gaithersburg, MD. Semiconductor Electronics Div.
Physics for Device Simulations and Its Verification by Measurements.
Final rept.
H. S. Bennett, and J. R. Lowney. 1994, 41p.
Pub. in Semiconductors, v59 pt2 p33-73 1994.

Keywords: *Computerized simulation, *Transistors, Silicon transistors, Bipolar transistors, Quantum mechanics, Energy bands, Gallium arsenides, Carrier mobility, Calibration, Phonons, Plasmons, Reprints.

The motivations for using computers to simulate the electrical characteristics of transistors are discussed. Our work and that of others in the area of device physics and modeling are described. We compare conventional device physics with an alternative approach to device physics that is more directly traceable to quantum-mechanical concepts. We then apply this new approach to quasi-neutral regions, space-charge regions, and regions with high levels of carrier injection. Examples of applying quantum-mechanically-based device physics to energy band diagrams for bipolar transistors are given. The limits for using theoretical results from uniform media in numerical simulations of devices with large concentration gradients are discussed. Calculations of the effective intrinsic carrier concentrations for gallium arsenide and silicon are also given, along with published data. In addition, calculations of the mobilities for GaAs that are based in part on quantum-mechanical phase shifts are compared with published data. We then conclude with a discussion of the requirements for verifying and calibrating device simulators for the submicrometer domain.

02,340
PB95-152997 Not available NTIS
National Inst. of Standards and Technology (EEEL), Gaithersburg, MD. Semiconductor Electronics Div.
Experimental Study of Reverse-Bias Failure Mechanisms in Bipolar Mode JFET (BMFET).
Final rept.
G. Busatto. 1993, 7p.
Pub. in Proceedings of Power Electronics Specialists Conference, Seattle, WA., June 20-24, 1993, p482-488.

Keywords: *Field effect transistors, *Bipolar transistors, *Breakdown(Electronic threshold), *Avalanche breakdown, Nondestructive tests, Failure(Electronics), Integrated circuits, Layout, Reprints, Power transistors, Second breakdown, Reverse bias.

A systematic, non-destructive, experimental study of the bipolar mode FET (BMFET) behavior during its failure is presented. The variation of the reverse bias safe operating area (RBSOA) for an inductive load with different bias conditions is described. It is shown that the device breakdown is strongly dependent on the reverse current gain. On the basis of the experimental results, insight into the physics of the failure mechanisms is given, and it is shown that most of the RBSOA limitations appear to result from device lay-out problems.

02,341
PB95-153359 Not available NTIS
National Inst. of Standards and Technology (MEL), Gaithersburg, MD. Precision Engineering Div.
Integration of Scanning Tunneling Microscope Nanolithography and Electronics Device Processing.
Final rept.
J. A. Dagata, W. Tseng, J. Bennett, H. Harary, E. A. Dobisz, and J. Schneir. 1992, 9p.
Pub. in Jnl. of Vacuum Science and Technology A 10, n4 p2105-2113 Jul/Aug 92.

Keywords: *Integrated circuits, Scanning tunneling microscopy, Molecular beam epitaxy, Quantum electronics, Semiconductor devices, Fabrication, Reprints, *Nanoelectronics, *Nanolithography, Reactive ion etching.

The emerging field of nanoelectronics demands innovative methods to fabricate nanometer-scale structures. Such structures will play a critical role in the quantum-effect device physics of future highly integrated circuit architectures. An integrated approach to compound semiconductor nanostructure fabrication based on scanning tunneling microscope (STM) nanolithography, molecular-beam epitaxy, and reactive ion etching techniques is described. The critical elements of this approach, which have been demonstrated recently, are reviewed. Prospects for the coevolutionary development of nanoelectronics and STM-based fabrication and characterization are considered.

02,342
PB95-153656 Not available NTIS
National Inst. of Standards and Technology (EEEL), Gaithersburg, MD. Semiconductor Electronics Div.
Performance of Commercial CMOS Foundry-Compatible Multijunction Thermal Converters.
Final rept.
M. Gaitan, J. Kinard, and D. X. Huang. 1993, 3p.
See also PB95-153664.
Pub. in Proceedings of International Conference on Solid-State Sensors and Actuators (7th), Yokohama, Japan, June 7-10, 1993, p1012-1014.

Keywords: *Microwave sensors, *Voltage measuring instruments, Electric current meters, Electric power meters, Computer aided design, Alternating current, Very large scale integration, Low costs, Integrated circuits, Performance, Electrical measurement, CMOS, Reprints, *Thermal converters, Multijunction thermal converters, MOSIS service.

We report on the performance of multijunction thermal converters (MJTCs) fabricated using commercial CMOS integrated circuit (IC) foundries through MOSIS. Calibration testing shows that the devices are suitable for the measurement of ac voltage, current, and power for frequencies above audio using conventional thermal transfer techniques. These devices show promise for applications as low-cost, high-precision RF and microwave power sensors with integrated electronics. The fabrication methodology allows easy integration with VLSI microcircuits using standard design libraries leading to low-cost, foundry-independent products.

02,343
PB95-153664 Not available NTIS
National Inst. of Standards and Technology (EEEL), Gaithersburg, MD. Semiconductor Electronics Div.
Multijunction Thermal Converters by Commercial CMOS Fabrication.
Final rept.
M. Gaitan, J. Suehle, J. R. Kinard, and D. X. Huang. 1993, 2p.
See also PB95-153656.
Pub. in Proceedings of Institute of Electrical and Electronics Engineers Instrumentation/Measurement Technology Conference, Irvine, CA., May 17-20, 1993, p243-244.

Keywords: Electrical measurement, Commercial sector, Fabrication, Transfer characteristics, Alternating current, Direct current, CMOS, Reprints, *Thermal converters, Multijunction thermal converters.

New multijunction thermal converters fabricated in a commercial CMOS foundry are described and the results of measurements of their ac-dc transfer characteristics are given.

02,344
PB95-153805 Not available NTIS
National Inst. of Standards and Technology (EEEL), Gaithersburg, MD. Semiconductor Electronics Div.
Modeling Buffer Layer IGBTs for Circuit Simulation.
Final rept.
A. R. Hefner. 1993, 10p.
Pub. in Proceedings of Power Electronics Specialists Conference, Seattle, WA., June 20-24, 1993, p60-69.

Keywords: *Bipolar transistors, Application specific integrated circuits, Mathematical models, Dynamic properties, Reprints, *Insulated gate bipolar transistors, Circuit simulators, Buffer layers.

The dynamic behavior of commercially available buffer layer IGBTs is described. It is shown that buffer layer IGBTs become much faster at high voltages than nonbuffer layer IGBTs with similar low voltage characteristics. Because the fall times specified in manufacturers' data sheets do not reflect the voltage dependence of switching speed, a new method of selecting devices for different circuit applications is suggested. A buffer layer IGBT model is developed and implemented into the Saber circuit simulator, and a procedure is developed to extract the model parameters for buffer layer IGBTs. It is shown that the new buffer layer IGBT model can be used to describe the dynamic behavior and power dissipation of buffer layer IGBTs in user-defined application circuits.

02,345
PB95-161014 Not available NTIS
National Inst. of Standards and Technology (EEEL), Gaithersburg, MD. Semiconductor Electronics Div.
Simulating the Dynamic Electro Thermal Behavior of Power Electronic Circuits and Systems.
Final rept.
A. R. Hefner, and D. L. Blackburn. 1993, 10p.
Pub. in Institute of Electrical and Electronics Engineers Transactions on Power Electronics 8, n4 p376-385 Oct 93.

Keywords: *Electronic circuits, *Electrical networks, *Thermal analysis, Temperature distribution, Mathematical models, Semiconductor devices, Chips(Electronics), Heat sinks, Integrated circuits, Electric current, Voltage, Reprints, *Circuit simulators, Thermal networks.

A methodology is presented for simulating the dynamic electrothermal behavior of power electronic circuits and systems. In the approach described, the simulator solves for the temperature distribution within the semiconductor devices, packages, and heat sinks (thermal network) as well as the currents and voltages within the electrical network. The thermal network is coupled to the electrical network through the electrothermal models for the semiconductor devices. The electrothermal semiconductor device models calculate the electrical characteristics based upon the instantaneous value of the device silicon chip surface temperature and calculate the instantaneous power dissipated as heat within the device. The thermal network describes the flow of heat from the chip surface through the package and heat sink and thus determines the evolution of the chip surface temperature used by the semiconductor device models.

02,346
PB95-161022 Not available NTIS
National Inst. of Standards and Technology (EEEL), Gaithersburg, MD. Semiconductor Electronics Div.
Thermal Component Models for Electro-Thermal Network Simulation.
Final rept.
A. R. Hefner, and D. L. Blackburn. 1993, 11p.
Pub. in Proceedings of Institute of Electrical and Electronics Engineers SEMI-THERM Symposium (9th), Austin, TX., February 2-4, 1993, p88-98.

Keywords: *Electronic circuits, *Electrical networks, *Thermal analysis, Temperature distribution, Temperature measurement, Semiconductor devices, Integrated circuits, Heat sinks, Electric current, Voltage, Reprints, *Circuit simulators, Thermal networks.

A procedure is given for developing thermal component models for electro-thermal network simulation. In the new electro-thermal network simulation methodology, the simulator solves for the temperature distribution within the semiconductor devices, packages, and heat sinks (thermal network) as well as the currents and voltages within the electrical network. Examples of electro-thermal network simulations are given, and the temperature measurement methods used to validate the thermal component models are described.

02,347
PB95-161576 Not available NTIS
National Inst. of Standards and Technology (EEEL), Boulder, CO. Electromagnetic Technology Div.
Verification of Commercial Probe-Tip Calibrations.
Final rept.
R. B. Marks, and D. F. Williams. 1993, 5p.
Pub. in Automatic Radio Frequency Techniques Group (ARFTG) Conference Digest (42nd), San Jose, CA., December 2-3, 1993, p37-41.

Keywords: *Integrated circuits, *Electric probes, *Calibration, Electrical measurement, Electronics laboratories, Verification, Accuracy, Industry, Reprints, *Probe tip calibration, *Wafer probe stations, Scattering parameters, On wafer calibration, On wafer probes.

We present results of a verification procedure useful in evaluating the accuracy of probe-tip scattering parameter measurements. The procedure was applied to calibrations and measurements performed in industrial laboratories. Actual measurement discrepancies, due primarily to calibration errors, are directly compared to bounds determined by the comparison method. The results demonstrate the utility of the verification technique as well as serious flaws, particularly at high frequencies, in some conventional calibrations.

02,348
PB95-162129 Not available NTIS
National Inst. of Standards and Technology (MEL), Gaithersburg, MD. Precision Engineering Div.
X-ray Mask Metrology: The Development of Linewidth Standards for X-ray Lithography.
Final rept.
M. T. Postek, J. R. Lowney, A. E. Viadar, R. D. Larrabee, W. J. Keery, and E. Marx. 1993, 15p.
Pub. in Proceedings of Society of Photo-Optical Instrumentation Engineers: Electron-Beam, X-ray, and Ion-Beam Submicrometer Lithographies for Manufacturing III, San Jose, CA., March 1-2, 1993, v1924 p435-449.

Keywords: *Integrated circuits, *Dimensional measurement, *Line width, *Lithography, *Standards, Scanning electron microscopy, Monte Carlo method, Electron beams, Metrology, Reprints, *X ray lithography, *X ray masks, Transmitted electrons, Secondary electrons.

The calibration of masks used in X-ray lithography has been successfully accomplished in the scanning electron microscope (SEM) by using the transmitted scanning electron detection technique. This has been made possible because these masks present a measurement subject different from most (if not all) other objects used in semiconductor processing because the support membrane is, by design, X-ray transparent. This characteristic can be used as an advantage in electron beam-based mask metrology because, depending upon the incident electron beam energies, substrate composition and substrate thickness, the membrane can also be essentially electron transparent. The areas of the mask where the absorber structures are located are essentially X-ray opaque as well as electron opaque. Viewing the sample from a perspective below an X-ray mask (by placing the detector beneath the mask) provides excellent electron signal contrast between the absorber structure and the base membrane. Thus, the mask can be viewed in the transmitted electron detection mode of the SEM and precise, potentially accurate dimensional measurements can be made. Monte Carlo modeling of the transmitted electron signal was used to support this work in order to determine the optimum electron detector position and characteristics. This work represents the potential for the first accurate linewidth measurement standard measured at NIST in the SEM as well as the potential for linewidth standards for the X-ray lithography community.

02,349
PB95-163663 Not available NTIS
National Inst. of Standards and Technology (EEEL), Boulder, CO. Electromagnetic Fields Div.
Comparison of Three Techniques for the Precision Measurement of Amplifier Noise.
Final rept.
D. F. Wait. 1992, 2p.
Pub. in Proceedings of Conference on Precision Electromagnetic Measurements, Paris, France, June 9-12, 1992, p252-253.

Keywords: *Microwave amplifiers, *Electromagnetic noise measurement, Electrical measurement, Superhigh frequency, X band, Precision, Radiometers, Comparison, Reprints, *Amplifier noise.

This paper discusses three new measurement techniques and the experimental results for precision four-parameter amplifier noise measurements. Two different measurement systems were used with two different types of low-noise, X-band amplifiers. The current measurement accuracy is about + or - 0.2 dB.

02,350
PB95-163671 Not available NTIS
National Inst. of Standards and Technology (EEEL), Boulder, CO. Electromagnetic Fields Div.
Measurement Accuracies for Various Techniques for Measuring Amplifier Noise.
Final rept.
D. F. Wait. 1992, 10p.
Pub. in Proceedings of the ARFTG Conference Digest (39th), Albuquerque, NM., June 5, 1992, p43-52.

Keywords: *Microwave amplifiers, *Electromagnetic noise measurement, Electrical measurement,

Superhigh frequency, X band, Microwave radiometers, Accuracy, Reprints, *Amplifier noise, Automatic network analyzers.

The National Institute of Standards and Technology (NIST) has a program to develop an amplifier noise calibration service. Extensive measurements of the noise for different types of low-noise, X-band (8 - 12 GHz) amplifiers were made. This paper concentrates on the accuracy of measuring generalized noise figure for various techniques using the NIST 8 - 12 GHz noise calibration radiometer and a commercial automatic network analyzer.

02,351
PB95-163697 Not available NTIS
National Inst. of Standards and Technology (EEEL), Boulder, CO. Electromagnetic Fields Div.
Planar Resistors for Probe Station Calibration.
Final rept.
D. K. Walker, D. F. Williams, and N. Morgan. 1992, 9p.
Pub. in ARFTG Conference Digest (40th), Orlando, FL., December 3-4, 1992, p1-9.

Keywords: *Film resistors, Electrical impedance, Planar structures, Equivalent circuits, Photoresist coatings, Nickel chromium alloys, Integrated circuits, Residues, Reprints, *Wafer probe stations, On wafer probes, On wafer calibration.

This paper investigates the effects of variations in sheet resistance, geometry, distance from the probe tip, and fabrication processes on the impedance of planar nickel-chromium resistors. Resistor reactance is a strong function of film resistance, but depends only weakly on geometry and distance from the probe tip. Photoresist contamination in the resistive film induces more complicated impedance behavior, even at low frequencies. The impact on circuit design and time- and frequency-domain calibrations is considered in light of these results.

02,352
PB95-163945 Not available NTIS
National Inst. of Standards and Technology (EEEL), Boulder, CO. Electromagnetic Fields Div.
Calibrating On-Wafer Probes to the Probe Tips.
Final rept.
D. F. Williams, and R. B. Marks. 1992, 8p.
Pub. in Proceedings of the ARFTG Conference Digest (40th), Orlando, FL., December 3-4, 1992, p136-143.

Keywords: *Integrated circuits, *Electric probes, *Calibration, Electrical measurement, Microwave circuits, Accuracy, Reprints, *Probe tip calibration, *Wafer probe stations, Scattering parameters, On wafer probes, On wafer calibration.

This paper investigates the accuracy of on-wafer scattering-parameter calibrations at the probe tips. Data show the extent to which certain probe-tip calibrations are consistent with one another and applicable to the characterization of devices or circuits fabricated on different wafers or embedded in different transmission-line media. Calibrations to the probe tips are especially well suited to lower-frequency microwave measurements. Further results demonstrate conditions under which probe-tip calibrations fail.

02,353
PB95-163952 Not available NTIS
National Inst. of Standards and Technology (EEEL), Boulder, CO. Electromagnetic Technology Div.
LRM Probe-Tip Calibrations with Imperfect Resistors and Lossy Lines.
Final rept.
D. F. Williams, and R. B. Marks. 1993, 4p.
Pub. in Proceedings of ARFTG Conference Digest (42nd), San Jose, CA., December 2-3, 1993, p32-36.

Keywords: *Integrated circuits, *Electric probes, *Calibration, Electrical measurement, Microwave circuits, Broadband, Reprints, *Probe tip calibration, *Wafer probe stations, Scattering parameters, On wafer calibration, On wafer probes.

The line-reflect-match calibration is extended, without significant loss of measurement accuracy, to accommodate imperfect match standards and lossy lines typical of monolithic microwave integrated circuits. We characterize the match and line standards using an additional line standard of moderate length. The new method provides a practical means of obtaining accurate, wideband calibrations with compact standard sets.

02,354
PB95-164174 Not available NTIS
National Inst. of Standards and Technology (EEEL), Gaithersburg, MD. Electricity Div.
Anomalous Behavior of a Quantized Hall Plateau in a High-Mobility Si Metal-Oxide-Semiconductor Field-Effect Transistor.
Final rept.
K. Yoshihiro, C. T. Van Degrift, M. E. Cage, and D. Yu. 1992, 11p.
Pub. in Physical Review B 45, n24 p14 204-14 214, 15 Jun 92.

Keywords: *Field effect transistors, *MOSFET, *Electrical resistance, High electron mobility transistors, Silicon transistors, Metastable state, Electrical measurement, Anomalies, Reprints, *Quantum Hall effect, Millikelvin temperature.

Measurements at 14 T and 340 mK of the quantized Hall resistance of the i = 4 plateau of a Si metal-oxide-semiconductor field-effect transistor (Si-MOSFET) made with a precision of 0.005 ppm and an accuracy of 0.015 ppm revealed unexpected irregularities. Smooth variations of + or - 0.04 ppm were observed across the plateau even though the Si-MOSFET had a mobility of 1.2 m(squared)/V s and a diagonal resistivity less than 0.002 ppm of the plateau resistivity. Furthermore, measurements over a period of several months indicated that the plateau shape is metastable. A variety of possible causes for these phenomena are discussed, but none provides a satisfactory explanation.

02,355
PB95-164273 Not available NTIS
National Inst. of Standards and Technology (EEEL), Gaithersburg, MD. Semiconductor Electronics Div.
Electrical Test Structure for Improved Measurement of Feature Placement and Overlay in Integrated Circuit Fabrication Processes.
Final rept.
R. A. Allen, and C. E. Schuster. 1993, 3p.
Pub. in Proceedings of the Government Microcircuit Applications Conference (GOMAC), New Orleans, LA., November 1-5, 1993, p159-161.

Keywords: *Integrated circuits, *Semiconductor devices, *Alignment, Potentiometers(Resistors), Microwave circuits, Millimeter waves, Process control, Gallium arsenides, Metrology, Overlays, CMOS, Reprints, *Test structures.

The modified voltage-dividing potentiometer has previously been demonstrated to have a resolution of under 10 nm when applied to short-loop, single-level processes. This test structure has recently been applied to several full cycle processes, which we are reporting here for the first time. In this paper we describe the successful demonstration of test vehicle implementations and test results obtained from applying the new design to a GaAs Microwave/Millimeter Wave Monolithic Integrated Circuits (MIMIC) process and a CMOS/Bulk process. The demonstrated success in these substantially different processes indicates that these results should apply to a wide range of semiconductor fabrication environments.

02,356
PB95-164356 Not available NTIS
National Inst. of Standards and Technology (EEEL), Gaithersburg, MD. Semiconductor Electronics Div.
Effect of Annealing Ambient on the Removal of Oxide Precipitates in High-Dose Oxygen Implanted Silicon.
Final rept.
S. Seraphin, S. J. Krause, P. Roitman, D. S. Simons, and B. F. Cordts. 1991, 3p.
Sponsored by National Science Foundation, Washington, DC.
Pub. in Applied Physics Letters 59, n23 p3003-3005, 2 Dec 91.

Keywords: Ion implantation, Oxygen additions, Oxynitrides, Annealing, Ambience, Reprints, *Oxide removal, *SIMOX, Oxide precipitates.

The effect of annealing ambient on the precipitate removal processes in high-dose oxygen implanted silicon (separation by implantation of oxygen (SIMOX)) has been studied with transmission electron microscopy, electron energy-loss spectroscopy, and secondary ion mass spectroscopy. The rate of removal of oxide precipitates from the top silicon layer in SIMOX is higher during annealing in argon than in nitrogen. The removal is reduced in nitrogen due to the formation of an oxynitride complex at the precipitate surfaces which inhibits oxygen diffusion across the interfaces. Similar effects have been observed for oxide precipitation during nitrogen ambient annealing in bulk silicon.

02,357
PB95-164679 Not available NTIS
National Inst. of Standards and Technology (MSEL), Gaithersburg, MD. Ceramics Div.
Influence of Lattice Mismatch on Indium Phosphide Based High Electron Mobility Transistor (HEMT) Structures Observed in High Resolution Monochromatic Synchrotron X-Radiation Diffraction Imaging.
Final rept.
B. Steiner, J. Comas, W. Tseng, and U. Laor. 1993, 6p.
Sponsored by National Aeronautics and Space Administration, Washington, DC.
Pub. in Materials Research Society Symposia Proceedings, v281 p127-132 1993.

Keywords: *High electron mobility transistors, *Crystal defects, Molecular beam epitaxy, Synchrotron radiation, Monochromatic radiation, X-ray diffraction, High resolution, Indium phosphides, Substrates, Reprints, *Lattice mismatch.

The formation of mismatch dislocations in layered semiconductor structures was found recently in high resolution monochromatic synchrotron x-radiation diffraction images to be correlated with characteristics of the substrate as well as with the layer thickness and degree of lattice mismatch of nonpseudomorphic layers. We have now extended these studies to examine the accommodation to strain as a function of lattice mismatch in a series of high electron mobility transistor (HEMT) structures grown by molecular beam epitaxy (MBE) on indium phosphide substrates. Five distinct types of irregularity are observed: (1) lattice warping, (2) the formation of a nonpseudomorphic layer, (3) the formation of extended arrays of linear mismatch dislocations at the interface between the substrates and nonpseudomorphic layer, (4) the formation of oval regions of tweed-like local lattice variation imbedded among these arrays, (5) extended tweed-like local lattice variation over large peripheral areas in which the formation of straight mismatch dislocation arrays is not observed.

02,358
PB95-169397 (Order as PB95-169371, PC A07/MF A02)
National Inst. of Standards and Technology, Gaithersburg, MD.
Optical Characterization in Microelectronics Manufacturing.
S. Perkowitz, D. G. Seiler, and W. M. Duncan. 1994, 36p.
Prepared in cooperation with Texas Instruments, Inc., Dallas.
Included in Jnl. of Research of the National Institute of Standards and Technology, v99 n5 p605-640 Sep/Oct 94.

Keywords: *Semiconductor devices, *Manufacturing, *Quality control, Polarimetry, Infrared spectroscopy, Raman Spectra, Photoluminescence.

The six techniques described in the paper (ellipsometry, infrared spectroscopy, microscopy, modulation spectroscopy, photoluminescence, and Raman scattering) were chosen because they are currently or potentially widely used in the industry; they measure a broad array of semiconductor parameters; and they operate in different regions of the electromagnetic spectrum. The discussion of each technique indicates the basic semiconductor quantities measured, gives the scientific basis of the technique, and indicates how the measurement is made.

02,359
PB95-169405 (Order as PB95-169371, PC A07/MF A02)
National Inst. of Standards and Technology, Gaithersburg, MD.
Critical Issues in Scanning Electron Microscope Metrology.
M. T. Postek. 1994, 32p.
Included in Jnl. of Research of the National Institute of Standards and Technology, v99 n5 p641-672 Sep/Oct 94.

Keywords: *Integrated circuits, *Precision, *Manufacturing, Electron microscopy, Secondary emission, Metrology.

During the manufacturing of present-day integrated circuits, certain measurements must be made of the submicrometer structures composing the device with a high degree of repeatability. Optical microscopy, scanning electron miscroscopy, and the various forms of scanning probe microscopies are major microscopical techniques used for this submicrometer metrology. New techniques applied to scanning electron microscopy have improved some of the limitations of this technique and time will permit even further improvements. The paper reviews the current state of scanning electron microscope (SEM) metrology in light of many of these recent improvements.

02,360
PB95-170395 PC A03/MF A01
National Inst. of Standards and Technology (EEEL), Gaithersburg, MD. Semiconductor Electronics Div.
Electronics and Electrical Engineering Laboratory Technical Progress Bulletin Covering Laboratory Programs, July to September 1994 with 1994/1995 EEEL Events Calendar.
J. M. Rohrbaugh. Nov 94, 37p, NISTIR-5529.
See also PB95-143186.

Keywords: *Electrical measurement, *Superconducting devices, *Microelectronics, *Metrology, *Bibliographies, High temperature superconductors, Electromagnetic interference, Dimensional measurement, YBCO superconductors, Josephson junctions, Integrated circuits, Microwave equipment, Integrated optics, Video equipment, Mangetic materials, Optical fibers, Photodetectors, Semiconductors, Antennas, Abstracts, SOI(Semiconductors), SIMOX.

This is the forty-eighth issue of a quarterly publication providing information on the technical work of the National Institute of Standards and Technology, Electronics and Electrical Engineering Laboratory. This issue of the EEEL Technical Progress Bulletin covers the third quarter of calendar year 1994. Abstracts are provided by technical area for both published papers and papers approved by NIST for publication. Major subject headings include the following: Fundemental Electrical Measurements; Semiconductor Microelectronics; Signal Acquisition, Processing, and Transmission; Electrical Systems; Electromagnetic Interference; Product Data Systems; Video Technology.

02,361
PB95-175097 Not available NTIS
National Inst. of Standards and Technology (EEEL), Gaithersburg, MD. Semiconductor Electronics Div.
Status and Trends in Power Semiconductor Devices.
Final rept.
D. L. Blackburn. 1993, 7p.
Pub. in Proceedings of IECON '93 Institute of Electrical and Electronics Engineers International Conference on Industrial Electronics, Lahaina, Maui, Hawaii, November 15-19, 1993, p619-625.

Keywords: *Semiconductor devices, Electronic packaging, Chips(Electronics), Semiconductor materials, Bipolar transistors, Integrated circuits, Silicon carbides, Electric power, Simulation, Wafers, Trends, Reprints.

A brief description of some recent developments that affect the application of power semiconductor devices is given. Developments in 'chips', packages, simulation, and new materials are included.

02,362
PB95-175337 Not available NTIS
National Inst. of Standards and Technology (EEEL), Gaithersburg, MD. Semiconductor Electronics Div.
Evidence for a Deep Electron Trap and Charge Compensation in Separation by Implanted Oxygen Oxides.
Final rept.
J. F. Conley, P. M. Lenahan, and P. Roitman. 1992, 7p.
Sponsored by Office of Naval Research, Arlington, VA. and Defense Nuclear Agency, Washington, DC.
Pub. in Institute of Electrical and Electronics Engineers Transactions on Nuclear Science 39, n6 p2114-2120 Dec 92.

Keywords: *Electron traps, Electron spin resonance, Ion implantation, Oxygen additions, Reprints, *SOI(Semiconductors), *SIMOX.

We present direct evidence for the creation of deep electron traps in Separation by IMplantation of OXygen buried oxides. In addition, we present combined electrical and electron spin resonance evidence which demonstrate that at least some positively charged paramagnetic E' centers are compensated by negatively charged centers. Finally, we present evidence which strongly suggests that a substantial fraction of the deep electron traps are coupled to E' centers.

02,363
PB95-175345 Not available NTIS
National Inst. of Standards and Technology (EEEL), Gaithersburg, MD. Semiconductor Electronics Div.
New Test Structure for Nanometer-Level Overlay and Feature-Placement Metrology.
Final rept.
M. W. Cresswell, R. A. Allen, L. W. Linholm, E. C. Teague, C. H. Ellenwood, and W. B. Penzes. 1994, 6p.
Pub. in Institute of Electrical and Electronics Engineers Transactions on Semiconductor Manufacturing 7, n3 p266-271 Aug 94.

Keywords: *Microelectronics, *Overlays, *Lithography, Semiconductor devices, Integrated circuits, Process control, Measurement, Photomasks, Metrology, Reprints, Test structures.

A new electrical test structure for overlay measurement has been evaluated by replicating arrays of its complementary components from two different photomasks into a conducting film on a quartz substrate. The features resulting from images projected from the first mask were used as a reference grid which was calibrated by the NIST line-scale interferometer. A first subset of the relative placements of the images projected from the second mask, which were derived from the electrical overlay measurements and the reference grid, agreed to within 13 nm with corresponding measurements made directly by the line-scale interferometer over distances up to 13.5 mm. A second comparison made at another substrate location indicated that gradients of projected feature linewidths across the exposure site may need to be measured, and corrected for, in the electrical extraction of overlay.

02,364
PB95-175824 Not available NTIS
National Inst. of Standards and Technology (EEEL), Gaithersburg, MD. Semiconductor Electronics Div.
Defect Pair Formation by Implantation-Induced Stresses in High-Dose Oxygen Implanted Silicon-on-Insulator Material.
Final rept.
J. D. Lee, J. C. Park, D. Venables, S. J. Krause, and P. Roitman. 1994, 6p.
Pub. in Materials Research Society Symposia Proceedings, v316 p753-758 1994.

Keywords: *Crystal dislocations, Transmission electron microscopy, X ray diffraction, Crystal dislocations, Ion implantation, Temperature dependence, Integrated circuits, Oxygen additions, Doped materials, Microstructure, Annealing, Strains, Silicon, Stresses, Reprints, *SOI(semiconductors), *SIMOX.

Defect microstructure and the near-surface strain of high-dose oxygen implanted silicon-on-insulator material (SIMOX) were investigated as a function of dose, implant temperature, and annealing temperature by transmission electron microscopy and high resolution x-ray diffraction. Dislocation half loops (DHLs) begin to form by stress assisted climb at a critical stress level due to implantation-induced damage. DHLs evolve into through-thickness defect (TTD) pairs by expansion during annealing. Both DHL and TTD-pair density increase with higher implant dose and lower implant temperature. Possible methods for defect density reduction are suggested based on the results of this study.

02,365
PB95-176285 Not available NTIS
National Inst. of Standards and Technology (EEEL), Boulder, CO. Electromagnetic Fields Div.
On-Wafer Impedance Measurement on Lossy Substrates.
Final rept.
D. F. Williams, and R. B. Marks. 1994, 2p.
Pub. in Institute of Electrical and Electronics Engineers Microwave and Guided Wave Letters 4, n6 p175-176 Jun 94.

Keywords: *Electrical impedance, *Impedance measurement, Characteristic impedance, Transmission lines, Planar structures, Resistors, Wafers, Reprints, Silicon substrates, Scattering parameters.

This paper introduces a new method for measuring impedance parameters in transmission lines fabricated on lossy or dispersive dielectrics. The method, which uses an independent calibration to provide an impedance reference, compares well with conventional techniques when applied to lossless substrates. The effectiveness of the technique is illustrated for resistors fabricated on lossy silicon substrates.

02,366
PB95-176301 Not available NTIS
National Inst. of Standards and Technology (EEEL), Gaithersburg, MD. Semiconductor Electronics Div.
Interaction of Stoichiometry, Mechanical Stress, and Interface Trap Density in LPCVD Si-rich SiNx-Si Structures.
Final rept.
S. C. Witczak, M. Gaitan, J. S. Suehle, M. C. Peckerar, and D. I. Ma. 1994, 10p.
Pub. in Solid-State Electronics 37, n10 p1695-1704 1994.

Keywords: *Silicon nitrides, Chemical vapor deposition, X ray diffraction, Rutherford scattering, Dielectric films, Electron traps, Hole traps, Backscattering, Stoichiometry, Interfaces, Capacitors, Stresses, Wafers, Reprints.

Mechanical and electrical properties were correlated in LPCVD SiN(x)-Si structures through the characterization of six wafers patterned with MNS capacitors whose insulator films were deposited rich in Si under various processing conditions. The samples were measured for mechanical stress at the Si-SiN(x) interface with X-ray diffraction. The deposited SiN(x) films were measured for stoichiometry by Rutherford backscattering spectroscopy. Low-temperature C-V measurements were used for the first time to estimate Si-SiN(x) interface trap densities in the capacitors. The interface trap densities were confirmed with the aid of a model based on a numerical analysis of the capacitor small-single response. The measurement results indicate that an increase in the Si/N ratio in the insulating films was accompanied by a decrease in the film tensile stress. Those SiN(x) films made sufficiently rich in Si were successfully deposited under compressive stress. Furthermore, a decrease in the magnitude of the stress was accompanied by a decrease in interface trap densities, suggesting that interfacial mechanical stress may be influential in the formation of Si-SiN(x) interface traps. Interface trap densities were lowest in those structures whose insulating films were deposited under compression.

02,367
PB95-180568 Not available NTIS
National Inst. of Standards and Technology (EEEL), Gaithersburg, MD. Semiconductor Electronics Div.
Microelectronic Test Structures for Feature Placement and Electrical Linewidth Metrology.
Final rept.
L. W. Linholm, R. A. Allen, and M. W. Cresswell. 1994, 28p.
Pub. in Handbook of Critical Dimension Metrology and Process Control, vCR52 p91-118 1994.

Keywords: *Integrated circuits, *Microelectronics, *Line width, *Lithography, Overlays, Reviews, Reprints, *Test structures, Registration.

This paper presents a critical review of electrical test methods for determining feature placement with total measurement uncertainties below 10 nm and electrical linewidth for sub-half micrometer design linewidths with measurement precision below 1 nm. Microelectronic test structures are electrical devices that are used to determine selected tool, process, device, material, or circuit parameters by means of electrical tests. They are supported by a variety of commercial test equipment often found in semiconductor manufacturing facilities. They provide low-cost, post-patterning metrology for determining both feature placement and electrical linewidth. Properly characterized test structures and measurement methods provide an economic means of determining the critical parameters needed to develop, control, and operate the next generation of patterning tools.

02,368
PB95-180808 Not available NTIS
National Inst. of Standards and Technology (MEL), Gaithersburg, MD. Precision Engineering Div.
Accuracy in Integrated Circuit Dimensional Measurements.
Final rept.
J. E. Potzick. 1993, 10p.
Pub. in Proceedings of Society of Photo-Optical Instrumentation Engineers: Critical Review of IC Metrology

and Process Control, Monterey, CA., September 28-29, 1993, p1-10.

Keywords: *Integrated circuits, *Photomasks, *Dimensional measurement, Calibration, Metrology, Length, Accuracy, Reprints.

The measurement of critical dimensions of features on integrated circuits and photomasks is modeled as the comparison of the images of the test object and of a standard object in a measuring device. A length measuring instrument is then a comparator. The calibration of the standard and the conditions necessary for a valid comparison are discussed. The principles discussed here apply to many other types of measurement as well.

02,369
PB95-202610 Not available NTIS
National Inst. of Standards and Technology (EEEL), Boulder, CO. Electromagnetic Fields Div.
Dielectric Properties of Materials at Cryogenic Temperatures and Microwave Frequencies.
Final rept.
R. G. Geyer. 1994, 2p.
Pub. in Proceedings of Conference on Precision Electromagnetic Measurements Digest, Boulder, CO., June 27-July 1, 1994, p350-351.

Keywords: *Tetrafluoroethylene resins, *Polystyrene, *Quartz, *Teflon, Dielectric properties, Dielectric materials, Microwave frequencies, Temperature range 0065-0273 K, Temperature range 0273-0400 K, Room temperature, Single crystals, Permittivity, Microelectronics, Substrates, Reprints, Dielectric measurements, Rexolite.

The permittivity and dielectric loss tangent of single-crystal quartz, cross-linked polystyrene (Rexolite), and polytetrafluoroethylene (Teflon) were measured at microwave frequencies and at temperatures of 77 K and 300 K using a dielectric resonator technique. Application of high-temperature superconducting (HTS) films at the endplates of the dielectric resonator made it possible to determine dielectric loss tangents of about 7 X 10(exp -6) at 77 K. Two permittivity tensor components for uniaxially anisotropic crystalline quartz were measured. Although the permittivities at 77 K changed very little from their room temperature values at 300 K, large changes in dielectric losses were observed. The decreased loss characteristics of these microelectronic substrates can markedly improve the performance of many microwave devices at cryogenic temperatures.

02,370
PB95-203170 Not available NTIS
National Inst. of Standards and Technology (EEEL), Gaithersburg, MD. Semiconductor Electronics Div.
Electrical Method for Determining the Thickness of Metal Films and the Cross-Sectional Area of Metal Lines.
Final rept.
H. A. Schafft, S. Mayo, S. N. Jones, and J. S. Suehle. 1994, 7p.
Pub. in Proceedings of the Integrated Reliability Workshop, Lake Tahoe, CA., October 16-19, 1994, p5-11.

Keywords: *Integrated circuits, *Metal films, *Film thickness, *Dimensional measurement, Circuit interconnections, Reliability(Electronics), Aluminum alloys, Test methods, Microelectronics, Electromigration, Metallizing, Reprints, Thickness measurement, Resistance measurement, Test structures.

The electrical thickness of an aluminum-alloy metallization can be determined from resistance measurements of a van der Pauw cross structure at two temperatures, with corrections for the deviation from Matthiessen's rule and for thermal expansion. Thickness determinations, made in this way, agree with those made with a calibrated scanning electron microscope (SEM) to within the uncertainty of the instrument. The electrical cross-sectional area of metal lines can be determined by making resistance measurements at two temperatures.

02,371
PB95-203188 Not available NTIS
National Inst. of Standards and Technology (EEEL), Gaithersburg, MD. Semiconductor Electronics Div.
JEDEC 'TCR' Interlaboratory Experiment: Lessons Learned.
Final rept.
H. A. Schafft, J. S. Suehle, and J. Albers. 1994, 8p.
Pub. in Proceedings of the Integrated Circuit Reliability Workshop, Lake Tahoe, CA., October 16-19, 1994, p12-19.

Keywords: *Integrated circuits, Interlaboratory comparisons, Thermal resistance, Joule heating, Line width, Measurement, Precision, Wafers, Standards, Reprints, *Temperature coefficient of resistance, Silicon substrates.

Described are the results of an interlaboratory experiment involving wafer-level measurements intended to do the following: (1) to determine the precision and bias of both the JEDEC Standard Test Method (JESD33) for determining the temperature coefficient of resistance (TCR) and joule heating of a metal line and the ASTM standard (F1261) for measuring the electrical width of a metal line; (2) to assess the reproducibility of measuring the temperature drop across the interface between the silicon substrate and the hot chuck; and (3) to obtain a temperature calibration of the hot chucks used by the participating laboratories.

02,372
PB95-208724 PC A04/MF A01
National Inst. of Standards and Technology (EEEL), Gaithersburg, MD. Semiconductor Electronics Div.
Electronics and Electrical Engineering Laboratory Technical Progress Bulletin Covering Laboratory Programs, October to December 1994 with 1995 EEEL Events Calendar.
J. M. Rohrbaugh. Mar 95, 56p, NISTIR-5608.
See also PB95-170395.

Keywords: *Electrical engineering, *Semiconductor devices, *Metrology, Signal processing, Electrooptics, Reliability.

This is the forty-ninth issue of a quarterly publication providing information on the technical work of the National Institute of Standards and Technology, Electronics and Electrical Engineering Laboratory. This issue of the EEEL Technical Progress Bulletin covers the fourth quarter of calendar year 1994. Abstracts are provided by technical area for both published papers and papers approved by NIST for publication.

02,373
PB95-242277 PC A03/MF A01
National Inst. of Standards and Technology (EEEL), Gaithersburg, MD. Semiconductor Electronics Div.
Electronics and Electrical Engineering Laboratory Technical Publication Announcements Covering Laboratory Programs, January to March 1995 with 1995 EEEI Events Calendar.
J. M. Rohrbaugh. Jun 95, 17p, NISTIR-5669.
See also PB95-231841.

Keywords: *Electrical measurement, *Superconducting devices, *Microelectronics, *Metrology, *Bibliographies, Antennas, Video equipment, Optical fibers, Semiconductors, Superconductors, Magnetic materials, Electromagnetic interference, Electrical engineering, Lasers, Microwave equipment, Electronics, Abstracts.

This is the forty-fourth issue of a quarterly publication providing information on the technical work of the National Institute of Standards and Technology, Electronics and Electrical Engineering Laboratory. This issue of the EEEL Technical Publication Announcement covers the first quarter of calendar year 1995. Abstracts are provided by technical areas for papers published. Major subject headings include the following: Fundamental Electrical Measurements; Semiconductor Microelectronics; Signal Acquisition, Processing, and Transmission; Electrical Systems; Electromagnetic Interference; Law Enforcement Standards; Video Technology.

02,374
PB95-260766 PC A05/MF A01
National Inst. of Standards and Technology (EEEL), Gaithersburg, MD. Semiconductor Electronics Div.
Semiconductor Measurement Technology: HOTPAC. Programs for Thermal Analysis Including Version 3.0 of the TXYZ Program, TXYZ30, and the Thermal MultiLayer Program, TML.
Special pub.
J. Albers. Aug 95, 96p, NIST/SP-400-96.
Also available from Supt. of Docs. as SN003-003-03351-1.

Keywords: *Semiconductor devices, *Integrated circuits, *Thermal analysis, *Computer programs, Models, Heat transmission, Steady flow, Steady state, Thermal conductivity, Temperature, Area, Surface temperature, Average, Semiconductor(Materials), TXYZ3.0, TXYZ computer program, HOTPAC software package, Line averaging, Area averaging.

This report presents and discusses a number of recent developments in the steady-state thermal analysis of multiple-layer structures. These include: (1) analytical evaluation of line and area average temperatures, and (2) a recursion relation technique for calculating the steady-state surface temperature of a multilayer structure with an arbitrary number of layers. The application of the analytic averaging to the TXYZ code is incorporated in the updated code, TXYZ30, while the multilayer recursion relation solution along with analytic averaging are included in the Thermal Multilayer code, TML. Both of these are contained in the HOTPAC software package. The first part of this report contains a discussion of the general elements of the multiple-layer thermal model. This is presented in some detail for the case of the Kokkas three-layer problem and the associated TXYZ code. The previous update of the code, TXYZ20, is also discussed.

02,375
PB95-261947 (Order as PB95-261897, PC A07/MF A02)
National Inst. of Standards and Technology, Gaithersburg, MD.
Using Quantized Breakdown Voltage Signals to Determine the Maximum Electric Fields in a Quantum Hall Effect Sample.
M. E. Cage, and C. F. Lavine. 1995, 8p.
Included in Jnl. of Research of the National Institute of Standards and Technology, v100 n3 p269-276 May/Jun 95.

Keywords: *Quantum electronics, *Hall effect, *Electrical faults, *Electric fields, Electrical measurement, Electron plasma, Landau damping, Two dimensional flow, Dissipation, Quantum Hall Effect, National Institute of Standards and Technology, Quantized voltage states, Quasi-elastic inter-Landau level scattering.

We estimate the maximum values of the electric field across the width of a GaAs/AlGaAs heterostructure quantum Hall effect sample at several currents when the sample is in the breakdown regime. This estimate is accomplished by measuring the quantized longitudinal voltage drops along a length of the sample and then employing a quasi-elastic inter-Landau level scattering (QUILLS) model to calculate the electric field. We also present a pictorial description of how QUILLS transitions occuring between states distributed across the sample width can be detected as voltage signals along the sample length.

02,376
PB96-102017 Not available NTIS
National Inst. of Standards and Technology (EEEL), Gaithersburg, MD. Semiconductor Electronics Div.
Exact Recursion Relation Solution for the Steady-State Surface Temperature of a General Multilayer Structure.
Final rept.
J. Albers. 1995, 8p.
Pub. in Institute of Electrical and Electronics Engineers Transactions on Components, Packaging, and Manufacturing Technology, ptA18 n1 p31-38 Mar 95.

Keywords: *Semiconductor devices, *Fourier analysis, *Laplace equation, Electric conductivity, Surfaces, Thermal conductivity, Temperature, Steady state, Heat flow, Layers, Reprints, Multiple layers.

A recursion relation technique has been used in the past to determine the surface potential from the multilayer electrical Laplace equation. This has provided for a vastly simplified evaluation of the electrical spreading resistance and four-probe resistance. The isomorphism of the multilayer Laplace equation and the multilayer steady-state heat flow equation suggests the possibility of developing a recursion relation applicable to the multilayer thermal problem. This recursive technique is developed and is shown to provide the surface temperature of the multilayer steady-state heat flow equation.

02,377
PB96-102363 Not available NTIS
National Inst. of Standards and Technology (EEEL), Gaithersburg, MD. Semiconductor Electronics Div.

MEMS in Standard CMOS VLSI Technology.
Final rept.
M. Gaitan. 1995, 5p.
Pub. in Proceedings of Annual Conference on Information Sciences and Systems (29th), Baltimore, MD., March 22-24, 1995, p169-173.

Keywords: *Fabrication, *Very large scale integration, *Integrated circuits, *CMOS, Microelectronics, Micromechanics, Metal oxide semiconductors, Thermoelectric materials, Sensors, Computer aided design, Reprints, *Microelectromechanics, MEMS, CAD, IC.

The methodology for the design and fabrication of a class of thermo-electro-mechanical devices and systems that can be fabricated in a commercial CMOS foundry environment is presented. The fabrication technique allows the monolithic integration of the micromechanical devices with CMOS VLSI circuits using standard design methods. Microheating elements and thermoelectric sensors are presented as examples of the application of this technique.

02,378
PB96-102702 Not available NTIS
National Inst. of Standards and Technology (EEEL), Gaithersburg, MD. Semiconductor Electronics Div.
Model for Determining the Density and Mobility of Carriers in Thin Semiconducting Layers with Only Two Contacts.
Final rept.
J. R. Lowney. 1995, 5p.
Pub. in Jnl. of Applied Physics 78, n2 p1008-1012, 15 Jul 95.

Keywords: *Carriers, *Magnetoresistance, Reprints, Density, Mobility, Semiconductors, Electrical measurement, Coallocation, Hall effect.

A new method for determining the carrier densities and mobilities in a thin semiconducting layer was recently described. It is based on fitting the transverse magnetoresistance of the layers as a function of magnetic field, and it requires only two contacts. To improve the accuracy and generalize the procedure to multicarrier systems, a computer code was written to solve for the magnetoresistance as a function of magnetic field and the length-to-width ratio of a rectangular sample. A nonlinear-least-squares fit was made to the results of the computer model for a single-carrier system. The results for multicarrier systems are discussed. This method is especially useful as a monitor for improving the quality control of the electrical characteristics of thin conducting layers in finished devices. The code is also useful for interpreting standard four-terminal measurements as well.

02,379
PB96-102710 Not available NTIS
National Inst. of Standards and Technology (EEEL), Gaithersburg, MD. Semiconductor Electronics Div.
MONSEL-II: Monte Carlo Simulation of SEM Signals for Linewidth Metrology.
Final rept.
J. R. Lowney. 1995, 6p.
See also PB95-111522.
Pub. in Microbeam Analysis 4, p131-136 1995.

Keywords: *Integrated circuits, *Dimensional measurement, *Line width, Reprints, Scanning electron microscopy, Monte Carlo method, Electron scattering, Computerized simulation, *MONSEL-I computer code.

This is a guide to the FORTRAN code MONSEL-II, which is a Monte Carlo simulation of the transmitted, backscattered, and secondary electron signals in a scanning electron microscopy (SEM) associated with lines with a trapezoidal cross section. The lines are deposited on a multilayer substrate. The primary purpose of the code is to interpret the actual linewidths from measured SEM signals. However, it can be used for many other purposes such as corresponding image analysis in transmission electron microscopy.

02,380
PB96-102876 Not available NTIS
National Inst. of Standards and Technology (EEEL), Gaithersburg, MD. Semiconductor Electronics Div.
Buffer Layer Modulation-Doped Field-Effect-Transistor Interactions in the Al0.33Ga0.67As/GaAs Superlattice System.
Final rept.
J. G. Pellegrino, C. A. Richter, J. A. Dura, B. Roughani, P. M. Amirtharaj, and S. B. Qadri. 1995, 5p.
Pub. in Jnl. of Vacuum Science and Technology A 13, n3 p787-791 May/Jun 95.

Keywords: *Electron transport, Superlattices, X ray diffraction, Mobility, Reprints, *Field effect transistors, *Molecular beam epitaxy, MODFET(Modulation Doped Field Effect Transistors).

The correlation between the structural and transport properties for a series of high-quality modulation-doped field-effect transistor (MODFET) structures was made for various growth temperatures. X-ray reflectivity, x-ray diffraction, and magnetotransport measures were used to assess structural quality and transport parameters. Four samples with growth temperatures in the range 500-630 degrees C were examined. The results show a correlation exists between the measured electron mobility and the quality of the interface width, as measured from satellite peaks of the buffer layer. In addition, these results show, for the first time to the best of our knowledge, that a direct correlation can be made between x-ray reflectivity structural measurements and measured electron mobility of high-quality gallium-arsenide-based MODFETs. Both x-ray and transport results suggest a higher-quality structure was obtained at higher growth temperatures.

02,381
PB96-102926 Not available NTIS
National Inst. of Standards and Technology (EEEL), Gaithersburg, MD. Semiconductor Electronics Div.
TDDB Characterization of Thin SiO2 Films with Bimodal Failure Populations.
Final rept.
J. Prendergast, J. S. Suehle, P. Chaparala, E. Murphy, and M. Stephenson. 1995, 7p.
Pub. in Proceedings of the International Reliability Physics Symposium, Las Vegas, NV., April 4-6, 1995. p124-130.

Keywords: *Silicon dioxide, *Dielectric breakdown, Reprints, Time dependence, Reliability(Electronics), Dielectric films, Field acceleration models.

For many years Time Dependent Dielectric Breakdown (TDDB) has been the subject of much controversy. Two different field dependencies have been observed and several acceleration models have been suggested. Of the two most popular models one predicts that the log t50% is proportional to the electric field (E) (1 - 3) while the other predicts that it is proportional to the reciprocal of the electrical field (1/E) (4-6). This paper will help to explain the discrepancies in the electric field dependence observed and demonstrate distinct differences in the TDDB behavior between extrinsic dielectric breakdown.

02,382
PB96-112206 Not available NTIS
National Inst. of Standards and Technology (EEEL), Gaithersburg, MD. Semiconductor Electronics Div.
Effect of Anneal Temperature on Si/Buried Oxide Interface Roughness on SIMOX.
Final rept.
G. Jacobs, A. Genis, and L. P. Allen. 1995, 2p.
Pub. in Proceedings of the Institute of Electrical and Electronics Engineers SOI Conference, Nantucket Island, MA., October 3-6, 1994, p49-50.

Keywords: *Temperature dependence, *Silicon, Reprints, Roughness, *SIMOX, Atomic force microscopy, SOI(Semiconductors).

Fully depleted, thin film silicon-on-insulator SIMOX devices are attractive for their short channel characteristics and high speed compared with bulk silicon. Their potential for applications in low power devices and circuitry places extreme demands upon the starting SIMOX substrate material. Threshold voltage control for fully depleted SOI devices has been recognized as a key issue for realization of fully depleted SOI technology. To that end, examination of the interface roughness between the device silicon layer and the buried oxide of the SOI structure is an active area of materials research and development. In this work, we have used atomic force microscopy (AFM) to measure the interface roughness of SIMOX SOI substrates as a function of anneal parameters. This study has shown that the silicon/buried oxide interface roughness is a strong function of the post implant annealing temperature.

02,383
PB96-112248 Not available NTIS
National Inst. of Standards and Technology (PL), Boulder, CO. Time and Frequency Div.
New Model of 1/F Noise in Baw Quartz Resonators.
Final rept.
F. L. Walls, P. H. Handel, R. Besson, and J. J. Gagnepain. 1992, 7p.
Pub. in Proceedings of the Institute of Electrical and Electronics Engineers Frequency Control Symposium, Hershey, PA., May 27-29, 1992, p327-333.

Keywords: *Quartz resonators, *Resonators, *Noise, Reprints, Models, Bulk acoustic wave devices, 1/f noise, Electronic noise, Quantum 1/f effect.

The paper presents a new model for predicting the 1/f (flicker) frequency noise in quartz resonators as a function of the unloaded resonator quality factor Q and volume under the electrodes for bulk acoustic wave (BAW) resonators. The functional form of this model originates from a quantum 1/f theory for scattering of phonons from the primary oscillator mode. Using this new model, we are able to match the 1/f frequency noise observed in the best quartz controlled oscillators and resonators. Quite unexpectedly, this model indicates that the amplitude of 1/f frequency noise might be improved by making resonators with smaller electrodes. BVA resonators show approximately a factor of 3 improvements in 1/f frequency noise (Sy(f)) over electroded resonators with the same unloaded Q-factor and electrode volume.

02,384
PB96-112297 Not available NTIS
National Inst. of Standards and Technology (EEEL), Boulder, CO. Electromagnetic Fields Div.
Substrate and Thin Film Measurements.
Final rept.
C. A. Jones. 1994, 13p.
Pub. in Proceedings of Wireless Workshop, Phoenix/Scottsdale/Chandler, AZ., October 16-19, 1994, p1-3.

Keywords: *Substrates, *Thin films, *Electromagnetic properties, Reprints, Microwaves, Measurements, Dielectric constants, Loss tangents.

This paper describes the use of cavity resonators, coaxial probes, capacitive measurements and dielectric resonators for characterizing the electromagnetic properties of substrates and thin films.

02,385
PB96-112313 Not available NTIS
National Inst. of Standards and Technology (EEEL), Gaithersburg, MD. Electricity Div.
Surging the Upside-Down House: Looking into Upsetting Reference Voltages.
Final rept.
T. S. Key, and F. D. Martzloff. 1994, 6p.
Pub. in Proceedings of the International Conference on Power Quality (3rd): End-Use Applications and Perspectives, Amsterdam, The Netherlands, October 24-27, 1994, p1-6.

Keywords: *Surges, *Electronic equipment, *Circuit protection, *Voltage regulations, *Residential buildings, Telephones, Cable television, Communication equipment, Electric fuses, Power supply circuits, Wiring, Overvoltage, Voltage regulation, Retrofitting, Reprints.

Electronic equipment with two input ports-power and communications-can be exposed to damaging differences of voltage across the two ports during surge events. Two exposure scenarios of producing such differences of voltages are explained and illustrated by measurements performed in a replica of a residential or light commercial installation of power, telephone, and cable TV wiring. Several mitigation methods are described, and one possible retrofit solution is shown.

02,386
PB96-113311 PC A09/MF A03
National Inst. of Standards and Technology, Gaithersburg, MD.
Journal of Research of the National Institute of Standards and Technology, July/August 1995. Volume 100, Number 4. Special Issue: The Gaseous Electronics Conference Radio-Frequency Reference Cell.
1995, 196p.
See also PB96-113329 through PB96-113436 and PB95-261897. Color illustrations reproduced in black and white. Also available from Supt. of Docs. as SN703-027-00065-2.

Keywords: *Research and development, *Metrology, *Standards, *Meetings, RF systems, Microelectronics, Gases, Kinetics, Spectroscopy, Plasmas(Physics), Di-

agnostic techniques, Cells, *Gaseous electronics, NIST(National Institute of Standards and Technology).

No abstract available.

02,387
PB96-113329 (Order as PB96-113311, PC A09/ MF A03)
National Inst. of Standards and Technology, Gaithersburg, MD.
Gaseous Electronics Conference RF Reference Cell: An Introduction.
J. K. Olthoff, and K. E. Greenberg. 1995, 13p.
Prepared in cooperation with New Mexico Univ., Albuquerque.
Included in Jnl. of Research of the National Institute of Standards and Technology, v100 n4 p327-339 Jul/ Aug 95.

Keywords: *Microelectronics, *Gases, *Standards, *Cells, Plasma etching, Radio frequencies, Reactors, Research and development, Diagnostic techniques, *Gaseous electronics, Reference cell, NIST(National Institute of Standards and Technology).

This paper provides an introduction to the Gaseous Electronics Conference (GEC) RF Reference Cell, and to the articles published in this Special Issue of the Journal of Research of the National Institute of Standards and Technology. A brief summary of the history and purpose of the Reference Cell concept is presented, and recent changes to the GEC Cell design are documented. The paper concludes with highlights of research performed on GEC Cells, and with an appendix of all known publications that present research performed on GEC Cells.

02,388
PB96-113337 (Order as PB96-113311, PC A09/ MF A03)
National Inst. of Standards and Technology, Gaithersburg, MD.
Current and Voltage Measurements in the Gaseous Electronics Conference RF Reference Cell.
M. A. Sobolewski. 1995, 11p.
Included in Jnl. of Research of the National Institute of Standards and Technology, v100 n4 p341-351 Jul/ Aug 95.

Keywords: *Microelectronics, *Gases, *Standards, *Cells, *Meetings, Electric current, Diagnostic techniques, Electric discharges, Plasmas(Physics), Radio frequencies, Electrical impedance, Electrical measurement, Comparison, *Gaseous electronics, Reference cell, NIST(National Institute of Standards and Technology).

Measurements of the electrical characteristics of discharges in the Gaseous Electronics Conference Radio-Frequency Reference Cell are reviewed here. Topics include: common sources of error in the measurements; comparisons of current and voltage data among GEC cells; the effects of gas impurities, surface conditions and the external circuitry on the reproducibility of the electrical characteristics; and comparisons of current and voltage data with results of other measurements.

02,389
PB96-113345 (Order as PB96-113311, PC A09/ MF A03)
National Inst. of Standards and Technology, Gaithersburg, MD.
Optical Emission Spectroscopy on the Gaseous Electronics Conference RF Reference Cell.
J. R. Roberts. 1995, 19p.
Included in Jnl. of Research of the National Institute of Standards and Technology, v100 n4 p353-371 Jul/ Aug 95.

Keywords: *Microelectronics, *Gases, *Standards, *Cells, *Meetings, Light emission, Plasmas(Physics), Radio frequency discharge, Spectroscopy, Calibrating, *Gaseous electronics, Reference cell, NIST(National Institute of Standards and Technology).

A summary of the experimental observations of the optical emission from the Gaseous Electronics Conference (GEC) rf Reference Cell plasma will be discussed. Spatially and temporally resolved results are provided for various reference and nonreference conditions, including etching type plasmas. These measurements provide a detailed description of the temporal evolution of optical emission from different excited atomic states within different atomic and ionic species, as well as their radial and axial distributions. Some of the measurements have been placed on a absolute radiometric scale to provide comparisons to model calculations.

02,390
PB96-113352 (Order as PB96-113311, PC A09/ MF A03)
Sandia National Labs., Albuquerque, NM.
Optical Diagnostics in the Gaseous Electronics Conference Reference Cell.
G. A. Hebner, and K. E. Greenberg. 1995, 10p.
Contracts KC-03-01-03, DE-AC04-94AL85000
Prepared in cooperation with New Mexico Univ., Albuquerque. Dept. of Chemical and Nuclear Engineering.
Sponsored by Department of Energy, Washington, DC. Office of Basic Energy Sciences.
Included in Jnl. of Research of the National Institute of Standards and Technology, v100 n4 p373-382 Jul/ Aug 95.

Keywords: *Microelectronics, *Gases, *Standards, *Cells, *Meetings, Plasmas(Physics), Absorption, Argon, Electric discharges, Radio frequencies, Electric fields, Helium, Fluorescence, Metastable state, Diagnostic techniques, Plasma processing, NIST(National Institute of Standards and Technology).

A number of laser-induced fluorescence and absorption spectroscopy studies have been conducted using Gaseous Electronics Conference Reference Cells. Laser-induced fluorescence has been used to measure hydrogen atom densities, to measure argon metastable spatial profiles, to determine the sheath electric field, and to infer the electron density and temperature. Absorption spectroscopy, using lamp sources and diode lasers, has been used to measure metastable atom densities in helium and argon discharges and fluorocarbon densities in silicon etching discharges. The experimental techniques and sample results of these investigations are reviewed.

02,391
PB96-113360 (Order as PB96-113311, PC A09/ MF A03)
National Inst. of Standards and Technology, Gaithersburg, MD.
Studies of Ion Kinetic-Energy Distributions in the Gaseous Electronics Conference RF Reference Cell.
J. K. Olthoff, R. J. Van Brunt, and S. B. Radovanov. 1995, 18p.
Included in Jnl. of Research of the National Institute of Standards and Technology, v100 n4 p383-400 Jul/ Aug 95.

Keywords: *Microelectronics, *Gases, *Standards, *Cells, *Meetings, Argon plasma, Oxygen plasma, Irradiation, Kinetic energy, Mass spectroscopy, Radio frequencies, Electric discharges, *Gaseous, Reference cell, Argon-oxygen plasmas, Ion energy analyzers, NIST(National Institute of Standards and Technology).

A review is presented of kinetic-energy distribution measurements for ions striking grounded surfaces in a gaseous Electronics Conference (GEC) rf Reference Cell. Two experimental arrangements that have been used to measure ion energies in the GEC Cell are described, and a comparison of their performance under different operating conditions is presented. Significant results from ion-energy analysis in the Reference Cell are highlighted, including evidence of effects due to surface conditions on ion sampling, verification of electrical behavior of the cell, inferences about ion-molecule reactions indicated by the shapes of measured ion kinetic-energy distributions (IEDs), and the use of measured IEDs for the validation of theoretical models. The paper concludes with a detailed study of IEDs measured for rf plasmas generated in mixtures of argon and oxygen, using both experimental arrangements.

02,392
PB96-113378 (Order as PB96-113311, PC A09/ MF A03)
Texas Univ. at Dallas, Richardson.
Microwave Diagnostic Results from the Gaseous Electronics Conference RF Reference Cell.
L. J. Overzet. 1995, 14p.
Grant NSF-ECS-9257383
Sponsored by National Science Foundation, Arlington, VA.
Included in Jnl. of Research of the National Institute of Standards and Technology, v100 n4 p401-414 Jul/ Aug 95.

Keywords: *Microwave transmission, *Microelectronics, *Gases, *Cells, *Meetings, Electron density, Electric discharges, Microwave interferometers, Reactors, Diagnostic techniques, Plasmas(Physics), Time dependence, *Gaseous electronics, Reference cell, NIST(National Institute of Standards and Technology).

Three groups have published electron density data taken in the Gaseous Electronics Conference (GEC) reference reactor using microwave interferometry. The agreement in the data from these groups at higher pressures is excellent especially when one considers that the GEC reactors involved have some key differences. The electron densities compare favorably in argon, helium, and nitrogen above 33.3 Pa (250 mTorr); but, the measurements tend to diverge some at 13.3 Pa (100 mTorr) and in 133 Pa helium above approximately 200 mA. It is speculated that the latter difference occurs as the discharges change from a bulk ionization or a-mode to a secondary electron emission or y-mode, and that this transition occurs at lower voltages and currents for reactors with aluminum electrodes than it does for those with stainless steel electrodes. In addition, time resolved electron densities are presented.

02,393
PB96-113386 (Order as PB96-113311, PC A09/ MF A03)
Dublin City Univ. (Ireland). Dept. of Physics.
Langmuir Probe Measurements in the Gaseous Electronics Conference RF Reference Cell.
M. B. Hopkins. 1995, 11p.
Included in Jnl. of Research of the National Institute of Standards and Technology, v100 n4 p415-425 Jul/ Aug 95.

Keywords: *Microelectronics, *Gases, *Standards, *Cells, *Meetings, Electrostatic probes, Plasma diagnostics, Reactors, Radio frequencies, *Gaseous electronics, Reference cell, NIST(National Institute of Standards and Technology).

The use of a Langmuir probe system in two GEC cells is reviewed. The major problems associated with probe diagnostics and GEC cell are outlined and discussed. While the data base is still insufficient to give definitive values for many parametes, a number of standard measurements are put forward. The plasma density in argon is 9 x 10(exp 9)/cubic cm (plus or minus 20%) at an applied rf voltage of 250 V (500 V peak to peak) and a gas pressure of 13.3 Pa (100 mTorr). The electron density scales linearly with applied voltage. The plasma to ground sheath resistance is shown to be very important with a value of 810 Ohms in argon at a pressure of 13.3 Pa (100 mTorr) and discharge current of 0.1 A. The value of plasma to ground resistance scales inversely with discharge current and sublinear with pressure.

02,394
PB96-113394 (Order as PB96-113311, PC A09/ MF A03)
Sandia National Labs., Albuquerque, NM.
Inductively Coupled Plasma Source for the Gaseous Electronics Conference RF Reference Cell.
P. A. Miller, G. A. Hebner, K. E. Greenberg, P. D. Pochan, and B. P. Aragon. 1995, 13p.
Contract DE-AC04-94AL85000
Prepared in cooperation with New Mexico Univ., Albuquerque. Dept. of Chemical and Nuclear Engineering. and Applied Physics, Inc., Albuquerque, NM. Sponsored by Department of Energy, Washington, DC. and SEMATECH, Austin, TX.
Included in Jnl. of Research of the National Institute of Standards and Technology, v100 n4 p427-439 Jul/ Aug 95.

Keywords: *Microelectronics, *Gases, *Standards, *Cells, *Meetings, Plasma density, Electrostatic probes, Coupling, Plasmas(Physics), Plasma potential, *Gaseous electronics, Reference cell, NIST(National Institute of Standards and Technology).

In order to extend the operating range of the GEC RF Reference Cell, we developed an inductively coupled plasma source that replaced the standard parallel-plate upper-electrode assembly. Voltage and current probes, Langmuir probes, and an 80 GHz interferometer provided information on plasmas formed in argon, chlorine, and nitrogen at pressures from 0.1 Pa to 3 Pa. For powers deposited in the plasma from 20 W to 300 W, the source produced peak electron densities between 10(exp 10)/cubic cm and 10(exp 12)/cubic cm and electron temperatures near 4eV. The electron density peaked on axis with typical full-width at half maximum of 7 cm to 9 cm. Discharges in chlorine and nitro-

gen had biomodal operation that was clearly evident from optical emission intensity. A dim mode occurred at low power and a bright mode at high power. The transition between modes had hysteresis.

02,395
PB96-113402 (Order as PB96-113311, PC A09/MF A03)
Michigan Univ., Ann Arbor. Dept. of Nuclear Engineering.
Reactive Ion Etching in the Gaseous Electronics Conference RF Reference Cell.
M. L. Brake, J. T. P. Pender, M. J. Buie, P. D. Pochan, P. A. Miller, A. Ricci, and J. Soniker. 1995, 8p.
Contracts DE-AC04-94AL85000, DE-FI04-89AL588772
Prepared in cooperation with Sandia National Labs., Albuquerque, NM. Sponsored by Department of Energy, Washington, DC. and SEMATECH, Austin, TX. Included in Jnl. of Research of the National Institute of Standards and Technology, v100 n4 p441-448 Jul/Aug 95.

Keywords: *Microelectronics, *Gases, *Standards, *Cells, *Meetings, Electric discharges, Plasma etching, Wafers, Rates(Per time), Depth, Radio frequencies, *Gaseous electronics, Reference cell, Reactive ion etching, NIST(National Institute of Standards and Technology).

This paper describes the results of using the GEC reference cell as a reactive ion etcher. Silicon wafers with layers of polysilicon and silicon dioxide on crystalline silicon patterns with photoresist have been investigated with fluorine and chlorine chemistries. Scanning electron microscopy (SEM), profilometry, and refraction techniques were used to determine the etch parameters such as etch rate, uniformity and selectivity. The discharges are in general monitored by measuring the optical emission spectroscopy and the bias voltages. Depending upon the discharge and chemistry conditions, similar etch rates and etch patterns of different GEC cells were obtained.

02,396
PB96-113410 (Order as PB96-113311, PC A09/MF A03)
New Mexico Univ., Albuquerque. Dept. of Chemical and Nuclear Engineering.
Dusty Plasma Studies in the Gaseous Electronics Conference Reference Cell.
H. M. Anderson, and S. B. Radovanov. 1995, 14p.
Contract DE-AC04-76DP00789
Sponsored by Department of Energy, Washington, DC. and Sandia National Labs., Albuquerque, NM.
Included in Jnl. of Research of the National Institute of Standards and Technology, v100 n4 p449-462 Jul/Aug 95.

Keywords: *Microelectronics, *Gases, *Standards, *Cells, *Meetings, Radio frequencies, Electric discharges, Plasmas(Physics), Dust, Particles, Plasma clouds, Lasers, Light scattering, Trapping, Statistical analysis, *Gaseous electronics, Reference cells, LLS(Laser light scattering), DLLS(Dynamic laser light scattering), NIST(National Institute of Standards and Technology).

A number of important investigations into the formation, growth, charging, transport and consequences of particulate due in plasmas have been made using the Gaseous Electronics Conference Reference Cell as the reactor test-bed. The greatest amount of work to data has been directed toward a better understanding of the role that electrostatic, ion drag, neutral fluid drag and gravitational forces play in governing the dynamic behavior of particles cloud motion. Also, statistical correlation's in the fluctuation of scattered laser light intensity (dynamic laser light scattering (DLLS)) can be used to determine information about particle size, motion, and growth dynamics. New results from DLSS experiments performed in the Reference Cell are presented that show process-induced dust particles confined in an electrostatic trap exhibit low-frequency oscillatory motion consistent with charge density wave (CDW) motion predicted for strongly coupled Coulomb liquids.

02,397
PB96-113428 (Order as PB96-113311, PC A09/MF A03)
Scientific Research Associates, Inc., Glastonbury, CT.
One-Dimensional Modeling Studies of the Gaseous Electronics Conference RF Reference Cell.
T. R. Govindan, and M. Meyyappan. 1995, 10p.
Contract DOC-50-DKNA-3-00143
Sponsored by Department of Commerce, Washington, DC.
Included in Jnl. of Research of the National Institute of Standards and Technology, v100 n4 p463-472 Jul/Aug 95.

Keywords: *Microelectronics, *Gases, *Standards, *Cells, *Mathematical models, *Meetings, Plasmas(Physics), Fluid mechanics, Transport properties, Kinetics, Radio frequencies, Electric discharges, One dimensional, *Gaseous electronics, Reference cell, Hybrid model, NIST(National Institute of Standards and Technology).

A review of the one-dimensional modeling studies in the literature of the Gaseous Electronics Conference (GEC) reference plasma reactor is presented. Most of the studies are based on the fluid model description of the discharge and some utilize hybrid fluid-kinetic schemes. Both models are discussed here briefly. The models provide a basic understanding of the discharge mechanisms and reproduce several critical discharge features observed experimentally.

02,398
PB96-113436 (Order as PB96-113311, PC A09/MF A03)
Houston Univ., TX. Dept. of Chemical-Petroleum Engineering.
Two-Dimensional Self-Consistent Radio Frequency Plasma Simulations Relevant to the Gaseous Electronics Conference RF Reference Cell.
D. P. Lymberopoulos, and D. J. Economou. 1995, 22p.
Grant NSF-CTS-9216023
Sponsored by National Science Foundation, Arlington, VA., Robert A. Welch Foundation, Houston, TX. and SEMATECH, Austin, TX.
Included in Jnl. of Research of the National Institute of Standards and Technology, v100 n4 p473-494 Jul/Aug 95.

Keywords: *Plasmas(Physics), *Simulation, *Microelectronics, *Gases, *Standards, *Cells, *Meetings, Argon plasma, Electric discharges, Mathematical models, Radio frequencies, Two dimensional, *Gaseous electronics, Reference cell, RF discharges, NIST(National Institute of Standards and Technology).

Over the past few years multidimensional self-consistent plasma simulations including complex chemistry have been developed which are promising tools for furthering our understanding of reactive gas plasmas and for reactor design and optimization. These simulations must be benchmarked against experimental data obtained in well-characterized systems such as the Gaseous Electronics Conference (GEC) reference cell. Two-dimensional simulations relevant to the GEC Cell are reviewed in this paper with emphasis on fluid simulation.

02,399
PB96-117692 PC A05/MF A01
National Inst. of Standards and Technology (EEEL), Gaithersburg, MD. Semiconductor Electronics Div.
Semiconductor Measurement Technology: Test Structure Implementation Document: DC Parametric Test Structures and Test Methods for Monolithic Microwave Integrated Circuits (MMICs).
Special pub.
C. E. Schuster. Sep 95, 96p, NIST/SP-400-97.
Also available from Supt. of Docs. as SN003-003-03368-5. See also PB92-154640. Sponsored by Defense Advanced Research Projects Agency, Arlington, VA. and Air Force Wright Aeronautical Labs., Wright-Patterson AFB, OH.

Keywords: *Integrated circuits, *Semiconductor devices, *Microwave circuits, *Metrology, Gallium arsenides, Microelectronics, Fabrication, Expert systems, Microwave frequency converters, Communication equipment, Millimeter waves, Test methods, Test structures, MMIC, Monolithic Microwave Integrated circuits.

This document describes a set of microelectronic test structure designs for manufacturers of GaAs MMIC devices. These designs enable the dc measurement of process and device parameters that can be used to diagnose, monitor, compare, and predict the performance of the fabrication process or the devices produced. The test structure designs are embodied in a computer-aided design library known as NISTGAAS, which contains 8 types of test structures, implemented in 125 combinations of process layer and size and based on a 2 x 6 probe-pad array. Any design, once fabricated on a wafer, can be probed using commonly available commercial parametric test system equipment. This document specifies how to implement and test each type of test structure and how to analyze the results. It also provides guidance on how to apply the set of test structures at the wafer level. Although NISTGAAS was designed for the process described in this document, it was also designed and demonstrated to be adaptable for other MMIC processes. Since NISTGAAS contains cell designs rather than a chip design, it provides a flexible test structure methodology that also provides the MMIC community with a common reference point for assessing process and device performance.

02,400
PB96-119300 Not available NTIS
National Inst. of Standards and Technology (EEEL), Gaithersburg, MD. Semiconductor Electronics Div.
Characterization of Two-Dimensional Dopant Profiles: Status and Review.
Final rept.
A. C. Diebold, M. Kump, J. J. Kopanski, and D. G. Seiler. 1994, 20p.
Pub. in Proceedings of the Electrochemical Society, Miami, FL., October 10-14, 1994, v94-33 p78-97.

Keywords: *Transistors, *Computer-aided design, *Models, Verification, Calibrating, Two dimensional, Dopes, Simulation, Microscopy, Spatial resolution, Spectroscopic analysis, Reprints, *Scanning probe methods.

Process and device simulators are being used for the technology computer-aided design (TCAD) of 0.25-micrometers gate-length transistors predicted to begin manufacture in 1998. This paper compares and reviews the status of inverse modeling and direct physical analysis methods to obtain two-dimensional dopant profiles for verification and calibration of these TCAD simulators. Spatial resolution, dopant accuracy, and concentration range requirements are discussed. Direct characterization methods include scanning probe microscopies (scanning capacitance microscopy, scanning tunneling microscopy combined with 'spectroscopy,' Mu-spreading resistance probe, scanning Kelvin probe microscopy, and scanning potential microscopy), electron holography, and tomographic secondary ion mass tomographic spectroscopy.

02,401
PB96-119516 Not available NTIS
National Inst. of Standards and Technology (EEEL), Gaithersburg, MD. Semiconductor Electronics Div.
Oxidation of SiC.
Final rept.
J. J. Kopanski. 1992, 9p.
Pub. in Properties of Silicon Carbide, Book Chapter 5.2, p121-129.

Keywords: *Oxidation, *Silicon carbides, Metal oxide semiconductors, Mis(Semiconductors), Chemical vapor deposition, Epitaxy, Wafers, Vacuum deposition, Sublimation, Electrical properties, Semiconductors(Materials), Ceramics, Reprints, Thermal oxidation.

Thermal oxidation of the two most common forms of single-crystal silicon carbide with potential for semiconductor electronics applications is discussed: 3C-SiC formed by heteroepitaxial growth by chemical vapor deposition on silicon, and 6H-SiC wafers grown in bulk by vacuum sublimation or the Lely method. SiC is also an important ceramic and abrasive that exists in many different forms. Its oxidation has been studied under a wide variety of conditions. Thermal oxidation of SiC for semiconductor electronic applications is discussed in the following section. Insulating layers on SiC, other than thermal oxide, are discussed in Section C, and the electrical properties of the thermal oxide and metal-oxide-semiconductor capacitors formed on SiC are discussed in Section D.

02,402
PB96-119524 Not available NTIS
National Inst. of Standards and Technology (EEEL), Gaithersburg, MD. Semiconductor Electronics Div.

Defect Formation Mechanism Causing Increasing Defect Density during Decreasing Implant Dose in Low-Dose Simox.
Final rept.
J. D. Lee, J. C. Park, S. Krause, and P. Roitman. 1994, 2p.
Pub. in Proceedings of the International IEEE SOI Conference, Nantucket Island, Massachusetts, October 3-6, 1994, p69-70.

Keywords: *Large scale integration, *Defects, *Quality control, Oxygen, Ion implantation, Dosage, Crystal dislocations, Production costs, Wafers, Reprints, SIMOX wafers, Defect density, Defect formation mechanisms.

Silicon-on-insulator material synthesized by oxygen implantation (SIMOX) is a leading candidate for advanced large scale integrated circuit applications due to thickness uniformity and moderate defect density. In the past few years, there has been a significant reduction of the defect density by optimizing processing conditions. Today, commercial SIMOX wafers are available by single implant at a high dose of 1.8 x 10(exp 18)/square cm (defect density about 10(exp 6)/square cm), single implant at a low-dose of -0.5 x 10(exp 18)/square cm (defect density less than 10(exp 3)/square cm), and multiple implants/anneals (defect density less than 10(exp 4)/square cm). Studies on defect formation mechanisns may suggest further modification of the processing conditions for both production cost and material quality.

02,403
PB96-122460 Not available NTIS
National Inst. of Standards and Technology (EEEL), Gaithersburg, MD. Electricity Div.
Progress on the Quantized Hall Resistance Recommended Intrinsic/Derived Standards Practice.
Final rept.
R. E. Elmquist. 1995, 7p.
Pub. in National Conference on Standards Laboratories, Dallas, TX., July 16-20, 1995, p647-653.

Keywords: *Electrical resistance, *Device characterization, Fundamental constant, Electron gas, Reprints, *Quantum Hall effect.

The quantized Hall resistance (QHR) standard requires characterization test which determine if and how a particular QHR device should be used as an intrinsic standard. The initial characterization at a qualified QHR laboratory would provide the following: (1) Verification that the device resistance was approximately equal to that of other QHR devices under prescribed conditions; (2) Assurance that the QHR device meets recognized quality construction standards; (3) Determination of the effect of temperature in the range below 1.5k; (4) Determination of the approximate magnetic flux density which must be applied to measure the QHR standard. The device could than be used as a standard in another laboratory, which would be expected to characterize the device using procedures which are given in the Recommended Instrinsic/Derived Standards Practice. Some of the laboratory procedures are described.

02,404
PB96-122668 Not available NTIS
National Inst. of Standards and Technology (EEEL), Gaithersburg, MD. Semiconductor Electronics Div.
Development of a Standard Reference Material for Measurement of Interstitial Oxygen Concentration in Semiconductor Silicon by Infrared Absorption.
Final rept.
B. G. Rennex, J. R. Ehrstein, and R. I. Scace. 1994, 1p.
See also PB95-125076.
Pub. in Extended Abstract of the Meeting of the Electrochemical Society (186th), Miami, FL., October 9-14, 1994, Abstract No. 469, p738.

Keywords: *Calibration standards, *Semiconductors(Materials), *Oxygen, *Concentrations(Composition), Silicon, Interstices, Infrared spectrophotometers, Certification, Reprints, Standard Reference Material, SRM-2551, FTIR(Fourier Transform Infrared Radiation).

A Standard Reference Material, SRM-2551, has been prepared, measured, and certified for the determination of institial oxygen concentration in semiconductor silicon. Its purpose is to assist users in the calibration of infrared spectrophotometers used to measure the 1107 cm -1 oxygen peak. The SRM uncertainty is 0.17% for the low-oxygen specimens, 0.13% for the medium-oxygen specimens, and 0.12% for the high-oxygen specimens.

02,405
PB96-122692 Not available NTIS
National Inst. of Standards and Technology (MSEL), Gaithersburg, MD. Polymers Div.
Electronics Packaging Materials Research at NIST.
Final rept.
M. A. Schen, G. T. Davis, F. I. Mopsik, J. R. Manning, C. A. Handwerker, D. T. Read, W. L. Wu, and W. E. Wallace. 1995, 13p.
Pub. in Materials Research Society Symposium Proceedings, San Francisco, CA., April 17-21, 1995, v390 p19-31.

Keywords: *Electronic packaging, *Metrology, *Research programs, Electronic components, Microelectronics, Circuit interconnections, Technology innovation, Research management, Reprints, US NIST, Coefficient of thermal expansion.

The Materials Science and Engineering Laboratory at NIST has augmented its laboratory-based research in support of the U.S. commercial microelectronics industry by expanding its efforts in electronics packaging, interconnection, and assembly (P/I/A) materials technologies. In conjunction with industry, university, and other government agency partners, these new NIST efforts target materials technology issues that underlie the priorities contained within the various electronics industry technology roadmaps. A dominant aspect of the laboratory P/I/A program focuses on the in-situ metrology and data needs associated with the materials and complex material assembles which comprise today's microelectronic components and circuits.

02,406
PB96-122841 Not available NTIS
National Inst. of Standards and Technology (CAML), Gaithersburg, MD. Applied and Computational Mathematics Div.
Parallel Monte Carlo Simulation of MBE Growth.
Final rept.
I. M. Beichl, Y. A. Teng, and J. L. Blue. 1995, 7p.
Pub. in International Parallel Processing Symposium (9th), Santa Barbara, CA., April 25-28, 1994, p46-52.

Keywords: *Monte Carlo method, *Parallel processing, *Molecular beam epitaxy, Algorithms, Crystal growth, Computerized simulation, Computer software, Sequences(Mathematics), Reprints, MBE(Molecular beam epitaxy).

We present a parallel algorithm for Monte Carlo simulation of molecular beam epitaxial growth (MBE) focusing on the software we have developed and the experiences gained. An efficient sequential method to do MBE simulation was developed that uses a single binary tree to store the rates of occurence of all possible events at a given time. The challenge was to find a way to adapt this method to a parallel machine.

02,407
PB96-123674 Not available NTIS
National Inst. of Standards and Technology (EEEL), Gaithersburg, MD. Semiconductor Electronics Div.
Nano-Defects in Commercial Bonded SOI and SIMOX.
Final rept.
D. K. Sadana, J. Lasky, H. J. Hovel, K. Petrillo, and P. Roitman. 1994, 2p.
Pub. in Proceedings of the International Institute of Electrical and Electronics Engineers SOI Conference, Nantucket Island, MA., October 3-6, 1994, p111-112.

Keywords: *Crystal defects, *Defects, Reprints, *SIMOX, *SOI(Semiconductors), Nano defects.

Two new classes of defects have been identified in commercial SIMOX, plasma thinned BSOI and BESOI materials. The first class of defects are revealed when the materials are treated in concentrated HF, and their density is in the range 10 to the 2nd power - 10 to the third power cm -2. The second class of defects densities of 10 to the 4th power - 10 to the 5th power cm -2 are present in both plasma thinned BSOI and BESOI after Secco etching. The defect densities in SIMOX after the secco etching were 10 to the 6th power - 10 to the 7th power cm -2 which was expected.

02,408
PB96-135017 Not available NTIS
National Inst. of Standards and Technology (EEEL), Boulder, CO. Electromagnetic Technology Div.
Thermal Isolation of High-Temperature Superconducting Thin Films Using Silicon Wafer Bonding and Micromachining.
Final rept.
C. A. Bang, J. P. Rice, M. I. Flik, D. A. Rudman, and M. A. Schmidt. 1993, 5p.
Pub. in Jnl. of Microelectromechanical Systems, v2 n4 p160-164 Dec 93.

Keywords: *High temperature superconducting, *Superconductors, *Wafer bonding, *Micromachining, Thin films, Silicon, Reprints, Thermal isolation, Micromachining.

Using a new micromachining technology, thermally isolated thin films of high-temperature superconductor have been microfabricated. The intended application for these structures is in infrared bolometers. A silicon wafer bonding process produces a low thermal mass island of single-crystal silicon on a silicon nitride membrane which provides thermal isolation. The silicon can act as a seed for the epitaxial growth of YBa2Cu3O7 on a yttria-stabilized zirconia buffer layer. This paper describes the overall concept of the thermally isolated device, and demonstrates that the micromachined structure can be fabricated with high-quality superconducting films.

02,409
PB96-135181 Not available NTIS
National Inst. of Standards and Technology (EEEL), Boulder, CO. Electromagnetic Technology Div.
Growth of Epitaxial KNbO3 Thin Films.
Final rept.
T. M. Graettinger, P. A. Morris, A. Roshko, D. J. Lichtenwalner, A. F. Chow, A. I. Kingon, and O. Auciello. 1994, 12p.
Pub. in Materials Research Society Symposium Proceedings, San Francisco, CA., April 5-7, 1994, v341 p265-276.

Keywords: *Epitaxial growth, *Ion beams, *Thin films, Reprints, Morphology, Sputtering, MOCVD.

KNbO3 possesses high nonlinear optical coefficients making it a promising material for frequency conversion of infrared light into the visible wavelength range using integrated optical devices. While epitaxial thin films of KNbO3 have previously been grown using ion beam sputtering, defects (i.e. grain boundaries, domains, surface roughness) in these films resulted in high optical losses and no measurable in-plane birefringence. Previous films were grown on MgO substrates, which have a greater than 4% lattice mismatch with KNbO3. In the work reported here, the authors have grown films on MgO, MgAl2O4, NdGaO3, and KTaO3 to investigate the role of lattice mismatch on the resulting film quality. Films have also been grown with and without oxygen ion assistance. The orientations, morphologies, and defects in the films were examined using x-ray diffraction and AFM to determine their relationships to the growth conditions and substrate lattice mismatch.

02,410
PB96-135355 Not available NTIS
National Inst. of Standards and Technology (EEEL), Boulder, CO. Electromagnetic Technology Div.
Effects of Etching on the Morphology and Surface Resistance of YBa2Cu3O7-delta Films.
Final rept.
A. Roshko, S. E. Russek, K. A. Trott, J. S. Martens, D. Zhang, S. C. Sanders, and M. E. Johansson. 1995, 4p.
Pub. in Institute of Electrical and Electronics Engineers Transactions on Applied Superconductivity, v5 n2 p1733-1736 Jun 95.

Keywords: *Yttrium oxides, *Thin films, Reprints, Microwaves, *Atomic force microscopy, YBCO, RHEED, HTS.

The changes in surface morphology and surface resistance of sputtered and laser ablated YBa2Cu3O7-sigma films both before and after etching have been examined. Six different etchants were used: citric acid, nitric acid, Br-methanol, EDTA, disodium EDTA, and ion milling. The surface morphologies of the films were examined by reflection high energy electron diffraction (RHEED) and atomic force microscopy (AFM), both before and after etching. The surface resistance (Rs) was measured at 94 GHz using a confocal resonator. An amorphous layer was found on the film surfaces after exposure to air. A few of the etches restored some of the surface crystallinity, but most caused increases in the overall surface roughness. Several of

the wet etches attacked dislocations. Ion milling caused the largest degradation of surface crystallinity and a corresponding increase in (Rs). Some of the chemical etches increased R, by less than 15%.

02,411
PB96-135389 Not available NTIS
National Inst. of Standards and Technology (EEEL), Boulder, CO. Electromagnetic Fields Div.
LRM Probe-Tip Calibrations Using Nonideal Standards.
Final rept.
D. F. Williams, and R. B. Marks. 1995, 4p.
See also PB95-163952.
Pub. in Institute of Electrical and Electronics Engineers Transactions on Microwave Theory and Techniques, v43 n2 p466-469 Feb 95.

Keywords: *Integrated circuits, *Electric probes, *Calibration, Electrical measurement, Reprints, Microwave circuits, Broadband, *Probe tip calibration, *Wafer probe stations.

The line-reflect-match calibration is enhanced to accommodate imperfect match standards and lossy lines typical of monolithic microwave integrated circuits. The authors characterize the match and line standards using an additional line standard of moderate length. The new method provides a practical means of obtaining accurate, wideband calibrations with compact standard sets. Without the enhancement, calibration errors due to imperfection in typical standards can be severe.

02,412
PB96-137765 Not available NTIS
National Inst. of Standards and Technology (EEEL), Boulder, CO. Electromagnetic Fields Div.
Microwave Dielectric Properties of Anisotropic Materials at Cryogenic Temperatures.
Final rept.
R. G. Geyer, and J. Krupka. 1995, 3p.
Pub. in Institute of Electrical and Electronics Engineers Transactions on Instrumentation and Measurement, v44 n2 p329-331 Apr 95.

Keywords: *Cryogenics, Dielectric properties, Microwave frequencies, Permittivity, Reprints, Crystals, Superconductors, *Anisotropic materials, Dielectric resonators.

The permittivity and dielectric loss tangent of crosslinked polystyrene (Rexolite), polytetrafluoroethylene (Teflon), and single-crystal quartz were measured at microwave frequencies and at temperatures of 77 K and 300 K using a dielectric resonator technique. Dielectric loss tangents as low as 7 x 10 to the minus 6th power at 77 K were determined by applying high-temperature superconducting (HTS) films as the endplates of the dielectric resonator. Two permittivity tensor components for uniaxially anisotropic crystalline quartz were measured. Although the permittivities at 77 K changed very little from their room temperature values at 300 K, large changes in dielectric losses were observed. The decreased losses of these microelectronic substrates can markedly improve the performance of many microwave devices at cryogenic temperatures.

02,413
PB96-137807 Not available NTIS
National Inst. of Standards and Technology (EEEL), Gaithersburg, MD. Semiconductor Electronics Div.
Use of Monte Carlo Modeling for Interpreting Scanning Electron Microscope Linewidth Measurements.
Final rept.
J. R. Lowney. 1995, 6p.
Pub. in Scanning, v17 p281-286 1995.

Keywords: *Line width, *Lithography, Monte Carlo method, Electron beams, Metrology, Reprints, *X ray lithography, *Scanning electron microscopy.

A scanning electron microscope (SEM) can be used to measure the dimensions of the microlithographic features of integrated circuits. However, without a good model of the electron-beam/specimen interaction, accurate edge location cannot be obtained. A Monte Carlo code has been developed to model the interaction of an electron beam with one or two lines lithographically produced on a multilayer substrate. The purpose of the code is to enable one to extract the edge position of a line from SEM measurements. It is based on prior codes developed at the National Institute of Standards and Technology, but with a new formulation for the atomic scattering cross sections and the inclusion of a method to simulate edge roughness or rounding. The code is currently able to model the transmitted and backscattered electrons, and the results from the code have been applied to the analysis of electron transmission through gold lines on a thin silicon subtrate, such as is used in an x-ray lithographic mask. Significant reductions in backscattering occur because of the proximity of a neighboring line.

02,414
PB96-138433 Not available NTIS
National Inst. of Standards and Technology (EEEL), Gaithersburg, MD. Semiconductor Electronics Div.
Electrical Characterization of Integrated Circuit Metal Line Thickness.
Final rept.
S. Mayo, and H. A. Schafft. 1995, 8p.
Pub. in Solid-State Electronics, v38 n12 p1993-2000 1995.

Keywords: *Aluminum, *Film thickness, *Integrated circuits, Interconnect lines, Metallization, Reprints, Matthiessen's rule.

Resistance measurements of thin aluminum-silicon alloy lines, 10 and 30 microm wide, were made at various temperatures in the 9.2-295.5 K range. Deviations from Matthiessen's rule were observed over the whole temperature range. At temperatures near room ambient data for these lines are in good agreement with those reported for aluminum-copper alloy wires. A formalism was developed to calculate line thickness and cross-sectional area from electrical resistance data. Line thickness calculations are in good agreement with thickness data measured via scanning electron microscopy. The stress distributions in these lines were modeled by using finite element stress analysis. The results show large stress gradients localized at the line edge region, whereas at the central part of the line there is a high stress value and a low stress gradient. In submicrometer lines the whole line body is under large stress gradients.

02,415
PB96-141106 Not available NTIS
National Inst. of Standards and Technology (EEEL), Boulder, CO. Optoelectronics Div.
Cross-Sectional Photoluminescence and Its Application to Buried-Layer Semiconductor Structures.
Final rept.
D. T. Schaafsma, and D. H. Christensen. 1995, 6p.
Pub. in Jnl. of Applied Physics, v78 n2 p694-699 Jul 95.

Keywords: *Semiconductors, *Photoluminescence, Quantum wells, Lasers, Emission spectra, Reprints, Burried-layers, VCSEL.

We present an overview of a cross-sectional scanning microphotoluminescence technique that is used to examine various buried-layer semiconductor structures for which traditional surface-normal techniques cannot yield sufficient information or must be coupled with time-consuming and painstaking processes such as wet etching. This technique has a wide range of application; two-- defect-driven interdiffusion in quantum wells and the modificaton of spontaneous emission from quantum wells in vertical-cavity surface-emitting lasers (VCCSELs)-are discussed here. The data obtained using this method can be used to distinguish emission spectra from quantum wells as little as one micrometer apart in depth and a few nanometers different in wavelength. The comparison of normal incidence with cross-sectional data from VCSELs can be used to more effectively optimize the match between cavity resonance and quantum well emission in high-Q devices.

02,416
PB96-146634 Not available NTIS
National Inst. of Standards and Technology (MSEL), Gaithersburg, MD. Reactor Radiation Div.
In-situ Neutron Reflectivity of MBE Grown and Chemically Processed Surfaces and Interfaces.
Final rept.
J. A. Dura, and C. F. Majkrzak. 1996, 6p.
Pub. in Proceedings of International Workshop on Semiconductor Characterization: Present Status and Future Needs, Gaithersburg, MD., January 30-February 2, 1995, p549-554 1996.

Keywords: *Molecular beam epitaxy, *Neutron sources, *Reflectivity, Crystal growth, Semiconductor devices, Quantitative analysis, Isotopic labeling, Composition(Property), Xray analysis, Comparative evaluations, Reprints, MBE(Molecular beam epitaxy), In situ neutron reflectivity.

Several properties make neutron reflectivity particularly suited to investigations of semiconductor structures produced by both molecular beam epitaxy (MBE) and chemical means. Reflectivity can provide quantitative information about composition, layer thickness and interface width. Since the scattering length for neutrons depends upon nuclear interactions, in contrast to x-rays, a large difference in scattering length can occur between systems of similar atomic number and one can employ isotope tagging at a particular fabrication step to determine its effect in the finished structure. In this paper we describe a new facility for in-situ neutron reflectivity and related measurements within a MBE chamber, review the principles underlying reflectivity and grazing angle diffraction, discuss the unique capabilities of neutrons in comparison with X-rays, and give some examples of applications in which neutron reflectivity can be uniquely utilized.

02,417
PB96-146774 Not available NTIS
National Inst. of Standards and Technology (MEL), Gaithersburg, MD. Precision Engineering Div.
Progress Toward Accurate Metrology Using Atomic Force Microscopy.
Final rept.
T. McWaid, J. Schneir, J. S. Villarrubia, R. Dixson, and V. W. Tsai. 1996, 5p.
Pub. in Semiconductor Characterization Present Status and Future Needs, p313-317 1996.

Keywords: *Metrology, *Accuracy, *Microscopy, Semiconductors(Materials), Roughness, Microstructure, Calibration standards, Reprints, AFM(Atomic force microscopy), Critical dimension.

Accurate metrology using atomic force microscopy (AFM) requires accurate control of the tip position, an estimate of the tip geometry and an understanding of the tip-surface interaction forces. We describe recent progress at National Institute of Standards and Technology (NIST) towards accurate AFM metrology. We begin with a brief introduction to the potential applications of accurate AFM metrology within the semiconductor industry. Next, we describe the technological infrastructure required before industry personnel can successfully use AFM for repeatable, reproducible, and accurate measurements. NIST's programmatic response to the identified needs is then outlined. We give particular attention to the development of a calibrated atomic force microscope (C-AFM), since the development of this instrument is essential to the successful completion of most of our specific projects.

02,418
PB96-148044 Not available NTIS
National Inst. of Standards and Technology (EEEL), Boulder, CO. Electromagnetic Technology Div.
Josephson D/A Converter with Fundamental Accuracy.
Final rept.
C. A. Hamilton, C. J. Burroughs, and R. L. Kautz. 1995, 3p.
See also AD-A110 081/7.
Pub. in Institute of Electrical and Electronics Engineers Transactions on Instrumentation and Measurement, v44 n2 p223-225 Apr 95.

Keywords: *Josephson junctions, *Converters, Electric potential, Standards, Accuracy, Arrays, Reprints, Voltage standard.

A binary sequence of series arrays of shunted Josephson junctions is used to make a 14-b D/A converter. With 13 bias lines, any step number in the range -8192 to +8192 - 1.2V to + 1.2V can be selected in the time required to stabilize the bias current (a few microseconds). The circuit is a fast accurate dc reference, and it makes possible the digital synthesis of ac waveforms whose amplitudes derive directly from the internationally accepted definition of the volt.

02,419
PB96-148051 Not available NTIS
National Inst. of Standards and Technology (EEEL), Boulder, CO. Electromagnetic Technology Div.
Performance and Reliability of NIST 10-V Josephson Arrays.
Final rept.
C. A. Hamilton, and C. J. Burroughs. 1995, 3p.
Pub. in Institute of Electrical and Electronics Engineers Transactions on Instrumentation and Measurement, v44 n2 p238-240 Apr 95.

Keywords: *Josephson junctions, *Reliability, *Arrays, Superconductivity, Electric potential, Standards, Fabrication, Niobium, Lead(Metal), Aluminum oxides, Niobium oxides, Reprints.

This paper reviews eight years of fabrication of 10-V Josephson array chips at National Institute of Standards and Technology (NIST), and the performance and reliability of these chips at 22 different standards laboratories. Failure mechanisms and statistical data on failure rates are presented for devices made with both Nb/Nb2O5/Pb and Nb/Al2O3/Nb junctions.

02,420
PB96-148168 Not available NTIS
National Inst. of Standards and Technology (EEEL), Gaithersburg, MD. Semiconductor Electronics Div.
Measurement of Patterned Film Linewidth for Interconnect Characterization.
Final rept.
L. W. Linholm, R. A. Allen, M. W. Cresswell, H. A. Schafft, J. A. Kramar, E. C. Teague, R. N. Ghoshtagore, and S. Mayo. 1995, 4p.
Pub. in Proceedings of the Institute of Electrical and Electronics Engineers Conference on Microelectronic Test Structures, Nara, Japan, March 22-25, 1995, v8 p23-26 Mar 95.

Keywords: *Integrated circuits, *Microelectronics, Semiconductors(Materials), Electrical measurement, Resisters, Test equipment, Conductors, Line width, Reprints.

Test results from high-quality electrical and physical measurements on the same cross-bridge resistor test structure with approximately vertical sidewalls have shown differences in linewidth as great as 90 nm for selected conductive films. These differences were independent of design linewidth. As dimensions become smaller, the accurate measurement of the patterned conductor width is necessary to assure predictable timing performance of the interconnect system as well as control of critical device parameters.

02,421
PB96-155478 Not available NTIS
National Inst. of Standards and Technology (EEEL), Gaithersburg, MD. Semiconductor Electronics Div.
Methodology for the Certification of Reference Specimens for Determination of Oxygen Concentration in Semiconductor Silicon by Infrared Spectrophotometry.
Final rept.
B. G. Rennex, J. R. Ehrstein, and R. I. Scace. 1996, 6p.
Pub. in Jnl. of the Electrochemical Society, v143 n1 p258-263 1996.

Keywords: *Silicon, *Semiconductors, Fourier transform spectrometers, Interstitial, Oxygen, Reprints, Standards, FTIR.

The methodology and experiment for certification of reference specimens for determining interstitial oxygen concentration in semiconductor silicon are reported. These reference specimens are intended for calibration of infrared spectrophotometers which measure the 1107 cm to the minus 1 power oxygen peak in silicon to enable users to improve their measurement agreement. Based on an earlier international Grand Round Robin study, this measurement agreement is at best 5.4% (2(sigma)). Industry requirements for measurement comparison are much more demanding, and a methodology to satisfy those requirements is described. The most important aspect of this methodology is to reduce interlaboratory variation by the use of a single infrared instrument for certification. The certification uncertainty depends primarily on the improved repeatability of this instrument. Other sources of uncertainty were nonuniformity in both oxygen concentration and thickness over the specimen area, and variations in residual oxygen among the float-zone specimens which provided zero-oxygen reference for the reference sets. These various sources were combined in quadrature to arrive at 2(sigma) estimates of uncertainty under 0.2% at three oxygen levels.

02,422
PB96-156070 Not available NTIS
National Inst. of Standards and Technology (EEEL), Gaithersburg, MD. Semiconductor Electronics Div.
Micromachined Display Output for a Cellular Neural Network.
Final rept.
R. Yentis, C. Zincke, M. E. Zaghloul, and M. Gaitan. 1995, 4p.
Pub. in Proceedings of the Institute of Electrical and Electronics Engineers International Symposium on Circuits and Systems, Seattle, Washington, April 30-May 3, 1995, p660-663.

Keywords: *Neural networks, *Display devices, *Computer-aided design, Integrated circuits, Microelectronics, Chips(Electronics), CMOS, Input/output processing, Very large scale integration, Sensors, Design analysis, Reprints, *Micromachining, MOSIS system, MEMS(Microelectromechanical System).

A major problem with current Cellular Neural Networks is that the size of the network is partially limited by the number of input/output pins. This paper address this issue by combining a thermal pixel with the output of each cell. The output of all of the cells can then be seen in parallel with the aid of a thermal camera of other device located off-chip. THe layout for the cell is given and discussed. The chip was fabricated through the MOSIS service.

02,423
PB96-160668 Not available NTIS
National Inst. of Standards and Technology (PL), Gaithersburg, MD. Physics Lab. Office.
Interfaces in Mo/Si Multilayers.
Final rept.
J. M. Slaughter, P. A. Kearney, D. W. Schulze, E. B. Saloman, R. N. Watts, C. M. Falco, and C. R. Hills. 1990, 10p.
Pub. in Society of Photo-Optical Instrumentation Engineers X-ray/EUV Optics for Astronomy, Microscopy, Polarimetry, and Projection Lithography, San Diego, CA., July 9-13, 1990, v1343 p73-82.

Keywords: *Interfaces, *Reflective coatings, *Molybdenum, *Silicon, Epitaxy, Surface properties, X ray diffraction, Synchrotron radiation, Spectroscopic analysis, Chemical analysis, Reprints.

Mo/Si multilayer mirrors with high peak reflectivities have been fabricated in many laboratories. This material pair works very well for wavelengths between 125 Angstroms adn 250 Angstroms, and is therefore very useful in optics for astronomy and microscopy. However, complete understanding of the properties of these structures is presently limited by lack of understanding of the details of the interfaces. We report results from a study of Mo/Si interfaces performed with state-of-the-art surface science instruments and electron microscpoy. Low-angle x-ray diffraction and synchrotron radiation characterization results for multilayers prepared under a variety of conditions are reported.

02,424
PB96-160718 Not available NTIS
National Inst. of Standards and Technology (MEL), Gaithersburg, MD. Precision Engineering Div.
Metrology Standards for Advanced Semiconductor Lithography Referenced to Atomic Spacings and Geometry.
Final rept.
E. C. Teague, L. W. Linholm, M. W. Cresswell, F. E. Scire, J. S. Villarrubia, J. S. Jun, W. B. Penzes, and J. A. Kramar. 1993, 5p.
Pub. in Proceedings of the Institute of Electrical and Electronics Engineers International Conference on Microelectronic Test Structures, v6 p213-217 Mar 93.

Keywords: *Metrology, *Images, Semiconductors(Materials), Lithography, Masks, Heterodyning, Microelectronics, Reprints, CD metrology, Image placement, Mask metrology, Overlay error, Nanometrology.

This paper outlines how the needs for calibrating the positional accuracy of features on an X-ray mask membrane or an opticalreticle can be addressed by application of a high-accuracy coordinate metrology system known as the NIST Molecular Measuring Machine (M-Cubed). Based on scanning tunneling microscopy and state-of-the-art heterodyne optical interferometry, the measurements of M-cubed are referenced to fundamental standards of length and angle and with the atomic-resolution of its scanning tunneling microscope probe will be validated against the interatomic spacings and geometry of single crystal surfaces.

02,425
PB96-160726 Not available NTIS
National Inst. of Standards and Technology (MEL), Gaithersburg, MD. Precision Engineering Div.
Nanometrology.
Final rept.
E. C. Teague. 1991, 37p.
Pub. in AIP Conference Proceedings 241, Scanned Probe Microscopy, Santa Barbara, CA., January 1-11, 1991, p1-37 Feb 91.

Keywords: *Metrology, Heterodyning, Transducers, Flexing, Bearings, Microscopy, Interferometry, Reprints, Nanometrology, Probe geometry, Scanning tunneling microscopy.

Nanometrology is defined here as the science of measuring the dimensions of objects or object features to uncertainties of one nanometer or less. Four major tasks of nanometrology are examined: realizing a metric in the measurement space; establishing the metric in a coordinate reference frame; generating and measuring repeatable motion relative to the coordinate reference frame; and linking the testpiece to the coordinate reference frame/metric by a probe. Optical scales, x-ray interferometry, heterodyne interferometry, Fabry-Perot etalons, impedance-based transducers, and STM scales are evaluated as possible means to realize a metric.

02,426
PB96-160783 Not available NTIS
National Inst. of Standards and Technology (MEL), Gaithersburg, MD. Precision Engineering Div.
Scanned Probe Microscopies: Opportunities and Issues in Metrology.
Final rept.
E. C. Teague. 1991, 4p.
Pub. in Scanning Probe Microscopies: STM and Beyond, Proceedings 241, Santa Barbara, CA., January 1-11, 1991, 4p Feb 91.

Keywords: *Metrology, *Integrated circuits, *Trends, Electronics industry, Microelectronics, Surfaces, Geometry, Microscopy, Scanning, Requirements, Reprints, Frequency metrology, Atomically-flat surfaces, Scanned probe microscopy.

Projections about manufacturing trends in the integrated circuit industry are made which indicate that by 2001 uncertainty requirements for dimensional metrology will be less than 1 nanometer. Brief arguments are presented that new scanning probe microscopes offer many opportunities to meet this need because they have the potential of reducing the uncertainty of locating a feature on a testpiece and because they provide new access to the highly ordered atomic structure of crystal surfaces. Such access has much potential for giving greatly increased accuracy for generating reference lines and geometry against which motion of machine elements can be measured and characterized. The need for large-area, atomically-flat surfaces is discussed.

02,427
PB96-163787 Not available NTIS
National Inst. of Standards and Technology (EEEL), Gaithersburg, MD. Semiconductor Electronics Div.
High-Accuracy Principal-Angle Scanning Spectroscopic Ellipsometry of Semiconductor Interfaces.
Final rept.
N. V. Nguyen, D. Chandler-Horowitz, J. G. Pellegrino, and P. M. Amirtharaj. 1996, 5p.
Pub. in Proceedings of the International Workshop on Semiconductor Characterization: Present Status and Future Needs, Gaithersburg, MD., January 30-February 2, 1995, p438-442 1996.

Keywords: *Semiconductor interfaces, *Principal angle, Reprints, Interfaces, *Spectroscopic ellipsometry, Strain roughness.

A high-performance spectroscopic ellipsometer has been custom built, in house at NIST, based on the commonly used rotating-analyzer configuration. The data accuracy was highly enhanced by using the principal-angle scanning technique. This technique requires an accurate setting of the angle of incidence which is accomplished by an interferomter and high-precision goniometers for the sample stage and the polarizer. For each wavelength, the principal angle of incidence was automatically searched to obtain a 90s phase shift of the polarized light upon reflection, i.e., delta = 90 degrees, and the polarizer azimuth was set to psi. At this condition, the ac component of detected intensity is near a null. With zone averaging, systematic errors such as the detector nonlinearity, and the

analyzer and polarizer calibration constants, are minimized. To illustrate the use and capability of this system, the authors use the results of a recent study of the optical properties of SiO2/Si system and, in particlar, the transitional region, defined as an interlayer between the thermally grown SiO2/Si system and, in particular, the transitional region, defined as an interlayer between the thermally grown SiO2 film and the Si substrate. In this study, the complex dielectric function and the thickness of the interlayer were determined.

02,428
PB96-164025 Not available NTIS
National Inst. of Standards and Technology (EEEL), Gaithersburg, MD. Semiconductor Electronics Div.
Enhanced Voltage-Dividing Potentiometer for High-Precision Feature Placement Metrology.
Final rept.
R. A. Allen, M. W. Cresswell, C. H. Ellenwood, and L. W. Linholm. 1996, 6p.
Pub. in Institute of Electrical and Electronics Engineers Transactions on Instrumentation and Measurement, v45 n1 p136-141 Feb 96.

Keywords: *Metrology, *Potentiometer, Reprints, Voltage dividing, Spatial separations, Voltage dividing.

Enhancements to the voltage-dividing potentiometer, an electrical test structure for measuring the spatial separations of pairs of conducting features, are presented and discussed. These enhancements reduce or eliminate systematic errors which can otherwise lead to uncertainties as large as several hundred nanometers. These systematic errors, attributed by modeling to asymmetries at certain intersections of conducting features in the test structure, are eliminated by modifications to the test structure and test procedures.

02,429
PB96-164173 Not available NTIS
National Inst. of Standards and Technology (EEEL), Gaithersburg, MD. Semiconductor Electronics Div.
Modeling Buffer Layer IGBT's for Circuit Simulation.
Final rept.
A. R. Hefner. 1995, 13p.
See also PB95-153805.
Pub. in Institute of Electrical and Electronics Engineers Transactions on Power Electronics, v10 n2 p111-123 Mar 95.

Keywords: *Bipolar transistors, Application specific integrated circuits, Mathematical models, Dynamic properties, Reprints, *Insulated gate bipolar transistors, Circuit simulators, Buffer layers.

The dynamic behavior of commercially available buffer layer IGBT's described. It is shown that buffer layer IGBT's become much faster at high voltages than nonbuffer layer IGBT's with similar low voltage characteristics. Because the fall times specified in manufactures' data sheets do not reflect the voltage dependence of switching speed, a new method of selecting devices for different circuit applications is suggested. A buffer layer IGBT model is developed and implemented into the Saber circuit simulator, and a procedure is developed to extract the model parameters for buffer layer IGBT's. It is shown that the new buffer layer IGBT model can be used to describe the dynamic behavior and power dissipation of buffer layer IGBT's in user-defined application circuits. The results of the buffer layer IGBT model are verified using commercially available IGBT's.

02,430
PB96-164249 Not available NTIS
National Inst. of Standards and Technology (EEEL), Gaithersburg, MD. Semiconductor Electronics Div.
Microelectronic Test Structures for Overlay Metrology.
Final rept.
L. W. Linholm, R. A. Allen, and M. W. Cresswell. 1995, 3p.
See also PB95-180568.
Pub. in Nikkei Microdevices, p63-65 1995.

Keywords: *Microelectronics, *Overlays, *Positioning, *Alignment, Integrated circuits, Process control, Registration, Line width, Measurement, Lithography, Very large scale integration, Requirements, Metrology, Reprints, *Test structures, Test chips.

Control of image placement has been and is expected to remain one of the most important challenges required in the manufacturing of advanced microelectronic devices. The metrology to monitor and evaluate the performance of lithographic tools with those capabilities is lagging. Electrical test structures provide low-cost, post-patterning metrology for overlay that is routinely available during the advanced stages of process development and during manufacturing.

02,431
PB96-167192 Not available NTIS
National Inst. of Standards and Technology (EEEL), Gaithersburg, MD. Semiconductor Electronics Div.
Optical Characterization of Materials and Devices for the Semiconductor Industry: Trends and Needs.
Final rept.
S. Perkowitz, D. G. Seiler, and W. M. Bullis. 1996, 3p.
Pub. in Proceedings of the International Workshop on Semiconductor Characterization: Present Status and Future Needs, Gaithersburg, MD., January 30-February 2, 1995, p422-424 1996.

Keywords: *Semiconductors, *Optical characterization, Surveys, Processes, Devices, Reprints, Contactless, Nondestructive methods.

Contactless, nondestructive optical methods are used to characterize materials, process, and devices in the semiconductor industry. In response to industrial needs, the Semiconductor Electronics Division of the National Institute of Standards and Technology conducted a survey of the need for use of optical characterization methods within the semiconductor industry. Data from forty-two firms were analyzed to show the impact of the methods, what they measure, their range and precision, and their cost. A significant finding of the study is the need expressed by many industrial users for imporved standards and test methods for optical characterization.

02,432
PB96-175856 PC A07/MF A02
National Inst. of Standards and Technology (EEEL), Gaithersburg, MD. Semiconductor Electronics Div.
NIST List of Publications, LP 103, March 1996. National Semiconductor Metrology Program.
J. Walters. Mar 96, 102p.

Keywords: *US NIST, *Documents, Bibliographies, Semiconductors(Materials), Semiconductor industry, Metrology, Software.

This List of Publication includes all paper relevant to semiconductor technology published by NIST staff, including work of the National Semiconductor Metrology Program, the Semiconductor Electronics Division, and other parts of NIST having independent interests in semiconductor metrology. Bibliographic information is provided for publications from 1990 through 1995. Within each year, citations of published papers are listed alphabetically by first author. Indexes are provided by topic area and by author. Publications are referred to in the Topic and Author Indexes according to publication year and citation number (i.e., 95-3 refers to the third publication in the year 1995). A listing of software available from the Semiconductor Electronics Division is given on page 57, along with contacts for additional information and for copies of the computer programs.

02,433
PB96-176458 Not available NTIS
National Inst. of Standards and Technology (EEEL), Gaithersburg, MD. Semiconductor Electronics Div.
Novel Magnetic Field Characterization Techniques for Compound Semiconductor Materials and Devices.
Final rept.
C. A. Richter, D. G. Seiler, J. G. Pellegrino, W. F. Tseng, and W. R. Thurber. 1996, 5p.
Pub. in Proceedings of the International Workshop on Semiconductor Characterization: Present Status and Future Needs, Gaithersburg, MD., January 30-February 2, 1995, p673-677 1996.

Keywords: *Semiconductors, *Magnetic fields, Reprints, *Foreign technology, *Magnetoresistance, 2D electron gas, Magnetophonon effect, Universal conductance fluctuations, Shubnikov-de Haas oscillations.

Quantum-mechanical effects observed in the magnetoresistance of semiconductor devices and materials give important information such as carrier density, scattering rates, and band structure parameters. However, the small size of these effects often limits their observation and subsequently their practical use. The purpose of this paper is to show how these quantum mechanical effects can be more easily observed and used as characterization tools by modulating the applied magnetic field, which can increase the sensitivity of magnetotransport measurements.

02,434
PB96-176722 Not available NTIS
National Inst. of Standards and Technology (EEEL), Boulder, CO. Electromagnetic Fields Div.
Microwave Characterization of Flip-Chip MMIC Components.
Final rept.
R. B. Marks, J. A. Jargon, C. K. Pao, and C. P. Wen. 1995, 8p.
See also PB96-176730 and PB96-176748.
Pub. in Electronic Components and Technology Conference (45th), Las Vegas, NV., May 21-24, 1995, p343-350.

Keywords: *Microwave circuits, MIM(Semiconductors), Transmission lines, Capacitors, Calibration, Standards, Computer-aided design, Data bases, Reprints, *MMIC(Monolithic Microwave Integrated Circuits), *Monolithic Microwave Integrated Circuits, *Flip-chip technology, Coplanar waveguide, Circuit models, On wafer measurement, Spiral inductors.

The authors apply custom calibration standards and software to the accurate on-wafer measurement of MIM capacitors and spiral inductors on flip-chip coplanar-waveguide MMICs. The authors suggest equivalent circuit models and document their deficiencies. The results are applicable to the development of an accurate CAD database.

02,435
PB96-176730 Not available NTIS
National Inst. of Standards and Technology (EEEL), Boulder, CO. Electromagnetic Fields Div.
Microwave Characterization of Flip-Chip MMIC Interconnections.
Final rept.
R. B. Marks, J. A. Jargon, C. K. Pao, and C. P. Wen. 1995, 4p.
See also PB96-176722 and PB96-176748.
Pub. in International Microwave Symposium, Orlando, FL., May 14-19, 1995, v3 p1463-1466.

Keywords: *Microwave circuits, MIM(Semiconductors), Transmission lines, Capacitors, Calibration, Standards, Computer-aided design, Data bases, Reprints, *MMIC(Monolithic Microwave Integrated Circuits), *Monolithic Microwave Integrated Circuits, *Flip-chip technology, Coplanar waveguide, Circuit models, On wafer measurement, Spiral inductors.

The report accurate on-wafer measurements of transmission lines on flip-chip coplanar-wave-guide MMICs. The results are applicable to the development of an accurate CAD database. The authors also report and apply a new technique for the measurement of transmission line capacitance.

02,436
PB96-176748 Not available NTIS
National Inst. of Standards and Technology (EEEL), Boulder, CO. Electromagnetic Fields Div.
Electrical Measurements of Microwave Flip-Chip Interconnections.
Final rept.
R. B. Marks, J. A. Jargon, C. K. Pao, and C. P. Wen. 1995, 6p.
See also PB96-176722 and PB96-176730.
Pub. in ISHM '95 Proceedings, International Symposium on Microelectronics, Los Angeles, CA., October 24-26, 1995, p424-429.

Keywords: *Microwave circuits, MIM(Semiconductors), Circuit interconnections, Electrical measurement, Transmission lines, Capacitors, Calibration, Standards, Computer-aided design, Data bases, Reprints, *MMIC(Monolithic Microwave Integrated Circuits), *Monolithic Microwave Integrated Circuits, *Flip-chip technology, Coplanar waveguide, Circuit models, On wafer measurement, Spiral inductors.

The authors apply custom calibration standards and software to the accurate on-wafer measurement of components on flip-chip coplanar-waveguide MMICs. The authors characterize transmission lines, MIM capacitors, and spiral inductors and develop equivalent circuit models. The results are applicable to the development of an accurate CAD database.

02,437
PB96-179445 Not available NTIS

National Inst. of Standards and Technology (PL), Gaithersburg, MD. Molecular Physics Div.
Theory for Quantum-Dot Quantum Wells: Pair Correlation and Internal Quantum Confinement in Nanoheterostructures.
Final rept.
G. W. Bryant. 1995, 4p.
Pub. in Physical Review B, v52 n24 pR16997-17000, 15 Dec 95.

Keywords: *Binding energy, *Quantum wells, *Oscillator strength, Quantum dots, Correlation, Exciton, HgS, Reprints.

Spherical quantum-dot-quantum-well nanocrystallites, with internal radial quantum-well band profiles, can now be fabricated. Pair states in these nanoheterostructures are determined by electron-hole attraction, global confinement in the dot, and local confinement within the well. Configuration-interaction calculations using effective-mass models with screened pair interaction give accurate exciton energies for CDs/HgS quantum-dot quantum wells. Binding energy and pair correlation are suppressed but pair-oscillator strengths are enhanced by adding a HgS quantum well to a CDs quantum dot.

02,438
PB96-179478 Not available NTIS
National Inst. of Standards and Technology (EEEL), Gaithersburg, MD. Semiconductor Electronics Div.
Time-Dependent Dielectric Breakdown of Intrinsic SiO2 Films under Dynamic Stress.
Final rept.
P. Chaparala, J. S. Suehle, C. Messick, and M. Roush. 1995, 9p.
See also PB94-185956.
Pub. in Proceedings of the Institute of Electrical and Electronics Engineers International Integrated Reliability Workshop, Lake Tahoe, CA., October 22-25, 1995, p104-112.

Keywords: *Dielectric breakdown, *Silicon dioxide, Temperature dependence, High temperature, Integrated circuits, Reprints, Electric fields, Dielectric files, Thin films, Field acceleration models.

The authors present time-dependet dielectric breakdown (TDDB) characteristics for 9, 15, and 22 nm silicon dioxide films stressed under dc, unipolar, and bipolar pulsed bias conditions. The authors' results indicate that the increased lifetime observed under pulsed stress conditions diminishes as the stress electric field and oxide thickness are reduced. TDDB data under pulse bias conditions exhibit similar field and temperature dependencies as under static stress. C-V measurements indicate that lifetime enhancement only occurs for electric fields and thickness where charge trapping is significant.

02,439
PB96-179510 Not available NTIS
National Inst. of Standards and Technology (PL), Gaithersburg, MD. Electron and Optical Physics Div.
Improved Dose Metrology in Optical Lithography.
Final rept.
C. L. Cromer, T. B. Lucatorto, T. R. O'Brian, and M. Walhout. 1996, 6p.
Pub. in Solid State Technology, v39 n4 p75-80 Apr 96.

Keywords: *Metrology, *Laser annealing, *Ultraviolet radiation, Optical properties, Photoresistors, Radiometers, Semiconductors, Microelectronics, Calibration standards, Standardization, Reprints, *Optical lithography, Critical dimensions, Irradiance measurement, Laser etching, Microlithography.

Maintaining critical dimensions (CDs) in optical lithography requires careful control over the UV/DUV dose applied to a photoresist, especially as CDs become smaller. To meet the growing need for a UV-measurement infrastructure in the semiconductor industry, the National Institute of Standards and Technology (NIST) is improving its primary radiometric standards by an order of magnitude, reducing the absolute uncertainty in irradiance measurements to about 0.5% in the 100-400 nm range. Parallel improvements in transfer standards and source calibrations will allow the dissemination of highly accurate radiometric scales directly to industry.

02,440
PB96-186093 Not available NTIS
National Inst. of Standards and Technology (EEEL), Gaithersburg, MD. Semiconductor Electronics Div.
New Physics-Based Model for Time-Dependent-Dielectric-Breakdown.
B. Schlund, J. Suehle, C. Messick, and P. Chaparala. 1995, 9p.
Pub. in Proceedings of the Institute of Electrical and Electronics Engineers International Integrated Reliability Workshop Final Report, Lake Tahoe, CA., October 22-25, 1995, p72-80.

Keywords: *Silcon dioxide, Reliability(Electronics), Reprints, Dielectric films, Time dependence, *Time-Dependent Dielectric Breakdown, *Thin dielectric reliability.

A new, physics based model for time dependent dielectric breakdown has been developed, and is presented along with test data obtained by NIST on oxides provided by National Semiconductor. Testing included Fields from 5.6 MV/cm to 12.7 MV/cm, and temperatures ranging from 60 degrees C to 400 degrees C. The physics, mathematical model and test data, all confirm a linear, rather than an inverse field dependence. The primary influence on oxide breakdown was determined to be due to the dipole interaction energy of the field with the orientation of the molecular dipoles in the dielectric. The resultant failure mechanism is shown to be the formation and coalescence of vacancy defects, similar to that proposed by Dumin et al.

02,441
PB96-190038 Not available NTIS
National Inst. of Standards and Technology (PL), Gaithersburg, MD. Atomic Physics Div.
Microlithography by Using Neutral Metastable Atoms and Self-Assembled Monolayers.
Final rept.
K. K. Berggren, A. Bard, J. L. Wilbur, J. J. McClelland, S. L. Rolston, W. D. Phillips, M. Prentiss, G. M. Whitesides, J. D. Gillaspy, and A. G. Helg. 1995, 3p.
Pub. in Science, v269 p1255-1257 Sep 95.

Keywords: *Lithography, *Microstructures, *Metastable atoms, Gold, Etching, Surfaces, Aqueous solutions, Argon, Reprints, *Atom lithography, Microlithography, SAMs(Self-assembled monolayers).

Lithography can be performed with beams of neutral atoms in metastable excited states to pattern self-assembled monolayers (SAMs) of alkanethiolates on gold. An estimated exposure of a SAM of dodecanethiolate (DDT) to 15 to 20 metastable argon per DDT molecule damaged the SAM sufficiently to allow penetration of an aqueous solution of ferricyanide to the surface of the gold. This solution etched the gold and transformed the patterns in the SAMs into structures of gold; these structures had edge resolution of less than 100 nanometers. Regions of SAMs as large as 2 square centimeters were patterned by exposure to a beam of metastable argon atoms. These observations suggest that this system may be useful in new forms of micro- and nanolithography.

02,442
PB96-200365 Not available NTIS
National Inst. of Standards and Technology (PL), Boulder, CO. Time and Frequency Div.
Design Criteria for BJT Amplifiers with Low I/f AM and PM Noise.
Final rept.
E. S. Ferre-Pikal, F. L. Walls, and C. W. Nelson. 1995, 10p.
Pub. in Institute of Electrical and Electronics Engineers International Frequency Control Symposium, San Francisco, CA., May 31-June 2, 1995, p305-314.

Keywords: *Bipolar transistors, *Amplifiers, Design criteria, Junction transistors, Electric circuits, Noise, Reprints.

In this paper, the authors discuss guidelines for designing linear bipolar junction transistor (BJT) amplifiers with low 1/f amplitude modulation (AM) and phase modulation (PM) noise. These guidelines are derived from a new theory that relates AM and PM noise to transconductance fluctuations, junction capacitance fluctuations, and circuit architecture. The authors analyze the noise equations of each process for a common emitter (CE) amplifier and use the results to suggest amplifier designs that minimize the 1/f noise while providing other required attributes such as high gain. Although the authors use a CE amplifier as an example, the procedure applies to other configurations as well. Experimental noise results for several amplifier configurations are presented.

02,443
PB96-200845 Not available NTIS
National Inst. of Standards and Technology (MSEL), Gaithersburg, MD. Ceramics Div.
Overview of U.S. Government Advanced Packaging Programs.
Final rept.
J. A. Carpenter, J. Evans, E. B. Hakim, C. Pagel, D. Palmer, J. Lyke, and N. J. Naclerio. 1993, 6p.
Pub. in Proceedings of the International Conference and Exhibition on Multichip Modules, Denver, CO., April 14-16, 1993, p495-500.

Keywords: *Electronic packaging, *Interagency coordination, Photonics, Circuit interconnections, US DOD, US DOE, US DOC, NASA, Government/industry relations, Reprints, Multichip module.

An overview is provided of non-classified advanced electronics packaging programs, particularly those involving multichip module (MCM) technologies, sponsored and performed by the U.S. Departments of Defense, Energy, and Commerce and the National Aeronautics and Space Administration (NASA), and how those programs are coordinated among one another and with U.S. industry.

02,444
PB96-200969 Not available NTIS
National Inst. of Standards and Technology (EEEL), Gaithersburg, MD. Semiconductor Electronics Div.
Monte Carlo Simulation of Scanning Electron Microscope Signals.
Final rept.
J. R. Lowney. 1996, 6p.
Pub. in Scanning, v18 p301-306 1996.

Keywords: *Scanning electron microscopes, *Monte Carlo, *Metrology, Linewidth, Lithography, Reprints.

Two computer codes for simulating the backscattered, transmitted, and secondary-electron signals for targets in a scanning electron microscope are described. The frist code, MONSEL-II, has a model target consisting of three parallel lines on a three-layer substrate, while the second, MONSEL-III, has a model target consisting of a two-by-two array of finite lines on a three-layer substrate. Elastic electron scattering is determined by published fits to the Mott cross section. Both plasmon-generated electrons and ionized valence electrons are included in the secondary production. An adjustable quantity, called the residual energy loss rate, is added to the formula of Joy and Luo to obtain the measured secondary yield. The codes show the effects of signal enhancement due to edge transmission, known as blooming, as well as signal reduction due to neighboring lines, known as the 'black-hole' effect.

02,445
PB96-201074 Not available NTIS
National Inst. of Standards and Technology (MEL), Gaithersburg, MD. Precision Engineering Div.
Report on the NIST Low Accelerating Voltage SEM Magnification Standard Interlaboratory Study.
Final rept.
M. T. Postek, A. E. Vladar, S. Jones, and W. J. Keery. 1993, 18p.
Pub. in Integrated Circuit Metrology, Inspection and Process Control VII, San Jose, CA., March 2-4, 1993, p268-285.

Keywords: *Dimensional measurements, *Scanning electron microscopy, *Standards, Line widths, Lithography, Reprints, *Magnification standards, Nanofabrication, Standard reference materials.

NIST is in the process of developing a new scanning electron microscope (SEM) magnification calibration reference standard useful at both high and low accelerating voltages. This standard will be useful for all applications to which the SEM is currently being used, but it has been specifically tailored to meet many of the particular needs of the semiconductor industry. A small number of test samples with the pattern were prepared on silicon substrates using electron beam lithography at the National Nanofabrication Facility at Cornell University. The structures were patterned in titanium/palladium with maximum nominal pitch structures of approximately 3000 micrometers scaling down to structures with minimum nominal pitch of 0.4 micrometer. Eighteen of these samples were sent out to a total of 35 university, research, semiconductor and other industrial laboratories in an interlaboratory study. The purpose of the study was to test the SEM instrumentation and to review the suitability of the sample

design. The laboratories were asked to take a series of micrographs at various magnifications and accelerating voltages designed to test several of the aspects of instrument performance related to general SEM operation and metrology. If the instrument in the laboratory was used for metrology, the laboratory was also asked to make specific measurements of the sample. In the first round of the study (representing 18 laboratories), data from 35 instruments from several manufacturers were obtained and the second round yielded information from 14 more instruments. The results of the analysis of the data obtained in the study are presented in the paper.

02,446
PB96-201090 Not available NTIS
National Inst. of Standards and Technology (MEL), Gaithersburg, MD. Precision Engineering Div.
Scanning Electron Microscope Metrology.
Final rept.
M. T. Postek. 1993, 45p.
See also PB95-169405.
Pub. in Handbook of Critical Dimension Metrology and Process Control, Monterey, CA., September 28-29, 1993, p46-90.

Keywords: *Integrated circuits, *Precision, *Manufacturing, Electron microscopy, Secondary emission, Metrology, Reprints.

During the manufacturing of present-day integrated circuits, certain meausrements must be made of the submicrometer structures composing the device with a high degree of precision. Optical microscopy, scanning electron microscopy and the various forms of scanning probe microscopies are major microscopical techniques used for submicrometer metrology. New techniques applied to scanning electron microscopy have improved some of the limitations of this technique and time will permit even further improvements. This presentation will review the current state of scanning electron microscope (SEM) metrology in light of many of these recent improvements.

02,447
PB96-201108 Not available NTIS
National Inst. of Standards and Technology (MEL), Gaithersburg, MD. Precision Engineering Div.
SEM Linewidth Metrology of X-ray Lithography Masks.
Final rept.
M. T. Postek, J. R. Lowney, A. E. Vladar, R. D. Larrabee, W. J. Keery, and E. Marx. 1993, 5p.
Pub. in American Society of Mechanical Engineers, v8 p78-82 1993.

Keywords: *Scanning electron microscopy, *Metrology, *Lithography masks, X rays, Measurements, Reprints.

Accurate dimensional metrology of the submicrometer gold absorber structures of x-ray masks can be accomplished in the scanning electron microscope (SEM). This is possible because the x-ray masks present a measurement object that is unique from most other objects viewed in the SEM. This is because the silicon support membrane is, by design, x-ray transparent. The characteristic can be used as a distinct advantage in electron beam-based mask metrology since, depending upon the incident electron beam energies, substrate composition and substrate thickness, the membrane can also be essentially electron transparent. The area of the mask where the absorber structures are located are essentially x-ray opaque, as well as, electron opaque. Viewing the sample from a perspective below the mask, by placing an electron detector beneath the mask, provides excellent electron signal contrast between the absorber structure and the base membrane.

02,448
PB96-201132 Not available NTIS
National Inst. of Standards and Technology (EEEL), Gaithersburg, MD. Semiconductor Electronics Div.
New Physics-Based Model for Time-Dependent- Dielectric-Breakdown.
Final rept.
B. Schlund, J. S. Suehle, C. Messick, and P. Chaparala. 1996, 8p.
See also PB96-186093.
Pub. in Proceedings of the International Reliability Physics Conference, Dallas, TX., April 30-May 2, 1996, p84-92.

Keywords: *Dielectric breakdown, *Oxides, Time dependence, Mathematical models, Linear systems, Crystal defects, Reprints.

A new physics-based model for time dependent dielectric breakdown has been developed, and is presented along with test data obtained by NIST on oxides provided by National Semiconductor. Testing included fields from 5.4 MV/cm to 12.7 MV/cm, and temperatures ranging from 60C to 400C. The physics, mathematical model, and test data, all confirm a linear, rather than an inverse field dependence. The primary influence on oxide breakdown was determined to be due to the dipole interaction energy of the field with the orientation of the molecular dipoles in the dielectric. The resultant failure mechanism is shown to be the formation and coalescence of vacancy defects, similar to that proposed by Dumin et al.

02,449
PB96-204102 Not available NTIS
National Inst. of Standards and Technology (EEEL), Gaithersburg, MD. Semiconductor Electronics Div.
Electric Field Dependent Dielectric Breakdown of Intrinsic SiO2 Films Under Dynamic Stress.
Final rept.
P. Chaparala, J. S. Suehle, C. Messick, and M. Roush. 1996, 6p.
See also PB96-179478.
Pub. in Proceedings of the Institute of Electrical and Electronics Engineers International Reliability Physics Conference, Dallas, TX., April 30-May 2, 1996, p61-66.

Keywords: *Dielectric breakdown, *Silicon dioxide, Temperature dependence, Reprints, High temperature, Integrated circuits, Electric fields, Thin films, Oxides, Time-dependent.

Time-dependent dielectric breakdown (TDDB) characteristics are reported for 6.5 nm,, 9nm, 15 nm, and 22 nm intrinsic silicon dioxide films stressed under dc and bipolar pulsed stress conditions for a wide range of electric fields and temperatures. The authors results show that the increased ifetime observed under bipolar pulsed stress conditions diminishes as the stress electric field and oxide thickness are reduced. Similar electric field and temperature dependencies of TDDB are observed under both static and dynamic stress conditions. It is observed that lifetime enhancement only occurs for electric fields and thicknesses where charge trapping is significant. Contradictory to the convention notion, TDDB tests on intrinsic thin oxides indicate that static stress testing cannot be considered as a conservative test of bipolar stressing for estimating oxide reliability. These results also confirm the existence of two separate failure mechanisms for TDDB that are function of electric field and oxide thickness.

02,450
PB96-204136 Not available NTIS
National Inst. of Standards and Technology (EEEL), Gaithersburg, MD. Semiconductor Electronics Div.
Hybrid Optical-Electrical Overlay Test Structure.
Final rept.
M. W. Cresswell, R. A. Allen, L. W. Linholm, W. F. Guthrie, and A. W. Gurnell. 1996, 4p.
Pub. in Proceedings of the Institute of Electrical and Electronics Engineers International Conference on Microelectronic Test Structures, Trento, Italy, March 26-28, 1996, v9 p9-12.

Keywords: *Semiconductors, *Test structure, Reprints, Lithography, Metrology, Overlay.

The purpose of this work is to explore the use of electrical test structures for calibrating optical overlay instruments with respect to certain application-dependent errors which are otherwise expected to become a serious impediment to realization of the goals of the National Technology Roadmap for Semiconductors over the next decade. A new hybrid test structure, from which overlay measurements can be extracted electricallty, as well as by optical instruments used for inspecting production wafers, has been designed and fabricated with built-in overlay values ranging from -60 to +60 nm. Structures patterned in a single conducting film and having critical-dimension (CD) design-rules ranging from 1.0 to 2.0 micrometers have been tested. Electrical overlay parameters, derived from multiple step-and-repeat exposure-site measurements, generally match the corresponding optical parameters to within several nanometers, subject to nominal quality of the pattern-replication process. The paper focuses on the analysis of electrical measurements, their dependence on CD design rules, and their comparison with the corresponding measurements made both by a commercial optical-overlay instrument and by a coordinate-measurement system having measurements traceable to absolute dimensional standards.

02,451
PB97-110134 Not available NTIS
National Inst. of Standards and Technology (EEEL), Gaithersburg, MD. Semiconductor Electronics Div.
Characterization of Two-Dimensional Dopant Profiles: Status and Review.
Final rept.
A. C. Diebold, M. R. Kump, J. J. Kopanski, and D. G. Seiler. 1996, 6p.
See also PB96-119300.
Pub. in Jnl. of Vacuum Science and Technology B, v14 n1 p196-201 Jan/Feb 96.

Keywords: *Transistors, *Computer aided design, *Models, Verification, Calibrating, Two dimensional, Dopes, Simulation, Microscopy, Spatial resolution, Spectroscopic analysis, Scanning probe methods, Reprints.

The National Technology Roadmap for Semiconductors calls for development of two- and three-dimensional dopant profiling methods for calibration of technology computer-aided design process simulators. The authors have previously reviewed 2D dopant profiling methods. In the particle, the authors briefly review methods used to characterize etched transistor cross sections by expanding the previous discussion of scanned probe microscopy methods. They also mention the need to participate in the ongoing comparison of analysis results for test structures that the authors have provided the community.

02,452
PB97-111439 Not available NTIS
National Inst. of Standards and Technology (EEEL), Gaithersburg, MD. Semiconductor Electronics Div.
Double Modulation and Selective Excitation Photoreflectance for Characterizing Highly Luminescent Semiconductor Structures and Samples with Poor Surface Morphology.
Final rept.
P. M. Amirtharaj, D. Chandler-Horowitz, and D. P. Bour. 1996, 12p.
Pub. in Proceedings of the Material Research Society Fall Meeting, Boston, MA., November 25-29, 1995, v406 p229-240 1996.

Keywords: *Double-modulation, *Lasers, *Photoreflectance, *Semiconductors, Quantum-well, Selective-excitation, Reprints.

Photoreflectance (PR) is a powerful, contactless, and nondestructive technique capable of probing interband electronic transitions and built-in electric-fields at the surface and in interface regions in semiconductor materials and microstructures. It has been widely used as a characterization too. Howevr, its application to highly luminscent systems, such as quantum-well (QW) lasers and samples with poor surface morphology has been limited because of the difficulty in minimizing the interference from the luminescence and the pump beam that is scattered from the surface. The authors present a double modulation procedure where both the probe and pump beams are modulated which allows the PR component to be completely separated from the luminescence and scattered contributions. The separation is achieved through the appropriate choice of modulation frequencies and specially designed tuned amplifiers. A complete PR system, along with the necessary circuits, is presented. In addition, the authors have also exploited the freedom provided by the system to choose any pump wavelength to selectively modulate specific regions of the multilayer structure (QW, barrier, and cladding layer) and extract detailed information regarding the properties of each layer.

02,453
PB97-111462 Not available NTIS
National Inst. of Standards and Technology (EEEL), Gaithersburg, MD. Semiconductor Electronics Div.
Mechanism of Defect Formation in Low-Dose Oxygen Implanted Silicon-on-Insulator Material.
Final rept.
S. Bagchi, J. D. Lee, S. J. Krause, and P. Roitman. 1996, 6p.
Pub. in Jnl. of Electronic Materials, v25 n1 p7-12 1996.

Keywords: *Silicon islands, *Defect formation, Dislocation half-loop, Stacking fault pyramide, Threading dislocation, Reprints, SIMOX.

The defects and microsructure of low-dose (less than 0.7 x 10 to the 18th power cm to the minus 2 power), oxygen-implanted silicon-on-insulator (SIMOX) material were investigated as a function of implant dose and

annealing temperature by plan-view and cross-sectional transmission electron microscopy. The threading-dislocations in low-dose (0.2 approximately 0.3 x 10 to the 18 power cm to the minus 2 power), annealed SIMOX originate from unfaulting of long (approximately 10 micrometer), shallow (0.3 micrometer), extrinsic stacking faults generated during the ramping stage of annealing. As dose increases, the defect density is reduced and the structure of the buried oxide layer evolves dramatically. It was found that there is a dose window which gives a lower defect density and a continuous buried oxide with a reduced density of Si islands and the buried oxide.

02,454
PB97-111827 Not available NTIS
National Inst. of Standards and Technology (EEEL), Gaithersburg, MD. Semiconductor Electronics Div.
Electrical Test Structures Replicated in Silicon-on-Insulator Material.
Final rept.
M. W. Cresswell, J. J. Sniegowski, R. N. Ghoshtagore, J. S. Villarrubia, R. A. Allen, and L. W. Linholm. 1996, 18p.
Pub. in Proceedings of Society of Photo-Optical Instrumentation Engineers Metrology, Inspection and Process Control for Microlithography X, Santa Clara, CA., March 10-15, 1996, v2725 p659-676.

Keywords: *Silicon, *Electrical measurement, *Calibration, Semiconductors(Materials), Integrated circuits, Line width, Test equipment, Standards, Microelectronics, Reprints, MEMS(Microelectromechanical systems), Microelectromechanical systems.

Measurements of the linewidths of submicrometer features made by different metrology techniques have frequently been characterized by differences of up to 90 nm. The purpose of the work reported here is to address the special difficulties that this phenomenon presents to the certification of reference materials for the calibration of linewidth-measurement instruments. Accordingly, a new test structure has been designed and fabricated, and has undergone preliminary tests. Its distinguishing characteristics are assured cross-sectional profile geometries with known side-wall slopes, surface planarity, and compositional uniformity when it is formed in mono-crystalline material at selected orientations to the crystal lattice. To allow the extraction of electrical linewidth, the structure is replicated in a silicon film of uniform conductivity which is separated from the silicon substrate by a buried oxide layer. The utilization of a silicon-on-insulator (SOI) substrate further allows the selective removal of substrate material from local regions below the reference features, thus facilitating measurements by optical and electron-beam transmission microscopy. The combination of planar feature surfaces having known side-wall slopes is anticipated to eliminate factors which are believed to be responsible for methods divergence in linewidth measurements, a capability which is a prerequisite for reliable certification of the linewidths of features on reference materials.

02,455
PB97-112296 Not available NTIS
National Inst. of Standards and Technology (EEEL), Gaithersburg, MD. Semiconductor Electronics Div.
Interdigitated Stacked P-I-N Multiple Quantum Well Modulator.
Final rept.
X. R. Huang, S. K. Cheung, A. N. Cartwright, A. L. Smirl, and W. F. Tseng. 1996, 3p.
Pub. in Institute of Electrical and Electronics Engineers Photonics Technology Letters, v8 n9 p1172-1174 Sep 96.

Keywords: *Quantum wells, *Optical absorption, *Modulators, Lasers, Interdigitated, Hetero, Reprints.

The authors demonstrate low-voltage operation of a strained InGaAs-GaAs interdigitated hetero n-i-p-i modulator (or stacked SEED) that is grown and fabricated using a shadow-mask growth technique for making the metal contacts to the n- and p-layers separately. An absorption change of 6 x 10 to the 3rd power cm to the minus 1 with an applied bias as low as approximately 1 V is observed in an unoptimized structure. Optical switching of the unbiased structure is also demonstrated.

02,456
PB97-119283 Not available NTIS
National Inst. of Standards and Technology (EEEL), Gaithersburg, MD. Semiconductor Electronics Div.
Micromachined Coplanar Waveguides in CMOS Technology.
Final rept.
V. Milanovic, M. Gaitan, E. D. Bowen, and M. E. Zaghloul. 1996, 3p.
Pub. in Institute of Electrical and Electronics Engineers Microwave and Guided Wave Letters, v6 n10 p380-382 Oct 96.

Keywords: *CMOS, *Micromachining, *Coplanarity, *Waveguides, Lossy media, Transmission loss, Phase velocity, Magnetic dispersion, Substrates, Silicon, Reprints.

Coplanar waveguides were fabricated in standard complimentary metal-oxide semiconductor (CMOS) with post-processing micromachining. IC's were designed with commercial CAD tools, fabricated through the MOSIS service, and subsequently suspended by maskless top-side etching. Absence of the lossy silicon substrate after etching results in significantly improved insertion loss characteristics, dispersion characteristics, ad phase velocity. Measurement were performed at frequencies from 1 to 40 GHz, before and after micromachining. These show improvement in loss characteristics of orders of magnitude.

02,457
PB97-122428 Not available NTIS
National Inst. of Standards and Technology (EEEL), Gaithersburg, MD. Semiconductor Electronics Div.
Application of the Collocation Method in Three Dimensions to a Model Semiconductor Problem.
Final rept.
J. F. Marchiando. 1996, 12p.
Pub. in International Jnl. for Numerical Methods in Engineering, v39 p1029-1040 1996.

Keywords: *Semiconductors, *Collocation, Mathematical models, Three dimensional, Boundary value problems, Reprints, Poisson's equation.

A research code has been written to solve an elliptic system of coupled non-linear partial differential equations of conservation form on a rectangularly shaped three-dimensional domain. The code uses the method of collocation of Gauss points with tricubic Hermite piecewise continuous polynomial basis functions. The system of equations is solved by iteration. The system of non-linear equations is linearized, and the system of linear equations is solved by iterative methods. When the matrix of the collocation equations is duly modified by using a scaled block-limited partial pivoting procedure of Gauss elimination, it is found that the rate of convergence of the iterative method is significantly improved and that a solution becomes possible. The code is used to solve Poisson's equation for a model semiconductor problem. The electric potential distribution is calculated in a metal-oxide-semiconductor structure that is important to the fabrication of electron devices.

02,458
PB97-122527 Not available NTIS
National Inst. of Standards and Technology (EEEL), Gaithersburg, MD. Semiconductor Electronics Div.
Characterization of Time-Dependent Dielectric Breakdown in Intrinsic Thin SiO2.
Final rept.
J. S. Suehle, and P. Chaparala. 1996, 9p.
See also PB96-179478.
Pub. in Microelectronics Jnl., v27 p657-665 1996.

Keywords: *Dielectric breakdown, *Silicon dioxide, Temperature dependence, High temperature, Integrated circuits, Electric fields, Dielectric files, Thin films, Reprints, *Foreign technology.

Time-dependent dielectric breakdown data collected from 6.5-, 9-, 15-, 20-, and 22.5-nm-thick SiO2 films are presented. The failure distributions are of single mode with no apparent extrinsic population. The logarithm of the median-test-time-to-failure, log(t50) is described by a linear electric-field dependence. Contrary to reports in earlier studies, the field-acceleration parameter is observed to be insensitive to temperature and has a value to approximately 1.0 decade/Mv/cm for the range of oxide thicknesses studied. Capacitance-voltage studies indicate that there is no strong correlation between oxide trapped charges and time-to-failure under constant voltage stress conditions.

ENERGY

Batteries & Components

02,459
PB96-164231 Not available NTIS
National Inst. of Standards and Technology (EEEL), Gaithersburg, MD. Electronics and Electrical Engineering Lab. Office.
Rechargeable Batteries for Personal/Portable.
Final rept.
A. G. Lieberman, L. Eliason, and K. Higgins. 1995, 16p.
Sponsored by National Inst. of Justice, Washington, DC.
Pub. in Rechargeable Batteries for Personal/Portable Transceivers, NIJ Standard-0221.01, 16p Sep 95.

Keywords: *Test methods, *Requirements, *Nickel-cadmium batteries, *Radio equipment, Storage batteries, Performance tests, Transmitter receivers, Radio communication, Walkie talkies, Portable equipment, Reprints, *Rechargeable batteries.

The purpose of this document is to establish performance requirements and test methods for rechargeable (secondary) batteries used in personal/portable transceivers by law enforcement agencies. The scope of this standard is limited to nickel-cadmium secondary batteries.

Electric Power Production

02,460
PB94-161817 PC A03/MF A01
National Inst. of Standards and Technology (NEL), Gaithersburg, MD. Center for Building Technology.
Earthquake Resistant Construction of Electric Transmission and Telecommunication Facilities Serving the Federal Government Report.
F. Y. Yokel. Feb 90, 48p, NISTIR-89/4213, FEMA-202.
Sponsored by Federal Emergency Management Agency, Washington, DC.

Keywords: *Telecommunication, *Electric power generation, *Earthquake resistant structures, Seismic design, Design standards, Building codes, Telephone systems, Television systems, Radio communication, Computer networks, Transmission lines, Power transmission, Soil-structure interactions, Earthquake engineering, Lifeline systems.

The vulnerability of electrical transmission and telecommunication facilities to damage in past earthquakes, as well as available standards and technologies to protect these facilities against earthquake damage are reviewed. An overview is presented of measures taken by various Federal agencies to protect electrical transmission and telecommunication facilities against earthquake hazards. It is concluded that while most new facilities which are owned and operated by Federal agencies are presently designed to provide some, though not necessarily adequate, earthquake resistance, there generally is no effort to retrofit existing facilities. No evidence was found of requirements to protect electrical transmission and communication facilities which have major contractual obligations to serve the Federal Government and only limited seismic design requirements are stipulated for electrical transmission systems constructed with Federal funding.

02,461
PB95-188850 PC A03/MF A01
National Inst. of Standards and Technology (EEEL), Gaithersburg, MD. Electricity Div.
Evaluation of the Economic Impacts Associated with the NIST Power and Energy Calibration Services.
A. N. Link. Jan 95, 27p, NISTIR-5565.
See also DE94010428. Prepared in cooperation with North Carolina Univ. at Greensboro. Dept. of Economics.

Keywords: *Electric power, *Calibration, *Economic impacts, Benefit cost analysis, Government policies, Watt hour meters, Electric utilities, Evaluation, Power and Energy Calibration Project, Federal laboratories, US NIST.

It is well established in the economics literature that investments in measurement-related technology research by Federal laboratories represents an important resource commitment to the innovation process, and that these investments have a significant impact on economic growth. The purpose of this study is to identify, and quantify where possible, the net economic benefits associated with the NIST Power and Energy Calibration Project. The NIST services from the project that are considered in this report are: (1) maintenance of the national standard for the watthour; (2) research to lower the level of uncertainty associated with watthour revenue meters; (3) general technical support to industry associated with measurement activities. For this particular study, the calculation of a benefit-to-cost ratio is believed to be the most reliable evaluation metric. This ratio is computed as the ratio of benefits (received by economic units directly dependent on the activities of the NIST power and energy calibration services) to the costs to society to generate those benefits, namely the cost to operate the Power and Energy Calibration Project. An alternative metric, an internal rate of return measure, is also presented in this report in order to facilitate a comparison of the benefit-to-cost result to the results from similar studies.

02,462
PB96-147913 PC A05/MF A01
National Inst. of Standards and Technology (EEEL), Gaithersburg, MD. Electricity Div.
Technical Impact of the NIST Calibration Service for Electrical Power and Energy.
J. D. Ramboz, and F. D. Martzloff. Dec 95, 68p, NISTIR-5564.
See also PB95-188850.

Keywords: *Electric power meters, *Electrical measurement, *Calibration, Economic analysis, Watt hour meters, Standards, Power measurement, Electric utilities, NIST(National Institute of Standards and Technology).

A survey was conducted to assess the economic impact of the NIST Power and Energy Calibration service. Information was sought from electric utilities, manufacturers, testing laboratories, and Public Utilities Commissions on the structure of their operations and the economic aspects of the existence of traceability to National Standards by NIST. The information returned by the respondents was not sufficiently comprehensive and consistent to allow broad generalization leading to reliable assessment of the economic impact of the NIST services. However, the technical impact of these services was sufficiently documented to present this report describing the infrastructure and the relationships among the stakeholders.

Electric Power Transmission

02,463
PB94-172061 Not available NTIS
National Inst. of Standards and Technology (EEEL), Gaithersburg, MD. Electricity Div.
Coordinating Cascaded Surge Protection Devices: High-Low versus Low-High.
Final rept.
J. S. Lai, and F. D. Martzloff. 1993, 8p.
Pub. in Institute of Electrical and Electronics Engineers Transactions on Industry Applications 29, n4 p680-687 Jul/Aug 93. See also PB92-159664.

Keywords: *Cascaded elements, *Circuit protection, *Surges, Reliability(Electronics), Varistors, Standards, Electric fuses, Coordination, Reprints.

Cascading surge protection devices located at the service entrance of a building and near the sensitive equipment is intended to ensure that each device shares the surge stress in an optimum manner to achieve reliable protection of equipment against surges impinging from the utility supply. However, depending on the relative clamping voltages of the two devices, their separation distance, and the waveform of the impinging surges, the coordination may or may not be effective. The paper provides computations with experimental verification of the energy deposited in the devices for a matrix of combinations of these three parameters. Results show coordination to be effective for some combinations and ineffective for some others, which is a finding that should reconcile contradictory conclusions reported by different authors making different assumptions. From these results, improved coordination can be developed by application standards writers and system designers.

02,464
PB94-216488 Not available NTIS
National Inst. of Standards and Technology (EEEL), Gaithersburg, MD. Electricity Div.
Cascading Surge-Protective Devices: Options for Effective Implementation.
Final rept.
F. D. Martzloff, and J. S. Lai. 1992, 8p.
Sponsored by Electric Power Research Inst., Palo Alto, CA.
Pub. in Proceedings of International Conference on Power Quality (2nd): End-Use Applications and Perspectives, Atlanta, GA., September 28-30, 1992, pC-11:1-C-11:8.

Keywords: *Cascaded elements, *Circuit protection, *Surges, Arresters, Computerized simulation, Standards, Overvoltage, Reprints.

The basic and critical parameters for a successful coordination of cascaded surge-protective devices include the relative voltage clamping of the two devices, their electrical separation through wiring inductance, and the actual waveform of the impinging surge. The authors examine in detail the implications of the situation resulting from the present uncoordinated application of devices with low clamping voltage at the end of branch circuits and devices with higher clamping voltage at the service entrance. As an alternative, several options are offered for discussion, that might result in effective, reliable implementation of the cascaded protection concept.

02,465
PB94-216496 Not available NTIS
National Inst. of Standards and Technology (EEEL), Gaithersburg, MD. Electricity Div.
Coordinating Cascaded Surge-Protective Devices: An Elusive Goal.
Final rept.
F. D. Martzloff, and J. S. Lai. 1992, 4p.
Pub. in Electrical Business, p1-4 Sep 92.

Keywords: *Cascaded elements, *Circuit protection, *Surges, Reliability(Electronics), Overvoltage, Lightning protection, Standards, Reprints.

Cascading two or more surge-protective devices located at the service entrance of a building and near sensitive load equipment is done to ensure that each device shares the surge stress in a manner commensurate with its rating. The final purpose is to achieve reliable protection of equipment against surges impinging from the utility supply, as well as internally generated surges. Coordination may or may not be effective, depending upon the relative clamping voltages of the two devices, their separation distance, and the waveform of the impinging surge. The article presents the results of computations, confirmed by measurements of the energy deposited in the devices for combinations of these three parameters. From these results, a suggestion is made on a possible approach to a coordinated scheme. However, without consensus among interested parties, some questions remain on the likelihood of ensuring coordination for all possible circumstances.

Engine Studies (Energy Related)

02,466
PB95-200218 PC A07/MF A02
Southwest Research Inst., San Antonio, TX. Engine, Fuel, and Vehicle Research Div.
Evaluation of Wear Resistant Ceramic Valve Seats in Gas-Fueled Power Generation Engines. Topical Report, December 1991-April 1994.
R. W. Burrahm, R. J. Branecky, P. C. Sui, M. C. Shen, J. P. Latusek, and S. M. Hsu. Dec 94, 127p, SWRI-4770, GRI-94/0411.
Contract GRI-5091-288-2319
Color illustrations reproduced in black and white. Prepared in cooperation with National Inst. of Standards and Technology (MSEL), Gaithersburg, MD. Ceramics Div. Sponsored by Gas Research Inst., Chicago, IL.

Keywords: *Ceramics, *Wear resistance, *Engine wear, *Engine valves, *Diesel engines, *Electric generators, Life cycle costs, Engine failures, Economic analysis, Maintenance costs, Structural analysis, Finite element method, Natural gas.

This project is directed at the reduction of valve recession in natural gas-fueled engines. Ceramic valve seat inserts have been procured, installed in a Caterpillar G3516 natural gas generator set, and tested for 1000 hours. Two different silicon nitride materials are being utilized for the valve seats in addition to stock Eatonite metallic inserts. Three valve face materials are being tested. These include stock Caterpillar stellite 1 faced, stellite 6 faced, and unfaced valves. A test matrix was used to allow comparison of all three valve face materials in combination with all three insert materials. The testing is scheduled to continue for an additional 7000 hours. No problems have been encountered with the test materials. In general, it has been shown that two types of silicon nitride materials have at least short term durability in engine operation. Neither material has exhibited any deficiencies thus far. An economic analysis spreadsheet has been created to calculate potential cost savings potential using ceramic valve seat inserts. Valve recession data for the first 1000 hours shows expected trends. Exhaust valve positions are wearing more than intake valve positions. If the intake positions and all positions with unfaced valve are ignored, then ceramic inserts paired with Stellite 1 valves show the most wear.

Environmental Studies

02,467
PB94-212388 Not available NTIS
National Inst. of Standards and Technology (EEEL), Gaithersburg, MD. Electricity Div.
Investigation of S2F10 Production and Mitigation in Compressed SF6-Insulated Power Systems.
Final rept.
D. R. James, I. Sauers, G. D. Griffin, K. L. Stricklett, F. Y. Chu, J. R. Robins, H. D. Morrison, R. J. Van Brunt, and J. K. Olthoff. 1993, 13p.
Pub. in Institute of Electrical and Electronics Engineers Electrical Insulation Magazine 9, n3 p29-40, 51, May/Jun 93.

Keywords: *Sulfur fluorides, *Electric power distribution, *Insulation, *Toxic substances, *Circuit breakers, Air pollution, Electrical insulation, Byproducts, Operation, Maintenance, Electric discharges, Reprints.

A Cooperative Research and Development Agreement (CRADA) has been established to study the production and mitigation of S2F10 (disulfur decafluoride), one of a number of toxic by-products formed in electrical discharges in the insulating gas SF6. The particular concern for S2F10 is due to its highly toxic nature, the Ceiling Limit Value being 10 parts per billion (ppb, or 1 part in 10 to the 8th power) and the need for development of sensitive detection techniques down to this level. There are a large number of SF6 gas-insulated electric power systems already in service in North America, particularly circuit breakers. SF6 is extensively used as an insulation and current interruption medium in power circuit breakers, compressed gas transmission lines and various components in substations. Ensuring the safe operation and maintenance of this equipment is an important issue for utilities, government agencies, and manufacturers.

02,468
PB96-155528 Not available NTIS
National Inst. of Standards and Technology (EEEL), Gaithersburg, MD. Electricity Div.
Investigation of S2F10 Production and Mitigation in Compressed SF6- Insulated Power Systems.
Final rept.
I. Sauers, G. D. Griffin, D. R. James, K. L. Stricklett, H. D. Morrison, F. Y. Chu, M. F. Frechette, R. J. Van Brunt, and J. K. Olthoff. 1995, 27p.
See also PB94-212388. Sponsored by Electric Power Research Inst., Palo Alto, CA. and Department of Energy, Washington, DC.
Pub. in Oak Ridge National Laboratory, Oak Ridge, Tennessee Report No. ORNL/M-4314, v1 27p Oct 95.

Keywords: *Sulfur fluorides, *Electric power distribution, *Insulation, Toxic substances, Circuit breakers, Reprints, Air pollution, Electrical insulation.

A Cooperative Research and Development Agreement (CRADA) was established in 1991 to study the production and mitigation of S2F10 (disulfur decafluoride), one of a number of toxic by-products formed by electrical discharges in the insulating gas SF6. Since compressed SF6 is extensively used as an insulation and current interruption medium in electric power equipment, ensuring the safe operation and maintenance of this equipment is an important issue for utilities, government agencies, and manufacturers. The particular concern for S2F is due to (1) its highly toxic nature: the Threshold Limit Value - Ceiling (TLV-C) is 10 ppbv (1 ppbv = 1 part in 10 to the 9th power by volume = 1nL/L), the level which can not be exceeded during any part of the working exposure; and (2) the lack of sensitive detection techniques down to the TLV-C.

Fuels

02,469
AD-A279 952/6 PC A09/MF A02
National Bureau of Standards, Gaithersburg, MD.
National Standard Petroleum Oil Tables.
4 Mar 36, 185p.

Keywords: *Oils, *Standards, Petroleum industry, Scale, Specific gravity, Densimeters, Tables(Data), Weight, Temperature.

The tables given are based on an investigation of American petroleum oils carried out by the National Bureau of Standards, and the arrangement is largely according to the recommendations of a committee appointed by the American Petroleum Institute to represent the petroleum industry. In order to overcome the confusion that has existed in the petroleum-oil industry by reason of the use of two so-called Baume scales for light liquids, the American Petroleum Institute, the U. S. Bureau of Mines, and the National Bureau of Standards, in December 1921, agreed to recommend that in the future only the scale based on the modulus 141.5 be used in the petroleum-oil industry, and that it be known as the A. P. I. scale. The relation of degrees A. P. I. to specific gravity is expressed by the formula.

02,470
DE94004399 PC A02/MF A01
National Inst. of Standards and Technology (CSTL), Gaithersburg, MD.
Development of Measurement Capabilities for the Thermophysical Properties of Energy-Related Fluids. Annual Report, December 1, 1990--November 30, 1991.
Progress rept.
1991, 10p, DOE/ER/13823-T2.
Contract AI05-88ER13823
Sponsored by Department of Energy, Washington, DC.

Keywords: *Liquid Fuels, *Lubricants, *Measuring Instruments, *Refrigerants, *Working Fluids, Aqueous Solutions, Calorimetry, Densimeters, Density, Design, Dielectric Properties, Enthalpy, Phase Studies, Physical Properties, Progress Report, Thermal Conductivity, Thermodynamic Properties, Viscosimeters, Viscosity, *Thermophysical properties, EDB/400102, EDB/440800.

The objectives of this project are to develop state-of-the-art experimental apparatus that can be used to measure the thermophysical properties of a wide range of fluids and fluid mixtures important to the energy, chemical, and energy-related industries and to carry out carefully selected benchmark measurements on key systems. The measurement capabilities to be developed include new apparatus for transport properties, thermodynamic properties, phase equilibria properties, and dielectric properties. The specific measurement capabilities to be developed are: thermal conductivity apparatus; vibrating wire viscometer; dual-sinker densimeter; high-temperature vibrating tube densimeter; dynamic phase equilibria apparatus; apparatus for dilute solutions; total-enthalpy flow calorimeter; and dielectric constant apparatus. The research also includes benchmark experimental measurements on pure and mixed alternative refrigerants and their mixtures with lubricants, on aqueous solutions, and on carefully selected systems consisting of species of diverse size (methane + neopentane) and polarity (methane + ammonia) that are important for the development of predictive models for energy-related fluids.

02,471
DE94008991 PC A02/MF A01
National Inst. of Standards and Technology, Boulder, CO. Thermodynamics Div.
Low Temperature H(sub 2)S Separation Using Membrane Reactor with Redox Catalyst.
J. J. Pellegrino, M. Ko, and L. Watts. 1993, 9p, CONF-931156-41.
Contract AI21-86MC23120
Fuels Technology Contractors' Review Meeting, Morgantown, WV (United States), 16-18 Nov 1993. Sponsored by Department of Energy, Washington, DC.

Keywords: *Chemical Reactors, *Desulfurization, *Natural Gas, *Separation Processes, Hydrogen sulfides, Catalysts, Design, Membranes, Oxidation, Sodium Hydroxides, *Gas pipelines, EDB/030300.

A low temperature redox catalyst is combined with an H(sub 2)S selective membrane to create a composite-catalytic-membrane-reactor (CCMR) to help reach pipeline-quality natural gas H(sub 2)S levels of below 4 ppM. The goal of this program is to identify the apparent kinetic and mass transfer parameters for the CCMR. Using these kinetic and mass transfer parameters a preliminary process design can be made to ascertain the potential of this technology for replacement of conventional amine scrubbing and Claus sulfur recovery processes. In pursuit of this goal the project contains the following activities: construction of reactor and mass transfer equipment suitable for accurate measurements and safe handling of pure H(sub 2)S; initial proof-of-concept experiments with a prototype CCMR; obtain literature data and develop thermodynamic models for multicomponent natural gas components' solubility in electrolyte solutions; make physical and chemical measurements on the catalyst; obtain kinetic data using a 3-phase slurry reactor; obtain kinetic data for a catalytic membrane under varying mass transfer conditions; develop mathematical models to guide experimental work and for interpretation of results; optimize the permselective membrane part of the CCMR using commercially available materials; further proof-of-concept experiments with an optimized CCMR; and develop preliminary process design and economic analysis for the use of a CCMR in gas clean-up.

02,472
PB94-146677 PC A03/MF A01
National Inst. of Standards and Technology (CSTL), Boulder, CO. Thermophysics Div.
Thermophysical Properties of Fluids for the Gas Industry. Final Report, February 1, 1988-August 31, 1993.
T. J. Bruno, and W. M. Haynes. Nov 93, 20p, GRI-93/0396.
Contract GRI-5088-260-1700
See also PB93-207470. Sponsored by Gas Research Inst., Chicago, IL.

Keywords: *Fluids, *Thermophysical properties, *Natural gas, Gas industry, Equations of state, Experimental design, Mathematical models, Hydrocarbons, Detectors.

The U.S. gas industry standard for computing thermophysical properties is the A.G.A. Transmission Measurement Committee Report No. 8 equation of state (AGA 8). The report summarized the results from several experimental, theoretical, and modeling programs directed at the extensive evaluation of the accuracy with which various types of natural gas physical properties can be calculated using AGA 8 and related methods. The most important results were the assembly of benchmark data sets for speed of sound, viscosity, fugacity, heat capacity, critical region PVT, mixture compressibilities, and vapor pressure measurements for natural gas fluids.

02,473
PB94-193802 PC A08/MF A02
Purdue Univ., Lafayette, IN. Thermal Sciences and Propulsion Center.
Structure and Radiation Properties of Pool Fires.
Final rept. 1 Sep 91-31 Aug 92.
M. Klassen, and J. P. Gore. Aug 92, 156p, NIST/GCR-94/651.
Grant NIST-60NANB1D1169
Sponsored by National Inst. of Standards and Technology (BFRL), Gaithersburg, MD.

Keywords: *Radiative heat transfer, *Fuels, Burning rate, Combustion, Data analysis, Spectral emission, Burners, Heat flux, Soot, Heat measurement, *Pool fires.

An experimental and theoretical study of radiative feedback, burning rates, radiative heat loss fractions, and flame heights for pool fires with diameters ranging from 4.6 cm to 100 cm was completed. Transient measurements of soot and temperature distributions were obtained in 7.1 cm and 30 cm heptane and toluene fires using a three-wavelength emission/absorption probe. The heat release rates of the fires varied from 0.6 kW to 2,166 kW allowing a study over a wide range. A variety of fuels were tried but most of the measurements were restricted to methanol, heptane, and toluene as representatives of the alcohols, paraffins and aromatics. Radiative feedback was measured using a new in situ purged optical probe inserted at the level of the fuel surface. Measurements of reflection of energy from the fuel surface were also obtained.

02,474
PB94-199254 Not available NTIS
National Inst. of Standards and Technology (NML), Gaithersburg, MD. Chemical Thermodynamics Div.
Calculation of Higher Heating Values of Biomass Materials and Waste Components from Elemental Analyses.
Final rept.
T. J. Buckley. 1991, 13p.
Pub. in Resources, Conservation and Recycling 5, n4 p329-341 Aug 91.

Keywords: *Biomass, *Waste utilization, *Calorific value, *Hazardous materials, Comparison, Performance evaluation, Chemical analysis, Numerical analysis, Experimental design, Fuels, Reprints, Standard reference materials, Vondracek formula.

Higher heating values on a dry basis (HHV2) measured and those calculated from elemental analyses of over 140 biomass and waste component materials have been compared. The data was evaluated by six higher heating value formulas. The Vondracek formula was found to give the best agreement between calculated and measured heating values over a wide range (10 to 47 MJ/kg). This was evident by the good linear correlation between measured and calculated HHV2's. Standard reference materials also have been evaluated and shown generally to give good agreement. The calculation of higher heating values from elemental analyses is a good check for the reliability of a material's composition and heating value measurements in most cases. Materials with differences between calculated and measured higher heating values in excess of 6 percent should be considered suspect and examined closely.

02,475
PB94-206646 PC A05/MF A02
Southwest Research Inst., San Antonio, TX. Nondestructive Evaluation Science and Technology Div.
Assessment of Technology for Detection of Stress Corrosion Cracking in Gas Pipelines. Final Report, July 1993-March 1994.
A. E. Crouch, C. M. Teller, J. L. Fisher, G. M. Light, and C. M. Fortunko. Apr 94, 99p, GRI-94/0145.
Contract GRI-5093-271-2639
Prepared in cooperation with National Inst. of Standards and Technology, Boulder, CO. Sponsored by Gas Research Inst., Chicago, IL.

Keywords: *Nondestructive tests, *Natural gas pipelines, *Stress corrosion, Cracking(Fracturing), Wipers, Inspection, Technology assessment, Electromagnetic waves, ILI(In-line inspection), Smart pigs.

The objective of the project was to assess the nondestructive evaluation (NDE) technology that may be applied to natural gas steel pipelines for the detection of stress corrosion cracking (SCC). In particular, the application of such technology would be from the inside of the pipe while the pipeline is in service, and inspection commonly called in-line inspection (ILI). The assessment focused on two basic NDE methods, ultrasonics and electromagnetics (including magnetic flux leakage). A third technology was data acquisition/analysis systems. Based on the experience of British Gas (BG) and others doing SCC inspections in different industries, crack discrimination is the important challenge for any such inspection system.

02,476
PB94-211596 Not available NTIS

National Inst. of Standards and Technology (NEL), Gaithersburg, MD. Fire Science and Engineering Div.
Estimate of Flame Radiance via a Single Location Measurement in Liquid Pool Flames.
Final rept.
A. Hamins, M. Klassen, J. Gore, and T. Kashiwagi. 1991, 6p.
Pub. in Combustion and Flame 86, n3 p223-228 1991.

Keywords: *Radiative heat transfer, *Fuels, *Flames, *Heat loss, Radiative transfer, Heat transmission, Radiant heating, Combustion, Heat flux, Reprints, *Pool fires.

A method for estimating the radiative heat loss fraction is developed for non-premixed flames in a poor fire configuration. An experimental investigation of small to intermediate pool flames shows that a particular location can be determined such that a single radiance measurement yields an adequate estimate of the radiative heat loss fraction. The procedure is tested on a variety of fuels which yield flames over a wide range of luminosities and values of radiative heat loss fraction.

02,477
PB94-211604 Not available NTIS
National Inst. of Standards and Technology (NEL), Gaithersburg, MD. Fire Science and Engineering Div.
Measurement of Radiative Feedback to the Fuel Surface of a Pool Fire.
Final rept.
A. Hamins, M. Klassen, J. Gore, and T. Kashiwagi. 1990, 4p.
Pub. in Chem. Phys. Processes Combust., p58/1-58/4 1990.

Keywords: *Radiative heat transfer, *Fuels, *Surfaces, Radiant heating, Heat flux, Radiative transfer, Heat transmission, Methanol, Combustion, Reprints, *Pool fires, *Heat feedback.

The measurement of the radiative heat feedback to the fuel surface of fires burning in a pool fire configuration is discussed. Radiative feedback in a 30cm methanol pool is compared to total heat feedback. Measurements show that the radiative flux decreases from pool center towards the pool edge.

02,478
PB95-108544 Not available NTIS
National Inst. of Standards and Technology (NML), Gaithersburg, MD. Chemical Process Metrology Div.
Combustion of Methanol and Methanol/Dodecanol Spray Flames.
Final rept.
C. Presser, A. K. Gupta, C. T. Avedisian, and H. G. Semerjian. 1992, 7p.
Pub. in Jnl. of Propulsion and Power 8, n3 p553-559 May/Jun 92.

Keywords: *Methanol, *Combustion, *Spraying, *Flame propagation, Lasers, Velocity distribution, Drops(Liquids), Interferometry, Mixtures, Size determination, Reprints.

The structure of methanol and methanol/dodecanol mixture spray flames has been examined. The mixture was studied in order to obtain evidence for the occurrence of microexplosions. Droplet size and velocity measurements were carried out under burning conditions using phase/Doppler interferometry. Laser sheet beam photography was used to observe the global features of the spray within the nonluminous portion of the flames. Droplet size and velocity distributions near the nozzle exit were found to be similar and monomodal for both fuels. Further downstream in the mixture flame the velocity distribution became bimodal near the spray boundary along with a change in size distribution to smaller droplets and an increase in number density. These results suggest that microexplosions may occur in 50/50 mixtures of methanol/dodecanol spray flames.

02,479
PB95-108551 Not available NTIS
National Inst. of Standards and Technology (NML), Gaithersburg, MD. Chemical Process Metrology Div.
Study of Droplet Transport in Alcohol-Based Spray Flames Using Phase/Doppler Interferometry.
Final rept.
C. Presser, A. K. Gupta, C. T. Avedisian, and H. G. Semerjian. 1990, 5p.
Pub. in Proceedings of Annual Conference Extended Abstracts ILASS-Americas (4th), Hartford, CT., May 21-23, 1990, p243-247 1990.

Keywords: *Alcohol fuels, *Atomization, *Spraying, *Transport, *Flame propagation, Vaporization, Combustion, Combustion products, Particulates, Inteferometry, Reprints.

Studies with alternative fuels (i.e., methanol and ethanol) are of particular interest because of the current initiative to gradually replace the limited supply of conventional fossil fuels (i.e., gasoline, heating oils, etc.). Alcohol-based fuels are attractive, since they burn more cleanly and represent a potential to reduce the environmental impact of combustion processes. Investigation of the effect of alcohol fuels on spray and flame characteristics (i.e., droplet size and velocity) is important since chemical and physical properties of the fuel have a significant influence upon droplet atomization, vaporization, transport, combustion, and pollutant and particulate formation processes. The paper examines the effects of physical and chemical properties of two alcohol fuels on droplet transport processes of swirling spray flames. Experiments were carried out with methanol and a miscible mixture of methanol/1-dodecanol. The mixture fuel was selected to investigate the possibility of microexplosions in spray flames. Droplet size and velocity distributions were obtained using a phase/Doppler system. Laser sheet beam photography was also used to observe the internal features of pressure-atomized spray flames.

02,480
PB95-108569 Not available NTIS
National Inst. of Standards and Technology (NML), Gaithersburg, MD. Chemical Process Metrology Div.
Structure of a Swirl-Stabilized Kerosene Spray Flame.
Final rept.
C. Presser, A. K. Gupta, and H. G. Semerjian. 1990, 4p.
Sponsored by Department of Energy, Washington, DC.
Pub. in Proceedings of Fall Technical Meeting Chemical and Physical Processes in Combustion, Orlando, FL., December 3-5, 1990, p81-1-81-4.

Keywords: *Kerosene, *Swirling, *Spraying, *Flames, Velocity distribution, Atomization, Drops(Liquids), Laser doppler velocimeters, Combustion, Reprints.

The interaction of the fuel spray with the surrounding combustion air, in particular near the spray boundary, affects its combustion and emission characteristics. Near the spray boundary, droplets of many different sizes, traveling at different velocities, are expected to be found. In addition, combustion air swirl affects fuel/air mixing and modifies the entire spray pattern. Therefore, spatially and temporally resolved information about the effect of swirl on droplet properties, especially near the spray boundary, is important for understanding the structure of sprays and spray flames. The results presented demonstrate the strong interaction between the spray droplets and the combustion air flow, which significantly modifies the flame structure. They also demonstrate the need to assess the effect of instrument characteristics, such as dynamic range and system gain, on the measurements for determination of accurate mean flow properties.

02,481
PB95-126314 Not available NTIS
National Inst. of Standards and Technology (NEL), Gaithersburg, MD. Structures Div.
Ashland Tank Collapse Investigation.
Final rept.
J. L. Gross, J. H. Smith, and R. N. Wright. 1989, 19p.
See also PB95-126322.
Pub. in Jnl. of Performance of Constructed Facilities 3, n3 p144-162 Aug 89.

Keywords: *Storage tanks, *Structural failure, *Steel structurers, *Fractures(Materials), *Steels, *Brittleness, *Accident investigations, Crack propagation, Structural analysis, Welded joints, Fracture strength, Toughness, Pennsylvania, Cracking(Fracturing), Fuel tanks, Construction materials, Fuel oils, Collapse, Reprints, *Welded steel tanks, *Floreffe Terminal, Ashland Petroleum Company, Reconstruction.

On January 2, 1988, a four million gallon capacity oil storage tank at the Ashland Petroleum Company Floreffe Terminal near West Elizabeth, Pennsylvania, collapsed as it was being filled to capacity for the first time since its reconstruction. The tank had been dismantled in Cleveland, Ohio, after more than 40 years of service and reconstructed at the Floreffe site in 1986. The National Institute of Standards and Technology (NIST) conducted an independent investigation into the physical cause of the Ashland tank collapse. It was determined that the failure was caused by a brittle fracture of the tank shell that initiated from a defect which existed prior to reconstruction of the tank. Complete rupture of the tank shell occurred because the steel did not possess adequate toughness at the operating temperature to prevent brittle fracture propagation. The collapse shows the importance of using steel with sufficient fracture toughness to prevent propagation of a brittle fracture in tanks whose sudden failure would mean unacceptable human, environmental or economic losses.

02,482
PB95-126322 Not available NTIS
National Inst. of Standards and Technology (NEL), Gaithersburg, MD. Structures Div.
Ashland Tank-Collapse Investigation: Closure by Authors.
Final rept.
J. L. Gross, J. H. Smith, and R. N. Wright. 1991, 2p.
See also PB95-126314.
Pub. in Jnl. of Performance of Constructed Facilities 5, n2 p150-151 May 91.

Keywords: *Storage tanks, *Structural failure, *Steel structures, *Fractures(Materials), *Steels, *Brittleness, *Accident investigations, Crack propagation, Structural analysis, Welded joints, Fracture strength, Toughness, Pennsylvania, Cracking(Fracturing), Fuel tanks, Construction materials, Fuel oils, Collapse, Reprints, *Welded steel tanks, *Floreffe Terminal, Ashland Petroleum Company, Reconstruction.

This Closure addresses several issues raised in a discussion of the paper titled, 'Ashland Tank Collapse Investigation,' (PB95-126314) which appeared in the Journal of Performance of Constructed Facilities, ASCE. That article related to the structural failure of a four million gallon capacity oil storage tank at the Ashland Petroleum Company Floreffe Terminal as it was being fueled to capacity for the first time since its reconstruction.

02,483
PB95-136644 PC A03/MF A01
National Inst. of Standards and Technology (CSTL), Boulder, CO. Thermophysics Div.
Constituents and Physical Properties of the C6+ Fraction of Natural Gas. Topical Report, April-June 1994.
T. J. Bruno. Aug 94, 40p, NISTIR-5212, GRI-94/0274.
Contract GRI-5093-260-2720
Sponsored by Gas Research Inst., Chicago, IL.

Keywords: *Natural gas, *Chemical composition, *Physical properties, Data bases, Gas chromatography, Chemical analysis, Quality assurance, Thermophysical properties, Hydrocarbons, Thermodynamics, Odorants, Treatment compounds.

The U.S. gas industry relies upon gas chromatographic analysis to obtain detailed gas compositional information needed for determining phase equilibrium behavior, thermophysical properties, and compliance with gas quality and safety engineering specifications. Analysis of the C(6+) fraction constituents of natural gas is technically complex and expensive. The assembly of a physical properties database for known C(6+) fraction constituents is needed to facilitate the development of improved chromatographic separation procedures for analyzing raw and processed natural gas streams for compliance with gas quality and end use specifications. The report provides a critically reviewed compilation of physical properties data for 132 hydrocarbon compounds identified as being native constituents of natural gas, 21 gas treatment compounds, and 23 gas odorant compounds.

02,484
PB95-140950 Not available NTIS
National Inst. of Standards and Technology (MSEL), Gaithersburg, MD. Polymers Div.
Chemical and Microbiological Problems Associated with Research on the Biodesulfurization of Coal.
Final rept.
G. J. Olson, and R. M. Kelly. 1991, 11p.
Pub. in Resources, Conservation and Recycling 5, n2-3 p183-193 Apr 91.

Keywords: *Coal, *Desulfurization, *Biological treatment, *Air pollution abatement, *Sulfur inorganic compounds, *Sulfur organic compounds, Microorganisms, Microbiology, Biochemistry, Chemistry, Removal, Thermophiles, Reprints.

The study of microbial processes for the removal of organic and inorganic sulfur from coals is complicated by the lack of direct methods of measurement for organic sulfur content and the related incomplete understanding of the specific forms of organic sulfur in coal. In addition, the accessibility of specific chemical groups in the coal matrix to microorganisms and their enzymes is uncertain, raising questions about the nature and validity of model compound studies. Thus, interpretation of data from numerous efforts focused on the microbial removal of inorganic and organic sulfur from coals remains controversial. The discussion here reviews recent developments in the chemical characterization of coal sulfur related to bioprocessing research and describes some of our recent efforts in involving sulfur transformations by hyperthermophilic archaebacteria.

02,485
PB95-141099 Not available NTIS
National Inst. of Standards and Technology (CSTL), Boulder, CO. Thermophysics Div.
Process Gas Chromatography Detector for Hydrocarbons Based on Catalytic Cracking.
Final rept.
S. L. Outcalt, H. Ingham, and T. J. Bruno. 1992, 13p.
Sponsored by Gas Research Inst., Chicago, IL.
Pub. in Process Control and Quality 2, p357-369 1992.

Keywords: *Thermopiles, *Gas chromatography, *Catalytic cracking, *Hydrocarbons, *Detectors, Fuels, Temperature measurement, Thermocouples, Catalysis, Reprints, *Hydrocarbon detectors.

A detector has been designed and built for the gas chromatographic detection of hydrocarbon species, especially in plant or on-line applications. Detection of the temperature change that occurs as a result of the catalytic cracking of hydrocarbons is the functional basis of the detector. The main component of this detector is a thermopile bundle constructed with type-K thermocouple wire. The sensing junctions of the thermopile are coated with a catalyst made up of a silicon dioxide-aluminum oxide-zeolite mixture. The temperature change associated with catalytic cracking occurs predominantly on the catalyst surface and is measured by the thermopile. The thermopile is directly connected to an electronic integrator, and provides a signal as a result of the temperature change. The tests that were performed to characterize the performance capabilities of the detector are reported. In addition, variable parameters were studied to determine the optimal conditions for obtaining the greatest sensitivity of the detector. The catalytic cracking detector is a very simple, inexpensive, and rugged device and is proposed as a potential alternative to other detectors for use in field or plant environments.

02,486
PB95-150447 Not available NTIS
National Inst. of Standards and Technology (BFRL), Gaithersburg, MD. Fire Safety Engineering Div.
Estimate of the Effect of Scale on Radiative Heat Loss Fraction and Combustion Efficiency.
Final rept.
J. C. Yang, A. Hamins, and T. Kashiwagi. 1994, 6p.
Pub. in Combustion Science and Technology 96, p183-188 1994.

Keywords: *Burning rate, *Thermal radiation, *Heat loss, *Scaling factor, *Fuel combustion, *Combustion efficiency, Flames, Radiative heat transfer, Heat transmission, Diameters, Combustion control, Reprints, *Pool fires, *Flame height, Fuel fires.

The effect of fire size on radiative heat loss fraction kappa(sub r) and combustion efficiency kappa(sub a) was examined by an analysis of scale for pool flames with varying diameter (D). Correlations between D and kappa(sub r) or kappa(sub a) were obtained. For 0.1m < D < 1m, kappa(sub r) and kappa(sub a) are relatively constant and independent of D. For larger pool diameters, kappa(sub r) decreases with increasing D.

02,487
PB95-150900 Not available NTIS
National Inst. of Standards and Technology (NEL), Gaithersburg, MD. Fire Measurement and Research Div.
Optical Measurements of Atomic Hydrogen, Hydroxyl, and Carbon Monoxide in Hydrocarbon Diffusion Flames.
Final rept.
P. J. H. Tjossem, and K. C. Smyth. 1988, 4p.
Pub. in Chem. Phys. Processes Combust., p8/1-8/4 1988.

Keywords: *Diffusion flames, *Laser induced fluorescence, *Hydrogen, *Hydroxyl radicals, *Hydrocarbons, *Carbon monoxide, Methane, Ionization, Concentration(Composition), Multiphoton absorption, Polarization, Reprints.

Recent quantitative OH(-) measurements and relative data for H atoms and CO are presented for a CH4/air diffusion flame. These results have been obtained using absorption, laser-induced fluorescence, and multiphoton ionization technique.

02,488
PB95-163374 Not available NTIS
National Bureau of Standards (IMSE), Gaithersburg, MD. Polymers Div.
Microbial Degradation of Polysulfides and Insights into Their Possible Occurrence in Coal.
Final rept.
L. Tilstra, G. J. Olson, G. Eng, and R. M. Kelly. 1990, 16p.
Pub. in Proceedings of International Symposium on the Biological Processing of Coal (1st), Orlando, FL., May 1-3, 1990, p3.27-3.42.

Keywords: *Microbial degradation, *Biodeterioration, *Polysulfides, *Coal, *Air pollution abatement, Desulfurization, Sulfur-oxidizing bacteria, Thiobacillus oxidans, Reduction(Chemistry), Oxidation, Biological treatment, Microorganisms, Reprints, Sulfur reducing bacteria.

Sulfur-oxidizing mesophilic (Thiobacillus thiooxidans) and sulfur-reducing hyperthermophilic (pyrococcus, Pyrodictium and others) bacteria are used as probes of specific forms of sulfur coal. When these bacteria are grown in medium with elemental sulfur or simple polysulfides (e.g., methyl trisulfide, cystine), easily measured products which are diagnostic of desulfurization are produced. As part of this research, we have synthesized model compounds which might more closely approximate some of the forms in which sulfur occurs in coal. These include: (1) organic sulfur model compounds which have bulky chemical groups surrounding the sulfur atoms and (2) polymeric polysulfides. Tests on these polysulfides will clarify the ability of the above bacteria to oxidize or reduce various forms of sulfur. The studies are also providing information as to the potential for these microorganisms to serve as probes of specific functional groups in coal and for the microbiological removal of sulfur from coal. Our approach could be extended to studies of large model compounds containing sulfur in other types of linkages such as heterocyclic rings.

02,489
PB95-168449 Not available NTIS
National Inst. of Standards and Technology (TS), Gaithersburg, MD. Office of Standards Services.
Method of Sale for CNG Paves Way to Greater Public Acceptance.
Final rept.
C. S. Brickenkamp. 1994, 1p.
Pub. in Natural Gas Fuels Magazine, p47 Sep 94.

Keywords: *Compressed gases, *Sales, *Marketing, Gas fuels, Liquid fuels, Comparisons, Selling, Cost analysis, Market research, Alternative fuels, Reprints, *Gasoline gallon equivalent, Compressed natural gas.

The article describes the National Conference on Weights and Measures adoption of the Gasoline Gallon Equivalent (GGE) as the method of sale for compressed natural gas (CNG) when sold at reatil as an engine fuel. The GGE is defined as 5.660 Pounds CNG. This amount of CNG approximates the equivalent energy of a gallon of gasoline.

02,490
PB95-175188 Not available NTIS
National Inst. of Standards and Technology (CSTL), Boulder, CO. Thermophysics Div.
Measurement of Diffusion in Fluid Systems: Applications to the Supercritical Fluid Region.
Final rept.
T. J. Bruno. 1994, 5p.
Pub. in Jnl. of Thermophysics and Heat Transfer 8, n2 p329-333 1994.

Keywords: *Diffusion coefficient, *Aviation fuels, *Supercritical fluids, *Chromatography, Thermophysical properties, Diffusion, Concentration(Composition), Solubility, Binary mixtures, Chemical analysis, Nuclear magnetic resonance, Light scattering, Reprints.

In this article, the experimental procedures that are applicable to the measurement of diffusion in supercritical fluid solutions will be reviewed. This topic is of great importance to the proper design of advanced aircraft and turbine fuels, since the fuels on these aircraft may sometimes operate under supercritical fluid conditions. More specifically, we will consider measurements of the binary interaction diffusion coefficient D(sub 12) of a solute (species 1) and the solvent (species 2). In this discussion the supercritical fluid will be species 2, and the solute, species 1, will be at a relatively low concentration, sometimes approaching infinite dilution. After a brief introduction to the concept of diffusion, we will discuss in detail the use of chromatographic methods, and then briefly treat light scattering, nuclear magnetic resonance spectra, and physical methods.

02,491
PB95-175212 Not available NTIS
National Inst. of Standards and Technology (CSTL), Boulder, CO. Thermophysics Div.
Fugacity Coefficients of Hydrogen in (Hydrogen + Butane).
Final rept.
T. J. Bruno, and S. L. Outcalt. 1993, 10p.
Sponsored by Gas Research Inst., Chicago, IL.
Pub. in Jnl. of Chemical Thermodynamics 25, p1061-1070 1993.

Keywords: *Evanescence, *Hydrogen, *Butanes, *Fugacity, Thermodynamic properties, Permeability, Membranes, Gas flow, Transpiration, Binary mixtures, Reprints, *Fugacity coefficients.

The fugacity coefficients of hydrogen in (hydrogen + butane) were measured as a function of composition with a physical-equilibrium technique at (temperature, pressure) pairs of (433.15 K, 3.39 MPa), (473.15 K, 3.38 MPa), (473.15 K, 22.65 MPa), and (523.15 K, 3.42 MPa). The physical-equilibrium technique involved the use of an experimental chamber that was divided into two separate regions by a semipermeable membrane through which hydrogen, but not butane, could permeate. Measurement of the gas pressures on each side of the membrane, in addition to a measurement of the composition and the system temperature, allowed the calculation of the fugacity and fugacity coefficient of hydrogen in the mixture. The qualitative features of the measurements are discussed, and comparisons are made with predictions obtained from the Redlich-Kwong and Peng-Robinson models.

02,492
PB95-253571 PC A03/MF A01
National Inst. of Standards and Technology (TS), Gaithersburg, MD. Weights and Measures Program.
Advanced Mass Calibration and Measurement Assurance Program for State Calibration Laboratories.
K. L. Fraley, and G. L. Harris. Jun 95, 28p, NISTIR-5672.

Keywords: *Mass, *Calibrating, *Design, *Standards, Metrology, Laboratories, State government, Surveillance, Precision, Measurement, *Mass standards, US NIST, Surveillance tests, Measurement assurance.

This publication provides guidelines for evaluating data from the advanced mass calibration and for establishing measurement assurance programs in state metrology laboratories. The NIST Office of Weights and Measures (OWM) will use these guidelines when evaluating data for laboratories requesting technical support or accreditation at this level.

02,493
PB95-256335 PC A04/MF A01
National Inst. of Standards and Technology, Gaithersburg, MD.
Sliding Vane Flow Conditioner Tests in a 100 Diameter Long 10 inch Natural Gas Orifice Meter at Pacific Gas and Electric. Topical Report, 1990-1992.
J. W. Stuart. Oct 92, 58p, GRI-92/0576.
Contract GRI-5088-271-1680
Prepared in cooperation with Pacific Gas and Electric Co., San Francisco, CA. Sponsored by Gas Research Inst., Chicago, IL.

Keywords: *Natural gas, *Orifice meters, *Flow measurement, Field tests, Gas flow, Vanes, Gas pipelines, High pressure, Technical assistance, Standards, Orifice flow, *Sliding vanes.

Sliding vane tests in a 10-inch, high pressure, natural gas test loop conducted at the Pacific Gas and Electric company in January 1991 are documented in this volume. The work is part of cooperative research in flow conditioning aimed offer technical support for revisions of industry standards in gas metering.

02,494
PB96-122437 Not available NTIS
National Inst. of Standards and Technology (CSTL), Boulder, CO. Thermophysics Div.
Thermophysical Properties of Fluids for the Gas Industry.
Final rept.
T. J. Bruno, and W. M. Haynes. 1992, 12p.
Contract GRI-5088-260-1700
See also PB94-146677. Sponsored by Gas Research Inst., Chicago, IL.
Pub. in Gas Research Institute Annual Report, Jan-Dec 92, 12p.

Keywords: *Fluids, *Thermophysical properties, *Natural gas, Gas industry, Equations of state, Experimental design, Mathematical models, Hydrocarbons, Detectors, Reprints.

The U.S. gas industry standard for computing thermophysical properties is the A.G.A. Transmisson Measurement Committee Report No. 8 equation of state (AGA 8). This report summarized the results from several experimental, theoretical, and modeling programs directed at the extensive evaluation of the accuracy with which various types of natural gas physical properties can be calculated using AGA 8 and related methods. The most important results were the assembly of benchmark data sets for speed of sound, viscocity, fugacity, heat capacity, critical region PVT, mixture compressibilities, and vapor pressure measurements for natural gas fluids. When tested against these benchmark properties data, the AGA 8 equation of state model was found to be generally accurate within plus or minus 0.1% for sound speeds (and densities) and within plus or minus 0.03% for compressibilities over the ranges of pressure, temperature, and composition that encompass the major region of custody transfer or natural gas. Work was also completed on the fabrication and testing of a prototype catalytic cracking detector for the selective detection of hydrocarbons; a U.S. patent was awarded for this invention with the assignment to GRI.

02,495
PB96-141379 Not available NTIS
National Inst. of Standards and Technology (CSTL), Gaithersburg, MD. Inorganic Analytical Research Div.
Determination of Sulfur in Fossil Fuels by Isotope Dilution Thermal Ionization Mass Spectrometry.
Final rept.
W. R. Kelly, P. J. Paulsen, K. E. Murphy, R. D. Vocke, and L. T. Chen. 1994, 9p.
Pub. in Analytical Chemistry, v66 n15 p2505-2513 Aug 94.

Keywords: *Fossil fuels, *Sulfur, *Chemical composition, Coal, Petroleum products, Kerosene, Chemical analysis, Mass spectroscopy, Isotope dilution, Ionization potential, Reprints, Standard reference materials.

Total sulfur has been measured in 13 petroleum and 14 coal Standard Reference Materials (SRMs) by isotope dilution thermal ionization mass spectrometry. Samples were spiked with enriched stable S-34 and conbusted in sealed Carius tubes using nitric and hydrochloric acids. The oxidized sulfur was reduced to H2S, precipitated as As2S3, and then dissolved in an ammoniacal solution of As2O3. A portion of this solution, equivalent to 1.5 micrograms of sulfur, was added to a single Re filament coated wth silica gel. The amount of sulfur in the samples was determined from the S-32/S-34 ratio by mesuring the As(75)S(32)/As(75)S(34) molecular ions in a Faraday detector. The total uncertainty (95 percent confidence interval) for homogeneous materials such as oils is about 0.5 percent, and for less homogeneous materials such as coals is 1 - 4 percent.

02,496
PB96-155486 Not available NTIS
National Inst. of Standards and Technology (CSTL), Gaithersburg, MD. Organic Analytical Research Div.
Development of Gas Standards from Solid 1,4-dichlorobenzene.
Final rept.
G. C. Rhoderick. 1995, 7p.
Pub. in Jnl. of Chromatography A, v710 p229-235 1995.

Keywords: *Natural gas, Liquified, Recrystalize, Response factor, Solid, Reprints, *Foreign technology, *Gas standards.

For over fifteen years the National Institute of Standards and Technology (NIST) has been preparing gas standards containing volatile organic compounds at sub micro mol/mol (ppm) concentrations. These standards have been prepared using organic compounds that are either gases or liquids at room temperature. A microgravimetric technique was developed previously to prepare standards containing these compounds in treated aluminum gas cylinders using a one step dilution. Requests were received to prepare gas standards containing the compound 1,4-dichlorobenzene. These requests posed a major problem in that 1,4-dichlorobenzene is a solid at room temperature. Research was undertaken using the microgravimetric procedure to determine if it was feasible to prepare gas standards from solid phase compounds. In the first stage of research the liquid phase compound 1,2-dichlorobenzene previously studied at NIST in gas mixtures was used as an internal standard. Results from analyses of a pepared gas standard showed that the response factor on a gas chromatograph flame-ionization detector for 1,3-dichlorobenzene was 3% less than that for 1,2-dichlorobenzene.

02,497
PB96-155494 Not available NTIS
National Inst. of Standards and Technology (CSTL), Gaithersburg, MD. Organic Analytical Research Div.
Measurement of Atmospheric Methyl Bromide Using Gravimetric Gas Standards.
Final rept.
G. C. Rhoderick. 1995, 4p.
Pub. in Environmental Science and Technology, v29 n11 p2797-2800 Nov 95.

Keywords: *Methyl bromide, Samples, Calibration, Regression analysis, Reprints, *Gravimetric standards, Ozone layer.

Methyl bromide (CH3Br) is the largest source of gaseous bromine in the atmosphere. Methyl bromide is, therefore, environmentally important due to its potential to contribute to the loss of the stratospheric ozone layer through catalytic destruction. Several sets of atmospheric bethyl bromide measurements have been reported, but little has been reported on the calibration standards used to determine those values. For years, the National Institute of Standards and Technology (NIST) has prepared gravimetric gas standards containing methyl bromide at the low parts per billion (ppb; 10 to the minus 9th power mol/mol) level. These standards have been used by federal and state governments in urban air monitoring programs.

02,498
PB96-167234 Not available NTIS
National Inst. of Standards and Technology (CSTL), Boulder, CO. Thermophysics Div.
Viscosity of Defined and Undefined Hydrocarbon Liquids Calculated Using an Extended Corresponding-States Model.
Final rept.
M. E. Baltatu, R. A. Chong, and M. L. Huber. 1996, 9p.
Pub. in International Jnl. of Thermophysics, v17 n1 p213-221 1996.

Keywords: *Petroleum fractions, Reprints, *Foreign technoloogy, *Viscosity prediction, *Corresponding states.

We predict the viscosity of petroleum fractions using extended corresponding states. Our model builds upon the TRAPP procedure, which is the most advanced approach to predict transport properties of straight-chain nonpolar hydrocarbons and their mixtures. We perform comparisons with experimental viscosity data for pure hydrocarbons, treating them as nonstandard components; we find deviations of 10-15%. We also extend the model to predict the transport properties of petroleum fractions and compare with an experimental database of more than 80 crude oils, including highly aromatic petroleum fractions. The model predicts the viscosity of the crude oil fractions within experimental uncertainty.

02,499
PB96-176664 Not available NTIS
National Inst. of Standards and Technology (CSTL), Boulder, CO. Thermophysics Div.
New Data and Correlations for the Custody Transfer of Natural Gas Liquids.
Final rept.
J. F. Ely, W. M. Haynes, C. D. Holcomb, and J. W. Magee. 1995, 19p.
Pub. in Proceedings of the Gas Processors Association Annual Convention (74th), San Antonio, TX., March 13-15, 1995, p35-53.

Keywords: *Natural gas liquids, *Thermophysical properties, *Liquid phases, *Phase transformations, Compressed natural gas, Phase studies, Phase equilibria, Vapor phases, Equations of state, Volume, Mixtures, Density(Mass/Volume), Reprints, Coexisting density, Corresponding states, Vapor liquid equilibria.

This report presents new experimental density measurements and density prediction models for natural gas liquids. Experimentally, vibrating tube densimeters have been used to measure coexisting densities for ethane, propane, n-butane, isopentane, n-pentane, and isohexane and for binary mixtures of ethane+propane, propane+n-butane, and n-butaine+n-pentane. The density measurements were combined with simultaneous vapor-liquid equilibrium measurements using a vapor and liquid recirculation phase-equilibrium apparatus at temperatures from 240 K to either 410 K or the critical temperature of the system, whichever is less. Isothermal data were obtained for the binary mixtures over the entire composition range for each of the systems. Also, an isochoric gas expansion technique has been used to carry out (p,p,T) measurements on two binary mixtures of ethane + propane with mol fractions of 0.35 and 0.65 and one binary mixture of propane+n-butane with a propane mol fraction of 0.61.

02,500
PB97-119267 Not available NTIS
National Inst. of Standards and Technology (CSTL), Gaithersburg, MD. Process Measurements Div.
Internal Droplet Circulation Induced by Surface-Driven Rotation.
Final rept.
C. M. Megaridis, J. T. Hodges, J. Xin, J. M. Day, and C. Presser. 1994, 14p.
Pub. in International Jnl. of Heat and Fluid Flow, v15 n5 p364-377 Oct 94.

Keywords: *Droplets, *Rotation, *Liquid circulation, Circulation, Numerical models, Fluid transport, Spherical liquid volume, Rotation, Reprints.

The paper presents a combined theoretical/experimental study of internal liquid circulation induced by droplet surface rotation. A numerical model is presented first, examining the fluid transport within a spherical liquid volume whose surface is subjected to rotation about a central axis. The model predicts that the steady-state motion established from spatially nonuniform surface rotation has a helical character and bears little resemblance to the toroidal internal flows developed within droplets under axisymmetric conditions. Similar internal flow patterns are predicted for temporally varying surface rotation occuring during droplet spin-up or spin-down. Planar laser-induced fluorescence is employed to provide high-resolution images of fluid flow developed within millimeter-sized suspended droplets that are exposed to steady laminar air streams to induce repeatable surface rotation. The predicted spiral flow patterns are corroborated by the pendant droplet visualization experiments, and suggest that nonuniform rotation or transient spinning may significantly alter internal droplet dynamics.

Heating & Cooling Systems

02,501
PB94-140407 PC A08/MF A02
National Inst. of Standards and Technology (BFRL), Gaithersburg, MD.
Computer Programs for Simulation of Lighting/HVAC Interactions.
G. N. Walton. Dec 93, 156p, NISTIR-5322.
See also PB91-144386. Sponsored by Department of Energy, Washington, DC., and Electric Power Research Inst., Palo Alto, CA.

Keywords: *Space HVAC systems, *Lighting systems, *Computerized simulation, *Buildings, Coefficients, Algorithms, Interactions, Heat transfer, Cooling load, Energy audits, Thermal measurements, HLITE computer program, VLITE computer program, National Institute of Standards and Technology.

The report describes two computer programs developed for the analysis of lighting/HVAC interactions: HLITE and VLITE. VLITE is used to compute the coefficients (view factors) describing radiation interchange between surfaces. These coefficients are used in a thermal network model which is solved by HLITE for

transient temperatures and cooling loads. These programs are research tools. HLITE is based on a simple finite volume model for heat transfer combined with sufficiently short time steps to permit explicit time integration in most of the simulation. Controls are modeled in a manner emulating the operation of controls in real buildings. The accuracy of the mathematical solution is appropriate to the models used and data available resulting in a fast, flexible simulation tool.

02,502
PB94-143344 PC A04/MF A01
National Inst. of Standards and Technology (BFRL), Gaithersburg, MD. Building Environment Div.
Evaluation of GSA Maintenance Practices of Large Centrifugal Chillers and Review of GSA Refrigerant Management Practices.
J. Y. Kao. Jan 94, 51p, NISTIR-5336.
Sponsored by Public Buildings Service, Washington, DC.

Keywords: *Centrifugal pumps, *Refrigerating machinery, *Refrigerants, US GSA, Maintenance, Inspection, Nondestructive tests, Air pollution control, CFC(Chlorofluorocarbons).

The study contains two major subjects involving maintenance of large centrifugal chillers in the General Services Administration (GSA) facilities. The first part is to use nondestructive testing (NDT) techniques for chiller testing and maintenance. NDT techniques investigated are visual inspection, leak testing, vibration analysis, infrared thermal testing, eddy current testing, oil analysis, and acoustic emission testing. With the exception of acoustic emission testing, all other techniques are recommended for GSA chiller maintenance. The second part of the study is about refrigerant management.

02,503
PB94-218559 PC A04/MF A01
National Inst. of Standards and Technology (BFRL), Gaithersburg, MD. Building Environment Div.
Study of Heat Pump Performance Using Mixtures of R32/R134a and R32/R125/R134a as 'Drop-In' Working Fluids for R22 with and Without a Liquid-Suction Heat Exchanger.
P. I. Rothfleisch, and D. A. Didion. Dec 93, 65p, NISTIR-5321.

Keywords: *Heat pumps, *Refrigerants, *Working fluids, Heat exchangers, Performance(Engineering), Heat transfer, Uncertainty, Mathematical models, Thermodynamic cycles, Residential buildings.

A ductless mini-split residential heat pump with a modified indoor coil was utilized to compare the performance of R22 and a mixture of 34% R32/66% R134a by weight. This test was intended to serve as an indicator of 'drop-in' performance so the system was optimized for each refrigerant by varying only the charge mass and expansion valve setting. At the 27.8 C (82 F) cooling test condition the capacity and COP of the mixture were 94% and 90% of the values for R22, respectively. Additional tests were conducted with a liquid-suction intracycle heat exchanger. The modified system was operated with both single-phase and two-phase refrigerant entering the low pressure side of the liquid-suction heat exchanger. The addition of the liquid-suction heat exchanger showed a minimal performance improvement with the performance of the two-phase variation being slightly higher. The best performing liquid-suction heat exchanger variant (two-phase refrigerant on the low pressure side) was also run with a ternary mixture of 30% R32/10% R125/60% R134a, by weight. The results for this mixture were similar to the binary mixture.

02,504
PB95-105524 PC A03/MF A01
National Inst. of Standards and Technology (BFRL), Gaithersburg, MD. Building Environment Div.
Predicting the Energy Performance Ratings of a Family of Type I Combination Appliances.
S. T. Liu, and G. E. Kelly. Aug 93, 30p, NISTIR-5250.
Sponsored by Department of Energy, Washington, DC. Office of Codes and Standards.

Keywords: *Housing(Dwellings), *Space heaters, *Water heaters, *Energy efficiency, Water heating, Boilers, Thermal efficiency, Space heating, Comuterized simulation, *ANSI/ASHRAE Standard 124-1991, *Combination appliances.

ANSI/ASHRAE Standard 124-1991 specifies the laboratory tests and the calculation procedure for estimating seasonal and annual performance of combination appliances which are designed to provide both space heating and water heating. A boiler that includes a tankless coil for water heating is covered by those sections in ASHRAE Standard 124 that pertain to Type I combination appliances. In an effort to minimize the test burdens on manufacturers, a computer simulation study was conducted to determine if a subset of a family series of Type I combination appliances could be tested and used to predict the performance of the rest of the appliances in the family. Computer simulation was conducted on a family of five different size boilers with an identical tankless coil to calculate their Combined Annual Efficiency (CAE) as specified in ASHRAE Standard 124. To this end, the Energy Factor (EF) for water heating and the Annual Fuel Utilization Efficiency (AFUE) for space heating were calculated. For the water heating test that was simulated, daily hot water draw volumes of 243.4 liters (64.3 gal.) and 454.2 liters (120 gal.) were used. The results showed that for the five boilers, the AFUE for space heating differed by less than 1 percent.

02,505
PB95-220521 PC A03/MF A01
National Inst. of Standards and Technology (BFRL), Gaithersburg, MD. Building Environment Div.
Performance Testing of a Family of Type I Combination Appliance.
S. T. Liu, G. E. Kelly, and C. P. Terlizzi. Apr 95, 34p, NISTIR-5626.
Sponsored by Department of Energy, Washington, DC.

Keywords: *Space HVAC systems, *Performance evaluation, Boilers, Tests, Hot water heating, Energy efficiency.

In an effort to minimize the test burdens on manufacturers, a family series of gas-fired hot water boilers were tested to determine if a subset of a family series of Type I combination appliances could be tested and used to predict the performance of the rest of the appliances in the family series. Tests were conducted on a family series of three different size boilers with an identical indirectly heated storage tank to determine their Combined Annual Efficiency (CAE) as specified in ASHRAE Standard 124.

02,506
PB96-135066 Not available NTIS
National Inst. of Standards and Technology (CSTL), Gaithersburg, MD. Thermophysics Div.
Shape of the Temperature-Entropy Saturation Boundary.
Final rept.
G. Morrison. 1994, 10p.
Pub. in International Jnl. of Refrigeration, v17 n7 p494-503 1994.

Keywords: *Compression, *Diagrams, *Entropy, Reprints, Refrigerants, Saturation, Substitute, Temperature.

The phase diagram in temperature-entropy space plays an important role in the visualization, design and analysis of operating cycles in refrigerators and heat pumps. The shape of the phase boundary in this space varies dramatically from one material to another. The origin of these differences is shown to be a consequence of molecular structure. Relationships of varying accuracy are developed to estimate the slope of the vapour branch of the T-S diagram.

Miscellaneous Energy Conversion & Storage

02,507
PB95-155586 PC A99/MF A06
National Inst. of Standards and Technology (MSEL), Gaithersburg, MD. Materials Reliability Div.
Composite Struts for SMES Plants.
Rept. for May 91-Nov 92.
R. P. Reed, and J. D. McColskey. Oct 94, 624p, NISTIR-5024.
Contract DNA-IACRO-91-854
Prepared in cooperation with Cryogenic Materials, Inc., Boulder, CO. Sponsored by Defense Nuclear Agency, Washington, DC.

Keywords: *Epoxy matrix composites, *Glass fiber reinforced plastics, *Struts, *Composite structures, *Magnetic energy storage equipment, Structural components, Stress analysis, Strains, Tensile properties, Modulus of elasticity, Composite materials, Displacement, Fatigue tests, Mechanical properties, Thermal conductivity, *Superconducting Magnetic Energy Storage Plants.

This report summarizes NIST research efforts in the development of composite struts for Superconducting Magnetic Energy Storage plants (SMES). Large SMES plants require radial structural support from the superconducting coils to the outer walls to assist in restraining the coil cool-down and Lorentz forces. The struts proposed for this structural support must have good axial compressive strength and low axial thermal conductivity, as well as low cost. A variety of E-glass fibers, resins, lay-up angles and manufacturing methods were evaluated in the course of this program, at temperatures ranging from 295 to 76K. Analysis methods are presented that describe the response of fiber-reinforced cylinders and end fitting designs to axially varying mechanical and thermal loads. Finally, failure-mode and tube design studies were conducted in order to optimize support tube-design based on minimum cross-sectional area with allowable strain values input as design constraints.

Policies, Regulations & Studies

02,508
PB94-206018 PC A04/MF A01
National Inst. of Standards and Technology (CAML), Gaithersburg, MD. Office of Applied Economics.
Energy Prices and Discount Factors for Life-Cycle Cost Analysis 1994. Annual Supplement to NIST Handbook 135 and NBS Special Publication 709.
S. R. Petersen. Oct 93, 64p, NISTIR-85-3273-8.
See also PB87-180253, PB88-138227, PB94-500055 and report for 1993, PB92-238633. Sponsored by Department of Energy, Washington, DC. Federal Energy Management Program Staff.

Keywords: *Energy conservation, *Prices, *Life cycle costs, *Cost analysis, Federal buildings, Residential buildings, Economic analysis, Present worth, Fuels, Price index, Electric appliances, Energy supplies, Tables(Data).

This is the 1994 annual edition of energy prices and discount factors for performing life-cycle cost analyses of energy conservation and renewable energy projects. It supports the Federal life-cycle costing methodology by updating the energy price projections and discount factors that are described, explained, and illustrated in NIST Handbook 135 (HB 135). It supports private-sector life-cycle costs analysis by updating the energy price indices that are described, explained, and illustrated in NBS Special Publication 709 (SP 709). It also supports the Energy Conservation Mandatory Performance Standards for New Federal Residential Buildings (10 CFR 435) by providing a table of factors for updating appliance label values.

02,509
PB95-105011 PC A04/MF A01
National Inst. of Standards and Technology (CAML), Gaithersburg, MD. Office of Applied Economics.
Energy Price Indices and Discount Factors for Life-Cycle Cost Analysis 1995. Annual Supplement to NIST Handbook 135 and NBS Special Publication 709. (Revised).
S. R. Petersen. Oct 94, 56p, NISTIR-85/3273-9.
See also PB94-206018. Sponsored by Federal Energy Management Program, Washington, DC.

Keywords: *Life cycle costs, *Cost analysis, *Prices, *Energy conservation, Federal buildings, Residential buildings, Fuels, Economic analysis, Electric appliances, Present worth, Price index, Energy supplies, Tables(Data).

This is the 1995 annual edition of energy price indices and discount factors for performing life-cycle cost analyses of energy conservation and renewable energy projects. It supports the Federal life-cycle costing methodology by updating the energy price projections and discount factors that are described, explained, and illustrated in the National Institute of Standards and Technology (NIST) Handbook 135 (HB 135). It supports private-sector life-cycle cost analysis by updating the energy price indices that are described, explained, and illustrated in NBS Special Publication 709 (SP

709). It also supports the Energy Conservation Mandatory Performance Standards for New Federal Residential Buildings (10 CFR 435) by providing a table of factors for updating appliance label values.

02,510
PB96-162441 PC A05/MF A01
National Inst. of Standards and Technology (BFRL), Gaithersburg, MD. Office of Applied Economics.
Energy Price Indices and Discount Factors for Life-Cycle Cost Analysis 1996. Annual Supplement to NIST Handbook 135 and NBS Special Publication 709. (Revised).
S. R. Petersen. Oct 95, 69p, NISTIR-85/3273-10.
See also PB95-105011. Sponsored by Federal Energy Management Program, Washington, DC.

Keywords: *Life cycle costs, *Cost analysis, *Prices, *Energy conservation, Federal buildings, Residential buildings, Fuels, Economic analysis, Electric appliances, Present worth, Price index, Energy supplies, Tables(Data).

This is the 1996 annual edition of energy price indices and discount factors for performing life-cycle cost analyses of energy and water conservation and renewable energy projects. It supports the federal life-cycle costing methodology by updating the energy price projections and discount factors that are described, explained, and illustrated in NIST Handbook 135 (HB 135). It supports private-sector life-cycle cost analysis by updating the energy price indices that are described, explained, and illustrated in NBS Special Publication 709 (SP 709). It also supports the Energy Conservation Mandatory Performance Standards for New Federal Residential Buildings (10 CFR 435) by providing a table of factors for updating appliance label values.

02,511
PB96-172317 PC A10/MF A02
National Inst. of Standards and Technology (BFRL), Gaithersburg, MD. Office of Applied Economics.
Life-Cycle Costing Manual for the Federal Energy Management Program. 1995 Edition.
Handbook.
S. K. Fuller, and S. R. Petersen. Feb 96, 176p, NIST/HB-135.
Also available from Supt. of Docs. as SN003-003-03373-1. Supersedes PB88-138227. Sponsored by Federal Energy Management Program, Washington, DC.

Keywords: *Federal buildings, *Life cycle costs, *Energy management, Energy conservation, Economic analysis, Cost benefit analysis, Cost effectiveness, Water conservation, Investments, Capitalized costs, Renewable energy sources, Public buildings, Manuals, Energy economics.

Handbook 135 is a guide to understanding the life-cycle cost (LCC) methodology and criteria established by the Federal Energy Management Program (FEMP) for the economic evaluation of energy and water conservation projects and renewable energy projects in all federal buildings. The purpose of this handbook is to facilitate the implementation of the FEMP rules by explaining the LCC method, defining the measures of economic performance used, describing the assumptions and procedures to follow in performing evaluations, giving examples, and noting NIST computer software available for computation and reporting purposes.

02,512
PB96-210745 PC A05/MF A01
National Inst. of Standards and Technology (BFRL), Gaithersburg, MD. Office of Applied Economics.
Energy Price Indices and Discount Factors for Life-Cycle Cost Analysis 1997. Annual Supplement to NIST Handbook 135 and NBS Special Publication 709. (Revised).
S. R. Petersen. Jul 96, 68p, NISTIR-85-3273-11.
See also PB96-162441. Sponsored by Federal Energy Management Program, Washington, DC.

Keywords: *Life cycle costs, *Cost analysis, *Prices, *Energy conservation, Federal buildings, Residential buildings, Fuels, Electric appliances, Energy supplies, Economic analysis, Present worth, Price index, Tables(Data).

This report is the FY 1997 edition of energy price indices and discount factors for performing life-cycle cost analyses of energy and water conservation and renewable energy projects in federal facilities. It supports the federal life-cycle costing methodology by updating the energy price projections and discount factors that are described, explained, and illustrated in NIST Handbook 135 (HB 135, Life-Cycle Costing Manual for the Federal Energy Management Program (PB96-172317)). It supports private-sector life-cycle cost analysis by updating the energy price indices that are described, explained, and illustrated in NBS Special Publication 709 (SP 709 (PB87-180253)). It also supports the Energy Conservation Mandatory Performance Standards for New Federal Residential Building (10 CFR 435) by providing a table of factors for updating appliance label values.

Reserves

02,513
PB96-119755 Not available NTIS
National Inst. of Standards and Technology (EEEL), Gaithersburg, MD. Electricity Div.
Procedure for Measuring Trace Quantities of S2F10, S2OF10, and S2O2F10 in SF6 Using a Gas Chromatograph-Mass Spectrometer.
Final rept.
R. J. Van Brunt, J. K. Olthoff, K. L. Stricklett, and D. J. Wheeler. 1995, 8p.
Pub. in Proceedings of the International Symposium on Gaseous Dielectrics (7th), Knoxville, TN., April 24-28, 1994, p441-448 1995.

Keywords: *Gas chromotography, *Mass spectrometers, *Trace quantities, Reprints, Procedures.

The compounds S2F10, S2OF10, and S2O2F10 are formed by decomposition of gaseous sulfur hexafluoride (SF6) in electrical discharges. The species S2F10 is known to be highly toxic to humans, and there is recent evidence that S2O2F10 may also be very toxic. There is, therefore, an interest in having analytical methods to detect these compounds in compressed SF6 at trace levels down to 10 parts in 10 to the 9th power by volume (10 ppbv). Two chromatographic methods have been used to direct these compounds at the 10 ppbv level or lower. The first method developed by Sauers and coworkers is based on a cryogenic enrichment procedure first proposed by Janssen, and uses a gas chromatograph with an electron-capture detector. The second method, which is the focus of the present work, utilizes a gas chromatograph-mass spectrometer (GC/MS) with a thermal-chemical converter. The purposes of the present work are: (1) to define a procedure for using the CC/MS method to make fast, reliable measurement of trace S2F10, S2OF10, and S2O2F10 in pressurized SF6; (2) to discuss the major sources of error that can be encountered in using the method; and (3) to discuss the factors that limit the sensitivity such as interference from other compounds.

Solar Energy

02,514
PB94-211075 Not available NTIS
National Inst. of Standards and Technology (PL), Boulder, CO. Quantum Physics Div.
Plasma Chemistry in Disilane Discharges.
Final rept.
J. R. Doyle, D. A. Doughty, and A. Gallagher. 1992, 10p.
Contract SERI-XG-1-1216
Pub. in Jnl. of Applied Physics 71, n10 p4771-4780, 15 May 92. Sponsored by Solar Energy Research Inst., Golden, CO.

Keywords: *Silanes, *Radio frequency discharge, *Plasma chemistry, *Amorphous silicon, Silicon solar cells, Semiconducting films, Reprints, Disilanes.

We have measured the initial silane and polysilane product yields from disilane decomposition in rf and dc discharges, at 25 and 250 C and 20 Pa (0.15 Torr) pressure as typically used for alpha-Si:H film deposition. From analyses of these yields we conclude that the initial Si2H6 fragmentation pattern is SiH3 + SiH2 + H (91 + or - 9%) and H3SiSiH + 2H (9 + or - 9%), that the primary product of the H + Si2H6 reaction is SiH4 + SiH3, and that SiH3 is the dominant radical causing film growth. We have measured a radical-surface reaction probability of 0.34 + or - 0.03, very similar to that observed for SiH3 in SiH4 discharges. We report a spatial distribution of emission indicative of a gamma-regime discharge. From deposition on glass fibers strung between the electrodes, we find that highly strained alpha-Si:H film is produced everywhere except on or near the electrodes, suggesting that energetic ion impact is necessary to yield useful films in disilane discharges.

ENVIRONMENTAL POLLUTION & CONTROL

General

02,515
PB94-172533 Not available NTIS
National Inst. of Standards and Technology (CAML), Gaithersburg, MD. Statistical Engineering Div.
Replicate Measurements for Data Quality and Environmental Modeling.
Final rept.
W. Liggett. 1994, 32p.
Pub. in Handbook of Statistics, v12 p71-102 1994.

Keywords: *Environmental research, *Mathematical models, *Replicating, Statistical analysis, Multivariate analysis, Experimental design, Measurement, Reprints, *Data quality.

Replicate measurements can be used to improve sampling and measurement procedures and thereby data quality and to select an environmental model that agrees reasonably with the data. The implications for study design of these uses of replicates and corresponding statistical analysis methods are presented. The statistical analysis methods presented for quality improvement and model selection are especially appropriate for environmental studies. The quality improvement method discussed is a multivariate method generalized to include estimation of a power transformation for each constituent measurement. The model selection method discussed employs a bootstrap based on replicates that is applicable to models fit by robust estimation.

02,516
PB94-172806 Not available NTIS
National Inst. of Standards and Technology (CSTL), Gaithersburg, MD.
Current Activities Within the National Biomonitoring Specimen Bank.
Final rept.
S. A. Wise, B. Koster, J. Langland, and R. Zeisler. 1993, 12p.
Pub. in The Science of the Total Environment 139/140, p1-12 1993. Sponsored by Environmental Protection Agency, Washington, DC., National Oceanic and Atmospheric Administration, Rockville, MD., and Department of the Interior, Washington, DC.

Keywords: *Tissue banks, *Bioaccumulation, *Marine mammals, *Water pollution effects(Animals), Pollution monitoring, Biological accumulation, Data collection, Environmental monitoring, Terrestrial ecosystems, Specimens, Organic compounds, Contamination, Quality assurance, Reprints.

The National Institute of Standards and Technology (NIST) has been involved in biological environmental specimen banking activities since 1979. These activities, which are known collectively as the National Biomonitoring Specimen Bank (NBSB), include the banking of a variety of specimens (human liver, sediment, mussels/oysters, fish tissue and marine mammal tissues) from several different projects supported by different government agencies. The two most recent projects, the Alaska Marine Mammal Tissue Archival Project (AMMTAP) and the National Marine Mammal Tissue Bank (NMMTB), focus on the collection, banking and analysis of marine mammal tissues and they

are part of a comprehensive plan to address marine mammal monitoring, specimen banking and quality assurance of analytical measurements associated with contaminant analyses in marine mammals.

02,517
PB94-185527 Not available NTIS
National Inst. of Standards and Technology (CAML), Gaithersburg, MD. Statistical Engineering Div.
Scientific Protocols in Statistical Standards for Environmental Studies.
Final rept.
W. Liggett. 1993, 6p.
Pub. in Proceedings of American Statistical Association Conference on Quality and Product, San Francisco, CA., p38-43, 1993.

Keywords: *Environmental surveys, *Mathematical models, *Statistical inference, *Protocols, Statistical analysis, Randomization, Measurement, Errors, Experimental design, Reprints.

In environmental studies, the validity of the probability model that underlies statistical inference often depends on the operation of physical mechanisms. Deliberate randomization, although important, often cannot remove this dependence. Traditionally, statisticians have considered the impact of physical mechanisms on study conclusions to be the responsibility of scientific collaborators. Because scientists are guided by values other than the validity of probability models, statisticians must take responsibility themselves. Thus, statisticians must understand the relevant physical mechanisms so that they can develop scientific protocols that result in statistically-tractable probability models. As a practical approach, statisticians can become involved in the design and execution of pilot studies with the aim of resolving probability-model issues. Pilot studies adequate in this regard are necessary as a basis for environmental statistical standards.

02,518
PB94-198330 Not available NTIS
National Inst. of Standards and Technology (TS), Gaithersburg, MD. Standard Reference Materials Program.
Standard Reference Materials for Dioxins and Other Environmental Pollutants.
Final rept.
R. Alvarez. 1991, 7p.
Pub. in Science of the Total Environment 104, n1-2 p1-7 1991.

Keywords: *Dioxins, *Chemical analysis, *Environmental pollution, *Pollutants, Chemical composition, Certification, Concentration(Composition), Calibrating, Analytical techniques, Pesticides, Isotopic labeling, Physical properties, Chlorine organic compounds, Reprints, *Standard reference materials, National Intitute of Standards and Technology.

The National Institute of Standards and Technology issues approximately 1100 Standard Reference Materials (SRMs) certified for chemical composition or physical properties. A number of these SRMs have been developed to assist chemists in analyzing environmental samples more reliably for chlorinated dioxins and other organic pollutants. Certification of the pollutant concentration in a natural matrix SRM is based on concordant analyses by the NIST Organic Analytical Research Division using at least two independent methods. For a calibration solution, such as SRM 1614, Dioxin (2,3,7,8-TCDD) in Isooctane, certification is based on agreement of the calculated concentration based on the gravimetric preparation and the concentration as determined experimentally. SRM 1614 also includes a (13)C-labeled 2,3,7,8-TCDD for use as an internal standard in methods based on gas chromatography/mass spectrometry. The certified concentrations, in ng/g, are 98.3 + 3.3 for the unlabeled dioxin and 95.6 + or - 1.5 for the labeled dioxin. The certificates for SRM 1588, Organics in Cod Liver Oil, and SRM 1589, Polychlorinated Biphenyls (As Aroclor 1260) in Human Serum, provide noncertified concentrations of dioxins. Concentrations of chlorinated dioxins in two urban particulate SRMs have been reported in the literature.

02,519
PB94-206364 PC A08/MF A02
National Inst. of Standards and Technology (BFRL), Gaithersburg, MD.
U.S. Green Building Conference, 1994.
Special pub.
A. H. Fanney, K. M. Whitter, A. E. Traugott, and L. N. Simon. Jun 94, 153p, NIST/SP-863.
Also available from Supt. of Docs. as SN003-003-03274-3. Proceedings of a conference held in Gaithersburg, MD. on February 16-17, 1994.

Keywords: *Buildings, *Environmental engineering, *Meetings, Construction materials, Indoor air pollution, Carbon dioxide, Technology transfer.

The report constitutes the proceedings of the Green Building Conference held in Gaithersburg, Maryland, February 16-17, 1994. The conference was co-sponsored by the National Institute of Standards and Technology (NIST) and the U.S. Green Building Council (USGBC). Over 450 individuals attended the conference representing building product manufacturers, building owners and managers, environmental groups, utilities, contractors, builders, architects, engineers, and the local, state, and the federal governments. The conference provided an opportunity to acquire practical, useful information on green buildings, resources, and guidelines.

02,520
PB95-147146 PC A09/MF A02
National Inst. of Standards and Technology (TS), Gaithersburg, MD.
Opportunities for Innovation: Pollution Prevention.
D. E. Edgerly. Aug 94, 181p, NIST/GCR-93/659.
Grant 50SBNB3C7626

Keywords: *Pollution abatement, *Waste recycling, *Small businesses, *Waste disposal, *Industrial wastes, Automotive industry, Chemical industry, Paper industry, Textile industry, Paints, Coatings, Degreasing, Dyes, Dyeing, Printing, Office equipment, *Medium-sized businesses, Opportunities for innovation, Waste minimization, Pollution prevention, Waste reduction.

The objective was to identify technological opportunities within a number of selected industries and/or manufacturing/finishing processes, to reduce pollution. These industries/processes were selected as representative of and applicable to the broad range of U.S. manufacturing businesses. These include: metals coating (i.e., painting) which is widely done in a number of major industries, including the automotive industry; metals degreasing; recyclability of office equipment; chemical manufacturing; printing; textiles dye and dyeing; and the pulp and paper industry. Additionally, the promulgation of new regulations, requiring companies to change their historical manufacturing and waste generating/disposal practices, will continue to create technological needs and opportunities for savvy businesses to develop solutions.

02,521
PB95-161394 Not available NTIS
National Inst. of Standards and Technology (TS), Gaithersburg, MD. Office of Technology Evaluation and Assessment.
Encouraging Environmentally-Aware Inventions.
Final rept.
G. P. Lewett. 1993, 17p.
Sponsored by International Federation of Inventors' Associations, Geneva (Switzerland).
Pub. in Proceedings of Conference Invention and Protection of the Environment, Tunis, Tunisia, September 20-25, 1993, p1-17.

Keywords: *Environmental protection, *Research and development, *Technology transfer, *Inventions, Pollution abatement, Environmental research, Technology innovation, Commercialization, Appropriate technology, Research programs, Research management, Reprints, *Energy Related Inventions Program, Environmental aspects, Environmental considerations.

The paper provides a review of the Energy-Related Inventions Program to indicate how its experience can be utilized to stimulate invention of environmentally-oriented inventions. It also briefly describes federal programs which generate new environmental technologies.

02,522
PB95-164026 Not available NTIS
National Inst. of Standards and Technology (CSTL), Gaithersburg, MD. Organic Analytical Research Div.
Standard Reference Materials for the Determination of Trace Organic Constituents in Environmental Samples.
Final rept.
S. A. Wise. 1993, 44p.
Pub. in Environmental Analysis: Techniques, Applications and Quality Assurance, Chapter 12, p403-446 1993.

Keywords: *Organic compounds, *Chemical analysis, *Reference standards, *Certification, Polychlorinated biphenyls, Polycyclic aromatic hydrocarbons, Pesticides, Trace amounts, Test methods, Analytical techniques, Reprints, *Environmental samples, Standard reference materials.

Since 1980, NIST has issued a number of Standard Reference Materials (SRMs) for the determination of trace level organic contaminants such as polycyclic aromatic hydrocarbons (PAHs), polychlorinated biphenyls (PCBs), and chlorinated pesticides. This chapter describes these SRMs and the analytical techniques used for the certification measurements for these materials. The certified and noncertified concentrations for the PAHs, PCBs, and pesticides are summarized for the most recent natural matrix SRMs.

02,523
PB95-164042 Not available NTIS
National Inst. of Standards and Technology (CSTL), Gaithersburg, MD. Organic Analytical Research Div.
Liquid Chromatographic Determination of Polycyclic Aromatic Hydrocarbon Isomers of Molecular Weight 278 and 302 in Environmental Standard Reference Materials.
Final rept.
S. A. Wise, A. Deissler, and L. C. Sander. 1993, 16p.
Pub. in Polycyclic Aromatic Compounds 3, p169-184 1993.

Keywords: *Liquid column chromatography, *Polycyclic aromatic hydrocarbons, *Reference standards, *Quantitative chemical analysis, Isomers, Chromatographic analysis, Fluorescence spectroscopy, Extraction columns, Pollution sampling, Particulates, Sediments, Coal tar, Reprints, *Environmental samples, Standard reference materials, Dibenzopyrenes, Dibenzoanthracenes, Dibenzofluoranthenes.

Polycyclic aromatic hydrocarbons (PAHs) of molecular weight (MW) 278 (dibenzanthracene isomers) and 302 (dibenzopyrene/dibenzofluoranthene isomers) are seldom measured in environmental samples. A multidimensional liquid chromatography (LC) procedure was developed for the quantification of isomers of MW 278 and 302. Using the multidimensional LC procedure, six isomers of MW 278 and nine isomers of MW 302 were quantified in four environmental Standard Reference Materials (SRMs): coal tar (SRM 1597), air particulate matter (SRMs 1648 and 1649), and marine sediment (SRM 1941).

02,524
PB95-220513 PC A03/MF A01
National Inst. of Standards and Technology (TS), Gaithersburg, MD. Office of Standards Services.
ISO Environmental Management Standardization Efforts.
M. H. Saunders. Apr 95, 18p, NISTIR-5638.

Keywords: *ISO, *Standardization, *Environmental protection, Environment management, Manufacturing, Product development, Process control(Industry), Design criteria, Design analysis, Life cycle costs, Labeling, Auditing, Performance evaluation, Recommendations, *Life cycle analysis, Process management, Product standards.

The International Organization for Standardization (ISO) is currently developing a family of environmental management standards which address management systems and the environmental aspects of products in the areas of life cycle assessment and labeling. These standards have the potential to exert a significant influence on the design, manufacture, and marketing of products. They are also likely to affect the type of environmental data gathered by businesses and how those data are communicated internally and externally.

02,525
PB95-253605 PC A04/MF A01
National Inst. of Standards and Technology (BFRL), Gaithersburg, MD.

International Green Building Conference and Exposition (2nd). Held in Big Sky, Montana on August 13-15, 1995.
Special pub.
A. H. Fanney, K. M. Whitter, and T. B. Cohn. Aug 95, 63p, NIST/SP-888.
Also available from Supt. of Docs. as SN003-003-03349-9. See also PB94-206364.

Keywords: *Buildings, *Pollution abatement, *Meetings, Design analysis, Construction materials, Operation and maintenance, Building materials, Energy efficiency, Environmental engineering, Space HVAC systems, Landscaping, Demolition, Economic analysis, Technology innovation, Green buildings, Life cycle assessment, Building design.

The report constitutes the proceedings of the Green Building Conference held in Big Sky, Montana, August 13-15, 1995. The conference focused on the design, construction, operation, maintenance, and demolition of buildings in an environmental and cost-efficient manner.

02,526
PB96-112354 Not available NTIS
National Inst. of Standards and Technology (CSTL), Gaithersburg, MD. Inorganic Analytical Research Div.
Application of a Novel Slurry Furnace AAS Protocol for Rapid Assessment of Lead Environmental Contamination.
Final rept.
M. S. Epstein, S. M. Smith, and J. J. Breen. 1995, 6p.
Pub. in American Chemical Society Book, Chapter 30, p265-270 1995.

Keywords: *Lead(Metal), *Absorption spectroscopy, *Analytical methods, *Chemical analysis, Furnaces, Slurries, Atomization, Sampling, Sample preparation, Environmental pollution, Environmental monitoring, Public health, Health hazards, Reprints, *Atomic absorption.

Threats to public health must be identified and quickly eliminated by officials who have the proper information to make educated decisions. Instances of environmental injustice, where minority and low-income populations are subject to disproportionately high and adverse human health or environmental risks, need to be identified and corrected. Analytical science plays the pivotal role in providing data for environmental decision-making, from site hazard assessment, through evaluation of remediation efforts, and finally in the appraisal of pollution prevention technology.

02,527
PB96-112370 Not available NTIS
National Inst. of Standards and Technology (CSTL), Gaithersburg, MD. Analytical Chemistry Div.
Considerations in the Design of an Environmental Specimen Bank: Experiences of the National Biomonitoring Specimen Bank Program.
Final rept.
S. A. Wise, and B. J. Koster. 1995, 7p.
Pub. in Environmental Health Perspectives, v103 sup3 p61-67 Apr 95.

Keywords: *Tissue banks, *Reference standards, *Environmental monitoring, *Bioassay, Chemical analysis, Inorganic chemistry, Organic chemistry, Sampling, Bioaccumulation, Marine mammals, Fishes, Animal tissues, Humans, Biological effects, Cryogenic storage, Quality assurance, Reprints, National Biomonitoring Specimen Bank.

Since 1979 the National Institute of Standards and Technology (NIST) have been involved in environmental specimen banking activities as part of the National Biomonitoring Specimen Bank (NBSB). These activities have focused on the development of procedures for the collection, processing, analysis, and long-term storage of a variety of environmental specimens including: human liver, mussels and oysters, fish tissue (liver and muscle), marine mammal tissues (blubber, liver, and kidney), and marine sediments. The experiences of the NBSB, the issues that should be addressed in the design and operation of a valid specimen bank program are presented.

02,528
PB96-158662 PC A03/MF A01
National Inst. of Standards and Technology (TS), Gaithersburg, MD. Office of Standards Services.
ISO Environmental Management Standardization Efforts.
Technical note.
M. H. Saunders. Feb 96, 25p, NISTIR-5638-1.
Supersedes PB95-220513.

Keywords: *ISO, *Standardization, *Environmental protection, Environment management, Product development, Process control(Industry), Design criteria, Design analysis, Life cycle costs, Labeling, Auditing, Performance evaluation, Recommendations, *Life cycle analysis, Process management, Product standards.

The International Ogranization for Standardization (ISO) is currently developing a family of 'environmental management' standards which address management systems and the environmental aspects of products in the areas of life cycle assessment and labelling. These standards have the potential to exert a significant influence on the design, manufacture and marketing of products. They are also likely to affect the type of environmental data gathered by businesses and how those data are communicated internally and externally. The report outlines the current state of development of these planned ISO standards and also covers developments relating to third party certification of environmental management systems.

02,529
PB97-114359 PC A05/MF A01
Trade Promotion Coordinating Committee, Washington, DC. Environmental Trade Working Group.
India: Environmental Technologies Export Market Plan.
Final rept.
Oct 96, 64p.

Keywords: *India, *Pollution control equipment, *Environmental protection, *Market research, Water treatment, Waste water treatment, Air pollution control, Hazardous materials, Solid waste management, Sanitary engineering, Pollution monitoring, Pollution sampling, Infrastructure, Energy efficiency, Renewable energy sources, Exports, Financing, Market analysis, Technology transfer, International trade, Economic analysis, Export trade information.

Table of Contents:
Introduction and Objectives;
Market Overview;
Environmental Market Segments;
Routes to the Market;
Financing;
Financing Agencies and U.S. Government Programs;
Appendix A - Environmental Management in India;
Appendix B - U.S. Contracts for India;
Appendix C - Key Contacts in India;
Appendix D - Selected Publications;
Appendix E - Key Internet Web Sites;
and Appendix F - Environmental Trade Working Group Key Contacts.

02,530
PB97-118715 Not available NTIS
National Inst. of Standards and Technology (CAML), Gaithersburg, MD. Statistical Engineering Div.
Pilot Studies for Improving Sampling Protocols.
Final rept.
W. S. Liggett, and K. G. W. Inn. 1996, 18p.
Pub. in Principles of Environmental Sampling, p185-202 1996.

Keywords: *Environmental research, *Sampling, *Measurement, Experimental design, Protocols, Selectivity, Optimization, Sensitivity, Specificity, Statistical analysis, Statistical inference, Reprints.

Development of an environmental sampling and measurement protocol by means of experiments is feasible. The experiments require dissimilar plots, each of which is large enough for execution of a set of alternative protocols, but the experiments do not require that the property of interest be known for the plots. This chapter discusses the statistical framework for such experiments: what constitutes a proper set of alternative protocols, how the protocol responses can be used to estimate relative performance, and how the best protocol can be determined.

02,531
PB97-121826 PC A12/MF A03
National Inst. of Standards and Technology (BFRL), Gaithersburg, MD.
International Green Building Conference and Exposition (3rd). Held in San Diego, California on November 17-19, 1996. (Reannouncement with new abstract).
Special pub.
A. H. Fanney, and P. R. Svincek. Nov 96, 230p, NIST/SP-908.
Also available from Supt. of Docs. as SN003-0003-03433-9. See also report on 2nd conference, PB95-253605. Sponsored by American Inst. of Architects, Washington, DC., San Diego Gas and Electric Co., CA. and American Society of Landscape Architects, Washington, DC.

Keywords: *Buildings, *Pollution abatement, *Energy efficiency, *Meetings, Environmental engineering, Design analysis, Construction materials, Building materials, Energy conservation, Operation and maintenance, Space HVAC systems, Photovoltaic cells, Solar cells, Indoor air quality, Technology innovation, Economic analysis, Real estate, Insurance, Financial management, Green buildings, Life cycle assessment, Building design, Sustainability.

Sessions within the conference and corresponding papers within these proceedings focused on the role of cheif officers in bringing green products and services to market; A review of the U.S. Green Building Council's Leadership in Energy and Environmental Design Building Rating System; A review of the latest international green building projects including examples of commercial, industrial, historical, retail, office, academic, and residential projects; The selection of sustainable building materials; An overview of the latest practices in energy conservation; A world overview of solar photovoltaic components and systems; Commercial, residential, and legal indoor air quality issues; Design tools and resources that are applicable to green buildings including the Internet, 3D design visualization, computer simulations, and the Department of Energy's energy simulation programs; and The implications of green buildings on the real estate, financial, and insurance industries. (Reannouncement with new abstract).

Air Pollution & Control

02,532
PB94-143542 PC A05/MF A01
National Inst. of Standards and Technology, Gaithersburg, MD.
Ground-Based Smoke Sampling Techniques Training Course and Collaborative Local Smoke Sampling in Saudi Arabia.
Final rept. Aug 92-Aug 93.
N. P. Bryner, and B. A. Benner. Jan 94, 94p, NISTIR-5306.

Keywords: *Air pollution sampling, *Smoke, *Oil wells, *Fires, Particulates, Saudi Arabia, Health, Kuwait.

Smoke and gaseous emissions such as those generated by multiple oil-well fires can significantly impact the health of the local population. To assess the immediate risk to public health, the chemical and physical properties of the smoke and gaseous emissions must be quickly characterized. Local sampling via portable gas analyzers, filters and pumps, and particle sizing instrumentation provides real-time characterization of pollutant levels. These analyses provide a snapshot of the physical and chemical properties of the aerosols sampled in Saudi Arabia, but due to the very limited number of samples, they do not provide a reasonable basis for estimating the short- or long-term health risk due to exposure to smoke and gaseous emissions.

02,533
PB94-146636 PC A04/MF A01
National Inst. of Standards and Technology (CAML), Gaithersburg, MD. Applied and Computational Mathematics Div.
Modulation of Fossil Fuel Production by Global Temperature Variations, 2.
B. W. Rust, and F. J. Crosby. Jan 94, 64p, NISTIR-5332.
See also PB83-182592.

Keywords: *Fossil fuels, *Atmospheric temperature, *Northern Hemisphere, *Air pollution, Production, Climatic changes, Global warming, Variations, Mathematical models, Graphs(Charts), Gaia hypothesis, Rust-Kirk model.

The report includes the inverse modulation of global fossil production by variations in Northern Hemispheric temperatures. The present study incorporates recent revisions and extensions of the fuel production record and uses a much improved temperature record. The authors show that the new data are consistent with the predictions of the original Rust-Kirk model which they then extend to allow for time lag between variations in the temperature and the corresponding responses in fuel production. The modulation enters the new model through the convolution of a lagged averaging function with the temperature time-series. The authors also include explicit terms to account for the perturbations caused by the Great Depression and World War II. The final model accounts for 99.84% of the total variance in the production record. This modulation represents a feedback which is consistent with the carbon dioxide problem; climate change; fossil fuel production; global warming Gaia hypothesis; temperature variations.

02,534
PB94-155587 PC A04/MF A01
National Inst. of Standards and Technology (NML), Gaithersburg, MD. Center for Chemical Technology.
Sulfur Dioxide Capture in the Combustion of Mixtures of Lime, Refuse-Derived Fuel, and Coal.
Final rept.
K. L. Churney, and T. J. Buckley. Nov 90, 59p, NISTIR-4443.
Sponsored by Department of Energy, Washington, DC. Biofuels and Municipal Waste Technology Div.

Keywords: *Refuse derived fuels, *Sulfur dioxide, *High sulfur coal, *Cocombustion, *Air pollution control, Calcium oxides, Fly ash, Chlorine, Manganese oxides, Sorbents, Tests, Combustion chambers.

Chlorine and sulfur mass balance studies have been carried out in the combustion of mixtures of lime, refuse-derived fuel, and coal in the NIST multikilogram capacity batch combustor. The catalytic effect of manganese dioxide on the trapping of sulfur dioxide by lime was examined. Under the authors conditions, only 4% of the chlorine was trapped in the ash and no effect of manganese dioxide was observed. Between 42 and 14% of the total sulfur was trapped in the ash, depending upon the lime concentration. The effect of manganese dioxide on sulfur capture was not detectable. The temperature of the ash was estimated to be near 1200 deg C, which was in agreement with that calculated from sulfur dioxide capture thermodynamics.

02,535
PB94-161635 PC A03/MF A01
Maryland Univ., College Park.
Rare-Earth Isotopes as Tracers of Particulate Emissions: An Urban Scale Test.
Final rept.
J. M. Ondov, W. R. Kelly, J. Z. Holland, P. J. Paulsen, Z. C. Lin, and S. A. Wight. Jan 91, 43p, CBRM-TR-91-2.
See also PB91-195347. Prepared in cooperation with National Inst. of Standards and Technology (NML), Gaithersburg, MD. Center for Analytical Chemistry. Sponsored by Maryland Dept. of Natural Resources, Annapolis. Chesapeake Bay Research and Monitoring Div. and Maryland Power Plant Research Program, Annapolis.

Keywords: *Tracer techniques, *Isotopic labeling, *Particulates, *Rare earth elements, *Air pollution, Urban areas, Feasibility studies, Coal fired power plants, Fly ash, Flue gases, Concentration(Composition), Neodymium 148, Field tests.

The particulate emissions of a 100 MW(e) coal-fired power plant were successfully tagged with enriched rare-earth isotopes on three occasions during the month of August, 1988. On 28 August, an 8-hour release was made using 94% isotopically pure 148Nd injected at a rate of 61 mg/hr and 14 ambient aerosol samples collected along a 72 degree arc 20-km distant from the plant were analyzed by pulse-counting thermal-ionization mass spectrometry for excess 148Nd and naturally-occurring (total) Nd background. The results were in good agreement with Gaussian plume model predictions. We conclude that the experiment and preliminary results successfully demonstrate the feasibility of using an enriched rare-earth isotopes as tracers of emissions from coal-fired power plants. The large signal-to-noise ratios achieved here are sufficient for tracing particles over much larger distances.

02,536
PB94-164381 PC A05/MF A01
National Inst. of Standards and Technology (BFRL), Gaithersburg, MD.
CONTAM93 User Manual.
G. N. Walton. Mar 94, 80p, NISTIR-5385.

Keywords: *User manuals (Computer programs), *Indoor air pollution, *Air flow, *Buildings, Environmental transport, Spatial distribution, Ventilation, Contaminants, Algorithms, Requirements, Air quality, Environmental engineering, *CONTAM93 computer program, CONTAM computer program, CONTAMX computer program, Multizone analysis.

This manual describes the use of two computer programs for analyzing the air movement and indoor air quality in multizone buildings. The first program CONTAM is used to create and edit the building description including data for all features relating to airflow or to the generation and removal of contaminants. It uses a graphic interface to establish the spatial relationship of these features. These data along with weather data are used by the program CONTAMX to calculate the airflows and dynamic levels of indoor contaminants. The results of the calculation may be reviewed graphically in CONTAM and printable files may be generated. Together these two programs are called CONTAM93.

02,537
PB94-194388 PC A04/MF A01
National Inst. of Standards and Technology (BFRL), Gaithersburg, MD.
CONTAM88 Building Input Files for Multi-Zone Airflow and Contaminant Dispersal Modeling.
J. B. Fang, and A. K. Persily. Jun 94, 53p, NISTIR-5440.

Keywords: *Indoor air pollution, *Air flow, *Buildings, Computerized simulation, Algorithms, Ventilation, Contaminants, Computer files, Dispersants, Data bases, Infiltration(Fluids), *CONTAM88 computer program, *Multi-zone air flow, *Contaminant dispersal modeling.

Input files for the multi-zone airflow and contaminant dispersal computer program CONTAM88 are described for four large buildings. The files were developed for a twelve-story multi-family residential building, a five-story mechanically-ventilated office building with an atrium, a seven-story mechanically-ventilated office building with an underground parking garage, and a one-story school building. The physical characteristics of each building and its idealization as a multi-zone airflow system are described. These input files enable a user to employ CONTAM88 to study airflow and contaminant dispersal in these large buildings without developing building idealizations and inputting them into CONTAM88. Results of selected computer simulations are presented to demonstrate the effects of wind speed, indoor-outdoor temperature difference, and the percentage of outdoor air intake in the supply air on air change rates and interzonal airflows for these four buildings. Appendices are also included that contain a building component leakage database useful in multizone airflow modeling and updated information on the use of CONTAM88.

02,538
PB94-199874 Not available NTIS
National Inst. of Standards and Technology (BFRL), Gaithersburg, MD. Building Environment Div.
Environmental Evaluation of a New Federal Office Building.
Final rept.
W. S. Dols, A. K. Persily, and S. J. Nabinger. 1993, 9p.
Pub. in Proceedings of IAQ 92 Environments for People Conference, San Francisco, CA., October 19-21, 1992, p85-93. Sponsored by General Services Administration, Washington, DC.

Keywords: *Indoor air pollution, *Office buildings, *Air pollution monitoring, *Federal buildings, *Air quality, Environmental engineering, Ventilation, Concentration(Composition), Carbon dioxide, Carbon monoxide, Radon, Formaldehyde, Volatile organic compounds, Performance evaluation, Reprints, Overland(Missouri).

A study of the environmental performance of three new office buildings is being conducted, involving long-term monitoring of building ventilation rates and indoor levels of selected pollutants, both before occupancy and during early occupancy. This paper describes the effort in a seven-story office building in Overland, Missouri. The measurement results discussed in this paper include tracer gas decay measurements of ventilation rates and the concentrations of carbon dioxide, carbon monoxide, radon, formaldehyde, and volatile organic compounds (VOCs).

02,539
PB95-108825 Not available NTIS
National Inst. of Standards and Technology (NEL), Gaithersburg, MD. Building Environment Div.
Ventilation Rates in Office Buildings.
Final rept.
A. Persily. 1989, 9p.
Sponsored by Geological Survey, Reston, VA., General Services Administration, Washington, DC., and Department of Energy, Washington, DC.
Pub. in Proceedings of the ASHRAE/SOEH Conference on IAQ 89 The Human Equation: Health and Comfort, San Diego, CA., April 17-20, 1989, p128-136.

Keywords: *Ventilation, *Office buildings, *Air quality, *Thermal confort, *Indoor air pollution, *Flow measurement, Design criteria, Air flow, Performance evaluation, Standards, Tracer techniques, Reprints.

The ventilation rate of an office building impacts the building air quality in terms of both thermal comfort and pollutant levels. The National Institute of Standards and Technology has been studing ventilation in office buildings for several years. The research has included the measurement of ventilation rates in 14 office buildings for periods on the order of one year, and has produced a data set of about 3000 ventilation measurements under a range of weather and building operation conditions. These data are a unique source of actual ventilation rate measurements in office buildings, and are the subject of the paper. The data provides an indication of current practice. Although the ventilation rates vary considerably among the buildings and for each individual structure, many of the buildings have ventilation rates below recommended levels and/or design values during significant portions of the year.

02,540
PB95-126066 Not available NTIS
National Inst. of Standards and Technology (BFRL), Gaithersburg, MD. Fire Safety Engineering Div.
Dispersion and Deposition of Smoke Plumes Generated in Massive Fires.
Final rept.
A. F. Ghoniem, X. Zhang, O. M. Knio, H. Baum, and R. Rehm. 1993, 19p.
Sponsored by Minerals Management Service, Herndon, VA.
Pub. in Jnl. of Hazardous Materials 33, p275-293 1993.

Keywords: *Plumes, *Fires, *Smoke, *Environment effects, *Trajectories, *Computational fluid dynamics, Deposition, Buoyancy, Environmental pollution, Dispersion, Pollution transport, Equations of motion, Wind direction, Air pollution, Reprints, *Buoyant smoke plumes.

Massive fires resulting from the uncontrolled burning of crude oil from spills or industrial accidents produce large smoke-laden buoyant plumes which rise in the wind direction before they equilibrate within a stably stratified atmosphere. Beyond this point, the plume material cools by entrainment and the plume becomes negatively buoyant due to the heavy smoke loading. The trajectory of the descending plume, which determines the ground distribution of smoke, is the subject of this paper. A computational model for the simulation of large-scale smoke plumes resulting from such fires is developed and applied to investigate the effects of the plume initial properties on its trajectory and smoke deposition patterns. Attention is focused on the descent and dispersion of wind-driven plumes in a homogeneous atmosphere, and the smoke deposition on flat terrain. Results show that the plume dynamics in the cross-wind direction are dominated by two buoyantly generated, coherent, streamwise vortices which distort the plume cross section into a kidney-shaped structure. The strength of the two vortices and their separation increases as the plume falls. The plume width grows under the action of these vortices at a rate which increases as the plume settles on the ground, leading to a smoke footprint which does not resemble the prediction of Gaussian dispersion models.

02,541
PB95-138129 PC A04/MF A01
National Inst. of Standards and Technology (TS), Gaithersburg, MD. National Voluntary Lab. Accreditation Program.

National Voluntary Laboratory Accreditation Program: Bulk Asbestos Analysis.
Handbook.
E. B. Steel, J. Verkouteren, and D. F. Alderman. Aug 94, 72p, NIST/HB-150/3.
Also available from Supt. of Docs. as SN003-003-03288-3. See also PB94-178225.

Keywords: *Asbestos, *Laboratories, *Certification, *Polarized light, *Microscopy, Requirements, Licensure, Methodology, Standardization, Performance evaluation, Quality assurance, Administrative procedures, National Voluntary Laboratory Accreditation Program, US NIST.

The handbook presents the specific requirements that laboratories must comply with in order to be accredited under the National Voluntary Laboratory Accreditation Program (NVLAP) for Bulk Asbestos Analysis. Details are provided regarding the on-site assessment and proficiency testing requirements for laboratories analyzing bulk samples by means of polarized light microscopy.

02,542
PB95-150140 Not available NTIS
National Inst. of Standards and Technology (BFRL), Gaithersburg, MD. Building Environment Div.
Study of Ventilation and Carbon Dioxide in an Office Building.
Final rept.
S. J. Nabinger, A. K. Persily, and W. S. Dols. 1994, 10p.
Sponsored by Public Buildings Service, Washington, DC.
Pub. in American Society of Heating, Refrigerating and Air-Conditioning Engineers Transactions 100, pt2 10p 1994.

Keywords: *Office buildings, *Ventilation, *Carbon dioxide, *Indoor air quality, Air flow rates, Air circulation, Air infiltration, Flow measurement, Tracer techniques, Air pollution monitoring, Indoor air pollution, Space HVAC systems, Reprints, Air exchange rates.

Ventilation rates and indoor carbon dioxide levels were monitored for two years in a new office building near St. Louis, Missouri. These measurements were made to assess the operation and performance of the ventilation system in this building and to investigate the relationship between indoor carbon dioxide levels and air change rates. Ventilation rates were measured with the tracer gas decay technique using an automated measuring system. Indoor carbon dioxide concentrations were also measured with an automated system. The relationship between the indoor carbon dioxide levels and the building air change rates was similar to that seen in other office buildings. This discussion points out limitations in the use of equilibrium analysis of carbon dioxide concentrations in office buildings.

02,543
PB95-151189 Not available NTIS
National Inst. of Standards and Technology (NML), Gaithersburg, MD. Gas and Particulate Science Div.
Guidelines for Refractive Index Measurements of Asbestos.
Final rept.
J. R. Verkouteren, J. M. Phelps, and E. B. Steel. 1989, 5p.
Pub. in Microbeam Anal. 24, p429-433 1989.

Keywords: *Asbestos, *Refractive index, *Optical measurement, *Guidelines, Chrysotile, Amosite, Crocidolite, Polarized light, Microscopy, Calibration standards, Reference standards, Reprints, Standard reference materials, Focal screening, Dispersion staining, Becke line technique.

Refractive index is one of the primary optical properties used to identify minerals using polarized light microscopy. Through the association with the Bulk Asbestos Laboratory Accreditation Program, the authors have received requests from hundreds of Laboratories for technical assistance in the area of bulk asbestos analysis. Many of these requests are for information on the measurement of refractive index, specifically using the focal screening (dispersion staining) and Becke line techniques. The authors have developed Standard Reference Materials (SRMs) of chrysotile, amosite, and crocidolite (SRM1866) to serve laboratories as primary calibration standards for the measurement of the optical properties of asbestos, including refractive index. These materials will be discussed and used as examples to explain the application of focal screening and the Becke line technique to refractive index measurement.

02,544
PB95-162095 Not available NTIS
National Inst. of Standards and Technology (BFRL), Gaithersburg, MD. Building Environment Div.
Ventilation, Carbon Dioxide and ASHRAE Standard 62-1989.
Final rept.
A. K. Persily. 1993, 4p.
Pub. in American Society of Heating, Refrigeration and Air-Conditioning Engineers Jnl. 35, n7 p40-44 Jul 93.

Keywords: *Ventilation, *Carbon dioxide, *Air quality standards, *Indoor air quality, Commercial buildings, Office buildings, Indoor air pollution, Air flow, Flow rates, Flow measurement, Air infiltration, Air circulation, Air pollution monitoring, Space HVAC systems, Reprints, *ASHRAE Standard 62-1989.

The article is an attempt to reduce some of the confusion concerning the issues of ventilation, carbon dioxide and ASHRAE Standard 62-1989 that has been evident in numerous discussions of indoor air quality. The article presents a brief discussion of how indoor carbon dioxide levels are related to ventilation rates, including the potential for using these indoor concentrations to determine outdoor airflow rates. The role of carbon dioxide is Standard 62, specifically the significance of the 1000 ppm guideline is also discussed. Much of the discussion in the article is specific to mechanically-ventilated office buildings, but many of the conclusions are relevant to other building types.

02,545
PB95-162277 Not available NTIS
National Inst. of Standards and Technology (NML), Gaithersburg, MD. Gas and Particulate Science Div.
Development of a Gas Standard Reference Material Containing Eighteen Volatile Organic Compounds.
Final rept.
G. C. Rhoderick. 1991, 8p.
Pub. in Fresenius' Jnl. of Analytical Chemistry 341, n9 p524-531 Nov 91.

Keywords: *Reference standards, *Gas analysis, *Quantitative chemical analysis, Gas chromatography, Gravimetric analysis, Microanalysis, Flame ionization, Electron-capture detectors, Interlaboratory comparisons, Calibrating, Certification, Reprints, *Volatile organic compounds, Standard reference materials.

A procedure to prepare primary gas cylinder standards for eighteen volatile organic compounds (VOC's) at the 1-15 nmol/mol (ppb) level was developed. These gas standards were evaluated over a period of 2 years and were determined stable and accurate. This research resulted in the development of Standard Reference Material (SRM) 1804 containing these 18 volatile organic compounds in nitrogen at a nominal concentration of 5 ppb for each compound.

02,546
PB95-162285 Not available NTIS
National Inst. of Standards and Technology (NML), Gaithersburg, MD. Gas and Particulate Science Div.
Stability/Instability of Gas Mixtures Containing 1,3-Butadiene in Treated Aluminum Gas Cylinders.
Final rept.
G. C. Rhoderick. 1990, 9p.
Pub. in Proceedings of 1990 EPA/A&WMA International Symposium on Measurement of Toxic and Related Air Pollutants, Raleigh, NC., May 1990, p709-717.

Keywords: *Butadienes, *Stability, *Gas cylinders, *Binary mixtures, *Calibration standards, Nitrogen, Air pollution, Chemical analysis, Quantity ratio, Concentration(Composition), Reprints, *Aluminum gas cylinders, *1,3-Butadiene.

The Gas Metrology Research Group of the National Institute of Standards and Technology (NIST), has been involved in research and development of gas standards of volatile toxic organic compounds for many years. Over thirty toxic organic compounds have been studied in gas mixtures contained in high pressure aluminum gas cylinders with specially treated interior surfaces. Almost all compounds studied to date have shown very good long term stability at the parts-per-billion (ppb, nanomole/mole) to parts-per-million (ppm, micromole/mole) range. One exception, 1,3-butadiene, is a compound that many scientists and policy makers are very interested in measuring in the environment. The author discusses data obtained over several years for gas mixtures of 1,3-butadiene in nitrogen, at concentrations of 2 ppm, 100 ppb, and 10 ppb. The data demonstrate that mixtures of 1,3-butadiene at the 2 ppm level have remained stable for over three years. However, gas mixtures of 1,3-butadiene at the 10 ppb level have shown decreases in concentration of more than 70% over a two-year period. Decreases in the concentration of 1,3-butadiene have been observed immediately after the preparation of the gas mixture in several cylinders. This indicates that gas mixtures of 1,3-butadiene are not stable at the ppb levels and therefore are not reliable as accurate calibration standards.

02,547
PB95-163622 Not available NTIS
National Inst. of Standards and Technology (NML), Gaithersburg, MD. Gas and Particulate Science Div.
Standards for Atmospheric Measurements.
Final rept.
R. A. Velapoldi, and W. D. Dorko. 1990, 7p.
Pub. in Fresenius Jnl. of Analytical Chemistry 338, n4 p479-485 1990.

Keywords: *Air pollution sampling, *Chemical analysis, *Reference standards, *Quality control, Air pollutants, Gas analysis, Atmospheric chemistry, Interlaboratory comparisons, Quality assurance, Accuracy, Standardization, Reprints, Standard reference materials.

The effects of global climate change and air pollutants on the earth and human population, have made the measurement of atmospheric gaseous and particulate species as well as kinetic rate constants for modeling of utmost importance. The paper reviews: (1) the philosophy and process of the development, preparation, and certification of gas Standard Reference Materials (SRM's) at the National Institute of Standards and Technology; (2) some of the SRM's currently available, with a listing of their components, concentrations, and specific uses; (3) the results of a recent laboratory intercomparison; (4) a brief discussion of some of the measurements and SRM research currently in progress; and finally (5) some ideas for new standards that might be needed in the future.

02,548
PB95-163705 Not available NTIS
National Inst. of Standards and Technology (NML), Gaithersburg, MD. Chemical Kinetics Div.
Atmospheric Reactivity of alpha-Methyl-Tetrahydrofuran.
Final rept.
T. J. Wallington, W. O. Siegal, R. Liu, M. J. Kurylo, Z. Zhang, and R. E. Huie. 1990, 4p.
Pub. in Environmental Science and Technology 24, n10 p1596-1599 1990.

Keywords: *Atmospheric chemistry, *Air pollution, *Fuel additives, Biomass, Volatile organic compounds, Environmental impact, Hydroxyl radicals, Reaction kinetics, Exhaust emissions, Reprints, *Furan/methyltetrahydro.

Biomass derived alpha-methyl-tetrahydrofuran, MTHF, has been proposed as an automotive fuel additive. Since MTHF is a volatile organic compound, the environmental impact of evaporation to the atmosphere needs to be considered if this compound is to be used in substantial quantities in such applications. The major loss process of MTHF in the atmosphere is expected to occur via reaction with hydroxyl radicals (OH), hence we have conducted a study of the kinetics of the reaction of OH radicals with MTHF using both absolute (flash photolysis resonance fluorescence) and relative rate techniques. The absolute rate experiments were performed over the temperature range 240-400 K at total pressures of 35 torr of argon; the relative rate experiments were conducted at 295 K in 740 torr of synthetic air. The results from both techniques were in good agreement.

02,549
PB95-163754 Not available NTIS
National Inst. of Standards and Technology (NML), Gaithersburg, MD. Gas and Particulate Science Div.
Measurement of the Uniformity of Particle Deposition of Filter Cassette Sampling in a Low Velocity Wind Tunnel.
Final rept.
C. C. Wang, R. A. Fletcher, E. Steel, and J. W. Gentry. 1990, 4p.
Pub. in Jnl. of Aerosol Science 21, nS1 pS621-S624 1990.

Keywords: *Air pollution sampling, *Aerosols, *Wind tunnels, Indoor air pollution, Asbestos, Wind velocity, Bias, Error analysis, Reprints.

Microscopic particle counting is often employed for determining airborne fiber concentrations. Wind tunnel testing was used to determine whether there is a systematic sampling bias for anisokinetic and non-isoaxial conditions. Low wind velocities (0.2 - 0.5 m/s) were employed to simulate indoor air environments.

02,550
PB95-169041 Not available NTIS
National Inst. of Standards and Technology (CSTL), Boulder, CO. Thermophysics Div.
Membrane Gas Separation for a Fluidized-Bed Incinerator.
Final rept.
J. J. Pellegrino, D. M. Stull, and B. W. Logsdon. 1993, 5p.
Pub. in Proceedings of the American Filtration Society Meeting, Chicago, IL., May 3-6, 1993, p390-394.

Keywords: *Hazardous materials, *Low level radioactive wastes, *Incinerators, *Air pollution control, Fluidized beds, Membranes, Separation processes, Permeability, Combustion products, Carbon dioxide, Oxygen, Nitrogen, Water, Reprints, Gas permeation.

For their proposed fluidized-bed incineration process, EG&G Rocky Flats' technical staff are considering the possible scenario of placing a 'molecular filter' (a gas separation membrane) system on their stack gases. The permeate through the membrane would principally be the products of combustion: CO2 and H2O, and the retentate is circulated back to the incinerator as the fluidizing gas. Data were obtained for cellulose acetate and polyamide membranes using a CO2-rich stream with N2 and O2. Additional measurements were made to provide some basis for estimating the fate and effect of contaminants. Gas permeation measurements, with both types of membranes, were made on streams that contained trace C(sub 1)-C(sub 3) contaminants. These latter measurements were also made with cellulose acetate samples which had been exposed to saturated organic solvent vapors for extended periods.

02,551
PB95-175659 Not available NTIS
National Inst. of Standards and Technology (CSTL), Gaithersburg, MD. Surface and Microanalysis Science Div.
Sources of Urban Contemporary Carbon Aerosol.
Final rept.
L. M. Hildemann, D. Klinedinst, G. A. Klouda, L. A. Currie, and G. R. Cass. 1994, 12p.
Pub. in Environmental Science and Technology 28, n9 p1565-1576 1994.

Keywords: *Aerosols, *Carbonaceous materials, *Air pollution sources, *Urban areas, Carbon, Carbon 12, Carbon 14, Fossil fuels, Particulates, Exhaust emissions, Anthropogenic sources, Air pollution sampling, Air pollutants, Los Angeles, Reprints, Emission inventories.

Emissions from the major sources of fine carbonaceous aerosol in the Los Angeles basin atmosphere have been analyzed to determine the amounts of the C-12 and C-14 isotopes present. From these measurements, an inventory of the fossil carbon and contemporary carbon particle emissions to the Los Angeles atmosphere has been created. Using a mathematical model for atmospheric transport, predictions are made of the atmospheric fine particulate fossil carbon and contemporary carbon concentrations expected due to primary source emissions. It is concluded that the high fraction of contemporary carbon measured historically in Los Angeles is not due to local emission sources of biogenic material; rather, it is due to a combination of local anthropogenic pollution sources and background marine aerosol advected into the city.

02,552
PB95-176004 Not available NTIS
National Inst. of Standards and Technology (BFRL), Gaithersburg, MD. Building Environment Div.
Limits of CO2 Monitoring in Determining Ventilation Rates.
Final rept.
A. K. Persily. 1994, 4p.
Pub. in TAB Jnl., p19-22 1994.

Keywords: *Carbon dioxide, *Ventilation, *Indoor air pollution, *Air pollution monitoring, Air infiltration, Air flow, Flow rates, Concentration(Composition), Concentration rates, Buildings, Reprints, ASHRAE Standard 62-1989.

The article is an attempt to reduce some of the confusion concerning the issues of ventilation, carbon dioxide (CO2), and ASHRAE Standard 62-1989 that has been evident in recent discussions of indoor air quality. The article presents a brief discussion of how indoor CO2 levels are related to ventilation rates, including the use of indoor concentration measurements to determine outdoor air flow rates. The role of carbon dioxide in Standard 62, specifically the significance of the 1,000 ppm guideline, is also discussed. The article primarily addresses mechanically ventilated office buildings, but many of the statements are also relevant to other building types.

02,553
PB95-176012 Not available NTIS
National Inst. of Standards and Technology (BFRL), Gaithersburg, MD. Building Environment Div.
Ventilation Effectiveness Measurements in Two Modern Office Buildings.
Final rept.
A. K. Persily, W. S. Dols, and S. J. Nabinger. 1993, 6p.
Contract DE-AI01-91CE21042
Sponsored by Department of Energy, Washington, DC.
Pub. in Proceedings of Indoor Air '93, Helsinki, Finland, July 4-8, 1993, p195-200.

Keywords: *Office buildings, *Ventilation, *Indoor air pollution, *Air infiltration, Air flow, Flow rates, Flow measurement, Air quality, Air intakes, Space HVAC systems, Reprints, Air change effectiveness.

Ventilation effectiveness measurements were made in two office buildings employing the age-of-air approach. The objective of these tests was to study the applicability of the associated tracer gas procedures in mechanically ventilated office buildings. Experimental issues were investigated including the ability to establish a uniform tracer concentration at the start of the test and the relationship of ventilation system configuration and system operation on the test procedure. The test results indicate good mixing of the ventilation air within the occupied space. In addition, experience was obtained with the measurement procedures that will assist the development of a standardized approach to measuring ventilation effectiveness in the field.

02,554
PB95-178893 PC A05/MF A01
National Inst. of Standards and Technology (BFRL), Gaithersburg, MD. Building Environment Div.
Indoor Air Quality Impacts of Residential HVAC Systems. Phase 2.A Report: Baseline and Preliminary Simulations.
S. J. Emmerich, and A. K. Persily. Jan 95, 80p, NISTIR-5559.
See also Phase 1 Report, PB95-135596. Sponsored by Consumer Product Safety Commission, Washington, DC.

Keywords: *Air pollution monitoring, *Indoor air pollution, *Space HVAC systems, *Baseline measurements, Residential buildings, Air pollutants, Air intakes, Air infiltration, Air flow, Flow measurement, Ventilation, Air pollution control, Mathematical models, Computerized simulation.

NIST is performing whole building airflow and contaminant dispersal computer simulations with the program CONTAM93 to assess the ability of modifications of central forced-air heating and cooling systems to control pollutant sources relevant to the residential environment. The report summarizes the results of Phase II.A of this project, which consisted of three major efforts: baseline simulations of contaminant levels without indoor air quality (IAQ) controls, design of the IAQ control retrofits, and preliminary simulations of contaminant levels with the IAQ control retrofits. In Phase II.B of the study, all of the baseline cases will be modified to incorporate the IAQ control retrofits. The retrofit results will then be compared to the baseline results to evaluate the effectiveness of the retrofits.

02,555
PB95-180238 Not available NTIS
National Inst. of Standards and Technology (BFRL), Gaithersburg, MD. Building Environment Div.
Application of a Multizone Airflow and Contaminant Dispersal Model to Indoor Air Quality Control in Residential Buildings.
Final rept.
S. J. Emmerich, A. K. Persily, and G. N. Walton. 1994, 15p.
Pub. in Proceedings of the AIVC Conference (15th): The Role of Ventilation, Buxton, Great Britian, September 27-30, 1994, p493-507 1994.

Keywords: *Air flow, *Indoor air pollution, *Residential buildings, *Air quality, *Computerized simulation, Ventilation, HVAC systems, Air circulation, Air pollution control, Tracer studies, Contaminants, Reprints, *CONTAM93 model, Contaminant dispersal models, Multi-zone air flow.

A new multizone airflow and contaminant dispersal model CONTAM93 is described, along with a demonstration of its application in a study of ventilation and contaminant control in single-family residential buildings. While CONTAM93 is based on existing theory of network airflow analysis and contaminant dispersal, the model employs a unique graphic interface for data input and display. The interface uses a sketchpad to describe the connections between zones and icons to represent zones, openings, ventilation system components, and contaminant sources and sinks. The model, its graphic interface and plans for its further development are described. As a demonstration of the capabilities of CONTAM93, the paper describes a study of ventilation and contaminant control in eight single-family residential buildings. The overall objective of the effort is to study the impact of residential HVAC systems on indoor air quality (IAQ). This paper describes the study and the use of CONTAM93 to calculate whole building air change rates for a range of weather conditions and to simulate fan pressurization and tracer gas decay tests in the houses.

02,556
PB95-198735 PC A04/MF A01
National Inst. of Standards and Technology (BFRL), Gaithersburg, MD. Building Environment Div.
Measurements of Indoor Pollutant Emissions from EPA Phase II Wood Stoves.
S. J. Nabinger, A. K. Persily, K. S. Sharpless, and S. A. Wise. Feb 95, 68p, NISTIR-5575.
Sponsored by Consumer Product Safety Commission, Washington, DC. Directorate for Health Sciences.

Keywords: *Stoves, *Air pollution sampling, *Indoor air pollution, *Residential buildings, Polycyclic aromatic hydrocarbons, Particulates, Emission factors, Waste gases, Particle size, Air pollution monitoring, *Wood burning appliances.

Measurements of indoor pollutant emissions were made for four wood stoves meeting the U.S. Environmental Protection Agency (EPA) Phase II emission requirements in a 37 sq. m (400 sq. ft) test house at National Institute of Standards and Technology (NIST). The stoves were operated in a manner consistent with typical residential use and in accordance with the manufacturers' instructions. Three tests were conducted for each stove, with each test lasting approximately ten hours. During the tests some of the following quantities monitored included: combined gaseous and particulate phase concentrations of individual polycyclic aromatic hydrocarbons (PAH) averaged over the test period, including benzo(a)pyrene (BAP); and, indoor and outdoor air temperature and relative humidity. Based on these measurements, emission rates of the individual PAH compounds were determined for each test.

02,557
PB95-220422 PC A03/MF A01
National Inst. of Standards and Technology (BFRL), Gaithersburg, MD. Building Environment Div.
Computer Simulations of Airflow and Radon Transport in Four Large Buildings.
J. B. Fang, and A. K. Persily. Apr 95, 50p, NISTIR-5611.
Sponsored by Environmental Protection Agency, Washington, DC. Office of Air and Radiation.

Keywords: *Air flow, *Radon, *Indoor air quality, *Computerized simulation, Ventilation, Air infiltration, Air circulation, Radionuclide migration, Leakage, Flow rates, Air intakes, Space HVAC systems, Temperature measurement, Spatial distribution, Flow models.

Computer simulations of airflow and radon transport in four large buildings are performed using the multi-zone airflow and pollutant transport model CONTAM88. These buildings include a twelve-story multi-family residential building, a five-story mechanically ventilated office building with an atrium, a seven-story mechanically ventilated office building with an underground parking garage, and a one-story mechanically ventilated school building. Interzone airflow rates and radon concentrations are predicted in these buildings as a function of wind speed and direction, indoor-outdoor temperature difference, and ventilation system operation. Ventilation system factors that are studied include the operation of exhaust fans in the apartment

building and variations in the percent outdoor air intake in the office buildings. Simulations in the office buildings are also made with the ventilation systems off and with variations in the balance of the supply and return airflow rates.

02,558
PB95-255899 PC A05/MF A01
Yale Univ., New Haven, CT. School of Architecture.
New Mass Transport Elements and Components for the NIST IAQ Model.
J. W. Axley. Jul 95, 90p, NIST/GCR-95/676.
Sponsored by National Inst. of Standards and Technology (BFRL), Gaithersburg, MD. Building Environment Div.

Keywords: *Indoor air pollution, *Air flow, *Air pollution dispersion, *Mathematical models, Aerosols, Particles, Air circulation, Environmental transport, Mass transport, Flow measurement, Contaminants, Filtration, Ventilation, Computerized simulation, Contaminant dispersal models.

This report presents new mass transport elements for the next generation of the NIST IAQ Model that may be used to model (1) homogenous (bulk-air) chemistry within well-mixed chamber, (2) aerosol mass transport within well-mixed chambers and fractional particle filtration in building filtration devices, and (3) heterogeneous (surface-related) physical processes and chemical transformations including those governing the behavior of gas-phase air cleaning devices. In an effort to maintain rigor, generality, and flexibility, each transport process is formulated in terms of the elemental mass transport step that together govern the overall process. In this way, the more complex processes may be represented as component equations that are assembled from fundamental element equations.

02,559
PB96-106877 PC A05/MF A01
National Inst. of Standards and Technology (BFRL), Gaithersburg, MD. Building Environment Div.
Indoor Air Quality Impacts of Residential HVAC Systems Phase II.B Report: IAQ Control Retrofit Simulations and Analysis.
S. J. Emmerich, and A. K. Persily. Sep 95, 94p, NISTIR-5712.
Sponsored by Consumer Product Safety Commission, Bethesda, MD.

Keywords: *Indoor air pollution, *Air pollution monitoring, *Air flow, *Space HVAC systems, Air infiltration, Air intakes, Flow measurement, Retrofitting, Residential buildings, Vents, Ambient air quality, Air pollutants, Ventilation systems, Heating systems, Computerized simulation, Graphs(Charts).

The National Institute of Standards and Technology (NIST) performed a preliminary study of the potential for using central forced-air heating and cooling system modifications to control indoor air quality (IAQ) in residential buildings. The objective of this effort was to provide insight into the use of state-of-the-art IAQ models to evaluate such modifications, the potential of these modifications to mitigate residential IAQ problems, the pollutant sources they are most likely to impact, and their potential limitations. This study was not intended to determine definitively whether the IAQ control options studied are reliable and cost-effective. The report summarizes the results on Phase II.B of this project, which consisted of three main efforts: computer simulations of contaminant levels with IAQ control retrofits, evaluation of the effectiveness of the IAQ control retrofits, and development of recommendations for future research.

02,560
PB96-109566 PC A03/MF A01
National Inst. of Standards and Technology (BFRL), Gaithersburg, MD. Office of Applied Economics.
EMISS: A Program for Estimating Local Air Pollution Emission Factors Related to Energy Use in Buildings: User's Guide and Reference Manual.
Final rept.
S. R. Petersen. Oct 95, 36p, NISTIR-5704.
Sponsored by Federal Energy Management Program, Washington, DC.

Keywords: *Emission factors, *Energy use, *Air pollution monitoring, Buildings, Energy consumption, Energy conservation, Heating systems, Regional analysis, Life cycle costs, Nitrous oxide, Sulfur dioxide, Carbon dioxide, Electric power, Distillates, Natural gas, Coal, Liquified natural gas, Residual fuels, Fossil fuels, Combustion, Sulfur content, User guides, EMISS computer program, End users.

EMISS is a computer program used to generate data files with regional or local air pollution emission factors for use with the Nist BLCC (Building Life-Cycle Cost) program. BLCC uses these emission factors to calculate air pollution emissions associated with energy use in buildings and reductions in those emissions attributable to energy conservation measures. Emission factors for fossil fuels can be regionalized or localized by specifying the percentage of sulfur in the fuel, the heating content of the fuel, and the end-use combustion process at the building site. A data base with state-specific electricity emission factors and U.S. average sulfur content of fossil fuels provides default data for use in setting up a regional emission factors file.

02,561
PB96-117221 Not available NTIS
National Inst. of Standards and Technology (CSTL), Gaithersburg, MD. Analytical Chemistry Div.
Analysis by a Combination of Gas Chromatography and Tandem Mass Spectrometry: Development of Quantitative Tandem-in-Time Ion Trap Mass Spectrometry: Isotope Dilution Quantification of 11-Nor-Delta-9-Tetrahydro cannabinol-9-Carboxylic Acid.
Final rept.
C. S. Phinney, and M. J. Welch. 1995, 5p.
Pub. in Rapid Communications in Mass Spectrometry, v9 p1056-1060 1995.

Keywords: *Toxic substances, *Mass spectrometers, Reprints, Sampling, Organic compounds, Quantitative analysis, *Drug analysis, Tandem Mass Spectrometry.

Collision-induced dissociation (CID) was performed in an ion-trap mass spectrometer to investigate quantification by isotope dilution and gas chromatography coupled with tandem mass spectrometry (GC/MS/MS). The operating system software was modified to allow simultaneous CID of two ions differing only slightly in mass/charge ratios. Simultaneous excitation of the base peaks of the parent compound and its deuterated analog in a co-eluting GC peak leads to quantitative and reproducible formation of daughter ions. Changing conditions in the mass analyzer as the GC peak elutes required broadening of the CID excitation frequency pattern. This had to be done so that relatively uniform dissociation energy would be imparted to both parent ions during the concentration changes associated with the elution of a GC peak. A commonly measured human metabolite of marijuana, 11-nor-delta-9-tetrahydro cannabinol-9-carboxylic acid, was analyzed in freeze-dried urine. The mean value, 14.0 equal to or greater than 0.61 (1 standard deviation) ng/mL, agrees very well with the GC/MS mean measured value of 14.1 equal to or greater than 0.45 ng/mL. The overall coefficient of variation for the individual ion-trap MS/MS sample measurements is 4.3%.

02,562
PB96-122650 Not available NTIS
National Inst. of Standards and Technology (BFRL), Gaithersburg, MD. Building Environment Div.
Few Caveats on Carbon Dioxide Monitoring.
Final rept.
A. P. Persily. 1994, 4p.
Pub. in Indoor Air Quality Jnl., v1 n4 p22-25 1994.

Keywords: *Carbon dioxide, *Air pollution monitoring, *Indoor air pollution, Commercial buildings, Ecological concentration, Air flow, Air circulation, Ventilation systems, Space HVAC systems, Tracer techniques, Errors, Reprints.

While techniques exist to relate indoor carbon dioxide concentrations to building ventilation, they are not as simple as sometimes suggested. Some of the techniques can yield reliable results when used correctly, while others can result in serious errors. Using any of these approaches requires that one understands the technique and the following factors are considered: the outdoor carbon dioxide concentration; the number of people in the building and the rate at which they generate carbon dioxide; variations in the number of occupants within the building and over time; variations in the carbon dioxide concentration within the building; the measurement uncertainty of the carbon dioxide monitor being used; ventilation system operation prior to and during the measurements; and, indoor sources of carbon dioxide other than the occupants.

02,563
PB96-135124 Not available NTIS
National Inst. of Standards and Technology (CSTL), Gaithersburg, MD. Organic Analytical Research Div.
Distinguishing the Contributions of Residential Wood Combustion and Mobile Source Emissions Using Relative Concentrations of Dimethylphenanthrene Isomers.
Final rept.
B. A. Benner, S. A. Wise, L. A. Currie, R. B. Zweidinger, R. K. Stevens, C. W. Lewis, G. A. Klouda, and D. B. Klinedinst. 1995, 8p.
Pub. in Environmental Science and Technology, v29 n9 p2382-2389 Sep 95.

Keywords: *Air pollution sources, *Combustion products, *Emissions, Particulates, Polycylic aromatic hydrocarbons, Emission factors, Gas chromatography, Mass spectroscopy, Carbon 13, Carbon 14, Ecological concentration, Vehicle air pollution, Wood burning appliances, Air pollution monitoring, Reprints, *Dimethylphenanthrenes.

As part of the United States Environmental Protection Agency's Integrated Air Cancer Project, air particulate matter samples collected in Boise, ID, were analyzed by gas chromatography with mass spectrometric detection (GC-MS) and apportioned between their two main sources: residential wood combustion (RWC) and motor vehicle (MV) emissions. The technique used for distinguishing the source contributions involved comparison of the concentration of 1,7-dimethylphenanthrene (1,7-DMP), a polycyclic aromatic hydrocarbon (PAH) emitted primarily by burning soft woods (e.g., pines), with that of a PAH emitted in modest concentrations by both RWC and MV sources, 2,6-dimethylphenanthrene (2,6-DMP). These results were then compared with the mean 1,7-DMP/2,6-DMP ratio of 48 samples collected in a roadway tunnel, with any enrichment in the Boise sample ratios over the mean tunnel ratio attributable to the RWC source. These resulting RWC contributios were compared with fraction RWC results obtained by radiocarbon measurements (C-14/C-13) of the same extracts from Boise, with generally good correlations between the two techniques observed, suggesting that the methods are comparable when used to distinguish emissions of MVs from RWC of soft woods.

02,564
PB96-146642 Not available NTIS
National Inst. of Standards and Technology (BFRL), Gaithersburg, MD. Building Environment Div.
Effectiveness of a Heat Recovery Ventilator, an Outdoor Air Intake Damper and an Electrostatic Particulate Filter at Controlling Indoor Air Quality in Residential Buildings.
Final rept.
S. J. Emmerich, and A. K. Persily. 1995, 13p.
Pub. in Air Infiltration and Ventilation Centre Conference (16th), Palm Springs, CA., September 19-22, 1995, p263-275 1995.

Keywords: *Residential buildings, *Ventilation systems, *Indoor air pollution, Space HVAC systems, Ventilators, Heat recovery, Air intakes, Dampers, Electrostatic precipitators, Filters, Air flow, Air infiltration, Particulates, Air pollution control, Reprints.

A preliminary study of the potential for using central forced-air heating and cooling system modifications to control indoor air quality (IAQ) in residential buildings was performed. The main objective was to provide insight into the potential of three IAQ control options to mitigate residential IAQ problems, the pollutant sources the controls are most likely to impact, and the potential limitations of the controls. Another important objective was to identify key issues related to the use of multizone models to study residential IAQ and to identify areas for follow-up work.

02,565
PB96-146659 Not available NTIS
National Inst. of Standards and Technology (BFRL), Gaithersburg, MD. Building Environment Div.
Multizone Modeling of Three Residential Indoor Air Quality Control Options.
Final rept.
S. J. Emmerich, and A. K. Persily. 1995, 8p.
Pub. in Building Simulation '95, International IBPSA Conference (4th), Madison, WI., August 14-16, 1995, p213-220.

Keywords: *Indoor air pollution, *Air pollution control, *Space HVAC systems, Computerized simulation, Heating systems, Cooling systems, Ventilation systems, Residential buildings, Environmental transport, Ecological concentration, Air flow, Electrostatic

precipitators, Filters, Heat recovery, Ventilators, Air intakes, Dampers, Reprints.

The impact of central forced-air heating and cooling system modifications on the levels of selected pollutants in single-family houses was evaluated by simulating pollutant concentrations due to a variety of sources in eight houses with typical HVAC systems. Simulations were performed with a multizone airflow and pollutant transport model and were repeated with the systems modified to include an electrostatic particulate filter, a heat recovery ventilator, and an outdoor air intake damper. The system modification reduced the pollutant levels in the houses for some cases; however, the results also demonstrated potential limitations in both the simulation method and the performance of the devices.

02,566
PB96-147392 PC A05/MF A01
National Inst. of Standards and Technology (TS), Gaithersburg, MD. National Voluntary Lab. Accreditation Program.
Airborne Asbestos Analysis: National Voluntary Laboratory Accreditation Program.
Handbook.
S. Turner, E. B. Steel, and D. F. Alderman. Oct 95, 83p, NIST/HB-150-13.
Also available from Supt. of Docs.

Keywords: *Asbestos, *Air pollution, *Chemical analysis, *Handbooks, Electron microscopy, Airboric wastes, Test methods, Performance tests, Procedures, Requirements, Site survey, Laboratories, *National Voluntary Laboratory Accreditation Program, NIST(National Institute of Standards and Technology), TEM(Transmission electron microscopy).

Any laboratory (including commercial, manufactor, university, or federal, state, or local government laboratory) that performs the test method that comprises the Airborne Asbestos Analysis Program many apply for National Voluntary Laboratory Accreditation Program (NVLAP) accreditation. Accreditation will be granted to a laboratory that satisfactorily fulfills the conditions for accreditation defined in NIST Handbook 150, NVLAP Procedures and General Requirements, which contain Title 15, Part 285 of the Code of Federal Regulations. These conditions include satisfactory performance in selected proficiency testing as required, and fulfilling the on-site assessment requirements, including resolution of identified deficiencies. The names of NVLAP-accredited laboratories are published in the NVLAP annual directory and other media to which information is regularly provided.

02,567
PB96-165782 PC A08/MF A02
National Inst. of Standards and Technology (BFRL), Gaithersburg, MD. Building Environment Div.
Multizone Modeling of Three Residential Indoor Air Quality Control Options.
S. J. Emmerich, and A. K. Persily. Mar 96, 145p, NISTIR-5801.
Supersedes PB95-135596, PB95-178893 and PB96-106877. Sponsored by Consumer Product Safety Commission, Washington, DC. Directorate of Engineering Science.

Keywords: *Indoor air quality, *Heating systems, *Cooling systems, *Residential buildings, Space HVAC systems, Indoor air pollution, Central systems, Ventilation systems, Air flow, Air infiltration, Flow measurement, Particulates, Microorganisms, Nitrogen dioxide, Carbon monoxide, Filtration, Electrostatic precipitators, Dampers, Heat recovery equipment, Computerized simulation, *Multizone analysis, Forced air, Volatile organic compounds.

The National Institute of Standards and Technology (NIST) performed a preliminary study of the use of central forced-air heating and cooling system modifications to control indoor air quality (IAW) in residential buildings. The objective of the effort was to provide insight into the use of state-of-the-art multizone airflow and IAQ models to evaluate such modifications, the potential of these modifications to mitigate residential IAW problems, the pollutant sources they are most likely to impact, and their potential limitations. The multizone airflow and pollutant transport program CONTAM93 was used to simulate the pollutant concentrations due to a variety of sources in eight buildings with typical HVAC systems under different weather conditions. Three indoor air quality control technologies were incorporated into the house models to determine their effectiveness in controlling the modeled pollutant sources. The technologies include the following: electrostatic particulate filtration, heat recovery ventilation, and an outdoor air intake damper on the forced-air system return.

02,568
PB96-167812 PC A04/MF A01
National Inst. of Standards and Technology (BFRL), Gaithersburg, MD. Building Environment Div.
Study to Determine the Existence of an Azeotropic R-22 'Drop-In' Substitute.
M. S. Kim, G. Morrison, W. J. Mulroy, and D. A. Didion. Mar 96, 50p, NISTIR-5784.
See also PB92-149814. Sponsored by Electric Power Research Inst., Palo Alto, CA. and Korea Science and Engineering Foundation.

Keywords: *Refrigerants, *Environmental chemical substitutes, *Azeotropes, Cooling systems, Mixtures, Cyclopropane, Butanes, Propane, Refrigeration, Computerized simulation, Heat pumps, HFC-134a, HCFC(Hydrochlorofluorocarbon), CFC(Chlorofluorocarbon).

The reduction in chlorofluorocarbon (CFC) and hydrochlorofluorocarbon (HCFC) production and the scheduled phase-out of these ozone depleting refrigerants requires the development and determination of environmentally safe refrigerants for use in heat pumps, water chillers, air conditioners, and refrigerators. Azeotropic mixtures are attractive as alternative refrigerants because they behave very nearly as pure materials. A simple correlative scheme that allows one to judge whether or not an azeotrope is likely in a binary refrigerant mixture is discussed. This paper presents laboratory and computer simulation model evaluation of two of the azeotropic refrigerant mixtures which are identified, HFC-134a (1,1,1,2-tetrafluoroethane) with R-C290 (Propane) and HFC-134a with R-600a (Isobutane), in a generic heat pump apparatus. A third azeotropes mixture, HFC-134a with R-C290 (Cyclopropane) is examined by computer simulation only.

02,569
PB97-111249 Not available NTIS
National Inst. of Standards and Technology (BFRL), Gaithersburg, MD. Building Environment Div.
Relationship between Indoor Air Quality and Carbon Dioxide.
Final rept.
A. K. Persily. 1996, 6p.
Pub. in Indoor Air '96, the International Conference on Indoor Air Quality and Climate (7th), Nagoya, Japan, July 21-26, 1996, v2 p961-966.

Keywords: *Carbon monoxide, *Indoor air pollution, *Air pollution monitoring, Commercial buildings, Air flow, Flow rates, Air circulation, Air infiltration, Odors, Ventilation, Ecological concentration, Reprints, Air exchange rates.

The paper describes the relationship of indoor CO2 concentrations to building air quality and ventilation, with a focus on how CO2 can be used to evaluate air quality and ventilation performance. While CO2 concentrations do not provide a comprehensive indication of indoor air quality, they can be used to assess the acceptability of a space in terms of human body odor. Also, under some circumstances, CO2 can be used to evaluate building ventilation, specifically air change rates and percent outdoor air intake.

02,570
PB97-113203 Not available NTIS
National Inst. of Standards and Technology (BFRL), Gaithersburg, MD. Building Environment Div.
CONTAM94: A Multizone Airflow and Contaminant Dispersal Model with a Graphic User Interface.
Final rept.
G. N. Walton. 1995, 6p.
Pub. in Building Simulation '95: Proceedings of the Conference of International Building Performance Simulation Association (4th), Madison, WI., August 14-16, 1995, p674-679.

Keywords: *Air flow, *Contaminants, *Indoor air pollution, Air circulation, Air pollution monitoring, Environmental transport, Graphical user interface, Computerized simulation, Algorithms, Computer models, Reprints, CONTAM94 model, Multizone buildings.

CONTAM94 is an airflow and contaminant migration analysis program combining algorithms for modeling airflow and contaminant dispersal in multizone buildings. It employs a simplified graphic description of the building for both data entry and the presentation of simulation results. It can handle buildings containing a large number of zones.

02,571
PB97-114227 PC A05/MF A01
National Inst. of Standards and Technology (BFRL), Gaithersburg, MD. Building Environment Div.
Carbon Monoxide Dispersion in Residential Buildings: Literature Review and Technical Analysis.
A. K. Persily. Oct 96, 71p, NISTIR-5906.
Sponsored by National Fire Protection Association, Quincy, MA.

Keywords: *Carbon monoxide, *Air pollution dispersion, *Residential building, *Indoor air pollution, Air circulation, Ventilation, Air flow, Flow rates, Diffusion models, Rooms, Air pollution monitoring, Tracer techniques, Detection, Exposure, Environmental engineering, Computerized simulation, Literature surveys.

While the use of CO detectors can decrease the likelihood of exposure to such CO levels, questions exist concerning the installation of these devices in residential buildings, primarily with regards to the location and number of detectors. A literature review and technical analysis was conducted to assess information on CO dispersion in residential buildings that could support the development of guidance on detector installation. The review covered a number of issues including CO concentration measurements in residential buildings, sources of indoor CO, mixing within and between rooms, tracer gas techniques for assessing building airflow, and computer models of air movement and contaminant dispersal in buildings. The material obtained in the literature review is discussed, and a technical analysis of the issues related to CO dispersion in residential buildings is presented.

02,572
PB97-118749 Not available NTIS
National Inst. of Standards and Technology (BFRL), Gaithersburg, MD. Building Materials Div.
Materials-Science Based Approach to Phenol Emissions from a Flooring Material in an Office Building.
Final rept.
J. W. Martin, A. K. Persily, F. R. Guenther, E. Byrd, L. Oakley, T. Nguyen, and W. S. Liggett. 1996, 6p.
Pub. in Indoor Air '96, International Conference on Indoor Air Quality and Climate (7th), Nagoya, Japan, July 21-26, 1996, v2 p109-114.

Keywords: *Office buildings, *Phenols, *Floors, *Indoor air pollution, Epoxy resins, Emissions, Building materials, Chemical analysis, Physical properties, Reprints, Volatile organic compounds.

It was hypothesized that phenol emissions from an epoxy floor-leveling material were the source of the complaints. A materials-science based study was performed to ascertain whether phenol, or any other volatile organic compounds, was being emitted from the floor-leveling material. The chemical composition and physical properties of the leveling material were determined using a variety of analytical procedures typical of a materials-science based approach. It was concluded that the floor-leveling material contained phenol, and that the measured concentrations ranged from 0.25% to 0.52% of the material's mass.

02,573
PB97-118806 Not available NTIS
National Inst. of Standards and Technology (BFRL), Gaithersburg, MD. Building Environment Div.
Issues in the Field Measurement of VOC Emission Rates.
Final rept.
A. K. Persily. 1996, 6p.
Pub. in Indoor Air '96, International Conference on Indoor Air Quality and Climate (7th), Nagoya, Japan, July 21-26, 1996, v2 p49-54.

Keywords: *Emissions, *Indoor air pollution, *Air pollution monitoring, Ecological concentration, Mass balance, Absorption, Desorption, Design analysis, Computerized simulation, Reprints, *Volatile organic compounds.

The measurement of VOC emission rates in the field can be valuable in indoor air quality research, in evaluations of the indoor air quality impacts of design, and in the diagnosis of indoor air quality problems. The paper reviews the mass balance theory employed in field measurements of VOC emission rates. Some concerns associated with these measurements are dis-

cussed including the assumption of equilibrium VOC concentrations and the neglect of adsorption and desorption of VOC on building surfaces. Computer simulations are described that provide an order-of-magnitude assessment of the impacts of these issues.

02,574
PB97-122352 Not available NTIS
National Inst. of Standards and Technology (CSTL), Gaithersburg, MD. Surface and Microanalysis Science Div.
Radiocarbon Measurements of Atmospheric Volatile Organic Compounds: Quantifying the Biogenic Contribution.
Final rept.
G. A. Klouda, C. W. Lewis, R. A. Rasmussen, R. K. Stevens, L. A. Currie, D. J. Donahue, A. J. T. Jull, R. L. Seila, G. C. Rhoderick, and R. L. Sams. 1996, 8p.
Pub. in Environmental Science and Technology, v30 n4 p1098-1105 Jun 96.

Keywords: *Carbon 14, *Natural emissions, *Air pollution sampling, *Biomass, Air pollution sources, Ozone, Precursors, Ecological concentration, Atmospheric chemistry, Photochemistry, Urban areas, Photochemical reactions, Data quality, Quality control, Reprints, *Volatile organic compounds, Atlanta(Georgia).

The radiocarbon C-14 abundance of atmospheric volatile organic compounds (VOC) gives a quantitative estimate of contributions from biomass and fossil-mass sources, important information for effective regulation of ozone precursors. The authors report the details of a methodology to perform such measurements and the first exploratory C-14 results on VOC fractions separated from two composited urban tropospheric air samples, collected during the summer (1992) in Atlanta, GA. The results of these experiments, designed to (1) evaluate the entire C-14 VOC measurement process and (2) obtain reliable estimates of biogenic contributions to atmospheric VOC, emphasize how important controls are throughout this multi-step chemical process to ensure quality data.

Environmental Health & Safety

02,575
PB95-140117 Not available NTIS
National Inst. of Standards and Technology (PL), Gaithersburg, MD. Ionizing Radiation Div.
Radiation Accident at an Industrial Accelerator Facility.
Final rept.
D. A. Schauer, B. M. Coursey, C. E. Dick, M. F. Desrosiers, A. D. Jacobson, W. L. McLaughlin, and J. M. Puhl. 1993, 10p.
Sponsored by Navy Health Sciences Education and Training Command, Bethesda, MD.
Pub. in Health Physics 65, n2 p131-140 1993.

Keywords: *Radiation accidents, *Occupational safety and health, *Radiation injuries, *Industrial medicine, *Accident investigations, Industrial accidents, Occupational exposure, Radiation dosage, Partial body irradiation, Accelerators, Biological radiation effects, Radiation heating, Materials processing reactors, Reprints.

On 11 December 1991, a radiation overexposure occurred at an industrial radiation facility in Maryland. The radiation source was a 3-MV potential drop accelerator designed to produce high electron beam currents for materials-processing applications. During maintenance on the lower window pressure plate, an operator placed his hands, head, and feet in the beam. This was done with the filament voltage of the electron source turned 'off,' but with the full accelerating potential on the high voltage terminal. The operator's body, especially his extremities and head, were exposed to electron dark current. In an attempt to reconstruct the accident, radiochromic film and alanine measurements were made with the accelerator operated at two beam currents. Electron paramagnetic resonance spectrometry, which measures the concentration of radiation-induced paramagnetic centers in calcified tissues, was used to estimate the dose to the victim's extremities.

Radiation Pollution & Control

02,576
PB94-165602 PC A09/MF A03
National Inst. of Standards and Technology (BFRL), Gaithersburg, MD.
Measurement and Determination of Radon Source Potential: A Literature Review.
A. B. Tanner. Apr 94, 199p, NISTIR-5399.

Keywords: *Radon, *Air pollution sources, *Indoor air pollution, Natural radioactivity, Radium, Soil gases, Soil-structure interactions, Radionuclide migration, Mapping, Buildings, Diffusion, Permeability, Flow rates, Site characterization, Foundations, Construction materials, Regional analysis, Soil tests, Activity levels.

Radon source potential may be estimated for areas of a nation, state, county, housing development, or building lot. The critical characteristics of the soil are its radium concentration, emanation coefficient, permeability to gas, and diffusion coefficient for radon under typical conditions. This report summarizes and evaluates available information on radon potential mapping and site-specific characterization. More than 100 reports have been found that bear on radon potential mapping, and indicate fair to good agreement with indoor radon results where correlations have been possible.

02,577
PB94-185782 Not available NTIS
National Inst. of Standards and Technology (BFRL), Gaithersburg, MD. Building Materials Div.
Expansion of Cementitious Materials Exposed to Sulfate Solutions.
Final rept.
J. R. Pommersheim, and J. R. Clifton. 1994, 6p.
Pub. in Materials Research Society Symposia Proceedings, v333 p363-368 1994. Sponsored by Nuclear Regulatory Commission, Washington, DC.

Keywords: *Cements, *Concretes, *Radioactive waste disposal, *Environmental effects, *Sulfates, *Low-level radioactive wastes, Underground storage, Construction materials, Environmental protection, Degradation, Exposure, Diffusion, Crack propagation, Reprints.

Disposal of low-level radioactive waste in concrete vaults buried underground is being considered in the United States and a potentially significant degradation process is sulfate attack. The results of experimental studies and of modeling of the kinetics of sulfate attack of cement-based materials are given. It was concluded that the expansion process involves a two-stage mechanism. The first stage is likely to be diffusion controlled and the second stage appears to be acceleratory due to the development and spread of cracks.

02,578
PB96-190103 Not available NTIS
National Inst. of Standards and Technology, Gaithersburg, MD. Occupational Health and Safety Div.
Response Comparison of Electret Ion Chambers, LiF TLD, and HPIC.
Final rept.
T. Hobbs, P. Kotrappa, J. Tracy, and B. Biss. 1996, 8p.
Pub. in Radiation Protection Dosimetry, v63 n3 p181-188 1996.

Keywords: *Dosimeters, *Electrets, *Environmental monitoring, Ionization chambers, Radiation measuring instruments, Dielectrics, Thermoluminescent, Reprints.

During each quarter of 1991 electret ion chambers, (nai)LiF(6)LiF, and (7)LiF thermoluminescence dosimeters, all integrating ionizing radiation monitors, were placed at a location in the grounds of the National Institute of Standards and Technology. One group was exposed to the total ambient field, while a second group was sealed for testing a method of protection against radon gas instrusion. A high-pressure ion chamber at the same location provided another measure of the field. Simultaneously with the environmental response test, other sealed and unsealed groups of electret ion chambers and thermoluminescence dosemeters were exposed during each quarter to discrete exposures from calibrated sources of (60)Co and (137)Cs. All responses were evaluated at the end of each quarter. The results indicated that the electret ion chamber gave results comparable to thermoluminescence dosemeters for routine environmental monitoring. No significant difference was found for any monitor type when sealed results were compared with unsealed results.

Solid Wastes Pollution & Control

02,579
AD-A279 133/3 PC A03/MF A01
National Bureau of Standards, Gaithersburg, MD.
Recommendations for the Disposal of Carbon-14 Wastes.
1952, 21p.

Keywords: *Carbon, *Hazardous wastes, Biological agents, Chemical compounds, *Waste disposal.

No abstract available.

02,580
AD-A301 258/0 PC A04/MF A01
National Bureau of Standards, Gaithersburg, MD.
Performance of Plastic Packaging for Hazardous Materials Transportation. Part 1. Mechanical Properties.
Final rept. Jun 75-Jun 76.
J. M. Crissman, C. M. Guttman, and L. J. Zapas. Oct 76, 53p, DOT/MTB/OHMO-76/4.
Contract DOT-AS-50074

Keywords: *Packaging, *Hazardous materials, *Polyethylene plastics, Test and evaluation, Density, Vibration, Transportation, Static loads, Cracking(Fracturing), Damage assessment, Brittleness, Failure(Mechanics), Compressive strength, Regulations, Thermal stresses, Shipping containers.

This report, prepared for the U. S. Department of Transportation, contains background information useful in evaluating the performance of plastic packagings for hazardous materials transportation, insofar as mechanical properties are concerned. Current DoT regulations and test methods are reviewed, as well as testing procedures from other organizations and countries. Also included are recommendations to modify current DoT regulations to make test methods more quantitative Finally, experimental data are presented which represent the initial stage of a study it is hoped will ultimately lead to the establishment of criteria upon which the long time behavior of plastic containers can be predicted based on short time tests. (AN).

02,581
PB94-199882 Not available NTIS
National Inst. of Standards and Technology (NML), Gaithersburg, MD. Chemical Thermodynamics Div.
Assessing the Credibility of the Calorific Content of Muncipal Solid Waste.
Final rept.
E. S. Domalski, K. L. Churney, A. E. Ledford, T. J. Buckley, R. C. Paule, M. L. Reilly, J. C. Colbert, and S. S. Bruce. 1991, 4p.
Pub. in Pure and Applied Chemistry 63, n10 p1415-1418 1991.

Keywords: *Municipal wastes, *Calorific value, *Heat of combustion, *Heat measurement, Solid wastes, Calorimeters, Performance evaluation, Sample preparation, Reprints.

A study has been carried out to establish the limits of reliability of the calorific content of municipal solid waste (MSW) by the bomb calorimetric procedure currently used in commercial test laboratories. This procedure involves using gram-size samples derived from MSW that have been processed down to a particle size of 2 mm or less. Critics argue that one cannot sample a multi-ton quantity of MSW and extract gram-size samples which are representative of the entire gross sample. They argue further that processing down to 2 mm or less significantly alters the composition of the sample. In order to test the bomb calorimetric procedure, a multi-kg capacity combustion flow calorimeter was designed and constructed for the determination of the enthalpies of combustion of kilogram-size samples of MSW in flowing oxygen near atmospheric pressure.

02,582
PB95-140968 Not available NTIS
National Inst. of Standards and Technology (MSEL), Gaithersburg, MD. Polymers Div.

Bioleaching of Cobalt from Smelter Wastes by 'Thiobacillus ferrooxidans'.
Final rept.
G. J. Olson, C. K. Sakai, E. J. Parks, and F. E. Brinckman. 1990, 4p.
Pub. in Jnl. of Industrial Microbiology 6, n1 p49-52 Sep 90.

Keywords: *Waste treatment, *Materials recovery, *Cobalt, *Biological treatment, *Leaching, Microorganisms, Smelting, Mattes, Solubility, Reprints, Thiobacillus ferrooxidans.

The bioleaching of cobalt from domestic, industrial smelter wastes was studied. Thiobacillus ferrooxidans solubilized Co from sulfidic dross furnace mattes. At pulp densities of 4%, up to 600 mg of Co per liter of leaching solution was released from nickel matte, corresponding to removal of about two-thirds of the original amount of Co in the matte. Bioleaching methods may be useful as a component of a process for solubilization and recovery of Co from sulfidic smelter mattes.

Water Pollution & Control

02,583
PB95-104907 PC A06/MF A02
National Inst. of Standards and Technology (BFRL), Gaithersburg, MD. Fire Safety Engineering Div.
In Situ Burning Oil Spill Workshop Proceedings. Held in Orlando, Florida on January 26-28, 1994.
Special pub.
N. H. Jason. Aug 94, 112p, NIST/SP-867.
Also available from Supt. of Docs. as SN003-003-03290-5. See also PB94-101839. Sponsored by Minerals Management Service, Herndon, VA.

Keywords: *Meetings, *Oil spills, *In-situ combustion, *Fire tests, *Burning rate, *Water pollution control, Crude oil, Regulations, State government, Legal aspects, Louisiana, Decision making, Environmental research, Public health, Smoke.

This workshop is part of the U.S. Minerals Management Service's continuing effort to ensure the relevance of their research program to the needs of the user community. Specific emphasis was given to environmental and operational implications of in situ burn response technology. The goals of the In Situ Oil Burning workshop were: to present the state of knowledge to representatives of industry, government, and research organizations; to review the present status guidelines for use of in situ burning as an oil spill response method; and to prioritize research and information needs to support decisions on the use of in situ burning of oil spills.

02,584
PB95-140091 Not available NTIS
National Inst. of Standards and Technology (CSTL), Gaithersburg, MD. Organic Analytical Research Div.
Comparison of Methods for Gas Chromatographic Determination of PCBs and Chlorinated Pesticides in Marine Reference Materials.
Final rept.
M. Schantz, R. Parris, J. Kurz, K. Ballschmiter, and S. Wise. 1993, 13p.
Pub. in Fresenius J. Anal. Chem. 346, p766-778 1993.

Keywords: *Gas chromatography, *Water pollution detection, *Marine environments, *Polychlorinated biphenyls, *Pesticides, *Chemical analysis, Chlorine organic compounds, Comparison, Marine biology, Water pollution effects, Sediments, Reprints, *Standard reference materials, *Certified reference materials, SRM 1588, SRM 1941, SRM 1974, CRM 349, CRM 350.

Three gas-chromatographic (GC) columns with different selectivity (DB-5, DB-1701, and C-18) and two different GC detectors (electron-capture and mass-spectrometric) were used to analyze three Standard Reference Materials (SRMs), which are available from the National Institute of Standards and Technology (NIST), and two Certified Reference Materials (CRMs) which are available from the Community Bureau of Reference (CBR), for polychlorinated biphenyl (PCB) congeners and chlorinated pesticides. The materials analyzed were: SRM 1588, Organics in Cod Liver Oil; SRM 1941, Organics in Marine Sediment; SRM 1974, Organics in Mussel Tissue (Mytilus edulis); CRM 349, Chlorobiphenyls in Cod Liver Oil; and CRM 350, Chlorobiphenyls in Mackerel Oil. Results are reported.

02,585
PB95-140109 Not available NTIS
National Inst. of Standards and Technology (CSTL), Gaithersburg, MD. Organic Analytical Research Div.
NIST Standard Reference Materials (SRMs) for Polychlorinated Biphenyl (PCB) Determinations and Their Applicability to Toxaphene Measurements.
Final rept.
M. M. Schantz, R. M. Parris, and S. A. Wise. 1993, 8p.
Pub. in Chemosphere 27, n10 p1915-1922 1993.

Keywords: *Polychlorinated biphenyls, *Pesticides, *Environmental surveys, *Chemical analysis, *Toxaphene, *Water pollution detection, Chlorine organic compounds, Water pollution effects, Marine environments, Rivers, Sediments, Air pollution detection, Dust, Interlaboratory comparisons, Marine biology, Reprints, *Standard reference materials, SRM 1588, SRM 1939, SRM 1941, SRM 1974, SRM 1945, SRM 1649.

In the past five years the National Institute of Standards and Technology (NIST) has developed several Standard Reference Materials (SRMs) to assist in the validation of measurements of polychlorinated biphenyl (PCB) congeners and chlorinated pesticides in environmental samples. The following natural matrix SRMs have been issued: SRM 1588, Organics in Code Liver Oil; SRM 1939, PCB Congeners in River Sediment; SRM 1941, Organics in Marine Sediment; SRM 1974, Organics in Mussel Tissue (Mytilus edulis); and SRM 1945, Whale Blubber. Recently, SRM 1649 has been analyzed for selected PCB congeners and chlorinated pesticides. Toxaphene measurements have not been made at NIST for these SRMs; however, these SRMs represent the environmental matrices that are typically analyzed for toxaphene. Recommended values for toxaphene concentrations could be established on any of these materials through interlaboratory comparison exercises involving laboratories experienced in making toxaphene measurements. In this paper we describe these SRMs and discuss their suitability as potential reference materials for toxaphene measurements.

02,586
PB95-161402 Not available NTIS
National Inst. of Standards and Technology (CSTL), Gaithersburg, MD. Organic Analytical Research Div.
Development of the National Marine Mammal Tissue Bank.
Final rept.
T. Lillestolen, N. Foster, and S. Wise. 1993, 11p.
Pub. in Science of the Total Environment 139/140, p97-107 1993.

Keywords: *Marine mammals, *Animal tissues, *Tissue banks, *Bioaccumulation, Bioassay, Water pollution effects(Animals), Biological accumulation, Chemical analysis, Contaminants, Water pollutants, Environmental monitoring, Quality assurance, Reference standards, Reprints, *National Marine Mammal Tissue Bank, Standard reference materials.

The National Marine Mammal Tissue Bank (NMMTB) has been established as part of a comprehensive effort to obtain reliable information on contaminant levels in marine mammal tissues. A four component program consisting of the NMMTB, stranding networks, monitoring and quality assurance has been developed. The development and current status of the NMMTB and its relationship to the other three components will be described.

02,587
PB95-163747 Not available NTIS
National Inst. of Standards and Technology (BFRL), Gaithersburg, MD. Fire Safety Engineering Div.
In situ Burning of Oil Spills: Mesoscale Experiments and Analysis.
Final rept.
W. D. Walton, D. D. Evans, K. B. McGrattan, D. Madrzykowski, A. D. Putorti, R. G. Rehm, H. Koseki, E. J. Tennyson, H. R. Baum, and W. H. Twilley. 1993, 56p.
Sponsored by Minerals Management Service, Herndon, VA.
Pub. in Proceedings of the Arctic and Marine Oil Spill Program Technical Seminar (16th), Calgary, Alberta, Canada, June 7-9, 1993, p679-734.

Keywords: *Oil spills, *Fire tests, *In situ combustion, *Burning rate, Crude oil, Combustion properties, Combustion kinetics, Oil-water interfaces, Plumes, Particulates, Oil pollution control, Water pollution control, Reprints, Smoke yield.

A series of six mesoscale and one large laboratory fire experiments were performed to measure the burning characteristics of Louisiana crude oil on water in a pan. Results of the measurements for burning rate and smoke emissions are compared to those from previous burns of various scales. Predictions of smoke plume trajectory and particulate deposition at ground level from the Large Eddy Simulation (LES) model developed as part of this research effort are presented. LES is a steady-state three-dimensional calculation of smoke plume trajectory and smoke particulate deposition based on a mixed finite difference and Langrangian particle tracking method.

02,588
PB95-164034 Not available NTIS
National Inst. of Standards and Technology (CSTL), Gaithersburg, MD. Organic Analytical Research Div.
Quality Assurance of Contaminant Measurements in Marine Mammal Tissues.
Final rept.
S. A. Wise. 1993, 11p.
Pub. in Proceedings of Symposium on Coastal and Ocean Management (8th): Coastal Zone '93, New Orleans, LA., July 19-23, 1993, p2531-2541.

Keywords: *Marine mammals, *Animal tissues, *Bioaccumulation, *Chemical analysis, *Quality assurance, Water pollution effects(Animals), Biological accumulation, Bioassay, Standardization, Interlaboratory comparisons, Tissue banks, Reference standards, Reprints, Standard reference materials.

The National Institute of Standards and technology (NIST), in conjunction with the National Oceanic and Atmospheric Administration (NOAA) is developing a program to improve the quality and comparability of analytical measurements for contaminants in marine mammal tissues. This quality assurance program consists of the (1) preparation of marine mammal tissue control materials, (2) interlaboratory comparison exercises, and (3) development of standard reference materials. The development and status of the program is described.

02,589
PB95-171344 PC A05/MF A01
National Inst. of Standards and Technology (CSTL), Gaithersburg, MD. Organic Analytical Research Div. National Marine Fisheries Service, Silver Spring, MD. Office of Protected Resources.
Alaska Marine Mammal Tissue Archival Project: Specimen Inventory.
B. J. Koster, S. A. Wise, and P. R. Becker. Nov 94, 78p, NISTIR-5462.
See also PB91-184796 and PB92-143718. Prepared in cooperation with National Marine Fisheries Service, Silver Spring, MD. Office of Protected Resources.

Keywords: *Marine mammals, *Animal tissues, *Tissue banks, *Bioassay, *Reference standards, *Water pollution effects(Animals), Whales, Seals(Mammals), Bioaccumulation, Biological accumulation, Chemical analysis, Environmental monitoring, Alaska, *Standard reference materials, Sea lions.

The Alaska Marine Mammal Tissue Archival Project (AMMTAP) was initiated in 1987 to aid in the monitoring of contaminants in the Alaskan environment. The tissue samples are then archived in the National Biomonitoring Specimen Bank (NBSB) at the National Institute of Standards and Technology (NIST). In the NBSB, the tissues are stored in vapor phase liquid nitrogen freezers until required for analysis. This document contains the current inventory of the AMMTAP archive. Included in the inventory is information such as: species, location collected, morphometries, tissues collected and dispositions of the tissue, i.e., archived or homogenized for analysis. This document contains the records for the collection of tissue from 94 animals samples between July 87 - October 93.

02,590
PB95-209870 PC A06/MF A02
National Inst. of Standards and Technology (CSTL), Gaithersburg, MD.

Concentrations of Chlorinated Hydrocarbons, Heavy Metals and Other Elements in Tissues Banked by the Alaska Marine Mammal Tissue Archival Project.
P. R. Becker, E. A. Mackey, M. M. Schantz, B. J. Koster, S. A. Wise, D. C. G. Muir, R. Demiralp, and R. R. Greenberg. Mar 95, 124p, NISTIR-5620.
See also PB92-143718 and PB95-171344. Prepared in cooperation with Department of Fisheries and Oceans, Winnipeg (Manitoba). Freshwater Inst.

Keywords: *Marine mammals, *Animal tissues, *Chemical analysis, *Biological accumulation, *Bioassay, Bioaccumulation, Water pollution effects(Animals), Whales, Seals(Mammals), Heavy metals, Polychlorinated biphenyls, Trace elements, Chlorinated hydrocarbons, Pesticides, Muscles, Kidney, Liver, Neutron activation analysis, Tissue banks, Environmental monitoring, Alaska, Bioconcentration, Blubber.

The National Oceanic and Atmospheric Administration maintains two marine mammals tissue banks within NIST's National Biomonitoring Specimen Bank. The document is the second report in the NIST Interagency Report Series in which analytical data on samples collected and banked as part of the Alaska Marine Mammal Tissue Archival Project are summarized. Results for inorganic constituents in liver tissues from 15 bulukha whales, 14 ringed seals, 3 bowhead whales, 3 beared seals, and 1 spotted seal, and for organic contaminants in blubber tissues from 12 belukha whales are presented and discussed.

02,591
PB96-111737 Not available NTIS
National Inst. of Standards and Technology (CSTL), Gaithersburg, MD.
Quantitative Analysis of Selected PCB Congeners in Marine Matrix Reference Materials Using a Novel Cyanobiphenyl Stationary Phase.
Final rept.
B. R. Hillery, J. E. Girard, M. M. Schantz, and S. A. Wise. 1995, 8p.
Pub. in Jnl. of High Resolution Chromatography, v18 p89-96 Feb 95.

Keywords: *Polychlorinated biphenyls, *Quantitative chemical analysis, *Marine mammals, *Reference standards, Water pollution effects(Animals), Bioaccumulation, Bioassay, Environmental monitoring, Gas chromatography, Fish oils, Cod liver oil, Fishes, Whales, Reprints, Cyanobiphenyls, Stationary phase, Blubber, Mackerel.

A novel p,p-cyanobiphenyl stationary phase (p-cyanobiphenyl, p-allyloxy methlpolysiloxane) has been evaluated for the GC investigation of polychlorinated biphenyls (PCBs). Several PCB congeners which coelute on the phases typically used for PCB analysis (e.g. 5% phenyl methylpolysiloxane) are separated on the p,p-cyanobiphenyl phase, including the hexachlorobiphenyl congers PCB 163, PCB 164, and PCB 138. In this work, a p,p-cyanobiphenyl stationary phase was used to measure selected PCB congeners in two Standard Reference Materials (SRMs) available from the National Institute of Standards and Technology (NIST), and two Certified Reference Materials (CRMs) available from the Community Bureau of Reference (BCR). The materials analyzed were SRM 1588, Organics in Cod Liver Oil; SRM 1945, Organics in Whale Blubber; CRM 349, Chlorobiphenyls in Cod Liver Oil; and CRM 350, Chlorobiphenyls in Macherel Oil. Concentrations are reported for several PCB congeners which coelute on the 5% phenyl methylpolysiloxane, including PCB 163 and PCB 164.

02,592
PB96-111778 Not available NTIS
National Inst. of Standards and Technology (CSTL), Gaithersburg, MD. Analytical Chemistry Div.
Certification of Polycyclic Aromatic Hydrocarbons in a Marine Sediment Standard Reference Material.
Final rept.
S. A. Wise, M. M. Schantz, B. A. Benner, M. J. Hays, and S. B. Schiller. 1995, 8p.
Pub. in Analytical Chemistry, v67 n7 p1171-1178, 1 Apr 95.

Keywords: *Polycyclic aromatic hydrocarbons, *Environmental monitoring, *Reference standards, *Chemical analysis, *Analytical methods, Isomers, Water pollution effects, Test methods, Gas chromatography, Mass spectroscopy, Separation techniques, Fluorescence spectroscopy, Liquid chromatography, Sampling, Certification, Reprints, *Marine sediments, Standard reference materials.

Four different analytical techniques were used for the determination of polycyclic aromatic hydrocarbons (PAHs) in a new marine sediment reference material, SRM 1941 a, Organics in Marine Sediment. These procedures were based on reversed-phase liquid chromatography (LC) with fluorescence detection, a multidimensional LC procedure, and gas chromatography/mass spectrometry on two stationary phases with different selectivity for the separation of PAH isomers. The results from these four aproaches were in good agreement and were combined to provide certified concentrations for 23 PAHs, which represents the largest number of certified concentrations for PAHs in any natural matrix SRM.

02,593
PB96-123690 Not available NTIS
National Inst. of Standards and Technology (CSTL), Gaithersburg, MD. Organic Analytical Research Div.
Certification of Standard Reference Material (SRM) 1941a, Organics in Marine Sediment.
Final rept.
M. M. Schantz, B. A. Benner, M. J. Hays, R. Demiralp, R. R. Greenberg, S. B. Schiller, G. G. Lauenstein, S. A. Wise, W. R. Kelly, and R. D. Vocke. 1995, 8p.
Pub. in Analytical Chemistry, v352 p166-173 1995.

Keywords: *Bottom sediments, *Water pollution effects, *Chemical analysis, *Reference standards, Environmental monitoring, Certification, Marine environments, Pesticides, Polychlorinated biphenyls, Polycylic aromatic hydrocarbons, Aliphatic hydrocarbons, Organic carbon, Trace elements, Sulfur, Gas chromatography, Mass spectroscopy, Reprints, Marine sediments, Standard reference materials.

SRM 1941a, Organics in Marine Sediment, has been recently issued with certified concentrations 23 polycyclic aromatic hydrocarbons, 21 polychlorinated biphenyl congeners, 6 chlorinated pesticides, and sulfur. Noncertified concentrations have been also reported for additional PAHs, PCB congeners, and chlorinated pesticides and for percent total organic carbon (TOC), aliphatic hydrocarbons, and trace elements. SRM 1941a is the most extensively characterized natural matrix SRM issued by the National Institute of Standards and Technology (NIST).

02,594
PB96-131560 PC A03/MF A01
National Inst. of Standards and Technology (BFRL), Gaithersburg, MD.
Smoke Plume Trajectory from In situ Burning of Crude Oil in Alaska: Field Experiments.
K. B. McGrattan, W. D. Walton, A. D. Putorti, D. D. Evans, W. H. Twilley, and J. McElroy. Nov 95, 42p, NISTIR-5764.
See also PB94-114519. Sponsored by Alaska State Dept. of Environmental Conservation, Juneau. Div. of Spill Prevention and Response.

Keywords: *Oil spills, *In situ combustion, *Smoke, *Plumes, Atmospheric diffusion, Burning rate, Emulsions, Particulates, Combustion kinetics, Combustion properties, Crude oil, Oil pollution control, Water pollution control, Field tests, Fire tests, Comparison, LES(Large Eddy Simulation).

In the present report, experimental data collected at two sets of mesoscale burns are compared with the results of the LES model run using the recorded meteorological and physical conditions. The two experiments are the Newfoundland Offshore Burn Experiment (NOBE), Aug. 1993, and the Alaska Clean Seas Burning of Emulsions, Sept. 1994. Each series of burns was conducted under different conditions, and different data collection techniques were employed at each. The results show that the predictions of the LES model are in good agreement with the experimental measurements, given the uncertainty if the input parameters.

02,595
PB96-167127 Not available NTIS
National Inst. of Standards and Technology (CSTL), Gaithersburg, MD. Analytical Chemistry Div.
Trace Element Concentrations in Cetacean Liver Tissues Archived in the National Marine Mammal Tissue Bank.
Final rept.
E. A. Mackey, R. Demiralp, P. R. Becker, S. A. Wise, R. R. Greenberg, and B. J. Koster. 1995, 17p.
See also PB95-161402.
Pub. in Science of the Total Environment, v175 p25-41 1995.

Keywords: *Bioaccumulation, *Marine mammals, *Trace elements, Dolphins, Reprints, *Foreign technology, Harbor porpoise, Neutron activation analysis, Pilot whales, Specimen banking.

The National Biomonitoring Specimen Bank (NBSB), a collaborative project of several U.S. government agencies, includes marine mammal tissues collected for the Alaska Marine Mammal Tissue Archival Project (AMMTAP) and the National Marine Mammal Tissue Bank (NMMTB). Tissues were collected from 139 animals representing 13 species of marine mammals from around the U.S. Recently, concentrations for up to 30 elements in liver tissues of nine long-finned pilot whales (Globicephala melas), six harbors porpoises (Phocoena phocoena), and four white-sided dolphins (Lagenorhyunchus acutus) from the NMMTB were measured using instrumental neutron activation analysis. Results from analysis of these tissues are presented, compared with results for liver tissues from other marine mammals from the AMMTAP, and compared with published values.

02,596
PB96-167275 Not available NTIS
National Inst. of Standards and Technology (CSTL), Gaithersburg, MD. Inorganic Analytical Research Div.
Relationship of Silver with Selenium and Mercury in the Liver of Two Species of Toothed Whales (Odontocetes).
Final rept.
P. R. Becker, E. A. Mackey, R. Demiralp, B. J. Koster, S. A. Wise, R. Suydam, and G. Early. 1995, 10p.
Pub. in Marine Pollution Bulletin, v30 n4 p262-271 1995.

Keywords: *Bioaccumulation, *Marine mammals, *Water pollution effects(Animals), Liver, Mercury, Selenium, Silver, Reprints, *Foreign technology, *Instrumental neutron activation analysis, Pilot whale, Beluga whale.

Liver specimens archived in the National Biomonitoring Specimen Bank from beluga whales, Delphinapterus leucas, and from Alaska and pilot whales, Globicephala melas, from the North Atlantic were analysed for silver, selenium and total mercury. Silver concentrations in beluga whales were one to three orders of magnitude higher than the concentrations in pilot whales and those reported elsewhere for the other marine mammals. The concentrations of silver in the livers of beluga whales were the same or in some instances higher than the concentrations of selenium or mercury. Like mercury, silver was positively correlated with selenium in both pilot and beluga whales. This suggests a possible role for selenium in the accumulation and storage of silver in both species of whales, and raises questions about the potential for silver at such high concentrations to affect radical-scavenging enzyme systems in these marine mammals.

02,597
PB96-200993 Not available NTIS
National Inst. of Standards and Technology (BFRL), Gaithersburg, MD. Fire Safety Engineering Div.
Smoke Plume Trajectory from In situ Burning of Crude Oil: Field Experiments.
Final rept.
K. B. McGrattan, R. J. Ferek, and E. E. Uthe. 1995, 6p.
See also PB96-131560.
Pub. in International Conference on Fire Research and Engineering, Orlando, FL., September 10-15, 1995, p47-52.

Keywords: *Oil spills, *In situ combustion, *Atmospheric diffusion, *Combustion products, Smoke, Plumes, Particulates, Atmospheric transport, Burning rate, Combustion kinetics, Oil pollution control, Fire tests, Reprints.

There is growing interest in the environmental consequences of large fires, since the transport of combustion products by a windblown fire plume can distribute potentially hazardous materials over a wide area. Pools of burning oil and other petroleum products are of particular concern due to the vast flow of these materials through the global economy and because of the fragility of the environment in many regions where oil is extracted or transported. The present work is part of a larger study of a closely related issue, the feasibility of cleaning up oil spills on water through burning.

02,598
PB97-119226 Not available NTIS

National Inst. of Standards and Technology (CSTL), Gaithersburg, MD. Analytical Chemistry Div.
National Status and Trends Program Specimen Bank: Sampling Protocols, Analytical Methods, Results, and Archive Samples.
Final rept.
G. Lauenstein, A. Cantillo, B. Koster, R. Zeisler, S. Wise, M. Schantz, and S. Stone. 1996, 168p.
See also PB89-175855.
Pub. in NOAA Technical Memorandum NOS ORCA 98, v98 168p 1996.

Keywords: *Sediments, *Tissue banks, *Environmental monitoring, *Reference standards, *Animal tissues, Aquatic animals, Fish, Oysters, Mussels, Marine mammals, Biological effects, Bioaccumulation, Bioassay, Chemical analysis, Sampling, Quality assurance, Reprints, National Status and Trends Program.

The National Oceanic and Atmospheric Administration's (NOAA) National Status and Trends (NS&T) Program monitoring components, the National Benthic Surveillance and Mussel Watch Projects, have archived tissues and sediments in a specimen bank since 1985 and 1986, respectively. Additional samples were archived after the Exxon Valdez oil spill in Prince Williams Sound, Alaska. Samples from the Environmental Protection Agency's Mussel Watch Program, collected from 1976 to 1978, were added to the NS&T Specimen Bank in 1992. Contaminant analyses were performed to provide additional data on environmental quality and to ensure that data existed for sample stability studies. Samples in the NS&T Specimen Bank are available for retrospective analyses should a contaminant or group of contaminants be identified that was introduced into the environment during the years of the NS&T Program or during the EPA's Mussel Watch Program but that were not previously measured.

HEALTH CARE

Health Care Technology

02,599
PB96-160544 Not available NTIS
National Inst. of Standards and Technology (CSL), Gaithersburg, MD. Advanced Systems Div.
Prototyping a Graphical User Interface for DHCP.
Final rept.
W. J. Majurski, R. E. Dayhoff, and D. L. Maloney. 1992, 11p.
Pub. in MUMPS Computing: MUG Proceedings Issue, Phoenix, AZ., June 15-19, 1992, 11p.

Keywords: *Biomedical measurement, *Graphical user interface, *Computer programs, Computer graphics, Image processing, Software engineering, Operating systems(Computers), Reprints, DHCP(Decentralized Hospital Computing Program), Medical imaging, X windows, MIMPS(Massachusetts General Hosptial Utility Multi-Programming System).

We have started looking at how a large end user application, the Department of Veterans Affairs' DHCP, can adapt to this changing environment. We describe a minimal prototype X window binding that we have constructed and modifications to several DHCP subsystems to adapt to it. We then discuss the types of changes that may be needed to adapt DHCP to a graphical user interface environment.

INDUSTRIAL & MECHANICAL ENGINEERING

General

02,600
PB94-196029 PC A03/MF A01
National Inst. of Standards and Technology (TS), Gaithersburg, MD. Metric Program.
Federal Metric Progress in 1993.
G. P. Carver. Apr 94, 15p, NISTIR-5413.
See also PB89-114490.

Keywords: *Metric systems, Handbooks, Units of measurement, Government agencies, Interagency cooperation, National government.

During 1993, cooperation among the federal agencies on interagency issues led to more uniform metric transition approaches. Individually, agencies made significant progress in implementing metric use in their programs. However, the amount of progress by different agencies also showed significant variation. Cooperative progress included; Acquisition Guidelines; Functional subcommittees; Strategic Approach; Public Affairs; Metric Transition Plan Revision; Expanded Agency-Industry Cooperation; and Federal Standard 376.

02,601
PB94-206307 PC A02/MF A01
National Inst. of Standards and Technology (TS), Gaithersburg, MD. Metric Program.
Metric Path to Global Markets and New Jobs: A Question-and-Answer and Thematic Discussion.
G. P. Carver. Jun 94, 9p, NISTIR-5463.

Keywords: *Metric system, *Job creation, Global aspects, Government policies, Exports, Competitiveness, International trade.

The logic for use of the metric system in the United States is strongest when metric use is viewed as an element of our national economic infrastructure, as an investment in efficiency, and as a necessity for internatioal competitiveness.

02,602
PB95-226916 PC A05/MF A01
National Inst. of Standards and Technology (CSTL), Gaithersburg, MD. Process Measurements Div.
Laser Doppler Velocimeter Studies of the Pipeflow Produced by a Generic Header.
Technical note.
T. T. Yeh, and G. E. Mattingly. Apr 95, 79p, NIST/TN-1409.
Also available from Supt. of Docs.

Keywords: *Flow measurement, *Flow meters, Fluid flow, Installation effects, LDV, Header flow.

The report presents recent results obtained in a consortium-sponsored research program on flowmeter installation effects being conducted at NIST-Gaithersburg, MD. The piping element tested and reported here is generic header which has a specific arrangement of one inlet and two outlets. LDV velocity measurements are reported for the pipeflows produced downstream of the header with and without a conventional 19-tube concentric tube bundle flow conditioner. The results indicate that the secondary flow produced by the generic header is very similar to that produced by the closely-coupled double elbows out-of-plane piping configuration. The axial velocities are slower than the ideal flow near the pipe center and higher near the walls. Transverse velocity distributions show a very strong swirl eddy flow pattern produced by this header. This swirl eddy is relatively stable and organized and its dissipation is slower than that observed for the double elbows out-of-plane. The 19-tube tube bundle is quite effective in reducing the transverse velocities associated with the energetic, swirl flow from this header. Several profile indexes are introduced and presented for the header flow to characterize its swirl, profile peakness and flow displacements. These indexes can also be used to develop criteria for improving flow meter performance in the outlet piping from this header.

02,603
PB95-255824 PC A03/MF A01
National Inst. of Standards and Technology (BFRL), Gaithersburg, MD. Building Environment Div.
Simple Method of Composition Shifting with a Distillation Column for a Heat Pump Employing a Zeotropic Refrigerant Mixture.
P. I. Rothfleisch. Jul 95, 30p, NISTIR-5689.
Sponsored by Department of Energy, Washington, DC. Building Equipment Div. and Environmental Protection Agency, Research Triangle Park, NC. Air and Energy Engineering Research Lab.

Keywords: *Refrigerants, *Air conditioning equipment, *Heat pumps, Refrigerating, Chemical composition, Distillation, Columns(Process engineering), Zeotropic mixtures.

The work presents a simplified method of controlling heat pump capacity by shifting the composition of a zeotropic refrigerant mixture with a distillation column. Simplicity is achieved by incorporating the distillation column into the typical suction accumulator used by residential heat pumps. A U.S. patent has been applied for under the title Accumulator Distillation Insert for Zeotropic Mixtures. An experimental system employing this distillation concept has been evaluated in the laboratory for zeotropic mixtures of R32/134a (30/70) and R32/125/134a (23/25/52). For the binary mixture the circulating refrigerant composition was shifted to R32/134a (54/46). For the ternary mixture the circulating refrigerant composition was shifted to R32/125/134a (36/36/28).

02,604
PB96-123146 Not available NTIS
National Inst. of Standards and Technology (EEEL), Gaithersburg, MD. Electricity Div.
Effects of Nonmodel Errors on Model-Based Testing.
Final rept.
G. N. Stenbakken. 1995, 5p.
Pub. in Proceedings of Instrumentation and Measurement Technology Conference, Waltham, MA., April 24-26, 1995, p38-42.

Keywords: *Confidence intervals, Simulation, Testing, Empirical modeling, Reprints, *Nonmodel errors, Prediction intervals.

In previous work, methods have been developed for efficient testing of components and instruments that are based on models of these units. These methods allow for the full behavior of these units to be predicted from a small but efficient set of test measurements. Such methods can significantly reduce the testing cost of such units by reducing the amount of testing required. But these methods are valid only as long as the model accurately represents the behavior of the unit. Previous papers on this subject described many methods for developing accurate models and using them to develop efficient test methods. However, they gave little consideration to the problem of testing units which change their behavior after the model has been developed, for example, as a result of changes in the manufacturing process. Such changed behavior is referred to as nonmodel behavior or nonmodel error. When units with this new behavior are tested with these more efficient methods, their predicted behavior can show significant deviations from their true behavior. This paper describes how to analyze the data taken at the reduced set of measurements to estimate the uncertainty in the model predictions, even when the device has significant nonmodel error. Results of simulation are used to verify the accuracy of the estimates and to show the expected.

02,605
PB96-165956 PC A04/MF A01
National Inst. of Standards and Technology (BFRL), Gaithersburg, MD. Building Environment Div.
Enhancement of R123 Pool Boiling by the Addition of N-Hexane.
M. A. Kedzierski. Mar 96, 45p, NISTIR-5780.
See also PB96-128129. Sponsored by Department of Energy, Washington, DC.

Keywords: *Pool boiling, Hexanes, Heat transfer, Thermal conductivity, Surface treatment, Heat flux, Mixtures, Natural convection, Thermodynamic properties, Performance tests, *N-hexane, *R-123 refrigerant.

The paper presents the heat transfer data used to file international patent WO 94/18282. The data consisted of pool boiling performance of a GEWA-T(trademark) surface for three fluids: (1) pure R123, (2) R123/n-hexane (99/1), and (3) R123/n-hexane (98/2). The heat flux and the wall superheat were measured for each fluid at 277.6 K. The observations were used to describe various boiling modes on the GEWA-T(trademark) surface. The addition of hexane to pure R123 caused a simultaneous reduction in the bubble diameter and increase in the site density. The increase in site density enhanced the boiling despite the reduction in bubble size. Presumably, the site density enhancement was caused by a layer enriched in hexane at the heat transfer surface. The addition of hexane to R123 also improved natural convection.

02,606
PB96-210893 PC A07/MF A02
National Inst. of Standards and Technology (CSTL), Gaithersburg, MD. Process Measurements Div.
Flowmeter Installation Effects Due to a Generic Header.
Technical note.
T. T. Yeh, and G. E. Mattingly. Jul 96, 111p, NIST/TN-1419.
Also available from Supt. of Docs. as SN003-003-03415-1.

Keywords: *Flowmeters, *Orifice flow, *Installation, Orifice meters, Turbines, Orifices, Flow measurement, Inlets, Outlets, Pipe flow, Fluid flow, Discharge coefficient, Performance evaluation, Graphs(Charts), Tables(Data), *Headers.

This report presents recent results obtained in a consortium-sponsored research program on flowmeter installation effects being conducted at NIST-Gaithersburg, MD. The piping element tested and reported here is a generic header which has a specific arrangement of one inlet and two outlets. The results reported here are for the outlet nearest the inlet operated fully open with the other outlet fully closed. The meter performance measured in this outlet are reported with and without the installation of a conventional 19-tube concentric tube bundle flow conditioner.

Environmental Engineering

02,607
PB95-216917 PC A03/MF A01
National Inst. of Standards and Technology (BFRL), Gaithersburg, MD. Building Environment Div.
Theoretical Evaluation of the Vapor Compression Cycle with a Liquid-Line/Suction-Line Heat Exchanger, Economizer, and Ejector.
P. A. Domanski. Mar 95, 41p, NISTIR-5606.

Keywords: *Air conditioning, *Ejectors, *Heat exchangers, Refrigeration, Heat transfer, Feedwater heaters, Efficiency, *Vapor compression cycle, Liquid-line/suction-line heat exchange.

The report presents a theoretical analysis of three vapor compression cycles which are derived from the Rankine cycle by incorporating a liquid-line/suction-line heat exchanger, economizer, or ejector. These addendums to the basic cycle reduce throttling losses using different principles, and they require different mechanical hardware of different complexity and cost. The theoretical merits of the three modified cycles were evaluated in relation to the reversed Carnot and Rankine cycle. Thirty-eight fluids were included in the study using the Carnahan-Starling-DeSantis equation of state. In general, the benefit of these addendums increases with the amount of the throttling losses realized by the refrigerant in the Rankine cycle.

Hydraulic & Pneumatic Equipment

02,608
PB95-128906 PC A04/MF A01
National Inst. of Standards and Technology (CSTL), Boulder, CO. Process Measurements Div.
Uncertainty Analysis of the NIST Nitrogen Flow Facility.
Technical note.
J. L. Scott, and M. A. Lewis. Mar 94, 56p, NIST/TN-1364.
Supersedes COM-71-150325. Also available from Supt. of Docs. as SN003-003-03294-8. See also PB93-159465.

Keywords: *Test facilities, Cryogenic equipment, Cryogenic fluids, Liquid nitrogen, Gas flow, Mass flow, Error analysis, Statistical analysis, Orifice meters, Flow meters, Sensitivity, Buoyancy, Density, *Nitrogen flow facility, *Measurement uncertainty, Discharge coefficients, US NIST.

An uncertainty analysis of the National Institute of Standards and Technology nitrogen flow facility was performed. The facility functions as a cryogenic flow calibration laboratory and as an applied research laboratory for high pressure nitrogen gas flow measurement. The report includes the analysis of uncertainty in instrumentation, liquid nitrogen mass flow, gaseous nitrogen mass flow determined by a system turbine meter, and the uncertainty in orifice meter discharge coefficient calculation using a defined propagation of errors technique. Uncertainties determined by statistical and non-statistical means are presented separately.

02,609
PB95-175832 Not available NTIS
National Inst. of Standards and Technology (CSTL), Gaithersburg, MD. Thermophysics Div.
PC-Based Spinning Rotor Gage Controller.
Final rept.
J. P. Looney, F. G. Long, D. F. Browning, and C. R. Tilford. 1994, 8p.
Pub. in Review of Scientific Instruments 65, n9 p3012-3019 Sep 94.

Keywords: *Pressure measurement, *Vacuum gages, *Rotor dynamics, Vacuum apparatus, Measuring instruments, Rotors, Signal processing, Data analysis, Controllers, Reprints, *Spinning rotor gage controllers.

The spinning rotor gage (SRG) is a molecular drag vacuum gage. Commercial versions are available that operate between about 10(exp -4) and 1 Pa. In this paper we describe the design, and present performance data for a new SRG controller that uses a plug-in peripheral board and a personal computer (PC) to perform all control, signal processing, and data analysis functions. This controller offers several advantages over those presently available, including the simultaneous operation of multiple SRGs (at least four SRGs with a single PC), complete software control of all operating parameters, and significantly improved low-pressure performance.

Industrial Safety Engineering

02,610
PB95-174975 PC A04/MF A01
National Inst. of Standards and Technology (BFRL), Gaithersburg, MD. Fire Science Div.
Protection of Data Processing Equipment with Fine Water Sprays.
Annual rept. Sep 93-Sep 94.
W. Grosshandler, D. Lowe, K. Notarianni, and W. Rinkinen. Oct 94, 60p, NISTIR-5514.
See also PB93-219780. Sponsored by Fire Administration, Emmitsburg, MD.

Keywords: *Data processing equipment, *Fire protection, *Sprinkling, Fire fighting, Drops(Liquids), Size determination, Spraying, Nozzle geometry, Concentration(Composition), Velocity distribution, Fire extinguishing agents, Electronic equipment, *Fine water sprays, Halon 1301.

The major objective of the work presented here has been to determine how a fine water spray compares to a gaseous agent in extinguishing fires in data processing equipment, an environment typically protected by halon 1301. A scaled-down, generic electronics package was designed and a chamber built to contain the water spray to emulate the physical system of interest. The mock electronics cabinet is 0.5 m wide, 0.2 m deep and 0.4 m high. The fuel is a 3 mm thick plate of poly(methyl methacrylate), placed vertically in an aluminum frame centered among a number of aluminum circuit boards. The limitations imposed by the different transport phenomena associated with droplet versus gas dispersion have been investigated. The influence on extinguishing efficiency of the nozzles geometry, the location relative to the fire, the water application rate, and the amount of shielding surrounding the fire within the simulated cabinet are all parameters which have been examined. A gaseous agent, CF3H is used for comparison. A phase-Doppler particle analyzer measured the droplet size distribution and velocity. The water pressure has a significant effect on the size of the region in which a fire can be effectively suppressed. By contrast, similar fires in all geometric configurations can be successfully extinguished with CF3H as long as the concentrations in the chamber are close to those recommended in NFPA 2001.

02,611
PB95-270062 PC A03/MF A01
National Inst. of Standards and Technology (BFRL), Gaithersburg, MD.
Proceedings of the 1995 Workshop on Fire Detector Research. Held on February 6-7, 1995.
W. L. Grosshandler. Jun 95, 46p, NISTIR-5700.
See also PB95-189452.

Keywords: *Fire detection systems, *Research and development, *Meetings, Technology assessment, Smoke, Fire safety.

A workshop was convened February 6 and 7, 1995, to indentify the needs of users and specifiers of fire detection systems which are not currently being met by the U.S. fire protection industry. A series of experts from industry, government, certifying organizations and academia were invited to review the various applications for fire detection systems and to discuss recent development that could impact the future of the industry. The speakers were divided into focused panels of users and specifiers, systems and components manufactureres, regulators and certifiers, and researchers. Small working groups were convened after the panel discussions to identify critical research issues, concentrating on sensors, signal processing, systems integration and regulations.

Job Environment

02,612
PB97-122485 Not available NTIS
National Inst. of Standards and Technology (PL), Gaithersburg, MD. Ionizing Radiation Div.
Overview of a Radiation Accident at an Industrial Accelerator Facility.
Final rept.
D. A. Schauer, B. M. Coursey, C. E. Dick, M. F. Desrosiers, A. D. Jacobson, W. L. McLaughlin, and J. M. Puhl. 1994, 4p.
See also PB95-140117. Sponsored by Armed Forces Radiobiology Research Inst., Bethesda, MD.
Pub. in Advances in the Biosciences, v94 p321-324 1994.

Keywords: *Accelerator facilities, *Accident investigations, *Occupational safety and health, Industrial accidents, Occupational exposure, Radiation dosage, Radiation injuries, Partial body irradiation, Dosimetry, Biological radiation effects, Radiation accidents, Reprints, Dose reconstruction, EPR(Electron Paramagnetic Resonance).

On 11 December 1991, a radiation overexposure occurred at an industrial radiation facility in Gaithersburg, Maryland. During maintenance on the lower window pressure plate, an operator placed his hands, head, and feet in the beam. The operator's body, especially his extremities and head, were exposed to electron dark current. After prolonged periods of inactivity, particularly after the vacuum in the accelerator tube is lost, an electron beam current can be present even if the electron filament is cold or dark.

Laboratory & Test Facility Design & Operation

02,613
AD-A279 240/6 PC A03/MF A01

National Bureau of Standards, Gaithersburg, MD.
Standard Samples and Reference Standards Issued by the National Bureau of Standards.
31 Aug 54, 28p, NBS-CIRC-552.

Keywords: *Standards, *Scientific literature, Sampling, Circular, Periodicals, Weight, Procurement, Tables(Data), Chemical composition, Physical properties, Metals, Ceramic materials, Chemicals, Spectroscopy, Ph factor, Viscosity, Melting point, Density, Refractive index, Heat of combustion, *Reference standards, *Standard samples, Fees, Ores.

No abstract available.

02,614
AD-A279 948/4 PC A05/MF A01
National Bureau of Standards, Gaithersburg, MD.
Reference Tables for Thermocouples.
H. Shenker, J. I. Lauritzen, R. J. Corruccini, and S. T. Lonberger. 27 Apr 55, 89p.

Keywords: *Thermocouples, Tables(Data), Platinum, Rhodium, Copper, Electrical measurement, Calibration, Reference tables, Constantan, Chromel, Temperature measuring instruments.

No abstract available.

02,615
AD-A279 949/2 PC A05/MF A01
National Bureau of Standards, Gaithersburg, MD.
Corrected Optical Pyrometer Readings.
D. E. Poland, J. W. Green, and J. L. Margrave. 21 Apr 61, 77p.

Keywords: *Pyrometers, Optical properties, Conversion, Emissivity, Tables(Data), *Temperature measurement.

The table of corrected optical pyrometer readings enables optical pyrometer users to convert observed temperature immediately to the true temperature, if the effective emissivity of the material being observed is known. The table gives observed temperatures from 1,000 to 3,000 K in increments of 5 degrees, from 3,000 to 5,000 K in increments of 10 degrees, from 5,000 to 10,000 K in increments of 50 degrees, and from 10,000 to 39,900 K in increments of 100 degrees. For these, true temperatures are tabulated for 49 emissivities ranging from 0.02 to 0.98 in increments of 0.02. These calculations were made on a 650 electronic computer using Planck's law, and the value c sub 2 =1,438 cm deg for the radiation constant.

02,616
AD-A280 086/0 PC A03/MF A01
National Bureau of Standards, Gaithersburg, MD.
Federal Basis for Weights and Measures: A Historical Review of Federal Legislative Effort, Statutes, and Administrative Action in the Field of Weights and Measures in the United States.
R. W. Smith. 5 Jun 58, 27p.

Keywords: *Measurement, Weight, Federal law, Standardization, Standards, Length, Mass, Capacity(Quantity), *Weights and measures, Government policies.

No abstract available.

02,617
AD-A280 278/3 PC A08/MF A02
National Bureau of Standards, Gaithersburg, MD.
Guide to Instrumentation Literature.
W. G. Brombacker, J. F. Smith, and L. M. Van der Pyl. 14 Dec 55, 162p, NBS-567.

Keywords: *Instrumentation, *Literature surveys, *Measuring instruments, Standards, Abstracts, Bibliographies, Scientific literature, Biology, Medicine, Engineering, Electronics, Physics, Chemistry, *Guides, *Source list.

No abstract available.

02,618
AD-A280 562/0 PC A03/MF A01
National Bureau of Standards, Gaithersburg, MD.
Precision Laboratory Standards of Mass and Laboratory Weights.
T. W. Lashof, and L. B. Macurdy. 20 Aug 54, 28p.

Keywords: *Laboratory equipment, *Weight, *Standards, *Mass, *Balances, Precision, Calibration.

No abstract available.

02,619
AD-A286 618/4 PC A03/MF A01
National Bureau of Standards, Boulder, CO.
Design and Construction of a Liquid Hydrogen Temperature Refrigeration System.
D. B. Chelton, J. W. Dean, and B. W. Birmingham. 12 Jan 60, 42p, TN-38.

Keywords: *Refrigeration systems, *Liquid hydrogen, *Low temperature, *Bubble chambers, Design criteria, Construction, Circuits, Control systems, Heat exchangers, Physics, Nuclear instrumentation.

No abstract available.

02,620
DE93019682 PC A02/MF A01
National Inst. of Standards and Technology, Boulder, CO. Thermodynamics Div.
Development of a Dual-Sinker Densimeter for High-Accuracy Fluid P-V-T Measurements. Appendix A.
M. O. McLinden, and N. V. Frederick. 1993, 8p, CONF-9305134-3-APP.A.
Contract AI05-88ER13823
Symposium on Energy Engineering Sciences (11th), Argonne, IL (United States), 3-5 May 1993. Sponsored by Department of Energy, Washington, DC.

Keywords: *Densimeters, Design, Pressure Measurement, Temperature Measurement, Thermostats, Volume, EDB/440500.

A dual-sinker densimeter to very accurately measure the pressure-volume-temperature (P-V-T) properties of fluids over a temperature range of 80 K to 520 K and at pressures up to 35 MPa is in the final stages of development at NIST. The density of a fluid is determined by measuring the difference in the buoyancy forces experienced by two sinkers of identical mass, surface area, and surface material, but very different volumes. The buoyancy forces on the sinkers are transmitted to a semi-microbalance by means of a magnetic suspension coupling. This paper reviews the principle of the measurement and describes the overall design of the system.

02,621
DE95005780 PC A03/MF A01
National Inst. of Standards and Technology (NEL), Gaithersburg, MD. Automated Production Technology Div.
Minutes of the CAALS Workshop on modularity and communications standards.
G. W. Kramer. 1991, 11p, DOE/EW/50009-T2.
Contract AI01-90EW50009
Sponsored by Department of Energy, Washington, DC.

Keywords: *Measuring Instruments, Communications, Equipment Interfaces, Meetings, Standards, EDB/426000.

This Workshop was organized similarly to the previous meeting. After a presentation on Instrument Interfacing, three of the four Working Groups met individually. The Strategic Planning Committee did not meet at this Workshop, but it held a meeting in April; the minutes of that meeting are included. The Physical link and Transport Committee has defined the requirements for the link connecting modules to their controller, examined a new ASTM standard for low-level communication, and is determining what fits into to the various layers of the ISO model. The Module Requirements Group has proposed a process control model, has defined the core functionality, and has listed the requirements for a Standard Laboratory Module. The Software Engineering Group proposed that a document detailing the CAALS Modularity Architectural Specification be prepared and presented a working outline. The future structure and charters of the committees and the decision making criteria of the Workshop itself were questioned. These items will be examined in greater detail at the next Workshop.

02,622
N95-15937/2 (Order as N95-15919/0, PC A11/MF A03)
National Inst. of Standards and Technology, Gaithersburg, MD.
Numeric Data Distribution: The Vital Role of Data Exchange in Today's World.
M. W. Chase. 14 Sep 94, 2p.
In NASA, Washington, Fourth Annual International Acquisitions Workshop: Access to Multiple Media Worldwide 2 p.

Keywords: *Accuracy, *Dimensional measurement, *Information dissemination, *Measure and integration, *Numerical data bases, *Reference systems, *Reliability, *Standards, Chemical properties, Feedback, On-line systems, Physical properties.

The major aim of the NIST Standard Reference Data Program (SRD) is to provide critically evaluated numeric data to the scientific and technical community in a convenient and accessible form. A second aim of the program is to provide feedback into the experimental and theoretical programs to help raise the general standards of measurement. By communicating the experience gained in evaluating the world output of data in the physical sciences, NIST/SRD helps to advance the level of experimental techniques and improve the reliability of physical measurements.

02,623
PB94-138989 PC A18/MF A04
National Inst. of Standards and Technology, Gaithersburg, MD.
Report of the National Conference on Weight and Measures (78th). Held in Kansas City, MO. on July 18-22, 1993.
Special pub.
C. S. Brickenkamp, and A. H. Turner. Oct 93, 425p, NIST/SP-854.
Also available from Supt. of Docs. as SN003-003-03245-0. Library of Congress catalog card no. 26-27766.

Keywords: *Weight measurement, *Metrology, *Meetings, US NIST, Regulations, Laws(Legislation), Standards, Quality control, Kansas City(Missouri), Legal metrology.

The 78th Annual Meeting of the National Conference on Weights and Measures (NCWM) was held July 18 through 22, 1993, at the Ritz-Carlton Hotel, Kansas City, Missouri. The theme of the Meeting was 'Excellence Through Standards'. Reports by the standing and annual committees of the Conference comprise the major portion of the publication, along with the addresses delivered by Conference officials and other authorities from government and industry. Special meetings included those of the Metrologists, the Associate Membership Committee, the Retired Officials Committee, the Scale Manufacturers' Association, the American Petroleum Institute, the Industry Committee on Packaging and Labeling, the regional weights and measures associations, the National Association of State Departments of Agriculture Weights and Measures Division and the National Council on State Metrication.

02,624
PB94-142478 PC A03/MF A01
National Inst. of Standards and Technology (CSTL), Gaithersburg, MD. Process Measurements Div.
Assessment of Uncertainties of Calibration of Resistance Thermometers at the National Institute of Standards and Technology.
G. F. Strouse, and W. L. Tew. Jan 94, 19p, NISTIR-5319.
See also PB93-159465.

Keywords: *Resistance thermometers, *Calibration, International agreements, Temperature scales, Platinum, Estimates, *Measurement uncertainty, ITS-90, US NIST.

The National Institute of Standards and Technology (NIST) has adopted a new policy for the expression of measurement uncertainty, effective 1 January 1994, that is consistent with recommendations from the Comite International des Poids et Mesures. Using this new method of expressing uncertainties, this paper gives the expanded uncertainties for NIST-calibrated resistance thermometers (from 0.65 K to 1234.93 K) that are suitable as either defining interpolating devices of the International Temperature Scale of 1990 (ITS-90) or as scale transfer thermometers.

02,625
PB94-142510 PC A03/MF A01
National Inst. of Standards and Technology (CSTL), Gaithersburg, MD. Process Measurements Div.
Assessment of Uncertainties of Liquid-in-Glass Thermometer Calibrations at the National Institute of Standards and Technology.
J. A. Wise. Jan 94, 23p, NISTIR-5341.
See also PB89-128888 and PB94-142478.

Keywords: *Temperature measurement, *Thermometers, *Calibration, Calibration standards, Uncertainty, *Liquid-in-glass thermometers, US NIST.

By January 1, 1994, the method recommended by the International Committee of Weights and Measures in

1981 for expressing uncertainties for calibrations will be implemented at the National Institute of Standards and Technology. This paper explains how the Type A and Type B standard uncertainties and the combined uncertainty for liquid-in-glass thermometer calibrations are computed.

02,626
PB94-160785 PC A03/MF A01
National Inst. of Standards and Technology (MEL), Gaithersburg, MD.
Comparison of Finite Element and Analytic Calculations of the Resonant Modes and Frequencies of a Thick Shell Sphere.
D. E. Gilsinn, H. J. Hansen, Y. Xu, M. Huerta-Garnica, and E. C. Teague. May 91, 24p, NISTIR-4568.
Prepared in cooperation with Tianjin Univ. (China). and Centro de Investigacion y de Estudios Avanzados, Mexico City.

Keywords: High resolution, Dimensional measurement, Boundary value problems, Finite element analysis, Spherical shells, Resonant frequency, Simulation, Vibration, Comparison, *Coordinate measuring machines, *Molecular Measuring Machine, Normal mode analysis.

An ultra-high accuracy planar coordinate measuring machine, called the Molecular Measuring Machine (M(sup 3)) is being built at the National Institute of Standards and Technology (NIST). The design goal is to achieve a spatial resolution of 0.1 nm over an area of 50 mm X 50 mm. This goal requires that gravity loading and vibration response of a complicated mechanical structure be modeled to a high accuracy. Finite element analysis (FEA) was applied in the design of M(sup 3) as analytical modeling of the complicated structure was precluded. In order to achieve confidence in a specific FEA package, normal mode analysis results for a thick spherical shell that represented a first approximation to the M(sup 3) structure were compared to those predicted by another FEA package and to analytic results of the thick shell problem. The analytic model predicted degenerate modes due to the structural symmetry of the sphere. These were confirmed subsequently by both of the FEA packages. The FEA and analytic results differ by less than 5%.

02,627
PB94-160850 PC A03/MF A01
National Inst. of Standards and Technology (TS), Gaithersburg, MD. National Voluntary Lab. Accreditation Program.
NVLAP Procedures U.S. Code of Federal Regulations. Title 15, Subtitle A, Chapter 2, Part 7. (Effective December 1984; Amended September 1990).
J. Horlick, and H. M. Richmond. Nov 90, 22p, NISTIR-4493.

Keywords: *Laboratories, *Accreditation, Administrative procedures, Requirements, Quality assurance, *National Voluntary Laboratory Accreditation Program, *NVLAP system.

The NVLAP Procedures are a part of the U.S. Code of Federal Regulations and set forth the conditions under which the National Voluntary Laboratory Accreditation Program (NVLAP) will function. The Procedures contain general information about NVLAP, requirements for establishing a program in a specific field of testing, the process for accrediting a laboratory, and conditions and criteria for accreditation. NVLAP is a system for accrediting testing laboratories found competent to perform specific tests and types of tests. Competence is defined as the ability of a laboratory to meet conditions and conform to criteria specified in the Procedures as tailored and interpreted for the test methods, types of test methods, products, services, or standards for which the laboratory seeks accreditation.

02,628
PB94-161932 PC A03/MF A01
National Inst. of Standards and Technology (MSEL), Gaithersburg, MD. Polymers Div.
Recertification of the Standard Reference Material 1475A, a Linear Polyethylene Resin.
C. M. Guttman, and J. R. Maurey. Oct 93, 36p, NISTIR-5199.
See also PB93-159465.

Keywords: *Certification, *Calibration standards, *Polyethylenes, *References(Standards), US NIST, Quality assurance, Performance testing, Melt viscosity, Chromatographic analysis, Size determination, Organic polymers, Molecular weight, *Standard reference material 1475A, Measurement uncertainty.

The size exclusion chromatography (SEC) and the melt flow rate of Standard Reference Material (SRM) 1475a, a polyethylene resin, were determined and compared with measurements on the samples of SRM 1475. Within the errors of the measurements by SEC and melt flow rate, the measured characteristics of the SRM 1475a are identical to those of SRM 1475.

02,629
PB94-173754 PC A03/MF A01
National Inst. of Standards and Technology (MEL), Gaithersburg, MD. Factory Automation Systems Div.
Process for Selecting Standard Reference Algorithms for Evaluating Coordinate Measurement Software.
M. E. A. Algeo, and C. Diaz. Jan 94, 15p, NISTIR-5374.
See also PB93-149623 and PB94-163029.

Keywords: *Metrology, *Computer program verification, Computer applications, Computer software, Measuring instruments, Dimensional measurement, Calibrating, Coordinates, Data analysis, US NIST, Tests, Performance evaluation, *CMS, *Coordinate measuring systems, *SRA, *Standard reference algorithm, ATEP(Algorithm Testing and Evaluation Program), ATS(Algorithm Testing System).

The report is directed towards the dimensional metrology community interested in standardizing geometric fitting algorithms used in coordinate measuring systems (CMSs) and is intended to stimulate suggestions for establishing a standard reference algorithm (SRA) selection process. An acceptance procedure for evaluating and selecting the SRAs is identified. The SRA selection process provides control of variation among national reference algorithms and ensures addressing the needs of industry. It is envisioned as a two-stage process: an alpha phase conducted by the National Institute of Standards and Technology (NIST) and a beta phase of public review. The report describes the details of both phases and provides a summary of related activities.

02,630
PB94-178225 PC A03/MF A01
National Inst. of Standards and Technology (TS), Gaithersburg, MD. National Voluntary Lab. Accreditation Program.
National Voluntary Laboratory Accreditation Program: Procedures and General Requirements.
Handbook.
J. L. Cigler, and V. R. White. Mar 94, 44p, NIST/HB-150.
Also available from Supt. of Docs. as SN003-003-03260-3.

Keywords: *US NBS, *Laboratories, Certification, Procedures, Requirements, Calibration standards, Standardization, Licensure, Methodology, Accuracy, Performance evaluation, Government policies, *National Voluntary Laboratory Accreditation Program, NVLAP, NIST(National Institute of Standards and Technology).

NIST Handbook 150 is intended for information and use by staff of accredited laboratories, those seeking accreditation, other laboratory accreditation systems, users of laboratory services, and others needing information on the requirements for accreditation under the National Voluntary Laboratory Accreditation Program (NVLAP). It presents the basic procedures and general accreditation requirements of NVLAP for use in accrediting calibration and testing laboratories. This handbook contains Part 285 of Title 15 of the U.S. Code of Federal Regulations (CFR) plus all general procedures, criteria, and policies formerly contained in the individual NVLAP technical handbooks and separately published NVLAP policies.

02,631
PB94-185147 Not available NTIS
National Inst. of Standards and Technology (MSEL), Gaithersburg, MD. Metallurgy Div.
High-Temperature Laser-Pulse Thermal Diffusivity Apparatus.
Final rept.
A. Cezairliyan, T. Baba, and R. Taylor. Mar 94, 25p.
Pub. in International Jnl. of Thermophysics 15, n2 p317-341 Mar 94.

Keywords: *Thermal diffusivity, *High temperature tests, *Temperature measuring instruments, Radiative heat transfer, Thermophysical properties, Thermal properties, Boundary conditions, Transport properties, Pulsed lasers, Uncertainity, Reprints, *Laser pulse method.

A high-temperature laser-pulse apparatus for the measurement of thermal diffusivity in the temperature range from 1,500 to 2,500 K has been designed, constructed, and tested at the National Institute of Standards and Technology. A curve-fitting method is introduced by which the entire experimental temperature history curve is fitted with the theoretical curve under the boundary condition of radiative heat losses. The new apparatus and the curve-fitting method permit thermal diffusivity measurements with an uncertainty of not more than 3%.

02,632
PB94-186848 PC A06/MF A02
National Inst. of Standards and Technology (EEEL), Gaithersburg, MD.
Optical Fiber Sensors: Accelerating Applications in Navy Ships.
G. W. Day, P. S. Lovely, H. K. Whitesel, and R. K. Hickernell. May 94, 105p, NISTIR-5018.
Prepared in cooperation with Naval Surface Warfare Center, Annapolis, MD.

Keywords: *Naval vessels, *Fiber optics transmission lines, Pressure gages, Temperature measuring instruments, Cost analysis, Multiplexing, Military technology, Control systems, Specifications, Economic analysis, Signal processing, Damage assessment, Commercialization, Market research, *Optical fiber sensors.

The Navy needs new sensors for shipboard machinery monitoring and control, condition-based maintenance, and damage assessment. Optical fiber sensors are strongly preferred because of their immunity to electrical disturbances, as well as potential size, weight, and performance advantages. But despite well over a decade of development and promise, relatively few optical fiber sensors available today can meet the Navy's needs with acceptable performance and cost. This report examines the reasons and recommends strategies to help the Navy achieve its goals. Some of the recommendations confirm approaches that the Navy is already implementing. Optical fiber sensors have very valuable potential advantages, but those that the Navy can use may remain too expensive to be deployed if the Navy uses traditional methods of writing specifications and soliciting development and procurement bids. For this reason, the study focuses on cooperation with industry and promoting commercial off-the-shelf and dual-use technology.

02,633
PB94-187630 PC A03/MF A01
National Inst. of Standards and Technology (TS), Gaithersburg, MD. Metric Program.
Metric for Success.
G. P. Carver. May 94, 18p, NISTIR-5425.

Keywords: *Metric system, *Metrication, International system of units, Standards, United States, Federal agencies, Metrology, Units of measurement, Government/industry relations, National government, History, NIST(National Institute of Standards and Technology).

The federal agencies are working with industry to ease adoption of the metric system. The goal is to help U.S. industry to compete more successfully in the global marketplace, increase exports, and create new jobs. The strategy is to use federal procurement, financial assistance, and other business-related activities to encourage voluntary conversion. Based upon the positive experiences of firms and industries that have converted, federal agencies have concluded that metric use will yield long-term benefits that are beyond any one-time costs or inconveniences. It may be time for additional steps to move the Nation out of its dual-system comfort zone and to continue the progress toward metrication. The report includes Metric Highlights in U.S. History.

02,634
PB94-198819 Not available NTIS
National Inst. of Standards and Technology (NML), Gaithersburg, MD. Thermophysics Div.
Milliwatt Mixer for Small Fluid Samples.
Final rept.
R. F. Berg, and N. P. De Luca. 1991, 3p.
Pub. in Review of Scientific Instruments 62, n2 p527-529 1991.

Keywords: *Mixers, Milliwatt power range, Low power, Thermal stability, Fluoroform, Methanol, Mixing, Samples, Reprints, *Fluid mixers.

Mixing without excessive heating is sometimes needed for temperature-sensitive fluids. We modified an inexpensive low-frequency electronic filter based on a mechanical resonator to produce a compact (16 mm) and low-power (1-3 mW) mixer for low viscosity fluids. Tests made in air and methanol at room temperature and in fluoroform near its critical point are compared against the predictions of an electromechanical model.

02,635
PB94-199999 Not available NTIS
National Inst. of Standards and Technology (CSTL), Gaithersburg, MD. Thermophysics Div.
Millisecond-Resolution Pulse Heating System for Specific-Heat Measurements at High Temperatures.
Final rept.
A. Cezairliyan. 1992, 35p.
Pub. in Compendium of Thermophysical Property Measurements Methods, Chapter 17, v2 p483-517 1992.

Keywords: *Specific heat, *High temperature tests, *Test methods, *Pulse heating, Experiment design, Errors, Temperature measurement, Thermophysical properties, Test facilities, Reprints.

In the first volume of this Compendium, a general description and a brief survey of the pulse techniques, utilizing resistive self-heating of the specimen, for the measurement of specific heat at high temperatures were given. The presentation covered techniques over a wide regime of time response: from nearly a second to submicrosecond resolution. Most of the techniques were of an exploratory nature and were developed for specific immediate applications. However, as a result of extensive research performed during the last 25 years, the millisecond-resolution pulse heating technique for specific-heat measurements has reached a mature stage. The objective of the present chapter is to give details of the millisecond-resolution technique developed in the Dynamic Measurements Laboratory of the U.S. National Institute of Standards and Technology (NIST), formerly the U.S. National Bureau of Standards (NBS). The presentation includes a description of the measurement system, measurement procedure, consideration of various phenomena that affect the design and operation of the system, estimate of errors, and discussion summarizing recent improvements and additions to the overall system.

02,636
PB94-200003 Not available NTIS
National Inst. of Standards and Technology (CSTL), Gaithersburg, MD. Thermophysics Div.
High-Speed Spatial Scanning Pyrometer.
uinal rept.
A. Cezairliyan, R. F. Chang, G. M. Foley, and A. P. Miiller. 1993, 9p.
Pub. in Review of Scientific Instruments 64, n6 p1584-1592 Jun 93.

Keywords: *Pyrometers, *Spectral emission, *Temperature measurement, Linear arrays, Line spectra, Temperature measuring instruments, Errors, Tungsten, Thermophysical properties, Reprints.

A high-speed spatial scanning pyrometer has been designed and developed to measure spectral radiance temperatures at multiple target points along the length of a rapidly heating/cooling specimen in dynamic thermophysical experiments at high temperatures (above about 1800 K). The design, which is based on a self-scanning linear silicon array containing 1024 elements, enables the pyrometer to measure spectral radiance temperatures (nominally at 650 nm) at 1024 equally spaced points along a 25-mm target length. The elements of the array are sampled consecutively every 1 microsecond thereby permitting one cycle of measurements to be completed in approximately 1 ms. The pyrometer output is recorded digitally with a full-scale resolution of 0.025% every 1 microsecond. Procedures for calibration and temperature measurement as well as the characteristics and performance of the pyrometer are described. The details of sources and estimated magnitudes of possible errors are given. An example of measurements of radiance temperatures along the length of a tungsten rod, during its cooling following rapid resistive pulse heating, is presented.

02,637
PB94-211364 Not available NTIS
National Inst. of Standards and Technology (MEL), Gaithersburg, MD. Precision Engineering Div.
Advanced Angle Metrology System.
Final rept.
W. T. Estler, and Y. H. Queen. 1993, 4p.
Pub. in Annals of the CIRP 42, n1 p573-576 1993.

Keywords: *Metrology, Calibration, Resolution, Accuracy, Reprints, *Angle measurement, *AAMACS system, US NIST.

We describe the new Advanced Automated Master Angle Calibration System (AAMACS) at the U. S. National Institute of Standards and Technology. The heart of this system is a set of three stacked concentric indexing tables with 832, 729, and 625 teeth respectively. The system is fully error corrected and achieves a full-circle positioning accuracy of + or - 0.02 arc-seconds with an angular positioning resolution of 0.0034 arc-seconds. System accuracy is limited by autocollimator noise. We will describe the error mapping process and the use of the system for high-accuracy autocollimator calibrations.

02,638
PB94-211687 Not available NTIS
National Inst. of Standards and Technology (TS), Gaithersburg, MD. Weights and Measures Program.
Ensuring Accuracy and Traceability of Weighing Instruments.
Final rept.
G. L. Harris. 1993, 8p.
Pub. in American Society for Testing and Materials Standardization News, p44-51 Apr 93.

Keywords: *Weight indicators, Weight measurement, Calibration, Metrology, Balances, Accuracy, Reprints, Mass standards, ISO 9000, Accreditation, Traceability.

The paper reviews available standards, guides, recommended practices, and publications to provide both a general overview of available reference material and recommendations related to ensuring accuracy and traceability of weighing instruments. References are promulgated by the following organizations: (1) National Institute of Standards and Technology; (2) National Conference on Weights and Measures; (3) International Organization for Legal Metrology; (4) International Standards Organization; (5) Instrument Society of America for Testing and Materials.

02,639
PB94-211695 Not available NTIS
National Inst. of Standards and Technology (NEL), Gaithersburg, MD. Precision Engineering Div.
Particle Size Standards and Their Certification at NIST.
Final rept.
A. W. Hartman. 1991, 9p.
Pub. in Proceedings of Measurement Science Conference, Anaheim, CA., January 31-February 1, 1991, 9p.

Keywords: *Particle size, Particle size distribution, Electron microscopy, Certification, Microspheres, Reprints, Standard reference materials, US NIST.

An overview is given of the National Institute of Standards and Technology's (NIST's) Standard Reference Materials (SRMs) for particle size and of the techniques used in their certification.

02,640
PB94-212370 Not available NTIS
National Inst. of Standards and Technology (CSTL), Gaithersburg, MD. Thermophysics Div.
Intercomparison of the Effective Areas of a Pneumatic Piston Gauge Determined by Different Techniques.
Final rept.
K. K. Jain, C. D. Ehrlich, J. C. Houck, and J. K. N. Sharma. 1993, 9p.
Pub. in Meas. Sci. Technol. 4, p249-257 1993.

Keywords: *Pneumatic equipment, *Pressure gages, *Manometers, Calibration, Measuring instruments, Test methods, Pressure measurement, Uncertainty, Reprints, *Piston gages.

A variety of primary measurement techniques is now available for the measurement of pressure to 1 MPa and above. To ascertain the systematic uncertainty, if any, which exists in the measured pressure using the individual techniques, it is best to perform direct intercomparisons of primary instruments. However, when direct intercomparison is not possible, the next best alternative is to use a highly stable, reproducible transfer artifact such as a simple piston gage. Such intercomparisons are described here, utilizing a piston gage calibrated by a mercury manometer (with 0.1 MPa full-scale pressure), four large diameter 'dimensional' piston gages from two different manufacturers (all with 1 MPa full-scale pressure), and a controlled clearance piston gage (with 7 MPa full-scale pressure). The area ratio derived from dimensional measurements on two of the large diameter gages, when compared with the ratio obtained from measurements traceable to a manometer, agrees within 1 part per million (ppm). For one of the large diameter piston gages, the area value obtained from the manometer agrees within 3 ppm with its dimensional area, and within 10 ppm with the value obtained by its direct calibration against the controlled clearance piston gage.

02,641
PB94-216306 Not available NTIS
National Inst. of Standards and Technology (NML), Gaithersburg, MD.
Models and Interactions.
Final rept.
J. Mandel. 1991, 5p.
Pub. in Jnl. of Testing and Evaluation 19, n5 p398-402 1991.

Keywords: *Experimental data, Interlaboratory comparisons, Analysis of variance, Data analysis, Graphic methods, Test methods, Models, Reprints, Two way tables.

It is shown that the classical analysis of variance for two-way tables, with mean squares for rows, columns and interaction, is often a hindrance to understanding. For interlaboratory data resulting from the study of a test method, a row-linear model is generally more appropriate. However, in practice, a material-by-material analysis of such data, involving minimal prior assumptions, is the most appropriate way of dealing with interlaboratory test data. The importance of graphics is illustrated.

02,642
PB94-219060 PC A04/MF A01
National Inst. of Standards and Technology (TS), Gaithersburg, MD. National Voluntary Lab. Accreditation Program.
National Voluntary Laboratory Accreditation Program: Energy Efficient Lighting Products.
Handbook.
L. S. Galowin, W. Hall, and W. J. Rossiter. Jul 94, 74p, NIST/HB-150/1.
Also available from Supt. of Docs as SN003-003-03279-4. See also PB94-178225.

Keywords: *Energy efficiency, *Laboratories, *Accreditation, *Tests, Lighting equipment, Procedures, Methodology, Requirements, Calibration standards, Quality, Energy policy, *EEL program, *Energy Efficient Lighting program, *NVLAP(National Voluntary Laboratory Accreditation Program), *National Voluntary Laboratory Accreditation Program, US NIST.

The purpose of this handbook is to set out procedures and technical requirements for the National Voluntary Laboratory Accreditation Program (NVLAP) accreditation of laboratories which perform test methods covered by the Energy Efficient Lighting (EEL) Products program. It complements and supplements the NVLAP programmatic procedures and general requirements found in NIST Handbook 150 (PB94-178225). The interpretive comments and additional requirements contained in this handbook make the general NVLAP criteria specifically applicable to the EEL program.

02,643
PB94-219326 PC A05/MF A02
National Inst. of Standards and Technology, Gaithersburg, MD.
Journal of Research of the National Institute of Standards and Technology. May/June 1994. Volume 99, Number 3.
B. N. Taylor, and D. R. Harris. 1994, 100p.
See also PB94-219334 through PB94-219409 and PB94-219219. Also available from Supt. of Docs. as SN703-027-00058-0.

Keywords: *Resistors, *Standards, *Calibrating, Voltmeters, Electrical resistance meters, Hall effect, Drift(Instrumentation).

Contents:
Articles:
Sources of Uncertainty in a DVM-Based Measurement System for a Quantized Hall Resistance Standard;

A dc Method for the Absolute Determination of Conductivities of the Primary Standard KCl Solutions from 0 deg C to 50 deg C;
Three-Axis Coil Probe Dimensions and Uncertainties During Measurement of Magnetic Fields from Appliances;
Improved Automated Current Control for Standard Lamps;
Refractive Indices of Fluids Related to Alternative Refrigerants;
A Theoretical Analysis of the Coherenece-Induced Spectral Shift Experiments of Kandpal, Vaishya, and Joshi;
Comments on the paper 'Wolf Shifts and Their Physical Interpretation Under Laboratory Conditions' by K. D. Mielenz;
Reply to Professor Wolf's comments on my paper on Wolf shifts;
Errata--Erratum:
Precision Comparison of the Lattice Parameters of Silicon Monocrystals;
Conference Reports--Workshop on Characterizing Diamond Films III;
Briefs.

02,644
PB94-219342 (Order as PB94-219326, PC A05/MF A02)
National Inst. of Standards and Technology, Gaithersburg, MD.
dc Method for the Absolute Determination of Conductivities of the Primary Standard KCl Solutions from 0C to 50C.
Y. C. Wu, W. F. Koch, D. Feng, E. Arvay, A. Tomek, L. A. Holland, and E. Juhasz. 1994, 6p.
Prepared in cooperation with National Office of Measures, Budapest (Hungary).
Included in Jnl. of Research of the National Institute of Standards and Technology, v99 n3 p241-246 May/Jun 94.

Keywords: *Standards, *Conductivity, *Potassium chloride, Electrical resistivity, Tests, Aqueous electrolytes.

A new method for the absolute determination of electrolytic conductivity based on direct current and potentio-metric measurements is described. The unique design of the cell uses a removable center section whose length and cross-sectional area are accurately known. Two pairs of matched Ag, AgCl electrodes are used in a four terminal mode of resistance measurement. Measurements of the electrolytic conductivity of primary standard potassium chloride solution using this novel dc conductance cell are compared with the currently adopted IUPAC and OIML recommendations. In addition, measurements have been made of the electrolytic conductivity of a solution of potassium chloride having a molality of 1 mol/kg (mole KCl per kilogram H2O). The values so obtained over the temperature range of 0 deg C to 50 deg C are recommended as the new primary standards for electrolytic conductivity.

02,645
PB95-103826 PC A02/MF A01
National Inst. of Standards and Technology (CSTL), Gaithersburg, MD. Process Measurements Div.
New Expressions of Uncertainties for Humidity Calibrations at the National Institute of Standards and Technology.
P. H. Huang, and J. R. Whetstone. Jun 94, 9p, NISTIR-5455.

Keywords: *Humidity measurement, *Calibration, *Uncertainty, Error analysis, Mixing ratios, Dew point, Tables(Data), US NIST.

Beginning January 1, 1994, the National Institute of Standards and Technology (NIST) requires all calibration reports to state the uncertainties according to the new policy. Reference is to be made to some published document. Uncertainties of calibration results are expressed using the method described in the 'Guide to the Expression of Uncertainty in Measurement' (NIST Technical Note 1297). This report explains how each component of the combined standard uncertainty was determined for providing the expanded uncertainties of humidity parameters.

02,646
PB95-107280 Not available NTIS
National Inst. of Standards and Technology (TS), Gaithersburg, MD. Office of Measurement Services.
Should NIST Accredit U.S. Calibration Laboratories.
Final rept.
S. D. Rasberry, and J. D. Simmons. 1991, 11p.
Pub. in Proceedings of Measurement Science Conference, Anaheim, CA., January 31-February 1, 1991, 11p.

Keywords: Measurement, Standards, Reprints, *Calibration laboratories, *Laboratory accreditation, *Accreditation, Reference materials, Traceability, US NIST.

For nine decades the National Institute of Standards and Technology (NIST), and under its former name the National Bureau of Standards, has followed one model of providing traceability to National standards of measurement. In that model NIST offers calibration and reference material services, and leaves entirely to users of those services the burden of maintaining and demonstrating traceability. In this talk the authors explore the possibility of a new model. The NIST services mentioned above would be continued as would the feature of user responsibility for traceability. What would be added is accreditation by NIST of laboratory calibration competence, conformance to quality laboratory standards, and proficiency in providing calibration services. A NIST 'home' for such a system already exists in the National Voluntary Laboratory Accreditation Program (NVLAP) which currently accredits about 1000 testing laboratories. At least four pressures are building to move in this direction. They include (1) company quality programs aimed at the highest level of attainment; (2) customer requirements (including those of Federal executive branch departments); (3) requirements for accreditation as mandated in new laws; and (4) international trade requirements resulting from EC-92 developments.

02,647
PB95-108502 Not available NTIS
National Inst. of Standards and Technology (MEL), Gaithersburg, MD. Precision Engineering Div.
Metrology Model for Submicrometer Dimensional Measurements.
Final rept.
J. Potzick. 1993, 10p.
Pub. in Proceedings of Measurement Science Conference, Anaheim, CA., January 20-22, 1993, p1-10.

Keywords: *Dimensional measurement, *Length, Planar structures, Calibration, Metrology, Standards, Comparison, Precision, Accuracy, Models, Reprints, Nanostructures, Traceability.

A model for the accurate dimensional measurement of small planar objects is developed in terms of the comparison of the images of the test object and a standard object in a measuring device. A length measuring instrument is thus a comparator. The calibration of the standard and the conditions necessary for a valid comparison are discussed. The principles discussed here apply to many other types of measurement as well.

02,648
PB95-108700 Not available NTIS
National Inst. of Standards and Technology (NEL), Gaithersburg, MD. Automated Production Technology Div.
Vibration Laboratory Automation at NIST with Personal Computers.
Final rept.
B. F. Payne. 1990, 15p.
Pub. in Proceedings of National Computer Systems Laboratory Workshop and Symposium, Washington, DC., August 19-23, 1990, p41-55.

Keywords: *Vibration measurement, *Automation, *Personal computers, Accelerometers, Calibration, Standards, Laboratories, Measuring instruments, Vibration simulators, Shakers, High level languages, Reprints, US NIST.

The National Institute of Standards and Technology (NIST) provides calibration services for vibration pickups over a wide frequency range. Two experimental test measurement setups have been automated, each using a personal computer. One measurement system is for calibration of vibration shakers that uses an absolute reciprocity method, and the shaker is calibrated by measuring the changes in the electrical admittance of the shaker as a function of the mass attached to the shaker table. The second measurement system is for accelerometer calibration by comparison of a test accelerometer to a standard shaker which has been calibrated by an absolute method. These automated measurement systems make use of modern high level languages, one in Pascal and one in 'C'. The paper also gives some comparisons of the use of personal computers and technical laboratory computers.

02,649
PB95-143087 PC A03/MF A01
National Inst. of Standards and Technology (PL), Gaithersburg, MD.
Guidelines for Evaluating and Expressing the Uncertainty of NIST Measurement Results. 1994 Edition.
Technical note.
B. N. Taylor, and C. E. Kuyatt. Sep 94, 34p, NIST/TN-1297.
Supersedes PB93-159465. Also available from Supt. of Docs. as SN003-003-03292-1.

Keywords: Confidence level, Error analysis, Guidelines, Uncertainty, Standards, Accuracy, Precision, *Measurement uncertainty, ISO Guide, US NIST.

This Technical Note succinctly presents, in the context of the NIST Policy on Statements of Uncertainty Associated with Measurement Results, those aspects of the ISO Guide to the Expression of Uncertainty in Measurement that will be of most use to the NIST staff and others in implementing that policy, which is included as Appendix C. In this second (1994) edition of Technical Note (TN) TN 1297, Appendix D has been added to clarify and provide additional guidance on a number of topics in response to questions asked since the publication of the first (1993) edition.

02,650
PB95-150884 Not available NTIS
National Inst. of Standards and Technology (CSTL), Gaithersburg, MD. Thermophysics Div.
Vacuum Gauges and Partial Pressure Analyzers.
Final rept.
C. R. Tilford. 1993, 4p.
Pub. in Jnl. of Physics: Condens. Matter 5, pA81-A84 1993.

Keywords: *Vacuum gages, *Gas analysis, Partial pressure, Measuring instruments, Pressure measurement, Vacuum apparatus, Ionization gages, Reprints, Capacitance diaphragm gages, Partial pressure analyzers, Residual gas analyzers.

This paper briefly reviews the characteristics of several important vacuum instruments; capacitance diaphragm gauges, ionization gauges, spinning rotor gauges, and partial pressure or residual gas analyzers.

02,651
PB95-162202 Not available NTIS
National Inst. of Standards and Technology (NEL), Gaithersburg, MD. Precision Engineering Div.
Dimensional Characterization of Small Bores: A Survey.
Final rept.
J. Raja, and R. Veale. 1990, 10p.
Pub. in Proceedings of Measurement Science Conference, Anaheim, CA., February 8-9, 1990, 10p.

Keywords: *Holes, *Cavities, *Dimensional measurement, Methodology, Precision, Diameters, Waveguides, Reprints, CMM(Coordinate measuring machines).

The measurement of small bores is now and has always been a difficult measurement problem. The problem is especially difficult when the length to diameter ratio of the bore is large. This paper presents a survey of the various techniques now in use as well as other methods which have been developed in the past. It lists the advantages, disadvantages, and expected accuracy which can be achieved using the various methods. Current work using coordinate measuring machines to characterize the internal dimensions of waveguides is also described.

02,652
PB95-162434 Not available NTIS
National Inst. of Standards and Technology (MSEL), Gaithersburg, MD. Ceramics Div.
Loading Device for Fracture Testing of Compact Tension Specimens in the Scanning Electron Microscope.
Final rept.
J. Rodel, J. F. Kelly, M. R. Stoudt, and S. J. Bennison. 1991, 7p.
Pub. in Scanning Microscopy 5, n1 p29-35 Mar 91.

Keywords: *Loading rate, *Fractography, *Scanning electron microscopy, Loads(Forces), Crack propagation, Aluminum oxide, Ceramics, Performance evaluation, Design criteria, Case studies, Reprints, Piezoelectric translators.

A loading device for compact tension specimens allowing fracture experiments in the scanning electron microscopy (SEM) has been designed. Its key elements are a piezoelectric translator for applying controlled displacements to the loading points on the specimen and a load cell to measure applied loads. The effective transmission of displacement from the piezoelectric driver to the specimen was found to be the major mechanical design problem. The peripheral equipment include a function generator and a high voltage amplifier to drive the piezoelectric translator as well as a video overlay and standard video equipment to record the image continuously during the course of the experiment. A case study on alumina describes qualitative observations on the toughening mechanism, crack-interface bridging, operating in this material. Quantitative information pertaining to the closure stresses associated with this toughening mode can be obtained by measuring the crack profile.

02,653
PB95-163093 Not available NTIS
National Inst. of Standards and Technology (MEL), Gaithersburg, MD. Precision Engineering Div.
Two New Probes for a Coordinate Measuring Machine.
Final rept.
J. Stone, L. Carroll, G. Caskey, J. Rose, K. Lau, S. Phillips, and R. Resnick. 1993, 4p.
Pub. in Proceedings of the ASPE Annual Meeting (8th), Seattle, WA., November 7-12, 1993, p82-85.

Keywords: *Measuring instruments, *Probes, Dimensional measurement, Accuracy, Reprints, *CMM(Coordinate measuring machines), *Coordinate measuring machines, Analog probes, Touch-trigger probes.

We have performed tests of the measuring capabilities of two new analog probes used with coordinate measuring machines. Both probes are capable of sub-micrometer accuracies. The first is an LVDT-based three-dimensional analog probe with a range of 0.1 mm and a resolution of 0.025 micrometers. We found that the repeatability of the probe is 0.04 micrometers (1 standard deviation) and three-dimensional errors are less than 0.5 micrometers at small deflections. The second probe is a non-contact capacitance probe. The probe stylus is a precision ball mounted on the end of a hypodermic needle; the probe detects the position of a nearby surface through measuring the capacitance between the surface and the ball. The probe can be used as a true analog probe or it can simulate the operation of a touch-trigger probe, generating a trigger pulse when the reading exceeds a threshold value. The repeatability in analog mode is 0.05 micrometers and the repeatability as a touch-trigger probe is 0.1 micrometers. Used as a touch-trigger probe in three dimensions, the probe accuracy is about 1.3 micrometers.

02,654
PB95-164703 Not available NTIS
National Inst. of Standards and Technology (NML), Boulder, CO. Chemical Engineering Science Div.
Cryogenics.
Final rept.
L. L. Sparks. 1993, 20p.
Sponsored by American Society for Testing and Materials, Philadelphia, PA.
Pub. in Manual on the Use of Thermocouples in Temperature Measurement, Chapter 11, p214-233 1993.

Keywords: *Temperature dependence, *Thermocouples, *Cryogenic temperature, Magnetic fields, Thermoelectricity, Reprints, Reference tables, ITS-90.

Successful use of thermocouples for absolute or differential temperature measurement at low temperatures requires that particular attention be paid to thermocouple sensitivity and to the relative importance of thermoelectric effects such as dilute impurities, strain, and inhomogeneity. An important subset of cryogenic temperature measurement involves magnetic-field environments. Thermocouple types and the magnetic-field effect on the thermoelectric sensitivity are discussed. Reference tables based on ITS-90 are given for zero-field applications.

02,655
PB95-168506 Not available NTIS
National Inst. of Standards and Technology (CSTL), Gaithersburg, MD. Thermophysics Div.
Look at Uncertainties over Twenty Decades of Pressure Measurement.
Final rept.
C. D. Ehrlich. 1994, 10p.
Pub. in Proceedings of VIII IMEKO World Congress, Torino, Italy, September 5-9, 1994, p1941-1950.

Keywords: *Pressure measurement, *Uncertainity, Transducers, Pressure gages, Accuracy, Test facilities, Test methods, Reprints.

A wide variety of instrumentation is required to perform state-of-the-art pressure measurements over the almost 20 decade range of pressure that is used in science and industry today. The uncertainties associated with such measurements similarly span a wide range, from several parts in a million near atmospheric pressure to around 10% or more at both pressure extremes. This paper provides an overview of the techniques, instrumentation and uncertainties associated with the most common primary measurements of pressure practiced today. A discussion of some of the more prominent types of pressure gages and transducers in the various pressure regimes is also included.

02,656
PB95-169819 PC A20/MF A04
National Inst. of Standards and Technology (TS), Gaithersburg, MD. Weights and Measures Program.
Report of the National Conference on Weights and Measures (79th). Held in San Diego, California on July 17-21, 1994.
Special pub.
C. S. Brickenkamp, and A. H. Turner. Nov 94, 458p, NIST/SP-870.
Also available from Supt. of Docs. as SN003-003-03306-5. Library of Congress catalog card no. 26-27766. See also PB94-138989.

Keywords: *Weight measurement, *Metrology, *Meetings, Regulations, Laws(Jurisprudence), Standards, Quality control, US NBS, Safety, Scale(Ratio), Training, Mass flowmeters, San Diego(California), Legal metrology, Grain moisture.

The 79th Annual Meeting of the National Conference on Weights and Measures (NCWM) was held July 17 through 21, 1994, at the Doubletree Hotel at Horton Plaza, San Diego, California. The theme of the meeting was 'Consensus Through Communication.' Reports by the standing and annual committees of the Conference comprise the major portion of this publication, along with the addresses delivered by Conference officials and other authorities from government and industry. Special meetings included those of the Metrologists, the Associate Membership Committee, the Retired Officials Committee, the Scale Manufacturers' Association, the American Petroleum Institute, the Industry Committee on Packaging and Labeling, and the regional weights and measures associations.

02,657
PB95-175014 Not available NTIS
National Inst. of Standards and Technology (CSTL), Gaithersburg, MD. Thermophysics Div.
Influence of the Filament Potential Wave Form on the Sensitivity of Glass-Envelope Bayard-Alpert Gages.
Final rept.
P. J. Abbott, and J. P. Looney. 1994, 6p.
Pub. in Jnl. of Vacuum Science and Technology A 12, n5 p2911-2916 Sep/Oct 94.

Keywords: *Bayard-Alpert ionization gages, *Waveforms, *Sensitivity, *Filaments, Controllers, Vacuum gages, Nonlinearity, Glass, Pressure gages, Reprints.

Nonlinearities of about 10%-15% in the sensitivity of glass envelope Bayard-Alpert gages (BA gages) have been observed in the pressure range 10(exp -7) to 10(exp -2) Pa. These nonlinearities were studied in modified BA gage tubes with platinum coatings on their inner glass surfaces by measuring the equilibrium potential of the platinum coating as a function of pressure. The sensitivities of the gage systems (gage tube plus controller) were found to depend on the inner surface potential, and this potential was found to depend on pressure and on the details of the filament potential waveform provided by the gage controller. It was found that the nonlinearities could be minimized by holding the inner surface to a fixed direct-current (dc) potential, by modifying the alternating-current filament potential wave form, or by using a controller that provides a noise-free dc filament-heating current.

02,658
PB95-180428 Not available NTIS
National Inst. of Standards and Technology (BFRL), Gaithersburg, MD. Building Environment Div.
Design and Machining of Copper Specimens with Micro Holes for Accurate Heat Transfer Measurements.
Final rept.
M. A. Kedzierski, and J. L. Worthington. 1993, 16p.
Pub. in Experimental Heat Transfer 6, p329-344 1993.

Keywords: *Drilling, *Micromachining, *Temperature measurement, *Copper, Thermocouples, Experiment design, Temperature distribution, Uncertainty, Errors, Reprints, Micro holes.

This article presents a technique that has been developed specifically for drilling 0.5334-mm-diameter, 19-mm-deep holes in copper for use in temperature measurement. The holes accept thermocouples, which are used for the measurement of the temperature gradient and the wall temperature of the specimen. Errors due to the intrusion of the probe, and the finite size and mass of the probe, are reduced as the diameter of the probes is reduced. A machining procedure for drilling deep micro holes in copper cannot be found in conventional texts; this article advocates holes that are deeper than those traditionally recommended. This article is written for both machinists and experimentalists. Both heat transfer and machining criteria are considered. The necessary equipment and their specifications are discussed. Special attention is given to specifying drilling speeds, feed rates, and lubricants. Step-by-step drilling instructions are given. An analysis is performed to reveal the important parameters for reducing the errors associated with the uncertainty in the location, the relative position of the thermocouples, and the individual temperature measurements.

02,659
PB95-180998 Not available NTIS
National Inst. of Standards and Technology (CSTL), Gaithersburg, MD. Thermophysics Div.
Measurement of Very-Low Partial Pressures.
Final rept.
C. R. Tilford. 1994, 6p.
Pub. in Jnl. of the Vacuum Society of Japan 37, n9 p667-672 1994.

Keywords: *Pressure measurement, *Ultrahigh vacuum, *Partial pressure, *Residual gas, Measuring instruments, Sensitivity, Mass spectrometers, Gas analysis, Vacuum apparatus, Vapor pressure, Ionization gages, Reprints.

The measurement of partial pressures in the ultra high and extreme high vacuum ranges (below about 10(exp -6)) is important for residual gas analysis and the measurement of low-pressure constituents (both contaminants and deliberate additions) in higher-pressure process gases. Mass-spectrometer type instruments--partial pressure or residual gas analyzers (PPAs and RGAs)--are generally used for this purpose. Typically, these instruments consist of an electron-impact ionizer, a quadrupole mass filter, and an ion detector. This paper discusses these elements and other factors that determine the very-low-pressure performance of these instruments--detection limits, mass resolution, and stability and pressure-dependence of the sensitivity. Particular attention is paid to ion-source design and operating parameters, the coupling of ions between the ionizer and the mass analyzer, and the influence of the total pressure on partial pressure sensitivities.

02,660
PB95-181004 Not available NTIS
National Inst. of Standards and Technology (CSTL), Gaithersburg, MD. Thermophysics Div.
Process Monitoring with Residual Gas Analyzers (RGAs): Limiting Factors.
Final rept.
C. R. Tilford. 1994, 5p.
Pub. in Surface and Coatings Technology 68/69, p708-712 1994.

Keywords: *Pressure measurement, *Partial pressure, *Gas analysis, *Residual gas, Mass spectrometers, Calibration, Metrology, Vacuum apparatus, Sensitivity, Reprints, *Residual gas analyzers.

Many vacuum processes are limited by low-level impurities introduced with process gases or generated with-

in the process chamber. Specific impurities are often monitored using residual gas analyzers (RGAs) or partial pressure analyzers (PPAs), most commonly, mass spectrometers of the quadrupole type. Unfortunately, the performance of these instruments can be affected significantly by a number of instrument and vacuum environment variables, so that the sensitivities of even calibrated instruments can differ significantly from expected values. These variables include ion source parameters, total pressure and prior exposure to active gases. The magnitude of the deviations in sensitivity varies for different instruments, but can reach orders of magnitude in extreme cases. This paper reviews the important factors affecting instrument performance, illustrates the magnitude of the effects for different instruments, recommends instrument test procedures, and suggests operating parameters and procedures that can minimize these effects.

02,661
PB95-189478 PC A05/MF A01
National Inst. of Standards and Technology (TS), Gaithersburg, MD. National Voluntary Lab. Accreditation Program.
National Voluntary Laboratory Accreditation Program: POSIX. Portable Operating System Interface.
Handbook.
J. Horlick, and M. M. Gray. Jan 95, 76p, NIST/HB-150/7.
Also available from Supt. of Docs as SN003-003-03317-1. See also PB94-178225 and FIPS PUB 151-2.

Keywords: *Laboratories, *Requirements, Certification, Procedures, Calibration standards, Standardization, Management, Auditing, Personnel, Equipment, Tests, *POSIX(Portable Operating System Interface), *Portable Operating System Interface, *NVLAP(National Voluntary Laboratory Accreditation Program), *National Voluntary Laboratory Accreditation Program, US NIST.

The handbook presents the technical requirements of the National Voluntary Laboratory Accreditation Program (NVLAP) for the Portable Operating System Interface (POSIX program). It is intended for information and use by staff of accredited laboratories, those laboratories seeking accreditation, other laboratory accreditation systems, users of laboratory services, and others needing information on the requirements for accreditation under the POSIX program. This publication supplements NIST Handbook 150, 'NVLAP Procedures and General Requirements' (PB94-178225) which contains Part 285 of Title 15 of the U.S. Code of Federal Regulations (CFR) plus all general NVLAP procedures, criteria, and policies.

02,662
PB95-203444 Not available NTIS
National Inst. of Standards and Technology (MEL), Gaithersburg, MD. Precision Engineering Div.
Morphological Estimation of Tip Geometry for Scanned Probe Microscopy.
Final rept.
J. S. Villarrubia. 1994, 14p.
Pub. in Surface Science 321, p287-300 1994.

Keywords: *Tips, *Scanning tunneling microscopy, *Morphology, *Image processing, Geometry, Surface properties, Mathematical models, Image analysis, Reprints, *Atomic force microscopy.

Morphological constraints inherent in the imaging process limit the possible shapes of the tip with which any given tunneling microscope or atomic force microscope image could have been taken. Broad tips do not produce narrow image protrusions. Therefore, feature sizes within the image may be used to place an upper bound on the size of the tip. In this paper, mathematical morphology is used to derive, for each point on an image, a corresponding bounding surface for the tip. The actual tip must be equal to or smaller than the largest tip which satisfies all of the constraints. Example calculations are performed, demonstrating that if the imaged specimen contains sharp features and high relief, the tip shape deduced by this method will be a good estimate of the actual one. Once known, the tip geometry can be deconvoluted from images to recover parts of the actual surface which were accessible to the tip.

02,663
PB95-242293 PC A04/MF A01
National Inst. of Standards and Technology (MEL), Gaithersburg, MD. Manufacturing Systems Integration Div.
ISO TC 184/SC4 Reference Manual.
J. D. Wellington, and B. M. Smith. Jun 95, 61p, NISTIR-5665.

Keywords: *Standardization, *Manuals, Procedures, Research projects, Administration, Manufacturing, Digital systems, Technology transfer, International cooperation, International standards.

The reference manual contains background information on the International Organization for Standardization (ISO) and its Technical Committee 184. It gives a detailed explanation of the technical work of TC 184's Subcommittee 4 (TC 184/SC4) and information on the working groups and advisory committees that carry out that technical work.

02,664
PB95-242376 PC A06/MF A02
National Inst. of Standards and Technology (TS), Gaithersburg, MD. National Voluntary Lab. Accreditation Program.
National Voluntary Laboratory Accreditation Program: Electromagnetic Compatibility and Telecommunications. FCC Methods.
E. R. Lindstrom, and J. Horlick. Apr 95, 118p, NIST/HB-150-11.
Also available from Supt. of Docs. as SN003-003-03339-1. See also PB94-178225.

Keywords: *Laboratories, *Certification, *Handbooks, Requirements, Electronics laboratories, Telecommunication, Standards, Test methods, Electric devices, Measurements, *Federal Communications Commission, NVLAP(National Voluntary Laboratory Accreditation Program), ECT(Electromagnetic Compatibility and Telecommunications), ECT LAP, US NIST.

NIST Handbook 150-11 presents the technical requirements of the National Voluntary Laboratory Accreditation Program (NVLAP) for accreditation under the Electromagnetic Compatibility and Telecommunications (ECT) LAP. There are two program handbooks for he ECT LAP. The handbook covers test methods used to demonstrate compliance with FCC requirements given in Title 47 of the U.S. Code of Federal Regulations (CFR), Telecommunication, Part 15, Digitial Devices, and FCC Part 68, Analog and Digital. A second program handbook, NIST Handbook 150-14, describes the requirements for test methods in Military Standards 461/462, Electromagnetic Compatibility. Program handbooks are intended for information and use by staff of accredited laboratories and laboratories seeking accreditation, other laboratory accreditation systems, users of laboratory services, and others needing information on the requirements for accreditation.

02,665
PB95-242400 PC A03/MF A01
National Inst. of Standards and Technology (MEL), Gaithersburg, MD. Precision Engineering Div.
Measuring Long Gage Blocks with the NIST Line Scale Interferometer.
Technical note.
J. S. Beers. May 95, 24p, NIST/TN-1410.
Also available from Supt. of Docs. as SN003-003-03341-3. See also PB93-146645.

Keywords: *Interferometers, Length, Silicon dioxide, Measuring instruments, Uncertainty, Dimensions, Manufacturing, US NIST, Long gage blocks, Line scale interferometer.

An improved technique is described for temporarily converting long gage blocks into line scales so they can be measured by fringe counting (dynamic) interferometry in the National Institute of Standards and Technology (NIST) line scale interferometer. The new process employs fuzed silica rather than the previously used steel conversion gage blocks. Conversion blocks are pairs of small (26 mm) gage blocks with graduation lines on their side faces. The new conversion blocks have a number of advantages as shown by experimental evidence.

02,666
PB95-251658 PC A03/MF A01
National Inst. of Standards and Technology (MEL), Gaithersburg, MD. Manufacturing Systems Integration Div.
Algorithm Testing and Evaluation Program for Coordinate Measuring Systems: Testing Methods.
C. Diaz. Jul 95, 34p, NISTIR-5686.
See also PB95-231833.

Keywords: *Tests, *Metrology, *Computer program verification, Computer applications, Computer software, Measuring instruments, Data analysis, Calibrating, Coordinate measuring systems, Algorithm testing and evaluation program, Standard reference algorithm.

The Algorithm Testing and Evaluation Program for Coordinate Measuring Systems (ATEP-CMS) is a NIST Special Test service offered through the Office of Measurement Services Calibration Program. ATEP-CMS evaluates the performance of data analysis software used in coordinate measuring systems (CMSs). The report details the CMS testing and evaluating methods that ATEP-CMS uses to test and evaluate the performance of CMS software. The report is intended as a guide to procedures for ATEP-CMS testing personnel.

02,667
PB95-251716 PC A08/MF A02
National Inst. of Standards and Technology (MEL), Gaithersburg, MD. Precision Engineering Div.
Gage Block Handbook.
Monograph.
T. Doiron, and J. S. Beers. Jun 95, 160p, NIST/MONO-180.
Also available from Supt. of Docs.

Keywords: *Calibrating, *Measuring instruments, *Metrology, Interferometers, Standards, Length, Statistical quality control, Comparison, *Gage blocks.

Calibration of gage blocks is one of the oldest and most sophisticated measurements in dimensional metrology. This work explains gage blocks are calibrated by both interferometry and mechanical comparison at the National Institute of Standards and Technology. The basic physical and geometrical properties, and the limitations on calibration caused by these properties are explained. All known sources of uncertainty are discussed along with the methods used to estimate these uncertainties. Finally, the measurement assurance program used to control the calibrations processes are explained with estimates of the process parameters.

02,668
PB95-254439 PC A03/MF A01
National Inst. of Standards and Technology (MSEL), Gaithersburg, MD.
Materials Science and Engineering Laboratory Annual Report, December 1993.
Dec 93, 30p.

Keywords: *US NIST, *Laboratories, Metallurgy, Ceramics, Polymers, Reliability, Standards, Radiation.

Contents:
An overview of NIST's Materials Science and Engineering Laboratory, including the:
Metallurgy Division;
Ceramics Division;
Polymers Division;
Materials Reliability Division;
Reactor Radiation Division;
and Office of Intelligent Processing of Materials.

02,669
PB95-255840 PC A03/MF A01
National Inst. of Standards and Technology (MEL), Gaithersburg, MD. Precision Engineering Div.
NIST SRM 9983 High-Rigidity Ball-Bar Stand. User Manual.
D. Sawyer, S. D. Phillips, G. Caskey, P. Snoots, B. Borchardt, and D. Ward. Jun 95, 16p, NISTIR-5659.

Keywords: *Performance evaluation, Rigidity, Assembly, Manuals, *CMMs(Coordinate Measuring Machines), *Coordinate Measuring Machines, *Ball-bar stands, US NIST, SRM 2083, SRM 9983.

The National Institute of Standards and Technology (NIST) SRM 9983 high rigidity ball bar stand is designed to support a ball bar for coordinate measuring machine (CMM) performance evaluation. This document is a user manual for NIST SRM 9983. The manual contains the complete instructions for assembling and using the stand.

02,670
PB95-261897 PC A07/MF A02
National Inst. of Standards and Technology, Gaithersburg, MD.
Journal of Research of the National Institute of Standards and Technology, May/June 1995. Volume 100, Number 3.
1995, 127p.
See also PB95-261905 through PB95-261962 and PB95-169371. Also available from Supt. of Docs. as SN-703-027-00064-4.

Keywords: *Standards, *Metrology, *Research projects, US NBS, Magnetic properties, Electric properties, Interlaboratory comparisons, Calibration standards, Optical filters, Electromagnetic absorption, Radio frequencies, Isotope ratio, National Institute of Standards and Technology.

No abstract available.

02,671
PB95-267944 PC A02/MF A01
National Inst. of Standards and Technology (TS), Gaithersburg, MD. National Voluntary Lab. Accreditation Program.
National Voluntary Laboratory Accreditation Program (NVLAP): Commercial Products Testing.
Handbook.
L. I. Knab. Jul 95, 9p, NIST/HB-150/16.
Also available from Supt. of Docs. as SN003-003-03355-3. See also PB94-178225.

Keywords: *Laboratories, *Accreditation, *Test facilities, Paints, Plastics, Papers, Plumbing, Seals(Stoppers), Sealers, Test methods, Policies, NVLAP, Commercial products.

National Institute of Standards and Technology (NIST) Handbook 150-16 presents the technical requirements of the National Voluntary Laboratory Accreditation Program (NVLAP) for Commercial Products Testing. It is intended for information and use by staff of accredited laboratories, those laboratories seeking accreditation, other laboratory accreditation systems, users of laboratory services, and others needing information on the requirements for accreditation under the Commercial Products Testing program.

02,672
PB95-270039 PC A22/MF A04
National Inst. of Standards and Technology (MSEL), Gaithersburg, MD. Ceramics Div.
Ceramic Powders Characterization: Results of an International Laboratory Study.
Special pub.
S. G. Malghan, S. M. Hsu, R. G. Munro, and L. S. H. Lum. Jul 95, 514p, NIST/SP-879.
Also available from Supt. of Docs. as SN003-003-03337-5. See also PB92-171446.

Keywords: *Ceramics, *Powder(Particles), *Interlaboratory comparisons, *Germany(Unified), *Sweden, *United States, Morphology, Physical properties, Chemical properties, Test methods, Comparative evaluations, Statistical quality control, Phase, Chemical composition, Chemical analysis, Industries, Universities, Federal agencies, Laboratories.

This report contains the results of an international interlaboratory comparison program (round-robin) of powder characterization under the auspices of International Energy Agency (IEA). The results include the contributions of 25 industrial, university and governmental laboratories in the Federal Republic of Germany, Sweden and the United States. These laboratories surveyed a variety of methods for the characterization of physical properties and chemical characteristics of ceramic starting powders. For the first time, data from various measurement methods are available for critical comparison. Results of the same method from different laboratories are also provided. Recommendations for future studies are drawn from results of the present round-robin.

02,673
PB96-103080 Not available NTIS
National Inst. of Standards and Technology (CSTL), Gaithersburg, MD. Thermophysics Div.
Comments on the Stability of Bayard-Alpert Ionization Gages.
Final rept.
C. R. Tilford, A. R. Filippelli, and P. J. Abbott. 1995, 3p.
Pub. in Jnl. of Vacuum Science and Technology, v13 n2 p485-487 Mar/Apr 95.

Keywords: *Bayard-Alpert gages, *Stability, Ionization gages, Measuring instruments, Tests, Experimental data, Reprints.

A recent group of three articles presents stability testing results for ionization gages, discusses the causes of gage instability, and describes a new type of Bayard-Alpert (BA) ionization gage. Although the authors are in general agreement with the analysis of gage instability presented by Bills, they are concerned that the test results of Arnold and Borichevsky and the discussion in all three references imply instabilities for existing types of BA gages that are much larger than they find to be the case. Here the authors briefly describe their experience with BA gage stability, indicate why they think their results are different from those of Arnold and Borichevsky, and describe the operating conditions that they believe will result in improved stability.

02,674
PB96-113550 (Order as PB96-113535, PC A05/MF A01)
National Physical Lab., Teddington (England).
Intercomparison of the ITS-90 Radiance Temperature Scales of the National Physical Laboratory (U.K.) and the National Institute of Standards and Technology.
G. Machin, B. C. Johnson, C. Gibson, and R. L. Rusby. 1994, 6p.
Prepared in cooperation with National Inst. of Standards and Technology, Gaithersburg, MD.
Included in Jnl. of Research of the National Institute of Standards and Technology, v99 n6 p731-736 Nov/Dec 94.

Keywords: *Temperature scales, *Radiance, *Interlaboratory comparisons, Calibration standards, Pyrometers, Quality assurance, Temperature measurement, United States, United Kingdom, NIST(National Institute of Standards and Technology), ITS-90.

An intercomparison of radiance temperature scales has been performed by the National Physical Laboratory (NPL) and the National Institute of Standards and Technology (NIST) using a standard transfer pyrometer operating at a wavelength of approximatelly 1000 nm. It was found that the radiance temperature scales established by the two laboratories were in agreement to 0.1% or better of the temperature over the range 1000 degrees C to 2500 degrees C.

02,675
PB96-123138 Not available NTIS
National Inst. of Standards and Technology (MEL), Gaithersburg, MD. Precision Engineering Div.
Stylus Flight in Surface Profiling.
Final rept.
J. F. Song, and T. V. Vorburger. 1994, 14p.
Pub. in International Mechanical Engineering Congress and Exposition, Chicago, IL., June 6-11, 1994, Manufacturing Science and Engineering, v68 n1 p161-174.

Keywords: *Surface properties, *Flight, *Profile, Roughness, Slope, Specimen, Stylus, Surface, Waveform, Reprints.

In this paper, theoretical and experimental work on stylus flight is described. Experiments on the surfaces of different roughness specimens with sinusoidal, rectangular, triangular and random waveforms support the theoretical model, which predict stylus flight from the traversing speed, stylus force, stylus radius and parameters of the surface.

02,676
PB96-123567 Not available NTIS
National Inst. of Standards and Technology (CSTL), Gaithersburg, MD. Thermophysics Div.
Long-Term Stability of Bayard-Alpert Gauge Performance: Results Obtained from Repeated Calibrations against the National Institute of Standards and Technology Primary Vacuum Standard.
Final rept.
A. R. Fillippelli, and P. J. Abbott. 1995, 5p.
Pub. in Jnl. of Vacuum Science and Technology, vA 13 n5 p2582-2586 Sep/Oct 95.

Keywords: *Bayard-Alpert ionization gages, *Calibration, *Reference standards, Vacuum gages, Vacuum apparatus, Ultrahigh vacuum, Interlaboratory comparisons, Laboratory tests, Stability, Time, Utilization, Reprints.

This article presents and briefly discusses information on the long-term stability of the sensitivity of Bayard-Alpert ionization gages with time and use, derived from an analysis of data for Bayard-Alpert gauge calibrations performed at the National Institute of Standards and Technology over a ten year period.

02,677
PB96-135025 Not available NTIS
National Inst. of Standards and Technology (MSEL), Gaithersburg, MD. Metallurgy Div.
Radiance Temperatures (in the Wavelength Range 523-907 nm) of Group IVB Transition Metals Titanium, Zirconium, and Hafnium at Their Melting Points by a Pulse-Heating Technique.
Final rept.
A. Cezairliyan, J. L. McClure, and A. P. Miiller. 1994, 17p.
Pub. in International Jnl. of Thermophysics, v15 n5 p993-1009 1994.

Keywords: *Metals, *Melting points, *Temperature measurement, Reprints, *Radiance temperatures, *Pulse heating.

The melting-point radiance temperatures (at six wavelengths in the range 523-907 nm) of the Group IVB transition metals titanium, zirconium, and hafnium were measured by a pulse-heating technique. The method is based on rapid resistive self-heating of the specimen from room temperature to its melting point in less than 1s and on simultaneously measuring the specimen radiance temperatures every 0.5 ms with a high-speed six-wavelength pyrometer. Melting was manifested by a plateau in the radiance temperature-versus-time function for each wavelength. The melting-point radiance temperatures for a given specimen were determined by averaging the measured temperatures along the plateau at each wavelength.

02,678
PB96-160239 Not available NTIS
National Inst. of Standards and Technology (TS), Gaithersburg, MD. Office of Standards Services.
U.S. Government Accreditation and Conformity Assessment System Evaluation.
Final rept.
W. G. Leight. 1993, 20p.
Pub. in Conformity Assessment Conference, Gaithersburg, MD., July 14, 1993, 20p.

Keywords: *Laboratories, *Certification, *Standards, Conformity, Accreditation, Testing, Requirements, International trade, Federal government, United States, Reprints, US NIST.

The National Institute of Standards and Technology has since its earliest days been concerned with standards and conformity assessment, with regard to both the physical standards of measurement and documentary standards covering products and testing. We perform calibration services, issue standard reference materials and standard reference data, and conduct many other standards-related activities.

02,679
PB96-160841 Not available NTIS
National Inst. of Standards and Technology (CSTL), Gaithersburg, MD. Process Measurements Div.
Executive Summary: Proceedings of the Workshop on the Measurement of Transient Pressure and Temperature.
Final rept.
V. E. Bean, and G. J. Rosasco. 1992, 8p.
See also PB92-183680.
Pub. in Proceedings of the Workshop on the Measurement of Transient Pressure and Temperature, Gaithersburg, MD., April 23-24, 1991, p1-8 Apr 92.

Keywords: *Pressure measurement, *Meetings, Temperature measurement, Military requirements, Explosion effects, Pressure transducers, Shock waves, High pressure, Calibration, Transients, Standards, Reprints.

The Workshop on the Measurement of Transient Pressure and Temperature was held at the National Institute of Standards and Technology (NIST), Gaithersburg, MD, on 23-24 April 1991. There were 77 attendees, 55% from government and 45% from the private sector. Aerospace, automotive, and instrumentation manufacturers were present along with engineers from primate sector and government (Army, Navy, Air Force, and NASA) research organizations. The Army, Navy and NASA primary standards laboratories also were represented. The workshop drew international attention with participants from Taiwan, Sweden, Austria, and France. Only France currently offers transient pressure calibrations as part of their national measurement system. The purpose of the workshop was to identify current and emerging measurement problems and needs for transient pressure and temperature measurements, to explore scientific and technical barriers, and opportunities for achieving measurement accuracy goals, and to assist in the formulation of an appropriate role for NIST.

02,680
PB96-161666 Not available NTIS

National Inst. of Standards and Technology (MEL), Gaithersburg, MD. Precision Engineering Div.
Verification of Revised Water Vapour Correction to the Index of Refraction of Air.
Final rept.
J. Beers, and T. Doiron. 1992, 2p.
Pub. in Metrologia, v29 p315-316 1992.

Keywords: *Environmental compensation, *Refractive indexes, Reprints, Humidity, *Foreign technology, *Edlen equation, Wavelength correction.

The Edlen equation has become the standard method of relating the index of refraction of air to the air temperature, pressure and humidity. The recent suggestion for improvements in the humidity dependence by Birch and Downs has been verified at the 0.633 micrometers He-Ne laser wavelength using the line scale interferometer at the National Institute of Standards and Technology (NIST).

02,681
PB96-165840 PC A15/MF A03
National Inst. of Standards and Technology (TS), Gaithersburg, MD. Weights and Measures Program.
Report of the National Conference on Weights and Measures (80th) as Adopted by the 80th National Conference on Weights and Measures, 1995. Held in Portland, Maine on July 16-20, 1995.
Special pub.
G. M. Ugiansky, and A. H. Turner. Feb 96, 307p, NIST/SP-894.
Also available from Supt. of Docs. as SN003-003-03379-1. See also PB96-166616.

Keywords: *Weight measurement, *Metrology, *Meetings, Regulations, Laws(Jurisprudence), Standards, Quality control, US NBS, Safety, Beale(Ratio), Portland(Maine), Legal metrology, Grain moisture.

The 80th Annual Meeting of the National Conference on Weights and Measures (NCWM) was held July 16 through 20, 1995, at the Holiday Inn By the Bay, Portland, Maine. The theme of the meeeting was 'Quality Partnerships and Programs through Education.' Reports by the standing and annual committees of the Conference comprise the major portion of this publication, along with the addresses delivered by Conference officials and other authorities from government and industry. Special meetings included those of the Metrologists, the Associate Membership Committee, the Retired Officials Committee, the Scale Manufacturers' Association, the American petroleum Institute, the Industry Committee on Packaging and Labeling, the regional weights and measures associations, and the National Association of State Departments of Agriculture Weights and measures associations, and the National Association of State Departments of Agriculture Weights and Measures Division.

02,682
PB96-178926 PC A03/MF A01
National Inst. of Standards and Technology (TS), Gaithersburg, MD. Weights and Measures Program.
Specifications and Tolerances for Reference Standards and Field Standard Weights and Measures. 2. Specifications and Tolerances for Field Standard Measuring Flasks.
Handbook.
G. L. Harris. 1996, 18p, NIST/HB-105/2.
Supersedes COM-71-50065. Also available from Supt. of Docs. as SN003-003-03406-1. See also PB90-232752.

Keywords: *Flasks, *Standards, Specifications, Tolerances(Mechanics), Measurement, Handbooks, Weight measurement, Volumetric analysis.

Field standard volumetric flasks and graduated cylinders as described herein are intended to be used by weights and measures officials, manufacturers and distributors of liquid products, research and testing laboratories, and others concerned with accurate measurements of the volume of liquids. This handbook volumetric flasks with graduated necks and graduated cylinders for legal metrology applications as 'field standards.'

02,683
PB96-179544 Not available NTIS
National Inst. of Standards and Technology (MEL), Gaithersburg, MD. Automated Production Technology Div.
Testing the Sensitivity of Accelerometers Using Mechanical Shock Pulses Under NIST Special Publication 250 Test No. 24040S.
Final rept.
D. J. Evans. 1995, 15p.
Pub. in American Society of Mechanical Engineers International Mechanical Engineering Congress and Exposition, San Francisco, CA., November 12-17, 1995, p1-15.

Keywords: *Accelerometers, *Shock tests, *Mechanical vibration, Piezoelectric transducers, Calibration standards, Sensitivity, Reference standards, Acceleration, Inteferometry, Shock(Mechanics), Shock absorbers, Frequency analysis, Test and evaluation, Reprints, Drop-ball apparatus.

The complex sensitivity of a laboratory reference piezoelectric accelerometer in combination with a charge amplifier is obtained by comparison against two NIST standards which are calibrated periodically by reciprocity and by interferometric techniques. For each condition of test, a dynamic signal (FFT) analyzer is used to obtain estimates of the complex frequency response function (complex voltage output of the system under test relative to that of the reference system) and the coherence function from rms trispectral averages, as well as to obtain time averages of the complex linear spectra of the voltage outputs of the system under test and the reference system. Together with the calibrated complex sensitivity of the reference system, these spectra may then be used to estimate the magnitude of the sensitivity of the system under test as a function of frequency, and to obtain an estimate of the magnitude of the peak output voltage of the system under test relative to the magnitude of the peak acceleration for each condition of test.

02,684
PB96-179569 Not available NTIS
National Inst. of Standards and Technology (MEL), Gaithersburg, MD. Automated Production Technology Div.
Ultrasound Power Measurement Techniques at NIST.
Final rept.
S. E. Fick. 1995, 6p.
Pub. in American Society of Mechanical Engineers Congress and Exposition, San Francisco, CA., November 12-17, 1995, p1-6.

Keywords: *Ultrasonic wave transducers, *Power measurement, *Calibration, Ultrasonic radiation, Power meters, Pulse generators, Power levels, Electronic switching, Reprints, US NIST.

This paper tells how ultrasound power levels between 100 microwatts and 25 watts at frequencies between 0.5 MHz and 200 HMz are measured at NIST. Ultrasonic radiation pressure, the phenomenon most commonly used by ultrasound power meters, is described in the context of an instrument devised at NIST to minimize all known associated components of uncertainty. Also, described are an electronic switching technique for high precision pulse generation, and a calibration transfer technique which bases replicated ultrasound power levels on measurements of dc voltage.

02,685
PB96-201116 Not available NTIS
National Inst. of Standards and Technology (BFRL), Gaithersburg, MD. Fire Science Div.
Low Heat-Flux Measurements: Some Precautions.
Final rept.
A. F. Robertson, and T. J. Ohlemiller. 1995, 16p.
Pub. in Fire Safety Jnl., v25 n2 p109-124 1995.

Keywords: *Heat fluxes, *Measurement errors, Radiation, Gages, Sensors, Reprints, *Foreign technology.

Simple experiments are described for the purpose of illustrating measurement errors and their avoidance during use of Gardon or Schmidt-Boelter total heat flux sensors. These errors can assume serious proportions of the observed signal at flux levels below about 15 kW/sq. m. They result from two sources, both a consequence of the flux gage's temperature relative to its surrounding: firstly, convective heating of the gage by the boundary layer from hot surfaces surrounding it and second, heat exchange with the ambient environment by radiation and convection. Some proposals are made for standardizing measurement methods, but it seems unlikely that errors in measurement can be completely eliminated. It thus becomes important for users of experimentally derived data to understand the limitations which may exist in the data reported.

02,686
PB96-210141 PC A10/MF A03
National Inst. of Standards and Technology (TS), Gaithersburg, MD. Office of Standards Services.
Proceedings of the Open Forum on Laboratory Accreditation at the National Institute of Standards and Technology, October 13, 1995.
Special pub.
W. Leight, and L. Galowin. 1996, 195p, NIST/SP-902.
Also available from Supt. of Docs. as SN003-003-03418-5.

Keywords: *Accreditation, United States, Meetings, Trade associations, Organization, Tests, *Laboratory accreditation, NIST(National Institute of Standards and Technology).

The American National Standards Institute (ANSI), ACIL (formerly the American Council of Independent Laboratories), and NIST co-sponsor an informal Laboratory Accreditation Working Group (LAWG) composed of representatives of laboratories, their governmental and private sector customers, accreditation bodies, and those public and private sector institutions that require laboratory accreditation. At a Forum on October 13, 1995, reports were presented by sectoral interests, along with a Vision and Principles proposed by the LAWG Steering Committee, aimed at developing a consensus for the formation of an integrated, cost effective infrastructure for laboratory accreditation in the United States, mutual recognition of qualified bodies, and facilitation of trade based on test results from competent bodies. These Proceedings are a transcript of papers presented and ensuing floor discussions at the Forum.

02,687
PB96-214705 PC A07/MF A02
National Inst. of Standards and Technology (TS), Gaithersburg, MD. Weights and Measures Program.
State Weights and Measures Laboratories: Program Handbook.
G. L. Harris. Jul 96, 113p, NIST/HB-143.
Supersedes PB85-183358. Also available from Supt. of Docs. as SN003-003-03420-7.

Keywords: *Laboratories, *States(United States), *Accreditation, *Calibration standards, Metrology, Units of measurement, Weight, Tolerances(Mechanics), Standardization, Accuracy, Requirements, Procedures, Tests, Criteria, Handbooks, State services, State Standards Program.

As part of its program to encourage a high degree of technical and professional competence in such activities, the National Institute of Standards and Technology (NIST) Office of Weights and Measures (OWM) has developed performance standards and formalized procedures for voluntary accreditation of State legal metrology laboratories. This Handbook describes the procedures followed in accrediting State (and a few other jurisdictional) legal metrology laboratories for competence.

02,688
PB96-215074 PC A20/MF A04
National Inst. of Standards and Technology, Gaithersburg, MD. Office of Standards Services.
Directory of U.S. Private Sector Product Certification Programs.
Special pub. (Final).
C. W. Hyer. Jul 96, 446p, NIST/SP-903.
Supersedes PB90-161712. Also available from Supt. of Docs. as SN003-003-03414-2.

Keywords: *Consumer products, *Product inspection, *Directories, *United States, Inspection, Certification, Specifications, Quality assurance, Accreditation, Tests, Registration, Standards, Private sector, Listings, Conformity assessment.

This document presents information on 178 private sector groups in the United States which engage in product certification activities. Entries describe the type and purpose of each organization, the nature of the activity, a pictorial representation of the organization's mark (if available), products certified, standards used, certification requirements, any accreditation or recognition by a U.S. or foreign private sector or government agency, availability of services, methods of cost determination, and other relevant details.

02,689
PB97-108575 PC A04/MF A01

National Inst. of Standards and Technology (EEEL), Gaithersburg, MD. Electricity Div.
NIST High-Accuracy Sampling Wattmeter.
Technical note.
G. N. Stenbakken, and A. Dolev. Aug 96, 50p, NIST/TN-1420.
Portions of this document are illegible in microfiche products. Also available from Supt. of Docs. as SN003-003-03422-3.

Keywords: *Wattmeters, Ammeters, Voltmeters, Power measurement, Product development, Engineering drawings, US NIST.

A high-accuracy sampling wattmeter was developed at the National Institute of Standards and Technology (NIST) to investigate the feasibility of using waveform sampling techniques for making very accurate power measurements at frequencies from 50 Hz to 1000 Hz. The goal of this effort was to develop an instrument having a full scale measurement uncertainty over these frequencies of less than plus or minus 50 micro W/W. The prototype instrument that came out of the development was used to demonstrate the accuracy achievable with the digital sampling method. The new high-accuracy sampling wattmeter was built around a wideband instrument developed earlier at NIST.

02,690
PB97-110217 Not available NTIS
National Inst. of Standards and Technology (TS), Gaithersburg, MD.
Examination Procedure Outlines: Keys to Solving the Handbook 44 Puzzle.
Final rept.
J. Koenig. 1993, 5p.
Pub. in Weighing and Measurement, p26-30 Aug 93.

Keywords: *Standards, *Weight measurement, Meters, Procedures, Safety notes, Scales, Reprints, *Examination Procedure Outlines(EPOs), Handbook 44.

The article covers the development, organization, and use of the Examination Procedure Outlines (EPO's) published by the National Conference on Weights and Measures in cooperation with the National Institute of Standards and Technology (NIST). EPO's are outlines of requirements from the General Code and specific device codes of NIST Handbook 44, Specifications Tolerances, and Other Technical Requirements for Weighing and measuring Devices, that apply to a certain category of commerical devices, such as vehicle scales or motor-fuel dispensers. They are used by State and local weights and measures officials as well as device manufacturers and service companies to check a devices compliance with legal requirements.

02,691
PB97-110266 Not available NTIS
National Inst. of Standards and Technology (CSTL), Gaithersburg, MD. Process Measurements Div.
Current Status and Trends in Temperature Measurements at NIST, Cooperative Projects and New Mutual Agreement between NIST and IMGC.
Final rept.
B. W. Mangum. 1992, 11p.
Pub. in Proceedings of the Italy/USA Metrology Seminar, Torino, Italy, May 5-8, 1992, p1-11.

Keywords: *Temperature measurements, *Standards, Thermometry, Reprints, *Foreign technology, *International Temperature Scale of 1990, National Institute of Standards and Technology.

In the brief paper, the authors will discuss the status of the current realization of the International Temperature Scale of 1990 (ITS-90)I over its entire range associated with contact thermometry, various development projects, and the current research. Then, they will address the trends in temperature measurements at the National Institute of Standards and Technology (NIST), discuss some cooperative projects between NIST and the Istituto de Metrologia 'G. Colonnetti' (IMGC), and conclude with a brief discussion of the Mutual Agreement between NIST and IMGC on Equivalence of National Scales of Temperature.

02,692
PB97-111850 Not available NTIS
National Inst. of Standards and Technology (TS), Gaithersburg, MD. Calibration Program.
Measurement Comparability, Traceability, and Measurement Assurance Programs.
Final rept.
S. Dittmann. 1996, 6p.
Pub. in Metrology for the Americas Symposium, Miami, FL., November 6-10, 1995, p1-6 1996.

Keywords: *Reference standards, *Tracer techniques, *Interlaboratory comparisons, Metrology, Measurement, Accuracy, Standardization, Quality assurance, Reprints.

The paper presents three parts of a national metrology system - a system linked to other nations (e.g., trading partners) and to the local industries, and one in which industries having common metrology needs are strongly linked. The three parts of this system are measurement comparability, traceability, and assurance.

02,693
PB97-118368 Not available NTIS
National Inst. of Standards and Technology (MSEL), Gaithersburg, MD. Metallurgy Div.
Issues in High-Speed Pyrometry.
Final rept.
A. Cezairliyan, and F. Righini. 1996, 8p.
Pub. in Metrologia, v33 p299-306 1996.

Keywords: *Temperature measurements, *Pyrometry, Radiation thermometry, High temperatures, Optica, Reprints, *Foreign technology, *High-speed techniques.

A brief summary is given of the developments in optical techniques for rapid temperature measurement during the last three decades in two national laboratories, the National Institute of Standards and Technology in the USA and the Instituto di Metrologia 'G. Colonnetti' in Italy. Results of research conducted in originating and advancing the state-of-the-art in high-speed (millisecond- and microsecond-resolution) pyrometry for measurement of temperatures in the range 1000 K to 5000 K are discussed. The main emphasis is on several key issues related to high-speed pyrometry including: high-speed operation, calibration of pyrometers, determination of true temperature and high-temperature reference points. Anticipated future directions in research, developments and applications in high-speed pyrometry are briefly discussed.

02,694
PB97-118376 Not available NTIS
National Inst. of Standards and Technology (MSEL), Gaithersburg, MD. Metallurgy Div.
Simultaneous Measurement of Normal Spectral Emissivity by Spectral Radiometry and Laser Polarimetry at High Temperatures in Pulse-Heating Experiments: Application to Molybdenum and Tungsten.
Final rept.
A. Cezairliyan, S. Krishnan, and J. L. McClure. 1996, 19p.
Pub. in International Jnl. of Thermophysics, v17 n6 p1455-1473 Nov 96.

Keywords: *High-speed measurements, *Spectral radiometry, *Laser polarimetry, High temperatures, Molybdenum, Pulse heating, Pyrometry, Reprints.

Spectral radiometry and laser polarimetry are two independent methods for measurement of spectral emissivity of materials. In the paper, a high-speed system is described for the rapid measurements of normal spectral emissivity of a specimen based on the simultaneous utilization of the two techniques. One of the goals of the work is to ascertain the reliability of the laser polarimetry technique in measurement of normal spectral emissivity at high temperatures. To accomplish this, normal spectral emissivity, in the vicinity of 0.633 m, of molybdenum and tungsten were measured by the two techniques in the temperature range 2000-2800 K. The results obtained by the two techniques are in agreement with 1%. The total uncertainty (two standard-deviation level) in measurement of emissivity by either spectral radiometry or laser polarimetry technique is estimated to be not more than plus or minus 2%.

02,695
PB97-119101 Not available NTIS
National Inst. of Standards and Technology, Gaithersburg, MD. Office of the Director.
Design of Technically Complex Facilities.
Final rept.
S. R. Hogan. 1996, 50p.
Pub. in American Institute of Architects Symposium: Building Performance, Defining the Architect's Role, Washington, DC., April 12-13, 1996, 50p.

Keywords: *Advanced technology laboratory, *Design criteria, Laboratories, Research facilities, Environmental control, Temperature control, Product management, Metrology, Reprints, US NIST.

NIST's new Advanced Technology Laboratory (ATL) has a program goal to create the most environmentally stable laboratory in the world, in support of NIST's mission in basic research and measurement standards. The presentation will outline NIST and its place in the global measurement community, an overview of the new ATL design, a focus on several areas of research for which the new ATL is critical, and a presentation on the research project itself.

02,696
PB97-121610 PC A08/MF A02
National Inst. of Standards and Technology (TS), Gaithersburg, MD. Office of Information Services.
Science, Technology, and Competitiveness: Retrospective on a Symposium in Celebration of NIST's 90th Anniversary and the 25th Anniversary of the Gaithersburg Laboratories, November 14-15, 1991.
Special pub.
G. W. Hixenbaugh. Oct 96, 138p, NIST/SP-837.
Color illustrations reproduced in black and white. Also available from Supt. of Docs. as SN003-003-3431-2.

Keywords: *Meetings, *Federal agencies, *Research and development, Government agencies, Standards, Technoogy, Robotics, Fiber optics, Tomography, Fire protection, Competition, *US NIST, Gaithersburg(Maryland).

This symposium held in observance of the 90th anniversary of the National Institute of Standards and Technology and the 25th anniversary of NIST's Gaithersburg, MD, laboratories. The first day's program included sessions on emerging technologies, proprietary vs. non-proprietary research, educating the workforce, and the view from the U.S. Congress. On the second day NIST directors and researchers described some of the latest research at the Institute. Topics included advanced technology; competitiveness; computational geometry; computer performance, fire research; artificial intelligence and robotics; the history of NIST and the future of NIST; optical technology; science education; and surface science.

Manufacturing Processes & Materials Handling

02,697
PB94-176666 PC A09/MF A02
Northwestern Univ., Evanston, IL. BIRL Industrial Research Lab.
Opportunities for Innovation: Advanced Surface Engineering.
W. D. Sproul, and K. O. Legg. May 94, 191p, NIST/GCR-94/640-1.
Grant NIST-60NANB32D1223
See also PB94-100278. Sponsored by National Inst. of Standards and Technology, Gaithersburg, MD.

Keywords: *Surface finishing, *Technology innovation, *Coating processes, State of the art, Quality control, Deposition, Sputtering, Plating, Spray coating, Heat treatment, Ion implantation, Cathode sputtering, Chemical vapor deposition, Laser applications, Diamonds, Nitriding, *Advanced technology, Diamond films, Plasma enhanced chemical vapor deposition.

Over the last 20 years more advanced surface treatments have been developed. While some have been widely deployed (physical vapor deposition, chemical vapor deposition, thermal spray, and plasma nitriding, for example), others are less commonly used, or are just beginning to appear commercially (including ion implantation, diamond coating, and laser coating). The purpose of this volume is to provide information on the basics of advanced surface engineering processes to small businesses, especially to those not currently directly involved with the technology, in order to make them aware of the current state of the art. Each chapter has been written by an industrial expert in the particular area, and following the basic description of the technology are sections outlining the needs of the surface treatment (such as better controls, improved materials, or better knowledge of fundamental processes) and the future markets that can be expected to open. Meeting these needs and exploiting these new markets is likely to be best done by the combined efforts of present providers with companies whose experience lies in entirely different areas, and it is this type of cross-fertilization that this volume seeks to promote.

02,698
PB95-162004 Not available NTIS
National Inst. of Standards and Technology (MSEL), Gaithersburg, MD. Polymers Div.
Comparison of the Unidirectional and Radial In-Plane Flow of Fluids Through Woven Composite Reinforcements.
Final rept.
R. S. Parnas, and A. J. Salem. 1993, 12p.
Pub. in Polymer Composites 14, n5 p383-394 Oct 93.

Keywords: *Flow distribution, *Woven composites, *Resin transfer molding, *Fluid flow, Fiber composites, Comparison, Glass fiber reinforced plastics, Newtonian fluids, Preforms, Reinforcing fibers, Reprints.

The in-plane flow of fluids through dense fibrous woven reinforcements was studied to aid the development of constitutive models for use in simulations of composite fabrication by resin transfer molding. As a first part of this effort, both one-dimensional and radial flow experiments were conducted with Newtonian fluids in several woven glass fabrics. Analysis of the one-dimensional flow experiments shows that the two experimental techniques are often, but not always, consistent, and both techniques suggest a relationship between the physical structure of the reinforcement and the mathematical structure of the permeability tensor. Preform features at the laminar and interlaminar scales were hypothesized to influence the experimental results.

02,699
PB96-122981 Not available NTIS
National Inst. of Standards and Technology (MEL), Gaithersburg, MD. Automated Production Technology Div.
Effects of Spindle Dynamic Characteristics on Hard Turning.
Final rept.
K. Harper, M. Davies, and A. Donmez. 1995, 4p.
Pub. in International Precision Engineering Seminar Proceeding (8th), Compiegne, France, May 15-19, 1995, 4p.

Keywords: *Machining, *Lathes, *Precipitation hardening, Manufacturing, Mechanical properties, Spindles, Reprints, *Foreign technology.

Error motions between the tool and workpiece during cutting operations affect the surface finish of the final products. These error motions arise from a number of different sources including asynchronous axial machine and process vibrations, tool wear, and tool edge build up. In this work, the error motions and dynamic characteristics of a tapered-roller bearing spindle with adjustable bearing preload were measured, and their effect on hard turned surfaces was assessed.

02,700
PB96-160494 Not available NTIS
National Inst. of Standards and Technology (MEL), Gaithersburg, MD. Automated Production Technology Div.
Evaluation of a Tapered Roller Bearing Spindle for High-Precision Hard Turning Applications.
Final rept.
M. A. Donmez, K. Harper, L. Greenspan, Y. Matsumoto, and L. Keller. 1993, 6p.
Pub. in Annual Meeting of the American Society for Precision Engineering (8th), Seattle, WA., November 7-12, 1993, 6p.

Keywords: *Spindles, *Maching, *Axes of rotation, Precision, Defects, Roller bearings, Metrology, Reprints, *Hard turning.

In this study, we are to evaluate a spindle which consisted of a pair of high precision tapered roller bearings including a HYDRA-RIB tapered roller bearing. Roller bearing spindles are used for applications that require high bearing stiffness, and can be good candidates for applications such as precision hard turning. For evaluation purposes, we have classified our measurements into four categories: axis of rotation errors, thermal growth, static stiffness, and dynamic stiffness and damping. In this presentation, we will focus on the axis of rotation error measurements. In addition to evaluating the performance of the spindle, we will show that the axis of rotation error measurements can also be used to help diagnose, analyze and improve the spindle design.

Nondestructive Testing

02,701
PB94-172111 Not available NTIS
National Inst. of Standards and Technology (CAML), Gaithersburg, MD. Applied and Computational Mathematics Div.
Infinite Divisibility and the Identification of Singular Waveforms.
Final rept.
A. S. Carasso. 1992, 14p.
Pub. in Proceedings of Conference on Probabilistic and Stochastic Methods in Analysis, with Applications, Ciocco, Italy, July 14-27, 1991, p273-286 1992.

Keywords: *Ultrasonic tests, Nondestructive tests, System identification, Wave propagation, Elastic waves, Volterra equations, Stochastic processes, Waveforms, Reprints, Flaw detection, Impulse response, Deconvolution, Divisibility.

Infinitely divisible probability density functions on the half-line t = or > 0 form a convolution semigroup on t = or > 0, as they describe stochastic processes with stationary, non-negative, independent increments. A subclass D of such densities are C(sup infinity) functions on the whole t-line when extended by zero for t < 0. Such functions may be viewed as physically realizable, causal, C(sup infinity) approximations to the Dirac delta-function, with further positivity properties. The use of such probe waveforms for system identification is particularly advantageous in transient wave propagation problems, where the system's impulse response is typically highly singular. An ill-posed deconvolution problem must be solved to recover the system's response; the semigroup and positivity properties of the input probe enable the deconvolution problem to be implemented as a Cauchy problem or a diffusion equation. The approach allows the analyst to monitor the gradual and systematic development of sharp singularities in the presence of noise. One important context where this theory applies is ultrasonic flaw detection in nondestructive evaluation.

02,702
PB94-191640 PC A03/MF A01
National Inst. of Standards and Technology (MEL), Gaithersburg, MD. Ultrasonics Group.
NIST Calibration of ASTM E127-Type Ultrasonic Reference Blocks.
J. A. Slotwinski, and G. V. Blessing. May 94, 49p, NISTIR-5430.
See also PB-258 105.

Keywords: *Calibrating, *Standards, Ultrasonic wave transducers, Underwater acoustics, Ultrasonic tests, Nondestructive tests, *Ultrasonic reference blocks, Aluminum alloy 7075, US NIST.

This document describes the procedures and instrumentation used by the National Institute of Standards and Technology (NIST) in calibrating aluminum ultrasonic reference blocks. The Ultrasonics Group performs this calibration service for technological and industrial customers. The calibration is based on the American Society of Testing and Materials (ASTM) recognized practice for calibrating aluminum reference blocks, designated E127-92a. Instructions for requesting calibrations of ultrasonic reference blocks are contained in Appendix I of this document. The NIST ultrasonic reference block calibration service was originated in the late 1970's, and is described in the NBS Technical Note 924 (PB258105). At that time the application of one master block for use as a reference standard was considered to be a temporary or interim measure. Today NIST uses this master block to set the ultrasonic system sensitivity in all calibrations of ultrasonic reference block sets. In addition, there are several newly implemented practices employed for checking the calibration system characteristics, both over a period of years and in preparation for a particular calibration. This current document updates the NBS Technical Note 924 in describing these practices for our calibration procedure.

02,703
PB96-103098 Not available NTIS
National Inst. of Standards and Technology (EEEL), Gaithersburg, MD. Semiconductor Electronics Div.
Comparison of Techniques for Nondestructive Composition Measurements in CdZnTe Substrates.
Final rept.
S. P. Tobin, J. P. Tower, P. W. Norton, V. C. Lopes, W. M. Duncan, A. J. Syllaios, C. K. Ard, N. C. Giles, R. Balasubramanian, A. B. Bollong, T. W. Steiner, D. K. Bowen, B. K. Tanner, D. Chandler-Horowitz, and P. M. Amirtharaj. 1995, 10p.
Pub. in Jnl. of Electronic Materials, v24 n5 p697-705 1995.

Keywords: *Nondestructive tests, *Alloys, *Photoluminescence, Semiconductors(Materials), Optical measurement, Chemical composition, Lattice parameters, Cadmium alloys, X ray diffraction, Precision, Accuracy, Comparative evaluations, Variations, Epitaxy, Reprints, Photoreflectance.

The authors report an overview and a comparison of nondestructive optical techniques for determining alloy composition x in Cd, Zn, Te substrates for HgCdTe epitaxy. The methods for single-point measurements include a new x-ray diffraction technique for precision lattice parameter measurements using a standard high-resolution diffractometer, room-temperature photoreflectance, and low-termperature photoluminescence. The authors compare measurements on the same set of samples by all three techniques. Comparisons of precision and accuracy, with a discussion of the strengths and weaknesses of different techniques, are presented.

02,704
PB96-111786 Not available NTIS
National Inst. of Standards and Technology (MSEL), Boulder, CO. Materials Reliability Div.
Contributions of Out-of-Plane Material to a Scanned-Beam Laminography Image.
Final rept.
T. A. Siewert, and M. A. Austin. 1994, 6p.
Sponsored by Harry Diamond Labs., Adelphi, MD.
Pub. in Materials Evaluation, v52 n10 p1193-1198 Oct 94.

Keywords: *X ray inspection, *Nondestructive tests, *Image resolution, Blurring, Focusing, Gray scale, Quality, Scanning, Beams(Radiation), Reprints, *Laminography, *X ray laminography, *Out-of-plane.

The authors studied the edge of a thin step wedge with a scanned-beam laminography system to learn how material above and below the plane of focus contributes to the image. The edge of a planar, 0.5 mm (0.02 in.) Thick lead sheet with large x and y dimensions was centered in the field of view. Images were captured as the lead sheet was moved in 0.075 mm (0.003 in.) Steps above and below the plane of focus of the system. The blurring (measured as its width on the image) was no more than 0.1 mm (0.004 in., or the system resolution) when the sheet was in focus and increased linearly with the deviation from focus. Blurring of out-of-plane objects is an essential feature of this laminography system, and is used to minimize the contribution to the image from material above and below the plane of focus. The authors also imaged various three-dimensional structures to show the ability of laminography to resolve different planes of focus.

02,705
PB96-141023 Not available NTIS
National Inst. of Standards and Technology (MSEL), Boulder, CO. Materials Reliability Div.
Void Shape in Sintered Titanium.
Final rept.
H. Ledbetter, M. Dunn, S. Kim, and R. Fields. 1995, 7p.
Pub. in Review of Progress in Quantitative Nondestructive Evaluation, v14 p1633-1639 1995.

Keywords: *Sound velocities, *Titanium, Ultrasonics, Deformation, Reprints, *Void shapes.

Void shape in sintered materials is important because the shape affects both physical and plastic-deformation problem. For example, the mechanical stress distribution around a disc-shaped void differs drastically from that around a spherical void. Thompson, Spitzig, and coworkers made ultrasonic studies on compacted iron. Haynes reviewed the general topic of mechanical properties of sintered materials. Because voids are small, three-dimensional, and essentially empty space between grains, their geometry determination presents formidable problems. Here, we take an indirect approach to void shape: measure longitudinal-wave and transverse-wave sound velocities, use a solid-mechan-

ics model that predicts effective ('composite') sound velocities from matrix sound velocities and occlusion phase geometry, use model inversely to estimate void shape.

02,706
PB96-154596 PC A05/MF A01
National Inst. of Standards and Technology (EEEL), Gaithersburg, MD. Semiconductor Electronics Div.
Semiconductor Measurement Technology: Survey of Optical Characterization Methods for Materials, Processing, and Manufacturing in the Semiconductor Industry.
Special pub.
W. M. Bullis, S. Perkowitz, and D. G. Seiler. Dec 95, 54p, NIST/SP-400-98.
Also available from Supt. of Docs. as SNO03-003-03381-2. Prepared in cooperation with Emory Univ., Atlanta, GA.

Keywords: *Semiconductor devices, *Optical measurement, *Silicon, Ellipsometry, Infrared spectroscopy, Interferometry, Photoluminescance, Optical microscopy, Raman spectroscopy, Scutterometry, Microelectronics, Test methods, Surveys.

Contactless, nondestructive optical methods are used to characterize many critical properties of materials, processes, and devices in the semiconductor industry. To determine the extent of use and the relative importance of various opticals methods in the industry, the Smeiconductor Electronics Division of the National Institute of Standards and Technology conducted a survey of this field. The survey also sought to identify both advantages and limitations of these techniques as well as future requirements for and anticipated use of optical characterization methods within the semiconductor industry. Data from 42 firms were analyzed to show the impact of the methods, what they measure, their range and precision, and their cost. A significant finding of the study is the need expressed by many industrial users for improved standards and test methods for optical characterization, especially in the area of film thickness and composition.

02,707
PB96-190327 Not available NTIS
National Inst. of Standards and Technology (MSEL), Boulder, CO. Materials Reliability Div.
Ultrasonic Methods.
Final rept.
R. B. Thompson, W. Y. Lu, and A. V. Clark. 1996, 30p.
Pub. in Handbook of Measurement of Residual Stresses, Chapter 7, p149-178 1996.

Keywords: *Ultrasonic tests, *Residual stress, *Stress measurement, Nondestructive tests, Acoustic properties, Elastic properties, Reprints, Acoustoelastic measurement, Through-thickness.

The average stress is determined in the region through which the waves propagate, as indicated by the cross-hatching: (1) through-thickness pulse-echo; (2) through-thickness pitch-catch; and (3) surface pitch-catch.

Quality Control & Reliability

02,708
PB94-199064 Not available NTIS
National Inst. of Standards and Technology (NEL), Gaithersburg, MD. Statistical Engineering Div.
Statistical Quality Control Technology in Japan.
Final rept.
K. O. Bowen, T. H. Hopp, R. N. Kacker, and R. J. Lundegard. 1991, 7p.
Pub. in Chance 4, p15-21 1991.

Keywords: *Quality control, *Japan, *Technology assessment, Industries, Laboratories, Government agencies, Reprints, *Foreign technology, *Statistical quality control, US NIST, TQC(Total Quality Control).

From May 17 to June 1, 1989, a survey team organized by the National Institute of Standards and Technology visited Japan to assess research and application of statistical quality control technology. The team explored the philosophy and conduct of total quality control (TQC) in Japanese industries, government laboratories, and national agencies. The philosophy and practice of TQC in Japan is quite different from that of the U.S. industries.

Tooling, Machinery, & Tools

02,709
PB94-206109 PC A03/MF A01
National Inst. of Standards and Technology (MEL), Gaithersburg, MD. Precision Engineering Div.
User's Guide to NIST SRM 2084: CMM Probe Performance Standard.
Special pub.
G. W. Caskey, S. D. Phillips, B. R. Borchardt, D. E. Ward, and D. S. Sawyer. Jun 94, 32p, NIST-SP-260-120.
Also available from Supt. of Docs. as SN003-003-03275-1.

Keywords: *Dimensional measurement, *Standards, *Probes, Machine tools, User manuals, Performance, Uncertainty, Metrology, Calibration, Spheres, Mounts, Design, *Standard reference materials, *Coordinate measuring machines.

National and international published standards on the performance evaluation of coordinate measuring machines (CMMs) require various artifacts to facilitate testing of these machines. Standard Reference Material (SRM) 2084, developed by the National Institute of Standards and Technology, is a calibrated 10mm diameter sphere and mount designed to aid in CMM, and specifically CMM probe, performance assessment. This publication serves as a users' manual, with general instructions on the care and use of SRM 2084. Reference to relevant tests in the ASME B89.1.12M-1990 CMM performance standard as well as several performance issues not addressed in the Standard are presented.

02,710
PB95-203303 Not available NTIS
National Inst. of Standards and Technology (PL), Boulder, CO. Quantum Physics Div.
Low-Frequency, Active Vibration Isolation System.
Final rept.
R. Stebbins, D. Newell, S. Richman, J. Mason, P. Bender, and J. Faller. 1994, 11p.
Sponsored by National Science Foundation, Arlington, VA.
Pub. in Proceedings of Society of Photo-Optical Instrumentation Engineers: Vibration Monitoring and Control, San Diego, CA., July 28-29, 1994, v2264 p27-37.

Keywords: *Vibration isolators, Extremely low frequency, Infrasonic frequencies, Seismic noise, Ground motion, Control systems, Active control, Performance, Design, Reprints.

We are developing an active vibration isolation system for reducing the disturbing effects of ground motion about six orders of magnitude between 1 and 30 Hz. The system consists of three cascaded stages, each comprising a suspended platform on which are located seismometers and actuators for six degrees of freedom. Our goal is to reduce the vibration noise to (1 x 10(exp -13) x (1 Hz/f)(sup 2.5) + 3 x 10(exp -15))m/Hz(sup 1/2) on the third stage. We have built and tested the initial stage, which is intended to reduce our laboratory noise level to that of a quiet site. The design, control system models, measured performance and current limitations for this stage are presented. The two main stages require a vacuum environment and interferometric readout. The design and models for the main stages are also presented.

LIBRARY & INFORMATION SCIENCES

General

02,711
PB94-198488 Not available NTIS
National Inst. of Standards and Technology (CSL), Gaithersburg, MD. Advanced Systems Div.
Dilemma-Preservation versus Access.
Final rept.
T. C. Bagg. 1993, 5p.
Pub. in Preservation Research and Development - Round Table Proceedings, Washington, DC., September 28-29, 1992, p57-61 1993. Sponsored by Library of Congress, Washington, DC.

Keywords: *Data storage, *Information management, *Media, Preserving, Access, Indexes (Documentation), Information retrieval, Digital data, Papers, Microfilm, Reprints.

The dilemma is to find suitable techniques and media to preserve information now stored on media with a short life expectancy. A stable recording media such as an acid free buffered paper on microfilm, where the information is in human readable form and has access suitable to its needs, is the best solution today. Information requiring frequent access should be indexed and stored in a digital form for rapid automated retrieval with a back-up on a permanent medium. Today's digital systems, which are essential for rapid access, are not suitable for preservation because of the continuous changes in computer technology.

02,712
PB95-125837 Not available NTIS
National Inst. of Standards and Technology (CSL), Gaithersburg, MD. Systems and Software Technology Div.
Important Papers in the History of Document Preparation Systems: Basic Sources.
Final rept.
R. Furuta. 1992, 26p.
Pub. in Electronic Publishing 5, n1 p19-44 Mar 92.

Keywords: *Documents, *Text processing, *Computer applications, Format, Data processing, Text editors, Reprints.

This report provides a narrative description of influential papers that discuss computer-based document preparation systems. The report's focus is on the systems actually used to prepare documents--editors and formatters, and the goal is to provide an introduction to the papers that have been influential on the community of researchers who investigate such systems.

02,713
PB96-157896 Not available NTIS
National Inst. of Standards and Technology (BFRL), Gaithersburg, MD. Fire Safety Engineering Div.
Evolution of a United States Information System.
Final rept.
N. H. Jason. 1993, 10p.
Pub. in Proceedings of the inFIRE Annual Conference, Norwood, MA., April 28-30, 1993, p89-98.

Keywords: *Bibliographic databases, *Computer networks, *Fire research, Information dissemination, Reprints, Internet.

As part of the current information activities in the United States, the Conference for Exploration of a National and Engineering Information Service is discussed, in addition to the Internet and the proposed NREN (National Research Education Network). Challenges to the fire community to bridge the information gap are presented.

02,714
PB96-157904 Not available NTIS
National Inst. of Standards and Technology (BFRL), Gaithersburg, MD. Fire Safety Engineering Div.

Information Transfer in the 21st Century.
Final rept.
N. H. Jason. 1993, 10p.
Pub. in Proceedings of the International Fire Information Conference (1st), Moreton-in-Marsh, Gloustershire, England, April 27-May 1, 1992, p133-142 1993.

Keywords: *Fire research, *Information transfer, Politics, Libraries, Reprints, *Foreign technology.

The impact of technological advances and some political events are discussed in the context of current information activities. Several examples of new and exciting projects in information technology in print and nonprint activities are presented. The role of the information professional and specifically the future role of fire libraries concludes the discussion.

Information Systems

02,715
N94-31228/7 PC A06/MF A02
National Inst. of Standards and Technology, Gaithersburg, MD.
Putting the Information Infrastructure to Work: Report of the Information Infrastructure Task Force Committee on Applications and Technology.
May 94, 116p, NIST/SP-857, ISBN-0-16-043188-3.

Keywords: *Communication networks, *Computer networks, *Information systems, Technology utilization, Commerce, Computers, Education, Environmental monitoring, Libraries, Manufacturing, Public health, Technology assessment.

The Committee on Applications and Technology of the Information Infrastructure Task Force is charged with coordinating efforts to develop, demonstrate, and promote applications of information technology in several diverse areas and to develop and recommend technology strategies and policy to accelerate the implementation of the National Information Infrastructure (NII). The goal of this document is to focus the public debate on the uses of the NII and the benefits of advanced computing and communications technologies. Seven applications papers are presented which address manufacturing, electronic commerce, health care, education and lifelong learning, environmental monitoring, libraries, and government service delivery. In each of these papers a description of the application arena is given along with a summary of the current information technology uses, short and long term goals, and issues related to how these goals could be achieved.

02,716
N94-36858/6 (Order as N94-36853/7, PC A10/MF A03)
National Inst. of Standards and Technology, Gaithersburg, MD.
Open System Environment Procurement.
G. Fisher. Aug 94, 43p.
In National Aeronautics and Space Administration, NASA Sti Program Coordinating Council Twelfth Meeting: Standards p 116-158.

Keywords: *Computer networks, *Government procurement, *Information systems, *Standards, Data bases, Data transfer (Computers), Proposals.

Relationships between the request for procurement (RFP) process and open system environment (OSE) standards are described. A guide was prepared to help Federal agency personnel overcome problems in writing an adequate statement of work and developing realistic evaluation criteria when transitioning to an OSE. The guide contains appropriate decision points and transition strategies for developing applications that are affordable, scalable and interoperable across a broad range of computing environments. While useful, the guide does not eliminate the requirement that agencies possess in-depth expertise in software development, communications, and database technology in order to evaluate open systems.

02,717
N95-15938/0 (Order as N95-15919/0, PC A11/MF A03)
National Inst. of Standards and Technology, Gaithersburg, MD.
National Center for Standards and Certification Information: Service and Programs.
J. Overman. 14 Sep 94, 7p.
In NASA, Washington, Fourth Annual International Acquisitions Workshop: Access to Multiple Media Worldwide 7 p.

Keywords: *Certification, *Information dissemination, *Information systems, *International cooperation, *Libraries, *Regulations, *Standards, Commerce, Competition, Directories, Documentation.

The National Center for Standards and Certification Information (NCSCI) provides information on U.S., foreign and international voluntary standards, government regulations, and conformity assessment procedures for non-agricultural products. The Center serves as a referral service and focal point in the United States for information on standards and standards-related information. NCSCI staff respond to inquiries, maintain a reference collection of standards and standards-related documents, and serve as the U.S. inquiry point for information to and from foreign countries.

02,718
PB94-172194 Not available NTIS
National Inst. of Standards and Technology (NCSL), Gaithersburg, MD. Systems and Network Architecture Div.
Formal Multi-Layer Test Methodology and Its Application to OSI.
Final rept.
J. P. Favreau, R. J. Linn, and S. Nightingale. 1989, 18p.
Pub. in Proceedings of International Conference on Formal Description Techniques for Distributed Systems and Communications Protocols (2nd), Vancouver, Canada, December 5-8, 1989, p375-392 1990.

Keywords: *Tests, *Specifications, File management systems, Protocols, Reprints, *OSI, *Open Systems Interconnection, FTAM(File Transfer and Management), Estelle specification language, ASN1(Abstract Syntax Notation One), FTP(File Transfer Protocol).

A multi-layer test methodology is introduced which takes advantage of the emergence of formal specification methods. Protocols are specified using Estelle and Abstract Syntax Notation One. Then, the Estelle specifications are augmented in with the logic necessary for testing. In this methodology, test cases are stimuli which are injected into the augmented protocol machines. This methodology has been applied successfully to the design and implementation of a test system for FTAM/FTP gateways. Results are presented for FTAM/FTP gateway testing, FTAM interoperation testing, and evaluation of a commerical FTAM test system which is under development.

02,719
PB94-172202 Not available NTIS
National Inst. of Standards and Technology (NCSL), Gaithersburg, MD. Systems and Network Architecture Div.
ISO/IEC Workshop on Worldwide Recognition of OSI Test Results Regional Progress - North America.
Final rept.
J. P. Favreau. 1993, 13p.
Pub. in Proceedings of ISO/IEC Worldwide Recognition of Open Systems Interconnection Test Results Workshop, Brussels, Belgium, November 2-4, 1993, 13p.

Keywords: *Tests, *North America, Certification, Accreditation, Standardization, Information systems, Reprints, *OSI, *Open Systems Interconnection, GOSIP(Government OSI Profile), IGOSS(Industry/Government Open Systems Specification).

This paper presents a summary of the developments in North America towards harmonization of testing and certification/registration in the information technology field. The current status follows an intense period of activity to develop North American regional strategies favorable to future multilateral recognition of national/regional certificates/registers on a global basis. Special emphasis is given to the consolidation of profiles via the design the Industry/Government Open Systems Specification (IGOSS), the quality improvement of the Government Open System Interconnection Profile (GOSIP) Testing Program and the creation of the North American Open Systems Testing and Certification Policy Council as the basic steps towards achieving worldwide recognition of test results.

02,720
PB94-172335 Not available NTIS
National Inst. of Standards and Technology (CSL), Gaithersburg, MD. Advanced Systems Div.
Bringing Natural Language Information Retrieval Out of the Closet.
Final rept.
D. K. Harman, and G. T. Candela. Jul 90, 7p.
Pub. in SIGCHI Bulletin 22, n1 p42-48 Jul 90.

Keywords: *Information retrieval, *Natural language processing, Information systems, Prototypes, Man computer interface, Human factors engineering, Access, Tests, Response time(Computers), Reprints.

A prototype information retrieval system was developed that gives users fast and easy access to textual information. The system uses a statistical ranking methodology that allows a user to input a query using only natural language, such as a sentence or a noun phrase, with no special syntax required. The system returns a set of text titles or descriptions, ranked in order of likely relevance to the query. The user can then select one or more titles for further examination of the corresponding text. The prototype was tested by over forty users.

02,721
PB94-172921 Not available NTIS
National Inst. of Standards and Technology (CSL), Gaithersburg, MD. Systems and Software Technology Div.
Porting Multimedia Applications to the Open System Environment.
Final rept.
R. D. Schneeman. 1992, 9p.
Pub. in Institute of Electrical and Electronics Engineers Software 9, n6 p39-47 Nov 92.

Keywords: *Computer program portability, Computer program transferability, Standards, US NIST, Reprints, *OSE, *Open System Environment, *Multimedia.

Organizations in both industry and government are rapidly moving toward the Open System Environment (OSE), which is based on standards for information technology. Part of that transition means migrating existing software to that environment. Those overseeing OSE migration projects need implementation strategies that use available standards to initiate such transitions. My colleagues and I at the National Institute of Standards and Technology's Computer Systems Laboratory have been researching software approaches to such strategies.

02,722
PB94-207354 PC A03/MF A01
National Inst. of Standards and Technology (MEL), Gaithersburg, MD. Factory Automation Systems Div.
World Wide Web and Mosaic: User's Guide.
C. I. Schlenoff. Jun 94, 16p, NISTIR-5453.

Keywords: *Information systems, *Information retrieval, Computer networks, Documents, Protocols, User manuals, *WWW(World Wide Web), *World Wide Web, *Mosaic software package, US NIST, Internet, Wide area networks.

The National Institute of Standards and Technology (NIST) is moving forward in providing and accessing information through the World Wide Web (WWW) by using the Mosaic software package. The WWW is a seamless world in which all information, from any source, can be accessed in a simple and consistent manner. Mosaic is a networked information discovery, retrieval, and collaboration tool used to view documents available through the WWW. This document was created for the following purposes: to help new users become more familiar with the WWW concept; to demonstrate how to use Mosaic and its capabilities; and to provide a pointer to other documents further describing the WWW and Mosaic.

02,723
PB95-103719 PC A07/MF A02
National Inst. of Standards and Technology (CSL), Gaithersburg, MD. Advanced Systems Div.
Framework for National Information Infrastructure Services.
O. G. Farah, W. Majurski, W. McCoy, R. Schneeman, D. Cypher, J. Pottmeyer, and W. Jansen. Jul 94, 148p, NISTIR-5478.
Prepared in cooperation with Defense Information Systems Agency, Arlington, VA.

Keywords: *Computer networks, *Information technology, Information systems, Telecommunication, On-

line systems, Information management, Information services, Information flow, Information transfer, Information dissemination, Information processing, Information retrieval, Information needs, User needs, Delivery systems, *National Information Infrastructure, Information superhighways, Electronic delivery.

The document provides an initial description of a framework for National Information Infrastructure (NII) Services (hereafter referred to as the Services Framework), motivated by emerging information technologies. The original goal of the document was to define an architecture for NII services. Instead, the document represents a less ambitious attempt to define a framework within which architectures of NII services can be discussed. The Services Framework as presented herein is intended to serve as a point of departure for discussing the definition, scope, and alignment of NII services.

02,724
PB95-128641 PC A08/MF A01
National Inst. of Standards and Technology, Gaithersburg, MD. Office of Information Services.
Databases Available in the Research Information Center of the National Institute of Standards and Technology.
Special pub.
D. Cunningham. Sep 94, 158p, NIST/SP-869.
Supersedes PB94-114568. Also available from Supt. of Docs. as SN003-003-03284-1.

Keywords: *Data bases, *Information services, Information systems, Indexes(Documentation), Subject indexing, Directories, Vendors, CD-ROM, Tables(Data), *US NIST.

Databases available online in the Research Information Center of the National Institute of Standards and Technology (NIST) are listed by acronym and by full title. In addition, descriptions of the databases, dates covered, producers, hard copy counterpart, principal sources and vendors are listed. A list of CD-ROM databases, a general subject index, a cross reference index, and a full text database list are also supplied.

02,725
PB95-154738 PC A06/MF A02
National Inst. of Standards and Technology (CSL), Gaithersburg, MD. Systems and Software Technology Div.
User Study: Informational Needs of Remote National Archives and Records Administration Customers.
Special pub.
J. Moline, and S. Otto. Nov 94, 123p, NIST/SP-500/221.
Also available from Supt. of Docs. as SN003-003-03305-7.

Keywords: *Data acquisition, *User needs, *Information services, Customer service, Access, Information needs, Delivery systems, Records management, Information retrieval, Information systems, *National Archives and Records Administration, User surveys, Government services.

The National Archives and Records Administration (NARA) possesses a vast wealth of information and records holdings from the Federal Government, which documents the history of the American people. The purpose of this particular study was to conduct a survey to investigate the information and records needs of citizens who lack direct access to NARA's facilities and determine how to best meet those needs. The basic question answered is what remote users of the National Archives want in the way of information and materials and how they want to receive it.

02,726
PB95-168555 Not available NTIS
National Inst. of Standards and Technology (CSL), Gaithersburg, MD. Information Systems Engineering Div.
Coping with Different Retrieval Methods in Next Generation Networks.
Final rept.
D. Flater, and Y. Yesha. 1994, 7p.
Pub. in Proceedings of the International Conference on Parallel and Distributed Computer Systems (7th), Las Vegas, NV., October 6-8, 1994, p549-555.

Keywords: *Query languages, *Information retrieval, *Search profiles, *Computer networks, Natural language processing, Information systems, Data storage systems, Heuristic methods, Systems engineering, Man computer interfaces, Statistical analysis, Reprints.

Methods of information retrieval that rely on automated indexing, automated classification, and/or analysis of natural language queries are often categorically condemned by proponents of traditional retrieval methods. With statistical retrieval, a powerful and expressive query language is processed with limited success; with traditional retrieval, a less expressive query language is processed with 100% success. Some feel that a battle must be fought to decide what sort of information retrieval will serve the needs of the world. The challenge is to support both kinds of retrieval in an information space that is too large for global indexing.

02,727
PB95-168605 Not available NTIS
National Inst. of Standards and Technology (PL), Boulder, CO. Time and Frequency Div.
Using Archie to Find Files on the INTERNET.
Final rept.
J. M. Gilligan. 1992, 2p.
Pub. in Optics and Photonics News, p61, 64, Dec 92.

Keywords: *Data transfer(Computers), Data retrieval, Data transmission, Computer networks, Data links, Protocol(Computers), Reprints, *Archie, *FTP(File Transfer Protocol), *File transfer protocol, INTERNET.

The document provides a beginner's guide to using Archie, a database of computer files available by anonymous FTP on the Internet.

02,728
PB95-168720 Not available NTIS
National Inst. of Standards and Technology (PL), Boulder, CO. Time and Frequency Div.
Retrieving Articles from the Internet (without a UNIX Workstation). Part 1. File Formats and Software Tools.
Final rept.
W. M. Itano. 1994, 2p.
Contract ONR-N00014-89-J-1467
See also Part 2, PB95-168738. Sponsored by Office of Naval Research, Arlington, VA.
Pub. in Optics and Photonics News 5, n9 p36, 43, Sep 94.

Keywords: *Information retrieval, *Data retrieval, *Software tools, *Computer networks, Information transfer, Data transmission, Man computer interfaces, Data storage, Document storage, Reprints, *File format, *INTERNET.

File formats commonly used for electronic storage of Internet-accessible documents (TEX and PostScript) are discussed. File archiving, compression, and encoding formats used to reduce storage requirements and to facilitate transmission by electronic mail are discussed also. Sources for non-commercial software for processing electronic documents having these formats on IBM-compatible computers are listed.

02,729
PB95-168738 Not available NTIS
National Inst. of Standards and Technology (PL), Boulder, CO. Time and Frequency Div.
Retrieving Articles from the Internet (without a UNIX Workstation). Part 2. An Example.
Final rept.
W. M. Itano. 1994, 2p.
See also Part 1, PB95-168720.
Pub. in Optics and Photonics News 5, n10 p61, 67, Oct 94.

Keywords: *Information sources, *Information retrieval, *Data retrieval, *Computer networks, Information transfer, Data transmission, Man computer interfaces, Data storage, Document storage, Software tools, Reprints, *INTERNET, File format.

Some Internet sources for scientific and technical documents are described. A detailed example of retrieving a document from an Internet host computer and converting it to printed format on an IBM-compatible computer is given.

02,730
PB95-182275 PC A05/MF A01
National Inst. of Standards and Technology (CSL), Gaithersburg, MD. Computer Security Div.
Keeping Your Site Comfortably Secure: An Introduction to Internet Firewalls.
Special pub.
J. P. Wack, and L. J. Carnahan. Dec 94, 92p, NIST/SP-800/10.
Also available from Supt. of Docs. as SN003-003-03313-8. See also PB94-139045.

Keywords: *Computer security, *Data processing security, Information systems, Computer networks, Local area networks, Access control, Computer privacy, Authentication, Telecommunication, *Internet, TCP/IP(Transmission Control Protocol/Internet Protocol).

This document provides an overview of the Internet and security-related problems. It then provides an overview of firewall components and the general reasoning behind firewall usage. Several types of network access policies are described, as well as technical implementations of these policies. Lastly, the document contains pointers and references for more detailed information. The document is designed to assist users in understanding the nature of Internet-related problems and what types of firewalls will solve or alleviate specific problems. Users can then use this document to assist in purchasing or planning a firewall.

02,731
PB95-219218 PC A04/MF A01
National Inst. of Standards and Technology (CSL), Gaithersburg, MD. Systems and Software Technology Div.
Electronic Access: Blueprint for the National Archives and Records Administration.
Special pub.
J. Moline, and S. Otto. Apr 95, 66p, NIST/SP-500/227.
Also available from Supt. of Docs. as SN003-003-03330-8. See also PB95-217014.

Keywords: *Information storage, *Information retrieval, *Records management, *Strategic planning, Access to information, Information dissemination, Preservation, Primary sources, Computer system design, Information networks, Optical scanning, *Electronic Access Project, *National Archives and Records.

The Electronic Access Project of the National Archives and Records Administration (NARA) had three main tasks. They were to design a methodology for exploring the informational needs of remote customers, to survey the targeted population, and to develop a blueprint for NARA's long-term information delivery systems that would enable NARA to meet their customers' needs. This report covers the last task. It discusses the findings of the user study as they influence the design of an electronic access system for the National Archives and Records Administration and presents a blueprint for meeting the users' needs.

02,732
PB95-231908 PC A04/MF A01
National Inst. of Standards and Technology (NCSL), Gaithersburg, MD. Systems and Network Architecture Div.
Guidelines for the Evaluation of X.500 Directory Products.
Special pub.
J. Tebbutt. May 95, 74p, NIST/SP-500/228.
Also available from Supt. of Docs. Sponsored by Department of Agriculture, Washington, DC.

Keywords: *Distributed data bases, *Information systems, Performance evaluation, Access control, Data processing security, Computer networks, Data storage, Relational data bases, Data base management systems, *X500 Directory.

The document provides readers with the means to evaluate various X.500 products and make informed choices as to which available products best match the requirements of their organizations. The document is aimed at procurement officials, systems administration staff and others involved in the process of obtaining or recommending X.500 products for use in their organizations.

02,733
PB96-131545 PC A03/MF A01
National Inst. of Standards and Technology (CSL), Gaithersburg, MD. Systems and Software Technology Div.
Defining Environment Integration Requirements.
B. Cuthill, and M. Zelkowitz. May 95, 34p, NISTIR-5654.
See also PB94-143401 and PB95-143145.

Keywords: *Software engineering, *Information systems, *Requirements, Automation, Computer networks, Information flow, Systems management, Software tools, Systems engineering, Corporate information management, Integrated systems, Distributed computer systems, Interfaces, Data management, Organizational structure, *Enterprise integration, Enter-

prise modeling, ITEM(Information Technology Engineering and Measurement).

This paper discusses the use of enterprise and process modeling to classify the features of the enterprise process, its automation and the external stimuli on the enterprise that effect enterprise choices for tool and environment integration. This report focuses on the use of metadata and message types as mechanisms for integrating environments. This report includes an example of generating metadata and messaging requirements in the software development domain.

02,734
PB96-139407 PC A07/MF A02
National Inst. of Standards and Technology (TS), Gaithersburg, MD. Office of Information Services.
Databases Available in the Research Information Center of the National Institute of Standards and Technology (December 1995).
Special pub.
D. Cunningham. Dec 95, 150p, NIST/SP-895.
Supersedes PB95-128641. Also available from Supt. of Docs. as SN003-003-03383-9.

Keywords: *Data bases, *Information centers, Information services, Directories, Subject indexing, Indexes(Documentation), CD-ROMs, Vendors, Tables(Data), *US NIST.

Databases available online in the Research Information Center of the National Institute of Standards and Technology (NIST) are listed by acronym and by full title. In addition, descriptions of the databases, dates covered, producers, hard copy counterpart, principal sources and vendors are listed. A list of CD-ROM databases, a general subject index, a cross reference index, and a full text database sources and vendors are listed. A list of CD-ROM databases, a general subject index, a cross reference index, and a full text database list are also supplied.

02,735
PB96-147053 Not available NTIS
National Inst. of Standards and Technology (TS), Gaithersburg, MD. Office of Information Services.
General Types of Information Services.
Final rept.
P. W. Berger. 1992, 13p.
Sponsored by Engineering Foundation, New York. and Council on Library Resources, Inc., Washington, DC.
Pub. in Proceedings of the Conference on a National Engineering Information Service (NENGIS), Palm Coast, FL., June 14-19, 1992, p351-363.

Keywords: *Information services, Information systems, Library services, Data systems, Reprints, National Engineering Information System, Data services, Analytic services.

The report provides a description and evaluation of four types of information services: Library Services, Specialized Information Services, Data Services, and Analytic Services.

02,736
PB96-160536 Not available NTIS
National Inst. of Standards and Technology (CSL), Gaithersburg, MD.
Copyright and Information Services in the Context of the National Research and Education Network.
Final rept.
R. J. Linn. 1994, 12p.
Pub. in Intellectual Property Project Proceedings, v1 n1 p9-20 Jan 94.

Keywords: *Copyrights, *Property rights, *Requirements, Information services, Information dissemination, Computer networks, Legal aspects, Authentication, Systems management, Reprints, National Resource and Education Networks, High Performance Computing Act of 1991, Public Law 102-194, Digital signatures.

The High Performance Computing Act (HPCA) of 1991 (P.L. 102-194) places unenforcable requirements to protect copyrights and intellectual property rights on the National Research and Education Network (NREN). This paper discusses the roles and responsibilities of the NREN and associated information services; technical approaches to authentication, redistribution and authorization of use of electronic documents over the NREN; and an amendment to the high Performance Computing Act.

02,737
PB96-160866 Not available NTIS
National Inst. of Standards and Technology (CSL), Gaithersburg, MD.
Information Technology Standards in a Changing World: The Rose of the Users.
Final rept.
J. H. Burrows. 1993, 8p.
Pub. in Computer Standards and Interfaces, v15 p49-56 1993.

Keywords: *Information technology, *Interoperability, *User requirements, Information systems, Integrated systems, Standards, Interfaces, Reprints, Open Systems Interconnection.

Standards for information technology (IT) systems are important to users in effectively applying IT and carrying out the business of their organizations. Users need standards to interconnect products developed by different vendors and to move software, data ad applications from one system to another. However, the formal standards development process does not always respond to user needs in a timely way. The cost and complexity of the process often inhibits direct user participation over the long period of time needed to develop standards. Users also have difficulty applying the standards when they are developed in a fragmented and non-integrated fashion.

02,738
PB96-167846 PC A05/MF A01
National Inst. of Standards and Technology, Gaithersburg, MD.
Data Communications Strategy.
J. Mulvenna, and T. Boland. Jan 96, 62p, NISTIR-5793.
Sponsored by Internal Revenue Service, Arlington, VA.

Keywords: *Interoperability, *Computer networks, Network management, Computer architecture, Distributed computer systems, Data transfer(Computers), Data transmission, File management systems, Procurement, Protocols, Standards, Interfaces, Information retrieval, Data processing security, *Open systems interconnection, *Data communication systems, Internet.

The absence of a single solution for providing worldwide computer interoperability places more responsibility on procurement authorities to make the right choice. In order to make intelligent procurement decisions, procurement authorities need to be informed about the provided services and marketplace acceptance of computer networking products. The document provides technical, managerial, and procurement personnel with some of the factors that need to be considered when making procurment decisions.

02,739
PB96-183041 PC A03/MF A01
National Inst. of Standards and Technology (CSL), Gaithersburg, MD.
X.500 Directory Schema Design Handbook.
C. A. Warnar, and J. Tebbutt. Apr 96, 25p, NISTIR-5819.
See also PB95-231908.

Keywords: *Distributed data bases, *Information systems, *Directories, Performance evaluation, Data processing security, Computer networks, Design, Relational databases, Database management systems, *X500 Directory.

This document contains a high level schema description including a description of the schema components, the storage of schema information in the Directory Information Tree (DIT), and the tailoring of the schema components to meet an organization's needs. Pilot projects and other work in the area of schema design are reviewed and summarized.

Operations & Planning

02,740
PB95-181152 Not available NTIS
National Inst. of Standards and Technology (CSL), Gaithersburg, MD. Advanced Systems Div.
Prototype Information Retrieval System to Perform a Best-Match Search for Names.
Final rept.
N. E. Willman. 1994, 11p.
Sponsored by Social Security Administration, Washington, DC.
Pub. in Proceedings of RIAO 94' Conference on Intelligent Multimedia Information Retrieval Systems and Management, New York, NY., October 11-13, 1994, p751-761.

Keywords: *Information retrieval, *Information systems, Performance evaluation, Pattern recognition, Errors, Prototypes, Ranking, Reprints, *Proper names.

Personal names are often used as keywords in searches to retrieve information. The presence of misspellings and other errors in names can make an exact match of a keyword and a search query impossible. In these cases, it is necessary to be able to retrieve personal names that are similar to that of the personal name given in the search query. In addition, if an interactive search is required, it is necessary to retrieve matches quickly and to rank them in terms of their similarity to the search query. This paper discusses a prototype information retrieval system which was developed to test the feasibility of such a search, and the experimental results obtained using this system.

02,741
PB95-232633 PC A03/MF A01
National Inst. of Standards and Technology (TS), Gaithersburg, MD. Office of Information Services.
Abstract and Index Collection in the Research Information Center of the National Institute of Standards and Technology.
Special pub.
D. Cunningham. May 95, 40p, NIST/SP-884.
Supersedes PB94-152204. Also available from Supt. of Docs. as SN003-003-03340-5.

Keywords: *Abstracts, *Indexes(Documentation), Technical reports, Information centers, Subject indexing, Data bases, Sources, Publishing, *National Institute of Standards and Technology.

An alphabetical arrangement of abstracts and indexes available in the Research Information Center (RIC) of the National Institute of Standards and Technology (NIST) is listed by most current title of the publication. Other information includes description of the abstract or index, RIC holdings, principal sources, publisher or association, corresponding RIC database and CD-ROM availability and the classification number. A general subject and former title/database name index follow the main text of the report.

02,742
PB97-118665 Not available NTIS
National Inst. of Standards and Technology (CSL), Gaithersburg, MD. Information Access and User Interface Div.
Lab Report Special Section: Natural Language Processing and Information Retrieval Group Information Access and User Interfaces Division, National Institute of Standards and Technology.
Final rept.
D. Harman. 1995, 5p.
Pub. in SIGIR Forum, v29 n2 p6-10 Oct 95.

Keywords: *Natural language processing, *Text processing, *Information retrieval, Knowledge-based systems, Search structuring, Access, User needs, Automation, Human-computer interface, Reprints, US NIST, Electronic text.

The Natural Language Processing and Information Retrieval Group was formed in 1994 at the National Institute of Standards and Technology (NIST) in recognition of the importance of managing the ever-increasing amount of electronically available text. The formal objective of the group is 'to work with industry, academia and other government agencies to promote the use of more effective and efficient techniques for manipulating (largely) unstructured textual information, especially the browsing, searching, and presentation of the information'.

02,743
PB97-118673 Not available NTIS
National Inst. of Standards and Technology (CSL), Gaithersburg, MD. Information Access and User Interface Div.
Panel: Building and Using Test Collections.
Final rept.
D. Harman. 1996, 3p.
Pub. in Proceedings of the Annual International ACM SIGIR Conference on Research and Development in Information Retrieval (19th), SIGIR '96, Zurich, Switzerland, August 18-22, 1996, p335-337.

Keywords: *Information retrieval, *Text processing, *Documents, *Data collection, Knowledge-based sys-

tems, Search structuring, Multimedia, Computer languages, Semantics, Syntax, Reprints.

The panel, emphasizing audience participation, focuses on issues in building and using test collections for information retrieval. The panel presents an opportunity to share experiences gained from past test collection building and usage to help guide the development of these new test collections.

Reference Materials

02,744
PB94-152204 PC A03/MF A01
National Inst. of Standards and Technology, Gaithersburg, MD.
Abstract and Index Collection in the Research Information Center of the National Institute of Standards and Technology.
Special pub.
D. Cunningham. Jan 94, 41p, NIST-SP-859.
Also available from Supt. of Docs. as SN003-003-03250-6.

Keywords: *Abstracts, *Indexes(Documentation), Technical reports, Information centers, Subject indexing, Data bases, Sources, Publishing, *National Institute of Standards and Technology.

An alphabetical arrangement of abstracts and indexes available in the Research Information Center (RIC) of the National Institute of Standards and Technology (NIST) is listed by most current title of the publication. Other information includes description of the abstract or index, RIC holdings, principal sources, publisher or association, corresponding RIC database and CD-ROM availability and the classification number. A general subject and former title/database name index follow the main text of the report.

02,745
PB94-178068 PC A12/MF A03
National Inst. of Standards and Technology (TS), Gaithersburg, MD. Office of Information Services.
NIST Serial Holdings, 1994.
Special pub. (Final).
S. A. Sanders. Apr 94, 270p, NIST/SP-777-94-ED.
Supersedes PB94-120847. Also available from Supt. of Docs. as SN003-003-03261-1.

Keywords: *Periodicals, *Catalogs(Documentation), *Collection, *Information centers, *Bibliographies, Standards, Libraries, *National Institute of Standards and Technology, *NIST.

This publication contains bibliographic information on approximately 5,000 titles held in the NIST Research Information Center, representing current and noncurrent journals, periodicals, annuals, memoirs, proceedings and transactions.

02,746
PB95-188926 PC A12/MF A03
National Inst. of Standards and Technology (TS), Gaithersburg, MD. Office of Information Services.
NIST Serial Holdings, 1995.
Special pub. (Final).
S. A. Sanders. Feb 95, 271p, NIST/SP-777-95.
Supersedes PB94-178068. Also available from Supt. of Docs. as SN003-003-03319-7.

Keywords: *US NIST, *Periodicals, *Catalogs(Documentation), *Bibliographies, Standards, Libraries.

The publication contains bibliographic information on approximately 5,000 titles held in the NIST Research Information Center, representing current and noncurrent journals, periodicals, annuals, memoirs, proceedings and transactions.

02,747
PB95-226692 PC A05/MF A01
National Inst. of Standards and Technology (PL), Gaithersburg, MD.
Guide for the Use of the International System of Units (SI).
Special pub.
B. N. Taylor. Apr 95, 87p, NIST-SP-811.
Supersedes PB92-116383. Also available from Supt. of Docs. as SN003-003-03329-4.

Keywords: *International system of units, *Metric system, *Conversion tables, Units of measurement.

The guide is a practical tool for the use of NIST authors in the preparation of manuscripts in conformance with the NIST policy that requires the use of the International System of Units for all publications.

02,748
PB96-172523 PC A13/MF A03
National Inst. of Standards and Technology (TS), Gaithersburg, MD. Office of Information Services.
NIST Serial Holdings, 1996.
Special pub.
S. A. Sanders. Feb 96, 270p.
Supersedes PB95-188926. Also available from Supt. of Docs. as SN003-003-03394-4.

Keywords: *US NIST, *Periodicals, Documents.

This publication contains bibliographic information on approximately 5,000 titles held in the NIST Research Information Center, representing current and noncurrent journals, periodicals, annuals, memoirs, proceedings and transactions.

MANUFACTURING TECHNOLOGY

General

02,749
AD-A286 683/8 PC A03/MF A01
National Bureau of Standards, Boulder, CO.
Helium Refrigeration and Liquefaction Using a Liquid Hydrogen Refrigerator for Precooling.
Technical note.
D. B. Shelton, J. W. Dean, T. R. Strobridge, B. W. Birmingham, and D. B. Mann. 27 Jan 60, 36p.

Keywords: *Helium, *Refrigeration systems, *Liquefaction, *Liquid hydrogen, Circuits, Evaporators, Heat exchangers, Hydrogen, Production, Requirements, Temperature, Low temperature, Gases, *Precooling, Refrigerators.

Consideration is given to the use of a hydrogen refrigerator to assist in the production of temperatures below those obtained with hydrogen. A hydrogen refrigerator is used to maintain a precooling evaporator at or near 21 deg K in a helium gas circuit. The helium circuit may be arranged to produce liquid for external use or to produce refrigeration between 21 deg K and 4. 2 deg K in a closed system. Charts have been developed that show the requirements of the composite helium - hydrogen system and the effect of heat exchanger performance. The relative quantities of refrigeration (hydrogen and helium) at various temperature levels have been determined.

02,750
PB94-165966 PC A06/MF A02
National Inst. of Standards and Technology (MEL), Gaithersburg, MD.
Publications of the Manufacturing Engineering Laboratory Covering the Period January 1989-September 1992.
C. Albus. Nov 92, 115p, NISTIR-4974.
See also PB93-123041.

Keywords: *Bibliographies, *US NIST, Dimensional measurement, Robotics, Artificial intelligence, Production engineering, Information systems, Metrology, Primary standards, Calibrating, Precision, Sensors, Automation, *Manufacturing Engineering Laboratory.

The mission of the Manufacturing Engineering Laboratory (MEL) is to bring the resources of the National Institute of Standards and Technology to bear on the standards and measurement problems associated with America's discrete parts manufacturing. To fulfill this mission MEL conducts active programs of research in the areas of: High-precision dimensional measurement and precision engineering; Robotics and intelligent machines; Manufacturing data description, data administration, and information processing; and Sensors for manufacturing processes. This list of publications reflects the diversity of scientific and technical problems which have been attacked over the past fourteen years in fulfillment of the Laboratory's mission.

02,751
PB95-140943 Not available NTIS
National Inst. of Standards and Technology (CSTL), Gaithersburg, MD. Process Measurements Div.
Heat Transfer in Thin, Compact Heat Exchangers with Circular, Rectangular, or Pin-Fin Flow Passages.
Final rept.
D. A. Olson. 1992, 10p.
Contract NLRC-L7400C
Sponsored by National Aeronautics and Space Administration, Hampton, VA. Langley Research Center.
Pub. in Jnl. of Heat Transfer 114, p373-382 May 92.

Keywords: *Heat transfer, *Pressure gradients, *Channel flow, *Flow geometry, Heat flux, Friction factor, Reynolds number, Nusselt number, Helium, Gas flow, Viscosity, Thermal conductivity, Reprints, *Compact heat exchangers.

We have measured heat transfer and pressure drop of three thin, compact heat exchangers in helium gas at 3.5 MPa and higher, with Reynolds numbers of 450 to 36,000. The flow geometries for the three heat exchanger specimens were: circular tube, rectangular channel, and staggered pin fin with tapered pins. The specimens were heated radiatively at heat fluxes up to 77 W/sq cm. Correlations were developed for the isothermal friction factor as a function of Reynolds number, and for the Nusselt number as a function of Reynolds number and the ratio of wall temperature to fluid temperature. The specimen with the pin internal geometry had significantly better heat transfer than the other specimens, but it also had higher pressure drop. For certain conditions of helium flow and heating, the temperature more than doubled from the inlet to the outlet of the specimens, producing large changes in gas velocity, density, viscosity, and thermal conductivity. These changes in properties did not affect the correlations for friction factor and Nusselt number in turbulent flow.

02,752
PB95-169082 Not available NTIS
National Inst. of Standards and Technology (CSTL), Gaithersburg, MD. Process Measurements Div.
Energy Flows in an Orifice Pulse Tube Refrigerator.
Final rept.
W. Rawlins, R. Radebaugh, P. Bradley, and K. Timmerhaus. 1993, 8p.
Pub. in Advances in Cryogenic Engineering, v39 ptB p1449-1456 1993.

Keywords: *Mass flow, *Flow measurement, Enthalpy, Refrigerators, Entropy, Heat flux, Refrigerating machinery, Reprints, *Orifice pulse tube refrigerators, *Energy flow, *Enthalpy flow.

A technique which allows for the instantaneous measurements of mass flow rate and temperature in an orifice pulse tube refrigerator (OPTR) during actual operation has been developed recently. This paper presents the values of enthalpy, entropy, and work fluxes at the cold end of the pulse tube evaluated from these measurements. They are thermodynamically self consistent within 1%. An analytical model describing the operation of an OPTR was developed at the National Institute of Standards and Technology (NIST) in the late 1980's. This model assumes adiabatic performance of the pulse tube and purely sinusoidal mass flow rates, temperature, and pressure oscillations in the OPTR. The experimentally measured enthalpy flux varies from 60% to 85% of that predicted by the adiabatic model. The experimental work reported here also gives values for various phase relationships that are needed for some calculations with the analytical model.

02,753
PB95-169090 Not available NTIS
National Inst. of Standards and Technology (CSTL), Gaithersburg, MD. Process Measurements Div.
Graded and Nongraded Regenerator Performance.
Final rept.
W. Rawlins, K. D. Timmerhaus, R. Radebaugh, J. Gary, and P. Bradley. 1993, 13p.
Sponsored by National Aeronautics and Space Administration, Moffett Field, CA. Ames Research Center.

Pub. in Proceedings of International Cryocooler Conference (7th), Santa Fe, NM., November 17-19, 1992, p471-483 1993.

Keywords: *Regenerators, *Cooling systems, *Performance testing, Regeneration(Engineering), Refrigerating machinery, Cryogenic cooling, Temperature measurement, Heat loss, Mass flow, Effectiveness, Performance evaluation, Reprints, *Pulse tube refrigerators.

A method to measure regenerator performance, in situ, in an orifice pulse tube refrigerator has been successfully developed. This was accomplished by inserting two, 2 mm long, tungsten wires with diameters of 4 micrometers perpendicular to the fluid flow at the cold end of the regenerator. The paper compares the performance between two different regenerators constructed from stainless steel mesh: one with a graded mesh (where three different mesh sizes are used for the matrix material) and another with a single mesh size throughout. Both expeirmental and numerical model results are presented. The numerical model indicated that there was only a very slight advantage to using a graded mesh in a generator, whereas experiments showed the graded mesh regenerator to have a slightly higher ineffectiveness.

02,754
PB95-188835 PC A11/MF A02
National Inst. of Standards and Technology (MEL), Gaithersburg, MD.
Program of the Manufacturing Engineering Laboratory, 1995. Infrastructural Technology, Measurements, and Standards for the U.S. Manufacturing Industries.
G. P. Carver. Feb 95, 241p, NISTIR-5599.
See also PB94-165966.

Keywords: *Metrology, Dimensional measurement, Production engineering, Artificial intelligence, Automation, Robotics, Standards, *Manufacturing Engineering Laboratory, US NIST.

The National Institute of Standards and Technology (NIST) Manufacturing Engineering Laboratory works with the U.S. manufacturing industries to develop and apply infrastructural technology, measurements, and standards to meet their needs. This report summarizes the resources, objectives, needs addressed, accomplishments, and plans for the projects carried out by the Manufacturing Engineering Laboratory in support of U.S. industry.

02,755
PB95-198750 PC A04/MF A01
National Inst. of Standards and Technology (MEL), Gaithersburg, MD. Factory Automation Systems Div.
Apparel Manufacturing Glossary for Application Protocol Development.
M. E. Read. Feb 95, 60p, NISTIR-5572.
Sponsored by Defense Logistics Agency, Alexandria, VA.

Keywords: *Clothing industry, *Manufacturing, *Dictionaries, Pattern making, Standards, Specifications, APs(Application Protocols), APDES(Apparel Product Data Exchange Standard), STEP(Standard for the Exchange of Product Model Data).

A glossary of terms used in apparel manufacturing, specifically those used in the pattern-making process, are listed verbatim from six primary sources. These terms are needed in the development of new, International Organization for Standardization (ISO) Standard for the Exchange of Product Model Data (STEP) application protocols for the apparel industry. The purpose of this report is to present to the apparel industry a working set of terms and meanings from the published literature, and to act as a catalyst in the development of a set of consensus terms and meanings.

02,756
PB96-136973 PC A03/MF A01
National Inst. of Standards and Technology (BFRL), Gaithersburg, MD.
Effect of Inclination on the Performance of a Compact Brazed Plate Condenser and Evaporator.
M. A. Kedzierski. Nov 95, 33p, NISTIR-5767.
Sponsored by Trane Co., La Crosse, WI.

Keywords: *Heat exchanges, *Refrigerating machinery, Schematic diagrams, Refrigerants.

The origins of the compact brazed plate heat exchanger (CBE) began in the 1920's with the first commercially successful gasketed-plate heat exchangers (Saunders, 1988). Milk producers and other food and drink processors satisfied hygiene requirements by periodically disassembling and cleaning the gasketed-plates. Applications for the compact brazed plate heat exchangers (CBEs) have increased in recent years. Currently, the compactness of the CBE drives its use as refrigerant evaporators and condensers. The purpose of this study was to identify the performance degradation associated with tilting a CBE from the designed vertical position.

02,757
PB96-163621 Not available NTIS
National Inst. of Standards and Technology (MEL), Gaithersburg, MD. Precision Engineering Div.
Gage Block Standards, Measurement Capabilities and Laboratory Accreditation.
Final rept.
T. Doiron. 1992, 12p.
Pub. in NCSL Workshop and Symposium, August 1992, p183-194.

Keywords: *Gage blocks, *Interlaboratory tests, Reprints, Accuracy, Error budget, Standards, *Laboratory accreditation.

As the United States begins to seriously consider laboratory accreditation for calibration labs, the calibration of gage blocks (one of the most accurate and sophisticated of industrial measurements) has been suggested as the prototype dimension laboratory accreditation. One of the technical problems in implementing laboratory accreditation is determining the laboratory accuracy which is adequate for calibration systems. The author will discuss some of the problems inherent in the classifcation schemes of both the US and ISO standards and their relation to the current state of the art for gage block calibration.

02,758
PB96-190293 Not available NTIS
National Inst. of Standards and Technology (MEL), Gaithersburg, MD. Precision Engineering Div.
Increasing the Value of Atomic Force Microscopy Process Metrology Using a High-Accuracy Scanner, Tip Characterization, and Morphological Image Analysis.
Final rept.
J. Schneir, J. S. Villarrubia, T. H. McWaid, V. W. Tsai, and R. Dixson. 1996, 7p.
Pub. in Jnl. of Vacuum Science and Technology, v14 n2 p1540-1546 Mar/Apr 96.

Keywords: *Metrology, Tip, Manufacturing, Scanners, Image analysis, Reprints, *Atomic force microscopes.

Atomic force microscopes are being used increasingly for process metrology. As a case study, the measurement by atomic force microscope of a soda lime glass optical disk patterned using optical lithography and reactive plasma etching is examined. The atomic force microscope used for this measurement has a highly accurate scanner system. The X, Y, and Z axes are calibrated using laser interferometry. To determine the shape of the tip used a commercially available tip calibration artifact was imaged both before and after the measurement. The image was corrected for the tip shape using mathematical morphology. The value of the atomic force microscope measurement is defined to be the impacts of the metrology on the product or process. It is shown that the value of atomic force microscopy process metrology on an optical disk is increased by using an accurate scanner, tip characterization, and morphological image analysis; however, the cost per measurement in increased as well. In general, the characteristics of the metrology required depends on the secific manufacturing process being supported.

02,759
PB96-190368 Not available NTIS
National Inst. of Standards and Technology (MEL), Gaithersburg, MD. Precision Engineering Div.
Scanned Probe Microscope Tip Characterization Without Calibrated Tip Characterizers.
Final rept.
J. S. Villarrubia. 1996, 4p.
Pub. in Jnl. of Vacuum Science and Technology B, v14 n2 p1518-1521 Mar/Apr 96.

Keywords: *Metrology, Morphology, Reprints, *Atomic force microscopes, *Blind reconstruction, Scanned probe microscopy, Scanning tunneling microscopy.

In scanned probe microscopy the image is a combination of information from the sample and the tip. In order to reconstruct the true surface geometry, it is necessary to know the actual tip shape. It has been proposed that this shape may be constructed from images of 'tip characterizer' artifacts of independently known shape. The requirements for this strategy-dimensional uncertainty and instability of the characterizer small compared to the tip size-are not trivial. An alternative is 'blind reconstruction', which requires no information about the characterizer geometry apart from that contained within its image, yet produces an outer bound on the tip shape which for appropriately chosen characterizers is a good approximation. With blind reconstruction dimensional instability of characterizers is less problematical, and characterizer measureability is no longer a constraint, so more complex distributed characterizer has a known shape, blind reconstruction and the known-characterizer method may be combined.

02,760
PB96-195276 PC A11/MF A03
National Inst. of Standards and Technology (MEL), Gaithersburg, MD.
Program of the Manufacturing Engineering Laboratory, 1996. Infrastructural Technology, Measurements, and Standards for the U.S. Manufacturing Industries.
May 96, 218p, NISTIR-5845.
See also report for 1995, PB95-188835.

Keywords: *Metrology, Dimensional measurement, Production engineering, Standards, Calibration, Robotics, Automation.

The NIST Manufacturing Engineering Laboratory works with the U.S. manufacturing industries to develop and apply infrastructural technology, measurements, and standards to meet their needs. This report summarizes the Manufacturing Engineering laboratory in support of U.S. industry.

02,761
PB96-201157 Not available NTIS
National Inst. of Standards and Technology (MEL), Gaithersburg, MD. Automated Production Technology Div.
Ultrasonic NDE of Sprayed Ceramic Coatings.
Final rept.
J. A. Slotwinski, and G. V. Blessing. 1996, 8p.
Pub. in Review of Progress in Quantitative Nondestructive Evaluation, v15 p1613-1620 1996.

Keywords: *Ceramic coatings, *Plasma spray, *Nondestructive evaluation, Alumina, Elastic moduli, Ultrasonics, Zirconia, Reprints.

Thermal spraying of protective coatings has been in use since 1917 when the initial application was the spraying of zinc layers onto steel structures to prevent corrosion. In the 1970's plasma-spray technology was first used with the introduction of vacuum plasma-spraying. Today, gases such as argon and nitrogen (sometimes with an additional gas such as helium or hydrogen) are often used in plasma-spray guns. In plasma-spraying an electric-arc discharge heats the gas stream to high temperature (equal to or greater than 10,000 K), turning it into a plasma. The gas exits the spray-gun at high speed (approx. 200 m/s to 600 m/s) towards the material to be coated. Material powder (often carried by a second gas stream) is injected into the plasma stream, where it melts into liquid droplets. These droplets are carried onto the target surface, where they rapidly cool (approx. 10 to the sixth power K/s) into solid, flat splats. A layer of material can be built up by repeated spraying of the same surface area.

02,762
PB97-116107 PC A03/MF A01
National Inst. of Standards and Technology (BFRL), Gaithersburg, MD.
Intracycle Evaporative Cooling in a Vapor Compression Cycle.
B. S. Kim, and P. A. Domanski. Sep 96, 28p, NISTIR-5873.
Sponsored by Department of Energy, Washington, DC. Office of Building Technology.

Keywords: *Evaporative cooling, *Vapor compression refrigeration cycle, Heat pumps, Refrigerating, Buildings, Air conditioning.

The temperature glide of zeotropic mixtures during phase change provides the opportunity to limit throttling losses of the refrigeration cycle by intracycle evaporative cooling of the refrigerant leaving the condenser. Intracycle evaporative cooling is similar to the

use of the liquid-line/suction-line heat exchanger with the difference that a two-phase low-pressure refrigerant, instead of superheated vapor, is used to subcool the high-pressure liquid leaving the condenser. Intracycle evaporative cooling was evaluated by a semi-theoretical simulation model and in the NIST's Small Breadboard Heat Pump at the cooling mode operating condition typical for a water-to-water residential heat pump. The capacity, coefficient of performance (COP), pressures, and temperature profiles of refrigerant and heat-transfer fluid in the heat exchangers are reported. The laboratory measured improvement of the COP was 4.0% for R-32/152a, 3.6% for R-407C, and 1.8 percent for R-23/152a.

02,763
PB97-118681 Not available NTIS
National Inst. of Standards and Technology (MEL), Gaithersburg, MD. Automated Production Technology Div.
Transient Analysis of a Line-Focus Transducer Probing a Liquid/Solid Interface.
Final rept.
N. N. Hsu, D. Xiang, S. E. Fink, and G. V. Blessing. 1996, 8p.
Pub. in Review of Progress in Quantitative Nondestructive Evaluation, Seattle, WA., July 30-August 4, 1995, p995-1002 1996.

Keywords: *Line-focus transducer, *Transient ultrasonic wave, Materials, Reprints, Time-domain Green's function, Transducer response function, Ultrasonic tests, Liquid-solid interfaces.

The use of a line-focus ultrasonic transducer in a vertical scanning reflection acoustic microscope system is well known for quantitative materials characterization. The technique relies on the measurement of the reflected radio frequency tone burst echo emplitude, V, as a function of amount of defocus, z, and analysis of the interference minima of the V(z) curve to obtain various interface wave speeds. The technique uses well developed theory representing fixed frequency ultrasound generated and detected by a cylindrical lens in the frequency domain. The authors have developed a large aperture lensless line-focus transducer which is highly efficient and has a bandwidth wide enough to allow the generation and detection of narrow transient pulses. From this transducer placed in water near a solid sample, the resulting echo waveforms have multiple features which can be interpreted as the arrival of specularly reflected axial ray and leaky surface waves. Using this transducer, the authors have developed a time-resolved and polarization-sensitive testing tehcnique for materials characterization. The objective of the paper is to provide a theoretical basis for interpretation and analysis of these time domain waveforms.

02,764
PB97-122576 Not available NTIS
National Inst. of Standards and Technology (MEL), Gaithersburg, MD. Automated Production Technology Div.
Material Characterization By a Time-Resolved and Polarization-Sensitive Ultrasonic Technique.
Final rept.
D. Xiang, N. N. Hsu, and G. V. Blessing. 1996, 8p.
Pub. in Review of Progress in Quantitative Nondestructive Evaluation, Seattle, WA., July 30-August 4, 1995, v15 p1431-1438 1996.

Keywords: *Ultrasonic microscopy, *Transducers, Leaky waves, Reprints, *Line-focus transducer, PVDF transducers.

Acoustic microscopy provides materials characterization by measuring the leaky surface wave speed and attenuation in sample materials. These measurements may be interpreted by analyzing a V(z) curve, which is a record of the voltage of the transducer as a function of the defocus distance z between the focal point and sample surface. Since the V(z) curve results from the interference between the leaky surface waves and the direct-reflected wave in a tone-burst mode of operation, the fast Fourier transform (FFT) technique is commonly used to analyze the V(z) curve in the frequency domain. While this manner of acoustic microscopy utilizes a small aperture lens and high frequency tone bursts in order to obtain high spatial resolution, the system cost is greater than the alternative short-pulse broadband systems. Furthermore, high spatial resolution is not necessary for many practical measurements, for example in the case of composite materials.

02,765
PB97-122584 Not available NTIS
National Inst. of Standards and Technology (MEL), Gaithersburg, MD. Automated Production Technology Div.
Design, Construction and Application of a Large Aperture Lens-Less Line-Focus PVDF Transducer.
Final rept.
D. Xiang, N. N. Hsu, and G. V. Blessing. 1996, 7p.
Pub. in Ultrasonics, v34 p341-347 1996.

Keywords: *Transducers, *Materials characterization, Reprints, *Green's function, *PVDF transducers, *Line-focus transducers.

A large aperture lens-less line-focus transducer for materials characterization is described. The transducer design is based on a time-domain Green's function formalism, which also yields good theoretical corroboration of the experimental results. The transducer construction is readily achieved by conforming commercial polyvinylidene fluoride (PVDF) film to a cylindrical (convex) surface, followed by casting a tungsten-powder-loaded epoxy resin backing material into an attached housing. This transducer can be used to characterize sample material properties by simultaneously measuring surface wave speeds and bulk wave transit times, from which the thickness and anisotropy may be deduced.

Computer Aided Design (CAD)

02,766
PB94-139649 PC A03/MF A01
National Inst. of Standards and Technology, Gaithersburg, MD.
Security Considerations for SQL-Based Implementations of STEP.
L. E. Bassham, and W. T. Polk. Oct 93, 26p, NISTIR-5283.
See also PB89-168009, PB93-113637 and PB94-104585.

Keywords: *Computer security, Computer aided design, Computer aided manufacturing, Distributed processing, Data management, Standards, Access control, Data integrity, *PDES(Product Data Exchange using STEP), STEP(Standard for the Exchange of Product Model Data), SQL database language, RDA(Remote Database Access).

The Database Language SQL (SQL) is a standard interface for accessing and manipulating relational databases. As such, SQL can be used in many different operational environments, with correspondingly different needs for security. One specific application of this standard is in the field of Product Data Exchange using STEP (PDES). This paper examines the security implications of the versions of the SQL standard as used to implement STEP. STEP does not imply any particular security policy, so a variety of security policies are examined. The paper has been written as a companion document to the National Institute of Standards and Technology's (NTIS's) general SQL security document, 'Security Issues in the Database Language SQL', and references that document frequently.

02,767
PB94-154325 PC A03/MF A01
National Inst. of Standards and Technology, Gaithersburg, MD.
APDE Demonstration System Architecture. National PDES Testbed Report Series.
S. N. Clark, and A. B. Feeney. Jan 93, 21p, NISTIR-5318.
See also PB93-208114. Sponsored by Assistant Secretary of Defense (Production and Logistics), Washington, DC. Computer-aided Acquisition and Logistic Support Program.

Keywords: *Computer aided design, *Computer aided manufacturing, Standards, Prototypes, Systems engineering, *APDE(Application Protocol Development Environment), *Application protocols, STEP(Standard for the Exchange of Product Model Data), PDES(Product Data Exchange using STEP), ARM(Application Reference Model), AIM(Application Interpreted Model).

The National Product Data Exchange using STEP (PDES) Testbed project at the National Institute of Standards and Technology (NIST) is focused on the development and implementation of the emerging international Standard for the Exchange of Product model data (STEP). One sub-project within the Testbed is the effort to establish an Application Protocol Development Environment (APDE). The report describes the architecture of a prototype system which will be built at NIST to demonstrate some of the features needed in an APDE and some approaches to providing these features. The demonstration system will focus on a specific step in the AP development process, namely Application Reference Model (ARM) interpretation. The functionality demonstrated is based on specifications documented in an earlier report.

02,768
PB94-154358 PC A03/MF A01
National Inst. of Standards and Technology (MEL), Gaithersburg, MD. Factory Automation Systems Div.
Variant Design for Mechanical Artifacts-A State of the Art Survey.
Internal rept.
J. E. Fowler. Feb 94, 28p, NISTIR-5356.

Keywords: *Computer aided design, Reasoning, Specifications, Feature extraction, Mathematical models, Standards, *Variant design, STEP(Standard for the Exchange of Product Model Data).

Variant design refers to the technique of adapting existing design specifications to satisfy new design goals and constraints. Specific support of variant design techniques in current computer aided design systems would help to realize a rapid response manufacturing environment. A survey of approaches supporting variant design is presented. Capabilities used in current commercial computer aided design systems are discussed along with approaches used in recent research efforts. Information standards applicable to variant design are identified as well. Barriers to variant design in current systems are identified and ideas are presented for augmentation of current systems to support variant design.

02,769
PB94-159795 PC A04/MF A01
National Inst. of Standards and Technology (MEL), Gaithersburg, MD. Factory Automation Systems Div.
Structural EXPRESS Editor.
T. R. Kramer, K. C. Morris, and D. A. Sauder. Aug 92, 73p, NISTIR-4903.
See also PB90-269507. Prepared in cooperation with Catholic Univ. of America, Washington, DC. Dept. of Mechanical Engineering.

Keywords: *Editing routines, Computer aided design, Computer aided manufacturing, Standards, Interactive systems, Data structures, Algorithms, *EXPRESS modeling language, *STEP (Standard for the Exchange of Product Model Data), PDES(Product Data Exchange using STEP), SEXE(Structural EXPRESS Editor).

EXPRESS is the official information modeling language of the next generation of product information standards, commonly referred to as STEP or Standard for the Exchange of Product Model Data. This paper presents a Structural EXPRESS Editor (SEXE), which has two parts: an Interactive Editor, and a Translation Module. The Interactive Editor was built using a tool called the Data Probe Editor (DPE) Builder and is an interactive, friendly editor with which a user defines the structure of an EXPRESS schema. The output of the Interactive Editor is a STEP exchange file that is translated into EXPRESS by the Translation Module, a software system written in LISP. The paper describes the DPE Builder and both parts of SEXE. The editor is assessed and EXPRESS editors, generally, are discussed. Alternative representations of EXPRESS are presented. A few issues in information modeling highlighted in the course of building the editor are discussed.

02,770
PB94-160868 PC A05/MF A01
Catholic Univ. of America, Washington, DC.
Issues and Recommendations for a STEP Application Protocol Framework. National PDES Testbed.
T. R. Kramer, M. E. Palmer, and A. B. Feeney. 17 Jan 92, 90p, NISTIR-4755.
Contract NANB9H0923
See also PB92-112374. Sponsored by National Inst. of Standards and Technology, Gaithersburg, MD. and Assistant Secretary of Defense (Production and Logistics), Washington, DC. Computer-aided Acquisition and Logistic Support Program.

Keywords: Product development, Standards, Protocols, Computer aided design, Computer aided manufacturing, Tests, Standardization, *STEP(Standard for the Exchange of Product Model Data), *APs(Application Protocols), PDES(Product Data Exchange Using STEP), AIM(Application Interpreted Model).

Technical experts are developing the next generation product information exchange standards, called the Standard for the Exchange of Product Model Data (STEP). The STEP project is using the application protocol (AP) methodology for defining the information requirements of industry and for specifying standards for representing these requirements. Several APs have already been drafted. Before the AP methodology is expanded to address more complex problems, and before any more AP projects are initiated, the fundamental methods for developing and testing APs must be completed and proven. This report provides a description of application protocols, a summary of AP development issues (supplemented by discussions and case studies in the appendices), a listing of the relevant documentation and issues papers, and recommendations for resolving the identified issues. This includes recommendations on functional requirements for an AP framework, elements of AP structure, coordination of AP development, and AP classification. This report provides a baseline study for subsequent work on an AP Framework by members of the STEP community.

02,771
PB94-163482 PC A03/MF A01
National Inst. of Standards and Technology, Gaithersburg, MD.
Validation Testing System Requirements. National PDES Testbed Report Series.
K. C. Morris, M. McLay, and P. J. Carr. Sep 91, 32p, NISTIR-4676.
See also PB88-235452 and PB92-123090. Sponsored by Assistant Secretary of Defense (Production and Logistics), Washington, DC. Computer-aided Acquisition and Logistic Support Program.

Keywords: *Software engineering, *Requirements, Product development, Models, Tests, Computer software, Software tools, Data flow analysis, Interfaces, *VTS(Validation Testing System), PDES(Product Data Exchange using STEP), STEP(Standard for the Exchange of Product Model Data), ISO(International Standards Organization).

This document describes requirements for software to support the testing of information models for validity and correctness. The requirements provide a basis for the software development to support the Validation Testing System (VTS) within the National PDES Testbed. This document describes the software needs as currently known for a complete validation testing system. It identifies the scope of the VTS software, presents functional requirements for the proposed system, describes the data flow, environment, external interfaces, performance, and documentation requirements of the system, and prioritizes the requirements for the purpose of implementing the proposed system.

02,772
PB94-219086 PC A04/MF A01
Information Assets, Inc., Houston, TX.
Framework for Information Technology Integration in Process Plant and Related Industries.
W. G. Beazley, and J. B. Chapman. Jul 94, 74p, NIST/GCR-94/657.
See also PB87-209052. Sponsored by National Inst. of Standards and Technology (BFRL), Gaithersburg, MD. Building Environment Div.

Keywords: *Industrial plants, *Automation, *Petrochemistry, Design, Construction, Operation, Engineering, Constraints, Data processing, Digital data, Benefit cost analysis, Computer aided design, Computer aided manufacturing.

Initially, the report presents a constraint framework that can identify all the root constraints and their associated activities for the engineering, construction, and operation of a petrochemical plant. Second, it demonstrates how the constraint framework leads to functional models of design that can be traced directly to the constraints they address. This avoids some of the problems in basing models on design tasks assigned within phases. Third, it demonstrates how external constraints do, in fact, influence design and how to analyze their influence. Fourth, it discusses some of the data that is produced to document that the constraints have been satisfied. It provides a list of some of the tools that support the creation and maintenance of these data sets. Last, it discusses the business case for 3D design and for digital Piping and Instrumentation Drawings (P&ID) delivery.

02,773
PB95-105052 PC A03/MF A01
National Inst. of Standards and Technology (MEL), Gaithersburg, MD. Factory Automation Systems Div.
Formulation of Position on U.S. Standards Role in Enterprise Integration.
H. M. Bloom. Aug 94, 43p, NISTIR-5484.

Keywords: *Standards, *Product development, United States, Government policies, Technology innovation, Computer aided design, Computer aided manufacturing, *Enterprise integration, PDES(Product Data Exchange using STEP), STEP(Standard for the Exchange of Product Model Data), US NIST, IGES(Initial Graphics Exchange Specification), US PRO.

This paper gives a brief overview of the concepts of enterprise integration, defines a national strategy for enterprise integration (EI) that involves not only standards bodies but also the government and industry groups with an interest in EI technology and standards, and proposes that one specific standards organization, the US PRO that oversees the Initial Graphics Exchange Specification (IGES) Product Data Exchange using STEP (PDES) Organization, develop a new extended scope that will tackle the EI standards issues. Finally, a business case for US PRO involvement in EI is discussed, first through the identification of key issues requiring resolution, and then through listing the pros and cons of extending the scope to enterprise integration framework standards. As reference information to support the paper, the key government and industrial groups that are involved in EI-related technology development programs are described along with the organizations that have a stake in the standards process.

02,774
PB95-107314 Not available NTIS
National Inst. of Standards and Technology (NEL), Gaithersburg, MD. Factory Automation Systems Div.
Summary and Notes of the Joint ISO/IGES/PDES Organization Technical Committee Meeting. Held in Albuquerque, New Mexico on October 15-20, 1989.
Final rept.
S. R. Ray, and G. R. Rinaudot. 1989, 85p.
Pub. in Joint IGES/PDES/ISO Meeting Minutes, Albuquerque, NM., October 15-20, 1989, p1-85.

Keywords: *Computer aided design, *Computer aided manufacturing, *Standards, Automation, Reprints, *IGES(Initial Graphics Exchange Specification), *Initial Graphics Exchange Specification, *PDES(Product Data Exchange using STEP), *Product Data Exchange using STEP, STEP(Standard for the Exchange of Product Model Data), ISO(International Organization for Standardization).

The document is a summary of the Initial Graphics Exchange Specification/Product Data Exchange using STEP (IGES/PDES) Organization General Assembly meeting and the IGES/PDES technical committee meetings held in Albuquerque, New Mexico, on October 15th - 20th, 1989.

02,775
PB95-125829 Not available NTIS
National Inst. of Standards and Technology (NEL), Gaithersburg, MD. Factory Automation Systems Div.
National PDES Testbed: An Overview.
Final rept.
C. M. Furlani. 1989, 8p.
Pub. in Proceedings of Annual Conference on University Programs in Computer-Aided Engineering, Design, and Manufacturing (7th), Laramie, WY., July 23-26, 1989, p1-8.

Keywords: *Computer aided design, *Computer aided manufacturing, *Data transfer(Computers), *Standards, Tests, Reprints, *PDES(Product Data Exchange Specification), Product Data Exchange using STEP, STEP(Standard for the Exchange of Product Model Data), AMRF(Automated Manufacturing Research Facility), US NIST.

A description of the National PDES Testbed which has recently been established at the National Institute of Standards and Technology (NIST) to provide support for industry and government projects in developing and testing the Product Data Exchange Specification (PDES), the next generation of data interchange standards for automated manufacturing. An overview of the Automated Manufacturing Research Facility (AMRF), which provides the foundation for the Testbed, is included.

02,776
PB95-136347 PC A03/MF A01
National Inst. of Standards and Technology, Gaithersburg, MD.
Challenges to the National Information Infrastructure: The Barriers to Product Data Sharing. National PDES Testbed Report Series.
D. A. Sauder, M. J. Mitchell, and A. B. Feeney. 15 Sep 94, 13p, NISTIR-5498.
See also PB93-208114. Sponsored by CALS Evaluation and Integration Office, Washington, DC.

Keywords: *Computer aided design, *Computer aided manufacturing, *Standards, Data processing, Product development, Data management, Specifications, *STEP(Standard for the Exchange of Product Model Data), *Standard for the Exchange of Product Model Data, NII(National Information Infrastructure), SGML(Standard Generalized Markup Language), US NIST.

Industry has a need to share data among functions within its own enterprise and among its suppliers and partners. A standard specification for manufacturing data is needed that can support the entire product development and support life-cycle. The emerging international standard called the Standard for the Exchange of Product Model Data (STEP) is addressing this need by specifying what data is needed within industrial application areas, how it should be represented, and how it should be exchanged. The Application Protocol Development Environment (APDE) is a software project at the National Institute of Standards and Technology (NIST) designed to facilitate the development, acceptance, and use of STEP. The paper discusses the status of STEP, barriers to the development, acceptance, and use of STEP, and the benefits of using STEP in industry. Aspects of the APDE project are also discussed including current status, lans for a STEP information base, use of the Standard Generalized Markup Language (SGML) for facilitating the information base, barriers to the project, and expected benefits for STEP.

02,777
PB95-137790 PC A02/MF A01
National Inst. of Standards and Technology (MEL), Gaithersburg, MD. Factory Automation Systems Div.
STEP On-Line Information Service (SOLIS). The IGES/PDES Organization.
G. R. Rinaudot. Oct 94, 9p, NISTIR-5511.
See also PB91-159756.

Keywords: *Information services, *On-line systems, Standards, Product development, Computer aided design, Computer aided manufacturing, *STEP(Standard for the Exchange of Product Model Data), *Standard for the Exchange of Product Model Data, US NIST, SOLIS(STEP On-Line Information Service), IGES(Initial Graphics Exchange Specification), PDES(Product Data Exchange using STEP).

This document contains an overview and describes the objectives of the STEP (STandard for the Exchange of Product model Data) On-Line Information Service (SOLIS). This report is also intended to provide a general explanation of this service and its capabilities. The service is provided and maintained by the National Institute of Standards and Technology (NIST), Manufacturing Engineering Laboratory (MEL), IGES/PDES (Initial Graphics Exchange Specification/Product Data Exchange using STEP) Office in the Factory Automation Systems Division. SOLIS enhances the ability to gain consensus on STEP by expanding the availability of the draft standards, supporting documents, and software used by the community of experts who are contributing to this standard.

02,778
PB95-143103 PC A03/MF A01
National Inst. of Standards and Technology (MEL), Gaithersburg, MD. Factory Automation Systems Div.
SGML Environment for STEP.
L. Phillips, and J. Lubell. 22 Jun 94, 36p, NISTIR-5515.
See also PB94-114501 and PB94-150919. Sponsored by Assistant Secretary of Defense (Production and Logistics), Washington, DC. Computer-aided Acquisition and Logistic Support Program.

Keywords: *Documents, *Standards, Parsers, Text processing, *STEP(Standard for the Exchange of

Product Model Data), *Standard for the Exchange of Product Model Data, *SGML(Standard Generalized Markup Language), *Standard Generalized Markup Language, US NIST, APDE(Application Protocol Development), DTD(Document Type Definition).

The paper provides an in-depth discussion of the components of a proposed Standard Generalized Markup Language (SGML) environment for the Standard for the Exchange of Product Model Data (STEP). Section one introduces the SGML environment for STEP and provides a definition of SGML and its applicability to STEP. Section two provides a background discussion of the Application Protocol Development Environmental (APDE) project and its relationship to the SGML environment for STEP. Section three provides additional basic concepts in SGML. Section four provides further discussion on the benefits of using SGML and the rationale for choosing SGML for STEP. Section five provides a detailed overview of the components of an SGML environment for STEP. Finally, section six concludes with an overview of the lessons learned, current status, and the near-term and long-term future plans for the STEP SGML environment.

02,779
PB95-154688 PC A03/MF A01
National Inst. of Standards and Technology (MEL), Gaithersburg, MD. Factory Automation Systems Div.
Initial NIST Testing Policy for STEP: Beta Testing Program for AP 203 Implementations. National PDES Testbed Report Series.
M. J. Mitchell. 3 Nov 94, 25p, NISTIR-5535.
Also available from Supt. of Docs. Sponsored by CALS Evaluation and Integration Office, Washington, DC.

Keywords: *Tests, Policies, Protocols, Programs, Laboratories, Methodology, Standards, Computer aided design, Product development, *STEP(STandard for the Exchange of Product model data), *STandard for the Exchange of Product model data, *US NIST, Conformance testing, ITI(Industrial Technology Institute), Application protocols.

The standard for Product Data Representation and Exchange, ISO 10303, defines a neutral, computer-interpretable representation for describing product data in a manner that is independent from any particular system. This standard is more commonly known as STEP, STandard for the Exchange of Product model data. This document describes the policy and procedures for a 'beta' conformance testing program for one of the application protocols: Configuration Controlled 3D Design for Mechanical Parts and Assemblies (ISO 10303-203). However, the concepts described are applicable to ISO 10303 in general, and the characteristics of the longer term testing program are described. This document describes the policy and procedures used by the National Institute of Standards and Technology (NIST) and the Industrial Technology Institute (ITI) for the Beta STEP Conformance Testing Program. The objective of this beta program is to develop an acceptable degree of confidence in the test methods and procedures.

02,780
PB95-171427 PC A03/MF A01
National Inst. of Standards and Technology (CSL), Gaithersburg, MD. Information Systems Engineering Div.
Initial Graphics Exchange Specification (IGES): Procedures for the NIST IGES Validation Test Service.
J. A. Schneider, and L. S. Rosenthal. Dec 94, 36p, NISTIR-5541.

Keywords: *Tests, Computer aided design, Computer aided manufacturing, Data transfer(Computers), Preprocessors, Federal information processing standards, *CALS, *IGES(Initial Graphics Exchange Specification), *Initial Graphics Exchange Specification, Continuous Acquisition and Life-Cycle Support, Computer-aided Acquisition and Logistics Support, US NIST, Postprocessors, Conformance testing.

This document provides general procedures for the National Institute of Standards and Technology's (NIST) Initial Graphics Exchange Specification (IGES) Validation Test Service. The NIST IGES Validation Test Service provides a way of determining the degree to which an implementation conforms to the FIPS PUB 177, which adopts the ANSI standard (ASME/ANSI Y14.26M-1989) in its entirety. The NIST IGES Validation Test Service also provides a way of determining the degree to which an implementation confirms to the Continuous Acquisition and Life-Cycle Support (CALS) specification, MIL-D-28000, Class II subset. The goal of the NIST Validation Test Service is to maximize the probability of successful data exchange between dissimilar CAD/CAM systems. The document is divided into two testing programs: preprocessor and postprocessor testing. The procedures are organized into four sections: an introduction, general procedures, and specific procedures for the two testing programs.

02,781
PB95-180543 Not available NTIS
National Inst. of Standards and Technology (MEL), Gaithersburg, MD. Factory Automation Systems Div.
Concepts of the NIST EXPRESS Server.
Final rept.
D. Libes. 1994, 6p.
Pub. in Proceedings of International Workshop on Services in Distributed and Networked Environments (SDNE) (1st), Prague, Czech Republic, June 27-28, 1994, 6p.

Keywords: *Remote consoles, Computer aided design, Computer aided manufacturing, Compilers, Electronic mail, File structures, Software tools, Reprints, *EXPRESS, *US NIST, PDES(Product Data Exchange using STEP), STEP(Standard for the Exchange of Product Model Data).

The National Institute of Standards and Technology (NIST) has built numerous software toolkits and applications for manipulating STEP and EXPRESS data. The NIST EXPRESS Server is a computational facility at NIST, which provides the ability to run these toolkit-based applications remotely without installing them locally. Users e-mail EXPRESS Schemas and other data files to the Server. The Server runs the requested applications on the files and returns any diagnostics or output, also by e-mail. Applications requiring interaction can either be returned via e-mail so that they can be run locally, or run remotely by telnet or rlogin across the Internet.

02,782
PB95-242285 PC A04/MF A01
National Inst. of Standards and Technology (EEEL), Gaithersburg, MD. Electricity Div.
Operating Procedures and Life Cycle Documentation for the Initial Graphics Exchange Specification.
G. F. Morea, E. Reid, and C. Parks. 22 Jun 95, 62p, NISTIR-5666.

Keywords: *Changes, *Editing, *Standards, Administrative procedures, Documentation, Record keeping, Standardization, Computer aided design, Data processing, Data transfer(Computers), Concurrent engineering, *IGES(Initial Graphics Exchange Specification), *Initial Graphics Exchange Specification.

The purpose of this document is to provide a record of the underlying rationale and the detailed procedures by which the Initial Graphics Exchange Specification (IGES) is changed, new versions are approved, and the document itself is edited, maintained, and published by the IGES Project of the IGES/PDES Organization (IPO). The document also defines the life cycle documentation supporting these activities and provides guidance for its use, including record keeping requirements, to provide evidence of compliance with these procedures. Procedures given in this document are intended to be supplementary to and consistent with the documented procedures of the General Assembly of the IPO for the IGES Project. In general, procedures in this document are at a more detailed, working level.

02,783
PB95-253563 PC A03/MF A01
National Inst. of Standards and Technology (MEL), Gaithersburg, MD. Manufacturing Systems Integration Div.
Product Models and Virtual Prototypes in Mechanical Engineering.
M. J. Pratt. May 95, 22p, NISTIR-5650.
Presented at the IFIP Working Group 5.10 Workshop on Virtual Prototyping, Providence, RI., September 21-23, 1994.

Keywords: *Product development, *Models, *Prototypes, *Mechanical engineering, Virtual reality, Computerized simulation, Computer graphics, Computer aided design, Computer aided manufacturing, Systems integration, Production engineering, Knowledge based systems, Feature extraction.

The paper gives an overview of some of the modeling and virtual prototyping techniques used in product realization, with emphasis on the mechanical engineering field. It is pointed out that virtual prototypes, in the commonly accepted sense of computer models permitting realistic graphical simulation, represent only one class amongst the many types of computer models used in design and planning for manufacture. Each such model is usually created for some comparatively narrow purpose, and one of the major problems faced by developers of product realization systems concerns the transmutation of one type of model into another. A related problem is that of interpretation by any model of information generated by interrogations of another model. These difficulties are compounded by the increasing presence in such models of semantic information concerning different aspects of the intended functionality or manufacturing requirements of the modelled artifact.

02,784
PB95-267860 PC A03/MF A01
National Inst. of Standards and Technology (MEL), Gaithersburg, MD. Factory Automation Systems Div.
Design Engineering Research at NIST.
K. W. Lyons, and P. F. Brown. May 94, 22p, NISTIR-5464.

Keywords: *Design, *US NIST, *Production engineering, Research management, Technology transfer, Research and development.

The National Institute of Standards and Technology (NIST) has established an Engineering Design Laboratory (EDL) to assist in determining the best practices and methods to design new products and processes. This paper includes a description of issues facing designers and outlines research activities that are currently being done, or are planned, at NIST.

02,785
PB96-141049 Not available NTIS
National Inst. of Standards and Technology (MEL), Gaithersburg, MD. Manufacturing Systems Integration Div.
Object-Oriented Tel/Tk Binding for Interpreted Control of the NIST EXPRESS Toolkit in the NIST STEP Application Protocol Development Environment.
Final rept.
D. Libes, and S. N. Clark. 1995, 14p.
Pub. in Proceedings of the EXPRESS User Group Workshop (EUG '95), Grenoble, France, October 21-22, 1995, p1-14.

Keywords: *Software tools, *Object-oriented programming, *Standards, Computer aided design, Computer aided manufacturing, Systems engineering, Protocols, Reprints, PDES(Product Data Exchange using STEP), National PDES Testbed, STEP(Standard for the Exchange of Product model data), APDE(Application Protocol Development Environment), TCL(Tool Command Language), TCL programming language, TK(Task knowledge).

The National Institute of Standards and Technology (NIST) has built numerous software toolkits and applications for manipulating STEP and EXPRESS data. These toolkits are traditionally used as compiled libraries which are linked to other complied modules. This paper describes a binding allowing the toolkit interfaces to be called from interpreted scripts. This significantly reduces the time required to construct and compile new applications. An X11 extension allows the construction of graphic elements, providing easy creation and integration of existing applications into X graphic user interfaces. We describe how the combination of bindings has been used to construct a STEP Application Protocol Development Environment.

02,786
PB96-154539 PC A03/MF A01
National Inst. of Standards and Technology (MEL), Gaithersburg, MD. Manufacturing Systems Integration Div.
Guidelines for the Development of Mapping Tables.
A. B. Feeney, and D. Craig. 16 Nov 95, 24p, NISTIR-5716.
Prepared in cooperation with Product Data Integration Technology, Long Beach, CA.

Keywords: *Computer aided language, *Computer aided manufacturing, *Standards, Data processing, Product development, Data management, *STEP(Standard for the Exchange of Product Model Data), APDE(Application Protocol Development Environment).

The mapping table is a pivotal component of an application protocol (AP). The mapping table documents the traceability of the application information requirements between the specification of these requirements in clause 4 of the AP and the application interpreted model (AIM) that documents how standardized constructs are applied to satisfy these requirements in clause 5. The document is intended to provide guidance to application protocol development teams on the creation of mapping tables. Additionally, the document may aid reviewers and implementors of APs in understanding mapping tables. The document describes the methodology for producing a complete mapping table, focusing on the development of the mapping table content. Specifics on style, format, boiler plate text, and other presentation issues are provided in the Supplementary directives for the drafting and presentation of ISO 10303 (Supplementary directives). Additional guidance on other areas of AP development is found in the Guidelines for development and approval of STEP application protocols.

02,787
PB96-154976 PC A03/MF A01
National Inst. of Standards and Technology (CSL), Gaithersburg, MD.
STandard for the Exchange of Product Model Data (STEP): Procedures for NIST STEP Validation.
L. S. Rosenthal. Nov 95, 19p, NISTIR-5771.
See also PB95-154688.

Keywords: *Tests, Policies, Protocols, Programs, Laboratories, Standards, Computer aided design, Product development, *STEP(Standard for the Exchange of Product Model Data), Standard for the Exchange of Product Model Data, Conformance testing, Application protocols, ITI(Industrial Technology Institute), ISO 10303.

The standard for Product Data Representation and Exchange, ISO 10303, defines a neutral, computer-interpretable representation for describing product data in a manner that is independent from any particular system. This standard is more commonly known as STEP, Standard for the Exchange of Product model data and it is designed to support a wide range of design, engineering, and product support applications. STEP was adopted verbatim as an American National Standard (ANS) titled Product Data Exchange using Step, ANSI USPRO 200. Support for specific applications is provided through an Application Protocol. This document provides general procedures for the National Institute of Standards and Technology's (NIST) STEP FIPS Validation Service. The Validation Service provides a way of determining the degree to which an implementation conforms to the proposed STEP FIPS. The goal of the Validation Service is to maximize the probability of successful interchange among systems which implement the same STEP applications protocol.

02,788
PB96-160965 Not available NTIS
National Inst. of Standards and Technology (CSL), Gaithersburg, MD. Information Systems Engineering Div.
Template-Driven Systems Development with IDEF: Enterprise Standards for Reuse.
Final rept.
M. H. Law. 1992, 10p.
Pub. in IDEF Users Group Business Process Design: A Strategy for Corporate Information Management, Washington, DC., October 19-22, 1992, p1-10.

Keywords: *Software reuse, *Systems approach, *Integrated systems, Computer-aided design, Computer-aided manufacturing, Software engineering, Software reliability, Object-oriented programming, Parameterization, Standards, Reprints, IDEF(Integrated Definition), CASE(Counter-Aided Software Engineering), System development, Domain analysis, Life cycles(Software).

This paper addresses the use of reusable template-driven architectures to improve system and software development methods with an extended IDEF. Extended IDEF is proposed as a family of modeling techniques that has been integrated with the proposed Federal Information Processing Standards (FIPS) for IDEFO and IDEFIX, and extended to offer more support for the system and software development lifecycle. Integrated through a metamodel, Extended IDEF will present a number of distinct views to users working in different aspects of the lifecycle, such as activity modeling, data modeling, object modeling, state/event modeling, etc. Integration through the metamodel is intended to maintain the critical relationships among the IDEF techniques; extension through the lifecycle is intended to expand the utility of IDEF.

02,789
PB96-165402 PC A11/MF A03
National Inst. of Standards and Technology (BFRL), Gaithersburg, MD. Building Environment Div.
Group 1 for the Plant Spatial Configuration STEP Application Protocol.
S. W. Kline, M. E. Palmer, W. Burkett, and J. Skeels. Jun 95, 202p, NISTIR-5675.
Prepared in cooperation with Product Data Integration Technology, Long Beach, CA.

Keywords: *Computer aided manufacturing, *Industrial plants, *Computer aided design, *Standards, Standard tools, Pipes tubes, Models, *STEP(Standard for the Exchange of Product Model Data), ISO 1303, Standard for the the Exchange of Product Model Data, Application protocols, Spatial distribution.

The document specifies the scope and information requirements of the STEP application protocol (AP) for the exchange of spatial configuration information of plant systems with a central emphasis on piping systems. It specifies the information required to construct a piping system, including the shape, material, and arrangements of the system components. It also specifies requirements for the physical aspects of other plant systems (e.g., structure) needed to design and layout the piping system. The document includes the application activity model (AAM) and application reference model (ARM) for this AP. The document was submitted to ISO TC184/SC4 and to international experts for review and comment on the scope and requirements of the AP. Additional clauses and annexes and refinements will be added to the AP after the completion of the ISO Committee Draft for Comment review.

02,790
PB96-183231 PC A03/MF A01
National Inst. of Standards and Technology (MEL), Gaithersburg, MD. Manufacturing Systems Integration Div.
Aspects of a Product Model Supporting Apparel Virtual Enterprises.
P. O. Denno. 16 Apr 96, 15p, NISTIR-5821.
See also PB96-128194.

Keywords: *Clothing industry, *Computer aided design, Computer aided manufacturing, Data transfer, Patterns, Tests, Models, Data structures, Data exchange, Standard, Product data, Textile industry, STEP(Standard for the Exchange of Product Model Data).

Emerging computer technology, including an infrastructure for virtual enterprises and more capable apparel product development software, is providing an opportunity to reinvent how apparel is produced. The development of an information-rich and unambiguous garment product model would help realize this opportunity. This product model would improve the effectiveness of product development software and enhance the industry's ability to distribute work in virtual enterprises. This paper suggests what such a product model should contain, how it can be developed and how it would be utilized throughout the product development life cycle to enable apparel virtual enterprises.

02,791
PB96-202320 PC A03/MF A01
National Inst. of Standards and Technology (MEL), Gaithersburg, MD. Manufacturing Systems Integration Div.
Application Protocol Information Base World Wide Web Gateway.
Technical rept.
J. Lubell. 31 Jul 96, 27p, NISTIR-5868.

Keywords: *Documents, *Standards, Parsers, Text processing, Information retrieval, *STEP(Standard for the Exchange of Product Model Data), Standard for the Exchange of Product Model Data, SGML(Standard Generalized Markup Language), Standard Generalized Markup Language, APID(Application Protocol Information Base), Application Protocol Information Base, Internet, World Wide Web, HTML, Browsers.

The Application Protocol Information Base (APIB) is an on-line repository of documents for the Standard for the Exchange of Product Model Data (STEP, officially ISO 10303-Product Data Representation and Exchange). STEP Application Protocols are standards that are intended to be implemented in software systems, and Integrated Resources are used by them as building blocks. Application Protocols and Integrated Resources are represented in the Standard Generalized Markup Language (SGML) in the APIB in order to facilitate efficient information search and retrieval. This paper describes a World Wide Web gateway to the APIB, implemented using the Common Gateway Interface(CGI) standard. The APIB gateway allows STEP developers to efficiently search for ISO 10303 standards and supporting information. The only client software required to use the APIB gateway is a third party web browser.

02,792
PB97-111561 Not available NTIS
National Inst. of Standards and Technology (MEL), Gaithersburg, MD. Manufacturing Systems Integration Div.
Representing Designs with Logic Formulations of Spatial Relations.
Final rept.
S. C. Chase. 1996, 9p.
Pub. in International Conference on Artificial Intelligence in Design (AID) (4th): Workshop Notes, Visual Representation, Reasoning and Interaction in Design, Stanford University, CA., June 22-27, 1996, p1-9.

Keywords: *Logic programming, *Computer-aided design, *Representations, Computer graphics, Feature extraction, Pattern recognition, Shape, Geometry, Parameterization, Formalism, Computer models, Specifications, Reprints, *Spatial relations.

A new method of describing designs by combining the paradigms of shape algebras and predicate logic representations is presented. Representing shapes and spatial relations in first order predicate logic provides a natural, intuitive method of developing complete computer systems for reasoning about designs. Shape algebraic representations provide several advantages over more traditional geometric representations. The method described involves the definition of a large set of high level design relations from a small set of simple structures and spatial relations.

02,793
PB97-111579 Not available NTIS
National Inst. of Standards and Technology (MEL), Gaithersburg, MD. Manufacturing Systems Integration Div.
Using Logic to Specify Shapes and Spatial Relations in Design Grammars.
Final rept.
S. C. Chase. 1996, 4p.
Pub. in International Conference on Artificial Intelligence in Design (AID) (4th): Workshop Notes, Grammatical Design, Stanford University, CA., June 22-27, 1996, p1-4.

Keywords: *Computer-aided design, *Pattern recognition, *Shape, *Geometry, Computer graphics, Feature extraction, Representations, Parameterization, Logic programming, Formalism, Computer models, Specifications, Reprints, Spatial relations.

The use of predicate logic formulations of shape and spatial relations provides a natural, intuitive way to extend shape representations of the shape grammar formalism to provide generalized, parametric grammars.

02,794
PB97-112320 Not available NTIS
National Inst. of Standards and Technology (MEL), Gaithersburg, MD. Precision Engineering Div.
Combining Interactive Exploration and Optimization for Assembly Design.
Final rept.
G. J. Kim, and S. Szykman. 1996, 12p.
Pub. in American Society of Mechanical Engineers Design Engineering Technical Conference and Computers in Engineering Conference, Irvine, CA., August 18-22, 1996, p1-12.

Keywords: *Computer aided design, *Tools, Optimization, Standards, Quality assurance, Reprints.

The paper presents an integrated framework for assembly design. The framework allows the designer to represent knowledge about the design process and constraints, as well as information about the artifact being designed, design history and rationale. Because the complexity of assembly design leads to extremely large design spaces, adequately supporting design space exploration is a key issue that must be addressed. This is achieved in part by allowing the designer to use both top-down and bottom-up ap-

proaches to assembly design. Exploration of the design space is further enabled by incorporating a simulated annealing-based optimization tool that allows the designer to rapidly complete partial designs, refine complete designs, and generate multiple design alternatives.

02,795
PB97-113096 Not available NTIS
National Inst. of Standards and Technology (MEL), Gaithersburg, MD. Manufacturing Systems Integration Div.
Improving the Design Process by Predicting Downstream Values of Design Attributes.
Final rept.
S. Szykman. 1996, 9p.
Pub. in Proceedings of the American Society of Mechanical Engineers Design Engineering Technical Conference and Computers in Engineering Conference, Irvine, CA., August 18-22, 1996, p1-9.

Keywords: *Computer-aided design, *Product development, Design analysis, Design criteria, Feature extraction, Attributes, Specifications, Automation, Computer tools, Computer models, Reprints, *Design process.

The paper presents a computational approach to developing design space models that are utilized to improve the design process by predicting values of downstream design attributes based on information available at early stages, such as preliminary design specifications. The predictive models are similar in function, though not in form, to the internal (mental) models created by experienced designers; however, the advantages of these models are that it may be possible to construct them in the absence of a designer's internal models, and that they can be passed on to and used by less experienced designers. Once created, the computational models aid designers in exploration of design alternatives and to reduce design costs and product development time.

02,796
PB97-114268 PC A03/MF A01
National Inst. of Standards and Technology (MEL), Gaithersburg, MD. Manufacturing Systems Integration Div.
Interoperability Requirements for CAD Data Transfer in the AutoSTEP Project.
S. P. Frechette. Mar 96, 28p, NISTIR-5844.

Keywords: *Computer aided design, *Computer aided manufacturing, *Automotive engineering, Production planning, Questionnaires, Standards, Networks, Development, Communications, Packaging, Information exchange, Motor vehicles, Interoperability, *STEP(Standard for the Exchange of Product Model Data), *Standard for the Exchange of Product Model Data, ISO10303.

This document describes user requirements for implementing STEP in a production environment for packaging applications used in the auto industry. The main purpose of the document is to report the results of a requirements survey of AutoSTEP project participants concerning the implementation of STEP in production practice.

02,797
PB97-116073 PC A99/MF A06
National Inst. of Standards and Technology (BFRL), Gaithersburg, MD.
Group 1 for the Process Engineering Data STEP Application Protocol.
S. W. Kline, M. E. Palmer, N. Appel, and M. Gilbert. Oct 96, 656p, NISTIR-5909.
Prepared in cooperation with Product Data Integration Technology, Long Beach, CA.

Keywords: *Computer aided design, *Computer aided manufacturing, Product development, Automation, Standards, Production planning, Specifications, Process engineering, Systems engineering, Protocols, *PDES(Product Data Exchange using STEP), Concurrent engineering, STEP(Standard for the Exchange of Product Model Data), ISO(International Standards Organization), ISO10303.

The document specifies the scope and information requirements of the STEP application protocol (AP) for the exchange of process engineering data with a central emphasis on process design and major equipment. It specifies the information required to exchange process engineering and conceptual design information for process plants. The information forms the conceptual basis for the specification, selection, and operation of process plant equipment over the plant life cycle. The AP supports continuous and batch processes, process simulations, stream data, unit operations, conceptual design requirements for major process equipment, and conceptual process control strategies. The document includes the application activity model (AAM) and application reference model (ARM) for this AP. The document was submitted to ISO TC184/SC4 and to international experts for review and comment on the scope and requirements of the AP. The document follows the format and clause numbering scheme prescribed for this type of International organization for Standardization (ISO) standard. Additional clauses and annexes and refinements will be added to the Ap after the completion of the ISO Group 1 review.

02,798
PB97-118764 Not available NTIS
National Inst. of Standards and Technology (MEL), Gaithersburg, MD. Manufacturing Systems Integration Div.
Capabilities for Product Data Exchange.
Final rept.
M. J. Mitchell. 1996, 7p.
Pub. in Proceedings of an International Multidisciplinary Conference Intelligent Systems: A Semiotic Perspective, Capabilities for Product Data Exchange, 7p 1996.

Keywords: *Computer-aided design, *Computer-aided manufacturing, Reprints, Product development, Standards, Specifications, Data management, Communication, Integrated systems, ISO, *STEP(Standard for the Exchange of Product Model Data), *Standard for the Exchange of Product Model Data, *PDES(Product Data Exchange Specification), *Product Data Exchange Specifications.

The paper describes the need for standardized representations of product information which are suitable for electronic communication between engineering and manufacturing functions. It then describes how a single international standard, ISO 10303 - Product data representation and exchange, has been designed to meet this industrial need. The benefits of STEP and the scope of the standard are presented. A high level technical description is given; this includes a description of the segments of the standard that can be used by readers to determine if the standard satisfies any of their company's needs for product data exchange. Key players in the development and implementation of STEP along with sources of additional information are provided.

02,799
PB97-122410 Not available NTIS
National Inst. of Standards and Technology (MEL), Gaithersburg, MD. Manufacturing Systems Integration Div.
SC4 Short Names Registry.
Final rept.
J. Lubell. 1996, 15p.
See also PB95-242293.
Pub. in Express User Group International Conference, Toronto, Canada, October 5-6, 1996, p1-15.

Keywords: *Registries, *Standardization, *Software tools, Computer-aided manufacturing, Computer-aided design, Digital systems, Procedures, Standards, Reprints, Data types, Product Data Exchange, SQL(Structured Query Language), STEP(Standard for the Exchange of Product Model Data), EXPRESS programming language.

The paper describes a software environment recently implemented for maintaining a registry of unique short names for each of the entity data types within each of the EXPRESS schemas in the ISO TC184/SC4 standards. The new environment replaces an inefficient application and has already provided time savings for both the registry's administrator and editors of SC4 standards. It is also improving the quality of SC4 standards.

Computer Aided Manufacturing (CAM)

02,800
FIPSPUB183 PC E07
National Inst. of Standards and Technology (CSL), Gaithersburg, MD.
Integration Definition for Function Modeling (IDEF0); Category: Software Standard; Subcategory: Modeling Techniques.
21 Dec 93, 94p.
Also available from Supt. of Docs. See also AD-B062 465 and AD-A181 952.
Three ring vinyl binder also available; North American Continent price $7.00; all others write for quote.

Keywords: *Computer aided manufacturing, *Management information systems, Scheduling, Shops(Work areas), Integrated systems, Computer applications, Graphical languages, Functions, *IDEF0(Integration Definition for Function Modeling), Software standards, Modeling techniques, Business process improvement, Activity modeling.

The standard is based on the Air Force Wright Aeronautical Laboratories Integrated Computer-Aided Manufacturing (ICAM) Architecture, Part II, Volume IV -- Function Modeling Manual (IDEF0), June 1981 (AD-B062 457). The standard describes the IDEF0 modeling language (semantics and syntax), and associated rules and techniques, for developing structured graphical representations of a system or enterprise. Use of this standard permits the construction of models comprising system functions (activities, actions, processes, operations), functional relationships, and data (information or objects) that support systems integration. The standard is the reference authority for use by system or enterprise modelers required to utilize the IDEF0 modeling technique, by implementors in developing tools for implementing the technique, and by other computer professionals in understanding the precise syntactic and semantic rules of the standard.

02,801
PB94-100278 PC A07/MF A02
Rensselaer Polytechnic Inst., Troy, NY.
Opportunities for Innovation: Advanced Manufacturing Technology.
C. F. Rancourt, and G. R. Simons. Jul 92, 136p, NIST/GCR-92/610-1.
Grant NANB0D1071
Sponsored by National Inst. of Standards and Technology, Gaithersburg, MD.

Keywords: *Manufacturing, *Technology assessment, *Technology utilization, Computer aided manufacturing, Computer aided design, Competition, Numerical control, Machining, Automation, Assembling, Total quality management, Statistical analysis, Data acquisition, Data processing, Integrated systems, Systems engineering, Process planning, EDI(Electronic Data Interchange), CNC(Computer Numerical Control).

Contents:
- The Fit and Interaction of Competitiveness and Manufacturing Technology;
- Computer-Aided Design;
- Computer-Aided Process Planning and Group Technology;
- Electronic Data Interchange;
- CNC Machining;
- Automated Assembly;
- Statistical Quality Methods;
- Quality Measurement Techniques:
- Data Acquisition and Processing;
- Systems Integration.

02,802
PB94-142460 PC A03/MF A01
National Inst. of Standards and Technology (MEL), Gaithersburg, MD. Robot Systems Div.
Enhanced Machine Controller Architecture Overview.
F. M. Proctor, and J. Michaloski. Dec 93, 26p, NISTIR-5331.

Keywords: *Computer aided manufacturing, *Controllers, Numerical control, Machine tools, Systems engineering, Computer architecture, Workstations, EMC(Enhanced Machine Controller), RCS(Real-time Control System), National Institute of Standards and Technology.

The National Institute of Standards and Technology (NIST) Enhanced Machine Controller program has defined an architecture for controllers, with an emphasis on machine tools. The architecture defines a set of components and their interfaces. The objective is to reduce the cost of controller development, installation, maintenance, and integration by defining a framework for building controllers from commercial off-the-shelf components.

02,803
PB94-142502 PC A03/MF A01

National Inst. of Standards and Technology (CSL), Gaithersburg, MD. Systems and Software Technology Div.
Applying Virtual Environments to Manufacturing.
S. Ressler. Jan 94, 28p, NISTIR-5343.

Keywords: *Manufacturing, Computer graphics, Man computer interface, Technology assessment, Computer applications, Case studies, *Virtual environments, Synthetic environments, Virtual reality.

This document presents a high level overview on the use of Virtual Environments for manufacturing applications. A brief introduction of the many component technologies used to create 'virtual environments' gives the reader enough background for discussion. The terms virtual environment, virtual reality and synthetic environments all refer to the concepts of placing a human inside a synthetic or virtual environment and allowing interaction with the environment in a number of ways. In recent years applications of virtual environments are beginning to appear. In addition to the basics of the various technologies, information on where to go to get more information on these technologies is also included. A series of case studies illustrating the use of virtual environments for a variety of manufacturing applications is presented.

02,804
PB94-142791 PC A12/MF A03
National Inst. of Standards and Technology, Gaithersburg, MD.
Feasibility Study: Reference Architecture for Machine Control Systems Integration.
T. R. Kramer, and M. K. Senehi. Nov 93, 255p, NISTIR-5297.
See also PB91-240796 and PB92-112242. Prepared in cooperation with Catholic Univ. of America, Washington, DC.

Keywords: *Computer aided manufacturing, *Control systems, *Integrated systems, Systems engineering, Industrial plants, Computer architecture, Hierarchies, Models, Feasibility studies, National Institute of Standards and Technology, RCS(Real-time Control System), MSI(Manufacturing System Integration).

The Manufacturing Engineering Laboratory (MEL) at the National Institute of Standards and Technology (NIST), has been conducting research on control of mechanical systems for more than sixteen years. The Robot Systems Division has developed an architecture, the Real-time Control System (RCS) which focuses on providing real-time control of equipment. The Factory Automated Systems Division has developed the Manufacturing System Integration (MSI) architecture which focuses on providing information integration with factory production systems. While the architectures share some common features such as the use of hierarchical control and task decomposition, there are also differences. This report documents the work performed in assessing the feasibility of combining the RCS and MSI architectures into a single reference architecture. The report is written primarily for the team of researchers charged with developing the joint architecture. It includes a literature survey, a framework for developing the joint architecture, a detailed set of issues about architectures and control architectures, and a preliminary sketch of the joint architecture.

02,805
PB94-160819 PC A03/MF A01
National Inst. of Standards and Technology (MEL), Gaithersburg, MD. Factory Automation Systems Div.
Technical Program of the Factory Automation Systems Division 1993.
H. M. Bloom, and L. W. Masters. Jul 93, 49p, NISTIR-5225.
See also report for 1992, PB92-205392.

Keywords: *Automation, *Industrial plants, *Data base management systems, *Standards, Interfaces, Research and development, Computer aided manufacturing, Industries, National Institute of Standards and Technology, Concurrent engineering, STEP(Standard for the Exchange of Product Model Data), PDES(Product Data Exchange using STEP).

The report describes the 1993 technical program of the Factory Automation Systems Division (FASD), one of five technical divisions in the Manufacturing Engineering Laboratory (MEL), within the National Institute of Standards and Technology (NIST). MEL supports the U.S. mechanical manufacturing industry through research and measurement services that are oriented toward a modern automated environment. The mission of FASD is to provide a focus for national research and standards efforts related to information systems for manufacturing. In carrying out its mission, the Division contributes to the strength of manufacturing in the United States and to the ability of the United States to remain competitive in world markets. The Division provides leadership in the development of national and international standards relating to information technology and manufacturing systems to meet U.S. industry needs for the twenty-first century. The work is organized around five key technologies: Enterprise Integration, Product Data Exchange, FCIM Processes, Communications and Networking, and Database and Database Management. Typical outputs for the Division include: draft specifications for future standards, journal papers describing research results, prototype software systems that demonstrate proof-of-concept, test methodologies for supporting the implementation of standards and testbeds for use by NIST, industry, and academia.

02,806
PB94-161924 PC A03/MF A01
National Inst. of Standards and Technology (MEL), Gaithersburg, MD. Factory Automation Systems Div.
Bibliography on Apparel Sizing and Related Issues.
Y. T. Lee. Feb 94, 25p, NISTIR-5365.
Contract DLA-A708
See also PB93-158665. Sponsored by Defense Logistics Agency, Alexandria, VA. Mfg. Engineering Branch.

Keywords: *Clothing, *Anthropometry, *Size determination, *Bibliographies, Measurement, Clothing industry, Standards, APDES(Apparel Product Data Exchange Specification).

Anthropometric data and sizing systems is an important component of apparel quality. Apparel can not be top quality unless it fits satisfactorily the potential wearers. Much research has been conducted on this topic area. Some of these research results are documented but scattered. The purpose of the report is to collect these documentation/references for the quick use of apparel researchers who are studying sizing and its related issues. The report presents an annotated bibliography for apparel sizing and related issues. The report lists full bibliographic reference data and a brief abstract or summary for each technical paper or book. The literature collection for the bibliography includes documents from books, journals, reports, and national and international standards.

02,807
PB94-162831 PC A04/MF A01
National Inst. of Standards and Technology, Gaithersburg, MD. Automated Mfg. Research Facility.
U.S. Navy Coordinate Measuring Machines: A Study of Needs.
D. C. Stieren, R. C. Veale, H. H. Harary, and S. C. Feng. Dec 93, 55p, NISTIR-5379.
Contract N00014-92-F-0082
Sponsored by Naval Research Lab., Washington, DC. Navy Manufacturing Technology Program.

Keywords: *Metrology, *Computer aided manufacturing, *Dimensional measurement, *Weapon systems, Inspection, Navy, Measuring instruments, Quality assurance, Surveys, Production engineering, *Coordinate Measuring Machines, Integrated manufacturing.

This report presents the results of a one year study of Coordinate Measuring Machine (CMM) technology at US Navy manufacturing facilities, both in-house and contractor. The study was sponsored by the Navy Manufacturing Technology (ManTech) program through the NIST Automated Manufacturing Research Facility (AMRF) and was conducted by technical staff members of the NIST Manufacturing Engineering Laboratory (MEL). The results of the study are an analysis of the state-of-the-practice in the Navy regarding CMM utilization specifically with respect to weapon system manufacture. The results of the study are also an analysis of the Navy's needs in CMM technologies.

02,808
PB94-163490 PC A09/MF A02
National Inst. of Standards and Technology (MEL), Gaithersburg, MD. Robot Systems Div.
NIST Support to the Next Generation Controller Program: 1991 Final Technical Report.
J. S. Albus, R. Quintero, F. Proctor, N. Tarnoff, T. Kramer, J. Michaloski, and N. Dagalakis. Jul 92, 188p, NISTIR-4888.

Keywords: *Process control, *Computer aided manufacturing, *Controllers, Technology assessment, Air force, Control systems, Real time systems, Deburring, Chamfering, Data structures, Knowledge bases(Artificial intelligence), Robots, Software engineering, Automation, Machine tools, *National Institute of Standards and Technology, PDES(Product Data Exchange using STEP), STEP(Standard for the Exchange of Product Model Data).

This report covers work performed by the National Institute of Standards and Technology (NIST) Robot Systems Division between October 1, 1990 and December 31, 1991 in continuation of work previously undertaken by NIST during FY90 for the U.S. Air Force Next Generation Controller Program (NGC).

02,809
PB94-164183 PC A04/MF A01
National Inst. of Standards and Technology (MSEL), Gaithersburg, MD.
Intelligent Processing of Materials, Technical Activities 1993 (NAS-NRC Assessment Panel, April 21-22, 1994).
1994, 74p, NISTIR-5312.
See also report for 1992, PB94-112430.

Keywords: *Materials, *Process control, *Artificial intelligence, Metals, Alloys, Ceramics, Polymers, Monitoring, Sensors, Nondestructive tests, Arc welding, Aerospace environment, Eddy current tests, Metal sheets, Research projects.

The 1993 report of the Office of Intelligent Processing of Materials continued to focus on cooperative programs with industry and includes projects on metals and alloys, ceramics, polymers and polymer blends. The report also summarizes research on sensors for potential applications to process monitoring.

02,810
PB94-172681 Not available NTIS
National Inst. of Standards and Technology (NEL), Gaithersburg, MD. Robot Systems Div.
AMRF Composite Fabrication Workstation.
Final rept.
R. J. Norcross, W. R. Bunch, and R. D. Kilmer. 1990, 6p.
Pub. in Proceedings of International Symposium on Robotics and Manufacturing (3rd): Research, Education, and Applications, British Columbia, Canada, July 18-20, 1990, p655-660.

Keywords: *Thermosetting plastics, *Workstations, *Robots, *Computer aided manufacturing, *Fiber reinforced composites, Manipulators, Robotics, Composite materials, Real time, Matrix materials, Control systems, Reprints.

The Robot Systems Division of the National Institute of Standards and Technology (NIST) has initiated development of an advanced manufacturing workstation for the fabrication of composite parts. The focus of this project will be the application of sensor-based hierarchically controlled robot systems to automated fiber placement of thermoplastic composite materials. In such a system, continuous fiber reinforced thermoplastic polymer is fed from a spool and applied onto a mandrel or part form. The orientation of the fiber is based on the part's geometry and structural design. As the composite material is applied, it is heated to melt the polymer matrix, and then consolidates in place as it cools. The intention of this project is to demonstrate that the use of fiber placement via two cooperating robot manipulators and in-situ consolidation, can provide the capability to efficiently produce complex shaped composite parts.

02,811
PB94-172780 Not available NTIS
National Inst. of Standards and Technology (IMSE), Gaithersburg, MD. Office of Nondestructive Evaluation.
Intelligent Processing of Materials.
Final rept.
H. T. Yolken. 1992, 10p.
Pub. in Flight-Vehicle Materials, Structures, and Dynamics Technologies - Assessment and Future Directions, Chapter 15, p375-384 1992. See also PB94-112430.

Keywords: *Process control, *Computer aided manufacturing, *Nondestructive testing, *Composite materials, Microstructure, Artificial intelligence, Sensors, Signal processing, Control systems, Reprints, *Intelligent processing.

Advanced materials are capable of providing outstanding or specialized properties, or combinations of properties, that cannot be obtained in conventional materials. These unique properties are the result of the sophisticated microstructure that is designed and built into the materials. However, advanced materials generally require unusual and difficult to control processing operations in order to achieve their unique microstructures. A promising direction towards overcoming these difficulties involves intelligent processing of materials. This approach controls the microstructure in contrast to conventional materials processing where process variables such as temperature and pressure are automatically controlled to preselected values. In an intelligent processing system advanced nondestructive evaluation (NDE) sensors are utilized to characterize the evolution microstructure of the material in real time. Moreover, these data and data from conventional process variable sensors are transmitted to a computerized decision-making system. This computer system transmits control signals based on the sensor data, a process model, and process data.

02,812
PB94-187655 PC A03/MF A01
National Inst. of Standards and Technology (MEL), Gaithersburg, MD. Factory Automation Systems Div.
State-of-the-Art Survey of Methodologies for Representing Manufacturing Process Capabilities.
M. E. A. Algeo. Mar 94, 30p, NISTIR-5391.

Keywords: *Computer aided manufacturing, *Processes, Data management, Industrial plants, Resources, Standards, Mathematical models, Data bases, State of the art, Methodologies.

Representations of manufacturing process capabilities are essential for the integration of manufacturing applications as well as the dynamic management of factory data. The survey presents methodologies for describing and using such information within the domain of discrete parts manufacturing. Current practices in industry are identified. Standards and research efforts related to representing manufacturing process capabilities also are described. Finally, a course of action for advancing current practices is presented.

02,813
PB94-187739 PC A03/MF A01
National Inst. of Standards and Technology (MEL), Gaithersburg, MD. Factory Automation Systems Div.
Body Dimensions for Apparel.
Y. T. T. Lee. Apr 94, 30p, NISTIR-5411.
See also PB93-158665. Sponsored by Defense Logistics Agency, Alexandria, VA.

Keywords: *Clothing industry, *Anthropometry, *Body measurement(Biology), Body size(Biology), Computer aided manufacturing, Patterns, Pattern making, Fitting, Sizing, Size determination, APDES(Apparel Product Data Exchange Standard).

This report represents a compilation of body dimensions that are used in the manufacturing and fitting of apparel. It is the result of a comparison of five body measurements reports, including documentations of national and international apparel sizing standards. The information in this report will provide the basis for the development of the information model of made-to-measure pattern making. It will also contribute to the conducting of future body measurements surveys and the development of new or improved sizing standards for apparel.

02,814
PB94-187788 PC A03/MF A01
Catholic Univ. of America, Washington, DC. Dept. of Mechanical Engineering.
NIST RS274/NGC Interpreter Version 1.
T. R. Kramer, F. M. Proctor, and J. L. Michaloski. Apr 94, 32p, NISTIR-5416.
See also PB94-163490. Sponsored by National Inst. of Standards and Technology (MEL), Gaithersburg, MD. Robot Systems Div.

Keywords: *Computer aided manufacturing, *Numerical control, *Interpreters, Machining, Input out put processing, Process control, Models, NGC(Next Generation Controller), NIST(National Institute of Standards and Technology).

An interpreter has been written which reads numerical control code and produces calls to a set of canonical machining functions. The output of the interpreter can be used to drive a 3-axis machining center. This report describes version 1 of the interpreter.

02,815
PB94-191715 PC A06/MF A02
National Inst. of Standards and Technology (MEL), Gaithersburg, MD.
Control Entity Interface Specification.
S. Wallace, M. K. Senehi, E. Barkmeyer, S. Ray, and E. K. Wallace. Sep 93, 116p, NISTIR-5272.
See also PB91-240796.

Keywords: *Computer aided manufacturing, *Control systems, *Interfaces, *Specifications, Integrated systems, Hierarchies, Production planning, Models, Production control, NIST(National Institute of Standards and Technology), MSI(Manufacturing Systems Integration), Job control.

This document is concerned with defining the details of the interfaces for control entities which are incorporated into an integrated system that conforms to the National Institute of Standards and Technology (NIST) Manufacturing Systems Integration (MSI) architectural model as revised in 1992. The purpose of this document is twofold: to document the progress and current status of the MSI architecture's control entity interfaces and to provide designers and implementors with specifications for an MSI architectural compliant control entity. Section 2 provides an overview of the MSI project. Section 3 discusses production plans in the context of the interaction between planners and job controllers. Section 4 discusses generic data objects which are common to several of the 5 control entity interfaces. Sections 5-9 detail the 5 different control entity interfaces: the planning interface, the job control interface, the planning-to-job-control interface, the guardian planning interface and the guardian job control interface. Section 10 gives an example scenario of how the different messages from the 5 interfaces work together.

02,816
PB94-194552 PC A03/MF A01
National Inst. of Standards and Technology (MEL), Gaithersburg, MD. Factory Automation Systems Div.
Visualization Applications for Manufacturing: A State-of-the-Art Survey. Final Report.
H. T. Moncarz. May 94, 35p, NISTIR-5427.

Keywords: *Computer aided manufacturing, *Computer graphics, *Technology assessment, *Scientific visualization, Standards, Production engineering, Computerized simulation, Data transmission, Algorithms, Software tools, State of the art, Surveys, Product development, *Rapid response manufacturing.

A state-of-the-art (SOTA) survey was performed for visualization software applications (VAs) in the context of a rapid response manufacturing (RRM) environment. VAs are standalone, commercially-available products, that have sophisticated capabilities for interactively visualizing data. The data includes geometry, image, and scientific data. VAs' capabilities to visualize data can be advantageously applied to manufacturing if VAs are integrated within RRM. In general, integration enables any RRM process to access data from other RRM processes in the product life cycle. However, having access to data isn't necessarily useful if it is too overwhelming for a human to use it. VAs offer the potential for users to cognitively integrate the data from multiple RRM processes to make sense of it and to intelligently use it. This SOTA describes the capabilities of VAs and methods for integrating them within RRM to ultimately enable the full potential of VAs to be realized.

02,817
PB94-199932 Not available NTIS
National Inst. of Standards and Technology (NEL), Gaithersburg, MD. Factory Automation Systems Div.
Implementing a Transition Manager in the AMRF Cell Controller.
Final rept.
B. A. Catron. 1993, 5p.
Pub. in the Proceedings of International Conference CAD/CAM Robotics and Factories of the Future (3rd), Southfield, MI., August 14-17, 1988, v3 p42-46.

Keywords: *Computer aided manufacturing, *Controllers, Control systems, Synchronism, Process control, Integrated systems, Automation, Remote control, Reprints, *Transition management, AMRF(Automated Manufacturing Research Facility), US NIST.

The Transition Manager is one of several managers which are responsible for providing functionality to the cell controller in the Automated Manufacturing Research Facility (AMRF) at the National Institute of Standards and Technology. The cell controller implementation of the Transition Manager is based on a model developed at the University of Virginia (UVA). This model provides identical functionality at each level of the AMRF control hierarchy. The paper outlines the changes and additions which were needed in order to integrate the Transition Manager into the AMRF cell controller. An extension to the model is also proposed to allow more flexibility in the automated remote control capabilities. The extension to the UVA model will allow the cell controller the flexibility of controlling resources and then releasing the resource when finished.

02,818
PB94-199940 Not available NTIS
National Inst. of Standards and Technology (NEL), Gaithersburg, MD. Factory Automation Systems Div.
Generic Manufacturing Controllers.
Final rept.
B. A. Catron, and B. H. Thomas. 1989, 3p.
Pub. in Proceedings of Institute of Electrical and Electronics Engineers International Symposium on Intelligent Control, Arlington, VA., August 24-26, 1988, p742-744.

Keywords: *Computer aided manufacturing, *Controllers, *Software reuse, Integrated systems, Process control, Computer program portability, Reprints, AMRF(Automated Manufacturing Research Facility), US NIST.

The cost of developing software for the factory is continuing to increase due in part to the problems of integrating equipment and controllers from multiple vendors. A consistent philosophy is needed for designing reusable code for integrating manufacturing control systems. Development of a 'generic controller' will minimize the problem of redundant software. An outline of a generic controller architecture is discussed and key concepts are identified. A generic controller is under development at the Automated Manufacturing Research Facility at the National Institute of Standards and Technology. The implementation is outlined and future work identified.

02,819
PB94-213758 PC A05/MF A01
National Inst. of Standards and Technology (MEL), Gaithersburg, MD.
Technical Program Description Systems Integration for Manufacturing (SIMA).
H. M. Bloom. Jul 94, 94p, NISTIR-5476.
See also PB91-193367 and PB93-189801.

Keywords: *Computer aided manufacturing, *Integrated systems, *Standards, Data transfer(Computers), Interfaces, Computer aided design, Product development, Prototypes, Specifications, Systems engineering, *SIMA(Systems Integration for Manufacturing Applications), *Systems Integration for Manufacturing Applications, STEP(Standard for the Exchange of Product Model Data), US NIST, AMSANT(Advanced Manufacturing System and Networking Testbed).

The National Institute of Standards and Technology (NIST) has established an Advanced Manufacturing System and Networking Testbed (AMSANT) which supports research and development (R&D) in high-performance manufacturing systems and testing high-performance computer and networking hardware and software in a manufacturing environment. A standards-based data exchange effort for computer integrated manufacturing will focus on improving data exchange among computer aided design, process and manufacturing activities. This new program, Systems Integration for Manufacturing Applications (SIMA), is part of the government's High Performance Computing and Communications Initiative. Applications may include enterprise integration for manufacturing applications, integrated product/process design, simulation and agile manufacturing. Prototype systems, and interface specifications will be communicated to appropriate standards organizations. The report describes the objectives of the program and highlights the projects to be initiated in FY94 and proposed for FY95.

02,820
PB95-144549 PC A06/MF A02
National Inst. of Standards and Technology (MEL), Gaithersburg, MD. Factory Automation Systems Div.
Reference Architecture for Machine Control Systems Integration: Interim Report.
M. K. Senehi, T. R. Kramer, J. Michaloski, W. G. Rippey, S. Wallace, R. Quintero, and S. R. Ray. Oct 94, 111p, NISTIR-5517.
See also PB94-142791. Prepared in cooperation with Catholic Univ. of America, Washington, DC.

Keywords: *Computer aided manufacturing, *Control systems, *Integrated systems, Automation, Systems engineering, Industrial plants, Hierarchies, Models, Protocols, US NIST.

The Manufacturing Engineering Laboratory (MEL) at the National Institute of Standards and Technology (NIST) has been conducting research on control of mechanical systems for more than sixteen years. The Robot Systems Division and Factory Automation Systems Division have been working jointly for over a year to develop a reference architecture for computer integrated control of mechanical systems, drawing on the best of past work in both divisions. The architecture is not yet complete, and work on the architecture is continuing. This report describes the architecture in its current, incomplete state. The architecture is a hierarchical control architecture aimed at the domain of discrete parts manufacturing, including considerations of data systems, communications systems, planning, resource allocation, real-time control, and error recovery.

02,821
PB95-150827 Not available NTIS
National Inst. of Standards and Technology (NEL), Gaithersburg, MD. Factory Automation Systems Div.
Using Grafcet to Design Generic Controllers.
Final rept.
B. H. Thomas, and C. R. McLean. 1988, 10p.
Pub. in Proceedings of International Conference on Computer Integrated Manufacturing, Troy, NY., May 23-25, 1988, p110-119.

Keywords: *Computer aided manufacturing, *Controllers, *Systems engineering, Control systems, Software engineering, Parallel processing, Process control, Software reuse, Reprints, Grafcet programming language.

The purpose of this paper is to outline some ways Grafcet is being used to help design generic controllers within the Automated Manufacturing Research Facility. Grafcet is a powerful graphical language for expressing control flow and allows the expression of both parallel and sequential control logic. The paper describes the rationale for using Grafcet as a design tool for expressing software for a generic controller. Grafcet helps the designer determine: modularization of the code, functions that can be performed in parallel, communication flow, and problems in control flow.

02,822
PB95-151908 Not available NTIS
National Inst. of Standards and Technology (NEL), Gaithersburg, MD. Automated Production Technology Div.
Integration of Real-Time Process Planning for Small-Batch Flexible Manufacturing.
Final rept.
C. Yang, and K. Lee. 1989, 5p.
Pub. in Proceedings of IASTED International Symposium on Robotics and Manufacturing (12th), Santa Barbara, CA., November 13-18, 1989, p230-234.

Keywords: *Computer aided manufacturing, *Process control, *Planning, Automation, Control systems, Hierarchies, Task complexity, Task planning(Robotics), Workstations, Machine tools, Reprints.

Automation of just-in-time, small-lot, mixed-batch manufacturing at the workcell level is a topic of interest in Flexible Manufacturing Systems (FMS) research today. The control processes involved in producing different parts in small batches can be very complex. This paper describes a method of generating the process plan in real time based on part manufacturing attributes and execution of the plan by a three-level hierarchical controller. This method is currently implemented in the workstation controller for the Mare Island Flexible Manufacturing Workstation (MIFMW), a small-batch workcell designed for just-in-time, untended operation.

02,823
PB95-162335 Not available NTIS
National Inst. of Standards and Technology (MSEL), Gaithersburg, MD. Metallurgy Div.
Development of Adaptive Control Strategies for Inert Gas Atomization.
Final rept.
S. D. Ridder, S. A. Osella, P. I. Espina, and F. S. Biancaniello. 1990, 10p.
Pub. in MD (Intell. Process. Mater.) 21, p79-88 1990.

Keywords: *Atomizers, *Particle size, *Process control, *Metal powders, Real time operations, Artificial intelligence, Expert systems, Supersonic flow, Cinematography, Gas flow, Rare gases, Adaptive control, Particulates, Controllers, High speed, Monitors, Reprints, SiGMA method.

The Supersonic inert Gas Metal Atomization (SiGMA) technique produces ultra-fine (< 45 micrometer median particle diameter), rapidly solidified metal powder via high energy gas atomization. Research at the National Institute of Standards and Technology (NIST, formerly NBS) on SiGMA has focused on providing this system the ability to monitor and control particle size during atomization. The process controller currently under development for SiGMA includes a novel real-time particle size measurement sensor (incorporating an adaptive pattern recognition scheme) into a multiple level I/O command interface. The modular nature of both the hardware and software design will be adaptable to other particulate producing equipment. Gas and liquid flow imaging, gas flow modeling, real-time particle size measurement and process control will be discussed.

02,824
PB95-162343 Not available NTIS
National Inst. of Standards and Technology (IMSE), Gaithersburg, MD. Metallurgy Div.
Process Modeling and Control of Inert Gas Atomization.
Final rept.
S. D. Ridder, S. A. Osella, P. I. Espina, and F. S. Biancaniello. 1990, 18p.
Pub. in Proceedings of Thermal Structures Conference, Charlottesville, VA., November 13-15, 1990, p383-400.

Keywords: *Atomizing, *Particle size, *Process control, Real time operations, Artificial intelligence, Expert systems, Rare gases, Gas flow, Particulates, Controllers, Reprints.

Research at the National Institute of Standards and Technology (NIST, formerly NBS) on gas atomization has focused on providing this process the ability to monitor and control particle size during atomization. Studies included gas and liquid flow imaging, gas flow modeling, real-time particle size measurement and process control. The process controller incorporates a multi-level expert system shell and a novel real-time particle size measurement sensor (incorporating an adaptive pattern recognition scheme). The modular nature of both the hardware and software design is adaptable to other particulate producing equipment.

02,825
PB95-173555 PC A11/MF A03
National Inst. of Standards and Technology (MEL), Gaithersburg, MD. Intelligent Systems Div.
Workshop on the Application of Virtual Reality to Manufacturing. Final Report. Held in Gaithersburg, Maryland on August 9, 1994.
E. W. Kent. Dec 94, 227p, NISTIR-5543.

Keywords: *Computer aided manufacturing, *Virtual reality, *Human factors engineering, Man computer interface, Protocols, Interactive systems, Distributed processing, Surveys, Graphs(Charts), US NIST.

The Intelligent Systems Division (ISD) of the Manufacturing Engineering Laboratory (MEL) at the National Institute of Standards and Technology (NIST) is committed to the standardization of protocols for the application of information and interface technology for the virtual and distributed manufacturing of discrete parts. As part of this effort, ISD is developing an initiative in human interfaces in manufacturing, emphasizing the integration of human factors, virtual reality, and manufacturing systems technologies. A one-day workshop, was held on 9 August 1994 to examine the application of information and interface technology for the virtual and distributed manufacturing of discrete parts. The purpose of this report is to document the workshop, including presentations, participant discussions, and the results of working group deliberations.

02,826
PB95-181228 Not available NTIS
National Inst. of Standards and Technology (CAML), Gaithersburg, MD. Statistical Engineering Div.
Analysis of Autocorrelations in Dynamic Processes.
Final rept.
N. F. Zhang, and J. F. Polland. 1994, 15p.
Pub. in Technometrics 36, n4 p354-368 Nov 94.

Keywords: *Autoregressive processes, *Process control, *Data analysis, Error detection codes, Mass balance, Material balance, Autocorrelation, Time series analysis, Mathematical models, Reprints.

Data collected by process information and control systems are almost always correlated due to process dynamics combined with short sampling times. The traditional time series approach for dealing with autocorrelated data has been to model the autocorrelation. This modeling effort is substantially more difficult than simply treating the time series as a sequence of independent data. In this article, we develop and demonstrate a methodology that yields insight into the error introduced by not modeling the autocorrelation of the process data when performing material balances around process equipment. This work shows that in many cases data analysis (e.g., gross-error detection) can be done using the simplified models.

02,827
PB95-217097 PC A03/MF A01
National Inst. of Standards and Technology (MEL), Gaithersburg, MD.
Japan Technology Program Assessment. Simulation: State-of the-Art in Japan.
A. Jones. Mar 95, 37p, NISTIR-5614.
See also PB95-171112. Sponsored by Assistant Secretary for Technology Policy (Commerce), Washington, DC. Japan Technology Program.

Keywords: *United States, *Japan, *Technology transfer, Computerized simulation, Computerized manufacturing, Industries, Government policies, *Foreign technology, Translations.

The report summarizes the current state-of-the-art of simulation in Japan, and provides some insight into the future directions the Japanese are likely to pursue. It is divided into three parts. In part one, the authors provide a translation of a paper that was published in Journal of the Operations Research Society of Japan by Shigeki Umeda and Susumu Morito. In part two, they provide a copy of the paper by Shigeki Umeda which is contained in the proceedings of the recently held conference on New Directions in Simulation for Manufacturing and Communications. These authors have graciously agreed to allow their papers to be included in the report. In part three, the authors provide comments from five US researchers who attended the conference on New Directions in Simulation for Manufacturing and Communications.

02,828
PB95-231866 PC A05/MF A01
National Inst. of Standards and Technology (MEL), Gaithersburg, MD.
Conceptual Design Plan for the National Advanced Manufacturing Testbed.
Special pub.
M. M. Hessel. Apr 95, 87p, NIST/SP-882.
Also available from Supt. of Docs. as SN003-003-03336-7.

Keywords: *Manufacturing, *Government/industry relations, Computer aided manufacturing, Demonstration projects, US NIST, Distributed manufacturing, Testbeds, Advanced manufacturing.

The National Advanced Manufacturing Testbed (NAMT) Program provides a collaborative context for helping U.S. manufacturers achieve a competitive advantage. It is a national industry-government teaming program designed to leverage private sector and federal investments, expertise and facilities to accelerate the development and implementation of technologies for distributed and virtual manufacturing (DVM). The objective of the NAMT program is to establish and operate a distributed, multinode, multi-project testbed among industry, government agencies and universities. This testbed will facilitate coordination between individual projects and development and demonstra-

tion of industry-defined scenarios which advance DVM technologies to support integration and interoperability among suppliers, vendors and manufacturers.

02,829
PB95-251708 PC A03/MF A01
National Inst. of Standards and Technology (MEL), Gaithersburg, MD. Manufacturing Systems Integration Div.
Information Technologies Make Business Sense for the Custom Therapeutic Footwear Industry.
H. T. Moncarz. Jun 95, 12p, NISTIR-5673.
Presented at a workshop held in Charleston, SC. in March 1994.

Keywords: *Footwear industry, *Information technology, *Computer aided manufacturing, Shoes, Orthopedic equipment, Therapeutic uses, Design analysis, Process control, Production engineering, Product development, Standards, Requirements, Data transmission, Technology utilization, Life cycle analysis, STEP(Standard for the Exchange of Product Model Data).

The commercialization and integration of emerging technologies for custom therapeutic footwear (CTF) manufacturing will provide economic and health-care benefits to the nation and will improve responsiveness to consumer desires. Using STEP Application Protocols (APs), complex product information can be unambiguously transferred throughout the virtual and distributed, multi-enterprise marketplace that is anticipated for the future CTF industry. In that marketplace, information representing foot shapes, shoe lasts (forms for footwear manufacturing), orthopedic insets, and the patterns that comprise the footwear pieces must be transferred among different organizations. This paper will describe that marketplace, and type of STEP APs required, and possible business scenarios.

02,830
PB96-112008 Not available NTIS
National Inst. of Standards and Technology (MEL), Gaithersburg, MD. Factory Automation Systems Div.
Production Management Information Model for Discrete Manufacturing.
Final rept.
S. R. Ray, and S. Wallace. 1995, 15p.
Pub. in Production Planning and Control, v6 n1 p65-79 1995.

Keywords: *Computer aided manufacturing, *Production management, *Management information systems, Automation, Integrated systems, Control systems, Systems design, Production planning, Production control, Resource allocation, Process control, Scheduling, Specifications, Hierarchies, Mathematical models, Reprints, Manufacturing Systems Integration, NIAM(Nijssens Information Analysis Model), Systems architecture.

The Manufacturing Systems Integration (MSI) project at the National Institute of Standards and Technolgy is developing a system architecture that incorporates an integrated production planning and control environment. This paper presents the production management information model within the MSI project. The main focus of the model is to identify and characterize the relationships between orders and workpieces, to identify the information necessary to achieve workpieces, to identify the information necessary to achieve workpiece tracking and to identify the information necessary to achieve resource requirements specifications for process plans.

02,831
PB96-112685 PC A07/MF A02
National Inst. of Standards and Technology, Gaithersburg, MD.
Requisite Elements, Rationale, and Technology Overview for the Systems Intergration for Manufacturing Applications (SIMA) Program. Background Study.
E. J. Barkmeyer, T. H. Hopp, M. J. Pratt, and G. R. Rinaudot. Sep 95, 133p, NISTIR-5662.
See also PB94-213758.

Keywords: *Computer aided manufacturing, *Integrated systems, Product development, Systems engineering, Software, Cost estimates, Standards, *SIMA(Systems Integration for Manufacturing Applications), *Systems Integration for Manufacturing Applications.

The report--which documents the findings of a background study of industry needs in the area of manufacturing systems integration--defines the initial MSE project focus in detail and sets the technical direction for project efforts. The report also describes the principal types of product realization software applications now in use, reviews efforts within manufacturing industry towards developing integration solutions, discusses relevant research trends in the field of product realization, and surveys standards which may be applicable to the work of the MSE project. A brief review is also given of some potentially relevant supporting technologies from the realm of information technology.

02,832
PB96-122759 Not available NTIS
National Inst. of Standards and Technology (MEL), Gaithersburg, MD. Manufacturing Systems Integration Div.
Roadmap for the Computer Integrated Manufacturing (CIM) Application Framework.
Final rept.
S. L. Stewart, and J. A. St. Pierre. 1995, 21p.
Pub. in SEMATECH Roadmap for the Computer Integrated Manufacturing (CIM) Application Framework, p1-21 May 95.

Keywords: *Object oriented systems, *Systems engineering, *Production management, Computer software, Computer aided manufacturing, Integrated systems, Data management, Interfaces, Frameworks, Specifications, Technology transfer, Reprints, *CIM(Computer Integrated Manufacturing), *Computer Integrated Manufacturing.

This technology transfer reports on the first year of a joint project between the National Institute of Standards and Technology (NIST) and SEMATECH. It includes a roadmap for promoting adoption of the SEMATECH Computer Integrated Manufacturing (CIM) Framework as an industry standard. The CIM Framework is an object-oriented software infrastructure that creates a common environment for integrating applications and sharing information in production environments. The roadmap consists of the following stages: specifications; consensus; standardization; and testing/certification. Each stage is described in detail in the document.

02,833
PB96-128228 PC A03/MF A01
National Inst. of Standards and Technology (MEL), Gaithersburg, MD. Manufacturing Systems Integration Div.
Overview of the Manufacturing Engineering Toolkit Prototype.
M. J. Iuliano. Oct 95, 12p, NISTIR-5730.

Keywords: *Software tools, *Computer aided manufacturing, *Prototypes, Standards, Interfaces, Validation, Systems integration, Systems approach, Systems engineering, Software engineering, Life(Durability), Applications programs(Computers), METK(Manufacturing Engineering Toolkit).

A computer-aided Manufacturing Engineering Toolkit (METK) prototype is currently under development at the National Institute of Standards and Technology (NIST). The toolkit is being used to identify the integration standards and issues which must be addressed to implement plug-compatible environments in the future. The toolkit consists of commercial-off-the-shelf (COTS) manufacturing software applications housed together on a high speed computer workstation. The purpose of the CAME project at NIST is to provide an integrated framework, operating environment, common databases, and interface standards for manufacturing engineering software applications. This paper describes an initial METK prototype.

02,834
PB96-136965 PC A10/MF A03
National Inst. of Standards and Technology (MEL), Gaithersburg, MD. Manufacturing Systems Integration Div.
Computer-Aided Manufacturing Engineering Forum (1st). Technical Meeting Proceedings. Held in Gaithersburg, Maryland on March 21-22, 1995.
M. Smith, and S. Leong. Mar 95, 211p, NISTIR-5699.
Sponsored by Naval Research Lab., Washington, DC. Navy Manufacturing Technology Program.

Keywords: *Computer aided manufacturing, *Meetings, *Planning, Data processing, Process control, Validation, Integrated systems, Systems engineering, Metals, Machines, Materials handling, Models, Concurrent engineering.

Although many software tools are currently available for manufacturing engineers, they do not work together and cannot be readily integrated. This lack of integration significantly diminishes the productivity of manufacturing engineers, reduces the quality of their work, and increases the time it takes to plan the production of a part. The Manufacturing Engineering Tool Kit project is attempting to develop an integrated tool kit. This tool kit will be used to generate a process plan for production and to validate the engineering data package and process plan prior to release to production. The application software tools are based on commercially available off-the shelf products. This paper describes the validation requirements for the engineering data package and the categories and types of data errors compiled from a need analysis from the industry end users.

02,835
PB96-147954 PC A05/MF A01
Catholic Univ. of America, Washington, DC. Dept. of Mechanical Engineering.
NIST RS274KT Interpreter.
T. R. Kramer, and F. Proctor. 26 Oct 95, 58p, NISTIR-5738.
Grant NIST-70NANB2H1213
See also PB94-187788. Sponsored by National Inst. of Standards and Technology (MEL), Gaithersburg, MD. Intelligent Systems Div.

Keywords: *Computer aided manufacturing, *Numerical control, *Interpreters, Machining, Process control, Models, Computer programs, Software engineering, NGC(Next Generation Controller), National Institute of Standards and Technology, RS274KT interpreter.

The NIST 'RS274KT interpreter' is a software system which reads numerical control code in the 'KT' dialect of the RS274 numerical control language and produces calls to a set of canonical machining functions. The output of the interpreter can be used to drive a Kearney and Trecker 800 4-axis machining center. The report describes the RS274KT interpreter.

02,836
PB96-147962 PC A04/MF A01
National Inst. of Standards and Technology (MEL), Gaithersburg, MD. Manufacturing Systems Integration Div.
Product Realization Process Modeling: A Study of Requirements, Methods and Research Issues.
K. W. Lyons, M. R. Duffey, and R. C. Anderson. Jun 95, 48p, NISTIR-5745.
Prepared in cooperation with George Washington Univ., Washington, DC.

Keywords: *Computer aided manufacturing, *Process models, *Product development, Computerized simulation, Industrial plants, Electromechanical devices, Materials handling, Artificial intelligence, Automation.

The purpose of the document is to identify and document key requirements, industry practices, and research questions which should drive new methods and computer tools for process modeling of product realization. It addresses a wide range of industry-relevant modeling issues to help focus discussion on future research directions and its intended audience are modeling researchers and practitioners in industry, universities, and other federal agencies. Although process modeling methods have been applied to many types of development efforts (e.g., software engineering, VLSI), our sole focus in the report is realization of discrete electro-mechanical products.

02,837
PB96-154521 PC A02/MF A01
National Inst. of Standards and Technology (MEL), Gaithersburg, MD.
Machine Performance Standard Provides Opportunity to Improve Quality and Productivity.
C. D. Lovett. Dec 95, 8p, NISTIR-5775.
Sponsored by American Society of Mechanical Engineers, Washington, DC.

Keywords: *Process control, *Machine tools, *Computer aided manufacturing, Measurement, Performance evaluation, Standards, Quality control.

Evaluating manufacturing capability and monitoring any decrease in performance of CNC machines may provide some trends of manufacturing process variables which can be used for estimating better control over the manufacturing process. This in turn could lead to improved quality and a reduction in manufacturing

lead time. A performance standard for CNC machining centers and a draft standard for turning centers provide methods for evaluating performance of machines comparative analysis as well as ongoing assessment of machine tool performance.

02,838
PB96-154877 PC A08/MF A02
National Inst. of Standards and Technology (MEL), Gaithersburg, MD. Manufacturing Systems Integration Div.
NIST SIMA Interactive Management Workshop. Held in Fort Belvoir, Virginia on November 14-16, 1994.
C. Johnson, S. Frechette, and M. Luce. Sep 95, 127p, NISTIR-5717.

Keywords: *Computer aided manufacturing, *Integrated systems, *Workshops, Product development, Systems engineering, Software, Standards, *SIMA(Systems Integrated for Manufacturing Applications), *Systems Integrated for Manufacturing Applications.

The Manufacturing Systems Integration Divison (MSID) hosted a workshop November 14-16, 1994, on Systems Integrations for Manufacturing Application (SIMA). The workshop was held at the Defense Systems Mangement College (DSMC) in Fort Belvoir, Virginia. A total of 27 people participated in the workshop including representatives from industry, industry consortia, other government manufacturing programs, and the Natioanl Institute of Standards and Technology (NIST). The focus of the workshop was to identify critical problems and actions that can be taken to solve these problems in the context of advancing information technology for manufacturing systems and improving the effectiveness of related programs. This document contains diagrams that illustrate relationships between problems and actions related to removing barriers to manufacturing systems integration. In addition, it contains a description of the Interactive Management process that was used to facilitate the NIST SIMA workshop at Fort Belvoir, Virginia.

02,839
PB96-160437 Not available NTIS
National Inst. of Standards and Technology (MEL), Gaithersburg, MD. Automated Production Technology Div.
Quality in Automated Manufacturing.
Final rept.
D. S. Blomquist. 1991, 34p.
Pub. in Control and Dynamic Systems, v45 p163-196 Aug 91.

Keywords: *Computer-aided manufacturing, *Dimensional measurement, *Automation, Process control, Computerized control systems, Machine tools, Real-time systems, Integrated systems, Quality control, Error correcting codes, Reprints, Coordinate measuring machines, Initial Graphics Exchange Specifications.

The Quality in Automation (QIA) program is described at the Manufacturing Engineering Laboratory of the National Institute of Standards and Technology (NIST). The purpose of the QIA program is to develop a quality control and quality assurance system that exploits deterministic metrology principles in an automated manufacturing environment, producing small batches with commercially available and affordable equipment. This 'deterministic manufacturing' is based on the premise that most errors occuring in the manufacturing process are repeatable, thus predictable. The QIA program combines statistical process control methods with on-machine sensing and gauging, real-time error compensation and distributed processing to produce parts of consistently high quality.

02,840
PB96-160486 Not available NTIS
National Inst. of Standards and Technology (MEL), Gaithersburg, MD. Automated Production Technology Div.
Development of a New Quality Control Strategy for Automated Manufacturing.
Final rept.
M. A. Donmez. 1992, 12p.
Pub. in Proceedings of Manufacturing International 1992, MI92 Technologies, Economics, Information for Global Partnership Realignments, Dallas, TX., March 19-April 1, 1992, 12p.

Keywords: *Computer-aided manufacturing, *Machine tools, *Quality control, *Automation, Process control, Computerized control systems, Real time systems, Inspection, Error corection, Accuracy, Reprints.

A new quality control strategy is being developed at the Manufacturing Engineering Laboratory of the National Institute of Standards and Technology (NIST) with a project called Quality In Automation (QIA). The objective of this strategy is to demonstrate that the likelihood of producing defective parts can be dramatically reduced through better control of the manufacturing process. The QIA project is an effort to develop and implement a real-time, on-line quality control/quality assurance system to improve the quality of the parts produced in a small-batch, automated manufacturing environment using commercially available and affordable equipment. In order to obtain high-quality parts consistently, we are building a three-layered control strategy around the metal cutting process. These three control layers are: real-time, process-intermittent, and post-process.

02,841
PB96-165428 PC A03/MF A01
National Inst. of Standards and Technology (MEL), Gaithersburg, MD. Manufacturing Systems Integration Div.
Machining Process Planning Activity Model for Systems Integration.
S. C. Feng. Mar 96, 26p, NISTIR-5808.
See also PB96-112685.

Keywords: *Machining, *Planning, *Models, Computer aided manufacturing, Systems analysis, Software engineering, *STEP(Standard for the Exchange of Product Model Data), *Standard for the Exchange of Product Model Data.

A key issue of integrating process planning systems with design systems and production planning systems is how to overcome barriers in data exchange and sharing amongst software systems. A machining process planning activity model was developed at NIST to address some of the barriers. The model represents functional components and data requirements in process planning systems. The purpose of the model is to create the context in which data requirements and data flow for NC machining process planning are defined. The model was developed as a unification of many previously developed process planning activity models.

02,842
PB96-165980 PC A08/MF A02
National Inst. of Standards and Technology (MEL), Gaithersburg, MD. Automated Production Technology Div.
PIECS: A Software Program for Machine Tool Process-Intermittent Error Compensation.
H. T. Bandy, and D. E. Gilsinn. Mar 96, 140p, NISTIR-5797.

Keywords: *Machine tools, *Automation, *Error correction codes, Computer aided manufacturing, Numerical control, Feedback control, Coding, Cutting tools, Quality control, Algorithms, Real time, PIECS computer program, C programming language.

This report documents software, called PIECS, that performs process-intermittent error compensation for a turning center. The program is a part of a larger three loop control architecture that includes a real-time geometric-thermal error compensation, loop and a post-process loop. In process-intermittent error compensation, a part is measured by on-machine gauging after a semifinish cut which uses the same cutting parameters (speed, feed, and depth of cut) as are used in the finish cut, to reproduce process-dependent errors such as cutting-force induced tool or part deflection. During gauging a touch-trigger probe signal indicates that the part surface has been contacted. The coordinates of the points are then transformed to the part coordinate system and compared to the corresponding nominal coordinates so that errors may be determined. The error vector is defined as having its head at the measured coordinates of the gauged point and its tail at the nominal coordinate for that point. Since the philosophy chosen in this program is to compensate process-intermittent errors by changing the position and orientation of features, least squares curve fitting through the ends of the error vectors is used to determine the adjusted tool curve. The compensation curve becomes the tool path for the corresponding feature for the finish cut. The report includes a description of the program algorithm, the input and output data sets as well as descriptions of each of the C-programming language functions that compose PIECS. A listing of the program is included in the appendix.

02,843
PB96-183058 PC A04/MF A01
National Inst. of Standards and Technology (MEL), Gaithersburg, MD. Manufacturing Systems Integration Div.
Procedure for Product Data Exchange Using STEP Developed in the AutoSTEP Pilot.
D. A. Rosenfeld, and S. Dhar. Apr 96, 33p, NISTIR-5833.
Prepared in cooperation with Industrial Technology Inst., Ann Arbor, MI. Center for Electronic Commerce.

Keywords: *Automotive industry, *Product models, *Information exchange, *Computer aided manufacturing, Standards, Computer aided design, Interoperability, Production planning, Information systems, Motor vehicles, *STEP(Standard for the Exchange of Product Model data), *Standard for the Exchange of Product Model data, ISO 10303, STEP AP203.

The AutoSTEP Pilot Project, directed by the Automotive Industry Action Group (AIAG), is an effort whose goal is to promote the use of STEP (STandard for the Exchange of Product model data) as a neutral mechanism for product data exchange within the automotive industry. To explore and demonstrate the capabilities of STEP, AutoSTEP organized a number of trading pairs to exchange product model data represented in STEP Application Protocol 203, configuration controlled design conformance class six, or data represented with advanced boundary representation (b-rep). Model data would be transferred from one company's CAD system to its partner company's system via STEP. AutoSTEP Phase One organized pairs of automotive companies and their first-tier suppliers, and involved exchanges relating to packaging applications. Later phases will include exchanges of product model data relating to other applications, and will extend the information exchange further down the supply chain. Exchange results are logged in a database, and reports assessing the results will be produced. This document provides a complete description of the product model data exchange scenario envisioned for transactions using STEP, both in general and in the context of the AutoSTEP Pilot. It outlines the entire process that model data undergoes in STEP exchanges, and it identifies the significant metrics throughout the process. It also provides forms and tables for the benefit of the AutoSTEP participants to assist them in performing exchanges and logging metrics.

02,844
PB96-193735 PC A05/MF A01
National Inst. of Standards and Technology (MEL), Gaithersburg, MD. Manufacturing Systems Integration Div.
Systems Integration for Manufacturing Applications Program 1995 Annual Report.
J. E. Fowler, and M. E. Luce. May 96, 56p, NISTIR-5839.
See also PB94-213758 and PB96-154877.

Keywords: *Computer aided manufacturing, *Integrated systems, *Standards, Data transfer(Computers), Systems engineering, Technology transfer, Interfaces, Computer aided design, Product development, Prototypes, Specifications, *SIMA(Systems Integration for Manufacturing Applications), *Systems Integration for Manufacturing Applications(SIMA).

The Systems Integration for Manufacturing Applications (SIMA) Program is NIST's coordinating focus for manufacturing activities supporting the High Performance Computing and Communications/Information Infrastructure Technology and Applications initiative. The document summarizes the organizational structure of the program, provides descriptions of the technical projects comprising the program, and highlights accomplishments for those projects for FY94 and FY95.

02,845
PB96-195334 PC A11/MF A03
National Inst. of Standards and Technology (MEL), Gaithersburg, MD. Manufacturing Systems Integration Div.
Computer-Aided Manufacturing Engineering Forum (2nd). Technical Meeting Proceedings. Held in Gaithersburg, Maryland on August 22-23, 1995.
M. Smith, and S. Leong. May 96, 202p, NISTIR-5846.
See also PB96-136965. Prepared in cooperation with Naval Research Lab., Washington, DC. Navy Manufacturing Technology Program.

Computer Aided Manufacturing (CAM)

Keywords: *Computer aided manufacturing, *Meetings, Planning, Data processing, Process control, Integrated systems, Systems engineering, Materials handling, Concurrent engineering, Computerized simulation.

The paper reports results of the Computer-Aided Manufacturing Engineering (CAME) Forum Second Technical Meetings held in August 1995. This meeting built on work completed since the first technical meeting held in March 1995. The meeting brought together software developers, manufacturing technology managers and engineers, and university researchers to address important issues related to developing a Manufacturing Engineering Tool Kit (METK). The meeting was organized around three major segments. During the first segment, NIST computer scientists and engineers updated participants on the status of ongoing METK development work. Presentations were given on issues regarding the manufacturing data validation methodology, business case and implementation plan, and system architecture and tools integration. An overview was given on the Systems Integration for Manufacturing Applications (SIMA) Production System Engineering project. The METK baseline pilot system was demonstrated to the Forum attendees. The second segment used breakout groups to solicit ideas and feedback from meeting attendees on the issues discussed in the presentation topics. In the third segment, breakout groups prepared outbriefs and presented results to all meeting participants.

02,846
PB97-110472 Not available NTIS
National Inst. of Standards and Technology (MEL), Gaithersburg, MD. Automated Production Technology Div.
Compensation of Errors Detected by Process-Intermittent Gauging.
Final rept.
H. T. Bandy, and D. E. Gilsinn. 1995, 4p.
Pub. in Proceedings of the American Society for Precision Engineering Annual Meeting, October 15-20, 1995, v12 p440-443.

Keywords: *Machine tools, *Automation, *Error correction codes, Computer aided manufacturing, Numerical control, Feedback control, Cutting tools, Quality control, Algorithms, Real time, Metals, Reprints.

The paper describes a software design for implementing compensation of errors detected by process-intermittent gauging. This is the function of one control loop in the three-loop Quality In Automation (QIA) architecture that is under development at the National Institute of Stadards and Technology (NIST) (Donmez, 1992). Process-intermittent error compensation is useful for improving the accuracy of metal cutting processes on turning or machining centers (Brandy, 1991). During machining processes, errors due to tool wear, tool deflection, part deflection, etc., are independent of the accuracy of the machine tool itself, and can, therefore, be measured using the machine tool. The approach discussed here is to reduce those process errors. The term process-intermittent refers to inspection occurring during an interval between the semifinish and finish machining processes. Although in-process measurement techniques may allow uninterrupted machining (Fan, 1991), process intermittent inspection has advantages. For instance, a simple measurement device such as a tough-trigger probe may be used instead of the more intrusive apparatus required for measurement during active machining. Also, since a complete profile of the error pattern may be obtained in advance of finish machining, computational filters may be applied to the compensating tool path to minimize the effects of measurement irregularities.

02,847
PB97-110480 Not available NTIS
National Inst. of Standards and Technology (MEL), Gaithersburg, MD. Automated Production Technology Div.
Data Management for Error Compensation and Process Control.
Final rept.
H. T. Bandy, and D. E. Gilsinn. 1995, 10p.
Pub. in Proceedings Reprint, Modeling, Simulation, and Control Technologies for Manufacturing, Philadelphia, PA., October 25-26, 1995, v2596 p114-123.

Keywords: *Machine tools, *Automation, *Error correction codes, Computer aided manufacturing, Numerical control, Feedback control, Data management, Cutting tools, Metals, Quality control, Reprints.

Strategies for managing data flow are described for a system which controls processes to compensate machine tool and process errors. A CAD representation of the part is the basis for generating the data used in the processes and analyses. A process-oriented view of part features is used for tracking data regarding design, part programming, manufacture, error compensation, and inspection. Part ID and file name nomenclature have been developed to facilitate data identification. All data are stored in a database, enabling error trends over time to be studied so that error compensation algorithms may be refined.

02,848
PB97-112551 Not available NTIS
National Inst. of Standards and Technology (EEEL), Gaithersburg, MD. Electricity Div.
Exploring the Low-Frequency Performance of Thermal Converters Using Circuit Models and a Digitally Synthesized Source.
Final rept.
N. Oldham, M. E. Parker, B. Bell, and S. Avramov-Zamurovic. 1996, 2p.
Pub. in Conference on Precision Electromagnetic Measurements, CPEM '96 Conference Digest, Braunschweig, Germany, June 17-20, 1996, p495-496.

Keywords: *Electrical measurement, *Low frequency, Standards, Electrical networks, Temperature control, Tests, Reprints, *Thermal voltage converters, Voltage standards, Thermal converters.

Low-frequency tracking errors of thermal voltage converters are described and estimated using circuit models. A digitally synthesized source is used to confirm ac-dc differences in the 0.001 Hz to 40 Hz range.

02,849
PB97-113781 PC A03/MF A01
National Inst. of Standards and Technology (EEEL), Gaithersburg, MD.
Conformance Testing and Specification Management.
Rept. for Jun 95-Jun 96.
J. A. St. Pierre, K. G. Brady, and S. L. Stewart. Sep 96, 21p, NISTIR-5879.
Contract SEMATECH-95101037
Sponsored by SEMATECH, Austin, TX.

Keywords: *Conformance testing, *Object oriented programs, *Production management, Computer software, Computer aided manufacturing, Specifications, CIM(Computer Integrated Manufacturing), Computer Integrated Manufacturing, JAVA programming language, CORBA(Common Object Request Broker Architecture), Common Object Request Broker Architecture, Electronic.

This is the final report for the second year of a joint project between the National Institue of Standards and Technology (NIST) and SEMATECH. It presents the results from investigation in two areas that were proposed in the first year report: conformance testing and specification management. In conformance testing, a number of technologies are reviewed with special emphasis on using Java and Corba to develop a conformance testing environment. For specification management, technologies were reviewed for ways to use a single format with multiple uses and multiple distribution formats. This task looked at pragmatic solutions to the problem of maintaining complex documents with multiple uses through combinations of radily available software.

02,850
PB97-116123 PC A06/MF A01
National Inst. of Standards and Technology (MEL), Gaithersburg, MD. Manufacturing Systems Integration Div.
Unified Process Specification Language: Requirements for Modeling Process.
C. Schlenoff, A. Knutilla, and S. Ray. Sep 96, 78p, NISTIR-5910.

Keywords: *Computer aided manufacturing, *Process control, *Software tools, Production management, Scheduling, Systems integration, Industrial plants, Automation, Life cycles, PSL(Process Specification Language), Process Specification Language.

A wide range of applications deal with the manipulation and expression of collections of activities. Examples include project management, workflow management, business process reengineering, product realization process modeling, process planning, production scheduling, simulation, and Computer Aided Software Engineering, each of which is supported by some combination of graphical programming and control languages, Petri nets, PERT charts or other representation methodology. Each of these applications serves a specific audience and need, and focuses on particular aspects of a process. Nevertheless, much could be gained by sharing information among applications. One of the primary obstacles to such integration is the lack of any common representation of what is really the common underlying concept of process. The objective of the work described here is an investigation of the feasibility of a unifying specification of process which is applicable to all of the above applications, yet powerful and robust enough to meet each set of requirements. The document represents the results of the first phase of the work - that of researching the process representational requirements for design/manufacturing process life-cycle applications. These requirements are categorized into four categories; core, outer core, plug-ins, and application, which aided in describing the role of the requirements in the overall challenge of process representation.

Computer Software

02,851
PB95-155578 PC A09/MF A03
National Inst. of Standards and Technology (TS), Gaithersburg, MD.
Opportunities for Innovation: Software for Manufacturing.
D. E. Edgerly. Aug 94, 194p, NIST/GCR-94/658.

Keywords: *Manufacturing, *Computer software, Technology innovation, Computer applications, Models, Data management, Information management, Knowledge bases(Artificial intelligence), Computer aided design, Computer aided manufacturing, Numerical control, Total quality management, Software engineering.

The purpose of this Monograph is to survey the existing software applicable to the manufacturing enterprises, to identify the gaps and the opportunities for software developers to close these gaps. Information technology is constantly growing and adapting. This Monograph proposes directions for this growth and is a snapshot of current conditions, to be used as a starting guide.

Engineering Materials

02,852
PB95-162889 Not available NTIS
National Inst. of Standards and Technology (MSEL), Gaithersburg, MD. Materials Reliability Div.
Welding for Cryogenic Service.
Final rept.
T. A. Siewert, and C. N. McCowan. 1993, 4p.
Pub. in ASM Materials Handbook, v6 p1016-1019 Dec 93.

Keywords: *Cryogenics, *Welding, Mechanical properties, Aluminum, Nickel, Stainless steels, Materials, Reprints.

The report summarizes the factors that affect weld metal strength and toughness for cryogenic service. It provides advice on how to produce welds that match the properties of the wrought structural material.

Job Environment

02,853
PB95-161907 Not available NTIS
National Inst. of Standards and Technology (BFRL), Gaithersburg, MD. Fire Science Div.
Water Mist Fire Suppression Workshop Summary.
Final rept.
K. A. Notarianni. 1993, 2p.
Pub. in Society of Fire Protection Engineers Bulletin, p8-9 Summer 1993.

Keywords: *Sprays, *Fire suppression, *Commercialization, *Fire extinguishing agents, Workshops, Water vapor, Spraying, Fire fighting, Drop size, Technology assessment, Reprints, *Water mist.

The water mist fire suppression workshop was organized to facilitate the commercialization of water mist technology. The imminent lack of availability of halon fire suppressants has sparked worldwide efforts in developing other fire fighting agents. Water mist systems are potential replacements in many industrial uses, as well as in new markets, such as commercial passenger aircraft. Speakers presented state-of-the-art papers on the incentives of using misting sprays, the advances in spray drop size measurement and the engineering criteria for water mist fire suppression systems. Three papers discussed projects demonstrating the use of water mist systems in aircraft, marine, and telecommunications applications. The speakers and attendees were divided into three panels: Research Needs; End-Use Criteria; Marketing. The proceedings brings together the recommendations of each panel and the individual technical papers.

Joining

02,854
AD-A279 121/8 PC A04/MF A01
National Bureau of Standards, Gaithersburg, MD.
Screw-Thread Standards for Federal Services, 1957. Part 3.
1957, 75p.

Keywords: *Screw threads, *Standards, Nuts(Fastenings), Handbooks, Tolerances(Mechanics), Sizes(Dimensions).

No abstract available.

02,855
AD-A279 290/1 PC A10/MF A03
National Bureau of Standards, Gaithersburg, MD.
Screw-Thread Standards for Federal Services, 1957. Part 1.
Nov 60, 215p, NBS-HB-H28-PT-1.

Keywords: *Screw threads, *Standards, Gages, Handbooks, Screws, Fasteners, Couplers, Joints, Threaded products, Federal services.

No abstract available.

02,856
PB94-185873 Not available NTIS
National Inst. of Standards and Technology (MSEL), Boulder, CO. Materials Reliability Div.
International Institute of Welding: Report on 1992 Actions.
Final rept.
T. Siewert. Dec 92, 3p.
Pub. in Materials Evaluation 50, n12 p1389-1392 Dec 92. See also report for 1993, PB94-185881.

Keywords: *Welding, *Meetings, *Nondestructive tests, *Quality assurance, *Standardization, Inspection, Standards, Weldments, Defects, Test methods, Quality control, Reprints, International Institute of Welding.

Commission V on Quality Control and Quality Assurance of Welded Products handles inspection and quality issues for the International Institute of Welding. The activities of this commission are important to the nondestructive evaluation industry because the annual meetings serve as an international review of research activities and many of its draft standards are forward to the International Organization for Standards (ISO) for international approval. Thus, this summary of the meeting provides an up-to-date review of research in other countries and advance notice of standardization activities. This commission has activities in many areas, with subcommissions that cover major techniques for nondestructive inspection (x-ray, ultrasonic, electrical, magnetic, and optical techniques) and groups with interests in inspection of offshore construction, in significance of defects, and in quality assurance in welding technology. This year, Commission V met for three days and sponsored a seminar on the fourth. Thirty delegates and experts from sixteen countries attended the meetings. Following are reports of the subcommissions and working groups, in the order of presentation.

02,857
PB94-185881 Not available NTIS
National Inst. of Standards and Technology (MSEL), Boulder, CO. Materials Reliability Div.
International Institute of Welding: Report on 1993 Actions.
Final rept.
T. A. Siewert. 1994, 4p.
Pub. in Materials Evaluation 52, n1 p44, 46, 47, and 49 Jan 94. See also report for 1992, PB94-185873.

Keywords: *Welding, *Meetings, *Nondestructive tests, *Quality assurance, *Standardization, Inspection, Standards, Weldments, Defects, Test methods, Quality control, Reprints, International Institute of Welding.

Commission V on Quality Control and Quality Assurance of Welded Products handles inspection and quality issues for the International Institute of Welding (IIW). The activities of this commission are important to the nondestructive evaluation industry because the annual meetings serve as an international review of research activities. Many of its draft standards are forwarded to the International Organization for Standards (ISO) for international approval. Thus, this summary of the meeting provides an up-to-date review of research in other countries and advance notice of standardization activities.

02,858
PB94-185899 Not available NTIS
National Inst. of Standards and Technology (MSEL), Boulder, CO. Materials Reliability Div.
Through-the-Arc Sensing for Monitoring Arc Welding.
Final rept.
T. A. Siewert, R. B. Madigan, T. P. Quinn, and M. A. Mornis. 1993, 4p.
Pub. in Proceedings of International Conference on Trends in Welding Research (3rd), Gatlinburg, TN., June 1-5, 1992, p1037-1040 1993. Sponsored by Department of the Navy, Washington, DC.

Keywords: *Monitoring, *Quality control, Real time operation, Signal processing, Video signals, Welding machines, Wear, Algorithms, Process control(Industry), Reprints, *Through-the-arc sensing, *Pulsed gas metal arc welding.

Current and voltage records for pulsed gas metal arc welding were captured at data collection rates up to 9 kHz, then correlated with a high-speed video image of the arc. Loss of shielding gas coverage and contact tube wear caused characteristic changes in the current and voltage records. Change in contact-tube-to-work distance or change in the droplet transfer mode, also affected the current and voltage records. Algorithms were developed which use the current and voltage signals to automatically detect these undesirable welding conditions or variations in the welding procedure. The algorithms were incorporated in a computerized data collection and analysis system for real-time monitoring of the weld.

02,859
PB94-210143 PC A03/MF A01
National Inst. of Standards and Technology (TS), Gaithersburg, MD. Office of Standards Services.
Program Handbook: Requirements for Obtaining NIST Approval/Recognition of a Laboratory Accreditation Body Under P.L. 101-592. The Fastener Quality Act.
R. L. Gladhill. Aug 94, 49p, NISTIR-5428.

Keywords: *Fasteners, *Quality control, *Laboratories, *Accreditation, Requirements, Product inspection, Methodology, Tests, Costs, Foreign government, Private organizations, *US NIST, Fastener Quality Act, Public Law 101-592.

On November 16, 1990 the United States Congress enacted the Fastener Quality Act, P.L. 101-592 (The Act). The Act requires the establishment of procedures and conditions for the accreditation of laboratories engaged in the inspection and testing of certain fasteners entered into commerce within the United States. This document describes the National Institute of Standards and Technology (NIST) process to evaluate accreditation bodies as required by section 6 of the Act. The text of this handbook provides specific NIST interpretations of the general requirements. It explains the procedures, conditions, and requirements for gaining NIST approval/recognition.

02,860
PB95-147922 PC A06/MF A02
National Inst. of Standards and Technology (MEL), Gaithersburg, MD. Automated Production Technology Div.
Portsmouth Fastener Manufacturing Workstation. User's Manual.
V. J. Lee, L. J. Fronczek, R. J. Gavin, and K. B. Lee. Feb 93, 116p, NISTIR-5507.
See also PB94-118221. Sponsored by Naval Research Lab., Washington, DC. Navy Manufacturing Technology Program.

Keywords: *Fasteners, *Computer aided manufacturing, *Workstations, Control systems, UNIX(Operating system), Man machine systems, Computer software, Operators(Personnel), User manuals(Computer programs), US NIST, AMRF(Automated Manufacturing Research Facility).

A user manual is written for the integrated fastener manufacturing workstation which was jointly developed in the Automated Manufacturing Research Facility at the National Institute of Standards and Technology (NIST) by the Automated Production Technology Division and Portsmouth Naval Shipyard. The manual is intended to be used to train the operators or machinists to run the computer-controlled workstation. The workstation is controlled by a complex UNIX-based control system and requires operator interactions with the computer, machine and gaging devices. The workstation software is developed with ease of operation in mind and provides an operator-friendly environment for the machinists who usually have very little experience with computers, particularly a UNIX multitasking, multi-window system. The manual describes the workstation, the software, and operation procedures and leads the operator to order part batches, examine status and perform diagnostics.

02,861
PB95-162855 Not available NTIS
National Inst. of Standards and Technology (MSEL), Gaithersburg, MD. Materials Reliability Div.
Status Report: AWS Standards for Identifying Arc Welds (A91.1) and Recording Weld Data (A9.2).
Final rept.
T. A. Siewert. 1993, 4p.
Pub. in Proceedings of International Conference on Computerization of Welding Information IV, Orlando, FL., November 3-6, 1992, p3-6 1993.

Keywords: *Arc welding, *Data bases, Data processing, Standards, Materials specifications, Physical properties, Reprints, PQR, NDE data, Property data, Standard formats.

Standard formats are being developed for a wide range of data associated with materials and their properties. Two committees have cooperated in the development of two standards for welds, one covering the identification of welds (unique identification of a specific weld, as well as details on the preparation of the weld) and the other covering the properties and inspection of welds. Separation of the data into these two categories makes the standards compatible with the formats developed by E49 for other materials. The report provides more details on these standards.

02,862
PB95-162863 Not available NTIS
National Inst. of Standards and Technology (MSEL), Gaithersburg, MD. Materials Reliability Div.
Computers in Welding: A Primer.
Final rept.
T. A. Siewert, R. B. Madigan, and T. P. Quinn. 1994, 5p.
Pub. in Welding Jnl., p39-43 Feb 94.

Keywords: *Welding, *Computers, *Computer applications, Computer components, Computer hardware, Computer software, Reprints.

The article is a basic summary of computer concepts and components. If you haven't started to use computers yet, use this article to gain a basic understanding. If you feel somewhat comfortable with computers, you can use this article as a review, but it also may help you develop a plan to upgrade your skills and knowledge. We have added recommendations for further reading and a section on terms and definitions at the end to help you learn the jargon.

02,863
PB95-162871 Not available NTIS
National Inst. of Standards and Technology (MSEL), Gaithersburg, MD. Materials Reliability Div.

Through-the-Arc Sensing for Real-Time Measurement of Gas Metal Arc Weld Quality.
Final rept.
T. A. Siewert, R. B. Madigan, T. P. Quinn, and M. A. Mornis. 1992, 9p.
Sponsored by Department of the Navy, Washington, DC.
Pub. in Proceedings of International Conference on Computerization of Welding Information IV, Orlando, FL., November 3-6, 1992, p198-206.

Keywords: *Gas metal arc welding, *Quality control, *Real time operations, Computer systems programs, Electric potential, Electric current, Records, Detection, Reprints, Droplet transfer, Voltage records, Current records.

The voltage drop across the arc in gas metal arc welding is affected by droplet transfer, spatter formation, and many other arc characteristics. The current is affected in a similar manner. The authors collected voltage and current records with a high-speed data acquisition system, and correlated features in the records to various welding problems. Interruption in the shielding gas coverage, wear of the contact tube, change in the contact-tube-to-work distance, and change in the droplet transfer mode were detected through this sensing strategy. These effects were developed into general correlations and incorporated into a computerized data collection and analysis system.

02,864
PB95-163614 Not available NTIS
National Inst. of Standards and Technology (MEL), Gaithersburg, MD. Precision Engineering Div.
Variations in Size Measurements by Indicating Gaging Systems.
Final rept.
R. Veale, A. Strang, and C. Hsiao-Yu. 1994, 13p.
Pub. in Proceedings of the 1994 Measurement Science Conference, Pasadena, CA., January 27-28, 1994, p1-13.

Keywords: *Size determination, *Dimensional measurement, *Screw threads, Measuring instruments, Pitch(Inclination), Gages, Tests, Reprints, Pitch diameters.

The National Institute of Standards and Technology has investigated the efficacy of indicating gaging systems used to measure pitch diameter and functional size of threaded fasteners. Three external systems and four internal systems, representing four manufacturers, were used in the test. Twenty-seven external threads and eleven internal threads were measured. Some of the samples were purposely produced with form errors near and beyond product tolerances. The study shows that when the form errors are outside the product tolerances, indicating gages from different manufacturers give different results and do not always match the values obtained by alternate methods. Results of the tests are presented in tabular form.

02,865
PB95-189460 PC A03/MF A01
National Inst. of Standards and Technology (CAML), Gaithersburg, MD. Applied and Computational Mathematics Div.
Lubrication Theory for Reactive Spreading of a Thin Drop.
R. J. Braun, B. T. Murray, W. J. Boettinger, and G. B. McFadden. Dec 94, 50p, NISTIR-5557.

Keywords: *Soldering, *Lubrication, *Capillary flow, *Drops, Mass transfer, Transport properties, Solder, Concentration(Composition), Marangoni convection, Heat transfer, Temperature gradients.

Solder drops spreading on metallic substrates are a reactive form of the wetting problem. A metallic component may diffuse into the metal substrate and form intermetallics. This reaction with the substrate may affect the bulk transport in the spreading drop via coupling with the flow field via the Marangoni effect. Motivated by this situation, we extend a lubrication theory for the spreading of thin drops in the presence of gravity and thermocapillarity to include mass transport and solutocapillarity. We use an approximate solute profile in the drop to derive coupled evolution equations for the free surface shape and concentration field. Numerical solutions for the non-reactive (single component) drop agree well with previous theory. Including reactive effects in the model affects the flow patterns and spreading rates at relatively early times; but by the end of the spreading, solutal effects have died out in the model. We compare our results with some experimental results.

02,866
PB95-198743 PC A03/MF A01
National Inst. of Standards and Technology (MSEL), Boulder, CO. Materials Reliability Div.
IIW Commission V Quality Control and Quality Assurance of Welded Products Annual Report 1994/95.
T. A. Siewert. Mar 95, 35p, NISTIR-5034, IIW-V-1046-95.
Sponsored by International Inst. of Welding.

Keywords: *Quality assurance, *Quality control, *Weld tests, *Welded joints, Standards, Radiography, Welding, Inspection, Nondestructive tests, Standards, Test methods, Standardization, *International Institute of Welding.

The Annual Report 1994/1995 for Commission V, Quality Control and Quality Assurance of Welded Products, of the International Institute of Welding is presented. It includes (a) minutes, resolutions, and the future program adopted at its Annual Assembly in September 1994, (b) the organization, officials, and delegates, (c) schedules of meetings, and (d) the status of documents published by Commission V. It reviews current research and work on standardization.

02,867
PB95-209300 PC A04/MF A01
National Inst. of Standards and Technology (MSEL), Boulder, CO. Materials Reliability Div.
Droplet Transfer Modes for a MIL 100S-1 GMAW Electrode.
P. R. Heald, R. B. Madigan, T. A. Siewert, and S. Liu. Oct 91, 54p, NISTIR-3976.
See also PB91-174250. Prepared in cooperation with Colorado School of Mines, Golden. and Phillips Co., Borger, TX. Sponsored by David Taylor Research Center, Annapolis, MD. Programmable Automated Welding System Program.

Keywords: *Gas metal arc welding, *Welding electrodes, *Drops, *Mass transfer, Weldments, Standard deviation, Weld metal, Data acquisition, Computer applications, Computer aided manufacturing, MIL 100S-1 electrode.

Welds were made with a 1.2-mm-diameter MIL 100S-1 electrode using Ar-2% O2 shielding gas to investigate the effects of contact-tube-to-work distance (13, 19, and 25 mm) on metal transfer. The transfer modes were identified by the sound of the arc, images from a laser back-lit high-speed video system, and digital records of the voltage and current fluctuations. The spray transfer region was mapped on a current-voltage plot, with a range that included the boundaries of adjacent transfer modes. The metal transfer mode boundaries shifted with an increase in contact-tube-to-work distance. Increasing the contact-tube-to-work distance from 13 mm to 19 mm required a 15 mm/s increase in the wire feed rate for the globular-to-drop-spray transition.

02,868
PB95-253589 PC A03/MF A01
National Inst. of Standards and Technology (MSEL), Gaithersburg, MD. Reactor Radiation Div.
Determination of the Residual Stresses Near the Ends of Skip Welds Using Neutron Diffraction and X-ray Diffraction Procedures.
P. C. Brand, G. E. Hicho, and H. J. Prask. Jun 95, 40p, NISTIR-5671.
Also pub. as National Inst. of Standards and Technology (MSEL), Gaithersburg, MD. Metallurgy Div. rept. no. REPT-29.

Keywords: *Residual stress, *X ray diffraction, *Neutron diffraction, *Metal plates, Spot welds, Welding, Stress analysis, Stress distribution, Nondestructive tests, Stress measurement.

Welding is known to be a significant factor in the formation of residual stresses. Residual stresses are suspected as the reason for the occurrence of leaks in some railroad tank cars that had stiffeners welded to them. Residual stresses at the surface and in the bulk of metals can be measured non-destructively by x-ray and neutron diffraction respectively. In this report the results of such non-destructive residual stress measurements on one-pass, skip, bead-on plate welds are presented. The plate specimens used for this investigation contained two beads that represent the skip weld process. Of the full weld bead only positions close to the end of the first and the start of the second bead are investigated. The results show longitudinal tensile stresses and compressive transverse and perpendicular residual stresses in the region close to both the weld end and the weld start.

02,869
PB96-131461 PC A06/MF A02
National Inst. of Standards and Technology (MSEL), Gaithersburg, MD. Materials Reliability Div.
Control of Gas-Metal-Arc Welding Using Arc-Light Sensing.
R. B. Madigan, T. P. Quinn, and T. A. Siewert. Nov 95, 120p, NISTIR-5037.
See also AD-A177 893.

Keywords: *Gas metal arc welding, *Feedback control, Automation, Models, Process control, Radiation, Sensors, Arc length, Droplet-transfer frequency, National Institute of Standards and Technology.

In this development of closed-loop control of the gas-metal-arc welding process using light emitted by the arc, two process parameters were controlled in real time: arc length and droplet-transfer frequency. An arc-length sensor and controllers to regulate arc length and to actuate welding current were developed. The transfer frequency depended on current, wire-feed speed, and electrode extension, these results led to the design of a transfer-frequency controller.

02,870
PB96-135058 Not available NTIS
National Inst. of Standards and Technology (MSEL), Boulder, CO. Materials Reliability Div.
Mathematical Models of Transport Phenomena Associated with Arc-Welding Processes: A Survey.
Final rept.
P. G. Jonsson, J. Szekely, R. T. C. Choo, and T. P. Quinn. 1994, 22p.
Pub. in Modelling Simulation Materials Science and Engineering, v2 p995-1016, 1994.

Keywords: *Arc models, *Welding, Surveys, Reprints, Mathematical models, Process control, GNAW, GTAW.

A comprehensive survey is presented of research on transport phenomena, that is, heat flow, fluid flow, mass transfer, and electrodynamics, associated with arc welding. Both gas-metal arc-welding (GMAW) and gas-tungsten arc welding (GTAW) systems are considered, and appropriate emphasis is placed on the intrinsic differences between these systems. The topics discussed include the behavior of the arc, and its interaction with both the electrode and the surrounding medium, on the one hand, and the behavior of the weld pool on the other. The limited work done on the coupling between arcs, electrodes, and weld pools is also discussed, as are some process-control issues, but the problems of thermal stress evolution and stress-induced deformation in the solid state are not treated. A critical discussion of the comparison between model predictions and experimental measurements is a key feature of the presentation, which concludes with a discussion of the critical problems that still need to be addressed.

02,871
PB96-135074 Not available NTIS
National Inst. of Standards and Technology (MSEL), Boulder, CO. Materials Reliability Div.
Electrode Extension Model for Gas Metal Arc Welding.
Final rept.
T. P. Quinn, R. B. Madigan, and T. A. Siewert. 1994, 8p.
Pub. in Welding Research Supplement, p241s-248s Oct 94.

Keywords: *Welding, *Electrode extensions, Reprints, Transfer functions, Temperature profiles, Spray transfer mode, *Describing functions, GMAW, Electrode feed speed.

The electrode extension during gas metal arc welding is predicted using a one-dimensional model of the melting electrode. Jouile heating in the electrode, heat directly applied to the end of the electrode from the condensing electrons, and heat transferred from the droplet, together with conduction along the electrode are considered. The thermal conductivity, the thermal diffusivity, and the electrical resistivity of the electrode material are allowed to bary with temperature. The steady-state electrode extension is predicted to an accuracy of 1.9 mm (0.074 in.). The onset of short-circuiting as the current is decreased for a given electrode feed speed is predicted within 9%. Dynamic anal-

ysis shows that the gas metal arc welding process acts as a low-pass filter for electrode extension with respect to the square of the current (proportional to power) and with respect to electrode feed speed. As the mean welding current is increased, the electrode extension (or arc length if the contact-tube-to-work distance is constant) has a smaller response to perturbations in the current or electrode feed speed. The quasi-linear transfer functions between electrode extension and current squared and between electrode extension and electrode feed speed can be described by one zero, two pole parametric fits. The transfer functions are linear in the amplitude of the excitation up to 10% of the mean excitation. The model transfer functions were verified with experiments.

02,872
PB96-135330 Not available NTIS
National Inst. of Standards and Technology (MSEL), Boulder, CO. Materials Reliability Div.
Contact Tube Wear Detection in Gas Metal Arc Welding.
Final rept.
T. P. Quinn, R. B. Madigan, M. A. Mornis, and T. A. Siewert. 1995, 7p.
Pub. in Welding Research Supplement, p115s-121s Apr 95.

Keywords: *Wear tests, *Gas metal arc welding, *Welding current, *Sensors, Reprints, Weldments, Welding electrodes, Wear, Robots, Sliding contact, Tube wear detection.

A real-time algorithm has been developed to detect contact tube wear during gas metal arc welding. The integral from 0.3 to 4 Hz of the power spectral density of voltage (constant current and pulsed current power sources) or current (constant voltage power sources) is called the wear parameter and is used to measure wear. The contact tube is predicted to be worn when the parameter grows nonlinearly or exceeds a threshold. For 11 contact tubes worn by welding on a rotating pipe, the wear parameter predicted the observed increase in the area of the contact tube's exit bore of 140% of the original area within a standard deviation of 20%. Welds were made with a constant voltage power source and with a pulsed current power source at two different voltages. The pulsed current welds were made with and without automatic voltage control by wire feed speed and with and without weaving in a V-groove. No significant differences were detected between the wear parameters for all test welds, indicating that the algorithm can be used under these welding conditions.

02,873
PB96-138540 Not available NTIS
National Inst. of Standards and Technology (MSEL), Boulder, CO. Materials Reliability Div.
Report on 1994 Actions of the International Institute of Welding.
Final rept.
T. A. Siewert. 1995, 4p.
See also PB94-185881.
Pub. in Materials Evaluation, p396-399 Mar 95.

Keywords: *Welding, *Meetings, *Nondestructive tests, *Quality assurance, *Standardization, Inspection, Standards, Weldments, Defects, Test methods, Reprints, International Institute of Welding.

Commission V covers issues of weld inspection and quality control for the International Institute of Welding. The report summarizes the information presented at the 1994 Annual Assembly: descriptions of both research and draft ISO standards being developed from the research data. The information comes from the various multinational subcommissions, working groups, and task groups within Commission V. Thus, this summary provides an up-to-date review of research activities in other countries than the US and advanced notice of standardization activities.

02,874
PB96-158076 Not available NTIS
National Inst. of Standards and Technology (MSEL), Gaithersburg, MD. Materials Reliability Div.
International Institute of Welding: Report on 1995 Actions.
Final rept.
T. Siewert. 1995, 4p.
See also PB96-138540.
Pub. in Materials Evaluation, v53 n12 p1380-1383 Dec 95.

Keywords: *Welding, *Inspection, *Nondestructive tests, *Stadards, Weldments, Test methods, Defects, Quality assurance, Quality control, Radiology, Ultrasonic tests, Standardization, Reprints, International Institute of Welding, Radioscopy.

This report summarizes the information presented at the 1995 Annual Assembly, descriptions of both research and draft ISO standards having been developed from the research data. The information comes from the various multinational sub-commissions, working groups, and task groups within Commission V. This summary provides an up-to-date review of research activities in other countries and advance notice of standardization activities.

02,875
PB96-158084 Not available NTIS
National Inst. of Standards and Technology (MSEL), Gaithersburg, MD. Materials Reliability Div.
What's Available in Welding Software.
Final rept.
T. A. Siewert. 1995, 5p.
Pub. in Welding Jnl., p39-43 Nov 95.

Keywords: *Welding, *Computer software, Weldments, Computerized simulation, Expert systems, Reference materials, Mathematical calculations, Standards, Reprints.

Welding software is making large strides in sophistication and power, as the developers take advantage of the latest hardware technology and new software concepts. The list includes current software, a short summary of its capabilities, and where to buy it.

02,876
PB96-160676 Not available NTIS
National Inst. of Standards and Technology (TS), Gaithersburg, MD. Lab. Accreditation Program.
Implementation of the Fastener Quality Act.
Final rept.
S. W. Stiefel. 1993, 7p.
See also PB94-210143.
Pub. in National Board of Boiler and Pressure Vessel Inspectors Proceedings, General Meeting (62nd), San Diego, CA., May 3-7, 1993, p63-69.

Keywords: *Implementation, *Quality control, Fasteners, Product inspection, Laboratory procedures, Test methods, Requirements, Accreditation, Certification, Reprints, *Fastner Quality Act, Pubic Law 101-592.

This presentation describes: the objective of Public Law 101-592, (the fastener Quality Act), various requirements and responsibilities under that act, the status of the procedures required for implementation, and the process being used at the National Institute of Standards and Technology (NIST) to develop the laboratory accreditation program for those laboratories that will be doing the testing under the act.

02,877
PB96-183124 PC A04/MF A01
National Inst. of Standards and Technology (MEL), Gaithersburg, MD. Intelligent Systems Div.
Proceedings of NIST Workshop: Industry Needs in Welding Research and Standards Development. Held on August 15-16, 1995.
W. G. Rippey. Apr 96, 32p, NISTIR-5822.

Keywords: *Welding, *Standards, *Meetings, US NIST, Research and development, Gaithersburg(Maryland).

Thirty-two attendees representing technology users, technology providers, private and university research, and government gathered for this two-day workshop on welding technology. The attendees defined twelve sub-topics. The top four ranked, indicating where Industry has the strongest needs, were: Interface standards for data exchange, Electrical and mechanical interface standards, Predictive process models and knowledge base, Simulation and off-line programming.

02,878
PB96-186028 Not available NTIS
National Inst. of Standards and Technology (MSEL), Boulder, CO. Materials Reliability Div.
Ultrasonic Sensing of GMAW: Laser/EMAT Defect Detection System.
Final rept.
N. M. Carlson, J. A. Johnson, E. D. Larsen, and A. Van Clark. 1992, 13p.
See also DE92017916.
Pub. in International Conference on Welding Research Trends in Welding Technology (3rd), ASM International, Metals Park, OH., p2-14 1992.

Keywords: *Defects, *Gas Metal-Arc Welding, Transducers, Computerized control systems, Reprints, Data acquisition systems, Detection, Feedback, Monitoring, Nondestructive analysis, Personal computers, *Ultrasonography, Welded joints.

In-process ultrasonic sensing of welding allows detection of weld defects in real-time (1). For a sensing effort to be practical in a production environment, a noncontracting ultrasonic system is developed. The system components are a pulsed laser for ultrasound generation and an electromagnetic acoustic transducer (EMAT) for ultrasound reception. A personal computer (PC)-based system acquires and analyzes data to determine the quality of the welding process on a pass-by-pass basis. The laser/EMAT system interrogates an area in the weld volume where defect conditions are most likely to occur. This area of interest is computer calculated on a pass-by-pass basis using weld planning information provided by the off-line programmer (OLP). The absence of a signal level above threshold in the computer calculated time interval indicates a disruption of the sound path to the EMAT due to the presence of a defect condition. The ultrasonic sensor system then provides an input signal to the weld controller about the defect condition.

02,879
PB96-186077 Not available NTIS
National Inst. of Standards and Technology (MSEL), Boulder, CO. Materials Reliability Div.
Well-Shielded EMAT for On-Line Ultrasonic Monitoring of GMA Welding.
Final rept.
A. V. Clark, S. R. Schaps, and C. M. Fortunko. 1992, 3p.
Pub. in Proceedings of Institute of Electrical and Electronics Engineers Ultrasonics Symposium, Orlando, FL., 1991, 3p 1992.

Keywords: *Acoustics, *Ultrasonics, *Welding, Reprints, *EMATs.

A hybrid laser/EMAT system is currently being developed for pass-by-pass inspection of weldment defects. The laser source is inherently broadband, whereas the EMAT is a narrow-band detector. The authors review some of the theory used to develop an optimized EMAT system for use with a laser source. The EMAT will be used close to a welding torch. The welding system has a 40 kHz (fundamental) switching power supply. This gives rise to severe electromagnetic interference (EMI). The authors review the means of temperature- and EMI-hardening used to develop a practical EMAT system for this environment. They developed a balanced system of counter-wound coil and differential preamplifier which greatly suppressed EMI. Other measures, such as multiple shielding, bandpass filtering, and attention to grounds, were used. The system gives about 32 dB signal-to-noise ratio, when operated 125 mm from a welding torch.

02,880
PB96-191366 PC A04/MF A01
National Inst. of Standards and Technology (MSEL), Boulder, CO. Materials Reliability Div.
IIW Commission V Quality Control and Quality Assurance of Welded Products, Annual Report 1995/96.
T. A. Siewert. Apr 96, 36p, NISTIR-5044, IIW-V-1059-96.
See also report for 1994/95, PB95-198743. Sponsored by International Inst. of Welding.

Keywords: *Welding, *Quality control, Nondestructive tests, Inspection, Eddy current tests, Ultrasonic tests, Meetings, US NIST.

The Annual Report 1995-96 for Commission V, Quality Control and Quality Assurance of Welded Products, of the International Institute of Welding includes (1) minutes, resolutions, and the future program adopted at its Annual Assembly in June 1995, (2) the organization, officials, and delegates, (3) schedules of meetings, and (4) the status of documents published by Commission V. It reviews current research and work on standardization.

02,881
PB97-114185 PC A06/MF A01
National Inst. of Standards and Technology (TS), Gaithersburg, MD. National Voluntary Lab. Accreditation Program.

Joining

National Voluntary Laboratory Accreditation Program (NVLAP): Fasteners and Metals.
Handbook.
D. F. Alderman. Aug 96, 76p, NIST/HB-150-18.
Also available from Supt. of Docs. as SN003-003-03421-5.

Keywords: *Fasteners, *Quality control, Standards, Tests, Laboratories, Accreditation, Chemical analysis, Metallography, Corrosion resistance, US NIST.

NIST Handbook 150-18 presents the technical requirements of the National Voluntary Laboratory Accreditation Program (NVLAP) for Fasteners and Metals. It is intended for information and use by staff of accredited laboratories, those laboratories seeking accreditation, other laboratory accreditation systems, users of laboratory services, and others needing information on the requirements for accreditation under the Fastners and Metals program. This publication supplements the Fasteners Quality Act (PL 101-592) as amended by the National Technology Transfer and Advancement Act (PL 104-113) and its implementing regulations as described in Title 15, Part 280 of the U.S. Code of Federal Regulations, and NIST Handbook 150, NVLAP Procedures and General Requirements (which contains all general NVLAP procedures, criteria, and policies).

Manufacturing, Planning, Processing & Control

02,882
PB94-185493 Not available NTIS
National Inst. of Standards and Technology (MEL), Gaithersburg, MD. Robot Systems Div.
Issues Concerning Material Removal Shape Element Volumes (MRSEVs).
Final rept.
T. R. Kramer. 1994, 13p.
Pub. in International Jnl. of Computer Integrated Manufacturing 7, n3 p139-151 1994.

Keywords: *Machining, Numerical control, Metal cutting, Computer aided manufacturing, Automation, Shape, Subroutine libraries, Reprints, *MRSEVs(Material removal shape element volumes), *Material removal shape element volumes, PDES(Product Data Exchange using STEP), STEP(Standard for the Exchange of Product Model Data).

In machining discrete parts, material removal shape element volumes (MRSEVs) may be used to convey shape information from process planning to NC-programming. This paper discusses 16 issues regarding MRSEVs and presents, in summary form, a proposed library of MRSEVs for three-axis machining.

02,883
PB95-147906 PC A04/MF A01
National Inst. of Standards and Technology (MEL), Gaithersburg, MD. Factory Automation Systems Div.
Program Requirements to Advance the Technology of Custom Footwear Manufacturing.
H. T. Moncarz. Oct 94, 56p, NISTIR-5521.

Keywords: *Footwear, *Orthopedic equipment, *Manufacturing, *Research and development, *Meetings, Shoes, Technology innovation, Prototypes, Cost effectiveness, US NIST.

The National Institute of Standards and Technology (NIST) and the South Carolina Research Authority (SCRA) co-hosted the first Custom Footwear Manufacturing Workshop in Charleston, SC on March 10-11, 1994. At the workshop we discussed the potential creation of a nationwide, collaborative research and development (R&D) effort to benefit the American footwear industry. We discussed applicable technologies for custom and therapeutic footwear manufacturing, related business requirements, national impacts on the economy and health care, and potential strategies to launch a nationwide R&D effort. We decided that our best strategy will be to concentrate initial efforts on the technology requirements of therapeutic footwear. We believe that the proper development, commercialization, and particularly, the integration of the advanced technologies discussed will enable the cost-effective design, manufacture, and distribution of therapeutic footwear. This report documents the workshop and is intended as a starting point to initiate the R&D program proposed.

02,884
PB95-171112 PC A03/MF A01
National Inst. of Standards and Technology (MEL), Gaithersburg, MD. Precision Engineering Div.
Japan Technology Program Assessment: Precision Engineering/Precision Optics in Japan.
C. J. Evans. Dec 94, 18p, NISTIR-5491.

Keywords: *Precision, *Machining, *Optics, *Japan, Technology assessment, Manufacturing, Lithography, Research and development, Technology innovation, Metrology, Precision engineering, National Institute of Standards and Technology.

The report, based on two visits to Japan, discusses the structure of precision engineering research and development in Japan, and current directives in precision machining, precision optics and advanced lithography.

02,885
PB95-210167 PC A03/MF A01
Catholic Univ. of America, Washington, DC. Dept. of Mechanical Engineering.
Issues Concerning Material Removal Shape Element Volumes (MRSEVs).
T. R. Kramer. 26 Mar 92, 32p, NISTIR-4804.
Contract NIST-70NANB9H0923
See also PB94-185493. Sponsored by National Inst. of Standards and Technology (MEL), Gaithersburg, MD. Intelligent Systems Div.

Keywords: *Machining, *Numerical control, Metal cutting, Computer aided manufacturing, Automation, Subroutine libraries, Shape, Production control, Material forming, *Material removal shape element volumes.

In machining discrete parts, Material Removal Shape Element Volumes (MRSEVs) may be used to convey shape information from process planning to numerically controlled (NC) programming. This paper discusses sixteen issues regarding MRSEVs and presents, in summary form, a proposed library of MRSEVs for 3-axis machining.

02,886
PB96-109525 PC A03/MF A01
National Inst. of Standards and Technology (CAML), Gaithersburg, MD. Statistical Engineering Div.
Agile Manufacturing from a Statistical Perspective.
R. G. Easterling. Oct 95, 44p, NISTIR-5573.
Also pub. as Sandia National Labs., Albuquerque, NM. New Initiatives Dept. rept. no. SAND95-1552. Prepared in cooperation with Sandia National Labs., Albuquerque, NM. New Initiatives Dept.

Keywords: *Manufacturing, *Industrial management, *Systems analysis, Industrial plants, Product development, Industrial plants, Statistics, Research programs, Agile manufacturing.

The objective of agile manufacturing is to provide the ability to quickly realize high-quality, highly-customized, in-demand products at a cost commensurate with mass production. More broadly, agility in manufacturing, or any other endeavor, is defined as change-proficiency--the ability to thrive in an evironment of unpredictable change. This report discusses the general direction of the agile manufacturing initiative, including research programs at the National Institute of Standards and Technology (NIST), the Department of Energy, and other government agencies, but focuses on agile manufacturing from a statistical perspective. The role of statistics can be important because agile manufacturing requires the collection and communication of process characterization and capability information, much of which will be data-based. The statistical community should initiate collaborative work in this important area.

02,887
PB96-112693 PC A99/MF E08
National Inst. of Standards and Technology (MEL), Gaithersburg, MD.
Proceedings of the Annual Manufacturing Technology Conference (2nd): Toward a Common Agenda. Held in Gaithersburg, Maryland on April 18-20, 1995.
Special pub.
C. Albus. Aug 95, 913p, NIST/SP-886.
Also available from Supt. of Docs as SN003-003-03361-8. See also report for 1994, PB95-206181.

Keywords: *Manufacturing, *Meetings, *Proceedings, US NIST, State of the art, Market research, Aerospace industry, Electronics industry, Automotive industry, Construction industry, Food industry, Textile industry, Gaithersburg(Maryland).

This conference helped to define the major elements of a common manufacturing agenda that involves the efforts of government, industry, academia and workforce organizations. The conference built on the progress made at last year's priority-setting conference on manufacturing technology, which attracted more than 600 participants.

Quality Control & Reliability

02,888
PB94-136009 PC A11/MF A03
National Inst. of Standards and Technology, Gaithersburg, MD.
NIST Handbook 44, 1994: Specifications, Tolerances and Other Technical Requirements for Weighing and Measuring Devices as Adopted by the 78th National Conference on Weights and Measures 1993.
Handbook.
H. V. Oppermann, and T. G. Butcher. Oct 93, 230p, NIST/HB-44.
Supersedes PB93-213106. Also available from Supt. of Docs. as SN003-003-03242-5.

Keywords: *Weight measurement, *Tolerances(Mechanics), *Measuring instruments, *Metrology, *Handbooks, Liquid level indicators, Water meters, Weight indicators, Grains(Food), Dimensional measurement, Hydrocarbons, Fuel tanks, Specifications, Liquefied petroleum gases, Length, Grain moisture, Taximeters.

Handbook 44 was first published in 1949, having been preceeded by similar handbooks of various designations and in several forms beginning in 1918. This 1994 edition was developed by the Committee on Specifications and Tolerances of the National Conference on Weights and Measures, with the assistance of the Office of Weights and Measures of the National Institute of Standards and Technology. It includes amendments adopted by the 78th annual meeting of the National Conference on Weights and Measures, 1993. Handbook 44 is published in its entirety each year following the annual meeting of the National Conference on Weights and Measures.

02,889
PB94-160835 PC A05/MF A01
National Inst. of Standards and Technology, Gaithersburg, MD.
National Type Evaluation Program: Index of Device Evaluations by Company. NCWM Publication 5 Part A (Second Edition).
K. Newell. 8 May 90, 86p, NISTIR-4333.

Keywords: *Metrology, Indexes(Documentation), Performance evaluation, *National Type Evaluation Program.

The publication contains the listing of all devices that have been evaluated under the National Type Evaluation Program (NTEP) since January 1, 1986 to May 8, 1990. It replaces the first Edition and Supplements 1, 2, and 3.

02,890
PB94-163029 PC A03/MF A01
National Inst. of Standards and Technology (MEL), Gaithersburg, MD. Factory Automation Systems Div.
Concept for an Algorithm Testing and Evaluation Program at NIST.
C. Diaz. Jan 94, 14p, NISTIR-5366.
See also PB90-148362.

Keywords: *Dimensional measurement, *Data analysis, *Computer program integrity, Metrology, Coordinates, Computer software, Algorithms, Computer program verification, Standards, National Institute of Standards and Technology.

This report proposes a National Institute of Standards and Technology (NIST) service for testing and evaluating coordinate measuring systems (CMS) software. This program addresses industry's need for a formal mechanism that tests data analysis software used in CMSs. The NIST Algorithm Testing and Evaluation Program (ATEP) combines the NIST Algorithm Testing System (ATS), test procedures based on emerging na-

tional standards, and control over the ATS reference algorithms. This report presents a concept for this formal mechanism to provide testing methods and tools to test and evaluate CMS data analysis software.

02,891
PB94-163466 PC A03/MF A01
National Inst. of Standards and Technology (MEL), Gaithersburg, MD. Factory Automation Systems Div.
Models, Managing Models, Quality Models: An Example of Quality Management.
J. E. Tyler. Dec 91, 20p, NISTIR-4738.
See also PB91-193367.

Keywords: *Product development, *Quality, *Management, *Standards, Models, Data bases, Technology innovation, Design standards, Production models, Commerce, Competition, International trade, STEP(Standard for the Exchange of Product Model Data), PDES(Product Data Exchange using STEP), Malcolm Baldrige National Quality Award, IGES(Initial Graphics Exchange Specification), ISO(International Organization for Standardization), Quality levels, Model assessment, Information models, Data models.

Quality is an increasingly important element in competitiveness. This paper will focus on strategies used by an international standards committee for improving the development of its complex standard. The paper outlines an approach for use within the standards-making community. Aside from the standards-making community, any organization interested in establishing quality metrics and quality thresholds to assess technical quality should find this paper useful. An overview of a methodology for evaluating the technical quality of information and data models is also included. Quality management techniques for models are described along with management's role in ensuring that high quality models are produced. Many basic concepts of the Malcolm Baldrige National Quality Award were used in building the foundation for this new approach to standards development.

02,892
PB94-164043 PC A06/MF A02
National Inst. of Standards and Technology (CSTL), Gaithersburg, MD. Thermophysics Div.
NIST Measurement Services: NIST Pressure Calibration Service.
Special pub.
V. E. Bean. Feb 94, 102p, NIST-SP-250-39.
Also available from Supt. of Docs. as SN003-003-03249-2.

Keywords: *Pressure measurement, *Primary standards, *Calibration, Quality control, Uncertainty, *Pressure Calibration Service, *Piston gages, US NIST.

This report is the documentation for the NIST pressure calibration service. Topics discussed include design philosophy and theory of pressure primary standard piston gages, uncertainties of the primary standards, uncertainties of NIST transfer standard piston gages, calibration quality control, methods of piston gage calibration, and international intercomparisons of pressure measurement. A sample calibration report is included as an appendix.

02,893
PB94-169760 Not available NTIS
National Inst. of Standards and Technology, Gaithersburg, MD.
Uncertainties in Dimensional Measurements Made at Nonstandard Temperatures.
D. A. Swyt. 1994, 14p.
Included in Jnl. of Research of the National Institute of Standards and Technology, v99 n1 p31-44 Jan/Feb 94.

Keywords: *Dimensional measurement, *Length, Temperature effects, Tolerances(Mechanics), Thermal expansion, Uncertainty, Metrology, Reprints, Reference temperature.

The report examines the effects of uncertainties in temperature and coefficient of thermal expansion on the expanded uncertainty of length dimensional measurements made away from the international standard reference temperature of 20 C for artifact standards and workpieces of various materials. Specific cases examined deal with (1) uncertainties of thermal-expansion coefficients associated with values given in engineering references, standard reference data, standard reference materials and direct measurements; and (2) uncertainties of part temperature measurements associated with realizing the International Temperature Scale of 1990 (ITS-90) and determining part temperatures relative to ITS-90 with the principal types of thermometry and achievable levels of temperature control.

02,894
PB94-185683 Not available NTIS
National Inst. of Standards and Technology (MEL), Gaithersburg, MD. Precision Engineering Div.
Development of a Calibrated Atomic Force Microscope.
Final rept.
T. H. McWaid, and J. Schneir. 1994, 6p.
Pub. in Proceedings of the ASPE Conference, Tucson, AZ., 1994, 6p.

Keywords: *Microscopes, Process control, Calibration, Metrology, Operation, Height, Pitch(Inclination), Design, Reprints, *Atomic force microscopes, Atomic force microscopy.

Advances in the manufacture of integrated circuits, x-ray optics, magnetic read-write heads, optical data storage media, razor blades, etc. require advances in ultraprecision metrology. Each of these industries is currently investigating the use of Atomic Force Microscopy (AFM) to improve the precision and accuracy of their manufacturing process control measurements. To facilitate the use of AFM for manufacturing, we are developing a specially designed AFM system that we call the Calibrated AFM (C-AFM). The C-AFM will be used to calibrate artifacts which, in turn, can be used to calibrate commercial AFMs. The system design goals are first presented. The critical electro-mechanical and metrology issues involved in the design, construction, and operation of the C-AFM are then summarized. The current status and performance of the instrument is then presented. The effects of stage stiffness on system performance are discussed in depth. Finally, plans for the future development of the instrument are summarized.

02,895
PB94-207727 PC A07/MF A02
National Inst. of Standards and Technology, Gaithersburg, MD. Office of Weights and Measures.
State Weights and Measures Laboratories: State Standards Program Description and Directory. 1994 Edition.
Special pub.
G. L. Harris. Jun 94, 132p, NIST/SP-791.
Supersedes PB93-217529. Also available from Supt. of Docs. as SN003-003-03272-7.

Keywords: *Laboratories, *Standards, *Directories, Units of measurement, States(United States), Puerto Rico, Virgin Islands, Tolerances(Mechanics), Calibration, Tests, *State services, *Weights and measures, National Type Evaluation Program, State Standards Program, Accreditation.

The support of its mission to promote uniform standards of measurement throughout the United States, the National Institute of Standards and Technology (NIST) received funding in 1965 to provide new standards of mass, length, and volume to State weights and measures laboratories. This program, called the (New) State Standards Program, also provided the equipment needed to perform calibration in these measurement areas. Part I describes the accreditation program whereby NIST accredits State weights and measures laboratories. Part II is the directory of State weights and measures laboratories and lists the services they provide to State and local weights and measures agencies as well as to industry. The directory is intended to assist potential users of the laboratory services in locating and obtaining needed measurement services.

02,896
PB94-216132 Not available NTIS
National Inst. of Standards and Technology, Gaithersburg, MD. Office of Product Standards Policy.
Performance Standards: The Pro's and Con's.
Final rept.
D. R. Mackay. 1985, 3p.
Pub. in Proceedings of American Water Works Association Annual Conference, Washington, DC., June 23-27, 1985, p403-405.

Keywords: *Performance tests, *Standards, Requirements, Reprints.

This paper defines the characteristics of performance standards, describes the promotion of the use of such standards and discusses the positive and negative aspects of performance standards. The purpose of this paper is to acquaint more people with the subject of performance standards.

02,897
PB95-108809 Not available NTIS
National Inst. of Standards and Technology (MEL), Gaithersburg, MD. Precision Engineering Div.
Evolution of Automatic Line Scale Measurement at the National Institute of Standards and Technology.
Final rept.
W. B. Penzes, and J. S. Beers. 1990, 18p.
Pub. in IMEKO Proceedings of the Symposium on Measurement and Inspection in Industry by Computer Aided Laser Metrology, Balatonfured, Hungary, September 24-27, 1990, p1-18.

Keywords: *Dimensional measurement, *Length, Laser interferometry, Historical aspects, Data acquisition, Automation, Uncertainty, Accuracy, Stability, Correction, Reprints, Laser metrology, US NIST.

The paper describes automatic length scale measurement by laser interferometry at NIST. It will show the continuous progress in measurement technique, instrumentation, and, consequently, measurement accuracy since 1965 to the present time. The discussion will include the latest improvement in stability, and the new yaw and pitch correction of the subcarriage. Changes in the measurement process including the automatic environmental data acquisition and the interferometer deadpath correction are also described.

02,898
PB95-108858 Not available NTIS
National Inst. of Standards and Technology (NEL), Gaithersburg, MD. Precision Engineering Div.
Some Considerations for Interim Testing of Coordinate Measuring Machine Performance Using a Specific Artifact.
Final rept.
S. D. Phillips, and B. Borchardt. 1991, 13p.
Pub. in Proceedings of the Measurement Science Conference, Anaheim, CA., January 31-February 1, 1991, 13p.

Keywords: *Tests, Dimensional measurement, Metrology, Errors, Process control, Quality assurance, Reprints, *CMMs(Coordinate Measuring Machines), *Coordinate Measuring Machines, Machine Checking Gage.

The use of a specific artifact, known as the Machine Checking Gage, is examined for use as an interim test of Coordinate Measuring Machine (CMM) performance. The results of several tests using this gage on two different CMMs is reported. Suggestions for making the test more robust and informative are described.

02,899
PB95-108866 Not available NTIS
National Inst. of Standards and Technology (NEL), Gaithersburg, MD. Precision Engineering Div.
Development of an Automated Part Inspection System Using the DMIS Standard.
Final rept.
S. D. Phillips, D. C. Stieren, and J. G. Salsbury. 1990, 10p.
Pub. in Proceedings of the Conference on Precision Metrology with Coordinate Measurement Systems, San Jose, CA., September 18-19, 1990, 10p.

Keywords: *Dimensional measurement, *Inspection, *Automation, Computer aided design, Standards, Measuring instruments, Reprints, DMIS(Dimensional Measuring Interface Specification), CMMs(Coordinate Measuring Machines), US NIST.

The recently approved dimensional measuring interface specification (DMIS) standard is briefly reviewed. An inspection system which incorporates this standard is being developed at the National Institute of Standards and Technology (NIST), and the implementation of DMIS is outlined. It closes with a discussion of the benefits and limitations of such a system and a summary of the inspection process.

02,900
PB95-125704 Not available NTIS
National Inst. of Standards and Technology (MSEL), Boulder, CO. Materials Reliability Div.

High-Sensitivity Acoustic Emission Sensor/Preamplifier Subsystems.
Final rept.
C. M. Fortunko, M. A. Hamstad, and D. W. Fitting. 1993, 17p.
Pub. in Review of Progress in Quantitative Nondestructive Evaluation, v12 17p 1993.

Keywords: *Acoustic emission, *Piezoelectric ceramics, *Ultrasonic wave transducers, Failure analysis, Nondestructive tests, Ultrasonics, Acoustic measurement, Preamplifiers, Ultrasonic tests, Reprints.

An experimental study was conducted to evaluate the suitability of five piezoelectric materials for use in high-sensitivity, broadband (10 kHz-2 MHz) acoustic-emission (AE) 'point' sensors. The scope of the study included effects of the material parameters and preamplifier input-impedance characteristics. Computer-model predictions were compared with results of measurements. The NIST Standard Reference Material (SRM) 'conical' transducer was used as a reference high-performance sensor. The experimental study was carried out using 'pinducers' made of: PZT-5A, lead metaniobate, x-cut quartz, 36 deg Y-cut LiNbO3, and PVDF. It is shown that materials exhibiting the highest dielectric constant are best suited for high-performance AE sensor applications.

02,901
PB95-136354 PC A03/MF A01
National Inst. of Standards and Technology (MEL), Gaithersburg, MD. Factory Automation Systems Div.
Sensitivity of Three-Point Circle Fitting.
T. H. Hopp. Sep 94, 14p, NISTIR-5501.

Keywords: *Inspection, *Metrology, *Curve fitting, Dimensional measurement, Circles(Geometry), Coordinates, Estimating, *CMMs(Coordinate Measuring Machines), *Coordinate Measuring Machines.

This paper establishes to first order the sensitivity of the center coordinates and radius of a circle through three points in terms of small, random perturbations of those points. This problem arises in the estimation of measurement errors from coordinate measurement systems. Formulas developed herein express the uncertainty of circle parameters as functions of point measurement uncertainty and the arc angle between points. We show that for practical measurement procedures, task uncertainties depend only on the mean and variance of the point measurement errors and are essentially independent of their statistical distribution.

02,902
PB95-140455 Not available NTIS
National Inst. of Standards and Technology (MSEL), Gaithersburg, MD.
Nondestructive Evaluation and Materials Processing.
Final rept.
L. H. Schwartz. 1991, 16p.
Pub. in Review of Progress in Quantitative Nondestructive Evaluation, v10A p35-50 1991.

Keywords: *Nondestructive tests, *Test methods, Ultrasonic tests, Polymers, Process control, Heat treatment, Research, Eddy currents, Fluorescence, Aluminum alloys, Reprints, *Intelligent processing of materials, US NIST.

A brief introduction to this paper will be given describing the relationship of materials science to the industrial challenge facing the United States and the role of the National Institute of Standards and Technology (NIST) in helping to meet this challenge. The main portion of the talk will deal with the important role of Nondestructive Evaluation (NDE) in the processing of materials. NDE research and engineering at NIST aimed at developing sensors for such applications will be discussed and illustrated by the following examples: fluorescent sensors for polymer processing, ultrasonic sensors for high Tc superconductor heat treatment, and eddy current probes for aluminum processing. The focus on the intelligent processing of materials will be illustrated by examples involving high pressure gas atomization and hot isostatic processing of metal powders. Future directions of the NIST program will be presented.

02,903
PB95-146379 PC A11/MF A03
National Inst. of Standards and Technology (TS), Gaithersburg, MD. Office of Standards Services.
NIST Handbook 44, 1995: Specifications, Tolerances and Other Technical Requirements for Weighing and Measuring Devices as Adopted by the 79th National Conference on Weights and Measures 1994.
H. V. Oppermann, and T. G. Butcher. Oct 94, 240p, NIST/HB-44.
Supersedes PB94-136009. Also available from Supt. of Docs. as SN003-003-03298-1.

Keywords: *Weight measurement, *Measuring instruments, *Handbooks, Liquid level indicators, Time measuring instruments, Weight indicators, Dimensional measurement, Tolerances(Mechanics), Liquefied petroleum gases, Water meters, Grains(Food), Cryogenic fluids, Hydrocarbons, Specifications, Containers, Odometers, Flowmeters, Ammonia, Length, Volume, Fabrics, Rope, Wire, Milk, Grain moisture, Taximeters.

Handbook 44 was first published in 1949, having been preceded by similar handbooks of various designations and in several forms beginning in 1918. This 1995 edition was developed by the Committee on Specifications and Tolerances of the National Conference on Weights and Measures with the assistance of the Office of Weights and Measures of the National Institute of Standards and Technology. It includes amendments adopted by the 79th annual meeting of the National Conference on Weights and Measures in 1994. Handbook 44 is published in its entirety each year following the annual meeting of the National Conference on Weights and Measures.

02,904
PB95-151916 Not available NTIS
National Inst. of Standards and Technology (MSEL), Gaithersburg, MD. Materials Reliability Div.
Ultrasonic Technique for Sizing Voids Using Area Functions.
Final rept.
J. Yang, and L. J. Bond. 1992, 6p.
Sponsored by British Council, London (England).
Pub. in IEE Proceedings-A 139, n2 p45-50 Mar 92.

Keywords: *Voids, *Ultrasonic tests, *Size determination, Dimensional measurement, Nondestructive tests, Approximation, Size(Dimensions), Backscattering, Reprints.

A technique is reported for determining the sizes of voids in structural materials by the inversion of backscattered ultrasonic signals using the area function formula. The formulation of this method is based on the Born approximation which is a weak scattering approximation, but it is shown to work well for voids. Results for extracting the radii of spherical voids, or the tangent plane distances of spheroidal voids are presented, using theoretical and experimental scattering data.

02,905
PB95-152179 Not available NTIS
National Inst. of Standards and Technology (NEL), Gaithersburg, MD. Precision Engineering Div.
Automated Optical Roughness Inspection.
Final rept.
J. H. Zimmerman, T. V. Vorburger, and H. T. Moncarz. 1989, 13p.
Pub. in Proceedings of Society of Photo-Optical Instrumentation Engineers: Optical Testing and Metrology II, v954 p252-265 1989.

Keywords: *Surface roughness, *Inspection, *Computer aided manufacturing, *Optical measuring instruments, Light scattering, Robots, Robotics, Surface properties, Process control, Controllers, Quality control, Reprints, *Surface Roughness Instrument Controllers.

This paper describes the theory and implementation of automated optical roughness inspection. Our work has been accomplished at the Inspection Workstation (IWS) in the Automated Manufacturing Research Facility (AMRF) at the National Bureau of Standards. The Surface Roughness Instrument Controller (SRIC) supervises the automated optical roughness inspection of parts. This controller is an integrated, data-driven, hierarchical control software system. The SRIC controls two pieces of equipment--the surface roughness instrument (SRI) and the automatic dial indicator (ADI). The SRI is a photo-optical surface roughness inspection device which monitors surface roughness by measuring the angular distribution of light scattered from the surface of a part. Its tasks are coordinated with those of the IWS inspection robot. Using the SRI optical signals as sensory input, the robot properly aligns the part in front of the SRI so that a valid optical scattering reading is obtained. The ADI is used to help the robot to position the part in front of the SRI for its initial reading. The SRIC uses the optical data obtained to estimate values of roughness average and root mean square roughness for parts machined in the AMRF.

02,906
PB95-163077 Not available NTIS
National Inst. of Standards and Technology (NEL), Gaithersburg, MD. Precision Engineering Div.
Automated Inspection: The Integration of National Standards and Commercial Products at NIST.
Final rept.
D. C. Stieren, and S. Phillips. 1991, 7p.
Sponsored by Miami Univ., Coral Gables, FL. Dept. of Industrial Engineering.
Pub. in Productivity and Quality Management Frontiers-III, p330-336 1991.

Keywords: *Automated inspection, *Integrated systems, *Dimensional measurement, Computer aided design, Computer aided manufacturing, Measuring instruments, Standards, Interfaces, Reprints, *US NIST, Manufactured parts, Coordinate measuring machines, IGES(Initial Graphics Exchange Specification), Postprocessing.

An automated inspection system for manufactured parts is being implemented within the Quality in Automation program at the National Institute of Standards and Technology. The project is a cooperative research effort among NIST and six U.S. industrial firms to correct the traditional problems associated with post-process gauging procedures, and closes the loop for these procedures from the production of a CAD representation of a part to the analysis of inspection results for that part.

02,907
PB95-164455 Not available NTIS
National Inst. of Standards and Technology (MSEL), Gaithersburg, MD. Materials Reliability Div.
X-Ray Image Quality Indicator Designed for Easy Alignment.
Final rept.
T. A. Siewert, and M. W. Austin. 1992, 4p.
Pub. in Materials Evaluation, p1069-1072 Sep 92.

Keywords: *X-ray inspection, *Welded joints, *Image processing, *X-ray imagery, Image analysis, Quality control, Radiography, Imaging techniques, Nondestructive tests, Reprints, *Image quality indicator.

A new image quality indicator (IQI) design is proposed that is particularly suitable for fundamental measurements of image unsharpness. The design is that of a thin strip, with its larger cross-sectional dimension aligned parallel to the beam at some location along the strip. One end of the strip is given a half twist so some section near the center of the strip is perfectly aligned with the beam, without requiring the careful alignment as with some IQI designs. A strip configuration is apt because it is available for many materials at low cost and in thin dimensions. Our report describes preliminary evaluation of the concept using a steel strip with cross-sectional dimensions of 0.07 by 3 mm.

02,908
PB95-164463 Not available NTIS
National Inst. of Standards and Technology (MSEL), Gaithersburg, MD. Materials Reliability Div.
Through-the-Arc Sensing for Measuring Gas Metal Arc Weld Quality in Real Time.
Final rept.
T. Siewert, B. Madigan, T. Quinn, and M. Mornis. 1992, 4p.
Pub. in Materials Evaluation, p314-318 Nov 92.

Keywords: *Arc welding, *Electrical measurement, *Real time, *Quality control, Drop transfer, Shielding, Wear, Electric current, Voltage, Data acquisition, Monitoring, Inspection, Reprints, *Through-the-arc sensing, *Gas metal arc welding.

The voltage drop across the arc in gas metal arc welding is affected by droplet transfer, spatter formation, and many other arc characteristics, and the current is affected in a similar manner. We collected voltage and current records with a high-speed data acquisition system, and correlated features in the records to various welding problems. Interruption in the shielding gas coverage, wear of the contact tube, change in the contact-tube-to-work, distance, and change in the droplet

transfer mode were detected through this sensing strategy. These effects were developed into general correlations and incorporated into a computerized data collection and analysis system.

02,909
PB95-174470 PC A09/MF A02
National Inst. of Standards and Technology (TS), Gaithersburg, MD. Weights and Measures Program.
Uniform Laws and Regulations in the Areas of Legal Metrology and Motor Fuel Quality, 1994 as Adopted by the 79th National Conference on Weights and Measures 1994.
Handbook.
J. A. Koenig, and K. S. Butcher. Dec 94, 183p, NIST/HB-130-1995.
Supersedes PB93-125086. Also available from Supt. of Docs. as SN003-003-03308-1.

Keywords: *Weight measurement, *Regulations, *Handbooks, Packaging, Standardization, Revisions, Automotive fuels, Consumer affairs, Commodities, Labels, Prices, Food, Sales, Metrology, Law(Jurisprudence).

The handbook compiles the latest Uniform Laws and Regulations and related interpretations and guidelines adopted by the National Conference on Weights and Measures (NCWM). At the 1983 annual meeting, the NCWM voted to change the title of Handbook 130 and the titles of the Laws and Regulations compiled in the handbook. The edition includes amendments adopted at the annual meetings in 1993 and 1994. The Conference recommends adoption and promulgation by weights and measures jurisdictions of these Uniform Laws and Regulations as updated in the handbook.

02,910
PB95-175451 Not available NTIS
National Inst. of Standards and Technology (MEL), Gaithersburg, MD. Factory Automation Systems Div.
Dimensional Inspection Planning Based on Product Data Standards.
Final rept.
S. C. Feng. 1994, 10p.
Pub. in Proceedings of International Conference on Concurrent Engineering (1st): Research and Applications, Pittsburgh, PA., August 29-31, 1994, p333-342.

Keywords: *Dimensional measurement, *Inspection, *Standards, Computer aided design, Models, Information processing, Planning, Computer aided manufacturing, Reprints, *DMIS(Dimensional Measuring Interface Standard), *Dimensional Measuring Interface Standard, STEP(Standard for the Exchange of Product Model Data), CMMs(Coordinate Measuring Machines).

This paper describes an activity model for dimensional inspection planning that bridges the gap between product design and the dimensional measurement of manufactured products. Functionally, this model specifies requirements for developing a part of a product data exchange standard that enables design, inspection resource, and measurement data to be exchanged among computer aided design systems, computer aided process planning systems, and coordinate measuring systems. A set of diagrams has been generated to represent the activity and its sub-activities, inputs, outputs, controls, and mechanisms, when such inspection planning is based on technologies of product data exchange, process planning, and information modeling.

02,911
PB95-180816 Not available NTIS
National Inst. of Standards and Technology (MEL), Gaithersburg, MD. Precision Engineering Div.
Improving Photomask Linewidth Measurement Accuracy via Emulated Stepper Aerial Image Measurement.
Final rept.
J. E. Potzick. 1994, 8p.
Pub. in Society of Photo-Optical Instrumentation Engineers Photomask Technology and Management 10, n47 p1-8 Sep 94.

Keywords: *Photomasks, *Dimensional measurement, *Line width, Integrated circuits, Uncertainty, Chromium, Accuracy, Reprints.

The most significant contribution to uncertainty in the measurement of photomask linewidths is the rough shape of the edge of the etched chrome lines. This uncertainty can be greatly reduced if the emulated stepper aerial image of the feature is measured instead of its geometric linewidth. That is: measure what the photomask does, not what it is. Phase-shift and other kinds of mask can be measured in the same way.

02,912
PB95-189494 PC A03/MF A01
National Inst. of Standards and Technology (CSL), Gaithersburg, MD.
Proceedings Report of the International Invitation Workshop on Development Assurance. Held in Ellicott City, Maryland on June 16-17, 1994.
P. Toth. Jan 95, 35p, NISTIR-5590.

Keywords: *Quality assurance, *Product development, Product inspection, Evaluation, Competition, Models, Methodology, *Developmental assurance, US NIST.

Ninety-eight participants from the US, EC, Canada, and Japan representing government agencies, both defense and civil, private corporations, evaluators, users, and vendors of trusted products met to discuss the concept of developmental assurance. The majority of the participants felt that the concept of developmental assurance was valid. The participants recommended that all future developmental assurance work take place on the international level. The developmental assurance concept must first be proven at the lower levels of trust. Developmental assurance may provide a level of assurance that approaches the current C2/E2. If this is possible, developmental assurance may then be extended to the higher levels of trust. Developmental assurance may not replace third party evaluations completely but may help to speed up the evaluation process. Developmental assurance in combination with third party evaluation may provide a useful level of assurance in a more reasonable period of time.

02,913
PB95-209862 PC A03/MF A01
National Inst. of Standards and Technology (MEL), Gaithersburg, MD. Precision Engineering Div.
Design, Specification and Tolerancing of Micrometer-Tolerance Assemblies.
D. A. Swyt. Mar 95, 27p, NISTIR-5615.
See also PB92-164680.

Keywords: *US NIST, *Metrology, *Tolerances(Mechanics), Electronics industry, Automobile industry, Specifications, Engines.

Increasing numbers of economically important products manufactured by U.S. companies are comprised of assemblies of component parts which have macroscopic dimensions and microscopic tolerances. Micrometer-tolerance assemblies include not only integrated-circuit devices and mangetic-memory read-write heads, but automobile-engine systems, including fuel injectors, hydraulic valve lifters and even piston and cylinder assemblies. Focusing on these, this paper: (1) reports examples of micrometer-tolerance assemblies; (2) discusses strategies in design, specification, and tolerancing (DS&T) which some companies have adopted for the manufacture of such assemblies; and (3) identifies generic-technology, measurement, and standards issues in DS&T associated with that manufacture.

02,914
PB95-210589 PC A04/MF A01
National Inst. of Standards and Technology (MEL), Gaithersburg, MD. Precision Engineering Div.
Interim Testing Artifact (ITA): A Performance Evaluation System for Coordinate Measuring Machines (CMMs). User Manual.
A. T. Singer, J. L. Land, S. D. Phillips, G. Caskey, D. Ward, P. Snoots, B. Faust, D. Sawyer, and B. Borchardt. Feb 95, 74p, NISTIR-5602.

Keywords: *Dimensional measurement, *Measuring instruments, *Inspection, *Performance evaluation, Kinematics, Manufacturing, Tests, Pneumatic equipment, Components, User manuals, CMMs(Coordinate Measuring Machines), ITA(Interim Testing Artifact).

Coordinate Measuring Machines (CMMs) have emerged as the primary tool for manufactured part dimensional inspection. However, models which completely characterize CMM errors are not currently available. The Interim Testing Artifact (ITA) was developed at the National Institute of Standards and Technology (NIST) to help CMM users determine the performance of their CMMs. This document is a user manual which contains the complete instructions for the assembly, use and maintenance of the ITA.

02,915
PB95-231833 PC A03/MF A01
National Inst. of Standards and Technology (MEL), Gaithersburg, MD. Manufacturing Systems Integration Div.
Algorithm Testing and Evaluation Program for Coordinate Measuring Systems: Long Range Plan.
C. Diaz. May 95, 16p, NISTIR-5651.
See also PB94-163029.

Keywords: *Data analysis, *Computer program, *Dimensional measurement, Algorithms, Metrology, Coordinates, Computer software, Standards, National Institute of Standards and Technology.

The report is a long range plan for the NIST Algorithm Testing and Evaluation Program (ATEP). ATEP is a Special Test Service provided at NIST through the Office of Measurements Services Calibrations Program. ATEP is a serivce for testing and evaluating data analysis software found in coordinate measuring systems. The purpose of the long range plan is to outline the projected evolution of the service so that the service will evolve systematically.

02,916
PB95-251666 PC A03/MF A01
National Inst. of Standards and Technology (MEL), Gaithersburg, MD. Manufacturing Systems Integration Div.
User's Guide for the Algorithm Testing System Version 2.0.
D. A. Rosenfeld. Jun 95, 44p, NISTIR-5674.
See also PB93-175990.

Keywords: *Verification inspection, *Fitting, *Geometry, *Computer program verification, Algorithms, Computer software, Data analysis, Graphical user interface, Input output processing, Online systems, User manuals(Computer programs), ATEP(Algorithm Testing and Evaluation Program), CMS(Coordinate Measuring Systems), US NIST.

The Algorithm Testing System (ATS) is a software system which support the Algorithm Testing and Evaluation Program for Coordinate Measuring Systems (ATEP-CMS). ATEP-CMS is a National Institute of Standards and Technology (NIST) special test service for evaluating the performance of CMS geometric fitting software. ATEP-CMS uses the ATS to analyze such software. The ATS typically performs such an analysis by generating data sets, applying its own fitting routines to fit geometries onto the datasets, and comparing its own fit results to the fit results of the software under test for the same data. The ATS provides the above capabilities, and extensive on-line help. The report provides a user's guide for the ATS. It introduces the overall design and functionality of the ATS and guides the user through a number of hands-on tutorials.

02,917
PB95-255832 PC A03/MF A01
National Inst. of Standards and Technology (MEL), Gaithersburg, MD. Intelligent Systems Div.
Integrated Vision Touch-Probe System for Dimensional Inspection Tasks.
M. Nashman, W. Rippey, T. H. Hong, and M. Herman. Jun 95, 18p, NISTIR-5678.

Keywords: *Verification inspection, *Dimensional measurement, *Computer vision, *Tactile sensors(Robotics), Control systems, Real time operation, Hierarchies, Image processing, CMMs(Coordinate Measuring Machines), NGIS(Next Generation Inspection System).

The paper discusses the integration of vision and touch sensors in a coordinate measuring machine (CMM) controller used for dimensional inspection tasks. A real-time hierarchical control system is presented in which a vision system extracts positions of features. The probe is tracked by the vision system as it scans surfaces so that its motion can be visually served. Minimalist sensor-derived representations, involving only task-specific information, are used in this process. Although the camera itself remains incalibrated, a real-time calibration of very limited scope is performed each processing cycle to transform the task-specific image informaiton into 3-D information as feedback to guide the probe. The ability to integrate vision and touch sensors for CMM tasks promises expanded capabilities for flexible inspection data acquisition.

02,918
PB95-267928 PC A03/MF A01
National Inst. of Standards and Technology (MEL), Gaithersburg, MD. Precision Engineering Div.

Estimation of Measurement Uncertainty of Small Circular Features Measured by CMMs.
S. D. Phillips, B. Borchardt, and W. T. Estler. Aug 95, 16p, NISTIR-5698.

Keywords: *Dimensional measurement, *Accuracy, *Estimating, Circular plates, Algorithms, Metrology, Geometry, Uncertainty, Graphs(Charts), *CMMs(Coordinate Measuring Machines), *Coordinate Measuring Machines.

This paper examines the measurement uncertainty of small circular features as a function of the sampling strategy, i.e., the number and distribution of measurement points. Specifically, we examine measuring a circular feature using a three-point sampling strategy in which the angular distance between the points varies from widely spaced, 120 degrees, to closely grouped, a few degrees. Both theoretical and experimental results show that the measurements uncertainty is a strong function of the sampling strategy. The uncertainty is shown to vary by four orders of magnitude as a function of the angular distribution of the measurement points. A conceptual framework for theoretically estimating the measuring uncertainty is described and a good agreement with experiment is obtained when the measurements are consistent with the assumptions of the theoretical model.

02,919
PB96-115019 PC A04/MF A01
National Inst. of Standards and Technology, Gaithersburg, MD. Standards Application and Assistance Program.
Standards Setting in the European Union: Standards Organization and Officials in EU Standards Activities.
Special pub.
R. A. Rensberger, and R. van de Zande. Sep 95, 74p, NIST/SP-891.
Also available from Supt. of Docs. as SN003-003-03369-3. Prepared in cooperation with European Union, Brussels (Belgium).

Keywords: *European Union, *Standards, *Requirements, Certification, Test facilities, Standardization, Organizations, Specifications, Telecommunication, Electrotechnology, Quality assurance, International trade.

The guide includes a brief history of the role of standards in the European Union and the lastest information on the EU's harmonization directives for implementing the 'New Approach' and the Global Approach for harmonizing technical regulations and standards to reduce barriers to trade. The standards guide also contains information on the three key European standards organizations that are mandated by the EU Commission to draft European technical standards; information on European testing and certification activities; and a list of EU officials with standards-related responsibilities.

02,920
PB96-123401 Not available NTIS
National Inst. of Standards and Technology (TS), Gaithersburg, MD. Metric Program.
Federal Labs Have Key Role in Metrication.
Final rept.
R. Richter. 1995, 2p.
Pub. in NEWSLINK: A Monthly Publication of the Federal Laboratory Corsortium for Technology Transfer (FLC), v11 n5 p2-3 May 95.

Keywords: *Metrication, *Federal agencies, *International trade, Laboratories, Standards, Metric system, Metrology, SI units, International system of units, Exports, Reprints, Market competition.

As international trade becomes more competitive, the slightest disadvantage quickly is translated into lost opportunities. Many U.S. exporters may find themselves at a competitive disadvantage because of the incompatibility between the metric standards used in world markets and many U.S. standards which remain nonmetric.

02,921
PB96-128236 PC A03/MF A01
National Inst. of Standards and Technology (MEL), Gaithersburg, MD. Manufacturing Systems Integration Div.
User's Guide to 'SuperFit' Modeling Software for CMM Probe Lobing.
T. H. Hopp. Oct 95, 12p, NISTIR-5720.

Keywords: *Dimensional measurement, *Computer programs, Data analysis, Inspection, User manuals, *CMM(Coordinate Measuring Machines), *Coordinate Measuring Machines, Superfit Modeling Software.

Superfit is a software package developed by the National Institute of Standards and Technology (NIST) that fits a model of probe lobing to coordinate data obtained by probing a calibration ball. It runs under the Microsoft Windows(TM) 3.1 operating system. This document describes how to use the Superfit software.

02,922
PB96-128244 PC A03/MF A01
National Inst. of Standards and Technology (MEL), Gaithersburg, MD. Manufacturing Systems Integration Div.
Reference Manual for the Algorithm Testing System Version 2.0.
D. A. Rosenfeld. Oct 95, 44p, NISTIR-5722.
See also PB95-251666.

Keywords: *User manuals, *Dimensional measurement, *Data analysis, Computer program integrity, Metrology, Coordinates, Algorithms, Computer software tests, Computer program verification, Coordinate measuring systems, Geometric fitting software.

The Algorithm Testing System (ATS) is a software system which supports the Algorithm Testing and Evaluation Program for Coordinate Measuring Systems (ATEP-CMS). ATEP-CMS is a NIST Special Test Service for evaluating the performance of CMS geometric fitting software. The ATS typically performs an analysis by generating data sets, applying its own fitting routines to fit geometrics onto the data sets, and comparing its own fit results to the fit results of the software under test for the same data. This report is a reference manual for the ATS. It documents fully the usuage of the ATS, describes in detail the data generation and analysis capabilities of the ATS, and defines the naming conventions used by the ATS.

02,923
PB96-155429 Not available NTIS
National Inst. of Standards and Technology (TS), Gaithersburg, MD. Standards in Trade Program.
Metrology and Regional Trade Pacts.
Final rept.
H. Oppermann. 1995, 7p.
Pub. in Metrology for the Americas Symposium, Miami, FL., November 6-8, 1995, p1-7.

Keywords: *Dimensional measurements, *Standards, *International trade, Specifications, Metrology, Regulations, Laboratories, Accreditation, Reprints, Trade agreements, Technical barriers.

International investment and trade are driving forces for national economies, building a sound industrial base, and developing jobs. However, as tariffs have decreased, technical barriers have become significant as potential impediments to trade. These technical barriers are often the result of technical regulations (mandatory standards). Some of the major technical barriers to trade stem from product standards, conformity assessment, laboratory accreditation, and demonstrating traceability to national laboratories.

02,924
PB96-160684 Not available NTIS
National Inst. of Standards and Technology (MEL), Gaithersburg, MD. Precision Engineering Div.
New Concepts of Precision Dimensional Measurement for Modern Manufacturing.
Final rept.
D. A. Swyt. 1991, 52p.
See also PB91-240812.
Pub. in Control and Dynamic Systems, v45 p111-162.

Keywords: *Dimensional measurement, *Accuracy, *Precision, *Machine tools, Manufacturing, Process control, Integrated systems, Measuring instruments, Tolerance(Mechanics), Specifications, Metrology, Error analysis, Reprints, Coordinate measuring machines.

A hallmark of modern products is the high precision of the dimensions of their functional parts - high, that is, compared to that of their less-modern contemporaries. Modern products of this century are video cassette recorders, the precision of whose parts allows read-write heads to be aerodynamically flown over the recording medium at misrcoscopic altitudes.

02,925
PB96-160759 Not available NTIS
National Inst. of Standards and Technology (TS), Gaithersburg, MD. Office of Technology Information.
Metrology.
Final rept.
J. J. Ulbrecht. 1991, 1p.
Pub. in Academic Press Dictionary of Science, 1p Fall 91.

Keywords: *Metrology, Units of measurement, Weight, Standardization, Reprints.

Metrology is the field of knowledge concerned with measurement. While all scientific disciplines impact on human life in one way or another, the interaction with weigts and measures runs like a continuous line through everybody's life.

02,926
PB96-166616 PC A13/MF A03
National Inst. of Standards and Technology, Gaithersburg, MD. Office of Weights and Measures.
NIST Handbook 44, 1996: Specifications, Tolerances, and Other Technical Requirements for Weighing and Measuring Devices as Adopted by the 80th National Conference on Weights and Measures, 1995.
T. G. Butcher, C. Cotsoradis, and T. L. Grimes. Jan 96, 252p.
Supersedes PB95-146379.

Keywords: *Weight measurement, *Measuring instruments, *Handbooks, Metrology, Liquid level indicators, Time measuring instruments, Weight indicators, Dimensional measurement, Tolerances(Mechanics), Liquified petroleum gases, Water meters, Grains(Food), Cryogenic fluids, Hydrocarbons, Fuel tanks, Specifications, Containers, Odometers, Flowmeters, Ammonia, Length, Volume, Grain moisture, Taximeters.

Handbook 44 was first published in 1949, having preceded by similar handbooks of various designations and several forms, beginning in 1918. This 1996 edition was developed by the Committee on Specifications and Tolerances of the National Conference on Weights and Measures, with the assistance of the Office of Weights and Measures of the National Institute of Standards and Technology (NIST). It includes amendments adopted by the 80th annual meeting of the National Conference on Weights and Measures in 1995. Handbook 44 is published in its entirety each year following the annual meeting of the National Conference on Weights and Measures.

02,927
PB96-172309 PC A12/MF A03
National Inst. of Standards and Technology (TS), Gaithersburg, MD. Weights and Measures Program.
Uniform Laws and Regulations in the Areas of Legal Metrology and Motor Fuel Quality as Adopted by the 80th National Conference on Weights and Measures 1995. 1996 Edition.
Handbook.
J. A. Koenig, K. S. Butcher, and T. L. Grimes. Jan 96, 231p, NIST/HB-130-1996.
Supersedes 1995 Edition, PB95-174470. Also available from Supt. of Docs. as SN003-003-03391-0.

Keywords: *US NIST, *Weight measurement, *Law(Jurisprudence), Regulations, Handbooks, Automotive fuels, Consumer affairs, Packaging, Standardization, Commodities, Price, Labels, Food, Sales.

This handbook compiles the latest Uniform Laws and Regulations and related interpretations and guidelines adopted by the National Conference on Weights and Measures (NCWM). At the 1983 Annual Meeting, the NCWM voted to change the title of Handbook 130 and the titles of the Laws and Regulations compiled in this handbook. The former title of the handbook was 'Model State Laws and Regulations.' 'Model State' was changed to 'Uniform' in the titles to reflect that these Laws and Regulations are (1) intended to be standards rather than just guidelines, and (2) intended for adoption by political subdivisions other than States when deemed appropriate. The compilation itself was approved by the NCWM in 1979. This edition includes amendments adopted at the Annual Meeting in 1995.

02,928
PB97-110423 Not available NTIS
National Inst. of Standards and Technology (MEL), Gaithersburg, MD. Precision Engineering Div.

Present and Future Standard Specimens for Surface Finish Metrology.
Final rept.
T. V. Vorburger, J. F. Song, E. Marx, B. R. Scace, and T. R. Lettieri. 1992, 4p.
Pub. in International Symposium on Optical Fabrication Testing and Surface Evaluation, Society of Photo-Optical Instrumentation Engineers, v1720 p78-81 Feb 92.

Keywords: *Surface profiling, *Metrology, Bidirectional reflectance, Roughness average, Sinusoidal, Spatial wavelength, Reprints, *Standard reference materials.

The accurate measurement of surface finish requires standard specimens to calibrate and check the operation of the measuring instruments. This is true both for profiling techniques such as the stylus and area averaging techniques such as light scattering. For profiling stylus instruments, the international standard ISO 5436 has enumerated four types of standard specimens which may be classified as step height specimens, periodic roughness specimens, random roughness specimens, and specimens for checking probe tip resolution. A draft of a related U.S. standard uses the same taxonomy. For light scattering instruments, the use of standard specimens are discussed in the ASTM standard for total integrated scatter. In addition, several ad hoc standard specimens have been used in an interlaboratory comparison of instruments that measure the bidirectional reflectance distribution function (BRDF). The group has developed a series of specimens, known as Standard Reference Materials (SRMs), for calibrating stylus profiling instruments. The authors are also in the process of developing a series of profile specimens for calibrating the linearity of BRDF instruments. Both types of specimens have sinusoidal profiles and are discussed in turn.

Research Program Administration & Technology Transfer

02,929
PB94-211844 Not available NTIS
National Inst. of Standards and Technology, Gaithersburg, MD. Office of the Director.
Importance of Measurement in Technology-Based Competition.
Final rept.
H. Hellwig. 1990, 4p.
Pub. in Institute of Electrical and Electronics Engineers Transactions on Instrumentation and Measurement 39, n5 p685-688 1990.

Keywords: *Measurement, *Manufacturing, *Technology innovation, *Quality assurance, Metrology, Measuring instruments, Production, Productivity, Online systems, Reprints.

In this paper, measurement challenges are related to the changes taking place in emerging technologies, quality and production. The act of measurement is increasingly associated with the process rather than the product. As a result, the role of measurement is becoming proactive and anticipatory. Measurements are increasingly done on-line and at the place of need within the production process. Measurement problems must be addressed early in the research and development phase; and the purpose of measurement must be seen as assuring good product at all times as opposed to the traditional role of measurement which was focussed on eliminating bad products.

02,930
PB95-206181 PC A22/MF A04
National Inst. of Standards and Technology (MEL), Gaithersburg, MD.
Proceedings of the Manufacturing Technology Needs and Issues: Establishing National Priorities and Strategies Conference. Held in Gaithersburg, Maryland on April 26-28, 1994.
Special pub.
C. F. Albus, and J. D. Meyer. Feb 95, 510p, NIST/SP-877.
Also available from Supt. of Docs. as SN003-003-03320-1. Sponsored by Department of Defense, Washington, DC.

Keywords: *Meetings, *Manufacturing, *Technology assessment, *Government policies, Government/industry relations, Priorities, User needs, Industries, Competition, Government agencies, Programs, Technology innovation, Small businesses.

The conference addressed the many challenges and opportunities confronting manufacturers. Presentations were made by representatives from a host of manufacturing industries, each of which has been trying to chart its course for the future by developing a 'road map' of technology directions and needs. The conference was a unique opportunity to examine the spectrum of manufacturing industries, identify the commonalities and differences, and start assessing the value of road maps. The conference also provided a glimpse of the full spectrum of government programs in manufacturing technology. The ultimate goal was to develop a plan for moving forward to assure that the United States maintains a strong, dynamic manufacturing sector that is globally competitive and capable of meeting national challenges. Among other themes, the papers reflect growing government collaboration with industry, increasing cooperation within and among federal agencies, expanded technical agendas in government, and experimentation with innovative government programs.

02,931
PB96-109491 PC A11/MF A03
National Inst. of Standards and Technology (MEL), Gaithersburg, MD.
Joint DoD/NIST Workshop on International Manufacturing Systems Research and Development. Held in Rockville, Maryland on November 3-5, 1992. Proceedings.
Special pub.
J. D. Meyer. Oct 95, 244p, NIST/SP-873.
Also available from Supt. of Docs as SN003-003-03344-8. Sponsored by Assistant Secretary of Defense (Production and Logistics), Washington, DC.

Keywords: *Manufacturing, *Research and development, *Meetings, US NIST, Computer aided manufacturing, Competition, North America, Europe, Asia, International cooperation, Rockville(Maryland), CIM(Computer Integrated Manufacturing).

An international workshop was held in Rockville, Maryland, on November 3-5, 1992, to discuss major research and development programs in manufacturing systems technology. In addition to individual R&D programs and technology sources in North America, Western Europe, Eastern Europe, and Asia, the workshop participants also discussed R&D needs, priorities, underlying motivations, and opportunities for international collaboration. Approximately 25 leading experts attended the workshop, which was co-sponsored by the U.S. Department of Defense's Manufacturing Technology Program.

Robotics/Robots

02,932
PB94-172046 Not available NTIS
National Inst. of Standards and Technology (NEL), Gaithersburg, MD. Robot Systems Div.
Toward a Reference Model Architecture for Real-Time Intelligent Control Systems (ARTICS).
Final rept.
J. S. Albus, and R. Quintero. 1990, 8p.
Pub. in Proceedings of International Symposium on Robotics and Manufacturing (3rd): Research, Education, and Applications, British Columbia, Canada, July 18-20, 1990, p243-250.

Keywords: *Control systems, *Robotics, *Real time systems, Artificial intelligence, Automation, Technology innovation, Technology transfer, Government/industry relations, Computer architecture, Models, Systems engineering, Reprints, ARTICS(Architecture for Real-Time Intelligent Control Systems).

The paper presents a concept for the development of a reference model open-system architecture for real-time, sensory interactive, intelligent machine systems. Central to the notion is a desire to accelerate technological development, technology transfer and commercialization of world class control system products in the field of robotics, intelligent machines, and automation. A plan is outlined whereby a reference model Architecture for Real-Time Intelligent Control Systems (ARTICS) can be defined through the cooperative efforts of industry, academia, and government. As envisioned, ARTICS would be a series of evolving guidelines specifying an infrastructure of hardware components, software components, interfaces, communications protocols and application development tools. An ARTICS reference model would make it possible for industry to develop and market a diverse line of control system components which could be interchangeable and realizable on many different vendors' intelligent machine systems platforms.

02,933
PB94-173010 Not available NTIS
National Inst. of Standards and Technology (MEL), Gaithersburg, MD. Robot Systems Div.
World Model Registration for Effective Off-Line Programming of Robots.
Final rept.
N. Tarnoff, A. Jacoff, and R. Lumia. 1990, 8p.
Pub. in Proceedings of International Symposium on Robotics and Manufacturing (3rd): Research, Education, and Applications, British Columbia, Canada, July 18-20, 1990, p783-790.

Keywords: *Robots, *Computer programming, *Manufacturing, Trajectories, Robot dynamics, Control systems, Off line systems, Calibrating, US NIST, Reprints, *World models, AMRF(Automated Manufacturing Research Facility).

The paper discusses progress in world model calibration and environmental modeling of sensory information in the context of the Off-Line Programming (OLP) project at the National Institute of Standards and Technology's (NIST) Automated Manufacturing Research Facility (AMRF). The project began in 1988 to demonstrate an integrated OLP implementation. The baseline OLP system accepts IGES CAD data, enables graphical simulation of objects and devices and produces VAL II robot trajectories. The robot trajectories, however, are based on a world model that is inherently inaccurate. A basic OLP system and most existing commercial OLP systems, therefore, are more effective only as a prototyping tool. Consequently, the authors are now developing the new OLP system into a production tool for generating robust robot control programs. The authors recently completed work on world model calibration and environmental modeling of force and torque in an attempt to improve world model registration of the real world.

02,934
PB94-213162 Not available NTIS
National Inst. of Standards and Technology (NEL), Gaithersburg, MD. Robot Systems Div.
Hierarchical Ada Robot Programming System (HARPS): A Complete and Working Telerobot Control System Based on the NASREM Model.
Final rept.
S. Leake, T. Green, S. Cofer, and T. Sauerwein. 1989, 7p.
Pub. in Proceedings of Institute of Electrical and Electronics Engineers International Conference on Robotics and Automation, Scottsdale, AZ., May 14-19, 1989, p1022-1028.

Keywords: *Telerobotics, *Control systems, Real time, Robots, Robot sensors, Teleoperators, Computer vision, Software engineering, Software tools, Reprints, *NASREM(NASA Standard Reference Model), *NASA Standard Reference Model, Ada programming language, HARPS(Hierarchical Ada Robot Programming System), US NIST.

The Hierarchical Ada Robot Programming System (HARPS) is a telerobot control system which can perform some simple but useful tasks: this capability is demonstrated by performing an ORU exchange demo. HARPS is based on the National Institute of Standards and Technology (NIST) NASA Standard Reference Model (NASREM) model. The primary programming language for all developed software is Ada, and the project incorporated a number of different Computer Aided Software Engineering (CASE) development tools. NASREM was found to be a valid and useful model for building a telerobot control system: Its hierarchical and distributed structure creates a very natural and logical flow for developing and implementing large, complex, and robust control systems. Similarly, the ability of Ada to create and enforce abstraction was found to enhance the implementation of such a control system. The CASE tools utilized showed some promise in helping to design a large system which processed a tremendous amount of data involving very complex computations and relationships. An overview of NASREM, the ORU exchange demo, the HARPS system, and the development tools used in HARPS is given in this paper.

02,935
PB94-217098 PC A05/MF A01
National Inst. of Standards and Technology (MEL), Gaithersburg, MD. Intelligent Systems Div.
Publications of the Intelligent Systems Division (Previously Robot Systems Division) Covering the Period January 1971-April 1994.
D. L. F. Russell. Jul 94, 80p, NISTIR-5474.

Keywords: *Automation, *Robotics, *Artificial intelligence, *Bibliographies, Computer aided manufacturing, Robot dynamics, Control systems, Real time, Interactive systems, Software engineering, Construction, Mining, Documents, AMRF(Automated Manufacturing Research Facility), US NIST, MEL(Manufacturing Engineering Laboratory), Intelligent Systems Division.

This document consists of a list of publications by the staff of the Intelligent Systems Division, Manufacturing Engineering Laboratory (MEL), National Institute of Standards and Technology (NIST) for the period of January 1971 through April 1994. Publications cover research done by the division in the areas of intelligent machines and systems, robotics, real-time sensory-interactive control, open-systems architectures, software development techniques, world modeling, construction, mining and automated manufacturing systems.

02,936
PB95-164133 Not available NTIS
National Inst. of Standards and Technology (NEL), Gaithersburg, MD. Robot Systems Div.
Integrated Mobile Robot System for Testing Vision Algorithms.
Final rept.
H. H. Yakali, D. Raviv, and M. Herman. 1990, 8p.
Pub. in Proceedings of Conference on Recent Advances in Robotics (3rd), Boca Raton, FL., July 2-3, 1990, 8p.

Keywords: *Robot dynamics, *Computer vision, Robots, Robotics, Algorithms, Robot sensors, Real time, Image processing, Workstations, Tests, Reprints.

We describe an integrated real-time vision-based closed-loop system which will serve as a platform for testing vision-based navigation algorithms. The system consists of several subsystems: a charge coupled device (CCD) camera, a Pipelined Image Processing Engine (PIPE) real-time image processor, a SUN3/160 workstation and a DENNING mobile robot. We detail each of the subsystems, and the communications between them. Finally, we describe an algorithm used to test the system and discuss future work.

02,937
PB95-198677 PC A03/MF A01
National Inst. of Standards and Technology (MEL), Gaithersburg, MD. Intelligent Systems Div.
Real-Time Obstacle Avoidance Using Central Flow Divergence and Peripheral Flow.
D. Coombs, M. Herman, T. Hong, and M. Nashman. Feb 95, 22p, NISTIR-5605.

Keywords: *Robot dynamics, *Obstacle avoidance, *Computer vision, Real time, Robotics, Navigation, Image processing, Flow visualization, Control systems, PIPE(Pipelined Image Processing Engine).

The lure of using motion vision as a fundamental element in the perception of space drives this effort to use flow features as the sole cues for robot mobility. Real-time estimates of image flow and flow divergence provide the robot's sense of space. The robot steers down a conceptual corridor, comparing left and right peripheral flows. Large central flow divergence warns the robot of impending collisions at 'dead ends.' When this occurs, the robot turns around and resumes wandering. Behavior is generated by directly using flow-based information in the 2-D image sequence; no 3-D reconstruction is attempted. Active mechanical gaze stabilization simplifies the visual interpretation problems by reducing camera rotation. By combining corridor following and dead-end deflection, the robot has wandered around the lab at 30 cm/s for as long as 20 minutes without collision. The ability to support this behavior in real-time with current equipment promises expanded capabilities as computational power increases in the future.

02,938
PB95-242350 PC A09/MF A02
National Inst. of Standards and Technology (MEL), Gaithersburg, MD. Intelligent Systems Div.
Unified Telerobotic Architecture Project (UTAP) Standard Interface Environment (SIE), May 1995.
J. Michaloski, R. Russell, T. E. Wheatley, S. Lee, R. D. Steele, R. Lumia, and P. G. Backes. May 95, 179p, NISTIR-5658.
Prepared in cooperation with Jet Propulsion Lab., Pasadena, CA. and New Mexico Univ., Albuquerque. Sponsored by Air Force Systems Command, Kelly AFB, TX. Robotics and Automation Center of Excellence.

Keywords: *Artificial intelligence, *Robot control, *Robotics, *Teleoperators, Computer architecture, Standards, Interfaces, Terminology, Definitions, Robot sensors, Draft standard.

The Unified Telerobotic Architecture Project (UTAP) open architecture is intended for operator-supervised, teleoperated and shared control robotic maintenance tasks. The basic premise is to augment, not replace, the human operator by blending the individual skills of each into a system - the human's superior cognition and pattern recognition, and the robot's tireless, precise, and repeatable, motion. Further, many of the tasks are unsafe and hazardous. This document describes the UTAP architecture and a standard environment and Application Programming Interface for the architecture. The document presents a discussion of the Interface Framework including the reasoning process applied to the interface definition. It also presents a UTAP configuration and classification strategy. It describes the UTAP information model used for representing the interface data. The UTAP interfaces, including the format, types, syntax, semantics and significant features of operation are presented. Appendix I describes the architecture and module functionality. Appendix II summarizes the UTAP interface messages, and Appendix III contains specific definitions for each of the UTAP interfaces. Appendix IV contains profiles for the Remote modules in the system. Appendix V discusses a sample scenario for a refurbishing task, and then presents an overview of the message traffic.

02,939
PB96-154562 PC A03/MF A01
National Inst. of Standards and Technology (MEL), Gaithersburg, MD. Intelligent Systems Div.
Image Gradient Evolution: A Visual Cue for Danger.
H. Liu, T. H. Hong, M. Herman, and R. Chellappa. Oct 95, 19p, NISTIR-5728.
Prepared in cooperation with Maryland Univ., College Park. Center for Automation Research.

Keywords: *Computer vision, *Position sensing, *Collision avoidance, Autonomous navigation, Robot dynamics, Robot sensors, Motion perception, Three dimensional motion, Optical flow(Image analysis), Image processing, Divergence, Image analysis, Artificial intelligence, *Image gradient.

This paper is concerned with the task of visual motion-based navigation. A critical requirement of the task is the ability to estimate 3-D depth and motion from visual information. We present a new concept called image gradient evolution (IGE), which utilizes the change of image spatial gradients over time as a threat cue; an approaching object induces 2-D expanding motion and causes the image spatial structure to stretch so the image gradients decrease. Based on this idea, our method offers a one-step solution directly from image gradients, instead of from optical flow and its derived properties.

02,940
PB96-183173 PC A06/MF A01
National Inst. of Standards and Technology (MEL), Gaithersburg, MD. Intelligent Systems Div.
Scale-Space-Based Visual-Motion-Cue for Autonomous Navigation.
S. R. Kundur, D. Raviv, and E. Kent. Feb 96, 96p, NISTIR-5790.
Grant NSF-IRI-9115939
Prepared in cooperation with Florida Atlantic Univ., Boca Raton. Sponsored by National Science Foundation, Arlington, VA. Div. of Information, Robotics and Intelligent Systems.

Keywords: *Computer vision, *Autonomous navigation, *Robotics, Collision avoidance, Image analysis, Three dimensional bodies, Artificial intelligence, Image processing, Algorithms, Cameras, Visual perception, Computer motion.

This paper presents a new visual motion cue, the authors call the Hybrid Visual Threat Cue (HVCT) that provides some measure for a change in relative range as well as absolute clearances, between a 3D surface and a fixated observer in motion. The visual field associated with the HVTC can be used to demarcate the regions around a moving observer into safe and danger zones of varying degree, which may be suitable for autonomous navigation tasks, in particular collision avoidance and maintenance of clearance. The HVTC is independent of the 3D environment and needs almost no a-priori information about it. It is rotation independent, and is measured in (time(sup -1)) units. When there is a relative motion between a fixation point on a 3D surface and an observer, the perceived texture details the image vary. The rate at which the details vary provides an indication of the observer's relative motion with respect to the 3D surface. Scale space representation which is a multiscale approach provides a concrete way to analyze the variations of image details The authors derive a relation between the relative temporal variations of the image inner scale and the HVTC. A practical method to extract the HVTC from a sequence of images of a 3D textured surface obtained by a fixated, fixed-focus monocular camera in motion is also presented. A global dissimilarity measure is extracted directly from the raw data of the gray level of textured images from which the HVTC is obtained. This approach of extracting the HVTC is independent of the type of 3D surface texture and needs no optical flow information, 3D reconstruction, segmentation, feature tracking. It needs almost no camera calibration. This algorithm to extract the HVTC was applied to a set of twelve different texture patterns (of 3D scenes) from the Brodatz's album, where the authors observed a similar behavior for most of the textures.

02,941
PB96-193727 PC A05/MF A01
Florida Atlantic Univ., Boca Raton.
Novel Active-Vision-Based Motion Cues for Local Navigation.
S. R. Kundur, and D. Raviv. Feb 96, 65p, NISTIR-5791.
Grant NSF-IRI-9115939
Sponsored by National Inst. of Standards and Technology (MEL), Gaithersburg, MD. Intelligent Systems Div. and National Science Foundation, Arlington, VA. Div. of Information, Robotics and Intelligent Systems.

Keywords: *Robots, *Autonomous navigation, *Computer vision, *Collision avoidance, Sensors, Controllers, Cameras, Image processing, Visual perception, Real time operation.

In the absence of a-priori information about the information an autonomous mobile robot relies on sensory information to make local judgments about its surrounding. Generation of a local collision-free path based on sensory data plays an important role in the control of the robot's motion. The paper presents a novel active vision-based approach for generating local collision-free paths for mobile robot navigation in indoor as well as outdoor environments. Two measurable visual motion cues that provide some measure for a relative change in range as well clearance between a 3D surface and fixated observed in motion are described. These visual cues are independent of the 3D environment and need no a-priori knowledge about it. For each visual motion cue, there is a visual field surrounding the moving observer. In other words, there are imaginary 3D surfaces attached to the observer that move with it, each of which correspond to a value of the cue. These visual fields can be used to demarcate regions around a moving observer into safe and danger zones of varying degree to make local decisions about the sterring as well as speed commands to the mobile robot. We describe a practical method to extract these cues from a sequence of images. This approach needs no feature tracking between images and almost no camera calibration.

Tooling, Machinery, & Tools

02,942
PB94-135621 PC A03/MF A01
National Inst. of Standards and Technology, Gaithersburg, MD.
Open Architectures for Machine Control.
F. M. Proctor, B. Damazo, C. Yang, and S. Frechette. Dec 93, 20p, NISTIR-5307.

Keywords: *Machine tools, *Controllers, *Standards, Interactive graphics, Man machine systems, Error cor-

recting devices, Modular structures, Extensibility, Workstations, Computer architecture, National Institute of Standards and Technology, EMC(Enhanced Machine Controller), NURBS(Non-Uniform Rational B-Splines).

A major impediment to improving the performance and functionality of machine tools is the limited access that users or third parties have to the internals of the machine controller. This limit has suppressed the emergence of a community of third-party vendors who could provide a wide range of applications at competitive prices. The result is that users are often faced with all-or-nothing compromises when choosing controllers, and are restricted to the original controls vendors for everything from spare parts to software. Machine tool users would benefit from an open architecture that can serve as both a target for innovative third party product development, and as a specification which produces multiple competitive sources for interoperable products. The National Institute of Standards and Technology has initiated a project which will demonstrate the feasibility of open architectures for machine control. This project, the Enhanced Machine Controller (EMC), has selected several target applications which improve the accuracy and ease of use of machine tool controllers: selectable look-and-feel, tool management, alternate part programming languages, spline-based motion, on-machine inspection, and thermal-geometric error compensation.

02,943
PB94-186673 PC A07/MF A02
National Inst. of Standards and Technology, Gaithersburg, MD.
Prediction of Geometric-Thermal Machine Tool Errors by Artificial Neural Networks.
D. E. Gilsinn, and M. A. Donmez. Apr 94, 149p, NISTIR-5367.
Sponsored by Naval Research Lab., Washington, DC. Navy Manufacturing Technology Program.

Keywords: *Machine tools, *Error correction codes, *Neural nets, Conjugate gradient method, Optimization, Cutting machines(Tools), Algorithms, Artificial neural networks, Fortran programming language, Gradient descent method.

In machining operations, the precision of the workpiece dimensions depends on the accuracy of the relative position of the cutting tool and the workpiece. Among the key factors that affect the accuracy of this relative position are the geometric errors of the machine tool and the thermal effects on these geometric errors. Recent work on developing models to predict volumetric errors on NC lathes has led to a synthesis technique that combines the modeling of individual axis related geometric-thermal components by way of a rigid body kinematic model to produce predicted errors in the work volume of the machine. An alternative method of modeling these component errors is described in this report. Neural network computing is shown to be a viable technique for developing mappings between machine tool component error measurements and the vector consisting of both a component slide position and the temperature state of the machine as reported by the thermal sensors. The conjugate gradient algorithm, used to compute the optimum neural network weights for the machine tool error components, is described. A case study of the mapping results for one component error of an actual NC lathe is given. Finally, the source codes for the neural network algorithm and the conjugate gradient algorithm are given in FORTRAN.

02,944
PB94-199858 Not available NTIS
National Inst. of Standards and Technology (NEL), Gaithersburg, MD. Precision Engineering Div.
Computer Vision Based Tool Setting Station.
Final rept.
T. D. Doiron. 1989, 12p.
Contract DE-AI05-85OR21584
Pub. in Proceedings of VISION '89 Conference, Chicago, IL., April 24-27, 1989, p8/61-8/72. Sponsored by Department of Energy, Washington, DC.

Keywords: *Computer vision, *Tools, *Metrology, Calibrating, Edge detection, Cameras, Reprints.

In order to use a computer vision system for high accuracy gaging, the intensity array reported to the computer from the camera must correspond closely to the geometry of the part to be measured. To verify this correspondence for two different vision systems, a number of tests are reported and discussed. A number of effects due to the camera sensor geometry, the type of edge finder employed, the thermal properties of the camera, and the interface method used between the camera and computer are explored.

02,945
PB95-107231 Not available NTIS
National Inst. of Standards and Technology (NEL), Gaithersburg, MD. Automated Production Technology Div.
Real Time Compensation for Tool Form Errors in Turning Using Computer Vision.
Final rept.
G. Nobel, M. Alkan Donmez, and R. Burton. 1990, 8p.
Pub. in Proceedings of Society of Photo-Optical Instrumentation Engineers - Dimensional Stability, San Diego, CA., July 12-13, 1990, v1335 p186-193.

Keywords: *Turning(Machining), *Errors, *Computer vision, Real time, Cutting tools, Algorithms, Numerical control, Inspection, Reprints, CMMs(Coordinate Measuring Machines).

Deviations from the circular shape of the cutting edge of a single-point turning tool cause form errors in the workpiece during contour cutting. One can compensate for these tool-form errors by determining the size of the effective deviation at a particular instant during cutting, and then adjusting the position of the cutting tool accordingly. An algorithm for the compensation of tool-nose-radius errors in real time has been developed and implemented on a CNC turning center. A previously developed computer-vision-based tool-inspection system is used to determine the size of the deviations. Information from this system is fed to the error compensation computer which modifies the tool path in real time. Workpieces were cut utilizing the compensation system and were inspected on a coordinate measuring machine. Significant improvements in workpiece form were obtained.

02,946
PB95-152088 Not available NTIS
National Inst. of Standards and Technology (NEL), Gaithersburg, MD. Precision Engineering Div.
Displacement Method for Machine Geometry Calibration.
Final rept.
G. Zhang, R. Ouyang, B. Lu, A. Donmez, B. Borchardt, R. Capparelli, R. Hocken, and R. Veale. 1988, 17p.
Pub. in CIRP Annals 38, n1 17p 1988.

Keywords: *Displacement measurement, *Machine tools, *Calibration, Three dimensional, Error analysis, Metrology, Interferometry, Reprints, *Coordinate measuring machines.

It is shown that the volumetric errors of a three-axis machine tool or measuring machine can be determined by measuring the displacement error along 22 lines in the machine work zone. Pitch and yaw are derived from measuring the displacement error on two parallel lines for each axis. The squareness and straightness errors are determined by measuring two diagonals and one additional line. Roll errors are derived from the straightness errors on two parallel planes. Formulae for calculating these components of error and also the three-dimensional positioning error at any particular point are given. Experiments done at both Tianjin and NBS show that this method simplifies machine calibration, reduces the equipment needed, and can improve accuracy.

02,947
PB95-154720 PC A07/MF A02
National Inst. of Standards and Technology (MSEL), Gaithersburg, MD. Metallurgy Div.
Review and Upgrading of Military Fastener Test Standard MIL-STD-1312.
S. R. Low. Sep 94, 147p, NISTIR-5524.
Contract MIPR-2-0117
Also available from Supt. of Docs. Sponsored by Defense Industrial Supply Center, Philadelphia, PA.

Keywords: *Test methods, *Military standards, *Fasteners, Durability, Fastenings, Tensile strength, Mechanical properties, Military equipment, Shear stresses, Tension, Fatigue tests(Mechanics), *MIL-STD-1312.

The National Institute of Standards and Technology (NIST) has conducted a study of United States Military Standard MIL-STD-1312, Fastener Test Methods. Military Standard MIL-STD-1312 is a unified compilation of over 35 individual fastener test methods for determining the capability of fasteners to withstand various environmental and mechanical conditions encountered in service. Each of the individual fastener test methods is itself a fastener test standard, and is designated with its own document number. For this study, only selected test methods which prescribe certain mechanical tests for fasteners were reviewed. These test methods were evaluated and recommendations formulated for upgrading or replacing them to reflect the current state-of-the-art.

02,948
PB95-168902 Not available NTIS
National Inst. of Standards and Technology (CSTL), Boulder, CO. Process Measurements Div.
Design Equations and Scaling Laws for Linear Compressors with Flexure Springs.
Final rept.
E. Marquardt, R. Radebaugh, and P. Kittel. 1993, 22p.
Sponsored by National Aeronautics and Space Administration, Moffett Field, CA. Ames Research Center.
Pub. in Proceedings of International Cryocooler Conference (7th), Santa Fe, NM., November 17-19, 1992, p783-804 1993.

Keywords: *Scaling laws, *Design criteria, *Refrigerant compressors, Seals(Stoppers), Electric motors, Mathematical models, Springs, Refrigerating machinery, Refrigerators, Reprints, *Flexural springs.

Linear-resonant compressors with flexure springs and clearance seals have recently been developed for use in long-life Stirling and pulse tube refrigerators. This paper describes a set of equations that are used to design the various components in the compressor given specified performance criteria. The components considered are the moving-coil linear motor, the mass of the moving components, the magnet assembly, the flexure springs, and the clearance seals. Both radially and axially magnetized magnets are analyzed and the criteria for selection are developed. Methods for reducing the compressor size and mass are discussed as well as the influence of the stroke-to-diameter ratio on the design of flexure springs. The design equations have allowed the development of scaling laws for linear motor compressors covering a wide range of compressor sizes from 3 watts to 4 kilowatts.

02,949
PB95-169207 Not available NTIS
National Inst. of Standards and Technology (CSTL), Boulder, CO. Process Measurements Div.
Comparing NIST-B 50 mm Orifice Meter Gas Data to the ANSI Equation.
Final rept.
J. L. Scott. 1993, 7p.
Pub. in Proceedings of Fluid Engineering Conference Fluid Measurement and Instrumentation Forum, Washington, DC., June 20-24, 1993, p13-19.

Keywords: *Orifice meters, *Flowmeters, *Flow distortion, Orifice flow, Flow measurement, Reynolds number, Discharge coefficient, Orifices, Reprints.

A revised equation for computing discharge coefficients in orifice meters has been adopted by the American National Standards Institute (ANSI). The empirical data base used to develop this equation did not include gaseous fluid measurements for the 50 mm orifice meter. New experimental data that extend the Reynolds number range of the data base have been generated using nitrogen gas in this meter size. These new data are compared to the discharge coefficients calculated from the equation and to the original, lower Reynolds number data. The comparisons are beta ratio dependent, but, in general, the comparisons between the new data and the original data are quite good for all the beta ratios tested. Work was sponsored by Gas Research Institute (GRI).

02,950
PB95-203287 Not available NTIS
National Inst. of Standards and Technology (MEL), Gaithersburg, MD. Precision Engineering Div.
Geometric Characterization of Rockwell Diamond Indenters.
Final rept.
J. F. Song, F. F. Rudder, T. V. Vorburger, J. H. Smith, A. W. Hartman, and B. R. Scace. 1994, 6p.
Pub. in Proceedings of IMEKO World Congress (13th) 'From Measurement to Innovation', Torino, Italy, September 5-9, 1994, v1 p779-784.

Keywords: *Calibration, Rockwell hardness, Uncertainty, Pens, Microform, Reprints, *Diamond indenters, Surface finish.

By using a stylus instrument, a series of calibration and check standards, and calibration and uncertainty calculation procedures, we have calibrated Rockwell diamond indenters with traceability to fundamental measurements. The combined measurement uncertainties (95%) of the calibration are less than 1/10 of the tolerance requirements of calibration grade Rockwell diamond indenters. Our combined measurement uncertainties are: + or - 0.4 micrometer in least squares radius, + or - 0.01 deg in cone angle, and + or - 0.023 deg in holder axis alignment. The profile deviation from least squares radius and cone flank straightness is also calibrated. Engineering features of the diamond indenter's surface finish, such as surface roughness, and flat or sharp-shaped spherical tip are explored and quantified.

02,951
PB95-203295 Not available NTIS
National Inst. of Standards and Technology (MEL), Gaithersburg, MD. Precision Engineering Div.
Microform Calibrations in Surface Metrology.
Final rept.
J. F. Song, F. F. Rudder, T. V. Vorburger, J. H. Smith, A. W. Hartman, and B. R. Scace. 1995, 10p.
Pub. in Int. Jnl. Mach. Tools Manufact. 35, n2 p301-310 1995.

Keywords: *Microform, *Calibration, Rockwell hardness, Measurement, Uncertainty, Pens, Reprints, *Surface metrology, Diamond indenters, Surface texture.

Microform calibrations include the measurement of complex profile forms and position errors of micrometer scale in combination with the measurement of deviations from specified profile and surface texture of profile segments. Tolerances on the profile form are specified and may correspond geometrically to surface texture parameters. One example of microform calibration is the calibration of Rockwell diamond indenters used for hardness testing of materials. Previously reported measurement techniques do not meet the stringent microform calibration requirements for Rockwell diamond indenters. Inadequate microform calibration of hardness indenters may be one factor resulting in significant interlaboratory differences in results from Rockwell hardness tests. By using a stylus instrument, in combination with a series of calibration and check standards and calibration and measurement uncertainty calculation procedures, we have calibrated Rockwell diamond indenters in accordance with the definitions specified in ISO and ASTM standards. Our procedures for conducting microform calibration yield total measurement uncertainties less than ten percent of the tolerance values specified in ISO and ASTM standards. In this paper, the general calibration requirements, calibration and check standards, and calibration and uncertainty procedures that we use in performing microform calibrations are introduced. Some general considerations on stylus radius correction, data fitting, calibration traceability, uncertainty and reproducibility are also discussed.

02,952
PB95-203451 Not available NTIS
National Inst. of Standards and Technology, Gaithersburg, MD. Program Office.
Post-Process Control of Machine Tools.
Final rept.
T. V. Vorburger, K. W. Yee, B. R. Scace, and F. F. Rudder. 1994, 15p.
Pub. in Manufacturing Review 7, n3 p252-266 Sep 94.

Keywords: *Machine tools, *Control, *Automation, Quality assurance, Real time, Error detection codes, Process control, Reprints, US NIST, QIA(Quality in Automation), Post-process.

The automated control of machine-tool accuracy is discussed based on a quality architecture that is being implemented at the National Institute of Standards and Technology (NIST) under the Quality in Automation (QIA) project. The quality architecture contains three control loops: real-time, process-intermittent, and post-process. This paper highlights the post-process loop, although the QIA project emphasizes the measurement and control of process variables to control the quality of the product, post-process dimensional measurements of the finished product play a role in the system and may be used for correction of certain variables. The strategy for the post-process loop includes classification schemes for the adjustable parameters in the system, for the error diagnostics, and for the error model of the machine tool.

02,953
PB95-242301 PC A04/MF A01
National Inst. of Standards and Technology (MEL), Gaithersburg, MD. Automated Production Technology Div.
Precision in Machining: Research Challenges.
H. A. Soons, and S. L. Yaniv. May 95, 57p, NISTIR-5628.

Keywords: *Machining, *Technology innovation, *Precision, Machine tools, Errors, Accuracy, Closed loop systems, Metrology, Production control, Manufacturing, Tolerances(Mechanics), Research and development.

This report looks at critical research needs for leading-edge technology developments in machining and precision that are important to the competitiveness of the US discrete-part industry. Key driving forces in manufacturing are identified. These include the increased demand for higher speed, greater flexibility, greater precision, automation, advanced materials, and the emergence of new processes. Infrastructural developments required for improvements in and control of manufacturing precision are discussed. Research challenges in machine tool characterization, machine tool performance enhancement, closed-loop precision manufacturing, process modeling, high speed machining and costs of precision are identified.

02,954
PB96-111695 Not available NTIS
National Inst. of Standards and Technology (MEL), Gaithersburg, MD. Precision Engineering Div.
Fabrication of Optics by Diamond Turning.
Final rept.
R. L. Rhorer, and C. J. Evans. 1995, 13p.
Pub. in Handbook of Optics, Chapter 41, p41.1-41.13 1995.

Keywords: *Optics, *Fabrication, *Diamonds, *Tools, Wear, Technology utilizing, Cost effectiveness, Cutting tools, Reprints, *Diamond turning.

Single point diamond turning is a cost effective method of fabricating aspheric and specialty optics. Tool wear is a major limit for certain materials. The range of applications of diamond turning, and the factors to consider in selecting an optical fabrication strategy are reviewed.

02,955
PB96-135363 Not available NTIS
National Inst. of Standards and Technology (CAML), Gaithersburg, MD. Statistical Engineering Div.
Proposed Changes to Charpy V-Notch Machine Certification Requirements.
Final rept.
J. D. Splett, and J. C. M. Wang. 1995, 13p.
Pub. in Symposium on Pendulum Impact Machines: Procedures and Specimens for Verification, Montreal, Quebec, Canada, May 18-19, 1994, p182-194 May 95.

Keywords: *Certification programs, Reprints, Impact testing, Requirements, *Charpy V Notch machines, *Pendulum impact machines, Notched bar testing.

In 1989 the administration of the Charpy V-Notch Certification Program was assumed by the National Institute of Standards and Technology. The United States Army originated the program to insure the measurement integrity of Charpy V-notch machines across the country. The program has been operated for many years using candidate machine acceptance limits which can possibly be traced to a 1955 paper by Driscoll, however, the original statistical justification for using these acceptance criteria has been lost or never existed. A statistical analysis of recent certification program data indicates that the existing candidate machine acceptance limits should be modified. In this paper, the authors will discuss and justify potential changes to candidate machine acceptance limits.

02,956
PB96-141189 Not available NTIS
National Inst. of Standards and Technology (EEEL), Boulder, CO. Electromagnetic Technology Div.
Effect of Magnetic Field Orientation on the Critical Current of HTS Conductor and Coils.
Final rept.
J. P. Voccio, A. J. Rodenbush, C. H. Joshi, J. W. Ekin, and S. L. Bray. 1995, 4p.
Pub. in Institute of Electrical and Electronics Engineers Transactions on Applied Superconductivity, v5 n2 p1822-1825 Jun 95.

Keywords: *High-Tc superconductors, *Magnetic fields, Magnet coils, Reprints, Conductors, Silver, Temperature, *Critical current.

The critical current of short samples of HTS multifilamentary conductor and ring-shaped coils has been measured at helium temperatures with varying magnetic field orientation with respect to the conductor. The samples and coil conductor consist of a multifilamentary composite of BSCCO-2223 filaments in a silver matrix. Short conductor samples were tested in a variable temperature system with up to 8 T background field using a sample rotational system. Ring-shaped coils made from the sample type of conductor were exposed to a large background field at liquid helium temperatures and critical current was measured with the ring located at various axial positions within the bore.

02,957
PB96-155551 Not available NTIS
National Inst. of Standards and Technology (MEL), Gaithersburg, MD. Precision Engineering Div.
Metrology Approach to Unifying Rockwell C Hardness Scales.
Final rept.
J. F. Song, J. H. Smith, and T. V. Vorburger. 1995, 13p.
Pub. in Proceedings of the International Symposium on Hardness Testing in Theory and Practice (9th), Dusseldorf, Germany, November 23-24, 1995, p19-31.

Keywords: *Rockwell hardness, *Calibration, Microforms, Etching, Diamond pyramid hardness tests, Indentation hardness tests, Verification, Metrology, Uncertainty, Reference standards, Reprints, *Diamond indenters, Traceability.

Current Rockwell C hardness scales (HRC) are unified by performance comparisons. Unless a reliable metrology approach is used for the direct verification of standard hardness machines and diamond indenters, the unified hardness scale may exhibit a systematic offset from the true value of the harness scale. Based on the recently developed NIST microform calibration system, a metrology approach is suggested to unify Rockwell C hardness scales. The true value and reference-value scales are defined. It is proposed to use the reference standards, including standard hardness machines and NIST standard-grade Rockwell diamond indenters, to create, maintain, and reproduce the reference-value scale for the metrology-based Rockwell hardness standard system, and to overcome the systematic offset in existing performance-based hardness scales.

02,958
PB96-155569 Not available NTIS
National Inst. of Standards and Technology (MEL), Gaithersburg, MD. Precision Engineering Div.
Stylus Technique for the Direct Verification of Rockwell Diamond Intenders.
Final rept.
J. F. Song, F. F. Rudder, T. V. Vorburger, and J. H. Smith. 1995, 10p.
Pub. in Proceedings of the International Symposium on Hardness Testing in Theory and Practice (9th), Dusseldorf, Germany, November 23-24, 1995, p129-138.

Keywords: *Rockwell hardness, *Calibration, *Pens, Etching, Microforms, Diamond pyramid hardness tests, Indentation hardness tests, Metrology, Verification, Uncertainty, Reference standards, Reprints, *Diamond indenters.

Based on a stylus technique, a microform calibration system was developed at NIST for the direct verification of Rockwell diamond indenters. The least-squares radius and profile deviations, cone angle and cone flank straightness, and the holder axis alignment error can be calibrated with traceability to fundamental measurements. The calibration requirements, instrument setup, calibration and check standards, calibration and uncertainty procedure, and the calibration results are described. Based on this calibration system, the use of the NIST standard-grade Rockwell diamond indenters is also suggested for the establishment of the

reference-value scale for a metrology-based Rockwell hardness standard system and for the unification of Rockwell hardness standards.

02,959
PB96-160569 Not available NTIS
National Inst. of Standards and Technology (MEL), Gaithersburg, MD. Automated Production Technology Div.
Integrated Inspection System for Improved Machine Performance.
Final rept.
J. Mou, and M. A. Donmez. 1993, 10p.
Pub. in Proceedings of Society of Photo-Optical Instrumentation Engineers, Vision, Sensors, and Control for Automated Manufacturing Systems, Boston, MA., September 9-10, 1993, v2063 p22-31.

Keywords: *Machine tools, *Displacement measurement, *Inspection, *Precision, Computerized control systems, Process control, Accuracy, Quality control, Error analysis, Calibration, Data analysis, Algorithms, Reprints, CNC(Computer Numerical Control).

An integrated inspection system for improving the accuracy of CNC machine tools is proposed. The sysem described in this paper emphasizes the integration of the on-machine inspection and analysis techniques with the information coming from post-process inspection. The proposed system utilizes the information from both post-process and on-machine inspection to improve machine performance automatically. Algorithms are derived for analyzing the post-process and on-machine inspection data to identify residual systematic errors and relate them to the machine performance. Various data analysis algorithms and techniques are compared. A feature comparison approach is developed to relate the dimensional and form errors of a manufactured workpiece to the systematic machine tool errors. Inverse kinematics technique and statistical methods are used to identify and characterize the contribution of each geometric error component. A self tuning algorithm is also proposed to fine tune the geometric-thermal model.

02,960
PB97-113898 PC A05/MF A01
National Inst. of Standards and Technology (MEL), Gaithersburg, MD. Precision Engineering Div.
Static Structural Analysis of a Reconfigurable Rigid Platform Supported by Elastic Legs.
F. F. Rudder. Jun 96, 62p, NISTIR-5885.

Keywords: *Machine tools, *Foundations, Platforms, Joints(Junctions), Supports, Positioning devices(Machinery), Metrology.

The report describes a static structural analysis of a rigid planar platform supported by elastic legs. The platform deformations are computed relative to a specified platform position and orientation. The analysis considers deformations due to static platform loads, non-uniform temperatures of the legs, and manufacturing errors of each leg length. The model was developed as a tool to assist in the interpretation of metrology data and the development of an error budget for the NIST Octahedral Hexapod Milling Machine.

02,961
PB97-116206 PC A03/MF A01
National Inst. of Standards and Technology (MEL), Gaithersburg, MD. Office of Manufacturing Programs.
Standards Promote Credibility and Technology Transfer: The Need for Greater Industry Support of Technical Committees.
C. D. Lovett. Oct 96, 13p, NISTIR-5899.

Keywords: *Technology transfer, *Standards, *Machining, Machine tools, International trade, Competition, Technical organizations, International Standards Organization.

The intent of this paper is to call attention to the need for greater industry participation in both national and international standards committees. This need is described by giving an overview of U.S. standardization by the voluntary consensus-based process and describing some of the benefits of participating in standards-developing committees. The U.S. National Machining Center Standards Committee is cited as an example of a voluntary consensus-based process, involving cooperation among industry, government and academia.

Tribology

02,962
PB94-172731 Not available NTIS
National Inst. of Standards and Technology (MSEL), Gaithersburg, MD. Ceramics Div.
Considerations on Data Requirements for Tribological Modeling.
Final rept.
A. W. Ruff. 1991, 16p.
Pub. in Tribological Modeling for Mechanical Designers, ASTM STP 1105, p127-142 1991.

Keywords: *Tribology, *Data bases, Mechanical engineering, Lubrication, Test methods, Friction, Wear, Materials, Models, Design, Reprints.

An idealized database for tribology is described that contains numeric data with characteristics needed for use in modeling approaches in tribology. Tribological data on materials are considered in detail, and other types of required data are identified. Testing methodologies for obtaining data are examined. Priority areas for future work in data gathering and data evaluation in tribology are suggested.

02,963
PB94-211018 Not available NTIS
National Inst. of Standards and Technology (MSEL), Gaithersburg, MD. Ceramics Div.
Tribological Characteristics of Alpha-Alumina at Elevated Temperatures.
Final rept.
X. Dong, S. Jahanmir, and S. M. Hsu. 1991, 9p.
Pub. in Jnl. of American Ceramic Society 74, n5 p1036-1044 1991.

Keywords: *Aluminum oxide, *Tribology, *Mechanical properties, High temperature tests, Friction, Performance evaluation, Wear, Ceramics, Reprints.

The tribological characteristics of alpha-alumina sliding on a similar material under dry sliding conditions are divided into four distinct regimes. At low temperatures, T < 200 C, tribochemical reactions between alumina surface and water vapor in the environment control the tribological performance. At temperatures above 800 C, formation of silicon oxide layers on the wear track, by viscous flow and diffusion of the grain boundary phase, reduces the coefficient of friction to 0.4; and the wear coefficient is reduced to a value less than .000001. The results of the wear tests and observations of the fundamental mechanisms controlling the tribological behavior of this material are consolidated in a simple wear transition diagram. The wear transition diagram can be used for the identification of wear mechanisms and the transition boundaries.

02,964
PB94-212057 Not available NTIS
National Inst. of Standards and Technology (MSEL), Gaithersburg, MD. Ceramics Div.
Tribochemical Reaction of Stearic Acid on Copper Surface Studied by Surface Enhanced Raman Spectroscopy.
Final rept.
Z. S. Hu, S. M. Hsu, and P. S. Wang. 1992, 6p.
Pub. in Tribology Transactions 35, n3 p417-422 1992.

Keywords: *Tribology, *Lubricants, *Copper, *Stearic acid, *Surface chemistry, Chemical reactions, Raman spectroscopy, Chemisorption, Wear, Reprints, Cupric stearate, Hexadecane.

Micro-Raman, back-scattered by Ar ion laser, was used to study the tribochemical reaction of copper surface and hexadecane containing 0.4 weight percent stearic acid. The characteristic Raman signals of cupric stearate at 1,547, 623, 288, and 243 wavenumbers were detected during the reaction and the formation of cupric stearate confirmed. The tribochemical reaction was initiated by the formation of a chemisorbed stearic acid on the native oxide film of the copper surface. This chemisorbed stearic acid is in the form of monomer and is approximately perpendicular to the copper surface. The native oxide film is necessary for this chemisorption to occur. Further wearing of the surface converts the chemisorbed stearic acid into cupric stearate.

02,965
PB94-212362 Not available NTIS
National Inst. of Standards and Technology (MSEL), Gaithersburg, MD. Ceramics Div.
Tribology Education: Present Status and Future Challenges.
Final rept.
S. Jahanmir, and F. E. Kennedy. 1991, 3p.
Pub. in Jnl. of Tribology 113, n2 p229-231 1991.

Keywords: *Tribology, *Education, *Mechanical engineering, *Lubrication, Recommendations, Surveys, Forecasting, Friction, Wear, Reprints, *Research Committee on Tribology, American Society of Mechanical Engineering.

The ASME-Research Committee on Tribology has been concerned that some of today's engineering students may not be learning enough about fundamentals of tribology. A survey of engineering schools was conducted to assess the current status of tribology education at universities. The survey results were presented and discussed at a panel session on Tribology Education. The panel consisted of an invited group of distinguished tribologists representing academia, industry, and federal government. A set of recommendations was prepared based on the presentations and the discussions that followed. Since only a small fraction of engineering colleges offer any treatments on tribology in their curricula, it is recommended that tribology fundamentals be incorporated in the course offerings to prepare the engineering students for future advanced technical developments.

02,966
PB95-164158 Not available NTIS
National Inst. of Standards and Technology (MSEL), Gaithersburg, MD. Ceramics Div.
Asperity-Asperity Contact Mechanisms Simulated by a Two-Ball Collision Apparatus.
Final rept.
T. N. Ying, and S. M. Hsu. 1993, 9p.
Pub. in Wear 169, p33-41 1993.

Keywords: *Wear, *Test methods, *Friction, Wear resistance, Interfaces, Friction measurement, Wear tests, Tribology, Reprints, *Two-ball collision test apparatus, *Asperity.

Wear of materials is controlled by asperity-asperity contacts. Since the asperities are of uneven height, the stresses imposed by different pairs of asperities necessarily are unequal. When two surfaces come together, there is a distribution of the contact stresses. In a wear experiment, we measure wear by measuring the cumulative wear across the interface from the beginning of the experiment, and we measure friction by measuring the average friction of all the asperity contacts across the interface at the particular instance in time. The friction and wear characteristics at the asperity level have interested the tribology community for a long time. Data at that level, however, are difficult to obtain and the conditions that lead to a single asperity wear event are not understood. This paper describes the design and construction of a two-ball collision test apparatus to simulate asperity contacts. Materials used include steels, brass, and aluminum of different hardness and elasticity. Dynamic friction and wear of the collision were measured under dry, paraffin oil lubricated conditions. The results suggested that at a coefficient of 0.4, wear of the asperity contact occurred. A simple plain strain model confirmed the observations that under certain conditions, asperity wear should occur at a coefficient of 0.39.

02,967
PB95-180949 Not available NTIS
National Inst. of Standards and Technology (MSEL), Boulder, CO. Materials Reliability Div.
Tribometer for Measurements in Hostile Environments.
Final rept.
A. J. Slifka, D. K. Chaudhuri, R. Compos, and J. D. Siegwarth. 1993, 6p.
Sponsored by National Aeronautics and Space Administration, Huntsville, AL. George C. Marshall Space Flight Center.
Pub. in Wear 170, p39-44 1993.

Keywords: *Friction measurement, *Wear tests, Coefficient of friction, Friction, Tribology, Test facilities, Measuring instruments, Wear, Reprints, *Tribometers.

A tribometer at the National Institute of Standards and Technology in Boulder, Colorado is used to measure the coefficient of friction and the wear rate for various specimens in a controlled atmosphere of oxygen or non-corrosive gas. The wide range of demonstrated operating temperature of 80 to 1030 K is presently unavailable in any commercial apparatus. The machine

use ball-on-flat or ring-on-flat specimen geometries for comparison of conforming and non-conforming contacts. The apparatus is described and some test results are compared with known values.

MATERIALS SCIENCES

General

02,968
AD-A301 675/5 PC A14/MF A03
National Bureau of Standards, Boulder, CO.
Weatherability of Plastic Materials.
M. R. Kamal. Feb 67, 306p.
Proceedings on Weatherability of Plastic Materials, Applied Polymer Symposia, Number 4, Gaithersburg, MD 8-9 Feb 67.

Keywords: *Polymers, *Plastics, *Weatherproofing, *Weathering, *Meetings, Crystal structure, Ultraviolet radiation, Weather, Aging(Materials), Degradation, Exposure, Laminates, Polystyrene, Atmospheric temperature, Copolymers, Embrittlement, Glass, Light sources, Rain, Oxidation, Radiation absorption, Light transmission, Photochemical reactions, Pigments, Accelerated testing, Elongation, Carbon black, Reinforcing materials, Humidity, Polyester plastics, Polyethylene plastics, Polyvinyl chloride, Sunlight, Plastic coatings, Radiant intensity, Durability, Photooxidation.

The growth of the plastics industry in recent years has been accompanied with a significant expansion in the outdoor application of plastic materials.

02,969
PB94-162534 PC A05/MF A01
National Inst. of Standards and Technology (MSEL), Gaithersburg, MD.
Materials Science and Engineering Laboratory Annual Report, 1993. NAS-NRC Assessment Panel, April 21-22, 1994.
Rept. for 1 Oct 92-30 Sep 93.
L. H. Schwartz, and H. L. Rook. Apr 94, 86p, NISTIR-5311.
See also PB94-112430.

Keywords: *Technology innovation, Research and development, Personnel, Technology transfer, Laboratories, Research management, Research projects, Reviews, *Materials Science and Engineering Laboratory, *MSEL, National Institute of Standards and Technology.

The Report contains background information on resources, activities, and representative highlights of the Materials Science and Engineering Laboratory (MSEL). The report includes a summary of the strategic plan of MSEL and the technical areas proposed for future emphasis.

02,970
PB94-172939 Not available NTIS
National Inst. of Standards and Technology (MSEL), Gaithersburg, MD.
Industry and Government-Laboratory Cooperative R and D: An Idea Whose Time Has Come.
Final rept.
L. H. Schwartz. Sep 90, 2p.
Pub. in MRS Bulletin 15, n9 p4-5 Sep 90.

Keywords: *Materials, *Research and development, *Cooperation, Government/industry relations, Joint ventures, Technology innovation, Technology transfer, Reprints, CRADAS(Cooperative Research and Development Agreements).

The article explores the role that Federal Laboratories can play in addressing the area of materials processing via joint technology development with industry. The discussion includes a brief description of the Technology Transfer Act of 1988 and the mechanism of Cooperative Research and Development Agreements (CRADAS) created therein. These CRADAS are an ideal vehicle with which to pursue such joint technology development.

02,971
PB94-198884 Not available NTIS
National Inst. of Standards and Technology (MSEL), Gaithersburg, MD. Polymers Div.
Diffraction Imaging of Polycrystalline Materials.
Final rept.
D. R. Black, H. E. Burdette, M. Kuriyama, and R. D. Spal. 1991, 8p.
Pub. in Jnl. of Materials Research 6, n7 p1469-1476 1991.

Keywords: *X-ray diffraction, *Imaging techniques, Residual stress, Crystal defects, Grain size, Polycrystalline, Strains, Shape, Reprints, *Diffraction imaging, Industrial materials.

For the characterization of industrial materials, a new diffraction imaging technique is proposed and applied to obtain direct information about individual grains and their size and shape distributions and, in turn, strains in materials. Unlike traditional powder diffractometry, the highly parallel and monochromatic beam available from a synchrotron x-ray source is employed to observe and measure diffraction images from individual grains and component particles in consolidated materials prepared by various processes. Unlike traditional diffractometry, this new technique provides the ability to measure shape, size and strain without model based analyses. The spatial distribution of strain within individual grains, displayed as a diffraction image (topograph), indicates the presence of defects, such as dislocations, subgrain boundaries and precipitates, and sheds new light on the origins of residual strains (stresses) in industrial materials. The resolution of the imaging system used is limited to particles 1 micrometer or larger due to diffraction broadening and the resolution of the recording medium.

02,972
PB94-200227 Not available NTIS
National Inst. of Standards and Technology (MSEL), Gaithersburg, MD. Ceramics Div.
Crack Growth Resistance of Strain-Softening Materials under Flexural Loading.
Final rept.
T. J. Chuang. 1993, 4p.
Pub. in Proceedings of American Society of Civil Engineers Structure Congress, Indianapolis, IN., April 29, 1991, p466-469.

Keywords: *Crack propagation, *Flexural properties, *Strain(Mechanics), *Brittle materials, Loads(Forces), Flexural strength, Mechanical properties, Toughness, Deformation, Reprints, Subcritical crack growth.

The subcritical crack growth resistance of a bend bar is investigated for a group of brittle materials exhibiting strain-softening behavior. Based on a nonlinear constitutive law ascribed to the process zone ahead of the crack tip in a strain gradient field, the evolution of the process zone size, crack length and applied load is predicted for a given deformation history. The results showed that the crack growth resistance or toughness increases to a peak, then decays precipitously to zero as the crack grows towards the compressive edge, in qualitative agreement with experimental data. The fact that the K value, in general, never reaches a plateau suggests that a bend bar geometry is not suitable for K(sub IC) measurement.

02,973
PB94-218567 PC A04/MF A01
National Inst. of Standards and Technology (MSEL), Gaithersburg, MD. Metallurgy Div.
NIST Workshop on Nanostructured Material (1st): Report of an Industrial Workshop Conducted by the National Institute of Standards and Technology. Held in Gaithersburg, Maryland on May 14-15, 1992.
Internal rept.
R. D. Shull. Mar 94, 56p, NISTIR-5456.

Keywords: *Meetings, Particle size, Composite materials, Information transfer, Synthesis(Chemistry), Industries, Phase studies, Physical properties, Thermodynamics, Mechanical properties, Corrosion, Processing, *Nanomaterials, *Nanostructures, *Advanced materials, Nanocomposites.

This workshop, the 'First NIST Workshop on Nanostructured Materials,' was the first of a series of workshops on the synthesis, characterization, properties, and applications of nanostructured materials to be held every three years at NIST. The workshop was organized to bring together people from industry, federal agencies, and universities to: (1) expedite the flow of information in the field, (2) identify key synthesis and processing methods with scalability potential, (3) acquaint the various communities with the unique properties of nanostructured materials, (4) assist industry in identifying potential application areas, and (5) identify needed areas of study. The workshop also was planned because of the recognition that in order for the U.S. to take advantage of the promise these materials hold, a concerted effort in this area is needed early. The workshop could highlight this need and provide directions for a concerted effort. Finally, it was felt that the workshop would provide NIST with additional guidance in directing its own programmatic initiative in the area.

02,974
PB95-150108 Not available NTIS
National Inst. of Standards and Technology (MSEL), Gaithersburg, MD. Metallurgy Div.
Method for Determining Both Magnetostriction and Elastic Modulus by Ferromagnetic Resonance.
Final rept.
R. D. McMichael. 1994, 3p.
Pub. in Jnl. of Applied Physics 75, n10 p5650-5652, 15 May 94.

Keywords: *Modulus of elasticity, *Ferromagnetic resonance, *Magnetostriction, Ferromagnetic materials, Elastic properties, Bending, Substrates, Ferromagnetism, Strains, Anisotrophy, Nickel, Polymers, Magnetic properties, Reprints.

The magnetostriction constant lambda(sub s) includes a combination of both elastic constants C(sub ij) and magnetoelastic coupling constants B(sub i). To provide information on both C(sub ij) and B(sub i), a method for measurement of both lambda(sub s) and the elastic modulus Y of thin films has been developed using ferromagnetic resonance (FMR). As in prior FMR schemes for measuring lambda(sub s), a strain is produced in the film by bending the substrate, and the resulting anisotropy field is measured. However, by using a triangular polymer beam as a substrate, three important advantages are obtained (1) the triangular beam shape has uniform strain along its surface, (2) the polymer material supports large strains (> 10(exp -3)) without breaking, and (3) the low elastic modulus of the beam allows measurement of the sample elastic modulus through variation of the sample aspect ratio. Measurements on Ni foils yield values of lambda(sub s) and Y which fall within the scatter of literature data.

02,975
PB95-162525 Not available NTIS
National Inst. of Standards and Technology (NML), Gaithersburg, MD. Standard Reference Data.
Access Paths for Materials Databases: Approaches for Large Databases and Systems.
Final rept.
J. Rumble. 1991, 10p.
Pub. in Computerization and Networking of Materials Databases: Second Volume, ASTM STP 1106, p132-141 1991.

Keywords: *Materials, *Databases, *Information retrieval, Information systems, Man computer interfaces, Graphical user interface, User requirements, User needs, Query languages, Reprints, Access paths, Search strategies.

Materials databases can contain widely differing data records in terms of the size and number of data elements, depending on the types of data. Acceptance of materials databases depends on user interfaces containing search strategies that will find answers to queries as needed by engineers and scientists. The paper will outline typical access paths (search strategies) from three points of view: first, simple and complex matching; second, specification of multiple criteria; and third, search refinement.

02,976
PB95-196697 PC A06/MF A02
National Inst. of Standards and Technology (MSEL), Gaithersburg, MD.
Materials Science and Engineering Laboratory Annual Report, 1994. NAS-NRC Assessment Panel, April 6-7, 1995.
Rept. for 1 Oct 93-30 Sep 94.
L. H. Schwartz. Apr 95, 103p, NISTIR-5577.
See also PB94-162534.

Keywords: *Research and development, Research management, Technology innovation, Research

projects, Organizational structure, Laboratories, Resources, Technology transfer, *US NIST, *MSEL(Materials Science and Engineering Laboratory), *Materials Science and Engineering Laboratory.

The report contains background information on the vision, mission, priority-setting process, implementation and organization of The National Institute of Standards and Technology's (NIST's) Materials Science and Engineering Laboratory (MSEL), as well as accomplishments and impacts, resources, activities, and technology transfer for the Laboratory.

02,977
PB95-267985 PC A05/MF A01
National Inst. of Standards and Technology (TS), Gaithersburg, MD. National Voluntary Lab. Accreditation Program.
National Voluntary Laboratory Accreditation Program: Thermal Insulation Materials.
Handbook.
L. I. Knab. May 95, 80p, NIST/HB-150-15.
Also available from Supt. of Docs. as SN003-003-03354-5. See also PB88-152541.

Keywords: *Thermal insulation, *Insulating materials, *Laboratories, Materials testing, Test methods, Requirements, Certification, Procedures, Calibration standards, Standardization, Equipment, Management, Auditing, Personnel, NVLAP(National Voluntary Laboratory Accreditation Program).

NIST Handbook 150-15 presents the technical requirements of the National Voluntary Laboratory Accreditation Program (NVLAP) for Thermal Insulation Materials. It is intended for information and use by staff of accredited laboratories, those laboratories seeking accreditation, other laboratory accreditation systems, users of laboratory services, and others needing information on the requirements for accreditation under the Thermal Insulation Materials program.

02,978
PB96-112677 PC A11/MF A03
National Inst. of Standards and Technology (MSEL), Gaithersburg, MD.
Glimpse of Materials Research in China: A Report from an Interagency Study Team on Materials Visiting China from June 19, 1995 to June 30, 1995.
Special pub.
S. M. Hsu, and L. H. Schwartz. Sep 95, 233p, NIST/SP-893.
Portions of text in Chinese. Also available from Supt. of Docs. as SN003-003-03370-7.

Keywords: *Materials, *Research programs, *China, International cooperation, Research and development, Electronics, Polymers, Electrooptics, Semiconductor devices, Ceramics, Tribology, Universities, *Foreign technology.

During the period June 16, 1995 to June 30, 1995, an interagency delegation of materials scientists from the Department of Commerce (DOC), Department of Energy (DOE), National Aeronautical and Space Administration (NASA), and the National Science Foundation (NSF) visited China and Hong Kong to explore areas for possible cooperation in materials research between the two countries under the general science and technology agreement. Recognizing the daunting task of assessing the state-of-the-art in a nation with so vast a scientific and academic structure as China, the study team's itinerary was organized to split into four smaller teams which began together in Beijing, spread out to visit separate locations and then met again in Shanghai. The visit ended at the Hong Kong University of Science and Technology (HKUST) which graciously provided facilities for the drafting of this report. The itineraries of these four teams (Appendix E) allowed for visits to 30 institutions in a period of a week and one half. Reports describing each of these visits are assembled in Appendix F, and should be referred to for detailed description.

02,979
PB96-119243 Not available NTIS
National Inst. of Standards and Technology (MSEL), Gaithersburg, MD.
Evolution Equations for Phase Separation and Ordering in Binary Alloys.
Final rept.
J. W. Cahn, and A. Novick-Cohen. 1994, 33p.
Pub. in Jnl. of Statistical Physics, v76 n3/4 p877-909 1994.

Keywords: *Alloys, *Phase separation, *Phase ordering, Reprints, Equations, Binary alloys, Allen-Cahn equations, Cahn-Hilliard equations.

The authors explore two phenomenological approaches leading to systems of coupled Cahn-Hilliard and Cahn-Allen equations for describing the dynamics of systems which can undergo first-order phase separation and order-disorder transitions simulateneously, starting from the same discrete lattice free energy function. In the first approach, a quasicontinuum limit is taken for this discrete energy and the evolution of the system is then assumed to be given by gradient flow. In the second approach, a discrete set of gradient flow evolution equations is derived for the lattice dynamics and a quasicontinuum limit is then taken. The authors demonstrate in the context of BCC Fe-Al binary alloys that it is important that variables be chosen that accommodate the variations in the average concentration as well as the underlying ordered structure of the possible coexistent phases. Only then will the two approaches lead to roughly the same continuum descriptions.

02,980
PB96-119698 Not available NTIS
National Inst. of Standards and Technology (MSEL), Gaithersburg, MD. Reactor Radiation Div.
Neutron Techniques in Materials Science and Related Disciplines.
Final rept.
J. M. Rowe, and H. J. Prask. 1995, 14p.
Pub. in Proceedings of Society of Photo-Optical Instrumentation Engineers: Neutrons and Their Applications, Crete, Greece, June 12-18, 1994, v2339 p304-317 1995.

Keywords: *Materials science, *Neutron activation analysis, Neutrons, Reprints, Depth profiling, Diffraction, Inelastic scattering, Reflectometry, *Foreign technology.

Thermal and cold neutron probes provide researchers in such fields as materials science, physics, chemistry, and biology information that often can be obtained by no other means. The main focus of this paper will be on recent studies at NIST which illustrate how thermal and cold neutrons are utilized for materials research.

02,981
PB96-136981 PC A08/MF A02
National Inst. of Standards and Technology (MSEL), Gaithersburg, MD. Metallurgy Div.
Metallurgy Technical Activities 1994 (NAS-NRC Assessment Panel, April 6-7, 1995).
E. N. Pugh, and S. C. Hardy. 1995, 151p, NISTIR-5582.

Keywords: *Metallurgy, *Properties, *Metrology, *Research projects, Government/industry relations, Metal matrix composites, Intermetallics, Superconductors, Corrosion, Electrodeposition, Mechanical properties, Magnetic materials, High temperature, Advanced materials, National Institute of Standards and Technology.

This report summarizes the FY 1994 activities of the Metallurgy Division, National Institute of Standards and Technology (NIST). These activities center on structure-processing-properties relations of metals and alloys, on methods of measurement, and on the generation and evaluation of critical materials data. Efforts comprise studies of metals processing and process sensors; advanced materials - including metal matrix composites, intermetallic alloys, and superconductors; corrosion and electrodeposition; mechanical properties; magnetic materials; and high temperature reactions.

02,982
PB96-160213 Not available NTIS
National Inst. of Standards and Technology (EEEL), Gaithersburg, MD. Semiconductor Electronics Div.
Effect of Intermediate Thermal Processing on Microstructural Changes of Oxygen Implanted Silicon-on-Insulator Material.
Final rept.
J. D. Lee, J. C. Park, S. J. Krauss, P. Roitman, and M. K. El-Ghor. 1992, 6p.
Pub. in Proceedings of the Materials Research Society Symposium, Boston, MA., December 2-6, 1991, v235 p133-138 1992.

Keywords: *Annealing, Defects, Reprints, *SIMOX, *Silicon on insulator, Transmission electron microscopy.

The microstructural changes in oxygen implanted silicon-on-insulator material (SIMOX) at intermediate annealing steps and the changes by rapid thermal annealing (RTA) were studied with transmission electron microscopy. Defects found in as-implanted SIMOX, including multiply faulted defects, short stacking faults, and (113) defects, were all removed in anneals from 900 degrees C to 1100 degrees C. The threading dislocations in annealed materials from at these temperatures during thermal ramping. RTA shows that the microstructure is significantly influenced by the ramp rate. The very high ramp rate in RTA results in very flat interfaces and a buried oxide layer with no Si islands, but significantly increases the defect density. Overall, the results show that intermediate thermal processing steps strongly affect the final microstructure of SIMOX material.

02,983
PB96-160262 Not available NTIS
National Inst. of Standards and Technology (EEEL), Gaithersburg, MD. Semiconductor Electronics Div.
Interface Roughness, Composition, and Alloying of Low-Order AlAs/GaAs Superlattices Studies by X-ray Diffraction.
Final rept.
W. R. Miller, J. G. Pellegrino, and J. Comas. 1993, 6p.
Pub. in Proceedings of the Materials Research Society Symposium, 1992, v280 p265-270 1993.

Keywords: *Interface roughness, Superlattices, Reprints, *X ray diffractometry, AlAs/GaAs, Heterostructures, Migration enhanced epitaxy.

Low-order, monolayer by monolayer (1x1) AlAs/GaAs superlattices grown by MBE using different growth techniques have been studied by X-ray diffractometry. High-resolution multiple-crystal diffractometry was used to study diffraction features near the (004) peaks due to the substrate and epilayers. Using this technique, we have investigated the effect of growth techniques on the strain and tilt of the superlattices. High-resolution X-ray diffraction (HRXRD) results suggest that the sample grown by migration-enhanced epitaxy (MEE) is more highly strained and has more tilt than the same superlattice sample grown using the interrupted growth (IG) technique.

02,984
PB96-160429 Not available NTIS
National Inst. of Standards and Technology (MSEL), Gaithersburg, MD. Reactor Radiation Div.
Instrumental Smearing Effects in Radially Symmetric Small-Angle Neutron Scattering by Numerical and Analytical Methods.
Final rept.
J. G. Barker, and J. S. Pedersen. 1995, 9p.
Pub. in Jnl. of Applied Crystallography, v28 p105-114 1995.

Keywords: *Resolution functions, Reprints, *Foreign technology, *Small angle neutron scattering, Smearing shadowing, Beamstop shadowing.

A numerical calculation method for determining the resolution functions for radially symmetric collimation and scattering is described. In the present approach, the total number of integrations is reduced to four by use of the radial symmetry of the geometry. Futhermore, the beam-stop shadowing effect is included exactly. A typical calculation can be completed in minutes on current personal computers. An interactive computer program allows the user to enter the experimental parameters such as aperture size and wavelength spread, allowing smearing calculations to be handled rountinely as a 'black box' operation. The exact smearing treatment is compared both to an improved technique involving Gaussian resolution functions where corrections for the beam stop are included and to results from Monte Carlo simulations. In most experiments, the use of a Gaussian distribution to approximate the resolution is preferred on account of its ease of calculation. But in a few cases, such as Porod scattering, the present more extensive numerical calculation or inclusion of the developed beam-stop-shadowing correction factors into a Gaussian scheme are needed for an adequate prediction of the smearing effects.

02,985
PB96-161823 Not available NTIS
National Inst. of Standards and Technology (MSEL), Gaithersburg, MD.
Lattice Statics of Interfaces and Interfacial Cracks in Bimaterial Solids.
Final rept.
V. K. Tewary, and R. Thomson. 1991, 39p.
Pub. in Jnl. of Materials Research, p1-39 1991.

Keywords: *Composites, *Films, *Fracture, Reprints, Interfaces, Calculation, Green's function.

A method for calculating a lattice statics Green's function is described for a bimaterial lattice or a bicrystal containing a plane interface. The method involves creation of two half space lattices containing free surfaces and then joining them to form a bicrystal. The two half space lattices may have different structures as in a two phase bicrystal or may be of the same type but joined at different orientations to form a grain boundary interface. The method is quite general but, in this paper, has been applied only to a simple model bicrystal formed by two simple cubic lattices with nearest neighbor interactions. The bimaterial Green's function is modified to account for an interfacial crack which is used to calculate the displacement field due to an applied external force. It is found that the displacement field, as predicted by the lattice theory, does not have the unphysical oscillations predicted by the continuum theory.

02,986
PB96-161922 Not available NTIS
National Inst. of Standards and Technology (MSEL), Gaithersburg, MD.
Correlations between Flaw Tolerance and Reliability in Zirconia.
Final rept.
M. J. Readey, C. L. McCallen, P. D. McNamara, and B. R. Lawn. 1993, 5p.
Pub. in Jnl. of Materials Science, v28 p6748-6752 1993.

Keywords: *Flaw tolerance, *Zirconia, Reliability, Indentations, Reprints, *Weibull modulus, R-curve.

Interrelations between flaw tolerance and reliability in Y-TZP, Ce-TZP and Mg-PSZ ceramics are investigated. Indentation-strength tests indicate an enhanced flaw tolerance with increasing R-curve behaviour from tetragonal goes to martensite transformation. The Weibull modulus of unindented specimens increases with the enhanced tolerance. However, even the most tolerant zirconias show persistent scatter in strength, implying that variability in material microstructure may be as important a factor in reliability evaluation in these materials as variability in flaw size.

02,987
PB96-161997 Not available NTIS
National Inst. of Standards and Technology (MSEL), Gaithersburg, MD.
Whither Computational Materials Science. Some Thoughts from the Mechanical Properties Front.
Final rept.
R. Thomson. 1993, 6p.
Pub. in Computational Materials Science, v2 p137-142 1994.

Keywords: *Elasticity theory, Mechanical properties, Reprints, Computations, Fractures, *Computational materials science.

A claim is made that analysis will remain important and become a useful ally in helping computational materials science live up to its ultimate potential. Examples are given in the mechanical properties area where numerical simulations have been able to parameterize and mark out areas of validity for elasticity theory. The important role of developing asymptomic paths from one level or category of theory to another is discussed.

02,988
PB96-163613 Not available NTIS
National Inst. of Standards and Technology (MSEL), Gaithersburg, MD.
Fracture in Multilayers.
Final rept.
P. Anderson, I. H. Lin, and R. Thompson. 1992, 6p.
Pub. in Scripta Metallurgica, 6p 1992.

Keywords: *Fractures, *Multilayers, *Interfaces, Reprints, *Foreign technology, *Green's functions.

Fracture in multilayers is a subject about which very little is known. One of the only papers on the mechanisms of interfacial fracture of multilayers at the microstructural scale is that by Hirth and Evans. General references to the experimental literature are given in the paper by Lashmore and Foecke in this series. The main thrust of this paper, however, will be the discussion and interpretation of a single observation of an interfacial crack in a Cu/Ni multilayer by Lashmore, and since the theory is so little developed, the authors will often be projecting what the authors know about interfacial cracking into the multilayer world. For presentation of the results by Lashmore, again, see the paper in this series by lashmore and Foecke. Some preliminary interpretation of this micrograph is reported in Reference, based on extrapolation from dislocation emission theory in homogeneous solids. It was suggested there that the fracture toughness of multilayers may be higher than in the corresponding homogeneous materials because emitted dislocations will shield the crack more forcefully due to the limited mobility of shielding glide dislocations in the multilayer.

02,989
PB96-163696 Not available NTIS
National Inst. of Standards and Technology (MSEL), Gaithersburg, MD.
Cracks and Dislocations in Face-Centered Cubic Metallic Multilayers.
Final rept.
D. S. Lashmore, and R. Thomson. 1992, 8p.
Pub. in Jnl. of Materials Science, v7 n9 p2379-2386 Sep 92.

Keywords: *Coherent interfaces, Reprints, *Dislocation emission, *Interfacial fracture, Metallic multilayers.

In this paper, the authors have demonstrated that very perfect thin multilayers of the Cu/Ni system can be prepared with coherent interfaces if the layer modulation wavelength is in the 10 nm range. At modulation thickness above about 60 nm, the interfaces become incoherent. The authors have injected a crack into a coherent interface in the 10 nm case which has generated dislocations into the interface forming the crack plane, as well as into the layers adjacent to the crack plane. The dislocations injected into the crack plane presumably from misfit dislocations on that interface, and are grouped so close to the crack tip that individual dislocations are not completely imaged. The dislocations injected into the adjacent layers are distributed rather widely. The authors have analyzed the dislocation emission from a crack in the fcc geometry appropriate to the multilayers using a simplified elastic theory developed for cracks in homogeneous materials. The mixed mode loading which the misfit stresses are expected to produce lead one to expect these materials to be ductile and to have high toughness. Very high dislocation densities on the crack plane near the crack, however, may lead to a brittle mode of failure, which is beyond the purview of the elastic theory. The dislocations are observed to have strong interactions with alternating interfaces in the multilayers, and this effect could be due to elastic bunching of the dislocations at alternating interfaces caused by the misfit stress.

02,990
PB96-164223 Not available NTIS
National Inst. of Standards and Technology (MSEL), Boulder, CO. Materials Reliability Div.
Compressibility of Polycrystal and Monocrystal Copper: Acoustic-Resonance Spectroscopy.
Final rept.
H. Ledbetter, S. Kim, C. Fortunko, and P. Heyliger. 1996, 7p.
Pub. in International Jnl. of Thermophysics, v17 n1 p263-269 Jan 96.

Keywords: *Bulk-modulus, *Compressibility, *Copper, Reprints, *Elastic constants, Ultrasonics.

Using a method used mainly by geophysicists for small specimens-acoustic-resonance spectroscopy (ARS)-we measured the elastic-stiffness constants of centimeter-size copper specimens with rectangular-parallelepiped shapes. The polycrystal consisted of heavily twinned 75-micromoles crystallites. From the specimens' macroscopic resonance-vibration frequencies (midkilohertz to low-megahertz), we calculated the least-squares elastic-stiffness coefficients, two and three for the two cases. Using the same specimens, we augmented the ARS measurements with conventional pulse-echo-method measurements. Using rod specimens, we measured the Young modulus E and torsional modulus G, and we calculated the bulk modulus B. The less direct and less familiar ARS method gives the same results as a usual pulse-echo method and a rod-resonance method.

02,991
PB96-176516 Not available NTIS
National Inst. of Standards and Technology (PL), Boulder, CO. Quantum Physics Div.
Growth and Nucleation of Hydrogenated Amorphous Silicon on Silicon (100) Surfaces.
Final rept.
D. M. Tanenbaum, A. Laracuente, and A. C. Gallagher. 1995, 6p.
Pub. in Materials Research Society Symposium Proceedings, v377 p143-148 1995.

Keywords: *Dynamic scaling, *Nucleation, Islanding, Reprints, *Nanoparticulates, A-SiiH.

A scanning tunneling microscope (STM) has been used to study the topology of the surfaces of a series of thin hydrogenated amorphous silicon (a-Si:H) films deposited by rf discharge from pure silane. The substrates were atomically flat, oxide-free, single-crystal Si(100). Films were grown in our laboratory and transferred to the STM with no air exposure between growth and measurement. A series of thin films between 1 and 50 nm in thickness reveals the initial growth stage of a-Si:H on Si(100). Initial nucleation and islanding can be seen on these films. The surface has a distribution of island sizes. The rms roughness and a surface lateral correlation length were measured as functions of film thickness. The rms roughness grows sublinearly with thickness from 0.3-0.5 nm as the film thickness is raised from 1 to 50 nm. The lateral size of the surface features also grows with film thickness. The growth of the roughness and correlation length can be compared with the dynamic scaling model. In addition, the topographs reveal occasional structures of larger size and low density on the film surface. These structures are nanoparticles of silicon deposited from the plasma during film growth. The frequency of these features scales with film thickness, and represents 10 to the minus 5th power - 10 to the minus 4th power of the total film volume.

02,992
PB96-179577 Not available NTIS
National Inst. of Standards and Technology (MSEL), Gaithersburg, MD. Reactor Radiation Div.
Design of a High-Flux Backscattering Spectrometer for Ultra-High Resolution Inelastic Neutron Measurements.
Final rept.
P. M. Gehring, C. W. Brocker, and D. A. Neumann. 1995, 6p.
Pub. in Materials Research Society Symposium Proceedings, v376 p113-118 1995.

Keywords: *Nuetron measurements, *Backscattering spectrometers, Design, Reprints, High-flux, Ultra-high resolution.

The authors discuss the design of a new backscattering spectrometer to be installed at the Cold Neutron Research Facility at the National Institute of Standards and Technology. Si (111) crystals cover both monochromator and analyzer which are spherically bent to a radius of curvature of approxmately 2 m to focus the incident and scattered neutron beams. The bending increases the intrinsic lattice gradient of Si beyond its Darwin limit, resulting in an energy resolution of approximately 0.75 mueV FWHM. The monochromator is Doppler-driven, allowing users access to a dynamic range of plus or minus 60 mueV. The elastic Q-range covers 0.15 to 1.8 Angstroms to the minus one power. The most novel aspect of this design lies in the incorporation of a phase-space transform chopper. This device rotates at 4700 rpm while neutrons are Bragg-diffracted from sets of pyrolytic graphite crystals affixed to its periphery. The process enhances the neutron flux at the backscattering energy of 2.08 meV, but at the expense of a larger horizontal divergence. Computer simulations indicate a resultant flux increase of order 3 should be obtained.

02,993
PB96-180039 Not available NTIS
National Inst. of Standards and Technology (MSEL), Gaithersburg, MD.
Diffusion of Water along 'Closed' Mica Interfaces.
Final rept.
R. Horn, K. T. Wan, S. Courmont, and B. R. Lawn. 1996, 3p.
Pub. in Jnl. of Colloid and Interface Science, v159 p509-511 1993.

Keywords: *Adhesion, *Cracks, *Mica, Fracture, Humidity, Reprints, Interface diffusion.

The responses of internal cracks at recontacted mica interface to change in external humidity are reported and analyzed. Cracks on interfaces reformed in lattice registry remain effectively stationary; cracks formed at

interfaces with a twist misorientation expand and contract reversibly with increasing and decreasing humidity. The results indicate that the internal cracks in the misoriented configuration are accessible to atmospheric water, which diffuses along the dilated interface and lowers the interface energy, but remain impervious to other constituent molecules of air.

02,994
PB96-180054 Not available NTIS
National Inst. of Standards and Technology (MSEL), Gaithersburg, MD. Polymers Div.
Synthesis of Hybrid Organic-Inorganic Materials from Interpenetrating Polymer Network Chemistry.
Final rept.
C. L. Jackson, B. J. Bauer, A. I. Nakatani, and J. D. Barnes. 1996, 7p.
Pub. in Chemistry of Materials, v8 n3 p727-733 1996.

Keywords: *Polymer networks, *Acrylate, Synthesis, Sol-gel, Scattering, Reprints, *Interpenetrating polymer network, Transmission electron microscopy.

Organic-inorganic interpenetrating polymer networks were synthesized with an SiO2 phase made by sol-gel chemistry and the organic phase made from poly(2-hydroxyethyl acrylate). The resultant morphologies were characterized by small-angle scattering and electron microscopy. When the vinyl polymerization is more rapid than the sol-gel reaction, gross phase separation occurs giving a heterogeneous structure. For comparable rates of the two polymerizations, the specimens have a dendritic morphology on the scale of 0.5 micro m. The more rapid formation of the silica phase relative to the organic network produces rigid and optically transparent materials, with a finely divided structure as seen by transmission electron microscopy. The glass content of these materials is about 0.15 g/g and the sizes of the SiO2-rich domains are 100 Angstroms or less. Addition of tetrakis(2-(acryloxy)ethoxy)silane was also studied and found to promote phase mixing between the organic and inorganic phases.

02,995
PB96-180104 Not available NTIS
National Inst. of Standards and Technology (MSEL), Gaithersburg, MD. Polymers Div.
Composition and Solubility Product of a Synthetic Calcium Hydroxyapatite.
Final rept.
M. Markovic, B. O. Fowler, M. S. Tung, and E. S. Lagergren. 1996, 12p.
Pub. in Mineral Scale Formation and Inhibition, Washington, DC., August 21-26, 1995, p271-282.

Keywords: *Calcium hydroxyapatite, *Chemical analysis, *Solubility products, Composition, Reprints, Statistical analysis, Thermal analysis.

Synthetic calcium hydroxyapatites (HA's) have, in general, excellent biocompatibility with tooth and bone tissues, and they are frequently used as biomedical materials. The properties of synthetic HA's depend strongly on preparative conditions. They are well known to be variable and the composition deviates from the stoichiometric HA formula. Ca10(POa)6(OH)2, that comprises the unit-cell content. In order to properly characterize these HA's, accurate determinations of complete chemical composition, unit-cell parameters, solubility, surface area, crystallinity, etc., are needed. The focus of this paper is on the procedures and methods for accurate and precise determinations of two important parameters, the Ca/P molar ratio and solubility product, of a HA that was prepared and characterized in the author's group for use as a HA reference material (HA-RM).

02,996
PB96-180245 Not available NTIS
National Inst. of Standards and Technology (MSEL), Gaithersburg, MD.
Effect of Chemical Interaction on Barenblatt Crack Profiles in Brittle Solids.
Final rept.
K. T. Wan, and B. R. Lawn. 1992, 7p.
Pub. in Acta Metallurgica Materials, v40 n12 p3331-3337 1992.

Keywords: *Brittle solids, *Chemical interactions, Cohesive zone, Reprints, Bareblatt profile, Crack-tip field, Molecular wedge.

A self-consistent solution for continuum-slit Barenblatt cracks with interactive chemistry is presented. Environmental species entering the crack mouth are limited in their transport along the ever-narrowing interface by molecular size restrictions. The ensuing cohesion zone behind the tip consists of three regions: an extended far region of weak solid-fluid-solid attraction; a small intermediate region of strong solid-fluid-solid repulsion; and an exclusinary near-tip intrinsic region of strong solid-solid attraction. To facilitate an analytical solution of the equations for the crack-opening displacements, the cohesion stresses are taken to be uniformly distributed within each of these zones. The magnitudes of these stresses are expressed in terms of the intersurface energies that define equilibrium crack states, for virgin and healed interfaces. Illustrative calculations of the crack profiles are given for the well-documented mica-water system. It is shown that the penetrating species cause a significant local bulge in the repulsion region, consistent with Thomson's picture of a molecular wedge.

02,997
PB96-180252 Not available NTIS
National Inst. of Standards and Technology (MSEL), Gaithersburg, MD.
Pressurized Internal Lenticular Cracks at Healed Mica Interfaces.
Final rept.
K. T. Wan, R. G. Horn, S. Courmont, and B. R. Lawn. 1993, 9p.
Pub. in Jnl. of Materials Research, v8 n5 p1128-1136 May 93.

Keywords: *Adhesion, *Fracture mechanics, *Interface cracks, Mica, Reprints, Lenticular flaws, Pressure difference.

The equilibrium states of internal penny cracks at interfaces in thin-sheet bodies are investigated. Consideration is given to cracks held open by a center-loading force from an entrapped particle in combination with a uniform pressure from a fixed mass of entrapped gas. A fracture mechanics analysis indicates that under these conditions the crack are stable, but are amendable to growth from an enhancement in net pressure (increase in internal pressure or decrease in external pressure) or effective particle size. Essential details of the theory are confirmed by experiments on linticular crack at healed interfaces in muscovite mica. The results are pertinent to flaw responses in brittle ceramic systems where structural integrity is an issue.

02,998
PB96-180286 Not available NTIS
National Inst. of Standards and Technology (PL), Gaithersburg, MD. Radiometric Physics Div.
Development of Neutral-Density Infrared Filters Using Metallic Thin Films.
Final rept.
Z. M. Zhang, R. U. Datla, and L. M. Hanssen. 1995, 6p.
Pub. in Materials Research Society Symposium Proceedings, v374 p117-122 1995.

Keywords: *Infrared filters, *Optical density, Optical properties, Spectrometers, Reprints.

Broadband infrared filters with uniform spectral transmittance are used for spectrometer calibration and other applications. However, commercially available neutral-density filters with optical density (OD) greater than 2 exhibit significant variations in OD over the wavelength region from 2 micrometers to 25 micrometers. In this work, the authors found a single-layer alloy film that, for appropriate thicknesses, yields a flat transmittance for OD near 3 and 4. The transmittance and reflectance of the filters were measured using a Fourier-transform infrared spectrometer. The optical constants of the alloy films were obtained from transmittance and reflectance measurements, which can be used for future design optimization.

02,999
PB96-183082 PC A07/MF A02
National Inst. of Standards and Technology (MSEL), Gaithersburg, MD. Materials Reliability Div.
Materials Reliability. Technical Activities, 1995.
H. I. McHenry, and T. A. Siewert. Apr 96, 107p, NISTIR-5748.
See also report for 1995, PB93-173466.

Keywords: *Research projects, *Materials, Quality, Reliability, Safety, Process control, Metrology, Welding, Casting, Thermomechanical treatment, Microstructure, Steels, Metals, Ultrasonic tests, Physical properties, Nondestructive tests.

Contents:
Division Organization;
Introduction;
Highlights;
Research Staff;
Technical Activities;
Intelligent Processing of Materials;
Ultrasonic Characterization of Materials;
Micrometer-Scale Measurements for Materials Evaluation;
Other Projects;
Outputs and Interactions;
Recent Publications;
Technical and Professional Committee Leadership;
Industrial and Academic Interactions;
and Appendix:
Organizational Charts.

03,000
PB96-186135 Not available NTIS
National Inst. of Standards and Technology (MSEL), Gaithersburg, MD. Polymers Div.
What Is a 'Standard Reference Material' - What Is Any Reference Material.
Final rept.
J. A. Tesk, and J. Colbert. 1996, 3p.
Pub. in Newsletter of the Society of Biomaterials, The Torch, v18 n1 p6-7 and 17, Jan/Feb 96.

Keywords: *Standards, Reprints, *Standard Reference Material, *Certified Reference Material, *NIST Reference Materials, ISO Reference Materials.

One of the pressing topics of discussion at the 1995 meeting of the Biomaterials Society Standards Committee (SC) was the need for Reference Materials (RMs). As discussions proceeded, however, it became apparent that some members of the SC were unaware of the different kinds of RMs that can be obtained and that the significance of their differences lies in their intended applications. This situation is not unique to SC members; it appears to be prevalent to varying degrees throughout the scientific and engineering community, including the Biomaterials Society at large. The fact is that there are two classifications of reference materials, readily distinguished by their definitions, which prescribe the kind of technical information that is supplied with them when they are acquired.

03,001
PB96-186168 Not available NTIS
National Inst. of Standards and Technology (MSEL), Gaithersburg, MD. Reactor Radiation Div.
Neutron and Raman Spectroscopies of 134 and 134a Hydrofluorocarbons Encaged in Na-X Zeolite.
Final rept.
T. J. Udovic, J. M. Nicol, R. R. Cavanagh, C. P. Grey, D. R. Corbin, J. J. Rush, and M. K. Crawford. 1995, 6p.
Pub. in Materials Research Society Symposium Proceedings, v376 p751-756 1995.

Keywords: *Hydrofluorocarbon, *Neutron spectroscopy, *Raman spectroscopy, Refrigerants, Reprints, Inelastic neutron scattering, Nax zeolite.

Inelastic neutron scattering methods were used in conjunction with Raman spectroscopy to probe the vibrational density of states of the hydrofluorocarbons (HFCs) 134 (HF2C-CF2H) and 134a (F3C-CFH2) adsorbed in the cages of dehydrated Na-X zeolite. A comparison of the vibrational spectra of the encaged HFC species with those of their gas-phase analogs indicates that the HFCs adsorb nondissociatively at room temperature and are most likely associated with Na cations in the supercages at the Sm sites. Guest-hose interactions are manifested by adsorption-induced perturbations of the gas-phase torsional and C-H stretching vibrations and the presence of additional features presumably due to low-energy whole-molecule vibrations and adsorbate-coupled zeolite framework vibrations. Moreover, although the 134 trans conformer is favored by 5 kJ/mole in the gas phase at 300 K, the gauche conformer seems to be more prevalent in the zeolite at this temperature and below. This suggests that a sizeable fraction of the Na-X adsorption sites provides a stabilizing configuration for the otherwise higher-energy gauche conformation, perhaps due to hydrogen-bonding interactions with the zeolite framework.

03,002
PB96-190335 Not available NTIS
National Inst. of Standards and Technology (MSEL), Boulder, CO. Materials Reliability Div.

General

Charpy Specimen Tests at 4 K.
Final rept.
R. L. Tobler, and A. Bussiba. 1992, 8p.
Pub. in International Cryogenic Materials Conference (9th), Huntsville, AL., June 11-14, 1991, Advances in Cryogenic Engineering (Materials), v38 p217-224 1992.

Keywords: *Austenitic steels, *Fracture toughness, Impact tests, Mechanical properties, Materials, Standards, Reprints, *Cryogenic test procedures.

The paper describes nonstandard methods of testing Charpy specimens at 4 K. We show that the initial temperature can be achieved using a helium flow method with U-type as well as C-type machines. Unfortunately, heating during impact loading weakens the correlation with quasistatic fracture toughness parameters. Alternative test procedures using fatigue precracked specimens were not fully satisfactory, either: (1) Precracking reduces the impact energy by 35-54%, but the specimen heating is still significant; (2) slow bending curtails the heating most effectively, but then the desired simplicity of a screening test is lost.

03,003
PB96-195284 PC A09/MF A02
National Inst. of Standards and Technology (MSEL), Gaithersburg, MD. Metallurgy Div.
Metallurgy. Technical Activities, 1995.
Rept. for 1 Oct 94-30 Sep 95.
E. N. Pugh, and S. C. Hardy. 1995, 163p, NISTIR-5750.
See also PB96-136981.

Keywords: *Metallurgy, *Metrology, *Research projects, Mechanical properties, Electronic packaging, Metallurgy, Electrochemistry, Alloys, Steels, Electrodeposition, Corrosion, Intermetallics, IPM(Intelligent processing of materials), Advanced materials, Nanomaterials.

The report describes the technical activities of the Metallurgy Division in 1995. The format this year is different from that in preceding years in that the descriptions of the Division's projects are grouped under major Materials Science and Engineering Laboratory (MSEL) program rather than under specific Groups. Partial Table of Contents: Intelligent Processing of Materials; High-Tc Superconductivity; Electronic Packaging and Interconnection; Nanostructured Materials; Dental and Medical Materials; MSEL Other; Metals Processing; Metals Data and Characterization.

03,004
PB96-200159 Not available NTIS
National Inst. of Standards and Technology (MSEL), Boulder, CO. Materials Reliability Div.
Scanning Electron Microscopy Observations of Misfit Dislocations in Epitaxial In0.25Ga0.75As on GaAs(001).
Final rept.
R. R. Keller, and J. M. Phelps. 1996, 3p.
Pub. in Jnl. of Materials Research, v11 n3 p552-554 Mar 96.

Keywords: *Scanning electron microscopes, *Dislocations, *Epitaxial films, Thin films, Electron channeling, Reprints, Kikuchi patterns, Backscattered electrons.

Dislocations in the misfit epitaxial film system In0.25Ga0.75As on GaAs(001) were imaged using a modified electron channeling contrast technique in a LaB6 SEM. We obtained images at an incident beam energy of 30 KeV, a beam divergence of less than 1 mrad and a specimen tilt of 70 degrees in conjunction with a movable scintillator detector mounted at a take-off angle of approximately 3 degrees to 5 degrees. We achieved a spatial resolution of approximately 80 to 100 nm with this technique. Such resolution allowed rapid imaging of clusters consisting of only a few closely spaced dislocations in a 55 nm thick film. At such small film thicknesses, we did not require accurate knowledge of the incident beam direction in order to obtain sufficiently strong channeling contrast for qualitative characterization. The observed defect arrangements included features that we believe represent clustered threading segments.

03,005
PB96-200761 Not available NTIS
National Inst. of Standards and Technology (MSEL), Boulder, CO. Materials Reliability Div.
Elastic Constants and Microcracks in YBa2Cu3O7.
Final rept.
Y. Shindo, H. Ledbetter, and H. Nozaki. 1995, 4p.
Pub. in Jnl. of Materials Research, v10 n1 p7-10 Jan 95.

Keywords: *Elastic constants, *Microcracks, *Superconductors, Polycrystalline, Crack density, Crack aspect ratio, Reprints, Oxide superconductors.

We analyze theoretically the effect of microcracks and voids on the apparent elastic constants of polycrystalline YBa2Cu3O7. Using measurements by Holcomb and Mayo, we calculate crack density and crack aspect ratio. We obtain reasonable intrinsic elastic constants. For the bulk modulus, for example, we predict values close to these obtained by neutron-diffraction studies: 123 GPa for a polycrystal and 122 GPa for a monocrystal.

03,006
PB96-200910 Not available NTIS
National Inst. of Standards and Technology (BFRL), Gaithersburg, MD. Building Materials Div.
Precision of Marchall Stability and Flow Test Using 6-in. (152.4-mm) Diameter Specimens.
Final rept.
P. S. Kandhal, Y. Wu, F. Parker, and P. A. Spellerberg. 1996, 6p.
Pub. in Jnl. of Testing and Evaluation (JTEVA), v24 n1 p20-25 Jan 96.

Keywords: *Stones, *Marshall stability, Percent voids, Precision statement, Marshall flow, Reprints, Large stone mixes.

Earlier studies have shown that the repeatability of Marshall stability, flow, and air voids content measurements on 6-in. (152.5-mm) diameter specimens of large stone mixes is better than the repeatability on 4-in. (101.6-mm) diameter specimens. A round robin study involving twelve participating laboratories was conducted to provide information for developing a precision statement for the ASTM Test Method for Resistance to Plastic Flow of Bituminous Mixtures Using Marshall Apparatus (6 inch-Diameter Specimen) (D 5581). Difference two-sigma (d2s) limits were developed to determine acceptable single and multilaboratory differences for bulk specific gravity, percent voids, Marshall stability, and Marshall flow measurements. Analysis of other data collected during the study indicated that stability and flow measurements are not sensitive to minor differences in various 6-in. (152.4-mm) diameter breaking heads currently in use.

03,007
PB96-204045 Not available NTIS
National Inst. of Standards and Technology (MSEL), Gaithersburg, MD. Ceramics Div.
Guide to Locating and Accessing Computerized Numeric Materials Databases.
Final rept.
E. F. Begley, and S. J. Dapkunas. 1993, 6p.
Pub. in Jnl. of Materials Engineering and Performance, v2 n6 p881-886 1993.

Keywords: *Materials, *Data bases, *Statistical data, Access, Data retrieval, Information retrieval, Information dissemination, Reprints.

The article provides the materials engineer and component designer a guide to these sources including the data available and the points of contact for gaining access.

03,008
PB96-204086 Not available NTIS
National Inst. of Standards and Technology (MSEL), Gaithersburg, MD. Ceramics Div.
NIST/NCMS Program on Electronic Packaging: First Update.
Final rept.
J. A. Carpenter, B. Dickens, K. G. Kreider, G. J. Piermarini, D. T. Read, R. D. Evans, J. R. Manning, and R. L. Mattis. 1992, 16p.
Pub. in Proceedings of the Conference of the International Electronics Packaging Society (IEPS), Austin, TX., September 27-30, 1992, p449-464.

Keywords: *Electronic packaging, *Metrology, *Quality control, Manufacturing, Circuit interconnections, Printed circuit boards, Measurement, Reliability analysis, Reprints, Materials properties.

In 1992 the National Institute of Standards and Technology (NIST) expanded its intramural efforts on development of metrology for microelectronics packaging and interconnection. The new intramural projects concentrate on development or refinement of metrology for measuring the properties of the materials as they actually exist in modern packaging and interconnection, and not as measured on idealized or bulk specimens. Also, work begin in 1991 accelerated a major consortium effort led by the National Center for Manufacturing Species (NCMS) and jointly supported by the consortium members and the NIST Advanced Technology Program (ATP) to develop new materials and production technology for printed wiring boards. This is an update on the progress of those efforts.

03,009
PB96-214754 PC A05/MF A01
National Inst. of Standards and Technology (MSEL), Gaithersburg, MD.
Materials Science and Engineering Laboratory Annual Report, 1995. Technical Activities.
Rept. for 1 Oct 94-30 Sep 95.
L. H. Schwartz, and H. L. Rook. 1995, 68p, NISTIR-5746.
See also PB95-196697.

Keywords: *Research and development, Research management, Technology innovation, Research projects, Organizational structure, Laboratories, Resources, Technology transfer, *US NIST, *MSEL(Materials Science and Engineering Laboratory), *Materials Science and Engineering Laboratory(MSEL).

The 1995 Annual Report was organized to assist the NAS-NAE-NRC Board on Assessment and intended to be used as background information at the annual review meeting. Coupled with the more detailed technical reports of the divisions of MSEL, this report describes the activities, accomplishments, output and impacts of the MSEL during the period of Fiscal Year 1995 (October 1, 1994 to September 30, 1995).

03,010
PB97-111587 Not available NTIS
National Inst. of Standards and Technology (MSEL), Gaithersburg, MD. Reactor Radiation Div.
Neutron Diffraction Texture Study of Deformed Uranium Plates.
Final rept.
C. S. Choi, and M. Staker. 1996, 6p.
Pub. in Jnl. of Materials Science, v31 p3397-3402 1996.

Keywords: *Uranium plates, *Neutron diffraction, Orientational distribution functions, Deformation, Reprints.

The texture of two depleted uranium (DU) samples, labelled DUWR and DUWRs, were studied by neutron diffraction. DUWR was prepared by warm rolling of a cast ingot, and DUWR2 was prepared by adding 20% tensile strain to the warm-rolled DUWR. Complete three-dimensional orientation distribution functions were determined using four neutron pole figures for the DUWR, and using six neutron pole figures for the DUWR2 sample, by the WIMV method of the program popLA. The textures of the two samples were essentially identical to each other. They could be described by a twisted helical density tube spiralling continously along the psi-axis of the Euler space. The projection of the backbone of the density tube along the Bragg angle-axis cast a linear shadow running parallel to the diagonal of the integral-psi plane, which could be defined by a integral = psi + 90 degrees (and integral = psi + 270 degrees) relation. The helical tube was confined within narrow Braggs angle-angle limits, from 14 degrees to 30 degrees with the peak orientation at (103) (010).

Adhesives & Sealants

03,011
PB94-212222 Not available NTIS
National Inst. of Standards and Technology (MSEL), Gaithersburg, MD. Polymers Div.

Micromechanics of Fracture in Rubber-Toughened Epoxies.
Final rept.
D. L. Hunston, H. Mizumachi, and W. McDonough. 1990, 6p.
Pub. in Proceedings of International Conference on Adhesion '90 (4th), Cambridge, England, September 10-12, 1990, p37/1-37/6.

Keywords: *Crack propagation, *Adhesive bonding, *Epoxy resins, *Fractures(Materials), *Micromechanics, Adhesives, Deformation, Bonded joints, Failure, Fracture mechanics, Mechanical properties, Reprints.

Previous work has shown the importance of the crack-tip deformation zone in determining the fracture energies for both samples of bulk adhesive and the corresponding adhesive joints. To gain a better understanding of deformation zone development, the crack-tip events in compact tension specimens of bulk adhesive were monitored during loading and failure. The results show no clear onset point for crack growth but rather a gradual acceleration. Moreover, in regions of stable crack growth, the size of the deformation zone correlates with the crack velocity. This has important implications for failure criteria.

03,012
PB96-183249 PC A05/MF A01
National Inst. of Standards and Technology (BFRL), Gaithersburg, MD. Building Materials Div.
Performance of Tape-Bonded Seams of EPDM Membranes: Comparison of the Peel Creep-Rupture Response of Tape-Bonded and Liquid-Adhesive-Bonded Seams.
Building science series.
W. J. Rossiter, M. G. Vangel, E. Embree, K. M. Kraft, and J. F. Seiler. May 96, 70p, NIST/BSS-175.
Also available from Supt. of Docs. as SN003-003-03411-8.

Keywords: *Adhesive tapes, *Roofs, Seams(Joints), Creep rupture tests, Construction materials, EPDM(Ethylene Propylene Diene Terpolymer).

A study was conducted to compare the creep-rupture response (i.e., time-to-failure or TTF) of tape-bonded and liquid-adhesive-bonded seams of EPDM (ethylene-propylene-diene terpolymer) roofing membranes. Two commercial tape systems (i.e., tape and primer) and one liquid adhesive were applied to well-cleaned EPDM rubber.

Carbon & Graphite

03,013
PB94-185022 Not available NTIS
National Inst. of Standards and Technology (MSEL), Gaithersburg, MD. Metallurgy Div.
Thermal Diffusivity of POCO AXM-5Q1 Graphite in the Range 1500 to 2500 K Measured by a Laser-Pulse Technique.
Final rept.
T. Baba, and A. Cezairliyan. 1994, 22p.
Pub. in International Jnl. of Thermophysics 15, n2 p343-364 Mar 94.

Keywords: *Graphite, *Thermal diffusivity, *Temperature measuring instruments, Radiative heat transfer, Thermophysical properties, Thermal properties, Boundary conditions, Transport properties, Pulsed lasers, Uncertainity, Reprints, *Laser pulse method.

The thermal diffusivity of POCO AXM-5Q1 graphite was measured in the temperature range 1,500 to 2,500 K utilizing the laser-pulse technique. The uncertainty of the values is estimated to be no more than 3%. The measured values are compared with the results of other investigators.

03,014
PB94-211471 Not available NTIS
National Inst. of Standards and Technology (MSEL), Gaithersburg, MD. Ceramics Div.
Analysis of Thermal Wave Propagation in Diamond Films.
Final rept.
A. Feldman, H. P. R. Frederikse, and S. Norton. 1990, 11p.
See also PB94-211489.
Pub. in Proceedings of Society of Photo-Optical Instrumentation Engineers Diamond Opt. 3, v1325 p304-314 1990.

Keywords: *Diamond films, *Thermal diffusivity, Chemical vapor deposition, Thermal conductivity, Thick films, Thin films, Wave propagation, Heating, Reprints, Photothermal radiometry, Thermal waves.

The use of photothermal radiometry to obtain the thermal diffusivity of CVD diamond is analyzed. The finite size of the heating beam and the radiation detector are taken into account. Heating a finite circularly symmetric region of the specimen surface is compared with uniform heating of the specimen surface. Thermal wave propagation in thick and thin diamond films in vacuum, in air, and on several substrate materials is modelled.

03,015
PB94-211489 Not available NTIS
National Inst. of Standards and Technology (MSEL), Gaithersburg, MD. Ceramics Div.
Thermal Wave Propagation in Diamond Films.
Final rept.
A. Feldman, H. P. R. Frederikse, and S. Norton. 1991, 6p.
See also PB94-211471.
Pub. in Proceedings of International Conference on New Diamond Science and Technology (2nd), Washington, DC., September 23-27, 1990, p881-886 1991.

Keywords: *Diamond films, *Thermal diffusivity, Chemical vapor deposition, Thermal conductivity, Wave propagation, Computation, Reprints, Photothermal radiometry, Thermal waves.

Photothermal radiometry, one of several methods based on the propagation of thermal waves, is a convenient noncontact technique to measure the thermal diffusivities of diamond films. Results of calculations for thermal wave propagation in diamond films are presented. Taken into account are the thickness of the film, the substrate material, the presence of air, the presence of a black absorbing layer, the finite size of the heating beam, and the finite size of the infrared detector used to measure the thermal energy emitted by the specimen.

03,016
PB95-162392 Not available NTIS
National Inst. of Standards and Technology (MSEL), Gaithersburg, MD. Ceramics Div.
Lineshape Analysis of the Raman Spectrum of Diamond Films Grown by Hot-Filament and Microwave-Plasma Chemical-Vapor Deposition.
Final rept.
L. H. Robins, E. N. Farabaugh, and A. Feldman. 1990, 13p.
Pub. in Jnl. of Materials Research 5, n11 p2456-2468 1990.

Keywords: *Crystal growth, *Crystal defects, *Raman spectroscopy, *Chemical vapor deposition, Atomic energy levels, Photoluminescence, Thin films, Diamonds, Reprints, *Diamond films.

Raman spectra were measured in 48 different polycrystalline diamond forms grown by hot-filament and microwave-plasma chemical vapor deposition, and one gem-quality diamond, and characterized by fitting the data to a model lineshape function. The lineshape function contains the following three components: a narrow symmetric line at -1333/cm, the Raman line of diamond; a broad symmetric band at -1520/cm due to s doublet p-bonded carbon; and a slowly varying background due to photoluminescence (PL). Four spectral parameters are observed to change in a correlated manner from one specimen to another: (1) the linewidth of the diamond Raman line, which varies from 3 to 30/cm; (2) the intensity in the tails of the diamond line, several halfwidths away from the peak; (3) the intensity of the s doublet p-bonded carbon band, relative to the diamond line, which varies from -0 to 1; and (4) the intensity of the PL background, relative to the diamond line, which varies from 0.03 to 9. The observed correlations suggest that these changes in the Raman spectrum are caused by a common set of defects.

03,017
PB95-162400 Not available NTIS
National Inst. of Standards and Technology (MSEL), Gaithersburg, MD. Ceramics Div.
Studies of Defects in Diamond Films and Particles by Raman and Luminescence Spectroscopies.
Final rept.
L. H. Robins, E. N. Farabaugh, and A. Feldman. 1990, 12p.
Pub. in Proceedings of Society of Photo-Optical Instrumentation Engineers: Diamond Opt. 3, v1325 p130-141 1990.

Keywords: *Crystal growth, *Crystal defects, *Raman spectroscopy, *Chemical vapor deposition, Atomic energy levels, Diamonds, Cathodoluminescence, Luminescence, Photoluminescence, Thin films, Reprints, *Diamond films.

Diamond films grown under a variety of deposition conditions in hot-filament or microwave-plasma chemical vapor deposition (CVD) reactors were characterized by Raman and cathodoluminescence (CL) spectroscopies. The magnitudes of the following four Raman spectral features were observed to vary from specimen to specimen in a correlated manner: (1) the linewidth of the diamond Raman line; (2) the intensity of the tails of the diamond Raman line at several halfwidths from the peak; (3) the intensity ratio of the s doublet p-bonded carbon Raman band to the diamond Raman line; and (4) the intensity ratio of the broad photoluminescence (PL) background that underlies the Raman spectrum to the diamond Raman peak. We suggest that each of these features varies with the abundance of s doublet p-bonded carbon. A model of competing recombination between two sets of defects is proposed to explain the inverse correlation.

03,018
PB95-162418 Not available NTIS
National Inst. of Standards and Technology (MSEL), Gaithersburg, MD. Ceramics Div.
Surface Roughness Evaluation of Diamond Films Grown on Substrates with a High Density of Nucleation Sites.
Final rept.
L. H. Robins, E. P. Whitenton, E. N. Farabaugh, and A. Feldman. 1991, 6p.
Pub. in Proceedings of International Conference New Diamond Science and Technology (2nd), Washington, DC., September 23-27, 1990, p619-624 1991.

Keywords: *Crystal growth, *Nucleation, *Chemical vapor deposition, *Surface roughness, Substrates, Diamonds, Scanning tunneling microscopy, Wet methods, Dry methods, Spectrum analysis, Polishing, Scanning electron microscopy, Profilometers, Thin films, Raman spectroscopy, Reprints, *Diamond films.

Diamond films were deposited on silicon substrates which were seeded with diamond by either of two techniques, abrasive dry polishing or wet polishing. Depositions were carried out in a microwave-plasma chemical vapor deposition (CVD) reactor. Films were characterized by scanning electron microscopy (SEM) imaging. Raman spectroscopy, optical transmittance and reflectance spectroscopy, stylus profilometry, and scanning tunneling microscope (STM) surface profilometry.

03,019
PB96-119714 Not available NTIS
National Inst. of Standards and Technology (MSEL), Boulder, CO. Materials Reliability Div.
Tribological Behavior of 440/Diamond-Like-Carbon Film Couples.
Final rept.
A. J. Slifka, R. Compos, R. Wei, P. Wilbur, and D. K. Chaudhuri. 1992, 6p.
Pub. in Advanced Earth-to-Orbit Propulsion Technology, Huntsville, AL., May 19-21, 1992, p398-403, NASA CP-3174.

Keywords: *Coatings, *Diamond, *Tribology, Reprints, Friction, Wear.

Diamond-Like-Carbon films were characterized for their tribological properties. Films were made on 440C substrates by first sputter-depositing an intermediate layer of SiC, then extracting 450 eV carbonacceous ions to produce the diamond-like-carbon film. The intermediate SiC layer provides adhesions between 440C and the diamond-like-carbon film, and also provides the necessary nucleation sites for diamond-like-carbon film formation. Films were prepared in three thicknesses, 0.5, 1, and 2 micrometer, and tested at two temperatures, liquid oxygen (-184 deg C) and room temperature (25 degrees C). A coefficient of friction of 0.03 was measured in an oxygen environment. Specific wear rates that are two orders of magnitude lower than for 440C on 440C were measured. Data are

Carbon & Graphite

presented for 440C on diamond-like-carbon, 440C on 440C, and Si3N4 on 440C, for comparison.

03,020
PB96-119748 Not available NTIS
National Inst. of Standards and Technology (MSEL), Gaithersburg, MD. Reactor Radiation Div.
Structural and Magnetic Properties of CuCl2 Graphite Intercalation Compounds.
Final rept.
M. Suzuki, I. S. Suzuki, C. R. Burr, K. Koga, D. G. Wiesler, and N. Rosov. 1994, 12p.
Pub. in Physical Review B, v50 n13 p9188-9199, 1 Oct 94.

Keywords: *Electrochemical cells, *Copper chlorides, Reprints, Catalysts, Electric conductors, Cathodes, *Graphite intercalation compounds.

Structural and magnetic properties of stage-1, stage-2, and stage-3 CuCl2 graphite intercalation compounds (GIC's) were studied by means of x-ray, electron- and neutron-diffraction, dc magnetic susceptibility, and electron spin resonance (ESR) measurements. The Cu2+ ions form an isosceles triangular lattice with one short side and two longer sides. The in-plate dc magnetic susceptibility shows Cure-Weiss behavior above 150 K, a broad maximum around 62-65 K, indicative of low-dimensional magnetic correlations, and a Curie-type behavior below 20 K, attributable to paramagnetic inhomogeneities in the sample.

03,021
PB97-112601 Not available NTIS
National Inst. of Standards and Technology (MEL), Gaithersburg, MD. Precision Engineering Div.
Chemical Aspects of Tool Wear in Single Point Diamond Turning.
Final rept.
E. Paul, C. J. Evans, A. Mangamelli, M. L. McGlauflin, and R. S. Polvani. 1996, 16p.
Pub. in Precision Engineering, v18 p4-19 1996.

Keywords: *Nickel alloys, *Electro deposited coatings, *Diamonds, *Tools, *Wear, Cutting, Machining, Reprints.

A hypothesis is proposed that ascrbies chemical wear of diamond tools to the presence of unpaired d electrons in the sample being machined. The hypothesis is used to explain a range of results for metals, alloys, and other materials including 'electroless' nickel. The hypothesis is further tested by experiments presented here on the machining of a range of high purity elements. The implications for diamond turnability of other materials are discussed.

Ceramics, Refractories, & Glass

03,022
AD-A244 582/3 PC A02/MF A01
National Inst. of Standards and Technology, Gaithersburg, MD.
Effect of Green Density and the Role of Magnesium Oxide Additive on the Densification of Alumina Measured by Small-Angle Neutron Scattering. (Reannouncement with New Availability Information).
G. G. Long, S. Krueger, and R. A. Page. Jul 91, 9p, ARO-26123.3-MS.
Contract ARO-MIPR-102-90
Pub. in Jnl. of the American Ceramic Society, v74 n7 p1578-1584 Jul 91.

Keywords: *Aluminum oxides, Additives, Density, Green(Color), Magnesium oxides, Microstructure, Neutron scattering, Porous materials, Sintering, Reprints, Alumina, Small angle scattering, Densification.

Small angle neutron scattering measurements were used to examine the effect of green density and the role of MgO additive on the evolution of the porous microstructure of alumina during intermediate- and final-stage sintering. It was found that the initial connectivity in the green state plays a dominant role in establishing the channel diameters during the intermediate stage of sintering, and contributes also to determining the onset density at which the final stage of sintering begins. The role of MgO as a sintering aid lies, at least in part, in prolonging the stability of intermediate stage sintering such that the body achieves greater density before the transition to final-stage sintering after which isolated pores are formed.

03,023
AD-A249 178/5 PC A03/MF A01
National Inst. of Standards and Technology, Gaithersburg, MD.
Evolution of the Pore Size Distribution in Final-Stage Sintering of Alumina Measured by Small-Angle X-ray Scattering. (Reannouncement with New Availability Information).
S. Krueger, G. G. Long, D. R. Black, D. Minor, and P. R. Jemian. 10 Oct 91, 11p, ARO-26123.4-MS.
Contract MIPR-ARO-102-90
Pub. in Jnl. of the American Ceramic Society, v74 n10 p2538-2546 Oct 91.

Keywords: *Aluminum oxides, *Sintering, *X ray scattering, Magnesium oxides, Doping, Ceramic materials, High resolution, Density, Entropy, Neutron scattering, Reprints, *Pore size distribution, Alumina, Magnesia, Small angle.

Small-angle X-ray scattering was used to follow the evolution of the pore size distribution during final-stage sintering of alumina and of alumina doped with 0.25 wt% magnesia. The volume-weighted (Guinier) results indicate that the effective size of the largest pores increases as the body goes from 97% to more than 99% dense. The surface-area-weighted (Porod) results show that the median size of the smallest pores decreases slightly over the same density range. Taken together, these data indicate that the pore size distribution becomes broader as final-stage densification proceeds. This was confirmed by a maximum entropy analysis, which was used to derive pore size distributions directly from the data. Finally, the evolution of the pore size distributions in alumina, with and without sintering aid, were compared.

03,024
AD-A249 179/3 PC A02/MF A01
National Inst. of Standards and Technology, Gaithersburg, MD.
Characterization of the Densification of Alumina by Multiple Small-Angle Neutron Scattering. (Reannouncement with New Availability Information).
S. Krueger, G. G. Long, and R. A. Page. 1991, 10p, ARO-26123.2-MS.
Contract MIPR-ARO-102-90
Pub. in Acta Crystallographica, vA47 p282-290 1991.

Keywords: Density, Microstructure, Neutron scattering, Sintering, Reprints, *Aluminum oxide, Small angle scattering.

Multiple small-angle neutron scattering was used to follow the evolution of the pore-size distribution in alpha-Al2O3 through the intermediate and final stages of sintering. This new technique enables the study of microstructure in the 0.08-10 micro size regime, which is the size range of importance for many materials systems, without needing to increase the resolution of currently available small-angle scattering instruments. The microstructure evolution results indicate a nearly constant effective pore radius for the alumina throughout the intermediate sintering stage, ranging from 0-19 micro at 54% of theoretical density to 0- 17 micro at 79% dense. As the alumina densifies further, there is a transition region after which the effective pore radius grows rapidly to 0.6 micro at 97-5% dense.

03,025
AD-A249 510/9 PC A03/MF A01
National Inst. of Standards and Technology, Gaithersburg, MD.
Small-Angle Neutron Scattering Characterization of Processing/Microstructure Relationships in the Sintering of Crystalline and Glassy Ceramics. (Reannouncement with New Availability Information).
G. G. Long, S. Krueger, R. A. Gerhardt, and R. A. Page. Dec 91, 11p, ARO-26123.5-MS.
Contract MIPR-ARO-102-90
Pub. in Jnl. Mater. Res., v6 n12 p2706-2715, Dec 91.

Keywords: *Neutron scattering, *Sintering, *Ceramic materials, Microstructure, Polycrystalline, Reprints, *Glassy silica, *Crystalline ceramics, Porosity, SANS(Small Angle Neutron Scattering).

Small-angle neutron scattering measurements were used to examine the pore microstructure evolution of glassy silica and polycrystalline alpha-alumina as a function of sintering. It was shown that the two major sintering mechanisms, viscous flow and surface and volume diffusion, lead to very different microstructure evolution signatures in terms of the average pore size as a function of density. However, with respect to topology, the evolution of the porosity per unit surface area as a function of density is remarkably similar in the two systems.

03,026
DE94013170 PC A02/MF A01
National Inst. of Standards and Technology, Gaithersburg, MD.
Ceramic Characterization.
M. D. Vaudin, E. R. Fuller, J. P. Cline, and A. L. Dragoo. 1987, 7p, CONF-8710535.
Contract AI05-85OR21569
Ceramic characterization for international standards meeting, Dearborn, MI (United States), 26 Oct - 1 Nov 1987. Sponsored by Department of Energy, Washington, DC.

Keywords: *Silicon Carbides, Electron Microscopy, Grain Boundaries, Microstructure, Standards, X-Ray Diffraction, EDB/360202.

Objective of this task is to measure and characterize the ceramic properties (crystalline phase composition, grain boundary properties, residual stresses) of a series of standard ceramic specimens to assist in developing international standards for ceramic characterization. This report describes electron microscopy of the microstructure and grain boundaries of ESK silicon carbide; supporting x-ray diffraction data for the bulk phase composition is included.

03,027
DE94013486 PC A03/MF A01
National Inst. of Standards and Technology, Gaithersburg, MD.
Densification of Nano-Size Powders. 1994 Report.
Progress rept.
W. Chen, S. G. Malghan, J. S. Dapkunas, G. Piermarini, and A. Pechenik. 1994, 12p, DOE/OR/22041-2.
Contract AI05-92OR22041
Sponsored by Department of Energy, Washington, DC.

Keywords: *Aluminium Oxides, *Silicon Nitrides, Compacting, Density, Fabrication, Hot Pressing, Powders, Progress Report, Sintering, Vickers Hardness, EDB/360201.

Green compacts from a nano-size silicon nitride powder were fabricated having density up to 67% of theoretical at 2.8 GPa pressure using liquid nitrogen and pentane as compaction lubricant media. Pressureless sintering of these transparent samples did not promote further densification beyond that obtained for the green state. To further increase the density of these samples, a hot-pressing device was designed. In a series of experiments, hot-pressing of these samples at.0.5 to 1.0 GPa and 800 C, followed by pressureless sintering at 1400 C was studied. The resulting silicon nitride ceramic had a Vickers hardness of 9.0 GPa while transparency under visible light was maintained. Without the use of hot pressing, the hardness obtained was 5.8 GPa. In addition, the effect of compaction pressure on densification was studied for nano-size Al(sub 2)O(sub 3) to further understand factors contributing to achieving high green densities. The dense Al(sub 2)O(sub 3) green samples were pressureless sintered to near full density at temperatures several hundred degrees lower than those needed for sintering low density green material.

03,028
DE94013593 PC A03/MF A01
National Inst. of Standards and Technology (IMSE), Gaithersburg, MD.
Equipment for Investigation of Cryogenic Compaction of Nanosize Silicon Nitride Powders. 1993 Report.
Progress rept.
W. Chen, G. J. Piermarini, S. J. Dapkunas, S. G. Malghan, and A. Pechenik. 1993, 11p, DOE/OR/22041-T1.
Contract AI05-92OR22041
Sponsored by Department of Energy, Washington, DC.

Keywords: *Presses, *Silicon Nitrides, Calibration, Compacting, Computerized Control Systems, Design, Lubricants, Nitrogen, Particle Size, Progress Report, EDB/360201.

This paper describes a highly-specialized system for studies of time-dependent compaction of nanosize sili-

con nitride powders under a variety of atmospheres and at temperatures ranging from 77 to 1,000 K. The system incorporates a screw-driven press (10 ton capacity) with a piston-cylinder type die and can produce decylindrical powder compacts, 3 mm in diameter and approximately 1 mm in thickness, using pressures up to 3 GPa. The system is computer-controlled and permits accurate measurements of the sample volume, and, after appropriate calibration, can determine the rate and degree of densification of the compacting powder as pressure is applied. Frictional forces between the piston and the die are measured during the compaction process. For calibration of the system, powders with known volume-change accompanied by phase transition under pressure were studied, and good agreement with published results was demonstrated. Several Si(sub 3)N(sub 4) samples have been compacted and sintered at 1,300 to 1,600 C. A maximum random packing density of 64% has been obtained using liquid nitrogen as a lubricant medium at pressure lower than 2.5 GPa. Both green samples and sample sintered at temperatures to 1,500 C exhibited visual transparency under visible light.

03,029
DE95013505 PC A05/MF A01
National Inst. of Standards and Technology (MSEL), Gaithersburg, MD. Ceramics Div.
Low temperature fabrication from nano-size ceramic powders.
E. J. Gonzalez, G. J. Piermarini, and B. Hockey.
1995, 79p, DOE/OR/22041-T2.
Contract AI05-92OR22041
Sponsored by Department of Energy, Washington, DC.

Keywords: *Aluminium Oxides, *Silicon Nitrides, Compacting, Equations, Mechanical Properties, Microstructure, Powder Metallurgy, Processing, Sintering, EDB/360201, EDB/360203, EDB/360202.

The objective of the compaction process is to produce a dense green-state compact from a nanosize powder that subsequently can be sintered at high temperatures to form a dense ceramic piece. High density in the green-state after pressing is of primary importance for achieving high densities after sintering. Investigation of the compaction behavior of ceramic powders, therefore, is an important part of characterization of raw ceramic powders and evaluation of their compaction behavior, analysis of interaction between particles, and the study of microstructure of green body (unsintered) during pressure-forming processes. The compaction of nanosize ceramic particles into high density green bodies is very difficult. For the nanosize materials used in this study (amorphous Si(sub 3)N(sub 4) and (gamma) Al(sub 2)O(sub 3)), there is no evidence by TEM of partial sintering after synthesis. Nevertheless, strong aggregation forces, such as the van der Waals surface forces of attraction, exist and result in moderate precursor particle agglomeration. More importantly, these attractive surface forces, which increase in magnitude with decreasing particle size, inhibit interparticle sliding necessary for particle rearrangement to denser bodies during subsequent compaction. Attempts to produce high density green body compacts of nanosize particles, therefore, generally have been focused on overcoming these surface forces of attraction by using either dispersive fluids or high pressures with or without lubricating liquids. In the present work, the use of high pressure has been employed as a means of compacting nanosize powders to relatively high green densities.

03,030
N94-35335/6 PC A07/MF A02
National Inst. of Standards and Technology, Gaithersburg, MD.
Classification of Advanced Technical Ceramics.
S. Schneider. Jul 93, 128p.

Keywords: *Ceramics, *Chemical composition, *Chemical properties, *Classifications, Data bases, Utilization, Ceramic coatings, Ceramic fibers, Ceramic matrix composites, Glass, Information dissemination, Porous materials, Powder (Particles).

This document presents the basis and scheme for a unified classification system for advanced (technical) ceramics. The utility of the classification system is multi-fold. Its use is advantageous at the company level for purposes involving assembly of design and materials property databases, or tabulation of inventories, or invoicing. Industry can use the system for gathering and sorting trend data on market behavior or R&D expenditures, or for literature categorization. At the government level, the system can be used for gathering national and international economic data, or other vital statistics, or for determining demographics of the field. The classification system is based on defining advanced technical ceramics as 'a highly engineered, high performance, predominately non-metallic, inorganic, ceramic material having specific functional attributes.' This excludes commodity products, such as building materials and refractories. Five hundred different product types are identified as advanced technical ceramics in this classification. The classification is a non-hierarchical, matrix-type scheme accessible by a number of entry and retrieval routes to build relational databases. The classification provides a machine readable coding system built upon four independent descriptor fields (application, chemical character and product form, processing, and property data) and corresponding subdivisions that may be sequenced in order to match the users preference.

03,031
PB94-162591 PC A10/MF A03
National Inst. of Standards and Technology (MSEL), Gaithersburg, MD. Ceramics Div.
Ceramics Technical Activities, 1993 (NAS-NRC Assessment Panel April 21-22, 1994).
1994, 215p, NISTIR-5313.
See also PB93-173508.

Keywords: *Research projects, *Ceramics, Data bases, Mechanical properties, Standards, Composite materials, Powder(Particles), Optical materials, Electronics, Glass, Surface properties, Thin films, Superconductors, Tribology, *National Institute of Standards and Technology, Advanced materials, Synchrotron radiation.

In 1993 the Ceramics Division continued to emphasize a technical program directly relevant to the needs of U.S. industry. The program is made up of tasks which involve standard materials development, construction of evaluated databases, and laboratory research focused on topics that address the dominant issues affecting commercialization of advanced ceramics, namely, processing costs and reliability. In accord with the strategic plan laid out by the Materials Science and Engineering Laboratory, the Ceramics Division is continuing to expand its direct involvement with industrially related research issues. Standard materials and data activities continue to represent an important portion of the Division's program. Three new Standard Reference Materials were developed this year, and an evaluated database on high Tc superconducting materials was begun in collaboration with a Japanese laboratory.

03,032
PB94-172434 Not available NTIS
National Inst. of Standards and Technology (MSEL), Gaithersburg, MD. Polymers Div.
Error Propagation Biases in the Calculation of Indentation Fracture Toughness for Ceramics.
Final rept.
J. R. Kelly, M. E. Cohen, and J. A. Tesk. 1993, 4p.
Pub. in Jnl. of the American Ceramic Society 76, n10, p2665-2668 Oct 93.

Keywords: *Ceramics, *Bias, *Fracture(Mechanics), *Error analysis, Cracks, Mechanical properties, Toughness, Regression analysis, Loads(Forces), Monte Carlo method, Reprints.

Indentation fracture toughness models generally share the derived parameter Pc (exp -3/2), where P is the indentation load and c the measured crack length. Biases, inherent to error propagation through this nonlinear transformation (c to c(exp 3/2)), can be introduced into calculated values for K(sub Ic) depending upon the amount of averaging of crack length data performed prior to the transformation. The work utilizes Monte Carlo simulations to evaluate the bias in K(sub Ic) calculated using both mean and linear regression methods. Significant positive biases were demonstrated when using mean-based calculations where coefficients of variation (cv) in c exceeded 10%. Regression methods produced significantly less bias. With cv < 10% or when c is averaged per load, both methods produce essentially unbiased estimates for K(sub Ic).

03,033
PB94-172970 Not available NTIS
National Inst. of Standards and Technology (MSEL), Gaithersburg, MD. Ceramics Div.
Surface Forces and Adhesion between Dissimilar Materials Measured in Various Environments.
Final rept.
D. T. Smith, and R. G. Horn. 1990, 7p.
Pub. in Materials Research Society Symposia Proceedings, v170 p3-9 1990. Sponsored by Office of Naval Research, Arlington, VA.

Keywords: *Surface chemistry, *Adhesion, *Solids, *Dissimilar materials bonding, Materials science, Liquid phases, Vapor phases, Silicon dioxide, Mica, Ceramics, Reprints, Israelachvili surface force apparatus.

The Israelachvili surface force apparatus has been used extensively over the past decade to make detailed measurements of surface forces and adhesion between very smooth solids in various liquid and vapor environments. Most of those measurements have been made with mica surfaces, but the authors have recently developed a method of preparing smooth silica surfaces for use in place of the micra. The silica surfaces adhere in dry and humid atmospheres, but do not adhere when immersed in water. The use of a second material not only broadens the scope of the Israelachvili technique, but also enables studies of forces and adhesion between dissimilar materials. In this work, the authors present the results of measurements of adhesion in air and forces in aqueous solution between two silica surfaces; they also report preliminary results of the adhesion between a mica surface and a silica surface.

03,034
PB94-185378 Not available NTIS
National Inst. of Standards and Technology (MSEL), Gaithersburg, MD. Ceramics Div.
Contact Electrification Induced by Monolayer Modification of a Surface and Relation to Acid-Base Interactions.
Final rept.
R. G. Horn, D. T. Smith, and A. Grabbe. 1993, 2p.
Pub. in Nature 366, p442-443, 2 Dec 93.

Keywords: *Surface chemistry, *Electrification, *Electric contacts, *Layers, *Acid-base equilibrium, *Silicon dioxide, Reprints, Adhesion, Coatings, Revisions, pH, Polarization(Charge separation), Ion atom interactions, Surface force apparatus.

Electrical charge separation following contact between two materials (contact electrification or the triboelectric effect) is well known to occur between different materials as a consequence of their different electronic structures. Here the authors show that the phenomenon occurs between two surfaces of the same material if one is coated with a single chemisorbed monolayer. The authors use the surface force apparatus to study contact electrification and adhesion between two silica surfaces, one coated with an amino-silane. The presence of this monolayer results in significantly enhanced adhesion between the surfaces, owing to electrostatic attraction following contact electrification, in accord with Derjaguin's electrostatic theory of adhesion. These observations demonstrate a link between acid-base interactions and contact electrification.

03,035
PB94-198843 Not available NTIS
National Inst. of Standards and Technology (MSEL), Gaithersburg, MD. Reactor Radiation Div.
Analysis of SANS from Controlled Pore Glasses.
Final rept.
N. F. Berk, C. J. Glinka, W. Haller, and L. C. Sander. 1990, 6p.
Pub. in Materials Research Society Symposia Proceedings Neutron Scattering Materials Science, v166 p409-414 1990.

Keywords: *Porous materials, *Glass, Small angle scattering, Neutron scattering, Probability density functions, Computerized simulation, Morphology, Silica, Reprints.

Small angle neutron scattering measurements have been performed on several samples of silica controlled pore glasses with pore sizes ranging from roughly 7 to 30 nm. The scattering intensity is strongly peaked at small Q and shows approximate Porod law behavior at large Q. Contrast variation measurements have shown that the pore space in these samples is entirely interconnected and thus forms a bicontinuous microstructure. The scattering data have been analyzed using the leveled wave method based on an early scheme for representing two-phase microstructures resulting from spinodal decomposition. The authors determined model probability density

functions by fitting the SANS data with the leveled wave scattering function and then used these to construct leveled wave images of the corresponding porous structures.

03,036
PB94-200110 Not available NTIS
National Inst. of Standards and Technology (MSEL), Gaithersburg, MD.
Cavitation Damage During Flexural Creep of SiAlON-YAG Ceramics.
Final rept.
C. F. Chen, S. M. Wiederhorn, and T. J. Chuang. 1991, 5p.
Pub. in Jnl. of the American Ceramic Society 74, n7 p1658-1662 Jul 91.

Keywords: *Ceramics, *Sialon, *Creep properties, *Cavitation, Flexing, High temperature tests, Tensile strength, Density measurement, Stress analysis, Reprints.

Cavitation damage in flexure bars crept at 1,170 C was studied by a density measurement technique. The cavity density within the flexure beams could be approximated by a linear function of position from the tensile surface. A threshold stress for cavitation damage is suggested from the results of this study. Below the threshold tensile stress, cavitation ceases, whereas above the threshold, cavitation damage is in the form of wedge-shaped cracks at grain-boundary triple junctions. Cavitation is not observed in compression for the conditions used in this study. From a stress analysis of the flexure bars, a cavitation threshold of 55 MPa is estimated for this material.

03,037
PB94-200268 Not available NTIS
National Inst. of Standards and Technology (MSEL), Gaithersburg, MD. Ceramics Div.
Analysis of Creep in a Si-SiC C-Ring by Finite Element Method.
Final rept.
T. J. Chuang, Z. D. Wang, and D. Wu. 1992, 6p.
Contract GRI-TPSU-NBS-1302-37922
Pub. in Jnl. of Engineering Materials and Technology 114, p311-316 Jul 92. Sponsored by Gas Research Inst., Chicago, IL.

Keywords: *Creep buckling, *Finite element method, *Silicon carbides, Stress distribution, Stress relaxation, Creep properties, Creep tests, Displacement, Stress strain relations, Reprints.

The long-term creep deformation of a siliconized silicon carbide ceramic C-ring subjected to a compression load at 1300 C in air is studied by the finite element method. Based on asymmetric creep responses observed under uniaxial creep tests, multidirectional constitutive equations in power-law form are derived using the parameters of effective stress/strain. The elastic solutions are first solved and used as a guide to reach the final mesh design and as initial conditions. Solving the initial value problem in which equilibrium and constitutive equations are satisfied at all times, this model gives time-history of stresses and displacements. Fair agreements were obtained in load-point displacement rate, damage zone, neutral axis locations, stress relaxation and redistribution when compared with simple curved beam theory and experimental data. As common with other nonlinear problems, the convergence of the finite element solutions strongly depends on the time as well as the finess of the element size, particularly at the regions where principal stresses are close to the threshold stress for creep damage.

03,038
PB94-200656 Not available NTIS
National Inst. of Standards and Technology (MSEL), Gaithersburg, MD. Ceramics Div.
Transient Subcritical Crack-Growth Behavior in Transformation-Toughened Ceramics.
Final rept.
R. H. Dauskardt, W. C. Carter, D. K. Veirs, and R. O. Ritchie. 1990, 10p.
Pub. in Acta Metallurgica et Materialia 38, n11 p2327-2336 1990. Sponsored by Department of Energy, Washington, DC.

Keywords: *Crack propagation, *Ceramics, *Fatigue(Mechanics), *Transients, Transformations, Loads(Forces), Fracture(Mechanics), Cracking(Fracturing), Mechanical properties, Reprints, *Subcritical crack growth.

Transient subcritical crack-growth behavior following abrupt changes in the applied load are studied in transformation-toughened ceramics. A mechanics analysis is developed to model the transient nature of transformation shielding of the crack tip, Ks, with subcritical crack extension following the applied load change. Conditions for continued crack growth, crack growth followed by arrest, and no crack growth after the load change, are considered and related to the magnitude and sign of the applied load change and to materials properties such as the critical transformation stress. Using experimentally derived steady-state subcritical crack-growth relationships for cyclic fatigue in a transformation-toughened Mg-PSZ, the analysis is found to provide similar trends in Ks and accurate prediction of the post load-change transient crack-growth behavior compared to experimentally measured data.

03,039
PB94-212750 Not available NTIS
National Inst. of Standards and Technology (MSEL), Gaithersburg, MD. Ceramics Div.
Imaging of Fine Porosity in a Colloidal Silica: Potassium Silicate Gel by Defocus Contrast Microscopy.
Final rept.
H. Kerch, F. Cosandey, and R. Gerhardt. 1993, 14p.
Pub. in Jnl. of Non-Crystalline Solids 152, p18-31 1993.

Keywords: *Silicon dioxide, *Porosity, *Potassium silicates, *Gels, Transmission electron microscopy, Image processing, Fines, Colloids, Reprints.

The fine porosity present in a 10:90 colloidal silica:potassium silicate gel was imaged in the transmission electron microscope by the technique of defocus contrast microscopy. With this imaging method it is possible to detect very small pores (> or = 1 nm) and to obtain an accurate measure of their size and distribution. The technique allows independent measurement of the spatial location, morphology and size of the pores in the gel. Specifically, defocus contrast proves that the colloidal gel exhibits two pore populations in the micro- and mesopore range: a fine porous texture which is found uniformly across the gel particles, and larger pores with an interconnected globular morphology. This result, together with data from previous studies, showed that the gel composition possesses a polydisperse distribution of porosity which extends to many length scales. The influence of the gel structure on the resultant nitrogen sorption data is also discussed.

03,040
PB94-212958 Not available NTIS
National Inst. of Standards and Technology (MSEL), Gaithersburg, MD. Ceramics Div.
Observed and Theoretical Creep Rates for an Alumina Ceramic and a Silicon Nitride Ceramic in Flexure.
Final rept.
R. F. Krause. 1992, 4p.
Pub. in Jnl. of the American Ceramic Society 75, n5 p1307-1310 1992.

Keywords: *Aluminum oxide, *Silicon nitrides, *Ceramics, *Creep rate, *Flexing, Comparison, Compressive properties, Tensile properties, Reprints.

Observed creep curvature rates are compared to theoretical rates for both an alumina ceramic at 1,000 C and a silicon nitride ceramic at 1,200 C in four-point flexure. The observed rates have been calculated from published rise-displacement rates, and the theoretical rates have been calculated from published power-law parameters for compressive and tensile creep, which differ appreciably for these ceramics. Although both compressive and tensile creep measurements are easier to analyze than flexural creep measurements, the latter are usually less expensive and easier to conduct. The present work shows the usefulness of flexural creep tests to verify the accuracy of compressive and tensile creep tests.

03,041
PB94-216025 Not available NTIS
National Inst. of Standards and Technology (MSEL), Gaithersburg, MD. Ceramics Div.
Structures of Vapor-Deposited Yttria and Zirconia Thin Films.
Final rept.
G. G. Long, D. R. Black, A. Feldman, D. K. Tanaka, Z. Zhang, E. N. Farabaugh, and R. D. Spal. 1992, 7p.
Pub. in Thin Solid Films 217, p113-119 1992.

Keywords: *Zirconium oxides, *Yttrium oxides, *Crystal structure, X-ray absorption, Ceramic coatings, Bulk materials, Thin films, Porosity, Comparison, Reprints, Electron beam evaporation.

The structures of think films of zirconia and yttria, deposited by electron beam evaporation, have been examined by X-ray absorption fine structure (XAFS) analysis. It was found that the structure of the yttria film was similar to that of bulk yttria, which is a cubic oxide phase. The zirconia film, however, possessed a structure different from that of the bulk material. An analysis of the zirconia film data indicated a structure with a predominant tetragonal phase. Although lower coordination numbers were found in the films than in the standard powder specimens, it was not clear from the extended fine structure whether this deficit was due to film porosity observed in prior work or to the disorder that is generally observed in films. An analysis of the near-edge structure, however, suggested that porosity, rather than disorder, was present in the films. In addition, the K-edge positions observed for both the zirconia and the yttria films were higher in energy by approximately 3 eV than the corresponding K-edge in the powder specimens, indicating that the films may be more insulating than the standard bulk material.

03,042
PB94-216249 Not available NTIS
National Inst. of Standards and Technology (MSEL), Gaithersburg, MD. Ceramics Div.
Statistical Analysis of Parameters Affecting the Measurement of Particle-Size Distribution of Silicon Nitride Powders by Sedigraph (Trade Name).
Final rept.
S. G. Malghan, L. S. H. Lum, E. Lagergren, J. Kelly, and R. N. Kacker. 1992, 10p.
Pub. in Powder Technology 73, p275-284 1992.

Keywords: *Silicon nitrides, *Particle size distribution, *Powder(Particles), *Statistical analysis, Sedimentation, Experimental design, Surfactants, Regression analysis, Ultrasonic frequencies, Reprints, *Sedigraph method.

The need to achieve repeatability in the measurement of particle size distribution of submicron particles of silicon nitride powders, and its dependence on the appropriate application of deagglomeration forces and subsequent stabilization of particles from reforming into agglomerates are discussed. An analysis of parameters affecting the particle size distribution measurement by Sedigraph(Trademark), a gravity sedimentation method, is presented and major parameters are identified. Statistical factorial design of experiments was used to determine the influence of various parameters such as ultrasonic power, time and energy, type of surfactant, and concentration of surfactant in a suspension on particle size determination. The results were analyzed using statistical techniques such as graphical and least squares regression. This analysis led to the calculation of main and interaction effects of the major parameters mentioned above. Depending on the ultrasonic power level selected for a powder, the interaction effects between ultrasonic power, ultrasonic time, and surfactant concentration for the two types of surfactants were identified.

03,043
PB94-216264 Not available NTIS
National Inst. of Standards and Technology (MSEL), Gaithersburg, MD. Ceramics Div.
Characterization of Phase and Surface Composition of Silicon Carbide Platelets.
Final rept.
S. G. Malghan, M. Vaudin, J. P. Cline, M. K. Jain, P. S. Wang, and L. S. H. Lum. 1991, 9p.
Pub. in Ceram. Trans. Adv. Compos. Mater. 19, p253-261 1991.

Keywords: *Silicon carbides, *Surface properties, *Phase studies, Ceramics, Surface chemistry, X-ray diffraction, Carbon, Washing, Transmission electron microscopy, Photoelectron spectroscopy, X-ray spectroscopy, Electrokinetics, Reprints, *Platelets(Materials).

Silicon carbide platelets manufactured by a carbothermic reduction process were characterized for bulk phase composition and surface properties by transmission electron microscopy (TEM), X-ray diffraction (XRD), X-ray photoelectron spectroscopy (XPS) and electrokinetic sonic amplitude (ESA). These studies indicated that the platelets consisted of 4H and 6H polytypes as major phases, and 39H, 15R and 7H as minor phases. The XRD established the percent weight ratio of 4H to 6H as 57 to 43. The ESA and XPS techniques identified differences between the sur-

face properties of two types of platelets--acid washed and unwashed. The surface of the platelets was found to contain several forms of carbon. The thickness of the oxygen layer on the two types of platelets was calculated using Si 2p photoelectron data.

03,044
PB94-216272 Not available NTIS
National Inst. of Standards and Technology (MSEL), Gaithersburg, MD. Ceramics Div.
Deposition of Colloidal Sintering-Aid Particles on Silicon Nitride.
Final rept.
S. G. Malghan, P. S. Wang, A. Sivakumar, and P. Somasundaran. 1993, 18p.
Pub. in Composite Interfaces 1, n3 p193-210 1993.

Keywords: *Silicon nitrides, *Deposition, *Surface chemistry, *Colloids, Powder(Particles), Electrokinetics, Zirconium oxides, Yttrium oxides, Photoelectron spectroscopy, Sintering, X-ray spectroscopy, Substrates, Auger electron spectroscopy, Particle size, Reprints.

The deposition of alumina (Al2O3) and yttria (Y2O3) particles on silicon nitride (Si3N4) by electrostatic and electrosteric interactions was studied using acoustophoretic measurements. The characteristics of Si3N4, Al2O3, and Y2O3 powders in an aqueous environment were studied by measuring the electrokinetic sonic amplitude (ESA), and appropriate conditions for deposition by adsorption were identified. The deposition of Al2O3, Y2O3, and Y(NO3)3 on Si3N4 particles was conducted at different pH values where these chemically dissimilar particles exhibit electrical charges of opposite sign. The deposition studies indicated that the particle size has a strong effect on the amount of coating on Si3N4 particles. The presence of polyacrylic acid as an electrosteric stabilizer for Si3N4 had no measurable effect on Al2O3 adsorption. The shift of the isoelectric point of Si3N4 with Al2O3 showed that the total quantity of Al2O3 adsorbed on Si3N4 reached a maximum at approximately 75% coverage of the total surface area of Si3N4. Bremsstrahlung-excited Auger electron spectroscopy (AES) results showed that the as-received Si3N4 powder has a native oxide film of 8.9 A. The presence and relative differences in the surface composition of coated particles were established using X-ray photoelectron spectroscopy (XPS).

03,045
PB94-216587 Not available NTIS
National Inst. of Standards and Technology (MSEL), Gaithersburg, MD. Ceramics Div.
Rapid Hot Pressing of Ultra-Fine PSZ Powders.
Final rept.
M. D. Matthews, and A. Pechenik. 1991, 7p.
Pub. in Jnl. of the American Ceramic Society 74, n7 p1547-1553 1991.

Keywords: *Powder(Particles), *Zirconium oxides, *Yttrium oxides, *Compacting, *Densification, High temperature superconductors, Hot pressing, Deformation, Fines, Mechanical properties, Scanning electron microscopy, Transmission electron microscopy, X-ray diffraction, Reprints.

The process of compaction and densification of ultrafine powder of partially-stabilized zirconia with 3 mole % of Y2O3 (Y3-PSZ) during rapid hot pressing was investigated. Special apparatus was designed to allow rapid application of 1.6 GPa of quasi-isostatic pressure at temperatures of 1,100-1,300 C to powder compacts encapsulated in glass under vacuum. Pressure was applied for 10 seconds, then the samples were rapidly cooled, removed from glass and characterized using scanning electron microscopy (SEM), transmission electron microscopy (TEM) and X-ray diffraction. Density and mechanical properties of the prepared materials were measured and compared with that of similar materials fabricated via conventional hot pressing.

03,046
PB95-125746 Not available NTIS
National Inst. of Standards and Technology (IMSE), Gaithersburg, MD. Ceramics Div.
Environmentally Enhanced Fracture of Ceramics.
Final rept.
S. W. Freiman. 1988, 11p.
Sponsored by Office of Naval Research, Arlington, VA.
Pub. in Materials Research Society Symposia Proceedings, v125 p205-215 1988.

Keywords: *Ceramic materials, *Glass, *Single crystals, *Fracture(Mechanics), *Stress corrosion, Mechanical properties, Crack propagation, Cracking(Fracturing), Polycrystalline, Bonding, Reprints.

This paper presents a review of our current understanding of environmentally induced crack growth in glasses, single crystals, and polycrystalline ceramics. It is shown that the rate of crack growth is controlled by the chemical activity of the active species in the environment as well as by the crack tip stress. A molecular model of a stress-induced chemical reaction between vitreous silica and water is described, and the implications of this model for predicting the effects of other chemical species on crack growth are discussed. Effects of chemical changes both in the bonding in the solid as well as in the reacting solutions on the crack growth mechanism are elucidated. Finally, the complicating effects of multigrain arrays on crack extension in polycrystalline ceramics are pointed out.

03,047
PB95-140208 Not available NTIS
National Inst. of Standards and Technology (MSEL), Gaithersburg, MD.
New Materials, Advanced Ceramics and Standards.
Final rept.
S. Schneider. 1991, 6p.
Pub. in Key Engineering Materials 53-55, p480-485 1991.

Keywords: *Ceramics, *Standards, *Classifications, *Materials science, Materials tests, Comparison, Mechanical tests, Structural engineering, Marketing, Reprints, *Advanced materials.

Today's technological world might well be termed the age of new materials for industrial needs that now require engineered materials that perform totally new functions or old functions in much better ways. Unfortunately, companion standards development has not kept pace with technology advances and this lack represents one of the more important technical unknowns in the commercial market equation. For advanced ceramics the problem is acute for currently there are no consensus standards that allow national or international comparisons. While the standards needs are diverse and product specific, there are two areas that crosscut all advanced ceramic product lines. First, there is an international need for a unified classification system that uniquely categories an array of advanced products by a series of set apart features, like application and materials chemistry. Second, there is need for a set of mechanical test standards to assure the structural reliability of advanced ceramics. This paper presents a perspective on these issues and problems, in the context of the age of new materials.

03,048
PB95-140570 Not available NTIS
National Inst. of Standards and Technology (MSEL), Gaithersburg, MD. Ceramics Div.
Phase Equilibria in the Systems CaO-CuO and CaO-Bi2O3.
Final rept.
R. S. Roth, N. M. Hwang, C. J. Rawn, B. P. Burton, and J. J. Ritter. 1991, 4p.
Pub. in Jnl. of the American Ceramic Society 74, n9 p2148-2151 1991.

Keywords: *Bismuth oxides, *Calcium oxides, *Copper oxides, Binary mixtures, Polymorphism, Superconductors, Reprints, *Calcium bismuthates, *Copper bismuthates, Phase equilibrium.

New data are presented on the phase equilibria of the binary systems CaO-CuO and CaO-Bi2O3. Corrected compositions are reported for Ca4Bi6O13 and Ca2Bi2O5 and a new high temperature polymorph is reported for Ca2Bi2O5. The composition and decomposition temperatures for Ca(1-x)CuO2 are given for both air and one atmosphere oxygen.

03,049
PB95-161303 Not available NTIS
National Inst. of Standards and Technology (MSEL), Gaithersburg, MD. Ceramics Div.
Tensile Creep of a Silicon Nitride Ceramic.
Final rept.
R. F. Krause, and S. M. Wiederhorn. 1994, 6p.
Pub. in Key Engineering Materials 89-91, p619-624 1994.

Keywords: *Silicon nitrides, *Ceramic materials, *Tensile creep, Failure, Least squares method, Strain rate, Fatigue(Materials), Tensile properties, Reprints.

The tensile creep behavior of a hot isostatically pressed silicon nitride ceramic containing 6 percent yttria was characterized at temperatures between 1250 and 1400 C and applied stresses between 72 and 250 MPa. Creep extension of specimens with nominal 10 mm gage length was measured by laser extensometry, showing final extensions between 20 and 200 micrometers. Secondary creep strain rates varied from 0.3 to 3000 Gs(exp -1). Some tests ended with specimen failure between 1 and 500 h, but other tests were discontinued after 1000 up to 2500 h without failure. A least-squares fit of the Norton and Arrhenius functions to 31 strain-rate tests yielded a stress exponent of 8.4 + or - 0.9 and an activation energy of 1310 + or - 140 kJ/mol. A Monkman-Grant function was fitted to represent strain rate versus failure time.

03,050
PB95-161501 Not available NTIS
National Inst. of Standards and Technology (MSEL), Gaithersburg, MD. Ceramics Div.
Analysis of Physical Properties of Ceramic Powders in an International Interlaboratory Comparison Program.
Final rept.
S. G. Malghan, S. M. Hsu, A. L. Dragoo, H. Hausner, and R. Pompe. 1991, 16p.
Sponsored by Department of Energy, Washington, DC.
Pub. in Proceedings of International Symposium on Ceramic Materials and Components for Engines (4th), p920-935 1992.

Keywords: *Interlaboratory comparisons, *Physical properties, *Ceramics, *Powder(Particles), International cooperation, Particle size distribution, Surface properties, Area, Density(Mass/volume), Reprints.

Accuracy in the measurement of physical characteristics of ceramic starting powders is a critical factor in the control and reproducibility of powder processing unit operations. An international interlaboratory comparison program on powders characterization has been in progress under the auspices of the International Energy Agency. In this paper, the results of powder characterization effort on five powders by 25 industrial, university and governmental laboratories are presented. Selected results of density, specific surface area, and particle size distribution are presented and discussed in terms of factors affecting these measurements. The reasons for the discrepancies in the data are outlined.

03,051
PB95-162681 Not available NTIS
National Inst. of Standards and Technology (IMSE), Gaithersburg, MD.
Recent VAMAS Activity in Ceramics.
Final rept.
L. H. Schwartz, and B. Steiner. 1990, 3p.
Pub. in Ceramic Bulletin 69, n3 p312-314 1990.

Keywords: *Ceramics, *Mechanical tests, *Standards, Fracture tests, Mechanical properties, Hardness tests, Classifying, Wear tests, International coordination, Reprints, *Advanced materials, VAMAS(Versailles Project on Advanced Materials and Standards).

Current activity dealing with ceramics in the Versailles Project on Advanced Materials and Standards (VAMAS) is reviewed. The activity includes enhanced environmental fracture testing, hardness testing, wear testing, and classification. The nature of VAMAS is described.

03,052
PB95-163069 Not available NTIS
National Inst. of Standards and Technology (MSEL), Gaithersburg, MD.
Real-Time Small-Angle X-Ray Scattering Study of the Early Stage of Phase Separation in the SiO2-BaO-K20 System.
Final rept.
G. B. Stephenson, W. K. Warburton, W. Haller, and A. Bienenstock. 1991, 21p.
Pub. in Physical Review B 43, n16 p13417-13437 1991.

Keywords: *X-ray scattering, *Phase separation(Materials), *Silicates, Small angle scattering, Spinodal decomposition, Glass, Real time operations, Silicon dioxide, Barium oxides, Potassium oxides, Amorphous materials, Deformation, Reprints.

Time-resolved small-angle x-ray scattering was used to study the early stage of phase separation in a silicate system. Scattering patterns were acquired in real time as a sample was quenched in situ from a temperature T1 in the single-phase region directly to a tem-

perature T2 in the two-phase region and held isothermally. This was made possible by using the high x-ray intensity from a synchrotron radiation source, a fast position-sensitive detector based on a photodiode array, a sample heater capable of rapid quenches, and an appropriate sample composition. The composition studied, 90-mole-% SiO2, 5-mole-% BaO, and 5-mole-% K2O, undergoes subliquidus phase separation at temperatures below 1,021 K to form alkali-rich and alkali-poor amorphous phases. This is the best agreement between experiment and spinodal decomposition theory yet demonstrated for any system. For amorphous systems in particular, these results provide direct evidence that deformation is the rate-limiting step for the interdiffusion of network-forming and network-modifying species over the short length scales involved in the early stage of phase separation.

03,053
PB95-164570 Not available NTIS
National Inst. of Standards and Technology (MSEL), Gaithersburg, MD. Ceramics Div.
Measuring Contact Charge Transfer at Interfaces: A New Experimental Technique.
Final rept.
D. T. Smith. 1991, 18p.
Contract N0014-88-F-0034
Sponsored by Office of Naval Research, Arlington, VA.
Pub. in Jnl. of Electrostatics 26, p291-308 1991.

Keywords: *Surface energy, *Electric charge, *Charge transfer, *Ceramics, *Solid-solid interfaces, Experimental design, Silicon dioxide, Mica, Materials science, Interfaces, Test chambers, Charge density, Reprints.

A new experimental technique has been developed for measuring the amount of electric charge transferred when two dissimilar surfaces are brought into contact and separated without lateral motion in a controlled environment. The primary surfaces studied, silica and mica, are prepared with very low surface roughness (average roughness less than 0.5 nm); the macroscopic contact area, which can be measured directly, is therefore a better measure of microscopic contact area than is typically the case in contact electrification experiments, and the surface charge density can be more accurately determined. Observations reported include (1) the transfer of charge densities as high as .01 C/sq m after only a few contacts of a mica and silica surface in dry air or N2 gas at room temperature and (2) a reduction in transferred charge density in the silica-mica system as the relative humidity of the air in the environmental chamber is increased from 0% to 98%. The technique also permits the study of the rate at which the surface charge decays under various environmental conditions.

03,054
PB95-175493 Not available NTIS
National Inst. of Standards and Technology (MSEL), Gaithersburg, MD. Ceramics Div.
Fabrication of Transparent gamma-Al2O3 from Nanosize Particles.
Final rept.
M. R. Gallas, B. Hockey, A. Pechenik, and G. J. Piermarini. 1994, 6p.
Pub. in Jnl. of the American Ceramic Society 77, n8 p2107-2112 Aug 94.

Keywords: *Aluminum oxides, Transmission electron microscopy, Temperature dependence, Pressure dependence, Heat treatment, Transparence, Hardness, Compacting, Temperature range 0065-0273 K, Room temperature, Reprints, Diamond anvils, Nanomaterials.

The compaction and heat-treatment behavior of nanosize gamma-Al2O3 powder (average diameter = 20nm) was studied. A diamond anvil high-pressure cell was used to compact the powder at pressures up to 3 GPa, both in air at room temperature and under liquid nitrogen, followed by pressureless heat treatment at 800 C. For all conditions studied, the fabricated compacts were optically transparent. X-ray diffraction confirmed retention of the gamma-phase. The compacts were also characterized before and after heat treatment by microhardness measurements and by transmission electron microscopy. For both ambient and cryogenic compaction, sample hardness increased with pressure, and heat treatment resulted in about a 50% increase in hardness independent of the initial green-state value. Samples compacted in LN2 were significantly harder (up to 9.6 GPa) than those compacted in air.

03,055
PB95-175568 Not available NTIS
National Inst. of Standards and Technology (MSEL), Gaithersburg, MD. Ceramics Div.
Polyelectrolytes as Dispersants in Colloidal Processing of Silicon Nitride Ceramics.
Final rept.
V. A. Hackley, and S. G. Malghan. 1993, 2p.
Pub. in Polymer Preprints 34, n1 p1024-1025 Mar 93.

Keywords: *Silicon nitrides, *Ceramics, *Colloiding, *Dispersants, *Polyelectrolytes, Powder(Particles), Sintering, Carboxylates, High temperature tests, Rheology, Homogeneity, Reprints.

Colloidal processing of submicron powders has become increasingly important in the commercial production of structural ceramic shapes. Silicon nitride is one of the materials of choice for high temperature load-bearing applications such as turbines and bearings for heat engines. To obtain chemical and microstructural homogeneity in the final sintered product, the powders must be dispersed at high solid loadings (up to 60% by volume) and then consolidated and dried. Carboxylate polyelectrolytes are routinely added to aqueous slurries to act as dispersants and obtain suitable rheological properties. Recipes for slurry preparation are often determined by trial and error, without specific knowledge of the complex interactions between solution, polyelectrolyte and colloidal particles. We have examined the electrostatic component of these interactions for PAA and PMMA using an electroacoustic technique and adsorption isotherms. These results are correlated with polymer structure and molecular weight and with the fluidity of dense slurries.

03,056
PB95-175576 Not available NTIS
National Inst. of Standards and Technology (MSEL), Gaithersburg, MD. Ceramics Div.
Surface Chemical Interactions of Si3N4 with Polyelectrolyte Deflocculants.
Final rept.
V. A. Hackley, R. Premachandran, and S. G. Malghan. 1994, 4p.
Pub. in Key Engineering Materials 89-91, p679-682 1994.

Keywords: *Silicon nitrides, *Colloiding, *Surface chemistry, *Polyelectrolytes, *Deflocculating, Electroacoustics, Solid solutions, Interfaces, Particle size distribution, Cations, Anions, pH, Concentration(Composition), Molecular weight, Polyacrylic acids, Reprints, Poly(diamine epoxychlorohydrin), Ammonium poly(methacrylate).

The interaction of organic polyelectrolyte deflocculants at the Si3N4 solid-solution interface was investigated using electroacoustic measurements, polymer adsorption and particle size distribution analysis. One cationic and two anionic polymers were studied: quaternized poly(diamine epoxychlorohydrin), ammonium poly(methacrylate) and poly(acrylic acid), respectively. Electrostatic interactions are emphasized as a function of pH, concentration and molecular weight.

03,057
PB95-175584 Not available NTIS
National Inst. of Standards and Technology (MSEL), Gaithersburg, MD. Ceramics Div.
Effects of Soxhlet Extraction on the Surface Oxide Layer of Silicon Nitride Powders.
Final rept.
V. A. Hackley, P. S. Wang, and S. G. Malghan. 1993, 7p.
Pub. in Materials Chemistry and Physics 36, p112-118 1993.

Keywords: *Silicon nitrides, *Powder(Particles), *Surface chemistry, *Cleaning, *Colloids, *Oxide films, Electroacoustics, Isoelectronic sequence, pH, X ray spectroscopy, Auger spectroscopy, Interfaces, Solid solutions, Reprints, *Soxhlet extraction.

An aqueous soxhlet extraction procedure was used to surface-clean five commercial silicon nitride powders. The solid-solution interface properties were characterized before and after extraction by electrokinetic sonic amplitude measurements. The isoelectric point pH(sub iep) was found to increase significantly for some powders after treatment. The powder surface was analyzed using X-ray photoelectron spectroscopy and X-ray induced Auger electron spectroscopy before and after extraction. The surface oxygen content and oxide layer thickness decrease after treatment. A linear correlation was found between oxide thickness and pH(sub iep) which yields a pristine pH(sub iep) of about 9.7 for the unoxidized Si3N4 particle.

03,058
PB95-180931 Not available NTIS
National Inst. of Standards and Technology (BFRL), Gaithersburg, MD. Building Materials Div.
Calculation of the Thermal Conductivity and Gas Permeability in a Uniaxial Bundle of Fibers.
Final rept.
D. J. Skamser, D. P. Bentz, R. T. Coverdale, H. Jennings, D. L. Johnson, M. S. Spotz, and N. Martys. 1994, 12p.
Contract N00014-90-J-4020
Sponsored by Defense Advanced Research Projects Agency, Arlington, VA. and Office of Naval Research, Arlington, VA.
Pub. in Jnl. of the American Ceramic Society 77, n10 p2669-2680 1994.

Keywords: *Ceramic fibers, *Permeability, *Thermal conductivity, *Transport properties, Gas flow, Bundles, Microstructure, Thermophysical properties, Conduction(Heat transfer), Algorithms, Ceramics, Stokes law(Fluid mechanics), Reprints.

A model of the local microstructure of a bundle of fibers is simulated and used as the basis for calculations of transport properties. This, in turn, can be used in a macroscopic model of the chemical vapor infiltration process. An expanding/overlapping circle representation of the microstructure simulates the deposition of matrix in a uniaxial bundle of fibers. An iterative heat conduction algorithm is used to calculate the transverse thermal conductivity based on the thermal conductivities of the solid and gas phases. The permeability of gas through the microstructure is calculated for flow both parallel and transverse to overlapping cylinders using a Strokes equation and assuming a Darcy's law behavior. Both the simulations of the microstructure and associated calculations of the transport properties compare favorably with experimental data.

03,059
PB95-202750 Not available NTIS
National Inst. of Standards and Technology (MSEL), Gaithersburg, MD.
Stability and Surface Energies of Wetted Grain Boundaries in Aluminum Oxide.
Final rept.
D. Y. Kim, S. M. Wiederhorn, B. J. Hockey, C. A. Handwerker, and J. E. Blendell. 1994, 10p.
Pub. in Jnl. of the American Ceramic Society 77, n2 p444-453 Feb 94.

Keywords: *Aluminum oxide, *Grain boundaries, *Free energy, *Stability, *Surfaces, Crystal lattices, Interfaces, Wettability, Microstructure, Reprints.

The stability of a calcium-aluminum-silicate liquid film between two near-basal plane surfaces of sapphire at 1650 C was studied. Samples were prepared having an average basal misorientation across the interface of 6-7 deg about (10-10). Three types of interfaces were observed: faceted, solid-liquid interfaces; low-angle grain boundaries consisting of aligned arrays of dislocations; and boundaries consisting of alternating regions of dislocations and faceted solid-liquid interfaces. The type of interface observed depended on the orientation of the interface and could be predicted by using a construction based on Wulff shapes. Because the type of interface depends on crystal alignment and interface angle, these results suggest an absolute method of determining the surface free energy of wetted boundaries.

03,060
PB95-203758 PC A04/MF A01
Pennsylvania State Univ., University Park. Center for Advanced Materials.
Structural Ceramics Database. Topical Report, June 1989-May 1991.
E. F. Begley, and R. G. Munro. May 91, 65p, CAM-9201, GRI-92/0042.
Contracts GRI-5084-238-1302, GRI-TPSU-NBS-1302-379
Prepared in cooperation with National Inst. of Standards and Technology (MSEL), Gaithersburg, MD. Ceramics Div. Sponsored by Gas Research Inst., Chicago, IL.

Keywords: *Ceramics, *Information systems, *Data bases, *Research projects, *Structural engineering,

Physical properties, Chemical properties, Criteria, High temperature tests, Implementation, Heat resistant materials, *Structural Ceramics Database System, *Advanced materials.

The objective of the project was to strengthen the link between the development of new materials in research laboratories and the application of these materials by design engineers. The medium for improving this link is a user-friendly database on materials properties of advanced ceramics. Papers containing data appropriate for the structural ceramics database (SCD) were identified by a computerized search of the open technical literature. Acceptance criteria were applied during careful review of the papers. At the end of this process, approximately seventy-five papers remained. Material and property information were extracted and evaluated by experts within the Ceramics Division at NIST who were particularly concerned with assessing the material specifications, the measurement methods and procedures, and the reliability of the data. Concurrently, user-friendly database software was developed to manage the data on personal computers. With this software, users can easily find the properties of a given material or identify materials that meet specified property values. After completion of code development and data entry, test sites were selected to review the database system.

03,061
PB95-210498 PC A03/MF A01
National Inst. of Standards and Technology (MSEL), Gaithersburg, MD. Ceramics Div.
Room-Temperature Flexure Fixture for Advanced Ceramics.
G. D. Quinn. Aug 92, 22p, NISTIR-4877.
See also PB92-222959.

Keywords: *Ceramics, *Test facilities, *Fixtures, *Temperature effects, Flexural strength, Room temperature, Standards, Design criteria, Mechanical properties, Loads(Forces), *Advanced materials.

A test fixture for the measurement of the flexure strength of advanced ceramic specimens is presented. This report presents a four-point flexure fixture that is in accordance with the requirements of U.S. Army MIL STD 1942 and ASTM C 1161. These standards prescribe specific specimen and fixture sizes, tolerance, and alignment requirements. The standards specify that the fixture must have sufficient articulation to ensure even line-loading pins. The fixture is designed so that it can be set up and aligned easily and quickly (about 30 minutes). The fixture in this report is intended for use with flat and parallel specimens.

03,062
PB95-220547 PC A05/MF A02
National Inst. of Standards and Technology (MSEL), Gaithersburg, MD. Ceramics Div.
Evaluation of Thermal Wave Imaging for Detection of Machining Damage in Ceramics.
L. Wei, H. H. K. Xu, and S. Jahanmir. Mar 95, 100p, NISTIR-5645.
Contract DE-AC05-840R21400
Color illustrations reproduced in black and white. Sponsored by Department of Energy, Washington, DC. Office of Transportation Technologies. and Martin Marietta Energy Systems, Inc., Oak Ridge, TN.

Keywords: *Ceramics, *Machining, *Damage assessment, *Imaging techniques, Grinding(Material removal), Cracks, Subsurface investigations, Nondestructive tests, Performance tests, Aluminum oxide, Silicon nitrides, *Thermal wave imaging.

The feasibility of a thermal wave imaging technique is evaluated for the detection and characterization of machining damage in ceramics. First, a well-defined crack system produced by Vickers indentation is used to examine the characteristic response of thermal wave signals to different forms of cracks (i.e., median/radial and lateral). The results clearly indicate that thermal wave imaging can be used for the detection of surface and subsurface cracks in ceramics. Thermal wave imaging is then conducted on the surfaces of ground alumina and the cross-section of scratched silicon nitride. Careful examinations of the thermal wave images confirm that this technique can be used to detect the grinding-induced subsurface microcracks. The limitations of the thermal wave imaging technique in the detection of small cracks and precautions regarding choosing appropriate sets of imaging parameters are pointed out.

03,063
PB95-256053 PC A04/MF A01
National Inst. of Standards and Technology (MSEL), Gaithersburg, MD. Ceramics Div.
Applications of Diamond Films and Related Materials: International Conference (3rd). Held in Gaithersburg, Maryland on August 21-24, 1995. Supplement to NIST Special Publication 885.
A. Feldman, W. A. Yarbrough, M. Murakawa, Y. Tzeng, and M. Yoshikawa. 1995, 52p, NISTIR-5692-SUP.
See also PB95-255204. Prepared in cooperation with Auburn Univ., AL., Pennsylvania State Univ., University Park. and Nippon Inst. of Tech., Saitama. Sponsored by Tokyo Inst. of Tech. (Japan).

Keywords: *Diamonds, *Thin films, *Technology utilization, *Meetings, Raman spectra, Spectroscopic analysis, Vapor deposition, Epitaxy, Crystal defects, Crystal lattices, Crystal growth, Polycrystals, Cutting tools, Degradation, Annealing, Adhesion, Electrical resistivity, CVD(Chemical vapor deposition).

This supplement contains ten papers which had not been included in the conference proceedings of the Applied Diamond Conference 1995 (ADC'95) due to late arrival. In addition, the supplement contains two errata that correct two papers that appear in the proceedings.

03,064
PB96-102975 Not available NTIS
National Inst. of Standards and Technology (MSEL), Gaithersburg, MD. Reactor Radiation Div.
X-ray Powder Diffraction from Carbon Nanotubes and Nanoparticles.
Final rept.
D. Reznik, C. H. Olk, D. A. Neumann, and J. R. D. Copley. 1995, 9p.
Pub. in Physical Review B, v52 n1 p116-124 Jul 95.

Keywords: *Powders, *Diffraction, Reprints, X ray diffraction, Interlayers, Cross section, *Nanomaterials.

We report detailed x-ray powder-diffraction measurements on a sample consisting of approximately 60 carbon nanotubes and approximately 40 carbon nanoparticles. These measurements demonstrate the existence of short-range interlayer stacking correlations. Our calculations show that such correlations should not be observable in idealized models of nanotubes. The observation of short-range interlayer correlations can be explained if many of the nanotubes and nanoparticles have polygonal cross sections, largely consisting of flat regions having graphitic interlayer correlations. This polygonization is almost certainly driven by the van der Waals interactions responsible for the AB AB stacking in crystalline graphite.

03,065
PB96-102983 Not available NTIS
National Inst. of Standards and Technology (MSEL), Gaithersburg, MD. Ceramics Div.
Damage Processes in Ceramics Resulting from Diamond Tool Indentation and Scratching in Various Environments.
Final rept.
A. W. Ruff, H. Shin, and C. J. Evans. 1995, 12p.
Pub. in Wear Jnl. 181-183, p551-562 1995.

Keywords: *Ceramic materials, *Diamonds, Reprints, Damage, Tools, Scratching, *Foreign technology.

Studies have been carried out to determine the influence of different chemical environments and tool shapes on damage produced during diamond tool scratching and indenting of two advanced ceramics: chemical-vapor-deposited silicon carbide and a composite aluminum oxide-titanium carbide. A nanoindentation/scratching apparatus was used in a controlled-load mode for the studies. Two diamond tool shapes were used: a wedge with -45 degrees rake and 0.5 mm radius curved edge, and a Vickers pyramid. The environments studied were: air, water, mineral oil, mineral oil + stearic acid and two commercial water-based fluids. It was of interest to identify damage mechanisms, critical loads for initiation of severe damage, specific scratching energies and the effect on damage of the different tool shapes.

03,066
PB96-111646 Not available NTIS
National Inst. of Standards and Technology (CSTL), Gaithersburg, MD. Surface and Microanalysis Science Div.
Photodesorption Dynamics of CO from Si(111): The Role of Surface Defects.
Final rept.
P. M. Chu, S. A. Buntin, L. J. Richter, and R. R. Cavanagh. 1994, 6p.
Pub. in Surface Science, v321 p127-132 1994.

Keywords: *Silicon, *Carbon monoxide, *Desorption, *Surface defects, Etching, Ion beams, Annealing, Diagnostic techniques, Photochemical reactions, Reprints, *Photodesorption.

Laser-induced desorption of CO from an ion beam etched and annealed Si(111) surface is reported. State-resolved measurements of the desorbed CO reveal very high translational and vibrational energy contents, with the rotational excitation being quite low. The results suggest that the CO photodesorption is derived from CO bound to ion beam etch-induced active defect site(s) on the Si(111)7x7 surface that are only minimally influenced by either the ion beam etching conditions or the anneal. Comparison of the photoyields at 266 and 355 nm suggests that the desorption mechanism cannot be described using existing models for thermal- or carrier-mediated processes.

03,067
PB96-111703 Not available NTIS
National Inst. of Standards and Technology (MSEL), Gaithersburg, MD. Ceramics Div.
Silicon Nitride Boundary Lubrication: Lubrication Mechanism of Alcohols.
Final rept.
R. S. Gates, and S. M. Hsu. 1995, 9p.
See also PB95-213583 and PB96-111711.
Pub. in STLE Tribology Transactions, v38 n3 p645-653 1995.

Keywords: *Silicon nitrides, *Lubrication, *Alcohols, *Wear tests, Chemical reactions, Chemical analysis, Boundaries, Friction, Tribology, Wear, Alkoxides, Reprints, *Boundary lubrication, GPC-GFAA analysis, Silicon alkoxides.

This paper describes the lubrication mechanism of alcohols with silicon nitride under boundary lubrication conditions. Dynamic wear tests and static chemical reaction studies were conducted to study the chemical interaction between alcohols and silicon nitride. Direct evidence of chemical reactions occurring between alcohols and silicon nitride was collected. Gel-permeation-chromat ography-graphite- furnace-atomic-absorption (GPC-GFAA) analysis detected the presence of high molecular weight (HMW), silicon-containing, metallo-organic compounds in the wearing contact. Secondary ion mass spectrometry (SIMS) analysis of the reactionproducts from wear tests revealed the formation of silicon alkoxides. These alkoxide subsequently reacted to form HMW products which had been independently verified as capable of lubricating silicon nitride surfaces.

03,068
PB96-111711 Not available NTIS
National Inst. of Standards and Technology (MSEL), Gaithersburg, MD. Ceramics Div.
Silicon Nitride Boundary Lubrication: Effect of Oxygenates.
Final rept.
R. S. Gates, and S. M. Hsu. 1995, 12p.
See also PB96-111703.
Pub. in STLE Tribology Transactions, v38 n3 p607-617 1995.

Keywords: *Silicon nitrides, *Wear tests, *Lubrication, Oxygen compounds, Boundaries, Friction, Tribology, Wear, Lubricating oils, Alcohols, Reprints, *Boundary lubrication, BTF(Ball-on-three-flat), Oxygenates.

A ball-on-three-flat (BTF) wear tester was used to investigate the boundary lubricating characteristics of oxygenates on a commercial silicon nitride. A wide variety of oxygen-containing compounds were tested neat and/or at 1% by weight in a paraffin oil. Compounds containing hydroxyl functional groups were more effective compared to a base case of neat paraffin oil. Decreases of up to 58% in friction coefficient, and 95% in wear were obtained. In most cases, films were observed in and around the wear scar, suggesting chemical reactions had taken place in the contact. Additional wear tests, conducted using neat shorter-chain linear primary alcohols, i.e., 6-10 carbons, demonstrated boundary lubrication protection, with longer chain length providing better antiwear performance.

03,069
PB96-111919 Not available NTIS

National Inst. of Standards and Technology (MSEL), Gaithersburg, MD. Reactor Radiation Div.
Small Angle Neutron Scattering Study of the Structure and Formation of Ordered Mesopores in Silica.
Final rept.
C. J. Glinka, J. M. Nicol, G. D. Stucky, Q. Huo, E. Ramli, and D. I. Margolese. 1995, 6p.
Pub. in Materials Research Society Symposia Proceedings, v371 p47-52 1995.

Keywords: *Porous materials, *Neutron scattering, *Silica, Reprints, Small angle scattering, Molecular sieves, Mesoporous materials.

The nanoscale structure and synthesis mechanisms of a recently developed class of inorganic mesoporous materials with ordered arrays of uniform mesopores have been investigated by small angle neutron scattering (SANS). SANS measurements with solvents imbibed into the pores to vary the scattering contrast demonstrate that the low angle diffraction peaks from these materials are entirely due to the pore structure and that the pores are fully accessible to both aqueous and organic solvents. SANS measurements on the concentrated cationic surfactant and silicate that the existence of preassembled supramolecular arrays that mimic the final pore structure is not essential for the synthesis of these materials.

03,070
PB96-112339 Not available NTIS
National Inst. of Standards and Technology (MSEL), Boulder, CO. Materials Reliability Div.
Torsion Modulus and Internal Friction of a Fiber-Reinforced Composite.
Final rept.
H. Ledbetter, and M. Lei. 1994, 2p.
Pub. in Jnl. of Applied Physics, v76 n5 p3212-3213 1994.

Keywords: *Fiber composites, *Glass fiber reinforced plastics, *Epoxy matrix composites, Reprints, Torsional stress, Elastic properties, Ultrasonics, Internal friction.

By a kilohertz-frequency resonance method, we determined the torsion modulus and internal friction of a uniaxially fiber-reinforced composite. The composite was composed of glass fibers in an epoxy-resin matrix. We studied three fiber contents: 0.41 and 49 vol %. The internal friction failed to fit a classical free-damped-oscillator model where one assumes a linear rule-of-mixture for three quantities: oscillator mass, force constant, and mechanical-resistance constant. The torsion modulus approximately fits a plane-wave scattering ensemble-average model. The microstructure showed strong fiber-distribution nonhomogeneity. Considering this nonhomogeneity yielded a better agreement between model and observation. Thus, torsion-modulus measurements provide a method to detect and quantify fiber-distribution nonhomogeneity.

03,071
PB96-122510 Not available NTIS
National Inst. of Standards and Technology (MSEL), Gaithersburg, MD. Ceramics Div.
Epitaxial Growth of BaTiO3 Thin Films at 600C by Metalorganic Chemical Vapor Deposition.
Final rept.
D. L. Kaiser, M. D. Vaudin, L. D. Rotter, C. S. Hwang, R. B. Marinenko, J. G. Gillen, Z. L. Wang, and J. P. Cline. 1995, 3p.
Pub. in Applied Physics Letters, v66 n21 p2801-2803 May 95.

Keywords: *Barium compounds, Chemical vapor deposition, Reprints, Thin films, Temperature, *Epitaxial growth.

BaTiO3 thin films were grown epitaxially on (100) MgO substrates by metalorganic chemical vapor deposition (MOCVD) at a temperature of 600 degrees C. This substrate temperature is the lowest reported temperature for the growth of epitaxial BaTiO3 films by an MOCVD process. The films had a cube-cube orientation relationship with the substrate and were oriented with an a-axis perpendicular to the substrate plane. Nanoscale energy dispersive x-ray spectrometry measurements showed no evidence of interdiffusion between the film and substrate.

03,072
PB96-122999 Not available NTIS
National Inst. of Standards and Technology (MSEL), Gaithersburg, MD. Ceramics Div.
Chemically Assisted Machining of Si3N4.
Final rept.
C. J. Hsy, J. C. Wang, and S. M. Hsu. 1995, 17p.
Pub. in Proceedings of the CIMTEC (8th): High Performance Materials in Engine Technology, Faenza, Italy, June 28-July 4, 1994, p497-513.

Keywords: *Silicon nitride, *Ceramics, Cutting, Hydration, Machining, Surface chemistry, Surfac films, Reprints, *Chemical assisted machining.

Ceramics are hard and brittle. Machining such materials is time-consuming, difficult, and expensive. Current machining technology requires ultra-stiff tools, diamond-bonded wheels, and low material removal rate to minimize surface damage. This study demonstrates the feasibility of a novel ceramic machining concept that utilizes tribo-chemical reactions at the tool-workpiece interface to reduce the stress and minimize the surface damage. A series of cutting tests using a diamond wheel on silicon nitride with different chemical compounds has been conducted. Results suggest that by using different chemistries, the material removal rate and the surface finish of the machined Si3N4 surface can be significantly altered. Halogenated hydrocarbons show significant improvement over some commercial machining fluids currently in use.

03,073
PB96-123575 Not available NTIS
National Inst. of Standards and Technology (MSEL), Gaithersburg, MD. Ceramics Div.
Electrokinetic Sonic Analysis of Silicon Nitride Suspensions.
Final rept.
V. A. Hackley, R. S. Premachandran, and S. G. Malghan. 1992, 8p.
Pub. in American Chemical Society, p141-148 1992.

Keywords: *Electroacoustics, *Silicon nitrides, Isoelectric point, Electrokinetics, Reprints, Interfacial chemistry.

In colloidal processing of ceramic slips, reactions occurring at the solid-solution interface play a dominant role in the dispersion properties. Electrokinetic sonic amplitude (EsA) measurements have been used to characterize the aqueous interfacial chemistry of Si3N4 suspensions. The ESA signal is proportional to the dynamic mobility and depends on the colloid shear-plane potential. Samples were subjected to acidic and alkaline soxhlet extraction, then titrated potentiometrically. Variations in the ESA signal and isoelectric pH indicate differences in the surface charge behavior of each powder. These differences may arise from surface contamination by specifically absorbed ionic species or modification of potential determining surface sites as a result of treatment history. This paper is intended to provide hands-on information regarding the electrokinetic sonic analysis of aqueous ceramic dispersions.

03,074
PB96-135132 Not available NTIS
National Inst. of Standards and Technology (BFRL), Gaithersburg, MD. Building Materials Div.
Modelling Drying Shrinkage of Cement Paste and Mortar. Part 1. Structural Models from Angstroms to Millimeters.
Final rept.
D. P. Bentz, D. A. Quenard, V. Baroghel-Bouny, E. J. Garboczi, and H. M. Jennings. 1995, 9p.
Pub. in Materials and Structures, v28 p450-458 1995.

Keywords: *Calcium silicates, *Hydrates, *Drying, *Shrinkage, Cements, Pases, Mortars(Material), Concretes, Physical properties, Sorption, Sorptive properties, Microstructure, Models, Simulation, Reprints.

The nanostructure of calcium silicate hydrate (C-S-H) gel contributes to many physical properties of concrete, including the important engineering properties of creep and shrinkage. A set of structural models for this gel and computational techniques for their validation have been developed. The basic nanostructure of C-S-H is conceived as a self-similar agglomeration of spherical particales at two levels (diameters of 5 nm and 40 nm). Computational techniques are presented for simulating transmission electron microscopy images and computing sorption characteristics of the model nanostructures. Agreement with available experimental data is reasonable. The development of these nanostructural models is a first step in a multiscale approach to computing the drying shrinkage of model cement-based materials. Such an approach will provide a better understanding of the relationships between microstructure and the shrinkage behavior of these systems.

03,075
PB96-160411 Not available NTIS
National Inst. of Standards and Technology (MSEL), Gaithersburg, MD. Ceramics Div.
Analysis of Small-Angle Scattering Data Dominated by Multiple Scattering for Systems Containing Eccentrically Shaped Particles or Pores.
Final rept.
A. J. Allen, and N. F. Berk. 1994, 14p.
Pub. in Jnl. of Applied Crystallography, v27 p878-891 1994.

Keywords: *Neutron scattering, *Porous ceramics, Sintering, Microstructure, Reprints, *X ray scattering, Multiple small angle scattering.

A previously developed formalism to interpret the beam broading due to multiple small-angle scattering of a collimated beam of radiation in condensed matter is extended to treat the case of nonspherical scattering particles or pores. The new formalism concerns the situation where coherent single-particle scattering is incoherently, or stochastically, compounded by a random system of spheroidal particles, of any given mean aspect ratio, in a uniform matrix. By appropriate transformation of axes to reflect a spherroidal particle symmetry, Bethe's analysis of scattering when the sample thickness greatly exceeds the scattering mean free path is combined with the dynamical analysis of single-particle scattering to model the beam broadening arising from a system containing nonspherical scattering objects. For the range of experimental parameters used in practical small-angle scattering studies of technological materials such as porous ceramics, it is shown that, while the previous formulation suffices for spheres, globules and even short capillary pores, the variation in beam broadening as a function of incident wavelength exhibits distinguishable signatures for systems in which a collapsed planar or extreme capillary scattering morphology predominates.

03,076
PB96-161765 Not available NTIS
National Inst. of Standards and Technology (MSEL), Gaithersburg, MD. Ceramics Div.
Friction Processes in Brittle Fracture.
Final rept.
B. Lawn. 1992, 29p.
Pub. in Fundamentals of Friction: Macroscopic and Microscopic Processes, Braunlage, July-August 1991, p137-165 1992.

Keywords: *Brittle materials, *Fiber reinforced composites, Reprints, Fracture, Friction, Strength, Toughness, *Foreign technology, *Contact cracks, Interface chemistry.

In this paper the authors consider the interrelations between friction and fracture in highly brittle materials. First, they examine frictional effects in the mechanics of crack formation at elastic and elastic-plastic contacts on brittle surfaces. Then they consider how fundamental intersurface forces manifest themselves as 'internal friction' at crack interfaces in 'model' solids like mica and glass, with special reference to environmental chemistry. Finally, the authors examine the controlling role of frictional processes in the strength and toughness of modern ceramic systems.

03,077
PB96-163704 Not available NTIS
National Inst. of Standards and Technology (MSEL), Gaithersburg, MD.
Model for Microcrack Initiation and Propagation beneath Hertzian Contacts in Polycrystalline Ceramics.
Final rept.
B. R. Lawn, N. P. Padture, F. Guiberteau, and H. Cai. 1994, 11p.
Pub. in Acta Metallurgica Materials, v42 n5 p1683-1693 1994.

Keywords: *Microcrack, *Crack propagation, *Ceramics, Fracture mechanics, Reprints, Initiation, *Foreign technology, Shear faults.

A fracture mechanics model of damage evolution within Hertzian stress fields in heterogeneous brittle ceramics is developed. Discrete microcracks generate from shear faults associated with the heterogeneous ceramic microstructure; e.g. in polycrystalline alumina, they initiate at the ends of intergrain twin lamellae and extend along intergrain boundaries. Unlike the well-de-

fined classical cone fracture that occurs in the weakly tensile region outside the surface contact in homogeneous brittle solids, the fault-microcrack damage in polycrystalline ceramics is distributed within a subsurface shear-compression zone below the contact. The shear faults are modelled as sliding interfaces with friction, in the manner of established rock mechanics descriptions but with provision for critical nucleation and matrix restraining stresses. This allows for constrained microcrack pop-in during the loading half-cycle. Ensuing stable microcrack extension is then analyzed in terms of a K-field formulation. For simplicity, only mode I extension is considered specifically here, although provision exists for including mode II. The compressive stresses in the subsurface field constrain microcrack growth during the loading half-cycle, such that enhanced extension occurs during unloading.

03,078
PB96-163795 Not available NTIS
National Inst. of Standards and Technology (MSEL), Gaithersburg, MD.
Model for Toughness Curves in Two-Phase Ceramics. 2. Microstructural Variables.
Final rept.
N. P. Padture, J. L. Runyan, S. J. Bennison, L. M. Braun, and B. R. Lawn. 1993, 7p.
Pub. in Jnl. of the American Ceramic Society, v76 n9 p2241-2247 Sep 93.

Keywords: *Damage accumulation, *Microstructural design, Reprints, Strength, *Fracture mechanics model, Toughness curve, Two-phase composites.

The fracture mechanics analysis of Part I is here extended to consider the effects of volume fraction and scale of second-phase particles on the toughness-curve properties of ceramic-matrix composites. Increasing these variables enhances the flaw tolerance of the material, but only up to certain limits, beyond which bulk microcracking occurs. These limits define domains of damage accumulation and potential strength degradation by microcrack coalesence. In the familiar approximation of elliptical crack-wall profiles, the authors show that the principal effects of increasing volume fraction (or expansion mismatch) and particle size is to enhance the slope and scale of the T-curve, respectively.

03,079
PB96-179429 Not available NTIS
National Inst. of Standards and Technology (MSEL), Gaithersburg, MD. Ceramics Div.
Objective Evaluation of Short-Crack Toughness Curves Using Indentation Flaws: Case Study on Alumina-Based Ceramics.
Final rept.
L. M. Braun, S. J. Bennison, and B. R. Lawn. 1992, 9p.
Pub. in Jnl. of the American Ceramic Society, v75 n11 p3049-3057 Nov 92.

Keywords: *Alumina, *Flaw tolerance, Reprints, *Indentation strength, Aluminum titanate, Toughness curves, Two phase composite.

An objective methodology is developed for evaluating toughness curves (T-curves) of ceramics using identation flaws. Two experimental routes are considered: (1) conventional measurement of inert strength as a function of indentation load; (2) in situ measurement of crack size as a function of applied stress. Central to the procedure is a proper calibration of the indentation coefficients that determine the K-field of indentation cracks in combined residual-contact and applied-stress loading, using data on an appropriate base material with single-valued toughness. Tests on a fine-grain alumina serve to demonstrate the approach.

03,080
PB96-179452 Not available NTIS
National Inst. of Standards and Technology (MSEL), Gaithersburg, MD.
Deformation and Fracture of Mica-Containing Glass-Ceramics in Hertzian Contacts.
Final rept.
H. Cai, M. A. Kalceff, and B. R. Lawn. 1994, 9p.
Pub. in Jnl. of Materials Research, v9 n3 p762-770 Mar 94.

Keywords: *Hertzian contact, Deformation, Machinability, Microfracture, Reprints, Glass-ceramic, Shear fault.

The Hertzian indentation response of a machinable mica-containing glass-ceramic is studied. Relative to the highly brittle base glass from which it is formed, the glass-ceramic shows evidence of considerable 'ductility' in its indentation stress-strain response. Section views through the indentation sites reveal a transition from classical cone fracture outside the contact area in the bae glass to accumulated subsurface deformation-microfracture in the glass-ceramic. The deformation is attributed to shear-driven sliding at the weak interfaces between the mica flakes and glass matrix. Extensile microcracks initiate at the shear-fault interfaces and propagate into the matrix, ultimately coalescing with neighbors at adjacent mica flakes to effect easy material removal. The faults are subject to strong compressive stresses in the Hertzian field, suggesting that frictional tractions are an important element in the micromechanics. Bend-test measurements on indented specimens show that the glass-ceramic, although weaker than its base glass counterpart, has superior resistance to strength degradation at high contact loads. Implications of the results in relation to microstructural design of glass-ceramics for optimal toughness, strength, and wear and fatigue properties are discussed.

03,081
PB96-179460 Not available NTIS
National Inst. of Standards and Technology (MSEL), Gaithersburg, MD.
Flaw Tolerance and Toughness Curves in Two-Phase Particulate Composites: SiC/Glass System.
Final rept.
H. Cai, N. P. Padture, B. M. Hooks, and B. R. Lawn. 1994, 9p.
Pub. in Jnl. of the European Ceramic Society, v13 p149-157 1994.

Keywords: *Composites, *Flaw tolerances, Glass, Reprints, *Foreign technology, Indentation-strength, Silicon carbide, Toughness-curve.

Flaw-tolerance and associated toughness-curve (T-curve) characteristics in SiC/glass particle/matrix composites are studied. Two glass compositions, chosen to produce composites at extremes of high (H) and low (L) thermal expansion mismatch relative to the SiC particles, are investigated. In-situ observations of crack extension from indentation flaws reveal widely different responses: in the L composite the path is relatively undistorted from the planar geometry, with trans-particle fractures: in the H composite the path deflects strongly around the particles, with consequent interfacial bridge formation and activity in the crack wake. Surface fracture patterns produced by spherical indenters confirm the implied transition from transparticle to inter-particle with increasing internal residual stress, and point to a potential degradation in short-crack properties like wear and fatigue. Indentation-strength measurements also show different characteristics in the two composites: minor flaw tolerance in the L material, consistent with a single-valued, 'rule of mixtures' toughness: major tolerance in the H material, consistent with a pronounced T-curve. The T-curves themselves are deconvoluted from the indentation-strength data for each composite and analyzed.

03,082
PB96-179593 Not available NTIS
National Inst. of Standards and Technology (MSEL), Gaithersburg, MD. Polymers Div.
Wear of Enamel against Glass-Ceramic, Porcelain, and Amalgam.
Final rept.
L. A. George, and F. C. Eichmiller. 1996, 8p.
Pub. in Ceramic Transactions Series: Challenges in Ceramic Development, Manufacture, and Commercialization, v66 p181-188 1996.

Keywords: *Amalgam, *Betz-quartz, *Glass-ceramic, *Wear, Enamel, Procelain, Reprints.

The wear of human enamel opposing certain dental materials is a problem in restorative dentistry. A wear study was carried out on enamel that was in contact with three dental restorative materials, a beta-quartz glass-ceramic, a fused porcelain (Ceramco, Inc., Burlington, NJ), and a dispersed phase amalgam (Dispersalloy, Johnson & Johnson, Skillman, NJ). Twenty-seven human teeth tooled to form enamel cones were randomly assigned to the three restorative materials. Three groups of 9 enamel cones each were abraded against sample disks of each material. The test was carried out on a two-body, unidirectional, rotary wear testing machine. The wear of the enamel was evaluated by measurement of the volume of enamel lost during testing. The average wear volumes lost (cm cubed) for the enamel were: glass-ceramic, 5.0 x 10 to the minus 5 power (s = 2.1 x 10 to the minus 5 power); porcelain, 5.2 x 10 to the minus 4 power (s = 5.4 x 10 to the minus 4 power); amalgam, 3.5 x 10 to the minus 5 power (s = 1.8 x 10 to the minus 5 power). Comparison of the mean worn volume of enamel lost for the three materials, by the Turkey method of multiple comparisons with a significance level of 5%, indicated no significant difference between only the enamel worn against glass-ceramic and against amalgam. The results indicate that beta-quartz glass-ceramic material would produce less wear to opposing enamel than traditional fused porcelains. The wear of enamel opposing glass-ceramic should be equivalent to that resulting from contact with amalgam.

03,083
PB96-179601 Not available NTIS
National Inst. of Standards and Technology (MSEL), Gaithersburg, MD.
Effect of Grain Size on Hertzian Contact Damage in Alumina.
Final rept.
F. Guiberteau, N. P. Padture, and B. R. Lawn. 1994, 7p.
Pub. in Jnl. of the American Ceramic Society, v77 n7 p1825-1831 1994.

Keywords: *Alumina, *Damage accumulation, Deformation, Grain size, Microfracture, Reprints, *Hertzian contact.

The role of microstructural scale on deformation-microfracture damage induced by contact with spheres is investigated in monophase alumina ceramics over a range 3-48 um in grain size. Measurement of a universal indentation stress-strain curve indicates a critical contact pressure approximately 5 GPa, above which irreversible deformation occurs in alumina. A novel sectioning technique identifies the deformation elements as intragrain shear faults, predominantly crystallographic twins, within a confining subsurface zone of intense compression-shear stress. The twins concentrate the shear stresses at the grain boundaries and, above a threshold grain size, initiate tensile intergranular microcracks. Below this threshold size, classical Hertzian cone fractures initiate outside the contact circle.

03,084
PB96-180013 Not available NTIS
National Inst. of Standards and Technology (MSEL), Gaithersburg, MD.
Indentation Fatigue: A Simple Cyclic Hertzian Test for Measuring Damage Accumulation in Polycrystalline Ceramics.
Final rept.
F. Guiberteau, N. P. Padture, H. Cai, and B. R. Lawn. 1996, 14p.
Pub. in Philosophical Magazine A, v68 n5 p1003-1916 1993.

Keywords: *Alumina, *Damage accumulation, *Ceramics, Fatigue, Internal stress, Microfracture, Reprints, Hertzian contact.

A simple Hertzian contact procedure for investigating cyclic fatigue damage in brittle polycrystalline ceramics is described. Repeat loading of a shperical indenter on a coarse alumina ceramic produces cumulative mechanical damage. The mode of damage is one of deformation-induced intergranular microfracture, leading ultimately at large numbers of cycles and high contact pressures to severe grain dislodgement. In contrast to the classical Hertzian cone cracks that form in more homogeneous materials in the regions of tensile stress outside the contact circle, the damage in the coarse-grain alumina develops in a zone of high shear stress and hydrostatic compression beneath the contact circle. The fatigue damage is evident in inert environments, confirming the mechanical nature of the process, although exposure to moisture accelerates the effect. The relatively modest degradation in failure stress with number of repeat contacts for indented flexure specimens suggests that conventional strength and toughness testing procedures may not always provide sensitive indications of the extent of damage that can be incurred in concentrated loading.

03,085
PB96-180088 Not available NTIS
National Inst. of Standards and Technology (MSEL), Gaithersburg, MD.

Model for Toughness Curves in Two-Phase Ceramics. 1. Basic Fracture Mechanics.
Final rept.
B. R. Lawn, N. P. Padture, L. M. Braun, and S. J. Bennison. 1996, 6p.
See also PB96-163795.
Pub. in Jnl. of the American Ceramic Society, v76 n9 p2235-2240 1993.

Keywords: *Crack bridging, Strength, Reprints, *Fracture mechanics model, Microstructural design, Toughness-curve, Two-phase composites.

A fracture mechanics model is presented for the toughening of ceramics by bridging from second-phase particles, resulting in toughness curve (T-curve) behavior. It is assumed that the second-phase particles are in a state of residual thermal expansion dilatational mismatch relative to the matrix. In the long-crack region, these stresses augment frictional sliding stresses at the interphase boundaries, enhancing the crack resistance; in the short-crack region, the same stresses drive the crack, diminishing the crack resistance. The principal manifestation of these countervailing influences is a reduced sensitivity of strength to initial flaw size, i.e., an increased flaw tolerance.

03,086
PB96-180278 Not available NTIS
National Inst. of Standards and Technology (MSEL), Gaithersburg, MD.
Transient Creep Behaviour of Hot Isostatically Pressed Silicon Nitride.
Final rept.
S. M. Wiederhorn, B. J. Hockey, D. C. Cranmer, and R. Yeckley. 1993, 9p.
Pub. in Jnl. of Materials Science, v28 p445-453 1993.

Keywords: *Creep rupture, *Silicon nitride, *Ceramics, Lifetime, Reprints.

Transient creep is shown to dominate the high-temperature behavior of a grade of hot isostatically pressed silicon nitride containing only 4 wt% Y2O3 as a sintering aid. Contributing factors to transient creep are discussed and it is concluded that the most likely cause of long-term transient creep in the present study is intergranular sliding and interlocking of silicon nitride grains. In early stages of creep, devitrification of the intergranular phase, and intergranular flow of that phase may also contribute to the transient creep process. The occurrence of transient creep precluded the determination of an activation energy on the as-received material. However, after creep in the temperature range 1330-1430 degrees C for times exceeding approximately 1100 h, an apparent activation energy of approximately 1260 kJ mol to the minus 1 power was measured. It is suggested that the apparent activation energy for creep is determined by the mobility and concentration of diffusing species in the intergranular glassy phase. The time-to-rupture was found to be a power function of the minimum strain rate, independent of applied stress or temperature. Hence, creep-rupture behavior followed a Monkman-Grant relation. A strain rate exponent of -1.12 was determined.

03,087
PB96-193677 PC A11/MF A03
National Inst. of Standards and Technology (MSEL), Gaithersburg, MD. Ceramics Div.
Ceramics Technical Activities, 1995.
S. W. Freiman, and S. J. Dapkunas. 1995, 211p, NISTIR-5747.
See also PB94-162591.

Keywords: *Ceramics, *Research projects, Mechanical properties, Standards, Ceramic coatings, Microstructure, Superconductors, Powder(Particles), Surface properties.

Current programs of the Ceramics Division are reviewed.

03,088
PB96-200829 Not available NTIS
National Inst. of Standards and Technology (MSEL), Gaithersburg, MD. Ceramics Div.
Multimedia Tutorial on Phase Equilibria Diagrams.
Final rept.
E. F. Begley, and C. G. Lindsay. 1993, 2p.
Pub. in Innovations in Ceramic Education, v72 n12 p103-104 Dec 93.

Keywords: *Phase diagrams, *Multimedia, Computer applications, Video tapes, Ceramics, Physical properties, Phase studies, Chemical composition, Vapor phases, Crystal structure, Solid phases, Reprints, *Phase equilibria, US NIST.

In materials research, the phase diagram is a critical processing tool describing the relationship between temperature, chemical composition, and gaseous environment to the crystalline phases that should appear. The Ceramics Div. at the National Institute of Standards and Technology has initiated the development of innovative, distributable, multimedia software incorporating digital video interactive (DVI) technology to assist in the understanding and use of these diagrams.

03,089
PB96-204060 Not available NTIS
National Inst. of Standards and Technology (MSEL), Gaithersburg, MD. Ceramics Div.
Need for Advanced Characterization Techniques in Product Manufacturing: A Case Study on Ceramic Matrix Composites.
Final rept.
L. M. Braun. 1996, 5p.
Contract DE-AI05-920422014
Sponsored by Department of Energy, Washington, DC.
Pub. in Ceramic Product Development, Manufacture, and Commercialization, p213-217 1996.

Keywords: *Ceramics, *Composites, Reprints, Interfaces, Fiber-reinforced, Properties.

The capability of industry to manufacture reliable and cost-effective fiber-reinforced ceramic matrix composites requires detailed characterization and control of the composite properties. Advanced characterization techniques, including in situ characterization of material properties, offer the potential for process control, quality control, and lifetime monitoring. Advanced characterization techniques currently being developed to aid in the manufacture and scientific understanding of ceramic components are discussed.

03,090
PB96-204110 Not available NTIS
National Inst. of Standards and Technology (MSEL), Gaithersburg, MD. Ceramics Div.
Diffusive Crack Growth at a Bimaterial Interface.
Final rept.
T. J. Chuang, J. L. Chu, and S. Lee. 1995, 6p.
Contract NASA-C082000-R
Sponsored by National Aeronautics and Space Administration, Cleveland, OH. Lewis Research Center.
Pub. in AIAA/ASME/ASCE/AHS/ASC Structures, Structural Dynamics and Materials Conference (33rd), Dallas, TX., April 13-15, 1992, p2964-2969 1995.

Keywords: *Crack growth, *Ceramic composites, Reprints, Creep rupture, *Bimaterial interface, Energy release rate, High temperature fracture, Interfacial crack.

The diffusional microcrack growth behavior in a bimaterial system is investigated with an aim at estimating service life of advanced ceramic composites under creep-rupture conditions. The crack is assumed to grow via a coupled surface and grain-boundary diffusion under steady state conditions. The tensile stress distribution along the interface ahead of the moving crack tip is solved, and it is found that a new length parameter exists as a scaling factor for which the solution becomes identical to the single phase case when plotted on the nondimensional physical plane. In contrast to the elastic stress solution which shows singularity at the tip, together with oscillatory character away from the tip, the creep stresses have a peak value away from the tip due to a wedging effect and interfacial sliding eliminates stress oscillation resulting in a decoupling between mode I and mode II loading. The solution ties the far-field loading parameter to the crack tip conditions in terms of the unknown crack velocity to give a specific V-K relationship. It is shown that an exponent of 12 in the conventional crack growth power law emerges at the higher applied stress range.

03,091
PB96-204128 Not available NTIS
National Inst. of Standards and Technology (MSEL), Gaithersburg, MD. Ceramics Div.
Life Prediction of a Continuous Fiber Reinforced Ceramic Composite Under Creep Conditions.
Final rept.
T. J. Chuang. 1993, 12p.
Contract NASA-C-82000-R
Sponsored by National Aeronautics and Space Administration, Cleveland, OH. Lewis Research Center.
Pub. in Fatigue and Fracture of Aerospace Structural Materials, ASME 1993, v36 p73-84 1993.

Keywords: *Ceramics, *Composites, *Creep rupture, Fiber-reinforced, Cavity growth, Damage mechanics, Engine materials, Life prediction, Reprints.

The paper is concerned with development of a lifetime prediction methodology for a unidirectional fiber reinforced ceramic composite subjected to creep conditions. A continuum damage mechanics approach is adopted in which constitutive creep laws incorporating damage are constructed based on micromechanical modeling. A unit cell model is established to take advantage of the periodic feature of the material. The model which entails two elements (one representing the fiber phase and the other the matrix phase) connected in parallel is subjected to a constant stress applied in the fiber direction. From the requirements of equilibrium and compatibility, a system of simultaneous differential equations was derived for the dependent variables: stress, strain and damage as functions of time, with the initial conditions given by the elastic state of the material. The algorithm for solving this time-dependent problem was given in a flow chart from which the lifetime limited by creep can be computed. The results suggested that creep life is strongly dependent on applied stress, temperature and volume fraction of the fibers.

03,092
PB96-204185 Not available NTIS
National Inst. of Standards and Technology (MSEL), Gaithersburg, MD. Ceramics Div.
Bulk Modulus and Young's Modulus of Nanocrystalline gamma-Alumina.
Final rept.
M. R. Gallas, and G. J. Piermarini. 1994, 4p.
Pub. in Jnl. of the American Ceramic Society, v77 n11 p2917-2920 Nov 94.

Keywords: *Nanocrystalline ceramic, *Bulk modulus, *Young's modulus, Reprints, Compression, Gamma-alumina, Diamond anvil cell, Energy dispersive x-ray.

Compression measurements were performed for the first time on nanocrystalline gamma-alumina utilizing a diamond anvil cell (DAC) and the energy dispersive X-ray diffraction method. The cubic unit cell (alpha=0.7924 nm) for gamma-alumina was found to have a volume compression of about 2.4% over the pressure range from ambient to 3.8 GPa at room temperature under both hydrostatic and nonhydrostatic conditions. Using the first-order Bridgman equation and the Birch equation of state, the isothermal bulk modulus (B0) was determined to be 162 plus or minus 14 GPa and Young's modulus (E) was estimated to be 253 plus or minus 22 GPa assuming a Poisson's ratio for gamma-alumina of 0.24 plus or minus 0.2.

03,093
PB96-204524 Not available NTIS
National Inst. of Standards and Technology (MSEL), Gaithersburg, MD.
Creep and Creep Rupture of Structural Ceramics.
Final rept.
S. M. Wiederhorn, B. J. Hockey, and T. J. Chuang. 1991, 22p.
Pub. in NATO Advanced Research Workshop on 'Toughening Mechanisms in Quasi-Brittle Materials', Evanston, IL., July 1990, p555-576 1991.

Keywords: *Ceramics, *Crack growth, *Creep, Reprints, Rupture, Strength cavitation, *Foreign technology.

Structural ceramics are often two phase materials, in which rigid refractory grains, fibers, or whiskers are bonded by a less refractory matrix. At elevated temperatures, creep occurs by deformation of the matrix, resulting in the localization of stresses along grain boundaries, followed by cavitation and eventually be structural failure of the ceramic. The sequence of events prior to failure depends on the grain size and the amount of bonding matrix within the solid. Large amounts of matrix phase reduce constraints at grain boundaries, and thus the stresses that cause cavitation. Large grains, fibers or whiskers provie easy paths for crack growth, so that, once initiated, cracks readily propagate to failure. In structural ceramics, failure time can be expressed as a power function of the creep rate; the coefficient and exponent of the power function are determined by the failure mechanism. In the paper, models for creep rupture of ceramics are presented for cavity coalescence and for crack growth as primary failure processes. The model for cavity coalescence, in particular, is used to rationalize creep rupture data for a two phase ceramic that fails by cavity coalescence.

03,094
PB96-204532 Not available NTIS
National Inst. of Standards and Technology (MSEL), Gaithersburg, MD.
Fracture Mechanism Maps: Their Applicability to Silicon Nitride.
Final rept.
S. M. Wiederhorn, G. D. Quinn, and R. Krause. 1994, 26p.
See also AD-A220 428.
Pub. in Life Prediction Methodologies and Data for Ceramic Materials, ASTM STP 1201, p36-61 1994.

Keywords: *Ceramic materials, *Fracture(Mechanics), *Hot pressing, *Silicon nitrides, Reprints, Crack propagation, Creep, Failure, Fatigue(Materials), Flexual properties, Magnesium oxides.

Fracture mechanism maps provide means of assessing the structural reliability of ceramics at elevated temperatures. They can be used to summarize large quantities of data dealing with effects of load, temperature and environment on component lifetime. they also can be used to generate a design envelope that defines stress allowables for a given application. In this paper, the authors review the history and philosophy behind fracture mechanism maps and then discuss methods of obtaining such maps in an efficient manner. Based on data obtained in simple tensile tests, these methods are illustrated for one of the newer grades of silicon nitride. The map is then used to compare this material with a high temperature structural alloy, and another, older grade of silicon nitride. Finally, the authors discuss the use of fracture mechanism maps for design.

03,095
PB97-110027 Not available NTIS
National Inst. of Standards and Technology (MSEL), Gaithersburg, MD.
Flaw-Insensitive Ceramics.
Final rept.
S. J. Bennison, N. P. Padture, J. L. Runyan, and B. R. Lawn. 1991, 5p.
Pub. in Philosophical Magazine Letters, v64 n4 p191-195 1991.

Keywords: *Ceramics, *Flaw insensitivity, Bridging, Microstructures, Processing, Reliability, Reprints.

Ceramics are notorious for their 'brittleness', i.e. the sensitivity of mechanical strength to flaws on the microstructural scale. The association notion of the 'critical flaw' has dominated design considerations concerning structural reliability and materials processing of ceramic components. The accounts for the trend over the last decade towards a processing strategy of elimination strength-degrading flaws at source. Here the authors propose a fundamentally different approach, that of processing ceramics with crack-impeding elements integrated into the indigenous microstructures, such that any pre-existing or service-induced flaws are effectively stabilized. Strength data on a tailored alumina/aluminium-titanate material demonstrate the capacity of the approach to produce simple ceramics with unique flaw insensitivity.

03,096
PB97-110258 Not available NTIS
National Inst. of Standards and Technology (MSEL), Gaithersburg, MD.
Tension/Compression Creep Asymmetry in Si3N4.
Final rept.
W. E. Luecke, and S. M. Wiederhorn. 1994, 6p.
Pub. in Key Engineering Materials, v89-91 p587-592 1994.

Keywords: *Cavitation, *Creep, *Silicon nitride, Tension, Compression, Reprints, *Foreign technology.

The authors have deformed a commercial HIP-ed silicon nitride in both tension and compression at 1430 degrees C at stresses between 40 and 300 MPa. The material creeps up to 100 times faster in tension than in compression. The stress dependence of the tensile strain rate is not characterized by a single stress exponent, rising from about two at low stresses to about five at higher stresses. When stressed in tension, the material responds by cavitating, with the cavitation contributing signifciantly to the tensile strain. In compression, however, the material exhibits a stress exponent of unity, and cavitation is almost completely suppressed. The asymmetry in creep behavior between tension and compression is due to the dilatation of the material.

03,097
PB97-110282 Not available NTIS
National Inst. of Standards and Technology (MSEL), Gaithersburg, MD. Ceramics Div.
Characterizing Materials Properties for Ceramic Matrix Composites.
Final rept.
R. G. Munro. 1991, 8p.
Pub. in Proceedings of the Advanced Materials and Processing Technology Workshop on Ceramic Matrix Composites, Alexandria, VA., August 1-2, 1991, Part 2, p2-153-2-160.

Keywords: *Ceramics, *Composites, Data bases, Material properties, Matrix materials, Reprints.

The requirements for the effective reporting of materials property data for ceramic matrix composites are reviewed. The discussion focuses on bicomponent materials consisting of a reinforcement that is distributed in a ceramic matrix. The reinforcement may be short, whisker-like crystallites or long fibers with large length-to-diameter ratios. Examples are given to illustrate the sometimes dramatic and the sometimes subtle significance of the information requirements.

03,098
PB97-110290 Not available NTIS
National Inst. of Standards and Technology (MSEL), Gaithersburg, MD. Ceramics Div.
Database Development and Management (Project A.2.2): The Annual Report for 1992-1993.
Final rept.
R. G. Munro, and E. F. Begley. 1993, 6p.
Pub. in Projects within the Center for Advanced Materials: 1992-1993 Annual Report to the Gas Research Institute, Center for Advanced Materials, 6p 1993.

Keywords: *Data bases, *Ceramics, *Structural ceramics, High temperature, Development, Management, Reprints.

The Database Development and Management Project is directed towards the production and dissemination of a computerized database of materials properties for advanced, high-temperature, structural ceramics. The principle output of the project is the Structural Ceramics Database which is provided in a user-friendly software package that operates on DOS-based personal computers. The database is distributed worldwide via the NIST Standard Reference Data Program. The report discusses how the scope of the database has expanded in the current year, from the thermal and mechanical properties of silicon carbides and silicon nitrides, to a more extensive coverage of the thermal, mechanical, and chemical corrosion properties of structural ceramic oxides, carbides, and nitrides in general.

03,099
PB97-110308 Not available NTIS
National Inst. of Standards and Technology (MSEL), Gaithersburg, MD. Ceramics Div.
Role of Corrosion in a Material Selector Expert System for Advanced Structural Ceramics.
Final rept.
R. G. Munro. 1995, 9p.
Pub. in American Society for Testing and Materials Special Publication, p127-135 1995.

Keywords: *Ceramics, *Structural ceramics, *Corrosion, Expert systems, Heat exchangers, High temperature, Data bases, Material selection, Knowledge base, Reprints.

The primary goal in the development of advanced structural ceramics has been to provide high-strength, corrosion-resistant materials for use in high-temperature, aggressive environments. Much of the developmental effort has focused on heat exchangers for use in industrial gas- or coal-fueled systems with temperatures on the order of 1200 to 1400 degrees C. While ceramics are often popularly described as inert to chemical degradation, the corrosion resistance of these materials actually ranges from excellent to very poor, depending especially on the compositions of the environment and the materials selector expert system for advanced ceramics. The present paper examines the development of a set of rules for a material selector expert system based on relations among composition, microstructure, transport processes, operating conditions, and corrosion. The concurrent information requirements that must be provided in a computerized materials property database are discussed also.

03,100
PB97-110316 Not available NTIS
National Inst. of Standards and Technology (MSEL), Gaithersburg, MD. Ceramics Div.
Variances in the Measurement of Ceramic Powder Properties.
Final rept.
R. G. Munro, S. G. Malghan, and S. M. Hsu. 1995, 10p.
Pub. in Jnl. of Research of the National Institute of Standards and Technology, v100 n1 p51-60 Jan/Feb 95.

Keywords: *Ceramic powder, *Variances, Characterization, Composition, Density, Particle size, Surface areas, Round robin, Reprints.

Variances in the measurement of properties used to characterize ceramic powders are discussed in the context of the International Energy Agency's study. Annex II, Subtask 2, which includes chemical and physical measurements for five powders: two grades of silicon nitride, and one grade each of silicone carbide, silicon, and ziconia. The analysis presented here includes results for 39 properties reported by 25 laboratories using approximately 700 samples of the powders. Measurement uncertainties are discussed in the contexts of measurement variations within given laboratories (within-laboratory variance, sometimes called repeatability), among different laboratories (between-laboratory variance, also called reproducibility), and among different measurement techniques (between-methods variance). The analysis shows that the between-laboratory variance tends to be significantly greater than either the within-laboratory or the between-methods variances. The implication of this results is that the most important improvements in powder characterization measurements may be achieved through the standardization of the measurement methodologies.

03,101
PB97-110324 Not available NTIS
National Inst. of Standards and Technology (MSEL), Gaithersburg, MD.
Flaw-Tolerance and Crack-Resistance Properties of Alumina-Aluminum Titanate Composites with Tailored Microstructures.
Final rept.
N. P. Padture, S. J. Bennison, and H. M. Chan. 1993, 9p.
Pub. in Jnl. of the American Ceramic Society, v76 n9 p2312-2320 Sep 93.

Keywords: *Alumina, *Aluminum titanate, Mechanical properties, Microstructure, Processing, Reprints, *Flaw tolerance, *Crack resistance.

The microstructures of alumina-aluminum titanate (A-AT) composites have been tailored with the intent of altering their crack-resistance (R- or T-curve) behavior and resulting flaw tolerance. Specifically, two microstructural parameters which influence grain-localized crack bridging, viz., (1) internal residual stresses and (2) microstructural titanate was added to alumina to induce intense internal residual stresses from extreme thermal expansion mismatch. It was found that A-AT composites with uniformly showed significantly improved flaw tolerance over single-phase alumina. Coarsening of the duplex microstructure via grain growth scaling was relatively ineffective in improving the flaw tolerance further. Onset of spontaneous microcracking precluded further exploitation of this scaling approach. Therefore, an alternative approach to coarsening was developed, in which a uniform distribution of large alumina grains was incorporated within a fine-grain A-AT matrix ('duplex-bimodal'), via a powder processing route. The duplex-bimodal composites yielded excellent flaw tolerance with steady-state toughness of approximately 8 MPa-m(1/2). A qualitative model for microstructure development in these duplex-bimodal composites is presented.

03,102
PB97-110332 Not available NTIS
National Inst. of Standards and Technology (MSEL), Gaithersburg, MD.
In situ-Toughened Silicon Carbide.
Final rept.
N. P. Padture. 1994, 5p.
Pub. in Jnl. of the American Ceramic Society, v77 n2 p519-523 Feb 94.

Keywords: *Silicon carbide, Sintering, Microstructure, Reprints, Yttrium aluminum garnet, Crack-wake bridging, Fracture toughness.

A new processing strategy based on atmospheric pressure sintering is presented for obtaining dense SiC-based materials with microstructures consisting of (1)

uniformly distributed elongate-shape alpha-SiC grains and (2) relatively high amounts (20 vol%) of second-phase yttrium aluminum garnet (YAG). This strategy entails the sintering of beta-SiC powder doped with alpha-SiC, Al2O3, and Y2O3. The Al2O3 and Y2O3 aid in the liquid-phase sintering of SiC and form in situ YAG, which has a significant thermal expansion mismatch with SiC. During a subsequent grain-growth heat treatment, it is postulated that the alpha-SiC 'seeds' assist in controlling in situ growth of the elongated alpha-SiC grains.

03,103
PB97-110340 Not available NTIS
National Inst. of Standards and Technology (MSEL), Gaithersburg, MD.
Postfailure Subsidiary Cracking from Indentation Flaws in Brittle Materials.
Final rept.
N. P. Padture. 1993, 7p.
Pub. in Jnl. of Materials Research, v8 n6 p1411-1417 Jun 93.

Keywords: *Ceramics, *Cracking, *Indentation, Fracture, Lateral-cracks, Glass, Reprints.

Vickers indentation sites in ceramics have been examined after specimen failure from medial-radial indentation cracks. Evolution of a newcracking pattern of 'ortho-lateral' cracks, originating at the intact corners of the Vickers indentation and running orthogonal to the classic-lateral cracks and parallel to the new fracture surface, has been observed. In some instances postfailure extension of the classic-lateral cracks toward the surface was also observed. Enhanced residual tensile stress from relaxation of constraints on the indentation-plastic cavity by the generation of a fracture surface is postulated to drive the subsidiary cracking. A simple qualitative model to explain this phenomenon is presented. Possible implications of such postfailure subsidiary cracking on residual-stress-driven flaws, postmortem fractography, and wear in ceramics are discussed.

03,104
PB97-110456 Not available NTIS
National Inst. of Standards and Technology (MSEL), Gaithersburg, MD.
High Temperature Structural Reliability of Silicon Nitride.
Final rept.
S. M. Wiederhorn, G. D. Quinn, and R. Krause. 1994, 6p.
Pub. in Key Engineering Materials, v89-91 p575-580 1994.

Keywords: *Ceramics, *Silicon nitride, *Reliability, Strength, Creep, Fracture maps, Reprints, *Foreign technology.

Structural reliability of ceramics at elevated temperatures is often determined by crack growth, or by creep induced cavitation. Ceramics that fail in this manner fit a Monkman-Grant relation, in which the time to failure is represented as a power las function of the creep rate. In the paper the authors show that the Monkman Grant approach can be used to obtain fracture maps for characterizing creep and creep rupture behavior at high temperatures. Maps are presented for ceramics currently being considered for turbine or heat exchanger applications. Attributes of current grades of silicon nitride are compared.

03,105
PB97-110464 Not available NTIS
National Inst. of Standards and Technology (MSEL), Gaithersburg, MD.
Tensile Creep Testing of Structural Ceramics.
Final rept.
S. M. Wiederhorn, R. Krause, and D. C. Cranmer. 1991, 8p.
See also PB93-166619.
Pub. in Annual Automotive Technology Development Contractors Coordination Meeting, Dearborn, MI., October 28-31, 1991, p1-8.

Keywords: *Ceramics, *Creep tests, Loads(Forces), Mechanical properties, Tension tests, Test methods, Deformation, Strains, Fractures(Materials), Mechanical tests, Reprints.

In order to use structural ceramics in heat engines, their high temperature properties must be characterized. Temperatures as high as 1400 degrees C are expected, hence, test equipment capable of this temperature will be needed. Furthermore, as the dominant wear-out mechanism for high temperature applications is creep rupture, test equipment must not only be capable of high temperatures and stresses, but must be stable and must be able to sustain applied stresses for extended periods of time. In the paper, the authors discuss an inexpensive tensile tests apparatus that can be used to collect creep data for the prediction of component lifetime. They use this equipment to collect creep and creep rupture data on two grades of silicon nitride. They also demonstrate the general tendency of silicon nitride ceramics to follow a Monkman-Grant type of stress rupture behavior. The tendency permits a simple design methodology to be used for lifetime prediction.

03,106
PB97-112247 Not available NTIS
National Inst. of Standards and Technology (MEL), Gaithersburg, MD. Precision Engineering Div.
Chip Morphology, Tool Wear and Cutting Mechanics in Finish Hard Turning.
Final rept.
M. A. Davies, Y. Chou, and C. J. Evans. 1996, 6p.
Pub. in Annals of the CIRP, v45 n1 p77-82 Jan 96.

Keywords: *Machining, *Boron nitrides, *Wear, Cutting tools, Models, Reprints, Cubic baron nitrides.

Topography of surfaces produced in finish hard turning using cubic boron nitride (CBN) tools is affected by a large number of factors including tool wear and the mechanics of the chip formation process. The paper shows first that tool wear rates are affected by interactions between the world material and binder phase of the CBN tool. For finish hard turning, low CBN content, ceramic binder tools give longer lives and better finish than high CBN content metallic binder tools. For low CBN tools, wear rate is directly related to the microstructure of the work material and to the CBN grain size. SEM studies suggest that chip morphology is independent of work material microstructure, but varies with tool wear. Orthogonal cutting tests show that, above a critical speed, segmented chips are formed by catastrophic localized shear and that chip segmentation spacing may be reflected in a mdoulation of the machined surface. Segment spacing is a function of depth of cut, rake angle, and surface speed, approaching a limiting value with speed. Specific cutting energies decrease with speed, also approaching an asymptote. A simple mechanical model gives reasonable predictions of segment spacing along the original surface, although a full thermo-plastic model will be required to account for other aspects of the chip formation process.

03,107
PB97-115802 PC A05/MF A01
National Inst. of Standards and Technology (BFRL), Gaithersburg, MD. Building Materials Div.
Multi-Scale Picture of Concrete and Its Transport Properties: Introduction for Non-Cement Researchers.
E. J. Garboczi, and D. P. Bentz. Oct 96, 53p, NISTIR-5900.
Color illustrations reproduced in black and white.

Keywords: *Concretes, *Microstructure, Computerized simulation, Cements, Mortars(Material), Digital techniques, Silicate cements, Porosity, Hydration, Composite materials, US NIST.

Concrete is a multi-length scale composite material. From the nanometer to the millimeter scale, it is a random composite, and a different random composite at each length scale. Percolation processes play a key role in the microstructure of concrete, and help to describe the overall dependence of transport properties like ionic diffusivity on the microstructure. Computer models have been developed to describe the microstructure and transport properties, as the randomness of the material precludes most (but not all) analytical formulations. The overall description of concrete, over six orders of magnitude of length scales, in terms of computer models, precolation theory, and composite ideas is of interest to those studying other random materials as well, like ceramics and rocks. This report is written to present the ideas for concrete in such a way so as to be accessible to the non-cement researcher. It is hoped that these ideas will prove to be useful in other materials.

03,108
PB97-118731 Not available NTIS
National Inst. of Standards and Technology (MSEL), Gaithersburg, MD.
Sources of Strain-Measurement Error in Flag-Based Extensometry.
Final rept.
W. E. Luecke, and J. D. French. 1996, 10p.
Pub. in Jnl. of the American Ceramic Society, v79 n6 p1617-1626 Jun 96.

Keywords: *Strain measurement, *Extensometry, Advanced ceramics, Creep errors, Flag-based, Reprints.

The paper examines the sources of error in strain measurement using flag-based extensometry that uses either scanning laser or electroptical extensometers. These errors fall into two groups: errors in measuring the true gauge length of the specimen, which arise from the method of attachment of the flags, and errors arising from unanticipated disortions of the specimen during testing. The sources of errors of the first type include gauge-length errors from nonparallel flags and uncertainties in the true attachment point of the flag. During the test, strain-measurement errors of the second type can arise from horizontal translation of nonparallel flags, flag rotation that is induced by slippage, and flag motion from bending of the gauge length.

03,109
PB97-122220 Not available NTIS
National Inst. of Standards and Technology (MSEL), Gaithersburg, MD. Reactor Radiation Div.
Antiferromagnetic Interlayer Correlations in Annealed Ni80Fe20/Ag Multilayers.
Final rept.
J. A. Brochers, P. M. Gehring, R. W. Erwin, T. L. Hylton, K. R. Coffey, M. A. Parker, J. K. Howard, J. F. Ankner, and C. F. Majkrzak. 1996, 13p.
Pub. in Physical Review B, v54 n14 p9870-9882 Oct 96.

Keywords: *Annealing, *Antiferromagnetics, *Diffraction, Interlayers, Multilayers, X ray diffraction, Cross section, Reprints.

Sputtered Ni80Fe20/Ag multilayers, annealed postgrowth, exhibit giant magnetoresistance (GMR) with pronounced field sensitivity. The authors have characterized a series of Ni80Fe20(20 Angstroms/Ag(40 Angstroms)) multilayers annealed at temperatures ranging from 305 to 335 degrees C using x-ray and polarized neutron reflectivity techniques. For all of the samples, specular x-ray measurements reveal that the laterally averaged interfaces between the Ni80Fe20 and Ag layers are not well defined. The growth-plane morphology of the multilayers, determined from off-specular x-ray diffraction, shows a dependence on annealing temperature. Specular and off-specular polarized neutron reflectivity data indicate that the GMR in the annealed samples does not arise from long-range antiferromagnetic alignment of coherent ferromagnetic sheets, as generally observed in related materials. Instead, annealing promotes the formation of planar ferromagnetic domains of micrometer size within each Ni80Fe20 layer that are antiferromagnetically correlated along the growth axis. The length scales of these domains are consistent with a model in which weak dipolar forces dominate the interactions between them.

03,110
PB97-122337 Not available NTIS
National Inst. of Standards and Technology (MSEL), Gaithersburg, MD. Reactor Radiation Div.
Small Angle Neutron Scattering Study of the Structure and Formation of MCM-41 Mesoporous Molecular Sieves.
Final rept.
C. J. Glinka, J. M. Nicol, G. D. Stucky, Q. Huo, J. B. Higgins, M. E. Leonowicz, E. Ramli, and D. Margolese. 1996, 6p.
Pub. in Jnl. of Porous Materials, v3 p93-98 1996.

Keywords: *Porous materials, *Neutron scattering, *Molecular sieves, Mesopores, Liquid crystals, Reprints, Mesoporous sieves.

The nanoscale structure and synthesis mechanisms of the MCM-41 class of inorganic mesoporous materials have been investigated by small angle neutron scattering (SANS). SANS measurements with solvents imbibed in the pores to vary the scattering contrast demonstrate that the low angle diffraction peaks from these materials are entirely due to the pore structure and that the pores are fully accessible to both aqueous and organic solvents. Static and shear flow SANS measurements on the concentrated cationic surfactant and silicate precursor solutions typically used in the synthesis

of the mesopore materials indicate that the existence of preassembled supramolecular arrays that mimic the final pore structure is not essential for the synthesis of these materials.

03,111
PB97-122477 Not available NTIS
National Inst. of Standards and Technology (MSEL), Gaithersburg, MD. Ceramics Div.
Nanoindentation and Instrumented Scratching Measurements on Hard Coatings.
Final rept.
A. W. Ruff. 1996, 3p.
Pub. in American Society for Testing and Materials Publication - Effect of Surface Coatings and Treatments on Wear, vSTP1278 p124-126 1996.

Keywords: *Ceramics, *Coatings, *Elastic modulus, Hardness, Indentation, Surface treatments, Scratching, Reprints, Plasma sprayed coatings.

Elastic, plastic, and cracking properties of ZrO2, a ZrO2-metal composite, and a Ni-NiO composite, all plasma-sprayed as coatings on metallic substrates, have been studied. Data comparisons were made with bulk ZrO2, bulk nickel, and single-crystal silicon as reference materials. A nanoindentation and scratching apparatus was used for the measurements. Three different indenter and scratching tool shapes were used: 200 micrometers radius sphere, Vickers four-sided pyramid, and a 45 degree wedge with a 0.5-mm radius curved edge. During indentation, over a load range of 10 mN to 1 N, continuous load versus depth data were obtained in each case to permit analysis for material hardness and elastic modulus. The loading curve data are used to calculate hardness, and the unloading curve data are used to calculate elastic modulus. The analytical models used are described and compared. An alternate method for deriving elastic modulus from the initial portion of the loading curve is described. Comparison among the results for different tool shapes will be discussed.

03,112
PB97-122501 Not available NTIS
National Inst. of Standards and Technology (MSEL), Gaithersburg, MD. Ceramics Div.
Wear Modeling of Si-Based Ceramics.
Final rept.
M. C. Shen, and S. M. Hsu. 1996, 6p.
Pub. in Proceedings of the International Tribology Conference, Yokohama, Japan, October 29-November 2, 1995, p403-408 1996.

Keywords: *Ceramics, *Wear mechanics, *Silicon compounds, Fracture, Models, Carbides, Nitrides, Reprints, *Foreign technology.

Existing ceramic wear models have been evaluated against a large set of wear data of a Si3N4 and a SiC under dry sliding condition. The wear data cover a wide range of speeds and loads. The data include various wear mechanisms: deformation, fracture, and severe fracture corresponding to milk wear, severe, and ultra-severe wear regimes. Transition zones separate individual wear regimes. The wear models are assessed for their ability to predict both the level of wear and the locations of the wear transitions. The fracture models predict well in the severe wear regime but deviate from the data in the milk and ultra-severe wear regimes. In predicting the locations of wear transitions, the mild-to-severe wear transitions can be predicted reasonably well. The severe-to-ultra-severe wear transition in both materials can be successfully described by a critical velocity model. This suggests that thermal-shock-induced fracture damages are responsible for the existence of the ultra-severe wear regime. Consequently, a modified model was developed to include the thermal shock stresses.

03,113
PB97-122592 Not available NTIS
National Inst. of Standards and Technology (MSEL), Gaithersburg, MD. Ceramics Div.
Chemical Effect in Ceramics Grinding.
Final rept.
T. N. Ying, and S. M. Hsu. 1996, 6p.
Pub. in Proceedings of the International Tribology Conference, Yokohama, Japan, October 29-November 2, 1995, p1725-1730 1996.

Keywords: *Ceramics, *Coolants, *Machining rate, Particles, Diamond wear, Silicon nitride, Reprints, *Foreign technology.

Ceramics are tough and hard and require diamond tooling to machine or cut. The chemical effects of coolants in ceramic grinding have received relatively little attention. The paper describes various chemical effects of coolants on machining rates, surface finish, and explains why some chemistries can improve grinding rates of tough ceramics several order of magnitudes.

Coatings, Colorants, & Finishes

03,114
AD-A310 087/2 PC A03/MF A01
National Bureau of Standards, Gaithersburg, MD.
Volatile Corrosion Inhibitors.
Dec 64, 15p.
Availability: Document partially illegible.

Keywords: *Corrosion, *Corrosion inhibition, *Volatility, *Packing materials, Test and evaluation, Materials, Steel, Coatings, External, Storage, Oils, Paper, Water vapor.

Significant reports covering the period since 1962 were selected for this study, with reference to relevant earlier works. Recent government RD on volatile corrosion inhibitors (VCI) has generally proceeded along three lines: extension of tests defining the protective value of these materials for longer storage periods to steel equipment, tolerances of various nonferrous materials and finishes toward tarnishing or corrosion by these materials, and effectiveness of exterior packaging materials in extending use of these inhibitors to more severe exposures of water vapor and liquid. Volatile corrosion inhibitors in the form of salts, dissolved in oils, or coated on paper within enclosed shipment parcels or storage spaces offer improved corrosion protection to hare steel while it is in a ready condition for withdrawal and immediate use.

03,115
PB94-160801 PC A03/MF A01
National Inst. of Standards and Technology (MSEL), Gaithersburg, MD. Polymers Div.
Cylinder Wipe Air-Drying Intaglio Ink Vehicles for U.S. Currency Inks.
Annual rept.
B. Dickens, B. J. Bauer, and W. R. Blair. Jan 91, 29p, NISTIR-4498.
See also PB90-112343 and PB91-144345. Sponsored by Department of the Treasury, Washington, DC. Office of Research and Technical Services.

Keywords: *Alkyd resins, *Inks, *Synthesis(Chemistry), Polymers, Drying oils, Pentaerythritol esters, Linseed oil, Sebacic acid, Succinic acid, Performance tests, Thermosetting resins, Curing, Drying, *Intaglio ink resins.

A family of air-dry intaglio resin alkyds has been developed. The alkyds are based on pentaerythritol, sebacic, acid, linseed oil fatty acids and succinic anhydride. In laboratory tests, intaglio inks made from these resins washed well and cured to satisfactorily resistant films. Industrial quantities for press trials have been synthesized by a third party. A second series of resins has also been developed. These resins are based on tripentaerythritol, linseed oil fatty acids and succinic anhydride. Satisfactory washing and solvent resistance are obtained in laboratory tests. A third series of resins based on poly(vinyl alcohol) was synthesized but did not appear to be satisfactory for industrial development. The temperature program is important in the synthesis of alkyds. The influence of temperature has been studied so that satisfactory resins can be made industrially in minimum time.

03,116
PB94-199338 Not available NTIS
National Inst. of Standards and Technology (NEL), Gaithersburg, MD. Chemical Process Metrology Div.
Gas Phase Reactions Relevant to Chemical Vapor Deposition: Optical Diagnostics.
Final rept.
D. B. Burgess. 1990, 6p.
Pub. in Materials Research Society Symposia Proceedings, v168 p137-142 1990.

Keywords: *Chemical vapor deposition, *Vapor phases, *Reaction kinetics, *Optical tests, Silanes, Silicon, Silicon nitrades, Laser applications, Photolysis, Fabrication, Emission, Decomposition reactions, Nucleation, Ammonia, Silicon hydrides, Reprints, Laser induced fluorescence.

Laser photolysis, optical emission, and laser-induced fluorescence (LIF) were used to study laser driven decomposition processes in the gas phase pertaining to the systems: SiH4 -> Si (s) and SiH4 + NH3 -> Si3N4 (s). These processes are important to silicon/silicon-nitride chemical vapor deposition, flame-driven gas phase silicon-particle nucleation, and laser-induced processes for materials fabrication. UV laser photolysis was used to generate SiHx and NHx species from silane and ammonia. A number of photo-fragments were identified by emission from excited states. The rate of reaction of NH2 with silane was measured using LIF to detect NH2 as a function of time following photolysis of ammonia.

03,117
PB94-199346 Not available NTIS
National Inst. of Standards and Technology (NEL), Gaithersburg, MD. Chemical Process Metrology Div.
Gas Phase Reactions Relevant to Chemical Vapor Deposition: Numerical Modeling.
Final rept.
D. Burgess, and M. R. Zachariah. 1990, 6p.
Pub. in Materials Research Society Symposia Proceedings, v169 p31-36 1990.

Keywords: *Chemical vapor deposition, *Mathematical models, *Vapor phases, *Reaction kinetics, Laser applications, Particles, Nucleation, Concentration(Composition), Fabrication, Temperature, Silicon, Silicon nitrides, Decomposition, Silanes, Reprints, Chemical reation mechanisms.

Numerical modeling of gas phase chemical kinetic was used to investigate reactions following silane decomposition to suggest experimental conditions and to interpret concentration measurements. The effects of concentration and temperature gradients on kinetic pathways and reactive intermediates were studied. These processes are relevant to silicon and silicon-nitride chemical vapor deposition (CVD), to flame-driven gas phase particle nucleation, and to laser-induced processes for materials fabrication.

03,118
PB94-200540 Not available NTIS
National Inst. of Standards and Technology (IMSE), Gaithersburg, MD. Ceramics Div.
Perspective on Fiber Coating Technology.
Final rept.
D. C. Cranmer. 1988, 4p.
Contract N00014-86-F-0096
Pub. in Ceram. Eng. Sci. Proc. 9, n9-10 p1121-1124 1988. Sponsored by Strategic Defense Initiative Organization, Washington, DC. Innovative Science and Technology.

Keywords: *Coating processes, *Fibers, *Deposition, Ceramic fibers, Carbon fibers, Composite materials, Reprints.

A variety of techniques exist for depositing coatings on ceramic and carbon fibers. The paper reviews several of these techniques and their advantages and disadvantages and points out several deficiencies in uniformly and reproducibly coating the fibers.

03,119
PB94-215704 PC A03/MF A01
National Inst. of Standards and Technology (BFRL), Gaithersburg, MD.
Diffusion of Cations Beneath Organic Coatings on Steel Substrate.
J. Pommersheim, T. Nguyen, Z. Zhang, and C. Lin. Apr 93, 42p, NISTIR-5102.
Prepared in cooperation with Bucknell Univ., Lewisburg, PA. Dept. of Chemical Engineering. and Xiamen Univ. (China). Dept. of Chemistry.

Keywords: *Polymeric films, *Steels, *Corrosion mechanisms, Cations, Diffusion, Transport properties, Organic coatings, Substrates, Sodium, Mathematical models, Computer codes, US NBS, National Institute of Standards and Technology.

Theoretical and experimental studies were carried out for the transport of cations in the channel between a polymer coating and a metal substrate from a defect in the absence of an electrical applied potential. The model consists of two stages: an initial period during which ions diffuse in the coating/metal interfacial 'channel' and adsorb on the coating surface and a propagation period during which ions also diffuse into the coating. The mathematical models were solved to predict the cation concentration and flux under the coating and the relative rate of diffusion between initial and propa-

gation periods. Model parameter values were derived from the results of an experiment conducted in a specially designed diffusion cell. The results also indicated that during the propagation period, the rate limiting step was the lateral diffusion along the coating/metal interface rather than diffusion through the coating.

03,120
PB94-216447 Not available NTIS
National Inst. of Standards and Technology (NEL), Gaithersburg, MD. Building Materials Div.
Non-Osmotic, Defect-Controlled Cathodic Disbondment of a Coating from a Steel Substrate.
Final rept.
J. Martin, E. Embree, and W. Tsao. 1990, 9p.
Sponsored by Naval Civil Engineering Lab., Port Hueneme, CA.
Pub. in Jnl. of Coatings Technology 62, n790 p25-33 1990.

Keywords: *Coatings, *Blistering, *Surface defects, Steels, Substrates, Cracking(Fracturing), Stress corrosion tests, Protective coatings, Barrier coatings, Reprints, *Cathodic disbondment model.

A non-osmotic, defect-controlled cathodic disbondment model is proposed for explaining experimental results which were inconsistent with an osmotically controlled disbondment process. The proposed model attempts to integrate the physics of blister initiation and growth (that is, the development of internal stresses and the fracture of the coating from the substrate as the blister grows in size) with the better elucidated chemistry of blister growth. The proposed model has many features which are analogous to the buckling and stress corrosion cracking models proposed for other materials. It also provides an alternative explanation for the well-known barrier-effect in coatings.

03,121
PB95-108734 Not available NTIS
National Inst. of Standards and Technology (MSEL), Gaithersburg, MD. Ceramics Div.
Interface Modification and Characterization of Silicon Carbide Platelets Coated with Alumina Particles.
Final rept.
P. T. Pei, J. F. Kelly, and S. G. Malghan. 1993, 11p.
Pub. in Colloids and Surfaces A: Physicochemical and Engineering Aspects 70, p277-287 1993.

Keywords: *Coating processes, *Surface chemistry, *Silicon carbides, *Aluminum oxide, *Interfaces, Surface coating, Particle size, Colloids, Flocculation, Scanning electron microscopy, Additives, Electrodynamics, Aluminum coatings, Reprints.

A colloidal-chemistry-based technique was developed for interface modification of silicon carbide platelets (SiCp) by coating with alumina particles. The coating process utilizes electrostatic and/or electrosteric interactions between the particles to promote heterocoagulation. Since an understanding of the chemical interface between the SiCp and alumina is important for improving the coating process, the powders were characterized by the measurement of the electrokinetic sonic amplitude (ESA). The major factors studied were particle size, type of alumina, presence of polyacrylate surfactant, and concentration of alumina in the coating slip. The surface coverage and morphology of the alumina coating on SiCp was determined quantitatively by scanning electron microscopy (SEM). The results indicate that around pH 5.8, the surface charge difference between SiCp and alumina was the largest and the coating of alumina on SiCp was feasible. The SEM data showed that surface coverage was uniform, and the highest surface coverage on SiCp was 66% when the surface area ratio of alumina to SiCp was 250% in the suspension. No significant improvement of the coating rate was observed by the addition of a polyacrylate for dispersion of SiCp. The concentration of alumina in the slip exhibited a strong influence on the amount of surface coverage on SiCp.

03,122
PB95-140893 Not available NTIS
National Inst. of Standards and Technology (NEL), Gaithersburg, MD. Building Materials Div.
In situ Measurements of Chloride Ion and Corrosion Potential at the Coating/Metal Interface.
Final rept.
T. Nguyen, and C. Lin. 1990, 4p.
Pub. in Proceedings of the Annual Meeting of the Adhesion Society (13th), (Extended Abstract), Savannah, GA., February 18-21, 1990, 4p.

Keywords: *Metal coatings, *Chlorides, *Corrosion, *In situ measurement, *Steels, Chemical attack, Chemical reactions, Interfaces, Metal-metal bonding, Corrosion tests, Reprints, *Corrosion potential.

One of the main reasons for the lack of a complete understanding of corrosion and adhesion failures of a coated metal is the lack of analytical instrumentation to probe the behaviors of corrosive agents at the coating/steel interface. We have developed a procedure based on microelectrodes for studying in situ the behaviors of potential and chloride ions at a coating/metal interface. The procedure requires an attachment of a Cl(-) selective microelectrode at the coating/metal interface, thus allowing direct measurements of Cl(-) concentration and corrosion potential changes at localized areas under a coating. Although it is intricate to prepare these microelectrodes, the procedure provided very useful information for mechanistic studies of corrosion under coatings, as well as for transport studies of Cl(-) ions through a coating on metal. The procedure should also be very useful for studying the roles of Cl(-) in localized corrosion.

03,123
PB95-140927 Not available NTIS
National Inst. of Standards and Technology (MSEL), Gaithersburg, MD. Metallurgy Div.
Aging Effects on XRF Measurements of Solder Coatings.
Final rept.
F. Ogburn, and H. J. Brown. 1988, 2p.
Pub. in Plating and Surface Finishing, p58-59 Nov 88.

Keywords: *Aging(Materials), *X ray fluorescence, *Solders, *Metal coatings, Metastable state, Thickness, Degradation, Nondestructive tests, Errors, Lead alloys, Tin alloys, Reprints.

The use of fluorescent x-ray methods to measure the thickness and composition of electroplated solder coatings is subject to measurable errors associated with the spontaneous decomposition of the metastable state of the freshly deposited coating. The rate of change at room temperature drops off with time, but is evident for at least 90 days.

03,124
PB95-146387 PC A05/MF A01
National Inst. of Standards and Technology (BFRL), Gaithersburg, MD.
Methodologies for Predicting the Service Lives of Coating Systems.
Building science series.
J. W. Martin, S. C. Saunders, F. L. Floyd, and J. P. Wineburg. Oct 94, 78p, NIST/BSS-172.
Also available from Supt. of Docs. as SN003-003-03291-3. See also PB88-175542. Prepared in cooperation with Washington State Univ., Pullman. Dept. of Pure and Applied Mathematics. and Duron Paints and Wallcoverings, Beltsville, MD. Sponsored by Federal Highway Administration, Washington, DC. and Du Pont de Nemours (E.I.) and Co., Philadelphia, PA. Marshall Labs.

Keywords: *Organic coatings, *Service life, *Environmental effects, *Life tests, *Coating processes, Reliability, Durability, Exposure, Life(Durability), Criteria, Fault trees, Time series analysis, Aging tests(Materials), Pollution abatement.

Over the last two decades, the organic coatings industry has undergone rapid technological and structural changes. These changes have been induced by legislative actions such as restrictions pertaining to hazardous chemicals, toxic effluents, and volatile organic compounds. The consequence of these changes has been the displacement of almost all commercially-important, well-established coatings (largely high-solvent coatings) by newer systems, the formulation and application of which are based on different chemistries and technologies. This report reviews the attributes of the service life prediction problem which are common to all materials, components, and systems in an effort to establish a set of criteria for assessing the adequacy of existing or proposed service life prediction methodology for coating systems. The current durability methodology and the reliability-based methodology are then evaluated against these criteria. The proposed criteria include the ability to (1) handle high variability in the time-to-failure data for nominally identical coated panels exposed in the same service environment, (2) analyze multivariate and censored time-to-failure data, (3) establish a connection between laboratory and field exposure results, and (4) quantitatively predict the service life of a coating system exposed in its intended service environment.

03,125
PB95-176087 Not available NTIS
National Inst. of Standards and Technology (MSEL), Gaithersburg, MD. Ceramics Div.
Modified Surface Layers and Coatings.
Final rept.
A. W. Ruff. 1994, 11p.
Pub. in Tribology in the USA and the Former Soviet Union: Studies and Applications, Chapter 3.5, p197-207 1994.

Keywords: *Surface properties, *Ceramic coatings, *Layers, *Tribology, Lubrication, Finishes, Ceramic materials, Self lubricating materials, Surface finishing, Residual stress, Adhesion, Reprints.

The use of advanced surface modification and coating methods to improve tribological characteristics of materials is an important development in recent years. Considerable effort is being expended on development of new coating materials, both hard and soft, on new techniques of alteration of near-surface material, and on important questions of coating adhesion, and system residual stresses. This Chapter will briefly mention some of the current areas of research and development in the U.S., although space limitations and lack of information on proprietary methods will not permit a thorough discussion. In addition, examples of two techniques of surface improvement will be described.

03,126
PB96-123211 Not available NTIS
National Inst. of Standards and Technology (MSEL), Gaithersburg, MD. Ceramics Div.
Anisotropy of the Surfaces of Pores in Plasma Sprayed Alumina Deposits.
Final rept.
J. Ilavsky, A. J. Allen, G. G. Long, C. C. Berndt, A. N. Goland, S. Krueger, and H. Herman. 1995, 6p.
Contract DE-AC02-76CH00016
Sponsored by Department of Energy, Washington, DC.
Pub. in Proceedings of Thermal Spraying (ITSC '95) - Current Status and Future Trends, Kobe, Japan, May 22-26, 1995, p483-488.

Keywords: *Plasma sprayed alumina, *Pore surface area, *Neutron scattering, Porosity, Reprints.

Porosity is an important factor in determining the physical properties of plasma sprayed deposits. A significant fraction (2 - 15%) of the deposit volume consists of voids. These voids are in the form of pore between the splats and around any inclusions (unmelted particles) that may be present, and in the form of cracks within the splats. Neither the pores nor the cracks are spherical in shape, and the splat structure is circularly symmetric only when viewed from the spray direction. The microstructure of a plasma sprayed deposit contains significant anisotropy in the void shapes and there may be significant alignment of some of these shapes along particular directions. In this research, the voids in plasma sprayed deposits were investigated by measuring the specific surface areas of the voids from the terminal slope of small-angle neutron scattering, i.e., Porod scattering, by the deposits, and by means of mercury intrusion porosimetry. The results indicate that much of the void surface area is found perpendicular to the substrate and is associated with cracks. The second population of voids is found mostly parallel with the substrate and is associated with interlamellar pores. The surface areas measured by means of porosimetry were smaller than the surface areas derived from scattering, and were probably influenced by the presence of closed porosity, by the void model and by the low precision for measuring small voids.

03,127
PB96-123237 Not available NTIS
National Inst. of Standards and Technology (MSEL), Gaithersburg, MD. Polymers Div.
Flow-Induced Structure in Polymers: Chapter 16. Shear-Induced Changes in the Order-Disorder Transition Temperature and the Morphology of a Triblock Copolymer.
Final rept.
C. L. Jackson, F. A. Morrison, A. I. Nakatani, K. A. Barnes, C. C. Han, J. W. Mays, and M. Muthukumar. 1994, 13p.
Pub. in Symposium of the National Meeting of the American Chemical Society (208th), Washington, DC., August 21-25, 1994, p233-245.

Keywords: *Copolymers, Reprints, *Triblock copolymer, Transition temperature, Steady shear flow.

An overview of ongoing research on a triblock copolymer subjected to steady-shear flow is presented. The

copolymer is composed of polystyrene-polybut adiene-polystyrene (23 st% polystyrene-degrees) with cylindrical morphology in the quiescient state. The order-disorder transition (ODT) was studied by in-situ SANS in a couette geometry as a function of temperature and shear rate. We observed that the ODT temperature shifted upward by 20 degrees C as the shear rate was increased from - 0.1 to 25 s to the minus 1. Sheared samples were also quenched and studied by transmission electron microscopy. A unique shear-induced morphology was found and tentatively identified as a transformation from the original p31m space group to a p3m1 space group of lower symmetry, similar to a martensitic transformation in metals.

03,128
PB96-154984 PC A04/MF A01
National Inst. of Standards and Technology (BFRL), Gaithersburg, MD. Building Materials Div.
Development of a Test Method for Leaching of Lead from Lead-Based Paints Through Encapsulants.
T. Nguyen, M. E. McKnight, and E. Byrd. Feb 96, 40p, NISTIR-5783.
Sponsored by Department of Housing and Urban Development, Washington, DC. Office of Lead-Based Paint Abatement and Poisoning Prevention.

Keywords: *Lead(Metal), *Leaching, *Encapsulation, *Test methods, *Lead coatings, Chemical analysis, Paints, Acetic acid, Diffusion, Polymers, Standards, Pollution abatement, Toxic substances.

Lead in paints is one of the major sources of lead poisoning in children. Polymeric encapsulant is considered a viable approach for controlling the hazards associated with lead-based paints. Encapsulant is considered a viable approach for controlling the hazards associated with lead-based paints. This study aimed to provide a technical basis for the development of a standard test method for lead leaching through polymeric encapsulants. The effects of pigment type and concentration in the film, chemical types and pH of leaching solutions, and encapsulants of different generic resins on the leaching of lead from a lead-based film with and without an encapsulant covering it were investigated.

03,129
PB97-110431 Not available NTIS
National Inst. of Standards and Technology (MEL), Gaithersburg, MD. Precision Engineering Div.
Proposed Coating Technology Consortium. (National Coil Coaters Association Fall Conference). Held in Rosemont, Illinois in September 1992.
Final rept.
T. Vorburger. 1993, 4p.
Pub. in Coil Lines, v1 n3 4p Mar 93.

Keywords: *Coatings, Appearance, Consortium, Defects, Film thickness, Inspection, Reprints, *National Institute of Standards and Technology.

At NCCA's Fall Conference in Rosemont, IL, this past September, attendees heard about a proposed consortium to improve coating technology. The consortium is being organized at the National Institute of Standards and Technology (NIST) in Gaithersburg, MD, but will be directed by a board composed mainly of industrial members.

03,130
PB97-118772 Not available NTIS
National Inst. of Standards and Technology (MSEL), Gaithersburg, MD. Polymers Div.
Shear-Induced Changes in the Order-Disorder Transition Temperature and the Morphology of a Triblock Copolymer.
Final rept.
A. I. Nakatani, F. A. Morrison, C. L. Jackson, M. Muthukumar, C. C. Han, J. F. Douglas, and J. W. Mays. 1996, 15p.
See also PB96-123237.
Pub. in Jnl. of Macromolecular Science: Chemistry Physics Reviews in Macromolecular Chemistry and Physics, nB35 p489-503 1996.

Keywords: *Copolymers, Reprints, *Triblock copolymer, Transition temperature, Steady shear flow.

A summary of the work on a triblock copolymer under steady shear is presented. The experiments were conducted using small-angle neutron scattering (SANS), as a function of shear rate and temperature, and transmission electron microscopy (TEM) on quenched specimens. The triblock copolymer is composed of polystyrene d8/polybutadiene/polystyrene-d8, and the ordered microstructure normally consists of hexagonally packed cylinders. Two temperature-dependent, characteristic shear rates, gamma(c1) and gamma(c2), are identified from the scattering results. The first characteristic shear rate identifies the shear rate required to go from a disordered state to an ordered state, while the second characteristic shear rate is interpreted as the shear rate necessary to produce a different ordered morphology.

Composite Materials

03,131
PB94-160066 PC A13/MF A03
National Inst. of Standards and Technology (MSEL), Gaithersburg, MD. Polymers Div.
Report on the Workshop on Manufacturing Polymer Composites by Liquid Molding. Held in Gaithersburg, Maryland on September 20-22, 1993.
R. S. Parnas, A. J. Salem, K. N. Kendall, and M. V. Bruschke. Feb 94, 284p, NISTIR-5373.
Prepared in cooperation with General Electric Corporate Research and Development, Schenectady, NY. and Ford Motor Co., Dearborn, MI.

Keywords: *Meetings, *Composite materials, *Molding techniques, *Composite fabrication, Permeability, Binders(Materials), Molding materials, Design, Mathematical models, Validation, Fiber composites, Reinforcing materials, Heat transfer, Rheology, Kinetics, *Liquid composite molding, Standard reference materials.

The report documents the workshop on manufacturing composites by liquid molding, held at NIST September 20-22, 1993. The workshop was jointly sponsored by NIST, Ford, and General Electric, and attracted a diverse international group of participants from Industry, University and government. Eight invited lectures were presented, and then the workshop divided into five discussion groups to focus on particular issues. A small number of critical issues were identified, including preform deformation inside and outside of the mold, high speed processing, and the establishment of standard reference materials, data, and test methods.

03,132
PB94-172848 Not available NTIS
National Inst. of Standards and Technology (IMSE), Gaithersburg, MD.
High Temperature Degradation of Structural Composites.
Final rept.
S. M. Wiederhorn, and B. J. Hockey. 1991, 16p.
Contract DE-AI05-850R21569
Pub. in Advanced Structural Inorganic Composites, p365-380 1991. Sponsored by Department of Energy, Washington, DC.

Keywords: *Ceramic matrix composites, *Creep properties, *Thermal degradation, *Structural components, Toughness, Failure(Mechanics), Whisker composites, Cavitation, Fracture(Mechanics), Mechanical properties, Reprints.

Ceramic matrix composites are being developed to improve the toughness of ceramics in structural applications. Modest success has been experienced in manufacturing ceramic matrix composites for which it is possible to double the room temperature toughness while still retaining the high strength of the untoughened material. As many of these new composites are expected to be used at high temperatures, their mechanical behavior at both high and low temperature must be characterized. In the paper, creep and creep rupture of both particulate and whisker reinforced ceramic matrix composites are discussed. Principal findings of experimental investigations on these materials indicate: (1) resistance to creep deformation is greater in compression than in tension; (2) the creep rupture lifetime follows a Monkman-Grant behavior in which the lifetime can be expressed as a power function of the steady state creep rate; (3) the principal mechanism of failure in creep is interfacial cavitation. Cavities nucleate at interfaces and then grow into full facet cavities. Failure occurs either by the growth or the linkage of these cavities to form critical size cracks in the composite.

03,133
PB94-185279 Not available NTIS
National Inst. of Standards and Technology (MSEL), Boulder, CO. Materials Reliability Div.
Selection of Appropriate Ultrasonic System Components for NDE of Thick Polymer-Composites.
Final rept.
C. M. Fortunko, and D. W. Fitting. 1990, 8p.
Pub. in Review of Progress in Quantitative Nondestructive Evaluation, v10B 8p 1990.

Keywords: *Polymer matrix composites, *Ultrasonic flaw detection, *Test methods, Ultrasonic tests, Bandwidth, Construction materials, Transducers, Fibers, Polymers, Nondestructive tests, Pulse generators, Reprints.

In certain marine applications, thick polymer-composite materials may have to endure different operating environments than those experienced in traditional aerospace applications. In particular, structures made of such materials may experience very large compressive and bending forces. To prevent in-service failure, appropriate NDE methods and instrumentation are needed to characterize the state of the material. Specifically, in addition to detecting high-contrast anomalies (cracks and delaminations) it may be of interest to determine the pore content, measure the fiber volume, assess the severity of fiber waviness, and the like. The NDE requirements of thick marine composites cannot be met by using traditional ultrasonic instrumentation, particularly in the pulse-echo mode. For example, conventional ultrasonic instruments often lack features that permit effective pulse-echo operation below 1 MHz and have limited dynamic range. In this paper, we describe specific approaches that overcome the above limitations. Specifically, we describe a particularly effective transmit/receive circuit configuration that offers large dynamic range greater than 60 dB, wide bandwidth (100 kHz - 60 MHz), and fast recovery. We also describe the design of a very-low-noise, high-impedance input preamplifier. We found that this preamplifier is particularly useful for conditioning signals generated by very small ('phase insensitive') receiver transducers.

03,134
PB94-198645 Not available NTIS
National Inst. of Standards and Technology (MSEL), Gaithersburg, MD. Ceramics Div.
Matrix Grain Bridging Contribution to the Toughness of Whisker Reinforced Ceramics.
Final rept.
P. F. Becher, E. R. Fuller, and P. Angelini. 1991, 5p.
Pub. in Jnl. of the American Ceramic Society 74, n9 p2131-2135 1991.

Keywords: *Ceramic matrix composites, *Whisker composites, *Fracture strength, Composite materials, Reinforcing fibers, Silicon carbides, Aluminum oxide, Matrix materials, Grain size, Mechanical properties, Reprints.

The fracture toughness of whisker reinforced noncubic ceramic matrices increases with increase in matrix grain size, d, as well as increased whisker content. An analytical description for a grain bridging toughening contribution is derived which is combined with the whisker bridging contribution to describe the toughness of such composites. Results for SiC whisker reinforced alumina composites confirm the predicted d 1/2 dependence of the fracture toughness.

03,135
PB94-199361 Not available NTIS
National Inst. of Standards and Technology (MSEL), Gaithersburg, MD. Ceramics Div.
Interface Properties for Ceramic Composites from a Single Fiber Pull-Out Test.
Final rept.
E. P. Butler, E. R. Fuller, and H. M. Chan. 1990, 8p.
Pub. in Materials Research Society Symposia Proceedings, v170 p17-24 1990.

Keywords: *Ceramic matrix composites, *Interfaces, *Surface properties, *Fiber composites, Silicon carbides, Borosilicates, Friction measurement, Shear strength, Fracture properties, Thermal expansion, Reprints, *Pull-Out test.

An experimental approach has been developed using a single fiber pull-out test to measure the intrinsic materials properties of a ceramic composite interface. These properties are determined from the force-displacement curve, which is directly related to reinforcement toughening of composites via a fiber-debonding and frictional pull-out process. These interface properties were evaluated for a model composite system

of continuous SiC fibers with various surface treatments in a borosilicate glass matrix. For the processing conditions used the interface fracture toughness and the interface frictional shear resistance, were found to be 1.0 + or - 0.5 J/sq m and 3.3 + or - 0.6 MPa, respectivley, for as-received fibers. Experiments conducted with long embedded fiber lengths to be deconvolved into an interface friction coefficient of acid washed fibers has an increased interface toughness, 3.6 + or - 0.1 J/sq m, and friction coefficient, 0.08 + or - 0.02, but approximately the same initial clamping matrix thermal expansion mismatch and from measurements of the stress birefringence of glass were in general agreement with this value.

03,136
PB94-199536 Not available NTIS
National Inst. of Standards and Technology (MSEL), Gaithersburg, MD. Ceramics Div.
Micro-Mechanical Aspects of Asperity-Controlled Friction in Fiber-Toughened Ceramic Composites.
Final rept.
W. C. Carter, E. P. Butler, and E. R. Fuller. 1991, 6p.
Pub. in Scripta Metallurgica et Materialia 25, n3 p579-584 1991. Sponsored by Department of Energy, Washington, DC.

Keywords: *Ceramic matrix composites, *Reinforcing fibers, *Mechanical properties, *Friction, Cracking(Fracturing), Ceramic bonding, Interfaces, Matrix materials, Fiber composites, Ceramic fibers, Reprints.

Evidence for the presence of asperities at the sliding interface of a ceramic-fiber composite is presented. The origins of different types of asperities are discussed. A micro-mechanical model for the role of the interfacial asperities is developed and related to measured quantities. Asperities play a direct role in the behavior of the debonded tip, but only indirectly enhance the dominate fracture mechanism which is strain-energy-release by friction along the mode II crack flank.

03,137
PB94-200235 Not available NTIS
National Inst. of Standards and Technology (MSEL), Gaithersburg, MD. Ceramics Div.
Generic Model for Creep Rupture Lifetime Estimation on Fibrous Ceramic Composites.
Final rept.
T. J. Chuang. 1992, 17p.
Contract NASA-C-82000-R
Pub. in Fracture Mechanics of Ceramics, v10 p441-457 1992. Sponsored by National Aeronautics and Space Administration, Cleveland, OH. Lewis Research Center.

Keywords: *Ceramic matrix composites, *Fiber composites, *Fracture mechanics, *Creep rapture strength, *Fatigue life, Crack initiation, Life(Durability), Ceramic fibers, Creep properties, Mechanical properties, Toughness, Reprints.

Because of their high strength and toughness at elevated temperatures, fiber reinforced ceramic composites have become potential candidates for the next generation of turbine engine materials for aerospace applications. A generic model is proposed for assessing lifetime of this class of materials when subjected to long-term creep rupture conditions. This two dimensional model consists of interfacial cracks growing beween square grains and rectangular fibers in the direction normal to the principal tensile stress axis. Neglecting transient effects, the total lifetime is derived based on the criterion that rupture is due to coalescence of adjacent cracks. It is found that lifetime is inversely proportional to crack growth rate, volume fraction, and aspect ratio of the fibers; but extremely sensitive to the applied stress owing to the high power of the V-K(sub I) law. This lifetime estimation seems to be in fair agreement with the creep rupture data of SiCw/Si3N4 composite with 0 and 30 vo1% reinforcement tested at 1250 C in air. Furthermore, TEM performed on the post crept specimens revealed that creep damage is predominantly in the form of microcracks at matrix/matrix as well as fiber/matrix interfaces, approximately in accord with the model simulation.

03,138
PB94-200243 Not available NTIS
National Inst. of Standards and Technology (MSEL), Gaithersburg, MD. Ceramics Div.
Asymmetric Tip Morphology of Creep Microcracks Growing Along Bimaterial Interfaces.
Final rept.
T. J. Chuang, J. L. Chu, and S. Lee. 1992, 9p.
Pub. in Acta Metall. Mater. 40, n10 p2683-2691 1992.

Keywords: *Microcracking, *Interfaces, *Crack propagation, *Composite materials, Elastic properties, Deformation, Diffusivity, Laminates, Morphology, Dihedral angle, Reprints, *Bimaterials.

The asymmetric tip morphology of a creep microcrack propagating along a bimaterial interface is presented based on the assumptions that the near-tip shapes are developed from surface diffusion controlled crack growth and that a steady state prevails. Following Chuang and Rice, a single master curve still can adequately describe the near-tip shapes to within 6% accuracy, but four cases of crack-tip morophology emerge depending on the ratio of surface to interfacial free energy and diffusivity of the adjoining phases. For fixed ratios of the two surface diffusivities, crack tip morphology maps in the space of specific surface energies are constructed with which areas associated with each individual case are indicated. Predicted cases on a set of bimaterial systems are tabulated and discussed. TEM photos of creep crack tips in alumina and silicon nitride are presented for illustration. The information given here is essential to a coupled analysis diffusion and elastic deformation at a composite interface which may ultimately yield predictions of the delamination rate between the reinforcing phase and the matrix phase as a function of applied stress, temperature and other relevant materials' constants.

03,139
PB94-200532 Not available NTIS
National Inst. of Standards and Technology (MSEL), Gaithersburg, MD. Ceramics Div.
Assessment of Testing Methodology for Ceramic Matrix Composites.
Final rept.
D. C. Cranmer. 1991, 8p.
Pub. in Ceram. Trans. Adv. Compos. Mater., v19 p1003-1010 1991.

Keywords: *Ceramic matrix composites, *Materials testing, *Mechanical properties, Assessments, Sample preparation, Interlaboratory comparisons, Strength, Creep tests, Fatigue tests, Whisker composites, Ceramics, Reprints.

An assessment of strength, creep, and fatigue measurement techniques for ceramic matrix composites is made. Many of the techniques available for composites testing are reviewed. Tensile tests, not flexure, should be used for experimental measurements, and different tests are needed for material development and system design. Careful attention must be paid to specimen preparation. Tests used for monolithic ceramics can be used for whisker-reinforced materials. Interlaboratory comparisons are also needed to determine the reproducibility and limitations of the methodology as well as material behavior.

03,140
PB94-200649 Not available NTIS
National Inst. of Standards and Technology (MSEL), Boulder, CO. Materials Reliability Div.
Elastic Properties of Uniaxial-Fiber Reinforced Composites: General Features.
Final rept.
S. Datta, H. Ledbetter, and M. Lei. 1991, 6p.
Pub. in Nondestructive Evaluation and Material Properties of Advanced Materials, p23-28 1991.

Keywords: *Fiber composites, *Elastic properties, *Reinforcing fibers, Modulus of elasticity, Poisson ratio, Matrix materials, Fiber volume fraction, Reinforcing materials, Mechanical properties, Reprints, Scattered-plane-wave model, Ensemble-average model, Elastic constants.

The authors consider the complete set of elastic constants of composites comprising isotropic uniaxial fibers in an isotropic matrix. Such materials exhibit transverse-isotropic symmetry and five independent elastic constants, and the authors calculate and display all these constants over the entire fiber-volume-fraction range, 0.0-1.0. They also consider some practical elastic constants such as the principal Young moduli and the principal Poisson ratios. Except for one principal Poisson ratio, all other elastic constants show negative departures from a linear rule-of-mixture. Because one often uses sound velocities to study such materials, the authors give results for the four principal sound velocities.

03,141
PB94-211778 Not available NTIS
National Inst. of Standards and Technology (MSEL), Gaithersburg, MD. Ceramics Div.
Effect of Microstructure on the Wear Transition of Zirconia-Toughened Alumina.
Final rept.
C. He, Y. S. Wang, J. S. Wallace, and S. M. Hsu. 1993, 8p.
Pub. in Wear 162-164, p314-321 1993.

Keywords: *Ceramic matrix composites, *Microstructure, *Wear tests, *Aluminum oxide, *Zirconium oxides, Mechanical properties, Lubrication, Particle size distribution, Environmental effects, Fractures(Materials), Reprints.

The mechanical properties of alumina ceramics can be improved by the addition of pure or partially stabilized zirconia particles. In the present study, the wear characteristics of zirconia-toughened alumina (ZTA) composites under a non-reactive fluid (paraffin oil) lubricated condition were investigated. The wear transition load (i.e. the load at which a rapid increase in wear occurs) increased with increasing zirconia content up to 20 vol.%. The transition from mild to fracture-controlled wear of ZTA depends on the material properties (e.g. hardness, elastic modules), the contact conditions (e.g. hertzian stress, coefficients of friction) and the microstructure of the material. The effect of the microstructure on wear was demonstrated and a Hall-Petch-type relationship between the microfracture stresses and the grain size was found. The effect of the grain size distribution on the wear transition load was also shown.

03,142
PB94-211984 Not available NTIS
National Inst. of Standards and Technology (MSEL), Gaithersburg, MD. Ceramics Div.
Tensile Creep of Whisker Reinforced Silicon Nitride.
Final rept.
B. J. Hockey, S. M. Wiederhorn, W. Liu, J. G. Baldoni, and S. T. Buljan. 1991, 9p.
Pub. in Jnl. of Materials Science 26, n14 p3931-3939, 15 Jul 91.

Keywords: *Whisker composites, *Silicon nitrides, *Tensile creep, Tensile properties, Reinforcing fibers, Ceramics, Creep properties, Mechanical properties, Tensile deformation, Cavitation, Reprints.

In this paper we discuss the creep and creep rupture behavior of a grade of hot pressed silicon nitride reinforced with 30v/o SiC whiskers. The material was tested in both tension and compression at temperatures ranging from 1100 C to 1250 C for periods as long as 1000 hr. Principal findings were: (1) transient creep due to devitrification of the intergranular phase dominates high temperature creep behavior; (2) at high temperatures and stresses, cavitation at the whisker/silicon nitride interface enhances the creep rate and reduces the lifetime of the silicon nitride composite; (3) resistance to creep deformation is greater in compression than in tension; (4) the time to rupture is a power function of the creep rate, so that the temperature and stress dependence of the failure time is determined solely by the temperature and stress dependence of the creep rate.

03,143
PB94-212453 Not available NTIS
National Inst. of Standards and Technology (MSEL), Gaithersburg, MD. Metallurgy Div.
Status of Electrocomposites.
Final rept.
C. E. Johnson, and M. Browning. 1990, 24p.
Pub. in Proceedings of the American Electroplaters and Surface Finishers Annual Technical Conference, Boston, MA., July 9-12, 1990, p1203-1226.

Keywords: *Electrochemistry, *Metal matrix composites, *Intermetallics, Coatings, Electrodeposition, Electroforming, Matrix materials, Hot pressing, Mechanical properties, Reprints.

This presentation is intended to discuss the current state of the art in the use of electrochemical techniques for the fabrication of metal and intermetallic matrix composites. Electroforming techniques are being evaluated for fabrication of near net-shape composite structures, for example, reusable rocket thrust chambers. Copper and nickel coated fibers are presently being used in polymer matrix composites for the pur-

pose of EMI shielding. If sufficiently thick, the coated fibers can be consolidated into metal matrix composites by hot pressing without the need for infusion of additional metal. Electrocoatings are also used as diffusion barriers to protect carbon fibers from degradation at high temperatures due to carbide formation and dissolution of carbon into the matrix alloy. Another use of electroplating is to provide improved fiber/matric interfacial adhesion. Multilayer fiber coatings (e.g. Fe/Cu/Al) can provide gradual transitions in the coefficient of thermal expansion and/or Young's modulus. These techniques can greatly improve the mechanical and thermal properties of the composites. Metal matrix composites which combine high stiffness and strength with low specific gravity are of particular interest in applications such as transportation (e.g. air and space craft, automobiles) and high speed machinery (e.g. textile machinery, drive shafts).

03,144
PB94-213204 Not available NTIS
National Inst. of Standards and Technology (MSEL), Boulder, CO. Materials Reliability Div.
Thermal Expansion of an SiC Particle-Reinforced Aluminum Composite.
Final rept.
H. Ledbetter, and M. Austin. 1991, 9p.
Pub. in International Jnl. of Thermophysics 12, n4 p731-739 Jul 91.

Keywords: *Metal matrix composites, *Aluminum graphite composites, *Thermal expansion, Extensometers, Silicon carbides, Elastic properties, Microstructure, Single crystals, Thermophysical properties, Neutron diffraction, Reprints.

Using a push-rod dilatometer, we measured between 76 and 390 K the thermal expansion of a particle-reinforced-composite wrought plate obtained by powder-metallurgy methods. The particles, 30% by volume, consisted of monocrystals of alpha-SiC with sizes near 10 micrometers. The matrix consisted of a 6061 aluminum alloy with original particle sizes near 20 micrometers. We found the perpendicular thermal expansivity, alpha 3, higher by 26% than the in-plane thermal expansivity, alpha 1 approximately equal to alpha 2. These values differ from a rule-of-mixture prediction by -3 and -23%, respectively. All three alpha components lie outside the Rosen-Hashin bounds. Levin's isotropic model agrees within 10% with the alpha 1-alpha 2-alpha 3 average. Both the anisotropy and the bounds violation result from microstructural nonhomogeneity arising from processing. Rosen and Hashin's transverse-isotropic-symmetry relationships account approximately for these effects by introducing the anisotropic elastic constants. Using neutron diffraction, we determined that the SiC particles are textureless.

03,145
PB94-216728 Not available NTIS
National Inst. of Standards and Technology (MSEL), Gaithersburg, MD. Polymers Div.
Review of Cure Monitoring Techniques for On-Line Process Control.
Final rept.
W. G. McDonough, B. M. Fanconi, F. I. Mopsik, and D. L. Hunston. 1990, 8p.
Pub. in Proceedings of Annual ASM/ESD Advanced Composites Conference (6th), Materials Park, OH., October 8-11, 1990, p637-644.

Keywords: *Process control(Industry), *Polymer matrix composites, *Curing, *Monitoring, *Nondestructive tests, Spectroscopy, Quality control, Real time operations, Inspection, Fluorescence, Ultrasonics, Reprints.

A driving force for implementation of on-line process control is the need to improve the efficiency and reliability of polymer composite processing. A critical element in process control is on-line process monitoring. This paper reviews and compares the most important techniques currently under development, i.e. dielectric, ultrasonic, optical and spectroscopic monitoring methods. A number of technical and scientific issues that must be addressed for these techniques to reach their full potential are identified. The chief technical barrier is to adapt the methods to operate in the harsh environment of a factory with industrial grade resin systems. The major scientific barrier is a need to improve our ability both to interpret the information provided by the sensor and translate this data into process control information. Although these issues are challenging, many programs are currently underway to address them so the future for on-line process control of composites looks very bright.

03,146
PB94-219243 (Order as PB94-219219, PC A06/MF A02)
National Inst. of Standards and Technology, Gaithersburg, MD.
Physics Required for Prediction of Long Term Performance of Polymers and Their Composites.
G. B. McKenna. 1994, 21p.
Included in Jnl. of Research of the National Institute of Standards and Technology, v99 n2 p169-189 Mar/Apr 94.

Keywords: *Polymers, *Glass transition temperature, *Composite materials, *Viscoelasticity, Stress relaxation, Mechanical properties, Mathematical models, Predictions, Performance tests, Temperature, Volume, Constitutive equations, Material clocks, Nonlinearity, National Institute of Standards and Technology.

The long term performance of polymers and their composites is an important aspect of their increasing use in engineering applications. Temporal, thermal, and mechanical stresses can all contribute to the deterioration of performance. Here we examine the concepts of the physics of glassy polymers and how they are important in developing constitutive equations that describe their volume/temperature/stress time response. The understanding of such response forms the basis of the prediction of long term performance.

03,147
PB94-780129 AV E99
Minnesota Technology, Inc., Minneapolis, MN.
Polymer Composites Workshop. Held in Winona, Minnesota on April 29-30, 1992 (Video).
Audio-Visual.
J. Wright. 4 Jun 92, 5 VHS videos.
See also PB92-182658. Sponsored by National Inst. of Standards and Technology (TS), Gaithersburg, MD. This video package contains 5 VHS videos with a total viewing time of approximately 8 hrs, 45 minutes.

Keywords: *Polymer matrix composites, *Composite materials, *Meetings, Technology innovation, Filament winding, Financing, Small businesses, Contact molding, Manufacturers, Maintenance, Compression molding, Injection molding, Pultrusion process, Video tapes, Minnesota Technology, National Institute of Standards and Technology.

The set of five video tapes covers the Polymer Composites Workshop held in Winona, Minnesota on April 29-30, 1992. Presentations include: Minnesota Technology, Inc.; The NIST Perspective; The Regional Perspective; Filament Winding; Regional and National Funding Sources for Small Businesses; Contact Molding; Opportunities for Interaction Between Primary Manufacturing Companies and Small Business; Composite Repair; Compression Molding/Class A Resin Transfer; Injection Molding; Reaction Injection Molding; Structural Resin Transfer Molding; Pultrusion.

03,148
PB95-125696 Not available NTIS
National Inst. of Standards and Technology (IMSE), Boulder, CO. Fracture and Deformation Div.
Appropriate Ultrasonic System Components for NDE of Thick Polymer Composites.
Final rept.
C. M. Fortunko, and D. W. Fitting. 1991, 8p.
Pub. in Review of Progress in Quantitative Nondestructive Evaluation, v10B p2105-2112 1991.

Keywords: *Ultrasonic tests, *Polymer matrix composites, *Ultrasonic flow detection, Acoustic measurement, Nondestructive tests, Signal processing, Preamplifiers, Ultrasonic wave transducers, Fiber volume fraction, Cracks, Fiber composites, Delaminating, Reprints.

In certain marine applications, thick polymer-composite materials may have to endure different operating environments than those experienced in traditional aerospace applications. In particular, structures made of such materials may experience very large compressive and bending forces. To prevent in-service failure, appropriate NDE methods and instrumentation are needed to characterize the state of the material. Specifically, in addition to detecting high-contrast anomalies (cracks and delamination), it may be of interest to determine the pore content, measure the fiber volume, assess the severity of fiber waviness, and the like. In this paper we describe specific approaches that overcome the limitations of conventional ultrasonic instrumentation. Specifically, we describe a particularly effective transmit/receive circuit configuration that offers large dynamic range (greater than 60 dB), wide bandwidth (100 kHz - 60 MHz), and fast recovery. We also describe the design of a very-low-noise, high impedance input preamplifier. We found that this preamplifier is particularly useful for conditioning signals generated by very small ('phase insensitive') receiver transducers.

03,149
PB95-125811 Not available NTIS
National Inst. of Standards and Technology (MSEL), Gaithersburg, MD. Ceramics Div.
Determination of Fiber-Matrix Interfacial Properties of Importance to Ceramic Composite Toughening.
Final rept.
E. R. Fuller, E. P. Butler, and W. C. Carter. 1991, 19p.
Sponsored by Department of Energy, Washington, DC.
Pub. in Toughening Mechanisms in Quasi-Brittle Materials, p385-403 1991.

Keywords: *Ceramic composites, *Fiber composites, Mechanical properties, Interfaces, Silicon carbides, Borosilicate glass, Toughness, Shear strength, Reprints, *Debonding, *Single fiber pull-out test.

The fiber-matrix interface is investigated for its role during fiber debonding and pull-out and its effect on the toughening of ceramic composites. Possible interface debonding criteria (critical interface shear strength; interface toughness, or critical energy-release rate, and asperity interlock) are considered. The interfacial and mechanical properties of a model SiC-fiber, borosilicate-glass-matrix composite system are measured by a single fiber pull-out test. Initial stresses are determined by photoelastic methods.

03,150
PB95-140828 Not available NTIS
National Inst. of Standards and Technology (MSEL), Gaithersburg, MD. Metallurgy Div.
Surface Energy Reduction in Fibrous Monotectic Structures.
Final rept.
A. C. Sandlin, and R. J. Schaefer. 1991, 6p.
Pub. in Metallurgical Transactions A 22, n8 p1881-1886 1991.

Keywords: *Surface energy, *Directional solidification(Crystals), *Monotectic alloys, *Metal matrix composites, Grain boundaries, Morphology, Lead alloys, Aluminum alloys, Copper alloys, Microstructure, Metal fibers, Reprints.

A study has been made of the morphology of directionally solidified Cu-Al-Pb monotectic alloys. The structure consisted of a hexagonal array of Pb rods in a Cu-based matrix. In addition, highly-curved grain boundaries in the Cu-based matrix with lens-shaped Pb fibers on the boundary and a 'denuded zone', depleted of Pb rods, were observed. Existence of these boundaries is shown to reduce the overall surface energy of the system leading to the formation of the highly-curved grain boundaries.

03,151
PB95-140935 Not available NTIS
National Inst. of Standards and Technology (BFRL), Gaithersburg, MD. Fire Safety Engineering Div.
One- and Two-Sided Burning of Thermally Thin Materials.
Final rept.
T. Ohlemiller, and J. Shields. 1993, 8p.
Contract NLRC-C-32003-R
Sponsored by National Aeronautics and Space Administration, Cleveland, OH. Lewis Research Center.
Pub. in Fire and Materials 17, p103-110 1993.

Keywords: *Burning rate, *Composite materials, *Fire tests, *Flammability, Flame propagation, Temperature dependence, Heat flux, Fire safety, Combustion, Reprints.

The rate of heat release from a thermally thin material burning on both sides will be more than twice the value seen when only one side is burning. Two simplified models demonstrate that this is a consequence of the Arrhenius temperature dependence of the gasification rate of the solid. Experiments carried out on three composite materials over a range of incident heat fluxes confirm this effect. It is inferred that a further consequence of this heat release enhancement is an increased tendency for concurrent flame spread in the two-sided burning case. Materials whose application could lead to two-sided burning should thus be as-

sessed in this mode to obtain a true picture of their flammability potential.

03,152
PB95-143293 PC A03/MF A01
National Inst. of Standards and Technology (BFRL), Gaithersburg, MD. Fire Science Div.
Investigation into the Flammability Properties of Honeycomb Composites.
Special pub.
M. R. Nyden, and J. E. Brown. Oct 94, 23p, NISTIR-5509.

Keywords: *Polymers, *Composite materials, *Aircraft construction materials, *Flammability, *Aircraft fires, Fire resistant materials, Ignition, Burning rate, Honeycomb structures, Formaldehyde, Sandwich structures, Absorption spectra, Combustion, *Honeycomb composites.

The study, which is the subject of this report, was carried out in two stages. The objective of the first phase was to investigate the effect of electron beam irradiation and grafting on polymer flammability. The time to ignition and the rate-of-heat-release were measured for the combustion of a series of samples in which a fire resistant polymer was used to protect the surface of a more flammable polymer. The flammability properties of honeycomb composite materials, which are currently used in the interior cabin compartments of commercial aircraft, were examined in the second phase of this project. Analyses of the gases evolved during the thermal degradation of the components indicated that the phenol-formaldehyde resin makes a significant contribution to the flammability of these composites. The possibility that a more fire resistant formulation could be developed was examined by testing a series of resins which differed in the relative amounts of phenol and formaldehyde used in the reaction mixtures. The flammabilities of resins synthesized in excess phenol were measurably less than those synthesized in excess formaldehyde.

03,153
PB95-151528 Not available NTIS
National Inst. of Standards and Technology (MSEL), Gaithersburg, MD. Ceramics Div.
Measuring Matching Wear Scars on Balls and Flats.
Final rept.
E. P. Whitenton, and D. E. Deckman. 1989, 18p.
Pub. in Surface Topography 2, p205-222 1989.

Keywords: *Wear tests, *Aluminum oxides, *Profilometers, Profiles, Topography, Lubrication, Surface properties, Reprints, *Wear scars, Ball-on-three flat wear tests, Four-ball wear tests.

Four-ball and ball-on-three-flat wear tests are often performed to assess the tribological performance of lubricants and materials. Test results are described by the worn volume and or topography parameters of the balls or flats. As a general rule, relatively little effort goes into quantifying the wear scar of the top ball even though there is often useful information there. A computer-controlled profiling machine is described to measure the topography of the top ball and the bottom balls or flats. Several techniques are examined to turn this topographic information into useful parameters and aids for assessing the interaction between the balls or flats.

03,154
PB95-152294 Not available NTIS
National Inst. of Standards and Technology (MSEL), Gaithersburg, MD.
Creep Rupture of MoSi2/SiCp Composites.
Final rept.
J. D. French, S. M. Wiederhorn, and J. J. Petrovic. 1994, 6p.
Pub. in Materials Research Society Symposia Proceedings, v322 p203-208 1994.

Keywords: *Creep rupture strength, *Ceramic matrix composites, *Silicon carbides, Composite materials, Creep properties, Creep tests, Ductility, Molybdenum compounds, Reprints, *Molybdenum disilicide.

We studied the creep rupture of a series of MoSi2 materials reinforced with SiC particles. Particulate contents were in the range of O to 40 volume percent. Temperature and stress ranges were 1050 C to 1200 C and 10 MPa to 50 MPa, which gave failures ranging from 1 hour to 1500 hours. The creep curves show an extensive tertiary regime, accounting for 25-95% of the total lifetime. Tertiary creep increases with increasing stress and temperature. Cavitation occurs throughout the creep life, and tertiary creep is associated with the linkage of cavities into large cracks. The creep life improves with increasing SiC particle content, with a concurrent loss of creep ductility. Significant improvement occurs only when the particle content is greater than 30 volume percent. Our studies suggest that the creep and creep rupture behavior of MOSi2 can be further improved by increasing the content of SiC particles.

03,155
PB95-152880 Not available NTIS
National Inst. of Standards and Technology (MSEL), Boulder, CO. Materials Reliability Div.
Residual Stresses in Aluminum-Mullite (alpha-Alumina) Composites.
Final rept.
D. Balzar, and H. Ledbetter. 1993, 9p.
Pub. in Advances in X-ray Analysis, p489-497 1993.

Keywords: *X-ray diffraction, *Metal matrix composites, *Residual stress, *Aluminum alloys, *Particulate reinforced composites, *Aluminum oxides, Strains, Matrix materials, Reinforcing materials, Anisotropy, Tensile properties, Reprints, Rietveld refinement.

We studied particle-reinforced 6061-aluminum-alloy composites with particle volume fractions ranging from 0 to 0.25. The mullite particles are approximately sphericai and contain embedded alpha-alumina phase. We obtained lattice parameters of all three phases in the composites and starting materials by using Rietveld refinement of x-ray diffraction patterns. In all three phases stresses are tensile and approximately of the same magnitude, contradicting a requirement for mechanical equilibrium. Stresses increase with both increasing particle size and volume fraction. Measurements of extracted-from-composites particles showed no evidence of a possible chemical reaction at the matrix-particle interface. The matrix is (111) and (100) textured, but measurements of elastic constants reveal only small anisotropy. Thus, explanation of the mechanical-equilibrium violation remains uncertain.

03,156
PB95-161295 Not available NTIS
National Inst. of Standards and Technology (MSEL), Gaithersburg, MD. Ceramics Div.
Flat and Rising R-Curves for Elliptical Surface Cracks from Indentation and Superposed Flexure.
Final rept.
R. F. Krause. 1994, 7p.
Pub. in Jnl. of the American Ceramic Society 77, n1 p172-178 1994.

Keywords: *Whisker composites, *Aluminum oxides, *Silicon carbides, *Surface cracks, *Flexing, *Indentation, Fracture strength, Deformation, Stress intensity factors, Surface properties, Loads(Forces), Cracking(Fracturing), Defects, Reprints, *R-curves, *Superposed flexure.

Flat and rising R-curves, fracture resistance versus crack extension, were determined for a sintered 99% alpha-silicon carbide and for a hot-pressed composite of 25 wt% silicon carbide whiskers and alumina, respectively. The R-curves were evaluated from a combination of measured crack lengths, which were produced over a range of Vickers indentation loading, and of measured strengths, which were correlated either with the indentation flaws or with the most severe natural flaws or flexure specimens. A published analysis of the stress-intensity factor for a surface crack in flexure was interpreted to show that the crack front takes the form of a semiellipse where both the ratio of the minor to major radii and the configuration coefficient itself decrease with increasing crack extension. A power-law function of the indentation load was fitted to the product of an effective configuration coefficient and the flexural strength to evaluate the R-curves. When the configuration coefficient is assumed constant, a customary practice, the R-curves appear to have steeper rises. The assumed constancy of the coefficient of the indentation driving force may also have an effect on R-curves, but the effect would be much less.

03,157
PB95-161378 Not available NTIS
National Inst. of Standards and Technology (MSEL), Boulder, CO. Materials Reliability Div.
Elastic Properties of Al2O3/Al Composites: Measurements and Modeling.
Final rept.
H. Ledbetter, and S. Datta. 1991, 6p.
Pub. in Damage and Oxidation Protection in High Temperature Composites AD, v25-2 p83-88 1991.

Keywords: *Metal matrix composites, *Elastic properties, *Particulate reinforced composites, Reinforcing materials, Composite materials, Aluminum oxides, Aluminum, Modulus of elasticity, Shear properties, Poisson ratio, Acoustic velocity, Reprints.

We considered seven Al2O3-particle-reinforced Al-matrix composites with particle volume fractions ranging from 0 to 0.24. At ambient temperature, we measured the elastic constants by two dynamic methods: kHz resonance and MHz pulse-echo-superposition. We report the usual elastic-constant set: bulk, shear, Young moduli, and Poisson ratio. The microstructures show a random distribution of spherical particles, from specimen to specimen ranging from 30 to 100 micrometers. The highest observed Young-modulus anisotropy was 1.04. To model this system, we used the long-wavelength limit of a plane-wave ensemble-average method. Measurements and modeling agree well: the average disagreement in the Young modulus is about one percent. As expected, except for the Poisson ratio, all measurements fall below a linear rule-of-mixture.

03,158
PB95-161824 Not available NTIS
National Inst. of Standards and Technology (MSEL), Gaithersburg, MD. Polymers Div.
Thermoacoustic Technique for Determining the Interface and/or Interply Strength in Polymeric Composites.
Final rept.
W. L. Wu. 1990, 5p.
Pub. in Society for the Advancement of Material and Process Engineers Jnl. 26, n2 p11-15 1990.

Keywords: *Polymer matrix composites, *Graphite composites, *Thermal analysis, *Acoustic emission, Fiber composites, Laser heating, Interfacial energy, Debonding(Materials), Mechanical properties, Reprints.

Local heating was applied on polymeric composites reinforced with graphite fibers to induce interfacial debonding events and the acoustic emissions associated with the debonding events were monitored. Correlations among some of the acoustic parameters and the interfacial strength were observed. The possibility of adopting this scheme to determine interfacial strength in composites is delineated.

03,159
PB95-162012 Not available NTIS
National Inst. of Standards and Technology (MSEL), Gaithersburg, MD. Polymers Div.
Interaction between Micro and Macroscopic Flow in RTM Preforms.
Final rept.
R. S. Parnas, A. J. Salem, T. A. K. Sadiq, H. P. Wang, and S. G. Advani. 1994, 15p.
Pub. in Composite Structures 27, p93-107 1994.

Keywords: *Porous materials, *Composite materials, *Resin transfer molding, *Flow distribution, *Preforms, Resin matrix composites, Fiber composites, Microparticles, Macromolecules, Permeability, Reprints.

Both experimental and modeling results are presented to convey the wide span of length scales over which flow in porous media can occur in a single material. Flow in such heterogeneous porous media are shown to be important in composites processing because the structure of fibrous reinforcements contains multiple length scales. Flow phenomena that arise due to material heterogeneity have been shown to include void formation and to explain the differences observed between measurements of the 'wet' permeability and the 'dry' permeability. The work presented indicates that the heterogeneous reinforcement structure may also contribute to the differences observed in permeability measurements carried out by the radial flow and the one-dimensional flow methods. The concept of heterogeneous porous media is also extended to the molecular level by considering the flow problem in a reinforcement sized with grafted macromolecules.

03,160
PB95-162194 Not available NTIS
National Inst. of Standards and Technology (MSEL), Gaithersburg, MD. Ceramics Div.
Fracture Toughness of Advanced Ceramics at Room Temperature: A Vamas Round-Robin.
Final rept.
G. Quinn. 1993, 9p.
Sponsored by Department of Energy, Washington, DC. Office of Transportation Systems Utilization.

Pub. in Ceramic Engineering and Science Proceedings 14, n7-8 p92-100 1993.

Keywords: *Ceramic matrix composites, *Fracture strength, Mechanical properties, Ceramic materials, Test methods, Standards, Silicon nitrides, Toughness, Fracture mechanics, Reprints.

The VAMAS project is an international collaboration for prestandardization research. The participating countries are Canada, France, Germany, Italy, Japan, the United Kingdom, the United States, and the Commission of European Communities. Technical Working Area No. 3, Ceramics, has the objective of undertaking research on the reliability and reproducibility of test procedures for advanced technical ceramics. The Japan Fine Ceramics Center (JFCC) in 1988 organized a VAMAS round-robin to evaluate fracture toughness by three methods on two advanced ceramics. The three methods are schematically illustrated. Preliminary results from thirteen of the participating twenty-two laboratories have been previously reported. A comprehensive, more recent report with the results of the five United States laboratories has been prepared. The five USA laboratories were: NIST, NASA-Lewis, Worcester Polytechnic Institute, Allied-Signal, Norton-St. Gobain. The present paper highlights the principal results of the project.

03,161
PB95-162533 Not available NTIS
National Inst. of Standards and Technology (MSEL), Gaithersburg, MD. Ceramics Div.
Fabrication of Flaw-Tolerant Aluminum-Titanate-Reinforced Alumina.
Final rept.
J. L. Runyan, and S. J. Bennison. 1991, 7p.
Pub. in Jnl. of the European Ceramic Society 7, n2 p93-99 1991.

Keywords: *Particulate reinforced composites, *Aluminum oxide, *Fabrication, *Defects, *Ceramic composites, Composite materials, Ceramics, Crack propagation, Crack arrest, Grain structure, Microstructure, Reprints, *Aluminum titanates.

Fabrication and flaw tolerance properties of particulate aluminum-titanate-reinforced alumina composites have been studied. High-density (-99% theoretical) composites with controlled microstructures are readily produced via a conventional ceramics processing scheme utilizing starting powders of alpha-alumina and beta-aluminum titanate. Indentation-strength measurements demonstrate certain composites exhibit unusually pronounced flaw tolerance behavior. Direct observations of crack evolution from Vickers indentations during loading reveal strong stabilization of cracks with sizes in the millimeter range. It is concluded that this stabilization gives rise to the flaw tolerance properties and results from pronounced crack-resistance (R-curve) behavior. Grain-localized crack bridging is strongly active in this system and is believed to be a major contributor to the R-curve properties.

03,162
PB95-163325 Not available NTIS
National Inst. of Standards and Technology (IMSE), Boulder, CO. Fracture and Deformation Div.
Elastic Green's Function for a Bimaterial Composite Solid Containing a Free Surface Normal to the Interface.
Final rept.
V. K. Tewary. 1991, 17p.
Pub. in Jnl. of Materials Research 6, n12 p2592-2608 1991.

Keywords: *Composite materials, *Greens function, Fracture(Mechanics), Stress analysis, Series(Mathematics), Numerical solution, Singularity, Anisotropy, Integrals, Cracks, Reprints, Hilbert problems, Free surfaces.

Elastic plane strain Green's function is calculated for an anisotropic bimaterial composite solid containing a free surface normal to the interface. An exact integral representation is obtained for the Green's function which is evaluated numerically. The integral is also evaluated analytically which gives a series representation for the Green's function. The singularities in the stress field associated with the presence of the free surface are identified and discussed. For the purpose of illustration, the formalism is applied to a cubic solid containing a Sigma-5 grain boundary.

03,163
PB95-163333 Not available NTIS
National Inst. of Standards and Technology (IMSE), Boulder, CO. Fracture and Deformation Div.
Green's Function for Generalized Hilbert Problem for Cracks and Free Surfaces in Composite Materials.
Final rept.
V. K. Tewary. 1991, 7p.
Pub. in Jnl. of Materials Research 6, n12 p2585-2591 1991.

Keywords: *Composite materials, *Greens function, Vectors(Mathematics), Fracture mechanics, Stress analysis, Eigenfunctions, Cracks, Reprints, *Hilbert problems, Free surfaces.

Green's function for a generalized vector Hilbert problem is calculated which can be used to solve the Hilbert problem with any integrable inhomogeneity. The Green's function is obtained by using a complex transform defined by eigenfunctions of the homogeneous Hilbert problem. This method should be particularly convenient for the stress analysis of anisotropic composite materials containing cracks and free surfaces.

03,164
PB95-163341 Not available NTIS
National Inst. of Standards and Technology (IMSE), Boulder, CO. Fracture and Deformation Div.
Generalized Plane Strain Analysis of a Bimaterial Composite Containing a Free Surface Normal to the Interface.
Final rept.
V. K. Tewary, and R. D. Kriz. 1991, 14p.
Pub. in Jnl. of Materials Research 6, n12 p2609-2622 1991.

Keywords: *Composite materials, *Stress analysis, *Binary systems(Materials), *Solid-solid interfaces, Fracture(Mechanics), Laminates, Grain boundaries, Strain distribution, Green's functions, Plane waves, Elastic properties, Reprints.

The elastic plane strain Green's function calculated in earlier papers is modified to account for the generalized plane strain and applied to calculate the stress and the displacement field in a bimaterial composite containing a free surface normal to the interface which is subjected to an out of plane load. The result is obtained in terms of a closed integral representation which is evaluated numerically as well as analytically. The method is applied to a cubic solid containing a Sigma-5 grain boundary and to fiber reinforced laminated composites. The singularities in the stress are identified and discussed.

03,165
PB95-163929 Not available NTIS
National Inst. of Standards and Technology (IMSE), Gaithersburg, MD.
Creep and Creep Rupture of Ceramic Matrix Composites.
Final rept.
S. M. Wiederhorn. 1992, 26p.
Pub. in Flight-Vehicle Materials, Structures, and Dynamics: Assessment and Future Directions, v3 p239-264 1992.

Keywords: *Creep rupture strength, *Ceramic matrix composites, Matrix materials, Whisker composites, Creep properties, Aluminum oxides, Asymmetry, Ceramics, Silicon carbides, Silicon nitrides, Reprints.

Ceramic matrix composites are being developed to improve the toughness of ceramics in structural applications. As many of these new materials are expected to be used at high temperatures, their mechanical behavior at both high and low temperature must be characterized. In this paper, creep and creep rupture of both particulate and whisker reinforced ceramic matrix composites are discussed. Creep in these materials tends to be asymmetric, creep occurring faster in tension than in compression. Also, extended transient creep occurs for those materials that react with the air or undergo phase transformations. The creep rupture lifetime of ceramic matrix composites may be expressed as a power function of the creep rate regardless of load or test temperature, which implies that improvement in lifetime can be achieved solely by reducing the rate of creep in these materials. Structural use of these materials seems to be limited to about 1300 C at the present time.

03,166
PB95-203220 Not available NTIS
National Inst. of Standards and Technology (MSEL), Gaithersburg, MD. Polymers Div.
Environmental Durability of Glass-Fiber Composites.
Final rept.
C. L. Schutte. 1994, 59p.
Pub. in Materials Science and Engineering R13, n7 p265-323, 15 Nov 94.

Keywords: *Environmental effects, *Fiber composites, *Polymer matrix composites, *Durability, Degradation, Polymer chemistry, Stress analysis, Moisture, Temperature, Reprints.

Durability of glass-fiber/polymer composites is dictated by the durability of the components: glass fiber, matrix, and the interface. Environmental attack by moisture, for example, can degrade the strength of the glass fiber; plasticize, swell, or microcrack the resin; and degrade the fiber/matrix interface by either chemical or mechanical attack. The relative rates of these degradation processes are a function of the chemistry of the resin, temperature, length of time of exposure, degree of stress (whether cyclic or static), chemistry and morphology of coating of coupling agent on the glass fiber, and type of glass fiber. Several examples illustrate how the chemistry and morphology of the coatings of coupling agents that are on the glass fiber influence the strength and durability of the interfacial region.

03,167
PB96-102397 Not available NTIS
National Inst. of Standards and Technology (BFRL), Gaithersburg, MD. Building Materials Div.
Geometrical Percolation Threshold of Overlapping Ellipsoids.
Final rept.
E. J. Garboczi, K. A. Snyder, J. F. Douglas, and M. R. Thorpe. 1995, 10p.
Pub. in Physical Review E, v52 n1 p819-828 Jul 95.

Keywords: *Percolation, *Composite materials, Porous materials, Ellipsoids, Shapes, Thresholds, Microstructure, Reprints.

A recurrent problem in material science is the prediction of the percolation threshold of suspensions and composites containing complex-shaped constituents. The authors consider an idealized material built up from freely overlapping objects randomly placed in a matrix, and numerically compute the geometrical percolation threshold p(sub c) where the objects first form a continuous phase. Ellipsoids of revolution, ranging from the extreme oblate limit of platelike particles to the extreme prolate limit of needlelike particles, are used to study the influence of object shape on the value of p(sub c). The reciprocal threshold 1/p(sub c)(p(sub c) equals the critical volume fraction occupied by the overlapping ellipsoids) is found to scale linearly with the ratio of the larger ellipsoid dimension to the smaller dimension in both the needle and plate limits.

03,168
PB96-103163 Not available NTIS
National Inst. of Standards and Technology (MSEL), Gaithersburg, MD. Ceramics Div.
Wear Transitions in Monolithic Alumina and Zirconia-Alumina Composites.
Final rept.
Y. S. Wang, C. He, B. J. Hockey, P. I. Lacey, and S. M. Hsu. 1994, 9p.
Pub. in Wear 181-183, p156-164 1995.

Keywords: *Aluminum oxide, *Zirconium oxides, *Composite materials, *Tribology, Wear, Microstructure, Grain size, Phase transformations, Residual stress, Ceramics, Toughness, Reprints.

The tribological properties of composite materials can be improved by its specially designed microstructure. Four zirconia-alumina composites (ZrO2-Al2O3) and a monolithic alumina were compared under paraffin oil lubricated wear test to investigate the effect of grain size, the residual stress and the phase transformation on the wear transitions. The tensile stress on the contact surface has been identified as the dominant stress which initiates the fracture wear of brittle materials. Wear transition occurs in the brittle materials when the tensile stress at the contact exceeds the critical value. The effect of zirconia content on the mean grain size of alumina and the wear transition resistance of the materials are presented.

03,169
PB96-109509 PC A17/MF A04
National Inst. of Standards and Technology (MSEL), Boulder, CO. Materials Reliability Div.

Composite Materials for Offshore Operations: Proceedings of the International Workshop (1st). Held in Houston, Texas on October 26-28, 1993.
Special pub.
S. S. Wang, and D. W. Fitting. Aug 95, 400p, NIST/SP-887.
Also available from Supt. of Docs as SN003-003-03357-0. Prepared in cooperation with Houston Univ., TX. Sponsored by Minerals Management Service, Washington, DC.

Keywords: *Composite materials, *Offshore drilling, *Meetings, Petroleum industry, Fiberglass reinforced plastics, Fabrication, Construction, Safety, Tubes, Technology assessment, Research and development, Government policies.

The eight working group sessions focused on topics selected by the international steering committee of the workshop: (1) fabrication, construction, maintenance, and repair; (2) material performance, damage tolerance, durability, and environmental degradation; (3) structural design, optimization, testing, and reliability; (4) nondestructive evaluation; condition monitoring and inspection; (5) flammability and fire retardation; (6) facilities and secondary structural applications; (7) advanced applications; and (8) certification issues and policy concerns. In each group, leading experts, invited by the steering committee, made presentations and guided and stimulated the discussions. This proceedings describes the scope, the organization, and the program of the workshop. It contains a summary, recommendations reported by the steering committee representatives, invited lectures, keynote addresses, and most of the papers presented in the working-group sessions. Also included are a list of working-group chairs and panelists and their discussion summaries. A list of registered workshop participants is given at the end of this volume.

03,170
PB96-119318 Not available NTIS
National Inst. of Standards and Technology (MSEL), Gaithersburg, MD. Polymers Div.
Intrinsic Viscosity and the Polarizability of Particles Having a Wide Range of Shapes.
Final rept.
J. F. Douglas, and E. J. Garboczi. 1995, 69p.
Pub. in Advances in Chemical Physics, vXCI p85-153 1995.

Keywords: *Mixtures, *Composite materials, *Solids, *Liquids, Shapes, Visocity, Polarization, Particles, Virial coefficients, Refractivity, Wave scattering, Reprints.

The intrinstic viscosity (Nu) and the electric alpha(sub e) and magnetic alpha(sub m) polarizabilities of objects having general shape are required in the calculation of some of the most basic properties (viscosity, refracture index, dielectric constant, magnetic permeability, thermal and electrical conductivity, and others) can often be expressed in terms of these functionals of object shape. These virial coefficients also provide basic input into effective medium theories describing higher concentration mixtures. We present an argument that the ratio of (Nu) and alpha(sub e) (the average electric polarizability tensor trace) is an invariant to a good approximation.

03,171
PB96-122577 Not available NTIS
National Inst. of Standards and Technology (MSEL), Gaithersburg, MD.
Cavitation Contributes Substantially to Tensile Creep in Silicon Nitride.
Final rept.
W. E. Luecke, S. M. Wiederhorn, B. J. Hockey, R. F. Krause, and G. G. Long. 1995, 12p.
Pub. in Jnl. of the American Chemical Society, v78 n8 p2085-2096 Mar 95.

Keywords: *Silicon nitride, *Tensile creep, *Cavitation, Dilation, Reprints.

During tensile creep of a hot isostatically pressed (HIPed) silicon nitride, the volume fraction of cavities increases linearly with strain; these cavities produce nearly all of the measured strain. In contrast, compressive creep in the same stress and temperature range produces very little cavitation. A stress exponent that increases with stress characterizes the tensile creep response, while the compressive creep response exhibits a stress dependence of unity. Futhermore, under the same stress and temperature, the material creeps nearly 100 times faster in tension than in compression. Transmission electron microscopy (TEM) indicates that the cavities formed during tensile creep occur in pockets of residual crystalline silicate phase located at silicon nitride multigrain junctions. Small-angle X-ray scattering (SAXS) from crept material quantifies the size distribution of cavities observed in TEM and demonstrates that cavity addition, rather than cavity growth, dominates the cavitation process. These observations are in accord with a model for creep based on the deformation of granular materials in which the microstructure must dilate for individual grains to slide past one another. During tensile creep the silicon nitride grains remain rigid; cavitation in the multigrain junctions allows nitride grain boundary sliding accommodates this expansion and leads to extension of the specimen. In compression, where cavitation is suppressed, deformation occurs by solution-reprecipitation of silicon nitride.

03,172
PB96-123542 Not available NTIS
National Inst. of Standards and Technology (MSEL), Gaithersburg, MD. Polymers Div.
Modification of the Phase Stability of Polymer Blends by Diblock Copolymer Additivies.
Final rept.
J. Dudowicz, K. F. Freed, and J. F. Douglas. 1995, 12p.
Pub. in Macromolecules, n28 p2276-2287 1995.

Keywords: *Composite materials, *Polymer blends, Phase separation(Materials), Reprints, *Diblock copolymer additives.

The addition of a third component to a binary mixture usually alters the critical temperature and critical composition for phase seperation. In practice, these shifts can be large, leading to both increasing and decreasing of the phase stability of the mixture. Lattice cluster theory calculations show that the addition of a small amount of A-b-B dibock copolymer to an A/B polymer blend shifts the phase boundary as 'impurities' do in other fluid mixtures. The novel feature associated with the dilution of the blend by a diblock copolymer additive is that both stabilization and destabilization can be achieved for certain conditions merely by 'tuning' the asymmetry of the block lengths in the diblock copolymer. More substantial shifts are found in the phase diagram of a blend (polystyrene/poly(vinyl menthyl ether)) exhibiting a lower critical solution temperature. We also examine the relation between the shifts in the critical temperature and in the critical composition shift when the block copolymer is nearly symmetric, but no simple relation seems to exist for asymmetric diblock copolymers.

03,173
PB96-126206 (Order as PB96-126180, PC A05/MF A01)
National Inst. of Standards and Technology, Gaithersburg, MD.
Mixing Plate-Like and Rod-Like Molecules with Solvent: A Test of Flory-Huggins Lattice Statistics.
E. A. Di Marzio, A. J. M. Yang, and S. C. Glotzer. 1995, 14p.
Prepared in cooperation with Armstrong World Industries, Lancaster, PA.
Included in Jnl. of Research of the National Institute of Standards and Technology, v100 n2 p173-186 Mar/Apr 95.

Keywords: *Solvents, Lattice dynamics, Layered silicates, Liquid crystals, Flory Huggins theory, Discotic phase, Plate-rod transition, Rod-rod transition.

Boehm and Martire have shown that the Flory-Huggins (FH) lattice model applied to mixtures of squares and rigid rods in solvent on a two dimensional lattice gives different results depending on whether rods or squares are placed first onto the lattice. This correct derivation places the validity of the FH model itself into question since the final result should be independent of the order of placement. An analysis of the FH model in terms of Poisson statistics suggests an alternative formula for the probability of successfully placing a rectangle into an area partially filled with other rectangles, which when incorporated into the FH counting procedure gives the exact thermodynamic result for the tiling of squares (i.e., no solvent and no rods).

03,174
PB96-141270 Not available NTIS
National Inst. of Standards and Technology (BFRL), Gaithersburg, MD. Building Materials Div.
Unreacted Cement Content in Macro-Defect-Free Composites: Impact on Processing-Structure-Property Relations.
Final rept.
P. G. Desai, J. A. Lewis, and D. P. Bentz. 1994, 8p.
Pub. in Jnl. of Materials Science, v29 n24 p6445-6452 1994.

Keywords: *Cements, *Counstruction materials, Fracture(Mechanics), Reprints, Ceramic materials, Moisture, Physical properties, Defect analysis, Flexural properties, MDF(Macro defect-free) cements.

The effect of unreacted cement content on the processing, structure, and properties of macro-defect-free (MDF) composites fabricated from calcium aluminate cement (CAC), alpha-alumina (Al2O3), and polyvinyl alcohol-acetate (PVAA) has been investigated. Three systems were formed with inital CAC:Al2O3 ratios of 50:50, 35:65, and 25:75 by volume in their respective formulations. The amount of unreacted cement was reduced from 68.1 vol% which is present in standard (100% CAC) MDF cement, to 14.9 vol% for composites with an initial CAC: Al2O3 ratio of 25:75, while the hydration product content was reduced from 18.1 vol% to 11.4 vol% for these respective systems. A hard core/soft shell continuum percolation model was used to determine that alumina substitution did not significantly affect the percolative nature of the interphase and bulk polymer regions. However, experiments showed that the reduction in unreacted cement content through Al2O3 substitution affected both the processing and microstructural features of these composites.

03,175
PB96-146873 Not available NTIS
National Inst. of Standards and Technology (MSEL), Gaithersburg, MD. Polymers Div.
Influence of an Impenetrable Interface on a Polymer Glass-Transition Temperature.
Final rept.
W. E. Wallace, J. H. van Zanten, and W. L. Wu. 1995, 4p.
Pub. in Physical Review E, v52 n4 pR3329-R3332 Oct 95.

Keywords: *Glass transition temperature, *Polymers, Substrate effects, Thermal expansion, Thin films, Reprints.

The thermal expansion of polystyrene thin films, supported on hydrogen-terminated silicon substrates, is measured by x-ray reflectivity. Films on the order of 400 Angstroms and thinner show no glass transition up to at least 60 degrees C above the bulk glass-transition temperature, while a break in the thickness versus temperature curve, signaling the glass transition and the onset of bulk behavior, is observed for thicker films. This increase in the glass-transition temperature is in contrast to similar studies on the silicon native-oxide surface where a decrease in the glass-transition temperature is observed. This illustrates the importance of the character of the substrate surface in determining thin film behavior.

03,176
PB96-146881 Not available NTIS
National Inst. of Standards and Technology (MSEL), Gaithersburg, MD. Metallurgy Div.
Electrodeposited Cobalt-Tungsten as a Diffusion Barrier between Graphite Fibers and Nickel.
Final rept.
N. S. Wheeler, and D. S. Lashmore. 1995, 7p.
Pub. in Jnl. of Composites Technology and Research, v17 n4 p301-307 Oct 95.

Keywords: *Cobalt base alloys, *Composites, *Diffusion, Tungsten, Nickel, Coatings, Reprints.

An electrodeposited cobalt alloy coating have a composition of 7.1 plus or minus 0.8 at % tungsten was developed to serve as a diffusion barrier between graphite fibers and nickel. A nickel matrix was electrodeposited around the fibers, and the results composite was annealed in vacuum under various time/temperature conditions. The coating was shown to inhibit interdiffusion for up to 24 h at 800 degrees C. This represents an improvement of 200 degrees over the uncoated fibers.

03,177
PB96-167200 Not available NTIS
National Inst. of Standards and Technology (MSEL), Gaithersburg, MD. Polymers Div.

Analysis of Transverse Flow in Aligned Fibrous Porous Media.
Final rept.
F. R. Phelan, and G. Wise. 1996, 10p.
Pub. in Composites Part A, v27A n1 p25-34 1996.

Keywords: *Fibrous porous media, *Porous media, Reprints, *Foreign technology, Darcy's law, Lubrication theory, Permeability prediction, Structure property relationships.

The permeability of preform materials used in liquid moulding proceses such as resin transfer moulding and structural reaction injection moulding is a complex function of weave pattern, packing characteristics, tow structure and intra-tow properties. The development of tools for predicting permeability as a function of these parameters is of great practical importance because such capability would speed process design and optimization, and provide a step towards establishing processing-performance relations. In this study, transverse flow in aligned fibrous porous media has been investigated. A semi-analytical model based on lubrication analysis is derived to predict the effect of tow shape and intra-tow permeability on the overall bed permeability for flow through rectangular arrays of porous elliptical cylinders. The Brinkman equation is used to model flow inside the porous structures, and the Stokes equation to model flow in the open media between the structures. The model predictions are verified by comparing with rigorous finite element calculations. The model shows that the influence of the intra-tow permeability on the overall bed permeability increases with inter-tow packing, and increasing degree of tow ellipticity. The influence is particularly critical for 'stacked' geometers for which previous models predict a zero permeability. A method for predicting intra-tow permeability is also proposed and investigated by comparing the model predications for overall bed permeability with some experimental data for flow in a model porous medium. The comparison shows that use of the method enables the experimentally measured permeability value to be properly bounded.

03,178
PB96-176656 Not available NTIS
National Inst. of Standards and Technology (MSEL), Boulder, CO. Materials Reliability Div.
Estimation of the Orientation Distribution of Short-Fiber Composites Using Ultrasonic Velocities.
Final rept.
M. L. Dunn, and H. Ledbetter. 1996, 9p.
Pub. in Jnl. of the Acoustical Society of America, v99 n1 p283-291 Jan 96.

Keywords: *Composites, *Fiber reinforced composites, *Ultrasonic velocities, Reprints, Orientation distribution function, SiC/AL composite.

A method for estimating the orientation distribution function (ODF) of short-fiber composites using measured ultrasonic velocities is presented. The method is based on the coupling of (1) a forward micromechanics model of the effective ultrasonic velocities of the textured composite in terms of the coefficients in an expansion of the ODF in generalized spherical harmonics, (2) an inversion algorithm to obtain the coefficients of the ODF from the measured velocities and the forward model. The approach is used to determine the ODF coefficients for a transversely isotropic short-fiber SiC/Al metal-matrix composite. The ODF coefficients obtained by inversion of ultrasonic velocities agree reasonably with those obtained from neutron-diffraction pole figures. Corresponding elastic constants predicted with these coefficients also agree well with independently measured elastic constants.

03,179
PB96-180260 Not available NTIS
National Inst. of Standards and Technology (MSEL), Gaithersburg, MD.
Fracture of Silicon Nitride and Silicon Carbide at Elevated Temperatures.
Final rept.
S. M. Wiederhorn, A. B. Fields, and B. J. Hockey. 1994, 10p.
Pub. in Materials Science and Engineering, vA176 p51-60 1994.

Keywords: *Ceramic matrix composites, *Statistics, *Fracture(Mechanics), Silicon nitride, Silicon carbide, High temperature, Damage, Failure(Mechanics), Tension, Stresses, Strain(Mechanics), Reprints, *Foreign technology.

High temperature fracture of structural ceramics often results from creep and creep-related processes. Creep cavitation in particular plays an important role in the failure process, resulting in crack nucleation and crack growth prior to failure. Equations modeling cavitation and crack growth mechanisms are consistent with the Monkman-Grant behavior observed for structural ceramics. Both the mechanism of fracture and the mode of crack growth are affected by the test geometry. In flexure, cracks tend to remain stable because of stress relaxation near the tensile surface of test specimens. In tensile specimens, stress relaxation due to cavity formation occurs in the vicinity of crack tips. Intermittent crack growth results, in which the density of cavities at the crack tip has to reach a critical level for the occurrence of crack motion. Crack growth occurrs by microcrack nucleation and linkage with the dominant crack.

03,180
PB96-183207 PC A04/MF A01
National Inst. of Standards and Technology (MSEL), Gaithersburg, MD. Polymers Div.
Hygrothermal Effects on the Performance of Polymers and Polymeric Composites: A Workshop Report. Held in Gaithersburg, Maryland on September 21-22, 1995.
M. Y. M. Chiang, and G. B. McKenna. Apr 96, 42p, NISTIR-5826.

Keywords: *Polymers, *Composite materials, *Meetings, Moisture, Performance, Models, Osmosis, Microelectronics, Packaging, Films, Automotive industry, *Hygrothermal effect.

This report contains the highlights of the presentations and discussions at the NIST/Industry/Academe Workshop: Hygrothermal Effects on the Performance of Polymers and Polymeric Composites that took place on 21 and 22 September 1995 at the Hilton Hotel, Gaithersburg, Maryland. The workshop was organized by the Polymers Division of the Materials Science and Engineering Laboratory (MSEL) at the National Institute of Standards and Technology (NIST). Sponsorshop was provided by the Center for Theoretical and Computational Materials Science in MSEL. This workshop brought together 46 attendees; including (10) invited speakers, fifteen (15) representatives from the academic community, eighteen (18) companies and several Divisions within NIST, to define the state-of-the art in hygrothermal issues in polymers and polymeric composites.

03,181
PB96-190087 Not available NTIS
National Inst. of Standards and Technology (MSEL), Boulder, CO. Materials Reliability Div.
Hemispherical Test Fixture for Measuring the Wavefields Generated in an Anisotropic Solid.
Final rept.
D. W. Fitting, and C. M. Fortunko. 1991, 6p.
Pub. in Ultrasonics Symposium, Lake Buena Vista, Florida, December 8-11, 1991, p831-836.

Keywords: *Wave propagation, *Anistropy, *Solids, Directivity, Composite materials, Radiation, Patterns, Ultransonic tests, Reprints, Wavefields, Christoffel equation.

Recently, a closed-form representation for the exact solution of the Chirstoffel equation for wave propagation in an anisotropic solid has been derived. This development and the need to know the wavefield generated during ultrasonic inspection of composites has prompted the design and fabrication of an experimental system for measurement of wavefields in such materials. In the test fixture, a source transducer is affixed to the flat portion of a hemisphere of the anisotropic solid. A receiving transducer having a large field of view (FOV) is scanned over the surface of the hemisphere by a motorized C-arm, mapping out the wavefield generated in the specimen. The hemispherical shape of the test specimen permits scanning the wavefield over nearly a full 2pi solid angle, an improvement over the limited angular range afforded by a flat panel of the anisotropic solid. In this paper, the authors report the result of preliminary experiments designed to evaluate the fixture.

03,182
PB96-200175 Not available NTIS
National Inst. of Standards and Technology (MSEL), Boulder, CO. Materials Reliability Div.

Orthotropic Elastic Constants of a Boron-Aluminum Fiber-Reinforced Composite: An Acoustic-Resonance-Spectroscopy Study.
Final rept.
H. Ledbetter, C. Fortunko, and P. Heyliger. 1995, 5p.
Pub. in Jnl. of Applied Physics, Chapter 78, v3 p1542-1546 Aug 95.

Keywords: *Composites, *Elastic constants, Model calculations, Reprints, Fiber reinforcements, Ultrasonic resonance spectroscopy.

Acoustic-resonance spectroscopy was used to determine the complete elastic constants of a uniaxial-fiber-reinforced metal-matrix composite: boron-aluminum. This material exhibits orthotropic macroscopic symmetry and, therefore, nine indepedent elastic stiffnesses Cij. The off-diagonal elastic constants (C12, C13, C23), which contain large errors when measured by conventional methods, were especially focused on. Good agreement emerged among present results, a previous pulse-echo study, and theoretical predictions using a plane-scattered-wave ensemble-average model. Attempts to measure the internal-friction 'tensor' failed.

03,183
PB96-200803 Not available NTIS
National Inst. of Standards and Technology (MSEL), Gaithersburg, MD.
Tensile Creep of Silicide Composites.
Final rept.
S. M. Wiederhorn, R. J. Gettings, D. E. Roberts, C. Ostertag, and J. J. Petrovic. 1992, 7p.
Pub. in Materials Science and Engineering, vA155 p209-215 1992.

Keywords: *Creep, *Silicides, *Composites, High temperatures, Tensile creep, Reprints, Molybdenum disilicide.

A study has been conducted on the creep behavior of a silicide composite consisting of 50 mol.% MoSi2 and WSi2 reinforced with SiC whiskers. Activation energies for creep in compression and tension were 312 kJ mol to the minus 1 power and 557 kJ mol to the minus 1 power respectively. Stress exponents for creep were 3.2 in tension and 2.3 in compression. These values lie within the range of values obtained by other investigators. The creep resistance of the composite is considerably better than that of current alloys used in heat engines. Most of this improvement comes from the addition of SiC whiskers to the base alloy. It is suggested that the addition of higher concentrations of whiskers or particles would result in additional improvement of the creep behavior of silicide composites.

03,184
PB96-210695 PC A04/MF A01
National Inst. of Standards and Technology (BFRL), Gaithersburg, MD. Building Materials Div.
Materials Aspects of Fiber-Reinforced Polymer Composites in Infrastructure.
J. W. Chin. Aug 96, 47p, NISTIR-5888.

Keywords: *Polymer composites, *Civil engineering, Retrofitting, Composite materials, Highway bridges, Corrosion, Beams(Supports), Maintenance, Reviews.

This paper provides a review of the technical literature pertaining to materials aspects of fiber-reinforced polymer (FRP) composites in infrastructural and other civil engineering applications. The main focus is placed upon the durability, chemical and mechanical aspects of structures reinforced with or constructed from FRP materials. Categories which are addressed include marine applications, structural shapes, joining/fastening, reinforced concrete and rehabilitation/retrofitting of structures. Effects of moisture, salt water, alkalinity and mechanical loading on the performance of FRP components are emphasized.

03,185
PB97-112478 Not available NTIS
National Inst. of Standards and Technology (CSTL), Gaithersburg, MD. Process Measurements Div.
In situ Characterization of Vapor Phase Growth of Iron Oxide-Silica Nanocomposites: Part 1. 2-D Planar Laser-Induced Fluorescence and Mie Imaging.
Final rept.
B. K. McMillin, P. Biswas, and M. R. Zachariah. 1996, 10p.
Pub. in Jnl. of Materials Research, v11 n6 p1552-1561 Jun 96.

Composite Materials

Keywords: *Fluorescence, *Laser scattering, *Nanocomposites, *Vapor phase, In situ analysis, Mie imaging, Reprints, Iron oxide silica.

Planar laser-based imaging measurements of fluorescence and particle scattering have been obtained during flame synthesis of iron-oxide/silica superparamagnetic nanocomposites. The theory and application of laser-induced fluorescence, the spectroscopy of FeO(g), and the experimental approach for measurement of gas phase precursors to particle formation are discussed. The results show that the vapor phase FeO concentration rapidly rises at the primary reaction front of the flame and is very sensitive to the amount of precursor added, suggesting nucleation-controlled particle growth. The FeO vapor concentration in the main nucleation zone was found to be insensitive to the amount of silicon precursor injected, indicating that nucleation occurred independently for the iron and silicon components. Light scattering measurements indicate that nanocomposite particles sinter faster than single component silica, in agreement with TEM measurements.

Corrosion & Corrosion Inhibition

03,186
DE94017332 PC A02/MF A01
National Inst. of Standards and Technology (MSEL), Gaithersburg, MD.
Comparison of the Corrosion Rates of FeAl, Fe(sub 3)Al and Steel in Distilled Water and 0.5 M Sodium Chloride. Technical Report Number 2, January--March 1991.
Progress rept.
R. E. Ricker, and J. L. Fink. Aug 91, 9p, DOE/OR/21941-T2.
Contract AI05-90OR21941
Sponsored by Department of Energy, Washington, DC.

Keywords: *Aluminium Alloys, *Carbon Steels, *Iron Base Alloys, *Sodium Chlorides, *Corrosive Effects, Water, Comparative Evaluations, Corrosion, Experimental Data, Intermetallic Compounds, Progress Report, Tables(data), *Corrosion tests, EDB/360105.

The corrosion rate of an Fe(sub 3)Al alloy (FA117) and an FeAl (FA362) alloy in distilled water and 0.5 M NaCl was determined and compared to two low carbon steels. The results demonstrate that the corrosion rate of these two intermetallic compounds were more than an order of magnitude less than that of the two steels in both of the environments. The corrosion rates of the two iron aluminides were not significantly different.

03,187
PB94-198348 Not available NTIS
National Inst. of Standards and Technology (MSEL), Gaithersburg, MD. Metallurgy Div.
Evaluation of Corrosion Data: A Review.
Final rept.
D. B. Anderson. 1992, 12p.
Pub. in Computer Modeling in Corrosion, American Society for Testing and Materials Special Technical Publication 1154, p162-173 1992.

Keywords: *Corrosion, *Materials, *Environmental effects, *Industrial plants, Exposure, Field tests, Atmospheric corrosion, Electrochemical corrosion, Pitting, Concentration cell corrosion, Cracks, Reprints.

The needs, objectives, and techniques for evaluation of material property data are reviewed with respect to their applicability to certain types of corrosion data. Examples of approaches that have been taken for data generated from exposures in natural environments and industrial processes are described to illustrate methods used for characterizing the materials, the environment and exposure conditions, the measurement techniques used to describe these components, and the delineation of controlling factors with respect to specific forms of corrosion.

03,188
PB94-198876 Not available NTIS
National Inst. of Standards and Technology (MSEL), Gaithersburg, MD. Metallurgy Div.
Modeling Polarization Curves and Impedance Spectra for Simple Electrode Systems.
Final rept.
U. Bertocci, and R. E. Ricker. 1992, 19p.
Pub. in Proceedings of Symposium on Computer Modeling for Corrosion, San Antonio, TX., November 12-13, 1990, n1154 p143-161 1992.

Keywords: *Electrochemical corrosion, *Electrodes, *Impedance, *Electrolytic polarization, *Spectrum analysis, Models, Steady states, Impedance measurement, Reprints.

A method for modeling the behavior of electrochemical systems based on electrode kinetics instead of equivalent circuits is developed and examples of the application of this modeling method to three electrochemical systems are presented. It is shown that the behavior of simple, as well as relatively complex, electrochemical systems can be modeled on desktop computers yielding impedance spectra as a function of input quantities that describe steady state electrode kinetics and the electrode potential. This approach, since it is based on quantities that describe the kinetics of the actual processes that occur at the electrode, has the advantage over other approaches of having a built-in physical interpretation. The impedance plots produced in this way can give a feeling of what to expect experimentally, and can be useful in testing hypotheses, in establishing reasonable ranges for quantities not easily accessible to measurement, and in suggesting experimental strategies.

03,189
PB94-213345 Not available NTIS
National Inst. of Standards and Technology (NEL), Gaithersburg, MD. Building Materials Div.
Relation between AC Impedance Data and Degradation of Coated Steel. 1. Effects of Surface Roughness and Contamination on the Corrosion Behavior of Epoxy Coated Steel.
Final rept.
C. Lin, T. Nguyen, and M. McKnight. 1992, 18p.
Pub. in Progress in Organic Coatings 20, n2 p169-186 1992.

Keywords: *Surface roughness, *Degradation, *Corrosion, *Steels, *Epoxy resins, *Contamination, Substrates, Protective coatings, Environment effects, Organic compounds, Reprints, AC impedance spectroscopy.

The effects of surface roughness and contamination on the corrosion behaviors of epoxy coated steel substrate were investigated using AC impedance spectroscopy. The results of the AC impedance spectroscopy were analyzed using equivalent circuit model to discern the different steps of the corrosion processes of coated steel. Two kinds of corrosion of coated steel, which can be discerned by AC impedance spectroscopy, were observed depending on surface treatment. The area of coating deficiency that causes rapid corrosion of coated metal could be calculated accurately from the AC impedance data as verified by scanning electron microscopy (SEM) and computer image analyses. Interpretations for the experimental results were suggested and the factors dominating the protective properties of an organic coating were discussed.

03,190
PB95-152096 Not available NTIS
National Inst. of Standards and Technology (MSEL), Gaithersburg, MD.
Interaction between Dislocations and Intergranular Cracks.
Final rept.
H. Zhang, A. H. King, and R. Thomson. 1991, 10p.
Pub. in Jnl. of Materials Research 6, n2 p314-323 1991.

Keywords: *Dislocations(Materials), *Intergranular corrosion, *Emission, Isotropic media, Crack propagation, Cracking(Fracturing), Surface properties, Crack tips, Reprints.

The elastic interactions of dislocations and intergranular cracks in isotropic materials have been studied. In the first part of the paper, a model based on Rice-Thomson theory is established under which the conditions for dislocation emission and crack propagation can be described in terms of an emission surface, cleavage surface and loading line in the local k-space associated with a mixed mode intergranular crack. For a given crack, the local k-field changes with the emission of dislocations from the crack tip, which alters the balance of cleavage and emission. In the second part, we present experimental results of in situ TEM observation of intergranular cracks in molybdenum. Alternating brittle crack propagation and dislocation emission is observed. The number of emitted dislocations corresponding to each crack propagation is in good agreement with the calculated values.

03,191
PB95-162327 Not available NTIS
National Inst. of Standards and Technology (MSEL), Gaithersburg, MD. Metallurgy Div.
Evidence of Film-Induced Cleavage by Electrodeposited Rhodium.
Final rept.
R. E. Ricker, J. L. Fink, and E. Escalante. 1993, 7p.
Pub. in Corrosion-Deformation Interactions, p734-740 1993.

Keywords: *Stress corrosion cracking, *Cleavage, *Electrodeposition, *Rhodium, Crack tips, Fracture(Mechanics), Brittleness, Crack propagation, Metal powder, Cracking(Fracturing), Reprints.

Transgranular stress corrosion cracking (T-SCC) has been the subject of numerous investigations, but there is no universally accepted mechanism for this form of crack propagation. One of the mechanisms that has been proposed for T-SCC is film induced cleavage. According to this mechanism, T-SCC cracks propagate by discontinuous micro-cleavage initiated by the corrosion films that form at the crack tip. A critical hypothesis in this postulated mechanism is that when the crack in the surface layer reaches the matrix, it will continue to propagate in a brittle manner in the normally ductile matrix for some distance before it arrests. The objective of this work was to unambiguously evaluate this hypothesis by electrodepositing Rh, a metal which normally cleaves at room temperature, on samples of pure Ni, which does not normally cleave, and then deform these samples and examine the resulting cracks and the morphology of the cracks at the Rh/Ni interface.

03,192
PB95-162475 Not available NTIS
National Inst. of Standards and Technology (NEL), Gaithersburg, MD. Building Materials Div.
Sorption of Moisture on Epoxy and Alkyd Free Films and Coated Steel Panels.
Final rept.
H. N. Rosen, and J. W. Martin. 1991, 9p.
Pub. in Jnl. of Coatings Technology 63, n792 p85-93 Jan 91.

Keywords: *Sorption, *Moisture, *Protective coatings, *Steels, *Corrosion, Degradation, Corrosion inhibition, Diffusion, Moisture content, Isotherms, Humidity, Corrosion prevention, Epoxy compounds, Reprints.

Adsorption isotherm curves at 23 C were determined for alkyd and epoxy free films and coated steel panels as well as for alkyd 'pocket' panels, consisting of an unadhered film surrounding steel panels. The isotherms consisted of a linear portion to about 75% relative humidity (RH) followed by a rapidly rising portion to 100% RH. A model assuming weak bonding forces between paint film and water with microvoid condensation at high RH gave an excellent fit to the data. Transient adsorption and desorption data on the approach to equilibrium conditions showed differences between alkyd and epoxy coatings. Surface boundary layer resistance was significant for alkyd films and sorption followed Fickian models. For the epoxy coating, surface resistance was not significant and moisture movement was non-Fickian.

03,193
PB96-148036 Not available NTIS
National Inst. of Standards and Technology (BFRL), Gaithersburg, MD. Building Materials Div.
Water Permeability and Chloride Ion Diffusion in Portland Cement Mortars: Relationship to Sand Content and Critical Pore Diameter.
Final rept.
P. Halamickova, R. J. Detweiler, D. P. Bentz, and E. J. Garboczi. 1995, 13p.
Pub. in Cement and Concrete Research, v25 n4 p790-802 1995.

Keywords: *Porosity, *Mortars(Material), *Portland cements, Interfaces, Construction materials, Diffusion, Ions, Chlorides, Percolation, Permeability, Cements, Sands, Reprints, Mercury intrusion porosimetry, Pore structure.

The pore structure of hydrated cement in mortar and concrete is quite different from that of neat cement

paste. The porous transition zones formed at the aggregate-paste interfaces affect the pore size distribution. The effect of the sand content on the development of pore structure, the permeability to water, and the diffusivity of chloride ions was studied on portland cement mortars. Mortars of two water-to-cement ratios and three sand volume fractions were cast together with pastes and tested at degrees of hydration ranging from 45 to 70%. An electrically-accelerated concentration cell test was used to determine the coefficient of chloride ion diffusion while a high pressure permeability cell was employed to assess liquid permeability. The data set provides an opportunity to directly examine the application of the Katz-Thompson relationship to cement-based materials.

Elastomers

03,194
AD-A307 789/8 PC A03/MF A01
National Bureau of Standards, Washington, DC. Inst. for Applied Technology.
Synthesis of Thermally Stable Elastomers.
Apr 66, 21p.

Keywords: *Elastomers, *Thermal stability, Polymers, High temperature, Synthesis(Chemistry), Anhydrides, Nitrogen, Siloxanes, Chemical bonds, Silicon, Ethers, Inhibitors, Phenyl radicals, Silicates, Fluorohydrocarbons, Dienes, Diepoxides, Epoxides, Silicarbanes, Polyphenylether, Metallosiloxane, Silazanes.

Significant reports covering the period since 1960 were selected for this study with reference to relevant earlier works. Recent Government-sponsored research and development (RD) in high temperature elastomers has been directed along two lines: (1) new polymer synthesis and (2) evaluation of compounds to improve the thermal stability of current elastomers. Progress has been made in each of these areas. Large groups of inorganic and semi-inorganic polymer systems were evaluated. Systems included silazanes, siloxanes, and fluorocarbons.

03,195
PB95-107033 Not available NTIS
National Inst. of Standards and Technology (MSEL), Gaithersburg, MD. Polymers Div.
Localization Model of Rubber Elasticity: Comparison with Torsional Data for Natural Rubber Networks in the Dry State.
Final rept.
G. B. McKenna, J. F. Douglas, K. M. Flynn, and Y. Chen. 1991, 7p.
Pub. in Polymer 32, n12 p2128-2134 1991.

Keywords: *Natural rubber, *Elastic properties, *Crosslinking, Strain energy methods, Vulcanizing, Elastomers, Thermodynamics, Free energy, Plastic analysis, Torsion, Networks, Reprints, Gaylord-Douglas Localization Model, Free energy density function.

Previously reported results from determinations of the first derivative of the elastic contribution to the free energy density function for dicumyl peroxide crosslinked natural rubber were analyzed within the context of the Gaylord-Douglas 'localization model' of rubber elasticity. It was found that the dry state properties of the rubbers are well described by the localization model and that the non-classical contribution to rubber elasticity arising from the confinement of network chains by surrounding chains varies according to the theory. The only other parameter in the model, the prefactor to a classical term, was set to the classical phantom value assuming a tetrafunctional network and that each dicumyl peroxide molecule decomposed to form one crosslink.

Fibers & Textiles

03,196
PB94-216256 Not available NTIS
National Inst. of Standards and Technology (MSEL), Gaithersburg, MD. Ceramics Div.
Coating of Fibers by Colloidal Techniques in Ceramic Composites.
Final rept.
S. G. Malghan, D. B. Minor, P. S. Wang, and C. P. Ostertag. 1990, 11p.
Pub. in Ceramic Engineering and Science Proceedings 11, n9-10 p1674-1684 1990.

Keywords: *Ceramic fibers, *Silicon carbides, *Ceramic composites, *Deposition, Composite materials, Colloids, Surface chemistry, Aluminum oxide, Fiber composites, Powder(Particles), Reprints.

A process for coating silicon carbide fibers with alumina particulates for control of interface characteristics in the sintering of fiber reinforced composites is described. The process is based on colloidal slurry processing techniques, in which the fibers are allowed to take up a positive surface charge, while the alumina particles are imparted a negative surface charge. When the oppositely charged fibers and particles are brought together, the particles deposit on the surface of fibers. Some unique features of the process, as well as characteristics of the resultant coating are described. Process variables of the coating technique that control the coating morphology, thickness and adherence to the fiber are examined.

03,197
PB95-108676 Not available NTIS
National Inst. of Standards and Technology (MSEL), Gaithersburg, MD. Polymers Div.
Effect of Heterogeneous Porous Media on Mold Filling in Resin Transfer Molding.
Final rept.
R. S. Parnas, and F. R. Phelan. 1991, 8p.
Pub. in Society for the Advancement of Material and Process Engineers Quarterly 22, n2 p53-60 Jan 91.

Keywords: *Fluid flow, *Resin transfer molding, *Molding techniques, *Flow characteristics, *Fibers, Preforms, Porous media, Permeability, Curing, Polymers, Heterogeneity, Bundles, Reprints.

A model for fluid flow in the resin transfer molding (RTM) process is developed. The model takes into account two competing flow processes which occur simultaneously: the macroscopic flow of the resin through the preform and the impregnation of the individual fiber bundles which make up the preform. The model predicts the entrapment of air in the fiber bundles and the subsequent formation of voids in the cured part. In addition, the competition between the two flow processes leads to transient phenomena in which mold inlet pressure continues to rise even after the flow front has reached the outlet of the mold. This result agrees qualitatively with experimental data and has implications regarding the use of D'Arcy's law to model transient mold filling processes with heterogeneous preforms.

03,198
PB96-128194 PC A03/MF A01
National Inst. of Standards and Technology (MEL), Gaithersburg, MD. Manufacturing Systems Integration Div.
Extensions of the Prototype Application Protocol of Ready-to-Wear Apparel Pattern Making.
Y. T. Lee. Oct 95, 44p, NISTIR-5727.
See also PB93-158665. Sponsored by Defense Logistics Agency, Alexandria, VA.

Keywords: *Clothing industry, *Computer aided design, Computer aided manufacturing, Data transfer(Computers), Patterns, Prototypes, Pattern making, Tests, Models, Data structures, Data exchange, Specifications, Standards, Product data, Information modeling, *Application protocols, *Standard for the Exchange of Product Model Data(STEP), *STEP(Standard for the Exchange of Product Model Data), *EXPRESS language, EXPRESS-G computer program, Apparel industry.

A prototype application protocol for ready-to-wear pattern making was developed for the communication of pattern pieces and related information between various computer aided design (CAD) systems. The basic methodology for the application protocol is the Standard for the Exchange of Product Model Data (STEP). STEP is an emerging international standard, the result of an effort to develop a mechanism for digitally representing the physical and functional characteristics of a product throughout the product's life cycle. The STEP application protocol addresses a specific application area and contains an information model written in the conceptual modeling language EXPRESS. The experience gained through the implementation of the prototype application protocol and recommendations received from apparel researchers provided us useful input to improve the prototype application protocol. The report presents a revised version of the information model using both the EXPRESS language and the EXPRESS-G graphical notation. An application activity model that defines the scope and information requirements of the prototype application protocol is also presented in this report. Neither the EXPRESS-G diagrams nor the application activity model was shown in the original prototype application protocol report.

03,199
PB96-193792 PC A06/MF A01
National Inst. of Standards and Technology (MEL), Gaithersburg, MD. Manufacturing Systems Integration Div.
Survey of Standards for the U.S. Fiber/Textile/Apparel Industry.
C. G. Pawlak. Apr 96, 94p, NISTIR-5823.
See also PB93-139095.

Keywords: *Textile industry, *Clothing industry, *Surveys, *Technology utilization, Design standards, Fibers, Textiles, Test methods, Industries, Integration systems, Standards, Specifications, *Apparel clothing.

The report documents a survey of standards relevant to the U.S. Fiber/Textile/Apparel (FTA) industry. The standards are discussed in four main groups--integration standards, test methods, quality standards, and standard reference data and materials. The Appendix of the report lists the titles of all standards found, grouped together by the organization responsible for them. Those organizations are also listed along with contact information for them. The report attempts to bring together useful information concerning FTA standards as a starting point to support the industry in intelligently planning future standards' development efforts.

Iron & Iron Alloys

03,200
AD-A279 759/5 PC A04/MF A01
National Inst. of Standards and Technology, Gaithersburg, MD.
Characterization of the Hydrogen Induced Cold Cracking Susceptibility at Simulated Weld Zones in HSLA-100 Steel.
M. R. Stoudt, and R. E. Ricker. Apr 94, 73p, NISTIR-5408.

Keywords: *Welding, *Cracks, *Low alloy steels, Simulation, Hydrogen, Navy, Microstructure, Martensite, Carbon, Precipitation, Strength(Mechanics), Toughness, Hardening, Mechanical properties, Strain(Mechanics), Sea water, Corrosion, Electrochemistry, *HY-100 Steel, *HSLA-100 Steel, Characterization, Fugacities, HY(High Yield), HSLA(High Strength Low Alloy), Susceptibility.

The relative susceptibilities to hydrogen induced cold cracking were evaluated for HY-100, a steel presently in service in naval applications and for HSLA-100. The martensitic microstructure of the HY-100 undergoes wide variations in the heat affected zone during welding which strongly influence the resistance of that alloy to cold cracking. The HSLA-100, a low carbon, precipitation hardened steel with similar strength and toughness to that of the HY-100, possesses a significantly lower degree of hardenability which results in minimal microstructural variations in the heat affected zone under the same simulated welding conditions. The mechanical properties of the base metal and the heat affected zone created during a simulated, single welding pass were characterized by the slow strain rate technique for both steels in an inert environment and in artificial seawater under free corrosion and controlled hydrogen fugacities. The electrochemical behaviors of both steels were also evaluated in artificial seawater.

03,201
PB94-172087 Not available NTIS
National Inst. of Standards and Technology (MSEL), Gaithersburg, MD. Metallurgy Div.

Monte Carlo and Mean-Field Calculations of the Magnetocaloric Effect of Ferromagnetically Interacting Clusters.
Final rept.
L. H. Bennett, R. D. McMichael, L. J. Swartzendruber, R. D. Shull, and R. E. Watson.
1992, 2p.
Pub. in Jnl. of Magnetism and Magnetic Materials 104-107, p1094-1095 1992. See also DE91014792.

Keywords: *Ferromagnetic materials, *Monte Carlo method, *Curie temperature, *Magnetic properties, Magnetic moments, Entropy, Solid clusters, Ferromagnetism, Mean-field theory, Reprints, *Magnetocaloric effect.

The magnetic entropy change of a ferromagnet induced by an application of a magnetic field is greatest in the temperature region near the Curie point, and the magnitude of the effect is expected to rise monotonically with the size of the individual moments which make up the material. The authors explore the case of nanocomposite materials with ferromagnetically interacting clusters having large cluster magnetic moments as a function of cluster size. As cluster size increases, both Monte Carlo and mean-field calculations show a decrease in the entropy change at T(c) for a given applied field and constant total magnetic moment, and an increase in the entropy change well above T(c). In addition, for the first time, the authors present a comparison of the results of mean-field and Monte Carlo calculations of the magnetocaloric effect in classical Heisenberg ferromagnets. Previous calculations of the magnetocaloric effect have taken the mean-field approach, which is known to underestimate the spontaneous magnetization below T(c). These issues are relevant to devices employing magnetic refrigeration.

03,202
PB94-172251 Not available NTIS
National Inst. of Standards and Technology (CAML), Gaithersburg, MD. Applied and Computational Mathematics Div.
PC-Based Prototype Expert System for Data Management and Analysis of Creep and Fatigue of Selected Materials at Elevated Temperatures.
Final rept.
J. T. Fong, and B. Bernstein. 1990, 4p.
Pub. in Proceedings of International Conference on Computer Applications to Materials Science and Engineering, CAMSE-'90, Tokyo, August 1990 p65-68. Sponsored by Illinois Inst. of Tech., Chicago.

Keywords: *Creep properties, *Expert systems, *Data management, *Fatigue(Mechanics), *Stainless steel, *High temperature, Data bases, Mechanical properties, Algorithms, Stresses, Strains, Information systems, Viscoelasticity, Computer programs, Materials, Fatigue life, Reprints, LPA PROLOG Professional Computer Program, CFD Expert System.

An engineering expert system named CFD for storing, analyzing, and assessing experimental data of the creep and fatigue properties of a class of structural materials at elevated temperatures is presented. The system is coded in micro-PROLOG, a PC version (1.4) of a commercially-available software named LAP PROLOG Professional and is implemented on an IBM-PC-XT or compatible with DOS 2.11 or up. The system is menu-driven and is designed to assist a computer-unsophisticated user in managing creep and fatigue data for a variety of materials at various temperature, stress or strain levels. To illustrate the feasibility of this prototype system, selected data of AISI 304 stainless steel (fatigue life vs. hold time at 593 C) and AISI 316 stainless steel (stress relaxation test at 700 C) are examined and plotted. Based on the linear theory of viscoelasticity, the stress relaxation data are used to predict creep properties using a numerical algorithm due to Hopkins and Hamming (1957).

03,203
PB94-172541 Not available NTIS
National Inst. of Standards and Technology (MSEL), Boulder, CO. Materials Reliability Div.
Nitrogen Effect on Elastic Constants of f.c.c. Fe-18Cr-19Mn Alloys.
Final rept.
S. Lin, and H. Ledbetter. 1993, 5p.
Pub. in Materials Science and Engineering A167, p81-85 1993. Sponsored by Department of Energy, Washington, DC. Office of Fusion Energy.

Keywords: Iron base alloys, Chromium alloys, Manganese alloys, Bulk modulus, Elastic properties, FCC lattices, Interstitials, Nitrogen, Reprints, *Iron alloy 18Cr 19Mn.

Previously, the authors studied the effects of interstitial carbon-plus-nitrogen (C + N) on the elastic constants of f.c.c. Fe-18Cr-10Ni-1Mn alloys. Consistent with a volume increase, all the elastic stiffnesses decrease with increasing C + N. The present alloys show different behavior: although volume increases, interstitial nitrogen atoms increase the bulk modulus. The peculiar bulk-modulus-electron-concentration behavior (B vs. n(sub e) of 3d electron elements is described. At first B increases with increasing n(sub e); beyond a critical concentration, B decreases rapidly. Application of Ducastelle's model (bandstructure and repulsion energies) shows that interstitial nitrogen increases the bandstructure contribution to the bulk modulus.

03,204
PB94-172715 Not available NTIS
National Inst. of Standards and Technology (MSEL), Boulder, CO. Materials Reliability Div.
Microstructure and Tensile Properties of Microalloyed Steel Forgings.
Final rept.
P. T. Purtscher, and Y. W. Cheng. 1993, 10p.
Pub. in Proceedings of Iron and Steel Society's Mechanical Working Conference, Montreal, Canada, October 1992, p331-340 1993.

Keywords: *Steels, *Tensile properties, *Microstructure, *Forging, Austenite, Ferrites, Deformation, Metalworking, Strain rate, Grain size, Hardness, Mechanical properties, Simulation, Cooling, Pearlite, Automotive components, Reprints, *Microalloying.

Forging is studied by thermomechanical simulation of the process variables on the microstructure, hardness, and tensile properties of medium-C, ferrite plus pearlite steel with V or Nb additions, steels used for forged automotive components. Experiments were carried out on a test machine with a load capacity of 500kN and capable of high strain rates. The prior austenite grain size increases as the reheat temperature goes up from 950 to 1210 C and decreases with applied strain up 50%. The prior austenite grain size of the Nb- and V-treated steels are nearly equal. As the cooling rate after deformation decreases from 1.9 to 0.8 C/s, the ferrite content increases. Deformation reduces the prior austenite grain size and increases the ferrite content. The hardness, yield, ultimate, and fracture stresses are not a strong function of reheating and deformation temperature or strain, but are lowered by about 10% when the cooling rate is reduced.

03,205
PB94-185394 Not available NTIS
National Inst. of Standards and Technology (MSEL), Gaithersburg, MD. Metallurgy Div.
Effect of Backfill and Atomizing Gas on the Powder Porosity and Mechanical Properties of 304L Stainless Steel.
Final rept.
G. M. Janowski, F. S. Biancaniello, G. E. Hicho, R. J. Fields, and S. D. Ridder. 1993, 6p.
Pub. in P/M in Aerospace, Defense and Demanding Applications, p363-370 1993.

Keywords: *Stainless steel-304L, *Powder metallurgy, *Porosity, *Mechanical properties, Austenitic steels, Atomization, Argon, Nitrogen, Particle size distribution, Reprints, Backfill gas.

A series of nitrogenated austenitic stainless steels was produced by gas atomization and HIP consolidation using various combinations of nitrogen and argon as the melt chamber backfill gas and as the atomizing gas. Analysis of the gas-only flow patterns and the physical properties of nitrogen and argon suggest that their atomization behavior should be quite comparable. The similar particle size distributions support this hypothesis and indicate that the liquid metal ligament and sheet break-up were unaffected by gas type. It was found that the nitrogen content of the powder was largely controlled by the backfill gas and that the fraction of hollow particles was determined by the atomization gas. The nitrogen content of the standard 304L alloy was 0.15 wt % when processed using nitrogen for both backfilling and atomizing, and a modified version of 304L with 23 wt % Cr contained 0.21 wt % nitrogen when processed in the same manner. Hardness, yield strength, and the ultimate tensile strength of the HIP consolidated powders were improved with the addition of nitrogen while retaining significant tensile elongation (about 40%).

03,206
PB94-185675 Not available NTIS
National Inst. of Standards and Technology (MSEL), Gaithersburg, MD. Metallurgy Div.
Langevin Approach to Hysteresis and Barkhausen Modeling in Steel.
Final rept.
R. D. McMichael, L. J. Swartzendruber, and L. H. Bennett. 15 May 93, 3p.
Pub. in Jnl. of Applied Physics 73, n10 p5848-5850, 15 May 93.

Keywords: *Carbon steels, *Hysteresis, *Barkhausen effect, Stochostic processes, Electromagnetism, Rolling(Metallurgy), Ferromagnetic materials, Magnetic properties, Metastable state, Reprints.

To represent the multiplicity of metastable states in a bulk ferromagnetic material with domain-wall pinning effects, fluctuations in the domain-wall energies are described in terms of an ensemble of stochastic Langevin functions. The model parameters used are a correlation length, a rms value for the amplitude of the fluctuations in the domain-wall energy gradient, and a 'demagnetizing factor.' The model generates both hysteresis loops and Barkhausen effect (BE) jump size distributions. Jump size distributions were determined experimentally for low-carbon rolled sheet steel with the field applied both parallel and perpendicular to the rolling direction. Both the model and the experimental BE jump size distributions show a power-law behavior for small jumps and a rapid cutoff at large jump sizes.

03,207
PB94-200136 Not available NTIS
National Inst. of Standards and Technology (MSEL), Boulder, CO. Materials Reliability Div.
Hot-Deformation Apparatus for Thermomechanical Processing Simulation.
Final rept.
Y. W. Cheng, and H. I. McHenry. 1988, 8p.
Pub. in Proceedings of International Symposium on Physical Simulation of Welding, Hot Forming, and Continuous Casting, Canada, p1-8 1988.

Keywords: *Hot working, *Quenching(Cooling), *Thermomechanical treatments, *Simulation, Reprints, Hardening(Materials), Heat treatment, High strength steels, Microstructure, Deformation, *Thermomechanical processing, *Steel-ASTM-A710.

A hot-deformation apparatus designed to simulate thermomechanical processing of steel plates is described, and some initial results for a study on controlled rolling followed by direct quenching (CR-DQ) of ASTM A710 steel are presented. The apparatus has the following features: a servohydraulic load frame with a 250 kN capacity in tension or compression; a variable-actuator traveling speed up to 500 mm/s; a multiple-strike capability with controllable displacements and strain rates; a maximum heating rate of 150 deg. C/s with a 10 kW induction heater (for a cylindrical steel specimen mm in diameter and 18 mm in height); a maximum cooling rate of 25 deg C/s with helium-gas cooling; and vacuum to 1.33 x 10(exp-3) Pa (1 x 10 (exp-5) torr) within 25 min. Experimental results indicated that the hardenability of the steel increased with a simplified CR/DQ processing. The CR/DQ processed specimens showed variation of microstructure within the specimen due to nonuniform deformation during compression. Mechanisms that contributed to the increase of hardenability are discussed.

03,208
PB94-211927 Not available NTIS
National Inst. of Standards and Technology (MSEL), Gaithersburg, MD. Metallurgy Div.
Determination of the Prior-Austenitic Grain Size of Selected Steels Using a Molten Glass Etch.
Final rept.
G. E. Hicho, L. C. Smith, C. A. Handwerker, and D. A. Kauffman. 1991, 11p.
Pub. in Jnl. of Heat Treating 9, n1 p37-47 1991.

Keywords: *Austenitic stainless steels, *Grain size, *Heat treatment, Microstructure, Austenite, Precipitates, Etching, Glass, Grain boundaries, Reprints.

A hot etching procedure was used to reveal the prior-austenitic grain size of several steels. Etching experiments, using molten glass, were conducted on a HSLA precipitation hardened steel, two alloy steels, and a control-rolled steel. Experiments were also conducted

on the HSLA precipitation hardenable steel in order to determine the effects of prolonged heating on the austenite grain size. For comparison purposes, the austenite grain size of the HSLA precipitation hardenable steel, as a function of temperature, was determined using a hot-stage microscope. Photomicrographs of the various steels showing the microstructures obtained using chemical etchants are also presented. A comparison of prior-austenitic grain sizes which were determined using the molten glass etch and chemical etches is shown.

03,209
PB94-212396 Not available NTIS
National Inst. of Standards and Technology (MSEL), Gaithersburg, MD. Metallurgy Div.
Beneficial Effects of Nitrogen Atomization on an Austenitic Stainless Steel.
Final rept.
G. M. Janowski, F. S. Biancaniello, and S. D. Ridder. 1992, 10p.
Pub. in Metallurgical Transactions A 23A, p3263-3272 Dec 92.

Keywords: *Austenitic stainless steels, *Atomization, *Nitrogen, Copper alloys, Hardness, Powder metallurgy, Porosity, Hot pressing, Nickel alloys, Reprints.

Fully dense nitrogenated austenitic stainless steels were produced by gas atomization and HIP consolidation. The base alloy, 304L, contained about 0.15 weight percent nitrogen when melted under a nitrogen atmosphere, and a modified version of 304L with 23 weight percent Cr contained 0.21 weight percent nitrogen. A series of experiments using various combinations of N2 and Ar as the melt chamber backfill gas and atomizing gas demonstrated that the nitrogen content of the powder was largely controlled by the backfill gas and that the fraction of hollow particles was determined by the atomization gas. The hollow powder particles, which are common in inert-gas atomized materials, were virtually eliminated in the nitrogen atomized powders. Additional atomizing experiments using copper and a nickel-base superalloy indicate that low gas solubility in the metal leads to gas entrapment. Hardness and compression behavior (yield strength and flow stress) are substantially improved with the addition of nitrogen. The results of this study suggest that the properties of nitrogenated stainless steels fabricated in this manner are comparable to other high nitrogen austenitic alloys.

03,210
PB94-213188 Not available NTIS
National Inst. of Standards and Technology (MSEL), Boulder, CO. Materials Reliability Div.
Dynamics vs. Static Young's Moduli: A Case Study.
Final rept.
H. Ledbetter. 1993, 2p.
Pub. in Materials Science and Engineering A165, pL9-L10 1993.

Keywords: *Austenitic stainless steels, *Dynamic modulus of elasticity, *Modulus of elasticity, Static tests, Dynamic tests, Mechanical properties, Uncertainty, Elastic properties, Case studies, Reprints.

For one material, a 316LN austenitic steel, a comparison is made between the Young's modulus measured statically with usual commercial equipment and that measured dynamically at mega-hertz frequencies. The first gives a + or - 6% uncertainty; the second a + or - 0.5% uncertainty. The two Young's moduli, 207 GPa (static) and 202 GPa (dynamic), agree within the statistical bounds of the static measurement, 195 GPa and 219 GPa, the extreme static values being 178 GPa and 229 GPa. Simple thermodynamics that shows the difference between dynamic and static elastic constants is also presented.

03,211
PB94-213212 Not available NTIS
National Inst. of Standards and Technology (MSEL), Boulder, CO. Materials Reliability Div.
Cast-Iron Elastic Constants: Effect of Graphite Aspect Ratio.
Final rept.
H. Ledbetter, and S. Datta. 1992, 4p.
Pub. in Zeitschrift fuer Metallkunde 83, n3 p195-198 1992.

Keywords: *Cast iron, *Elastic properties, Bulk modulus, Shear modulus, Young modulus, Aspect ratio, Poisson ratio, Graphite, Reprints, Scattered plane wave method.

Using a scattered-plane-wave ensemble-average model developed for composite materials, we calculated the effective elastic constants of cast iron. We focused on the effect of graphite-particle aspect ratio on the Young modulus. Between model and observation, we found good agreement. Oblate spheroidal graphite flakes lower the elastic stiffness much more than do spheres. To obtain good model-measurement agreement, one must use graphite's lower third-order-bound (Kroner-bound) elastic constants. Besides the Young modulus, we give calculated results for all the other usual quasi-isotropic elastic constants: shear modulus, Poisson ratio, and bulk modulus.

03,212
PB95-108759 Not available NTIS
National Inst. of Standards and Technology (NML), Gaithersburg, MD. Gas and Particulate Science Div.
Apparent Bias in the X-Ray Fluorescence Determination of Titanium in Selected NIST SRM Low Alloy Steels.
Final rept.
P. A. Pella, R. B. Marinenko, J. A. Norris, and A. Marlow. 1991, 4p.
Pub. in Applied Spectroscopy 45, n2 p242-245 1991.

Keywords: *X-ray fluorescence, *Titanium, *Low alloy steels, *Chemical analysis, Standards, Calibrating, Emission spectroscopy, Metallurgy, Comparison, Electron microprobe analysis, Reprints, *SRM 1165, *SRM 1264, Standard reference materials.

X-ray fluorescence (XRF) results of analysis of titanium in National Institute of Standards and Technology (NIST) SRM 1165 and 1264 low alloy steels were found to be significantly different from the certified values. These differences appear to be unique to the XRF results since results from other methods such as emission spectroscopy did not show any discrepancies. The microhomogeneity of selected samples was examined by electron probe microanalysis and revealed the presence of titanium inclusions containing varying amounts of zirconium, niobium, and tantalum. Differences in metallurgical uniformity is believed to be the major cause of apparent XRF bias in these SRM's. XRF analysis of the new 1760 series alloys indicates that these are more accurate for purposes of calibration than the 1160 series and 1260 series for such elements as titanium.

03,213
PB95-153235 Not available NTIS
National Inst. of Standards and Technology (MSEL), Boulder, CO. Materials Reliability Div.
Ultrasonic Measurement of Sheet Anisotropy and Formability.
Final rept.
A. V. Clark, R. B. Thompson, R. C. Reno, G. V. Blessing, and D. Matlock. 1989, 7p.
Pub. in Proceedings of International Congress and Exposition, Detroit, MI., February 27-March 3, 1989, p89-95.

Keywords: *Metal sheets, *Anisotrophy, *Modules of elasticity, *Steels, *Ultrasonic tests, Resonant frequencies, Textures, Nondestructive tests, Process control, Mechanical properties, Tensile properties, Reprints, *Formability, Electromagnetic-acoustic transducers.

The anisotropy of Young's modulus in steel sheet is closely related to the r-value. Commercially available instrumentation is often used to predict formability by measuring the resonant frequencies of coupons cut at 0, 45, and 90 degrees to the rolling direction. This paper describes recent advances in instrumentation to acquire equivalent information nondestructively, with possibility of on-line process control. The technique uses electromagnetic-acoustic transducers (EMAT's) to excite and detect ultrasonic guided waves propagating in the plane of the sheet. Theories of wave propagation relate the velocities of these waves to Young's modulus anisotropy or to the orientation distribution coefficients (ODC's) describing the texture. The paper reviews the principles of the measurement and then presents correlations of the elastic anisotropy, as deduced by the ultrasonic instrumentation, with tensile measurements of r. Measurements of Young's modulus anisotropy and neutron diffraction measurements of ODC's are also included.

03,214
PB95-161261 Not available NTIS
National Inst. of Standards and Technology (MSEL), Gaithersburg, MD. Materials Reliability Div.
Cryogenic Toughness of Austenitic Stainless Steel Weld Metals: Effect of Inclusions.
Final rept.
A. O. Kluken, C. N. McCowan, and T. A. Siewert. 1992, 19p.
Pub. in Microstructural Science, v20 p45-63 1992.

Keywords: *Cryogenic equipment, *Welded joints, *Austenitic stainless steels, *Toughness, *Inclusions, Voids, Fractures(Materials), Fractography, Mechanical properties, Microstructure, Image analysis, Impurities, Crack initiation, Reprints.

The present investigation studies the effect of the volume fraction inclusion and size distribution of inclusions on the cryogenic (4 K) toughness of austenitic stainless steel weld metals. Two weld series with systematic variations in the volume fraction of inclusions were made by varying the oxygen potential of the shielding gas at a constant heat input. To obtain differences in the size distribution of inclusions, at a given volume fraction of inclusions, the heat input was varied. The subsequent examinations of the welds involved both optical microscopy and scanning electron microscopy. Automatic image analysis was used to determine the inclusion volume fraction and size distribution. The results from these examinations revealed that the arithmetic mean three-dimensional inclusion diameter increased with increasing volume fraction of inclusions. Moreover, for one of the weld series, a shift in the chemical composition of inclusions from spherical manganese silicates to predominantly angular chromium oxides was also observed with increasing content of weld-metal oxygen. Fracture toughness testing of the welds showed that the energy required to initiate and propagate cracks decreased as inclusion volume fraction increased. Fractographic examinations revealed that all specimens failed in a ductile manner with fracture surfaces exhibiting typical ductile dimple morphologies.

03,215
PB95-175253 Not available NTIS
National Inst. of Standards and Technology (MSEL), Boulder, CO. Materials Reliability Div.
Friction and Oxidative Wear of 440C Ball Bearing Steels Under High Load and Extreme Bulk Temperatures.
Final rept.
D. K. Chauduri, A. J. Slifka, and J. D. Siegwarth. 1993, 14p.
Contract NASA-H-01026D
Sponsored by National Aeronautics and Space Administration, Washington, DC.
Pub. in Wear 160, p37-50 1993.

Keywords: *Steels, *Sliding friction, *Wear, Temperature range 0065-0273 K, Temperature range 0273-0400 K, Temperature range 0400-1000 K, Temperature dependence, Coefficient of friction, Ball bearings, Oxidation, Reprints, Steel 440C.

Unlubricated sliding friction and wear of 440C steels in an oxygen environment have been studied under a variety of load, speed and temperature ranging from approximately -185 to 675 C. A specially designed test apparatus with a ball-on-flat geometry has been used for this purpose. The observed dependencies of the initial coefficient of friction, the average dynamic coefficient of friction, and the wear rate on load, speed, and test temperatures have been examined from the standpoint of existing theories of friction and wear. High contact temperatures are generated during the sliding friction causing rapid oxidation and localized surface melting. A combination of fatigue, delamination, and loss of hardness due to tempering of the martensitic structure is responsible for the high wear rate observed and the coefficient of friction.

03,216
PB96-123393 Not available NTIS
National Inst. of Standards and Technology (MSEL), Boulder, CO. Materials Reliability Div.
Prediction of the Strength Properties for Plain-Carbon and Vanadium Micro-Alloyed Ferrite-Pearlite Steel.
Final rept.
P. T. Purtscher, Y. W. Cheng, and R. P. Foley. 1995, 10p.
Pub. in Mechanical Working and Steel Processing Conference Proceedings (36th), ISS-AIME, Baltimore, MD., October 1994, v32 p279-288 1995.

Keywords: *Steels, *Alloying, *Fracture mechanics, Microstructure, Carbon steels, Toughness, Strength, Regression analysis, Reprints, Composite deformation theory.

Composite deformation theory is examined and applied to the case of ferrite and pearlite microstructures. The goal of this paper is to use the basic microstructural features (grain size and volume fraction of ferrite, and interlamellar spacing of pearlite) to predict as much of the stress-strain curve as possible, and from the stress-strain curve, to calculate strength. Two different deformation schemes are examined for the prediction of stress-strain curves: first, strain partitioning between ferrite and pearlite, and second, equal strain in ferrite and pearlite. The strain partitioning case can be used to predict the yield strength when the ferrite volume fraction is greater than about 33%. When the volume fraction of ferrite is less than about 15%, an equal-strain deformation scheme can be used to predict the flow curve up the uniform strain (both yield and ultimate strengths). Strengthening from microalloy precipitation can be incorporated by adding the assumed additional strengthening to the flow curves for the two phases.

03,217
PB96-135140 Not available NTIS
National Inst. of Standards and Technology (MSEL), Gaithersburg, MD.
Catastrophic Failures Propagate Field of Fracture Mechanics.
Final rept.
R. L. Blumberg. 1995, 2p.
Pub. in Materials Research Society Bulletin, v20 n8 p74-75 Aug 95.

Keywords: *Fracture mechanics, *Stresses, *Failure(Mechanics), Wires, Stress-strain relations, Failure analysis, Mechanical properties, Reprints, Size effect, Fracture analysis, Flaws.

The development of fracture mechanics dates back five centuries to Leonardo da Vinci, who carried out experiments on the fracture of iron wire. He demonstrated that the strength of a piece of wire varies inversely with its length; long wires are weaker, on average, while short wires are stronger. This behavior, better known today as the size effect, supported the theory that wire fracture is initiated by rare flaws. A longer piece of wire is more likely to contain a larger flaw that causes fracture at a lower critical stress.

03,218
PB96-161971 Not available NTIS
National Inst. of Standards and Technology (MSEL), Gaithersburg, MD.
Fundamentals of Fracture: A 1993 Prologue, and Other Comments.
Final rept.
R. Thomson. 1994, 7p.
See also PB86-189131.
Pub. in Materials Science and Engineering, vA176 p1-7 1994.

Keywords: *Fracture(Materials), Dislocations(Materials), Reprints, Cracks, Fracture(Mechanics), *Foreign technology.

In the first of this paper, I discuss the trends in fracture science as it is reflected in the papers given at this and the past three conferences on the fundamentals of fracture. In the second part of the paper, I present some results carried out by myself and callaborators on certain atomic aspects of fracture in a simple two-dimensional hexagonal lattice, i.e. the dislocation emission criterion, the non-local shift in the emission criterion caused by the shielding of dislocations already present, and the structure and some properties of the interfacial crack.

03,219
PB96-190194 Not available NTIS
National Inst. of Standards and Technology (MSEL), Gaithersburg, MD. Materials Reliability Div.
Charpy Impact Test as an Evaluation of 4 K Fracture Toughness.
Final rept.
H. Nakajima, K. Yoshida, H. Tsuji, M. M. Morra, R. G. Ballinger, R. L. Tobler, and I. S. Hwang. 1992, 9p.
Pub. in International Cryogenic Materials Conference Publication, Huntsville, AL., June 11-14, 1991, Advances in Cryogenic Engineering (Materials), v38 p207-215 1992.

Keywords: *Cryogenics, *Austenite, *Alloys, *Impact tests, *Fracture properties, Toughness, Mechanical properties, Standards, Tests methods, Low temperature tests, Reprints, Austenitic structural alloys, Charpy test.

A 4 K Charpy test is defined as a Charpy test in which the initial temperature of a specimen is 4 K. Two methods, a glass Dewar method and a flow method, are compared in this study to demonstrate that both provide consistent results as long as an initial specimen temperature is the same. An improved correlation between the Charpy absorbed energy and the fracture toughness at 4 K is also examined to clarify the limitation of Charpy test applications at cryogenic temperatures.

03,220
PB96-190251 Not available NTIS
National Inst. of Standards and Technology (MSEL), Boulder, CO. Materials Reliability Div.
Prediction of Strengthening Due to V Additions in Direct-Cooled Ferrite-Pearlite Forging Steels.
Final rept.
P. T. Purtscher, Y. Cheng, R. Kuziak, and R. P. Foley. 1996, 11p.
Pub. in Mechanical Working and Steel Processing Conference (37th), Hamilton, Ontario, Canada, October 1995, p405-415 1996.

Keywords: *Forging steels, *Thermodynamic modeling, Vanadium, Yield strength, Microstructure, Solubility products, Reprints.

Two different approaches predict the yield-strength increment (deltaYS) due to V additions in ferrite-pearlite forging steels. The first is based on the cooling rate and on the V and N contents dissolved in austenite before transformation to ferrite. The second is based on the V available for precipitations strengthening in ferrite. Based on comparisons between the prediction schemes and measured results in the literautre for a range of compositions and forging variables, both approaches predict similar trends. There is no consistently better agreement with the measured deltaYS for one approach than for the other. Considering the reheat/deformation temperatures typically used in industrial practice, the first approach based on V and N dissolved in austenite is preferred.

03,221
PB96-190269 Not available NTIS
National Inst. of Standards and Technology (MSEL), Boulder, CO. Materials Reliability Div.
Temperature-Induced Transition in Ductile Fracture Appearance of a Nitrogen-Strengthened Austenitic Stainless Steel.
Final rept.
P. T. Purtscher, G. Krauss, and D. K. Matlock. 1993, 9p.
Pub. in Metallurgical Transactions A, v24A p2521-2529 Nov 93.

Keywords: *Stainless steel, *Cryogenic properties, Reprints, Ductile fracture, Shear fracture, Sigma phase, Void nucleation.

A nitrogen-strengthened autenitic stainless steel was tested in uniaxial tension at room temperature (295 K) and in liquid nitrogen (76 K). A transition in ductile fracture appearance from a cup-cone fracture at room temperature to shear fracture at cryogenic temperature is observed and correlated to deformation behavior and micromechanisms (void nucleation and strain localization) of fracture. The flow stresses, fracture stresses, and strain hardening rates are all higher at liquid nitrogen temperature compared to those at room temperature, and the significant increases in platic flow stresses are accompanied by planar deformation mechanisms. At both temperatures, primary void nucleation is observed mainly at scattered, large patches of sigma phase, and initial primary void growth is associated with tensile instability (necking) in the specimen. Postuniform elongation at 195 K leads to secondary void growth and coalescence is highly localized and does not contribute to macroscopic elongation. At 76 K, uniform strain increases, total strain decreases, and strain location into shear bands between the primary voids and the surface of the neck leads directly to failure. Secondary void nucleation, growth, and coalescence are limited to shear bands and also do not contribute to the macroscopic elongation. The observations of void nucleation are characterized in terms of a continuum analysis for the interfacial stress at void-nucleating particles. The critical interfacial stress for void nucleation at the lower temperature correlates with the increased flow properties of the matrix.

03,222
PB96-190285 Not available NTIS
National Inst. of Standards and Technology (MSEL), Boulder, CO. Materials Reliability Div.
Ductile Fracture and Tempered Martensite Embrittlement of 4140 Steel.
Final rept.
J. A. Sanders, P. T. Purtscher, D. K. Matlock, and G. Krauss. 1992, 10p.
Pub. in Speich Symposium Proceedings, Iron and Steel Society Meeting, Montreal, Canada, October 1992, p67-76.

Keywords: *Ductile fracture, *Fractography, *Steel, Strain hardening, Tensile properties, Void nucleation, Reprints, Tempered martensite embrittlement.

Specimens of martensitic 4140 steel were tempered at 200, 300, and 400 degrees C and subjected to uniaxial tensile testing and fractographic examination. Ductility does not increase as flow stresses decrease with increasing tempering temperature. This manifestation of tempered martensite embrittlement is related to the introduction of new void-nucleating carbide particles by high temperature tempering and the effect of the particle distributions on ductile fracture. Calculations of void-nucleating stresses at the interfaces of carbide particles at fracture, incorporating the effects of macroscopic changes during necking, were made. The effect of changing particle distributions on these calculations are discussed.

03,223
PB96-190343 Not available NTIS
National Inst. of Standards and Technology (MSEL), Boulder, CO. Materials Reliability Div.
Fatigue Crack Thresholds of a Nickel-Iron Alloy for Superconductor Sheaths at 4 K.
Final rept.
R. L. Tobler, and I. S. Hwang. 1994, 8p.
Pub. in Advances in Cryogenic Engineering, v40 p1315-1322 1994.

Keywords: *Fracture mechanics, *Nickel base superalloy, Liquid helium, Fatigue tests, Cryogenic properties, Reprints, Superconductor conduit, Austenitic alloys.

Short crack simulation (SCS) tests were used to characterize the fatigue crack growth rates da/dN and thresholds deltaK(Th) of a Ni-Fe superalloy proposed for conduit sheath applications in superconducting magnets at 4 K. Experiments described demonstrate the reproducibility of the SCS data and confirm that this alloy has a relatively high fatigue crack growth rate threshold at 4 K. The effects of plate thickness and thermal treatment (650 degrees C, 180 h) on near-threshold fatigue properties are minor compared with a strong cryogenic temperature effect that increases the fatigue threshold from about 2 MPa.m(to the one half power) at room temperature to 9 or 10 MPa.m(to the one half power) at 4 K.

03,224
PB96-190350 Not available NTIS
National Inst. of Standards and Technology (MSEL), Boulder, CO. Materials Reliability Div.
Mechanical Properties and Warm Prestress of Ultra-Low Carbon Steel at 4 K.
Final rept.
R. L. Tobler, L. M. Ma, and R. P. Reed. 1991, 8p.
Pub. in Supercollider III, Proceedings of the Supercollider Symposium (3rd), p139-146 1991.

Keywords: *Steel, *Fracture toughness, Ferritis steel, Cryogenic properties, Prestress effect, Tension tests, Warm prestress, Reprints, Low carbon steel.

The yield strength of ultra-low carbon steel increases from 137 MPa at 195 K to 705 MPa at 4 K. In liquid helium the material is brittle and cleaves in tension. Consequently it is difficult or impossible to properly fatigue-precrack toughness specimens for test at 4 K. We precracked a series of compact specimens at room temperature and then fractured them at 4 K. The toughness measurements at 4 K are affected by precracking at 295 K, and they provide only an estimate of K(Ic) for this steel: 15 MPa M(to the one half power). The tensile properties of the steel at 295 and 4 K are reported, and the effects of prestress on the tensile and fracture properties at 4 K are discussed.

Lubricants & Hydraulic Fluids

03,225
PB95-125969 Not available NTIS

National Inst. of Standards and Technology (MSEL), Gaithersburg, MD. Ceramics Div.
Control of Friction and Wear of Alpha-Alumina with a Composite Solid-Lubricant Coating.
Final rept.
A. Gangopadhyay, and S. Jahanmir. 1990, 8p.
Pub. in Proceedings of a Conference on Tribology of Composite Materials, Oak Ridge, TN., May 1-3, 1990, p337-344.

Keywords: *Aluminum oxide, *Solid lubricants, *Ceramics, *Friction reduction, *Wear resistance, High temperature lubricants, Tribology, Alternatives, Performance evaluation, Coatings, Coefficient of friction, Reprints, *Advanced materials.

The successful utilization of advanced structural ceramic materials as tribological components in high temperature engine applications requires friction coefficients in the range of 0.1 to 0.2. The low values of friction coefficients are needed for energy conservation and control of the wear rate, since it has been shown that the wear of ceramics is adversely affected by friction. Presently, liquid lubricants are not available for the high temperature applications. Solid-lubricant coatings appear as a viable alternative to achieve a low friction coefficient. In the present study, the tribological characteristics of a multicomponent solid-lubricant coating deposited on alumina is investigated up to a temperature of 800 C, and compared with that of uncoated alumina.

03,226
PB95-213583 PC A18/MF A04
National Inst. of Standards and Technology (MSEL), Gaithersburg, MD. Ceramics Div.
Boundary Lubrication of Silicon Nitride.
Special pub.
R. S. Gates, and S. M. Hsu. Feb 95, 408p, NIST/SP-876.
Also available from Supt. of Docs. as SN003-003-03316-2. See also PB91-236711. Sponsored by Department of Energy, Washington, DC.

Keywords: *Tribology, *Boundary lubrication, *Ceramics, *Silicon nitrides, Friction, Wear tests, Alcohols, Silicon compounds, Alkoxides, Fluid-solid interactions, Surface chemistry, Organic compounds, Oxygen, Phosphorus, Sulfur, Nitrogen, Halogens.

Successful use of advanced ceramics in many tribological applications requires an understanding of the physical, chemical, and mechanical properties of the material. This report describes a systematic study to investigate the effects of selected organic chemical compounds on the friction and wear of silicon nitride under boundary lubrication conditions. A broad range of chemistries were investigated. Results are grouped according to predominant chemical compound class as oxygen, phosphorus, halogen, sulfur, and nitrogen-containing chemistries.

03,227
PB96-119466 Not available NTIS
National Inst. of Standards and Technology (MSEL), Gaithersburg, MD. Ceramics Div.
Mechano-Chemical Model: Reaction Temperatures in a Concentrated Contact.
Final rept.
S. M. Hsu, M. C. Shen, E. E. Klaus, H. S. Cheng, and P. I. Lacey. 1994, 10p.
Pub. in Wear, v175 p209-218 1994.

Keywords: *Boundary lubrication, *Models, *Wear tests, *Tribology, *Surface chemistry, Chemical reactions, Fluid mechanics, Hydrodynamics, Kinetics, Degradation, Temperature, Wear, Reprints, *Contact mechanics.

Successful boundary lubrication is essential in the design and operation of many components. The lubrication process is complex and it involves contact mechanics, fluid mechanics, tribochemistry, and material deformation and fracture. Two schools of thought have emerged over the years in examining the mechanisms and modeling of boundary lubrication. The chemical school believes that chemical reactions at the rubbing surfaces control the efficacy of the lubrication process. The mechanical school believes that while chemistry is a factor, hydrodynamics, elastohydrodynamics (EHD), and micro-EHD can account for most of the load-bearing mechanisms, so at least in design, they are the principal issues. This paper attempts to bring the two schools together to examine a common set of experimental data. The experiments involved running wear tests on a four-ball wear tester using microliter of lubricant until seizure. Lubricant degradation and breakdown are therefore a factor in the wear test. The key to both models is the temperatures in the contest. This paper describes the two models and focuses on the temperatures in the contact. The temperatures calculated from the two models differ significantly.

Materials Degradation & Fouling

03,228
DE93041307 PC A06/MF A02
National Inst. of Standards and Technology (MSEL), Gaithersburg, MD. Ceramics Div.
Review of Corrosion Behavior of Ceramic Heat Exchanger Materals: Corrosion Characteristics of Silicon Carbide and Silicon Nitride. Final Report, September 11, 1992--March 11, 1993.
Progress rept.
R. G. Munro, and S. J. Dapkunas. 1993, 103p, DOE/PC/92179-T1.
Contract AI22-92PC92179
Sponsored by Department of Energy, Washington, DC.

Keywords: *Heat Exchangers, *Silicon Carbides, *Silicon Nitrides, *Corrosion Resistance, Ashes, Flexural Strength, Gases, Liquid Metals, Materials, Molten Salts, Oxidation, Progress Report, Protective Coatings, Reviews, Slags, Temperature Range 1000-4000 K, EDB/360205.

The present work is a review of the substantial effort that has been made to measure and understand the effects of corrosion with respect to the properties, performance, and durability of various forms of silicon carbide and silicon nitride. The review encompasses corrosion in diverse environments, usually at temperatures of 1000C or higher. The environments include dry and moist oxygen, mixtures of hot gaseous vapors, molten salts, molten metals, and complex environments pertaining to coal ashes and slags.

03,229
PB94-172368 Not available NTIS
National Inst. of Standards and Technology (MSEL), Gaithersburg, MD. Ceramics Div.
Wear Mechanism Maps of Ceramics.
Final rept.
S. M. Hsu, P. I. Lacey, Y. S. Wang, and S. W. Lee. 1990, 10p.
Pub. in Advances in Engineering Tribology, SP-31, p123-132 1990. Sponsored by Gas Research Inst., Chicago, IL.

Keywords: *Wear tests, *Ceramic fibers, *Tribology, *Metal matrix composites, Lubrication, Comparison, Polycrystalline, Composite materials, Reinforcing fibers, Plastic deformation, Fractures(Materials), Reprints.

The wear mechanisms of polycrystalline ceramics have been studied using wear map methodology. Wear of ceramic materials was examined under a wide range of speed and load to identify different wear regimes, and to establish the critical operating limits. The methodology also facilitates comparison among different materials under various systems parameters such as dry sliding, non-reactive fluids, and reactive fluids. The present study compares the wear mechanisms of alumina, silicon nitride, partially stabilized zirconia, and silicon carbide whisker reinforced alumina. Particular attention is given to the location of the transition zone from mild plastic deformation to rapid fracture controlled wear and the concomitant increase in wear rate.

03,230
PB94-172400 Not available NTIS
National Inst. of Standards and Technology (MSEL), Gaithersburg, MD. Ceramics Div.
Fracture Mechanics Analysis of Near-Surface Cracks.
Final rept.
S. Jahanmir, J. W. Dally, and Y. M. Chen. 1990, 6p.
Pub. in Proceedings of Japan International Tribology Conference, Nagoya, Japan, October 29-November 1, 1990, p581-586.

Keywords: *Ceramics, *Wear tests, *Fracture mechanics, *Crack propagation, Tribology, Photoelasticity, Particles, Stress intensity factors, Surfaces, Materials testing, Reprints.

The purpose of the analysis is to develop a qualitative understanding on the propagation of cracks relevant to the formation of wear particles in an elastically deforming stress field. A shallow subsurface crack oriented parallel to the boundary and a vertical surface-breaking crack were analyzed. Three different series of photoelastic experiments were conducted on each crack type and results for the stress intensity factors for both the opening mode and the shearing mode were determined. The relative signs of K(I) and K(II), which depend on the location of crack tip with respect to the point of load application, were used to predict the crack trajectories. The implications of these results on the process of wear particle formation in elastically deforming materials, such as ceramics, are discussed.

03,231
PB94-172749 Not available NTIS
National Inst. of Standards and Technology (MSEL), Gaithersburg, MD. Ceramics Div.
Wear of Selected Materials and Composites Sliding against MoS2 Films.
Final rept.
A. W. Ruff, and M. B. Peterson. 1993, 6p.
Pub. in Wear 162-164, p492-497 1993. See also PB93-138949. Sponsored by Research and Development Lab., Wright-Patterson, OH.

Keywords: *Wear tests, *Molybdenum disulfide, *Composite materials, *Films, *Tribology, *Vacuum coating, Friction tests, Coatings, Solid lubricants, Roller bearings, Space environments, Physical vapor deposition, Reprints.

Improved vacuum deposition methods are now available to produce dense, suitability oriented, durable films of molybdenum disulfide on substrates appropriate for tribological applications. It is of interest to examine materials in sliding contact with such films in order to identify optimum combinations, and to improve further tribological performance of the system. Results of wear and friction measurements are presented to a number of materials including self-lubricating composites sliding against four different types of vacuum-deposited MoS2 films. The testing program utilized a controlled environment, pin-on-ring tribometer, with load and speed conditions appropriate to a possible application. Differences in wear over four orders of magnitude, and friction up to a factor of seven times, were measured among the materials. One application area of interest for these material combinations would be as ball retainers in rolling element bearings for space satellite systems.

03,232
PB94-187317 PC A03/MF A01
National Inst. of Standards and Technology (BFRL), Gaithersburg, MD.
Sulfate Attack of Cementitious Materials: Volumetric Relations and Expansions.
J. R. Clifton, and J. M. Pommersheim. Apr 94, 24p, NISTIR-5390.
Prepared in cooperation with Bucknell Univ., Lewisburg, PA.

Keywords: *Cements, *Concretes, *Sulfates, *Environmental effects, *Mathematical models, Hydration, Expansion, Volume, Chemical composition, Density(Mass/volume), Gypsum, Construction materials, Tricalcium aluminate, Chemical reaction mechanisms, Ettringite.

A model was developed which predicts the conditions under which volumetric expansion of cementitious materials are most likely and the amount of expansion expected. Model parameters include concrete composition, phase densities, water-cement ratio, degree of hydration, extent of expansive reaction and reaction stoichiometry. The model was applied to several different reactions involving sulfate attack of concrete, including gypsum and ettringite formation reactions. The model predicted that ettringite formation from monosulfate would not cause general expansion. However, local expansion could occur if ettringite occupied the same space vacated by reacting monosulfate. The model predicted that if sufficient unhydrated tricalcium aluminate (C3A) was available in mature cement paste and it reacted with gypsum to form ettringite, the reaction could cause expansion at low water-to-cement ratios.

03,233
PB94-212354 Not available NTIS
National Inst. of Standards and Technology (MSEL), Gaithersburg, MD. Ceramics Div.

Materials Degradation & Fouling

Mechanism of Mild to Severe Wear Transition in Alpha-Alumina.
Final rept.
S. Jahanmir, and X. Dong. 1992, 9p.
Pub. in Jnl. of Tribology 114, n3 p403-411 1992.

Keywords: *Aluminum oxide, *Wear, *Friction factor, *Coefficient of friction, Temperature, Ceramics, Tribology, Fractures(Materials), Reprints.

Friction and wear experiments were conducted on high purity alpha-alumina sliding against a similar material in air under different contact loads and at temperatures ranging from 23 C to 900 C. Experimental results indicate that tribochemical reactions between water vapor and alpha-alumina at room temperature produce aluminum hydroxide which result in relatively low coefficients of friction and low wear rates. Both the coefficient of friction and the wear rate of alumina were low at intermediate temperatures (200 C to 800 C), if the contact stress was below a threshold value. Above this load, wear occurred by fracture, the wear coefficient exceeded a value of .0001, and the coefficient of friction increased to 0.90. At 900 C, the coefficient of friction was 0.40 and the wear coefficient was reduced to .0001, because of the formation of a silicon-rich layer on the wear track. A contact mechanics model based on linear elastic fracture mechanics indicated that the propagation of cracks from pre-existing flaws controls the onset of catastrophic wear in the intermediate temperature range.

03,234
PB94-213014 Not available NTIS
National Inst. of Standards and Technology (CSTL), Gaithersburg, MD. Process Measurements Div.
Iridium Oxide Thin-Film Stability in High-Temperature Corrosive Solutions.
Final rept.
K. Kreider. 1991, 5p.
Pub. in Sensors and Actuators B 5, p165-169 1991.

Keywords: *Iridium oxides, Temperature range 0400-1000, Radioactive waste facilities, Underground facilities, High temperature, Aluminum oxide, Thin films, pH meters, Substrates, Stability, Reprints, Sputtered films.

The stability of sputtered iridium oxide films is investigated after exposure to pH 4, 7, and 10 solutions at 200 C (15 bar) and 245 C (40 bar). These reactively sputtered films are being considered as pH-sensing electrodes in high-temperature high-pressure saline solutions such as those found underground in potential nuclear repositories. The sputtered iridium oxide films (SIROF) have a linear response of approximately 53-58 mV per pH at room temperature under a wide range of solution conditions. Other advantages include their ruggedness, small size, high voltage/low impedance output, and the low cost of fabrication. To evaluate their stability, the films are exposed in a Teflon-lined bomb for up to 70 h at high temperature. The pH testing of 50 samples includes cycling between pH 2 and pH 12 before and after exposure. Changes of the potential intercept and the slope are most severe after acidic conditions at 250 C. It is found that ion-assisted deposition helps to maintain film adherence and continuity on the alumina substrates during exposure to 200 C solutions.

03,235
PB95-107041 Not available NTIS
National Inst. of Standards and Technology (MSEL), Gaithersburg, MD. Polymers Div.
Aging in Glasses Subjected to Large Stresses and Deformations.
Final rept.
G. B. McKenna, M. M. Santore, A. Lee, and R. S. Duran. 1991, 8p.
Pub. in Jnl. of Non-Crystalline Solids 131, p497-504 1991.

Keywords: *Glass, *Aging(Materials), *Dilatometry, Viscoelasticity, Torsion, Deformation, Creep, Glass transition temperature, Kinetics, Thermodynamics, Reprints, Erasure, Rejuvenation, Volume recovery.

Physical aging studies near to the conventional glass transition temperature Tg were made using a model epoxy glass. Nonlinear viscoelastic responses were measured after quenching the samples from above Tg to below it. The physical aging response in creep in simple extension was studied as a function of stress magnitude and in stress relaxation in torsion at a function of deformation magnitude. In each test the time t(star) for the aging time shift factor to approach a constant value was determined and found to be independent of the stress or deformation magnitude. These results are interpreted to mean that large mechanical stimuli do not alter the underlying therodynamic state of the glass and aging is not 'erased' by the large stresses or deformations.

03,236
PB95-140588 Not available NTIS
National Inst. of Standards and Technology (MSEL), Gaithersburg, MD. Ceramics Div.
Critical Factors in Non-Lubricated, Non-Abrasive Wear Testing.
Final rept.
A. W. Ruff. 1992, 6p.
Pub. in Jnl. of Friction and Wear 13, n1 p48-53 1992.

Keywords: *Wear tests, *Test methods, *Nondestructive tests, *Standardization, Tribology, Morphology, Wear, Friction, Wear resistance, Reprints, *Non-abrasive wear testing.

Some wear testing approaches used in research and in standardized testing are discussed, along with data from several interlaboratory studies of wear. Four critical factors are suggested to explain the relatively high variation in measured wear properties from three prominent test geometries and methods. The factors are: uniform wear scar morphology, wear debris retention in the contact, test system dynamic stiffness, and specimen shape. Further research efforts are needed to better identify and understand these factors, so that the test methods can be improved and the wear data obtained using them are more accurate and useful.

03,237
PB95-140596 Not available NTIS
National Inst. of Standards and Technology (IMSE), Gaithersburg, MD. Polymers Div.
Tribological Data: Needs and Opportunities.
Final rept.
A. W. Ruff. 1989, 6p.
Sponsored by Department of Energy, Washington, DC.
Pub. in Proceedings of the International Congress on Tribology (5th), Helsinki, Finland, June 12-15, 1989, p26-31 .

Keywords: *Tribology, *Data bases, *Information systems, Information retrieval, Wear, Data retrieval, Information transfer, Data processing, Friction, Information management, Reprints, *ACTIS data base.

Many opportunities exist today for evaluated tribology data and information to influence material selection, component design, predictive model development, and planning of research and development programs for new materials and understanding. In order for tribology databases to have a significant impact, there is need for improved standards of tribological measurement, and for new standards of data systems themselves. Basic considerations applying to tribology data and information are presented and discussed in this paper. Current developments in the U.S. in a joint government-private sector activity concerned with a comprehensive data and information system for tribology, ACTIS, are also described.

03,238
PB95-162517 Not available NTIS
National Inst. of Standards and Technology (MSEL), Gaithersburg, MD. Ceramics Div.
Introduction to ASTM 1199 'Wear Test Selection for Design and Application'.
Final rept.
1993, 2p.
Pub. in Tribology: Wear Test Selection for Design and Application, ASTM STP 1199, 2p 1993.

Keywords: *Wear tests, *Experimental design, *Test methods, *Standards, Design analysis, Test facilities, Erosion, Wear, Tribology, Reprints, *ASTM STP 1199.

ASTM's Committee on Wear and Erosion has sponsored numerous symposia in subject areas such as wear, solid particle erosion, and wear modeling. The focus of those symposia and the resulting Special Technical Publications (STPs) involved numerous scientific and engineering subjects, as well as the area of test methodology. One important area that has not been covered so far is the connection between laboratory testing and actual operating performance of systems or components. The connection between laboratory testing, test results, and final design and performance is a crucial one in the practical application of tribology science and engineering.

03,239
PB95-163796 Not available NTIS
National Inst. of Standards and Technology (MSEL), Gaithersburg, MD. Ceramics Div.
Wear Model for Alumina Sliding Wear.
Final rept.
Y. S. Wang, S. M. Hsu, and R. G. Munro. 1990, 6p.
Pub. in Proceedings of Japan International Tribology Conference, Nagoya, October 29-November 1, 1990, p1225-1230.

Keywords: *Aluminum oxide, *Wear tests, *Mathematical models, *Sliding friction, *Microstructure, Ceramics, Tribology, Lubrication, Tensile stress, Loads(Forces), Velocity, Reprints.

A wear model incorporating microstructural effects has been developed to understand the wear data of alumina sliding on alumina under dry, paraffin oil lubricated, and water lubricated conditions. The model accounts for the wear transitions which were observed under different speeds and loads. A normalized tensile stress delta(sub max)/delta(sub D) is proposed as a critical parameter to explain wear transitions.

03,240
PB95-164067 Not available NTIS
National Inst. of Standards and Technology (MSEL), Gaithersburg, MD. Ceramics Div.
Molecular Orbital Study of Water Enhanced Crack Growth Process.
Final rept.
W. Wong-Ng, G. S. White, and S. W. Freiman. 1990, 4p.
Pub. in Materials Research Society Extended Abstract (EA-23), p11-14 1990.

Keywords: *Silicon dioxide, *Environmental effects, *Molecular orbitals, *Crack propagation, *Water immersion, Covalent bonds, Self consistent field, Chemical bonds, Atomic properties, Ions, Strains, Reprints.

To further our understanding of the mechanism of environmentally enhanced crack growth, molecular orbital calculations (MO) using the ab initio self-consistent field (SCF) technique have been employed to investigate the effect of applied strain on the atomic charges, bond overlap population and ionic character of the Si-O bond at the crack tip of silica. Pyrosilicic acid H6Si2O7 with eclipsed conformation has been employed as the model molecule. Strain effects up to 30% were simulated in terms of bond stretching and angle distortion.

03,241
PB96-141395 Not available NTIS
National Inst. of Standards and Technology (MSEL), Boulder, CO. Materials Reliability Div.
Artificial Crack in Steel: An Ultrasonic-Resonance-Spectroscopy and Modeling Study.
Final rept.
H. Ledbetter, P. Heyliger, K. Pei, S. Kim, and C. Fortunko. 1995, 7p.
Pub. in Review of Progress in Quantitative Nondestructive Evaluation, v14 p2019-2025 1995.

Keywords: *Cracks, *Steels, *Spectroscopy, Ultrasonics, Reprints, Defect detection, Finite element method, Ritz method, Natural-vibration frequencies.

The problem of detecting and characterizing cracks in solids is a major research area involving contributions from mathematics, physics, mechanics, and materials science. In the present study the authors approached this problem from both measurement and modeling viewpoints. In the measurements, the authors used ultrasonic-resonance spectropscopy to determine the macroscopic-vibration-frequency shifts caused by an artificial (electromachined) crack. The modeling used a finite-element method to approximate the macroscopic vibration frequencies of a cracked solid. As a check, the authors used the Ritz method to calculate the frequencies of the noncracked solid.

Miscellaneous Materials

03,242
AD-A302 669/7 PC A04/MF A01
Optical Materials, Inc., Cambridge, MA.
Preliminary Subject and Authors Index to Compilations of Data on Properties of Materials.
J. G. Beckerley. 1966, 47p, NBS-9058.
Contract CST-1321
ADA302670.

Keywords: *Materials, *Subject indexing, Commerce, Technology transfer, Chemistry, Engineering, Physics, Space sciences, Standards, Mathematics, Telecommunications, Industrial research, Physical sciences, Scientists, Applied mechanics.

This report is intended for use in conjunction with NBS Report 9057, Preliminary List of References Containing Compilations of Data on Properties of Materials. It contains two parts: (1) a preliminary subject index; and (2) a name index of authors, editors, translators, and corporate sponsors.

03,243
AD-A302 670/5 PC A05/MF A01
Optical Materials, Inc., Cambridge, MA.
Preliminary List of References Containing Compilations of Data on Properties of Materials.
J. G. Beckerley. 1966, 66p, NBS-9057.
Contract CST-1321
ADA302669.

Keywords: *Materials, *Bibliographies, *Scientific literature, Commerce, Technology transfer, Chemistry, Engineering, Physics, Space sciences, Standards, Mathematics, Telecommunications, Industrial research, Physical sciences, Applied mechanics.

This preliminary list contains 1,000 references in alphabetical order by author or editor. The references contain compilations of numerical data on the physical properties of materials.

03,244
DE93019683 PC A02/MF A01
National Inst. of Standards and Technology (NEL), Gaithersburg, MD. Thermophysics Div.
Dielectric Studies of Fluids with Reentrant Resonators. Appendix B.
A. R. H. Goodwin, and M. R. Moldover. 1993, 10p, CONF-9305134-4-APP.B.
Contract AI05-88ER13823
Symposium on Energy Engineering Sciences (11th), Argonne, IL (United States), 3-5 May 1993. Sponsored by Department of Energy, Washington, DC.

Keywords: *Dielectric Properties, Mixtures, Calibration, Cavity Resonators, Fluids, Fluorine Compounds, Measuring Methods, Phase Transformations, RF Systems, Temperature Dependence, *Refrigerants, EDB/420400.

We have used a reentrant radio-frequency (rf) cavity as a resonator operating near 375 MHz to measure changes in the dielectric constant of fluids within it. The utility of these measurements was demonstrated by determining the dipole moment of 1,1,1,2,5,3-hexafluoropropane, a candidate replacement refrigerant (denoted R236ea) and by detecting the phase boundaries in the mixture ((I-x)C(sub 2)H(sub 6) + xCO(sub 2)), for the mole fraction x = 0.492. The densities of the coexisting phases of the mixture, were determined using the Clausius-Mossotti relation which has errors on the order of 0.5 % in this application. To test the accuracy of the present techniques, the rf resonator was calibrated with helium and then used to redetermine the molar polarizability A(sub c) of argon. The results were in excellent agreement with published values. Our design of the recent resonator makes it suitable for use with corrosive fluids at temperatures up to 400(degrees)C.

03,245
DE94004236 PC A03/MF A01
National Inst. of Standards and Technology, Boulder, CO. Thermodynamics Div.
Thermophysical Properties of HFC-143a and HFC-152a. Quarterly Report, 1 July 1993--30 September 1993.
Progress rept.
W. M. Haynes. Oct 93, 27p, DOE/CE/23810-22A.
Contract FG02-91CE23810
Sponsored by Department of Energy, Washington, DC.

Keywords: *Freons, *Refrigerants, Compiled Data, Data Compilation, Density, Equations of State, Physical Properties, Progress Report, Specific Heat, Thermodynamic Properties, Vapor Pressure, Volume, Tables(data), *Thermophysical properties, EDB/360606.

Numerous fluids have been identified as promising alternative refrigerants, but much of the information needed to predict their behavior as pure fluids and as components in mixtures does not exist. In particular, reliable thermophysical properties data and models are needed to predict the performance of the new refrigerants in heating and cooling equipment and to design and optimize equipment to be reliable and energy efficient. Objective of this project is to provide highly accurate, selected thermophysical properties data for refrigerants HFC-143a (CH(sub 3)CF(sub 3)) and HFC-152a (CH(sub 3)CHF(sub 2)) and to use these data to fit complex equations of state and detailed transport property models. The new data will fill gaps in the existing data sets and resolve problems and uncertainties that exist in and between the data sets.

03,246
DE94017738 PC A03/MF A01
National Inst. of Standards and Technology (NEL), Gaithersburg, MD. Thermophysics Div.
Development of Measurement Capabilities for the Thermophysical Properties of Energy-Related Fluids. Annual Report, December 1, 1993--November 30, 1994.
Progress rept.
17 Aug 93, 24p, DOE/ER/13823-T3.
Contract AI05-88ER13823
Sponsored by Department of Energy, Washington, DC.

Keywords: *Refrigerants, *Measuring Instruments, Calorimeters, Densimeters, Dielectric Properties, Phase Studies, Progress Report, Solutions, Thermal Conductivity, Viscosimeters, *Thermophysical properties, EDB/440800.

Objectives are to develop state-of-the-art experimental apparatus for measuring the thermophysical properties of a wide range of fluids and fluid mixtures important to the energy, chemical, and energy-related industries, and carry out benchmark measurements on key systems. Measurement capabilities to be developed cover transport properties, thermodynamic properties, phase equilibria properties, and dielectric properties. The new apparatus will make it possible to study a wide range of complex fluid systems under conditions that have been previously inaccessible. Specific measurement capabilities to be developed are: Thermal Conductivity Apparatus, Vibrating Wire Viscometer, Dual-Sinker Densimeter, High-Temperature Vibrating Tube Densimeter, Dynamic Phase Equilibria Apparatus, Apparatus for Dilute Solutions, Total-Enthalpy Flow Calorimeter, Dielectric Constant Apparatus. The research also includes benchmark experimental measurements on pure and mixed alternative refrigerants, aqueous solutions, and carefully selected systems consisting of species of diverse size (methane + neopentane) and polarity (methane + ammonia) important for development of predictive models for energy-related fluids. (ERA citation 19:030826)

03,247
DE95002261 PC A02/MF A01
National Inst. of Standards and Technology, Boulder, CO.
Thermophysical properties of HCFC alternatives. Quarterly report, 1 July 1994--30 September 1994.
Progress rept.
W. M. Haynes. Oct 94, 6p, DOE/CE/23810-48A.
Contract FG02-91CE23810
Sponsored by Department of Energy, Washington, DC.

Keywords: *Refrigerants, Performance, Progress Report, *Thermophysical properties, EDB/420400, EDB/320106.

Numerous fluids and fluid mixtures have been identified as promising alternatives to the HCFC refrigerants, but, for many of them, reliable thermodynamic data do not exist. In particular, reliable thermodynamic properties data and models are needed to predict the performance of the new refrigerants in heating and cooling equipment and to design and optimize equipment to be reliable and energy efficient. The objective of this project is to measure, with high accuracy, selected thermodynamic properties data for two pure refrigerants and nine refrigerant blends; these data will be used to fit equations of state and other property models which can be used in equipment design. The new data will fill in gaps in the existing data and resolve problems and differences that exist in and between existing data sets. Most of the studied fluids and blends are potential replacements for HCFC-22 and/or R502; in addition, one pure fluid and one blend are potential replacements for CFC-13 in low temperature refrigeration applications.

03,248
DE95011238 PC A03/MF A01
National Inst. of Standards and Technology (BFRL), Gaithersburg, MD.
Lean flammability limit as a fundamental refrigerant property. Phase 1, Interim technical report, 1 October 1994--31 March 1995.
C. Womeldorf, M. King, and W. Grosshandler. 31 Mar 95, 30p, DOE/CE/23810-58.
Contract FG02-91CE23810
Sponsored by Department of Energy, Washington, DC.

Keywords: *Refrigerants, Chlorofluorocarbons, Flammability, Testing, EDB/320106.

Due to the ozone-depleting effects of commonly used chlorofluorocarbon refrigerants, safe environmentally-friendly replacements must be found. HFC-32 (CH(sub 2)F(sub 2)) and other hydrochlorofluorocarbons are potential candidates; however, in contrast with the CFCs, many of these compounds are flammable. Testing the flammability limits of these hydrochlorofluorocarbons using traditional ASTM E-681 methods has produced a range of limits depending upon the vessel and ignition source used. This project demonstrates the feasibility of defining a fundamental flammability limit of HFC-32, that occurs at the limit of a zero strain rate and is independent of ignition source. Using a counterflow twin-flame burner to define extinction points for different strain rates, an extrapolation to zero strain rate is performed. Using this technique, preliminary results on the lean flammability limit of HFC-32 and the critical flammability ratio of HFC-125 (C(sub 2)HF(sub 5)) in ETC-32 are reported.

03,249
DE96010433 PC A04/MF A01
National Inst. of Standards and Technology (CSTL), Boulder, CO. Thermophysics Div.
Thermophysical properties of HCFC alternatives. Quarterly report, October 1--December 31, 1995.
PROGRESS REPT.
W. M. Haynes. Jan 96, 32p, DOE/CE/23810-66A.
Contract FG02-91CE23810
Sponsored by Department of Energy, Washington, DC.

Keywords: *Refrigerants, Air Conditioners, Chemical Composition, Chlorofluorocarbons, Density, Experimental Data, Fluorinated Aliphatic Hydrocarbons, Liquids, Material Substitution, Measuring Instruments, Progress Report, Refrigerating Machinery, Thermodynamic Model, Thermodynamic Properties, Vapor Pressure, Vapors, Tables(data), EDB/400201, EDB/320106, EDB/320302.

Numerous fluids and fluid mixtures have been identified as promising alternatives to the HCFC refrigerants, but, for many of them, reliable thermodynamic data do not exist. In particular, reliable thermodynamic properties data and models are needed to predict the performance of the new refrigerants in heating and cooling equipment and to design and optimize equipment to be reliable and energy efficient. The objective of this project is to measure, with high accuracy, selected thermodynamic properties data for two pure refrigerants and nine refrigerant blends; these data will be used to fit equations of state and other property models which can be used in equipment design. The new data will fill in gaps in the existing data and resolve problems and differences that exist in and between existing data sets. Most of the studied fluids and blends are potential replacements for HCFC-22 and/or R502; in addition, one pure fluid and one blend are potential replacements for CFC-13 in low temperature refrigeration applications.

03,250
DE96010579 PC A05/MF A01
National Inst. of Standards and Technology (CSTL), Boulder, CO. Thermophysics Div.
Thermophysical properties of HCFC alternatives. Quarterly report, April 1--June 30, 1995.
PROGRESS REPT.
W. M. Haynes. Jul 95, 68p, DOE/CE/23810-61A.
Contract FG02-91CE23810
Sponsored by Department of Energy, Washington, DC.

Keywords: *Refrigerants, Air Conditioners, Chlorofluorocarbons, Compiled Data, Density, Equilibrium, Experimental Data, Liquids, Material Substitution, Mixtures, Progress Report, Refrigerating Machinery, Sound Waves, Specific Heat, Thermodynamic Model, Thermodynamic Properties, Vapor Pressure, Vapors, Velocity, Tables(data), EDB/400201, EDB/320106, EDB/320302.

Numerous fluids and fluid mixtures have been identified as promising alternatives to the HCFC refrigerants, but, for many of them, reliable thermodynamic data do not exist. In particular, reliable thermodynamic prop-

erties data and models are needed to predict the performance of the new refrigerants in heating and cooling equipment and to design and optimize equipment to be reliable and energy efficient. The objective of this project is to measure, with high accuracy, selected thermodynamic properties data for two pure refrigerants and nine refrigerant blends; these data will be used to fit equations of state and other property models which can be used in equipment design. The new data will fill in gaps in the existing data and resolve problems and differences that exist in and between existing data sets. Most of the studied fluids and blends are potential replacements for HCFC-22 and/or R502; in addition, one pure fluid and one blend are potential replacements for CFC-13 in low temperature refrigeration applications.

03,251
PB94-172426 Not available NTIS
National Inst. of Standards and Technology (BFRL), Gaithersburg, MD. Building Environment Div.
Simultaneous Visual and Calorimetric Measurements of R11, R123, and R123/Alkylbenzene Nucleate Flow Boiling.
Final rept.
M. A. Kedzierski. 1993, 7p.
Pub. in Proceedings of NHTC Session on Alternative Refrigerants in Heat Transfer Equipment, Atlanta, GA., August 8-13, 1993, 7p. See also PB94-120756. Sponsored by Department of Energy, Washington, DC.

Keywords: *Refrigerants, *Nucleate boiling, *Environmental chemical substitutes, *Air pollution abatement, Mixtures, Performance standards, Lubricants, Freons, Chlorohydrocarbons, Fluorohydrocarbons, Benzenes, Heat measurement, Visual inspection, Reprints, Methane/trichlorofluoro, Ethane/dichloro-trifluoro, R11, R123.

Bubble formation during horizontal flow boiling of trichloromethane (R11), 1,1-dichloro-2,2,2-trifluoroethane (R123) and two R123/alkylbenzene lubricant mixtures was investigated both visually and calorimetrically. Locally measured heat transfer coefficients were taken simultaneously with high speed motion picture images of the boiling process. The addition of a small amount (0.55%) of alkylbenzene to R123 increases the number of active nucleation sites by approximately 5 sites/sq cm which corresponds to a 12% to 50% increase in the site density. The increase in the site density contributed to the enhancement of the heat transfer coefficient of the R123/0.55% alkylbenzene mixture over that of the pure 123. Further increase in the amount of alkylbenzene to the R123 reduces the number of active sites to below that of pure R123 to approximately the value for that of R11. Consequently, the 0.55% lubricant mass fraction mixture exhibited a heat transfer coefficient that was larger than that of the 2% lubricant mass fraction mixture.

03,252
PB94-199775 Not available NTIS
National Inst. of Standards and Technology (NEL), Gaithersburg, MD. Building Environment Div.
Role of Refrigerant Mixtures as Alternatives to CFCs.
Final rept.
D. A. Didion, and D. B. Bivens. 1990, 13p.
Pub. in International Jnl. of Refrigeration 13, n3 p163-175 May 90. See also PB92-170836.

Keywords: *Refrigerants, *Working fluids, *Azeotropes, Heat transfer fluids, Cooling systems, Refrigeration, Solutions(Mixtures), Air pollution abatement, Mixtures, Reprints, *Near-azeotropes, *Zeotropes.

A review of the state-of-the-art of refrigerant mixtures is presented. The categories of azeotropes, near-azeotropes and zeotropes are discussed separately as to their advantages as a refrigerant system working fluid and as to their requirements for adaptation. It may be possible to find azeotropes and near-zeotropes which could be candidates for alternatives for existing systems as well as new systems with little or no change in system performance. Zeotropes are not applicable for existing systems but offer the potential for significant performance improvements if the new systems are redesigned so as to incorporate the zeotropic attributes of two phase flow temperature glide and variable composition. Whereas, the azeotropes and near-azeotropes development are likely to have impact on the immediate ozone depletion crisis, the development will take longer but will be necessary for the greenhouse warming crisis.

03,253
PB94-199783 Not available NTIS
National Inst. of Standards and Technology (NEL), Gaithersburg, MD. Building Environment Div.
Role of R22 in Refrigerating and Air Conditioning Equipment.
Final rept.
D. A. Didion, R. Cohen, and D. R. Tree. 1990, 27p.
Pub. in Proceedings of the International Colloquium of Brussels 'Refrigeration and CFCs', p128-154 1990.

Keywords: *Refrigerants, *Refrigerating machinery, *Air conditioning equipment, *Chlorofluorocarbons, Reprints, Heat transfer fluids, Economic analysis, Working fluids, Ozone depletion, Air pollution abatement, *R 22, Hydrofluorocarbons.

Refrigerant 22 is shown to be, like many other HCFC refrigerants, one of depletion potential, as a class, HCFC refrigerants, especially R22, are part of the interim solutions for the substitution of CFC refrigerants. Until refrigerants with no ozone depletion potential are developed and equipment designed and produced in quantity to use these refrigerants, the HCFC refrigerants will remain an important and vital refrigerant class. Except in a few applications, other factors such as global warming potential and efficiency, toxicity, safety, materials compatibility, and commercial availability of the refrigerant and of the refrigerating and air conditioning equipment make immediate replacement of R22 and all other HCFC refrigerants impossible. For some applications commitment of major capital investments and log lead times for design and production of new machinery systems using existing atmospherically benign alternatives are needed. Other applications require research for new refrigerants without ozone depletion potential, a process without a guarantee of success. The immediate replacement of R22 systems is not a viable choice.

03,254
PB94-199791 Not available NTIS
National Inst. of Standards and Technology (CSTL), Boulder, CO. Thermophysics Div.
Measurements of the Viscosities of Saturated and Compressed Fluid 1-chloro-1,2,2,2-tetrafluoroethane (R124) and Pentafluoroethane (R125) at Temperatures between 120 and 420 K.
Final rept.
D. E. Diller, and S. M. Peterson. 1993, 12p.
Contract DE-A101-91CE23808
Pub. in International Jnl. of Thermophysics 14, n1 p55-66 Jan 93. Sponsored by Department of Energy, Washington, DC.

Keywords: *Viscosity, *Refrigerants, *Fluids, *Compressible fluids, *Saturation(Chemistry), Temperature dependence, Fluorohydrocarbons, Pressure, Volume, Reprints, *Ethane/chloro-tetrafluoro, *Ethane/pentafluoro, Molar volume, R125, R124.

The shear viscosities of saturated and compressed fluid 1-chloro-1,2,2,2-tetrafluoroethane (R124) and pentafluoroethane (R125) have been measured with two torsional crystal viscometers at temperatures between 120 and 420 K and at pressures up to 50 MPa. At small molar volumes, the fluidity (reciprocal viscosity) increases linearly with molar volume at fixed temperature and weakly with temperature at fixed volume. We have described this behavior with simple empirical equations and have compared the data of Shankland and of Ripple with them. The data of Ripple are in good agreement with our data for both fluids.

03,255
PB94-199890 Not available NTIS
National Inst. of Standards and Technology (NEL), Gaithersburg, MD. Building Environment Div.
Simplified Cycle Simulation Model for the Performance Rating of Refrigerants and Refrigerant Mixtures.
Final rept.
P. A. Domanski, and M. O. McLinden. 1993, 8p.
Pub. in International Jnl. of Refrigeration 15, n2 p81-88 1992. See also PB93-130383. Sponsored by Environmental Protection Agency, Washington, DC. and Electric Power Research Inst., Palo Alto, CA.

Keywords: *Refrigerants, *Thermodynamic properties, *Models, *Computerized simulation, Equations of state, Mixtures, Computer programs, Transport properties, Heat pumps, Refrigerators, Vapor compression refrigeration cycle, Reprints.

A simulation program, CYCLE11, which is useful for the preliminary evaluation of the performance of refrigerants and refrigerant mixtures in the vapor compression cycle is described. The program simulates a theoretical vapor-compression cycle and departures from the theoretical cycle as occur in a heat pump and in a refrigerator. The cycles are prescribed in terms of the temperatures of the external heat transfer fluids with the heat exchangers generalized by their average effective temperature differences. The isenthalpic expansion process is assumed. The program includes a rudimentary model of a compressor and a representation of the suction line and liquid line heat exchange. Refrigerant thermodynamic properties are calculated using the Carnahan-Starling-DeSantes equation-of-state. Refrigerant transport properties are not included in the simulations. The program can generate merit ratings of refrigerants for which limited measurement data are available. An example of simulation results stresses the need for careful application of simplified models and consideration for the involved assumptions.

03,256
PB94-212081 Not available NTIS
National Inst. of Standards and Technology (CSTL), Boulder, CO. Thermophysics Div.
Equation of State Formulation of the Thermodynamic Properties of R134a (1,1,1,2-Tetrafluoroethane).
Final rept.
M. L. Huber, and J. F. Ely. 1992, 8p.
Pub. in International Jnl. of Refrigeration 15, n6 p393-400 1992.

Keywords: *Thermodynamic properties, *Refrigerants, Specific heat, Volume, Mathematical models, Equations of state, Vapor pressure, Density, Temperature, Reprints, *R134a, *Tetrafluoroethane.

New correlations for the thermodynamic properties of R134a are presented. A classical equation for the molar Helmholtz energy is used with temperature and density as the independent variables. The equation is accurate for both the liquid and vapor phases at pressures up to 70 MPa, and for a temperature range from the triple point to 450 K. Temperatures are given on the new International Temperature Scale of 1990 (ITS 90). The equation was developed by using experimental data for pressure-volume-temperature properties, isochoric heat capacity, second virial coefficients, speed of sound and coexistence properties. Comparisons with experimental data and with two other equations of state are given. Ancillary equations representing the saturated liquid and vapor densities and the vapor pressure are also presented.

03,257
PB94-212099 Not available NTIS
National Inst. of Standards and Technology (CSTL), Boulder, CO. Thermophysics Div.
Prediction of Viscosity of Refrigerants and Refrigerant Mixtures.
Final rept.
M. L. Huber, and J. F. Ely. 1992, 10p.
Sponsored by Department of Energy, Washington, DC.
Pub. in Fluid Phase Equilibria 80, p239-248 1992.

Keywords: *Viscosity, *Refrigerants, Mixtures, Equations of state, Thermodynamic properties, Mathematical models, Mass, Boundary conditions, Reprints, R134a, Tetrafluoroethane.

We have developed a predictive corresponding states model for the viscosity of pure refrigerants and refrigerant mixtures. The model uses extended corresponding states with R134a (1,1,1,2-tetrafluoroethane) as the reference fluid. The model uses equilibrium shape factors and an equivalent substance reducing ratio (ESRR) for the viscosity which involves the molecular mass. The 'mass' ESRR is found using viscosity data along the saturation boundary. We have fit these mass ESRR's to a general form involving reduced temperature and a structural factor. In addition, we have determined a set of universal coefficients for the mass ESRR that can be used to predict the viscosity of any halocarbon refrigerant given the critical parameters and the structural parameter. We give sample results comparing the model predictions with experimental data for pure fluids and a refrigerant mixture.

03,258
PB94-212107 Not available NTIS
National Inst. of Standards and Technology (CSTL), Boulder, CO. Thermophysics Div.

Prediction of the Thermal Conductivity of Refrigerants and Refrigerant Mixtures.
Final rept.
M. L. Huber, D. G. Friend, and J. F. Ely. 1992, 13p.
Sponsored by Department of Energy, Washington, DC.
Pub. in Fluid Phase Equilibria 80, p249-261 1992.

Keywords: *Refrigerants, *Mixtures, *Thermal conductivity, Thermodynamic properties, Working fluids, Mathematical models, Uncertainty, Reprints, R134a, Tetrafluoroethane.

We use an extended corresponding states model to predict the thermal conductivity of pure halocarbon refrigerants and refrigerant mixtures. The model uses R134a (1,1,1,2-tetrafluoroethane) as the reference fluid, and we present a correlation, including critical enhancement, for the thermal conductivity of R134a. We give sample results comparing the model predictions with experimental data for pure halocarbon refrigerants and refrigerant mixtures; typically, the uncertainty of the predictions is 5-10 percent.

03,259
PB94-212701 Not available NTIS
National Inst. of Standards and Technology (BFRL), Gaithersburg, MD. Building Environment Div.
Causes of the Apparent Heat Transfer Degradation for Refrigerant Mixtures.
Final rept.
M. A. Kedzierski, J. H. Kim, and D. A. Didion. 1992, 10p.
Sponsored by Electric Power Research Inst., Palo Alto, CA. and Department of Energy, Washington, DC.
Pub. in Proceedings of National Heat Transfer Conference and Exhibition (28th), San Diego, CA., August 9-12, 1992, p149-158.

Keywords: *Thermal degradation, *Refrigerants, *Heat transfer coefficients, Mixtures, Evaporation, Heat transfer, Working fluids, Mass transfer, Nucleate boiling, Reprints.

This paper presents an investigation into the causes of the apparent heat transfer degradation associated with horizontal-annular flow evaporation of refrigerant mixtures. The apparent heat transfer degradation is the difference between the measured heat transfer coefficient and the heat transfer coefficient that would be obtained from a linear interpolation of the single component values. The degradation is apparent since the linearly interpolated values have no physical basis. For horizontal-annular flow evaporation, most of the heat transfer degradation is a consequence of the use of the locally uniform equilibrium temperature in the measurement and calculation of the heat transfer coefficient. In reality, both circumferential and radial composition gradients can exist within the liquid film which cause temperature distributions that deviate significantly from a uniform saturation temperature. If the actual liquid-vapor interface temperatures (local vapor temperatures) were used in the calculation of the measured heat transfer coefficient for the impose heat flux condition, most of the apparent degradation would not exist. The remainder of the heat transfer degradation is due to nonlinear mixture property effects. Previously published measured heat transfer coefficients for three mixtures were investigated.

03,260
PB94-219375 (Order as PB94-219326, PC A05/MF A02)
National Inst. of Standards and Technology, Boulder, CO.
Refractive Indices of Fluids Related to Alternative Refrigerants.
T. J. Bruno, M. A. Wood, and B. N. Hansen. 1994, 4p.
Included in Jnl. of Research of the National Institute of Standards and Technology, v99 n3 p263-266 May/Jun 94.

Keywords: *Refrigerants, *Refractivity, Ethane, Ethylene, Ethers, Propane, Halohydrocarbons, Propyne.

As part of a comprehensive program to develop suitable methods of chemical analysis for alternative refrigerants and their products, the authors have compiled a database of spectral, chromatographic, and physical property data that can aid in compound identification. As a small part of this effort, they have measured the refractive indices of a number of such fluids for which data were unavailable. The measurements were performed on a commercially available, digital Abbe refractometer that was modified for the relatively low temperature measurements (0 deg C to 20 deg C) that are sometimes required with these samples.

03,261
PB95-107298 Not available NTIS
National Inst. of Standards and Technology (CSTL), Gaithersburg, MD. Process Measurements Div.
Resistance Thermometers with Fast Response for Use in Rapidly Oscillating Gas Flows.
Final rept.
W. Rawlins, K. D. Timmerhaus, and R. Radebaugh. 1992, 4p.
Pub. in Temperature - Its Measurement and Control in Science and Industry, v6 p471-474 1992.

Keywords: *Thermometers, *Oscillating flow, *Cryogenic cooling, *Refrigerators, *Working fluids, Temperature measurement, Effectiveness, Coolers, Gas flow, Refrigerating machinery, Reprints.

The paper describes a resistance thermometer that permits instantaneous measurement of gas temperatures with the use of a 4 micrometer diameter tungsten wire mounted on heavier wire supports. This configuration provides sufficient strength to survive oscillating flows of helium gas up to 30 Hz at pressures up to 2.2 MPa. The probes are small enough to fit perpendicular to the flow in 3 mm diameter stainless steel tubes. Custom fittings designed to support the resistance thermometers introduce very little void volume to the system. Response time of the probes is approximately 260 microseconds, which permits resolution of temperature oscillations up to 30 Hz with negligible phase shifts. A very nearly linear response for these resistance thermometers is obtained from 80 K to 400 K. Sensitivity of these thermometers decreases rapidly below about 60 K. Results of dynamic temperature measurements obtained at the cold end of a pulse tube refrigerator will be shown.

03,262
PB95-143301 PC A05/MF A02
National Inst. of Standards and Technology (BFRL), Gaithersburg, MD. Building Environment Div.
Visual Measurement Technique for Analysis of Nucleate Flow Boiling.
M. A. Kedzierski, J. M. Crowder, A. M. Jacobi, and L. W. Zhang. Oct 94, 99p, NISTIR-5519.
See also PB93-120756.

Keywords: *Refrigerants, *Nucleate boiling, *Flow visualization, *Image analysis, Heat flux, Computer programs, Flow rate, Heat transfer, Bubbles, Vaporization, *Visual measurement.

This report provides a record of a visual measurement technique for the analysis of the bubbles formed by nucleate flow boiling. The purpose of measuring these bubbles is to extend the understanding of the boiling process. By studying the behavior of these vapor bubbles, a better understanding of the physics controlling boiling heat transfer will be gained. The boiling of refrigerants is simultaneously filmed with a high speed 16mm camera while heat transfer measurements are taken. These tests are performed over a range of heat fluxes and flow velocities in order to study the effect of these conditions on the bubble dynamics. The analysis of the 16mm films evolved from a manual to a computer assisted system, and finally to a digital image analysis system. The following is an overview of the filming apparatus and the bubble measurement schemes.

03,263
PB95-168688 Not available NTIS
National Inst. of Standards and Technology (CSTL), Boulder, CO. Thermophysics Div.
Reference Data for the Thermophysical Properties of Cryogenic Fluids.
Final rept.
W. M. Haynes, and D. G. Friend. 1994, 10p.
Pub. in Advances in Cryogenic Engineering, v39 p1865-1874 1994.

Keywords: *Cryogenic fluids, *Refrigerants, *Thermophysical properties, *Reference materials, Thermodynamic properties, Pressure, Temperature, Volume, Specific heat, Thermal conductivity, Equations of state, Transport properties, Technology transfer, Reprints, *Standard reference materials, US NIST, Phase equilibria, Sound speed profile.

The Thermophysics Division of the National Institute of Standards and Technology has long been involved in providing standard reference data for the thermophysical properties of cryogenic fluids. Comprehensive experimental facilities have been used to provide accurate data for Pressure-Vapor-Temperature (PVT) relations, heat capacities, sound speeds, phase equilibria, and transport properties for a large variety of well characterized cryogenic fluid systems. This critically evaluated information on the thermophysical properties of fluids and fluid mixtures of cryogenic interest is used for custody transfer applications and for efficient design and operation of cryogenic processes in the chemical, natural gas, aerospace, environmental, refrigeration, and other energy related industries.

03,264
PB95-168878 Not available NTIS
National Inst. of Standards and Technology (CSTL), Boulder, CO. Thermophysics Div.
Measurements of Molar Heat Capacity at Constant Volume (Cv) for 1,1,1,2-Tetrafluoroethane (R134a).
Final rept.
J. W. Magee. 1992, 9p.
Pub. in International Jnl. of Refrigeration 15, n6 p372-380 1992.

Keywords: *Specific heat, *Fluorohydrocarbons, *Refrigerants, Calorimetry, Temperature dependence, Pressure dependence, Triple point, Phase transformations, Thermodynamic properties, Liquid phases, Vapor phases, Reprints, *R134a, *1,1,1,2-Tetrafluoroethane.

The molar heat capacity at constant volume was measured by applying an adiabatic method. Heat capacities at 310 state conditions were measured. Measurements were made on liquid in equilibrium with its vapor, and on compressed liquid samples of 1,1,1,2-tetrafluoroethane (R134a), at temperatures from 172 to 343 K with pressures as high as 35 MPa. In the course of these measurements, a determination of the triple point temperature (169.85 + or - 0.01 K) was made. For the high purity (0.9999 +) sample, results were obtained for two-phase, saturated liquid and single phase molar heat capacities as a function of measured temperature, pressure and density. The maximum probable uncertainty of the heat capacity values is estimated not to exceed + or - 0.5%.

03,265
PB95-168886 Not available NTIS
National Inst. of Standards and Technology (CSTL), Boulder, CO. Thermophysics Div.
Vapour Pressure Measurements on 1,1,1,2-Tetrafluoroethane (R134a) from 180 to 350 K.
Final rept.
J. W. Magee, and J. B. Howley. 1992, 3p.
Pub. in International Jnl. of Refrigeration 15, n6 p362-364 1992.

Keywords: *Vapor pressure, *Fluorohydrocarbons, *Refrigerants, Thermodynamic properties, Temperature dependence, Reprints, *1,1,1,2-Tetrafluoroethane, *R134a.

Measurements of vapor pressures were made for 1,1,1,2-tetrafluoroethane (R134a) from 180 to 350 K by using a static cell. Temperatures were measured with a platinum resistance thermometer to within an accuracy of + or - 0.03 K. Pressures were measured with calibrated oscillating quartz-crystal pressure transducers with uncertainties estimated to range from 0.02 to 1.8 kPa.

03,266
PB95-168936 Not available NTIS
National Inst. of Standards and Technology (CSTL), Boulder, CO. Thermophysics Div.
Annex 18: An International Study of Refrigerant Properties.
Final rept.
M. O. McLinden. 1994, 4p.
Pub. in IEA Heat Pump Centre Newsletter 12, n1 p28-31 Mar 94.

Keywords: *Fluorohydrocarbons, *Refrigerants, *Environmental chemical substitutes, *Thermophysical properties, Thermodynamic properties, Transport properties, Research programs, International cooperation, Alternatives, Reprints, *Hydrochlorofluorocarbons, Halons, Hydrofluorocarbons.

The article highlights the activities of Annex 18 'Thermophysical Properties of the Environmentally Accpetalbe Refrigerants', which was established in 1990. The objectives of the Annex are to foster coordination and cooperation among researchers in this field and to determine thermophysical properties leading to internationally accepted formulations for the leading al-

ternative refrigerants. Tasks in support of these goals have included surveys of research, compilations of data, evaluations of equations of state, and the preparation of properties bulletins for HFC-134a and HCFC-123.

03,267
PB95-168951 Not available NTIS
National Inst. of Standards and Technology (CSTL), Boulder, CO. Thermophysics Div.
Development of a Dual-Sinker Densimeter for High-Accuracy Fluid P-V-T Measurements.
Final rept.
M. O. McLinden, and N. V. Frederick. 1993, 16p.
Sponsored by Department of Energy, Washington, DC.
Pub. in Proceedings of Symposium on Energy Engineering Sciences (11th), Argonne, IL., May 3-5, 1993, p63-69 1994.

Keywords: *Refrigerants, *Thermophysical properties, *Fluorohydrocarbons, *Environmental chemical substitutes, Thermodynamic properties, Transport properties, Boiling points, Specific heat, Thermal conductivity, Equations of state, Vapor pressure, Triple point, Pressure, Volume, Temperature, Alternatives, Reprints, *Hydrofluorocarbons, Phase equilibria, Sound speed profile.

The status and available data for several of the leading 'new' or alternative refrigerants are summarized. The data considered include triple point, normal boiling point, and critical point parameters; the temperature dependence of the vapor pressure, ideal gas heat capacity, and saturated liquid density. Also considered are single phase Pressure-Vapor-Temperature (p-V-T), heat capacity, sound speed, viscosity, and thermal conductivity data. The fluids of interest are the HFCs 23, 32, 125, 134a, 134, 143a, and 152a.

03,268
PB95-168969 Not available NTIS
National Inst. of Standards and Technology (CSTL), Boulder, CO. Thermophysics Div.
Need for, and Availability of, Working Fluid Property Data: Results from Annexes XIII and XVIII.
Final rept.
M. McLinden, and L. Vamling. 1993, 12p.
Pub. in Heat Pumps for Energy Efficiency and Environmental Progress, p115-126 1993.

Keywords: *Working fluids, *Thermodynamic properties, *Transport properties, Heat pumps, Equations of state, Refrigerants, Sensitivity analysis, Accuracy, Reprints, R134a, R123.

In these days of transition to new, more environmentally friendly working fluids, there is a definite need for good data and models of basic thermodynamic and transport properties of both pure compounds and mixtures to be used for cycle calculations and equipment redesign. Two annexes of the IEA Program on Advanced Heat Pumps have dealt with such data, namely Annex XIII--State and Transport Properties of High Temperature Working Fluids and Nonazeotropic Mixtures and Annex XVIII--Thermophysical Properties of the Environmentally Acceptable Refrigerants. In this paper, highlights of these two annexes are presented. A sensitivity analysis (from Annex XIII) gives an estimate of how accurately these basic data need to be known to reach a certain accuracy in heat pump coefficient of performance (COP) and heating or cooling capacity calculations. This analysis points out the importance of measured property data. Other projects to be highlighted are a comparison of equations of state with experimental density, vapor pressure, and heat capacity data for mixtures (XIII), a survey of current research on the properties of the 'new' refrigerants (XVIII), and an evaluation of equations of state for R134a and R123 which will lead to an international bulletin for the properties of these two alternative refrigerants (XVIII).

03,269
PB95-169058 Not available NTIS
National Inst. of Standards and Technology (CSTL), Boulder, CO. Thermophysics Div.
Measurement of the Thermal Properties of Electrically Conducting Fluids Using Coated Transient Hot Wires.
Final rept.
R. A. Perkins. 1994, 8p.
Sponsored by Department of Energy, Washington, DC.
Pub. in Proceedings of the Symposium on Energy Engineering Sciences (12th), Argonne, IL., April 27-29, 1994, p90-97.

Keywords: *Thermal conductivity, *Fluorohydrocarbons, Thermal properties, Supercritical fluids, Refrigerants, Temperature dependence, Thermophysical properties, Reprints, *R134a, *Electrically conducting fluids, Transient hot wire technique.

Measurements of fluid thermal properties using the transient hot-wire technique are described. When bare hot wires are used in electrically conducting fluids, there are additional measurement uncertainties due to the formation of electric double layers on the surfaces of the wires and the cell wall. If the electrical conductivity of the fluid is large enough, there is also significant power generation in the fluid. These measurement uncertainties can be eliminated by electrically insulating the hot wires with a thin film. The use of tantalum hot wires with an anodized layer of tantalum pentoxide is demonstrated with measurements on nonpolar argon and polar 1,1,1,2-tetrafluoroethane (R134a). Although coated tantalum hot wires have been used previously in a transient mode to measure the thermal conductivity of liquids, this work is the first demonstration of the use of coated wires to measure thermal conductivity in the liquid, vapor, and supercritical gas phases.

03,270
PB95-169272 Not available NTIS
National Inst. of Standards and Technology (CSTL), Gaithersburg, MD. Thermophysics Div.
Measurements of the Vapor Pressures of Difluoromethane, 1-Chloro-1,2,2,2-Tetrafluoroethane, and Pentafluoroethane.
Final rept.
L. A. Weber, and A. M. Silva. 1994, 5p.
Pub. in Jnl. of Chemical and Engineering Data 39, n4 p808-812 Oct 94.

Keywords: *Refrigerants, *Fluorohydrocarbons, *Thermophysical properties, Vapor pressure, Boiling points, Temperature measurement, Ebulliometry, Measuring methods, Reprints, *Difluoromethane, *Tetrafluoroethane, *Pentafluoroethane, R32, R124, R125.

The report presents new measurements of the vapor pressures of dibluoromethane (R32) from 235 to 265 K, of 1-chloro-1,2,2,2-tetrafluoroethane (R124) from 220 to 286 K, and of pentafluoroethane (R125) from 218 to 286 K. Overall, pressures ranged from 13 to about 950 kPa. The report also presents vapor pressures of R125, calculated via thermodynamic relationships, for temperatures down to 170 K (2.3 kPa). The report also discusses the azeotropic mixture of R125 with chloropentafluoroethane (R115), and the authors correct their data for a small R115 impurity.

03,271
PB95-175154 Not available NTIS
National Inst. of Standards and Technology (CSTL), Gaithersburg, MD. Thermophysics Div.
Vapor Pressures and Gas-Phase PVT Data for 1-Chloro-1,2,2,2-Tetrafluoroethane (R124).
Final rept.
S. J. Boyes, and L. A. Weber. 1994, 18p.
Contract DE-FG02-91CE23810
Sponsored by Department of Energy, Washington, DC.
Pub. in International Jnl. of Thermophysics 15, n3 p443-460 May 94.

Keywords: *Fluorohydrocarbons, *Refrigerants, *Thermodynamic properties, Vapor pressure, Volume, Temperature, Gases, Vapor phases, Phase studies, Thermophysical properties, Reprints, Ethane/chlorotetrafluoro, Hydrofluorocarbons, R124, Virial coefficients.

The authors present new data for the vapor pressure and Pressure-Vapor-Temperature (PVT) surface of 1-chloro-1,2,2,2-tetrafluoroethane (designated R124 by the refrigeration industry) in the temperature range 278-423 K. The PVT data are for the gas phase at densities up to 1.5 times the critical density. Correlating equations are given for the vapor pressures from 220 K to the critical temperature, 395.43 K, and for the PVT surface at densities up to approximately 0.5 times the critical density. Second and third virial coefficients have been derived from the PVT measurements.

03,272
PB95-175196 Not available NTIS
National Inst. of Standards and Technology (CSTL), Boulder, CO. Thermophysics Div.
Retention of Halocarbons on a Hexafluoropropylene Epoxide Modified Graphitized Carbon Black. Part 1. Methane-Based Compounds.
Final rept.
T. J. Bruno, and M. Caciari. 1994, 10p.
Pub. in Jnl. of Chromatography A 672, p149-158 1994.

Keywords: *Refrigerants, *Chlorofluorocarbons, *Fluorocarbons, *Thermodynamic properties, Methane compounds, Halohydrocarbons, Chemical analysis, Gas chromatography, Temperature, Thermophysical properties, Carbon black, Environmental chemical substitutes, Reprints, *Halocarbons, Hexafluoropropylene, Tetrafluoromethane.

The retention characteristics of eight methane-based chlorofluorocarbon and fluorocarbon fluids have been studied as a function of temperature on a stationary phase consisting of a 5% (w/w) coating of a low-molecular-mass polymer of hexafluoropropylene epoxide on a graphitized carbon black. The fluids that were studied include chlorotrifluoromethane (R-13), tetrafluoromethane (R-14), dischlorofluoromethane (R-21), chlorodifluoromethane (R-22), trifluoromethane (R-23), difluoromethane (R-32), chloromethane (R-40), and fluoromethane (R-41). Qualitative features of the data are examined, and trends are identified. In addition, the data were fit to linear models for the purpose of predicting retention behavior of these compounds to facilitate chromatographic analysis.

03,273
PB95-175386 Not available NTIS
National Inst. of Standards and Technology (CSTL), Boulder, CO. Thermophysics Div.
Measurements of the Viscosities of Saturated and Compressed Liquid 1,1,1,2-Tetrafluoroethane (R134a), 2,2-Dichloro-1,1,1-Trifluoroethane (R123) and 1,1-Dichloro-1-Fluoroethane (R141b).
Final rept.
D. E. Diller, A. S. Aragon, and A. Laesecke. 1993, 12p.
Pub. in Fluid Phase Equilibria 88, p251-262 1993.

Keywords: *Compressible fluids, *Refrigerants, *Viscosity, *Saturation(Chemistry), Fluorohydrocarbons, Temperature dependence, Shear flow, Volume, Reprints, *Ethane/tetrafluoro, *Ethane/dichloro-difluoro, *Ethane/dichloro-fluoro, RI34a, R123, R141b, Molar volume.

The shear viscosity coefficients of saturated and compressed liquid 1,1,1,2-tetrafluoroethane (R134a), 2,2-dichloro-1,1,1-trifluoroethane (R123) and 1,1-dichloro-1-fluoroethane (R141b) have been measured with a torsional crystal viscometer at temperatures between 170 and 320 K and at pressures up to 30 MPa. The fluidities (reciprocal viscosity) increase linearly with molar volume at fixed temperature and increase weakly with temperature at fixed volume. We have correlated our data using empirical fluidity-volume-temperature equations and have compared the data of others with the equations.

03,274
PB95-175691 Not available NTIS
National Inst. of Standards and Technology (CSTL), Boulder, CO. Thermophysics Div.
Coexisting Densities, Vapor Pressures and Critical Densities of Refrigerants R-32 and R-152a, at 300 - 385 K.
Final rept.
C. D. Holcomb, V. G. Niesen, L. J. Van Poolen, and S. L. Outcalt. 1993, 13p.
Contract DE-FG02-91CE23810
Sponsored by Department of Energy, Washington, DC.
Pub. in Fluid Phase Equilibria 91, p145-157 1993.

Keywords: *Refrigerants, *Critical point, *Vapor pressure, *Thermodynamic properties, Fluorohydrocarbons, Thermophysical properties, Equations of state, Phase studies, Temperature dependence, Pressure dependence, Density(Mass/Volume), Reprints, *Difluoromethane, *Difluoroethane, R32, R152a, Hydrofluorocarbons, Coexisting density, Critical density.

Experimental measurement for the vapor pressures and coexisting densities are presented for the refrigerants R-32 (difluoromethane) and R-152a (1,1-difluoroethane) from 300 K to near their respective critical points. In addition, the coexisting density measurements have been analyzed to determine an internally consistent critical density using the critical liquid volume fraction method. Experimental results have been

correlated and are in good agreement with existing literature values for each compound.

03,275
PB95-175717 Not available NTIS
National Inst. of Standards and Technology (CSTL), Boulder, CO. Thermophysics Div.
Predictive Extended Corresponding States Model for Pure and Mixed Refrigerants Including an Equation of State for R134a.
Final rept.
M. L. Huber, and J. F. Ely. 1994, 14p.
Sponsored by Department of Energy, Washington, DC.
Pub. in Rev. Int. Froid 17, n1 p18-31 1994.

Keywords: *Refrigerants, *Thermophysical properties, *Equations of state, *Fluorohydrocarbons, Thermodynamic properties, Saturation, Boundary conditions, Mixtures, Phase equilibria, Phase studies, Liquid phases, Vapor phases, Density(Mass/Volume), Reprints, *R134a, *Tetrafluoroethane, Hydrofluorocarbons.

The authors have developed a predictive corresponding states model for the thermophysical properties of pure refrigerants and refrigerant mixtures. The bulk phase properties such as the density, enthalpy and entropy are predicted using the principle of extended corresponding states, incorporating a recent 32-term modified Benedict-Webb-Rubin correlation for the R134a (1,1,1,2-tetrafluoroethane) reference fluid. In the work the authors present the coefficients for density-independent shape-factor correlations for 21 refrigerants, and a set of universal coefficients that can be used with any refrigerant given only the critical parameters and the acentric factor. The authors show comparisons with experimental density data for each of the 21 refrigerants. They also demonstrate the use of generalized coefficients for shape factors where only the critical parameters and acentric factors are known. In addition, they present comparisons of the volume prediction for two binary refrigerant mixtures and one ternary refrigerant mixture.

03,276
PB95-176236 Not available NTIS
National Inst. of Standards and Technology (CSTL), Gaithersburg, MD. Thermophysics Div.
Estimating the Virial Coefficients of Small Polar Molecules.
Final rept.
L. A. Weber. 1994, 22p.
Pub. in International Jnl. of Thermophysics 15, n3 p461-482 May 94.

Keywords: *Refrigerants, *Thermophysical properties, Density, Thermodynamic properties, Estimating, Mathematical models, Evanescence, Halogenated hydrocarbons, Reprints, *Virial coefficients, *Fugacity coefficients, *Small polar molecules.

We adapt existing models for estimating the second and third virial coefficients of small molecules to the halogenated methanes and ethanes. We compare the results with the abundant new, high-quality PVT data resulting from the search for alternative refrigerants. The present model provides an accurate method for calculating densities, and therefore it should provide reliable thermodynamic properties and fugacity coefficients. We give equations and parameters useful for estimating the properties of pure refrigerants and their mixtures when no PVT data are available.

03,277
PB96-117775 PC A99/MF E08
National Inst. of Standards and Technology (BFRL), Gaithersburg, MD. Fire Science Div.
Fire Suppression System Performance of Alternative Agents in Aircraft Engine and Dry Bay Laboratory Simulations. SP890: Volume 1.
Special pub.
R. G. Gann. Nov 95, 792p, NIST/SP-890-V1.
Also available from Supt. of Docs. as SN003-003-03371-5. See also PB96-117783. Sponsored by Wright Lab., Wright-Patterson AFB, OH., Naval Air Systems Command, Washington, DC. and Federal Aviation Administration Technical Center, Atlantic City, NJ.

Keywords: *Aircraft engines, *Fire suppression, *Environmental chemical substitutes, *Materials substitution, Halons, Alternatives, Aircraft fires, Engine nacelles, Inflight, Fire extinguishing agents, Fire fighting, Performance evaluation, Chemical properties, Thermodynamic properties, Physical properties, Combustion kinetics, Fire tests, Fire research, Aviation safety, Dry bays.

This report documents the development of knowledge (1) to differentiate among chemicals, leading to selections of the optimal currently available options for in-flight fire suppression, and (2) to assist in the development of engineering design criteria and suppression system certification.

03,278
PB96-117783 PC A99/MF A06
National Inst. of Standards and Technology (BFRL), Gaithersburg, MD. Fire Science Div.
Fire Suppression System Performance of Alternative Agents in Aircraft Engine and Dry Bay Laboratory Simulations. SP 890: Volume 2.
Special pub.
R. G. Gann. Nov 95, 639p, NIST/SP-890-V2.
Also available from Supt. of Docs. as SN003-003-03372-3. See also PB96-117775. Sponsored by Wright Lab., Wright-Patterson AFB, OH., Naval Air Systems Command, Washington, DC. and Federal Aviation Administration Technical Center, Atlantic City, NJ.

Keywords: *Aircraft engines, *Fire suppression, *Environmental chemical substitutes, *Materials substitution, Halons, Alternatives, Aircraft fires, Engine nacelles, Inflight, Fire extinguishing agents, Fire fighting, Performance evaluation, Chemical properties, Thermodynamic properties, Physical properties, Combustion kinetics, Fire tests, Fire research, Aviation safety, Dry bays.

This report documents the development of knowledge (1) to differentiate among chemicals, leading to selections of the optimal currently available options for in-flight fire suppression, and (2) to assist in the development of engineering design criteria and suppression system certification.

03,279
PB96-119573 Not available NTIS
National Inst. of Standards and Technology (CSTL), Boulder, CO. Thermophysics Div.
Physical Properties of Alternatives to the Fully Halogenated Chlorofluorocarbons.
Final rept.
M. O. McLinden. 1989, 24p.
See also N92-15436/8.
Pub. in Scientific Assessment of Stratospheric Ozone, Chapter 2, v2 p7-30 1989.

Keywords: *Chlorofluorocarbons, *Physical properties, *Thermophysical properties, Thermodynamic properties, Triple point, Boiling points, Temperature, Solubility, Vapor pressure, Critical point, Density(Mass/Volume), Liquid phases, Hydrolysis, Reprints.

The properties of nine halogenated hydrocarbons are collected from a variety of sources, including unpublished data, evaluated and correlated. Considered are the triple point, normal boiling point, and critical point parameters and the temperature dependence of the vapor pressure, saturated liquid density, solubility in water and hydrolysis rates. The fluids, which are potential alternatives to the fully-halogenated chlorofluorocarbons, are R125, R22, R134a, R152a, R124, R142b, R123 and R141b; also included is the solvent menthyl choroform.

03,280
PB96-122114 (Order as PB96-117767, PC A08/MF A02)
National Inst. of Standards and Technology, Gaithersburg, MD.
Microform Calibration Uncertainties of Rockwell Diamond Indenters.
J. F. Song, F. F. Rudder, T. V. Vorburger, and J. H. Smith. 1995, 19p.
Included in Jnl. of Research of the National Institute of Standards and Technology, v100 n5 p543-561 Sep/Oct 95.

Keywords: *Rockwell hardness, *Calibration standards, Reprints, Metals, Data covariances, Diamond pyramid hardness tests, Geometry, Mechanical tests, NIST(National Institute of Standards and Technology).

National and international comparisons in Rockwell hardness tests show significant differences. Uncertainties in the geometry of the Rockwell diamond indenters are largely responsible for these differences. By using a stylus instrument, with a series of calibration and check standards, and calibration and uncertainty calculation procedures, we have calibrated the microform geometric parameters of Rockwell diamond indenters. These calibrations are traceable to fundamental standards. Under ISO and NIST guidelines for expressing measurement uncertainties, the calibration and uncertainty calculation procedures, error sources, and uncertainty components are described, and the expanded uncertainties are calculated.

03,281
PB96-146626 Not available NTIS
National Inst. of Standards and Technology (CSTL), Gaithersburg, MD. Thermophysics Div.
Interaction Coefficients for 15 Mixtures of Flammable and Non-Flammable Components.
Final rept.
D. R. Defibaugh, and G. Morrison. 1995, 6p.
Pub. in International Jnl. of Refrigeration, v18 n8 p518-523 1995.

Keywords: *Refrigerants, *Thermodynamic properties, Environmental chemical substitutes, Alternatives, Equations of state, Interfacial tension, Pressure dependence, Temperature dependence, Ethanes, Propanes, Butanes, Liquid phases, Vapor phases, Flammability, Reprints, *Interaction coefficients.

Bubble pressures were measured for 15 binary mixtures, each composed mainly of one flammable and one non-flammable component. The mixtures were trichlorofluoromethane + isopentane, pentafluoroethane + 1,1,1-trifluoroethane, 1,1-dichloro-2,2,2-trifluoroethane + (1,1-dichloro-1-fluoroethane or isopentane), 1,1,1,2-tetrafluoroethane + (1,1-difluoroethane or propane or cyclopropane or isobutane), difluoromethane + (pentafluoroethane or 1,1,1,2-tetrafluoroethane or 1,1-difluoroethane). Also studied were mixtures of 1,1-difluoroethane + (cyclopropane or propane or butane or isobutane), which comprise two flammable components. The bubble pressures were used to determine interaction coefficients that characterize the non-ideal behavior of these fluid mixtures. The interaction coefficients are used in equation-of-state models for the thermodynamic properties of refrigerant mixtures.

03,282
PB96-159710 Not available NTIS
National Inst. of Standards and Technology (BFRL), Gaithersburg, MD. Fire Science Div.
Agent Screening for Halon 1301 Aviation Replacement.
Final rept.
W. Grosshandler, R. Gann, A. Hamins, J. Yang, M. Zachariah, M. Nyden, and W. Pitts. 1993, 9p.
Pub. in International CFC and Halon Alternatives Conference, October 20-22, 1993, Washington, DC., 9p.

Keywords: *Environmental chemical substitutes, *Fire extinguishing agents, *Aircraft fires, Halons, Bicarbonates, Halohydrocarbons, Combustion kinetics, Two phase flow, Thermodynamic properties, Combustion chemistry, Fire suppression, Reprints, Halon 1301.

A comprehensive experimental program is described in which eleven gaseous agents and sodium bicarbonate powder have been screened, so that the best three candidates for subsequent full scale air craft fire extinguishment evaluation can be identified. Because the effectiveness of a fire supression agent is known to be related to its thermodynamic properties, its behavior during two-phase flow, its interaction with flame chemistry, the timing of its release and the nature of the fire, a series of carefully designed experiments was conducted to examine each of these factors.

03,283
PB96-159728 Not available NTIS
National Inst. of Standards and Technology (BFRL), Gaithersburg, MD. Fire Science Div.
Validation of a Turbulent Spray Flame Facility for the Assessment of Halon Alternatives.
Final rept.
W. Grosshandler, C. Presser, and D. Lowe. 1993, 8p.
Sponsored by Department of the Air Force, Wright-Patterson AFB, OH.
Pub. in Proceedings of the 'Halon Alternatives Technical Working Conference', Albuquerque, NM., May 12, 1993, 8p.

Keywords: *Environmental chemical substitutes, *Fire extinguishing agents, *Aircraft fires, Material alternatives, Fire fighting, Fuel sprays, Turbulent flow, Fluorocarbons, Halohydrocarbons, Fire suppression,

Flame propagation, Halons, Atomization, Reprints, Hydrochlorofluorocarbons.

The work discussed in this paper is part of a large effort at NIST focused on finding an alternative to halon 1301 for application to aircraft engine nacelle and dry bay in-flight fire protection. Alternative chemical compounds are sought which will perform similarly to halon 1301, and which do not create unacceptable safety, environmental, or systems compatibility problems. A cup burner, an opposed flow diffusion flame, a turbulent spray flame, and a deflagration/detonation tube are used to rank the relative combustion suppression effectiveness.

03,284
PB96-164033 Not available NTIS
National Inst. of Standards and Technology (CSTL), Boulder, CO. Thermophysics Div.
Retention of Halocarbons on a Hexafluoropropylene Epoxide-Modified Graphitized Carbon Black. 4. Propane-Based Compounds.
Final rept.
T. J. Bruno, K. H. Wertz, and M. Caciari. 1995, 10p.
See also Part 1, PB95-175196.
Pub. in Jnl. of Chromatography A, v708 p293-302 1995.

Keywords: *Refrigerants, *Chlorofluorocarbons, *Fluorocarbons, *Thermodynamic properties, Methane compounds, Halohydrocarbons, Chemical analysis, Gas chromatography, Temperature, Thermophysical properties, Reprints, *Foreign technology.

The retention Characteristics of 25 propane-based bromofluorocarbon, chlorocarbon, chlorofluorocarbon, and fluorocarbon fluids have been studied as a function of temperature on a stationary phase consisting of a 5% (m/m) coating of a low-molecular-mass polymer of hexafluoropropylene epoxide on a graphitized carbon black adsorbent. Measurements were performed at 0, 20, 40 and 60 degrees C for R-245ca and R-245cb. Measurements were performed at 40, 60, 80, and 100 degress C for R-227ca, R-227ea, R-236ea, R-236fa, R-245fa, and R-263fb. Measurements were performed at 40, 60, 80 and 100 degrees C for R-217ba, R-254cb and R-1243b, and at 60, 80, 100 and 120 degrees C for R-280da and R-217caB1. Measurements were performed at 80, 100, 120, and 140 degrees C for R-215aa, R-216ba, R253fb, R-262da, and R-270aa. Measurements were performed at 100, 120, 140 and 160 degrees C for R-215ba, R-225ca, R-225cb, R-243db, R-270da, R-270fa, and R-270fa, and R-270fb. Relative retentions as a function of temperature were calculated with respect to the retentions of tetrafluoromethane (R-14) and hexafluoroethane (R-116). Qualitative features of the data are examined, and trends are identified. In addition, the relative retention data were fitted to linear models for the purpose of predicting retention behavior of these compounds to facilitate chromatographic analysis.

03,285
PB96-164165 Not available NTIS
National Inst. of Standards and Technology (BFRL), Gaithersburg, MD. Fire Science Div.
In Search of Alternative Fire Suppressants.
Final rept.
W. L. IGrosshandler. 1995, 8p.
Pub. in Thermal Science and Engineering Symposium in Honor of Chancello Chang-Lin Tien, Berkeley, CA., November 1995, p275-282.

Keywords: *Fire extinguishing agents, *Alternatives, *Aircraft fires, Environmental chemical substitutes, Material substitution, Fire suppresion, Fire fighting, Performance evaluation, Effectiveness, Halons, Reprints, Halon 1301.

Halons had been the agents of choice for numerous fire protection applications because of their inherent ability to inhibit flames at low concentrations with no residue while exhibiting a number of additional strongly positive attributes. To avoid costly mistakes in choosing replacements for aircraft applications, research has been conducted to determine the performance of different agents in extinguishing aircraft-type fires. This paper describes the major elements of the overall program and the rationale of how an alternative to halon 1301 was chosen for aircraft applications.

03,286
PB96-167309 Not available NTIS
National Inst. of Standards and Technology (CSTL), Boulder, CO. Thermophysics Div.
Retention of Halocarbons on a Hexafluoropropylene Epoxide-Modified Graphitized Carbon Black. 3. Ethene-Based Compounds.
Final rept.
T. J. Bruno, and M. Caciari. 1994, 7p.
See also PB95-175196 and PB96-164033.
Pub. in Jnl. of Chromatography A, v686 p245-251 1994.

Keywords: *Refrigerants, *Chlorofluorocarbons, *Fluorocarbons, *Thermodynamic properties, Chemical analysis, Reprints, Gas chromatography, Temperature, Thermophysical properties, *Foreign technology, *Halocarbons, Relative retention.

The retention characteristics of 11 ethene-based chlorofluorocarbon, bromochlorofluorocarbon and fluorocarbon fluids have been studied as a function of temperature on a stationary phase consisting of a 5% (m/m) coating of a low-molecular-mass polymer of hexafluoropropylene epoxide on a graphitized carbon black absorbent. Measurements were performed at -20, 0, 20 and 40 deg C for trifluoroethene (R-1123), 1.1-difluoroethene(R1132a), and fluoroethene (R-1112a), chlorotrifluoroethene (R-113), 2-chloro-1,1-difluoroethene (R-1122), 1-chloro-1-fluoroethene (R1121a), 2-bromo-1,1-difluoroethene (R-1122B1) and bromoethene (Vinly bromide, R-1140B1). Measurements were performed at 60, 80, 100, and 120 deg C fortrans-1,2-dichloro- 1,2-difluoroethene (R1112t) and cis-1,2-dichloro- 1,2-difluoroethene (R-1112c). Net retention volumes, corrected to a column temperature of 0 deg C, were calculated from retention time measurements, the logarithms of which were fitted againstreciprocal thermodynamic temperature.

03,287
PB96-175724 Not available NTIS
National Inst. of Standards and Technology (BFRL), Gaithersburg, MD. Fire Science Div.
Suppression of High-Speed C2H4/Air Flames with C1-Halocarbons.
Final rept.
G. Gmurczyk, and W. Grosshandler. 1994, 7p.
Sponsored by Department of the Air Force, Wright-Patterson AFB, OH.
Pub. in International Symposium on Combustion (25th), Irvine, CA., July 31-August 5, 1994, p1497-1503.

Keywords: *Fire suppression, *Halogenated hydrocarbons, *Combustion kinetics, Fire extinguishing agents, Halons, Performance evaluation, Turbulent flow, Flame propagation, Detonations, Flames, Thermodynamic properties, Heat flow, Reprints, Turbulent flames.

A primary objective of the work has been to determine the relative suppression efficiencies of different agents under highly dynamic situations, without the undue influence of either the ignition event or the mixing of the agent into the flame front. This was accomplished by generating a highly turbulent flame/quasi detonation in the driver section, which contain no suppressant, followed by measurements of the velocity and pressure ratio as the wave front entered the test section of the tube, which contained suppressant premixed with the same fuel/air combination. The experimental facility was successfully employed to clearly discriminate among the dynamic characteristics of the five compounds, revealing behavior distinct from what was observed in companion studies using atmospheric nonpremixed flames. The suppression process is strongly influenced by the concentration of an agent, the structure and composition of a agent molecule, and the composition of the combustible mixture itself.

03,288
PB96-175732 Not available NTIS
National Inst. of Standards and Technology (BFRL), Gaithersburg, MD. Fire Science Div.
Effectiveness of Halon Alternatives in Suppressing Dynamic Combustion Process.
Final rept.
W. L. Grosshandler, C. Presser, and G. Gmurczyk. 1995, 21p.
Pub. in American Chemical Society Halon Replacements: Technology and Science Symposium, Washington, DC., August 21-25, 1994, p204-224 1995.

Keywords: *Aircraft fires, *Fire extinguishing agents, *Environmental chemical agents, *Combustion kinetics, Fire suppression, Alternatives, Halons, Fluorocarbons, Fire fighting, Fuel sprays, Turbulent flow, Thermodynamic properties, Detonations, Reprints, Explosiveness.

C3F8 is shown to require the least storage volume among twelve fluorocarbons for suppressing a quasi-detonation. CF3I performs the best of the gaseous suppressants evaluated in a spray burner. Two experimental facilities are describes as part of an effort to identify suitable replacements for CF3Br is aircraft applications. A turbulent spray burner simulates the hazards associated with a ruptured fuel line in an engine nacelle or dry bay. A deflagration/detonation tube evaluates the ability of a gaseous agent to attenuate the pressure build-up and Mach number of a quasi-detonation.

03,289
PB96-175740 Not available NTIS
National Inst. of Standards and Technology (CSTL), Gaithersburg, MD. Process Measurements Div.
Halon Thermochemistry: 'Ab Initio' Calculations of the Enthalpies of Formation of Fluoromethanes.
Final rept.
R. J. Berry, D. R. F. Burgess, M. R. Nyden, M. R. Zachariah, and M. Schwartz. 1995, 6p.
Pub. in Jnl. of Physical Chemistry, v99 n47 p17145-17150 1995.

Keywords: *Fluorocarbons, *Thermochemistry, *Calculation methods, Thermodynamic properties, Thermophysical properties, Quantum chemistry, Molecule molecule interactions, Chemical bonds, Molecular orbitals, Reprints, *Enthalpy of formation.

Atomic equivalent (AEQ), BAC-MP4, G2(MP2), G2, CBS-4, CBS-Q, and CBS-QCI/APNO molecular orbital calculations were used to calculate enthalpies of formation in the series of fluoromethanes, CH(sub x)F(sub(4-x)),x = 0-4. Enthalpies of formation calculated with the G2(MP2) and G2 procedures exhibited systematic deviations from experiment which were linearly dependent upon the number of C-F bonds in the molecule. This technique had no significant effect on the quality of results from the AEQ, BAC-MP4, and CBS-4 methods.

03,290
PB96-176417 Not available NTIS
National Inst. of Standards and Technology (BFRL), Gaithersburg, MD. Fire Science Div.
Interaction of HFC-125, FC-218 and CF3I with High Speed Combustion Waves.
Final rept.
W. L. Grosshandler, and G. Gmurczyk. 1995, 9p.
Sponsored by Naval Air Systems Command, Washington, DC.
Pub. in International CFC and Halon Alternatives and Exhibition: Stratospheric Ozone Protection for the 90's, Washington, DC., October 23-25, 1995, p635-643.

Keywords: *Aircraft fires, *Fire extinguishing agents, *Combustion kinetics, Halogenated hydrocarbons, Fire suppression, Environmental chemical substitutes, Alteratives, Flame propagation, Fuel sprays, Propane, Thermodynamic properties, Halons, Overpressure, Reprints, *Turbulent flames, Explosiveness, Ethenes.

Live-fire full-scale testing has been conducted at Wright-Patterson Air Force Base to identify an agent to replace CF3 Br (halon 1301) for suppressing fires in military aircraft dry bays. High pressures motivated the current study to determine the initial conditions which would lead to dangerous situations, and to explore a less extreme regime more representative of a realistic threat. Based upon over a hundred experiments with modified facility, it was possible to reconfirm the conclusion that FC-218 provides the most consistent performance over the widest range of fuel/air mixtures and tube geometries. The CF3I has the greatest positive impact at low partial pressure fractions, but exhibits non-monotonic behavior of flame speed and shock pressure ratio at increasing concentrations. The dangerously high over-pressures previously exhibited by HFC-125 were not observed during suppression under more moderate (and realistic) combustion conditions.

03,291
PB96-176425 Not available NTIS
National Inst. of Standards and Technology (BFRL), Gaithersburg, MD. Fire Science Div.
Suppression of Ignition Over a Heated Metal Surface.
Final rept.
A. Hamins, P. Borthwick, and C. Presser. 1995, 5p.
Pub. in International Conference on Fire Research and Engineering, Orlando, FL., September 10-15, 1995, p77-81.

Keywords: *Fire suppression, *Halogenated hydrocarbons, *Metals, *Surfaces, Fire extinguishing agents, Halons, Performance evaluation, Flames, Temperature, Combustion kinetics, Heat flow, Heat transmission, Thermal radiation, Thermodynamic properties, Fire fighting, Radiant heat flow, Reprints.

The objective of this work is to investigate the effectiveness of various agents in suppressing flame ignition. Experiments were conducted to determine the amount of agent needed to suppress the ignition of a gaseous propane flow over a heated metal disk. The metal surface was heated by a regulated power supply which provided up to 200 W. With the fuel and oxidizer flowing, flame ignition occurred in a repeatable fashion by increasing the power through the metal disk. Various amounts of agent were added to the air flow and the temperature of the heated metal disk was measured at flame ignition using an optical pyrometer. The effectiveness of N2, HFC-125, HFC-227 and CF3I were compared in suppressing the ignition event.

03,292
PB96-176680 Not available NTIS
National Inst. of Standards and Technology (CSTL), Boulder, CO. Thermophysics Div.
Viscosity of 1,1,1,2,3,3-Hexafluoropropane and 1,1,1,3,3,3-Hexafluoropropane at Saturated-Liquid Conditions from 262 K to 353 K.
Final rept.
A. Laesecke, and D. R. Defibaugh. 1996, 4p.
Pub. in Jnl. of Chemical and Engineering Data, v41 n1 p59-62 1996.

Keywords: *Refrigerants, *Viscosity, *Propanes, Alternatives, Material substitution, Environmental chemical substitutes, Volume, Vapor pressure, Free energy, Reprints, 1-1-1-2-3-3-hexafluoropropane, 1-1-1-3-3-3-hexafluoropropane, R236ea, R236fa, Corresponding states, Saturated liquids.

Viscosities are reported for two fluorinated propane isomers in the saturated-liquid state at temperatures from 262 K to 353 K. The compounds are 1,1,1,2,3,3-hexafluoropropane (R236ea) and 1,1,1,3,3,3-hexafluoropropane (R236fa). The measurements were performed in a capillary viscometer designed for fluids with vapor pressures above ambient. A free-volume model was used to correlate the experimental results, and they were also compared with predictions from an extended corresponding states model.

03,293
PB96-176755 Not available NTIS
National Inst. of Standards and Technology (CSTL), Boulder, CO. Thermophysics Div.
Report of the Refrigeration, Air Conditioning and Heat Pumps Technical Options Committee.
Final rept.
M. O. McLinden, G. Angelino, D. Arnaud, J. M. Calm, E. Preisegger, R. Tillner-Roth, K. Watanabe, P. Weiss, and S. Bhaduri. 1995, 24p.
Pub. in Assessment of the United Nations Environment Programme Montreal Protocol on Substances That Deplete the Ozone Layer, p31-54 1995.

Keywords: *Refrigerants, *Enviromental chemical substitutes, *Thermophysical properties, Chlorofluorocarbons, Alternatives, Material substitution, Thermodynamic properties, Flammability, Toxicity, Reprints, Material compatibility.

The properties of refrigerants that may serve as replacements to the chlorofluorocarbons (CFCs) are considered. The characteristics required of a refrigerant are reviewed, and the data needed to evaluate possible alternative refrigerants are summarized. These data include thermophysical properties, toxicity and flammability data, materials compatibility information, and parameters characterizing environmental consequences. The available data for 45 potential replacement refrigerants are summarized.

03,294
PB96-176805 Not available NTIS
National Inst. of Standards and Technology (CSTL), Boulder, CO. Thermophysics Div.
International Standard Equation of State for the Thermodynamic Properties of Refrigerant 123 (2,2-Dichloro- 1,1,1-Trifluoroethane).
Final rept.
B. A. Younglove, and M. O. McLinden. 1994, 49p.
Pub. in Jnl. of Physical and Chemical Reference Data, v23 n5 p731-779 1994.

Keywords: *Refrigerants, *Equations of state, *Thermodynamic properties, Alternatives, Material substitution, Enviroinmental chemical substitutes, Ethanes, Vapor pressure, Critical temperature, Specific heat, Density(Mass/Volume), Standardization, Reprints, 2-2-dichloro-1-1-1-trifluoroethane, R123, Correlation density, Heat capacity, Speed of sound.

A modified Benedict-Webb-Rubin (MBWR) equation of state has been developed for Refrigerant 123 (2,2-dichloro- 1,1,1-trifluoroethane) basedon recently measured thermodynamic property data and data available fromthe literature. Single-phase pressure-volume-temperature (PVT), heat capacity, and sound speed data, as well as second virial, vapor pressure, and saturated liquid and saturated vapor density data, were used with multiproperty linear least squares fitting techniques to fit the 32 adjustable coefficients of the MBWR equation. Coefficients for the equation of state and for ancillary equations representing the vaporpressure, saturated liquid and saturated vapor densities, and ideal gas heat capacity are given.

03,295
PB96-190095 Not available NTIS
National Inst. of Standards and Technology (MSEL), Boulder, CO. Materials Reliability Div.
Mapping the Droplet Transfer Modes for an ER100S-1 GMAW Electrode.
Final rept.
P. R. Heald, R. B. Madigan, T. A. Siewert, and S. Liu. 1994, 7p.
See also PB91-174250.
Pub. in Welding Jnl., p38s-44s Feb 94.

Keywords: *Gas metal arc welding, *Electrodes, Spray transfer, Electric potential, Mapping, Transferring, Reprints, CTWD, GMAW(Gas metal arc welding), Metal transfer modes, Wire feed rate.

Welds were made with a 1.2-mm-diameter AWS ER100S-1 electrode using Ar-2% O2 shielding gas to map the effects of contact-tube-to-work distance (13, 19 and 25 mm), current, voltage, and wire feed rate on metal transfer. The droplet transfer modes were identified for each map by both the sound of the arc and images from a laser back-lit high-speed video system. The modes were correlated to digital records of the voltage and current fluctuations. The maps contain detailed information on the spray transfer mode, including the boundaries of drop spray modes. The metal transfer mode boundaries shifted with an increase in contact-tube-to-work distance.

03,296
PB96-190145 Not available NTIS
National Inst. of Standards and Technology (MSEL), Boulder, CO. Materials Reliability Div.
Power Characteristics in GMAW: Experimental and Numerical Investigation.
Final rept.
P. G. Jonsson, J. Szekely, R. B. Madigan, and T. P. Quinn. 1995, 10p.
Pub. in Welding Jnl., p93s-102s Mar 95.

Keywords: *Power, *Gas metal arc welding, Numerical analysis, Electric power distribution, Input, Models, Electric potential, Reprints, GMAW(Gas metal arc welding), Arc column, Arc length.

The voltage and power distributions in gas metal arc welding (GMAW) were studied both experimentally and numerically. The principal voltage drop takes place in the arc, which also constitutes the dominant power contribution. Within the arc, the dominating voltage contributions are from the arc column and the cathode fall, while the anode fall and the electrode regions are less significant. The power input to the arc column increases with both increasing current and increasing arc length. These results indicate that it is critical to control the arc length in order to control the power input to the system.

03,297
PB96-190160 Not available NTIS
National Inst. of Standards and Technology (MSEL), Boulder, CO. Materials Reliability Div.
Sensing Droplet Detachment and Electrode Extension for Control of Gas Metal Arc Welding.
Final rept.
R. B. Madigan, T. P. Quinn, and T. A. Siewert. 1993, 4p.
Pub. in International Trends in Welding Science and Technology, Gatlinburg, TN., June 1-5, 1992, p999-1002 1993.

Keywords: *Gas metal arc welding, *Electrodes, Currents, Electric potential, Detectors, Luminous intensity, Transferring, Drops(Liquid), Frequencies, Reprints, GMAW(Gas metal arc welding), Arc length, Arc current.

An arc light intensity sensor, in conjunction with voltage and current sensors, was evaluated to detect droplet detachment and electrode extension under spray transfer welding conditions. Arc length, electrode extension and droplet transfer frequency were obtained from high-speed video images of the process and correlated to arc current and arc light intensity measurements. The arc light intensity sensor was able to detect droplet frequency from variations in arc light intensity caused by changes in arc length due to droplet detachment. Arc length could be estimated using this regression within 1 mm with current ranging from 180 to 300 A and arc length ranging from 4 to 12 mm.

03,298
PB96-201033 Not available NTIS
National Inst. of Standards and Technology (CSTL), Gaithersburg, MD. Chemical Kinetics and Thermodynamics Div.
Temperature Dependence of the Gas and Liquid Phase Ultraviolet Absorption Cross Sections of HCFC-123 (CF3CHCl2) and HCFC-142b (CH3CF2Cl).
Final rept.
A. K. Nayak, T. J. Buckley, M. J. Kurylo, and A. Fahr. 1996, 8p.
Pub. in Jnl. of Geophysical Research, v101 nC4 p9055-9062 Apr 96.

Keywords: *Thermal properties, *Temperature dependence, *Ultraviolet absorption, *Absorption cross sections, Chlorofluorocarbons, Halogenated hydrocarbons, Vapor phases, Liquid phases, Wavelengths, Reprints, *HCFC-123, *HCFC-142b.

The absorption cross sections for HCFC-123 (CF3CHCl2) and HCFC-142b (CH3CF2Cl) have been measured in the gas and liquid phases over the temperature range of about 220-330 K. The liquid phase results were converted into effective gas phase cross sections using a wavelength shift procedure, thereby extending the gas phase cross sections to longer wavelengths. The results are compared with other available data and lend increased confidence in atmospheric lifetime calculations for these important industrial alternatives to the fully halogenated chlorofluorocarbons.

03,299
PB97-118384 Not available NTIS
National Inst. of Standards and Technology (CSTL), Gaithersburg, MD. Thermophysics Div.
Thermodynamic Properties of CF3-CHF-CHF2, 1,1,1,2,3,3-Hexafluoropropane.
Final rept.
D. R. Defibaugh, K. A. Gillis, M. R. Moldover, J. W. Schmidt, and L. A. Weber. 1996, 25p.
Pub. in Fluid Phase Equilibria, v122 p131-155 1996.

Keywords: *Thermodynamic properties, Vapor pressure, Equations of state, Density(Mass/Volume), Refractive index, Critical temperature, Acoustic velocity, Surface tension, Specific heat, Critical pressure, Gas phases, Liquid phases, Phase studies, Ideal gas, Refrigerants, Refrigerating machinery, Environmental chemical substitutes, Reprints, *Hexafluoropropane, *HFC-236ea, Critical density.

The authors report the thermodynamic properties of 1,1,1,2,3,3-Hexafluoropropane (known in the refrigeration industry as HFC-236ea) in the temperature and pressure region commonly encountered in thermal machinery. The properties are based on measurements of the vapor pressure, the density of the compressed liquid (PVT), the refractive index of the saturated liquid and vapor, the critical temperature, the speed of sound in the vapor phase, and the capillary rise. From these data, the authors deduce the ideal-gas heat-capacity, the saturated liquid and vapor densities, the equation of state of the vapor phase, the surface tension, and estimates of the critical pressure and density. The data determine the coefficients for a Carnahan-Starlings-DeSantis (CSD) equation of state.

03,300
PB97-118392 Not available NTIS
National Inst. of Standards and Technology (CSTL), Gaithersburg, MD. Thermophysics Div.

Miscellaneous Materials

Thermodynamic Properties of CHF2-CF2-CHF, 1,1,2,2,3-Pentafluoropropane.
Final rept.
D. R. Defibaugh, K. A. Gillis, M. R. Moldover, J. W. Schmidt, and L. A. Weber. 1996, 10p.
Pub. in International Jnl. of Refrigeration, v19 n4 p284-294 1996.

Keywords: *Thermodynamic properties, Vapor pressure, Equations of state, Density(Mass/Volume), Refractive index, Critical temperature, Acoustic velocity, Surface tension, Specific heat, Critical pressure, Gas phases, Liquid phases, Phase studies, Ideal gas, Refrigerants, Refrigerating machinery, Environmental chemical substitutes, Reprints, *Pentafluoropropane, *HFC-245ca.

The authors report the thermodynamic properties of 1,1,2,3,3-pentafluoropropane (known in the refrigeration industry as HFC-245ea) in the temperature and pressure region commonly encountered in thermal machinery. The properties are based on measurements of the vapor pressure, the density of the compressed liquid, the refractive index of the saturated liquid and vapor, the critical temperature, the speed of sound in the vapor phase, and the capillary rise. From these data, the authors deduce the ideal-gas heat-capacity, the saturated liquid and vapor densities, the equation of state of the vapor phase, the surface tension, and estimates of the critical pressure and density. The data determine the coefficients for a Carnahan-Starlings-DeSantis (CSD) equation of state.

03,301
PB97-122261 Not available NTIS
National Inst. of Standards and Technology (CSTL), Gaithersburg, MD. Physical and Chemical Properties Div.
Environmental Aspects of Halon Replacements: Considerations for Advanced Agents and the Ozone Depletion Potential of CF3I.
Final rept.
P. S. Connell, D. E. Kinnison, D. J. Bergmann, R. G. Daniel, C. K. Williamson, A. W. Miziolek, R. E. Huie, K. O. Patten, and D. J. Wuebbles. 1996, 15p.
Pub. in Halon Options Technical Working Conference, Albuquerque, NM., May 7-9, 1996, p585-609.

Keywords: *Environmental chemical substitutes, *Physical properties, *Chemical properties, *Environmental impacts, Halons, Materials replacement, Atmospheric reactivity, Chemical reactivity, Biodegradation, Iodine fluorides, Ozone depletion, Environmental persistance, Bioaccumulation, Biosphere, Reprints, *Trifluoromethyl iodide.

The introduction of a new chemical species into the environment raises the question of the ultimate fate of that compound. In most cases, any compound which is introduced into the environment can undergo various transformations, physical and chemical. Of considerable importance is accumulation in the biosphere, which can take place when the chemical is lipid soluble. In this case, the concentration of the substance through the food chain becomes important. In concert with these physical transformations are chemical transformations such as oxidation, photolysis, hydrolysis, and complexation. It is important to understand both the rates and the mechanisms of these transformations in order to evaluate the environmental impact of a chemical species which may be introduced into the environment.

Nonferrous Metals & Alloys

03,302
AD-A279 180/4 PC A04/MF A01
National Bureau of Standards, Gaithersburg, MD.
Thermal Conductivity of Metals and Alloys at Low Temperatures. A Review of the Literature.
R. L. Powell, and W. A. Blanpied. 1 Sep 54, 72p.

Keywords: *Metals, *Alloys, *Thermal conductivity, *Low temperature, Construction materials, Dielectrics, Crystals, Chemical elements, Solids, Tables(Data), *Reviews.

No abstract available.

03,303
AD-A286 675/4 PC A04/MF A01
National Inst. of Standards and Technology, Boulder, CO. Cryogenic Engineering Lab.
Cryogenic Materials Data Handbook.
W. L. Burriss, and J. L. Mason. 14 Nov 61, 60p.
Contract AF-04(647)-59-3

Keywords: *Aluminum, *Thermal properties, *Cryogenics, *Mechanical properties, Strength(Mechanics), Handbooks.

No abstract available.

03,304
AD-A294 088/0 PC A04/MF A01
National Inst. of Standards and Technology, Gaithersburg, MD.
Electrochemical Synthesis of Metal and Intermetallic Composites.
D. S. Lashmore, C. R. Beauchamp, C. E. Johnson, T. Moffat, and J. L. Mullen. 24 Feb 94, 72p.

Keywords: *Aluminum alloys, *Electrochemistry, *Manganese alloys, Metals, Reprints, Synthesis, Structural properties, Composite materials, Patents, Intermetallic compounds, Electrodeposition, Molten salts, Compilations, Pat cl 205/176.

Partial contents: Formation of the Al-Mn icosahedral phase by electrodeposition; The electrodeposition of an Aluminum-Manganese metallic glass from molten salts; Phase formation in electrodeposited and thermally annealed Al-Mn alloys; Structural study of electrodeposited Aluminum-Manganese alloys; Patents: Metal-coated fiber compositions containing alloys barrier layer; Cooperative research and development agreement. jg (abstract is modified and taken from document titles.).

03,305
AD-A306 625/5 PC A04/MF A01
National Inst. of Standards and Technology, Gaithersburg, MD.
Fracture Testing of Large-Scale Thin-Sheet Aluminum Alloy.
Final rept.
R. DeWit, R. J. Fields, S. R. Low, D. E. Harne, and T. Foecke. Feb 96, 32p, DOT/FAA/AR-95/11.
Contract DTGFA03-92-Z-00018

Keywords: *Aluminum alloys, *Fracture(Mechanics), *Sheets, *Thinness, Test and evaluation, Optical equipment, Models, Panels, Cracks, Sites, Test methods, Strength(Mechanics), Tension, Strain gages, Plastic properties, Linkages, Diagrams, Magnetic tape, Video tapes, Test fixtures, Motion picture film, R-curve, Antibuckling, Msd(Multiple site damage), Multiple site damage.

A series of fracture tests on large-scale, precracked, aluminum alloy panels were carried out to examine and characterize the process by which cracks propagate and link up in this material. Extended grips and test fixtures were specially designed to tension load the panel specimens in a 1780-kN capacity universal testing machine. Single sheets of bare 2024-T3 aluminum alloy, approximately 4 m high, 2.3 m wide, and 1 mm thick were fabricated with simulated through cracks oriented horizontally at midheight. Using existing information, a test matrix was set up to explore regions of failure controlled by fracture mechanics, with additional tests near the boundary between plastic collapse and fracture. In addition, a variety of multiple site damage (MSD) configurations were included to distinguish between various proposed linkage mechanisms. All tests but one used antibuckling guides. Three specimens were fabricated with a single central crack, six others had multiple cracks on each side of the central crack, and one had a single crack but no antibuckling guides. The results of each fracture event were recorded on various media: film, video, computer, magnetic tape, and occasionally optical microscope. The video showed the crack tip with a load meter in the field of view, using motion picture film for one tip and super VHS video tape for the other. The computer recorded the output of the testing machine load cell, the stroke, and the twelve strain gages at 1.5-second intervals. A wideband FM magnetic tape recorder was used to record data from the same sources. The data were analyzed by two different procedures: (1) the plastic zone model based on the residual strength diagram and (2) the R-curve.

03,306
DE94017331 PC A03/MF A01
National Inst. of Standards and Technology (MSEL), Gaithersburg, MD.
Evaluation of the Environmentally Induced Fracture Resistance of Ductile Nickel Aluminide. Technical Report Number 1, Final report. October-December 1990.
Progress rept.
R. E. Ricker, U. Bertocci, J. L. Fink, and M. R. Stoudt. Jul 91, 21p, DOE/OR/21941-T1.
Contract AI05-90OR21941
Sponsored by Department of Energy, Washington, DC.

Keywords: *Aluminium Alloys, *Nickel Base Alloys, *Fracture Properties, Aluminium Chlorides, Boron Additions, Corrosion, Experimental Data, Hafnium Additions, Hydrogen Embrittlement, Iron Additions, Nickel Chlorides, PH Value, Progress Report, Sodium Chlorides, Sodium Sulfates, Tables(data), EDB/360103, EDB/360105.

Slow-strain-rate tensile tests and electrochemical experiments were performed in different aqueous solutions on ductile nickel aluminide, Ni(sub 3)Al+B, in order to evaluate the possibility of environmentally induced fracture of this material in neutral pH solutions as a result of hydrogen absorption. Two different processes were postulated that could lead to hydrogen absorption and embrittlement: (1) local acidification due to hydrolysis of the corrosion reaction products and (2) hydrogen reduction during the potential transient that accompanies film rupture and repair. Experiments were designed to evaluate each of these possibilities. First, slow strain rate tests were conducted in solutions with varying concentrations of metal ions and pH to determine the critical metal ion concentration and pH that result in hydrogen absorption and embrittlement of this material. Second, the potential transient that follows the mechanical rupture of the protective surface film in different solutions was measured and the minimum potential during the transient was compared to the potential that results in a hydrogen fugacity large enough to cause cracking. The results indicate that hydrogen reduction, absorption, and embrittlement are not to be expected in neutral solutions as a result of local acidification during crevice corrosion or film rupture during crack propagation or cyclic loading.

03,307
DE94017351 PC A02/MF A01
National Inst. of Standards and Technology (MSEL), Gaithersburg, MD. Metallurgy Div.
Evaluation of the Electrochemical Behavior of Ductile Nickel Aluminide and Nickel in a pH 7.9 Solution. Technical Report Number 3, April-June 1991.
D. M. Gram, U. Bertocci, and R. E. Ricker. Aug 91, 10p, DOE/OR/21941-T3.
Contract AI05-90OR21941
Sponsored by Department of Energy, Washington, DC.

Keywords: *Aluminium Alloys, *Nickel Base Alloys, *Electrochemistry, Nickel, Doped Materials, Intermetallic Compounds, EDB/360104, EDB/400400.

The electrochemical behavior of ductile nickel aluminide has been examined in neutral solutions. Features observed in a certain potential range were characterized, and the potentiodynamic sweep parameters affecting them identified. Nickel aluminide behaves essentially as pure nickel; however, small differences were observed.

03,308
DE94018566 PC A01/MF A01
National Inst. of Standards and Technology, Gaithersburg, MD.
Study of Laser Resonance Ionization Mass Spectrometry Using a Glow Discharge Source.
X. Xiong, J. M. R. Hutchinson, J. D. Fassett, W. A. Bowman, K. R. Hess, T. B. Lucatorto, and F. J. Schima. 1994, 5p, DOE/ER/60447-T6.
Contract AI05-86ER60447
Sponsored by Department of Energy, Washington, DC.

Keywords: *Aluminium Base Alloys, *Copper Alloys, *Iron Alloys, Atomization, Data Acquisition Systems, Dye Lasers, Mass Spectrometers, Resonance Ionization Mass Spectroscopy, EDB/400102.

The mass spectra of a metal alloy sample consisting of Al, Cu and Fe were studied using both glow discharge mass spectrometry (GDMS) and resonance ionization mass spectrometry (RIMS). Particular emphasis was placed on the reduction of isobaric interferences and discrimination between those ions formed by the discharge and those formed by the laser radiation.

03,309
N94-25124/6 (Order as N94-25120/4, PC A11/MF A03)
National Inst. of Standards and Technology, Gaithersburg, MD.
Dynamic Measurements of Thermophysical Properties of Metals and Alloys at High Temperatures by Subsecond Pulse Heating Techniques.
A. Cezairliyan. Nov 93, 15p.
In NASA. Lewis Research Center, Workshop on the Thermophysical Properties of Molten Materials p 71-85.

Keywords: *High temperature environments, *Pulse heating, *Thermophysical properties, *Liquid alloys, *Liquid metals, Dynamic characteristics, Electric potential, Electrical resistivity, Enthalpy, Phase transformations, Specific heat, Temporal resolution, Thermal expansion, Heat of fusion, Interfacial tension, Liquidus, Microgravity, Solidus, Spectral emission.

Rapid (subsecond) heating techniques developed at the National Institute of Standards and Technology for the measurements of selected thermophysical and related properties of metals and alloys at high temperatures (above 1000 C) are described. The techniques are based on rapid resistive self-heating of the specimen from room temperature to the desired high temperature in short times and measuring the relevant experimental quantities, such as electrical current through the specimen, voltage across the specimen, specimen temperature, length, etc., with appropriate time resolution. The first technique, referred to as the millisecond-resolution technique, is for measurements on solid metals and alloys in the temperature range 1000 C to the melting temperature of the specimen. It utilizes a heavy battery bank for the energy source, and the total heating time of the specimen is typically in the range of 100-1000 ms. Data are recorded digitally every 0.5 ms with a full-scale resolution of about one part in 8000. The properties that can be measured with this system are as follows: specific heat, enthalpy, thermal expansion, electrical resistivity, normal spectral emissivity, hemispherical total emissivity, temperature and energy of solid-solid phase transformations, and melting temperature (solidus). The second technique, referred to as the microsecond-resolution technique, is for measurements on liquid metals and alloys in the temperature range 1200 to 6000 C. It utilizes a capacitor bank for the energy source, and the total heating time of the specimen is typically in the range 50-500 micro-s. Data are recorded digitally every 0.5 micro-s with a full-scale resolution of about one part in 4000. The properties that can be measured with this system are: melting temperature (solidus and liquidus), heat of fusion, specific heat, enthalpy, and electrical resistivity. The third technique is for measurements of the surface tension of liquid metals and alloys at their melting temperature. It utilizes a modified millisecond-resolution heating system designed for use in a microgravity environment.

03,310
N95-14548/8 (Order as N95-14522/3, PC A20/MF A04)
National Inst. of Standards and Technology, Gaithersburg, MD.
Convection and Morphological Stability During Directional Solidification.
S. R. Coriell, A. A. Chernov, B. T. Murray, and G. B. Mcfadden. Aug 94, 6p.
In NASA. Lewis Research Center, Second Microgravity Fluid Physics Conference p 175-180.

Keywords: *Anisotropy, *Binary alloys, *Convection, *Directional solidification (Crystals), *Interface stability, *Phase stability (Materials), Crystallography, Destabilization, Germanium alloys, Melts (Crystal growth), Morphology, Shear flow, Silicon alloys, Traveling waves.

For growth of a vicinal face at constant velocity, the effect of anisotropic interface kinetics on morphological stability is calculated for a binary alloy. The dependence of the interface kinetic coefficient on crystallographic orientation is based on the motion and density of steps. Anisotropic kinetics give rise to traveling waves along the crystal-melt interface, and can lead to a significant enhancement of morphological stability. The stability enhancement increases as the orientation approaches a singular orientation and as the solidification velocity increases. Shear flows interact with the traveling waves and, depending on the direction of the flow, may either stabilize or destabilize the interface. Specific calculations are carried out for germanium-silicon alloys.

03,311
N95-19494/0 (Order as N95-19468/4, PC A24/MF A04)
National Inst. of Standards and Technology, Gaithersburg, MD.
Fracture Behavior of Large-Scale Thin-Sheet Aluminum Alloy.
R. Dewit, R. J. Fields, L. Mordfin, S. R. Low, and D. Harne. Sep 94, 21p.
Contract DTFA03-92-Z-00018
In NASA. Langley Research Center, FAA/NASA International Symposium on Advanced Structural Integrity Methods for Airframe Durability and Damage Tolerance, Part 2 p 963-983.

Keywords: *Aluminum alloys, *Cracks, *Failure, *Fracture mechanics, *Fracturing, *Metal sheets, *Residual strength, Crack tips, Field of view, Loads (Forces), Magnetic recording, Microscopy, Strain gages.

A series of fracture tests on large-scale, pre-cracked, aluminum alloy panels is being carried out to examine and to characterize the process by which cracks propagate and link up in this material. Extended grips and test fixtures were specially designed to enable the panel specimens to be loaded in tension, in a 1780-kN-capacity universal testing machine. Twelve panel specimens, each consisting of a single sheet of bare 2024-T3 aluminum alloy, 3988 mm high, 2286 mm wide, and 1.016 mm thick are being fabricated with simulated through-cracks oriented horizontally at mid-height. Using existing information, a test matrix has been set up that explores regions of failure that are controlled by fracture mechanics, with additional tests near the boundary between plastic collapse and fracture. In addition, a variety of multiple site damage (MSD) configurations have been included to distinguish between various proposed linkage mechanisms. All tests but one use anti-buckling guides. At this writing seven specimens have been tested. Three were fabricated with a single central crack, three others had multiple cracks on each side of the central crack, and one had a single crack but no anti-buckling guides. Each fracture event was recorded on film, video, computer, magnetic tape, and occasionally optical microscopy. The visual showed the crack tip with a load meter in the field of view, using motion picture film for one tip and SVHS video tape for the other. The computer recorded the output of the testing machine load cell, the stroke, and twelve strain gages at 1.5 second intervals. A wideband FM magnetic tape recorder was used to record data from the same sources. The data were analyzed by two different procedures: (1) the plastic zone model based on the residual strength diagram; and (2) the R-curve. The first three tests were used to determine the basic material properties, and these results were then used in the analysis of the two subsequent tests with MSD cracks. There is good agreement between measured values and results obtained from the model.

03,312
PB94-158268 PC A03/MF A01
National Inst. of Standards and Technology (CAML), Gaithersburg, MD. Applied and Computational Mathematics Div.
Boundary Conforming Grid Generation System for Interface Tracking.
B. V. Saunders. Feb 94, 22p, NISTIR-5352.

Keywords: *Liquid-solid interfaces, Mapping(Transformations), Binary alloys, Tensor products, Spline functions, Coordinates, Directional solidification, Grid generation(Mathematics).

The development of an algebraic grid generation system that tracks a solid-liquid interface during directional solidification of a binary alloy is discussed. A single mapping, constructed with tensor product B-splines, is proposed for calculations of both shallow and deep solidification cells. The initial spline coefficients for the coordinate mapping are modified to minimize a discrete functional that regulates the smoothness and orthogonality of the mesh. The use of transfinite blending function interpolation to obtain an initial grid is examined.

03,313
PB94-172707 Not available NTIS
National Inst. of Standards and Technology (MSEL), Gaithersburg, MD. Metallurgy Div.
Effects of Elastic Stress on Phase Equilibrium in the Ni-V System.
Final rept.
M. J. Pfeifer, P. W. Voorhees, and F. S. Biancaniello. 1994, 6p.
Pub. in Scripta Metallurgica et Materialia 30, No. 6, p743-748 1994.

Keywords: *Elastic properties, *Stress analysis, *Phase diagrams, Nickel base alloys, Vanadium alloys, Phase transformations, Precipitation(Chemistry), Chemical equilibrium, Phase coherence, Transition points, Reprints, *Nickel vanadium, Congruent points.

Using our predictions of the effects of elastic stresses on the phase diagram of an alloy displaying a congruent point as a guide we studied experimentally the effects of elastic stress on the Ni-V phase diagram in the neighborhood of the Ni-V--> Ni3V congruent point. The Ni-V--> Ni3V transformation has been well studied and displays a congruent point at 25 at % V, 1,045 C. These experiments have shown that the effects of elastic stress on phase equilibrium is observable in the Ni-V system.

03,314
PB94-172764 Not available NTIS
National Inst. of Standards and Technology (IMSE), Gaithersburg, MD. Fracture and Deformation Div.
Reaction Sensitivities of Al-Li Alloys and Alloy 2219 in Mechanical-Impact Tests.
Final rept.
N. J. Simon, J. D. McColskey, R. P. Reed, and C. Gracia-Salcedo. 1991, 23p.
Pub. in Flammability Sensitivity of Materials in Oxygen-Enriched Atmospheres, ASTM STP 111, p193-215 1991. See also AD-A242 956.

Keywords: *Impact tests, *Flammability, Aluminum alloys, Lithium alloys, Chemical properties, Chemical reactions, Cracking(Fracturing), Mechanical tests, Deformation, Reprints, *Aluminum-Lithium alloys, *Oxygen compatibility.

Open-cup and pressurized mechanical impact tests were conducted at White Sands Test Facility (WSTF) on Al-Li alloys (2090, 8090, and WL049) and Al Alloy 2219 in various tempers. Pressure, drop height (potential energy), and environment (gaseous (GOX) or liquid (LOX)) oxygen were variables in the test program. Reactions were detected in all alloys. The reaction sensitivity was found to vary with specimen absorbed energy. Large, macroreactions occurred on specimen shear lips, a region that has very high deformation and is exposed to striker pin-specimen friction. Small, microreactions were found to occur over many areas of the specimen. The effects of the test variables (pressure, drop height, LOX, GOX) on the frequency of macro- and microreactions is discussed. It is shown that the energy for fracture is always less than, or equal to, the energy for (oxygen) reaction.

03,315
PB94-172913 Not available NTIS
National Inst. of Standards and Technology (MSEL), Gaithersburg, MD. Metallurgy Div.
Intelligent Processing of Hot Isostatic Pressing.
Final rept.
R. J. Schaefer. 1990, 11p.
Pub. in Proceedings of Thermal Structures Conference (1st), Charlottesville, VA., November 13-15, 1990, p401-411.

Keywords: *Hot pressing, *Process control, *Metals, *Intermetallic compounds, *Sensors, Microstructure, Metalworking, Artificial intelligence, Powder metallurgy, Mechanical working, Hot working, Reprints, *Intelligent processing, *Hot isostatic pressing.

Successful hot isostatic pressing (HIP) of metal or intermetallic powders requires that the product meet many goals with respect to shape, density, microstructure and cost. The development of sensors which can detect sample characteristics during HIP consolidation and process models which can predict how the sample characteristics will respond to changes in its environment raises the possibility of active control based on these characteristics. The report describes intelligent processing of hot isostatic pressing.

03,316
PB94-172962 Not available NTIS
National Inst. of Standards and Technology (MSEL), Boulder, CO. Fracture and Deformation Div.

Temperature Increases in Aluminum Alloys during Mechanical-Impact Tests for Oxygen Compatibility.
Final rept.
N. J. Simon, and R. P. Reed. 1991, 14p.
Pub. in Flammability Sensitivity of Materials in Oxygen-Enriched Atmospheres, ASTM STP 111, p367-380 1991.

Keywords: *Impact tests, *Aluminum alloys, *Fracture(Mechanics), *Temperature gradients, Thermal analysis, Cracking(Fracturing), Mechanical tests, Strain rate, Deformation, Reprints.

In mechanical-impact testing of Al-Li alloys and Al alloy 2219 for oxygen compatibility, specimens absorb a significant amount of energy in a short time. The absorbed energy is sufficient to crack and, in many cases, produce large fractures (splits) in the specimens. The high strain rate from impact results in the formation of adiabatic shear bands under adiabatic conditions in the deformed areas. Large local temperature increases in the specimens occur during deformation. Localized melting is more prevalent in alloy 2219, compared to Al-Li alloys. Microreactions also occur more frequently in 2219, but larger, macroreactions occur more readily in the Al-Li alloys. Estimates of temperature increases assuming macroscopic homogeneous deformation during impact are presented. Characteristic times to propagate a thermal transient and to complete the mechanical deformation process are estimated. The difference between the alloy systems in this characteristic time to propagate a thermal disturbance is used to discuss the sizes and frequencies of macro- and microreactions.

03,317
PB94-198694 Not available NTIS
National Inst. of Standards and Technology (MSEL), Gaithersburg, MD. Metallurgy Div.
Coherent Precipitates in the BCC/Orthorhombic Two Phase Field of the Ti-Al-Nb System.
Final rept.
L. A. Bendersky, W. J. Boettinger, and A. Roytburd. 1991, 11p.
Pub. in Acta Metallurgica et Materialia 39, n8 p1959-1969 1991.

Keywords: *Aluminum intermetallics, *Niobium intermetallics, *Titanium intermetallics, Transmission electron microscopy, Binary systems(Materials), Orthorhombic lattices, Bcc lattices, Precipitates, Reprints.

Alloys of composition Ti2AlNb and Ti4AlNb3, cooled from 1400 C and equilibrated at 700 C for 26 days, were both found to consist of two phases: the Ti- and Nb-rich bcc phase and the orthorhombic phase based on Ti2AlNb. Depending on the alloy composition, each phase was observed as a precipitate with a plate morphology in the matrix of the other phase. In both cases, the phases share a common direction, (left bracket)011(right bracket)(bcc) (left bracket)001(right bracket)(ort), and interface (habit plane, (2(-1)1)(bcc) (1(-1)0)(ort). Geometrical patterns of plates of the different orientational variants were also observed. Analysis of the orientation relation, habit plane and plate patterns are consistent with the concept of a strain-type transition even though long range diffusion is required.

03,318
PB94-198702 Not available NTIS
National Inst. of Standards and Technology (MSEL), Gaithersburg, MD. Metallurgy Div.
Crystallographic Characterization of Some Intermetallic Compounds in the Al-Cr System.
Final rept.
L. A. Bendersky, R. S. Roth, J. T. Ramon, and D. Shechtman. 1991, 6p.
Pub. in Metallurgical Transactions A 22, n1 p5-10 1991.

Keywords: *Aluminum intermetallics, *Crystal structure, Transmission electron microscopy, X-ray diffraction, Hexagonal lattices, Monoclinic lattices, Single crystals, Lattice parameters, Reprints, *Chromium intermetallics.

Two Al-Cr compounds known in literature as the nu and epsilon phases were studied in the present work by precession camera single crystal x-ray diffraction and transmission electron microscopy (TEM). The results are different from those reported in the literature. The epsilon phase was found to be hexagonal P6(3)/mmc, with lattice parameters a=2.01 nm and c=2.48 nm. The phase is believed to be isomorphous to the Al4Mn nu phase. The nu phase has monoclinic (pseudo-orthorhombic) C centered Bravais lattice with a(3) approx.=1.76 nm, b(3) approx.=3.05 nm, c(3) approx.=1.76 nm and beta approx.=90 deg. Single crystal of the nu phase are usually twinned.

03,319
PB94-198850 Not available NTIS
National Inst. of Standards and Technology (MSEL), Gaithersburg, MD. Reactor Radiation Div.
Structures of Sodium Metal.
Final rept.
R. Berliner, H. G. Smith, J. R. D. Copley, and J. Trivisonno. 1992, 12p.
Pub. in Physical Review B 46, n22 p14 436-14 447, 1 Dec 92. Sponsored by Department of Energy, Washington, DC.

Keywords: *Martensitic transformation, *Sodium, Neutron diffraction, Neutron scattering, Inelastic scattering, Stacking faults, Temperature dependence, Temperature range 0013-0065 K, Cryogenic temperature, Reprints.

The martensitic transformation in sodium metal has been studied using neutron-diffraction and neutron-inelastic-scattering techniques. In two separate experiments the transformation was observed on cooling near 32 K. Measurements of the diffuse scattering, diffraction linewidths, quasielastic scattering, and the temperature dependence of the Sigma(4)(left bracket)hh0(right bracket) phonon energies above the transformation show no evidence of transformation precursors. The sodium martensite appears as 24 rhombohedral variants, four about each bcc (110), with reflections from their basal planes at (1.018, 0.92, + or - 0.06), (0.92, 1.018, + or - 0.06), and equivalent points. The layer stacking order of the variants is fixed by their relationship to the host bcc material. The crystallography of the low-temperature phase is shown to be a complex mixture of stacking-fault-affected rhombohedral polytypes of a particular 'almost-hexgonal' structure. These form a ladder of structures connected, one to another, by stacking faults. As the martensite is warmed and before the complete reversion to a bcc structure, the relative fraction of the different martensite phases changes. Near 55 K, the longest-period polytypes are the most stable.

03,320
PB94-198900 Not available NTIS
National Inst. of Standards and Technology (MEL), Gaithersburg, MD. Automated Production Technology Div.
Dynamic Shear Modulus Measurements with Four Independent Techniques in Nickel-Based Alloys.
Final rept.
G. V. Blessing, A. Wolfenden, V. K. Kinra, M. R. Harmouche, P. Terranova, Y. T. Chen, and V. Dayal. 1992, 3p.
Pub. in Jnl. of Testing and Evaluation 20, n4 p321-323, Jul 92.

Keywords: *Nickel alloys, *Shear properties, *Modulus of elasticity, *Vibration tests, *Nondestructive tests, Vibrational stress, Frequencies, Resonance testing, Mechanical properties, Resonant frequency, Reprints.

Experimental results are presented, on a round-robin basis, to study the effect of vibrational frequency on the dynamic shear moduli of two metals, Inconel 600 and Incoloy 907. Four separate laboratories, each using a different experimental technique, obtained results over the nominal frequency range of 7 kHz to 10 MHz. A brief discussion and comparison of the four techniques, both resonant and pulse, are included. No significant differences were observed for each alloy's modulus over this frequency range.

03,321
PB94-198934 Not available NTIS
National Inst. of Standards and Technology (MSEL), Gaithersburg, MD. Metallurgy Div.
Thermodynamic Constraints on Non-Equilibrium Solidification of Ordered Intermetallic Compounds.
Final rept.
W. J. Boettinger. 1991, 5p.

Keywords: *Intermetallic compounds, *Order-disorder transformations, *Solidification, Thermodynamic properties, Temperature, Trapping(Charged particles), Interfaces, Equilibrium, Freezing, Reprints.

Thermodynamic constraints on permissible values of temperature, liquid composition, solid composition and long range order parameter at the freezing interface during non-equilibrium solidification of intermetallic phases are defined in terms of the liquid and solid free energy functions.

03,322
PB94-198942 Not available NTIS
National Inst. of Standards and Technology (MSEL), Gaithersburg, MD. Metallurgy Div.
Disorder Trapping in Ni2TiAl.
Final rept.
W. J. Boettinger, L. A. Bendersky, J. Cline, J. A. West, and M. J. Aziz. 1991, 4p.
Pub. in Materials Science and Engineering A 133, p592-595 Mar 91.

Keywords: *Nickel intermetallics, *Solidification, *Trapping(Charged particles), Interfaces, Melting, Intermetallic compounds, Equilibrium, Order-disorder transformations, Reprints.

Pulsed laser melting and rapid resolidification can induce disorder trapping in Ni2AlTi at the solidification interface. The alloy formed from the melt with the nonequilibrium L2 structure and subsequently transformed to the equilibrium L2(sub 1) Heusler structure during cooling to room temperature.

03,323
PB94-199353 Not available NTIS
National Inst. of Standards and Technology (MSEL), Gaithersburg, MD. Metallurgy Div.
LMTO/CVM and LAPW/CVM Calculations of the Nickel Aluminide/Nickel Titanium Pseudobinary Phase Diagram.
Final rept.
B. P. Burton, J. E. Osburn, and A. Pasturel. 1991, 6p.
Pub. in Materials Research Society Symposia Proceedings, v213 p107-112 1991.

Keywords: Order disorder transformations, Aluminum intermetallics, Nickel intermetallics, Titanium intermetallics, Phase diagrams, Reprints, *Nickel aluminides, *Nickel titanium, *Nickel aluminum titanium, Augmented plane wave method, Cluster variation method.

Linear Muffin Tin Orbital and Linearly Augmented Plane Wave calculations of equations of state were performed for observed and hypothetical ordered structures in the NiAl-NiTi System. Total energies were parameterized in both the Connolly and Williams and epsilon-G approximations, and the resulting parameters were used to calculate theoretical phase diagrams by the cluster variation method. Third nearest neighbor Al-Ti pairwise interactions are predicted to be strongly repulsive, and to be the major cause of observed immiscibility between B2 and L2(1) phases.

03,324
PB94-199403 Not available NTIS
National Inst. of Standards and Technology (IMSE), Gaithersburg, MD.
Modeling the Evolution of Structure in Unstable Solid Solution Phases by Diffusional Mechanisms.
Final rept.
J. W. Cahn. 1991, 9p.
Pub. in Scandinavian Jnl. of Metallurgy 20, n1 p9-17 1991.

Keywords: *Crystal-phase transformation, *Solid solutions, *Diffusion theory, Reprints, Nonlinear differential equations, Order disorder transformations, Spinodal decomposition, Difference equations, Mathematical models, Alloys.

Certain phase changes evolve entirely by atom rearrangements among neighboring sites in a crystal structure, and can be understood through the formulation and solution of a realistic diffusion equation. A portion of the 1956 thesis by Mats Hillert, published in 1961 under the title 'A Solid-solution Model for Inhomogeneous Systems', is the seminal theoretical paper in this subject. It deals with solid solutions that have atoms confined to lattice points with a one-dimensional concentration variation, that are unstable to ordering or phase separation, and that evolve entirely by atom exchanges. The results of the theory were applied to his experimental observations on a spinodal alloy. Subsequent theoretical studies have extended the theory to include many factors that make the theory more realistic. Among them is another of Mats Hillert's themes; the introduction of the effects of stresses that result from the diffusional processes.

03,325
PB94-199429 Not available NTIS

National Inst. of Standards and Technology (IMSE), Gaithersburg, MD.
Stability, Microstructural Evolution, Grain Growth, and Coarsening in a Two-Dimensional Two-Phase Microstructure.
Final rept.
J. W. Cahn. 1991, 11p.
Pub. in Acta Metallurgica et Materialia 39, n10 p2189-2199 1991.

Keywords: *Grain growth, Binary systems(Materials), Grain boundaries, Two dimensional, Surface energy, Microstructure, Polycrystalline, Coarseness, Interfaces, Stability, Reprints.

The stability of microstructural features and how this affects grain growth and coarsening in a two-dimensional polycrystalline two-phase material with isotropic energies for the two grain boundaries and the interphase interface is examined using classical concepts of classical capilarity and surface energy driven processes. A catalog of stable microstructural features depends on surface-energy ratios; it is shown to include a four-grain junction that is stable for a range of surface-energy ratios, and, for a given set of ratios, is stable over a range of angles. It is the grain boundary analog of the line junctions among four phases, discussed by Gibbls. Three-grain junctions and grain boundaries had been known to have a limited range of stability. Inferences about grain growth, coarsening, and evolving morphology are obtained from the integrated curvature of the bounding surface of a grain, which depends on the number and phase of neighboring grains, as well as the order of their arrangement. Under some conditions, a dispersion of grains of a boundary phase will tend to a uniform size; this phase resists coarsening.

03,326
PB94-199866 Not available NTIS
National Inst. of Standards and Technology (NEL), Gaithersburg, MD. Precision Engineering Div.
Measuring the Stability of Three Copper Alloys.
Final rept.
T. Doiron, J. Stoup, P. Snoots, and G. Chaconas. 1990, 8p.
Pub. in Proceedings of Society of Photo-Optical Instrumentation Engineers, San Diego, CA., July 12-13, 1990, v1335 p45-52.

Keywords: *Dimensional stability, *Copper alloys, *Experimental design, Dimensional measurement, Measuring instruments, Length, Probability theory, Error analysis, Brass, Beryllium copper, Reprints, Tellurium copper alloys.

In the paper the authors report measurements of the dimensional stability of samples of brass, beryllium copper, and tellurium copper taken over an 18 month time span. Of the materials, brass was the most stable, decreasing slightly in length at the rate of 1 part per million per year (ppm/y) with an uncertainty (3) of about 1 ppm/y. Tellurium copper shrank at an average rate of 2.4 ppm/y and beryllium copper at the rate of 5.8 ppm/y. In order to measure the instrumental uncertainty there were 4 samples of each material were measured, and the measurement scheme was designed to detect and correct for thermal drift during measurements. The experiment design and the problems associated with these measurements and their associated uncertainties are discussed.

03,327
PB94-200326 Not available NTIS
National Inst. of Standards and Technology (MSEL), Gaithersburg, MD. Metallurgy Div.
Micromechanics of Densification and Distortion.
Final rept.
R. B. Clough, and R. J. Schaefer. 1990, 17p.
Pub. in Proceedings of International Conference on Isostatic Pressing (4th), Stratford-upon-Avon, UK, November 5-7, 1993, p38.1-38.17. Sponsored by Defense Advanced Research Projects Agency, Arlington, VA.

Keywords: *Metal powder, *Hot isostatic pressing, *Densification, *Distortion, Compacting, Shear stress, Plastic properties, Finite element method, Porous materials, Powder metallurgy, Reprints.

While compaction under purely isostatic pressure is distortion-free, the introduction of shear stresses, e.g. by the canister, can cause a change in shape of a powder compact. The paper describes a plasticity theory for both shape and volume change of compacts. It is first formulated at a level sufficiently general to apply to both porous and particulate media. It is then combined with the Ashby micromechanical plasticity model for powder compaction, modified to allow for work-hardening, and applied to particulate compacts. It tests favorably against experimental data for a variety of powder compacts in uniaxial and isostatic stress states. The theory of Gurson for porous materials does not fit this data from particulate materials very well. The effect of shear stresses, generated by the containment cansiter, on shape change is then examined using data from copper powder compacts in copper canisters. The theory is available for finite element modeling.

03,328
PB94-200441 Not available NTIS
National Inst. of Standards and Technology (MSEL), Gaithersburg, MD. Metallurgy Div.
Effects of Crystalline Anisotropy and Buoyancy-Driven Convection on Morphological Stability.
Final rept.
S. R. Coriell, G. B. McFadden, and R. F. Sekerka. 1990, 8p.
Pub. in Proceedings of F. Weinberg International Symposium on Solidification Processing, Hamilton, Ontario, August 27-29, 1990, p44-51.

Keywords: *Tin base alloys, *Binary alloys, Indium alloys, Thermal conductivity, Fluid flow, Anisotropy, Convection, Stability, Reprints, *Directional solidification.

The effect of anisotropy of thermal conductivity and buoyancy-driven convection on morphological stability during directional solidification of a binary alloy is considered. Results are presented for dilute alloys of indium in tin. The onset of instability depends on crystallographic orientation, and can be oscillatory in time under certain conditions. Buoyancy-driven flow can result in a long wavelength instability that enhances morphological instability.

03,329
PB94-200474 Not available NTIS
National Inst. of Standards and Technology (IMSE), Gaithersburg, MD. Metallurgy Div.
Assessment of the Al-Sb System.
Final rept.
C. A. Coughanowr, U. R. Kattner, and T. J. Anderson. 1990, 10p.
Contract DE-FG05-86ER45276
Pub. in CALPHAD 14, n2 p193-202 1990. Sponsored by Department of Energy, Washington, DC.

Keywords: *Thermodynamic properties, *Phase diagrams, *Thermochemistry, Assessments, Antimony containing alloys, Aluminum alloys, Binary alloys, Reprints, *Aluminum antimony alloys.

An assessment of the thermochemistry and phase diagram data for the Al-Sb system using the Lukas optimization program is presented. A comparison between the Redlich-Kister and associate models is made.

03,330
PB94-203593 PC A03
National Inst. of Standards and Technology, Boulder, CO.
Cryogenic Properties of Silver.
D. R. Smith, and F. R. Fickett. Jan 94, 14p, NIST/TN-1363.
Also available from Supt. of Docs as SN003-003-03265-4.

Keywords: *Cryogenics, *Silver, *Charts, Precious metals, Mechanical properties, Thermodynamic properties, Tensile properties, Resistivity, Low temperature, Cryochemistry, Stress-strain relationships.

The chart presents several cryogenic properties of silver.

03,331
PB94-211091 Not available NTIS
National Inst. of Standards and Technology (MSEL), Gaithersburg, MD. Metallurgy Div.
Ordered omega-Derivatives in a Ti-37.5Al-2ONb at% Alloy.
Final rept.
L. A. Bendersky, B. P. Burton, W. J. Boettinger, and F. S. Biancaniello. 1990, 6p.
Pub. in Scripta Metallurgica et Materialia 24, n8 p1541-1546 1990.

Keywords: *Titanium containing alloys, *Titanium intermetallics, Molecular structure, Ternary compounds, Aluminum intermetallics, Niobium intermetallics, Transmission electron microscopy, Reprints, *Titanium aluminum niobium, *Omega phase.

In the present work we report finding a new Ti-Al-Nb phase which is apparently a more ordered derivative of the B82 phase. The phase was found as fine precipitates in the presumably B8(2) matrix in Ti-37.5Al-20Nb at% alloy. A possible structure of the new phase will be discussed based on the results of electron diffraction and high-resolution microscopy.

03,332
PB94-211638 Not available NTIS
National Inst. of Standards and Technology (MSEL), Gaithersburg, MD. Metallurgy Div.
Energy and Migration of Grain Boundaries in Polycrystals.
Final rept.
C. Handwerker. 1993, 11p.
Pub. in Interfaces: Structures and Properties, Chapter 20, p339-349 1993.

Keywords: *Grain boundaries, *Microstructure, *Polycrystals, *Physical properties, *Diffusion, Scanning electron microscopy, Electron diffraction, Backscattering, Surfaces, Reprints.

A challenge in the field of microstructure evolution is to understand the physical processes that govern microstructure evolution and the relationship between microstructure and the resulting physical properties of the polycrystal. In this paper two new scanning electron microscope (SEM) techniques for measuring two fundamental characteristics of grain boundaries are described. A metal reference line technique (MRL) has been developed for measuring surface-grain boundary dihedral angles from thermal grooves at a sample surface using an SEM. The second technique is the electron backscattered diffraction pattern (EBDP) for measuring grain texture and grain-grain misorientations.

03,333
PB94-211646 Not available NTIS
National Inst. of Standards and Technology (MSEL), Gaithersburg, MD. Metallurgy Div.
Fabrication of Platinum-Gold Alloys in Pre-Hispanic South America: Issues of Temperature and Microstructure Control.
Final rept.
C. Handwerker, H. Lechtman, R. Marinenko, D. Bright, and D. Newbury. 1991, 16p.
Pub. in Materials Research Society Symposia Proceedings, v185 p649-664 1991.

Keywords: *Metallurgy, *Platinum alloys, *Gold alloys, *Temperature, *Microstructure, Sintering, Electron microscopy, Phase diagrams, Chemical composition, Fabrication, Historical aspects, Reprints.

The microstructures and compositions of sintered Pt-Au objects from La Tolita, Ecuador, and of experimentally simulated Pt-Au alloy samples were analyzed using new electron microprobe microanalysis (EPMA) techniques and data from the Pt-Au phase diagram in an effort to determine the fabrication temperatures used by Pre-Hispanic South American smiths. A comparison of EPMA results from the simulated materials with the corresponding results from the La Tolita Pt-Au objects suggests that the Pt-Au objects were never heated as high as 1100 C and probably never contained a liquid phase. As illustrated by this comparison, the qualitative and quantitative information provided by these new digital acquisition and display techniques far exceeds what conventional line scan and x-ray dot maps could provide.

03,334
PB94-212040 Not available NTIS
National Inst. of Standards and Technology (NML), Gaithersburg, MD. Chemical Process Metrology Div.
In-situ Fume Particle Size and Number Density Measurements from a Synthetic Smelt.
Final rept.
J. C. L. Hsu, C. Presser, and D. T. Clay. 1990, 9p.
Pub. in Proceedings of American Institute of Aeronautics and Astronautics/American Society of Mechanical Engineers Thermophysics and Heat Transfer Conference, Seattle, WA., June 18-20, 1990, p67-75.

Keywords: *Particle size distribution, *Smelting, Polarization, Density, Fumes, Sodium, Potassium, Light scattering, Reprints.

In Kraft recovery furnaces, significant fuming takes place of sodium and potassium. It is essential to quan-

tify the fume generation rate because fume particles coat heat transfer tubes and plug flue gas passages. To address this problem an ensemble light scattering technique, based on measurement of the polarization ratio, was used to measure fume particle size and number density from a synthetic Kraft smelt. This in-situ nonintrusive technique is used because of its application to high density particle-laden flows. Measurements were also carried out at different scattering angles in order to determine the imaginary part of the particle complex refractive index. In addition, fume particle size distributions obtained from scanning electron microscope images were correlated with the log-normal distribution function. Results indicated that an increase in nitrogen flow rate generated smaller fume particles, while a higher air flow rate produced larger fume particles. In addition, increased nitrogen flow rate increased fume mass density, but the air flow rate had a negligible effect. The fume particle geometric mean diameter (Dg) was found to vary with gas flow rate between values of 0.2 and 0.3 m, and number density varied between 3 x 10(exp 7) and 2 x 10(exp 8) particles/cc.

03,335
PB94-212586 Not available NTIS
National Inst. of Standards and Technology (MSEL), Gaithersburg, MD. Metallurgy Div.
Development in the Theory and Analysis of Eddy Current Sensing of Velocity in Liquid Metals.
Final rept.
A. H. Kahn, and L. C. Phillips. 1992, 12p.
Pub. in Res. Nondestr. Eval. 4, p237-248 1992.

Keywords: *Velocity measurement, *Liquid metals, *Eddy currents, Magnetic properties, Nondestructive tests, Magnetic fields, Velocity distribution, Magnetic coils, Flow measurement, Reprints, *Electromagnetic flowmeters.

We have performed a theoretical study of the magnetic fields produced by a single turn ac coil encircling a moving conductive rod or tube of flowing liquid metal. A solution exact to first order in the velocity has been obtained as a closed-form integral. Radial variation of the velocity profile is included. The solution allows a calculation of the voltages induced in two secondary coils wired in opposition for application as a velocimeter. With secondary coils wired in series, the calculation provides the classical impedance vs. frequency curves which allow determination of sample conductivity and diameter. The solution has been used to optimize design for a sensor to be used for monitoring speed and tube bore diameter in a liquid metal atomizer system. An additional solution has been obtained for arbitrary magnitude of velocity, but for constant velocity profile.

03,336
PB94-212636 Not available NTIS
National Inst. of Standards and Technology (MSEL), Gaithersburg, MD. Metallurgy Div.
Thermodynamic Calculation of the Ternary Ti-Al-Nb System.
Final rept.
U. R. Kattner, and W. J. Boettinger. 1992, 9p.
Pub. in Materials Science and Engineering A152, p9-17 1992.

Keywords: *Ternary alloy systems, *Titanium alloys, *Aluminum alloys, *Niobium alloys, Phase diagrams, Thermodynamics, Computation, Reprints, Phase equilibrium.

Phase equilibria of the ternary Ti-Al-Nb system are dominated by the large range of homogeneity of (beta-Ti,Nb), the binary intermetallic compounds of the Nb-Al and Ti-Al systems and the formation of two ternary compounds. The available ternary experimental data, together with a thermodynamic extrapolation of the ternary system from the binary systems, have been used to calculate the ternary phase diagram. The model descriptions of the Gibbs energies of most of these compounds are given by the existing calculations of the binary systems. In order to model a phase which is present in only one binary system, but has a ternary homogeneity range, a hypothetical phase with the same structure was analytically described for each binary system. Such a phase would, of course, be metastable in the other binary systems. Constraints on the Gibbs energies of formation were derived from the crystal structures of the corresponding ordered compounds. These same constraints were employed for the corresponding phases in the ternary system. In a final optimization step, ternary parameters were introduced and adjusted to the available experimental data. The as-derived description of the ternary Ti-Al-Nb system can be used to estimate single or multiphase fields and thermodynamic quantities where no experimental data are yet available. It is also useful as an indicator of problem areas for which additional experimental data are required.

03,337
PB94-212644 Not available NTIS
National Inst. of Standards and Technology (MSEL), Gaithersburg, MD. Metallurgy Div.
Thermodynamic Assessment and Calculation of the Ti-Al System.
Final rept.
U. R. Kattner, J. C. Lin, and Y. A. Chang. 1992, 10p.
Pub. in Metallurgical Transactions A 23A, p2081-2090 Aug 92.

Keywords: *Binary alloy systems, *Titanium alloys, *Aluminum alloys, Least squares method, Phase diagrams, Thermodynamics, Intermetallics, Computation, Reprints.

A thermodynamic description of the Ti-Al system has been developed. Three different analytical descriptions were used to describe the three different types of phases occurring in the Ti-Al system: the stoichiometric compounds, the disordered solution phases, and the ordered intermetallic compounds which have homogeneity ranges. A least-squares technique was used to optimize the thermodynamic quantities of the analytical description using experimental data available in the literature. The calculated phase diagram, as well as the thermodynamic functions, agree well with the critically evaluated experimental data from the literature.

03,338
PB94-216694 Not available NTIS
National Inst. of Standards and Technology (IMSE), Boulder, CO. Fracture and Deformation Div.
Recommended Changes in ASTM Test Methods D2512-82 and G86-84 for Oxygen-Compatibility Mechanical Impact Tests on Metals.
Final rept.
G. W. McColskey, R. P. Reed, N. J. Simon, and J. W. Bransford. 1991, 28p.
Pub. in Flammability and Sensitivity of Materials in Oxygen-Enriched Atmospheres, American Society for Testing and Materials Special Technical Publication 1111, v5 p126-153 1991.

Keywords: *Test methods, *Impact tests, *Aluminum alloys, *Lithium alloys, *Flammability, Energy absorption, Oxygen, Sensitivity, Ignition, Absorbers(Materials), Metals, Interlaboratory comparisons, Reprints, ASTM Test Method D2512-82, ASTM Test Method G86-84, Oxygen compatibility mechanical impact tests.

A cooperative test program to assess the oxygen compatibility of aluminum-lithium alloys with White Sands Test Facility (WSTF), Marshall Space Flight Center (MSFC), and the National Institute of Standards and Technology (NIST) led to assessment of the mechanical impact test by NIST. There were substantially different variations in test parameters between the test laboratories; some of these led to significant variability in the actual energy absorbed by the specimens. Therefore, test results varied widely. To reduce the large disparities in interlaboratory test results, a number of changes are recommended in the current ASTM test standards.

03,339
PB95-107322 Not available NTIS
National Inst. of Standards and Technology (MSEL), Gaithersburg, MD. Ceramics Div.
Electric Field Effects on Crack Growth in a Lead Magnesium Niobate.
Final rept.
A. S. Raynes, G. S. White, and S. W. Freiman. 1990, 14p.
Sponsored by Office of Naval Research, Arlington, VA.
Pub. in Ceram. Trans. 15, p129-142 1990.

Keywords: *Crack propagation, *Electric fields, *Lead compounds, *Niobates, *Magnesium compounds, Strain(Mechanics), Field strength, Electrodes, Fracturing, Reprints, Electrostrictive strain.

The influence of an applied electric field on crack extension in a lead magnesium niobate ceramic was investigated in order to evaluate possible effects of electrostrictive strain on crack propagation. Cracks were generated by indenting polished specimen surfaces equidistant between imbedded parallel electrodes. The field was applied before indentation and maintained for the duration of the measurement. Results showed that cracks emanating from indentations perpendicular to the applied field were consistently shorter than those from indentations made with no field present. No effect of field was observed on cracks parallel to the field. Crack length also appeared to depend on the indentation location relative to the electrodes. A qualitative model explaining these results is proposed.

03,340
PB95-107348 Not available NTIS
National Inst. of Standards and Technology (IMSE), Boulder, CO. Fracture and Deformation Div.
Macro- and Microreactions in Mechanical-Impact Tests of Aluminum Alloys.
Final rept.
R. P. Reed, C. N. McCowan, J. D. McColskey, and N. J. Simon. 1991, 20p.
Pub. in Proceedings of the Symposium on Flammability and Sensitivity of Materials in Oxygen-Enriched Atmospheres, Cocoa Beach, FL., May 14-16, 1991, ASTM STP 1111, p240-259.

Keywords: *Aluminum alloys, *Lithium alloys, *Impact tests, *Accelerated life tests, Morphology, Metallography, Liquid oxygen, Oxygen, Pressure, Reprints, Macroreactions, Microreactions.

Open-cup and pressurized mechanical-impact tests have been conducted at White Sands Test Facility on selected tempers of Al-Li alloys (2090, 8090, WL049), and Al alloy 2219. Both liquid (LOX) and gaseous (GOX) oxygen environments were used and pressure and drop height (potential energy) were varied in each environment. Reactions were observed in all alloys and tempers on both sides of the specimens. Reaction sizes, morphologies, and locations were characterized using a magnifying glass (2X power), a light microscope (5 to 100X), and a scanning electron microscope (100 to 3000X). Photomicrographs of various types of macro- and microreactions are presented and discussed. The variety of sizes of reactions poses a serious problem for the definition of a reaction in standards documents for LOX and GOX mechanical-impact qualification testing. This dilemma is discussed.

03,341
PB95-107355 Not available NTIS
National Inst. of Standards and Technology (IMSE), Boulder, CO. Fracture and Deformation Div.
Influence of Specimen Absorbed Energy in LOX Mechanical-Impact Tests.
Final rept.
R. P. Reed, N. J. Simon, J. R. Berger, and J. D. McColskey. 1991, 18p.
Pub. in Proceedings of Symposium on Flammability and Sensitivity of Materials in Oxygen-Enriched Atmospheres, Cocoa Beach, FL., May 14-16, 1991, ASTM STP 1111, p381-398.

Keywords: *Impact tests, *Aluminum alloys, *Lithium alloys, *Energy absorption, Fracture mechanics, Liquid oxygen, Potential energy, Deformation, Strain(Mechanics), Reprints.

In mechanical impact tests, the potential energy of the plummet is divided between energy absorbed by the specimen, the plummet kinetic energy of rebound, and various losses in the test machine. Thus, all of the potential (or drop height) energy is not transferred to the specimen. The fracture and deformation characteristics and the reactability of metal specimens are dependent on the amount of energy that the specimen absorbs. The absorbed energy may be calculated either from knowledge of the potential energy and rebound height (assuming losses are negligible), or from the depth of striker-pin penetration into the specimen. The depth measurement gives an estimate of specimen strain; a reasonable estimate of force exerted on the specimen during deformation allows calculation of the work of deformation. The effects of the absorbed energy on fracture and deformation characteristics and on reactions in Al-Li alloys and alloy 2219 are discussed.

03,342
PB95-108577 Not available NTIS
National Inst. of Standards and Technology (NML), Gaithersburg, MD. Chemical Process Metrology Div.

Parametric Investigation of Metal Powder Atomization Using Laser Diffraction.
Final rept.
C. Presser, S. Huzarewicz, F. Biancaniello, S. D. Ridder, and H. G. Semerjian. 1990, 5p.
Pub. in Proceedings of Annual Conference on Extended Abstracts ILASS-Americas (4th), Hartford, CT., May 21-23, 1990, p187-191.

Keywords: *Atomization, *Powder metals, *Particle size distribution, *Size determination, *Diffraction analysis, Reprints, Powder metallurgy, Solidification, Flow velocity, Microstructure, *Laser diffraction.

Special properties of rapidly solidified metal powders that are of particular interest to materials engineers include improved chemical homogeneity, novel microstructures, increased solubility and spherically smooth surfaces. These properties have a strong dependence on the solidification rate, and therefore on the particle size. Inert gas pressure, nozzle design and gas/melt flow rates can be used to control powder size, once the particular characteristics of a system are understood. A size, once the particular characteristics of a system are understood. A state-of-the-art sensor system is therefore required to provide high-speed, nonintrusive measurements of particle characteristics for process feedback and control. To address this challenge, a commercially-available particle size analyzer, based on laser diffraction is used to monitor the powder stream in the exhaust section of the Supersonic Inert Gas Metal Atomizer (SiGMA) at NIST. A line-of-sight measurement technique is preferred over one with a discrete point measurement, since this technique provides particle size information which is more representative of the entire flow stream passing through the atomizer exhaust section.

03,343
PB95-126355 Not available NTIS
National Inst. of Standards and Technology (MSEL), Gaithersburg, MD. Metallurgy Div.
Effect of Mn Content on the Microstructure of Al-Mn Alloys Electrodeposited at 150C.
Final rept.
B. Grushko, and G. R. Stafford. 1988, 5p.
Pub. in Israel Jnl. of Technology 24, n3-4 p523-527 1988.

Keywords: *Aluminum manganese alloys, *Electrodeposition, *Microstructure, *Manganese additions, Fused salts, X-ray diffraction, Substrates, Electron microscopy, Reprints.

Al-Mn alloys with compositions ranging between 0-50 wt% Mn were electrodeposited at 150 C onto copper substrates from a chloroaluminate molten salt electrolyte with controlled additions of MnCl2. The results of examination by scanning electron microscopy (SEM), transmission electron microscopy (TEM), energy dispersive x-ray analysis (EDAX) and x-ray diffraction are presented.

03,344
PB95-141057 Not available NTIS
National Inst. of Standards and Technology (NEL), Gaithersburg, MD. Factory Automation Systems Div.
Intelligent Control of an Inert Gas Atomization Process.
Final rept.
S. A. Osella, S. D. Ridder, F. S. Biancaniello, and P. I. Espina. 1991, 4p.
Pub. in Jnl. of the Minerals Metals and Materials Society 43, n1 p18-21 1991.

Keywords: *Metal powder, *Gas atomization, *Controllers, *Artificial intelligence, Process control, Computer aided manufacturing, Atomizers, Control systems, Rare gases, Feedback control, Cybernetics, Heuristic methods, Reprints, US NIST.

Intelligent control is an attempt to specify the function of a controller in ways which mimic the decision-making capabilities of humans. The National Institute of Standards and Technology's (NIST) program on Intelligent Processing of Metal Powders is a multi-disciplinary research initiative investigating the application of intelligent control technologies to improve the state-of-the-art of metal powder manufacturing. This paper reviews the design of NIST's supersonic inert gas metal atomizer control system.

03,345
PB95-147914 PC A04/MF A01
National Inst. of Standards and Technology (CAML), Gaithersburg, MD. Applied and Computational Mathematics Div.
Phase-Field Model for Solidification of a Eutectic Alloy.
A. A. Wheeler, G. B. McFadden, and W. J. Boettinger. Sep 94, 52p, NISTIR-5523.

Keywords: *Eutectic alloys, *Solidification, *Phase transformations, Liquid-soil interfaces, Crystallization, Concentration(Composition), Mathematical models, *Phase field models.

In this paper we discuss two phase-field models for solidification of a eutectic alloy, a situation in which a liquid may transform into two distinct solid phases. The first is based on a regular solution model for the solid with a chemical miscibility gap. This model suffers from the deficiency that, in the sharp interface limit, it approximates a free-boundary problem in which the surface energy of the solid/solid interface is zero and consequently mechanical equilibrium at a trijunction requires that the solid/solid interface has zero dihedral angle (locally planar). We propose a second model which uses two order parameters to distinguish the liquid phase and the two solid phases. We provide a thermodynamically consistent derivation of this phase-field model which ensures that the local entropy production is positive. We conduct a sharp interface asymptotic analysis of the liquid/solid phase transition and show it is governed by a free-boundary problem in which both surface energy and interface kinetics are present. Finally, we consider a sharp interface analysis of a stationary trijunction between the two solid phases and the liquid phase, from which we recover the condition that the interfacial surface tensions are in mechanical equilibrium (Young's equation). This sharp interface analysis compares favorably with numerical solutions of the phase-field model appropriate to a trijunction.

03,346
PB95-151346 Not available NTIS
National Inst. of Standards and Technology (MSEL), Gaithersburg, MD. Polymers Div.
New Alloys Show Extraordinary Resistance to Fracture and Wear.
Final rept.
R. M. Waterstrat. 1992, 4p.
Sponsored by American Dental Association Health Foundation, Chicago, IL.
Pub. in Jnl. of the American Dental Association 123, p33-36 Dec 92.

Keywords: *Zirconium alloys, *Palladium alloys, *Ruthenium alloys, *Wear resistance, *Fracture strength, Implantation, Dental equipment, Medical equipment, Performance evaluation, Crack propagation, Reprints.

A newly invented alloy of zirconium, palladium and ruthenium holds great promise for use in high-strength orthodontic wires, dental and medical implants, and in other applications because of its extraordinary fracture-toughness and wear resistance. Cracks produced experimentally in alloy samples are apparently prevented from propagating by internal stress-induced transformations that occur at the crack tips. This type of behavior has been observed previously in certain industrial ceramics and alloy steels but is a relatively rare phenomenon. ADA and government scientists at the National Institute of Standards and Technology are particularly excited about the alloy because of the insights it might offer on the wear process mechanism and because of its practical implications.

03,347
PB95-151684 Not available NTIS
National Inst. of Standards and Technology (MSEL), Gaithersburg, MD. Metallurgy Div.
Investigation into a Practical Grain Growth Model for Hot Isostatic Pressing.
Final rept.
J. J. Wiassich, and R. B. Clough. 1989, 6p.
Sponsored by Defense Advanced Research Projects Agency, Arlington, VA. and Air Force Office of Scientific Research, Bolling AFB, DC.
Pub. in Proceedings of International Conference on Hot Isostatic Pressing (2nd): Theory and Applications, Gaithersburg, MD., June 7-9, 1989, p123-128.

Keywords: *Grain growth, *Hot isostatic pressing, *Metals, Grain structure(Metallurgy), Sintering, Copper, Microstructure, Diffusion, Pressing(Forming), Reprints.

This paper describes an investigation into a practical model of grain growth for coupling with a microstructural model of densification during Hot Isostatic Pressing (HIP). Grain growth affects densification through plastic yielding and diffusive mechanisms, which are grain size dependent. Depending on the HIP conditions, grain growth can increase or inhibit densification. The grain growth formulation stated here contains relatively well-established parameters for many materials. Coupled with the densification model it executes rapidly on modest computer resources, making the models amenable for further study into the effects of microstructural coarsening on densification. The grain growth model was compared to experiments using OFHC copper compacts that were sintering. Results show that the grain growth model can yield good results but is necessarily sensitive to the value for the activation energy of volume self diffusion.

03,348
PB95-152229 Not available NTIS
National Inst. of Standards and Technology (MSEL), Gaithersburg, MD. Ceramics Div.
Hybrid Method for Determining Material Properties from Instrumented Micro-Indentation Experiments.
Final rept.
Y. M. Chen, A. W. Ruff, and J. W. Dally. 1994, 8p.
Sponsored by National Science Foundation, Arlington, VA. and Office of Naval Research, Arlington, VA.
Pub. in Jnl. Materials Research 9, n5 p1314-1321 May 94.

Keywords: *Indentation, *Copper, *Micromechanics, *Impact tests, Deformation, Finite element method, Penetration, Computational grids, Plastic properties, Elastic properties, Reprints, *EPIC computer program, *Hybrid methods.

The impact code EPIC was employed to study the relationship between the applied force and the penetration depth in a micrometer-scale indentation experiment with oxygen free high conductivity (OFHC) copper. EPIC is an elastic-plastic finite element code that uses a Lagrangian formulation and triangular mesh, which can accommodate large deformation without the need to remesh during the computation process. By fitting the force-penetration curves for a triangular indenter with second degree polynomials, it was demonstrated that the fit changed with two material constants in the constitutive equation. A systematic procedure for determining the material constants is described that is based on matching either the slope or the curvature of the force penetration depth curves from numerical simulation and experiments. It is concluded that material constants can be determined from indentation data obtained using pyramidal or spherical indenters as well as a flat-ended indenter.

03,349
PB95-161782 Not available NTIS
National Inst. of Standards and Technology (MSEL), Gaithersburg, MD. Metallurgy Div.
Ultrasonic Method for Reconstructing the Two-Dimensional Liquid-Solid Interface in Solidifying Bodies.
Final rept.
F. A. Mauer, S. J. Norton, Y. Grinberg, D. Pitchure, and H. N. G. Wadley. 1991, 7p.
Pub. in Metallurgical Transactions B 22, n4 p467-473 1991.

Keywords: *Solidification, *Ultrasonic tests, *Aluminum, Tomography, Time of flight spectrometers, Strands, Fluid boundaries, Least squares method, Reprints, *Liquid-solid interfaces.

A method is demonstrated for reconstructing the two-dimensional boundary of the liquid core in a solidifying strand of aluminum using ultrasonic time-of-flight data. Approximating the boundary by an ellipse leads to a model that can be used to calculate the time-of-flight along any path in the plane of the ellipse. The shape and location of the ellipse are specified by four free parameters. A least-squares algorithm is then used to find the set of four parameters that provides the best fit to the measured time-of-flight data on ten intersecting paths through the strand. For a strand with a 6 inch square cross section, the agreement between the actual interface and the computed interface was within about + or - 2%. Reference data for the temperature dependence of longitudinal velocity for solid 1110 aluminum are included.

03,350
PB95-163028 Not available NTIS
National Inst. of Standards and Technology (NEL), Gaithersburg, MD. Applied and Computational Mathematics Div.

Effects of Elastic Stress on the Stability of a Solid-Liquid Interface.
Final rept.
B. J. Spencer, S. H. Davis, G. B. McFadden, and P. W. Voorhees. 1990, 2p.
Sponsored by National Science Foundation, Washington, DC. and National Aeronautics and Space Administration, Washington, DC.
Pub. in Applied Mechanics Reviews 43, n5 pS54-S55 May 90.

Keywords: *Liquid-solid interface, Binary alloys, Stability, Reprints, *Crystal-melt interface, Directional solidification, Elastic stresses.

The effects of elastic stress on the stability of solid-liquid interfaces under a variety of conditions are discussed. In the cases discussed, the nonuniform composition field in the solid, which accompanies either the melting process or the development of a perturbation on the solid-liquid interface during solidification, generates nonhydrostatic stresses in the solid. Such compositionally generated elastic stresses have been shown experimentally to induce a solidifying solid-liquid interface to become unstable. We are in the process of analyzing the effects of these stresses on the conditions for morphological stability of a directionally solidified binary alloy.

03,351
PB95-164620 Not available NTIS
National Inst. of Standards and Technology (MEL), Gaithersburg, MD. Precision Engineering Div.
Surface Texture.
Final rept.
J. F. Song, and T. V. Vorburger. 1992, 12p.
Pub. in Metals Handbook, v18 p334-345 1992.

Keywords: *Surface roughness, Metal working, Automotive components, Power spectra, Autocorrelation, Measurement, Calibration, Skewness, Tribology, Profiles, Pens, Uses, Reviews, Reprints, *Surface texture, Surface topography.

The field of surface texture measurement is reviewed with emphases on stylus techniques and applications to tribology and related problems. We define a number of useful surface statistical parameters including roughness average, rms roughness, skewness, and peak spacing as well as the power spectral density and autocorrelation functions. The strengths and limitations of stylus instruments are discussed in detail, along with procedures for calibrating them. Practical applications of these measurements include the study of lip seals, the study of wear by standard techniques, and many other problems in the automotive and metal working industries.

03,352
PB95-168415 Not available NTIS
National Inst. of Standards and Technology (EEEL), Boulder, CO. Electromagnetic Technology Div.
Effect of Microstructure on Phase Formation in the Reaction of Nb/Al Multilayer Thin Films.
Final rept.
K. Barmak, K. R. Coffey, D. A. Rudman, and S. Foner. 1992, 6p.
Sponsored by Department of Energy, Washington, DC.
Pub. in Materials Research Society Symposia Proceedings, v230 p61-66 1992.

Keywords: *Aluminum, *Niobium, Metal films, Thin films, Microstructure, Reprints, *Interfacial reactions, Phase formation, Multilayers.

We investigated the phase formation sequence in the reaction of multilayer thin films of Nb/Al with overall compositions of 25 and 33 at.% Al. We report novel phenomena which distinguish thin-film reactions unequivocally from those in bulk systems. For sufficiently thin layers, composition and stability of product phases are found to deviate significantly from that predicted from the equilibrium phase diagram. We demonstrate that in the Nb/Al system, the length scales below which such deviations occur is about 150 nm. We believe that these phenomena occur due to the importance of grain boundary diffusion and hence microstructure in these thin films.

03,353
PB95-168456 Not available NTIS
National Inst. of Standards and Technology (EEEL), Boulder, CO. Electromagnetic Technology Div.
First Phase Formation Kinetics in the Reaction of Nb/Al.
Final rept.
K. R. Coffey, K. Barmak, D. A. Rudman, and S. Foner. 1992, 6p.
Sponsored by Department of Energy, Washington, DC.
Pub. in Materials Research Society Symposia Proceedings, v230 p55-60 1992.

Keywords: *Niobium, Aluminum, Transmission electron microscopy, X ray diffraction, Metal films, Thin films, Calorimetry, Annealing, Aluminum intermetallics, Niobium intermetallics, Reprints, *Interfacial reactions, Phase formation, Niobium aluminides, Multilayers.

Phase formation kinetics in the reaction of Nb/Al multilayered thin films were investigated using scanning calorimetry, x-ray diffraction, and transmission electron microscopy. The first phase to form upon annealing the Nb/Al layered structure is the NbAl3 intermetallic. Its formation is clearly identified by the calorimetry to be a two-stage process, which has been modeled as the nucleation and three-dimensional growth to coalescence of the product phase in the plane of the initial interface, followed by the thickening of the product layer by one-dimensional growth perpendicular to the interface plane. For the initial reaction stage the reaction front velocity is higher than can be supported by diffusional transport within the lattice adjacent to the moving interface. Thus diffusion along nonequilibrium interfaces must be the growth mechanism. The large volume fraction consumed during the initial reaction stage indicates a lower nucleation site density than expected at a Nb/Al interface at local equilibrium, suggesting that the interface transport is reducing the driving force for nucleation.

03,354
PB95-176103 Not available NTIS
National Inst. of Standards and Technology (MSEL), Gaithersburg, MD. Reactor Radiation Div.
Small Angle Neutrons Scattering from Nanocrystalline Palladium as a Function of Annealing.
Final rept.
P. G. Sanders, J. R. Weertman, J. G. Barker, and R. W. Siegel. 1993, 6p.
Pub. in Scripta Metallurgica et Materialia 29, p91-96 1993.

Keywords: *Neutron scattering, *Palladium, *Crystal defects, *Grain boundaries, Small angle scattering, Particle size, Mechanical properties, Crystal structure, Reprints, *Nanocrystalline materials.

Nanocrystalline materials, with grain sizes on the order of nanometers, have many interesting properties as a result of having confining grain sizes and a significant fraction of their atoms in grain boundary regions. Nanocrystalline materials may be synthesized by inert gas condensation and compaction, as developed by Gleiter and co-workers. While this processing method is very effective, it does produce specimens containing defects of various sizes. Evidence for the presence of these defects in nanocrystalline metals includes substantial deviations from theoretical density, positron lifetime measurements, and small angle neutron scattering (SANS) measurements. Previous SANS results have been interpreted primarily in terms of scattering from low density grain boundaries, although the contribution from pores has also been recognized. The presence of such defects is believed to have a strong influence on the apparent strength of nanocrystalline metals; therefore, any comprehensive study of mechanical behavior should include detailed information on the defect structure of the material. As part of a study of mechanical properties and their correlation with changes in internal structure, SANS measurements were made on a series of nanocrystalline palladium (n-Pd) samples. Preliminary results of the study are described.

03,355
PB95-181111 Not available NTIS
National Inst. of Standards and Technology (CAML), Gaithersburg, MD. Applied and Computational Mathematics Div.
Morphological Development of Second-Phase Particles in Elastically-Stressed Solids.
Final rept.
P. W. Voorhees, G. B. McFadden, and W. C. Johnson. 1992, 14p.
Grant NSF-DMR89-57219
Sponsored by National Science Foundation, Washington, DC., National Aeronautics and Space Administration, Washington, DC., and Defense Advanced Research Projects Agency, Arlington, VA.
Pub. in Acta Metall. Mater. 40, n11 p2979-2992 1992.

Keywords: *Particle shape, Boundary integral method, Particle motion, Thermodynamics, Coarseness, Elasticity, Morphology, Anisotropy, Dynamics, Reprints, Two phase systems, Ostwald ripening, Particle coarsening.

We examine the equilibrium shape and the dynamics of the morphological evolution of a coherent misfitting particle in an elastically anisotropic medium. No a priori assumptions are made on the possible particle morphologies; the particle evolves in a manner consistent with both the diffusion and elastic fields surrounding the particle and the thermodynamics of interfaces in stressed solids. Through these calculations we find the thermodynamically stable equilibrium shape of a misfitting particle. By thermodynamically stable we mean that all the equilibrium conditions, elastic, chemical and interfacial are satisfied simultaneously, in contrast to previous treatments which determined the equilibrium shape by minimizing the sum of the elastic and interfacial energies for certain classes of particle shapes. We find that the equilibrium particle morphologies are not simple geometric shapes, have fourfold symmetry and a continuously varying interfacial curvature with position along the interface. Furthermore, the results show that the times required for a particle to evolve to its equilibrium morphology are likely to be within those which are accessible experimentally. In addition, we develop a general approach for determining the equilibrium shape of a particle in an elastically stressed solid.

03,356
PB96-102207 Not available NTIS
National Inst. of Standards and Technology (MSEL), Gaithersburg, MD. Metallurgy Div.
Radiance Temperatures (in the Wavelength Range 523-907 nm) of Group IV B Transition Metals Titanium, Zirconium, and Hafnium at Their Melting Points by a Pulse-Heating Technique.
Final rept.
A. Cezairliyan, J. L. McClure, and A. P. Miller. 1994, 18p.
Sponsored by National Aeronautics and Space Administration, Washington, DC.
Pub. in International Jnl. of Thermophysics, v15 n5 p993-1009 1994.

Keywords: *Emissivity, *Transition metals, *Melting points, *Pulse heating, Temperature measurement, Radiant flux density, Hafnium, Titanium, Zirconium, High temperature, Reprints.

The melting-point radiance temperatures (at six wavelengths in the range 523-907 nm) of the Group IVB transition metals titanium, zirconium, and hafnium were measured by a pulse-heating technique. The method is based on rapid resistive self-heating of the specimen from room temperature to its melting point in less than 1 s and on simultaneously measuring the specimen radiance temperatures every 0.5 ms with a high-speed six-wavelength pyrometer. Melting was manifested by a plateau in the radiance temperature-versus-time function for each wavelength. The melting-point radiance temperatures for a given specimen were determined by averaging the measured temperatures along the plateau at each wavelength.

03,357
PB96-103007 Not available NTIS
National Inst. of Standards and Technology (CAML), Gaithersburg, MD. Applied and Computational Mathematics Div.
Boundary Conforming Grid Generation System for Interface Tracking.
Final rept.
B. V. Saunders. 1995, 17p.
See also PB94-158268.
Pub. in Computers and Mathematics with Applications 29, n10 p1-17 1995.

Keywords: *Liquid solid interfaces, Reprints, Mapping(Transformations), Binary alloys, Tensor products, Spline functions, Coordinates, Directional solidification, Grid generation(Mathematics).

The development of an algebraic grid generation system to track a solid-liquid interface during directional solidification of a binary alloy is discussed. A single mapping, constructed with tensor product B-splines, is proposed for calculations of both shallow and deep solidification cells. The initial spline coefficients for the coordinate mapping are modified to minimize a discrete functional that regulates the smoothness and

orthogonality of the mesh. The use of transfinite blending function interpolation to obtain an initial grid is examined.

03,358
PB96-109558 PC A06/MF A02
National Inst. of Standards and Technology, Gaithersburg, MD.
Factors Significant to Precracking of Fracture Specimens.
C. G. Interrante, and J. J. Filliben. Nov 89, 102p, NISTIR-89/4214.

Keywords: *Fracture tests, *Impact tests, *Titanium, *Aluminum, *Steels, Standards, Cracking(Fracturing), Toughness, Fatigue(Materials), Stress analysis, Bend tests.

The significance of four controlled variables in the technique used to precrack Charpy specimens is determined by analyses of seven response variables computed from results of slow-bend tests of metallic materials. The results can be summarized in three major conclusions: (1) All seven computed responses are linearly related to crack size and the sensitivity to crack size depends on the choice of response parameter and on the material. (2) Precracking at either very high or very low levels of stress-intensity factor KF, are to be avoided. (3) For the three methods of notch preparation, the effects of notch preparation were largely not significant. This work is the result of a study conducted by ASTM Task Group E24.03.03 and members of eight participating laboratories.

03,359
PB96-115050 PC A04/MF A01
National Inst. of Standards and Technology (MSEL), Gaithersburg, MD. Office of Intelligent Processing of Materials.
Intelligent Processing of Materials, Technical Activities 1994 (NAS-NRC Assessment Panel, April 6-7, 1995).
Annual rept.
D. E. Hall, and G. Birnbaum. 7 Apr 95, 70p, NISTIR-5578.
See also report for 1993, PB94-164183.

Keywords: *Materials, *Gas atomization, *Controllers, *Artificial intelligence, Process control, Computer-aided manufacturing, Atomizers, Control systems, Rare gases, Ceramics, Metal powders, Polymers, Sensors, Grinding(Material removal), Research programs, Ultrasonic tests, Nondestructive tests.

This report discusses the technical activities during 1994 of the projects supported by the Office of Intelligent Processing of Materials in the Materials Science and Engineering Laboratories. The activities include large consortia and other large programs in metals and alloys, ceramics, polymer and polymer blends sensor research involving thermal wave and ultrasonic evaluation of ceramic grinding damage, eddy current temperature measurement during hot rolling of aluminum sheet, and metal sensors in the microstructural engineering of steel.

03,360
PB96-123203 Not available NTIS
National Inst. of Standards and Technology (PL), Gaithersburg, MD. Ionizing Radiation Div.
Study of Laser Resonance Ionization Mass Spectrometry Using a Glow Discharge Source.
Final rept.
X. Xiong, J. M. R. Hutchinson, J. D. Fassett, W. A. Bowman, K. R. Hess, T. B. Lucatorto, and F. J. Schima. 1995, 4p.
See also DE94018566.
Pub. in AIP Conference Proceedings, Bernkastel-kues, Germany, July 1994, v329 p316-319 1995.

Keywords: *Aluminum base alloys, *Copper alloys, *Iron alloys, Atomization, Data acquisition systems, Dye lasers, Mass spectrometers, Reprints, *Foreign technology.

The mass spectra of a metal alloy sample consisting of Al, Cu and Fe were studies using both glow discharge mass spectrometry (GDMS) and resonance ionization mass spectrometry (RIMS). Particular emphasis was placed on the reduction of isobaric interferences and discrimination between those ions formed by the discharge and those formed by the laser radiation.

03,361
PB96-126198 (Order as PB96-126180, PC A05/MF A01)
National Institute of Standards and Technology, Boulder, CO.
Low-Temperature Properties of Silver.
D. R. Smith, and F. R. Fickett. 1995, 53p.
Included in Jnl. of Research of the National Institute of Standards and Technology, v100 n2 p119-171 Mar/Apr 95.

Keywords: *Mechanical properties, *Silver, Temperature, Physical properties, Conductivity, Cryogenics, Superconductors, Thermodynamics.

Pure silver is used extensively in the preparation of high-temperature superconductor wires, tapes, films, and other configurations in which the silver not only shields the superconducting material from the surrounding materials, but also provides a degree of flexibility and strain relief, as well as stabilization and low-resistance electrical contact. Silver is relatively expensive, but at this stage of superconductor development, its unique combination of properties seems to offer the only reasonable means of achieving usable lengths of conductor. In this role, the low-temperature physical (electrical, thermal, magnetic, optical) and mechanical properties of the silver all become important. Here the authors present a collection of properties data extracted from the cryogenic literature and, to the extent possible, selected for reliability.

03,362
PB96-134954 PC A05/MF A01
National Inst. of Standards and Technology, Gaithersburg, MD.
Journal of Research of the National Institute of Standards and Technology, September-October 1993. Volume 98, Number 5.
B. N. Taylor, and D. R. Harris. 1993, 96p.
See also PB94-108529.

No abstract available.

03,363
PB96-135231 Not available NTIS
National Inst. of Standards and Technology (MSEL), Boulder, CO. Materials Reliability Div.
Effects of Copper, Nickel and Boron on Mechanical Properties of Low-Alloy Steel Weld Metals Deposited at High Heat Input.
Final rept.
A. O. Kluken, T. A. Siewert, and R. Smith. 1994, 7p.
Pub. in Welding Research Supplement, p193s-199s Aug 94.

Keywords: *Weld metal, *Heat, *Fracture resistance, *Submerged arc welding, Reprints, Mechanical properties, Tensile strength, High heat input.

The authors studied the effects of copper, nickel and boron on the mechanical properties of low-alloy steel weld metals deposited at high heat input (4.8 kJ/mm) by the submerged arc process. The copper and nickel contents of the welds were systematically varied within the ranges of 0.03 to 0.89 wt-% Cu and 0.01 to 1.54 wt-% Ni. In addition, several of these copper and nickel combinations were duplicated with welds containing 36 to 44 ppm B. Tensile testing revealed yieled strengths in the range from 462 to 546 Mpa, and ultimate tensile strengths from 638 to 869 Mpa. The weld metal Charpy V-notch (CVN) data showed a 35 J transition temperature, ITT, ranging from -28 to 55 C. Upon adding boron, patches of intergranular fracture were present on the CVN fracture surfaces. This was particularly true when boron was added at the higher copper and nickel levels. Qualitative metallographic examinations revealed the presence of extensive amounts of particles at the prior austenite grain boundaries in boron containing welds. Furthermore, adding boron at the higher copper and nickel levels promoted the formation of the MAC (martensite-austenite-carbide) microconstituent. Also nickel seemed to promote formation of MAC in reheated weld metal. At this high heat input (4.8 kJ/mm), additions of copper, nickel and boron did not improve the mechanical properties.

03,364
PB96-141015 Not available NTIS
National Inst. of Standards and Technology (MSEL), Boulder, CO. Materials Reliability Div.
Elastic Constants and Internal Friction of Polycrystalline Copper.
Final rept.
H. Ledbetter, C. Fortunko, and P. Heyliger. 1995, 2p.
See also PB87-111662.
Pub. in Jnl. of Materials Research, v10 n6 p1352-1353 Jun 95.

Keywords: *Elastic properties, *Copper, Internal friction, Reprints, Ultrasonics, Vibrations, Spectroscopy, Koehler-Granato-Lucke model.

Using ultrasonic-resonance spectroscopy (URS), we measured the elastic constant C and companion internal friction Q-1 of isotropic polycrystalline copper. The annealed material was 0.9999 pure with equiaxed heavily twinned grains averaging about 75 micrometers diameter. The URS method offers the principal advantage of point contact or loose coupling, thus there was no contribution from a transducer-specimen bond and only small contributions from transducers and fixture. A second advantage is one measurement for all elastic constants and all associated internal frictions. The C's agree with established values. The Q-1's are much lower than pulse-echo-method values. Comparison of measured Q-1 with the Koehler-Granato-Lucke model permits estimating an effective dislocation-loop length. Q-1 (shear) exceeds Q-1 (Longitudinal) by a factor of about 1.5.

03,365
PB96-141122 Not available NTIS
National Inst. of Standards and Technology (MSEL), Boulder, CO. Materials Reliability Div.
Effect of Charpy V-Notch Striker Radii on the Absorbed Energy.
Final rept.
T. A. Siewert, and D. P. Vigliotti. 1995, 13p.
Pub. in Pendulum Impact Machines, p140-152 May 95.

Keywords: *Impact tests, *Energy absorption, Fracture mechanics, Strain(Mechanics), Reprints, Charpy V-notch, Striker radius.

The two most common Charpy V-notch striker designs (8-mm and 2-mm radii on the striking edge) were compared using verification (reference-grade) impact specimens. Other variables in the test matrix included two different brands of U-type pendulum machines and four different specimen energy ranges (near 18, 45, 100, and 200 J). In this comparative study, we found a very small difference betwenn the two striker designs and an even smaller difference between the two brands of machines. At 200 J, the difference between the two striker designs was about 10 J. This difference might not be important in most production testing, but must be considered in verification testing where the acceptable range may be 5 percent. The standard deviations of absorbed energy for the two strikes were similar, except at 200 J were the 2-mm striker produced standard deviations about 3 times higher than the 8-mm striker.

03,366
PB96-146857 Not available NTIS
National Inst. of Standards and Technology (MSEL), Gaithersburg, MD. Reactor Radiation Div.
Inelastic Neutron Scattering Study of Hydrogen in Nanocrystalline Pd.
Final rept.
U. Stuhr, H. Wipf, T. J. Udovic, J. Weissmuller, and H. Gleiter. 1995, 4p.
Pub. in NanoStructured Materials, v6 p555-558 1995.

Keywords: *Neutron scattering, *Palladium, *Grain boundaries, Crystal structure, Reprints, *Foreign technology, *Nanocrystalline materials.

The vibrational excitations and the position of hydrogen in nanocrystalline Pd was investigated by neutron spectroscopy. This study was restricted to low hydrogen concentrations where no hydrogen precipitation was observed at room temperature. The experiments show that most of the hydrogen is incorporated in the grain boundaries and at the inner surfaces of the grains. Surface modes of the hydrogen can be identified. Compared to coarse-grained Pd, no change in the hydrogen solubility was found for the lattice regions of the nanocrystalline Pd.

03,367
PB96-161807 Not available NTIS
National Inst. of Standards and Technology (MSEL), Gaithersburg, MD.
Nonlocal Effects of Existing Dislocations on Crack-Tip Emission and Cleavage.
Final rept.
V. Shastry, P. M. Anderson, and R. Thomson. 1994, 16p.
Pub. in Jnl. of Materials Research, v9 n3 p812-827 Mar 94.

Keywords: *Ductile brittle transition, *Crack propagation, Cleavage, Emission, Reprints, Fractures(Materials), *Dislocations(Materials).

This paper investigates the criterion for a ductile-to-brittle transition in materials, due to nonlocal shielding effects at the crack tip when the dislocation free zone (DFZ) size is small. It is found that both cleavage and emission criteria are altered by nonlocal shielding, but that the emission shift is dominant, and is always in the direction to increase the local critical stress intensity for emission, kIIe. The nonlocal shift varies with the sum sigma(gamma(sub us)dj) to the negative 3/2, over each dislocation (j), where gamma(sub us) is the unstable stacking fault energy, and dj is the distance from each dislocation to the crack tip. When there is a pileup of many shielding dislocations against a barrier near the crack tip, the total shift for the pileup varies as (gamma(sub us)d) to the minus 1 power. The most likely candidates for a brittle transition induced by the nonlocal shift are materials where barriers to dislocation motion exist within 10-100 nanometers of the crack tip, such as in thin films, multilayers, or ultrafine grain materials.

03,368
PB96-169057 PC A05/MF A01
National Inst. of Standards and Technology, Gaithersburg, MD.
Journal of Research of the National Institute of Standards and Technology, September/October 1993. Volume 98, Number 5.
1993, 96p.
See also PB96-169065 through PB96-169081 and PB94-108529. Also available from Supt. of Docs. as SN703-027-00054-7.

Keywords: *Titanium alloys, *Aluminum alloys, *Niobium alloys, *Crystal-phase transformations, *Silicon carbides, *Silicon nitrides, *Corrosion, BCC lattices, HCP lattices, Orthorhombic lattices, Transmission electron microscopy, Heat exchangers, Combustion, Coal, Slags, Ashes, Integrated Services Digital Network.

Contents:
- Articles--Transformation of BCC and B2 High Temperature Phases to HCP and Orthorhombic Structures in the Ti-Al-Nb System. Part I--Microstructural Predictions Based on a Subgroup Relation Between Phases;
- Transformation of BCC and B2 High Temperature Phases to HCP and Orthorhombic Structures in the Ti-Al-Nb System. Part II--Experimental TEM Study of Microstructures;
- Corrosion Characteristics of Silicon Carbide and Silicon Nitride. Conference Reports--North American Integrated Services Digital Network (ISDN) Users' Forum (NIUF);
- News Briefs.

03,369
PB96-169057 PC A06/MF A01
National Inst. of Standards and Technology, Gaithersburg, MD.
Journal of Research of the National Institute of Standards and Technology, September/October 1993. Volume 98, Number 5.
1993, 96p.
See also PB96-169065 through PB96-169081 and PB96-108529. Supersedes PB96-134954. Also available from Supt. of Docs. as SN-703-027-00054-7.

Keywords: *Titanium alloys, *Aluminum alloys, *Niobium alloys, *Crystal-phase transformations, *Silicon carbides, *Silicon nitrides, *Corrosion, BCC lattices, HCP lattices, Orthorhombic lattices, Transmission electron microscopy, Heat exchangers, Combustion, Coal, Slags, Ashes, *Integrated Services Digital Network.

Contents:
- Calibration of Electret-Based Integral Radon Monitors Using NIST Polyethylene-Encapsulated 226Ra/222Rn Emanation (PERE) Standards;
- Microstructural Characterization of Cobalt-Tungsten Coated Graphite Fibers;
- On Using Collocation in Three Dimensions and Solving a Model Semiconductor Problem;
- Precision Tests of a Quantum Hall Effect Device DC Equivalent Circuit Using Double-Series and Triple-Series Connections;
- Analysis of the (5d2 + 5d6s) - 5d6p Transition Arrays of Os VII and Ir VIII, and the 6s 2S-6p2P Transitions of Ir IX.

03,370
PB96-169065 (Order as PB96-169057, PC A05/MF A01)
National Inst. of Standards and Technology, Gaithersburg, MD.
Transformation of BCC and B2 High Temperature Phases to HCP and Orthorhombic Structures in the Ti-Al-Nb System. Part 1. Microstructural Predictions Based on a Subgroup Relation between Phases.
L. A. Bendersky, A. Roytburd, and W. J. Boettinger. 1993, 23p.
Included in Jnl. of Research of the National Institute of Standards and Technology, v98 n5 p561-583 Sep/Oct 93.

Keywords: *BCC lattices, *Orthorhombic lattices, Phases, Reprints, Structural relations, *Domain structures, Elastic accommodation, Space group relations.

Possible paths for the constant composition coherent transformation of BCC or B2 high temperature phases to low temperature HCP or Orthorhombic phases in the Ti-Al-Nb system are analyzed using a sequence of crystallographic structural relationships developed from subgroup symmetry relations. Symmetry elements lost in each step of the sequence determine the possibilities for variants of the low symmetry phase and domains that can be present in the microstructure. The orientation of interdomain interfaces is determined by requiring the existence of a strain-free interface between the domains.

03,371
PB96-169073 (Order as PB96-169057, PC A05/MF A01)
National Inst. of Standards and Technology, Gaithersburg, MD.
Transformation of BCC and B2 High Temperature Phases to HCP and Orthorhombic Structures in the Ti-Al-Nb System. Part 2. Experimental TEM Study of Microstructures.
L. A. Bendersky, and W. J. Boettinger. 1993, 22p.
Included in Jnl. of Research of the National Institute of Standards and Technology, v98 n5 p585-606 Sep/Oct 93.

Keywords: *BCC lattices, *Orthorhombic lattices, Phases, Reprints, Structural relations, *Domain structures, Elastic accomodation, Space group relations.

Possible transformation paths that involve no long range diffusion and their corresponding microstructural details were predicted by Bendersky, Roytburd, and Boettinger for Ti-Al-Nb alloys cooled from the high temperature BCC/B2 phase field into close-packed orthorhombic or hexagonal phase fields. These predictions were based on structural and symmetry relations between the known phases. In the present paper experimental TEM results show that two of the predicted transformation paths are indeed followed for different alloy compositions.

03,372
PB96-169081 (Order as PB96-169057, PC A05/MF A01)
National Inst. of Standards and Technology, Gaithersburg, MD.
Corrosion Characteristics of Silicon Carbide and Silicon Nitride.
R. G. Munro, and S. J. Dapkunas. 1993, 25p.
Included in Jnl. of Research of the National Institute of Standards and Technology, v98 n5 p607-631 Sep/Oct 93.

Keywords: *Corrosion, *Silicon carbides, *Silicon nitrides, Ashes, Reprints, Ceramics, Coal.

The present work is a review of the substantial effort that has been made to measure and understand the effects of corrosion with respect to the properties, performance, and durability of various forms of silicon carbide and silicon nitride. The review encompasses corrosion in diverse environments, usually at temperatures of 1000 degrees C or higher. The environments include dry and moist oxygen, mixtures of hot gaseous vapors, molten salts, molten metals, and complex environments pertaining to coal ashes and slags.

03,373
PB96-186069 Not available NTIS
National Inst. of Standards and Technology (MSEL), Boulder, CO. Materials Reliability Div.
Sensor System for Intelligent Processing of Hot-Rolled Steel.
Final rept.
A. V. Clark, M. G. Lozev, B. J. Filla, and L. J. Bond. 1994, 8p.
Pub. in International Symposium on Nondestructive Characterization of Materials VI (6th), Honolulu, HI., June 7-11, 1993, p29-36 1994.

Keywords: *Acoustics, *Intelligent processing, *Steel, Ultrasonics, Reprints.

Microstructural engineering offers a means of reducing cycle time and improving product quality with reduced energy cost. Process modelling of hot-rolling of steel has advanced to the point where key metallurgical parameters (e.g. austenite grain size) can be predicted from computer models if other process parameters such as temperature are known. However, a need still remains to develop on-line sensors because sensors can rapidly acquire data for model validation, and could be combined with a process control strategy in feedforward or feedback loops. The authors report a study to develop an on-line sensor for autenite grain size measurement at temperatures up to 1000 degrees C. They are developing a system for measurement of attenuation in ultrasonic waves propagating through hot steel samples. Existing theories allow the authors to infer grain size for attenuation measurement. The authors' system consists of a high temperature transducer acoustically coupled to a high strength, low loss buffer rod. The rod is to be pressed against a hot steel specimen sufficiently good contact to transmit ultrasound into the specimen. To avoid plastic deformation of the specimen, they implement computer control of the load applied to the buffer rod. Attenuation measurements were performed at room temperature on specimens of known grain size. Good agreement with optically measured grain size was obtained. The system is now being assembled for measurement at elevated temperatures.

03,374
PB96-190236 Not available NTIS
National Inst. of Standards and Technology (MSEL), Boulder, CO. Materials Reliability Div.
Aluminum-Lithium Alloys: Evaluation of Fracture Toughness by Two Test Standards, ASTM Method E 813 and E 1304.
Final rept.
P. T. Purtscher, J. D. McColskey, and E. S. Drexler. 1992, 21p.
Pub. in Standard Technical Publication 1172, p110-130 1992.

Keywords: *Aluminum lithium alloys, *Fracture toughness, Standards, Cryogenic properties, Declaminations, Reprints, Alloy 2219.

Fracture toughness of three aluminum-lithium alloys and Alloy 2219 (a total of nine different plates) was measured with two different types of specimens and methods: (1) compact specimens using ASTM E 813 and (2) chevron-notched short-bar specimens using ASTM E 1304. The properties were measured in two orientations (T-L and L-T) and at three temperatures (295, 76, and 4 K). In general, the short-bar specimens exhibited a higher fracture toughness than the compact specimens. The difference between the two procedures was relatively constant, independent of test orientation and strength. However, when the specimens exhibited extensive declamations on the fracture surface, the compact specimens had a higher fracture toughness than the short bar specimens. The difference in fracture toughness measured by the two procedures is explained in terms of the alloys' crack growth behavior.

03,375
PB96-190244 Not available NTIS
National Inst. of Standards and Technology (MSEL), Boulder, CO. Materials Reliability Div.
Light-Weight Alloys for Aerospace Applications II.
Final rept.
P. T. Purtscher, and E. S. Drexler. 1991, 11p.
Pub. in Light-Weight Alloys for Aerospace Applications II, New Orleans, LA., February 17-21, 1991, p65-75.

Keywords: *Aluminum alloys, *Fracture toughness, *Aerospace, Aluminum lithium, Chevron-notch, Cryogenic properties, Mechanical properties, Reprints.

The mechanical properties of Al-Li alloys and alloy 2219 were measured in the through-thickness direction. The toughness was evaluated in the S-L and S-T orientations according to ASTM Method E 1304 with

chevron-notched specimens, 13 mm thick and 19 mm wide. The test temperatures were 295, 76, and 4 K. Each alloy was tested after different thermomechanical processing to vary the strength at a given temperature. The ultimate strength for all the materials increased with decreasing test temperature. The toughness varied significantly with chemical compositionn and aging treatment, but were inconsistent with respsect to test temperature.

03,376
PB96-204193 Not available NTIS
National Inst. of Standards and Technology (MSEL), Gaithersburg, MD. Ceramics Div.
Cavity Evolution during Tensil Creep of Si3N4.
Final rept.
W. Luecke, S. M. Wiederhorn, B. J. Hockey, and G. G. Long. 1993, 6p.
Pub. in Materials Research Society Symposium Proceedings, Boston, MA., November 30-December 3, 1992, v287 p467-472 1993.

Keywords: *Silicon nitride, *Creep, *Cavities, Reprints, Lifetime, Rupture, Monkman-Grant.

The authors have characterized the evolution of cavities during tensile creep of a Y2O3-hot isostatically pressed Si3N4, using precision density measurements, small angle x-ray scattering (SAXS) and transmission electron microscopy (TEM). The cavities ae bimodally distributed in size. Lenticular, 200 nm-size cavities are common, and lie primarily on two-grain boundaries. Irregularly shaped 500-1000 nm size cavities are rare and lie at multi-grain junctions, but comprise approximately half of the total volume fraction of cavities. Although the material shows a continuous decrease in strain rate with strain, the cavity volume fraction evolves linearly with strain. Cavities account for approximately 85% of the total strain at any point during creep.

03,377
PB96-204466 Not available NTIS
National Inst. of Standards and Technology (MSEL), Gaithersburg, MD. Ceramics Div.
Experimental Assessment of Crack-Tip Dislocation Emission Models for an Al67Cr8Ti25 Intermetallic Alloy.
Final rept.
W. G. Meng, M. D. Vaudin, M. F. Bartholomeusz, and J. A. Wert. 1995, 13p.
Pub. in Metallurgical and Materials Transactions A, v26A p329-341 Feb 95.

Keywords: *Dislocation emission, Reprints, Cleavage, *Intermetallic alloys, Electron backscatter pattern, Grain orientations.

A potential explanation for the cleavage fracture of intermetallic alloys with low or moderate critical resolved shear stress (CRSS) is the existence of an energy barrier for crack-tip dislocation emission, as described by models that analyze the energetics of dislocation emission from crack tips. In the present study, an intermetallic alloy with the L1(2) crystal structure, Al67Cr8Ti25, has been used to experimentally assess th predictions of the Rice-Thomson dislocation-emission model. The assessment is performed in two ways. First, model predictions of a fracture mode transition at elevated temperature are compared with experimental results. Bend tests performed at temperatures in the range of 293 to 1061 K reveal that the fracture mode of Al67Cr8Ti25 changes from predominately cleavage fracture at room temperature to a mixed mode of cleavage and intergranular fracture at intermediate temperatures and then to predominantly intergranular fracture at high temperatures. Second, model predictions of the effect of grain orientation on the fracture mode are compared with experimental results.

03,378
PB97-119366 Not available NTIS
National Inst. of Standards and Technology (MSEL), Gaithersburg, MD. Metallurgy Div.
Electronic Structure and Phase Equilibria in Ternary Substitutional Alloys.
Final rept.
A. J. S. Traiber, P. E. A. Turchi, R. M. Waterstrat, and S. M. Allen. 1996, 23p.
See also DE93013848.
Pub. in Jnl. of Physics: Condensed Matter, n8 p6357-6379 1996.

Keywords: *Iron alloys, *Titanium alloys, *Vanadium alloys, Binary alloy systems, Electronic structure, Mixing, Perturbation theory, Phase stability, Reprints, *Foreign technology, *Ternary alloy systems.

A reliable and consistent scheme for studying phase equilibria in ternary substitutional alloys based on the tight-binding approximation is presented. With the electronic parameters obtained from linear muffin-tin orbital calculations, the authors show that the computed densities of states and band structures compare well with those obtained from more accurate ab initio calculations. Disordered alloys are studied within the tight-binding coherent-potential approximation formalism extended to multi-component alloys. The energetics of ordered systems is obtained through effective-pair interactions computed with the general perturbation method. Finally, partially ordered alloys are studied with a novel simplification of the molecular coherent-potential approximation combined with the general perturbation method.

Plastics

03,379
PB94-211166 Not available NTIS
National Inst. of Standards and Technology (MSEL), Gaithersburg, MD. Polymers Div.
Torsional Dilatometer for Volume Change Measurements on Deformed Glasses: Instrument Description and Measurements on Equilibrated Glasses.
Final rept.
R. S. Duran, and G. B. McKenna. 1990, 27p.
Pub. in Jnl. of Rheology 34, n6 p813-839 1990.

Keywords: *Epoxy resins, *Volume, *Extensometers, *Torsion, Glass, Design criteria, Deformation, Rheology, Glass transition temperature, Aging tests(Materials), Performance evaluation, Reprints.

An automated mercury dilatometer has been designed and built for the purpose of making volume change measurements on cylindrical samples subjected to torsional deformations. In its current configuration the instrument takes readings of torque, normal force and volume change upon application of a twist at one end of the sample. Here we describe the instrument and preliminary measurements on epoxy glasses which have been equilibrated by annealing near to the glass transition. Our results show that the volume of the sample tested at temperatures ranging from T(sub g)-10 to T(sub g) increases upon application of a torsional deformation. This result is contrary to results reported in the literature for samples tested well below T(sub g).

03,380
PB94-213501 Not available NTIS
National Inst. of Standards and Technology (BFRL), Gaithersburg, MD. Fire Science Div.
Investigation of the Thermal Stability and Char-Forming Tendency of Cross-linked Poly(methyl methacrylate).
Final rept.
S. M. Lomakin, J. E. Brown, R. S. Breese, and M. R. Nyden. 1993, 15p.
Pub. in Polymer Degradation and Stability 41, p229-243 1993.

Keywords: *Polymethyl methacrylate, *Thermal stability, *Charring, Combustion products, Crosslinking, Thermal degradation, Pyrolysis, Thermographs, Thermogravimetric analysis, Reprints.

The thermal degradation of two network copolymers of methyl methacrylate was studied as a function of the chemical nature of the cross-linking agent and the frequency of cross-links. Unlike the linear homopolymer, both the trimethylolpropane triacrylate and trimethylolpropane trimethacrylate networks were found to char when burned. The corresponding derivative thermograms indicate that there are dramatic differences in the thermal degradation of these polymers even in the absence of oxygen. These differences are interpreted in terms of a simple model for the kinetics of depolymerization.

03,381
PB95-126363 Not available NTIS
National Inst. of Standards and Technology (MSEL), Gaithersburg, MD. Polymers Div.
Influence of Physical Aging on the Yield Response of Model DGEBA + Poly(propylene oxide) Epoxy Glasses.
Final rept.
C. G'Sell, and G. B. McKenna. 1992, 11p.
Pub. in Polymer 33, n10 p2103-2113 1992.

Keywords: *Aging tests(Materials), *Epoxy resins, *Polyoxypropylene, *Laminated glass, Kinetics, Plastic flow, Temperature, Crosslinking, Plasticity tests, Plastic analysis, Stress analysis, Reprints, DGEBA(Diglcidyl ether of Bisphenol).

Cylindrical specimens were prepared from two DGEBA + amine-terminated PPO networks of different crosslink density and subjected to quenching and isothermal aging treatments at different temperatures and aging times in the range from 0.1 to 1000 hours, The changes in the structure of the glasses during the aging towards equilibrium was subsequently assessed by the measurement of the yield stress in uniaxial compression at the same temperature as the aging. From the influence of temperature and strain rate on the above phenomena, the kinetics of physical aging were examined quantitatively in terms of the time-aging time-temperature equivalence principle. The results suggest that the increase in yield stress on aging is correlated to volume recovery and to the induced increase of the relaxation times as the polymeric glass evolves towards its equilibrium state.

03,382
PB95-140018 Not available NTIS
National Inst. of Standards and Technology (MSEL), Gaithersburg, MD. Polymers Div.
Volume Recovery in Epoxy Glasses Subjected to Torsional Deformations: The Question of Rejuvenation.
Final rept.
M. M. Santore, R. S. Duran, and G. B. McKenna. 1991, 5p.
Pub. in Polymer 32, n13 p2377-2381 1991.

Keywords: *Laminated glass, *Epoxy resins, *Aging tests(Materials), *Deformation, Dilatometry, Torsion, Mechanical properties, Volume, Viscoelasticity, Kinetics, Stress relaxation, Reprints, *Rejuvenation.

Torsional dilatometry was used to examine the mechanical properties of an epoxy glass during physical aging, i.e. after a quench from above the glass transition temperature to slightly below it. Volume changes in the sample were measured simultaneously with the viscoelastic responses in stress relaxation experiments as functions of the deformation magnitude. In this epoxy, the torsional deformations induce volume expansions which relax on a time scale similar to those of the torque relaxation. Mechanical stimuli only momentarily disrupt the volume evolution following a quench: the underlying volume recovery kinetics, which are much slower than the mechanical torque or volume relaxation, remain unaltered. Both the independence of t* of the magnitude of the strain and the fact that the volume recovery after a quench remains unaltered in spite of the imposition of mechanical deformations support the argument that mechanical stimuli neither alter the underlying (nonequilibrium) thermodynamic state of the glass nor erase physical aging.

03,383
PB95-140026 Not available NTIS
National Inst. of Standards and Technology (MSEL), Gaithersburg, MD. Polymers Div.
Torsional Relaxation and Volume Response during Physical Aging in Epoxy Glasses Subjected to Large Torsional Deformations.
Final rept.
M. M. Santore, and G. B. McKenna. 1991, 6p.
Pub. in Materials Research Society Symposia Proceedings 215, p81-86 1991.

Keywords: *Laminated glass, *Epoxy resins, *Aging tests(Materials), *Deformation, Dilatometry, Torsion, Mechanical properties, Volume, Viscoelasticity, Stress relaxation, Reprints, *Rejuvenation.

We present torsional dilatometry experiments to simultaneously measure torque relaxation and volume recovery in an epoxy glass quenched from above its glass transition temperature to below it. Two strain histories are employed: one with strains of equal sizes and a second where small strains follow a large one. The baseline for the thermally induced volume recovery is insensitive to intermittent torsional strains whose magnitude can be well into the non-linear regime. The torque relaxations from equal intermittent mechanical

stimuli can be superposed by a time-aging time shift in a way that indicates fast changes cease to occur at approximately 10,000 seconds after the quench, a 'mechanical equilibration' time. Stimuli of different sizes can confound superposition via nonlinear effects, but do not affect the ultimate volume recovery of the glass or its mechanical equilibration time. Our results show the signature of rejuvenation; however, this may result from the nonlinear response of the material in a nonisochoric strain history. Our data firmly show that mechanical stimuli do not erase aging or rejuvenate this epoxy.

03,384
PB95-140901 Not available NTIS
National Inst. of Standards and Technology (MSEL), Gaithersburg, MD. Polymers Div.
Using Torsional Dilatometry to Measure the Effects of Deformations on Physical Aging.
Final rept.
M. Santore, R. Duran, and G. McKenna. 1990, 1p.
Pub. in Abstracts of Papers of the American Chemical Society 200, 344p Aug 90.

Keywords: *Aging tests(Materials), *Epoxy resins, *Deformation, *Laminated glass, Dilatometry, Torsion, Mechanical properties, Volume, Reprints, *Rejuvenation.

An epoxy glass was studied via torsional dilatometry to test the 'rejuvenation' hypothesis, i.e. that large deformations retard physical aging. For example, rejuvenation predicts that samples subjected to deformations after a quench to below Tg will contract more slowly than those quenched without subsequent deformations. The model further implies that the mechanical properties should evolve more slowly toward equilibrium when deformations are imposed during aging. Our torsional dilatometry tests both premises: Simultaneous measurements of volume recovery and torque relaxation suggest that the application of large deformations does not directly influence the physical aging process. However, we do observe an interesting effect: the equilibration time based on the time required for the mechanical properties to cease evolving is at least one order of magnitude shorter than that evidenced by the volume recovery measurements.

03,385
PB95-202990 Not available NTIS
National Inst. of Standards and Technology (MSEL), Gaithersburg, MD. Reactor Radiation Div.
Hydration in Semicrystalline Polymers: Small-Angle Neutron Scattering Studies of the Effect of Drawing in Nylon-6 Fibers.
Final rept.
N. S. Murthy, and W. J. Orts. 1994, 9p.
Grant NSF-DMR-9122444
Sponsored by National Science Foundation, Arlington, VA.
Pub. in Jnl. of Polymer Science: Part B, Polymer Physics 32, p2695-2703 1994.

Keywords: *Hydration, *Small angle scattering, *Nylon fibers, *Nylon 6, *Drawing, Neutron scattering, Thermoplastic resins, Amorphous materials, Crystallinity, Water, Polymer physics, Reprints.

Water absorbed by nylons appears to be partitioned into interlamellar and interfibrillar spaces. The amount of water in the interfibrillar region remains essentially unchanged with increasing draw ratio, whereas that in the interlamellar regions decreases with draw ratio; the latter accounts for the decrease in the water uptake in the drawn fibers. These results suggest that the amount of the amorphous material in the interfibrillar regions remains unchanged during drawing, and the increase in the crystallinity during drawing results from the incorporation of the amorphous chain segments in the interlamellar regions into the crystalline lamellae. Further, the interfibrillar water is more tightly bound than the interlamellar water. The length of the longitudinal channels into which water diffuses is about the same as that of the fibrils, and increases from ca. 1500 to 2000 A upon drawing. The longitudinal channels are highly oriented even in undrawn fibers, and their misorientation increases from 5 degrees to 15 degrees upon drawing. These channels can be described as surface fractals of dimension 3.4-3.6.

03,386
PB95-226866 PC A03/MF A01
National Inst. of Standards and Technology (PL), Gaithersburg, MD. Radiometric Physics Div.
Standard Reference Materials: Polystyrene Films for Calibrating the Wavelength Scale of Infrared Spectrophotometers - SRM 1921.
Special pub.
D. Gupta, L. Wang, L. M. Hanssen, J. J. Hsia, and R. U. Datla. Apr 95, 49p, NIST/SP-260-122.
Also available from Supt. of Docs.

Keywords: *Polystyrene, *Fourier transformation, *Infrared spectrophotometers, Chemical analysis, Calibration standards, Optical measuring instruments, Standardization, Wavelengths.

Standard Reference Material (SRM) 1921 is a matte finish polystyrene film and is intended for use in calibrating the wavelength scale of spectrophotometers in the infrared (IR) spectral region from 545.49 cm exp(-1) to 3082.19 cm exp(-1) (18.332 micrometers to 3.2445 micrometers). Thirteen absorption peak positions obtained using a center-of-gravity method are certified. The expanded uncertainty value associated with these peak values are between 0.06 cm exp(-1) and 0.66 cm exp(-1), except for 1.84 at 2850.13 cm exp(-1) and 12.29 at 545.49 cm exp(-1). This publication describes the IR spectrophotometer, instrument calibration, SRM material, measurement procedure, calibration of polystyrene films, and uncertainty determination.

03,387
PB96-123369 Not available NTIS
National Inst. of Standards and Technology (MSEL), Gaithersburg, MD. Polymers Div.
Flow-Induced Structure in Polymer. Chapter 1. An Introduction to Flow-Induced Structures in Polymers.
Final rept.
A. I. Nakantani. 1995, 19p.
Pub. in National Meeting of the American Chemical Society (208th), Washington, DC., August 21-25, 1994, p1-19.

Keywords: *Polymers, Morphology, Blends, Solutions, Melts, Multicomponent systems, Reprints, *Flow induced structures.

An overview of flow-induced structures in polymers is presented and recent references to research in the areas of polymer solutions, homopolymer melts, polymer blends, block copolymers and multi-component systems, and liquid crystalline polymers are given. The research area of flow-induced structures in polymers has expanded with the advent of in-situ measuring techniques. Studies of this type are useful for probing fundamental issues such as chain deformation, shifts in phase behavior, and the formation of novel shear-induced structures. The applications addressed include the kinetics of morphology evolution and the relationship between ultimate properties and morphology.

03,388
PB96-123377 Not available NTIS
National Inst. of Standards and Technology (MSEL), Gaithersburg, MD. Polymers Div.
Flow-Induced Structure in Polymers. Chapter 17. Phase-Separation Kinetics of a Polymer Blend Solution Studied by a Two-Step Shear Quench.
Final rept.
A. I. Nakatani, D. S. Johnsonbaugh, and C. C. Han. 1995, 17p.
Pub. in Symposium of the National Meeting of the American Chemical Society (208th), Washington, DC., August 21-25, 1994, p246-262 1995.

Keywords: *Polymers, Shear quench, Light scattering, Reprints, *Flow induced structures, Phase separation kinetics.

A polystyrene (PS) and polybutadiene (PB) blend (50:50 by weight) dissolved in dioctyl phthalate (DOP) (8% total polymer by weight) was subjected to a two-step shear quench with a delay time between the two shear rates examine the phase separation kinetics by light scattering. The time dependence of the peak maximum position, qm, and the intensity of the peak maximum, I(qm), were measured. The growth rate after cessation from the second shear rate was unaffected by the delay time. The mechanism for the coarsening parallel to flow was coupled to the extent of coarsening which occurred normal to the flow direction during the second shear rate.

03,389
PB96-159777 Not available NTIS
National Inst. of Standards and Technology (BFRL), Gaithersburg, MD. Fire Safety Engineering Div.
Effects of Sample Mounting on Flammability Properties of Intumescent Polymers.
Final rept.
T. Kashiwagi, and T. G. Cleary. 1993, 23p.
Pub. in Fire Safety Jnl., v20 n3 p203-225 1993.

Keywords: *Fire resistant materials, *Polymers, *Flammability testing, *Heat release rate, Sample preparation, Flame propagation, Burning rate, Radiative heat transfer, Heat flux, Combustion products, Fireproofing, Soot, Calorimetry, Heat of combustion, Reprints.

Various flammability properties of polycarbonate samples were measured with the cone calorimater and lateral ignition and flame spread (LIFT) devices at various external fluxes. Four different sample mountings were used with the cone calorimeter to investigate the effects of sample mounting on the flammability properties of these samples. The mounting configurations allowed the intumesced char to rise free. The results show that peak heat release rate curves were significantly affected by the sample mounting configuration but total heat released, effective heat of combustion, and soot yield were not significantly affected by the sample mounting configuration but total heat released, effective heat of combustion, and soot yield were not significantly affected. Tow sample mounting configurations were used, the standard method and the standard method with the addition of a wire grid to retain intumesced char. Significant differences in flame spread rates were observed between the two sample mounting configurations with and without the grid.

03,390
PB96-180229 Not available NTIS
National Inst. of Standards and Technology (MSEL), Gaithersburg, MD. Polymers Div.
Advances in the Measurement of Polymer CTE: Micrometer- to Atomic-Scale Measurements.
Final rept.
M. Schen, F. I. Mopsik, W. Wu, G. T. Davis, W. Guthrie, W. E. Wallace, and N. C. Beck Tan. 1996, 3p.
Pub. in Polymer Preprints, v37 n1 p180-182 Mar 96.

Keywords: *Polymer films, *Thermomechanical analyzer, Capacitance, Coefficient, Metrology, Reprints, *Coefficient or thermal expansion, X-ray reflectivity, Electronic packaging.

Today's microelectronics products rely heavily on the use of polymeric materials; whether to package and protect the integrated circuit or to manufacture printed wiring boards and assemblies. In this work, NIST is pursuing a three-pronged strategy to improve the quality of measurement techniques and resulting data for characterizing the out-of-plane, or z-axis, coefficient of thermal expansion (CTE) of polymer films. The strategy consists of effecting evolutionary improvements in commonly used measurement techniques and standards for measuring CTE using the thermomechanical analyzer (TMA), introducing revolutionary improvements in measuring CTE by developing and applying a new NIST capacitance technique that has vastly improved sensitivity and accuracy over the TMA or existing capacitance-based approaches, and utilizing X-ray reflectivity measurements to understand the behavior of ultra-thin polymer films (50 to 1000A).

03,391
PB97-112262 Not available NTIS
National Inst. of Standards and Technology (MSEL), Gaithersburg, MD. Polymers Div.
Lattice Model of a Hydrogen-Bonded Polymer Blend.
Final rept.
E. K. Hobbie, and C. C. Han. 1996, 11p.
Pub. in Jnl. of Chemical Physics, v105 n2 p738-748 Jul 96.

Keywords: *Polymer blends, *Hydrogen bonding, *Lattice models, Phase diagrams, Concentration, Mean-fields, Reprints.

A mean-field lattice model is used to investigate some possible aspects of the low-temperature behavior of a lower critical solution temperature (LCST) polymer blend made miscible by a dilute distribution of a hydrogen-bonding comonomer. The nature of the binding interaction is examined for both a random comonomer distribution and for the case of identically end-modified chains. For the latter case, competition between the interaction responsible for the immiscibility of the homopolymer components and the attraction due to hydrogen bonding leads to a stable intermediate

phase. For random distributions, polydispersity in the binding interaction restricts this intermediate phase to an extremely narrow window in reduced temperature, consistent with a 'smeared' transition. The free-energy landscape contains local minima separated by energy barriers.

03,392
PB97-112304 Not available NTIS
National Inst. of Standards and Technology (MSEL), Gaithersburg, MD. Polymers Div.
Vitrification and Crystallization of Organic Liquids Confined to Nanoscale Pores.
Final rept.
C. L. Jackson, and G. B. McKenna. 1996, 10p.
Pub. in Chemistry of Materials, v8 n8 p2128-2137 1996.

Keywords: *Organic liquids, *Nanoscale pores, O-terphenyl, Vitrification, Crystallization, Benzyl alcohol, Calorimetry, Glass transition temperature, Reprints.

The effect of finite size on the solidification of o-terphenyl and benzyl alcohol confined in model controlled pore glass (CPG) materials is described. These two organic liquids form either amorphous glasses or crystalline solids in the bulk upon cooling, depending on the rate of cooling and other factors. The solidification behavior of the liquid in the pores was studied as a function of pore diameter (4-73 nm), chemical surface treatment of the CPG and the degree of pore filling, by differential scanning calorimetry (DSC). The authors observe that the glass transition Tg, shifts to a lower temperature as pore size decreases. This shift is independent of the degree of pore filling for both o-terphenyl and benzyl alcohol, suggesting that a reduction in bulk density or a negative pressure effect is not the cause of the observed shift. The crystallization behavior of o-terphenyl and benzyl alcohol is also altered by confinement and strongly depends on the pore size and degree of pore filling.

03,393
PB97-112486 Not available NTIS
National Inst. of Standards and Technology (MSEL), Gaithersburg, MD. Polymers Div.
Evidence of Crosslinking in Methyl Pendent PBZT Fiber.
Final rept.
V. R. Mehta, S. Kumar, M. B. Polk, T. D. Dang, D. L. Vanderhart, and F. E. Arnold. 1996, 11p.
Pub. in Jnl. of Polymer Science, Part B, Polymer Physics, v34 p1881-1891 1996.

Keywords: *Crosslinking, *Methyl pendant PBZT, *Fibers, Reprints, Poly(p-phenylene benzobis thiazole).

In order to influence the compressive strength of the rigid rod polymeric fibers, methyl pendent poly (p-phenylene benzodisthiazole) fibers have been heat treated in the 400 to 550 degrees C temperature range in air and in nitrogen for varying times to achieve intermolecular crosslinking. These fibers have been examined using Fourier transform infrared (FTIR) spectroscopy, (13)C solid-state nuclear magnetic resonance (NMR) swelling behavior, and scanning electron microscopy. (13)C NMR has also been carried out on solutions of as-spun fibers. Fibers heat-treated at 400 degrees C, both in nitrogen and in air, up to heat-treatment times of 60 min are insoluble in 99% chlorosulfonic acid, however, no direct evidence of crosslinking has been obtained for these fibers using spectroscopic techniques, suggesting that in these fibers the degree of crosslinking must be very low. Evidence that methyl groups are precursors to certain crosslinks was first seen via a weak methylene resonance in (13)C solid state NMR, corresponding to about 2% of the the original methyl intensity, in a sample heat-treated at 450 degrees C in air.

03,394
PB97-112494 Not available NTIS
National Inst. of Standards and Technology (MSEL), Gaithersburg, MD. Polymers Div.
Relaxation After a Temperature Jump Within the One Phase Region of a Polymer Mixture.
Final rept.
G. Merkle, B. Bauer, and C. Han. 1996, 4p.
Pub. in Jnl. of Chemical Physics, v104 n23 p9647-9650 Jun 96.

Keywords: *Polymer blends, *Hydrogen bonding, *Spinodal decomposition, Small angle neutron scattering, Concentration fluctuation growth, Reprints.

Small-angle neutron scattering was used to observe the relaxation of the structure factor from a smaller to a larger fluctuation state after a temperature jump within the one-phase region of a miscible polymer blend. The blend studied is a 60/40 by weight mixture of a hydrogen bonded polymer blend which consists of hydroxy modified dueterated polystyrene and poly(butylmethacrylate). A peak clearly evolved during the transition from the initial state at Ti to the final state at Tf as predicted by linear as well as nonlinear theories. This relaxation process, which took more than 10 h, could be represented reasonably well by a simple linear approximation of the Chn-Hilliard-Cook (CHC) theory without involving nonlinear calculations for the evolution of the dynamic structure factor. The measurement offers an alternative method for estimating the order parameter relaxation rate in the one-phase region. Also, this demonstrates experimentally the correct relaxation (to a higher fluctuation state) mechanism predicted by the linear theory of CHC type.

03,395
PB97-113088 Not available NTIS
National Inst. of Standards and Technology (MSEL), Gaithersburg, MD. Polymers Div.
Dimensional Crossover in the Phase Separation Kinetics of Thin Polymer Blend Films.
Final rept.
L. Sung, A. Karim, J. F. Douglas, and C. C. Han. 1996, 4p.
Pub. in Physical Review Letters, v76 n23 p4368-4371 1996.

Keywords: *Thin films, *Phase separation, *Spinodal decomposition, Blend, Crossovers, Reprints.

The kinetics of phase separation in thin polymer blend films of polystyrene and polybutadiene on a silicon substrate is examined by optical microscopy of the free film boundary. The observations on 1000 and 200 Angstroms films are consistent with a crossover from three- to two-dimensional spinodal decomposition kinetics in the (off-critical) viscous hydrodynamic regime. In this stage of phase separation the exponent n, characterizing the scale R(t) approximately tn of the coarsening pattern, is predicted to change from 1 to a value near 0.46 upon lowering the dimensionality.

03,396
PB97-118400 Not available NTIS
National Inst. of Standards and Technology (MSEL), Gaithersburg, MD. Polymers Div.
Swelling and Growth of Polymers, Membranes and Sponges.
Final rept.
J. F. Douglas. 1996, 13p.
Pub. in Physical Review E, v54 n3 p2677-2689 Sep 96.

Keywords: *Polymers, *Membranes, *Sponges, Network swelling, Wiener sheet, Reprints, Branched polymers, Blocked copolymers.

Polymers can be formed into a wide range of structures depending on the monomer chemistry and the kinetic conditions of growth. A general model of polymers have higher-order connectivity is introduced that reduces to flexible linear polymers, membranes, and sponges as special cases. This 'Wiener sheet' model, which extends the conventional Wiener path model of linear polymers, is argued to describe various classes of branched polymers, as well as different types of interacting random surfaces. For example, lattice animals and percolation clusters are considered to be perforated sheets whose large-scale dimensions are described by the Wiener sheet model with excluded volume interactions. To within the approximations of the model calculations, the properties of the Wiener sheet 'membrane' are consistent with this correspondence. The influence of the excluded volume and the kinetics of growth of membrane and sponge structures are treated at a Flory-level approximation, although the Wiener sheet model should admit to a renormalization-group treatment as in the case of linear polymers. Predictions of the self-interacting Wiener sheet model are contrasted with an alternative and complementary random surface model introduced by Nelson and co-workers and are compared with recent simulations and experiment.

Refractory Metals & Alloys

03,397
PB94-172590 Not available NTIS
National Inst. of Standards and Technology (CSTL), Gaithersburg, MD. Thermophysics Div.
Radiance Temperature (in the Wavelength Range 519-906 nm) of Tungsten at Its Melting Point by a Pulse-Heating Technique.
Final rept.
A. P. Miiller, and A. Cezairliyan. 1993, 14p.
Pub. in International Jnl. of Thermophysics 14, n3 p511-524 1993. Sponsored by National Aeronautics and Space Administration, Washington, DC.

Keywords: *Tungsten, *Melting point, *Radiation pyrometers, Wavelengths, Radiance, Heating, Temperature measurement, Surface temperature, Thermophysical properties, Uncertainty, Reprints.

Radiance temperatures (at six wavelengths in the range 519-906 nm) of tungsten at its melting point were measured by a pulse-heating technique. The method is based on rapid resistive self-heating of the specimen from room temperature to its melting point in less than 1 s; and on simultaneously measuring the specimen radiance temperatures every 0.5 ms with a high-speed six-wavelength pyrometer. Melting was manifested by a plateau in the radiance temperature versus time function for each wavelength. The melting-point radiance temperatures for a given specimen were determined by averaging the measured temperatures along the plateau at each wavelength. The melting-point radiance temperatures for tungsten were determined by averaging the results at each wavelength for 10 specimens (standard deviation in the range 0.5-1.1K, depending on the wavelength) as follows: 3319 K at 519 nm, 3236 K at 615 nm, 3207 K at 652 nm, 3157 K at 707 nm, 3078 K at 808 nm, and 2995 K at 906 nm. Based on estimates of the random and systematic errors arising from pyrometry and specimen conditions, the total uncertainty in the reported values is about + or - 7 K at 653 nm and + or - 8 K at the other wavelengths.

03,398
PB94-200011 Not available NTIS
National Inst. of Standards and Technology (CSTL), Gaithersburg, MD. Thermophysics Div.
Wavelength Dependence of Normal Spectral Emissivity of High-Temperature Metals at Their Melting Point.
Final rept.
A. Cezairliyan, A. P. Miiller, F. Righini, and A. Rosso. 1991, 8p.
Pub. in High Temperatures - High Pressures 23, p325-332 1991. Sponsored by National Aeronautics and Space Administration, Washington, DC.

Keywords: *Refractory metals, *Spectral emittance, *Melting point, *Emissivity, *Wavelengths, Thermophysical properties, Literature surveys, Spectral emission, Spectral lines, Line spectra, Molybdenum, Niobium, Tantalum, Reprints.

The literature data on normal spectral emissivity of selected high-temperature metals at their melting points are reviewed. This study is motivated by recent results published by a major laboratory which show a common wavelength-independent behavior for the emissivity (in the wavelength range 500-1,000 nm) of several high-temperature metals (including V, Nb, Mo, Ta, and W) at their melting points. Based on the present study of accurate data for Ni, Ti, V, Nb, Mo, Ta, and W reported in the literature, it is concluded that the normal spectral emissivity of these high-temperature metals at their melting points is not constant but decreases with increasing wavelength in the range 400-1,000 nm.

03,399
PB94-200169 Not available NTIS
National Inst. of Standards and Technology (MSEL), Gaithersburg, MD. Reactor Radiation Div.
Textures of Tantalum Metal Sheets by Neutron Diffraction.
Final rept.
C. S. Choi, H. J. Prask, and J. Orosz. 1993, 8p.
Pub. in Jnl. of Materials Science 28, p3283-3290 1993.

Keywords: *Tantalum, Neutron diffraction, Metal sheets, Orientation, Texture, Reprints.

The orientation distributions of six tantalum samples, TaPA, TaG1, TaG2, TaQ2-S1, TaQ2-S2 and TaQ2-S4, were studied by neutron diffraction and ODF analy-

Refractory Metals & Alloys

sis. The TaPA specimen is a commercial tantalum sheet with an unknown fabrication history. The TaG1 and TaG2 were fabricated from a powder metallurgical ingot by uniaxial compression, and the TaQ2 type samples were fabricated from commercial stock by similar uniaxial forging. TaQ2-S1 is the section closest to the center of the forged disc, S2 is the intermediate section, and S4 is the section adjacent to the periphery.

03,400
PB94-216686 Not available NTIS
National Inst. of Standards and Technology (CSTL), Gaithersburg, MD. Thermophysics Div.
Measurement of the Heat of Fusion of Tungsten by a Microsecond-Resolution Transient Technique.
Final rept.
J. L. McClure, and A. Cezairliyan. 1993, 7p.
Sponsored by National Aeronautics and Space Administration, Washington, DC.
Pub. in International Jnl. of Thermophysics 14, n3 p449-455 1993.

Keywords: *Heat of fusion, *Refractory metals, *Pulse heating, *Tungsten, High temperature, Melting, Transients, Reprints.

A microsecond-resolution pulse-heating technique was used for the measurement of the heat of fusion of tungsten. The method is based on rapid (100 to 125 microseconds) resistive self-heating of a specimen by a high-current pulse from a capacitor discharge system and measuring current through the specimen and voltage across the specimen as functions of time. Melting of a specimen is manifested by changes in the slope of the electrical resistance versus time function. The time integral of the power absorbed by a specimen during melting yields the heat of fusion. Measurements gave a value of 48.7 kJ/mol for the heat of fusion of tungsten with an estimated maximum uncertainty of + or - 6%. The electrical resistivity of solid and liquid tungsten at its melting temperature was also measured.

03,401
PB95-202388 Not available NTIS
National Inst. of Standards and Technology (MSEL), Gaithersburg, MD. Reactor Radiation Div.
Application of ODF to the Rietveld Profile Refinement of Polycrystalline Solid.
Final rept.
C. S. Choi, E. F. Baker, and J. Orosz. 1994, 9p.
Pub. in Advances in X-ray Analysis, v37 p49-57 1994.

Keywords: *Nodular iron, *Tungsten, Diffraction patterns, Polycrystalline, Texture, Reprints, *Rietveld method, Orientation distribution functions.

The Rietveld profile refinement method is probably the most popular technique used for the crystallographic characterization of materials including crystal structures and phase analysis, but it has been used mostly with ideal powder sample, not with textured polycrystals, because effects of strong and complex textures. Most technological materials are fabricated by using thermo-mechanical forming processes, which inevitably produce strong and complex preferential orientations of the crystallites. Consequently, the diffraction patterns of a given technological material are not unique but vary considerably with the measuring direction, with intensity variations as large as factors of hundreds, depending on the degree of texture. Part I of this study describes the determination of the orientation distribution function (ODF) and its application to the Rietveld profile refinement of the highly textured tungsten sample. Part II demonstrates the application of the Rietveld method to the quantitative analysis of the austempered ductile irons.

Wood & Paper Products

03,402
PB94-162500 PC A03/MF A01
National Inst. of Standards and Technology (TS), Gaithersburg, MD. Office of Standards Services.
Voluntary Product Standard PS 20-94. American Softwood Lumber Standard.
Mar 94, 45p, NIST/PS-20/94.
Supersedes PB87-158564. Also available from Supt. of Docs as SN003-003-03257-3. Sponsored by American Lumber Standards Committee, Germantown, MD.

Keywords: *Softwoods, *Lumber, *Standards, *Measurement, Requirements, Sizes, Quality, Classifying, Marking, Inspection, Surface roughness, Industries, US NIST, Certification, Design criteria, Maintenance, Voluntary standards.

The Standard pertains to softwood lumber. It establishes standard sizes and requirements for development and coordination of the lumber grades of the various species, the assignment of design values when called for, and the preparation of grading rules applicable to each species. It provides for implementation of the Standard through an accreditation and certification program to assure uniform industry-wide grade marking and inspection. It establishes principal trade classifications and lumber sizes for yard, structural, factory and shop use and provides for the classification, measurement, grading and grade marking of rough and dressed sizes of lumber items. Terms and procedures are defined to provide a basis for the use of uniform methods in the grading, inspection, measurement, and description of softwood lumber. It also includes the organization and functions of the American Lumber Standard Committee, the Board of Review, and the National Grading Rule Committee. Commercial names of the principal softwood species, definitions of terms used in describing standard grades of lumber and commonly used industry abbreviations are also provided.

03,403
PB94-212404 Not available NTIS
National Inst. of Standards and Technology (NEL), Gaithersburg, MD. Fire Science and Engineering Div.
Rate of Heat Release of Wood Products.
Final rept.
M. Janssens. 1991, 22p.
Pub. in Fire Safety Jnl. 17, n3 p217-238 1991.

Keywords: *Wood, *Fires, *Heat transfer, Burning rate, Calorimeters, Ignition, Combustion, Mathematical models, Pyrolysis, Reprints.

The importance of energy release rate in a fire is illustrated. Two ways are identified to calculate rate of heat release in compartment fires from wood products used as interior finish: (1) use of detailed mathematical models of wood pyrolysis and combustion; (2) use of experimental bench-scale rate of heat release data. Available wood pyrolysis models are briefly reviewed. The second option is looked at in more detail. Rate of heat release data is presented and analyzed for 22 different wood products which were tested on the NIST Cone Calorimeter over the past 6 years. The experimental data cover two orientations, a range of irradiance levels, conditioned and oven dried samples and wood species covering a wide range of densities. Oven dry density is used as the key independent variable to analyze the data. Some important conclusions are drawn concerning the influence of density, conditioning, irradiance and specimen orientation on the rate of heat release. Further analysis and more data are required to confirm the results and to provide an answer to the questions which could not be resolved.

03,404
PB95-125712 Not available NTIS
National Inst. of Standards and Technology (IMSE), Boulder, CO. Fracture and Deformation Div.
Examination of Objects Made of Wood Using Air-Coupled Ultrasound.
Final rept.
C. M. Fortunko, M. C. Renken, and A. Murray. 1990, 5p.
Pub. in Proceedings of Institute of Electrical and Electronics Engineers Ultrasonics Symposium, Honolulu, HI., December 4-7, 1990, p1099-1103.

Keywords: *Wood, *Ultrasonic flow detection, *Grain boundaries, Nondestructive tests, Ultrasonic radiation, Ultrasonic tests, Acoustic measurement, Acoustic velocity, Acoustic properties, Wave propagation, Reprints.

The speed of ultrasound is approximately 330 m/sec in air and 1500 m/sec in water. Many materials exhibit surface-acoustic-wave velocities in the 300-1500 m/sec range. For this reason, air appears to be the ideal coupling fluid for exciting and detecting flexural waves, which are generally slower than surface acoustic waves, and shear waves. Air coupling may also be ideal for launching and detecting the quasi-longitudinal plate wave in materials which can exhibit very low longitudinal phase velocities, such as balsa wood (800 m/sec). In this paper, we describe an experimental, air-coupled, ultrasonic measurement system that can be used to study the propagation of MHz signals in wooden plates ranging in thickness from 3mm to 25mm. Also, we report experimental measurements of the amplitude of through-transmitted, narrow-band, 0.5 MHz signals as a function of the angle of incidence for different grain orientations.

03,405
PB95-170429 PC A04/MF A01
National Inst. of Standards and Technology (TS), Gaithersburg, MD. National Voluntary Lab. Accreditation Program.
National Voluntary Laboratory Accreditation Program (NVLAP): Wood Based Products.
Handbook.
L. I. Knab, L. S. Galowin, W. J. Rossiter, and W. A. Hall. Nov 94, 74p, NIST/HB-150-9.
Also available from Supt. of Docs. as SN003-003-03307-3. See also PB94-178225.

Keywords: *Laboratories, *Certification, *Wood products, *US NBS, Requirements, Procedures, Manuals, Quality assurance, Standardization, Licensure, Methodology, Calibration standards, Government policies, NVLAP(National Voluntary Laboratory Accreditation Program), National Institute of Standards and Technology, NIST.

National Institute of Standards (NIST) Handbook 150-9 presents the technical requirements of the National Voluntary Laboratory Accreditation Program (NVLAP) for Wood Based Products. It is intended for information and use by staff of accredited laboratories, those laboratories seeking accreditation, other laboratory accreditation systems, users of laboratory services, and others needing information on the requirements for accreditation under the Wood Based Products program. The publication supplements NIST Handbook 150, NVLAP Procedures and General Requirements, which contains Part 285 of Title 15 of the U.S. Code of Federal Regulations (CFR) plus all general NVLAP procedures, criteria, and policies.

03,406
PB96-178900 PC A04/MF A01
National Inst. of Standards and Technology (TS), Gaithersburg, MD. Office of Standards Services.
Voluntary Product Standard PS 1-95 Construction and Industrial Plywood.
B. M. Meigs. Mar 96, 48p.
Supersedes PB84-216449, Product Standard PS 1-83. Also available from Supt. of Docs. as SN003-003-03404-5. Sponsored by Engineered Wood Association, Tacoma, WA.

Keywords: *Plywood, *Standards, Test methods, Specifications, Building codes, Definitions, Veneers.

The Standard pertains to construction and industrial plywood. It provides requirements for the principal types and grades, and it covers wood species, veneer grading, glue bonds, panel construction and workmanship, dimensions and tolerances, grade marking, moisture content, and packing of plywood intended for construction and industrial uses. It includes test methods to determine product compliance and a glossary of trade terms and definitions. A quality certification program and information regarding reinspecting practices are also provided. The Standard, a revision of Voluntary Product Standard PS 1-83, Construction and Industrial Plywood, was developed by the Standing Committee for Voluntary Product Standard PS 1-83 in accordance with procedures of the U.S. Department of Commerce.

MATHEMATICAL SCIENCES

General

03,407
DE95017761 PC A03/MF A01
National Inst. of Standards and Technology, Gaithersburg, MD.

Report of the Federal Internetworking Requirements Panel.
31 May 94, 45p, DOE/ER/25188-T1.
Contract AI02-93ER25188
Sponsored by Department of Energy, Washington, DC.

Keywords: *Computer Networks, Computers, Performance Testing, Procurement, Recommendations, Security, Specifications, Standards, EDB/990200.

The Federal Internetworking Requirements Panel (FIRP) was established by the National Institute of Standards and Technology (NIST) to reassess Federal requirements for open systems networks and to recommend policy on the Government's use of networking standards. The Panel was chartered to recommend actions which the Federal Government can take to address the short and long-term issues of interworking and convergence of networking protocols--particularly the Internet Protocol Suite (IPS) and Open Systems Interconnection (OSI) protocol suite and, when appropriate, proprietary protocols. The Panel was created at the request of the Office of Management and Budget in collaboration with the Federal Networking Council and the Federal Information Resources Management Policy Council. The Panel's membership and charter are contained in an appendix to this report.

Algebra, Analysis, Geometry, & Mathematical Logic

03,408
PB94-152725 PC A03/MF A01
National Inst. of Standards and Technology (CAML), Gaithersburg, MD.
Growth Surface for the Slopes at the Boundary of a Polygon.
J. Bernal. Feb 94, 22p, NISTIR-5344.

Keywords: *Computational geometry, Polygons, Slopes, Algorithms, Fortran, Theorems, Voronoi diagrams, Growth surfaces.

In this paper, we describe the growth surface for the slopes at the boundary of a polygon, and present a brute force algorithm for computing it.

03,409
PB94-172053 Not available NTIS
National Inst. of Standards and Technology (CAML), Gaithersburg, MD. Applied and Computational Mathematics Div.
Monte Carlo Approach to the Approximation of Invariant Measures.
Final rept.
F. Y. Hunt. 1994, 23p.
Pub. in Random and Computational Dynamics 2, n1 p111-133 1994. See also PB93-159069.

Keywords: Monte Carlo method, Numerical solution, Approximation, Optimization, Convergence, Reprints, *Invariant measures, Frobenius-Perron operator, Ulam method.

Approximation of absolutely continuous measures of maps of the interval and the closely related tasks of computing Lyapunov exponents and metric entropy are accomplished in principle by iterating the map to produce a sufficiently long trajectory. There is an alternative approach based on approximating the fixed point of the Frobenius-Perron operator. The authors present a Monte-Carlo implementation of the original piecewise constant method proposed by Ulam. This method has the advantage of not requiring explicit evaluation of the elements of the approximate Frobenius-Perron operator. Convergence rates of Ulam's method and some recently proposed higher order variants are discussed. Finally Ulam's scheme is used to estimate the leading Lyapunov exponent of a one dimensional map with an absolutely continuous measure.

03,410
PB94-198660 Not available NTIS
National Inst. of Standards and Technology (CAML), Gaithersburg, MD. Applied and Computational Mathematics Div.
Computing S(alpha) Using Symbolic Monte Carlo.
Final rept.
I. M. Beichl, and F. Sullivan. 1992, 7p.
Pub. in Physica D 60, p358-364 1992.

Keywords: *Computation, Monte Carlo method, Mapping(Transformations), Numerical solution, Reprints, Entropy functions, Symbolic dynamics.

We describe a method for carrying out a computation of the entropy function of the invariant set of a particular class of maps. We illustrate the method for the case of the quadratic and the Feigenbaum map. Elementary consequences of the symbolic dynamics associated with a map f lead to an algorithm that is a novel application of the Monte Carlo method. To sample, we use the fact that the salient features of the thermodynamic properties of the map are captured by its symbolic dynamics. In the symbolic domain, samples are chosen by manipulating character strings, rather than by performing floating-point calculations. Therefore, exact symbolic answers can be obtained by purely combinatorial methods. These symbolic answers then provide a recipe for performing high-precision numerical computations.

03,411
PB94-216744 Not available NTIS
National Inst. of Standards and Technology (NEL), Gaithersburg, MD. Mathematical Analysis Div.
Boundary Integral Method for the Simulation of Two-Dimensional Particle Coarsening.
Final rept.
G. B. McFadden, P. W. Voorhees, R. F. Boisvert, and D. I. Meiron. 1986, 28p.
Pub. in Jnl. of Scientific Computing 1, n2 p117-144 1986.

Keywords: *Boundary integral method, Time dependence, Two dimensional, Free boundaries, Integral equations, Iterative methods, Binary alloys, Coarseness, Simulation, Reprints, Ostwald ripening, Particle coarsening.

A boundary integral method for the solution of a time-dependent free-boundary problem in a two-dimensional, multiply-connected, exterior domain is described. The method is based on an iterative solution of the resulting integral equations at each time step, with the initial guesses provided by extrapolation from previous time steps. The method is related to a technique discussed by Baker for the study of water waves. The discretization is chosen so that the solvability conditions required for the exterior Dirichlet problem do not degrade the convergence rate of the iterative solution procedure. Consideration is given to the question of vectorizing the computation. The method is applied to the problem of the coarsening of two-dimensional particles by volume diffusion.

03,412
PB95-126165 Not available NTIS
National Inst. of Standards and Technology (MEL), Gaithersburg, MD. Automated Production Technology Div.
Constructing Invariant Tori for Two Weakly Coupled van der Pol Oscillators.
Final rept.
D. E. Gilsinn. 1993, 20p.
Pub. in Nonlinear Dynamics 4, p289-308 1993.

Keywords: *Van der Pol differential equation, Partial differential equations, Fast Fourier transforms, Perturbation theory, Periodic functions, Nonlinear systems, Approximation, Toruses, Algorithms, Reprints, *Van der Pol oscillators, Invariant tori.

An algorithm is developed for the construction of an invariant torus of a weakly coupled autonomous oscillator. The system is put into angular standard form. The determining equations are found by averaging and are solved for the approximate amplitudes of the torus. A perturbation series is then constructed about the approximate amplitudes with unknown coefficients as periodic functions of the angular variables. A sequence of solvable partial differential equations is developed for determining the coefficients. The algorithm is applied to a system of nonlinearly coupled van der Pol equations and the first order coefficients are generated in a straightforward manner. The approximation shows both good numerical accuracy and reproducibility of the periodicities of the van der Pol system. A comparative analysis of integrating the van der Pol system with integrating the phase equations from the angular standard form on the approximate torus shows numerical errors of the order of the perturbation parameter epsilon = 0.05 for integrations of up to 10,000 steps. Applying fast Fourier transforms (FFT) to the numerical periodicities generated by integrating the van der Pol system near the torus reveals the same predominant frequencies found in the perturbation coefficients. Finally an expected rotation number is found by integrating the phase equations on the approximate torus.

03,413
PB95-126249 Not available NTIS
National Inst. of Standards and Technology (EEEL), Boulder, CO. Electromagnetic Technology Div.
Accuracy of Eigenvalues: A Comparison of Two Methods.
Final rept.
I. C. Goyal, R. L. Gallawa, and A. K. Ghatak. 1993, 7p.
Pub. in Jnl. of Mathematical Physics 34, n3 p1169-1175 Mar 93.

Keywords: *Differential equations, *Eigenvalues, Boundary value problems, Variational methods, Numerical solution, Perturbation, Comparative evaluations, Matrices, Estimates, Accuracy, Reprints, Langer method, WKB method.

The problem of estimating the eigenvalues lambda of the equation (second derivative of psi with respect to x) + (lambda)f(x)psi(x) = 0, where f(x) is smooth and positive in the closed interval (0,l) and the imposed boundary conditions are psi(0) = psi(l) = 0 is revisited. Two methods, the Wentzel-Kramers-Brillouin (WKB) method and Langer's method, which until very recently has been virtually ignored, are compared. The variational principle further improves the accuracy of the eigenvalues. The results obtained when the WKB and Langer's results are used as trial functions with the variational principle are also compared. Results are given in tabular form.

03,414
PB95-180923 Not available NTIS
National Inst. of Standards and Technology (BFRL), Gaithersburg, MD. Structures Div.
Melnikov Function and Homoclinic Chaos Induced by Weak Perturbations.
Final rept.
E. Simiu, and M. Frey. 1993, 3p.
Pub. in Physical Review E 48, n4 p3190-3192 Oct 93.

Keywords: *Nonlinear differential equations, *Duffing differential equation, Dynamical systems, Perturbation, Chaos, Reprints, Melnikov functions, Homoclinic orbits.

The effect of noise on the possible occurrence of chaos in systems with a homoclinic orbit (e.g., the Duffing equation) was recently considered by Bulsara, Schieve, and Jacobs (Phys. Rev. A 41, 668 (1990)), and Schieve and Bulsara (Phys Rev. A 41, 1172 (1990)), who adopted an approach based on a redefinition of the Melnikov function. We show that this redefinition is unsatisfactory and leads to incorrect results.

03,415
PB95-198933 PC A03/MF A01
National Inst. of Standards and Technology (CAML), Gaithersburg, MD. Applied and Computational Mathematics Div.
Inserting Line Segments into Triangulations and Tetrahedralizations.
J. Bernal. Mar 95, 27p, NISTIR-5596.

Keywords: *Computational geometry, *Triangulation, *Tetrahedrons, Algorithms, Three dimensional models, Two dimensional models, *Segment insertion, Edge swapping, Delaunay triangulations, Voronoi diagrams.

In this paper, we further develop an algorithm by Bernal, De Floriani, and Puppo, for inserting a line segment into a Constrained Delaunay triangulation. The new version of the algorithm inserts the line segment in exactly the same manner in which the old version does but has the additional capability that it does not delete the triangles intersected by the line segment but transforms them through edge-swapping. A 3-dimensional version of the algorithm without the optimization step for the Delaunay property is also presented for attempting to insert a line segment into a tetrahedralization. It is shown that for certain cases the failure of the 3-dimensional algorithm to insert a line segment is an indication that it can not be done. Finally, 3-dimensional problems that can be approached algorithmically as 2-dimensional problems are identified.

03,416
PB95-202354 Not available NTIS
National Inst. of Standards and Technology (CAML), Gaithersburg, MD. Applied and Computational Mathematics Div.

Algebra, Analysis, Geometry, & Mathematical Logic

Overcoming Hoelder Continuity in Ill-Posed Continuation Problems.
Final rept.
A. S. Carasso. 1994, 23p.
Pub. in Society for Industrial and Applied Mathematics Jnl. on Numerical Analysis 31, n6 p1535-1557 Dec 94.

Keywords: *Partial differential equations, Fast Fourier transforms, Image processing, Banach space, Numerical stability, Numerical solution, Computation, Reprints, *Image deblurring, Ill posed problems, Holder continuity, SECB constant, Tikhonov-Miller regularization.

Many ill-posed continuation problems in partial differential equations obey a logarithmic convexity inequality and can be stabilized in an appropriate Banach space by imposing an a priori bound on the solutions. The present paper analyzes the effects of prescribing a physically motivated supplementary constraint, the so-called slow evolution from the continuation boundary (SECB) constraint. When the SECB constraint is applicable, there results an improved stability estimate. This theoretical result is valid for a large class of ill-posed continuation problems. The computational significance of this result is demonstrated in the latter half of the paper. An important class of image deblurring problems is reformulated as a backwards-in-time continuation problem for a generalized diffusion equation. A quadratic functional on L(sup 2)(R(sup 2)) is constructed for which the SECB deblurred image is the unique minimizer. An explicit formula is then obtained for SECB restoration in the Fourier transform domain, leading to a fast, practical, numerical restoration procedure involving fast Fourier transform (FFT) algorithms. For a 512 X 512 image, SECB restoration requires about 20 seconds of cpu time on current desktop workstations.

03,417
PB96-119557 Not available NTIS
National Inst. of Standards and Technology (CAML), Gaithersburg, MD. Applied and Computational Mathematics Div.
Numerical Evaluation of Special Functions.
Final rept.
D. W. Lozier, and F. W. J. Olver. 1994, 47p.
Pub. in Proceedings of Symposia in Applied Mathematics, Vancouver, British Columbia, August 9-13, 1993, v48 p79-125.

Keywords: *Numerical analysis, *Functions(Mathematics), *Computer software, Approximation, Algorithms, Transcendental functions, Applications of mathematics, Computer applications, Reprints, *Special functions, Mathematical software.

Higher transcendental functions continue to play varied and important roles in investigations by engineers, mathematicians, scientists and statisticians. The purpose of this paper is to assist in locating useful approximations and software for the numerical generation of these functions, and to offer some suggestions for future developments in this field.

03,418
PB96-122858 Not available NTIS
National Inst. of Standards and Technology (CAML), Gaithersburg, MD. Applied and Computational Mathematics Div.
Slow Evolution from the Boundary: A New Stabilizing Constraint in Ill-Posed Continuation Problems.
Final rept.
A. S. Carasso. 1994, 5p.
Pub. in Proceedings of Symposia in Applied Mathematics, American Mathematical Society, Vancouver, Canada, August 8-14, 1993, v48 p269-273 1994.

Keywords: *Noise reduction, *Boundary value problems, Image resolution, Blurring, Constraints, Differential equations, Applications of Mathematics, Reprints, *Ill-posed continuation, Holder continuity, SECB constraint, Tikhonov-Miller regularization, Image deblurring.

A new a-priori constraint sharply reduces noise contamination in ill-posed continuation problems. One application concerns a significant class of image deblurring problems that can be formulated as ill-posed time-reversed parabolic initial value problems.

03,419
PB96-122874 Not available NTIS
National Inst. of Standards and Technology (EEEL), Gaithersburg, MD. Electricity Div.
Bounds on Frequency Response Estimates Derived from Uncertain Step Response Data.
Final rept.
J. P. Deyst, and T. M. Souders. 1995, 6p.
Pub. in Institute of Electrical and Electronics Engineers Instrumentation and Measurement Technology Conference Proceedings, Waltham, MA., April 24-26, 1995, p252-257.

Keywords: *Frequency response, *Probability theory, *Dynamic response, Estimates, Boundaries, Step functions, Time, Reprints, Electrical measurment, Simulation, *Uncertainty bounds, Time domain.

A system's frequency response can be estimated from measurements of its step response; however, many error sources affect the accuracy of such estimates. This paper investigates the effects of incertainty in the knowledge of the step response. Methods for establishing uncertainty bounds for the frequency response estimates are developed, based on the corresponding time-domain uncertainties associated with the step-like waveform. Two methods are described. One is a provable upper bound that is often very conservative. The other is more realistic, but it is based on an unproved conjecture. End effects that influence the bounds are also considered. A simulated example of the bounds is presented.

03,420
PB96-155577 Not available NTIS
National Inst. of Standards and Technology (EEEL), Gaithersburg, MD. Electricity Div.
Effects of Nonmedel Errors on Model-Based Testing.
Final rept.
G. N. Stenbakken. 1995, 5p.
Pub. in Institute of Electrical and Electronics Engineers Instrumentation/Measurement Conference, IMTC '95, Watham, MA., April 24-26, 1995, p38-42.

Keywords: *Confidence intervals, Efficient testing, Simulation, Reprints, Empirical modeling, Nonmodel error, Prediction intervals.

In previous work, methods have been developed for efficient testing of components and instruments that are based on models of these units. These methods allow for the full behavior of these units to be predicted from a small but efficient set of test measurements. Such methods can significantly reduce the testing cost of such units by reducing the amount of testing required. But these methods are valid only as long as the model accurately represents the behavior of the units. Previous papers on this subject described many methods for developing accurate models and using them to develop efficient test methods. However, they gave little consideration to the problem of testing units which change their behavior after the model has been developed, for example, as a result of changes in the manufacturing process. Such changed behavior is referred to as nonmodel behavior or nonmodel error. When units with this new behavior are tested with these more efficient methods, their predicted behavior can show significant deviations from their true behavior. This paper describes how to analyze the data taken at the reduced set of measurements to estimate the uncertainty in the model predictions, even when the device has significant nonmodel error. Results of simulation are used to verify the accuracy of the estimates and to show the expected variation in the results for many modeling variables.

03,421
PB96-165931 PC A03/MF A01
National Inst. of Standards and Technology (CAML), Gaithersburg, MD. Applied and Computational Mathematics Div.
Basic Linear Algebra Operations in SLI Arithmetic.
M. A. Anuta, D. W. Lozier, N. Schabanel, and P. R. Turner. Mar 96, 20p, NISTIR-5811.

Keywords: *Linear algebra, Algebra, *SLI arithmetric, Computer arithmetric, Level-index arithmetic.

Symmetric level-index arithmetic was introduced to overcome recognized limitations of floating-point systems, most notably overflow and underflow. The original recursive algorithms for arithmetic operations could be parallelized to some extent, particularly when applied to extended sums of products, and a SIMD software implementation of some of these algorithms is described. The main purpose of this paper is to present parallel SLI algorithms for arithmetic and basic linear algebra operations.

03,422
PB96-193750 PC A04/MF A01
National Inst. of Standards and Technology (CAML), Boulder, CO. Applied and Computational Mathematics Div.
Hybrid Gauss-Trapezoidal Quadrature Rules.
B. K. Alpert. Jul 96, 36p, NISTIR-5048.
Sponsored by Defense Advanced Research Projects Agency, Arlington, VA.

Keywords: *Gaussian quadrature, *Convergence, Functions(Mathematics), Numerical methods, Numerical analysis, Algorithms.

A new class of quadrature rules for the integration of both regular and singular functions is constructed and analyzed. For each rule the quadrature weights are positive and the class includes rules of arbitrarily high order convergence. The quadratures result from alterations to the trapezoidal rule, in which a small number of nodes and weights as the ends of the integration interval are replaced. The new nodes and weights are determined so that the asymptotic expansion of the resulting rule, provided by a generalization of the Euler-Maclaurin summation formula, has a prescribed number of vanishing terms. The superior performance of the rules is demonstrated with numerical examples and application to several problems is discussed.

03,423
PB97-110167 Not available NTIS
National Inst. of Standards and Technology (PL), Gaithersburg, MD. Ionizing Radiation Div.
Exact Series Solution to the Epstein-Hubbell Generalized Elliptic Type Integral Using Complex Variable Residue Theory.
Final rept.
J. D. Evans. 1993, 17p.
Pub. in Applied Mathematics and Computation, v53 p173-189 1993.

Keywords: *Complex variable, *Disk source, *Elliptic-type integral, Radiation field, Residue theory, Series solution, Reprints, Epstein-Hubbell integral.

In the paper, complex variable residue theory is used to arrive at an exact infinite series solution to the Epstein-Hubbell integral. This method of solution is differnet from those used to derive previous solutions to the Epstein-Hubbell integral, but produces exactly equivalent results. Several sets of numerical data are included that verify the results. Additional information on the improvement of convergence will be forthcoming at a later date.

03,424
PB97-111488 Not available NTIS
National Inst. of Standards and Technology (CAML), Gaithersburg, MD. Applied and Computational Mathematics Div.
Heap of Data.
Final rept.
I. Beichl, and F. Sullivan. 1996, 4p.
Pub. in Institute of Electrical and Electronics Engineers Computational Science and Engineering, v3 n2 p11-14, Summer 1996.

Keywords: *Data structures, *Extremum values, Data processing, Maxima, Minima, Mathematical computations, Algorithms, Reprints.

The authors discuss the heap, a data structure that allows one to keep track of the maximum or minimum dynamically.

Operations Research

03,425
PB94-152709 PC A03/MF A01
National Inst. of Standards and Technology (CAML), Gaithersburg, MD.
Submissions to a Planned Encyclopedia of Operations Research on Computational Geometry and the Voronoi/Delaunay Construct.
I. Beichl, J. Bernal, C. Witzgall, and F. Sullivan. Jan 94, 17p, NISTIR-5349.
Sponsored by Institute for Defense Analysis, Bowie, MD. Supercomputing Research Center.

Keywords: *Computational geometry, Operations research, Computer applications, Encyclopedias, Set

theory, Polygons, *Voronoi diagrams, *Delaunay triangulation.

This report contains two submissions to a prospective Encyclopedia of Operations Research. The first submission covers an entry on 'Computational Geometry'. The second submission addresses both the Voronoi Diagram and its dual, the Delaunay triangulation, and is therefore termed the 'Voronoi/Delaunay Construct'. The latter plays such an important role in Computational Geometry and has so many potential applications in Operations Research, that a separate entry appears justified. Both submissions refer to other entries which may be included in the planned Encyclopedia.

03,426
PB94-198959 Not available NTIS
National Inst. of Standards and Technology (NEL), Gaithersburg, MD. Scientific Computing Div.
Algorithmic Enhancements to the Method of Centers for Linear Programming Problems.
Final rept.
P. T. Boggs, P. D. Domich, J. R. Donaldson, and C. Witzgall. 1989, 13p.
Pub. in ORSA Jnl. on Computing 1, n3 p159-171 1989.

Keywords: *Linear programming, Algorithms, Optimization, Convergence, Trajectory analysis, Ordinary differential equations, Two dimensional models, Reprints, *Method of centers, Interior point method.

Interior point algorithms to solving linear programming problems are considered. The techniques are derived from a continuous version of Huard's method of centers that yields a family of trajectories in the feasible region that all converge to an optimal solution. The tangential direction of these trajectories is the dual affine direction. Deficiencies in some of these trajectories are discussed, and the need to recenter is argued. Several new algorithms that use the dual affine direction and a recentering direction in a multi-direction approach are then derived. The most promising of these algorithms is based on minimizing the cost function on a sequence of two-dimensional cross sections of the feasible region. Numerical results are presented.

03,427
PB94-212347 Not available NTIS
National Inst. of Standards and Technology (NEL), Gaithersburg, MD. Center for Manufacturing Engineering.
Guidelines for Reporting Results of Computational Experiments. Report of the Ad hoc Committee.
Final rept.
R. H. F. Jackson, P. T. Boggs, S. G. Nash, and S. Powell. 1991, 13p.
Pub. in Mathematical Programming 49, p413-425 1991.

Keywords: *Mathematical programming, *Experimentation, *Reporting, *Guidelines, Algorithms, Computation, Technology transfer, Parallel processing, Reprints.

Controversy often surrounds the reporting of results from scientific experimentation. Guidelines for the reporting of the results of experimentation have helped to reduce some common errors and to clarify some issues for all concerned. As experience grows in new areas, such as the reporting of the results of computational experiments, it is natural to attempt to update and revise the guidelines to stimulate further discussion and to improve the reporting of results. In this spirit, the Council of the Mathematical Programming Society asked the Committee on Algorithms (COAL) to reconsider the existing guidelines and to offer extensions and modifications as deemed necessary. The proliferation of powerful desktop workstations, microcomputers, mainframes, supercomputers, and novel machines with some form of parallel architecture, will continue to place increasing pressure on developers of algorithms to support their ideas with the results of computational experiments. Our hope is that we can supply a document that authors, editors, and referees can agree upon, and one that can provide a solid basis for the presentation of results.

03,428
PB94-215688 PC A04/MF A01
Clemson Univ., SC. Dept. of Mathematical Sciences.
Time Dependent Vector Dynamic Programming Algorithm for the Path Planning Problem.
Master's thesis.
M. R. Wilson. Dec 93, 70p, NIST/GCR-93/636.
Grant NANB0D1023
Portions of this document are not fully legible. Sponsored by National Inst. of Standards and Technology (BFRL), Gaithersburg, MD.

Keywords: *Dynamic programming, *Paths, *Operations research, Planning, Mathematical models, Algorithms, Vector processing, Fires, Buildings, Escape systems, Computer programs.

Dynamic programming is a modeling technique used for the decision making process. This method can be used to find the set of nondominated paths in a network with time dependent vector costs. In this report a dynamic programming algorithm and its implementation are discussed. An application to a fire egress problem is also included.

03,429
PB95-180089 Not available NTIS
National Inst. of Standards and Technology (CAML), Gaithersburg, MD. Applied and Computational Mathematics Div.
Interior-Point Method for Linear and Quadratic Programming Problems. (NIST Reprint).
Final rept.
P. T. Boggs, P. D. Domich, J. E. Rogers, and C. Witzgall. 1991, 9p.
See also PB91-187815.
Pub. in Committee on Algorithms Newsletter 19, p32-40, 1 Apr 91.

Keywords: *Quadratic programming, Linear programming, Iteration, Algorithms, Mathematical programming, Reprints, *Interior point methods, Method of centers.

We have been working on a particular class of interior point methods for solving linear programming problems for several years. Our methods combine several search directions that are readily computed at each iteration. The final step is then calculated by computing the step that solves the original problem restricted to the subspace spanned by these several directions. In this paper we propose an extension of these ideas to the case of convex quadratic programming.

03,430
PB95-180097 Not available NTIS
National Inst. of Standards and Technology (CAML), Gaithersburg, MD. Applied and Computational Mathematics Div.
Convergence Properties of a Class of Rank-Two Updates. (NIST Reprint).
Final rept.
P. T. Boggs, and J. W. Tolle. 1994, 26p.
Contract AFOSR-ISSA-90-0004
See also PB91-187799. Sponsored by Air Force Office of Scientific Research, Bolling AFB, DC.
Pub. in Society for Industrial and Applied Mathematics Jnl. of Optimization 4, n2 p262-287 May 94.

Keywords: *Optimization, *Convergence, *Numerical analysis, Algorithms, Approximation, Iteration, Matrices(Mathematics), Newton methods, Sequences(Mathematics), Reprints.

Many optimization algorithms generate, at each iteration, a pair (I(sub K), H(sub K)) consisting of an approximation to the solution I(sub K) and a Hessian matrix approximation H(sub K) that contains local second-order information about the problem. Much is known about the convergence of I(sub K) to the solution of the problem, but relatively little is known about the behavior of the sequence of matrix approximations. The sequence H(sub K), generated by the extended Broyden class of updating schemes independently of the optimization setting in which they are used, is analyzed. Various conditions under which convergence is assured are derived, and the structure of the limits is delineated. Rates of convergence are also obtained. These results extend and clarify those already in the literature.

03,431
PB96-179528 Not available NTIS
National Inst. of Standards and Technology (CAML), Gaithersburg, MD. Statistical Engineering Div.
Move-to-Root Rule for Self-Organizing Trees with Markov Dependent Requests.
Final rept.
R. P. Dobrow. 1996, 15p.
Pub. in Stochastic Analysis and Applications, v14 n1 p73-87 1996.

Keywords: *Search profiles, *Self organizing systems, *Heuristic methods, *Data structures, Markov chains, Eigenvalues, Search theory, Probability distribution functions, Trees(Mathematics), Costs, Reprints, Binary search trees, Move-to-root rule.

The move-to-root (MTR) heuristic is a self-organizing rule which attempts to keep a binary search tree in near-optimal form. It is a tree analogue of the well-studied move-to-front (MTF) scheme. The authors study a Markov move-to-root (MMTR) model, where the sequence of record requests is a Markov chain, and analyze several characteristics of the tree chain, including the stationary distribution, eigenvalues, and stationary expected search cost.

Statistical Analysis

03,432
PB95-104956 PC A11/MF A03
National Inst. of Standards and Technology (CAML), Gaithersburg, MD. Statistical Engineering Div.
Extreme Value Theory and Applications: Proceedings of the Conference on Extreme Value Theory and Applications, Volume 3. Held in Gaithersburg, Maryland in May 1993.
Special pub.
J. Galambos, J. Lechner, E. Simiu, and C. Hagwood. Aug 94, 244p, NIST/SP-866.
Also available from Supt. of Docs. as SN003-003-03280-8.

Keywords: *Statistical analysis, *Meetings, Weibull density functions, Statistical distributions, Order statistics, Markov chains, Wind velocity, Reliability, Corrosion, Quantiles, *Extreme value theory.

These 27 manuscripts make up Volume III of the Proceedings of the National Institute of Standards and Technology (NIST) Conference on Extreme Value Theory. They have been selected for their important contribution to a number of specialized topics. Partial Contents: On the Record Values from Univariate Distributions; Composite Sampling and Extreme Values; Extremal Sojourn Times for Markov Chains; Extreme Analysis of Wave Pressure and Corrosion for Structural Life Prediction; The Point-Process Approach to the Directional Analysis of Extreme Wind Speeds; Approximate Extreme Value Analysis for a Rigid Block Under Seismic Excitation; Large Deviations for Order Statistics; Extreme Values in Business Interruption Insurance.

03,433
PB95-125761 Not available NTIS
National Inst. of Standards and Technology (CAML), Gaithersburg, MD. Statistical Engineering Div.
Noise-Induced Chaos and Phase Space Flux.
Final rept.
M. Frey, and E. Simiu. 1993, 20p.
Pub. in Physica D 63, p321-340 1993.

Keywords: *Dynamical systems, Stochastic processes, Random noise, Phase space, Excitation, Chaos, Reprints.

We study the effect of additive noise on near-integrable second-order dynamical systems whose unperturbed flows have homoclinic or heteroclinic orbits. The noise is represented by a type of Shinozuka stochastic process capable of arbitrarily closely approximating Gaussian noise with any specified spectrum. We derive a formula for the flux factor applicable for any asymptotic mean stationary excitation. This derivation shows that, to first order, the effect of the external excitation on the system is mediated by a linear filter associated with the system homoclinic or heteroclinic orbit. It also shows that the stationary mean distribution of the filtered excitation determines the average phase space flux. This is true for both random and nonrandom excitations and indicates that, for the dynamical systems considered here, these two classes of excitation play substantially equivalent roles in the promotion of chaos.

03,434
PB95-150405 Not available NTIS
National Inst. of Standards and Technology (CAML), Gaithersburg, MD. Statistical Engineering Div.

Tolerance Intervals for the Distribution of True Values in the Presence of Measurement Errors.
Final rept.
C. M. Wang, and H. K. Iyer. 1994, 9p.
Pub. in Technometrics 36, n2 p162-170 May 94.

Keywords: *Statistical distributions, Confidence limits, Approximation, Variance(Statistics), Mathematical models, Growth, Reprints, *Tolerance intervals.

A tolerance-interval procedure for a distribution is derived based on mutually independent statistics. Application to the construction of tolerance intervals for the distribution of true values when observations are contaminated with measurement errors is explained. This includes the problem of constructing tolerance intervals in some growth-curve models. Numerical examples are given to illustrate the procedures.

03,435
PB95-151296 Not available NTIS
National Inst. of Standards and Technology (NEL), Gaithersburg, MD. Statistical Engineering Div.
Approximate Confidence Intervals on Linear Combinations of Expected Mean Squares.
Final rept.
C. M. Wang. 1992, 13p.
Pub. in Jnl. of Statistical Computation and Simulation 43, p229-241 1992.

Keywords: *Confidence limits, *Variance(Statistics), Mean square values, Approximation, Probability theory, Mathematical models, Simulation, Reprints.

In this article, we develop new procedures for obtaining approximate confidence intervals on linear combinations of the expected mean squares. The proposed approximations are indexed by a 'tuning' constant. By choosing the appropriate constant, which can be easily determined from data, we show that the proposed methods produce confidence intervals that maintain the stated confidence level. Numerical examples compare the performance to other approximations.

03,436
PB95-151304 Not available NTIS
National Inst. of Standards and Technology (NEL), Gaithersburg, MD. Statistical Engineering Div.
Approximate Confidence Intervals on Positive Linear Combinations of Expected Mean Squares.
Final rept.
C. M. Wang. 1991, 16p.
Pub. in Communications in Statistics - Simulation 20, n1 p81-96 1991.

Keywords: *Confidence limits, *Variance(Statistics), Mean square values, Approximation, Probability theory, Reprints.

In this article, we develop new procedures for obtaining approximate confidence intervals on positive linear combinations of the expected mean squares. The proposed approximations, in many cases, are the weighted average of liberal and conservative confidence limits. By choosing the appropriate weight, which can be easily determined from data, we show that the proposed methods produce confidence intervals with confidence coefficients very close to the stated level. Numerical examples compare the performance to other approximations.

03,437
PB95-151312 Not available NTIS
National Inst. of Standards and Technology (CAML), Gaithersburg, MD. Statistical Engineering Div.
Ranges of Confidence Coefficients for Confiedence Intervals on Variance Components.
Final rept.
C. M. Wang. 1990, 14p.
Pub. in Communications in Statistics - Simulation 19, n4 p1165-1178 1990.

Keywords: *Confidence limits, Variance(Statistics), Mathematical models, Approximation, Reprints.

The among variance component is the balanced one-factor nested components-of-variance model is of interest in many fields of application. Expect for an artificial method that uses a set of random numbers which is of no use in practical situations, an exact-size confidence interval on the among variance has not yet been derived. This paper provides a detailed comparison of three approximate confidence intervals which possess certain desired properties and have been shown to be the better methods among many available approximate procedures. Specifically, the minimum and the maximum of the confidence coefficients for the one- and two-sided intervals of each method are obtained. The expected lengths of the intervals are also compared.

03,438
PB95-152286 Not available NTIS
National Inst. of Standards and Technology (CAML), Gaithersburg, MD. Statistical Engineering Div.
Representing a Large Collection of Curves: A Case for Principal Points.
Final rept.
B. D. Flury, and T. Tarpey. 1993, 3p.
Pub. in American Statistician 47, n4 p304-306 1993.

Keywords: *Cluster analysis, *Principal components analysis, Curves, Reprints, Principal points.

A principal component-based method of selecting a few representative curves from a large collection of curves was previously proposed. We suggest a solution based on estimation of principal points.

03,439
PB95-153524 Not available NTIS
National Inst. of Standards and Technology (CAML), Gaithersburg, MD. Statistical Engineering Div.
Constant-Width Calibration Intervals for Linear Regression.
Final rept.
K. R. Eberhardt, and R. W. Mee. 1994, 9p.
Pub. in Jnl. of Quality Technology 26, n1 p21-29 Jan 94.

Keywords: *Linear regression, *Calibrating, Regression analysis, Mathematical models, Confidence limits, Independent variables, Dependent variables, Probability theory, Reprints, Tolerance intervals.

Calibration, in the sense of inverse regression, is widely used in measurement science and other applications. For univariate regression models, simultaneous calibration intervals enable one to construct confidence intervals for the unobserved values of the independent variable corresponding to an unlimited sequence of future observations of the dependent variable. The intervals considered have the interpretation that if the initial training sample belongs to a specified set G of 'good' outcomes, the conditional coverage probability for each future confidence interval will be at least the nominal value. The set G is constructed to occur with high probability. All methods for constructing calibration intervals currently in the literature are conservative in that they are obtained from simultaneous tolerance intervals for which the actual confidence level exceeds the nominal level. This work develops constant-width simultaneous tolerance intervals for which the bound on the nominal coverage probabilities is exact under normality. The resulting confidence intervals represent an attractive balance between efficiency and simplicity for linear calibration problems.

03,440
PB95-160594 PC A13/MF A03
National Inst. of Standards and Technology, Gaithersburg, MD.
Journal of Research of the National Institute of Standards and Technology, July/August 1994. Volume 99, Number 4. Special Issue: Extreme Value Theory and Applications. Proceedings of the Conference on Extreme Value Theory and Applications, Volume 2. Held at Gaithersburg, Maryland, in May 1993.
May 93, 296p.
Also available from Supt. of Docs. See also PB94-219326 and PB95-104956.

Keywords: *Extreme-value problems, *Failure analysis, *Corrosion, *Meetings, Extremum values, Ocean waves, Radiation damage, Weibull density functions, Spacecraft electronic equipment, Microelectronics, Sequences(Mathematics), Multivariate analysis, Ground motion, Loads(Forces), Fatigue limit, Risk analysis, Wind velocity, Aerosols, Floods, Ozone, Uses, *Extreme value theory, Bayesian analysis, Seismic risk.

It appears that the authors live in an age of disasters: the Mississippi and the Missouri rivers flood millions of acres, earthquakes hit Tokyo and California, airplanes crash due to mechanical failure, and powerful windstorms cause increasingly costly damage. While these may seem to be unexpected phenomena to the man in the street, they are actually happening according to well defined rules of science known as extreme value theory. The Proceedings are published in three Volumes. Volume I, published by Kluwer Academic Publishers, contains papers of general interest in extreme value theory and practice. Volume II, this Special Issue of the NIST Journal of Research, contains papers deemed by the Committee to be most directly relevant to NIST's mission. Volume III, NIST Special Publication 866, contains papers selected for their important contribution to a number of specialized topics. Applications considered in Volume II include damage because of ocean waves, high winds, seismic waves, ionizing radiation, floods, and corrosion.

03,441
PB95-180352 Not available NTIS
National Inst. of Standards and Technology (CAML), Gaithersburg, MD. Statistical Engineering Div.
Existence and Nonexistence Theorems of Finite Diameter Sequential Confidence Regions for Errors-in-Variables Models.
Final rept.
J. T. Hwang, and H. Liu. 1992, 11p.
Pub. in Statistics and Probability Letters 13, p45-55 1992.

Keywords: Stopping rules(Mathematics), Principal components analysis, Sequential analysis, Confidence limits, Existence therorems, Reprints, *Errors in variables models.

In errors-in-variables models, confidence sets (or intervals) for the key parameters with finite diameter and with asymptotic coverage probabilities greater than some nominal level 1-alpha have been constructed. Do these sets have good coverage probabilities for any fixed sample size. The answer may be no. In fact, in these models, any finite diameter confidence sets have zero minimum coverage probability, no matter how large the sample size is as long as it is fixed. The results apply to various models, including most linear and nonlinear errors-in-variables and inverse regression problems. Sequential approach appears to lie in between fixed-sample and asymptotic approaches. It seems to be interesting to investigate whether it is possible to construct good sequential confidence sets. In the paper, we focus on the errors-in-variables models and show that the answer is negative for K-stage, for any finite positive interger K, sequential sampling. However, the answer is positive for fully sequential sampling.

03,442
PB95-181103 Not available NTIS
National Inst. of Standards and Technology (CAML), Gaithersburg, MD. Statistical Engineering Div.
Moments of the Quartic Assignment Statistic with an Application to Multiple Regression.
Final rept.
D. F. Vecchia, and H. K. Iyer. 1991, 17p.
Pub. in Communications in Statistics - Theory and Methods 20, n10 p3253-3269 1991.

Keywords: *Distribution moments, Nonparametric statistics, Statistical tests, Regression analysis, Permutations, Computation, Reprints, *Assignment models, Pearson distributions.

We present the first three exact moments of the symmetric quartic assignment statistic. Efficient computational formulas have been derived to overcome severe difficulties in third moment calculations. Two examples illustrate applications of the quartic assignment statistic: evaluation of significant 'clustering' or 'mixing'; and distribution-free tests for equality of several planar regression models. This article extends previous results on the cubic assignment statistic in Iyer and Vecchia (1989).

03,443
PB95-203360 Not available NTIS
National Inst. of Standards and Technology (CAML), Gaithersburg, MD. Statistical Engineering Div.
Two Principal Points of Symmetric, Strongly Unimodal Distributions.
Final rept.
T. Tarpey. 1994, 5p.
Pub. in Statistics and Probability Letters 20, p253-257 1994.

Keywords: *Statistical distributions, Cluster analysis, Mixtures, Variance(Statistics), Optimization, Reprints, *Principal points, Self-consistent points.

Examples illustrate that splitting a symmetric, unimodal distribution into two groups so as to minimize the sum of the within-group variances does not always occur at the mean. Strong unimodality is shown to be a suffi-

cient condition for the optimal cutpoint to occur at the mean.

03,444
PB95-203436 Not available NTIS
National Inst. of Standards and Technology (CAML), Gaithersburg, MD. Statistical Engineering Div.
Outlier-Resistant Methods for Estimation and Model Fitting.
Final rept.
D. F. Vecchia, and J. D. Splett. 1994, 10p.
Pub. in ISA Transactions 33, p411-420 1994.

Keywords: *Mathematical models, *Curve fitting, *Estimating, *Outliers(Statistics), Least squares method, Estimators, Robustness(Mathematics), Regression analysis, Computer software, Reprints, LMS(Least Median of Squares).

Least squares is perhaps the most widely used technique for model fitting. In this article, we illustrate the poor performance of least squares when there are spurious values, or outliers, in a sequence of measurements. A brief overview of three well-known classes of robust alternatives to the least-squares mean is presented. For robust regression, a recent proposal called least median of squares (LMS) is described. LMS regression is compared to least-squares regression in an example involving the estimation of optical fiber geometry. References are provided for software that is available for robust estimation techniques surveyed in this article.

03,445
PB96-111802 Not available NTIS
National Inst. of Standards and Technology (CAML), Gaithersburg, MD. Statistical Engineering Div.
Taguchi's Parameter Design: A Panel Discussion.
Final rept.
B. Abraham, J. Mackay, J. A. Nelder, R. N. Kacker, J. Sacks, W. J. Welch, T. J. Lorenzen, A. C. Shoemaker, K. L. Tsui, R. H. Myers, G. G. Vining, S. Taguchi, J. M. Lucas, C. F. Wu, G. Box, and M. S. Phadke. 1992, 35p.
Pub. in Technometrics, v34 n2 p127-161 May 92.

Keywords: *Parameters, *Statistical analysis, *Experimental design, Analysis of variance, Factoral design, Reliability, Variations, Quality assurance, Quality control, Process control, Signal-to-noise ratio, Performance evaluation, Reprints.

The statistical techniques used by Taguchi to implement parameter design have been the subject of much debate, however, and there has been considerable research aimed at integrating the parameter-design principles with well-established statistical techniques. On the other hand, Taguchi and his colleagues feel that these research efforts by statisticians are misguided and reflect a lack of understanding of the engineering principles underlying Taguchi's methodology. This panel discussion provides a forum for a technical discussion of these diverse views. A group of practitioners and researchers discuss the role of parameter design and Taguchi's methodology for implementing it. The topics covered include the importance of variation reduction, the use of noise factors, the role of interactions, selection of quality characteristics, signal-to-noise ratios, experimental strategy, dynamic systems, and applications. The discussion also provides an up-to-date overview of recent research on alternative methods of design and analysis.

03,446
PB96-135090 Not available NTIS
National Inst. of Standards and Technology (CAML), Gaithersburg, MD. Statistical Engineering Div.
Principal Points and Self-Consistent Points of Symmetric Multivariate Distributions.
Final rept.
T. Tarpey. 1995, 13p.
Pub. in Jnl. of Multivariate Analysis, v53 n1 p39-51 Apr 95.

Keywords: *Elliptical distributions, *Multivariate distributions, Reprints, *Principal points, Self consistent points, Unimodal distributions.

Principal points and self-consistent points are cluster means of a distribution and represent a generalization of the population mean from one to several points. Principal points and self-consistent points are studied for a class of strongly symmetric multivariate distributions. Elliptical distributions belong to the class of strongly symmetric distributions. Several results are given for principal points and self-consistent points of strongly symmetric multivariate distributions. One result relates self-consistent points to principal component subspaces. Another result provides a sufficient condition for any set of self-consistent points lying on a line to be symmetric to the mean of the distribution.

03,447
PB96-137740 Not available NTIS
National Inst. of Standards and Technology (CAML), Gaithersburg, MD.
Churchill Eisenhart, 1913-1994.
Final rept.
J. M. Cameron, and J. R. Rosenblatt. 1995, 2p.
Pub. in American Statistician, v49 n3 p243-244 Aug 94.

Keywords: Statistics, Biographies, Reprints, *Obituaries, *Churchill Eisenhart.

This document is an obituary for Churchill Eisenhart, 1913-1994.

03,448
PB96-141163 Not available NTIS
National Inst. of Standards and Technology (CAML), Gaithersburg, MD. Statistical Engineering Div.
Anova Estimates of Variance Components for a Class of Mixed Models.
Final rept.
M. G. Vangel. 1995, 6p.
Pub. in Proceedings of the Section on Physical and Engineering Sciences, Toronto, Canada, August 13-18, 1994, p91-96 1995.

Keywords: *Analysis of variance, Reprints, *Variance estimates, *Henderson method, Quadratic form, Singular value decomposition.

This article examines a simple and intuitively appealing way to estimate variance components in mixed models: perform as many ordinary least squares regressions as there are variance components, using dummy variables for all but one random effect in each regression. By equating these residual sums of squares to their expectations, unbiased estimates of all of the variance components can be obtained. This approach is a special case of Method 3 of Henderson (1953). For a class of 'nearly balanced' nested mixed models, having no interactions involving both fixed and random effects, the exact distributions (under normality) of residual sums of squares are derived.

03,449
PB96-141171 Not available NTIS
National Inst. of Standards and Technology (CAML), Gaithersburg, MD. Statistical Engineering Div.
One-Sided beta-Content Tolerance Intervals for Mixed Models.
Final rept.
M. G. Vangel. 1995, 7p.
Pub. in Proceedings of the Section on Physical and Engineering Sciences, Toronto, Canada, Chapel Hill, NC., June 13-15, 1994, Birmingham, AL., p200-206 1995.

Keywords: *Mathematical models, *Confidence limits, Variance(Statistics), Reprints, Approximation, *Material strength.

Lower confidence limits on lower tail quantiles of a population of material strength measurements are routinely used to characterize the strength of a material, particularly in air craft design. Composite materials typically exhibit considerable between-batch variability, so that the approach discussed in this article could have important applications. For example, if three batches of five specimens each are tested at each of four temperatures, and it is desired to determine as a function of temperature a lower confidence limit on the tenth percentile of the population corresponding to the strength of a specimen chosen at random from a randomly selected batch, then the proposed methodology could be applied.

03,450
PB97-118707 Not available NTIS
National Inst. of Standards and Technology (CAML), Gaithersburg, MD. Statistical Engineering Div.
Developing Measurement for Experimentation.
Final rept.
W. Liggett. 1996, 26p.
Pub. in Statistics in Quality, Chapter 10, p179-204 1996.

Keywords: *Experimental design, *Measurement, *Sensitivity, *Selectivity, Multivariate analysis, Analysis of variance, Accuracy, Estimating, Statistical analysis, Statistical inference, Reprints, *Homoscedasticity.

Measurement consists of producing, for each unit measured, a response related to the unit property in question. The response may be multivariate. Development of a measurement system entails experiments involving responses obtained from sets of test units, with each set consisting of nearly identical units. These experiments require a variety of statistical approaches, which this chapter brings together.

MEDICINE & BIOLOGY

Biochemistry

03,451
DE96014476 PC A05/MF A01
National Inst. of Standards and Technology, Gaithersburg, MD.
Small genomes: New initiatives in mapping and sequencing. Workshop summary report.
K. McKenney, and F. Robb. 1993, 57p, CONF-9307232-SUMM.
Contract AI02-93ER61622
Small genomes: new initiatives in mapping and sequencing, Rockville, MD (United States), 5-7 Jul 1993. Sponsored by Department of Energy, Washington, DC.

Keywords: *DNA Sequencing, *Genetic Mapping, Biotechnology, Man, Meetings, EDB/550400, EDB/550200.

The workshop was held 5--7 July 1993 at the Center for Advanced Research in Biotechnology (CARB) and hosted by the University of Maryland Biotechnology Institute (UMBI) and the National Institute of Standards and Technology (NIST). The objective of this workshop was to bring together individuals interested in DNA technologies and to determine the impact of these current and potential improvements of the speed and cost-effectiveness of mapping and sequencing on the planning of future small genome projects. A major goal of the workshop was to spur the collaboration of more diverse groups of scientists working on this topic, and to minimize competitiveness as an inhibitory factor to progress.

03,452
PB94-172145 Not available NTIS
National Inst. of Standards and Technology (IMSE), Gaithersburg, MD. Polymers Div.
Calcium Phosphate Precipitation in Liposomal Suspensions.
Final rept.
E. D. Eanes. 1990, 10p.
Pub. in Materials Research Society Symposia Proceedings, v174 p15-24 1990. Sponsored by National Inst. of Dental Research, Bethesda, MD.

Keywords: *Liposomes, *Calcium phosphates, *Mineralization, Artificial membranes, Bones, In vitro analysis, Phosphatidycholines, Cholesterol, pH, Reprints, Diacetylphosphates.

Artificial lipid vesicles (liposomes) provide an in vitro approach for microencapsulating calcium phosphate precipitation reactions in a manner similar to that which occurs in matrix vesicles, the initial loci for extracellular mineralization in many skeletal tissues. Apatitic precipitates readily form within the aqueous interiors of liposomes prepared from phosphatidycholine, dicetylphosphate, and cholesterol when the liposomal membranes enclosing pH 7.4 buffered PO4 solutions are made permeable to external Ca2+ with ionophores. If the external Ca solution is rendered metastable with PO4, the apatitic precipitates rapidly expand to outside the liposomes as well. The present paper describes the basic features of liposomal mineralization and presents some specific examples on how compositional alterations in the liposomal membrane and external Ca solution can affect the progress of this mineralization.

03,453
PB94-172509 Not available NTIS

National Inst. of Standards and Technology (MSEL), Gaithersburg, MD. Reactor Radiation Div.
Characterization of the Binding of Gallium, Platinum, and Uranium to Pseudomonas Fluorescens by Small-Angle X-ray Scattering and Transmission Electron Microscopy.
Final rept.
S. Krueger, G. J. Olson, D. Johnsonbaugh, and T. J. Beveridge. 1993, 9p.
Pub. in Applied and Environmental Microbiology 59, n12 p4056-4064 Dec 93.

Keywords: *Gallium, *Platinum, *Uranium, *Pseudomonas fluorescens, *Radiation scattering, *Electron microscopy, *Binding sites, X rays, Cell membrane, Particle size, Peptidoglycans, Reprints.

Small-angle X-ray scattering (SAXS) was used to determine the binding of Ga, U, and Pt to Pseudomonas fluorescens in aqueous buffer. Atomic absorption spectrophotometry was used to quantify the heavy metals during bulk analysis, whereas transmission electron microscopy of whole mounts and thin sections was used to determine the locations of the cell-bound metal precipitates, as well as their sizes and physical structures. Energy-dispersive X-ray spectroscopy confirmed the compositions and identities of the precipitates and helped show that they were associated primarily with the envelope layers of the bacteria. Unlike Ga and Pt, which were located only at the cell surface, U was also found intracellularly in approximately 10% of the cells. The cytoplasmic location ultimately killed and lysed the cells. Surface-bound Ga and U were spread over the entire cell envelope (outer membrane-peptidoglycan-plasma membrane complex), whereas Pt was associated only with the lipopolysaccharide-rich, external face of the outer membrane. SAXS confirmed these data and showed that the bacteria were metal-enshrouded particles that were 1.0 to 1.5 micrometers in diameter. SAXS also provided a statistically significant representation of the bound metal precipitates, which ranged in size from 10 nm to 1 micrometers. The correlation between the microscopic data and the scattering data was extremely good. Since SAXS is performed in an aqueous milieu, it yields a more representative picture of the physical state of the metal bound to cell surfaces.

03,454
PB94-198249 Not available NTIS
National Inst. of Standards and Technology (CSTL), Gaithersburg, MD. Biotechnology Div.
Calorimetric Determination of the Standard Transformed Enthalpy of a Biochemical Reaction at Specified PH and pMg.
Final rept.
R. A. Alberty, and R. N. Goldberg. 1993, 11p.
Pub. in Biophysical Chemistry 47, p213-223 1993.

Keywords: *Chemical equilibrium, *pH, *Metals, *Ions, *Heat of reaction, Reprints, Calorimetry, Hydrogen ions, Enthalpy, Biochemistry, *Metallic ions.

In a biochemical reaction there is generally a change in the binding of hydrogen ions and metal ions. Therefore, calorimetric measurements of enthalpies of reaction have to be adjusted for the enthalpies of reaction of the hydrogen ions and metal ions produced or consumed with the buffer. It can be shown that this yields the standard transformed enthalpy of reaction that determines the change in the apparent equilibrium constant (written in terms of sums of concentrations of species of a reactant) with temperature at the chosen pH and concentration of free metal ion. The derivations are based on the assumption that the changes in pH and free metal ion concentrations in the calorimetric experiment are small. This assumption is experimentally realized if a solution is well buffered for hydrogen and metal ions. The derived equations are discussed in terms of the implications they have for the performance and interpretation of calorimetric measurements.

03,455
PB94-199593 Not available NTIS
National Inst. of Standards and Technology (CSTL), Gaithersburg, MD. Biotechnology Div.
Thermodynamic Analysis of Heparin Binding to Human Antithrombin.
Final rept.
S. DeLauder, F. P. Schwarz, J. Williams, and D. H. Atha. 1992, 9p.
Pub. in Biochimica et Biophysica Acta 1159, p141-149 1992.

Keywords: *Heparin, *Antithrombin III, *Thermodynamics, Binding sites, Differential scanning calorimetry, Protein denaturation, Protein folding, Reprints.

The binding of heparin to human antithrombin III (ATIII) was investigated by titration calorimetry (TC) and differential scanning calorimetry (DSC). TC measurements of homogeneous high-affinity pentasaccharide and octasaccharide fragments of heparin in 0.02 M phosphate buffer and 0.15 M sodium chloride (pH 7.3) yielded binding constants of (7.1 + or - 1.3) times 10 to the fifth power/M and (6.7 + or - 1.2) times 10 to the sixth power/M, respectively, and corresponding binding enthalpies of -48.3 + or - 0.7 and -54.4 + or - 5.4 kJ/mol. The binding enthalpy of heparin in phosphate buffer (0.02 M, 0.15 M NaCl, pH 7.3) was estimated from TC measurements to be -55 + or - 10 kJ/mol, while the enthalpy in Tris buffer (0.02 M, 0.15 M NaCl, pH 7.3) was -18 + or - 2 kJ/mol. The heparin-binding affinity was shown by fluorescence measurements not to change under these conditions. The 3-fold lower binding enthalpy in Tris can be attributed to the transfer of a proton from the buffer to the heparin-ATIII complex. DSC measurements of the ATIII unfolding transition exhibited a sharp denaturation peak at 329 + or - 1 K with a van 't Hoff enthalpy of 951 + or - 89 kJ/mol, based on a two-state transition model and a much broader transition from 333 to 366 K. The transition peak at 329 K accounted for 9-18% of the total ATIII. At sub-saturate heparin concentrations, the lower temperature peak became bimodal with the appearance of a second transition peak at 336 K. At saturate heparin concentration only the 336 K peak was observed. This supports a two domain model of ATIII folding in which the lower stability domain (329 K) binds and is stabilized by heparin.

03,456
PB94-211042 Not available NTIS
National Inst. of Standards and Technology (NML), Gaithersburg, MD.
Molar Absorptivities of Bilirubin (NIST SRM 916A) and Its Neutral and Alkaline Azopigments.
Final rept.
B. T. Doumas, B. W. Perry, R. B. McComb, K. L. J. Vink, J. C. Koedam, R. C. Paule, A. Kessner, and H. L. Vader. 1990, 4p.
Pub. in Clinical Chemistry 36, n9 p1698-1701 1990.

Keywords: *Pigments, *Azo compounds, *Bilirubin, *Absorptivity, Interlaboratory comparisons, Reprints, *Standard reference materials.

Three laboratories in the U.S. and two in the Netherlands determined molar absorptivities (epsilon) of bilirubin from the National Institute of Standards and Technology (NIST, the former National Bureau of Standards), Standard Reference Material SRM 916a. In caffeine reagent average epsilon values were 50,060 and 48,980 L times mol(sup -1) times cm(sup -1) at 432 and 457 nm, respectively. The epsilon value of the blue azopigment, obtained with the reference method for total serum bilirubin was 76,490 L times mol(sup -1) times cm(sup -1) at 598 nm. When the addition of alkaline tartrate was omitted, the molar absorptivity of the red azopigment was 56,600 L times mol(sup -1) times cm(sup -1) at 530 nm.

03,457
PB94-211190 Not available NTIS
National Inst. of Standards and Technology (MSEL), Gaithersburg, MD. Polymers Div.
Mixed Phospholipid Liposome Calcification.
Final rept.
E. D. Eanes. 1992, 4p.
Sponsored by National Inst. of Dental Research, Bethesda, MD.
Pub. in Bone and Mineral 17, p269-272 1992.

Keywords: *Liposomes, *Phospholipids, *Calcification, Precipitation, Phosphatidylserines, Sphingomyelins, Reprints.

Synthetic lipid vesicle (liposome) suspensions have been used to experimentally model many of the calcium phosphate precipitation steps observed in matrix vesicle (MV) calcification. In particular, precipitate development in liposomes can be made to preferentially follow the progression seen in MV, i.e. to occur initially in intraliposomal spaces and then to expand into the surrounding suspending medium. This paper reviews results from studies by us which show that certain phospholipid constituents of the liposomal membrane can modulate this progression. Of greatest relevance to MV calcification is the observation that phosphatidylserine and sphingomyelin, two lipids selectively enriched in MV, slow the expansion of the precipitation from inside to outside the liposome.

03,458
PB94-212602 Not available NTIS
National Inst. of Standards and Technology (NML), Gaithersburg, MD. Ionizing Radiation Div.
Modification of Deoxyribose-Phosphate Residues by Extracts of Ataxia Telangiectasia Cells.
Final rept.
L. R. Karam, P. Calsou, W. A. Franklin, T. Lindahl, R. B. Painter, and M. Olsson. 1990, 8p.
Pub. in Mutation Research 236, n1 p19-26 1990.

Keywords: *Ataxia telangiectasia, *Deoxyribose, *Phosphates, Molecular weight, Cell line, pH, Chromatography, Xeroderma pigmentosum, Bloom syndrome, Friedreich's ataxia, Werner's syndrome, Reprints.

The release of DNA 5'-terminal deoxyribose-phosphate residues from enzymatically incised apurinic/apyrimidinic sites by human cell extracts has been under investigation. During the course of these studies, we observed that ataxia telangiectasia cell extracts modify deoxyribose-phosphate (dRp) residues by converting them to an adduct form, dRp-X, which shows altered chromatographic properties on high pressure liquid chromatography (HPLC) analysis. The chemical nature of the adduct is as yet unknown, but dRp-X is stable to both heat and acid. The modification requires an enzymatic activity and a low-molecular weight cofactor. Extracts of normal cells contain a dialyzable inhibitor that suppresses the reaction occurring with ataxia telangiectasia cell extracts. Formation of dRp-X has been observed in 7 out of 7 ataxia telangiectasia lymphoblastoid lines which represent at least 3 genetic complementation groups. Similar modification of dRp did not occur with extracts of cells of normal origin, nor those representing Fanconi's anemia, xeroderma pigmentosum, Bloom's syndrome, Werner's syndrome or Friedreich's ataxia.

03,459
PB94-212800 Not available NTIS
National Inst. of Standards and Technology (CSTL), Gaithersburg, MD. Biotechnology Div.
Apparent Molar Heat Capacities and Apparent Molar Volumes of Aqueous Glucose at Temperatures from 298.15 K to 327.01 K.
Final rept.
N. Kishore, R. N. Goldberg, and Y. B. Tewari. 1993, 13p.
Pub. in Jnl. of Chemical Thermodynamics 25, p847-859 1993.

Keywords: *Glucose, *Aqueous solutions, *Specific heat, *Density(Mass/Volume), *Volume, Temperature dependence, Thermodynamic properties, Error analysis, Reprints, *Molar volume, Thermodynamic excess properties.

Specific heat capacities, apparent molar heat capacities, densities, and apparent molar volumes were determined for aqueous glucose over the temperature range 298.15 to 327.O K. The molal concentrations of the solutions ranged from 0.20 to 1.54 mol/kg. The results were used to calculate c(sub p,2,m)(sup o) and V(sub 2,m)(sup o) for glucose at 298.15 K and the first and second derivatives of these quantities with respect to temperature. The first virial coefficient in the expression for the excess molar volume was determined. The results were compared with published data. A discussion of systematic errors attributable to instrumental errors, sample impurities, and incomplete anomeric and relaxation in the solutions is given.

03,460
PB94-213113 Not available NTIS
National Inst. of Standards and Technology (CSTL), Gaithersburg, MD. Biotechnology Div.
Thermochemistry of the Reactions between Adenosine, Adenosine 5'-monophosphate, Inosine, and Inosine 5'-monophosphate; the Conversion of L-histidine to (Urocanic Acid+Ammonia).
Final rept.
J. W. Larson, Y. B. Tewari, and R. N. Goldberg. 1993, 18p.
Pub. in Jnl. of Chemical Thermodynamics 25, p73-90 1993.

Keywords: *Adenosine monophosphates, *Thermochemistry, *Chemical equilibrium, *Inosine monophosphate, *Thermodynamic properties, Gibbs free energy, Entropy, Enthalpy, Calorimetry, Histidine, Catalysis, Enzymes, Biochemistry, Reprints, Deamination, Dephosphorylation.

The results of equilibrium and calorimetric measurements are reported for a series of enzyme-catalyzed

reactions involving deamination of adenosine-5'-monophosphate (AMP), adenosine, and L-histidine and the dephosphorylation of AMP and inosine-5'-monophosphate. The data have been analyzed with a model that described the complex equilibria in solution. Values for the standard molar enthalpies, Gibbs free energies, and entropy changes of the reactions were calculated and discussed in relation to thermodynamic cycle calculations involving the substances and other reactions of a chemically similar nature.

03,461
PB94-216363 Not available NTIS
National Inst. of Standards and Technology (NML), Gaithersburg, MD. Chemical Process Metrology Div.
Energy Transduction between a Concentration Gradient and an Alternating Electric Field.
Final rept.
V. S. Markin, T. Y. Tsong, R. D. Astumian, and B. Robertson. 1990, 5p.
Pub. in Jnl. of Chemical Physics 93, n7 p5062-5066 1990.

Keywords: *Signal transduction, *Electric fields, *Proteins, Conformational changes, Gradients, Concentration(Composition), Membranes, Reprints, *Electroconformational coupling, *Alternating electric fields, Membrane transduction.

A four-state transport protein that has electric charges that move concomitantly with conformational changes can transduce energy in either direction between an alternating membrane potential and a concentration gradient. An alternating electric potential of very large amplitude is considered, and the rapid-equilibrium approximation is used for the conformational changes. This permits deriving simple expressions for the transport flux, the power supplied by the alternating potential, and the power applied to the concentration gradient.

03,462
PB95-140497 Not available NTIS
National Inst. of Standards and Technology (CSTL), Gaithersburg, MD. Biotechnology Div.
Determining Mobility from Homodyne ac Electrophoretic Light Scattering.
Final rept.
B. Robertson, and J. Hubbard. 1992, 4p.
Pub. in Jnl. of Colloid and Interface Science 153, n2 p457-460, 15 Oct 92.

Keywords: Light scattering, Correlation functions, Alternating current, Electric fields, Suspensions, Reprints, *Electrophoretic mobility, Homodyne measurement.

The homodyne correlation function for light scattered from a suspension of particles in an oscillating field is derived, assuming there are two species of particles of the same size but with different mobilities. If the mobility of one species is known, the mobility of the other can be determined from the modulation of the correlation function. This method of determining mobility is insensitive to thermal convection effects, electroosmotic flow, and mechanical vibrations.

03,463
PB95-150801 Not available NTIS
National Inst. of Standards and Technology (CSTL), Boulder, CO. Biotechnology Div.
Thermochemistry of the Hydrolysis of L-arginine to (L-citrulline + Ammonia) and of the Hydrolysis of L-arginine to (L-ornithine + Urea).
Final rept.
Y. B. Tewari, N. Kishore, S. A. Margolis, R. N. Goldberg, and T. Shibatani. 1993, 13p.
Pub. in Jnl. of Chemical Thermodynamics 25, p293-305 1993.

Keywords: *Arginine, *Heat measurement, *Hydrolysis, *Thermochemistry, Thermodynamics, Urea, Metabolic processes, Models, Chemical reactions, Enzymes, Ammonia, Catalysis, Biotechnology, Reprints, *Molar enthalpy, Microcalorimetry, L-arginine.

Molar enthalpies of reaction for the hydrolysis of L-arginine(aq) to (L-ornithine(aq) + urea(aq)) and for the hydrolysis of L-arginine(aq) to (L-citrulline(aq) + ammonia(aq)) have been measured by microcalorimetry. These reactions are catalyzed, respectively, by arginase and by arginine deiminase. The effects of variations in pH, temperature, and ionic strength of the molar enthalpies of reaction were studied. The results have been analyzed with a model which accounts for the complex equilibria in solution. The results are discussed in terms of thermodynamic-cycle calculations and in terms of the metabolic urea cycle.

03,464
PB95-162707 Not available NTIS
National Inst. of Standards and Technology (NML), Gaithersburg, MD. Chemical Thermodynamics Div.
Biological Thermodynamic Data for the Calibration of Differential Scanning Calorimeters: Dynamic Temperature Data on the Gel to Liquid Crystal Phase Transition of Dialkylphosphatidylcholine in Water Suspensions.
Final rept.
F. P. Schwarz. 1991, 19p.
Pub. in Thermochimica Acta 177, p285-303 Apr 91.

Keywords: *Lipids, *Thermodynamics, *Heat measurement, Transition temperature, Specific heat, Transition points, Enthalpy, Liquid crystals, Chemical energy, Reprints, Diakylphosphatidylcholine, Differential scanning calorimetry, Gel to liquid crystal transition.

Heat capacity measurements of the gel to liquid crystalline transition of phosphocholine lipid suspensions in buffer solutions were performed by a differential scanning calorimeter over a range of experimental conditions. Since the temperatures at the transition peak maxima, i.e. transition temperatures, were observed to increase linearly with scan rate due to the response time of the DSC, they were corrected to zero scan rate and found to agree closely with the literature values.

03,465
PB95-162715 Not available NTIS
National Inst. of Standards and Technology (NML), Gaithersburg, MD. Chemical Thermodynamics Div.
Thermodynamics of the Binding of Galactopyranoside Derivatives to the Basic Lectin from Winged Bean (Psophocarpus Tetrogonolobus).
Final rept.
F. P. Schwarz, K. D. Puri, and A. Surolia. 1991, 7p.
Pub. in Jnl. of Biological Chemistry 266, n36 p24344-24350 1991.

Keywords: *Thermodynamics, *Beans, *Heat measurement, Carbohydrates, Chemical energy, Chemical bonds, Bonding, Transition points, Transition temperature, Reprints, *Galactopyranoside, Winged bean, Psophocarpus tetrogonolobus, Lectin, Differential scanning calorimetry, Binding energy.

The thermodynamics of the binding of galactose derivatives to the basic agglutinin from winged bean (WBAI) in PBS (0.02 M sodium phosphate and 0.15 M sodium chloride) have been investigated from 298.15 to 333.15 K by titration calorimetry and at the denaturation temperature by differential scanning calorimetry (DSC). WBAI is a dimer with one binding site per each identical sub-unit. The thermal transition consisted of two overlapping peaks over the pH range 5.6 to 7.4.

03,466
PB95-163192 Not available NTIS
National Inst. of Standards and Technology (NML), Gaithersburg, MD. Chemical Thermodynamics Div.
Glucose Permease of Bacillus Subtilis Is a Single Polypeptide Chain That Functions to Energize the Sucrose Permease.
Final rept.
S. L. Sutrina, P. Reddy, M. H. Saier, and J. Reizer. 1990, 9p.
Sponsored by California Univ., San Diego, La Jolla. Dept. of Biology.
Pub. in Jnl. of Biological Chemistry 265, n30 p8581-8589 1990.

Keywords: *Bacillus subtilis, *Peptides, Sucrose, Glucose, Biological transport, Phosphorylation, Cell membrane, Phosphoenolpyruvate, Protein conformation, Reprints, *Glucose permease, *Sucrose permease.

Biochemical, immunological and sequence analyses demonstrated that the glucose permease of Bacillus subtilis, the glucose-specific Enzyme II of the phosphoenolpyruvate-dependent phosphotransferase system (PTS), is a single polypeptide chain with a C-terminal Enzyme III-like domain. A flexible hydrophilic linker, similar in length and amino acid composition to linkers previously identified in other regulatory or sensory transducing proteins, functions to tether the Enzyme III(glc)-like domain of the protein to the membrane-embedded Enzyme II(glc). Evidence is presented demonstrating that the Enzyme III(glc)-domain of the glucose permease plays a dual role and functions in the transport and phosphorylation of both glucose and sucrose. The sucrose permease appears to lack a sucrose-specific Enzyme III-like domain or a separate, soluble III(scr) protein. Enzyme II(scr) was capable of utilizing the III(glc)-like domain of the glucose permease regardless of whether the III(glc) polypeptide was provided as a purified, soluble protein, as a membrane-bound protein within the same membrane as Enzyme II(scr), or as a membrane-bound protein within membrane fragments different from those bearing Enzyme II(scr). These observations suggest that the III(glc)-like domain is an autonomous structural unit that assumes a conformation independent of the hydrophobic, N-terminal intramembranal domain of Enzyme II(glc).

03,467
PB95-163820 Not available NTIS
National Inst. of Standards and Technology (CSTL), Gaithersburg, MD. Thermophysics Div.
Affinity Chromatography on Inorganic Support Materials.
Final rept.
H. H. Weetall. 1993, 22p.
Pub. in Molecular Interactions in Bioseparations, Chapter 3, p27-48 1993.

Keywords: *Biochemistry, *Supports, *Inorganic compounds, *Ligands, Chromatographic analysis, Chemical bonds, Separations, Purification, Antigens, Antibodies, Enzymes, Nucleic acids, Reviews, Reprints, *Affinity chromatography.

Inorganic support materials have been used for chromatography for over 75 years. However, it is only been within the last 25 years that these materials have been applied to affinity separations in which the affinity ligand is covalently bonded to the support. This review will cover the application of inorganic silicas and metal oxides for coupling to ligands of various types for the isolation and purification of antigens, antibodies, enzymes, nucleic acids and related species. Specific protocols for the activation and coupling of ligands are presented. The review will not cover ion chromatography or use of hydrocarbon bonded phases for protein isolations, nor will it cover the application of ion exchange as a separation and purification method on inorganic supports. The review contains 77 references.

03,468
PB95-164547 Not available NTIS
National Inst. of Standards and Technology (MSEL), Gaithersburg, MD. Polymers Div.
Membrane-Mediated Precipitation of Calcium Phosphate in Model Liposomes with Matrix Vesicle-Like Lipid Composition.
Final rept.
D. Skrtic, and E. D. Eanes. 1992, 11p.
Sponsored by National Inst. of Dental Research, Bethesda, MD.
Pub. in Bone and Mineral 16, p109-119 1992.

Keywords: *Calcium phosphates, *Membrane lipids, *Liposomes, *Precipitation(Chemistry), pH, Divalent cations, Phospholipids, In vivo analysis, Minerals, Biochemistry, Reprints, *Matrix vesicles, Apatite/hydroxy, Serine/phosphatidyl, Sphingomyelin.

The present study examined calcium phosphate precipitation in aqueous suspensions of artificial liposomes which closely resembled matrix vesicles (MV) in membrane lipid composition. At 22 C, the liposomes per se did not initiate precipitation in the suspending medium for up to 120 h when the latter was made supersaturated with respect to hydroxyapatite (2.25 mM Ca(2+), 1.5 mM PO4, 240 mosmol, pH 7.4). Likewise, the suspending medium remained stable for up to 72 h when precipitation was induced within the aqueous interiors of the liposomes by encapsulating pH 7.4-buffered 50 mM PO4 solutions in the interior spaces and making the enclosing membranes permeable to external solution Ca(2+) ions with the ionophore X-537A. However, extraliposomal precipitation readily occurred under these latter conditions when phosphiatidylserine (PS) and sphingomyelin (Sph) were deleted from the MV-like lipid formulation used to prepare the liposomes. These results suggest that lipidic membrane constituents such as PS and Sph may have a controlling influence on MV-mediated calcification in vivo by affecting the release of intravesicularly formed mineral crystals into the extracellular matrix space where they can subsequently grow and proliferate.

03,469
PB95-169223 Not available NTIS
National Inst. of Standards and Technology (MSEL), Gaithersburg, MD. Polymers Div.
Effect of 1-Hydroxyethylidene-1,1-Bisphosphonate on Membrane-Mediated Calcium Phosphate Formation in Model Liposomal Suspensions.
Final rept.
D. Skrtic, and E. D. Eanes. 1994, 11p.
Sponsored by National Inst. of Dental Research, Bethesda, MD.
Pub. in Bone and Mineral 26, p219-229 1994.

Keywords: *Calcium phosphates, *Membrane lipids, *Liposomes, Dental materials, Mineralization, Precipitation(Chemistry), Biochemistry, Physicochemical properties, In vivo analysis, Phosphatidylserines, Matrix bands, Reprints, *Ethylidene bisphosphonate/hydroxy.

The bisphosphonate, 1-hydroxyethylidene-1,1-bisphosphonate (HEBP), was examined for its effect on calcium phosphate precipitation in pH 7.4, 22 C suspensions of 7:2:1 phosphatidylcholine (PC):dicetylphosphate (DCP):cholesterol (Chol) and 7:1:1 PC:phosphatidylserine (PS):Chol liposomes. HEBP (0.5-50 micromol/l) in the suspending medium had little, if any, effect on precipitation that formed inside phosphate-rich (50 mmol/l) aqueous interiors of liposomes as a result of ionophore (X-537A) driven 2.25 mmol/l Ca(2+) influxes from the medium. These results provide a possible physicochemical explanation for the suppression of matrix vesicle initiated mineralization in ectopically-induced osteoid tissue of HEBP treated mice. In particular, the liposome results suggest that membrane phosphatidylserine interactions with mineral may enhance HEBP's effectiveness in vivo.

03,470
PB95-180782 Not available NTIS
National Inst. of Standards and Technology (CSTL), Gaithersburg, MD. Biotechnology Div.
Supported Phospholipid/Alkanthiol Biomimetic Membranes: Insulating Properties.
Final rept.
A. L. Plant, M. Gueguetchkeri, and W. Yap. 1994, 8p.
Pub. in Biophysical Jnl. 67, p1126-1133 Sep 94.

Keywords: *Phospholipids, *Lipid bilayers, *Artificial membranes, Spectroscopy, Electron transfer, Gold, Melittin, Dielectrics, Insulation resistance, Conductivity, Resistance, Reprints, *Alkanethiol monolayers.

A novel model lipid bilayer membrane is prepared by the addition of phospholipid vesicles to alkanethiol monolayers on gold. This supported hybrid bilayer membrane is rugged, easily and reproducibly prepared in the absence of organic solvent, and is stable for very long periods of time. We have characterized the insulating characteristics of this membrane by examining the rate of electron transfer and by impedance spectroscopy. Supported hybrid bilayers formed from phospholipids and alkanethiols are pinhole-free and demonstrate measured values of conductivity and resistivity which are within an order of magnitude of that reported for black lipid membranes. Capacitance values suggest a dielectric constant of 2.7 for phospholipid membranes in the absence of organic solvent. The protein toxin, melittin, destroys the insulating capability of the phospholipid layer without significantly altering the bilayer structure. This model membrane will allow the assessment of the effect of lipid membrane perturbants on the insulating properties of natural lipid membranes.

03,471
PB96-102728 Not available NTIS
National Inst. of Standards and Technology (CSTL), Gaithersburg, MD. Biotechnology Div.
Bacteriorhodopsin Retains Its Light-Induced Proton-Pumping Function After Being Heated to 140C.
Final rept.
E. P. Lukashev, and B. Robertson. 1995, 4p.
Pub. in Bioelectrochemistry and Bioenergetics 37, p157-160 1995.

Keywords: *Photochemical reactions, *Protons, Reprints, Pumping, High temperature, Reactions, Photosynthetic bacteria, Membrane transport, *Bacteriorhodopsin, *Halobacterium.

Films of purple membrane of Halobacterium salinarium have been reported to keep their two-dimensional hexagonal lattice structure and their optical absorbance spectrum even after being heated to 140 degrees C for two days. Tests of the light-induced proton-pumping function of the bacteriorhodopsin (bR) molecule in the purple membrane were not reported. The present paper describes measurements of the light-induced proton-pumping by films of wild-type and D96H-mutant bR at room temperature after the films were heated to high temperatures. The measurements show that cycling bR through 140 deg C does not reduce its proton-pumping ability.

03,472
PB96-102900 Not available NTIS
National Inst. of Standards and Technology (CSTL), Gaithersburg, MD. Biotechnology Div.
Phospholipid/Alkanethiol Bilayers for Cell-Surface Receptor Studies by Surface Plasmon Resonance.
Final rept.
A. L. Plant, M. Brigham-Burke, E. C. Petrella, and D. J. O'Shannessy. 1995, 7p.
Pub. in Analytical Biochemistry 226, p342-348 1995.

Keywords: *Phospholipids, *Lipid bilayers, *Artificial membranes, Reprints, Electron transfer, Conductivity, Resistance, Dielectrics, *Alkanethiol monolayers.

Supported hybrid bilayer membranes (HBM) composed of a monolayer of phospholipid and a monolayer of alkanetiol associated with a thin gold film on glass are useful as model lipid bilayer membranes for studying membrane receptor-ligand and cell-cell binding events by surface plasmon resonance (SPR). Measurements of specific binding of proteins and lipid vesicles to well-defined HBMs have been performed under conditions or continuous flow using a commercial SPR instrument (BIAcore). HBMs are shown to be stable in flow and to block nonspecific adsorption of proteins to the alkanethiol/gold surface. The use of such supported lipid bilayers in flow provides a means of conducting equilibrium and kinetic studies of models of ligand-cell and cell-cell interactions with receptors or ligands in a membrane environment. Compared to the extended dextran polymer layer that is currently used for surface modification of BIAcore 'sensor chips,' the described HBMs provide a well-defined surface that will permit less ambiguous modeling of these important biological interactions.

03,473
PB96-111976 Not available NTIS
National Inst. of Standards and Technology (CSTL), Gaithersburg, MD. Biotechnology Div.
Detection of Aromatic Compounds Based on DNA Intercalation Using an Evanescent Wave Biosensor.
Final rept.
P. C. Pandey, and H. H. Weetall. 1995, 6p.
Sponsored by Environmental Protection Agency, Washington, DC.
Pub. in Analytical Chemistry, v67 n5 p787-792, 1 Mar 95.

Keywords: *Deoxyribonucleic acids, *Biosensors, *Aromatic compounds, Reprints, Flow injection analysis, *Intercalation, Wave sensors, Fluorophore, Fluorescence radiation.

A flow injection analysis system coupled with an evanescent wave biosensor employing total international reflection of fluorescence radiation for the detection of the compounds that intercalate within DNA is reported. A highly fluorescent intercalator, ethidium bromide, has been used as the reference compounds for the detection. The evanescent wave biosensor was developed using immobilized double-strand DNA (daDNA) over the surface of a cylindrical wave guide. The response of the DNA-modified fiber is significantly higher than the responce obtained with an unmodified fiber. The response of the biosensor at a constant concentration of ethidium bromide increases on increasing the concentration of immobilized dsDNA. At the steady-state response of the biosensor, obtained at a constant concentration of ethidium bromide, there is a decrease in the response to the injection of another DNA intercalator that competes for the intercalation sites on the dsDNA, displacing the ethidium bromide. This is immediately followed by recovery of the steady-state response. The decrease in the sensor response is a linear function of the concentrations of injected intercalator. Responce curves for 9, 10-anthraquinone-2, 6-disulfonic acid, remazol brillant blue, decacyclene, and 4', 6-diamidino-2-phenylindole dihydrochloride are reported.

03,474
PB96-112040 Not available NTIS
National Inst. of Standards and Technology (CSTL), Gaithersburg, MD. Biotechnology Div.
Physicochemical Characterization of Low Molecular Weight Heparin.
Final rept.
D. Atha, B. Coxon, V. Reipa, and A. Gaigalas. 1995, 5p.
Pub. in Jnl. of Pharmaceutical Sciences, v84 n3 p360-364 Mar 95.

Keywords: *Heparin, *Light scattering, Reprints, Anticoagulants, Physicochemistry, HPLC, Raman spectroscopy.

Nuclear magnetic resonance spectroscopy (NMR), Raman spectroscopy, dynamic light scattering (DLS) and high performance exclusion chromatography (HPLC) were used to characterize two different commercial preparations of low molecular weight heparin produced by peroxide cleavage using nitrous acid. Proton NMR showed that the contamination by dermatam sulfate varied from 2% in the material produced by deaminative cleavage using nitrous acid, to 4% for the material produced by peroxide cleavage. The Raman spectra of the nitrous acid produced material showed an equivalent amount of O - sulfation to that in the material produced by peroxide, but about a 10% reduction in the content of N-sulfated glucosamine, as expected from the deamination reaction. DLS and HPLC indicated the presence of less than 0.2% of very high molecular weight/aggregate material for the peroxide preparation as compared to 1% for the nitrous acid prepared material. The weight average molecular weight (Mw) determined from HPLC was 5900 Da for the nitrous acid prepared material and 6850 Da for the peroxide produced material. The number average molecular weight (Mn) calculated from this data was 5200 Da for the nitrous acid preparation and 5300 Da for the peroxide produced material. In addition, the nitrous acid prepared material exhibited a much narrower size distribution of oligomeric species, as evidenced by the polydispersity (MwMn) of 1.1 for the nitrous acid prepared material, as compared with a value of 1.3 for the peroxide prepared material.

03,475
PB96-112305 Not available NTIS
National Inst. of Standards and Technology (MSEL), Gaithersburg, MD. Reactor Radiation Div.
Small Angle Neutron Scattering Studies of Structural Characteristics of Argarose Gels.
Final rept.
S. Krueger, A. P. Andrews, and R. Nossal. 1994, 10p.
Pub. in Biophysical Chemistry, v53 p85-94 1994.

Keywords: *Neutron scattering, *Gels, Reprints, Structural analysis, *Agarose.

The 30 m small angle neutron scattering facility at the National Institutes of Standards and Technology has been used to examine neutron scattering from agarose gels formed in D(2)O. Differential scattering cross sections have been acquired over a continuous range of Q between 0.005 and 0.3 Angstroms to the minus 1.power. Subtle changes in gel structure are observed when pre-gelation agarose concentration is varied. Similarly, except when the gelling solution is rapidly cooled to a low temperature, the rate at which the gels are formed does not seem to have much effect. Clearer evidence of structural rearrangement is observed when the solvent quality is changed by the addition of dimethyl sulfoxide, or when the temperature of the gel is elevated above 70 degrees C. These data are consistent with a description of a randomly structured polymer network containing discrete self-similar, hydrogen-bonded, junctions normally of minimal thickness = 35-40 Angstroms.

03,476
PB96-122569 Not available NTIS
National Inst. of Standards and Technology (MSEL), Gaithersburg, MD. Reactor Radiation Div.
Extending the Angular Range of Neutron Reflectivity Measurements from Planar Lipid Bilayers: Applications to a Model Biological Membrane.
Final rept.
S. Krueger, J. F. Ankner, S. K. Staija, M. Colombini, C. F. Majkrzak, and D. Gurley. 1995, 5p.
Pub. in Langmuir, v11 n8 p3218-3222 1995.

Keywords: *Lipids, *Neutron reflectivity, *Membranes, Measurement, Mitochondria, Reprints.

A novel experimental setup has been used to measure the specularly reflected neutron intensity from a model biological membrane containing components from the outer membrane of Neurospora crassa mitochondria. The specular reflectivity from a single bilayer membrane, formed by the fusion of vesicles onto a phospholipid monolayer supported on a flat substrate, was measured in both D2O and H20 solvents. In D2O solvent, reflected neutron intensities down to 10 to the minus 6 power were measured for wavevector transfers out to 0.25 A-1. A symmetric model for the neutron scattering length density profile perpendicular to the bilayer surface was constructed based on fits to the D2O data. The overall bilayer thickness was found to be 43 plus or minus 2 A. The individual lipid head group and hydrocarbon tail layer thickness were 7.5 plus or minus 1.4 and 28.0 plus or minus 2.8 A, respectively. The fitted results are consistent with the H2O data. The integrity of the model membrane bilayer was confirmed by comparing its measured reflectivity to that obtained from a single lipid bilayer consisting of soybean phospholipids (asolectin) which was deposited on a flat substrate by the Langmuir-Blodgett technique.

03,477
PB96-123344 Not available NTIS
National Inst. of Standards and Technology (CSTL), Gaithersburg, MD. Biotechnology Div.
Optical Control of Enzymatic Conversion of Sucrose to Glucose by Bacteriorhodopsin Incorporated into Self-Assembled Phosphatidylcholine Vesicles.
Final rept.
M. F. McCurley, and S. A. Glazier. 1995, 5p.
Pub. in Analytica Chimica Acta, v311 p211-215 1995.

Keywords: *Enzymatic methods, *Vesicles, Bacteriorhodopsin, Invertase, Reprints.

This report describes an alternative method to modulate enzyme activity optically through pH modulation. Bacteriorhodopsin (BR) is used to regulate the activity of an enzyme which it does not naturally regulate. In this study BR controlled the pH-dependent conversion of sucrose to glucose by the enzyme, invertase. BR is oriented in the wall of phosphatidylcholine vesicles so that at pH values greater than 4-5 it pumps protons into the vesicles and at pH values less than 4 it pumps protons out of the vesicle when illuminated with light of the proper wavelength. The bulk-solution pH correspondingly changes as a result. At an intial pH of 5.57 the change in pH of the solution due to pumping by the bacteriorhodopsin-vesicle complex was 0.17 pH units. To study this effect on the enzyme, samples containing BR vesicles and invertase were assayed for enzyme activity under dark and illuminated conditions. It was found that changes in enzyme activity, upon illumination, were generally larger than predicted for the corresponding changes in the bulk solution pH generated by the BR vesicles.

03,478
PB96-155460 Not available NTIS
National Inst. of Standards and Technology (CSTL), Gaithersburg, MD. Biotechnology Div.
Mapping Domains in Proteins: Dissection and Expression of 'Escherichia coli' Adenylyl Cyclase.
Final rept.
P. Reddy, J. Hoskins, and K. McKenney. 1995, 5p.
Pub. in Analytical Biochemistry, n231 p282-286 1995.

Keywords: Oligonucleotides, Reprints, *Protein expression, *Domains, PRE expression vector.

The authors have used the pRE expression vector containing the Escherichia coli adenylyl cyclase gene (cya) with the unique NdeI restriction site CATATG at the initiation codon in conjunction with a family of self-complimentary oligonucleotides to create amino- and carboxy-terminal domains in adenylyl cyclase. The three sets of oligonucleotides contain a TAA translation stop condon in all reading frames flanked by the NdeI restriction endonuclease sequence and one or two nucleotides (5' NNCATATGTTAATTAATTAACATATGNN 3'). Ligation of one of these annealed oliognucleotides into a restriction site or creation of 5' TAA/CATATG 3' translation stop/NdeI restriction site along a gene in the pRE expression vector facilitates the premature termination of protein synthesis thus yielding amino-terminal domains. Removal of a fragment of the gene corresponding to the amino-terminal portion by NdeI restriction and ligation brings the 3' end of the gene in frame with the initiator ATG. With this strategy, expression of the carboxyl-terminal domain of a protein is possible which is otherwise not as simple as the expression of the amino-terminal domain. The feasibility of expression of any domain of protein is demonstrated using the cya gene to create several amino- and carboxyl-terminal domains of adenylyl cyclase.

03,479
PB96-164132 Not available NTIS
National Inst. of Standards and Technology (CSTL), Gaithersburg, MD. Biotechnology Div.
Novel Activities of Human Uracil DNA N-glycosylase for Cytosine-Derived Products of Oxidative DNA Damage.
Final rept.
M. Dizdaroglu, A. Karakaya, P. Jaruga, G. Slupphaug, and H. E. Krokan. 1996, 5p.
See also PB96-110747.
Pub. in Nucleic Acids Research, v24 n3 p418-422 1996.

Keywords: *DNA damage, *Deoxyribonucleic acids, *Enzyme kinetics, Reprints, Isodialuric acid, Hydroxyl radical.

Uracil DNA N-glycosylase is a repair enzyme that releases uracil from the DNA. A major function of this enzyme is presumably to protect the genome from premutagenic uracil resulting from deamination of cytosine in DNA. Here, we report that human uracil DNA N-glycosylase also recognizes three uracil derivatives that are generated as major products of cytosine in DNA by hydroxyl radical attack or other oxidative processes. DNA substrates were prepared by y-irradiation of DNA in aerated aqueous solution and incubated with human uracil DNA N-glycosylase, heat-inactivated enzyme or buffer. Ethanol-precipitated DNA and supernatant fractions were then separated.

03,480
PB96-167226 Not available NTIS
National Inst. of Standards and Technology (CSTL), Gaithersburg, MD. Biotechnology Div.
Structural Analysis of Heparin by Raman Spectroscopy.
Final rept.
D. H. Atha, A. K. Gaigalas, and V. Reipa. 1996, 5p.
Pub. in Jnl. of Pharmaceutical Sciences, v85 n1 p52-56 Jan 96.

Keywords: *Heparin, *Raman spectroscopy, Anticoagulants, Reprints, Physicochemistry.

The Raman spectra of commercially available heparin disaccharide standards exhibit bands associated with the N-sulfate and the 6-O-sulfate groups of the glucosamine and the 2-O-sulfate of the iduronic acid. The N-sulfate has a strong band at 1039 cm to the minus one. The 6-O-sulfate and the 2-O-sulfate exhibit bands at 1055 and 1065 cm to thh minus one, respectively. The pattern of these modes, which are assigned to the symmetric SO3 vibrations, was supported by semiempirical quantum mechanical calculations. The above bands were identified in the Raman spectrum of a commercial preparation of porcine mucosal heparin and were used to determine the relative proportion of the N-sulfate, 6-O-sulfate, and 2-O-sulfate groups in the heparin molecule. The information, which is complementary to that obtained by NMR spectroscopy, is of particular importance in relation to biological activity.

03,481
PB96-167382 Not available NTIS
National Inst. of Standards and Technology (CSTL), Gaithersburg, MD. Biotechnology Div.
New Method for the Detection and Measurement of Polyaromatic Carcinogens and Related Compounds by DNA Intercalation.
Final rept.
J. J. Horvath, M. Gueguetchkeri, A. Gupta, D. Penumatchu, and H. H. Weetall. 1995, 17p.
Sponsored by Environmental Protection Agency, Research Triangle Park, NC. Atmospheric Research and Exposure Assessment Lab.
Pub. in National Meeting of the American Chemical Society (209th), Anaheim, CA., April 2-6, 1995, Biosensor and Chemical Sensor Technology, Process Monitoring and Control, ACS Symposium Series, Chapter 5, v613 p44-60.

Keywords: *Deoxyribonucleic acids, *Fluorescence, Measurement, Polarization, Reprints, *Polyaromatic carcinogens, DNA intercalation.

A simple and sensitive method for detection and quantification of carcinogens and related polyaromatic compounds by DNA intercalation has been devised. The experimental technique is based on the phenomenon of DNA intercalation using fluorescence polarization for quantitative measurements. The assay architecture is analogous to a protocol presently used for competitive immunoassays, whereby an intercalating dye of fluorochrome would compete with or be displaced by the analyte (test compound). Our competitive binding assay utilizes DNA binding sites and a fluorescent intercalating dye. The carcinogenic analytes investigated were benzo(a)pyrene, dibenz(a,h)anthracene, dibenz(a,j)anthracene, benz(a)anthracene, benzo(j)fluoranthene, benzidine, aniline, parathion, pentachlorophenol and nitrobenzene. The non-carcinogenic hydrocarbons studies were naphthalene, anthracene, phenanthrene, benzo(k)fluoranthene and 1,2,3,4,5,6,7, 8-octahydronaphthalene. The intercalating dyes examined were acridine orange, ethidium bromide, proflavin and 4,6-diamidino 2-phenylindale chloride (DAPI). Of the compounds studied, only the single ring compounds gave a negative response. All the other compounds investigated displaced the intercalated dye molecule. It has been determined that molecules require at least two adjacent benzene rings for intercalation to occur. The detection limits of this analytical method were between 10 to the minus 5th power mol/L and 10 to the minus 8 power mol/L for all materials tested.

03,482
PB96-190020 Not available NTIS
National Inst. of Standards and Technology (CSTL), Gaithersburg, MD. Analytical Chemistry Div.
Investigations of Sulfur Interferences in the Extraction of Methylmercury from Marine Tissues.
Final rept.
M. K. Behlke, P. C. Uden, and M. M. Schantz. 1996, 2p.
Pub. in Analytical Communications, v33 p91-92 Mar 96.

Keywords: *Gas chromatography, *Calibration standards, *Sulfur, Methyl compounds, Mercury(Metal), Atomic spectra, Emission, Marine biology, Tissues(Biology), Reprints.

Gas chromatography with element-specific atomic emission detection was used to investigate sulfur interferences in the quantification of methylmercury in marine tissues. The elimination of sulfur-containing species by treatment with copper powder was confirmed by sulfur-specific atomic emission detection.

03,483
PB96-200886 Not available NTIS
National Inst. of Standards and Technology (CSTL), Gaithersburg, MD. Biotechnology Div.
Quantitative Determination of Oxidative Base Damage in DNA by Stable Isotope-Dilution Mass Spectrometry.
Final rept.
M. Dizdaroglu. 1993, 6p.
Pub. in Federation of European Biochemical Societies Letter, v315 n1 p1-6 1993.

Keywords: *Radiation damage, *DNA, *Spectrometry, Free radical, Hydroxyl radical, Modified base, Reprints, *Foreign technology, Isotope-labeled analogue, Selected-ion monitoring.

For understanding of the role of oxidative DNA damage in biological processes such as mutagenesis and carcinogenesis, it is essential to identify and quantify the type of DNA damage in cells. This can be achieved by gas chromatography/mass spectrometry. The present study describes the quantification of modified bases in DNA by isotope-dilution mass spectrometry with the use of stable isotope-labeled analogues as internal standards. A number of isotopically labeled DNA bases were synthesized. The mass spectra of their trimethylsilyl derivatives were recorded. Calibration plots were obtained for known quantities of modified bases and their isotope-labeled analogues. Quantification of various modified DNA bases by isotope-dilution mass spectrometry was demonstrated in isolated chromatin exposed to ionizing radiation. The results indicate that gas chromatography/stable isotope-dilution mass spectrometry is an ideally suited technique for selective and sensitive quantification of modifed bases in DNA.

03,484
PB96-200894 Not available NTIS
National Inst. of Standards and Technology (CSTL), Gaithersburg, MD. Biotechnology Div.

Biochemistry

Commentary: The Measurement of Oxidative Damage to DNA by HPLC and GC/MS Techniques.
Final rept.
B. Halliwell, and M. Disdaroglu. 1992, 13p.
Pub. in Free Rad. Res. Comms., v16 n2 p75-87 1992.

Keywords: *DNA, *Hydroxyl radical, Singlet oxygen, Mass spectrometry, Reprints, *Foreign technology, 8-hydroxyguanine, Electro-chemical detection.

Oxidative damage to DNA has been measured by quantitating 8-hydroxy-2'-deoxyguanosine (8-OHdGuo) after enzymic digestion of DNA, followed by HPLC separation and electrochemical detection. Alternatively, 8-hydroxyguanine (and a wide range of other base-derived products of free radical attack) may be measured after acidic hydrolysis of DNA or chromatin, followed by derivatization and gas-chromatography/mass spectrometry. Both techniques have comparable sensitivity, but GC/MS enables determination of a wide variety of chemical changes to all four DNA bases and it can be applied to DNA-protein complexes. However, the two techniques do not always give similar results. Potential reasons for this are discussed. Greater attention of methodological questions is required before using measurement of 8-OHdGuo as a 'routine' marker of oxidative DNA damage in vivo.

03,485
PB96-200928 Not available NTIS
National Inst. of Standards and Technology (CSTL), Gaithersburg, MD. Biotechnology Div.
Intercomparison of DNA Sizing Ladders in Electrophoretic Separation Matrices and Their Potential for Accurate Typing of the D1S80 Locus.
Final rept.
M. C. Kline, J. W. Redman, D. J. Reeder, and D. L. Duewer. 1996, 9p.
Pub. in Applied and Theoretical Electrophoresis, v6 p33-41 1996.

Keywords: *DNA, *Separation matrices, Acrylamide, Agarose, Basepair, Genetic markers, Quantitative analysis, Reprints, Electrophoretic mobility, Polymerase chain reaction.

The 100-1,000 basepair size typical of PCR-amplified DNA fragments demands high resolution electrophoretic gels for the adequate characterization of small differences among samples. We have studied the behavior of a number of commercial sizing ladders in three ladders in three classes of separation systems: polyacrylamides with discontinuous buffer, proprietary acrylamides with continuous buffer, and agarose-like materials with continuous buffer. None of the ladders examined perform adequately in any of these systems using vendor-supplied nominal ladder component basepair sizes. All ladders successfully types D1S80 alleles after calibration with the allelic ladder (replacing the nominal size values with the least squares estimate of allele/matrix-specific apparent sizes). Some ladders and matrices are qualitatively better than others. No one ladder proved consistently better than others; a polyacrylamide gell with ribose modifier provided the most precise results in the study. Appropriate allelic ladders or a well defined subset of known alleles can serve as the calibration system.

03,486
PB97-119374 Not available NTIS
National Inst. of Standards and Technology (CSTL), Gaithersburg, MD. Biotechnology Div.
Positive and Negative Cooperativities at Subsequent Steps of Oxygenation Regulate the Allosteric Behavior of Multistate Sebacylhemoglobin.
Final rept.
R. Unger, A. Razynska, H. Kwansa, J. Collins, C. Fronticelli, M. Braxenthaler, J. Moult, X. Ji, G. Gilliland, Z. Gryczynski, and E. Bucci. 1996, 8p.
Pub. in Biochemistry, v35 p3418-3425 1996.

Keywords: *Hemoglobin, Blood proteins, Oxygenation, Regulations, Reprints, *Allosteric effectors, Oxygen affinity, Sebacylhemoglobin.

Cross-linked human hemoglobin (Hba) is obtained by reaction with bis(3,5-dibromosalicyl) sebacate. Peptide maps and crystallographic analyses confirm the presence of the 10 carbon atom long sebacyl residue cross-linking the two beta82 lysines of the beta-cleft (DecHb). The Adair's constants, obtained from the oxygen binding isotherms, show that at the first step of oxygenation normal hemoglobin and DecHb have a very similar oxygen affinity. In DecHb negative binding cooperativity is present at the second step of oxygenation, which has an affinity 27 times that of the second step. Positive cooperativity is present at the third binding step, whose affinity is 380 times that of the second step. The fourth binding step shows a weak negative cooperativity with an affinity one-half that of the third step. Crystals of deoxy-DecHb diffracted to 1.9 Angstroms resolution. The electron density map of deoxy-DecHb indicates the presence of the 10 carbon bridge between the beta82 lysines.

Botany

03,487
PB95-126280 Not available NTIS
National Inst. of Standards and Technology (NML), Gaithersburg, MD. Inorganic Analytical Research Div.
Dissolution Problems with Botanical Reference Materials.
Final rept.
R. R. Greenberg, H. M. Kingston, R. L. Watters, and K. W. Pratt. 1990, 5p.
Pub. in Fresenius Jnl. of Analytical Chemistry 338, n4 p394-398 1990.

Keywords: *Botany, *Dissolving, *Analytical techniques, *Chemical analysis, Trace elements, Absorption, Adsorption, Particulates, Leaves(Botany), Plants(Botany), Reprints, *Standard reference materials.

As part of the analytical research leading to the certification of the new Apple and Peach Leaves Standard Reference Materials (SRMs), a study was undertaken to evaluate different sample dissolution techniques for losses of analyte species. Possible loss mechanisms include absorption or adsorption of analyte elements at the walls of the sample decomposition vessels, and the formation or persistence of insoluble particulate material during sample dissolution. Results of this study indicated that significant fractions of some elements were present on particles after acid dissolution, despite visual indications that dissolution was complete. In addition, large amounts of some elements remained in the platinum crucibles used to fuse samples with lithium metaborate.

03,488
PB96-147061 Not available NTIS
National Inst. of Standards and Technology (CSTL), Gaithersburg, MD. Biotechnology Div.
Rapid Method for the Isolation of Genomic DNA from 'Aspergillus fumigatus'.
Final rept.
N. Bir, A. Paliwal, K. Muralidhar, P. Reddy, and P. Usha Sarma. 1995, 11p.
Pub. in Preparative Biochemistry, n25(4) p171-181 1995.

Keywords: *Deoxyribonucleic acids, Genomes, Diagnosis, Reprints, *Aspergillus fumigatus, Polymerase chain reaction.

A majority of Aspergillus induced diseases are reported to be caused by Aspergillus fumigatus. In immunocompromized and post transplant cases it can lead to invasive aspergillosis. Due to this the molecular fingerprinting of aspergillus isolates by RFLP analysis and development of DNA diagnostic probes are gaining importance. Different methodologies are being adopted for extraction of the genomic DNA from fungus. The existing procedures for isolation of DNA are time consuming and range from several hours to few days. The most difficult step in the isolation of DNA from aspergillus species is to disrupt the tough chitin rich cell wall without causing damage to genomic DNA. The authors report here a rapid method for extraction of genomic DNA based on the cleavage of chitin with chirinase. The subsequent modification steps included are lysis and microwave treatment.

03,489
PB96-167267 Not available NTIS
National Inst. of Standards and Technology (CSTL), Gaithersburg, MD. Inorganic Analytical Research Div.
Recent Developments in NIST Botanical SRMs.
Final rept.
D. A. Becker, and T. E. Gills. 1995, 3p.
See also PB93-153153.
Pub. in Fresenius J. Analytical Chemistry, v352 p163-165 1995.

Keywords: *Drying techniques, *Homogeneity, Reprints, *Foreign technology, *Standard reference materials, *Botanical reference materials, Jet-milling techniques, Reference material preparation, Trace element analysis.

The National Institute of Standards and Technology (NIST) (formerly the Natioanl Bureau if Standards (NBS)) issued the first botanical reference material certified for elemental content in January 1971, as Standard Reference Material (SRM) 1571, Orchard Leaves. In the following years a total of nine additional botanical certified reference materials have been issued by NIST. Each of these materials was certified for major, minor and trace elements except for SRM 2695, certified for fluorine only. Botanical SRMs issued since 1991 are significantly improved over previous materials in a number of ways. Probably the most significant change is the use of a jet-milling process to grind them to extremely fine particles. This has resulted in botanical SRMs wth significantly improved homogeneity. These NIST reference materials are described with information on homogeneity, drying techniques and grit content.

03,490
PB97-119036 Not available NTIS
National Inst. of Standards and Technology (CSTL), Gaithersburg, MD. Nuclear Methods Group.
Results of the ASTM Nuclear Methods Intercomparison on NIST Apple and Peach Leaves Standard Reference Materials.
Final rept.
D. A. Becker. 1993, 15p.
Pub. in Jnl. of Radioanalytical and Nuclear Chemistry, Articles, v168 n1 p169-183 1993.

Keywords: *Botany, *Analytical techniques, *Chemical analysis, Plants(Botany), Leaves(Botany), Trace elements, Comparisons, Absorption, Adsorption, Reprints, *Foreign technology, Standard reference materials.

The ASTM Task Group on Nuclear Methods of Chemical Analysis (E10.052.12) has conducted a trace element intercomparison among some of its members over the past two years. Eight non-NIST laboratories submitted data using nuclear techniques, with a total of 111 values for the apple leaves and 116 values for the peach leaves, on 46 to 50 elements, respectively. This intercomparison provided a unique opportunity for the analyical laboratories, because the analytical values submitted could be later compared to the NIST certified values. For the seven elements which were certified by NIST and had three or more intercomparison values, the results showed that: (1) 61% of all 56 intercomparison values submitted had results whose stated uncertainty overlapped the uncertainty limits of the NIST certified values, and (2) less than 6% of the intercomparison values had means which fell outside plus or minus 20% of the NIST values. In general, the intercomparison values submitted showed excellent agreement with the NIST values. However, many reported uncertainties accompanying intercomparison values appeared overly optimistic.

Clinical Chemistry

03,491
PB94-198579 Not available NTIS
National Inst. of Standards and Technology (CSTL), Gaithersburg, MD. Inorganic Analytical Research Div.
Regulation of Lithium and Boron Levels in Normal Human Blood: Environmental and Genetic Considerations.
Final rept.
R. M. Barr, W. B. Clarke, R. M. Clarke, R. G. Downing, J. Venturelli, and G. R. Norman. 1993, 6p.
Pub. in Jnl. of Laboratory and Clinical Medicine 121, n4 p614-619 Apr 93.

Keywords: *Lithium, *Boron, *Blood chemical analysis, *Genetics, *Environmental health, Mass spectroscopy, Carrier proteins, Water supply, Twins, Reprints.

Blood lithium levels may be both genetically and environmentally regulated. The genetic component is evidenced mainly from studies in twins who were either normal or had a manic-depressive disorder. An environmental contribution is adduced from the relationship between the blood lithium level and the amount of the element ingested. No such information is available for boron, another element present in ultra trace amounts in human blood. Unusually high levels of lithium and

boron in the waters of northern Chile offer an opportunity to study the genetic and environmental regulation of these elements in the blood of healthy subjects. Samples of blood (n = 40) and water (n = 47) were collected at seven locations in the province of Tarapaca. Most of the healthy subjects were Aymara who had been resident in the respective communities for at least 3 years. Because some of the individual subjects (n = 15) were first-degree relatives, a genetic component to the regulation of blood levels was explored. The variance in blood levels of lithium and boron was significantly greater between than within families ($p < 0.0001$). There are environmental and apparent genetic contributions to the regulation of blood levels of lithium and boron in healthy human subjects.

03,492
PB94-199379 Not available NTIS
National Inst. of Standards and Technology (NML), Gaithersburg, MD. Organic Analytical Research Div.
Determination of 3-Quinuclidinyl Benzilate (Qnb) and Its Major Metabolites in Urine by Isotope Dilution Gas Chromatography Mass Spectrometry.
Final rept.
G. D. Byrd, R. C. Paule, L. C. Sander, H. T. Bausum, L. T. Sniegoski, and E. White. 1992, 6p.
Pub. in Jnl. of Analytical Toxicology 16, n3 p182-187 1992. Sponsored by Army Medical Bioengineering Research and Development Lab., Fort Detrick, MD.

Keywords: *Urinalysis, *Quinuclidinyl benzilate, *Metabolites, *Hallucinogens, Mass fragmentography, Isotopes, Chemical analysis, Reprints, *3-Quinuclidinol, *Benzilic acid.

In response to the scheduled destruction of U. S. military stockpiles of the hallucinogenic agent 3-quinuclidinyl benzilate (BZ), a specific confirmatory test for human exposure to BZ was developed. The amount of the parent compound in the urine as well as the two major metabolites, 3-quinuclidinol (Q) and benzilic acid (BA), was determined since the exact relationship between BZ dose and levels of BZ and its metabolites in urine is not well known. BZ was determined in urine samples spiked at a target level of 0.5 ng/mL and the metabolites Ba and Q were determined at a target level of 5 ng/mL. The variabilities in the method are more or less evenly distributed between three imprecision categories (GC/MS measurement, sample preparation, and sample). The imprecision of a single measurement is about 15% for each analyte. The method developed uses solid phase extraction to isolate each analyte from the urine and isotope dilution GC/MS for quantitation. Each analyte is converted to its trimethylsilyl derivative for analysis. The analytical method was tested on 8 different urines spiked with known amounts of analytes near the target levels, at ten times the target levels, and blank (unspiked) urine samples.

03,493
PB94-200201 Not available NTIS
National Inst. of Standards and Technology (CSTL), Gaithersburg, MD. Organic Analytical Research Div.
Determination of Oltipraz in Serum by High-Performanace Liquid Chromatography with Optical Absorbance and Mass Spectrometric Detection.
Final rept.
R. G. Christensen, and W. Malone. 1992, 6p.
Pub. in Jnl. of Chromatography 584, p207-212 1992. Sponsored by National Cancer Inst., Bethesda, MD.

Keywords: *Pesticides, *Blood chemical analysis, High pressure liquid chromatography, Mass spectroscopy, Isotopes, Reference standards, Reprints, *Oltipraz.

Three methods have been developed for the analysis of Oltipraz in serum. A method suitable for routine use employs spiking with a homologous internal standard, off-line solid-phase extraction, high-performance liquid chromatographic separation, and optical absorbance detection at 450 nm. Method detection limit is about 1 ng/ml. A second method, less susceptible to bias from co-eluting interferences, uses a stable isotope-labeled internal standard, similar extraction and separation, and detection by thermospray mass spectrometry. Method detection limit is about 0.2 ng/ml. A third method was developed which can be used without specially synthesized internal standards. it uses on-line solid-phase extraction, with quantification by comparison with external standards. Method detection limit is about 3 ng/ml. Good agreement was observed between these methods and with similar and different methods run in other laboratories. Calibration curves were linear over the entire range which was investigated, i.e., up to 500 ng/ml. Coefficients of variation were similar for all three methods, being about 5%.

03,494
PB94-213493 Not available NTIS
National Inst. of Standards and Technology (CSTL), Gaithersburg, MD. Organic Analytical Research Div.
Liposome-Based Flow-Injection Immunoassay for Determining Theophylline in Serum.
Final rept.
L. Locascio-Brown, A. Plant, R. Chesler, R. Durst, M. Kroll, and M. Rudell. 1993, 6p.
Pub. in Clinical Chemistry 39, p386-391 1993.

Keywords: *Liposomes, *Flow injection analysis, *Theophylline, *Blood chemical analysis, *Immunoassay, Competitive binding, Fluorescence polarization immunoassay, Antibodies, Reprints.

We developed a method for quantitatively determining theophylline in serum, using a heterogeneous immunoassay called flow-injection immunoanalysis. The reaction involves competition between serum theophylline and theophylline-labeled liposomes. Separation occurs on a solid-phase reactor column containing immobilized antibody to theophylline incorporated in a flow-injection system. Subsequent lysis of the bound liposomes provides sensitive detection of the analyte. Effective regeneration of the immobilized antibody activity allows the reactor to be reused for hundreds of sequential samples. Comparison of the results of the flow-injection immunoassay method with results obtained with a commercially available fluorescence polarization method showed an excellent correlation.

03,495
PB94-216330 Not available NTIS
National Inst. of Standards and Technology (NML), Gaithersburg, MD. Organic Analytical Research Div.
Ascorbic and Dehydroascorbic Acids Measured in Plasma Preserved with Dithiothreitol or Metaphorphoric Acid.
Final rept.
S. A. Margolis, R. C. Paule, and R. G. Ziegler. 1990, 6p.
Pub. in Clinical Chemistry 36, n10 p1750-1755 Oct 90.

Keywords: *Ascorbic acid, *Dehydroascorbic acid, *Blood chemical analysis, *Dithiothreitol, *Blood preservation, Reference standards, pH, Temperature, Lyophilization, Accuracy, Precision, Stability, Reprints, *Metaphosphoric acid.

The accurate and precise measurement of ascorbic and dehydroascorbic acids in human plasma requires reference materials of demonstrable stability and homogeneity, and analytical methodology of demonstrable accuracy and precision. We have developed a rapid (8 min.), accurate (gravimetric and assessed values agree) and precise (CV<2%) method for ascorbic acid analysis. The stability and homogeneity of lyophilized plasma samples supplemented with ascorbic acid and dithiothreitol is sufficient for the materials to be used as control or reference materials. Plasma samples supplemented with ascorbic acid and dehydroascorbic acid, and preserved with 5% metaphosphoric acid were used to develop an assay for dehydroascorbic acid and to study the stability of both ascorbic and dehydroascorbic acid under these conditions. The assay consists of measuring the native ascorbic acid, then reducing the dehydroascorbic acid at neutral pH with dithiothreitol and measuring the total ascorbic acid. The metaphosphoric acid treated samples were shown to be stable at -70 C and the stability decreased with temperature over the range of 4 to 50 C.

03,496
PB95-108767 Not available NTIS
National Inst. of Standards and Technology (NML), Gaithersburg, MD. Gas and Particulate Science Div.
Secondary Target X-Ray Excitation for In vivo Measurement of Lead in Bone.
Final rept.
P. A. Pella, and C. G. Soares. 1991, 6p.
Sponsored by Agency for Toxic Substances and Disease Registry, Atlanta, GA.
Pub. in Advances in X-ray Analysis 34, p293-298 1991.

Keywords: *Lead(Metal), *In vivo analysis, *Toxic substances, *X-ray analysis, *Bones, Biomedical measurement, Radiation dosage, Pollution sources, Excitation, Reprints.

Secondary target x-ray excitation (L-shell) was explored for possible application in x-ray systems designed for in vivo measurement of lead in bone (e.g. tibia bone) for screening purposes. Since x-ray output from secondary targets is due mostly to characteristic x-rays and is many times lower than from direct excitation from high power tubes, it was of interest to measure the x-ray dose. This consisted of the experimental measurement of the x-ray fluorescence followed by appropriate conversion to an effective equivalent dose. Minimum detection limits were calculated using simulated bone samples (i.e. bone ash) using different instrumental configurations. An overlay of lucite was used to simulate the absorption of the skin layer.

03,497
PB95-151486 Not available NTIS
National Inst. of Standards and Technology (NML), Gaithersburg, MD. Organic Analytical Research Div.
How to Verify Reference Materials.
Final rept.
M. Welch. 1989, 4p.
Pub. in Forensic Urine Drug Testing, pp1, 5-7, Jun 89.

Keywords: *Reference standards, *Verification, *Urinalysis, *Quantitative chemical analysis, Laboratory tests, Test methods, Accuracy, Calibration, Quality control, Quality assurance, Laboratories, Reliability, Reprints.

The article describes the type of reference materials available for laboratories conducting urine drug testing. It describes how laboratories can check their standards to assure accuracy in their methods. Some description is provided on how NIST determines the purity of standard reference materials. The laboratories doing the drug testing do not have the time, facilities, or expertise to test their standards as thoroughly as is done at NIST. Some recommendations are provided concerning testing that these laboratories can and should perform on their standards.

03,498
PB95-161980 Not available NTIS
National Inst. of Standards and Technology (CSTL), Gaithersburg, MD. Biotechnology Div.
Amperometric Flow-Injection Analysis Biosensor for Glucose Based on Graphite Paste Modified with Tetracyanoquinodimethane.
Final rept.
P. C. Pandey, S. A. Glazier, and H. H. Weetall. 1993, 5p.
Pub. in Analytical Biochemistry 214, p233-237 1993.

Keywords: *Flow injection analysis, *Glucose, *Biosensors, Immobilized enzymes, Reproducibility of results, Oxidation, Reduction(Chemistry), Graphite, Blood, Humans, Reprints, *Tetracyanoquinodimethane.

A biosensor system using flow injection analysis (FIA) has been developed for the analysis of glucose in human serum. The system consists of the enzyme glucose oxidase incorporated into graphite paste modified with the electroactive material tetracyanoquinodimethane (TCNQ). Data are presented to show the effect of sample injection volume and flow rate on the response of the FIA sensor. The biosensor exhibited excellent reproducibility for 800 injections. The loss of response after 800 injections was due to leaching of TCNQ from the graphite paste. Each assay takes 3 min giving a sample throughput of 20 per hour at a flow rate of 30 ml/h. The sensor was applied to the determination of glucose in human serum. The glucose measurements are in good agreement with those of a commercially available spectrophotometric method. Data showing the effect of interfering substances, ascorbic acid and acetaminophen, on the response of the sensor are also reported.

03,499
PB95-176160 Not available NTIS
National Inst. of Standards and Technology (CSTL), Gaithersburg, MD. Organic Analytical Research Div.
Certification of Morphine and Codeine in a Human Urine Standard Reference Material.
Final rept.
S. S. C. Tai, R. G. Christensen, R. C. Paule, L. C. Sander, and M. J. Welch. 1994, 6p.
Pub. in Jnl. of Analytical Toxicology 18, p7-12 Jan/Feb 94.

Keywords: *Urinalysis, *Reference standards, *Morphine, *Codeine, *Chemical analysis, Humans, Urine, Gas chromatography, Mass spectroscopy, Test methods, Analytical techniques, Certification, Reprints, *Standard reference materials, SRM 2381.

Clinical Chemistry

The National Institute of Standards and Technology has developed and certified a Standard Reference Material, SRM 2381, for use in testing for bias in determinations of morphine and codeine in human urine. Three different analytical methods, employing GC/MS, LC/MS, and MS/MS, were used to certify the concentrations of each analyte. Results from the three methods were in good agreement and, therefore, were statistically combined to yield certified values of 138,293, and 578 ng/mL for morphine and 134,283, and 591 for codeine.

03,500
PB95-176251 Not available NTIS
National Inst. of Standards and Technology (CSTL), Gaithersburg, MD. Organic Analytical Research Div.
Interlaboratory Comparison Studies on the Analysis of Hair for Drugs of Abuse.
Final rept.
M. J. Welch, L. T. Sniegoski, and C. C. Allgood. 1993, 9p.
Contracts IAA-89-IJ-CX-A031, RA-ND-92-36
Sponsored by National Inst. of Justice, Washington, DC. and National Inst. on Drug Abuse, Rockville, MD.
Pub. in Forensic Science International 63, p295-303 1993.

Keywords: *Hair, *Drug abuse, *Test methods, *Quantitative chemical analysis, *Interlaboratory comparisons, Laboratories, Detection, Cocaine, Morphine, Gas chromatography, Mass spectroscopy, Enzyme digestion, Acid extraction, Analytical techniques, Drug users, Reprints, Benzoylecgonine.

Eleven laboratories interested in the analysis of human hair for drugs of abuse participated in a study to determine how well drugs could be detected and quantified in hair. Samples sent to the participating laboratories included hair from drug users, drug-free hair, and hair into which drugs had been soaked. For the first exercise, the hair samples were sent as powders; for the second, they were in the form of short segments. Results from these studies have shown that the laboratories, with a few exceptions, have performed very well qualitatively. Various approaches were used to liberate drugs from the hair, with the most commonly used, acid extractions and enzyme digestions, producing similar results.

03,501
PB95-176269 Not available NTIS
National Inst. of Standards and Technology (CSTL), Gaithersburg, MD. Organic Analytical Research Div.
Hair Analysis for Drugs of Abuse: Evaluation of Analytical Methods, Environmental Issues, and Development of Reference Materials.
Final rept.
M. J. Welch, L. Sniegoski, C. Allgood, and M. Habram. 1993, 10p.
Sponsored by National Inst. of Justice, Washington, DC. and National Inst. on Drug Abuse, Rockville, MD.
Pub. in Jnl. of Analytical Toxicology 17, p389-398 Nov/Dec 93.

Keywords: *Hair, *Drug users, *Quantitative chemical analysis, *Detection, *Biomarkers, *Reference standards, Cocaine, Morphine, Codeine, Drug abuse, Certification, Test methods, Analytical techniques, Gas chromatography, Mass spectroscopy, Acid extraction, Enzyme digestion, Reprints, *Standard reference materials.

Methods for extraction of cocaine, some of its metabolites, morphine, and codeine from hair and methods for analyzing the extracts have been investigated. Results of these studies have shown that extractions with 0.1N HCl are efficient at removing the target compounds from hair and appear to be as effective as enzymatic digestions that dissolve the hair. To assist laboratories in evaluating the accuracy of their methods, two human hair reference materials with recommended concentrations of cocaine, benzoylecgonine, morphine, and codeine determined by GC/MS have been developed.

03,502
PB95-200648 PC A07/MF A02
National Inst. of Standards and Technology (CSTL), Gaithersburg, MD. Organic Analytical Research Div.
Methods for Analysis of Cancer Chemopreventive Agents in Human Serum.
Special pub.
J. B. Thomas, and K. E. Sharpless. Feb 95, 136p, NIST/SP-874.
Also available from Supt. of Docs. as SN003-003-03321-9. Sponsored by National Cancer Inst., Bethesda, MD. Div. of Cancer Prevention and Control.

Keywords: *Trace elements, *Quantitative analysis, *Serums, Analytical chemistry, Neoplasms, Carotenoids, Vitamins, Blood, Plasma, Glycyrrhetinic acid, Ascorbic acid, Dehydroascorbic acid, Vitamin K, Liquid chromatography, Measurement, Quality assurance, *Chemopreventive agents, Oltipraz, 4-Hydroxyphenylretinamide.

The purpose of this manual is to summarize several years of methods development and refinement for the measurement of selected fat- and water-soluble vitamins, carotenoids, oltipraz, and glycyrrhetinic acid in serum and plasma as part of the National Institute of Standards and Technology (NIST)/National Cancer Institute (NCI) Micronutrients Measurement Quality Assurance Program. The manual is divided into six sections, each containing a series of publications pertaining to the measurement of the specified analyte(s). A summary of factors that are important to the method performance for each procedure is provided. This summary is included to help the analyst focus on the steps needed to implement each procedure.

03,503
PB96-119706 Not available NTIS
National Inst. of Standards and Technology (CSTL), Gaithersburg, MD. Organic Analytical Research Div.
History of NIST's Contributions to Development of Standard Reference Materials and Reference and Definitive Methods for Clinical Chemistry.
Final rept.
R. Schaffer, G. N. Bowers, and R. S. Melville. 1995, 7p.
Pub. in Clinical Chemistry, v41 n9 p1306-1312 1995.

Keywords: *Calibration, *Clinical chemistry, Chloride, Reprints, Cholesterol, Creatinine, Glucose, Lithium, Calcium, Standard Reference Materials, National Institute of Standards and Technology.

The issuance of cholesterol as a Standard Reference Material (SRM) in 1967 started the National Institute of Standards and Technology (NIST; then named the National Bureau of Standards) on a major effort to help clinical laboratories establish and improve the quality of measurements they make. NIST now issues three kinds of SRMs for that purpose: analyte samples of certified purity as primary standards, serum samples having certified analyte concentrations as accuracy controls, and materials certified for calibrating instruments. In working with clinical laboratory scientists to establish Reference Methods (RMs) for measuring the analytes NIST developed Definitive Methods (DMs) to use for evaluating RM accuracy and then used the DMs for assigning analyte values to its SRMs. The development of SRMs and DMs is discussed.

03,504
PB96-120555 PC A18/MF A04
National Inst. on Drug Abuse, Rockville, MD.
Hair Testing for Drugs of Abuse: International Research on Standards and Technology.
E. J. Cone, M. J. Welch, and M. B. G. Babecki. 1995, 412p, NIH/PUB-95-3727.
Prepared in cooperation with National Inst. of Standards and Technology, Gaithersburg, MD.

Keywords: *Hair, *Drug users, *Quantitative chemical analysis, Detection, Certification, Test methods, Analytical techniques, Gas chromatography, Mass spectroscopy, Acid extraction, Enzyme digestion, *Standard reference materials.

Partial Contents:
- Introduction and Overview:
- National Institute on Drug Abuse Special Publication on Hair Analysis for Drugs of Abuse;
- Mechanisms of Incorporation of Drugs Into Hair and the Interpretation of Hair Analysis Data;
- How Environmental Drug Exposure Can Affect Hair Testing for Drugs of Abuse;
- Testing Human Hair for Opiates and Cocaine by Gas Chromatography/Mass Spectrometry After Acid or Enzyme Hydrolysis;
- Capillary Electrophoresis:
- A Novel Tool for Toxicological Investigation:
- Its Potential in the Analysis of Body Fluids and Hair;
- Comparison of Different Extraction Procedures for Drugs in Hair of Drug Addicts;
- Human Scalp Hair as Biopsy Material Suitable for Quantitative Analysis in Therapeutic Drug Monitoring;
- Neonatal Hair Analysis:
- A Tool for the Assessment of In Utero Exposure to Drugs.

03,505
PB96-123807 Not available NTIS
National Inst. of Standards and Technology (CSTL), Gaithersburg, MD. Organic Analytical Research Div.
NIST Reference Materials to Support Accuracy in Drug Testing.
Final rept.
M. J. Welch, P. Ellerbe, S. S. C. Tai, L. C. Sander, C. S. Phinney, R. G. Christensen, and L. T. Sniegoski. 1995, 5p.
Pub. in Fresenius Jnl. of Analytical Chemistry, v352 p61-65 1995.

Keywords: *Drug abuse, *Reference standards, *Quantitative chemical analysis, *Detection, Hair, Urinalysis, Drug users, Interlaboratory comparisons, Accuracy, Quality assurance, Test methods, Analytical techniques, Cocaine, Morphine, Marijuana, Codeine, Mass spectroscopy, Gas chromatography, Reprints, Standard reference materials.

The National Institute of Standards and Technology (NIST) supports accuracy in drugs of abuse testing by proving Standard Reference Materials (SRMs) with certified concentrations of drugs of abuse in urine- and hair-based reference materials. NIST, working in collaboration with the College of American Pathologist (CAP), has developed urine-based SRMs for marijuana metobolite, cocaine metabolite, morphine and codeine, and morphine glucuronide and CAP Reference Materials for amphetamines and phencyclidine. Certification measurements performed at NIST involve two independent methods for each analyte, one of which always uses GC/MS with the other usually being an LC method with either MS or UV detection. Work has recently been completed on a seven component drug in urine SRM. In addition NIST conducts research in the analysis of hair for drugs of abuse. To assist laboratories testing hair for that purpose, NIST has developed two drugs in hair reference materials.

03,506
PB96-138425 Not available NTIS
National Inst. of Standards and Technology (CSTL), Gaithersburg, MD. Organic Analytical Research Div.
Determination of Vitamin K1 in Serum Using Catalytic-Reduction Liquid Chromatography with Fluorescence Detection.
Final rept.
W. A. MacCrehan, and E. Schonberger. 1995, 9p.
Pub. in Jnl. of Chromatography B, Biomedical Applications, v670 p209-217 1995.

Keywords: *Vitamin K, *Fluorescence detection, *Chromatography, Phylloquinone, Reverse phase separation, Solid phase fractionation, Reprints.

A new method for the liquid chromatographic-fluorescene determination of serum vitamin K, is described using reduction of the K-quinone to the fluorescent K-hydroquinone. The reduction reaction occurs 'on-line' in the LC system using a catalytic reducer column and an alcohol mobile phase as reductant. A procedure for serum determination utilizes a liquid-liquid serum lipid extraction followed by normal-phase fractionation on a solid-phase extraction cartridge. The final measurement uses a reversed phase (C18) seperation with a ethanol-methanol mobile phase and provides a detection limit of approximately 20 pg/ml.

03,507
PB96-159785 Not available NTIS
National Inst. of Standards and Technology (CSTL), Gaithersburg, MD. Inorganic Analytical Research Div.
Development of a Standard Reference Material for ISE Measurements of Sodium and Potassium.
Final rept.
W. F. Koch, and R. C. Paule. 1989, 10p.
Pub. in IFCC Workshop, Stresa 1988, v10 p99-108 1989.

Keywords: *Blood, *Ion selective electrodes, Potassium, Reprints, Potentiometry, Serium, Sodium, Ultrafiltration, *Interlaboratory test, Standard Reference Material.

A research project, sponsored by the National Committee for Clinical Laboratory Standards and funded by eight manufacturers of clinical potentiometric instruments, is being conducted in the Electroanalytical Research Group at the National Institute of Standards and Technology (NIST, formerly NBS). The goal of this research is to bring conformity to the direct potentiometric measurements of sodium and potassium in human serum through the development of ref-

erence materials. Currently, different manufacturers of clinical analyzers each recommend their own calibration standards. These materials range from simple aqueous solutions to complex mixtures containing bovine serum albumin. Hence, different electrolyte values for the same sample of human serum analyzed by different instruments are not uncommon. A series of four interlaboratory tests has been carried out to quantify the problem and to identify the most suitable reference materials. Ideally, an accurate calibration standard should simulate the actual sample to minimize the effects of liquid junction, activity, protein volume, and other factors that affect the electrode potential. It also should also be easy to prepare in large quantities, be stable for long periods, and be convenient to use in hospital laboratory environment.

03,508
PB96-160692 Not available NTIS
National Inst. of Standards and Technology (CSTL), Gaithersburg, MD. Organic Analytical Research Div.
Certification of Phencyclidine in Lyophilized Human Urine Reference Materials.
Final rept.
S. S. C. Tai, R. G. Christensen, K. Coakley, M. J. Welch, P. Ellerbe, and T. Long. 1996, 7p.
Pub. in Jnl. of Analytical Toxicology, v20 p43-49 Jan/Feb 96.

Keywords: *Drug abuse, *Calibration standards, *Quantitative chemical analysis, *Urine, Concentration(Composition), Test methods, Spectroscopic analysis, Chromatographic analysis, Certification, Interlaboratory comparisions, Reprints, PCP(Phencyclidine), SEM 1511, CAP PCP RM.

The Natioanl Institute of Standards and Technology (formerly the National Bureau of Standards), in cooperation with the College of American Pathologists (CAP), has certified the concentrations of phencyclidine (PCP) in two new reference materials (RMs). One of these materials is Standard possibility of undetected bias, two independent analytical methods, employing gas chromatography-mass spectrometry and liquid chromatography-mass spectrometry and liquid chromatography-mass spectrometry, were used to certify PCP in these materials. Results from the two methods were in good agreement and were statistically combined to yield certified values.

03,509
PB97-110449 Not available NTIS
National Inst. of Standards and Technology (CSTL), Gaithersburg, MD. Analytical Chemistry Div.
Interlaboratory Studies on the Analysis of Hair for Drugs of Abuse: Results from the Fifth Exercise.
Final rept.
M. J. Welch, and L. T. Sniegoski. 1996, 19p.
See also PB95-176251.
Pub. in Forensic Science International, p1-19 1996.

Keywords: *Hair, *Drug abuse, *Test methods, *Quantitative chemical analysis, *Interlaboratory comparisons, Laboratories, Detection, Cocaine, Morphine, Gas chromatography, Mass spectroscopy, Reprints, *Foreign technology.

Fourteen laboratories interested in the analysis of human hair for drugs of abuse participated in a fifth interlaboratory study to determine how well drugs could be detected and quantified in hair. The drugs of above included cocaine, benzoylecgonine, cocaethylene, codeine, morphine, and 6-monoacetylmorphine. The size hair samples analyzed included three in the form of short segments and three in a powder form and included hair from drug users, drug-fortified hair (drug-free hair into which drugs had been soaked), and drug-free hair. Results from the study show that the laboratories performed well qualitatively, particularly for drug levels above 0.5 ng/mg. While there was significant scatter in quantitative results, results were less scattered overall than had been seen previously. Various methods were used to extract the drugs from the hair, and the most commonly used approaches (i.e., acid extraction, methanol extractions, and enzyme digestions) have comparable results. For analysis of the extracts, gas chromatography/mass spectrometry (GC/MS) was used by all but one laboratory, which used a radioimmunoassay (RIA). Of the laboratories using GC/MS, some produced consistently good results, while others produced poorer quality results.

03,510
PB97-111322 Not available NTIS
National Inst. of Standards and Technology (CSTL), Gaithersburg, MD. Analytical Chemistry Div.
Interlaboratory Studies on the Analysis of Hair for Drugs of Abuse: Results from the Fourth Exercise.
Final rept.
L. T. Sniegoski, and M. J. Welch. 1996, 6p.
Pub. in Jnl. of Analytical Toxicology, v20 p242-247 Jul/Aug 96.

Keywords: *Drug abuse, *Reference materials, *Quantitative chemical analysis, *Detection, *Hair, Drug users, Interlaboratory comparisons, Accuracy, Quality assurance, Test methods, Analytical techniques, Cocaine, Morphine, Codeine, Mass spectroscopy, Gas chromatography, Reprints, Benzoylecgonine, Cocaethylene, Monoacetylmorphine.

Fourteen laboratories interested in the analysis of human hair for drugs of abuse participated in a fourth interlaboratory study to determine how well drugs could be detected and quantitated in hair. The drugs of abuse included cocaine, benzoylecgonine, cocaethylene, codeine, morphine, and 6-monoacetylmorphine. The hair samples analyzed were in the form of short segments and included hair from drug users, soaked hair (drug-free hair into which drugs had been soaked), and drug-free hair. Results from the study show that the laboratories performed well qualitatively, but that there was a large amount of scatter in quantitative results.

03,511
PB97-112445 Not available NTIS
National Inst. of Standards and Technology (CSTL), Gaithersburg, MD. Analytical Chemistry Div.
Measurement of Ascorbic Acid in Human Plasma and Serum: Stability, Intralaboratory Repeatability, and Interlaboratory Reproducibility.
Final rept.
S. A. Margolis, and D. L. Duewer. 1996, 6p.
See also PB92-154442.
Pub. in Clinical Chemistry, v42 n8 p1257-1262 1996.

Keywords: *Ascorbic acid, *Blood chemical analysis, *Metaphosphoric acid, Blood plasma, Bias, Dithiothreitol, Liquid chromatography, Repeatability, Reproducibility, Reprints.

The authors demonstrate that total ascorbic acid (TAA, the sum of ascorbic acid and dehydroascorbic acid) in property prepared human plasma is stable at -70 degrees C for at least 6 years when preserved with dithiothreitol. TAA in human plasma or serum preserved with metaphosphoric acid degrades slowly, at the rate of no more than 1% per year. As assessed from the stability data and from data obtained from 23 laboratories over a period of greater than 2 years, the intralaboratory repeatability of TAA measurements is approximately 2 micromol/L, irrespective of TAA concentration. Nonchromatographic analytical methods involving dinitrophenylhydrazine and o-phenylenediamine yield biased results relative to chromatographic methods.

03,512
PB97-119333 Not available NTIS
National Inst. of Standards and Technology (CSTL), Gaithersburg, MD. Analytical Chemistry Div.
Liquid Chromatographic Determination of Carotenoids in Human Serum Using an Engineered C30 and a C18 Stationary Phase.
Final rept.
K. E. Sharpless, T. J. Brown, L. C. Sander, and S. A. Wise. 1996, 9p.
Pub. in Jnl. of Chromatography B: Biomedical Applications, v678 p187-195 Oct 96.

Keywords: *Trace elements, *Serums, *Quantitative analysis, Carotenoids, Liquid chromatography, Blood, Plamsa, Carbon, Reprints, *Chemopreventive agents.

A C30 stationary phase was specifically engineered for carotenoid separations, and carotenoid measurements using this column are compared with those obtained using a somewhat more conventional C18 column. Both methods were used to contribute measurements for the certification of carotenoids in Standard Reference Material 968b, Fat-Soluble Vitamins and Cholesterol in Human Serum. Analytes were extracted from the serum into hexane. Measurements on the C18 column were made using a gradient of acetonitrile, methanol, and ethyl acetate, which is described in detail elsewhere. Measurements on the C30 column were made using a graident of water, methanol, and methyl tert.-butyl ether.

Clinical Medicine

03,513
AD-A279 120/0 PC A04/MF A01
National Bureau of Standards, Gaithersburg, MD.
Report of the International Commission on Radiological Units and Measurements (ICRU), 1956.
10 Apr 57, 53p.

Keywords: *Radiology, *Measurement, *Handbooks, *Radiation dosage, *Radiation measuring instruments, Dose rate, Dosimetry, Radiation protection, Materials, Health physics instrumentation, ICRU(International Commissionon Radiological Units).

No abstract available.

03,514
PB94-185642 Not available NTIS
National Inst. of Standards and Technology (PL), Gaithersburg, MD. Ionizing Radiation Div.
Use of a Radiochromic Detector for the Determination of Stereotactic Radiosurgery Dose Characteristics.
Final rept.
W. L. McLaughlin, C. G. Soares, J. A. Sayeg, A. Wu, A. H. Maitz, E. C. McCullough, and R. W. Kline. 1994, 10p.
Pub. in Med. Phys. 21, n3 p379-388 Mar 94.

Keywords: *Radiosurgery, *Radiotherapy dosage, *Detectors, Gamma rays, Densitometry, Lasers, Quality control, Precision, Resolution, Dosimetry, Reprints, *Radiochromic films.

The measurement of absorbed dose as well as dose distributions (profiles and isodose curves) for small radiation fields (as encountered in stereotactic surgery) has been difficult due to the usual large detector size or densitometer aperture (> 1 mm) relative to the radiation field (as small as 4 mm). The radiochromic direct-imaging film, when read with a scanning laser microdensitometer (laser beam diameter 0.1 mm), overcomes this difficulty and has advantages over conventional film in providing improved precision, better tissue equivalence, greater dynamic range, higher spatial resolution, and room light handling. As a demonstration of suitability, the calibrated radiochromic film has been used to measure the dose characteristics for the 18-, 14-, 8-, and 4-mm fields from the gamma-ray stereotactic surgery units at the Mayo Clinic and the University of Pittsburgh. Intercomparisons of radiochromic film with conventional methods of dosimetry and vendor-supplied computational dose planning system values indicate agreement to within + or - 2%. The dose, dose profiles, and isodose curves obtained with radiochromic film can provide high-spatial-resolution information of value for acceptance testing and quality control of dose measurement and/or calculation.

03,515
PB94-198470 Not available NTIS
National Inst. of Standards and Technology (NML), Gaithersburg, MD. Organic Analytical Research Div.
Nutritional Status and Growth in Juvenile Rheumatoid Arthritis.
Final rept.
M. C. Bacon, P. H. White, D. J. Raiten, O. A. Levander, M. L. Taylor, R. N. Lipnick, S. Sami, N. Craft, and S. Margolis. 1990, 10p.
Pub. in Seminars in Arthritis and Rheumatism 20, n2 p97-106 1990.

Keywords: *Nutrition, *Growth abnormalities, Reprints, Anthropometry, Biochemistry, Vitamin and mineral preparations, Blood proteins, Nutritional requirements, *Juvenile rheumatoid arthritis.

Juvenile rheumatoid arthristis (JRA) has been associated with short stature. However, the specific cause is unknown. One hypothesis is that altered growth is due to inadequate nutrition. The authors looked at 34 children with JRA and 9 healthy controls using 3-day diet records, anthropometric measures and biochemical analysis of plasma protein, vitamin and mineral levels. The children with JRA were compared between groups according to type of JRA: systemic, polyarticular and pauciarticular. Significant differences in growth and biochemical status were found. Those with polyarticular or systemic types of JRA had lower levels of zinc, vitamins A and C, and retinol binding protein. No direct relationship between intake and plasma levels of nutrients was found. However, alterations in nutritional needs according to disease type and severity could not be ruled out.

03,516
PB94-198827 Not available NTIS
National Inst. of Standards and Technology (NML), Gaithersburg, MD. Ionizing Radiation Div.
Standard Reference Materials (SRM's) for Measuring Genetic Damage.
Final rept.
D. S. Bergtold, E. Holwitt, and M. G. Simic. 1990, 3p.
Pub. in Fresenius Jnl. of Analytical Chemistry 338, n4 p383-385 1990.

Keywords: *DNA damage, *Radiotherapy, Biological markers, Reprints, *Standard reference materials, Hydroxyl radical, Thymine glycol, Thymidine glycol.

Standard reference materials (SRM's) were designed for the measurement of radiolytic products resulting from OH radical reaction with DNA in patients treated by radiation therapy. Deuterated thymine glycol and thymidine glycol are proposed as such SRM's; the synthesis of the former is described in detail. They might be of importance for optimizing the therapy.

03,517
PB94-219227 (Order as PB94-219219, PC A06/MF A02)
National Inst. of Standards and Technology, Gaithersburg, MD.
Sealed Water Calorimeter for Measuring Absorbed Dose.
S. R. Domen. 1994, 21p.
Included in Jnl. of Research of the National Institute of Standards and Technology, v99 n2 p121-141 Mar/Apr 94.

Keywords: *Calorimeters, *Radiation doses, *Water, Dissolved gases, Calorimetric dosemeters, Measuring instruments, Temperature effects, Thermistors, Exothermic reactions, Endothermic reactions, Heat defect, Convective barrier, National Institute of Standards and Technology.

The sealed water calorimeter is intended for direct measurement of absorbed dose to water. This calorimeter was used for a series of approximately 3700 measurements to investigate the so-called heat defect, that is, anomalous endothermic or exothermic effects caused by dissolved gases. The three systems investigated were high-purity water saturated with N2, H2, and mixtures of H2/O2. The repeatability of measurements of absorbed dose rates for the (60)Co teletherapy beam was studied with different water fillings and accumulated absorbed dose. Measurements with the H2/O2 system varied with accumulated absorbed dose. Based on the measurements and theoretical considerations, it appears that the H2-saturated system is the best choice for eliminating the heat defect. Measurements with both the N2- and H2-saturated systems are in good agreement with those determined with a graphite and graphite-water calorimeter (for which there is no heat defect).

03,518
PB95-164604 Not available NTIS
National Inst. of Standards and Technology (PL), Gaithersburg, MD. Ionizing Radiation Div.
Measurement of Radial Dose Distributions Around Small Beta Particle Emitters Using High Resolution Radiochromic Foil Dosimetry.
Final rept.
C. G. Soares, and W. L. McLaughlin. 1993, 6p.
Pub. in Radiation Protection Dosimetry 47, n1/4 p367-372 1993.

Keywords: *Radiation doses, *Beta particles, *Ophthalmology, Calibrating, Densitometry, Dosimetry, Strontium 90, Yttrium 90, Cobalt 60, Thulium 170, Reprints, *Radiochromic foils.

A method is described for the direct measurement of the radial dose distributions around small (from several mm down to tens of micrometers in diameter) beta particle emitters. The method employs the high resolution readout of radiochromic dye foils. These foils form a blue image upon irradiation and require no processing to stabilize the image. The color change (in units of absorbance) is nearly linear with absorbed dose over a range of 10 Gy to 1000 Gy and the response to electrons is nearly identical to (60)Co gamma radiation which makes the system easy to calibrate. Readout is performed with a laser scanning densitometer with a 100 micrometer spot size which can be stepped in increments of 40 micrometers in two dimensions. Examples of the results of measurements of (90)Sr/(90)Y eye applicators as well as particle sources of (90)Sr/(90)Y, (60)Co, and (170)Tm are given.

03,519
PB96-102280 Not available NTIS
National Inst. of Standards and Technology (CSTL), Gaithersburg, MD. Analytical Chemistry Div.
Isotope Dilution Mass Spectrometry as a Candidate Definitive Method for Determining Total Glycerides and Triglycerides in Serum.
Final rept.
P. Ellerbe, L. T. Sniegoski, and M. J. Welch. 1995, 8p.
Pub. in Clinical Chemistry, v41 n3 p397-404 1995.

Keywords: *Isotope dilution, *Mass spectrometers, *Glycerol, *Cholesterol, Triglycerides, Isotope ratio, Test methods, Tracer techniques, Isotope applications, Gas chromatography, Blood serum, Humans, Reprints.

A new isotope dilution mass spectrometric method for total glycerides and triglycerides in human serum is described. Total glycerides are defined as the sum of tri-, di-, and monoglycerides plus free glycerol; triglycerides are defined as the pure triglyceride species. In both determinations, serum samples are supplemented by additon of (13C3) tripalmitin, processed, derivatized, and the abundance ratios of selected ions are determined. The CV for a single measurement ranged from 0.35% to 0.72%, and the relative SEM ranged from 0.10% to 0.34%; there was no significant bias in the measurements. The combination of high precision and absence of significant bias in the results qualify this method for consideration as a Definitive Method as defined by the National Committee for Clinical Laboratory Standards.

03,520
PB96-179486 Not available NTIS
National Inst. of Standards and Technology (EEEL), Gaithersburg, MD. Electronics and Electrical Engineering Lab. Office.
Preliminary Investigation of Oleoresin Capsicum.
Final rept.
R. G. Christensen, and D. E. Frank. 1995, 20p.
Sponsored by National Inst. of Justice, Washington, DC.
Pub. in Preliminary Investigation of Oleoresin Capsicum, NIJ Report 100-95, 20p, 15 Apr 95.

Keywords: *Medicinal plants, *Peppers, *Oleoresins, Chemical composition, Toxicity, Reprints.

This report documents a preliminary investigation into the anlaytical characterization of Oleoresin Capsicum (OC), an oily extract of hot peppers that is increasingly used in law enforcement applications. Being a natural product, it is subject to variations in composition. The characteristic hot sensation or pungency is quantified in the industry in terms of 'Scoville Heat Units,' (SU). SU is defined as the dilution at which the pungency can barely be detected by a trained taster. Pure capsaicin, the most pungent constituent, has an SU value of 16 times 10 to the sixth power mL/g (milliliters of diluent per gram of base material). Recently, OC has come into use as a pain-producing agent in aerosol sprays used in an attempt to subdue violent individuals. This use raises the question of how to assign an objective index of potency to these sprays. Published information on the pharmacology of capsaicinoid compounds has been studied to examine correlations between pungency and pain production. Experiments in the analytical chemistry of OC have been carried out to check the feasibility of determining the concentrations of the pungent constituents.

03,521
PB97-110092 Not available NTIS
National Inst. of Standards and Technology (PL), Gaithersburg, MD. Ionizing Radiation Div.
Needs for Brachytherapy Source Calibrations in the United States.
Final rept.
B. M. Coursey, L. J. Goodman, D. D. Hoppes, C. G. Soares, J. T. Weaver, R. Loevinger, and W. L. McLaughlin. 1992, 5p.
Pub. in Nuclear Instruments and Methods in Physics Research, vA312 p246-250 1992.

Keywords: *Brachytherapy, *Dosimetry, *Gamma rays, Radiation, Radionuclides, Standards, Therapy, Reprints, *Foreign technology.

Brachytherapy sources of beta and gamma radiation ('brachy' is from the Greek, meaning 'near') have a long history of use in interstitial, intracavitary, intraluminal, and ocular radiation therapy. In the past the US national standards for these sources were often specified in activity of milligram radium equivalent. With the introduction of new radionuclide sources to replace radium. Source strength calibrations are now expressed as air kerma rate at a meter. In the paper, the authors review the NIST standards for brachytherapy sources, list some of the common radionuclides and source encapsulations in use in the US radiology community, and describe the latest NIST work, in collaroation with several US medical institutions, on a method of two-and three-dimensional dose mapping of brachytherapy sources using radiochromic films.

03,522
PB97-110100 Not available NTIS
National Inst. of Standards and Technology (PL), Gaithersburg, MD. Ionizing Radiation Div.
Radioassays of Yttrium-90 Used in Nuclear Medicine.
Final rept.
B. M. Coursey, J. M. Calhoun, and J. T. Cessna. 1993, 7p.
Pub. in International Jnl. of Nuclear Medicine and Biology, v20 p693-699 1993.

Keywords: *Nuclear medicine, *Radioassays, Standards, Liquid scintillation, Gamma counters, Dose calibrators, Reprints, *Foreign technology, *Yttrium-90, Cerenkov counting.

Yttrium-90 radioassays are required in nuclear medicine at the gigabecquerel activity level (Gbq) for measuring injected activity, and at the becquerel level for measuring individual tissue samples in biodistribution studies. A method of standardizing 90Y for activity using high-efficiency liquid-scintillation counting is described. Solution standards were used to establish the calibration factors for commercial radionuclide-calibrators. Detection efficiencies are also presented for liquid-scintillation counting. NaI(Ti) bremsstrahlung counting and Cerenkov counting.

03,523
PB97-110159 Not available NTIS
National Inst. of Standards and Technology (PL), Gaithersburg, MD. Ionizing Radiation Div.
Problem of Convection in the Water Absorbed Dose Calorimeter.
Final rept.
S. R. Domen, A. Krauss, and M. Roos. 1991, 9p.
Pub. in Thermochimica Acta, v187 p225-233 1991.

Keywords: *Absorbed dose, *Calorimeters, *Convection, Convective barrier, Convective cooling, Thermistor water, Reprints, *Foreign technology.

The water absorbed dose calorimeter allows the water absorbed dose, the measure and in radiotherapy, to be measured in accordance with its definition. Its application, however, requires the suppression convection. In the present paper the authors investigate how far the convection problem may be solved by mechanical means, for the case of 60C-gamma radiation.

Cytology, Genetics, & Molecular Biology

03,524
PB94-172319 Not available NTIS
National Inst. of Standards and Technology (CSTL), Gaithersburg, MD. Biotechnology Div.
beta-D-Glucosyl-Hydroxymethyluracil: A Novel Modified Base Present in the DNA of the Parastic Protozoan T. brucei.
Final rept.
J. Gommers-Ampt, F. Van Leeuwen, A. de Beer, J. Kowalak, P. Crain, P. Borst, J. Vliegenthart, and M. Dizdaroglu. 1993, 8p.
Pub. in Cell 75, p1129-1136, 17 Dec 93.

Keywords: *Protozoan DNA, *Trypanosoma brucei, *Nucleotides, Surface antigens, Gene expression, Telomere, Reprints, *Uracil/5-((beta-D-glycopyranosyl oxy)-methyl).

We have previously shown that the DNA of the unicellular eukaryote T. brucei contains about 0.1% of a novel modified base, called J. The presence of J correlates with a DNA modification associated with the silencing of telomeric expression sites for the variant sur-

face antigens of trypanosomes. Here we show that J is 5-((beta-D-glucopyranosyloxy)-methyl)-uracil (shortened to beta-D-glucosyl-hydroxymethyluracil), a base not previously found in DNA. We discuss putative pathways for the introduction of this base modification at specific positions in the DNA and the possible contribution of this modification to repression of surface antigen gene expression.

03,525
PB94-199825 Not available NTIS
National Inst. of Standards and Technology (CSTL), Gaithersburg, MD. Biotechnology Div.
Oxidative Damage to DNA in Mammalian Chromatin.
Final rept.
M. Dizdaroglu. 1992, 12p.
Pub. in Mutation Research 275, p331-342 1992. Sponsored by Department of Energy, Washington, DC.

Keywords: *DNA damage, *Chromatin, Mammals, Ionizing radiation, Hydrogen peroxide, Toxicology, Mass fragmentography, Cross-linking reagents, Cultured cells, In vivo analysis, In vitro analysis, Reprints.

Efforts have been made to characterize and measure DNA modifications produced in mammalian chromatin in vitro and in vivo by a variety of free radical-producing systems. Methodologies incorporating the technique of gas chromatography/mass spectrometry have been used for this purpose. A number of products from all four DNA bases and several DNA-protein cross-links in isolated chromatin have been identified and quantitated. Product formation has been shown to depend on the free radical-producing system and the presence or absence of oxygen. A similar pattern of DNA modifications has also been observed in chromatin of cultured mammalian cells treated with ionizing radiation or H2O2 and in chromatin of organs of animals treated with carcinogenic metal salts.

03,526
PB94-199833 Not available NTIS
National Inst. of Standards and Technology (CSTL), Gaithersburg, MD. Biotechnology Div.
Modification of DNA Bases in Chromatin of Intact Target Human Cells by Activated Human Polymorphonuclear Leukocytes.
Final rept.
M. Dizdaroglu, R. Olinski, J. Doroshow, and S. Akman. 1993, 4p.
Pub. in Cancer Research 53, p1269-1272, 15 Mar 93.

Keywords: *DNA damage, *Tetradecanoylphorbol acetate, *Pharmacology, *Chromatin, *Leukocytes, Hydroxy compounds, Deoxyribonucleic acids, Mass fragmentography, Guanine, Adenine, Free radicals, In vivo analysis, Reprints.

The authors investigated whether phorbol-12-acetate-13-myristate (PMA)-activated human polymorphonuclear leukocytes (PMNs) induce base modifications in target cell DNA in vivo. Human PMNs produced 9.4 + or - 0.8 (SD) nmol of H2O2/10 to the sixth power cells during 50 min of exposue to 2 micrograms/ml PMA and 13.7 + or - 2.8 nmol/10 to the sixth power cells during exposure to PMA plus 5 mM NaN3. Neither nonstimulated PMNs, nor PMA alone, nor NaN3 alone induced base modifications in chromatin-associated DNA of human Ad293 cells above control levels, when assayed by gas chromatography/mass spectrometry with selected-ion monitoring, However, a 60-min exposure to 1.7 + or - 0.4 times 10 to the sixth power PMNs/ml in the presence of 2 micrograms/ml PMA induced a 2-3-fold increase in the level of all modified bases detected by gas chromatography/mass spectrometry with selected-ion monitoring. The guanine-derived products 8-hydroxyguanine and 2,6-diamino-4-hydroxy-5-formamidopyrimidine, and the adenine-derived product 4,6-diamino-5-formamidopyrimidine were induced to the highest levels among those bases detected. These data demonstrate that exposure to activated PMNs causes DNA base modifications in target cells in vivo typical of those induced by hydroxyl radical attack. The induction of potentially promutagenic modified bases may contribute to the mutagenicity of activated PMNs.

03,527
PB94-200375 Not available NTIS
National Inst. of Standards and Technology (CSTL), Boulder, CO. Biotechnology Div.
Salt-PEG Two-Phase Aqueous Systems to Purify Proteins and Nucleic Acid Mixtures.
Final rept.
K. D. Cole. 1992, 12p.
Pub. in Proceedings of Frontiers in Biochemistry II, Boulder, CO., June 17-21, 1990, p340-351 1992.

Keywords: *Proteins, *Nucleic acids, *Purification, Deoxyribonucleic acids, pH, Polyethylene glycols, Salts, Molecular weight, Protein denaturation, Reprints.

This paper examines the effect of variables on protein and nucleic acid partitioning in aqueous two-phase extraction systems composed of salt and polyethylene glycol (PEG). The variables that can be changed in these systems include: pH, PEG concentration, PEG molecular mass, salt type, salt concentration and addition of protein denaturants such as chaotropic salts and detergents. Methods for the preparation of high molecular mass DNA from crude mixtures are described. These methods offer the advantages of simplicity, speed and use of nontoxic materials.

03,528
PB94-216322 Not available NTIS
National Inst. of Standards and Technology (CSTL), Gaithersburg, MD. Organic Analytical Research Div.
Hydrolysis of Proteins by Microwave Energy.
Final rept.
S. A. Margolis, L. Jassie, and H. M. Kingston. 1991, 3p.
Pub. in Jnl. of Automatic Chemistry 13, n3 p93-95 May/Jun 91.

Keywords: *Bovine serum albumin, *Hydrolysis, *Microwaves, Valine, Isoleucine, Automation, Reprints.

Microwave energy, at manually-adjusted, partial power settings has been used to hydrolyze bovine serum albumin at 125 C. Hydrolysis was complete within 2 h, except for valine and isoleucine which were completely liberated within 4 h. The amino acid destruction was less than that observed at similar hydrolysis conditions with other methods and complete hydrolysis was achieved more rapidly. These results provide a basis for automating the process of amino acid hydrolysis.

03,529
PB95-150793 Not available NTIS
National Inst. of Standards and Technology (CSTL), Gaithersburg, MD. Biotechnology Div.
Application of Thermodynamics to Biotechnology.
Final rept.
Y. B. Tewari, and R. N. Goldberg. 1991, 10p.
Pub. in Proceedings of International Enzyme Biotechnology Symposium, Veracruz, Mexico, October 1991, p1-10.

Keywords: *Thermodynamics, *Biotechnology, Temperature, Osmolar concentration, Heat, Enthalpy, Gibbs free energy, Chemical reactions, Reprints.

High product yield is important for the successful commercialization of any chemical reaction. The factors influencing the product yields are temperature, ionic strength, pH, and the concentrations of the substrates and cofactors. Thermodynamics plays an important role in understanding the interrelationships between these various factors. Thus, a knowledge of the Gibbs energy, enthalpy, and heat capacity change can be used to calculate the optimal product yield. This, in turn, is important in assessing the economic viability of the reaction. Thermodynamic data also provides the amount of heat evolved or absorbed in a reaction and defines the energy costs for that reaction. Thus, a reaction can be carried out under optimal condition to ensure maximum life and activity of the enzyme. In consideration of these points, a thermodynamic assessment will be made for several enzyme-catalyzed reactions of industrial importance.

03,530
PB95-151403 Not available NTIS
National Inst. of Standards and Technology (CSTL), Boulder, CO. Biotechnology Div.
Preparation of Immobilized Proteins Covalently Coupled Through Silane Coupling Agents to Inorganic Supports.
Final rept.
H. H. Weetall. 1993, 32p.
Pub. in Applied Biochemistry and Biotechnology 41, p157-188 1993.

Keywords: *Proteins, *Silane, Enzymes, Antibodies, Antigens, Molecular weight, Reprints, *Inorganic supports, Immobilization(Chemistry), Sol-gel.

Enzymes were first immobilized on inorganic supports through silane coupling agents over 25 yr ago. Since that initial report, literally hundreds of laboratories have utilized this methodology for the immobilization of enzymes, antigens, antibodies, receptors, and other high and low mol wt compounds. Today silane coupling is one of the commonly used techniques in the arsenal of the biochemist for the binding of material of all sorts to inorganic surfaces. Inorganic materials come in a variety of shapes, sizes, and characteristics. Sol-gel entrapped enzymes are also produced by the application of silane technology by the polymerization of the silane to form glass-like materials with entrapped protein. This review will discuss the general preparation and characterization of silane coupled proteins with special emphasis on enzymes and describe in detail the actual methods for the silanization and specific chemical coupling of proteins to the silanized carrier.

03,531
PB95-151411 Not available NTIS
National Inst. of Standards and Technology (CSTL), Gaithersburg, MD. Biotechnology Div.
Method for the Assay of Hydrolytic Enzymes Using Dynamic Light Scattering.
Final rept.
H. H. Weetall, and A. K. Gaigalas. 1993, 6p.
Pub. in Applied Biochemistry and Biotechnology 41, p139-144 1993.

Keywords: *Enzymes, *Light scattering, Hydrolysis, Colloids, Substrate specificity, Reprints.

Dynamic light-scattering techniques have been successfully used for the assay of several hydrolytic enzymes. The enzymes were assayed using substrate-coated colloidal particles. Hydrolysis of the substrate coat causes destabilization of the particles followed by particle aggregation. The rate of particle aggregation can be related to the initial concentration of added enzyme.

03,532
PB95-151429 Not available NTIS
National Inst. of Standards and Technology (CSTL), Gaithersburg, MD. Biotechnology Div.
Bacteriorhodopsin Immobilized in Sol-Gel Glass.
Final rept.
H. Weetall, B. Robertson, D. Cullin, J. Brown, and M. Walch. 1993, 3p.
Pub. in Biochimica et Biophysica Acta 1142, p211-213 1993.

Keywords: *Bacteriorhodopsin, Light, pH, Spectroscopy, Reprints, *Sol-gel glass.

The 96N mutant of bacteriorhodopsin (BR) has been successfully trapped in a sol-gel glass. The protein retains its light-sensitive properties when immobilized at pH 9.0. Spectroscopic studies on the immobilized BR shows properties similar to those observed when in suspension.

03,533
PB95-151544 Not available NTIS
National Inst. of Standards and Technology (NML), Gaithersburg, MD. Chemical Thermodynamics Div.
Function of DnaJ and DnaK as Chaperones in Origin-Specific DNA Binding by RepA.
Final rept.
S. Wickner, J. Hoskins, and K. McKenney. 1991, 3p.
Pub. in Nature 350, n6314 p165-167, 14 Mar 91.

Keywords: *Heat-shock proteins 60, *Heat-shock proteins 70, *Origin of replication, *Deoxyribonucleic acids, *DNA-binding proteins, Escherichia coli, Cell membrane, Biological transport, Plasmids, Phage lambda, Protein folding, Reprints.

Heat-shock proteins are normal constituents of cells whose synthesis is increased on exposure to various forms of stress. They are interesting because of their ubiquity and high conservation during evolution. Two families of heat-shock proteins, hsp60s and hsp70s, have been implicated in accelerating protein folding and oligomerization and also in maintaining proteins in an unfolded state, thus facilitating membrane transport. The Escherichia coli hsp70 analogue, DnaK, and two other heat-shock proteins, DnaJ and GrpE, are required for cell viability at high temperatures and are involved in DNA replication of phage lambda and plasmids P1 and F. These three proteins are involved in replication in vitro of P1 DNA along with many host replication proteins and the P1 RepA initiator protein. RepA exists in a stable protein complex with DnaJ containing a dimer each of RepA and DnaJ. We report

here that DnaK and DnaJ mediate an alteration in the P1 initiator protein, rendering it much more active for oriP1 DNA binding.

03,534
PB95-151833 Not available NTIS
National Inst. of Standards and Technology (NML), Gaithersburg, MD. Organic Analytical Research Div.
Potentiometric Enzyme-Amplified Flow Injection Analysis Detection System: Behavior of Free and Liposome-Released Peroxidase.
Final rept.
T. G. Wu, J. M. Bellama, and R. A. Durst. 1989, 18p.
Pub. in Analytical Letters 22, n5 p1107-1124 1989.

Keywords: *Flow injection analysis, *Potentiometric analysis, *Liposomes, *Peroxidases, *Enzymes, Electrodes, Immunochemistry, Reprints, Triton X-100.

A flow injection analysis (FIA) system was designed for the determination of free and liposome-released peroxidase activity. The inclusion of an extra washing channel in the FIA system provided a solution to problems of electrode fouling and slow recovery of response. The addition of Triton X-100 to acetate buffer resulted in an effective and reliable wash solution, and improved the electrode recovery rate by a factor of three. The sensitivity also increases by about 20% for the enzyme with 3 mU activity by using the wash solution containing Triton X-100. Based on 16 replicate measures of the solution containing 3 mU enzyme, the relative standard deviation of the enzyme determination was 1.5%. Based on the sensitivity obtained with this prototype FIA system, it should be possible to adapt this approach to an immunochemical-based flow injection analysis system capable of measuring an analyte at the femtomole level.

03,535
PB95-153425 Not available NTIS
National Inst. of Standards and Technology (CSTL), Gaithersburg, MD. Biotechnology Div.
Substrate Specificity of the Escherichia coli Endonuclease III: Excision of Thymine- and Cytosine-Derived Lesions in DNA Produced by Radiation-Generated Free Radicals.
Final rept.
M. Dizdaroglu, J. Laval, and S. Boiteux. 1993, 7p.
Pub. in Biochemistry 32, n45 p12105-12111 1993.

Keywords: *Substrate specificity, *Escherichia coli, *Deoxyribonucleic acids, *Thymine, *Cytosine, *Ionizing radiation, Free radicals, Mass fragmentography, DNA damage, DNA repair, Reprints, *Endonuclease III.

The excision of modified bases from DNA by Escherichia coli endonuclease III was investigated. Modified bases were produced in DNA by exposure of dilute buffered solutions of DNA to ionizing radiation under oxic or anoxic conditions. The technique of gas chromatography/mass spectrometry (GC/MS) was used to identify and quantify 16 pyrimidine- and purine-derived DNA lesions. DNA substrates were incubated either with the native enzyme or with the heat-inactivated enzyme. Subsequently, DNA was precipitated. Pellets were analyzed by GC/MS after hydrolysis and derivatization. Supernatant fractions were analyzed after derivatization without hydrolysis. The results provided unequivocal evidence for the excision by E. coli endonuclease III of a number of thymine- and cytosine-derived lesions from DNA. None of the purine-derived lesions was excised by endonuclease III. The present work extends the substrate specificity of E. coli endonuclease III to another thymine-derived and four cytosine-derived lesions. It is the first investigation of the substrate specificity of this repair enzyme in the context of a large number of pyrimidine- and purine-derived lesions in DNA.

03,536
PB95-163036 Not available NTIS
National Inst. of Standards and Technology (CSTL), Gaithersburg, MD. Biotechnology Div.
Electrophoretic Separations of Polymerase Chain Reaction: Amplified DNA Fragments in DNA Typing Using a Capillary Electrophoresis-Lased Induced Fluorescence System.
Final rept.
K. Srinivasan. 1993, 9p.
Sponsored by National Inst. of Justice, Washington, DC.
Pub. in Jnl. of Chromatography A 652, p83-91 1993.

Keywords: *Polymerase chain reaction, *Deoxyribonucleic acids, *Fluorescence spectroscopy, Lasers, Ultraviolet spectroscopy, Apolipoproteins B, Alleles, Viral DNA, Bacteriophages, Reprints, *Capillary electrophoresis.

Analysis of polymerase chain reaction (PCR)-amplified DNA fragments for human identification requires high-resolution separation and efficient detection of amplified alleles. Capillary electrophoresis (CE) with its speed, automation, high resolution and efficiency shows promise for analyzing the amplified DNA fragments. CE with UV detection, however, suffers from lack of detector sensitivity owing to the limited detection path length of the capillary. By the use of intercalating dyes (TOTO and YOYO) a laser-induced fluorescence (LIF) detection system can provide much greater sensitivity for detecting DNA fragments. Femtogram quantities of dsDNA (Phi X174 HaeIII restriction digest mixture) per nanoliter of injected volume have been detected. Application of CE-LIF to analysis of PCR-amplified DNA fragments from three different genetic loci (apolipoprotein B, VNTR locus D1S80, mitochondrial DNA) is shown here. Further, the resolving power of a polymer-network capillary separation system is compared to that of a capillary-gel separation system.

03,537
PB95-163291 Not available NTIS
National Inst. of Standards and Technology (NML), Gaithersburg, MD. Chemical Process Metrology Div.
Electropermeabilization of Cell Membranes: Effect of the Resting Membrane Potential.
Final rept.
E. Tekle, R. D. Astumian, and P. B. Chock. 1990, 6p.
Pub. in Biochemical and Biophysical Research Communications 172, n1 p282-287 1990.

Keywords: *Cell membrane, *Membrane potential, Electric fields, 3T3 cells, Fluorescent dyes, Plants(Botany), Electroporation, Erythrocyte membrane, Reprints.

Electric field induced permeabilization of cell membranes is a potentially important technique for biomedical research. Its application includes gene transfection and cell hybridization. To study the mechanism of this process, Mehrle et al. monitored the uptake of fluorescent indicator by plant protoplasts (Avena Mesophyll) and showed the permeabilization occurs predominantly on the hemisphere facing the positive electrode. However, Dimitrov and Sowers using erythrocyte ghosts loaded with fluorescent-labeled dextran demonstrated that the probes exit through the hemisphere facing the negative electrode. They proposed that electopores were symmetrically formed and electroosmosis is the dominant mechanism for molecular exchange in electroporation. To resolve these 'apparent' controversial observations, we conducted a systematic study of electroporation of NIH3T3 cells with varying electric field strength, waveform and frequency. Results indicate the electropermeabilization of cell membranes is affected by its resting potential and electroosmosis is not the dominant mechanism for the cellular uptake of foreign molecules in electroporation.

03,538
PB95-163382 Not available NTIS
National Inst. of Standards and Technology (NML), Boulder, CO. Chemical Engineering Science Div.
Gravity Dependent Processes and Intracellular Motion.
Final rept.
P. Todd. 1991, 5p.
Contract NASA-W-16985
Sponsored by National Aeronautics and Space Administration, Washington, DC.
Pub. in ASGSB Bulletin 4, n2 p35-39 Jul 91.

Keywords: *Gravity, *Cells(Biology), *Cell movement, Cytoskeleton, Acceleration, Energy metabolism, Reprints.

The application of simple (and complicated) physical principles to the action of gravitational acceleration inside the cell depends heavily on our understanding of the physical properties of the cell interior. While substantial progress has been made in the last decade on understanding cytoskeletal structure and bioenergetics, the dynamics of intracellular and intercellular forces requires considerable further study.

03,539
PB95-163911 Not available NTIS
National Inst. of Standards and Technology (NML), Gaithersburg, MD. Center for Chemical Technology.
Deletion Analysis of the Mini-P1 Plasmid Origin of Replication and the Role of E.coli DnaA Protein.
Final rept.
S. Wickner, J. Hoskins, D. Chattoraj, and K. McKenney. 1990, 6p.
Pub. in Jnl. of Biological Chemistry 265, n20 p1622-1627 1990.

Keywords: *Plasmids, *Origin of replication, *Sequence deletion, *Escherichia coli, Binding sites, In vivo analysis, Adenine nucleatides, Deoxyribonucleic acids, Bacteriophages, Reprints, *DnaA proteins.

The mini-PI plasmid origin of replication is contained on a 246 base pair (bp) piece of DNA. At one end there are five 19 bp binding sites for the PI initiator protein, RepA and near the other end there are two 9 bp DnaA protein binding sites. To further define the limits of the origin we cloned the origin region in M13 and constructed deletions of either end. We sequenced the DNA and tested the RF 1 DNA of the deletion phages for their ability to support RepA-dependent DNA replication in an in vitro system. The origin that is functional in vitro could be reduced to 202 bp. It includes three intact and one incomplete RepA binding sites at one end and the two DnaA binding sites at the other end. When the two naturally occurring DnaA binding sites were replaced with one or two synthetic sites, only the construction containing two sites was active in vitro. We found that the minimal origin that is functional in vivo contains all of the five RepA and the two DnaA binding sites. Mini-PI plasmid replication both in vivo and in vitro requires two initiator proteins, the Escherichia coli DnaA protein and the PI RepA protein. We have found that the ADP form of DnaA is as active as the ATP form of the protein in the in vitro replication of mini-PI. In contrast, only the ATP form is active for in vitro replication of plasmids carrying the E. coli origin.

03,540
PB95-175394 Not available NTIS
National Inst. of Standards and Technology (CSTL), Gaithersburg, MD. Biotechnology Div.
Chemical Determination of Oxidative DNA Damage by Gas Chromatography-Mass Spectrometry.
Final rept.
M. M. Dizdaroglu. 1994, 15p.
Sponsored by Department of Energy, Washington, DC.
Pub. in Methods in Enzymology 234, p3-17 1994.

Keywords: *DNA damage, *Mass fragmentography, Nucleosides, Oxidation, Nuclear proteins, Cross-linking(Chemistry), Free radicals, Isotopes, Reprints.

Measurement of oxidative DNA damage by gas chromatography-mass spectrometry (GC/MS) is described. The use of GC/MS with selected-ion monitoring facilities unequivocal identification and quantification of a large number of modified bases, nucleosides and DNA-protein cross-links that are produced in DNA or nucleoprotein by free radicals or by other DNA-damaging agents. Recently available stable isotope-labeled compounds permit precise quantification at low analyte concentrations. Methodologies involved are presented and discussed in detail.

03,541
PB95-175899 Not available NTIS
National Inst. of Standards and Technology (CSTL), Gaithersburg, MD. Biotechnology Div.
Optical Biosensor Using a Fluorescent, Swelling Sensing Element.
Final rept.
M. F. McCurley. 1994, 7p.
Pub. in Biosensors and Bioelectronics 9, p527-533 1994.

Keywords: *Fluorescence, *Gels, *Polymers, *Fluorometry, Biotechnology, Fiber optics, Swelling, Enzymes, Crosslinking, Amines, Glucose oxidase, Reprints, *Optical biosensors.

An optical sensor based on coupling the swelling of a polymer gel to a change in fluorescence intensity is discussed. A fluorophore, an amine functional group and the enzyme glucose oxidase were each incorporated into a crosslinked polymer gel, which was formed on the end of a fiber optic rod. While the amount of fluorophore remains constant, the gel volume changes in response to a change in the ionization state of the amine moiety. This change is related to glucose concentration. These effects were examined along with subsequent changes in the fluorescence of the gel.

03,542
PB95-175923 Not available NTIS

National Inst. of Standards and Technology (CSTL), Gaithersburg, MD. Surface and Microanalysis Science Div.
Interlaboratory Comparison of Autoradiographic DNA Profiling Measurements. 1. Data and Summary Statistics.
Final rept.
J. L. Mudd, F. S. Baechtel, D. L. Duewer, S. D. Leigh, H. K. Liu, L. A. Currie, and D. J. Reeder. 1994, 15p.
Pub. in Analytical Chemistry 66, n20 p3303-3317, 15 Oct 94.

Keywords: *Deoxyribonucleic acids, *Autoradiography, *Interlaboratory comparisons, Reference standards, Restriction fragment length polymorphism, Base composition, Reproducibility of results, Methods, Least-squares analysis, Reprints.

The data obtained during an interlaboratory precision study sponsored by the Technical Working Group of DNA Analysis Methods are summarized. These data are representative of DNA restriction fragment length polymorphism (RFLP) autoradiographic measurements using laboratory protocols based upon procedures validated by the Federal Bureau of Investigation. Measurement reproducibility for a given RFLP fragment is a nonlinear function of the fragment's size, with the logarithm of the sample standard deviation (SD) approximately proportional to fragment size. The least-squares estimate of this relationship for fragments composed of 600 to 11,000 DNA base pairs (bp) is SD = 10.4 x 10(sup (bp/8300)). Among-analyst and among-laboratory differences appear to contribute about equally to the variance in RFLP measurements. Autoradiographic imaging is a relatively small component of the overall variance for fragments < or = 10,000 bp. Currently available data are sufficient to establish reliable tolerances for the expected interlaboratory variation for any given RFLP band size in this size range, assuming that relevant laboratories continue to use RFLP analysis protocols that are within the current 'statistical population' (i.e., protocols similar to those used by the laboratories that participated in the interlaboratory study). This consistency may best be maintained through appropriate use of Standard Reference Materials, internal quality assurance programs, and external proficiency demonstrations.

03,543
PB96-110747 Not available NTIS
National Inst. of Standards and Technology (CSTL), Gaithersburg, MD. Biotechnology Div.
Novel Activity of E. coli uracil DNA N-glycosylase Excision of Isodialuric Acid (5,6-dihydroxyuracil), a Major Product of Oxidative DNA Damage, from DNA.
Final rept.
T. Zastawny, P. Doetsch, and M. Dizdaroglu. 1995, 4p.
Sponsored by Department of Energy, Washington, DC.
Pub. in FEBS Letters 364, p255-258 1995.

Keywords: *Carcinogenesis, *E. coli, *DNA, Enzymes, DNA repair, Hydroxyl radicals, Isodialuric acid, Oxidation, Damage, Uracil glycosylase, Reprints, E. coli uracil, Isodialuric acid, N-glycosylase.

The authors describe a novel activity of E. coli uracil DNA N-glycosylase (UNG) that excises isodialuric acid from DNA. Isodialuric acid is formed in DNA as a major oxidative product of cytosine. DNA substrates, which were prepared by gamma-irradiation, were incubated with UNG. Following precipitation of DNA, analyses of pellets and supernatant fractions by gas chromatography/mass spectrometry showed an efficient excision of isodialuric acid from DNA by UNG. None of the other 15 identified DNA base lesions was excised. The excision of isodialuric acid indicates that the non-aromaticity of a substrate may not be a limiting factor for UNG.

03,544
PB96-112081 Not available NTIS
National Inst. of Standards and Technology (CSTL), Gaithersburg, MD. Biotechnology Div.
Rapid pH Change Due to Bacteriorhodopsin Measured with a Tin-Oxide Electrode.
Final rept.
B. Robertson, and E. P. Lukashev. 1995, 11p.
Pub. in Biophysical Jnl., v68 p1507-1517 Apr 95.

Keywords: *Bacteriorhodopsin, *Electrodes, Measurements, pH, Photosynthetic bacteria, Sensitivity, Membranes, Reprints, Tin oxide electrodes.

The photocurrent transient generated by bacteriorhodopsin (bR) on a tin-oxide electrode is due to pH change and not to charge displacement as previously assumed. Films of either rendomly oriented of highly oriented purple membranes were deposited on transparent electrodes made of tin-oxide-coated glass. The membranes contained either wild-type or D96N-mutant bR. When excited with yellow light through the glass, the bR pumps protons across the menbrane. The results is a rapid local pH change as well as a charge displacement. Experiments with these films show that it is the pH change rather than the displacement that produces the current transient. The calibration for the transient pH measurement is given. The sensitivity of a tin-oxide electrode to a transient pH change is very much larger than its sensitivity to a steady-state pH change.

03,545
PB96-112123 Not available NTIS
National Inst. of Standards and Technology (CSTL), Gaithersburg, MD. Analytical Chemistry Div.
Interlaboratory Comparison of Autoradiographic DNA Profiling Measurements. 2. Measurement Uncertainty and Its Propagation.
Final rept.
D. L. Duewer, L. A. Currie, D. J. Reeder, J. L. Mudd, S. D. Leigh, and H. K. Liu. 1995, 12p.
See also Part 1, PB95-175923.
Pub. in Analytical Chemistry, v67 n7 p1220-1231 1995.

Keywords: *Deoxyribonucleic acids, *Autoradiography, *Interlaboratory comparisons, Reprints, Reference standards, Base composition, Measurement, *Band size.

Identifying the intrinsic sources of measurement uncertainty greatly facilitates control and further optimization of a measurement system. We have developed a model which quantitatively describes the observed interlaboratory variability autoradiographic DNA band sizing. The model focuses on optical imaging measurements of band position and the calibration techniques used to convert measured band position to reported band size. The imaging components of measurement variability is described as a 0.05-02.% standard deviation in determining the relative location of sample and calibration bands on a given film image. While developed solely with optical imaging information, the model is consistent with interlaboratory band sizing measurement variability observed with pristine samples. This interlaboratory variability can be modeled as a 0.2-0.4% standard deviation in the relative positions of sample and calibration bands across different electrophoretic gels. Further band sizing protocol standardization among laboratories would thus be expected to achieve at best a 2-fold reduction in interlaboratory.

03,546
PB96-123500 Not available NTIS
National Inst. of Standards and Technology (CSTL), Gaithersburg, MD. Biotechnology Div.
Optical Properties of Triton X-100-Treated Purple Membranes Embedded in Gelatin Films.
Final rept.
D. W. Cullin, N. N. Vsevolodov, T. V. Dyukova, and H. H. Weetall. 1995, 8p.
See also PB96-119284.
Pub. in Supramolecular Science, v2 p25-32 1995.

Keywords: *Purple membranes, *Holography, *Geletin films, Optical properties, Reprints, *Bacteriorhodopsin.

The purple membrane (PM) of the microorganism Halobacterium salinarium contains a hexagonally packed monolayer of the light-sensitive protein, bacteriorhodopsin (BR). The optical characteristics of gelatin-immobilized PMs depend strongly on the chemical environment of the PMs in the matrix. Here we present photoinduced absorptive and holographic characteristics of gelatin-embedded PMs solubilized with the non-ionic detergent, Triton X-100. The BR/detergent interaction was shown to slow the M-to-initial state transition of the photocycle and to increase the photosensitivity of the BR films. The lifetime of the holographic grating in Triton X-100-treated BR films was 2-3 times greater, when compared to the unmodified sample. Holographic grating growth times in BR films were shown to change depending on the extent of solubilization. The measured holographic sensitivity appeared to maximize in the range of Triton X-100/BR molar ratios from 15:1 to 25:1. The possible advantages of solubilized PM films as they are applied to optoelectronic devices are discussed.

03,547
PB96-135041 Not available NTIS
National Inst. of Standards and Technology (CSTL), Gaithersburg, MD. Biotechnology Div.
In situ Fluorescence Cell Mass Measurements of 'Saccharomyces cerevisiae' Using Cellular Tryptophan.
Final rept.
J. J. Harvath, S. A. Glazier, and C. J. Spangler. 1993, 5p.
Pub. in Biotechnology Progress, Nov/Dec Issue, v9 p666-670 1993.

Keywords: *Spectroscopy, *Fluorescence, *Bioreactors, In situ, Sensors, Fermentation, Reprints, *Cell mass.

This work describes a new spectroscopic optical fiber/rod technique for in situ real time measurement of cell mass and product concentrations in bioreactors using intrinsic fluorescence. The variable excitation/emission wavelength capability of this sensor allows for the species-selective measurement during fermentations. Cell mass (tryptophan) and product concentrations (pyridoxine) have been measured during fermentations of Saccharomyces cerevisiae. The effects of varying substrate concentration and oxygen concentration on the observed cell mass signals are eliminated by direct measurement of cell mass, as opposed to indirect measurement schemes such as those using NADH fluorescence. The sensor is robust and able to undergo many cycles of in situ steam sterilization without degradation, and its fluorescence signal is linear with concentration for all species studied in this work. Tryptophan fluorescence from yeast is shown to be a better measure of cell mass than NADH fluorescence.

03,548
PB96-137799 Not available NTIS
National Inst. of Standards and Technology (MSEL), Gaithersburg, MD. Reactor Radiation Div.
Low-Frequency Excitations of Oriented DNA.
Final rept.
H. Grimm, P. M. Gehring, S. M. Shapiro, R. Kahn, and A. Rupprecht. 1995, 3p.
See also DE95000629.
Pub. in Physica B Condensed Matter, v213-214 p780-782 1995.

Keywords: *DNA, *Excitations, Thermal neutrons, Thermodynamic properties, Neutron scattering, Reprints, Proton self-correlations, Time-of-flight.

The self-correlation spectrum of DNA hydrogens has been measured by thermal neutron scattering for two orientations of the helical axis in the temperature range 200K equal to or less than T equal to or less than 300 K. Typical spectra for glass formers are observed which show that DNA hydrogens become increasingly delocalized above T equals 200 K. This self-correlation is essentially isotropic. Anisotropic contributions to the scattering are identified as being due too compressional waves along the helix and the low-lying optical band observed in Raman scattering. Both modes show strong coupling to relaxational modes at the zone center (10th layer line). It is argued that the observability of the optical band at this position is due to an antiparallel displacement of the base-pair centers along the helix direction.

03,549
PB96-160478 Not available NTIS
National Inst. of Standards and Technology (CSTL), Gaithersburg, MD. Biotechnology Div.
Novel DNA N-Glycosylase Activity of E. coli T4 Endonuclease V That Excises 4,6-Diamino-5-Formamidopyrimidine from DNA, a UV-Radiation- and Hydroxyl Radical-Induced Product of Adenine.
Final rept.
M. Dizdaroglu, T. H. Zastawny, J. R. Carmical, and R. S. Lloyd. 1996, 8p.
Pub. in Mutation Research DNA Repair, v362 p1-8 1996.

Keywords: *Deoxyribonucleic acids, *Mutagenesis, Reprints, *Foreign technology, UV-radiation, Hydroxyl radical.

We report on a novel activity of T4 endonuclease V. This enzyme is well known to be specific for the excision of pyrimidine dimers from UV-irradiated DNA. In this work, we show that T4 endonuclease V excises 4.6-diamino-5-for-mamidopyrimidine from DNA. 4,6-Diamino-5-formamidopyrimidine is formed as a product of adenine in DNA upon action of hydroxyl radicals and upon UV-irradiation. DNA substrates were prepared by UV-or y-irradiation of DNA in aqueous solution. DNA substrates were incubated either with active

T4 endonuclease V or with heat-inactivated T4 endonuclease V or without the enzyme. After incubation, DNA was precipitated and supernatant fractions were separated. Supernatant fractions after derivatization, and pellets after hydreolysis and derivatization were analyzed by gas chromatography/isotopedilution mass spectrometry. The results provide evidence for the excision of 4.6-diamino-5-formamidopyrimidine by T4 endonuclease V from both y-annd UV-irradiated DNA. Kinetics of excision were also determined. Fifteen other pyrimidine-and purine-derived base lesions that were identified in DNA samples were not substrates for this enzyme. It was concluded that, in addition to its well known activity for pyrimidine photodimers, T4 endonuclease V possesses an N-glycosylase activity for a major UV-radiation- and hydroxyl radical-induced monomeric product in DNA.

03,550
PB96-161641 Not available NTIS
National Inst. of Standards and Technology (CSTL), Gaithersburg, MD. Biotechnology Div.
Genetically Engineered Pores for New Materials.
Final rept.
H. Bayley, S. Beznukhov, J. J. Kasianowicz, M. Krishnasastry, and B. Walker. 1992, 1p.
See also PB96-161658.
Pub. in Materials Research Society (Abstracts), Boston, MA., Nov/Dec 92, p568 Fall 92.

Keywords: *Exotoxins, *Hemolysis, *Ion channels, Reprints, Dynamics, Ion transport, Proteins, Protons, Noise analysis, Staphylococcus aureus.

Alpha-Hemolysin (alphaHL), which is secreted by Staphylococcus aureus as a single polypeptide chain of 293 amino acids, is capable of self-assembling into hexameric pores -1.1 nm in internal diameter. Based on an understanding of the assembly mechanism and the functional properties of the pore, genetic manipulation and chemical modification will be used to construct new pores with potential applications in novel materials, such as monolayer coatings for selective electrodes. Details of the mechanism of self-assembly are being revealed by the isolation of mutant of recombinant alphaHL that become arrested at various stages in assembly, alphaHL first binds to membranes as a monomer, which undergoes a conformational change. It is then converted to a non-conducting hexamer and finally to the open pore.

03,551
PB96-161658 Not available NTIS
National Inst. of Standards and Technology (CSTL), Gaithersburg, MD. Biotechnology Div.
Genetically Engineered Pore as a Metal Ion Biosensor.
Final rept.
J. J. Kasianowicz, B. Walker, M. Krishnasastry, J. Aghajanian, and H. Bayley. 1993, 1p.
See also PB96-161641.
Pub. in Materials Research Society (Abstracts), Boston, MA., Nov/Dec 1993, p480 Fall 93.

Keywords: *Biosensors, *Divalent cations, *Heavy metals, Reprints, Ion channels, Proteins, Toxins.

The authors are investigating the potential use of proteins that form pores in cell membranes as biosensors for heavy metals in the aqueous phase. Specifically, the authors are producing genetically engineered versions of the alpha-hemolysin (alphaHL) from Staphlococcus aureus with properties that are sensitive to low concentrations of divalent cations. For example, in contrast to wild-type alphaHL, the assembly of one mutant (alphaHL-H5: residues 130-134 inclusive replaced with His) into pores was inhibited by Zn squared concentrations as low as 1.0 micro M as judged by its ability to lyse rabbit RCBs and to increase the conductance of planar lipid bilayer membranes. Previously, the authors demonstrated two intermediates in the assembly of alphaHL a membrane-bound monomer and a hexameric prepore complex. Zn squared can act pn the alpha HL-H5 prepore complex to inhibit pore formation.

03,552
PB96-167093 Not available NTIS
National Inst. of Standards and Technology (CSTL), Boulder, CO. Thermophysics Div.
Determination of Total Protein Adsorbed on Solid (Membrane) Surface by a Hydrolysis Technique: Single Protein Adsorption.
Final rept.
M. K. Ko, K. D. Cole, and J. Pellegrino. 1994, 10p.
Pub. in Jnl. of Membrane Science, v93 p21-30 1994.

Keywords: *Adsorption, *Fouling organisms, *Proteins, Analytical methods, Reprints, Lactoglobulin, Hydrolysis, Polycarbonate, Ultrafiltration, *Biofouling, Bovine serum albumin.

We developed a new analytical technique for single protein adsorption in the context of basic studies on membrane fouling. This method simply combines two well-established techniques. HCl hydrolysis and reaction of the resultant amino acids with ninhydrin (10 to the minus 6th power M sensitivity). The HCl hydrolysis step, using 6 N HCl solution, breaks up the adsorbed protein into its constituent amino acids by hydrolyzing the peptide bonds, resulting in complete removal of the absorbed protein from the surface. After the HCl hydrolysis, the condition of the hydrolysate is adjusted for the ninhydrin derivatization by mixing with 6 N NaOH and 6 m sodium acetate. The optimal pH for the ninhydrin derivatization reaction of the hydrolysate is approx. 6. This technique uses an unmodified protein and determines protein loading on the membrane's surface (external and/or pore wall), under static or filtration environments, in a consistent manner. This method provides an absolute measurement of the total protein adsorbed and holds good promise for high sensitivity, accuracy, and reproducibility at a relatively low cost. Other amino acid analytical techniques (such as flourescence and HPLC) may be used to eliminate artifacts, improve sensitivity, and extend the aproach to multi-protein adsorption.

03,553
PB96-167408 Not available NTIS
National Inst. of Standards and Technology (CSTL), Gaithersburg, MD. Biotechnology Div.
Genetically Engineered Pores as Metal Ion Biosensors.
Final rept.
J. Kasianowicz, B. Walker, M. Krishnasastry, and H. Bayley. 1994, 7p.
See also PB96-161641.
Pub. in Materials Research Society Symposium Proceedings, v330 p217-223 1994.

Keywords: *Hemolysin, *Dynamic range, Longevity, Response time, Selectivity, Sensitivity, Reprints, Staphylococcus aureus.

We are adapting proteins that form pores in lipid bilayers for use as components of biosensors. Specifically, we have produced genetically engineered variants of the alpha-hemolysin (alpha HL) from Staphylococcus aureus with properties that are sensitive to low concentrations of divalent cations. For example, the pore-forming activity of one mutant (alpha HL-H5: residues 130-134 inclusive replaced with histidine) is inhibited by Zn2+ at concentrations as low as 1 micromoles, as judged by the reduction in its ability to lyse rabbit red blood cells and to increase the conductance of planar lipid bilayer membranes. When alpha HL-H5 is added to the aqueous phase bathing one side of a planar membrane, the subsequent addition of 100 micromoles Zn2+ to either side blocks the pores that form. This result suggests that at least part of the mutated region lines the channel lumen. Ca2+ and Mg2+ do not block the channel and therefore the H5 mutation confers a degree of analyte specificity to the alpha HL pore.

03,554
PB96-176557 Not available NTIS
National Inst. of Standards and Technology (CSTL), Gaithersburg, MD. Biotechnology Div.
Pore-Forming Protein with a Metal-Actuated Switch.
Final rept.
B. Walker, J. Kasianowicz, M. Krishnasastry, and H. Bayley. 1994, 8p.
Pub. in Protein Engineering, v7 n5 p655-662 1992.

Keywords: *Histidine, *Mutagenesis, Pores, Sensors, Zinc, Reprints, Divalent metal ion.

Staphylococcal alpha-hemolysin, a pore-forming exotoxin, is a poplypeptide of 293 amino acids that is secreted by Staphylococcus aureus as a water-soluble monomer. It assembles to form hexameric pores in lipid bilayers. Previous studies of pore formation have established the involvement of a central glycine-rich loop. Here, we show that when five consecutive histidine residues replace amino acids 130-134 at the midpoint of the loop, they provide a switch with which pore activity can be (1) turned off by micromolar concentrations of divalent zinc ions and (2) turned back on with the chelating agent EDTA.

03,555
PB96-190129 Not available NTIS
National Inst. of Standards and Technology (CSTL), Gaithersburg, MD. Biotechnology Div.
Repair of Products of Oxidative DNA Base Damage in Human Cells.
Final rept.
P. Jaruga, and M. Dizdaroglu. 1996, 6p.
Pub. in Nucleic Acids Research, v24 n8 p1389-1394 1996.

Keywords: *Deoxyribonucleic acid, *Damage, *Oxidation, *Cells(Biology), Humans, Hydroxyl radical, Mutagenesis, Kinetics, Hydrogen peroxide, Reprints, DNA repair, Repair kinetics, 8-Hydroxyguanine.

Oxidative DNA damage is the most frequent type of damage encountered by aerobic cells and may play an important role in biological processes such as mutagenesis, carcinogenesis and aging in humans. Oxidative damage generates a myriad of modifications in DNA. The authors investigated the cellular repair of DNA base damage products in DNA of cultured human lymphoblast cells, which were exposed to oxidative stress by by H2O2. This DNA-damaging agent is known to cause base modifications in genomic DNA of mammalian cells. The results showed a significant formation of these DNA base products upon H2O2-treatment of cells.

03,556
PB97-111983 Not available NTIS
National Inst. of Standards and Technology (CSTL), Gaithersburg, MD. Biotechnology Div.
DNA Damage and DNA Sequence Retrieval from Ancient Tissues.
Final rept.
M. Hoss, P. Jaruga, T. H. Zastawny, M. Dizdaroglu, and S. Paabo. 1996, 4p.
Pub. in Nucleic Acids Research, v24 n7 p304-307 1996.

Keywords: *DNA damage, Bones, Tissues, Archeological remains, Hydroxyl radical, Reprints, *Foreign technology, 8-hydroxyguanine.

Gas chromatography/mass spectrometry (GC/MS) was used to determine the amounts of eight oxidative base modifications in DNA extracted from 11 specimens of bones and soft tissues, ranging in age from 40 to 50,000 years. Among the compounds assayed hydantoin derivatives of pyrimidines were quantitatively dominant. From five of the specimens endogenous ancient DNA sequences could be amplified by PCR. The DNA from these specimens contained substantially lower amounts of hydantoins than the six specimens from which no DNA could be amplified. Other types of damage, e.g., oxidation products of purines, did not correlate with the inability to retrieve DNA sequences. Furthermore, all samples with low amounts of damage and from which DNA could be amplified stemmed from regions where low temperatures have prevailed throughout the burial period of the specimens.

03,557
PB97-119382 Not available NTIS
National Inst. of Standards and Technology (CSTL), Gaithersburg, MD. Biotechnology Div.
DnaJ, DnaK, and GrpE Heat Shock Proteins are Required in 'ori'P1 DNA Replication Solely at the RepA Monomerization Step.
Final rept.
S. Wickner, D. Skowyra, J. Hoskins, and K. McKenney. 1992, 5p.
Pub. in Proc. Natl. Acad. Sci., v89 p10345-10349 Nov 92.

Keywords: *Heat shock proteins, *Deoxyribonucleic acids, *Replication, *Monomerization, DNA, Escherichia coli, Cell membrane, Biological transport, Reprints.

The authors have found that three Escherichia coli heat shock proteins, DnaK (the hsp 70 homolog), DnaJ, and GrpE, function in oriP1 DNA replication in vitro solely to activate DNA binding by the replication initiator protein RepA. Activation results from the conversion of P1 or P7 RepA dimers to monomers that bind with high affinity to the origin of replication of plasmid P1. Thus, the essential role of these three heat shock proteins in this replication system is to change the quaternary structure of a single protein, RepA.

Dentistry

03,558
PB94-160843 PC A06/MF A01
National Inst. of Standards and Technology (MSEL), Gaithersburg, MD. Polymers Div.
Properties and Interactions of Oral Structures and Restorative Materials. Annual Report for Period October 1, 1990 to September 30, 1991.
J. A. Tesk, J. M. Antonucci, J. W. Stansbury, Y. Matsuya, H. Kikuchi, K. Asaoka, J. Tang, S. M. Keeny, and M. Y. Chiang. May 92, 125p, NISTIR-4841.
Contract NIDR-Y01-DE30001
See also PB93-198836. Sponsored by National Inst. of Dental Research, Bethesda, MD.

Keywords: *Dental materials, *Permanent dental restoration, Biocompatible materials, Composite materials, Cements(Adhesives), Adhesives, Alloys, Fluorescent dyes, Sealants, Chemical analysis.

The research described herein is designed to achieve a number of objectives leading to improved dental restorative materials, techniques and applications of dental materials science for improved delivery of health care. The bulk of the research is related in one manner or another to dental composites, cements, adhesives, and sealants. Composite research focuses on improvements through the development of durable resin matrices, stronger, durable coupling between fillers and resins (defining the best overall combination of components) and optimal curing systems. A major emphasis of the programs is on the synthesis and applications of monomers which reduce polymerization shrinkage through the use of expanding monomers (or monomers which undergo much less shrinkage than conventional monomers). A second distinct area of effort focuses on dental alloy and ceramic systems. Weibull statistics and finite element stress analysis are employed for the determination of the strengths of ceramic and ceramic-metal systems as affected by processing parameters and thermo-mechanical properties.

03,559
PB95-150710 Not available NTIS
National Inst. of Standards and Technology (MSEL), Gaithersburg, MD. Polymers Div.
Deposition of Loosely Bound and Firmly Bound Fluorides on Tooth Enamel by an Acidic Gel Containing Fluorosilicate and Monocalcium Phosphate Monohydrate.
Final rept.
S. Takagi, L. C. Chow, and B. A. Sieck. 1992, 7p.
Sponsored by American Dental Association Health Foundation, Chicago, IL.
Pub. in Caries Research 26, p321-327 1992.

Keywords: *Dental enamel, *Fluorides, *Mouthwashes, *Deposition, Enamel, Gels, Dental caries, Sodium fluorides, Tooth remineralization, In vivo analysis, Reprints, Phosphate fluoride, Calcium phosphate hydrate, Sodium hexafluorosilicate.

The amounts of loosely bound fluoride (F) deposited on human enamel by 4-min and 2-hour treatments with either acidulated phosphate fluoride (APF) or a monocalcium phosphate monohydrate and sodium hexafluorosilicate (MCPM-SHFS)-containing gel were measured with the use of a constant-composition F washing method. Enamel biopsies conducted before treatment and after washing were used to determine the firmly bound F uptake. The results showed that the MCPM-SHFS treatments produced significantly more loosely bound F than did the APF treatments. The 4-min treatment with either APF or MCPM-SHFS did not produce significant firmly bound F deposition, but the 2-hour treatments did, with that produced by MCPM-SHFS being significantly greater. The MCPM-SHFS gel, which had the same F content as APF and which may be applied to the proximal tooth surfaces in vivo without the use of a tray, has the potential to be more efficacious than APF because it deposits greater amounts of both loosely bound and firmly bound F.

03,560
PB95-150967 Not available NTIS
National Inst. of Standards and Technology (MSEL), Gaithersburg, MD. Polymers Div.
Influence of Natural and Synthetic Inhibitors on the Crystallization of Calcium Oxalate Hydrates.
Final rept.
B. B. Tomazic, M. E. Sheehan, and G. H. Nancollas. 1992, 10p.
Sponsored by American Dental Association Health Foundation, Chicago, IL.
Pub. in World Jnl. Urol. 10, p216-225 1992.

Keywords: *Crystallization, *Reaction kinetics, *Dentistry, Polyacrylates, Molecular weight, Urine, Crystal growth, Crystal lattices, Ions, Heparins, Reprints, *Calcium oxalate hydrate, Polyaspartic acid, Polyglutamic acid.

The kinetics of crystallization of calcium oxalate monohydrate was studied in the presence of polyacrylate, and the growth of both this salt and the trihydrate was investigated in the presence of polyaspartic acid, polyglutamic acid, and heparin. We monitored the crystallization reactions either by following the change in lattice-ion concentrations as a function of time or by maintaining constant supersaturation via the replacement of lattice ions during the experiments. In addition, the crystallization reactions of calcium oxalate monohydrate, dihydrate, and trihydrate were studied in the presence of urine fractions (5%, v/v) separated by molecular weight in the range of 1000-50000 Da from whole urine.

03,561
PB95-151205 Not available NTIS
National Inst. of Standards and Technology (MSEL), Gaithersburg, MD. Polymers Div.
Distribution of Fluoride in Saliva and Plaque Fluid After a 0.048 mol/L NaF Rinse.
Final rept.
G. L. Vogel, C. M. Carey, and J. Ekstrand. 1992, 5p.
Sponsored by American Dental Association Health Foundation, Chicago, IL.
Pub. in Jnl. of Dental Research 71, n9 p1553-1557 Sep 92.

Keywords: *Dental plaque, *Fluorides, *Saliva, *Microanalysis, Tooth, Sodium fluorides, Mouthwashes, Dental caries, Dental care, Reprints.

An ultramicro method has recently been described for measurement of plaque-fluid fluoride concentration. This method was used: (1) for exploration of the variation in fluoride concentration of plaque fluid collected from the same buccal tooth sites following a 0.048 mol/L NaF (0.2%) rinse, and (2) for examination of the distribution of fluoride in plaque fluid and saliva within one hour after this rinse. Results indicated an average coefficient of variation (CV) of 31% for plaque-fluid fluoride in triplicate samples recovered simultaneously from the buccal-proximal region of two teeth after the rinse. The variations suggest that an examination of plaque-fluid fluoride from specific tooth regions may be essential for understanding the effects of fluoride on the site-specificity of caries.

03,562
PB95-153052 Not available NTIS
National Inst. of Standards and Technology (MSEL), Gaithersburg, MD. Polymers Div.
Publication and Presentation Abstracts, 1993. (Published by Paffenbarger Research Center and Center of Excellence for Materials Science Research).
Final rept.
M. W. Chalkley, and W. A. Marjenhoff. 1993, 68p.
Sponsored by American Dental Association Health Foundation, Chicago, IL.
Pub. in Dental Materials Research Highlights, 68p Oct 93.

Keywords: *Dental materials, *Research projects, *Technology innovation, *Medical research, *Abstracts, Dental cements, Dental implantation, Biocompatible materials, Adhesives, Composite materials, Sealants, Temporary dental restoration, Permanent dental restoration, Dentistry, Reprints, Paffenbarger Research Center.

The report is a compilation of abstracts published by Paffenbarger Research Center and Center of Excellence for Materials Science Research staff in 1992.

03,563
PB95-153169 Not available NTIS
National Inst. of Standards and Technology (MSEL), Gaithersburg, MD. Polymers Div.
Effects on Whole Saliva of Chewing Gums Containing Calcium Phosphates.
Final rept.
L. C. Chow, S. Takagi, R. J. Shern, B. A. Sieck, T. H. Chow, and K. K. Takagi. 1994, 7p.
Sponsored by American Dental Association Health Foundation, Chicago, IL.
Pub. in Jnl. of Dental Research 73, n1 p26-32 Jan 94.

Keywords: *Chewing gum, *Calcium phosphates, *Salivation, *Tooth remineralization, Additives, Weight, pH, Calcium, Phosphates, Reprints, Dicalcium phosphate anhydrous, Calcium phosphate hydrate, Tetracalcium phosphate.

To evaluate chewing gums as a vehicle to increase salivary mineral saturation levels and enhance salivation, monocalcium phosphate monohydrate (MCPM) and an equimolar mixture of tetracalcium phosphate (TTCP) with dicalcium phosphate anhydrous (DCPA) were chosen as experimental chewing gum additives. The saliva samples collected every 2 min were analyzed for weight, pH, and total calcium (Ca) and phosphate (P) concentrations. The degree of saturation of tooth mineral was significantly increased by both experimental gums, with the greater increase being produced by the TTCP-DCPA gum. The MCPM gum produced a significantly greater saliva flow and a lower salivary pH than did the control and TTCP-DCPA gums. The results suggest that the experimental gums may be useful for promoting remineralization in general and for inducing salivation in xerostomic patients.

03,564
PB95-164448 Not available NTIS
National Inst. of Standards and Technology (MSEL), Gaithersburg, MD. Polymers Div.
Procedure for the Study of Acidic Calcium Phosphate Precursor Phases in Enamel Mineral Formation.
Final rept.
C. Siew, S. E. Gruninger, L. C. Chow, and W. E. Brown. 1992, 5p.
Sponsored by American Dental Association Health Foundation, Chicago, IL.
Pub. in Calcified Tissue International 50, p144-148 1992.

Keywords: *Dental enamel, *Acidification, *Minerals, Magnesium, Calcium phosphates, Fluorides, Biochemistry, Hydrolysis, In vitro analysis, In vivo analysis, Reprints, *Octacalcium phosphate, Apatite/hydroxy.

Considerable evidence suggests that an acidic calcium phosphate, such as octacalcium phosphate (OCP) or brushite, is involved as a precursor in enamel and other hard tissue formation. Additionally, there is in vitro evidence suggesting that fluoride accelerates and magnesium inhibits the hydrolysis of OCP to hydroxyapatite (OHAp). As the amount of OCP or brushite in enamel cannot be measured directly in the presence of an excess of hydroxyapatite, a procedure was developed that allows for their indirect in vivo quantification as pyrophosphate. This permits study of the effects of fluoride and magnesium ions on enamel mineral synthesis.

03,565
PB95-164505 Not available NTIS
National Inst. of Standards and Technology (MSEL), Gaithersburg, MD. Polymers Div.
Effects of Aluminum Oxalate/Glycine Pretreatment Solutions on Dentin Permeability.
Final rept.
M. D. Simpson, J. A. Horner, P. D. Brewer, F. Eichmiller, and D. H. Pashley. 1992, 5p.
Sponsored by American Dental Association Health Foundation, Chicago, IL.
Pub. in American Jnl. of Dentistry 5, n6 p324-328 Dec 92.

Keywords: *Dentin permeability, *Glycine, *Solutions, In vitro analysis, pH, Buffers, Reprints, *Aluminum oxalate, *Pretreatments, Smear layers.

Aluminum oxalate buffered with glycine to pH 0.5 - 2.5 has been proposed as a dentin pretreatment for the Gluma bonding system. In this experiment, the effects of 1-minute treatments of smear layers with these aluminum oxalates on the permeability of human dentin were determined in vitro. The aluminum oxalate solutions at pH 0.5 - 1.5 removed most of the original smear layer but occluded the tubules with crystalline deposits which decreased dentin permeability. Those solutions used at pH 2.0 and 2.5 increased dentin permeability. All dentin pretreatments increased dentin permeability when measured after a 24-hour storage period, especially the solutions at pH 2.0 and 2.5. The SEM correlates of these permeability changes indicated that these solutions remove the smear layer but reocclude the tubules with precipitates which are probably different forms of calcium oxalate, aluminum phosphate and calcium phosphates.

03,566
PB95-175907 Not available NTIS

National Inst. of Standards and Technology (MSEL), Gaithersburg, MD. Polymers Div.
Interaction of Chlorhexidine Digluconate with and Adsorption of Chlorhexidine on Hydroxyapatite.
Final rept.
D. N. Misra. 1994, 7p.
Sponsored by American Dental Association Health Foundation, Chicago, IL.
Pub. in Jnl. of Biomedical Materials Research 28, p1375-1381 1994.

Keywords: *Adsorption, *Hydroxyapatites, *Reaction kinetics, *Chlorhexidine, *Mouthwashes, *Dentistry, Dental cements, Aqueous solutions, Oral hygiene, Precipitation(Chemistry), Solubility, Reprints, *Chlorhexidine digluconate.

It is well known that chlorhexidine digluconate provides an effective microbicidal activity during oral rinsing, and therefore, it was considered worthwhile to investigate its interaction with hydroxyapatite on a fundamental level. The kinetics of uptake (or reaction) of the compound from aqueous solutions by synthetic hydroxyapatite was studied at 23 C for four time periods by monitoring its concentration. All of the experimental facts can be qualitatively explained on the basis of the solubility considerations of hydroxyapatite and of chlorhexidine phosphate, the reaction product that slowly precipitates out of the solution. To explore the nature of interaction, the uptake of chlorhexidine base was studied from p-dioxane and it is irreversible. The uptake is total below a threshold equilibrium concentration and constant above it.

03,567
PB96-102140 Not available NTIS
National Inst. of Standards and Technology (MSEL), Gaithersburg, MD. Polymers Div.
Remineralization of Root Lesions with Concentrated Calcium and Phosphate Solutions.
Final rept.
L. C. Chow, and S. Takagi. 1995, 6p.
Sponsored by American Dental Association Health Foundation, Chicago, IL.
Pub. in Dental Materials Jnl., v14 n1 p31-36 Jun 95.

Keywords: *Teeth, *Enamels, *Calcium phosphates, Solutions, Diffusion, Caries, Teeth roots, Holes(Openings), Reprints, *Remineralization, Lesions, Root caries.

Remineralization of enamel lesions in vitro by use of sequential treatments with an alkaline (pH 9) phosphate (1 mol/L) solution and slightly acidic (pH 6) calcium (1 mol/L) solution was reported to be relatively ineffective. An analysis of the diffusion processes that may occur during the remineralization treatments suggested that the driving force for diffusion of Ca into the lesion can be increased by making the calcium solution more alkaline than the phosphate solution. In the present study this modified treatment procedure was evaluated for remineralizing root lesion in vitro.

03,568
PB96-119250 Not available NTIS
National Inst. of Standards and Technology (MSEL), Gaithersburg, MD. Polymers Div.
Publications and Presentation Abstracts, 1995. (Published by Paffenbarger Research Center and Center of Excellence for Materials Science Research).
Final rept.
M. W. Chalkley, and W. A. Marjenhoff. 1995, 61p.
See also report for 1993, PB95-153052. Sponsored by American Dental Association Health Foundation, Gaithersburg, MD. Paffenbarger Research Center.
Pub. in Dental Materials Research Highlights, 1995 Publications and Presentation Abstracts, p1-61 Oct 95.

Keywords: *Dental materials, *Research projects, *Technology innovation, *Medical research, *Abstracts, Dental cements, Dental implantation, Biocompatible materials, Adhesives, Composite materials, Temporary dental restoration, Permanent dental restoration, Reprints, Paffenbarger Research Center.

This report is the annual compilation of abstracts published or accepted for publication by Paffenbarger Research Center and Center of Excellence for Materials Science Research staff thus far in 1995.

03,569
PB96-119722 Not available NTIS
National Inst. of Standards and Technology (MSEL), Gaithersburg, MD. Polymers Div.
In vitro Fracture Behavior of Ceramic and Metal-Ceramic Restorations.
Final rept.
T. B. Smith, J. R. Kelly, and J. A. Tesk. 1994, 7p.
Pub. in Jnl. of Prosthodontics, v3 n3 p138-144 Sep 94.

Keywords: *Dental ceramics, Reprints, In vitro analysis, Failure analysis, Metal ceramics.

Failed crowns and failure load data were studied to gain insights into the fracture behavior of prosthesis under incaisal-directed, load-to-failure testing. Incisor crowns (n-68) were fabricated: two all-ceramic groups (feldspathic veneer on high-strength core), differing in core design, and two metal-ceramic groups, differing in metal oxidation time (30 seconds v 3 minutes). Crowns were loaded to failure on their indisal edge. Gross visual, microscopic, and elemental microprobe analyses of failed crowns were coupled with Weibull analysis of the failure load data.

03,570
PB96-123666 Not available NTIS
National Inst. of Standards and Technology (MSEL), Gaithersburg, MD. Polymers Div.
Intensive Swimming: Can It Affect Your Patients' Smiles.
Final rept.
K. J. Rose, and C. M. Carey. 1995, 5p.
Pub. in Jnl. of the American Dental Association, v126 p1402-1406 Oct 95.

Keywords: *Teeth, *Discoloration, *Swimming, Dental calculus, Calculi, Dental enamel, Pellicle, Chemical reactions, Oral intake, Chlorination, Exposure, Reprints, Pool water.

Athletes who swim intensively, such as those who swim laps more than six hours a week, may develop unusual yellowish brown or dark brown stains on their teeth. The authors hypothesize that long-term contact of the teeth with swimming pool water, as well as the mixture of oral fluids with swimming pool water, leads to the formation of these deposits. The authors report two cases of development of such stains.

03,571
PB96-135215 Not available NTIS
National Inst. of Standards and Technology (MSEL), Gaithersburg, MD. Polymers Div.
Effect of Supersaturation on Apatite Crystal Formation in Aqueous Solutions at Physiologic pH and Temperature.
Final rept.
K. Ishikawa, E. D. Eanes, and M. S. Tung. 1994, 8p.
Pub. in Jnl. of Dental Research, v73 n8 p1462-1469 Aug 94.

Keywords: *Apatites, *Calcification, *Crystal size, Reprints, Supersaturation, X ray diffraction.

The importance of supersaturation in the dynamics of apatite precipitation from aqueous solutions is well-established. To determine whether this parameter has a comparable impact on the concomitant development of the textural properties of this phase, such as crystal size and shape, the authors investigated mineral accretion in synthetic solutions seeded with 0.67 g/L apatite over a range of supersaturations at pH 7.4 and 37 degrees C. A dual specific-ion electrode-controlled titration method was used to maintain the seeded reactions under the following solution conditions: 1.0 to 1.8 mmol/L Ca2+, 0.67 to 1.2 mmol/L total phosphate (PO4), Ca/PO4 (initial) = 1.5, 143 mmol/L KNO3, and 10 mmol/L HEPES. Samples were collected for chemical and textural analyses when the seed apatite was reduced by new accretions to 1/2, 1,4. 1/8, 1/16, and 1/32 of the total solids in suspension. All new accretions were found to be apatitic. At the lowest supersaturation, accretion occurred primarily by growth of the seed crystals. However, at the highest supersaturation examined, the crystals at the end of the experiments were actually smaller, on average, than the original seeds, even though the total mass increased 32-fold. The results suggest that proliferation of new crystals supplanted growth of the seed crystals as supersaturation was increased. The results also suggest that differences in tissue fluid supersaturation may contribute to the large disparity in dimensions between dentin and enamel apatite crystals.

03,572
PB96-147012 Not available NTIS
National Inst. of Standards and Technology (MSEL), Gaithersburg, MD. Polymers Div.
Bioactive Polymeric Dental Materials Based on Amorphous Calcium Phosphate.
Final rept.
J. M. Antonucci, D. Skrtic, and E. D. Eanes. 1994, 2p.
Pub. in Polymer Preprints, v35 n2 p460-461 1994.

Keywords: *Calcium phosphates, *Dental cements, Tooth remineralization, Physiologic calcification, Phototchemical reactions, Monomers, Amorphous compounds, Hydroxyapatites, Composite materials, Physicochemical properties, Biochemistry, Dental materials, Reprints, *Bioactive materials, Coupling agents, HAP(Hydroxyapatite).

Amorphous calcium phosphate (ACP) is an important intermediate in HAP formation, has received far less attention as a biomaterial. The two principal reasons for this are ACP's high solubility in aqueous media and its rapid conversion to HAP. These very properties, however, suggest its use as a bioactive filler in polymeric materials, e.g., composites, sealants, adhesives, that can preserve teeth against demineralization and possibly promote remineralization of defective tooth structure. In this study, several visible light curable composites based on several acrylic monomer systems and a stablized ACP were prepared, polymerized and evaluated for their ability to release calcium and phosphate ions in the presence of an aqueous environment in a sustained fashion and at levels adequate to favor HAP formation.

03,573
PB96-147020 Not available NTIS
National Inst. of Standards and Technology (MSEL), Gaithersburg, MD. Polymers Div.
Remineralizing Dental Composites Based on Amorphous Calcium Phosphate.
Final rept.
J. M. Antonucci, D. Skrtic, and E. D. Eanes. 1995, 2p.
Pub. in Polymer Preprints, Anaheim, California 1995 Meeting, v36 n1 p779-780 1995.

Keywords: *Calcium phosphates, *Mineralization, *Dental cements, Precipitation(Chemistry), Tooth remineralization, Physiologic calcification, Dental caries, Polymerization, Amorphous compounds, Composite materials, Hydroxyapatites, Biochemistry, Dental materials, Reprints, Acrylic monomers, HAP(Hydroxyapatite).

Amorphous calcium phosphate (ACP) has some unique properties that make it ideal for use as a remineralizing agent in polymeric composites. In this study, visible light curable composites based on an acrylic monomer system and either a stabilized ACP or a HAP particulate filler were evaluated for sustained release of Ca(2+) and PO4 ions into aqueous media at levels adequate for HAP formation, and for their abilities to remineralize caries-like lesions in extracted bovine incisors.

03,574
PB96-147095 Not available NTIS
National Inst. of Standards and Technology (MSEL), Gaithersburg, MD. Polymers Div.
Dynamics of Calcium Phosphate Precipitation.
Final rept.
E. D. Eanes. 1992, 17p.
Pub. in Calcification in Biological Systems, Chapter 1, p1-17 1992.

Keywords: *Calcium phosphates, *Precipitation(Chemistry), *Dental cements, Physicochemical properties, Biochemistry, Mineralization, Physiologic calcification, In vivo analysis, Synthetic materials, Dental materials, Reprints.

Many of the physicochemical principles of crystal nucleation and growth relevant to understanding biomineralization dynamics have been elucidated by solution studies on synthetic calcium phosphate analogs. These studies have also helped to delimit the range of action of specific biological substances. e.g., matrix macromolecules, that may be involved in initiating and regulating mineral formation in vivo. Together with our present knowledge of the ultrastructural features of skeletal mineral and mineral-matrix associations, these synthetic studies have provided valuable insight into biomineral formation and the physiological constraints placed on it. This chapter reviews current knowledge in these areas.

03,575
PB96-155544 Not available NTIS

National Inst. of Standards and Technology (MSEL), Gaithersburg, MD. Polymers Div.
Polymeric Calcium Phosphate Composites with Remineralization Potential.
Final rept.
D. Skrtic, E. D. Eanes, and J. M. Antonucci. 1995, 16p.
Pub. in Industrial Biotechnological Polymers, Chapter 25, p393-408 1995.

Keywords: *Teeth, *Enamels, *Calcium phosphate, Composites, Reprints, *Remineralization.

Calcium phosphates constitute an increasingly important class of inorganic dental materials. Their excellent compatibility with both hard and soft tissues as well as with other dental materials, especially polymeric resins and acids, has led to a number of possible prophylactic, prosthetic and restorative uses. Crystalline calcium phosphates such as hydroxyapatite (HAP) and various di-, tri- and tetracalcium phosphates have received the greatest consideration for such purposes. Less attention in this regard has been given to the possible use of amorphous calcium phosphate (ACP), an important intermediate in the formation of apatite, as a dental material. One reason for this neglect is that the relatively high solubility of ACP and its conversion to apatite in aqueous environments poses limitations in applications where structural, mechanical and chemical stabilities are desired. These same properties, however, may make ACP suitable as a potential mineralizing agent. When compounded with appropriate polymeric resins, ACP's bioactivity may be particularly useful in enhancing the performance of sealants and adhesives in preventing tooth demineralization or promoting its remineralization when defective.

03,576
PB96-164082 Not available NTIS
National Inst. of Standards and Technology (MSEL), Gaithersburg, MD. Polymers Div.
Publication and Presentation Abstracts, 1995.
Final rept.
M. W. Chalkley, and W. A. Marjenhoff. 1995, 61p.
See also PB95-153052. Sponsored by American Dental Association Health Foundation, Chicago, IL.
Pub. in Dental Materials Research Highlights, p1-61 Oct 95.

Keywords: *Dental materials, *Research projects, *Technology innovation, *Medical research, *Abstracts, Dental cements, Dental implantation, Biocompatible materials, Adhesives, Composite materials, Sealants, Temporary dental restoration, Permanent dental restoration, Reprints, Paffenbarger Research Center.

This fourth compilation of Publication and Presentation Abstracts provides a summary of research conducted at the American Dental Association Health Foundation's (ADAHF) Paffenbarger Research Center (PRC) and the National Institute of Dental Research (NIDR) - funded Center of Excellence for Materials Science Research (CEMSR) during the past year.

03,577
PB96-176623 Not available NTIS
National Inst. of Standards and Technology (MSEL), Gaithersburg, MD. Polymers Div.
Publication and Presentation Abstracts, 1994.
Final rept.
M. W. Chalkley, and W. A. Marjenhoff. 1994, 74p.
See also report for 1993, PB95-153052 and report for 1995, PB96-164082.
Pub. in Dental Materials Research Highlights, p1-74 1994.

Keywords: *Dental materials, *Research projects, *Technology innovation, *Medical research, *Abstracts, Dental cements, Dental implantation, Biocompatible materials, Adhesives, Composite materials, Sealants, Temporary dental restoration, Permanent dental restoration, Dental equipment, Biomedical radiography, Mirrors, Resins, Reprints, Paffenbarger Research Center.

The American Dental Association (ADA) Health Foundation presents this third annual compilation of Publication and Presentation Abstracts of the Paffenbarger Research Center (PRC) and Center of Excellence for Materials Science Research. Among the innovations emanating from the ADA-NIST alliance are the panoramic radiograph; the turbine contra-angle handpiece; rhodium front-surface dental mirrors; dental composites; the first radiopaque mineral fillers (glasses) for composite restorative materials; and pit and fissure sealant resins and orthodontic bracket bonding resins.

03,578
PB96-180237 Not available NTIS
National Inst. of Standards and Technology (MSEL), Gaithersburg, MD. Polymers Div.
Fluoride Analytical Methods.
Final rept.
P. Venkateswarlu, and G. Vogel. 1996, 13p.
Sponsored by American Dental Association Health Foundation, Chicago, IL.
Pub. in Fluoride in Dentistry, Chapter 2, p27-39 1996.

Keywords: *Dental, *Fluoride, Soil, Tissue, Analysis, Fluorine, Foods, Research, Reprints, *Foreign technology.

The emergence of fluoridation of public water supplies as a safe and economic mass caried-control measure was based on epidemiologic studies and on the concurrent elucidation of the tranpsort and metabolism of fluoride, the mechanism of action of fluoride compounds, their biological effects, and the environmental aspects of fluorides. The success of these studies depended, among other things, on the development of sound fluoride analytical methods. This involved fluorine analysis of water, soil, minerals, vegetation, foods and a host of other biological materials such as bone, teeth (enamel, dentin, cementum), body fluids (urine, blood, saliva) and soft tissues (kidney, liver, muscle).

03,579
PB96-204052 Not available NTIS
National Inst. of Standards and Technology (MSEL), Gaithersburg, MD. Polymers Div.
New Surface-Active Comonomer for Adhesive Bonding.
Final rept.
R. L. Bowen, P. S. Bennett, R. J. Groh, M. Farahani, and F. C. Eichmiller. 1996, 5p.
Pub. in Jnl. of Dental Research, v75 n1 p606-610 Jan 96.

Keywords: *Adhesive bonding, *Amines, *Dentin, Reprints, Monomers, Chemical properties, Physical properties, Hydrogen atoms, Methyl groups.

Previous studies have indicated that chemical and physical characteristics of aromatic amines can be influenced by the nature of their substituents. The experimental question examined in the present study relates to the effects of replacing specific hydrogen atoms with methyl groups in a surface-active comonomr utilized in adhesive bonding protocols. N-2-propionic acid-N-3-(2-hydroxy- 1-methacryloxy)propyl=3, 5-dimethylaniline sodium salt (N35A) was synthesized by an addition reaction of glycidyl methacrylate with the sodium salt of N-(3,5-dimethylphenyl)alanine, which was formed by alkaline hydrolysis of ethyl-N-(3,5-dimethylphenyl)alanate that was prepared by condensation ofethyl-2-bromopropionate with 3,5-dimethylaniline.

03,580
PB97-111595 Not available NTIS
National Inst. of Standards and Technology (MSEL), Gaithersburg, MD. Polymers Div.
Calcium Phosphate Cements.
Final rept.
L. C. Chow, and S. Takagi. 1996, 13p.
See also PB92-144443. Sponsored by American Dental Association Health Foundation, Chicago, IL.
Pub. in Cements Research Progress 1994, the American Ceramic Society, v8 p189-201 1996.

Keywords: *Cements, *Calcium phosphate cements, Biomaterials, Hydroxyapatite, Mechanical strength, Setting time, Reprints.

Since their development in 1987 (1), self-hardening calcium phosphate cements (CPC) have been a subject of considerable interest in biomaterials research. The first CPC's consisted of tetracalcium phosphate (Ca4(PO4)2O or TTCP) and anhydrous dicalcium phosphate (CaHPO4 or DCPA), or TTCP and dicalcium phosphate dihydrate (ChH-PO4.2H2O or DCPD). These cements set in about 30 minutes after mixing the powder with water or dilute acid (e.g., 25 mmol/L H3PO4) and develop sufficient mechanical strength for many clinical applications.

03,581
PB97-112510 Not available NTIS
National Inst. of Standards and Technology (MSEL), Gaithersburg, MD. Polymers Div.
Adsorption of Polyacrylic Acids and Their Sodium Salts on Hydroxyapatite: Effect of Relative Molar Mass.
Final rept.
D. N. Misra. 1996, 8p.
Sponsored by American Dental Association Health Foundation, Chicago, IL.
Pub. in Jnl. of Colloid and Interface Science, Article No. 0380, v181 p289-296 1996.

Keywords: *Polyacrylics, *Hydroxyapatites, *Molar mass, Molecular conformation, Acids, Salts, Adsorption, Langmuir plot, Molecular association, Reprints.

The effect of molar mass on the adsorptive properties of polyacrylic acids and their sodium salts (polymers) has an important bearing on the adhesive mechanisms of restorative resins based on these or similar polymers. The adsorption isotherms of the aqueous solution of polymers were determined on synthetic hydroxyapatite at room temperature to elucidate the role of physico-chemical factors involved in the process. The adsorption of lower molar mass (<90,000) polyacrylic acids shows that the isotherms first rise, reach a maximum, then decrease. In contrast, a higher molar mass (250,000) polyacrylic acid shows no maximum and follows a regular isotherm. The adsorption isotherms of sodium polyacrylates are regular, do not exhibit any maxima, and merge into each other for higher molar mass salts (>60,000). The adsorption is irreversible for the acids as well as for the salts. The concentrations of calcium and phosphate ions were also determined in the filtrates in order to establish any possible correlation with the adsorbed amounts of polymers. The self-association of the polyacrylic molecules by intermolecular hydrogen bonding that may be responsible for the decrease in adsorption at higher concentrations may not play a significant role for higher molar mass acids where individual molecules can fold on themselves as intramolecular hydrogen bonding becomes more dominant.

03,582
PB97-118624 Not available NTIS
National Inst. of Standards and Technology (MSEL), Gaithersburg, MD. Polymers Div.
Posterior Restorative Materials Research.
Final rept.
F. C. Eichmiller, and W. A. Marjenhoff. 1996, 4p.
Pub. in California Dental Association Jnl., v24 n9 p73-76 Sep 96.

Keywords: *Dental materials, *Biocompatible materials, *Teeth, Calcium phosphates, Resins, Silver alloys, Glass ceramics, Protective coatings, Polymerization, Shrinkage, Permanent dental restoration, Temporary dental restoration, Dental implantation, Reprints.

Novel materials and cutting-edge technologies developed at the American Dental Association Dental Health Foundation Center of Excellence for Materials Science Research are discussed. The search for better posterior restorative materials continues.

03,583
PB97-119010 Not available NTIS
National Inst. of Standards and Technology (MSEL), Gaithersburg, MD. Polymers Div.
Surface Roughness of Glass-Ceramic Insert. Composite Restorations: Assessing Several Polishing Techniques.
Final rept.
M. J. Ashe, G. A. Tripp, F. C. Eichmiller, L. A. George, and J. C. Meiers. 1996, 6p.
Pub. in Jnl. of the American Dental Association, v127 n10 p1495-1500 1996.

Keywords: *Ceramics, *Composites, Polishing, Profilometry, Surface roughness, Reprints.

The authors compared the effectiveness of seven polishing methods on glass-ceramic insert-composite restorations placed in plastic resin squares. The polishing methods used carbide dental finishing burs and diamond polishing paste, diamond abrasive finishing burs and diamond polishing paste, diamond abrasive finishing burs and composite resin finishing disks, diamond abrasive finishing burs and composite resin polishing points, diamond abrasive finishing burs only, diamond abrasive finishing burs followed by resin impregnated disks and an aluminum oxide polishing abrasive past, and diamond abrasive finishing burs followed by diamond polishing paste. All systems achieved comparable smoothness except the carbide finishing burs, which damaged the insert-composite margin.

Dentistry

03,584
PB97-119309 Not available NTIS
National Inst. of Standards and Technology (MSEL), Gaithersburg, MD. Polymers Div.
Interaction of Citric Acid with Hydroxyapatite: Surface Exchange of Ions and Precipitation of Calcium Citrate.
Final rept.
D. N. Misra. 1996, 8p.
Sponsored by American Dental Association Health Foundation, Chicago, IL.
Pub. in Jnl. of Dental Research, v75 n6 p1418-1425 1996.

Keywords: *Calcium citrate, *Hydroxyapatite, *Citric acid, *Surface exchange, Formation, Interactions, Peridontal regeneration, Restorative bonding, Reprints.

The use of citric acid is efficacious and distinctive in the demineralization of dentinal root surfaces for periodontal regeneration and in the etching and conditioning of enamel or dentin for bonding restorative resins. To decipher the role of citric acid in these applications, it is important to have a basic understanding of its interaction with synthetic hydroxyapatite. The uptake or removal of citrate ions from aqueous solutions of citric adic (4 to 100 mmol/L, 10 mL) by hydroxyapatite (1 g) was studied at 22 degrees C after a given reaction period (from 3 hr to 11 days) by immediate spectrophotometric monitoring of the concentration of the filtrates (214 nm). The concentrations of calcium, phosphate and hydrogen ions were also determined in the same solutions. The interaction: (1) is a time-independent ionic exchange process with the substrate when the initial acid-concentrations are dilute (4 to 12.5 mmol/L), and (2) is a reactive process that is time-dependent for higher acid concentrations. The exchange process shows an adsorption of about one citrate ion per (100) face of the unit cell of hydroxypatite for a maximally exchanged surface.

03,585
PB97-122238 Not available NTIS
National Inst. of Standards and Technology (MSEL), Gaithersburg, MD.
Publication and Presentation Abstracts, 1996.
Final rept.
M. W. Chalkley, and W. A. Marjenhoff. 1996, 61p.
See also PB96-164082. Sponsored by American Dental Association Health Foundation, Chicago, IL.
Pub. in 1996 Publication and Presentation Abstracts, 61p 1996.

Keywords: *Dental materials, *Research projects, *Technology innovation, *Medical research, *Abstracts, Dental cements, Dental implantation, Biocompatible, Adhesives, Polymers, Composite materials, Sealants, Crystallography, Temporary dental restoration, Permanent dental restoration, Clinical medicine, Reprints.

The abstracts presented in the volume provide a summary of much of the research conducted during the past year at the American Dental Association Health Foundation's (ADAHF) Paffenbarger Research Center (PRC) and the National Institute of Dental Research (NIDR)-funded Center of Excellence for Materials Science Research (CEMSR). PRC research is primarily conducted in four areas: dental chemistry, polymer chemistry, clinical research, and dental crystallography.

Immunology

03,586
PB94-200185 Not available NTIS
National Inst. of Standards and Technology (NML), Gaithersburg, MD. Organic Analytical Research Div.
Planar Waveguide Optical Sensors.
Final rept.
S. Choquette, L. Locascio-Brown, and R. A. Durst. 1990, 9p.
Pub. in Proceedings of Sensors Expo, Chicago, IL., September 11-13, 1990, p206A-1-206A-9.

Keywords: *Theophylline, *Optical waveguides, Planar structures, Fluorescence, Liposomes, Sensors, Reprints, *Ammonium ions, Immunosensors, Flow injection analysis.

The report addresses on-going research involving the development of optical waveguides as analytical sensors. Optical waveguides were fabricated in our laboratory using a metal ion diffusion method, and were employed in independent assays for ammonium and theophylline. The assay for ammonium ion was performed in a flow injection analysis (FIA) system in which the waveguide was used as the detector for an absorbance-based measurement. Detection limits of this assay were 300 M, and the throughput for the system was 60 samples per hour. As a fluorescence sensor, anti-theophylline was immobilized to the surface of the waveguide to create an immunospecific sensor for theophylline. Immunospecific binding of theophylline derivatized liposomes has been demonstrated, and work is progressing on developing a competitive assay for theophylline using planar waveguides.

Microbiology

03,587
PB94-212024 Not available NTIS
National Inst. of Standards and Technology (NML), Gaithersburg, MD. Chemical Process Metrology Div.
In situ On-Line Optical Fiber Sensor for Fluorescence Monitoring in Bioreactors.
Final rept.
J. J. Horvath, and C. J. Spangler. 1992, 17p.
Pub. in Front. Bioprocess. 2, Proc., p99-115 1992.

Keywords: *Bioreactors, *Fluorescence spectroscopy, *Optical fibers, On-line systems, Pyridoxine, Tryptophan, NAD, Riboflavin, Saccharomyces cerevisiae, Reprints.

This work examines the fluorescence properties of natural cell components such as tryptophan, pyridoxine, NADH, and riboflavin in batch fermentations of S. cerevisiae. Measurements were made using both an external flow-thru cuvette loop and an in-situ optical fiber/rod sensor. Pyridoxine gave the largest fluorescence signal; the spectrum of pyridoxine overlaps that of NADH, complicating its interpretation. A good correlation was found between the dry weight of yeast and on-line fluorescence measurements of pyridoxine and tryptophan. The pyridoxine signal was linear with the dry mass of yeast and the tryptophan signal showed absorption effects starting at a dry mass of 0.5 g/l in the cuvette. No deviations were observed with the in-situ optical fiber/rod.

03,588
PB96-161732 Not available NTIS
National Inst. of Standards and Technology (CSTL), Gaithersburg, MD. Biotechnology Div.
Current Fluctuations Reveal Protonation Dynamics and Number of Ionizable Residues in the alpha-Toxin Channel.
Final rept.
J. J. Kasianowicz, and S. M. Bezrukov. 1993, 1p.
Pub. in Biophysical Jnl., v64 pA344 Feb 93.

Keywords: *Ion channels, *Ion transport, *Noise analysis, Reprints, Proteins, Protons, Dynamics.

The I-V relationship of channels formed by Staphlococcus aureus alpha-toxin is pH dependent. To understand the nature of this effect, the authors measured the fluctuations in current through the open channel as a function of pH. The low frequency noise levels in NaCl solutions exhibits a single, well-defined peak over the range 4.5 less than pH less than 7.5. The noise can be described theoretically assuming the channel has several ionizable sites that bind protons with first-order kinetics. In the model, the association of a proton with each of the binding sites in the channel is assumed to increase the conductance in a stepwise manner. Data analysis shows that the residues responsible for the pH dependent noise have a PKa = 5.5. Moreover, the rate constants for the association and dissociation of protons are kg = 8 10 to the 9th power M to the minus 1 power S to the minus 1 power, and KD = 10 to the 5th power, respectively.

03,589
PB96-161757 Not available NTIS
National Inst. of Standards and Technology (CSTL), Gaithersburg, MD. Biotechnology Div.
Protonation Dynamics in an Ion Channel Pore.
Final rept.
J. J. Kasianowicz, and S. M. Bezrukov. 1993, 1p.
Pub. in International Biophysics Conference (11th), Budapest, Hungary, July 25-30, 1993, p136.

Keywords: *Alpha toxin, *Ion channels, *Noise analysis, Reprints, Protons, Rate constant, Spectral analysis, *Foreign technology, Diffusion limited reactions, Ionizable group, Protein structure.

Staphylococcus aureus alpha-hemolysin (alpha-HL) forms channels that have a pH dependent I-V relationship. To evaluate the rate constants for these protonation reactions, the authors measured the fluctuations in current through fully open alpha-HL channels as a function of pH in the presence of 1M NaCl. Spectral analysis shows that the data are well described by a model in which protons bind independently to n ionizable residues with first-order kinetics and that pK = 5.5, kon = 8 10 to the 9th power M to the minus 1 power S to the minus 1 power, koff = 2.5 10 to the 4th power S to the minus 1 power and n = 4 (Phys. Rev. Lett. 70). The value the authors obtain for the association rate constant, kon, is similar to the values measured by Eigen and co-workers for reactions between H+ and free carboxyl or imidazole groups, which suggests that the protonation reactions inside these pores are diffusion limited.

03,590
PB96-163639 Not available NTIS
National Inst. of Standards and Technology (CSTL), Gaithersburg, MD. Biotechnology Div.
Autofluorescence Detection of 'Escherichia coli' on Silver Membrane Filters.
Final rept.
S. A. Glazier, and H. H. Weetall. 1994, 5p.
Pub. in Jnl. of Microbiological Methods, v20 p23-27 1994.

Keywords: *Bacteria, Reprints, Escherichia coli, *Foreign technology, *Autofluorescence, *Epifluorescence.

This report describes the measurement of the limit of detection of the bacterium, Escherichia coli, on the surface of membrane filters employing autofluorescence. Investigation of detection of E. coli by this method was prompted by NASA's need for a method which could detect, principally, fecal coliforms in initially sterile storage water on-board the space station. This method was examined, with E. coli as a model, because it could be conducted rapidly with little or no need for disposables, large amounts of instrumentation, or constant human involvement. The autofluorescence of E. coli collected on the surface of silver membrane filters was quantitated by epifluorescence microscopy and related to a viable count of the bacteria. The fluorescence was excitated using a broad region of ultraviolet radiation from a mercury arc lamp (approx. 250-400 nm) examined in the wavelength region of 495 nm and higher through a long pass optical filter. From these measurements, the limit of detection of viable E. coli collected on the membrane filters was fewer than 550 plus or minus 32 viable bacteria or 170,000 plus or minus 10,000/ml in terms of solution concentration.

03,591
PB96-163647 Not available NTIS
National Inst. of Standards and Technology (CSTL), Gaithersburg, MD. Biotechnology Div.
Bacterial Enumeration in Storage Water.
Final rept.
S. A. Glazier, and H. H. Weetall. 1993, 33p.
Pub. in Bacterial Enumeration in Storage Water, 33p, 17 Feb 93.

Keywords: *Bacteria, *Water analysis, *Fluorescence, Reprints, Enumeration, Microscopy.

This report describes the progress of a NASA funded project. The goal of this project is the enumeration of bacteria which are present in storage water. This work is part of NASA's efforts to prepare environmental monitoring systems for the space station currently under construction. A prototype system for enumeration of bacteria in storage water is proposed based on the fluorescence detection of single bacterial cells collected on a membrane filter. This method of bacterial detection was chosen because it conveniently concentrates the bacteria from the water and enumerates them without the need for disposable reagents and supplies. The report describes the model enumeration system proposed, explains the origins of bacterial cells by laser confocal microscopic imaging, explores the possibility of distinguishing between live and dead bacteria based on their native fluorescence, and details progress on the construction of a simple, compact bacterial enumeration system.

03,592
PB96-201017 Not available NTIS

National Inst. of Standards and Technology (CSTL), Gaithersburg, MD. Biotechnology Div.
Escherichis coli Cyclic AMP Receptor Protein Mutants Provide Evidence for Ligand Contacts Important in Activation.
Final rept.
J. Moore, M. Kantorow, D. Vanderzwaag, and K. McKenney. 1992, 6p.
Pub. in Jnl. of Bacteriology, v174 n24 p8030-8035 Dec 92.

Keywords: *Protein mutants, *Ligand contacts, *Receptor proteins, Activation, Escherichis coli, Reprints, Cyclic AMP.

The three-dimensional model of the Escherichia coli cyclic AMP (cAMP) receptor protein (CRP) shows that several amino acids are involved as chemical contacts for binding cAMP. We have constructed and characterized mutants at four of these positions, E72, R82, S83, and R123. The mutations were made in wild-type crp as well as a cAMP-independent crp, crp(star). The activities of the mutant proteins were characterized in vivo for their ability to activate the lac operon. These results provide genetic evidence to support that E72 and R82 are essential and S83 and R123 are importnat in the activation of CRP by cAMP.

Nutrition

03,593
PB95-151692 Not available NTIS
National Inst. of Standards and Technology (TS), Gaithersburg, MD. Office of Measurement Services.
Mixed Diet Reference Materials for Nutrient Analysis of Foods: Preparation of SRM-1548 Total Diet.
Final rept.
W. R. Wolf, G. V. Iyengar, and J. T. Tanner. 1990, 3p.
Sponsored by Department of Agriculture, Beltsville, MD. and Food and Drug Administration, Washington, DC.
Pub. in Fresenius Jnl. of Analytical Chemistry 338, n4 p473-475 1990.

Keywords: *Food analysis, *Chemical analysis, *Diets, *Trace elements, *Nutritive value, Nutrients, Human nutrition, Fats, Proteins, Cholesterol, Caloric requirements, Reprints, *Standard reference materials, *SRM 1548.

Several mixed component diet materials have been available for use as Reference Materials for determination of elemental contents in foods. Wide acceptance of these materials has resulted in supplies being no longer available. A new mixed food material, SRM 1548 Total Diet has been prepared and characterized for a number of elemental and organic constituents of nutritional concern. SRM 1548 was prepared from foods obtained from collections of the USFDA's Total Diet Study, which are representative of foods consumed by the US population. SRM 1548 has been composited from these foods, proportional to a representative daily intake. The composited foods were blended, freeze-dried, reblended and bottled in six gram sample size. Homogeneity studies were carried out along with certification analyses for elements, cholesterol, caloric, and proximate content. This material is available from NIST and will be useful for multipurpose determinations of constituents in the naturally occurring range in foods and food related materials.

Occupational Therapy, Physical Therapy, & Rehabilitation

03,594
PB96-147814 PC A05/MF A01
National Inst. of Standards and Technology (CSL), Gaithersburg, MD. Information Access and User Interface Div.
Virtual Environments for Health Care. A White Paper for the Advanced Technology Program (ATP), the National Institute of Standards and Technology.
Special pub.
J. Moline. Nov 95, 60p, NISTIR-5740.

Keywords: *Virtual reality, *Health, Surgery, Therapy, Education, Databases, Rehabilitation, *Augmented reality, *Telemedicine.

This report surveys the state of the art in applications of virtual environments (VE) and related technologies for healthcare. After a brief introduction, terms are defined and a review of the healthcare applications is presented. The report also discusses the value-added of these application, their limitations, and areas of current research and development concerning virtual environments for healthcare. Applications of virtual environments and related technologies are being developed for healthcare in the following areas: surgical procedures (remote surgery or telepresence, augmented or enhanced surgery, and planning and simulating procedures before surgery), medical therapy, medical diagnosis and monitoring (telemedicine), preventive medicine and patient education, medical education and training, visualization of massive medical databases, skills enhancement and rehabilitation, and architectural design for healthcare facilities. Virtual environments are benefiting healthcare. To date, the developments have improved the quality of healthcare and in the future will result in substantial cost savings. Tools are being refined or developed which respond to needs of present VE systems. However, additional large scale research is necessary in the following areas: users' studies, use of robots for teleoperated procedures, enhancing system reality, and improving system functionality.

Pathology

03,595
PB96-201140 Not available NTIS
National Inst. of Standards and Technology (MSEL), Gaithersburg, MD. Polymers Div.
In vitro Inhibition of Membrane-Mediated Calcification by Novel Phosphonates.
Final rept.
D. Skrtic, N. Eidelman, G. Golomb, E. Breuer, and E. D. Eanes. 1996, 8p.
Pub. in Calcified Tissue International, v58 p347-354 1996.

Keywords: *Bone disorders, *Calcium metabolism, *Hydroxyapatite, Reprints, Geminal bisphosphonates.

The effects of a series of novel phosphonates on the kinetics of mineral development in an ionophore-primed 7:2:1 phosphatidylcholine (PC): dicetylphosphate (DCP): cholesterol (Chol) liposomal model system are reported. When present at 2.5 micro mol/L or 25 micro mol/L concentrations in the solution surrounding the liposomes, the investigated phosphonates did not significantly delay the initial formation of hydroxyapatite-like calcium phosphate salts (HAP) within the liposomes or the penetration of HAP crystals through the enclosing membranes. However, the phosphonates variably retarded the subsequent growth and proliferation of the HAP crystals once they became directly exposed to the phosphonate-containing solution. The effectiveness of phosphonates in inhibiting extraliposomal precipitation strongly depended on their structure. The inhibitory action on active surface growth sites of released intraliposomal crystals was found to be the most effective if the phosphonate molecule contained two phosphonic groups linked to the same C atom. At a phosphonate concentration of 25 micro mol/L the following general order of effectiveness was established: geminal bisphosphonate equal to or greater than geminal tetrakisphosphonate greater than bisacylphosphonates greater than monoacylphosphonate greater than bisalkylphosphonate.

Pharmacology & Pharmacological Chemistry

03,596
PB94-172467 Not available NTIS
National Inst. of Standards and Technology (CSTL), Gaithersburg, MD. Biotechnology Div.
Thermodynamics of the Hydrolysis of Penicillin G and Ampicillin.
Final rept.
N. Kishore, Y. B. Tewari, W. T. Yap, and R. N. Goldberg. 1994, 12p.
Pub. in Biophysical Chemistry 49, p163-174 1994.

Keywords: *Penicillin G, *Ampicillin, *Thermodynamics, *Hydrolysis, Calorimetry, High performance liquid chromatography, Enthalpy, beta-Lactamase, Reprints.

Apparent equilibrium constants and calorimetric enthalpies of reaction have been measured for the beta-lactamase catalyzed hydrolysis of penicillin G(aq) and ampicillin(aq) to penicillinoic acid(aq) and to ampicillinoic acid(aq), respectively. High-pressure liquid-chromatography and microcalorimetery were used to perform these measuremens. Calorimetric enthalpies of reaction for the beta-lactamase catalyzed hydrolysis of cephalosporin C have also been measured but the reaction products have not been identified and the measured enthalpies cannot be assigned to a specific reaction. Acidity constants for ampicillin, penicillin G, ampicillinoic acid, and penicillinoic acid are also reported. A strain of energy of 116 kJ mol for the beta-lactam ring is obtained from thermochemical data.

03,597
PB95-175444 Not available NTIS
National Inst. of Standards and Technology (CSTL), Gaithersburg, MD. Organic Analytical Research Div.
Determination of Amphetamine and Methamphetamine in a Lyophilized Human Urine Reference Material.
Final rept.
P. Ellerbe, T. Long, and M. J. Welch. 1993, 6p.
Pub. in Jnl. of Analytical Toxicology 17, p165-170 May/Jun 93.

Keywords: *Amphetamine, *Methamphetamine, *Urine, *Reference standards, Mass fragmentography, Clinical chemistry, Humans, Freeze drying, Isotope dilution, Reprints, Heptafluorobutyryl derivative, N-trifluoroacetyl-1-prolyl chloride.

The concentrations of amphetamine and methamphetamine in a new lyophilized human urine reference material (RM) were determined at the National Institute of Standards and Technology, in cooperation with the College of American Pathologists. In order to minimize the possibility of undetected bias, two different methods were developed. Both methods were based on isotope-dilution gas chromatography/mass spectrometry (GC/MS) with a deuterium-labeled standard. The first method used a solid phase extractor (SPE) to isolate the analytes, followed by the forming the heptafluorobutyryl (HFB) derivatives for measurement by GC/MS. The second method used another kind of SPE to isolate the analytes, followed by forming the N-trifluoroacetyl-1-prolyl chloride (TPC) derivatives for measurement by GC/MS. The RM consists of three levels of amphetamine, three levels of methamphetamine, and a blank. For amphetamine, the concentrations are 291, 558, and 1081 ng/mL of human urine. For methamphetamine, the concentrations are 311, 573, and 1137 ng/mL of human urine.

03,598
PB96-119383 Not available NTIS
National Inst. of Standards and Technology (CSTL), Gaithersburg, MD. Biotechnology Div.
Physical Characterization of Herparin by Light Scattering.
Final rept.
A. K. Gaigalas, J. B. Hubbard, R. LeSage, and D. H. Atha. 1995, 5p.
Pub. in Jnl. of Pharmaceutical Science, v84 n3 p355-359 Mar 95.

Keywords: *Heparins, *Light scattering, *Transport properties, Physical properties, Anticoagulants, Size determination, Diffusion coefficient, Charge density, Electric charge, Reprints.

Dynamic and electrophoretic light scattering were used to measure the size and charge heterogeneity of a

commercial preparation of heparin. For this preparation of porcine mucosal heparin (M(sub r) = 10-20 kDa), the diffusion coefficient was 1.2 plus or minus 0.5 x 10(exp -8) square cm/s and the mobility was 4.4 plus or minus 0.9 x 10(exp -4) square cm/V s for an unfiltered solution at 22 deg. C in distilled water. This diffusion constant is 2 orders of magnitude smaller than expected for a molecule the size of heparin. A fast diffusion component of 5.8 plus or minus 1.0 x 10(exp -7) square cm/s, corresponding to the individual molecule, was observed in the presence of 2 M NaCl, where single molecule motion is better observed. This indicates that a portion of the heparin population is in an aggregated state, which produces a higher scattering intensity than individual heparin molecules. The electrophoretic light-scattering measurements also indicate that the aggregate scattering species have very similar surface charge densities resulting from the aggregates being formed from heparin molecules. These results can provide a framework to interpret future light-scattering data for various preparations of heparin.

Psychiatry

03,599
AD-A280 082/9 PC A06/MF A02
National Bureau of Standards, Gaithersburg, MD.
Screw-Thread Standards for Federal Services, 1957. Handbook H28 (1957), Part 2. Revised.
Apr 62, 114p.

Keywords: *Screw threads, *Standards, Gages, Handbooks, Screws, Fasteners, Couplers, Joints, Threaded products, Federal services.

No abstract available.

Public Health & Industrial Medicine

03,600
PB94-154382 PC A04/MF A01
National Inst. of Standards and Technology (BFRL), Gaithersburg, MD. Building Materials Div.
Source of Phenol Emissions Affecting the Indoor Air of an Office Building.
Technical note.
J. W. Martin, F. R. Guenther, T. Nguyen, L. Oakley, W. S. Liggett, and E. Byrd. Feb 94, 53p, NISTIR-5353.
Sponsored by General Services Administration, Washington, DC.

Keywords: *Phenols, *Indoor air pollution, *Office buildings, Occupational exposure, Building materials, Epoxy compounds, Floors, Occupational safety and health, Chemical analysis, Industrial hygiene, Environmental surveys, *Silver Spring(Maryland), Leveling materials.

For several years, National Oceanic and Atmospheric Administration (NOAA) employees occupying Floors 3 through 5 of the Silver Spring Metro Center Building One (SSMC-1) in Silver Spring, MD have complained about ailments which they have associated with poor indoor air quality. NOAA and the General Services Administration (GSA) commissioned at least six indoor air quality surveys to seek the causes of these complaints. In one of the later surveys (5), it was concluded that phenol emissions from an epoxy floor-leveling material used in leveling the floor slabs were causing the indoor air quality complaints from Floors 3 through 5. To obtain an independent analysis and assessment, NOAA and GSA asked the National Institute of Standards and Technology (NIST) to ascertain whether phenol (or any other volatile organic compound) was being emitted from the epoxy floor-leveling material and, if so, to recommend remedial actions for mitigating or eliminating the emissions.

03,601
PB94-172038 Not available NTIS
National Inst. of Standards and Technology (BFRL), Gaithersburg, MD. Building Materials Div.
Lead Abatement in Buildings and Related Structures.
Final rept.
K. Ashley, and M. E. McKnight. 1993, 8p.
Pub. in American Society for Testing and Materials Standardization News, p32-39 Dec 93.

Keywords: *Lead(Metal), *Health hazards, *Buildings, *Lead poisoning, Children, Legislation, Guidelines, Government agencies, Reprints.

The subject of lead-containing painted surfaces has received a great deal of attention in recent years. Much of this interest has been fueled by the potential hazard that this toxic metal poses to the developmental capabilities and health of young children. New federal and state guidelines and legislation concerning lead have spurred many activities in government agencies, academia, and the private sector. In 1988, the Agency for Toxic Substances and Disease Registry (ATSDR) provided, in a report to Congress, a comprehensive review of the health risks that lead in anthropogenic sources pose to children. In 1991, the Centers for Disease Control (CDC) reduced the 'level of concern' of childhood blood lead concentrations from 25 to 10 micrograms per deciliter. According to the CDC report, millions of children in the United States are believed to be at risk of lead poisoning.

03,602
PB94-195047 PC A22/MF A04
National Inst. for Occupational Safety and Health, Cincinnati, OH. Div. of Standards Development and Technology Transfer.
Documentation for Immediately Dangerous to Life or Health Concentrations (IDLHs).
H. R. Ludwig, S. G. Cairelli, and J. J. Whalen. May 94, 523p.
See also PB95-100368.

Keywords: *Occupational safety and health, *Acute exposure, *Toxicity, Regulations, Air pollution effects(Humans), Respirators, Toxic substances, Hazardous materials, Concentration(Composition), Classifications, Air pollution effects(Animals), Lethal doses, Respiration, *IDLH(Immediately Dangerous to Life or Health), *Immediately Dangerous to Life or Health, LC(Lethal concentration).

The 'immediately dangerous to life or health air concentration values (IDLHs)' used by the National Institute for Occupational Safety and Health (NIOSH) as respirator selection criteria were first developed in the mid-1970's. This report is a compilation of the rationale and sources of information used by NIOSH during the original determination of 387 IDLHs and their subsequent review and revision in 1994.

03,603
PB95-100368 PC$14.00/MF A04
National Inst. for Occupational Safety and Health, Cincinnati, OH. Div. of Standards Development and Technology Transfer.
NIOSH Pocket Guide to Chemical Hazards.
Jun 94, 457p.
Also pub. as National Inst. for Occupational Safety and Health, Cincinnati, OH. Div. of Standards Development and Technology Transfer rept. no. DHHS/PUB/NIOSH-94-116. Also available from Supt. of Docs.

Keywords: *Occupational safety and health, *Chemical compounds, *Health hazards, *Handbooks, Industrial hygiene, Exposure, Chemical properties, Physical properties, Concentration(Composition), Classifications, Toxic substances, Signs and symptoms, First aid, Nomenclature, Identifying, Tables(Data), Exposure limits, Listings.

This guide is intended as a source of general industrial hygiene information for workers, employers, and occupational health professionals. It presents key information and data in abbreviated tabular form for 677 chemicals or substance groupings (e.g., manganese compounds, tellurium compounds, inorganic tin compounds, etc.) that are found in the work environment. The industrial hygiene information found in the Guide should help users recognize and control occupational chemical hazards. The chemicals or substances contained in this revision include all substances for which the National Institute for Occupational Safety and Health (NIOSH) has recommended exposure limits (RELs) and those with permissible exposure limits (PELs) as found in the Occupational Safety and Health Administration (OSHA) General Industry Air Contaminants Standard (29 CFR 1910.1000). This revision includes updated sampling and analytical methods, updated Department of Transportation (DOT) identification and guide numbers, current exposure limits, revised respirator selections, and revised IDLH (immediately dangerous to life or health concentration) values.

03,604
PB95-267779 PC A02/MF A01
National Inst. for Occupational Safety and Health, Cincinnati, OH. Div. of Standards Development and Technology Transfer.
NIOSH Comments to DOL on Risk Estimates from the Cadmium Cohort Study by L. Stayner, February 7, 1992.
7 Feb 92, 8p.

Keywords: *Occupational safety and health, *Testimony, *Risk assessment, *Cadmium, Epidemiology, Carcinogenesis, Mortality, Occupational exposure, Pulmonary neoplasms, Models, CAS 7440439.

This testimony includes a table summarizing the risk estimates from fitting the multistage model to a specific cadmium (7440439) cohort study. The risk estimates from fitting the multistage model to the cadmium study were intermediate between estimates derived from fitting the Cox and Poisson regression models. NIOSH further notes that the risk estimates from the Cost and Poisson models are about 50% higher than the estimates in the risk assessment report submitted earlier by NIOSH. The lifetime risk was calculated over the entire life span rather than the median life span. Lung cancer rates were used rather than respiratory cancer rates. NIOSH assumed a five stage model for the analysis, as this is the number of stages generally observed in other multistage analyses of lung cancer. The model was fit by varing the stage affected by cadmium exposure and the model fit best when NIOSH assumed that cadmium affected the third stage.

Radiobiology

03,605
AD-A279 132/5 PC A03/MF A01
National Bureau of Standards, Gaithersburg, MD.
X-ray Protection.
1955, 50p.

Keywords: *X rays, *Handbooks, *Radiation protection, Radiation shielding, Electromagnetic radiation, Ionizing radiation, Occupational exposure, MPD(Maximum Permissible Dose), Maximum permissible dose.

No abstract available.

03,606
AD-A279 181/2 PC A03/MF A01
National Bureau of Standards, Gaithersburg, MD.
X-ray Protection Design.
H. O. Wyckoff, and L. S. Taylor. 9 May 52, 41p.

Keywords: *X rays, *Radiation protection, Installation, Protective equipment.

No abstract available.

03,607
AD-A279 261/2 PC A04/MF A01
National Bureau of Standards, Gaithersburg, MD.
Protection Against Radiations from Radium, Cobalt-60, and Cesium-137.
1 Sep 54, 67p, NBS-HB-54.

Keywords: *Radium, *Radiation protection, *Cobalt 60, *Cesium 137.

No abstract available.

03,608
AD-A279 281/0 PC A05/MF A01
National Bureau of Standards, Gaithersburg, MD.
Permissible Dose from External Sources of Ionizing Radiation.
24 Sep 54, 89p.

Keywords: *Ionizing radiation, Dose rate, X rays, Radium.

No abstract available.

03,609
AD-A280 281/7 PC A04/MF A01

National Bureau of Standards, Gaithersburg, MD.
Maximum Permissible Amounts of Radioisotopes in the Human Body and Maximum Permissible Concentrations in Air and Water.
20 Mar 53, 51p, HANDBOOK-52.

Keywords: *Human body, Concentration(Chemistry), Radiation protection, Air, Water, *Radioactive air pollutants, *Radioactive water pollutants, *Radioisotopes.

No abstract available.

03,610
AD-A280 282/5 PC A06/MF A02
National Bureau of Standards, Gaithersburg, MD.
Maximum Permissible Body Burdens and Maximum Permissible Concentrations of Radionuclides in Air and in Water for Occupational Exposure.
5 Jun 59, 104p, HANDBOOK-69.

Keywords: *Radiation protection, *Exposure(Physiology), *Human body, *Radioactive air pollutants, *Radioactive water pollutants, *Radioisotopes.

No abstract available.

03,611
AD-A286 681/2 PC A05/MF A01
National Bureau of Standards, Gaithersburg, MD.
Protection Against Neutron Radiation Up to 30 Million Electron Volts.
Handbook.
22 Nov 57, 95p.

Keywords: *Radiation, *Neutron radiography, *Radiation protection, Voltage, Electron irradiation.

No abstract available.

03,612
DE94014709 PC A01/MF A01
National Inst. of Standards and Technology (NEL), Gaithersburg, MD.
Ionizing radiation-induced DNA damage and its repair in human cells. Progress report, (April 1, 1993--February 28, 1994).
1994, 3p, DOE/ER/60826-T1.
Contract AI05-89ER60826
Sponsored by Department of Energy, Washington, DC.

Keywords: Endonucleases, Biochemical Reaction Kinetics, Carbon 13, Cytosine, Deuterium Compounds, Gas Chromatography, Guanine, Mass Spectroscopy, Molecular Biology, Nitrogen 15, Progress Report, Radiolysis, Standards, Thymine, Uracils, *DNA damage, *DNA repair, *Ionizing radiation, EDB/560120, EDB/550200, Cells(Biology).

The excision of radiation-induced lesions in DNA by a DNA repair enzyme complex, namely the UvrABC nuclease complex, has been investigated. Irradiated DNA was treated with the enzyme complex. DNA fractions were analyzed by gas chromatography/isotope-dilution mass spectrometry. The results showed that a number pyrimidine- and purine-derived lesions in DNA were excised by the UvrABC nuclease complex and that the enzyme complex does not act on radiation-induced DNA lesions as a glycosylase. This means that it does not excise individual base products, but it excises oligomers containing these lesions. A number of pyrimidine-derived lesions that were no substrates for other DNA repair enzymes investigated in our laboratory were substrates for the UvrABC nuclease complex.

03,613
DE95007065 PC A01/MF A01
National Inst. of Standards and Technology (IMSE), Gaithersburg, MD.
Electron transport calculations with biomedical and environmental applications. Final report, December 23, 1992--January 31, 1994.
PROGRESS REPT.
S. M. Seltzer. 1995, 5p, DOE/ER/61529-T1.
Contract AI02-93ER61529
Sponsored by Department of Energy, Washington, DC.

Keywords: *Man, *Radiation Hazards, *Radiation Transport, Biological Radiation Effects, Dosimetry, Mathematical Models, Progress Report, EDB/560100.

The general objective of this project has been to carry out studies of radiation interactions with matter, and of radiation transport in bulk media, in order to generate basic radiological physics information needed as input for: Biomedical radiation dosimetry, Assessment of radiation hazards in nuclear technology, Modeling of biological radiation action. This work has included the development of transport-theoretic methods, the compilation and critical evaluation of the underlying single-scattering cross sections, and the application of the transport methods to radiological physics problems. The project carried out for DOE has been closely related to other projects of the Radiation Interactions and Dosimetry Group of the Ionizing Radiation Division supported in-house by NIST (radiation standards for medical and industrial applications). It has shared with these projects mathematical methods, computer programs, and cross section data bases. The support from DOE has covered approximately 20% of the activities in the radiation transport area by the Radiation Theory Task. The research for DOE was carried out by S. M. Seltzer and M. J. Berger.

03,614
DE96007979 PC A02/MF A01
National Inst. of Standards and Technology (PL), Gaithersburg, MD. Ionizing Radiation Div.
Experimental assessment of absorbed dose to mineralized bone tissue from internal emitters: An electron paramagnetic resonance study.
M. F. Desrosiers. 1994, 7p, DOE/EH/89334-T1.
Contract AI01-93EH89334
Sponsored by Department of Energy, Washington, DC.

Keywords: *Electron spin resonance, *Bone Tissues, Humans, Radiation Doses, EDB/560161, EDB/560151, EDB/560101.

EPR resonances attributable to radiation-induced centers in hydroxyapatite were not detectable in bone samples supplied by the USTUR. These centers are the basis for imaging and dose assessment. Presumable, the short range of the alpha particles emitted precluded the formation of appreciable amounts of hydroxyapatite centers. However, one bone sample did offer a suggestion of hydroxyapatite centers and newly-developed methods to extract this information will be pursued.

03,615
PB94-185139 Not available NTIS
National Inst. of Standards and Technology (PL), Gaithersburg, MD. Ionizing Radiation Div.
Systematics of Alpha-Particle Energy Spectra and Lineal Energy (Y) Spectra for Radon Daughters.
Final rept.
R. S. Caswell, L. R. Karam, and J. J. Coyne. 1994, 4p.
Pub. in Radiation Protection Dosimetry 52, n1-4 p377-380 1994. Sponsored by Department of Energy, Washington, DC.

Keywords: *Bronchi, *Radon, *Alpha particles, *Biological radiation effects, *Daughter products, Carcinogenesis, Cells(Biology), Cell nucleus, Polonium 218, Polonium 214, Reprints, *Y spectra.

This study is concerned with the irradiation of target cells by alpha particles from radon daughters deposited in the bronchial airways, which may lead to cellular damage and carcinogenesis. Alpha particle energy spectra and y spectra at cell nuclei have been calculated for cell depths between 10 and 70 micrometers for the radon daughter nuclei, (218)Po, (214)Po, and for mixtures of the two. Calculations were performed for airways of diameters 1.130, 0.651, 0.435, and 0.198 cm (generations 2, 4, 6, and 10 of the Yeh and Schum morphometry). The y spectra assume a site size of 5 micrometers: the changes in the spectra are studied as functions of particular parameters. This information is useful as input to biophysical models of radon induced carcinogenesis. The significance of this work for the radon biological effectiveness problem is discussed.

03,616
PB94-199643 Not available NTIS
National Inst. of Standards and Technology (PL), Gaithersburg, MD. Ionizing Radiation Div.
EPR Bone Dosimetry: A New Approach to Spectral Deconvolution Problems.
Final rept.
M. F. Desrosiers. 1993, 4p.
Pub. in Applied Radiation and Isotopes 44, n1/2 p81-84 1993.

Keywords: *Bones, *Dosimetry, Electron paramagnetic resonance, Radiation accidents, Reprints.

Electron paramagnetic resonance (EPR) dosimetry was used to assess the dose to bone samples from radiation accident victims. Complications in the measurement process arose from overlapping resonances of multiple paramagnetic centers. A computer fitting routine was developed to enhance measurement of the EPR signal of interest, thereby improving the precision of the dose assessment.

03,617
PB94-199668 Not available NTIS
National Inst. of Standards and Technology (PL), Gaithersburg, MD. Ionizing Radiation Div.
Experimental Validation of Radiopharmaceutical Absorbed Dose to Mineralized Bone Tissue.
Final rept.
M. F. Desrosiers, M. J. Avila, D. A. Schauer, B. M. Coursey, and N. J. Parks. 1993, 6p.
Pub. in Applied Radiation and Isotopes 44, n1/2 p459-464 1993.

Keywords: *Radiopharmaceuticals, *Bones, *Dosimetry, *Physiologic calcification, Clinical trials, Electron paramagnetic resonance, Reprints.

Therapeutic and palliative uses of bone-seeking radiopharmaceuticals are undergoing clinical trials for human subjects. Radiation dosimetry for these applications is based on the Medical Internal Radiation Dosimetry (MIRD) schema. An experimental method for dosimetry of bone tissue based on electron paramagnetic resonance (EPR) spectrometry is described. Preliminary results for beagle bone exposed to radiopharmaceuticals under clinical conditions have indicated that the EPR dose measurements give approximately the calculated dose, but suggest that the dose distribution may be non-uniform.

03,618
PB94-199676 Not available NTIS
National Inst. of Standards and Technology (NML), Gaithersburg, MD. Ionizing Radiation Div.
Radiation Doses.
Final rept.
M. F. Desrosiers, B. M. Coursey, M. J. Avila, and N. J. Parks. 1991, 2p.
Pub. in Nature 349, n6307 p287-288 1991. Sponsored by California Univ., Davis. Lab. for Energy-Related Health Research.

Keywords: *Radiation dosage, *Radiopharmaceuticals, *Dosimetry, Dogs, Bones, Electron paramagnetic resonance, Holmium 166, Reprints.

A radiopharmaceutical containing holmium-166m was administered to a beagle. A bone sample was removed and examined by electron paramagnetic resonance (EPR) spectroscopy. Radiation-induced paramagnetic centers were detected in the bone tissue. The goal of these and future studies will be to quantify these centers in terms of dose and correlate this estimate with theoretical estimates.

03,619
PB94-199700 Not available NTIS
National Inst. of Standards and Technology (PL), Gaithersburg, MD. Ionizing Radiation Div.
New EPR Dosimeter Based on Polyvinylalcohol.
Final rept.
M. F. Desrosiers, J. M. Puhl, and W. L. McLaughlin. 1993, 2p.
Pub. in Applied Radiation and Isotopes 44, n1/2 p325-326 1993.

Keywords: *Dosimetry, *Polyvinyl alcohol, Electron paramagnetic resonance, Dose-response relationships, Reprints.

A new dosimetry system based on the electron paramagnetic resonance (EPR) response of polyvinyl alcohol is presented. The dose response was measured from 10-100,000 Gy and the persistence of the signal was monitored over a period of 14 days.

03,620
PB94-211273 Not available NTIS
National Inst. of Standards and Technology (NML), Gaithersburg, MD. Ionizing Radiation Div.
National Quality Assurance Program for Personnel Radiation Dosimetry: A Case History.
Final rept.
E. H. Eisenhower. 1988, 11p.
Pub. in Proceedings of the National Conference of Standards Laboratories Workshop and Symposium on Competitiveness in a World Market, Washington, DC., August 14-18, 1988, p18-1 - 18-11.

Keywords: *Quality assurance, *Personnel dosimetry, *Radiation dosage, *Dosimetry, *Performance standards, Ionizing radiation, Occupational safety and health, Standards, Radiation protection, Health physics, Exposure, Case studies, Reprints.

The estimated 1.3 million workers who are potentially exposed to ionizing radiation in the United States must be monitored for exposure by wearing personnel dosimeters. Accurate measurement of radiation doses received by workers is needed because of the health, economic, and legal consequences of exposure to radiation. Because of a general concern about the reliability of reported doses, government and industry groups made several attempts during 25 years to establish dosimetry performance standards. In 1973 the Conference of Radiation Control Program Directors stated that the necessary degree of reliability was not being achieved, in spite of attempts to provide reliability testing of personnel dosimetry services. This paper describes the subsequent development of a national program which now accredits personnel dosimetry processors that satisfy a prescribed level of performance. Reasons are given why the present program is successful, in contrast to earlier attempts.

03,621
PB94-211430 Not available NTIS
National Inst. of Standards and Technology (MSEL), Gaithersburg, MD. Polymers Div.
New Method for Shielding Electron Beams Used for Head and Neck Cancer Treatment.
Final rept.
M. Farahani, F. C. Eichmiller, and W. L. McLaughlin. 1993, 5p.
Pub. in Medical Physics 20, n4 p1237-1241 Jul/Aug 93.

Keywords: *Head and neck neoplasms, *Electron beams, *Radiation shielding, *Radiotherapy, Copper, Silver, Resin matrix composites, Catalysts, Reprints.

Shields and stents of metals with high atomic number, which are custom cast in molds from the melt, are the materials most widely used to protect surrounding tissues during treatment of skin or oral lesions with therapeutic electron beams. An improved fabrication method is to mix a polysiloxane-metal composite, which is readily cast at room temperature by combining a metal-powder/polysiloxane resin mixture with a hardening catalyst. The purpose of the present study is to compare the shielding effectiveness of two different metal-polysiloxane composites with that of conventional cast Lipowitz metal (50.1% Bi, 26.6% Pb, 13.3% Sn, 10% Cd). Also, a 2(sup 3) factorial experiment was run to investigate the effects and interactions of metal particle size (20-micrometers vs 100-micrometers diameter), the atomic weight of the metal (304 stainless steel vs 70% Ag, 30% Cu alloy), and the presence or absence of a layer of unfilled polymer added to the forward-scatter side of the shield. The composites of different thicknesses were made by blending 90% (w/w) metal powder separately with 10% polysiloxane base and catalyst. A thin GafChromic (TM) dosimeter film was placed between the shielding material and a polystyrene base to measure the radiation shielding effect of composite disc samples irradiated with a 6-MeV electron beam normal to the flat surface of the disc. The results show that composite shields with the metal of higher atomic weight and density (Ag-Cu) combined with an additional unfilled layer are more effective than the stainless-steel composite with a similar additional unfilled layer, in terms of diminishing the dose at the surface of the polystyrene backing material.

03,622
PB94-212933 Not available NTIS
National Inst. of Standards and Technology (NML), Gaithersburg, MD. Ionizing Radiation Physics Div.
Summary of the Proceedings of the Workshop on Standard Phantoms for In-vivo Radioactivity Measurement.
Final rept.
G. H. Kramer, and K. G. W. Inn. 1991, 2p.
Pub. in Health Physics 61, n6 p893-894 1991.

Keywords: *Meetings, *Anatomic models, *Standards, *Radioactivity, In vivo analysis, Quality assurance, Chest, Thyroid gland, Bone and bones, Tissue distribution, Reprints.

A three-day workshop on Standard Phantoms for In-vivo Radioactivity Measurements was co-sponsored by the Bureau of Radiation and Medical Devices, the National Institute of Standards and Technology (NIST), U.S. Nuclear Regulatory Commission, and the U.S. Department of Energy and held at NIST. It was established at the workshop that: (1) Standards Writing Groups must be organized to specify requirements for Torso, BOMAB, Thyroid, and Bone phantoms; (2) quality assurance of all manufacturing and radioactivity loading stages must include and stress documentation and be traceable to NIST; (3) radionuclides identified by the ANSI N13.30 draft standard are satisfactory; (4) the present Torso, BOMAB, and Thyroid reference phantoms are satisfactory as starting points for standard phantom research, development, and specification, and a set of 5, 10, 15 year old and 95 percent adult male is sufficient to fulfill the needs of the community; and (5) radionuclides should be homogeneously distributed in the phantoms.

03,623
PB95-128658 PC A06/MF A02
National Inst. of Standards and Technology, Gaithersburg, MD. National Voluntary Lab. Accreditation Program.
National Voluntary Laboratory Accreditation Program: Ionizing Radiation Dosimetry.
Handbook.
P. R. Martin. Aug 94, 116p, NIST/HB-150-4.
Also available from Supt. of Docs. as SN003-003-03286-7. See also PB94-178225.

Keywords: *Personnel dosimetry, *Dosimetry, *Laboratories, *Handbooks, Dosimeters, Beta dosimetry, Gamma dosimetry, X-ray dosimetry, Standardization, Performance evaluation, Assessments, Calibration, Test methods, Government policies, *National Voluntary Laboratory Accreditation Program, *NVLAP program, *Ionizing radiation dosimetry, Traceability, US NIST.

NIST Handbook 150-4 presents the technical requirements of the National Voluntary Laboratory Accreditation Program (NVLAP) for Ionizing Radiation Dosimetry (formerly called the Personnel Radiation Dosimetry program). It is intended for information and use by staff of accredited laboratories, those laboratories seeking accreditation, other laboratory accreditation systems, users of laboratory services, and others needing information on the requirements for accreditaton under the Ionizing Radiation Dosimetry program. This publication supplements NIST Handbook 150, NVLAP Procedures and General Requirements, (PB94-178225) which contains Part 285 of Title 15 of the U.S. Code of Federal Regulations (CFR) plus all general NVLAP procedures, criteria, and policies. Handbook 150-4 contains information that is specific to the Dosimetry program and does not duplicate information contained in the Procedures and General Requirements. It is organized to cross-reference with Handbook 150; for example, Section 285.3 of Handbook 150 presents the description and goal of NVLAP, whereas Section 285.3 of Handbook 150-4 presents the description of the Dosimetry program. Where there is no material specific to the field of accreditation, the section number is omitted.

03,624
PB95-152260 Not available NTIS
National Inst. of Standards and Technology (PL), Gaithersburg, MD. Ionizing Radiation Div.
Neutron Energy Deposition on the Nanometer Scale.
Final rept.
J. J. Coyne, and R. S. Caswell. 1992, 4p.
Contract DE-A105-86ER60389
Sponsored by Department of Energy, Washington, DC. Office of Health and Environmental Research.
Pub. in Radiation Protection Dosimetry 44, n1/4 p49-52 1992.

Keywords: Monte Carlo method, Tissues(Biology), Energy transfer, Neutrons, Radiation transport, Reprints, *Neutron dosimetry.

We have incorporated the synthesis of Monte Carlo results for proton tracks of Wilson, Metting, and Paretzke into our analytic method neutron microdosimetry code. Both 'crossers' and 'passers' are included. Results are calculated for neutrons in the energy range 1.05 MeV to 14.5 MeV for site diameters 2 nm to 1 micrometer.

03,625
PB95-152344 Not available NTIS
National Inst. of Standards and Technology (PL), Gaithersburg, MD. Ionizing Radiation Div.
Microdosimetry and Cellular Radiation Effects of Radon Progency in Human Bronchial Airways.
Final rept.
W. Hofmann, M. Noesterer, M. G. Menache, J. J. Coyne, D. J. Crawford-Brown, and R. S. Caswell. 1994, 5p.
Sponsored by Department of Energy, Washington, DC. Office of Energy Research. and Health Effects Research Lab., Research Triangle Park, NC.
Pub. in Radiation Protection Dosimetry 52, n1-4 p381-385 1994.

Keywords: *Radon, *Biological radiation effects, *Microdosimetry, *Dose response relationships, *Bronchi, Alpha particles, Daughter products, Radionuclide migration, Respiration, Radiation induced neoplasms, Lung neoplasms, Carcinogenesis, Cells(Biology), Risk assessment, Humans, Reprints, *Cell damage.

The microdosimetric interaction model simulates individual interactions of alpha particles with nuclei of sensitive target cells in human bronchial airway generations 2, 4, 6 and 10. For a normalized source density of Po 218 and Po 214 alpha particles, number of hits, microdosimetric spectra and related parameters for cell nuclei located at various depths in bronchial epithelium are calculated. The lineal energy spectrum is a spherical nuclear target is then converted into probabilities for cell killing, mutation and transformation by multiplying the single event chord length distribution with event specific effect probabilities per unit track length as a function of LET. These effect probabilities are finally weighted by the depth-density distributions of basal and secretory cells. The predicted transformation probability is compared with other physical indicators of lung cancer risk, such as dose, dose equivalent, biologically weighted dose, mean lineal energy, and number of alpha particle hits.

03,626
PB95-153375 Not available NTIS
National Inst. of Standards and Technology (PL), Gaithersburg, MD. Ionizing Radiation Div.
Extrapolation Chamber Measurements on (90)Sr + (90)Y Beta-Particle Ophthalmic Applicator Dose Rates.
Final rept.
J. O. Deasy, and C. G. Soares. 1994, 9p.
Pub. in Medical Physics 21, n1 p91-99 Jan 94.

Keywords: *Ophthalmology, *Radiation doses, *Beta dosimetry, *Extrapolation chambers, Strontium 90, Yttrium 90, Monte Carlo method, Electrodes, Accumulators, Ionizing radiation, Reprints, *Ophthalmic applicators, Collector electrodes.

Aspects of extrapolation chamber dose-rate measurements of (90)Sr + (90)Y beta-particle ophthalmic applicators are examined in this report, including the proper choice of collector electrode size, the gap width over which the measurement should be done, the effect of the entrance window materials, and the stopping-power ratio. Experiments, a simple analytic model for the effect of chamber geometry and nonzero gap width, and more detailed Monte Carlo simulations were used. The variation of the planar flux density as a function of angle for a thick (90)Sr + (90)Y source was measured and used as input for the model. From Monte Carlo simulation, the dose rate for tissue irradiation falls off by 8% between the surface and a depth of 7 mg/sq cm. The derivative of chamber ionization as a function of gap width, needed for the dose-rate calibration, increases rapidly as the gap width decreases, typically by a factor of about 2 between gap widths of 1.5 and 0.15 mm. The backscattering effect increases the derived surface dose by a factor of 1.46. A satisfactory dose-rate extrapolation is obtained from gap widths of 0.1-0.25 mm, where the total ionization current is observed to be nearly linear in gap width.

03,627
PB95-161741 Not available NTIS
National Inst. of Standards and Technology (CSTL), Gaithersburg, MD. Biotechnology Div.
DNA Base Damage Generated In vivo in Hepatic Chromatin of Mice upon Whole Body y-Irradiation.
Final rept.
T. Mori, Y. Hori, and M. Dizdaroglu. 1993, 6p.
Sponsored by Department of Energy, Washington, DC.
Pub. in International Jnl. of Radiation Biology 64, n6 p645-650 1993.

Keywords: *DNA damage, *Liver, *Chromatin, *Gamma rays, Dose-response relationships, Mutagenesis, Carcinogenesis, Mass fragmentography, Reprints, Hydroxyl radicals.

DNA base lesions in hepatic chromatin formed upon whole-body irradiation of mice were studied. After gamma-irradiating (20-470 Gy) and killing animals, chromatin was isolated from their livers and analyzed by gas chromatography-mass spectroscopy (GC-MS). Five pyrimidine- and five purine-derived DNA lesions were identified and quantified. There were 5-hydroxy-5-methylhydantoin, 5-hydroxycytosine, 5-(hydroxymethyl)uracil, 4,6-diamino-5-formamidopyrimidine, 7,8-dihyro-8-oxoadenine, 2-hydroxy-adenine, 2,6-diamino-4-hydroxy-5-formamidopyrimidine, 7,8-dihydro-8-oxoguanine, thymine glycol and 5,6-dihydroxy-uracil. Except for the latter two, the amounts of these compounds were increased significantly over control levels in the dose range of 100-470 Gy. Above 200 Gy, a deviation from linearity was observed, although the yields were increased in most cases up to 470 Gy. The modified bases that were identified are typically produced by hydroxyl radical attack on the DNA bases. This may indicate a role for hydroxyl radicals in their formation in vivo. These lesions may play a role in the biological consequences of ionizing radiation such as mutagenesis and carcinogenesis.

03,628
PB95-162632 Not available NTIS
National Inst. of Standards and Technology (PL), Gaithersburg, MD. Ionizing Radiation Div.
Radiation Process Data: Collection, Analysis, and Interpretation.
Final rept.
M. C. Saylor, S. W. Baryschpolec, L. M. Hurwitz, and W. L. McLaughlin. 1993, 21p.
Sponsored by Johnson and Johnson, New Brunswick, NJ.
Pub. in Proceedings of International Kilmer Memorial Conference on Sterilization of Medical Products, Brussels, Belgium, June 13-15, 1993, p240-260.

Keywords: *Dosimetry, *Sterilization, *Data processing, Digital systems, Surveys, Radiation measuring instruments, Digital computers, Ultraviolet radiation, Reprints, Industrial sterilization.

Prior to 1984, the capital expense tended to limit radiation-based sterilization technology's access to affordable, state-of-the-art digital technology in the form of programmable logic controllers (PLCs), computers and manufacturing-oriented programming languages. These components were utilized, however, in selected device manufacturing and pharmaceuticals sectors. The paper reviews key aspects of the role of radiation process data collection, analysis and interpretation at present and in the near future as radiation sterilization technologies continue to evolve.

03,629
PB95-164554 Not available NTIS
National Inst. of Standards and Technology, Gaithersburg, MD. Occupational Health and Safety Div.
Characterization of a Health Physics Instrument Calibration Range.
Final rept.
L. A. Slaback, and C. G. Jones. 1988, 9p.
Pub. in Proceedings of Midyear Topical Meeting on Instrumentation (22nd), San Antonio, TX., December 4-8, 1988, p281-288.

Keywords: *Health physics, *Measuring instruments, *Calibrating, *Test facilities, *Occupational safety and health, Cesium 137, Radiation dosage, Radiation protection, Radiation shielding, Alternatives, Attenuators, Filtration, Reprints.

The radiation field of an instrument calibration facility consisting of a 4m range and an 80 Ci Cs-137 source with various attenuators was characterized in terms of secondary field components such as backscatter and buildup; intensity of the radiation beam versus distance; actual effective energy of the filtered beams; useful field size and useful calibration distance as a function of detector size. The relative effectiveness of the attenuators with respect to an unfiltered beam is consistent at distances greater than one meter. At distances less than this, the relative effectiveness of the filters is not constant with up to an 8% change under certain conditions. Aluminum filtration was added to lead attenuators to correct for low energy emissions. This paper examines the scattered environment for a relatively small calibration room (3m x 7m) and presents it as a viable alternative to a large facility. A PC computer program is available which fits the calibration data that are described here.

03,630
PB95-168472 Not available NTIS
National Inst. of Standards and Technology (PL), Gaithersburg, MD. Ionizing Radiation Div.
Angular Variation of the Personal Dose Equivalent, Hp(0.07), for Beta Radiation and Nearly Monoenergetic Electron Beams: Preliminary Results.
Final rept.
T. A. da Silva, and C. G. Soares. 1994, 12p.
Pub. in Proceedings of Conference on Radiation Protection and Dosimetry (4th), Orlando, FL., October 23-27, 1994, p175-186.

Keywords: *Beta particles, *Electron beams, Reprints, *Personal dose equivalent, Angular dependence, Monoenergetic.

Using the NIST standard beta-particle radiation sources, as well as the NIST nearly-monoenergetic electron beams, the angular variation of the personal dose equivalent, H(sub p)(0.07), was experimentally determined. Measurements were performed with the NIST standard extrapolation chambers, and with thermoluminescent detectors covered with 7-mg/sq cm thickness of tissue equivalent material on a slab phantom. Extrapolation chamber correction factors, which are functions of energy and angle of incidence, were determined.

03,631
PB95-175428 Not available NTIS
National Inst. of Standards and Technology (PL), Gaithersburg, MD. Ionizing Radiation Div.
Interpreting the Readings of Multi-Element Personnel Dosimeters in Terms of the Personal Dose Equivalent.
Final rept.
M. Ehrlich, and T. Soodprasert. 1994, 13p.
Pub. in Radiation Protection Management 11, n3 p39-51 May/Jun 94.

Keywords: *Multi-element analysis, *Personnel dosimetry, *Dose equivalents, *Occupational exposure, Dosemeters, Radiation dose units, Radiation monitoring, Calibration, Performance evaluation, Algorithms, Reprints, Angle dependence, Energy dependence, Photon dosimeters.

In 1989, one of the authors (M.E.) suggested an algorithm for extending the well-known method of evaluating the readings of multi-filter and/or multi-element photon personnel dosimeters to take into account the dependence of their response both on energy and on angle, as is required for an interpretation in terms of the operational quantity 'personal dose equivalent.' This algorithm was tested on a widely used commercial photon dosimeter. At irradiation levels at which the dosimeter's less sensitive elements of low atomic numbers can be employed, the algorithm was found to be unnecessary for the interpretation of the readings in terms of the personal dose equivalent at a depth of 10 mm in tissue, over the entire photon-energy range and angles of photon incidence up to 60 deg.

03,632
PB95-175915 Not available NTIS
National Inst. of Standards and Technology (CSTL), Gaithersburg, MD. Biotechnology Div.
Ionizing Radiation Causes Greater DNA Base Damage in Radiation-Sensitive Mutant M10 Cells That in Parent Mouse Lymphoma L5178Y Cells.
Final rept.
T. Mori, and M. Dizdaroglu. 1994, 6p.
Sponsored by Department of Energy, Washington, DC.
Pub. in Radiation Research 140, p85-90 1994.

Keywords: *DNA damage, *Mutation, *Ionizing radiation, *Radiation tolerance, Dose-response relationships, Lymphoma, Cultured tumor cells, Chromatin, Mass fragmentography, Pyrimidines, Reprints.

The DNA base damage in radiation-sensitive mutant M10 cells and parent mouse lymphoma L5178Y cells was studied. Cells were exposed to ionizing radiation in the dose range of 48 to 400 Gy. Chromatin was isolated from cells and analyzed by gas chromatography-mass spectrometry. Ten DNA base products were identified and quantified. A dose-dependent formation of the products was observed. The yields of products in M10 cells were up to threefold greater than in L5178Y cells. Of the products measured, formamidopyrimidines had the highest difference in their yields between the two cell lines. The greater initial DNA base damage in M10 cells may play a role in their hypersensitivity to ionizing radiation.

03,633
PB96-102645 Not available NTIS
National Inst. of Standards and Technology (PL), Gaithersburg, MD. Ionizing Radiation Div.
Intercomparison Study of (237)Np Determination in Artificial Urine Samples.
Final rept.
S. C. Lee, J. M. Robin Hutchinson, K. G. W. Inn, and M. Thein. 1995, 9p.
Pub. in Health Physics, v68 n3 p350-358 1995.

Keywords: *Neptunium 237, *Radioassay, *Bioassay, *Urine, Urinalysis, Occupational exposure, Biological accumulation, Excretion, Radiochemical analysis, Qualitative chemical analysis, Alpha detection, Alpha particles, Coprecipatation, Anion exchanging, Reprints, Inductively coupled plasma mass spectroscopy.

An intercomparison study of low-level Np-237 determination in artificial urine samples has been carried out. The purpose of this study was to find the 'optimal' method presently available for use in a routine in-vitro radiobioassay program for occupationally exposed workers. The solutions were submitted to 10 alpha-particle and 10 inductively coupled plasma-mass spectrometry (ICP-MS) laboratories of which six and four laboratories, respectively, returned results. The best results obtained by ICP-MS were comparable with but not better than the most accurate results obtained by alpha-particle spectrometry. Alpha-particle spectrometry measurements overall gave consistently better agreement with known values.

03,634
PB96-123708 Not available NTIS
National Inst. of Standards and Technology (PL), Gaithersburg, MD. Ionizing Radiation Div.
Comparison of NIST and Manufacturer Calibrations of (90)Sr+(90)Y Ophthalmic Applicators.
Final rept.
C. G. Soares. 1995, 7p.
Pub. in Medical Physics, v22 n9 p1487-1493 1995.

Keywords: *Calibration, *Radiation doses, Strontium 90, Yttrium 90, Ionizing radiation, Reprints, *Ophthalmic applications, National Institutes of Standards and Technology.

Since the resumption of the NIST calibration service for 90Sr + 90Y beta-particle ophthaimic applicators, 65 sources have been calibrated using the revised technique (C. G. Soares, Med. Phys. 18, 787-793(1991)). For 59 of these sources, the manufacturer's calibration results were available for comparison to the NIST calibration results were available for comparison to the NIST calibration results. The 59 sources represent eight different manufactures, only one of which is still selling new sources. Manufacturer calibration dates range from the present back to 1954. The resuls of the comparisons are presented, broken down by both manufacturer and calibration date: there are interesting and significant trends in both, with average differences of 20% not uncommon. The obsolete unit, 'roentgen-equivalent-beta' (reb), in which some of the manufacturer calibrations are expressed, is discussed, and a factor (0.00982 Gy reb sub -1) for its conversion to absorbed dose is suggested.

03,635
PB96-141288 Not available NTIS
National Inst. of Standards and Technology (PL), Gaithersburg, MD. Ionizing Radiation Div.
Research and Development Activities in Electron Paramagnetic Resonance Dosimetry.
Final rept.
M. F. Desrosiers, G. Burlinska, P. Kuppusamy, F. P. Auteri, M. R. McClelland, C. E. Dick, W. L. McLaughlin, J. Zweier, and D. M. Yaczko. 1995, 4p.
Pub. in International Meeting on Radiation Processing (9th), Istanbul, Turkey, September 11-16, 1994, Radiation Physics and Chemistry, v46 n4-6 p1181-1184 Oct 95.

Keywords: *Irradiation, Electron paramagnetic resonance, Reprints, Gamma rays, Electron beams, Quartz, *Foreign technology, *Dosimetry, *Alanine, Spin trapping.

This work describes ongoing activities in Electron Paramagnetic Resonance (EPR) dosimetry at the National Institute of Standards and Technology. Progress in the commercialization of the alanine-EPR system will be discussed along wih basic research in high-dose dosimetry, including EPR imaging.

03,636
PB96-146782 Not available NTIS

Radiobiology

National Inst. of Standards and Technology (PL), Gaithersburg, MD. Ionizing Radiation Div.
Investigation of Applicability of Alanine and Radiochromic Detectors to Dosimetry of Proton Clinical Beams.
Final rept.
D. Nichiporov, V. Kostijuchenko, J. M. Puhl, C. E. Dick, W. L. McLaughlin, T. Kojima, B. M. Coursey, S. Zink, D. L. Bensen, and M. F. Desrosiers. 1995, 8p.
Pub. in Applied Radiation and Isotopes, v46 n12 p1355-1362 Dec 95.

Keywords: *Alanine, *Dosimetry, *Proton accelerators, Detectors, Films, Proton beams, Radiotherapy, Radiation dosage, Interlaboratory comparisons, Clinical medicine, Reprints, Radiochromic films, LET.

Cancer therapy studies using proton accelerators are underway in several major medical centers in the U.S., Russia, Japan and elsewhere. To facilitate dosimetry intercomparisons between these laboratories, alanine-based detectors produced at the National Institue of Standards and Technology and commercially available radiochromic films were studied for their possible use as passive transfer dosimeters for clinical proton beams. Evaluation of characteristics of these instruments, including the LET dependence of their response of proton energy, was carried out at the Institute of Theoretical and Experimental Physics.

03,637
PB96-160254 Not available NTIS
National Inst. of Standards and Technology (PL), Gaithersburg, MD. Ionizing Radiation Div.
External Gamma-ray Counting of Selected Tissues from a Thorotrast Patient.
Final rept.
C. W. Mays, R. L. Aamodt, K. G. W. Inn, V. G. Iyengar, F. J. Schima, L. S. Slaback, J. W. Tracy, T. P. Lynch, K. L. Mossman, D. R. Brown, and R. R. Greenberg. 1992, 8p.
Pub. in Workshop Proceedings, Health Physics, v63 n1 p33-40 1992.

Keywords: *Health physics, Patients, Dose, Tissue sampling, Reprints, *Thorotrast.

Results of gamma-ray measurements of selected tissues from a patient who was injected with Thorotrast almost 36 y ago are reported. The purposes of this study were: (1) to determine the relative tissue distribution and activities of specific radionuclides in the Th decay chain, specifically Ra (as measured by Ac), Pb, and Ra (measured directly and as measured by Pb), and (2) to evaluate the level of radioactive disequilibrium among the daughter products. The spleen and liver had the highest concentrations of radioactivity. Bone also appears to be a long-term sink for Th daughter products based on estimates from a small portion of one rib. Larynx and esophagus contained measurable activity, which may have been due to their proximity to the 'Thorotrastoma.'

03,638
PB97-110035 Not available NTIS
National Inst. of Standards and Technology (PL), Gaithersburg, MD. Ionizing Radiation Div.
Radon in the Lung.
Final rept.
R. S. Caswell, and L. R. Karam. 1993, 7p.
See also PB95-152344.
Pub. in Radon Research Notes, p6-12 Nov 93.

Keywords: *Radon, *Lungs, *Dose response relationships, Bronchi, Respiration, Computer codes, Reprints, *Cell damage, RADONA.

A computer code, RADONA (radon-analytic), has been developed to investigate the physics of the interaction of radon in the lung. This code (1) calculates the slowing-down spectra of alpha particles at the locations of the cells in the bronchial epithelium and (2) calculates y (lineal energy) spectra at specified cell depths and for site sizes in the range of 0.5 to 10 micrometers. The authors are primarily concerned with cylindrical airways.

03,639
PB97-110373 Not available NTIS
National Inst. of Standards and Technology (PL), Gaithersburg, MD. Ionizing Radiation Div.
EPR Dosimetry of Cortical Bone and Tooth Enamel Irradiated with X and Gamma Rays: Study of Energy Dependence.
Final rept.
D. A. Schauer, M. F. Desrosiers, F. G. Le, S. M. Seltzer, and J. M. Links. 1994, 8p.
Sponsored by Navy Health Sciences Education and Training Command, Bethesda, MD. and Department of Energy, Washington, DC. Office of Health and Environmental Research.
Pub. in Radiation Research, v138 p1-8 1994.

Keywords: *X rays, *Tooth enamel, *Cortical bone, *Dosimetry, Energy dependent, Gamma rays, Reprints.

Previous investigators have reported that the radiation-induced EPR signal intensity in compact or cortical bone increases up to a factor of two with decreasing photon energy for a given absorbed dose. If the EPR signal intensity was dependent on energy, it could limit the application of EPR spectrometry and the additive reirradiation method to obtain dose estimates. The authors have recently shown that errors in the assumptions governing conversion of measured exposure to absorbed dose can lead to similar 'apparent' energy-dependence results. They hypothesized that these previous results were due to errors in the estimated dose in bone, rather than the effects of energy dependence per se. To test this hypothesis the authors studied human adult cortical bone from male and female donors ranging in age from 23 to 95 years, and bovine tooth enamel, using 34 and 138 keV average energy X-ray beams and (137)Cs (662 keV) and (60)Co (1250 keV) gamma rays.

03,640
PB97-110381 Not available NTIS
National Inst. of Standards and Technology (PL), Gaithersburg, MD. Ionizing Radiation Div.
Exposure-to-Absorbed-Dose Conversion for Human Adult Cortical Bone.
Final rept.
D. A. Schauer, S. M. Seltzer, and J. M. Links. 1993, 5p.
Sponsored by Navy Health Sciences Education and Training Command, Bethesda, MD. and Department of Energy, Washington, DC. Office of Health and Environmental Research.
Pub. in Applied Radiation and Isotopes, v44 n3 p485-489 1993.

Keywords: *Bones, *Photons, Humans, Dose-absorbed, Exposure, Reprints, F-factors, Mass energy-absorption coefficients.

The conversion of measured exposure to absorbed dose at a point in bone, under conditions of electron equilibrium, involves a factor (the f-factor) which is proportional to the ratio of the spectrum-averaged photon energy-absorption coefficient for bone to that for air. The paper gives mass energy-absorption coefficients and f-factors for three compositions of human adult compact or cortical bone recommended in publications by the ICRU and ICRP, for photon energies from 1 keV to 1.5 MeV. Spectrum-averaged f-factor results reflect: (1) the rather large differences due to the differing calcium contents among the recommended compositions for bone; and (2) the generally poor predictions obtained when replacing a broad energy spectrum by an equivalent photon energy.

03,641
PB97-119259 Not available NTIS
National Inst. of Standards and Technology (PL), Gaithersburg, MD. Ionizing Radiation Div.
Novel Radiochromic Films for Clinical Dosimetry.
Final rept.
W. L. McLaughlin, J. M. Puhl, M. Al-Sheikhly, A. Kovacs, L. Wojnarovits, D. F. Lewis, C. A. Christou, and A. Miller. 1996, 6p.
Pub. in Radiation Protection Dosimetry, v66 n1-4 p263-268 1996.

Keywords: *Dosimetry, Radiotherapy, Radiation dosage, Clinical medicine, Absorption, Gamma rays, Reprints, *Foreign technology, *Radiochromic films.

New transparent radiochromic films, GafChromic MD-55 and NMD-55, which turn from colorless to deep blue upon irradiation, have been designed particularly for measuring radiation therapy absorbed doses (1 Gy to 100 Gy). They are also useful for high resolution mapping of dose distributions, radiographic imaging, treatment planning dosimetry, beam penumbra measurements, and interface dosimetry with ionizing photons, electrons and protons. The gamma ray responses are linear with dose in terms of increase of optical absorbance at 670.633, and 600 nm and are independent of absorbed dose rate and relative humidity. The radiochromic images show a slight gradual post-irradiation increase in absorbance especially during the first 24 h. In addition, there is a small but predictable variation of sensitivity with temperature, both during iraddiation and during spectrophotometry. The films also have a slight sensitivity to ultraviolet radiation (250 to 350 nm) in direct sunlight. Experiments with X ray beams show no appreciable energy dependence relative to dose in water at photon energies greater than 100 keV, but they have a sensitivity that gives readings of about 60% of the dose in water for photons at 20 to 40 keV.

03,642
PB97-122246 Not available NTIS
National Inst. of Standards and Technology (PL), Gaithersburg, MD.
Flat and Curved Crystal Spectrography for Mammographic X-ray Sources.
Final rept.
C. T. Chantler, R. D. Deslattes, A. Henins, and L. T. Hudson. 1996, 14p.
Pub. in British Jnl. of Radiology, v69 p636-649 Jul 96.

Keywords: *X ray, *Mammography, *Spectrography, Crystals, Voltage calibration, Analytical equations, Reprints.

The demand for improved spectral understanding of mammographic X-ray sources and non-invasive voltage calibration of such sources has led to research into applications using curved crystal spectroscopy. Recent developments and the promise of improved precision and control are described. Analytical equations are presented to indicate effects of errors and alignment problems in the flat and curved crystal systems. These are appropriate for all detection systems. Application to and testing of spectrographic detection (using standard X-ray film) is presented. Suitable arrangements exist which can be used to measure X-ray tube voltages well below 1 kV precision in the operating range of 20-35 kV.

03,643
PB97-122444 Not available NTIS
National Inst. of Standards and Technology (CSTL), Gaithersburg, MD. Biotechnology Div.
DNA Base Damage in Lymphocytes of Cancer Patients Undergoing Radiation Therapy.
Final rept.
R. Olinski, T. H. Zastawny, M. Foksinski, M. Dizdaroglu, W. Windorbska, and P. Jaruga. 1996, 9p.
Pub. in Cancer Letters, v106 p207-215 1996.

Keywords: *Radiation therapy, *DNA damage, *Lymphocytes, Patients, Cancer, Free radicals, Hydroxyl radical, Reprints, *Foreign technology.

The authors investigated DNA base damage in genomic DNA of lymphocytes of cancer patients undergoing radiation therapy. Lymphocyte chromatin samples were analyzed by gas chromatography/isotope-dilution mass spectrometry for DNA base damage. The results provided evidence for formation of typical hydroxyl radical-induced base modifications in genomic DNA of lymphocytes. Different levels of DNA products in individuals were observed and, in the case of some patients, there was no significant product formation, possibly resulting from differences between individuals and between the types of radiation exposures. Decreases in product levels after an initial increase by radiation exposure were observed. This may indicate the removal of modified bases from lymphocyte DNA by cellular repair.

Toxicology

03,644
PB94-182003 Not available NTIS
National Inst. of Standards and Technology (CSTL), Gaithersburg, MD. Biotechnology Div.

Tert-Butyl Hydroperoxide-Mediated DNA Base Damage in Cultured Mammalian Cells.
Final rept.
S. Altman, T. Zastawny, L. Randers, J. Remacle, M. Dizdaroglu, G. Rao, Z. Lin, and J. Lumpkin. 1994, 10p.
Contract NIH-RR-06562
Pub. in Mutation Research 306, p35-44 1994. Sponsored by National Institutes of Health, Bethesda, MD.

Keywords: *DNA damage, *Mutagens, Cultured cells, Mass spectrometry, Escherichia coli, Dose-response relationships, Hybridomas, Free radical scavengers, Chromatin, Reprints, *Tert-butyl hydroperoxide.

Tert-Butyl hydroperoxide has been utilized to study the effect of oxidative stress on living cells; however, its effect on DNA bases in cells has not been characterized. In the present work, we have investigated DNA base damage in mammalian cells exposed to this organic hydroperoxide. SP2/0 derived murine hybridoma cells were treated with 4 concentrations of tert.-butyl hydroperoxide for varying periods of time. Chromatin was isolated from treated and control cells and subsequently analyzed by gas chromatography-mass spectrometry with selected-ion monitoring for DNA-base damage. Quantification of damaged DNA bases was achieved by isotope-dilution mass spectrometry. The amounts of 8 products were significantly higher than control levels in cells treated with tert.-butyl hydroperoxide at a concentration range of 0.01-0.1 mM. At concentrations from 1.0 to 10 mM, product formation was inhibited and the amounts of products were similar to those in control cells. The bimodal nature of the dose-response may be qualitatively analogous to previous reports of bimodal killing of E. coli bacteria by hydrogen peroxide. The nature of the identified DNA base lesions suggests the involvement of the hydroxyl radical in their formation. The inhibition of product formation at high concentrations of tert.-butyl hydroperoxide may be explained by the scavenging of tert.-butoxyl radical by tert.-butyl hydroperoxide resulting in inhibition of oxidative stress. The plausibility of the scavenging mechanism was evaluated with a mathematical simulation of the dose-response for DNA damage in solutions containing hydrogen peroxide.

03,645
PB94-198231 Not available NTIS
National Inst. of Standards and Technology (CSTL), Gaithersburg, MD. Biotechnology Div.
Copper Ion-Mediated Modification of Bases in DNA in Vitro by Benzoyl Peroxide.
Final rept.
S. A. Akman, T. W. Kensler, J. H. Doroshow, and M. Dizdaroglu. 1993, 4p.
Pub. in Carcinogenesis 14, n9 p1971-1974 1993.

Keywords: *DNA damage, *Copper, *Mutagens, *Benzoyl peroxide, In vitro analysis, Ions, Mass fragmentography, Free radical scavengers, Dimethyl sulfoxide, Reprints.

The mouse skin tumor promoter benzoyl peroxide (BzPO), in conjunction with Cu(I), causes promutagenic damage in DNA. Because free radical intermediates are produced by the reaction of BzPO with Cu(I), the authors sought to determine whether BzPO plus Cu(I) caused DNA base damage typical of that caused by the hydroxyl radical. A broad range of modified DNA bases were measured by GC-MS with selected-ion monitoring after exposure of purified plasmid pCMV beta gal DNA to BzPO + or - Cu(I). Exposure to BzPO/Cu(I) caused up to 20-fold increases in the levels of adenine-derived modified bases, up to 4-fold increases in guanine- and cytosine-derived modified bases, and only a <2-fold increase in thymine-derived modified bases. The guanine-derived modified base 8-hydroxyguanine was elevated to the highest net amount. Exposure to BzPO alone or Cu(I) alone induced only minor (< <2-fold) DNA base modification. Also, benzoic acid, the major non-radical metabolite of BzPO, or BzPO plus Fe(II) were ineffective at inducing DNA base modification. The hydroxyl radical scavenger dimethyl sulfoxide inhibited BzPO/Cu(I)-induced base modification by 10-50%. These data suggest that the reaction of BzPO with Cu(I) generates hydroxyl radical or a similarly reactive intermediate which causes DNA base damage. This damage may be responsible for BzPO/Cu(I)-mediated mutagenesis.

03,646
PB94-212628 Not available NTIS
National Inst. of Standards and Technology (CSTL), Gaithersburg, MD. Biotechnology Div.

Nickel(II)-Mediated Oxidative DNA Base Damage in Renal and Hepatic Chromatin of Pregnant Rats and Their Fetuses. Possible Relevance to Carcinogenesis.
Final rept.
K. Kasprzak, B. Diwan, J. Rice, M. Dizdaroglu, M. Misra, and R. Olinski. 1992, 7p.
Pub. in Toxicology 5, n6 p809-815 Nov/Dec 92.

Keywords: *DNA damage, *Nickel, *Liver, *Kidney, *Teratogens, *Chromatin, Carcinogens, Fetus, Oxidation, Reprints.

DNA base damage was studied in renal and hepatic chromatin of nickel(II)-injected pregnant female F344/NCr rats and their fetuses under conditions leading to initiation of sodium barbital-promotable renal tumors, but not liver tumors, in the male offspring. Pregnant rats were given a total of 90 or 180 micromol of nickel(II) acetate/kg body wt in a single ip dose on day 17 or in 2 or 4 ip doses between days 12 and 18 of gestation. Control rats received 180 micromol of sodium acetate/kg body wt. The animals were killed 24 or 48 h after the last injection. Chromatin was isolated from livers and kidneys from both adults and fetuses and analyzed by gas chromatography/mass spectrometry with selected ion monitoring. Eleven products derived from the purine and pyrimidine bases in DNA bases were identified and quantified. Nickel(II) exposure increased the content of these products, especially those derived from purines, in both renal and hepatic chromatin of pregnant rats. The major difference between these two organs was the content of 8-OH-Gua, which increased greatly in the kidney but remained unchanged in the liver. In the corresponding fetal organs, the relative increases in 8-OH-Gua were comparable to the findings in adults. Fetal kidney DNA was relatively higher in pyrimidine-derived products (especially thymine glycol and 5-hydroxyhydantoin) and lower in purine-derived products (except for 8-OH-Gua) than fetal hepatic DNA. No consistent dose effect of nickel(II) on the amounts of the DNA base products recovered from either organ was observed in either the dams or their fetuses. The present results indicate possible involvement of oxidative DNA base damage in the mechanism of nickel(II) carcinogenesis in the rat kidney.

03,647
PB95-150025 Not available NTIS
National Inst. of Standards and Technology (CSTL), Gaithersburg, MD. Biotechnology Div.
Oxidative DNA Base Damage in Renal, Hepatic, and Pulmonary Chromatin of Rats After Intraperitoneal Injection of Cobalt (II) Acetate.
Final rept.
K. Kasprzak, T. Zastawny, S. North, J. Rice, M. Dizdaroglu, C. Riggs, and B. Diwan. 1994, 7p.
Pub. in Chemical Research in Toxicology 7, n3 p329-335 May/Jun 94.

Keywords: *DNA damage, *Chromatin, *Liver, *Kidney, *Lung, *Mutagens, Rats, Mass fragmentography, Sex factors, Oxidation, Carcinogens, Reprints, *Cobalt acetate.

DNA base damage was studied in renal, hepatic, and pulmonary chromatin of male and female F344/NCr rats that had been given either 50 or 100 micromol of Co(II) acetate/kg body wt in a single ip dose and killed 2 or 10 days later. Control rats received 200 micromol of sodium acetate/kg body wt. Chromatin was isolated from organs and analyzed by gas chromatography/mass spectrometry with selected ion monitoring. Eleven products derived from purine and pyrimidine bases in DNA were quantified. The response was organ-specific. Eight of the DNA base products in renal chromatin of CO(II)-treated rats, five in hepatic chromatin, and two in pulmonary chromatin were increased by 30% to more than 200% over control levels with increasing CO(II) dose. The renal and hepatic, but not pulmonary, DNA base damage tended to increase with time. No significant differences in response were found between male and female rats. The bases determined were typical products of hydroxyl radical attack on DNA, suggesting a role for this radical in the mechanism(s) of DNA damage caused by Co(II) in vivo. Some of these bases have been shown previously to be promutagenic. The present results imply involvement of oxidative DNA damage in Co(II)-induced genotoxic and carcinogenic effects.

03,648
PB95-150363 Not available NTIS
National Inst. of Standards and Technology (CSTL), Gaithersburg, MD. Biotechnology Div.

DNA Base Modifications in Renal Chromatin of Wistar Rats Treated with a Renal Carcinogen, Ferric Nitrilotriacetate.
Final rept.
S. Toyokuni, T. Mori, and M. Dizdaroglu. 1994, 6p.
Sponsored by Department of Energy, Washington, DC.
Pub. in International Jnl. of Cancer 57, p123-128 1994.

Keywords: *DNA damage, *Carcinogens, *Chromatin, *Kidney, Wistar rats, Mass fragmentography, Proximal kidney tubules, Necrosis, Mutagens, Carcinogenesis, Reprints, *Ferric nitrilotriacetate.

Ferric nitrilotriacetate (Fe-NTA) causes renal proximal tubular necrosis, a consequence of iron ion-mediated free-radical-associated damage, that finally leads to a high incidence of renal adenocarcinoma in male rats and mice. We have investigated the levels of typical hydroxyl radical-induced DNA base modifications in renal chromatin of male Wistar rats treated with a single or repeated administrations of Fe-NTA. Five pyrimidine-derived and 5 purine-derived modified DNA bases were identified and quantified by gas chromatography/mass spectrometry with selected-ion monitoring. The amounts of most of these compounds were significantly increased over control levels in renal chromatin of Fe-NTA-treated rats as measured 3 and 24 hrs after treatment. Elevated levels of modified bases were accompanied by proximal tubular necrosis. Presence of modified DNA bases concomitant with necrosis and regeneration of the renal proximal tubules may be a critical step in Fe-NTA-induced carcinogenesis.

03,649
PB96-112115 Not available NTIS
National Inst. of Standards and Technology (CSTL), Gaithersburg, MD. Biotechnology Div.
Treatment of Wistar Rats with a Renal Carcinogen, Ferric Nitrilotriacetate, Causes DNA-Protein Cross-Linking between Thymine and Tyrosine in Their Renal Chromatin.
Final rept.
S. Toyokuni, T. Mori, H. Hiai, and M. Dizdaroglu. 1995, 5p.
Pub. in International Jnl. of Cancer, v62 p309-313, 14 Sep 95.

Keywords: *DNA damage, *Carcinogens, *Chromatin, *Kidney, Reprints, Wistar rats, Carcinogenesis, Necrosis, Proximal kidney tubules, *Ferric nitrilotriacetate.

Ferric nitrilotriacetate (Fe-NTA) induces renal proximal tubular damage associated with lipid peroxidation and oxidative DNA base modifications that finally leads to a high incidence of renal adenocarcinoma in rodents. In the present study, we report on the in vivo formation of DNA-protection cross-links (DPCs) involving thymine and tyrosine in the renal chromatin of Wistar rats treated with single or repeated i.p. administration of Fe-NTA. Analyses of chromatin samples by gas chromatography/mass spectrometry revealed a significant increase in the amount of 3-((1,3-dihydro- 2,4-dioxopyrimidin- 5-yl)-methyl)-L-tyrosine (Thy-Tyr cross-link) 23 and 48 hr after the administration of Fe-NTA. At19th day of FE-NTA treatment, the amount of Thy-Tyr cross-link decreasedto the control level, indicating the presence of cellular repair activity. Thy-Tyr cross-link may play a role in the genetic alteration of this renal carcinogenesis model, since mitoses for reregeneration of renal proximal tubules were closely associated with the increase in DPCs.

03,650
PB96-123260 Not available NTIS
National Inst. of Standards and Technology (CSTL), Gaithersburg, MD. Biotechnology Div.
Further Development of the N-Gas Mathematical Model: An Approach for Predicting the Toxic Potency of Complex Combustion Mixtures.
Final rept.
B. C. Levin, E. Braun, M. Navarro, and M. Paabo. 1995, 19p.
Pub. in Fire and Polymers II, Chapter 20, p293-311 Oct 95.

Keywords: *Combustion, Mathematical models, Carbon dioxide, Carbon monoxide, Complex mixtures, Hydrogen chloride, Hydrogen cyanide, Toxicity, Reprints, *N-gas model.

A methodology has been developed for predicting smoke toxicity based on the toxicological interactions of complex fire gas mixtures. This methodology consists of burning materials using a bench-scale method that simulates realistic fire conditions, measuring the concentrations of the following primary fire gases - CO,

CO2, O2, HCN, HCl, Hbr, and NO2 - and predicting the toxicity of the smoke using an empirical mathematical model called the N-Gas Model. The model currently in use is based on toxicological studies of the first six of the above listed primary gases both as individual gases and complex mixtures. The predicted toxic potency (based on this N-Gas Model) is checked with a small number of animal (Fischer 344 male rats) tests to assure than an unanticipated toxic gas was not generated. The results indicate whether the smoke from a material or product is extremely toxic (based on mass consumed at the predicted toxic level) or unusually toxic (based on mass consumed at the predicted toxic level) or unusually toxic (based on the gases deemed responsible). The predictions based on bench-scale laboratory tests have been verified with full-scale room burns of a limited number of materials of widely differing characteristics chosen to challenge the system.

03,651
PB96-137724 Not available NTIS
National Inst. of Standards and Technology (CSTL), Gaithersburg, MD. Biotechnology Div.
Formation of DNA-Protein Cross-Links in Cultured Mammalian Cells Upon Treatment with Iron Ions.
Final rept.
S. A. Altman, T. H. Zastawny, L. Randers-Eichhorn, M. Dizdaroglu, G. Rao, M. A. Cacciuttolo, and S. A. Akman. 1995, 6p.
Pub. in Free Radical Biology and Medicine, v19 n6 p897-902 1995.

Keywords: *DNA-binding proteins, *Crosslinking, *Chromatin, *Iron, Toxicity, Reprints, Hydroxyl radical, Oxidative stress, Free radicals, Thymine-tyrosine crosslinks.

Formation of DNA-protein crosslinks (DPCs) in mammalian cells upon treatment with iron or copper ions was investigated. Cultured murine hybridoma cells were tested with Fe(II) or Cu(II) ions by addition to the culture medium at various concentrations. Subsequently, chromatin samples were isolated from treated and control cells. Analyses of chromatin samples by gas chromatography/mass spectrometry after hydrolysis and derivatization revealed a significant increase over the background amount of 3-((1,3-dihydro- 2,4-dioxopyrimidin- 5-yl)-methyl)-L-tyrosine (Thy-Tyr crosslink) in cells treated with Fe(II) ions in the concentration range of 0.01 to 1 mM. In contrast Cu(II) ions at the same concentrations did not produce this DPC in cells. No DNA base damage was observed in cells treated with Cu(II) ions, either. Preincubation of cells with ascorbic acid or coincubation with dimethyl sulfoxide did not significantly alleviate the Fe(II) ion-mediated formation of DPCs. In addition, a modified fluorometric analysis of DNA unwinding assay was used to detectDPCs formed in cells. Fe(II) ions caused significant formation of DPCs, but CU(II) ions did not. The nature of the Fe(II)-mediated DPCs suggeststhe involvement of the hydroxyl radical in their formation. The Thy-Tyr crosslink may contribute to pathological processes associated with free radical reactions.

03,652
PB96-161740 Not available NTIS
National Inst. of Standards and Technology (CSTL), Gaithersburg, MD. Biotechnology Div.
Protonation Dynamics of the alpha-Toxin Ion Channel from Spectral Analysis of pH-Dependent Current Fluctuations.
Final rept.
J. J. Kasianowicz, and S. M. Bezrukov. 1995, 12p.
Pub. in Biophysical Jnl., v69 p94-105 Jul 95.

Keywords: *Conductance fluctuations, *Amino acids, *Noise analysis, Reprints, *Deuterium isotope effects, Ionization dynamics, Protein ion channels.

To probe protonation dynamics inside the fully open alpha-toxin ion channel, the authors measured the pH-dependent fluctuations in its current. In the presence of 1 M NaCl dissolved in H2O and positive applied potentials (from the side of protein addition), the low frequency noise exhibited a single well defined peak between pH 4.5 and 7.5. A simple model in which the current is assumed to change by equal amounts upon the reversible protonation of each of N identical ionizable residues inside the channel describes the data well. These results, and the frequency dependence of the spectral density at higher frequencies, allow the authors to evaluate the effective pK = 5.5, as well as the rate constants for the reversible protonation reactions: kon = 8 x 10 to the 9th power M to the minus 1 power S to the minus 1 power and Koff = 2.5 x 10 to the 4th power S to the minus 1 power. The estimate of kon is only slightly less than the diffusion-limited values measured by others for protonation reactions for free carboxyl or imidazole residues. Substitution of H2O by D2O caused a 3.8-fold decrease in the dissociation rate constant and shifted the pK to 6.0. The decrease in the ionization rate constants caused by H2O/D3O substitution permitted the reliable measurement of the characteristic relaxation time over a wide range of D+ concentrations and voltages. The dependence of the relaxation time on D+ concentration strongly supports the first order reaction model.

MILITARY SCIENCES

General

03,653
PB95-189510 PC A03/MF A01
National Inst. of Standards and Technology (CSL), Gaithersburg, MD. Computer Security Div.
Assessment of the DOD Goal Security Architecture (DGSA) for Non-Military Use.
A. E. Oldehoeft. Nov 94, 34p, NISTIR-5570.
See also PB94-170362 and PB95-109203. Sponsored by Defense Information Systems Agency, Arlington, VA.

Keywords: *US DOD, *Computer security, *Commercial sector, Systems engineering, Data processing security, Standards, Computer networks, Information systems, Telecommunication, Computer systems hardware, Computer software, *DGSA(DoD Goal Security Architecture), *DoD Goal Security Architecture, ISO(International Standards Organization), ISA(Internet Security Architecture), DCE(Distributed Computing Environment).

The purpose of this study is to assess the potential of the DOD Goal Security Architecture (DGSA) as a model and framework for the development of non-military computer information security architectures. To achieve this goal, this study presents an overview of the DGSA and provides a cursory comparison of some of the features of the DGSA with several prominent, proposed non-military security architectures including: the International Standards Organization (ISO); SESAME; the Internet Security Architecture (ISA); and Open Systems Foundation (OSF) Distributed Computing Environment (DCE). The study concludes the DGSA has the potential for being applicable in both the civilian and commercial sectors. However, there are some attending restrictions that may prevent its acceptance. These restrictions are detailed in the Summary Observations.

03,654
PB95-203790 PC A03/MF A01
National Inst. of Standards and Technology (MEL), Gaithersburg, MD. Intelligent Systems Div.
Robotics Application to Highway Transportation. Volume 1. Final Report.
Rept. for Sep 92-Nov 93.
E. W. Kent. Jan 95, 34p, FHWA/RD-94/053.
Contract DTFH61-92-Y-00160
See also PB95-170551, PB95-171633 and PB95-193173. Sponsored by Federal Highway Administration, McLean, VA. Office of Advanced Research.

Keywords: *Air Force training, *United States Air Force Academy, *Career development, Military training, Air Force planning, Air Force personnel, Education, Schools, Careers, Curriculum development, Military personnel, Military planning.

The Office of the Registrar, Academic Affairs Division (DFRC) publishes the Curriculum Handbook at the beginning of each calendar year. Together with the USAFA Catalog published by the Office of Administrations (RR), it documents the curriculum of the United States Air Force Academy as approved by the Academy Board. The Curriculum Handbook contains general information concerning graduation requirements, academic registration procedures, course offerings, academic majors, and academic probation.

03,655
PB96-119649 Not available NTIS
National Inst. of Standards and Technology (EEEL), Boulder, CO. Electromagnetic Fields Div.
NIST and the Navy: Past, Present and Future.
Final rept.
G. R. Reeve, and D. S. Friday. 1995, 9p.
Sponsored by American Society of Naval Engineers, Alexandria, VA. and Society of Logistics Engineers, New Carrollton, MD.
Pub. in Proceedings of the Test and Calibration Symposium, Washington, DC., November 30-December 1, 1994, p229-237.

Keywords: *Navy, *Interagency cooperation, US DOD, Technology innovation, Naval research, Research support, Research programs, Support services, Program management, History, Reprints, *US NIST.

The National Institute of Standards and Technology (NIST) has had an historic and fruitful relationship with the Department of Defense, its predecessors, and the three military services, particularly the Navy. In this paper, we will outline some of the historic support, current collaborations, and what areas of technology may require our support for the Navy of the future.

Logistics, Military Facilities, & Supplies

03,656
AD-A280 223/9 PC A06/MF A02
National Bureau of Standards, Gaithersburg, MD.
1950 Supplement to Screw-Thread Standards for Federal Services. 1944.
20 Mar 51, 119p.

Keywords: *Federal law, *Standards, *Screw threads, Handbooks, Department of Defense.

No abstract available.

03,657
PB94-962000 Contact NTIS for subscription information and price.
National Inst. of Standards and Technology, Gaithersburg, MD.
CALS-Automated Interchange of Technical Information.
Irregular repts.
1994, open series.
Supersedes PB93-962000.
Paper copy available on Standing Order, deposit account required (minimum deposit $100 U.S., Canada, and Mexico; all others $200). Single copies also available in paper copy or microfiche.

Keywords: *Standards, *Specifications, Digital data, Manuals, Computer graphics, Computer aided design, Computer aided manufacturing, File management systems, Automation, Information processing, *CALS(Computer-aided Acquisition and Logistics Support).

The publication is the parent document for a family of military specifications through which the Computer-aided Acquisition and Logistics Support (CALS) standards will be published. It provides the 'enveloping' rules for organizing files of digital data into a complete document--for example, a technical manual composed of MIL-M 28001 text, MIL-D-28003 Vector Graphics, and MIL-R-28001 Raster Graphics.

03,658
PB94-962100 Contact NTIS for subscription information and price.
National Inst. of Standards and Technology, Gaithersburg, MD.
CALS-Digital Representation for Communication of Product Data: IGES Application Subsets.
Irregular repts.
1994, open series.
Supersedes PB93-962100.
Paper copy available on Standing Order, deposit account required (minimum deposit $100 U.S., Canada, and Mexico; all others $200). Single copies also available in paper copy or microfiche.

Keywords: *Computer aided design, Computer aided manufacturing, Graphic arts, Numerical control, Engineering drawings, Data transmission,

*CALS(Computer-aided Acquisition and Logistics Support), *IGES(Initial Graphics Exchange Specification).

The publication defines subsets of the Initial Graphics Exchange Specification (IGES) for technical illustration, engineering drawings, electrical/electronic applications, and numerical control manufacturing, IGES is a neutral format for digital interchange of Product Definition Data between dissimilar computer aided design systems.

03,659
PB94-962200 Contact NTIS for subscription information and price.
National Inst. of Standards and Technology, Gaithersburg, MD.
CALS-Markup Requirements and Generic Style Specifications for Electronic Printed Output and Exchange of Text.
Irregular repts.
1994, open series.
Supersedes PB93-962200.
Paper copy available on Standing Order, deposit account required (minimum deposit $100 U.S., Canada, and Mexico; all others $200). Single copies also available in paper copy and microfiche.

Keywords: *Publishing, *Automation, Text processing, Computer aided design, Computer aided manufacturing, *CALS(Computer-aided Acquisition and Logistics Support), Department of Defense.

The publication defines standard Department of Defense (DoD) requirements for all steps involved in automated publishing of page-oriented (i.e., printed) technical publications. For exchange of source data (prior to document composition it defines a common implementation of the Standard Generalized Markup Language (SGML). For composition processing functions, it defines an Output Specification of typographic tags and format rules, and for display of the composed document, it provides options for use of commercial Page Description languages.

03,660
PB94-962300 Contact NTIS for subscription information and price.
National Inst. of Standards and Technology, Gaithersburg, MD.
CALS-Raster Graphics Representation Binary Format Requirements.
Irregular repts.
1994, open series.
Supersedes PB93-962300.
Paper copy available on Standing Order, deposit account required (minimum deposit $100 U.S., Canada, and Mexico; all other $200). Single copies also available in paper copy or microfiche.

Keywords: *Computer aided design, *Computer graphics, File management systems, Documents, Facsimile communication, Image processing, Standards, Computer aided manufacturing, *CALS(Computer-aided Acquisition and Logistics Support), Department of Defense.

The publication defines Department of Defense (DoD) technical requirements for raster (bit-map) graphics that have been compressed to reduce file size and transmission time. Computer-aided Acquisition and Logistics Support (CALS) must apply raster graphics to both office documents and facsimiles (for which the international standard that MIL-R-28002 implements was prepared), and for engineering drawings and other oversize documents. An option is included to use tiling, in which the raster image is divided into a series of tiles that can be individually processed to reduce throughout and terminal storage requirements.

03,661
PB94-962400 Contact NTIS for subscription information and price.
National Inst. of Standards and Technology, Gaithersburg, MD.
CALS-Digital Representation for Communication of Illustration Date: CGM Application Profile.
Irregular repts.
1994, open series.
Supersedes PB93-962400.
Paper copy available on Standing Order, deposit account required (minimum deposit $100 U.S., Canada, and Mexico; all others $200). Single copies also available in paper copy or microfiche.

Keywords: *Computer aided design, *Computer graphics, Manuals, Graphic arts, Work stations, Digital data, Two dimensional models, Computer aided manufacturing, *CALS(Computer-aided Acquisition and Logistics Support), Computer graphics metafile.

The publication defines use of Computer Graphics Metafile (CGM) for two dimensional vector (line segment) picture descriptions or illustrations in technical manuals. Whereas Initial Graphics Exchange Specification (IGES) has its principal use within computer-aided design, CGM is becoming widely available for authoring and graphic art work stations.

03,662
PB94-962500 Contact NTIS for subscription information and price.
National Inst. of Standards and Technology, Gaithersburg, MD.
CALS-Department of Defense Computer Aided Acquisition Logistic Support (CALS).
Irregular repts.
1994, open series.
Supersedes PB93-962500.
Paper copy available on Standing order, deposit account required (minimum deposit $100 U.S., Mexico, and Canada; all others $200). Single copies also available in paper copy or microfiche.

Keywords: *Weapons system, *Logistics management, Acquisition, Information services, Contract administration, Computer aided design, Computer aided manufacturing, *CALS(Computer-aided Acquisition and Logistics Support), Department of Defense.

The guide assists weapon system acquisition managers to understand when, where, and how to apply Computer-Aided Acquisition and Logistics Support (CALS) capabilities efficiently to support their information interchange and access requirements, and how to define their functional requirements for integration of the contractor process (such as Reliability and Maintainability analysis) that create and use the information.

03,663
PB94-962600 Contact NTIS for subscription information and price.
National Inst. of Standards and Technology, Gaithersburg, MD.
CALS-Contractor Integrated Technical Information Service (CITIS), Functional Requirements.
Irregular repts.
1994, open series.
Supersedes PB93-962600.
Paper copy available on Standing Order, deposit account required (minimum deposit $100 U.S., Canada, and Mexico; all others $200). Single copies also available in paper copy or microfiche.

Keywords: *Information services, *Requirements, On line systems, Contractors, US DOD, *CALS(Computer-aided Acquisition and Logistics Support), *CITIS(Contractor Integrated Technical Information Service).

The publication describes functional requirements for the Department of Defense's (DoD's) new Computer-Aided Acquisition and Logistics Support (CALS) acquisition policy which gives preference to contractor information services and online access instead of data deliverables. Contractor Integrated Technical Information Service (CITIS) addresses how DoD will buy information services instead of what form the deliverable will be in, whether paper or digital based. it defines things a contractor must do, such as planning, analysis, and submitting proposals and things the service must do, such as managing data, and providing access to the data tailored to meet a government Concept of Operations.

03,664
PB95-105029 PC A04/MF A01
National Inst. of Standards and Technology (CAML), Gaithersburg, MD. Office of Applied Economics.
Present Worth Factors for Life-Cycle Cost Studies in the Department of Defense (1995).
Final rept.
S. R. Petersen. Oct 94, 63p, NISTIR-4942-2.
See also PB94-109238. Sponsored by Assistant Secretary of Defense (Production and Logistics), Washington, DC.

Keywords: *Life cycle costs, *Present worth, *Energy supplies, *Military facilities, Benefit cost analysis, Economic analysis, Energy conservation, Buildings, Construction, Return on investment, Cost engineering, Fuels, Regional analysis, Department of Defense, Tables(Data), Military Construction Program.

This document provides 47 tables of present worth factors to be used in computing the present worth of future costs (or cost reductions) in economic analyses of design decisions for projects in the Department of Defense (DoD) Military Construction Program. These factors are especially useful for the life-cycle cost analysis of investments in buildings or building systems which are intended to reduce future operating, maintenance, repair, replacement, and energy costs over the life of the facility. The tables include present worth factors for both one-time costs and annually recurring costs, based on the Federal Energy Management Program (FEMP) discount rate of 3.0% (FY 1995) for energy-related studies and on the Office of Management and Budget (OMB) discount rate of 2.5% and 2.8% for short-term and long-term non-energy studies, respectively. Forecasts of future energy prices used in the calculation of present worth factors for energy costs were provided by the Energy Information Administration.

03,665
PB95-162723 Not available NTIS
National Inst. of Standards and Technology (NEL), Gaithersburg, MD. Robot Systems Div.
Vehicle-Command Center Communications in a Robotic Vehicle System.
Final rept.
H. A. Scott. 1992, 18p.
Pub. in Automation in Construction 1, n3 p267-284 Dec 92.

Keywords: *Ground vehicles, *Automatic control, *Robotics, Remote control, Communications central, Army, Real time operations, Data links, Telecommunication, Reprints, Remote vehicles, Robotic vehicles, Real time control, Remote data links.

The U.S. Army Laboratory Command is developing a testbed for cooperative, real-time control of multiple land vehicles from a remotely located command center. The paper analyzes the characteristics of the communication link between the vehicle and the remote command center. Areas addressed include the communication technology, the information content and required rates, the control system communication requirements, communications support of the development effort and examination of available standards.

03,666
PB95-962000 Contact NTIS for subscription information and price.
National Inst. of Standards and Technology, Gaithersburg, MD.
CALS-Automated Interchange of Technical Information.
Irregular repts.
1995, open series.
Supersedes PB94-962000.
Paper copy available on Standing Order, deposit account required (minimum deposit $100 U.S., Canada, and Mexico; all others $200). Single copies also available in paper copy or microfiche.

Keywords: *Standards, *Specifications, Digital data, Manuals, Computer graphics, Computer aided design, Computer aided manufacturing, File management systems, Automation, Information processing, *CALS(Continuous Acquisition and Life-Cycle Support).

The publication is the parent document for a family of military specifications through which the Continuous Acquisition and Life-Cycle Support (CALS) standards will be published. It provides the 'enveloping' rules for organizing files of digital data into a complete document--for example, a technical manual composed of MIL-M 28001 text, MIL-D-28003 Vector Graphics, and MIL-R-28001 Raster Graphics.

03,667
PB95-962100 Contact NTIS for subscription information and price.
National Inst. of Standards and Technology, Gaithersburg, MD.
CALS-Digital Representation for Communication of Product Data: IGES Application Subsets.
Irregular repts.
1995, open series.
Supersedes PB94-962100.
Paper copy available on Standing Order, deposit account required (minimum deposit $100 U.S., Canada, and Mexico; all others $200). Single copies also available in paper copy or microfiche.

Keywords: *Computer aided design, Computer aided manufacturing, Graphic arts, Numerical control, Engi-

neering drawings, Data transmission, *CALS(Continuous Acquisition and Life-Cycle Support), *IGES(Initial Graphics Exchange Specification).

The publication defines subsets of the Initial Graphics Exchange Specification (IGES) for technical illustration, engineering drawings, electrical/electronic applications, and numberical control manufacturing, IGES is a neutral format for digital interchange of Product Definition Data between dissimilar computer aided design systems.

03,668
PB95-962200 Contact NTIS for subscription information and price.
National Inst. of Standards and Technology, Gaithersburg, MD.
CALS-Markup Requirements and Generic Style Specifications for Electronic Printed Output and Exchange of Text.
Irregular repts.
1995, open series.
Supersedes PB94-962200.
Paper copy available on Standing Order, deposit account required (minimum deposit $100 U.S., Canada, and Mexico; all others $200). Single copies also available in paper copy and microfiche.

Keywords: *Publishing, *Automation, Text processing, Computer aided design, Computer aided manufacturing, *CALS(Continuous Acquisition and Life-Cycle Support), Department of Defense.

The publication defines standard Department of Defense (DoD) requirements for all steps involved in automated publishing of page-oriented (i.e., printed) technical publications. For exchange of source data (prior to document composition it defines a common implementation of the Standard Generalized markup Language (SGML). For composition processing functions, it defines an Output Specification of typographic tags and format rules, and for display fo the composed document, it provides options for use of commercial Page Description languages.

03,669
PB95-962300 Contact NTIS for subscription information and price.
National Inst. of Standards and Technology, Gaithersburg, MD.
CALS-Raster Graphics Representation Binary Format Requirements.
Irregular repts.
1995, open series.
Supersedes PB94-962300.
Paper copy available on Standing Order, deposit account required (minimum deposit $100 U.S., Canada, and Mexico; all other $200). Single copies also available in paper copy or microfiche.

Keywords: *Computer aided design, *Computer graphics, File management systems, Documents, Facsimile communication, Image processing, Standards, Computer aided manufacturing, *CALS(Continuous Acquisition and Life-Cycle Support), Department of Defense.

The publication defines Department of Defense (DoD) technical requirements for raster (bit-map) graphics that have been compressed to reduce file size and transmission time. Continuous Acquisition and Life-Cycle Support (CALS) must apply raster graphics to both office documents and facsimiles (for which the international standard that MIL-R-28002 implements was prepared), anf for engineering drawings and other oversize documents. An option is included to use tiling, in which the raster image is divided into a series of tiles that can be individually processed to reduce throughout and terminal storage requirements.

03,670
PB95-962400 Contact NTIS for subscription information and price.
National Inst. of Standards and Technology, Gaithersburg, MD.
CALS-Digital Representation for Communication of Illustration Date: CGM Application Profile.
Irregular repts.
1995, open series.
Supersedes PB94-962400.
Paper copy available on Standing Order, deposit account required (minimum deposit $100 U.S., Canada, and Mexico; all others $200). Single copies also available in paper copy or microfiche.

Keywords: *Computer aided design, *Computer graphics, Manuals, Graphic arts, Work stations, Digital data, Two dimensional models, Computer aided manufacturing, *CALS(Continuous Acquisition and Life-Cycle Support), Computer graphics metafile.

The publication defines use of Computer Graphics Metafile (CGM) for two dimensional vector (line segment) picture descriptions or illustrations in technical manuals. Whereas Initial Graphics Excahnge Specification (IGES) has its principal use within computer-aided design, CGM is becoming widely available for authoring and graphic art work stations.

03,671
PB95-962500 Contact NTIS for subscription information and price.
National Inst. of Standards and Technology, Gaithersburg, MD.
CALS-Department of Defense Computer Aided Acquisition Logistic Support (CALS).
Irregular repts.
1995, open series.
Supersedes PB94-962500.
Paper copy available on Standing order, deposit account required (minimum deposit $100 U.S., Mexico, and Canada; all others $200). Single copies also available in paper copy or microfiche.

Keywords: *Weapons system, *Logistics management, Acquisition, Information services, Contract administration, Computer aided design, Computer aided manufacturing, *CALS(Continuous Acquisition and Life-Cycle Support), Department of Defense.

The guide assists weapon system acquisition managers to understand when, where, and how to apply Computer-Aided Acquisition and Logistics Support (CALS) capabilities efficiently to support their information interchange and access requirements, and how to define their functional requirements for integration of the contractor process (such as Reliability and Maintainability analysis) that create and use the information.

03,672
PB95-962600 Contact NTIS for subscription information and price.
National Inst. of Standards and Technology, Gaithersburg, MD.
CALS-Contractor Integrated Technical Information Service (CITIS), Functional Requirements.
Irregular repts.
1995, open series.
Supersedes PB94-962600.
Paper copy available on Standing Order, deposit account required (minimum deposit $100 U.S., Canada, and Mexico; all others $200). Single copies also available in paper copy or microfiche.

Keywords: *Information services, *Requirements, On line systems, Contractors, US DOD, *CALS(Continuous Acquisition and Life-Cycle Support), *CITIS(Contractor Integrated Technical Information Service).

The publication describes functional requirements for the Department of Defense's (DoD's) new Continuous Acquisition and Life-Cycle Support (CALS) acquisition policy which gives preference to contractor information services and online access instead of data deliverables. Contractor Integrated Technical Information Service (CITIS) addresses how DoD will buy information services instead of what form the deliverable will be in, whether paper or digital based. it defines things a contractor must do, such as planning, analysis, and submitting proposals and things the service must do, such as managing data, and providing access to the data tailored to meet a government Concept of Operations.

03,673
PB96-106869 PC A04/MF A01
National Inst. of Standards and Technology (CAML), Gaithersburg, MD. Office of Applied Economics.
Present Worth Factors for Life-Cycle Cost Studies in the Department of Defense (1996).
S. R. Petersen. Oct 95, 62p, NISTIR-4942-3.
See also report for 1995, PB95-105029. Sponsored by Federal Energy Management Program, Washington, DC.

Keywords: *US DOD, *Life cycle costs, *Energy supplies, Present worth, Cost analysis, Economic analysis, Cost engineering, Return on investment, Cost reduction, Cost estimates, Fuels, Natural gas, Electric power, Disillates, Residual oils, Liquefied petroleum gas, Steam, Coal, Tables(Data), Military Construction Program.

This document provides 47 tables of present worth factors to be used in computing the present worth of future costs (or cost reductions) in economic analyses of design decisions for projects in the DOD Military Construction Program. These factors are especially useful for the life-cycle cost analysis of investments in buildings or building systems which are intended to reduce future operating, maintenance, repair, replacement, and energy costs over the life of the facility. The tables include present worth factors for both one-time costs and annually recurring costs, based on the FEMP discount rate of 4.1% (FY 1996) for energy-related studies and on the OMB discount rate of 4.6% and 4.9% for short-term and long-term non-energy studies, respectively. Forecasts of future energy prices used in the calculation of present worth factors for energy costs were provided by the Energy Information Administration.

03,674
PB96-112651 PC A04/MF A01
National Inst. of Standards and Technology (NCSL), Gaithersburg, MD. Systems and Network Architecture Div.
Federal Implementation Guideline for Electronic Data Interchange: ASC X12 003040 Transaction Set 838 Trading Partner Profile (Vendor Registration), Implementation Convention.
Special pub.
J. P. Favreau. Aug 95, 61p, NIST/SP-881/1.
Also available from Supt. of Docs. as SN003-003-00363-4. See also PB96-111190, AD-A263 350/1 and AD-A263 445/9.

Keywords: *Computer programs, *Information exchange, *Acquisitions, Standards, Databases, Logistics management, Industries, Corporations, Procurement, *EDI(Electronic Data Interchange), *Electronic Data Interchange.

The ASC X12 003040 Transaction Set 838, Trading Partner (Vendor Registration), Implementation Convention defines the Federal Government interpretation of the use of ASC X12 003040 standards. This implementation convention provides the information necessary for the user to be able to develop an interface program between the computer application and the ASC X12 translator.

03,675
PB96-155023 PC A05/MF A01
National Inst. of Standards and Technology (EEEL), Boulder, CO. Electromagnetic Fields Div.
TEM/Reverberating Chamber Electromagnetic Radiation Test Facility at Rome Laboratory.
M. L. Crawford, B. F. Riddle, and D. G. Camell. Jan 96, 75p, NISTIR-5002.

Keywords: *Reverberation chambers, *Electromagnetic testing, Electromagnetic susceptibility, Vulnerability, Test facilities, Performance evaluation, Radio frequencies, Electromagnetic pulses, Rome Air Development Center, Griffis Air Force Base, Weapons systems, Magnetic permeability, Electric equipment.

This report summarizes the measurement and evaluation of a TEM/reverberating chamber. This chamber was developed as a single, integrated facility for testing radiated electromagnetic compatibility/vulnerability (EMC/V) of large systems over the frequency range of 10 kHz to 18 GHz or higher. The facility consists of a large shielded enclosure configured as a transverse electromagnetic (TEM) transmission line-driven reverberating chamber. TEM mode test fields are generated at frequencies below multimode cutoff, and mode-stirred test fields are generated at frequencies above multimode cutoff. The report discusses the basis for such a development including the theoretical concepts, the advantages and limitations, the experiments approach for evaluating the operational parameters, and the procedures for using the chamber to perform EMC/V measurements. Both the chamber's cw and pulsed rf characteristics are measured and analyzed.

NATURAL RESOURCES & EARTH SCIENCES

Cartography

03,676
PB94-172079 Not available NTIS
National Inst. of Standards and Technology (TS), Gaithersburg, MD. Metric Program.
Metrication.
Final rept.
G. P. Carver. 1993, 6p.
Pub. in Point of Beginning magazine, p74-78, 81, Oct/Nov 93. See also PB93-188969.

Keywords: *Surveying(Geographic), *Mapping, *Metrication, Government policies, Metric system, Standardization, Conversion, USA, Reprints.

The metric system is one key to success in the global marketplace, where non-metric products are becoming increasingly unacceptable. Procurement is the primary federal tool for encouraging and helping U.S. industry to convert voluntarily to the metric system. Common sense, based upon the knowledge, experience, and needs of an industry, should be the determinant in choosing a practical conversion approach. In the United States, besides the perceived unwillingness of the customer, and certain legal definitions in some states, there are no major impediments to conversion of surveying and mapping to metric units. Instead, there are good reasons for changing, including an opportunity to rethink many industry standards and to take advantage of size standardization. Also, when surveying and mapping services adopt the metric system, they will come into conformance with federal agencies engaged in similar activities.

03,677
PB95-150942 Not available NTIS
National Inst. of Standards and Technology (NCSL), Gaithersburg, MD. Information Systems Engineering Div.
Standards: A Cardinal Direction for Geographic Information Systems.
Final rept.
H. Tom. 1988, 11p.
Pub. in Proceedings of Annual Conference of the Regional Information Systems Association (26th), Los Angeles, CA., August 7-11, 1988, v2 p142-152.

Keywords: *Geographic information systems, *Computer applications, *Standards, Computer aided mapping, Automatic mapping, Digital data, Systems integration, Interoperability, Reprints, Digital spatial applications.

Geographic Information Systems reflect the changing role of computer technology within earth science disciplines. Successful use of computer technology includes the ability to interchange or interface computer data, software, and hardware. This ability, in large part, is predicated on standards. Intensifying the need for standards is the changing use of computer technology to provide information. Standardization of fundamental parameters and the implementation, integration, and support of standards facilitate system integration and interoperability. A clear understanding of standards is decisive in determining the impact of geographic information systems. The focus is primarily on the applicability, strategy, and commitment regarding standards pertaining to geographic information systems.

03,678
PB95-163390 Not available NTIS
National Inst. of Standards and Technology (NCSL), Gaithersburg, MD. Information Systems Engineering Div.
Geographic Information Systems Standards: A Federal Perspective.
Final rept.
H. Tom. 1990, 3p.
Pub. in GIS World 3, n2 p50-52 1990.

Keywords: *Geographic information systems, *Computer aided mapping, *Standards, Automatic mapping, Digital data, Computer applications, Systems integration, Interoperability, Information technology, Reprints, Digital spatial data.

Spatial data standards are associated with defining, describing, and processing spatial data. Information technology (IT) standards are generic computer standards. IT standards specifically implemented or generically configured for GIS usage can also be considered GIS standards. The adaptation of IT standards provides GIS with an existing set of common computer standards for enabling integration within a GIS. These standards also facilitate interoperability between different GIS or between a GIS and its overall corporate computer environment.

03,679
PB96-135108 Not available NTIS
National Inst. of Standards and Technology (CSL), Gaithersburg, MD. Information Systems Engineering Div.
Spatial Information and Technology Standards Evolving.
Final rept.
H. Tom. 1991, 3p.
Pub. in 1991-92 International GIS Sourcebook, Chapter 3, p422-424 Aug 91.

Keywords: *Digital data, *Geographic information systems, *Standards, Computer aided mapping, Automatic mapping, Systems integration, Interoperability, Computer applications, Reprints, Digital spatial data.

Standards typically evoke different responses in observers. Such a range of reactions also is experienced in the world of GIS standards. Support at both ends of this spectrum is evident, yet a balanced perspective of GID standards is lacking.

03,680
PB96-159629 Not available NTIS
National Inst. of Standards and Technology (TS), Gaithersburg, MD. Metric Program.
METRICATION: An Economic Wake-Up Call for Surveyors and Mappers.
Final rept.
G. P. Carver. 1993, 8p.
See also PB93-188969.
Pub. in Point of Beginning (P.O.B.), v19 n1 p74-81 Oct 93.

Keywords: *Mapping, *Surveying, *Metric system, Metrication, Measurement, Conversion, International system of units, Cartography, Reprints.

The 'modernized' metric system is the international System of Units or SI (from the French Le Systeme Internationale d'Unites). It includes the product standards and preferred sizes that are accepted by industries and governments throughout the world.

Geology & Geophysics

03,681
PB94-198686 Not available NTIS
National Inst. of Standards and Technology (PL), Boulder, CO. Quantum Physics Div.
Integrated Laser Doppler Method for Measuring Planetary Gravity Fields.
Final rept.
P. L. Bender. 1992, 10p.
Pub. in Proceedings of International Association of Geodesy Symposium on Gravity Field Determination from Space and Airborne Measurements, Vienna, Austria, August 20, 1991, p63-72 1992.

Keywords: *Gravitational fields, *Earth gravitation, *Lunar gravitation, *Planetary gravitation, Polar orbits, Satellite tracking, High resolution, Geodynamics, Reprints, Laser doppler techniques.

Four main approaches have been applied to, or studied extensively for use in, high-resolution determination of the global gravity fields of the Earth, other planets, or the Moon. These approaches are the following: laser or microwave tracking of spacecraft orbiting the Earth; microwave tracking from the Earth of spacecraft orbiting other planets or the Moon; satellite-to-satellite microwave tracking; and gravity gradiometry from an orbiting spacecraft. The paper will discuss another possibility which has been studied much less extensively. It is the use of integrated laser Doppler measurements between two spacecraft in essentially the same nearly polar orbit. In this case, the shot noise in the measurement system can be extremely low, even for 5 cm diameter transmit and receive apertures and 1 milliwatt of laser power. For the highest accuracy, it is assumed that a Disturbance Reduction System would be used to strongly reduce the disturbing forces on a freely floating and carefully shielded test mass inside each spacecraft. As one example, the authors take 50 km spacecraft separation and a spurious acceleration level of 5 x 10(sup -10) m/s(sup 2)/Hz(sup 0.5) from 0.005 to 0.1 Hz. The achievable accuracy with laser Doppler measurements is then expected to be 10(sup -5) Eotvos/Hz(sup 0.5) in this frequency range for the difference of the line-of-sight test mass accelerations divided by the spacecraft separation.

03,682
PB95-175030 Not available NTIS
National Inst. of Standards and Technology (MSEL), Boulder, CO. Materials Reliability Div.
Crystal Structure and Compressibility of 3:2 Mullite.
Final rept.
D. Balzar, and H. Ledbetter. 1993, 5p.
Pub. in American Mineralogist 78, p1192-1196 1993.

Keywords: *Mullite, *Crystal structure, *Compressibility, X ray diffraction, Ionic crystals, Crystal models, Bulk modulus, Ultrasonic radiation, Aluminum oxide, Silicon dioxide, Reprints.

The crystal structure of 3:2 mullite (3Al2O3 (center dot) 2SiO2) has been refined by Rietveld refinement of X-ray powder diffraction data. The average structure is described successfully by previously published models for 2:1 mullite. Bond lengths of tetrahedral cations are slightly shorter, because of the smaller ionic radii of Si(4+) relative to Al(3+). Using ultrasonic methods, we determined the bulk modulus (reciprocal compressibility). The result, 174 GPa, is slightly lower than that of a prediction based on a rigid-ion ionic crystal model: 190 GPa.

03,683
PB95-202495 Not available NTIS
National Inst. of Standards and Technology (PL), Boulder, CO. Quantum Physics Div.
Lunar Laser Ranging: A Continuing Legacy of the Apollo Program.
Final rept.
J. O. Dickey, P. L. Bender, J. E. Faller, J. G. Ries, P. J. Shelus, C. Veillet, A. L. Whipple, J. R. Wiant, J. G. Williams, C. F. Yoder, Newhall, and R. L. Ricklefs. 1994, 9p.
See also PB91-203026.
Pub. in Science 265, p482-490, 22 Jul 94.

Keywords: *Lunar rangefinding, *Geodynamics, Apollo 11 flight, Laser range finders, Equivalence principle, Lunar rotation, Gravitation, Moon, Uses, Reprints.

On 21 July 1969, during the first manned lunar mission, Apollo 11, the first retroreflector array was placed on the moon, enabling highly accurate measurements of the Earthmoon separation by means of laser ranging. Lunar laser ranging (LLR) turns the Earthmoon system into a laboratory for a broad range of investigations, including astronomy, lunar science, gravitational physics, geodesy, and geodynamics. Contributions from LLR include the three-orders-of-magnitude improvement in accuracy in the lunar ephemeris, a several-orders-of-magnitude improvement in the measurement of the variations in the moon's rotation, and the verification of the principle of equivalence for massive bodies with unprecedented accuracy. Lunar laser ranging analysis has provided measurements of the Earth's precession, the moon's tidal acceleration, and lunar rotational dissipation. These scientific results, current technological developments, and prospects for the future are discussed.

03,684
PB95-202651 Not available NTIS
National Inst. of Standards and Technology (PL), Boulder, CO. Quantum Physics Div.
Calibration of a Superconducting Gravimeter Using Absolute Gravity Measurements.
Final rept.
J. Hinderer, N. Florsch, J. Makinen, H. Legros, and J. E. Faller. 1991, 7p.
Pub. in Geophys. Jnl. Int. 106, p491-497 1991.

Keywords: *Gravimeters, *Calibration, Superconducting devices, Sensitivity analysis, Uncer-

tainty, Precision, Tests, Reprints, *Superconducting gravimeters, Absolute gravity.

A 24 hr continuous parallel registration between an absolute free-fall gravimeter and a relative cryogenic gravimeter is analyzed. Different adjustment procedures (L(1), L(2) norms) are applied to the sets of absolute and relative readings in order to estimate the value of the calibration factor of the superconducting meter, as well as its uncertainty. In addition, a sensitivity test is performed to investigate the influence of some parameters (like the laser frequency and its short-term drift) upon this factor. The precision in the calibration factor is found to be better than 1 per cent, but systematic effects related to the short time interval may add another one and half per cent uncertainty. From preliminary results, it appears that this calibration experiment leads to a close agreement between the values of the gravimetric factor for the reference tidal wave O(1) observed with the superconducting meter and the theoretical value (Dehant-Wahr body tide + ocean loading).

03,685
PB95-203048 Not available NTIS
National Inst. of Standards and Technology (PL), Boulder, CO. Quantum Physics Div.
Continuous Gravity Observations Using Joint Institute for Laboratory Astrophysics Absolute Gravimeters.
Final rept.
T. M. Niebauer, and J. E. Faller. 1992, 9p.
Pub. in Jnl. of Geophysical Research 97, nB9 p12,427-12,435, 10 Aug 92.

Keywords: *Gravimeters, *Gravity, Calibration, Correction, Reprints, Absolute gravity.

We discuss two different 1-month gravity records taken with two different Joint Institute for Laboratory Astrophysics (JILA) gravimeters. These records were corrected for the effects of Earth tides, ocean loading, local and global barometric effects, and polar motion. These data allowed precise determinations of the local air pressure admittance. We also obtained a value for the second-order gravimetric factor which agreed with the theoretical value to about 0.3% where the predominant uncertainty is the ocean load modeling. We note that absolute gravimeters have a sensitivity to time varying gravity that is comparable to that obtained with superconducting relative gravimeters. The sensitivity of these data emphasizes the need for better modeling of ocean loads, air pressure effects, and even man-made environmental noise.

03,686
PB96-102611 Not available NTIS
National Inst. of Standards and Technology (PL), Boulder, CO. Time and Frequency Div.
Measurement and Interpretation of Tidal Tilts in a Small Array.
Final rept.
M. L. Kohl, and J. Levine. 1995, 13p.
Pub. in Jnl. of Geophysical Research, v100 nB3 p3929-3941, 10 Mar 95.

Keywords: *Tiltmeters, *Strain measurement, Reprints, Geodynamics, Boreholes, Sensitivity, *Earth tides, Tilt tides.

Strain-induced tilts caused by variations in materials properties can produce large perturbations in the tilt field near a material discontinuity. This is evidenced in data from a closely spaced array of borehole tiltmeters that has been operating at Pinon Flat Geophysical Observatory in southern California since 1987. The array is composed of three borehole tiltmeters located at depths of 24, 36, and 120 m. The tiltmeters have a sensitivity of a few nanoradians. Tidal measurements show differences between the boreholes of up to 50%. The largest percent difference occurs in the semidiurnal band where the tilt field measured in the 36-m borehole differs by approximately 10 nrad at the M2 frequency. This difference has been modeled as a strain-induced tilt caused by the weathering layer.

03,687
PB96-102660 Not available NTIS
National Inst. of Standards and Technology (PL), Boulder, CO. Time and Frequency Div.
Measurement of Very Low Frequency Vibrations.
Final rept.
J. Levine. 1994, 10p.
Pub. in Proceedings of Society of Photo-Optical Instrumentation Engineers: Vibration Monitoring and Control, San Diego, CA., July 28-29, 1994, v2264 p160-169.

Keywords: *Low frequency vibrations, *Tiltmeters, *Strain measurement, Reprints, Boreholes, Geodynamics, Sensitivity, Laser strainmeter.

We have developed a number of instruments that are capable of measuring vibrations at very low frequencies (below 1 Hz). Two of these instruments are a laser strainmeter, which can respond to strains with frequencies ranging from 0 to about 100 Hz and a borehole tiltmeter which can respond to deflections of the vertical or horizontal accelerations in the frequency range from 0 to about 1 Hz. We have also modified commercial gravity meters (vertical accelerometers) and have used them to make measurements at comparable frequencies. Most of our work has been motivated by geophysical considerations including the dynamics of the earth in seismically active regions, but the instrumentation might also be useful in vibration monitoring for other purposes.

03,688
PB96-102991 Not available NTIS
National Inst. of Standards and Technology (PL), Boulder, CO. Quantum Physics Div.
Intracomparison Tests of the FG5 Absolute Gravity Meters.
Final rept.
G. S. Sasagawa, F. Klopping, T. M. Niebauer, J. E. Faller, and R. L. Hilt. 1995, 4p.
Pub. in Geophysical Research Letters 22, n4 p461-464, 15 Feb 95.

Keywords: *Gravimeters, *Calibration, Reprints, *Absolute gravity.

The FG5 series absolute gravimeters have an estimated instrumental accuracy of 1-2 microGal. A number of instrument comparisons were conducted with six FG5 instruments over a period of 9 months; the predecessor series JILA4 instrument was also used. The standard deviation of mean g values (averaged over 24-48h), as observed by different instruments, is 1.8 microGal. Observations taken within 48 h typically agree within 2 microGal, and the maximum observed disagreement is 6 microGal for two observations taken 37 days apart.

03,689
PB96-137732 Not available NTIS
National Inst. of Standards and Technology (CSTL), Gaithersburg, MD. Thermophysics Div.
Temperature and Frequency Dependence of Anelasticity in a Nickel Oscillator.
Final rept.
R. F. Berg. 1995, 6p.
Pub. in Review of Scientific Instruments, v66 n9 p4665-4670 Sep 95.

Keywords: *Creep, *Rock mechanics, Flexural properties, Oscillators, Transfer function, Reprints, *Anelasticity.

The frequency dependance of the real and imaginary parts of a nickel oscillator's transfer function is described over 3 decades in frequency by the use of simple expressions. These expressions incorporate only the resonance frequency w0, the quality factor Q, and a characteristic exponent Beta determined by a single measurement of creep. They are based on the ansatz phi (w) = Q(-1)(w/w0)-Beta, where psi is the imaginary part of the spring constant. Over a 100 K range of temperature T, the exponent Beta=0.18 was constant even though Q(T) changed by a factor of 8. These expressions are potentially useful for accurately describing a mechanical oscillator whose transfer function must be modeled at frequencies far below w0. Examples include accelerometers based on a flexure element and suspensions for interferometric gravitational wave detectors.

03,690
PB96-165972 PC A05/MF A01
Colorado School of Mines, Golden. Div. of Engineering.
Preliminary Processing of the Lotung LSST Data.
S. D. Glaser, and A. L. Leeds. Mar 96, 59p, NIST/GCR-96/690.
Contract NIST-60NANB4D1677
See also PB93-178606. Sponsored by National Inst. of Standards and Technology (BFRL), Gaithersburg, MD.

Keywords: *Soil mechanics, *Nuclear power plants, *Earthquake engineering, *Soil structure interactions, Soil dynamics, Soil profiles, Seismic effects, Earthquakes, Ground motion, Seismic waves, Strain measurement, Site characterization, Earthquake magnitude, Piezometers, Data collection, Data processing, Lotung(Taiwan).

Possibly the best set of data for earthquake excitation of soils exists for the test site operated by the Electric Power Research Institute (EPRI) and the Taiwan Power Company at Lotung Taiwan. At this site, two locations are instrumented with three-component accelerometers at depths of 47, 17, 11, 6 meters, and at the surface. One array is in the free-field while the other is adjacent to a one-quarter scale nuclear containment vessel. The site is also well instrumented with piezometers at various depths and locations. The report summarizes the data and signal processing that was done to the EPRI Lotung data at the Colorado School of Mines. The over 2000 files were organized into MATLAB experiments by event. The provided acceleration data were carefully double integrated to yield velocity and displacement time history records.

03,691
PB96-214747 PC A13/MF A03
Bechtel Corp., San Francisco, CA.
Energy-Based Method for Liquefaction Potential Evaluation. Phase 1. Feasibility Study.
F. Ostadan, N. Deng, and I. Arango. Aug 96, 264p, NIST/GCR-96/701.
Figures in this document may not be legible in microfiche. Sponsored by National Inst. of Standards and Technology (BFRL), Gaithersburg, MD.

Keywords: *Liquefaction, *Ground motion, *Earthquakes, Pore pressure, Strain measurement, Earthquake magnetic, Seismic waves, Strain energy release rate, Strain rate, Shear strain, Vibration dampling, Stress-strain relations, Acceleration, Sands, Seismic effects, Soil sampling, Laboratory tests, Soil mechanics.

The purpose of this study is to evaluate the feasibility of the development and application of the strain energy method for general use. The study is expected to continue with two additional phases that will develop generic strain energy, liquefaction curves as a function of the most relevant soil properties and generic strain energy demand as a function of seismicity data and a wide range of site soil data and profiles. The limited scope of the feasibility study did not permit laboratory testing for the purpose of the strain energy computation. Available laboratory data were used for this purpose.

Hydrology & Limnology

03,692
PB96-202452 PC A04/MF A01
National Oceanic and Atmospheric Administration, Ann Arbor, MI. Great Lakes Environmental Research Lab.
Lake Erie Water Temperature Data, Put-in-Bay, Ohio, 1918-1992.
Technical memo.
M. J. McCormick. Aug 96, 41p, NOAA-TM-ERL-GLERL-97.
See also PB96-202445.

Keywords: *Lake Erie, *Water temperature, *Data collections, Great Lakes, Ohio, Trends, Climate change, Graphs(Charts), Put-In-Bay(Ohio).

Water temperature data from several sites around the Great Lakes were obtained to determine if any regional climatic changes or trends could be detected based upon these data sets. This technical memorandum contains data for Put-In-Bay, Ohio on Lake Erie. Water temperature data were measured at the Put-In-Bay fish hatchery on South Bass Island on Western Lake Erie. The hatchery data were collected by the Ohio Department of Natural Resources, Lake Erie Fisheries Unit, Sandusky Bay, from 1918 through 1992.

03,693
PB96-204425 Not available NTIS
National Inst. of Standards and Technology (MSEL), Gaithersburg, MD. Ceramics Div.
Adhesion, Contact Electrification, and Acid-Base Properties of Surfaces.
Final rept.
A. Grabbe, D. T. Smith, and R. G. Horn. 1995, 8p.
See also PB93-125235.

Pub. in AMP Jnl. of Technology, v4 p95-102 Jun 95.

Keywords: *Electrification, *Electrical insulation, *Adhesion, *Static electricity, Reprints, Silicon dioxide, Mica, Charge transport, Electric discharges.

When two different materials contact and separate, an electrical charge transfer from one surface to the other can take place because of the different electronic structures of the two materials. In the paper, it is shown that the same can occur between two surfaces of the same material, if one of the two surfaces carries a monolayer of a chemi-sorbed species. A surface force apparatus is used for studying contact electrification and resulting adhesion between two surfaces. It is shown that the interaction between a silica surface presenting an amine, i.e., basic, termination to a silanol terminated, i.e., acidic surface, is vastly greater than between two ordinary silica surfaces. The increased adhesion demonstrates the connection between acid-base interactions and contact electrification.

Mineral Industries

03,694
PB94-185386 Not available NTIS
National Inst. of Standards and Technology (NEL), Gaithersburg, MD. Robot Systems Div.
Task Decomposition Methodology for the Design of a Coal Mining Automation Hierarchical Real-Time Control System.
Final rept.
H. M. Huang, and R. Quintero. 1990, 9p.
Pub. in Proceedings of the International Institute of Electrical and Electronics Engineers Symposium on Intelligent Control, p884-892 1990. Sponsored by Bureau of Mines, Pittsburgh, PA.

Keywords: *Coal mining, *Control systems, Reprints, Hierarchies, Automation, Real time systems, Planning, Artificial intelligence, Sumps, Coal mines, *Task decomposition.

The paper describes a systematic approach to hierarchical task decomposition and planning. Such a methodology can be used to design a complex system which receives goals from the external world, performs intelligent planning, and commands the actuators to achieve the goals. The application of this task decomposition methodology is illustrated in the paper through the design of a coal mining automation hierarchical real-time control system.

03,695
PB94-193976 PC A04/MF A01
Purdue Univ., Lafayette, IN. Thermal Sciences and Propulsion Center.
Investigation of Oil and Gas Well Fires and Flares.
Final rept.
P. Dutta, Y. R. Sivathanu, and J. P. Gore. Jun 94, 68p, NIST/GCR-94/653.
Grant NIST-60NANB1D1172
Sponsored by National Inst. of Standards and Technology (BFRL), Gaithersburg, MD.

Keywords: *Natural gas wells, *Diffusion flames, *Oil wells, *Radiative heat transfer, Atomizers, Soot, Heat flux, Burners, Sprayers, Mathematical models, Jet flow, *Well fires, *Well flares, Effervescent atomization.

A theoretical and experimental study of jet flames with applications to large fires resulting from oil well and gas well accidents is reported. The results have been used in the interpretation of the single point radiation heat flux data collected around well fires in Kuwait. Based on the high liquid loading involved in actual well fires, a new device called effervescent atomizer/burner was successfully designed, constructed and tested during the grant period. Measurements of flame heights, radiative heat loss fractions, emission temperatures, and path integrated transmittances were completed for nine crude oil and methane/air flames in the 10-20 KW range. The significant accomplishments during the grant include: (1) Development of a technique to find total radiative heat loss from turbulent jet flames based on measurements of heat flux at a single location; (2) Design and successful operation of an effervescent atomizer/burner. The burner also allows laboratory measurements of such flames for the first time; and (3) Study of global properties of the high liquid loading jet flames have shown that their lengths are affected by two-phase flow effects and that their soot loading and radiant output is lower than equivalent pool flames.

03,696
PB94-203429 PC A02/MF A01
National Inst. of Standards and Technology (MEL), Gaithersburg, MD. Robot Systems Div.
Integration of Servo Control into a Large-Scale Control System Design: An Example from Coal Mining.
J. A. Horst. Jun 94, 10p, NISTIR-5446.

Keywords: *Continuous miners, *Systems integration, *Servocontrol, *Motion simulators, *Robotics, *Coal mining, Control systems design, Systems engineering, Cutting machines, Controllers, Mining engineering, Computerized simulation, Autonomous navigation, Mathematical models, *Real-time Control Systems, Coal interface detection, Proportional-plus-Integral-plus Derivative controllers.

Closed loop control of cutting drum height of a continuous mining machine (CM) using a coal interface detection (CID) sensor is described. The control is accomplished using a discrete-time Proportional-plus-Integral-plus-Derivative (PID) controller. The mining machine, sensor, and mine environment are simulated. The dynamic model of the cutting drum arm (boom) and motors is described and a discrete time version of the solution to the plant equation of boom angle and angular velocity is derived. Cutting drum height control is placed in the context of an existing large-scale Real-time Control System (RCS) for CM control, simulation, and animation. RCS is a paradigm for defining, describing, and designing intelligent control systems developed at the Robot Systems Division of the National Institute of Standards and Technology (NIST).

03,697
PB94-203536 PC A03/MF A01
National Inst. of Standards and Technology (MEL), Gaithersburg, MD. Robot Systems Div.
Environment Simulation for a Continuous Mining Machine.
J. A. Horst. Jun 94, 11p, NISTIR-5449.

Keywords: *Continuous miners, *Mining equipment, *Coal mining, *Motion simulators, *Robotics, Computerized simulation, Mining engineering, Systems engineering, Cutting machines, Mathematical models, Controllers, Autonomous navigation, Collisions.

A simulator is described for the motion of a continuous mining machine (CM) in a coal mine. Of special interest is the motion of the CM following collision with an immovable obstacle in the mine. This type of constrained motion effected our choice of presentation of the CM and its environment. The CM is represented as a two dimensional polygonal hull and the mine obstacles are given two separate representations, certainty grids and obstacle boundary curves, each of which efficiently perform specific tasks. The object boundary curve representation is most useful for determining motion following a collision and the certainty grid is most useful for determining whether and where a collision has occurred.

03,698
PB94-212065 Not available NTIS
National Inst. of Standards and Technology (NEL), Gaithersburg, MD. Robot Systems Div.
Hierarchical Real-Time Control System for Use with Coal Mining Automation.
Final rept.
H. M. Huang. 1990, 12p.
Sponsored by Bureau of Mines, Pittsburgh, PA.
Pub. in Proceedings of Conference on the Use of Computers in the Coal Industry (4th), Morgantown, WV., June 20-22, 1990, p3-14.

Keywords: *Coal mining, *Automation, *Real time operation, *Hierarchies, *Control systems, Signal processing, Systems engineering, Artificial intelligence, Man machine systems, Reprints.

This paper describes a systematic approach to the design of a hierarchical control system for mining automation. In particular, the methodology can be used to design a complex system which receives goals from the external world, evaluates the current world situation through an interactive sensory data assimilation process, performs intelligent planning, and commands the actuators to achieve its goals. The operator interaction capability is also emphasized.

03,699
PB96-210760 PC A07/MF A02
National Inst. of Standards and Technology (BFRL), Gaithersburg, MD. Structures Div.
Report of a Workshop on Requalification of Tubular Steel Joints in Offshore Structures. Held in Houston, Texas on September 5-6, 1995.
Final rept.
A. W. Taylor. Jun 96, 105p, NISTIR-5877.
Sponsored by Minerals Management Service, Herndon, VA. Technology Assessment and Research Branch.

Keywords: *Offshore structures, *Joints(Junctions), *Meetings, Pipes(Tubes), Inspection, Loads(Forces), Stress analysis, Houston(Texas).

This report is a summary of a workshop title Requalification of Tubular Steel Joints in Offshore Structures, held September 5 and 6, 1995 in Houston, Texas. The workshop was sponsored by the U.S. Minerals Management Service, and the National Institute of Standards and Technology. This report contains the papers presented at the workshop, summary of the workshop discussions, and the conclusions reached by the workshop participants. The major issues discussed at the workshop included tubular joint characterization, computational methods, tubular joint failure definition/condition, condition assessment, and code requirements/technology transfer.

Natural Resource Surveys

03,700
PB94-203528 PC A02/MF A01
National Inst. of Standards and Technology (MEL), Gaithersburg, MD. Robot Systems Div.
Continuous Mining Machine Control Using the Real-Time Control System.
J. A. Horst, and A. J. Barbera. Jun 94, 10p, NISTIR-5448.
Prepared in cooperation with Advanced Technology and Research Corp., Laurel, MD.

Keywords: *Continuous miners, *Real time operation, *Control systems design, *Coal mining, *Motion simulators, *Robotics, Mining equipment, Underground mining, Computerized simulation, Systems engineering, Mining engineering, Controllers, Autonomous navigation, *Real-time Control Systems.

Application of the Real-time Control System (RCS) reference model to a simulated underground coal mining machine is described. RCS is characterized by explicit software modules that perform tasks decomposition, sensory processing, and world modeling functions at different hierarchical levels. We use a detailed and sharply defined approach to RCS design characterized by task-oriented problem analysis, generic software objects, rule-based control (using finite state machines), cyclic execution of manually scheduled processes, and generic communications interfaces.

NAVIGATION, GUIDANCE, & CONTROL

Navigation Systems

03,701
PB94-211885 Not available NTIS
National Inst. of Standards and Technology (NEL), Gaithersburg, MD. Robot Systems Div.
Real-Time Vision for Autonomous and Teleoperated Control of Unmanned Vehicles.
Final rept.
M. Herman, J. S. Albus, and T. H. Hong. 1991, 36p.
Sponsored by Army Research Lab., Adelphi, MD. and Defense Advanced Research Projects Agency, Arlington, VA.
Pub. in Active Perception and Robot Vision, 36p 1991.

Keywords: *Autonomous navigation, *Computer vision, *Real time operation, *Telerobotics, Remotely piloted

vehicles, Architecture(Computers), Robotics, Control systems design, Hierarchies, Teleoperators, Pattern recognition, Video compression, Reprints, *Unmanned vehicles.

This paper focuses on two related topics: a control system architecture that unifies autonomous and teleoperated control of unmanned vehicles, and examples of how real-time vision processing fits into this architecture. The National Institute of Standards and Technology (NIST) hierarchical real-time control system architecture and its application to unmanned vehicles is presented. The paper then discusses recent work at NIST in real-time vision for both teleoperated and autonomous vehicles. For teleoperated vehicles, we describe a system for video compression for low data rate remote vehicle driving. For autonomous vehicles, we describe passive range extraction from optical flow for applications such as target extraction and identification, vehicle driving, and terrain mapping. We also describe how each of these vision systems fits into the control system architecture.

03,702
PB94-211893 Not available NTIS
National Inst. of Standards and Technology (NEL), Gaithersburg, MD. Robot Systems Div.
Real-Time Vision for Unmanned Vehicles.
Final rept.
M. Herman, J. S. Albus, and T. H. Hong. 1990, 12p.
Sponsored by Army Research Lab., Adelphi, MD. and Defense Advanced Research Projects Agency, Arlington, VA.
Pub. in Proceedings of Sensors Expo, Chicago, IL., September 1990, p206c-1-206c-12.

Keywords: *Autonomous navigation, *Computer vision, *Real time operation, *Telerobotics, Architecture(Computers), Robotics, Remotely piloted vehicles, Control systems design, Teleoperators, Pattern recognition, Video compression, Reprints, *Unmanned vehicles.

This paper provides examples of how real-time vision may be used for controlling both teleoperated and autonomous vehicles. For teleoperated vehicles, we describe a system for video compression for low data rate remote vehicle driving. For autonomous vehicles, we describe passive range extraction from optical flow for applications such as target extraction and identification, vehicle driving, and terrain mapping.

03,703
PB95-220414 PC A03/MF A01
National Inst. of Standards and Technology (MEL), Gaithersburg, MD. Intelligent Systems Div.
Outline of a Multiple Dimensional Reference Model Architecture and a Knowledge Engineering Methodology for Intelligent Systems Control.
H. M. Huang. Apr 95, 18p, NISTIR-5643.

Keywords: *Underwater navigation, *Submarines, *Real time operations, *Automatic control, Computer systems programs, Systems engineering, Controllers, Simulations, Computer models, *Autonomous navigation.

The authors outline a multiple dimensional reference model architecture and a methodology for representing and developing intelligent systems. The reference model architecture features multiple dimensions enabling modeling the multiple aspects of complex systems. The canonical form within this framework facilitates open and scalable system architecture. The well-defined structures facilitate efficient knowledge engineering processes. We describe a submarine automation model performing real-time control to illustrate the application of this reference model architecture.

NUCLEAR SCIENCE & TECHNOLOGY

General

03,704
PB96-157847 Not available NTIS
National Inst. of Standards and Technology (PL), Gaithersburg, MD. Electron and Optical Physics Div.
Laser-Synchrotron Hybrid Experiments: A Photon to Tickle, A Photon to Poke.
Final rept.
D. L. Ederer, J. E. Rubensson, D. R. Mueller, J. Jai, Q. Y. Dong, T. A. Callcott, G. L. Carr, G. P. Williams, C. J. Hirschmugl, S. Etemad, A. Inam, D. B. Tanner, R. Shuker, and W. L. O'Brien. 1992, 7p.
Pub. in Nuclear Instruments and Methods in Physics Research, Section A, vA319 p250-256 1992.

Keywords: *Laser synchrotron coincidence, *Infrared absorption, *Pulse synchronization, Reprints, AL2O3 exciton, Nanosecond scale dynamical process, Phase shifting pulses.

In this paper we present the preliminary results from a new experimental technique to synchronize the pulses from a mode-locked Nd-YAG laser to the light pulses in the VUV storage ring at the National Synchrotron Light Source (NSLS). We describe a method to electronically change the delay time between the laser pulses and the synchrotron pulses. We also illustrate a method to overlap the synchrontron pulses with the laser pulses in space and time. Preliminary results will be presented for two experiments.

Fusion Devices (Thermonuclear)

03,705
PB95-147351 PC A18/MF A04
National Inst. of Standards and Technology (MSEL), Gaithersburg, MD. Materials Reliability Div.
Irradiation Damage in Inorganic Insulation Materials for ITER Magnets: A Review.
N. J. Simon. Sep 94, 424p, NISTIR-5025.
See also PB93-206928. Sponsored by Department of Energy, Washington, DC. Office of Fusion Energy.

Keywords: *Thermonuclear reactor materials, *Iter tokamak, *Superconducting magnets, *Electrical insulation, *Radiation damage, *Literature surveys, Aluminum oxide, Aluminum nitrides, Magnesium oxides, Silicon dioxide, Zirconium oxides, Porcelain, Mica, Spinel, Quartz, Toroidal configuration, Neutron irradiation, Crystal defects, Amorphous materials, Ceramics, Magnesium aluminates, Amorphization.

A literature search on the irradiation resistance of inorganic insulators for the ITER toroidal field superconducting magnets is reported. The materials included Al2O3, AlN, MgO, porcelain, SiO2, MgAl2O4, ZrO2, and mica. No in situ measurements of the 4-K compressive, shear, and electrical breakdown strengths after 4-K neutron irradiation were retrieved. Limited optical and thermal property measurements made on these insulators after cryogenic irradiations indicate that recovery occurs in ceramic oxides at ambient temperatures. Host atom amorphization has been demonstrated in Al2O3 at 77 K, but was not successful at 300 K. Apparently, host ion amorphization does not occur in most ceramic oxides at 300 K. Amorphization has evidently not been attempted in AlN, MgO, or MgAl2O4 at 77 K. Silicate-bonded structures, such as mica, porcelain, and silica, do amorphize at ambient temperature and are, at present, considered unacceptable unless proven otherwise by in situ electrical and mechanical property testing after 4-K irradiation. Zirconia, even if stabilized, will probably transform under neutron irradiation and is, therefore, considered unsuitable. Mica layers delaminated under low energy electron bombardment. Natural mica layers are porous, owing to spontaneous and induced tracks from U impurities. Tracks caused a decrease in electrical breakdown strength. Simulation of neutron irradiation by other radiation species is also reviewed in this report.

03,706
PB95-198768 PC A10/MF A03
National Inst. of Standards and Technology (MSEL), Boulder, CO. Materials Reliability Div.
Cryogenic Properties of Inorganic Insulation Materials for ITER Magnets: A Review.
N. J. Simon. Dec 94, 218p, NISTIR-5030.
Sponsored by Department of Energy, Washington, DC. Office of Fusion Energy.

Keywords: *ITER tokamak, *Superconducting magnets, *Electrical insulation, Literature surveys, Electrical properties, Mechanical properties, Thermal properties, Aluminum nitrides, Aluminum oxides, Magnesium oxides, Silicon dioxide, Zirconium oxides, Porcelain, Cryogenics, Spinel, Mica, Reviews, Temperature range 0000-0013 K, Temperature range 0013-0065 K, Temperature range 0065-0273 K, Temperature range 0273-0400 K, Graphs(Charts), Magnesium aluminates.

Results of a literature search are reported on the cryogenic properties of candidate inorganic insulators for the toroidal field magnets of the International Thermonuclear Experimental Reactor. The materials investigated include: Al2O3, AlN, MgO, porcelain, SiO2, MgAl2O4, ZrO2, and mica. A graphical presentation is given of mechanical, elastic, electrical, and thermal properties between 4 and 300 K. A companion report reviewed the low temperature irradiation resistance of these materials.

Isotopes

03,707
PB96-159637 Not available NTIS
National Inst. of Standards and Technology (PL), Gaithersburg, MD. Ionizing Radiation Div.
System for Intercomparing Standard Solutions of Beta-Particle Emitting Radionuclides.
Final rept.
J. M. Calhoun, J. T. Cessna, and B. M. Coursey. 1992, 7p.
Pub. in Nuclear Instruments and Methods in Physics Research, Section A (ICRM Symposium Issue), Chapter A312, p114-120 1992.

Keywords: *Radioisotopes, *Beta particles, *Aqueous solutions, Technetium 99, Tritium, Carbon 14, Hexadecane, Liquid scintillation, Quantum efficiency, Comparisons, Radiochemistry, Reference standards, Reprints, *Standard reference materials.

A system for intercomparing standard solutions of pure beta-particle emitting radionuclides is described. The CIEMAT/NIS technique of beta-particle efficiency tracing is based on establishing a parameter in a simple calculational model, using a (H-3) standard with comparable quenching. Measurements were made under similar geometrical and quenching conditions for each radionuclide with a commercial scintillator and conventional liquid-scintillation counter with two phototubes operating in coincidence. The technique was then tested at different sites in the area using a set of flame-sealed vials and state-of-the-art liquid-scintillation counters.

03,708
PB96-159751 Not available NTIS
National Inst. of Standards and Technology (PL), Gaithersburg, MD. Ionizing Radiation Div.
International Radon-in-Air Measurement Intercomparison Using a New Transfer Standard.
Final rept.
J. M. R. Hutchinson, J. Cessna, R. Colle, and P. A. Hodge. 1992, 15p.
Pub. in Applied Radiation and Isotopes, Chapter 12, v43 n12 p175-189 1992.

Keywords: *Radon 222, *Interlaboratory comparisons, *Air sampling, Radiation monitoring, Photon emission scanning, Ionization chambers, Calibration standards, Standardization, Quality control, Reprints.

A new secondary measuring system for Rn22-in-air that can be used as a very efficacious transfer calibration standard for measurement intercomparisons be-

tween laboratories has been developed and extensively tested. The system is based on measurements of the photon emission rate of radon samples contained in spherical 35-mL glass ampoules with a NaI(Tl) well counter. The system is calibrated against the NIST pulse-ionization-chamber (PIC) national radon measuring system, and has an overall uncertainty of approximately 2 percent. An international intercomparison of 11 laboratories, including NIST, using this system was performed.

03,709
PB97-110084 Not available NTIS
National Inst. of Standards and Technology (PL), Gaithersburg, MD. Ionizing Radiation Div.
Liquid-Scintillation Counting Techniques for the Standardization of Radionuclides Used in Therapy.
Final rept.
B. M. Coursey, J. M. Calhoun, J. Cessna, M. P. Unterweger, D. B. Golas, and F. J. Schima. 1994, 5p.
Pub. in Nuclear Instruments and Methods in Physics Research A, v339 p26-30 1994.

Keywords: *Scintillation counting, *Nuclear medicine, *Radionuclides, Radiopharmaceuticals, Standards, Therapy, Reprints, *Foreign technology.

Radionuclides are increasingly used in therapeutic nuclear medicine. The CIEMAT/NIST method of standardizing high-energy beta-particle emitters is being applied to a list of candidate radionuclides developed by the US nuclear medicine community. Standards and standard methods are needed by the pharmaceutical manufacturers in North America before these nuclides can be widely distributed. Solutions standardized-by liquid-scintillation counting are used to establish counting efficiencies for Cerenkov counting and NaI(Tl) well crystals, and potentiometer settings for commercial radionuclide calibrators. Results are presented for a number of beta-particle-emitting radionuclides.

Nuclear Instrumentation

03,710
AD-A286 647/3 PC A05/MF A01
National Bureau of Standards, Gaithersburg, MD.
Measurement of Absorbed Dose of Neutrons, and of Mixtures of Neutrons and gamma rays.
G. S. Hurst, R. S. Caswell, F. C. Maienschein, H. H. Rossi, and J. A. Sayeg. 3 Feb 61, 94p, NBS-HB-75, NCRP-25.

Keywords: *Scintillation counters, Dosimetry, Gamma rays, Neutrons, Proportional counters, Ionization chambers, Radiation shielding, Inelastic scattering, Fast neutrons, Dosimeters, Handbooks, Photoelectric effect(Gamma rays), Radiation effects, Neutron scattering, *Neutron dosimetry, *Gamma dosimetry, Radiation doses.

No abstract available.

03,711
DE96010065 PC A03/MF A01
National Inst. of Standards and Technology, Gaithersburg, MD.
Improving measurement quality assurance for photon irradiations at Department of Energy facilities. Final technical report.
PROGRESS REPT.
1996, 24p, DOE/EH/89321-T1.
Contract AI01-93EH89321
Sponsored by Department of Energy, Washington, DC.

Keywords: *Calibration Standards, *Dosemeters, Personnel Dosimetry, Photon Beams, Progress Report, Quality Assurance, Radiation Protection, US DOE, X Radiation, EDB/440102.

For radiation-instrument calibration to be generally acceptable throughout the US, direct or indirect traceability to a primary standard is required. In most instances, one of the primary standards established at NIST is employed for this purpose. The Department of Energy Laboratory Accreditation Program (DOELAP) is an example of a program employing dosimetry based on the NIST primary photon-, beta particle- and neutron-dosimetry standards. The NIST primary dosimetry standards for bremsstrahlung were first established in the 1950s. They have been updated since then on several occasions. In the 1970s, Technical Committee 85 of the International Standards Organization (ISO) started its work on establishing sets of internationally acceptable, well-characterized photon beams for the calibration of radiation-protection instruments. It is the intent of this paper to make a detailed comparison between the current NIST and the most up-to-date ISO techniques. At present, 41 bremsstrahlung techniques are specified in ISO 4037 while NIST supports a total of 32 techniques. Given the existing equivalences, it makes sense to try to extend the NIST techniques to cover more of the ISO Narrow Spectrum and High Air-Kerma Rate Series. These extensions will also allow the possibility for use of ISO beam techniques in future revisions of the DOELAP standard, which has been suggested by DOE. To this end, NIST was funded by DOE to procure material and make adaptations to the existing NIST x-ray calibration ranges to allow NIST to have the capability of producing all the ISO bremsstrahlung techniques. The following sections describe the steps that were taken to achieve this.

03,712
PB95-126272 Not available NTIS
National Inst. of Standards and Technology (NML), Gaithersburg, MD. Ionizing Radiation Div.
Review of the USCEA/NIST Measurement Assurance Program for the Nuclear Power Industry.
Final rept.
D. H. Gray, D. B. Golas, and J. M. Calhoun. 1991, 9p.
Pub. in Radioact. Radiochem. 2, n1 pp30, 34-41 1991.

Keywords: *Nuclear power, *Radiation measurement, *Quality assurance, Electric power industry, Electric utilities, Energy sources, Laboratories, Proving, Tracing, Radioactivity, Reprints, *USCEA(US Council for Energy Awareness), *US Council for Energy Awareness, *US NIST.

Beginning in 1987 the U.S. Council for Energy Awareness (USCEA) in cooperation with the National Institute of Standards and Technology (NIST) established a measurement assurance program for the nuclear power industry. It was designed to serve the needs of the utility companies, source suppliers, and service laboratories which were not addressed by other programs in existence at that time. The program distributes various samples prepared at NIST to all participants, with the NIST value undisclosed until the measurement result from the participant is reported. In another part of the program, source suppliers also submit samples of their standards to NIST for verification and traceability. The mechanics of the program are described, and the results from the first three years of the program are summarized.

03,713
PB95-151106 Not available NTIS
National Inst. of Standards and Technology (PL), Gaithersburg, MD. Ionizing Radiation Div.
Electron and Proton Dosimetry with Custom-Developed Radiochromic Dye Films.
Final rept.
R. M. Uribe, C. Vargas-Aburto, W. L. McLaughlin, M. L. Walker, and C. E. Dick. 1993, 4p.
Sponsored by Kent State Univ., OH.
Pub. in Radiation Protection Dosimetry 47, n1/4 p693-696 1993.

Keywords: *Electron dosimetry, *Proton dosimetry, *Film dosimetry, MeV range 1-10, Electron irradiation, Proton irradiation, Fabrication, Sensitivity, Reprints, *Radiochromic dyes, *Radiochromic dosimeters.

The systematic study and identification of the mechanisms responsible for changes occurring in radiochromic dye films (RDFs) as a result of exposure to ionizing radiation, requires the possibility of varying a number of parameters during their fabrication. A series of RDFs were developed with thicknesses in the range of 15 to 60 micrometers. The amount of dye precursor and stabilizers was varied in a systematic way. A series of unexposed films was irradiated with 1 MeV electrons and 10 MeV protons. Optical characterization of the films was performed. Irradiations were carried out in the dose range from 0 to 440 kGy. The fabrication techniques, the irradiation procedures, and the optical characterization of the films are described. Conclusions are presented regarding the useful dose range for the RDFs, their sensitivity to different types of radiation, and a comparison is made with other similar film dosemeters used in the materials processing industry.

03,714
PB95-162954 Not available NTIS
National Inst. of Standards and Technology (NML), Gaithersburg, MD. Ionizing Radiation Div.
Dose Mapping of Radioactive Hot Particles Using Radiochromic Film.
Final rept.
C. G. Soares, B. M. Coursey, F. F. McWilliams, and M. J. Scannell. 1990, 2p.
Pub. in Radioact. Radiochem. 1, n2 p14, 16-17 1990.

Keywords: *Dosimetry, *Radioactivity, *Cobalt 60, Dosage, Films, Radioactive isotopes, Beta particles, Radiation protection, Reprints, Hot particles, Radiochromic films, Dose profile, Scanning densitometer.

An attempt to standardize hot particle beta dosimetry is addressed through the generation and characterization of (60)CO micro-spheres. An electrical arc, rapid solidification process of a cobalt alloy was used to produce uniform spherical particles of various diameters ranging from 50 to 250 microm. Neutron activation of these particles yielded essentially pure (60)CO in the microcurie range. The particles were characterized by physical size and activity; dose rates were determined using extrapolation chamber and radiochromic dye film measurements.

03,715
PB96-135173 Not available NTIS
National Inst. of Standards and Technology (PL), Gaithersburg, MD. Ionizing Radiation Div.
Anionic Triphenylmethane Dye Solutions for Low-Dose Food Irradiation Dosimetry.
Final rept.
N. B. El-Assy, Y. D. Chen, M. L. Walker, M. Al-Sheikhly, and W. L. McLaughlin. 1995, 9p.
Pub. in Radiation Physics and Chemistry, v45 n4-6 p1189-1197 Oct 95.

Keywords: *Dosimetry, *Food irradiation, Reprints, Gamma radiation, Radiation processing, *Foreign technology, *Dye bleaching, Fast Green FCF, Light Green SF, Radiolytic bleaching.

The radiolytic bleaching of aryl sulfonic-substituted para-diethyl-amino triphenylmethane dye solutions can be used for dosimetry in the absorbed dose range 10 to 400 Gy. The sulfonic anions provide solubility of these acid dyes in water. Two of these dyes are supplied as stable greenish-blue biological stains when dissolved in weakly-acidic aqueous solution. Light Green SF Yellowish and East Green FCF. They have, respectively, linear molar absorption coefficents of 7.14 x 10 to the 3rd power (at pH 5.4) and 10.0 x 10 to the 3rd power (at pH 4.2) sq. m. mol to the minus one power, when measured at the peaks of the primary absorption bands, 630 nm and 622 nm, respectively. The bleaching due to irradiation with gamma rays shows a linear function with a positive slope between the negative algorithm of the absorbance and the absorbed dose. The effect of pH on the response is studied, as well as the effects of light and temperature on pre- and post-irradiation stability. A mechanism, based mainly on radiolytic oxidation of the protonated phenolic or sulfonated phenyl group by OH, with the abstraction of H-atom to water, is postulated for neutral to slightly acidic aerated aqueous solutions.

03,716
PB96-135249 Not available NTIS
National Inst. of Standards and Technology (PL), Gaithersburg, MD. Ionizing Radiation Div.
Alcohol Solutions of Triphenyl-Tetrazolium Chloride as High-Dose Radiochromic Dosimeters.
Final rept.
A. Kovacs, L. Wojnarovits, N. B. El-Assy, M. L. Walker, W. L. McLaughlin, H. Y. Afeefy, and M. Al-Sheikhly. 1995, 9p.
Pub. in International Meeting on Radiation Processing (9th), Istanbul, Turkey, September 11-16, 1994, Radiation Physics and Chemistry, v46 n4-6 p1217-1225 Oct 95.

Keywords: *Radiochromic dosimeters, *Dosimetry, Reprints, Dyes, Formazan, Gamma rays, *Foreign technology, *Triphenyl tetrazolium chloride.

The radiolytic reduction of colorless tetrazolium salts in aqueous solution to the highly colored formazan dye is well-known acid-forming radiation chemical reaction. Radiochromic thin films and three-dimensional hydrocolloid gels have been used for imaging and mapping absorbed dose distributions. The high solubility of

Nuclear Instrumentation

2.3.5-triphenyl-tetrazolium chloride (TTC) in alcohols provides a useful liquid dosimeter (45 mM TTC in aerated ethanol) and shows a linear response of absorbance increase (lambda(sub max) = 480 nm) with dose over the range 1-16 kGy. The linear molar absorption coefficient lambda for the formazan at the absorption peak is 1.5 x 10 to the third power sq. m. mol to the minus one power, and the radiation chemical yield for the above solution is G (formazan) = 0.014 micromoles J to the minus 1 power. The irradiation temperature coefficient is about 0.8 percent per degree Celsius rise in temperature over the temperature range 0-30 degrees C but is much larger between 30 degrees and 60 degrees C.

03,717
PB96-135280 Not available NTIS
National Inst. of Standards and Technology (PL), Gaithersburg, MD. Ionizing Radiation Div.
Dosimetry Systems for Radiation Processing.
Final rept.
W. L. McLaughlin, and M. F. Desrosiers. 1995, 12p.
See also PB92-117118.
Pub. in International Meeting on Radiation Processing (9th), Istanbul, Turkey, September 11-16, 1994, Radiation Physics and Chemistry, v46 n4-6 p1163-1174 Oct 95.

Keywords: *Dosemeters, *Radiation monitors, *Calibration, *Quality assurance, Gamma dosimetry, Electron dosimetry, Calorimetric dosemeters, Radiation doses, Dose rates, Dose-response relationships, Thin films, Solids state devices, Reprints, Radiation processing.

Dosimetry serves important functions in radiation processing, where large absorbed doses and dose rates from photon and electron sources have to be measured with reasonable accuracy. Proven dosimetry systems are widely used to perform radiation measurements in development of new processes, validation, qualification, and verification (quality control) of established processes and archival documentation of day-to-day and plant-to-plant processing uniformity. Proper calibration and traceability of routine dosimetry systems to standards are crucial to the success of many large-volume radiation processes. Recent innovations and advances in performance of systems that enhance radiation measurement assurance and process diagnostics include dose-mapping media (new radiochomic film and solutions), optical waveguide systems for food irradiation, solid-state devices for real-time and passive dosimetry over wide dose-rate and dose ranges, and improved analytical instruments and data acquisitions.

03,718
PB96-135298 Not available NTIS
National Inst. of Standards and Technology (PL), Gaithersburg, MD. Ionizing Radiation Div.
Temperature and Relative Humidity Dependence of Radiochromic Film Dosimeter Response to Gamma and Electron Radiation.
Final rept.
W. L. McLaughlin, J. M. Puhl, and A. Miller. 1995, 7p.
Pub. in International Conference on Radiation Processing (9th), Istanbul, Turkey, September 11-16, 1994, Radiation Physics and Chemistry, v46 n4-6 p1227-1233 Oct 95.

Keywords: *Colorimetric dosemeters, *Environmental effects, *Temperature effects, *Relative humidity, Gamma dosimetry, Electron dosimetry, Radiation monitors, Electron beams, Radiation doses, Gamma radiation, Thin films, Reprints, Radiation processing.

Nylon-base radiochromic films are commercially-available, thin dosimeters that are widely used in radiation processing. Based on some earlier studies, their response functions have been reported to be dependent on the temperature and relative humidity during irradiation. The present study investigates differences in response over practical ranges of temperature, relative humidity, dose, and for different recent batches of films of both types. It is observed that for each new batch of film to be used for radiation processing, the effects of such parameters on response to both gamma rays and electrons should be investigated.

03,719
PB96-135306 Not available NTIS
National Inst. of Standards and Technology (PL), Gaithersburg, MD. Ionizing Radiation Div.
Real Time Monitoring of Electron Processors.
Final rept.
S. V. Nablo, D. R. Kneeland, and W. L. McLaughlin. 1995, 7p.
Pub. in International Meeting on Radiation Processing (9th), Istanbul, Turkey, September 11-16, 1994, Radiation Physics and Chemistry, v46 n4-6 p1377-1383 Oct 95.

Keywords: *Dosimeters, *Electron processors, Radiation dosage, Real time operation, Reprints, Diagnosis, Performance, *Foreign technology.

A real time radiation monitor (RTRM) has been developed for monitoring the dose rate (current density) of electron beam processors. The system provides continuous monitoring of processor output, electron beam uniformity, and an independent measure of operating voltage or electron energy. In view of the device's ability to replace labor-intensive dosimetry in verification of machine performance on a real-time basis, its application to providing archival performance data for in-line processing is discussed.

03,720
PB96-146725 Not available NTIS
National Inst. of Standards and Technology (PL), Gaithersburg, MD. Ionizing Radiation Div.
Orientation Effects on ESR Analysis of Alanine-Polymer Dosimeters.
Final rept.
T. Kojima, S. Kashiwazaki, H. Tachibana, W. L. McLaughlin, R. Tanaka, and M. F. Desrosiers. 1995, 5p.
Pub. in Applied Radiation and Isotopes, v46 n12 p1407-1411 Dec 95.

Keywords: *Dosimeters, *Elcetron paramagnetic resonance, *Alanine, *Polymers, Thin films, Orientation, Pressing(Forming), Extrusion, Shape, Reprints, ESR(Electron spin resonance), Film dosimeter, Rod dosimeter.

Orientation effects during electron spin resonance (ESR) measurement are studied on alanine-polymer dosimeters prepared by different molding procedures (press-molding or extrusion), and also according to different shapes (rods with different lengths and thin-films). The variation in ESR signal amplitude was measured by rotating a dosimeter around the vertical mid-axis and at a right angle to the magnetic field in the ESR cavity, at a temperature of 22 deg C. Orientation effects for rod dosimeters with both molding procedures (press and extrusion), and with different lengths, were negligible. Orientation effects on the film dosimeters can be eliminated, however, when they are positioned vertically and parallel to the mid-axis of the ESR cavity.

03,721
PB97-110514 Not available NTIS
National Inst. of Standards and Technology (PL), Gaithersburg, MD. Ionizing Radiation Div.
USCEA/NIST Measurement Assurance Programs for the Radiopharmaceutical and Nuclear Power Industries.
Final rept.
D. B. Golas. 1993, 16p.
See also PB95-126272.
Pub. in Proceedings of the Workshop on Measurement Quality Assurance for Ionizing Radiation, Gaithersburg, MD., March 16-18, 1993, p191-206.

Keywords: *Nuclear power plants, *Radiopharmaceuticals, *Radiation measurement, Radiation monitoring, Laboratories, Public utilities, Nuclear medicine, Tracer techniques, Dosimetry, Radiochemistry, Quality assurance, Reprints.

In cooperation with the U.S. Council for Energy Awareness (USCEA), the National Institute of Standards and Technology (NIST) supervises and administers two measurement assurance programs for radioactivity measurement traceability. One, in existence since the mid 1970s, provides traceability to suppliers of radiochemicals and radiopharmaceuticals, dose calibrators, and nuclear pharmacy services. The second program, begun in 1987, provides traceability to the nuclear power industry for utilities, source suppliers, and service laboratories. Each program is described, and the results of measurements of samples of known, but undisclosed activity, prepared at NIST and measured by the participants are presented.

03,722
PB97-122279 Not available NTIS
National Inst. of Standards and Technology (CSTL), Gaithersburg, MD.
Conference Report: Calorimetry Conference (50th).
Final rept.
E. S. Domalski, R. N. Goldberg, and P. A. G. O'Hare. 1996, 6p.
Pub. in Calorimetry Conference (50th), Gaithersburg, MD., July 23-28, 1995, Jnl. of Research of the National Institute of Standards and Technology, v101 n1 p63-68 1996.

Keywords: *Calorimetry, *Thermodynamics, *Meetings, Temperatures, Chemistry, Chemical engineering, Biochemistry, Reprints.

Calorimetry and thermodynamics are used in a wide variety of basic and applied sciences. This was reflected in the seemingly disparate topics dealt with at the conference: low- and high-temperature physics, inorganic and organic chemistry, solution chemistry, chemical engineering, biochemistry, and biology. Accordingly, the conference was organized into 11 symposia covering a variety of topics.

Radiation Shielding, Protection, & Safety

03,723
PB95-126132 Not available NTIS
National Inst. of Standards and Technology (NML), Gaithersburg, MD. Ionizing Radiation Div.
Neutron Leakage Benchmark for Criticality Safety Research.
Final rept.
D. M. Gilliam, V. Spiegel, C. M. Eisenhauer, J. Tang, E. Quang, and J. Briesmeister. 1990, 3p.
Pub. in Transactions of the American Nuclear Society 62, p340-342 1990.

Keywords: *Neutron leakage, *Criticality, Interlaboratory comparisons, Monte Carlo method, Fission neutrons, Neutron transport, Neutron sources, Californium 252, Subcriticality, Measurements, Benchmarks, Arrays, Water, Computation, Reprints.

An interlaboratory program has been undertaken to investigate the consistency of direct measurements and rigorous calculations of neutron leakage from a moderated fission neutron source for the purpose of improving the calculations of criticality for arrays of individually sub-critical components. The present work is intended to check the possibility that one problem with these calculations may be associated with the estimation of neutron leakage from individual components, which could lead to misrepresented source terms for other components of the array. Results of calculations and measurements are presented, and discrepancies are noted.

03,724
PB95-161121 Not available NTIS
National Inst. of Standards and Technology (MSEL), Gaithersburg, MD. Metallurgy Div.
Information Retrieval Using Key Words and a Structured Review.
Final rept.
C. G. Interrante, C. A. Messina, and A. C. Fraker. 1993, 10p.
Sponsored by Nuclear Regulatory Commission, Washington, DC. Div. of High-Level Waste Management.
Pub. in Standardizing Terminology for Better Communication: Practice, Applied Theory, and Results, ASTM STP 1166, p242-251 1993.

Keywords: *High level radioactive wastes, *Radioactive waste storage, *Information retrieval, *Databases, Information systems, Database management, Standardized terminology, Reviewing, Reliability, Literature surveys, Radioactive waste disposal, Containment systems, Failure mode analysis, Reprints, Controlled vocabulary.

A database has been developed to assist the Nuclear Regulatory Commission in assessing the efficacy of proposed plans for radionuclide containment for long-term storage of high-level nuclear waste (HLW). Important elements of this database are reviews and evaluations of available literature on a waste package for HLW. The review process and database have been developed and tailored to quickly provide information to answer questions about materials or components, about environments, and about interactions among the

components of a waste package. Descriptions are given of the structure of the database and of the document review process and methods of searching.

Radioactive Wastes & Radioactivity

03,725
PB95-220448 PC A04/MF A01
National Inst. of Standards and Technology (BFRL), Gaithersburg, MD. Structures Div.
Prediction of Cracking in Reinforced Concrete Structures.
N. J. Carino, and J. R. Clifton. Apr 95, 58p, NISTIR-5634.
Sponsored by Nuclear Regulatory Commission, Washington, DC.

Keywords: *Cracking(Fracturing), *Concrete structures, *Predictions, *Low-level radioactive wastes, Creep properties, Shrinkage, Construction materials, Radioactive waste disposal, Permeability, Tensile properties, Reinforced concrete.

The useful life of a buried concrete, containment structure for low level nuclear waste may be controlled by the loss of its load-bearing capacity or an increase in permeability. The latter factor is controlled by the general degradation of the concrete and by the presence of discrete cracks resulting from externally applied loads or from restraint to normal volume changes. To be able to predict the effects of cracks on permeability, it is necessary to understand the causes and mechanisms of discrete crack formation in reinforced concrete structures. The objective of this report is to provide an overview of the design and behavior of reinforced concrete members and to discuss the factors affecting the formation of cracks in hardened concrete.

03,726
PB95-231593 PC A05/MF A01
National Inst. of Standards and Technology (BFRL), Gaithersburg, MD. Building Materials Div.
4SIGHT Manual: A Computer Program for Modelling Degradation of Underground Low Level Waste Concrete Vaults.
K. A. Snyder, and J. R. Clifton. Jun 95, 80p, NISTIR-5612.
Sponsored by Nuclear Regulatory Commission, Washington, DC. Div. of Engineering.

Keywords: *Low-level radioactive wastes, *Radioactive waste disposal, *Underground disposal, *Concretes, *Performance evaluation, Service life, Leaching, Precipitation(Chemistry), Dissolution, Sulfates, Ion transport, Computer models, One-dimensional models, 4SIGHT computer program.

A computer program has been written to facilitate performance assessment of concrete vaults used in Low Level Waste (LLW) disposal facilities. The computer program is a numerical computer model of degradation in concrete. A one-dimensional finite different equation is used to propagate ions by precipitation/dissolution of available salts. The precipitation/dissolution of salts, in turn, changes the transport properties, which changes the rate of ion transport. The result is a model which incorporates the synergism of multiple degradation mechanisms.

03,727
PB95-260816 PC A03/MF A01
National Inst. of Standards and Technology (BFRL), Gaithersburg, MD. Building Materials Div.
Long-Term Performance of Engineered Concrete Barriers.
J. R. Clifton, J. M. Pommersheim, and K. Snyder. Jul 95, 22p, NISTIR-5690.
Prepared in cooperation with Bucknell Univ., Lewisburg, PA.

Keywords: *Low-level radioactive wastes, *Radioactive waste disposal, *Concretes, Service life, Sulfates, Leaching, Cracking(Fracturing), Accelerated tests.

This paper describes research being carried out at NIST on the long-term performance of concrete for constructing low-level nuclear waste (LLW) disposal facilities. Three major research needs have been identified which are: validation of service life models; development of performance criteria for materials and systems to repair concrete before closure of concrete vaults; and development of an expert system to disseminate knowledge on concrete durability for constructing concrete vaults.

Reactor Engineering & Nuclear Power Plants

03,728
NUREG/CP-0136 PC A16/MF A03
National Inst. of Standards and Technology, Gaithersburg, MD.
Proceedings of the Digital Systems Reliability and Nuclear Safety Workshop. Held in Rockville, Maryland on September 13-14, 1993.
D. R. Wallace, B. B. Cuthill, L. M. Ippolito, and L. Beltracchi. Mar 94, 356p, NIST-SP-500-216.
Also available from Supt. of Docs. Prepared in cooperation with Nuclear Regulatory Commission, Washington, DC. Office of Nuclear Regulatory Research.

Keywords: *Meetings, *Digital systems, *Reactor safety, *Nuclear power plants, Information exchange, Software engineering, Computer software, Computer software management, Program verification(Computers).

The United States Nuclear Regulatory Commission (NRC), in cooperation with the National Institute of Standards and Technology conducted the Digital Systems Reliability and Nuclear Safety Workshop on September 13-14, 1993, in Rockville, Maryland. The workshop provided a forum for the exchange of information among experts within the nuclear industry, experts from other industries, regulators and academia. The information presented at this workshop provided in-depth exposure of the NRC staff and the nuclear industry to digital systems design safety issues and also provided feedback to the NRC from outside experts regarding identified safety issues, proposed regulatory positions, and intended research associated with the use of digital systems in nuclear power plants. Technical presentations provided insights on areas where current software engineering practices may be inadequate for safety-critical systems, on potential solutions for development issues, and on methods for reducing risk in safety-critical systems. The report contains an analysis of results of the workshop, the papers presented, panel presentations, and summaries of discussions at this workshop.

03,729
PB95-151619 Not available NTIS
National Inst. of Standards and Technology (MSEL), Gaithersburg, MD. Reactor Radiation Div.
Liquid-Hydrogen Cold Neutron Source for the NBSR.
Final rept.
R. E. Williams, J. M. Rowe, and P. Kopetka. 1992, 3p.
Pub. in Transactions of the American Nuclear Society 66, p169-171 1992.

Keywords: *NBSR reactor, *Neutron sources, *Liquid hydrogen, *Cold neutrons, Research reactors, Neutron scattering, Thermosyphons, Moderators, Safety, Reprints.

The NBSR is a 20-MW research reactor operated by the National Institute of Standard and Technology. It was designed with a 55 cm diameter beam port for the purpose of installing a D20-ice cold neutron source, completed in 1987. A liquid hydrogen cold neutron source is being developed to replace the D20 ice in order to increase the cold-neutron yield. A simple, passively-safe system has been designed, with multiple barriers preventing air from mixing with hydrogen. A thermosiphon will be used to maintain the liquid hydrogen inventory in the moderator chamber. The hydrogen condenser is cooled by a 3.5-kW helium refrigerator. A ballast tank is connected to the condenser so the entire hydrogen inventory can expand freely into the tank, providing completely passive protection against refrigerator failures.

03,730
PB95-152955 Not available NTIS
National Inst. of Standards and Technology (MSEL), Gaithersburg, MD. Reactor Radiation Div.
Nuclear Heat Load Calculations for the NBSR Cold Neutron Source Using MCNP.
M. Blau, J. M. Rowe, and R. E. Williams. 1993, 2p.
Pub. in Transactions of the American Nuclear Society 69, p404-405 1993.

Keywords: *NBSR reactor, *Neutron sources, *Liquid hydrogen, *Moderators, Spherical configuration, Annular shape, Reactor cores, Heavy water, Monte Carlo method, Cold neutrons, Heating load, Computation, Reprints.

The existing D2O-ice cold neutron source in the 20-MW NBSR will be replaced in 1994 with a liquid-hydrogen (LH2) source to increase the yield of cold neutrons (lambda greater than 0.4 nm). Two series of Monte Carlo calculations using MCNP were performed to determine the optimum cold moderator geometry, and to verify its performance. Only the region near the cryostat was modeled for the first series of calculations, leading to the choice of a spherical annulus for the LH2 source. A complete MCNP model of the core was subsequently developed.

03,731
PB95-163978 Not available NTIS
National Inst. of Standards and Technology (MSEL), Gaithersburg, MD. Reactor Radiation Div.
Cold Neutron Gain Calculations for the NBSR Using MCNP.
Final rept.
R. E. Williams, M. Blau, and J. M. Rowe. 1993, 3p.
Pub. in Transactions of the American Nuclear Society 69, p401, 403-404 1993.

Keywords: *NBSR reactor, *Neutron sources, *Cold neutrons, Monte Carlo method, Mathematical models, Spherical configuration, Annular space, Liquid hydrogen, Reactor cores, Moderators, Gain, Reprints, MCNP model.

The existing D2O-ice cold neutron source in the 20-MW National Bureau of Standards reactor (NBSR) will be replaced in 1994 with a liquid-hydrogen (LH2) source to increase the yield of cold neutrons (lambda > 0.4 nm). Two series of Monte Carlo calculations using MCNP were performed to determine the optimum cold moderator geometry and to verify its performance. Only the region near the cryostat was modeled for the first series of calculations, leading to the choice of a spherical annulus for the LH2 source. A complete MCNP model of the core was subsequently developed.

03,732
PB95-209888 PC A08/MF A02
National Inst. of Standards and Technology (MSEL), Gaithersburg, MD. Reactor Radiation Div.
Reactor Radiation Technical Activities, 1994. NAS-NRC Assessment Panel, April 6-7, 1995.
J. M. Rowe, and T. M. Raby. 1994, 154p, NISTIR-5583.
See also PB92-133024.

Keywords: *Nuclear reactors, *Research projects, *Nondestructive tests, *Neutron activation analysis, Cold neutrons, Irradiation, Standards, Radioisotopes, Neutron radiography, Neutron diffraction, Crystal structure, Measurement, Calibrating, US NBS, Microanalysis, NBSR reactor, US NIST, Molecular dynamics.

This report summarizes all the programs which use the NIST reactor. It covers the period for October 1993 through September 1994. The programs range from the use of neutron beams to study the structure and dynamics of materials through nuclear physics and neutron standards to sample irradiations for activation analysis, isotope production, neutron radiography, and nondestructive evaluation.

03,733
PB96-138599 Not available NTIS
National Inst. of Standards and Technology (MSEL), Gaithersburg, MD. Reactor Radiation Div.
MCNP Model of the National Bureau of Standards Reactor (NBSR) Core.
Final rept.
R. E. Williams. 1995, 2p.
Pub. in Transactions of the American Nuclear Society, San Francisco, CA., October 29-November 2, 1995, v73 n0003-18x p397-398 1995.

Keywords: *NBSR reactor, *Reactors, *Cold neutrons, Monte Carolo method, Reactor cores, Reprints, *Criticality calculations, MCNP model, National Institute of Standards and Technology(NIST).

The National Bureau of Standards reactor (NBSR) is a 20-MW research reactor operated for the U.S. Department of Commerce at the National Institute of Standards and Technology in Gaithersburg, Maryland.

Earlier this year, a liquid hydrogen cold neutron source was installed in the NBSR to increase the yield of long wavelength (lambda equal to or greater than 0.4 nm) neutrons. As part of the design effort for the new cold source, Monte Carlo simulations of the core and the cryogenic beam port were performed using the MCNP code. The model has been steadily improved and, where possible, compared with measurements.

03,734
PB96-160890 Not available NTIS
National Inst. of Standards and Technology (CSL), Gaithersburg, MD. Systems and Software Technology Div.
Assessing Functional Diversity by Program Slicing.
Final rept.
K. B. Gallagher, J. R. Lyle, D. Wallace, and L. Ippolito. 1993, 1p.
Pub. in Transactions of the Water Reactor Safety Information Meeting (21st), Bethesda, MD., October 25-27, 1993, p9-1.

Keywords: *Nuclear power plants, *Electronic security, *Software engineering, Safety programs, Validation, Debugging(Computers), Computer program verification, Software reliability, Computer program integrity, Computer programming, Mathematical calculations, Reprints, *Program slicing, Functional diversity.

One of the most commonly invoked safeguards against design basis events in nuclear power plants is the use of functional diversity. When auditors for the United States Nuclear Regulatory Commission (NRC) examine safety systems for nuclear power plants, they also inspect the software embedded within the safety systems to ensure functional diversity. For computer software, this means that there is no common code shared among diverse computations. The steps the auditor must take include identifying the types of system hazards that could occur, using techniques, like fault tree analysis, to locate software that should be examined further, and then inspecting the code for diversity. This paper describes an approach using a concept called program slicing to support auditors.

03,735
PB96-161351 Not available NTIS
National Inst. of Standards and Technology (CSL), Gaithersburg, MD. Systems and Software Technology Div.
Analysis of Standards for the Assurance of High Integrity Software.
Final rept.
D. R. Wallace, D. R. Kuhn, L. M. Ippolito, and L. Beltracchi. 1992, 21p.
See also PB95-173084 and PB95-251674.
Pub. in International Symposium on Nuclear Power Plant Instrumentation and Control, Tokyo, Japan, May 18-22, 1992, p1-21.

Keywords: *Computer program integrity, *Computer program verification, *Validation, *Nuclear power plants, Software reliability, Software engineering, Configuration management, Safety programs, Standards, Specifications, Computer information security, Electronic security, Quality assurance, Reprints, High integrity.

This study examines standards, draft standards, and guidelines (all of which will hearafter be referred to as documents) that provide requirements for the assurance of software in safety systems in nuclear power plants. The study focuses on identifying the attributes necessary in a standard for providing reasonable assurance for software in nuclear systems. The documents vary widely in their requirements and the precision with the requirements are expressed. Recommendations are provided for guidance for the assurance of high integrity software.

03,736
PB96-161369 Not available NTIS
National Inst. of Standards and Technology (CSL), Gaithersburg, MD. Systems and Software Technology Div.
Control and Instrumentation: Standards for High-Integrity Software.
Final rept.
D. R. Wallace, D. R. Kuhn, L. M. Ippolito, and L. Beltracchi. 1994, 12p.
Pub. in Nuclear Safety, v35 n1 p86-97 Jan-Jun 94.

Keywords: *Nuclear power plants, *Electronic security, *Safety programs, *Software reliability, Software engineering, Computer program integrity, Configuration management, Computer information security, Standards, Requirements, Software development, Functional analysis, Quality assurance, Reprints, High integrity.

This article describes a study that examines standards, draft standrads, and guidelines (all of which will hereafterbe referred to as documents) that provide requirements for the assurance of software in safety systems in nuclear power plants. The study focuses on identifying, for developers of standards, the elements to be addressed in a standard for providing reasonable assurance of software in safety systems in nuclear power plants. The documents vary widely in their requirements and the precision with which the requirements are eexpressed. Recommendations are outlined for guidance for the assurance of high-integrity software.

03,737
PB96-161872 Not available NTIS
National Inst. of Standards and Technology (MSEL), Gaithersburg, MD. Reactor Radiation Div.
Upgrade and Modernization Projects at the NBSR.
Final rept.
R. E. Williams. 1995, 2p.
Pub. in Transactions of the American Nuclear Society, v72 n0003-018X p312-313 1995.

Keywords: *Heat exchangers, *Nuclear reactors, *Refueling system, Reprints, NBSR, Cold Neutron Research Facility(CNRF).

The National Bureau of Standards (now the National Institute of Standards and Technology (NIST)) reactor (NBSR), a 20-MW research reactor operated by NIST, has become the leading U.S. laboratory in research using nuclear methods. About 1000 scientists from 200 industries, government and foreign laboratories, and universities conducted experiments at the NBSR last year. Since 1990, when the first instruments in the Cold Neutron Research Facility (CNRF) became available, the number of research participants has doubled. A major program of modernization and facility upgrade was initiated to meet this growing demand and to ensure safe and reliable reactor operations for 30 additional yr.

03,738
PB96-167259 Not available NTIS
National Inst. of Standards and Technology (CSTL), Gaithersburg, MD. Analytical Chemistry Div.
New NIST Rapid Pneumatic Tube System.
Final rept.
D. A. Becker, R. M. Lindstrom, J. K. Langland, and R. R. Greenberg. 1996, 7p.
Pub. in Jnl. of Trace and Microprobe Techniques, v14 n1 p1-7 1996.

Keywords: *Neutron activation analysis, Neutron irradiation, Reprints, Epithermal irradiation, Nuclear reactors, *Foreign technology, *Pneumatic tube terminal, Rapid activation analysis.

The Nuclear Methods Group of NIST is developing a new rapid pneumatic tube irradiation system to be inserted into our 20 MW nuclear reactor. The terminal will be inserted into an existing horizontal pneumatic tube location, the only one of five pneumatic tubes which has not been operational since the reactor upgrade from 10 to 20 MW ten years ago. This new terminal will contain two irradiation locations, one at the tip in a void area between several fuel elements for epithermal fluence optimization, the second in a D2O tank midway in the terminal to optimize the thermal fluence. Estimated neutron fluence rates (in n-cm-2s-1) are 9E13 thermal/3E13 epithermal for the tip irradiation location inside the D2O tank.

03,739
PB96-176615 Not available NTIS
National Inst. of Standards and Technology (MSEL), Gaithersburg, MD. Reactor Radiation Div.
Magnetic Structure Determination for Annealed Ni80Fe20/Ag Multilayers Using Polarized-Neutron Reflectivity.
Final rept.
J. A. Borchers, P. M. Gehring, C. F. Majkrzak, K. R. Coffey, M. A. Parker, J. K. Howard, J. F. Ankner, and T. L. Hylton. 1995, 6p.
Pub. in Materials Research Symposium Proceedings, Boston, MA., November 1994, v386 p577-582 1995.

Keywords: *Magnetoresistance, *Neutron reflectivity, Reprints, *Antiferromagnetic coupling, Metallic multilayers.

Sputtered Ni80Fe20/Ag multilayers, annealed post-growth, show giant magnetoresistive (GMR) effects at unusually low magnetic fields (approx. 5 Oe). Structural characterization by cross-sectional TEM and x-ray diffraction indicates that the Ag preferentially diffuses into the Ni80Fe20 layers at the interfaces. Using polarized-neutron specular reflectivity, the authors have obtained magnetization depth profiles for a series of annealed (Ni80Fe20(20A)/Ag(40A))4 multilayers. Though GMR in related materials is associated with coherent antiferromagnetic alignment of the ferromagnetic layers, specular neutron data for the Ni80Fe20/Ag multilayers show no trace of half-order spin-flip intensity characteristic of this simple structure. In small applied fields, transverse scans at the half-order position show a broad feature which disappears upon saturation. These data suggest that while the Ni80Fe20 moments are antiferromagnetically correlated along the growth axis, the in-plane magnetic domains are only of micron-order size and are thus not apparent in a specular measurement.

03,740
PB96-176631 Not available NTIS
National Inst. of Standards and Technology (MSEL), Gaithersburg, MD. Reactor Radiation Div.
Energy Distributions of Neutrons Scattered from Solid C60 by the Beryllium Detector Method.
Final rept.
J. R. D. Copley, D. A. Neumann, and W. A. Kamitakahara. 1995, 9p.
Pub. in Canadian Jnl. of Physics, v73 p763-771 1995.

Keywords: *Fullereness, *Spectroscopy, Reprints, *Foreign technology, Internal mode dynamics, Neutron scattering, Vibrational spectrometer, C60.

The authors measured the energy distribution scattered from polycrystalline C60, using a high-resolution filter-analyzer spectrometer. In the energy range 30-90 meV (242-726 cm to the minus one power) the authors observed a rich spectrum that the authors fitted to a sum of 15 Gaussian functions, each of which is assigned to one or a set of several degenerate normal vibrational modes of the C60 molecule. The authors also observed two broad features in the energy range from 90-130 meV (726-1049 cm to the minus one power). The authors' results are generally in excellent agreement with published spectroscopic data. Detailed comparisons with the results of several first-principles calculations suggest that present-day theories can predict the internal vibrational frequencies of C60 rather well, at least in the 30-90 meV range of energies.

03,741
PB96-193644 PC A07/MF A02
National Inst. of Standards and Technology (MSEL), Gaithersburg, MD.
Reactor Radiation Technical Activities, 1995.
Rept. for Oct 94-Sep 95.
L. K. Clutter. 1996, 108p, NISTIR-5751.
See also PB95-209888.

Keywords: *Nuclear reactors, *Research projects, *Nondestructive tests, *Neutron activation analysis, Cold neutrons, Irradiation, Standards, Radioisotopes, Neutron radiography, Neutron diffraction, Crystal structure, Measurement, Calibrating, US NIST, Microanalysis.

The report summarizes all the programs that use the NIST reactor. It covers the period for October 1994 through September 1995. The programs range from the use of neutron beams to study the structure and dynamics of materials through nuclear physics and neutron standards to sample irradiations for activation analysis, isotope production, neutron radiography, and nondestructive evaluation.

03,742
PB96-193784 PC A07/MF A02
National Inst. of Standards and Technology (BFRL), Gaithersburg, MD. Fire Science Div.
Methodology for Developing and Implementing Alternative Temperature-Time Curves for Testing the Fire Resistance of Barriers for Nuclear Power Plant Applications.
L. Y. Cooper, and K. D. Steckler. May 96, 117p, NISTIR-5842.
Sponsored by Nuclear Regulatory Commission, Washington, DC. Office of Nuclear Reactor Regulation.

Keywords: *Nuclear power plants, *Barriers, *Fire protection, *Performance testing, Fire tests, Flammability, Ratings, Scenarios, Threats, Reactor safety, Fire safe-

ty, Exposure, Fire resistance, Test methods, Temperature-time curves, ASTM E 119 Standard.

The aim of the current study is to propose a methodology for developing and implementing NPP-specific descriptions of fire environments and associated ASTM-type furnace test methods. Here the terminology ASTM E 119-type test is used to refer to a test method that basically follows the ASTM E 119 test procedures, but where the ASTM E 119 standard temperature-time curve is replaced with a relevant, NPP-specific, alternative curve. The approach taken in the current study consists of three steps or tasks: (1) review the history of the ASTM E 119 temperature-time curve to assess its current applicability and limitations in simulating real fires; (2) review the history of efforts to develop alternative curves and the methodologies used; and (3) use the findings from (1) and (2), knowledge of NPP construction, fuel types and loads, and state-of-the-art fire science to propose a methodology for developing and implementing NPP-specific descriptions of fire environments and associated ASTM-type temperature-time curves and test methods.

Reactor Materials

03,743
PB96-148127 Not available NTIS
National Inst. of Standards and Technology (MSEL), Gaithersburg, MD. Ceramics Div.
High-Temperature Furnace for In situ Small-Angle Neutron Scattering during Ceramic Processing.
Final rept.
H. M. Kerch, H. E. Burdette, and G. G. Long. 1995, 7p.
Pub. in Jnl. of Applied Crystallography, v28 p604-610 1995.

Keywords: *Furnances, *Research and development, *Ceramics, Neutron scattering, Experimental data, Nuclear reactors, Sintering, Glasses, Silicon dioxide, Reprints, *Small angle neutron scattering, SANS, SANS furnace, MSANS.

The design and operation of a new research furnace, optimized for small-angle neutron scattering experiments at a steady-state nuclear reactor with a cold source, are presented. The apparatus enables the study of thermal processing of materials, such as the sintering behavior in ceramics, through the measurement of their microstructural parameters (e.g. pore sizes, pore volumes and pore surface areas) during thermal treatment. Small-angle neutron scattering measurements can be performed in situ in an oxidizing, reducing or neutral environment at temperatures up to 2000 K.

OCEAN SCIENCES & TECHNOLOGY

Biological Oceanography

03,744
PB95-162640 Not available NTIS
National Inst. of Standards and Technology (CSTL), Gaithersburg, MD. Organic Analytical Research Div.
Determination of PCBs and Chlorinated Hydrocarbons in Marine Mammal Tissues.
Final rept.
M. M. Schantz, B. J. Koster, S. A. Wise, and P. R. Becker. 1993, 23p.
Pub. in Science of the Total Environment 139/140, p323-345 1993.

Keywords: *Chlorinated aromatic hydrocarbons, *Marine animals, *Pesticides, Chromatographic analysis, Tissue culture, Liver, Kidney, Muscles, Mammals, Reprints, PCBs(Polychlorinated biphenyls), Blubber, Northern fur seal, Ringed seal, Belukha whale.

Selected tissues (blubber, liver, kidney and muscle) from marine mammals, which were collected as part of the Alaska Marine Mammal Tissue Archival Project (AMMTAP), were analyzed for polychlorinated biphenyl (PCB) congeners and chlorinated pesticides. Concentrations of these compounds in the different tissues were compared and blubber was selected as the primary tissue for organic contaminant analyses for the AMMTAP based on higher levels (1-2 orders of magnitude) in this tissue compared to liver, kidney and muscle.

03,745
PB96-103023 Not available NTIS
National Inst. of Standards and Technology (CSTL), Gaithersburg, MD. Organic Analytical Research Div.
Certification of Polychlorinated Biphenyl Congeners and Chlorinated Pesticides in a Whale Blubber Standard Reference Material.
Final rept.
M. M. Schantz, B. J. Koster, L. M. Oakley, S. B. Schiller, and S. A. Wise. 1995, 10p.
Pub. in Analytical Chemistry 67, n5 p901-910, 1 Mar 95.

Keywords: *Polychlorinated biphenyls, *Pesticides, *Whales, *Animal tissues, *Bioaccumulation, Marine mammals, Water pollution effects(Animals), Reference standards, Gas chromatography, Mass spectroscopy, Electron capture, Chemical analysis, Quality assurance, Reprints, *Blubber, Standard reference materials.

A Standard Reference Material (SRM) made from whale blubber has been developed for the validation of methods used for the determination of polychlorinated biphenyl (PCB) congeners and chlorinated pesticides. This material, which is a frozen blubber tissue homogenate, was analyzed using three different analytical techniques. These techniques were based on gas chromatography with electron capture detection on two stationary phases with different selectivity for the seperation of PCB congeners and gas chromatography with mass spectrometric detection. The results from these three techniques were in good agreement and were combined to provide certified concentrations for 27 PCB congeners and 15 chlorinated pesticides.

Marine Engineering

03,746
PB94-174505 PC A04/MF A01
National Inst. of Standards and Technology (MSEL), Gaithersburg, MD. Metallurgy Div.
Characterization of the Hydrogen Induced Cold Cracking Susceptibility at Simulated Weld Zones in HSLA-100 Steel.
M. R. Stoudt, and R. E. Ricker. 1994, 71p, NISTIR-5408.
See also AD-A224 341. Sponsored by Office of Naval Research, Arlington, VA.

Keywords: *Alloys, *Carbon steels, *Crack resistance, *Welding, *Naval vessels, Fracture(Mechanics), Fabrication, Impact strength, Hydrogen embrittlement, Cold forming, Mechanical properties, Structural steel, Strength(General), Corrosion, Sea water, Performance evaluation, Comparison, Strain rate, Tests, Electrochemistry.

The relative susceptibilities to hydrogen induced cold cracking were evaluated for HY-100, a steel presently in service in naval applications and for HSLA-100. The martensitic microstructure of the HY-100 undergoes wide variations in the heat affected zone during welding which strongly influence the resistance of that alloy to cold cracking. The HSLA-100, a low carbon, precipitation hardened steel with similar strength and toughness to that of the HY-100, possesses a significantly lower degree of hardenability which results in minimal microstructural variations in the heat affected zone under the same simulated welding conditions. The mechanical properties of the base metal and the heat affected zone created during a simulated, single welding pass were characterized by the slow strain rate technique for both steels in an inert environment and in artificial seawater under free corrosion and controlled hydrogen fugacities. The electrochemical behaviors of both steels were also evaluated in artificial seawater.

03,747
PB94-211877 Not available NTIS
National Inst. of Standards and Technology (NEL), Gaithersburg, MD. Robot Systems Div.
Intelligent Control for Multiple Autonomous Undersea Vehicles.
Final rept.
M. Herman, J. S. Albus, and T. H. Hong. 1990, 48p.
Pub. in Neural Networks for Control, Chapter 18, p427-474 1990.

Keywords: *Autonomous navigation, *Underwater vehicles, *Artificial intelligence, Neural nets, Architecture(Computers), Control systems design, Remotely piloted vehicles, Real time operation, Hierarchies, Robotics, Models, Reprints, *Multiple Autonomous Undersea Vehicles project, *MAUV project.

Intelligent control for autonomous vehicles in a natural, potentially hostile environment requires a system that integrates artificial intelligence with modern control theory, and that is implemented on parallel, possibly special-purpose hardware. Issues dealing with the requirements of such a system are discussed in the context of the Multiple Autonomous Undersea Vehicles (MAUV) project. The MAUV control system and its implementation are also presented. The goal of the MAUV project was to have multiple undersea vehicles exhibiting intelligent, autonomous, cooperative behavior. The MAUV control system is hierarchically structured and incorporates sensing, world modeling, planning and execution. The levels in the hierarchy include: mission, group, vehicle task, elemental action, primitive action, and servo. Issues of real-time planning and dynamic replanning in unstructured environments are discussed. A multi-level world model that supports real-time planning is also described. Finally, timing issues, implementation, and initial experimental results are presented.

03,748
PB95-251633 PC A03/MF A01
National Inst. of Standards and Technology (MEL), Gaithersburg, MD. Intelligent Systems Div.
Submarine Automation: Demonstration No. 5.
Rept. for Oct 92-Nov 93.
H. M. Huang, R. Quintero, and K. Young. 1995, 21p, NISTIR-5676, ARPA-7829-2.
See also PB93-184257. Prepared in cooperation with PdMA Corp., Rockville, MD. Sponsored by Defense Advanced Research Projects Agency, Arlington, VA.

Keywords: *Submarines, *Automation, *Demonstration projects, Computer applications, ARPA(Advanced Research Projects Agency).

The major objectives of this project are to: Demonstrate the application of the NIST RCS to submarine automation; and Refine and document the RCS methodology. This cycle of the submarine automation project emphasizes: Continuing investigating and developing the human computer interface (HCI); Expanding the submarine control system, the simulator, and the animator to include engineering supporting systems; Demonstrating reusing the existent automated maneuvering system software; and Refining the RCS methodology.

03,749
PB96-123112 Not available NTIS
National Inst. of Standards and Technology (BFRL), Gaithersburg, MD. Structures Div.
Stranding Experiments on Double Hull Tanker Structures.
Final rept.
J. L. Rodd, M. P. Phillips, and E. D. Anderson. 1994, 17p.
Pub. in Advanced (Unidirectional) Double-Hull Technical Symposium, Gaithersburg, MD., October 25-26, 1994, p1-17.

Keywords: *Oil tankers, *Double hulls, Ship structural components, Tanker ships, Ship hulls, Losses, Structural failures, Design analysis, Failure analysis, Crashworthiness, Ship accidents, Reprints, *Strandings, *Groundings.

Three different hull designs were evaluated in the 30,000-40,000 lon range: a baseline conventional double hull bottom with transverse and longitudinal framing, an advanced double hull (ADH) with unidirectional longitudinal web, and a variant of the AH design incorporating curved plates. A large fabricated 'rock' was used to indent each structure vertically, causing first rupture of the outer shell, and then rupture of the inner shell. Inner shell rupture occurred at model loads of up to 750,000 lbs, and the rock intrusion into the ship was nearly twice the double hull spacing. The results

are proving to be vital in validating numerical modeling tools needed to develop reliable design and analysis methods. In addition, efforts are already underway to develop an ADH crash worthiness system that can minimize or eliminate rupture of the inner shell during the high energy dissipation that occurs during a grounding.

03,750
PB96-155759 Not available NTIS
National Inst. of Standards and Technology (BFRL), Gaithersburg, MD. Structures Div.
Transitions to Chaos Induced by Additive and Multiplicative Noise.
Final rept.
E. Simiu, and M. Frey. 1994, 4p.
Pub. in Proceedings of the Toyota Conference (7th) 'Towards the Harnassing of Chaos', Amsterdam, p405-408 1994.

Keywords: *Noise, *Building technology, *Chaos, Reprints, Transitions, Stochastic processes, *Foreign technology.

For a class of multistable systems, deterministic and stochastic chaos are closely related mathematically; a necessary condition for the occurrence of noise-induced chaos with sensitive dependence on initial conditions can be derived from the generalized Melnikov function. Proof that this condition is applicable requires the approximate representation of the noise in the form of a modified Shinozuka process or other uniformly continuous and uniformly bounded processes. Additive and/or multiplicative Gaussian noise with any spectral density can be accommodated, as can other types of noises, including shot noise and non-Gaussian noise. We review recent results, including a successful verfication of our Melnikov-based approach against results based on a solution of the Fokker-Planck equation. We conclude by briefly describing ongoing research.

03,751
PB96-195516 PC A03/MF A01
National Inst. of Standards and Technology (MEL), Gaithersburg, MD. Intelligent Systems Div.
Operator Experience with a Hierarchical Real-Time Control System (RCS).
H. M. Huang. Jun 96, 19p, NISTIR-5862.

Keywords: *Submarines, *Real time control, Automatic control, Computer architecture, Human computer interface, Artificial intelligence, Knowledge bases, Computer programming, Underwater vehicles, Autonomous navigation.

The issue of operator interface in the RCS hierarchical control systems is the focus of this report. In a submarine automation project, the authors have studied the logical structure of the operator interface function and the way it should be integrated to existing systems. A design issue is to allow operators to be involved in system operations at in different degrees. In some situations, the operators are requested to perform certain manual operations and report the status back to the control systems. In some other situations, the operators are required to make some decisions for the controllers. At different control levels, operators require different information. A system developer may require total different types of information.

Physical & Chemical Oceanography

03,752
PB94-199122 Not available NTIS
National Inst. of Standards and Technology (MSEL), Gaithersburg, MD. Polymers Div.
Atmospheric and Marine Trace Chemistry: Interfacial Biomediation and Monitoring.
Final rept.
F. E. Brinckman, and G. J. Olson. 1990, 14p.
Pub. in Marine Chemistry 30, n1-3 p147-160 1990. Sponsored by International Union of Pure and Applied Chemistry, Stockholm (Sweden).

Keywords: *Air-water interfaces, *Metalloids, *Metals, *Marine chemistry, *Environmental monitoring, *Environmental impact assessments, Trace elements, Geochemistry, Biotechnology, State of the art, Natural emissions, Pollutants, Metal containing organic compounds, Reprints.

Valid monitoring and assessment of metals and metalloids active in our planetary environment is now established with analytical methodology employing ultratrace (microgram/L) molecular speciation of illustrative organometallic substances. During the past 20 years, such measurements have placed into realistic context the vital interplay betwen abiotic geochemical sources and man's technological effluents, in terms of the frequent rate-deterring and extensive biogeorganometallic chemistry dictating heavy element transport and speciation, especially at bioactive surface microlayers featuring heightened bioprocessing of both depositional and emissive fluxes of metals and metalloids. The report places its overview of this current state of art with air-sea measurement capability for monitoring such biogenic organometal(loid)s, within the context of independently established predictive mimetic aqueous chemistry of metals and metalloids, with implications for marine biotechnology.

ORDNANCE

Ammunition, Explosives, & Pyrotechnics

03,753
AD-A295 896/5 PC A03/MF A01
National Inst. of Standards and Technology (NML), Gaithersburg, MD. Molecular Physics Div.
Thermal Decomposition Pathways in Nitramine Propellants.
Final rept. 1 Jan 92-31 Dec 94.
F. J. Lovas, and R. D. Suenram. 4 Apr 95, 45p, ARO-29596.2-CH.
Contract ARO-MIPR-126-94

Keywords: *Thermal properties, *Propellants, *Decomposition, *Nitramines, Spectroscopy, Vapors, Test methods, Microwaves, Chemical composition, Amines, Organic compounds, Rdx, Reactants(Chemistry), Pyrolysis, Nitro radicals, Microwave spectroscopy, Pathways.

We have investigated intermediates and products in the thermal decomposition of RDX vapor, using a variety of experimental microwave techniques previously employed in our laboratory in studies of pyrolysis decomposition of organic amines. We used microwave spectroscopy to determine the chemical composition of the decomposition of nitramines by pyrolysis methods and identify the products in the thermal decomposition processes. The objective was to determine the validity of proposed decomposition mechanisms, and to identify new reaction products or pathways. jg p.1.

03,754
PB94-200177 Not available NTIS
National Inst. of Standards and Technology (MSEL), Gaithersburg, MD. Reactor Radiation Div.
Texture Study of Two Molybdenum Shaped Charge Liners by Neutron Diffraction.
Final rept.
C. S. Choi, H. J. Prask, J. Orosz, and E. L. Baker. 1993, 7p.
Pub. in Jnl. of Materials Science 28, p3557-3563 1993.

Keywords: *Shaped charges, *Cavity liners, *Molybdenum, Neutron diffraction, Conical bodies, Texture, Reprints.

The textures of two different conical shaped liners, fabricated by the same forging processes from arc-cast and powder-sintered ingots, were investigated by using neutron-diffraction measurements and three-dimensional orientation-distribution-function (ODF) analysis. The major textures of both liners could be described by the (111)<uvw> and (100)<uvw> type. The two liners had essentially identical texture at the 8 cm position (measured from the base of the cone) with strong sheet-type texture components, i.e. (111)<(-1)01>, (111)<(-1)10> and (100)<011>. However, the dominant textures at the 3 cm positions were <111> and <100> fiber textures with the fiber axes oriented parallel to the normal direction in both liners. A strong cube texture was observed at the 3 cm position of the arc-cast liner but it was not observed for the powder-sintered liner. The arch-cast liner had a generally higher degree of texture than the powder-sintered liner.

03,755
PB95-108437 Not available NTIS
National Inst. of Standards and Technology (MSEL), Gaithersburg, MD. Ceramics Div.
1,4-Dinitrocubane and Cubane under High Pressure.
Final rept.
G. J. Piermarini, S. Block, R. Damavarapu, and S. Iyer. 1991, 6p.
Pub. in Propellants, Explosives, Pyrotechnics 16, p188-193 1991.

Keywords: *High pressure tests, *Cubane, Chemical reactions, Phase transformations, Fourier transform spectrometers, Pyrolysis, Optical microscopy, Pyrotechnic devices, Reprints, *Cubane/dinitro, Energetic materials.

The effects of pressure on the chemical reactivity, phase behavior and thermal decomposition of energetic materials can be studied by a combination of measurement techniques in conjunction with a high pressure diamond anvil cell and the ruby fluorescence method of pressure measurement. These techniques include: (1) optical polarizing microscopy and (2) Fourier transform infrared (FTIR) spectroscopy. Recent results on the study of 1,4-dinitrocubane and cubane will be presented.

03,756
PB95-202396 Not available NTIS
National Inst. of Standards and Technology (MSEL), Gaithersburg, MD. Reactor Radiation Div.
Microstructure Study of Molybdenum Liners by Neutron Diffraction.
Final rept.
C. S. Choi, E. L. Baker, and J. Orosz. 1994, 8p.
Pub. in Nondestructive Characterization of Materials VI, p637-644 1994.

Keywords: *Shaped charges, *Cavity liners, Neutron diffraction, Microstructure, Molybdenum, Reprints, Orientation distribution functions, Plastic strain ratio, R values.

The crystallites orientation distributions of three different conical molybdenum shaped-charge liners, labeled C00, C20 and C40, fabricated with different thermo-mechanical treatment processes, were investigated by using neutron diffraction measurements and three-dimensional ODF (orientation distribution function) analysis. Two specimens were obtained from each liner, one from 25 mm below the apex and the other from 25 mm above the liner base. Results are discussed.

Armor

03,757
PB94-158573 PC A03/MF A01
National Inst. of Standards and Technology (EEEL), Gaithersburg, MD.
Study to Determine the Most Important Parameters for Evaluating the Resistance of Soft Body Armor to Penetration by Edged Weapons.
N. J. Calvano. Jul 93, 47p, NISTIR-4895.
See also PB87-105524. Sponsored by National Inst. of Justice, Washington, DC.

Keywords: *Body armor, *Puncture resistance, Blades, Knives, Police, Law enforcement officers, Protective clothing, Impact tests, Lightweight armor, Polyaramid fabrics.

The paper describes tests that were conducted to determine the most important parameters for measuring the resistance of soft body armor to penetration by edged weapons. Samples consisting of multiple layers of polyaramid fabric were tested against the following variables: blade, geometry, backing material, conditioning, impact angle, and velocity. Stab and slice tests were conducted. Some commercial armors were also tested. The commercial armors were constructed of ultra-high molecular weight polyethylene, polyaramid fabric, and combinations of ultra-high molecular weight polyethylene, polyaramid fabric, and titanium. Results

indicate that penetration is a strong function of blade geometry. Backing material, conditioning, and impact angle appeared to have only a minimal affect upon the results.

Combat Vehicles

03,758
N94-34037/9 (Order as N94-34019/7, PC A21/MF A04)
National Inst. of Standards and Technology, Gaithersburg, MD.
Ground Vehicle Control at NIST: From Teleoperation to Autonomy.
K. N. Murphy, M. Juberts, S. A. Legowik, H. A. Scott, S. Szabo, M. Nashman, and H. Schneiderman. Jan 94, 6p.
In NASA. Johnson Space Center, the Seventh Annual Workshop on Space Operations, Applications, and Research (Soar 1993), Volume 1 p 137-142.

Keywords: *Communication equipment, *Ground based control, *Inertial navigation, *Real time operation, *Teleoperators, Military operations, Radio communication, Communication networks, Highways, Measuring instruments, Steering, *Military vehicles, *Autonomous navigation.

NIST is applying their Real-time Control System (RCS) methodology for control of ground vehicles for both the U.S. Army Research Lab, as part of the DOD's Unmanned Ground Vehicles program, and for the Department of Transportation's Intelligent Vehicle/Highway Systems (IVHS) program. The actuated vehicle, a military HMMWV, has motors for steering, brake, throttle, etc. and sensors for the dashboard gauges. For military operations, the vehicle has two modes of operation: a teleoperation mode--where an operator remotely controls the vehicle over an RF communications network; and a semi-autonomous mode called retro-traverse--where the control system uses an inertial navigation system to steer the vehicle along a prerecorded path. For the IVHS work, intelligent vision processing elements replace the human teleoperator to achieve autonomous, visually guided road following.

03,759
PB95-163200 Not available NTIS
National Inst. of Standards and Technology (NEL), Gaithersburg, MD. Robot Systems Div.
Control System Architecture for a Remotely Operated Unmanned Land Vehicle.
Final rept.
S. Szabo, H. A. Scott, K. Murphy, and S. A. Legowik. 1990, 8p.
Pub. in Proceedings of Institute of Electrical and Electronics Engineers International Symposium on Intelligent Control (5th), Philadelphia, PA., September 5-7, 1990, p876-883.

Keywords: *Control systems, *Systems architecture, Military vehicles, Remote control, Teleoperators, Real time operation, Unmanned, Ground vehicles, Robot dynamics, Systems engineering, Reprints, *Mobile robots.

The U.S. Army Laboratory Command, as part of its Robotics Initiative, is developing a testbed for cooperative, real-time control of unmanned land vehicles. The National Institute of Standards and Technology is supporting this program by developing the vehicle control system using an architecture based on the Real-time Control System (RCS). RCS is a hierarchical, sensory-based control system, initially developed for the control of industrial robots and automated manufacturing systems. In this application, RCS controls all vehicle mobility functions, coordinates the operations of the other subsystems on the vehicle, and communicates between the vehicle and the remote operator control station. The paper reviews the overall control system architecture and the design of the mobility and communication functions.

Underwater Ordnance

03,760
PB95-182390 PC A05/MF A01
National Inst. of Standards and Technology (EEEL), Boulder, CO. Electromagnetic Fields Div.
Assessment of Data by a Second-Order Transfer Function.
Technical note.
D. G. Camell, and M. T. Ma. Oct 94, 78p, NIST/TN-1372.
Also available from Supt. of Docs. as SN003-003-03303-1. See also PB95-161485.

Keywords: *Electromagnetic interference, *Torpedoes, Electromagnetic pulses, Convolution integrals, Continuous radiation, Resonant frequency, Transfer functions, Laplace transformation, Linear systems, Approximation, Magnitude, Phase, Graphs(Charts), Impulse response.

A newly developed theory for predicting the response of a linear system to an electromagnetic pulse, based only on the measured continuous-wave magnitude, is applied to the problem of possible electromagnetic interferences at a sensitive part of a torpedo. The measured magnitude representing the system's transfer function is deduced first from the measured response at this sensitive point to a known cw source, supplied by the Naval Surface Warfare Center. We derive an analytic expression for the magnitude square of the transfer function to approximate the measured data and obtain a system transfer function in terms of the complex frequency, from which we predict the system's cw phase characteristics and its multiple solutions due to a given impulse source.

PHOTOGRAPHY & RECORDING DEVICES

Holography

03,761
PB96-119284 Not available NTIS
National Inst. of Standards and Technology (CSTL), Gaithersburg, MD. Biotechnology Div.
Holographic Properties of Triton X-100-Treated Bacteriorhodopsin Embedded in Gelatin Films.
Final rept.
D. W. Cullin, N. N. Vsevolodov, and T. V. Dyukova. 1995, 4p.
Pub. in BioSystems, v34 n2,3 p141-144 Jul 95.

Keywords: *Bacteria, *Thin films, *Gelatins, *Holographic spectroscopy, Surfactants, Biotechnology, Diffraction, Phases, Amplitudes, Kinetics, Concentration(Composition), Fabrications, Reprints, *Triton X-100, *Bacteriorhodopsin.

Bacteriorhodopsin (bR) thin films have been fabricated with varying amounts of the detergent Triton X-100 to measure the effects of this additive on the holographic performance of these thin films. Holographic spectroscopy is used to measure the effect of these detergents on the overall diffraction efficiency as well as on the phase and amplitude components of the overall signal. The diffracted rise and decay kinetics of these materials will also be presented as a function of varying detergent concentration. This research also studied the effect of this additive on the absorptive properties of bR-based thin films. Comparison of the two complimentary sets of data are drawn.

03,762
PB96-167366 Not available NTIS
National Inst. of Standards and Technology (EEEL), Boulder, CO. Electromagnetic Fields Div.
Planar Near-Field Measurements and Microwave Holography for Measuring Aperture Distribution on a 60 GHz Active Array Antenna.
Final rept.
J. Guerrieri, N. Canales, K. MacReynolds, and D. Tamura. 1995, 6p.
Pub. in Annual Meeting and Symposium (17th), Antenna Measurement Techniques 1995 Association, Williamsburg, VA., November 13-17, 1995, p295-300.

Keywords: *Amperture amplitude distribution, Reprints, *Planar near-field method, Aperture phase distribution, Black transform, Phase-shifter settings.

This paper discusses results of a recent attempt to measure aperture distribution of a small active steerable array antenna at 60 GHz using planar near-field measurements and the back transform. Using a procedure which exercises every phase shifter without steering the antenna beam, it is possible to isolate problems with individual bits in the phase shifters. From calculation of the aperture fields for each case we hope to infer the individual phase shifter bit loss. We will also discuss problems which arose in the measurement because of the short wavelength signal-to-noise ratio and small number of elements.

Recording Devices

03,763
PB95-180907 Not available NTIS
National Inst. of Standards and Technology (EEEL), Boulder, CO. Electromagnetic Technology Div.
Comparison of Magnetic Fields of Thin-Film Heads and Their Corresponding Bit Patterns Using Magnetic Force Microscopy.
Final rept.
P. Rice, B. Hallett, and J. Moreland. 1994, 3p.
Pub. in Institute of Electrical and Electronics Engineers Transactions on Magnetics 30, n6 p4248-4250 Nov 94.

Keywords: *Recording heads, *Magnetic fields, Imaging techniques, Thin films, Magnetization, Comparison, Reprints, Magnetic force microscopy, Magnetic imaging, Hard disks, Bit patterns.

We have used de-mode magnetic force microscopy to image the magnetic fringing fields of several thin-film heads and the bit patterns written with these heads. The images were taken with Si3N4 tips coated with 10-nm Fe and 5-nm Au. The heads and disks are typical industry standards. The heads had a variety of pole piece configurations. A large track separation was used so that the erase bands could be thoroughly studied. We were surprised to discover magnetic fields that correspond to layers in the alumina overcoat near the pole pieces. The magnetic force microscope images of the bit pattern show a definite twist at the track edge that points toward the trailing pole piece. We also observed disk magnetization patterns that remained after an ac erase procedure.

PHYSICS

General

03,764
AD-A278 130/0 PC A05/MF A01
National Bureau of Standards, Gaithersburg, MD.
Atomic Energy Levels As Derived from the Analyses of Optical Spectra. Volume 1. Section 1. The Spectra of Hydrogen, Deuterium, Helium, Lithium Beryllium, Boron, Carbon, Nitrogen, Oxygen, and Fluorine.
C. E. Moore. 15 Apr 48, 79p, NBS-CIRCULAR-467.

Keywords: *Atomic energy levels, *Atomic spectra, Atomic structure, Energy levels, Spectra, Optical analysis, Hydrogen, Deuterium, Helium, Lithium, Beryllium, Boron, Carbon, Nitrogen, Oxygen, Fluorine.

No abstract available.

03,765
AD-A278 139/1 PC A04/MF A01
National Bureau of Standards, Boulder, CO.
X-ray Attenuation Coefficients from 10 Kev to 100 Mev.
G. W. Grodstein. 30 Apr 57, 58p, NBS-CIRCULAR-583.

Keywords: *X rays, *Radiation attenuation, *Gamma rays, Narrow beams(Radiation), Photoelectric effect, Photons, Interactions, Attenuation coefficients.

A tabulation of attenuation coefficients of X-rays and gamma rays from 0.01 to 100 Mev for 29 materials is

presented. A summary of information on the probability of the basic interaction processes of photons with matter and a detailed analysis of experimental and theoretical evidence are included. Present information on the basic processes is adequate for many applications; however, improved theory and additional experimental data are needed in certain areas. A comparison of calculated and experimental coefficients points up this need.

03,766
AD-A279 282/8 PC A15/MF A03
National Bureau of Standards, Gaithersburg, MD.
Technologic Papers of the Bureau of Standards: Number 170. Pyrometric Practice.
P. D. Foote, C. O. Fairchild, and T. R. Harrison. 1948, 326p.

Keywords: *Optical pyrometers, *Measuring instruments, *Standards, Radiation pyrometers, High temperature, Thermometers, Melting point, Thermoelectricity, Resistance thermometers, Recording systems, *Temperature measurement, Technological papers.

No abstract available.

03,767
AD-A279 289/3 PC A03/MF A01
National Bureau of Standards, Gaithersburg, MD.
X-Ray Attenuation Coefficients from 10 kev to 100 Mev.
R. T. McGinnies. 30 Oct 59, 15p, NBS-CIRC-583-SUPP.

Keywords: *X-rays, X-ray scattering, Photons, Incoherent scattering, Attenuation, Coefficients, Absorption, Tables(Data), X-ray absorption.

No abstract available.

03,768
AD-A280 290/8 PC A04/MF A01
National Bureau of Standards, Gaithersburg, MD.
X-Ray Attenuation Coefficients from 10 KEV to 100 MEV.
G. W. Grodstein. 30 Apr 57, 58p.

Keywords: *X-ray absorption analysis, X-ray scattering, Cross sections, Radiation attenuation, Gamma ray absorption coefficients, Tables(Data), Water, Hydrogen, Potassium, Air, X-ray attenuation coefficients.

A tabulation of attenuation coefficients of X-rays and gamma rays from 0.01 to 100 Mev for 29 materials is presented. A summary of information on the probability of the basic interaction processes of photons with matter and a detailed analysis of experimental and theoretical evidence are included. Present information on the basic processes is adequate for many applications; however, improved theory and additional experimental data are needed in certain areas. A comparison of calculated and experimental coefficients points up this need. (Author).

03,769
AD-A281 167/7 PC A07/MF A02
National Bureau of Standards, Gaithersburg, MD.
Bibliography of the Physical Equilibria and Related Properties of Some Cryogenic Systems.
T. M. Flynn. May 60, 130p, NBS-TN-56.

Keywords: *Cryogenics, Bibliographies, Carbon dioxide, Carbon monoxide, Ethanes, Helium, Hydrogen, Methane, Mixtures, Nitrogen, Propane, Liquid phases, Vapor phases, Physical properties, Pressure, Volume, Temperature, *Physical equilibrium.

A bibliography of approximately 700 references is presented on the physical equilibria and related properties of several important cryogenic systems. The systems considered are the pure components and mixtures of: Hydrogen, Helium, Nitrogen, Carbon Dioxide, Carbon Monoxide, Methane, Ethane, and Propane.

03,770
AD-A286 701/8 PC A03/MF A01
National Bureau of Standards, Boulder, CO.
Precise Measurement of Heat of Combustion with a Bomb Calorimeter.
R. S. Jessup. 2 Sep 60, 28p.
Contract NBS-MONO-7

Keywords: *Heat of combustion, *Calorimeters, Measurement, Reprints, Standards, Liquids, Hydrocarbons, Fuels, Computations, Organic compounds, Chemical compounds, Solid fuels, Precision, Water, Combustion, Oxygen, Pressure, *Bomb calorimeter, Glass bulbs.

No abstract available.

03,771
AD-A292 502/2 PC A01/MF A01
National Bureau of Standards, Gaithersburg, MD.
Penetration and Diffusion of Hard X-rays through Thick Barriers. III. Studies of Spectral Distributions.
P. R. Karr, and J. C. Lamkin. 15 Dec 49, 3p.
Pub. in The Physical Review, v76 n12 p1843-1845, 15 Dec 49.

Keywords: *Gamma rays, *Spectral energy distribution, *Compton scattering, Mathematical models, Reprints, Thickness, Penetration, Barriers, Photons, Diffusion, Integral equations, Monochromatic light, Laplace transformation, Photon beams, Photoelectric effect(Gamma rays), Gamma ray spectra.

Two kinds of spectral distributions of gamma-rays are discussed. These are spectra found in an infinite medium with an uniformly distributed monochromatic source and equilibrium spectra obtained in an artificial penetration problem. Curves are shown for various media and for various energies of the source photons. The relations of these spectra to the general problem of gamma-ray penetration is discussed. (AN).

03,772
AD-A295 314/9 PC A01/MF A01
National Bureau of Standards, Gaithersburg, MD.
Further Calculations of X-ray Diffusion in an Infinite Medium.
L. V. Spencer, and F. Stinson. 15 Feb 52, 3p.
Pub. in Tax Physical Review, v85 n4 p662-664, 15 Feb 52.

Keywords: *X ray scattering, *Diffusion, Sources, Computations, Spectra, Polynomials, Expansion, Homogeneity, Reprints.

The problem of x-ray diffusion in an infinite homogeneous medium can be solved numerically by a method of expansion into suitable polynomial systems. This method has already been applied to determine the spectrum of scattered radiation as a function of distance from the radiation source for several cases of interest. This note presents further numerical applications of the polynomial method.

03,773
AD-A295 578/9 PC A03/MF A01
National Inst. of Standards and Technology (NML), Gaithersburg, MD. Molecular Physics Div.
Infrared and Near-Infrared Spectra of HCC and DCC Trapped in Solid Neon.
D. Forney, M. E. Jacox, and W. E. Thompson. 1995, 38p, ARO-30094.4-CH.
Contract ARO-MIPR-107-94
Pub. in Jnl. of Molecular Spectroscopy, v170 p178-214, 1995.

Keywords: *Trapping(Charged particles), *Solids, *Near infrared radiation, *Neon, *Infrared spectra, Reprints, Vibration, Vapor phases, Spectra, Shifting, Isotopes, Ground state, Absorption, Energy levels, Low frequencies, Chemical shifts.

Spectra have been recorded from 700 to 12 000/cm for HCC and DCC trapped in solid neon. In this region, which includes not only the ground-state absorptions but also all of the absorptions of appreciable intensity in the highly perturbed A (2)pi state, all of the matrix shifts are to lower frequencies, and none of them exceeds 30 /cm. The X(OnO) and X(On1) progressions of HCC, recently reported in the photoelectron spectrum of HCC-, also appear in the infrared spectrum. The spectra of the singly and doubly carbon-13 substituted species of HCC and of doubly carbon-13 substituted DCC are presented. Except in a few regions of very strong mixing of energy levels of the X and A states, correlations of the HCC and DCC bands with their carbon-13 substitution counterparts are possible, and the resulting isotopic shift data are useful in assigning the vibronic spectra. Assignments are proposed for a considerable number of HCC and DCC bands. These assignments are aided by the carbon-13 shift data, by the results of recent ab initio calculations, and, where they are available, by the upper-state symmetries of bands observed in the gas phase. Absorptions of C2, C2-, C4, HC4, HCCO, and C2H3 isolated in a neon matrix are also identified. jg.

03,774
AD-A296 061/5 PC A03/MF A01
National Inst. of Standards and Technology (NML), Gaithersburg, MD. Molecular Physics Div.
Spectroscopic Study of Reaction Intermediates and Mechanisms in Nitramine Decomposition and Combustion.
Final rept. 20 Mar 92-19 Mar 95.
M. B. Jacox. 20 May 95, 40p, ARO-30094.5-CH.
Contract ARO-MIPR-107-94

Keywords: *Spectroscopy, *Combustion, *Decomposition, *Nitramines, Water, Solids, Short range(Time), Spectra, Responses, Diagnostic techniques, Free radicals, Neon, Infrared spectra, Nitromethane, Photodecomposition, Molecular ions.

The infrared spectra of reaction intermediates trapped in solid neon were studied in order to support the development of diagnostics for short-lived species which are reaction carriers in nitramine decomposition and combustion and to derive information about reactions which are important in the condensed-phase decomposition of nitramines. Nitromethane and monomethylnitramine were used as model compounds in these studies. Evidence was obtained for the formation of water complexes with both of these species. The results support the water-catalyzed decomposition mechanism for nitramines that was proposed by Melius. Studies of the photodecomposition of isotopically substituted monomethylnitramine demonstrate that four different groups of products are formed. Tentative spectral assignments are made for the aci-isomer of monomethylnitramine and for CH3NHONO. The final photodecomposition products are CH4, NO, CH3OH, and N20. Other studies have provided evidence for the formation of a weakly bonded complex of H2 with H20, as well as spectral data for the HCC free radical and for the H20+, N02+, NO(2-), and NO(3-), molecular ions.

03,775
DE94005988 PC A02/MF A01
National Inst. of Standards and Technology (EEEL), Boulder, CO. Electromagnetic Technology Div.
Magnetic Characteristics and Measurements of Filamentary Nb-Ti Wire for the Superconducting Super Collider.
R. B. Goldfarb, and R. L. Spomer. 1989, 9p, CONF-890701-32.
Contract AI05-85ER40240
International cryogenic materials conference, Los Angeles, CA (United States), 24-28 Jul 1989. Sponsored by Department of Energy, Washington, DC.

Keywords: *Niobium Alloys, *Superconducting Super Collider, *Superconducting Wires, *Titanium Alloys, Evaluation, Magnetic Flux, Magnetic Properties, Magnetization, Superconducting Magnets, EDB/430300.

In synchrotron accelerator applications, such as the Superconducting Super Collider (SSC), superconducting magnets are cycled in magnetic field. Desirable properties of the magnets include field uniformity, field stability with time, small residual field, and fairly small energy losses upon cycling. This paper discusses potential sources of problems in achieving these goals, describes important magnetic characteristics to be considered, and reviews measurement techniques for magnetic evaluation of candidate SSC wires. Instrumentation that might be practical for use in a wire-fabrication environment is described. The authors report on magnetic measurements of prototype SSC wires and cables and speculate on causes for instability in multipole fields of dipole magnets constructed with such cables.

03,776
DE95004446 PC A03/MF A01
National Inst. of Standards and Technology (PL), Gaithersburg, MD. Electron and Optical Physics Div.
Electron-atom collision studies using optically state selected beams. Progress report, May 15, 1987--May 14, 1988.
R. J. Celotta, and M. H. Kelley. 15 Nov 88, 36p, DOE/ER/13520-T1.
Contract AI01-86ER13520
Sponsored by Department of Energy, Washington, DC.

Keywords: *Electron-Atom Collisions, *Sodium, EV Range 10-100, Elastic Scattering, Electron Reactions, Optical Pumping, Polarized Beams, Progress Report, EDB/664300, Electron spin polarization, Electron scattering.

This report discusses progress made during the current contract period on the authors research program

to study collisions between spin-polarized electrons and optically prepared atoms. The objective of this work is to stimulate a deeper theoretical understanding of the electron-atom interaction by providing more complete experimental measurements on colliding systems. By preparing the internal states of the collision partners before scattering, they are able to extract substantially more information about the scattering process than is available from more conventional measurements of differential cross sections. The authors are principally interested in observing the role played by spin in low energy electron-atom collisions. The additional information provided by these spin-dependent measurements can greatly enhance understanding of both exchange and the spin-orbit interaction in the scattering process. They have made substantial progress in the past three years in their measurements both of elastic and superelastic scattering of spin-polarized electrons from optically pumped sodium.

03,777
DE95004447 PC A03/MF A01
National Inst. of Standards and Technology (PL), Gaithersburg, MD. Electron and Optical Physics Div.
Electron-atom collision studies using optically state selected beams. Progress report, May 15, 1988--May 14, 1991.
R. J. Celotta, and M. H. Kelley. 15 Nov 90, 29p, DOE/ER/13520-T2.
Contract AI01-86ER13520
Sponsored by Department of Energy, Washington, DC.

Keywords: *Sodium, Electron reactions, EV Range 10-100, Elastic Scattering, Polarized Beams, Progress Report, *Electron-atom collisions, EDB/664300, Electron spin polarization, Electron scattering.

This report discusses progress made during the current contract period on the authors research program to study collisions between spin-polarized electrons and spin-polarized atoms. The objective of this work is to stimulate a deeper theoretical understanding of the electron-atom interaction by providing the most complete possible experimental characterization of the colliding system. Through the use of optical state preparation techniques to prepare both the incident electrons and atom in well-defined initial states, the authors are able to extract substantially more information about the scattering process than is available from more conventional measurements of differential scattering cross sections. Their primary interest is to study in detail the role played by spin in electron-atom collisions at low to intermediate energies. The additional information provided by these spin-dependent measurements greatly enhances understanding of both exchange and the spin-orbit interaction in the scattering process. During this three-year period they have made substantial progress in measurements of both elastic and superelastic scattering of spin-polarized electrons from optically pumped sodium. The elastic scattering measurements in particular were made possible by several important improvements to the experimental apparatus.

03,778
DE95011352 PC A03/MF A01
National Inst. of Standards and Technology, Boulder, CO.
Experimental plan to determine the performance of the Oak Ridge National Laboratory Cold Neutron Moderator. Final report, September 1, 1993--November 30, 1993.
PROGRESS REPT.
P. J. Giarratano, and J. D. Siegwarth. 10 Nov 93, 21p, DOE/OR/22121-T1.
Contract AI05-93OR22121
Sponsored by Department of Energy, Washington, DC.

Keywords: *Deuterium, *Moderators, Cold Neutrons, Hydraulics, Mathematical Models, Neutron Beams, Neutron Source Facilities, ORNL, Performance, Progress Report, Thermal Analysis, Thermodynamic Properties, Waste Heat, EDB/430100, EDB/663610.

This paper outlines an experimental plan to test the thermohydraulic concept of the proposed Oak Ridge National Laboratory Cold Neutron Moderator. The goals, approach, description of the experimental apparatus, and proposed budget and duration are presented.

03,779
N95-32323/4 (Order as N95-32319, PC A20/MF A04)
National Inst. of Standards and Technology, Boulder, CO.
Implementation of a Standard Format for GPS Common View Data.
M. A. Weiss, and C. Thomas. May 95, 14p.
In NASA. Goddard Space Flight Center, the 26TH Annual Precise Time and Time Interval (Ptti) Applications and Planning Meeting p 75-88.

Keywords: *Data processing, *Global positioning system, *Standardization, *Time signals, Receivers, Time measurement.

A new format for standardizing common view time transfer data, recommended by the Consultative Committee for the Definition of the Second, is being implemented in receivers commonly used for contributing data for the generation of International Atomic Time. We discuss three aspects of this new format that potentially improve GPS common-view time transfer: (1) the standard specifies the method for treating short term data, (2) it presents data in consistent formats including needed terms not previously available, and (3) the standard includes a header of parameters important for the GPS common-view process. In coordination with the release of firmware conforming to this new format the Bureau International des Poids et Mesures will release future international track schedules consistent with the new standard.

03,780
PB94-140605 (Order as PB94-140555, PC A06/MF A02)
National Inst. of Standards and Technology, Gaithersburg, MD.
Wavelengths and Energy Levels of Neutral Kr(84) and Level Shifts in All Kr Even Isotopes.
V. Kaufman. 1993, 8p.
Included in Jnl. of Research of the National Institute of Standards and Technology, v98 n6 p717-724 Nov/Dec 93.

Keywords: *Atomic energy levels, *Krypton 84, *Isotope effect, Spectral shift, Krypton 86, Krypton 82, Krypton 80, Krypton 78, Interferometry, Wavelengths.

Interferometrically-measured wavelengths of 109 lines of neutral Kr(84) are compared with those of Kr(86). Sixty energy levels of neutral Kr(84) derived from those wavelengths and 25 Kr(86)-Kr(84) isotope shifts previously measured are given along with their shifts from the energy levels of Kr(86). Twenty levels of each of Kr(82), Kr(80), and Kr(78) are also evaluated using isotope-shift information in the literature. The differences between the experimentally observed shifts and the normal mass shift leave large negative residuals which are accounted for by ionization energy differences and by the specific mass shift. It appears that the volume effect causes only a very small, if any, energy level shift.

03,781
PB94-142486 PC A03/MF A01
National Inst. of Standards and Technology (MEL), Gaithersburg, MD. Automated Production Technology Div.
Mass Unit Disseminated to Surrogated Laboratories Using the NIST Portable Mass Calibration Package.
R. M. Schoonover, J. E. Taylor, and J. Rothleder. Feb 94, 18p, NISTIR-5290.
See also PB89-132336.

Keywords: *Calibration, Interlaboratory comparisons, Primary standards, Portable equipment, Computer applications, Uncertainty, Balances, Buoyancy, *Mass standards, California State Laboratory, US NIST.

Over a ten-year period, three mass calibration packages were circulated to selected laboratories by the Mass Group at NIST. Initially the objective was to determine if the NIST mass calibration service could be disseminated to qualified users via a 'do-it-yourself' package. However, it became obvious that the technique could be very useful in the training of personnel and the examination of laboratories. The first package of 1-kilogram artifacts was circulated to see what problems might arise in their calibration. The second package was designed to overcome the difficulties encountered and to ensure the quality of the next package. The third and final package incorporates improvements and demonstrates the method with the calibration of the California State primary mass standards from 1 kg to 1 mg. This report looks briefly at the entire project experience with comments about the pitfalls and benefits of calibrations by surrogate laboratories and other likely uses of the method.

03,782
PB94-152691 PC A03/MF A01
National Inst. of Standards and Technology (CSTL), Gaithersburg, MD. Process Measurements Div.
Assessment of Uncertainties of Thermocouple Calibrations at NIST.
Internal rept.
D. Ripple, G. W. Burns, and M. G. Scroger. Jan 94, 37p, NISTIR-5340.

Keywords: *Thermocouples, *Calibration, Temperature measurement, Uncertainty, Estimates, International Temperature Scale of 1990, ITS-90, US NIST.

The uncertainties of thermocouple calibrations performed at the National Institute of Standards and Technology are described in this report, and they are expressed in a manner consistent with the newly-adopted NIST standard for the expression of uncertainties. The adoption of the International Temperature Scale of 1990 (ITS-90) has resulted in alterations in data analysis techniques that affect the uncertainties, and these are described also.

03,783
PB94-156957 PC A08/MF A02
Maryland Univ., College Park. Dept. of Mechanical Engineering.
Transient Cooling of a Hot Surface by Droplets Evaporation.
Final rept.
P. Tartarini, Y. Liao, C. Kidder, and M. di Marzo. Apr 93, 170p, NIST/GCR-93/623.
Contract NIST-NANB8H0840
Also pub. as Maryland Univ., College Park. Dept. of Mechanical Engineering rept. no. REPT-91-1. See also PB93-189421. Sponsored by National Inst. of Standards and Technology (BFRL), Gaithersburg, MD.

Keywords: *Fire suppression, *Evaporative cooling, *Spray cooling, *Cooling, *Surfaces, Computerized simulation, Thermal conductivity, Temperature distribution, Computer programs, Solid fuels, Transients, Aluminum, Conduction, Water, *Droplet-solid interactions, Macor.

The long term objective of the study of droplet-solid interaction is to obtain information applicable to the extinguishment of fire through a droplet array (e.g. spray). The solids of concern include low thermal conductivity materials, typical of fire applications. The research described hereafter constitutes portion of an extensive research program aimed at developing accurate droplet cooling models of burning solid fuel surfaces. This research is only concerned with the evaporation of single droplets on a hot surface. Limited experiments are also performed in the nucleate boiling range. This report consists of three different portions; each portion focuses on an independent issue of the research program. In Part A the major progresses in the numerical simulation of a single droplet evaporation are described. In Part B the experimental program conducted with radiant heat input for single droplets evaporating on Macor is described. In Part C a novel model is presented, which extends the single droplet results to a multi-droplet system.

03,784
PB94-163037 PC A03/MF A01
National Inst. of Standards and Technology, Gaithersburg, MD.
Examination of Parameters That Can Cause Error in Mass Determinations.
R. M. Schoonover, and F. E. Jones. Feb 94, 14p, NISTIR-5376.

Keywords: Weight measurement, Error analysis, Stainless steels, Platinum, Iridium, Silicon, Buoyancy, Uncertainty, Metrology, Comparison, Calibration, *Mass standards, Kilogram.

The parameters that can cause error in mass determinations are examined and estimates of the magnitude of consequent errors are given. We examine the possible errors in the embodiment of the kilogram in the platinum-iridium (Pt-Ir) artifact. We trace the propagation of errors from the Pt-Ir artifact to the system of stainless steel artifacts through mass comparison. We examine in detail such parameters as buoyancy corrections, including uncertainties in measurement of environmental variables.

03,785
PB94-163052 PC A03/MF A01
National Inst. of Standards and Technology, Gaithersburg, MD.

Electronic Balance and Some Gravimetric Applications. (The Density of Solids and Liquids, Pycnometry and Mass).
R. M. Schoonover, M. S. Hwang, J. Taylor, and C. Smith. c1993, 26p, NISTIR-5375.
See also PB91-112854. Prepared in cooperation with Industrial Technology Research Inst., Hsinchu (Taiwan). Center for Measurement Standards. and Aluminum Co. of America, Alcoa Center, PA. Alcoa Technical Center.

Keywords: *Density measurement, Pycnometers, Calibration, Gravimetry, Liquids, Solids, Water, Air, Silicon, Algorithms, *Electronic balances, Hydrostatic weighing, Pycnometry.

In recent years the electronic force balance has been perfected to a degree that it can replace the mechanical balance in both precision and capacity. Hence, the mechanical balance is rapidly disappearing from the scene. The work reported here describes the use of the electronic balance in some high precision gravimetric applications. The balance has been examined from the user's viewpoint and its use is illustrated in measuring solid and liquid densities and mass. The density assigned to a silicon crystal is in good agreement with its accepted value to within 2.4 ppm. Likewise, the water density measurements substantiate Kell's equation for the density of water near 23 degrees Celsius. (Copyright (c) ISA, 1993.)

03,786
PB94-163060 PC A03/MF A01
National Inst. of Standards and Technology, Gaithersburg, MD.
Piggyback Balance Experiment: An Illustration of Archimedes' Principles and Newton's Third Law.
R. M. Schoonover. Feb 94, 13p, NISTIR-5377.

Keywords: *Buoyancy, Weight measurement, Gravimetry, Force, Mass, Metrology, Newton third law, Archimedes principles, Electronic balances, Piggyback balance experiment, Mass measurement.

The lifting force of a fluid upon an immersed body was analyzed and reported by Archimedes in the third century B.C. In these modern times many people employed in metrology find it difficult to grasp the concept of buoyancy as it applies to mass measurement. Antiquated techniques in use today propagate ignorance of the concept. The modern electronic balance makes possible a simple, educational two-balance experiment that provides the observer with a clear picture of the buoyant force and Newton's third law. The experiment, when performed carefully, yields an excellent volume determination of the demonstration mass and brings together the SI units of mass, length and temperature and the derived units of force, pressure and density.

03,787
PB94-163078 PC A03/MF A01
National Inst. of Standards and Technology, Gaithersburg, MD.
Determination of Density of Mass Standards: Requirement and Method.
Conference proceedings.
R. M. Schoonover, M. S. Hwang, and R. Nater. Feb 94, 22p, NISTIR-5378.
See also PB91-112854. Prepared in cooperation with Industrial Technology Research Inst., Hsinchu (Taiwan). and Mettler-Toledo A.G., Greifensee (Switzerland).

Keywords: *Density measurement, Weight indicators, Error analysis, Calibration, Silicon, Hydrostatic weighing, Electronic balances.

The usual method of a mass assignment to an artifact is by comparing the forces exerted on a balance pan. The observed difference between the standard mass and the unknown object is then expressed as the solution of the two force equations and includes terms for their respective displacement volumes, i.e, densities. With the advent of commercially available balances with precision near the 1 part per billion level (ppb), the user must pay particular attention to the artifact density and its associated error if the available precision is to be meaningful. Described here is the need and a method to determine the artifact density with an error analysis that leads to the selection of the appropriate equipment. Measurements of a 200 g silicon crystal of known density were performed to demonstrate the accuracy of the method.

03,788
PB94-172152 Not available NTIS
National Inst. of Standards and Technology (CAML), Gaithersburg, MD.
Complete Reduction of the Euler-Poinsot Problem.
Final rept.
A. Deprit, and A. Elipe. 1993, 26p.
Pub. in Jnl. of the Astronautical Sciences 41, n4 p603-628 Oct-Dec 93.

Keywords: Rigid structures, Hamiltonians, Dynamics, Reprints, *Euler-Poinsot problem, Serret-Andoyer variables.

The authors propose a new way of defining the Serret-Andoyer variables that does not call on spherical trigonometry. The authors use those variables to present a complete solution of the Euler-Poinsot problem in the phase space determined by the components of the angular momentum along the principal axes of inertia. The authors use the solution to convert directly the Serret-Andoyer variables into action- and angle-variables, thereby making the Hamiltonian dependent on only two momenta.

03,789
PB94-172376 Not available NTIS
National Inst. of Standards and Technology (NML), Gaithersburg, MD. Atomic and Plasma Radiation Div.
Electron Screening Correction to the Self Energy in High-Z Atoms.
Final rept.
P. Indelicato, and P. J. Mohr. 1991, 3p.
Pub. in Proceedings of International Conference on Atomic Physics (12th), Ann Arbor, MI., July 31-August 3, 1990, p501-503 1991.

Keywords: Quantum electrodynamics, Coulomb field, Self-energy, Correction, Reprints, *Electron screening.

The paper describes a calculation of the electron screening effect on the self energy in an external Coulomb field, and gives preliminary results. The calculation is done to first order in the perturbing potential and to all orders in the strong Coulomb field.

03,790
PB94-172830 Not available NTIS
National Inst. of Standards and Technology (NML), Gaithersburg, MD. Atomic and Plasma Radiation Div.
New Critical Review of Experimental Stark Widths and Shifts.
Final rept.
W. L. Wiese, and N. Konjevic. 1991, 2p.
Pub. in Proceedings of International Conference on Spectral Line Shapes (10th), Austin, TX., 1990, v6 p63-64 1991.

Keywords: *Stark effect, Experimental data, Line broadening, Spectral lines, Positive ions, Neutral atoms, Reviews, Reprints.

A critical review and tabulation of the available experimental data on Stark widths and shifts for spectral lines of non-hydrogenic neutral atoms and positive ions has been carried out. The review covers the period from 1983 through the end of 1988 and represents a continuation of earlier critical reviews through the year 1982.

03,791
PB94-172855 Not available NTIS
National Inst. of Standards and Technology (PL), Gaithersburg, MD. Ionizing Radiation Div.
Measurement and Calibration of Large-Area Alpha-Particle Sources at NIST.
Final rept.
M. P. Unterweger, J. M. R. Hutchinson, and P. A. Hodge. 1994, 7p.
Pub. in Nuclear Instruments and Methods in Physics Research A 339, p109-115 1994.

Keywords: *Alpha sources, *Calibration, Plutonium 238, Plutonium 239, Monitoring, Alpha particles, Reprints, X-ray emission.

Work has been performed at NIST to develop and calibrate large-area (238)Pu alpha-particle sources and related measuring equipment. A large-area-source X-ray counting system and a 2pi(alpha) internal gas-proportional counting system were used for the primary calibration of these sources. Studies have been performed to relate these calibrations to the measurement of thin, large area (239)Pu sources, which are of primary interest but are generally unavailable in the necessary high specific activities required. Two systems have been characterized for the monitoring and measurement of large-area alpha sources: (1) a source-detector mounting unit developed at NIST to calibrate monitoring systems by mounting a standard source of plutonium at an accurately calibrated distance from the user's alpha-monitoring detector; (2) a diffused-junction silicon semiconductor detector which is used as a transfer standard from low to high activity of large-area alpha-particle sources. A determination of the L X-ray emission probability for (239)Pu has been made.

03,792
PB94-172889 Not available NTIS
National Inst. of Standards and Technology (NML), Gaithersburg, MD. Center for Atomic, Molecular and Optical Physics.
Report on the Meeting of the CCU (10th) (of the International Committee of Weights and Measures). Held on July 10-11, 1990.
Final rept.
B. N. Taylor. 1990, 1p.
Pub. in Metric Today 25, n4, 3, Jul/Aug 90.

Keywords: *Metric system, International system of units, Symbols, Meetings, Reprints, *Consultative Committee on Units, International Committee of Weights and Measures, Liter.

This is a brief summary of the 10th meeting of the Consultative Committee on Units (CCU) of the International Committee of Weights and Measures (CIPM) held 10-11 July 1990 at the International Bureau of Weights and Measures (BIPM). The topics covered at the meeting included revisions to the 5th edition of the brochure 'International System of Units (SI)' published by the BIPM, the symbol for the liter, and new SI prefixes for 10(sup -21), 10(sup 21), 10(sup -24), and 10(sup -24).

03,793
PB94-172897 Not available NTIS
National Inst. of Standards and Technology (NML), Gaithersburg, MD. Electron and Optical Physics Div.
National Institute of Standards and Technology Resonance Ionization Spectroscopy/Resonance Ionization Mass Spectroscopy Data Service.
Final rept.
E. B. Saloman. 1990, 4p.
Contract DE-AI05-86ER-60447
Pub. in Proceedings of International Symposium on Resonance Ionization Spectroscopy and Its Applications (5th), Varese, Italy, September 16-21, 1990, p45-48. Sponsored by Department of Energy, Washington, DC.

Keywords: *Resonance ionization mass spectroscopy, *Mass spectroscopy, *Data bases, Chemical analysis, Reprints, *Resonance ionization spectroscopy, US NIST.

A resonance ionization spectroscopy data service has been established at the National Institute of Standards and Technology. It publishes formatted data sheets which provide the atomic and laser physics information to apply RIS/RIMS to a given element. A first group of ten data sheets has been published. It covers As, B, Cd, C, Ge, Au, Fe, Pb, Si, and Zn. A second group has been submitted for publication. It covers Al, Ca, Cs, Cr, Co, Cu, Kr, Mg, Hg, and Ni. More will be produced in the future.

03,794
PB94-172905 Not available NTIS
National Inst. of Standards and Technology (PL), Gaithersburg, MD. Radiometric Physics Div.
Realization of New NIST Radiation Temperature Scales for the 1000 K to 3000 K Region, Using Absolute Radiometric Techniques.
Final rept.
R. D. Saunders, B. C. Johnson, V. Sapritsky, and K. D. Mielenz. 1992, 5p.
Pub. in ITS Measurement and Control in Science and Industry, Temperature, v6 p221-225 1992.

Keywords: *Temperature scales, *Temperature measurements, Temperature range 1000-4000 K, High temperature, Melting points, Uncertainty, Gold, Reprints, Radiance temperatures.

The National Institute of Standards and Technology (NIST) has developed a radiance temperature measurement technique using absolute optical detectors for measuring the freezing temperature of gold with a 3(sigma) uncertainty of + or - 0.34 K (K. D. Mielenz, R. D. Saunders, and J. B. Shumaker, J. Res. Natl. Inst. Stand. Technol. 95, 49 (1990)). The significance of this approach is discussed for the measurement of the radiance temperature of sources in the range of 1000 K to 3000 K, and a comparison of the current method,

complete with uncertainty estimates, is presented. The proposed experimental apparatus is described, and progress to date is reported.

03,795
PB94-172996 Not available NTIS
National Inst. of Standards and Technology (NML), Gaithersburg, MD. Center for Atomic, Molecular and Optical Physics.
Fine-Structure Constant.
Final rept.
B. N. Taylor. 1991, 7p.
Pub. in Numerical Data and Functional Relationships in Science and Technology - Units and Fundamental Constants in Physics and Chemistry, Chapter 3.2.9, p3-125 - 3-131 1991.

Keywords: *Sommerfeld constant, *Fundamental constants, Quantum electrodynamics, Josephson effect, Reprints, *Fine structure constant, Quantum Hall effect.

The paper briefly reviews the history of the fine-structure constant alpha and discusses its relationship to other fundamental constants and quantities of physics, including the Josephson and von Klitzing constants,the gyromagnetic ratio of the proton, and the electron magnetic moment anomaly. It summarizes and compares the values of alpha presently available having an uncertainty of 2 parts in 10(sup 7) or less, and briefly discusses the experiments from which they are obtained and their major sources of uncertainty. A list of useful references is given.

03,796
PB94-176088 PC A10/MF A03
National Inst. of Standards and Technology (PL), Gaithersburg, MD.
Physics Laboratory Technical Activities, 1993.
K. B. Gebbie. Mar 94, 224p, NISTIR-5363.
Presented to the Board on Assessment of NIST Programs, National Research Council, May 2-3, 1994. See also report for 1992, PB93-178648. Sponsored by National Research Council, Washington, DC. Board on Assessment of NIST Programs.

Keywords: *Physics, Atomic physics, Molecular physics, Fundamental constants, Frequency standards, Time standards, Quantum theory, Ionizing radiation, Calibration, Metrology, Radiometry, Optics, Electrons, Measurement, Progress report.

This report summarizes research projects, measurement method development, calibration and testing, and data evaluation activities that were carried out during calendar year 1993 in the NIST Physics Laboratory. These activities fall in the areas of electron and optical physics, atomic physics, molecular physics, radiometric physics, quantum metrology, ionizing radiation, time and frequency, quantum physics, and fundamental constants.

03,797
PB94-185295 Not available NTIS
National Inst. of Standards and Technology (PL), Gaithersburg, MD. Atomic Physics Div.
Investigation of LS Coupling in Boronlike Ions.
Final rept.
S. Glenzer, H. J. Kunze, J. Musielok, Y. K. Kim, and W. L. Wiese. 1994, 7p.
Pub. in Physical Review A 49, n1 p221-227 Jan 94.

Keywords: *L-S coupling, Reprints, Light elements, Transition probabilities, *Boron-like ions.

In order to test the validity of the LS-coupling approximation for light elements, the line-intensity ratios of the 3s-3p and 3p-3d multiplets in C II through F V and C II through Ne VI, respectively, have been investigated experimentally with emission sources. Also, calculations with multiconfiguration Dirac-Fock wave functions have been performed. Within the errors of the experimental procedure, no significant violations of the LS-coupling approximation were found for the lines of the 3s-3p and 3p-3d multiplets in C II through F V. However, in the case of Ne VI, small deviations of measured intensities from those obtained by applying the LS-coupling approximation were observed.

03,798
PB94-185311 Not available NTIS
National Inst. of Standards and Technology (EEEL), Boulder, CO. Electromagnetic Technology Div.
Anharmonic Oscillator Analysis Using Modified Airy Functions.
Final rept.
I. C. Goyal, S. Roy, A. K. Ghatak, and R. L. Gallawa. 1992, 4p.
Pub. in Canadian Jnl. of Physics 70, p1218-1221 1992.

Keywords: *Anharmonic oscillators, Reprints, Schrodinger equation, WKB approximation, Wave equations, Airy function, Numerical solution, WKB-J approximation.

The authors have applied the modified Airy function (MAF) method to the analysis of an anharmonic oscillator, characterized by the potential V(x) = k(x squared)/ 2 + alpha(x (sup 4)), k > 0, alpha > 0. The MAF method gives an accurate closed-form expression for the wave function as well as very accurate eigenvalues with much less numerical effort than the five-term (eighth-order) WKBJ approximation. The application of the first-order perturbation correction to the MAF eigenvalues makes them even more accurate than those obtained by the five-term WKBJ approximation.

03,799
PB94-185345 Not available NTIS
National Inst. of Standards and Technology (PL), Boulder, CO. Quantum Physics Div.
Backscattering in Electron-Impact Excitation of Multiply Charged Ions.
Final rept.
X. Q. Guo, E. W. Bell, J. S. Thompson, R. A. Phaneuf, A. C. H. Smith, G. H. Dunn, and M. E. Bannister. 1993, 10p.
Contract DE-A105-86ER53237
Pub. in Proceedings of International Conference on the Physics of Highly Charged Ions (6th), Manhattan, KS., September 28-October 2, 1992, p463-472 1993. Sponsored by Department of Energy, Washington, DC.

Keywords: *Electron-ion collisions, *Argon ions, Reprints, Multicharged ions, Electron scattering, Electron impact, Inelastic scattering, Backscattering, Excited states, Cross sections, Excitation.

For the first time, evidence for strong back-scattering of electrons during near threshold excitation of highly charged ions has been observed. By measuring the apparent cross section for the electron-impact excitation of Ar(7+)(3s->3p) as a function of center-of-mass velocity, over 90% of the inelastically scattered electrons were found to be deflected by more than 90 degrees in the center-of-mass frame. This unusual angular scattering has not been previously observed for atoms or ions, but may be typical for multiply charged ions. Our observation of backscattering has been confirmed recently by close-coupling calculations and distorted-wave calculations. Absolute total excitation cross sections measured in an energy range extending to 2.2 eV above threshold are also reported and are in agreement with close-coupling calculations.

03,800
PB94-185576 Not available NTIS
National Inst. of Standards and Technology (BFRL), Gaithersburg, MD. Fire Safety Engineering Div.
Intercomparison of Internal Proportional Gas Counting of (85)Kr and (3)H.
Final rept.
J. L. Makepeace, F. E. Clark, J. L. Picolo, M. P. Unterweger, N. Coursol, and E. Gunther. 1994, 6p.
Pub. in Nuclear Instruments and Methods in Physics Research A 339, p343-348 1994.

Keywords: *Krypton 85, *Tritium, Interlaboratory comparisons, Proportional counters, Uncertainty, Reprints, Intercomparison.

An international intercomparison of internal proportional gas counting of (85)Kr and (3)H has been carried out under the auspices of EUROMET, a European Collaboration in Measurement Standards. A sample of (85)Kr mixed with inactive krypton gas was measured at three laboratories and a sample of (3)H mixed with nitrogen gas was measured at four laboratories. In each case, agreement was achieved within the stated uncertainties. The experimental techniques employed at each of the participating laboratories are described and a statement of the results and conclusions is provided.

03,801
PB94-185709 Not available NTIS
National Inst. of Standards and Technology (PL), Gaithersburg, MD. Electron and Optical Physics Div.
Verification of the Ponderomotive Approximation for the ac Stark Shift in Xe Rydberg Levels.
Final rept.
T. R. O'Brian, J. B. Kim, G. Lan, T. J. McIlrath, and T. B. Lucatorto. 1994, 4p.
Pub. in Physical Review A 49, n2 pR649-R652 Feb 94. Sponsored by Department of Energy, Washington, DC.

Keywords: *Rydberg states, *Xenon, Alternating current, Laser radiation, Stark effect, Perturbation theory, Reprints.

We report direct measurements of the ac Stark shifts of Xe Rydberg levels in high-intensity laser fields (up to 6 GW/sq cm), demonstrating the expected near-ponderomotive behavior. These measurements provide extensive unambiguous evidence for the validity of perturbative calculations of the nonresonant ac Stark shift at these intensities.

03,802
PB94-185741 Not available NTIS
National Inst. of Standards and Technology (PL), Gaithersburg, MD. Ionizing Radiation Div.
Intermediate Structure in the Neutron-Induced Fission Cross Section of 236U.
Final rept.
W. E. Parker, J. E. Lynn, G. L. Morgan, N. W. Hill, P. W. Lisowski, and A. D. Carlson. 1994, 6p.
Pub. in Physical Review C 49, n2 p672-677 Feb 94.

Keywords: *Uranium 236 target, *Fission cross sections, *Neutron reactions, Intermediate structure, Intermediate resonance, Reprints.

Neutron-induced fission of (236)U has been measured at the Los Alamos Neutron Scattering Center with a white neutron source using a fast parallel plate ionization chamber at a flight path of about 56 m. In the resonance and the intermediate resonance region, very little of the previously reported structure was detected. Only five resonance structures were observed. Additionally, the width of the 5.45 eV resonance is approximately 100 times smaller than previously reported. An explanation for the discrepancies between old data and data reported here is discussed. New fission widths for resonances from 5.45 eV to 10.4 keV are reported. The new data are in agreement with theoretical estimates.

03,803
PB94-187713 PC A03/MF A01
National Inst. of Standards and Technology, Gaithersburg, MD.
Use of the Electronic Balance for Highly Accurate Direct Mass Measurements Without the Use of External Mass Standards.
R. M. Schoonover, and F. E. Jones. May 94, 20p, NISTIR-5423.

Keywords: Weight measurement, Calibration, Uncertainty, *Mass measurement, Electronic balances, Traceability.

The object of the paper is to show how to make highly accurate mass measurements using an appropriate electronic balance without the use of external mass standards. The method eliminates the need for a set of external mass standards and, therefore, the need to have these mass standards calibrated periodically at a standards laboratory. Traceability to NIST can be achieved by periodic calibration of the built-in mass standard of the balance by a standards laboratory and by self-verification of balance linearity and function. The method benefits the user with lower cost and a higher measurement rate. Presented here is a detailed analysis of the method, a determination of measurement uncertainty, and the traceability path. Lastly, the method is illustrated by specific examples including the calculation of uncertainty.

03,804
PB94-193760 PC A06/MF A02
National Inst. of Standards and Technology (PL), Gaithersburg, MD. Ionizing Radiation Div.
Bibliography of Photon Total Cross Section (Attenuation Coefficient) Measurements 10 eV to 13.5 GeV, 1907-1993.
J. H. Hubbell. May 94, 102p, NISTIR-5437.
See also PB87-116141.

Keywords: *Photon cross sections, *Far ultraviolet radiation, *X rays, *Gamma rays, *Bibliographies, Vacuum ultraviolet radiation, Extreme ultraviolet radiation, Absorption coefficients, Total cross sections, Bremsstrahlung, Attenuation coefficients.

A bibliography is presented of papers reporting absolute measurements of photon (XUV, x-ray, gamma-ray, bremsstrahlung) total interaction cross sections or attenuation coefficients for the elements and some compounds. The energy range covered is from 10 eV to above 10 GeV. These papers are part of the reference collection of the National Institute of Standards and Technology Photon and Charged Particle Data Center. They cover the period from 1907 through 1993 and into 1994. Thus this report is an update of the 1986 earlier report NBSIR 86-3461 (PB87-116141), and also includes additional papers dating back as far as 1966 which have since been found or brought to the attention of the author. Included with each reference are annotations specifying the energy range covered and the substances studied. This updated bibliography now includes 573 non-duplicative references to available measured data, plus 42 references to critical evaluations and review articles.

03,805
PB94-194073 PC A03/MF A01
National Inst. of Standards and Technology (BFRL), Gaithersburg, MD. Building Environment Div.
Single-Phase Heat Transfer and Pressure Drop Characteristics of an Integral-Spine-Fin Within an Annulus.
M. A. Kedzierski, and M. S. Kim. Jun 94, 37p, NISTIR-5454.
Sponsored by Department of Energy, Washington, DC. Building Equipment Div.

Keywords: *Fins, *Heat transfer, *Pressure gradients, *Annular flow, Nusselt number, Friction factor, Heat transfer coefficients, Mathematical models, Test facilities, Skin friction.

The laminar, single phase heat transfer and friction characteristics of an integral-spine-fin pipe within an annulus are presented. The heat-transfer coefficient was determined using a modified version of the Wilson Plot method. The test fluid was pumped through the annulus of a straight, 3m test section. Three fluids were investigated: (1) tap water, (2) 34% ethylene glycol/water mixture, and (3) 40% ethylene glycol/water mixture. These fluids produced a significant variation in the Prandtl number so that its exponential dependence could be determined. The annulus-Reynolds numbers were varied from 100 to 1400 to obtain the Reynolds number exponent. An empirical correlation for the Nusselt number was developed which accounts for the development of the thermal boundary layer. An empirical correlation for the friction factor is also presented. It is demonstrated that the spines enhance the heat transfer through additional surface area and fluid mixing.

03,806
PB94-198587 Not available NTIS
National Inst. of Standards and Technology (PL), Boulder, CO. Quantum Physics Div.
Characteristics of Light Emission After Low-Energy Electron Impact Excitation of Caesium Atoms.
Final rept.
K. Bartschat, U. Thumm, and D. W. Norcross. 1992, 6p.
Contract DE-A105-86ER53237
Pub. in Jnl. of Physics B: Atomic and Molecular Opt. Physics 25, pL641-L646 1992. Sponsored by Department of Energy, Washington, DC. Office of Energy Research.

Keywords: *Electron-atom collisions, *Polarized light, *Cesium, EV range 1-10, Electron scattering, Electron impact, Atomic excitations, Excited states, R matrix, Reprints.

Results of a recent calculation for e-Cs scattering, carried out in a fully relativistic (Dirac R-matrix) framework, are used to calculate the polarization of the light emitted by excited cesium atoms in an energy range from threshold to 2.7 eV. They are compared with previous semirelativistic Breit-Pauli calculations and the available experimental data. The results indicate that the Percival-Seaton theory approximating relativistic scattering amplitudes by recoupling amplitudes from a non-relativistic LS calculation is not valid for low-energy e-Cs scattering.

03,807
PB94-198835 Not available NTIS
National Inst. of Standards and Technology (MSEL), Gaithersburg, MD. Reactor Radiation Div.
Scattering Properties of the Leveled-Wave Model of Random Morphologies.
Final rept.
N. F. Berk. 1991, 11p.
Pub. in Physical Review A 44, n8 p5069-5079, 15 Oct 91.

Keywords: *Scattering, Light scattering, Neutron scattering, X-ray scattering, Random processes, Standing waves, Porous materials, Morphology, Reprints, Leveled wave model.

In the leveled-wave model, random porous morphologies are simulated by discrete maps of continuous stochastic standing waves generated by adding sinusoids over suitable distributions of wave vectors and phase constants. The mathematical structures obtained this way appear to be useful models for certain kinds of random geometries, such as the bicontinuous morphologies that occur in microemulsions and porous glasses. Properties of the leveled-wave method are developed, and the scattering behavior is derived. Scattering from an arbitrary three-phase system can be analyzed by adding different instances of scattering from a generalized film morphology in which the scattering phase is confined to the interior of the interspatial region bounded by two leveled-wave interfaces that are separated everywhere. General results for this interspace scattering are derived. Fractal surfaces, dimension 2 = or < D = or < 3, are incorporated into the leveled-wave scheme by using a wave-number distribution having an appropriate long-tailed asymptotic behavior. Scenarios are discussed for the scattering as D -> 2 from above and for D -> 3 from below. For D = 3 the asymptotic scattering falls faster than algebraically as the scattering wave vector Q -> infinity.

03,808
PB94-198918 Not available NTIS
National Inst. of Standards and Technology (PL), Gaithersburg, MD. Atomic Physics Div.
Evaluation of Two-Photon Exchange Graphs for Highly-Charged Heliumlike Ions.
Final rept.
S. A. Blundell, P. J. Mohr, W. R. Johnson, and J. Sapirstein. 1993, 12p.
Pub. in Physical Review A 48, n4 p2615-2626 Oct 93.

Keywords: *Multicharged ions, Quantum electrodynamics, Perturbation theory, Ground state, Graphs, Reprints, *Helium-like ions, Two photon exchange.

Contributions of one-loop ladder and crossed-ladder graphs to the ground-state energy of heliumlike ions are calculated in Furry representation QED. With the aid of a contour rotation, the graphs are evaluated to all orders in Z(alpha) in the range Z = 10-110. Particular attention is given to the relation of this work to recent many-body perturbation theory and configuration-interaction calculations.

03,809
PB94-198991 Not available NTIS
National Inst. of Standards and Technology (NML), Boulder, CO. Time and Frequency Div.
Liquid and Solid Atomic Ion Plasmas.
Final rept.
J. J. Bollinger, S. L. Gilbert, D. J. Heinzen, W. M. Itano, and D. J. Wineland. 1990, 11p.
Pub. in Proceedings of American Physical Society Topical Conference on Atomic Processes in Plasmas (7th), Gaithersburg, MD., October 2-5, 1989, p152-162 1990.

Keywords: Strongly coupled plasmas, Atomic spectroscopy, Laser spectroscopy, Ion storage, Atomic ions, Beryllium ions, Beryllium 9, Reprints, *Ion plasmas, Penning traps, Laser cooling.

Atomic ions which are stored in electromagnetic traps can be viewed as one component plasmas. When the ions are laser cooled they become strongly coupled (gamma > 100) and exhibit liquid-like and solid-like behavior. Experimental evidence for this behavior is discussed for nonneutral (9)Be(1+) ion plasmas stored in a Penning ion trap.

03,810
PB94-199080 Not available NTIS
National Inst. of Standards and Technology (NML), Gaithersburg, MD. Temperature and Pressure Div.
Precision Nuclear Orientation Measurements for Determining Mixed Magnetic Dipole/Electric Quadrupole Hyperfine Interactions.
Final rept.
W. D. Brewer, P. Roman, and H. Marshak. 1989, 7p.
Pub. in Hyperfine Interactions 51, n1-4 p1131-1137 Jun 89.

Keywords: *Terbium 160, Nuclear alignment, Oriented nuclei, Gamma radiation, Hyperfine structure, Single crystals, Temperature dependence, Magnetic dipole moments, Quadrupole moments, Temperature range 0000-0013 K, Least squares method, Reprints.

The authors report the temperature dependence of the gamma-ray anisotropies from oriented (160)Tb nuclei produced by neutron activation of the central portion of a high-purity single crystal Tb slab. The magnetically saturated sample was studied over a wide temperature range from 18 mK to 150 mK. The temperatures were determined using precision resistance thermometry with in situ calibration by a magnetically shielded six-element superconducting fixed point device. Temperature stability during data acquisition was better than 0.1%, and least-squares fitting of the resulting temperature dependences of 0 deg and 90 deg anisotropies allowed both the magnetic dipole and the electric quadrupole hyperfine interaction frequencies to be determined with good accuracy. The weighted averages for 18 gamma rays are nu(M) = 1393.8 (8.1) MHz and nu(P) = 178.0 (2.1) MHz, in excellent agreement with NMR results on ion-implemented samples.

03,811
PB94-199445 Not available NTIS
National Inst. of Standards and Technology (IMSE), Gaithersburg, MD. Office of Nondestructive Evaluation.
Collision-Induced Emission in the Fundamental Vibration-Rotation Band of H2.
Final rept.
G. E. Caledonia, R. H. Krech, T. Wilkerson, R. L. Taylor, and G. Birnbaum. 1991, 8p.
Pub. in Physical Review A 43, n11 p6010-6017 1991.

Keywords: *Atom-molecule collisions, *Hydrogen, Infrared spectra, Emission spectra, Band spectra, Shock waves, Temperature range 0273-0400, Temperature range 0400-1000, Dipole moments, Neon, Argon, Xenon, Reprints.

Measurements of collision-induced emission in the fundamental vibration-rotation band of hydrogen are presented for argon, xenon, and neon collision partners. These absolute, spectrally-resolved infrared measurements were performed at high densities behind reflected shock waves over the temperature range of 900 to 3,400 K. The emission was found to be dominated by Q branch transitions at high temperature due primarily to the dipole moment induced by the overlap between the electron clouds of the collision pair. The strength of this interaction was evaluated from the data and compared with similar evaluations determined from low temperature absorption studies.

03,812
PB94-199486 Not available NTIS
National Inst. of Standards and Technology (CAML), Gaithersburg, MD. Applied and Computational Mathematics Div.
Slowly Divergent Space Marching Schemes in the Inverse Heat Conduction Problem.
Final rept.
A. S. Carasso. 1993, 16p.
Pub. in Numerical Heat Transfer 23, ptB p111-126 1993.

Keywords: *Conduction, Reprints, One dimensional calculations, Finite difference theory, Rocket nozzles, Divergence, Lax-Richtmyer theory, Tikhonov regularization, Ill posed problems, Inverse problems.

Recently developed 'slowly divergent' space marching difference schemes, coupled with Tikhonov regularization, can solve the one-dimensional inverse heat conduction problem at values of the nondimensional time step (Delta)t(+) as low as (Delta)t(+) = 0.0003. A Lax-Richtmyer analysis is used to demonstrate dramatic differences in error amplification behavior among various space marching algorithms, for the same problem, on the same mesh; maximum error amplification factors may differ by more than 10 orders of magnitude at parameter values that are of interest in rocket nozzle applications. Slowly divergent schemes are characterized by their damping behavior at high frequencies. A widely used benchmark problem, where the surface

temperature gradient is a step function, provides a basis for evaluating Tikhonov-regularized marching computations.

03,813
PB94-199510 Not available NTIS
National Inst. of Standards and Technology (NML), Gaithersburg, MD. Ionizing Radiation Div.
Neutron Standard Cross Sections in Reactor Physics: Need and Status.
Final rept.
A. D. Carlson. 1990, 2p.
Pub. in Transactions of the American Nuclear Society 62, p525-526 1990.

Keywords: *Neutron cross sections, *Neutron reactions, *Reactor physics, *Standards, Uranium 235 target, Lithium 6 target, Helium 3 target, Boron 10 target, Gold, Carbon, Hydrogen, Reprints.

Topics covered include: highlights of the evaluation process for the ENDF/B-VI standards evaluation; relation of the standards to reactor physics; highlights of work done on standards since the completion of the standards evaluation.

03,814
PB94-199585 Not available NTIS
National Inst. of Standards and Technology (PL), Gaithersburg, MD. Atomic Physics Div.
Isotope Shifts and Hyperfine Splittings of the 398.8-nm Yb I Line.
Final rept.
K. Deilamian, J. D. Gillaspy, and D. E. Kelleher. 1993, 5p.
Pub. in Jnl. of the Optical Society of America B 10, n5 p789-793 May 93.

Keywords: *Ytterbium, *Spectral lines, *Isotope effect, Reprints, Hyperfine structure, Electron transitions, Line width, Ytterbium 168, Ytterbium 170, Ytterbium 171, Ytterbium 174, Photon burst spectroscopy.

We report the first observation to our knowledge of the 6s(2) Singlet S(0) - 6s6p singlet P(sub 1, sup 0) transition (398.8 nm) of (168)Yb. The relative position of this spectral line was directly determined by using a laser sideband technique to simultaneously probe pairs of lines. The hyperfine structure of (171)Yb and the isotope shifts of (170)Yb, and (171)Yb, and (174)Yb were determined to an accuracy of better than 6 MHz and found to differ by as much as 23 MHz from previous results. By using photon-burst spectroscopy to carry out these measurements, we obtained subnatural linewidths and fully resolved the (170)Yb and (171)Yb lines, which otherwise overlap in fluorescence.

03,815
PB94-199627 Not available NTIS
National Inst. of Standards and Technology (PL), Gaithersburg, MD. Quantum Metrology Div.
Experimental Aspects and Z-Dependent Systematics in One- and Two-Electron Ions and Single Vacancy Systems.
Final rept.
R. D. Deslattes. 1993, 7p.
Pub. in Physica Scripta T46, p9-15 1993.

Keywords: *X-ray spectra, *Multicharged ions, Reprints, Heavy ions, K lines, *Hydrogen-like ions, *Helium-like ions, Radiative corrections.

Some predominantly experimental considerations concerning both few electron highly charged ion spectra and inner-shell vacancy spectra are discussed in relation to the currently available theoretical approaches. For the cases of H-like and He-like spectra, theoretical machinery appears to be well in hand particularly in comparison to the relatively sparse experimental database which is also of limited accuracy in most cases. Owing particularly to some impressive recent theoretical progress on the problem of nearly neutral ions containing inner-shell vacancies, the traditional X-ray data suitably filtered and strengthened by modern measurements, appear to offer some quite useful insights in spite of their formidable complexity. With the advent of new storage ring facilities and advanced technology ion sources as well as a new effort on transuranic X-ray spectra, one can reasonably foresee an upcoming period of fruitful activity.

03,816
PB94-199734 Not available NTIS
National Inst. of Standards and Technology (PL), Boulder, CO. Quantum Physics Div.
Polarization of Light Emitted After Positron Impact Excitation of Alkali Atoms.
Final rept.
K. M. DeVries, K. Bartschat, R. P. McEachran, and A. D. Stauffer. 1992, 4p.
Grant NSF-PHY-9014103
Pub. in Jnl. of Physics B: At. Mol. Opt. Phys. 25, pL653-L656 1992. Sponsored by National Science Foundation, Arlington, VA.

Keywords: *Positron-atom collisions, *Alkali metals, *Polarized light, Reprints, Linear polarization, EV range 10-100, EV range 1-10, Excitation, Lithium, Sodium, Potassium, Rubidium, Percival-Seaton hypothesis, Close coupling approximation.

Recent two-state and five-state close-coupling calculations for positron-alkali scattering are used to predict the linear polarization of the resonance line (np) double P(0) -> (ns) double S emitted by the alkali atoms Li, Na, K and Rb after positron impact excitation. The collision energies considered range from threshold (about 2 eV) to 40 eV. The results are interpreted in terms of elementary collision theory, including depolarization of the line radiation through fine- and hyperfine-structure effects. Given the size of the polarizations predicted and the recent developments in positron physics, an experimental test of our results should be possible. This should provide an independent test of the theoretical model, in addition to the cross sections considered so far.

03,817
PB94-199742 Not available NTIS
National Inst. of Standards and Technology (NML), Gaithersburg, MD. Quantum Metrology Div.
Current Results and Future Prospects for a Neutron Lifetime Determination Using Trapped Protons.
Final rept.
M. S. Dewey. 1991, 13p.
Pub. in Proceedings of International Symposium on Capture Gamma-ray Spectroscopy and Related Topics (7th), Pacific Grove, CA., October 14-19, 1990, p774-786 1991.

Keywords: *Neutron lifetime, *Neutron decay, Reprints, Trapping(Charged particles), Neutron beams, Particle decay, Measurement, Protons, Penning traps.

The availability of an accurate value for tau(n) has important implications for tests of the standard V - A theory of semi-leptonic weak processes, cosmology, and astrophysics. The lack of agreement between values of g(A)/g(V) derived from recent lifetime measurements and values obtained from recent beta-decay asymmetry experiments hints at a problem with the current theoretical framework. In this neutron beam measurement, the lifetime is determined by counting decay protons stored in a Penning trap whose magnetic axis coincides with the neutron beam axis. The recent result, tau(r) = 893.5 + or - 5.3s, is based upon data accumulated during one reactor cycle at the Institut Laue-Langevin in Grenoble, France. In the next two years a final accuracy approaching 1s will be sought.

03,818
PB94-199841 Not available NTIS
National Inst. of Standards and Technology (PL), Boulder, CO. Quantum Physics Div.
Absolute Cross-Section Measurements for Electron-Impact Ionization of C1(+1).
Final rept.
N. Djuric, E. W. Bell, E. Daniel, and G. H. Dunn. 1992, 5p.
Contract DE-A105-86ER53237
Pub. in Physical Review A 46, n1 p270-274, 1 Jul 92. Sponsored by Department of Energy, Washington, DC. Office of Energy Research.

Keywords: *Electron-ion collisions, *Chlorine ions, Reprints, EV range 100-1000, EV range 10-100, Colliding beams, Cross sections, Electron impact, Ionization.

Absolute cross sections for electron-impact ionization of Cl(1+) have been measured from threshold to 200 eV with the use of the crossed-beams technique. The cross section shows a peak value of 12.8 x 10(sup -17) sq cm at about 70 eV. Results are compared to the semiempirical prediction formula of Lotz, with scaled cross sections for ions in the same isoelectronic sequence, and with other recent measurements. Expansion coefficients and formulas for generating ionization rate coefficients in the electron temperature range 10 thousand = or < T = or < 10 million K are presented.

03,819
PB94-199916 Not available NTIS
National Inst. of Standards and Technology (PL), Gaithersburg, MD. Ionizing Radiation Div.
Neutron Measurement Intercomparisons Sponsored by CCEMRI, Section 3 (Neutron Measurements).
Final rept.
R. S. Caswell, and V. E. Lewis. 1992, 6p.
Pub. in Radiation Protection Dosimetry 44, n1/4 p105-110 1992.

Keywords: Reprints, Interlaboratory comparisons, Neutron sources, Neutron fluence, Radiation sources, *Neutron measurement, Systematic errors, Intercomparison.

A large number of neutron measurement comparisons has been out under the sponsorship of Section III (Neutron Measurements) of the Consultative Committee for Measurement Standards of Ionizing Radiations (CCEMRI) since Section III became active in 1961. These have included a series of comparisons of radionuclide neutron source emission rate, neutron fluence, and neutron dose measurements with the participation of laboratories worldwide. The paper discusses these comparisons and what has been learned from them. Future plans of Section III and neutron measurement services available from BIPM to national laboratories are also given.

03,820
PB94-200078 Not available NTIS
National Inst. of Standards and Technology (PL), Gaithersburg, MD. Quantum Metrology Div.
Improvements in Computation of Form Factors.
Final rept.
C. T. Chantler. 1993, 8p.
Pub. in Radiation Physics and Chemistry 41, n4/5 p759-766 1993.

Keywords: *Form factors, EV range 10-100, EV range 100-1000, KeV range 1-10, KeV range 10-100, Dispersion relations, Cross sections, X rays, Computation, Reprints, Anomalous dispersion.

Tables for form factors and anomalous dispersion are of wide general use in the UV, X-ray and gamme-ray communities, and have existed for a considerable period of time. The generality of these works has entailed numerous simplifications compared to detailed relativistic S-matrix calculations. However, the latter calculations do not appear to give convenient tabular application for the range of Z and energy of general interest, whereas the former tables have large regions of limited validity throughout the range of Z and energies, and in particular have limitations with regard to extrapolation to energies outside tabulated ranges. Intermediate theoretical and procedural assumptions limit the precision and applicability of available tabulations and procedures. The paper identifies regions of Z and energy where these assumptions fail and the improvement which can be achieved by their avoidance, both in tabulated ranges and by extrapolation. Particular concern involves the application of the dispersion relation to derive Re(f) from photoelectric absorption cross-sections. Revised formulae can lead to significant qualitative and quantitative improvement, particularly above 30-60 keV energies, near absorption edges, or at 30-3000 eV energies.

03,821
PB94-200086 Not available NTIS
National Inst. of Standards and Technology (PL), Gaithersburg, MD. Quantum Metrology Div.
Photographic Response to X-Ray Irradiation. 1. Estimation of the Photographic Error Statistic and Development of Analytic Density-Intensity Equations.
Final rept.
C. T. Chantler. 1993, 27p.
Pub. in Applied Optics 32, n13 p2371-2397, 1 May 93. See also Part 2, PB94-200094 and Part 3, PB94-200102.

Keywords: *X rays, *Vacuum ultraviolet radiation, *Photographic analysis, Reprints, KeV range 01-10, KeV range 10-100, EV range 1-10, EV range 10-100, EV range 100-1000, Optical density, Photographic emulsions, Linearization, Estimates, Intensity, Beam foil spectra, DEF-392 emulsion.

Formulations for specular optical density as a function of incident x-ray intensity are shown to be inadequate, theoretically and compared with available data. Ap-

proximations assuming low intensities, grain densities, or energies yield significant error in typical emulsions. Unjustifiable simplifications limit analysis and consequent results. The avoidance of assumptions leads to models for rough and smooth emulsion surfaces, which correspond to Kodak 101-01 and DEF-392 emulsion types. The self-consistent use of spherical grains yields scaling that is dependent on emulsion roughness. The authors obtained improvement over standard formulations, avoiding the empirical character of earlier models and associated parameterization. The correlation of grain locations and occluded emulsion area is approximated within monolayer depths but neglected between layers. Effects of the incident angle from a broad source, scattering and photoelectrons are considered. The models presented herein apply to the vacuum UV and x-ray energies from 9eV to 20 keV and may be preferred over alternative models at lower energies, densities greater than unity, emulsions with high grain fractions, or where interpolation over energy ranges is desired.

03,822
PB94-200094 Not available NTIS
National Inst. of Standards and Technology (PL), Gaithersburg, MD. Quantum Metrology Div.
Photographic Response to X-Ray Irradiation. 2. Correlated Models.
Final rept.
C. T. Chantler. 1993, 13p.
Pub. in Applied Optics 32, n13 p2398-2410, 1 May 93. See also Part 1, PB94-200086 and Part 3, PB94-200102.

Keywords: *X rays, *Vacuum ultraviolet radiation, *Photographic analysis, Reprints, KeV range 01-10, KeV range 10-100, EV range 1-10, EV range 10-100, EV range 100-1000, Optical density, Photographic emulsions, Photographic grain, Statistics, Models, DEF-392 emulsion.

In the paper models from the first paper are generalized so that they include the correlation of attenuation coefficients and coverages with emulsion depth. They avoid further assumptions and can provide physically meaningful parameters (as opposed to earlier studies); thus closer agreement with experimental measurements is obtained. The difficulty in estimating correlated overlap functions is discussed. Error estimates resulting from grain statistics are generalized and computed in a self-consistent manner. Contributions to granularity from densitometer and grain statistics have been shown to be significant or dominant in most emulsion types. The formulation derives reliable error estimates. Correlated models are important for thick emulsions such as DEF-392, whereas integral formalisms may be as useful for thin emulsions. In agreement with the first paper, reciprocity failure appears to be negligible for UV or x-ray energies above 9eV.

03,823
PB94-200102 Not available NTIS
National Inst. of Standards and Technology (PL), Gaithersburg, MD. Quantum Metrology Div.
Photographic Response to X-Ray Irradiation. 3. Photographic Linearization of Beam-Foil Spectra.
Final rept.
C. T. Chantler, J. D. Silver, and D. D. Dietrich. 1993, 11p.
Pub. in Applied Optics 32, n13 p2411-2421, 1 May 93. See also Part 1, PB94-200086 and Part 2, PB94-200094.

Keywords: *X rays, *Photographic analysis, Reprints, Optical density, Linearization, Statistics, Models, Beam foil spectra.

In the paper models for the relation of specular density to incident (x-ray) intensity with uncertainties are applied to experimental data, indicating methods for the correction of additional effects. Linearization and error calculations are simplified by double linear interpolation, and the effect of this is quantified. Relative first-order intensities are determined directly. Secondary linearization or calculation for higher-order lines gives correction factors that yield absolute and relative higher-order intensity ratios. The effects of energy and angle on linearization are included. Densitometry uncertainty is estimated and quantified.

03,824
PB94-200334 Not available NTIS
National Inst. of Standards and Technology (CAML), Gaithersburg, MD. Statistical Engineering Div.
Analysis of Scattering Asymmetry Statistics When Background Corrected Counts Are Negative.
Final rept.
K. J. Coakley. 1993, 4p.
Pub. in Review of Scientific Instruments 64, n7 p1895-1898 Jul 93.

Keywords: *Signal processing, Reprints, Background noise, Confidence limits, Polarized beams, Scattering, Uncertainty, Asymmetry, Correction, Estimates, Poisson processes, Bootstrap technique.

An asymmetry statistic of physical interest is an estimate of the ratio of the difference and the sum of the Poisson rate parameters for two scattering processes. Typically, an additive background signal contributes to measurements of each signal. Background is measured in a third experiment. Data are corrected by subtracting measured background. When the measured background is larger than one of the other measurements, background-correlated counts are negative. For this case, it would seem that no useful information can be extracted from the experiment. Here, asymmetry and an associated uncertainty interval are estimated for such cases using a bootstrap approach.

03,825
PB94-200342 Not available NTIS
National Inst. of Standards and Technology (CAML), Gaithersburg, MD. Statistical Engineering Div.
Uncertainty Intervals for Polarized Beam Scattering Asymmetry Statistics.
Final rept.
K. J. Coakley, J. J. McCelland, M. H. Kelley, and R. L. Celotta. 1993, 7p.
Pub. in Review of Scientific Instruments 64, n7 p1888-1894 Jul 93.

Keywords: *Polarized beams, *Signal processing, Reprints, Monte Carlo method, Confidence limits, Asymmetry, Uncertainty, Statistics, Background noise, Correction, Bootstrap technique, Poisson processes.

In many scattering experiments, the quantity of most direct physical interest is a measure of the difference between two closely related scattering signals, each generated by a Poisson scattering process. The difference is often expressed in terms of an asymmetry statistic, that is, the difference normalized to the sum of the two signals, corrected for an additive background contribution. Typically, a propagation of errors approach is used to compute confidence intervals for asymmetry. However, these confidence intervals are not reliable in general. In this work, generally accurate confidence intervals for asymmetry are obtained using a parametric bootstrap approach. Based on the observed data, data are simulated using a Monte Carlo resampling scheme. The resampled data sets satisfy a constraint that ensures that background-corrected count rates are not negative.

03,826
PB94-200417 Not available NTIS
National Inst. of Standards and Technology (MSEL), Gaithersburg, MD. Reactor Radiation Div.
Acceptance Diagram Analysis of the Performance of Multidisk Neutron Velocity Selectors.
Final rept.
J. R. D. Copley. 1993, 10p.
Pub. in Nuclear Instruments and Methods in Physics Research A 332, p511-520 1993.

Keywords: Reprints, Neutron scattering, Neutron beams, Performance, Design, Algorithms, *Neutron velocity selectors, Acceptance diagrams, Multidisk rotors, Neutron monochromators.

Transmission and absorption properties of helical multidisk neutron velocity selectors can be calculated using the method of acceptance diagrams. In this approach, neutron trajectories are characterized by a transverse spatial coordinate and by a coordinate that is linearly related to wavelength and angle relative to the selector axis. It is then possible to classify neutron trajectories according to the number of absorbing sectors that they cross within the sector. In this way the authors can determine the extent to which a given selector is successful in eliminating neutrons that get through the selector other than via one of the intended helical channels. The authors describe the design algorithm for selectors such as those in use at the National Institute of Standards and Technology, and the authors discuss the properties of a selector built according to this algorithm. The authors also consider what happens when the direction of the neutron beam is reversed. The problem of optimizing the design of a multidisk velocity selector is briefly discussed.

03,827
PB94-200425 Not available NTIS
National Inst. of Standards and Technology (MSEL), Gaithersburg, MD. Reactor Radiation Div.
Acceptance Diagram Analysis of the Performance of Vertically Curved Neutron Monochromators.
Final rept.
J. R. D. Copley. 1991, 11p.
Pub. in Nuclear Instruments and Methods in Physics Research A301, p191-201 1991.

Keywords: Reprints, Neutron scattering, Neutron guides, Beam forming, Bragg reflection, Thermal neutrons, *Neutron monochromators, Acceptance diagrams.

Vertically curved monochromator crystals are commonly used to increase the intensity in thermal neutron scattering applications. Such devices are found on spectrometers installed both at nonreflecting beam tubes and at totally reflecting guide tubes. The authors present an analysis of the performance of vertically curved monochromators located at instruments of both types. The acceptance diagram approach gives considerable insight into the behavior of vertically curved monochromators. The analysis can be extended to more complicated systems, which closely represent what is acutally found at a neutron scattering installation.

03,828
PB94-200433 Not available NTIS
National Inst. of Standards and Technology (MSEL), Gaithersburg, MD. Reactor Radiation Div.
Joy of Acceptance Diagrams.
Final rept.
J. R. D. Copley. 1993, 16p.
Pub. in Jnl. of Neutron Research 1, n2 p21-36 1993.

Keywords: Reprints, Neutron scattering, Neutron guides, Ray tracing, Phase space, Collimators, *Acceptance diagrams, Neutron velocity selectors, Neutron monochromators.

An acceptance diagram is a convenient and instructive way to represent spatial/angular neutron distributions within a neutron scattering instrument. In complicated systems, ray-tracing is used to calculate acceptance diagrams whereas in simple systems an analytical approach is appropriate. In the latter case, the action of a device such as a collimator or reflecting guide corresponds to one or more rather simple operations on the entrance acceptance diagram. Acceptance diagrams can also be used to investigate the behavior of devices such as focusing monochromators and velocity selectors.

03,829
PB94-200482 Not available NTIS
National Inst. of Standards and Technology (NML), Gaithersburg, MD. Ionizing Radiation Div.
Assay of the Eluent from the Alumina-Based Tungsten-188-Rhenium-188 Generator.
Final rept.
B. M. Coursey, J. M. Calhoun, J. Cessna, M. P. Unterweger, D. B. Golas, A. P. Callahan, S. Mirzadeh, F. F. Knapp, D. D. Hoppes, and F. J. Schima. 1990, 9p.
Pub. in Radioact. Radiochem. 1, n4, 38, p42-49 1990.

Keywords: *Rhenium 188, Radiopharmaceuticals, Liquid scintillators, Decay schemes, Half life, Standardization, Tungsten 188, Radioisotopes, Reprints.

The alumina-based (188)W-(188)Re generator from ORNL can be eluted with saline to provide the (188)Re daughter as a short-lived high-energy beta-particle emitter which shows great promise for radiolabelling therapeutic radiopharmaceuticals. In this work, key parameters in the decay scheme of the (188)Re have been measured, and standard methods for quantitating the eluent have been developed. Rhenium-188 has been standardized for activity by the CIEMAT/NIST method of 4(pi)(beta) liquid-scintillation efficiency tracing with tritium, with an uncertainty (equivalent to one standard deviation) of 0.3%. Half-life measurements with a pressurized ionization chamber gave a T(1/2) = 17.01 + or - 0.01 hours. Photon emission rates were measured with semi-conductor detectors, and the probability of emission of the principal gamma ray at 155 keV was found to be P(gamma) = 0.1588 + or - 0.0011.

03,830
PB94-200490 Not available NTIS

National Inst. of Standards and Technology (PL), Gaithersburg, MD. Ionizing Radiation Div.
Standardization and Decay Scheme of Rhenium-186.
Final rept.
B. M. Coursey, J. Cessna, E. Garcia-Torano, D. H. Gray, D. D. Hoppes, J. M. Los Arcos, M. T. Martin-Casallo, F. J. Schima, M. P. Unterweger, D. B. Golas, and A. Grau Malonda. 1991, 5p.
Pub. in Applied Radiation and Isotopes 42, n9 p865-869 1991.

Keywords: *Rhenium 186, Liquid scintillators, Gamma radiation, Half life, Decay schemes, Standardization, Radioactivity, Reprints.

Rhenium-186 has been standardized for activity by the CIEMAT/NIST method of 4(pi)(beta) liquid-scintillation efficiency tracing with tritium, with an uncertainty (equivalent to 1 SD) of 1.61%. Half-life measurements with pressurized ionization chamber give a Tau(1/2) = 89.25 + or - 0.07 h. Photon emission rates were measured with semiconductor detectors, and the probability of emission of the principal gamme-ray at 137 keV was found to be P(gamma) = 0.0945 + or - 0.0016.

03,831
PB94-200615 Not available NTIS
National Inst. of Standards and Technology (NML), Gaithersburg, MD. Center for Radiation Research.
Accuracy-Weighted Variational Principle for Degenerate Continuum States.
Final rept.
M. Danos. 1990, 4p.
Pub. in Jnl. of Mathematical Physics 31, n11 p2588-2591 1990.

Keywords: Variational principles, Numerical solution, Ritz method, Accuracy, Reprints, *Degenerate states, Continuum states, Degeneracy.

A variational principle for continuum states is given which permits numerical solution by the Ritz method. It allows to maximize the accuracy of the solution in pre-selected regions of space, and also allows the selection of that solution from the perhaps infinitely degenerate solution set which is needed in the particular application.

03,832
PB94-200623 Not available NTIS
National Inst. of Standards and Technology (NML), Gaithersburg, MD. Center for Radiation Research.
Comprehensive Theory of Nuclear Effects on the Intrinsic Sticking Probability. 1.
Final rept.
M. Danos, L. C. Biedenharn, and A. Stahlhofen. 1989, 12p.
Pub. in AIP Conf. Proc. Muon-Catal. Fusion, v181 p308-319 1989. See also Part 2, PB94-200631.

Keywords: *Muon-catalyzed fusion, Nuclear fusion, Nuclear forces, Reprints, Intrinsic sticking fraction.

A comprehensive, inherently many-body, reaction theory for an accurate calculation of the intrinsic sticking fraction for (dt(mu)) fusion is outlined. The non-pertubative treatment of the long-range Coulomb force and its interference with the short range nuclear force is emphasized.

03,833
PB94-200631 Not available NTIS
National Inst. of Standards and Technology (NML), Gaithersburg, MD. Center for Radiation Research.
Comprehensive Theory of Nuclear Effects on the Intrinsic Sticking Probability. 2.
Final rept.
M. Danos, L. C. Biedenharn, and A. Stahlhofen. 1989, 10p.
Pub. in AIP Conf. Proc. Muon-Catal. Fusion, v181 p320-329 1989. See also Part 1, PB94-200623.

Keywords: *Muon-catalyzed fusion, Nuclear fusion, Reprints, Intrinsic sticking fraction.

An accurate calculation of the intrinsic sticking fraction for (dt(mu)) fusion requires the development of a comprehensive, non-perturbative, inherently many-body, reaction theory. The authors identify and discuss the key problems underlying their construction of this theory.

03,834
PB94-211109 Not available NTIS
National Inst. of Standards and Technology (PL), Boulder, CO. Quantum Physics Div.
Three-Vector Correlation Theory for Orientation/Alignment Studies in Atomic and Molecular Collisions.
Final rept.
J. P. J. Driessen, and L. Eno. 1992, 10p.
Contract NSF-PHY90-12244
Sponsored by National Science Foundation, Washington, DC.
Pub. in Jnl. of Chemical Physics 97, n8 p5532-5541, 15 Oct 92.

Keywords: *Molecular collisions, *Atomic collisions, Colliding beams, Cross sections, Orientation, Alignment, Calcium, Helium, Reprints.

The laboratory integral cross section under crossed-beam conditions is examined for collisions between a structured and an unstructured species, where the orientation (or alignment) of the initial and final states is determined with respect to arbitrarily configured laboratory axes. Three parameters are necessary to characterize the mutual orientation of the relevant axes in this case and these parameters then also characterize the cross section. The laboratory cross section is expanded in terms of a more fundamental (angle-independent) set of cross sections as determined in the so-called collision frame, where projections of the structured species are taken with respect to the direction of the initial relative velocity vector. Drawing upon a number of symmetry relations, we count the numbers of fundamental cross sections for arbitrary initial and final angular momenta. Then we consider the explicit dependence on angular parameters which can be anticipated for the laboratory cross section. Finally, we raise a number of experimental considerations in attempting to determine the fundamental cross sections. These considerations are 'fleshed out' by applying our cross-section analysis to a recent three-vector correlation experiment involving collisions between Ca and He.

03,835
PB94-211117 Not available NTIS
National Inst. of Standards and Technology (NML), Boulder, CO. Time and Frequency Div.
NIST Optically Pumped Cesium Frequency Standard.
Final rept.
R. E. Drullinger, D. J. Glaze, J. L. Lowe, and J. H. Shirley. 1991, 3p.
Pub. in Institute of Electrical and Electronics Engineers Transactions on Instrumentation and Measurement 40, n2 p162-164 1991.

Keywords: *Cesium frequency standards, *Frequency standards, Optical pumping, Performance, Design, Tests, Reprints, US NIST.

The National Institute of Standards and Technology is developing an optically-pumped, cesium-beam primary frequency standard. The design follows from an analysis of systematic errors found in cesium beam standards. The details of the design, performance of major sub-systems, and preliminary tests of the standard are presented.

03,836
PB94-211158 Not available NTIS
National Inst. of Standards and Technology (PL), Boulder, CO. Quantum Physics Div.
Early Dielectronic Recombination Measurements: Singly Charged Ions.
Final rept.
G. H. Dunn. 1992, 17p.
Contract DE-A105-86ER53237
Sponsored by Department of Energy, Washington, DC. Office of Energy Research.
Pub. in Recombination of Atomic Ions, p115-131 1992.

Keywords: *Dielectronic recombination, *Atomic ions, Electric fields, Cross sections, Magnesium ions, Calcium ions, Carbon ions, Autoionization, Measurement, Reviews, Reprints.

Dielectronic recombination (DR) cross sections measurements on singly charged ions are reviewed, including a perspective on events leading to the exciting breakthroughs that occurred in 1982-83 for the study of this process. The DR mechanism is discussed along with the effect of electric fields on the process. The measurements on Mg ions in variable fields and the measurements of the effects of fields on the inverse process of autoionization are cited as the definitive experimental work on the field effects on DR. The quite spectacular disagreements between theory and experiment for DR cross section in C and Ca ions remain a perplexing mystery.

03,837
PB94-211182 Not available NTIS
National Inst. of Standards and Technology (PL), Boulder, CO. Quantum Physics Div.
Fine Structure of Negative Ions of Alkaline-Earth-Metal Atoms.
Final rept.
V. A. Dzuba, V. V. Flambaum, G. F. Gribakin, and D. P. Sushkov. 1991, 5p.
Pub. in Physical Review A 44, n5 p2823-2827, 1 Sep 91.

Keywords: *Calcium ions, *Strontium ions, *Barium ions, *Radium ions, *Fine structure, Electron scattering, Spin orbit interactions, Negative ions, Perturbation theory, Reprints.

Fine-structure intervals np(sub 1/2)-np(sub 3/2) (np(sub 1/2) is the ground state) are calculated for negative ions using relativistic many-body perturbation theory: Ca(1-) 4p, 56/cm; Sr(1-) 5p, 178/cm; Ba(1-) 6p, about 460/cm; and Ra(1-) 7p, 1,341/cm. Comparison of the fine-structure interval with affinity: Ca(1-) 10%, Sr(1-) 22%, Ba(1-) 30%; for Ra(1-) the fine-structure interval is larger than the affinity. Thus the Ra(1-) (sup 7)p(sub 3/2) state is a resonance in the continuous spectrum with energy 0.018 eV. This means that the relativistic spin-orbit interaction plays a determining role in slow electron-radium scattering.

03,838
PB94-211265 Not available NTIS
National Inst. of Standards and Technology (NML), Gaithersburg, MD. Ionizing Radiation Div.
Slab Transmission and Reflection for Point Source and Point Detector.
Final rept.
C. M. Eisenhauer. 1990, 2p.
Pub. in Transactions of the American Nuclear Society 62, p449-450 1990.

Keywords: *Neutron transport, *Photon transport, Monte Carlo method, Gamma rays, Point sources, Polyethylene, Reflection, Slabs, Reprints.

Using Monte Carlo calculations, we show that the transmission of scattered neutrons or gamma rays from a point source, through a plane slab of infinite extent, to a point detector, depends on the orientation of the slab but varies very little with the slab position. This statement is also true for reflected radiation if the source is replaced by its image source and the results are interpreted in terms of a transmission problem. We also show that the transition from a slab of small extent (narrow beam conditions) to a slab of infinite extent (broad beam conditions) can be characterized by a simple function of the single scatter angle. This function, too, can be applied to reflected radiation by invoking the image source. Typical results are presented for polyethylene.

03,839
PB94-211406 Not available NTIS
National Inst. of Standards and Technology (NML), Gaithersburg, MD. Ionizing Radiation Div.
Anomalous Odd- to Even-Mass Isotope Ratios in Resonance Ionization with Broad-Band Lasers.
Final rept.
W. M. Fairbank, M. T. Spaar, J. E. Parks, and J. M. R. Hutchinson. 1989, 4p.
Contract DE-AI-05-86-ER-60447
Sponsored by Department of Energy, Washington, DC.
Pub. in Physical Review A 40, n4 p2195-2198, 15 Aug 89.

Keywords: *Molybdenum, *Tin, Laser radiation, Isotope ratio, Fractionation, Anomalies, Reprints, Resonance ionization.

The response of even- and odd-mass isotopes is found to be very different in several schemes for resonance ionization of Mo and Sn, even when the laser linewidth is greater than the span of the hyperfine structure and isotope shifts.

03,840
PB94-211414 Not available NTIS
National Inst. of Standards and Technology (PL), Boulder, CO. Quantum Physics Div.
Earth-Based Gravitational Experiments.
Final rept.
J. E. Faller. 1990, 4p.
Pub. in Proceedings of International Conference on General Relativity and Gravitation (12th), Boulder, CO., July 2-8, 1989, p345-348 1990.

Keywords: *Gravitation, General relativity, Ground based, Experimentation, Reprints.

Though historically, the solar system has been the principal area for testing theories of gravitation, we seem to be at the end of the golden age of solar-system tests (Reasenberg (1987)). The classical effects have now been measured within the limits of today's technology and further significant improvements cannot be expected in the near term. Future space-based experiments such as GPB, Gravity Probe B; LAGOS, Laser Gravitational-wave Observatory in Space; and POINTS, the (proposed) Astrometric Optical Interferometer, await further technological as well as engineering developments and logistic (launch) support to deliver them to the laboratory of space. Recent years have seen, however, ground-based gravitational experimentation undergo a resurgence, driven by new experimental capabilities and by new theoretical work.

03,841
PB94-211505 Not available NTIS
National Inst. of Standards and Technology (NML), Gaithersburg, MD. Radiometric Physics Div.
Photoionization of Small Molecules Using Synchrotron Radiation.
Final rept.
T. A. Ferrett, and A. C. Parr. 1988, 4p.
Pub. in Proceedings of Society of Photo-Optical Instrumentation Engineers - X-ray and Vacuum Ultraviolet Interaction Data Bases, Calculations, and Measurements, Los Angeles, CA., January 14-15, 1988, v911 p19-22.

Keywords: *Carbon monoxide, *Carbon dioxide, *Photoionization, EV range 10-100, Vibrational states, Synchrotron radiation, Angular distribution, High resolution, Molecular dynamics, Molecular ions, Autoionization, Reprints.

We report here new high-resolution vibrationally resolved studies of photoionization in the molecules CO and CO2 using synchrotron radiation in the photon-energy range 10-30 eV. The detailed decay dynamics of autoionizing resonances in CO and the origin of symmetry-forbidden vibrational transitions in the (C bar) state of CO2(1+) are discussed. These examples illustrate the need for experimental work with both high optical resolution and electron resolution sufficient to resolve the complex resonances in molecules and the vibrational dependence of molecular dynamics.

03,842
PB94-211554 Not available NTIS
National Inst. of Standards and Technology (NML), Gaithersburg, MD. Atomic and Plasma Radiation Div.
Atomic Transition Probability Ratios between Some Ar I 4s-4p and 4s-5p Transitions.
Final rept.
T. D. Hahn, and W. L. Wiese. 1990, 3p.
Pub. in Physical Review A 42, n9 p5747-5749 1990.

Keywords: *Argon, Atomic energy levels, Electron transitions, Transition probabilities, Visible spectra, Line spectra, Neutral atoms, Ratios, Reprints.

All recent determinations of the atomic transition probabilities for the prominent Ar I 4s-4p lines in the red part of the visible spectrum have been carried out separately from other determinations of the equally prominent 4s-5p lines in the blue part of the spectrum. A cross-connection of these data is thus desirable to establish their mutual consistency. We have measured several transition probability ratios for 4s-4p to 4s-5p transitions and find very close consistency.

03,843
PB94-211562 Not available NTIS
National Inst. of Standards and Technology (NML), Gaithersburg, MD. Atomic and Plasma Radiation Div.
Ion Broadening Parameters for Several Argon and Carbon Lines.
Final rept.
T. D. Hahn, and L. A. Woltz. 1990, 4p.
Pub. in Physical Review A 42, n3 p1450-1453 1990.

Keywords: *Line broadening, *Carbon, *Argon, Spectral lines, Neutral atoms, Asymmetry, Reprints, Ion broadening.

The ion broadening parameters of several argon and carbon spectral lines are determined by fitting asymmetric theoretical profiles to spectral line profiles obtained in a wall-stabilized arc.

03,844
PB94-211737 Not available NTIS
National Inst. of Standards and Technology (MSEL), Gaithersburg, MD. Metallurgy Div.
High Temperature.
Final rept.
J. W. Hastie, D. W. Bonnell, and J. B. Berkowitz. 1991, 6p.
Pub. in Encyclopedia of Physics, p497-502 1991.

Keywords: *High temperature, Temperature measurement, Materials, Flames, Fusion, Plasma, Reprints.

This article defines the condition of high temperature, its measurement, and its significance to physics and interdisciplinary areas of materials and chemical sciences.

03,845
PB94-211752 Not available NTIS
National Inst. of Standards and Technology (NML), Gaithersburg, MD. Radiation Source and Instrumentation Div.
Drill-Hearn-Gerasimov Sum Rule.
Final rept.
E. Hayward. 1992, 6p.
Pub. in Proceedings of Course (7th) and the Winter Course (2nd) of the International School of Intermediate Energy Nuclear Physics, L'Aquila and Folgaria, Italy, July 16-26, 1990 and January 27-February 3, 1991, p164-169 1992.

Keywords: *Sum rules, Dispersion relations, Optical theorem, Low-energy theorem, Reprints.

The Drell-Hearn-Gerasimov sum rule is derived and discussed. The much earlier work of Karliner is pointed out.

03,846
PB94-211760 Not available NTIS
National Inst. of Standards and Technology (NML), Gaithersburg, MD. Radiation Source and Instrumentation Div.
Polarizability of the Nucleon.
Final rept.
E. Hayward. 1992, 22p.
Pub. in Proceedings of Seventh Course and Second Winter Course of the International School of Intermediate Energy Nuclear Physics, L'Aquila and Folgaria, Italy, July 16-26, 1990 and January 27-February 3, 1991, p126-147 1992.

Keywords: *Neutrons, *Protons, Polarization characteristics, Absorption cross sections, Scattering cross sections, Low-energy theorem, Dispersion relations, Optical theorem, Nucleons, Reprints, Photon absorption.

The conflict between the polarizabilities of the nucleon derived from the total photon absorption cross section and the photon scattering cross section is discussed. The electric and magnetic dipole cross sections for the proton and neutron are illustrated. Expressions for the photon scattering cross sections for the proton and neutron are given including the scattering cross section for the point nucleon and for plane polarized incident photons. Possible explanations for this discrepancy are discussed.

03,847
PB94-211786 Not available NTIS
National Inst. of Standards and Technology (NML), Gaithersburg, MD. Molecular Physics Div.
Asymptotic Wave Function Splitting Procedure for Propagating Spatially Extended Wave Functions: Application to Intense Field Photodissociation of H2(+).
Final rept.
R. W. Heather. 1991, 14p.
Pub. in Computer Physics Communications 63, n1-3 p446-459 1991.

Keywords: *Hydrogen ions 2 plus, *Photodissociation, Wave functions, Reprints.

We describe an efficient procedure for propagating a spatially extended wave function evaluated on a small grid. The procedure involves the repeated splitting of the wave function into a part residing mainly in the interaction region (small fragment separation) and parts residing solely in the asymptotic region (large fragment separation), and propagating each part separately. The total wave function can be reassembled at a later time by adding the individual asymptotic pieces, propagated to a common final time with a free particle propagator, to the part of the wave function remaining in the interaction region. This procedure is well suited to propagation methods that evaluate the wave function on a spatial grid, because the amount of asymptotic region included in the grid, and therefore the computational effort, can be minimized (the smaller the asymptotic region, the more frequent the splitting).

03,848
PB94-211851 Not available NTIS
National Inst. of Standards and Technology (NML), Gaithersburg, MD. Electron and Optical Physics Div.
Design and Characterization of X-Ray Multilayer Analyzers for the 50 - 1000 eV Region.
Final rept.
B. L. Henke, E. M. Gullikson, J. Kerner, A. L. Oren, and R. L. Blake. 1990, 64p.
Pub. in Jnl. of X-ray Science and Technology 2, n1 p17-80 Mar 90.

Keywords: *X-ray optics, *Analyzers, EV range 100-1000, EV range 10-100, X-ray analysis, Spectroscopy, Reflectance, Design, Reprints.

Detailed absolute reflectivity characterizations are presented for selected examples of multilayers, which have been semi-empirically determined for Mica, KAP and the fabricated Langmuir-Blodgett and sputtered multilayer analyzers with d-spacings in the 10-200 A range. Design requirements for absolute spectrometry are established. Efficient analytical multilayer reflectivity models are derived and parameterized (based upon a modification of the Darwin-Prins model for the low-energy x-ray region) -- including, for the sputtered multilayers, parameters for defining interface structure. The dependence of the reflectivity characteristics, high-order Bragg diffraction suppression, and over-all efficiency upon the model parameters is analyzed. A special spectrograph and procedure for the absolute measurement of the relevant reflectivity characteristics are described. Detailed measurements and semi-empirical characterizations are presented.

03,849
PB94-212248 Not available NTIS
National Inst. of Standards and Technology (PL), Gaithersburg, MD. Quantum Metrology Div.
K alpha Transitions in Few-Electron Ions and in Atoms.
Final rept.
P. Indelicato. 1990, 12p.
Pub. in Proceedings of International Conference on X-ray and Inner-Shell Processes (15th), Knoxville, TN., July 1990, p591-602.

Keywords: *K lines, Atomic energy levels, Electron transitions, Heavy elements, Reprints, Hydrogen-like ions, Helium-like ions.

The study of the 1s level in heavy atoms or ions provides very important tests of QED and relativistic corrections in strong electromagnetic fields. Such studies have been conducted mainly by measuring 2p-1s transitions in one and two-electron ions and K transitions in atoms. In this paper I will discuss the status and the merit of the different approaches, and show detailed comparisons between experiment and theory in all three cases.

03,850
PB94-212271 Not available NTIS
National Inst. of Standards and Technology (PL), Boulder, CO. Time and Frequency Div.
Quantum Projection Noise: Population Fluctuations in Two-Level Systems.
Final rept.
W. M. Itano, J. C. Bergquist, J. J. Bollinger, F. L. Moore, M. G. Raizen, D. J. Wineland, J. M. Gilligan, and D. J. Heinzen. 1993, 17p.
Pub. in Physical Review A 47, n5 p3554-3570 May 93.

Keywords: *Quantum mechanics, *Ion storage, Laser spectroscopy, Frequency standards, Internal energy, Beryllium ions, Beryllium 9, Mercury ions, Mercury 199, Reprints, Penning traps, Ion traps, Quantum noise.

Measurements of internal energy states of atomic ions confined in traps can be used to illustrate fundamental properties of quantum systems, because long relaxation times and observation times are available. In the experiments described here, a single ion or a few identical ions were prepared in well-defined superpositions of two internal energy eigenstates. The populations of the energy levels were then measured. For an individual ion, the outcome of the measurement is uncertain, unless the amplitude for one of the two eigenstates is zero, and is completely uncertain when the magnitudes of the two amplitudes are equal. In one experiment,

a single (199)Hg(1+) ion, confined in a linear rf trap was prepared in various superpositions of two hyperfine states. In another experiment, groups of (9)Be(1+) ions, ranging in size from about 5 to about 400 ions, were confined in a Penning trap and prepared in various superposition states. The measured population fluctuations were greater when the state amplitudes were equal than when one of the amplitudes was nearly zero, in agreement with the predictions of quantum mechanics. These fluctuations, which we call quantum projection noise, are the fundamental source of noise for population measurements, with a fixed number of atoms. These fluctuations are of practical importance, since they contribute to the errors of atomic frequency standards.

03,851
PB94-212560 Not available NTIS
National Inst. of Standards and Technology (NML), Gaithersburg, MD. Molecular Physics Div.
Theory of Atomic Collisions at Ultracold Temperatures.
Final rept.
P. S. Julienne, R. Heather, and J. Vigue. 1991, 21p.
Pub. in Proceedings of International Conference on Atomic Physics (12th), Ann Arbor, MI., July 31-August 3, 1990, p116-136 1991.

Keywords: *Atomic collisions, Temperature range 0000-0013 K, Ionization, Sodium, Potassium, Rubidium, Cesium, Reprints, Ultracold atoms, Atom traps.

Recent developments in laser cooling and trapping of neutral atoms have opened the new field of atomic collisions at ultracold temperatures, T < 1 mK. There are many new challenges and opportunities for both theory and experiment. We will outline some of the key problems in this field, and present calculations on several collisional processes which have been observed in atom traps.

03,852
PB94-212651 Not available NTIS
National Inst. of Standards and Technology (EEEL), Boulder, CO. Electromagnetic Technology Div.
Chaos in a Computer-Animated Pendulum.
Final rept.
R. L. Kautz. 1993, 9p.
Pub. in American Jnl. of Physics 61, n5 p407-415 May 93.

Keywords: *Pendulums, *Chaos, Computer animation, Strange attractors, Symmetry breaking, Frequency multipliers, Josephson effect, Demonstrations, Trajectories, Reprints, Chaotic motion, State space.

A classroom demonstration based on computer animation illustrates chaotic motion in a driven pendulum. Generated by a 76 line BASIC program that runs on PC-compatible computers, the animation shows four simultaneous displays, including the pendulum and its trajectory in state space. The program can be used to illustrate periodic attractors, symmetry breaking, period doubling, and chaos.

03,853
PB94-212727 Not available NTIS
National Inst. of Standards and Technology (NML), Gaithersburg, MD. Atomic and Plasma Radiation Div.
Autoionizing Resonances in Electric Fields.
Final rept.
D. E. Kelleher, E. B. Saloman, and J. W. Cooper. 1991, 4p.
Pub. in Proceedings of International Conference on Coherent Radiation Processes in Strong Fields (1st), Washington, DC., June 18-22, 1990, p665-678 1991.

Keywords: *Autoionization, Electric fields, Direct current, Resonance, Reprints.

We present a brief overview of observed effects of d.c. electric fields on autoionizing resonances in the region above the first ionization threshold. The types of phenomena fall into three broad categories: (I) field broadening (and narrowing), (II) field-induced interferences and transitions, and (III) field-induced Stark manifolds. Theoretical methods for dealing with these phenomena have been developed, and comparisons with their predictions will be discussed.

03,854
PB94-212784 Not available NTIS
National Inst. of Standards and Technology (NML), Gaithersburg, MD. Atomic and Plasma Radiation Div.
Relativistic and Quantum Electrodynamic Effects in Highly-Charged Ions.
Final rept.
Y. K. Kim. 1990, 21p.
Pub. in AIP Conference Proceedings on At. Processes Plasmas, v206 p19-39 1990.

Keywords: *Multicharged ions, *Atomic structure, *Atomic spectra, Quantum electrodynamics, Relativistic effects, Transition probabilities, Lamb shift, Corrections, Reprints.

Recent spectroscopic data clearly indicate that both relativistic and quantum electrodynamic (QED) effects are indispensable in understanding the spectra of highly-charged ions. QED effects are discernible even in spectra involving M- and N-shell electrons. Current understanding and theoretical capability in predicting relativistic and QED corrections in atomic structure are reviewed.

03,855
PB94-212842 Not available NTIS
National Inst. of Standards and Technology (PL), Gaithersburg, MD. Atomic Physics Div.
Atomic Branching Ratio Data for Carbon-Like Ions.
Final rept.
J. Z. Klose, T. M. Deters, J. R. Fuhr, and W. L. Wiese. 1993, 6p.
Pub. in Jnl. of Quantitative Spectroscopy and Radiative Transfer (JQSRT) 50, n1 p1-6 1993.

Keywords: *Branching ratio, *Multicharged ions, Vacuum ultraviolet radiation, Transition probabilities, High temperature, Spectral lines, Calibration, Radiometry, Plasma, Reprints, *Carbon-like ions.

The branching-ratio technique for radiometric calibrations in the vacuum ultraviolet spectral region is briefly reviewed. A list of transitions suitable for use of the technique is given for carbon-like ions, along with pertinent data for their application.

03,856
PB94-213055 Not available NTIS
National Inst. of Standards and Technology (MSEL), Gaithersburg, MD. Ceramics Div.
High Resolution Hard X-Ray Microscope.
Final rept.
M. Kuriyama, R. Dobbyn, and R. Spal. 1990, 11p.
Pub. in Rigaku Jnl. 7, n2 p5-15 1990.

Keywords: Hard x radiation, X-ray optics, X-ray diffraction, X-ray detection, Modulation transfer function, Spatial resolution, High resolution, Microradiography, Tomography, Uses, Reprints, *X-ray microscopes, Microtomography, Multilayers.

A high resolution hard x-ray microscope is described. This system is capable of detecting line features as small as 0.5 micrometer in width. The spatial resolution determined by the modulation transfer function is 1.0 micrometer. Three types of two-dimensional image detectors are discussed and compared for use with hard x-rays in high resolution. Principles of x-ray image magnification are also discussed, based on x-ray optics and diffraction physics. The effect of the x-ray source size is discussed as an important factor limiting spatial resolution. Some examples of applications are demonstrated in microradiography and diffraction imaging (topography). High resolution tomography has now become a reality.

03,857
PB94-213063 Not available NTIS
National Inst. of Standards and Technology (CSTL), Boulder, CO. Thermophysics Div.
Thermal Conductivity of R134a.
Final rept.
A. Laesecke, R. A. Perkins, and C. A. Nieto de Castro. 1992, 12p.
Sponsored by Environmental Protection Agency, Washington, DC.
Pub. in Fluid Phase Equilibria 80, p263-274 1992.

Keywords: *Fluorohydrocarbons, *Thermal conductivity, Supercritical fluids, Refrigerants, Substitutes, Temperature dependence, Reprints, *R134a, Ethane/tetrafluoro.

Thermal conductivity measurements are reported for the alternative refrigerant 1,1,1,2-tetrafluoroethane (R134a). These measurements were made over the temperature range from 200 to 390 K at pressures to 70 MPa. Data are reported for the liquid, vapor, and supercritical fluid phases. A significant critical enhancement is observed for R134a. A thermal conductivity surface, which fits our data to + or - 3.8% at 95% confidence, is provided for R134a. Correlations are also provided for the saturated vapor and saturated liquid thermal conductivity of R134a. Comparisons are made with other available thermal conductivity data for the dilute gas, saturated vapor, and saturated liquid.

03,858
PB94-213154 Not available NTIS
National Inst. of Standards and Technology (MSEL), Gaithersburg, MD. Reactor Radiation Div.
Elastic Deformation of a Monolithic Perfect Crystal Interferometer: Implications for Gravitational Phase Shift Experiments.
Final rept.
H. P. Layer, and G. L. Greene. 1991, 5p.
Pub. in Physics Letters A 155, n8,9 p450-454, 27 May 91.

Keywords: *Gravitation, Finite element method, Elastic deformation, Phase shift, Distortion, Neutrons, Reprints, Silicon interferometers.

A calculation of the gravitationally induced distortion of a monolithic silicon interferometer using the finite element method has been used to analyze the data from a gravitational phase shift experiment using neutrons. The observed dependence of the X-ray phase shift on interferometer rotational angle has been reproduced. An additional interferometer distortion has been identified which can explain the discrepancy between the observed neutron phase shift and the theoretical value.

03,859
PB94-213238 Not available NTIS
National Inst. of Standards and Technology (NML), Gaithersburg, MD. Electron and Optical Physics Div.
Ultracold Collisions: Associative Ionization in a Laser Trap.
Final rept.
P. Lett, P. Jessen, C. Westbrook, P. Julienne, P. Gould, S. Rolston, and W. Phillips. 1991, 2p.
Sponsored by Office of Naval Research, Arlington, VA.
Pub. in Light Induced Kinetic Effects on Atoms, Ions and Molecules, p181-182 1991.

Keywords: Reprints, *Associative ionization, Laser cooling, Laser trapping, Ultracold atoms, Optical molasses.

Experimental investigations of associative ionization in a laser trap are reported. The recent prediction by Julienne of a laser intensity modified reaction rate has been confirmed. In addition, a new channel for the reaction involving long-range molecular states has been discovered.

03,860
PB94-213279 Not available NTIS
National Inst. of Standards and Technology (PL), Gaithersburg, MD. Quantum Metrology Div.
High-Energy Behavior of the Double Photoionization of Helium from 2 to 12 keV.
Final rept.
J. C. Levin, I. A. Sellin, B. M. Johnson, N. Berrah, Y. Azuma, H. G. Berry, D. H. Lee, D. W. Lindle, and R. D. Miller. 1993, 4p.
Sponsored by Department of Energy, Washington, DC.
Pub. in Physical Review A 47, n1 pR16-R19 Jan 93.

Keywords: *Photoionization, *Helium, KeV range 1-10, KeV range 10-100, Synchrotron radiation, Correlation, Reprints.

We report that the ratio of double-to-single photoionization of He at several photon energies from 2 to 12 keV. By time-of-flight methods, we find a ratio consistent with an asymptote at 1.5% + or - 0.2%, essentially reached by h(nu) approx = 4 keV. Fair agreement is obtained with older shake calculations of Byron and Joachain (Phys. Rev. 164, 1 (1967)), of Aberg (Phys. Rev. A 2, 1726(1970)), and with recent many-body perturbation theory (MBPT) of Ishihara, Hino, and McGuire (Phys. Rev. A 44, 6980 (1991)). The result lies below earlier MBPT calculations by Amusia et al. (J. Phys. B 8, 1248 (1975)) (2.3%), and well above semiempirical predictions of Samson (Phys. Rev. Lett. 65, 2861 (1990)), who expects no asymptote and predicts sigma (He(2+))/sigma(He(1+))=0.3% at 12 keV.

03,861
PB94-213337 Not available NTIS
National Inst. of Standards and Technology (NML), Gaithersburg, MD. Molecular Spectroscopy Div.

Molecular Spectroscopy.
Final rept.
D. R. Lide, and A. Weber. 1991, 17p.
Pub. in Encyclopedia of Physics, p737-753 1991.

Keywords: *Molecular spectroscopy, Rotational states, High resolution, Electronic spectra, Microwave spectra, Infrared spectra, Raman spectra, Laser spectroscopy, Perturbation, Reprints, Molecular constants.

This article is a revised version of an earlier one on molecular spectroscopy. Experimental techniques are discussed and the advantages of using narrow band lasers for high resolution investigations are illustrated.

03,862
PB94-213360 Not available NTIS
National Inst. of Standards and Technology (NML), Gaithersburg, MD. Quantum Metrology Div.
Polarized X-Ray Emission Spectroscopy.
Final rept.
D. W. Lindle, P. L. Cowan, T. Jach, R. E. LaVilla, and R. D. Deslattes. 1989, 5p.
Pub. in Nuclear Instruments and Methods in Physics Research B40-41, p257-261 Apr 89.

Keywords: *X-ray fluorescence, *X-ray spectroscopy, Polarization(Waves), Synchrotron radiation, Excited states, Methyl chloride, Reprints, Inner-shell spectroscopy, X-ray emission.

Strongly polarized x-ray fluorescence from gas-phase molecules has been observed by selectively exciting near core level ionization thresholds using monochromatized synchrotron radiation. Both the degree and the direction of the polarization are very sensitive to the incident excitation energy, and the symmetry of the occupied and unoccupied molecular orbitals involved in the excitation/fluorescence process. Illustration of the phenomenon will be made using Cl K-edge excitation on the molecule methyl chloride, CH3Cl. The possibility of extracting orientational, geometrical, and orbital-symmetry information directly from experiment will be discussed, and the importance of the rapid time scale of the x-ray fluorescence decay (about 10 fs), which effectively precludes disorientation effects, will be stressed. Expectations are that x-ray polarized fluorescence spectroscopy will enjoy wide applicability to, for example, solids, surfaces and interfaces, oriented molecules such as surface adsorbates, and active sites in macromolecules.

03,863
PB94-213378 Not available NTIS
National Inst. of Standards and Technology (NML), Gaithersburg, MD. Quantum Metrology Div.
Atomic, Molecular, and Optical Physics with X-rays.
Final rept.
D. W. Lindle, and B. Crasemann. 1991, 5p.
Pub. in Nuclear Instruments and Methods in Physics Research B 56-7, p441-445 May 91.

Keywords: *Molecular spectroscopy, *Atomic spectroscopy, *Synchrotron radiation, Synchrotron radiation sources, Advanced Light Source, X-ray sources, Uses, Reprints.

With the advent of third-generation synchrotron-radiation sources now being built, research in the area of atomic, molecular, and optical physics using x-rays from these insertion-device-based facilities is expected to experience a renaissance. Many of the most sought-after experimental goals in this area of research will become possible or even routine. To highlight some of the exciting possibilities, some specific examples are discussed, such as the x-ray and Auger resonant-Raman effect and polarized molecular x-ray emission. Plans for implementation of an x-ray synchrotron-radiation beamline dedicated to atomic, molecular, and optical physics at the Advanced Light Source are presented, with emphasis on the enhanced capabilities that will be available at this state-of-the-art facility.

03,864
PB94-216041 Not available NTIS
National Inst. of Standards and Technology (CSTL), Gaithersburg, MD. Inorganic Analytical Research Div.
Measurement of CO Pressures in the Ultrahigh Vacuum Regime Using Resonance-Enhanced Multiphoton-Ionization Time-of-Flight Mass Spectroscopy.
Final rept.
J. P. Looney, J. E. Harrington, K. C. Smyth, T. R. O'Brian, and T. B. Lucatorto. 1993, 10p.
Pub. in Jnl. of Vacuum Science and Technology A 11, n6 p3111-3120 Nov/Dec 93.

Keywords: *Carbon monoxide, *Pressure measurement, Time-of-flight method, Two photon absorption, Ultrahigh vacuum, Laser radiation, Photoionization, Reprints.

An evaluation is made of measurements of CO pressures in the UHV regime using resonance-enhanced multiphoton ionization coupled with time-of-flight mass spectroscopy (REMPI-TOFMS). It has been found that once the REMPI-TOFMS system has been calibrated, quantitative measurement of CO pressures as low as 10(sup -10) Pa is possible, even in overwhelming N2 backgrounds. With compensation for laser pulse energy variations, we find measurements with uncertainties of 10%-15% are possible for pressures down to 10(sup -7) Pa, and an ultimate detection limit for CO pressures of 10(sup -10) Pa for our measurement system. In this study, the REMPI-TOFMS system was calibrated using a pressure division technique along with a spinning rotor gage. The ionization of CO is achieved using 230 nm radiation to excite the B singlet Sigma(1+) state of CO at 10.8 eV via a two-photon absorption and then ionizing some of the excited state molecules by the absorption of an additional photon from the laser beam.

03,865
PB94-216124 Not available NTIS
National Inst. of Standards and Technology (CSTL), Gaithersburg, MD. Thermophysics Div.
Analytical Method of Determining the Heat Capacity at High Temperatures from the Surface Temperature of a Cooling Sphere.
Final rept.
R. A. MacDonald. 1992, 7p.
Pub. in High Temperature-High Pressures 24, p127-133 1992.

Keywords: *Specific heat, *Spheres, *Radiant cooling, *Surface temperature, *Molybdenum, Thermophysical properties, High temperature, Temperature dependence, Emissivity, Reprints, Time dependent temperature profiles.

The feasibility of determining thermophysical properties at high temperatures from measurements of the surface temperature of a radiating sphere is investigated. For a sphere initially maintained in a steady state but with no heat supplied after some time, t = 0, the subsequent temperature profile in the sphere has been calculated as a function of time. The material properties of the sphere: thermal conductivity, heat capacity at constant pressure, thermal expansion, and emissivity, are assumed to have a quadratic dependence on temperature over a limited temperature range (several hundred degrees). The sensitivity of the temperature profile to the material parameters has been examined for values representative of molybdenum. The surface temperature shows some sensitivity to the heat capacity and to the emissivity but it is quite insensitive to the thermal conductivity and thermal expansion. In spite of the rather small effect, a method for determining the heat capacity, given the surface temperature of the sphere as a function of time, has been developed on the basis of these calculations for the full range of temperature, 1500-3000 K.

03,866
PB94-216215 Not available NTIS
National Inst. of Standards and Technology (MSEL), Gaithersburg, MD. Reactor Radiation Div.
Supermirror Transmission Polarizers for Neutrons.
Final rept.
C. F. Majkrzak, V. Nunez, J. R. D. Copley, J. F. Ankner, and G. C. Greene. 1992, 17p.
Pub. in Proceedings of Society of Photo-Optical Instrumentation Engineers - Neutron Optical Devices and Applications, San Diego, CA., July 22-24, 1992, v1738 p90-106.

Keywords: *Polarizers, Polarization(Spin alignment), Cold neutrons, Thermal neutrons, Silicon coatings, Iron, Monochromators, Reprints, *Neutron polarizers, *Supermirrors, Accordion configuration.

We describe several geometrical configurations of supermirror arrays for polarizing cold and sub-thermal neutrons in transmission with high efficiency, which is particularly important in applications where several polarizers occur in series. The measured polarizing efficiency and reflectivity of Fe-Si supermirror coatings which can be used in these devices are also reported.

03,867
PB94-216439 Not available NTIS
National Inst. of Standards and Technology (PL), Boulder, CO. Quantum Physics Div.
Atomic Beam Splitters and Mirrors by Adiabatic Passage in Multilevel Systems.
Final rept.
P. Marte, P. Zoller, and J. Hall. 1992, 10p.
Sponsored by National Science Foundation, Washington, DC. and Office of Naval Research, Arlington, VA.
Pub. in Proceedings Foundations of Quantum Mechanics Workshop, Santa Fe, NM., June 1991, p298-307 1992.

Keywords: *Atomic beams, *Beam splitters, Beam optics, Laser spectroscopy, Raman effect, Deflection, Reprints, *Beam mirrors, Atomic interferometry.

We study atomic beam deflection by adiabatic passage between Zeeman ground-levels via Raman transitions induced by counterpropagating Sigma + - polarized lasers. We show that complete population transfer between the ground states can be achieved which corresponds to the scattering of the atomic wave packet into a single final momentum state by absorption and induced emission of laser photons. Although the lasers can be resonant, the excited state(s) are never populated during the adiabatic transfer which suppresses the effects of spontaneous emission and preserves the coherence of the atomic wave function. This scheme has attractive features as a beam splitter and mirror for atomic interferometry.

03,868
PB94-216611 Not available NTIS
National Inst. of Standards and Technology (NML), Gaithersburg, MD. Center for Radiation Research.
Theoretical Aspects of Tagged Photon Facilities.
Final rept.
L. C. Maximon. 1990, 17p.
Pub. in Proceedings of Seminar on Electromagnetic Interactions of Nuclei at Low and Medium Energies (7th), Moscow, USSR, December 12-14, 1988, p217-233 1990.

Keywords: *Tagged photon method, Polarization, Marking, Reprints.

The idea behind photon tagging is conceptually simple; a signal from a detector looking at one of the particles involved in the photon production process provides information on both the energy and the time of creation of each photon, thereby 'tagging' the energy of each of the photons in a continuous spectrum. A fast time coincidence between the signal from the tagging detector and the signal from the nuclear reaction product detector indicates that the reaction was initiated by the associated photon and serves to identify the energy of the photon that initiated the reaction. Three tagging techniques have been implemented at a number of accelerator laboratories.

03,869
PB94-216652 Not available NTIS
National Inst. of Standards and Technology (PL), Gaithersburg, MD. Electron and Optical Physics Div.
Determination of Complex Scattering Amplitudes in Low-Energy Elastic Electron-Sodium Scattering.
Final rept.
J. J. McClelland, S. R. Lorentz, R. E. Scholten, M. H. Kelley, and R. J. Celotta. 1992, 4p.
Sponsored by Department of Energy, Washington, DC.
Pub. in Physical Review A 46, n9 p6079-6082, 1 Nov 92.

Keywords: *Electron-atom collisions, *Sodium, Scattering cross sections, Scattering amplitudes, Electron scattering, Elastic scattering, EV range 1-10, EV range 10-100, Reprints.

Measurements of spin-resolved elastic electron-sodium scattering have been carried out at incident energies of 4.1 and 12.1 eV, and the ratio of triplet to singlet scattering cross sections has been obtained at each energy. The ratio is used to provide a determination of not only the magnitudes of the triplet and singlet amplitudes, but also the cosine of the relative phase difference between them. These determinations of magnitude and relative phase represent the most detailed characterization to date of electron-atom scattering from a 'one-electron' target.

03,870
PB94-216660 Not available NTIS
National Inst. of Standards and Technology (NML), Gaithersburg, MD. Electron and Optical Physics Div.

Laser Focusing of Atoms: A Particle Optics Approach.
Final rept.
J. J. McClelland, and M. R. Scheinfein. 1990, 1p.
Pub. in Proceedings of International Conference on Atomic Physics (12th), Ann Arbor, MI., July 29-August 3, 1990, 1p.

Keywords: *Atomic beams, *Focusing, Photon-atom interactions, Laser radiation, Reprints, Laser focusing, Atomic diffraction.

The use of a TEM(sub 01, sup *) ('donut') mode laser beam has been proposed as a means of focusing an atomic beam to extremely small spot sizes. In the initial analysis, Balykin and Letokhov showed that when a donut mode laser beam is focused to a small spot of order 1 micrometer, and an atom beam is passed concentrically through the focus, the dipole force on the atoms has the correct radial dependence to produce first order focusing. They then estimated the effects of atomic diffraction (due to the deBroglie wavelength of the atom), spherical and chromatic aberration, and diffusion arising from spontaneous emission. It was found that spot sizes of order a few Angstroms could be obtained with reasonable values for atomic beam collimation and monochromaticity, and laser power and detuning.

03,871
PB95-107025 Not available NTIS
National Inst. of Standards and Technology (PL), Boulder, CO. Quantum Physics Div.
Intermolecular HF Motion in Ar(sub n)HF Micromatrices (n=1,2,3,4,): Classical and Quantum Calculations on a Pairwise Additive Potential Surface.
Final rept.
A. McIlroy, and D. J. Nesbitt. 1992, 13p.
Grant NSF-CHE90-00641
Sponsored by National Science Foundation, Washington, DC.
Pub. in Jnl. of Chemical Physics 97, n9 p6044-6056, 1 Nov 92.

Keywords: *Hydrogen fluoride, *Argon, *High resolution, *Librational motion, Matrix isolation, Van der Waals Forces, Quantum mechanics, Three body problem, Isomers, Supersonic aircraft, Infrared radiation, Microwaves, Molecular interactions, Reprints, Argon clusters.

The availability of pairwise additive 'two-body' potentials for van der Waals systems from near-IR, far-IR and microwave data permits detailed prediction of librational behavior for isolated HF chromophores solvated by successive numbers of rare gas Ar atoms. The paper describes theoretical calculations of Ar(n)HF equilibrium structures and intermolecular HF vibrational frequencies based on an Ar(n)HF 'two-body' potential energy surface developed from previously determined Ar-Ar and Ar-HF potentials. Isomeric structures are predicted from local minima on these multidimensional surfaces, and are found to be in excellent qualitative agreement with near-IR observations of Ar(n)HF clusters with n=1,2,2, and 4 Ar atoms. Quantum mechanical calculations are performed for the HF librational and van der Waals stretching modes against a rigid Ar(n) frame. In the limit of sufficient Ar atoms to fill the first coordination sphere around the HF, the calculations indicate a nearly perfect concellation of angular anisotropy for HF librational motion, consistent with the nearly free internal rotation of the HF observed in cryogenic Ar matrices.

03,872
PB95-107363 Not available NTIS
National Inst. of Standards and Technology (PL), Gaithersburg, MD. Ionizing Radiation Div.
Thin Dyed-Plastic Dosimeter for Large Radiation Doses.
Final rept.
F. Abdel Rehim, S. Ebraheem, W. Z. Ba, and W. L. McLaughlin. 1992, 8p.
Pub. in Applied Radiation and Isotopes 43, n12 p1503-1510 1992.

Keywords: *Gamma dosimetry, *Film dosimetry, *Dosimeters, Polyvinyl chloride, Phthalocyanines, Polymeric films, Gamma radiation, Spectrophotometry, Performance, Stability, Dyes, Reprints, Radiation processing, Absorbed dose.

A commercially available, thin, dyed-plastic film (mean thickness 30 micrometers) having a transparent green color, changes color progressively to brown shades and then to a deep red shade upon irradiation at successively higher values of absorbed dose (gamma radiation) in the range 8-60 kGy. The analysis for dosimetry is made with spectrophotometric measurements (at visible light wavelengths) of pre-irradiation absorbance, A(0), and radiation-induced absorbance, A(1). Either the wavelength of the maximum of the absorption band that bleaches upon irradiation (wavelength = 425 nm) or the wavelengths of the maxima of the two overlapping radiation-induced absorption bands (wavelength = 525 or 556 nm) are used to make these measurements. The most reproducible calibration consists of the ratio, A(1)/A(0), at a given wavelength, as a function of the absorbed dose. The new film dosimeter is flexible, rugged, and relatively stable at temperatures between -80 C and +50 C, and in daylight. The radiation-induced color, in terms of the absorbance, A(1), at selected wavelengths, is unstable for about two days subsequent to irradiation, after which the values of A(1)/A(0) remain stable for at least several months, even under illumination with white fluorescent or indirect daylight.

03,873
PB95-108411 Not available NTIS
National Inst. of Standards and Technology (NML), Gaithersburg, MD. Center for Atomic, Molecular and Optical Physics.
Heterodyne Measurement of the Fluorescence Spectrum of Optical Molasses.
Final rept.
W. D. Phillips, C. I. Westbrook, R. N. Watts, P. D. Lett, P. L. Gould, S. L. Rolston, and C. E. Tanner. 1989, 4p.
Sponsored by Office of Naval Research, Arlington, VA.
Pub. in Proceedings of International Conference on Laser Spectroscopy (9th), Bretton Woods, NH., June 18-23, 1989, p8-11.

Keywords: *Resonance fluorescence, Experiment design, Line narrowing, Spectral analysis, Heterodyning, Measurement, Temperature range 0000-0013 K, Reprints, *Optical molasses, Laser cooling, Laser trapping, Atom traps.

The authors describe a heterodyne experiment to measure the spectrum of fluorescence of the atoms confined in optical molasses.

03,874
PB95-108692 Not available NTIS
National Inst. of Standards and Technology (NML), Gaithersburg, MD. Ionizing Radiation Div.
Preparation and Characterization of (6)LiF and (10)B Reference Deposits for the Measurement of the Neutron Lifetime.
Final rept.
J. Pauwels, R. Eykens, A. Lamberty, R. Scott, J. Byrne, P. Dawber, D. Gilliam, J. Van Gestel, and H. Tagziria. 1991, 8p.
Pub. in Nuclear Instruments and Methods in Physics Research A 303, n1 p133-140 1991.

Keywords: *Neutron lifetime, *Lithium fluorides, *Lithium 6, *Boron 10, Vacuum deposition, Preparation, Characteristics, Measurement, Deposits, Silicon, Wafers, Reprints.

In beam experiments, the achievement of an accurate neutron lifetime measurement depends heavily on the use of well characterized boron and/or lithium reference deposits to assess the neutron density. Sets of (6)LiF and (10)B reference deposits on silicon wafers were prepared by vacuum deposition using planetary rotating substrate holders. The uniformity of deposition was investigated using visible light spectrophotometry and accurate dimensional characterization was carried out on the basis of travelling microscope and talistep measurements. The results obtained agreed well with theoretical calculations based on the geometry of the evaporation system. The deposits prepared in successive evaporation runs were then characterized by neutron induced charged particle measurements calibrated by isotope dilution mass spectrometry. (6)Li and (10)B surface densities are certified with accuracies of 0.35-0.50% and 0.30-0.41%, respectively. An intercomparison of the (6)Li and (10)B calibrations confirms the consistency of the measurements.

03,875
PB95-108874 Not available NTIS
National Inst. of Standards and Technology (NML), Gaithersburg, MD. Center for Atomic, Molecular and Optical Physics.
Atoms in Optical Molasses.
Final rept.
W. D. Phillips, P. D. Lett, S. L. Rolston, C. Westbrook, C. Salomon, J. Dalibard, A. Clairon, S. Guellati, C. E. Tanner, and R. Watts. 1991, 10p.
Pub. in Proceedings of the Conference on Light Induced Kinetic Effects on Atoms, Ions and Molecules, Elba, Italy, May 2-5, 1990, p25-34.

Keywords: Temperature range 0000-0013 K, Temperature measurement, Neutral atoms, Reprints, *Optical molasses, Polarization gradient cooling, Laser cooling, Atom cooling, Sodium atoms, Cesium atoms, Atomic fountains, Laser trapping.

Temperature measurements on atoms released from optical molasses are found to agree very well with the predictions of the theoretical models of polarization gradient cooling. This agreement extends over a wide range of laser intensity and detuning and even covers values of those parameters where it was originally believed the cooling would not be effective. The lowest temperatures achieved in a 3-D optical molasses are 25 microK and 2.5 microK for sodium and cesium respectively. In each case, this is equivalent to an rms velocity of about three times the recoil velocity.

03,876
PB95-108882 Not available NTIS
National Inst. of Standards and Technology (NML), Gaithersburg, MD. Center for Atomic, Molecular and Optical Physics.
Atoms in Optical Molasses: Applications to Frequency Standards.
Final rept.
W. D. Phillips, P. D. Lett, S. L. Rolston, C. I. Westbrook, C. Salomon, J. Dalibard, A. Clairon, S. Guellati, C. E. Tanner, and R. N. Watts. 1990, 4p.
Pub. in Proceedings of the European Frequency and Time Forum (4th), Neuchatel, Switzerland, March 13-15, 1990, p273-276.

Keywords: *Frequency standards, *Time standards, Laser spectroscopy, Trapped particles, Quantum optics, Neutral atoms, Temperature range 0000-0013 K, Reprints, *Optical molasses, Laser trapping, Laser cooling, Ion traps, Atomic fountains.

Recent progress in laser cooling and trapping of neutral atoms is discussed with a view toward future applications to time and frequency standards. Advantages and discadvantages of neutral atom standards with respect to ion standards are discussed. Prospects for a neutral atom 'atomicfountain' clock are examined and appear to be promising.

03,877
PB95-108890 Not available NTIS
National Inst. of Standards and Technology (NML), Gaithersburg, MD. Center for Atomic, Molecular and Optical Physics.
Optical Molasses: Cold Atoms for Precision Measurements.
Final rept.
W. D. Phillips, P. D. Lett, S. L. Rolston, C. I. Westbrook, C. Salomon, J. Dalibard, A. Clairon, S. Guellati, C. E. Tanner, and R. N. Watts. 1991, 3p.
Sponsored by Office of Naval Research, Arlington, VA.
Pub. in Institute of Electrical and Electronics Engineers Transactions on Instrumentation and Measurement 40, n2 p78-80 Apr 91.

Keywords: Atomic spectroscopy, Frequency standards, Neutral atoms, Temperature range 0000-0013 K, Reprints, *Optical molasses, Laser cooling, Ultracold atoms, Cesium atoms, Precision measurements.

Reduction of atomic kinetic motion by laser cooling has important applications to atomic frequency standards and other precision measurements. The optical molasses technique, used for cooling neutral atoms, has produced temperatures below 3 microK for cesium atoms, corresponding to an rms velocity of about 13 mm/s. This is considerably lower than the lower limit originally thought to apply to laser cooling and is apparently the lowest kinetic temperature ever measured for three-dimensional cooling. New laser cooling mechanisms have been identified to explain the low temperature.

03,878
PB95-108908 Not available NTIS
National Inst. of Standards and Technology (NML), Gaithersburg, MD. Electron and Optical Physics Div.

Optical Molasses: The Coldest Atoms Ever.
Final rept.
W. Phillips, P. Lett, S. Rolston, C. Westbrook, C. Salomon, J. Dalibard, A. Clairon, S. Guellati, C. Tanner, and R. Watts. 1991, 3p.
Pub. in Physica Scripta T34, p20-22 1991.

Keywords: Temperature range 0000-0013 K, Atomic clocks, Doppler effect, Neutral atoms, Reprints, *Optical molasses, Laser cooling, Atom cooling, Sodium atoms, Cesium atoms, Ultracold atoms, Atomic fountains.

Optical molasses is a three-dimensional (3-D) configuration of laser beams used to laser-cool and to confine neutral atoms. Atoms laser cooled in optical molasses reach temperatures much lower than the limit given by the original theories of laser cooling based on the Doppler effect. This cooling below the Doppler-Cooling limit is now seen as being due to new laser cooling mechanisms not present in the original theories. The dependence of the atomic temperature on parameters such as laser intensity and detuning shows good agreement between calculations performed in 1-D and experiments performed in 3-D. For cooling of Na and Cs atoms, the lowest observed temperatures correspond to rms velocities between three and four times the single photon recoil velocity. For Cs the temperature is 2.5 + or - 0.6 microK and is the lowest temperature ever measured for 3-D cooling.

03,879
PB95-125639 Not available NTIS
National Inst. of Standards and Technology (NML), Gaithersburg, MD. Chemical Process Metrology Div.
Development of a Temperature Scale below 0.5 K.
Final rept.
W. E. Fogle, J. H. Colwell, and R. J. Soulen. 1990, 2p.
Pub. in Physica B 165, p33-34 Aug 90.

Keywords: *Temperature scales, *Cryogenic temperature, Temperature range 0000-0013 K, Temperature measurement, Noise thermometers, Melting points, Reprints, Fixed points.

We summarize our most recent results on the development of an absolute temperature scale below 0.5 K. It is the most recent of several experiments at our laboratory and represents both our best effort and the one in which all available thermometers were simultaneously and fully operational. Perhaps the most interesting conclusion reached by us so far is that the temperature scale below 15 mK may be quite different than has been developed by other laboratories, particularly those engaged in low-temperature physics projects such as (3)He research.

03,880
PB95-125886 Not available NTIS
National Inst. of Standards and Technology (PL), Boulder, CO. Quantum Physics Div.
Associative Ionization in Collisions of Slowed and Trapped Sodium.
Final rept.
A. Gallagher. 1991, 11p.
Pub. in Physical Review A 44, n7 p4249-4259, 1 Oct 91.

Keywords: *Atom-atom collisions, *Atomic collisions, Energy transfer, Ionization, Photoabsorption, Reprints, *Sodium atoms, Atom traps.

Collisions of trapped atoms occur over time intervals that are often longer than radiative lifetimes. This leads to radiative interruption of excited-state collision dynamics and constrains collisional interactions to atom pairs that are in close proximity at the time of excitation. Using classical dynamics, I show that this causes Na associative ionization to be dominated by a four-step process in which the longer-range Na(star)-Na interaction initiates inward motion that is completed as Na(star) + Na(star) --> Na2(1+) + e. Thus low-temperature associative ionization does not result from Na(star) + Na(star) collisions. I predict strong single- and two-wavelength dependencies, which have a molecular character due to the close proximity at the time of photoabsorption. These are amenable to experimental observation. I also calculate saturation that results from the depletion of interacting pairs. This produces very-low-power saturation and explains the associative ionization measurements of Gould et al. (Phys. Rev. Lett. 60, 788 (1988)).

03,881
PB95-126058 Not available NTIS
National Inst. of Standards and Technology (PL), Gaithersburg, MD. Atomic Physics Div.
Temperature of Optical Molasses for Two Different Atomic Angular Momenta.
Final rept.
C. Gerz, T. Hodapp, P. Jessen, C. Westbrook, K. Molmer, K. Jones, and W. Phillips. 1993, 6p.
Sponsored by Office of Naval Research, Washington, DC.
Pub. in Europhysics Letters 21, n6 p661-666 1993.

Keywords: Fokker-Planck equation, Isotope effects, Temperature dependence, Quantum optics, Neutral atoms, Rubidium 85, Rubidium 87, Reprints, *Rubidium atoms, Laser cooling, Optical molasses.

We have measured the temperature of laser-cooled Rb atoms in optical molasses as a function of laser intensity and detuning. For both (85)Rb and (87)Rb, cooled on the F = 3--> F' = 4 and F = 2 --> F' = 3 transitions, respectively, the temperatures are proportional to the ratio of laser power and detuning for a wide range of these parameters. We observe a small but significant difference between the two isotopes. We also show the results of three-dimensional semi-classical numerical calculations. Our results favor a model which includes atomic localization in optical standing waves.

03,882
PB95-126298 Not available NTIS
National Inst. of Standards and Technology (NML), Gaithersburg, MD. Quantum Metrology Div.
Some Aspects of Fundamental Neutron Physics.
Final rept.
G. L. Greene. 1990, 9p.
Pub. in Proceedings of Rencontre Moriond New Exotic Phenom., v25 p163-171 1990.

Keywords: *Neutron physics, Sommerfeld constant, Neutron lifetime, Cold neutrons, Fundamental constants, Reprints, Gravitational phase shift, Fine structure constants, Neutron interferometry.

Low energy neutrons provide a tool of great versatility in the investigation of fundamental interactions. Recent experimental work with 'cold' neutrons have addressed such issues as the study of weak interactions, nuclear physics and astrophysics. They have also been employed in the study of invariance principles and for the determination of fundamental constants. This contribution focuses on three particular areas of investigation which reflect this broad nature of neutron physics. The examples discussed include gravitational phase shift experiments with neutron interferometers, the measurement of the neutron lifetime, and the determination of the fine structure constant by a new method.

03,883
PB95-126405 Not available NTIS
National Inst. of Standards and Technology (PL), Boulder, CO. Quantum Physics Div.
Evidence for Significant Backscattering in Near-Threshold Electron-Impact Excitation of Ar(7+)(3s yields 3p).
Final rept.
X. Q. Guo, E. W. Bell, J. S. Thompson, R. A. Phaneuf, A. C. H. Smith, G. H. Dunn, and M. E. Bannister. 1993, 4p.
Contract DE-AI05-86ER53237
Sponsored by Department of Energy, Washington, DC. Office of Energy Research.
Pub. in Physical Review A 47, n1 pR9-R12 Jan 93.

Keywords: *Electron-ion collisions, *Electron scattering, *Backscattering, *Argon ions, Total cross sections, Multicharged ions, Electron impact, Excited states, Inelastic scattering, Excitation, R matrix, Reprints, Sodium-like ions.

Measurements of absolute total cross sections for electron-impact excitation of Ar(7+)(3s--> 3p) using a merged-beams electron-energy-loss technique show that near threshold, the inelastically scattered electrons are ejected primarily in the backward direction. This unusual angular scattering has not been previously observed for atoms or ions, but may be typical for multiply charged ions. The total cross sections, measured over an energy range to 2.2 eV above threshold, agree with seven-state R-matrix close-coupling calculations. Both close-coupling and distorted-wave calculations also confirm the backscattering observed in these measurements.

03,884
PB95-135570 PC A03/MF A01
National Inst. of Standards and Technology (CSTL), Boulder, CO. Process Measurements Div.
Thermal Hydraulic Tests of a Liquid Hydrogen Cold Neutron Source.
J. D. Siegwarth, D. A. Olson, M. A. Lewis, P. Kopetka, J. M. Rowe, and R. E. Williams. Jul 94, 28p, NISTIR-5026.

Keywords: *NBSR reactor, *Neutron sources, *Cold neutrons, *Moderators, Liquid hydrogen, Hydraulic tests, Thermal testing, Scale models, Thermosyphons.

We have built and tested a simplified full scale model of the planned liquid hydrogen moderator for the cold neutron source of the NIST reactor. The heat load to the liquid hydrogen will be removed to an external refrigerator by means of a thermosyphon. Our experiments showed that this system could be filled, would operate stably, and the gas volume in the moderator chamber would not exceed 20 percent. Results of the tests suggested some improvements to the original designs. The circulation of liquid hydrogen proved to be self-regulating even when the available liquid inflow rate was sufficient to flood the vapor line.

03,885
PB95-140059 Not available NTIS
National Inst. of Standards and Technology (PL), Gaithersburg, MD. Radiometric Physics Div.
Precision High Temperature Blackbodies.
Final rept.
V. I. Sapritsky, B. C. Johnson, R. D. Saunders, B. B. Klevnoy, V. I. Shapoval, I. A. Dmitriev, L. M. Buchnev, A. V. Prochorov, L. V. Vlasov, and K. A. Sudarev. 1993, 9p.
Pub. in Proceedings of Society of Photo-Optical Instrumentation Engineers: Ultraviolet Technology IV, San Diego, CA., July 20-21, 1992, v1764 p323-331 1993.

Keywords: *Blackbody radiation, *Radiation sources, Temperature range 1000-4000 K, High temperature, Ultraviolet radiation, Precision, Design, Reprints.

This paper reviews the research and design of high temperature blackbody sources for the temperature interval from 2000 K to 3000 K. Sources with large apertures are addressed specifically, as these are well suited to the important problem of spectral irradiance scale realizations.

03,886
PB95-140422 Not available NTIS
National Bureau of Standards (NML), Gaithersburg, MD. Ionizing Radiation Div.
Measurement of the (235)U(n,f) Reaction from Thermal to 1 keV.
Final rept.
R. A. Schrack. 1988, 4p.
Pub. in Proceedings of International Conference on Nuclear Data for Science and Technology, Mito, Japan, May 30, 1988, 4p.

Keywords: *Fission cross sections, *Neutron reactions, *Uranium 235, Milli eV range, EV range 01-10, EV range 10-100, EV range 100-1000, Accelerator facilities, Nuclear fission, Measurement, Boron 10, Reprints.

The neutron induced fission cross section for (235)U has been measured from .02 to 1000 electron volts at the NBS electron LINAC facility. This cross section, especially the integrals from 7.8 to 11 eV and from 100 to 1000 eV is widely used as a standard to normalize shape experiments. A special ion chamber incorporating both the (235)U foils and the (10)B foils used to monitor the neutron beam was built. The geometry of the chamber and the data taking system was designed to give the effect of a common environment and flight path so as to reduce or eliminate background and energy assignment problems. The shape measurements were normalized at thermal. Results are compared to other recent measurements, and ENDF/B-V.

03,887
PB95-140869 Not available NTIS
National Inst. of Standards and Technology (PL), Gaithersburg, MD. Atomic Physics Div.
Wavelengths and Isotope Shifts for Lines of Astrophysical Interest in the Spectrum of Doubly Ionized Mercury (Hg III).
Final rept.
C. J. Sansonetti, and J. Reader. 1993, 5p.
Sponsored by National Aeronautics and Space Administration, Washington, DC.
Pub. in Physical Review A 47, n4 p3080-3084 Apr 93.

Keywords: *Mercury ions, *Ultraviolet spectra, *Isotope effect, *Spectral shift, *Peculiar stars, Stellar spectra,

Mercury isotopes, Line spectra, Wavelengths, Radio frequency discharge, Multicharged ions, Reprints, Isotope abundance.

Wavelengths and isotope shifts have been measured for the 1738.4-, 1738.5-, 1740.2-, and 2354.2-A lines of Hg III with an uncertainty of 0.002 A. The lines were excited in a pulsed radio-frequency discharged and observed with a 10.7-m normal-incidence vacuum spectrograph. Observations were made with lamps containing natural Hg, (198)Hg, and (204)Hg. By using well-established relative isotope shifts, wavelengths of these four lines for (196)Hg, (200)Hg, (202)Hg, and the centers of gravity for (199)Hg and (201)Hg were also determined. The results provide important data for determining elemental and isotopic abundances of Hg from spectra of Hg-rich chemically peculiar stars.

03,888
PB95-140877 Not available NTIS
National Inst. of Standards and Technology (PL), Gaithersburg, MD. Atomic Physics Div.
Spectrum and Energy Levels of Triply Ionized Barium (Ba IV).
Final rept.
C. J. Sansonetti, J. Reader, A. Tauheed, and Y. N. Joshi. 1993, 6p.
Pub. in Jnl. of the Optical Society of America B 10, n1 p7-12 Jan 93.

Keywords: *Barium ions, *Atomic energy levels, *Ultraviolet spectra, Vacuum ultraviolet radiation, Ionization potentials, Electron transitions, Line spectra, Multicharged ions, Reprints.

The spectrum of Ba IV was observed with sliding sparks and low-inductance vacuum sparks on 10.7- and 3-m normal-incidence vacuum spectrographs. Thirty-nine lines between 463 and 923 A are classified as transitions between levels of the 5s(2)5p(5) doublet P ground term and levels of the 5s5p(6), 5s(2)5p(4)5d, and 5s(2)5p(4)6s configurations. These configurations are theoretically interpreted, and the energy parameters determined from least-squares fits to the observed levels are compared with Hartree-Fock calculations. The ionization energy is revised to 379,300 + or - 2700/cm (47.03 + or - O.33 eV).

03,889
PB95-141206 Not available NTIS
National Inst. of Standards and Technology (CSTL), Gaithersburg, MD. Inorganic Analytical Research Div.
Neutron Focusing Lens Using Polycapillary Fibers.
Final rept.
H. Chen, D. F. R. Mildner, and Q. F. Xiao. 1994, 3p.
Contracts DE-FG02-91ER81220, DE-FG02-91ER81411
Sponsored by Department of Energy, Washington, DC.
Pub. in Applied Physics Letters 64, n16 p2068-2070, 18 Apr 94.

Keywords: *Neutron beams, *Cold neutrons, *Focusing, Borosilicate glass, Grazing incidence, Thermal neutrons, Neutron transport, Mirrors, Lenses, Reprints, *Neutron focusing, Multiple reflection.

Multiple mirror reflection at small grazing angles from the smooth surfaces of the narrow channels of polycapillary fibers can be used to transport, bend, and focus thermal neutron beams. We report the results of the focusing of a polychromatic cold neutron beam using a compact lens of borosilicate fibers and with a focal distance of 57 mm. The intensity profile of the beam at the focus is approximately conical in shape with a full width at half-maximum of 0.49 mm, and with an average gain in intensity of about 20. These experimental results agree well with those obtained by computer simulation.

03,890
PB95-143194 PC A09/MF A02
Maryland Univ., College Park. Dept. of Mechanical Engineering.
Transient Cooling of a Hot Surface by Droplets Evaporation.
Final rept.
G. White, S. Tinker, and M. di Marzo. Dec 93, 178p, NIST/GCR-94/662.
Grant NIST-70NANB1H1173
See also PB90-227968. Sponsored by National Inst. of Standards and Technology (BFRL), Gaithersburg, MD.

Keywords: *Droplets, *Surface temperature, *Evaporative cooling, *Hot surfaces, Heat transfer, Computer programs, Heat flux, Green's function, Water, Vaporizing, Thermal conductivity, Numerical integration.

A computer code is developed and tested which simulates the transient evaporation of a single liquid droplet from the surface of a semi-infinite solid subject to radiant heat input from above. For relatively low temperature incident radiation, it is shown that the direct absorption of radiant energy by the droplet can be treated as purely boundary conditions, while a model for higher temperature incident radiation would require the addition of constant heat source terms. The heat equation is numerically coupled between the liquid and solid domains by using a predictor-corrector scheme. Three one-dimensional solution schemes are used within the droplet: a start-up semi-infinite medium solution, a tridiagonal Crank-Nicholson transient solution, and a steady-state solution. The solid surface temperatures at each time step are calculated through careful numerical integration of an axisymmetric Green's functions solution with the forcing function given by the past lower droplet surface and solid-vapor boundary heat fluxes. The time step is increased after a sensitive initial period to allow for reasonable run times. Two geometry models are included which give the droplet height as a function of current droplet volume and initial wetted radius; the second allows inclusion of the effects of initial contact angle and receding angle. Using water as the liquid and Macor, a low-thermal conductivity material, as the solid, the program output was compared to the experimental results in this line of research. They correlate well to the experiments in which the critical geometric shape factor and evaporation time were most easily measured.

03,891
PB95-150298 Not available NTIS
National Inst. of Standards and Technology (PL), Gaithersburg, MD. Quantum Metrology Div.
Resonance and Threshold Effects in Polarized X-Ray Emission from Atoms and Molecules.
Final rept.
S. H. Southworth. 1994, 6p.
Sponsored by Department of Energy, Washington, DC.
Pub. in Nuclear Instruments and Methods in Physics Research B 87, p247-252 1994.

Keywords: *X-ray spectra, *Polarized electromagnetic radiation, Inner-shell excitation, Molecular spectra, Atomic spectra, X-ray absorption, Molecular orbitals, Angular distribution, Threshold effects, K shell, Anisotropy, Resonance, Gases, Reprints, *X-ray emission.

Strongly anisotropic and polarized K-V (valence to K-vacancy) X-ray emission has been observed from gas-phase molecules following excitation of a K-shell electron to valence-like subthreshold resonances using a narrow bandwidth, linearly polarized X-ray beam. Distinctively different polarizations and angular distributions are observed for emission involving molecular orbitals of different symmetries. A classical model of the X-ray absorption/emission process accurately describes the observed radiation patterns. Relatively weak polarizations and anisotropies are observed following excitation of atomic subthreshold resonances, due to averaging over unresolved final states. However, resonance and threshold studies of atomic X-ray spectra illustrate the inelastic resonance scattering process and the onset of characteristic fluorescence.

03,892
PB95-150470 Not available NTIS
National Inst. of Standards and Technology (MSEL), Gaithersburg, MD. Reactor Radiation Div.
Grazing Incidence Prompt Gamma Emissions and Resonance-Enhanced Neutron Standing Waves in a Thin-Film.
Final rept.
H. Zhang, P. D. Gallagher, S. K. Satija, T. P. Russell, P. Lambooy, E. J. Kramer, F. S. Bates, R. M. Lindstrom, and R. L. Paul. 1994, 4p.
Pub. in Physical Review Letters 72, n19 p3044-3047, 9 May 94.

Keywords: *Neutron capture gamma rays, *Prompt gamma radiation, *Polymeric films, Grazing incidence, Thin films, Measurement, Gadolinium, Resonance, Reprints, *Neutron standing waves, Neutron depth profiling, Neutron reflectivity.

We report simultaneous measurements of neutron-capture prompt gamma emissions as well as neutron reflectivity on a polymer film with an embedded Gd layer. Enhanced gamma-ray signals and reduced neutron reflectivity were observed when the neutron standing waves were resonantly amplified in the film. Fitting of both the gamma-ray and reflectivity data is of significant aid in uniquely characterizing the depth profile of the polymer film as well as locating the Gd layer.

03,893
PB95-150546 Not available NTIS
National Inst. of Standards and Technology (PL), Boulder, CO. Quantum Physics Div.
Excitation of Balmer Lines in Low-Current Discharges of Hydrogen and Deuterium.
Final rept.
Z. Stokic, M. M. F. R. Fraga, J. Bozin, B. M. Jelenkovic, V. Stojanovic, and Z. L. Petrovic. 1992, 6p.
Pub. in Physical Review A 45, n10 p7463-7468, 15 May 92.

Keywords: *Gas discharges, *Hydrogen plasma, *Deuterium plasma, *Balmer lines, Electron-ion collisions, Electron impact, Gas ionization, Ionization coefficients, H alpha line, Excitation, Reprints.

Measurements have been made of electron-impact ionization and excitation of Balmer lines in low-current, steady-state discharges of hydrogen and deuterium. Results were obtained from spatial scans of H(alpha) lines for E/N ranging from 250 Td to 10 kTd. Here E is the electric field, N is the gas density, and 1 Td=10(exp -21) V meters squared. Ionization and excitation coefficients versus E/N are presented for E/N between 250 and 1,800 Td, and Nd (where d denotes the gap length) between 2.3 X 10(exp 22) and 1.7 X 10(exp 21) per square meter. Excitation coefficients obtained for H(alpha) and D(alpha) are placed on an absolute scale using a standard tungsten lamp calibrated against the blackbody radiation standard. The ionization coefficients are compared with previous experimental and theoretical data, while the excitation coefficients are compared with the calculated values.

03,894
PB95-150553 Not available NTIS
National Inst. of Standards and Technology (PL), Boulder, CO. Quantum Physics Div.
Fast Computer Evaluation of Radiative Properties of Hydrogenic Systems.
Final rept.
P. J. Storey, and D. G. Hummer. 1991, 13p.
Contract NASA-NAGW-766, Grant NSF-AST88-02937
Sponsored by National Aeronautics and Space Administration, Washington, DC. and National Science Foundation, Washington, DC.
Pub. in Computer Physics Communications 66, p129-141 1991.

Keywords: Hypergeometric functions, Einstein coefficients, Oscillator strengths, Computer calculations, Cross sections, Photoionization, Reprints, *Hydrogen-like ions, Gaunt factor.

Three subroutines are described for the very fast calculation of bound-bound, bound-free, and free-free cross-sections for nonrelativistic hydrogenic systems of arbitrary nuclear charge and reduced mass. The first two are essentially exact, being based on recursion relations which are known to be stable. The third evaluates the thermally-averaged free-free Gaunt factor by means of a two-dimensional Chebyshev expansion calculated by numerical evaluation of the cross-sections expressed as hypergeometric functions, augmented by other analytical approximations.

03,895
PB95-150629 Not available NTIS
National Inst. of Standards and Technology (PL), Gaithersburg, MD. Atomic Physics Div.
Improved Wavelengths for Prominent Lines of Cr XVI to Cr XXII.
Final rept.
J. Sugar, V. Kaufman, and W. L. Rowan. 1993, 3p.
Sponsored by Department of Energy, Washington, DC.
Pub. in Jnl. of the Optical Society of America B 10, n1 p13-15 Jan 93.

Keywords: *Chromium ions, *Ultraviolet spectra, *X-ray spectra, Extreme ultraviolet radiation, Soft x-rays, Multicharged ions, Spectral lines, Wavelengths, Atomic energy levels, TEXT devices, Reprints.

New measurements of 34 spectral lines of highly ionized Cr ions in the range of 100-280 A have been made with a wavelength uncertainty of + or - 5 mA. The light source was the TEXT tokamak at the University of Texas at Austin. Lines of Li-like to F-like Cr are included with visually estimated relative intensities, the

best previous measurements, and their energy-level classifications. The uncertainties of the best earlier measurements were reported as + or - 20-30 mA, but much larger errors were found in some cases.

03,896
PB95-150637 Not available NTIS
National Inst. of Standards and Technology (PL), Gaithersburg, MD. Atomic Physics Div.
Observation of Pd-Like Resonance Lines Through Pt(32+) and Zn-Like Resonance Lines of Er(38+) and Hf(42+).
Final rept.
J. Sugar, V. Kaufman, and W. L. Rowan. 1993, 3p.
Sponsored by Department of Energy, Washington, DC.
Pub. in Jnl. of the Optical Society of America B 10, n5 p799-801 May 93.

Keywords: *Erbium ions, *Ytterbium ions, *Hafnium ions, *Tungsten ions, *Platinum ions, *Resonance lines, Multicharged ions, Isoelectronic sequence, Plasma spectra, TEXT devices, Reprints, *Palladium-like ions, Zinc-like ions.

Spectra of highly ionized Er, Yb, Hf, W, and Pt were observed by injecting these elements into the plasma of the TEXT tokamak. Resonance lines of the 4d(10)-4d(9)4f transition array in the Pd I isoelectronic sequence were identified by comparison with plots of observed-minus-calculated transition energies. These plots were based on data previously known through Ho(21+). They were fitted to low-order polynomials that permitted accurate predictions of wavelengths to Bi(37+). In addition, resonance lines of Zn-like Er(38+) and Hf(42+) were observed.

03,897
PB95-150645 Not available NTIS
National Inst. of Standards and Technology (PL), Gaithersburg, MD. Atomic Physics Div.
Rb-Like Spectra: Pd X to Nd XXIV.
Final rept.
J. Sugar, V. Kaufman, and W. L. Rowan. 1992, 3p.
Sponsored by Department of Energy, Washington, DC.
Pub. in Jnl. of the Optical Society of America B 9, n11 p1959-1961 Nov 92.

Keywords: *Ultraviolet spectra, *Palladium ions, *Neodymium ions, Extreme ultraviolet radiation, Isoelectronic sequence, TEXT devices, Plasma spectra, Multicharged ions, Wavelengths, Reprints, *Rubidium-like ions.

Spectra of selected elements from Pd to Nd were observed with the TEXT tokamak at the University of Texas in Austin. Lines of the Rb I isoelectronic sequence were identified and wavelengths compared with calculated values obtained with the Cowan relativistic Hartree-Fock code. We made plots of observed minus calculated (O - C) transition energies in order to obtain smoothed wavelengths and interpolate values for elements not observed.

03,898
PB95-150652 Not available NTIS
National Inst. of Standards and Technology (PL), Gaithersburg, MD. Atomic Physics Div.
Rh I Isoelectronic Sequence Observed from Er(23+) to Pt(33+).
Final rept.
J. Sugar, V. Kaufman, and W. L. Rowan. 1993, 3p.
Sponsored by Department of Energy, Washington, DC.
Pub. in Jnl. of the Optical Society of America B 10, n11 p1977-1979 Nov 93.

Keywords: *Erbium ions, *Ytterbium ions, *Hafnium ions, *Tungsten ions, *Platinum ions, *X ray spectra, Soft x-rays, Multicharged ions, Isoelectronic sequence, TEXT devices, Plasma spectra, Metal films, Laser ablation, Reprints, *Rhodium-like ions.

The TEXT tokamak was used to obtain spectra of highly ionized Er, Yb, Hf, W, and Pt. Injection of these elements into the plasma was achieved by laser ablation of thin films of metal deposited on glass slides and mounted at the inner wall of the vessel. The spectra were photographed with a 2.2-m grazing-incidence spectrograph set at a grazing angle of 4 deg. These spectra occur in a very small wavelength interval, for example about 2 A at 50 A in W. In this spectral range we previously classified lines of the Ag and Pd isoelectronic sequences. We have now classified lines of the Rh isoelectronic sequence 4d(9)-4d(8)4f, which accounts for the remaining strong lines in this dense but well-resolved group. No lines of this array have previously been identified. They were classified by comparison of observed and calculated transition energies along the isoelectronic sequence.

03,899
PB95-150660 Not available NTIS
National Inst. of Standards and Technology (PL), Gaithersburg, MD. Atomic Physics Div.
Spectra of Ag I Isoelectronic Sequence Observed from Er(21+) to Au(32+).
Final rept.
J. Sugar, V. Kaufman, and W. L. Rowan. 1993, 5p.
Pub. in Jnl. of the Optical Society of America B 10, n8 p1321-1325 Aug 93.

Keywords: *Erbium ions, *Gold ions, *Hafnium ions, *Platinum ions, *Tungsten ions, *Ytterbium ions, *X-ray spectra, *Ultraviolet spectra, Extreme ultraviolet radiation, Soft x rays, Multicharged ions, Isoelectronic sequence, TEXT devices, Plasma spectra, Metal films, Laser ablation, Reprints, *Silver-like ions.

Spectra of highly ionized Er, Yb, Hf, W, Pt, and Au were observed with the TEXT tokamak at the University of Texas at Austin. These metals were injected into the tokamak plasma by laser ablation of thin-film targets. Spectra were photographed with a 2.2-m grazing-incidence spectrograph in the range 40-300 A. Three strong doublets of the Ag I isoelectronic sequence were identified: 4d(10)4f - 4d(9)4f(singlet P)4f doublet D, doublet F and doublet G. Interpolated and extrapolated wavelengths in this sequence were derived from plots of the difference between observed and calculated values for the transition energies. The correspondence of the W wavelengths with previously reported tokamak spectra is shown.

03,900
PB95-150769 Not available NTIS
National Inst. of Standards and Technology (PL), Gaithersburg, MD. Atomic Physics Div.
Analysis of the 5s(2)5p(2)-(5s5p(3)+5s(2)5p5d+5s(2)5p6s) Transitions of Four-Times Ionized Xenon (Xe V).
Final rept.
A. Tauheed, Y. N. Joshi, V. Kaufman, J. Sugar, and E. H. Pinnington. 1993, 5p.
Pub. in Jnl. of the Optical Society of America B 10, n4 p561-565 Apr 93.

Keywords: *Ultraviolet spectra, *Xenon ions, Far ultraviolet radiation, Electron transitions, Multicharged ions, Line spectra, Reprints.

The spectrum of xenon was photographed in the range 350-2000 A with 3-m normal-incidence and 10.7-m normal-incidence spectrographs. The source used in both cases was a gas-triggered spark. The Xe V spectrum was distinguished by observation of spectral changes with variation of spark current. The 5s(2)5p(2) - (5s5P(3) + 5s(2)5p5d + 5s(2)5p6s) transition array of Xe V was identified and analyzed. Calculations were carried out to assist in the analysis and to help us to interpret the results. An earlier analysis was revised and extended, and 73 lines are now classified. A value for the ionization energy of 436,700 + or - 400/cm was determined.

03,901
PB95-150868 Not available NTIS
National Inst. of Standards and Technology (PL), Boulder, CO. Quantum Physics Div.
Relativistic Effects in Spin-Polarization Parameters for Low-Energy Electron-Cs Scattering.
Final rept.
U. Thumm, K. Bartschat, and D. W. Norcross. 1993, 12p.
Contract DE-AI05-86ER53237
Sponsored by Department of Energy, Washington, DC. Office of Energy Research.
Pub. in Jnl. of Physics B: Atomic and Molecular Optical Physics 26, p1587-1598 1993.

Keywords: *Electron-atom collisions, *Electron scattering, *Cesium, Relativistic effects, Inelastic scattering, Elastic scattering, EV range 1-10, Polarized targets, R matrix, Excitation, Reprints, *Electron spin polarization.

Based on a recent Dirac R-matrix (close-coupling) calculation, we present results for various spin-polarization parameters for elastic and inelastic scattering of slow (E(kin) approx = or < 2 eV) polarized electrons from unpolarized and polarized neutral Cs atoms in their ground state. Our results allow for a quantitative estimate of the importance of relativistic effects, and our calculated parameters clearly deviated from predictions obtained by just jj-recoupling the results of a nonrelativistic calculation.

03,902
PB95-151122 Not available NTIS
National Inst. of Standards and Technology (EEEL), Gaithersburg, MD. Electricity Div.
Kinetic-Energy Distributions of K(+) in Argon and Neon in Uniform Electric Fields.
Final rept.
R. J. Van Brunt, and J. K. Olthoff. 1993, 3p.
Pub. in Proceedings of International Seminar on Electron and Ion Swarms (8th), Trondheim, Norway, July 15-17, 1993, p76-78.

Keywords: *Potassium ions, Mass spectroscopy, Kinetic energy, Electric fields, Drift tubes, Argon, Neon, Reprints, Ion energy analysis.

Kinetic-energy distributions have been measured for the K(1+) ions traveling in a drift tube in argon or neon buffer gases. Measurements were made at different electric field-to-gas density ratios (E/N). The distributions were observed to deviate from a Maxwellian dependence at high E/N for neon buffer gas.

03,903
PB95-151221 Not available NTIS
National Inst. of Standards and Technology (PL), Gaithersburg, MD. Atomic Physics Div.
Hyperfine Effects and Associative Ionization of Ultracold Sodium.
Final rept.
M. Wagshul, K. Helmerson, P. Lett, R. Heather, P. Jullienne, S. Rolston, and W. Phillips. 1993, 4p.
Sponsored by Office of Naval Research, Arlington, VA.
Pub. in Physical Review Letters 70, n14 p2074-2077, 5 Apr 93.

Keywords: *Atomic collisions, *Sodium, Hyperfine structure, Laser spectroscopy, Reprints, Associative ionization, Ultracold atoms, Laser cooling, Millikelvin temperature.

We observe a new resonance structure in the associative ionization spectrum of laser-cooled sodium due to the collision of two atoms in different ground hyperfine states. This associative ionization is due to doubly resonant excitation at moderate internuclear separation through intermediate molecular states. Substructure within this resonance is evidence for the role of molecular bound states in this process. We present calculations modeling the effect of ground-state hyperfine structure, the importance of which was unanticipated in earlier theoretical studies.

03,904
PB95-151239 Not available NTIS
National Inst. of Standards and Technology (PL), Boulder, CO. Quantum Physics Div.
Electron-Impact Excitation of Si(3+)(3S yields 3P) Using a Merged-Beam Electron-Energy-Loss Technique.
Final rept.
E. K. Wahlin, J. S. Thompson, G. H. Dunn, A. C. H. Smith, R. A. Phaneuf, and D. C. Gregory. 1991, 4p.
Contract DE-AI01-76PR06010
Sponsored by Department of Energy, Washington, DC.
Pub. in Physical Review Letters 66, n2 p157-160, 14 Jan 91.

Keywords: *Electron-ion collisions, *Silicon ions, Multicharged ions, Electron impact, Cross sections, Excitation, Reprints, Electron energy loss spectroscopy.

For the first time, absolute cross sections for electron-impact excitation of a multiple charged ion have been measured using an electron-energy-loss technique. Cross sections for e+Si(3+) 3s doublet S(1/2) --> e+Si(3+) 3p doublet P(1/2,3/2) - 8.88 eV have been measured with an accuracy of + or - 20% (at 90%-confidence level) over a narrow energy range (+ or - 0.6 eV) about the threshold energy with an energy resolution of 0.2 eV. Results are in good agreement with close-coupling calculations.

03,905
PB95-151254 Not available NTIS
National Inst. of Standards and Technology (PL), Gaithersburg, MD. Atomic Physics Div.
Magneto-Optical Trapping of Metastable Xenon: Isotope-Shift Measurements.
Final rept.
M. Walhout, H. J. L. Megens, A. Witte, and S. L. Rolston. 1993, 4p.
Sponsored by Office of Naval Research, Arlington, VA.
Pub. in Physical Review A 48, n2 pR879-R882 Aug 93.

Keywords: *Trapped particles, *Xenon isotopes, *Isotope effect, *Magnetooptics, Metastable state, Zeeman effect, Spectral shift, Hyperfine structure, Reprints, Atom traps, Laser cooling.

We have magneto-optically trapped the nine stable isotopes of xenon. Using the Zeeman slowing method to decelerate a beam of xenon atoms in the metastable 6s 3/2 (3/2)(sub 2) state (notation representing nl J(core) (K = J(core) + l)(sub J)), we load our trap to a collisionally limited density of more than 10(exp 10) atoms/cc. The two odd isotopes are trapped without a repumping frequency, even though they have hyperfine structure. The sensitivity of the trapping process to the laser frequency is exploited to make accurate measurements of the isotope shifts for the 6s 3/2 (3/2)(sub 2) --> 6p 3/2 (5/2)(sub 3) laser-cooling transition and of the hyperfine constants for (131)Xe.

03,906
PB95-151353 Not available NTIS
National Inst. of Standards and Technology (CSTL), Gaithersburg, MD. Thermophysics Div.
Measurements of the Virial Coefficients and Equation of State of the Carbon Dioxide + Ethane System in the Supercritical Region.
Final rept.
L. A. Weber. 1992, 22p.
Sponsored by Gas Research Inst., Chicago, IL.
Pub. in International Jnl. of Thermophysics 13, n6 p1011-1032 Nov 92.

Keywords: *Virial equation, *Binary mixtures, *Carbon dioxide, *Ethane, *Equations of state, Density(Mass/volume), Critical pressure, Critical temperature, Thermophysical properties, Temperature dependence, Reprints, Phase boundaries.

Gas-phase densities of the system carbon dioxide + ethane were measured with a Burnett apparatus at 320 K and at pressures up to approximately 10 MPa. Measurements were made on systems having carbon dioxide mole fractions of 0, 0.25166, 0.49245, 0.73978, and 1. Second and third virial coefficients were determined for each composition, and the cross virial coefficients were calculated. Comparisons were made with other recent high-quality measurements on this system. For each mixture composition PdT measurements were made on five isochores having densities within + or - 30% of the critical density. Temperatures varied from 288 to 320 K. The two-phase boundary was determined and estimates are given for Tc and Pc for each composition.

03,907
PB95-151494 Not available NTIS
National Inst. of Standards and Technology (NML), Gaithersburg, MD. Radiometric Physics Div.
High Resolution Angle Resolved Photoelectron Spectroscopy Study of N2.
Final rept.
J. B. West, M. A. Hayes, A. C. Parr, T. A. Ferrett, J. L. Dehmer, X. M. Hu, G. V. Marr, J. E. Hardis, and S. H. Southworth. 1990, 3p.
Pub. in Physica Scripta 41, n4 p487-489 1990.

Keywords: *Photoelectron spectroscopy, *Photoionization, *Nitrogen, Near infrared radiation, High resolution, Rydberg series, Nitrogen ions, Autoionization, Reprints.

This is a preliminary report on a series of measurements, using high optical resolution, on the photoionization of the nitrogen molecule in the wavelength region 740 - 780A where there are at least five Ryberg series converging onto the lst excited state of N2(1+) A doublet Pi(u). An advanced electron spectrometer system is used which provides measurements of the angular distribution parameter beta for three members of the ground state of the ion, on a wavelength mesh sufficient to show variations in beta over the width of the autoionizing lines. This study was undertaken to assist in the identification of these series, and to encourage further theoretical work on interaction between electronic and vibrational motion in the region of autoionizing resonances.

03,908
PB95-151502 Not available NTIS
National Inst. of Standards and Technology (NML), Gaithersburg, MD. Center for Atomic, Molecular and Optical Physics.
Laser Cooling.
Final rept.
C. I. Westbrook, and W. D. Phillips. 1991, 3p.
Pub. in McGraw-Hill Yearbook of Science and Technology, p208-210 1991.

Keywords: Temperature range 0000-0013 K, Range(Extremes), Atomic mobilities, Atomic clocks, Doppler effect, Limits, Reprints, *Laser cooling, Millikelvin temperature, Photon recoil.

Laser cooling can reduce the thermal motion of atoms in a gas. Such cooling has achieved temperatures less than one millikelvin. The traditional view of laser cooling involves the Doppler-effect induced velocity dependence of light absorption and predicts a limit on the lowest achievable temperature. The energy imparted to an atom from a single photon recoil also implies a separate limit. Recent experiments have shown that both of these limits can be broken with the help of new laser cooling mechanisms.

03,909
PB95-151551 Not available NTIS
National Inst. of Standards and Technology (NML), Gaithersburg, MD. Atomic and Plasma Radiation Div.
Comprehensive Spectroscopic Data Tabulations and Progress in the Compilation of Atomic Transition Probabilities.
Final rept.
W. L. Wiese. 1991, 10p.
Pub. in Jnl. de Physique IV 1, nC1 p287-296 Mar 91.

Keywords: *Atomic spectroscopy, *Transition probabilities, Atomic energy levels, Wavelengths, Reprints, *Spectroscopic data, Critical data tables, US NIST.

The critical data compilation work as well as the bibliographical efforts of two data centers on atomic spectroscopy at the National Institute of Standards and Technology (formerly the National Bureau of Standards) are briefly reviewed. A complete listing of all current compilations on wavelengths, energy levels and transition probabilities is given. A recently completed large tabulation of atomic transition probabilities for the Fe-group elements comprising about 18000 lines is discussed in some detail, and several data comparisons are presented in order to provide an impression of the current status of these atomic data.

03,910
PB95-151585 Not available NTIS
National Inst. of Standards and Technology (NML), Gaithersburg, MD. Atomic and Plasma Radiation Div.
Spectroscopic Data Tables for Highly-Ionized Atoms.
Final rept.
W. L. Wiese, J. R. Fuhr, W. C. Martin, A. Musgrove, and J. Sugar. 1991, 2p.
Pub. in Zeitschrift fur Physik D 21, pS147-S148 1991.

Keywords: *Atomic spectroscopy, *Multicharged ions, Atomic energy levels, Transition probabilities, Wavelengths, Tables(Data), Reprints, *Spectroscopic data, Critical data tables, US NIST.

Two data centers at the National Institute of Standards and Technology (NIST) are engaged in the critical compilation of atomic spectroscopic data including those for highly ionized atoms: the Atomic Energy Levels Data Center and the Data Center for Atomic Transition Probabilities. Several major compilations have been recently completed, centered on the iron-group elements.

03,911
PB95-151627 Not available NTIS
National Inst. of Standards and Technology (PL), Boulder, CO. Time and Frequency Div.
Trapped Atoms and Laser Cooling.
Final rept.
D. J. Wineland. 1992, 8p.
Pub. in Elementary Modern Physics, Chapter 4, p156-163 1992.

Keywords: *Trapped particles, Laser spectroscopy, Atomic spectroscopy, Atomic clocks, Ion storage, Textbooks, Reprints, *Laser cooling, Ion traps, Millikelvin temperature.

This short article is an 'essay' in the elementary physics text Physics by P.A. Tipler. It is intended as supplementary material to the regular text, but refers to the text material when appropriate. Topics discussed include atomic clocks, atomic spectroscopy, ion trapping, laser cooling, and laser spectroscopy.

03,912
PB95-151635 Not available NTIS
National Inst. of Standards and Technology (PL), Boulder, CO. Time and Frequency Div.

Spin Squeezing and Reduced Quantum Noise in Spectroscopy.
Final rept.
D. J. Wineland, J. J. Bollinger, W. M. Itano, F. L. Moore, and D. J. Heinzen. 1992, 4p.
Pub. in Physical Review A 46, n11 pR6797-6800, 1 Dec 92.

Keywords: *Atomic spectroscopy, Atomic clocks, Frequency standards, Reprints, Squeezed states(Quantum theory), Quantum noise, Correlated states.

We investigate the quantum-mechanical noise in spectroscopic experiments on ensembles of N two-level (or spin-1/2) systems where transitions are detected by measuring changes in state population. By preparing correlated states, here called squeezed spin states, we can increase the signal-to-nose ratio spectroscopy (by approximately N(exp 1/2) in certain cases) over that found in experiments using uncorrelated states. Possible experimental demonstrations of this enhancement are discussed.

03,913
PB95-151999 Not available NTIS
National Inst. of Standards and Technology (NML), Gaithersburg, MD. Chemical Process Metrology Div.
Multiphoton Ionization Spectroscopy Measurements of Silicon Atoms during Vapor Phase Synthesis of Ceramic Particles.
Final rept.
M. R. Zachariah, and R. G. Joklik. 1990, 7p.
Pub. in Jnl. of Applied Physics 68, n1 p311-317 1990.

Keywords: *Vapor phases, *Silicon, *Particle production, *Ceramics, *Ionization, *Chemical vapor deposition, Chemical reactors, Silanes, Spectrum analysis, Concentrating, Clumps, Particle size distribution, Reprints, *Silicon atoms, Multiphoton ionization spectroscopy.

Resonance Enhanced Multi-Photon Ionization spectroscopy has been applied to the problem of detection of gas phase species in a dense particle forming flow. Relative silicon atom profiles of an atmospheric pressure flame reactor producing silica particles have been made using a '2 + 1' ionization scheme. The results have shown that silicon atoms are confined to a very narrow time window in the reactor (less than 15 msec). In addition, the non-resonant background indicated the presence of ionizable clusters and could be a valuable tool for observing the presence and location of small clusters. The effect of varying silane loading changed both the location and magnitude of the silicon concentration observed. The results suggest that chain branching chemistry is important in the production of silicon and that enhancement of pyrolytic relative to oxidative processes occurs as the silane loading is increased.

03,914
PB95-152161 Not available NTIS
National Inst. of Standards and Technology (PL), Boulder, CO. Quantum Physics Div.
High-Precision Calculations of Cross Sections for Low-Energy Electron Scattering by Ground and Excited State of Sodium.
Final rept.
H. L. Zhou, D. W. Norcross, and B. L. Whitten. 1993, 10p.
Grant NSF-PHY86-04504
Sponsored by National Science Foundation, Washington, DC.
Pub. in Proceedings of International Symposium on Correlations and Polarization in Electronic and Atomic Collisions and (e,2e) Reactions (6th), Adelaide, Australia, July 18-21, 1992, p39-48.

Keywords: *Electron-atom collisions, *Electron scattering, *Sodium, Scattering cross sections, Excited states, Ground states, Precision, Orientation, Polarization(Spin alignment), Reprints.

We report progress in a detailed series of calculations intended to provide a comprehensive set of results against which a wide variety of completed, in progress, and proposed measurements can be compared. A high emphasis has been put on numerical accuracy, technical convergence in various parameters (e.g. state expansions and partial wave summations), and inclusion of physical effects (e.g. exchange and core polarization).

03,915
PB95-152203 Not available NTIS

National Inst. of Standards and Technology (NML), Gaithersburg, MD. Time and Frequency Div.
Atomic Oxygen Fine Structure Splittings with Tunable Far Infrared Spectroscopy.
Final rept.
L. R. Zink, K. M. Evenson, F. Matsushima, T. Nelis, and R. Robinson. 1991, 2p.
Pub. in Astrophysical Jnl. 371, n2 pL85-L86 1991.

Keywords: *Oxygen atoms, *Fine structure, Far infrared radiation, Infrared spectroscopy, Interstellar matter, Atmospheric composition, Ground states, Reprints.

We have measured the atomic oxygen (16)O ground state fine structure splittings using a tunable far infrared spectrometer. The triplet P(0) - triplet P(1) splitting is 2,060,069.09 (10) MHz and the triplet P(1) - triplet P(2) splitting is 4,744,777.49 (16) MHz. These frequencies are important for the study of the earth's atmosphere and the interstellar medium.

03,916
PB95-152245 Not available NTIS
National Inst. of Standards and Technology (CAML), Gaithersburg, MD. Statistical Engineering Div.
Effect of Splitting on Estimation of Emission Rate Profiles from Neutron Depth Profiling Spectra.
Final rept.
K. J. Coakley. 1994, 5p.
Pub. in Proceedings of 1993 Section on Physical and Engineering Sciences of the American Statistical Association, San Francisco, CA., August 8-12, 1993, p77-82 1994.

Keywords: Stopping rules(Mathematics), Iterative methods, Estimating, Reprints, *Neutron depth profiling, Cross validation, Data splitting, EM algorithm.

Based on Neutron Depth Profiling spectra, emission rate profiles are estimated using a data splitting and cross-validation approach. In the procedure, data are split into a variable number of parts. From each part, emission rate profiles are estimated using the iterative EM algorithm. The algorithm is halted according to a cross-validation criterion. The estimates from all parts are averaged. As the split becomes finer, the stopping point is reached sooner and the estimate gets smoother. Mean and variance curves are computed for simulated data. An experimental data set is analyzed.

03,917
PB95-152252 Not available NTIS
National Inst. of Standards and Technology (MSEL), Gaithersburg, MD. Reactor Radiation Div.
Analysis of the Effectiveness of Oscillating Radial Collimators in Neutron Scattering Applications.
Final rept.
J. R. D. Copley, and J. C. Cook. 1994, 11p.
Pub. in Nuclear Instruments and Methods in Physics Research A 345, p313-323 1994.

Keywords: *Neutron scattering, *Collimators, Time-of-flight method, Neutron diffraction, Transmissivity, Effectiveness, Reprints, Visibility functions, Radial collimators.

We describe a formalism which allows the transmission properties of oscillating radial collimators to be discussed using the concept of 'visibility' functions. We develop a small angle approximation to the theory which proves to be valuable in describing typical instrumental situations. Independent Monte Carlo (ray-tracing) simulations give very good agreement with analytical results and provide a means for investigating situations where an analytical treatment would be extremely complicated.

03,918
PB95-152906 Not available NTIS
National Inst. of Standards and Technology (PL), Boulder, CO. Quantum Physics Div.
Electron-Impact Ionization of In(+) and Xe(+).
Final rept.
E. W. Bell, N. Djuric, and G. H. Dunn. 1993, 6p.
Contract DE-A105-86ER53237
Sponsored by Department of Energy, Washington, DC.
Pub. in Physical Review A 48, n6 p4286-4291 Dec 93.

Keywords: *Electron-ion collisions, *Indium ions, *Xenon ions, Ionization cross sections, EV range 10-100, EV range 100-200, Electron impact, Excited states, Colliding beams, Autoionization, Reprints.

Absolute ionization cross sections for In(1+) and Xe(1+) by electron impact have been measured from below threshold to 200 eV using the crossed-beams technique. The cross sections for In(1+) were possibly enhanced by indirect ionization processes. The excitation of the ion from the 4d(10)5S(2) ground state to the 4d(9)5S(2)5P state followed by autoionization has been postulated. The In(1+) cross sections show a peak value at about 80 eV. The cross sections for Xe(1+) peak at a value at about 35 eV. Also presented are ionization-rate coefficients and fitting parameters for both ions for temperatures in the range 10(exp 4) K = or < T = or < 10(exp 7) K.

03,919
PB95-152922 Not available NTIS
National Inst. of Standards and Technology (CSTL), Gaithersburg, MD. Thermophysics Div.
Thermal Equilibration Near the Critical Point: Effects Due to Three Dimensions and Gravity.
Final rept.
R. F. Berg. 1993, 7p.
Contract NASA-C-32009-M
Sponsored by National Aeronautics and Space Administration, Washington, DC.
Pub. in Physical Review E 48, n3 p1799-1805 Sep 93.

Keywords: *Critical point, *Liquid-vapor interfaces, Density distribution, Thermodynamic properties, Heat transfer, Relaxation(Mechanics), Temperature gradients, Reprints, *Thermal equilibrium.

Two calculations are presented that clarify how the density profile equilibrates near the liquid-vapor critical point. Both use the equation of heat transfer recently improved to account for the large compressibility near the critical point. Previous work by others indicated that in one dimension the slowest mode of this equation relaxes at a rate four times faster than that predicted by the older, usual equation of heat transfer. However, this is not always true in higher dimensions. The first calculation demonstrates this for the cases of isobaric modes excited by temperature gradients in a rectangle and in a thin disk. For thin experimental cells with isothermal walls the slowest mode is accurately estimated by the usual heat-transfer equation. The second calculation indicates that gravity-induced stratification plays an insignificant role in determining the final relaxation rate. This is done by estimating the size of the V (center dot) Del P term in the improved heat-transfer equation.

03,920
PB95-152963 Not available NTIS
National Inst. of Standards and Technology (PL), Boulder, CO. Time and Frequency Div.
Electrostatic Modes of Ion-Trap Plasmas.
Final rept.
J. Bollinger, D. Heinzen, F. Moore, D. Dubin, W. Itano, and D. Wineland. 1993, 21p.
Sponsored by Office of Naval Research, Arlington, VA. and National Science Foundation, Washington, DC.
Pub. in Physical Review A 48, n1 p525-545 Jul 93.

Keywords: *Trapped particles, *Ion storage, Beryllium ions, Electrostatics, Reprints, Nonneutral plasmas, Ion plasmas, Ion traps, Laser cooling, Penning traps, Paul traps.

The electrostatic modes of a non-neutral plasma confined in a Penning or Paul (rf) trap are discussed in the limit that the Debye length is small compared to the plasma dimensions, and the plasma dimensions are small compared to the trap dimensions. In this limit, the plasma shape is spheroidal and analytic solutions exist for all of the modes. The solutions for the modes of a Paul-trap plasma are a special case of the modes of a Penning-trap plasma. A simple derivation of some of the low-order quadrupole modes is given. Experimental measurements of these mode frequencies on plasmas of laser-cooled Be(+) ions in a Penning trap agree well with the calculations. A general discussion of the higher-order modes is given. The modes provide a nondestructive method for obtaining information on the plasma density and shape. In addition, they may provide a practical limit to the density and number of charged particles that can be stored in a Penning trap.

03,921
PB95-153045 Not available NTIS
National Inst. of Standards and Technology (CSTL), Gaithersburg, MD. Thermophysics Div.
Dynamic Technique for Measuring Normal Spectral Emissivity of Electrically Conducting Solids at High Temperatures with a High-Speed Spatial Scanning Pyrometer.
Final rept.
A. Cezairliyan, and A. P. Miiller. 1993, 6p.
Sponsored by National Aeronautics and Space Administration, Washington, DC.
Pub. in International Jnl. of Thermophysics 14, n5 p1109-1114 1993.

Keywords: *Temperature measurement, *Spectral emission, *Molybdenum, Temperature range 1000-4000 K, High temperature, Optical measurement, Blackbody radiation, Electric conductors, Pyrometers, Emissivity, Reprints.

A dynamic (subsecond) technique is described for measuring normal spectral emissivity of electrically conducting solids at high temperatures, primarily in the range 1800 K up to near their melting point. The basic method involves resistively heating a tubular specimen from ambient temperature through the temperature range of interest in less than 1 s by passing an electrical current pulse through it, while using a high-speed spatial scanning pyrometer to measure spectral radiance temperatures along a 25-mm length on the specimen. This portion of the specimen includes a small rectangular hole that approximates a blackbody cavity. Measurements of spectral radiance temperature of the specimen surface as well as specimen true temperature enable the determination of the normal spectral emissivity of the surface via Planck's law. The applicability of the technique is demonstrated by measurements performed on molybdenum in the range 1900-2850 K.

03,922
PB95-153078 Not available NTIS
National Inst. of Standards and Technology (CSTL), Gaithersburg, MD. Inorganic Analytical Research Div.
Neutron Focusing Lens Using Polycapillary Fibers.
Final rept.
H. Chen, D. F. R. Mildner, and Q. F. Xiao. 1994, 3p.
Contracts DE-FG02-91ER81220, DE-FG02-91ER81411
Sponsored by Department of Energy, Washington, DC.
Pub. in Applied Physics Letters 64, n16 p2068-2070, 18 Apr 94.

Keywords: *Neutron beams, *Neutron transport, *Cold neutrons, Neutron guides, Grazing incidence, Borosilicate glass, Reprints, *Neutron focusing lenses, Neutron reflection, Polycapillary fibers.

Multiple mirror reflection at small grazing angles from the smooth surfaces of the narrow channels of polycapillary fibers can be used to transport, bend, and focus thermal neutron beams. We report the results of the focusing of a polychromatic cold neutron beam using a compact lens of borosilicate fibers and with a focal distance of 57 mm. The intensity profile of the beam at the focus is approximately conical in shape with a full width at half-maximum of 0.49 mm, and with an average gain in intensity of about 20. These experimental results agree well with those obtained by computer simulation.

03,923
PB95-153268 Not available NTIS
National Inst. of Standards and Technology (NML), Gaithersburg, MD. Center for Atomic, Molecular and Optical Physics.
New Mechanisms for Laser Cooling.
Final rept.
C. N. Cohen-Tannoudji, and W. D. Phillips. 1990, 8p.
Pub. in Physics Today 43, n10 p33-40 1990.

Keywords: Laser spectroscopy, Optical pumping, Trapped particles, Reprints, *Laser cooling, Millikelvin temperature, Photon recoil.

Well known physical effects, such as optical pumping and light-shifts, have unexpectedly conspired to improve, by orders of magnitude, the performances of laser cooling and to produce the lowest kinetic temperatures ever measured.

03,924
PB95-153433 Not available NTIS
National Inst. of Standards and Technology (PL), Gaithersburg, MD. Atomic Physics Div.
Hydrogen Balmer Alpha Line Shapes for Hydrogen-Argon Mixtures in a Low-Pressure rf Discharge.
Final rept.
S. Djurovic, and J. R. Roberts. 1993, 8p.
Pub. in Jnl. of Applied Physics 74, n11 p6558-6565, 1 Dec 93.

Keywords: *Hydrogen plasma, *Balmer lines, *Atom-atom collisions, *Ion-atom collisions, Radio frequency discharge, Line broadening, Doppler effect, Plasma spectra, Argon plasma, Line shape, Gas mixtures, Reprints, Reference cells.

The spectral and spatial profiles of atomic hydrogen emission (the Balmer lines H(alpha) and H(beta)) from a low-pressure rf (13.56 MHz) discharge in H2 + Ar mixtures have been studied. The plasma emission was observed in a direction normal to the applied electric field. The H(alpha) profiles exhibit central narrow components and wide components which are due to Doppler broadening. Comparisons of the H(alpha) profiles in a pure hydrogen plasma with those in H2 + Ar mixtures show that collisions of molecular hydrogen ions and hydrogen atoms with argon atoms play a significant role in the production of the H(alpha) profile shapes.

03,925
PB95-153532 Not available NTIS
National Inst. of Standards and Technology (CSTL), Gaithersburg, MD. Surface and Microanalysis Science Div.
Semiclassical Explanation of the Generalized Ramsauer-Townsend Minima in Electron-Atom Scattering.
Final rept.
W. F. Egelhoff. 1993, 4p.
Pub. in Physical Review Letters 71, n18 p2883-2886, 1 Nov 93.

Keywords: *Electron-atom collisions, *Ramsauer effect, Electron scattering, Reprints, Semiclassical methods.

The generalized Ramsauer-Townsend minima which occur, at certain scattering angles, in the intensity of electrons elastically scattered by atoms have been a subject of interest in atomic physics for over sixty years. While quantum mechanical calculations predict these minima with great accuracy, no clear, simple, intuitively appealing description of the underlying scattering processes has been given. It is shown here for the first time that simple semiclassical calculations provide such a description.

03,926
PB95-153615 Not available NTIS
National Inst. of Standards and Technology (PL), Gaithersburg, MD. Ionizing Radiation Div.
Polarization Effects on Multiple Scattering Gamma Transport.
Final rept.
J. E. Fernandez, J. H. Hubbell, A. L. Hanson, and L. V. Spencer. 1993, 52p.
Pub. in Radiation Physics and Chemistry 41, n4/5 p579-630 1993.

Keywords: *Polarization(Waves), *Gamma ray scattering, *X-ray scattering, *Photon-electron collisions, Polarized electromagnetic radiation, Photoelectron emission, Rayleigh scattering, Compton effect, Multiple scattering, Polarized beams, Backscattering, Reprints.

The scattering of X-rays and gamma-rays are events that have strong dependencies on the polarization of the incident and scattered photons. Because of this, scattering problems that can be solved without explicit reference to the state of polarization of the incident and scattered radiation are exceptional. This article reviews available information on polarization effects arising when photons in the X-ray and gamma-ray regime undergo photoelectric effect, coherent (Rayleigh) scattering and incoherent (Compton) scattering by atomic electrons. In addition to descriptions and discussion of these effects, we study the backscattering of gamma-rays from an infinite thickness target excited with a plane slant monodirectional and monochromatic source, using the Boltzmann transport theory and the mathematical representation of polarization introduced by Stokes. Results from this model, for both unpolarized and polarized gamma-ray sources, are compared with computations performed neglecting or averaging polarization effects, showing the limitations of such approximations.

03,927
PB95-161105 Not available NTIS
National Inst. of Standards and Technology (MSEL), Gaithersburg, MD. Reactor Radiation Div.
Crystal Structure of Annealed and As-Prepared HgBa2CaCu2O6+delta Superconductors.
Final rept.
Q. Huang, J. W. Lynn, R. L. Meng, and C. W. Chu. 1993, 9p.
Pub. in Physica C 218, p356-364 1993.

Keywords: *Electron beams, *Calibration, *Calorimeters, *Radiation doses, MeV range 1-10, MeV range 10-100, Temperature measurement, Industrial production, Thermistors, Reprints, *Graphite calorimeters, Radiation processing.

A multi-body graphite calorimeter has been designed for the absolute calibration of high-intensity electron beams in the energy regime of 2 to 12 MeV. This novel calorimeter consists of eight thermally and electrically insulated disks of high-purity graphite that serve as the active calorimetric bodies, arranged in a stacked array and oriented so that the flat surfaces are perpendicular to the electron-beam axis. Calibrated thermistors imbedded in the disks act as temperature sensors. The temperature of each disk is measured in real-time during irradiation by a scanning multichannel digital meter interfaced with a computer-based data acquisition system. The resultant data provide a depth-dose profile from which the electron energy can be calculated. Calorimeters of this type would be useful in standardizing the absorbed dose to passive routine dosimeters in the range of 100 Gy to 50 kGy, typical of that delivered by industrial processing electron beams.

03,928
PB95-161147 Not available NTIS
National Inst. of Standards and Technology (PL), Boulder, CO. Time and Frequency Div.
Quantum Measurements of Trapped Ions.
Final rept.
W. M. Itano, J. C. Bergquist, J. J. Bollinger, F. L. Moore, M. G. Raizen, D. J. Wineland, J. M. Gilligan, and D. J. Heinzen. 1993, 15p.
Sponsored by Office of Naval Research, Arlington, VA.
Pub. in Vistas in Astronomy 37, p169-183 1993.

Keywords: *Ion storage, *Quantum mechanics, Trapped particles, Beryllium ions, Mercury ions, Reprints, *Quantum measurements, Quantum jumps.

When a quantum state is subjected to a measurement and the state is not an eigenstate of the dynamical variable being measured, the outcome is unpredictable. Only the probabilities of the various possible outcomes are predicted by theory. This phenomenon is sometimes discussed in terms of 'wavefunction collapse.' Trapped ions can be used for real, as opposed to 'gedanken' demonstrations of this basic process. In the experiments described here, a single ion, or a few identical ions, were prepared in well defined superpositions of two internal energy eigenstates. The populations of the energy levels were then measured. When the state amplitudes were equal, the population fluctuations were greater than when one of the amplitudes was nearly zero, in agreement with the predictions of quantum mechanics. In other experiments, such as those with atomic beams, the number of atoms under observation fluctuates, and this obscures the fluctuations from other sources. However, if the number of atoms is small and constant, the fundamental quantum mechanical fluctuations can be observed.

03,929
PB95-161220 Not available NTIS
National Inst. of Standards and Technology (NML), Gaithersburg, MD. Molecular Physics Div.
Laser Assisted Collisions at Ultracold Temperatures.
Final rept.
P. S. Julienne, R. Heather, and J. Vigue. 1990, 15p.
Sponsored by Air Force Office of Scientific Research, Bolling AFB, DC.
Pub. in Spectral Line Shapes, v6 p191-205 1990.

Keywords: *Photon-atom collisions, *Atomic collisions, Molecular spectroscopy, Alkali metals, Bound state, Neutral atoms, Temperature range 0000-0013 K, Dimers, Reprints, Laser cooling, Laser trapping, Atom traps, Ultracold atoms, Millikelvin temperature, Associative ionization, Photoassociation spectroscopy.

Recent developments in laser cooling and trapping of neutral atoms have opened the new field of atomic collisions at ultracold temperatures, T < 1 mk. This field offers many new challenges and opportunities for both theory and experiment in the general area of spectral line shapes. We will outline here some of the key problems in this field, and present calculations on several collisional processes which have been observed in atom traps. First the very unusual energy, time and distance scales encountered in ultracold collisions will be described. Second, the molecular physics of excited plus ground alkali dimers will be examined, and the T-dependent rate coefficients will be calculated for processes which lead to loss of alkali atoms from an atom trap. Finally, a new kind of free-bound molecular spectroscopy, photoassociation spectroscopy, will be described which should permit the observation of long range molecular bound states extremely close to the molecular dissociation limit.

03,930
PB95-161527 Not available NTIS
National Inst. of Standards and Technology (NML), Gaithersburg, MD. Chemical Process Metrology Div.
Practical Applications of the ITS-90: Inherent Uncertainties.
Final rept.
B. W. Mangum, E. R. Pfeiffer, and G. F. Strouse. 1991, 12p.
Pub. in Proceedings of Measurement Science Conference, Anaheim, CA., January 31-February 1, 1991, 12p.

Keywords: *Temperature measurement, Temperature range 0013-0065 K, Temperature range 0065-0273 K, Temperature range 0273-0400 K, Temperature range 0400-1000 K, Resistance thermometers, Platinum, Error analysis, Calibration, Uncertainty, Reprints, *International Temperature Scale of 1990, *ITS-90, Fixed points.

We report results of a study of the non-uniqueness of the ITS-90 at temperatures in the range 13.8033 K to 933.473 K (660.323 C) of a variety of capsule-type and long-stem type standard platinum resistance thermometers (SPRTs). The capsule SPRTs were calibrated by comparison techniques and at some fixed points of the ITS-90; the long-stem SPRTs were calibrated at the relevant defining fixed points. In addition, we present results on subrange inconsistencies for several partly overlapping ranges of the ITS-90. Error propagation curves and errors introduced by extrapolations will be discussed also.

03,931
PB95-161634 Not available NTIS
National Inst. of Standards and Technology (PL), Gaithersburg, MD. Ionizing Radiation Div.
ESR-Based Analysis in Radiation Processing.
Final rept.
W. L. McLaughlin, M. F. Desrosiers, and M. C. Saylor. 1993, 27p.
Sponsored by Johnson and Johnson, New Brunswick, NJ.
Pub. in Proceedings of International Kilmer Memorial Conference on the Sterilization of Medical Products, Brussels, Belgium, June 13-15, 1993, p213-239.

Keywords: *Electron spin resonance, *Dosimetry, Radiation doses, Radiation effects, Nuclear medicine, Sterilization, Food irradiation, Polymers, Alanines, Uses, Reprints, *Radiation processing, *ESR dosimetry.

Electron spin resonance (ESR) spectrometry has attracted attention in radiation processing. Not only is ESR analysis of alanine achieving success as a reference dosimetric system, but ESR also provides a means of evaluating short- and long-term effects of radiation on polymers, composites and ceramics, and in the post-irradiation analysis and imaging of absorbed dose in teeth and bone. The broad range of doses (10(exp -1) - 10(exp 8) Gy) and dose rates (up to 10(exp 8) Gy/s) measurable with relatively high precision and accuracy, and the small size, ruggedness, and inexpensiveness of sensor materials, such as L-alpha-alanine pellets and films and other sensor materials (e.g., hydroxyapatite, sugar, quartz, cellulose, etc.), make ESR dosimetry attractive for radiation sterilization dosimetry, radiation treatment planning, nuclear medicine dosimetry, food irradiation and the study of radiation effects on materials. Within the next few years, there may well be impact of this ESR-based analysis on international radiation standards practices and 2D and 3D imaging of radiation dose distributions, especially as the trend toward lowering the cost of the analytical equipment and simplifying its operation continues. ESR dosimetry may, in fact, be the future method of choice for interlaboratory transfer metrology, process validation, and measurement quality assurance.

03,932
PB95-161667 Not available NTIS
National Inst. of Standards and Technology (CSTL), Gaithersburg, MD. Thermophysics Div.
Measurement of Surface Tension of Tantalum by a Dynamic Technique in a Microgravity Environment.
Final rept.
A. P. Miiller, and A. Cezairliyan. 1993, 13p.
Pub. in International Jnl. of Thermophysics 14, n5 p1063-1075 1993.

Keywords: *Interfacial tension, *Tantalum, *Weightlessness simulation, *High temperature, Melting points, Research aircraft, Dynamic tests, Thermophysical properties, Reprints.

A dynamic technique has been used in a microgravity environment to measure the surface tension of tantalum at its melting point. The basic method involves resistively heating a tubular specimen from ambient temperature to temperatures above its melting point in about 1 s by passing an electrical current pulse through it, while simultaneously measuring the pertinent experimental quantities with millisecond resolution. A balance between the magnetic and the surface tension forces acting on the specimen is achieved by splitting the current after it passes through the specimen tube and returning a fraction of the current along the tube axis and the remaining fraction concentrically outside of the specimen. Values for surface tension are determined from measurements of the equilibrium dimensions of the molten specimen tube and the magnitudes of the currents. Rapid melting experiments were performed during microgravity simulations with NASA's KC-135 aircraft and the results were analyzed, yielding a value of 2.07 + or - 0.06 N/m for the surface tension of tantalum at its melting point.

03,933
PB95-161774 Not available NTIS
National Inst. of Standards and Technology (PL), Gaithersburg, MD. Electron and Optical Physics Div.
Spin-Resolved Elastic Scattering of Electrons from Sodium.
Final rept.
S. R. Lorentz, R. E. Scholten, J. J. McClelland, M. H. Kelley, and R. J. Celotta. 1993, 7p.
Sponsored by Department of Energy, Washington, DC.
Pub. in Physical Review A 47, n4 p3000-3006 Apr 93.

Keywords: *Electron-atom collisions, *Sodium, Polarization(Spin alignment), Optical pumping, EV range 1-10, EV range 10-100, Electron scattering, Elastic scattering, Asymmetry, Reprints.

Angle-resolved ratios of the separate triplet and singlet spin channel cross sections have been measured for elastic scattering of spin-polarized electrons from optically pumped spin-polarized sodium atoms. The triplet-to-singlet ratios are reported at incident energies of 4.1, 10.0, and 20.0 eV for scattering angles from 20 deg to 140 deg. The data demonstrate that spin-exchange scattering plays an important role in the description of electron scattering from sodium at these energies. Comparisons are made with the results of several close-coupling theoretical calculations.

03,934
PB95-161840 Not available NTIS
National Inst. of Standards and Technology (PL), Gaithersburg, MD. Atomic Physics Div.
sigma+-sigma- Optical Molasses in a Longitudinal Magnetic Field.
Final rept.
M. Walhout, J. Dalibard, S. L. Rolston, and W. D. Phillips. 1992, 11p.
Sponsored by Office of Naval Research, Arlington, VA.
Pub. in Jnl. of the Optical Society of America B 9, n11 p1997-2007.

Keywords: Fokker-Planck equation, Diffusion coefficient, Magnetic fields, Numerical solution, Magnetooptics, Reprints, *Optical molasses, *Atom cooling, Polarized gradient cooling, Atom traps.

We investigate the effect of a longitudinal magnetic field on the orientational cooling mechanism that operates both in sigma(+) - sigma(-) optical molasses and in a magneto-optical trap. For an atom with different Lande g factors in its ground and excited states, single-photon scattering and stimulated Raman scattering are resonant at different field-dependent velocities. The sharp polarization-gradient feature in the force-versus-velocity curve may therefore be translated to a velocity at which the Doppler force is dominant. In addition to this, we find that the momentum diffusion coefficient can grow as the field is increased. By numerically solving a semiclassical Fokker-Planck equation, we show that these effects lead to a field-induced inhibition of efficient sub-Doppler cooling for atoms with unequal g factors. Our treatment also enables us to discuss other phenomena that are accessible only if both Doppler and polarization-gradient effects are included in the calculation.

03,935
PB95-161964 Not available NTIS
National Inst. of Standards and Technology (EEEL), Gaithersburg, MD. Electricity Div.
Kinetic-Energy Distributions of Ions Sampled from Argon Plasmas in a Parallel-Plate, Radio-Frequency Reference Call.
Final rept.
J. K. Olthoff, R. J. Van Brunt, S. B. Radovanov, J. A. Rees, and R. Surowiec. 1994, 11p.
Pub. in Jnl. of Applied Physics 75, n1 p115-125 Jan 94.

Keywords: *Radio frequency discharge, *Gas discharges, *Argon ions, Argon plasma, Kinetic energy, Reprints, Reference cells.

Kinetic-energy distributions are presented for ions sampled from 13.56-MHz discharges in argon in a capacitively-coupled, parallel-plate, Gaseous Electronics Conference (GEC) radio-frequency reference cell. The cell was modified to allow sampling of ions through an orifice in the grounded electrode. Kinetic-energy distributions are presented for Ar(1+), Ar(2+), Ar2(1+), and ArH(1+), and several trace ions for plasma pressures ranging from 1.3 Pa, where ion-atom collisions in the plasma sheath are not important, to 33.3 Pa, where collisions are important. Applied peak-to-peak radio-frequency (rf) voltages of 50, 100, and 200 V were used, and the current and voltage waveforms at the powered electrode were measured. Dependences of the ion fluxes, mean energies, and kinetic-energy distributions on gas pressure and applied rf voltage are interpreted in terms of possible ion-collision processes.

03,936
PB95-162053 Not available NTIS
National Inst. of Standards and Technology (PL), Gaithersburg, MD. Quantum Metrology Div.
Production and Characterization of Ion Beam Sputtered Multilayers.
Final rept.
J. Pedulla, and R. D. Deslattes. 1994, 11p.
Pub. in Society of Photo-Optical Instrumentation Engineers Proceedings, v2011 p299-309 Jan 94.

Keywords: *X-ray optics, Extreme ultraviolet radiation, Sputtering, Polishing, Reprints, Ion beam deposition, Multilayers.

We report on the application of low pressure ion beam sputtering combined with simultaneous (neutralized) ion beam polishing to the production of multilayer structures for x-ray optics. Initial examination of these structures by high resolution diffractometry at 0.154 nm indicates that the structures exhibit a high degree of structural perfection.

03,937
PB95-162574 Not available NTIS
National Inst. of Standards and Technology (NML), Gaithersburg, MD. Electron and Optical Physics Div.
Labeling Conventions in Isoelectronic Sequences - Reply.
Final rept.
E. B. Saloman, and Y. K. Kim. 1990, 2p.
Pub. in Physical Review A 42, n3 p1824-1825 1990.

Keywords: *Isoelectronic sequence, Atomic energy levels, Relativistic effects, Multicharged ions, Electron correlation, Labelling, Reprints, *Sulfur-like ions.

We agree with the Comment by Maniak and Curtis (Phys. Rev. Al (1990)) that qualitative isoelectronic behavior of low-lying energy levels of sulfur-like ions with high nuclear charges, Z, can easily be understood using single jj configuration labels. However, such labels are, in general, useful only for high-Z ions. We do not recommend mixing numerical results from multiconfiguration calculations with those from single configuration calculations because such a mixed usage may introduce artificial discontinuities in Z dependence, defeating the main advantage of studies along an isoelectronic sequence.

03,938
PB95-162657 Not available NTIS
National Inst. of Standards and Technology (NML), Gaithersburg, MD. Electron and Optical Physics Div.
Surface Magnetic Microstructural Analysis Using Scanning Electron Microscopy with Polarization Analysis (SEMPA).
Final rept.
M. R. Scheinfein, J. Unguris, D. T. Pierce, and R. J. Celotta. 1990, 2p.
Pub. in Proceedings of International Congress for Electron Microscopy (12th), Seattle, WA., August 12-18, 1990, p216-217.

Keywords: *Electron microscopes, *Magnetic materials, *Polarization, Ferromagnetism, Microstructure, Images, Domain walls, Secondary emission, Electrons, Reprints, SEMPA(Scanning electron microscope with polarization analysis), Scanning electron microscope, Secondary electrons.

High resolution imaging of magnetic microstructure has important ramifications for both fundamental studies of magnetism and the technology surrounding the magnetic recording industry. A focused beam of electrons excites secondary electrons on a ferromagnet's surface. The secondaries leave the solid with an electron spin polarization which is characteristic of the net spin density in the ferromagnet. This is related directly to the sample magnetization. By scanning the beam and analyzing the secondary electron spin polarization at each point, a magnetization map of the ferromagnet's surface is generated.

03,939
PB95-162970 Not available NTIS
National Inst. of Standards and Technology (NML), Gaithersburg, MD. Chemical Process Metrology Div.
Systematic Studies of the Effect of a Bandpass Filter on a Josephson-Junction Noise Thermometer.
Final rept.
R. J. Soulen, W. E. Fogle, and J. H. Colwell. 1991, 4p.
Pub. in Institute of Electrical and Electronics Engineers Transactions on Magnetics 27, n2 p2920-2923 1991.

Keywords: *Bandpass filters, *Noise temperature, *Superconductivity, Temperature measurement, Temperature scales, Fixed points(Mathematics), Variance(Statistics), Josephson junctions, Reprints, *Noise thermometers, SQUID noise thermometer.

The authors present the results of an extensive study of the effect of a filter upon the performance of a resistive SQUID noise thermometer used to define an absolute temperature scale below 1 K. Agreement between the model for this effect and the experimental results indicates that the temperature scale defined by this noise thermometer is accurate to 0.1%.

03,940
PB95-162988 Not available NTIS
National Inst. of Standards and Technology (CSTL), Gaithersburg, MD. Process Measurements Div.
Systematic Studies of the Effect of a Post-Detection Filter on a Josephson-Junction Noise Thermometer.
Final rept.
R. J. Soulen, W. E. Fogle, and J. H. Colwell. 1990, 2p.
Pub. in Physica B 165, p111-112 Aug 90.

Keywords: *Filters, *Noise temperature, *Thermometers, Temperature measurement, Temperature scales, Audio frequencies, Reprints, *Noise thermometers, SQUID noise thermometer.

The authors present the results of an extensive study of the effect of a filter upon the performance of a resistive SQUID noise thermometer used to define an absolute temperature scale below 1 K. Agreement between the theory and the experiment indicates that the scale defined by this noise thermometer is accurate to 0.1%.

03,941
PB95-163226 Not available NTIS
National Inst. of Standards and Technology (NML), Gaithersburg, MD. Ionizing Radiation Div.
Problems Related to the Determination of Mass Densities of Evaporated Reference Deposits.
Final rept.
H. Tagziria, J. Pauwels, J. Verdonk, D. M. Gilliam, R. D. Scott, J. Byrne, P. Dawber, J. Van Gestel, and R. Eykens. 1991, 10p.
Pub. in Nuclear Instruments and Methods in Physics Research A 303, n1 p123-132 1991.

Keywords: Experiment design, Lithium fluorides, Lithium 6, Boron 10, Reprints, *Reference deposits, Surface density, Mass density.

The accurate characterization of the surface density of thin deposits is of highest importance in certain experiments. However, if accuracies better than + or - 0.5% are to be quoted, careful consideration of secondary effects is necessary, as these effects may generate serious errors. The details of the radial surface density distribution, the formation of edge effects, and the evaluation of effective deposit diameters are discussed for the case of measurements and observations made

during the preparation and characterization of (6)LiF and (10)B reference deposits, which were employed in a recent determination of the free neutron lifetime. Theoretical considerations are in excellent agreement with the experimental data obtained.

03,942
PB95-163283 Not available NTIS
National Inst. of Standards and Technology (NML), Gaithersburg, MD: Center for Atomic, Molecular and Optical Physics.
How Accurate Are the Josephson and Quantum Hall Effects and QED.
Final rept.
B. N. Taylor, and E. R. Cohen. 1991, 5p.
Pub. in Physics Letters A 153, n6-7 p308-312 1991.

Keywords: *Quantum electrodynamics, *Josephson effect, Fundamental constants, Sommerfeld constant, Accuracy, Reprints, *Quantum Hall effect, Von Klitzing constant, Fine structure constant.

We assess the accuracy of the theories of the Josephson and quantum Hall effects by testing precisely the exactness of the theoretically predicted relations K(J) = 2e/h and R(K) = h/e(squared), where K(J) and R(K) are the phenomenological Josephson and von Klitzing constants, respectively. Using the reported results of the most accurate determinations of various fundamental constants and related quantities currently available, we find K(J)/(2e/h) = 1 - (219 + or - 103) X 10(exp -9) and R(K)/(h/e(squared)) = 1 + (60 + or - 22) X 10(exp -9). If, as theory predicts, the relations are assumed to be exact, quantum electrodynamics (QED) may be tested precisely by comparing the QED value of the inverse fine-structure constant obtained from the electron magnetic moment anomaly, with the essentially QED-independent value derived from all of the other data.

03,943
PB95-163879 Not available NTIS
National Inst. of Standards and Technology (NML), Gaithersburg, MD. Center for Atomic, Molecular and Optical Physics.
Measurements of Fluorescence from Cold Atoms: Localization in Three-Dimensional Standing Waves.
Final rept.
C. I. Westbrook, P. S. Jessen, C. E. Tanner, R. N. Watts, W. D. Phillips, P. D. Lett, and S. L. Rolston. 1991, 16p.
Pub. in AIP Conf. Proc. At. Phys. 12, v233 p89-104 1991.

Keywords: *Resonance fluorescence, Optical heterodyning, Three dimensional, Standing waves, Power spectra, Reprints, *Ultracold atoms, Doppler velocity spectroscopy, Optical molasses, Laser cooling, Laser trapping.

We have developed a heterodyne detector to measure the power spectrum of the resonance fluorescence from laser cooled atoms. With this detector we have demonstrated that cooled atoms can be localized in a three-dimensional optical standing wave. We have also used it to measure the temperature of the atoms in optical molasses and our results are consistent with those measured by other methods.

03,944
PB95-163887 Not available NTIS
National Inst. of Standards and Technology (NML), Gaithersburg, MD. Center for Atomic, Molecular and Optical Physics.
Localization of Atoms in a Three-Dimensional Standing Wave.
Final rept.
C. I. Westbrook, R. N. Watts, C. E. Tanner, P. D. Lett, P. L. Gould, S. L. Rolston, and W. D. Phillips. 1990, 4p.
Pub. in Physical Review Letters 65, n1 p33-36 1990.

Keywords: Optical heterodyning, Resonance fluorescence, Standing waves, Three dimensional, Reprints, *Sodium atoms, *Atom traps, Optical molasses, Dicke narrowing, Laser cooling, Laser trapping.

We have a heterodyne technique to observe the spectrum of resonance fluorescence from sodium atoms in optical molasses. The spectra show a very narrow feature which we attribute to Dicke narrowing of the fluorescence of atoms localized to less than a wavelength in three dimensional potential wells.

03,945
PB95-163986 Not available NTIS
National Inst. of Standards and Technology (NML), Gaithersburg, MD. Inorganic Analytical Research Div.
Measurement of the (93)Nb(n,2n) (92m)Nb Cross Section in a (235)U Fission Spectrum.
Final rept.
T. G. Williamson, and G. P. Lamaze. 1990, 5p.
Sponsored by Virginia Univ., Charlottesville. Dept. of Nuclear Engineering and Engineering Physics.
Pub. in Proceedings of ASTM-EURATOM Symposium (7th) on Reactor Dosimetry, Strasbourg, France, August 27-31, 1990, p371-375.

Keywords: *Niobium 93 target, *Neutron reactions, *Neutron cross sections, Neutron monitors, Fast neutrons, Fission spectra, Metastable state, Radioactivation, Dosimetry, Uranium 235, Niobium 92, Reprints.

When niobium is used as a fast neutron monitor, the isotopes (93m)Nb and (92m)Nb are produced. Much interest has been placed on the (93)Nb(n,n') (93m)Nb reaction because of the long half life of the product isotope and the low threshold energy of the reaction. On the other hand, the (93)Nb(n,2n) (92m)Nb reaction product has a half life of 10.1 days and the reaction has a threshold energy of about 9 MeV. It is useful for relatively short irradiations and for cases in which information is desired about high energy neutrons, such as in fusion applications. The spectrum-averaged cross section for the reaction (93)Nb(n,2n) (92m)Nb in a (235)U fission spectrum has been measured. The measured value is 0.433 + or - 0.017 mb. Comparisons are made with calculated values.

03,946
PB95-164497 Not available NTIS
National Inst. of Standards and Technology (NEL), Gaithersburg, MD. Center for Manufacturing Engineering.
Metrology.
Final rept.
J. A. Simpson. 1991, 3p.
Pub. in Encyclopedia of Physics, p723-725 1991.

Keywords: *Metrology, Units of measurement, Nomenclature, Interferometry, Quality control, Symbols, Mass, Time, Reprints, Weights and measures.

Metrology is the science of measurement, and if broadly construed would encompass the bulk of experimental physics. The term is usually used in a more restricted sense to refer to that portion of measurement science used to provide, maintain, and disseminate a consistent set of units; to provide support for the enforcement of equity in trade by weights and measures laws; or as an adjunct to quality control in manufacturing.

03,947
PB95-164646 Not available NTIS
National Inst. of Standards and Technology (PL), Boulder, CO. Quantum Physics Div.
Validation of the Inverse Square Law of Gravitation Using the Tower at Erie, Colorado, USA.
Final rept.
C. Speake, J. Faller, J. Y. Cruz, and J. C. Harrison. 1990, 3p.
Sponsored by Defense Mapping Agency, Fairfax, VA.
Pub. in Gravity, Gradiometry, and Gravimetry, Symposium No. 103, Edinburgh, Scotland, August 8-10, 1989, p17-19 1990.

Keywords: *Gravitation, *Gravity, Basic interactions, Validation, Measurement, Towers, Tests, Reprints, Inverse square laws, Fifth force.

Eckhardt et al (1988) point out that gravity measurements on towers provide a straightforward way of testing Newton's inverse square law of gravitation, whose validity in the distance range of 10-1000 m has been repeatedly questioned during the last decade. Eckhardt et al (loc. cit.) and Romaides et al (1989) have interpreted their measurements on the 600 m WTVD tower in North Carolina as evidence for non-Newtonian gravitation. This paper describes a similar experiment using a 300 m meteorological tower at Erie on the plains of Colorado some 20 km east of Boulder. Gravity was measured at eight levels and, in contrast with the results from North Carolina, these measurements are in excellent agreement with values obtained by upward continuation of surface values using Newton's inverse square law.

03,948
PB95-168514 Not available NTIS
National Inst. of Standards and Technology (PL), Boulder, CO. Time and Frequency Div.
Interference in the Resonance Fluorescence of Two Trapped Atoms.
Final rept.
U. Eichmann, J. C. Bergquist, J. J. Bollinger, M. G. Raizen, D. J. Wineland, J. M. Gilligan, and W. M. Itano. 1994, 6p.
Pub. in Proceedings of International Conference on Laser Spectroscopy (11th), Hot Springs, VA., June 13-18, 1993, p43-48 1994.

Keywords: *Optical interference, *Resonance fluorescence, Trapped particles, Polarization(Waves), Laser radiation, Mercury ions, Ion storage, Reprints, Laser cooling, Atom traps, Complementarity.

We report the observation of interference in the resonance fluorescence of two localized atoms irradiated by laser light. The fringe visibility can be explained in terms of X-ray scattering by a harmonic crystal and by simple 'which-path' arguments for the scattered photons. Polarization-sensitive detection of the resonance fluorescence demonstrates complementarity without invoking the position-momentum uncertainty relation.

03,949
PB95-168698 Not available NTIS
National Inst. of Standards and Technology (MEL), Gaithersburg, MD. Precision Engineering Div.
Force Calibrations in the Nanonewton Regime.
Final rept.
L. P. Howard, and E. C. Teague. 1994, 5p.
Pub. in Proceedings of American Society for Precision Engineering Annual Meeting, Cincinnati, OH., October 2-7, 1994, p13-17.

Keywords: *Atomic force microscopy, *Calibration, Electrical measurement, Prototypes, Tribology, Pens, Reprints, *Force measurement, *Nanohardness, NanoNewton forces, Nanotechnology, Force balances.

The paper describes an instrument and experiments for calibrating forces encountered with atomic force microscopes (AFMs) and nanohardness instruments. Calibration needs of such instruments are examined and a prototype calibration instrument is briefly introduced. Our force balance performs nulling measurements using a capacitance gage for displacement detection, a magnet and coil actuator for application of nulling forces and a Proportional Integral Derivative (PID) control system. Experiments using electrical power measurements to calibrate the force balance magnet and coil actuator are described. Our experiments were modeled after Absolute Ampere and kilogram comparisons to S1 electrical units. Actual applied forces of tens of microNewtons were compared against the electrical calibrations to an agreement of approximately 3%. For forces of tens of microNewtons, type A uncertainties of approximately 14 nN were observed with estimated type B uncertainties of about 1.7% as a coefficient of variation (CV).

03,950
PB95-168746 Not available NTIS
National Inst. of Standards and Technology (PL), Boulder, CO. Time and Frequency Div.
Laser Cooling of Trapped Ions.
Final rept.
W. M. Itano, J. C. Bergquist, J. J. Bollinger, and D. J. Wineland. 1992, 19p.
Sponsored by Office of Naval Research, Arlington, VA. and Air Force Office of Scientific Research, Bolling AFB, DC.
Pub. in Proceedings of International School of Physics: Laser Manipulation of Atoms and Ions, Varenna, Italy, July 9-19, 1991, p519-537 1992.

Keywords: *Ion storage, Trapped particles, Atomic spectroscopy, Hyperfine structure, Laser spectroscopy, Reprints, *Laser cooling, Nonneutral plasmas, Penning traps, Paul traps.

Laser cooling techniques which have been applied to trapped ions are reviewed. We describe cooling in terms of mode coupling by a parametric drive. Experiments and theory which illustrate Doppler cooling, resolved-sideband cooling, and Sisyphus cooling are described. Differences of laser cooling in Penning and Paul traps are discussed. Sympathetic cooling of one ion species by another is also discussed.

03,951
PB95-168910 Not available NTIS
National Inst. of Standards and Technology (EEEL), Boulder, CO. Electromagnetic Technology Div.

Metrological Accuracy of the Electron Pump.
Final rept.
J. M. Martinis, M. Nahum, and H. D. Jensen. 1994, 4p.
Sponsored by Office of Naval Research, Arlington, VA.
Pub. in Physical Review Letters 72, n6 p904-907, 7 Feb 94.

Keywords: Electron pumping, Electron tunneling, Error analysis, Metrology, Accuracy, Reprints, *Electron pumps.

We have operated a five-junction electron pump with an error for transferring electrons of approximately 0.5 part per 10(exp 6). The error predicted from existing theory is several orders of magnitude smaller, thus implying that our present understanding of the Coulomb blockade is incomplete. We conjecture that the errors arise from photon-assisted tunneling, where the photon energy is supplied by noise from the environment.

03,952
PB95-169322 Not available NTIS
National Inst. of Standards and Technology (PL), Boulder, CO. Time and Frequency Div.
Recent Experiments on Trapped Ions at the National Institute of Standards and Technology.
Final rept.
D. J. Wineland, J. C. Bergquist, J. J. Bollinger, J. M. Gilligan, M. G. Raizen, D. J. Heinzen, C. S. Weimer, C. H. Manney, W. M. Itano, and F. L. Moore. 1992, 15p.
Sponsored by Office of Naval Research, Arlington, VA. and Air Force Office of Scientific Research, Bolling AFB, DC.
Pub. in Proceedings of International School of Physics: Laser Manipulation of Atoms and Ions, Varenna, Italy, July 9-19, 1991, p553-567 1992.

Keywords: *Ion storage, Trapped particles, Hyperfine structure, Atomic spectroscopy, Laser spectroscopy, High resolution, Radiation pressure, Optical spectra, Beryllium ions, Beryllium 9, Mercury ions, Mercury 199, Reprints, Laser cooling, Penning traps, Paul traps.

These lecture notes summarize the work performed by the Ion Storage group of NIST in the year preceeding July, 1991. Specific topics discussed are (1) the measurement of a hyperfine pressure shift in (9)Be(1+); (2) construction and testing of a Paul trap with linear geometry; (3) density limitations in a Penning trap; (4) a search for anomalous spin-dependent forces using spectroscopy of (9)Be(1+) ions; (5) the theory of Sisyphus cooling for a bound atom; (6) the observation of 'atomic projection' noise; (7) a precision measurement of the g(j) factor of Mg(1+); (8) subharmonic excitation of a single electron; (9) observation of time varying radiation pressure forces; and (10) high resolution optical spectroscopy of (199)Hg(1+) ions.

03,953
PB95-169330 Not available NTIS
National Inst. of Standards and Technology (PL), Boulder, CO. Time and Frequency Div.
High-Resolution Atomic Spectroscopy of Laser-Cooled Ions.
Final rept.
D. J. Wineland, J. C. Bergquist, J. J. Bollinger, J. M. Gilligan, M. G. Raizen, C. S. Weimer, C. H. Manney, W. M. Itano, and F. L. Moore. 1992, 14p.
Sponsored by Office of Naval Research, Arlington, VA. and Air Force Office of Scientific Research, Bolling AFB, DC.
Pub. in Proceedings of International School of Physics: Laser Manipulation of Atoms and Ions, Varenna, Italy, July 9-19, 1991, p539-552 1992.

Keywords: *Ion storage, *Atomic spectra, Atomic spectroscopy, High resolution, Hyperfine structure, Laser spectroscopy, Beryllium ions, Beryllium 9, Mercury ions, Mercury 199, Reprints, Laser cooling, Penning traps, Paul traps, Nonneutral plasmas.

Techniques for obtaining high-resolution atomic spectra of laser-cooled ions are illustrated by on-going experiments at NIST. In one experiment, an rf oscillator is locked to a nuclear spin-flip hyperfine transition (frequency approx = 3.03 X 10(exp 8) Hz) in (9)Be(1+) ions which are stored in a Penning trap and sympathetically laser-cooled. Stability is better than 3 X 10(exp -12) tau (sup -1/2) and uncertainty in Doppler shifts is estimated to be less than 5 X 10(exp -15). In a second experiment, a stable laser is used to probe an electric quadrupole transition (frequency approx = 1.07 X 10(exp 15) Hz) in a single laser-cooled (199)Hg(1+) ion stored in a Paul trap. The measured Q value of this transition is approximately 10(exp 13). Future possible experiments are also discussed.

03,954
PB95-169348 Not available NTIS
National Inst. of Standards and Technology (PL), Boulder, CO. Time and Frequency Div.
Laser-Cooled Positron Source.
Final rept.
D. J. Wineland, C. S. Weimer, and J. J. Bollinger. 1993, 11p.
Pub. in Hyperfine Interactions 76, p115-125 1993.

Keywords: *Positron sources, Ion storage, Beryllium ions, Beryllium 9, Feasibility, Reprints, Laser cooling, Penning traps, Millikelvin temperature, Nonneutral plasmas.

We examine, theoretically, the feasibility of producing a sample of cold (= or < 4 K), high-density (approx 10(exp 10)/cc) positrons in a Penning trap. We assume (9)Be(1+) ions are first loaded into the trap and laser-cooled to approximately 10 mK where they form a uniform density column centered on the trap axis. Positrons from a moderator are then injected into the trap along the direction of the magnetic field through an aperture in one endcap of the trap so that they intersect the (9)Be(1+) column. Positron/(9)Be(1+) Coulomb collisions extract axial energy from the positrons and prevent them from escaping back out the entrance aperture. Cooling provided by cyclotron radiation and sympathetic cooling with the laser-cooled (9)Be(1+) ions causes the positrons to eventually coalesce into a cold column along the trap axis. We present estimates of the efficiency for capture of the positrons and estimates of densities and temperatures of the resulting positron column. Positrons trapped in this way may be interesting as a source for antihydrogen production, as an example of a quantum plasma, and as a possible means to produce a bright beam of positrons by leaking them out along the axis of the trap.

03,955
PB95-175022 Not available NTIS
National Inst. of Standards and Technology (PL), Gaithersburg, MD. Ionizing Radiation Div.
Multi-Stage, Position Stabilized Vibration Isolation System for Neutron Interferometry.
Final rept.
M. Arif, D. E. Brown, G. L. Greene, R. Clothier, and K. Littrell. 1994, 7p.
Pub. in Proceedings of Society of Photo-Optical Instrumentation Engineers: Vibration Monitoring and Control, San Diego, CA., July 28-29, 1994, v2264 p20-26.

Keywords: *Vibration isolators, Computerized control systems, Pneumatic servomechanisms, Degrees of freedom, Proximity devices, Interferometers, Inclinometers, Metrology, Design, Reprints, *Neutron interferometry, CNRF facility, US NIST.

A two stage, position stabilized vibration isolation system has been constructed and is now in operation at the Cold Neutron Research Facility of the National Institute of Standards and Technology, Gaithersburg, Md. The system employs pneumatic isolators with a multiple input/multiple output pneumatic servo system based upon pulse width modulation control loops. The first stage consists of a 40,000 kg reinforced concrete table supported by pneumatic isolators. A large environmentally isolated laboratory enclosure rests on the concrete table. The second stage consists of a 3000 kg granite optical table located within the enclosure and supported by another set of pneumatic isolators. The position of the two stages is monitored by proximity sensors and inclinometers with 12 degrees of freedom. The system controls 12 independent pneumatic airsprings. The signals from these sensors are fed into a personal computer based control system. The control system has maintained the position of the two stages to better than 1 micrometer in translation and 5 (micro)rad in orientation for a period of a few months. A description of the system and its characteristics is given.

03,956
PB95-175105 Not available NTIS
National Inst. of Standards and Technology (PL), Boulder, CO. Time and Frequency Div.
Experimental Results on Normal Modes in Cold, Pure Ion Plasmas.
Final rept.
J. Bollinger, D. Heinzen, F. Moore, D. Wineland, C. Weimer, and W. M. Itano. 1993, 6p.
Sponsored by Office of Naval Research, Arlington, VA.
Pub. in Proceedings of Conference on Strongly Coupled Plasma Physics, Rochester, NY, August 17-21, 1992, p393-398 1993.

Keywords: *Ion storage, *Beryllium ions, Strongly coupled plasmas, Cold plasmas, Beryllium 9, Trapping(Charged particles), Reprints, Electrostatic modes, Normal modes, Nonneutral plasmas, Penning traps, Ion plasmas, Ion traps.

Experimental measurements of some of the low order electrostatic modes of a nonneutral plasma of (9)Be(1+) ions stored in a Penning trap are discussed. The ions are laser-cooled and typically are strongly coupled with couplings as large as 200 to 300. The measured mode frequencies agree well with a cold fluid calculation. The modes provide a nondestructive method for obtaining information on the plasma density and shape. In addition, the mode excitation by field asymmetries may provide a practical limit to the density and number of charged particles that can be stored in a Penning trap. Future measurements of the damping of the modes should provide information on the plasma viscosity in a strongly correlated plasma.

03,957
PB95-175113 Not available NTIS
National Inst. of Standards and Technology (PL), Boulder, CO. Time and Frequency Div.
Non-Neutral Ion Plasmas and Crystals, Laser Cooling, and Atomic Clocks.
Final rept.
J. J. Bollinger, D. J. Wineland, and D. H. E. Dubin. 1994, 12p.
Sponsored by Office of Naval Research, Arlington, VA.
Pub. in Phys. Plasmas 1, n5 p1403-1414 May 94.

Keywords: *Ion storage, *Atomic clocks, Strongly coupled plasmas, Brillouin flow, Trapping(Charged particles), Reprints, Penning traps, Paul traps, Ion plasmas, Ion traps, Millikelvin temperature, Laser cooling, Nonneutral plasmas.

Experimental work which uses Penning and Paul traps to confine non-neutral ion plasmas is discussed. Penning traps use a static uniform magnetic field and a static electric field to confine ions. The Paul trap uses the ponderomotive force from inhomogeneous radio-frequency fields to confine ions to a region of minimum field strength. In many atomic physics experiments, these traps are designed to produce a harmonic restoring force for small numbers of stored ions (< 10,000). Under these conditions and at low temperatures, both traps produce plasmas with simple shapes whose mode properties can be calculated exactly. Laser cooling has been used to reduce the temperature of trapped ions to less than 10 mK with ion spacings less than 20 micrometers. At such temperatures and interion spacings, the Coulomb potential energy between nearest neighbor ions is greater than the ion thermal energy and the ions exhibit spatial correlations characteristic of a liquid or crystal. Laser beams also apply a torque which, by changing the plasma angular momentum, changes the plasma density. Atomic clocks are an important application of ion trap plasmas. Better control of the plasma dynamics will reduce fluctuations in the relativistic time dilation, yielding better clocks.

03,958
PB95-176137 Not available NTIS
National Inst. of Standards and Technology (PL), Gaithersburg, MD. Quantum Metrology Div.
Electron-Ion-X-ray Spectrometer System.
Final rept.
S. H. Southworth, M. A. MacDonald, T. LeBrun, and R. D. Deslattes. 1994, 5p.
Contract DE-W-31-109-ENG-38
Sponsored by Department of Energy, Washington, DC.
Pub. in Nuclear Instruments and Methods in Physics Research A 347, p499-503 1994.

Keywords: *Electron spectrometers, *Mass spectrometers, *X ray spectrometers, *Spectrometers, Inner-shell excitation, Electron spectroscopy, Ion spectroscopy, X ray spectroscopy, Coincidence spectrometry, Fluorescence spectroscopy, Synchrotron radiation, Electron spectra, Design, Reprints.

We describe a spectrometer system developed for electron, ion, and X-ray spectroscopy of gas-phase atoms and molecules following inner-shell excitation by tunable synchrotron radiation. The instrumentation and experimental methods are discussed, and examples are given of electron spectra and coincidence spectra between electrons and fluorescent X-rays.

03,959
PB95-176244 Not available NTIS
National Inst. of Standards and Technology (PL), Boulder, CO. Time and Frequency Div.
Electrostatic Modes as a Diagnostic in Penning-Trap Experiments.
Final rept.
C. S. Weimer, J. J. Bollinger, F. L. Moore, and D. J. Wineland. 1994, 12p.
Sponsored by Office of Naval Research, Arlington, VA.
Pub. in Physical Review A 49, n5 p3842-3853 May 94.

Keywords: *Electron clouds, Diagnostic techniques, Reprints, *Electrostatic modes, Nonneutral plasmas, Penning traps.

A subset of the electrostatic modes of a cold cloud of electrons, a non-neutral electron plasma, trapped in a Penning trap has been observed and identified using a recent theoretical model. The detection of these modes is accomplished using electronic techniques which could apply to any ion species. The modes are observed in the low-density, low-rotation limit of the cloud where the cloud approaches a two-dimensional charged disk. We observe both axially symmetric and asymmetric drumhead modes. The shape, rotation frequency, and density of the cloud are found in a real-time nondestructive manner by measuring the frequency of these modes. In addition, it is found that radio-frequency sideband cooling compresses the cloud, increasing its density. The ability to measure and control the density of a trapped ion cloud might be useful for experiments on low-temperature ion-neutral-atom collisions, recombination rates, and studies of the confinement properties of non-neutral plasmas.

03,960
PB95-176293 Not available NTIS
National Inst. of Standards and Technology (PL), Boulder, CO. Time and Frequency Div.
Squeezed Atomic States and Projection Noise in Spectroscopy.
Final rept.
D. J. Wineland, J. J. Bollinger, W. M. Itano, and D. J. Heinzen. 1994, 22p.
Sponsored by Office of Naval Research, Arlington, VA.
Pub. in Physical Review A 50, n1 p67-88 Jul 94.

Keywords: *Atomic spectroscopy, Atomic clocks, Trapped particles, Reprints, *Squeezed states(Quantum theory), Quantum noise, Atom traps.

We investigate the properties of angular-momentum states which yield high sensitivity to rotation. We discuss the application of these 'squeezed-spin' or correlated-particle states to spectroscopy. Transitions in an ensemble of N two-level (or, equivalently, spin-1/2) particles are assumed to be detected by observing changes in the state populations of the particles (population spectroscopy). When the particles' states are detected with 100% efficiency, the fundamental limiting noise is projection noise, the noise associated with the quantum fluctuations in the measured populations. If the particles are first prepared in particular quantum-mechanically correlated states, we find that the signal-to-noise ratio can be improved over the case of initially uncorrelated particles. We have investigated spectroscopy for a particular case of Ramsey's separated oscillatory method where the radiation pulse lengths are short compared to the time between pulses.

03,961
PB95-180055 Not available NTIS
National Inst. of Standards and Technology (PL), Gaithersburg, MD. Radiometric Physics Div.
Inner-Valence States CO(+) between 22 eV and 46 eV Studied by High Resolution Photoelectron Spectroscopy and ab Initio CI Calculations.
Final rept.
P. Baltzer, M. Lundqvist, B. Wannberg, M. A. Hayes, J. B. West, M. R. F. Siggel, A. C. Parr, J. L. Dehmer, L. Karlsson, and M. Larsson. 1994, 18p.
Contract DE-W-31-109-ENG-38
Sponsored by Department of Energy, Washington, DC.
Pub. in Jnl. of Physics B: Atomic and Molecular Optical Physics 27, p4915-4932 1994.

Keywords: *Carbon monoxide, Photoelectron spectroscopy, Vibrational spectra, Vibrational states, Angular distribution, High resolution, Branching ratio, EV range 10-100, Molecular ions, Synchrotron radiation, Rydberg states, Helium ions, Photoionization, Reprints.

Photoionization of the CO molecule and inner-valence states of CO(1+) between 22 and 45 eV have been studied by means of photoelectron spectroscopy using both synchrotron radiation and He II radiation. Vibrational structure has been resolved in many bands up to 45 eV. CASSCF (complete active space self-consistent field) and MRCI (multireference configuration interaction) calculations of potential curves in the 22-30 eV range have been performed and these have been used to predict vibrational levels and Franck-Condon factors. In this energy range three valence states, have been identified, and spectroscopic constants have been determined for the first two of these. Above 30 eV, all valence states have been found to be repulsive. In addition to the broad bands expected for these states, several progressions of narrow lines are observed, most probably reflecting transitions to Rydberg states.

03,962
PB95-180295 Not available NTIS
National Inst. of Standards and Technology (CAML), Gaithersburg, MD. Applied and Computational Mathematics Div.
Laplace's Equation and the Dirichlet-Neumann Map in Multiply Connected Domains. (NIST Reprint).
Final rept.
A. Greenbaum, L. Greengard, and G. B. McFadden. 1993, 12p.
See also DE91011069. Sponsored by National Aeronautics and Space Administration, Washington, DC. Microgravity Science and Applications Div. and Defense Advanced Research Projects Agency, Arlington, VA.
Pub. in Jnl. of Computational Physics 105, n2 p267-278 Apr 93.

Keywords: *Laplace equation, Boundary integral method, Dirichlet problem, Integral equations, Iterative methods, Computational fluid dynamics, Computation, Matrices, Reprints, Ostwald ripening.

A variety of problems in materials science and fluid dynamics require the solution of Laplace's equation in multiply connected domains. Integral equation methods are natural candidates for such problems as they discretize the boundary alone, require no special effort for free boundaries, and achieve superalgebraic convergence rates on sufficiently smooth domains in two space dimensions, regardless of shape. Current integral equation methods for the Dirichlet problem, however, require the solution of M independent problems of dimension N, where M is the number of boundary components and N is the total number of points in the discretization. In this paper, we present a new boundary integral equation approach, valid for both interior and exterior problems, which requires the solution of a single linear system of dimension N + M. We solve this system by making use of an iterative method (GMRES) combined with the fast multipole method for the rapid calculation of the necessary matrix vector products. For a two-dimensional system with 200 components and 100 points on each boundary, we gain a speedup of a factor of 100 from the new analytic formulation and a factor of 50 from the fast multipole method.

03,963
PB95-180436 Not available NTIS
National Inst. of Standards and Technology (PL), Gaithersburg, MD. Atomic Physics Div.
Atomic Branching Ratio Data for Oxygen-Like Species.
Final rept.
J. Z. Klose, T. M. Deters, J. R. Fuhr, and W. L. Wiese. 1994, 19p.
See also PB94-212842.
Pub. in Jnl. of Quantitative Spectroscopy and Radiative Transfer 52, n5 p601-619 1994.

Keywords: *Branching ratio, Vacuum ultraviolet radiation, Transition probabilities, High temperature, Spectral lines, Neon ions, Oxygen atoms, Radiometry, Plasma, Reprints, *Oxygen-like ions.

The branching ratio technique for radiometric calibrations in the vacuum ultraviolet spectral region is briefly reviewed. Lists of transitions suitable for use of the technique are given for oxygen-like species (O I and Ne III) along with pertinent data for their application.

03,964
PB95-180600 Not available NTIS
National Inst. of Standards and Technology (CSTL), Gaithersburg, MD. Thermophysics Div.
Laser Photoionization Measurements of Pressure in Vacuum.
Final rept.
J. P. Looney. 1994, 8p.
Pub. in Jnl. of the Vacuum Society of Japan 37, n9 p703-710 1994.

Keywords: *Pressure measurement, *Ultrahigh vacuum, Laser applications, Reprints, *Laser photoionization.

For some time, laser photoionization has been used to detect low concentrations of atoms, molecules, and radical intermediates in a variety of applications, including analytical chemistry, combustion, plasma and CVD diagnostics. Several of these studies have shown that laser photoionization has the fundamental sensitivity and selectivity necessary for species-specific partial pressure measurement in the ultrahigh vacuum regime. This body of work has, in part, spurred interest in the application of laser photoionization to measurements of pressures in the UHV regime. In this paper we discuss the results of the recent research conducted at NIST on the use of laser photoionization for quantitative pressure measurements and the factors which limit the pressure measurements based upon this technique.

03,965
PB95-180790 Not available NTIS
National Inst. of Standards and Technology (PL), Boulder, CO. Time and Frequency Div.
Progress on a Cryogenic Linear Trap for (199)Hg(+) Ions.
Final rept.
M. E. Poitzsch, J. C. Bergquist, W. M. Itano, and D. J. Wineland. 1994, 3p.
Sponsored by Office of Naval Research, Arlington, VA.
Pub. in Proceedings of Institute of Electrical and Electronic Engineers International Frequency Control Symposium, Boston, MA., June 1-3, 1994, p744-746.

Keywords: *Ion storage, *Mercury ions, Mercury 199, Temperature range 0000-0013 K, Extremely high frequency, Frequency standards, Prototypes, Reprints, *Ion traps, Laser cooling.

We have observed linear 'crystals' of up to tens of laser-cooled (199)Hg (I+) ions in a new cryogenic linear rf ion trap that operates at liquid helium temperature and is designed for use as a prototype 40.5 GHz frequency standard with high accuracy and stability.

03,966
PB95-180915 Not available NTIS
National Inst. of Standards and Technology (EEEL), Boulder, CO. Electromagnetic Technology Div.
Flexible-Diaphragm Force Microscope.
Final rept.
P. Rice, and J. Moreland. 1994, 2p.
Pub. in Jnl. of Vacuum Science and Technology B 12, n4 p2465-2466 Jul/Aug 94.

Keywords: *Atomic force microscopy, *Diaphragms(Mechanics), *Microscopes, Scanning tunneling microscopy, Disc recording systems, Polyamide resins, Low temperature, Flexibility, Reprints, Surface topography, Hard disks.

A flexible polyimide diaphragm was used in place of the usual cantilever for atomic force microscopy. Images of hard disk surface features are presented, demonstrating the practicality of the method.

03,967
PB95-180956 Not available NTIS
National Inst. of Standards and Technology (PL), Gaithersburg, MD. Ionizing Radiation Div.
Comparison of NIST and ISO Filtered Bremsstrahlung Calibration Beams.
Final rept.
C. G. Soares, and M. Ehrlich. 1994, 16p.
Contract DE-AI01-93EH89321
Sponsored by Department of Energy, Washington, DC.
Pub. in Proceedings of Conference on Radiation Protection and Dosimetry (4th), Orlando, FL., October 23-27, 1994, p457-472.

Keywords: *Bremsstrahlung, X ray spectra, Interlaboratory comparisons, Calibration, Standards, Revisions, ISO, Reprints, US NIST.

A detailed comparison is made between the 32 currently available National Institute of Standards and Technology (NIST) bremsstrahlung techniques and the 41 International Standards Organization (ISO) brems-

strahlung techniques recommended for use in the latest revision of ISO Standard 4037. The comparison is made in terms of measured and theoretical spectral distributions, and measured half-value layers. Some historical background on the choice of the respective techniques is also given. With the goal of greater international uniformity, a program is underway at NIST to implement the ISO techniques. The scope of the work and the current status of this effort is presented.

03,968
PB95-180964 Not available NTIS
National Inst. of Standards and Technology (PL), Gaithersburg, MD. Ionizing Radiation Div.
Calibration of Dosimeters for the Cryogenic Irradiation of Composite Materials Using an Electron Beam.
Final rept.
A. Spindel, M. L. Tupper, W. L. McLaughlin, H. L. Whittaker, and T. Overett. 1994, 4p.
Contract DE-AC35-89ER40486
Sponsored by Department of Energy, Washington, DC.
Pub. in Nuclear Instruments and Methods in Physics Research B 94, p150-153 1994.

Keywords: *Electron dosimetry, *Dosimeters, *Calibration, Superconducting composites, Superconducting magnets, Temperature range 0000-0013 K, MeV range 10-100, Radiation effects, Electron irradiation, Electron beams, Accelerators, Reprints, Radiochromic films.

In order to evaluate materials such as superconducting magnet components for use in the high-dose radiation environment of the large recirculating charged-particle accelerators such as CERN's Large Hadron Collider (Switzerland/France), CEBAF (Virginia), HERA (Hamburg, Germany), Fermilab's Tevatron (Illinois), and the recently cancelled Superconducting Super Collider (Texas), a study of the radiation resistance of these materials was carried out. These materials must withstand absorbed doses as large as 10(exp 7) Gy at a temperature of 4 K and were tested under these conditions using an electron beam from a 20 MeV linear accelerator. This paper describes the dosimetry at such very large doses and how the dose was delivered to the samples.

03,969
PB95-181244 Not available NTIS
National Inst. of Standards and Technology (PL), Boulder, CO. Time and Frequency Div.
High-Resolution Diode-Laser Spectroscopy of Calcium.
Final rept.
A. S. Zibrov, R. W. Fox, R. Ellingsen, G. M. Tino, L. Hollberg, C. S. Weimer, and V. L. Velichansky. 1994, 5p.
Sponsored by Air Force Office of Scientific Research, Bolling AFB, DC.
Pub. in Applied Physics B 59, p327-331 1994.

Keywords: *Laser spectroscopy, *Calcium, Semiconductor lasers, High resolution, Line width, Visible radiation, Reprints, *Frequency references.

Saturated-absorption signals on the calcium 657 nm transition are observed by direct absorption using diode lasers and a high flux atomic-beam cell. Linewidths as narrow as 65 kHz are observed with a high signal-to-noise ratio. Prospects for using this system as a compact wavelength/frequency reference are considered.

03,970
PB95-202214 Not available NTIS
National Inst. of Standards and Technology (PL), Boulder, CO. Quantum Physics Div.
Core Potentials for Quasi-One-Electron Systems.
Final rept.
B. J. Albright, K. Bartschat, and P. R. Flicek. 1993, 8p.
Grant NSF-PHY-9014103
Sponsored by National Science Foundation, Washington, DC.
Pub. in Jnl. of Physics B: Atomic and Molecular Optical Physics 26, p337-344 1993.

Keywords: *Atomic structure, Ionization potentials, Electron orbitals, Barium ions, Cesium, Indium, Sodium, Thallium, Reprints, Core potentials.

We have developed a method to calculate core potentials for quasi-one-electron systems and the corresponding single electron orbitals. It is shown that the approximate inclusion of exchange effects between the valence electrons and the core removes the unphysical structure in the potential function that is characteristic for potentials calculated by only including the effect of core polarization due to the valence electrons. Excellent agreement with experimental ionization potentials is achieved, and example results for various systems such as Na, Cs, Ba(1+), In and Tl are presented.

03,971
PB95-202248 Not available NTIS
National Inst. of Standards and Technology (PL), Boulder, CO. Quantum Physics Div.
Reduction of Light-Assisted Collisional Loss Rate from a Low-Pressure Vapor-Cell Trap.
Final rept.
M. H. Anderson, W. Petrich, J. R. Ensher, and E. A. Cornell. 1994, 4p.
Grant NSF-PHY90-12244
Sponsored by National Science Foundation, Arlington, VA. and Office of Naval Research, Arlington, VA.
Pub. in Physical Review A 50, n5 pR3597-R3600 Nov 94.

Keywords: *Rubidium 87, Trapped particles, Laser radiation, Magnetooptics, Lifetime, Reduction, Losses, Reprints, *Atom traps, Collisional energy transfer.

We have demonstrated an order of magnitude increase in the number and in the lifetime of magneto-optically trapped (87)Rb atoms collected from a low-pressure vapor. The improvement results from the reduction of light-assisted collision losses and is achieved by shelving the atomic population into the lower hyperfine ground state. Large fractional populations of the lower hyperfine ground state have been obtained by blocking the hyperfine repumping light in the region of the trapped atoms and by application of laser light that optically pumps the atoms into that state. We have observed trap lifetimes in excess of 700 s at our highest vacuum levels. At the rubidium pressure that maximizes the product of the number and lifetime of trapped atoms we observe a lifetime of 240 s with 5 X 10(exp 7) trapped atoms, under conditions for which an ordinary magneto-optical trap has a lifetime of only 14 s with 3 X 10(exp 6) atoms.

03,972
PB95-202271 Not available NTIS
National Inst. of Standards and Technology (PL), Boulder, CO. Quantum Physics Div.
Resonance Structure and Absolute Cross Sections in Near-Threshold Electron-Impact Excitation of the 4s(2) (1)S yields 4s4p (3)P Intercombination Transition in Kr(6+).
Final rept.
M. E. Bannister, X. Q. Guo, T. M. Kojima, and G. H. Dunn. 1994, 3p.
Contract DE-A105-86ER53237
Sponsored by Department of Energy, Washington, DC.
Pub. in Physical Review Letters 72, n21 p3336-3338, 23 May 94.

Keywords: *Electron-ion collisions, *Krypton ions, Total cross sections, Multicharged ions, Electron transitions, Electron impact, Excitation, Reprints, Zinc-like ions.

First measurements of absolute total cross sections for electron-impact excitation of an intercombination transition to a nonradiating state of an ion are reported. The cross sections for near-threshold excitation of the 4s(2) singlet S --> 4s4p triplet P transition of Kr(6+) are dominated by dielectronic resonances. The measurements can serve as a benchmark for theoretical predictions by dielectronic resonance structure in the excitation of multicharged ions.

03,973
PB95-202289 Not available NTIS
National Inst. of Standards and Technology (PL), Boulder, CO. Quantum Physics Div.
Short-Range Correlation and Relaxation Effects on the (6p(2))(1)SO Autoionizing State of Atomic Barium.
Final rept.
K. Bartschat, and C. H. Greene. 1993, 8p.
Sponsored by National Science Foundation, Washington, DC.
Pub. in Jnl. of Physics B: Atomic and Molecular Optical Physics 26, pL109-L116 1993.

Keywords: *Photoionization, *Autoionization, *Barium, Excited states, R matrix, Correlation, Relaxation, Reprints, Basis sets.

The discrepancy between previous R-matrix calculations using fixed boundary conditions and the eigenchannel method for the photoionization spectrum of barium is resolved. In particular, it is shown that the position of the (6p(2)) singlet S(0) resonance that results in a maximum of the experimental photoionization cross section near 44,800/cm relative to the (s(2)) singlet S(0) ground state of barium cannot be obtained by a standard close-coupling expansion involving only physical bound states; instead, the correct representation of short-range correlation effects and the relaxation of the 6p orbital requires the inclusion of doubly excited configurations of the continuum-continuum type.

03,974
PB95-202297 Not available NTIS
National Inst. of Standards and Technology (PL), Boulder, CO. Quantum Physics Div.
Connection between Superelastic and Inelastic Electron-Atom Collisions Involving Polarized Collision Partners.
Final rept.
K. Bartschat, and D. H. Madison. 1993, 2p.
Sponsored by National Science Foundation, Washington, DC.
Pub. in Physical Review Letters 48, n1 p836-837 Jul 93.

Keywords: *Electron-atom collisions, *Polarized beams, *Sodium, Electron transitions, Electron scattering, Elastic scattering, Inelastic scattering, Polarization(Spin alignment), Low energy, Reprints.

It is shown how the results of a recent experiment by Jiang, Zuo, Vuskovic, and Bederson (Phys. Rev. Lett. 68, 915 (1992)), who investigated low-energy electron scattering from laser-excited polarized sodium atoms in the initial (3p) doublet P(sub 3/2, sup 0) (F = 3, M(F) = 3) state, can be related to the inelastic 3S --> 3P transition involving initially unpolarized electron and atom beams. Hence, this method can provide an independent check of the traditional electron-scattering experiment with unpolarized beams.

03,975
PB95-202305 Not available NTIS
National Inst. of Standards and Technology (PL), Boulder, CO. Quantum Physics Div.
Femtosecond Time-Resolved Molecular Multiphoton Ionization: The Na2 System.
Final rept.
T. Baumert, M. Grosser, R. Thalweiser, and G. Gerber. 1991, 4p.
Pub. in Physical Review Letters 67, n27 p3753-3756, 30 Dec 91.

Keywords: *Sodium, Multi-photon processes, Molecular ions, Molecular beams, Excited states, Diatomic molecules, Autoionization, Reprints, *Multiphoton ionization, Femtosecond pulses, Time-of-flight spectroscopy.

We report here the first experimental study of femtosecond time-resolved molecular multiphoton ionization. Femtosecond pump-probe techniques are combined with time-of-flight spectroscopy to measure transient ionization spectra of Na2 in a molecular-beam experiment. The wave-packet motions in different molecular potentials show that incoherent contributions from direct photoionization of a singly excited state and from excitation and autoionization of a bound doubly excited molecular state determine the observed transient ionization signal.

03,976
PB95-202362 Not available NTIS
National Inst. of Standards and Technology (MSEL), Gaithersburg, MD. Reactor Radiation Div.
Roles of Local Classical Acceleration and Spatial Separation in the Neutral Particle Analogs of the Aharonov-Bohm Phases.
Final rept.
R. C. Casella. 1994, 5p.
Pub. in Physical Review Letters 73, n22 p2941-2945, 28 Nov 94.

Keywords: *Aharonov-Bohm effect, Neutral particles, Quantum theory, Acceleration, Spin, Reprints, Neutron interferometry.

The author shows that neither local nonuniform classical acceleration nor spatial separation of the quantized spin components plays an essential role in a number of neutron interferometer experiments designed to detect phases phi(+-)(B, E) akin to the Aharonov-Bohm phases. These neutral particle phases, which simply manifest quantum interference in spin space, can also

be detected by single beams, as exemplified by a recent breakthrough experiment by Sangster et al.

03,977
PB95-202438 Not available NTIS
National Inst. of Standards and Technology (PL), Boulder, CO. Quantum Physics Div.
Analyses of Recent Experimental and Theoretical Determinations of e-H2 Vibrational Excitation Cross Sections: Assessing a Long-Standing Controversy.
Final rept.
R. W. Crompton, and M. A. Morrison. 1993, 27p.
Grant NSF-PHY-9108890
Sponsored by National Science Foundation, Washington, DC.
Pub. in Australian Jnl. of Physics 46, p203-229 1993.

Keywords: *Electron-molecule collisions, *Hydrogen, Vibrational states, Colliding beams, Cross sections, Reprints, Vibrational excitation.

During the last four years, we have undertaken a major effort to resolve a serious, long-standing discrepancy between various experimental and theoretical determinations of the cross section for the upsilon(0) = 0 --> upsilon = 1 vibrational excitation of H2. This effort has involved crossed electron-beam molecular-beam measurements of relative angular distributions, measurements of transport coefficients in mixtures of H2 and various rare gases, and ab initio theoretical calculations using a vibrational close-coupling formalism with an exact treatment of non-local exchange effects. The discrepancy remains unresolved--a fact with potentially wide-ranging consequences for beam experiments, theory, and the unfolding of inelastic electron-molecule cross sections from swarm data. New analyses of the transport data and the application of a new method of extrapolating angular distributions beyond the range of measurement sheds light on this disagreement and its implications.

03,978
PB95-202446 Not available NTIS
National Inst. of Standards and Technology (PL), Boulder, CO. Quantum Physics Div.
Test of Newton's Inverse Square Law of Gravitation Using the 300-m Tower at Erie, Colorado.
Final rept.
J. Y. Cruz, J. C. Harrison, C. C. Speake, P. T. Keyser, J. E. Faller, J. Makinen, R. B. Beruff, T. M. Niebauer, and M. P. McHugh. 1991, 20p.
Pub. in Jnl. of Geophysical Research 96, nB12 p10,073-20,092, 10 Nov 91.

Keywords: *Gravitation, *Gravity, Basic interactions, Measurement, Validation, Towers, Tests, Reprints, Inverse square laws, Fifth force.

Gravity was measured at eight different heights on a 300-m meteorological tower, using electrostatically nulled LaCoste and Romberg gravimeters. The observed values were corrected for tides, temperature, and gravimeter screw errors, and tested for systematic effects due to (wind-induced) tower motion (no such effects were found). These corrected results were compared with values predicted by means of Newton's inverse square law from surface gravity values. The differences exhibit no systematic trends, and their rms value is only 10 microGal, well within the errors of the experiment, as the estimated measurement errors increase from 9 microGal at the lowest platform to 14 microGal at the top and those of the predictions from 10 microGal to 23 microGal. These results set new constraints on the magnitude of any non-Newtonian gravitational force; if such a force is derived from a Yukawa potential, the absolute value of alpha must be less than 0.001 for lambda = 1,000 m.

03,979
PB95-202453 Not available NTIS
National Inst. of Standards and Technology (PL), Boulder, CO. Quantum Physics Div.
Three-Vector Correlation Study of Orientation and Coherence Effects in Na(3p, (2)P1/2 inversely maps (2)P3/2)+He: Semiclassical and Quantum Calculations.
Final rept.
R. de Vivie-Riedle, J. P. J. Driessen, and S. R. Leone. 1993, 16p.
Grant NSF-PHY90-12244
Sponsored by National Science Foundation, Washington, DC.
Pub. in Jnl. of Chemical Physics 98, n3 p2038-2053, 1 Feb 93.

Keywords: *Atom-atom collisions, *Atomic collisions, *Sodium, Atomic energy levels, Electron transitions, MeV range 10-100, MeV range 100-1000, Colliding beams, Fine structure, Laser radiation, Cross sections, Quantum mechanics, Polarization, Orientation, Coherence, Alignment, Correlation, Helium, Reprints.

Multistructure cross sections, of both conventional and coherence types, are calculated for the fine structure transition Na(doublet P(1/2)<--doublet P(3/2)) + He in an energy range of 10-200 meV. The cross sections are related to conditions of a crossed beams experiment in which the three controlled vectors are the initial relative velocity and the two polarization directions of excitation and probe laser beams. Both semiclassical and quantum mechanical calculations are performed. The semiclassical method is employed to interpret and visualize the collision mechanism leading to the multistructure cross sections. In addition, the validity of the approximations used in the semiclassical model is investigated.

03,980
PB95-202503 Not available NTIS
National Inst. of Standards and Technology (PL), Boulder, CO. Quantum Physics Div.
Absolute Cross-Section Measurements for Electron-Impact Single Ionization of Se(+) and Te(+).
Final rept.
N. Djuric, E. W. Bell, and G. H. Dunn. 1994, 5p.
Contract DE-A105-86ER53527
Sponsored by Department of Energy, Washington, DC. Office of Fusion Energy.
Pub. in International Jnl. of Mass Spectroscopy and Ion Processes 135, p207-211 1994.

Keywords: *Electron-ion collisions, *Selenium ions, *Tellurium ions, Electron impact, Colliding beams, Cross sections, EV range 10-100, EV range 100-1000, Ionization, Reprints, Arsenic-like ions, Antimony-like ions.

The crossed beams technique has been used to measure absolute cross-sections for the single ionization of Se(1+) and Te(1+) at electron energies from threshold to 200eV. The peak cross-sections obtained are 16.6 x 10(exp -17)sq cm at about 53eV for Se(1+) and 24.3 x 10(exp -17)sq cm at about 43eV for Te(1+). The measured Se(1+) cross-sections are bracketed from above by directionization cross-sections from configuration-averaged distorted-wave calculations of Pindzola (unpublished work) and from below by results using the single parameter semi-empirical formula of Lotz (Z. Phys., 216 (1968) 241), with both calculations giving results in moderate agreement with the measurements. In contrast, comparisons of measured Te(1+) cross-sections with similar calculations are generally poor. Ionization-rate coefficients for a Maxwellian electron-temperature distribution calculated from the experimental data presented.

03,981
PB95-202511 Not available NTIS
National Inst. of Standards and Technology (PL), Boulder, CO. Quantum Physics Div.
Crossed-Beams Measurements of Absolute Cross Sections for Electron Impact Ionization of S(+).
Final rept.
N. Djuric, E. W. Bell, and G. H. Dunn. 1993, 5p.
Contract DE-A105-86ER53237
Sponsored by Department of Energy, Washington, DC. Office of Energy Research.
Pub. in International Jnl. of Mass Spectrometry and Ion Processes 123, p187-191 1993.

Keywords: *Electron-ion collisions, *Sulfur ions, EV range 10-100, EV range 100-1000, Electron impact, Cross sections, Colliding beams, Ionization coefficients, Reprints, Phosphorus-like ions.

Absolute cross sections for electron impact ionization of S(1+) have been measured in the electron energy range from 30-250eV using the crossed beams technique. Results are compared with scaled cross sections from other P-like ions, with a semiempirical formula and with other recently reported measurements. Expansion coefficients and formulas for generating ionization rate coefficients in the electron temperature range 10,000 K = or < T = or < 1 million K are presented.

03,982
PB95-202529 Not available NTIS
National Inst. of Standards and Technology (PL), Boulder, CO. Quantum Physics Div.
Absolute Cross Sections for Electron-Impact Single Ionization of Si(+) and Si(2+).
Final rept.
N. Djuric, E. W. Bell, X. Q. Guo, M. E. Bannister, M. S. Pindzola, D. C. Griffin, G. H. Dunn, and R. A. Phaneuf. 1993, 8p.
Contract DE-A105-86ER53237
Sponsored by Department of Energy, Washington, DC. Office of Fusion Energy.
Pub. in Physical Review A 47, n6 p4786-4793 Jun 93.

Keywords: *Electron-ion collisions, *Silicon ions, Electron impact, Cross sections, Colliding beams, Ionization, Reprints, Aluminum-like ions, Magnesium-like ions.

Absolute cross sections for electron-impact single ionization of Si(1+) and Si(2+) have been measured using crossed beams of ions and electrons and calculated using a configuration-average distorted-wave method. Corrections have been made for metastable components and small fractions of nitrogen impurities in the incident ion beams. Excitation-autoionization measurably enhances the cross sections of both Si(1+) and Si(2+). Ionization rate coefficients and fitting parameters are presented for the experimental data.

03,983
PB95-202545 Not available NTIS
National Inst. of Standards and Technology (PL), Boulder, CO. Quantum Physics Div.
n-Vector Correlations in Collision Dynamics with Atomic Orbital Alignment: The Importance of Coherence Denoting Azimuthal Structure for n (greater than or equal to) 3.
Final rept.
J. P. J. Driessen, and S. R. Leone. 1992, 11p.
Pub. in Jnl. of Physical Chemistry 96, n15 p6136-6146 1992.

Keywords: *Atomic collisions, *Calcium, Vectors(Mathematics), Atomic orbitals, Polarized light, Laser radiation, Energy transfer, Orientation, Alignment, Coherence, Reprints.

An introduction is presented of vector correlations in collision experiments involving atomic orbital alignment or orientation. At present, aligned or oriented species can be prepared (or probed) with 'relative' ease using polarized laser beams. First, an extensive expose of the necessary mathematical formalisms for two- and three-vector correlations is given, and then experimental examples for atomic Ca are discussed to elucidate the theory. It is demonstrated both theoretically and experimentally that azimuthal structure about the initial relative velocity vector (called coherence) becomes important when three or more vector quantities are controlled in the collision process.

03,984
PB95-202552 Not available NTIS
National Inst. of Standards and Technology (PL), Boulder, CO. Quantum Physics Div.
Resonant Two-Color Detachment of H(-) with Excitation of H(n=2).
Final rept.
N. Y. Du, A. F. Starace, and N. A. Cherepkov. 1993, 13p.
Contract DE-FG02-88ER13955
Sponsored by Department of Energy, Washington, DC.
Pub. in Physical Review A 48, n3 p2413-2425 Sep 93.

Keywords: *Hydrogen ions, *Electron detachment, *Photodetachment, Polarized light, Cross sections, Negative ions, Excitation, Reprints, Two photon processes.

The cross sections for resonant two-color, two-photon detachment of H(1-) with excitation of the degenerate H(2s) and H(2p) levels are calculated within a semiempirical adiabatic hyperspherical representation. The first photon, with energy omega(1) = 0.4017 au, is resonant with the well-known Feshbach (sup 1)P(sup o) resonance below the H(n = 2) threshold. The second photon, with energy omega(2) = or > 0.12605 au, scans the energy region above the H(n = 2) threshold over which long-range dipole-field-induced cross-section oscillations are predicted to occur. Such Gailitis-Damburg oscillations have not yet been observed experimentally. Results for various pairs of light polarization for the two photons are presented.

03,985
PB95-202578 Not available NTIS
National Inst. of Standards and Technology (PL), Gaithersburg, MD. Electron and Optical Physics Div.

Numerical Solution of the Nonlinear Schroedinger Equation for Small Samples of Trapped Neutral Atoms.
Final rept.
M. A. Edwards, and K. Burnett. 1995, 5p.
Grant NSF-PHY-9206769
Sponsored by National Science Foundation, Arlington, VA.
Pub. in Physical Review A 51, n2 p1382-1386 Feb 95.

Keywords: *Schrodinger equation, Nonlinear differential equations, Bose-Einstein condensation, Trapped particles, Neutral atoms, Numerical solution, Reprints, *Atom traps, Laser traps, Laser cooling, Gross-Pitaevskii equation.

We present a numerical technique to solve the time-independent nonlinear Schrodinger equation with an external potential. We apply it to the case of a dilute Bose-condensed assembly of trapped neutral atoms where the potential varies on the same scale as the condensate. This situation should soon be accessible to experimental observation.

03,986
PB95-202594 Not available NTIS
National Inst. of Standards and Technology (PL), Boulder, CO. Quantum Physics Div.
Long-Range Parity-Nonconserving Interaction.
Final rept.
V. V. Flambaum. 1992, 6p.
Grant NSF-PHY89-04035
Sponsored by National Science Foundation, Washington, DC.
Pub. in Physical Review A 45, n9 p6174-6179, 1 May 92.

Keywords: *P invariance, *Parity, Weak interactions, Polarization characteristics, Charged particles, Vectors(Mathematics), Molecules, Atoms, Solids, Interactions, Reprints.

There is a long-range parity-nonconserving (PNC) interaction between a charged particle and a composite system (atom, nucleus) induced by the usual contact weak interaction inside this system: U = (H X E)(dot)(beta(sub nu)) approx. = 1/R(sup 4) or 1/R(sup 5), where R is distance, E and H are electric and magnetic fields of the particle, and J and B(beta(sub nu)) are the angular momentum and PNC vector polarizability of the system. The mechanisms of enhancement of PNC vector polarizability are considered. PNC effects in atoms, molecules, and solids are discussed (P-odd and T-even electric dipole moment, P-odd electric field, etc).

03,987
PB95-202628 Not available NTIS
National Inst. of Standards and Technology (PL), Boulder, CO. Quantum Physics Div.
Quantum Mechanics of a Solid-State Bar Gravitational Antenna.
Final rept.
L. P. Grishchuk. 1992, 8p.
Pub. in Physical Review D 45, n8 p2601-2608, 15 Apr 92.

Keywords: *Gravitational wave antennas, *Quantum mechanics, Absorption cross sections, Solid state devices, Bars, Reprints.

A quantum-mechanical treatment of a bar gravitational antenna is presented. The theory takes into account the crystalline structure of the bar and collective behavior of its mass elements. The low-frequency and high-frequency (Debye) modes of oscillations are considered. It is shown that the quantum-mechanical derivation of the absorption cross section of the gravitational antenna agrees totally with the classical result. The recent claims of a significant (six orders of magnitude) quantum-mechanical enhancement of the cross section are shown to be incorrect.

03,988
PB95-202701 Not available NTIS
National Inst. of Standards and Technology (PL), Boulder, CO. Quantum Physics Div.
Modified Effective Range Theory as an Alternative to Low-Energy Close-Coupling Calculations.
Final rept.
W. A. Isaacs, and M. A. Morrison. 1992, 23p.
Grant NSF-PHY-8505438
Sponsored by National Science Foundation, Washington, DC.
Pub. in Jnl. of Physics B: Atomic and Molecular Optical Physics 25, p703-725 1992.

Keywords: *Electron-molecule collisions, *Effective range theory, *Hydrogen, *Nitrogen, Electron scattering, Cross sections, Low energy, Feasibility, Reprints.

We investigate the feasibility of using modified effective range theory to 'project' results of theoretical scattering calculations to energies so low that such calculations are numerically intractable. In particular, this theory, as developed by Fabrikant in the body-frame fixed-nuclei formulation of electron scattering from non-polar molecules, provides expansions of the reactance matrix that enable determination of the scattering length (and other parameters as needed) and total cross sections with greater accuracy and over a larger range of energies than do conventional implementations of such expansions for the total cross section. We have explored the viability, accuracy and potential problems of this stratagem for the e-H2 and e-N2 systems; in both cases, careful use of these expansions enables calculation of highly accurate cross sections at very low energies without resource to numerically problematic, CPU-intensive close-coupling calculations.

03,989
PB95-202719 Not available NTIS
National Inst. of Standards and Technology (PL), Boulder, CO. Quantum Physics Div.
Slow-Electron Collisions with CO Molecules in an Exact-Exchange Plus Parameter-Free Polarization Model.
Final rept.
A. Jain, and D. W. Norcross. 1992, 13p.
Contract DE-FC05-85ER-250000
Sponsored by Department of Energy, Washington, DC. Office of Energy Research.
Also pub. as Physical Review A 45, n3 p1644-1656, 1 Feb 92.

Keywords: *Electron-molecule collisions, *Carbon monoxide, Electron scattering, Electron collisions, Milli EV range, EV range 1-10, Momentum transfer, Cross sections, Reprints.

We report low-energy (0.001 to 10-eV) electron-CO scattering cross sections obtained using an exact-exchange (via a separable-exchange formulation) plus a parameter-free correlation-polarization model in the fixed-nuclei approximation (FNA). The differential, total, and momentum-transfer cross sections are reported for rotationally elastic, inelastic, and summed processes. To remove the limitations of the FNA with respect to the convergence of total and differential cross sections, the multipole-extracted-adiabatic-nuclei approximation is used.

03,990
PB95-202727 Not available NTIS
National Inst. of Standards and Technology (PL), Boulder, CO. Quantum Physics Div.
Superconducting Resonator and a Cryogenic GaAs Field-Effect Transistor Amplifier as a Single-Ion Detection System.
Final rept.
S. R. Jefferts, T. Heavner, P. Hayes, and G. H. Dunn. 1993, 4p.
Grant NSF-PHY90-12244
Sponsored by National Science Foundation, Washington, DC.
Pub. in Review of Scientific Instruments 64, n3 p737-740 Mar 93.

Keywords: *Ion detection, Field effect transistors, Transistor amplifiers, Gallium arsenides, Superconducting devices, Resonators, Inductors, Reprints, *Single ion detectors.

A current measuring system capable of detecting single ions is described. The detector operates at a frequency of nominally 900 kHz and uses a superconducting inductor with high Q(Q approx = 8,500) and a cryogenic GaAs field-effect transistor (FET) amplifier with noise temperature less than 0.3 K. Noise measurements of the FET are presented, along with details of the construction of the superconducting inductor.

03,991
PB95-202818 Not available NTIS
National Inst. of Standards and Technology (PL), Boulder, CO. Quantum Physics Div.
Probing Bose-Einstein Condensed Atoms with Short Laser Pulses.
Final rept.
M. Lewenstein, and L. You. 1993, 4p.
Pub. in Physical Review Letters 71, n9 p1339-1342, 30 Aug 93.

Keywords: Bose-Einstein condensation, Light scattering, Light pulses, Laser radiation, Reprints, *Atom traps, Optical probes.

We propose a method of probing a system of cooled atoms in a trap using short laser pulses. Above the critical temperature for Bose-Einstein condensation, such a system scatters very weakly. Coherent scattering occurs primarily in the forward direction. Below the critical temperature, the number of scattered photons increases dramatically and the scattered light is emitted in the solid angle determined by the size of the condensate.

03,992
PB95-202867 Not available NTIS
National Inst. of Standards and Technology (PL), Boulder, CO. Quantum Physics Div.
Variationally Stable Treatment of Two- and Three-Photon Detachment of H(-) Including Electron-Correlation Effects.
Final rept.
C. Liu, B. Gao, and A. F. Starace. 1992, 14p.
Pub. in Physical Review A 46, n9 p5985-5998, 1 Nov 92.

Keywords: *Hydrogen ions, Electron affinity, Electron correlation, Electron detachment, Negative ions, Hyperspheres, Reprints, Keldysh approximation, Hyperspherical coordinates.

A variationally stable, adiabatic hyperspherical treatment of two- and three-photon detachment of H(1-) is presented. Results are compared with analytic predictions of a zero-range potential model of H(1-). Detailed comparisons are made also with other theoretical results which include the effects of electron correlations. We predict analytically (and demonstrate numerically) an extreme sensitivity of the theoretical predictions to any errors in the value of the electron affinity employed. In an Appendix we show that the low-intensity limit of the Keldysh treatment of detachment of an electron bound in a zero-range potential agrees with the results of a perturbative treatment.

03,993
PB95-202883 Not available NTIS
National Inst. of Standards and Technology (PL), Boulder, CO. Quantum Physics Div.
Alignment in Two-Step Pulsed Laser Excitation of Rydberg Levels in Light Atoms: The Example of Sodium.
Final rept.
K. B. MacAdam, and M. A. Morrison. 1993, 14p.
Grants NSF-PHY-9122377, NSF-PHY-9108890
Sponsored by National Science Foundation, Washington, DC.
Pub. in Physical Review A 48, n2 p1345-1358 Aug 93.

Keywords: *Rydberg states, *Sodium, Atomic energy levels, Laser radiation, Pulsed lasers, Density matrix, Excitation, Alignment, Atomic orbitals, Reprints.

Aligned atomic Rydberg states of sodium can be prepared using two-step excitation from the ground state by linearly polarized pulsed lasers. Information that is normally inaccessible, e.g., sublevel partial cross sections in charge-transfer experiments, can be obtained when aligned targets are used. The calculations of orbital alignment must carefully allow for fine and hyperfine structure, laser linewidths, pulse widths and delays, sublevel coherences, and other factors. In this paper we derive the orbital alignments and time-averaged d-state sublevel populations for 3 doublet S(1/2)-->3 doublet P(J sub 1)-->n doublet D excitations in Na using angular-momentum and density-matrix methods. We consider both quadrupole alignment A(sup (2)) and hexadecapole alignment A(sup (4)), with excitation through either J(1)=1/2 or 3/2 intermediate states considered on the same footing. We show sublevel populations for absolute values of M(L)=0, 1, and 2 analytically and graphically.

03,994
PB95-202917 Not available NTIS
National Inst. of Standards and Technology (PL), Boulder, CO. Quantum Physics Div.
Threshold Electron Excitation of Na.
Final rept.
B. Marinkovic, P. Wang, and A. Gallagher. 1992, 5p.
Contract DE-FG02-87ER13720
Sponsored by Department of Energy, Washington, DC. Office of Energy Research.
Pub. in Physical Review A 46, n5 p2553-2557, 1 Sep 92.

Keywords: *Electron-atom collisions, *Sodium, Electron collisions, Electronic states, Threshold effects, Excited states, Excitation, Reprints, Collisional energy transfer.

Electron collisional excitation of the 4D, 5D, 4P, and 6S states of Na has been measured with about 30-meV energy resolution. Very rapid, unresolved threshold onsets are seen for all but the 4P state, and a near-threshold resonance is suggested by the 5D data. However, only weak undulations in the cross sections are observed above threshold.

03,995
PB95-202958 Not available NTIS
National Inst. of Standards and Technology (PL), Boulder, CO. Quantum Physics Div.
Collisional Energy Transfer between Excited-State Strontium and Noble-Gas Atoms.
Final rept.
D. A. Miller, L. You, J. Cooper, and A. Gallagher. 1992, 7p.
Grant NSF-PHY90-12244
See also PB91-204164. Sponsored by National Science Foundation, Washington, DC.
Pub. in Physical Review A 46, n3 p1303-1309, 1 Aug 92.

Keywords: *Atomic collisions, *Strontium, Atomic energy levels, Oscillator strengths, Excited states, Pulsed lasers, Radiative lifetime, Transition probabilities, Rare gases, Reprints, Collisional energy transfer.

Inert-gas induced collisional transfer between the first four excited states of Sr has been measured by determining excited-state densities following pulsed laser excitation of the 5 singlet P state. We observe 5 singlet P collisional transfer exclusively to the 4 triplet D state, with (about 800 K) rate coefficients ranging from 0.24 to 2.0 X 10(exp -11)cc/s for the various gases. We also measure 4 singlet D(2) transfer primarily to the 4 triplet D state, with rate coefficients of 0.65 to 6.8 X 10(exp -11)cc/s. The 4 triplet D state radiative lifetime is observed to be 2.9 + or - 0.2 microsec.

03,996
PB95-202974 Not available NTIS
National Inst. of Standards and Technology (PL), Boulder, CO. Quantum Physics Div.
Importance of Bound-Free Correlation Effects for Vibrational Excitation of Molecules by Electron Impact: A Sensitivity Analysis.
Final rept.
M. A. Morrison, and W. K. Trail. 1993, 13p.
Grant NSF-PHY90-12244
Sponsored by National Science Foundation, Washington, DC.
Pub. in Physical Review A 48, n4 p2874-2886 Oct 93.

Keywords: *Electron-molecule collisions, *Hydrogen, Electron scattering, Electron impact, Colliding beams, Cross sections, Sensitivity analysis, Correlation, Reprints, Vibrational excitation.

One of the most interesting, important, and problematic components of interaction potentials for electron-atom and -molecule scattering arises from many-body effects in the near-target region. Such 'core-polarization' effects are of particular concern for vibrational-excitation calculations, where these short-range bound-free correlation and nonadiabatic velocity-dependent effects have remained resistant to rigorous treatment, being represented instead by approximations or model potentials. In order to provide guidance for assessing such potentials and insight into the nature of these many-electron effects, we have investigated the sensitivity to core polarization of total, momentum-transfer, rotational-excitation, and vibrational-excitation e-H2 cross sections. The sensitivity analysis for the latter cross section also comments on a long-standing, severe discrepancy between cross sections determined in various crossed-beam experiments and by transport analysis of swarm data for this simplest electron-neutral-molecule system.

03,997
PB95-203030 Not available NTIS
National Inst. of Standards and Technology (PL), Boulder, CO. Quantum Physics Div.
Energy-Pooling Collisions in Barium.
Final rept.
J. A. Neuman, A. Gallagher, and J. Cooper. 1994, 9p.
Grant NSF-PHY90-12244
Sponsored by National Science Foundation, Arlington, VA.
Pub. in Physical Review A 50, n2 p1292-1300 Aug 94.

Keywords: *Barium, *Atomic collisions, Atomic energy levels, Excited states, Energy transfer, Reprints, Rate coefficients.

Rate coefficients for energy-pooling collisions between low-lying excited states of Ba have been measured. The 6s6p triplet P(1) level in Ba is pumped by a cw diode laser, and radiative decay and collisions with buffer-gas atoms also populate the 5d6s (singlet D) and 5d6s (triplet D) metastable levels. The densities of these low-lying excited states are measured by the absorption of lines from a Ba hollow-cathode lamp, and the states populated by energy-pooling collisions are studied by comparing their fluorescence intensity to that of the laser-excited level. The rate coefficients are on the order of gas-kinetic rates, and they are not strongly dependent on energy defect, spin changes, or angular-momentum changes.

03,998
PB95-203097 Not available NTIS
National Inst. of Standards and Technology (PL), Boulder, CO. Quantum Physics Div.
Relative Photoionization and Photodetachment Cross Sections for Particular Fine-Structure Transitions with Application to Cl 3s-subshell Photoionization.
Final rept.
C. Pan, and A. F. Starace. 1993, 10p.
Grant NSF-PHY-9108002
Sponsored by National Science Foundation, Washington, DC.
Pub. in Physical Review A 47, n1 p295-304 Jan 93.

Keywords: *Photoionization, *Photodetachment, *Chlorine, Branching ratio, Cross sections, Electron transitions, Fine structure, Negative ions, Positive ions, Reprints.

The relative photoionization cross section for starting from a particular fine-structure level of the initial state of an atomic system and leading to a particular fine-structure level of the residual ion is presented for the case of atomic systems having one open subshell using a simple theoretical model in which emphasis is placed on the analysis of geometrical effects. This model parametrizes photoionization cross sections in terms of LS-dependent, single-configuration dynamical amplitudes, unlike previous treatments which assume LS-independent transition amplitudes from the start. In special cases our general formulas are shown to reduce to those of previous workers. We highlight photoionization of inner s subshells in open-shell atoms and show that when the total angular momenta for the initial atomic and final ionic fine-structure levels differ by more than 1/2 then such transitions are quasiforbidden. This prediction is tested in detail for the case of Cl 3s-subshell photoionization by comparison of our single-configuration results with the multiconfiguration, eigenchannel R-matrix results of Robicheaux and Greene. All of our results apply also to photoionization of open-shell positive ions or photodetachment of open-shell negative ions.

03,999
PB95-203105 Not available NTIS
National Inst. of Standards and Technology (PL), Boulder, CO. Quantum Physics Div.
Behavior of Atoms in a Compressed Magneto-Optical Trap.
Final rept.
W. Petrich, M. H. Anderson, J. R. Ensher, and E. A. Cornell. 1994, 4p.
Grant NSF-PHY90-12244
Sponsored by National Science Foundation, Arlington, VA. and Office of Naval Research, Arlington, VA.
Pub. in Jnl. of the Optical Society of America B 11, n8 p1332-1335 Aug 94.

Keywords: Trapped particles, Laser radiation, Magnetic fields, Magnetooptics, Reprints, *Atom traps, Laser cooling.

We investigate the behavior of a cloud of atoms in a magneto-optical trap, which--after collection--is compressed when the field gradients of the trap magnetic field are increased. We measure sizes and shapes of the atom cloud as a function of laser detuning, magnetic field gradient, and number of trapped atoms. A transient density increase of more than an order of magnitude has been achieved. Moreover, reproducible Gaussian density distributions are observed at large detunings and intermediate magnetic-field gradients, permitting an accurate determination of density.

04,000
PB95-203113 Not available NTIS
National Inst. of Standards and Technology (PL), Boulder, CO. Quantum Physics Div.
Dielectronic Capture Processes in the Electron-Impact Ionization of Sc(2+).
Final rept.
M. S. Pindzola, T. W. Gorczyca, N. R. Badnell, G. Hofmann, B. Weissbecker, K. Tinschert, E. Salzborn, A. Muller, G. H. Dunn, D. C. Griffin, and M. Stenke. 1994, 6p.
Pub. in Physical Review A 49, n2 p933-938 Feb 94.

Keywords: *Electron-ion collisions, *Electron capture, *Scandium ions, Ionization cross sections, Electron impact, Colliding beams, Excited states, Reprints.

Theoretical and experimental results are presented for the electron-impact ionization of Sc(2+) in the near-threshold energy region where strong resonance features due to dielectronic capture processes are found. The indirect ionization contributions are calculated in the close-coupling approximation. Both absolute and scan measurements for the ionization cross section are obtained in a crossed-beams experimental geometry. The overall agreement between theory and experiment is good, once a sufficient number of singly excited states are included in the close-coupling expansion. The additional states allow a proper theoretical determination of the decay pathways available to the resonances formed following dielectronic capture of the incident electron.

04,001
PB95-203147 Not available NTIS
National Inst. of Standards and Technology (PL), Boulder, CO. Quantum Physics Div.
Charge Cloud Distribution of Heavy Atoms After Excitation by Polarized Electrons.
Final rept.
A. Raeker, K. Blum, and K. Bartschat. 1993, 18p.
Grant NSF-PHY-901414103
Sponsored by National Science Foundation, Washington, DC.
Pub. in Jnl. of Physics B: Atomic, Molecular and Optical Physics 26, p1491-1508 1993.

Keywords: *Electron-atom collisions, Polarized beams, Electron impact, Heavy elements, Charge distribution, Multipoles, Mercury, Thallium, Reprints, Electron spin polarization.

We consider the charge cloud distribution of heavy atoms after impact excitation by polarized electrons. A general formula in terms of state multipoles is derived and interpreted with regard to ratios of principal axes and three independent angles of rotation. Finally, the theory is illustrated by numerical results for excitation of mercury and thallium.

04,002
PB95-203162 Not available NTIS
National Inst. of Standards and Technology (PL), Boulder, CO. Quantum Physics Div.
Pulsed Laser Photolysis Time-Resolved FT-IR Emission Studies of Molecular Dynamics.
Final rept.
S. A. Rogers, and S. R. Leone. 1993, 8p.
Contract DE-FG02-883413860
Sponsored by Department of Energy, Washington, DC.
Pub. in Applied Spectroscopy 47, n9 p1430-1437 1993.

Keywords: *Molecular dynamics, Pulsed lasers, Excimer lasers, Energy transfer, Photolysis, Molecular collisions, Chemical radicals, Reprints, Fourier transform infrared spectroscopy, Argon fluoride lasers, Photofragmentation.

Time-resolved Fourier transform infrared (FT-IR) emission experiments are used to study photofragmentation processes, single collision reactions, energy transfer events, and laser-initiated radical-radical reactions. In the experimental apparatus, a 200-Hz ArF excimer laser is coupled to a commercial 0.01/cm resolution Fourier transform infrared spectrometer. Fringes from the He:Ne reference laser are used for time synchronization of the laser pulses to the FT-IR mirror retardation. We report here on the comprehensive details of our experimental apparatus and discuss several of the processes studied with the use of this apparatus.

04,003
PB95-203261 Not available NTIS

National Inst. of Standards and Technology (PL), Boulder, CO. Quantum Physics Div.
Laser Preparation and Probing of Initial and Final Orbital Alignment in Collision-Induced Energy Transfer Ca(4s5p,(1)P1) + He yields Ca(4s5p,(3)P2) + He.
Final rept.
C. J. Smith, J. P. J. Driessen, L. Eno, and S. R. Leone. 1992, 13p.
Grant NSF-PHY90-12244
Sponsored by National Science Foundation, Washington, DC.
Pub. in Jnl. of Chemical Physics 96, n11 p8212-8224, 1 Jun 92.

Keywords: *Atom-atom collisions, *Atomic collisions, *Calcium, Atomic energy levels, Atomic orbitals, Angular momentum, Colliding beams, Cross sections, Laser radiation, Pulsed laser, Polarized light, Alignment, Correlation, Helium, Reprints.

In a crossed beam atomic energy transfer experiment, relative cross sections are measured between initial and final magnetic substates of atomic orbitals in a three vector correlation experiment. A pulsed laser beam prepares Ca(4s5p singlet P(1)) in a single magnetic sublevel (vertical stroke)j(1)m(i)> with respect to the laser polarization vector. Subsequent collision with He at a well-defined relative velocity yields Ca(4s5p triplet P(2)). The near-resonant Ca(4s5P triplet P(2)) is probed by a second polarized pulsed laser, revealing its magnetic sublevel (vertical stroke)j(2)m(f)> distribution with respect to the probe laser polarization vector. The experiment is analyzed in the collision frame where the direction of the initial relative velocity vector serves as the quantization axis.

04,004
PB95-203279 Not available NTIS
National Inst. of Standards and Technology (PL), Boulder, CO. Quantum Physics Div.
Initial and Final Orbital Alignment Probing of the Fine-Structure-Changing Collisions among the Ca (4s)(1)(4p)(1), (3)PJ States with He: Determination of Coherence and Conventional Cross-Sections.
Final rept.
C. J. Smith, E. M. Spain, M. J. Dalberth, S. R. Leone, and J. P. J. Driessen. 1993, 11p.
Grant NSF-PHY90-12244
Sponsored by National Science Foundation, Washington, DC. Div. of Physics.
Pub. in Jnl. of the Chemical Society, Faraday Transactions 89, n10 p1401-1411 1993.

Keywords: *Atom-atom collisions, *Atomic collisions, *Calcium, Atomic energy levels, Atomic orbitals, Laser radiation, Polarized light, Fine structure, Orientation(Direction), Cross sections, Alignment, Helium, Colliding beams, Reprints, Collisional energy transfer.

A laser pump-probe experiment is used to study the orbital alignment effects, orientation effects and vector correlations of collisional transfer of the Ca (4s)(1)(4p)(1), triplet P(1) state to the Ca (4s)(1) (4p)(1), triplet P(2,0) levels. The experiment is configured in a single-collision crossed-beam arrangement between Ca and He, and multi-structure cross-sections are determined using appropriate combinations of linear and circular laser light for the pump/probe steps. Real and imaginary parts of coherence cross-sections are obtained along with the conventional population cross-sections for the m(1) --> m(2) magnetic sublevel transitions into the triplet P(2) level.

04,005
PB95-203402 Not available NTIS
National Inst. of Standards and Technology (PL), Boulder, CO. Quantum Physics Div.
Angle-Differential and Momentum-Transfer Cross Sections for Low-Energy Electron-Cs Scattering.
Final rept.
U. Thumm, and D. W. Norcross. 1993, 12p.
Contract DE-A105-86ER53237
Sponsored by Department of Energy, Washington, DC. Office of Energy Research.
Pub. in Physical Review A 47, n1 p305-316 Jan 93.

Keywords: *Electron-atom collisions, *Cesium, Electron scattering, Elastic scattering, Inelastic scattering, Momentum transfer, EV range 170, Electron collisions, Cross sections, Relativistic effects, Excitation, Reprints.

Based on a previous Dirac R-matrix calculation, we have derived elastic and inelastic angle-differential and elastic momentum-transfer cross sections for slow electrons (E(kin) = or < 2.8 eV) colliding with neutral Cs atoms. Our results for the angle-differential cross sections are in good agreement with scaled experimental data and, depending on the incident electron energy, in qualitative or fair quantitative agreement with previously published theoretical work. The inelastic angle-differential cross sections for sextet p(1/2) and sextet p(3/2) excitation differ by more than a statistical branching ratio due to relativistic effects. For the momentum-transfer cross sections, we hope to resolve existing discrepancies in the literature and to provide more reliable input for transport calculations.

04,006
PB95-203410 Not available NTIS
National Inst. of Standards and Technology (PL), Boulder, CO. Quantum Physics Div.
Relativistic R-Matrix Calculations for Electron - Alkali-Metal-Atom Scattering: Cs as a Test Case.
Final rept.
U. Thumm, and D. W. Norcross. 1992, 22p.
Contract DE-A105-86ER532337
Sponsored by Department of Energy, Washington, DC. Office of Energy Research.
Pub. in Physical Review A 45, n9 p6349-6370, 1 May 92.

Keywords: *Electron-atom collisions, *Alkali metals, *Cesium, Milli EV range, EV range 1-10, Electron scattering, Electron collisions, Relativistic effects, Cross sections, R matrix, Low energy, Multiplets, Reprints.

We have reformulated the Dirac R-matrix method for low-energy electron scattering by (effectively) one-electron, alkali-metal-like systems and developed an independent computer program for this special purpose. A highly accurate and relativistic representation of the target was used to perform a multichannel close-coupling calculation of cross sections for electron scattering. Our results include the negative-ion affinity and elastic, inelastic, and total cross sections for incident electrons with 0 to 2.8 eV kinetic energy. We find that core-polarization and relativistic effects lead to multiplets of very narrow triplet P(j), J = 0,1,2 shape resonances: the effect of the induced core polarization on the electron-electron correlation leads to 6s6p triplet P(sub j, sup 0) resonances in contrast to previously predicted bound states of Cs(1-), and relativistic interactions are responsible for the autoionizing decay of 6p(2) triplet P(J) states below the first excitation threshold.

04,007
PB95-203477 Not available NTIS
National Inst. of Standards and Technology (PL), Boulder, CO. Quantum Physics Div.
Short-Pulse Detachment of H(-) in the Presence of a Static Electric Field.
Final rept.
Q. Wang, and A. F. Starace. 1993, 4p.
Grant NSF-PHY-9108002
Sponsored by National Science Foundation, Washington, DC.
Pub. in Physical Review A 48,m n3 pR1741-R1744 Sep 93.

Keywords: *Hydrogen ions, *Electron detachment, *Photodetachment, Electric fields, Negative ions, Cross sections, Laser radiation, Reprints, Laser photoionization.

Quantum interference effects occurring in photodetachment of H(1-) in the presence of a uniform, static electric field are shown theoretically to be controllable through use of short laser pulses having characteristic times comparable to photodetached electron reflection times. In particular, calculated cross sections for single-photon detachment by two laser pulses that are delayed and phase shifted relative to one another are shown to oscillate as a function of the relative phases of the laser pulses at fixed photodetached electron energy.

04,008
PB95-203493 Not available NTIS
National Inst. of Standards and Technology (PL), Boulder, CO. Quantum Physics Div.
Oscillator Strengths and Radiative Branching Ratios in Atomic Sr.
Final rept.
H. G. C. Werij, C. H. Greene, C. E. Theodosiou, and A. Gallagher. 1992, 13p.
Grant NSF-PHY90-12244
Sponsored by National Science Foundation, Washington, DC.
Pub. in Physical Review A 46, n3 p1248-1260, 1 Aug 92.

Keywords: *Oscillator strengths, *Strontium, Transition probabilities, Branching ratio, R matrix, Reprints, Radiative transitions.

Tables of radiative transition rates (A) are provided for allowed singlet and triplet transitions between Sr states below n approx. = 11. These are obtained from a combination of R-matrix, multichannel-quantum-defect-theory (MQDT), and modified Coulomb-approximation calculations, plus branching-ratio measurements. Measurements of some spin-changing branchings and of the 4 singlet D(2) - 5 singlet S(0) quadrupole transition rate are also reported. Lifetime and A-value measurements from the literature are included in the tables and compared to the calculations. These and the present measurements provide the most comprehensive test to date of calculated transition probabilities for divalent atoms. The MQDT calculation achieves 0-20% agreement with experiment in the great majority of cases tested.

04,009
PB95-203600 Not available NTIS
National Inst. of Standards and Technology (PL), Boulder, CO. Quantum Physics Div.
Suppression of Ionization in One- and Two-Dimensional Model Calculations.
Final rept.
L. You, J. Mastowski, and J. Cooper. 1992, 7p.
Grant NSF-PHY90-12244
Sponsored by National Science Foundation, Washington, DC.
Pub. in Physical Review A 45, n5 p3203-3209, 1 Mar 92.

Keywords: One-dimensional calculations, Two-dimensional calculations, Two dimensional models, Mathematical models, Multi-photon processes, Reprints, *Ionization suppression, Multiphoton ionization.

We study numerically ionization from a model atom induced by a strong high-frequency field. Both one- and two-dimensional models are considered. We discuss the physics of ionization suppression in strong fields and point out the differences between one- and higher-dimensional models. We also discuss the applicability of classical modeling.

04,010
PB95-203816 Not available NTIS
National Inst. of Standards and Technology (PL), Boulder, CO. Quantum Physics Div.
Precision Lifetime Measurements of Cs 6p (2)P1/2 and 6p (2)P3/2 Levels by Single-Photon Counting.
Final rept.
L. Young, W. T. Hill, S. J. Sibener, C. E. Wieman, S. R. Leone, S. D. Price, and C. E. Tanner. 1994, 8p.
Contract DE-W-31-109-ENG-38
Sponsored by National Science Foundation, Arlington, VA. and Department of Energy, Washington, DC.
Pub. in Physical Review A 50, n3 p2174-2181 Sep 94.

Keywords: *Atomic energy levels, *Cesium, Mode locked lasers, Excited states, Atomic beams, P invariance, Lifetime, Parity, Reprints, Titanium sapphire lasers, Femtosecond pulses, Photon counting.

Time-correlated single-photon counting is used to measure the lifetimes of the 6p doublet P(1/2) and 6p doublet P(3/2) levels in atomic Cs with accuracies of approx. 0.2-0.3%. A high-repetition-rate, femtosecond, self-mode-locked Ti:sapphire laser is used to excite Cs produced in a well-collimated atomic beam. The time interval between the excitation pulse and the arrival of a fluorescence photon is measured repetitively until the desired statistics are obtained. The lifetime results are 34.75(7) and 30.41(10) ns for the 6p doublet P(1/2) and 6p doublet P(3/2) levels, respectively. These lifetimes fall between those extracted from ab initio many-body perturbation-theory calculations by Blundell, Johnson, and Sapirstein (1991) and V. A. Dzuba et al (1989) and are in all cases within 0.9% of the calculated values. The measurement errors are dominated by systematic effects, and methods to alleviate these and to approach an accuracy of 0.1% are discussed. The technique is a viable alternative to the fast-beam laser approach for measuring lifetimes with extreme accuracy.

04,011
PB95-203824 Not available NTIS
National Inst. of Standards and Technology (PL), Boulder, CO. Quantum Physics Div.

Hyperfine-Structure Studies of Zr II: Experimental and Relativistic Configuration-Interaction Results.
Final rept.
L. Young, C. A. Kurtz, D. R. Beck, and D. Datta.
1993, 9p.
Contract DE-W-31-109-ENG-38
Sponsored by Department of Energy, Washington, DC. Office of Basic Energy Sciences.
Pub. in Physical Review A 48, n1 p173-181 Jul 93.

Keywords: *Zirconium ions, *Hyperfine structure, Atomic energy levels, Atomic spectroscopy, Atomic structure, Metastable state, Electric moments, Quadrupole moments, Experimental data, Zirconium 91, Reprints, Ab initio calculations.

We report an experimental and theoretical study of the hyperfine structure (hfs) in various metastable levels in (91)Zr II. Hyperfine structures in 11 levels arising from the 4d(3) and 4d(2)5s configurations were measured using the laser-rf double-resonance method in a collinear laser-ion-beam geometry. The hfs A and B constants were measured to a precision of 4 and 11 kHz, respectively. Less precise values for hfs constants for nine upper levels in the 4d(2)5p configuration were derived from optical spectra. Theoretically, the A and B constants for the metastable levels having J=0.5 and 1.5 were calculated using a relativistic configuration-interaction (RCI) approach. The calculations confirm a previous report that the level at 17,614.00/cm reported in Moore's Atomic Energy Levels, Vol. II (US Government Printing Office, Washington, DC, 1971) is spurious.

04,012
PB95-203840 Not available NTIS
National Inst. of Standards and Technology (PL), Boulder, CO. Quantum Physics Div.
Improved Hyperfine Measurements of the Na NP Excited State Through Frequency-Controlled Dopplerless Spectroscopy in a Zeeman Magneto-Optic Laser Trap.
Final rept.
M. Zhu, C. W. Oates, and J. L. Hall. 1993, 3p.
Contract N00014-89-J-1227, Grant NSF-PHY90-12244
Sponsored by National Science Foundation, Washington, DC. and Office of Naval Research, Arlington, VA.
Pub. in Optics Letters 18, n14 p1186-1188, 15 Jul 93.

Keywords: *Sodium, Atomic spectroscopy, Excited states, Hyperfine structure, High resolution, Frequency standards, Magnetooptics, Reprints, *Atom traps, Laser traps, Dopplerless spectroscopy.

We report what is to our knowledge the first Dopplerless high-resolution optical spectroscopy based on unperturbed atoms left nearly at rest when a vapor cell magneto-optic trap is switched off. A lambda = 285 nm beam excited the 3s --> 5p transition in our sample of laser trapped/cooled Na atoms from which we collected fluorescence. Excited-state 5 doublet P(3/2) and 5 doublet P(1/2) hyperfine interaction constants are derived with 4- and 47-fold increases, respectively, in accuracy. Future prospects for vapor-cell based optical spectroscopy and frequency standards are considered.

04,013
PB95-220539 PC A06/MF A02
National Inst. of Standards and Technology (PL), Gaithersburg, MD. Ionizing Radiation Div.
Tables of X-ray Mass Attenuation Coefficients and Mass Energy-Absorption Coefficients 1 keV to 20 MeV for Elements Z = 1 to 92 and 48 Additional Substances of Dosimetric Interest.
J. H. Hubbell, and S. M. Seltzer. May 95, 116p, NISTIR-5632.

Keywords: *X rays, *Gamma rays, KeV range 1-10, KeV range 10-100, KeV range 100-1000, MeV range 1-10, MeV range 10-100, Gamma dosimetry, X-ray dosimetry, Radiation shielding, Chemical elements, Bremsstrahlung, Tables(Data), Graphs(Charts), *Mass attenuation coefficients, *Mass energy-absorption coefficients.

Tables and graphs of the photon mass attenuation coefficient mu/rho and the mass energy-absorption coefficient my(en)/rho are presented for all of the elements Z=1 to 92, and for 48 compounds and mixtures of radiological interest. The tables cover energies of the photon (x ray, gamma ray, bremsstrahlung) from 1 keV to 20 MeV. The mu/rho values are taken from the current photon interaction database at the National Institute of Standards and Technology, and the mu(en)/rho values are based on the new calculations by Seltzer described in Radiation Research 136, 147 (1993). These tables of my/rho and mu(en)/rho replace and extend the tables given by Hubbell in the International Journal of Applied Radiation and Isotopes 33, 1269 (1982).

04,014
PB95-242384 PC A04/MF A01
National Inst. of Standards and Technology, Gaithersburg, MD.
DETAN 95: Computer Code for Calculating Spectrum-Averaged Cross Sections and Detector Responses in Neutron Spectra.
C. M. Eisenhauer. Mar 95, 70p, NISTIR-5622.

Keywords: *Neutron cross sections, *Neutron spectra, *Programming manuals, Neutron detectors, Spectrum analysis, Personnel dosimetry, Fission spectra, Response functions, Computer programs, Tables(Data), Computation, *DETAN 95 computer code.

DETAN 95 is a computer code for converting an input neutron spectrum to a spectrum or detector response function expressed in arbitrary energy-group structure. The input spectrum may be expressed either in analytic form or in some energy-group structure. The code also calculates spectrum-averaged neutron cross sections or responses for neutron personnel detectors. The code includes 625-group neutron cross sections for a number of reactions common to materials dosimetry. Other energy-dependent cross sections or response functions supplied by the user may be used to calculated spectrum-averaged values.

04,015
PB95-255923 PC A03/MF A01
National Inst. of Standards and Technology (CSTL), Gaithersburg, MD. Process Measurements Div.
Reproducibility of the Temperature of the Ice Point in Routine Measurements.
Technical note.
B. W. Mangum. Jun 95, 27p, NIST/TN-1411.
Also available from Supt. of Docs. as SN003-003-03347-2.

Keywords: *Temperature measurement, *Water, Resistance thermometers, Triple point, Reproducibility, *Ice point, Fixed points.

This note presents results on the reproducibility and temperature of the ice point of water. The data were obtained over the years 1963 to 1970, in 1992 and in 1995. The data from 1963 to 1970 are from resistance measurements of a standard platinum resistance thermometer in ice points, made for the purpose of obtaining the reference value for the thermometer to be used for determining temperatures of calibration of liquid-in-glass thermometers. In 1992 and in 1995, measurements of the temperature of the ice point were made, using water (and ice) from different sources. The value of the temperature determined for the ice point prepared from the authors' highest-purity water is in excellent agreement with that determined previously. Also, the reproducibility of routine measurements at the ice point are consistent with what has been generally accepted, but heretofore undocumented.

04,016
PB95-261905 (Order as PB95-261897, PC A07/MF A02)
Bureau International des Poids et Mesures, Sevres (France).
Determining the Magnetic Properties of 1 kg Mass Standards.
R. S. Davis. 1995, 17p.
Included in Jnl. of Research of the National Institute of Standards and Technology, v100 n3 p209-225 May/Jun 95.

Keywords: *Magenetic properties, *Mass, *Metrology, Calibration standards, Magnetic permeability, US NBS, National Institute of Standards and Technology, Susceptometer.

Magnetic interactions may lead to errors in precision mass metrology. An analytical description of such magnetic errors is presented in which the roles of both the volume magnetic susceptibility and permanent magnetization are discussed. The same formalism is then used to describe in detail the calibration and operation of a susceptometer developed at the Bureau International des Poids et Mesures (BIPM).

04,017
PB96-102058 Not available NTIS
National Inst. of Standards and Technology (PL), Boulder, CO. Quantum Physics Div.
Merged-Beams Energy-Loss Technique for Electron-Ion Excitation: Absolute Total Cross Sections for O(5+) (2s yields 2p).
Final rept.
E. W. Bell, X. Q. Guo, J. L. Forand, J. S. Thompson, G. H. Dunn, M. E. Bannister, D. C. Gregory, R. A. Phaneuf, A. C. H. Smith, A. Muller, C. A. Timmer, E. K. Wahlin, B. D. DePaola, D. S. Belic, K. Rinn, and D. R. Swenson. 1994, 12p.
Contract DE-A105-86ER53237
Sponsored by Department of Energy, Washington, DC.
Pub. in Physical Review A 49, n6 p4585-4596 Jun 94.

Keywords: *Beams(Radiation), *Energy dissipation, *Electron-ion coupling, Cross sections, Oxygen, Ionization, Backscattering, Spectroscopy, Reprints, *Merged beams, O(5+).

A merged-beams electron-energy-loss technique is described, by which absolute cross sections can be measured for near-threshold electron-impact excitation of multiple charged ions. The experimental data are in good agreement with a seven-state close-coupling throughout the energy range of the experiment. Results agree with calculations showing that more than 90% of the electrons causing excitation are ejected in the backward direction in the center-of-mass frame. This backscattering is shown in both quantum-mechanical and semiclassical calculations. Evidence is observed for high-lying metastable autoionizing states with a life-time of approximately 0.9 microseconds which are made to ionize by electron impact.

04,018
PB96-102074 Not available NTIS
National Inst. of Standards and Technology (CAML), Gaithersburg, MD. Applied and Computational Mathematics Div.
Faster Monte Carlo Simulations.
Final rept.
J. L. Blue, I. Beichl, and F. Sullivan. 1995, 2p.
See also PB95-136370.
Pub. in Physical Review E 51, n2 pR867-R868 Feb 95.

Keywords: *Monte Carlo method, *Simulation, Crystal growth, Kinetics, Computerized simulation, Equilibrium equations, Reprints, Computer time.

For Monte Carlo simulations of systems of size M, either kinetic simulations or equilibrium simulations that use the method of Bortz, Kalos, and Liebowitz the best computer time per event has been O(M(sup 1/2)). The authors present two methods whose computer time per event is O(M(sup 1/k)) or O(logM). In practice, for typical simulation sizes, K = 4 or K = 5 is fastest, requiring even less computer time than the O(logM) method. For typical simulation sizes, the authors are able to achieve speedup factor of 5 to 7 over the O(M(sup 1/2)) technique.

04,019
PB96-102090 Not available NTIS
National Inst. of Standards and Technology (CSTL), Gaithersburg, MD. Thermophysics Div.
Vapour Pressures and Gas-Phase (p, rho n, T) Values for CF3CHF2{R125).
Final rept.
S. J. Boyes, and L. A. Weber. 1995, 12p.
Pub. in Jnl. of Chemical Thermodynamics 27, p163-174 1995.

Keywords: *Vapor pressure, *Gases, *Fluorinated celiphatic hydrocarbons, Refrigerants, Pressure, Temperature, Density(Mass/volume), Virial equation, Thermodynamic properties, Reprints, *Pentafluoroethane, R125 refrigerant.

The authors present new vapor pressures and the (p, p(sub n), T) surface of CF3CHF2 (pentafluoroethane, designated R125 by the refrigeration industry) in the temperature range T = 273 K to 363 K. The (p, p(sub n), T) measurements are for the gas phase at densities up to approximately the critical density. The static vapor pressures reported here have been combined with previous ebulliometric measurements made in this laboratory at lower temperatures. Correlating equations are given for the vapour pressures from T = 220 K to the critical temperature: T(sub c) - 339.30 K. A virial equation has been used to correlate the (p, p(sub n), T) surface at amount-of-substance densities up to 1600 mol/cubic m. Second and third virial coefficients have been derived from the (p, p(sub n), T) measurements.

04,020
PB96-102124 Not available NTIS

National Inst. of Standards and Technology (PL), Gaithersburg, MD. Quantum Metrology Div.
Energy Dependences of Absorption in Beryllium Windows and Argon Gas.
Final rept.
C. T. Chantler, and J. L. Staudenmann. 1995, 4p.
Pub. in Review of Scientific Instruments 66, n2 p1651-1654 Feb 95.

Keywords: *Energy dependence, *Beryllium, *Argon, *Absorption, Gas detectors, Coefficients, Synchrotron radiation, X rays, Form factors, Particle properties, Reprints.

In part of an ongoing work on x-ray form factors, new absorption coefficients are being evaluated for all elements, across the energy range from below 100 eV to above 100 keV. These new coefficients are applied herein to typical problems in synchrotron radiation stations, namely the use of beryllium windows and argon gas detectors. Results are compared with those of other authors. The electron-ion pair production process in ionization chambers is discussed, and the effects of 3d-element impurities are indicated.

04,021
PB96-102199 Not available NTIS
National Inst. of Standards and Technology (MSEL), Gaithersburg, MD. Reactor Radiation Div.
Transmission Properties of Short Curved Neutron Guides. Part 1. Acceptance Diagram Analysis and Calculations.
Final rept.
J. R. D. Copley. 1995, 9p.
Pub. in Nuclear Instruments and Methods in Physics Research A, v355 p469-477 1995.

Keywords: *Transmittance, *Neutron guides, Neutron reflectors, Beam acceptance, Optical properties, Gamma rays, Performance evaluation, Reprints, *Curved guide, *Acceptance diagrams, Ray-tracing.

A curved neutron guide is considered 'short' if there are direct lines of sight through the device. Such guides have the disadvantage that they transmit high energy neutrons and gamma rays, which are generally unwanted, as well as the desired low energy neutrons. Nevertheless short curved guides have several uses at thermal neutron research facilities because they can be combined with sections of straight guide to produce composite guides through which there is no line of sight. The authors analyze the transmission properties of short curved neutron guides using the method of acceptance diagrams, and they present the results of several calculations of their performance.

04,022
PB96-102330 Not available NTIS
National Inst. of Standards and Technology (BFRL), Gaithersburg, MD. Structures Div.
Fluctuations in Probability Distribution on Chaotic Attractors.
Final rept.
M. Franaszek. 1995, 7p.
Pub. in Physics Letters A 203, p115-121 1995.

Keywords: *Probability distribution functions, *Variations, *Chaos, *Strange attractors, Perturbation, Periodic variations, Noise, Amplitudes, Time series analysis, Stochastic processes, Reprints.

Fluctuations in probability distribution are used to study the influence of a weak periodic perturbation on chaotic system. A detailed analysis of one very long time series reveals a great sensitivity to external perturbation. The case of large amplitude stochastic perturbation is also discussed. It is shown that the fractal geometry of an experimental attractor may be visualized up to length scales smaller than noise amplitude.

04,023
PB96-102348 Not available NTIS
National Inst. of Standards and Technology (PL), Boulder, CO. Quantum Physics Div.
Kinetics and Dynamics of Vibrationally State Resolved Ion-Molecule Reactions: (14)N2(+)(v=1 and 2) and (15)N2(+)(v=0,1 and 2) with (14)N2.
Final rept.
M. J. Frost, S. Kato, V. M. Bierbaum, and S. R. Leone. 1994, 9p.
Contract AFOSR-FA9620-92J-0072, Grant NSF-PHY90-12244
Sponsored by Air Force Office of Scientific Research, Bolling AFB, DC. and National Science Foundation, Washington, DC.
Pub. in Jnl. of Chemical Physics 100, n9 p6359-6367, 1 May 94.

Keywords: *Charge transfer, *Ions, *Reaction kinetics, Molecular interactions, Nitrogen isotopes, Lasers, Ionic reactions, Vibration, Reprints.

Vibrationally state-selected measurements of the kinetics and dynamics of 14N2(1+)(nu = 1 and 2) and 15N2(1+)(nu = 0, 1, and 2) in collisions with (14)N2 are made using a selected ion flow tube (SIFT), laser induced fluorescence (LIF) technique at thermal energies. Kinetics are measured by monitoring the LIF signal amplitudes of N2(1+)(nu) as a function of (14)N2 concentration, added after ion injection. By comparison with the known N2(1+)(nu = 1) + Ar rate, the (15)N2(1+)(nu = 0) + 14N2 rate constant is found to be one-half of the Langevin collision rate or 4.2 + or - 0.2 x 10(exp -10) cubic cm/molecule/s. This suggests that the reaction proceeds via an N4(1+) energized adduct in which charge is shared on a time scale shorter than the adduct lifetime. The removal rates of (14)N2(1+)(nu = 1 and 2) reactions by (14)N2 are also found to proceed at one-half of the Langevin collision rate. Thus product channels that remove vibrational energy from the ion upon dissociation of the adduct account for 50% of the collision probability.

04,024
PB96-102744 Not available NTIS
National Inst. of Standards and Technology (CSTL), Gaithersburg, MD. Thermophysics Div.
Analytical Method for Determining Thermal Conductivity from Dynamic Experiments.
Final rept.
R. A. MacDonald. 1995, 8p.
Sponsored by National Aeronautics and Space Administration, Washington, DC.
Pub. in International Jnl. of Heat and Mass Transfer, v38 n14 p2549-2556 1995.

Keywords: *Thermal conductivity, *Rods, *Tungsten, Temperature dependence, Specific heat, Surface temperature, Profiles, Cylindrical bodies, High temperature, Partial differential equations, Heat transmission, Radiative heat transfer, Thermodynamics, Reprints.

The temperature profile along a cylindrical rod or tube as it cools has been obtained by numerical solution of the second-order time-dependent partial differential equation for heat conduction. The surface temperature is calculated for given temperature dependent values of the heat capacity, hemispherical total emissivity, thermal expansion and thermal conductivity and, by adjusting the thermal conductivity, is fitted to experimental temperature profiles from preliminary measurements on a cooling cylindrical tungsten rod. The surface temperature of the rod is quite sensitive to the thermal conductivity but the accuracy of the predicted thermal conductivity cannot be assessed without further experimentation.

04,025
PB96-102751 Not available NTIS
National Inst. of Standards and Technology (PL), Gaithersburg, MD. Quantum Metrology Div.
Evolution of X-ray Resonance Raman Scattering into X-ray Fluorescence from the Excitation of Xenon Near the L3 Edge.
Final rept.
M. A. MacDonald, S. H. Southworth, J. C. Levin, T. Lebrun, Y. Azuma, P. L. Cowan, B. A. Karlin, A. Henins, and R. D. Deslattes. 1995, 6p.
Pub. in Physical Review A, v51 n5 p3598-3603 May 95.

Keywords: *Xenon, *Raman spectra, *X ray fluorescence, Synchrotron radiation, Absorption spectra, Edges, Experimental data, Reprints, Absorption edge, L3 edge.

Near an absorption edge, x-ray emission cannot be treated separately from the absorption process itself; a scattering formalism must be used. Experimental data have been recorded showing x-ray emission from xenon following excitation by tunable synchrotron radiation below and above the L3 absorption edge. Complete data sets are presented for Xe La1,2 and Lbeta2,15 emission from 10 eV below to 40 eV above the L3 edge. In accord with the resonant-inelastic-scattering model, the observed x-ray emission evolves from resonant Raman scattering into characteristic fluorescence as the excitation energy is scanned from below to above the absorption edge.

04,026
PB96-102850 Not available NTIS
National Inst. of Standards and Technology (EEEL), Gaithersburg, MD. Electricity Div.
Effect of Electrode Material on Measured Ion Energy Distributions in Radio-Frequency Discharges.
Final rept.
J. K. Olthoff, R. J. Van Brunt, and S. B. Radovanov. 1995, 3p.
Pub. in Applied Physics Letters, v67 n4 p473-475, 24 Jul 95.

Keywords: *Electrodes, *Ions, *Radio frequency discharge, Reprints, Ion energy analysis, Distribution, Discharges, Surface charging.

Evidence is presented for a significant influence of electrode surface material and condition on the measurement of the kinetic energies of ions sampled from discharges through a orifice in the electrode. Significant differences in ion energy shifts and/or discrimination of low-energy ions are found using aluminum and stainless-steel electrodes in a radio-frequency (rf) discharge cell. It is argued that the observed differences in energy shifts may be attributable in part to differences in charging oxide layers on the electrode surface around the sampling orifice.

04,027
PB96-102918 Not available NTIS
National Inst. of Standards and Technology (CSTL), Gaithersburg, MD. Surface and Microanalysis Science Div.
Energy Calibration of X-ray Photoelectron Spectrometers: Results of an Interlaboratory Comparison to Evaluate a Proposed Calibration Procedure.
Final rept.
C. J. Powell. 1995, 12p.
Pub. in Surface and Interface Analysis, v23 p121-132 1995.

Keywords: *Spectrometers, *Calibration, Reprints, Copper, Gold, Silver, X rays, Photoelectrons, *Foreign technology, *Binding energy.

Results are reported of an interlaboratory comparison conducted to evaluate a proposed procedure for calibration of the binding energy (BE) scales on x-ray photoelectron spectrometers. The calibration was performed at two points on the BE scale (the Au 4f7/2 and Cu 2p3/2 lines) and checks were made of the assumption of BE-scale linearity from measurements on other lines. It is shown here that small offsets can arise if peaks are located with assumed backgrounds on non-zero slope or if multipeak fits are made to Cu L3VV and Ag M4VV Auger spectra.

04,028
PB96-102942 Not available NTIS
National Inst. of Standards and Technology (PL), Gaithersburg, MD. Atomic Physics Div.
Time-Resolved Balmer-Alpha Emission from Fast Hydrogen Atoms in Low Pressure, Radio-Frequency Discharges in Hydrogen.
Final rept.
S. B. Radovanov, K. Dzierzega, J. R. Roberts, and J. K. Olthoff. 1995, 3p.
Pub. in Applied Physics Letters, v66 n20 p2637-2639, 15 May 95.

Keywords: *Hydrogen, *Radiofrequency discharges, Reprints, Atoms, Balmer lines, Low pressure, *Doppler broadened emission.

Doppler-broadened H(alpha) emission (656.28 nm) detected from a 13.56 MHz, parallel-plate, radio-frequency discharge in hydrogen indicates the presence of fast excited H atoms throughout the discharge volume. Time and spatially resolved measurements of the Doppler-broadened emission indicate that the fast H atoms are formed primarily at the surface of the powered electrode with kinetic energies exceeding 120 eV.

04,029
PB96-102959 Not available NTIS
National Inst. of Standards and Technology (EEEL), Gaithersburg, MD. Electricity Div.
Ion Kinetic-Energy Distributions and Balmer-alpha (Halpha) Excitation in Ar-H2 Radio-Frequency Discharges.
Final rept.
S. B. Radovanov, J. K. Olthoff, R. J. Van Brunt, and S. Djurovic. 1995, 12p.
Pub. in Jnl. of Applied Physics, v78 n2 p746-757, 15 Jul 95.

Keywords: *Radiofrequency charges, *Gas discharges, *Argon ions, Reprints, Hydrogen, Balmer lines, Neutrals, Electrodes, Ion kinetic energy.

Excited neutrals and fast ions produced in a 13.56 MHz radio-frequency discharge in a 90% argon -10% hydro-

gen gas mixture was investigated, respectively, by spatially and temporally resolved optical emission spectroscopy, and by mass-resolved measurements of ion kinetic energy distributions at the grounded electrode. The electrical characteristics of the discharge were also measured and comparisons are made with results obtained for discharges in pure H2 under comparable conditions. Measurements of Balmer-alpha emission show Doppler-broadened emission that is due to the excitation of fast atomic hydrogen neutrals formed from ion neutralization processes in the discharge.

04,030
PB96-103106 Not available NTIS
National Inst. of Standards and Technology (PL), Boulder, CO. Quantum Physics Div.
Low-Energy-Electron Collisions with Sodium: Elastic and Inelastic Scattering from the Ground State.
Final rept.
W. K. Trail, M. A. Morrison, H. L. Zhou, K. B. MacAdam, T. L. Goforth, D. W. Norcross, B. L. Whitten, and K. Bartschat. 1994, 26p.
Sponsored by National Science Foundation, Arlington, VA.
Pub. in Physical Review A 49, n5 p3620-3645 May 94.

Keywords: *Cross sections, *Electron-atom collisions, *Elastic scattering, *Inelastic scattering, Sodium, R matrix, Angular momentum, Electron diffraction, Experimental data, Data bases, Reprints.

The electron-Na system is the prototype for nonrelativistic scattering of a charged particle from a quasi-one-electron system. At scattering energies below several eV, e-Na cross sections are particularly sensitive to the exchange interaction and manifest a rich variety of near-threshold structures in various spin channels. By applying the nonperturbative coupled-channel R-matrix method in carefully converged calculations the authors have generated a comprehensive data base of accurate scattering quantitities for studying these phenomena and for comparison to present and future experimental data. In addition to conventional integrated and differential cross sections, the authors consider partial cross sections for changes in the projection of the spin and orbital angular momentum of the Na valence electron, comparing results for all these quantities to experimental data where available.

04,031
PB96-103122 Not available NTIS
National Inst. of Standards and Technology (PL), Boulder, CO. Time and Frequency Div.
Aging, Warm-Up Time and Retrace; Important Characteristics of Standard Frequency Generators.
Final rept.
J. Vanier, J. J. Gagnepain, W. J. Riley, F. L. Walls, and M. Granveaud. 1992, 9p.
Pub. in Proceedings of Institute of Electrical and Electronics Engineers Frequency Control Symposium, Hershey, PA., May 22-29, 1992, p807-815 1992.

Keywords: *Frequency, *Standards, *Pulse generators, Frequency measurement, Environmental effects, Sensitivity, Aging(Materials), Reporting, Reprints, Retrace, Warm-up.

The report is an effort to produce an IEEE standard providing guidelines for standardized methods of defining, measuring and reporting environmental sensitivities of precision frequency generators. The present report covers the subject of aging, warm-up time and retrace.

04,032
PB96-110739 Not available NTIS
National Inst. of Standards and Technology (PL), Boulder, CO. Quantum Physics Div.
Intensity-Dependent Scattering Rings in High Order Above-Threshold Ionization.
Final rept.
B. Yang, K. J. Schafer, B. Walker, L. F. DiMauro, K. C. Kulander, and P. Agostini. 1993, 4p.
Sponsored by Department of Energy, Washington, DC.
Pub. in Physical Review Letters 71, n23 p3770-3773, 6 Dec 93.

Keywords: *Photoionization, *Electron scattering, *Xenon, *Krypton, Photoelectrons, Angular distribution, Ponderomotive forces, Electrodynamics, Rings, Wave functions, Reprints, Multiphoton processes, Photoelectron angular distributions.

Angular distributions of high energy photoelectrons from Xe and Kr, excited by a 50 ps, 1.05 micro m laser, are presented. In Xe, strong, narrow, rings about 45 deg. off the polarization axis appear in a limited energy range centered around U(sub p), where U(sub p) is the ponderomotive energy. This effect is much weaker in Kr. Single active electron calculations agree well with these observations. The authors conclude that the rings result from single-electron ionization dynamics, most likely involving rescattering from the ion core of the tunneling component of the continuum wave function.

04,033
PB96-111612 Not available NTIS
National Inst. of Standards and Technology (PL), Gaithersburg, MD. Ionizing Radiation Div.
Monte Carlo and Analytic Methods in the Transport of Electrons, Neutrons, and Alpha Particles.
Final rept.
R. S. Caswell, and S. M. Seltzer. 1994, 17p.
Pub. in Computational Approaches in Molecular Radiation Biology, p115-131 1994.

Keywords: *Alpha particles, *Monte Carlo method, Photons, Electrons, Neutrons, Biological effects, Computer programs, Radiation transport, Energy, Deposition, Reprints.

In this paper the authors discuss Monte Carlo calculational methods and analytic methods, and methods combining features of both, developed over the past decades at the National Institute of Standards and Technology. These include the Monte Carlo program ETRAN for electrons and photons developed by Berger and Seltzer: the neutron analytic method developed by Caswell and Coyne, and the incorporation into that program of the synthesis of Monte Carlo results for proton tracks of Wilson and Paretzke. Some comparisons with experimental results and with other calculations are given. Also, some applications of the calculational results to the prediction of biologial effects using biophysical models are given.

04,034
PB96-111661 Not available NTIS
National Inst. of Standards and Technology (CAML), Gaithersburg, MD. Applied and Computational Mathematics Div.
Nonequilibrium Thermodynamic Theory of Viscoplastic Materials.
Final rept.
B. Bernstein, and J. T. Fong. 1993, 9p.
Pub. in Jnl. of Applied Physics, v74 n4 p2220-2228, 15 Aug 93.

Keywords: *Thermodynamic equilibrium, *Elasticity, Mechanical properties, Thermodynamic properties, Entropy, Free energy, Creep, Fatigue, Models, Reprints.

A nonequilibrium thermodynamic theory for predicting the mechanical behavior of materials beyond the elastic range is formulated. The theory incorporates the idea of a concealed parameter alpha, originally due to Bridgman where the constitutive equation are governed by (1) a thermodynamic potential such as a generalized Gibbs function, G, or Helmholtz free-energy function, F, each with an explicit dependence on alpha and (2) a prescription for alpha, the time rate of change of alpha, such that alpha is directly proportional to the negative of G(sub alpha) or F(sub alpha), the partial derivative of G or F with respect to alpha, respectively.

04,035
PB96-111828 Not available NTIS
National Inst. of Standards and Technology (MSEL), Gaithersburg, MD. Reactor Radiation Div.
Vibrational Excitations and the Position of Hydrogen in Nanocrystalline Palladium.
Final rept.
U. Stuhr, H. Wipf, T. J. Udovic, J. Weissmuller, and H. Gleiter. 1995, 12p.
Pub. in Jnl. of Physics: Condensed Matter, v7 p219-230 1995.

Keywords: *Palladium, *Hydrogen atoms, *Vibrational spectroscopy, Position(Location), Grain boundaries, Solubility, Crystal lattices, Neutron scattering, Absorption, Reprints, *Nanocrystals, *Hydrogen absorption.

The vibrational excitations and the position of hydrogen in nanocrystalline palladium were investigated by means of inelastic neutron-scattering and H solubility measurements. The study focuses on the H concentration regime (less than or equal to 4.8 at.% H) where, at room temperature, no precipitation of the H in a hydride phase (Beta-phase) was observed. In this concentration regime, the solubility measurements show an enhanced H solubility relative to coarse-grained Pd. The neutron-scattering experiments show that this additional H is incorporated in the grain boundaries and at the surface of the grains. Surface modes of H at approximately 90 and 120 meV were identified. Compared to coarse-grained Pd, no change in the H solubility was found for the crystal lattice of the nanosized grains.

04,036
PB96-111836 Not available NTIS
National Inst. of Standards and Technology (MSEL), Gaithersburg, MD. Reactor Radiation Div.
Magnetic Structure and Spin Dynamics of the Pr and Cu in Pr2CuO4.
Final rept.
I. W. Sumarlin, J. W. Lynn, T. Chattopadhyay, J. L. Peng, S. N. Barilo, and D. I. Zhigunov. 1995, 15p.
Pub. in Physical Review B, v51 n9 p5824-5838, 1 Mar 95.

Keywords: *Magnetic properties, *Spin dynamics, *Praseodymium, *Copper, Crystal structure, Magnons, Atomic interactions, Velocity, Phase diagrams, Temperature dependence, Zero point energy, Field theory, Neutron scattering, Reprints, *Zero-field ordered moment.

Neutron-scattering techniques have been used to study the magnetic structure and spin dynamics of the Pr and Cu spins in Pr2CuO4. In the ordered state the Cu spin-wave velocity c has been determined to be 0.85 + or - 0.08 eV Angstroms, which corresponds to an in-plane nearest-neighbor exchange constant J = 130 + or - 13 meV. A spin-wave gap of approximately 5 meV has been observed, corresponding to a reduced anisotropy constant alpha(sub parrallel sign) = (J - J(sup xy))/J of about 2 x 10(exp -4). In the paramagnetic regime the evolution of the Cu spin-correlation length with temperature is adequately described by the renormalized classical theory for the quantum nonlinear sigma model.

04,037
PB96-111885 Not available NTIS
National Inst. of Standards and Technology (PL), Boulder, CO. Quantum Physics Div.
Electron-Ion Collisions in the Plasma Edge.
Final rept.
G. H. Dunn. 1992, 15p.
Pub. in Nuclear Fusion A and M Suppl., v2 p25-39 1992.

Keywords: *Electron ion collisions, *Data bases, Reprints, Plasma diagnostics, Modelling, Fusion plasmas, *Plasma edge.

The electron-ion collisional database required for modelling and diagnostics of the fusion plasma edge is briefly examined from the points of view of (1) experimental and theoretical means for obtaining the data, (2) relevant physical processes, (3) limitations on the data, and (4) availability and quality of the data for relevant species. Both molecular and atomic ions are considered.

04,038
PB96-111992 Not available NTIS
National Inst. of Standards and Technology (EEEL), Boulder, CO. Electromagnetic Technology Div.
Comparison of Photodiode Frequency Response Measurements to 40 GHz between NPL and NIST.
Final rept.
A. D. Gifford, D. A. Humphreys, and P. D. Hale. 1994, 2p.
Pub. in Electronics Letters, v31 n5 p397-398, 2 Mar 95.

Keywords: *Photodiodes, Measurements, Reprints, Comparison, *Frequency responses.

The authore report the first comparison, at the national standards level, of photodiode frequency response measurements at wavelengths of 1,285, 1319 and 1.531 micrometers. A photodiode was measured up to 40GHz and the results were normalized to 1.319 micrometers using a model of the device. The average scatter in the results was plus or minus 0.12dB (2omega) below 20GHz and plus or minus 0.21dB from 20 to 33GHz.

04,039
PB96-112073 Not available NTIS

National Inst. of Standards and Technology (PL), Boulder, CO. Time and Frequency Div.
Quantum-Limited Cooling and Detection of Radio-Frequency Oscillations by Laser-Cooled Ions.
Final rept.
D. J. Heinzen, and D. J. Wineland. 1990, 18p.
Pub. in Physical Review A, v42 n5 p2977-2994, 1 Sep 90.

Keywords: *Radio frequency detection, Reprints, Quantum measurements, Mass spectroscopy, *Ion traps, *Laser cooling, Squeezed states.

A single trapped ion, laser cooled into its quantum ground state of motion, may be used as a very-low-temperature detector of radio-frequency signals applied to the trap end caps. If the signal source is a resonant oscillator of sufficiently high Q, the source may also be placed in its quantum ground state by coupling to the ion. Parametric couplings may be used to cool and detect source modes other than the mode directly coupled to the ion. A theoretical analysis of these cooling and detection processes is presented, and as an example, their application to single trapped electron and proton spectroscopy is examined. Squeezing and low noise detection of one quadrature component of the source oscillation are also discussed. The techniques discussed here may lead to radio-frequency measurements of improved accuracy and sensitivity. Cooling and detection of vibrations of macroscopic oscillators also appear possible.

04,040
PB96-112164 Not available NTIS
National Inst. of Standards and Technology (PL), Boulder, CO. Time and Frequency Div.
Precise Spectroscopy for Fundamental Physics.
Final rept.
W. M. Itano, J. C. Bergquist, J. J. Bollinger, F. L. Moore, M. G. Raizen, D. J. Wineland, J. M. Gilligan, and D. J. Heinzen. 1993, 10p.
Pub. in Hyperfine Interactions, v78 p211-220 1993.

Keywords: *Beryllium ions, *Ion storage, Reprints, Lorentz invariance, Spin, Interactions, Quantum mechanics.

We have applied experimental techniques that were developed for use in atomic frequency standards and clocks to investigations of local Lorentz invariance, the linearity of quantum mechanics, and anomalous long-range-spin-dependent forces. These experiments used a hyperfine transition in 9Be+ ions in a Penning trap. Recently, we have studied hyperfine transitions in 199Hg+ ions in a linear rf trap. Hg+ ions might be used for similar investigations in the future.

04,041
PB96-112347 Not available NTIS
National Inst. of Standards and Technology (CSTL), Gaithersburg, MD. Inorganic Analytical Research Div.
Analytical Applications of Guided Neutron Beams.
Final rept.
R. M. Lindstrom, E. A. Mackey, and R. L. Paul. 1994, 7p.
Pub. in Biological Trace Element Research, p47-53 1994.

Keywords: *Cold neutrons, *Neutron guides, Reprints, Neutron beams, Neutron scattering, Prompt gamma radiation, *Foreign technology.

Guided beams of thermal and cold neutrons have become available to analysts at several reactors during the past decade. The very pure beams from these guides have led to lower backgrounds and higher sensitivities for prompt-gamma activation analysis (PGAA), and thus to new applications for this technique. For analytical accuracy, the details of neutron scattering within the sample need to be taken into account; this consideration is especially important for most materials of biological origin.

04,042
PB96-119631 Not available NTIS
National Inst. of Standards and Technology (PL), Gaithersburg, MD. Quantum Metrology Div.
Strangeness Flow Difference in Nuclear Collisions at 15A and 200A GeV.
Final rept.
J. Rafelski, and M. Danos. 1994, 4p.
Pub. in Physical Review C, v50 n3 p1684-1687 Sep 94.

Keywords: *Nuclear collisions, Reprints, Particle production, *Strangeness flow.

The authors show existence of an important difference between strange-particle production in Si-Au collisions at 15A GeV (AGS) and in S-A collisions at 200A GeV (CERN), with A=32 and A=0(200).

04,043
PB96-119763 Not available NTIS
National Inst. of Standards and Technology (EEEL), Boulder, CO. Electromagnetic Technology Div.
VAMAS Intercomparison of Critical Current Measurements on NB3Sn Superconductors: A Summary Report.
Final rept.
H. Wada, C. R. Walters, L. F. Goodrich, and Tachikawa. 1994, 10p.
See also PB89-202147.
Pub. in Cryogenics, v34 n11 p899-908 1994.

Keywords: Reprints, Electrical measurement, *Superconducting wires, *Niobium stannides, *Critical current, Niobium tin, Interlaboratory comparisons.

The paper is a summary of an international collaboration endorsed by VAMAS to study problems associated with critical current measurements in Nb3Sn superconductors and provide guidelines for a standard measurement. Two series of critical current measurements were implemented. In the fifth series, three different sample conductors were used and participants made measurements using their own techniques. As a result, coefficients of variation for these samples at 12 T turned out the be 8-29.9%. A major source of these variations was attributed to strain sensitivity of the Nb3Sn conductors. Thus, the second series of measurements were done on one sample conductor and under specified measurement conditions, particularly in terms of specimen strain. The coefficient of variation decreased to 2.2%, which is regarded as a reasonable base for future establishment of an international standard measurement method.

04,044
PB96-119789 Not available NTIS
National Inst. of Standards and Technology (PL), Boulder, CO. Time and Frequency Div.
High-Order Multipole Excitation of a Bound Electron.
Final rept.
C. S. Weimer, F. L. Moore, and D. J. Wineland. 1993, 4p.
Pub. in Physical Review Letters, v70 n17 p2553-2556, 26 Apr 93.

Keywords: *Multipole excitation, Reprints, *Parametric processes, Penning trap, Single electron.

The nonlinear resonant response of a bound electron to a time-varying spatially inhomogeneous electric field was studied experimentally. By use of the artifical atom 'geonium' (an electron bound in a Penning trap), the authors observed up to ninth-order multiple (pentacosiododecapole) coherent excitation of the electron's magnetron motion, and up to third-order (octuple) excitation of the cyclotron motion. Also, by applying two fields simultaneously, the authors have observed coherent stimulated Raman Excitation of the electron's motion.

04,045
PB96-122106 (Order as PB96-117767, PC A08/MF A02)
National Inst. of Standards and Technology, Gaithersburg, MD.
Potential and Current Distributions Calculated Across a Quantum Hall Effect Sample at Low and High Currents.
M. E. Cage, and C. F. Lavine. 1995, 13p.
Included in Jnl. of Research of the National Institute of Standards and Technology, v100 n5 p529-541 Sep/Oct 95.

Keywords: *Hall effect, *Quantum theory, Potential, Charge distribution, Current distribution, Electron gas, Reprints, NIST(National Institute of Standards and Technology).

The potential and current distributions are calculated across the width of a quantum Hall effect sample for applied currents between 0 microA and 225 microA. For the first time, both a confining potential and a current-induced charge-redistribution potential are used. The confining potential has a parabolic shape, and the charge-redistribution potential is logarithmic. The solution for the sum of the two types of potentials is unique at each current, with no free parameters. The calculated potential distributions are in excellent agreement with contactless electro-optic effect laser beam measurements of Fontein et al.

04,046
PB96-122148 (Order as PB96-117767, PC A08/MF A02)
National Inst. of Standards and Technology, Gaithersburg, MD.
Third Generation Water Bath Based Blackbody Source.
J. B. Fowler. 1995, 9p.
Included in Jnl. of Research of the National Institute of Standards and Technology, v100 n5 p591-599 Sep/Oct 95.

Keywords: *Blackbody radiation, *Apertures, Reprints, Cavities, Emissivity, Temperature, Reflectance, Radiometry, Measuring instruments, NIST(National Institute of Standards and Technology).

A third generation water bath based blackbody source has been designed and constructed in the Radiometric Physics Division at the National Institute of Standards and Technology, Gaithersburg, MD. The goal of this work was to design a large aperture blackbody source with improved temporal stability and reproducibility compared with earlier designs, as well as improved ease of use. These blackbody sources operate in the 278 K to 353 K range with water temperature combined standard uncertainties of 3.5 mK to 7.8 mK. The calculated emissivity of these sources is 0.9997 with a relative standard uncertainty of 0.0003. With 50 mm limiting aperture at the cavity; entrance, the emissivity increases 0.99997.

04,047
PB96-122742 Not available NTIS
National Inst. of Standards and Technology (PL), Boulder, CO. Quantum Physics Div.
Orbital Alignment and Vector Correlations in Inelastic Atomic Collisions.
Final rept.
E. M. Spain, C. J. Smith, M. J. Dalberth, and S. R. Leone. 1993, 9p.
Pub. in International Conference on the Physics of Electronic and Atomic Collisions (18th), Invited Papers, Aarhus, Denmark, v295 p675-683 Jul 93.

Keywords: *Calcium, *Inelastic scattering, *Atomic collisions, Atomic orbitals, Alignment, Coherence, Vector analysis, Lasers, Reprints.

We present a brief commentary on two-, three-, and four-vector correlations in the inelastic scattering of orbitally aligned calcium atoms.

04,048
PB96-122916 Not available NTIS
National Inst. of Standards and Technology (PL), Boulder, CO. Quantum Physics Div.
Atom Cooling and Trapping, and Collisions of Trapped Atoms.
Final rept.
A. Gallagher. 1992, 14p.
Pub. in International Conference on the Physics of Electronic and Atomic Collisions (17th), Invited Papers, Brisbane, Australia, July 10-16, 1991, Section 3, p139-152.

Keywords: *Atomic collisions, *Energy transfer, Sodium, Densities, Temperatures, Reprints, *Foreign technology, Atom cooling, Trapped atoms.

Methods currently used to optically cool and trap atoms, and the resulting trap densities and temperatures are discussed. Next, the types of cold-atom collision processes that occur in these traps are discussed, with emphasis on their differences compared to more familiar atomic collisions at thermal and higher energies. A semiclassical model and calculations for trap-loss and associative ionization, due to excited state collisions of these very cold atoms, is then described.

04,049
PB96-123476 Not available NTIS
National Inst. of Standards and Technology (EEEL), Gaithersburg, MD. Electricity Div.
Noise Characteristics Below 1 Hz of Zener Diode-Based Voltage Reference.
Final rept.
A. F. Clark, and R. L. Steiner. 1995, 90p.
Pub. in Bulletin of the American Physical Society Meeting, San Jose, CA., March 13-17, 1995, v40 n1 90p.

Keywords: *Calibration, *Low frequency noise, *Voltage reference, Zener diode, Reprints.

The short- and mid-term noise of voltage references based on Zener diodes are the limiting factors in the accuracy of their application as voltage standards. Although these references are relatively rugged, survive the rigors of shipping, and have predictable long-term behavior, they do have noise in the voltage output values with a time dependence about the same as the desired measurement intervals. We have characterized several of these references in the frequency range of 10 to the minus 1 power to 10 to the minus 6 power Hz (time intervals of seconds to months) by direct comparison to a Josephson array voltage standard at the 10 and 1 volt level with nanvolt precision. Several distincty different regions of noise characteristics are observed. Comparisons are made with 1/f and other expected behaviors and resulting accuracy limitations discussed.

04,050
PB96-123518 Not available NTIS
National Inst. of Standards and Technology (PL), Gaithersburg, MD. Atomic Physics Div.
Search for Small Violations of the Symmetrization Postulate in an Excited State of Helium.
Final rept.
K. Deilamian, J. D. Gillaspy, and D. E. Kelleher. 1995, 4p.
Pub. in Physical Review Letters, v74 n24 p4787-4790 Jun 95.

Keywords: *Excited states, *Helium, *Laser spectroscopy, Reprints, Pauli Exclusion Principles, Symmetrization postulate.

We have searched for the existence of the permutation symmetric 1s2siS state of helium in an atomic beam. Such a state directly violates the symmetrization postulate (SP) of quantum mechanics and implies a breakdown of the Pauli exclusion principle. Our data constrain recent SP-violating models at the 5 ppm level. This is the first experiment to look systematically for an SP-violating state with no multiple occupancy of a quantum state.

04,051
PB96-123658 Not available NTIS
National Inst. of Standards and Technology (EEEL), Gaithersburg, MD. Electricity Div.
Ion Kinetics and Symmetric Charge-Transfer Collisions in Low-Current, Diffuse (Townsend) Discharges in Argon and Nitrogen.
Final rept.
S. B. Radovanov, R. J. Van Brunt, and J. K. Olthoff. 1995, 11p.
Pub. in Physical Review E, v51 n6 p6036-6046 Jun 95.

Keywords: *Discharge, *Argon, *Nitrogen, Gas mixture, Hydrogen, Ion energy, Optical emission, Radio frequency, Reprints, Balmer alpha, Doppler broadened emission.

Translational kinetic-energy distributions of mass-selected ions have been measured in diffuse, low-current Townsend-type discharges at high electric field-to-gas density ratios (E/N) in the range of 1 x 10 to the minus 18 -2 x 10 to the minus 17 Vm2 (1-20 kTd). The discharges were generated in Ar and N2 under uniform-field conditions and ion energies were measured using a cylindrical-mirror energy analyzer coupled to a quadrupole mass spectrometer. The mean ion energies determined from measured energy distributions of Ar+ in Ar and N2+ in N2 are compared with the mean energies predicted from solutions of the Boltzmann transport equation based on the assumption that symmetric resonant charge transfer is the predominant ion-neutral interaction. The results for Ar+ and N2+ are consistent with predictions made using a constant (energy independent) cross section for which an effective ion temperature can be defined. However, for both ions, the measured mean energies tend to fall increasingly below the predicted values as E/N increases.

04,052
PB96-123799 Not available NTIS
National Inst. of Standards and Technology (PL), Gaithersburg, MD. Atomic Physics Div.
Relativistic Modifications of Charge Expansion Theory.
Final rept.
A. W. Weiss, and Y. K. Kim. 1995, 7p.
Pub. in Physical Review A, v51 n6 p4487-4493 Jun 95.

Keywords: *Atomic structure, Relativistic effects, Reprints, *Electron correlation, *Charge expansion theory.

We examine the effects of relativity on the high-Z (where Z denotes nuclear charge) behavior of isoelectronic sequences and the modifications require of the traditional charge expansion theory. We propose that the idea of a complex be refined as the set of all configurations with the same occupation of angular-momentum quantum numbers j as well as the same principal quantum numbers n. This leads to asymptotic, high-Z grouping of states that might cut across the conventional LS-coupled states, grouping together levels from different configurations, as long as the n and j occupation numbers remain the same. This regrouping substantially reduces the asymptotic configuration interaction from the predicted by a nonrelativistic theory. Frequently correlation configurations that are significant in low-Z ions disappear entirely in high-Z ions.

04,053
PB96-128129 PC A04/MF A01
National Inst. of Standards and Technology (BFRL), Gaithersburg, MD. Building Environment Div.
Calorimetric and Visual Measurements of R123 Pool Boiling on Four Enhanced Surfaces.
M. A. Kedzierski. Nov 95, 62p, NISTIR-5732.
Sponsored by Department of Energy, Washington, DC.

Keywords: *Pool building, *Heat transfer, Surface treatment, *Electric resistance heating, R-123 refrigerant, TURBO-B tubes.

Pool boiling of R-123 on four commercial enhanced surfaces was investigated both calorimetrically and visually. The four surfaces were: (1) Turbo-BIITM-LP, (2) High-FluxTM, (3) GEWA-KTM, and (4) GEWA-TTM. The surfaces were either machined or soldered onto a flat thick OFHC copper plate. This permitted 20 sheathed thermocouples to be embedded in the copper for accurate heat transfer measurements. The difference between electric resistance and fluid heating was investigated. The fluid heating condition results in heat fluxes that are as much as 32% greater than those obtained by electric resistance heating. Hysterisis effects near the results in heat fluxes that are as much as 32% greater than those obtained by electric resistance heating. Hysterisis effects near the onset of nucleate boiling were also investigated. The boiling was visually recorded with 16mm high speed film. Mechanistic descriptions of the boiling activity are given for each surface.

04,054
PB96-135256 Not available NTIS
National Inst. of Standards and Technology (PL), Gaithersburg, MD. Ionizing Radiation Div.
Oscillometric and Conductometric Analysis of Aqueous and Organic Dosimeter Solutions.
Final rept.
A. Kovacs, I. Slezsak, W. L. McLaughlin, and A. Miller. 1995, 5p.
Pub. in International Meeting on Radiation Processing (9th), Istanbul, Turkey, September 11-16, 1994, v46 n4-6 p1211-1215 Oct 95.

Keywords: *Chlorobenzene, *Dosimetry, *Conductivity, Reprints, *Foreign technology, *Ethanol monochlorobenzene, Electron beam dosimetry, Gamma ray dosimetry, Oscillometry.

Conductometric and oscillometric evaluation methods have earlier been developed to determine absorbed dose in the ethanol-monochlorobenzene dosimeter solution. Recent investigations on the same solution as well as on alanine solutions included the study of the possible use of different type 'conductometric' electrodes and the study of the effect of frequency on the sensitivity of the method. On the basis of these investigations an oscillometric reader has been designed and tested. The same evaluation methods have been tested on the irradiated aqueous alanine solutions, aiming also at the study of the applicable concentration of the alanine solute and the dose (1 to 50 kGy) and dose-rate range using both electron and gamma radiation.

04,055
PB96-135272 Not available NTIS
National Inst. of Standards and Technology (PL), Gaithersburg, MD. Ionizing Radiation Div.
Calorimeters for Calibration of High-Dose Dosimeters in High-Energy Electron Beams.
Final rept.
W. L. McLaughlin, M. L. Walker, and J. C. Humphreys. 1995, 8p.
Pub. in International Meeting on Radiation Processing (9th), Istanbul, Turkey, September 11-16, 1994, Radiation Physics and Chemistry, v46 n4-6 p1235-1242 Oct 95.

Keywords: *Calorimeters, *Electron beams, Reprints, Dosimeters, Calibration, Radiation processing, *Foreign technology, *Beam calibration.

Graphite calorimeters in both single-slab and modular multiple-slab disk geometries have been designed and used for measuring absorbed doses in graphite in intense electron beams of 2 to 12 MeV energy. The modular system has also been used with two to eight graphite elements to measure electron-beam depth-dose curves and to calibrate the response functions of radiochromic-film and alanine-pellet dosimeters. An advantage of this new design is that such calibrations can be accomplished without requiring electron-beam current or charge monitoring, since the calorimeter modules adjacent to the dummy graphic element used to hold the dosimeters during calibration provide simultaneous calorimetric dose monitoring. Temperature-dependence corrections for dosimeter response are also simplified in this way.

04,056
PB96-138441 Not available NTIS
National Inst. of Standards and Technology (PL), Gaithersburg, MD. Atomic Physics Div.
Observation and Visible and uv Magnetic Dipole Transitions in Highly Charged Xenon and Barium.
Final rept.
C. A. Morgan, F. G. Serpa, E. Takacs, J. Sugar, J. R. Roberts, C. M. Brown, U. Feldman, E. S. Meyer, and J. D. Gillaspy. 1995, 4p.
Pub. in Physical Review Letters, v74 n10 p1716-1719 Mar 95.

Keywords: *Ions, *Charged ions, Reprints, *Atomic spectroscopy, *Electron Beam Ion Trap(EBIT).

The authors have observed an unusual transition which is predicted to result in visible and near-uv emission from very highly charged titaniumlike ions spanning the entire upper half of the periodic table. Measurements of the wavelengths of the 3d45D2-5D3 transitions in Ba+34 and Xe+32 are in surprisingly poor agreement with ab initio calculations. This work was carried out in an electron beam ion trap and demonstrates that such a device can be an important tool for visible spectroscopy of highly charged ions.

04,057
PB96-138466 Not available NTIS
National Inst. of Standards and Technology (PL), Gaithersburg, MD. Atomic Physics Div.
Atomic Transition Probabilities and Tests of the Spectroscopic Coupling Scheme for N I.
Final rept.
J. Musielok, W. L. Wiese, and G. Veres. 1995, 10p.
Pub. in Physical Review A, v51 n5 p3588-3597 May 95.

Keywords: Emission, Spectrum, Reprints, *Atomic transition probabilities, *Spectroscopic coupling, LS-coupling, Neutral nitrogen.

With a wall-stabilized arc source, the authors have measured the relative transition probabilities of 100 lines of neutral nitrogen in the visible and near-infrared spectrum and have normalized their data to an absolute scale utilizing four recent lifetime results. The authors estimate that the expanded uncertainties of their data are in the range of plus or minus 11-15%. For a number of 3s-3p and 3p-3d multiplets. They have measured complete sets of lines and observe that most 3p-3d multiplets show considerable departure from LS coupling, while the 3s-3p multiplets adhere to it within plus or minus 20%. Agreement between intermediate coupling calculations and their experimental data for the 3p-3d multiplets is noticeably better, but significant differences are still encountered for two multiplets originating from the 3d4P level.

04,058
PB96-146675 Not available NTIS
National Inst. of Standards and Technology (EEEL), Boulder, CO. Electromagnetic Fields Div.
Electric Dipole Excitation of a Long Conductor in a Lossy Medium.
Final rept.
D. A. Hill. 1995, 19p.
Pub. in Electromagnetics, v15 p301-319 1995.

Keywords: *Electric charge, *Dipoles, *Conductors, Electormagnetic wave transmission, Lossy media, Frequencies, Numerical analysis, Reprints.

Excitation of currents on an infinitely long conductor is analyzed for horizontal electric dipole or line sources and for plane-wave, far-field source. Any of these sources can excite strong currents which produce strong scattered fields for detection. Numerical results for these sources indicate that long conductors produce a strong anomaly over a broad frequency range. The conductor can be either insulated or bare, to model either ungrounded or grounded conductors.

04,059
PB96-146683 Not available NTIS
National Inst. of Standards and Technology (EEEL), Gaithersburg, MD. Electricity Div.
Evidence for Inelastic Processes for N(+)3 and N(+)4 from Ion Energy Distributions in He/N2 Radio Frequency Glow Discharges.
Final rept.
H. H. Hwang, J. K. Olthoff, R. J. Van Brunt, S. B. Radovanov, and M. J. Kushner. 1996, 6p.
Pub. in Jnl. of Applied Physics, v79 n1 p93-98 Jan 96.

Keywords: *Ion distribution, *Radio frequency discharge, *Glow discharges, Microelectronics, Gases, Mixtures, Helium, Nitrogen, Inelastic collisions, Interactions, Fabrication, Reprints, IEDs(Ion energy distributions), Ion molecule reactions.

The ion energy distributions (IEDs) striking surfaces in rf glow discharges are importatnt in the context of plasma etching during the fabrication of microelectronics devices. In discharge sustained in molecular gases of multicomponent gas mixtures, the shape of the IED and the relative magnitudes of the ion fluxes are sensitive to ion-molecule collisions which occur in the presheath and sheath. Ions which collisionlessly traverse the sheaths or suffer only elastic collisions arrive at the substrate with a measurably different IED than do ions which undergo inelastic collisions. In this article we present measurements and results from parametric calculations of IEDs incident on the grounded electrode of a rf glow discharge sustained in a He/N2 gas mixture while using a Gaseous Electronics Conference Reference Cell (33.3 Pa, 13.56 MHz).

04,060
PB96-148069 Not available NTIS
National Inst. of Standards and Technology (EEEL), Boulder, CO. Electromagnetic Fields Div.
Accuracy in Time Domain Transmission Line Measurements.
Final rept.
L. A. Hayden, and R. B. Marks. 1994, 3p.
Pub. in Institute of Electrical and Electronics Engineers Topical Meeting on Electrical Performance of Electronic Packaging (3rd), Monterey, CA., November 2-4, 1994, p176-178.

Keywords: *Transmission lines, *Signals, *Time, Accuracy, Joining, Signal generators, Network analysis, Measurement, Reprints, *Time domain, TDNA(Time domain network analysis).

This paper examines time domain methods for characterizing signal propagation in uniform transmission lines. The impact of the limitations associated with time domain instrumentation and methodologies are examined and guidelines for minimizing errors are presented.

04,061
PB96-148176 Not available NTIS
National Inst. of Standards and Technology (EEEL), Boulder, CO. Electromagnetic Fields Div.
High-Speed Interconnection Characterization Using Time Domain Network Analysis.
Final rept.
R. B. Marks, D. C. DeGroot, and J. A. Jargon. 1995, 5p.
Pub. in Advancing Microelectronics, v22 n6 p35-39 Nov/Dec 95.

Keywords: *Time, *Calibration standards, *Packaging, *Microelectronics, Network analysis, Errors, Joining, Measurement, Reprints, *Time domain, TDNA(Time Domain Network Analysis).

Time domain network analysis (TDNA) has become a realistic competitor to conventional automatic network analyzers. Off-line processing of data from fast digital sampling oscilloscopes can provide measurements of network parameters with an accuracy that is acceptable for many packaging and interconnection problems at frequencies from dc to over 10 GHz. Since many packaging laboratories have ready access to the required instruments, TDNA brings many advanced measurement capabilities into the hands of engineers to whom a conventional network analyzer is unavailable.

04,062
PB96-155502 Not available NTIS
National Inst. of Standards and Technology (EEEL), Boulder, CO. Optoelectronics Div.
Simultaneous Laser-Diode Emission and Detection for Fiber-Optic Sensor Applications.
Final rept.
K. B. Rochford, and A. H. Rose. 1995, 3p.
Pub. in Optics Letters, v20 n20 p1205-1207 Oct 95.

Keywords: *Detectors, Polarization, Responsitivity, Emission, Detection, Reprints, *Fiber optic sensors, *Laser diodes.

The simultaneous emission and detection of radiation with a semiconductor laser is investigated. Measured signal-to-noise ratios of up to 56 dB demonstrate that self-detecting devices are adequate for sensor applications with discrete measurands. The authors observed a strong polarization dependence, which can cause response fluctuations, and suggest methods to minimize these fluctuations. This technique could be used for lower-cost sensors without splitters and detectors.

04,063
PB96-155775 Not available NTIS
National Inst. of Standards and Technology (BFRL), Gaithersburg, MD. Structures Div.
Necessary Condition for Homoclinic Chaos Induces by Additive Noise.
Final rept.
E. Simiu, M. Frey, and M. Grigoriu. 1992, 8p.
Pub. in Proceedings of the International Conference on Computational Stochastic Mechanics (1st), Corfu, Greece, September 17-19, 1991, p889-896 1992.

Keywords: *Chaos, *Noise, Reprints, *Foreign technology, Duffing equation, Dynamical systems, Homoclinic orbits, Nonlinear differential equations.

The effect of noise on the possible occurrence of chaos in systems with a homoclinic orbit was recently investigated in the literature on the bais of a redefinition of the Melnikov function. The purpose of this note is to show that, even in the case of deterministic equations, this redefinition is not consistent with the geometry of the perturbed orbits and would therefore lead to incorrect solutions. The possibility is then explored in developing a necessary condition for the occurrence of homoclinic chaos in forced systems perturbed additively by a commonly used approximate representation of white noise.

04,064
PB96-156047 Not available NTIS
National Inst. of Standards and Technology (CSTL), Gaithersburg, MD. Thermophysics Div.
Model for Calculating Virial Coefficients of Natural Gas Hydrocarbons with Impurities.
Final rept.
L. A. Weber. 1995, 12p.
Pub. in Fluid Phase Equilibria, v111 p15-26 1995.

Keywords: *Activity coefficient, Vapor pressure, Reprints, *Foreign technology, *Ebulliometry, *Refrigerant mixtures, Vapor liquid equilibrium.

A model for calculating second and third virial coefficients, originally developed to describe the behavior of polar halocarbon refrigerants and their mixtures, has been applied to systems of natural gas hydrocarbons and their common impurities, namely H2S, H2O, CO2, CO, and N2. It can be used to correlate data, point out probable errors and provide predictions where data are nonexistent or unreliable. It also provides a means for calculating accurate gas-phase densities, thermodynamic properties, fugacities, and 'calculated data' which can be incorporated into global equations of state for phase equilibrium calculations. Examples are shown for some of the pure components and for the binary systems C2H6 + H2S and CH4 + H2O. In the case H2O, terms are included that account for association. Comparisons are made with available data, and predicted values are shown where no data exist.

04,065
PB96-156203 Not available NTIS
National Inst. of Standards and Technology (PL), Gaithersburg, MD. Electron and Optical Physics Div.
Simple Variable Line Space Grating Monochromator for Synchrotron Light Source Beamlines.
Final rept.
T. A. Callcott, W. L. O'Brien, J. J. Jia, R. N. Watts, D. R. Mueller, Q. Y. Dong, and D. L. Ederer. 1992, 7p.
Pub. in Nuclear Instruments and Methods in Physics Research, vA319 p128-134 1992.

Keywords: *Monochromators, *Spectrometers, Synchrotrons, Vacuum ultraviolet, Reprints, Soft x ray, Varied line spaced grating.

In this paper, the authors present and analyze an improved spectrometer design that has evolved from studies of the focal properties of transmission gratings in converging light beams. This design uses a variable line space grating at a fixed angle of incidence to focus the diffracted light in one dimension, producing resolutions in excess of 1000 over a large wavelength region. Attractive features of this concept include high throughput, simple wavelength scanning, simple optical elements (plane gratings and plane and toroidal mirrors), and relatively inexpensive realizations. After presenting a mathematical analysis of the primary design features, the authors discuss implementations of this design both as a spectrometer and as two versions of beamline monochromators. Design parameters for the two monochromators will be given.

04,066
PB96-157813 Not available NTIS
National Inst. of Standards and Technology (CAML), Gaithersburg, MD. Statistical Engineering Div.
Modeling Detector Response for Neutron Depth Profiling.
Final rept.
K. J. Coakley, R. G. Downing, G. P. Lamaze, C. Ronning, H. C. Hofsass, and J. Biegel. 1995, 8p.
Pub. in Nuclear Instruments and Methods in Physics Research, Section A, vA366 p137-144 1995.

Keywords: *Detector response, Semiconductors, Straggling, Reprints, *Foreign technology, *Neutron depth profiling, Diamond-like carbon, Statistical modeling.

In Neutron Depth Profiling (NDP), inferences about the concentration profile of an element in a material are based on the energy spectrum of charged particles emitted due to specific nuclear reactions. The detector response function relates the depth of emission to the expected energy spectrum of the emitted particles. Here, the detector response function is modeled for arbitrary source and detector geometries based on a model for the stopping power of the material, energy straggling, multiple scattering and random detector measurement error. At the the NIST Cold Neutron Research Facility, a NDP spectrum was collected for a diamond-like carbon (DLC) sample doped with boron. A vertical slit was placed in front of the detector for collimation. Based on the computed detector response function, a model for the depth profile of boron is fit to the observed NDP spectrum. The contribution of straggling to overall variability was increased by multiplying the Bohr Model prediction by a ramp factor. The adjustable parameter in the ramp was selected to give the best agreement between the fitted profile and the expected shape of the profile. The expected shape is determined from experimental process control measurements.

04,067
PB96-157839 Not available NTIS
National Inst. of Standards and Technology (PL), Gaithersburg, MD. Electron and Optical Physics Div.
Al L2,3 Core Excitons in AlxGa1-x as Studied by Soft-X-ray Reflection and Emission.
Final rept.
Q. Y. Dong, W. L. O'Brien, J. J. Jia, T. A. Callcott, and D. L. Ederer. 1992, 7p.
Pub. in Physical Review B, v46 n23 p15 116-15 122 Dec 92.

Keywords: *X ray emission, Reprints, *Aluminum gallium arsenide, Absorption spectra, Core exciton.

The Al L2.3 soft-x-ray reflection and emission spectra of AlxGa1-xAs have been measured for x between 0.17 and 1.0. The valence-band maximum was monitored via the emission spectra using a fit based on band-structure parameters. The dominant features in the reflection spectra are produced by the L2.3 core excitons. Since both the reflection spectra and emission spectra were obtained using the same soft-x-ray spectrometer, the energies of the excitons above the

valence-band maximum are acurately obtained. The known values of the optical band gap, as a function of x, are then used to determine the core exciton binding energy. The core excitons are found to follow and lie above the conduction-band minimum by 0.3 eV as the Al composition changes. Our results are compared to various core exciton theories and to previous experiments.

04,068
PB96-157870 Not available NTIS
National Inst. of Standards and Technology (CAML), Gaithersburg, MD. Statistical Engineering Div.
Stochastic Modeling of a New Spectrometer.
Final rept.
C. Hagwood, K. Coakley, A. Negiz, and K. Ehara. 1995, 17p.
Pub. in Aerosol Science and Technology, n23 p611-627 1995.

Keywords: *Aerosol spectrometers, Equations, Reprints, *Stochastic differential, *Transfer function, Exit probability.

A new spectrometer for classifying aerosol particles according to specific masses is being considered (Ehara et at. 1995). The spectrometer consists of concentric cylinders which rotate. The instrument is designed so that an electric field is established between the cylinders. Thus, aerosol particles injected into the spectrometer are subjected to a centrifugal force and an electric force. Depending on the balance between these two forces, as well as Brownian motion, charged particles either pass through the space between the cylinders or stick to either cylinder wall. Particles which pass through are detected. Given the rotation rate, voltage drop and physical dimensions of the device, we calculate the probability of detection in terms of particle density, diameter and charge.

04,069
PB96-157912 Not available NTIS
National Inst. of Standards and Technology (PL), Gaithersburg, MD. Electron and Optical Physics Div.
Soft-X-ray-Emission Investigation of Cobalt Implanted Silicon Crystals.
Final rept.
J. J. Jia, T. A. Callcott, W. L. O'Brien, J. E. Rubensson, D. L. Ederer, Z. Tan, F. Namavar, J. I. Budnick, Q. Y. Dong, and D. R. Mueller. 1991, 5p.
Pub. in Jnl. of Applied Physics, v69 n11 p7800-7804 Jun 91.

Keywords: *X ray emissions, *Semiconductors, Core excitation, Silicide, Reprints, Band structure, Ion implantation.

The Si L2,3 emission spectra of silicon crystals implanted with Co at doses of (1-8) x 10 to the 17th power Co/cm2 have been examined using soft-x-ray-emission (SXE) spectroscopy. At the lowest dose, the spectra are little modified from that of crystalline Si, indicating that only a small fraction of Si is in the form of silicides within the probe depth of SXE spectroscopy. For higher doses and implant profiles with Co extending to the surface, there is clear evidence ordered CoSi2 combined with richer Co phases, but little evidence for pure Si or for ordered regions of CoSi.

04,070
PB96-157920 Not available NTIS
National Inst. of Standards and Technology (PL), Gaithersburg, MD. Electron and Optical Physics Div.
Soft-X-ray-Emission Spectra of Solid Kr and Xe.
Final rept.
J. J. Jia, W. L. O'Brien, T. A. Callcott, D. R. Mueller, D. L. Ederer, Q. Y. Dong, and J. E. Rubensson. 1991, 4p.
Pub. in Physical Review Letters, v67 n6 p731-734 Aug 91.

Keywords: *Electron structure, *X ray emissions, Reprints, *Rare gas solids.

We present the first soft-x-ray-emission spectra for solid Kr (4p-3d) and Xe (5p-4d) that are free of complicating satellite spectra. Monochromatic synchrotron-radiation excitation is used to suppress the satellites. The data are analyzed to determine the P3/2 bandwidth for both elements; these results are compared with both photoemission data and available theoretical calculations. Bandwidths are found to be larger than those predicted by most electronic structure calculations.

04,071
PB96-157938 Not available NTIS
National Inst. of Standards and Technology (PL), Gaithersburg, MD. Electron and Optical Physics Div.
Soft-X-ray-Emission Studies of Bulk Fe3Si, FeSi, and FeSi2, and Implanted Iron Silicides.
Final rept.
J. J. Jia, T. A. Callcott, W. L. O'Brien, D. L. Ederer, Z. Tan, J. I. Budnick, Q. Y. Dong, and D. R. Mueller. 1992, 6p.
Pub. in Physical Review B, v46 n15 p9446-9451 Oct 92.

Keywords: *Electronic structure, *Iron silicides, *X ray emissions, Reprints, Iron implanted silicon, Partial density.

Bulk iron silicides and implanted iron silicides have been studied by soft-x-ray emission (SXE) spectroscopy. The Si L2,3 emission spectra of these materials are measured. For bulk silicides, these spectra provide a measure of s- and d-type partial density of states (PDOS) localized on the Si sites. We compare them with available band-structure calculations and also with photoemission measurements. For implanted systems, the Si L2,3 emission spectra provide useful information about the silicide formation process with the variation of implant doses.

04,072
PB96-157946 Not available NTIS
National Inst. of Standards and Technology (PL), Gaithersburg, MD. Electron and Optical Physics Div.
Influence of Coadsorbed Potassium on the Electron-Stimulated Desorption of F(+), F(-), and F(*) from PF3 on Ru(0001).
Final rept.
S. A. Joyce, C. Clark, V. Chakarian, T. E. Madey, P. Nordlander, B. Maschhoff, H. S. Tao, D. K. Shuh, and J. A. Yarmoff. 1992, 9p.
Pub. in Physical Review B, v45 n24 p14 264-14 272 Jun 92.

Keywords: *Charge transfer, *Fluorine, *Photoemission, Ruthenium, Reprints, PF3, Stimulated desorption.

The electron-stimulated-desorption ion angular distributions (ESDIAD) of positive ions, negative ions, and metastable species from PF, and K coadsorbed on a Ru(0001) surface are measured. In the absence of K, only positive- and negative-ion ESDIAD is observed, showing highly anisotropic, off-normal fluorine-ion emission (F+, F-) from PF3, which demonstrates that PF bonds are inclined away from the surface normal. In the presence of K, ESDIAD patterns of F+, F-, and metastable F(star) display only normal emission, suggesting a reorientation or chemical reaction which results in fluorine bonding perpendicular to the surface. Thermal desorption spectrometry, Auger electron spectroscopy, and soft-x-ray photoemission (SXPS) are used to determine the surface chemistry as an aid in intepreting the ESDIAD results. The SXPS data show that in the presence of potassium, PF3 dissociates, possibly forming KF-like species, which suggests that an alkali-metal-induced chemical reaction is responsible for the changes observed in ESDIAD. The yields of the various desorbed fluorine species vary strongly with potassium coverage; the results for F- and F(star) are interpreted in terms of a charge-transfer model.

04,073
PB96-157953 Not available NTIS
National Inst. of Standards and Technology (PL), Gaithersburg, MD. Electron and Optical Physics Div.
RIS Measurement of AC Stark Shifts and Photoionization Cross Sections in Calcium.
Final rept.
J. B. Kim, X. Xiong, T. R. O'Brian, T. J. McIlrath, and T. B. Lucatorto. 1992, 4p.
Pub. in Inst. Phys. Conf. Ser. No. 128, RIS 92, Santa Fe, NM., May 24-29, 1992, p59-62.

Keywords: *Calcium, Reprints, *AC Stark shifts, Intense laser fields, Multiphoton ionization, Photo-ionization, Resonance ionization spectroscopy, Rydberg levels.

The ac Stark shifts of four high-lying Ca levels in intense laser fields (10 to the 8th power to 10 to the 10th power W/sq. cm) are studied using two-photon ionization spectroscopy. The two-photon Rabi rates and photoionization cross sections for excited states are also measured, and compared to values obtained from detailed modeling of the RIS profiles. Although three Rydberg levels studied display the expected pondermotive energy shifts, a fourth doubly-excited level deviates significantly from the ponderomotive behavior.

04,074
PB96-157979 Not available NTIS
National Inst. of Standards and Technology (PL), Gaithersburg, MD. Electron and Optical Physics Div.
Comment On: Two-Photon Absorption Series of Calcium.
Final rept.
J. R. Krumrine, A. Musgrove, and T. B. Lucatorto. 1995, 2p.
Pub. in Canadian Jnl. of Physics, v73 p403-404 1995.

Keywords: *Calcium, *Energy levels, *Laser spectroscopy, Series, Spectra, Quantum defects, Reprints, *Foreign technology.

Using two-photon absorption laser spectroscopy of calcium, Makdisi and Bhatia presented a well-resolved series that they tentatively assigned as 4S2 1S0 - 4snf 1F3 (n = 33 - 59). We find this assignment to be erroneous. Calculations of quantum defects and a comparison of their observed energy levels with previously determined values reveal that the spectra actually represent the 4s2 1S0 - 4snp 1P1 series (n = 34 - 60).

04,075
PB96-157987 Not available NTIS
National Inst. of Standards and Technology (PL), Gaithersburg, MD. Electron and Optical Physics Div.
Laser Modification of Ultracold Collisions: Experiment.
Final rept.
P. D. Lett, P. S. Jessen, W. D. Phillips, P. L. Gould, S. L. Rolston, and C. I. Westbrook. 1991, 4p.
Pub. in Physical Review Letters, v67 n16 p2139-2142 Oct 91.

Keywords: *Atomic collisions, *Laser cooling, Optical molasses, Trapped atoms, Reprints, *Ultracold atoms, Associative ionization, Laser trapping, Low energy collisions.

Julienne recently predicted a dramatic laser-intensity-dependent modification of the associative ionization (AI) rate in ultracold collisions. We observe such a modification, but with a behavior inconsistent with the originally proposed mechanism. Furthermore, we find resonant structure in the spectrum of AI rate versus laser frequency, showing the importance of molecular bound states in the AI process. These observations are explained in a new theoretical treatment by Julienne and Heather (preceding Letter).

04,076
PB96-158019 Not available NTIS
National Inst. of Standards and Technology (PL), Gaithersburg, MD. Electron and Optical Physics Div.
Barium Contributions to the Valence Electronic Structure of YBa2Cu3O7-delta, PrBa2Cu3O7-delta, and Other Barium-Containing Compounds.
Final rept.
D. R. Mueller, J. S. Wallace, J. J. Jia, T. A. Callcott, K. E. Miyano, T. A. Ederer, W. L. O'Brien, and Q. Y. Dong. 1995, 7p.
Pub. in Physical Review B, v52 n13 p9702-9708 Oct 95.

Keywords: *Barium partial density, *Photon beam excitation, *Soft x ray emission, Reprints, BaF2, BaTiO3, PrBa2Cu307, YBA2Cu307.

Monochromatic photon beams were used to excite barium NIV,V soft x-ray emission spectra from YBa2Cu3O7-delta, prBa2Cu3O7-delta, BaF2, and BaTiO3. Near threshold excitation was used to demonstrate that small contributions to the barium NV and NIV emission spectra in the energy region above the 5p-->4d core-core transitions do not arise as satellite emission from transitions in multiply excited atoms but rather occur as a result of transitions from the valence states. The emission spectrum of YBa2Cu3O7-delta and PrBa2Cu3O7-delta reveals a contribution to the electronic density of states at the barium site in the region near the Fermi level. The YBa2Cu3O7-delta compound is a superconductor and PrBa2Cu3O7-delta is an insulator. It has been proposed that the difference between them is due to mixing of praseodymium and barium among the sites occupied by yttrium and barium, with an accompanying change in electronic structure. However, the authors' measurements indicate that the barium partial density of states for the two compounds are essentially identical.

04,077
PB96-158027 Not available NTIS

National Inst. of Standards and Technology (PL), Gaithersburg, MD. Electron and Optical Physics Div.
Cooper M(sub II,III) X-ray-Emission Spectra of Copper Oxides and the Bismuth Cuprate Superconductor.
Final rept.
D. R. Mueller, J. Wallace, D. L. Ederer, Q. Y. Dong, T. A. Callcott, J. J. Jia, and W. L. O'Brien. 1992, 6p.
Pub. in Physical Review B, v46 n17 p11 069-11 074 Nov 92.

Keywords: *Cupric oxide, *Electron density, Cuprous oxide, Reprints, *X ray fluorescence, Superconductivity bismuth cuprate.

Photon-excited soft x-ray emission spectra for CuO, Cu2O, and bismuth cuprate in the region of the Cu 3d-->3p transitions were measured to obtain bulk-sensitive electronic partial density-of-states information. For CuO and Cu2 transitions from the valence levels into the Mn and Mm levels were clearly resolved. The emission features were separated by the 2.3-eV spin-orbit interaction of the copper 3p1/2 and 3p3/2 states and appeared in the statistical intensity ratio. The copper Mm emission spectrum of the superconductor is broader than the spectra CuO and Cu2O. For all three compounds the shape of the Mm emission spectrum extracted from the data is qualitively similar to calculations of the copper single-particle local density of states. No evidence of multiplet structure was observed in the emission spectrum of CuO in spite of the open d shell in the ground state. The measurements are compared with published copper L emission data and photoemission results.

04,078
PB96-158035 Not available NTIS
National Inst. of Standards and Technology (PL), Gaithersburg, MD. Electron and Optical Physics Div.
RIS Measurements of the AC Stark Shift.
Final rept.
T. O'Brian. 1993, 2p.
Pub. in Resonances (Newsletter of the Institute for Resonance Ionization Spectroscopy), v1 n3 p2-3 Spring 1993.

Keywords: *Spectroscopy, Reprints, *Ac Stark shift, *Rydberg atoms, Resonance ionization spectroscopy.

The ac Stark shift in xenon Rydberg levels is directly measured using resonance ionization spectroscopy. The authors report excellent agreement between the measured shifts and the near-ponderomotive shifts predicted by detailed theory of the resonant ionization process.

04,079
PB96-158043 Not available NTIS
National Inst. of Standards and Technology (PL), Gaithersburg, MD. Electron and Optical Physics Div.
Intermediate Coupling in L2-L3 Core Excitons of MgO, Al2O3, and SiO2.
Final rept.
W. L. O'Brien, J. J. Jia, Q. Y. Dong, D. L. Mueller, D. L. Ederer, T. A. Callcott, and J. E. Rubensson. 1991, 6p.
Pub. in Physical Review B, v44 n3 p1013-1018 Jul 91.

Keywords: *Absorption spectra, *Reflection spectra, *Exciton, Measurement, Reprints, MgO, AL203, SiO2.

The L23 reflection spectra for single-crystal MgO, alpha-Al2O3, and alpha-SiO2 are measured. These reflection spectra are used to generate absorption spectra that agree well with electron-total-yield and electron-energy-loss measurements. Exciton features are shown to exist in the band gap by comparing the valence-band maximum plus optical band gap to the observed transition energies. The energy splitting on the L2-L3 excitons, as seen in reflection, is clearly resolved for Al2O3 and SiO2, while in electron-total-yield measurements the doublets are not resolved for Al2O3. This resolution allows the calculation of the exchange energy using intermediate-coupling theory.

04,080
PB96-158092 Not available NTIS
National Inst. of Standards and Technology (PL), Gaithersburg, MD. Electron and Optical Physics Div.
New NIST/ARPA National Soft X-ray Reflectometry Facility.
Final rept.
C. Tarrio, R. N. Watts, T. B. Lucatorto, J. Jia, M. Haass, and T. A. Calcott. 1994, 6p.
Pub. in Jnl. of X-ray Science and Technology, v4 p96-101 1994.

Keywords: *Lithography, *Metrology, Monochromator, Reflectometry, Synchrotron, Reprints, *Soft x ray.

The authors have recently begun a series of upgrades to the NIST/ARPA National Reflectometry Facility at the Synchrotron Ultraviolet Radiation Facility. The facility currently consists of a new monochromator and the original sample manipulator which allows the authors to measure optical components less than 10 cm in diameter. The monochromator offers high throughput and modest resolution over the wavelength range 3.5-40 nm. In the next year the authors will be installing a sample manipulator that will be able to accommodate the much larger optics that will be used in future x-ray projection lithography and astronomy instruments. The authors offer preliminary measurements of the throughput and resolution of the new monochromator.

04,081
PB96-159678 Not available NTIS
National Inst. of Standards and Technology (EEEL), Gaithersburg, MD. Semiconductor Electronics Div.
Boron-Implanted 6H-SiC Diodes.
Final rept.
M. Ghezzo, D. M. Brown, E. Downey, J. Kretchmer, and J. J. Kopanski. 1993, 3p.
Pub. in Applied Physics Letters, v63 n9 p1206-1208 Aug 93.

Keywords: *Ion implantation, Reprints, *High temperature electronics, SiC, Silicon carbide.

Ion implanted planar p-n junctions are important for silicon carbide discrete devices and integrated circuits. Conversion to p-type of n-type 6H-SiC was observed for the first time using boron implantation. Diodes were fabricated with boron implants at 25 and 1000 degrees C, followed by 1300 degrees C post-implant annealing in a furnace. The best diodes measured at 21 degrees C exhibited an ideality factor of 1.77, reverse bias leakage of 10 to the minus 10th power A/sq. cm. at -- 10 V, and a record high (for a SiC-implanted diode) breakdown voltage of -- 650 V.

04,082
PB96-159801 Not available NTIS
National Inst. of Standards and Technology (CSTL), Gaithersburg, MD. Surface and Microanalysis Science Div.
Dynamics of Hydrogen Interactions with Si(100) and Si(111) Surfaces.
Final rept.
K. W. Kolasinski. 1995, 57p.
Pub. in International Jnl. of Modern Physics B, v9 n21 p2753-2809 1995.

Keywords: *Internal state distribution, *Molecular beam scattering, Reaction dynamics, Reprints, Silicon, Adsorption, Desorption, Hydrogen, *Foreign technology, Disilane.

Experimental and theoretical work probing the dynamics of dissociative adsorption and recombinative desorption of hydrogen at Si(100) and Si(111) surfaces is reviewed. Whereas molecular beam experiments demonstrate that molecular excitations do aid in overcoming a substantial activation barrier toward adsorption, desorbed molecules are found to 'have a total energy content only slightly above the equilibrium expectation at the surface temperature. A consistent interpretation of the ad/desorption dynamics is arrived at which requires neither a violation of microscopic reversibility nor defect-mediated processes. An essential element of this model is that surface atom relaxations play an essential role in the dynamics such that different portions of the potential energy hypersurface govern the results of adsorption and desorption experiments. The 'lost' energy, i.e. that portion of the activation energy not evident in the total energy of the desorbed molecules, is deposited in the surface coordinates where it is inaccessible to experiments that probe the desorbates final state.

04,083
PB96-160221 Not available NTIS
National Inst. of Standards and Technology (EEEL), Gaithersburg, MD. Semiconductor Electronics Div.
Stacking Fault Pyramid Formation and Energetics in Silicon-on-Insulator Material Formed by Multiple Cycles of Oxygen Implantation and Annealing.
Final rept.
J. D. Lee, J. C. Park, D. Venables, S. J. Krause, and P. Roitman. 1993, 3p.
Pub. in Applied Physics Letters, v63 n24 p3330-3332, 13 Dec 93.

Keywords: *Silicon defects, Reprints, *Silicon on insulator, Oxygen implanted silicon, Stacking faults, Transmission electron microscopy.

The defect microstructure of silicon-on-insulator wafers produced by multiple cycles of oxygen implantation and annealing was studied with transmission electron microscopy. The dominant defects are stacking fault pyramids (SFPs), 30-100 nm wide, located at the upper buried oxide interface at a density of approx. 10 to the 6th power cm to the minus 2 power. The defects are produced by the expansion and interaction of narow stacking fault (NSF) ribbons pinned to residual precipitates in the top silicon layer. Consideration of the energetics of the transformaion from a collection of four NSF ribbons to a single SFP indicates that the reaction is energetically favorable below a critical NSF length. Thus small defects are stable as SFPs while large defects are stable as NSF ribbons.

04,084
PB96-160247 Not available NTIS
National Inst. of Standards and Technology (EEEL), Gaithersburg, MD. Semiconductor Electronics Div.
RII Spectroscopy of Trap Levels in Bulk and LPE Hg1-xCdxTe.
Final rept.
C. L. Littler, X. N. Song, Z. Yu, D. G. Seiler, J. L. Elkind, and J. R. Lowney. 1993, 5p.
Pub. in Semiconductor Science and Technology, v8 pS317-S321 1993.

Keywords: *Magnetoabsorption, *Liquid phase epitaxy, One photon, Trap levels, Impurities, Defects, Reprints, *Foreign technology, HgCdTe, Mercury interstitials.

Resonant impact ionization (RII) spectroscopy, a new technique for studying low concentrations of trap levels in narrow-gap Hg(1-x)Cd(x)Te, has been used to investigate impurity and defect levels in both bulk and liquid phase epitaxy (LPE) crystals of this ternary material. Mercury interstitials, deliberately introduced into bulk samples with x equals 0.22 and x equals 0.24, provide direct evidence for the formation of trap levels near 45 and 61 meV above the valence band edge for these x-value samples. The 61meV level in the x equals 0.24 (Eg =121 meVat 5 K) sample is seen to enhance the transition strength of resonant two-photon magneto-absorption (TPMA) observed at high fields by acting as a near-resonant intermediate state for the two-photon process. In the LPE material, samples which have received just a post-anneal in an Hg-saturated atmosphere show strong (RII) structure due to defect levels at equals 60 meV above the valence band, whereas samples which are both doped with indium and post-annealed show only intrinsic one-photon magneto-absorption structure.

04,085
PB96-160296 Not available NTIS
National Inst. of Standards and Technology (PL), Gaithersburg, MD. Electron and Optical Physics Div.
Phonon Relaxation in Soft-X-ray Emission of Insulators.
Final rept.
W. L. O'Brien, J. Jia, Q. Y. Dong, D. L. Ederer, D. R. Mueller, C. C. Kao, T. A. Callcott, and K. E. Miyano. 1993, 4p.
Pub. in Physical Review B, v47 p140-143 1993.

Keywords: *Insolators, *Phonons, Photon excitation, Reprints, Soft x ray emission, Stoke shift, Synchrotron radiation.

Phonon-relaxation effects on the L2.3 soft-x-ray emission of MgO, Al2O3, and SiO2 are measured by comparing soft-x-ray emission spectra to photoelectron spectra. The observed shifts of the soft-x-ray emission spectra relative to the photoelectron spectra are identified as Stokes shifts and are described in terms of partial phonon relaxation. The observed Stokes shifts are 0.5, 0.9, and 1.2 eV for MgO, Al2O3, and SiO2, respectively. Similar measurements on Mg, Al, and Si show no detectable Stokes shift within the experimental uncertainty of 0.2 eV. The larger Stokes shifts observed in the oxides are due to the longer core-hole lifetime, the faster phonon relaxation, and larger phonon relaxation energy in the oxides.

04,086
PB96-160312 Not available NTIS
National Inst. of Standards and Technology (PL), Gaithersburg, MD. Atomic Physics Div.

Laser-Cooled Neutral Atom Frequency Standards.
Final rept.
S. L. Rolston, and W. D. Phillips. 1991, 9p.
Pub. in Proceedings of the Institute of Electrical and Electronics Engineers, v79 n7 p943-951 Jul 91.

Keywords: *Atomic fountain, *Frequency standards, *Laser cooling, Microwave standards, Optical clock, Reprints, Two-photon spectroscopy.

Recent advances in laser cooling, including temperatures as low a few microkelvin, and the demonstration of the ability to launch atoms while maintaining these low temperatures, now allows the realization of atomic fountain frequency standards. An analysis of a Cs microwave fountain predicts potential stability anmd accuracy improvements of a factor of 100 over present laboratory standards, with an ultimate accuracy near 10 to the 16th power. An optical frequency standard based on a two-photon transition in xenon is analyzed and shown to have potential stability 5 orders of magnitude better than current Cs standards, and a possible accuracy of 10 to the 18th power. Neutral atom frequency standards will have much better signal-to-noise (S/N) ratios than ion standards, but suffer from large systematic effects, making the two technologies complementary in many ways.

04,087
PB96-160338 Not available NTIS
National Inst. of Standards and Technology (PL), Gaithersburg, MD. Electron and Optical Physics Div.
Improved Reflectometry Facility at the National Institute of Standards and Technology.
Final rept.
C. Tarrio, R. N. Watts, T. B. Lucatorto, J. Jia, M. Haass, and T. A. Calcott. 1993, 6p.
Pub. in Society of Photo-Optical Instrumentation Engineers Proceedings of the International Society for Optical Engineering; Multilayer and Grazing Incidence X-ray EUV Optics II, San Diego, CA., July 14-16, 1993, v2011 p534-539.

Keywords: *Extreme ultraviolet, *Lithography, *Reflectometers, Optics, Reprints, Monochromator, Soft x ray, Synchrotron.

We have recently completed construction of a high throughput, modest resolution soft x-ray monochromator installed at the Synchrotron Ultraviolet Radiation Facility of the National Institute of Standards and Technology. Although this monochromator will be used primarily to characterize the optical properties of multilayer-coated x-ray optics, the versatility of the instrument will enable us to measure such properties as reflectivity, transmission, diffraction, and scatter of a variety of component. We present measurements of monochromator throughput and resolution.

04,088
PB96-160379 Not available NTIS
National Inst. of Standards and Technology (PL), Gaithersburg, MD. Electron and Optical Physics Div.
NIST Metrology for Soft X-ray Multilayer Optics.
Final rept.
R. N. Watts, D. L. Ederer, T. B. Lucatorto, and M. Isaacson. 1991, 3p.
Pub. in OSA Proceedings on Soft-X-ray Projection Lithography, Monterey, CA., April 10-12, 1991, v12 p142-144.

Keywords: *X ray optics, *Nanostructure, *Lithography, Reflectivity, Multilayers, Metrology, Figure, Reprints.

We describe the capabilities of the exciting NIST soft X-ray reflectometry program and outline our proposed new characterization facility.

04,089
PB96-160445 Not available NTIS
National Inst. of Standards and Technology (PL), Gaithersburg, MD. Electron and Optical Physics Div.
Appearance Intensities for Multiply Charged Ions in a Strong Laser Field.
Final rept.
M. Brewczyk, K. Rzazewski, and C. W. Clark. 1995, 6p.
Pub. in Physical Review A, v52 n2 p1468-1473 Aug 95.

Keywords: *Nonlinear optics, Ionization, Reprints, Atoms, Lasers, *Thomas-Fermi model.

We study multiple ionization of atoms by a strong laser field using a time-dependent approach based on the Thomas-Fermi model. The evolution of the electron density under the influence of transient, linearly polarized radiation field is determined by numerical solution of hydrodynamic equations on a two-dimensional grid. We find a threshold 'appearance intensity' for a given charge state, i.e., the laser intensity at which such a charge state first appears, which is in reasonable agreement with experimental results for high charge states.

04,090
PB96-160700 Not available NTIS
National Inst. of Standards and Technology (MEL), Gaithersburg, MD. Precision Engineering Div.
Generating and Measuring Displacements Up to 0.1 m to an Accuracy of 0.1 nm: Is It Possible.
Final rept.
E. C. Teague. 1993, 42p.
Pub. in Society of Photo-Optical Instrumentation Engineers Handbook 'The Technology of Proximal Probe Lithography', Part 3, p322-363 Jun 93.

Keywords: *Metrology, *Displacement, Workplace layout, Interferometry, Accuracy, Motion studies, Lithography, Reproducibility, Reprints, Positioning uncertainty, Abbe offset, Proximal probe lithography.

Four major tasks of accurate positioning are examined: generating highly repeatable motion in a workspace, constructing a metrology frame from highly-stable, accurate lines and planes, realizing a metric in the workspace, and linking the workpiece to the coordinate system with a probe. Optical scales, x-ray interferometry, optical heterodyne interferometry, Fabry-Perot etalons, and impedance-based transducers are evaluated as possible means to realize a metric. The major error sources, practical limitations, and guidelines for establishing a coordinate reference frame are described. The repeatability of sliding bearings and flexure bearings is examined and this combined with cosine and Abbe offset errors is used to estimate uncertainties in generating and measuring linear motion. Finally, the effects of probe-substrate forces and energies of interactions on positioning accuracy are discussed.

04,091
PB96-161617 Not available NTIS
National Inst. of Standards and Technology (MEL), Gaithersburg, MD. Precision Engineering Div.
Residual Error Compensation of a Vision-Based Coordinate Measuring Machine.
Final rept.
M. V. Ananda, J. Raja, T. Doiron, and J. Zimmerman. 1993, 5p.
Pub. in Proceedings of the American Society for Precision Engineering Fall Meeting, p66-70 1993.

Keywords: *Calibration, *Metrology, Reprints, *Dimensional metrology, Error compensation, Grid plate.

The commercial equipment for measuring lithography patterns has reached an accuracy level which makes it difficult to provide two dimensional artifact of higher accuracy for use as calibration standards. Because of the simpler nature of one-dimensional measurements, it is still possible to measure one line of a grid plate to a higher accuracy than is possible using the two dimensional measurement machines. The main idea of this paper is to introduce the idea of using a partially calibrated grid plate (one of two lines calibrated) and a series of measurements of the whole plate on the two dimensional machine to produce a calibration of both the grid plate and the machine. The authors' procedure involves measurement of a grid plate in three specified orientation. The measurement data is used to build an error compensation model. The following sections give a brief description. Software compensation of a coordinate measuring machine has become an accepted practice to enhance the accuracy of a CMM. In addition to parametric error compensation schemes, research work in self calibration schemes have also been carried out in recent years. Hocken and Borchardt used the measurements of an artifact in two specified orientations to model squareness and scale error. Belforte, et al. Developed a model that included the twenty one error components. They used legendre polynomials to model the errors. The self calibration methods eliminate the need for calibrated artifacts, but require the dimensional stability of the artifacts during the measurement. Raugh has also developed a method that falls under this category. The authors' method is an extension of the Hocken-Borchardt method.

04,092
PB96-161674 Not available NTIS
National Inst. of Standards and Technology (CSTL), Gaithersburg, MD. Biotechnology Div.
Current Noise Reveals Protonation Kinetics and Number of Ionizable Sites in an Open Protein Ion Channel.
Final rept.
S. M. Bezrukov, and J. J. Kasianowicz. 1993, 4p.
Pub. in Physical Review Letters, v70 n15 p2352-2355 Apr 93.

Keywords: *Ionization, *Kinetics, *Noise analysis, Reprints, Protons, *Foreign technology, Protein structure.

In analogy to current fluctuations found in solid state electronic microstructure devices, excess noise generated by the reversible ionization of sites in a transmembrane ionic channel was observed. By analyzing the pH-dependent fluctuations in the current through fully open single channels formed by the alpha-toxin protein, the authors were able to evaluate the protonation rate constants, the number of sites participating in the protonation process, and the effect of recharging a single site on the channel conductance.

04,093
PB96-161682 Not available NTIS
National Inst. of Standards and Technology (CSTL), Gaithersburg, MD. Biotechnology Div.
Noise Analysis of Ionization Kinetics in a Protein Ion Channel.
Final rept.
S. M. Bezrukov, and J. J. Kasianowicz. 1993, 4p.
Pub. in Proceedings of the International Conference on Noise Analysis in Physical Systems and 1/f Fluctuations (12th), p677-680 1993.

Keywords: *Chemical reactions, *Ion channel, *Noise analysis, Current, Reprints, Fluctuations, Kinetics, Ionization, Protein structure, Spectral density.

The authors observed excess current noise generated by the reversible ionization of sites in a transmembrane protein ion channel, which is analogous to current fluctuations found recently in solid state microstructure electronic devices. Specifically the current through fully open single channel formed by Staphylococcus aureus alpha-toxin show pH dependent fluctuations. The authors show that noise analysis of the open channel current can be used to evaluate the ionization rate constants, the number of sites participating in the ionization process, and the effect of recharging a single site on the channel conductance.

04,094
PB96-161708 Not available NTIS
National Inst. of Standards and Technology (PL), Gaithersburg, MD. Ionizing Radiation Div.
Measurement of the Neutron Lifetime.
Final rept.
M. S. Dewey, D. M. Gilliam, W. M. Snow, and G. L. Greene. 1992, 8p.
See also PB91-118026. Sponsored by Department of Energy, Washington, DC.
Pub. in Proceedings of the Weak and Electromagnetic Interactions in Nuclei Conference, Dubna, Russia, 1992.

Keywords: *Neutrons, Measurement, Counting, Reprints, Penning traps, Lifetime.

Neutron beta-decay is a proto-typical semi-leptonic weak interaction whose rate is of considerable theoretical importance. Accurate measurements of the neutron decay rate along with Big Bang nucleosynthesis calculations and measurements of light element abundances constrain the number of light neutrino species, Nv. This constraint currently agrees with the number of neutrino species inferred from the recent precision measurements of the decay width of the Z boson. A resolution of the current disagreement among experimental values for the neutron lifetime Tn, the neutron beta asymmetry An, and fr-values of pure Fermi O+ goes to O+ superallowed beta-transitions might require extensions to the Standard Model. In the coming year the authors hope to improve by a factor of four the accuracy of their previous measurement of the neutron lifetime (5.3 goes to approximately 1.5s). The current status and future prospects for the measurement are discussed.

04,095
PB96-161716 Not available NTIS
National Inst. of Standards and Technology (MEL), Gaithersburg, MD. Precision Engineering Div.

SPC Artifact for Automated Solder Joint Inspection.
Final rept.
T. Doiron, D. A. Pinsky, S. Chen, and M. Plott. 1993, 8p.
Pub. in Measurement, v12 p1-8 1993.

Keywords: *Solder joints, *Inspections, Reprints, *Foriegn technology, Dimensional metrology, Interim artifact, Statistical process control.

Automated inspection of printed wiring assemblies, particularly those using surface mount technology, has become practical with the advent of high-speed vision processing for dimensional measurements on each feature coupled with artificial intelligence tools to make decisions based on the measurements. In this paper the authors present accuracy tests of such a system based on the measurement of known artifacts which simulate the geometry of typical solder joints.

04,096
PB96-161724 Not available NTIS
National Inst. of Standards and Technology (MEL), Gaithersburg, MD. Precision Engineering Div.
Length Metrology of Complimentary Small Plastic Rulers.
Final rept.
D. T. Doiron, and T. D. Doiron. 1994, 7p.
Pub. in Proceedings of the Measurement Science Conference, Pasadena, CA., January 1994, 7p.

Keywords: *Measurement systems, *Rulers, *Metrology, Reprints, *Scale error standards.

The national measurement system concerns the relationships between individual measurements and the specific units of measure. In some cases, gage blocks for example, there are standards, a large body of scientific research, and considerable effort taken to trace the accuracy of blocks used in manufacturing back to the unit of length. The international trend to laboratory accreditation (NVLAP, NAMAS, etc.) is a formalization of the idea of assuring measurement accuracy by assessment of laboratory practice and evaluation of a measurement system's relation to the unit of length.

04,097
PB96-161781 Not available NTIS
National Inst. of Standards and Technology (CSTL), Gaithersburg, MD. Biotechnology Div.
Nonequilibrium Statistical Mechanics.
Final rept.
B. Robertson. 1993, 2p.
Pub. in Physics and Probability, p251-260 1993.

Keywords: *Statistical mechanics, *Temperature, *Thermodynamics, Reprints, *Foreign technology, *Nonequilibrium entropy, *Correlation function, Projection operators.

The derivation of the equations of nonequilibrium statistical mechanics is reviewed. These exact closed equations are valid for nonlinear systems arbitrarily far from equilibrium. In the short-correlation-time and local limit they reduce to the equations of nonequilibrium thermodynamics with molecular expression for the transport coefficients.

04,098
PB96-161799 Not available NTIS
National Inst. of Standards and Technology (PL), Gaithersburg, MD. Ionizing Radiation Div.
Measurement of the (10)B(n, alpha1gamma)(7)Li Cross Section in the 0.3 to 4 MeV Neutron Energy Interval.
Final rept.
R. A. Schrack, O. A. Wasson, D. C. Larson, J. K. Dickens, and J. H. Todd. 1992, 3p.
Pub. in Nuclear Data for Science and Technology, Forschungszentrum Julich, Federal Republic of Germany, May 13-17, 1991, p507-509 1992.

Keywords: *Germanium detector, *Neutron standards, Cross sections, Reprints, *Foreign technology, *Black detectors, Monte Carlo.

A relative cross section measurement of the 10B(n, alpha, gamma)7Li cross section was made using the ORELA neutron source. The reaction was measured by observing the 478 keV photon using a 30% efficiency germanium detector. The neutron flux was monitored with a high efficiency plastic scintillator. Data analysis required the use of extensive Monte Carlo calculations for corrections to the data. The measured cross section differs as much as 40% from the ENDF/B-VI evaluation for neutron energies greater than 1.5 MeV.

04,099
PB96-161864 Not available NTIS
National Inst. of Standards and Technology (MSEL), Gaithersburg, MD. Polymers Div.
Gas Absorption during Ion-Irradiation of a Polymer Target.
Final rept.
W. E. Wallace, T. T. Chiou, J. B. Rothman, and R. J. Composto. 1995, 5p.
Pub. in Nuclear Instruments and Methods in Physics Research B, v103 p435-439 May 95.

Keywords: *Blistering, *Polyimide, *Gas absorption, Reprints, Water absorption, *Foreign technology, *Ion beam modification.

The presence of a high partial pressure of deuterated water in the vacuum of the scattering chamber of an MeV ion accelerator system was shown to promote the incorporation of deuterium into a thin polyimide target subjected to 1.3 MeV 4He+ irradiation. When the background pressure in the chamber was low, 2.7 x 10 to the minus 5th power Pa (2 x 10 to the minus 7th power Torr), the polyimide was shown by forward recoil spectrometry to evolve hydrogen when ion bombarded. This was an expected, and commonly observed phenomenon. However, when the pressure in the scattering chamber was raised to 1.3 x 10 to the minus 2 power Pa(1 x 10 to the minus 4 power Torr) by the addition of D2O vapor through a leak valve, deuterium was readily incorporated into the target in the ion-irradiated area. The degree to which the polyimide film absorbed gas from the vacuum of the scattering chamber was unexpected. The deuterium/hydrogen atomic concentration ratio reached 0.235 after a dose of 3.5 x 10 to the 15th power ions/sq. cm. The absorption of deuterium was accompanied by blistering in the polyimide at high ion fluences.

04,100
PB96-161989 Not available NTIS
National Inst. of Standards and Technology (MSEL), Gaithersburg, MD.
Interfacial Crack in a Two-Dimensional Hexagonal Lattice.
Final rept.
R. Thomson, and S. J. Zhou. 1994, 11p.
Pub. in Physical Review B, v49 n1 p44-54 Jan 94.

Keywords: *Crack propagation, Fracture, Interfaces, Dislocation, Reprints, *Interfacial crack, *Lattices.

In this paper we compare a set of atomic calculations of interfacial crack structure and properties with the predictions of an augmented elastic theory. Our intent is to critique the elastic predictions, especially the mode conversion and displacement closure oscillation features of the elastic theory. A simple physical picture is developed based on a crack stability diagram, using two sets of stress intensity axes. The first set is the normal applied stress intensity K and the second is a local stress intensity factor k, defined to describe the physics of the core region. The Griffith condition is different from that for dislocation emission. In each case, the effective core size is much smaller than the physical core size, which means that the mode shift at the crack tip is considerably larger than would be expected on the basis of linear elasticity. However, with appropriately defined condition is also surprisingly well satisfied in the mode-II emission configuration. The crack is found never to exhibit displacement oscillations, in part, because of the necessary condition that the Griffith condition be satisfied at the crack tip, and in part because the amount of shear in the core is limited by dislocation emission.

04,101
PB96-162003 Not available NTIS
National Inst. of Standards and Technology (MSEL), Gaithersburg, MD.
Dislocation Core-Core Interaction and Peierls Stress in a Model Hexagonal Lattice.
Final rept.
S. J. Zhou, A. E. Carlsson, and R. Thomson. 1994, 6p.
Pub. in Physical Review B, Condensed Matter, Third Series, v49 n10 p6451-6456 Mar 94.

Keywords: *Dislocation core, Fracture, Reprints, *Lattices, *Atomistic calculations, Peierls Stress.

A series of atomistic calculations is performed in order to explore dislocation core-core interactions and the Peierls stress in a model hexagonal lattice. The method of calculation is the lattice Green's function method, using several pair potentials with variable parameters. We confirm that dislocation cores broaden as a pair of dislocations with opposite sign move closer to each other. Continuum theories are surprisingly accurate in describing the dislocations-dislocation interaction force even in the range of strong core-core overlap. However, our atomistic calculations show that while the relation between the Peierls stress and dislocation width is exponential as the Peierls-Nabarro model predicts, that model underestimates the Peierls stress by nearly a factor of 10 to the 4th power.

04,102
PB96-163746 Not available NTIS
National Inst. of Standards and Technology (PL), Gaithersburg, MD. Electron and Optical Physics Div.
Charge-Transfer-Induced Multiplet Structure in the N4,5O2,3 Soft-X-ray Emission Spectrum of Lanthanum.
Final rept.
D. R. Mueller, C. W. Clark, D. L. Ederer, Q. Y. Dong, T. A. Callcott, J. J. Jia, and W. L. O'Brien. 1995, 5p.
Pub. in Physical Review A, v52 n6 p4457-4461 Dec 95.

Keywords: *Lanthanum, *Multiplet structures, *Emission spectrum, Reprints, *Soft x-ray emission spectra.

Soft-x-ray emission spectra for the La N4.5O2.3 transitions in lanthanum aluminate LaAlO3 include contributions from several relatively intense multiplet lines near 80 eV. The appearance of this spectrum contrasts sharply with the three diagram lines observes for the N4.5O2.3 emission spectrum of Ba in BaF2. An atomic model of the La N4.5O2.3 transition, assuming single occupancy of the 4f shell by a spectator electron, provides a good approximation of the measured spectrum. Emission features due to the low-energy 3P0 and 3D0 terms of the 4d94f configuration are also apparent in the laAlO3 emission spectra, but not in emission spectra from BaF2. Reflection measurements indicate that the 4f level is not occupied in the ground state in LaAlO3. The data suggest that charge transfer from ligand orbitals following creation of a 4d vacancy prior to the emission process is the predominant mechanism giving rise to the required 4f occupancy.

04,103
PB96-163761 Not available NTIS
National Inst. of Standards and Technology (CSTL), Boulder, CO. Thermophysics Div.
Non-Newtonian Flow between Concentric Cylinders Calculated from Thermophysical Properties Obtained from Simulations.
Final rept.
A. P. Narayan, J. C. Rainwater, and J. M. Hanley. 1995, 7p.
Pub. in International Jnl. of Thermophysics, v16 n2 p347-353 Mar 95.

Keywords: *Colloidal suspension, *Rheology, Reprints, *Foreign technology, *Couette flow, Shear thickening, Soft sphere fluid, Weissenberg effect.

A study of the Weissenburg effect (rod climbing in a stirred system) based on nonequilibrium molecular dynamics (NEMD) is reported. Simulation results from a soft-sphere fluid are used to obtain a self-consistent free-surface profile of the fluid of finite compressibility undergoing Couette flow between concentric cylinders. A numerical procedure is then applied to calculate the height profile for a hypothetical fluid with thermophysical properties of the soft-sphere liquid and of a dense colloidal suspension. The height profile calculated is identified with shear thickening and the forms of the visometric functions. The maximum climb occurs between the cylinders rather than at the inner cylinder.

04,104
PB96-163779 Not available NTIS
National Inst. of Standards and Technology (EEEL), Gaithersburg, MD. Semiconductor Electronics Div.
2D-Scanning Capacitance Microscopy Measurements of Cross-Sectioned VLSI Teststructures.
Final rept.
G. Neubauer, and A. Erickson. 1996, 4p.
Pub. in Proceedings of the International Workshop on Semiconductor Characterization: Present Status and Future Needs, Gaithersburg, MD., January 30-February 2, 1995, p318-321 1996.

Keywords: *Microscopy, Measurements, Reprints, Electrical data, Topographic data, *Scanning capacitance microscopy, 2-D dopant profiling.

The authors have developed a setup which uses scanning capacitance microscopy (SCM) to obtain electrical data of cross-sectioned samples while simultaneously acquiring conventional topographical AFM data. The results presented here include 2D SCM maps of cross-sections of blanket implanted, annealed Si wafers as well as test structures on Si. The authors found the technique to be sensitive over several orders of magnitude of carrier density concentrations less than E15 to E20 atoms/sq. cm., with a lateral resolution of 20-150 nm, depending on probe tip and dopant level. The authors find excellent agreement of total implant depth obtained from SCM signals of cross-sectioned samples with conventional Secondary Ion Mass Spectrometry (SIMS) profiles of the same sample.

04,105
PB96-167119 Not available NTIS
National Inst. of Standards and Technology (CSTL), Gaithersburg, MD. Analytical Chemistry Div.
Loss-Free Counting at IRI and NIST.
Final rept.
R. M. Lindstrom, M. J. J. Ammerlaan, and S. S. Then. 1996, 9p.
Pub. in Jnl. of Trace and Microprobe Techniques, v14 n1 p67-75 1996.

Keywords: *Gamma spectrometry, Accuracy, Reprints, *Foreign technology, *Loss free counting, Neutron activation analysis.

Loss-free counting has been successfully implemented for neutron activation analysis with short-lived nuclides at the Interfaculty Reactor Institute (IRI) and at the Natioanl Institute of Standards and Technology (NIST). In the system built at IRI, the LFC is integrated through a buffer module to a Unix workstation; the NIST system uses standard Canberra equipment and VMS software. Procedures are described for the calibration and validation of LFC in these two environments, with emphasis on accuracy and on control of the quality of the measurements.

04,106
PB96-167317 Not available NTIS
National Inst. of Standards and Technology (CSTL), Boulder, CO. Thermophysics Div.
Dynamic Scaling in an Aggregating 2D Lennard-Jones System.
Final rept.
B. D. Butler, H. J. M. Hanley, D. Hansen, and D. J. Evans. 1995, 4p.
Pub. in Physical Review Letters, v74 n22 p4468-4471 May 95.

Keywords: *Fractal aggregation, *Gelaton, Molecular dynamics, Reprints, Scaling, Spinodal decomposition.

The evolution of a 2D Lennard-Jones system, quenched from the fluid to below the triple point, is simulated by molecular dynamics. We show that the structure factor obeys the scaling relation S(q/qm(t)) approx. qm(t)-dfS(q/qm). Here qm is the location of the low angle peak in S(q), df equals 1.85 plus or minus 0.05 is a fractal dimension, and S(q/qm) is a time-independent characteristic function which peaks at qm. The quenching process is thermodynamically similar to the formation of a gel from a sol. Hence the relation suggests that a characteristic fractal dimension of even a dense gel can be derived from measurements of the time evolution of S(q).

04,107
PB96-167341 Not available NTIS
National Inst. of Standards and Technology (MSEL), Gaithersburg, MD. Ceramics Div.
Preparation and Crystal Structure of Sr5TiNb4O17.
Final rept.
A. R. Drews, W. Wong-Ng, R. S. Roth, and T. A. Vanderah. 1996, 10p.
Pub. in Materials Research Bulletin, v31 n2 p153-162 1996.

Keywords: *Ceramics, *Crystal growth, *X ray diffraction, Reprints, Crystal structure.

The compound Sr5TiNb4O17 was prepared and its crystal structure determined by single-crystal X-ray diffraction. This compound crystallizes with an orthorhombic unit cell (space group Pnnm (No. 58); a equals 5.6614(4), b equals 32.515(7), c equals 3.9525(3) Angstroms; Z equals 2). The structure consists of alternating perovskite-like slabs offset with respect to each other by a/2 and c/2. The Sr2+ ions occupy two 12-fold coordinated sites within the slabs and a distorted (7 + 1)-fold coordinated site in the gap separating the slabs. Nb5+ and Ti4+ are distributed among the octahedral sites of the sperovskite slabs with preferential odering of Ti4+ on octahedral sites on the center of the slabs adjacent to the gap. This compound is the n equals 5 member of a structural series AnBnO(3n + 29) (A equal Sr; B equal Ti, Nb) where n is the number of perovskite layers within each slab.

04,108
PB96-172358 PC A11/MF A03
National Inst. of Standards and Technology (PL), Boulder, CO. Time and Frequency Div.
Trapped Ions and Laser Cooling 4: Selected Publications of the Ion Storage Group of the Time and Frequency Division, NIST, Boulder, Colorado.
Technical note.
J. C. Bergquist, J. J. Bollinger, W. M. Itano, C. R. Monroe, and D. J. Wineland. Jan 96, 205p, NIST/TN-1380.
Also available from Supt. of Docs. as SN003-003-03395-2. See also PB92-189547. Sponsored by Office of Naval Research, Arlington, VA. and Army Research Office, Research Triangle Park, NC.

Keywords: *Ion storage, *Trapped particles, Atoms, Lasers, Cooling, Atomic clocks, Spectroscopy, Frequency standards, Lights scattering, Plasmas(Physics), Cryogenics, Laser cooling, Atomic spectroscopy, NIST(National Institute of Standards and Technology).

This collection of papers represents the work of the Ion Storage Group, Time and Frequency Division, National Institute of Standards and Technology, from May 1992 to January 1996. It follows the collections of papers contained in NBS Technical Note 1086, Trapped Ions and Laser Cooling (June 1985), NIST Technical Note 1324, Trapped Ions and Laser Cooling II (September 1988), and NIST Technical Note 1353, Trapped Ions and Laser Cooling III (April 1992).

04,109
PB96-176490 Not available NTIS
National Inst. of Standards and Technology (CSTL), Gaithersburg, MD. Process Measurements Div.
Electrical Characteristics of Argon Radio Frequency Glow Discharges in an Asymmetric Cell.
Final rept.
M. A. Sobolewski. 1995, 17p.
Pub. in Institutue of Electrical and Electronics Engineers Transactions on Plasma Science, v23 n6 p1006-1022 Dec 95.

Keywords: *Current, *Discharges, Diagnostics, Electrical, Impedance, Plasma, Radio frequency, Voltage, Reprints, *Gaseous Electronics Conference.

Measurements of the current and voltage at both electrodes of a parallel-plate, capacitively coupled RF discharge cell (the Gaseous Electronics Conference Reference Cell) were combines with measurements of the voltage on a wire inserted into the glow region between the electrodes, for argon discharges at pressures of 1.3-133 Pa and peak-to-peak applied voltages equal to or less than 400 V. Together, these measurements determined the RF voltage, current, impedance, and power of each sheath of the plasma. Simple power laws were found to describe changes in sheath impedances observed as voltage and pressure were varied. An equivalent circuit model for the electrical behavior of the discharge was obtained. The equivalent circuit model can be used to relate the electrical data to plasma properties such as electron densities, ion currents, and sheath widths. The results differ from models previously proposed for asymmetric RF discharges, and the implications of this disagreement are discussed.

04,110
PB96-176540 Not available NTIS
National Inst. of Standards and Technology (EEEL), Boulder, CO. Optoelectronics Div.
Automated Measurement of Nonlinearity of Optical Fiber Power Meters.
Final rept.
I. Vayshenker, S. Yang, X. Li, and T. R. Scott. 1995, 8p.
Pub. in Society of Photo-Optical Instrumentation Engineers: Photodetectors and Power Meters II, Sand Diego, CA., July 11-12, 1995, v2550 p12-19.

Keywords: *Optical fibers, *Fiber optics, Nonlinearity, Power calibration, Power meter, Reprints.

We have developed a system for measuring the nonlinearity of optical power meters or detectors over a dynamic range of more than 60 dB at telecommunications wavelengths. This system uses optical fiber components and is designed to accommodate common optical power meters and optical detectors. It is based on the triplet superposition method. The system also measures the range discontinuity between neighboring power ranges or scale settings of the optical power meter. We have developed an algorithm to treat both the nonlinearity and the range discontinuity in a logically consistent manner. Measurements with this system yield correction factors for powers in all ranges. The measurement system is capable of producing results which have standard deviations as low as 0.02%. With slight modification the system can operate over a 90 dB dynamic range at telecommunications wavelengths. This measurement system provides accurate determination of optical power meter or detector nonlinearity; the characterized detectors then can be used for such applications as absolute power and attenuation measurements.

04,111
PB96-176698 Not available NTIS
National Inst. of Standards and Technology (CSTL), Boulder, CO. Thermophysics Div.
Small-Angle Neutron Scattering (SANS) Study of Worm-Like Micelles Under Shear.
Final rept.
M. Y. Lin, H. J. M. Hanley, G. C. Straty, S. K. Sinha, D. G. Peiffer, and M. W. Kim. 1994, 10p.
Pub. in International Jnl. of Thermophysics, v15 n6 p1169-1178 Nov 94.

Keywords: *Neutron scattering, *Shear alignment, Anisotropy, Couette flow, Polymers, Rods, Reprints, *Foreign technology, *Small angle neutron scattering, Polydispersity, Worm-like micelles.

The structure of a cationic worm-like cylindrical micelle was investigated by SANS (small-angle neutron scattering). Intensities from 0.1% by weight solutions in D2O, at rest and under shear, were measured on the NIST Cold Neutron Research Facility 30-m spectrometer in the wave vector range 0.03 equal to or less than Q (nm to the minus one power) equal to or less than 2.0. Scattered intensity patterns from the solutions subjected to shears equal to or greater than 40 s to the minus one power showed pronounced anisotropy, but such anisotropy could not be detected below this apparent threshold shear. The threshold was characterized by a relaxation time since anisotropy was detected only after several minutes of shearing. In contrast, the anisotropy was apparent immediately the shear was applied at the higher shears. The data were analyzed based on the assumption that the micelles behave as rigid rods. Estimates of the radii and length under shear are given. Polydispersity in rod length is discussed, and the authors argue that it contributes significantly to the scattering patterns.

04,112
PB96-180021 Not available NTIS
National Inst. of Standards and Technology (MSEL), Gaithersburg, MD. Reactor Radiation Div.
Dynamics of Mu(+) in Sc and ScHx.
Final rept.
F. N. Gygax, A. Amato, R. Feyerherm, T. J. Udovic, G. Solt, A. Schenck, and I. S. Anderson. 1996, 4p.
Pub. in Jnl. of Alloys and Compounds, v231 p248-251 1995.

Keywords: *Muon spin rotations, *Crystals, Relaxation rate, Reprints, Dynamics, Locations, Magnetic fields.

Muon spin rotation (microSR) experiments on single-crystal samples of ScHx, with x = 0, 0.05, and 0.10 and 0.25, were performed in order to investigate the muon location and possible systematic variations in muon dynamics in these systems. The angular and magnetic field dependence of the microSR relaxation rates shows that at temperatures below 50 K the muon is localized at the interstitial tetrahedral (T) sites. The results for pure Sc, covering a wide range of high and low fields, are coherent with the picture that the muon performs fast tunnelling between two adjacent T sites, separated by 2z = 0.18c, above and below the a-b plane. This value for the muon position along the c axis is remarkably near the sz = 0.194c found for D in Sc by neutron diffraction. The anisotropy of the relaxation rate at low magnetic fields varies sensitively with the H concentration, indicating a change in the ratio of the radial, muon-induced and the partly inherent, uniaxial electric field gradients at the position of the Sc nuclei.

04,113
PB96-180062 Not available NTIS
National Inst. of Standards and Technology (MSEL), Gaithersburg, MD. Polymers Div.
Electrostatic Rigidity of Polyelectrolytes from Reparametrization Invariance.
Final rept.
A. L. Kholodenko, J. F. Douglas, and T. A. Vilgis. 1996, 7p.
Pub. in Macromolecules Theory Simul., v5 p121-127 1996.

Keywords: *Persistence length, *Polyelectrolytes, Electrostatics, Rigidity, Reprints, *Reparametrization invariance.

The persistence length of a polyelectrolyte chain can be represented as lp = lo + le where lo is the bare persistence and le is the electrostatic contribution coming from the effects of electrostatic chain self-interactions. Using a reparametrization-invariant path integral model of semiflexible polymers the authors find that le depends on the ionic strength I as le approximately I to the minus 1/2. This result accords with experimental observations and recent Monte Carlo simulations. Reparametrization-invariance is apparently an essential constraint in selecting acceptable models of semiflexible polymers.

04,114
PB96-180096 Not available NTIS
National Inst. of Standards and Technology (EEEL), Gaithersburg, MD. Electricity Div.
Quantum Hall Effect-Based Resistance Standard: Capabilities and Implementation.
Final rept.
K. C. Lee. 1996, 6p.
See also PB95-171419.
Pub. in NASA Metrology and Calibration 1995, Proceedings of the Annual Workshop (18th), Greenbelt, MD., April 18-20, 1995, p1-6.

Keywords: *Digital multimeter, Reprints, *Quantum Hall effect, *Resistance standard.

In order to support modern 8 and one-half digit digital multimeters and high accuracy calibrators capable of delivering uncertainties of the order of parts per million (ppm), primary standards laboratories must be able to provide calibration uncertainties less than 0.1 ppm. Quantum Hall effect-based resistance standards can provide these low uncertainties, but at present require very sophisticated and costly equipment. This talk describes the quantum Hall effect (QHE), the equipment necessary to use it as a resistance standard, and some of the challenges in making a QHE-based resistance standard commercially viable.

04,115
PB96-180112 Not available NTIS
National Inst. of Standards and Technology (EEEL), Gaithersburg, MD. Semiconductor Electronics Div.
Assessing MOS Gate Oxide Reliability on Wafer Level with Ramped/Constant Voltage and Current Stress.
Final rept.
A. Martin, J. Suehle, P. Chaparala, C. Messick, P. O'Sullivan, and A. Mathewson. 1996, 11p.
Pub. in Proceedings of the Institute of Electrical and Electronics Engineers International Integrated Reliability Workshop Final Report, Lake Tahoe, CA., October 22-25, 1996, p81-91.

Keywords: *Accelerated testing, *Oxide breakdown, Reliability, Reprints, *MOS gate oxides.

In this study time to breakdown distributions are compared for MOS gate oxides which were stressed with a constant voltage (or current) stress or a pre-stressing voltage (or current) ramp followed by a constant voltage (or current) stress. Results show clearly that a pres-stress can increase time to breakdown. This increase is discussed and it is shown that it is dependent on oxide thickness, pre-stressing ramp rate and the processing conditions. The current-time (or voltage-time) characteristics of the constant stress are investigated and it is observed that charge trapping in the oxide is the reason for the time to breakdown increase. The pre-stressed oxide clearly shows a different initial charge trapping characteristic than the non pre-stressed oxide. The measurement results are discussed and it will be demonstrated that the common understanding of oxide breakdown cannot explain the observed results. Therefore, a new parameter will be proposed which is related to oxide degradation and breakdown and which has to be considered in combined ramped/constant stress measurements.

04,116
PB96-180120 Not available NTIS
National Inst. of Standards and Technology (PL), Gaithersburg, MD. Atomic Physics Div.
Designations of ds(2)p Energy Levels in Neutral Zirconium, Hafnium, and Rutherfordium (Z=104).
Final rept.
W. C. Martin, and J. Sugar. 1996, 4p.
Pub. in Physical Review A, v53 n3 p1911-1914 Mar 96.

Keywords: *Atomic energy levels, *Electron configuration, *Energy-level calculations, Atomic spectroscopy, Hafnium, Level designation, Rutherfordium, Reprints.

The authors have examined available data for the odd-parity energy-level structures in Zr and Hf, stimulated by the designations of four predicted 6d7s27p levels in the homologous atom rutherfordium (Rf, Z = 104) by Eliav et al. (Phys. Rev. Lett. 74, 1079 (1995)). The authors point out some errors and deficiencies in the Zr data and give the results of Hartree-Fock calculations for Hf 5d6s26p-6p and Rf 6d7s27p levels. Configuration interactions within the (d + s)3p complexes were included. The resulting eigenvectors allow meaningful LS-coupling designations for most of the levels belonging mainly to Hf 5d6s26p and for most of the predicted Rf levels belonging mainly to 6d7s27p. Some changes in the designations assigned to these levels in the literature are suggested: in particular, the lowest level of both Hf 5d626p and Rf 6d7s27p is most appropriately designated 3F02. The authors point out the need for systematic whole-row studies of the low odd-parity configurations in 4d- and 5d-shell spectra.

04,117
PB96-180203 Not available NTIS
National Inst. of Standards and Technology (PL), Gaithersburg, MD. Atomic Physics Div.
Hyperfine Structure Investigations and Identification of New Energy Levels in the Ionic Spectrum of (147)Pm.
Final rept.
R. Otto, H. Huhnermann, J. Reader, and J. F. Wyart. 1996, 13p.
Pub. in Jnl. of Physics B, Atomic and Molecular Physics, v28 p3615-3627 1995.

Keywords: *Energy levels, *Hyperfine structures, *Promethium, Spectrum, Reprints.

Hyperfine structure splittings have been measured for 75 lines of singly ionized promethium 147 PmII with a hollow cathode discharge and a Fabry-Perot interferometer. Magnetic dipole and electric quadrupole splitting factors A and B have been determined for 10 levels of the 4f56s configuration, 2 levels of 4f5d, and 57 upper undesignated levels. The A-factors are in general agreement with calculated values. With the aid of Hartree-Fock calculations and Zeeman-effect data, four new levels of the 4f5(6H)5d7K term were located. The strong lines terminating on these 7K levels originate from levels of 4f5(6H)6p7I, which were already known, but had not been designated. An unidentified line at 556.17 nm previously observed with collinear laser ion-beam spectroscopy is now classified as 4f5(6H)5d 7K6-4f5(6H)6p7I5.

04,118
PB96-180211 Not available NTIS
National Inst. of Standards and Technology (PL), Gaithersburg, MD. Atomic Physics Div.
Measurements of the Resonance Lines of (6)Li and (7)Li by Doppler-Free Frequency-Modulation Spectroscopy.
Final rept.
C. J. Sansonetti, B. Richou, R. Engleman, and L. J. Radziemski. 1995, 7p.
Pub. in Physical Review A, v52 n4 p2686-2688 Oct 95.

Keywords: *Atomic spectra, *Isotope shift, *Laser spectroscopy, Lithium, Wavelengths, Reprints.

Using Doppler-free frequency-modulation spectroscopy, the authors have measured most of the hyperfine components and the centers of gravity of the D1 line of 7Li and the D2 line of 6Li. By using previously measured fine- and hyperfine-structure splittings, the authors have also determined centers of gravity for the D2 line of 7li and the D1 line of 6Li. The present results are more accurate than previously reported values by a factor of more than 100. The wave numbers are 7Li D2: 14,903.983,468 (14) cm to the minus 1 power; 7Li D1: 14,903.648,130 (14) cm to the minus 1 power; 6Li D2: 14.903.632,116(18) cm to the minus 1 power; 6Li D1: 14,903.296,792 (23) cm to the minus 1 power. Values for the isotope shifts of the resonance lines of 0.351,338 (21) cm to the minus 1 power for the D1 line and 0.351,352 (15) cm to the minus 1 power for the D2 line have been derived. All uncertainties represent a 95% level of confidence.

04,119
PB96-186085 Not available NTIS
National Inst. of Standards and Technology (PL), Gaithersburg, MD. Ionizing Radiation Div.
Alpha-Particle and Electron Capture Decay of (209)Po.
Final rept.
F. J. Schima, and R. Colle. 1996, 5p.
Pub. in Nuclear Instruments and Methods in Physics Research A, v369 p498-502 Feb 96.

Keywords: *Electron capture decay, Alpha decay, Reprints, Photon spectrometry, Radioactivity, *Foreign technology, *Internal conversion coefficients, Bismuth-209, Lead-205, Polonium-209.

Gamma-ray and K alpha X-ray emissions have been measured from a very pure 209 Po source containing less than 0.13% 208 Po activity and no detectable 210 Po (equal to or less than (2 x 10 to the minus 4 power)%). The alpha-particle emission rate for this source has previously been determined. Data are presented that confirm alpha decay to the 205 Pb excited level at 262.8 keV, with an alpha-particle emission probability (+ or - standard uncertainty) of 0.00559 + or - 0.00008. The ratio of K-shell electron capture to total electron capture for the second forbidden unique electron capture decay to the 896.6 keV level in 209 Bi was determined to be 0.594 + or - 0.018. The electron capture decay fraction was found to be 0.00454 + or - 0.00007, while the probabilities per decay for the 896.6, 262.8, and 260.5 keV gamma rays and the Bi K alpha and PB K alpha X-rays were measured as 0.00445 + or - 0.00007. 0.00085 + or - 0.00002, 0.00254 + or - 0.00003, 0.00202 + or - 0.00005, and 0.00136 + or - 0.00005, respectively.

04,120
PB96-186101 Not available NTIS
National Inst. of Standards and Technology (PL), Gaithersburg, MD. Ionizing Radiation Div.
Scattered Fractions of Dose from 18 and 25 MV X-ray Radiotherapy Linear Accelerators.
Final rept.
J. Shobe, J. E. Rodgers, P. L. Taylor, J. Jackson, and G. Popescu. 1996, 3p.

Keywords: *Radiotherapy, *Linear accelerator scatter, Neutrons, Shielding, Reprints, *Foreign technology, *Scattered fractions of dose.

Over the years, measurements have been made at few energies to estimate the scattered fraction of dose from the patient in medical radiotherapy operations. This information has been a useful aid in the determination of shielding requirement for these facilities. With these measurements, known characteristics of photons, and various other known parameters, Monte Carlo codes are being used to calculate the scattered fractions and hence the shielding requirements for the photons of other energies commonly used in radiotherapeutic applications. The National Institute of Standards and Technology (NIST) acquired a Sagittaire medical linear accelerator (linac) which was previously located at the Yale-New Haven Hospital. This linac provides an x-ray beam of 25 MV photons and electron beams with energies up to 32 MeV. The housing on the gantry was permanently removed from the accelerator during installation. A varian Clinac 1800 linear accelerator was used to produce the 18 MV photons at the Frederick Memorial Hospital Regional Cancer Therapy Center in Frederick, MD. This paper presents a study of the photon dose scattered from a patient in typical radiation treatment situations as it relates to the dose delivered at the isocenter in water. The results of these measurements will be compared to Monte Carlo calculations. Photon spectral measurements were not made at this time. Neutron spectral measurements were made on this Saggitaire machine in its previous location and that work was not repeated here, made at this time. Neutron spectral measurements were made on this Sagittaire machine in its previous location and that work was not repeated here, although a brief study of the neutron component of the 18 and 25 MV linacs was performed utilizing thermoluminescent dosimetry (TLD) to determine the isotropy of the neutron dose.

04,121
PB96-186127 Not available NTIS
National Inst. of Standards and Technology (PL), Gaithersburg, MD. Electron and Optical Physics Div.
Coarsening of Unstable Surface Features during Fe(001) Homoepitaxy.
Final rept.
J. A. Stroscio, D. T. Pierce, M. D. Stiles, and A. Zangwill. 1995, 4p.
Pub. in Physical Review Letters, v75 n23 p4246-4249 Dec 95.

Keywords: *Surface morphology, *Epitaxial growth, Reprints, STM, RHEED, Fe homoepitaxy, Non self-affine surface, Nonequilibrium growth.

The evolution of the surface potential during homoepitaxial growth of Fe(001) is studied by scanning tunneling microscopy and reflection high energy electron diffraction. The observed morphology exhibits a non-self-affine collection of moundlike features that maintain their shape but coarsen as growth proceeds. The characteristic feature separation L is set in the submonolayer regime and increases with thickness t as L(t) approx. t 0.16 plus or minus 0.04. During the coarsening phase, the mounds are characterized by a magic slope and a lack of reflection symmetry. These observations are shown to be described by a continuum growth equation without capillarity.

04,122
PB96-190152 Not available NTIS
National Inst. of Standards and Technology (PL), Gaithersburg, MD. Atomic Physics Div.
Atomic Branching Ratio Data for Nitrogen-Like Species.
Final rept.
J. Z. Klose, J. R. Fuhr, and W. L. Wiese. 1996, 18p.
Pub. in Jnl. of Quantitative Spectroscopy and Radiative Transfer (JQSRT), v55 n4 p413-430 1996.

Keywords: *Atoms, *Branching ratio, High temperature, Nitrogen ions, Plasmas(Physics), Spectral lines, Vacuum ultraviolet radiation, Transition probabilities, Radiometry, Reprints, *Nitrogen-like ions.

The branching ratio technique for radiometric calibrations in the vacuum ultra-violet spectral region is briefly reviewed. Lists of transitions suitable for use with the technique are given for nitrogen-like species (NI, O II, and NeIV) along with pertinent data for their application.

04,123
PB96-200290 Not available NTIS
National Inst. of Standards and Technology (PL), Boulder, CO. Quantum Physics Div.
Comment on <<A Dynamic Electric Trap for Ground-State Atoms>>.
Final rept.
E. A. Cornell. 1995, 2p.
Grant NSF-PHY90-12244
Sponsored by National Science Foundation, Arlington, VA.
Pub. in Europhysics Letters, v30 n7 p439-440 1995.

Keywords: *Trapping(Charged particles), Electric fields, Dynamics, Gravitational fields, Ground state, Equilibrium(General), Reprints, *Atom traps, *Foreign technology.

Riis and Barnett have examined the motion of a polarizable atom in the electric field in the vicinity of a sphere with time-arying charge. The configuration they examined may be experimentally useful but their paper propagates a common misconception about the mechanism of dynamic stabilization. Dynamic stabilization is an important techique in atom and ion trapping, and the purpose of the comment is to clear up the misconception.

04,124
PB96-200316 Not available NTIS
National Inst. of Standards and Technology (PL), Boulder, CO. Quantum Physics Div.
Alignment Probing of Rydberg States by Stimulated Emission.
Final rept.
E. M. Spain, M. J. Dalberth, P. D. Kleiber, J. P. J. Driessen, S. R. Leone, and S. S. Op de Beek. 1995, 10p.
Grant NSF-PHY90-12244
Sponsored by National Science Foundation, Arlington, VA.
Pub. in Jnl. of Chemical Physics, v102 n24 p9522-9531, 22 Jun 95.

Keywords: *Calcium, *Collision, Lasers, Alignment, Reprints, *Rydberg states.

The possibility of probing the collisions of aligned Rydberg atoms by stimulated emission is assessed with studies of a polarized state and a new measurement of a collisional alignment effect in atomic Ca. The stimulated emission method uses a laser to dump the desired state to a lower level which subsequently fluoresces. The technique can be used to obtain populations and polarization dependent information. First, the method is tested by applying it to an aligned Ca(4s17d1D2) state. Alignment curves are measured when the initial state is prepared with both parallel and perpendicular relative polarizations. The experimentally observed alignment compares well with that derived from theoretical considerations of a saturated stimulated transition. Second, a two-vector collisional alignment experiment (initial state and relative velocity vector) is performed to study the energy transfer process and alignment effects are measured by both stimulated emission and conventional direct fluorescence detection.

04,125
PB96-200357 Not available NTIS
National Inst. of Standards and Technology (PL), Boulder, CO. Quantum Physics Div.
Pairwise and Nonpairwise Additive Forces in Weakly Bound Complexes: High Resolution Infrared Spectroscopy of ArnDF (n=1,2,3).
Final rept.
J. T. Farrell, S. Davis, and D. J. Nesbitt. 1995, 16p.
Pub. in Jnl. of Chemical Physics, v103 n7 p2395-2411 1995.

Keywords: *Spectroscopy, *Intermolecular forces, Infrared, Reprints, *Nonpairwise additive forces, Potential energy surface, Vander Waals, Argon hydrogen fluoride.

High resolution infrared spectra of the vDF=1<-0 stretch in ArnDF (n=1-3) have been recorded using a slit-jet infrared spectrometer. Analysis of the rotationally resolved spectra provides vibrationally averaged geometries and vibrational origins for a DF chromophore sequentially 'solvated' by Ar atoms. Calculations using pairwise additive Ar-Ar and Ar-DF potentials predict lowest energy equilibrium structures consistent with the vibrationally averaged geometries inferred spectroscopically. Variational calculations by Ernesti and Hutson using pairwise additive potentials predict rotational constants which are in qualitative agreement with, but consistently larger than, the experimental values. The inclusion of nonpairwise additive (three-body) terms improves the agreement, though still not to within the uncertainty of the pair potentials.

04,126
PB96-200720 Not available NTIS
National Inst. of Standards and Technology (PL), Boulder, CO. Quantum Physics Div.
Stable, Tightly Confining Magnetic Trap for Evaporative Cooling of Neutral Atoms.
Final rept.
W. Petrich, M. H. Anderson, J. R. Ensher, and E. A. Cornell. 1995, 4p.
Pub. in Physical Review Letters, v74 n17 p3352-3355 Apr 95.

Keywords: *Magnetic traps, *Evaporative cooling, Atoms, Reprints, *Bose condensation, Orbiting potential.

We describe a new type of magnetic trap whose time-averaged, orbiting potential (TOP) supplies tight and harmonic confinement of atoms. The TOP trap allows for long storage times even for cold atom samples by suppressing the loss due to nonadiabatic spin flips which limits the storage time in an ordinary magnetic quadrupole trap. In preliminary experiments on evaporative cooling of 87Rb atoms in the TOP trap, we obtain a phase-space density enhancement of up to 3 orders of magnitude and temperatures as low as 200 nK.

04,127
PB96-200944 Not available NTIS
National Inst. of Standards and Technology (EEEL), Gaithersburg, MD. Electricity Div.
Quantum Hall Effect-Based Resistance Standard (Quantum Hall Res).
Final rept.
K. C. Lee. 1996, 18p.
See also PB96-180096.
Pub. in Proceedings of the Annual National Aeronautics and Space Administration Metrology and Calibration Workshop (19th), NASA Kennedy Space Center, FL., February 26-March 1, 1996, p577-594.

Keywords: *Digital multimeter, Temperatures, Magnetic fields, Reprints, *Quantum Hall effect, *Resistance standard.

The present technology for observing the quantum Hall effect requires that a quantum Hall resistor (QHR) be maintained at temperatures below 1.4 K, and in magnetic fields between 5 T and 15 T. Furthermore, in contrast with wire-wound standard resistors that can pass milli-amperes of current, present quantum Hall resistors are limited to currents between 25 micro Angstroms and 60 micro Angstroms. This means that expensive cryogenic systems and super conducting solenoids are required to produce the conditions for the QHE to be observed. The very limited current-carrying capacity of present QHRs requires highly specialized and complex measurement systems that can compare the low voltages developed across them to the voltages developed across the resistors being calibrated. The primary objective of the project is to develop QHRs that can operate at lower magnetic fields, higher temperatures, and higher currents, in order to reduce the costs and complexity of the cryogenic system and the measurement system. A secondary objective is to develop and improve simple measurement techniques that can calibrate wire-wound resistors using QHRs with combined relative uncertainties less than 0.1 ppm, even with the present limitations on the current that can be passed through the devices.

04,128
PB96-200985 Not available NTIS
National Inst. of Standards and Technology (EEEL), Gaithersburg, MD. Semiconductor Electronics Div.
New Oxide Degradation Mechanism for Stresses in the Fowler-Nordheim Tunneling Regime.
Final rept.
A. Martin, J. S. Suehle, P. Chaparala, P. O'Sullivan, and A. Mathewson. 1996, 10p.
Pub. in Proceedings of the International Reliability Physics Conference, Dallas, TX., April 30-May 2, 1996, p67-76.

Keywords: *Oxides, *Tunneling, Reliability, Degradation, Stresses, Reprints, *Fowler-Nordheim.

In the study, voltage and current stress measurements in the Fowler-Nordein regime, performed on gate oxides (9nm-28nm), indicated that a ramped pre-stress prior to a constant stress can increase the time to breakdown in some cases. In the literature oxide breakdown is said to be related to a fixed amount of trapped oxide charge or to a fixed amount of generated traps in the oxide. However, these models cannot explain our experimental observations. Current-time, current-charge, voltage-time characteristics and results of high frequency pre-stresses have been extensively studied in order to gain information about the charge trapping properties of the virgin and pre-stressed oxides. It is concludes from experimental results that the rate of initial positive charge build up in the oxide during the constant stress is a key factor for oxide degradation and breakdown.

04,129
PB96-201066 Not available NTIS
National Inst. of Standards and Technology (MEL), Gaithersburg, MD. Precision Engineering Div.
Modification of a Commercial SEM with a Computer Controlled Cathode Stabilized Power Supply.
Final rept.
M. T. Postek, W. J. Keery, and A. E. Vladar. 1993, 4p.
Pub. in Scanning, v15 p208-211 1993.

Keywords: *Accelerating voltage, *Scanning electron microscopes, Anode, Cathode, Computer control, Reprints, Wehnelt.

Modification of the high-voltage circuitry of the thermionic electron gun of a commercial scanning electron microscope (SEM) to a fully computer-controlled, cathode-stabilized system is described. The modification permits automatic filament saturation and monitoring. Using this system, variations and drifts in the emission current over time can be adjusted and compensated automatically with a feedback loop in the computer-controlled system. This change also enables the accurate determination and setting of the primary electron beam energy. Therefore, the accelerating voltage is known for comparison to Monte Carlo computer modeling of the electron beam specimen interaction.

04,130
PB96-201173 Not available NTIS
National Inst. of Standards and Technology (PL), Gaithersburg, MD. Electron and Optical Physics Div.
Spin-Dependent Interface Transmission and Reflection in Magnetic Multilayers (Invited).
Final rept.
M. D. Stiles. 1996, 6p.
Pub. in Jnl. of Applied Physics, v79 n8 p5805-5810 Apr 96.

Keywords: *Interface transmission, *Magnetic multilayers, Reflection, Exchange coupling, Reprints, Magnetoresistance, Magnetotransport.

First-principles calculations of transmission and reflection from Ag/Fe, Au/Fe, Cu/Co, and Cu/Ni interfaces show very strong spin dependence that differs significantly from expectations based on free electron approximations. The results can be used to understand both the giant magnetoresistance and the oscillatory exchange coupling observed in magnetic multilayers of these materials. The spin dependent of the reflection probabilities is strong enough to give a large giant magnetoresistance even if there is no spin-dependent defect scattering. The calculated reflection amplitudes determine the strength of the oscillatory exchange coupling.

04,131
PB96-201207 Not available NTIS
National Inst. of Standards and Technology (PL), Gaithersburg, MD. Radiometric Physics Div.
Vibrationally Resolved Photoelectron Angular Distributions and Branching Ratios for the Carbon Dioxide Molecule in the Wavelength Region 685-795 Angstrom.
Final rept.
J. B. West, M. A. Hayes, M. R. F. Siggel, A. C. Parr, J. E. Hardis, J. L. Dehmer, and P. M. Dehmer. 1996, 12p.
Pub. in Jnl. of Chemical Physics, v104 n11 p3923-3934 Mar 96.

Keywords: *Branching ratios, *Asymmetry parameters, *Spectroscopy, Cross sections, Ionization, Reprints, Photoelectron spectroscopy.

Measurements of vibrational branching ratios and photoelectron angular distributions have been made in the regions for the Tanaka-Ogawa, Linkholm, and Henning series for the CO2 molecule. The behavior of these parameters was found to be sensitive to which particular resonance is excited, with considerable intensity going into vibrational modes other than the symmetric stretch. An initial analysis of some of the data taken is presented.

04,132
PB96-204094 Not available NTIS
National Inst. of Standards and Technology (PL), Gaithersburg, MD. Electron and Optical Physics Div.
Nanostructure Fabrication via Laser-Focused Atomic Deposition (Invited).
Final rept.
R. J. Celotta, R. Gupta, R. E. Scholten, and J. J. McClelland. 1996, 5p.
Pub. in Jnl. of Applied Physics, v79 n8 p6079-6083 Apr 96.

Keywords: *Nanostructure, *Atomic deposition, Reprints, Fabrication, Atoms, *Laser focusing.

Nanostructured materials and devises will play an important role in a variety of future technologies, including magnetics. The authors describe a method for nanostructure fabrication based on the use of laser light to focus neutral atoms. The method uses neither a mask nor a resist, but relies on the direct deposition of atoms to form permanent structures. Since the atomic de Broglie wavelength is of picometer order, the size of structurs produced is not significantly limited by diffraction, as in optical lithography. Lines as narrow as 38 nm full width at half maximum spaced by 213 nm have been produced and the authors have demonstrated the production of a two-dimensional array of dots. The highly parallel process of nanostructure formation and the intrinsic accuracy of the optical wavelength that determines structure spacing suggest a number of interesting applications, including calibration standards for various types of microscopy, lithography, and micromeasurement systems. Possible magnetic applications include the production of arrays of magnetic elements, laterally structures giant magnetoresistive devices, and the patterning of magnetic media.

04,133
PB96-204144 Not available NTIS
National Inst. of Standards and Technology (PL), Gaithersburg, MD. Electron and Optical Physics Div.
Properties of a Bose-Einstein Condensate in an Anisotropic Harmonic Potential.
Final rept.
M. Edwards, R. J. Dodd, C. W. Clark, P. A. Ruprecht, and K. Burnett. 1996, 4p.
Pub. in Physical Review A, v53 n4 pR1950-R1953 Apr 96.

Keywords: *Laser cooling, Reprints, Lifetime, Rubidium, Vortex, *Bose-Einstein condensation, Non-linear Schrodinger equation.

The authors present results on the size, density, chemical potential, and lifetime of a Bose-Einstein condensate as a function of a number of condensate atomes for parameters appropriate to the time-averaged orbiting potential trap in which a Bose condensate of 87Rb atoms was recently formed. These results were obtained by solving the time-independent nonlinear Schrodinger equation with anisotropic harmonic trapping potential. The authors also find vortex solutions for the trap and the critical rotation frequency required for their formation.

04,134
PB96-204201 Not available NTIS
National Inst. of Standards and Technology (PL), Gaithersburg, MD. Radiometric Physics Div.
Mode-Locked Lasers for High-Accuracy Radiometry.
Final rept.
T. R. Gentile, and C. L. Cromer. 1996, 3p.
Pub. in Metrologia, v32 p585-587 1995/96.

Keywords: *Radiometry, *Lasers, Reprints, Cryogenics, Linearity, Mode-locked laser, NIST.

The use of a mode-locked laser as a source for high-accuracy calibration of transfer standards to a cryogenic radiometer is discussed. The critical issue is the relative response of the transfer standard to the mode-locked laser light as compared with continuous-wave laser light. As a first test, the author have measured the linearity of the response of silicon photodiode light-trapping detectors using mode-lock laser light at a wavelength of 532 nm.

04,135
PB97-110175 Not available NTIS
National Inst. of Standards and Technology (PL), Gaithersburg, MD. Electron and Optical Physics Div.
Stable Silicon Photodiodes for Absolute Intensity Measurements in the VUV and Soft X-ray Regions.
Final rept.
E. M. Gullikson, R. Korde, L. R. Canfield, and R. E. Vest. 1996, 4p.
Pub. in Jnl. of Electron Spectroscopy and Related Phenomena, v80 p313-316 1996.

Keywords: *X-rays, *Photodiodes, Silicon, Vacuum ultraviolet, Absolute detectors, Reprints, *Foreign technology.

Stable silicone photodiodes with 100% internal quantum efficiency have been developed for the vacuum ultraviolet and soft x-ray regions. It is demonstrated that the response of these detectors can be reasonably well represented by a simple model for photon energies above 40 eV. The measured efficiency is consistent with a constant electron-hole pair creation energy for Si above 40 eV. Radiation damage is demonstrated to result in loss of carriers to recombination at the front surface. The uniformity of the diodes is shown to be better than 0.1% RMS at 110 eV.

04,136
PB97-110191 Not available NTIS
National Inst. of Standards and Technology (CSTL), Gaithersburg, MD. Biotechnology Div.
Hydrodynamic Friction of Arbitrarily Shaped Brownian Particles.
Final rept.
J. B. Hubbard, and J. F. Douglas. 1993, 4p.
Pub. in Physical Review E, v47 n5 pR2983-R2986 May 93.

Keywords: *Brownian motion, *Hydrodynamic friction, Capacitance, Wiener sausage, Reprints.

The authors present a simple and accurate method of estimating the translational hydrodynamic friction on rigid Brownian particles of arbitrary shape. The Brownian friction coefficient f take the form f=6(pi)nC(omega), where C(omega) is mathematically equivalent to the electrostatic capacitance of the particle omega in units where the caacity of a sphere equals its radius. This formula is particularly useful for particles consisting of a few globular subunits, for which slender body approximations are not very accurate.

04,137
PB97-110399 Not available NTIS
National Inst. of Standards and Technology (PL), Gaithersburg, MD. Ionizing Radiation Div.
Calculation of Photon Mass Energy-Transfer and Mass Energy-Absorption Coefficients.
Final rept.
S. M. Seltzer. 1993, 24p.
See also PB92-181106.
Pub. in Radiation Research, v136 p147-170 1993.

Keywords: *Photons, *Energy absorption, *Energy transfer, Bremsstrahlung, Cross sections, Calculations, Reprints, Positron annihilation.

Calculations of mass energy-transfer and mass energy-absorption coefficients for photon energies from 1 keV to 100 MeV have been developed, based on a re-examination of the processes involved after the initial photon interaction. The probabilities for the initial interaction are from the current photon interaction cross-section database at the National Institute of Standards and Technology. The calculation then take into account (1) electron binding effects on the Compton-scattered photon distribution; (2) the complete cascade of fluorescence emission after ionization events in any atomic subshell, including those associated with incoherent scattering and triplet production; and (3) the radiative energy losses of the secondary electrons and positrons slowing down in the medium, including the emission of bremsstrahlung, characteristic x-rays from impact ionization, and positron in-flight as well as at-rest annihilation quanta. Consideration of the processes in (3) goes beyond the continuous-slowing-down approximation and includes the effects of energy-loss straggling. Results for the mass energy-absorption coefficient are compared with those from recent tabulations.

04,138
PB97-110407 Not available NTIS
National Inst. of Standards and Technology (PL), Gaithersburg, MD. Ionizing Radiation Div.
Electron-Photon Monte Carlo Calculations: The ETRAN Code.
Final rept.
S. M. Seltzer. 1991, 24p.
Pub. in Applied Radiation and Isotopes, v42 n10 p917-941 1991.

Keywords: *Photons, *Electrons, Positron, Bremsstrahlung, Reprints, *Foreign technology, *ETRAN code, Monte Carlo transport code.

The paper briefly describes the Monte Carlo code ETRAN, developed for the solution of coupled electron-photon transport problems. The authors focus on the multiple-scattering distributions and underlying cross sections that form the basis of current versions of ETRAN, without details on sampling algorithms or numerical procedures.

04,139
PB97-110563 Not available NTIS
National Inst. of Standards and Technology (MEL), Gaithersburg, MD. Precision Engineering Div.
Point Charges, Radiation Reaction, and Quantum Mechanics.
Final rept.
E. Marx. 1993, 5p.
Pub. in Institute of Electrical and Electronic Engineers EMC Symposium, Anaheim, CA., August 17-21, 1992, p508-512 1993.

Keywords: *Point charges, *Radiation reactions, *Quantum mechanics, Electrodynamics, Reprints, Aharonov-Bohm effect, Cerenkov radiation.

Moving point charges generate nonsinusoidal electromagnetic fields, and the motion of the charges is in turn determined by the fields. The full dynamical problem includes radiation reaction, which is discussed here. Nonsinusoidal fields are also associated with relativistic quantum mechanics, where the notion of causality is extended. Cerenkov radiation and the Aharonov-Bohm effect are two other topics.

04,140
PB97-110571 Not available NTIS
National Inst. of Standards and Technology (MEL), Gaithersburg, MD. Precision Engineering Div.
Positronium in Relativistic Quantum Mechanics.
Final rept.
E. Marx. 1992, 11p.
Pub. in Jnl. of the Franklin Institute, v329 n5 p869-879 1992.

Keywords: *Quantum mechanics, *Positronium, Bound states, Pair annihilation, Electromagnetic interactions, Reprints, Klein-Gordan equation.

The problem of bound states of a charged particle and its antiparticle is formulated in the framework of the relativistic quantum mechanics of a single scalar particle interacting with the electromagnetic field. The Coulomb interaction between the particle and the antiparticle gives rise to the bound states, and the coupling of the wave function to the radiation field is responsible for the decay of the pair into electromagnetic energy. The contribution of a pion-pion interaction is discussed briefly. The theory is extended to the spin-1/2 electron.

04,141
PB97-110589 Not available NTIS
National Inst. of Standards and Technology (MEL), Gaithersburg, MD. Precision Engineering Div.
Relativistic Quantum Mechanics of Interacting Particles.
Final rept.
E. Marx. 1992, 17p.
Pub. in Jnl. of the Franklin Institute, v329 n4 p637-653 1992.

Keywords: *Quantum mechanics, *Particles, *Electromagnetic interactions, Probability amplitudes, Field theory, Identical particles, Reprints, Klein-Gordon equation.

The relativistic quantum mechanics of several charged scalar particles interacting with a dynamical electromagnetic field is presented in the framework of the many-amplitudes formalism. Each particle and its antiparticle are represented by a seaparate wave function that satisfies the Klein-Gordon equation and which contributes to the charge-current density that is a source of the electromagnetic field. The probability amplitude for several particles or antiparticles is the symmetrized product of the single-particle probability amplitudes.

04,142
PB97-110605 Not available NTIS
National Inst. of Standards and Technology (MEL), Gaithersburg, MD. Precision Engineering Div.
Spinor Equations in Relativistic Quantum Mechanics.
Final rept.
E. Marx. 1992, 13p.
Pub. in Jnl. of Mathematical Physics, v33 n6 p2290-2302 Jun 92.

Keywords: *Quantum mechanics, *Spinor equations, Wave functions, Formulas, Weyl equations, Reprints.

A set of two first-order equations for classical spinor fields are used to formulate the relativistic quantum mechanics (RQM) of a single massive spin-one half particle. These equations are generalized Weyl equations and they are not equivalent to the Dirac equation. They lead to a conserved charge that is not positive definite, thus allowing for a probabilistic interpretation fo the wave function in RQM. The charge is also conserved when the fields interact with a scalar field through the charge-current densities.

04,143
PB97-111256 Not available NTIS
National Inst. of Standards and Technology (PL), Gaithersburg, MD. Atomic Physics Div.
Beam Line for Highly Charged Ions.
Final rept.
A. I. Pikin, C. A. Morgan, E. W. Bell, J. D. Gillaspy, L. P. Ratliff, and D. A. Church. 1996, 6p.
Pub. in Review of Scientific Instruments, v67 n7 p2528-2533 Jul 96.

Keywords: *Beam lines, *Ion optics, *Highly charged ions, Electron beams, Reprints, Electron beam ion trap.

The design and operation of a beam line for transporting and charge-to mass selecting highly charged ions extracted from the National Institute of Standards and Technology electron beam ion trap (EBIT) are described. This beam line greatly extends the range of experiments possible at this facility. Using the transport system, pure beams of low-energy, highly charged ions up to Xe(44+) have been produced with substantially higher fluxes than previously reported from an EBIT source. Design choices and computer modeling for the various components of the beam line are explained in detail.

04,144
PB97-111264 Not available NTIS
National Inst. of Standards and Technology (EEEL), Gaithersburg, MD. Semiconductor Electronics Div.
Quantum Conductance Fluctuations in the Larger-Size-Scale Regime.
Final rept.
C. A. Richter, D. G. Seiler, and J. G. Pellegrino. 1996, 5p.
Pub. in Physical Review B, v53 n19 p13 086-13 090 May 96.

Keywords: *Conductance, *Fluctuations, Heterostructure, Magnetoresistance, Mesoscopic, Reprints, *GaAs/AlGaAs, UCF.

The authors report the results of experimental studies of 'universal' conductance fluctuations in a variety of millimeter-sized GaAs/AlxGal-xAs heterostructures. The ability to observe these mesoscopic fluctuations in traditionally macroscopic semiconductor devices is due to the enhanced sensitivity of the magnetic field modulation measurement technique, which allows a coherent interference effect to be observed and studied in the large-size-scale regime where both the sample length and width are much greater than the quantum scattering lengths.

04,145
PB97-111306 Not available NTIS
National Inst. of Standards and Technology (EEEL), Boulder, CO. Electromagnetic Technology Div.
Size Effects and Giant Magnetoresistance in Unannealed NiFe/Ag Multilayer Stripes.
Final rept.
S. C. Sanders, R. W. Cross, S. E. Russek, A. Roshko, and J. O. Oti. 1996, 3p.
Pub. in Jnl. of Applied Physics, v79 n8 p6240-6242 Apr 96.

Keywords: *Magnetoresistance, *Magnetostatics, Annealing, Barkhausen noise, Multilayers, Size effects, Thin films, Reprints, NiFe/Ag.

The authors have observed giant magnetoresistance (GMR) in unannealed NiFe/Ag multilayer thin-film stripes. Rectangular stripes having constant thickness and a constant 11:1 length-to-width aspect ratio, but varying widths down to 0.5 micrometers were measured. Two types of multilayer configurations were tested, a system of five NiFe/Ag bilayers with 5.5-nm-thick Ag spacer layers, and a system of nine bilayers with 4.4-nm-thick Ag layers. In contrast to the characterstics of annealed NiFe/Ag multilayer stripes, the unannealed stripes produced increasing GMR ratios for decreasing stripe sizes, with the 0.5-micrometer-wide stripe of the five-bilayer system exhibiting a deltaR/R of 2.5%. Barkhausen noise and response broadening also increased with decreasing stripe size, however. The results are discussed in terms of magnetostatic coupling of the NiFe layers within the stripes.

04,146
PB97-111413 Not available NTIS
National Inst. of Standards and Technology (CSTL), Gaithersburg, MD. Thermophysics Div.
Commercial Helium Permeation Leak Standards: Their Properties and Reliability.
Final rept.
P. J. Abbott, and S. A. Tison. 1996, 5p.
Pub. in Jnl. of Vacuum Science and Technology A, v14 n3 p1242-1246 May/Jun 96.

Keywords: *Helium, *Permeation leaks, Decay rates, Stability, Properties, Reliability, Reprints.

Standard leaks or leak artifacts are used extensively in industrial and research environments, typically for the calibration of helium leak detectors. The most commonly used leak is the helium permeation type, which uses a glass, quartz, or polymer barrier to restrict the flow of helium via diffusion. Physical leaks, on the other hand, use a physically restrictive element to limit the flow. The article will discuss the properties and reliability of helium permeation standard leaks, based on eight years of accumulated calibration data. Physical helium leaks will not be discussed since relatively few have been calibrated at the National Institute of Standards and Technology.

04,147
PB97-111421 Not available NTIS
National Inst. of Standards and Technology (MSEL), Gaithersburg, MD.
Extrapolation of the Heat Capacity in Liquid and Amorphous Phases.
Final rept.
J. Agren, B. Cheynet, M. T. Clavaguera-Mora, U. Kattner, F. Sommer, K. Hack, and J. Hertz. 1996, 32p.
Pub. in Calphad, v19 n4 p449-480 1995.

Keywords: *Amorphouse phases, *Heat capacity, Extrapolation, Liquid phase, Phase stability, Two-states model, Reprints.

Various methods of extrapolating the thermodynamic properties of the liquid will be discussed. A phenomenological method based on polynomials as well as a more physical method based on an extended two-state Schottky formalism will be presented and their application to some substances will be demonstrated.

04,148
PB97-111496 Not available NTIS
National Inst. of Standards and Technology (EEEL), Boulder, CO. Electromagnetic Technology Div.
Pulse-Driven Programmable Josephson Voltage Standard.
Final rept.
S. P. Benz, and C. A. Hamilton. 1996, 3p.
Pub. in Applied Physics Letters, v68 n22 p3171-3173 May 96.

Keywords: *Josephson junctions, *Voltage standards, Digital-to-analog converters, Programmable pulses, Pulses, Reprints.

A voltage standard based on a series array of pulse-biased, nonhysteretic Josephson junctions is proposed. The output voltage can be rapdily and continuously programmed over a wide range by changing the pulse repetition frequency. Simulations relate the circuit margins to pulse height, width, and frequency. Experimental results on a prototype circuit confirm the expected behavior.

04,149
PB97-111868 Not available NTIS
National Inst. of Standards and Technology (MSEL), Gaithersburg, MD. Reactor Radiation Div.
X-ray Reflectivity Determination of Interface Roughness Correlated with Transport Properties of (AlGa)As/GaAs High Electron Mobility Transistor Devices.
Final rept.
J. A. Dura, J. G. Pellegrino, and C. A. Richter. 1996, 3p.
Pub. in Applied Physics Letters, v69 n8 p1134-1136 Aug 96.

Keywords: *X ray reflectivity, *Aluminum gallium arsenide, *Gallium arsenide, Interface roughness, Mobility, Molecular beam epitaxy, Transport properties, Reprints.

To explore the role of interface scattering in high electron mobility transistor (HEMT) device performance, a series of samples consisting of both a superlattice and a HEMT structure were grown by molecular beam epitaxy (MBE) at temperatures ranging from 500 to 630 degrees C. Hall measurements indicate a trend toward higher mobilities in samples growth at higher temperatures. Subsequent x-ray reflectivity measurements were made, and the data were fitted by least-squares refinement of a calculated reflectivity curve determined from a model of the sample structure to obtain the composition profile along the growth direction. These results indicate smoother interfaces for the samples with higher mobilities.

04,150
PB97-111934 Not available NTIS
National Inst. of Standards and Technology (MSEL), Gaithersburg, MD. Polymers Div.
Intrinsic Conductivity of Objects Having Arbitrary Shape and Conductivity.
Final rept.
E. J. Garboczi, and J. F. Douglas. 1996, 12p.
Pub. in Physical Review E, v53 n6 p6169-6180 1996.

Keywords: *Intrinsic conductivity, *Conductivity, Arbitrary, Shapes, Reprints.

The authors study the electrical conductivity omega of a dispersion of randomly oriented and positioned particle inclusions having common shape and conductivity omega(p), suspended in an isotropic homogeneous matrix of conductivity omega(0). For this problem, the mixture conductivity is a scalar and the authors concentrate on the leading order concentration virial coefficient, the 'intrinsic conductivity' (omega). Results for (omega) are summarized for limiting cases where there is a large mismatch between the conductivities of the inclusions and the suspending matrix. For a general particle shape, the authors then treat the more difficult case of arbitrary relative conductivity delta equal or minus omega(p)/omega(0) through the introduction of a Pade approximant that incorporates (exact or numerical) information for (omega(delta)) in the delta -> infinity, delta -> 0+, and delta approximately 1 limits. Comparison of this approximation for (omega(delta)) to exact and finite element calculations for a variety of particle shapes in two and three dimensions shows excellent agreement over the entire range of delta. This relation should be useful for inferring particle shape and property information from conductivity measurements on dilute particle dispersions. The leading order concentration virial coefficient for other mixture properties (thermal conductivity, dielectric constant, refractive index, shear modulus, bulk modulus, viscosity, etc.) are equally well described by a similar Pade approximant.

04,151
PB97-111942 Not available NTIS
National Inst. of Standards and Technology (MSEL), Gaithersburg, MD. Reactor Radiation Div.
Observation of Two Length Scales Above (T sub N) in a Holmium Thin Film.
Final rept.
P. M. Gehring, A. Vigliante, D. F. McMorrow, G. Helgesen, R. A. Cowley, R. C. C. Ward, M. R. Wells, D. Gibbs, and C. F. Majkrzak. 1996, 7p.
Pub. in Physica B, v221 p398-404 1996.

Keywords: *Thin films, *Holmium, Two length scales, Neutron scattering, Reprints, *Foreign technology.

Two-axis neutron-scattering measurements on a 1 micrometer thick holmium film reveal the presence of two magnetic correlation lengths above TN that are qualitatively similar to those recently observed in X-ray and neutron scattering studies of bulk holmium and terbium. The scattering profile is well described by a broad Lorentzian plus a narrow Lorentzian-squared line-shape with widths that, for temperatures sufficiently close to TN, differ by a factor of ten or more.

04,152
PB97-112239 Not available NTIS
National Inst. of Standards and Technology (PL), Gaithersburg, MD. Quantum Metrology Div.
Systematic Correction in Bragg X-ray Diffraction of Flat and Curved Crystals.
Final rept.
C. T. Chantler, and R. D. Deslattes. 1995, 25p.
Pub. in Review of Scientific Instruments, v66 n11 p5123-5147 Nov 95.

Keywords: *Systematic corrections, *Bragg x-ray diffraction, *Crystals, Curved crystals, Flat crystals, Refractive index shifts, Spectral wavelengths, Foreign technology, Reprints.

Measurements of spectral wavelengths in Bragg diffraction from crystals often require refractive index corrections to allow a detailed comparison of experiment with theory. These corrections are typically 100-300 ppm in the x-ray regime, and simple estimates may sometimes be accurate to 5% or better. The inadequacies of these estimates are discussed. Even with a possibly improved index of refraction estimate, this correction is insufficient since additional systematics in the diffraction process occur at or above this level. For example, asymmetries of diffraction profiles with pi-polarized radiation or due to three-beam diffraction can approach the magnitude of refractive index corrections for flat or curved crystals. The depth of penetration of the x-ray field inside curved crystals, the shift of the mean angle to the diffracting planes, and lateral shifts around the crystal surface are rarely considered but can dominate over refractive index corrections, particularly for high-order diffraction or medium-energy x rays. Shifts and nonlinearities arise when diffracting surfaces lie off the Rowland circle, and exhibit strong and rapidly varying angular dependencies.

04,153
PB97-112346 Not available NTIS
National Inst. of Standards and Technology (EEEL), Boulder, CO. Electromagnetic Technology Div.
Bias Current Dependent Resistance Peaks in NiFe/Ag Giant Magnetoresistance Multilayers.
Final rept.
L. S. Kirschenbaum, C. T. Rogers, P. D. Beale, S. E. Russek, and S. C. Sanders. 1996, 3p.
Pub. in Applied Physics Letters, v68 n22 p3099-3101 May 96.

Keywords: *Thin films, *Magnetoresistance, *Currents, Multilayers, Peaks, Magnetic fields, Reprints, NiFe-Ag.

The authors show that thin-film Ni82Fe18/Ag multilayer structures display multiple peaks in their magnetoresistance curves when biased at current densities above 10(6) A/cm(2). These peaks appear for annealed and unannealed structures, and their number is correlated with the number of NiFe layers. At high bias currents, the peak positions shift linearly with the internal magnetic field created by the bias current. The peak positions extrapolate to nonzero fields at zero bias currents, providing an upper bound on the magnetic layer-layer coupling strength of J(0) approximately equal to 10(-20) J (k(B) x 700 K). The peak positions do not shift with temperature over the range 200-375 K; their widths narrow with increasing temperature. The single-domain magnetic moment micro is estimated as 10 17 J/T from the peak widths of approximately 0.8 kA/m.

04,154
PB97-112387 Not available NTIS
National Inst. of Standards and Technology (MSEL), Gaithersburg, MD. Reactor Radiation Div.
Isolated Spin Pairs and Two-Dimensional Magnetism in SrCr(sub 9p)Ga(sub 12-9p)O19.
Final rept.
S. H. Lee, C. Broholm, G. Aeppli, A. Taylor, T. G. Perring, and B. Hessen. 1996, 4p.
Pub. in Physical Review Letters, v76 n23 p4424-4427 Jun 96.

Keywords: *Neutron scattering, *Ligand environment, *Magnetism, Sub-lattices, Dispersionless, Inelasticity, Reprints.

The authors show by inelastic neutron scattering that the frustrated magnet SrCr9pGa12-9pO19 (p = 0.92(5)) has dispersionless magnetic excitations at energies 18.6(1) and 37.2(5) meV. The wave vector and temperature dependence of the excitations as well as the ratio 1:2 of excitation energies is perfectly accounted for by isolated antiferromagnetically exchange coupled pairs of spins s = 3/2. Consideration of the layered structure of magnetic chromium ions and the ligand environment indicates that these pairs are adjacent spins in neighboring triangular lattice planes which separate two-dimensional sublattices of interacting kagome-triangle-kagome layers.

04,155
PB97-112403 Not available NTIS
National Inst. of Standards and Technology (PL), Gaithersburg, MD. Molecular Physics Div.
Matrix Isolation Study of the Interaction of Excited Neon Atoms with O3: Infrared Spectrum of O((sub 3)(-)) and Evidence for the Stabilization of O2...O((sub 4)(+)).
Final rept.
C. L. Lugez, W. E. Thompson, and M. E. Jacox. 1996, 8p.
Pub. in Jnl. of Chemical Physics, v105 n6 p2153-2160 Aug 96.

Keywords: *Neon atoms, *Matrix isolation, Infrared spectrum, Photodissociation, Photionization, Reprints.

When a Ne:O3 sample is codeposited at approximately 5 K with neon atoms that have been excited in a microwave discharge, the most prominent infrared absorptions of the resulting solid are contributed by trans- and cyc-O4(=) and by O3(-). The failure to detect infrared absorptions of O3(+) is consistent with the initial formation of that species in one or more dissociative excited states. The v3 absorption of O3(-) appears at 796.3 cm(-1), close to its position in earlier argon-matrix experiments in which photoionization of an alkali metal atom provided the electron source and in which diffusion of the atomic cation would result in the stabilization of appreciable M+O3(-). The identification of O3(-) isolated in solid neon is supported by observations of O3(-) generated from isotopically substituted Ne:O2:N2O samples, also codeposited with excited neon atoms. An upper bound of 810 cm to the minus 1 power is estimated for the gas-phase band center of v3 of O3(-). Infrared absorption which grow on mild warmup of the sample are tentatively assigned to an O2...O4(+) complex.

04,156
PB97-112429 Not available NTIS
National Inst. of Standards and Technology (MSEL), Gaithersburg, MD. Reactor Radiation Div.
Unconventional Ferromagnetic Transition in La(sub 1-x)Ca(sub x)MnO3.
Final rept.
J. W. Lynn, R. W. Erwin, J. A. Borchers, Q. Huang, and A. Santoro. 1996, 4p.
Pub. in Physical Review Letters, v76 n21 p4046-4069 May 96.

Keywords: *Quasielastic component, *Polycrystalline, Isotropic, Ferromagnetic, Despersion relation, Reprints.

Neutron scattering has been used to study the magnetic correlations and long wavelength spin dynamics of La(l-x)Ca(x)MnO3 in the ferromagnetic regime (0 equal to or less than 1/2). For x = 1/3 (T(C)=250 K) where the magnetoresistance effects are largest the system behaves as an ideal isotropic ferromagnet at low T, with a gapless (less than 0.04 meV) dispersion relation E = Dq2 and D(T-0) approximately equal to 170 meV Angstroms. However, an anomalous strongly field-dependent diffusive component develops above approximately 200 K and dominates the fluctuation spectrum at T -> T(C). This component is not present at lower x.

04,157
PB97-112585 Not available NTIS
National Inst. of Standards and Technology (EEEL), Boulder, CO. Electromagnetic Technology Div.
Modeling Effects of Temperature Annealing on Giant Magnetoresistive Response in Discontinuous Multilayer NiFe/Ag Films.
Final rept.
J. O. Oti, and Y. K. Kim. 1996, 3p.
Pub. in Jnl. of Applied Physics, v79 n8 p5596-5598 Apr 96.

Keywords: *Magnetoresistance, *Grain clusters, *Multilayer films, Anisotropy, Exchange, Magnetostatic, Reprints.

The giant magnetoresistive (GMR) behaviors of discontinuous double-layer giant magnetoresistive films with different microstructure arising from different annealing conditions, are calculated using a numerical micromagnetic model. The effect of magnetic grain growths in the perpendicular and lateral directions in the magnetic layers, and the formation and growth of grain clusters were studied. The GMR responses of the films are analyzed in terms of magnetostatic interactions between the magnetic layers and the microstructural geometric effects on the transport properties of the samples.

04,158
PB97-112593 Not available NTIS
National Inst. of Standards and Technology (EEEL), Boulder, CO. Electromagnetic Technology Div.
Simulating Device Size Effects on Magnetization Pinning Mechanisms in Spin Valves.
Final rept.
J. O. Oti, R. W. Cross, S. E. Russek, and Y. K. Kim. 1996, 3p.
Pub. in Jnl. of Applied Physics, v79 n8 p6386-6388 Apr 96.

Keywords: *Spin valves, *Magnetization, Anisotropy, Exchange, Magnetoresistance, Magnetostatic, Reprints.

The effects of magnetostatic interactions on the giant magnetoresistive (GMR) response of NiFe/Cu/NiFe spin valves are studied using an analytical model. The model is applicable to devices small enough for the magnetic layers to exhibit single-domain behavior. Devices having lengths in the track-width direction of 10 micrometers and interlayer separations of 4.5 nm are studied. Stripe heights are varied from 0.5 to 2 micrometers. The magnetization of one magnetic layer is pinned by a transverse pinning field that is varied from 0 to 24 kA/m (300 Oe). GMR curves for transverse fields are calculated. At zero external field and magnetization of the layers shows a tendency to align themselves antiparallel in the transverse direction. This

results in an offset from the ideal biasing of the device. Broadening of the curves due to shape anisotropy occurs with decreasing stripe height and increasing magnetic layer thickness, and the magnetization in the pinned layer becomes less stable.

04,159
PB97-113021 Not available NTIS
National Inst. of Standards and Technology (PL), Gaithersburg, MD. Radiometric Physics Div.
Results of a NIST/VNIIOFI Comparison of Spectral-Radiance Measurements.
Final rept.
R. D. Saunders, C. E. Gibson, K. D. Mielenz, B. B. Khlevnoy, S. N. Mekhontsev, C. D. Harchenko, V. I. Sapritsky, and K. A. Sudarev. 1996, 5p.
Pub. in Metrologia, v32 p449-453 1995/96.

Keywords: *Spectral radiance, *Radiometry, Temperature scales, Intercomparison, Ribbon filament lamps, Reprints, NIST/VNIIOFI.

A comparison of the spectral-radiance scales of the National Institute of Standards and Technology (NIST) and the All-Russian Research Institute for Optophysical measurements (NVIIOFI) was carried out in 1989 and 1990. The spectral range of the comparison was between 240 nm and 2400 nm. The transfer standards were argon-filled tungsten ribbon filament lamps. The NIST/VNIIOFI agreement was 0.5% to 1% in the 240 nm to 800 nm range, and better than 0.5% between 900 nm and 2400 nm. On average, the spectral radiances measured at the NVIIOFI were slightly higher than the NIST values.

04,160
PB97-113070 Not available NTIS
National Inst. of Standards and Technology (MSEL), Gaithersburg, MD. Reactor Radiation Div.
Colossal Magnetoresistance without Mn(3+)/Mn(4-) Double Exchange in the Stoichiometric Pyrochlore Tl2Mn2O7.
Final rept.
M. A. Subramanian, B. H. Toby, A. P. Ramirez, G. H. Kwei, W. J. Marshall, and A. W. Sleight. 1996, 4p.
Pub. in Science, v273 p81-84 Jul 96.

Keywords: *Magnetic structure, *Magnetoresistance, *Neutron diffraction, Pyrochlore, Single crystal diffraction, Reprints.

Structural analysis with powder neutron and single-crystal x-ray diffraction data for a sample of the Tl2Mn2O7 pyrochlore, exhibiting colossal magnetoresistance (CMR), shows no deviations from ideal stoichiometry. Furthermore, the analysis gives an Mn-O distance of 1.90 Angstroms, significantly shorter than the Mn-O distances in the range 1.94 to 2.00 Angstroms observed in phases based on LaMnO3 perovskites which show CMR. Both the stoichiometry and shorter Mn-O dsitance in Tl2Mn2O7 indicate oxidation states very close to Tl2Mn2O7. Thus Tl2Mn2O7 has neither mixed valency for a double exchange magnetic interaction or a Jahn-Teller cation such as Mn(3+). Both were thought to play an essential role in CMR materials. The authors propose an alternate mechanism for CMR in Tl2Mn2O7 based on magnetic ordering driven by superexchange and strong spin fluctuation scattering above Tc. Thus the pyrochlores represent a distinct new class of CMR materials.

04,161
PB97-113104 Not available NTIS
National Inst. of Standards and Technology (PL), Gaithersburg, MD. Atomic Physics Div.
Polarization Measurements on a Magnetic Quadrupole Line in Ne-Like Barium.
Final rept.
E. Takacs, E. S. Meyer, J. D. Gillaspy, L. T. Hudson, R. D. Deslattes, C. M. Brown, J. M. Laming, J. R. Roberts, and C. T. Chantler. 1996, 9p.
Pub. in Physical Review A, v54 n2 p1342-1350 Aug 96.

Keywords: *Polarization, *X ray spectroscopy, Measurement, Charged ions, Reprints, *Electron beam ion trap(EBIT).

The authors have measured the absolute polarization of the (2p(-1)3/2 3s1/2)J=2 to (2p6)J=0 Ne-like barium M2 line, excited in an electron beam ion trap (EBIT) at a variety of energies. The authors find strong evidence for the existence of resonant excitation processes which are not explained by collisional-radiative calculations even when the polarization arising from impact excitation is included. At energies well away from where the resonances occur, the agreement between experiment and theory is good.

04,162
PB97-113161 Not available NTIS
National Inst. of Standards and Technology (PL), Gaithersburg, MD. Radiometric Physics Div.
Comparison of Filter Radiometer Spectral Responsivity with the NIST Spectral-Irradiance and Illuminance Scales.
Final rept.
B. K. Tsai, B. C. Johnson, R. D. Saunders, and C. L. Cromer. 1996, 5p.
Pub. in Metrologia, v32 p473-477 1995/96.

Keywords: *Scales, *Radiometers, *Spectral comparator, *Photometers, Detectors, Filters, Illuminance, Irradiance, Quartz halogen lamp, Reprints, *Foreign technology.

Narrowband filter radiometers are being used in the development of a new method of irradiance scale realization at the National Institute of Standards and Technology (NIST). To improve the accuracy of the current spectral-irradiance scale, the authors propose to eliminate several steps from the calibration process and to use the filter radiometers and a high-temperature black body in realizing the scale. Ultimately, the filter radiometers will be calibrated against a trap detector measured at the NIST High Accuracy Cryogenic Radiometer, which maintains an expanded uncertainty at 633 nm of 0.0266% for a coverage factor of k = 2. In the work, the filter and detector were calibrated as a unit using the NIST Detector Comparator Facility, and the aperture areas were measured by flux comparison with a uniform source. Six filter radiometers covering the spectral range 350 nm to 1100 nm were used to measure a known irradiance source; the measurements agreed with predictions to within 1%.

04,163
PB97-113229 Not available NTIS
National Inst. of Standards and Technology (CSTL), Gaithersburg, MD. Thermophysics Div.
Design of a High-Pressure Ebulliometer, with Vapor-Liquid Equilibrium Results for the Systems CHF2Cl + CF3-CH3 and CF3-CH2F + CH2F2.
Final rept.
L. A. Weber, and A. M. Silva. 1996, 16p.
Pub. in International Jnl. of Thermophysics, v17 n4 p873-888 Jul 96.

Keywords: *Ebulliometers, *Phase equilibrium, *Refrigerant mixtures, Activity coefficient, Reprints, Chlorodifluoromethane, Difluoromethane, 1-1-1-trifluoroethane, 1-1-1-2-tetrafluoroethane.

The authors give a description of the design and operation of a new high-pressure metal ebulliometer which is capable of operating at pressures to at least 3 MPa in the range 220-400 K. Infinite dilution activity coefficients are presented for the system CHF2Cl = CF3-CH3 at 275 K and for the system CF3-CH2F = CH2F2 at 260, 280, and 300 K. The Wilson activity coefficient model and a virial coefficient model are applied to these systems, and the phase equilibrium conditions are calculated. The results are shown to agree well with predicted and with published measured values. The excess enthalpy is calculated and compared with results using a Peng-Robinson equation of state. Vapor densities of the dew curves are given.

04,164
PB97-113278 Not available NTIS
National Inst. of Standards and Technology (MSEL), Gaithersburg, MD. Reactor Radiation Div.
Diffraction of Neutron Standing Waves in Thin Films with Resonance Enhancement.
Final rept.
H. Zhang, S. K. Satija, P. D. Gallagher, C. P. Flynn, J. F. Ankner, J. A. Dura, and K. Ritley. 1996, 5p.
Pub. in Physica B, v221 p450-454 1996.

Keywords: *Thin films, *Standing waves, *Neutrons, Diffraction, Resonance, Reprints.

Diffraction on neutron standing waves in thin films has been demonstrated for the first time with experiments on an epitaxial Y/Gd/Y/Nb/Al2O3 sample. Resonance enhancement in the diffraction intensity has been observed. The new diffraction scheme for neutrons and x-rays provides an oscillatory spatial concentration in thin films, in contrast to the evanescent diffraction which provides an exponential concentration. It also discriminates against diffraction background from substrate, and may be especially useful when diffraction in transmission geometry is not available due to high absorption of substrate.

04,165
PB97-114474 PC A04/MF A01
National Inst. of Standards and Technology (PL), Gaithersburg, MD. Ionizing Radiation Div.
Experimentally Measured Total X-ray Attenuation Coefficients Extracted from Previously Unprocessed Documents Held by the NIST Photon and Charged Particle Data Center.
J. H. Hubbell. Sep 96, 37p, NISTIR-5893.

Keywords: *Bibliographies, *Photon cross sections, *X-rays, Tables(Data), Nuclear data collections, Data bases.

This report lists and annotates 47 previously unprocessed original-source documents held by the NIST Photon and Charged Particle Data Center (PCPDC), containing experimentally measured absolute values of the mass attenuation coefficient, or total photon interaction cross section for one or more elemental materials. The data from these documents had not been previously extracted for purposes of entering into the PCPDC x-ray attenuation measurement data base. Tables of the extracted data, with all photon energies converted to multiples of eV (electron volts), and all photon cross sections converted to units of barns/atom, are given. In some cases, photon wavelengths in angstroms or nm (nanometers) are given in the source documents instead of photon energies, in which case the reciprocal conversion to photon energies (in eV) has been made. A total of 3735 data points were extracted and are presented.

04,166
PB97-118657 Not available NTIS
National Inst. of Standards and Technology (PL), Gaithersburg, MD. Molecular Physics Div.
Bimolecular Interactions in (Et)3SiOH:Base:CCl4 Hydrogen-Bonded Solutions Studied by Deactivation of the Free OH-Stretch Vibration.
Final rept.
W. T. Grubbs, T. P. Dougherty, and E. J. Heilweil. 1995, 4p.
Pub. in Jnl. of the American Chemical Society, v117 n48 p11989-11992 1995.

Keywords: *Bimolecular reaction, *Hydrogen bonding, Complexes, Diffusing control, Infrared, Picoseconds, Reprints, Time-resolved spectroscopy, Vibrational relaxation.

Picosecond infrared (PI) pump-probe measurements of the OH-stretch (v=1) population lifetime were performed for uncomplexes (Et)3SiOH present in dilute, room temperature, tertiary (Et)3SiOH:base:CCl4 hydrogen-bonded solutions (base = acetonitrile, tetrahydrofuran, and pyridine). When base is present in solution, the intrinsic OH-stretch T1 vibrational population lifetime (183 plus or minus 6 ps for (Et)3SiOH in CCl4) is reduced by bimolecular (Et)3SiOH:base hydrogen-bonding encounters. The base concentration dependence of the 'free' OH-stretch vibrational deactivation rate is analyzed by a Stern-Volmer kinetic model and a least-squares fit to all the data yielded a single rate constant k(BM)=1.2 plus or minus 0.2 x 10 to the 10th power dm to the 3rd power mole(-1)s(-1) for (Et)3SiOH:base bimolecular encounters. This vlaue is in agreement with estimate sfor the bimolecular diffusion limit, k(BM) was found to be the same for all (Et)3SiOH:base interactions studied, suggesting that the bimolecular OH-stretch deactivation mechanism is relatively insensitive to the proton-accepting strength of the base.

04,167
PB97-118699 Not available NTIS
National Inst. of Standards and Technology (MSEL), Gaithersburg, MD. Metallurgy Div.
Radiance Temperatures at 1500 nm of Niobium and Molybdenum at Their Melting Points by a Pulse-Heating Technique.
Final rept.
E. Kaschnitz, and A. Cezairliyan. 1996, 10p.
See also PB92-154095.
Pub. in International Workshop on Subsecond Thermophysics (4th), Koln, Germany, June 27-29, 1995, International Jnl. of Thermophysics, v17 n5 p1069-1078 Sep 96.

Keywords: *Niobium, *Temperature measurement, Pulse heating, High temperature, Near infrared radiation, Visible radiation, Melting, Reprints, *Foreign technology, *Radiance temperatures.

Radiance temperatures at 1500 nm of niobium and molybdenum at their melting points were measured by a pulse-heating technique. The method is based on rapid resistive self-heating of the strip-shaped specimen from room temperature to its melting point in less than 1 s and measuring the specimen radiance temperature every 0.5 nm with a high-speed infrared pryometer. Melting of the specimen was manifested by a plateau in the radiance temperature-versus-time function. The melting-point radiance temperature for a given specimen was determined by averaging the measured values along the plateau. A total of 12 to 13 experiments was performed for each metal under investigation. The melting-point radiance temperatures for each metal were determined by averaging the results of the individual specimens.

04,168
PB97-118723 Not available NTIS
National Inst. of Standards and Technology (PL), Gaithersburg, MD. Radiometric Physics Div.
Microwave Spectrum and Structure of CH2O-H2O.
Final rept.
F. J. Lovas, and C. L. Lugez. 1996, 4p.
Pub. in Jnl. of Molecular Spectroscopy, Article No. 0210, v179 p320-323, 1996.

Keywords: *Microwave spectrum, *Dipole moment, Dimer, Formaldehyde, Structure, Water, Reprints, *Formaldehyde-water complex, Rotational spectrum.

The microwave spectrum of the formaldehyde-water complex (CH2O-H2O) has been studied with a pulsed-beam Fourier transform Fabry-Perot cavity spectrometer. Both a-type and b-type transitions were observed for each of the isotopic species studied. To provide additional structural information, the spectra of H2O, HDO, and D2O substituents combined with H2CO and D2CO were assigned. Measurement of the dipole moment components yielded the values micro a=3.379(13) x 10 to the minus 30 power C.m(micro a=1.043(4)D) and micro b=2.54(20) x 10 to the minus 30 power C.m (micro b=0.76(6)D) and indicated that the dipole moment vectors are anti-aligned. The molecular structure derived from the moments of inertia has a center of mass separation of 2.00(3)Angstroms with the C2v symmetry axes of the monomers oriented at 19.3 degrees from parallel with the dipole moments opposed. The complex is quite strongly bound with a harmonic pseudodiatomic stretching force constant, k2=8.93 N/m, and hydrogen bond lengths of approximately 2.68 Angstroms between the water oxygen atom and a CH2 hydrogen atom, and 2.03 Angstroms between a water hydrogen atom and the oxygen atom of H2CO. Expanded uncertainties (coverage factor k = 2 i.e., two standard deviations) are shown in parentheses for each experimental value reported above.

04,169
PB97-118756 Not available NTIS
National Inst. of Standards and Technology (PL), Gaithersburg, MD. Ionizing Radiation Div.
Colour Centres in LiF for Measurement of Absorbed Doses Up to 100 MGy.
Final rept.
W. L. McLaughlin. 1996, 4p.
Pub. in Radiation Protection Dosimetry, v66 n1-4 p197-200 1996.

Keywords: *Lithium fluoride, *Dosimeters, *Radiation damage, Measurements, Absorbed doses, Reprints.

Radiation damage studies on electronic components, polymers, composites, ceramics, metals, and insulating materials exposed to very large doses of ionizing photons and particles (i.e. electrons, protons, and neutrons) require reproducible and accurate passive dosimetry. Absorbed doses in the range 10 to the 2nd power - 2 x 10 to the 6th power Gy have previously been measured with optical quality, undoped LiF by spectrophotometry of radiation-induced absorption bands of stable color centers. These include the relatively stable F center (247 nm), M center (443 nm), R1 center (315 nm), R2 center (374 nm), and N2 center (547 nm). It is now possible to extend this range to 10 to the 8th power Gy by spectrophotometry of the N1 center (517 nm) and an 'X' Center (785 nm). These dosemeters can be used from cryogenic (4 K) to relatively high radiation temperatures (up to 500 K). the radiation-induced coloration can be bleached for reuse of the dosemeters by a two hour thermal annealing treatment at 830 K.

04,170
PB97-118798 Not available NTIS
National Inst. of Standards and Technology (PL), Gaithersburg, MD. Molecular Physics Div.
Rotational Spectra of CH3CCH-NH3, NCCCH-NH3, and NCCCH-OH2.
Final rept.
R. M. Omron, A. R. Hight Walker, G. Hilpert, G. T. Fraser, and R. D. Suenram. 1996, 9p.
Pub. in Jnl. of Molecular Spectroscopy, v179 p85-93 1996.

Keywords: *Cyanoacetylene, *Hydrogen bonding, *Methlacetylene, Microwave spectroscopy, Complexes, Reprints.

Microwave spectra of NCCCH-NH3, CH3CCH-NH3, and NCCCH-OH2 have been recorded using a pulsed-nozzle Fourier-transform microwave spectrometer. The complexes NCCCH-NH3 are found to have symmetric-top structures with the acetylenic proton hydrogen-bonded to the nitrogen of the NH3. The data for CH3CCH-NH3 are further consistent with free or nearly free internal rotation of the methyl top against the ammonia top. For NCCCH-OH2, and acetylenic proton is hydrogen-bonded to the oxygen of the water. The complex has a dynamical C2 structure, as evidenced by the presence of two nuclear-spin modifications of the complex. The hydrogen bond lengths and hydrogen-bond stretching force constants are 2.212 Angstroms and 10.8N/m, 2.322 Angstroms and 6.0N/m, and 2.125 Angstroms and 9.6N/m, for NCCCH-NH3, CH3CCH-NH3, and NCCCH-OH2, respectively. For the cyanoacetylene complexes, these bond lengths and force constants lie between the values for the related hydrogen cyanide and acetylene complexes of NH3 and H2O. The NH3 bending and weak-bond stretching force constants of CH3CCH-NH3 are less than those found in NCCCH-NH3, NCH-NH3, and HCCH-NH3, suggesting that the hydrogen bonding interaction is particularly weak in CH3CCH-NH3. The weakness of this hydrogen bond is partially a consequence of orientation of monomer electric dipole moments in the complex. In CH3CCH-NH3 the antialigned monomer dipole moments leads to a repulsive dipole-dipole interaction energy, while in NCH-NH3 and NCCCH-NH3 the aligned dipoles give an attraction interaction.

04,171
PB97-119028 Not available NTIS
National Inst. of Standards and Technology (PL), Gaithersburg, MD. Ionizing Radiation Div.
Effect of Formulation Changes on the Response to Ionizing Radiation of Radiochromic Dye Films.
Final rept.
M. Barcelo, R. M. Uribe, W. L. McLaughlin, and G. Belmont. 1996, 6p.
Pub. in Radiation Protection Dosimetry, v66 n1-4 p237-242 1996.

Keywords: *Film dosimetry, *Gamma radiation, *Radiochromic films, Ultraviolet radiation, Radiation processing, Reprints, *Foreign technology, Pararosaniline cyanide.

Radiochromic dye films have been studied with the purpose of optimizing the formulation in order to increase their sensitivity to ultraviolet and ionizing radiation. The films consist of certain substituted triphenylmethane leucodyes incorporated in an acid solution with polyacetal resins, which can be cast into thin, colorless, tansparent films. Upon irradiation they become deeply colored due to dye formation (without development); they are analyzed for dosimetry by absorption spectrophotometry at the visible wavelength of maximum absorption, in terms of increase of absorbance versus delivered absorbed dose. Response functions were obtained for different films, in which the concentrations of each of the constituents, the dye precursors, as well as the types of acids and solvents were varied. A new formulation is suggested for radiochromic dye films useful in the dose range from 5 kGy to 35 kGy.

04,172
PB97-119051 Not available NTIS
National Inst. of Standards and Technology (PL), Gaithersburg, MD. Ionizing Radiation Div.
Measurements of the (235)U(n,f) Cross Section in the 3 to 30 MeV Neutron Energy Region.
Final rept.
A. D. Carlson, O. A. Wasson, P. W. Lisowski, J. L. Ullmann, and N. W. Hill. 1991, 3p.
Pub. in Proceedings of the International Conference on Nuclear Data for Science and Technology, Julick, FRG, May 13-17, 1991, p518-520.

Keywords: *Standard cross section, *Neutron energy, *Fission chamber, Telescopes, Measurements, Fluence, Reprints, *Foreign technology.

To improve the accuracy of the 235U(n,f) cross section, measurements have been made of this standard cross section at the target 4 facility at Los Alamos National Laboratory (LANL). The data were obtained at the 20-meter flight path of that facility. The fission reaction rate was determined with a fast parallel plate ionization chamber and the neutron fluence was measured with an annular proton recoil telescope. The measurements provide the shape of the 235U(n,f) cross section relative to the hydrogen scattering cross section for neutron energies from about 3 to 30 MeV neutron energy. The data have been normalized to the very accurately known value near 14 MeV. The results are in good agreement with the ENDF/B-VI evaluation up to about 15 MeV neutron energy. Above this energy differences as large as 5% are observed.

04,173
PB97-119069 Not available NTIS
National Inst. of Standards and Technology (PL), Gaithersburg, MD. Ionizing Radiation Div.
Measurements of the (237)Np(n,f) Cross Section.
Final rept.
A. D. Carlson, W. E. Parker, P. W. Lisowski, N. W. Hill, K. Meggers, G. L. Morgan, and S. J. Seestrom. 1994, 7p.
Sponsored by Department of Energy, Washington, DC.
Pub. in American Society for Testing and Materials-Euration Symposium on Reactor Dosimetry (8th), Vail, CO., August 29-September 3, 1993, p704-710 Dec 94.

Keywords: *Fission cross section, *Neutron scattering, *Dosimetry, Measurements, Resonance, Reprints.

Measurements have been made of the neutron induced fission cross section of 237Np(n,f) at the Los Alamos Neutron Scattering Center utilizing a white neutron source and a fast parallel multiplate ionization chamber. The 10B(n,a) standard cross section was used to establish the energy dependence of the neutron fluence and a very accurately known fission resonance integral for 235U was used for normalization. The measurements in the resonance region, from 5 eV to 5 keV, indicate that the ENDF.B-VI values are too low by about a factor of three.

04,174
PB97-119077 Not available NTIS
National Inst. of Standards and Technology (CSTL), Gaithersburg, MD. Thermophysics Div.
Influence of Envelopes Geometry on the Sensitivity of 'Nude' Ionization Gauges.
Final rept.
A. R. Filippelli. 1996, 5p.
Pub. in Jnl. of Vacuum Science and Technology A, v14 n5 p2953-2957 Sep/Oct 1996.

Keywords: *Envelopes, *Ionization gauges, *Extractors, Nude, Sensitivity, Reprints, Bayard-Alpert.

This article presents the results of some measurements of the influence of envelope size and shape on the N2 sensitivity of two nominally identical 'nude' extractor ionization gauges, and three common 'nude' versions of the Bayard-Alpert ionization gauge. Measurement were made over the pressure range 10 to the minus 7 power - 10 to the minus 1 power Pa, using typical gauge operating parameters and with vacuum chamber and gauge envelope at ground potnetial. Sensitivity values corresponding to three different envelopes used in this work differed by as much as a factor of 2 (comparing maximum value to minimum value for each gauge) for the Bayard-Alpert gauges. For the extractor gauges, the diferences were as large as 7%.

04,175
PB97-119085 Not available NTIS
National Inst. of Standards and Technology (PL), Gaithersburg, MD. Ionizing Radiation Div.
Mass Assay and Uniformity Test of Boron Targets by Neutron Beam Methods.
Final rept.
D. M. Gilliam, G. P. Lamaze, M. S. Dewey, and G. L. Greene. 1993, 5p.
Pub. in Nuclear Instruments and Methods in Physics Research A, v334 p149-153 1993.

Keywords: *Ionization chambers, *Neutron beams, *Boron targets, Deposits, University, Vacuum evaporation, Reprints.

The areal densities (g/cm2) of enriched boron and lithium fluoride targets were compared to those of reference deposits from the Central Bureau of Nuclear Measurements (CBNM, Geel, Belgium) by charged-particle counting at the NIST Research Reactor. The

uniformity of the target thicknesses was also investigated by scans with a small-diameter, intense neutron beam. The neutron uniformity measurements agree satisfactorily with previously reported interferometric results and no pattern of uniformity variation except the expected, small radial dependence was found. In a separate series of measurements, the boron areal density ratios of a number of the deposits were determined using a new double ionization chamber. The new double ionization chamber permits a comparison of two targets directly without a beam monitor and without sensitivity to the exact placement of the samples. The new device needs only a very simple data acquisition system and requires less neutron beam intensity than the previously employed systems with arrays of surface barrier detectors. The ionization chamber counting losses from the combined effects of self-absorption and sub-threshold pulse-height formation were determined by comparison with ratio measurements made by the conventional surface barrier detector technique.

04,176
PB97-119275 Not available NTIS
National Inst. of Standards and Technology (MSEL), Gaithersburg, MD. Reactor Radiation Div.
Orientational Fluctuations, Diffuse Scattering, and Orientational Order in Solid C60.
Final rept.
K. H. Michel, and J. R. D. Copley. 1996, 4p.
Pub. in Proceedings of the International Winterschool on Electronic Properties of Novel Materials Fullerenes and Fullerene Nanostructures, p1-4 1996, World Scientific.

Keywords: *Diffuse scattering, *Mode coupling, *Fluctuations, *Orientational disorder, Scattering cross section, Carbon, Reprints, *Foreign technology.

The authors present a theory of the orientational dynamics of solid C60 which takes into account the coupling of orientational modes belonging to various symmetries and manifolds. More coupling strongly enhances the transition temperature and the discontinuity of the order parameter at the first order phase transition to the Pa3 structure. The diffuse scattering intensity in the disordered phase is calculated and compared with experiments.

04,177
PB97-122345 Not available NTIS
National Inst. of Standards and Technology (CSTL), Gaithersburg, MD. Process Measurements Div.
Generalized Optical Theorem for On-Axis Gaussian Beams.
Final rept.
G. Gouesbet, C. Letellier, G. Grehan, and J. T. Hodges. 1996, 21p.
Pub. in Optics Communications, v125 p137-157 1996.

Keywords: *Optical theorems, *Beams, *Gaussian beams, Plane waves, Finite scatters, Reprints, *Foreign technology.

The optical theorem for an incident plane was interacting with a finite scatterer is generalized to the case of on-axis Gaussian beams, taken as examples of shaped beams. The results are restricted in the paper to homogeneous spheres. The beams are defined by using (1) the standard description (2) the localized approximation and (3) the modified localized approximation. Rigorous expressions generalizing the classical plane wave case expression are given and numerically discussed. A recently proposed approximation is investigated in order to point out assumptions underlying its validity.

04,178
PB97-122360 Not available NTIS
National Inst. of Standards and Technology (PL), Gaithersburg, MD. Atomic Physics Div.
Measurement of the Atomic Na(3P) Lifetime and of Retardation in the Interaction between Two Atoms Bound in a Molecule.
Final rept.
K. M. Jones, P. S. Julienne, P. D. Lett, C. J. Williams, W. D. Phillips, and E. Tiesinga. 1996, 5p.
Pub. in Europhysics Letters, v35 n2 p85-90 1996.

Keywords: *Atomic interactions, *Lifetimes, *Retardation, Atoms, Molecules, Measurements, Reprints, *Foreign technology.

From molecular spectroscopy of the Na2 purely long-range O-g state the authors determine the Na(3P) lifetime and measure the predicted but previously unobserved effect of retardation in the interaction between two atoms. The lifetime tau(P3/2)=16.230(16) ns helps to remove a longstanding discrepancy between experiment and theory. Electron cloud overlap is unimportant in the O-g state (R greater than 55ao) and the spectrum is calculated, ab initio, from atomic properties. By measuring the binding energies the 120 MHz correction due to retardation of the resonant-dipole R-3 interaction is confirmed.

04,179
PB97-122386 Not available NTIS
National Inst. of Standards and Technology (BFRL), Gaithersburg, MD. Building Environment Div.
Single-Phase Heat Transfer and Pressure Drop Characteristics of an Integral-Spine Fin Within an Annulus.
Final rept.
M. A. Kedzierski, and M. S. Kim. 1996, 10p.
See also PB94-194073.
Pub. in Jnl. of Enhanced Heat Transfer, v3 n3 p201-210 1996.

Keywords: *Fins, *Heat transfer, *Pressure gradients, *Annular flow, Nusselt number, Friction factor, Heat transfer coefficients, Mathematical models, Test facilities, Reprints.

The laminar, single-phase heat transfer and friction characteristics of a porcupine-like surface (integral-spine fin) within an annulus are presented. The heat-transfer coefficient was determined using a modified version of the Wilson Plot method on a 3 m test section. Three fluids were investigated: (1) water, (2) 34% ethylene glycol/water mixture, and (3) 40% ethylene glycol/water mixture. These fluids produced a sufficient variation in the Prandtl number, so that its exponential dependence could be determined. The annulus Reynolds numbers were varied from 100 to 1400 to obtain the Reynolds number exponent. An empirical correlation for the Nusselt number that accounts for the development of the thermal boundary layer is presented. An empirical correlation for the Fanning friction factor is also provided. It is shown that the spines enhance the heat transfer through additional surface area and fluid mixing.

04,180
PB97-122436 Not available NTIS
National Inst. of Standards and Technology (PL), Gaithersburg, MD. Ionizing Radiation Div.
Complex Time Dependence of the EPR Signal of Irradiated L-alpha-alanine.
Final rept.
V. Y. Nagy, and M. F. Desrosiers. 1996, 5p.
Pub. in Applied Radiation Isotopes, v47 n8 p789-793 1996.

Keywords: *Alanine, *EPR signal, Irradiation, Amplitude, Measurements, Reprints, *Foreign technology, *Complex time dependence.

Measurements of the EPR signal amplitude of gamma-irradiated L-alpha-alanine with use of an adjacent reference sample have revealed variations in the signal intensity within hours and days after irradiation. The character of the time dependence of the amplitude varies with dose and the amplitude changes reach 1-1.5%. This observation favors the hypothesis that irradiated alanine contains several paramagnetic centers. Usefulness of adjacent reference samples in alanine dosimetry is also demonstrated.

Acoustics

04,181
PB94-172137 Not available NTIS
National Inst. of Standards and Technology (MEL), Gaithersburg, MD. Automated Production Technology Div.
Ultrasonic Measurements of Surface Roughness.
Final rept.
G. V. Blessing, J. A. Slotwinski, D. G. Eitzen, and H. M. Ryan. 1 Jul 93, 5p.
Pub. in Applied Optics 32, n19 p3433-3437, 1 Jul 93.

Keywords: *Surface roughness, *Ultrasonic tests, *Profilometers, Wave propagation, Sound transmission, Test methods, Surface properties, Real time, Process control, Acoustic properties, Scattering, Reflection, Reprints.

Pulsed ultrasound propagating in water was used at megahertz carrier frequencies (nominally 10-50 MHz) to reflect and scatter from rough surfaces in the same way as light. We have considered noncontact ultrasonic techniques as complementary to optical techniques in several ways: (a) for specific applications such as wet surfaces, (b) for rougher surfaces with average roughness, Ra > or = 0.1 micrometer, and (c) for (simultaneous) profilometry by time-of-flight measurements. Stylus and ultrasonic data are compared. An example of application to the manufacturing environment is for on-line, real-time sensor feedback and process control in the cutting or grinding of metals and ceramics.

04,182
PB94-199007 Not available NTIS
National Inst. of Standards and Technology (MSEL), Boulder, CO. Materials Reliability Div.
Absorption of Ultrasonic Waves in Air at High Frequencies (10-20 MHz).
Final rept.
L. J. Bond, C. H. Chiang, and C. M. Fortunko. 1992, 10p.
Pub. in Jnl. Acoust. Soc. Am. 92, n4 p2006-2015 Oct 92.

Keywords: *Ultrasonic radiation, *Acoustic absorption, *Air, MHz range 01-100, Acoustic measurement, Acoustic velocity, Acoustic waves, High frequency, Room temperature, Reprints.

A high power and sensitive gated radio-frequency (rf) measurement system has been used to determine the absorption of compressional waves in air, in the frequency range from 10-20 MHz. The measured absorption, between 80 and 90 kPa and at room temperature (15 deg C to 25 deg C), has been found to be in good agreement with that predicted, by extrapolation, from low-frequency (below 1 MHz) data for the combination of the classical and rotational loss effects. The velocity of ultrasound in air in the frequency range from 10-18 MHz has also been measured and is in good agreement with that predicted from theory. Normalized velocity and attenuation data plotted against Knudsen numbers and a rarefaction parameter are in good agreement with those obtained at reduced pressure and lower frequencies.

04,183
PB94-199015 Not available NTIS
National Inst. of Standards and Technology (MSEL), Boulder, CO. Materials Reliability Div.
Absorption of Sound in Gases between 10 and 25 MHz: Argon.
Final rept.
L. J. Bond, C. H. Chiang, C. M. Fortunko, and J. D. McColskey. 1991, 5p.
Pub. in Proceedings of Ultrasonics Symposium, Orlando, FL., December 5-8, 1991, p1069-1073.

Keywords: *Ultrasonic radiation, *Acoustic absorption, *Argon, MHz range 01-100, Acoustic measurement, Acoustic velocity, Temperature dependence, Pressure dependence, High frequency, Reprints.

A measurement system has been developed to investigate the technology required for high-power gas-coupled ultrasonics and the phenomenology of finite-amplitude of ultrasonic waves in gases at high frequencies (> 10 MHz) and pressures up to 10 MPa (100 bar). In this paper, results of measurements of compression wave absorption and velocity in argon between 10 and 25 MHz, with various combinations of pressure, temperature and power level are presented. For small-amplitude waves, the resulting data are in good agreement with that calculated using ideal gas equations and fundamental thermophysical gas constants. At higher power levels, non-linear phenomena are observed.

04,184
PB94-199023 Not available NTIS
National Inst. of Standards and Technology (MSEL), Boulder, CO. Materials Reliability Div.
Interaction of Rayleigh Waves with a Rib Attached to a Plate.
Final rept.
L. J. Bond, and J. Taylor. 1991, 8p.
Pub. in Ultrasonics 29, p451-458 Nov 91.

Keywords: *Rayleigh waves, *Wave propagation, *Acoustic emissions, Plates, Ribs, Surface acoustic waves, Models, Finite difference method, Interactions, Reprints.

An analysis of the interaction of a pulse of Rayleigh waves on a plate with a rectangular flange or rib at-

tached in the far field of its acoustic emission (AE) source is presented. A finite difference (FD) model is used to give numerical visualizations of the development of the complete wave-field propagating through the structure and also to give displacement data for selected points. An 'energy partition model', for Rayleigh wave propagation across the rib has been developed and is described. Ray theory wave arrival time calculations are given for the propagation of various mode-converted components transmitted across the flange. A series of experimental measurements of AE wave propagation across a T-butt welded rib on a plate were made and these are compared with the model predictions. The practical implications of these findings for acoustic emission monitoring of large structures of complex shape are discussed.

04,185
PB94-212537 Not available NTIS
National Inst. of Standards and Technology (MSEL), Gaithersburg, MD. Metallurgy Div.
Ultrasonic Spectroscopy of Metallic Spheres Using Electromagnetic-Acoustic Transduction.
Final rept.
W. L. Johnson, S. J. Norton, F. Bendec, and R. Pless. 1992, 6p.
Pub. in J. Acoust. Soc. Am. 91, n5 p2637-2642 May 92.

Keywords: *Ultrasonic spectroscopy, Vibrational spectra, Resonant frequency, Magnetic fields, Elastic properties, Aluminum, Spheres, Reprints.

An ultrasonic technique for studying vibrational resonant modes of metallic spheres is presented. The technique employs electromagnetic-acoustic transduction with a configuration consisting of a sample surrounded by a coil in a static magnetic field. Resonance spectra from 0.5 to 4.5 MHz with the coil axis parallel and perpendicular to the magnetic field are measured for a 3.145-mm-diam sphere of polycrystalline 2024 aluminum. Elastic constants calculated from the resonant peak frequencies are consistent with results obtained using an ultrasonic pulse-echo system. This new technique has advantages over pulse-echo and conventional resonance techniques for experiments where high absolute accuracy is necessary or where samples are heated far above room temperature.

04,186
PB95-151957 Not available NTIS
National Inst. of Standards and Technology (CSTL), Boulder, CO. Thermophysics Div.
Speed-of-Sound Measurements in Liquid and Gaseous Air.
Final rept.
B. A. Younglove, and N. V. Frederick. 1993, 9p.
Pub. in International Jnl. of Thermophysics 13, n6 p1033-1041 Nov 92.

Keywords: *Acoustic velocity, *Acoustic resonators, *Air, *Acoustic measurements, *Time of flight spectrometers, Sound waves, Sound transmission, Isotherms, Vapor phases, Reprints, *Liquified air, AIRPROPS model.

The speed of sound in air has been measured along isotherms for a 'standard air' mixture (0.7811 N2 + 0.2097 O2 + 0.0092 Ar) in the gas and liquid phases at pressure to 14 MPa. A cylindrical resonator was used in the vapor and supercritical gas phases, and a time-of-flight system was used for measurements of the liquid phase. Data were obtained for the liquid phase at 90, 100, 110, 120, and 130 K. Data were taken at 110, 120, 130, 135, 140, 150, 200, and 300 K in the vapor and supercritical gas phases. These experimental results were compared to a predictive computer model, namely, AIRPROPS.

04,187
PB95-162905 Not available NTIS
National Inst. of Standards and Technology (MSEL), Gaithersburg, MD. Metallurgy Div.
Leady Axisymmetric Modes in Infinite Clad Rods. Part 1.
Final rept.
J. A. Simmons, E. Drescher-Krasicka, and H. N. G. Wadley. 1992, 30p.
Pub. in Jnl. of the Acoustical Society of America 92, n2 p1061-1090 1992.

Keywords: *Waves, *Clad metals, *Rods, *Computation, Composite materials, Reinforcing materials, Wave propagation, Phase velocity, Nondestructive tests, Aluminum, Silicon carbides, Reprints, Leaky waves, Clad rods, Radial-axial modes, Ultrasonic waves, Interface waves.

A detailed computational study is presented for the radial-axial modes-both leaky and non-leaky-in an infinitely clad isotropic rod. The complex phase velocities of leaky modes are located using an application of the argument principle. Particle orbits are determined, and leaky modes are shown to have an asymptotic leakage angle away from the interface. By using the homotopic methods of varying densities and elastic constants, clad-rod modes are compared with those in a bare rod. The topology of the clad-rod mode dispersion diagram differs qualitatively from that of a bare rod, even when the cladding has negligible density, with no velocity cutoffs and with wave mode knitting. Comparison is also given with modes occuring in a cladding without a rod present (a tunnel) and for a planar interface. Most leaky modes can be correlated with rod modes; only a limited number of tunnel modes exist. Energy flow contours within modes are also calculated. The local energy velocity, which generalizes group velocity, can vary considerably in the radial direction for bare rod modes. For leaky modes the contours are quite complex due to the cylindrical geometry, giving rise to apparent shifts in wave position across the interface.

04,188
PB95-182234 PC A05/MF A01
National Inst. of Standards and Technology (TS), Gaithersburg, MD. National Voluntary Lab. Accreditation Program.
National Voluntary Laboratory Accreditation Program Acoustical Testing Services.
Handbook.
P. R. Martin, and R. J. Peppin. Dec 94, 88p, NIST/HB-150-8.
Also available from Supt. of Docs. as SN003-003-03314-6. See also PB91-107524. Sponsored by Nuclear Regulatory Commission, Rockville, MD.

Keywords: *Acoustic testing, *Acoustic measurement, *Laboratories, Acoustic absorption, Acoustic attenuation, Sound transmission, Noise reduction, Performance evaluation, Test methods, Ear protection, Hearing, Calibration, National Voluntary Laboratory Accreditation Program, NVLAP program.

NIST Handbook 150-8 presents the technical requirements of the National Voluntary Laboratory Accreditation Program (NVLAP) for Acoustical Testing Services. It is intended for information and use by staff of accredited laboratories, those laboratories seeking accreditation, other laboratory accreditation systems, users of laboratory services, and others needing information on the requirements for accreditation under this program. This publication supplements NIST Handbook 150, NVLAP Procedures and General Requirements, which contains Part 285 of Title 15 of the U.S. Code of Federal Regulations (CFR) plus all general NVLAP procedures, criteria, and policies. Handbook 150-8 contains information that is specific to the Acoustical Testing Services program and does not duplicate information contained in the Procedures and General Requirements. It is organized to cross-reference with Handbook 150; for example, Section 285.3 of Handbook 150 presents the description and goal of NVLAP, whereas Section 285.3 of Handbook 150-8 presents the description of the Acoustical Testing Services program. Where there is no material specific to the field of accreditation, the section number is omitted.

04,189
PB96-102413 Not available NTIS
National Inst. of Standards and Technology (CSTL), Gaithersburg, MD. Thermophysics Div.
Thermodynamic Properties of Two Gaseous Halogenated Ethers from Speed-of-Sound Measurements: Difluoromethoxy-Difluoromethane and 2-Difluoromethoxy- 1,1,1-Trifluoroethane.
Final rept.
K. A. Gillis. 1994, 27p.
Contracts N000249OMP33493, DW13935108-01-0
Sponsored by Department of the Navy, Washington, DC. and Environmental Protection Agency, Washington, DC.
Pub. in International Jnl. of Thermophysics 15, n5 p821-847 Sep 94.

Keywords: *Thermodynamic properties, *Halohydrocarbons, *Ethers, *Gases, *Acoustic velocity, Specific heat, Ideal gas, Virial coefficients, Intermolecular forces, Reprints, Difluoromethoxy-difluoromethane, 2-Difluoromethoxy- 1-1-1-trifluoroethane.

The authors present measurements of the speed of sound in gaseous difluoromethoxy-difluoromethane (CHF2-O-CHF2) and 2-difluoromethoxy- 1,1,1-trifluoroethane (CF3-CH2-O-CHF2). These measurements were performed in an all-metal apparatus between 255 and 384 K. The authors have obtained ideal-gas heat capacities and second acoustic virial coefficients from analysis of these measurements. Two methods of correlating the second acoustic virial coefficients, a squarewell model of the intermolecular interaction and a function due to Pitzer and Curl, are presented.

04,190
PB96-204508 Not available NTIS
National Inst. of Standards and Technology (MEL), Gaithersburg, MD. Automated Production Technology Div.
Determination of Acoustic Center Correction for Type LS2aP Condensor Microphones.
Final rept.
R. P. Wagner, and V. Nedzelnitsky. 1995, 1p.
Pub. in Jnl. of the Acoustical Society of America, v98 n5 pt2 p2917 Nov 95.

Keywords: *Acoustical instruments, *Microphones, Reprints, Calibration, Acoustic center.

Acoustic center corrections for microphones are necessary for accurate free-field calibration by the reciprocity technique. Such correction for several pairs of the relatively new type LS2aP microphone (IEC Std. 1094-1: 1992) were obtained by utilizing the theoretical inverse relationship between the sound pressure amplitude at the receiving microphone and the distance between the acoustic centers of the source and receiving microphones. For a nominally 10-V sinusoidal rms excitation of the source microphone, source-to-receiver voltage ratios were measured with a dynamic signal analyzer at 500 Hz intervals in the extended frequency range (2 to 50)kHz. This procedure allowed all the data for a microphone pair to be gathered within several hours as a function of microphone diaphragm separation at 10-mm intervals from 101 to 311 mm. At each frequency, these ratios were corrected for atmospheric effects, including attenuation of sound, and then fit to a straight line (ratio versus diaphragm separation). Acoustic center corrections were calculated from the derived values of the fit parameters. These corrections agree with appropriately scaled values (IEC Publication 486-1974) for 'l-in.' microphones with recessed diaphragms. Physical phenomena that cause small deviations from the linear fits will be discussed along with uncertainty estimate, and effects of spatially truncating data.

04,191
PB96-204516 Not available NTIS
National Inst. of Standards and Technology (MSEL), Gaithersburg, MD. Ceramics Div.
Thermal Wave NDE of Advanced Materials Using Mirage Effect Detection.
Final rept.
L. Wei, and G. S. White. 1993, 8p.
Pub. in Proceedings of the International Conference on Photoacoustics, Maine, 1993, p1-8.

Keywords: *Meetings, *Mirage detection, *Thermal waves, Reprints, Advanced materials, Nondestructive evaluation, Thermal property.

The dramatic improvement in modern materials has driven the search for improved measurement techniques, for both the detection of flaws which will prevent or limit applications and for the evaluation of basic physical parameters of the materials themselves. The mirage thermal wave technique has been used successfully to meet both requirements. Because thermal waves are sensitive to changes in the heat flow in a material, the thermal wave technique is complementary to techniques such as ultrasonics and light scattering measurements, which are sensitive to changes in elastic and optical properties, respectively.

Fluid Mechanics

04,192
AD-A278 249/8 PC A03/MF A01
National Bureau of Standards, Gaithersburg, MD.
Characteristics of Turbulence in a Boundary Layer with Zero Pressure Gradient.
P. S. Klebanoff. 1955, 22p, NASA-L-1247.

Keywords: *Turbulent boundary layer, *Pressure gradients, Turbulent flow, Zero pressure gradients.

No abstract available.

04,193
AD-A286 680/4 PC A04/MF A01
National Bureau of Standards, Gaithersburg, MD.
Survey of the Literature on Heat Transfer from Solid Surfaces to Cryogenic Fluids.
Technical note.
R. J. Richards, W. G. Steward, and R. B. Jacobs.
Oct 61, 51p.

Keywords: *Cryogenics, *Fluids, *Heat transfer, *Solids, *Surfaces, *Low temperature, *Bibliographies, Computations, Formulations, Literature surveys, Liquid helium, Liquid hydrogen, Liquid oxygen, Convection, Nucleate boiling.

A bibliography of 156 references on heat transfer from solid surfaces to fluids and related phenomena is presented. Heat transfer data obtained from experimental work on cryogenic fluids are presented in graphical form. The theoretical and empirical formulations appearing in the references are presented. In those cases where sufficient information is available to make numerical computations, the formulations are presented graphically to permit comparison with the results of the experimental work.

04,194
AD-A297 391/5 PC A03/MF A01
National Bureau of Standards, Gaithersburg, MD.
Air Flow in the Boundary Layer of an Elliptic Cylinder.
G. B. Schubauer. 1939, 25p, NBS-652.
Document partially illegible.

Keywords: *Air flow, *Boundary layer, Velocity, Position(Location), Intensity, Turbulence, Turbulent flow, Turbulent boundary layer, Variations, Cylindrical bodies, Scale, Airspeed, Transitions, Hot wire, Ellipses.

The boundary layer of an elliptic cylinder of major and minor axes 11.78 and 3.98 inches, respectively, was investigated in an air stream in which the turbulence could be varied. Conditions were arranged so that the flow was two-dimensional with the major axis of the ellipse parallel to the undisturbed stream. Speed distributions across the boundary layer were determined with a hot-wire anemometer at a number of positions about the surface for the lowest and highest intensities of turbulence, with the air speed in both cases sufficiently high to produce a turbulent boundary layer over the downstream part of the surface. The magnitude and the frequency of the speed fluctuations in the boundary layer were also measured by the use of the conventional type of hot-wire turbulence apparatus. Stream turbulence was found to affect both the nature of transition from to turbulent flow in the layer and the position on the surface at which transition occurred. Transition was then investigated in detail with stream turbulence of several different scales and intensities. It was found that the position of transition could be expressed as a function of the intensity divided by the fifth root of the scale. (KAR) P.5.

04,195
DE94017817 PC A02/MF A01
National Inst. of Standards and Technology (NEL), Gaithersburg, MD. Thermophysics Div.
Ebulliometers for Measuring the Thermodynamic Properties of Fluids and Fluid Mixtures.
L. A. Weber, and A. M. Silva. 1994, 8p, CONF-9404137-5.
Contract AI05-88ER13823
Symposium on Energy Engineering Sciences (12th), Argonne, IL (United States), 27-29 Apr 1994. Sponsored by Department of Energy, Washington, DC.

Keywords: *Boiling Points, *Fluids, *Temperature Measurement, *Thermodynamic properties, Design, Measuring Instruments, Measuring Methods, Mixtures, Vapor Pressure, EDB/440500.

The design and operation of two ebulliometers is described. One is constructed of glass and is used for measuring vapor pressures of fluids at low reduced temperatures and pressures. The other is constructed of metal. It can be used for vapor pressure measurements, and also for the study of fluid mixture thermodynamics through the determination of the activity coefficients at infinite dilution. The advantages and potential problems associated with ebulliometers are described, and typical results are given for the properties of alternative refrigerants.

04,196
PB94-160736 PC A04/MF A01
National Inst. of Standards and Technology (CSTL), Gaithersburg, MD. Process Measurements Div.
Summary Report of NIST's Industry-Government Consortium Research Program on Flowmeter Installation Effects with Emphasis on the Research Period, January-September 1991: The Reducer.
G. E. Mattingly, and T. T. Yeh. Feb 92, 58p, NISTIR-4779.
See also PB92-149848 and PB94-149855.

Keywords: *Flow meters, *Pipe flow, Flow measurement, Turbulence, Reynolds number, Velocity distribution, Orifice meters, Orifices, Pipes(Tubes), Research programs.

This report presents recent results obtained in a consortium-sponsored research program on flowmeter installation effects being conducted at NIST-Gaithersburg, MD. The objective of this research program is to produce improved flowmeter performance when meters are installed in non-ideal conditions. Ideal meter installation conditions are those where long straight lengths of constant diameter piping precede the meter locations. Actual installations seldom conform to these conditions. This research effort has also included experimental studies of the flow into and out of several tube bundle flow conditioners. These results have produced, for the first time, detailed descriptions of the effects these devices have on swirling pipe flows. Specifically, this report contains measurements of the pipeflows produced downstream of the conventional reducer. Results are given for the performance characteristics of a range of orifice meter geometries and a specific turbine meter in these pipe flows. Also included are the velocity profile measurements downstream of the tee used as an elbow and several arrangements of tube bundles installed downstream of the single elbow and the tee used as an elbow.

04,197
PB94-198405 Not available NTIS
National Inst. of Standards and Technology (CSTL), Boulder, CO. Thermophysics Div.
Transient Methods for Thermal Conductivity.
Final rept.
M. J. Assael, C. A. Nieto de Castro, H. M. Roder, and W. A. Wakeham. 1991, 32p.
Pub. in Measurement of the Transport Properties of Fluids, Chapter 7, p163-194 1991.

Keywords: *Thermal conductivity, *Transport properties, *Hot wire, *Fluids, *Measuring instruments, Accuracy, Reliability, Thermophysical properties, Temperature measurement, Reprints.

The chapter summarizes the transient hot-wire technique for the measurement of thermal conductivity of fluids. A description is given for specific examples of instruments of proven reliability for both electrically conducting and electrically non-conducting fluids. The theory and working equations of the method are given, as is the accuracy of the technique.

04,198
PB94-211380 Not available NTIS
National Inst. of Standards and Technology (CSTL), Boulder, CO. Thermophysics Div.
Conditions for Existence of a Reentrant Solid Phase in a Sheared Atomic Fluid.
Final rept.
D. J. Evans, S. T. Cui, H. J. M. Hanley, and G. C. Straty. 1992, 4p.
Sponsored by Department of Energy, Washington, DC.
Pub. in Physical Review A 46, n10 p6731-6734, 15 Nov 92.

Keywords: Small angle scattering, Neutron scattering, Molecular dynamics, Suspensions, Simulation, Shear rate, Reprints, *Atomic fluids.

A nonequilibrium molecular-dynamics method is proposed to simulate the behavior of simple fluids under high shear rates. A thermostat that makes no assumptions regarding the form of the streaming velocity of the fluid is introduced. Simulations are carried out for a Weeks-Chandler-Andersen dense liquid. With the form of the streaming velocity partially or wholly constrained, we find evidence for a reentrant solid or string phase, but the phase disappears if constraints are removed. Small-angle neutron-scattering data from a sheared colloidal suspension are presented. There is no evidence of a steady-state shear-induced structure in the suspension.

04,199
PB94-212420 Not available NTIS
National Inst. of Standards and Technology (CSTL), Gaithersburg, MD. Thermophysics Div.
Global Thermodynamic Behavior of Fluid Mixtures in the Critical Region.
Final rept.
G. X. Jin, S. Tang, and J. V. Sengers. 1993, 15p.
Contract DE-FG05-88ER13902
Sponsored by Department of Energy, Washington, DC.
Pub. in Physical Review E 47, n1 p388-402 Jan 93.

Keywords: *Fluids, *Thermodynamic properties, *Mixtures, *Critical point, Equations of state, Free energy, Ethane, Carbon dioxide, Thermophysical properties, Reprints.

In a previous publication (Z. Y. Chen, A. Abbaci, S. Tang, and J. V. Sengers, Phys. Rev. A 42, 4470 (1990)) a renormalized Landau expansion was constructed for the thermodynamic free energy of one-component fluids that incorporates the crossover from singular thermodynamic behavior at the critical point to regular behavior far away from the critical point. In the present paper the approach is extended to obtain a crossover free energy for binary fluid mixtures in the region around the vapor-liquid critical line. The thermodynamic equations thus obtained are compared with experimental equation-of-state and specific-heat data for mixtures of carbon dioxide and ethane.

04,200
PB94-212818 Not available NTIS
National Inst. of Standards and Technology (NML), Gaithersburg, MD. Chemical Process Metrology Div.
Evolution of a Turbulent Boundary Layer Induced by a Three-Dimensional Roughness Element.
Final rept.
P. S. Klebanoff, W. G. Cleveland, and K. D. Tidstrom. 1992, 87p.
Sponsored by Calspan Field Services, Inc., Arnold AFS, TN. AEDC Div.
Pub. in Jnl. of Fluid Mechanics 237, p101-187 Apr 92.

Keywords: *Turbulent boundary layer, *Boundary layer transition, *Vortex generators, *Roughness, Reynolds number, Vortices, Unsteady flow, Steady flow, Three dimension flow, Vortex shedding, Reprints.

An experimental investigation of the transition from a laminar to a fully-developed turbulent boundary layer induced by a three dimensional roughness element in a zero pressure gradient boundary layer, incorporating an extensive bibliography, is described. The critical roughness Reynolds number at which turbulence is regarded as originating at the roughness was determined for the roughness elements herein considered and evaluated in the context of data existing in the literature. The effect of a steady and oscillatory free stream velocity on eddy shedding was also investigated and whether the eddy shedding is governed by an inflectional instability is examined. Distributions of mean velocity and turbulence intensity demonstrating the evolution toward a fully developed turbulent boundary layer were measured at various Reynolds numbers. A two region model is postulated for the evolutionary change toward a fully developed turbulent boundary layer: an inner region where the turbulence is generated by the complex interaction near the surface of hairpin eddies with pre-existing stationary vortices, and an outer region where the hairpin eddies deform and generate turbulent vortex rings. The structure of the resulting fully developed turbulent boundary layer is discussed in the light of the proposed model for the evolutionary process.

04,201
PB95-105540 PC A05/MF A01
National Inst. of Standards and Technology (CSTL), Gaithersburg, MD. Process Measurements Div.
Flow Conditioner Tests for Three Orifice Flowmeter Sizes.
Technical note.
J. L. Scott, and M. A. Lewis. May 94, 87p, NIST/TN-1367.
Also available from Supt. of Docs. as SN003-003-03287-5. Sponsored by Gas Research Inst., Chicago, IL.

Keywords: *Orifice flow, *Flowmeters, Flow measurement, Discharge coefficient, Flow resistance, Orifices, Pipe flow, Turbulent flow, Reynolds number, *Flow conditioners, Beta ratio.

Tests sponsored by the Gas Research Institute were performed with orifice flowmeters of three nominal

sizes: 52, 104, and 154 mm (2, 4, and 6 in). Tests with the 52 mm orifice meter included establishing a baseline curve for 6 beta ratios and then conducting flow conditioner performance tests with an elbow located 17 pipe diameters (17D) upstream of the orifice plate. Results from this laboratory indicate that beta ratios of 0.54 or less do not require flow conditioning in this configuration and the 19 tube bundle flow conditioner at 12D produces the best results for larger beta ratios. For the 104 mm orifice meter in the same piping configuration, flow conditioning is necessary for beta ratios of 0.55 and greater. Meter performance is less sensitive to the location of the 7 tube bundle than the 19 tube bundle flow conditioner, but the influence of the flange tape location is greater. Testing of two beta ratios in the 154 mm orifice meter in a baseline configuration and with a tee located 18D from the orifice plate indicates that placing a 19 tube bundle flow conditioner at 12D produces discharge coefficients equivalent to those measured in baseline conditions. Flow rates for all tests were in the turbulent regime.

04,202
PB95-107256 Not available NTIS
National Inst. of Standards and Technology (MSEL), Gaithersburg, MD. Metallurgy Div.
Reconstructing Stratified Fluid Flow from Reciprocal Scattering Measurements.
Final rept.
S. J. Norton. 1991, 6p.
Pub. in Jnl. of the Acoustical Society of America 89, n6 p2567-2572 1991.

Keywords: *Fluid flow, *Acoustic scattering, *Stratification, Inhomogeneity, Wave propagation, Flow measurement, Acoustic properties, Defects, Acoustic signals, Reprints.

The authors show how an inversion formula can be derived for reconstructing the magnitude and direction of stratified fluid flow from two scattering measurements. The measurements are recorded by transmitting an acoustic pulse from a source below the region of stratified flow and then recording the scattered wave at another point horizontally displaced from the source. A second measurement is performed with the source and receive interchanged and the result is subtracted from the first scattering measurement. This difference is, within the Born approximation, independent of scattering that arises from stationary inhomogeneities and thus solely sensitive to scattering due to flow. As a by-product, the sum of the two scattering measurements with source and receiver interchanged yields a quantity sensitive only to scattering from stationary inhomogeneities. This allows the stationary inhomogeneities to be recovered independently of flow.

04,203
PB95-125787 Not available NTIS
National Inst. of Standards and Technology (CSTL), Boulder, CO. Thermophysics Div.
Thermophysical Property Computer Packages from NIST.
Final rept.
D. G. Friend, M. L. Huber, and J. S. Gallagher. 1992, 6p.
Pub. in Proceedings of American Society of Mechanical Engineers Winter Annual Meeting Computerized Thermophysical Property Packages, Anaheim, CA., November 8-13, 1992, p13-18.

Keywords: *Thermophysical properties, *Data bases, *Fluids, *Mixtures, Working fluids, Cryogenic fluids, Refrigerants, Water, Transport properties, Reprints.

The Fluid Mixtures Data Center and the Thermophysics Division are currently supporting, and continuing development on several computerized packages to calculate the thermophysical properties of commercially important fluid systems. The NIST Thermophysical Properties of Hydrocarbon Mixtures Database (SUPERTRAPP) and the NIST Mixture Property Database (DDMIX) are based on extended corresponding states models. The NIST Thermophysical Properties of Fluids Database (MIPROPS) computes properties of 17 pure fluids, generally of cryogenic importance, based on validated wide ranging thermophysical properties correlations. The NIST Thermodynamic Properties of Refrigerants and Refrigerant Mixtures Database (REFPROP) computes thermodynamic and transport properties of existing as well as proposed environmentally acceptable alternative refrigeration fluids and mixtures. Finally, the NIST Thermophysical Properties of Water Database interactively calculates properties using the most recent formulation approved by the International Association for the Properties of Water and Steam.

04,204
PB95-143061 PC A06/MF A02
National Inst. of Standards and Technology (CSTL), Gaithersburg, MD. Process Measurements Div.
Summary Report of NIST's Industry-Government Consortium Research Program on Flowmeter Installation Effects: The 45 Degree Elbow.
Technical note.
T. T. Yeh, and G. E. Mattingly. Sep 94, 108p, NIST/TN-1408.
Also available from Supt. of Docs. as SN003-003-03296-4. See also PB94-160736.

Keywords: *Flow meters, *Pipe bends, *Pipe flow, *Meetings, Flow measurement, Turbulence, Velocity distribution, Orifice meters, Orifices, Pipes(Tubes), Government/industry relations, Research programs, Concentric tube bundle flow conditioners.

The report presents recent results obtained in a consortium-sponsored research program on flowmeter installation effects being conducted at National Institute of Standards and Technology (NIST)-Gaithersburg, MD, presented at the meeting of consortium participants in November 1992. This project is supported by an industry-government consortium and has been underway for several years. This piping element tested and reported here is the conventional 45 degree elbow; the conventional 19- and 7-tube concentric tube bundle flow conditioners were also tested. The LDV velocity measurements are reported for the pipeflows produced downstream of the 45 degree elbow with and without the 19-tube tube bundles. The performance characteristics of a range of orifice meters with various pressure tap geometries and a specific turbine meter are obtained downstream of the 45 degree elbow with and without the 19- and 7-tube bundle flow conditioners.

04,205
PB95-150280 Not available NTIS
National Inst. of Standards and Technology (BFRL), Gaithersburg, MD. Building Materials Div.
Cross-Property Relations and Permeability Estimation in Model Porous Media.
Final rept.
L. M. Schwartz, N. Martys, D. P. Bentz, E. J. Garboczi, and S. Torquato. 1993, 8p.
Sponsored by Department of Energy, Washington, DC.
Pub. in Physical Review E 48, n6 p4584-4591 Dec 93.

Keywords: *Porous materials, *Permeability, *Stokes law(Fluid mechanics), Solubility, Stokes flow, Diffusion, Nuclear magnetic resonance, Electrical resistivity, Reprints.

Results from a numerical study examining cross-property relations linking fluid permeability to diffusive and electrical properties are presented. Numerical solutions of the Stokes equations in three-dimensional consolidated granular packings are employed to provide a basis of comparison between different permeability estimates. Estimates based on the lambda parameter (a length derived from electrical conduction) and on d(sub c) (a length derived from immiscible displacement) are found to be considerably more reliable than estimates based on rigorous permeability bounds related to pore space diffusion. We propose two hybrid relations based on diffusion which provide more accurate estimates than either of the rigorous permeability bounds.

04,206
PB95-150892 Not available NTIS
National Inst. of Standards and Technology (CSTL), Gaithersburg, MD. Thermophysics Div.
Experimental Data and Theoretical Modeling of Gas Flows Through Metal Capillary Leaks.
Final rept.
S. A. Tison. 1993, 5p.
Pub. in Vacuum 44, n11/12 p1171-1175 1993.

Keywords: *Flow rate, *Capillary tubes, *Leak detectors, *Gas flow, Flow measurement, Leakage, Viscous flow, Vacuum gages, Vacuum apparatus, Slip flow, Calibration, Pressure measurement, Transition flow, Reprints.

Metal capillary tubes are commonly used as leak elements to admit known flows of gases into vacuum systems for calibration of vacuum gaging equipment. In many instances it is desired to generate flow rates over a range of three or more decades, preferably with a single leak element. The generation of flow rates over wide ranges is possible with metal capillary leaks, but in most cases the conductance of the leak element will need to be measured as a function of the relevant pressures due to the changing of the flow regimes. Many fits to experimental data and theoretical models exist for predicting the flow rate through tubes, but their validity is not well established in this study, measured conductances of stainless steel tubes for flow rate of 10(exp -8) to 10(exp -14) mol/s with several inert gases are compared with various experimental and theoretical models of gas flow in the molecular, viscous and transition flow regimes. Characteristics of crimped metal capillaries are also examined over this range of flows.

04,207
PB95-162301 Not available NTIS
National Inst. of Standards and Technology (BFRL), Gaithersburg, MD. Fire Science Div.
Global Density Effects on the Self-Preservation Behavior of Turbulent Free Jets.
Final rept.
C. Richards, and W. Pitts. 1993, 19p.
Pub. in Jnl. of Fluid Mech. 254, p417-435 1993.

Keywords: *Turbulent jets, *Free jets, *Jet mixing flow, *Density(Mass/volume), Jet flow, Turbulent flow, Concentration(Composition), Boundary conditions, Nozzle flow, Light scattering, Axisymmetric flow, Density measurement, Velocity distribution, Reprints, *Global density ratio, *Self-preservation behavior.

An experimental investigation was designed to test the hypothesis that all axisymmetric turbulent free jets become asymptotically independent of the source conditions and may be described by classical similarity analysis. Effects of initial conditions were studied by varying jet exit boundary conditions and the global density ratio. The exit velocity profile and turbulence level was changed by using both pipe and nozzle flow hardware. Initial density differences were imposed by using three gases: helium, methane, and propane. The scalar field (concentration) in the momentum-dominated regime of the far field (10 to 60 jet exit diameters downstream) of turbulent free jets was characterized using Rayleigh light scattering as the diagnostic. The results show that regardless of the initial conditions axisymmetric turbulent free jets decay at the same rate, spread at the same angle, and both the mean and r.m.s. values collapse in a form consistent with full self-preservation. The means and fluctuations follow a law of full self-preservation in which two virtual origins must be specified.

04,208
PB95-181145 Not available NTIS
National Inst. of Standards and Technology (CAML), Gaithersburg, MD. Applied and Computational Mathematics Div.
Convective Stability in the Rayleigh-Benard and Directional Solidification Problems: High-Frequency Gravity Modulation.
Final rept.
A. A. Wheeler, G. B. McFadden, B. T. Murray, and S. R. Coriell. 1991, 12p.
Sponsored by National Aeronautics and Space Administration, Washington, DC. and Defense Advanced Research Projects Agency, Arlington, VA.
Pub. in Physics of Fluids A 3, n12 p2847-2858 Dec 91.

Keywords: Rayleigh-Benard convection, Gravitational effects, Asymptotic series, Numerical solution, Flow stability, Solutes, Rayleigh number, Schmidt number, Reprints, *Directional solidification, Floquet theory.

The effect of vertical, sinusoidal, time-dependent gravitational acceleration on the onset of solutal convection during directional solidification is analyzed in the limit of large modulation frequency Omega. When the unmodulated state is unstable, the modulation amplitude required to stabilize the system is determined by the method of averaging, and is O(Omega). Comparison of the results from the averaged equations with numerical solutions of the full linear stability equations (based on Floquet theory) show that the difference is O(Omega(Sup 1/2)). When the unmodulated state is stable, resonant modes of instability occur at large modulation amplitude. These are analyzed using matched asymptotic expansions to elucidate the boundary-layer structure for both the Rayleigh-Benard and directional solidification configurations.

04,209
PB96-102520 Not available NTIS

National Inst. of Standards and Technology (MSEL), Gaithersburg, MD. Polymers Div.
Probabilistic Computation of Poiseuille Flow Velocity Fields.
Final rept.
F. Y. Hunt, J. F. Douglas, and J. Bernal. 1995, 16p.
Pub. in Jnl. of Mathematical Physics, v36 n5 p2386-2401 May 95.

Keywords: *Open channel flow, *Laminar flow, Probability theory, Fractals, Pipe flow, Cross sections, Torsion, Rigidity, Reprints.

Velocity fields for Poiseuille flow through tubes having general cross sections are calculated using a path integral method involving the first-passage times of random walks in the interior of the cross sectional domain of the pipe. This method is applied to a number of examples where exact results are available and to more complicated geometries of practical interest. These examples include a tube with 'fractal' cross section and open channel flows. The calculations demonstrate the feasibility of the probabilistic method for pipe flow and other applications having an equivalent mathematical description (e.g., torsional rigidity of rods, membrane deflection).

04,210
PB96-102579 Not available NTIS
National Inst. of Standards and Technology (MSEL), Gaithersburg, MD. Metallurgy Div.
Measurements of Thermophysical Properties of Nickel Near Its Melting Temperature by a Microsecond-Resolution Transient Technique.
Final rept.
E. Kaschnitz, J. L. McClure, and A. Cezairliyan. 1994, 10p.
Pub. in International Jnl. of Thermophysics 15, n4 p757-766 Jul 94.

Keywords: *Thermophysical properties, *Nickel, *Melting points, Electrical resistivity, Enthalpy, Heat of fusion, High temperature, Specific heat, Liquid phases, Pulse heating, Reprints, Transient techniques.

A microsecond-resolution capacitor discharge system was used to heat nickel specimens rapidly to temperatures several hundred degrees above the melting point. From time-resolved measurements of current, voltage, and radiance temperature, selected thermophysical properties of nickel at its melting temperature and in the liquid state were determined. The properties measured include enthalpy and electrical resistivity at the beginning and end of melting, heat of fusion, and enthalpy, specific heat capacity, and electrical resistivity in the liquid phase up to 2000 K.

04,211
PB96-113543 (Order as PB96-113535, PC A05/MF A01)
National Physical Lab., New Delhi (India).
Intercomparison between NPL (India) and NIST (USA) Pressure Standards in the Hydraulic Pressure Region Up to 26 MPa.
J. K. N. Sharma, K. K. Jain, C. D. Ehrlich, J. C. Houck, and D. B. Ward. 1994, 5p.
Prepared in cooperation with National Inst. of Standards and Technology, Gaithersburg, MD.
Included in Jnl. of Research of the National Institute of Standards and Technology, v99 n6 p725-729 Nov/Dec 94.

Keywords: *Hydraulic fluids, *Pressure, *Standards, Interlaboratory comparison, Pistons, Pressure measurement, India, United States, Pneumatics, Manometers, Pressure gages, NIST(National Institute of Standards and Technology).

Results are presented of an intercomparison of pressure measurements between the National Physical Laboratory (NPL), India, and the National Institute of Standards and Technology (NIST), USA, using piston guage pressure standards over the range 6 MPa to 26 MPa. The intercomparison, using the NPL piston gauge pressure standard, with a normal effective area of 8.4 x 10(exp-5) square m., and the NIST piston gauge pressure standard, with a nominal effective area of 2.0 x 10(exp-5) square m., was carried out at the NPL. The intercomparison data obtained show a relative difference of 1 x 10(exp-6) in the zero-pressure effective area A(sub 0) of the NPL standard as obtained by the NIST standard.

04,212
PB96-119565 Not available NTIS
National Inst. of Standards and Technology (CSTL), Gaithersburg, MD. Thermophysics Div.
Long-Lived Structures in Fragile Glass-Forming Liquids.
Final rept.
A. I. Mel'cuk, R. A. Ramos, H. Gould, W. Klein, and R. D. Mountain. 1995, 4p.
Pub. in Physical Review Letters, v75 n13 p2522-2525, 25 Sep 95.

Keywords: *Molecular structure, *Supercooling, *Liquids, *Glass, *Lennard-Jones potential, Computerized simulation, Clumps, Monte Carlo method, Thermodynamic properties, Thermal stability, Kinetics, Two dimensional, Reprints, *Molecular dynamics, *Fragile glass, Voronoi analysis.

We present molecular dynamics results for the existence of long-lived clusters near the glass transition in a two component, two-dimensional Lennard-Jones supercooled liquid. Several properties of this system are similar to a mean-field glass-forming liquid near the spinodal. This similarity suggests that the glass 'transition' in the supercooled liquid is associated with an incipient thermodynamic instability. Our results also suggest that single particle properties are not relevant for characterizing the instability, but are relevant to the kinetic transition that occurs at a lower temperature than the glass transition.

04,213
PB96-122726 Not available NTIS
National Inst. of Standards and Technology (BFRL), Gaithersburg, MD. Structures Div.
Non-Gaussian Noise Effects on Reliability of Multistable Systems.
Final rept.
E. Simiu, and M. Grigoriu. 1993, 7p.
Pub. in Proceedings of the International Conference on Offshore Mechanics and Arctic Eng., OMAE (12th), Glargow, Scotland, June 20-24, 1993, v2 p65-71 1993.

Keywords: *Chaos, *Noise, *Dynamical systems, *Ocean engineering, Stability, Elastic properties, Nonlinear systems, Stochastic processes, Branching(Mathematics), Reliability, Reprints, *Non-gaussian effects, Fluidelasticity.

For certain types of compliant structures the designer must consider limit states associated with the onset of fluidelastic instability. For a wide class of dynamical systems, a fundamental connection between deterministic and stochastic chaos allows the application of this condition to obtain probabilities that chaotic motions with jumps cannot occur in multistable systems excited by processes with tail-limited marginal distributions.

04,214
PB96-123427 Not available NTIS
National Inst. of Standards and Technology (CAML), Gaithersburg, MD. Applied and Computational Mathematics Div.
Lubrication Theory for Reactive Spreading of a Thin Drop.
Final rept.
R. J. Braun, B. T. Murray, W. J. Boettinger, and G. B. McFadden. 1995, 14p.
See also PB95-189460.
Pub. in Phys. Fluids, v7 n8 p1797-1810 Aug 95.

Keywords: *Contact line, *Lubrication theory, Reactive spreading, Solder, Reprints, *Foreign technology.

Solder drops spreading on metallic substrates are a reactive form of the wetting problem. A metallic component may diffuse in the liquid toward a metal substrate, where it is consumed by a reaction that forms a solid intermetallic phase. The resulting spatial variation in the composition of the drop may cause composition gradients along the free surface of the drop. Together with any thermal gradients along the free surface. Marangoni effects may, in turn, modify the bulk transport in the spreading drop. Motivated by this situation, we extend lubrication theory for the spreading of thin drops in the presence of gravity and thermocapillarity to include mass transport and equations for the free surface shape and concentration field. Numerical solutions for the nonreactive (single component) drop agree well with previous theory. In the reactive case, we are only able to compute results for parameters outside of the range for solder materials. Including reactive effects in the model impacts the flow patterns and spreading rates at relatively early times; but by the end of the spreading, solutal effects have died out in the model.

04,215
PB96-123534 Not available NTIS
National Inst. of Standards and Technology (MSEL), Gaithersburg, MD. Polymers Div.
Book Review: Aspects and Applications of the Random Walk.
Final rept.
J. Douglas. 1995, 4p.
Pub. in Jnl. of Statistical Physics, v79 n1-2 p497-500 1995.

Keywords: *Random walk, *Hydrodynamics, *Computational fluid dynamics, Random processes, Phase transitions, Dynamical systems, Equilibrium, Stochastic processes, Numerical analysis, Mathematical models, Reviews, Reprints.

Scientists have often pondered the 'unreasonable effectiveness' of mathematics in describing the complex cooperative phenomena which occur at many scales in our physical environment - processes ranging from subatomic to cosmic dimensions. The success of random walk models, and the limit theorems associated with these walks, in describing the origin of various kinds of cooperative phenomena (phase transitions, fluid flow,..) is similarly remarkable and we can expect the perspective and tools of random walk theory to offer clues into the microscopic origin of large-scale regularities in the natural world and into the success of hydrodynamic mathematical models introduced to describe dynamic and equilibrium cooperative phenomena.

04,216
PB96-156013 Not available NTIS
National Inst. of Standards and Technology (CSTL), Gaithersburg, MD. Thermophysics Div.
Improved Gas Flow Measurements for Next-Generation Processes.
Final rept.
S. A. Tison. 1996, 5p.
Pub. in Proceedings of the International Workshop on Semiconductor Characterization: Present Status and Future Needs, Gaithersburg, MD., January 30-February 2, 1995, p497-501 1996.

Keywords: *Gas flow, Semiconductors, Meters, Reprints, Mass flow controller.

Many semiconductor processes require stable and known flows of gas be delivered to the processing chamber. Gas types and flow rates are process dependent, but it is clear that next-generation processes will require flow measurements that are two to three decades lower than current requirements. Specifically, the Semi-Sematech-sponsored Mass Flow Controller Working Group recently identified the need for flow measurements with an accuracy of 1% or better to be extended to cover the range 7 x 10 to the minus 8th power to 7 x 10 to the minue 5th power mol/s (0.1 to 100 sccm, standard cubic centimeters per minute). At least two problems must be overcome if this goal is to be attained. Achieving 1% accuracy in the process chamber will require reference standards with an accuracy of 0.2% or better, but adequate reference standards do not exist over this range. Further, the thermal mass flow controllers (TMFCs) used to measure and control the process gases are generally calibrated with nitrogen and 'corrected' for other gases, but the correction factors are not well understood and of questionable reliability. The National Institute of Standards and Technology (NIST) is addressing both of these problems by developing new flow standards and by investigating the performance of TMFCs. This paper will present data on the performance of five TMFCs, from different manufacturers, with full scale rangers of 1.5 x 10 to the minus 6th power mol/s to 3.7 x 10 to the minus 6th power mol/s (2 to 5 sccm).

04,217
PB96-161880 Not available NTIS
National Inst. of Standards and Technology (CSTL), Gaithersburg, MD. Thermophysics Div.
Electric Field Effects on a Near-Critical Fluid in Microgravity.
Final rept.
G. Zimmerli, R. A. Wilkinson, R. A. Ferrell, H. Hao, and M. R. Moldover. 1995, 6p.
See also N95-25878.
Pub. in Proceedings of the National Heat Transfer Conference (30th), Portland, OR., August 6-8, 1995, v3 p121-126.

Keywords: *Critical flow, *Electric fields, *Electrostriction, *Microgravity, Reprints, Sulfur hexafluoride, Meetings, Critical point, Density distribution, Interferometry.

The authors have studied the effects of an electric field on a sample of SF6 fluid in the vicinity of the liquid-

vapor critical point. The authors measured the isothermal increase of the density of a near-critical sample as a function of the applied electric field. In agreement with theory, this electrostriction effect diverges near the critical point as the isothermal compressibility diverges. Also as expected, turning on the electric field in the presence of density gradients can induce flow within the fluid, in a way analogous to turning on gravity. These effects were observed in a microgravity environment by using the Critical Point Facility which flew onboard the Space Shuttle Columbia in July 1994 as part of the Second International Microgravity Laboratory Mission. Both visual and interferometric images of two separate sample cells were obtained by means of video downlink.

04,218
PB96-176789 Not available NTIS
National Inst. of Standards and Technology (CSTL), Gaithersburg, MD. Process Measurements Div.
Thermal Anemonetry for Mass Flow Measurement in Oscillating Cryogenic Gas Flows.
Final rept.
W. Rawlins, R. Radebaugh, and K. D. Timmerhaus. 1993, 7p.
Pub. in Review of Scientific Instruments, v64 n11 p3229-3235 Nov 93.

Keywords: *Oscillating flow, *Anemometers, Reprints, Pulse tube refrigerator, Cryocoolers, Constant temperature anemometer, Resistance temperature detectors.

Constant temperature anemometers and resistance temperature detectors have been adapted to measure the instantaneous mass flow rates and tempeatures in oscillating gasflows at frequencies up to 30 Hz and temperatures down to 70 K. These devices were used to study the behavior of the oscillating working fluid (helium) in a regenerative refrigerator called an orifice pulse tube refrigerator with little instrusion in the system. The probes have proved to be very robust with no probe breakage even under the severe operating conditions imposed by the oscillating mass flow. Calibration procedures are presented for correcting the anemometer output associated with the oscillating temperatures and pressures in such systems. Under these conditions the sensors appear to have an uncertainty of less than 1.6%. Typical results obtained with these sensors are presented in this paper. These sensors could be used in many other applications for studies of oscillating systems where instantaneous mass flow rates and temperatures are required.

04,219
PB96-180195 Not available NTIS
National Inst. of Standards and Technology (BFRL), Gaithersburg, MD. Fire Science Div.
Tomographic Reconstruction of the Moments of Local Probability Density Functions in Turbulent Flow Fields.
Final rept.
M. R. Nyden, P. Vallikul, and Y. R. Sivathanu. 1996, 12p.
Pub. in Jnl. of Quantative Spectroscopy Radiation Transfer, v55 n3 p345-356 1996.

Keywords: *Turbulent flow, *Flow fields, *Probability density functions, Turbulent heat transfer, Turbulent jets, Flame propagation, Jet mixing flow, Jet flow, Propenes, Algorithms, Numerical flow visualization, Fourier transformation, Reprints, Ethenes.

An algorithm for the tomographic reconstruction of the individual moments of the probability density functions describing the local transmittance of radiation through a turbulent flow field is advanced. The new method, which is based on Fourier inversion, is applicable to asymmetric (as well as, to axiymmetric) flows. The validity of the method is examined by comparing reconstructed moments of the local probability functions in a buoyant propene/air flame and an ethene/air jet flame to the corresponding values obtained from optical probe measurements.

04,220
PB96-204417 Not available NTIS
National Inst. of Standards and Technology (CSTL), Gaithersburg, MD. Thermophysics Div.
Greenspan Acoustic Viscometer for Gases.
Final rept.
K. A. Gillis, J. B. Mehl, and M. R. Moldover. 1996, 8p.
Pub. in Review of Scientific Instruments, v67 n5 p1850-1857 May 96.

Keywords: *Viscometers, *Transport properties, Reprints, Viscosity, Speed-of-sound, Thermophysical properties, *Helmholtz resonators.

Double Helmholtz acoustic resonators, first proposed by Greenspan for measuring the viscosity of gases, were tested with helium, argon, and propane. Two different resonators were tested extensively with all three gases. For each of these instruments, the results for the viscosities of the three gases were consistent within plus or minus 5% at pressures spanning the range 25-1000 kPa. Without calibration, the viscosities deduced from one viscometer were systematically 1% larger than data from the literature; the viscositites from the second viscometer were systematically 3% larger than data from the literature. If the systematic differences were removed for each viscometer by calibration with a single gas at a single temperature and pressure, then nearly all the results for both instruments would have fallen within plus or minus 0.5% of the data from the literature. In these viscometers, the gases are in contact with robust metal parts only; thus, these instruments are applicable to a very wide variety of gases over a very wide range of temperatures.

04,221
PB97-111504 Not available NTIS
National Inst. of Standards and Technology (CSTL), Gaithersburg, MD. Thermophysics Div.
Internal Waves in Xenon Near the Critical Point.
Final rept.
R. F. Berg, M. J. Lyell, G. B. McFadden, and R. G. Rehm. 1996, 12p.
Pub. in Physics of Fluids, v8 n4 p1464-1475 Jun 96.

Keywords: *Critical points, *Internal waves, *Density profiles, Mode symmetry, Stratified fluid, Reprints, Brunt-Vaisala frequency.

Just above the liquid-vapor critical point, a fluid's large compressibility causes a stable stratification in which the density varied by as much as 10% in 1 cm. This stratification supports internal gravity waves which the authors observe with an oscillator immersed in a near-critical xenon sample. The authors found the number and frequencies of the observable modes depended on the sample cell's orientation, with only two modes seen in the horizontal cell. The frequencies of the two modes had different temperature dependences: with decreasing temperature, the higher frequency increased monotonically from 0.7 to 2.8 Hz, but the lower frequency varied nonmonotonically, with a maximum of 1.0 Hz at 20 mK above the critical temperature. These temperature dependences continued to 20 mK below the critical temperature, where the xenon was separated into liquid and vapor phases. The authors calculated these two frequencies by solving the eigenvalue problem of internal waves in a box containing a stratified fluid. The fluid's density profile was obtained from xenon's equation of state. The calculated and measured frequencies agree to within 15%. Analytical calculations based on simple approximations of the density profile provide insight into the observed temperature dependences.

Optics & Lasers

04,222
N94-23605/6 (Order as N94-23595/9, PC A21/MF A04)
National Inst. of Standards and Technology, Gaithersburg, MD.
Activities of NIST (National Inst. Of Standards and Technology).
1992, 14p.
In NASA. Goddard Space Flight Center, the Fifth Calibration/Data Product Validation Panel Meeting 14 p.

Keywords: *Black body radiation, *Calibrating, *Earth observing system (Eos), *Infrared radiometers, *Remote sensors, *Standardization, Instrument compensation, Radiance, Radiant flux density, Temperature measurement, US NIST.

The Radiometric Physics Division of the NIST is responsible for the national standards in radiation thermometry, spectroradiometry, photometry, and spectrophotometry; dissemination of these standards by providing measurement services to customers requiring calibrations of the highest accuracy; and conducting fundamental and applied research to develop the scientific basis for future measurement services. Its relevance to EOS/TIR calibration includes calibrating unknown blackbody for radiance using a well-characterized NIST blackbody source by matching the radiant fluxes with an IR radiometer. The TIR Round Robin is used to verify the calibration of the sources that are used for the absolute radiometric calibration of the individual EOS sensors.

04,223
PB94-140555 PC A06/MF A02
National Inst. of Standards and Technology, Gaithersburg, MD.
Journal of Research of the National Institute of Standards and Technology, November-December 1993. Volume 98, Number 6.
1993, 125p.
See also PB94-140563 through PB94-140605 and PB94-108529. Also available from Supt. of Docs. as SN703-027-00055-5.

Keywords: *Research, Atomic energy levels, Mass spectroscopy, Chlorine 36, Tritium, Thermodynamic properties, Infrared filters, Light scattering, Isotope effect, Krypton 84, Smoke, Standards, Accelerator mass spectroscopy.

Contents:
- (36)Cl/Cl Accelerator-Mass Spectrometry Standards--Verification of Their Serial-Dilution-Solution Preparations by Radioactivity Measurements;
- Pressure-Volume-Temperature Relations in Liquid and Solid Tritium;
- Filter Transmittance Measurements in the Infrared;
- On Two Numerical Techniques for Light Scattering by Dielectric Agglomerated Structures;
- Wavelengths and Energy Levels of Neutral Kr(84) and Level Shifts in All Kr Even Isotopes.

04,224
PB94-140589 (Order as PB94-140555, PC A06/MF A02)
National Inst. of Standards and Technology, Gaithersburg, MD.
Filter Transmittance Measurements in the Infrared.
A. L. Migdall, A. Frenkel, and D. E. Kelleher. 1993, 7p.
Included in Jnl. of Research of the National Institute of Standards and Technology, v98 n6 p691-697 Nov/Dec 93.

Keywords: *Infrared filters, Intermediate infrared radiation, Carbon dioxide lasers, Optical heterodyning, Laser radiation, Light modulation, Transmittance, Attenuators.

The authors have set up a novel direct detection system to measure filter transmittances over an attenuation range of at least 5 decades, with relative combined standard uncertainties as low as 0.5% (1 sigma) per decade, in the 9 micrometer to 11 micrometer spectral region. This system, using an apparatus originally designed for a heterodyne measurement of transmittance, achieves higher accuracy at the expense of a reduced dynamic range. The high modulation frequency and narrow bandwidth of the system allow thermal background radiation to be suppressed and high accuracy to be achieved. The authors correct for the non-ideal natures of the detector and attenuators. In particular, the detector position is scanned to reduce the effect of its spatial nonuniformity and the deflection of the transmitted beam caused by the nonparallel surfaces of the filter. The authors discuss the sources of systematic errors and the methodology to reduce their contribution.

04,225
PB94-140597 (Order as PB94-140555, PC A06/MF A02)
Pennsylvania State Univ., University Park. Dept. of Engineering Science and Mechanics.
Two Numerical Techniques for Light Scattering by Dielectric Agglomerated Structures.
A. Lakhtakia, and G. W. Mulholland. 1993, 18p.
Prepared in cooperation with National Inst. of Standards and Technology, Gaithersburg, MD.
Included in Jnl. of Research of the National Institute of Standards and Technology, v98 n6 p699-716 Nov/Dec 93.

Keywords: *Light scattering, *Smoke, Method of moments, Maxwells equations, Agglomerates, Combustion, Fires, Soot, Coupled dipole method, Dielectric spheres.

Smoke agglomerates are made of many soot spheres, and their light scattering response is of interest in fire research. The numerical techniques chiefly used for theoretical scattering studies are the method of moments and the coupled dipole moment. The two methods have been obtained in this tutorial paper directly from the monochromatic Maxwell curl equations and shown to be equivalent. The effects of the finite size of the primary spheres have been numerically delineated.

04,226
PB94-185246 Not available NTIS
National Inst. of Standards and Technology (PL), Gaithersburg, MD. Atomic Physics Div.
Spectrum and Energy Levels of Five-Times-Ionized Niobium (Nb VI).
Final rept.
J. O. Ekberg, and J. Reader. 1994, 13p.
Pub. in Jnl. of the Optical Society of America B 11, n3 p415-427 Mar 94. Sponsored by Department of Energy, Washington, DC.

Keywords: *Atomic energy levels, *Ultraviolet spectra, *Niobium ions, Vacuum ultraviolet radiation, Atomic spectra, Line spectra, Hyperfine structure, Ionization, Reprints, Krypton-line ions.

The spectrum of the kryptonlike ion Nb VI was observed from 325 to 2,700 A with sliding-spark discharges on 10.7-m normal-incidence and grazing-incidence spectrographs. Experimental energies were determined for all levels of the 4s(2)4p(6), 4s(2)4p(5)4d, 4f, 5s, 5p, 5d, 5g, 6s, and 4s4p(6)4d configurations as well as for some levels of the 4s(2)4p(5)6g and 6h configurations. A total of 303 lines are now classified as transitions between 99 observed levels. Large hyperfine splittings were found for several levels of the 4p(5)5s and 5p configurations. The observed configurations were theoretically interpreted by means of Hartree-Fock calculations and least-squares fits of the energy parameters to the observed levels. An improved value of the ionization energy was determined from the 4p(5)5g, 6g, and 6h configurations.

04,227
PB94-188240 PC A03/MF A01
National Inst. of Standards and Technology (PL), Gaithersburg, MD. Radiometric Physics Div.
NIST Response to the Fifth CORM Report on the Pressing Problems and Projected Needs in Optical Radiation Measurements.
A. C. Parr, and J. J. Hsla. May 94, 18p, NISTIR-5420.

Keywords: *Optical measurement, *Radiometry, *Metrology, Optical properties, Visible radiation, Infrared radiation, Infrared detectors, Irradiance, Reflectance, Photometry, *CORM(Council for Optical Radiation Measurements), Council for Optical Radiation Measurements, Standard reference materials, Spectroradiometry.

The Council for Optical Radiation Measurements (CORM) issued its Fifth Report in September 1989. Some of the concerns addressed in the CORM report required a response from NIST measurements services. Herein is documented NIST's endeavors to assist the optical radiation measurement community by acting on some of the CORM requests.

04,228
PB94-191707 PC A03/MF A01
National Inst. of Standards and Technology (PL), Gaithersburg, MD. Radiometric Physics Div.
Optical Metrology and More. Programs and Services of the Radiometric Physics Division, Physics Laboratory.
S. Bruce. May 94, 24p, NISTIR-5429.
Color illustrations reproduced in black and white.

Keywords: *Optical measurement, *Radiometry, Temperature range 1000-4000 K, Temperature measurement, Ultraviolet radiation, Visible radiation, Infrared radiation, Infrared detectors, Light scattering, Light sources, Calibration, Photometry, Metrology, *Radiometric Physics Division, US NIST.

The Radiometric Physics Division is the primary unit within NIST for carrying out the basic mission of promoting accurate and useful optical radiation measurements in the ultraviolet, visible, and infrared regions. This brochure describes the programs and projects that comprise the work represented by this division.

04,229
PB94-199098 Not available NTIS
National Inst. of Standards and Technology (PL), Gaithersburg, MD. Atomic Physics Div.
Development and Calibration of UV/VUV Radiometric Sources.
Final rept.
J. M. Bridges. 1993, 9p.
Pub. in Proceedings of Society of Photo-Optical Instrumentation Engineers - Ultraviolet Technology IV, San Diego, CA., July 20-21, 1992, v1764 p262-270 1993. Sponsored by Office of Space Science and Applications, Washington, DC.

Keywords: *Vacuum ultraviolet radiation, *Ultraviolet radiation, *Radiometry, *Calibration, SURF II storage ring, Electric arcs, Irradiance, Radiance, Reprints, Hydrogen arcs, Argon arcs, US NIST.

A program exists at NIST to calibrate radiometric sources for the spectral range from 118-350 nm. These include deuterium lamps, hollow-cathode lamps, RF-excited dimer lamps, and wall-stabilized argon arcs. Sources have been calibrated for and used by researchers in solar physics, astrophysics, atmospheric physics (ozone measurements), magnetically controlled fusion, and photobiology. The argon arcs were developed in our laboratory, and provide intense sources of both radiance and irradiance. Calibrations are performed relative to two primary sources, a wall-stabilized hydrogen arc and a 12,000 K black-body line arc, both developed in our laboratory. Also we recently have begun periodic calibrations on the NIST storage ring, SURF II, to ensure consistency between our respective radiometric bases. Various sources have been calibrated for space applications, including several which are flyable. Also, some development and testing of radiometers for semiconductor lithography were recently carried out with an intense argon arc source.

04,230
PB94-199163 Not available NTIS
National Inst. of Standards and Technology (PL), Gaithersburg, MD. Radiometric Physics Div.
Overview of Radiometric Program of the NIST Thermal Imaging Laboratory.
Final rept.
R. J. Bruening. 1991, 11p.
Pub. in Proceedings of MICOM Logistics Research and Development Workshop (2nd), Huntsville, AL., August 27-28, 1991, p503-513. Sponsored by Naval Warfare Assessment Center/Metrology Engineering Center, Corona, CA.

Keywords: *Radiometry, Infrared radiometers, Infrared detectors, Infrared cameras, Temperature range 0273-0400 K, Blackbody radiation, Heat pipes, Calibration, Reprints, Thermal Imaging Laboratory, US NIST.

Radiometric calibrations performed in the NIST Thermal Imaging Laboratory now support infrared detecting devices that operate in the temperature range of 0 to 100 C, including devices that produce pictures of ambient temperature scenes. The laboratory provides characterization of the temperature and temperature-differences of infrared blackbody sources, and characterization of radiometers. Research into the quantitative performance of infrared cameras, and use of higher temperature calibrated heat pipe sources (to 1000 C) is planned.

04,231
PB94-207636 PC A10/MF A03
National Inst. of Standards and Technology (EEEL), Boulder, CO. Electromagnetic Technology Div.
Technical Digest: Symposium on Optical Fiber Measurements (8th), 1994. Held in Boulder, Colorado on September 13-15, 1994.
Special pub. (Final).
G. W. Day, D. L. Franzen, and R. K. Hickernell. Sep 94, 233p, NIST/SP-864.
Also available from Supt. of Docs. as SN003-003-03277-8. See also PB93-102259. Prepared in cooperation with Lasers and Electro-Optics Society (IEEE), Piscataway, NJ. and Optical Society of America, Washington, DC.

Keywords: *Fiber optics, *Optical fibers, *Optical measurement, *Meetings, Optical polarization, Electrooptics, Transmission lines, Reviews, US NBS, Integrated optics, National Institute of Standards and Technology.

The Digest contains the manuscripts of 50 papers, 10 invited and 40 contributed, presented at the eighth Symposium on Optical Fiber Measurements, September 13-15, 1994 in Boulder, Colorado. The most significant theme of the symposium is the present importance of polarization measurements. More than 20% of the papers are concerned either with polarization measurements, especially polarization mode dispersion and polarization dependent loss, or the characterization of fibers and components with special polarization properties. Optical time-domain reflectometry (OTDR) measurements are another important theme, as they have been since the first Symposium in 1980, and the characterization of optical fiber amplifiers continues to be important. Nonlinear processes in fiber seem to be a growing interest. Approximately two thirds of the papers come from outside of the United States, up from about half at the seventh Symposium. Ten countries are represented in the program.

04,232
PB94-211224 Not available NTIS
National Inst. of Standards and Technology (NML), Gaithersburg, MD. Radiometric Physics Div.
Update on the Low Background IR Calibration Facility at the National Institute of Standards and Technology.
Final rept.
S. C. Ebner, A. C. Parr, and C. C. Hoyt. 1989, 12p.
Pub. in Proceedings of Society of Photo-Optical Instrumentation Engineers - Imaging Infrared: Scene Simulation, Modeling, and Real Image Tracking, Orlando, FL., March 30-31, 1989, v1110 p49-60.

Keywords: *Infrared sources, *Calibration, Temperature range 0013-0065 K, Blackbody radiation, Research facilities, Radiometry, Irradiance, Reprints, US NIST.

Details will be given about the recently completed facility for the calibration of infrared sources in a low background environment. The basic components of the facility are a large (60 cm diameter by 152 cm long) stainless steel vacuum chamber housed in a soft-wall cleanroom. A low background environment inside the chamber is achieved by cooling internal cryoshields to temperatures less than 20 K using a closed cycle helium refrigerator. Sources of up to 30 cm square can be inserted into the chamber for calibration. Total radiant power from the blackbodies is measured with an Absolute Cryogenic Radiometer. Plans will be discussed for future enhancement of the system allowing for measurement of spectral and angular distribution of the emitted radiation and possible experiments which could utilize the full capabilities of this system.

04,233
PB94-211232 Not available NTIS
National Inst. of Standards and Technology (PL), Gaithersburg, MD. Radiometric Physics Div.
Comparison of Regular Transmittance Scales of Four National Standardizing Laboratories.
Final rept.
K. E. Eckerle, J. Bastie, J. Zwinkels, V. Sapritsky, and A. Ulyanov. 1993, 6p.
Pub. in COLOR Research and Application 18, n1 p35-40 Feb 93.

Keywords: *Transmittance, International, Interlaboratory comparisons, Spectrophotometers, Standardization, Optical filters, Uncertainty, Reprints.

A comparison of the regular spectral transmittance scales of the National Institute of Standards and Technology (USA), Institut National de Metrologie (France), National Research Council (Canada), and All-Union Research Institute for Optical and Physical Measurements (CIS) was accomplished using neutral glass filters with transmittances ranging from approximately 0.92 to 0.001. Storing the filters for almost four years produced no conclusive evidence of improvement over a previous interchange between NIST and three different national standardizing laboratories when the filters were stored for only 30 days. The agreement ranges from 0.01% to 0.3% depending on the laboratory and the filter used. This interchange is part of an ongoing effort to obtain international standardization.

04,234
PB94-211349 Not available NTIS
National Inst. of Standards and Technology (PL), Gaithersburg, MD. Radiometric Physics Div.
Longterm Changes of Silicon Photodiodes and Their Use for Photometric Standardization.
Final rept.
G. Eppeldauer. 1990, 6p.
Pub. in Applied Optics 29, n15 p2289-2294, 20 May 90.

Keywords: *Photometry, *Photodiodes, Long term effects, Optical measurement, Silicon diodes, Standardization, Calibration, Accuracy, Reprints.

A secondary standard silicon photodiode matched with a V-lambda filter was calibrated against primary standard, self-calibrated inversion layer silicon photodiodes, to achieve a high accuracy photometer, according to the new definition of the candela (the photometric base unit). The measured several percent/year specular spectral reflectance change of the windowless primary standard photodiodes was eliminated by their repeated self-calibration. This self-calibration also eliminated the measured several tenth of a percent/year spectral response change of the secondary standard silicon photodiode. The secondary standard detector could be a nonunity quantum efficiency light detector. The spectral response calibration of the V-lambda matched detector of medium spectral mismatch against the absolute spectral responses of three self-calibrated photodiodes resulted in a standard deviation of 0.17% in luminous flux (lumen) calibration. Also illuminance (lux) and light intensity (candela) calibrations were derived from the above primary photometric calibration. It is shown that the V-lambda matched photometer with the above spectral calibration can be used for accurate photometric measurements for all kinds of light sources of known spectral power distribution.

04,235
PB94-211570 Not available NTIS
National Inst. of Standards and Technology (PL), Boulder, CO. Quantum Physics Div.
Dreams About the Next Generation of Super-Stable Lasers.
Final rept.
J. L. Hall, M. Zhu, and D. Hils. 1992, 8p.
Contracts AFOSR91-0283, N00014-89-J-1227
Sponsored by Office of Naval Research, Arlington, VA., National Science Foundation, Arlington, VA., and Air Force Office of Scientific Research, Bolling AFB, DC.
Pub. in Proceedings of International Conference on Laser Spectroscopy (10th), Font-Romeu, France, June 1991, p83-90 1992.

Keywords: *Laser stability, *Laser spectroscopy, High resolution, Beam cooling, Tunable lasers, Calcium, Silver, Reprints, Laser cooling.

Even if we propose using general, widely-tunable lasers for our ultra-resolution dream spectroscopy, we show that the S/N available from a cavity locking scheme is adequate to define sub-milliHertz laser linewidths. We prove that present External Stabilizer servo technology is adequate to track an error signal precisely enough that 97% of the emitted power lies within the narrow spectral feature defined by phase- or cavity-locking. Cavity stability of + or - 5 kHz for several weeks is documented, and efforts to eliminate the influence of laboratory vibrations are described. The paper concludes with a dream: application of these lasers to two delicious laser-cooled species, Ag and Ca.

04,236
PB94-211935 Not available NTIS
National Inst. of Standards and Technology (EEEL), Boulder, CO. Electromagnetic Technology Div.
Pump-Induced Dispersion of Erbium-Doped Fiber Measured by Fourier-Transform Spectroscopy.
Final rept.
R. K. Hickernell, K. Takada, M. Yamada, M. Shimizu, and M. Horiguchi. 1993, 3p.
Sponsored by Nippon Telegraph and Telephone Corp., Ibaraki. Opto-Electronics Labs.
Pub. in Optics Letters 18, n1 p19-21, 1 Jan 93.

Keywords: Near infrared radiation, Light amplifiers, Optical measurement, Doped materials, Erbium ions, Interferometry, Dispersion, Reprints, *Fiber amplifiers, Fourier transform spectroscopy, Group index.

We report the measurement of group index and dispersion in an erbium-doped fiber amplifier by Fourier transformation of low-coherence interferograms. In a germania-codoped fiber whose background dispersion was -14 ps/(km nm), we measured resonant gain-induced changes as high as 9 and -12 ps/(km nm) near 1.536 micrometers. The interferometric measurements agree with calculations based on a Kramers-Kronig transformation of absorption and emission spectra.

04,237
PB94-212511 Not available NTIS
National Inst. of Standards and Technology (NML), Gaithersburg, MD. Radiation Source and Instrumentation Div.
NIST-NRL Free-Electron Laser Facility.
Final rept.
R. G. Johnson, R. L. Ayres, J. B. Broberg, B. C. Johnson, E. R. Lindstrom, D. L. Mohr, J. E. Rose, J. K. Whittaker, N. D. Wilkin, M. A. Wilson, S. Penner, C. M. Tang, P. Sprangle, R. I. Cutler, and P. H. Debenham. 1990, 12p.
Pub. in Society of Photo-Optical Instrumentation Engineers - Free-Electron Lasers and Applications, Los Angeles, CA., January 18-19, 1990, v1227 p14-25.

Keywords: *Free electron lasers, *Research facilities, Naval Research Laboratory, Racetrack microtrons, Tunable lasers, Infrared lasers, Electron accelerators, Ultraviolet lasers, Wiggler magnets, Uses, Reprints, US NIST.

A free-electron laser (FEL) facility is being constructed at the National Institute of Standards and Technology (NIST) in collaboration with the Naval Research Laboratory (NRL). The FEL will be driven by the electron beam from the NIST racetrack microtron (RTM). The anticipated performance of the FEL is given. Initial operation of the FEL is scheduled for 1991. The NIST-NRL FEL will provide a powerful, tunable light source for research in biomedicine, materials science, physics, and chemistry.

04,238
PB94-212529 Not available NTIS
National Inst. of Standards and Technology (NML), Gaithersburg, MD. Radiation Source and Instrumentation Div.
Hybrid Undulator for the NIST-NRL Free-Electron Laser.
Final rept.
R. G. Johnson, D. L. Mohr, M. A. Wilson, B. Ng, K. M. Thomas, S. Penner, and F. C. Younger. 1990, 5p.
Pub. in Proceedings of International Free Electron Laser Conference (11th), Naples, FL., August 28-September 1, 1989, p592-596 1990.

Keywords: *Free electron lasers, *Wiggler magnets, Permanent magnets, Hybrid structures, Tunable lasers, Magnetic fields, Cobalt alloys, Samarium alloys, Reprints, US NIST.

The National Institute of Standards and Technology (NIST) and the Naval Research Laboratory (NRL) free electron laser (FEL) will use a 3.64-m hybrid undulator that is being constructed at Brobeck Division of Maxwell Laboratories. The undulator has a period of 2.8 cm, a variable gap with a 1.0-cm minimum, a peak magnetic field of 0.54 T, and a total number of periods of 130. The magnetic design uses SmCo permanent magnets and vanadium permendur pole pieces. Provision has been made to operate the undulator at half its length to enhance lasing at longer wavelengths. Remote control of gap and taper will permit on-line tuning of the wavelength. Vacuum chambers for both full and half length operation are available. The oval aperture of the vacuum chambers is 0.86 cm by 1.6 cm. A system to measure the magnetic field along the undulator is included in the structure. A full-scale, one-period model of the magnetic design has been tested and the results exceed specifications. The mechanical structure of the undulator is nearly complete as is the control system. Construction of the magnet assemblies is underway.

04,239
PB94-212545 Not available NTIS
National Inst. of Standards and Technology (EEEL), Boulder, CO. Electromagnetic Technology Div.
Beam Analysis Round Robin.
Final rept.
R. D. Jones, and T. R. Scott. 1992, 12p.
Pub. in Proceedings of Society of Photo-Optical Instrumentation Engineers - Laser Energy Distribution Profiles: Measurement and Applications, Boston, MA., November 16-18, 1992, v1834 p60-71.

Keywords: *Laser beams, Statistical analysis, Reprints, Beam analysis, Round robins.

We present the results of a round robin in which six U.S. manufacturers of beam analysis instruments participated. Following a procedure recommended by the International Organization for Standardization (ISO), participants used a camera, pinhole, slit, or knife-edge to determine several parameters characterizing the beam of a common laser source. Their results and ours are displayed graphically and analyzed statistically. Agreement on beam width measurements is in a range around five percent relative standard deviation while significantly less agreement exists for other quantities calculated within the ISO procedure.

04,240
PB94-212552 Not available NTIS
National Inst. of Standards and Technology (EEEL), Boulder, CO. Electromagnetic Technology Div.
Laser-Beam Analysis Pinpoints Critical Parameters.
Final rept.
R. D. Jones, and T. R. Scott. 1993, 8p.
Pub. in Laser Focus World, p123-130 Jan 93.

Keywords: *Laser beams, Beam profiles, Optical measurements, Reprints, Beam analysis.

We demonstrate the need for measuring laser beam parameters such as diameter, divergence and propagation constant. These terms are defined and methods for their measurement are described. We make the point that assumption of ideal beam properties can result in degraded optical performance.

04,241
PB94-213097 Not available NTIS
National Inst. of Standards and Technology (MEL), Gaithersburg, MD. Precision Engineering Div.
Normal-Incidence Complex-Index Refractometry.
Final rept.
R. D. Larrabee. 1992, 8p.
Pub. in Proceedings of Society of Photo-Optical Instrumentation Engineers - Laser-Induced Damage in Optical Materials, v1848 p86-93 1992.

Keywords: *Refractive index, *Refractivity, *Optical measurement, Electromagnetic absorption, Optical materials, Optical prisms, Complex numbers, Reprints.

Traditional refractometry of bulk transmissive optical materials is usually restricted to the lossless case where the material can be completely characterized by a real index of refraction. This paper is concerned with the measurement of both the real and the imaginary parts of the index of refraction (i.e., including any loss) using a single prism-shaped specimen of homogeneous material. The normal-incidence configuration is analyzed and discussed in this paper because of its mathematical simplicity compared to the minimum-deviation configuration. The measurement of the imaginary part of the index of refraction (i.e. loss) is practical when the longest and shortest optical paths through the prism differ by an absorption length or more. The measurement of the real part of the index can ignore loss and still be accurate to better than one part per million if the power absorption length in the prism material is longer than 60 wavelengths in that material. An equation to determine the real part of the index of refraction is given when the loss must be taken into consideration.

04,242
PB94-213246 Not available NTIS
National Inst. of Standards and Technology (NEL), Gaithersburg, MD. Precision Engineering Div.
Light Scattering from Glossy Coatings on Paper.
Final rept.
T. R. Lettieri, E. Marx, J. F. Song, and T. V. Vorburger. 1991, 9p.
Pub. in Applied Optics 30, n30 p4439-4447 1991.

Keywords: *Light scattering, *Surface roughness, *Coatings, Optical measurement, Laser radiation, Angular distribution, Autocorrelation, Texture, Pens, Reprints, Angle resolved scattering, Glossy paper.

The application of angle-resolved light scattering (ARLS) to the measurement of the surface roughness of coatings on glossy paper was investigated. To this end, ARLS patterns were measured for laser light scattered from several glossy paper samples, and these experimental patterns were compared to those calculated using a theoretical model based on plane-wave scattering from an isotropic, two-dimensional, rough surface. The calculated patterns were computed using, as input, mechanical stylus data for the rms roughnesses and the autocorrelation lengths of the coatings. For all of the paper samples measured, as well as for all of the incidence angles used, there was very good agreement between the experimental and the calculated patterns, indicating that ARLS may be used to determine the coating roughness parameters. As a check on these results, measurements were also made with a commercial optical surface probe; these data compared favorably with both the ARLS and the stylus results.

04,243
PB94-216520 Not available NTIS

National Inst. of Standards and Technology (NEL), Gaithersburg, MD. Precision Engineering Div.
Determination of Surface Roughness from Scattered Light.
Final rept.
E. Marx, L. X. Cao, and T. Vorburger. 1989, 4p.
Pub. in Proceedings of International Symposium Digest - Antennas and Propagation, San Jose, CA., June 26-30, 1989, v1 p192-195.

Keywords: *Surface roughness, *Light scattering, Optical measurement, Data processing, Autocorrelation, Pens, Reprints.

The surface roughness and correlation length are determined from measurements of scattered light by fitting the data of the spectrum calculated for a random rough surface. The results are compared to values determined from stylus measurements.

04,244
PB94-216538 Not available NTIS
National Inst. of Standards and Technology (MEL), Gaithersburg, MD. Precision Engineering Div.
Autocorrelation Functions from Optical Scattering for One-Dimensionally Rough Surfaces.
Final rept.
E. Marx, B. Leridon, T. R. Lettieri, J. F. Song, and T. V. Vorburger. 1993, 10p.
Pub. in Applied Optics 32, n1 p67-76, 1 Jan 93.

Keywords: *Surface roughness, *Light scattering, One dimensional, Fourier transformation, Autocorrelation, Pens, Reprints, Angle resolved scattering, Fraunhofer approximation.

The relationship between the height autocorrelation function of a one-dimensionally rough surface and the Fourier transform of the intensity distribution of the light scattered by that surface is tested experimentally. The theory is derived by using the Fraunhofer approximation, without recourse to the inconsistent Kirchhoff boundary conditions. In spite of the limitations imposed by the approximations used, the results obtained from optical data agree well with those obtained from stylus data, even for an autocorrelation length as small as the optical wavelength. However, this method should be limited to surfaces with rms roughness smaller than approximately 0.14 times the wavelength of light.

04,245
PB94-216546 Not available NTIS
National Inst. of Standards and Technology (NEL), Gaithersburg, MD. Precision Engineering Div.
Light Scattered by Coated Paper.
Final rept.
E. Marx, J. F. Song, T. V. Vorburger, and T. R. Lettieri. 1990, 9p.
Pub. in Proceedings of Society of Photo-Optical Instrumentation Engineers - Optical Testing and Metrology III: Recent Advances in Industrial Optical Inspection, San Diego, CA., July 8-13, 1990, v1332 p826-834.

Keywords: *Light scattering, *Surface roughness, *Coatings, Optical measurement, Laser radiation, Angular distribution, Autocorrelation, Profiles, Pens, Reprints, Angle resolved scattering, Glossy paper.

Angle-resolved light scattering (ARLS) was used to investigate the roughness of coatings on glossy paper. The angular spectra were measured for laser light scattered from several glossy paper samples, and these spectra were compared to those calculated using the Beckman model of a surface that is isotropic, random, and rough in two dimensions. A surface was characterized by its rms roughness and autocorrelation function, which were determined from surface profiles measured with a stylus instrument. There was very good agreement between the measured and the computed spectra. The surfaces are too rough to produce a specular beam and we cannot get an accurate value of the rms roughness from the angular spectrum, but ARLS provides information about the coating roughness when the measured spectra are compared to computed ones.

04,246
PB94-219391 (Order as PB94-219326, PC A05/MF A02)
National Inst. of Standards and Technology, Gaithersburg, MD.
Comments on the Paper 'Wolf Shifts and Their Physical Interpretation under Laboratory Conditions'.
K. D. Mielenz. 1994, 2p.
Included in Jnl. of Research of the National Institute of Standards and Technology, v99 n3 p281-282 May/Jun 94.

Keywords: *Spectral shift, Light transmission, Conservation laws, Spectroscopy, Radiometry, Diffraction, Coherence, Invariance, *Wolf shifts.

In a recent paper in the Journal of Research of the National Institute of Standards and Technology, K. D. Mielenz has criticized the generally accepted interpretation of a phenomenon discovered a few years ago, regarding frequency shifts of spectral lines due to coherence properties of sources. In these comments the authors show that much of the criticism is invalid.

04,247
PB94-219409 (Order as PB94-219326, PC A05/MF A02)
National Inst. of Standards and Technology, Gaithersburg, MD.
Reply to Professor Wolf's Comments on My Paper on Wolf Shifts.
K. D. Mielenz. 1994, 1p.
Included in Jnl. of Research of the National Institute of Standards and Technology, v99 n3 p283 May/Jun 94.

Keywords: *Spectral shift, Light transmission, Conservation laws, Spectroscopy, Radiometry, Diffraction, Coherence, Invariance, *Wolf shifts.

The authors addressed the following comments: (1) Does the spectrum of partially coherent light change on propagation in free space. (2) Do the theory of partial coherence and the classical Huyghens-Fresnel-Kirchhoff diffraction theory give different results in situations that involve incoherent physical sources. Which of them should be applied for solutions of practical problems. (3) Are traditional radiometric practices afflicted by previously unknown errors due to the partial coherence of light.

04,248
PB95-108684 Not available NTIS
National Inst. of Standards and Technology (PL), Boulder, CO. Quantum Physics Div.
Efficient Br(*) Laser Pumped by Frequency-Doubled Nd: YAG and Electronic-to-Vibrational Transfer-Pumped CO2 and HCN Lasers.
Final rept.
R. L. Pastel, G. D. Hager, H. C. Miller, and S. R. Leone. 1991, 5p.
Sponsored by Phillips Lab., Kirtland AFB, NM. and National Science Foundation, Washington, DC.
Pub. in Chemical Physics Letters 183, n6 p565-569, 13 Sep 91.

Keywords: *Carbon dioxide lasers, Intermediate infrared radiation, Near infrared radiation, Infrared lasers, Gas lasers, Optical pumping, Iodine bromides, YAG lasers, Photodissociation, Reprints, *Bromine lasers, *Hydrogen cyanide lasers.

A photolytic, repetitively pulsed Br(4 doublet P(1/2) - 4 doublet P(3/2)) laser at 2.714 micrometers is demonstrated by photodissociation of IBr at 532 nm using a frequency-doubled Nd:YAG pump laser. Pulse energies of 3 mJ at 10 Hz are achieved, resulting in a maximum pump energy conversion efficiency of 1.5%. The authors also demonstrate lasing on ro-vibrational transitions of CO2 at 4.3 micrometers and HCN at 3.9 micrometers by electronic-to-vibrational transfer from photolytically generated Br(star).

04,249
PB95-125910 Not available NTIS
National Inst. of Standards and Technology (EEEL), Boulder, CO. Electromagnetic Technology Div.
Complex Propagation Constants for Nonuniform Optical Waveguides: Calculations.
Final rept.
R. L. Gallawa. 1993, 4p.
Pub. in Microwave and Optical Technology Letters 6, n8 p490-493, 20 Jun 93.

Keywords: *Optical waveguides, *Optical fibers, *Fiber optics, Refractive index, Light transmission, Planar structures, Galerkin method, Attenuation, Reprints, Hermite-Gauss functions, Basis functions.

A method of calculating the complex propagation constant of a planar optical waveguide under very general but weakly guiding conditions is derived. The method, based on Galerkin's formalism using Hermite-Gaussian basis functions, allows a nonuniform and complex refractive index profile. The real and imaginary parts of the index are allowed to vary independently and arbitrarily as a function of position. The planar waveguide is used so the results can be compared with exact solutions. The method is more general than this, however, and can be used with any geometry. The results are inherently stationary.

04,250
PB95-125936 Not available NTIS
National Inst. of Standards and Technology (EEEL), Boulder, CO. Electromagnetic Technology Div.
Fiber Spot Size: A Simple Method of Calculation.
Final rept.
R. L. Gallawa, I. C. Goyal, and A. K. Ghatak. 1993, 6p.
Pub. in Jnl. of Lightwave Technology 11, n2 p192-197 Feb 93.

Keywords: *Optical fibers, *Fiber optics, Sizes(Dimensions), Symbolic programming, Radiation patterns, Galerkin method, Far field, Algorithms, Reprints, Laguerre-Gauss functions, Spot size, Mode field diameter.

The ability to integrate the Laguerre-Gauss functions in closed form is exploited to allow a simple but accurate evaluation of single-mode fiber spot size using Galerkin's method. The method avoids the need for numerical integration in a broad class of refractive-index profiles. Its simplicity depends on the use of a pattern-matching algorithm to avoid the numerical integration normally called for. The algorithm is very fast and gives exact results. The development of symbolic computer languages makes this approach especially easy. We used a symbolic program to predict the spot size and the far-field radiation pattern and compared the results with the exact values, getting excellent results.

04,251
PB95-125944 Not available NTIS
National Inst. of Standards and Technology (EEEL), Boulder, CO. Electromagnetic Technology Div.
Modal Properties of Circular and Noncircular Optical Waveguides.
Final rept.
R. L. Gallawa, I. C. Goyal, and A. K. Ghatak. 1992, 26p.
Pub. in Fiber and Integrated Optics 11, p25-50 1992.

Keywords: *Optical waveguides, Circular configuration, Rectangular configuration, Trigometric functions, Variational methods, Orthogonal functions, Galerkin method, Wave equations, Reprints, Laguerre-Gauss functions, Hermite-Gauss functions, Basis functions, Modal analysis.

We give a review and a comparison of recent methods of analyzing circular and noncircular optical waveguides. Comparison among competing methodologies is made as follows: Galerkin's method is used with Laguerre-Gauss basis functions in circular geometry to examine the modal solution in a step index fiber, and comparison with the exact solution is made. A W-fiber, which has no exact solution, is then examined. Rectangular geometry is considered, and discussion centers on the use of Galerkin's method using trigonometric basis functions and Hermite-Gauss basis functions. The difficulty arising from the use of basis functions that do not decay exponentially for large argument (trigonometric functions) is illustrated. Finally, a square step index waveguide is used to illustrate a comparison between a variational method that uses the Gaussian approximation as the starting point, and Galerkin's method using Hermite-Gauss basis functions. We conclude that the variational method does well in predicting the propagation constant beta but does not do well in predicting the modal field.

04,252
PB95-126082 Not available NTIS
National Inst. of Standards and Technology (EEEL), Boulder, CO. Electromagnetic Technology Div.
Frequency Stabilization of a Fiber Laser to Rubidium: A High-Accuracy 1.53 mu m Wavelength Standard.
Final rept.
S. L. Gilbert. 1993, 8p.
Pub. in Proceedings of Society of Photo-Optical Instrumentation Engineers Frequency-Stabilized Lasers and Their Applications, Boston, MA., November 16-18, 1992, v1837 p146-153 1993.

Keywords: *Erbium glass lasers, *Frequency stability, *Frequency standards, Near infrared radiation, Infrared spectroscopy, Electron transitions, Rubidium 87, Stabilization, Optical communication, Laser spectroscopy, Reprints, *Wavelength standards, Fiber lasers, Laser cooling, Atom traps.

Spectroscopy of the rubidium 5P(3/2) --> 4D(5/2) transition near 1.529 micrometers has been performed using a single-longitudinal-mode erbium-doped fiber laser. Rubidium atoms were laser-cooled and confined in a vapor-cell Zeeman optical trap. This produced a dense sample of cold atoms and reduced the Doppler broadening of the transition to less than the natural linewidth. Transition linewidths of 10 MHz were observed on the 5P(3/2) --> 4D(5/2) transition and the fiber laser was actively stabilized to the 5P(3/2), F = 3 --> 4D(5/2), F' = 3 line of (87)Rb.

04,253
PB95-126090 Not available NTIS
National Inst. of Standards and Technology (EEEL), Boulder, CO. Electromagnetic Technology Div.
Laser Cooling and Trapping for the Masses.
Final rept.
S. L. Gilbert, and C. E. Wieman. 1993, 7p.
Pub. in Optics and Photonics News, p8-14 Jul 93.

Keywords: Temperature range 0000-0013 K, Laser spectroscopy, Semiconductor lasers, Frequency standards, Trapped particles, Beam cooling, Uses, Reprints, *Laser cooling, *Laser trapping, Atoms traps, Wavelength standards, Fiber lasers.

In this article, we describe laser trapping techniques and discuss current applications of this technology, ranging from frequency and wavelength standards to basic physics research.

04,254
PB95-126256 Not available NTIS
National Inst. of Standards and Technology (EEEL), Boulder, CO. Electromagnetic Technology Div.
Approximate Solution to the Scalar Wave Equation for Optical Waveguides.
Final rept.
I. C. Goyal, R. L. Gallawa, and A. K. Ghatak. 1991, 5p.
Pub. in Applied Optics 30, n21 p2985-2989, 20 Jul 91.

Keywords: *Optical waveguides, *Wave equations, WKB approximation, Circular configuration, Planar structures, Integrated optics, Scalars, Reprints.

We consider an approximate solution to the wave equation appropriate to the optical waveguides encountered in practice. The refractive-index profile may be arbitrary, and the geometry may be two or three dimensional. A circular or a planar waveguide could thus be treated by this method. The technique is more accurate and more useful than the WKB method, which is often used in problems of this type, because the technique is valid even at the turning points, where the WKB solution fails. The fields and the propagation constraints of the lowest-order modes for two profiles are calculated, and they compare well with the exact solutions. The solutions that we proposed are, in fact, not new. However, insofar as we know, they are unknown and unused by the optics community.

04,255
PB95-128633 PC A03/MF A01
National Inst. of Standards and Technology (PL), Boulder, CO. Time and Frequency Div.
Sub-Doppler Frequency Measurements on OCS at 87 Thz (3.4 micrometers) with the CO Overtone Laser: Considerations and Details.
Technical note.
A. Dax, J. S. Wells, L. Hollberg, A. G. Maki, and W. Urban. Jul 94, 34p, NIST/TN-1365.
Also available from Supt. of Docs. as SN003-003-03285-9. Prepared in cooperation with Bonn Univ. (Germany, F.R.). Inst. fuer Angewandte Physik.

Keywords: *Carbon oxysulfide, *Frequency measurement, Intermediate infrared radiation, Carbon monoxide lasers, Optical heterodyning, Electron transitions, Calibration standards, Frequency synthesizers, *Carbonyl sulfide, Polarization spectroscopy, Saturated absorption spectroscopy.

The authors have investigated two techniques for making sub-Doppler frequency measurements with the CO overtone laser. They studied three OCS transitions whose frequencies overlap either directly with CO (Delta)v=2 overtone transition frequencies or with the overtone lines after they have been shifted by an acousto-optic modulator. The authors have investigated both conventional saturated-absorption and an optical heterodyne polarization. While they eventually used the latter technique for their measurements, it is too cumbersome to use as a conventional laser stabilization tool. Saturation absorption is considerably simpler and has potential for a more accurate measurement, if some technical problems are overcome. This becomes more important in the light of a potential use of the CO (Delta)v=2P(sub 26)(9) transition in a new frequency chain. This transition was used for the OCS P(27) 10(sup 0)1-00(sup 0)0 measurement. Polarization spectroscopic techniques with optical heterodyne detection were used to observe the features and then to provide the discriminant for locking the overtone laser to the OCS transitions. A CO2 laser synthesizer was used for the frequency measurement basis.

04,256
PB95-140158 Not available NTIS
National Inst. of Standards and Technology (EEEL), Boulder, CO. Electromagnetic Technology Div.
Metrology Applications of Mode-Locked Erbium Fiber Lasers.
Final rept.
J. B. Schlager, P. D. Hale, and D. L. Franzen. 1992, 1p.
Pub. in Proceedings of Conference on Precision Electromagnetic Measurements, Paris, France, June 9-12, 1992, 1p.

Keywords: *Mode locked lasers, *Erbium glass lasers, Near infrared radiation, Pulse compression, Light sources, Infrared lasers, Metrology, Solitons, Reprints, Fiber lasers, Femtosecond pulses, Optical sampling.

Mode-locked erbium fiber lasers (MLEFLs) are a compact source of short optical pulses around 1540 nm. NIST has developed an 'all' fiber design consisting of commercially available pigtailed components. Soliton pulse shaping helps produce sub-picosecond pulses. Characterization of high-speed detectors and fast optical waveforms has been realized using MLEFLs as a sampling pulse source.

04,257
PB95-140836 Not available NTIS
National Inst. of Standards and Technology (EEEL), Boulder, CO. Electromagnetic Technology Div.
Rare-Earth-Doped Waveguide Devices: The Potential for Compact Blue-Green Lasers.
Final rept.
N. A. Sanford, J. A. Aust, D. R. Larson, and K. J. Malone. 1992, 4p.
Pub. in Technical Digest Compact Blue-Green Lasers, Santa Fe, NM., February 20-21, 1992, p1-4.

Keywords: *Waveguide lasers, Lithium niobates, Doped materials, Electron transitions, Optical pumping, Visible radiation, Erbium, Reprints, *Blue green lasers, Titanium sapphire lasers.

Er-doped LiNbO3 channel waveguides produce efficient upconversion luminescence from two bands centered at 520 nm and 550 nm due to radiative decay from the doublet H(11/2) and quartet S(3/2) levels, respectively. The doping density of the rare earth was approximately 10(exp 19)/cu cm. Pumping experiments were performed near 800 nm and again near 970 nm with a cw Ti:sapphire laser. The excitation paths are given. The integrated luminescence efficiency, defined as the total visible output (guided and unguided) divided by the absorbed pump power in the waveguide, was approximately 1%. Laser action in the visible due to a single-wavelength pump appears to be prevented by parasitic nonradiative decay from the intermediate levels.

04,258
PB95-140844 Not available NTIS
National Inst. of Standards and Technology (EEEL), Boulder, CO. Electromagnetic Technology Div.
Linewidth Narrowing in an Imbalanced Y-Branch Waveguide Laser.
Final rept.
N. A. Sanford, J. A. Aust, K. J. Malone, and D. R. Larson. 1993, 3p.
Pub. in Optics Letters 18, n4 p281-283, 15 Feb 93.

Keywords: *Neodymium lasers, *Waveguide lasers, *Line narrowing, *Line width, Near infrared lasers, Optical pumping, Glass lasers, Reprints, Titanium sapphire lasers.

A Y-branch channel waveguide laser whose branch segments were mismatched in length by 2.4% was fabricated by electric-field-assisted ion exchange in Nd-doped, mixed alkali-silicate glass. The laser output wavelength was centered at 1057.3 nm, and the linewidth was 0.4 nm FWHM. Our similarly fabricated single-channel Fabry-Perot lasers and balanced Y-branch lasers display linewidths of 3-4 nm. Pumping was performed with a cw Ti:sapphire laser operating at 785 nm. The imbalanced Y-branch laser reached threshold with an absorbed pump power of 48 mW when a 2% transmitting output coupler was used. The slope efficiency was 2%. An extended cavity was used to imbalance the arms in a second laser by a ratio of 2.8:1. This device displayed a linewidth of approximately 3.7 GHz FWHM. The linewidth narrowing of these coupled-cavity lasers is analogous to that seen in a Michelson laser.

04,259
PB95-140851 Not available NTIS
National Inst. of Standards and Technology (EEEL), Boulder, CO. Electromagnetic Technology Div.
Nd:LiTaO3 Waveguide Laser.
Final rept.
N. A. Sanford, J. A. Aust, K. J. Malone, D. R. Larson, and A. Roshko. 1992, 3p.
Pub. in Optics Letters 17, n22 p1578-1580, 15 Nov 92.

Keywords: *Neodymium lasers, *Waveguide lasers, Near infrared radiation, Lithium tantalates, Infrared lasers, Wafers, Reprints.

Waveguide lasers operating near 1092 and 1076 nm were fabricated in Z-cut Nd-Ti codiffused LiTaO3. The Nd diffusion was at 1400 C for 120 h. Samples from two wafers were examined. The Nd film starting thickness was 7 nm in wafer 1 and 15 nm in wafer 2. Ti stripes, 8-15 micrometers wide, were diffused at 1500 C for 4 h for wafer 1 (130-nm stripe thickness) and 2 h for wafer 2 (100-nm stripe thickness). Pumping was at 750 nm. Threshold occurred at 330 mW of absorbed pump power for the best waveguides from wafer 1 and 100 mW for the best waveguides from wafer 2. The slope efficiency of the latter was 0.07%.

04,260
PB95-141123 Not available NTIS
National Inst. of Standards and Technology (NML), Gaithersburg, MD. Electron and Optical Physics Div.
Perturbative Calculation of the AC Stark Effect by the Complex Rotation Method.
Final rept.
L. Pan, K. T. Taylor, and C. W. Clark. 1991, 12p.
Pub. in Physical Review A 43, n11 p6272-6283 1991.

Keywords: *Stark effect, Frequency dependence, Multi-photon processes, Alternating current, Perturbation theory, Ground state, Hamiltonians, Greens function, Computation, Reprints, *Hydrogen atoms, Complex rotation method, Multiphoton ionization.

We have calculated the high-order AC Stark effect for the ground state of atomic hydrogen by applying Rayleigh-Schrodinger perturbation theory to a complex-rotated Hamiltonian. We present results for the level shift and multiphoton ionization rate, which include effects of above-threshold ionization.

04,261
PB95-150173 Not available NTIS
National Inst. of Standards and Technology (PL), Gaithersburg, MD. Radiometric Physics Div.
Integrating Sphere Simulation: Application to Total Flux Scale Realization.
Final rept.
Y. Ohno. 1994, 11p.
Pub. in Applied Optics 33, n13 p2637-2647, 1 May 94.

Keywords: *Optical measurement, Computerized simulation, Ray tracing, Light sources, Calibration, Photometry, Lumens, Reprints, *Luminous flux, *Integrating spheres.

A method is proposed for realizing the total flux scale of light sources by use of an integrating sphere with an opening to introduce a known amount of flux from a luminous intensity standard or a spectral irradiance standard lamp placed outside the sphere. Computer simulations were made on several models of an integrating sphere, designed to compare the total flux of a test lamp inside the sphere with the flux introduced from an external source. The author describes the theory and algorithm of the simulation, presents the results of the simulation for varying conditions of sphere geometry such as size and location of the baffles, internal source, and wall reflectance, and predicts that one of the models has sufficient accuracy to calibrate lamps for total flux.

04,262
PB95-150496 Not available NTIS

National Inst. of Standards and Technology (EEEL), Boulder, CO. Optical Electronic Metrology Group.
Multiwavelength Birefringent-Cavity Mode-Locked Fibre Laser.
Final rept.
H. Takara, S. Kawanishi, M. Saruwatari, and J. B. Schlager. 1992, 2p.
Sponsored by Yokosuka Electrical Communication Lab. (Japan). Transmission Systems Labs.
Pub. in IEE Electronics Letters 28, n25 p2274-2275 Dec 92 and Proceedings of Conference on Lasers and Electro-Optics, Anaheim, CA., May 10-15, 1992, p250.

Keywords: *Erbium glass lasers, *Mode locked lasers, *Ring lasers, Laser cavities, Light pulses, Picosecond pulses, Doped materials, Birefringence, Synchronism, Reprints, Multiwavelengths.

Generation of simultaneous four wavelength optical pulses is successfully demonstrated using a novel multiwavelength mode-locked Er(3+)-doped fiber ring laser with two 45 deg concatenated, birefringent fibers in the cavity. Wavelength separations of 0.9-2.7 nm and pulse durations of 28-55 ps are obtained.

04,263
PB95-150702 Not available NTIS
National Inst. of Standards and Technology (EEEL), Boulder, CO. Electromagnetic Technology Div.
Direct Dispersion Measurement of Highly-Erbium-Doped Optical Amplifiers Using a Low Coherence Reflectometer Coupled with Dispersive Fourier Spectroscopy.
Final rept.
K. Takada, T. Kitagawa, K. Hattori, R. Hickernell, M. Yamada, and M. Horiguchi. 1992, 3p.
Sponsored by Nippon Telegraph and Telephone Corp., Ibaraki. Opto-Electronics Labs.
Pub. in Electronics Letters 28, n20 p1889-1891, 24 Sep 92.

Keywords: *Light amplifiers, *Optical measurement, Optical fibers, Planar structures, Refractive index, Erbium additions, Doped materials, Wave dispersion, Reflectometers, Silica, Reprints, Fourier transform spectroscopy, Group delay.

The group delay and dispersion, including the erbium ion contributions, of the highly erbium-doped silica planar waveguide amplifier and multicomponent glass fiber amplifiers are directly measured at different pump powers using a low coherence reflectometer and dispersive Fourier spectroscopy. This method derives the refractive index spectra of these amplifiers directly from the produced reflectograms without any physical or mathematical assumptions. The dispersion of the planar waveguide amplifier at 500 mW pumping changes between +300 and -200 ps/km/nm with a 0.4 wt % erbium concentration.

04,264
PB95-150736 Not available NTIS
National Inst. of Standards and Technology (CSTL), Gaithersburg, MD. Surface and Microanalysis Science Div.
Use of Sum Rules on the Energy-Loss Function for the Evaluation of Experimental Optical Data.
Final rept.
S. Tanuma, C. J. Powell, and D. R. Penn. 1993, 15p.
Pub. in Jnl. of Electron Spectroscopy and Related Phenomena 62, p95-109 1993.

Keywords: *Optical data, *Sum rules, *Aluminum, *Iridium, *Molybdenum, *Silicon, *Titanium, *Tungsten, EV range 10-100, EV range 100-1000, Electron spectroscopy, Energy losses, Reprints, Energy loss functions.

We present an evaluation of optical data for Al, Si, Ti, Mo, W, and Ir based on two sum rules for the energy-loss function, the familiar f-sum rule and another sum rule based on a limiting form of the Kramers-Kronig integral. These sum rules were used to evaluate sets of energy-loss function data constructed first from tabulated optical data which have been supplemented by interpolations in the 40-100 eV range for Ti, Mo, W, and Ir. A second set of energy-loss function data was constructed for each material by substituting energy-loss function values calculated from the optical data of Windt et al. (Appl. Opt., 27(1988) 246, 279) in the 10-525 eV range. The deviations in the results of the sum-rule tests with the second set of optical data were about twice those found for the first set. We conclude that the first set of optical data is preferred over the second set.

04,265
PB95-151213 Not available NTIS
National Inst. of Standards and Technology (MEL), Gaithersburg, MD. Precision Engineering Div.
Regimes of Surface Roughness Measurable with Light Scattering.
Final rept.
T. V. Vorburger, E. Marx, and T. R. Lettieri. 1993, 8p.
Pub. in Applied Optics 32, n19 p3401-3408, 1 Jul 93.

Keywords: *Surface roughness, *Light scattering, *Optical measurement, Directional measurement, Angular distribution, Fourier transformation, Autocorrelation, Reflectance, Reprints, Angle resolved scattering.

In this paper we summarize a number of previous experiments on the measurement of the roughness of metallic surfaces by light scattering. We identify several regimes that permit measurement of different surface parameters and functions, and we establish approximate limits for each regime. Using a straightforward criterion, we calculate that the smooth-surface regime, in which the angular distribution of scattered light is closely related to the power spectral density of the roughness, ranges over 0 < sigma/lambda approx = or < 0.05, where sigma is the rms roughness and lambda is the optical wavelength. Above that, the surface autocorrelation function may be calculated from a Fourier transform of the angular distribution over 0 < sigma/lambda approx = or < 0.14. Then comes the specular regime where the specular beam can still be identified and measured over 0 < sigma/lambda approx = or < 0.3. For all of these regimes and for rougher surfaces too, the rms width of the scatter distribution is proportional to the rms slope of the surface.

04,266
PB95-151940 Not available NTIS
National Inst. of Standards and Technology (EEEL), Boulder, CO. Electromagnetic Technology Div.
Optical Fiber Geometry: Accurate Measurement of Cladding Diameter.
Final rept.
M. Young, S. E. Mechels, and P. D. Hale. 1993, 2p.
Pub. in Proceedings of Conference on Precision Electromagnetic Measurements, Paris, France, June 9-12, 1992, p202-203.

Keywords: *Optical fibers, *Optical microscopes, *Optical measurement, *Dimensional measurement, *Micrometers, Optical interferometers, Fiber optics, White light, Diameters, Artifacts, Reprints, *Claddings, Scanning confocal microscopes.

This paper reports progress toward developing an artifact standard for video microscopes devoted to measuring optical fiber geometry. Specifically, we have developed three devices, a contact micrometer, a scanning confocal microscope, and a white-light interference microscope, that are capable of absolute measurements with accuracy between 50 and 100 nm.

04,267
PB95-153334 Not available NTIS
National Inst. of Standards and Technology (MSEL), Gaithersburg, MD. Ceramics Div.
Moisture and Water-Induced Crack Growth in Optical Materials.
Final rept.
D. C. Cranmer, S. W. Freiman, G. S. White, and A. S. Raynes. 1990, 12p.
Pub. in Proceedings of Society of Photo-Optical Instrumentation Engineers: Optical Surfaces Resistant to Severe Environments, San Diego, CA., July 11-12, 1990, v1330 p152-163.

Keywords: *Optical materials, *Crack propagation, *Water erosion, *Moisture, Environment effects, Fracture properties, Fatigue(Materials), Sensitivity, Zinc sulfides, Silicon dioxide, Titanium dioxide, Glass, Reprints.

A number of optically important materials such as ZnS, SiO2, SiO2-TiO2, GaAs, and heavy metal fluoride (e.g., ZBLAN) glasses are subject to moisture- and/or liquid water-induced crack growth. A notable exception to this behavior appears to be Si. Such environmentally enhanced crack growth can lead to ultimate failure in service at stresses well below those expected from normal strength tests. The sensitivity of a material to water can be obtained by determining a crack growth parameter, N. This parameter can be combined with other easily obtainable fracture information which include measures of the strength and strength distribution to create a lifetime design diagram using fracture mechanics concepts. Methods for determining these fracture parameters including direct crack growth measurements and dynamic fatigue are reviewed, and the influence of environmental water on the materials is discussed. Crack growth mechanisms including physical (dielectric) and chemical reaction mechanisms are discussed, and lifetime design diagrams which can be used to determine stress levels in service are presented.

04,268
PB95-153714 Not available NTIS
National Inst. of Standards and Technology (EEEL), Boulder, CO. Electromagnetic Technology Div.
High-Resolution Spectroscopy of Laser-Cooled Rubidium in a Vapor-Cell Trap.
Final rept.
S. L. Gilbert. 1993, 1p.
Pub. in Proceedings of Quantum Electronics and Laser Science Conference, Baltimore, MD., May 2-7, 1993, p212.

Keywords: *Laser spectroscopy, *Rubidium, Erbium glass lasers, Near infrared radiation, Optical communication, High resolution, Electron transitions, Frequency stability, Trapped particles, Reprints, Fiber lasers, Atom traps, Laser cooling.

High resolution spectroscopy was performed using a 1.529 micrometer fiber laser to probe the 5P(3/2) --> 4D(5/2) transition in rubidium atoms confined in a vapor-cell trap. Line shapes and fiber laser stabilization are discussed.

04,269
PB95-153771 Not available NTIS
National Inst. of Standards and Technology (PL), Boulder, CO. Quantum Physics Div.
Frequency Stabilized Lasers: A Parochial Review.
Final rept.
J. L. Hall. 1993, 14p.
Contracts N00014-89-J-1227, AFOSR91-0283
Sponsored by Office of Naval Research, Arlington, VA., Air Force Office of Scientific Research, Bolling AFB, DC., and National Science Foundation, Washington, DC.
Pub. in Proceedings of Society of Photo-Optical Instrumentation Engineers: Frequency-Stabilized Lasers and Their Applications, Boston, MA., November 16-18, 1992, v1837 p2-15 1993.

Keywords: *Laser stability, *Frequency stability, Atomic clocks, Frequency standards, Laser spectroscopy, Laser cavities, High resolution, Uses, Reprints, Atomic interferometry, Atom traps.

This article is meant to serve as a useful introduction to the art of stabilized lasers, especially for those who are entering this activity from other fields. With the current explosion of interest in atom trapping techniques, we can look forward to major progress in the narrow-line laser/super-sharp absorber high resolution spectroscopy business. Applications range from atomic clocks to cold atom collision physics to tests of special relativity. The combination of ultra-stable lasers with cold atom interferometry will be especially powerful in offering new tests of atomic charge neutrality and of time reversal invariance via new limits on atomic electric dipole moments. Remarkably, a practical instrument for oil and gas prospecting might be based on a laser-diode/atom-interferometric measurement of local 'g'.

04,270
PB95-161204 Not available NTIS
National Inst. of Standards and Technology (PL), Gaithersburg, MD. Radiometric Physics Div.
Method of Realizing Spectral Irradiance Based on an Absolute Cryogenic Radiometer.
Final rept.
B. C. Johnson, C. Cromer, R. Saunders, V. Sapritsky, G. Dezsi, G. Eppeldauer, and J. Fowler. 1993, 7p.
Pub. in Metrologia 30, p309-315 1993.

Keywords: Blackbody radiation, Cryogenic temperature, Radiometers, Reprints, *Irradiance measurement.

A technique is presented for realizing spectral irradiance using a large-area, high temperature, uniform, black-body source and filter-radiometers that are calibrated using a High Accuracy Cryogenic Radiometer. The method will be studied by calibrating irradiance lamps with this new technique and comparing the results with those obtained by the method currently employed at the National Institute of Standards and Tech-

nology (NIST). Progress to date and preliminary results are presented. The ultimate goal of the program is to reduce the measurement uncertainties in the spectral irradiance scales that are made available to industry by calibrating deuterium and tungsten-halogen irradiance lamps.

04,271
PB95-161329 Not available NTIS
National Inst. of Standards and Technology (EEEL), Boulder, CO. Electromagnetic Technology Div.
Bending-Induced Phase Shifts in Dual-Mode Planar Optical Waveguides.
Final rept.
A. Kumar, and R. L. Gallawa. 1993, 3p.
Pub. in Optics Letters 18, n17 p1415-1417, 1 Sep 93.

Keywords: *Optical waveguides, *Bending, Refractive index, Phase shift, Planar structures, Dual mode, Reprints, Waveguide sensors.

We examine the manner in which the effective index for each of the two modes of a bent dual-mode planar waveguide changes with curvature. We find that the bending-induced changes in the effective indices depend strongly on core-cladding index contrast and the value of V. For waveguides with large contrast, the changes in effective indices are such that the change in the phase difference between the modes is positive (or negative) at large (or small) values of V. The change becomes zero at a V value that depends on the waveguide parameters and curvature. If the index contrast is small, the bending-induced phase difference may change sign with increase in curvature. This might help in ultimately explaining the bipolar phase shift seen in a recent experiment. The results of our study can be used to increase or decrease the bending sensitivity of dual-mode optical-waveguide sensors and devices.

04,272
PB95-161519 Not available NTIS
National Inst. of Standards and Technology (EEEL), Boulder, CO. Electromagnetic Technology Div.
Optical Fiber Geometry by Gray-Scale Analysis with Robust Regression.
Final rept.
L. Mamileti, C. M. J. Wang, M. Young, and D. F. Vecchia. 1992, 4p.
Pub. in Applied Optics 31, n21 p4182-4185, 20 Jul 92.

Keywords: *Optical fibers, *End effects, *Image analysis, Elliptical configuration, Regression analysis, Fiber optics, Geometry, Reprints, Gray scale.

We have used least-median-of-squares (LMS) regression to analyze gray-scale images of optical fiber ends. This regression is a form of robust regression that ignores outlying data points. We fitted ellipses to the images of each of two fiber ends by using LMS and least-sum-of-squares regression. The two methods yielded nearly identical results on a pristine fiber end, but the LMS method was far superior on a damaged fiber end, even though we made no effort to filter the outlying data points.

04,273
PB95-161949 Not available NTIS
National Inst. of Standards and Technology (PL), Gaithersburg, MD. Radiometric Physics Div.
Detector-Based Candela Scale and Related Photometric Calibration Procedures at NIST.
Final rept.
Y. Ohno, C. L. Cromer, J. E. Hardis, and G. Eppeldauer. 1994, 10p.
Pub. in Jnl. of the Illuminating Engineering Society, p89-98 1994.

Keywords: *Calibration, *Accuracy, *Luminosity, *Photometers, Light sources, Lumens, Detectors, Uncertainty, Standards, Luminous intensity, Spectrum analysis, Luminance, Illuminance, Flux density, Reprints, *Candela scale.

The candela scale, one of the SI base units, has been realized by using absolutely calibrated detectors rather than sources. A group of eight photometers were constructed using silicon photodiodes, precision apertures, and glass filters for V(lambda) match. Their absolute spectral responsivities were calibrated against the NIST absolute spectral responsivity scale. The measurement chain has been significantly shortened compared with the old scale based on a black body. This resulted in improving the calibration uncertainty to be 0.46% (2 sigma), a factor-of-2 improvement. This revision has made various photometric calibrations at NIST more versatile and flexible. Luminous intensity of light sources, ranging from 10(exp -3) to 10(exp 4) candelas, is directly calibrated with the standard photometers which have a linear response over that range. Illuminance meters are calibrated directly against the standard photometers. The luminance scale has also been realized on the detector base using an integrating sphere source. The total flux ranging from 10(exp -2) to 10(exp 5) lumens can be measured in a 2m integrating sphere using a photometer of the same design. These revisions accompanied significant improvement of the calibration accuracy.

04,274
PB95-162020 Not available NTIS
National Inst. of Standards and Technology (EEEL), Boulder, CO. Electromagnetic Technology Div.
Bragg Gratings in Optical Fibers Produced by a Continuous-Wave Ultraviolet Source.
Final rept.
H. Patrick, and S. L. Gilbert. 1993, 1p.
Pub. in Proceedings of Conference on Lasers and Electro-Optics, Baltimore, MD., May 2-7, 1993, p508.

Keywords: *Gratings(Spectra), *Optical fibers, Continuous radiation, Near ultraviolet radiation, Laser radiation, Frequency multipliers, Argon lasers, Germanium additions, Doped materials, Reprints, *Bragg gratings.

Bragg gratings with a reflectance of 50% were written in Ge-doped fiber by exposure to continuous-wave 244 nm light. The ultraviolet light was produced by frequency doubling argon-ion laser light in a buildup cavity.

04,275
PB95-162038 Not available NTIS
National Inst. of Standards and Technology (EEEL), Boulder, CO. Electromagnetic Technology Div.
Growth of Bragg Gratings Produced by Continuous-Wave Ultraviolet Light in Optical Fiber.
Final rept.
H. Patrick, and S. L. Gilbert. 1993, 3p.
Pub. in Optics Letters 18, n18 p1484-1486, 15 Sep 93.

Keywords: *Gratings(Spectra), *Optical fibers, Continuous radiation, Near ultraviolet radiation, Germanium additions, Doped materials, Refractive index, Reprints, *Bragg gratings.

We have written Bragg gratings of as much as 94% reflectance in germanium-doped optical fiber by two-beam interference of 244-nm continuous-wave UV light. We measured grating reflectance as a function of exposure time for UV light intensities ranging from 1.5 to 47 W/sq cm. The observed dependence of index modulation on time and intensity does not agree with the predictions of a model based on depletion of a defect population by one-photon absorption.

04,276
PB95-162350 Not available NTIS
National Inst. of Standards and Technology (PL), Boulder, CO. Quantum Physics Div.
Stabilization and Precise Calibration of a Continuous-Wave Difference Frequency Spectrometer by Use of a Simple Transfer Cavity.
Final rept.
E. Riedle, S. H. Ashworth, J. T. Farrell, and D. J. Nesbitt. 1994, 7p.
Grants NSF-CHE90-00641, NSF-PHY90-12244
Sponsored by National Science Foundation, Washington, DC.
Pub. in Review of Scientific Instruments 65, n1 p42-48 Jan 94.

Keywords: *Spectrometers, *Calibration, Continuous radiation, Difference frequency, Molecular spectra, Near infrared radiation, Intermediate infrared radiation, Helium neon lasers, Argon lasers, Ring lasers, Dye lasers, Frequency stability, Reprints, Transfer cavities.

A novel, simple, and inexpensive calibration scheme for a continuous-wave difference frequency spectrometer is presented, based on the stabilization of an open transfer cavity by locking onto the output of a polarization stabilized HeNe laser. High frequency, acoustic fluctuations of the transfer cavity length are compensated with a piezoelectric transducer mounted mirror, while long term drift in cavity length is controlled by thermal feedback. A single mode Ar(1+) laser, used with a single mode ring dye laser in the difference frequency generation of 2-4 micrometers light, is then locked onto a suitable fringe of this stable cavity, achieving a very small long term drift and furthermore reducing the free running Ar(1+) linewidth to about 1 MHz. The dye laser scan provides tunability in the difference frequency mixing process, and is calibrated by marker fringes with the same stable cavity. Due to the absolute stability of the marker cavity, precise frequency determination of near infrared molecular transitions is achieved via interpolation between these marker fringes. It is shown theoretically that the residual error of this scheme due to the dispersion of air in the transfer cavity is quite small, and experimentally that a frequency precision on the order of 1 MHz per hour is routinely obtained with respect to molecular transitions.

04,277
PB95-163606 Not available NTIS
National Inst. of Standards and Technology (PL), Boulder, CO. Time and Frequency Div.
Laser Spectroscopy of Carbon Monoxide: A Frequency Reference for the Far Infrared.
Final rept.
T. D. Varberg. 1992, 2p.
Pub. in Proceedings of Conference on Precision Electromagnetic Measurements, Paris, France, June 9-12, 1992, p145-146.

Keywords: *Carbon monoxide, *Laser spectroscopy, *Far infrared radiation, Rotational spectra, Frequency standards, Reprints, Reference materials.

The purely rotational spectrum of carbon monoxide in the far infrared has been accurately measured. The set of calculated transitions derived from a fit to these data forms the world's most accurate far infrared frequency reference.

04,278
PB95-164000 Not available NTIS
National Inst. of Standards and Technology (NML), Gaithersburg, MD. Center for Atomic, Molecular and Optical Physics.
XUV Characterization Comparison of Mo/Si Multilayer Coatings.
Final rept.
D. L. Windt, W. K. Waskiewicz, G. D. Kubiak, T. W. Barbee, and R. N. Watts. 1991, 9p.
Sponsored by A.T. and T. Bell Labs., Murray Hill, NJ.
Pub. in Proceedings of Society of Photo-Optical Instrumentation Engineers: X-ray/EUV Optics for Astronomy, Microscopy, Polarimetry, and Projection Lithography, San Diego, CA., July 9-13, 1990, v1343 p274-282 1991.

Keywords: *Optical coatings, *Reflectance, Extreme ultraviolet radiation, Comparative evaluations, Optical measurement, Soft x-rays, Reflectometers, Molybdenum, Silicon, Reprints, Multilayers, X-ray mirrors, Systematic errors.

The reflectance of seven Mo/Si multilayer coatings made at AT&T Bell Labs and at Lawrence Livermore National Laboratories (LLNL) have been measured using three different reflectometers, in order to determine whether reflectance measurements made using different reflectometers yield consistent results. By comparing the deduced adjustable parameters used to fit the measured reflectances with those calculated from a model based on recursive application of the modified Fresnel equations, we conclude that the measurements made with the three reflectometers are inconsistent. We attribute the discrepancies to systematic measurement errors, including those associated with the spectral purity of the incident radiation.

04,279
PB95-164182 Not available NTIS
National Inst. of Standards and Technology (EEEL), Boulder, CO. Electromagnetic Technology Div.
Vector Theory of Diffraction by a Single-Mode Fiber: Application to Mode-Field Diameter Measurements.
Final rept.
M. Young, and R. C. Wittman. 1993, 3p.
Pub. in Optics Letters 18, n20 p1715-1717, 15 Oct 93.

Keywords: *Optical fibers, *Wave diffraction, *Diffraction, Vector fields, Far field, Obliqueness, Integrals, Fiber optics, Reprints, Single mode fibers, Mode-field diameter, Obliquity factors.

We derive a far-field diffraction integral by (vector) electromagnetic theory; the result differs from the (scalar) Rayleigh-Sommerfeld or Kirchhoff result in that it depends on polarization. For unpolarized light, we derive a factor that replaces the usual obliquity factor. Omitting this factor can cause an error of the same order as the measurement uncertainty in determining

the mode-field diameter of a single-mode fiber from far-field data.

04,280
PB95-168464 Not available NTIS
National Inst. of Standards and Technology (EEEL), Boulder, CO. Electromagnetic Technology Div.
Interlaboratory Comparison of Polarization-Holding Parameter Measurements on High-Birefringence Optical Fiber.
Final rept.
R. M. Craig, D. Tang, and G. W. Day. 1993, 4p.
Pub. in Proceedings of Optical Fibre Measurement Conference, Torino, Italy, September 21-22, 1993, p177-180.

Keywords: *Optical fibers, Interlaboratory comparisons, Optical measurement, Polarization(Waves), Fiber optics, Birefringence, Reprints, H parameter.

We report the results of a preliminary interlaboratory comparison of polarization-holding parameter (h-parameter) measurements, in which seven participants measured three coils of fiber using the participants' normal procedures. The variations in results (one standard deviation) among the three coils ranged from 13% to 50%.

04,281
PB95-168548 Not available NTIS
National Inst. of Standards and Technology (PL), Boulder, CO. Time and Frequency Div.
New cw CO2 Laser Lines: The 9-mu m Hot Band.
Final rept.
K. M. Evenson, C. C. Chou, B. W. Bach, and K. G. Bach. 1994, 2p.
Pub. in Institute of Electrical and Electronics Engineers Jnl. of Quantum Electronics 30, n5 p1187-1188 May 94.

Keywords: *Carbon dioxide lasers, *Infrared spectra, Intermediate infrared radiation, Frequency measurement, Continuous radiation, Gratings(Spectra), Line spectra, Reprints.

We have made what we think is the first observation of the oscillation of the 9-micrometer hot-band lines 01(sup 1) --> (left bracket)11(sup 1)0, 03(sup 1)0(right bracket)(sub II) of CO2. We have observed 40 lines with a maximum power of 8 W. They will provide a new source of laser radiation for spectroscopy. The set of lines has been positively identified by directly measuring the frequencies of two of the lines with a heterodyne technique using a CO2 laser standard.

04,282
PB95-168571 Not available NTIS
National Inst. of Standards and Technology (EEEL), Boulder, CO. Electromagnetic Technology Div.
Mode Coupling and Loss on Tapered Optical Waveguides.
Final rept.
R. L. Gallawa, A. Kumar, and A. Weisshaar. 1994, 3p.
Pub. in Proceedings of Integrated Photonics Research Topical Meeting, San Francisco, CA., February 17-19, 1994, p57-59.

Keywords: *Optical waveguides, *Dielectric waveguides, Coupled modes, Galerkin method, Approximation, Tapering, Reprints.

Tapered dielectric waveguides have been analyzed using a variety of methods including coupled mode theory, a step tapered configuration, a method that uses a ray-optics model, and the beam propagation method. We also use a step taper approach, approximating the smooth taper with a series of discrete steps. Our method accounts for the interaction between modes and is capable of tracking the propagation through the taper by using an expansion of the field on each side of the step; we use basis functions that are known to approximate the field very accurately. Integration is avoided in evaluating the coupling efficiency across the step.

04,283
PB95-168589 Not available NTIS
National Inst. of Standards and Technology (EEEL), Boulder, CO. Electromagnetic Technology Div.
Symbolic Programming with Series Expansions: Applications to Optical Waveguides.
Final rept.
R. L. Gallawa, A. Kumar, and A. Weisshaar. 1994, 7p.
Pub. in Proceedings of Annual Review of Progress in Applied Computational Electromagnetics (10th), Monterey, CA., March 21-26, 1994, p475-481.

Keywords: *Optical waveguides, *Optical fibers, *Symbolic programming, Series expansion, Approximation, Eigenvalues, Eigenvectors, Reprints, Single mode fibers.

We discuss the utility of symbolic computer languages in the context of optical fiber analysis. The symbolic Mapping command, for example, is useful whenever a series expansion approach is used in eigenvalue problems if the basis functions are integrable in closed form. We show how this command allows a simple but accurate evaluation of single-mode fiber parameters in most cases of practical interest. The Replacement command is also demonstrated in tracking the variation of fiber operational parameters as a function of the V-parameter. The saving in CPU time is substantial.

04,284
PB95-168597 Not available NTIS
National Inst. of Standards and Technology (EEEL), Boulder, CO. Electromagnetic Technology Div.
Comparison of UV-Induced Fluorescence and Bragg Grating Growth in Optical Fiber.
Final rept.
S. L. Gilbert, and H. Patrick. 1994, 1p.
Pub. in Proceedings of Conference on Lasers and Electro-Optics, Anaheim, CA., May 8-13, 1994, v8 p244.

Keywords: *Optical fibers, *Fluorescence, Near ultraviolet radiation, Continuous radiation, Optical measurement, Time dependence, Refractive index, Gratings(Spectra), Doped materials, Germanium additions, Darkening, Reprints, *Bragg gratings.

We have measured the time dependence of the 400 nm fluorescence of Ge-doped optical fiber illuminated with continuous-wave 244 nm light. Our results differ from previous measurements that used pulsed 242 nm light.

04,285
PB95-168639 Not available NTIS
National Inst. of Standards and Technology (EEEL), Boulder, CO. Electromagnetic Technology Div.
Improved Variational Analysis of Inhomogeneous Optical Waveguides Using Airy Functions.
Final rept.
I. C. Goyal, R. L. Gallawa, and A. K. Ghatak. 1993, 4p.
Pub. in Jnl. of Lightwave Technology 11, n10 p1575-1578 Oct 93.

Keywords: *Optical waveguides, Variational methods, Airy function, Planar structures, Light transmission, Approximation, Inhomogeneity, Eigenvalues, Reprints.

Variational trial fields that are based on modified Airy functions are proposed to obtain the propagation characteristics of inhomogeneous planar optical waveguides. We compare with other recently proposed trial fields to demonstrate the improved accuracy obtained through the use of these Airy function trial fields. The probable reason that the proposed fields are better suited than others is that, unlike the others, they depend on the profile shape. The argument of the Airy function trial field is also sensitive to the rate of change of the profile. The fields are thus better matched to the exact field, improving the variational results.

04,286
PB95-168753 Not available NTIS
National Inst. of Standards and Technology (PL), Boulder, CO. Time and Frequency Div.
Light Scattered from Two Atoms.
Final rept.
W. M. Itano, U. Eichmann, J. C. Bergquist, M. G. Raizen, D. J. Wineland, J. J. Bollinger, and J. M. Gilligan. 1994, 8p.
Sponsored by Office of Naval Research, Arlington, VA.
Pub. in Proceedings of the International Conference on Lasers '93, Lake Tahoe, NV., December 6-9, 1993, p412-419 1994.

Keywords: *Optical interference, *Light scattering, Trapped particles, Laser radiation, Mercury ions, Ion storage, Photon-atom collisions, Quantum mechanics, Quantum optics, Reprints, Polarization dependence, Laser cooling, Atom traps, Complementarity.

We have observed interference fringes, like those in Young's classic experiment, in the laser light scattered by two trapped atoms. The interference fringes are present only in one polarization of the scattered light. The polarization dependence is related to the complementarity principle, which forbids the simultaneous observation of wave-like and particle-like aspects of light. The interference fringes are due to processes in which a single photon scatters from two atoms. We describe methods which might be used to observe other interference effects due to two photons scattering from two atoms.

04,287
PB95-168779 Not available NTIS
National Inst. of Standards and Technology (EEEL), Boulder, CO. Electromagnetic Technology Div.
Widths and Propagation of a Truncated Gaussian Beam.
Final rept.
R. D. Jones, and T. R. Scott. 1994, 12p.
Pub. in Proceedings of Workshop on Laser Beam Characterization (2nd), Berlin, Germany, May 30-June 1, 1994, p161-172.

Keywords: *Laser beams, Light transmission, Beam profiles, Near field, Far field, Slits, Irradiance, Truncation, Reprints, Gaussian beams, Beam divergence.

We calculated irradiance profiles resulting from the truncation of a gaussian beam by hard-edged slits transmitting 95 or 99 percent of the incident power. Three definitions--second moment, slit, and knife edge--were used to obtain widths of the near and far field profiles. From these widths, we calculated the propagation factors of the beam, with and without a lens. Second moment widths are indeterminate, due to their dependence on the extent of integration. Scanning slit and knife-edge widths are measurable, but do not, in general, fit the hyperbolic propagation equation. Least-squares fits of the measurements can result in propagation factors better than the ideal limit. Beam divergence values calculated from single beam width measurements, or from least-squares fits of many data, differ by several percent.

04,288
PB95-168795 Not available NTIS
National Inst. of Standards and Technology (EEEL), Boulder, CO. Electromagnetic Technology Div.
Bending-Induced Loss in Dual-Mode Rectangular Waveguides.
Final rept.
A. Kumar, and R. L. Gallawa. 1994, 3p.
Pub. in Optics Letters 19, n10 p707-709, 15 May 94.

Keywords: *Optical waveguides, Rectangular waveguides, Elliptical configuration, Dual mode, Reprints, Bending losses.

We examine how the bending-induced mode losses in a dual-mode rectangular-core waveguide vary with bend orientation. Bending about the minor axis (case (i)) and bending about the major axis (case (ii)) are considered. The second (LP(11)) mode is more lossy in case (i) than in case (ii), while the reverse is true for the first (LP(01)) mode. Further, in case (i) the LP(11)-mode loss is larger than than LP(01)-mode loss, but in case (ii) the LP(01)-mode loss is, surprisingly, larger than the LP(11)-made loss. LP(11)-mode loss is consistent with the recent experimental results. This study should be useful in designing efficient elliptical-core fiber components such as LP(11)-mode strippers based on differential mode loss of the first two modes.

04,289
PB95-168803 Not available NTIS
National Inst. of Standards and Technology (EEEL), Boulder, CO. Electromagnetic Technology Div.
Bent Rectangular Core Waveguides: An Accurate Perturbation Approach.
Final rept.
A. Kumar, and R. L. Gallawa. 1994, 5p.
Pub. in Microwave and Optical Technology Letters 7, n6 p281-285, 20 Apr 94.

Keywords: *Dielectric waveguides, *Optical waveguides, *Optical fibers, Rectangular waveguides, Perturbation theory, Waveguide bends, Reprints.

We discuss a method of evaluating the effective indices of quasi-modes of a bent rectangular core waveguide taking into account the correct dielectric constant of the corner regions, which is ignored in earlier methods. At small bend curvatures and low V values, the corner regions contribute much more to the effective index change than the bending itself. (Copyright(c) 1994 John Wiley & Sons, Inc).

04,290
PB95-169256 Not available NTIS

National Inst. of Standards and Technology (EEEL), Boulder, CO. Electromagnetic Technology Div.
Optical Power Meter Calibration Using Tunable Laser Diodes.
Final rept.
I. Vayshenker, X. Li, and T. R. Scott. 1994, 10p.
Pub. in Proceedings of National Computer Systems Laboratory Workshop and Symposium 'The Role of Metrology in a Changing World', Chicago, IL., July 31-August 4, 1994, p363-372.

Keywords: *Optical measurement, *Power meters, *Calibration, Near infrared radiation, Semiconductor lasers, Tunable lasers, Metrology, Standards, Reprints, *Optical power.

We describe a measurement system developed by NIST to calibrate optical power meters using either collimated-beam or connectorized-fiber configurations. This calibration system uses tunable laser diodes which operate in the three fiber optics windows of 850, 1,310, and 1,550 nm. This paper describes the standards, techniques, and systems involved in these calibrations.

04,291
PB95-169355 Not available NTIS
National Inst. of Standards and Technology (EEEL), Boulder, CO. Electromagnetic Technology Div.
Optical Detector Nonlinearity: A Comparison of Five Methods.
Final rept.
S. Yang, I. Vayshenker, X. Li, and T. R. Scott. 1994, 2p.
Pub. in Proceedings of Conference on Precision Electromagnetic Measurements Digest, Boulder, CO., June 27-July 1, 1994, p455-456.

Keywords: *Optical detectors, *Infrared detectors, *Power meters, Optical measurement, Mathematical models, Computerized simulation, Nonlinearity, Reprints, Optical power.

We derived a set of unified equations for five methods to evaluate nonlinearity of power meters and detectors. We performed computer simulations of these methods. The simulations assist in design of a measurement system to meet a target accuracy. Measurements verified the simulations.

04,292
PB95-169363 Not available NTIS
National Inst. of Standards and Technology (PL), Boulder, CO. Time and Frequency Div.
Far Infrared Laser Frequencies of (13)CD3OH.
Final rept.
L. R. Zink, G. P. Galvao, K. M. Evenson, and E. C. C. Vasconcellos. 1994, 2p.
Pub. in Jnl. of Quantum Electronics 30, n6 p1361-1362 Jun 94.

Keywords: *Laser radiation, *Methyl alcohol, *Methanol, Far infrared radiation, Infrared lasers, Optical pumping, Deuterium compounds, Carbon 13, Heterodyning, Reprints.

We have measured 30 far-infrared laser frequencies of optically pumped (13)CD3OH, 13 of which are new lines. The frequencies range from 0.5 to 4.9 THz with the majority between 0.75 and 1.5 THz. Two frequency stabilized CO2 lasers were used as standards for the heterodyne measurements.

04,293
PB95-169371 PC A07/MF A02
National Inst. of Standards and Technology, Gaithersburg, MD.
Journal of Research of the National Institute of Standards and Technology, September/October 1994. Volume 99, Number 5.
1994, 148p.
See also PB95-169389 through PB95-169405 and PB95-160594. Also available from Supt. of Docs. as SN703-027-00060-1.

Keywords: *Meetings, *US NIST, *Research and development, *Periodicals, Optics, Electron microscopes, Microelectronics, Systems engineering, Information systems, Standards, Computer security.

Contents include articles on Tilt Effects in Optical Angle Measurements; Optical Characterization in Microelectronics Manufacturing; and Critical Issues in Scanning Electron Microscope Metrology. Also, there are Conference Reports on the 16th National Computer Security Conference and Systems Integration Needs of U.S. Manufacturers. Various News Briefs are included as well.

04,294
PB95-169389 (Order as PB95-169371, PC A07/MF A02)
National Inst. of Standards and Technology, Gaithersburg, MD.
Tilt Effects in Optical Angle Measurements.
Y. H. Queen. 1994, 12p.
Included in Jnl. of Research of the National Institute of Standards and Technology, v99 n5 p593-604 Sep/Oct 94.

Keywords: *Calibrating, *Angles(Geometry), *Collimators, Tilt, Errors, Vector analysis, Tests.

Vector analysis is used to determine the quantitative error in angle calibration using autocollimators. This error is caused by tilt in the mount upon which the artifact is placed. For tilt angles that are less than 1 degree, the error can be simplified to be the product of a coefficient and three terms. The three terms are: (1) the square of the tilt, (2) the sine of the artifact's nominal angle, and (3) the cosine of the artifact's nominal angle plus two times the artifact's position angle. It is shown that the error can be eliminated by placing the artifact at designated periodic positions.

04,295
PB95-173068 PC A04/MF A01
National Inst. of Standards and Technology (EEEL), Boulder, CO. Electromagnetic Technology Div.
Video Microscopy Applied to Optical Fiber Geometry Measurements.
Technical note.
N. A. Brilliant, B. K. Alpert, and M. Young. Nov 94, 56p, NIST/TN-1369.
Also available from Supt. of Docs. as SN003-03310-3.

Keywords: *Fibers, *Optical equipment, *Microscopes, Fiber optics, Telecommunication, Micrometers, Measuring instruments, Gray scales, Coherence, Geometry, Images, *Video microscope, National Institute of Standards and Technology.

The report describes a video microscope used to measure the mean diameter and noncircularity of the cladding of optical fibers. Discribed is an unsuccessful attempt to perform absolute measurements. When the microscope was calibrated with a fiber of known diameter, however, the cladding diameter could be measured within 0.1 micro m.

04,296
PB95-175469 Not available NTIS
National Inst. of Standards and Technology (PL), Boulder, CO. Time and Frequency Div.
Optical Probing of Cold Trapped Atoms.
Final rept.
R. W. Fox, S. L. Gilbert, L. Hollberg, J. H. Marquardt, and H. G. Robinson. 1993, 3p.
Sponsored by Air Force Office of Scientific Research, Bolling AFB, DC. and Naval Command, Control and Ocean Surveillance Center, San Diego, CA.
Pub. in Optics Letters 18, n17 p1456-1458, 1 Sep 93.

Keywords: *Rubidium, *Cesium, Electron transitions, Excited states, Beam cooling, Neutral atoms, Semiconductor lasers, Glass lasers, Reprints, Laser trapping, Laser cooling, Atom traps.

Transitions between excited states of laser-cooled and laser-trapped rubidium and cesium atoms are probed by use of fiber and diode lasers. High-resolution Doppler-free spectra are detected by observation of the absorption and fluorescence of light from the intermediate level of two-step cascade systems. The optical double-resonance spectra show Autler-Townes splitting in the weak probe limit and more complicated spectra for a strongly coupled three-level system.

04,297
PB95-175477 Not available NTIS
National Inst. of Standards and Technology (PL), Boulder, CO. Time and Frequency Div.
High-Sensitivity Spectroscopy with Diode Lasers.
Final rept.
R. W. Fox, H. G. Robinson, A. S. Zibrov, J. Magyar, L. W. Hollberg, N. Mackie, and J. Marquardt. 1992, 6p.
Sponsored by National Aeronautics and Space Administration, Washington, DC. and Air Force Office of Scientific Research, Bolling AFB, DC.
Pub. in Proceedings of Society of Photo-Optical Instrumentation Engineers: Frequency-Stabilized Lasers and Their Applications, Boston, MA., November 16-18, 1992, v1837 p360-365.

Keywords: *Laser spectroscopy, *Semiconductor lasers, Laser stability, Laser cavities, Line spectra, Line width, Visible spectra, High sensitivity, High resolution, Red(Color), Calcium, Cesium, Reprints.

Linewidth reduction of an extended cavity diode laser at 657 nm was accomplished by negative feedback to an intra-cavity ADP crystal. High resolution (170 kHz wide) saturated absorption signals were recorded of the calcium intercombination line which is of interest for a frequency standard. The spectrum of the red 6 doublet P(3/2)-9 doublet S(1/2) cesium line in a magneto-optical cell trap was also investigated.

04,298
PB95-175501 Not available NTIS
National Inst. of Standards and Technology (EEEL), Boulder, CO. Electromagnetic Technology Div.
Calculated Fiber Attenuation: A General Method Yielding Stationary Values.
Final rept.
R. L. Gallawa, I. C. Goyal, and A. K. Ghatak. 1993, 5p.
Pub. in Jnl. of Lightwave Technology 11, n12 p1900-1904 Dec 93.

Keywords: *Optical fibers, *Transmission loss, *Refractive index, Galerkin method, Complex numbers, Fiber optics, Attenuation, Computation, Reprints.

A method of calculating the attenuation constant of an optical fiber under very general but weakly guiding conditions is derived. The method, based on Galerkin's formalism, allows a nonuniform and complex refractive-index profile. The real and imaginary parts of the refractive index are allowed to vary independently and arbitrarily as a function of radius. The result is the predicted complex propagation constant. The results are inherently stationary.

04,299
PB95-175519 Not available NTIS
National Inst. of Standards and Technology (EEEL), Boulder, CO. Electromagnetic Technology Div.
Fibre Splice Loss: A Simple Method of Calculation.
Final rept.
R. L. Gallawa, A. Kumar, and A. Weisshaar. 1994, 8p.
Pub. in Optical and Quantum Electronics 26, pS165-S172 1994.

Keywords: *Optical fibers, *Transmission loss, *Splices, Galerkin method, Fiber optics, Computation, Splicing, Eigenvectors, Reprints, Single mode fibers.

We evaluate the loss encountered when splicing between two circular single-mode fibers with unmatched parameters. Our method represents a significant improvement in simplicity over other methods, with only an insignificant degradation of accuracy. We use Galerkin's method, but expand the field of both fibers in terms of the same set of basis functions, leading to considerable simplicity: the overlap integral is simply the inner (dot) product of the eigenvectors. Integration is thus avoided. We assume that weakly guiding conditions prevail.

04,300
PB95-175881 Not available NTIS
National Inst. of Standards and Technology (PL), Boulder, CO. Time and Frequency Div.
Absolute Frequency Measurements of Methanol from 1.5 to 6.5 THz.
Final rept.
F. Matsushima, K. Evenson, and L. Zink. 1994, 14p.
Pub. in Jnl. of Molecular Spectroscopy 164, p517-530 1994.

Keywords: *Methanol, *Infrared spectra, *Frequency measurement, Far infrared radiation, Forbidden transitions, Carbon dioxide lasers, Rotational spectra, Reprints, Frequency references.

Frequencies of 445 CH3OH rotational transitions between 1.5 and 6.5 THz have been measured with an accuracy of one part in 10(exp 9). The far-infrared radiation used for the measurements was generated from the radiation of two CO2 lasers using a MIM diode as a nonlinear mixer. The high resolution and sensitivity of the spectrometer also enabled us to observe a series of forbidden Q-branch transitions ((Delta)n = 1 and (Delta)K = 0) for J = 12 to 26.

04,301
PB95-175949 Not available NTIS
National Inst. of Standards and Technology (MEL), Gaithersburg, MD. Precision Engineering Div.
Rapid Post-Polishing of Diamond-Turned Optics.
Final rept.
R. E. Parks, and C. J. Evans. 1994, 5p.
Pub. in Precision Engineering 16, n3 p223-227 Jul 94.

Keywords: *Polishing, Asphericity, Finishes, Reprints, *Optical surfaces, Diamond turning, Surface finish, Electroless nickel.

A simple technique for post-polishing single-point, diamond-turned optics is described. Synthetic fabric-faced laps are used. Surface finish converges to a limiting value set by process parameters. Lap construction and diamond grit size affects both convergence rate and ultimate finish.

04,302
PB95-176111 Not available NTIS
National Inst. of Standards and Technology (EEEL), Boulder, CO. Electromagnetic Technology Div.
High-Sensitivity Optical Sampling Using an Erbium-Doped Fiber Laser Strobe.
Final rept.
J. B. Schlager, P. D. Hale, and D. L. Franzen. 1993, 3p.
Pub. in Microwave and Optical Technology Letters 6, n15 p835-837 Dec 93.

Keywords: Near infrared radiation, Distributed feedback lasers, Erbium glass lasers, Mode locked lasers, Infrared lasers, High sensitivity, Picosecond pulses, Laser amplifiers, Real time, Light pulses, Stroboscopes, Reprints, *Optical sampling, Indium gallium arsenide phosphides.

Optical pulses at a repetition frequency of 1 GHz from a gain-switched InGaAsP distributed-feedback laser diode at 1.3 micrometers are optically sampled with compressed pulses from a mode-locked erbium-doped fiber laser amplifier. High signal-to-noise ratios down to 21-(micro)W average laser-diode power with temporal resolutions close to the sampling pulse duration of 4 ps are achieved. The sampled waveform is displayed at a repetition rate of 3 Hz or higher to give a real-time measurement.

04,303
PB95-176152 Not available NTIS
National Inst. of Standards and Technology (PL), Boulder, CO. Time and Frequency Div.
Improved Rubidium Frequency Standards Using Diode Lasers with AM and FM Noise Control.
Final rept.
C. Szekely, and R. E. Drullinger. 1992, 7p.
Pub. in Proceedings of Society of Photo-Optical Instrumentation Engineers: Frequency-Stabilized Lasers and Their Applications, Boston, MA., November 16-18, 1992, v1837 p299-305.

Keywords: *Rubidium frequency standards, *Frequency standards, Semiconductor lasers, Optical pumping, Noise reduction, Reprints.

Diode-laser-pumped, rubidium cell frequency standards have potential short-term stability that is vastly better than their lamp-pumped counterparts. However, AM and FM noise in monolithic laser diodes limit their performance. With extended-cavity, grating-feedback diode lasers, the AM and FM noise can be controlled. In the preliminary work reported here, we have used such a laser to make measurements in two different rubidium cell systems. Measured line Q and signal-to-noise ratios corresponding to sigma(sub y)(tau) = 4 X 10(exp -13) tau(sup -1/2) in a commercial, buffer gas type standard and sigma(sub y)(tau) = 2 X 10(exp -13) tau(sup -1/2) in an evacuated, wall-coated cell are demonstrated. We believe both of these numbers can be improved significantly in a fully engineered and optimized standard.

04,304
PB95-176186 Not available NTIS
National Inst. of Standards and Technology (PL), Boulder, CO. Time and Frequency Div.
Frequency-Stabilized LNA Laser at 1.083 mum: Application to the Manipulation of Helium 4 Atoms.
Final rept.
N. Vansteenkiste, C. Gerz, R. Kaiser, A. Aspect, L. Hollberg, and C. Salomon. 1991, 22p.
Pub. in Jnl. Phys. II France 1, p1407-1428 1991.

Keywords: *Ring lasers, Infrared lasers, Near infrared radiation, Gas discharges, Atomic beams, Metastable state, Frequency stability, Helium 4, Reprints, *Helium spectroscopy, Laser cooling, Optical molasses.

We describe a single mode LNA ring laser, which emits 60 mW at 1.083 micrometers. Thanks to a high frequency F.M. saturated absorption technique, this laser is directly locked to an atomic line in a (4)He discharge cell. The residual frequency jitter is 130 kHz. We then present two examples of laser manipulation of helium 4 atoms in the 2 triplet S(1) metastable state, using this laser : a density increase of the atomic beam by a factor of 8, with one-dimensional optical molasses, and a selective deflection of the metastable helium beam using a laser beam with curved wavefronts.

04,305
PB95-176228 Not available NTIS
National Inst. of Standards and Technology (PL), Boulder, CO. Time and Frequency Div.
Precise Optical Frequency References and Difference Frequency Measurements with Diode Lasers.
Final rept.
S. Waltman, A. Romanovsky, J. Wells, M. P. Sassi, H. G. Robinson, R. W. Fox, and L. Hollberg. 1992, 6p.
Sponsored by National Aeronautics and Space Administration, Washington, DC. and Air Force Office of Scientific Research, Bolling AFB, DC.
Pub. in Proceedings of Society of Photo-Optical Instrumentation Engineers: Frequency-Stabilized Lasers and Their Applications, Boston, MA., November 16-18, 1992, v1837 p386-391.

Keywords: *Frequency measurement, *Difference frequency, Near infrared radiation, Semiconductor lasers, Electron transitions, Schottky diodes, Wavelengths, Heterodyning, Reprints, Frequency references.

Heterodyne methods have been used in conjunction with molecular calculations to accurately determine the wavelengths of more than 35,000 infrared transitions. We have used high speed whisker contact Schottky diodes to extend this technology to the 0.8 micrometer spectral region. Using microwave harmonic mixing, we demonstrate that it is possible to detect beat notes between diode lasers to frequencies as high as 400 GHz.

04,306
PB95-176319 Not available NTIS
National Inst. of Standards and Technology (EEEL), Gaithersburg, MD. Office of Law Enforcement Standards.
Spectrally Smooth Reflectances That Match.
Final rept.
J. A. Worthey. 1994, 2p.
Pub. in Color Research and Application 19, n5 p395-396 Oct 94.

Keywords: *Spectral reflectance, Color vision, Illuminating, Reprints, Metamerism.

This letter to the editor is a comment on William A. Thornton, 'Intersections of spectral power distributions of lights that match,' Color Res. App. 18(6): 399-410. The present author expresses support for criticisms explained at length by two non-NIST authors in a separate letter. Thornton claims generality for a result that in fact depends on arbitrary assumptions.

04,307
PB95-180030 Not available NTIS
National Inst. of Standards and Technology (PL), Gaithersburg, MD. Radiometric Physics Div.
Rayleigh Scattering Limits for Low-Level Bidirectional Reflectance Distribution Function Measurements.
Final rept.
C. Asmail, J. Hsia, A. Parr, and J. Hoeft. 1994, 8p.
Pub. in Applied Optics 33, n25 p6084-6091, 1 Sep 94.

Keywords: *Light scattering, *Rayleigh scattering, Optical measurement, Optical paths, Angular distribution, Surfaces, Nitrogen, Helium, Air, Reprints, *Bidirectional scattering distribution functions, *BSDF(Bidirectional Scattering Distribution Function).

The objective is to estimate the Rayleigh limit in bidirectional reflectance distribution function (BRDF) measurements caused by air in the laboratory, the wavelength, and the path length of light in the receiver field of view. Moreover, we intend to show the trend for the reduction of this limit by introducing a medium with small refractive index and by using a longer wavelength. Although the BRDF typically describes the angular distribution of scattered light from surfaces, the expression describing the equivalent BRDF caused by the optical scattering from gas molecules in the optical path is derived through the use of the Rayleigh scattering theory. The instrumentation is described, and the experimental results of the equivalent BRDF caused by gas scattering from molecules in clear air, nitrogen, and helium gases are reported. These results confirm the trends of the prediction.

04,308
PB95-180048 Not available NTIS
National Inst. of Standards and Technology (EEEL), Boulder, CO. Electromagnetic Technology Div.
Passively Q-Switched Nd-Doped Waveguide Laser.
Final rept.
J. A. Aust, K. J. Malone, D. L. Veasey, N. A. Sanford, and A. Roshko. 1994, 3p.
Pub. in Optics Letters 19, n22 p1849-1851, 15 Nov 94.

Keywords: *Waveguide lasers, *Neodymium lasers, Solid state lasers, Q switched lasers, Infrared lasers, Glass lasers, Near infrared radiation, Intergrated optics, Reprints.

A passively Q-switched waveguide laser operating at 1.054 micrometers has been demonstrated in a Nd-doped phosphate glass. The channel waveguide was fabricated by K-ion exchange from a nitrate melt. Passively Q-switched pulses were achieved by placement of an acetate sheet containing an organic saturable-absorbing dye within the laser cavity. The resulting pulse train consisted of pulses with a FWHM of about 25 ns and peak powers of 3.04 W. With an 80% transmitting output coupler, cw operation of the laser provided a 5.2 mW of output power at 1.054 micrometers for 229 mW of absorbed 794-nm pump power.

04,309
PB95-180261 Not available NTIS
National Inst. of Standards and Technology (PL), Gaithersburg, MD. Radiometric Physics Div.
Broadband High-Optical-Density Filters in the Infrared.
Final rept.
A. Frenkel, and Z. M. Zhang. 1994, 3p.
Pub. in Optics Letters 19, n18 p1495-1497, 15 Sep 94.

Keywords: *Infrared filters, Intermediate infrared radiation, Near infrared radiation, Cadmium tellurides, Zinc selenides, Metal films, Thin films, Substrates, Broadband, Reprints, Lexan(Trademark), Multilayers.

A new concept for the design of broadband (2-25 micrometers and beyond) neutral-density filters in the infrared region without etaloning effects is proposed and demonstrated. One important aspect of the technique is to use metallic-thin-film (10-200-nm-thick) multilayer combinations deposited onto different substrates (ZnSe, CdTe, Lexan). Neutral-density filters with optical densities as high as 4 are designed and built in the broadband region (2-25 micrometers). Another key innovation is the use of ultrathin substrates (about 100 nm thick) for elimination of etaloning effects normally present in thick (>0.5-mm) substrates. Neutral-density filters with such ultrathin substrates are also designed and investigated.

04,310
PB95-180394 Not available NTIS
National Inst. of Standards and Technology (EEEL), Boulder, CO. Electromagnetic Technology Div.
Error Propagation in Laser Beam Spatial Parameters.
Final rept.
R. D. Jones, and T. R. Scott. 1994, 10p.
Sponsored by Army Test Measurements and Diagnostic Equipment Activity, Redstone Arsenal, AL.
Pub. in Optical and Quantum Electronics 26, p25-34 1994.

Keywords: *Laser beams, Light transmission, Beam profiles, Spatial distribution, Semiconductor lasers, Error analysis, Uncertainty, Reprints, Beam analysis.

We have performed a propagation-of-errors analysis on two methods used to determine the spatial parameters of a laser beam. We measured diameters of a diode laser beam focused by a 993 mm focal length lens. Measurement uncertainties of less than 1% can result in uncertainties greater than 200% in locating the beam waist of the laser. We compare the inherent uncertainties in the spatial parameters as obtained by the two methods. Longer focal length lenses and lens position can reduce this magnification of uncertainty, but would require large propagation distances.

04,311
PB95-180485 Not available NTIS
National Inst. of Standards and Technology (EEEL), Boulder, CO. Electromagnetic Technology Div.
Modal Characteristics of Bent Dual Mode Planar Optical Waveguide.
Final rept.
A. Kumar, R. L. Gallawa, and I. C. Goyal. 1994, 4p.
Pub. in Jnl. of Lightwave Technology 12, n4 p621-624 Apr 94.

Keywords: *Optical waveguides, *Waveguide bends, Planar structures, Modal response, Dual mode, Bending, Reprints.

Modal characteristics of bent dual-mode planar optical waveguides are obtained. The bending-induced changes in the modal power distribution is found to be quite different for the two modes. Surprisingly, unlike the fundamental mode, bending causes the fractional modal power for the second mode to increase in the inner core-half and to decrease in the outer core-half of the waveguide. Interestingly, this leads to a decrease in effective index of the second mode due to bending at sufficiently high V-values.

04,312
PB95-180634 Not available NTIS
National Inst. of Standards and Technology (PL), Boulder, CO. Time and Frequency Div.
Improved Molecular Constants and Frequencies for the CO2 Laser from New High-J Regular and Hot-Band Frequency Measurements.
Final rept.
A. G. Maki, C. C. Chou, K. M. Evenson, L. R. Zink, and J. T. Shy. 1994, 14p.
Pub. in Jnl. of Molecular Spectroscopy 167, p211-224 1994.

Keywords: *Carbon dioxide lasers, *Frequencies, Intermediate infrared radiation, Frequency measurement, Electron transitions, Carbon 12, Carbon 13, Oxygen 16, Oxygen 18, Reprints, Molecular constants.

New frequencies are given for the (12)C(16)O2, (13)C(16)O2, (12)C(18)O2, and (13)C(18)O2 regular band laser transitions and for the hot-band transitions of (12)C(16)O2. These frequencies are based on a new least-squares analysis of all of the frequency measurements of these four molecular species including new high-J measurements reported here and recent absolute frequency measurements. Fourteen new high-J transitions of the regular (12)C(16)O2 laser bands have been observed, the lasers have been stabilized with sub-Doppler saturated 4.3-micrometer fluorescence, and their frequencies have been measured. Nine of these transitions fill the gap between the 9.4- and 10.4-micrometer bands. New frequency measurements are reported for 84 hot-band lines, which were also included in the reanalysis of the CO2 laser transitions.

04,313
PB95-180709 Not available NTIS
National Inst. of Standards and Technology (PL), Boulder, CO. Time and Frequency Div.
Stabilization of 3.3 and 5.1 m Lead-Salt Diode Lasers by Optical Feedback.
Final rept.
M. Murtz, M. Schaefer, M. Schneider, U. Schiessl, M. Tacke, J. S. Wells, and W. Urban. 1992, 6p.
Sponsored by National Aeronautics and Space Administration, Washington, DC. Upper Atmospheric Research Program.
Pub. in Optics Communications 94, n6 p551-556 1994.

Keywords: *Semiconductor lasers, *Laser stability, Intermediate infrared radiation, Lead inorganic salts, Frequency stability, Line narrowing, Molecular spectroscopy, Infrared lasers, Tunable lasers, Feedback, Reprints.

Optical stabilization of tunable lead-salt diode lasers (TDL) in the mid-infrared is presented for the first time. By introducing an external feedback mirror both the linewidth is substantially narrowed and the frequency of the TDL is stabilized and controlled via this mirror in a frequency-offset locked scheme. We achieved narrowing of the linewidth by 1-2 orders of magnitude or better. The TDL is offset-locked to a CO gas laser by a heterodyne technique: the beatnote between the two lasers is used to control the length of the external resonator. By this scheme we gain the capability of absolute frequency measurements with sub-Doppler accuracy. The improved spectral properties of the diode laser provide a new tool for high-resolution molecular spectroscopy in the mid-infrared.

04,314
PB95-180857 Not available NTIS
National Inst. of Standards and Technology (PL), Gaithersburg, MD. Atomic Physics Div.
Laser-Produced and Tokamak Spectra of Lithiumlike Iron, Fe(23+).
Final rept.
J. Reader, J. Sugar, N. Acquista, and R. Bahr. 1994, 5p.
Sponsored by Department of Energy, Washington, DC.
Pub. in Jnl. of the Optical Society of America B 11, n10 p1930-1934 Oct 94.

Keywords: *Iron ions, *Ultraviolet spectra, Laser-produced plasma, Multicharged ions, Tokamak devices, Electron transitions, Extreme ultraviolet radiation, Line spectra, Energy levels, Reprints, *Lithium-like ions.

Spectra of highly ionized iron were generated in a laser-produced plasma and a tokamak. In the spectra from the laser-produced plasma, new lines of Fe(23+) were observed that were identified as 3s-4p, 3p-4d, and 3d-4f transitions. The measured wavelengths of these lines were combined with measurements of the 2s-2p resonance lines measured in the tokamak plasma and with earlier measurements of n = 2 to n = 3 transitions to yield an improved system of energy levels for Fe(23+). The measured wavelengths are compared with ab initio theoretical values calculated with a Dirac-Fock code. With the 4f energy levels, which are nearly hydrogenic, an improved ionization energy of 16,503,000 + or - 1400/cm (2046.11 + or - 0.17 eV) was determined.

04,315
PB95-180899 Not available NTIS
National Inst. of Standards and Technology (EEEL), Boulder, CO. Electromagnetic Technology Div.
Antenna-Coupled High-Tc Air-Bridge Microbolometer on Silicon.
Final rept.
J. P. Rice, E. N. Grossman, and D. A. Rudman. 1994, 3p.
Pub. in Applied Physics Letters 65, n6 p773-775, 8 Aug 94.

Keywords: *Bolometers, Temperature range 0065-0273 K, High temperature superconductors, Superconducting devices, Infrared detectors, Reprints, *Microbolometers, Silicon substrates.

An antenna-coupled high-T(c) superconducting microbolometer on a silicon substrate, operating at infrared wavelengths, is described. This detector incorporates a silicon-micromachined yttria-stabilized zirconia air bridge at the feed of a planar lithographic antenna to simultaneously minimize the thermal conductance and the heat capacity of the bolometer. At an operating temperature of 87.4 K, the optical responsivity measured using a 300-K blackbody source over a 0.2-2.9 THz bandwidth is 2900 V/W, the optical noise-equivalent power (NEP) is 9 X 10(exp -12) W/Hz(exp 1/2), and the time constant is <10 microsec. This NEP is nearly a factor of 2 lower than the previous record for a liquid-nitrogen-cooled thermal detector, and the time constant is several orders of magnitude shorter.

04,316
PB95-181236 Not available NTIS
National Inst. of Standards and Technology (PL), Gaithersburg, MD. Radiometric Physics Div.
Thermal Modeling of Absolute Cryogenic Radiometers.
Final rept.
Z. M. Zhang, R. U. Datla, S. R. Lorentz, and H. C. Tang. 1994, 6p.
Pub. in Jnl. of Heat Transfer 116, p993-998 Nov 94.

Keywords: *Infrared radiometers, *Radiometers, Finite element method, Resistance thermometers, Temperature sensors, Superconducting devices, Cryogenic temperature, Recommendations, Germanium, Reprints.

This work consists of a detailed thermal modeling of two different radiometers operated at cryogenic temperatures. Both employ a temperature sensor and an electrical-substitution technique to determine the absolute radiant power entering the aperture of a receiver. Their sensing elements are different: One is a germanium resistance thermometer, and the other is a superconducting kinetic-inductance thermometer. The finite element method is used to predict the transient and steady-state temperature distribution in the receiver. Recommendations are given based on the modeling for future improvement of the dynamic response of both radiometers.

04,317
PB95-202255 Not available NTIS
National Inst. of Standards and Technology (PL), Boulder, CO. Quantum Physics Div.
High-Efficiency, High-Power Difference-Frequency Generation of 0.9-1.5 mu m Light in BBO.
Final rept.
S. Ashworth, C. Iaconis, O. Votava, and E. Riedle. 1993, 6p.
Grant NSF-PHY90-12244
Sponsored by National Science Foundation, Washington, DC.
Pub. in Optics Communications 97, p109-114 1993.

Keywords: *Near infrared radiation, Difference frequency, High power, Nonlinear optics, Light pulses, Laser radiation, Neodymium lasers, YAG lasers, Dye lasers, Reprints, *Barium borates, Barium beta borates, Nanosecond pulses.

An efficient method for generation of high energy pulsed infrared light between 0.9 and 1.5 micrometers is described. The technique uses difference frequency mixing of pulsed, visible dye and Nd:YAG laser light in a 10 mm long BBO crystal. Quantum efficiencies of up to 23% and infrared pulse energies up to 4.5 mJ are demonstrated. The low shot-to-shot fluctuations of difference frequency generation in BBO make this technique an attractive alternative to the conventional optical parametric oscillator or Raman shifting methods that are currently used to access this spectral region.

04,318
PB95-202636 Not available NTIS
National Inst. of Standards and Technology (PL), Boulder, CO. Quantum Physics Div.
Failures of the Four-Wave Mixing Model for Cone Emission.
Final rept.
R. C. Hart, L. You, A. Gallagher, and J. Cooper. 1994, 7p.
Pub. in Optics Communications 111, p331-337 1994.

Keywords: Four wave mixing, Optical pumping, Blue(Color), Pulsed lasers, Dye lasers, Strontium, Vapors, Reprints, *Cone emission.

Strontium vapor is pumped by an unfocused, single-mode, pulsed dye laser tuned near the 461 nm resonance transition. With blue laser detuning the previously reported red-shifted conical emission is present. We simultaneously resolve in angle and in frequency the emissions from this intense, near-resonant pumping of a 'two-level' atom. This quantitative spectral and angular discrimination provides uniquely detailed measurements and demonstrates a serious lack of understanding of this highly nonlinear phenomenon.

04,319
PB95-202891 Not available NTIS
National Inst. of Standards and Technology (PL), Boulder, CO. Quantum Physics Div.
Narrow-Band Tunable Diode Laser System with Grating Feedback, and a Saturated Absorption Spectrometer for Cs and Rb.
Final rept.
K. B. MacAdam, A. Steinbach, and C. Wieman. 1992, 14p.
Contract N00014-91-J-1006, Grant NSF-PHY90-12244
Sponsored by Office of Naval Research, Arlington, VA.
Pub. in American Jnl. of Physics 60, n12 p1098-1111 Dec 92.

Keywords: *Semiconductor lasers, *Tunable lasers, *Spectrometers, Near infrared radiation, Red(Color), Absorption spectra, Atomic spectroscopy, Instruction manuals, Construction, Operation, Rubidium, Cesium, Reprints, Optical feedback.

Detailed instructions for the construction and operation of a diode laser system with optical feedback are presented. This system uses feedback from a diffraction grating to provide a narrow-band continuously tuneable source of light at red or near-IR wavelengths. These instructions include machine drawings for the parts to be constructed, electronic circuit diagrams, and prices and vendors of the items to be purchased. It is also explained how to align the system and how to use it to observe saturated absorption spectra of atomic cesium or rubidium.

04,320
PB95-203071 Not available NTIS
National Inst. of Standards and Technology (EEEL), Boulder, CO. Electromagnetic Technology Div.
Decrease of Fluorescence in Optical Fiber during Exposure to Pulsed or Continuous-Wave Ultraviolet Light.
Final rept.
H. Patrick, S. L. Gilbert, and A. Lidgard. 1994, 8p.
Pub. in Optical Materials 3, p209-216 1994.

Keywords: *Optical fibers, *Radiation effects, *Fluorescence, Near ultraviolet radiation, Refractive index, Germanium additions, Boron additions, Doped materials, Blue(Color), Silica, Reprints, Bragg gratings.

We exposed optical fibers to UV light and simultaneously measured the intensity of the blue fluorescence from the fiber core. Two silica glass fibers with different core dopants were investigated: a germanium-doped fiber and a germanium-boron-codoped fiber. The fibers were exposed transversely to pulsed or continuous-wave 244 nm light for times ranging from a few minutes to over an hour. For all UV intensities and exposure times used, the fluorescence decreased during UV exposure. For a given fiber, the fractional decrease in fluorescence seen from the side of the fiber was dependent only on the total UV fluence.

04,321
PB95-203352 Not available NTIS
National Inst. of Standards and Technology (PL), Boulder, CO. Quantum Physics Div.
Frequency Shifting of Pulsed Narrow-Band Laser Light in a Multipass Raman Cell.
Final rept.
R. Sussmann, T. Weber, E. Riedle, and H. J. Neusser. 1992, 7p.
Pub. in Optics Communications 88, p408-414 1992.

Keywords: *Laser radiation, *Frequency shift, *Raman effect, Molecular spectroscopy, High resolution, Light sources, Light pulses, Optical pumping, Carbon dioxide, Hydrogen, Benzene, Narrowband, Reprints.

A multipass cell is described which allows efficient stimulated Raman frequency shifting for low pump laser intensities and low gas pressures. The latter is important for Raman shifting of narrow-band Fourier-transform limited light pulses (Delta nu = 75 MHz). It is shown that frequency broadening of the Raman shifted light can be largely avoided in the Dicke narrowing regime at low pressures. For 75 MHz pump pluses and an H2 density of 2.5 amagat, we found a negligible broadening to 90 MHz of the stimulated Stokes light. This is far below the value of 250 MHz expected from spontaneous emission. The narrow-band Stokes pulses achieved in CO2 enabled us to measure the pressure shift coefficient (-0.71 X 10(sup -2)/cm/amagat) of this gas. It is demonstrated, for the example of benzene, that our technique provides a very practical light source for high resolution molecular spectroscopy.

04,322
PB95-203469 Not available NTIS
National Inst. of Standards and Technology (PL), Boulder, CO. Quantum Physics Div.
Resonance Fluorescence with Squeezed-Light Excitation.
Final rept.
R. Vyas, and S. Singh. 1992, 15p.
Sponsored by National Science Foundation, Washington, DC.
Pub. in Physical Review A 45, n11 p8095-8109, 1 Jun 92.

Keywords: *Resonance fluorescence, Parametric oscillators, Excitation, Reprints, Squeezed light.

Resonance fluorescence from a single two-level atom driven by a beam of squeezed light is studied in the weak-field limit. We consider the situation where the atom is coupled to the ordinary vacuum and only a few field modes corresponding to the driving field are squeezed. The field produced by the degenerate optical parametric oscillator is used as the driving field. Heisenberg equations of motion are solved in the steady-state and analytic expressions for the fluorescent-light intensity and the spectrum of fluorescent light are derived. We also consider photon statistics of fluorescent light. In particular, squeezing, antibunching, and sub-Poissonian statistics of fluorescent photons are discussed, and analytic expressions for the quadrature variance and the two-time intensity correlation function are presented. Contrary to the case of coherent excitation, the second-order intensity correlation function does not factorize. This and other differences are discussed, and curves are presented to illustrate the behavior of various quantities. We also present results for thermal excitation of the atom.

04,323
PB95-203543 Not available NTIS
National Inst. of Standards and Technology (PL), Boulder, CO. Quantum Physics Div.
High-Resolution Optical Multiplex Spectroscopy.
Final rept.
M. P. Winters, C. W. Oates, J. L. Hall, and K. P. Dinse. 1992, 9p.
Contract N00014-89-J-1227, Grant NSF-PHY90-12244
Sponsored by National Science Foundation, Washington, DC. and Office of Naval Research, Arlington, VA.
Pub. in Jnl. of the Optical Society of America B 9, n4 p498-506 Apr 92.

Keywords: *Laser spectroscopy, Laser radiation, Frequency stability, High resolution, Multiplexing, Iodine, Reprints, Stochastic excitation.

We report on recent refinements in the development of high-resolution optical multiplex spectroscopy using stochastic excitation. We discuss the attainment of higher excitation bandwidths through the use of faster digital noise sources and digital filtering techniques, the active suppression of residual amplitude modulation noise, laser-frequency stabilization using an external stabilizer, and the performance of various data-analysis methods.

04,324
PB95-203550 Not available NTIS
National Inst. of Standards and Technology (EEEL), Boulder, CO. Electromagnetic Fields Div.
Integral Occurring in Coherence Theory.
Final rept.
R. C. Wittmann, and B. K. Alpert. 1994, 1p.
Pub. in Society for Industrial and Applied Mathematics Review 36, n4 p655-62 Dec 94.

Keywords: *Coherent light, *Integrals, Bessel functions, Reprints.

We evaluate a multi-dimensional integral involving cylindrical Bessel functions. This integral arose during a study of optical coherence.

04,325
PB95-203584 Not available NTIS
National Inst. of Standards and Technology (PL), Boulder, CO. Quantum Physics Div.
Cone Emission from Laser-Pumped Two-Level Atoms. 1. Quantum Theory of Resonant Light Propagation.
Final rept.
L. You, J. Mostowski, and J. Cooper. 1992, 22p.
See also Part 2, PB95-203592. Sponsored by National Science Foundation, Washington, DC.
Pub. in Physical Review A 46, n5 p2903-2924, 1 Sep 92.

Keywords: Four wave mixing, Resonance fluorescence, Laser pumping, Quantum theory, Light transmission, Reprints, *Cone emission.

This is the first of a series of papers on the theory of cone emission from a laser-pumped two-level atomic medium. Starting from microscopic quantum theory for both the active medium and the field, equations for the slowly varying macroscopic quantities are derived. In the steady-state limit, which experimentally corresponds to cw excitation, we find that the sources for the paraxial fields of interest have a long coherence length despite the random nature of spontaneous emission. These radiation sources enter into the equations for the fields in the same form as the source generated by four-wave mixing and therefore may be considered as a 'spontaneous four-wave mixing,' since the photons emitted in the Rabi sidebands are correlated. This has far-reaching consequences on the physics of cone emission and also sheds some new light on the fluorescence from strongly driven atomic systems.

04,326
PB95-203592 Not available NTIS
National Inst. of Standards and Technology (PL), Boulder, CO. Quantum Physics Div.
Cone Emission from Laser-Pumped Two-Level Atoms. 2. Analytical Model Studies.
Final rept.
L. You, J. Mostowski, and J. Cooper. 1992, 14p.
See also Part 1, PB95-203584. Sponsored by National Science Foundation, Washington, DC.
Pub. in Physical Review A 46, n5 p2925-2938, 1 Sep 92.

Keywords: Four wave mixing, Spontaneous emission, Cherenkov radiation, Resonance fluorescence, Laser pumping, Models, Reprints, *Cone emission.

We establish a mechanism, which supports Cherenkov-type radiation, as a source of cone emission. This can be considered as an additional mechanism to the previously discussed four-wave mixing (4WM) and initial encoding and follow-up refraction effects. The radiation source is provided by spontaneous emission of the driven atoms at the frequencies of interest. Due to the medium dispersion, the pump field propagates faster than the phase velocity of the field that is generated at the Rabi sideband at lower frequency. Cherenkov radiation is then possible if the source has a long correlation length, which is indeed the case despite the random nature of spontaneous emission. Coherent superposition of the source for the lower-frequency field is in an off-axis direction given by the Cherenkov radiation condition. Differences between 4WM and Cherenkov-type models are consequently resolved.

04,327
PB95-203832 Not available NTIS
National Inst. of Standards and Technology (PL), Boulder, CO. Quantum Physics Div.
Stabilization of Optical Phase/Frequency of a Laser System: Application to a Commercial Dye Laser with an External Stabilizer.
Final rept.
M. Zhu, and J. L. Hall. 1993, 15p.
Contract N00014-89-J-1227, Grant NSF-PHY90-12244
Sponsored by Office of Naval Research, Arlington, VA. and National Science Foundation, Washington, DC.
Pub. in Jnl. of the Optical Society of America B 10, n5 p802-816 May 93.

Keywords: *Continuous wave lasers, *Dye lasers, *Laser stability, Phase locked systems, Frequency stability, Power spectra, Stabilization, Reviews, Reprints.

We present a comprehensive and quasi-tutorial review of the theory for analyzing the optical power spectrum of an optical field that has noise modulations of both the amplitude and the phase. We also present experimental results of the frequency stabilization of a commercial dye laser to a high-finesse Fabry-Perot cavity (0.49-Hz resulting full linewidth) and of the optical phase locking of the dye laser to a second reference laser (putting 97% of the optical power into the carrier) using an external stabilizer scheme. This external optical phase/frequency stabilization technique can be applied to virtually any cw laser system.

04,328
PB95-260758 PC A06/MF A02
National Inst. of Standards and Technology (PL), Gaithersburg, MD. Radiometric Physics Div.
45 deg/0 deg Reflectance Factors of Pressed Polytetrafluoroethylene (PTFE) Powder.
Technical note.
P. Y. Barnes, and J. J. Hsia. Jul 95, 110p, NIST/TN-1413.
Also available from Supt. of Docs. as SN003-003-03352-9.

Keywords: *Reflectance, *Standards, *Powder(Particles), *Polytetrafluoroethylene, Reflectometers, Synthetic resins, Difluoro compounds, Quality control, Optical measuring instruments, *Reflectance factors, PTFE resins.

Pressed polytetrafluoroethylene (PTFE) powder is used for 45 deg. /0 deg. reflectance factor standards. The radiometric and spectrophotometric measurements community such as the Council for Optical Radiation Measurements (CORM) has demonstrated the need for such a standard and its application to quality control and quantity assessment. This publication briefly describes the instrumentation used for the 45 deg./ 0 deg. reflectance factor measurements of pressed PTFE powder from 380 nm to 770 nm. Also, the variations of 45 deg./0 deg. reflectance factor with sample preparation and materials are discussed. The expanded uncertainty at a coverage factor of two for

the 45 deg./0 deg. reflectance factors of pressed PTFE powder range from 0.009 to 0.017.

04,329
PB95-261913 (Order as PB95-261897, PC A07/MF A02)
National Inst. of Standards and Technology, Gaithersburg, MD.
Intercomparison of Photometric Units Maintained at NIST (USA) and PTB (Germany), 1993.
Y. Ohno, and G. Sauter. 1995, 13p.
Prepared in cooperation with Physikalisch-Technische Bundesanstalt, Brunswick (Germany, F.R.). Abt. Optik und Photometrie.
Included in Jnl. of Research of the National Institute of Standards and Technology, v100 n3 p227-239 May/Jun 95.

Keywords: *Interlaboratory comparisons, *Calibration standards, *Photometers, *Luminous intensity, Lumens, Flux density, Canada, United States, Germany(Unified), Photometric responsivity, National Institute of Standards and Technology, PTB(Germany).

A bilateral intercomparison of photometric units between NIST, USA and PTB, Germany has been conducted to update the Knowledge of the relationship between the Photometric units diseminated in each country. The luminous intensity unit (cd) and the luminous flux unit (lm) maintained at both laboratories are compared by circulating transfer standard lamps. Also, the photometric responsivity s(sub v) is compared by circulating a lambda-corrected detector with a built-in current-to-voltage converter. The results show that the difference of luminous intensity unit between NIST and PTB, (PTB-NIST)/NIST, is 0.2% with a relative expanded uncertainty (coverage factor k=2) of 0.24%. The difference is reduced significantly from that at the 1985 CCPR intercomparison (0.9%).

04,330
PB96-102215 Not available NTIS
National Inst. of Standards and Technology (PL), Boulder, CO. Time and Frequency Div.
Sub-Doppler Frequency Measurements on OCS at 87 THz (3.4 mu m) with the CO Overtone Laser.
Final rept.
A. Dax, J. S. Wells, L. Hollberg, A. G. Maki, and W. Urban. 1994, 13p.
See also PB95-128633. Sponsored by National Aeronautics and Space Administration, Washington, DC.
Pub. in Jnl. of Molecular Spectroscopy 168, p416-428 1994.

Keywords: *Carbonyl compounds, *Sulfides, *Lasers, *Frequency measurement, Calibrating, Standards, Polarization, Molecular spectroscopy, Wavelengths, Tables(Data), Reprints, *Sub-Doppler frequencies.

Sub-Doppler frequency measurements have been made on three transitions of OCS in the 87-THz region (near 2900 1/cm). The CO overtone laser was used as the saturating laser. Polarization spectroscopic techniques utilizing optical heterodyne detection were used to observe the features and subsequently provide the discriminant for locking the overtone laser to the OCS transitions. A CO2 laser synthesizer was used to measure the frequency of the CO overtone laser and thereby measure the frequencies of the OCS lines. The resulting frequencies of the three new measurements are given. These new numbers have been fitted along with more than 5700 other data points in our OCS data bank and improved constants have been obtained. These latest constants are used to calculate updated calibration tables containing values with much smaller uncertainties; three such tables are included.

04,331
PB96-102553 Not available NTIS
National Inst. of Standards and Technology (EEEL), Boulder, CO. Optoelectronics Div.
Characterization of a Clipped Gaussian Beam.
Final rept.
1995, 15p.
Pub. in Proceedings of Society of Photo-Optical Instrumentation Engineers: Beam Control, Diagnostics, Standards, and Propagation, San Jose, CA., February 6-7, 1995, v2375 p360-374.

Keywords: *Laser beams, Light transmission, Beam profiles, Divergence, Irradiance, Wave propagation, Width, Slits, Diffraction, Reprints, Times diffraction limit.

The authors calculated irradiance distributions resulting from clipping a Gaussian beam with hard-edged slits transmitting 99 or 95 percent of the incident power. The authors determined the widths -- second moment (with 8- and 12-bit resolution), scanning slit, and knife-edge -- of these profiles at several distances from the source, both with and without a focusing lens. When using a lens, they had the option of determining the characterization parameters from two beam width measurements and one axial distance, or from a least-squares fit of several beam width measurements and axial distances. Finite resolution of irradiance, inherent in any measurement device, truncates integrals necessary for calculation of the second moment of irradiance distributions.

04,332
PB96-102736 Not available NTIS
National Inst. of Standards and Technology (PL), Boulder, CO. Quantum Physics Div.
Delivering the Same Optical Frequency at Two Places: Accurate Cancellation of Phase Noise Introduced by an Optical Fiber or Other Time-Varying Path.
Final rept.
L. S. Ma, P. Jungner, J. Ye, and J. L. Hall. 1994, 3p.
Sponsored by Office of Naval Research, Arlington, VA. and National Science Foundation, Arlington, VA.
Pub. in Optics Letters 19, n2 p1777-1779, 1 Nov 94.

Keywords: *Phase noise, *Doppler radar, Reprints, Cancellation, Noise, *Optical radar, Optical fiber.

Although a single-mode optical fiber is a convenient and efficient interface/connecting medium, it introduces phase-noise modulation, which corrupts high-precision frequency-based applications by broadening the spectrum toward the kilohertz domain. We describe a simple double-pass fiber noise measurement and control system, which is demonstrated to provide millihertz accuracy of noise cancellation.

04,333
PB96-102843 Not available NTIS
National Inst. of Standards and Technology (PL), Gaithersburg, MD. Radiometric Physics Div.
New Method for Realizing a Luminous Flux Scale Using an Integrating Sphere with an External Source.
Final rept.
Y. Ohno. 1995, 10p.
Pub. in Jnl. of the Illuminating Engineering Society 24, n1 p106-115 1995.

Keywords: *Luminous flux, *Optical measurement, Reprints, Lumens, Light sources, Computerized simulation, Integrating spheres, Calibration.

A method is proposed to realize a total luminous flux scale (lumens) using an integrating sphere with a known amount of flux introduced from an external source. The integrating sphere features an opening for a detector, a test lamp in its center, a baffle between the test lamp and the detector. A second opening is used to introduce flux from an external source, and is appropriately baffled from the test lamp. Flux from the external source is introduced into the sphere through limiting aperture of known area. The flux entering the sphere is determined from knowledge of the illuminance on the aperture plane and the area of the aperture. The total flux from the test lamp is deduced by comparison to the flux from the external source. Theoretical analysis was first made by computer simulation based on a ray tracing technique. Several integrating sphere designs were analyzed under various conditions, and based on the results of the simulation, an integrating sphere 50 cm in diameter was built to conduct experimental analysis. The characteristics of the sphere were measured and compared with the simulation results. The total luminous flux values of several miniature lamps measured with this method were found to agree within 0.5% with measurements using goniophotometric technique. This method can be applied also to realize a total spectral radiant flux scale.

04,334
PB96-111638 Not available NTIS
National Inst. of Standards and Technology (PL), Gaithersburg, MD. Atomic Physics Div.
Improved Wavelengths for Prominent Lines of Fe XX to Fe XXIII.
Final rept.
J. Sugar, and W. L. Rowan. 1995, 3p.
Pub. in Jnl. of the Optical Society of America B, v12 n8 p1403-1405, 13 Aug 95.

Keywords: *Iron, *Line spectra, *Wavelengths, Ionization, Laser plasmas, Intensity, Energy levels, Tokamak devices, Electron transitions, Charged particles, Reprints.

New measurements of 26 spectral lines of highly ionized Fe in the range of 91-263 Angstroms have been carried out with a wavelength uncertainty of + or - 5 mAngstroms. The light source was the TEXT tokamak at the University of Texas in Austin. Lines of Be-like, C-like, and N-like Fe are included, with visually estimated intensities, the best previous measurements, and energy-level classifications. Level values are derived from these wavelengths and from known magnetic dipole (M1) lines.

04,335
PB96-111950 Not available NTIS
National Inst. of Standards and Technology (EEEL), Boulder, CO. Electromagnetic Technology Div.
Glasses for Waveguide Lasers.
Final rept.
K. J. Malone, D. L. Veasey, N. A. Sanford, and J. S. Hayden. 1994, 13p.
Pub. in Proceedings of Society of Photo-Optical Instrumentation Engineers: Properties and Characteristics of Glass III, San Diego, CA., July 28-29, 1994, v2887 p75-87.

Keywords: *Glass, *Optical systems, Reprints, Ion exchange, Neodymium, Erbium, Waveguide lasers.

Waveguide lasers formed by ion exchange in rate-earth-doped glasses have emerged as an attractive new technology on the threshold of commercial insertion. These devices can be used as both laser oscillators and optical amplifiers. In this article, we review ion exchange and glass composition. We then discuss the performance of ion-exchanged waveguide lasers made in silicate and phosphate glasses.

04,336
PB96-113535 PC A05/MF A01
National Inst. of Standards and Technology, Gaithersburg, MD.
Journal of Research of the National Institute of Standards and Technology, November/December 1994. Volume 99, Number 6.
1994, 92p.
See also PB96-113543 through PB96-113584 and PB95-169371. Also available from Supt. of Docs.

Keywords: *Research and development, *Metrology, *Standards, Interlaboratory comparisons, Quality assurance, Pressure, Temperature, Optical equipment, Radiators, Magnetohydrodynamics, NIST(National Institute of Standard and Technology).

No abstract available.

04,337
PB96-113576 (Order as PB96-113535, PC A05/MF A01)
National Inst. of Standards and Technology, Gaithersburg, MD.
Beamcon III, a Linearity Measurement Instrument for Optical Detectors.
A. Thompson, and H. M. Chen. 1994, 5p.
Prepared in cooperation with Alabama Univ. in Huntsville. Dept. of Electrical and Computer Engineering.
Included in Jnl. of Research of the National Institute of Standards and Technology, v99 n6 p751-755 Nov/Dec 94.

Keywords: *Optical detection, *Beams(Radiation), *Linearity, Detectors, Radiation measuring instruments, Silicon, Photodiodes, *Beam addition method, NIST(National Institute of Standards and Technology).

The design and operation of Beamcon III, the latest linearity measurement instrument using the beam addition method in the detector metrology program at the National Institute of Standards and Technology, is described. The primary improvements in this instrument are the reduction of stray radiation to extremely low levels by using three well-baffled chambers, a larger dynamic range, and an additional source entrance port. A polynomial response function is determined from the data obtained by this instrument using a least-squeares method. The linearity of a silicon photodiode-amplifer detector system was determined to be within 0.054% (2 sigma estimate) over nine decades of signal.

04,338
PB96-119292 Not available NTIS
National Inst. of Standards and Technology (EEEL), Boulder, CO. Optoelectronics Div.

Magnetooptic Effects.
Final rept.
M. N. Deeter, G. W. Day, and A. H. Rose. 1995, 36p.
Pub. in CRC Handbook of Laser Science and Technology, Supplement 2: Optical Materials, Section 9.1, p367-402 1995.

Keywords: *Magnetooptics, *Faraday effect, *Kerr magnetooptical effect, Liquid crystals, Birefringence, Magnetohydrodynamics, Ferromagnetic materials, Paramagnetic materials, Diamagnetism, Ferrimagnetic materials, Antiferromagnetism, Reprints.

We review the orgins and applications of various magneto-optic effects, including the Faraday and Kerr effects, and magnetic linear birefringence. Mathematically, we show how all of these effects can be derived from a single dielectric tensor. We then consider the characteristics of magneto-optic effects in specific material classes, including diamagnetic, paramagnetic, ferromagnetic, ferrimagnetic, and antiferromagnetic materials. Relevant data for each class are summarized in tabular format. Finally, both scientific and commerical applications of magneto-optic materials are described.

04,339
PB96-119581 Not available NTIS
National Inst. of Standards and Technology (PL), Boulder, CO. Quantum Physics Div.
Doppler-Free Spectroscopy of Large Polyatomic Molecules and van der Waals Complexes.
Final rept.
H. J. Neusser, E. Riedle, T. Weber, and E. W. Schlag. 1992, 7p.
Pub. in Topics in Applied Physics, v70 p205-212 1992.

Keywords: *Tunable lasers, *Laser spectroscopy, *Benzene, *Polyatomic molecules, Spectral line width, Molecular structure, Energy distribution, Electronic spectra, Ultraviolet spectra, Van der Waals forces, Chemical bonds, Coupling, Reprints, *Doppler-free spectroscopy, Molecular clusters, Coriolis coupling.

It is shown that high-resolution spectroscopy with tunable dye lasers leads to rotationally resolved electronic spectra of large molecular systems. Two-photon absorption of narrow-band cw light in an external cavity eliminates Doppler broadening in the S(sub 1) inversely maps to S(sub 0) transition of the prototype organic molecule benzene. Several thousands of rotational lines in the room temperature spectrum are analyzed, providing spectroscopic constants with a hitherto inaccessible precision. Investigations of the homogeneous linewidth of individual rotational transitions reveals that Coriolis coupling plays an important role in the intramolecular energy redistribution process in this moloecule. Rotationally resolved UV spectra of benzene-noble-gas van der Waals clusters were measured. These measurements yield precise information on the van der Waals bond lengths and structures of these complexes.

04,340
PB96-119599 Not available NTIS
National Inst. of Standards and Technology (EEEL), Boulder, CO. Electromagnetic Technology Div.
Using Secondary Ion Mass Spectrometry (SIMS) to Characterize Optical Waveguide Materials.
Final rept.
S. W. Novak, J. M. Zavada, and K. Malone. 1994, 2p.
Pub. in Proceedings of the Annual MAS Meeting (28th), Microbeam Analysis Society, New Orleans, LA., July 31-August 5, 1994, p167-168.

Keywords: *Optical waveguides, *Mass spectroscopy, Measuring instruments, Lithium niobates, Oxides, Glass, Diffusion, Ion implantation, Refractivity, Titanium, Silver, Reprints, SIMS(Secondary Ion Mass Spectrometry).

Secondary ion mass spectrometry (SIMS) has proven to be a versatile technique to obtain depth resolved information on optical waveguides in materials such as LiNbO3, LiTaO3 and glasses. Optical waveguides are typically formed by diffusing an element into the material to cause a localized change in its refractive index. In LiNbO3 this is done using Ti indiffusion from a deposited metal film or proton exchange in an acid bath. Optical waveguides in glasses have been made using Ag indiffusion from AgNO3 solutions. SIMS instruments have been used to obtain depth profiles of planar waveguides using either a normal-incidence electron gun in a magnetic sector SIMS instrumental or a quadrupole-based SIMS instrument.

04,341
PB96-119623 Not available NTIS
National Inst. of Standards and Technology (PL), Boulder, CO. Time and Frequency Div.
Far Infrared Laser Frequencies of CH3OD and N2H4.
Final rept.
H. E. Radford, K. M. Evenson, F. Matushima, T. J. Sears, L. R. Zink, and G. P. Galvao. 1991, 6p.
Pub. in International Jnl. of Infrared and Millimeter Waves, v12 n10 p1161-1166 1991.

Keywords: *Lasers, *Methyl alcohol, *Hydrazine, Optical pumping, Reprints, Frequency measurements, Molecular laser lines.

The frequencies of 26 laser lines with wavelengths between 57 and 534 um have been measured in the optically pumped laser gases CH3OD and N2H4. A pair of stabilized cw 12CO2 lasers was used as a frequency standard for the heterodyne frequency measurements. Seven of the 26 lines are new.

04,342
PB96-119672 Not available NTIS
National Inst. of Standards and Technology (EEEL), Boulder, CO. Electromagnetic Technology Div.
Standard Polarization Components: Progress Toward an Optical Retardance Standard.
Final rept.
K. B. Rochford, P. A. Williams, A. H. Rose, G. W. Day, I. G. Clarke, and P. D. Hale. 1994, 7p.
Pub. in Society of Photo-Optical Instrumentation Engineers, Polarization Analysis and Measurement II, San Diego, CA., July 25-27, 1994, v2265 p2-8.

Keywords: *Birefringence, Reprints, Polarization, Metrology, Waveplate, *Optical retardance, Quartwave retarder.

NIST is developing a quarterwave linear retarder designed to have a retardance stable within 0.1 degree over a variety of operational and environmental conditions. In this paper the authors review several design strategies and early results of this effort. These have led to a promising prototype design consisting of a double rhomb TIR retarder constructed from a low stress-optic glass. The authors also review several measurement methods that are used in their evaluations.

04,343
PB96-119680 Not available NTIS
National Inst. of Standards and Technology (EEEL), Boulder, CO. Electromagnetic Technology Div.
Improved Annealing Technique for Optical Fiber.
Final rept.
A. H. Rose, Z. B. Ren, and G. W. Day. 1994, 4p.
Pub. in International Conference on Optical Fibre Sensors (10th), Glasgow, Scotland, UK, October 11-13, 1994, v2360 p306-309.

Keywords: *Birefringence, Reprints, *Foreign technology, *Current sensing, *Fiber annealing.

The authors demonstrate that twisting a fiber a few turns per meter before it is annealed largely eliminates the residual linear bierefringence. This dramatically improves the yield of annealed coils for current sensing and makes it possible to use fibers that previously could not be successfully annealed. It is believed that twisting is effective because the residual birefringence is associated with core ellipticity and this contribution is averaged to near zero by twisting. The authors also show the temperature stability of sensors made with this new technique.

04,344
PB96-119805 Not available NTIS
National Inst. of Standards and Technology (EEEL), Boulder, CO. Electromagnetic Technology Div.
Standard Reference Materials for Optical Fibers and Connectors.
Final rept.
M. Young. 1995, 2p.
Pub. in Proceedings: Optical Fiber Communication Conference, San Diego, CA., February 26-March 3, 1995, v8 p239-240.

Keywords: *Microscopes, *Optical fibers, Reprints, Conforal, Gray scale, Interference, Micrometers, Video, Communications.

This paper outlines the development of a standard of fiber cladding diameter and the three instruments - a micrometer, a scanning confocal microscope, and a white-light interference microscope - that were crucial to that development. An international round robin yielded agreement generally with 0.1 micometers. The authors are planning other artifact standards.

04,345
PB96-122643 Not available NTIS
National Inst. of Standards and Technology (EEEL), Boulder, CO. Electromagnetic Technology Div.
Decay of Bragg Gratings in Hydrogen-Loaded Optical Fibers.
Final rept.
H. Patrick, and S. L. Gilbert. 1995, 2p.
Pub. in OFC '95 Optical Fiber Communication, San Diego, CA., February 26-March 3, 1995, v8 p179-180 1995.

Keywords: *Optical fibers, *Hydrogen, *Gratings(Spectra), Annealing, Doping, Photosensitivity, Ultraviolet radiation, Reflectance, Reprints, Bragg gratings, Doped fibers, Hydrogen-loading.

Bragg gratings written in hydrogen-loaded optical fibers showed a larger decrease in reflectivity than gratings in non-hydrogen-loaded fibers after 10 hours at 100 degrees C and after 18 days at room temperature.

04,346
PB96-122957 Not available NTIS
National Inst. of Standards and Technology (EEEL), Boulder, CO. Electromagnetic Technology Div.
Growth Characteristics of Fiber Gratings.
Final rept.
S. L. Gilbert, and H. Patrick. 1994, 2p.
Pub. in Proceedings of the LEOS '94 Symposium on Photoinduced Devices in Optical Fibers and Waveguides (IEEE Lasers and Electro-Optics Society 1994 Annual Meeting), Boston, MA., October 31-November 3, 1994, p131-132.

Keywords: *Gratings, *Fiber optics, Bragg angle, Optical fibers, Ultraviolent radiation, Reprints, *Fiber gratings.

We have measured the time and UV intensity dependence of the growth of Bragg gratings in germanium-doped and germanium-boron-codoped optical fiber. We compare this with the change in blue fluorescence and theoretical predictions. We find that the index change during UV exposure is correlated with a decrease in fluorescence and that a simple one-photon model for defect absorption does not explain the time and intensity dependence of the grating growth.

04,347
PB96-122973 Not available NTIS
National Inst. of Standards and Technology (PL), Boulder, CO. Quantum Physics Div.
Introduction to Phase-Stable Optical Sources.
Final rept.
J. L. Hall, and M. Zhu. 1992, 32p.
Contract AFOSR91-0283, Grant NSF-PHY90-12244
Sponsored by National Science Foundation, Washington, DC., Air Force Office of Scientific Research, Bolling AFB, DC. and Office of Naval Research, Arlington, VA.
Pub. in Proceedings of the International School of Physics 'Enrico Fermi', Course CXVIII, Laser Manipulation of Atoms and Ions, Varenna, Italy, July 9-19, 1991, p671-702.

Keywords: *Lasers, Reprints, *Foreign technology, *Superstable lasers, High resolution laser spectroscopy, Laser cooled atoms.

This lecture deals with one of the impressive and exciting topics of our time--the development and application of superstable lasers. Their relevance to this school arises in large measure from the incipient marriage of such stable laser sources with the remarkable samples of free-floating quantum absorbers which can be assembled. Manipulated and cooled using light forces on atoms--the later forming the main course of our study here. In addition, such gas samples and stable laser sources represent now in many cases the tools of choice in ultra-precise experiments designed to test our cherished beliefs about the fundamental physical laws. Indeed, a large number of important and impressive measurements have already been carried out using stable-laser techniques. Still, many of us in the field believe that the best is just ahead, becoming freshly enabled in a significant number of examples by progress in the 'atom manipulation business'.

04,348
PB96-123609 Not available NTIS
National Inst. of Standards and Technology (EEEL), Boulder, CO. Electromagnetic Technology Div.
Optical Sampling Using Nondegenerate Four-Wave Mixing in a Semiconductor Laser Amplifier.
Final rept.
M. Jinno, J. B. Schlager, and D. L. Franzen. 1994, 2p.
See also PB96-122502.
Pub. in Electronics Letters, v30 n18 p1489-1490 Sep 94.

Keywords: *Laser amplifiers, Semiconductors, Reprints, *Multiwave mixing, *Optical sampling, High speed optical techniques.

Picosecond optical sampling using nondegenerate four-wave mixing in a semiconductor laser amplifier (SLA) is demonstrated for the first time. High-peak-power pulses and electrical gating of the SLA produce an optical sampling signal-to-noise ratio.

04,349
PB96-126180 PC A05/MF A01
National Inst. of Standards and Technology, Gaithersburg, MD.
Journal of Research of the National Institute of Standards and Technology, March/April 1995. Volume 100, Number 2.
1995, 96p.
See also PB96-126198, PB96-126206, and PB96-113535. Also available from Supt. of Docs.

Keywords: *Meetings, *Research and development, *Periodicals, *National Institute of Standards and Technology(NIST).

The Journal of Research of the National Institute of Standards and Technology features advances in measurement methodology and analyses consistent with the NIST responsibility as the nation's measurement science laboratory. It includes reports on instrumentation for making accurate and precise measurements in fields of physical science and engineering, as well as the mathematical models of phenomena which enable the predictive determination of information in regions where measurements may be absent. Papers on critical data, calibration techniques, quality assurance programs, and well-characterized reference materials reflect NIST programs in these areas. Special issues of the Journal are devoted to invited papers in a particular field of measurement science. Occasional survey articles and conference reports appear on topics related to the Institute's technical and scientific programs.

04,350
PB96-135199 Not available NTIS
National Inst. of Standards and Technology (PL), Boulder, CO. Quantum Physics Div.
Frequency-Stabilized Lasers: A Driving Force for New Spectroscopies.
Final rept.
J. L. Hall. 1994, 23p.
See also PB95-153771.
Pub. in 1992 International School of Physics 'Enrico Fermi', Italy, p217-239 1994.

Keywords: *Laser stability, *Laser spectroscopy, *Standards, Frequency stability, High resolution, Optical measurement, Laser cavities, Reprints, Saturated absorption spectroscopy.

It is particularly appropriate to consider the evolution of stabilized lasers within the context of a Fermi School concerned with the Frontiers of Laser Spectroscopy, as the stabilization of lasers has clearly provided one of the stimulating influences for the development of new spectroscopic methods.

04,351
PB96-137757 Not available NTIS
National Inst. of Standards and Technology (MEL), Gaithersburg, MD. Precision Engineering Div.
Visualization of Surface Figure by the Use of Zernike Polynomials.
Final rept.
C. J. Evans, R. E. Parks, P. J. Sullivan, and J. S. Taylor. 1995, 5p.
Pub. in Applied Optics, v34 n34 p7815-7819 Dec 95.

Keywords: *Interferometers, *Optical testing, Reprints, Zernike polynomials, Power spectral density.

Commercial software in modern interferometers used in optical testing frequently fit the wave-front or surface-figure error to Zernike polynomials; typically 37 coefficients are provided. We provide visual representation of these data in a form that may help optical fabricators decide how to improve their process or how to optimize system assembly.

04,352
PB96-138482 Not available NTIS
National Inst. of Standards and Technology (MEL), Gaithersburg, MD. Precision Engineering Div.
Test of a Slow Off-Axis Parabola at Its Center of Curvature.
Final rept.
R. E. Parks, C. J. Evans, and L. Shao. 1995, 5p.
Pub. in Applied Optics, v34 n31 Nov 95.

Keywords: *Optical testing, Interferometry, Reprints, *Zernike polynomials, *Off-axis aspherics.

The authors describe the interferometric testing of a slow (F/16 at the center of curvature) off-axis parabola, intended for use in an x-ray spectrometer, that uses a spherical wave front matched to the mean radius of the asphere. The authors find the figure error in the off-axis mirror by removing the theoretical difference between the off-axis segment and the spherical reference from the measured wave-front error. This center of curvature test is easy to perform because the spherical reference wave front has no axis and thus alignment is trivial. The authors confirm that the test results are the same as the double-pass null test for a parabola that uses a plane autocollimating mirror. They also determine that the off-axis section apparently warped as the result of being cut from the symmetric parent part.

04,353
PB96-140371 Not available NTIS
National Inst. of Standards and Technology (EEEL), Boulder, CO. Electromagnetic Technology Div.
Inexpensive Laser Cooling and Trapping Experiment for Undergraduate Laboratories.
Final rept.
C. Wieman, G. Flowers, and S. Gilbert. 1995, 14p.
Pub. in American Jnl. of Physics, v63 n4 p317-330 Apr 95.

Keywords: *Laboratories, Spectroscopy, Rubidium, Reprints, *Laser cooling, *Laser trapping, Vapor cell trap.

We present detailed instructions for the construction and operation of an inexpensive apparatus for laser cooling and trapping of ribidium atoms. This apparatus allows one to use the light from low power diode lasers to produce a magneto-optical trap in a low pressure vapor cell. We present a design which has reduced the cost to less than $3000 and does not require any matching or glassblowing skills in the construction. It has the additional virtues that the alignment of the trapping laser beams is very easy, and the rubidium pressure is conveniently and rapidly controlled. These features make the trap simple and reliable to operate, and the trapped atoms can be easily seen and studied. With a few milliwatts of laser power we are able to trap 4 x 10 to the 7th power atoms for 3.5 s in this apparatus. A step-by-step procedure is given for construction of the cell, setup of the optical system, and operation of the trap. A list of parts with prices and vendors is given in the Appendix.

04,354
PB96-140405 Not available NTIS
National Inst. of Standards and Technology (EEEL), Boulder, CO. Optoelectronics Div.
Thermal Modeling and Analysis of Laser Calorimeters.
Final rept.
Z. M. Zhang, D. J. Livigni, R. D. Jones, and T. R. Scott. 1995, 11p.
Pub. in ASME/AIAA National Heat Transfer Conference, Portland, OR., August 6-9, 1995, AIAA 95-3520, p1-11.

Keywords: *Calorimeters, *Laser radiation, Measurements, Thermal analysis, Reprints.

We performed detailed thermal analysis and modeling of the C-series laser calorimeters at the National Institute of Standards and Technology for calibrating laser power or energy meters. A finite-element method was employed to simulate the space and time dependance of temperature at the calorimeter receiver. The inequivalence in the temperature response caused by different spatial distributions of the heating power was determined. The inequivalence between electrical power applied to front and rear portions of the receiver is approximately 1.7 percent, and the inequivalence between the electrical and laser heating is estimated to be less than 0.05 percent. The computational results are in good agreement with experiments at the 1 percent level. The effects of the deposited energy, power duration, and relaxation time on the calibration factor and cooling constant were investigated. This paper provides information for the future design improvement on the laser calorimeters.

04,355
PB96-141031 Not available NTIS
National Inst. of Standards and Technology (EEEL), Boulder, CO. Optoelectronics Div.
Deep-UV Excimer Laser Measurements at NIST.
Final rept.
R. W. Leonhardt, and T. R. Scott. 1995, 12p.
Pub. in Society of Photo-Optical Instrumentation Engineers: The International Society for Optical Engineering, Santa Clara, CA., February 20-22, 1995, v2439 p448-459.

Keywords: *Eximer lasers, *Beamsplitters, *Calorimeters, Dosage, Reprints, Volume absorbers.

The National Institute of Standards and Technology has designed and built two electrically calibrated laser calorimeters as primary standards for absolute energy measurements at the wavelength of 248 nm. Under the sponsorship of SEMATECH, NIST developed the calorimeters to improve measurements of dose energy in excimer laser based microlithography. The calorimeter system can be used to calibrate transfer standards which in turn can be used to calibrate detectors employed for energy measurements of semiconductor wafer exposure. The excimer calorimeter uses a glass filter which functions as a volume absorber that allows collection of nanosecond pulses of laser radiation without suffering damage. The measurement range of the calorimeters is 0.3-25 J, but can be extended to 1 mJ with beamsplitters. Electrical calibration of the calorimeters shows a standard deviation in the calibration factor of less than 0.5 percent for entire energy range. The total uncertainty of typical power and energy meter calibrations is approximately 2 percent.

04,356
PB96-141072 Not available NTIS
National Inst. of Standards and Technology (PL), Gaithersburg, MD. Electron and Optical Physics Div.
Atom-Optical Properties of a Standing-Wave Light Field.
Final rept.
J. J. McClelland. 1995, 8p.
Pub. in Jnl. of the Optical Society of America B, v12 n10 p1761-1768 Oct 95.

Keywords: *Atomic optics, *Lithography, Lasers, Standing waves, Reprints, Dipole force, Paraxial approximation.

The focusing of atoms to nanometer-scale dimensions by a near-resonant standing-wave light field is examined from a particle optics perspective. The classical equation of motion for atoms traveling through the lens formed by a node of the standing wave is derived and converted to a spatial trajectory equation. A paraxial solution is obtained, which results in simple expressions for the focal properties of the lens, useful for estimating its behavior. Aberrations are also discussed, and an exact numerical solution of the trajectory equation is presented. The effects on focal linewidth of angular collimation and velocity spread in the atomic beam are investigated, and it is shown that angular collimation has much more significant effect than velocity spread, even when the velocity spread is thermal.

04,357
PB96-141197 Not available NTIS
National Inst. of Standards and Technology (EEEL), Boulder, CO. Electromagnetic Technology Div.
Vector and Quasi-Vector Solutions for Optical Waveguide Modes Using Efficient Galerkin's Method with Hermite-Gauss Basis Functions.
Final rept.
A. Weisshaar, R. L. Gallawa, and I. C. Goyal. 1995, 6p.
Pub. in Jnl. of Lightwave Technology, v13 n8 p1795-1800 Aug 95.

Keywords: *Optical waveguides, Galerkin method, Reprints, *Scalar approximation, *Polarization, Vector solution, Basis functions.

An efficient vector formulation and corresponding quasi-vector formulation for the analysis of optical

waveguides are presented. The proposed method is applicable to a large class of optical waveguides with general refractive index profile in a finite region of arbitrary shape and surrounded by a homogenous cladding. The vector formulation is based on Galerkin's procedure using Hermite-Gauss basis functions. It is shown that use of Hermite-Gauss basis functions leads to a significant increase in computational efficiency over trigonometric basis functions. The quasi-vector solution is obtained from the standard scalar formulation by including a polarization correction. The accuracy of the scalar, vector, and quasi-vestor solutions is demonstrated by comparison with the exact solution for the fundamental mode in a circular fiber. Comparison of the model solutions obtained with the various methods for optical wave-guides with square, rectangular, circular, and elliptical core demonstrate the accuracy and advantage of the quasi-vector solution.

04,358
PB96-147103 Not available NTIS
National Inst. of Standards and Technology (PL), Gaithersburg, MD. Radiometric Physics Div.
Absolute Response Calibration of a Transfer Standard Cryogenic Bolometer.
Final rept.
G. Eppeldauer, A. L. Migdall, T. R. Gentile, and C. L. Cromer. 1995, 11p.
Pub. in Proceedings Reprint, Society of Photo-Optical Instrumentation Engineers: The International Society for Optical Engineering, San Diego, CA., July 11-12, 1995, v2550 p36-46.

Keywords: *Bolometers, *Calibration, Standards, Reprints, Cryogenic radiometer, Infrared detector, Spectral response.

A cryogenic bolometer has been developed for use as a transfer standard in an ambient temperature infrared detector response comparator facility at the National Institute of Standards and Technology (NIST). Issues affecting calibration of the bolometer response were studied and a calibration procedure was developed. These issues included frequency dependence, stability, repeatability, and spectral flatness. The relative spectral response as determined from the reflectance of the bolometer absorber and the transmittance of the bolometer window. The bolometer calibration has been tied to the NIST primary standard High Accuracy Cryogenic Radiometer (HACR) using a silicon trap detector and a pyroelectric detector.

04,359
PB96-148028 Not available NTIS
National Inst. of Standards and Technology (EEEL), Boulder, CO. Electromagnetic Technology Div.
Partially Coherent Transmittance of Dielectric Lamellae.
Final rept.
E. N. Grossman, and D. G. McDonald. 1995, 7p.
Pub. in Optical Engineering, v34 n5 p1289-1295 May 95.

Keywords: *Dielectrics, *Lamella, *Transmittance, Interferometers, Fourier transformations, Coherence, Surface roughness, Microstructure, Reprints, Nonparallelism, Fabry-Perot fringes.

The authors derive an analytic formula for the transmittance of a dielectric lamella when the interference between successive internal reflections is only partially spatially coherent. This allows effects such as surface roughness and nonparallelism, which produce cumulative distortions in the phase front with each reflection, and which result in a loss of fringe contrast at high frequencies, to be accounted for quantitatively. The transmittance of a Si lamella agrees with the authors' formula to within the accuracy of the data, which is dominated by systematic instrumental effects.

04,360
PB96-154422 PC A05/MF A01
National Inst. of Standards and Technology (EEEL), Boulder, CO. Optoelectronics Div.
Optical Fiber, Fiber Coating, and Connector Ferrule Geometry: Results of Interlaboratory Measurement Comparisons.
Technical note.
T. J. Drapela, D. L. Franzen, and M. Young. Nov 95, 66p, NIST/TN-1378.
Also available from Supt. of Docs. as SN003-003-03384-7.

Keywords: *Interlaboratory comparisons, *Fibers, *Geometry, Calibration, Coatings, Optical fibers, Connectors, Glass fibers, Parameterization, Diameter, Standards, Fiber connectors ferrule, Geometric parameters, Pin gage, NIST(National Institute of Standards and Technology).

Interlaboratory measurement comparisons, dealing with geometrical parameters of optical fibers, fiber coatings, and fiber connector ferrules (including steel pin gages used to determine ferrule inside diameter), have been coordinated by National Institute of Standards and Technology (NIST). The international fiber (glass) geometry comparison showed better agreement among participants, for all measured parameters, than in previous comparisons. Many participants' test set were calibrated for fiber cladding diameter measurements by means of calibration artifacts from NIST or other national standards laboratories; there was significantly better agreement among those participants than among participants whose test sets were not calibrated. NIST is developing ferrule, pin gage, and coating calibration artifacts.

04,361
PB96-155437 Not available NTIS
National Inst. of Standards and Technology (EEEL), Boulder, CO. Optoelectronics Div.
Annealing of Bragg Gratings in Hydrogen-Loaded Optical Fiber.
Final rept.
H. Patrick, S. L. Gilbert, A. Lidgard, and M. D. Gallagher. 1995, 6p.
Pub. in Jnl. of Applied Physics, v78 n5 p2940-2945 Sep 95.

Keywords: *Annealing, *Optical fibers, Change, Reprints, *Bragg gratings, Photo induced index, Hydrogen loaded fiber.

The authors have conducted a detailed study of the thermal stability of Bragg gratings written in hydrogen-loaded and unloaded germanium-doped optical fiber. Interference of either continuous-wave or pulsed ultraviolet light was used to induce the index modulation gratings. Some gratings were kept at room temperature and others were annealed at fixed temperatures for 10-20 h. For temperatures between room temperature and 350 degrees C, gratings in the hydrogen-loaded fiber showed significantly greater decay than those in the unloaded counterpart. The ultraviolet-induced index modulation in hydrogen-loaded fiber was reduced by 40% after 10 h at 176 degrees C, whereas it was reduced by only 5% in unloaded fiber under the same conditions. The annealing behavior of gratings written using the pulsed source was identical to that of gratings written with the continuous-wave source, and the thermal stability of gratings in hydrogen-loaded fiber did not depend on the magnitude of the index modulation.

04,362
PB96-155445 Not available NTIS
National Inst. of Standards and Technology (EEEL), Boulder, CO. Optoelectronics Div.
Comparison of UV Photosensitivity and Fluorescence during Fiber Grating Formation.
Final rept.
H. Patrick, and S. Gilbert. 1995, 4p.
See also PB95-168597.
Pub. in Proceedings of the Photosensitivity and Quadratic Nonlinearity in Glass Waveguides, Fundamentals and Applications Topical Meeting, Portland, OR., September 9-11, 1995, p148-151.

Keywords: *Optical fibers, *Fluorescence, Near ultraviolet radiation, Reprints, Continuous radiation, Optical measurement, Fiber gratings, *Bragg gratings.

The authors have conducted a comparison of the UV photosensitivity of optical fiber with the blue fluorescence emitted during the exposure. In a survey of ten non-hydrogen-loaded germanium-doped fibers, the authors measured the UV photosensitivity and monitored the blue fluorescence during the growth of fiber gratings. The authors' goal was to determine whether the initial fluorescence, or the change in the fluorescence during exposure, is correlated with the index change. This provides insight into the underlying physical mechanism of UV-induced index change and also determines whether the blue fluorescence can be used as an indicator of the photosensitivity of a fiber.

04,363
PB96-157995 Not available NTIS
National Inst. of Standards and Technology (PL), Gaithersburg, MD. Electron and Optical Physics Div.
Configuration-Dependent AC Stark Shifts in Calcium.
Final rept.
Q. Li, T. R. O'Brian, T. B. Lucatorto, X. Xiong, T. J. McIlrath, and J. B. King. 1992, 3p.
Pub. in Optics Letters, v17 n19 p1373-1375 Oct 92.

Keywords: *Calcium, *Laser spectroscopy, Light shifts, Reprints, *AC stark effect, Configuration intervention, Rydberg levels.

The energy shifts caused by intense laser radiation (10 to the 8th power to 10 to the 10th power W/sq. cm) are investigated for several high-lying levels of calcium in order to determine the ac Stark shift of a loosely bound electron in a strong electromagnetic field. Energy shifts are measured for the closely spaced levels 4s9s 1S0. 4s8d 1D2. 4s10s 1S0. and 3d5s 1d2 by using resonance ionization spectroscopy. The levels associated with Rydberg configurations show the expected pondermotive energy shifts, but the 3d5s 1D2 shift is approximately half as large as the ponderomotive shifts.

04,364
PB96-159611 Not available NTIS
National Inst. of Standards and Technology (PL), Gaithersburg, MD. Electron and Optical Physics Div.
Soft-X-ray Damage to p-terphenyl Coatings for Detectors.
Final rept.
E. L. Benitez, M. L. Dark, D. E. Husk, S. E. Schnatterly, and C. Tarrio. 1994, 3p.
Pub. in Applied Optics, v33 n10 p1854-1856 Apr 94.

Keywords: *Detectors, *Soft x ray, Efficiency, Phosphor, Rerints, Reprints, P-terphenyl, Photoluminescence, Photon damage.

The organic phosphor p-terphenyl is used as a wavelength-converter coating in some soft-x-ray detectors. The authors have measured the absolute photoluminescent efficiency of p-terphenyl as a functon of incident photon energy from 36 to 191 eV. The authors have also measured changes in the efficiency caused by soft-x-ray fluence (total photons absorbed per unit area) at several photon energies in this range. The authors find that efficiency drops rapidly as a function of fluence, with the rate of decrease increasing with higher soft-x-ray energies.

04,365
PB96-159736 Not available NTIS
National Inst. of Standards and Technology (PL), Gaithersburg, MD. Electron and Optical Physics Div.
Influence of Electrical Isolation on the Structure and Reflectivity of Multilayer Coatings Deposited on Dielectric Substrates.
Final rept.
G. Gutman, J. Keem, J. Wood, C. Tarrio, and R. Watts. 1993, 4p.
Pub. in Applied Optics, v32 n34 p6981-6984 Dec 93.

Keywords: *Soft x ray, Characterization, Reprints, Substrates, Multilayers, Performance, *Electrically isolated.

Multilayers prepared with electrically isolated or grounded surfaces during deposition are shown to have dramatically different hard-x-ray, soft-x-ray, and neutron reflectivity characteristics. The effect has been observed for (100) silicon wafers, fused silica, and borate glass substrates of different sizes and with different surface roughness and flatness for multilayer structures prepared by rf and dc magnetron sputtering.

04,366
PB96-159744 Not available NTIS
National Inst. of Standards and Technology (PL), Gaithersburg, MD. Electron and Optical Physics Div.
New Method for Achieving Accurate Thickness Control for Uniform and Graded Multilayer Coatings on Large Flat Substrates.
Final rept.
G. Gutman, J. Keem, K. Parker, C. Tarrio, J. L. Wood, and R. Watts. 1993, 11p.
Pub. in Conference on Multilayer and Grazing Incidence X-ray/EUV Optics for Astronomy and Projection Lithography, No. 1742, San Diego, CA., July 19-22, 1992, p373-381.

Keywords: *Deposition, *Soft x ray, Multilayer, Sputtering, Uniformity, Reprints.

High performance in normal incidence Soft X-Ray optical systems requires accurate control of the d-spacing

across the surface of each mirror in the system. As a first step towards being able to fabricate any desired d-spacing variation, the authors demonstrate the ability to produce large (25 mm x 150 mm) flat Mo/Si multilayer coated mirrors with a d-spacing uniformity of +/ -0.4%. Instead of applying the approach most often taken to minimize the d-spacing variation physical shielding of the deposition source, the authors use a mask with a corrected profile positioned just in front of the rotating substrate to compensate for the non-uniform deposition flux. Results obtained from hard (lambda = 0.154nm) and soft (wavelength of interest) X-Ray mapping of the surface are presented along with a discussion of the technique used to control the d-spacing distribution.

04,367
PB96-160387 Not available NTIS
National Inst. of Standards and Technology (PL), Gaithersburg, MD. Electron and Optical Physics Div.
Upgraded Facility for Multilayer Mirror Characterization at NIST.
Final rept.
R. N. Watts, D. L. Ederer, R. D. Deslattes, C. J. Evans, T. V. Vorburger, T. B. Lucatorto, and W. T. Estler. 1991, 7p.
Pub. in Society of Photo-Optical Instrumentation Engineers 1547, Multilayer Optics for Advanced X-ray Application, San Diego, CA., July 21-26, 1991, p159-165.

Keywords: *Surface figure, *Reflectometry, Characterizations, Reprints, Diffractometry, Surface finish, XUV multilayer optics.

In response to the needs of the emerging field of normal incidence, soft X-ray optics, a field with applications ranging from extreme ultraviolet (XUV) solar imaging to X-ray lithography, the National Institute of Standards and Technology (NIST) has initiated an XUV multilayer and optical substrate characterization program. In this paper, we give an overview of the present capabilities of the NIST facility and discuss some of the proposed improvements, concentrating on the new soft X-ray reflectometry facility being built at the SURF-II electron storage ring.

04,368
PB96-160395 Not available NTIS
National Inst. of Standards and Technology (PL), Gaithersburg, MD. Electron and Optical Physics Div.
Soft X-ray Reflectometry Program at the National Institute of Standards and Technology.
Final rept.
R. Watts, T. Lucatorto, and C. Tarrio. 1993, 9p.
See also PB96-158092.
Pub. in Conference on Multilayer and Grazing Incidence X-ray/EUV Optics for Astronomy and Projection Lithography, No. 1742, San Diego, CA., July 19-22, 1992, p345-353 1993.

Keywords: *Monochromator, *Optics, *Reflectometers, Multilayer, Reprints, Reflectivity, Soft x ray.

In response to the metrology needs of the soft X-ray community, the National Institute of Standards and Technology (NIST) has initiated a program devoted to the characterization of multilayer coated optics in the 4 - 40 nm region. In this paper, we describe the synchrotron based XUV reflectometers in use and under construction at NIST. We review the characteristics of the Synchrotron Ultraviolet Radiation Facility storage ring (SURF II), dicuss the capabilities of the existing reflectometry facility, and present the final design parameters, expected performance, and construction status of a new reflectometry beam line.

04,369
PB96-161963 Not available NTIS
National Inst. of Standards and Technology (CSTL), Gaithersburg, MD. Process Measurements Div.
Electrical Measurements for Monitoring and Control of rf Plasma Processing.
Final rept.
M. A. Sobolewski, and J. R. Whetstone. 1993, 12p.
Pub. in Proceedings of the Society of Photo-Optical Instrumentation Engineers, San Jose, CA., September 21-23, 1992, Advanced Techniques for Integrated Circuit Processing II, v1803 p309-320 1993.

Keywords: *Gaseous electronics, *Electrical measurements, *Plasma, Argon, Current, Discharge, Reprints, Impedance, Real-time, Transient, Voltage.

We have investigated the possibility of using current and voltage measurements for real-time monitoring and control of radio-frequency discharges. Specifically, we have equipped a Gaseous Electronics Conference (GEC) rf Reference Cell with a computer-controlled measurement system that samples the voltage and current waveforms at the cell power input and Fourier analyzes these waveforms to obtain the amplitude and phase of their fundamental and harmonic components. The system accounts for errors introduced by the stray impedance of the cell, yielding corrected values that more accurately reflect the values of voltage and current at electrode surfaces in contact with the plasma. These corrected values are monitored to reveal changes in fundamental plasma parameters such as sheath voltages, sheath fields, and sheath (dark space) thickness. Futhermore, the corrected values serve as better control parameters than the raw values of voltage, current or power, measured externally. The time required for the acquisition and analysis of a pair of current and voltage waveforms is approximately one second, making these measurements suitable for real-time sensing and control applications.

04,370
PB96-163688 Not available NTIS
National Inst. of Standards and Technology (CSTL), Gaithersburg, MD. Biotechnology Div.
Elastic Scattering from Spheres under Non Plane-Wave Illumination.
Final rept.
J. T. Hodges, G. Grehan, C. Presser, and H. G. Semerjian. 1993, 15p.
Pub. in Laser Applications in Combustion and Combustion Diagnostics, Los Angeles, CA., January 16-23, 1993, SPIE Proceedings, v1862 n33 p294-308.

Keywords: *Light scattering, *Elastic scattering, Reprints, Measurements, Gaussian laser beams, Lorenz-Mie theory, Laser beam illumination.

Measurements of the scattered light intensity from individual droplets illuminated by focused Gausssian laser beams are presented. The results are compared with both the generalized Lorenz-Mie theory and classical Lorenz-Mie theory of elastic scattering. The data are shown to be consistent with the generalized theory. Besides experimental results, computations indicate that differences between the two theoretical approaches exist. It is shown that for sufficiently small beam diameter, characteristic of focused laser between the two theoretical approaches exist. It is shown that for sufficiently small beam diameter, characteristic of focused laser beam illumination, the departure of elastic scattering from that predicted by the classical Lorenz-Mie Theory can be significant.

04,371
PB96-164140 Not available NTIS
National Inst. of Standards and Technology (PL), Gaithersburg, MD. Electron and Optical Physics Div.
Population Trapping in Short-Pulse Multiphoton Ionization.
Final rept.
M. Edwards, and C. W. Clark. 1996, 12p.
Pub. in Optical Society of America B, v13 n1 p101-112 Jan 96.

Keywords: *Multiphoton ionization, Reprints, *Complex resonance energies, *Excitodion spectra, Floquet analysis, Photoelectron spectra, Population trapping.

We have studied population trapping in a one-dimensional model interacting with a short-pulse high-intensity laser, using Floquet analysis and direct numerical integration of the time-dependent Schrodinger equation for a range of peak pulse intensities. We find that photoelectrons are efficiently produced only by pulses whose peak intensities lie in a narrow range around the resonant intensity for a given intermediate state. Excited-state populations, however, are generated throughout a larger volume than are photoelectrons. Interpretations of recent experiments are examined in light of this result.

04,372
PB96-167325 Not available NTIS
National Inst. of Standards and Technology (EEEL), Gaithersburg, MD. Semiconductor Electronics Div.
Double-Modulation and Selective Excitation Photoreflectance for Wafer-Level Characterization of Quantum-Well Laser Structures.
Final rept.
D. Chandler-Horowitz, D. W. Berning, J. G. Pellegrino, J. H. Burnett, and P. M. Amirtharaj. 1996, 5p.
Pub. in Proceedings of the International Workshop on Semiconductor Characterization: Present Status and Future Needs, Gaithersburg, MD., January 30-February 2, 1995, p639-643 1996.

Keywords: *Laser structures, *Photoreflectance, Luminescence, Reprints, Pump beams, Bandgap, Double modulation, Quantum-well.

A double-modulation photoreflectance (PR) procedure is presented, where both the probe and pump beams are modulated, and the photoreflectance signal can be isolated from the luminescence and the scattered pump beam signals. The PR signal is separated from the other two signals through detection at the sum frequency. A careful choice of frequencies and specially design filters and tuned amplifiers were needed to achieve optimum operation. A couple system, along with the necessary circuits, is presented and applied to the characterization of a highly luminescent quantum-well laser structure. The freedom allowed by such a system to easily accommodate any pump wavelength is an important feature. We have exploited this added versatility, and the ordering of the bandgap of the multiple layers required in complex laser structures, to extract the bandgap and alloy composition of each of the constituent regions as well as the built-in strain in the pseudomorphic quantum-well.

04,373
PB96-175690 (Order as PB96-175666, PC A07/MF A02)
National Institute of Standards and Technology, Boulder, CO.
Theory of Electron Beam Moire.
D. T. Read, and J. W. Dally. 1996, 29p.
Prepared in cooperation with Maryland Univ., College Park. Dept. of Mechanical Engineering.
Included in Jnl. of Research of the National Institute of Standards and Technology, v101 n1 p47-76 Jan/Feb 96.

Keywords: *Experimental mechanics, *Electronic beams, Contract, Division, Fringe, Multiplication, Pitch, Rotation, Spatial frequency, Stress analysis, Reprints.

When a specimen surface carrying a high-frequency line grating is examined under a scanning electron microscope (SEM), moire fringes are observed at several different magnifications. The fringes are characterized by their spatial frequency, orientation, and contrast. These features of the moire pattern depend on the spatial frequency mismatch between the specimen grating and the raster scan lines, the diameter of the electron beam, and the detailed topography of the lines on the specimen.

04,374
PB96-176433 Not available NTIS
National Inst. of Standards and Technology (PL), Gaithersburg, MD. Radiometric Physics Div.
Realization of NIST 1995 Luminous Flux Scale Using the Integrating Sphere Method.
Final rept.
Y. Ohno. 1996, 10p.
See also PB96-102843.
Pub. in IESNA Annual Conference, New York, NY., August 1-4, 1995, Jnl. of the Illuminating Engineering Society, v25 n1 p13-22 1996.

Keywords: *Optical measurement, Lumens, Light sources, Calibration, Photometry, Radiant flux density, Scale, Units of measurement, Standards, Photometers, Reprints, *Luminous flux, Integrating spheres.

The NIST luminous flux scale was last realized in 1985 using a goniophotometer. A new theoretical method for luminous flux scale realization using an integrating sphere has been studied at NIST. An experimental realization predicted sufficient accuracy of this method for standards use. This method (called integrating sphere method) uses an integrating sphere with an opening to introduce a known amount of flux from an external source, which is compared to the liminous flux of an internal source to be calibrated.

04,375
PB96-176466 Not available NTIS
National Inst. of Standards and Technology (PL), Gaithersburg, MD. Atomic Physics Div.
Irradiances of Spectral Lines in Mercury Pencil Lamps.
Final rept.
J. Reader, C. J. Sansonetti, and J. M. Bridges. 1996, 6p.
See also PB96-176474.
Pub. in Applied Optics, v35 n1 p78-83, 1 Jan 96.

Keywords: *Irradiances, Reprints, *Mercury pencil lamps, *Spectral lines.

The irradiances of 37 spectral lines emitted by mercury pencil-type lamps were measured by comparison with calibrated continuum sources. The lines span the region 230 - 590 nm. For the 14 most prominent lines the absolute irradiances should be useful for radiometric calibrations at an uncertainty level of approx. 15% (95% confidence). The ratios of the irradiances for this same group of lines are significantly more reproducible; they should be useful at an uncertainty level of approx. 10%.

04,376
PB96-176474 Not available NTIS
National Inst. of Standards and Technology (PL), Gaithersburg, MD. Atomic Physics Div.
Wavelengths of Spectral Lines in Mercury Pencil Lamps.
Final rept.
C. J. Sansonetti, M. L. Salit, and J. Reader. 1996, 4p.

Keywords: *Wavelengths, Spectral lines, Reprints, *Fourier-transform spectroscopy, *Mercury pencil lamp.

The wavelengths of 19 spectral lines in the region 253-579 nm emitted by Hg pencil-type lamps were measured by Fourier-transform spectroscopy. Precise calibration of the spectra was obtained with wavelengths of 198 Hg as external standards. Our recommended values should be useful as wavelength-calibration standards for moderate resolution spectrometers at an uncertainty level of 0.0001 nm.

04,377
PB96-179536 Not available NTIS
National Inst. of Standards and Technology (MEL), Gaithersburg, MD. Precision Engineering Div.
Test Optics Error Removal.
Final rept.
C. J. Evans, and R. N. Kestner. 1996, 7p.
Pub. in Applied Optics, v35 n7 p1015-1021, 1 Mar 96.

Keywords: *Optical interferometers, *Instrument errors, *Geometrical aberrations, Optical tests, Optical measurement, Optical correction procedure, Symmetry, Surfaces, Wave fronts, Configuration management, Reprints, Zernike polynomials.

Wave-front or surface errors may be divided into rotational symmetric and nonrotationally symmetric terms. It is shown that if either the test part or the reference surface in an interferometric test is rotated to N equally spaced positions about the optical axis and the resulting wave fronts are averaged, then errors in the rotated member with angular orders that are not interger multiples of the number of positions will be removed.

04,378
PB96-179585 Not available NTIS
National Inst. of Standards and Technology (PL), Gaithersburg, MD. Radiometric Physics Div.
National Institute of Standards and Technology High-Accuracy Cryogenic Radiometer.
Final rept.
T. R. Gentile, J. M. Houston, J. E. Hardis, C. L. Cromer, and A. C. Parr. 1996, 13p.
Pub. in Applied Optics, v35 n7 p1056-1068 Mar 96.

Keywords: *Cryogenics, *Radiometry, Standards, Reprints, *Electrical substitution, National Institute of Standards and Technology, High-accuracy.

A high-accuracy cryogenic radiometer has been developed at the National Institute of Standards and Technology to serve as a primary standard for optical power measurements. This instrument is an electrical-substitution radiometer that can be operated at cryogenic temperatures to achieve a relatively standard uncertainty of 0.021% at an optical power level of 0.8 mW. The construction and operation of the high-accuracy cryogenic radiometer and the uncertainties in optical power measurements are detailed.

04,379
PB96-200704 Not available NTIS
National Inst. of Standards and Technology (PL), Boulder, CO. Quantum Physics Div.
Gravitational Sisyphus Cooling of (87)Rb in a Magnetic Trap.
Final rept.
N. R. Newbury, C. J. Myatt, E. A. Cornell, and C. E. Wieman. 1995, 4p.
Pub. in Physical Review Letters, v74 n12 p2196-2199 May 95.

Keywords: *Magnetic traps, *Laser cooling, *Nuetron atoms, Reprints.

We describe a method for cooling magnetically trapped 87Rb atoms by irreversibly cycling the atoms between two trapped states. The cooling force is proportional to gravity. The atoms are cooled to 1.5 micro K in the vertical dimension. We have extended this cooling method to two dimensions through anharmonic mixing, achieving a factor of 25 increase in the phase space density over an uncooled sample. The cooling method should be an important intermediate step toward achieving a Bose-Einstein condensate of Rb atoms.

04,380
PB96-200738 Not available NTIS
National Inst. of Standards and Technology (EEEL), Boulder, CO. Optoelectronics Div.
Self-Calibrated Intelligent Optical Sensors and Systems.
Final rept.
A. H. Rose, and J. C. Wyss. 1996, 7p.
Pub. in Proceedings of the Self-Calibrated Intelligent Optical Sensors and Systems Conference, Philadelphia, PA., October 25-26, 1996, v2594 p142-148 1996.

Keywords: *Temperature sensors, *Calibration, Self repairing devices, Computerized control systems, Reprints, *Optical thermometers, *Self calibration, Optical fiber sensors, Fiber optic sensors.

A computer controlled optical thermometer has been built to demonstrate a self-calibrating optical sensor. The self-calibrating thermometers records the temperature with a fiber-optic polarimetric temperature sensor. The wavelength sensitivity of the polarimetric sensor is used to facilitate the recalibration. The system contains an optical source which can be tuned over approximately a 9 nm wavelength range, and a monochromator to measure any shifts in the wavelength of the laser. The monochromator is calibrated with the spectrum of a neon discharge lamp.

04,381
PB96-201165 Not available NTIS
National Inst. of Standards and Technology (EEEL), Boulder, CO. Electromagnetic Technology Div.
Electronically Tunable Fiber Laser for Optical Pumping of (3)He and (4)He.
Final rept.
E. F. Stephens, H. Patrick, and S. L. Gilbert. 1996, 2p.
Pub. in Review of Scientific Instruments, v67 n3 p843-844 Mar 96.

Keywords: *Optical pumping, *Fiber lasers, *Helium, *Laser spectroscopy, Fiber grating, Neodymium, Reprints, Bragg grating, Nd-doped optical fiber.

We present in the paper a low threshold, highly stable, integrated fiber laser cavity that uses an electronically tunable internal Bragg grating. The fiber laser produced over 5 mW with a spectral width of about 5 GHz at 1083 nm. The laser was used to achieve 30% polarization of the 23S1 metastable states of 4He in a weak rf discharge cell. (Copyright (c) 1996 American Institute of Physics.)

04,382
PB97-108559 PC A04/MF A01
National Inst. of Standards and Technology (PL), Gaithersburg, MD. Optical Technology Div.
National Measurement System for Radiometry, Photometry, and Pyrometry Base Upon Absolute Detectors.
Technical note.
A. C. Parr. Sep 96, 37p, NIST/TN-1421.
Also available from Supt. of Docs. as SN003-003-03429-1.

Keywords: *Radiometers, *Photometry, *Pyrometry, Procedures, Calibrations, Cryogenic radiometers, National Institute of Standards and Technology.

Advancements in the performance and ease of use of absolute photodetectors based upon electrical substitution principals offers the possibility of a simplified and more accurate way to transfer the fundamental radiometric, photometric, and pyrometric units from NIST to the U.S. technical establishment. The history of electrical substitution radiometers at NIST is briefly reviewed and the implementation of the latest generation absolute cryogenic radiometer is discussed. Procedures to maintain fundamental units based upon a detector approach are reviewed in a general way with references to the technical literature for detailed discussion. It is proposed that NIST customers consider adopting the suggestions made in this technical note to simplify and improve their optical radiation based calibrations.

04,383
PB97-108583 PC A12/MF A03
National Inst. of Standards and Technology (EEEL), Boulder, CO. Optoelectronics Div.
Technical Digest: Symposium on Optical Fiber Measurements (9th), 1996. Held in Boulder, Colorado on October 1-3, 1996.
Special pub.
G. W. Day, D. L. Franzen, and P. A. Williams. Oct 96, 226p, NIST/SP-905.
Details in illustrations may not be fully legible in microfiche. Also available from Supt. of Docs. as SN003-003-03425-8. See also PB94-207636. Prepared in cooperation with Lasers and Electro-Optics Society (IEEE), Piscataway, NJ. and Optical Society of America, Washington, DC.

Keywords: *Fiber optics, *Optical fibers, *Optical measurement, *Meetings, Optical polarization, Electrooptics, Transmission lines, Reviews, Nonlinear optics, Integrated optics, National Institute of Standards and Technology.

Measurements of polarization mode dispersion (PMD) and nonlinear processes in optical fibers are two of the major topics in this digest of papers presented at the ninth Symposium on Optical Fiber Measurements, Held October 1-3, 1996, at the laboratories of the National Institute of Standards and Technology in Boulder, Co. Summaries of all the papers presented at the Symposium-10 invited and 39 contributed-are included. The statistical nature of PMD complicates its measurement and makes verification of accuracy difficult. This is reflected in the content of the papers, many of which focus on comparisons of measurement techniques. In wavelength division multiplexed systems employing optical amplification, high powers can be lead to problems from nonlinear processes such as Brillouin scattering and four-wave mixing. The importance of these issues is seen by the inclusion of several papers regarding the measurement of nonlinear coefficients and effective area. Strong international participation has been maintained, as about two thirds of the paper in this digest originated outside of the United States.

04,384
PB97-110209 Not available NTIS
National Inst. of Standards and Technology (MEL), Gaithersburg, MD. Precision Engineering Div.
Model of an Optical Roughness-Measuring Instrument.
Final rept.
A. B. Kiely, T. R. Lettieri, and T. V. Vorburger. 1991, 4p.
Pub. in Proceedings of the International Conference on the Metrology and Properties of Engineering Surfaces (5th), Leicester, England, April 1991, 4p.

Keywords: *Light scattering, *Optical metrology, Roughness, Surface finish, Texture, Models, Reprints.

The authors have developed a nonlinear model of a commercial optical instrument for measuring the root-mean-square slopes of rough surfaces. The model improves upon previous ones in that it accounts for certain instrumental factors which affect the optical roughness measurements.

04,385
PB97-110415 Not available NTIS
National Inst. of Standards and Technology (MEL), Gaithersburg, MD. Precision Engineering Div.
Optical Scattering from Moderately Rough Surfaces.
Final rept.
T. V. Vorburger, E. Marx, and T. R. Lettieri. 1991, 3p.
Pub. in ICO Topical Meeting on Atmospheric, Volume and Surface Scattering Propagation, Florence, Italy, August 27-30, 1991, p205-207.

Keywords: *Optical scattering, *Surface roughness, Light scattering, Optical metrology, Reprints, Fraunhofer diffraction.

Light-scattering techniques have become important tools for the study of surface finish, and several such techniques have been developed. The choice depends, among other factors, upon the degree of roughness: for very smooth surfaces a technique such as total integrated scatter can be used, while for rougher surfaces angle-resolved light scattering should be applicable. In the paper, the authors discuss some of the work being conducted at the National Institute of Standards and Technology which applies laser light scattering to the measurement and understanding of the topographic properties of moderately rough surfaces.

04,386
PB97-110506 Not available NTIS
National Inst. of Standards and Technology (MEL), Gaithersburg, MD. Precision Engineering Div.
Compensation for Errors Introduced by Nonzero Fringe Densities in Phase-Measuring Interferometers.
Final rept.
C. J. Evans. 1993, 4p.
Pub. in Annals of the CIRP, v42 n1 p577-580 1993.

Keywords: *Optical interferometers, *Instrument errors, *Geometric abberations, Optical tests, Optical measurement, Surfaces, Optical correction procedures, Reprints.

Interferometers offer rapid full aperture measurement of optics. Flats, spheres and conics can be measured to high accuracy with computer controlled systems using high density detectors. In principle, aspheres that depart from the base sphere or conic by several micrometers could also be measured. The paper demonstrates that substantial errors may be incurred and describes simple tests to evaluate the scale of those errors. The paper then discusses the error sources and presents a method for compensating for those errors.

04,387
PB97-110548 Not available NTIS
National Inst. of Standards and Technology (MEL), Gaithersburg, MD. Precision Engineering Div.
Light Scattering by Sinusoidal Surfaces: Illumination Windows and Harmonics in Standards.
Final rept.
E. Marx, T. R. Lettieri, and T. V. Vorburger. 1995, 9p.
Pub. in Applied Optics, v34 n7 p1260-1277 Mar 95.

Keywords: *Light scattering, *Sinusoidal surfaces, Windowing effects, Harmonics, Bidirectional reflectance, Distribution function, Reprints, Angle-resolved scattering.

Sinusoidal surfaces can be used as material standards to help calibrate instruments that measure the angular distribution of the intensity of light scattered by arbitrary surfaces, because the power in the diffraction peaks varies over several orders of magnitude. The calculated power in the higher-order diffraction peaks from sinusoidal surfaces expressed in terms of Bessel functions is much smaller than the values determined from angular distributions that are measured or computed from measured profiles, both of which are determined mainly by the harmonic contents of the profile. The finite size of the illuminated area, represented by an illumination window, gives rise to a background that is much larger than the calculated power in the higher-order peaks. For a rectangular window of a size equal to an even number of periods of the sinusoid, a computation of the power distribution produces minima at or near the location of the diffraction angles for higher-order diffraction angles.

04,388
PB97-110597 Not available NTIS
National Inst. of Standards and Technology (MEL), Gaithersburg, MD. Precision Engineering Div.
Sinusoidal Surfaces as Standards for BRDF Instruments.
Final rept.
E. Marx, T. R. Lettieri, T. V. Vorburger, and M. McIntosh. 1991, 7p.
Pub. in Proceedings Reprint, Optical Scatter: Applications, Measurement, and Theory, San Diego, CA., July 24-26, 1991, v1530 p15-21.

Keywords: *Sinusoidal surfaces, *Lasers, *Electromagnetic scattering, Diffraction peaks, Reprints, BRDF standards, Kirchhoff approximation.

The study of light scattered by sinusoidal surfaces shows that such a configuration can be used as a material standard to help calibrate instruments that measure the BRDF of arbitrary surfaces. Measured and computed values of the power scattered into the diffraction peaks show good agreement, and such calculations can be further improved and used to verify the standards.

04,389
PB97-111215 Not available NTIS
National Inst. of Standards and Technology (MEL), Gaithersburg, MD. Precision Engineering Div.
Windowing Effects on Light Scattering by Sinusoidal Surfaces.
Final rept.
E. Marx, and T. V. Vorburger. 1993, 14p.
Pub. in Proceedings Reprint, Optical Scattering: Applications, Measurement, and Theory II, San Diego, CA., v1995 p1-14 1993.

Keywords: *Sinusoidal surfaces, *Window functions, *Light scattering, Diffraction peaks, Rough surfaces, Reprints, BRDF.

A window function is used to represent the variation in the intensity of the radiation in a light beam. Windowing effects are factored into computations of the angular distribution of light scattered by a sinusoidal surface. These effects, as well as those of harmonics and noise, are shown for the angular distributions computed from simulated profiles. The integrated power in each diffraction peak computed for perfect sinusoids, measured profiles, and simulated profiles with different window functions is compared to that of a measured angular distribution.

04,390
PB97-111272 Not available NTIS
National Inst. of Standards and Technology (EEEL), Boulder, CO. Optoelectronics Div.
Magneto-Optic Rotation Sensor Using a Laser Diode as Both Source and Detector.
Final rept.
K. B. Rochford, and A. H. Rose. 1996, 4p.
Pub. in International Conference on Optical Fiber Sensors (11th), Sapporo, Japan, May 21-24, 1996, p686-689.

Keywords: *Detectors, *Fiber optic sensors, *Laser diodes, Rotation sensors, Self-detection, Reprints, *Foreign technology.

The authors show that a laser diode can serve as both the emitter and detector in a diffraction-based magneto-optic rotation sensor. Self-detection devices have sufficient linearity and stability for applications with discrete measurands. Signal-to-noise ratios greater than 50 dB (1 Hz bandwidth) are possible for binary measurands, and a fiber optic rotation sensor with a signal-to-noise ratio of 18 dB in a 1.25 kHz bandwidth is demonstrated.

04,391
PB97-111280 Not available NTIS
National Inst. of Standards and Technology (MEL), Gaithersburg, MD. Precision Engineering Div.
Laser Cooling and the Recoil Limit.
Final rept.
S. L. Rolston, P. D. Lett, and W. D. Phillips. 1989, 6p.
Pub. in Conference on Quantum Electronics and Laser Science, Baltimore, MD., April 24-28, 1989, Technical Digest Series, v12 6p.

Keywords: *Laser cooling, *Recoil limits, Cooling limits, Doppler cooling, Optical molasses, Radiation pressure, Reprints.

The effect of a finite recoil on the laser cooling process is studied with a Monte Carlo simulation. The authors find non-Maxwell-Boltzmann velocity distributions, and mean energies no lower than the recoil energy.

04,392
PB97-111330 Not available NTIS
National Inst. of Standards and Technology (MEL), Gaithersburg, MD. Precision Engineering Div.
Numerical Reference Models for Optical Metrology Simulation.
Final rept.
G. L. Wojcik, J. Mould, E. Marx, and M. P. Davidson. 1992, 13p.
Pub. in Society of Photo-Optical Instrumentation Engineers Microlithography '92: IC Metrology, Inspection, and Process Control VI, v1673-06 p1-13 1992.

Keywords: *Electromagnetic scattering, *Optical measurement, Integral equations, Finite element analysis, Maxwell equations, Computerized simulation, Reprints, Numerical reference models.

Optical modeling on the computer can aid R&D efforts to enhance metrology methods, and similarly for lithography, alignment, and particulate monitoring. However, full exploitation of optical modeling is hindered by the lack of appropriate benchmarks for verifying algorithms and evaluating approximations. To help remedy this situation the authors describe a preliminary set of scalar, 2D numerical reference models (NRMs). These include isolated thin and thick lines, periodic lines, and an isolated trench. Scattered fields are compared for three different solution methods, based on time-domain finite elements, boundary integrals, and a waveguide model. Correlation is good in general, although important differences are seen in both code accuracy and performance. NRM generalizations are suggested that accommodate 3D effects, imaging, and experiment verification.

04,393
PB97-111470 Not available NTIS
National Inst. of Standards and Technology (PL), Gaithersburg, MD. Electron and Optical Physics Div.
Closed Loop Controller for Electron-Beam Evaporators.
Final rept.
A. Band, and J. A. Stroscio. 1996, 4p.
Pub. in Review of Scientific Instruments, v67 n6 p2366-2369 Jun 96.

Keywords: *Evaporators, *Closed loop controllers, *Electron-beam heating, Instruments, Process controllers, Reprints.

A simple instrument for automatically controlling the deposition rate of an electron-beam evaporator is described. The design incorporates a commercially available, microprocessor based, proportional-integral-differential process controller that provides loop control and automatic determination of optimal poportional, integral, and differential loop constants. A logarithmic amplifier is used to linearize the overall loop response. The controller is used in conjunction with a compact electron-beam heated evaporator.

04,394
PB97-112254 Not available NTIS
National Inst. of Standards and Technology (CSTL), Gaithersburg, MD. Process Measurements Div.
Laser Bandwidth Effects in Quantitative Cavity Ring-Down Spectroscopy.
Final rept.
J. T. Hodges, J. P. Looney, and R. D. van Zee. 1996, 5p.
Pub. in Applied Optics, v35 n21 p4112-4116 Jul 96.

Keywords: *Lasers, *Spectroscopy, *Cavity ringdown, Absorption, Bandwidths, Oxygen, Reprints.

The authors have investigated the effects of laser bandwidth on quantitative cavity ring-down spectroscopy using the (r)R transitions of the b(v=0)<--X(v=0) band of molecular oxygen. It is found that failure to account properly for the laser bandwidth leads to systematic errors in the number of densities determined from measured ring-down signals. When the frequency-integrated expression for the ring-down signal is fitted and measured laser line shapes are used, excellent agreement between measured and predicted number densities is found.

04,395
PB97-112288 Not available NTIS
National Inst. of Standards and Technology (CSTL), Gaithersburg, MD. Process Measurements Div.
Forward Scattering of a Gaussian Beam by a Nonabsorbing Sphere.
Final rept.
J. T. Hodges, G. Grehan, G. Gouesbet, and C. Presser. 1995, 13p.
Pub. in Applied Optics, v34 n12 p2120-2132 Apr 95.

Keywords: *Gaussian beams, *Light scattering, *Spheres, Diffractions, Reprints, Lorenz-Mie theory.

The forward scattering of a Gaussian laser beam by a spherical particle located along the beam axis is analyzed with the generalized Lorenz-Mie theory (GLMT) and with diffraction theory. Forward-scattering and near-foward-scattering profiles from electrodynamically levitated droplets, 51.6 micrometers in diameter, are also presented and compared

with GLMT-based predictions. The total intensity in the forward direction, formed by the superposition of the incident and the scattered fields, is found to correlate with the particle-extinction cross section, the particle dimater, and the beam width. Based on comparison with the GLMT, the diffraction solution is accurate when beam widths that are approximately greater than or equal to the particle diameter are considered and when large particles that have an extinction efficiency near the asymptotic value of 2 are considered. However, diffraction fails to describe the forward intensity for more tightly focused beams. The experimental observations, which are in good agreement with GLMT-based predictions, reveal that the total intensity profile about the forward direction is quite sensitive to particle axial position within a Gaussian beam.

04,396
PB97-116057 PC A06/MF A01
National Inst. of Standards and Technology (EEEL), Boulder, CO. Electromagnetic Technology Div.
Metrology for Electromagnetic Technology: A Bibliography of NIST Publications.
A. G. Bradford. Sep 96, 79p, NISTIR-5051.
See also PB96-128269.

Keywords: *Superconductivity, *Electromagnetic fields, *Bibliographies, Cryogenics, Publishing, Employees, Scientists, Lasers, Optical communication, Metrology, US NIST.

This bibliography lists the publications of the personnel of the Electromagnetic Technology Division of NIST during the period from January 1970 through publication of this report. A few earlier references that are directly related to the present work of the Division are also included. The bibiliography includes publications in cryoelectronic metrology and superconductor and magnetic measurements.

04,397
PB97-118640 Not available NTIS
National Inst. of Standards and Technology (PL), Gaithersburg, MD. Radiometric Physics Div.
Realization of a Scale of Absolute Spectral Response Using the NIST High Accuracy Cryogenic Radiometer.
Final rept.
T. R. Gentile, J. M. Houston, and C. L. Cromer. 1996, 12p.
See also PB96-179585.
Pub. in Applied Optics, v35 n22 p4392-4403 Aug 96.

Keywords: *Cryogenics, *Radiometry, Standards, Reprints, *Electrical substitution, National Institute of Standards and Technology, High-accuracy.

Using the National Institute of Standards and Technology high-accuracy cryogenic radiometer (HACR), the authors have realized a scale of absolute spectral response between 406 and 920 nm. The HACR, an electrical-substitution radiometer operating at cryogenic temperatures, achieves a combined relative standard uncertainty of 0.021%. Silicon photodiode light-trapping detectors were calibrated against the HACR with a typical relative standard uncertainty of 0.03% at nine laser wavelengths between 406 and 920 nm. Modeling of the quantum efficiency of these detectors yields their responsivity throughout this range with comparable accuracy.

04,398
PB97-119390 Not available NTIS
National Inst. of Standards and Technology (EEEL), Boulder, CO. Optoelectronics Div.
Anomalous Relation between Time and Frequency Domain PMD Measurements.
Final rept.
P. A. Williams, and P. R. Hernday. 1995, 4p.
Pub. in Optical Fibre Measurement Conference (3rd), Liege, Belgium, September 25-26, 1995, 4p.

Keywords: *Polarization mode dispersion, *Fiber optics, *Optical fibers, Electrooptics, Fourier transform, Reprints, *Foreign technology, Differential group delay, Jones matrix eigenanalysis.

The authors report nearly simultaneous measurements of polarization mode dispersion (PMD) in various samples of highly mode-coupled single-mode fiber using the measurement methods of Jones matrix eigenanalysis (JME) and Fourier-transformed wavelength scanning. The ratio of the PMD values resulting from these two methods differs by approximately 10% from current theoretical predictions. The measurements are verified by demonstrating the theoretical agreement between the JME and wavelength scanning extremum counting results.

04,399
PB97-122212 Not available NTIS
National Inst. of Standards and Technology (EEEL), Gaithersburg, MD. Electricity Div.
Interface-Filter Characterization of Spectraradiometers and Colorimeters.
Final rept.
P. A. Boynton, Y. Ohno, and E. F. Kelley. 1996, 4p.
Pub. in Society for Information Display (SID) Symposium, Digest of Technical Papers, San Diego, CA., May 12-17, 1996, p207-210.

Keywords: *Spectroradiometers, *Colorimeters, *Filters, *Interface filters, Displays, Measurements, Reprints.

Spectroradiometers and colorimeters are used in display measurements to measure color in one of several color space coordinate systems. How accurately these instruments can measure the color coordinates can be simply tested by using interference filtes. Error sources within the measuring system are identified which could explain several observed anomalies.

04,400
PB97-122378 Not available NTIS
National Inst. of Standards and Technology (PL), Gaithersburg, MD. Electron and Optical Physics Div.
Large Local-Field Corrections in Optical Rotatory Power of Quartz and Selenium.
Final rept.
L. Jonsson, Z. H. Levine, and J. W. Wilkins. 1996, 4p.
Pub. in Physical Review Letters, v76 n8 p1372-1375 Feb 96.

Keywords: *Rotary powers, *Corrections, *Quartz, *Selenium, Local fields, Nonconductors, Calculations, Reprints.

The authors show that local fields can increase the rotatory power rho of nonconductors by a factor of 10--in contrast to the typical 10% effect in other properties. The authors present calculations for quartz and Se, and a general method to estimate the size of local-field corrections. Notably, only scalar local fields are needed despite the vector character of light. A self-energy-corrected local-density band structure yields corrections to rho of a factor of +7 in quartz and -4 in Se. These values are 30% above experiment for quartz, and, for one sign choice, within the 50% error bars for Se.

04,401
PB97-122469 Not available NTIS
National Inst. of Standards and Technology (PL), Gaithersburg, MD. Radiometric Physics Div.
Photonic Band-Structure Effects for Low-Index-Contrast Two-Dimensional Lattices in the Near Infrared.
Final rept.
A. Rosenberg, R. J. Tonucci, H. B. Lin, and E. L. Shirley. 1996, 4p.
Pub. in Physical Review B, v54 n8 pR5195-R5198 Aug 96.

Keywords: *Lattices, *Low index contrast, Attenuation, Two dimensional, Reprints, *Photonic band structure.

The authors demonstrate that two-dimensional periodic dielectric structures with low index contrast give rise to remarkable, easily measurable photonic band-structure effects. The structures consist of triangular arrays of glass cylinders embedded in a glass matrix, having centr-to-center nearest-neighbor separations from 1.08 micrometers to 0.54 micrometers. The cylinders and the matrix are composed of different glasses, but the difference between the indices of refraction is as low as 0.02 throughout the relevant spectral region. The attenuation features corresponding to the boundaries of the first Brillouin zone appear in the near-infrared, at photon energies between 0.4 eV and 0.9 eV.

Plasma Physics

04,402
DE94004400 PC A02/MF A01
National Inst. of Standards and Technology, Gaithersburg, MD.
Determination of Atomic Data Pertinent to the Fusion Energy Program. Progress Report for FY 92.
1992, 6p, DOE/ER/53237-T1.
Contract AI05-86ER53237
Sponsored by Department of Energy, Washington, DC.

Keywords: *Argon Ions, *Atoms, *Electron-Atom Collisions, *Electron-Ion Collisions, *Ions, *Oxygen Ions, *Thermonuclear Reactors, Calculation Methods, Cross Sections, Data Compilation, Energy Levels, Excitation, ITER Tokamak, Ionization, J Codes, Plasma Diagnostics, Plasma Impurities, Polarization, Progress Report, Research Programs, Scattering, Spectra, TEXT Devices, TFTR Tokamak, Wavelengths, EDB/700380.

In the pursuit of the general goal to provide essential atomic radiation and collision data for the fusion energy program, the following progress was achieved at NIST during FY 92: (1) identification of spectral lines of impurity in ions (from Er to Bi); (2) spectroscopic data compilations of critically evaluated wavelengths and energy levels of atoms and ions; (3) electron-ion collision experiments; (4) electron impact excitation theory; and (5) electron-impact ionization theory.

04,403
DE95011593 PC A02/MF A01
National Inst. of Standards and Technology, Gaithersburg, MD.
Measurements of quantum electrodynamic sensitive transitions in Na-like and Cu-like ions: Final report, 1 October 1993--29 September 1994.
PROGRESS REPT.
J. Reader. 1994, 7p, DOE/SF/20143-T2.
Contract FG03-93SF20143
Sponsored by Department of Energy, Washington, DC.

Keywords: *Iron Ions, *Laser-Produced Plasma, Cations, Emission Spectra, Energy Levels, Energy-Level Transitions, Experimental Data, ICF Devices, Modifications, Plasma Diagnostics, Progress Report, Research Programs, Theoretical Data, Tokamak Devices, X-Ray Lasers, Tables(data), EDB/700320, EDB/700380, EDB/426002.

The object of this research was to use the GDL laser at the Laboratory for Laser Energetics at the University of Rochester to measure the energies of spectral transitions that would be of importance for testing the accuracy of calculations used to predict properties of plasmas found in inertial fusion experiments as well as in tokamaks and x-ray lasers. The general method to be used for this experiment was to focus the beam from the GDL laser to a small point so as to create a laser-produced plasma of the material of interest. Light from the plasma was to be photographed with a 2.2-m grazing incidence spectrograph transported to Rochester from NIST. The region of observation was 10-300 angstroms. In the initial phase of the work, a series of spectrograms were made of highly ionized iron. For this, a special target chamber was fabricated at NIST and interfaced to the light beam from the GDL laser. The results for iron provided valuable data for Li-like iron, Fe(sup 23+). Fig. 2 shows an example of the spectrum obtained in the region of 30-40 angstroms. The lower spectrum shows intense lines of Fe(sup 23+), obtained by focusing the GDL beam tightly onto the target surface. For the upper spectrum the GDL beam was focused slightly in front of the target, producing lines of Fe(sup 23+) that are much reduced in intensity. The lines of Fe(sup 23+) in the 30-40 angstrom region were observed for the first time in this experiment. Measurement of their wavelengths provided the following comparison with ab initio values calculated with the Dirac-Fock quantum mechanics computer code of Desclaux. After completing the observations for Li-like iron, the GDL laser was shut down for the planned upgrade to much higher energy. Extensive work was undertaken to interface the NIST target chamber to the 30-cm-diameter beam of the upgraded GDL laser. The NIST system is now ready for use with the upgraded GDL laser.

04,404
PB94-172327 Not available NTIS
National Inst. of Standards and Technology (PL), Gaithersburg, MD. Atomic Physics Div.
Gaseous Electronics Conference Radio-Frequency Reference Cell: A Defined Parallel-Plate Radio-Frequency System for Experimental and Theoretical Studies of Plasma-Processing Discharges.
Final rept.
1994, 15p.
Pub. in Rev. Sci. Instrum. 65, n1 p140-154 Jan 94.

Keywords: *Radio frequency discharge, *Glow discharges, Electrical measurement, Interlaboratory comparisons, Argon plasma, Reprints, Reference cells.

A 'reference cell' for generating radio-frequency (rf) glow dicharges in gases at a frequency of 13.56 MHz is described. The reference cell provides an experimental platform for comparing plasma measurements carried out in a common reactor geometry by different experimental groups, thereby enhancing the transfer of knowledge and insight gained in rf discharge studies. The results of performing ostensibly identical measurements on six of these cells in five different laboratories are analyzed and discussed. Measurements were made of plasma voltage and current characteristics for discharges in pure argon at specific values of applied voltages, gas pressures, and gas flow rates. Data are presented on relevant electrical quantities derived from Fourier analysis of the voltage and current wave forms. Amplitudes, phase shifts, self-bias voltages, and power dissipation were measured.

04,405
PB94-185048 Not available NTIS
National Inst. of Standards and Technology (PL), Boulder, CO. Quantum Physics Div.
Physics and Prospects of Inertial Confinement Fusion.
Final rept.
M. M. Basko. 1993, 10p.
Pub. in Plasma Phys. Control. Fusion 35, pB81-B90 1993.

Keywords: *Inertial confinement fusion, Plasma confinement, Trends, Reprints, Prospects.

Some key physical aspects of the inertial confinement fusion (ICF) are discussed. The minimum scale of ICF microexplosions is determined by the ability to implode spherical shells with high radial convergence ratios C(R) and high initial aspect ratios A(RO). The attainable values of C(R) are limited by large-scale drive asymmetries, while the values of A(RO) are constrained by the Rayleigh-Taylor instability. Under the indirect drive approach to ICF, it is easier to achieve the required uniformity of the drive pressure, but the penalty is a factor 4-5 reduction of the target energy gain as compared to the direct drive option. Spark ignition is a crucial issue for indirect drive targets (at least for those to be used in power reactors), while the targets driven directly by heavy ion beams could, in principle, use a less demanding volume ignition scheme.

04,406
PB94-185717 Not available NTIS
National Inst. of Standards and Technology (EEEL), Gaithersburg, MD. Electricity Div.
Use of an Ion Energy Analyzer: Mass Spectrometer to Measure Ion Kinetic-Energy Distributions from RF Discharges in Argon-Helium Gas Mixtures.
Final rept.
J. K. Olthoff, R. J. Van Brunt, S. B. Radovanov, and J. A. Rees. 1994, 6p.
Pub. in IEE Proc.-Sci. Meas. Technol. 141, n2 p105-110 Mar 94.

Keywords: *Helium ions, *Argon ions, Radio frequency discharge, Mass spectroscopy, Metastable state, Kinetic energy, Helium plasma, Argon plasma, Gas mixtures, Semiconductors, Reprints, Ion energy analysis, Plasma processing.

A mass spectrometer equipped with an electrostatic ion energy analyzer has been used to measure the kinetic-energy distributions of ions sampled through an orifice in the grounded electrode of a parallel-plate radio-frequency (RF) discharge cell. Kinetic-energy distributions are presented for Ar(1+), Ar2(1+), Ar(2+), He(1+), and ArHe(1+) sampled from argon-helium plasmas with helium concentrations ranging from 0-95 mole percent, applied peak-to-peak RF voltages of 200 V, and gas pressures of 13.3 Pa. Variations in the ion kinetic-energy distributions and ion fluxes observed for different gas mixtures demonstrate the ability of this diagnostic technique to monitor plasma conditions and to investigate the ion kinetic processes occurring in the system.

04,407
PB94-211497 Not available NTIS
National Inst. of Standards and Technology (NML), Gaithersburg, MD. Quantum Metrology Div.
Magnetic Dipole Line from U LXXI Ground-Term Levels Predicted at 3200 Angstroms.
Final rept.
U. Feldman, P. Indelicato, and J. Sugar. 1991, 3p.
Pub. in Jnl. of the Optical Society of America B 8, n1 p3-5 Jan 91. Sponsored by Department of Energy, Washington, DC.

Keywords: *M1-transitions, *Uranium ions, Near ultraviolet radiation, Plasma diagnostics, Line spectra, Wavelengths, Reprints, Titanium-like ions.

Magnetic dipole (M1) lines above 2,500 A are convenient diagnostic tools for high-energy, low-density plasmas such as those of tokamaks. We found a sequence of such lines arising from transitions between two levels of the 3d(4) quintet D ground term of titanium-like ions. From Nd XXXIX to U LXXI, the calculated wavelengths range from 3,557 to 3,200 A with ionization energies of 2.7 to 8.2 keV. These lines have transition rates of 480 to 262/sec. The calculations were made with the multiconfiguration Dirac-Fock code of Desclaux (J. Phys. B 20, 651 (1987)).

04,408
PB94-212719 Not available NTIS
National Inst. of Standards and Technology (NML), Gaithersburg, MD. Atomic and Plasma Radiation Div.
Attempts at Extending the Unified Theory to Include Many-Body Effects.
Final rept.
D. E. Kelleher, and J. Cooper. 1990, 2p.
Pub. in Proceedings of International Conference on Spectral Line Shapes (10th), Austin, TX., June 25-29, 1990, p78-79.

Keywords: *Hydrogen plasma, Many-body problem, Ion collisions, Line broadening, Stark effect, Reprints, Hydrogen-like ions, Ion dynamics.

As a rule, hydrogen and hydrogen-like systems are the most sensitive to collisional Stark broadening in plasmas. The l-degeneracy in hydrogen gives rise to a first-order Stark effect. This same fact accounts for the long-range of the interaction between the hydrogenic radiator and the charged perturbers in the plasma, and thus for the fact that strong ion collisions which overlap in time are likely to occur, except at very low densities.

04,409
PB95-141008 Not available NTIS
National Inst. of Standards and Technology (EEEL), Gaithersburg, MD. Electricity Div.
Ion Kinetic-Energy Distributions in Argon rf Glow Discharges.
Final rept.
J. K. Olthoff, R. J. Van Brunt, and S. Radovanov. 1992, 9p.
Sponsored by SEMATECH, Austin, TX.
Pub. in Jnl. of Applied Physics 72, n10 p4566-4574, 15 Nov 92.

Keywords: *Argon ions, *Argon hydrides, *Glow discharges, Radio frequency discharge, Plasma sheaths, Charge exchange, Kinetic energy, Reprints.

Kinetic-energy distributions have been measured for different mass-selected ions sampled from 13.56 MHz rf glow discharges in argon inside a 'GEC rf reference cell.' The electrode geometry of this cell produces an asymmetric discharge and the cell is operated in a pressure regime where ion-molecule collisions in the sheath region of the discharge are significant. Ions are sampled from the side of the plasma perpendicular to the interelectrode axis using an electrostatic energy analyzer coupled to a quadrupole mass spectrometer. Kinetic-energy distributions for Ar(+), Ar2(+), Ar(++), and ArH(+) are presented as functions of applied rf voltage, gas pressure, and distance of the mass spectrometer entrance aperture from the edge of the electrodes.

04,410
PB95-151569 Not available NTIS
National Inst. of Standards and Technology (NML), Gaithersburg, MD. Atomic and Plasma Radiation Div.
Spectroscopic Data for Fusion Edge Plasmas.
Final rept.
W. L. Wiese. 1992, 7p.
Pub. in Nuclear Fusion 2, p7-13 1992.

Keywords: *Plasma diagnostics, *Spectroscopic analysis, Atomic energy levels, Atomic ions, Transition probabilities, Neutral atoms, Iron ions, Wavelengths, Tables(Data), Reprints, Fusion edge plasmas.

The status of spectroscopic data for neutral atoms and moderately charged atomic ions of interest to fusion edge plasmas is reviewed. A table is presented which lists references to all current critical compilations on energy levels, wavelengths and transition probabilities. The critical assessment of spectroscopic data is discussed mainly with respect to atomic transition probabilities, as the typical uncertainties for these are still quite large. For the specific case of neutral iron and its low ions (Fe I - Fe V), the scope and quality of evaluated spectroscopic data is discussed in detail.

04,411
PB95-151577 Not available NTIS
National Inst. of Standards and Technology (NML), Gaithersburg, MD. Atomic and Plasma Radiation Div.
Spectroscopic Diagnostics of Low Temperature Plasmas: Techniques and Required Data.
Final rept.
W. L. Wiese. 1991, 11p.
Pub. in Spectrochimica Acta B 46, n6-7 p831-841 1991.

Keywords: *Cold plasmas, *Plasma diagnostics, *Spectroscopic analysis, Atomic spectroscopy, Transition probabilities, Electron density, Stark effect, Argon, Iron, Reprints.

An overview of plasma diagnostic techniques based on atomic spectroscopy, interferometry, and laser scattering is given. Two widely used spectroscopic techniques--the Boltzmann-plot or slope method for excitation temperature measurements, and Stark width determinations for electron density measurements--are discussed in detail. As these techniques depend critically on the availability of accurate atomic data, specifically transition probabilities and Stark broadening parameters, the numerical data are reviewed with respect to availability and quality. For the important spectra of Ar I and Fe I, tables of the most accurate available transition probabilities--typically with uncertainties of + or - 10% or less--are given, which are based on very recent critical compilations. Some specific data needs are pointed out which would significantly contribute to improve the accuracy of the diagnostic techniques.

04,412
PB95-162962 Not available NTIS
National Inst. of Standards and Technology (CSTL), Gaithersburg, MD. Process Measurements Div.
Electrical Sensors for Monitoring rf Plasma Sheaths.
Final rept.
M. A. Sobolewski, and J. K. Olthoff. 1994, 11p.
Pub. in Proceedings of Society of Photo-Optical Instrumentation Engineers: Microelectronic Processes, Sensors, and Controls, Monterey, CA., September 27-29, 1992, v2091 p290-300 1994.

Keywords: *Plasma sheath, *Argon, *Radiofrequencies, Sensors, Glow discharges, Electric current, Electrical impedance, Electrical properties, Electric potential, Kinetics, Distribution functions, Reprints.

The authors have investigated the use of radio-frequency (rf) current and voltage measurements to monitor the electrical characteristics of rf plasmas and to predict changes in ion kinetic energy distributions. These studies were performed at 2.7 and 13.3 Pa (20 and 100 mTorr) in a Gaseous Electronics Conference (GEC) RF Reference Cell in mixtures of argon with oxygen, nitrogen and water. Simultaneous with the electrical measurements, the kinetic energy distributions of ions at the grounded electrode were obtained using a mass spectrometer equipped with an ion energy analyzer. It is expected that the measurement techniques described here could be extended to monitor the sheath above a wafer during plasma etching to obtain information about changes in the condition of the wafer surface and energies of ions bombarding it.

04,413
PB96-111927 Not available NTIS
National Inst. of Standards and Technology (EEEL), Gaithersburg, MD. Electricity Div.
Kinetic Energy Distribution of Ions Produced from Townsend Discharges in Neon and Argon.
Final rept.
M. V. V. S. Rao, S. B. Radovanov, R. J. Van Brunt, and J. K. Olthoff. 1995, 1p.
Pub. in International Conference on the Physics of Electronic and Atomic Collisions (19th), Whistler, British Columbia, Canada, July 26-August 1, 1994, p392 1995.

Keywords: *Gas discharges, *Kinetic energy, *Charge transfer, Argon, Neon, Reprints, Mass spectrometry, Townsend discharge, Electric fields, Ions.

Results are reported from measurements of the kinetic energy distributions of mass selected ions from diffuse, Townsend discharges in neon and argon at high electric field-to-gas density (E/N) ratios from 3 x 10 to the minus 18th power Vm2 to 6 x 10 to the minus 18th power Vm2. The ion energies were measured using a cylindrical mirror analyzer coupled to a quadruple mass spectrometer. The measured ion energy distributions are compared with predictions from solving the Boltzmann transport equation assuming that symmetric resonant charge transfer is the dominant ion-neutral interacton. Results for Ne+ in Ne show evidence of deviations from equilibrium.

04,414
PB96-119391 Not available NTIS
National Inst. of Standards and Technology (PL), Gaithersburg, MD. Atomic Physics Div.
Visible and UV Light from Highly Charged Ions: Exotic Matter Advancing Technology.
Final rept.
J. D. Gillaspy. 1995, 2p.
Pub. in Institute of Electrical and Electronics Engineers Leos Newsletter, v9 n4 p19-20 Aug 95.

Keywords: *Charged particles, *Ions, *Plasma diagnostics, Atomic properties, Spectroscopy, Nuclear fusion, Electron beams, Ion traps(Instrumentation), Reprints, HCIs(Highly charged ions), EBIT(Electron beam ion trap).

This news article discusses one of the applications of our research on highly charged ions: an optical diagnostic for extremely hot plasmas, such as those found in fusion devices. Our results were published in Phys. Rev. Letters earlier this year and are reviewed and updated, and put into perspective for a more general audience.

04,415
PB96-123351 Not available NTIS
National Inst. of Standards and Technology (EEEL), Gaithersburg, MD. Electricity Div.
Kinetic Energy Distributions of H(+), H2(+), and H3(+) from a Diffuse Townsend Discharge in H2 at High E/N.
Final rept.
M. V. V. S. Rao, R. J. Van Brunt, and J. K. Olthoff. 1995, 2p.
Pub. in International Symposium on Electron- and Photon-Molecule Collisions and Swarms, Berkley, CA., July 22-25, 1995, pH-9.

Keywords: *Hydrogen ions, *Gas discharges, Kinetic energy, Distribution functions, Townsend discharge, Reprints.

The translational kinetic-energy distributions of the predominant ions, H+, H2+, and H3+, formed in a diffuse Townsend discharge in H2 were measured for electric field-to-gas density ratios (E/N) from 7 x 10 to the minus 19th power Vm2 to 2 x 10 to the minus 18th power Vm2. The discharge was generated in a parallel-plate electrode gap for conditions corresponding to the 'left-hand' side of the Paschen minimum where the electric field in the gap is expected to be constant and uniform, i.e., the discharge is characterized by a well defined E/N. The discharge cell configuration and ion measurement system are similar to those described previously. The ions were sample through a 0.1 mm diameter orifice in the center of the stainless-steel cathode. Simultaneous analyis of ion energy and mass was performed using a cylindrical mirror analyzer coupled to a quadrupole mass spectrometer.

04,416
PB96-138532 Not available NTIS
National Inst. of Standards and Technology (EEEL), Gaithersburg, MD. Semiconductor Electronics Div.
Nonequilibrium Total-Dielectric-Function Approach to the Electron Boltzmann Equation for Inelastic Scattering in Doped Polar Semiconductors.
Final rept.
B. A. Sanborn. 1995, 9p.
Pub. in Physical Review B, v51 n20 p14 247-14 255 May 95.

Keywords: *Dielectric functions, *Semiconductors, Inelastic scattering, Reprints, *Doped polar semiconductors, Boltzmann equation.

The paper describes a simple and general method for deriving the inelastic collision term in the electron Boltzmann equation for scattering from a coupled electron-phonon system and applies the method to the case of doped polar semiconductors. In the Born approximation, the inelastic differential scattering rate W(inel) can be expressed in terms of the nonequilibrium total dynamic dielectric function, which includes both electronic and lattice contributions. Within the random-phase approximation W(inel) separates into two componenents: an electron-electron interaction containing the nonequilibrium distribution function for excitations of the electron gas and a Frohlich interaction including the phonon distribution function and self-energy due to polarization of the electrons. Each of these two interactions is screened by only the electronic part of the total dielectric function, which contains the high-frequency dielectric constant, unlike commonly used expressions that contain the static dielectric constant.

04,417
PB96-141130 Not available NTIS
National Inst. of Standards and Technology (EEEL), Boulder, CO. Electromagnetic Technology Div.
Apparatus for Resistance Measurement of Short, Small-Diameter Conductors.
Final rept.
C. A. Thompson. 1994, 3p.
Pub. in Institute of Electrical and Electronics Engineers Transactions on Instrumentation and Measurements, v43 n4 p675-677 Aug 94.

Keywords: *Electrical resistivity, *Conductors, Copper, Reprints, Fibers, Measurement, Resistance.

A system for determining the dc resistance of individual conductors 2 micrometers in diameter and 0.5-1 mm in length is described. The system uses a four-wire measurement, computerized data acquisition, and unique sample handling and contacting methods. To demonstrate system operation, data from measurements made on small-diameter copper wires are presented. These wires were first measured in long lengths on another system and then cut into short lengths and remeasured on this system. The results from these two measurement systems show that this system is an effective tool for determining the resistance per unit length of short, small-diameter conductors.

04,418
PB96-204458 Not available NTIS
National Inst. of Standards and Technology (MSEL), Gaithersburg, MD. Polymers Div.
Shear Suppression of Critical Fluctuations in a Diluted Polymer Blend.
Final rept.
E. K. Hobbie, A. I. Nakatani, H. Yajima, J. F. Douglas, and C. C. Han. 1996, 3p.
Pub. in Physical Review E, v53 n5 p4322-4324 May 96.

Keywords: *Phase separation, *Diluted blends, Reprints, Neutron scattering, Light scattering, *Fisher renormalization.

Small-angle neutron scattering has been combined with equilibrium dynamic light scattering to study shear-induced mixing in a diluted high-molecular-weight polymer blend. The data show an enhancement of critical fluctuations upon dilution and are found to collapse onto a universal scaling curve containing no free parameters. The scaling curve is motivated by the theoretical predictions of Onuki and Kawasaki for undiluted binary mixtures. The data also appear to suggest that 'Fisher renormalization' is relevant in this diluted pseudobinary polymer mixture, consistent with a previous dynamic-light-scattering study.

04,419
PB97-111231 Not available NTIS
National Inst. of Standards and Technology (MSEL), Gaithersburg, MD. Ceramics Div.
Characterization and Processing of Spray-Dried Zirconia Powders for Plasma Spray Application.
Final rept.
P. Pei, S. G. Malghan, S. J. Dapkunas, and P. H. Zajchowski. 1996, 9p.
Pub. in Jnl. of Thermal Spray Technology, v5 n3 p343-351 Sep 96.

Keywords: *Plasma spray, *Zirconia powder, *Spray dried powder, Powder characterization, Thermal barrier coatings, Thermal rupture test, Reprints.

The correlation between the performance of plasma spray coatings and feedstock powder properties is not fully understood. To demonstrate this correlation, eight spray-dried zirconia powders containing a mass fraction of 20% Y2O3(yttria) were characterized with respect to their physical, bulk chemical, and surface chemical properties. The same powders were plasma spray deposited as coatings, and their relative performance was evaluated using a thermal rupture test developed by Pratt and Whitney. The specific powder properties studied were chemical composition, binder content, particle size distribution, powder morphology, interface chemistry, thermogravimetry, phase composition, and specific surface area. Among the characterization data, the binder-related properties of the powder correlated most strongly with the thermal rupture test data. Specifically, higher binder contents were associated with poor thermal rupture test performance.

Radiofrequency Waves

04,420
AD-A292 471/0 PC A02/MF A01
National Bureau of Standards, Boulder, CO. Central Radio Propagation Lab.
Higher-Order Approximations in Ionospheric Wave-Propagation.
J. Feinstein. Jun 50, 10p.
Pub. in Jnl. of Geophysical Research, v55 n2 p161-170, Jun 50.

Keywords: *Approximation, *Ionospheric propagation, Velocity, Mathematical models, Electromagnetic fields, Ionosphere, Reprints, Vibration, Equations of motion, Time dependence, Electromagnetic wave transmission, Drift, Resonance, Perturbations, Transverse waves, Maxwells equations, Plane waves, Difference frequency.

It is found that the ionosphere, even when considered homogeneous, is a linear medium for the propagation of electromagnetic waves only as a first approximation. Second-order terms give rise to harmonics, and to sum and difference frequencies when low independent waves traverse the same physical region. These new frequencies are, in general, of the nature of forced vibrations, except in the case where their propagation characteristics are those of a natural mode capable of existing in the region. A resonance effect then occurs, the new wave increasing its energy at the expense of the interacting waves, and assuming an independent existence. While these effects couple energy from the primary wave, they do not affect its propagation characteristics. As a result of the degeneracy of the determinantal equation for the propagation constant, the introduction of any disturbing physical effects, such as a layer drift velocity, raises the degree of the equation, resulting not merely in changes in the values of the propagation constants of the usual modes, but, in addition, introducing new ones. For the usual disturbing effects encountered in the ionosphere, the energy content of these new modes is negligibly small. (AN).

04,421
PB94-211950 Not available NTIS
National Inst. of Standards and Technology (EEEL), Boulder, CO. Electromagnetic Fields Div.
Electromagnetic Scattering by a Periodic Surface with a Wedge Profile.
Final rept.
D. A. Hill. 1992, 18p.
Pub. in Electromagnetics 12, p247-264 1992.

Keywords: *Electromagnetic scattering, Polarization(Waves), Two dimensional, Numerical solution, Perturbation theory, Absorbers(Materials), Matrices, Electromagnetic absorption, Reprints, Dielectric wedges, Periodic surfaces, Extended boundary conditions, Ill-conditioned problems(Mathematics).

Two-dimensional scattering from a periodic surface with a wedge profile is treated for both TE and TM polarization. The interface can be either perfectly conducting or penetrable, and the extended boundary condition (EBC) is used in both cases. The method results in simple matrix elements and is easy to apply. Comparison with a perturbation solution shows that the EBC method has greater accuracy and a greater range of validity. Even so, EBC becomes numerically ill conditioned for surface heights that are a significant fraction of the period or the wavelength. Numerical results are presented for conservation of power, and some comparisons are made with previous results for sinusoidal surfaces. Some applications to rf absorber are also presented.

Radiofrequency Waves

04,422
PB94-216512 Not available NTIS
National Inst. of Standards and Technology (NEL), Gaithersburg, MD. Precision Engineering Div.
Alternative Single Integral Equation for Scattering by a Dielectric.
Final rept.
E. Marx. 1991, 4p.
Pub. in Proceedings of Antennas and Propagation Society Symposium 1991 Digest, London, Ontario, Canada, June 24-28, 1991, p1635-1638.

Keywords: *Electromagnetic scattering, *Integral equations, Boundary conditions, Cylindrical bodies, Helmholtz equations, Delta function, Dielectrics, Reprints.

A single integral equation for electromagnetic scattering by a dielectric cylindrical body is derived. The unknown is the jump in the auxiliary field across the boundary. The delta-function behavior of the derivative of the solution of the Helmholtz equation is studied in detail.

04,423
PB95-161675 Not available NTIS
National Inst. of Standards and Technology (EEEL), Gaithersburg, MD. Electricity Div.
ELF Electric and Magnetic Field Measurement Methods.
Final rept.
M. Misakian. 1993, 6p.
Pub. in Proceedings of International Symposium on Electromagnetic Compatibility, Dallas, TX., August 9-13, 1993, 6p.

Keywords: *Extremely low frequencies, *Magnetic fields, *Electric fields, *Frequency measurement, Harmonic generation, Harmonics, Measuring methods, Calibration, Instrumentation, Standards, Reprints, Power frequency, Harmonic fields.

The paper surveys the instrumentation, calibration procedures, measurement techniques, and standards which can be used to characterize extremely low frequency (ELF) electric and magnetic fields. While the focus of the paper is on power frequency and power frequency harmonic fields, the measurement methods discussed are appropriate in principle for other ELF frequencies.

04,424
PB95-261939 (Order as PB95-261897, PC A07/MF A02)
National Institute of Standards and Technology, Boulder, CO.
Low-Frequency Model for Radio-Frequency Absorbers.
J. Randa. 1995, 11p.
Included in Jnl. of Research of the National Institute of Standards and Technology, v100 n3 p257-267 May/Jun 95.

Keywords: *Law frequencies, *Radio frequencies, *Absorbers(Equipment), *Models, Electromagnetic absorption, Anechoic chambers, National Institute of Standards and Technology.

A simple model is developed to characterize the behavior of radio-frequency absorbers at low frequency. The absorber is represented by a flat, homogeneous, isotropic slab of lossy material, with effective constitutive parameters are determined by a fit to measured data. Excellent fits are obtained in the two applications considered. The model is intended for use in the characterization of absorber-lined chambers at low frequency.

04,425
PB96-112222 Not available NTIS
National Inst. of Standards and Technology (PL), Gaithersburg, MD. Ionizing Radiation Div.
Study of Multiple Scattering Background in Compton Scatter Imaging.
Final rept.
G. Barnea, C. E. Dick, A. Ginzburg, E. Navon, and S. M. Seltzer. 1995, 8p.
Pub. in NDT and E International, v28 n3 p155-162 1995.

Keywords: *Electromagnetic scattering, *Compton effect, Reprints, Monte Carlo method, Computerized simulation, *Foreign technology, *Multiple scattering.

The multiple scattering background in Compton scatter imaging at 662 keV is studied, both experimentally and by Monte Carlo radiation transport calculations as a function of the scattering angle, scattering material (aluminum, brass and tin) and object thickness. A double-peak structure was observed in the pulse-height distribution for the thicker brass and tin objects and at the larger scattering angles (90 degrees and 120 degrees). In addition to the Compton peak, a second peak appeared at a higher energy. Monte Carlo transport simulations have revealed the origin of the second peak: photons that have scattered exactly twice before reaching the detector. The ratio of the multiple-scattered radiation to the total radiation detected was calculated as a function of the energy-window width around the Compton peak and scattering angle. The results of this study may help in the design of future Compton scatter imaging apparatus.

04,426
PB96-138474 Not available NTIS
National Inst. of Standards and Technology (EEEL), Boulder, CO. Electromagnetic Fields Div.
Accurate Computations of Radar Cross Sections of Simple Objects.
Final rept.
L. A. Muth, and J. Gary. 1994, 5p.
Pub. in International Microwave Conference (10th) MIKON - 94, Ksiaz Castle, Poland, May 30-June 2, 1994, v1 p298-302.

Keywords: *Radar cross sections, *Measurement, Two dimensional models, Electromagnetic scattering, Boundary conditions, Impedance, Computational grids, Helmholtz equations, Error analysis, Reprints.

A comparison of two methods for the computation of the radar cross section is given. The first method is by Mei and the second by Keller and Givoli. Both direct methods solve a discrete version of the Helmholtz equation in a small domain containing the scatterer using absorbing outer boundary conditions. The solutions for a plane wave scattered from a two-dimensional infinite cylinder are better than 0.10 dB when compared to the analytic solutions.

04,427
PB96-148077 Not available NTIS
National Inst. of Standards and Technology (EEEL), Boulder, CO. Electromagnetic Fields Div.
Spatial Correlation Function for Fields in a Reverberation Chamber.
Final rept.
D. A. Hill. 1995, 1p.
Pub. in Institute of Electrical and Electronics Engineers Transactions on Electromagnetic Compatability, v37 n1 p1 Feb 95.

Keywords: *Plane waves, *Reverberation, *Chambers, Spatial filtering, Acoustic properties, Wave scattering, Correlation, Reprints, Reverberation chamber, Plane wave spectrum, Spatial correlation.

The plane-wave spectrum representation has been found useful for providing a mathematical description for the response of a receiving antenna or other test object in a reverberation chamber and for calculating the quality factor (Q) for reverberation chambers of arbitrary geometries. The purpose of this correspondence is to show that the plane-wave spectrum representation can also be used to provide a simple derivation for the spatial correlation function of the fields. The identical correlation function has been derived via a cavity mode representation and has been tested experimentally.

04,428
PB97-110274 Not available NTIS
National Inst. of Standards and Technology (MEL), Gaithersburg, MD. Precision Engineering Div.
Hypersingular Single Integral Equation and the Dielectric Wedge.
Final rept.
E. Marx. 1992, 4p.
Pub. in Institute of Electrical and Electronics Engineers Antennas and Propagation Society International Symposium, Chicago, IL., July 18-25, 1992, v4 p1865-1868, 1992 Digest.

Keywords: *Dielectric wedge, *Electromagnetic scattering, Far fields, Hypersingular integrals, Integral equations, Sharp edges, Reprints.

The theory of the behavior of electromagnetic fields near the edge of a dielectric wedge is poorly understood and disagrees with numerical results. Here the authors compute the fields scattered by a finite dielectric wedge and compared the results obtained by using two different integral equations. The unknown boundary function is either the jump n in the normal derivative of the auxiliary field across the boundary or the jump 0 in the field itself. In the latter case, one of the integrals is hypersingular.

04,429
PB97-110522 Not available NTIS
National Inst. of Standards and Technology (MEL), Gaithersburg, MD. Precision Engineering Div.
Causality and Maxwell's Equations.
Final rept.
E. Marx. 1993, 5p.
Pub. in Institute of Electrical and Electronics Engineers International EMC Symposium, Anaheim, CA., August 17-21, 1992.

Keywords: *Electromagnetic scattering, *Integral equations, Maxwell's equations, Algorithms, Reprints, *Causality.

Causality is addressed in the context of the principles of electromagnetism for nonsinusoidal fields. Topics include Maxwell's equations, integral equations for scattering, stepping-in-time algorithms, dispersive media, and Green's functions.

04,430
PB97-110530 Not available NTIS
National Inst. of Standards and Technology (MEL), Gaithersburg, MD. Precision Engineering Div.
Electromagnetic Scattering from a Dielectric Wedge and the Single Hypersingular Integral Equation.
Final rept.
E. Marx. 1993, 8p.
See also PB97-110274.
Pub. in Institute of Electrical and Electronics Engineers Transactions on Antennas and Propagation, v41 n8 p1001-1008 Aug 93.

Keywords: *Electromagnetic scattering, *Dielectrics, Integral equations, Reprints, Dielectric wedges.

Electromagnetic fields scattered by a finite dielectric wedge are computed using a hypersingular integral equation (HIE). The results are compared with those obtained previously using a singular integral equation (SIE) and with the theory that predicts that the fields near the edge of the wedge behave like static fields. The HIE produces more consistent results than the SIE, probably because the unknown boundary function tends to a constant near the edge instead of diverging. The two numerical methods agree reasonably well, and these results agree only in part with the static field behavior.

Solid State Physics

04,431
AD-A280 150/4 PC A05/MF A01
National Bureau of Standards, Gaithersburg, MD.
Atomic Energy Levels in Crystals.
Monograph rept.
J. L. Prather. 24 Feb 61, 90p.

Keywords: *Atomic energy levels, Crystals, Perturbations, Ions, Electrostatics, Charged particles, Symmetry, Angular momentum, Selection rules(Physics), Dipole moments, Magnetic dipoles, Quadrupole moment, Transitions, Absorption spectra, Optical properties, Nuclear electric moments, Spectroscopy, N-99057.

No abstract available.

04,432
DE95015476 PC A04/MF A01
National Inst. of Standards and Technology (EEEL), Boulder, CO. Electromagnetic Technology Div.
Electromechanical properties of superconductors for DOE fusion applications.
J. W. Ekin, S. L. Bray, C. L. Lutgen, and W. L. Bahn. Jan 94, 53p, NISTIR-5013.
Contract AI01-84ER52113
Sponsored by Department of Energy, Washington, DC.

Keywords: *Superconducting Magnets, *Superconductors, Current Density, Electromechanics, Leading Abstract, Magnetic Fields, Niobium Base Alloys, Stresses, Thermonuclear Reactors, Tin Alloys, EDB/700430, EDB/665412.

The electrical performance of many superconducting materials is strongly dependent on mechanical load. This report presents electromechanical data on a broad range of high-magnetic-field superconductors. The conductors that were studied fall into three general categories: Candidate conductors, experimental conductors, and reference conductors. Research on candidate conductors for fusion applications provides screening data for superconductor selection as well as engineering data for magnet design and performance analysis. The effect of axial tensile strain on critical-current density was measured for several Nb(sub 3)Sn candidate conductors including the US-DPC (United States Demonstration Poloidal Coil) cable strand and an ITER (International Thermonuclear Experimental Reactor) candidate conductor. Also, data are presented on promising experimental superconductors that have strong potential for fusion applications. Axial strain measurements were made on a V(sub 3)Ga tape conductor that has good performance at magnetic fields up to 20 T. Axial strain data are also presented for three experimental Nb(sub 3)Sn conductors that contain dispersion hardened copper reinforcement for increased tensile strength. Finally, electromechanical characteristics were measured for three different Nb(sub 3)Sn reference conductors from the first and second VAMAS (Versailles Project on Advanced Materials and Standards) international Nb(sub 3)Sn critical-current round robins. Published papers containing key results, including the first measurement of the transverse stress effect in Nb(sub 3)Sn, the effect of stress concentration at cable-strand crossovers, and electromechanical characteristics of Nb(sub 3)Al, are included throughout the report.

04,433
DE95016656 PC A01/MF A01
National Inst. of Standards and Technology, Boulder, CO.
VAMAS interlaboratory comparisons of critical current vs. strain in Nb(sub 3)Sn.
J. W. Ekin. 1989, 5p, CONF-8902131-3.
Contract AI01-84ER52113
Japan-US workshop on high field superconductors materials and standard procedures for high-field superconducting materials testing (6th), Boulder, CO (United States), 22-24 Feb 1989. Sponsored by Department of Energy, Washington, DC.

Keywords: *Niobium Base Alloys, *Tin Alloys, *Meetings, Comparative Evaluations, Critical Current, Current Density, Intermetallic Compounds, Magnetic Fields, Strains, Superconducting Magnets, Tensile Properties, Wire, EDB/360107, EDB/360103, EDB/665412.

A comparison is made of measurements of the effect of axial tensile strain on the critical current of multifilamentary Nb(sub 3)Sn superconductors by three different laboratories. Two of the laboratories used short sample testing apparatus wherein a straight section of conductor was cooled in a force-free state. One of the laboratories used a spring apparatus wherein a long sample was reacted in a coil shape and attached to a spring sample holder. The agreement between the results for the two laboratories that used the straight sample apparatus was quite good, within 15% for all three conductors at 15 T, except at very high strain for one conductor which had an upper critical field close to the measurement field. To make a comparison with the data obtained using the spring method, it was necessary to fit the data to the compressive prestrain determined using the straight-sample technique. With such a fit, the agreement was variable, between 15 and 25% depending on the conductor. Values of the prestrain and irreversible strain obtained from the straight sample data agreed within 0.06% and 0.05% respectively. Values of the maxi (strain-free) upper critical fields agreed within several tenths of a tesla.

04,434
DE95016659 PC A01/MF A01
National Inst. of Standards and Technology, Boulder, CO.
Transverse stress effect on the critical current of internal tin and bronze process Nb(sub 3)Sn superconductors.
J. W. Ekin, S. L. Bray, P. Danielson, D. Smathers, and R. L. Sabatini. 1989, 4p, CONF-8902131-2.
Contract AI01-84ER52113
Japan-US workshop on high field superconductors materials and standard procedures for high-field superconducting materials testing (6th), Boulder, CO (United States), 22-24 Feb 1989. Sponsored by Department of Energy, Washington, DC.

Keywords: *Niobium Alloys, *Tin Alloys, Comparative Evaluations, Critical Current, Fabrication, Intermetallics, Stresses, Superconducting Magnets, Tensile Properties, Wire, EDB/360107, EDB/360103, EDB/665412.

The effect of transverse stress on the critical current density, J(sub c), has been shown to be significant in bronze process Nb(sub 3)Sn, with the onset of significant degradation at about 50 Mpa. In an applied field of 10 T, the magnitude of the effect is about seven times larger for transverse stress than for axial tensile stress. In a subsequent study, similar results were observed in another bronze process Nb(sub 3)Sn conductor made by a different manufacturer. The mechanism accounting for the transverse stress effect and its large magnitude compared with the axial tensile effect is still the subject of speculation. In an attempt to better understand the nature of the effect, The authors have undertaken a series of experiments to determine whether the transverse stress effect depends on the grain morphology of the Nb(sub 3)Sn reaction layer in the superconductor. To do this, the authors have measured the effect in an internal tin conductor with excess tin, which yields a more equiaxed Nb(sub 3)Sn grain morphology than for bronze process Nb(sub 3)Sn, where the grains are more columnar. The results for the effect of transverse compression on the J(sub c) of a round bronze process Nb(sub 3)Sn wire are given. The data are probably applicable to a wide variety of Nb(sub 3)Sn conductors for magnet engineering.

04,435
PB94-145984 PC A01/MF A01
National Inst. of Standards and Technology, Boulder, CO.
Alternating-Field Susceptometry and Magnetic Susceptibility of Supercondoctors. Presented at Office of Naval Research Workshop on Magnetic Susceptibility of Superconductors and Other Spin Systems. Held in Berkeley Springs, West Virginia on 20 May 1991.
R. B. Goldfarb, M. Lelental, and C. A. Thompson.
Oct 91, 36p, NISTIR-3977.
Sponsored by Eastman Kodak Co., Rochester, NY.

Keywords: *Magnetic susceptibility, *Superconductors, High temperature superconductors, Superconducting films, Critical temperature, Critical current, Critical field, Meissner effect, Alternating current, Calibration, Diamagnetism, Demagnetization, Granular materials, Sensitivity, Design, Reviews, Bibliographies, *Susceptometers.

The review critically analyzes current practice in the design, calibration, sensitivity determination, and operation of alternating-field susceptometers, and examines applications in magnetic susceptibility measurements of superconductors. Critical parameters of the intrinsic and coupling components of granular superconductors may be deduced from magnetic susceptibility measurements. The onset of intrinsic diamagnetism corresponds to the initial decrease in electrical resistivity upon cooling, but the onset of intergranular coupling coincides with the temperature for zero resistivity. The lower critical field may be determined by the field at which the imaginary part of susceptibility increases from zero. Unusual features in the susceptibility of superconductor films, such as a magnetic moment that is independent of film thickness and the variation of susceptibility with angle, are related to demagnetization. Common misunderstandings of the Meissner effect, magnetic units, and formula conversions are discussed. There is a comprehensive summary of critical-state formulas for slabs and cylinders, including new equations for complex susceptibility in large alternating fields. Limitations on the use of the critical-state model for deducing critical current density are listed and the meaning of the imaginary part of susceptibility is considered.

04,436
PB94-160744 PC A03/MF A01
National Inst. of Standards and Technology (CAML), Gaithersburg, MD. Applied and Computational Mathematics Div.
Computation of Dendrites Using a Phase Field Model.
A. A. Wheeler, B. T. Murray, and R. J. Schaefer. Jul 92, 42p, NISTIR-4894.

Keywords: *Dendritic crystals, *Crystal growth, *Solidification, Finite difference theory, Mathematical models, Two-dimensional calculations, Numerical solution, Interfaces, Nickel, Spheres, Free boundary problems, Phase field models.

A phase field model is used to numerically simulate the solidification of a pure material. We employ it to compute growth into an undercooled liquid for a one-dimensional spherically symmetric geometry and a planar two-dimensional rectangular region. The phase field model equations are solved using finite difference techniques on a uniform mesh. For the growth of a sphere, the solutions from the phase field equations for sufficiently small interface widths are in good agreement with a numerical solution to the classical sharp interface model obtained using a Green's function approach. In two dimensions, we simulate dendritic growth of nickel with four-fold anisotropy and investigate the effect of anisotropy level on the growth of a dendrite. The quantitative behavior of the phase field model is evaluated for varying interface thickness and spatial and temporal resolution. Results are discussed.

04,437
PB94-161502 PC A08/MF A02
National Inst. of Standards and Technology (MSEL), Gaithersburg, MD. Reactor Radiation Div.
NIST Reactor: Summary of Activities October 1992 through September 1993.
Internal rpt.
C. L. O'Connor. Feb 94, 155p, NISTIR-5362.
See also PB93-162873.

Keywords: *NBSR reactor, Research reactors, Activation analysis, Cold neutrons, Crystal structure, Neutron diffraction, Neutron radiography, Nondestructive tests, Analytical chemistry, YBCO superconductors, Fullerenes, Hydrogen, Magnetism, Polymers, Macromolecules, Microstructure, Thin films, Neutron dosimetry, Multilayers.

This report summarizes all of the programs which use the NIST reactor. It covers the period for October 1992 through September 1993. The programs range from the use of neutron beams to study the structure and dynamics of materials through nuclear physics and neutron standards to sample irradiations for activation analysis, isotope production, neutron radiography, and nondestructive evaluation.

04,438
PB94-169745 Not available NTIS
National Inst. of Standards and Technology, Gaithersburg, MD.
Precision Comparison of the Lattice Parameters of Silicon Monocrystals.
E. G. Kessler, A. Henins, R. D. Deslattes, L. Nielsen, and M. Arif. 1994, 18p.
Included in Jnl. of Research of the National Institute of Standards and Technology, v99 n1 p1-18 Jan/Feb 94.

Keywords: *Lattice parameters, *Silicon, Interlaboratory comparisons, X-ray spectrometers, X-ray diffraction, Michelson interferometers, Bragg angle, Single crystals, Comparators, Monocrystals, Precision, Uncertainty, Reprints, US NIST.

The lattice spacing comparator established at the National Institute of Standards and Technology to measure the lattice spacing differences between nearly perfect crystals is described in detail. Lattice spacing differences are inferred from the measured differences in Bragg angles for different crystals. The difference in lattice spacing between silicon samples used at Physikalisch-Technische Bundesanstalt (PTB) and NIST has been measured with a relative uncertainty of 1 x 10(-8). The measurement is consistent with absolute lattice spacing measurements made at PTB and NIST. Components of uncertainty associated with systematic effects due to misalignments are derived and estimated.

04,439
PB94-172129 Not available NTIS
National Inst. of Standards and Technology (MSEL), Gaithersburg, MD.
RDFs and Fe-Fe Pair Correlations in an AlCuFe Icosahedral Alloy by Double Isotopic Substitution.
Final rept.
R. Bellissent, B. Mozer, Y. Calvayrac, D. Gratias, and J. W. Cahn. 1993, 4p.
Pub. in Jnl. of Non-Crystalline Solids 153/154, p1-4 1993.

Keywords: Aluminum copper alloys, Iron alloys, Neutron diffraction, Crystal structure, Reprints, *Quasicrystals, Icosahedral phase, Radial distribution functions.

Short range order in an AlCuFe quasicrystal was investigated using the double isotopic substitution of Fe in

order to determine partial radial distribution (pair correlation) functions of the system. The experiment was carried out on the 7c2 spectrometer at Orphee designed for studies of atomic local order in liquid and amorphous systems. Very accurate total radial distribution functions were calculated. All of the observed pair distances, up to about 10 A, are consistent with the atomic positions of the model proposed by Cornier-Quiquandon et al. (Phys. Rev. B44 (1991) 2071). Partial Fe-Fe pair correlation functions have been extracted and show that Fe atoms occupy only a subset of sites.

04,440
PB94-172210 Not available NTIS
National Inst. of Standards and Technology (NML), Gaithersburg, MD. Gas and Particulate Science Div.
Raman and Fluorescence Spectra Observed in Laser Microprobe Measurements of Several Compositions in the Ln-Ba-Cu-O System.
Final rept.
E. S. Etz, T. D. Schroeder, and W. Wong-Ng. 1990, 5p.
Pub. in Proceedings of Annual Conference of the Microbeam Analysis Society (25th), Seattle, WA., August 12-18, 1990, p243-247.

Keywords: *Superconductors, Rare earth compounds, Vibrational spectra, Raman spectra, Microanalysis, Microprobes, Fluorescence, Impurities, Reprints, Erbium barium cuprates, Europium barium cuprates.

The superconducting and related phases in the Ln-Ba-Cu-O system are investigated by Raman microprobe measurements to obtain their vibrational Raman spectra and any structure-specific fluorescence spectra from active lanthanide (Ln) or rare earth ions. These studies are aimed at relating the observed optical spectra to the compositional and structural aspects of these materials. Specific examples are discussed with special reference to the erbium and the europium analogs of the yttrium 1:2:3 superconductor. Highlighted are the results from certain phases that are known to constitute potential impurity phases in the superconducting compositions. The microanalytical implications of these results are discussed.

04,441
PB94-172475 Not available NTIS
National Inst. of Standards and Technology (MSEL), Gaithersburg, MD. Reactor Radiation Div.
Neutron-Spectroscopy Study of the Hydrogen Vibrations in Hydrogen-Doped YBa2Cu3Ox.
Final rept.
U. Knell, H. Wipf, H. J. Lauter, T. J. Udovic, and J. J. Rush. 1993, 7p.
Pub. in Jnl. of Phys.: Condens. Matter 5, p7607-7613 1993.

Keywords: *YBCO superconductors, Electron phonon interactions, Neutron spectroscopy, Orthorhombic lattices, Tetragonal lattices, Doped materials, Cryogenic temperature, Reprints, *Hydrogen vibrations.

The authors studied H vibrations in H-doped YBa2Cu3O(x)H(y) (y = 0.6) by neutron spectroscopy. Neutron spectra were taken at 10 and 14 K from both orthorhombic (x approx equals 6.9) and tetragonal (x approx equals 6.3) samples. The spectra exhibit large H-induced intensities in the energy range between 40 and 130 meV. In comparison to orthorhombic samples, the H vibrations in tetragonal samples are shifted to lower energies by about 11%. This shift is opposite to the spectral shift of the lattice vibrations between H-free orthorhombic and tetragonal YBa2Cu3O(x), frequently attributed to differences in the electron-phonon coupling. The results show that any such differences in the electron-phonon coupling are not apparent in the H vibrations. The results also support previous suggestions that the H occupies sites in the close neighborhood of the Cu(1) atomic planes.

04,442
PB94-172558 Not available NTIS
National Inst. of Standards and Technology (MSEL), Gaithersburg, MD. Reactor Radiation Div.
Structural and Magnetic Ordering in Iron Oxide/Nickel Oxide Multilayers by X-ray and Neutron Diffraction (Invited).
Final rept.
D. M. Lind, S. P. Tay, S. D. Berry, J. A. Borchers, and R. W. Ewrin. 1993, 6p.
Contract N00014-92-J-1356, Grant NSF-DMR-9206870
Pub. in Jnl. of Applied Physics 73, n10, p6886-6891, 15 May 93. Sponsored by Office of Naval Research, Arlington, VA. and National Science Foundation, Arlington, VA.

Keywords: *Iron oxides, *Nickel oxides, *Superlattices, Antiferromagnetic materials, X ray diffraction, Neutron diffraction, Magnetization, Thin films, Reprints, Magnetic ordering, Exchange interactions, Multilayers.

Presented are studies of the magnetic and structural ordering in superlattices composed of Fe3O4 and NiO, and their study by a variety of techniques including x-ray and neutron diffraction, and SQUID magnetometry, X-ray diffraction indicates that structures with individual layer thicknesses down to 8.5 A grow as single crystals in registry with the substrate lattice with a layer-thickness-dependent tetragonal lattice distortion due to epitaxial and interfacial lattice mismatch. The lattice coherence of the Fe3O4 layers, however, is degraded by stacking faults between adjacent spinel layers. Neutron diffraction indicates that the NiO orders antiferromagnetically along the (in brackets: 111) direction with a magnetic coherence that extends over several superlattice bilayers, and the presence of an enhancement in the NiO Neel temperature in thin layered superlattices. These results are compared with SQUID magnetometry, which shows large anisotropy energies, but a lack of favored magnetization direction, indicating that the magnetic ordering in these systems is dominated by the exchange coupling across the interfaces.

04,443
PB94-172665 Not available NTIS
National Inst. of Standards and Technology (IMSE), Gaithersburg, MD. Reactor Radiation Div.
Enhanced Curie Temperatures and Magnetoelastic Domains in Dy/Lu Super Lattices and Films.
Final rept.
R. S. Beach, J. A. Borehers, A. Matheny, B. Everitt, K. Pettit, J. J. Rhyne, C. P. Flynn, R. W. Erwin, and M. B. Salamon. 1993, 4p.
Pub. in Physical Review Letters 70, No. 22, pp3502-3505 May 31, 1993. Sponsored by National Science Foundation, Arlington, VA.

Keywords: *Dysprosium, *Lutetium, *Superlattices, Curie temperature, Magnetostriction, Thin films, Ferromagnetic materials, Alignment, Reprints.

We have grown high quality superlattices of Dy with nonmagnetic Lu and find that the 2.4% epitaxial compression nearly doubles the ferromagnetic T(c) of Dy with little change in the Neel temperature. A helimagnetic phase exists over a narrow temperature range. Below T(c) in superlattices, 300 A orthorhombic domains form despite epitaxial constraints, each with a magnetostrictive distortion comparable to that of bulk Dy. For the thinnest intervening Lu layers, individual ferromagnetic Dy blocks have parallel alignment; the remaining samples show antiparallel alignment, coherent over many bilayer periods.

04,444
PB94-173044 Not available NTIS
National Inst. of Standards and Technology (MSEL), Gaithersburg, MD. Reactor Radiation Div.
Dispersions of Magnetic Excitations of the Pr Ions in Pr2CuO4.
Final rept.
I. W. Sumarlin, J. W. Lynn, and T. Chattpadhyay. 1994, 5p.
Pub. in Physica C 219, p195-199 1994.

Keywords: *Superconductors, Praseodymium ions, Crystal field, Dispersion, Excitons, Reprints, *Praseodymium cuprates, Exchange interactions.

The authors have used inelastic neutron scattering techniques to measure the dispersion of the singlet-doublet magnetic excitons of the Pr(3+) ions in the singlet ground state system Pr2CuO4. The excitons exhibit significant dispersion both within the basal plane as well as along the c-axis direction, directly demonstrating the Pr-Pr exchange interactions. These exchange interactions must be mediated through the CuO2 layers involved in the formation of the superconducting state.

04,445
PB94-173069 Not available NTIS
National Inst. of Standards and Technology (PL), Gaithersburg, MD. Electron and Optical Physics Div.
Homoepitaxial Growth of Iron and a Real Space View of Reflection-High-Energy-Electron Diffraction.
Final rept.
J. A. Stroscio, D. T. Pierce, and R. A. Dragoset. 1993, 4p.
Pub. in Physical Review Letters 70, n23 p3615-3618, 7 Jun 93. Sponsored by Office of Naval Research, Arlington, VA.

Keywords: *Iron, *Epitaxial growth, Scanning tunneling microscopy, Whiskers(Single crystals), Electron diffraction, Surface diffusion, Temperature range 0273-0400 K, Temperature range 0400-1000 K, Metal films, Reprints.

The authors report real space views of the homoepitaxial growth of Fe on Fe(001) whiskers observed by scanning tunneling microscopy. A measure of the surface diffusion of the Fe atoms is obtained over the temperature range of 20-250 deg C. The effect of the diffusion kinetics is observed in the surface morphology as a decrease in the interface width with temperature. Measurements of reflection-high-energy-electron diffraction during growth allow a comparison of real and reciprocal space techniques.

04,446
PB94-185162 Not available NTIS
National Inst. of Standards and Technology (EEEL), Boulder, CO. Electromagnetic Technology Div.
Effects of Critical Current Density, Equilibrium Magnetization and Surface Barrier on Magnetization of High Temperature Superconductors.
Final rept.
D. X. Chen, R. W. Cross, and A. Sanchez. 1993, 9p.
Pub. in Cryogenics 33, n7 p695-703 1993.

Keywords: *High temperature superconductors, *Magnetization, YBCO superconductors, Critical current, Surface barrier, Mathematical models, Temperature range 0065-0273 K, Current density, Reprints, Yttrium barium cuprates.

An extended critical state model which includes the effects of bulk critical current density, equilibrium magnetization and surface barrier is developed for the magnetization of superconductors. The equilibrium magnetization and surface barrier are modeled by an applied field dependent surface supercurrent density j(sub s)(H), whose presence changes the boundary field of the bulk. The volume supercurrents flow with a density equal to the internal field dependent critical current density J(sub c)(H(sub i)). The magnetization M is produced by both supercurrents. For the M(H) curve computation, exponential-type J(sub c(H(sub i)) and j(sub s)(H) values are used for the general case of an infinite sample of rectangular cross-section. A comparison between the experimental magnetization curves of a sintered YBa2Cu3O7 superconductor at 76 K and the model fit shows that j(sub s)(H) is null for the coupling matrix, whereas a non-zero j(sub s)(H) is needed for the grains. The model fit for the irreversible magnetization of the grains is improved by including a surface barrier to the entry and exit of flux.

04,447
PB94-185329 Not available NTIS
National Inst. of Standards and Technology (EEEL), Gaithersburg, MD. Semiconductor Electronics Div.
Optical Conductivity of Single Crystals of Ba1-xMxBiO3(M=K, Rb, x=0.04, 0.37).
Final rept.
S. Guha, D. Peebles, V. Browning, M. Norton, T. Wieting, and D. Chandler-Horowitz. 1993, 11p.
Pub. in Jnl. of Superconductivity 6, n5 p339-349 1993.

Keywords: *Infrared reflectance, Reprints, Single crystals, Room temperature, Superconductors, Ellipsometry, Polarons, Phonons, *Potassium barium bismuthates, *Rubidium barium bismuthates, Optical conductivity.

Reflectance data (0.001-4.0 eV) from several large (a typical surface area 3 x 3 sq mm) single crystals of Ba(1 - x) K(x) BiO3 (x = 0.04, 0.37) (BKBO) and Ba(1 - x) Rb(x) BiO3 (x = 0.37) (BRBO) were obtained by Fourier Transform infrared (FTIR) and ellipsometric methods. Normal-state optical conductivities of these samples were obtained from infrared and ellipsometric measurements using a Kramers-Kronig transform. A broad mid-IR band was observed that peaked at 0.3 eV for BKBO and at 0.16 eV for BRBO at room temperature. Each band was fitted with two Lorentz oscillators. The optical mass of the charge carriers was obtained from a Drude fit, and was found to be large.

These overdamped charge carriers can be viewed as polarons with a large effective mass. An optic phonon mode at 325/cm was also observed in the metallic phase. Interpretations of low-temperature measurements on BKBO and BRBO were complicated due to the change of color of the sample from bluish-green to bronze-red. Upon warming, samples revert to their original bluish-green color.

04,448
PB94-185428 Not available NTIS
National Inst. of Standards and Technology (MSEL), Gaithersburg, MD. Metallurgy Div.
Interfacial Free Energies from Substrate Curvature Measurements of the Creep of Multilayer Thin Films.
Final rept.
D. Josell. 1994, 8p.
Pub. in Acta Metall. Mater. 42, n3 p1031-1038 1994.

Keywords: *Free energy, Creep properties, Thin films, Substrates, Interfaces, Reprints, Biaxial curvature, Multilayers.

The equilibrium biaxial curvature of a multilayer thin film adhering to a free standing substrate is determined when plastic flow is possible in the multilayer. The relationship found between the equilibrium biaxial curvature and the interfaces in the multilayer is modified to account for grain boundaries in the layers. Two possible experiments that use the resulting relationship to determine interfacial free energies are described.

04,449
PB94-185477 Not available NTIS
National Inst. of Standards and Technology (PL), Boulder, CO. Quantum Physics Div.
Temperature Dependence and Anharmonicity of Phonons on Ni(110) and Cu(110) Using Molecular Dynamics Simulations.
Final rept.
D. D. Koleske, and S. J. Sibener. 1993, 10p.
Pub. in Surface Science 298, p215-224 1993. Sponsored by National Science Foundation, Washington, DC. and Air Force Office of Scientific Research, Washington, DC.

Keywords: *Nickel, *Copper, *Phonons, Temperature dependence, Molecular dynamics, Surface potential, Simulation, Reprints, Anharmonicity.

Molecular dynamics simulations were performed for Ni(110) and Cu(110) using Finnis-Sinclair model potential. During the simulations the temperature dependencies of the mean-square displacements (MSD), the layer-by-layer stress tensors, and the surface phonon spectral densities were measured. The simulation results imply that the Ni(110) and Cu(110) surfaces do not extensively roughen before the onset of adatom-defect formation, and, in confirmation of experimental findings, that the rapid decrease of specular intensity for helium or electron scattering at elevated temperatures is due to the influence of anharmonicity in the surface potential.

04,450
PB94-185659 Not available NTIS
National Inst. of Standards and Technology (MSEL), Gaithersburg, MD. Metallurgy Div.
Enhanced Magnetocaloric Effect in Gd3Ga5-xFexO12.
Final rept.
R. D. McMichael, J. J. Ritter, and R. D. Shull. 15 May 93, 3p.
Pub. in Jnl. of Applied Physics 73, n10 p6946-6948, 15 May 93.

Keywords: Temperature range 0013-0065 K, Gadolinium-gallium garnet, Magnetic refrigerators, Solid clusters, Entropy, Reprints, *Gadolinium gallium ferrates, *Magnetocaloric effect, Cryogenic refrigerators, Exchange interactions, Nanostructures.

The working refrigerant material in the majority of magnetic refrigerators has been Gd3Ga5O12 (GGG) which has an upper temperature limit near 15 K. In this paper we report on the field-induced adiabatic magnetic entropy change, Delta S(sub m)(H,T), of a series of iron-substituted gadolinium garnets (GGIG) Gd3Ga(5-x)Fe(x)O12 which have the potential to increase the working temperature range or to reduce the field requirements of cryogenic magnetic refrigeration. Depending on Fe concentration, x, the entropy change of these materials at applied fields of 0.9 and 5.0 T is much greater than that of GGG, especially at temperatures above 15 K. At low Fe concentrations, the results are consistent with formation of magnetically ordered clusters of spins at low temperatures. Room temperature electron paramagnetic resonance measurements show that Fe(3+) ions mediate exchange interactions which are responsible for clustering at low temperatures.

04,451
PB94-185667 Not available NTIS
National Inst. of Standards and Technology (MSEL), Gaithersburg, MD. Metallurgy Div.
Magnetocaloric Effect in Rapidly Solidified Nd-Fe-Al-B Materials.
Final rept.
R. D. McMichael, R. D. Shull, L. H. Bennett, C. D. Fuerst, and J. F. Herbst. 1993, 7p.
Pub. in NanoStructured Materials 2, p277-283 1993.

Keywords: Magneto-thermal effects, Magnetic refrigerators, Magnetic fields, Neodynium containing alloys, Boron containing alloys, Aluminum alloys, Iron alloys, Temperature range 0273-0400 K, Temperature range 0400-1000 K, Temperature dependence, Magnetization, Entropy, Reprints, *Magnetocaloric effect, Rapid solidification.

We have measured the temperature and field dependence of the magnetization of several rapidly solidified Nd(0.14)(Fe(1-x)Al(x))(0.80)B(0.06) alloys in the 290-500 K temperature range at fields from 0 to 0.9 T. At room temperature the materials are ferromagnetic. Calculations of the magnetocaloric effect from the magnetization data clearly show a peak in the field-induced entropy change, Delta S, at a critical temperature T(p), which varies with aluminum content and is identified as the Curie temperature, T(c), by differential scanning calorimetry measurements. The magnitude, shape and width of the Delta S vs. T curves differ greatly from that predicted for elemental ferromagnets, but are consistent with curves predicted for magnetic nanocomposites. This similarity suggests that the magnetic moments are (1) grouped in clusters with moments on the order of 20 - 50 mu(sub B) and (2) that these materials may be potential candidates for high temperature magnetic refrigerants.

04,452
PB94-185840 Not available NTIS
National Inst. of Standards and Technology (EEEL), Gaithersburg, MD. Semiconductor Electronics Div.
Correction to the Decay Rate of Nonequilibrium Carrier Distributions Due to Scattering-in Processes.
Final rept.
B. A. Sanborn, B. Y. K. Hu, and S. Das Sarma. 1994, 3p.
Pub. in Physical Review B 49, n11 p7767-7769, 15 Mar 94.

Keywords: *Charge carriers, Electron scattering, Doped materials, Semiconductors, Correction, Reprints.

We show that, for doped semiconductor structures at nonzero temperatures, processes which scatter electrons into a state (vertical stroke) K > can contribute strongly to the decay of a nonequilibrium electron occupation of (vertical stroke) K >. For electrons, the decay rate gamma (K) is given by the sum of the total scattering-out and scattering-in rates of state (vertical stroke) K >. The scattering-in term is safely neglected in the nondegenerate and highly degenerate limits, but it increases gamma (K) of low-energy electrons injected into semidegenerate systems (between these limits) by the factor (1 - f(0)(K))(sup -1). We show that the degree of degeneracy of a system of fermions depends strongly on the system dimension, so that doped systems of reduced dimension can be semidegenerate, with the two scattering rates comparable, even at high temperature.

04,453
PB94-185857 Not available NTIS
National Inst. of Standards and Technology (MSEL), Gaithersburg, MD. Metallurgy Div.
Magnetocaloric Effect of Ferromagnetic Particles.
Final rept.
R. D. Shull. 1993, 2p.
Pub. in Institute of Electrical and Electronics Engineers Transactions on Magnetics 29, n6 p2614-2615 Nov 93.

Keywords: Magneto-thermal effects, Gadolinium-gallium garnet, Magnetic refrigerators, Superparamagnetism, Solid clusters, Entropy, Reprints, *Gadolinium gallium ferrates, *Magnetocaloric effect, Nanocomposites.

The entropy change accompanying the removal of an applied magnetic field (i.e., the magnetocaloric effect) has been calculated for a system of magnetic spins independent of each other and also clustered together into independently-acting magnetic particles. Mean-field theory calculations have also been made for interacting, single magnetic spins and also for interacting, magnetic particles. In both cases, there are found temperature and field regimes where the entropy changes are larger when the spins are coupled together into nanometer-sized magnetic particles. Entropy change data is shown for a new Gd3Ga(5-x)Fe(x)O(12) (X = or < 2.5) magnetic nanocomposite, confirming the calculations and possessing magnetocaloric effects larger than the presently preferred low temperature paramagnetic refrigerant, gadolinium gallium garnet.

04,454
PB94-185865 Not available NTIS
National Inst. of Standards and Technology (MSEL), Gaithersburg, MD. Metallurgy Div.
Viewpoint: Nanocrystalline and Nanophase Materials.
Final rept.
R. D. Shull. 1993, 4p.
Pub. in Jnl. of NanoStructured Materials 2, p213-216 1993.

Keywords: Nucleation, Magnetism, Metals, Ceramics, Reprints, *Nanomaterials, Nanocomposites, Nanophases.

Nanocrystalline materials represent one of the most active laboratories in recent times for the atomic tailoring of materials with specific properties and property combinations. However, it is still in its infancy; its emergence as a major materials science thrust has just begun. At this stage in its development, there have been glimpses of exciting new properties (e.g., superplasticity, giant magnetoresistance, transparency in opaque ceramics, enhanced homogeneity, unusually soft ferromagnetism, and giant magnetocaloric effects) possessed by materials containing some critical length which has been reduced to nanometer dimensions. But, for many of these cases, it still remains to be determined whether the property changes are due to new physics of the mechanisms at small dimensions or to an extension of larger-scale systematics to small sizes.

04,455
PB94-185923 Not available NTIS
National Inst. of Standards and Technology (PL), Gaithersburg, MD. Electron and Optical Physics Div.
Scaling of Diffusion-Mediated Island Growth in Iron-on-Iron Homoepitaxy.
Final rept.
J. A. Stroscio, and D. T. Pierce. 1994, 4p.
Pub. in Physical Review B 49, n12 p8522-8525, 15 Mar 94. Sponsored by Office of Naval Research, Arlington, VA.

Keywords: *Epitaxial growth, *Iron, Whiskers(Single crystals), Scanning tunneling microscopy, Critical size, Nucleation, Metal films, Scaling, Reprints, Homoepitaxy.

An analysis of the island size and separation distributions of Fe islands, observed in the initial stages of growth in the homoepitaxy of Fe on Fe(001) whiskers, shows scaling properties recently predicted in nucleation and growth theories. A critical size of one atom, where islands greater than the critical size undergo irreversible nucleation, is supported by the measured scaling functions for the Fe on Fe system in the temperature range of 20-250 C.

04,456
PB94-187663 PC A04/MF A01
National Inst. of Standards and Technology (MSEL), Gaithersburg, MD. Ceramics Div.
Workshop on Characterizing Diamond Films (3rd). Held in Gaithersburg, Maryland on February 23-24, 1994.
A. Feldman, S. Holly, C. A. Klein, and G. Lu. Apr 94, 56p, NISTIR-5418.
See also PB92-205426 and PB93-207157. Prepared in cooperation with Rockwell International, Canoga Park, CA., Raytheon Co., Lexington, MA. Research Div., and Norton Diamond Film, Northboro, MA.

Keywords: *Diamond films, *Meetings, Chemical vapor deposition, Thermal conductivity, Thermal diffusivity, Raman spectroscopy, Fracture properties, Thin films, Polycrystalline, Polishing, Brazing, Stresses, Strains, Standards.

The third in a series of workshops was held at NIST on February 23rd and 24th, 1994 to discuss the characterization of diamond films and the need for standards in diamond technology. The audience targeted for this workshop were producers and potential users of chemical vapor deposition (CVD) diamond technology in the United States. Three technical topics that have relevance to applications of CVD diamond films were discussed: characterizing brazing and polishing, standardization of thermal conductivity measurement, and characterizing stress, strain, and fracture.

04,457
PB94-198355 Not available NTIS
National Inst. of Standards and Technology (MSEL), Gaithersburg, MD. Reactor Radiation Div.
Combined Low- and High-Angle X-Ray Structural Refinement of a Co/Pt(111) Multilayer Exhibiting Perpendicular Magnetic Anisotropy.
Final rept.
J. F. Ankner, J. A. Borchers, R. F. C. Farrow, and R. F. Marks. 1993, 3p.
Pub. in Jnl. of Applied Physics 73, n10 p6427-6429, 15 May 93.

Keywords: *Cobalt, *Platinum, Molecular beam epitaxy, Magnetic anisotropy, X-ray diffraction, X-ray reflection, Metal films, Superlattices, Substrates, Interfaces, Sapphire, Reprints, Multilayers.

We have used Cu K(alpha) radiation to measure both specular reflectivity (000) and longitudinal Bragg diffraction (222) from a Co/Pt multilayer grown by molecular-beam epitaxy on a sapphire (0001) substrate. By refining both low- and high-angle profiles, we are able to separate the effects of surface morphology from microstructure. Our results indicate mixing at the interfaces consistent with the existence of alloy or compound formation.

04,458
PB94-198363 Not available NTIS
National Inst. of Standards and Technology (MSEL), Gaithersburg, MD. Reactor Radiation Div.
Magnetic Dead Layer in Fe/Si Multilayer: Profile Refinement of Polarized Neutron Reflectivity Data.
Final rept.
J. F. Ankner, C. F. Majkrzak, and H. Homma. 1993, 2p.
Pub. in Jnl. of Applied Physics 73, n10 p6436-6437, 15 May 93.

Keywords: *Silicon, *Iron, Polarized beams, Metal films, Antiferromagnetism, Interfaces, Thin films, Reprints, Neutron reflectivity, Polarized neutrons, Multilayers.

We have used polarized neutron reflectometry to study the magnetic structure of an Fe/Si multilayer film. By simultaneous refinement of both plus and minus reflectivities, we have extracted separate nuclear and magnetic scattering density profiles that include a 6-A-thick magnetically dead layer in Fe at the interface. This result supports the contention that the antiferromagnetic coupling reported in this system is mediated by the presence of Fe in the Si interlayers.

04,459
PB94-198421 Not available NTIS
National Inst. of Standards and Technology (MSEL), Gaithersburg, MD. Ceramics Div.
Weak-Link-Free Behavior of High Angle YBa2Cu3O7-x Grain Boundaries in High Magnetic Fields.
Final rept.
S. E. Babcock, X. Y. Cai, D. L. Kaiser, and D. C. Larbalestier. 1990, 3p.
Pub. in Nature 347, n6289 p167-169 1990.

Keywords: *YBCO superconductors, *Grain boundaries, High temperature superconductors, Transport properties, Critical current, Current density, Magnetic fields, Bicrystals, Reprints, *Yttrium barium cuprates, Weak links.

The transport properties across grain boundaries in several bi-crystals of YBa2Cu3O(7-delta) have been measured. In three cases, including two high angle grain boundaries, no weak link behavior was observed. These results remove an important restriction suggested by earlier thin film bi-crystal results, showing that at least some high angle grain boundaries can transmit supercurrents in high magnetic fields at 77 K. Such results are conceptually important in searching for ways to improve the J(ct) characteristics of bulk, polycrystalline high temperature superconductors for high field applications.

04,460
PB94-198512 Not available NTIS
National Inst. of Standards and Technology (MSEL), Boulder, CO. Materials Reliability Div.
Profile Fitting of X-Ray Diffraction Lines and Fourier Analysis of Broadening.
Final rept.
D. Balzar. 1992, 12p.
Pub. in Jnl. of Applied Crystallography 25, p559-570 1992.

Keywords: *X-ray diffraction, *Line broadening, Reprints, High temperature superconductors, Distribution functions, Fourier analysis, Lanthanum strontium cuprates, Warren-Averbach method, Voigt functions, Microstains.

The extraction of pure-specimen X-ray diffraction-line broadening is described using a convolution of the instrumental profile and an exact Voigt function. Real Fourier coefficients were computed from the Cauchy and Gauss integral breadths and were input for Warren-Averbach analysis. Smooth surface-weighted and volume-weighted column-length distribution functions were obtained and errors in root-mean-square strains as well as effective domain sizes were evaluated. The method was applied to two cubic structures with average volume-weighted domain sizes up to 3600 A as well as patterns of tetragonal and orthorhombic (La, Sr)2CuO4, which exhibit weak line broadenings and highly overlapping reflections. Comparison with the integral-breadth methods is given. Reliability of the method is discussed in the case of a cluster of overlapping peaks.

04,461
PB94-198520 Not available NTIS
National Inst. of Standards and Technology (MSEL), Boulder, CO. Materials Reliability Div.
Microstrains and Domain Sizes in Bi-Cu-O Superconductors: An X-Ray Diffraction Peak-Broadening Study.
Final rept.
D. Balzar, and H. Ledbetter. 1992, 2p.
Pub. in Jnl. of Materials Science Letters 11, p1419-1420 1992.

Keywords: *BSCCO superconductors, High temperature superconductors, X-ray diffraction, Size determination, Domains, Reprints, *Bismuth strontium calcium cuprates, Warren-Averbach method, Microstrains.

We present an x-ray diffraction peak-broadening analysis of three Bi-Cu-O high-T(c) superconductors. The diffraction line profiles were fitted with a convolution of instrumental and specimen functions. The specimen's particle size and strain contributions to the peak-broadening were analyzed with the Warren-Averbach method. We found that for both the 2212 and 2223 Bi-Cu-O superconductors, microstrain along the c-axis is larger than in the basal plane, because of larger stacking disorder. In the specimen containing both phases, strain is relieved by the macroscopic intergrowth of two phases within the same grain, and effective domain sizes are smaller than in one-phase specimens.

04,462
PB94-198538 Not available NTIS
National Inst. of Standards and Technology (MSEL), Boulder, CO. Materials Reliability Div.
Voigt-Function Modeling in Fourier Analysis of Size- and Strain-Broadened X-Ray Diffraction Peaks.
Final rept.
D. Balzar, and H. Ledbetter. 1993, 7p.
Pub. in Jnl. of Applied Crystallography 26, p97-103 1993.

Keywords: *X-ray diffraction, Reprints, Fourier analysis, Strains, *Voight functions, Warren-Averbach method.

With the assumption that both size- and strain-broadened profiles of the pure-specimen function are described with a Voigt function, it is shown that the analysis of Fourier coefficients leads to the Warren-Averbach method of separation of size and strain contributions. The analysis of size coefficients shows that the 'hook' effect occurs when the Cauchy content of the size-broadened profile is underestimated. The ratio of volume-weighted and surface-weighted domain sizes can range from about 1.31, for the minimum allowed Cauchy content, to 2, when the size-broadened profile is given solely by a Cauchy function. If the distortion coefficient is approximated by a harmonic term, mean-square strains decrease linearly with increasing the average distance. The local strain is finite only in the case of purely Gaussian strain broadening, because strains are then independent of averaging distance.

04,463
PB94-198553 Not available NTIS
National Inst. of Standards and Technology (NML), Gaithersburg, MD. Electron and Optical Physics Div.
Experimental Constraints on Some Mechanisms for High-Temperature Superconductivity.
Final rept.
T. W. Barbee, M. L. Cohen, and D. R. Penn. 1991, 7p.
Pub. in Physical Review B 44, n9 p4473-4479 1991.

Keywords: *High temperature superconductors, Electron phonon interactions, Isotope effect, Spectral shift, Transition temperature, Specific heat, Cuprates, Reprints.

Three years after its discovery, many mechanisms have been suggested to explain the phenomenon of high-temperature superconductivity (HTS) in oxides. We propose that experimental data, along with theoretical models, can place constraints on or exclude many of these mechanisms. The isotope shift a, the transition temperature T(o), the ratio of the electronic specific heat jump to the normal state specific heat (Delta)C/(gamma)T(o) and the superconducting gap ratio 2(Delta)/k(B)T(c) are considered. We find limits on the applicability of solely phonon-based and combined phonon-electronic mechanisms.

04,464
PB94-198744 Not available NTIS
National Inst. of Standards and Technology (MSEL), Gaithersburg, MD. Metallurgy Div.
Meissner, Shielding, and Flux Loss Behavior in Single-Crystal YBa2Cu3O6+x.
Final rept.
L. H. Bennett, L. J. Swartzendruber, and D. L. Kaiser. 1991, 2p.
Pub. in Jnl. of Applied Physics 69, n8 p4889-4890 1991.

Keywords: *Meissner effect, *Ytterbium compounds, Twinning, Flux(Rate), Crystal properties, Magnetic properties, Temperature, Reprints.

Meissner effect measurements were performed on a nearly cubic single crystal of YBCO, which exhibited a predominant (110) twin habit, by cooling the crystal from above T(c) to 10 k in an applied field, H, of 10 Oe. A significant difference was observed for H applied parallel and perpendicular to the c axis, but little difference could be seen for H perpendicular and parallel to the twin boundaries. After cooling from above T(c) in 10 Oe to 10 K, the field was reduced to zero. The magnetization changed sign, increasing by approx. 15 G, which is the value expected for complete flux expulsion by a crystal of this geometry. Magnetization measurements were then made as the temperature was raised back to 100 K. Again, there is a significant difference for the results with H parallel and perpendicular to the c axis, especially above 60 K, with only a small (but possibly meaningful) difference for perpendicular and parallel to the twin boundaries.

04,465
PB94-198751 Not available NTIS
National Inst. of Standards and Technology (NML), Gaithersburg, MD. Surface Science Div.
Magnetic Properties of Pd/Co Multilayers.
Final rept.
W. R. Bennett, C. D. England, D. C. Person, and C. M. Falco. 1991, 7p.
Pub. in Jnl. of Applied Physics 69, n8 p4384-4390 1991.

Keywords: *Palladium, *Cobalt, Reprints, Magnetic anisotropy, Temperature dependence, Domain walls, Metal films, Thin films, Interfaces, Magnetization, Multilayers.

Measurements of the magnetic anisotropy of a series of Pd/Co multilayers grown by magnetically enhanced dc triode sputter deposition revealed an interface contribution of 0.53 ergs/sq cm and a net volume anisotropy of -13.2 x 10(sup 6) ergs/cc. A characteristic reduction of perpendicular anisotropy for ultrathin Co layers (<4A) is explained by using a pair interaction model to evaluate a thickness dependence of the interface anisotropy. Temperature dependence of saturation

magnetization of a Pd(11A)/Co(7.8A) multilayer demonstrates complete mixing of Pd and Co by 380 C.

04,466
PB94-198769 Not available NTIS
National Inst. of Standards and Technology (NML), Gaithersburg, MD. Surface Science Div.
Concurrent Enhancement of Kerr Rotation and Antiferromagnetic Coupling in Epitaxial Fe/Cu/Fe Structures.
Final rept.
W. R. Bennett, W. Schwarzacher, and W. F. Egelhoff. 1990, 4p.
Pub. in Physical Review Letters 65, n25 p3169-3172 1990.

Keywords: *Kerr magnetooptical effect, *Antiferromagnetism, *Copper, *Iron, Metal films, Epitaxy, Reprints, Multilayers.

The authors report the observation of major enhancements in the magneto-optical polar Kerr rotation in the Fe/Cu/Fe system. These enhancements are as much as a factor of two greater than those anticipated due to recently reported plasma resonance effects. A close connection between these enhancements and antiferromagnetic coupling between the two Fe films is established by the observation of concurrent oscillations in the magnitude of these two effects as a function of Cu thickness.

04,467
PB94-198868 Not available NTIS
National Inst. of Standards and Technology (CAML), Gaithersburg, MD. Applied and Computational Mathematics Div.
Non-Equilibrium Thermodynamic Theory of Viscoplastic Materials.
Final rept.
B. Bernstein, and J. T. Fong. 1993, 9p.
Pub. in Jnl. of Applied Physics 74, n4 p2220-2228, 15 Aug 93.

Keywords: *Viscoplasticity, Constitutive equations, Continuum mechanics, Creep properties, Mechanical properties, Fatique(Materials), Thermodynamic, Irreversible processes, Reprints.

A nonequilibrium thermodynamic theory for predicting the mechanical behavior of materials beyond the elastic range is formulated. The theory incorporates the idea of a 'concealed' parameter alpha, originally due to Bridgman (Rev. Mod. Phys. 22, 56 (1950)), where the constitutive equations are governed by (1) a thermodynamic potential such as a generalized Gibbs function, G, or Helmholtz free-energy function, F, each with an explicit dependence on alpha, and (2) a prescription for (alpha dot), the time rate of change of alpha, such that (alpha dot) is directly proportional to the negative of G(alpha) or F(alpha), the partial derivative of G or F with respect to alpha, respectively. The theory is found to be consistent with (1) the second law of thermodynamics regarding entropy production; (2) the concept of Lyapunov stability at equilibrium; (3) the rule of invariance with respect to a transformation of parameters; and (4) the powerful law of invariance with respect to the Legendre transformation. Significance of the new formulation is discussed by solving a class of one-dimensional creep and fatigue modeling problems and by comparing the new theory with several similar approaches in the literature.

04,468
PB94-199031 Not available NTIS
National Inst. of Standards and Technology (EEEL), Boulder, CO. Electromagnetic Technology Div.
Intrinsic Stress in DC Sputtered Niobium.
Final rept.
P. A. A. Booi, C. A. Livingston, and S. P. Benz. 1993, 3p.
Pub. in Institute of Electrical and Electronics Engineers Transactions on Applied Superconductivity, n2 p3029-3031 Jun 93.

Keywords: *Niobium, Metal films, Direct current, Transition temperature, Stresses, Reprints, Target erosion, Sputtered films.

The intrinsic mechanical stress of dc magnetron-sputtered Nb films is characterized as a function of sputtering parameters and target erosion. The zero-stress point shifts to lower cathode voltages as the target erodes. The zero-stress point was always characterized by the same cathode current-Ar pressure relationship.

04,469
PB94-199072 Not available NTIS
National Inst. of Standards and Technology (CAML), Gaithersburg, MD. Applied and Computational Mathematics Div.
Asymptotic Behavior of Modulated Taylor-Couette Flows with a Crystalline Inner Cylinder.
Final rept.
R. J. Braun, G. B. McFadden, B. T. Murray, M. E. Selleck, S. R. Coriell, and M. E. Glicksman. 1993, 13p.
Pub. in Phys. Fluids A 5, n8 p1891-1903 Aug 93. See also PB93-139061.

Keywords: *Crystal growth, *Solidification, Coaxial configuration, Prandtl number, Asymptotic series, Hydrodynamics, Cylinders, Instability, Reprints, Crystal-melt interface, Taylor-Couette flow, Floquet theory.

The linear stability of a modulated Taylor-Couette system when the inner cylindrical boundary consists of a crystalline solid-liquid interface is considered. Both experimentally and in numerical calculations, it is found that the two-phase system is significantly less stable than the analogous rigid-walled system for materials with moderately large Prandtl numbers. A numerical treatment based on Floquet theory is described, which gives results that are in good agreement with preliminary experimental findings. In addition, this instability is further examined by carrying out a formal asymptotic expansion of the solution in the limit of large Prandtl number. It is surprising that the determination of the linear stability of the two-phase system is considerably simpler than that of the rigid-walled system, despite the complications introduced by the presence of the crystal-melt interface.

04,470
PB94-199148 Not available NTIS
National Inst. of Standards and Technology (MSEL), Gaithersburg, MD. Ceramics Div.
Microstructure and Ferroelectric Properties of Lead Zirconate-Titanate Films Produced by Laser Evaporation.
Final rept.
P. S. Brody, J. M. Benedetto, B. J. Rod, P. K. Schenck, C. K. Chiang, W. Wong-Ng, K. W. Bennett, and L. P. Cook. 1991, 4p.
Pub. in Proceedings of Institute of Electrical and Electronics Engineers Symposium on Applications of Ferroelectrics (7th), Urbana-Champaign, IL., June 6-8, 1990, p181-184 1991.

Keywords: *Lead zirconate titanates, *PZT, Reprints, Ferroelectric materials, Dielectric properties, Laser ablation, Thin films, Microstructure, Neodymium lasers, Polarization, X-ray diffraction, Silicon substrates.

Lead titanate-zirconate films were produced by laser-induced vaporization from a PZT target with the use of a focused q-switched Nd:YAG laser. Deposition was onto room-temperature platinum-covered silicon substrates. Although the films were initially amorphous as indicated by x-rays, they crystallized when annealed. EDX results showed that the film and targets were similar in composition. SEM and optical dark field micrographs showed a structure which might be interpreted as a sintered assemblage of particulate. A pattern of platinum electrodes was sputter deposited onto each sample to form parallel plate capacitors for investigating dielectric and ferroelectric properties. For a 2.5-micrometer-thick film annealed at 700 C, the relative dielectric constant was approximately that of the bulk target. Hysteresis loops were obtained. The remanent polarization was 5.1 microC/sq cm measured at a 160 kV/cm peak sinusoidal field.

04,471
PB94-199239 Not available NTIS
National Inst. of Standards and Technology (CAML), Gaithersburg, MD. Applied and Computational Mathematics Div.
Laser Melting of Thin Silicon Films.
Final rept.
L. N. Brush, G. B. McFadden, and S. R. Coriell. 1991, 21p.
Pub. in Jnl. of Crystal Growth 114, p446-466 1991.

Keywords: *Silicon films, Reprints, Laser-radiation heating, Liquid-solid interfaces, Boundary integral method, Boundary conditions, Numerical solution, Melting, Stability.

Thin silicon films on a cooled substrate are often found to develop two-phase lamellar structures upon radiative heating. Jackson and Kurtze developed a two-dimensional model for the process in which the heated film consists of alternating parallel bands of liquid and solid phases separated by planar solid-liquid interfaces. To understand the cellular or dendritic structures that sometimes are observed in these interfaces, they also performed a linearized morphological stability analysis and obtained the conditions for the growth or decay of infinitesimal perturbations to the interface. In this work the authors extend that analysis to finite amplitudes by developing a boundary integral representation of the thermal field, and obtain steady-state numerical solutions for nonplanar solid-liquid interfaces. Eigenvalue calculations to determine the linear stability of the nonplanar solutions are also performed. The effects of the lateral boundary conditions on the stability of the solutions are investigated as well.

04,472
PB94-199395 Not available NTIS
National Inst. of Standards and Technology (EEEL), Gaithersburg, MD. Electricity Div.
Quantized Dissipation of the Quantum Hall Effect at High Currents.
Final rept.
M. E. Cage. 1993, 3p.
Pub. in Institute of Electrical and Electronics Engineers Transactions on Instrumentation and Measurement 42, n2 p176-178 Apr 93. See also PB93-150712.

Keywords: *Hall effect, Two dimensional, Electric current, Electron gas, Quantization, Dissipation, Reprints, *Quantum Hall effect.

Quantized dissipative voltage states are observed when large currents are passed through a high-quality quantized Hall resistance device. These dissipative states are interpreted as occurring when electrons are excited to higher Landau levels and then return to the original Landau level. We show that the quantization is more complicated than previously thought. For example, the quantization can be a function of magnetic field. Therefore, the dissipative voltage quantization can, in general, be difficult to verify and determine.

04,473
PB94-199411 Not available NTIS
National Inst. of Standards and Technology (MSEL), Gaithersburg, MD.
Singularities in Minimum Surface Energy Problems and Their Influence in Surface Motion.
Final rept.
J. W. Cahn. 1992, 3p.
Pub. in Proceedings of Computational Crystal Growers Workshop, Minneapolis, MN., February 22-28, 1992, p28-30.

Keywords: *Minimal surfaces, *Surface energy, Reprints, Three dimensional, Singularity, Froth, Soap bubbles.

Singularities can arise in area minimizing problems in three dimensions when three or more contiguous volumes separated by surfaces are considered. In a soap froth, the catalog of singularities has two members: a trijunction curve, where three bubbles meet with the three surface separating them meeting with 120 degree dihedral angles along a curve, and a quadrijunction point, where four bubbles and four trijunctions curves meet along tetrahedral angles and where there are six surfaces, each spanning a pair of trijunction curves (Taylor). For the soap froth, all surfaces have the same energy per unit area, and thus surface energy minimization is the same as area minimization. Furthermore, no energy is assigned to the point or line singularities. Recent research has focussed on the singularities that arise when the problem is altered to add certain complications, some realistic and some hypothetical.

04,474
PB94-199635 Not available NTIS
National Inst. of Standards and Technology (NML), Gaithersburg, MD. Quantum Metrology Div.
Status of a Silicon Lattice Measurement and Dissemination Exercise.
Final rept.
R. D. Deslattes, and E. G. Kessler. 1991, 6p.
Pub. in Institute of Electrical and Electronics Engineers Transactions on Instrumentation and Measurement 40, n2 p92-97 1991.

Keywords: *Crystal lattices, *Silicon, Single crystals, Optical interferometers, Comparators, Reprints, X-ray interferometers.

Although no longer explicitly directed toward measurement of the Avogadro constant, we continue significant effort on lattice period measurement in monocrystalline silicon. There are currently operating an up-graded x-ray/optical interferometer and a recently established lattice comparator. We report the status of measurements with these two instruments.

04,475
PB94-199767 Not available NTIS
National Inst. of Standards and Technology (MSEL), Gaithersburg, MD. Polymers Div.
Hysteresis Measurements of Remanent Polarization and Coercive Field in Polymers.
Final rept.
B. Dickens, E. Balizer, A. S. DeReggi, and S. C. Roth. 1992, 7p.
Pub. in Jnl. of Applied Physics 72, n9 p4258-4264, 1 Nov 92. Sponsored by Naval Surface Warfare Center, Silver Spring, MD.

Keywords: *Polymers, *Ferroelectric materials, *Hysteresis, *Polarization(Charge separation), Reprints, Electric potential, Electric conductivity, *Remanent polarization, Coercive fields.

An experimental method is described which allows estimation of remanent polarization and coercive fields without assuming functional forms for the capacitive and electrical resistance terms. The method can be used to measure polarization in specimens with voltage-dependent conductivity (often arising from the presence of ions in the specimens), voltage-dependent capacitance, and significant amounts of space charge. It consists of: (1) performing bipolar current/voltage hysteresis loops to allow a steady state of remanent polarization and space charge to build up in the specimen, and (2) following a bipolar loop with two or more unipolar loops in the first unipolar loop. Both sinusoidal and linear time-dependent applied voltages may be used. Automatic data processing of hysteresis loops is described for cases in which specimen behavior may be considered to be ideal.

04,476
PB94-199924 Not available NTIS
National Inst. of Standards and Technology (PL), Gaithersburg, MD. Quantum Metrology Div.
Diffraction of X-rays at the Far Tails of the Bragg Peaks.
Final rept.
A. Caticha. 1993, 8p.
Contract AFOSR 88-0018
Pub. in Physical Review B 47, n1 p76-83, 1 Jan 93. Sponsored by Air Force Office of Scientific Research, Bolling AFB, DC. and Defense Advanced Research Projects Agency, Arlington, VA.

Keywords: *X-ray diffraction, Bragg reflection, Bragg angle, Reprints, Truncation rod scattering.

It is known that the kinematical and dynamical theories of diffraction by perfect crystals predict the same values for the intensities scattered into the vicinity of the Bragg peaks whenever those intensities are low. Here we address the question of whether this is also true throughout the region between two Bragg peaks. We show that the two theories give equivalent results for the weak intensities in the far tails of the Bragg peaks, provided better approximations for both the shape of the dispersion surface and the boundary conditions are used: One needs to take into account the asymptotic sphericity of the dispersion surface and the difference between electric and displacement fields. This results in a nontrivial transmission coefficient for the diffracted electric field as it leaves the crystal. By explicitly showing the equivalence of kinematical and dynamical results, this work provides additional theoretical support for the kinematical approach usually adopted to describe the so-called truncation-rod-scattering.

04,477
PB94-200045 Not available NTIS
National Inst. of Standards and Technology (NML), Gaithersburg, MD. Radiation Physics Div.
Electronic Correlations and Satellites in Superconducting Oxides.
Final rept.
K. J. Chang, M. L. Cohen, and D. R. Penn. 1988, 6p.
Pub. in Physical Review B38, n13 p8691-8696 1988.

Keywords: *YBCO superconductors, High temperature superconductors, Electron correlation, Band theory, S matrix, Satellites, Reprints, *Lanthanum strontium cuprates, *Yttrium barium cuprates.

The satellite observed at a binding energy of 12 to 13 eV below the Fermi level in the high T(c) oxide superconductors, La(2-x)Sr(x)CuO4 and YBa2Cu3O(7-delta), is viewed as originating from a state with two holes bound at the same Cu site. As in the case of Ni metal, the satellite is caused by an intra d-shell shake-up process into a Cu 3d(8) final state and its intensity is enhanced at resonance because of a super Koster-Kronig transition. Based on the t-matrix approach for the hole self-energy, the authors study the effect of electronic correlations on the one-electron band structure. They examine the position of the satellite and find a large Coulomb interaction energy of 5 eV at the Cu site when the experimental satellite position is duplicated by the theory. Since this energy is comparable with the 3d bandwidth, the two-hole bound state is a high energy excitation. This indicates that in the ground state a creation of two holes at the Cu site is unlikely and thus holes are formed at the O sites when Sr is substituted for La in La2CuO4 and when the oxidation is increased in YBa2CuO(7-delta).

04,478
PB94-200128 Not available NTIS
National Inst. of Standards and Technology (EEEL), Boulder, CO. Electromagnetic Technology Div.
Surface Barrier and Lower Critical Field in YBa2Cu3O7-delta Superconductors.
Final rept.
D. X. Chen, R. B. Goldfarb, R. W. Cross, and A. Sanchez. 1993, 5p.
Pub. in Physical Review B 48, n9 p6426-6430, 1 Sep 93.

Keywords: *YBCO superconductors, High temperature superconductors, Ginzburg-Landau theory, Temperature dependence, Surface barrier, Critical field, Magnetization, Reprints, *Yttrium barium cuprates.

The fields for first vortex entry and last vortex exit, H(1) and H(2), and the lower critical field H(C1) for a grain-aligned, sintered YBa2Cu3O(7-delta) superconductor have been determined from saturated magnetic-hysteresis loops using an extended critical-state model. For fields oriented along the grain c axis, H(1) increases with decreasing temperature, showing an upturn below 50 K, whereas H(2) remains small and positive, in general agreement with the theory of Bean-Livingston surface barriers. H(C1) has a Bardeen-Cooper-Schrieffer temperature dependence above 50 K, but it rises at low temperatures. For fields oriented in the ab plane, H(C1) has a similar temperature dependence, but surface barriers are not evident in the magnetization.

04,479
PB94-200144 Not available NTIS
National Inst. of Standards and Technology (CSTL), Gaithersburg, MD. Surface and Microanalysis Science Div.
X-Ray Photoelectron and Auger Electron Spectroscopy Study of Ultraviolet/Ozone Oxidized P2S5/(NH4)2S Treated GaAs(100) Surfaces.
Final rept.
M. Chester, T. Jach, and J. A. Dagata. 1993, 7p.
Pub. in Vacuum Science and Technology A 11, n3 p474-480 May/Jun 93.

Keywords: *Gallium arsenides, *Surface analysis, *Oxidation, X-ray photoelectron spectroscopy, Auger electron spectroscopy, Temperature dependence, Temperature range 0273-0400 K, Temperature range 0400-1000 K, Thermal stability, Passivation, Annealing, Reprints.

In the paper the authors discuss the results of a study undertaken to investigate the composition and thermal stability of ultraviolet/ozone oxidized, P2S5/(NH4)2S treated GaAs(100) surfaces. In particular, the authors have used x-ray photoelectron spectroscopy and Auger electron spectroscopy to probe the oxide and interface at room temperature and as a function of annealing temperature. The room temperature data indicate that S is buried between the oxide overlayer and the GaAs substrate. This oxide contains a variety of As and Ga bonding configurations which, after moderate annealing, are transformed into thermally more stable phases, such as As2O3 and Ga2O3. Complete desorption of the oxide occurs after annealing at 600 deg C. Annealing the as-oxidized surface to high temperatures also has a profound effect on the S.

04,480
PB94-200151 Not available NTIS
National Inst. of Standards and Technology (CSTL), Gaithersburg, MD.
Grazing-Incidence X-Ray Photoemission Spectroscopy Investigation of Oxidized GaAs(100): A Novel Approach to Nondestructive Depth Profiling.
Final rept.
M. J. Chester, T. Jach, and S. Thurgate. 1993, 5p.
Pub. in Jnl. of Vacuum Science and Technology B 11, n4 p1609-1613 Jul/Aug 93.

Keywords: *Gallium arsenides, *Surface analysis, X-ray photoelectron spectroscopy, Grazing incidence, Oxidation, Reprints, Depth profiles.

When a beam of x rays (about 1 keV) impinges on a flat surface at grazing angles (approx = or < 3 deg) the x rays undergo total external reflection. Under these conditions, the penetration depth of the x rays can become comparable to photoelectron escape depths and the photoelectron yields from the surface are enhanced. As the incidence angle of the x rays is increased, and x-ray penetration depth increases and the photoelectron yields contain a larger contribution from deeper layers within the sample. By exploiting this depth-dependence of photoelectron yields as a function of incident x-ray beam angle, it is possible to obtain information about the depth distribution of the photoelectron emitting atoms. The authors have used this novel application of grazing-incidence x-ray photoelectron spectroscopy (GIXPS) to study the ultraviolet oxidized GaAs(100) surface. Much insight into the composition and depth-dependence of these oxide phases can be obtained by directly comparing the spectra collected at different x-ray incidence angles.

04,481
PB94-200276 Not available NTIS
National Inst. of Standards and Technology (MSEL), Gaithersburg, MD. Reactor Radiation Div.
Incorporation of Gold into YBa2Cu3O7: Structure and Tc Enhancement.
Final rept.
M. Z. Cieplak, G. Xiao, C. L. Chien, W. Bryden, J. K. Stalick, J. J. Rhyne, A. Bakhshai, and D. Artymowicz. 1990, 9p.
Grant NSF-DMR88-22559
Pub. in Physical Review B 42 n10 p6200-6208, 1 Oct 90. Sponsored by National Science Foundation, Arlington, VA.

Keywords: *YBCO superconductors, *Doped materials, *Gold, Orthorhombic lattices, X-ray diffraction, Neutron diffraction, Transition temperature, Crystal structure, High temperature superconductors, Reprints, *Yttrium barium cuprates.

The structural and superconducting properties of gold-doped YBa2Cu3O7 compounds have been studied with x-ray and neutron diffraction, optical microscopy, weight-loss analysis, magnetization, and resistivity measurements. The solubility of Au in YBa2Cu3O7 is closed to 10 at. %, below which all samples are thermally stable up to the processing temperature (950 C). Metallic Au grains precipitate out when the Au content exceeds 10 at. %. Analysis of the x-ray and neutron-scattering intensities shows that Au substitutes for the Cu(1) chain site exclusively and has a probable valence state of Au(3+). The main effect of Au doping is a substantial uniaxial lattice expansion, while the orthorhombic structure is preserved. The authors present a detailed set of structural data including the Cu-O bond lengths and interplanar distances in a Au-doped sample. Unlike all other known dopants on Cu sites, the Au dopant is not detrimental to the superconducting properties. On the contrary, T(c) is slightly enhanced over that of YBa2Cu3O7. Such an enhancement, observed for the first time for a Cu site dopant, is intrinsic and reproducible. The authors discuss the possible causes of the T(c) increase and the features of Au dopant useful in the investigation of high-T(c) superconductivity.

04,482
PB94-200284 Not available NTIS
National Inst. of Standards and Technology (MSEL), Gaithersburg, MD. Reactor Radiation Div.
Unexpected Effects of Gold on the Structure, Superconductivity, and Normal State of YBa2Cu3O7.
Final rept.
M. Z. Cieplak, G. Xiao, C. L. Chien, J. K. Stalick, and J. J. Rhyne. 1990, 3p.
Grant NSF-DMR88-22559
Pub. in Applied Physics Letters 57, n9 p934-936 Aug 90. Sponsored by National Science Foundation, Arlington, VA.

Keywords: *YBCO superconductors, *Doped materials, *Gold, High temperature superconductors, X-ray diffraction, Neutron diffraction, Transition temperature, Crystal structure, Reprints, *Yttrium barium cuprates, Rietveld method.

Using high-resolution x-ray and neutron diffraction measurements, the authors have shown that gold can be doped into YBa2Cu3O7 (1:2:3) up to 10% per formula unit, exclusively at the Cu(1) sites. Au doping causes a larger uniaxial expansion along the c axis, accompanying an increase in the Cu(1)-O(1) bond length and a decrease in the Cu(2)-O(1) bond length. The superconducting transition temperature (T(c)) is enhanced upon Au doping and the normal-state transport properties are altered even for small levels of Au doping. The widely held belief in the inert nature of Au with regard to high T(c) superconductors is therefore invalid. These findings also raise questions concerning results using single crystals grown from gold crucibles.

04,483
PB94-200359 Not available NTIS
National Inst. of Standards and Technology (EEEL), Boulder, CO. Electromagnetic Technology Div.
High-Frequency Linear Response of Anisotropic Type-II Superconductors in the Mixed State.
Final rept.
M. W. Coffey. 1993, 9p.
Pub. in Physical Review B 47, n18 p12 284-12 287, 1 May 93.

Keywords: *Type 2 superconductors, *Superconductors, Penetration depth, High frequency, Effective mass, Response functions, Anisotropy, Complexity, Linearity, Tensors, Vortices, Reprints, Surface impedance.

Effective-mass anisotropy is incorporated into a self-consistent phenomenological theory of the high frequency electrodynamic response of type-II superconductors in the mixed state. The theory accounts for two-fluid effects, including a possible anisotropic normal-fluid contribution, in addition to nonlocal vortex interaction. The approach, applicable to the modeling of a wide range of complex response functions, is illustrated in the calculation of the complex penetration depths and surface impedance for uniaxially anisotropic type-II superconductors.

04,484
PB94-200367 Not available NTIS
National Inst. of Standards and Technology (EEEL), Boulder, CO. Electromagnetic Technology Div.
Nonlinear Response of Type-II Superconductors in the Mixed State in Slab Geometry.
Final rept.
M. W. Coffey. 1993, 4p.
Pub. in Physical Review B 47, n22 p15 298-15 301, 1 Jun 93. Sponsored by Department of Energy, Washington, DC.

Keywords: *Type 2 superconductors, *Superconductors, Penetration depth, Magnetic permeability, Boundary conditions, Electrical conductivity, Electrodynamics, Complexity, Nonlinearity, Vortices, Reprints.

The nonlinear response of a type-II superconductor of finite thickness arising from vortex motion is investigated. The results of the phenomenological theory extend the complex rf magnetic permeability and conductivity to a specific regime of nonlinear response. Explicit expressions for the complex penetration depths, amplitudes, fields, and densities for the second-harmonic response with various boundary conditions are presented.

04,485
PB94-200458 Not available NTIS
National Inst. of Standards and Technology (MSEL), Gaithersburg, MD.
Neutron Scattering Structural Study of AlCuFe Quasicrystals Using Double Isotopic Substitution.
Final rept.
M. Cornier-Quiquandon, R. Bellissent, Y. Calvayrac, B. Mozer, J. W. Cahn, and D. Gratias. 1993, 5p.
Pub. in Jnl. of Non-Crystalline Solids 153 and 154, p10-14 1993.

Keywords: *Crystal structure, Aluminum alloys, Copper alloys, Iron alloys, Correlation functions, Isotope exchange, Neutron diffraction, Reprints, *Quasicrystals, Icosahedral phase.

Neutron diffraction data with double isotopic substitution using two isotopes each of Fe and Cu has been obtained on six samples of quasicrystalline AlCuFe with a 6D face-centered icosahedral symmetry. Calculations of heteroatomic and homoatomic pair correlation functions for this structure have been made. The authors find that there is a localized position of copper on a 6D body center site which gives a clear but still qualitative picture of the structure with iron, copper, and aluminum chemically ordered and occupying successive concentric 'shells' in the large atom surfaces centered at the two major atomic positions, n(1) = left bracket 0, 0, 0, 0, 0, 0 right bracket and n(2) = left bracket 1, 0, 0, 0, 0, 0 right bracket, (indexed with respect to a primitive unit cell) in this 6D NaCl type structure. There is an indication that some of the aluminum is mixed with the iron (or is encapsulated in a small volume inside an iron surface).

04,486
PB94-200557 Not available NTIS
National Inst. of Standards and Technology (NML), Gaithersburg, MD. Electron and Optical Physics Div.
Anharmonic Phonons and the Isotope Effect in Superconductivity.
Final rept.
V. H. Crespi, M. L. Cohen, and D. R. Penn. 1991, 4p.
Pub. in Physical Review B 43, n16 p2921-2924 1991.

Keywords: *High temperature superconductors, *Phonons, High-Tc superconductors, Isotope effects, Electron phonon interactions, Schrodinger equation, Cuprates, Reprints, Anharmonicity.

Anharmonic ionic potentials are examined to study the unusual isotope effect exponents for the high-T(c) oxides. Numerical solutions of Schrodinger's equation for a double well potential produce electron-phonon coupling constants lambda in the range 1.5 to 4 for a material with a vanishing isotope effect parameter alpha. However, low phonon frequencies limit T(c). Within our approximations, double well potential cannot produce alpha, >1/2. However, a negative quartic perturbation to a harmonic well can increase alpha above 1/2. In the extreme strong coupling limit, alapha is 1/2 regardless of anharmonicity.

04,487
PB94-211059 Not available NTIS
National Inst. of Standards and Technology (NML), Gaithersburg, MD. Inorganic Analytical Research Div.
Measurement of Boron at Silicon Wafer Surfaces by Neutron Depth Profiling.
Final rept.
R. G. Downing, J. P. Levine, T. Z. Hossain, J. B. Russell, and G. P. Zenner. 1990, 3p.
Pub. in Jnl. of Applied Physics 67, n8 p3652-3654, 15 Apr 90.

Keywords: *Silicon, *Boron, Secondary ion mass spectroscopy, Concentration(Composition), Boron 10 target, Neutron reactions, Measurement, Aerosols, Surfaces, Wafers, Reprints, Neutron depth profiling.

The thermal neutron reaction (10)B(n, alpha)(7)Li is used to measure the boron concentration on the surface of silicon wafers. The technique, referred to as neutron depth profiling (NDP), requires no special sample preparation. Boron is determined on the as-received wafers at a level of 10(sup 12) to 10(sup 13) atoms/sq cm. A boron level of about 2 X 10(sup 12) atoms/sq cm is found at the wafer surface after oxidation, epitaxial, or polycrystalline silicon deposition. Additional measurements are given from SIMS measurements of multilayer structures on silicon also showing the presence of boron. Ambient air appears to be a significant source of the boron.

04,488
PB94-211174 Not available NTIS
National Inst. of Standards and Technology (NML), Gaithersburg, MD. Surface Science Div.
Brillouin Light Scattering Intensities for Thin Magnetic Films with Large Perpendicular Anisotropies.
Final rept.
J. R. Dutcher, W. F. Egelhoff, J. F. Cochran, and I. Jacob. 1989, 3p.
Pub. in Physical Review B 39, n14 p430-432 1989.

Keywords: *Magnetic films, *Light scattering, *Brillouin effect, Metal films, Thin films, Magnetization, Anisotropy, Copper, Iron, Reprints.

The intensity of light scattered from thermal magnetic waves in thin magnetic films with large perpendicular uniaxial anisotropies was calculated. The anisotropies were large enough to pull the magnetization out of the sample plane. The intensity of light scattered from the surface magnetic mode in a 3.0 monolayer thick fcc Fe film grown on Cu(001) was measured as a function of the applied in-plane d.c. magnetic field. The measured intensities are in excellent agreement with those calculated using the magnetic parameters determined from the measured values of the surface mode frequency. Both the frequency and intensity data indicate that the magnetization of the Fe film was perpendicular to the sample plane in zero applied field.

04,489
PB94-211216 Not available NTIS
National Inst. of Standards and Technology (EEEL), Gaithersburg, MD. Electricity Div.
Half-Integral Constant Voltage Steps in High-Tc Grain Boundary Junctions.
Final rept.
E. A. Early, A. F. Clark, and K. Char. 1993, 3p.
Pub. in Applied Physics Letters 62, n25 p3357-3359, 21 Jun 93.

Keywords: *Superconducting junctions, High temperature superconductors, YBCO superconductors, Grain boundaries, Superhigh frequency, Josephson effect, Magnetic fields, Reprints, Yttrium barium cuprates.

A novel effect from microwave radiation near 9.3 GHz applied to high-T(c) YBa2Cu3O(7-delta) single grain boundary junctions was observed. In addition to the usual Shapiro steps resulting from the ac Josephson effect, constant voltage steps with voltages halfway between the voltages of the Shapiro steps were present. The widths of these 'half-integral' steps were measured as a function of microwave power, and the influence of a magnetic field was investigated. From previous results on high-T(c) grain boundary junctions and a comparison of the results presented here with single- and multiple-junction effects in low-T(c) materials, we conclude that the half-integral steps are likely to be a result of grain boundaries being composed of multiple junctions in parallel.

04,490
PB94-211281 Not available NTIS
National Inst. of Standards and Technology (EEEL), Boulder, CO. Electromagnetic Technology Div.
Critical Magnetic-Field Angle for High-Field Current Transport in YBa2Cu3O7 at 76 K.
Final rept.
J. W. Ekin. 1992, 4p.
Pub. in Cryogenics 32, n11 p1089-1092 1992.

Keywords: *YBCO superconductors, *Critical current, High temperature superconductors, Temperature range 0065-0273 K, Flux pinning, Reprints, *Yttrium barium cuprates, High magnetic fields.

High magnetic field (0.5 T to 9 T) measurements of the in-plane transport critical current density J(c) of YBa2Cu3O7 at liquid nitrogen temperature are reported as a function of the orientation of magnetic field B with respect to the a,b-plane. In contrast to earlier results at lower fields (< 3 T), the measurements reported here at high fields reveal a J(c) versus angle curve with a head-and-shoulders shape with two angular regions having distinctly different behavior. For magnetic field oriented close to the a,b-plane, a sharp, narrow intrinsic-pinning peak in J(c) about the B perpendicular c-axis is observed; on either side of the peak, J(c) is still relatively high and nearly independent of magnetic field magnitude and angle. However, beyond a critical angle theta(c), the J(c) versus theta dependence crosses over to a markedly different behavior, characterized by a decrease in the sharpness of the voltage-current characteristic and a rapid decrease in J(c). To take advantage of the high, nearly field-independent J(c) on either side of the intrinsic pinning peak, magnet design will need to allow an adequate angular margin to avoid the pinning transition at theta(c).

04,491
PB94-211299 Not available NTIS
National Inst. of Standards and Technology (NEL), Boulder, CO. Electromagnetic Technology Div.
Superconducting Materials: Specification.
Final rept.
J. W. Ekin. 1992, 6p.
Pub. in Concise Encyclopedia of Magnetic and Superconducting Materials, p578-583 1992.

Keywords: *Superconductors, Mechanical properties, Critical current, Specifications, Stabilizers, Standards, Reprints.

The specification of superconductors is needed both in the purchase of practical superconductors, as well

as in the characterization of superconductor materials for research. In the case of research, the emphasis is usually in specifying parameters that are intrinsic to the material such as the critical temperature T(c) and upper critical field H(c2). In the case of procuring superconductors for practical applications, the primary concern is, rather, with the extrinsic parameters such as the physical shape of the conductor, critical current, matrix resistivity, and mechanical properties. The emphasis of this article is on practical superconductors and, consequently, specification of the extrinsic parameters. The extrinsic parameters are described under three general headings: physical, electrical, and mechanical specification.

04,492
PB94-211307 Not available NTIS
National Inst. of Standards and Technology (NEL), Boulder, CO. Electromagnetic Technology Div.
Transport Critical Current of Aligned Polycrystalline Yttrium Barium Copper Oxide (YBa2Cu3O7-delta).
Final rept.
J. W. Ekin. 1990, 4p.
Pub. in Prog. High Temp. Supercond. 25, p23-26 1990.

Keywords: *YBCO superconductors, *Critical current, High temperature superconductors, Magnetic fields, Direct current, Polycrystalline, Reprints, Yttrium barium cuprates, Grain boundaries, Weak links.

A study of grain alignment and its effect on the dc transport critical current in fine-grained bulk Y1Ba2Cu3O(7-delta) is reported in magnetic fields from 10(sup -4) T to 26 T. This paper presents a summary of the main results. The data are interpreted as evidence for two parallel components for intergranular current conduction, one consisting of weak-linked material, the other behaving like intrinsic intragranular material that is not weak-linked. A comparison with unaligned YBa2Cu3O7 indicates that the volume fraction of such nonweak-linked material is significantly enhanced by grain alignment, but still only 0.01 to 0.1% of the grain boundary area.

04,493
PB94-211315 Not available NTIS
National Inst. of Standards and Technology (EEEL), Boulder, CO. Electromagnetic Technology Div.
Effect of Axial Strain on the Critical Current of Ag-Sheathed Bi-Based Superconductors in Magnetic Fields Up to 25 T.
Final rept.
J. W. Ekin, D. K. Finnemore, Q. Li, J. Tenbrink, and W. Carter. 1992, 3p.
Pub. in Applied Physics Letters 61, n7 p858-860, 17 Aug 92.

Keywords: *BSCCO superconductors, *Critical current, *Axial strain, High temperature superconductors, Superconducting wires, Magnetic fields, Silver, Reprints, *Bismuth strontium calcium cuprates.

The irreversible strain limit epsilon(irrev) for the onset of permanent axial strain damage to Ag-sheathed Bi2Sr2Ca1Cu2O(8+x) and Bi2Sr2Ca2Cu3O(10+x) superconductors has been measured to be in the range of 0.2%-0.35%. This strain damage onset is about an order of magnitude higher than for bulk sintered Y-, Bi-, or Tl-based superconductors and is approaching practical values for magnet design. The measurements show that the value of epsilon(irrev) is not dependent on magnetic field, nor does the critical current depend on strain below epsilon(irrev) at least up to 25 T at 4.2 K. Both of these factors indicate that the observed strain effect in Ag-sheathed Bi-based superconductors is not intrinsic to the superconductor material. Rather, the effect is extrinsic and arises from superconductor fracture. Thus, the damage onset is amenable to further enhancement. Indeed, the data suggest that subdividing the superconductor into fine filaments or adding Ag to the superconductor powder prior to processing significantly enhances the damage threshold epsilon(irrev) to above 0.6%.

04,494
PB94-211323 Not available NTIS
National Inst. of Standards and Technology (EEEL), Boulder, CO. Electromagnetic Technology Div.
In situ Noble Metal YBa2Cu3O7 Thin-Film Contacts.
Final rept.
J. W. Ekin, S. E. Russek, C. C. Clickner, and B. Jeanneret. 1993, 3p.
Pub. in Applied Physics Letters 62, n4 p369-371, 25 Jan 93.

Keywords: *YBCO superconductors, *Electric contacts, High temperature superconductors, Thin films, Metal films, Silver, Gold, Reprints, *Yttrium barium cuprates, Ohmic contacts.

Thin-film contacts to YBa2Cu3O7 have been fabricated by an in situ noble-metal process and patterned down to 2X2 sq micrometers; at this small size, the contacts carry transport current over 10(sup 6) A/sq cm while maintaining a specific contact resistivity rho(sub c) in the 10(sup -8) to 10(sup -9) ohm sq cm range. No oxygen annealing was used in the processing, thus avoiding the problem of silver or gold agglomeration, as well as preserving a sharp interface for Josephson-device applications. Rho(sub c) was measured to increase only about 25% as temperature was increased from 4 to 90 K. The measurements were carried out on a series of film morphologies using both superconductor-normal metal and superconductor-normal metal-superconductor test structures; a carefully designed test pattern was used to correct for spreading conduction in the noble-metal contact layer. The contacts were ohmic with voltage-current characteristics that were linear over more than four orders of magnitude.

04,495
PB94-211356 Not available NTIS
National Inst. of Standards and Technology (IMSE), Gaithersburg, MD. Reactor Radiation Div.
Magnetoelasticity in Rare-Earth Multilayers and Films.
Final rept.
R. W. Erwin, J. J. Rhyne, J. Borchers, C. P. Flynn, M. B. Salamon, and R. Du. 1990, 6p.
Pub. in Proceedings of Neutron Scattering for Materials Science Symposium, Boston, MA., November 27-30, 1989, p133-138 1990.

Keywords: *Magnetostriction, *Dysprosium, *Yttrium, *Erbium, Phase transformations, Neutron scattering, Critical field, Metal films, Epitaxy, Reprints, Multilayers.

The magnetic structure has been measured with neutron scattering and SQUID magnetometry for a number of epitaxial multilayers and films of the magnetic rare-earths dysprosium and erbium grown with non-magnetic yttrium. In almost all cases the first order ferromagnetic phase transitions are suppressed, although the Neel temperatures are within 5% of the bulk values. The observed critical fields are explained by including epitaxial constraints with the bulk theory of magnetoelasticity.

04,496
PB94-211869 Not available NTIS
National Inst. of Standards and Technology (MSEL), Gaithersburg, MD. Reactor Radiation Div.
Fast-Ion Conduction and Disorder in Cation and Anion Arrays in Y2(ZryTi(1-y))2O7 Pyrochlores Induced by Zr Substitution: A Neutron Rietveld Analysis.
Final rept.
C. Heremans, B. J. Wuensch, J. K. Stalick, and E. Prince. 1993, 6p.
Pub. in Materials Research Society Symposium Proceedings, v293 p349-354 1993.

Keywords: *Order-disorder transformations, *Ionic conductivity, *Crystal structure, Zirconium additions, Reprints, Yttrium zirconate titanates, Rietveld method, Pyrochlore structure.

Structural refinements have been carried out on the Y2(Zr(y)Ti(1-y))2O7 system for increasing amounts of Zr substitution. The structure changes from an ordered pyrochlore structure (superstructure of the fluorite structure) to an anion-deficient fluorite structure. Separate processes govern the disordering of the cation and anion arrays. In particular, the anions begin to disorder at lower values of y than the cations. For intermediate compositions, a minor amount of fluorite phase coexists with the primary partially-disordered pyrochlore phase.

04,497
PB94-211919 Not available NTIS
National Inst. of Standards and Technology (MSEL), Boulder, CO. Materials Reliability Div.
Elastic Constants of Isotropic Cylinders Using Resonant Ultrasound.
Final rept.
P. R. Heyliger, A. Jilani, H. Ledbetter, R. G. Leisure, and C. L. Wang. 1993, 6p.
Pub. in Jnl. of Acoust. Soc. Am. 94, n3 p1482-1487 1993.

Keywords: *Resonant frequency, *Elastic properties, *Cylindrical bodies, *Isotropic media, Equations of motion, Ultrasonic frequencies, Free vibration, Solid mechanics, Reprints.

A method of ultrasonic resonance is used to determine the elastic constants of isotropic cylinders. As applied in this study, this method implies simultaneous application of approximate techniques to solve for the equations of motion of the cylinder and an experimental measurement of the natural frequencies of free vibration. Optimal estimates for the elastic constants are obtained by minimizing the differences between these values. Two separate examples are considered in this study, with promising results.

04,498
PB94-211992 Not available NTIS
National Inst. of Standards and Technology (MSEL), Gaithersburg, MD.
Microstructural Evolution in Two-Dimensional Two-Phase Polycrystals.
Final rept.
E. A. Holm, D. J. Srolovitz, and J. W. Cahn. 1993, 18p.
Pub. in Acta Metallurgica Materials 41, n4 p1119-1136 1993.

Keywords: *Microstructure, *Crystal growth, *Polycrystals, Crystal structure, Phase transformations, Crystallization, Thermodynamic properties, Crystal lattices, Crystal field theory, Reprints.

In two-dimensional polycrystals composed of alpha-phase and beta-phase grains the stability of three-grain junctions and four-grain junctions depends on the interfacial energies. A computer simulation which generates thermodynamically consistent microstructures for arbitrary interfacial energies has been used to investigate microstructural evolution in such polycrystals when phase volume is not conserved. Since grain shapes, phase volume, and phase arrangements are dictated by interfacial energies, clustered-, alternating-, isolated-, and single-phase microstructures occur in different interfacial energy regimes. Despite great differences in microstructure, polycrystals which contain only three-grain junctions evolve with normal grain growth kinetics. In contrast, structures containing flexible four-grain junctions eventually stop evolving. We conclude that two dimensional polycrystals continually evolve when grain junction angles are thermodynamically fixed, while grain growth ultimately ceases when grain junction angles may vary. Predictions concerning three-dimensional and phase-volume conserved systems are made.

04,499
PB94-212073 Not available NTIS
National Inst. of Standards and Technology (MSEL), Gaithersburg, MD. Reactor Radiation Div.
Neutron Powder Diffraction Study of the Crystal Structure of YSr2AlCu2O7.
Final rept.
Q. Huang, S. A. Sunshine, R. J. Cava, and A. Santoro. 1993, 8p.
Pub. in Jnl. of Solid State Chemistry 102, p534-541 1993.

Keywords: *Crystal structure, Orthorhombic lattices, Neutron diffraction, Reprints, *Yttrium strontium aluminum cuprates.

The structure of YSr2AlCu2O7 has been analyzed by neutron powder diffraction techniques. This compound crystallizes with space group P4/mmm symmetry and with lattice parameters a = 3.8646(1), c = 11.1139(3)A. The general structural features of YSr2AlCu2O7 are similar to those found for the 123 superconductor YBa2Cu3O(6+x), and in particular the sequence of layers is the same in the two materials, with SrO substituting for BaO. The Al ions substitute for the copper ions of the chain sites of the 123 parent structure and have tetrahedral coordination. The tetrahedra form chains propagating along the a and b axes on the basal plane of the unit cell. Thus the structure is made of short-range domains within which the local symmetry is orthorhombic. All of the oxygen atoms in this compound have a disordered configuration around the specialized positions of the 123 structure. This arrangement results in tilting of the CuO5 pyramids and in significant distortions of the coordination polyhedra of the other cations.

04,500
PB94-212149 Not available NTIS

National Inst. of Standards and Technology (PL), Gaithersburg, MD. Quantum Metrology Div.
Photoelectron Spectroscopic Study of the Valence and Core-Level Electronic Structure of BaTiO3.
Final rept.
L. T. Hudson, R. L. Kurtz, S. W. Robey, D. Temple, and R. L. Stockbauer. 1993, 7p.
Pub. in Physical Review B 47, n3 p1174-1180, 15 Jan 93.

Keywords: *Barium titanates, *Electronic structure, Photoelectron spectroscopy, Single crystals, Band theory, Photoemission, Valence, Surfaces, Reprints.

We present valence and core-level photoemission measurements from vacuum-fractured, single-crystal barium titanate. These results resolve contradictory measurements in the literature which have employed other methods of sample surface preparation. The valence-shell electronic structure is compared with previously published results of band structure and cluster calculations. Resonant photoemission is used to probe the covalent coupling between titanium and oxygen in the cubic and tetragonal phases of this ionic compound. Photoelectron spectra of the Ti 2p and O 1s core levels reveal the valence of these two ions to be TiO2-like. Valence, core, satellite, and Auger transitions are also assigned and tabulated.

04,501
PB94-212156 Not available NTIS
National Inst. of Standards and Technology (PL), Gaithersburg, MD. Quantum Metrology Div.
Surface Core-Level Shifts of Barium Observed in Photoemission of Vacuum-Fractured BaTiO3 (100).
Final rept.
L. T. Hudson, R. L. Kurtz, S. W. Robey, D. Temple, and R. L. Stockbauer. 1993, 7p.
Pub. in Physical Review B 47, n16 p10 832-10 838, 15 Apr 93.

Keywords: *Barium titanates, X-ray photoelectron spectroscopy, Ultraviolet spectroscopy, Electronic structure, Band theory, Photoemission, Oxides, Reprints, Core level shift.

When clean, vacuum-fractured surfaces of BaTiO3 are analyzed using ultraviolet and x-ray photoelectron spectroscopy (UPS and XPS), more than one set of barium core levels is observed. Sputtering the surface with ions removes lower-binding-energy intensity within the barium line shapes in UPS spectra while little change is noted in XPS. Sputtering of the surface also causes band bending and the creation of band-gap surface states of Ti 3d character. From a comparison of UPS and XPS Ba 4d line shapes from a vacuum-fractured surface, the lower-binding-energy component is assigned to barium with 12-fold oxygen coordination representative of bulk stoichiometry; the higher-binding-energy intensity originates from undercoordinated barium in the region of the sample surface. Reasonable values for the energy-dependent attenuation length of electrons in BaTiO3 are derived from the relative intensities of bulk and surface components using a simple model of electron attenuation.

04,502
PB94-212230 Not available NTIS
National Inst. of Standards and Technology (EEEL), Boulder, CO. Electromagnetic Technology Div.
Flux Expulsion at Intermediate Fields in Type-II Superconductors.
Final rept.
O. B. Hyun. 1993, 7p.
Pub. in Physica C 206, p169-175 1993.

Keywords: *BSCCO superconductors, *YBCO superconductors, *Niobium stannides, *Superconductors, High temperature superconductors, Type 2 superconductors, Temperature dependence, Critical current, Current density, Magnetic fields, Magnetic flux, Magnetization, Reprints, *Bismuth strontium calcium cuprates, *Yttrium barium cuprates.

The flux expulsion behavior at an intermediate field H was studied for type-II superconductors Nb3Sn, YBa2Cu3O7, and Bi2Sr2CaCu2O8. Based on a temperature-dependent critical-state model, magnetization as a function of temperature, M(T), for the zero-field-cooled (ZFC) measurement was used to predict flux expulsion in the field-cooled (FC) measurement and to construct the internal flux profiles for both ZFC and FC at an applied field of 1 T. The model includes empirical relations of the temperature dependence of the reversible magnetization, and the critical current density. Various M(T) patterns are demonstrated by the exponent n, varying from 2 for Nb3Sn to over 20 for Bi2Sr2CaCu2O8.

04,503
PB94-212263 Not available NTIS
National Inst. of Standards and Technology (EEEL), Boulder, CO. Electromagnetic Technology Div.
Offset Susceptibility of Superconductors.
Final rept.
T. Ishida, R. B. Goldfarb, A. B. Kos, and R. W. Cross. 1992, 4p.
Pub. in Physical Review B 46, n18 p12 080-12 083, 1 Nov 92.

Keywords: *High temperature superconductors, *YBCO superconductors, *Superconductors, Temperature dependence, Magnetic fields, Fourier analysis, Magnetometers, Reprints, *Yttrium barium cuprates, *Offset susceptibility.

The novel concept of offset susceptibility chi(0) is presented for superconductors in applied fields H(dc) + H(ac) sin (omega)t. Chi(0) represents the dc component of the time-dependent magnetization M(t). For sintered YBa2Cu3O7, chi(0) was measured as a function of H(ac), H(dc), and temperature using a Hall probe magnetometer and Fourier analysis. For intragranular diamagnetism, chi(0) behaves as the real part of complex fundamental susceptibility chi'(1), confirming a London-like field penetration. However, chi(0) arising from intergranular coupling is positive at temperatures just below the onset of the coupling transition, in good agreement with theoretical predictions of a simplified Kim critical-state model of magnetization.

04,504
PB94-212412 Not available NTIS
National Inst. of Standards and Technology (NML), Gaithersburg, MD. Electron and Optical Physics Div.
Local Partial Densities of States in Ni and Co Silicides Studied by Soft X-Ray Emission Spectroscopy.
Final rept.
J. J. Jia, T. A. Callcott, W. L. O'Brien, D. R. Mueller, D. L. Ederer, J. E. Rowe, Q. Y. Dong, and J. E. Rubensson. 1991, 8p.
Pub. in Physical Review B 43, n6 p4863-4870 1991.

Keywords: *Cobalt silicides, *Nickel silicides, X-ray spectroscopy, X-ray fluorescence, Soft x-rays, Emission spectra, Band theory, Reprints, Density of states.

The Ni and Co mono- and di-silicides are studied by soft x-ray emission spectroscopy. The Si L(2,3) spectra, which provide a measure of the partial densities of states of s and d angular momentum symmetry ((s+d)-PDOS) localized on the Si site, are compared with available theoretical calculations, and discussed in terms of the contribution of s electrons to the bonding. The Ni and Co M(2,3) emission spectra are also obtained, and analyzed to provide information about the d-PDOS localized at the metal site. These spectra are discussed in terms of p-d bonding in the silicides.

04,505
PB94-212578 Not available NTIS
National Inst. of Standards and Technology (NEL), Gaithersburg, MD. Statistical Engineering Div.
Efficient Experiment to Study Superconducting Ceramics.
Final rept.
R. N. Kacker, E. S. Sagergren, M. D. Hill, E. R. Fuller, W. Wong-Ng, and C. K. Chiang. 1991, 16p.
Pub. in Communications in Statistics, Theory and Methods 20, n2 p441-456 1991.

Keywords: *High temperature superconductors, Experimental design, Formulations, Collinearity, Processing, Approximation, Polynomials, Ceramics, Mixtures, Reprints, Scheffe method.

Materials formulation and processing research are important industrial processes and most materials know-how comes from physical experiments. Our impression, based on discussions with materials scientists, is that statistically planned experiments are infrequently used in materials research. This scientific and engineering area provides an excellent opportunity for both using the available techniques of statistically planned experiments, including mixture experiments, and identifying opportunities for collaborative research leading to further advances in statistical methods for scientists and engineers. This paper describes an application of Scheffe's (1958) simplex approach for mixture experiments to formulation of high-temperature superconducting compounds. This example has given us better appreciation of the needs of materials scientists and has provided us opportunities for further collaborative research.

04,506
PB94-212677 Not available NTIS
National Inst. of Standards and Technology (EEEL), Boulder, CO. Electromagnetic Technology Div.
Effect of Thermal Noise on Shapiro Steps in High-Tc Josephson Weak Links.
Final rept.
R. L. Kautz, R. H. Ono, and C. D. Reintsema. 1992, 3p.
Sponsored by Defense Advanced Research Projects Agency, Arlington, VA.
Pub. in Applied Physics Letters 61, n3 p342-344, 20 Jul 92.

Keywords: *Josephson junctions, Temperature range 0013-0065 K, Temperature range 0065-0273 K, High temperature superconductors, Monte Carlo method, YBCO superconductors, Thermal noise, Silver alloys, Gold alloys, Simulation, Reprints, *Shapiro steps, Weak links, Yttrium barium cuprates.

The amplitudes of Shapiro steps are measured at temperatures up to 77 K for a superconductor-normal metal-superconductor Josephson weak link fabricated from YBa2Cu3O(7-delta) with a Ag-Au alloy bridge. The step amplitudes are found to be in agreement with calculations based on the resistively shunted-junction model when the Johnson noise of the junction resistance is included.

04,507
PB94-212685 Not available NTIS
National Inst. of Standards and Technology (EEEL), Boulder, CO. Electromagnetic Technology Div.
Self-Heating in the Coulomb-Blockade Electrometer.
Final rept.
R. L. Kautz, G. Zimmerli, and J. M. Martinis. 1993, 11p.
Contract N00014-92-F-0003
Sponsored by Office of Naval Research, Arlington, VA.
Pub. in Jnl. of Applied Physics 73, n5 p2386-2396, 1 Mar 93.

Keywords: *Electron temperature, Electron-phonon coupling, Electron tunneling, Hot electrons, Electrometers, Aluminum, Reprints.

A detailed comparison between theory and experiment is used to demonstrate the presence of self-heating in the Coulomb-blockade electrometer. When three different heating models are considered, the best fit with experimental electrometer characteristics is obtained for a model in which the electron temperature of the island electrode is determined by heat transfer to the lattice via electron-phonon coupling. In the successful model, the temperature of the island electrons is related to the power dissipated in the island and the temperature of the phonons. The best fit between theory and experiment yields a value of electron-phonon coupling parameter for the electron-phonon coupling in aluminum. Our calculations show that the electron temperature of the island commonly exceeds 100 mK even when the lattice remains at 35 mK.

04,508
PB94-212743 Not available NTIS
National Inst. of Standards and Technology (MSEL), Gaithersburg, MD. Ceramics Div.
Compositional Homogeneity in Processing Precursor Powders to the Ba2YCu3O7-x High Tc Superconductor.
Final rept.
J. F. Kelly, and J. J. Ritter. 1992, 5p.
Pub. in Jnl. of Materials Research 7, n3 p580-584 1992.

Keywords: *YBCO superconductors, *Composition(Property), High temperature superconductors, Scanning electron spectroscopy, X-ray spectroscopy, Powder(Particles), Homogeneity, Processing, Precursor, Ceramics, Reprints, *Yttrium barium cuprates.

We have used scanning electron microscopy (SEM) and energy dispersive x-ray spectroscopy (EDS) to study compositional homogeneity at several stages in the processing of powders to the Ba2YCu3Ox high T(c) superconductor. We investigated the effects of solution pH and ionic concentration in the precipitation preparation of mixed hydroxycarbonates of Ba, Y, and Cu as precursor to the Ba2YCu3O(7-x) high T(c)

superconductor. Our results show that both powder homogeneity and particle morphology are strongly dependent on these parameters. Additionally, studies of the compacted powders by EDS mapping at successive stages of processing show the development of phase inhomogeneities, even in homogeneous starting powders.

04,509
PB94-212768 Not available NTIS
National Inst. of Standards and Technology (NML), Gaithersburg, MD. Electron and Optical Physics Div.
Correlations of Modulation Noise with Magnetic Microstructure and Intergranular Interactions for CoCrTa and CoNi Thin Film Media.
Final rept.
M. R. Khan, S. Y. Lee, S. L. Duan, D. E. Speliotis, M. R. Scheinfein, J. L. Pressesky, and N. Heiman. 1991, 3p.
Pub. in Jnl. of Applied Physics 69, n8 p4745-4747 1991.

Keywords: *Cobalt alloys, Chromium containing alloys, Nickel containing alloys, Tantalum containing alloys, Magnetic alloys, Magnetic anisotropy, Magnetic films, Remanent magnetism, Coercive force, Thin films, Demagnetization, Microstructure, Reprints, Modulation noise.

This paper reports on two thin film media alloys Co(86)Cr(12)Ta(2) and Co(75)Ni(25) which have very different noise characteristics. The magnetic microstructure of these films were observed with SEMPA. The variance of the magnetization across the transition region was calculated. The origin of anisotropy was determined by measuring the temperature coefficients of H(c) and M(s). The interaction strengths between grains, M(H), were obtained from the measurements of the reverse demagnetization remanence Md(H), and the forward magnetization remanence Mr(H). We found that the CoNi film showed a greater degree of interparticle interaction which may explain the observed cross-bit linkages in SEMPA image, larger RMS transition variation, and higher modulation noise.

04,510
PB94-213048 Not available NTIS
National Inst. of Standards and Technology (MSEL), Gaithersburg, MD. Ceramics Div.
Materials Science with SR Using X-Ray Imaging: Spatial-Resolution/Source Size.
Final rept.
M. Kuriyama. 1991, 12p.
Pub. in Nuclear Instruments and Methods in Physics Research 303, n3 p503-514 1991.

Keywords: *Materials science, *Synchrotron radiation, *X-ray imagery, Synchrotron radiation sources, X-ray diffraction, Spatial resolution, Single crystals, Microradiography, Polycrystalline, Reprints, Multilayers.

Some examples of applications of synchrotron radiation to materials science demonstrate the importance of microstructure information within structural as well as functional materials in order to control their properties and quality as designed for industrial purposes. To collect such information, x-ray imaging in quasi real time (50 - 100 sec time intervals) is required in either the microradiographic mode or the diffraction (in transmission) mode. New measurement technologies based on imaging are applied to polycrystalline materials, single crystal materials and multilayered device materials to illustrate what kind of synchrotron radiation facility is most desirable for materials science and engineering.

04,511
PB94-213089 Not available NTIS
National Inst. of Standards and Technology (CSTL), Gaithersburg, MD. Inorganic Analytical Research Div.
Analysis of Boron in CVD Diamond Surfaces Using Neutron Depth Profiling.
Final rept.
G. P. Lamaze, R. G. Downing, L. Pilione, A. Badzian, and T. Badzian. 1993, 6p.
Sponsored by Office of Naval Research, Arlington, VA.
Pub. in Applied Surface Science 65/66, p587-592 1993.

Keywords: *Diamond films, *Surface analysis, *Boron, Chemical vapor deposition, Concentration(Composition), Semiconducting films, Cold neutrons, Doped materials, Single crystals, Thin films, Reprints, Neutron depth profiling, Depth profiles, CNRF facility.

Neutron depth profiling (NDP) is a method of near surface analysis for isotopes that undergo neutron-induced positive Q-value charged particle reactions, e.g., (n,alpha), (n,p). Because of its large cross section and large Q-value, the (10)B(n,alpha)(7)Li reaction has been widely employed for NDP studies. We have used the NDP technique to study the concentration and distribution of boron in CVD diamond layers. The measurements were made using the new Cold Neutron Depth Profiling instrument at the NIST Cold Neutron Research Facility. The diamond samples were prepared at the Materials Research Laboratory at the Pennsylvania State University. The doped diamond single crystal films were grown by microwave plasma chemical vapor deposition from a mixture of methane, hydrogen and diborane. Natural type IIa crystals cut along the (001) plane were used as substrates. Results of the measurements are presented.

04,512
PB94-213121 Not available NTIS
National Inst. of Standards and Technology (IMSE), Gaithersburg, MD. Metallurgy Div.
Magnetic and Structural Properties of Electrodeposited Copper-Nickel Microlayered Alloys.
Final rept.
D. S. Lashmore, R. R. Oberle, L. H. Bennett, M. P. Dariel, L. Romankiw, L. Swartzendruber, and U. Atzmony. 1990, 11p.
Pub. in Proceedings of Symposium on Magnetic Materials, Processes, and Devices, Hollywood, FL., October 15-19, 1989, p347-357 1990.

Keywords: *Electrodeposited coatings, *Superlattices, X-ray diffraction, Magnetic properties, Magnetic films, Metal films, Thin films, Electrodeposition, Copper, Nickel, Reprints, Multilayers.

Magnetic measurements of Ni-Cu compositionally modulated alloys prepared by electrochemical deposition suggest a high degree of perfection is achieved. The magnetic behavior closely resembles that of bulk nickel and suggests little interdiffusion between the copper and the nickel. The high value of the saturation magnetization implies that no magnetic dead layer exists at the nickel/copper interface for wavelengths greater than 2.5 nm. A magnetic after effect has been found which increases with decreasing temperature and is a maximum at the coercive field. The electrochemical technique has progressed to the point where third order satellites are now commonly observed, suggesting a very square composition profile. Continuous layers of copper as thin as 5 A (about 2 monolayers) have been produced.

04,513
PB94-213196 Not available NTIS
National Inst. of Standards and Technology (MSEL), Boulder, CO. Materials Reliability Div.
Elastic Constants of Polycrystalline Y1Ba2Cu3Ox.
Final rept.
H. Ledbetter. 1992, 3p.
Pub. in Jnl. of Materials Research 17, n11 p2905-2907 Nov 92.

Keywords: *YBCO superconductors, *Elastic properties, High temperature superconductors, Ultrasonic radiation, Acoustic velocity, Debye temperature, Bulk modulus, Ionic crystals, Polycrystalline, Reprints, *Yttrium barium cuprates, Oxygen content.

We measured the elastic constants of polycrystalline Y1Ba2Cu3Ox with eleven oxygen contents varying from 6.2 to 6.9. Reported properties include sound velocities; bulk, shear, Young's moduli; Poisson ratio; Debye temperature. After correction to the void-free state, the measurements fail to show a systematic dependence on oxygen content. Focusing on the bulk modulus, all measurements fall below an ionic-crystal model prediction, by 5-50%. We attribute this macroscopic softness to either microcracks or weak grain-boundary mechanical linkages. For the case x = 6.9, we suggest a set of intrinsic elastic constants.

04,514
PB94-213220 Not available NTIS
National Inst. of Standards and Technology (MSEL), Boulder, CO. Materials Reliability Div.
Correlation between Tc and Elastic Constants of (La-M)2CuO4.
Final rept.
H. Ledbetter, S. Kim, and A. Roshko. 1992, 3p.
Pub. in Zeitschrift fuer Physikalische B - Condensed Matter 89, p275-277 1992.

Keywords: *Superconductors, High temperature superconductors, Electron phonon interactions, Ultrasonic radiation, Acoustic velocity, Debye temperature, Elastic properties, Transition temperature, Correlation, Reprints, *Lanthanum calcium cuprates, *Lanthanum barium cuprates, *Lanthanum strontium cuprates.

By an ultrasonic method, we measured the elastic constants of polycrystalline La(1.85)M(0.15)CuO4 with M=Ca, Ba, Sr. These materials show zero-resistance normal-superconductive transition temperatures of 19, 28, and 36 K. Versus T(c), all the elastic stiffnesses - bulk modulus, Young modulus, shear modulus - increase. Derived from the elastic constants and average atomic volume, the Debye temperature increases linearly with T(c). In conventional BCS superconductors, T(c) decreases with increasing 1 Theta(D).

04,515
PB94-213352 Not available NTIS
National Inst. of Standards and Technology (MSEL), Boulder, CO. Materials Reliability Div.
Elastic Constants and Debye Temperature of Y1Ba2Cu3Ox: Effect of Oxygen Content.
Final rept.
S. Lin, M. Lei, and H. Ledbetter. 1993, 4p.
Pub. in Materials Letters 16, p165-168 1993.

Keywords: *YBCO superconductors, *Elastic properties, High temperature superconductors, Ultrasonic radiation, Debye temperature, Bulk modulus, Temperature range 0000-0013 K, Temperature range 0013-0065 K, Temperature range 0065-0273 K, Temperature range 0273-0400 K, Polycrystalline, Reprints, *Yttrium barium cuprates, Oxygen content.

Using ultrasonic methods, we measured the elastic constants of polycrystalline Y1Ba2Cu3Ox between 295 and 4 K. For a single specimen, using vacuum annealing and oxygen annealing, we varied the oxygen content in four steps from x=6.2 to x=6.9. Elastic stiffnesses that depend mainly on shear modes increase monotonically with increasing oxygen content. Stiffnesses that depend on dilatation modes increase up to about x=6.7 and then decrease. The elastic Debye temperature, which depends mainly on shear modes, increases monotonically, in agreement with the specific-heat Debye temperature. An ionic-model calculation for the bulk modulus and Debye temperature predicts a monotonic increase for both. We conjecture that the irregular oxygen-content dependence of the dilatation-mode-related elastic constants arises from changes in copper-oxygen valences.

04,516
PB94-216116 Not available NTIS
National Inst. of Standards and Technology (MSEL), Gaithersburg, MD. Reactor Radiation Div.
Polarization Analysis of the Magnetic Excitations in Invar and Non-Invar Amorphous Alloys.
Final rept.
J. W. Lynn, N. Rosov, and G. Fish. 1993, 3p.
Pub. in Jnl. of Applied Physics 73, n10 p5369-5371, 15 May 93.

Keywords: *Invar, Phosphorus containing alloys, Boron containing alloys, Nickel alloys, Iron alloys, Polarized beams, Neutron scattering, Inelastic scattering, Amorphous materials, Spin waves, Ferromagnetic materials, Reprints, *Amorphous ferromagnets, Magnetic excitations, METGLAS 2826.

Conventional spin wave theory works remarkably well in describing the spin dynamics of both Invar and non-Invar isotropic ferromagnets, with the important exception that for Invar systems the magnetization decreases much more rapidly with temperature than can be explained based on the measured spin wave dispersion relations. We have been carrying out triple-axis polarized inelastic neutron scattering experiments on the amorphous ferromagnets Fe86B14 (Invar system) and Fe40Ni40P14B6 (METGLAS (R(circled)) 2826) in order to separate the longitudinal magnetic fluctuations from the transverse (spin wave) excitations, and thereby determine if the presence of longitudinal excitations might resolve this discrepancy. The present measurements exhibit longitudinal excitations below t(c), but in both materials. Possible interpretations of the results are discussed.

04,517
PB94-216207 Not available NTIS
National Inst. of Standards and Technology (IMSE), Gaithersburg, MD. Reactor Radiation Div.
Neutron Scattering Studies of Surfaces and Interfaces.
Final rept.
C. F. Majkrzak, and G. P. Felcher. 1990, 7p.
Pub. in MRS Bulletin 15, n11 p65-71 Nov 90.

Keywords: *Surfaces, *Interfaces, Neutron diffraction, Grazing incidence, Magnetic materials, Superconductors, Polymers, Reprints, Neutron reflectometry, Multilayers.

During the past decade, scientific and technological interest in the properties of surfaces and interfaces has grown at an astounding rate. Electron, atomic beam, and x-ray diffraction techniques have been used to study surface or near surface problems. Neutrons can also be used in many cases and because neutrons can distinguish between different isotopes of the same element, most notably hydrogen and deuterium, as well as couple to atomic magnetic moments via a dipolar interaction, they can be an indispensable and complementary probe. The purpose of this paper is to give a concise description of the methodology of neutron reflectometry, multilayer diffraction, and grazing angle diffraction, including specific examples of the characterization of magnetic, superconducting, and polymeric surfaces or interfaces.

04,518
PB94-216314 Not available NTIS
National Inst. of Standards and Technology (MSEL), Gaithersburg, MD. Reactor Radiation Div.
Crystal Structure of Pb2Sr2YCu3O8+delta with delta=1.32, 1.46, 1.61, 1.71, by Powder Neutron Diffraction.
Final rept.
M. Marezio, A. Santoro, J. J. Capponi, Q. Huang, R. J. Cava, and O. Chmaissem. 1992, 10p.
Pub. in Physica C 199, p365-374 1992.

Keywords: *Crystal structure, Neutron diffraction, Reprints, *Lead strontium yttrium cuprates, Oxygen content.

The structures of Pb2Sr2YCu3O(8 + delta) with delta = 1.46, 1.61, 1.71, have been determined by powder neutron diffraction data. As previously shown for Pb2Sr2YCu3O(9.32), the extra oxygen atoms are incorporated on the Cu layer sandwiched between two PbO layers. The structural refinements indicated that the most stable structure is that of Pb2Sr2YCu3O(9.5) in which the two possible oxygen sites on the Cu layer are filled up to 75%. These extra oxygen atoms give rise to superstructures and change the coordination of the cations belonging to the (PbO)(Cu)(PbO) blocks. In Pb2Sr2YCu3O(9.5) the Cu cations inside these blocks are surrounded by an oxygen pyramid, while the Pb cations are surrounded by seven, eight, or nine oxygen atoms, depending upon the specific site in the superstructure. At the same time, the valences of these cations increase from 1+ to 2+ for Cu and from 2+ to 4+ for half of the Pb. The oxidation of the Pb cations hinders the charge transfer from the CuO(1.5) layers to the superconducting (CuO2)(Y)(CuO2) blocks and the oxidation of Pb2Sr2YCu3O8 does not lead to a superconducting state. Every sample we analyzed should be considered either an oxygen-deficient compound or one containing an excess oxygen with respect to the Pb2Sr2YCu3O(9.5) structure.

04,519
PB94-216553 Not available NTIS
National Inst. of Standards and Technology (IMSE), Gaithersburg, MD. Fracture and Deformation Div.
Atomic Theory of Fracture of Brittle Materials: Application to Covalent Semiconductors.
Final rept.
K. Masuda-Jindo, V. K. Tewary, and R. Thomson. 1991, 14p.
Pub. in Jnl. of Materials Research 6, n7 p1553-1566 1991.

Keywords: *Brittle fracturing, *Atomic theory, *Silicon, Perturbation theory, Greens function, Chemical bonds, Semiconductors, Cracks, Reprints, LCAO theory.

Using the lattice Green's function approach and LCAO (linear combination of atomic orbitals) electron theory, we investigate the atomistic configuration and lattice trapping of cracks in Si. The LCAO electron theory coupled to second order perturbation (SOP) theory has been used to derive explicit expressions for the bond breaking non-linear forces between Si atoms. We calculate the cracked lattice Green's functions for a crack on the (111) plane and lying in the (110) direction. With the non-linear forces acting in a cohesive region near the crack tips, the crack structure is then calculated. The calculated structure possesses a crack opening at the Griffith load which should allow penetration of typical external molecules to the crack tip at the Griffith loading. Other consequences for chemical reactions at the crack tip are discussed in the light of these results. The lattice trapping is low, only a few percent of the Griffith load.

04,520
PB94-216678 Not available NTIS
National Inst. of Standards and Technology (PL), Gaithersburg, MD. Electron and Optical Physics Div.
Simple, Compact, High-Purity Cr Evaporator for Ultrahigh Vacuum.
Final rept.
J. J. McClelland, J. Unguris, R. E. Scholten, and D. T. Pierce. 1993, 2p.
Pub. in Jnl. of Vacuum Science and Technology A 11, n5 p2863-2864 Sep/Oct 93.

Keywords: *Evaporators, *Chromium, Ultrahigh vacuum, Metal films, Thin films, Filaments, Reprints.

A simple, compact Cr evaporator is constructed by electroplating Cr metal onto the tip of a W hairpin filament. At 5 cm from the evaporator, deposition rates up to 10 nm/min (flux approx = 10(sup 19) atoms/sq m/s) have been obtained, with total deposition thickness in excess of 400 nm. Auger analyses of thin films deposited in ultrahigh vacuum show impurities below detectability.

04,521
PB94-216736 Not available NTIS
National Inst. of Standards and Technology (NEL), Gaithersburg, MD. Applied and Computational Mathematics Div.
Effect of Modulated Taylor-Couette Flows on Crystal-Melt Interfaces: Theory and Initial Experiments.
Final rept.
G. B. McFadden, B. T. Murray, S. R. Coriell, M. E. Glicksman, and M. E. Selleck. 1992, 20p.
Pub. in Proceedings of IMA Workshop on the Evolution of Phase Boundaries, September 17-21, 1990, p81-100 1992.

Keywords: *Crystal growth, *Solidification, Cylindrical configuration, Free boundaries, Reprints, *Crystal-melt interface, *Taylor-Couette flow, Floquet theory, Two phase systems.

An important problem in the process of crystal growth from the melt phase is to understand the interaction of the crystal-melt interface with fluid flow in the melt. This area combines the complexities of the Navier-Stokes equations for fluid flow with the nonlinear behavior of the free boundary representing the crystal-melt interface. Some progress has been made by studying explicit flows that allow a base state corresponding to a one-dimensional crystal-melt interface with solute and/or temperature fields that depend only on the distance from the interface. This allows the strength of the interaction between the flow and the interface to be assessed by a linear stability analysis of the simple base state. The case of a time-periodic Taylor-Couette flow interacting with a cylindrical crystalline interface is currently being investigated both experimentally and theoretically; some preliminary results are given here. The results indicate that the effect of the crystal-melt interface in the two-phase system is to destabilize the system by an order of magnitude relative to the single-phase system with rigid walls.

04,522
PB95-107207 Not available NTIS
National Inst. of Standards and Technology (NML), Gaithersburg, MD. Gas and Particulate Science Div.
Monte Carlo Electron Trajectory Simulation of X-Ray Emission from Films Supported on Substrates.
Final rept.
D. E. Newbury, R. L. Myklebust, and E. B. Steel. 1990, 4p.
Pub. in Microbeam Anal. 25, p127-130, 1990.

Keywords: *Monte Carlo method, *X-ray analysis, Reprints, Thin films, Microanalysis, Electron probes, Silicon, Calibration standards, Trajectories, Simulation, Multicomponent targets, Scanning electron microscopy, National Institute of Standards and Technology, SRM 2063.

The development of a Monte Carlo electron trajectory simulation for application to scanning electron microscopy and x-ray microanalysis involves several possible choices of elastic scattering and energy loss models, as well as for inner shell ionization. The problem of establishing proper weighting for the simulation of multicomponent targets must also be considered. While there is an extensive base of pure element experimental data for comparison to calculations, relatively little data is available on multi-component targets.

04,523
PB95-107306 Not available NTIS
National Inst. of Standards and Technology (MSEL), Gaithersburg, MD. Ceramics Div.
Improved Crystallographic Data for Aluminum Niobate (AlNbO4).
Final rept.
C. J. Rawn, R. S. Roth, and H. F. McMurdie. 1991, 2p.
Pub. in Powder Diffr. 6, n1 p48-49 1991.

Keywords: *Lattice parameters, Least squares method, X-ray diffraction, Orthorhombic lattices, Single crystals, Reprints, *Aluminum niobates.

The compound AlNbO4 has been studied by single crystal x-ray precession photographs and x-ray powder diffraction. Unit cell dimensions were calculated using a least squares analysis that refined to a Delta 2 theta deg of no more than 0.03 deg. An orthorhombic cell was found with space group C2/m, a = 121558(5)A, B = 3.7345(2)A, c = 6.4886(3)A, and beta = 107.613(4) deg.

04,524
PB95-107371 Not available NTIS
National Inst. of Standards and Technology (MSEL), Gaithersburg, MD. Reactor Radiation Div.
Rietveld Analysis of NaxWO3+x/2.yH2O, Which Has the Hexagonal Tungsten Bronze Structure.
Final rept.
K. P. Reis, E. Prince, and M. S. Whittingham. 1992, 6p.
Pub. in Chem. Mater. 4, n2 p307-312 1992.

Keywords: *Sodium tungstates, *Crystal structure, Hexagonal lattices, Neutron diffraction, Hydrates, Deuterium compounds, Reprints, Rietveld method.

Powder neutron diffraction and Rietveld analysis were used to investigate the crystal structures of hydrated and deuterated samples of Na(x)WO(3+x/2)(dot)yH2O (x approx. = 0.17, y approx. = 0.23). The compound, which crystallizes with the symmetry of space group P6/mmm, is related to the hexagonal tungsten bronze structure but differs from it due to the presence of sodium and oxygen along the hexagonal tunnel. Some of the oxygens appear in the structure as water molecules. The oxygen is disordered along the z axis in the hexagonal cavity with sodium in the hexagonal window.

04,525
PB95-108429 Not available NTIS
National Inst. of Standards and Technology (PL), Gaithersburg, MD. Electron and Optical Physics Div.
Magnetic Moments in Cr Thin Films on Fe(100).
Final rept.
D. T. Pierce, R. J. Celotta, and J. Unguris. 1993, 3p.
Sponsored by Office of Naval Research, Arlington, VA.
Pub. in Jnl. of Applied Physics 73, n10 p6201-6203, 15 May 93.

Keywords: *Magnetic moments, *Chromium, Whiskers(Single crystals), Polarization(Spin alignment), Antiferromagnetic materials, Scanning electron microscopy, Spin waves, Metal films, Thin films, Epitaxy, Iron, Reprints, *Surface magnetism, Electron spin polarization, Secondary electrons.

The magnetism at the surface of a Cr film grown epitaxially on a Fe(100) whisker is observed as a function of Cr thickness by scanning electron microscopy with polarization analysis. Use of a wedge-shaped film of linearly increasing thickness allows the magnetism to be followed continuously for 75 Cr layers. Over the temperature range measured from just below the Neel temperature of bulk Cr, T(N), to 1.8 T(N), the surface magnetic moment is seen to persist and change direction with each additional Cr layer, but there are phase slips in this antiferromagnetic ordering. These are con-

sistent with an incommensurate spin density wave (SDW) in the Cr film having a wavelength of 40 layers at T(N). An irregularity in the antiferromagnetic stacking order in the first four layers is discussed and the behavior of the moments at the subsequent phase slip is examined. The limitations which prevent the determination of the surface magnetic moment from the spin polarization of secondary electrons are discussed.

04,526
PB95-108601 Not available NTIS
National Inst. of Standards and Technology (MSEL), Gaithersburg, MD. Reactor Radiation Div.
Mathematical Aspects of Rietveld Refinement.
Final rept.
E. Prince. 1993, 12p.
Pub. in Rietveld Method, Chapter 3, p43-54 1993.

Keywords: Least squares method, X-ray diffraction, Neutron diffraction, Crystal structure, Data processing, Reprints, *Rietveld method, Parameter estimation.

The method of least squares is a powerful technique for estimating the parameters of a model given a set of observations. In the Rietveld method, the observations are the intensities of neutrons or x-rays in a powder diffraction pattern, and the model predicts these intensities as a function of background, peakshape and crystallographic parameters. The loss of information due to overlapping peaks can be compensated for by incorporating additional information, such as chemical composition, noncrystallographic symmetry and rigid body motion, in the model by means of constraints and restraints. Careful attention to the efficiency and stability of refinement procedures is important. Statistical analysis can be used to assess the uncertainties in the parameters of a refined model and to compare two or more models.

04,527
PB95-125647 Not available NTIS
National Inst. of Standards and Technology (MSEL), Boulder, CO. Materials Reliability Div.
Asymmetry between Flux Penetration and Flux Expulsion in Tl-2212 Superconductors.
Final rept.
M. Foldeaki, H. Ledbetter, M. Paranthaman, H. M. Duan, and A. M. Hermann. 1993, 5p.
Pub. in Jnl. of Superconductivity 6, n3 p185-189 1993.

Keywords: *High temperature superconductors, Temperature range 0013-0065 K, Irreversible processes, Time dependence, Magnetic hysteresis, Flux pinning, Direct current, Single crystals, Polycrystals, Asymmetry, Reprints, *Thallium barium calcium cuprates.

dc magnetic hysteresis as well as flux penetration and flux expulsion were investigated in Tl(2-y)Ba2CaCu2O(8-x) polycrystals and monocrystals. All measurements were performed at 35 K and in the 0-5 T field range. Hysteresis measurements revealed an irreversibility field of about 2 T. Existing models predict identical field-cooled (fc) and zero-field-cooled (zfc) magnetizations and vanishing time dependence above this field. Although the identical fc and zfc magnetizations are in fact observed, the time dependence vanishes only for flux penetration after zero-field cooling; a remanence is preserved after field cooling and decays with a finite relaxation rate. Activation energies calculated on the basis of the thermal activation model display a pronounced field dependence, and are lower for flux penetration than for flux expulsion in high fields (H = or > 3 T) for all orientations. This behavior of extreme layered superconductors contradicts classical theoretical models and questions the original definition of the irreversibility line as well. All of our results are consistent with the recent theory of lock-in transition, and can be well interpreted by using those principles.

04,528
PB95-126033 Not available NTIS
National Inst. of Standards and Technology (MSEL), Gaithersburg, MD. Metallurgy Div.
Nature of (001) Tilt Grain Boundaries in YBa2Cu3O6+x.
Final rept.
F. W. Gayle, and D. L. Kaiser. 1991, 8p.
Pub. in Jnl. of Materials Research 6, n5 p908-915 1991.

Keywords: *YBCO superconductors, *Grain boundaries, High temperature superconductors, Crystal-phase transformations, Orthorhombic lattices, Tetragonal lattices, Twinning, Reprints, *Yttrium barium cuprates, Tilt boundaries.

Fifty-two facetted grain boundary segments ((left bracket) 001 (right bracket) tilt boundaries) in clusters of bulk-scale YBa2Cu3O(7-x) crystals having coincident c-axes were characterized by optical microscopy techniques. Grain boundary orientations were widely distributed, with a slight favoring of (110), (310), and (510) boundary planes. All grain boundaries, except those far from the symmetric condition and those with (110) facets, exhibited well-developed matching of the twin domains across the boundary. It is suggested that this newly-reported phenomenon of twin pattern matching occurs due to a local coordination of the tetragonal --> orthorhombic transformation strain across grain boundaries and may be beneficial with regard to electrical transport in highly-textured polycrystalline material.

04,529
PB95-126074 Not available NTIS
National Inst. of Standards and Technology (EEEL), Gaithersburg, MD. Electricity Div.
Cryogenic Precision Capacitance Bridge Using a Single Electron Tunneling Electrometer.
Final rept.
R. N. Ghosh, E. R. Williams, A. F. Clark, and R. J. Soulen. 1993, 2p.
Pub. in Proceedings of the International Conference on Low Temperature Physics (20th), Eugene, OR., August 4-11, 1993.

Keywords: *Capacitance bridges, *Electrometers, Cryogenic equipment, Precision, Design, Reprints, *Electron charge, Single electron tunneling.

The electronic charge can be determined by placing a known number of electrons on a calibrated capacitor and measuring the resulting voltage. Single electron tunneling (SET) electrometers with sufficient sensitivity for this application have been fabricated. We report on the design and preliminary results of a capacitance bridge experiment using an SET electrometer to measure two capacitors in a dilution refrigerator. This includes discussion of issues such as the leakage rate of a capacitor at cryogenic temperatures and the optimum coupling of the electrometer to the bridge circuit.

04,530
PB95-126116 Not available NTIS
National Inst. of Standards and Technology (NML), Gaithersburg, MD. Gas and Particulate Science Div.
Image Depth Profiling SIMS: An Evaluation for the Analysis of Light Element Diffusion in YBa2Cu3O7-x Single Crystal Superconductors.
Final rept.
G. Gillen, D. L. Kaiser, and J. S. Wallace. 1991, 8p.
Pub. in Surface and Interface Analysis 17, n1 p7-14 1991.

Keywords: *YBCO superconductors, Secondary ion mass spectroscopy, High temperature superconductors, Single crystals, Oxygen 18, Diffusion, Reprints, *Yttrium barium cuprates, Depth profiles.

An analytical strategy for quantifying the diffusion of (18)O in small, melt-grown single crystal YBa2Cu3O(7-x) superconductors by image depth profiling SIMS (Secondary Ion Mass Spectroscopy) is presented. This technique was used to obtain data for both in-depth (along the c axis) and lateral (in the ab plane) diffusion from one superconducting crystal. Cross sectional images, generated from the image depth profiling data, revealed features of the diffusion processes which would not have been apparent in a standard depth profile. Retrospective selected area depth profiling was used to remove the influence of background species, edge effects, and imperfections in the crystals, resulting in processed depth profiles with greater dynamic range. Finally, the influence of detector artifacts on the analytical results were evaluated.

04,531
PB95-126199 Not available NTIS
National Inst. of Standards and Technology (EEEL), Boulder, CO. Electromagnetic Technology Div.
Magnetic Measurement of Transport Critical Current Density of Granular Superconductors.
Final rept.
R. B. Goldfarb, R. W. Cross, L. F. Goodrich, and N. F. Bergren. 1993, 5p.
Pub. in Cryogenics 33, n1 p3-7 1993.

Keywords: *High temperature superconductors, *Critical current, Granular materials, Magnetic measurement, Current density, Magnetization, Reprints.

We describe two magnetic techniques that may be used to determine the transport critical current density J(ct) of granular superconductors by measuring the intergranular magnetization of a sample. In the first method, magnetization critical current density J(cm) is used to estimate J(ct) by isolating the intergranular magnetization and applying the critical state model. In the second method, magnetic detection is used to measure J(ct) directly: intergranular magnetization hysteresis loops are obtained while increasing a transport current through a sample. The critical current density J(ct) is that value of transport current density which causes the intergranular magnetization to collapse at a given magnetic field and temperature. Both methods give values of J(ct) in fair agreement with values obtained from conventional transport measurements of J(ct). Magnetization was measured with both extraction and Hall probe magnetometers.

04,532
PB95-126215 Not available NTIS
National Inst. of Standards and Technology (MSEL), Gaithersburg, MD. Metallurgy Div.
Inelastic Neutron Scattering Measurements of Phonons in Icosahedral Al-Li-Cu.
Final rept.
A. I. Goldman, C. Stassis, R. Bellissent, F. W. Gayle, H. Moudden, and N. Pyka. 1991, 4p.
Pub. in Physical Review B 43, n10 p8763-8766 1991.

Keywords: Aluminum copper alloys, Lithium alloys, Neutron scattering, Inelastic scattering, Icosahedrons, Reprints, *Quasicrystals, Phonon dispersion.

We describe the results of inelastic neutron scattering measurements on a single grain of the icosahedral alloy Al-Li-Cu. Within experimental error the acoustic phonon dispersion at small, but finite, q is independent of direction, confirming the isotropic elasticity expected for icosahedral crystals. By following the longitudinal phonon dispersion curve along a five-fold axis, we can identify the location of a 'quasi-Brillouin zone boundary.' Furthermore, the measurements suggest the presence of an optical or localized mode along the two-fold axis at approximately 10 meV.

04,533
PB95-126223 Not available NTIS
National Inst. of Standards and Technology (EEEL), Boulder, CO. Electromagnetic Technology Div.
n-Value and Second Derivative of the Superconductor Voltage-Current Characteristic.
Final rept.
L. F. Goodrich, A. N. Srivastava, M. Yuyama, and H. Wada. 1993, 4p.
Pub. in Institute of Electrical and Electronics Engineers Transactions on Applied Superconductivity 3, n1 p1265-1268 Mar 93.

Keywords: *Superconductors, High temperature superconductors, BSCCO superconductors, Critical current, Electric current, Transition points, Voltage, Copper, Simulators, Data acquisition, Reprints, Niobium titanium.

We studied the n-value (V varies as I(sup n)) and second derivative of V with respect to I, of the voltage-current curve of high and low temperature superconductors and superconductor simulators. We used these parameters for diagnosing problems with sample heating and data acquisition, and as indicators of the superconducting-to-normal state transition. The superconductor simulator may be useful in testing the measurement system integrity and reducing measurement variability as its characteristics are highly repeatable.

04,534
PB95-126389 Not available NTIS
National Inst. of Standards and Technology (NML), Gaithersburg, MD. Gas and Particulate Science Div.
Transition Metal Implants in In0.53GA0.47As.
Final rept.
S. M. Gulwadi, M. V. Rao, A. K. Berry, H. B. Dietrich, D. S. Simons, and P. H. Chi. 1991, 6p.
Pub. in Jnl. of Applied Physics 69, n8 p4222-4227 1991.

Keywords: *Indium gallium arsenides, *Ion implantation, Secondary ion mass spectroscopy, Semiconductor doping, Chromium ions, Iron ions, Phosphorus ions, Vanadium ions, Annealing, Reprints, Photoreflectance.

Single- and multiple-energy Fe, Cr, and V implants are performed into InGaAs. Annealing of the implanted InGaAs samples results in redistribution of the im-

planted atoms, as determined by secondary ion mass spectrometry. Coimplantation of Fe with P does not prevent this redistribution. A transport equation calculation of Fe-implantation-induced stoichiometric disturbances in InGaAs is done. The lattice quality of implanted InGaAs is investigated by photoreflectance measurements. Fe-implanted InGaAs has a resistivity close to the intrinsic limit, whereas Cr- and V-implanted InGaAs have a lower resistivity than the unimplanted material.

04,535
PB95-126397 Not available NTIS
National Inst. of Standards and Technology (NML), Gaithersburg, MD. Gas and Particulate Science Div.
Range Statistics and Rutherford Backscattering Studies on Fe-Implanted In0.53Ga0.47As.
Final rept.
S. M. Gulwadi, M. V. Rao, D. S. Simons, C. Caneau, H. B. Dietrich, O. W. Holland, and W. P. Hong. 1991, 6p.
Pub. in Jnl. of Applied Physics 69, n1 p162-167 1991.

Keywords: *Indium gallium arsenides, Secondary ion mass spectroscopy, KeV range 10-100, KeV range 100-1000, MeV range 1-10, Semiconductor doping, Doped materials, Radiation damage, Rutherford scattering, Ion implantation, Iron ions, Backscattering, Reprints, Amorphization.

Single-energy Fe-implantation at energies in the range 50 keV - 2 MeV to achieve a peak Fe-concentration of 1 - 2 X 10(exp 18)/cu cm is performed into undoped (n-type) In-GaAs layers grown on InP:Fe. The first four statistical moments of the Fe-profiles measured by secondary ion mass spectrometry are determined. The Pearson IV distribution calculated from these moments matches the implant-profile closely. Samples implanted with Fe to doses in the range 5 X 10(exp 12) - 2 X 10(exp 15)/sq cm at 380 keV are analyzed by Rutherford backscattering measurements to study ion-induced damage. For 380 KeV implants, amorphization takes place at a dose of = 6 X 10(exp 13)/sq cm.

04,536
PB95-136628 PC A03/MF A01
National Inst. of Standards and Technology (CAML), Gaithersburg, MD. Applied and Computational Mathematics Div.
xi-Vector Formulation of Anisotropic Phase-Field Models: 3-D Asymptotics.
A. A. Wheeler, and G. B. McFadden. 17 Oct 94, 25p, NISTIR-5505.
Sponsored by Bristol Univ. (England). School of Mathematics.

Keywords: *Solidification, Liquid-solid interfaces, Surface energy, Differential geometry, Asymptotic series, Vector analysis, Three dimensional, Anisotropy, *Phase field models, Allen-Cahn equation, Gibbs-Thomson equation, Xi vector.

In the paper the authors present a new formulation of a large class of phase-field models, which describe solidification of a pure material and allow for both surface energy and interface kinetic anisotropy, in terms of the Hoffman-Cahn xi-vector. The Hoffman-Cahn vi-vector has previously been used in the context of sharp interface models, where it provides an elegant tool for the representation and analysis of interfaces with anisotropic surface energy. The authors show that the usual gradient-energy formulations of ansotropic phase-field models are expressed in a natural way in terms of the vi-vector when approximately interpreted. The authors use this new formulation of the phase-field equations to provide a concise derivation of the Gibbs-Thomson-Herring equation in the sharp-interface limit in three dimensions.

04,537
PB95-140034 Not available NTIS
National Inst. of Standards and Technology (MSEL), Gaithersburg, MD. Reactor Radiation Div.
Defective Structures of Barium Yttrium Copper Oxide (Ba2YCu3Ox) and Ba2YCu3-yMyOz (M=Fe, Co, Al, Ga, ..).
Final rept.
A. Santoro. 1992, 44p.
Pub. in Chem. Supercond. Mater., p146-189 1992.

Keywords: *YBCO superconductors, *Crystal defects, High temperature superconductors, Vacancies(Crystal defects), Twinning, Substitutes, Reprints, *Yttrium barium cuprates, Oxygen transport.

The structural determination of Ba2YCu3O(x) for 6.8 = or < x = or < 7.0 was completed in several laboratories by Rietveld analysis of powder neutron diffraction data. The neutron diffraction experiments confirmed the space group Pmmm and the main structural features found by x-rays by Siegrest et al., but revealed that some of the oxygen assignments made in the x-ray studies were not entirely correct. The refined structural parameters obtained in four of these neutron diffraction analyses are given and the structure of Ba2YCu3O7.0 is schematically illustrated where it is compared with the parent structure of perovskite. Data collected at low temperatures revealed that no phase transitions take place in going from room temperature down to 5K.

04,538
PB95-140042 Not available NTIS
National Inst. of Standards and Technology (IMSE), Gaithersburg, MD. Reactor Radiation Div.
Neutron Powder Diffraction Study of the Structures of La1.9Ca1.1Cu2O6 and La1.9Sr1.1Cu2O6+Delta.
Final rept.
A. Santoro, F. Beech, and R. J. Cava. 1990, 6p.
Pub. in Materials Research Society Symposia Proceedings 166, p187-192 1990.

Keywords: *Crystal structure, Tetragonal lattices, Lattice parameters, Neutron diffraction, Superconductors, Reprints, *Lanthanum calcium cuprates, *Lanthanum strontium cuprates, Reitveld method, Powder diffraction.

The title compounds are structurally isomorphous and crystallize with the symmetry of space group I4/mmm. The lattice parameters are a = 3.8248(1), c = 19.4286(5)A for La(1.9)Ca(1.1)Cu2O6 and a = 3.8601(1), c = 19.9994(5)A for La(1.9)Sr(1.1)Cu2O(6 + delta). The structure can be easily derived from that of La2CuO4 by substituting the layers of composition CuO2 present in La2CuO4 with a block of three layers having composition and sequence (CuO2) - (R) - (CuO2), where R is Ca, Sr, and/or La. Although the general structural configuration is the same for the Ca and the Sr compounds, the distribution of the metal atoms is different in the two cases.

04,539
PB95-140067 Not available NTIS
National Inst. of Standards and Technology (MSEL), Gaithersburg, MD. Reactor Radiation Div.
Normal Modes and Structure Factor for a Canted Spin System: The Generalized Villain Model.
Final rept.
W. M. Saslow, and R. W. Erwin. 1992, 10p.
Pub. in Physical Review B 45, n9 p4759-4768, 1 Mar 92.

Keywords: Structure factors, Heisenberg model, Antiferromagnetism, Ferromagnetism, Spin waves, Hamiltonians, Reprints, *Villain model, Normal modes.

The generalized Villain model has a rich variety of possible structures, ranging from a pure ferromagnet to a pure antiferromagnet. In between these extremes, the system is canted. Using a Heisenberg exchange Hamiltonian and linearized spin-wave theory, we have studied the normal modes and structure factors for this model. The exchange ratio J'/J and the external field have both been varied. The effect of canted spin structures on the modes and structure factors is readily seen. We believe that it is now a practical matter to study the normal modes and structure factors for more complicated systems described by this type of model.

04,540
PB95-140471 Not available NTIS
National Inst. of Standards and Technology (MSEL), Gaithersburg, MD. Ceramics Div.
Study of the Hydroxycarbonate Precursor Route to the YBa2Cu3O7-x High Tc Superconductor.
Final rept.
J. J. Ritter, and J. F. Kelly. 1989, 8p.
Pub. in Proceedings of Symposium on High Temperature Superconducting Compounds: Processing and Related Properties, Las Vegas, NV., February 27-28, 1989, p303-310.

Keywords: *YBCO superconductors, *Precipitation(Chemistry), *Precursors, High temperature superconductors, Chemical composition, Synthesis(Chemistry), Particle size, Polycrystalline, Reprints, *Yttrium barium cuprates, Hydroxycarbonates.

The precipitation of the mixed hydroxycarbonates of Ba, Y and Cu as precursors to the YBa2Cu3O(7-x) high T(c) superconductor is an attractive route to this material. However, studies in our laboratory indicate that powder homogeneity is strongly dependent upon ionic concentrations and system pH. Moreover, we have assessed the composition of the precipitated moieties. These data have been incorporated into controlling the precipitation process in order to optimize particle size and powder homogeneity. Further processing of these powders has yielded polycrystalline solids with sharp transitions near 95K and high transport current densities.

04,541
PB95-140505 Not available NTIS
National Inst. of Standards and Technology (CSTL), Gaithersburg, MD. Surface and Microanalysis Science Div.
Substitution-Induced Midgap States in the Mixed Oxides RxBa1-ChiTiO3-Delta, with R=Y, La, and Nd.
Final rept.
S. W. Robey, L. T. Hudson, C. Eylem, and B. Eichorn. 1993, 7p.
Pub. in Physical Review B 48, n1 p562-568, 1 Jul 93.

Keywords: *Electronic structure, *Band theory, Photoelectron spectroscopy, Ultraviolet spectroscopy, Barium titanates, Binding energy, Substitutes, Reprints, *Yttrium barium titanates, *Lanthanum barium titanates, *Neodymium barium titanates, Metal insulator transition, Mixed oxides.

Changes induced in the electronic structure of BaTiO3 by substitutions of R=Y, La, or Nd for Ba to form the mixed oxides, R(x)Ba(1-x)TiO(3-delta) have been investigated using ultraviolet photoelectron spectroscopy. Substitution of formally R(3+) ions for Ba(2+) leads to the introduction of filled states in the band gap that are shown by resonant-photoemission measurements to have significant Ti 3d character, consistent with a Mott-Hubbard-insulator description for these oxides. Various contributions to the binding energy and width of these states are considered. It is suggested that the dominant factor is electron-electron correlation and this leads to the estimates U approx equals Delta approx equals 3 eV for this system, where U is the correlation energy for the 3d electrons and Delta is the charge-transfer energy.

04,542
PB95-140513 Not available NTIS
National Inst. of Standards and Technology (MSEL), Gaithersburg, MD. Reactor Radiation Div.
Incommensurate Magnetic Order in UPtGe.
Final rept.
R. A. Robinson, A. C. Lawson, J. W. Lynn, and K. H. J. Buschow. 1993, 4p.
Sponsored by Department of Energy, Washington, DC.
Pub. in Physical Review B 47, n10 p6138-6141, 1 Mar 93.

Keywords: Orthorhombic lattices, Platinum intermetallics, Ternary compounds, Neel temperature, Neutron diffraction, Magnetic moments, Reprints, *Uranium platinum germanides, *Magnetic ordering, Uranium intermetallics, Germanium intermetallics, Powder diffraction.

The orthorhombic uranium (1:1:1) ternary compound UPtGe has been studied by means of neutron powder diffraction, using both the time-of-flight method at a spallation source and the constant-wavelength reactor method. The material exhibits incommensurate magnetic order with q = (0,0.5543,0), with a uranium moment at the lowest temperature of 1.11 mu(sub B) and a Neel temperature of 51 K. The moments are confined to the bc plane, which includes the propagation vector for the incommensurate modulation, and they rotate within that plane as one moves parallel to the b axis. The magnitude of the ordered uranium moment is the only order parameter in the problem.

04,543
PB95-140521 Not available NTIS
National Inst. of Standards and Technology (MSEL), Gaithersburg, MD. Reactor Radiation Div.
Crystallographic and Magnetic Properties of UAuSn.
Final rept.
R. A. Robinson, J. W. Lynn, V. Nunez, A. C. Lawson, K. H. J. Buschow, and H. Nakotte. 1993, 5p.
Pub. in Physical Review B 47, n9 p5090-5094, 1 Mar 93.

Keywords: *Crystal structure, Antiferromagnetic materials, Gold intermetallics, Tin intermetallics, Neutron

diffraction, Magnetic properties, Reprints, *Uranium gold stannides, Uranium intermetallics, Powder diffraction, Uranium palladium stannides, Uranium copper stannides.

The uranium intermetallic compound UAuSn has been studied by means of neutron powder diffraction. It crystallizes in the CaIn2 structure type, with space group P6(3)/mmc, in agreement with previous x-ray work. Below 37 K, it exhibits long-range antiferromagnetic order, in a double-sized orthohexagonal magnetic unit cell. At the lowest temperature measured, the uranium moment is 1.10 mu(sub B). The magnetic structure is collinear with moments parallel to the orthorhombic b axis and the magnetic space group is C(p)m'cm'. We discuss the Au/Sn disorder in terms of metallic radii and discuss the consequences of this symmetry on the collinearity of the magnetic structure. These results are compared with work on the isostructural compounds UPdSn and UCuSn.

04,544
PB95-140539 Not available NTIS
National Inst. of Standards and Technology (EEEL), Boulder, CO. Electromagnetic Technology Div.
Influence of Deposition Parameters on Properties of Laser Ablated YBa2Cu3O7-Delta Films.
Final rept.
A. Roshko, D. A. Rudman, L. R. Vale, H. Beck, L. F. Goodrich, and J. Moreland. 1993, 4p.
Pub. in Institute of Electrical and Electronics Engineers Transactions on Applied Superconductivity 3, n1 p1590-1593 Mar 93.

Keywords: *YBCO superconductors, *Superconducting films, *Laser ablation, High temperature superconductors, Scanning tunneling microscopy, Temperature dependence, Transition temperature, Critical current, Substrates, Thin films, Reprints, *Yttrium barium cuprates, Lanthanum aluminates.

YBa2Cu3O(7-delta) films have been laser ablated under a variety of conditions, onto four different substrate materials. Using scanning tunneling microscopy, it was observed that the films grow by an island nucleation and growth mechanism. The properties of the films were studied as functions of the deposition conditions. Films on LaAlO3 had the best and most reproducible properties. The superconducting transition temperatures of films deposited on LaAlO3 proved to be fairly insensitive to the substrate temperature during deposition; T(c) > 90 K were obtained for films deposited over a temperature range from 760 to 850 C. The oxygen partial pressure during the deposition had a large effect on the transition temperature; the highest T(c)s were obtained for films deposited in 26.7 Pa (200 mTorr) oxygen.

04,545
PB95-140547 Not available NTIS
National Inst. of Standards and Technology (MSEL), Gaithersburg, MD. Reactor Radiation Div.
Magnetic Ordering of the Cu Spins in PrBa2Cu3O6+x.
Final rept.
N. Rosov, J. W. Lynn, G. Cao, J. E. Crow, J. W. O'Reilly, and P. Pernambuco-Wise. 1992, 8p.
Pub. in Physica C 204, p171-178 1992.

Keywords: Neel temperature, Neutron diffraction, Single crystals, Antiferromagnetic materials, Copper, Reprints, *Praseodymium barium cuprates, *Magnetic ordering.

Neutron diffraction has been employed to investigate the magnetic ordering of the Cu spins in a single crystal of PrBa2Cu3O(6+x). At small x we have observed a Neel temperature T(N) of 370 K, where both the chain and plane Cu spins order simultaneously. For x approx 0.6, the Cu planes still order at T(N) about 370 K; however, the ordering temperature of the chain spins has decreased to about 160 K. The observed intensities of the magnetic reflections cannot be explained by keeping the chain layer Cu spin direction in the ab plane; rather, the chain moments must have a component along the c direction. We discuss these results in light of recent optical reflectivity measurements on PrBa2Cu3O(6+x) by Takenaka et al. (Phys. Rev. B 46 (1992) 5833).

04,546
PB95-140554 Not available NTIS
National Inst. of Standards and Technology (MSEL), Gaithersburg, MD. Reactor Radiation Div.
Crystal Structure and Magnetic Ordering of the Rare-Earth and Cu Moments in RBa2Cu2NbO8(R=Nd,Pr).
Final rept.
N. Rosov, J. W. Lynn, H. B. Radousky, P. Klavins, R. N. Shelton, M. Bennahmias, and T. J. Goodwin. 1993, 9p.
Pub. in Physical Review B 47, n22 p15 256-15 265, 1 Jun 93.

Keywords: *Crystal structure, Neutron diffraction, Magnetic moments, Reprints, *Neodymium barium copper niobates, *Praseodymium barium copper niobates, *Magnetic ordering.

Using neutron diffraction, we have studied the crystal structure and magnetic ordering of the rare-earth and Cu moments in the layered perovskite systems NdBa2Cu2NbO8 (Nd 2:2:1:8) and PrBa2Cu2NbO8 (Pr 2:2:1:8). These are systems similar to R Ba2Cu3O(6+x) (R 1:2:3:(6+X)) for which the chain Cu-O layers have been fully replaced by layers of Nb-O octahedra. Powder profile refinements below 20 K show that both Nd 2:2:1:8 and Pr 2:2:1:8 are in space group I4/mcm, because the near-neighbor Nb-O octahedra are rotated about the c axis in opposite senses. The Cu moments are ordered below 375(10) K for Nd 2:2:1:8 and 340(15) K for Pr 2:2:1:8, with saturation moments in both cases of 0.5(1)mu(sub B). The near-neighbor Cu spins are aligned antiparallel, just as for the Cu 'plane' ordering in R 1:2:3:(6 + X).

04,547
PB95-140562 Not available NTIS
National Inst. of Standards and Technology (MSEL), Gaithersburg, MD. Reactor Radiation Div.
Quasielastic and Inelastic Neutron-Scattering Studies of ((CD3)3ND)FeCl3.2D2O: A One-Dimensional Ising Ferromagnet.
Final rept.
N. Rosov, J. W. Lynn, J. J. M. Williams, and C. P. Landee. 1993, 3p.
Pub. in Jnl. of Applied Physics 73, n10 p6081-6083, 15 May 93.

Keywords: Orthorhombic lattices, Cryogenic temperature, Hydrogen bonds, Deuterium compounds, Iron compounds, Neutron scattering, Inelastic scattering, One dimensional, Hydrates, Reprints, *Ferrous trimethylammonium chloride, Ising ferromagnets.

Ferrous trimethylammonium chloride (FeTAC) is a member of a family of compounds that consist of chains of bihalide-bridged metal ions aligned along the b axis of the orthorhombic unit cell. FeTAC orders three dimensionally below T(N) = 3.16 K, with the moments, which are canted from the b axis by approx 20 deg, coupled ferromagnetically along the b axis and staggered along the (left bracket) 101 (right bracket) direction. The order parameter follows the exact Onsager solution for a rectangular 2D Ising lattice below T/T(N) approx 0.95. However, quasielastic scattering measurements in the vicinity of T(N) show that the correlations do not evolve as do those of the 2D Ising antiferromagnets ErBa2Cu3O7 and K2CoF4. Above T(N), magnetic excitations along the b axis that follow the dispersion relation of a 1D ferromagnet with a gap of 3.7 meV have been observed.

04,548
PB95-140810 Not available NTIS
National Inst. of Standards and Technology (EEEL), Boulder, CO. Electromagnetic Technology Div.
Thermally Activated Hopping of a Single Abrikosov Vortex.
Final rept.
S. C. Sanders, J. Sok, D. K. Finnemore, and Q. Li. 1993, 5p.
Pub. in Physical Review B 47, n14 p8996-9000, 1 Apr 93.

Keywords: Joseph junctions, Lead(Metal), Metal films, Thin films, Flux pinning, Superconductors, Reprints, *Abrikosov vortices, Thermal activation.

Thermally activated hopping of a single Abrikosov vortex has been investigated for a thin Pb film that was decorated with an artificial pinning structure. To determine the location of the vortex, the Pb film is fabricated to be one electrode of a cross-strip superconductor/normal-metal/insulator/superconductor (SNIS') Josephson junction. Distortions in the Fraunhofer pattern specify the vortex location. As the temperature is raised toward T(c), the vortex depins from the artificial pinning site and reproducibly moves through the same sequence of other pinning sites before it leaves the function area of the Pb film. The first thermal depinning occurs when the order parameter of the bulk superconductor is about 20% of the T = O value. The trajectory is not random.

04,549
PB95-141016 Not available NTIS
National Inst. of Standards and Technology (NEL), Boulder, CO. Electromagnetic Technology Div.
Critical Current Behavior of Ag-Coated YBa2Cu3O7-x Thin Films.
Final rept.
R. H. Ono, J. A. Beall, T. E. Harvey, M. W. Cromar, L. F. Goodrich, J. Moreland, A. Roshko, T. C. Stauffer, C. D. Reintsema, and M. Johansson. 1991, 4p.
Pub. in Institute of Electrical and Electronics Engineers Transactions on Magnetics 27, n2 p1471-1474 Mar 91.

Keywords: *YBCO superconductors, *Superconducting films, *Critical current, High temperature superconductors, Current density, Laser ablation, Metal films, Thin films, Interfaces, Silver, Reprints, *Yttrium barium cuprates, Bilayers.

We have studied the behavior of high-quality YBa2Cu3O(7-delta) (YBCO) thin films with Ag overlayers. In some cases, the Ag was diffused into the high-T(c) film post-annealing. We chose to study Ag in detail because of its widespread use as contact metallization and our earlier studies of proximity effects in YBCO. The details of transport critical current measurements are presented. The Ag coatings can reduce normal state resistance while not degrading J(c).

04,550
PB95-141024 Not available NTIS
National Inst. of Standards and Technology (NEL), Boulder, CO. Electromagnetic Technology Div.
Magnetic Field Dependence of the Critical Current Anisotropy in Normal Metal-YBa2Cu3O7-delta Thin Film Bilayers.
Final rept.
R. H. Ono, L. F. Goodrich, J. A. Beall, M. E. Johansson, and C. R. Reintsema. 1991, 3p.
Pub. in Applied Physics Letters 58, n11 p1205-1207 1991.

Keywords: *YBCO superconductors, *Critical current, *Superconducting films, High temperature superconductors, Magnetic fields, Current density, Metal films, Thin films, Anisotropy, Laser ablation, Interfaces, Silver, Reprints, *Yttrium barium cuprates, Bilayers.

We have measured the transport critical current density (J(c)) in epitaxial-quality films of YBa2Cu3O(7-delta) which were covered by thin (10 nm) Ag films. The films, both with and without Ag, had J(c) values greater than 10(exp 6) A/sq cm in liquid nitrogen. The effect of the Ag was to greatly reduce the dependence of J(c) on external magnetic fields, but only in the case where the field was oriented in the plane of the film perpendicular to the c axis. It is unlikely that the effect is simply due to altered surface pinning, although qualitative agreement with critical state models is observed.

04,551
PB95-141065 Not available NTIS
National Inst. of Standards and Technology (EEEL), Boulder, CO. Electromagnetic Technology Div.
Micromagnetic Model of Dual-Layer Magnetic-Recording Thin Films.
Final rept.
J. O. Oti. 1993, 11p.
Pub. in Institute of Electrical and Electronics Engineers Transactions on Magnetics 29, n2 p1265-1275 Mar 93.

Keywords: *Magnetic films, Magnetic recording, Magnetic anisotropy, Thin films, Magnetostatics, Cobalt alloys, Reprints, Micromagnetic models, Exchange interactions.

A micromagnetic model of dual-layer magnetic-recording thin films is described. The model, which is capable of simulating magnetic layers having different magnetic and geometric properties, is applied to the study of the magnetic properties of dual-layer media characterized by a three-dimensional isotropic distribution of anisotropy axes in both layers, using parameters typical of cobalt-alloy films. In the absence of exchange interactions between the layers, a correlation is found between squareness ratios, average magnetostatic energy densities, and structural dimensions of the media. An in-phase magnetization reversal of the layers is found to occur with increasing interlayer exchange

coupling. A complex relationship is found between coercivity and media parameters.

04,552
PB95-141073 Not available NTIS
National Inst. of Standards and Technology (EEEL), Boulder, CO. Electromagnetic Technology Div.
Micromagnetic Simulations of Tunneling Stabilized Magnetic Force Microscopy.
Final rept.
J. O. Oti, and P. Rice. 1993, 3p.
Pub. in Jnl. of Applied Physics 73, n10 p5802-5804, 15 May 93.

Keywords: Electron tunneling, Magnetic films, Simulation, Images, Reprints, *Magnetic force microscopy, *Garnet films, Micromagnetics.

A micromagnetic model simulating the images produced by tunneling stabilized magnetic force microscopy is described. The images are related to the force interactions between the fringing fields from the imaged surface and stray fields from the sensing probe. The model, which allows for variations in the magnetization states of the probe, is used to examine the dependence of the interaction forces on varying probe-film separations for a magnetic garnet film. The results show that the images are sensitive to separation and that the changing probe magnetization plays an important role in determining the final image.

04,553
PB95-141081 Not available NTIS
National Inst. of Standards and Technology (EEEL), Boulder, CO. Electromagnetic Technology Div.
Experimental Verification of a Micromagnetic Model of Dual-Layer Magnetic Films.
Final rept.
J. O. Oti, and S. E. Russek. 1993, 3p.
Pub. in Jnl. of Applied Physics 73, n10 p5845-5847, 15 May 93.

Keywords: *Magnetic films, Thin films, Cobalt alloys, Nickel alloys, Magnetostatics, Chromium, Reprints, *Micromagnetic models, Exchange interactions, Multilayers.

A micromagnetic model has been used to characterize the magnetic properties of dual-layer magnetic films. The model calculations, with experimentally determined input parameters, have been compared with measurements on fabricated Co alloy dual-layer films. Calculations are done with a more general version of a previous micromagnetic model, modified to allow the variation of certain media parameters which were previously held constant. Each of the experimental media consists of a bilayer of 30-nm-thick Co(0.75) Ni(0.25) magnetic films separated by a Cr decoupling layer. The calculations predict a split in the coercivities of the layers for small Cr thicknesses which is observed experimentally. The model correlates an observed increase in media squareness ratio and coercivity, as the Cr thickness is increased, with diminishing exchange and magnetostatic interactions between the magnetic layers.

04,554
PB95-141149 Not available NTIS
National Inst. of Standards and Technology (NEL), Boulder, CO. Electromagnetic Technology Div.
Trapped Vortices in a Superconducting Microbridge.
Final rept.
G. S. Park, C. E. Cunningham, B. Cabrera, and M. E. Huber. 1991, 4p.
Sponsored by Stanford Univ., CA. Dept. of Physics.
Pub. in Institute of Electrical and Electronics Engineers Transactions on Magnetics 27, n2 p3021-3024 1991.

Keywords: Frequency dependence, Optical switching, Noise reduction, SQUID devices, Laser radiation, Light pulses, Magnetometers, Niobium, Reprints, *Flux vortices, *Flux trapping, Microbridges.

We are experimenting with optical switches for use in a noise reduction device for SQUID magnetometers. Laser light pulsed onto a Nb microbridge drives it momentarily normal and changes the quantum flux state of a superconducting circuit. For certain laser pulse parameters, a vortex is sometimes trapped in the microbridge and is detected by a SQUID coupled to the circuit. The trapping frequency and vortex position were studied using various waveforms.

04,555
PB95-141164 Not available NTIS
National Inst. of Standards and Technology (NML), Gaithersburg, MD. Surface Science Div.
Variation in Magnetic Properties of Cu/Fcc (001) Sandwich Structures.
Final rept.
W. Schwarzacher, J. Penfold, I. Jacob, R. F. Willis, W. Allison, R. C. Ward, and W. F. Egelhoff. 1989, 4p.
Pub. in Solid State Communications 71, n7 p563-566 1989.

Keywords: Polarization(Spin alignment), Magnetic moments, Fcc lattices, Sandwich structures, Magnetization, Copper, Magnetic films, Metal films, Thin films, Epitaxy, Reprints, *Ion films, Ultrathin films, Neutron reflection.

Spin-polarized neutron reflection is used to determine the magnetization of ultrathin epitaxial fcc Fe films sandwiches by Cu (001). A 3.0 ML film had a measured average magnetic dipole moment per atom of 1.9 + or - 0.6 Bohr magnetons/atom which is the highest value yet observed for an fcc Fe film and is consistent with the high spin-moment phase predicted for bulk fcc iron. This state appears to be unstable since increasing the film thickness or using a higher growth temperature leads to a considerable decrease in the observed moment.

04,556
PB95-150017 Not available NTIS
National Inst. of Standards and Technology (PL), Gaithersburg, MD. Electron and Optical Physics Div.
Effects of Interfacial Roughness on the Magnetoresistance of Magnetic Metallic Multilayers.
Final rept.
R. Q. Hood, L. M. Falicov, and D. R. Penn. 1994, 10p.
Contract DE-AC03-76SF00098
Sponsored by Department of Energy, Washington, DC.
Pub. in Physical Review B 49, n1 p368-377, 1 Jan 94.

Keywords: *Magnetoresistance, *Superlattices, Boltzmann equation, Chromium, Copper, Iron, Reprints, *Interface roughness, Magnetic multilayers.

The Boltzmann equation is solved for a system consisting of a ferromagnetic-normal-metallic multilayer. The in-plane magnetoresistance of Fe/Cr and Fe/Cu superlattices is calculated for (1) varying interfacial geometric random roughness with no lateral coherence, (2) correlated (quasiperiodic) roughness, and (3) varying chemical composition of the interfaces. The interplay between these three aspects of the interfaces may enhance or suppress the magnetoresistance, depending on whether it increases or decreases the asymmetry in the spin-dependent scattering of the conduction electrons. Properties of the interfaces relevant to the giant negative magnetoresistance are discussed.

04,557
PB95-150074 Not available NTIS
National Inst. of Standards and Technology (MSEL), Gaithersburg, MD. Reactor Radiation Div.
Magnetic Neutron Scattering (Invited).
Final rept.
J. W. Lynn. 1994, 5p.
Pub. in Jnl. of Applied Physics 75, n10 p6806-6810, 15 May 94.

Keywords: *Neutron scattering, *Magnetism, Neutron spectrometers, Inelastic scattering, Order parameters, Polarized beams, Critical point, Form factors, Uses, Reprints, Spin dynamics.

The application of neutron scattering techniques to magnetic problems is reviewed. We will first discuss diffraction techniques used to solve magnetic structures, as well as to measure magnetic form factors, order parameters, critical phenomena, and the scattering from low-dimensional systems. We will also discuss inelastic scattering techniques, including polarized beam methods, used to determine the spin dynamics of various materials. Information will be provided about the types of spectrometers available at the user-oriented national facilities located at Argonne National Laboratory, Brookhaven National Laboratory, Los Alamos National Laboratory, The National Institute of Standards and Technology, and Oak Ridge National Laboratory, as well as the spectrometers at the Missouri University Research Reactor.

04,558
PB95-150082 Not available NTIS
National Inst. of Standards and Technology (MSEL), Gaithersburg, MD. Reactor Radiation Div.
Polarization Analysis of the Magnetic Excitations in Fe65Ni35 Invar.
Final rept.
J. W. Lynn, N. Rosov, M. Acet, and H. Bach. 1994, 3p.
Pub. in Jnl. of Applied Physics 75, n10 p6069-6071, 15 May 94.

Keywords: *Invar, Iron alloys, Nickel containing alloys, Polarization characteristics, Polarized beams, Neutron beams, Spin waves, Temperature dependence, Single crystals, Amorphous materials, Comparative evaluations, Reprints, *Magnetic excitations.

Triple-axis inelastic polarized neutron measurements have been performed as a function of temperature on a single crystal of the Invar alloy Fe(65)Ni(35) to distinguish longitudinal from transverse magnetic excitations in the magnetically ordered phase. Well below the Curie temperature of 501 K the magnetic excitation spectrum is dominated by conventional transverse spin-wave excitations, which in fact follow the predictions of spin-wave theory very well. In particular, we find no evidence for propagating longitudinal excitations in this system, ir, sharp contrast to the behavior observed in the amorphous Invar Fe(86)B(14) material as well as the non-Invar amorphous system Fe(40)Ni(40)P(14)B(6).

04,559
PB95-150116 Not available NTIS
National Inst. of Standards and Technology (EEEL), Gaithersburg, MD. Electricity Div.
Superconducting Energy Gap of Bulk UBe13.
Final rept.
J. Moreland, A. F. Clark, R. J. Soulen, and J. L. Smith. 1994, 2p.
Pub. in Physica B 194-196, p1727-1728 1994.

Keywords: *Energy gap, *Superconductors, Superconducting junctions, Temperature dependence, BCS theory, Reprints, *Uranium beryllium, Point contacts, Uranium intermetallics, Beryllium intermetallics.

The superconducting energy gap, Delta, of bulk UBe13 was measured as a function of temperature. Junctions were made by breaking a narrow region of a specimen in a vacuum and then repositioning the broken ends to form a mechanically adjustable break junction point contact. We concluded that the 2 Delta(O)/k(B)T(c) = 4.2 by fitting the data to the BCS form, assuming a T(c) of 0.80 K.

04,560
PB95-150157 Not available NTIS
National Inst. of Standards and Technology (EEEL), Gaithersburg, MD. Semiconductor Electronics Div.
Spectroscopic Ellipsometry Determination of the Properties of the Thin Underlying Strained Si Layer and the Roughness at SiO2/Si Interface.
Final rept.
N. V. Nguyen, D. Chandler-Horowitz, P. M. Amirtharaj, and J. G. Pellegrino. 1994, 3p.
Pub. in Applied Physics Letters 64, n20 p2688-2690, 16 May 94.

Keywords: *Silicon dioxide, *Oxide films, Dielectric films, Ellipsometry, Substrates, Strains, Silicon, Reprints, *Interface roughness.

The existence of both the strain and microroughness at the interface of thermally grown SiO2 films on Si was ascertained unambiguously for the first time by high accuracy spectroscopic ellipsometry. The dielectric function of the interface was determined by a comprehensive data analysis procedure. By carefully examining the dielectric function obtained by our model, the strain was seen to cause a red shift of 0.042 eV of the interband critical point E(1) compared with the bulk silicon value. The thickness of the interface region was found to be 2.2 nm of which a significant part is due to the strain.

04,561
PB95-150165 Not available NTIS
National Inst. of Standards and Technology (CSTL), Gaithersburg, MD. Surface and Microanalysis Science Div.
Spot-Profile-Analyzing LEED Study of the Epitaxial Growth of Fe, Co, and Cu on Cu(100).
Final rept.
G. L. Nyberg, M. T. Kief, and W. F. Egelhoff. 1993, 11p.
Pub. in Physical Review B 48, n19 p14 509-14 519, 15 Nov 93.

Keywords: *Epitaxial growth, *Cobalt, *Copper, *Iron, Temperature range 0065-0273 K, Temperature range 0273-0400 K, Temperature dependence, Thermal diffusion, Metal films, Thin films, Microstructure, Substrates, Reprints, Low energy electron diffraction, Henzler rings, Ultrathin films.

The structure of epitaxial films of Fe, Co, and Cu grown at 80-300 K on Cu(100) has been investigated using a spot-profile-analyzing low-energy electron-diffraction (LEED) instrument. In all three systems rings appear around the substrate LEED spots, although the rings differ in intensity and in diameter depending upon the variables of film thickness and deposition temperature. Rings of this type have been studied extensively by Henzler et al and correlated with the mean separation between islands. Much can be inferred about the growth mechanism through a study of these Henzler rings. The rings contract radially with increasing deposition temperature or with increasing annealing temperature as thermally activated diffusion permits the formation of larger islands with greater distances between them. The value of the mean separation suggests that upon consideration these atoms do not come to rest at the immediate site of impact but instead experience some very transient type of mobility associated with the impact and accommodation process.

04,562
PB95-150181 Not available NTIS
National Inst. of Standards and Technology (PL), Gaithersburg, MD. Electron and Optical Physics Div.
Influence of Cr Growth on Exchange Coupling in Fe/Cr/Fe(100).
Final rept.
D. T. Pierce, J. A. Stroscio, J. Unguris, and R. J. Celotta. 1994, 9p.
Sponsored by Office of Naval Research, Arlington, VA.
Pub. in Physical Review B 49, n20 p14 564-14 572, 15 May 94.

Keywords: *Epitaxial growth, *Chromium, *Iron, Scanning electron microscopy, Scanning tunneling microscopy, Polarization characteristics, Temperature range 0273-0400 K, Exchange interactions, Metal films, Magnetization, Substrates, Reprints, Magnetic multilayers, Exchange coupling.

Scanning electron microscopy with polarization-analysis (SEMPA) measurements of the dependence of the oscillations of the exchange coupling in Fe/Cr/Fe(100) structures on the Cr growth temperature are correlated with the thickness fluctuations in Cr films measured by scanning tunneling microscopy (STM) at similar growth temperatures. Layer-by-layer growth was observed by STM for Cr deposition on very flat Fe(100) whiskers at deposition temperatures = or > 300 C. The SEMPA measurements of the magnetization of the Fe overlayer as a function of Cr spacer-layer thickness at this temperature could be simulated well by oscillatory coupling with periods 2.105 + or - 0.005d and 12 + or - 1d, where d is the layer spacing. Rougher Cr growth, limited by diffusion kinetics, occurs at lower growth temperatures giving a distribution of thicknesses in the growth front as determined by STM. We modeled the Fe magnetization for lower-temperature Cr growth by assuming that the exchange coupling at each discrete Cr thickness is the same as found for layer-by-layer growth. Important characteristic length scales and the role of biquadratic coupling in the SEMPA measurements are addressed.

04,563
PB95-150223 Not available NTIS
National Inst. of Standards and Technology (MSEL), Gaithersburg, MD. Reactor Radiation Div.
Temperature Dependence of the Magnetic Excitations in Ordered and Disordered Fe72Pt28.
Final rept.
N. Rosov, J. W. Lynn, J. Kastner, H. Bach, E. F. Wassermann, and T. Chattopadhyay. 1994, 3p.
Pub. in Jnl. of Applied Physics 75, n10 p6072-6074, 15 May 94.

Keywords: *Platinum containing alloys, *Iron alloys, Temperature dependence, Neutron scattering, Inelastic scattering, Single crystals, Spin waves, Reprints, *Magnetic excitations.

We have performed inelastic neutron scattering measurements of the long-wavelength spin wave excitations of both ordered and disordered Fe(72)Pt(28) single crystals below their critical temperatures, T(C) = 510 and 375 K, respectively. The spin waves followed the expected E = D(q squared) dependence, and the temperature-dependent spin stiffness D decreased as T/T(C)(exp 5/2), as expected for an isotropic ferromagnet. The extrapolated zero-temperature spin stiffness was D = 98(4) meV (A squared) and 107(1) me V (A squared) for the disordered and ordered alloy, respectively. These values are significantly higher than the zero-temperature stiffness as determined by magnetization measurements.

04,564
PB95-150272 Not available NTIS
National Inst. of Standards and Technology (PL), Gaithersburg, MD. Electron and Optical Physics Div.
Nanostructure Fabrication via Direct Writing with Atoms Focused in Laser Fields.
Final rept.
R. E. Scholten, J. J. McClelland, E. C. Palm, A. Gavrin, and R. J. Celotta. 1994, 4p.
Grant NSF-PHY93-12572
Sponsored by National Science Foundation, Arlington, VA.
Pub. in Jnl. of Vacuum Science and Technology B 12, n3 p1847-1850 May/Jun 94.

Keywords: Scanning electron microscopy, Atomic force microscopy, Laser radiation, Fabrication, Lithography, Chromium, Surfaces, Reprints, *Atomic manipulation, *Nanostructures, Atom optics, Laser cooling.

The techniques of atom optics can be applied during the deposition of atoms onto a surface to produce nanostructures. A laser is used to form a standing wave intensity pattern in front of the substrate. An atom beam, which has been collimated by optical means, is focused onto the substrate by dipole forces from the standing wave pattern so as to deposit a series of lines spaced by half the laser wavelength. We describe the fabrication of a Cr nanograting formed using this new technique. The experimental arrangement for deposition and the optical collimation of the atom beam are described. Scanning electron microscopy (SEM) and atomic force microscopy (AFM) images of the resulting nanostructures are presented.

04,565
PB95-150306 Not available NTIS
National Inst. of Standards and Technology (MSEL), Gaithersburg, MD. Ceramics Div.
Effect of a Crystal Monochromator on the Local Angular Divergence of an X-Ray Beam.
Final rept.
R. D. Spal. 1994, 7p.
Pub. in Acta Crystallographica A50, p295-301 1994.

Keywords: *X-ray monochromators, *X-ray optics, X-ray diffraction, Synchrotron radiation, Incident radiation, Divergence, Asymmetry, Collimation, Reprints.

The performance of an X-ray optical system often depends critically on the local angular divergence of the X-ray beam. For example, in systems for radiography, tomography and diffraction topography, the angular divergence of the incident beam at a point in the sample determines the limiting spatial resolution. In this paper, formulas are derived for the local divergence in the diffracted beam of the non-dispersive asymmetric reflection double-flat-crystal monochromator, illuminated by synchrotron or characteristic radiation. The formulas are analyzed to determine the general behavior of the local divergence as a function of the asymmetry factors of the crystal reflections. For synchrotron radiation, one surprising conclusion is that the local divergence of the magnifying monochromator is always greater than that of the symmetric monochromator, significantly so for even moderate magnification factors.

04,566
PB95-150314 Not available NTIS
National Inst. of Standards and Technology (PL), Gaithersburg, MD. Electron and Optical Physics Div.
Exchange Coupling in Magnetic Heterostructures.
Final rept.
M. D. Stiles. 1993, 21p.
Pub. in Physical Review B 48, n10 p7238-7258, 1 Sep 93.

Keywords: Exchange interactions, Fermi surfaces, Oscillations, Reprints, *Magnetic heterostructures, Magnetic multilayers, Exchange coupling.

Many structures consisting of magnetic layers separated by a nonmagnetic spacer layer show an oscillatory exchange coupling. This behavior is explained in terms of a simple model that shows that the Fermi surface of the spacer-layer material is responsible for the oscillatory coupling. The periods of the oscillatory coupling are set by extremal spanning vectors of the Fermi surface of the spacer-layer material. The strength of the coupling depends both on the geometry of the Fermi surface and on the reflection amplitudes for electrons scattering from the interfaces between the spacer layers and the magnetic layers. To test this and related models, the extremal spanning vectors and the associated Fermi-surface geometrical factors have been calculated for a large set of spacer-layer materials and interface orientations. These models are at least consistent with the experimental data. All measured oscillation periods are consistent with the calculated periods, but particularly for transition metals there are many more periods calculated than are seen experimentally.

04,567
PB95-150322 Not available NTIS
National Inst. of Standards and Technology (PL), Gaithersburg, MD. Electron and Optical Physics Div.
Growth of Iron on Iron Whiskers.
Final rept.
J. A. Stroscio, and D. T. Pierce. 1994, 6p.
Pub. in Jnl. of Vacuum Science and Technology B 12, n3 p1783-1788 May/Jun 94.

Keywords: *Epitaxial growth, *Iron, Whiskers(Single crystals), Scanning tunneling microscopy, Electron diffraction, Surface roughness, Surface diffusion, Temperature range 273-400 K, Temperature range 400-1000 K, Temperature dependence, Metal films, Thin films, Islands, Scaling, Reprints.

Real space views of the homoepitaxial growth of Fe on Fe(001) whiskers is reported, observed by scanning tunneling microscopy (STM), during the initial stages of growth. Scaling of the Fe island sizes and separation distribution are observed as a function of the diffusion rate to the deposition rate. A measure of the surface diffusion of the Fe atoms is obtained over the temperature range of 20-250 C from the temperature dependence of the island density. The effect of the diffusion kinetics is also observed in the surface morphology as a decrease in surface roughness with increasing temperature in thin Fe films. A comparison of real and reciprocal space techniques is obtained from a comparison of STM images and reflection-high-energy-electron-diffraction measurements during growth.

04,568
PB95-150330 Not available NTIS
National Inst. of Standards and Technology (PL), Gaithersburg, MD. Electron and Optical Physics Div.
Scanning Tunneling Microscopy Study of the Growth of Cr/Fe(001): Correlation with Exchange Coupling of Magnetic Layers.
Final rept.
J. A. Stroscio, D. T. Pierce, J. Unguris, and R. J. Celotta. 1994, 4p.
Sponsored by Office of Naval Research, Arlington, VA.
Pub. in Jnl. of Vacuum Science and Technology B 12, n3 p1789-1792 May/Jun 94.

Keywords: *Epitaxial growth, *Chromium, Scanning tunneling microscopy, Whiskers(Single crystals), Temperature range 400-1000 K, Temperature dependence, Electron diffraction, Exchange interactions, Film thickness, Metal films, Substrates, Reprints, Magnetic multilayers, Exchange coupling.

Scanning tunneling microscopy (STM) and reflection high-energy electron diffraction (RHEED) were used to study the epitaxial growth of Cr on Fe(001) whiskers as a function of the Fe whisker temperature during growth. The STM images give real space views of the morphology of Cr growth, which can be correlated with the nature of the RHEED intensity oscillations. Layer by layer growth is found for Cr deposition on an Fe(001) surface at 300 C, and very rough growth, limited by diffusion kinetics, is observed at lower temperatures. The variation in the interlayer exchange coupling in Fe/Cr/Fe sandwiches as a function of the thickness of the Cr interlayer, which has been found to depend strongly on the growth temperature of the Cr interlayer, can be explained by the thickness fluctuations determined from the STM measurements of Cr films grown at different temperatures.

04,569
PB95-150371 Not available NTIS
National Inst. of Standards and Technology (PL), Gaithersburg, MD. Electron and Optical Physics Div.
Oscillatory Exchange Coupling in Fe/Au/Fe(100).
Final rept.
J. Unguris, R. J. Celotta, and D. T. Pierce. 1994, 3p.
Sponsored by Office of Naval Research, Arlington, VA.

Pub. in Jnl. of Applied Physics 75, n10 p6437-6439, 15 May 94.

Keywords: *Epitaxial growth, *Gold, *Iron, Scanning electron microscopy, Polarization characteristics, Electron diffraction, Exchange interactions, Fermi surfaces, Metal films, Thin films, Substrates, Reprints, Magnetic multilayers, Exchange coupling.

Scanning electron microscopy with polarization analysis was used to investigate the interlayer exchange coupling in Fe/Au/Fe(100) sandwich structures. The films were epitaxially grown on single-crystal Fe(100) substrates. Electron diffraction measurements revealed that the Au spacer film grew with a surface reconstruction consistent with that observed for bulk Au crystals. The exchange coupling oscillates between primarily ferromagnetic and antiferromagnetic coupling for Au spacer layers up to 65 layers (13 nm) thick, but a significant biquadratic coupling component was also observed. The oscillatory coupling exhibited two components with periods of 2.48 + or - 0.05 layers (0.506 + or - 0.010 nm) and 8.6 + or - 0.3 layers (1.75 + or - 0.06 nm). The measured periods are in excellent agreement with those calculated from spanning vectors of the Au Fermi surface.

04,570
PB95-150413 Not available NTIS
National Inst. of Standards and Technology (EEEL), Gaithersburg, MD. Semiconductor Electronics Div.
Band-to-Band Photoluminescence and Luminescence Excitation in Extremely Heavily Carbon-Doped Epitaxial GaAs.
Final rept.
L. Wang, N. M. Haegel, and J. R. Lowney. 1994, 10p.
Grant NSF-DMR-8957215
Sponsored by National Science Foundation, Arlington, VA.
Pub. in Physical Review B 49, n16 p10 976-10 985, 15 Apr 94.

Keywords: *Gallium arsenides, *Photoluminescence, *Band structure of solids, Carbon additions, Doped crystals, Energy gap, Fermi level, Emission spectra, Epitaxy, Reprints, *Interband absorption, Bandgap narrowing, Density of states.

Heavily carbon-doped GaAs samples with doping levels as high as 4.1 X 10(exp 20)/cc were studied by photoluminescence and luminescence excitation spectroscopies. Luminescence and absorption band gaps were determined, from which the positions of the Fermi levels were deduced. A variety of factors which affect the observed emission spectra, including diffraction and refraction of the luminescence, substrate effects, and lattice contraction in the carbon-doped epilayer, were examined. A first-principles calculation was performed to calculate the density of states, the band gap, the Fermi energy, and the emission spectrum. Comparison of the calculation results with the experiments shows that the theoretical model we use is a good approximation for describing band structure for doping levels higher than 10(exp 20)/cc. However, the discrepancy between the measured and the calculated emission spectra indicates that the usual assumptions such as constant momentum matrix elements and quasiequilibrium distribution of photoexcited electrons in the conduction band may not be appropriate in treating the transition processes in highly degenerate semiconductors.

04,571
PB95-150512 Not available NTIS
National Inst. of Standards and Technology (CAML), Gaithersburg, MD. Applied and Computational Mathematics Div.
Self-Avoiding Surfaces, Topology, and Lattice Animals.
Final rept.
A. L. Stella, E. Orlandini, I. Beichl, T. L. Einstein, F. Sullivan, and M. C. Tesi. 1992, 4p.
Pub. in Physical Review Letters 69, n25 p3650-3653, 21 Dec 92.

Keywords: *Surfaces, Monte Carlo method, Cubic lattices, Topology, Simulation, Reprints, *Self-avoiding surfaces, Oct trees.

With Monte Carlo simulation, we study closed self-avoiding surfaces (SAS) of arbitrary genus on a cubic lattice. The gyration radius and entropic exponents are v = 0.506 + or - 0.005 and theta = 1.50 + or - 0.06, respectively. Thus, SAS behave like lattice animals (LA) or branched polymers at criticality. This result, contradicting previous conjectures, is due to a mechanism of geometrical redundancy, which is tested by exact renormalization on a hierarchical vesicle model. By mapping SAS into restricted interacting site LA, we conjecture v(sub theta) = 1/2 phi(sub theta) = 1, and theta(sub theta) = 3/2 at the LA theta point.

04,572
PB95-150587 Not available NTIS
National Inst. of Standards and Technology (PL), Gaithersburg, MD. Electron and Optical Physics Div.
Atomic Manipulation of Polarizable Atoms by Electric Field Directional Diffusion.
Final rept.
J. A. Stroscio, L. J. Whitman, R. A. Dragoset, and R. J. Celotta. 1992, 4p.
Pub. in Nanotechnology 3, p133-136 1992.

Keywords: *Alkali metals, Scanning tunneling microscopy, Electric fields, Gallium arsenides, Polarization, Semiconductors, Adsorbates, Diffusion, Cesium, Surfaces, Reprints, *Atomic manipulation, Nanostructures.

We present a brief summary of the properties of alkali metals on III-V(110) surfaces, as studied with the scanning tunneling microscope (STM). These include the non-metallic properties found in the one- and two-dimensional phases, and the directional diffusion of the alkali atoms due to the electric field gradient in the STM junction.

04,573
PB95-150595 Not available NTIS
National Inst. of Standards and Technology (PL), Boulder, CO. Quantum Physics Div.
Nanoscale Study of the As-Grown Hydrogenated Amorphous Silicon Surface.
Final rept.
G. C. Stutzin, R. M. Ostrom, A. Gallagher, and D. M. Tanenbaum. 1993, 10p.
Contract SERI-DD-1-11001-1(XG1-1216)
Sponsored by Solar Energy Research Inst., Golden, CO.
Pub. in Jnl. of Applied Physics 74, n1 p91-100, 1 Jul 93.

Keywords: *Amorphous silicon, *Surface analysis, *Silicon, Radio frequency discharge, Scanning tunneling microscopy, Gallium arsenides, Topography, Substrates, Single crystals, Reprints, Nanostructures.

A scanning tunneling microscope has been used to study the topography of the as-grown surface of device-quality, intrinsic, hydrogenated amorphous silicon deposited by rf discharge from silane. The substrates were atomically flat, oxide-free, single-crystal silicon or gallium arsenide. No evidence for island formation or nanoscale irregularities was seen in studies of 100-A-thick films on either silicon or gallium arsenide. The topography of 1000- and 4000-A-thick films has much variation; many regions can be characterized as 'rolling hills,' but atomically flat areas have also been observed nearby. Generally, it appears that surface diffusion plays a role in smoothing the film topography. In most regions, the observed slopes were 10% or less from horizontal, but some steep-sided valleys, indicating incipient voids, were observed. The effect of the finite size of the scanning tunneling microscope probe tip is considered; this has an effect on the observed images in some cases.

04,574
PB95-150686 Not available NTIS
National Inst. of Standards and Technology (MSEL), Gaithersburg, MD. Reactor Radiation Div.
Phonon Density of States in R2CuO4 and Superconducting R1.85Ce0.15CuO4 (R = Nd, Pr).
Final rept.
I. W. Sumarlin, J. W. Lynn, D. A. Neumann, J. L. Peng, Z. Y. Lin, J. J. Rush, and C. K. Loong. 1993, 10p.
Pub. in Physical Review B 48, n1 p473-482, 1 Jul 93.

Keywords: *Superconductors, *Phonons, Time-of-flight spectrometers, Neutron scattering, Inelastic scattering, Electron tunneling, Crystal field, Neodymium ions, Praseodymium ions, Excitation, Reprints, *Neodymium cerium cuprates, *Praseodymium cerium cuprates, *Neodymium cuprates, *Praseodymium cuprates, Density of states.

Inelastic-neutron-scattering measurements of the generalized phonon density of states (GDOS) for the electron-doped superconductors Nd(1.85)Ce(0.15)CuO4 and Pr(1.85)Ce(0.15)CuO4 have been carried out with the use of both a filter-detector method and time-of-flight spectroscopy. A measurement of the GDOS for the insulating Pr2CuO4 was also done for comparison with that of Pr(1.85)Ce(0.15)CuO4, while a more limited set of data was obtained for Nd2CuO4. We have also determined the ground-state crystal-field excitations associated with the rare-earth ions (Nd(3+), Pr(3+)).

04,575
PB95-150843 Not available NTIS
National Inst. of Standards and Technology (EEEL), Boulder, CO. Electromagnetic Technology Div.
Insulating Nanoparticles on YBa2Cu3O7-delta Thin Films Revealed by Comparison of Atomic Force and Scanning Tunneling Microscopy.
Final rept.
R. E. Thomson, J. Moreland, N. Missert, B. F. Cole, D. A. Rudman, and S. Sanders. 1993, 3p.
Pub. in Applied Physics Letters 63, n5 p614-616, 2 Aug 93.

Keywords: *High temperature superconductors, *Superconducting films, *YBCO superconductors, Atomic force microscopy, Scanning tunneling microscopy, Surface analysis, Thin films, Topography, Reprints, *Yttrium barium cuprates, Nanostructures.

The surface topography of YBa2Cu3O(7-delta) thin films has been studied with both atomic force microscopy (AFM) and scanning tunneling microscopy (STM). The AFM images reveal a high density of small distinct nanoparticles, 10-50 nm across and 5-20 nm high, which do not appear in STM images of the same samples. In addition, we have shown that scanning the STM tip across the surface breaks off these particles and moves them to the edge of the scanned area, where they can later be imaged with the AFM.

04,576
PB95-150850 Not available NTIS
National Inst. of Standards and Technology (MSEL), Gaithersburg, MD.
Lattice Imperfections Studied by Use of Lattice Green's Functions.
Final rept.
R. Thomson, S. Zhou, A. Carlsson, and V. Tewary. 1992, 10p.
Pub. in Physical Review B 46, n17 p10 613-10 622, 1 Nov 92.

Keywords: *Crystal defects, *Crack propagation, *Greens function, Crystal dislocations, Hexagonal lattices, Fractures(Materials), Numerical solution, Interfaces, Reprints.

This paper explores the use of lattice Green's functions for calculating the static structure of defects in lattices, in that the atoms of the lattice interact with their neighbors with an arbitrary nonlinear (short-range) potential. The method is hierarchical, in which Green's functions are calculated for the perfect lattice, for increasingly complicated defect lattices, and finally the nonlinear structure problem is iterated until a converged solution is found. As an illustration of the method, we report numerical calculations for an interfacial crack emitting dislocations from an interface between two joined two-dimensional hexagonal lattices. The supercell size was 4 x 10(exp 6), and the crack length was 101 lattice spacings. After the Green's functions were obtained for the defective lattice, the dislocation and crack structures were obtained in a minute or less, making possible detailed studies of the defects with various external loads, force laws, defect relative positions, etc., with negligible computer time.

04,577
PB95-151320 Not available NTIS
National Inst. of Standards and Technology (NEL), Gaithersburg, MD. Statistical Engineering Div.
Technique to Evaluate Benchmarks: A Case Study Using the Livermore Loops.
Final rept.
J. C. M. Wang, J. M. Gary, and H. K. Iyer. 1990, 16p.
Sponsored by Department of Energy, Washington, DC.
Pub. in International Jnl. of Superconductor Application 4, n4 p40-55 1990.

Keywords: Principle components analysis, Least squares method, Data reduction, Data analysis, Cluster analysis, Kernel functions, Superconductors, Reprints, *Livermore loops.

This paper is devoted to an analysis of the data from the Livermore kernels benchmark. We will show that in the sense of least squares prediction the dimension

of these data is rather small; a reduction of the data to dimension four has about the same predictive power as the original data. Two techniques are used that reduce the 72 kernel timings for each machine to a few scores by which the machine is characterized. The first is based on a principal component analysis, the second on a cluster analysis of the kernels. The validity of the reduction to lower dimension is checked by various means. The possible use of the Livermore data to predict the running time of larger codes is demonstrated.

04,578
PB95-151536 Not available NTIS
National Inst. of Standards and Technology (NML), Gaithersburg, MD. Electron and Optical Physics Div.
Manipulation of Adsorbed Atoms and Creation of New Structures on Room-Temperature Surfaces with a Scanning Tunneling Microscope.
Final rept.
L. J. Whitman, J. A. Stroscio, R. A. Dragoset, and R. J. Celotta. 1991, 5p.
Pub. in Science 251, n4998 p1206-1210, 8 Mar 91.

Keywords: Scanning tunneling microscopy, Room temperature, Indium antimonides, Gallium arsenides, Adsorbates, Semiconductors, Diffusion, Cesium, Surfaces, Alkali metals, Reprints, *Atomic manipulation, Nanostructures, Nanoclusters.

A general method of manipulating adsorbed atoms and molecules on room-temperature surfaces with the use of a scanning tunneling microscope is described. By applying an appropriate voltage pulse between the sample and probe tip, adsorbed atoms can be induced to diffuse into the region beneath the tip. The field-induced diffusion occurs preferentially toward the tip during the voltage pulse because of the local potential energy gradient arising from the interaction of the adsorbate dipole moment with the electric field gradient at the surface. Depending upon the surface and pulse parameters, cesium (Cs) structures from one nanometer to a few tens of nanometers across have been created in this way on the (110) surfaces of gallium arsenide (GaAs) and indium antimonide (InSb), including structures that do not naturally occur.

04,579
PB95-151700 Not available NTIS
National Inst. of Standards and Technology (MSEL), Gaithersburg, MD. Ceramics Div.
X-Ray Characterization of the Crystallization Process of High-Tc Superconducting Oxides in the Sr-Bi-Pb-Ca-Cu-O System.
Final rept.
W. Wong-Ng, C. K. Chiang, S. W. Freiman, M. D. Hill, L. P. Cook, and N. M. Hwang. 1990, 6p.
Pub. in Materials Research Society Symposia Proceedings, v169 p123-128 1990.

Keywords: *High temperature superconductors, *BSCCO superconductors, *Crystallization, Scanning electron microscopy, X-ray diffraction, Heat treatment, Lead additions, Microstructure, Glass, Reprints, *Bismuth lead strontium calcium cuprates.

Phase assemblages in two Sr-Bi-Pb-Ca-Cu-O glasses and their crystallization into glass-ceramics through a sequence of heat treatments are described. Samplers were heat treated at various temperature based on differential thermal analysis (DTA) of the as-quenched glasses. X-ray powder diffraction was used to identify the compounds in each sample; and the different phases formed in these two samples were compared. Results of microstructural characterization of selected samples using scanning electron microscopy are discussed.

04,580
PB95-151718 Not available NTIS
National Inst. of Standards and Technology (MSEL), Gaithersburg, MD. Ceramics Div.
Crystal Chemistry and Phase Equilibrium Studies of the BaO(BaCO3)-R2O3-CuO Systems. 5. Melting Relations in Ba2(Y,Nd,Eu)Cu3O6+x.
Final rept.
W. Wong-Ng, L. P. Cook, M. Hill, B. Paretzkin, and E. R. Fuller. 1990, 6p.
See also PB95-151742, Part 2, PB95-151734 and Part 4, PB95-151759.
Pub. in Materials Research Society Symposia Proceedings, v169 p81-86 1990.

Keywords: *YBCO superconductors, *Crystal chemistry, *High temperature superconductors, Scanning electron microscopy, X ray diffraction, Recrystallization, Europium additions, Neodymium additions, Melting, Grain growth, Microstructure, Reprints, Yttrium barium cuprates, Europium barium cuprates, Neodymium barium cuprates, Phase equilibrium, Ionic size.

The influence of the ionic size of the lanthanides R on melting relations of Ba2RCu3O(6+x), where R=Y, Eu and Nd, was studied and compared with that of a high T(c) superconductor mixed-lanthanide phase Ba2(Y(0.75)Eu(0.125)Nd(0.125))Cu3O(6+x). These materials have been characterized by a variety of methods including scanning electron microscopy (SEM). Single phase samples of Ba2(Y(0.75)Eu(0.125)Nd(0.125))Cu3O(6+x) were annealed at 1004, 1040, 1052, 1060, 1078, 1107 and 1160 C and quenched into a helium gas container cooled by liquid nitrogen. The SEM micrographs of these samples showed the progressive changes in features of the microstructures from sintering and grain growth through melting and then recrystallization from the melt. The addition of the SEM technique in conjunction with X-ray diffraction has been helpful in the study of phase equilibria in this system.

04,581
PB95-151726 Not available NTIS
National Inst. of Standards and Technology (MSEL), Gaithersburg, MD. Ceramics Div.
X-Ray-Diffraction Study of a Thermomechanically Detwinned Single Crystal of YBa2Cu3O6+x.
Final rept.
W. Wong-Ng, F. W. Gayle, D. L. Kaiser, S. F. Watkins, and F. R. Fronczek. 1990, 4p.
Pub. in Physical Review B 41, n7 p4220-4223, 1 Mar 90.

Keywords: *High temperature superconductors, *YBCO superconductors, *Crystal structure, Temperature range 0065-0273 K, Room temperature, X-ray diffraction, Single crystals, Orthorhombic lattices, Gold additions, Thermomechanics, Reprints, *Yttrium barium cuprates, Detwinning.

A twin-free single crystal of YBa2Cu3O(6+x) has been studied at room temperature and 115 K by x-ray diffraction analysis. The crystal was grown from an Y-Ba-Cu-O melt in a gold crucible, leading to a 2% substitution of Au for Cu. Twins were removed from the as-grown crystal by a novel thermomechanical process, resulting in an orthorhombic (Pmmm), single-domain crystal. Oxygen positions and occupancies in the Cu-O basal plane have been refined, showing that the O(5) site is completely vacant, and the O(4) atoms are offset from the crystallographic mirror plane positions by 0.15 A in a zig-zag fashion. Gold, which is a common impurity in crystals grown by the present technique, was found to occupy Cu(1) sites only. Weak superlattice reflections suggest a possible three-dimensional ordering of O and/or Au. To our knowledge, this paper reports the first high-resolution x-ray study of an intentionally detwinned, superconducting YBa2Cu3O(6+x) single crystal.

04,582
PB95-151734 Not available NTIS
National Inst. of Standards and Technology (MSEL), Gaithersburg, MD. Ceramics Div.
Crystal Chemistry and Phase Equilibrium Studies of the BaO-R2O3-CuO Systems. 2. X-Ray Characterization and Standard Patterns of BaR2CuO4, R=Lanthanides.
Final rept.
W. Wong-Ng, and B. Paretzkin. 1991, 3p.
See also PB95-151742, Part 4, PB95-151759 and Part 5, PB95-151718. Sponsored by Electric Power Research Inst., Palo Alto, CA.
Pub. in Powder Diffraction 6, n4 p187-189 Dec 91.

Keywords: *Rare earth compounds, *Crystal structure, *Crystal chemistry, Orthorhombic lattices, X-ray diffraction, Barium oxides, Reprints, Phase equilibrium.

The compounds BaR2O4, where R = La, Nd, Sm, Gd, Eu, Dy, Ho and Er have been prepared from a stoichiometric mixture of BaCO3 and lanthanide oxides, and characterized by X-ray powder diffraction. Standard X-ray patterns of these phases were prepared. In general, BaR2O4 crystallizes in the pervoskite-related CaFe2O4 structure which is orthorhombic with a space group Pnam. The cell parameters of these compounds from R = Er to La were found. When R = Tm, Lu and Yb, the BaO R2O3 composition produced the mixture Ba3R4O9 and the unreacted lanthanide oxide. Under the present experimental conditions, the compound BaRO3 was the predominant component when R = Ce, Pr, and Tb.

04,583
PB95-151767 Not available NTIS
National Inst. of Standards and Technology (MSEL), Gaithersburg, MD. Ceramics Div.
X-Ray Powder Diffraction Data for BaCu(C2O4)2.6H2O.
Final rept.
W. Wong-Ng, W. E. Rhine, and R. B. Hallock. 1991, 1p.
Pub. in Powder Diffraction 6, n1 p50 Mar 91.

Keywords: *Crystal structure, *X-ray diffraction, Hydrates, Reprints, *Barium copper oxalates, Powder patterns.

An indexed powder diffraction pattern and related crystallographic data are reported for a new phase, BaCu(C2O4)2 (dot) 6H2O, which was a major product in the coprecipitation of barium and copper oxalates.

04,584
PB95-152104 Not available NTIS
National Inst. of Standards and Technology (MSEL), Gaithersburg, MD. Reactor Radiation Div.
Coupled-Bilayer Two-Dimensional Magnetic Order of the Dy Ions in Dy2Ba4Cu7O15.
Final rept.
H. Zhang, J. W. Lynn, and D. E. Morris. 1992, 10p.
Pub. in Physical Review B 45, n17 p10 022-10 031, 1 May 92.

Keywords: *High temperature superconductors, *Dysprosium ions, Neutron scattering, Two dimensional, Antiferromagnetism, Reprints, *Dysprosium barium cuprates, *Magnetic ordering, Bilayers.

Neutron scattering has been used to investigate the magnetic ordering of the Dy ions in the superconducting (T(c) approx = 60 K) Dy2Ba4Cu7O15 (2:4:7) material. A modulated saw-tooth scattering profile is observed, indicative of a coupled-bilayer two-dimensional (2D) system in which the nearest-neighbor Dy spins within the a-b plane are coupled antiferromagnetically, with the moment direction along the c axis. The a-b-plane spin configuration is identical to the one which has been observed for the related DyBa2Cu3O7 (1:2:3) and Dy2Ba4Cu8O16 (2:4:8) materials. We anticipate that a similar coupled-bilayer 2D behavior should occur in other R2Ba4Cu7O15 systems (R = rare-earth element, except Er) which exhibit the same a-b-plane spin configuration as the Dy.

04,585
PB95-152302 Not available NTIS
National Inst. of Standards and Technology (MSEL), Gaithersburg, MD. Reactor Radiation Div.
Anomalous Dispersion and Thermal Expansion in Lightly-Doped KTa1-xNbxO3.
Final rept.
P. M. Gehring, H. Chou, S. M. Shapiro, J. Toulouse, D. Rytz, L. A. Boatner, J. A. Hriljac, and D. H. Chen. 1993, 12p.
Sponsored by Department of Energy, Washington, DC.
Pub. in Ferroelectrics 150, p47-58 1993.

Keywords: *Potassium tantalates, *Thermal expansion, Temperature dependence, Cryogenic temperature, X-ray diffraction, Neutron scattering, Inelastic scattering, Niobium additions, Lattice parameters, Cubic lattices, Single crystals, Anomalies, Reprints, *Potassium tantalate niobates, Phonon dispersion.

The temperature dependences of the lattice constant and TA phonon dispersion in dilute single crystals of KTa(1-x)Nb(x)O3 with 0.012 less than or equal to x less than or equal to 0.09 have been studied using x-ray diffraction and neutron scattering techniques, respectively. For x less than or equal to 0.06 an anomalous low-temperature expansion of the cubic lattice parameter is observed at a temperature T(sub min) that increases monotonically with Nb concentration, with no measurable change in symmetry down to 10 K. Concurrent with T(sub min) is a monogeneous broadening of the x-ray Bragg peaks which persists down to 10 K, as well as a strong relief of extinction seen by neutron diffraction. Inelastic neutron scattering measurements reveal that the coupling between TA and TO modes, first observed in pure KTaO3, is both wavevector and concentration dependent.

04,586
PB95-152328 Not available NTIS

National Inst. of Standards and Technology (MSEL), Gaithersburg, MD. Reactor Radiation Div.
Neutron-Scattering Studies of the Two Magnetic Correlation Lengths in Terbium.
Final rept.
K. Hirota, G. Shirane, P. M. Gehring, and C. F. Majkrzak. 1994, 12p.
Pub. in Physical Review B 49, n17 p11 967-11 978, 1 May 94.

Keywords: *Terbium, Transition temperature, Neutron scattering, Reprints, *Magnetic correlation lengths.

Extensive neutron-scattering experiments have been performed in order to characterize the nature of the two correlation lengths observed in Tb, a phenomenon common to Ho as well as SrTiO3. In the vicinity of the transition temperature, each of those crystals exhibits an anomalous two-component q profile in the critical scattering; the usual broad peak and an unexpected additional narrow peak. In order to clarify the spatial origin of the narrow component, the (0,0,delta) magnetic satellite peak of Tb has been closely examined using a very narrow neutron beam realized by a high spatial resolution reflectometer at the National Institute of Standards and Technology, which can produce well-defined beam widths of 0.3 mm and less. The small scattering angle (theta approx = 1.35 deg) and the narrow beam width result in an extraordinarily fine q and E resolution. As recently reported, we have confirmed that the intensity of the narrow component is enhanced near the edge of the crystal; it demonstrates that the major part is located within the near surface volume or 'skin' of the crystal.

04,587
PB95-152971 Not available NTIS
National Inst. of Standards and Technology (MSEL), Gaithersburg, MD. Reactor Radiation Div.
Comment on 'Phase Transitions in Antiferromagnetic Superlattices'.
Final rept.
J. A. Borchers, and R. W. Erwin. 1993, 1p.
Pub. in Physical Review B 48, n9 p6711, 1 Sep 93.

Keywords: *Phase transformations, *Antiferromagnetic materials, *Superlattices, Mean-field theory, Neutron diffraction, Cobalt oxides, Iron oxides, Nickel oxides, Reprints, Magnetic insulators.

Using a mean-field approach, Carrico and Camley (Phys. Rev. B 45, 13117 (1992)) have determined the magnetic behavior expected for superlattices consisting of uniaxial antiferromagnets. They state that the resulting phase transitions in a real system cannot be observed by standard, bulk measurements of the magnetization. In fact, the predictions of their model can be explicitly tested using neutron-diffraction techniques, which have already been applied toward the study of antiferromagnetic Ni0/CoO and Fe3O4/NiO superlattices.

04,588
PB95-153060 Not available NTIS
National Inst. of Standards and Technology (EEEL), Boulder, CO. Electromagnetic Technology Div.
Effects of Critical Current Density, Equilibrium Magnetization and Surface Barrier on Magnetization of High Temperature Superconductors.
Final rept.
D. X. Chen, R. W. Cross, and A. Sanchez. 1993, 9p.
Pub. in Cryogenics 33, n7 p695-703 1993.

Keywords: *High temperature superconductors, *High-TC superconductors, *Magnetization, Critical current, Current density, Surface barrier, YBCO superconductors, Reprints, Yttrium barium cuprates.

An extended critical state model which includes the effects of bulk critical current density, equilibrium magnetization and surface barrier is developed for the magnetization of superconductors. The equilibrium magnetization and surface barrier are modeled by an applied field dependent surface supercurrent density j(s)(H), whose presence changes the boundary field of the bulk. The volume supercurrents flow with a density equal to the internal field dependent critical current density J(c)(Hi). The magnetization M is produced by both supercurrents. For the M(H) curve computation, exponential-type J(c)(Hi) and j(s)(H) values are used for the general case of an infinite sample of rectangular cross-section. A comparison between the experimental magnetization curves of a sintered YBa2Cu3O7 superconductor at 76 K and the model fit shows that j(s)(H) is null for the coupling matrix, whereas a non-zero j(s)(H) is needed for the grains. The model fit for the irreversible magnetization of the grains is improved by including a surface barrier to the entry and exit of flux.

04,589
PB95-153128 Not available NTIS
National Inst. of Standards and Technology (CSTL), Gaithersburg, MD. Surface and Microanalysis Science Div.
Grazing-Incidence X-Ray Photoelectron Spectroscopy: A Novel Approach to Thin Film Characterization.
Final rept.
M. J. Chester, and T. Jach. 1993, 9p.
Pub. in Physical Review B 48, n23 p17-262 - 17-270, 15 Dec 93.

Keywords: *X-ray photoelectron spectroscopy, *Chemical composition, *Thin films, Concentration(Composition), Grazing incidence, Gallium arsenides, Gallium oxides, Interfaces, Reprints, Total external reflection, Multilayers.

At the energies of interest in x-ray photoelectron spectroscopy (XPS), total external reflection of the x-ray beam occurs from a smooth surface at small incidence angles. The penetration of the x rays into the material is strongly attenuated at these angles and surface sensitivity is enhanced in the XPS yields. As the incidence angle is increased, the x rays penetrate more deeply into the material and the XPS signal contains a larger contribution from the bulk. By exploiting this angle-dependent x-ray penetration depth, it is possible to obtain depth-dependent XPS spectra from which the concentration profiles of the photoelectron-emitting atoms can be inferred. In this paper we develop a general formalism for calculating grazing-incidence XPS (GIXPS) yields from multilayer media. A quantitative analysis of GIXPS spectra acquired from an oxidized GaAs(100) surface that was annealed to remove oxidized As will be discussed. The results show that this annealed oxide is composed of Ga2O3 and that the oxide-GaAs substrate interface is rough.

04,590
PB95-153250 Not available NTIS
National Inst. of Standards and Technology (EEEL), Boulder, CO. Electromagnetic Technology Div.
Transverse Thermomagnetic Effects in the Mixed State and Lower Critical Field of High-Tc Superconductors.
Final rept.
M. W. Coffey. 1993, 5p.
Pub. in Physical Review B 48, n13 p9767-9771, 1 Oct 93.

Keywords: *High temperature superconductors, *Thermomagnetic effects, Ettingshausen effect, Nernst effect, Type 2 superconductors, Critical field, Penetration depth, Temperature dependence, Thermodynamics, Vortices, Reprints.

Transverse thermomagnetic effects (Ettingshausen, Nernst effects) are discussed for a variety of phenomenological models of high-T(c) and other layered superconductors. The use of the temperature-dependent vortex-line energy in determining the transport entropy is stressed, leading to predictions and possibilities for additional experiments. The dynamics of both Abrikosov and Josephson vortices is considered.

04,591
PB95-153318 Not available NTIS
National Inst. of Standards and Technology (MSEL), Gaithersburg, MD. Metallurgy Div.
Morphological Stability.
Final rept.
S. R. Coriell, and G. B. McFadden. 1993, 73p.
Sponsored by National Aeronautics and Space Administration, Washington, DC. and Defense Advanced Research Projects Agency, Arlington, VA.
Pub. in Handbook of Crystal Growth, Chapter 12, v1 p785-857 1993.

Keywords: *Crystal growth, *Solidification, Liquid-solid interfaces, Binary alloys, Morphology, Stability, Reviews, Reprints, Crystal-melt interface.

During crystal growth, a smooth crystal-fluid interface is subject to instability and may become cellular or dendritic. Linear morphological stability theory described the conditions under which the interface becomes unstable. The theory is applicable to first order phase transformation in general, but in this article we will treat the growth of a crystal from a liquid phase. There are many reviews of morphological stability. In this article we will review the basic theory and discuss extension of the theory with emphasis on recent developments. A number of important topics will not be treated in this article, but will be covered in other articles in this volume. Effects of fluid flow are treated in the Chapter by Davis. Dendritic growth is treated in the Chapter by Billia and Trivedi. We will also assume that effects of crystalline anisotropy are small enough that facets or missing interface orientations do not occur.

04,592
PB95-153490 Not available NTIS
National Inst. of Standards and Technology (MSEL), Gaithersburg, MD. Reactor Radiation Div.
Epitaxial Integration of Single Crystal C60.
Final rept.
J. A. Dura, P. M. Pippenger, N. J. Halas, S. C. Moss, X. Z. Xiong, and P. C. Chow. 1993, 3p.
Sponsored by National Science Foundation, Washington, DC. and Office of Naval Research, Arlington, VA.
Pub. in Jnl. of Applied Physics Letters 63, n25 p3443-3445, 20 Dec 93.

Keywords: *Buckminsterfullerene, *Fullerenes, *Epitaxial growth, *Single crystals, Orientation(Direction), X-ray diffraction, Gallium antimonides, Thin films, Substrates, Antimony, Reprints, Low energy electron diffraction, Carbon films.

Single crystal thin films of (111) oriented C(60) are grown on epitaxial layers of single crystal antimony. The C(60)/Sb epitaxy is confirmed by low-energy electron diffraction which indicates that the (left bracket) (1-10) (right bracket) in-plane directions are parallel in the two layers. X-ray diffraction shows that the C(60) film is entirely (111) oriented and of high quality with sharp Bragg peaks and narrow mosaic spread. In this study, the Sb films were grown on GaSb, to which they are lattice matched; however, as Sb can be epitaxially grown on surfaces with a large lattice mismatch, this technique may be applied to integrate C(60) single crystals onto many substrates or devices with a surface having sixfold symmetry.

04,593
PB95-153540 Not available NTIS
National Inst. of Standards and Technology (EEEL), Boulder, CO. Electromagnetic Technology Div.
Even-Odd Asymmetry of a Superconductor Revealed by the Coulomb Blockade of Andreev Reflection.
Final rept.
M. T. Eiles, J. M. Martinis, and M. H. Devoret. 1993, 4p.
Contract NOOO14-92-F-0003
Sponsored by Office of Naval Research, Arlington, VA.
Pub. in Physical Review Letters 70, n12 p1862-1865, 22 Mar 93.

Keywords: *Superconductors, Superconducting junctions, Symmetry breaking, Asymmetry, Reprints, Single electron tunneling, Andreev reflection.

We have measured at low temperatures the current through a submicrometer superconducting island connected to two normal metal leads by ultrasmall tunnel junctions. As the bias voltage is lowered well below twice the superconducting energy gap, the current changes from being e periodic with gate charge to 2e periodic. This behavior is clear evidence that there is a difference in the total energy between the ground states of an even and odd number of electrons on the island. The 2e-periodic current peaks are the first observation of the Coulomb blockade of Andreev reflection.

04,594
PB95-153565 Not available NTIS
National Inst. of Standards and Technology (EEEL), Boulder, CO. Electromagnetic Technology Div.
Improved Uniaxial Strain Tolerance of the Critical Current Measured in Ag-Sheathed Bi2Sr2Ca1Cu2O8+x Superconductors.
Final rept.
J. W. Ekin, S. L. Bray, T. A. Miller, D. K. Finnemore, and J. Tenbrink. 1992, 3p.
Sponsored by Office of Naval Research, Arlington, VA.
Pub. in Advances in Cryogenic Engineering Materials, v38 ptB p1041-1043 1992.

Keywords: *High temperature superconductors, *BSCCO superconductors, Superconducting magnets, Critical current, Axial strain, Electromechanics, Tolerances, Silver, Reprints, *Bismuth strontium calcium cuprates.

Practical electromechanical properties of a high T(c) superconductor have been measured for Ag-sheathed Bi2Sr2Ca1Cu2O(8+x) superconductors at high magnetic fields up to 25 T. A melt-processed powder-in-tube Bi2Sr2Ca1Cu2O(8+x) conductor had an irreversible strain of 0.2% for the onset of permanent damage and a 50% critical-current-degradation strain of 0.36%. Measurements of a discontinuous filament melt-processed Ag-sheathed Bi2Sr2Ca1Cu2O(8+x) superconductor show an irreversible strain of 0.6% and a 50% degradation strain of about 1%. These strain damage thresholds are about an order of magnitude higher than for high-temperature superconductors made by bulk sintering and are reaching practical values for magnet design.

04,595
PB95-153649 Not available NTIS
National Inst. of Standards and Technology (EEEL), Boulder, CO. Electromagnetic Technology Div.
Surface Topography and Ordering-Variant Segregation in GaInP2.
Final rept.
D. J. Friedman, J. G. Zhu, A. E. Kibbler, J. M. Olson, and J. Moreland. 1993, 3p.
Contract DE-AC02-83CH10093
Sponsored by Department of Energy, Washington, DC.
Pub. in Applied Physics Letters 63, n13 p1774-1776, 27 Sep 93.

Keywords: Atomic force microscopy, Vapor phase epitaxy, Electron diffraction, Gallium arsenides, Substrates, Reprints, *Gallium indium phosphides, *Surface topography, Nomarski microscopy, Epilayers.

Using transmission electron diffraction dark-field imaging, atomic force microscopy (AFM), and Nomarski microscopy, we demonstrate a direct connection between surface topography and cation site ordering in GaInP2. We study epilayers grown by organometallic vapor-phase epitaxy on GaAs substrates oriented 2 deg off (100) towards (110). Nomarski microscopy shows that, we growth proceeds, the surface of ordered material forms faceted structures aligned roughly along left bracket 011 right bracket. A comparison with the dark-field demonstrates that the left bracket 1-11 right bracket and left bracket 11-1 right bracket ordering variants are segregated into complementary regions corresponding to opposite-facing facets of the surface structures. This observation cannot be rationalized with the obvious but naive model of the surface topography as being due to faceting into low-index planes. However, AFM reveals that the facets are in fact not low-index planes, but rather are tilted 4 deg from (100) towards (111)(sub B). This observation explains the segregation of the variants: the surface facets act as local (111)(sub B)-misoriented growth surfaces which select only one of the two variants.

04,596
PB95-153698 Not available NTIS
National Inst. of Standards and Technology (MSEL), Gaithersburg, MD. Reactor Radiation Div.
Origin of the Second Length Scale Above the Magnetic Spiral Phase of Tb.
Final rept.
P. M. Gehring, K. Hirota, C. F. Majkrzak, and G. Shirane. 1993, 4p.
Pub. in Physical Review Letters 71, n7 p1087-1090, 16 Aug 93.

Keywords: *Terbium, Neutron scattering, Line shape, Holmium, Reprints, Critical scattering.

High q-resolution neutron-scattering measurements of the critical scattering in Tb above the magnetic-spiral phase transition temperature T(s) exhibit a two-component line shape, as recently documented in Ho. This implies the existence of a second length scale. By using a narrow beam only 300 micrometers wide, and then translating the crystal through the beam, we have established that the origin of the second length scale lies within the near-surface volume or 'skin' of the Tb crystal. This is manifested by a large enhancement of the scattering intensity at the c-axis face of the cube-shaped crystal.

04,597
PB95-153722 Not available NTIS
National Inst. of Standards and Technology (EEEL), Boulder, CO. Electromagnetic Technology Div.
Volume Magnetic Hysteresis Loss of Nb3Sn Superconductors as a Function of Wire Length.
Final rept.
R. B. Goldfarb. 1993, 1p.
Sponsored by Department of Energy, Washington, DC.
Pub. in Proceedings of U.S.-Japan Workshop (8th) on High-Field Superconducting Materials, Wires and Conductors and Standard Procedures for High-Field Superconducting Wires Testing, Madison, WI., March 17-19, 1993, p72.

Keywords: *Superconducting wires, *Magnetic hysteresis, *Niobium stannides, Temperature range 0000-0013 K, SQUID devices, AC losses, Reprints, *Niobium ten, Multifilaments.

The magnetic hysteresis losses of samples of reacted multifilamentary Nb3Sn superconductor wire in coiled and straight geometries were measured at 4.1 K with a superconducting-quantum-interference-device (SQUID) magnetometer and an extraction dc magnetometer (DCM) for fields perpendicular to the wire axis. There were significant differences in the volume energy dissipation for the various samples. These differences are a function only of the length of the wire samples and are independent of whether the samples are straight segments or coils. As sample length increases from 2.6 mm, losses per total sample volume, for complete field cycles of + or - 3 T, increase nonlinearly from 0.19 to an asymptotic value of 0.43 MJ/cu m. A coiled sample with wire length 3 cm has 97% of the losses of a coiled sample with wire length 15 cm or greater. Losses are very length-dependent below 1 cm.

04,598
PB95-161113 Not available NTIS
National Inst. of Standards and Technology (PL), Gaithersburg, MD. Ionizing Radiation Div.
Calibration of High-Energy Electron Beams by Use of Graphite Calorimeters.
Final rept.
J. C. Humphreys, M. L. Walker, J. M. Puhl, C. E. Dick, and W. L. McLaughlin. 1993, 7p.
Pub. in Nuclear Instruments and Methods B 83, p563-569 1993.

Keywords: *High temperature superconductors, *Crystal structure, Tetragonal lattices, Neutron diffraction, Oxygen additions, Annealing, Temperature dependence, Reprints, *Mercury barium calcium cuprates.

Neutron profile refinements have been carried out on powders of as-prepared and oxygen annealed samples of the layered HgBa2CaCu2O(6 + delta)(1212) cuprate superconductors. The crystal structure is tetragonal P4/mmm over the range of temperatures 10 K to 298 K investigated, with no structural transitions of any kind being detected. The extra oxygen that electrically dopes these materials is found to reside in the centered position of the Hg plane, and no other excess oxygen is present in these samples. In addition, we found no conclusive evidence for mixing of the Hg and Cu cations. In the as-prepared sample we found delta = 0.22, while the oxygen content increased substantially to delta = 0.35 with annealing. This extra oxygen had only a small effect on the superconductivity, broadening the transition somewhat and shifting T(c) from 112 K to 120 K. The incorporation of extra oxygen also had the effect of constricting the lattice parameters by about 0.1%. The overall behavior is similar to the single-layer Hg-1201 system.

04,599
PB95-161139 Not available NTIS
National Inst. of Standards and Technology (EEEL), Boulder, CO. Electromagnetic Technology Div.
Harmonic and Static Susceptibilities of YBa2Cu3O7.
Final rept.
T. Ishida, R. B. Goldfarb, S. Okayasu, T. Arndt, W. Schauer, Y. Kazumata, and J. Franz. 1993, 29p.
Pub. in Materials Science Forum 137-139, p103-131 1993.

Keywords: *High-temperature superconductors, *Magnetic susceptibility, *YBCO superconductors, Alternating current, Direct current, Sintered materials, Superconducting films, Single crystals, Flux pinning, Temperature dependence, Thin films, Comparison, Reprints, *Yttrium barium cuprates, Gadolinium barium cuprates, Magnetic field dependence.

Intergranular properties of the sintered superconductor YBa2Cu3O7 have been studied in terms of complex harmonic magnetic susceptibility chi(sub n) = (chi prime)(sub n) - i(chi double prime)(sub n) (n integer) as well as DC susceptibility chi(dc). As functions of temperature T, (chi prime)(sub 1) and (chi, double prime)(sub 1) depend on both the AC magnetic-field amplitude H(ac) and the magnitude of a superimposed DC field H(dc). Only odd-harmonic susceptibilities are observed below the critical temperature, T(c), for zero H(dc) while both odd and even harmonics are observed for nonzero H(dc). With T constant, odd-harmonic susceptibilities are even functions of H(dc), whereas even-harmonic susceptibilities are odd functions of H(dc). In contrast, even-harmonic susceptibilities measured for a GdBa2Cu3O7 thin film and an YBa2Cu3O7 single crystal are not prominent due to missing weak links, whereas odd-harmonic susceptibilities are remarkable. A survey of several models for the harmonic response of superconductors is presented.

04,600
PB95-161154 Not available NTIS
National Inst. of Standards and Technology (CSTL), Gaithersburg, MD. Surface and Microanalysis Science Div.
Grazing Angle X-Ray Photoemission System for Depth-Dependent Analysis.
Final rept.
T. Jach, M. J. Chester, and S. M. Thurgate. 1994, 4p.
Pub. in Review of Scientific Instruments 65, n2 p339-342 Feb 94.

Keywords: *X-ray photoelectron spectroscopy, *X-ray spectrometers, *Gallium arsenides, *Surface analysis, Grazing incidence, Photoemission, Oxidation, Oxides, Reprints, Depth dependence, Depth profiles.

We have developed an x-ray photoelectron spectrometer system which combines an adjustable grazing incidence angle source with reflected beam detection. When operated about the critical angle, this combination permits a variation of the x-ray penetration depth which can be monitored by means of the reflectivity. At angles of incidence less than the critical angle, the sampling depth of the photoemission is diminished, but the photoemission from the surface is enhanced due to the constructive interference of the incident and reflected x-ray beams. When used with Mg K(alpha) radiation (E(sub gamma) = 1253.6 eV), the spectrometry system obtains useful distributions of chemical species in surface layers of 10-40 A thickness. We present data showing the depth dependence obtained with the spectrometer of different oxides in a sulfide-treated, oxidized GaAs (100) surface.

04,601
PB95-161279 Not available NTIS
National Inst. of Standards and Technology (MSEL), Gaithersburg, MD. Reactor Radiation Div.
Hydrogen in YBa2Cu3Ox: A Neutron Spectroscopy and a Nuclear Magnetic Resonance Study.
Final rept.
U. Knell, C. Heid, H. Wipf, H. J. Lauter, T. J. Udovic, and J. J. Rush. 1993, 5p.
Pub. in Zeitschrift fur Physikalische Chemie 179, p397-401 1993.

Keywords: *High temperature superconductors, *YBCO superconductors, *Hydrogen additions, Spin lattice relaxation, Nuclear magnetic resonance, Neutron spectroscopy, Neutron scattering, Inelastic scattering, Relaxation time, Vibrational spectra, Doped materials, Reprints, *Yttrium barium cuprates.

The high temperature superconductor YBa2Cu3O(x) absorbs considerable amounts of hydrogen if it is kept at elevated temperatures in a hydrogen gas atmosphere. In parallel neutron spectroscopic and nuclear magnetic resonance experiments, we studied the vibrational spectra and the spin lattice relaxation time of the protons in YBa2Cu3O(x) samples that were doped with hydrogen due to the absorption of hydrogen gas. Both the vibrational spectra and the spin lattice relaxation time are a sensitive probe for the local environment of the protons. We carried out analogous measurements on samples with a similar proton concentration due to the uptake of water vapor. These experiments demonstrated a totally different local environment of the protons. This fact is a strong indication that the protons absorbed from the hydrogen gas atmosphere did not react with the oxygen of the sample under formation of molecular water.

04,602
PB95-161451 Not available NTIS
National Inst. of Standards and Technology (NEL), Boulder, CO. Electromagnetic Technology Div.

Grain Alignment and Transport Properties of Bi2Sr2CaCu2O8 Grown by Laser Heated Float Zone Method.
Final rept.
J. Luo, X. P. Jiang, H. M. Chow, T. P. Orlando, D. A. Rudman, M. J. Cima, and J. M. Graybeal. 1991, 4p.
Pub. in Institute of Electrical and Electronics Engineers Transactions on Magnetics 27, n2 p1499-1502 Mar 91.

Keywords: *High temperature superconductors, *BSCCO superconductors, *Grain structure, *Critical current, Grain boundaries, Orientation(Direction), X-ray analysis, Temperature dependence, Transport properties, Zone melting, Float zones, Laser heating, Alignment, Anisotropy, Reprints, *Bismuth strontium calcium cuprates, Magnetic field dependence.

Single phase Bi2Sr2CaCu2O8 bulk superconductor (T(c) approx = 82 K) has been grown by laser heated floating zone method. The samples are highly textured with the grains, typically 100 micrometers in diameter and 0.5 cm long, elongated along the crystal a-axis which is the preferred growth direction. Our X-ray analysis and transport measurements indicate that the b, c axes are also orientated from grain to grain in the plane perpendicular to the growth direction. The upper limit of the misalignment between the grains is estimated to be less than 2 degrees from the measured upper critical field anisotropic ratio. The critical current density for such highly textured polycrystalline is anisotropic and limited mainly by the weak links at the grain boundaries. The grain boundary effects will be discussed on the basis of the measured temperature and magnetic field dependence of the critical current.

04,603
PB95-161600 Not available NTIS
National Inst. of Standards and Technology (NEL), Boulder, CO. Electromagnetic Technology Div.
Effects of Anneal Time and Cooling Rate on the Formation and Texture of Bi2Sr2CaCu2O8 Films.
Final rept.
M. M. Matthiesen, J. M. Graybeal, T. P. Orlando, J. B. Vander Sande, and D. A. Rudman. 1991, 4p.
Pub. in Institute of Electrical and Electronics Engineers Transactions on Magnetics 27, n2 p1223-1226 Mar 91.

Keywords: *High temperature superconductors, *Superconducting films, *BSCCO superconductors, Time dependence, Cooling rate, Microstructure, Annealing, Reprints, *Bismuth strontium calcium cuprates, Sputtered coatings, Surface texture.

The effects of anneal time and cooling rate on the formation and texturing of superconducting Bi2Sr2CaCu2O8 (BSCCO) films were investigated. Samples were prepared by sputter depositing amorphous BSCCO films, annealing them at 870 C in flowing 20% O2-80% Ar for 30, 60, or 180 minutes and then cooling them. Two cooling rates were investigated: a fast cool of 80 C/min and a slow cool of 9 C/min. It was observed that effective coupling between superconducting 2,212 grains occurs when films exhibit a minimum amount of (001) texturing. In addition, the nucleation and growth kinetics are significantly different for the isothermal and cooling regimes of thermal processing. Consequently, anneal time and cooling rate play distinct roles in the achievement of the appropriate texture and microstructure in the films: longer anneal times increase the volume fraction of the 2,212 phase while slower cooling rates enhance grain growth and texturing.

04,604
PB95-161618 Not available NTIS
National Inst. of Standards and Technology (PL), Gaithersburg, MD. Electron and Optical Physics Div.
Laser-Focused Atomic Deposition.
Final rept.
J. J. McClelland, R. E. Scholten, E. C. Palm, and R. J. Celotta. 1993, 4p.
Pub. in Science 262, p877-880, 5 Nov 93.

Keywords: Photon-atom collisions, Atomic force microscopy, Atomic beams, Standing waves, Laser radiation, Line width, Lithography, Substrates, Silicon, Reprints, *Atom optics, *Nanostructures, *Laser deposition, Laser focusing, Chromium atoms.

The ability to fabricate nanometer-sized structures that are stable in air has the potential to contribute significantly to the advancement of new nanotechnologies and our understanding of nanoscale systems. Laser light can be used to control the motion of atoms on a nanoscopic scale. Chromium atoms were focused by a standing-wave laser field as they deposited onto a silicon substrate. The resulting nanostructure consisted of a series of narrow lines covering 0.4 millimeter by 1 millimeter. Atomic force microscopy measurements showed a line width of 65 + or - 6 nanometers, a spacing of 212.78 nanometers, and a height of 34 + or - 10 nanometers. The observed line widths and shapes are compared with the predictions of a semiclassical atom optical model.

04,605
PB95-161659 Not available NTIS
National Inst. of Standards and Technology (MEL), Gaithersburg, MD. Precision Engineering Div.
Comparison of Elastic and Plastic Contact Models for the Prediction of Thermal Contact Conductance.
Final rept.
T. H. McWaid, and E. Marschall. 1993, 8p.
Pub. in Warme- und Stoffubertragung 28, p441-448 1993.

Keywords: *Contact resistance, *Thermal conductors, Plastic properties, Elastic properties, Plastic deformation, Microhardness, Thermal conductivity, Reprints, *Contact models, Asperity.

Experimentally determined thermal contact resistance (conductance) data are compared with predictions based on two different theories. One of the theories assumes elastic contact, while the other theory is based on the assumption of plastic contact. Even though the high plastic index calculated for the contacting surface suggested that contacting asperities would deform plastically, the experimental data generally agree better with the predictions obtained using the elastic contact model than with the predictions obtained using the plastic contact model.

04,606
PB95-161709 Not available NTIS
National Inst. of Standards and Technology (EEEL), Boulder, CO. Electromagnetic Technology Div.
Tunneling Spectroscopy of Thallium-Based High-Temperature Superconductors.
Final rept.
J. Moreland. 1994, 9p.
Pub. in Thallium-Based High-Temperature Superconductors, p569-577 1994.

Keywords: *High temperature superconductors, *Thallium compounds, Bound state, Interfaces, Reprints, *Thallium barium calcium cuprates, *Tunneling spectroscopy, *Electron tunneling spectroscopy.

This chapter focuses on electron tunneling spectroscopy (ETS) of the thallium based high-temperature superconductor (HTS) materials. A summary of published results is included with comments regarding interpretations of each measurement. Other phenomena that may have subsequent bearing on the interpretation of tunneling spectra are addressed briefly including a linear background conductance, Coulomb blockade effects, and bound states at superconductor/normal metal (SN) interfaces. This chapter does not address many of the Josephson like devices based on weak-links, point contacts, microbridges, or step-edge junctions.

04,607
PB95-161717 Not available NTIS
National Inst. of Standards and Technology (EEEL), Boulder, CO. Electromagnetic Technology Div.
Tunneling Stabilized Magnetic-Force Microscopy.
Final rept.
J. Moreland. 1993, 2p.
Pub. in Proceedings of the Annual Meeting of the Microscopy Society of America (51st), Cincinnati, OH., August 2-6, 1993, p1034-1035.

Keywords: Scanning tunneling microscopy, High temperature superconductors, Superconducting films, Magnetic flux, Domain walls, Magnetic recording, Reprints, *Magnetic force microscopy, Bloch walls, Garnet films.

Magnetic force microscopy (MFM) can be done by making a simple change in conventional scanning tunneling microscopy (STM) where the usual rigid STM tip is replaced with a flexible magnetic tip. STM images acquired this way show both the topography and the magnetic forces acting on the flexible tip. The z-motion of the STM piezo tube scanner flexes the tip to balance the magnetic force so that the end of the tip remains a fixed tunneling distance from the sample surface. We present a review of some 'tunneling-stabilized' MFM (TSMFM) images showing magnetic bit tracks on a hard disk, Bloch wall domains in garnet films, and flux patterns in high-T(c) superconductor films. The image resolution of TSMFM is routinely 0.1 micrometer using Au coated magnetic tips cut from Ni or Fe films. Recent results show that a TSMFM resolution of less than 40 nm is possible with micromachined cantilevers coated with a very thin Au-Fe bilayer.

04,608
PB95-161733 Not available NTIS
National Inst. of Standards and Technology (EEEL), Boulder, CO. Electromagnetic Technology Div.
Magnetic Force Microscopy of Flux in Superconductors.
Final rept.
J. Moreland, P. Rice, and A. Wadas. 1993, 4p.
Pub. in Proceedings of the International Workshop on Superconductivity, Hakodate, Japan, June 28-July 1, 1993, p77-80.

Keywords: *Magnetic flux, *Superconductors, Scanning tunneling microscopy, Imaging techniques, Image analysis, Penetration, Reprints, *Magnetic force microscopy.

We are developing a novel form of magnetic force microscopy (MFM) which is well suited for low-temperature imaging of magnetic flux lines penetrating superconductors. This method is based on standard scanning tunneling microscopy (STM) where the usual rigid tunneling tip is replaced with a flexible magnetic tip. We present a discussion of the interpretations of these images which includes theoretical aspects of MFM of flux lines in superconductors and experimental details regarding MFM which we believe are critical for flux imaging.

04,609
PB95-161832 Not available NTIS
National Inst. of Standards and Technology (MSEL), Gaithersburg, MD. Reactor Radiation Div.
New Exact Solution of the One-Dimensional Schrodinger Equation and Its Application to Polarized Neutron Reflectometry.
Final rept.
H. Zhang, and J. W. Lynn. 1993, 4p.
Pub. in Physical Review Letters 70, n1 p77-80, 4 Jan 93.

Keywords: *Schrodinger equation, *Superconductors, Penetration depth, One dimensional, Magnetization, Neutron scattering, Reprints, *Polarized neutron reflectometry.

An analytic expression for the polarized neutron reflectivity R(sup +,-) (theta, lambda) from a superconductor with penetration depth lambda is derived as an exact solution of the 1D Schroedinger equation in the continuum limit. The down-spin solution R(sup -) (theta, lambda) reveals a surprising oscillatory dependence on lambda within a narrow angular range immediately above the total reflection angle, and in fact vanishes when lambda and H satisfy certain conditions. This exact solution is applicable to other scattering problems with a general exponential dependence in the potential.

04,610
PB95-162111 Not available NTIS
National Inst. of Standards and Technology (CAML), Gaithersburg, MD. Applied and Computational Mathematics Div.
Micromagnetic Structure of Domains in Co/Pt Multilayers. 1. Investigations of Wall Structure.
Final rept.
R. Ploessl, J. N. Chapman, M. R. Scheinfein, H. Hoffmann, J. L. Blue, and M. Mansuripur. 1993, 7p.
Pub. in Jnl. of Applied Physics 74, n12 p7431-7437, 15 Dec 93.

Keywords: *Magnetic domains, *Domain walls, Electron microscopy, Metal films, Cobalt, Platinum, Reprints, Micromagnetics, Multilayers.

An analysis of the micromagnetic structure of domains and domain walls in Co/Pt multilayer films is reported. Magneto-optically written domains have been imaged in a scanning transmission electron microscope by using the modified differential phase contrast mode of Lorentz electron microscopy. These have been compared with computer-simulated images based on a two-dimensional model of a circular, perpendicular magnetized domain with a Bloch-like wall structure. Agreement is found for the domain and stray field contrast, but the absence of wall contrast in the experimental images indicates a more complex wall structure

in the multilayer than was assumed by the model. In a further series of calculations the magnetic microstructure of a Co/Pt multilayer was modeled by solving the Landau-Lifshitz-Gilbert equations. These suggest that the wall structure varies throughout the thickness of the multilayer, allowing significant saving of magnetostatic energy through the establishment of flux closure paths close to the walls, and are consistent with experimental observations.

04,611
PB95-162293 Not available NTIS
National Inst. of Standards and Technology (MSEL), Gaithersburg, MD. Reactor Radiation Div.
Magnetic Rare Earth Artificial Metallic Superlattices.
Final rept.
J. J. Rhyne, R. W. Erwin, J. A. Borchers, C. P. Flynn, M. B. Salamon, and R. Du. 1991, 20p.
Pub. in Proceedings of NATO Advanced Study Institute on the Science and Technology of Nanostructured Magnetic Materials, Crete, Greece, June 24-July 6, 1990, p117-136 1991.

Keywords: *Rare earth elements, *Superlattices, Magnetic anisotropy, Magnetic films, Magnetic materials, Magnetostriction, Exchange interactions, Neutron diffraction, Metal films, Magnetism, Reviews, Reprints, *Artificial superlattices, Multilayers.

Intense interest has been generated over the past several years in the growth and properties of layered magnetic materials, both from a fundamental point of view and for applications. For the purposes of this review, the term artificial metallic superlattice will be reserved for true three dimensionally coherent layered structures, while the term multilayer will be used for layered structures in which coherence is present in less than three dimensions. The recent refinements in computer-controlled molecular beam epitaxy (MBE) techniques for the growth of single crystal artificial superlattices of two or more distinct compositions have opened up vast possibilities for the production of tailor-made artificial superlattices with controlled film thicknesses down to atomic dimensions and with highly reproducible stacking sequences. This has provided previously unavailable opportunities to examine problems of interaction ranges, tunneling distances, and other coherent phenomena which are dependent on the superlattice periodicity. In particular, the development starting in 1984 of MBE growth procedures for single crystal rare earth metal superlattices has permitted prototypical tests for verifying many of the theoretical concepts of magnetic exchange, anisotropy, and magnetostriction effects in the rare earths which could not previously be examined in as controlled a way using conventional bulk materials.

04,612
PB95-162384 Not available NTIS
National Inst. of Standards and Technology (CSTL), Gaithersburg, MD. Surface and Microanalysis Science Div.
Resonant-Photoemission Investigation of the Heusler Alloys Ni2MnSb and NiMnSb.
Final rept.
S. W. Robey, L. T. Hudson, and R. L. Kurtz. 1992, 8p.
Pub. in Physical Review B 46, n18 p11 697-11 704, 1 Nov 92.

Keywords: *Electronic structure, *Photoemission, Heusler alloys, Magnetic alloys, Valence bands, Band theory, Binding energy, Reprints, *Nickel manganese antimonides, Density of states.

Photoemission was used to investigate the electronic density of states (DOS) in Ni2MnSb and NiMnSb. Comparisons with calculated band structures reveal reasonable agreement, but there are indications that the calculations overemphasize Ni 3d contributions at some binding energies. Resonant effects at the Mn 3p core threshold were employed to obtain information on the Mn 3d partial densities of states and these indicate that Mn 3d character is spread throughout the valence bands, in agreement with theory. These effects are strongest in the bottom of the valence band around a binding energy of 3.1 eV and produce structure which agrees well with the theoretical Mn 3d DOS, but are weak for other portions of the calculated Mn DOS. These results are discussed in the context of models for the formation of localized moments in these materials.

04,613
PB95-162442 Not available NTIS
National Inst. of Standards and Technology (MSEL), Gaithersburg, MD. Metallurgy Div.
Temperature Dependence of Vortex Twin Boundary Interaction in Yttrium Barium Copper Oxide (YBa2Cu3O6+x).
Final rept.
A. Roitburd, L. J. Swartzendruber, D. L. Kaiser, F. W. Gayle, and L. H. Bennett. 1990, 1p.
Pub. in Physical Review Letters 64, n24 p2962 1990.

Keywords: *High temperature superconductors, *YBCO superconductors, *Flux pinning, Temperature dependence, Temperature range 0065-0273 K, Magnetic fields, Twinning, Reprints, *Yttrium barium cuprates.

It is shown that the interaction energy between flux vortices and twin boundaries changes sign from negative to positive as the temperature is lowered. For small applied fields (H < 2Hc1) the crossover temperature is approximately 70 K.

04,614
PB95-162541 Not available NTIS
National Inst. of Standards and Technology (EEEL), Boulder, CO. Electromagnetic Technology Div.
Growth of Laser Ablated YBa2Cu3O7-delta Films as Examined by Rheed and Scanning Tunneling Microscopy.
Final rept.
S. E. Russek, A. Roshko, S. C. Sanders, J. Moreland, D. A. Rudman, and J. W. Ekin. 1993, 6p.
Contract DE-AI05-89ER14044
Sponsored by Department of Energy, Washington, DC.
Pub. in Materials Research Society Symposia Proceedings, v285 p305-310 1993.

Keywords: *High temperature superconductor, *Superconducting films, *YBCO superconductors, Scanning tunneling microscopy, Electron diffraction, Crystal growth, Laser ablation, Thin films, Morphology, Reprints, *Yttrium barium cuprates, Surface structure.

Using scanning tunneling microscopy (STM) and reflection high energy electron diffraction (RHEED) we have examined the growth morphology, surface structure, and surface degradation of laser ablated YBa2Cu30(7-delta) thin films. Films from 5 nm to I micrometer thick were studied. The films were deposited on MgO and LaAlO3 substrates using two different excimer laser ablation systems. Both island nucleated and spiral growth morphologies were observed depending on the substrate material and deposition rate used. The initial growth mechanism observed for a 5-10 nm thick film is replicated through different growth layers up to thicknesses of 200 nm. Beyond 200 nm, the films show some a-axis grains and other outgrowths. The thinnest films (5-10 nm) show considerable surface roughness on the order of 3-4 nm. For both growth mechanisms the ledge width remains approximately constant (about 30 nm) and the surface roughness increases as the film thickness increases.

04,615
PB95-162624 Not available NTIS
National Inst. of Standards and Technology (MSEL), Gaithersburg, MD. Reactor Radiation Div.
Description of Layered Structures: Applications to High Tc Superconductors.
Final rept.
A. Santoro. 1993, 6p.
Pub. in Jnl. of Alloys and Compounds 197, p153-158 1993.

Keywords: *Superconductors, *Oxides, *Classifying, Structural analysis, Chemical composition, Gradients, Crystal structure, Crystallography, Perovskites, Rock salt, Reprints.

The layered structures of the known superconducting copper oxides can be described in terms of alternating slices having the rock salt and perovskite structure. This layer by layer representation of the crystal structures of oxide superconductors offers a conventient method for classifying and comparing to one another these important materials, and for predicting new compounds which may exhibit interesting electronic properties.

04,616
PB95-162749 Not available NTIS
National Inst. of Standards and Technology (EEEL), Boulder, CO. Electromagnetic Technology Div.
Critical Current Density, Irreversibility Line, and Flux Creep Activation Energy in Silver-Sheathed Bi2Sr2Ca2Cu2Ox Superconducting Tapes.
Final rept.
D. Shi, Z. Wang, S. Sengupta, S. X. Dou, H. K. Liu, Y. C. Guo, M. Smith, and L. F. Goodrich. 1993, 3p.
Contract DE-W-31-109-ENG-38
Sponsored by Department of Energy, Washington, DC.
Pub. in Institute of Electrical and Electronics Engineers Transactions on Applied Superconductivity 3, n1 p1194-1196 Mar 93.

Keywords: *Superconductors, *Films, *Magnetism, Microstructure, Creep rate, Flux(Rate), Current density, Transport properties, Data processing, Magnetic hysteresis, Reprints, Flux creep.

Transport data, magnetic hysteresis and flux creep activation energy experimental results are presented for silver-sheathed high-Tc Bi2Sr2Ca2Cu3Ox superconducting tapes. The 110 K superconducting phase was formed by lead doping in a Bi-Sr-Ca-Cu-O system. The transport critical current density was measured at 4.0 K to be 0.7 x 10(5) A/sq. cm (the corresponding critical current is 74 A) at zero field and 1.6 x 10(4) A/sq. cm at 12 T for H(double vertical bars)ab. Excellent grain alignment in the a-b plane was achieved by a short-melting method, which considerably improved the critical current density and irreversibility line.

04,617
PB95-162780 Not available NTIS
National Inst. of Standards and Technology (MSEL), Gaithersburg, MD. Metallurgy Div.
Nanocomposite Magnetic Materials.
Final rept.
R. D. Shull, and L. H. Bennett. 1992, 6p.
Pub. in Nanostructured Materials 1, p83-88 1992.

Keywords: *Composite materials, *Magnetic materials, *Electrodeposition, Anisotropy, Glass, Magnetic properties, Magnetism, Copper, Nickel, Iron oxides, Silica gel, Sputtering, Reprints, Magnetic spin glass.

Composites of dissimilar materials wherein the sizes of the constituents are on the order of a few nanometers (Nanocomposites) are found to possess properties similar to, but different from, the properties of the individual constituents. When at least one of the constituents possesses a permanent magnetic moment, the magnetization statics and dynamics of the nanocomposite can be very different from that of the magnetic species in bulk form. In addition, the sensitivity of these magnetic properties to composition and morphology allows the class of magnetic nanocomposites to serve as a laboratory for the atomic engineering of materials with specific magnetic characteristics.

04,618
PB95-162798 Not available NTIS
National Inst. of Standards and Technology (MSEL), Gaithersburg, MD. Metallurgy Div.
Magnetocaloric Effect in Nanocomposites.
Final rept.
R. D. Shull, L. J. Swartzendruber, and L. H. Bennett. 1991, 15p.
Pub. in Proceedings of International Cryocoolers Conference (6th), Plymouth, MA., October 25-26, 1990, p231-245 1991.

Keywords: *Superconductors, *Magnetic properties, Microstructure, Magnetic field, Barium, Yttrium, Copper oxides, Currents, Vortices, Reprints, Twins, BaYCuO, Vortex pinning, Critical currents, Magnetocaloric effect.

The magnetic properties of nanocomposites containing extremely small magnetic particulates dispersed in a nonmagnetic matrix can be very different than those of the bulk magnetic material. Here we consider the consequences of such a microstructure on the magnetocaloric effect. Upon the application of an external magnetic field, the magnetic spins in a material tend to align with the field, thereby reducing the magnetic entropy of the spin system. Creation of a nanocomposite with many very small ferromagnetic regions provides an effective enhanced magnetic moment which can result in certain temperature and field ranges in an increased dT over that provided by either paramagnetic or ferromagnetic materials, with potential application to magnetic refrigeration.

04,619
PB95-162806 Not available NTIS

National Inst. of Standards and Technology (MSEL), Gaithersburg, MD. Polymers Div.
Preparation of 2-Dimensional Ultra Thin Polystyrene Film by Water Casting Method.
Final rept.
K. Shuto, Y. Oishi, T. Kajiyama, and C. C. Han.
1993, 10p.
Pub. in Polymer Jnl. 25, n3 p291-300 1993.

Keywords: *Thin films, *Polystyrene, *Neutron reactions, Electron microscopy, Neutron scattering, Polymers, Gyration, X rays, Reprints, TEM(Transmission electron microscopy), Water casting method, Tagged-polymer method, Radius of gyration.

The preparation condition of polystyrene (PS) ultra thin film by a water casting method was investigated on the basis of transmission electron microscopic (TEM) observations. Homogeneous ultra thin films were prepared from a 0.2-2.0 wt% cyclohexanone solution of PS owing to moderate spreadability of the solution on the water surface. The spreading state of the solution on the water surface depending on the dissipation speed of solvent and entanglements among PS chains were in strong relation to formation of the homogeneous ultra thin film. X-Ray interference measurements revealed that the thickness of the ultra thin film was smaller than the dimension of an unperturbed PS chain.

04,620
PB95-162822 Not available NTIS
National Inst. of Standards and Technology (MSEL), Gaithersburg, MD. Ceramics Div.
Ca1-xCuO2, a NaCuO2-Type Related Structure.
Final rept.
T. Siegrist, R. S. Roth, C. J. Rawn, and J. J. Ritter.
1990, 3p.
Pub. in Chemistry of Materials 2, n2 p192-194 1990.

Keywords: *Crystal structure, *Superconductors, X ray diffraction, Crystallography, Calcium, Copper oxides, Sodium, Reprints.

The crystal structure of Ca(1-x)CuO(2), a low temperature phase in the Ca-Cu-O system, has been studied by X-ray diffraction. The structure contains edge shared chains of CuO4 squares, forming linear (CuO2)-chains and is related to the NaCuO2-type. In contrast to the NaCuO2-type, the calcium atoms are not well localized and various superstructures caused by different Ca ordering are observed.

04,621
PB95-163002 Not available NTIS
National Inst. of Standards and Technology (NML), Gaithersburg, MD. Quantum Metrology Div.
Anisotropy of Polarized X-ray Emission from Atoms and Molecules.
Final rept.
S. H. Southworth, D. W. Lindle, R. Mayer, and P. L. Cowan. 1991, 5p.
Pub. in Nuclear Instruments and Methods in Physics Research B 56-7, p304-308 May 91.

Keywords: *Anisotropy, *Polarization, *X rays, Atoms, Molecules, X ray analysis, Reprints, X ray emission.

Strongly anisotropic, polarized Cl Kbeta x-ray emission has been observed from gas-phase CF3Cl following selective resonant excitation with a linearly polarized x-ray beam. Distinctively different polarizations and angular distributions result for emission involving molecular orbitals of different symmetries. A classical model of the x-ray absorption/emission process well describes the observed radiation patterns. A small anisotropy also was measured for Ar Kalpha emission following resonant excitation. The observation of only a small anisotropy in this case is attributed to the averaging out of the individual anisotropies from unresolved final states. The authors review the experimental methods and results and discuss theoretical models used to describe polarization and anisotropy effects in x-ray absorption and emission from atoms and molecules.

04,622
PB95-163358 Not available NTIS
National Inst. of Standards and Technology (EEEL), Boulder, CO. Electromagnetic Technology Div.
Observation of Insulating Nanoparticles on YBCO Thin-Films by Atomic Force Microscopy.
Final rept.
R. E. Thomson, J. Moreland, N. Missert, D. A. Rudman, and S. C. Sanders. 1993, 2p.
Pub. in Proceedings of International Workshop on Superconductivity, Hokkaido, Japan, June 28-July 1, 1993, p242-243.

Keywords: *High temperature superconductors, *YBCO superconductors, *Superconducting films, *Surface analysis, Scanning tunneling microscopy, Atomic force microscopy, Image analysis, Thin films, Reprints, *Yttrium barium cuprates, Surface topography, Nanostructures.

The surface topography of YBa2CU3O(7-delta) thin films was studied with both atomic force microscopy (AFM) and scanning tunneling microscopy (STM). The AFM images revealed a high density of small distinct nanoparticles, 10-50 nm across and 5-20 nm high, which did not appear in STM images of the same samples. Scanning the STM tip across the surface broke off particles and moved them to the edge of the scanned area, where they were later imaged with the AFM.

04,623
PB95-163366 Not available NTIS
National Inst. of Standards and Technology (NEL), Gaithersburg, MD. Building Materials Div.
Elastic Properties of Central-Force Networks with Bond-Length Mismatch.
Final rept.
M. F. Thorpe, and E. J. Garboczi. 1990, 13p.
Pub. in Physical Review B 42, n13 p8405-8417 1990.

Keywords: *Elastic properties, *Crystal lattices, *Crystal defects, Crystal structures, Bonding, Crystallography, Strain rate, Stress analysis, Reprints, *Bond-length mismatch.

We study a triangular network containing two kinds of Hooke springs with different natural lengths. If the two spring constants are the same, we can solve the model exactly and show that Vegard's law is obeyed, irrespective of whether the bonds are arranged randomly or in a correlated way. A more complete description of these networks is obtained through the mean lengths and length fluctuations associated with the two kinds of bonds, and the strain energy. The complete distribution of bond lengths is obtained numerically and shows an interesting and unexpected symmetry for the random case. Finally, we show that numerical results for a similar system, but with different force constants as well as different natural lengths, can be well accounted for by using an effective medium theory which reduces to the exact results when the two spring constants are made equal. We show that these lattices can be described very accurately up to about 50% length mismatches, when pleating occurs and the lattices develop local instabilities.

04,624
PB95-163499 Not available NTIS
National Inst. of Standards and Technology (MSEL), Gaithersburg, MD. Metallurgy Div.
Determination of Thermoactivation Parameters of Vortex Mobility in YBa2Cu3O7 Using Only Magnetic Measurements.
Final rept.
M. J. Turchinskaya, A. L. Roytburd, L. H. Bennett, L. J. Swartzendruber, and K. Sawano. 1991, 10p.
Pub. in Physica C 182, n4-6 p297-306 1991.

Keywords: *High temperature superconductors, *YBCO superconductors, Type 2 superconductors, Magnetic measurement, Magnetic induction, Activation energy, Time dependence, Single crystals, Reprints, *Yttrium barium cuprates, Vortex mobility.

A method for determination of the basic parameters of vortex mobility from the magnetic induction vs. time curve obtained from a zero-field cooled superconductor is presented. Three stages of magnetizing are considered. Measurement of the log-creep rate allows determination of the activation moment alpha, while the study of the kinetics during the approach to equilibrium provides the relaxation time r, and the equilibrium inductions B(o). Then the activation energy U can be calculated. These two stages were obtained both for three different samples of YBa2Cu3O7: a single crystal, a sintered powder, and a sample prepared by the quench-melt-growth (QMG) process. The QMG sample was perfect enough to give reliable quantitative results.

04,625
PB95-163556 Not available NTIS
National Inst. of Standards and Technology (PL), Gaithersburg, MD. Electron and Optical Physics Div.
SEMPA Studies of Oscillatory Exchange Coupling.
Final rept.
J. Unguris, D. T. Pierce, R. J. Celotta, and J. A. Stroscio. 1993, 12p.
Sponsored by Office of Naval Research, Arlington, VA.
Pub. in Magnetism and Structure in Systems of Reduced Dimension, p101-112 1993.

Keywords: *Exchange interactions, *Magnetism, Scanning electron microscopy, Whiskers(Single crystals), Fermi surfaces, Metal films, Polarization, Epitaxy, Iron, Chromium, Silver, Spacers, Reprints, Oscillatory coupling, Multilayers.

We have used scanning electron microscopy with polarization analysis (SEMPA) to investigate the magnetic exchange coupling between an Fe film and an Fe whisker separated by either a Cr or Ag spacer layer. The thickness dependence of the oscillatory coupling in these atomically well ordered, epitaxial films was precisely measured. The periodicity of exchange coupling is consistent with predictions based on Fermi surface spanning vectors of the interlayer material.

04,626
PB95-163564 Not available NTIS
National Inst. of Standards and Technology (MSEL), Gaithersburg, MD. Metallurgy Div.
Experimental Verification of a Vector Preisach Model.
Final rept.
F. Vajda, J. Oti, M. Pardavi-Horvath, L. H. Bennett, E. Della Torre, and L. J. Swartzendruber. 1991, 4p.
Pub. in Jnl. of Applied Physics 69, n8 p4501-4504 1991.

Keywords: *Magnetic recording, Remanent magnetism, Coercive force, Experimentation, Verification, Particulates, Reprints, *Preisach model, Angular dependence, Micromagnetics.

A vector moving Preisach model has been developed that describes partially oriented particulate media by pseudo-particles, consisting of a distribution of several basic particles with various orientations of easy axes. The model uses switching modes calculated by a micro-magnetic simulation of physical particles. In order to test this model, the angular dependence of the magnetic properties was measured by a VSM for several samples of commercial recording media that had different degrees of particle orientation. The experimental results are in good agreement with the orientation dependence of the squareness, remanence, and coercivity, as predicted by the model.

04,627
PB95-163721 Not available NTIS
National Inst. of Standards and Technology (NEL), Boulder, CO. Electromagnetic Technology Div.
High Critical Temperature Superconductor Tunneling Spectroscopy Using Squeezable Electron Tunneling Junctions.
Final rept.
T. Walsh, J. Moreland, R. H. Ono, T. Harvey, C. Reintsema, T. S. Kalkur, J. A. Beall, and M. Cromar. 1991, 4p.
Pub. in Institute of Electrical and Electronics Transactions on Magnetics 27, n2 p840-843 Mar 91.

Keywords: *High temperature superconductors, *Tunnel junctions, Electron tunneling, Temperature dependence, BSCCO superconductors, YBCO superconductors, Energy gap, Electrodes, Niobium, Cuprates, Reprints, Tunneling spectroscopy.

Tunneling spectroscopy measurements were performed on squeezable electron tunneling (SET) junctions using Bi-Sr-Ca-Cu-O, Y-Ba-Cu-O, and Nb electrodes in a variety of combinations. A zero-bias conductance peak has been seen repeatedly in the current-voltage (I(V)) and the conductance-voltage (G(V)) characteristics. A model is presented to explain this conductance peak in terms of quasi-particle tunneling, phase diffusion, and a supercurrent. Two additional structures have been seen repeatedly in I(V) and G(B). One of these structures has the characteristics of an energy gap feature. The other structure, which can mimic the gap feature, is explained in terms of the switching to the voltage state of a grain boundary junction that is in series with the SET junction. The dependence of these features upon temperature and the force applied to the junction are examined.

04,628
PB95-163739 Not available NTIS
National Inst. of Standards and Technology (NEL), Boulder, CO. Electromagnetic Technology Div.

Tunneling Measurement of the Zero-Bias Conductance Peak and the Bi-Sr-Ca-Cu-O Thin-Film Energy Gap.
Final rept.
T. Walsh, J. Moreland, R. H. Ono, and T. S. Kalkur. 1991, 4p.
Pub. in Physical Review Letters 66, n4 p516-519 1991.

Keywords: *High temperature superconductors, *Superconducting junctions, *Superconducting films, *BSCCO superconductors, *Energy gap, Temperature range 0000-0013 K, Quasi particles, Electron tunneling, Thin films, Reprints, *Bismuth strontium calcium cuprates.

We have used squeezable electron tunneling junctions, at 4 K, to examine the zero-bias conductance peak that has been found in high temperature superconductor tunnel junction spectra by a number of researchers. In addition, peaks in the differential conductance-voltage characteristic have been found repeatedly between 46 and 64 mV. We interpret the voltages at which these peaks occur to be the gap voltage 2 delta (4 K). The zero-bias conductance peak can be explained in terms of a supercurrent and thermal excitations, both quasi-particles and phase diffusion.

04,629
PB95-164224 Not available NTIS
National Inst. of Standards and Technology (MSEL), Gaithersburg, MD. Reactor Radiation Div.
Analytic Calculation of Polarized Neutron Reflectivity from Superconductors.
Final rept.
H. Zhang, and J. W. Lynn. 1993, 12p.
Pub. in Physical Review B 48, n21 p15 893-15 904, 1 Dec 93.

Keywords: *Superconducting films, *Superconductors, Polarized beams, Penetration depth, Angle of incidence, Schrodinger equation, Magnetic fields, Thick films, Meissner effect, Ferromagnetic materials, Magnetization, Reprints, *Neutron reflection, *Polarized neutron reflectometry.

We have obtained an analytic expression for the reflectivity R(sup + -)(theta, lambda) of polarized neutrons from a superconductor in the Meissner state, where lambda is the magnetic-field penetration depth and theta is the incident angle of the neutron beam. The result is derived as an exact solution of the 1D Schroedinger equation in the continuum limit, with an interaction potential. The solution for R(sup + -)(theta, lambda) reveals surprising features in its lambda dependence that have not been discovered in previous numerical studies. In particular, R(sup -)(theta, lambda) displays an oscillatory dependence on lambda within a narrow angular range immediately above the total reflection angle, instead of a monotonic dependence as inferred from earlier numerical calculations. The solution also reveals that complete transmission for the down-spin state (R(sup -)(theta, lambda) = 0) may occur when lambda and H (the applied magnetic field) satisfy certain conditions.

04,630
PB95-164240 Not available NTIS
National Inst. of Standards and Technology (IMSE), Gaithersburg, MD.
Dislocation Emission at Ledges on Cracks.
Final rept.
S. J. Zhou, and R. Thomson. 1991, 15p.
Pub. in Jnl. of Materials Research 6, n3 p639-653 1991.

Keywords: *Dislocations, *Emission, *Crack tips, *Ledges, Brittleness, Fracture(Mechanics), Cracking(Fracturing), Crack initiation, Solid mechanics, Reprints.

In this paper, we propose that, depending on their height, ledges on cracks can be efficient sources of dislocations at loadings well below the critical loading for homogeneous emission. Detailed three dimensional elastic calculations are presented supporting this proposition. There are two configurations for emission; one which blunts the crack, and one we call a jogging configuration. By our calculations, the blunting configuration should be the more efficient source; however, jogging dislocations are more frequently observed, experimentally. We find that the ledge is only a finite source of dislocations, in the sense that the ledge height decreases as the dislocations are emitted. The atomic configuration at the ledge is composed of finite lengths of real dislocations, which is the reason why such dislocations can be emitted easier than homogeneously produced dislocations. The stresses at the ledge tip produce a cloud of bound dislocations near the ledge, pinned at the ledge ends, so that the ledge crack configuration becomes delocalized. Delocalization of the pile-up dislocations in the jogging direction may explain why the jogging dislocations are more frequently seen. Implications for DFZ's and ductile transitions are discussed.

04,631
PB95-164257 Not available NTIS
National Inst. of Standards and Technology (IMSE), Gaithersburg, MD.
Shielding of Cracks in a Plastically Polarizable Material.
Final rept.
S. J. Zhou, and R. Thomson. 1991, 10p.
Pub. in Jnl. of Materials Research 6, n8 p1763-1772 1991.

Keywords: *Shielding, *Crack tips, *Fracture strength, *Dislocations, Plastic properties, Mechanical properties, Polarization(Waves), Dipoles, Emission, Brittleness, Reprints, *Plastically polarizable materials.

In this paper, we address some fundamental questions regarding the response of a crack to externally generated dislocations. We note that since dislocations formed at external sources in the material must be in the form of loops or dipoles, that the theory must be couched in terms of crack shielding in a plastically polarizable medium. There are strong analogies to dielectric theory. We prove two general theorems: (1) Dipoles formed in the emission geometry relative to a crack tip always antishield the crack, and (2) when dipoles are induced during uniform motion through a uniformly plastically polarizable material, then the shielding is always positive. We illustrate these general theorems with a number of special cases for fixed and polarizable sources. Finally, we simulate the self consistent time dependent response of a crack to a polarizable source as the crack moves past it. The results show the crack is initially antishielded, but that positive shielding always dominates during later stages of configuration evolution. The crack may be arrested by the source, or it may break away from it, depending upon the various parameters--source strength and geometry, dislocation mobility, Griffith condition for the crack, etc. The results indicate that the time dependence of crack shielding in the presence of a nonuniform density of sources will be very important in practical cases of brittle transitions in materials.

04,632
PB95-164406 Not available NTIS
National Inst. of Standards and Technology (PL), Gaithersburg, MD. Quantum Metrology Div.
Lattice Position of Si in GaAs Determined by X-Ray Standing Wave Measurements.
Final rept.
A. Shih, P. Cowan, S. Southworth, B. Karlin, F. Moore, E. Dobisz, H. Dietrich, L. Fotiadas, and C. Hor. 1993, 8p.
Pub. in Jnl. of Applied Physics 73, n12 p8161-8168, 15 Jun 93.

Keywords: *Gallium arsenides, *Silicon additions, Molecular beam epitaxy, Synchrotron radiation, Ion implantation, Thermal diffusion, Standing waves, Position finding, Crystal lattices, X-ray analysis, Doped crystals, Impurities, NSLS, Reprints, *Lattice sites.

The x-ray standing wave (XSW) technique was applied to determine the lattice location of Si impurity atoms in GaAs(100) crystals. The synchrotron radiation of X24A at the national synchrotron light source was used to set up backreflection XSW, an experimental geometry which drastically relaxes the otherwise stringent requirement on the lattice perfection. Specifically, the lattice sites were determined with respect to the (left bracket) 311 (right bracket) reflection planes which differentiate a Ga site from an As site. With the aid of an appropriate choice of the x-ray fluorescence filter, we were able to study GaAs(100) samples with very low levels of Si impurities. On a sample doped with 4 X 10(exp 18)/cc Si during the molecular-beam epitaxy growth, we found that the Si atoms predominantly occupied the Ga sites. On both an ion-implanted sample after annealing and a sample with Si impurities introduced by thermal diffusion, about 30% of the Si atoms occupied the Ga sites, and the rest occupied random sites. The As site occupation was less than 6%. Suggestions are made for further experiments with improved sensitivity.

04,633
PB95-164521 Not available NTIS
National Inst. of Standards and Technology (MSEL), Gaithersburg, MD. Reactor Radiation Div.
Field Dependence of the Magnetic Ordering of Cu in R2CuO4 (R = Nd, Sm).
Final rept.
S. Skanthakumar, J. W. Lynn, J. L. Peng, and Z. Y. Li. 1993, 3p.
Pub. in Jnl. of Applied Physics 73, n10 p6326-6328, 15 May 93.

Keywords: Neutron diffraction, Electron spin, Spin orientation, Copper, Reprints, *Neodymium cuprates, *Samarium cuprates, *Magnetic ordering, Magnetic field dependence.

We have used neutron diffraction techniques to study the field dependence of the magnetic ordering of Cu spins in R2CuO4 (R=Nd,Sm) in order to distinguish between the proposed collinear and noncollinear spin structures. In the proposed collinear spin structure, there are two separate domains with the spins either along the (110) or along the (1-10) directions, while in the noncollinear model there is a single domain with the alternate-layer spins along the (100) and (010) directions, respectively. If a magnetic field is applied along the (1-10), strong hysteresis effects are anticipated for the collinear spin structure due to domain repopulation, while such effects are not expected for the noncollinear spin structure. Our field dependent data do not show any hysteresis effects associated with the pure Cu ordering, which strongly suggest that the noncollinear spin structure is correct for the magnetic spin configuration of the Cu spins of both compounds. Hysteresis effects in a field are observed in Sm2CuO4 near and below the Sm ordering temperature, and these are most likely caused by the interaction between Sm and Cu sublattices.

04,634
PB95-164539 Not available NTIS
National Inst. of Standards and Technology (MSEL), Gaithersburg, MD. Reactor Radiation Div.
Observation of Noncollinear Magnetic Structure for the Cu Spins in Nd2CuO4-Type Systems.
Final rept.
S. Skanthakumar, J. W. Lynn, J. L. Peng, and Z. Y. Li. 1993, 4p.
Pub. in Physical Review B 47, n10 p6173-6176, 1 Mar 93.

Keywords: Spin orientation, Neutron diffraction, Electron spin, Copper, Reprints, *Neodymium cuprates, *Samarium cuprates, Magnetic field dependence, Magnetic ordering.

Field-dependent neutron-diffraction measurements have been taken on Nd2CuO4 and Sm2CuO4 in order to distinguish between the proposed collinear and noncollinear spin structures for the Cu ions. For magnetic fields applied along the (110) direction, both systems exhibit Bragg intensities that are continuous and reversible with H. For Nd2CuO4 we have also taken data for fields applied within an angle alpha of the (100) direction, and we have found that the intensities of the magnetic reflections increase or decrease depending on the sign of alpha. Both of these observations are only consistent with the noncollinear spin model.

04,635
PB95-164562 Not available NTIS
National Inst. of Standards and Technology (CSTL), Gaithersburg, MD. Surface and Microanalysis Science Div.
Reactive Coevaporation of DyBaCuO Superconducting Films: The Segregation of Bulk Impurities on Annealed MgO(100) Substrates.
Final rept.
R. V. Smilgys, S. W. Robey, C. K. Chiang, and T. J. Hsieh. 1993, 6p.
Pub. in Jnl. of Vacuum Science and Technology A 11, n4 p1361-1366 Jul/Aug 93.

Keywords: *Superconducting films, *Magnesium oxides, *Surface analysis, High temperature superconductors, Substrates, Thin films, Microstructure, Annealing, Impurities, Calcium, Reprints, *Dysprosium barium cuprates.

This article reports results from a study on the effect bulk impurities in MgO substrates may have when substrates are annealed to improve film microstructure and transport properties. DyBaCuO thin films are prepared by molecular beam reactive coevaporation on

both annealed and unannealed MgO(100). While predeposition annealing has led to improved film quality for some groups, under our conditions just the opposite occurs. We point out the existence of Ca segregation to the MgO surface as a factor that needs investigation because Ca is a common contaminant in commercially supplied MgO. Atomic force microscope images show decoration of annealed substrates with submicron size particles that may be composed of the segregated Ca. These particles seem to underlie the distinct differences seen in the surface microstructure of films on annealed and unannealed substrates.

04,636
PB95-168431 Not available NTIS
National Inst. of Standards and Technology (EEEL), Boulder, CO. Electromagnetic Technology Div.
In situ Observation of Surface Morphology of InP Grown on Singular and Vicinal (001) Substrates.
Final rept.
K. A. Bertness, C. Kramer, J. M. Olson, and J. Moreland. 1994, 6p.
Pub. in Jnl. of Electronic Materials 23, n2 p195-200 1994.

Keywords: *Indium phosphides, *Vapor phase epitaxy, Atomic force microscopy, Optical microscopy, Surface roughness, Orientation(Direction), Light scattering, Laser radiation, Substrates, Reprints, In situ monitoring, Surface topography.

Surface morphology of InP layers is monitored during organometallic vapor phase epitaxy using an in situ diffuse laser light scattering technique. Changes in the diffuse scatter signal are noted for several substrate orientations near the (001) plane and at various growth temperatures. The diffuse scatter signal is shown to be a semi-quantitative indicator of surface roughness through post-growth examination of the samples with phase contrast optical microscopy and atomic force microscopy. Singular substrates consistently have almost featureless surfaces and very little diffuse scattering during growth. Vicinal substrates display a more complicated morphological evolution which cannot be deduced from the diffuse scattering alone but which does produce characteristic changes in diffuse scattering.

04,637
PB95-168522 Not available NTIS
National Inst. of Standards and Technology (EEEL), Boulder, CO. Electromagnetic Technology Div.
Combined Josephson and Charging Behavior of the Supercurrent in the Superconducting Single-Electron Transistor.
Final rept.
T. M. Eiles, and J. M. Martinis. 1994, 280p.
Contract ONR-00014-92-F-0003
Sponsored by Office of Naval Research, Arlington, VA.
Pub. in Physical Review B 50, n1 p627-630, 1 Jul 94.

Keywords: *Josephson junctions, Josephson effect, Cooper pairs, Superconductivity, Reprints, *Single electron transistors, Coulomb blockage, Supercurrent, Nanoelectronics, Shapiro steps.

Measurements of two ultrasmall Josephson junctions connected in series show a supercurrent with magnitude much greater than previously reported for similar devices. The dependence of the supercurrent on gate charge shows agreement with predictions made by Averin and Likharev that are based on a conjugate relationship between the junction phase and charge variables. The transport of Cooper pairs through the two junctions makes the devices behave effectively as a single junction whose critical current is modulated by the gate charge.

04,638
PB95-168613 Not available NTIS
National Inst. of Standards and Technology (EEEL), Boulder, CO. Electromagnetic Technology Div.
Alternating-Field Susceptometry and Magnetic Susceptibility of Superconductors.
Final rept.
R. B. Goldfarb, and M. Lelental. 1991, 32p.
See also PB94-145984.
Pub. in Magnetic Susceptibility of Superconductors and Other Spin Systems, p49-80 1991.

Keywords: *Magnetic susceptibility, *Superconductors, Superconducting films, Alternating current, Granular materials, Critical field, Critical current, Meissner effect, Demagnetization, Thin films, Sensitivity, Operation, Calibration, Design, Reviews, Reprints, Susceptometers.

This review critically analyzes current practice in the design, calibration, sensitivity determination, and operation of alternating-field susceptometers, and examines applications in magnetic susceptibility measurements of superconductors. Critical parameters of the intrinsic and coupling components of granular superconductors may be deduced from magnetic susceptibility measurements. The onset of intrinsic diamagnetism corresponds to the initial decrease in electrical resistivity upon cooling, but the onset of intergranular coupling coincides with the temperature for zero resistivity. The lower critical field may be determined by the field at which the imaginary part of susceptibility increases from zero. Unusual features in the susceptibility of superconductor films, such as a magnetic moment that is independent of film thickness and the variation of susceptibility with angle, are related to demagnetization.

04,639
PB95-168621 Not available NTIS
National Inst. of Standards and Technology (EEEL), Boulder, CO. Electromagnetic Technology Div.
High Current Pressure Contacts to Ag Pads on Thin Film Superconductors.
Final rept.
L. F. Goodrich, A. N. Srivastava, T. C. Stauffer, A. Roshko, and L. R. Vale. 1994, 4p.
Pub. in Institute of Electrical and Electronics Engineers Transactions on Applied Superconductivity 4, n2 p61-64 Jun 94.

Keywords: *High temperature superconductors, *Superconducting films, *YBCO superconductors, *Electric contacts, *Contact resistance, Soldered joints, Critical current, Electrical resistance, Thin films, Indium, Silver, Reprints, *Yttrium barium cuprates, *Pressure contacts.

High current, low resistance, nonmagnetic, and nondestructive pressure contacts to Ag pads on YBa2Cu3O(7-delta) (YBCO) thin film superconductors were developed in this study. The contact resistance reported here includes the resistance of the current lead/Ag pad interface, the Ag pad/YBCO interface, and the bulk resistance of the contact material. This total contact resistance is the relevant parameter which determines power dissipation during critical-current measurements. It was found that regardless of the optimization of the Ag pad/YBCO interface through annealing, a pressure contact can yield a lower total resistance than a soldered contact. The lowest resistance obtained with pressure contacts was 3 (micro)ohms (for a 2 X 4 sq mm contact). These contacts may be useful for many different high temperature superconductor (HTS) studies where high-current contacts with low heating are needed.

04,640
PB95-168670 Not available NTIS
National Inst. of Standards and Technology (EEEL), Boulder, CO. Electromagnetic Technology Div.
Suitability of Metalorganic Chemical Vapor Deposition-Derived PrGaO3 Films as Buffer Layers for YBa2Cu3O7-x Pulsed Laser Deposition.
Final rept.
B. Han, D. A. Neumayer, T. J. Marks, V. P. Dravid, D. A. Rudman, and H. Zhang. 1993, 3p.
Pub. in Applied Physics Letters 63, n26 p3639-3641, 27 Dec 93.

Keywords: *YBCO superconductors, High temperature superconductors, Metalorganic chemical vapor deposition, Temperature range 0400-1000 K, Superconducting films, Perovskites, Precursor, Thin films, Substrates, Reprints, *Praseodymium gallates, *Yttrium barium cuprates, Lanthanum aluminates, Buffer layers.

Phase-pure thin films of the YBa2Cu3O(7-x) (YBCO) lattice matched and low loss tangent perovskite insulator PrGaO3 have been grown in situ on single-crystal (110) LaAlO3 substrates by metalorganic chemical vapor deposition (MOCVD). Films were grown at temperatures of 750-800 C using beta-diketonate precursors M(dpm)3 (M = Pr,Ga; dpm = dipivaloylmethanate). YBCO films were then grown on the MOCVD-derived PrGaO3 by pulsed laser deposition (PLD). Scanning electron microscopy reveals that the PrGaO3 films have smooth, featureless surfaces. As assessed by x-ray diffraction, the PrGaO3 films grow epitaxially on LaAlO3 with a high degree of (001) and/or (110) plane orientation parallel to the substrate surface, and the subsequent YBCO films grow with a (00l) orientation. Rocking curve and phi-scan analyses reveal that the PrGaO3 and YBCO films grow epitaxially. YBCO films grown by PLD on the MOCVD-derived PrGaO3 exhibit T(c) = 91 K and J(c) = 6 X 10(exp 6) A/sq cm at 77 K in zero field.

04,641
PB95-168829 Not available NTIS
National Inst. of Standards and Technology (MSEL), Boulder, CO. Materials Reliability Div.
Relationship between Bulk-Modulus Temperature Dependence and Thermal Expansivity.
Final rept.
H. Ledbetter. 1994, 5p.
Pub. in Physica Status Solidi (b) 181, p81-85 1994.

Keywords: *Bulk modulus, *Thermal expansion, Zero point energy, Temperature dependence, Debye temperature, Gruneisen constant, Elastic properties, Metals, Reprints.

The relationship between two anharmonic physical properties is considered: the bulk-modulus temperature dependence and the thermal expansivity. For the first, Varshni's relationship is used, which derives from an Einstein-oscillator model of crystals. For the second, a relationship from Slater is used with a similar basis. The ration of the two properties is found to be gamma + 1, where gamma denotes the usual Gruneisen parameter. Varshni's adjustable parameter s is interpreted in terms of the Gruneisen parameter, the Einstein temperature, and the atomic volume. Applied to metals, our relationship works well for those with s-p-electron bonding, but poorly for those where d-electrons contribute to bonding.

04,642
PB95-168837 Not available NTIS
National Inst. of Standards and Technology (MSEL), Boulder, CO. Materials Reliability Div.
Low-Temperature Elastic Constants of Y1Ba2Cu3O7.
Final rept.
H. Ledbetter, M. Lei, A. Hermann, and Z. Sheng. 1994, 7p.
Pub. in Physica C 225, p397-403 1994.

Keywords: *YBCO superconductors, *Elastic properties, High temperature superconductors, Temperature range 0000-0013 K, Temperature range 0013-0065 K, Temperature range 0065-0273 K, Temperature range 0273-0400 K, Temperature dependence, Polycrystalline, Ultrasonic tests, Bulk modulus, Shear modulus, Young modulus, Poisson ratio, Reprints, *Yttrium barium cuprates.

Using ultrasonic methods, we studied the 4-295 K elastic constants of a 'good' Y1Ba2Cu3O7 polycrystal. We report the bulk, shear, Young moduli and the Poisson ratio. Except for the Poisson ratio, all elastic constants show smooth temperature behavior. Near T(c) during cooling, the Poisson ratio decreases irregularly. Focusing on the bulk modulus B, we use simple thermodynamics to show that the harmonic-observed decrement at T = O corresponds to expectation, but the temperature effect dB/dT is too large by about a factor of two. We attribute the irregular slope to oxygen-atom reordering. Against many reports, our bulk-modulus value is approximately that found in monocrystals or that predicted by an ionic-crystal model calculation.

04,643
PB95-168977 Not available NTIS
National Inst. of Standards and Technology (EEEL), Boulder, CO. Electromagnetic Technology Div.
Microwave Properties of YBa2Cu3O7-x Films at 35 GHz from Magnetotransmission and Magnetoreflection Measurements.
Final rept.
E. K. Moser, W. J. Tomasch, M. J. McClorey, C. L. Petiette-Hall, S. M. Schwarzbek, J. K. Furdyna, and M. W. Coffey. 1994, 10p.
Sponsored by Department of Energy, Washington, DC.
Pub. in Physical Review B 49, n6 p4199-4208, 1 Feb 94.

Keywords: *YBCO superconductors, *Superconducting films, High temperature superconductors, Extremely high frequency, Microwave transmission, Temperature dependence, Type 2 superconductors, Penetration depth, Thin films, Substrates, Reprints, Magnetic field dependence, Surface impedance, Vortex dynamics, Lanthanum aluminates, Magnetoreflectance.

Microwave transmission and reflection measurements are performed simultaneously on thin films (approx 1,800 A) of YBa2Cu3O(7-x) having their c axis per-

pendicular to the LaAlO3 substrate. We determine power transmission and reflection fractions, Tau(T,H) and R(T,H), as functions of temperature and static magnetic field (O < H < 5.4 T), the latter being applied perpendicular to the film. A guided-wave model, which we develop for our experimental situation, is the basis of a computational algorithm that extracts quantitative values of the complex penetration depth (lambda bar), or alternatively the complex surface impedance Z(s), from Tau and R data. This inversion algorithm is successful when applied to test data generated from a phenomenological theory describing the electrodynamic response of a type-II superconductor. The procedure is applied to Tau(T,H) and R(T,H) measurements to infer the temperature- and field-dependent complex penetration depth (lambda bar)(T,H) that completely characterizes the superconductive film's electromagnetic response.

04,644
PB95-168993 Not available NTIS
National Inst. of Standards and Technology (EEEL), Boulder, CO. Electromagnetic Technology Div.
Hot-Electron Microcalorimeters for X-ray and Phonon Detection.
Final rept.
M. Nahum, J. M. Martinis, and S. Castles. 1993, 6p.
Pub. in Jnl. of Low Temperature Physics 93, n3/4 p733-738 1993.

Keywords: *X ray detectors, *Superconducting junctions, *Calorimeters, Electron temperature, Electron funneling, Hot electrons, Metal films, Dark matter, Tunnel junctions, Microcalorimetry, Prototypes, Reprints, *Phonon detectors, *Microcalorimeters.

We propose a novel hot-electron microcalorimeter for measurements of x-rays or phonons produced by the interaction of a high energy particle with the underlying substrate. This type of detector uses a normal metal film to absorb the incoming excitation which subsequently heats the electrons above the lattice temperature. The temperature of the electrons is measured from the current - voltage characteristics of a superconductor-insulator-normal metal tunnel junction, where part of the absorber forms the normal electrode. We present simple calculations of the energy sensitivity of the junction and of the ultimate performance of x-ray and phonon detectors. We also present preliminary measurements of prototype devices which were used to test the basic detector physics.

04,645
PB95-169017 Not available NTIS
National Inst. of Standards and Technology (EEEL), Boulder, CO. Electromagnetic Technology Div.
Proposed Antiferromagnetically Coupled Dual-Layer Magnetic Force Microscope Tips.
Final rept.
J. O. Oti, P. Rice, and S. Russek. 1994, 3p.
Pub. in Jnl. of Applied Physics 75, n10 p6881-6883, 15 May 94.

Keywords: Magnetic films, Exchange interactions, Antiferromagnetism, Magnetostatics, Resolution, Reprints, *Magnetic force microscopy, *Microscope tips, Dual layers, Micromagnetics.

A magnetic force microscope tip designed from dual-layer magnetic films of antiferromagnetically coupled magnetic layers is proposed. A theoretical analysis of the possible advantages of such a tip over conventional single-layer tips is given, using an extension to dual layers of a previously described micromagnetic model of single-layer tips. In contrast to single-layer tips, the magnetic domains of dual-layer tips are less sensitive to the fringing fields of the specimen, and the tips' stray fields are greatly reduced, thus minimizing the likelihood of erasure of the sample magnetization. These properties of dual-layer tips should lead to improved resolution of magnetic force microscopy images.

04,646
PB95-169025 Not available NTIS
National Inst. of Standards and Technology (EEEL), Boulder, CO. Electromagnetic Technology Div.
Magnetic and Magnetoresistive Properties of Inhomogeneous Magnetic Dual-Layer Films.
Final rept.
J. O. Oti, S. E. Russek, and S. C. Sanders. 1994, 3p.
Pub. in Jnl. of Applied Physics 75, n10 p6519-6521, 15 May 94.

Keywords: *Magnetoresistance, *Magnetic films, Magnetic anisotropy, Coercive force, Exchange interactions, Cobalt alloys, Nickel alloys, Metal films, Magnetostatics, Chromium, Simulation, Reprints, Dual layers, Micromagnetics, Multilayers.

Magnetic and magnetoresistive properties of sputtered Co alloy dual-layer films are compared with micromagnetic simulations. The simulations elucidate the details of the switching behavior of the dual-layer films as a function of the interlayer exchange and magnetostatic interactions. The simulations have led to a conceptual understanding of the coercive field splitting caused by the interlayer interactions. A calculation of the anisotropic magnetoresistance (AMR) has been included in the simulations. The AMR provides a second independent macroscopic quantity (in addition to the average magnetization) which can be measured and compared with the micromagnetic simulations. The AMR is more sensitive to the micromagnetic structure perpendicular to the applied field and is a better test of the accuracy of the micromagnetic model. The simulations qualitatively describe the measured AMR data on CoNi-Cr-CoNi dual layers.

04,647
PB95-169033 Not available NTIS
National Inst. of Standards and Technology (MSEL), Boulder, CO. Materials Reliability Div.
Enhanced Flux Pinning via Chemical Substitution in Bulk Superconducting T1-2212.
Final rept.
M. Paranthaman, M. Foldeaki, D. Balzar, A. M. Hermann, H. Ledbetter, and A. J. Nelson. 1994, 7p.
Pub. in Supercond. Sci. Technol. 7, p227-233 1994.

Keywords: *Flux pinning, High temperature superconductors, Temperature range 0000-0013 K, Penetration depth, Magnetic hysteresis, Magnesium additions, Direct current, Doped materials, Critical current, Crystal defects, Reprints, *Thallium barium calcium cuprates.

The flux-pinning characteristics in both pure and doped superconducting Tl2Ba2CaCu2O8 (referred to as Tl-2212) systems were studied via DC magnetic hysteresis as well as flux-penetration and flux-expulsion measurements. Our results demonstrate an increase in both intrinsic pinning and lock-in transition of flux lines as a result of increased density of atomic-size structural defects via Mg doping in Tl-2212.

04,648
PB95-169157 Not available NTIS
National Inst. of Standards and Technology (EEEL), Boulder, CO. Electromagnetic Technology Div.
Insulating Boundary Layer and Magnetic Scattering in YBa2Cu3O7-delta/Ag Interfaces Over a Contact Resistivity Range of 10(-8) - 10(-3) Omega cm(2).
Final rept.
S. C. Sanders, S. E. Russek, C. C. Clickner, and J. W. Ekin. 1994, 3p.
Contract ARPA-7975-01
Sponsored by Advanced Research Projects Agency, Arlington, VA.
Pub. in Applied Physics Letters 65, n17 p2232-2234, 24 Oct 94.

Keywords: *YBCO superconductors, *Electron tunneling, High temperature superconductors, Superconducting films, Electrical resistivity, Boundary layer, Thin films, Interfaces, Silver, Reprints, *Yttrium barium cuprates, Contact resistivity.

We have measured interface transport in thin-film YBa2Cu3O(7-delta)/Ag interfaces having resistivities ranging from 10(exp -8) to 10(exp -3) ohm sq cm. Analysis of the interface I-V data indicates that tunneling is the predominant transport mechanism even for the in situ interfaces having contact resistivities of 1-7 X 10(exp -8) ohm sq cm. Zero-bias conductance peaks are also observed for the entire range of interface resistivity. The similarity of the zero-bias conductance peaks among these widely varying interfaces suggests that the low-temperature interface transport is governed by the same mechanism in each case. These conductance peaks are analyzed in the framework of the Appelbaum-Anderson model for tunneling assisted by magnetic scattering from isolated magnetic spins in the interface.

04,649
PB95-171963 PC A05/MF A01
National Inst. of Standards and Technology (EEEL), Gaithersburg, MD. Electricity Div.
From Superconductivity to Supernovae: The Ginzburg Symposium. Report on the Symposium Held in Honor of Vitaly L. Ginzburg. Held in Gaithersburg, Maryland on May 22, 1992.
A. F. Clark, V. L. Ginzburg, L. P. Gor'kov, V. Z. Kresin, J. D. Kurfess, R. Ramaty, W. A. Little, and K. Kellermann. Nov 94, 79p, NISTIR-5556.

Keywords: *High temperature superconductors, *Gamma ray astronomy, *Meetings, High-Tc superconductors, Electron tunneling, Radio galaxies, Radio sources(Astronomy), Gamma ray observatory, Cosmic rays, Quasars, Cuprates, *Ginzburg symposium.

A one day symposium honoring Professor Vitaly L. Ginzburg and his many contributions to the world of physics was held at the National Institute of Standards and Technology. An additional purpose was to explore future directions for research in the context of his extensive involvement in the rapid developments in physics in the last fifty years. This transcription of the proceedings includes invited talks on some of those recent developments in such fields as superconductivity and astrophysics. Prof. Ginzburg's own address 'What problems of physics and astrophysics seem now to be especially important and interesting' was the focus for discussion on the future directions of physics research. Titles of the other papers given at the symposium are as follows: New Phenomena in Proximity Effect Tunneling in High TC Superconductors; Radio Galaxies, Quasars, and Superluminal Radio Sources; Exotic Properties of High TC Materials and the Ginzburg Parameter; Gamma Ray Astrophysics and Early Results of the Compton Observatory; Some Puzzles of the Normal State of High TC Oxides; Galactic Annihilation Radiation.

04,650
PB95-175089 Not available NTIS
National Inst. of Standards and Technology (EEEL), Boulder, CO. Electromagnetic Technology Div.
Thermal Noise in High-Temperature Superconducting-Normal-Superconducting Step-Edge Josephson Junctions.
Final rept.
S. J. Berkowitz, W. J. Skocpol, P. M. Mankiewich, P. A. Rosenthal, L. R. Vale, R. H. Ono, and N. A. Missert. 1994, 3p.
Pub. in Jnl. of Applied Physics 76, n2 p1337-1339, 15 Jul 94.

Keywords: *Josephson junctions, *Thermal noise, High temperature superconductors, YBCO superconductors, Reprints, Yttrium barium cuprates, RSJ model.

We have fabricated YBa2Cu3O(7-delta)-normal metal-YBa2Cu3O(7-delta) step-edge Josephson junctions that fit the resistively shunted junction model with Johnson-Nyquist thermal noise. The I-V curves are well fit over a large temperature range for junctions of varying critical current values. There is good agreement between the fitted thermal noise temperature and the measured ambient temperature. This is strong evidence that these junctions are not dominated by superconducting shorts longer than the superconducting coherence length.

04,651
PB95-175295 Not available NTIS
National Inst. of Standards and Technology (EEEL), Boulder, CO. Electromagnetic Technology Div.
Thin Film Reaction Kinetics of Niobium/Aluminum Multilayers.
Final rept.
K. R. Coffey, K. Barmak, D. A. Rudman, and S. Foner. 1992, 9p.
Pub. in Jnl. of Applied Physics 72, n4 p1341-1349, 15 Aug 92.

Keywords: *Aluminum alloys, *Niobium alloys, *Phase studies, Transmission electron microscopy, X ray diffraction, Reaction kinetics, Metal films, Thin films, Nucleation, Calorimetry, Superconductors, Reprints, *Niobium aluminides, Multilayers.

Phase formation kinetics in Nb/Al multilayered thin films having overall compositions of 25, 33, 50, and 75 at. % Al have been investigated using scanning calorimetry, x-ray diffraction, and cross-sectional transmission electron microscopy. The first phase to form upon annealing the Nb/Al layered structure of all samples is the NbAl3 intermetallic. Calorimetry clearly identifies the NbAl3 formation to be a two-stage process. The first stage is the formation of a planar layer

by nucleation and growth to coalescence while the second stage is the thickening of the planar layer. The next phase observed in samples of 25 and 33 at. % Al is the A15 superconducting phase, Nb3Al. The Nb3Al growth completes a first reaction stage similar to the NbAl3, but the subsequent thickening reaction stage is not observed without simultaneous Nb2Al growth. The high interface velocities derived from the calorimetry for formation of both NbAl3 and the A15 Nb3Al indicate that atomic transport must be by grain boundary diffusion.

04,652
PB95-175303 Not available NTIS
National Inst. of Standards and Technology (EEEL), Boulder, CO. Electromagnetic Technology Div.
Aspects of a Deformable Superconductor Model for the Vortex Mass.
Final rept.
M. W. Coffey. 1994, 9p.
Pub. in Jnl. of Low Temperature Physics 96, n1/2 p81-89 1994.

Keywords: *Superconductivity, Type 2 superconductors, Mathematical models, Temperature dependence, Critical field, Quasi-particles, Elasticity, Mass, Reprints, Vortex dynamics.

A deformable superconductor model for the vortex mass per unit length mu(sub d) in a type-II superconductor is discussed. A new identity for the inertial vortex mass in this model is presented which holds for an arbitrary quasiparticle fraction when the ionic displacement is irrotational. This result is used to show unphysical behavior in the temperature dependence of the ionic-strain-field vortex mass and is key in resolving this difficulty. A possibility for the experimental observation of the strain field mechanism is discussed.

04,653
PB95-175311 Not available NTIS
National Inst. of Standards and Technology (EEEL), Boulder, CO. Electromagnetic Technology Div.
Deformable Superconductor Model for the Fluxon Mass.
Final rept.
M. W. Coffey. 1994, 4p.
Pub. in Physical Review B 49, p9774-9777, 1 Apr 94.

Keywords: *Superconductivity, Type 2 superconductors, Mathematical models, Quasi-particles, Elasticity, Mass, Reprints, *Fluxons, Vortex dynamics.

Outstanding difficulties in a deformable type-II superconductor model for the fluxon inertial mass per unit length mu(sub d) are resolved. An identity for the inertial mass, valid for an arbitrary quasiparticle fraction when the ionic displacement field is irrotational, plays a critical role in the analysis. This approach avoids previously employed approximations, leading to qualitatively different results, including a fluxon mass which properly vanishes at the transition temperature and which has a greatly reduced magnitude. A framework for the solution of the elasticity equation for an isotropic superconductor is presented and the close relation between mu(sub d) and the ionic strain field is shown.

04,654
PB95-175352 Not available NTIS
National Inst. of Standards and Technology (EEEL), Boulder, CO. Electromagnetic Technology Div.
Increased Pinning Energies and Critical Current Densities in Heavy-Ion-Irradiated Bi2Sr2CaCu2O8 Single Crystals.
Final rept.
J. A. Cutro, D. A. Rudman, T. P. Orlando, A. E. White, E. M. Gyorgy, J. V. Waszczak, R. J. Felder, R. B. van Dover, and L. F. Schneemeyer. 1993, 3p.
Pub. in Applied Physics Letters 62, n7 p759-761, 14 Feb 93.

Keywords: *BSCCO superconductors, *Radiation effects, *Ion irradiation, *Flux pinning, *Critical current, Hydrogen ions 1 plus, Helium ions, Argon ions, Single crystals, Crystal defects, High temperature superconductors, Light ions, Heavy ions, Reprints, *Bismuth strontium calcium cuprates, Flux vortices.

We report a significant increase in the pinning energy of vortices in single-crystal Bi2Sr2CaCu2O8 when irradiated with heavy ions such as Ar(1+). This is in contrast with the results of light ion (H(1+), He(1+)) irradiations which give pinning energies comparable with those of unirradiated crystals. The stronger pinning is attributed to defects larger than point defects, e.g., clusters or amorphized regions. As a result of higher pinning energies, critical currents persist at markedly higher temperatures and fields.

04,655
PB95-175360 Not available NTIS
National Inst. of Standards and Technology (EEEL), Gaithersburg, MD. Semiconductor Electronics Div.
Characterization of the ZnSe/GaAs Interface Layer by TEM and Spectroscopic Ellipsometry.
Final rept.
R. Dahmani, L. Salamanca-Riba, D. P. Beesabathina, B. T. Jonker, N. V. Nguyen, and D. Chandler-Horowitz. 1993, 4p.
Grant NSF-DMR90-20304
Sponsored by National Science Foundation, Washington, DC.
Pub. in Materials Research Society Symposia Proceedings, v280 p271-274 1993.

Keywords: *Zinc selenides, *Gallium arsenides, *Interfaces, Transmission electron microscopy, Molecular beam epitaxy, Transition layers, Thin films, Ellipsometry, Substrates, Reprints.

The interface between ZnSe thin films and GaAs substrates is characterized by High Resolution Transmission Electron Microscopy and room temperature Spectroscopic Ellipsometry. The films were grown on (001) GaAs by Molecular Beam Epitaxy. A three-phase model is used in the reduction of the ellipsometric data, from which the presence of a transition layer of Ga2Se3, with a thickness of less than 1 nm, is confirmed. These results corroborate the high resolution transmission electron microscopy images obtained from the same samples.

04,656
PB95-175378 Not available NTIS
National Inst. of Standards and Technology (EEEL), Gaithersburg, MD. Semiconductor Electronics Div.
Determination of the Optical Constants of ZnSe Films by Spectroscopic Ellipsometry.
Final rept.
R. Dahmani, L. Salamanca-Riba, N. V. Nguyen, D. Chandler-Horowitz, and B. T. Jonker. 1994, 4p.
Grant NSF-DMR90-20304
Sponsored by National Science Foundation, Arlington, VA. and Office of Naval Research, Arlington, VA.
Pub. in Jnl. of Applied Physics 76, n1 p514-517, 1 Jul 94.

Keywords: *Zinc selenides, Molecular beam epitaxy, Semiconducting films, Dielectric properties, Complex numbers, Refractive index, Energy gap, Thin films, Gallium arsenides, Ellipsometry, Substrates, Reprints.

Spectroscopic ellipsometry was used to determine the real and imaginary parts of the dielectric function of ZnSe thin films grown on (001) GaAs substrates by molecular-beam epitaxy, for energies between 1.5 and 5.0 eV. A sum of harmonic oscillators is used to fit the dielectric function in order to determine the values of the threshold energies at the critical points. The fundamental energy gap was determined to be at 2.68 eV. The E(0) + Delta(0) and E(1) points were found to be equal to 3.126 and 4.75 eV, respectively. Below the fundamental absorption edge, a Sellmeir-type function was used to represent the refractive index. At the critical points, E(0) and E(0) + Delta(0), the fitting was improved by using an explicit function combining the contributions of these two points to the dielectric function.

04,657
PB95-175410 Not available NTIS
National Inst. of Standards and Technology (EEEL), Gaithersburg, MD. Electricity Div.
Evidence for Parallel Junctions Within High-Tc Grain-Boundary Junctions.
Final rept.
E. A. Early, R. L. Steiner, A. F. Clark, and K. Char. 1994, 10p.
Pub. in Physical Review B 50, n13 p9409-9418, 1 Oct 94.

Keywords: *Josephson junctions, High temperature superconductors, Alternating current, YBCO superconductors, Grain boundaries, Josephson effect, Parallel orientation, Microwaves, Reprints, Grain boundary junctions, Yttrium barium cuprates.

Half-integral constant voltage steps were observed in many high-T(c) grain-boundary Josephson junctions of YBa2Cu3O(7-delta) when a microwave field was applied. Five distinct observed behaviors of the widths of both integral and half-integral steps as a function of microwave amplitude, Delta I(dc)(I(ac)), are reproduced by simulations of two or three junctions in parallel. This provides quantitative evidence that a single high-T(c) grain-boundary junction is composed of several junctions in parallel. These junctions are formed by the overlap of superconducting filaments on either side of the grain boundary, and the spacing between ones with relatively large critical currents is approximately 20 micrometers.

04,658
PB95-175436 Not available NTIS
National Inst. of Standards and Technology (EEEL), Boulder, CO. Electromagnetic Technology Div.
Thermal Enhancement of Cotunneling in Ultra-Small Tunnel Junctions.
Final rept.
T. M. Eiles, G. Zimmerli, H. D. Jensen, and J. M. Martinis. 1992, 4p.
Contract ONR-N00014-92-F-0003
Sponsored by Office of Naval Research, Arlington, VA.
Pub. in Physical Review Letters 69, n1 p148-151, 6 Jul 92.

Keywords: *Electron tunneling, Tunnel junctions, Reprints, Single electron tunneling, Coulomb blockade, Thermal enhancement.

We have measured the cotunneling current below the Coulomb blockade threshold in a circuit of two ultra-small metallic tunnel junctions. The thermal enhancement of cotunneling, as well as the island-charge dependence, is in excellent agreement with theory. Circuit parameters were measured enabling theoretical and experimental values for the cotunneling current to be compared without adjustable parameters. This comparison yielded agreement within the 15% uncertainty to the experiment. Data showing the cotunneling current near the threshold voltage are also presented.

04,659
PB95-175543 Not available NTIS
National Inst. of Standards and Technology (EEEL), Boulder, CO. Electromagnetic Technology Div.
Standard Reference Devices for High Temperature Superconductor Critical Current Measurements.
Final rept.
L. F. Goodrich, A. N. Srivastava, and T. C. Stauffer. 1993, 7p.
Pub. in Cryogenics 33, n12 p1142-1148 1993.

Keywords: *High temperature superconductors, *Electrical measurement, *Critical current, BSCCO superconductors, High-Tc superconductors, Performance evaluation, Design, Reprints, *Standard reference devices.

Obtaining repeatable critical current measurements for a high temperature superconductor (HTS) is a challenging task, as HTSs are highly susceptible to degradation due to mechanical stress, moisture, thermal cycling and aging. This paper discusses the development of a high temperature superconducting standard reference device (SRD) to address these measurement concerns, and gives preliminary data on its characteristics. An SRD is an HTS specimen that has had its critical current /(c) non-destructively evaluated. Because HTSs are sensitive to mechanical alterations, minor changes in sample preparation or mounting procedure could yield large changes in the measured critical current. Preliminary data on SRDs made using Bi-based oxide tapes (2212) with an Ag substrate are presented. Differences between two consecutive measurements of /(c) can typically change by 40%; these deviations have been reduced to about 4%.

04,660
PB95-175725 Not available NTIS
National Inst. of Standards and Technology (EEEL), Boulder, CO. Electromagnetic Technology Div.
Experimental Aspects of Flux Expulsion in Type-II Superconductors.
Final rept.
O. B. Hyun. 1993, 5p.
Pub. in Physical Review B 48, n2 p1244-1248, 1 Jul 93.

Keywords: *YBCO superconductors, *Niobium stannides, High temperature superconductors, Type 2 superconductors, Temperature dependence, Experimental data, Meissner effect, Magnetic flux, Flux pinning, Magnetization, Diamagnetism, Reprints, *Yttrium barium cuprates.

Experimental aspects of flux expulsion in Nb3Sn and YBa2Cu3O7 type-II superconductors are presented. There is a clear distinction in magnetization between field-cooled measured-upon-cooling (FCC) and field-cooled measured-upon-warming (FCW) results. This thermal hysteresis, predicted in the temperature-dependent critical-state model at low fields by Clem and Hao, was observed for measuring fields up to about 0.5 T. The model explains the observation of increases in diamagnetism after field cooling and thermal cycling. The thermal hysteresis, together with weak links, accounts for the occurrence of a negative peak in FCW magnetization. The FCC-FCW bifurcation observed for a 0.1 mT field down to 5 K might imply that flux lines are not completely frozen below the temperature at which the lower critical field is equal to the measuring field, but are expelled from the sample even in the Meissner state.

04,661
PB95-175840 Not available NTIS
National Inst. of Standards and Technology (EEEL), Gaithersburg, MD. Semiconductor Electronics Div.
Magneto-Transport Properties of HgCdTe.
Final rept.
J. R. Lowney, J. S. Kim, and D. G. Seiler. 1994, 7p.
Pub. in EMIS Data Reviews, p264-270 1994.

Keywords: *Mercury cadmium tellurides, Shubnikov-de Haas effect, Hall effect, Magnetoresistivity, Reprints.

Magnetotransport techniques are widely used to characterize the electrical properties of HgCdTe. The Hall-effect method is the most common method of determining the carrier density and mobility of semiconductor materials. Multicarrier characterization techniques are needed for determination of carrier densities and mobilities in a multicarrier system present in layered-structures or in a variety of complex semiconductor materials. Because of the importance of these methods for proper electrical characterization of complex HgCdTe single crystals or layered-structures, we discuss this topic pedagogically with the primary objective of promulgation of this emerging tool to the HgCdTe characterization community. We also discuss magnetoresistance and magnetoresistance-based techniques such as the Shubnikov-de Haas effect and magnetophonon effect, which have been used to characterize HgCdTe materials. These techniques are capable of providing very accurate data if applied with care and proper analysis.

04,662
PB95-175865 Not available NTIS
National Inst. of Standards and Technology (EEEL), Boulder, CO. Electromagnetic Technology Div.
Effect in Environmental Noise on the Accuracy of Coulomb-Blockade Devices.
Final rept.
1993, 4p.
Contract ONR-N00014-92-F-0003
Sponsored by Office of Naval Research, Arlington, VA.
Pub. in Physical Review B 48, n24 p18 316-18 319, 15 Dec 93.

Keywords: Electron tunneling, Thermal noise, Performance, Accuracy, Reprints, *Coulomb blockade, Electron pumps.

We calculate how noise generated by a finite environmental impedance limits the ultimate performance of Coulomb-blockade devices and possible current or charge standards. We have expressed the environmental theory of the Coulomb blockade in terms of the spectral density of the voltage noise arising from the environment, and have calculated the resulting single-junction tunneling, and two-junction cotunneling rates. These rates are used to predict the tunneling rate of electrons through a five-junction pump and may explain the anomalously large rates that are observed experimentally.

04,663
PB95-175873 Not available NTIS
National Inst. of Standards and Technology (EEEL), Boulder, CO. Electromagnetic Technology Div.
Testing for Metrological Accuracy of the Electron Pump.
Final rept.
J. M. Martinis, M. Nahum, and H. D. Jensen. 1994, 2p.
Contract ONR-N00014-92-F-0003
Sponsored by Office of Naval Research, Arlington, VA.
Pub. in Physica B 194-196, p1045-1046 1994.

Keywords: Metrology, Accuracy, Tests, Reprints, *Electron pumps, Single electron tunneling, Coulomb blockage.

We have measured the electron leakage rate through a 5 junction electron pump. Our observed rate of about 0.3 e/s is several orders of magnitude larger than predicted by thermal activation or cotunneling rates. Our results may be explained by the environmental theory of the Coulomb blockade where noise from the environment causes photon assisted tunneling.

04,664
PB95-175931 Not available NTIS
National Inst. of Standards and Technology (EEEL), Boulder, CO. Electromagnetic Technology Div.
Numerical Micromagnetic Techniques and Their Applications to Magnetic Force Microscopy Calculations.
Final rept.
J. O. Oti. 1993, 6p.
Pub. in Institute of Electrical and Electronics Engineers Transactions on Magnetics 29, n6 p2359-2364 Nov 93.

Keywords: Exchange interactions, Magnetic anisotropy, Magnetic films, Numerical solution, Magnetostatics, Thin films, Reviews, Reprints, *Micromagnetics, Magnetic force microscopy.

Numerical micromagnetics is a flexible and powerful means of designing and characterizing magnetic devices. This paper presents an overview of numerical methods of solution of micromagnetics problems. The modeling of exchange, anisotropy and magnetostatic interaction fields in magnetic films, and micromagnetic modeling of magnetic force microscopy are discussed.

04,665
PB95-176061 Not available NTIS
National Inst. of Standards and Technology (EEEL), Boulder, CO. Electromagnetic Technology Div.
dc Magnetic Force Microscopy Imaging of Thin-Film Recording Head.
Final rept.
P. Rice, J. Moreland, and A. Wadas. 1994, 3p.
Pub. in Jnl. of Applied Physics 75, n10 p6878-6800, 15 May 94.

Keywords: *Recording heads, *Imaging techniques, Atomic force microscopy, Magnetic fields, Magnetic films, Thin films, Direct current, Tips, Reprints, Magnetic force microscopy, Surface topography.

Using a new form of magnetic force microscope (dc MFM), magnetic force images of a thin-film recording head have been made. Using dc MFM, atomic force microscope images are presented of the surface topography and magnetic forces taken simultaneously, allowing direct correlation of magnetic fields to the pole pieces. Magnetic force images of the head at typical head-to-disk spacings are presented. The tips used for these images had two different magnetic coatings.

04,666
PB95-176079 Not available NTIS
National Inst. of Standards and Technology (EEEL), Boulder, CO. Electromagnetic Technology Div.
High Temperature Superconductor-Normal Metal-Superconductor Josephson Junctions with High Characteristic Voltages.
Final rept.
P. A. Rosenthal, E. N. Grossman, R. H. Ono, and L. R. Vale. 1993, 3p.
Pub. in Applied Physics Letters 63, n14 p1984-1986, 4 Oct 93.

Keywords: *Josephson junctions, High temperature superconductors, Superconducting films, Submillimeter waves, Far infrared radiation, YBCO superconductors, Epitaxy, Reprints, Yttrium barium cuprates.

We have fabricated step edge superconductor-normal metal-superconductor microbridges using YBa2Cu3O(7-x) (YBCO) and noble metals with critical current-normal resistance (I(c)R(N)) products as high as 10 mV and normal resistances up to 38 ohms. Our fabrication process achieves high values of the I(c)R(N) product by exploiting the anisotropy in the properties of epitaxial YBCO films, allowing contact only between normal metal and superconductor through the crystalline axes which support the largest Josephson coupling. This results in a dramatic increase in the normal resistance of a junction without decreasing its critical current. We discuss the role of the superconductor-normal metal boundary resistance on the junction electrical properties. We have coupled submillimeter wave rf currents quasioptically into junctions integrated at the feeds of noble metal planar log periodic antennas and have induced up to 7 Shapiro steps in the current-voltage characteristics with a 760 GHz beam from a far infrared laser.

04,667
PB95-176095 Not available NTIS
National Inst. of Standards and Technology (EEEL), Boulder, CO. Electromagnetic Technology Div.
Surface Degradation of Superconducting YBa2Cu3O7-delta Thin Films.
Final rept.
S. E. Russek, S. C. Sanders, A. Roshko, and J. W. Ekin. 1994, 3p.
Contract ARPA-7975-01
Sponsored by Advanced Research Projects Agency, Arlington, VA.
Pub. in Applied Physics Letters 64, n26 p3649-3651, 27 Jun 94.

Keywords: *YBCO superconductors, *Superconducting films, *Surface reactions, *Contact resistance, High temperature superconductors, Scanning tunneling microscopy, Electron diffraction, Time dependence, Amorphous state, Surface layers, Thin films, Carbon dioxide, Vacuum, Nitrogen, Oxygen, Air, Reprints, *Yttrium barium cuprates, Surface degradation.

The surface degradation of c-axis oriented YBa2Cu3O(7-delta) thin films due to air, CO2, N2, O2, and vacuum exposure has been studied with reflection high-energy electron diffraction (RHEED), scanning tunneling microscopy, and contact resistivity measurements. The formation of an amorphous surface reaction layer upon exposure to air and CO2 is monitored with RHEED and correlated with an increase in contact resistivity. The contact resistivity of samples exposed to air increases with time. Surfaces exposed to CO2 show a similar degradation while surfaces exposed to N2 showed a slightly different degradation mechanism. Vacuum exposed surfaces show little increase in contact resistivity, indicating no long-term surface oxygen loss.

04,668
PB95-176129 Not available NTIS
National Inst. of Standards and Technology (BFRL), Gaithersburg, MD. Building Materials Div.
Transport and Diffusion in Three-Dimensional Composite Media.
Final rept.
L. M. Schwartz, F. Auzerais, J. Dunsmuir, S. Torquato, N. Martys, and D. P. Bentz. 1994, 9p.
Pub. in Physica A 207, p28-36 1994.

Keywords: *Diffusion, *Transport properties, *Porous materials, Permeability, Three dimensional models, Grain boundaries, Nuclear magnetic resonance, Porosity, Microstructure, Fluid flow, Reprints, *X ray microtomography.

We will review recent progress in our understanding of classical transport in porous media. Theoretical concepts will be illustrated with two distinct kinds of calculations. The first involve the grain consolidation model and are based on a particular multisize packing of spherical grains. The computational methods developed here are sufficiently accurate that we propose to combine them with direct measurements of the pore and grain geometry based on X-ray microtomography. Our preliminary results indicate that this approach may well play an important part in future studies of transport in porous media.

04,669
PB95-176210 Not available NTIS
National Inst. of Standards and Technology (EEEL), Boulder, CO. Electromagnetic Technology Div.
Magnetic Force Microscopy Images of Magnetic Garnet with Thin-Film Magnetic Tip.
Final rept.
A. Wadas, J. Moreland, P. Rice, and R. Katti. 1994, 3p.
Pub. in Applied Physics Letters 64, n9 p1156-1158, 28 Feb 94.

Keywords: *Ferrite garnets, *Magnetic domains, *Imaging techniques, Atomic force microscopy, Magnetic films, High resolution, Silicon nitrides, Substrates, Thin films, Tips, Reprints, Magnetic force microscopy, Surface topography.

We present magnetic force microscopy images of YGdTmGa/YSmTmGa magnetic garnet, using a thin

magnetic film deposited on Si3N5 atomic force microscopy tips. We have found correlations between the topography and the magnetic domain structure. We show that by using either magnetized Fe-Ni bilayer tips versus unmagnetized single layer Fe tips that the image contrast shows domains versus domain walls, respectively.

04,670
PB95-176327 Not available NTIS
National Inst. of Standards and Technology (EEEL), Boulder, CO. Electromagnetic Technology Div.
Noise in the Coulomb Blockade Electrometer.
Final rept.
G. Zimmerli, T. M. Eiles, R. L. Kautz, and J. M. Martinis. 1992, 3p.
Contract ONR-N00014-92-F-0003
Sponsored by Office of Naval Research, Arlington, VA.
Pub. in Applied Physics Letters 61, n2 p237-239, 13 Jul 92.

Keywords: *Electrometers, Tunnel junctions, Shot noise, Reprints, *Coulomb blockade electrometers, Single electron tunneling, Quantum noise.

We have measured the noise of a Coulomb blockade electrometer. Below 100 Hz, the noise referred to the input charge has a 1/f power spectrum with a charge noise of 3 X 10(exp -4) e/Hz(sup 1/2) and an energy sensitivity E(N) of 3 X 10(exp 4)(Planck's constant) at 10 Hz. The 1/f noise probably results from the stochastic occupation of charge traps which could in principle be eliminated. The theoretical noise floor is set by shot noise, and indirect measurements show that this contribution to E(N) can be as small as 1.5 (Planck's constant), suggesting that the electrometer will be a quantum limited amplifier if the 1/f noise can be eliminated.

04,671
PB95-176335 Not available NTIS
National Inst. of Standards and Technology (EEEL), Boulder, CO. Electromagnetic Technology Div.
Voltage Gain in the Single-Electron Transistor.
Final rept.
G. Zimmerli, R. L. Kautz, and J. M. Martinis. 1992, 3p.
Contract ONR-N00014-92-F-0003
Sponsored by Office of Naval Research, Arlington, VA.
Pub. in Applied Physics Letters 61, n2 p2616-2618, 23 Nov 92.

Keywords: Tunnel junctions, Voltage gain, Electrometers, Reprints, *Single electron transistors, Single electron tunneling, Coulomb blockade.

We report the first observation of voltage gain in the capacitively coupled single-electron transistor (SET). Using parallel-plate and interdigital geometries for the gate capacitor (C(g) = 1.2 and 0.4 fF) and ultrasmall tunnel junctions with capacitances near 0.2 fF, we find maximum voltage gains of 2.8 and 1.5, respectively. The leakage resistance of the gate is of the order 10(exp 12) ohms for the parallel-plate capacitor and greater than 10(exp 18) ohms for the interdigital capacitor.

04,672
PB95-180071 Not available NTIS
National Inst. of Standards and Technology (EEEL), Boulder, CO. Electromagnetic Technology Div.
Increased Transition Temperature in In situ Coevaporated YBa2Cu3O7-delta Thin Films by Low Temperature Post-Annealing.
Final rept.
S. J. Berkowitz, E. De Obaldia, K. F. Ludwig, R. H. Ono, J. A. Beall, L. R. Vale, D. A. Rudman, M. L. O'Malley, L. M. Drabeck, P. A. Polakos, W. J. Skocpol, and P. M. Mankiewich. 1994, 3p.
Pub. in Applied Physics Letters 65, n12 p1587-1589, 19 Sep 94.

Keywords: *YBCO superconductors, *Superconducting films, High-Tc superconductors, Transition temperature, Thin films, Annealing, Strains, Reprints, *Yttrium barium cuprates.

In situ coevaporated YBa2Cu3O(7-delta) thin films have a slightly depressed transition temperature T(c), though they have excellent radio-frequency surface resistance characteristics. These films consistently have less orthorhombic strain than laser ablated or post-annealed films. Low temperature (320-420 C) post-annealing of in situ coevaporated films in 100 kPa of O2 raised T(c) to values as high as 91.5 K with some increase in the orthorhombic strain. All measured thin films show less variation of T(c) with orthorhombic strain than does bulk material.

04,673
PB95-180170 Not available NTIS
National Inst. of Standards and Technology (EEEL), Boulder, CO. Electromagnetic Technology Div.
Crossover in the Pinning Mechanism of Anisotropic Fluxon Cores.
Final rept.
L. D. Cooley, A. Gurevich, and D. C. Larbalestier. 1994, 4p.
Sponsored by Department of Energy, Washington, DC.
Pub. in Proceedings of International Workshop on Critical Currents in Superconductors (7th), Alpbach, Austria, January 24-27, 1994, p573-576.

Keywords: *Flux pinning, *Superconductors, Josephson effect, Crystal defects, Anisotropy, Reprints, Fluxons.

We propose that thin planar defects have a strong magnetic flux-pinning force. Magnetic pinning results from the anisotropic nature of a fluxon when the core is situated in the plane of the defect, and is a consequence of nonlocal Josephson electrodynamics. Since the magnetic pinning force approaches the maximum core-pinning force, a crossover from core pinning to magnetic pinning is predicted when the proximity coupling becomes strong. This model is supported by flux-pinning measurements of an artificial pinning center superconductor.

04,674
PB95-180188 Not available NTIS
National Inst. of Standards and Technology (EEEL), Boulder, CO. Electromagnetic Technology Div.
Size and Self-Field Effects in Giant Magnetoresistive Thin-Film Devices.
Final rept.
R. W. Cross, S. E. Russek, S. C. Sanders, S. A. Hossian, M. R. Parker, and J. A. Barnard. 1994, 3p.
Pub. in Institute of Electrical and Electronics Engineers Transactions on Magnetics 30, n6 p3825-3827 Nov 94.

Keywords: *Magnetic devices, *Magnetoresistance, Sizes(Dimensions), Magnetic films, Metal films, Thin films, Magnetization, Cobalt alloys, Iron alloys, Nickel alloys, Copper, Silver, Reprints, Magnetic multilayers.

Giant magnetoresistance (GMR) was measured as a function of device size for patterned NiCoFe/Cu and NiFe/Ag films. For the quasi-granular NiCoFe/Cu films, the normalized maximum change in resistivity (Delta)rho/rho was 8% for most of the samples. For the NiFe/Ag films, antiparallel alignment was achieved through magnetostatic coupling, not exchange fields, with a (Delta)rho/rho of 4.5%. The films were patterned into stripes with Au current leads for size-effect measurements. The height of the stripes varied from 0.5 to 16 micrometers and the track width varied from 1 to 16 micrometers. Discrete switching events and anomalous low-field dips in the response were observed for both materials for small device sizes.

04,675
PB95-180204 Not available NTIS
National Inst. of Standards and Technology (EEEL), Boulder, CO. Electromagnetic Technology Div.
Novel Bulk Iron Garnets for Magneto-Optic Magnetic Field Sensing.
Final rept.
M. N. Deeter, S. Milian Bon, G. W. Day, G. Diercks, and S. Samuelson. 1994, 3p.
Pub. in Institute of Electrical and Electronics Engineers Transactions on Magnetics 30, n6 p4464-4466 Nov 94.

Keywords: *Ferrite garnets, Yttrium iron garnets, Bismuth additions, Gallium additions, Faraday effect, Frequency response, Response functions, Magneto-optics, Substitutes, Sensitivity, Reprints, *Magnetic field sensors.

We report measurements of the magneto-optic response function and frequency response for three bulk iron garnet crystals grown by a flux technique. The samples were the product of an intensive effort to develop iron garnet compositions with properties specifically optimized for magnetic field sensing. Sensitivity enhancement was achieved through both bismuth substitution (for increasing the saturation Faraday rotation) and gallium substitution (for reducing the saturation magnetization). Frequency response measurements indicate that bismuth substitution actually improves performance (compared to unsubstituted yttrium iron garnet) in contrast with gallium, which causes substantial degradation.

04,676
PB95-180220 Not available NTIS
National Inst. of Standards and Technology (CSTL), Gaithersburg, MD. Surface and Microanalysis Science Div.
X-ray Photoelectron and Auger Electron Forward Scattering: A Structural Diagnostic for Epitaxial Thin Films.
Final rept.
W. F. Egelhoff. 1994, 83p.
See also PB91-112136 and PB91-112136.
Pub. in Ultrathin Magnetic Structures I: An Introduction to Electronic, Magnetic, and Structural Properties, Chapter 5.2, p220-302 1994.

Keywords: *X ray photoelectron spectroscopy, *Auger electron spectroscopy, *Magnetic films, *Forward scattering, *Epitaxial growth, Electron-atom collisions, EV range 100-1000, Electron scattering, Stacking faults, Magnetism, Quantum mechanics, Thin films, Reviews, Reprints.

The technique of X-ray photoelectron and Auger electron forward scattering has developed in the past few years into one of the most valuable structural diagnostics for investigating the early stages of epitaxial thin-film growth. A review is given here of this technique with special emphasis on its application to epitaxial films of interest to the thin-film magnetism community. The aim of this review is to provide an easily readable, self-contained account directed primarily at experimentalists, with the hope of making forward scattering accessible to new or occasional users. Some familiarity with XPS and Auger spectroscopy is assumed, as is an elementary knowledge of quantum mechanics.

04,677
PB95-180253 Not available NTIS
National Inst. of Standards and Technology (MSEL), Gaithersburg, MD. Materials Reliability Div.
Magnetic Susceptibility of Pr2-xCexCuO4 Monocrystals and Polycrystals.
Final rept.
M. Foldeaki, H. Ledbetter, and Y. Hidaka. 1994, 8p.
See also PB92-175264.
Pub. in Jnl. of Magnetism and Magnetic Materials 138, p139-146 1994.

Keywords: *Magnetic susceptibility, *Superconductors, Temperature dependence, Crystal field, Single crystals, Polycrystals, Magnetic moments, Reprints, *Praseodymium cerium cuprates.

We measured the temperature dependence of the magnetic susceptibility of Pr(2-x)Ce(x)CuO4 monocrystals and polycrystals in the composition range x = 0-0.18. For all compositions, the susceptibility curves reveal strong crystal-field effects and are evaluated in terms of Van Vleck's equation for magnetic susceptibility. At temperatures above 100 K, the behavior could be described by a Curie-Weiss-like equation, the parameters of which allow us to characterize the crystal-field interactions. The concentration dependence of these parameters is much stronger in the monocrystals, with the apparent magnetic moment going through a sharp maximum near x = 0.1, the composition of the onset of superconductivity after a reducing anneal. The concentration dependence of the magnetic moment can be qualitatively interpreted as a contribution of charge-carrying spins in localized states, mainly through initiating Cu(2+)-Pr(3+) interactions. With increasing Ce, these additional spins can not remain localized, thus the magnetic moment decreases, and a reducing anneal results in superconductivity.

04,678
PB95-180287 Not available NTIS
National Inst. of Standards and Technology (MSEL), Gaithersburg, MD. Reactor Radiation Div.
Crystal Structure and Magnetic Properties of CuGeO3.
Final rept.
M. Green, M. Kurmoo, J. Stalick, and P. Day. 1994, 2p.
Pub. in Jnl. of the Chemical Society, Chemical Communications, p1995-1996 1994.

Keywords: *Crystal structure, Temperature range 0000-0013 K, Temperature range 0013-0065 K, Room temperature, Magnetic susceptibility, Magnetic properties, Neutron diffraction, Reprints, *Copper germanates, Rietveld method.

The crystal structure of CuGeO3, which has been reported to undergo a spin-Peierls transition at 14 K, is

determined by neutron powder diffraction at 300, 20 and 4.2 K and the structure refined in the space group Pmma at all three temperatures, ie without displacement of the Cu atoms from a uniform one-dimensional chain; anisotropic broadening of (h0l) reflections, observed in all three data sets, is successfully modeled by an orthorhombic micro-strain along a and c, i.e. perpendicular to Cu-Cu chains. Below 10 K the magnetic susceptibility fits very well to the Bulaevskii model, indicating a ratio of 0.69 between the Cu-Cu exchange constants in the dimerised chain and a mean exchange constant of 88 K.

04,679
PB95-180303 Not available NTIS
National Inst. of Standards and Technology (MSEL), Gaithersburg, MD. Reactor Radiation Div.
Observation of Oscillatory Magnetic Order in the Antiferromagnetic Superconductor HoNi2B2C.
Final rept.
T. E. Grigereit, J. W. Lynn, Q. Huang, J. J. Krajewski, W. F. Peck, A. Santoro, and R. J. Cava. 1994, 4p.
Grant NSF-DMR93-02380
Sponsored by National Science Foundation, Arlington, VA.
Pub. in Physical Review Letters 73, n20 p2756-2759, 14 Nov 94.

Keywords: *Superconductors, Temperature range 0000-0013 K, Phase transformations, Antiferromagnetic materials, Neutron scattering, Oscillations, Reprints, *Holmium nickel boron carbides, *Magnetic ordering.

The nature of the holmium order in the reentrant superconductor (T(c) = 7.5 K) HoNi2B2C is revealed by neutron scattering. Upon cooling, a transversely polarized oscillatory magnetic state is formed (T(M) approx = 8 K), characterized by a wave vector (0,0,Q(c)) where Q(c) approx = 0.05/A is only weakly dependent on temperature and field. At the reentrant superconducting transition (about 5 K), the amplitude of the oscillatory state abruptly decreases in favor of a commensurate antiferromagnet, whereby superconductivity is restored and coexists with antiferromagnetism at low temperatures.

04,680
PB95-180345 Not available NTIS
National Inst. of Standards and Technology (CAML), Gaithersburg, MD. Applied and Computational Mathematics Div.
Analytical Expressions for Barkhausen Jump Size Distributions.
Final rept.
F. Y. Hunt, and R. D. McMichael. 1994, 3p.
Pub. in Institute of Electrical and Electronics Engineers Transactions on Magnetics 30, n6 p4356-4358 Nov 94.

Keywords: *Barkhausen effect, Langevin equation, Markov chains, Random walk, Bessel functions, Reprints.

In previous calculations of Barkhausen jump size distributions, the Langevin equation was used to describe the pinning field h(c). In this paper, h(c) is modeled by discretized random walks which are used to obtain analytical expressions for the Barkhausen jump size distribution, P(tau). For a bounded random walk which reduces to the Langevin function in the continuum limit, P(tau) is a sum of exponentials which is compared to functions of the form P(tau) = tau(sup -alpha)exp(-tau/tau(0)). The scaling exponent changes from alpha approx = 1.5 for small jumps to alpha approx = 1.0 for jumps larger than the correlation length. For an unbounded random walk with exponentially distributed distances between steps in h(c), P(tau) is shown to be proportional to a modified Bessel function which, for long jumps, is asymptotically a pure power law, tau(exp -3/2). This suggests that the scaling exponent shift and the exponential cutoff are caused by correlations in h(c).

04,681
PB95-180402 Not available NTIS
National Inst. of Standards and Technology (EEEL), Boulder, CO. Electromagnetic Technology Div.
Quasipotential and the Stability of Phase Lock in Nonhysteretic Josephson Junctions.
Final rept.
R. L. Kautz. 1994, 7p.
Sponsored by Army Test Measurements and Diagnostic Equipment Activity, Redstone Arsenal, AL.
Pub. in Jnl. of Applied Physics 76, n9 p5538-5544, 1 Nov 94.

Keywords: *Josephson junctions, Josephson effect, Activation energy, Phase locked systems, Thermal noise, Stability, Reprints, Voltage standards, Johnson noise, State space, Quasipotentials.

The principle of minimum available noise energy is used to calculate the quasipotential over the state space of a nonhysteretic Josephson junction driven by a rf bias. This potential surface provides an intuitive picture of the dynamics of phase lock and defines a stability parameter, the activation energy for thermally induced phase slippage, which determines the optimum operating conditions for a proposed programmable voltage standard.

04,682
PB95-180410 Not available NTIS
National Inst. of Standards and Technology (EEEL), Boulder, CO. Electromagnetic Technology Div.
Large-Amplitude Shapiro Steps and Self-Field Effects in High-Tc Josephson Weak Links.
Final rept.
R. L. Kautz, S. P. Benz, and C. D. Reintsema. 1994, 3p.
Sponsored by Army Test Measurements and Diagnostic Equipment Activity, Redstone Arsenal, AL.
Pub. in Applied Physics Letters 65, n11 p1445-1447 Sep 94.

Keywords: *Josephson junctions, High-Tc superconductors, Temperature range 0013-0065 K, YBCO superconductors, Reprints, *Shapiro steps, Yttrium barium cuprates, Voltage standards, Weak links.

We determine contiguous Shapiro steps of orders 0 and 1 having amplitudes of 1 mA in a YBa2Cu3O(7-delta) step-edge junction operated at 38 K. A wide-junction model that includes self-field effects explains why the observed step amplitudes are smaller than expected from the resistively shunted point-junction model. In spite of their reduced amplitudes, the observed steps are suitable for use in a proposed rapidly programmable Josephson voltage standard.

04,683
PB95-180493 Not available NTIS
National Inst. of Standards and Technology (MSEL), Gaithersburg, MD. Materials Reliability Div.
Dependence of Tc on Debye Temperature Theta(sub D) for Various Cuprates.
Final rept.
H. Ledbetter. 1994, 2p.
Pub. in Physica C 235-240, p1325-1326 1994.

Keywords: *High-Tc superconductors, *Critical temperature, *Debye temperature, Temperature dependence, Mercury inorganic compounds, YBCO superconductors, BSCCO superconductors, Electron phonon interactions, Reprints, Thallium barium calcium cuprates, Lanthanum cuprates.

The author extends the T(c)-Theta(D) relationship established by Ledbetter and coworkers for La-O and Y-O, and by Dominec for Bi-O, to include Tl-O and Hg-O compounds. In BCS-McMillan materials, Theta(D) occurs both in the pre-exponential factor in the expression T(c) approx = Theta(D) exp (-1/lambda) and in McMillan's expression for the electron-phonon parameter lambda = C/M < omega squared > , where < omega > approx Theta(D). In BCS materials, T(c) increases with decreasing Theta(D), that is with lattice softening. In all five cuprate superconductors listed above, the opposite occurs: T(c) increases with lattice stiffening. From these results, the author draws two principal conclusions. First, T(c) depends on phonons because it depends on Theta(D), the quintessential phonon parameter. Second, the T(c)-Theta(D) relationship for high-T(c) oxide superconductors differs dramatically from that for conventional BCS materials.

04,684
PB95-180527 Not available NTIS
National Inst. of Standards and Technology (MSEL), Gaithersburg, MD. Materials Reliability Div.
Elastic Constants of a Material with Orthorhombic Symmetry: An Alternative Measurement Approach.
Final rept.
M. Lei, H. Ledbetter, and Y. Xie. 1994, 4p.
Pub. in Jnl. of Applied Physics 76, n5 p2738-2741, 1 Sep 94.

Keywords: *Elastic properties, Fiber reinforced composites, Orthorhombic lattices, Ultrasonic radiation, Measurement, Anisotropy, Reprints.

An alternative approach to measuring the complete anisotropic elastic constants C(ij)(S(ij)) of an orthorhombic-symmetry material is proposed. This approach requires measurements along only principal directions: 100. In this approach, a pulse-echo (megahertz-frequency) method was used to measure C(11), C(22), C(33), C(44), C(55), and C(66). A resonance (kilohertz-frequency) method was used to measure three elastic compliances: S(11), S(22), and S(33). Combining the C(ii) with the S(ii), the complete sets of C(ij) and S(ij) were obtained. This approach avoids the troublesome, error-prone determination of off-diagonal C(ij) (S(ij)) by the usual measurements along nonprincipal directions. The approach was applied to a boron-aluminum composite where the off-diagonal terms remain uncertain. In principle, the approach applies to any orthorhombic-symmetry material.

04,685
PB95-180659 Not available NTIS
National Inst. of Standards and Technology (PL), Gaithersburg, MD. Electron and Optical Physics Div.
Laser Focused Atomic Deposition.
Final rept.
J. J. McClelland, R. E. Scholten, R. Gupta, and R. J. Celotta. 1994, 4p.
Pub. in Proceedings of Society of Photo-Optical Instrumentation Engineers: Laser Techniques for Surface Science, Los Angeles, CA., January 27-29, 1994, v2125 p324-327.

Keywords: *Photon-atom interactions, Vapor deposition, Standing waves, Surface layers, Laser beams, Lithography, Arrays, Reprints, *Laser focusing, *Nanostructures, Chromium atoms, Silicon substrates, Atom optics, Microfabrication.

We have demonstrated the use of a standing-wave laser beam to focus chromium atoms as they deposit onto a silicon surface. A permanent array of Cr lines has been fabricated, with line width 65 nm, spacing 213 nm, and height 34 nm. The array covers an area of 0.4 mm x 1 mm, and was deposited in approximately 10 minutes. The lines made in this way constitute a proof-of-principle of an entirely new approach to nanostructure fabrication, with potential for extremely small feature size coupled with massive parallelism.

04,686
PB95-180717 Not available NTIS
National Inst. of Standards and Technology (MSEL), Gaithersburg, MD. Reactor Radiation Div.
Magnetic Properties of Single-Crystalline UCu3Al2.
Final rept.
H. Nakotte, E. Bruck, J. H. V. J. Brabers, V. Sechovsky, K. H. J. Buschow, A. V. Andreev, R. A. Robinson, A. Purwanto, J. W. Lynn, K. Prokes, and F. R. de Boer. 1994, 3p.
See also DE93016607.
Pub. in Institute of Electrical and Electronics Engineers Transactions on Magnetics 30, n2 p1217-1219 Mar 94.

Keywords: Temperature range 0000-0013 K, Aluminum intermetallics, Hexagonal lattices, Magnetic susceptibility, Neutron diffraction, Temperature dependence, Single crystals, Magnetic fields, Reprints, *Uranium copper aluminides, Copper intermetallics, Uranium intermetallics, Powder patterns.

UCu3Al2 crystallizes in an ordered variant of the hexagonal CaCu5 structure. By neutron powder-diffraction, the U atoms were found to occupy the 1a sites, while the 2c sites are occupied by Cu atoms only and a random occupation of the 3g sites by the remaining Cu and Al is found. The magnetic susceptibility, measured on a single crystal grown by the Czochralski tri-arc technique, is found to be maximal within the hexagonal basal plane with a maximum at about 10 K. For fields applied within the basal plane, the magnetization at 4.2 K exhibits a slight S-shape starting slightly below 15 T. No such anomalies are found for fields applied along the c-axis where the magnetic response is found to be much lower. No additional magnetic peaks, which could be related with long-range antiferromagnetic ordering, were detected in the neutron powder-patterns at low temperatures.

04,687
PB95-180725 Not available NTIS
National Inst. of Standards and Technology (EEEL), Boulder, CO. Electromagnetic Technology Div.
Epitaxial Growth and Characterization of the Ordered Vacancy Compound CuIn3Se5 on GaAs (100) Fabricated by Molecular Beam Epitaxy.
Final rept.
A. J. Nelson, M. Bode, G. Horner, K. Sinha, and J. Moreland. 1994, 5p.
Pub. in Materials Research Society Symposia Proceedings, v340 p599-603 1994.

Keywords: *Epitaxial growth, Molecular beam epitaxy, Transmission electron microscopy, Atomic force microscopy, X ray diffraction, Raman spectra, Gallium arsenides, Single crystals, Stacking faults, Energy gap, Photoluminescence, Substrates, Films, Reprints, *Copper indium selenides.

Epitaxial growth of the ordered vacancy compound (OVC) CuIn3Se5 has been achieved on GaAs (100) by molecular beam expitaxy (MBE) from Cu2Se and In2Se3 sources. Electron probe microanalysis and X-ray diffraction have confirmed the composition for the 1-3-5 OVC phase and that the film is single crystal CuIn3Se5 (100). Transmission electron microscopy (TEM) characterization of the material also showed it to be single crystalline. Structural defects in the layer consisted mainly of stacking faults. Photoluminescence (PL) measurements performed at 7.5 K indicate that the bandgap is 1.28 eV. Raman spectra reveal a strong polarized peak at 152/cm, which is believed to arise from the totally symmetric vibration of the Se atoms in the lattice. Atomic force microscopy reveals faceting in a preferred (100) orientation.

04,688
PB95-180881 Not available NTIS
National Inst. of Standards and Technology (MSEL), Gaithersburg, MD. Reactor Radiation Div.
High Resolution Inelastic Neutron Scattering Study of Phonon Self-Energy Effects in YBCO.
Final rept.
D. Reznik, B. Keimer, F. Dogan, and I. A. Aksay. 1994, 2p.
Pub. in Physica C 235-240, p1733-1734 1994.

Keywords: *YBCO superconductors, *Phonons, Temperature range 0013-0065 K, Temperature range 0065-0273 K, High resolution, Neutron scattering, Inelastic scattering, High-Tc superconductors, Self-energy, Single crystals, Reprints, *Yttrium barium cuprates.

We report preliminary results of the high resolution inelastic neutron scattering measurements of the 42.5 meV optical phonon branch in YBCO, whose behavior at momentum transfer q=0 has been extensively studied by Raman scattering. The experiment was done on a large (75g) single crystal of YBa2Cu3O(7-x) (T(c) approx = 90K) with the resolution of 2 meV (full width at half maximum). In cooling from 100K to 50K, we observe a small softening of the phonon energy at q=0.25, 0.25, 0, but no significant linewidth change.

04,689
PB95-180980 Not available NTIS
National Inst. of Standards and Technology (EEEL), Boulder, CO. Electromagnetic Technology Div.
Scanning Tunneling Microscopy of the Charge-Density-Wave Structure in 1T-TaS2.
Final rept.
R. E. Thomson, B. Burk, A. Zettl, and J. Clarke. 1994, 18p.
Contract DE-AC03-76F00098, Grant NSF-DMR90-17254
Sponsored by Department of Energy, Washington, DC., Office of Naval Research, Arlington, VA., and National Science Foundation, Arlington, VA.
Pub. in Physical Review B 49, n24 p16 899-16 916, 15 Jun 94.

Keywords: *Tantalum sulfides, Temperature range 0065-0273 K, Temperature range 0273-0400 K, Scanning tunneling microscopy, Fourier transformation, Domain structure, Reprints.

Using scanning tunneling microscopy (STM), we studied 1T-TaS2 in all four of its charge-density-wave (CDW) supporting phases over the temperature range 360-143 K. Special attention was given to the search for discommensurate structures and the distinguishing of true CDW discommensurations and domains from apparent discommensurations and domains formed by interference between the CDW and the atomic lattice. In the lowest-temperature commensurate (C) phase, we find that the CDW is in the commensurate configuration as expected. In the nearly commensurate (NC) phase, the CDW is in a true domain structure as evidenced by satellite spots in the Fourier transforms of the STM images. In the triclinic (T) phase, the STM data indicate that the CDW is in a striped domain phase, which is significantly different from the domain model previously proposed. Finally, in the high-temperature incommensurate (I) phase, we find unexpected satellite spots in the STM Fourier transforms, suggesting that a CDW modulation is also present in this phase.

04,690
PB95-181186 Not available NTIS
National Inst. of Standards and Technology (EEEL), Boulder, CO. Electromagnetic Technology Div.
Novel YBa2Cu3O7-x and YBa2Cu3O7-x/Y4Ba3O9 Multilayer Films by Bias-Masked 'On-Axis' Magnetron Sputtering.
Final rept.
J. H. Xu, G. G. Zheng, A. M. Grishin, J. Moreland, B. M. Moon, and K. V. Rao. 1994, 3p.
Pub. in Applied Physics Letters 64, n14 p1874-1876, 4 Apr 94.

Keywords: *YBCO superconductors, *Superconducting films, *Dielectric films, High temperature superconductors, Scanning tunneling microscopy, Strontium titanates, Magnetrons, Sputtering, Substrates, Reprints, *Yttrium barium cuprates, Lanthanum aluminates, Multilayers.

In situ YBa2Cu3O(7-x) (YBCO) films have been fabricated on SrTiO3 (001) and LaAlO3 (001) substrates by on-axis biased-radio-frequency magnetron sputtering in Ar-10% O2 at total pressures as low as 3 Pa (0.03 mbar) and a deposition rate 210 nm/h. Negative oxygen ion-resputtering has been considerably reduced by introducing a biased copper mask between the substrate and target. The surface morphology and physical properties of the films are greatly improved on applying a positive dc substrate bias with respect to grounded deposition chamber. We have obtained superconducting YBCO films with transport critical current as high as 10(exp 6) A/sq cm at 77 K and low normal-state resistivity by this approach. However, films deposited by negative dc bias under identical sputtering conditions are insulating. We identify the insulating films to be c-axis oriented Y4Ba3O9 (YBO) films. Furthermore, YBCO films could be grown on the YBO layers without any degradation of T(sub C) and c-axis orientation. This novel bias sputtering feature gives us a unique opportunity to produce superconductor/insulator, YBCO/YBO, multilayers from a single YBCO target.

04,691
PB95-202370 Not available NTIS
National Inst. of Standards and Technology (PL), Boulder, CO. Quantum Physics Div.
Laser Vacuum Ultraviolet Single Photon Ionization Probing of III-V Semiconductor Growth.
Final rept.
S. M. Casey, A. L. Alstrin, A. K. Kunz, and S. R. Leone. 1994, 10p.
Contract ACS-PRF-27135-AC6, Grant NSF-PHY90-12244
Sponsored by National Science Foundation, Arlington, VA. and Petroleum Research Fund, Washington, DC.
Pub. in Proceedings of Society of Photo-Optical Instrumentation Engineers - Ultraviolet Technology V, San Diego, CA., July 26-27, 1994, v2282 p39-48.

Keywords: *Molecular beam epitaxy, *Epitaxial growth, *Gallium arsenides, Time-of-flight mass spectrometers, Vacuum ultraviolet radiation, Neodymium lasers, YAG lasers, Laser radiation, Photoionization, Reprints.

Epitaxial growth of III-V semiconductor materials is probed in a molecular beam epitaxy reactor by single photon ionization of the gaseous fluxes using vacuum ultraviolet (VUV) laser radiation. The ninth harmonic of the Nd:YAG laser is produced by frequency tripling the output to 355 nm and then to 118 nm in a Xe/Ar mixture. Together with a time-of-flight mass spectrometer, this radiation is used to selectively probe the gaseous fluxes of Ga, As, As2, and As4 during molecular beam epitaxy of III-V materials. The essential aspects of the method and details of calibration procedures to obtain relative fluxes are described. Recent work to correlate the flux determinations with Reflection High Energy Electron Diffraction (RHEED) oscillations during GaAs epitaxial growth will be discussed.

04,692
PB95-202487 Not available NTIS
National Inst. of Standards and Technology (PL), Gaithersburg, MD. Quantum Metrology Div.
Early History and Future Outlook for the X-ray Crystal Density Method.
Final rept.
R. D. Deslattes. 1994, 7p.
Pub. in Metrologia 31, p173-179 1994.

Keywords: *Crystal structure, X ray diffraction, Historical aspects, Reprints, X ray interferometry, Avogadro constant.

It is useful to recall that the (late nineteenth-century) Baltimore Lectures of Lord Kelvin indicated that the likely sizes of atomic particles spanned almost two decades. Yet in the early years of the present century, Sir William Bragg's ansatz, together with the oil-drop e, gave the first reliable estimate of the scale of crystal interplanar spacings. The converse process of using an XRCD approach to obtain a value for the Avogadro constant was, prior to the advent of x-ray interferometry, limited by the need to connect optical and x-ray wavelengths before using the latter to estimate unit cell dimensions in crystals. Other limitations of these early measurements included the use of water as a density standard and the assignment of molar masses to individual specimens based on geochemical abundance averages. All these difficulties were overcome, in principle, with the application of x-ray/optical interferometry to the determination of lattice periods, the use of solid object density standards, and the determination of densities and isotopic abundances on individual monocrystalline specimens. While the present-day situation is addressed in other contributions to this workshop, the present essay attempts to place some of the early work in context and to look also to the future.

04,693
PB95-202560 Not available NTIS
National Inst. of Standards and Technology (MSEL), Gaithersburg, MD. Reactor Radiation Div.
Epitaxial Growth of Sb/GaSb Structures: An Example of V/III-V Heteroepitaxy.
Final rept.
J. A. Dura, A. Vigliante, T. D. Golding, and S. C. Moss. 1995, 7p.
Sponsored by Army Research Office, Research Triangle Park, NC.
Pub. in Jnl. of Applied Physics 77, n1 p21-27, 1 Jan 95.

Keywords: *Gallium antimonides, *Gallium arsenides, *Antimony, *Molecular beam epitaxy, *Epitaxial growth, Semiconducting films, X ray diffraction, Crystal growth, Reprints, Heteroepitaxial films, Heterostructures.

The requirements for heteroepitaxial growth of Sb on both GaSb and GaAs, and the subsequent growth of GaSb on Sb, using molecular-beam epitaxy are described. These systems serve as examples of the heteroepitaxy of group-V elements with III-V compounds, i.e., between materials using different bonding and possessing different electronic properties. The quality of the films was determined using high-resolution four-circle x-ray diffraction, and comparisons were made between different structures. GaSb was found to grow (III) oriented on Sb (III) with an inverted stacking sequence. A simple epitaxial model is proposed to explain this.

04,694
PB95-202602 Not available NTIS
National Inst. of Standards and Technology (PL), Boulder, CO. Quantum Physics Div.
Hole Dispersion and Enhancement of Antiferromagnetic Interaction of Localized Spins in High-Tc Superconductors.
Final rept.
V. V. Flambaum, and O. P. Sushkov. 1992, 7p.
Pub. in Physica C 190, p453-459 1992.

Keywords: *High-Tc superconductors, *Hole mobility, Spin spin interactions, Holes(Electron deficiencies), Effective mass, Hubbard model, Band theory, Antiferromagnetism, Cuprates, Reprints.

In the framework of the extended Hubbard model (copper-oxygen and oxygen-oxygen hopping), the energy and effective mass of a mobile hole is expressed in terms of hopping parameters and the correlators between spins of the background (S(n)S(n + 1)). Due to interaction of the mobile hole with localized holes, its effective mass increases about four times.

04,695
PB95-202768 Not available NTIS
National Inst. of Standards and Technology (MSEL), Boulder, CO. Materials Reliability Div.
Off-Diagonal Orthorhombic-Symmetry Elastic Constants.
Final rept.
S. Kim. 1994, 2p.
Pub. in Applied Physics Letters 65, n23 p2949-2950, 5 Dec 94.

Keywords: *Elastic properties, Orthorhombic lattices, Cubic lattices, Tetragonal lattices, Hexagonal lattices,

Ultrasonic radiation, Young modulus, Fiber composites, Gallium, Indium, Lithium, Zinc, Stiffness, Reprints.

We derive analytical expressions for off-diagonal elastic stiffnesses C(12), C(13), and C(23) in terms only of easily and precisely measurable diagonal elastic stiffnesses and Young moduli. We verify the expressions for several symmetry classes: cubic (Li), hexagonal (Zn), tetragonal (In), orthorhombic (Ga), and a weakly orthorhombic fiber composite: B/Al.

04,696
PB95-203063 Not available NTIS
National Inst. of Standards and Technology (PL), Boulder, CO. Quantum Physics Div.
Construction of Silicon Nanocolumns with the Scanning Tunneling Microscope.
Final rept.
R. M. Ostrom, D. M. Tanenbaum, and A. Gallagher. 1992, 3p.
Pub. in Applied Physics Letters 61, n8 p925-927, 24 Aug 92.

Keywords: Scanning tunneling microscopy, Construction, Reprints, *Silicon nanocolumns, *Nanostructures, Nanolithography, Nanotechnology.

Voltage pulses to a scanning tunneling microscope (STM) are used to construct silicon columns of 30-100 A diameter and up to 200 A height on a silicon surface and on the end of a tungsten probe. These nanocolumns have excellent conductivity and longevity, and they provide an exceptional new ability to measure the shapes of nanostructures with a STM. This construction methodology and these slender yet robust columns provide a basis for nanoscale physics, lithography, and technology.

04,697
PB95-203345 Not available NTIS
National Inst. of Standards and Technology (PL), Boulder, CO. Quantum Physics Div.
Deposition Rates in Direct Current Diode Sputtering.
Final rept.
G. C. Stutzin, K. Rozsa, and A. Gallagher. 1993, 10p.
Contract SERI-DD-1-11001-1
Sponsored by Solar Energy Research Inst., Golden, CO.
Pub. in Jnl. of Vacuum Science and Technology A 11, n3 p647-656 May/Jun 93.

Keywords: *Sputtering, Electric discharges, Direct current, Thin films, Silicon, Reprints, Deposition rates, Sputtered films.

A physical model for anode deposition rates in parallel-plate, dc-diode sputtering is presented and tested. The deposition rate has been measured as a function of the discharge voltage, the anode-cathode gap and the pressure, using silicon or molybdenum cathodes with argon. Deposition rates as high as 23 A/s were obtained using 3 kV, and it is shown that deposition efficiency is similar to that obtained with magnetrons. The deposition rate varies inversely with anode-cathode gap at constant pressure and voltage and almost linearly with power density for discharge voltages above a threshold which depends on the cathode material. These observations are explained by the model, which can be used to estimate the deposition rates for any cathode material and gas for which the ion sputtering yields are known. Potential advantages and complications of dc diode sputtering for thin film deposition are discussed, and optimum conditions for high, uniform deposition rates are described.

04,698
PB95-203378 Not available NTIS
National Inst. of Standards and Technology (MSEL), Gaithersburg, MD.
Linking Anisotropic Sharp and Diffuse Surface Motion Laws via Gradient Flows.
Final rept.
J. E. Taylor, and J. W. Cahn. 1994, 15p.
Sponsored by National Science Foundation, Arlington, VA. and Advanced Research Projects Agency, Arlington, VA.
Pub. in Jnl. of Statistical Physics 77, n1/2 p183-197 1994.

Keywords: *Surface diffusion, Partial differential equations, Laplacian, Curvature, Anisotropy, Reprints.

We compare four surface motion laws for sharp surfaces with their diffuse interface counterparts by means of gradient flows on corresponding energy functionals. The energy functionals can be defined to give the same dependence on normal direction for the energy of sharp plane surfaces as for their diffuse counterparts. The anisotropy of the kinetics can be incorporated into the inner product without affecting the energy functional.

04,699
PB95-203394 Not available NTIS
National Inst. of Standards and Technology (EEEL), Boulder, CO. Electromagnetic Technology Div.
Surface Modification of YBa2Cu3O7-delta Thin Films Using the Scanning Tunneling Microscope: Five Methods.
Final rept.
R. E. Thomson, J. Moreland, and A. Roshko. 1994, 13p.
Pub. in Nanotechnology 5, p57-69 1994.

Keywords: *YBCO superconductors, *Superconducting films, High temperature superconductors, Scanning tunneling microscopy, Thin films, Reprints, *Yttrium barium cuprates, *Surface modification, Nanolithography.

We have investigated using the scanning tunneling microscope (STM) as a tool for surface modification of YBa2Cu3O(7-delta) (YBCO) thin films and have identified five distinct methods whereby the STM tip can modify the superconductor surface. (i) By lowering the tunneling resistance we make the tip scratch or 'mill' the sample surface mechanically. (ii) By increasing the bias voltage above about 4 V we can modify the surface by an apparent electron beam damaging process. (iii) By increasing the bias voltage above 10 V and raising the tunneling current, we can cause a more dramatic effect which is probably due to a thermal process. (iv) By operating the STM in a damp carbon dioxide atmosphere we can cause the STM tip to etch the surface electrochemically. (v) Finally, we have some preliminary data suggesting that the high field under an extremely sharp tip displaces the oxygen atoms in the YBCO lattice. Examples of each of these techniques are shown and discussed.

04,700
PB95-220430 PC A09/MF A02
National Inst. of Standards and Technology (MSEL), Gaithersburg, MD. Reactor Radiation Div.
NIST Reactor: Summary of Activities, October 1993 through September 1994.
C. L. O'Connor. Apr 95, 184p, NISTIR-5594.

Keywords: *NBSR reactor, Research reactors, Activation analysis, Cold neutrons, Crystal structure, Neutron diffraction, Neutron radiography, Nondestructive tests, Boron nitrides, Surface chemistry, Polymers.

The report summarizes all the programs which use the NIST reactor. It covers the period for October 1993 through September 1994. The programs range from the use of neutron beams to study the structure and dynamics of matierls through nuclear physics and neutron standards to sample irradiations for activation analysis, isotope production, neutron radiography, and nondestructive evaluation.

04,701
PB95-255204 PC A99/MF E11
National Inst. of Standards and Technology, Gaithersburg, MD.
Proceedings of the Applied Diamond Conference 1995: Applications of Diamond Films and Related Materials International Conference (3rd). Held in Gaithersburg, Maryland, on August 21-24, 1995.
Special pub.
A. Feldman, Y. Tzeng, W. A. Yarbrough, M. Yoshikawa, and M. Murakawa. Aug 95, 975p, NIST/SP-885, ISBN-1-886843-01-5.
Also available from Supt. of Docs. See also PB95-256053. Prepared in cooperation with Pennsylvania State Univ., University Park., Nippon Inst. of Tech., Saitama., Auburn Univ., AL. and Tokyo Inst. of Technology (Japan).

Keywords: *Diamonds, *Thin films, *Meetings, Vapor deposition, Electron emission, Cutting tools, Crystallization, Nucleation, Optics, Brazing, Wear, Composite materials, Models.

Interest in commercializing diamond technology and related materials technologies continues to grow. This can be attested to by the large number of abstracts received for this meeting, the Third International Conference on the Applications of Diamond Films and Related Materials. More than 300 abstracts were received. Cutting tools coated with CVD diamond are of immediate commercial interest. Other applications, such as diamond windows and diamond heat spreaders, are developing but at a slower pace. Interest in cubic boron nitride is receiving more attention because of its resistance to oxidation and because it can be used on tools to machine ferrous materials.

04,702
PB96-102066 Not available NTIS
National Inst. of Standards and Technology (EEEL), Boulder, CO. Electromagnetic Technology Div.
Step-Edge and Stacked-Heterostructure High-Tc Josephson Junctions for Voltage-Standard Arrays.
Final rept.
S. P. Benz, C. D. Reintsema, R. H. Ono, G. F. Virshup, J. N. Eckstein, and I. Bozovic. 1995, 4p.
Sponsored by Department of the Army, Washington, DC., Naval Research Lab., Washington, DC. and Office of Naval Research, Arlington, VA.
Pub. in Institute of Electrical and Electronics Engineers Transactions on Applied Superconductivity, v5 n2 p2915-2918 Jun 95.

Keywords: *Josephson junctions, *Electric potential, *Arrays, *Transition temperature, Comparative evaluations, High temperature, Bias, YBCO superconductors, Epitaxy, Heterojunction devices, Electric current, Resistance, Reprints, SNS junctions, Shapiro steps, Voltage-standard arrays.

The authors have explored two high-transition temperature Josephson junction technologies for application in voltage standard arrays: step-edge junctions made with YBa2Cu3O(7-delta) and Au normal-metal bridges, and stacked series arrays of Josephson junctions in selectively doped, epitaxially grown Bi2Sr2CaCu2O8 heterostructures. For both kinds of junctions, Shapiro steps induced by a microwave bias were characterized as a function of power. The authors compare the two technologies with respect to critical current and normal resistance uniformity, maximum achievable critical current, critical-current normal resistance product, and operating temperature.

04,703
PB96-102157 Not available NTIS
National Inst. of Standards and Technology (EEEL), Gaithersburg, MD. Electricity Div.
Application of Single Electron Tunneling: Precision Capacitance Ratio Measurements.
Final rept.
A. F. Clark, N. M. Zimmerman, E. R. Williams, F. C. Wellstood, C. J. Lobb, R. J. Soulen, A. Amar, and D. Song. 1995, 3p.
Pub. in Applied Physics Letters, v66 n19 p2588-2590, 8 May 95.

Keywords: *Metrology, *Electron tunneling, *Capacitance, Capacitors, Electric bridges, Cryogenic equipment, Precision, Ratios, Electron spectroscopy, Superconductivity, Electrometers, Reprints, SET(Single electron tunneling).

A metrological application is reported of the single electron tunneling (SET) phenomena: a precise measurement of the ratio of two cryogenic capacitors. The measurement used a superconducting SET electrometer as the null detector for a capacitance bridge. A 3-ppm level of imprecision has been achieved in the measurement of the capacitance ratio from 100 to 1000 Hz. Further improvements can be made in the attempt to obtain an imprecision of 10(exp -8) at lower frequencies, sufficient for the metrological measurement of capacitance or the fine-structure constant using a SET pump.

04,704
PB96-102264 Not available NTIS
National Inst. of Standards and Technology (EEEL), Gaithersburg, MD. Electricity Div.
Physical Basis for Half-Integral Shapiro Steps in a DC SQUID.
Final rept.
E. A. Early, A. F. Clark, and C. J. Lobb. 1995, 13p.
Pub. in Physica C, v245 p308-320 1995.

Keywords: *SQUID(Detectors), *Direct current, *Josephson junctions, Alternating current, Dynamic characteristics, Equations of motion, Projectory analysis, Energy storage, Potential, Reprints, DC SQUID, AC Josephson effect, Shapiro steps.

The dynamics of a DC SQUID is analogous to the classical dynamics of a particle subject to conservative,

damping, and driving forces in two dimensions. The equations of motion define a trajectory on a potential-energy surface derived from the conservative forces, the components of which correspond to different forms of stored energy in the SQUID. In the presence of a periodic driving force, half-integral Shapiro steps are possible when the trajectory follows a zig-zag path between minima of the potential surface. This description of the dynamics in terms of a potential surface provides an intuitive, physical basis for previous simulation results on half-integral Shapiro step in a DC SQUID.

04,705
PB96-102272 Not available NTIS
National Inst. of Standards and Technology (EEEL), Boulder, CO. Electromagnetic Technology Div.
Stacked Series Arrays of High-Tc Trilayer Josephson Junctions.
Final rept.
J. N. Eckstein, I. Bozovic, G. F. Virshup, R. H. Ono, and S. P. Benz. 1995, 4p.
Pub. in Institute of Electrical and Electronics Engineers Transactions on Applied Superconductivity, v5 n2 p3284-3287 Jun 95.

Keywords: *Josephson junctions, *Molecular beam epitaxy, Phase locked systems, High temperature, Current density, Superconductors, Alternating current, Wafers, Layers, Reprints.

The authors report on the properties of stacked series arrays of trilayer Josephson junctions grown by atomic layer-by-layer molecular beam epitaxy. Trilayer Josephson junctions oriented so that the current travels in the c-axis direction have been described previously. Series arrays are made by placing more than one barrier layer in the Ba2Sr2CaCu2O8-based, (2212), epitaxial structure. Single molecular layers of 2212 doped with Dy to reduce the local carrier concentration are used as barriers, and are placed very close to each other, e.g., separated by only a few molecular layers of the superconducting phase. Phase locking of a.c. Josephson currents has been observed. The critical current density of such junctions has been observed to be very uniform on wafers that are free of second phase defects, and operation up to 60 K has been obtained.

04,706
PB96-102421 Not available NTIS
National Inst. of Standards and Technology (MSEL), Gaithersburg, MD. Reactor Radiation Div.
Lattice Dynamics of Ba1-xKxBiO3.
Final rept.
M. A. Green, K. Prassides, P. Day, and D. A. Neumann. 1995, 2p.
Pub. in Synthetic Metals, v71 p1619-1620 1995.

Keywords: *Crystal lattices, *Superconductivity, *Density measurement, Temperature, Doped materials, Energy gaps(Solid state), Energy levels, Transitions, Reprints.

Neutron weighted density-of-states measurements of Ba(1-x)K(x)Bi03 are presented which show pronounced changes as a function of both temperature and Bi oxidation states. Information is gained on both the structural and metal-insulator transitions occurring with increased potassium doping. Phonon anomalies associated with the appearance of a superconducting energy gap gives strong evidence of electron-phonon coupling and superconductivity via a conventional BCS mechanism.

04,707
PB96-102439 Not available NTIS
National Inst. of Standards and Technology (MSEL), Gaithersburg, MD. Reactor Radiation Div.
Structure and Conductivity of Layered Oxides (Ba,Sr)n+1(Sn,Sb)nO3n+1.
Final rept.
M. A. Green, K. Prassides, P. Day, and J. K. Stalick. 1995, 2p.
Pub. in Synthetic Metals, v71 p1617-1618 1995.

Keywords: *Crystal structure, *Superconductivity, *Neuron diffraction, Oxides, Metal powder, Energy gaps(Solid state), Hueckel theory, Barium oxides, Strontium compounds, Tin compounds, Antimony compounds, Reprints.

Structures of various members of the Ruddlesdon-Popper homologous series, (BaSr)n+1(Sn,Sb)nO3n+1 solved by Rietveld refinement of powder neutron diffraction data are summarized. Predictions of band gaps are made on the basis of extended Huckel calculations.

04,708
PB96-102447 Not available NTIS
National Inst. of Standards and Technology (MSEL), Gaithersburg, MD. Reactor Radiation Div.
Lattice Dynamics of Semiconducting, Metallic, and Superconducting Ba1-xKxBiO3 Studied by Inelastic Neutron Scattering.
Final rept.
M. A. Green, K. Prassides, D. A. Neumann, and P. Day. 1995, 6p.
Pub. in Chemistry of Materials, v7 p888-893 1995.

Keywords: *Crystal lattices, *Superconductors, *Semiconductors(Materials), *Neutron scattering, Chemical composition, Phase diagrams, Temperature, Energy levels, Phase transformations, Barium oxides, Potassium, Bismuth oxides, BCS theory, Reprints.

Inelastic neutron scattering has been used to study the lattice dynamics in Ba(1-x)KxBiO3 over a wide range of compositions, covering regions of the (composition (x), temperature (T)) phase diagram displaying semiconducting, metallic, and superconducting behavior. Modes are assigned using interatomic potentials calculations, which show good agreement with experiment. The oxygen phonon modes are very sensitive to changes in composition and oxidation state of the Bi ions. Phonon anomalies observed in both the oxygen TO bending (about 33 meV) and stretching (about 62 meV) modes as a function of temperature are discussed within the context of the BCS theory. Novel behavior is shown by the LO oxygen bending mode at about 42 meV that shows a strong dependence on composition, proposed to arise from the occurrence of structural phase transitions in this system.

04,709
PB96-102462 Not available NTIS
National Inst. of Standards and Technology (EEEL), Boulder, CO. Electromagnetic Technology Div.
30 THz Mixing Experiments on High Temperature Superconducting Josephson Junctions.
Final rept.
E. N. Grossman, L. R. Vale, D. A. Rudman, K. M. Evensen, and L. R. Zink. 1995, 4p.
Pub. in Institute of Electrical and Electronics Engineers Transactions on Applied Superconductivity, v5 n2 p3061-3064 Jun 95.

Keywords: *Josephson junctions, *Superconductors, *Heterodyning, *Hot electrons, High temperature, Infrared radiation, Signal mixing, Bias, Microwaves, Reprints, SNS Josephson junctions, High Tc Josephson junctions.

The authors have investigated YBz2Cu3O7-delta superconductor- normal-superconductor Josephson junctions as mixers of 30THz radiation. The authors have directly observed (2nd order) differencefrequencies from 10 MHz to 12.8 GHz between two CO2 laser lines. Applying a third microwave signal to the junction, the authors have observed CO2 laser difference frequencies up to 27 GHz. The d.c. bias dependence of the difference frequency signal, as well as other evidence, suggests two distinct mixing mechanisms: hot-electron mixing in the junction banks at high d.c. biases, and bolometric Josephson mixing at low d.c. biases. The latter is the first observation of Josephson mixing at CO2 laser frequencies in high-T(sub C) junctions. The Josephson mixing has generated observable mixing products up to 6th order.

04,710
PB96-102470 Not available NTIS
National Inst. of Standards and Technology (CSTL), Gaithersburg, MD. Inorganic Analytical Research Div.
Effect of Stoichiometry on the Phases Present in Boron Nitride Thin Films.
Final rept.
L. B. Hackenberger, L. J. Pilione, R. Messier, and G. P. Lamaze. 1994, 7p.
Pub. in Jnl. of Vacuum Science and Technology A 12, n4 p1569-1575 Jul/Aug 94.

Keywords: *Boron nitrides, *Thin films, *Stoichiometry, Nondestructive tests, Neutron absorption, Chemical composition, Solids, Phase, Chemical analysis, Reprints, NDP(Neutron depth profiling).

Boron nitride thin films were deposited by ion-assisted evaporation and characterized by neutron depth profiling (NDP), a nondestructive method for the compositional analysis of solids. The phases present in the films were determined by infrared spectroscopy. Examination of the data presented here and comparison with the work of other authors revealed that stoichiometric or nearly stoichiometric films contained the greatest amount of the cubic phase. This led to the proposition that film stoichiometry is one of the factors that stabilize cubic boron nitride in boron nitride thin films. A shift in the position of the cubic boron nitride infrared absorption was also observed by the present authors which was related to film stoichiometry.

04,711
PB96-102512 Not available NTIS
National Inst. of Standards and Technology (MSEL), Gaithersburg, MD. Reactor Radiation Div.
Oxygen Dependance of the Crystal Structure of HgBa2CuO4+ and Its Relation to Superconductivity.
Final rept.
Q. Huang, J. W. Lynn, Q. Xiong, and C. W. Chu. 1995, 9p.
Pub. in Physical Review B, v52 n1 p462-470 Jul 95.

Keywords: *Mercury oxides, *Crystal structure, *Superconductivity, Phase transformations, Mercury compounds, Oxygen, Barium, Copper, Lattice parameters, Doped crystals, Temperature, Reprints.

Powder neutron-diffraction profile refinement techniques have been used to investigate the oxygen dependence of the crystal structure and its effect on the superconducting phase transition in high-quality samples of the superconductor HgBa2CuO(4+delta) (0.04 less than or equal to delta less than or equal to 0.23). The sustem remains tetragonal (space group P4/mmm) over the full range of temperature (10-300 K) and oxygen concentration explored. The a-axis lattice parameter decreases smoothly with increasing delta, while the c-axis lattice parameter exhibits a maximum. The extra oxygen in the material is found to randomly occupy the centered O(3) site (1/2, 1/2, 0) in the Hg layer, and no other additional site for the extra oxygen was found in the structure. There is also no mixing of the cations on the Cu and Hg sites.

04,712
PB96-102538 Not available NTIS
National Inst. of Standards and Technology (EEEL), Boulder, CO. Electromagnetic Technology Div.
Self-Biasing Cryogenic Particle Detector Utilizing Electrothermal Feedback and a SQUID Readout.
Final rept.
K. D. Irwin, S. W. Nam, B. Cabrera, R. P. Welty, J. M. Martinis, B. Chugg, and S. G. Park. 1995, 4p.
Pub. in Institute of Electrical and Electronics Engineers Transactions on Applied Superconductivity, v5 n2 p2690-2693 Jun 95.

Keywords: *SQIDS(Detectors), *Radiation counters, *Phonons, Transitions, Edges, Tungsten, Thin films, Silicon, Substrates, Feedback, Temperature, Superconductors, Reprints.

The authors are developing and testing a new type of superconducting transition edge sensor for phonon mediated particle detection. This sensor consists of a superconducting tungsten thin film deposition on a silicon substrate. The temperature of the film is held constant within the superconducting transitions (T(sub c) = 70 mK) by a feedback process, with the substrate temperature well below the film temperature. Phonon energy deposited in the film is removed by a reduction in feedback Joule heating, which is measured using a series array of DC SQUIDs. The resulting signals show improvements in linearity and signal-to-noise ratio over the authors' previous transition edge sensors.

04,713
PB96-102546 Not available NTIS
National Inst. of Standards and Technology (CSTL), Gaithersburg, MD. Thermophysics Div.
Simulation of C60 Through the Plastic Transition Temperatures.
Final rept.
S. D. Johnson, R. D. Mountain, and P. H. E. Meijer. 1995, 3p.
Pub. in Jnl. of Physical Chemistry, v103 n3 p1106-1108 Jul 95.

Keywords: *Carbon 60, *Transition temperature, *Plastic properties, Molecular interactions, Solid phase, Phase transformations, Solid phase, Phase transformations, Models, Simulation, Charge distribution, Crystal structure, Reprints, Fullerene, Molecular dynamics.

An interaction model is presented that accounts for the phase transitions in a crystalline C60 at 90 and 250

K. This was obtained by a molecular dynamics simulation of the C60 crystal. These transitions are used as indirect evidence of the appropriateness of the charge distribution. Additional support of the proposed charge distribution comes from the agreement of multiple energies with theoretical considerations.

04,714
PB96-102587 Not available NTIS
National Inst. of Standards and Technology (EEEL), Boulder, CO. Electromagnetic Technology Div.
Phase Locking in Two-Dimensional Arrays of Josephson Junctions: Effect of Critical-Current Nonuniformity.
Final rept.
R. L. Kautz. 1995, 5p.
Pub. in Institute of Electrical and Electronics Engineers Transactions on Applied Superconductivity, v5 n2 p2702-2706 Jun 95.

Keywords: *Josephson junctions, *Microwave oscillators, *Phase locked systems, Arrays, Superconductivity, Numerical analysis, Simulation, Nonuniformity, Electric current, Reprints.

Numerical simulations are used to study mutual phase locking in two-dimensional arrays of Josephson junctions for parameters typical of successful millimeter-wave oscillators. Such arrays are shown to be very tolerant of random critical-current nonuniformities. However, comparison with an equivalent series array reveals that the locking between rows in a two-dimensonal array is principally due to feedback through the external load and not to internal coupling between rows.

04,715
PB96-102595 Not available NTIS
National Inst. of Standards and Technology (MSEL), Boulder, CO. Materials Reliability Div.
Tensile Deformation-Induced Microstructures in Free-Standing Copper Thin Films.
Final rept.
R. R. Keller, J. M. Phelps, and D. T. Read. 1994, 6p.
Pub. in Materials Research Society Symposia Proceedings, v338 p227-232 1994.

Keywords: *Thin films, *Copper, *Microstructure, *Tensile deformation, Dislocations(Materials), Fractures(Materials), Reliability, Electron microscopy, Loads(Forces), Plastic deformation, Reprints, TEM(Transmission electron microscopy).

Existing work in the mechanical behavior of thin films focuses mainly on measurement of macroscopic properties without string correlation to microstructural features. The authors used transmission electron microscopy (TEM) to characterize the microstructures of free-standing copper thin films both before and after monotonic tensile deformation in an ex-situ thin film tensile testing system, as well as during in-situ loading in the TEM. The defect structures contributing to plastic deformation were investigated with an emphasis on comparison to mechanisms known to operate in bulk copper. The thin film exhibited much lower ductility (approximately 1%) than that normally observed in bulk form (greater than 40%). The predominant plastic deformation mechanisms did not include the typical dislocation activity that occurs in bulk copper, but rather greatly inhibited dislocation interactions typical of stages I and II hardening only.

04,716
PB96-102603 Not available NTIS
National Inst. of Standards and Technology (EEEL), Boulder, CO. Electromagnetic Technology Div.
Magnetostriction and Giant Magnetoresistance in Annealed NiFe/Ag Multilayers.
Final rept.
Y. K. Kim, and S. C. Sanders. 1995, 3p.
Pub. in Applied Physics Letters 66, n8 p1009-1011, 20 Feb 95.

Keywords: *Magnetostriction, *Magnetoresistivity, *Annealing, *Thin films, Temperature dependence, Nickel compounds, Iron compounds, Gold, Stress relieving, Sensors, Magnetic tape, Recording heads, Reprints, GMR, Multilayers.

Magnetostriction data are reported for NiFe/Ag multilayer thin films displaying giant magnetoresistance. Magnetostriction and magnetoresistance were measured as functions of annealing temperature for NiFe/Ag samples having different numbers of NiFe/Ag bilayers and Ag spacer thicknesses. They varied systematically with annealing temperature in a manner consistent with residual stress reduction and microstructural changes such as grain-boundary diffusion and grain growth. Zero magnetostriction concurrent with high magnetoresistance ratio (5%) and field sensitivity (7.5%(kA/m)(0.6%/Oe)) was observed for an optimal multilayer configuration and annealing temperature. This combination of zero magnetostriction and high magnetoresistive response makes the NiFe/Ag multilayer system an attractive candidate for high-performance magnetic recording read-head sensors.

04,717
PB96-102819 Not available NTIS
National Inst. of Standards and Technology (PL), Boulder, CO. Time and Frequency Div.
Optically Stabilized Tunable Diode-Laser System for Saturation Spectroscopy.
Final rept.
M. Murtz, M. Schaefer, T. George, J. S. Wells, and W. Urban. 1995, 7p.
Pub. in Applied Physics B, v60 p31-37 1995.

Keywords: *Saturation spectroscopy, *Lead salt diode lasers, *Laser applications, Tunable lasers, Diodes, Lasers, Reprints, *Foreign technology, Optical Feedback.

We present an optically stabilized lead-salt diode-laser system which is the nucleus of a very-high resolution instrument for sub-Doppler molecular spectroscopy in the mid-infrared. By application of external optical feedback, we have narrowed the diode-laser linewidth by two orders of magnitude, yielding a spectral width of less than 200 kHz. The diode-laser frequency is stabilized and controlled via the external reflector by variable-frequency offset-locking the diode-laser to a CO laser frequency. This substantial improvement in the spectral properties enabled us to perform a Lamb-dip experiment on a carbonyl sulfide (OCS) absorption line near 1985 cm-1.

04,718
PB96-102827 Not available NTIS
National Inst. of Standards and Technology (EEEL), Boulder, CO. Electromagnetic Technology Div.
Electronic Microrefrigerator Based on a Normal-Insulator-Superconductor Tunnel Junction.
Final rept.
M. Nahum, T. M. Eiles, and J. M. Martinis. 1994, 3p.
Pub. in Applied Physics Letters, v65 n24 p2123-2125 Dec 94.

Keywords: *Tunneling(Electronics), *Superconductors, *Refrigerators, Reprints, Junctions, Electro phonon coupling.

We present measurements on a novel electronic microrefrigerator that can cool conduction electrons significantly below the lattice temperature. A normal-insulator-superconductor tunnel junction is used to extract electrons from the normal metal electrode whose energy is higher than the Fermi energy. Electrons with an average energy equal to the Fermi energy are returned to the metal by a superconducting contact. Consequently, the high-energy thermal excitations are removed from the normal metal, thus cooling the electrons. For lattice temperatures higher than 100 mK the data can be explained by a simple theory incorporating the BCS density of states in the superconducting electrode and the coupling between electrons and phonons. At lower temperatures our measurement suggests that the electron energies in the normal electrode depart strongly from an equilibrium distribution.

04,719
PB96-103015 Not available NTIS
National Inst. of Standards and Technology (EEEL), Boulder, CO. Electromagnetic Technology Div.
Superconducting Integrated Circuit Fabrication with Low Temperature ECR-Based PECVD SiO2 Dielectric Films.
Final rept.
J. E. Sauvageau, C. J. Burroughs, P. A. A. Booi, J. A. Koch, M. W. Cromar, and S. P. Benz. 1995, 7p.
Pub. in Institute of Electrical and Electronics Engineers Transactions on Applied Superconductivity 5, n2 p2303-2309 Jun 95.

Keywords: *Josephson junctions, *Integrated circuits, *Superconductors, *Fabrication, Low temperature, Very large scale integration, Thin films, Vapor deposition, Cyclotron resonance, Silicon dioxide, Experimental design, Statistical quality control, Reprints.

A superconducting integrated circuit fabrication process has been developed to encompass a wide range of applications such as Josephson voltage standards, VLSI scale array oscillators, SQUIDS, and kinetic-inductance-based devices. An optimal Josephson junction low temperature processing for all deposition and etching steps. This low temperature process involves an electron cyclotron resonance-based plasma-enhanced chemical vapor deposition of SiO2 films for interlayer dielectrics. Experimental design and statistical process control techniques have been used to ensure high quality oxide films. Oxide and niobiom etches include endpoint detection and controlled overetch of all films. An overview of the fabrication process is presented.

04,720
PB96-103056 Not available NTIS
National Inst. of Standards and Technology (PL), Boulder, CO. Quantum Physics Div.
Nanoscale Study of the Hydrogenated Amorphous Silicon Surface.
Final rept.
D. M. Tanenbaum, A. Laracuente, and A. C. Gallagher. 1994, 6p.
Contract NREL-XG-1-1216
See also PB95-150595. Sponsored by National Renewable Energy Lab., Golden, CO.
Pub. in Materials Research Society Symposia Proceedings, v336 p49-54 1994.

Keywords: *Surface roughness, *Films, *Silicon, Amorphous materials, Vapor deposition, Topology, Microscopy, Crystal growth, Voids, Substrates, Reprints, Hydrogenated amorphous silicon, Scanning tunneling microscopy.

A scanning tunneling microscope has been used to study the topology of the surface of device-quality, hydrogenated amorphous silicon deposited by rf discharge from silane or hot wire CVD. The substrates were oxide-free single-crystal silicon or GaAs. Films studied were either grown in the authors' laboratory and observed with no air exposure, or grown at other laboratories producing device-quality photovoltaic cells and viewed after air exposures of less than 30 minutes. Thin films (10 nm) representing early growth stages appear significantly smoother than the thicker films. The topology of thick films (greater than 50 nm) has large variations over individual samples. Overall surface roughness measured on sub-micron areas of the authors' films is very inhomogeneous.

04,721
PB96-103130 Not available NTIS
National Inst. of Standards and Technology (EEEL), Boulder, CO. Electromagnetic Technology Div.
Recent Results in Magnetic Force Microscopy.
Final rept.
A. Wadas, P. Rice, and J. Moreland. 1994, 5p.
Pub. in Jnl. of Applied Physics A, v59 p63-67 1994.

Keywords: *Microscopy, *Magnetic properties, Domain structure, Magnetic disks, Permalloy, Iron alloys, Single crystals, Topography, Reprints, *Atomic force microscopy, MFM(Magnetic force microscopy), Magnetic garnet.

The authors present domain wall images obtained by using Magnetic Force Microscope (MFM) on magnetic samples like: double layer of permalloy alloy, magnetic hard disk. BaFe12O19 single crystal and TGdTmGa/TSmTmGa magnetic garnet. The authors have imaged topography and magnetic forces of the same area. The Fe double- and single-layer thin films tips have been prepared to achieve high sensitivity (10(exp -12)N) and high resolution of MFM.

04,722
PB96-111679 Not available NTIS
National Inst. of Standards and Technology (EEEL), Boulder, CO. Electromagnetic Technology Div.
Stable Phase Locking in a Two-Cell Ladder Array of Josephson Junctions.
Final rept.
B. H. Larsen, and S. P. Benz. 1995, 3p.
Pub. in Applied Physics Letters, v66 n23 p3209-3211 Jun 95.

Keywords: *Josephson junctions, *Arrays, Magnetic fields, Stability, Numerical analysis, Oscillators, Reprints, *Phase locking.

The stability of the periodic solution of the two-cell ladder array has been numerically investigated in order to explore intrinsic phase-locking mechanisms relevant to arrays and stacked junction oscillators. In zero magnetic field the periodic in-phase solution of the system

is neutrally stable. However, this solution is stable over a finite voltage range when an applied control current exceeds a critical value. The dependence upon system parameters of the boundaries of the stable range and the critical control current is investigated. Finally, the influence of the control current on the microwave power in a typical range of stability is calculated.

04,723
PB96-111745 Not available NTIS
National Inst. of Standards and Technology (EEEL), Boulder, CO. Electromagnetic Technology Div.
Temperature Dependence and Magnetic Field Modulation of Critical Currents in Step-Edge SNS YBCO/Au Junctions.
Final rept.
N. Missert, L. R. Vale, R. H. Ono, R. E. Thomson, S. J. Berkowitz, C. D. Reintsema, and D. A. Rudman. 1995, 4p.
Pub. in Institute of Electrical and Electronics Engineers Transactions on Applied Superconductivity, v5 n2 p2969-2972 Jun 95.

Keywords: *Josephson junctions, *Critical current, *Temperature dependence, *Magnetic fields, Gold, Modulation, Electrical properties, Transport properties, Superconducting devices, YBCO superconductors, Reprints, Step-edge SNS YBCO/Au junctions.

The authors compare the electrical transport properties of superconductor-normal metal-superconductor SNS step-edge YBCO/Au junctions where the Au is deposited at 100 deg C and 600 deg C. For both types of junctions the authors observe Resistively Shunted Junctions (RSJ) current-voltage characteristics. The critical currents Ic in all cases are similar for a given YBCO thickness to step height ratio, while the normal resistance R(sub n) for the Au deposited at 600 C is consistently 25% lower. The normalized temperature dependence of the I(sub c)R(sub n) product is identical for all junctions with Au deposited at high temperatures and varies among junctions on a single chop for Au deposited at 100 deg C. Low magnetic field modulation of the critical current can show either the expected Fraunhoffer-like pattern or a double-junction modulation for both types of devices. The modulation period is consistently a factor of three lower for the high-temperature deposited Au.

04,724
PB96-111752 Not available NTIS
National Inst. of Standards and Technology (EEEL), Boulder, CO. Electromagnetic Technology Div.
Critical Current and Normal Resistance of High-Tc Step-Edge SNS Junctions.
Final rept.
C. D. Reintsema, R. H. Ono, G. Barnes, G. Kunkel, D. A. Rudman, L. R. Vale, N. Missert, P. A. Rosenthal, L. Borcherdt, and T. E. Harvey. 1995, 5p.
Pub. in Institute of Electrical and Electronics Engineers Transactions on Applied Superconductivity, v5 n2 p3405-3409 Jun 95.

Keywords: *Josephson junctions, *High temperature, *Critical current, *Electric conductivity, Superconducting devices, Geometry, Technology utilization, Reprints, High-Tc, Step-edge SNS junctions, I(sub C)R(sub n) product.

The authors have fabricated high-Tc superconductor-normal- superconductorJosephson junctions with a variety of controlled geometries and measuredthe resulting dependences of critical current and normal resistance. These studies show that the authors can adjust their junction parametersover orders of magnitude, thus allowing the authors to tailor the junctions for a variety of applications.

04,725
PB96-111794 Not available NTIS
National Inst. of Standards and Technology (MSEL), Gaithersburg, MD. Ceramics Div.
Crystal Structure of a New Monoclinic Form of Potassium Dihydrogen Phosphate Containing Orthophosphacidium Ion, (H4PO4)(sup+1).
Final rept.
M. Mathew, and W. Wong-Ng. 1995, 5p.
Pub. in Jnl. of Solid State Chemistry, v114 p219-223 1995.

Keywords: *Crystal structure, *Potassium inorganic compounds, *Phosphate inorganic compounds, *X ray diffraction, Hydrogen bonds, Ions, Lattice parameters, Monoclinic lattice, Three dimensional, Crystallography, Reprints, *Potassium dihydrogen phosphate, *Orthophosphacidium ion.

The crystal structure of a new monoclinic form of potassium dihydrogen phosphate, KH2PO4, has been determined by single crystal x-ray diffraction. Crystals are monoclinic, space group P2/c with a = 7.4399(7), b = 7.2634(9), c = 9.3629(13) Angstroms, Beta = 127.696(8) degrees, V = 400.35(9) cubic Angstroms, dm = 2.25, dc = 2.257 Mg/cubic m for Z = 4, mu = 17.9 cm(exp -1), F(000) = 272, T = 293 K. The structure was refined to R = 0.022 and Rw = 0.038 for 740 reflections with greater I than or equal to 3sigma(I).

04,726
PB96-112024 Not available NTIS
National Inst. of Standards and Technology (EEEL), Boulder, CO. Electromagnetic Technology Div.
Temperature and Field Dependence of Flux Pinning in NbTi with Aritificial Pinning Centers.
Final rept.
S. L. Wipf, and L. D. Cooley. 1994, 4p.
Pub. in Proceedings of the International Workshop on Critical Currents in Superconductors, Alpback, Austria, January 24-27, 1994, p613-616.

Keywords: *Flux pinning, *Superconducters, Reprints, Niobium titanium, Efficiency, Force, *Foreign technology.

An experimental study of artificial pinning centers in NbTi covered a large range of many parameters: size of pints from 65nm down to 7.7nm (Pins spaced at twice their size in hexagonal array), critical current densities at tempertures between 2K and Tc at fields up to Bc2. The objective of this paper is to understand mainly the field dependence of flux pinning in this material with a view to achieve optimal performance in a practical conductor. We conclude that in these samples the optimal pinning at 5T is between 14 and 28 nm pin size and that the pinning is within a factor of 4 plus or minus 1 of the ultimate possible.

04,727
PB96-112032 Not available NTIS
National Inst. of Standards and Technology (EEEL), Boulder, CO. Electromagnetic Fields Div.
Distribution of Dielectric Relaxation Times and the Moment Problem.
Final rept.
J. Baker-Jarvis, and M. D. Janezic. 1994, 2p.
Pub. in Proceedings of the Conference on Precision Electromagnetic Measurements (CPEM), Boulder, CO., June 27-July 1, 1994, p356-357.

Keywords: *Permittivity, Reprints, Maximum entry method, *Dielectric relaxation, *Moment problem.

A procedure for deconvolving time-dependent distribution functions from permittivity data is developed. The problem is reduced to solving an associated moment problem. This moment problem is then solved using a maximum-entropy procedure. A new algorithm for approximating the associated Lagrange multipliers in the distribution function is also outlined. The method is applied to permittivity modeling both for in-band and out-of-band regions. The numerical results indicate that the technique has potential for deconvolving the distribution function from the permittivity data.

04,728
PB96-112065 Not available NTIS
National Inst. of Standards and Technology (EEEL), Boulder, CO. Electromagnetic Technology Div.
SUSAN: SUperconducting Systems ANalysis by Low Temperature Scanning Electron Microscopy (LTSEM).
Final rept.
T. Doderer, D. Hoffman, R. P. Huebener, S. Lachenmann, D. Quenter, J. Schmidt, S. Stehle, J. Niemeyer, R. Popel, S. P. Benz, P. A. A. Booi, N. Kirchmann, and C. A. Krulle. 1993, 4p.
Pub. in Institute of Electrical and Electronics Engineers Transactions on Applied Superconductivity, v3 n1 p2724-2727 Mar 93.

Keywords: *Elecron microscopy, *Superconducting magnets, Reprints, Low temperature, Integrated circuits, *2D arrays, *Fluxon oscillations, *Josephson junctions.

We used the technique of Low Temperature Scanning Electron Microscopy for spatially resolved investigations of both Josephson junctions and superconducting integrated circuits during their operation with a spatial resolution of about 1 micrometer. Two examples of our studies will be presented. With single Josephson tunnel junctions of various geometries we studied different dynamics states such as fluxon oscillations or unidirectional flux flow. With an integrated circuit consisting of a two-dimensional array of tunnel junctions and an rf detection circuit we investigated the rf-properties of the coupling circuit and confirmed the existence of an impedance mismatch and a geometrical standing wave in the blocking capacitor.

04,729
PB96-112321 Not available NTIS
National Inst. of Standards and Technology (MSEL), Gaithersburg, MD. Polymers Div.
Measured Stopping Powers of Hydrogen and Helium in Polystyrene Near Their Maximum Values.
Final rept.
L. Leblanc, G. G. Ross, and W. E. Wallace. 1995, 6p.
Pub. in Nuclear Instruments and Methods in Physics Research B, v95 p457-462 1995.

Keywords: *Energy losses, *Backscattering, *Stopping power, Reprints, Ion beams, Polymers, Hydrogen, Helium.

Rutherford backscattering at two different angles on multilayer targets is used to measure the stopping powers of hydrogen and helium ions in polystyrene in the energy range near their maximum values. In the energy range from 40 to 300 keV/amu, the hydrogen stopping power reaches a maximum value of 9.8 eV/10 to the 15th power atoms/cm. sq. at 81 keV/amu. As the energy increases from 25 to 90 keV/amu, the helium stopping power increases from 15.7 to 26.0 eV/(10 to the 15th power atoms/cm.sq.). Identical results (in keV/amu energy units) were obtained for 2H and 1H, as well as for 4He and 3He. The hydrogen and helium measured stopping power values are compared to the results calculated from two empirical models (Bragg's rule and the cores-and-bonds model). A function has been fit to the experimental data, including those previosly published, which permits rapid calculation of the stopping powers.

04,730
PB96-113584 (Order as PB96-113535, PC A05/MF A01)
National Inst. of Standards and Technology, Gaithersburg, MD.
Spectroscopic Study of Quantized Breakdown Voltage States of the Quantum Hall Effect.
C. F. Lavine, M. E. Cage, and R. E. Elmquist. 1994, 8p.
Included in Jnl. of Research of the National Institute of Standards and Technology, v99 n6 p757-764 Nov/Dec 94.

Keywords: *Spectroscopic analysis, *Electric potential, *Electrical faults, *Hall effect, Quantum theory, Semiconductors(Materials), Electron gas, Spectra, Solid-state plasma, Energy losses, Dissipation factor, Histograms, Two dimensional, NIST(National Institute of Standards and Technology).

Quantized breakdown voltage states are observed in a second, wide, high-quality GaAs/AlGaAs sample made from another wafer, demonstrating that quantization of the longitudinal voltage drop along the sample is a general feature of the quantum Hall effect in the breakdown regime. The voltage states are interpreted in a simple energy conservation model as occuring when electrons are excited to higher Landau levels and then return to the original level. A spectroscopic study of these dissipative voltage states reveals how well they are quantized. The statistical variations of the quantized voltages increase linearly with quantum number.

04,731
PB96-117239 Not available NTIS
National Inst. of Standards and Technology (EEEL), Boulder, CO. Electromagnetic Technology Div.
Measurement of the Weak-Localization Complex Conductivity at 1 Ghz in Disordered Ag Wires.
Final rept.
J. B. Pieper, J. C. Price, and J. M. Martinis. 1992, 4p.
Pub. in Physical Review B, v45 n7 p3857-3860 Feb 92.

Keywords: *Magnetoconductance, Reprints, *Electron diffusion constant, *Weak localization.

The authors have measured the complex magnetoconductivity of disordered quasi-dimensional Ag wires at 1 GHz and at 200 Hz. Because 1 GHz is of the same order as the dephasing rate, the authors have been able to observe the frequency dependence

of weak localization. Both the real and imaginary parts of the conductivity at 1 GHz are in good agreement with theory. The data yield an accurate value for the electron diffusion constant, which is not well determined by dc measurements, and support the theory of weak localization at finite frequency.

04,732
PB96-119417 Not available NTIS
National Inst. of Standards and Technology (PL), Gaithersburg, MD. Electron and Optical Physics Div.
Nanofabrication of a Two-Dimensional Array Using Laser-Focused Atomic Deposition.
Final rept.
R. Gupta, J. J. McClelland, Z. J. Jabbour, and R. J. Celotta. 1995, 3p.
Pub. in Applied Physics Letters, Chapter 67, v10 p1378-1380, 4 Sep 95.

Keywords: *Chromium, *Deposition, *Laser radiation, *Lithography, *Atomic beams, Fabrication, Silicon, Substrates, Two dimensional, Arrays, Microstructure, Lithography, Reprints, *Atom lithography, Nanofabrication, Nanostructures.

Fabricaion of a two-dimensional array of nanometer-scale chromium features on a silicon substrate by laser-focused atomic deposition is described. Features 13 plus or minus 1 nm high and having a full-width at half maximum of 80 plus or minus 10 nm are fabricated in a square array with lattice constant 212.78 nm, determined by the laser wavelength. The array covers an area of approximately 100 micro m x 200 micro m. Issues associated with laser-focusing of atoms in a two-dimensional standing wave are discussed, and potential applications and improvements of the process are mentioned.

04,733
PB96-119441 Not available NTIS
National Inst. of Standards and Technology (MSEL), Gaithersburg, MD. Ceramics Div.
Effect of Sm2BaCuO5 on the Properties of Sintered (Bulk) YBa2Cu3O6+x.
Final rept.
M. D. Hill, J. E. Blendell, C. K. Chiang, L. Chacon, J. F. Kelly, L. H. Bennett, and J. J. Ritter. 1995, 5p.
Pub. in Physica C, n251 p361-365, 7 Jul 95.

Keywords: *Critical current, *Superconductors, *Sintering, Transport properties, Current density, Superconductivity, Solid solutions, Microstructure, Samarium, Barium oxides, Copper oxides, Yttrium oxides, Reprints, *YBCO superconductors, High temperature superconductors, Weale-links.

The addition of Sm2BaCuO5 to YBa2Cu3O(6+x) has been shown to increase the transport critical current density. Because Sm2BaCuO5 and CuO do not coexist at equilibrium, additions of Sm2BaCuO5 to YBa2Cu3O(6+x) cause a reaction with the Cu rich liquid phase usually present during sintering. This forms crystalline phases that do not completely cover the grain boundaries. Sm was found to be homogeneously distributed in the YBa2Cu3O(6+x), matrix. Additions of 5 mole% Sm2BaCuO5 and sintering temperatures of 950 deg. C are effective in increasing the transport critical current density.

04,734
PB96-119615 Not available NTIS
National Inst. of Standards and Technology (CSTL), Boulder, CO. Process Measurements Div.
Building a Better Crycooler.
Final rept.
R. Radebaugh. 1992, 4p.
Pub. in Superconductor Industry, p22-25 Fall 92.

Keywords: *Cryogenics, Reprints, Electronics, Pulse tube, Refrigeration, Superconductors, *Cryocoolers, Brayton, Gifford-McMahon, Joule-Thomson, Stirling.

The lack of satisfactory cryocoolers designed specifically for superconducting electronics has hindered the marketability of superconducting devices. This article reviews the current status of the five most common cryocoolers: Joule-Thomson, Brayton, Stirling, Gifford-McMahon, and pulse tubes. Advantages and disadvantages of each type of commercially available cryocoolers are given. Most of these cryocoolers have been developed for the cooling of infrared sensors and can sometimes be adapted for use with superconducting electronics. Current areas of research are discussed and some projections for the future are given.

04,735
PB96-119656 Not available NTIS
National Inst. of Standards and Technology (EEEL), Gaithersburg, MD. Semiconductor Electronics Div.
Mesoscopic Conductance Fluctuations in Large Devices.
Final rept.
C. A. Richter, D. G. Seiler, and J. C. Pellegrino. 1995, 4p.
Pub. in Workbook of the International Conference on the Physics of Semiconductors (22nd), Vancouver, British Columbia, Canada, August 15-19, 1994, v3 p1967-1970 1995.

Keywords: *Conductance, *Fluctuations, Reprints, *Mesoscopic.

An ac magnetic field modulation and lock-in amplifier technique was used to study 'universal' conductance fluctuations in GaAs/AlGaAs devices. The enhanced measurement sensitivity of this technique permits universal conductance fluctuations to be observed and studied in a new large-size-scale regime where devices have been considered macroscopic. It generally has been assumed that a finite temperature, coherent quantum interference effects could not be observed in devices of this large size.

04,736
PB96-119664 Not available NTIS
National Inst. of Standards and Technology (EEEL), Boulder, CO. Electromagnetic Technology Div.
Faraday Effect Sensors for Magnet Field and Electric Current.
Final rept.
K. B. Rochford, G. W. Day, M. N. Deeter, and A. H. Rose. 1994, 4p.
Pub. in Proceedings of DoD Fiber Optics '94, 'Optical Networks in the Concept of a Global Grid', McLean, VA., March 22-24, 1994, p21-24.

Keywords: *Faraday effect, Reprints, Iron garnets, Magnetic field sensors, Magneto-optics, Optical fiber sensors, *Electric current sensors.

Recent research at NIST has resulted in significant fundamental and practical improvements in magneto-optics sensors used to measure magnetic field and electric current. This paper reviews these developments and considers prospects for further gains.

04,737
PB96-122783 Not available NTIS
National Inst. of Standards and Technology (MSEL), Gaithersburg, MD. Polymers Div.
Novel Method for Determining Thin Film Density by Energy-Dispersive X-ray Reflectivity.
Final rept.
W. E. Wallace, and W. L. Wu. 1995, 3p.
Pub. in Applied Physics Letters, v67 n9 p1203-1205 Aug 95.

Keywords: *Thin films, *X ray density measurement, Reflectance, X rays, Wavelengths, Alignment, Silicon dioxide, Single crystals, Reprints, Spin-on-glass, Polysilsesquioxane.

A technique utilizing the reflection of x-rays to determine material density at flat surfaces is described. The effects of sample misalignment limit the accuracy of x-ray reflectivity as typically practiced. These effects may be properly accounted for by measuring the critical angle for reflection at many different x-ray wavelengths simultaneously from which an extrapolation of the position of the critical angle at infinite wavelength may be made. This extrapolation has the effect of correcting for sample misalignment. Use of the technique is demonstrated for single-crystal silicon surfaces and for silica spin-on-glass thin films.

04,738
PB96-123617 Not available NTIS
National Inst. of Standards and Technology (EEEL), Gaithersburg, MD. Semiconductor Electronics Div.
Characterization of Liquid-Phase Epitaxially Grown HgCdTe Films by Magnetoresistance Measurements.
Final rept.
J. S. Kim, D. G. Seiler, L. Colombo, and M. C. Chen. 1995, 6p.
Pub. in Jnl. of Electronic Materials, v24 n9 p1305-1310 1995.

Keywords: *Magnetoresistance, *Films, Epitaxy, Magnetic properties, Reprints, HgCdTe.

In this paper, we demonstrate that measurements of the magnetoresistance can be used as a valuable alternative to conventional characterization tools to study transport properties of advanced semiconducting materials, structures, or devices. We have measured magnetoresistance on two different systems, namely, three liquid-phase epitaxially grown HgCdTe Films and two GaAs-based high-electron-mobility-transistor (HEMT) structures. The results are analyzed by using a two-carrier model as a reference in the context of the reduced-conductivity-tensor scheme. The HEMT data are in quantitative agreement with the two-carrier model, but the HgCdTe data exhibit appreciable deviations from the model. The observed deviations strongly indicate a mobility spread and material complexity in the HgCdTe samples which are probably associated with inhomogeneities and the resulting anomalous electrical behavior.

04,739
PB96-123641 Not available NTIS
National Inst. of Standards and Technology (EEEL), Boulder, CO. Electromagnetic Technology Div.
Hot-Electron Microcalorimeters as High-Resolution X-ray Detectors.
Final rept.
M. Nahum, and J. M. Martinis. 1995, 3p.
See also PB95-168993.
Pub. in Applied Physics Letters, v66 n23 p3203-3205 Jun 95.

Keywords: *X-ray detectors, *Superconducting junctions, *Calorimeters, Electron temperature, Hot electrons, Metal films, Reprints, *Phonon detectors, *Microcalorimeters.

Measurements are presented on a novel microcalorimeter for the detectionof x-rays. This detector uses a normal metal film deposited on a thin membrane to absorb x-ray photons. The subsequent temperature rise of theelectrons is measured from the current-voltage characteristics of a normal-insulator-superconductor tunnel junction, where part of the absorber forms the normal electrode. A superconducting-quantum- interference-device is used as a low-noise high-bandwidth readout for the junction. We have measured an energy resolution of 22 eV full width at half-maximum and a time constant of 15micro s for a detector operating at 80 mK and having a 0.5 micrometer thick Au adsorber with an area of 100 x 100 micrometer square.

04,740
PB96-123773 Not available NTIS
National Inst. of Standards and Technology (EEEL), Boulder, CO. Optoelectronics Div.
Distributed Feedback Lasers in Rare-Earth-Doped Phosphate Glass.
Final rept.
D. L. Veasey, K. J. Malone, J. A. Aust, N. A. Sanford, and A. Roshko. 1995, 3p.
Pub. in Proceedings of the European Conference on Integrated Optics, Delft, The Netherlands, April 3-6, 1995, p579-581.

Keywords: *Grating, *Lasers, *Glass, Phosphate glass, Waveguide, Reprints, *Foreign technology.

We have successfully demonstrated waveguide lasers operating at 1056.1, 1058.2, and 1062.6 nm in Nd-doped phosphate glass. The waveguides were fabricated by potassium ion exchange from a nitrate melt. Distributed feedback grating patterns were holographically written at 458 nm in photoresist spun on the sample surfaces. The gratings were developed, coated with chromium at a 60-degree evaporation angle, and were then transferred into the glass by argon ion sputtering. Typical laser threshold was 32 mW of absorbed pump power at 805 nm with a corresponding slope efficiency of 2%.

04,741
PB96-131594 PC A04/MF A01
National Inst. of Standards and Technology (CAML), Gaithersburg, MD. Applied and Computational Mathematics Div.
Anisotropy of Interfaces in an Ordered Alloy: A Multiple-Order-Parameter Model.
R. J. Braun, J. W. Cahn, G. B. McFadden, and A. A. Wheeler. Apr 95, 70p, NISTIR-5641.
Prepared in cooperation with Delaware Univ., Newark. Dept. of Mathematical Sciences. Sponsored by Southampton Univ. (England). Faculty of Mathematical Studies.

Keywords: *Face centered cubic lattices, *Alloys, Anisotropy, Lattice parameters, Crystal symmetry, Phase transformations, Binary systems(Materials).

The authors develop a diffuse-interface theory of ordering of a binary alloy on a face-centered-cubic (FCC) crystal lattice. A continuum, multiple-order-parameter theory is used that incorporates the underlying symmetries of the FCC crystal in both the bulk and gradient-energy terms of the free energy. With the theory the authors are able to compute interphase and antiphase boundaries for general orientations with respect to the fixed crystal axes. The authors are able to compute the structure of these interfaces, which compare very well with previous calculations by Kikuchi and Cahn using the cluster variation method. For the parameters the authors have studied, they find that the anisotropy of the surface free energy is not sufficiently strong to cause edges or corners in equilibrium shapes.

04,742
PB96-135033 Not available NTIS
National Inst. of Standards and Technology (EEEL), Boulder, CO. Electromagnetic Technology Div.
Coexistence of Grains with Differing Orthorhombicity in High Quality YBa2Cu3O7-delta Thin Films.
Final rept.
E. I. de Obaldia, K. F. Ludwig, S. J. Berkowitz, P. M. Mankiewich, D. A. Rudman, A. Roshko, R. Moerman, L. Vale, R. H. Ono, A. M. Clark, and W. J. Skocpol. 1994, 3p.
Pub. in Applied Physics Letters, v65 n26 p3395-3397 Dec 94.

Keywords: *Thin films, *X ray diffraction, *Lasers, Reprints, *Pulsed laser deposition, YBCO.

High quality films of YBa2Cu3O7-sigma on LaAlO3 have been grown by pulsed-laser deposition at oxygen pressures of 2.4-54 Pa (25-400 mTorr). X-ray diffraction reveals the coexistence of grains that align with the substrate axes (axial grains). The axial grains are tetragonal while the diagonal grains achieve lattice parameters close to bulk YBa2Cu3O7. The relative proportion of axial grains accounts for the measured variations of normal-state conductance and superconducting critical current density from film to film, based on a simple two-dimensional model of randomly positioned, insulating axial grains.

04,743
PB96-135223 Not available NTIS
National Inst. of Standards and Technology (EEEL), Boulder, CO. Electromagnetic Technology Div.
Accuracy of the Electron Pump.
Final rept.
H. D. Jensen, and J. M. Martinis. 1992, 21p.
See also PB95-168910 and PB95-175873.
Pub. in Physical Review B, v46 n20 p407-427 Nov 92.

Keywords: Metrology, Reprints, Tests, Accuracy, *Electron pumps, Single electron tunneling, Coulomb blockage, Cotunneling.

The authors calculate the accuracy of the single electron pump numerically and analytically. With a biasing of the device that the authors describe as optimal, the accuracy is computed with finite temperature cotunneling rates that systematically include all possible cotunneling processes. A simple graphical representation of the operation of the pump illustrates when cotunneling processes become active. The authors show that the accuracy is limited by cotunneling, thermal activation, and operating the device at too high a frequency; simple approximation formulas are given for these errors. Metrological accuracy is attainable for devices with five or more junctions and with parameters that are experimentally attainable.

04,744
PB96-135348 Not available NTIS
National Inst. of Standards and Technology (EEEL), Boulder, CO. Electromagnetic Technology Div.
Mutual Phase Locking in Systems of High-Tc Superconductor-Normal Metal-Superconductor Junctions.
Final rept.
C. D. Reintsema, R. H. Ono, T. E. Harvey, N. Missert, and L. R. Vale. 1994, 11p.
Pub. in International Society for Optical Engineering, Los Angeles, CA., January 25-27, 1994, v2160 p208-218 Jul 94.

Keywords: *High temperature superconductors, *Superconductors, Reprints, *Phase locking, *SNS junctions.

The authors have investigated the interaction between high critical temperature (high-Tc) superconductor-normal metal-superconductor step-edge junctions coupled through a non-superconducting feedback loop. The authors have characterized the strength of the interaction as a function of frequency and temperature for both a circuit without a groundplane and an all high-Tc multilayer circuit incorporating a superconducting ground plane. The authors observed relative locking strengths (the ratio of the measured locking current IL to the junctions average critical current Ic) as large as IL/IC=9% and peak locking frequencies as high as 1.06 THz. The maximum temperature at which locking occurred was 35 K. An analysis of the temperature dependence of the locking current accounting for thermal fluctuations in the context of Johnson noise from resistive elements in the circuit agrees well with the authors' experimental observations.

04,745
PB96-135371 Not available NTIS
National Inst. of Standards and Technology (PL), Gaithersburg, MD. Electron and Optical Physics Div.
Influence of Thickness Fluctuations on Exchange Coupling in Fe/Cr/Fe Structures.
Final rept.
J. A. Stroscio, D. T. Pierce, J. Unguris, and R. J. Celotta. 1995, 8p.
Pub. in Ultimate Limits of Fabrication and Measurement, p181-188 1995.

Keywords: *Chromium, *Exchange coupling, *Magnetism, Reprints, Iron, Electron microscopy, Polarization, Microscopy, *Foreign technology.

Realizing the ultimate limits in fabrication requires the controlled placement of material at the single atomic layer limit. This precision is required for both semiconductor and magnetic devices, the two largest industries racing towards the Ultimate Limits in fabrication. In this report the authors summarize results on the effects of thickness fluctuations on the exchange coupling in Fe/Cr/Fe trilayer structures. This work demonstrates the importance of controlling thin film thickness at the single atomic layer level in magnetic systems.

04,746
PB96-137773 Not available NTIS
National Inst. of Standards and Technology (EEEL), Boulder, CO. Electromagnetic Technology Div.
Panel Discussion on Units in Magnetism.
Final rept.
R. B. Goldfarb. 1995, 12p.
Pub. in Magnetic and Electrical Separation, v6 p105-116 1995.

Keywords: *Magnetism, Units of measurement, Symbols, Reprints, Conversion factors.

An evening panel discussion on magnetic units, attended by 150 participants, was held at the 1994 Joint MMM-Intermag Conference in Albuquerque, New Mexico, USA. The season was organized by C.D. Graham, Jr., and moderated by R.B. Goldfarb. The panel members were asked to describe the use of magnetic units in the countries, and to make appropriate comments and recommendations. In addition to units, several panelists talked about distinction between magnetic induction B and magnetic field strength H, and the conversion of equations. After the panelists' opening statements, the floor was opened for questions and discussion from the audience. Below are the panelists' summaries of their remarks. By agreement with authors, this article is not subject to copyright.

04,747
PB96-138417 Not available NTIS
National Inst. of Standards and Technology (EEEL), Boulder, CO. Electromagnetic Technology Div.
Low Noise YBa2Cu3O7-x-SrTiO3-YBa2Cu3O7-x Mulitlayers for Improved Superconducting Magnetometers.
Final rept.
F. Ludwig, D. Koelle, E. Dantsker, J. Clarke, R. E. Thomson, D. T. Nemeth, and A. H. Miklich. 1995, 3p.
Pub. in Applied Physics Letters, v66 n3 p373-375 Jan 95.

Keywords: *Magnetometers, Multilayers, Noise, Trilayers, Reprints, *Flux transformers, YBCO.

We have fabricated YB2Cu3O7-x-SrTiO3-YBa2Cu3O7-x (YBCO-STO-YBCO) trilayers, in which each layer is patterned photolithographically, capping the first YBCO film with an in situ STO film. Atomic force microscopy demonstrates that the capping process dramatically improves the quality of the surface of the second layer, allowing the growth of an upper YBCO film with a substantially reduced level of low-frequency flux noise. A magnetometer with a multiturn flux transformer coupled to a dc superconducting quantum interference device achieved a magnetic field noise of 74 fT Hz-1/2 at 1 Hz, improving to 31 fT Hz-1/2 at 1 kHz.

04,748
PB96-138458 Not available NTIS
National Inst. of Standards and Technology (MSEL), Gaithersburg, MD. Reactor Radiation Div.
High-Energy Phonon Dispersion in La1.85Sr0.15CuO4.
Final rept.
A. H. Moudden, P. M. Gehring, G. Shirane, B. Hennion, Y. Endoh, I. Tanaka, H. Kojima, M. Matsuda, and L. Vasiliu-Doloc. 1995, 3p.
Pub. in Physica B Condensed Matter, v213-214 p72-74 1995.

Keywords: *Superconducting, Transverse, Longitudinal, Reprints, *Phonon dispersion.

The authors have measured two phonon-dispersion curves above 50 meV in a superconducting (Tc=33 K) single crystal of La1.8Sr0.15CuO4. In the normal phase (T=45 K), the authors show that the A1 mode compatible with the Raman A1g(425 cm-1) mode is weakly dispersive, falling from 53.7 meV at the zone center to about 51 meV at the zone boundary along the tetragonal (0.0) direction. For the A1 mode compatible with the infra-red A2u (480 cm to the minus one) mode, they observe a significant dispersion of the photonon energy which drops monotonically from 60 to 56 meV. The global features of these dispersion curves were similar to those previously reported in studies of both pure and 10% Sr doped La2CuO4. However significant differences in the shape of the dispersion of the highest A1 branch is shown, as well as a significant softening with increasing carrier concentration.

04,749
PB96-138524 Not available NTIS
National Inst. of Standards and Technology (EEEL), Gaithersburg, MD. Semiconductor Electronics Div.
Electron-electron Interactions, Coupled-Plasmon-Phonon Modes, and Mobility in n-Type GaAs.
Final rept.
B. A. Sanborn. 1995, 9p.
Pub. in Physical Review B, v51 n20 p14 256-14 264 May 95.

Keywords: *Electron scattering, Mobility, Reprints, *Electron-electron interactions, GaAs, Coupled modes, Boltzmann equation, Dynamic screening.

The paper investigates the mobility of electrons scattering from the coupled system of electrons and longitudinal-optical (LO) phonons in n-type GaAs. The Boltzmann equation is solved exactly for low electric fields by an iterative method, including electron-electron and electron-LO-phonon self-energy is treated in the plasmon-pole approximation. Scattering from ionized impurities screened in static RPA is calculated with phase-shift cross sections and scattering from RPA screened deformation potential and piezoelectric acoustic phonons is included in the elastic approximation. The results show that dynamic screening and plasmon-phonon coupling significantly modify inelastic scattering at low temperatures and densities. The effect on mobility is obscured by ionized impurity scattering in conventionally doped material, but should be important in modulation doped structures. For uncompensated bulk n-type GaAs, the RPA phase-shift model for electron-impurity scattering gives lower drift mobilities than the standard Thomas-Fermi or Born calculations, which are high compared to experiment.

04,750
PB96-138557 Not available NTIS
National Inst. of Standards and Technology (EEEL), Boulder, CO. Electromagnetic Technology Div.
Dependence of Contrast on Probe/Sample Spacing with the Magneto-Optic Kerr-Effect Scanning Near-Field Optical Microscope (MOKE-SNOM).
Final rept.
T. J. Silva, and A. B. Kos. 1995, 7p.
Pub. in Proceedings - The Society of Photo-Optical Instrumentation Engineering Near-Field Optics, San Diego, CA., July 9-10, 1995, v2535 p2-8 1995.

Keywords: *Light scattering, Near-field, Reprints, *Magneto-optic, Surface plasmons.

A magneto-optic Kerr-effect scanning near-field optical microscope is used to image a stripe domain wall in a Co/Pt multilayer sample. The microscope is an improved version of a type previously reported, which uses light scattering from surface plasmons in 20-40 nm Ag particles as a near-field probe. Data are presented for both the probe intensity and polarization contrast as a function of probe/sample spacing. Oscillatory behavior in both sets of data is reasonbly explained with a simplified model of optical interference.

04,751
PB96-138573 Not available NTIS
National Inst. of Standards and Technology (EEEL), Boulder, CO. Electromagnetic Technology Div.
Development of Highly Conductive Cantilevers for Atomic Force Microscopy Point Contact Measurements.
Final rept.
R. E. Thomson, and J. Moreland. 1995, 3p.
Pub. in Jnl. of Vacuum Science and Technology B, v13 n3 p1123-1125 May/Jun 95.

Keywords: *Cantilevers, Contact resistance, Point contact, Reprints, *Atomic force microscopy.

Several techniques for improving the electrical conductivity of micromachined silicon cantilevers for atomic force microscopy point contact measurements were investigated. The techniques studied included sputtering or evaporating thin layers of gold, platinum or silver onto the lower surface of the cantilever to create a conducting metal layer, and doping the cantilevers with phosphorus. It was found that the lowest resistance contacts to a gold surface can be made by the metal coated tips, which can make stable point contacts with resistances as low as 30 omega at a tip sample force of 15 mu N.

04,752
PB96-141098 Not available NTIS
National Inst. of Standards and Technology (EEEL), Boulder, CO. Electromagnetic Technology Div.
Evidence for Tunneling and Magnetic Scatttering at 'In situ' YBCO/Noble-Metal Interfaces.
Final rept.
S. C. Sanders, S. E. Russek, C. C. Clickner, and J. W. Ekin. 1995, 6p.
Pub. in Institute of Electrical and Electronics Engineers Transactions on Applied Superconductivity, v5 n2 p2404-2407 Jun 95.

Keywords: *Conductance, *Electrical transport, Contacts, Reprints, Tunneling, Interfaces, Noble metals, *YBCO superconductors.

We report low-temperature conductance data for in situ YBa2Cu3O7-sigma (YBCO)/Au, and YBCO/Pt planar c-axis interfaces. Analysis of the conductance data for these interfaces, which have resistivities as low as 1 x 10 to the minus 8th power omega-cm2, indicates that tunneling is the predominant transport mechanism. Zero-bias conductance peaks are present for all of the in situ interfaces. These peaks are analyzed in the framework of the Appelbaum model and are attributed to the presence of isolated magnetic spins at the interface. The presence and similarity of the peaks for each noble-metal overlayer supports the hypothesis that the magnetic spins are inherent to the YBCO surface.

04,753
PB96-141155 Not available NTIS
National Inst. of Standards and Technology (MSEL), Gaithersburg, MD. Reactor Radiation Div.
Neutron-Powder-Diffraction Study of the Long-Range Order in the Octahedral Sublattice of LaD2.25.
Final rept.
T. J. Udovic, Q. Huang, J. J. Rush, J. Schefer, and I. S. Anderson. 1995, 11p.
Pub. in Physical Review B, v51 n18 p12 116-12 126 1995.

Keywords: *Crystal structure, *Lanthanum deuteride, Neutron diffraction, Reprints, Rare earths, Long range order.

Neutron-powder-diffraction patterns of the superstoichiometric rare-earth dideuteride LaD2.25 were measured between 15 and 400 K. Profile refinements indicated that, above approximately 345 K, the LaD2.25 structure is cubic (Fm3m) with deuterium fully occupying the tetrahedral (t) interstices of the fcc La lattice and the excess deuterium occupying a portion of the octahedral (o) interstices with full statistical disorder. As the temperature is decreased below approximately 345 K, the LaD2.25 structure undergoes a transformation to tetragonal symmetry concomitant with the onset of deuterium long-range order (I4/mmm) in the o sublattice. Fully developed long-range order is established near 230 K and ideally corresponds to the occare-earth-deuterium systems possessing similar D/Metal stoichiometric ratios. This ordering is accompanied by an outward expansion of the cubic ensemble of eight t-site deuterium atoms surrounding each o-site deuterium (Do) atom. Moreover, the c-directed La-Do bond distances are decreased by a displacement of the La atoms toward the Do atoms.

04,754
PB96-141205 Not available NTIS
National Inst. of Standards and Technology (MSEL), Gaithersburg, MD. Reactor Radiation Div.
Photoluminescence Spectra of Epitaxial Single Crystal C60.
Final rept.
R. D. Averitt, P. M. Pippenger, V. O. Papanyan, N. J. Halas, J. A. Dura, and P. Nordlander. 1995, 6p.
Pub. in Chemical Physics Letters, n242 p592-597 Sep 95.

Keywords: *Epitaxial growth, *Single crystals, Thin films, Optical properties, Carbon, Temperature, Reprints, *Photoluminescence.

We report the photoluminescence spectrum of well characterized, epitaxially grown single crystal C60 thin fims. The highly regular and reproducible spectral features observed can be explained by a simple molecular model which takes into account enhanced coupling of an excited C60 molecule with its nearest neighbor. This model provides an identification of all the observed spectral features at low temperature including a qualitative understanding of the relative peak height ratios, as well as the observed temperature dependene of the PL spectrum.

04,755
PB96-141213 Not available NTIS
National Inst. of Standards and Technology (EEEL), Boulder, CO. Electromagnetic Technology Div.
Quench Energy and Fatigue Degradation Properties of Cu- and Al/Cu-Stablized Nb-Ti Epoxy-Impregnated Superconductor Coils.
Final rept.
S. L. Bray, J. W. Ekin, D. J. Waltman, and M. J. Supercynski. 1995, 4p.
Pub. in Institute of Electrical and Electronics Engineers Transactions on Applied Superconductivity, v5 ptl n2 p222-225 Jun 95.

Keywords: *Superconductors, *Coils, Superconducting devices, Reprints, Fatigue degradation, NbTi, Residual resistivity, Stability strain, Quench energy.

In comparative measurements of small-scale epoxy-impregnated Cu-stabilized and Al/Cu-stabilized Nb-Ti test coils at 4 K and 5 T, the heat energy required to quench the Al/Cu-stabilized coil was 4 to 12 times greater than for the Cu-stabilized coil, depending on the relative operating current. Also, the coils' stabilizer resistivity (p) was measured as a function of mechanical fatigue to test for strain-induced degradation. The p of the Cu-stabilized coil is relatively unaffected by fatigue, while that of the Al/Cu-stabilized coil increases with fatigue. However, in these coils, having a typical stabilizer:superconductor ratio of 4:1, the degradation of the Al/Cu-stablized coil beings to saturate after several hundred fatigue cycles; after 2000 fatigue cycles to 0.2% strain, the p of the Al/Cu-stabilized coil is still 2.6 times lower than the p of the Cu-stabilized coil.

04,756
PB96-141221 Not available NTIS
National Inst. of Standards and Technology (PL), Boulder, CO. Time and Frequency Div.
Atomic Iron in Its (5)D Ground State: A Direct Measurement of the J = 0 inverted arrow 1 and J = 1 inverted arrow 2 Fine-Structure Intervals (1.2).
Final rept.
J. M. Brown, and K. M. Evenson. 1995, 4p.
Pub. in Astrophysical Jnl., v441 pL97-L100 Mar 95.

Keywords: *Iron, *Magnetic resonance, Fine structure, Reprints, Atoms.

The J = 0 <- 1 and J = 1 <- 2 fine-structure transitions in atomic Fe in its grond 5D state have been detected in the laboratory by far-infared laser magnetic resonance. The fine-structure intervals have been measured accurately as 2696.3942(22) and 5519.9397(18) GHz, respectively; these values correspond to wavelengths of 111.18273 and 54.31082 micrometers, with an uncertainty of about 2 x time 10 to the minus 5th power micrometers.

04,757
PB96-141247 Not available NTIS
National Inst. of Standards and Technology (PL), Gaithersburg, MD. Electron and Optical Physics Div.
Using Atom Optics to Fabricate Nanostructures.
Final rept.
R. J. Celotta, J. J. McClelland, R. E. Scholten, and R. Gupta. 1995, 4p.
Pub. in Ultimate Limits of Fabrication and Measurement, p75-78 1995.

Keywords: Photon-atom collisions, Atomic force microscopy, Reprints, Microstructures, *Nanostructures, *Atom optics, Chromium atoms.

The drive for further miniaturization of electronic and magnetic devices continues to place increasing demands on the authors' abilities to fabricate very small structures and to understand and exploit the physical laws applicable in such devices. Optical lithographic techniques continue to be refined and limitations imposed by diffraction are driving the wavelength of the photons utilized toward the x-ray region. Still shorter wavelength particles, high energy electrons, are used for the highest resolution mask making. A logical extension of the progression would involve using atoms, because of their short de Broglie wavelength, as the pattern generating particle, either to expose a resist, or to deposit structures directly. The authors' are exploring how the techniques of atom optics, a field paralleling electron optics but utilizing neutral atoms instead of electrons, can be used to fabricate structures on the nanometer scale. This article is a brief summary of the authors' research on this topic. A more detailed treatment can be found elsewhere.

04,758
PB96-141312 Not available NTIS
National Inst. of Standards and Technology (EEEL), Boulder, CO. Electromagnetic Technology Div.
Oxygen Annealing of Ex-situ YBCO/Ag Thin-Film Interfaces.
Final rept.
J. W. Ekin, C. C. Clickner, S. E. Russek, and S. C. Sanders. 1995, 4p.
Pub. in Institute of Electrical and Electronics Engineers Transactions on Applied Superconductivity, v5 pt3 n2 p2400-2403 Jun 95.

Keywords: *YBCO superconductors, *Electric contacts, Thin films, Silver, Magnetic scattering, Reprints, *Anneling.

The resistivity of YBCO/Ag interfaces has been measured for different oxygen annealing temperatures for a series of ex-situ fabricated thin-film contacts having sizes ranging from 16 micrometers x 16 micrometers down to 4 micrometers x 4 micrometers. The interface resistivity began to decrease after annealing at 300 deg C for 10 minutes in one atmosphere oxygen. After annealing at 400 deg C, the contact resistivity decreased by several orders of magnitude to the 10 to the minus 7 power Omega-(cm)squared range. The 500-nm thick Ag layer showed massive surface diffusion and agglomeration for annealing temperatures above -400 deg C; this temperature thus represents a practical limit for oxygen annealing the TBCO/Ag interface system for more than 10 minutes. Rapid cooling of the chip after annealing led to a severe loss of critical current density in the YBCO layer, which could be restored by reannealing and cooling at a slower rate of 50 deg C/min.

04,759
PB96-141338 Not available NTIS
National Inst. of Standards and Technology (MSEL), Boulder, CO. Materials Reliability Div.
Ultrasonic-Resonance Spectroscopy of Bulk and Layered Solids.
Final rept.
C. Fortunko, H. Ledbetter, and P. Heyliger. 1995, 6p.
Pub. in International Symposium on Surface Waves in Solid and Layered Structures and National Conference on Acoustoelectronics, Moscow-St. Petersburg, May 17-23, 1994, p430-435 1995.

Keywords: *Resonat frequency, *Composites, Copper, Elastic constants, Layered solids, Thin films, Superconductors, Reprints, *Foreign technology, *Ultrasonic-resonance spectroscopy.

The authors used ultrasonic-resonance spectroscopy (URS) to determine the complete elastic-stiffness. The

authors show spectra for five materials: polycrystal and monocrystal copper, laminated composite B1/Al, a seven-layer structure aramid-epoxy/Al, a YBa2Cu3O7 superconductive film on a SrTiO3 substrate. Frequencies involved are 100 kHz - 5 MHz. Specimen sizes are approximately 1 cm. The URS approach offers the principal advantage of one measurement for a multicomponent tensor property: for orthotropic symmetry, nine independence components.

04,760
PB96-141346 Not available NTIS
National Inst. of Standards and Technology (PL), Gaithersburg, MD. Electron and Optical Physics Div.
Domain Structures in Magnetoresistive Granular Metals.
Final rept.
A. Gavrin, M. H. Kelley, J. Q. Xiao, and C. L. Chien. 1995, 3p.
Pub. in Applied Physics Letters, v66 n13 p1683-1685 Mar 95.

Keywords: *Electron microscopy, *Magnetioresistance, Metal alloys, Cobalt, Reprints, *Granular materials, Polarizaton analysis, Annealing.

The author imagined the magnetic domain structure of several heterogeneous CovAg1-x alloys by using scanning electron microscopy with polarization analysis. These images show that extended domain structures exist in both the as-deposited samples and in samples annealed at moderate temperatures. This suggests that a significant fraction of the cobalt in these materials does not contribute to the giant magnetoresistance. Only those samples annealed at 600 deg C and containing less than 40% cobalt by volume show no domain structure.

04,761
PB96-141387 Not available NTIS
National Inst. of Standards and Technology (EEEL), Boulder, CO. Electromagnetic Technology Div.
Theory of the Magneto-Optic Kerr Effect in the Near Field.
Final rept.
V. A. Kosobukin. 1995, 7p.
Pub. in Proceedings of the International Society for Optical Engineering Near-Field Optics, San Diego, CA., July 9-10, 1995, v2535 p9-15.

Keywords: *Magneto-optical effects, Kerr effect, Near field, Reprints, Light scattering, Surface plasmons.

A theory is developed for the magneto-optic Kerr effect (MOKE) excited via an optical near field. The model under consideration includes a semi-infinite ferromagnet and a small non-magnetic metal particle which is located nearby and possesses a long-living surface plasmon. A multiple-scattering formulation of the problem is given. Considering the Rayleigh scattering of light and the magneto-optical light polarization conversion as elementary events, all the essential optical processes are classified, and those which contribute to the near-field excitation, is treated self-consistently to all orders in light-matter interaction, and the magneto-optical interaction is described in the first order approximation of perturbation theory. The scattered light field is discussed with special emphasis on the change of optical polarization due to MOKE.

04,762
PB96-146691 Not available NTIS
National Inst. of Standards and Technology (EEEL), Boulder, CO. Electromagnetic Technology Div.
Low Magnetostriction in Annealed NiFe/Ag Giant Magnetoresistive Multilayers.
Final rept.
Y. K. Kim, S. C. Sanders, and S. E. Russek. 1995, 3p.
Pub. in Institute of Electrical and Electronics Engineers Transactions on Magnetics, v31 n6 p3964-3966 Nov 95.

Keywords: *Magnetoresistivity, *Annealing, *Thin films, Temperature dependence, Nickel compounds, Iron compounds, Silver, Sensors, Magnetic tape, Recording heads, Reprints, *Magnetorestriction, Multilayers.

Systematic changes were observed in magnetostriction and magnetoresistance ratio for NiFe/Ag multilayers as a function of annealing temperature. Optimal multilayer configurations (number of bilayers and Ag layer thickness) can be engineered to achieve zero magnetostriction concurrent with high magnetoresistance sensitivity. This feature makes the NiFe/Ag multilayers potentially useful for high-performance magnetic recording read-sensors.

04,763
PB96-146717 Not available NTIS
National Inst. of Standards and Technology (EEEL), Boulder, CO. Electromagnetic Technology Div.
Telegraph Noise in Silver-Permalloy Giant Magnetoresistance Test Structures.
Final rept.
L. S. Kirschenbaum, C. T. Rogers, S. E. Russek, and S. C. Sanders. 1995, 3p.
Pub. in Institute of Electrical and Electronics Engineers Transactions on Magnetics, v31 n6 p3943-3945 Nov 95.

Keywords: *Magnetoresistivity, *Noise, *Permalloys(Trademark), Magnetic domains, Ferromagnetic materials, Telegraph systems, Electrical properties, Reprints, GMR, RTF(Random telegraph fluctuator), Multilayers.

We report noise data for discontinuous Ni82Fe18/Ag multilayer test structures. Examination of the noise data for this material indicates that random telegraph fluctuator (RTF) noise of the resistance is the predominant noise source. Analysis of the RTF noise in these structures presents an opportunity to estimate magnetic domain or magnetic cluster strengths and the domain-domain interactions.

04,764
PB96-146824 Not available NTIS
National Inst. of Standards and Technology (MSEL), Gaithersburg, MD. Reactor Radiation Div.
Statistical Descriptors in Crystallography. 2. Report of a Working Group on Expression of Uncertainty in Measurement.
Final rept.
D. Schwarzenbach, S. C. Abrahams, H. D. Flack, E. Prince, and A. J. C. Wilson. 1995, 5p.
See also PB89-201826.
Pub. in Acta Crystallographica, vA51 p565-569 1995.

Keywords: *Crystallography, *Uncertainty analysis, *Terminology, Statistical mechanics, Experimental data, Computations, Standard deviation, Error analysis, Statistics, Nomenclature, Reprints.

The present publication updates an earlier report of the IUCr Subcommittee on Statistical Descriptors (Schwarzenbach, Abrahams, Flack, Gonschorek, Hahn, Huml, Marsh, Prince, Robertson, Rollett and Wilson (1989): Acta Cryst. A45, 63-75). This new report presents the concepts of standard uncertainty, of combined stanard uncertainty, and of Type A and Type B evaluations of standard uncertainties. It expands the earlier dictionary of statistical terms, recommends replacement of the term estimated standard deviation (e.s.d.) by standard uncertainty (s.u.) or by combined standard uncertainty (c.s.u.) in statements of the statistical uncertainties of data and results, and requests a complete description of the experimental and computational procedures used to obtain all results submitted to IUCr publications.

04,765
PB96-146832 Not available NTIS
National Inst. of Standards and Technology (CAML), Gaithersburg, MD. Computer Systems and Communications Div.
Stagnant Film Model of the Effect of Natural Convection on the Dendrite Operating State.
Final rept.
R. F. Sekerka, S. R. Coriell, and G. B. McFadden. 1995, 7p.
Pub. in Jnl. of Crystal Growth, v154 p370-376 Apr 95.

Keywords: *Dendritic crystals, *Crystal growth, *Films, *Mathematical models, Convection, Heat transfer, Nusselt number, Fluid dynamics, Reprints.

We develop a simple model of the influence of natural convection on the selection of the operating state (dendrite tip velocity, V, and tip radius, rho) for dendritic growth of a pure material. We hypothesize that the important aspects if natural convection can be accounted for by considering the global convection that would occur in the vicinity of a sphere of radius R that characterizes the size of a dendritic array that is growing from a point source. We estimate the thickness, delta, of a stagnant boundary layer surrounding this sphere by matching the value of the Nusselt number obtained from the heat transfer literature. We solve the steady-state problem of a paraboloidal dendrite at temperature T(sub M) growing toward a confocal paraboloid at temperature T(sub infinity) located at a distance delta from the tip.

04,766
PB96-147087 Not available NTIS
National Inst. of Standards and Technology (EEEL), Boulder, CO. Electromagnetic Technology Div.
Magnetoresistance of Thin-Film NiFe Devices Exhibiting Single-Domain Behavior.
Final rept.
R. W. Cross, J. O. Oti, S. E. Russek, T. Silva, and Y. K. Kim. 1995, 3p.
Pub. in Institute of Electrical and Electronics Engineers Transactions on Magnetics, v31 n6 p3358-3360 Nov 95.

Keywords: *Magnetoresistivity, *Thin films, Nickel compounds, Iron compounds, Magnetization, Hysteresis, Devices, Single domain, Reprints, Barkhausen.

Rectangular NiFe stripes as small as 1 x 5 microm were fabricated and characterized as a function of film thickness. Gold current leads were sputtered and patterned onto the stripes so that magnetoresistance measurements could be performed. A uniform in-plane magnetic field was applied transverse to the stripe length and at various angles from the perpendicular direction. For film thicknesses greater than 10 nm, the magnetoresistance for all of the devices had large jumps and hysteresis due to domain formation. As the thickness of the film decreased below 10 nm, the domain structure disappeared for stripe heights 2 microm or less. Theoretical calculations of the magnetization reversals were obtained using a numerical implementation of the Stoner-Wohlfarth model for the switching of a single-domain ellipsoidal particle.

04,767
PB96-147160 Not available NTIS
National Inst. of Standards and Technology (EEEL), Boulder, CO. Electromagnetic Technology Div.
II-3: Critical Current Measurement Methods: Quantitative Evaluation.
Final rept.
L. F. Goodrich, and A. N. Srivastava. 1995, 5p.
See also PB93-153369.
Pub. in Cryogenics, v35 VAMAS Supplement, pS19-S23 1995.

Keywords: *Superconductors, *Critical current, Electrical measurement, Comparative evaluations, Reprints, *Foreign technology, Thermal contraction.

The critical current Ic of a superconductor is a quantitative evaluation of its current carrying capacity, and is defined as the current at which a specified electric field criterion Ec, or resistivity criterion Pc is achieved in the specimen. Typical electric field and resistivity criteria are 10 to the minus one microm and 10 to the minus 14th power omega m, respectively. The voltage-current (V-I) characteristic of the superconductor can be modelled by the empirical equation V = V0(III0) sup n where I0 is the observed current at voltage V0. The value of n can be thought of as a 'figure of merit' for the conductor, and reflects the abruptness of the transition from the superconducting to the normal state, with typical values ranging from 10 to 100.

04,768
PB96-147178 Not available NTIS
National Inst. of Standards and Technology (EEEL), Boulder, CO. Electromagnetic Technology Div.
First VAMAS USA Interlaboratory Comparison of High Temperature Superconductor Critical Current Measurements.
Final rept.
L. F. Goodrich, J. A. Wiejaczka, A. N. Srivastava, T. C. Stauffer, and L. T. Medina. 1995, 4p.
Pub. in Institute of Electrical and Electronics Engineers Transactions on Applied Superconductivity, v5 pt1 n2 p552-555 Jun 95.

Keywords: *High-Tc superconductors, *Critical current, Comparative evaluations, Damage, Homogeneity, Routing, Standards, Reprints.

The authors conducted an interlaboratory comparison of critical current (Ic) measurements on Bi2Sr2Ca2Cu3O10 tapes (2223). The study includes measurements from six participating US laboratories, with NIST as the central, organizing laboratory. A number of specimens were prepared with different degrees of instrumentation to isolate sources of variability. Most of the specimens were pre-measured by NIST to reduce uncertainties due to sample variability. Different specimen routing patterns among the laboratories were implemented to isolate sources of variability due to the specimen's measurement history.

04,769
PB96-147186 Not available NTIS
National Inst. of Standards and Technology (EEEL), Boulder, CO. Electromagnetic Technology Div.
II-5: Thermal Contraction of Materials Used in Nb3Sn Critical Current Measurements.
Final rept.
L. F. Goodrich, and A. N. Srivastava. 1995, 4p.
Pub. in Cryogenics, v35 VAMAS Supplement, pS29-S32 1995.

Keywords: *Superconductors, Comparative evaluations, Contraction, Electrical measurement, Reprints, *Foreign technology, *Niobium stannoides, *Critical current.

It is typical for Nb3Sn-Cu superconductor specimens to be wound into coils on tubular measurement mandrels for critical current measurements. If the thermal contraction of the mandrel is different from that of the specimen, either tensile or compressive axial strain could develop upon cooling from room temperature to liquid helium temperature, thus affecting the measured critical current Ic1.2. The amount of strain depends on the magnitude of the differential contraction, the relative strength of the specimen and mandrel, and the mechanical coupling between the specimen and its mandrel.

04,770
PB96-147194 Not available NTIS
National Inst. of Standards and Technology (EEEL), Boulder, CO. Electromagnetic Technology Div.
USA Interlaboratory Comparison of Superconductor Simulator Critical Current Measurements.
Final rept.
L. F. Goodrich, J. A. Wiejaczka, A. N. Srivastava, T. C. Stauffer, and L. T. Medina. 1995, 4p.
Pub. in Institute of Electrical and Electronics Engineers Transactions on Applied Superconductivity, v5 n2 pt1 p548-551 Jun 95.

Keywords: *Superconductors, Comparative evaluations, Variability, Simulators, Standards, Reprints, *Critical current.

An interlaboratory comparison of critical current (Ic) measurements was conducted on the superconductor simulator, which is an electronic circuit that emulates the extremely nonlinear voltage-current characteristic of a superconductor. These simulators are high precision instruments, and are useful for establishing the integrity of part of a superconductor measurement system. The study includes measurements from participating US laboratories, with NIST as the central, organizing laboratory. This effort was designed to determine the sources of uncertainty in Ic measurements due to uncertainties in the measurement apparatus, technique, or the analysis system.

04,771
PB96-148010 Not available NTIS
National Inst. of Standards and Technology (EEEL), Boulder, CO. Electromagnetic Technology Div.
Microwave Noise in High-Tc Josephson Junctions.
Final rept.
E. N. Grossman, L. R. Vale, and D. A. Rudman. 1995, 3p.
Pub. in Applied Physics Letters, v66 n13 p1680-1682 Mar 95.

Keywords: *Josephson junctions, *YBCO superconductors, Noise, Mixing circuits, Heterodyning, Reprints, SNS junctions, Terahertz, Mixer.

The authors have measured the noise of YBa2Cu3O7-delta superconductor- normal-superconductor (SNS) junctions whose high normal-state resistances and characteristic frequencies make them suitable for THz frequency mixers. By directly measuring the 1 GHz powerspectral density delivered to a low-noise 50 Ohms radiometer system, thenoise could be measured over a wide range of dc voltage and temperature,without complications due to 1/f noise, and without invoking any specific model. The effective noise temperature of the normal resistanceis approximately equal to the physical temperature at high temperatures,but approaches a limiting value at low temperatures, implying an excess current noise of unknown origin.

04,772
PB96-148143 Not available NTIS
National Inst. of Standards and Technology (EEEL), Boulder, CO. Electromagnetic Technology Div.
V-6: Effects of Temperature Variation.
Final rept.
H. Kirchmayr, and L. F. Goodrich. 1995, 2p.
Pub. in Cryogenics, VAMAS Supplement, v35 pS99-S100 1995.

Keywords: *Superconductors, *Low temperature tests, *Interlaboratory comparisons, Temperature dependence, Liquid helium, Pressure, Cryostats, Reproducibility, Niobium stannides, Reprints, Critical current, Mandrel.

The critical current (Ic) of a NbTi or Nb3Sn superconductor specimen depends on its temperature. The pressure, and thus the liquid helium temperature, may vary between laboratories due to different altitudes and different cryostats used for the Ic measurement. Thus, it is necessary to study the temperature dependence of the specimen's critical current. This paper presents measurements of Ic as a function of temperature for tests carried out at the Technical University of Vienna (TUW) and the National Institute of Standards and Technology (NIST).

04,773
PB96-148150 Not available NTIS
National Inst. of Standards and Technology (EEEL), Gaithersburg, MD. Semiconductor Electronics Div.
Scanning Capacitance Microscopy Measurements and Modeling: Progress Towards Dopant Profiling of Silicon.
Final rept.
J. J. Kopanski, J. F. Marchiando, and J. R. Lowney. 1995, 8p.
Pub. in Proceedings of the International Workshop on the Measurement and Characterization of Ultra-Shallow Doping Profiles in Semiconductors (3rd), Research Triangle Park, NC., March 20-22, 1995, p9.1-9.8.

Keywords: *Microscopy, *Scanning, *Semiconductor devices, *Silicon, Dopes, Profiles, Experimental data, Models, Reprints, AFM(Atomic force microscope), SCM(Scanning capacitance microscope).

A scattering capacitance microscope (SCM) has been implemented by interfacing a commercial contact-mode atomic force microscope (AFM) with a high-sensitivity capacitance sensor. SCM has promise as a next-generation dopant-profiling technique because the measurement is inherently two dimensional, has a potential spatial resolution limited by tip diameter of at least 20 nm, and requires no current carrying metal-semiconductor contact. Different capacitance images have been made with the SCM of a variety of bulk-doped samples and in the vicinity of pn junctions and homojunctions. Also, a computer code has been written that can numerically solve Poisson's equation for a model SCM geometry by using the method of collocation of Gaussian points.

04,774
PB96-148184 Not available NTIS
National Inst. of Standards and Technology (EEEL), Boulder, CO. Electromagnetic Technology Div.
Effects of Substrate Surface Steps on the Microstructure of Epitaxial Ba2YCu3O7-x Thin Films on (001) LaAlO3.
Final rept.
P. C. McIntyre, M. J. Cima, and A. Roshko. 1995, 10p.
Pub. in Jnl. of Crystal Growth, v149 p64-73 1995.

Keywords: *Epitaxy, *YBCO superconductors, *Thin films, Critical temperature, High temperature, Substrates, Crystal growth, Morphology, Reprints.

The effect of steps in the (001) surface of LaAlO3 substrates on the microstructural evolution of heteroepitaxial Ba2YCu3O7(7-x) (BYC) thin films were characterized by high resolution transmission electron microscopy (TEM) and atomic force microscopy (AFM). Native substrate surface steps acted as nucleation sites for both the c-axis normal and c-axis in-plane (a-axis normal) orientations in BYC films prepared by post-deposition annealing of a precursor film. The density of c-axis in-plane BYC grains varied dramatically across the surface of the substrates. In several samples. The spatial pattern of c-axis in-plane regions present in the BYC films was similar to the twin structure present in the LaAlO3 substrates.

04,775
PB96-155585 Not available NTIS
National Inst. of Standards and Technology (PL), Gaithersburg, MD. Electron and Optical Physics Div.
Tunneling Spectroscopy of bcc(001) Surface States.
Final rept.
J. A. Stroscio, D. T. Pierce, A. Davies, and R. J. Celotta. 1995, 4p.
Pub. in Physical Review Letters, v75 n16 p2960-2963 Oct 95.

Keywords: *Tunneling spectroscopy, *Surface states, Band structure, Reprints, Bcc (001) surfaces, Cr, Fe.

The authors have discovered an intense, sharp feature in tunneling spectra of the Fe(001) and Cr(001) surfaces that derives from a bcc surface state near the Fermi level. Band-structure calculations show that this state is a general feature of bcc(001) surfaces, and that it originates from a nearly unperturbed d orbital extending out into the vacuum region. This general feature should permit chemical identification with atomic spatial resolution on bcc(001) surfaces. The surface state is in the minority spin band for Fe and Cr, so it should be useful for future spin-polarized tunneling experiments.

04,776
PB96-156104 Not available NTIS
National Inst. of Standards and Technology (MSEL), Gaithersburg, MD. Reactor Radiation Div.
Fast-Ion Conducting Y2(ZryTi1-y)2O7 Pyrochlores: Neutron Rietveld Analysis of Disorder Induced by Zr Substitution.
Final rept.
C. Heremans, B. J. Wuensch, J. K. Stalick, and E. Prince. 1995, 14p.
Pub. in Jnl. of Solid State Chemistry, v117 p108-121 1995.

Keywords: *Order-disorder transformations, *Ionic conductivity, *Crystal structure, Zirconium additions, Reprints, Yttrium zirconate titanates, Rietveld method, Pyrochlore structure.

The structure of Y2(ZrvTi1-y)2Ov solid solutions progressively changes, with increasing y, from an ordered pyrochlore structure space group Fd3m, to a deflect-fluorite structure space group Fm3m, at y = 0.90. The anion array consists of three independent sites O(1), O(2), and O(3), occupying positions 48f, 8a and 8b, respectively, of which 8b is unoccupied in a fully ordered pyrochlore. Rietveld powder-profile analysis of data collected with 1.5453-A thermal neutrons was used to determine the structure state of four samples with increasing Zr content (y = 0.30, 0.45, 0.60, and 0.90). Refinements that employed only the pyrochlore superstructure intensity data provided weighted profile residuals that ranged 8.06 to 8.67% compared with expected values of 7.13 to 7.87% derived from counting statistics.

04,777
PB96-161278 Not available NTIS
National Inst. of Standards and Technology (MSEL), Gaithersburg, MD. Ceramics Div.
Powder X-ray Diffraction Data for Ca2Bi2O5 and C4Bi6O13.
Final rept.
C. J. Rawn, R. S. Roth, and H. F. McMurdie. 1992, 3p.
Pub. in Powder Diffraction, v7 n2 p109-111 1992.

Keywords: *Crystal growth, Reprints, *X ray diffraction, *Space group symmetry, Unit cell dimensions, X ray powder diffraction, CA2Bi205, CA4Bi6013.

Single crystals and powder samples of Ca2Bi5O5 and Ca4Bi6O13 have been synthesized and studied using single crystal X-ray diffraction as well as X-ray and neutron powder diffraction. Unit cell dimensions were calculated using a least squares analysis that refined to a delta 2 theta of no more than 0.03 degrees. A triclinic cell was found with space group P1, a = 10.1222(7), b = 10.1466(6), c = 10.4833(7) Angstroms. Alpha = 116.912(5), Beta = 107.135(6) and gamma = 92.939(6), Z = 6 for the Ca2Bi2O5 compound. An orthorhombic cell was found with space group C2mm, a = 17.3795(5), b = 5.9419(2) and c = 7.2306(2) Angstroms, Z = 2 for the Ca4Bi6O13 compound.

04,778
PB96-161948 Not available NTIS
National Inst. of Standards and Technology (EEEL), Gaithersburg, MD. Semiconductor Electronics Div.

Business and Manufacturing Motivations for the Developing of Analytical Technology and Metrology for Semiconductors.
Final rept.
T. J. Shaffner, A. C. Diebold, R. C. McDonald, D. G. Seiler, and W. M. Bullis. 1996, 10p.
Pub. in Proceedings of the International Workshop on Semiconductor Characterization: Present Status and Future Needs, Gaithersburg, MD., January 30-February 2, 1995, p1-10 1996.

Keywords: *Semiconductors, *Metrology, *Circuit technology, Analytical technology, Characterization, Microelectronics, Process development, Reprints.

Semiconductor characterization is an indispensable enabler of all modern microelectronics and optoelectronic circuit, and is in the critical path for maintaining the steady decline in cost-per-function of silicon integrated circuit technology. It is also driving new developments in compound semiconductor materials and devices (III-V and II-VI). In this overview, we present a perspective on measurement technology relative to business and economic challenges of the semiconductor industry, and illustrate the key role metrology plays in modern process development and manufacturing. We also describe how new characterization techniques evolve for semiconductor applications.

04,779
PB96-164058 Not available NTIS
National Inst. of Standards and Technology (EEEL), Gaithersburg, MD. Semiconductor Electronics Div.
Use of Pressure for Quantum-Well Band-Structure Characterization.
Final rept.
J. H. Burnett, P. M. Amirtharaj, H. M. Cheong, B. Elman, W. Paul, and E. S. Koteles. 1996, 5p.
Pub. in Proceedings of the International Workshop on Semiconductor Characterization: Present Status and Future Needs, Gaithersburg, MD., January 30-February 2, 1995, p634-638 1996.

Keywords: *Spectroscopy, Reprints, GaAs, Heterostructure, Pressure, Stress, *Quantum-well, HgCdTe, Photoluminescence, Uniaxial pressure.

We discuss the use of externally applied pressure for determining the origin of the peaks in absorption spectra (and related spectra) of semiconductor heterostructures. This technique depends on the different effective mass dependences of the various types of heterostructure energy levels involved in absorption transitions, such as electron, heavy-hole, light-hole, exciton, and defect levels, and the dissimilar pressure dependences of the various masses. Measurements of the hydrostatic or uniaxial pressure dependences of the spectral peaks thus distinguish peaks associated with these different types of energy levels. The approach is demonstrated for GaAs/AlGaAs quantum wells and HgTe/HgCdTe superlattices using hydrostatic pressure. We also briefly discuss the use of externally applied uniaxial pressure for distinguishing heavy- and light-hole-related peaks, and using the heavy-hole/light-hole splitting for determining quantitatively the amount of built-in uniaxial strain in the heterostructure layers.

04,780
PB96-164074 Not available NTIS
National Inst. of Standards and Technology (PL), Gaithersburg, MD. Electron and Optical Physics Div.
SEMPA Studies of Exchange Coupling in Magnetic Multilayers.
Final rept.
R. J. Celotta, D. T. Pierce, and J. Unguris. 1995, 4p.
Pub. in MRS Bulletin, v20 n10 p30-33 Oct 95.

Keywords: *Exchange coupling, *Magnetic multilayers, Reprints, *Scanning electron microscopy, Reflection high energy diffraction, Scanning tunneling microscopy.

In the late 1980's, a number of exciting yet puzzling observations resulted from experiments investigating the coupling between two ferromagnetic layers separated by a nonferromagnetic spacer layer. A pioneering experiment by Grunberg et al. showed that Fe layers separated by a thin Cr spacer aligned with antiparallel magnetization, but with Au as the spacer layer, a parallel alignment occured. The long-range magnetic dipole from each layer would tend to explain antiparallel alignment; small pinholes in the spacer layer would produce parallel alignment. Alternatively, the layers might be coupled through the spacer-layer conduction electrons by the Ruderman-Kittel-Kasuya-Yosida (RKKY) effects. This was expected to produce an oscillation in coupling as the spacer thickness increased, that is an oscillation between parallel and antiparallel alignment. Oscillatory coupling was first observed by Parkin et al. Researchers had also found that, at spacer thickness where antiparallel alignment occured, the Fe/Cr/Fe system can exhibit a giant magnetoresistance (GMR) effect, that is, an anomalously large change in resistance when a magnetic field is applied. The potential technological importance of the GMR effect to magnetic sensing and magnetic information storage added further impetus to the already rapidly growing area of research in magnetic multilayers.

04,781
PB96-164207 Not available NTIS
National Inst. of Standards and Technology (EEEL), Gaithersburg, MD. Semiconductor Electronics Div.
Scanning Capacitance Microscopy Measurements and Modeling for Dopant Profiling of Silicon.
Final rept.
J. J. Kopanski, J. F. Marchiando, and J. R. Lowney. 1996, 5p.
See also PB96-148150.
Pub. in Proceedings of the International Workshop on Semiconductor Characterization: Present Status and Future Needs, Gaithersburg, MD., January 30-February 2, 1995, p308-312 1996.

Keywords: *Microscopy, *Scanning, *Seniconductor devices, *Silicon, Dopes, Profiles, Experimental data, Models, Reprints, AFM(Atomic force microscope), SCM(Scanning capacitance microscope).

A scanning capacitance microscope (SCM) for the two-dimensional profiling of dopants in silicon has been implemented by interfacing a commercial atomic force microscope (AFM) with a high densitivity capacitance sensor. The AFM is used to control the position of a conducting tip and measure surface topography, while other electonics are used to control and record a simultaneous measurement of the capacitance-voltage (C-V) response between the tip and a semiconductor. The operation of the SCM has been quantified by acquiring differential capacitance images of a variety of lateral pn-junctions and uniformly doped silicon samples. The shape of the C-V response between the AFM tip and oxidized silicon has been measured. Also, a computer code has been written to solve poisson's equation for the SCM geometry in three dimensions by using the method of collocation of Gaussian points. The purpose of the SCM modeling is to extract the dopant profile from the SCM measurement.

04,782
PB96-176763 Not available NTIS
National Inst. of Standards and Technology (MSEL), Gaithersburg, MD. Ceramics Div.
Reference Relations for the Evaluation of the Materials Properties of Orthorhombic YBa2Cu3Ox Superconductors.
Final rept.
R. G. Munro, and H. Chen. 1996, 6p.
Pub. in Jnl. of the American Ceramic Society, v79 n3 p603-608 1996.

Keywords: *Ceramics, *Superonductors, Reprints, Critical temperature, Lattice parameters.

Several expressions, suitable as reference relations, pertaining to the composition and temperature dependencies of the properties of orthorhombic YBA2Cu3Ox superconductors have been derived from statistical assessments of collections of data from independent experimental studies. Relations are given for (1) the critical temperature vs oxygen contents, (2) the lattice parameters at room temperature vs oxygen content, (3) the lattice parameters at fixed oxygen content vs temperature, (4) the anisotropic thermal expansion vs temperature, (5) the isotropic polycrystalline thermal expansion vs temperature, and (6) the mass density vs temperature.

04,783
PB96-176797 Not available NTIS
National Inst. of Standards and Technology (MSEL), Gaithersburg, MD. Reactor Radiation Div.
Characterization of the Structure of LaD2.50 by Neutron Powder Diffraction.
Final rept.
T. J. Udovic, Q. Huang, and J. J. Rush. 1996, 9p.
Pub. in Jnl. of Solid State Chemistry, Article No. 0096, v122 p151-159 1996.

Keywords: *Neutron diffraction, Reprints, *Lanthanum deuteride, Long range order, Metal hydride, Phase transition.

Neutron powder diffraction (NPD) measurements of the rare-earth deuteride LaD2.50 were undertaken between 10 and 430 K. Rietveld refinements indicated that, above approximately 385 K, the LaD2.50 structure is cubic (Fm3m) with deuterium fully occupying the terrahedral (t) interstices of the fcc La lattice and the excess deuterium occupying a portion of the octahedral (o) interstices with full statistical disorder. As the temperature is decreased below approximately 385 K, the LaD2.50 structure undergoes a tetragonal distortion concomitant with the onset of deuterium long-range order (I41amd) in the o sublattice, similar to previous structural results for the light-rare-earth deuterides RD2+x for 0.3 less than x less than 0.5. Fully developed long-range order is established in the vicinity of 200 to 230 K.

04,784
PB96-179494 Not available NTIS
National Inst. of Standards and Technology (MSEL), Gaithersburg, MD. Ceramics Div.
Texture Measurement of Sintered Alumina Using the March-Dollase Function.
Final rept.
J. P. Cline, M. D. Vaudin, J. E. Blendell, K. J. Bowman, N. Medendorp, C. A. Handwerker, and R. Jiggets. 1994, 6p.
Pub. in Advances in X-ray Analysis, v37 p473-478 1994.

Keywords: *Alumina, Texture, Reprints, *March-Dollase, *Pole figures, Rietveld refinement, X ray diffraction.

The Rietveld method entails the calculation of a powder diffraction pattern from crystallographic, microstructural and equipment characteristics. These characteristics are related to the form of the pattern through a series of model functions. The difference between an observed and calculated pattern is then minimized by sequentially refining the physical parameters contained within the model functions to obtain an accurate and precise desceiption of the specimen. A powder diffraction pattern from a specimen exhibiting crystallographic texture, or preferred orientation, will display intensity values which differ systematically from those calculated for a specimen of random orientation. This systematic discrepancy can be addressed by incorporating into the Rietveld refinement a model function for sample texture. A successful model for texture will accurately assess the phase abundance and degree of texture from both oriented and randomized specimens. In this study the authors use the March-Dollase model function to characterize texture development in sintered alumina with respect to processing variables and sintering time.

04,785
PB96-179551 Not available NTIS
National Inst. of Standards and Technology (MSEL), Gaithersburg, MD. Polymers Div.
Dielectric Behavior of a Polycarbonate/Polyester Mixture Upon Transesterification.
Final rept.
B. J. Factor, F. I. Mopsik, and C. C. Han. 1996, 3p.
Pub. in Macromolecules, v29 n6 p2318-2320 1996.

Keywords: *Dielectric spectroscopy, Polycarbonates, Polyesters, Reprints, *Transesterfication.

Dielectric relaxation spectroscopy provides a sensitive measure of the local environment surrounding molecular dipoles. In the examination of polymers, it is customary to record the complex dielectric constant e(star)(v)=e'(v)+ie'(v) as a function of frequency v. The form of the spectra can often be related to aspects of specimen structure. For example, the distribution of local environments that arise due to concentration fluctuations in polymer blends and diblock copolymers has been characterized using this technique. Further information concerning the dipolar magnitude as well as local geometric constraints can also be obtained through accurate measurement of the dielectric dispersion magnitude.

04,786
PB96-183090 PC A04/MF A01
National Inst. of Standards and Technology (MSEL), Gaithersburg, MD. Ceramics Div.

Workshop on Characterizing Diamond Films (4th). Held in Gaithersburg, Maryland on March 4-5, 1996.
A. Feldman, A. P. Malshe, and J. E. Graebner. Apr 96, 33p, NISTIR-5837.
See also report on 3rd Workshop, PB94-187663. Prepared in cooperation with Arkansas Univ., Little Rock.

Keywords: *Diamonds, *Films, *Meetings, Cutting tools, Adhesion, Chemical vapor deposition, Interlaboratory comparisons, Thermal conductivity, Thermal diffusivity, Tungsten carbides, Round robin tests.

The fourth in a series of workshops was held at NIST on March 4th and 5th, 1996 to discuss the characterization of diamond films and the need for standards in diamond technology. The audience targeted for this workshop were the producers and potential users of chemical vapor deposited (CVD) diamond technology in the United States. Two technical topics that have relevance to applications of CVD diamond were discussed; adhesion of CVD diamond to cutting tool materials and standardization of thermal conductivity measurement for heat spreading applications. A new round-robin of thermal conductivity measurements was planned which will utilize specimens having significantly better homogeneity than those used in a previous round robin.

04,787
PB96-190186 Not available NTIS
National Inst. of Standards and Technology (EEEL), Boulder, CO. Electromagnetic Technology Div.
Epitaxial Nucleation and Growth of Chemically Derived Ba2YCu3O7-x Thin Films on (001) SrTiO3.
Final rept.
P. C. McIntyre, M. J. Cima, and A. Roshko. 1995, 11p.
Pub. in Jnl. of Applied Physics, v77 n10 p5263-5272 May 95.

Keywords: *Epitaxy, *Nucleation, *Thin films, *YBCO superconductors, Growth, Organometallic compounds, Kinetics, Phase transformations, X rays, Microstructure, Barium oxides, Copper oxides, Yttrium oxides, Reprints.

The nucleation and growth kinetics of epitaxial Ba2YCu3O(7-x) thin films prepared on (001) SrTiO3 by postdeposition annealing of a chemically derived intermediate layer were investigated in specimens quenched from the growth anneal. The films were produced by spin-on deposition of a metal-organic precursor solution at room temperature and ambient pressure, and subsequent postdeposition annealing to form Ba2Ycu3O(7-x) (BYC). Integrated x-ray intensities of reflections from the majority, c-axis-normal epitaxial BYC in the films were analyzed as a function of time at annealing temperature. The linear transformation kinetics suggest the growth process is controlled by molecular processes at the BY/intermediate interface, and is not rate limited by diffusion.

04,788
PB96-193776 PC A03/MF A01
National Inst. of Standards and Technology (CAML), Gaithersburg, MD. Applied and Computational Mathematics Div.
Notion of a xi-Vector and a Stress Tensor for a General Class of Anisotropic Diffuse Interface Models.
A. A. Wheeler, and G. B. McFadden. Apr 96, 29p, NISTIR-5848.
Prepared in cooperation with Southampton Univ. (England). Faculty of Mathematical Studies.

Keywords: *Surface diffusion, *Anistropy, *Interfaces, *Stress tensors, Binary systems(Materials), Phase transitions, Vector analysis, Surface energy, Three dimensional, Phase field models, Gibbs-Thomson equation, Xi vectors.

The authors consider a general class of multiple-order-parameter models which represent the diffuse interface of a first-order phase transition with anisotropic surface energy and kinetics. They show that in the sharp interface limit, it is possible to construct a xi-vector and they derive the three-dimensional form of the Gibbs-Thomson equation. Moreover they develop the notion of a stress tensor for diffuse interface theories and show that it may be used to derive the equilibrium conditions for edges in interfaces as well as multiple functions. The authors also show that when edges form in the special case of a phase-field model, a weak shock forms in which the spatial derivatives of the phase field are not continuous, and they derive the jump conditions.

04,789
PB96-195268 PC A03/MF A01
National Inst. of Standards and Technology (EEEL), Gaithersburg, MD. Office of Microelectronics.
National Semiconductor Metrology Program, Project Portfolio FY 1996.
D. S. Yaney, and A. D. Settle-Raskin. Jun 96, 28p, NISTIR-5851.
See also PB96-175856.

Keywords: *Semiconductor devices, *Metrology, Integrated circuits, Dielectrics, Chemical analysis, Research projects, *Semiconductor materials, Calibration.

The National Semiconductor Metrology Program (NSMP) is a NIST-wide effort designed to meet the highest priority measurement needs of the semiconductor industry as expressed by the National Technology Roadmap for Semiconductors and other authoritative industry sources. The NSMP was established in 1994 with a strong focus on mainstream silicon CMOS technology and an ultimate funding goal of $25 million annually. Current annual funding of approximately $11 million supports the 23 internal projects which are summarized in this Project Portfolio booklet.

04,790
PB96-200183 Not available NTIS
National Inst. of Standards and Technology (EEEL), Boulder, CO. Electromagnetic Technology Div.
High-Tc Multilayer Step-Edge Josephson Junctions and SQUIDs.
Final rept.
N. Missert, T. E. Harvey, R. H. Ono, and C. D. Reintsema. 1993, 3p.
Pub. in Applied Physics Letters, v63 n12 p1690-1692 Sep 93.

Keywords: *Josephson junctions, *Yttrium barium copper oxides, *High temperature superconductors, Fabrication, Thin films, Strontium titanates, Neodymium oxides, Gadolinium oxides, Silver, Reprints, Superconducting Quantum Interference Devices, SQUIDS(Superconducting Quantum Interference Devices), Yttrium barium cuprates, SNS junctions.

The authors have developed a reliable process to fabricate high-quality YBa2Cu3O(7-x) (YBCO) superconductor normal metal-superconductor (SNS) step-edge junctions and SQUIDs over YBCO ground planes. These multilevel circuits employ thin films of SrTiO3 and NdGaO3 as the insulating layer between the active device and the ground plane and use Ag as the normal metal in the Josephson junction. The reproducibility and uniformity of the junctions are better than our single-level devices grown directly on step edges cut into single-crystal substrates. Here the critical current variation among junctions on a single wafer is less than a factor of 2. Junctions grown on thin-film step edges of SrTiO3 have critical currents near 2 MA at 4K, while those grown on NdGaO3 step edges have critical currents near 0.5 mA at 4 K.

04,791
PB96-200340 Not available NTIS
National Inst. of Standards and Technology (PL), Boulder, CO. Quantum Physics Div.
Collisions of Electrons with Highly-Charged Ions.
Final rept.
G. H. Dunn, N. Djuric, Y. S. Chung, M. Bannister, and A. C. H. Smith. 1995, 7p.
See also DE95007393.
Pub. in Nuclear Instruments and Methods in Physics Research B, v98 p107-113 1995.

Keywords: *Gold, *Multicharged ions, *Electron ion collisions, *Ion atom collisions, Electron cyclotron resonance, Excitation, Ion collisions, Ion sources, Ionization, Surfaces, Reprints, *Foreign technology.

The progress report, in addition to describing recent work in the authors' laboratory, highlights the general character and importance of electron collisions with highly-charged ions (HCI) and describes major advances in the field since the previous conference on the subject. Thus, while the authors' principle efforts are currently directed toward investigation of excitation of HCI, there have been very notable advances by others in the areas of ionization and recombination and an attempt is made to put these into context of the field in general. Also, for the first time, significant progress is now being made by others in experimental investigation of elastic scattering electrons from HCI.

04,792
PB96-200399 Not available NTIS
National Inst. of Standards and Technology (EEEL), Boulder, CO. Electromagnetic Technology Div.
Hot-Electron Microcalorimeter for X-ray Detection Using a Superconducting Transition Edge Sensor with Electrothermal Feedback.
Final rept.
K. D. Irwin, G. C. Hilton, J. M. Martinis, and B. Cabrera. 1996, 3p.
Pub. in Nuclear Instruments and Methods in Physics Research A, v370 p177-179 Apr 96.

Keywords: *X-ray detectors, *Superconductivity junctions, *Calorimeters, Electron temperature, Metal films, Hot electrons, Reprints, *Phonon detectors, *Micro calorimeters.

The authors investigate a hot-electron microcalorimeter for X-ray detection. The X-ray absorber consists of a normal metal film in thermal and electrical contact with a superconducting transition-edge sensor. The sensor is formed by a proximity-effect bilayer of aluminum and silver, with a sharp superconducting transition near 100 mK. Energy from X-rays absorbed in the normal film is removed by a reduction of the Joule heating in the proximity bilayer due to electrothermal feedback and measured using a SQUID. The feedback mode of operation allows the measurement of incident energy with no free parameters and should lead to improvement in detector resolution over existing hot-electron microcalorimeters.

04,793
PB96-200670 Not available NTIS
National Inst. of Standards and Technology (EEEL), Boulder, CO. Electromagnetic Technology Div.
Hot-Electron-Microcalorimeters with 0.25 mm(2) Area.
Final rept.
J. M. Martinis. 1996, 2p.
Pub. in Nuclear Instruments and Methods in Physics Research A, v370 p171-172 Apr 96.

Keywords: *X-ray detectors, *Superconducting junctions, *Calorimeters, Reprints, *Microcalorimeters, Phonon detectors.

The author presents measurements on hot-electron microcalorimeter with a normal-insulator superconductor tunnel-junction thermometer that is used for the detection of X-rays. With an absorber area of 0.5 mm by 0.5 mm, pulses of 20- micrometers in duration were observed that gave a 30 eV FWHM resolution for 6 keV X-rays and an 18 eV resolution for heat pulses. This detector has sufficient resolution, detector area, and speed to warrant application in materials analysis.

04,794
PB96-200712 Not available NTIS
National Inst. of Standards and Technology (EEEL), Boulder, CO. Electromagnetic Technology Div.
Controlling the Critical Current Density of High-Temperature SNS Josephson Junctions.
Final rept.
R. H. Ono, L. R. Vale, C. D. Reintsema, G. Kunkel, and S. J. Berkowitz. 1995, 3p.
Pub. in International Superconductive Electronics Conference (5th) (ISEC '95), Nagoya, Japan, September 18-21, 1995, p114-116.

Keywords: *Josephson junctions, *Current density, High temperature, Superconductors, Reprints, SNS junctions.

High-Tc Josephson junctions have been made using a step-edge super-conductor-normal-conductor (SNS) process where the critical current density has been controlled by the geometric length of the N region. The authors will discuss techniques for controlling the critical current while simultaneously adjusting the normal resistances.

04,795
PB96-200746 Not available NTIS
National Inst. of Standards and Technology (EEEL), Boulder, CO. Electromagnetic Technology Div.
Magnetic Flux Pinning in Epitaxial YBa2Cu3O7-delta Thin Films.
Final rept.
A. Roshko, L. F. Goodrich, D. A. Rudman, R. Moerman, and L. R. Vale. 1995, 4p.
Pub. in Jnl. of Electronic Materials, v24 n12 p1919-1922 1995.

Keywords: *Flux pinning, *Thin films, Morphology, Dislocations, Microstructures, Reprints, Scanning tunneling microscopy, Nucleation mechanism.

The influence of microstructure on the critical current density of laser ablated YBa2Cu3O7 thin films has been examined. Scanning tunneling microscopy was used to examine the morphologies of YBa2Cu3O7 films and the morphology data were then correlated with measurements of the critical current density. The films were found to grow by an island nucleation and growth mechanism. The critical current densities of the films are similar to those of films with screw dislocation growth, indicating that screw dislocation growth is not necessary for good pinning. The data suggest that the critical current density in applied magnetic field may be higher in films with higher densities of growth features.

04,796
PB96-201058 Not available NTIS
National Inst. of Standards and Technology (EEEL), Gaithersburg, MD. Semiconductor Electronics Div.
Time-Resolved Measurements of the Polarization State of Four-Wave Mixing Signals from GaAs Multiple Quantum Wells.
Final rept.
A. E. Paul, J. A. Bolger, A. L. Smirl, and J. G. Pellegrino. 1996, 10p.
Pub. in Jnl. of the Optical Society of America B, v13 n5 p1016-1025 May 96.

Keywords: *Gallium arsenides, *Aluminum gallium arsenides, *Quantum wells, *Polarization, Optical properties, Excitons, Reprints, Four wave mixing.

The complete polarization state of the degenerate four-wave mixing signal from a GaAs/Al2Ga1-xAs multiple quantum well is determined by time resolution of all four of its Stokes parameters as a function of the relative angle between the two linear input polarizations. The degree of ellipticity and the orientation of the polarization ellipse are both observed to vary dramatically in time, and the temporal evolution is found to be consistent with previous measurements of the time-integrated Stokes parameters and to provide new constraints for physical models. The results are shown to be qualitatively consistent with a phenomenological model requiring the inclusion of both many-body interactions and biexcitonic effects.

04,797
PB96-204474 Not available NTIS
National Inst. of Standards and Technology (MSEL), Gaithersburg, MD. Ceramics Div.
Alvin Van Valkenburg and the Diamond Anvil Cell.
Final rept.
G. J. Piermarini. 1993, 6p.
Pub. in High Pressure Research, v11 p279-284 1993.

Keywords: *High pressure, *Diamond anvil cells, Reprints, Infrared spectroscopy, Invention, X-ray diffraction, Ruby fluorescence.

A history of the development of the diamond anvil high pressure cell at the National Institute of Standards and Technology (formerly NBS) in the late 1950's is given along with a description of the contributions made by the four co-inventors of the device.

04,798
PB97-109011 PC A11/MF A03
National Inst. of Standards and Technology, Gaithersburg, MD.
Journal of Research of the National Institute of Standards and Technology, May/June 1996. Volume 101, Number 3. Special Issue: NIST Workshop on Crystallographic Databases.
1996, 224p.
See also PB97-109029 through PB97-109227 and PB96-177381. Also available from Supt. of Docs. as SN703-027-00070-9.

Keywords: *Crystallography, *Information systems, Crystal structure, Data base management.

Contents:
- CRYSTMET-The NRCC Metals Crystallographic Data File;
- Inorganic Crystal Structure Database (ICSD) and Standardized Data and Crystal Chemical Characterization of Inorganic Structure Types (TYPIX)--Two Tools for Inorganic Chemists and Crystallographers;
- Evaluation of Crystallographic Data with the Program DIAMOND;
- The Cambridge Structural Database (CSD): Current Activities and Future Plans;
- The Protein Data Bank: Current Status and Future Challenges;
- The Nucleic Acid Database: Present and Future;
- The Powder Diffraction File: Past, Present, and Future;
- NIST Crystallographic Databases for Research and Analysis;
- Conventional and Eccentric Uses of Crystallographic Databases in Practical Materials Identification Problems;
- Using NIST Crystal Data Within Siemens Software for Four-Circle and SMART CCD Diffractometers;
- Phase Identification in a Scanning Electron Microscope Using Backscattered Electron Kikuchi Patterns;
- The Biological Macromolecule Crystallization Database and NASA Protein Crystal Growth Archive;
- Investigations of the Systematics of Crystal Packing Using the Cambridge Structural Database;
- Troublesome Crystal Structures: Prevention, Detection, and Resolution;
- CIF (Crystallographic Information File): A Standard for Crystallographic Data Interchange;
- The Role of Journals in Maintaining Data Integrity: Checking of Crystal Structure Data in Acta Crystallographica;
- Electronic Publishing and the Journals of the American Chemical Society;
- How the Cambridge Crystallographic Data Center Obtains its Information;
- Data Import and Validation in the Inorganic Crystal Structure Database;
- World Wide Web for Crystallography; Workshop Highlights.

04,799
PB97-109029 (Order as PB97-109011, PC A11/MF A03)
National Research Council of Canada, Ottawa (Ontario). Scientific Numeric Database Service.
CRYSTMET: The NRCC Metals Crystallographic Data File.
G. H. Wood, J. R. Rodgers, S. R. Gough, and P. Villars. 1996, 11p.
Prepared in cooperation with Materials Phases Data Bank, Vitznau (Switzerland).
Included in Jnl. of Research of the National Institute of Standards and Technology, v101 n3 p205-215 May/Jun 96.

Keywords: *Crystallography, *Metals, *Minerals, *Information systems, Alloys, Intermatallic compounds, Numeric data, Crystal structure, Online systems, Searching, Software tools, Database management.

CRYSTMET is a computer-readable database of critically evaluated crystallographic data for metals (including alloys, intermerallics and minerals) accompanied by pertinent chemical, physical and bibliographic information. It currently contains about 60,000 entries and covers the literature exhaustively from 1913. Scientific editing of the abstracted entries, consisting of numerous automated entries, consisting of numerous automated and manual checks, is done to ensure consistency with related, previously published studies, to assign structure types where necessary and to help guarantee the accuracy of the data and related information. Analyses of the entries and their distribution across key journals as a function of time show interesting trends in the complexity of the compounds studied as well as in the elements they contain. Two applications of CRYSTMET are the identification of unknowns and the prediction of properties of materials. CRYSTMET is available either online or via license of a private copy from the Canadian Scientific Numeric Database Service (CAN/SND). The indexed online search and analysis system is easy and economical to use yet fast and powerful. Development of a new system is under way combining the capabilities of ORACLE with the flexibility of a modern interface based on the Netscape browsing tool.

04,800
PB97-109086 (Order as PB97-109011, PC A11/MF A03)
JCPDS-International Centre for Diffraction Data, Newtown Square, PA.
Powder Diffraction File: Past, Present, and Future.
D. K. Smith, and R. Jenkins. 1996, 13p.
Included in Jnl. of Research of the National Institute of Standards and Technology, v101 n3 p259-271 May/Jun 96.

Keywords: *Crystallography, *X-ray powder diffraction, *Information systems, Crystal structure, Database management.

The Powder Diffraction file has been thte primary reference for Powder Diffraction Data for more than half a century. The file is a collection of about 65,000 reduced powder patterns stored as sets of d/I data along with the appropriate crystallographic, physical and experimental information. This paper reviews the development and growth of the PDF and discusses the role of the ICDD in the maintenance and dissemination of the file.

04,801
PB97-109094 (Order as PB97-109011, PC A11/MF A03)
National Inst. of Standards and Technology, Gaithersburg, MD.
NIST Crystallographic Databases for Research and Analysis.
A. D. Mighell, and V. L. Karen. 1996, 8p.
Included in Jnl. of Research of the National Institute of Standards and Technology, v101 n3 p273-280 May/Jun 96.

Keywords: *Crystallography, *Information systems, *Information centers, Crystal structure, Chemical composition, Physical properties, Bibliographies, Software tools, US National Institute of Standards and Technology.

The NIST Crystal and Electron Diffraction Data Center builds a comprehensive database with evaluated chemical, physical, and crystallographic information on all types of well-characterized substances. The data are evaluated and standardized by specially designed computer programs as well as by experts in the field. From its master database, the Data Center produces NIST Crystal Data and an Electron Diffraction Database with over 220,000 and 81,000 entries, respectively. These distribution databases are made available to the scientific community via CD-ROM, scientific community via CD-ROM, scientific instruments and online systems. In addition, the Data Center has developed theory and software that can be used for establishing all types of lattice relationships, for the determination of symmetry, for the identification of unknowns using lattice matching techniques, and for data evaluation.

04,802
PB97-109102 (Order as PB97-109011, PC A11/MF A03)
Amoco Corp., Naperville, IL. Naperville Analytical Technical Lab. Services.
Conventional and Eccentric Uses of Crystallographic Databases in Practical Materials Identification Problems.
J. A. Kaduk. 1996, 14p.
Included in Jnl. of Research of the National Institute of Standards and Technology, v101 n3 p281-294 May/Jun 96.

Keywords: *Crystallography, *Materials, *Information systems, Crystal structure, Cobalt compounds, Copper aluminum barates, Magnesium chloride tetrahydrate, Palladium chlorides, Terephthalic acid, Vanadium phosphates, Uses, Database management.

The crystallographic database are powerfull and cost-effective tools for solving materials identification problems, both individually and in combination. Examples of the conventional and unconventional use of the databases in solving practical problems involving organic, coordination, and inorganic compounds are provided. The creation and use of fully-relational versions of the Powder Diffraction File and NIST Crystal Data are described.

04,803
PB97-109110 (Order as PB97-109011, PC A11/MF A03)
Siemens Energy and Automation, Madison, WI.
Using NIST Crystal Data within Siemens Software for Four-Circle and SMART CCD Diffractometers.
S. K. Byram, C. F. Campana, J. Fait, and R. A. Sparks. 1996, 6p.
Included in Jnl. of Research of the National Institute of Standards and Technology, v101 n3 p295-300 May/Jun 96.

Keywords: *Crystallography, *X-ray diffractometers, *Information systems, Information retrieval, Single crystals, Crystal structure.

NIST Crystal Data developed at The National Institute for Standards and Technology has been incorporated with Siemens single crystal software for data collection on four-circle and two-dimensional CCD diffractometers. Why this database is useful in the process of single crystal structure determination, and how the database is searched, are described. Ideas for future access to this and other databases are presented.

04,804
PB97-109128 (Order as PB97-109011, PC A11/ MF A03)
Sandia National Labs., Albuquerque, NM. Materials and Process Sciences Center.
Phase Identification in a Scanning Electron Microscope Using Backscattered Electron Kikuchi Patterns.
R. P. Goehner, and J. R. Michael. 1996, 8p.
Included in Jnl. of Research of the National Institute of Standards and Technology, v101 n3 p301-308 May/ Jun 96.

Keywords: *Crystallography, *Scanning election microscopy, *Microstructure, Crystal structure, Change coupled devices, Detectors, Metals, Welds, BKD(Backscatter Kikuchi diffraction), Backscatter Kikuchi diffraction.

Backscattered electron Kikuchi patterns (BEKP) suitable for crystallographic phase analysis can be collected in the scanning electron microscope (SEM) with a newly developed charge coupled device (CCD) based detector. Crystallographic phase identification using BEKP in the SEM is unique in that it permits high magnification images and BEKP's to be collected from a bulk specimen. The combination of scanning electron microscope (SEM) imaging, BEKP, and energy dispersive x-ray spectrometry holds the promise of a powerful new tool for materials science.

04,805
PB97-109169 (Order as PB97-109011, PC A11/ MF A03)
McMaster Univ., Hamilton (Ontario). Brockhouse Inst. for Materials Research.
CIF Crystallographic Information File: A Standard for Crystallographic Data Interchange.
I. D. Brown. 1996, 6p.
Included in Jnl. of Research of the National Institute of Standards and Technology, v101 n3 p341-346 May/ Jun 96.

Keywords: *Crystallography, *Information systems, *Standards, Dictionaries, Crystal structure, Databases.

The Crystallographic Information File (CIF) uses the self-defining STAR file structure. This requires the creation of a dictionary of data names and definitions. A basic dictionary of terms needed to describe the crystal structures of small molecules was approved in 1991 and is currently used for the submission of papers to Acta Crystallographica C. A number of extensions to this dictionary are in preparation. By storing the dictionary itself as a STAR file, the definitions and relationships in the CIF dictionary become computer interpretable. This offers many possibilities for the automatic handling of crystallographic information.

04,806
PB97-109177 (Order as PB97-109011, PC A11/ MF A03)
International Union of Crystallography, Chester (England).
Role of Journals in Maintaining Data Integrity: Checking of Crystal Structure Data in 'Acta Crystallographica'.
B. McMahon. 1996, 9p.
Included in Jnl. of Research of the National Institute of Standards and Technology, v101 n3 p347-355 May/ Jun 96.

Keywords: *Crystallography, *Journals, Quality control, Publications, Crystal structure, Error analysis.

Quality control of the papers in its journals is a major concern of the International Union of Crystallography. Recent technology development, not least the emergence of a standard data interchange file format, have facilitated the checking of numerical data in a paper, and its error-free transference to the printed page. Consequently, database holdings derived from IUCr journals will be of greater accuracy. Other publishers of crystallographic data may benefit from these innovations.

04,807
PB97-109185 (Order as PB97-109011, PC A11/ MF A03)
American Chemical Society, Washington, DC.
Electronic Publishing and the Journals of the American Chemical Society.
J. D. Spring, and L. R. Garson. 1996, 4p.
Included in Jnl. of Research of the National Institute of Standards and Technology, v101 n3 p357-360 May/ Jun 96.

Keywords: *Crystallography, *Journals, Crystal structure, Publications, Color graphics, Services, CD-ROMs, Electronic journals, American Chemical Society.

The American Chemical Society is developing a number of initiatives that implement emerging electronic technologies in order to provide a broad range of products and services to members and subscribers. Examples of products currently available, or under development, for access via the World Wide Web include supporting information for journals, Electronic ads, color graphics and entire journals. Other activities employ e-mail, CD-ROMs, and softcopy text.

04,808
PB97-109193 (Order as PB97-109011, PC A11/ MF A03)
Cambridge Crystallographic Data Centre (England).
How the Cambridge Crystallographic Data Centre Obtains Its Information.
D. G. Watson. 1996, 3p.
Included in Jnl. of Research of the National Institue of Standards and Technology, v101 n3 p361-363 May/ Jun 96.

Keywords: *Crystallography, *Journals, *Information systems, *Data validation, Publications, Crystal structure, Records(Files), Databases.

This paper is concerned with the acquisition of supplementary information, both hardcopy and electronic. Special arrangements with major journals are discussed and plans announced for the deposition of private communications using an electronic deposition form.

04,809
PB97-109201 (Order as PB97-109011, PC A11/ MF A03)
Fachinformationszentrum Karlsruhe, Gesellschaft fuer Wissenschaftlich-Technische Information m.b.H., Eggenstein-Leopoldshafen (Germany, F.R.).
Data Import and Validation in the Inorganic Crystal Structure Database.
H. Behrens. 1996, 9p.
Included in Jnl. of Research of the National Institute of Standards and Technology, v101 n3 p365-373 May/ Jun 96.

Keywords: *Crystallography, *Information systems, *Data validation, *Inorganic compounds, Crystal structure, Publications, Bibliometrics.

In the following paper the input procedures for the Inorganic Crystal Structure Database (ICSD) will be outlined. The input flow of the data is explained. Since the data have been excerpted from journal articles a bibliometric analysis of the relevant literature is presented. The types of data and the form in which they are recorded are discussed. Finally, illustrations are given of the importance of data checking and the data checking procedures are described in detail.

04,810
PB97-109219 (Order as PB97-109011, PC A11/ MF A03)
Geneva Univ. (Switzerland). Lab. de Cristallographie.
World Wide Web for Crystallography.
H. D. Flack. 1996, 6p.
Included in Jnl. of Research of the National Institute of Standards and Technology, v101 n3 p375-380 May/ Jun 96.

Keywords: *Crystallography, *Information systems, Crystal structure, *Internet, World Wide Web, Electronic publications.

Some characteristics of the World Wide Web (WWW) and its Virtual Library (W3VL) are described. Aspects of the setting up, maintenance, future development and objectives of the World Wide Web Virtual Library: Crystallography are detailed. An overview of the successful use of WWW in the organization of two crystallographic conferences and one entirely electronic conference is given. A revolution in scientific publication is under way with the introduction of WWW and CD-ROM technologies and a few of the points important to crystallography are touched upon. An application to distance teaching in crystallography is described. There is no mention of WWW applications to crystallographic databases in this paper as others at the Workshop have adequately described their work.

04,811
PB97-109227 (Order as PB97-109011, PC A11/ MF A03)
National Inst. of Standards and Technology, Gaithersburg, MD.
Workshop Highlights.
V. L. Karen, and A. Mighell. 1996, 1p.
Included in Jnl. of Research of the National Institute of Standards and Technology, v101 n3 p381-418 May/ Jun 96.

Keywords: *Crystallography, *Research projects, *Information systems, *Databases, Crystal structure, Workshops, Abstracts.

The ongoing computer revolution is causing changes in all crystallographic data activities and is blurring distinctions between what have traditional been independent efforts. As computer technology removes barriers in data storage, retrieval, and networking, unprecedented opportunities arise to achive the dream of all crystallographers: easy access to all crystallographic data. One topic stressed was the importance of quality throughout all stages of the data flow including collection, publication, and incorportaion into a database. A second major focus was software tools. Many users emphasized that use and accepatance of crystallographic databases by the general scientific community is directly related to the availability and quality of the search tools. A third theme was related to access and availability of all the information. Among the questions raised were: how data will be made available to the user community, and 'Who will be the power brokers in the future technologies. Issues such as these demonstrate the need among the representatives of the various data activities for future meetings to foster a continuing dialog. In addition, many attendees emphasized the need for much greater cooperation among the data centers, among the journals and the date centers, and among users and the data centers.

04,812
PB97-112411 Not available NTIS
National Inst. of Standards and Technology (MSEL), Gaithersburg, MD. Reactor Radiation Div.
Neutron Scattering Study of Antiferromagnetic Order in the Magnetic Superconductors RNi2B2C.
Final rept.
J. W. Lynn, Q. Huang, S. K. Sinha, R. Nagarajan, C. Godart, Z. Hossain, and L. C. Gupta. 1996, 3p.
Pub. in Physica B, v223 and 224 p66-68 1996.

Keywords: *Superconductors, *Neutron scattering, *Magnetic order, Reprints.

Neutron diffraction has been used to investigate the magnetic order and crystallography of RNi2B2C. For R = Dy the magnetic order that develops at 10 K consists of ferromagnetic sheets of spins in the tetragonal a-b plane which are stacked antiferromagnetically along the c-axis. An identical magnetic order is observed for R = Ho at low T, while from approximately 5 K to T(N) approximately equal to 8 K each layer along the c-axis is rotated by 163 degrees to form a spiral state, which strongly couples the magnetic order to the superconductivity. Small a-axis peaks are also observed in a narrow temperature range, but the c-axis-peaks are dominant. In ErNi2B2C(Tc = 11 K) an antiferromagnetic a-axis spin density wave stage develops below T(N) = 6.8 K, which readily coexists with the superconductivity indicating that weak coupling occurs between this type of magnetic state and the superconducting state. There is no evidence of magnetic order for either R = Ce or R = Y.

04,813
PB97-113286 Not available NTIS
National Inst. of Standards and Technology (EEEL), Gaithersburg, MD. Electricity Div.

Results of Capacitance Ratio Measurements for the Single Electron Pump-Capacitor Charging Experiment.
Final rept.
N. M. Zimmerman, A. F. Clark, and E. R. Williams. 1996, 2p.
See also PB96-102157.
Pub. in Conference on Precision Electromagnetic Measurements, Braunschweig, Germany, June 17-20, 1996, p505-506.

Keywords: *Metrology, *Electron tunneling, *Capacitance, Electric bridges, Precision, Ratios, Capacitors, Reprints, *Foreign technology, SET(Single electron tunneling).

The authors report on a metrological application of the single electron tunneling (SET) phenomena: a precise measurement of the ratio of two cryogenic capacitors. The measurement used a superconducting SET electrometer as the null detector for a capacitance bridge. They have achieved a 3-ppm level of imprecision in the measurement of capacitance ratio from 100 to 1000 Hz. They used custom-made cryogenic vacuum-gap capacitors, which have a leakage resistance of no less than 10(19) omega. Further improvements can be made in the attempt to obtain an imprecision of 10(-8) at lower frequencies, sufficient for the metrological measurement of capacitance or the fine-structure constant using an SET pump.

04,814
PB97-118335 Not available NTIS
National Inst. of Standards and Technology (EEEL), Gaithersburg, MD. Semiconductor Electronics Div.
Majority and Minority Electron and Hole Mobilities in Heavily Doped Gallium Aluminum Arsenide.
Final rept.
H. S. Bennett. 1996, 10p.
See also PB91-236968.
Pub. in Jnl. of Applied Physics, v80 n7 p3844-3853 Oct 96.

Keywords: *Gallium arsenides, *Electron mobility, *Hole mobility, Minority carriers, Semiconductor doping, Doped materials, Reprints.

The majority electron and minority hole mobilities were calculated in Gal-yAlyAs for donor densities between 10 to the 16th power and 10 to the 19th power to the minus 3 power. Similarly, the majority hole and minority electron mobilities were calculated for acceptor densities between 10 to the 16th power and 10 to the 20th power to the minus 3 power. The mole fraction of AlAs, y, varies between 0.0 and 0.3 in these calculations. All the important scattering mechanisms have been included. The ionized impurity and carrier-carrier scattering processes were treated with a quantum-mechanical, phase-shift analysis. These calculations are the first to use a phase-shift analysis for minority carriers scattering from majority carriers in ternary compounds such as Gal-yAlyAs. The results are in good agreement with experiment for majority mobilities and predict that at high dopant densities minority mobilities should increase with increasing dopant density for a short range of densities. This effect occurs because of the reduction of plasmon scattering and the removal of carriers from carrier-carrier scattering due to the Pauli exclusion principle.

04,815
PB97-119408 Not available NTIS
National Inst. of Standards and Technology (EEEL), Boulder, CO. Electromagnetic Technology Div.
Vortex Images in Thin Films of YBa2Cu3O(sub 7-x) and Bi2Sr2Ca1Cu2O(sub 8+x) Obtained by Low-Temperature Magnetic Force Microscopy.
Final rept.
C. W. Yuan, Z. Zheng, A. L. deLozanne, J. N. Eckstein, M. Tortonese, and D. A. Rudman. 1996, 4p.
Pub. in Jnl. of Vacuum Science and Technology, v14 n2 p1210-1213 Mar 96.

Keywords: *Microscopy, *Thin films, *Magnetic force microscopy, *Superconductors, High temperature, Vortices, Reprints.

The authors have imaged vortices in superconducting thin films with a low-temperature magnetic force microscope that utilizes microfabricated piezoresistive cantilevers with built-in tips. The films of YBa2Cu3O7-x and Bi2Sr2Ca1Cu2O8+x, are made by laser ablation and molecular beam epitaxy, respectively. The vortices usually appear as round features in the noncontact image with a diameter of about 1 micrometer or slightly less. In some cases the position of the vortices is correlated to defects observed in the topographic image of the same area. The vortices move sometimes, especially after taking a topographic (contact mode) scan.

04,816
PB97-122550 Not available NTIS
National Inst. of Standards and Technology (CAML), Gaithersburg, MD. Applied and Computational Mathematics Div.
Xi-Vector Formulation of Anisotropic Phase-Field Models: 3-D Asymptotics.
Final rept.
A. A. Wheeler, and G. B. McFadden. 1996, 15p.
Pub. in European Jnl. of Applied Mathematics, v7 p367-381 1996.

Keywords: *Solidification, Liquids-solid interfaces, Surface energy, Differential geometry, Asymptotic series, Vector analysis, Reprints, *Foreign technology, *Phase field models, Allen-Cahn equation, Gibbs-Thomson equation.

In the paper the authors present a new formulation of a large class of phase-field models, which describe solidification of a pure material and allow for both surface energy an interface kinetic anisotropy, in terms of the Hoffman-Cahn epsilon-vector. The Hoffman-Cahn epsilon-vector has previously been used in the context of sharp interface models, where it provides an elegant tool for the representation and analysis of interfaces with anisotropic surface energy. The authors show that the usual gradient-energy formulations of anisotropic phase-field models are expressed in a natural way in terms of the epsilon-vector when apprpriately interpreted. They use this new formulation of the phase-field equations to provide a concise derivation of the Gibbs-Thomson-Herring equation in the sharp-interface limit in three dimensions.

Structural Mechanics

04,817
PB94-198298 PC A01
National Inst. of Standards and Technology (NEL), Gaithersburg, MD. Structures Div.
Foias-Temam Approximations of Attractors for Galloping Oscillators.
Final rept.
B. Alibe, G. R. Cook, and E. Simiu. 1991, 5p.
Pub. in Proceedings of American Society of Civil Engineers Engineering Mechanics Specialty Conference, Mechanics Computing in 1990's and Beyond, Columbus, OH., May 20-22 1991, p781-785.

Keywords: *Oscillations, *Structural analysis, *Nonlinear equations, Nonlinear systems, Approximation, Self excitation, Structural engineering, Analysis(Mathematics), Reprints, *Autonomous galloping oscillators, *Foias-Temam approximation.

A method for the algebraic approximation of attractors recently developed by Foias and Temam is adapted for application to autonomous galloping oscillators. We compare results obtained by algebraic approximation on the one hand and numerical integration on the other. We conclude with an assessment of the limitations of the method as applied to our systems.

04,818
PB94-200250 Not available NTIS
National Inst. of Standards and Technology (MSEL), Gaithersburg, MD. Ceramics Div.
Application of a Simple Technique for Estimating Errors of Finite-Element Solutions Using a General-Purpose Code.
Final rept.
T. J. Chuang, J. T. Tang, and J. T. Fong. 1990, 11p.
Pub. in Proceedings of Pressure Vessels and Piping Conference, Nashville, TN., June 17-21, 1990, p105-115.

Keywords: *Fracture mechanics, *Error analysis, *Finite element method, *Stress analysis, Glass, Computational grids, Plates, Computerized simulation, Mathematical models, Estimates, Reprints.

A simple error-estimate technique using commercially available general purpose finite element codes to solve a class of engineering problems is presented. The technique is based on the assumption that the class of engineering problems to be solved can be simplified to a new class having known analytical solutions. A two-phase procedure is developed where a series of successively-refined mesh designs with acceptable error estimates for the simplified class of problems is used to guide the finite element modeling of the actual engineering problem. To illustrate the procedure, an application in the preliminary design of a circular glass plate with a center hole, a 3-sector configuration, and reinforcing beams at all edges of the sectors, is reported. Error estimates and rates of convergence for parameters of practical interest are derived from numerical results using a finite element code named ANSYS (versions 4.3A and 4.4) as implemented on a Sun3-110 workstation.

04,819
PB95-107330 Not available NTIS
National Inst. of Standards and Technology (MSEL), Boulder, CO. Materials Reliability Div.
Potential Drop in the Center-Cracked Panel with Asymmetric Crack Extension.
Final rept.
D. T. Read, and M. Pfuff. 1991, 11p.
Sponsored by GKSS - Forschungszentrum Geesthacht G.m.b.H., Hamburg (Germany, F.R.).
Pub. in International Jnl. of Fracture 48, p219-229 1991.

Keywords: *Crack propagation, *Fracture strength, *Electric potential, *Nondestructive tests, Tensile tests, Fracturing, Asymmetry, Panels, Calibration, Reprints, Johnson formula.

The well-known Johnson formula relates the electrical potential drop across a symmetric center crack in a current-carrying tensile panel to the crack length. To allow individual measurement of the crack growth at both ends of such a crack, the potential measured between contact points located on opposite sides and equidistant from the panel center line has been studied. Because this potential must ideally be identically zero for symmetric crack growth, it is termed the asymmetric potential. Its sign and magnitude are related to the direction and extent of asymmetric crack growth. It was found that contact points directly above the ends of the initial symmetric crack provide a signal which is well-suited to the determination of the asymmetry of the crack extension. This information is complementary to the total crack length information obtained using the Johnson formula. Experimental measurements and theoretical results were used to produce calibration formulae relating the asymmetric potential to the asymmetry of the crack dimensions in center-cracked panels.

04,820
PB95-162897 Not available NTIS
National Inst. of Standards and Technology (NEL), Gaithersburg, MD. Structures Div.
Algebraic Approximation of Attractors for Galloping Oscillators.
Final rept.
E. Simiu, G. R. Cook, and B. Alibe. 1991, 6p.
Pub. in Jnl. of Sound and Vibration 146, n1 p170-175 1991.

Keywords: *Oscillators, *Structural engineering, *Nonlinear algebraic equations, Oscillations, Numerical analysis, Nonlinear systems, Fluidelasticity, Dynamic structural analysis, Approximations, Analysis(Mathematics), Reprints, *Foias-Teman approximation, *Autonomous galloping oscillators, Attractors, Bilinear operator.

A constructive method for approximating attractors was recently developed by Foias and Temam, who applied it to systems in which the nonlinearity is due to a bilinear operator. The purpose of the note is to test the practical applicability of the method to autonomous galloping oscillators, in which the nonlinearity, is due to seventh degree polynomials. The authors give revised versions of two of the expressions given in the original method. They then compare results obtained by algebraic approximation on the one hand and numerical integration on the other. The authors conclude with an assessment of the limitations of the method as applied to the systems.

04,821
PB95-202347 Not available NTIS
National Inst. of Standards and Technology (MSEL), Gaithersburg, MD.

Exponentially Rapid Coarsening and Buckling in Coherently Self-Stressed Thin Plates.
Final rept.
J. W. Cahn, and R. Kobayashi. 1995, 14p.
Sponsored by Defense Advanced Research Projects Agency, Arlington, VA.
Pub. in Acta Metall. Mater. 43, n3 p931-944 1995.

Keywords: *Buckling, *Coarseness, *Nonlinear systems, *Thin plates, Diffusion, Elastic properties, Wetting, Stress analysis, Decomposition, Reprints.

The nonlinear equations that couple diffusion and stress are solved by computation for one-dimensional spinodal decomposition and coarsening in a thin plate. The vicinity of two critical values of the stress parameter are explored. At small values of elastic self-stresses, coarsening changes to exponentially fast from the exponentially slow dynamics expected for one-dimensions in the absence of stress. Coarsening is by rapid thickening of a single layer of a different phase from each of the two plate surfaces, leading to bending of the plate. Even though the diffusion equation is the same for bulk and thin plate and changes type at the coherent spinodal transition, in a thin plate the changes near this transition are gradual; the difference in behavior is due to the boundary conditions. Furthermore elasto-chemical equilibria through this transition are completely continuous. If the elastic term is large compared to the wetting term, surface wetting layers of phase of lower energy are found to disappear late in the coarsening.

04,822
PB96-111943 Not available NTIS
National Inst. of Standards and Technology (BFRL), Gaithersburg, MD. Structures Div.
Noise Modeling and Reliability of Behavior Prediction for Multi-Stable Hydroelastic Systems.
Final rept.
E. Simiu, and M. Frey. 1992, 6p.
Pub. in Proceedings of the International Conference on Offshore Mechanics and Arctic Eng. (OMAE) (11th), Alberta, Canada, June 7-12, 1992, Safety and Reliability, v2 p39-44.

Keywords: *Oscillators, *Hydroelasticity, Modelling, Noise, Hydrodynamics, Prediction, Behavior, Reprints, *Hydroelastic systems.

This paper reviews results of experiments conducted on a simple multi-stable hydroelastic (galloping) oscillator. These results show that a noise may cause a multi-stable hydroelastic system to exhibit chaotic behavior, and that in some instances such behavior cannot be predicted reliably unless noise effects are carefully accounted for. We then present results of a theoretical investigation of a simple, paradigmatic multi-stable system, the Duffing-Holmes oscillator. The results of this investigation show that for the system being considered, noise promotes the occurance of chaotic behavior associated with Smale horseshoes. This theoretical investigation is the first phase of an effort to develop analytical tools for predicting reliably the potential for chaotic behavior of actual hydroelastic systems such as deep-water compliant platforms.

04,823
PB96-122718 Not available NTIS
National Inst. of Standards and Technology (BFRL), Gaithersburg, MD. Structures Div.
Chaotic Motions of Coupled Galloping Oscillators and Their Modeling as Diffusion Progresses.
Final rept.
E. Simiu, G. R. Cook, and B. Alibe. 1991, 8p.
See also PB93-153245.
Pub. in International Conference on Applications of Statistics and Probability (6th), Mexico City, Mexico, June 17-21, 1991, v2 p993-1000.

Keywords: *Chaos, *Diffusion, *Oscillators, Models, Elastic properties, Stability, Stochastic processes, Differential equations, Structural engineering, Hydroelasticity, Reliability, Nonlinear systems, Reprints, *Galloping oscillators, *Fluidelasticity.

According to numerical investigations recently reported in the literature certain types of compliant offshore structures may experience undesirable hydroelastic responses, including chaotic responses. The question arises whether such responses can be predicted reliably by using current fluidelastic models. We addressed this question in the specific case of a paradigmatic, strongly nonlinear hydroelastic oscillator exhibits strongly chaotic behavior. It is then shown that modeling the hydroelastic system as a nonlinear diffusion process helps to improve substantially the reliability of the predictions.

04,824
PB96-160650 Not available NTIS
National Inst. of Standards and Technology (CAML), Gaithersburg, MD. Statistical Engineering Div.
Exits in Multistable Systems Excited by Coin-Toss Square-Wave Dichotomous Noise: A Chaotic Dynamics Approach.
Final rept.
Y. R. Sivathanu, C. Hagwood, and E. Simiu. 1995, 7p.
Pub. in Physical Review E, v52 n5 p4669-4675 Nov 95.

Keywords: *Stochastic processes, *Structural engineering, *Noise, Chaos, Construction, Functions(Mathematics), Functional analysis, Reprints, Melnikov function.

We consider a wide class of multistable systems perturbed by adissipative term and coin-toss square-wave dichotomous noise. These systems behave like their harmonically or quasiperiodically driven counterparts: depending upon the system parameters, the steady-state motion is confined to one well for all time or experiences exits from the wells. This similarity suggests the application to the stochastic systems of a Melnikov approach originally developed for the deterministic case. The noise induces a Melnikov process that may be used to obtain a simple condition guaranteeing the nonoccurrence of exits from a well.

PROBLEM-SOLVING INFORMATION FOR STATE & LOCAL GOVERNMENTS

Police, Fire, & Emergency Services

04,825
PB94-207461 PC A09/MF A02
National Inst. of Standards and Technology (BFRL), Gaithersburg, MD. Structures Div.
Northridge Earthquake 1994: Performance of Structures, Lifelines, and Fire Protection Systems.
Special pub.
D. Todd, N. Carino, R. M. Chung, W. D. Walton, J. D. Cooper, R. Nimis, H. S. Lew, and A. W. Taylor. May 94, 185p, NIST/SP-862.
Also available from Supt. of Docs. as SN003-003-03264-6. See also PB94-157666 and PB94-161114. Prepared in cooperation with Federal Highway Administration, Washington, DC.

Keywords: *Earthquake engineering, *Damage assessment, Highway bridges, California, Seismic design, Overpasses, *Northridge(California).

A magnitude 6.8 (Ms) earthquake centered under the community of Northridge in the San Fernando Valley shook the entire Los Angeles metropolitan area at 4:31 a.m. local time on Monday, January 17, 1994. Moderate damage to the built environment was widespread; severe damage included collapsed buildings and highway overpasses. A multi-agency team, organized under the auspices of the Interagency Committee on Seismic Safety in Construction and headed by the National Institute of Standards and Technology, arrived at the earthquake site within days of the event to document the effects of the earthquake. The team focused on the effects to the built environment, with the goal of capturing perishable data and quickly identifying situations deserving in-depth study. The report includes a summary of the team's observations.

SPACE TECHNOLOGY

General

04,826
PB96-161955 Not available NTIS
National Inst. of Standards and Technology (CSTL), Gaithersburg, MD. Process Measurements Div.
SSME LOX Duct Flowmeter Design and Test Results.
Final rept.
J. D. Siegwarth. 1994, 8p.
Pub. in Advanced Earth-to-Orbit Propulsion Technology 1994 NASA Conference, Huntsville, AL., May 17-19, 1994, Publication 3282, v1 p105-112.

Keywords: *Flowmeters, Liquid oxygen, Reprints, Water, *Space Shuttle, *Vortex, Vortex shedding.

A vortex shedding flowmeter designed to measure Liquid oxygen flow in the RS007031 duct of the Space Shuttle Main Engine has been built and tested using water and liquid nitrogen (LN2). The best meter performance was obtained with an elbow located a few diameters upstream and the vane axis perpendicular to the plane of the bend rather than with a long straight section upstream of the meter. At either the same flow velocity or the same Reynolds number, the meter performance was better for LN2 than for water. A flowmeter vane of circular cross section has been developed for the 28 mm branch of the RS007032 duct. The performance of these meters approaches that of commercial flowmeters.

Astronautics

04,827
N95-14084/4 (Order as N95-14062/0, PC A20/MF A04)
National Inst. of Standards and Technology, Gaithersburg, MD.
Partial Pressure Analysis in Space Testing.
C. R. Tilford. Nov 94, 13p.
In NASA. Goddard Space Flight Center, Eighteenth Space Simulation Conference: Space Mission Success Through Testing p 257-269. Sponsored by Jhu.

Keywords: *Contamination, *Gas pressure, *Instrument errors, *Measuring instruments, *Partial pressure, *Space environment simulation, Calibrating, Vacuum systems, Exposure, Handbooks, Pressure vessels, Quadrupoles, Residual gas, Sensitivity.

For vacuum-system or test-article analysis it is often desirable to know the species and partial pressures of the vacuum gases. Residual gas or Partial Pressure Analyzers (PPA's) are commonly used for this purpose. These are mass spectrometer-type instruments, most commonly employing quadrupole filters. These instruments can be extremely useful, but they should be used with caution. Depending on the instrument design, calibration procedures, and conditions of use, measurements made with these instruments can be accurate to within a few percent, or in error by two or more orders of magnitude. Significant sources of error can include relative gas sensitivities that differ from handbook values by an order of magnitude, changes in sensitivity with pressure by as much as two orders of magnitude, changes in sensitivity with time after exposure to chemically active gases, and the dependence of the sensitivity for one gas on the pressures of other gases. However, for most instruments, these errors can be greatly reduced with proper operating procedures and conditions of use. In this paper, data are presented illustrating performance characteristics for different instruments and gases, operating parameters are recommended to minimize some errors, and calibrations procedures are described that can detect and/or correct other errors.

04,828
N96-15584/1 (Order as N96-15552, PC A20/MF A04)

National Inst. of Standards and Technology, Gaithersburg, MD.
Ignition and Subsequent Transition to Flame Spread in a Microgravity Environment.
T. Kashiwagi, K. Mcgrattan, and H. Baum. Aug 95, 6p.
In NASA. Lewis Research Center, the 3RD International Microgravity Combustion Workshop p 207-212.

Keywords: *Computerized simulation, *Flame propagation, *Flames, *Flow distribution, *Gravitational effects, *Heat flux, *Ignition, *Microgravity, Extinguishing, Fire prevention, Fires, Three dimensional flow, Time dependence, Two dimensional flow.

The fire safety strategy in a spacecraft is (1) to detect any fire as early as possible, (2) to keep any fire as small as possible, and (3) to extinguish any fire as quickly as possible. This suggests that a material which undergoes a momentary, localized ignition might be tolerable but a material which permits a transition to flame spread would significantly increase the fire hazard. Therefore, it is important to understand how the transition from localized ignition to flame spread occurs and what parameters significantly affect the transition. The fundamental processes involved in ignition and flame spread have been extensively studied, but they have been studied separately. Some of the steady state flame models start from ignition to reach a steady state, but since the objective of such a calculation is to obtain the steady state flame spread rate, the calculation through the transition process is made without high accuracy to save computational time. We have studied the transition from a small localized ignition at the center of a thermally thin paper in a microgravity environment. The configuration for that study was axisymmetric, but more general versions of the numerical scheme have been developed by including the effects of a slow, external flow in both two and three dimensions. By exploiting the non-buoyant nature of the flow, it is possible to achieve resolution of fractions of millimeters for 3D flow domains on the order of 10 centimeters. Because the calculations are time dependent, we can study the evolution of multiple flame fronts originating from a localized ignition source. The interaction of these fronts determines whether or not they will eventually achieve steady state spread. Most flame spread studies in microgravity consider two-dimensional flame spread initiated by ignition at one end of a sample strip with or against a slow external flow. In this configuration there is only one flame front. A more realistic scenario involves separate, oppositely directed fronts in two dimensions, or a continuous, radially directed front in three dimensions. We present here some results of both the two and three dimensional codes.

04,829
PB96-103072 Not available NTIS
National Inst. of Standards and Technology (CSTL), Gaithersburg, MD. Thermophysics Div.
Partial Pressure Analysis in Space Testing.
Final rept.
C. R. Tilford. 1995, 6p.
See also N95-14084.
Pub. in Jnl. of the IES, p30-35 May/Jun 95.

Keywords: *Partial pressure, *Space, *Tests, Measuring instruments, Vacuum systems, Gases, Monitoring, Accuracy, Error, Calibrating, Quadrupoles, Filters, Reprints, *Space testings.

For vacuum-system or test-article analysis it is often desirable to know the species and partial pressures of the vacuum gases. Residual Gas or Partial Pressure Analyzers (PPAs) are commonly used for this purpose. These are mass spectrometer-type instruments, most commonly employing quadrupole filters. Depending on the instrument design, calibration procedures, and conditions of use, measurements made with these instruments can be accurate to within a few percent, or in error by two or more orders of magnitude. In this paper, data are presented illustrating performance characteristics for different instruments and gases, operating parameters are recommended to minimize some errors, and calibrations procedures are described that can detect and/or correct other errors.

Extraterrestial Exploration

04,830
PB95-163234 Not available NTIS
National Inst. of Standards and Technology (MSEL), Gaithersburg, MD. Materials Reliability Div.
In-Space Welding: Visions and Realities.
Final rept.
D. Tamir, T. Siewert, K. Matsubuchi, T. Eagar, L. Flanigan, and R. Su. 1993, 8p.
Pub. in Proceedings of Space Congress 'Yesterday's Vision is Tomorrow's Reality' (13th), Cocoa Beach, FL., April 27-30, 1993, p1-9 - 1-16.

Keywords: *Space industrialization, *Aerospace environments, *Welding, *Lunar exploration, Space shuttle missions, Space manufacturing, Space laboratories, Space stations, Space processing, Plasma arc welding, Laser welding, Gas tungsten arc welding, Electron beam welding, Space exploration, Reprints, Space Exploration Initiative.

This paper establishes the value of having an in-space welding capability and identifies its applications, both near-term for Shuttle-Spacelab missions and Space Station Freedom, and longer-term for the First Lunar Outpost and Manned Mission to Mars. The leading candidate technologies, consisting of Electron Beam, Gas Tungsten Arc, Plasma Arc, and Laser Beam, are examined against the criteria for an in-space welding system. Research and development work to date, striving to achieve an in-space welding capability, is reviewed. Finally, a series of strategic NASA flight experiments is discussed as the remaining development required for achieving a complete in-space welding capability, which can fully serve the Space Exploration Initiative. This paper summarizes the visions and realities associated with in-space welding.

Manned Spacecraft

04,831
PB94-194560 PC A03/MF A01
National Inst. of Standards and Technology (MEL), Gaithersburg, MD. Robot Systems Div.
Overview of NASREM: The NASA/NBS Standard Reference Model for Telerobot Control System Architecture.
J. S. Albus, R. Quintero, and R. Lumia. Apr 94, 14p, NISTIR-5412.
See also PB88-123773 and PB89-193940.

Keywords: *Architecture(Computers), *Robot control, *Space station freedom, *Telerobotics, Control systems design, Robots, Systems engineering, Memory(Computers), Computer systems design, *Computerized control systems, NASA/NBS standard reference model.

The NASA/NBS Standard Reference Model for Telerobot Control System Architecture (NASREM) was developed by the National Institute of Standards and Technology (NIST) for the National Aeronautics and Space Administration (NASA) to provide a software control system architecture guideline for use by development contractors charged with building the Flight Telerobot Servicer (FTS) control system as part of the Freedom Space Station project. The original NASREM document describes a conceptual or domain-independent architecture, and suggests the outline of a functional or domain-specific architecture for FTS. This paper presents an overview of the NASREM conceptual architecture and reviews subsequent work at NIST in defining a functional architecture for the servo and primitive levels. This work suggests outlines for software and hardware architecture specifications, and software development environments to complement the NASREM conceptual and functional architectures.

04,832
PB94-216082 Not available NTIS
National Inst. of Standards and Technology (NEL), Gaithersburg, MD. Robot Systems Div.
Evolution of the Flight Telerobotic Servicer.
Final rept.
R. Lumia. 1990, 4p.
Pub. in Proceedings of International Symposium on Artificial Intelligence, Robotics and Automation in Space, Kobe, Japan, November 18-20, 1990, p69-72.

Keywords: *Space Station Freedom, *Manipulators, Automation, Robotics, Robot control, Telerobotics, Reprints, *FTS(Flight Telerobotic Servicer), *Flight Telerobotic Servicer, NASREM(NASA/NIST Standard Reference Model).

The Flight Telerobotic Servicer (FTS) is a two armed manipulator which will be used to build and maintain Space Station Freedom. One of the goals of the project is to be able to upgrade the capabilities of the FTS by incorporating new technology. To achieve this goal the FTS is using the NASA/NIST Standard Reference Model for Telerobot Control System Architecture (NASREM) for its functional architecture. While using NASREM helps integrate new technology into the system, the decisions concerning the precise technology needing development must be addressed. In this paper, an approach to the technological evolution of the FTS will be explored. The approach begins with detailed scripts of representative FTS activities. These scripts are analyzed to determine the generic or common actions performed by the FTS. Then, technological alternatives are described in terms of a decision tree format.

04,833
PB95-151510 Not available NTIS
National Inst. of Standards and Technology (NEL), Gaithersburg, MD. Robot Systems Div.
Mapping Processes to Processors for Space-Based Robot Systems.
Final rept.
T. E. Wheatley. 1989, 4p.
Pub. in Institute of Electrical and Electronics Engineers International Conference on Systems Engineering, Fairborn, OH., August 24-26, 1989, p65-68.

Keywords: *Robots, *Space stations, *Computers, Resource allocation, Robot control, Telerobotics, Manipulators, Computer architecture, Algorithms, Servocontrol, Reprints.

The NASA/NBS Standard Reference Model for Telerobot Control System Architecture (NASREM) has been adapted by NASA for use in the Flight Telerobotic Servicer, a two armed telerobotic manipulator which will build and maintain the Space Station. NASREM provides the paradigm that allows standard interfaces to be defined so that functionally equivalent software and hardware modules can be interchanged. This paper examines the mapping of these logical modules onto a functional computer architecture. Interfaces must be first defined which are capable of supporting the algorithms in the literature. After interface definition, the specific computer architecture for the implementation can be determined. An example is shown mapping the SERVO level of NASREM onto a set of computers utilizing the knowledge of the dominant response time required to aid in the selection process.

04,834
PB96-111810 Not available NTIS
National Inst. of Standards and Technology (MSEL), Gaithersburg, MD. Materials Reliability Div.
Wear Mechanism Maps of 440C Martensitic Stainless Steel.
Final rept.
A. J. Slifka, T. J. Morgan, R. Compos, and D. K. Chaudhuri. 1993, 5p.
Pub. in Wear, v162-164 p614-168 1993.

Keywords: *Martensitic stainless steels, *Wear, *Tribology, *Space shuttle main engine, *Turbine pumps, *Liquid oxygen, Wear tests, Temperature, Loads(Forces), Velocity, Sliding friction, Oxidation, Reprints, SSME(Space Shuttle Main Engine), HPOTP(High Pressure Oxygen Turbopump), Wear maps, Wear mechanisms.

AISI 44OC martensitic stainless steel is the material of choice for the high pressure oxygen turbopump (HPOTP) of the space shuttle main engine (SSME). Tests have been done over a range of sliding speeds from 0.5 to 2.0 m/s, initial hertzian stresses from 0.915 to 3.66 GPa, and bulk temperatures from -184 deg. C (liquid oxygen temperature) to 760 deg. C. which cover the variations thought to exist in the HPOTP. Data are presented in the form of contour wear maps to allow a more direct view of the interdependencies of the major tribological variables that can be obtained with wear data presented vs. a single variable. Wear maps are used as a tool to aid in the determination of regions dominated by a given wear mode.

04,835
PB96-155809 Not available NTIS
National Inst. of Standards and Technology (BFRL), Gaithersburg, MD. Fire Safety Engineering Div.

Transition from Localized Ignition to Flame Spread Over a Thin Cellulosic Material in Microgravity.
Final rept.
K. B. McGrattan, K. Nakabe, H. R. Baum, and T. Kashiwagi. 1993, 4p.
Pub. in Eastern States Section of the Combustion Institute Technical Meeting, Princeton, NJ., October 1993, Book of Abstracts, p409-412.

Keywords: *Cellulose, *Fire prevention, *Ignition, Combustion, Flame spread, Reprints, Microgravity.

Ignition and flame spread processes are complicated by strong coupling between chemical reactions and transport processes, not only in the gas phase but also in the condensed phase. In most previous studies, ignition and flame spread were studied separately with the result that there has been little understanding of the transition from ignition to flame spread. In fire safety applications this transition is crucial to determine whether a fire will be limited to a localized, temporary burn or whether it will grow to become a large fire. In order to understand the transition to flame spread, the transient mechanisms of ignition and subsequent spread must be studied. However, there have been no definitive experimental or modeling studies because of the complexity of the buoyancy-induced flow near the heated sample surface. One must solve the full Navier-Stokes equations over an extended region to represent accurately the highly unstable buoyant plume and entrainment of surrounding gas. To avoid the complicated nature of the plume problem under normal gravity, previous detailed radiative ignition models were assumed to be one-dimensional or were applied at a stagnation point. Unfortunately, these models could not be extended to include the transition to flame spread.

04,836
PB96-160270 Not available NTIS
National Inst. of Standards and Technology (BFRL), Gaithersburg, MD. Fire Science Div.
Ignition and Subsequent Flame Spread Over a Thin Cellulosic Material.
Final rept.
K. Nakabe, H. R. Baum, and T. Kashiwagi. 1992, 13p.
Also available as N93-20205 (Order as N93-20178).
Pub. in International Microgravity Combustion Workshop (2nd), Cleveland, OH., September 15-17, 1992, p167-179.

Keywords: *Cellulose, *Fire prevention, *Fires, *Flame propagation, *Ignition, *Reduced gravity, Gravitation, Mathematical models, Buoyancy, Entrainment, Reprints, *Spacecraft construction materials.

Both ignition and flame spread on solid fuels are processes that not only are of considerable scientific interest but that also have important fire safety applications. Both types of processes, ignition and flame spread, are complicated by strong coupling between chemical reactions and transport processes, not only in the gas phase but also in the condensed phase. In most previous studies, ignition and flame spread were to flame spread studied separately with the result that there has been little understanding of the transition from ignition limited to flame spread. In fire safety applications this transistion is crucial to determine whether a fire will be limited to a localized, temporary burn or will transition into a growth mode with a potential to become a large fire. In order to understand this transition, the transient mechanisms of ignition and subsequent flame spread must be studied. However, there have been no definitive experimental or modeling studies, because of the complexity of the flow motion generated by buoyancy near the heated sample surface. One must solve the full Navier-Stokes equations over an extended region to represent accurately the highly unstable buoyant plume and entrainment of surrounding gas from far away.

04,837
PB96-160288 Not available NTIS
National Inst. of Standards and Technology (BFRL), Gaithersburg, MD. Fire Science Div.
Ignition and Transition to Flame Spread Over a Thermally Thin Cellulosic Sheet in a Microgravity Environment.
Final rept.
K. Nakabe, K. B. McGrattan, T. Kashiwagi, G. Kushida, H. R. Baum, and H. Yamashita. 1994, 14p.
See also PB96-155809.
Pub. in Combustion and Flame, v98 n4 p361-374 1994.

Keywords: *Cellulose, *Fire prevention, *Ignition, Combustion, Flame spread, Reprints, Microgravity.

An axisymmetric, time-dependent model is developed describing auto-ignition and subsequent transition to flame spread over a thermally-thin cellulosic sheet heated by external radiation in a quiescent microgravity environment. Due to the unique combination of a microgravity environment and low Reynolds number associated with the slow, thermally induced flow, the resulting velocity is taken as a potential flow. A one-step global gas phase oxidaton reaction and three global degradation reactions for the condensed phase are used in the model. A maximum external radiant flux of 5 W/sq. cm (Gaussian distribution) with 21%, 30%, and 50% oxygen concentrations is used in the calculations. The results indicate that autoignition is observed for 30% oxygen concentrations but the transition to the flame spread does not occur. For 50% oxygen the trransition is achieved. A detailed discussion of the transition from ignition to flame spread is given as an aid to understanding this process. Also, a comparison is made between the axisymmetric configuration and a two-dimensional (line source) configuration.

Space Safety

04,838
PB95-171039 PC A04/MF A01
National Inst. of Standards and Technology (PL), Gaithersburg, MD. Ionizing Radiation Div.
Updated Calculations for Routine Space-Shielding Radiation Dose Estimates: SHIELDOSE-2.
S. M. Seltzer. Dec 94, 59p, NISTIR-5477.
Contract NASA-T9311R
See also PB80-176860. Sponsored by National Aeronautics and Space Administration, Houston, TX. Lyndon B. Johnson Space Center.

Keywords: *Spacecraft shielding, *Radiation dosage, Extraterrestrial radiation, Electron irradiation, Proton irradiation, Bremsstrahlung, Cosmic rays, Aluminum, Graphite, Silicon, Water, Gallium arsenides, Air, Calcium fluorides, Silicon dioxide, Computer programs, Fortran, Graphs(Charts), *SHIELDOSE-2 computer program.

New, more-extensive, depth-dose distributions for electrons, electron-bremsstrahlung, and protons have been calculated, based on improvements in cross-section information since the development of the original SHIELDOSE code. The new database covers incident electron energies from 5 keV to 50 MeV, with the bremsstrahlung tail calculated for depths out to 50 g/sq cm, and incident proton energies from 10 keV to 10 GeV. Effects of nuclear interactions on proton depth-dose distributions in aluminum shields have been estimated, and options are provided to include these approximations in test calculations. In addition to the absorbed dose in aluminum, the dose in small volumes of graphite, Si, air, bone, CaF2, GaAs, LiF, SiO2, tissue or water can be evaluated. The functionality of new code is much the same as the old code; however, the resultant dose estimates as a function of depth in aluminum spacecraft can be somewhat different. Through the use of a companion code based on approximate transformations, results can be extended beyond the dose as a function of depth in plane slabs and at centers of solid spheres to include the dose at off-center points in a solid sphere and at the inner surface of spherical shells.

Spacecraft Trajectories & Flight Mechanics

04,839
PB96-102165 Not available NTIS
National Inst. of Standards and Technology (CAML), Gaithersburg, MD. Applied and Computational Mathematics Div.
Frozen Orbits for Satellites Close to an Earth-Like Planet.
Final rept.
S. Coffey, A. Deprit, and E. Deprit. 1994, 36p.
Pub. in Celestial Mechanics and Dynamical Astronomy 59, p37-72 1994.

Keywords: *Artificial satellites, *Satellite orbits, Hamiltonian functions, Inclination, Eccentricity, Mission planning, Space missions, Surveys, Reprints, *Satellite theory.

The authors say that a planet is Earth-like if the coefficient of the second order zonal harmonic dominates all other coefficients in the gravity field. This paper concerns the zonal problem for satellites around the Earth-like planet, all other perturbations excluded. By numerical continuation the authors have discovered three families of frozen orbits in the full zonal problem under consideration; (1) a family of stable equilibria starting from the equatorial plane and tending to the critical inclination; (2) an unstable family arising from the bifurcation at the critical inclination; (3) a stable family also arising from that bifurcation and terminating with a polar orbit. Except in the neighborhood of the critical inclination, orbits in the stable families have very small eccentricities, and are thus well suited for survey missions.

Unmanned Spacecraft

04,840
PB95-140984 Not available NTIS
National Inst. of Standards and Technology (EEEL), Gaithersburg, MD. Electricity Div.
Metrology Requirements of Future Space Power Systems.
Final rept.
J. K. Olthoff, and R. E. Hebner. 1989, 7p.
Sponsored by Defense Nuclear Agency, Washington, DC.
Pub. in Space Nuclear Power Systems, Chapter 11, p95-101 1992.

Keywords: *Spacecraft power supplies, *Metrology, Strategic defense initiative, Antimissile defense, Reliability, Calibration, Sensors, Reprints.

Anticipated metrology requirements of future space power systems have been researched in a program initiated at the National Institute of Standards and Technology. These requirements have been compared with existing state-of-the-art measurement capabilities, and inadequacies in present measurement techniques are discussed. Particular attention is paid to the difficulties of determining measurement reliabilities for long-term, unattended sensor operation.

04,841
PB96-179437 Not available NTIS
National Inst. of Standards and Technology (PL), Gaithersburg, MD. Radiometric Physics Div.
Organization and Implementation of Calibration in the EOS Project. Part 1.
Final rept.
J. J. Butler, and B. C. Johnson. 1996, 6p.
Pub. in The Earth Observer, v8 n1 p22-27 Jan/Feb 96.

Keywords: *Landsat satellites, *Radiometers, *Calibration, Remote sensors, Multispectral band scanners, Radiometric resolution, Spectral resolution, Satellite observation, Earth observations(From space), Data quality, Standardization, Testing, Comparison, Reprints.

The Earth Observing System (EOS) is an international multi-satellite program in global remote sensing of the Earth. The simultaneous goals of acquiring accurate data over many years and correctly identifying systematic effects depend crucially on: (1) calibrating all instruments against a set of recognized physical standards, (2) carefully characterizing the instruments' performances at the system level, (3) adhering to good measurement practices and established protocols, (4) intercomparing instrument measurements where possible, and (5) establishing traceability for all instruments to the common scale of physical quantities maintained at the national standards laboratories.

04,842
PB97-112213 Not available NTIS
National Inst. of Standards and Technology (PL), Gaithersburg, MD. Optical Technology Div.
Calibration in the Earth Observing System (EOS) Project. Part 2. Implementation.
Final rept.
J. J. Butler, and B. C. Johnson. 1996, 6p.
See also PB96-179437.
Pub. in The Earth Observer, p26-31 1996.

Keywords: *Earth observing system(EOS), *Radiometers, *Calibration, Satellite observation, Remote sensors, Radiometry, Requirements, Testing, Implementation, Remote sensing, Data quality, Reprints.

The article constitutes part 2 of a two-part article describing the overall organization and implementation of a calibration program in the EOS project based on requirements initially established in 1989. The article completes the description of the implementation of the program by outlining the EOS approaches to pre-flight and on orbit calibration.

04,843
PB97-113013 Not available NTIS
National Inst. of Standards and Technology (PL), Gaithersburg, MD. Optical Technology Div.
NIST Thermal Infrared Transfer Standard Radiometer for the Earth Observing System (EOS) Program.
Final rept.
J. P. Rice, and B. C. Johnson. 1996, 5p.
Pub. in The Earth Observer, p31-35 1996.

Keywords: *Earth observing system(EOS), *Infrared radiometers, *Calibration standards, Blackbody radiation, Infrared radiation, Thermometers, Temperature control, Heat transfer, Reprints.

A program to establish radiometric traceability between Earth Observing System (EOS) instrument calibration facilities and the National Institute of Standards and Technology (NIST) radiance scale is underway. To ensure the high accuracy required for instruments used in the National Aeronautics and Space Administration's (NASA's) EOS program, the output of the working standards will be compared to the radiance scale maintained at NIST. Plans are in place for NIST to provide similar radiometers for the EOS program: the Visible Transfer Radiometer (VXR), the Short-wave Infrared Transfer Radiometer (SWIXR), and the Thermal-infrared Transfer Radiometer (TXR). This article describes the TXR.

TRANSPORTATION

Air Transportation

04,844
PB94-213857 PC A06/MF A02
National Inst. of Standards and Technology (BFRL), Gaithersburg, MD.
Feasibility of Fire Evacuation by Elevators at FAA Control Towers.
J. H. Klote, B. M. Levin, and N. E. Groner. Aug 94, 112p, NISTIR-5445.
Prepared in cooperation with George Mason Univ., Fairfax, VA. Sponsored by Federal Aviation Administration, Washington, DC. Engineering and Environmental Safety Div.

Keywords: *Airport towers, *Air traffic control, *Fire safety, *Evacuating(Transportation), Elevators(Lifts), US FAA, Feasibility, Emergencies.

Throughout most of the world, warning signs next to elevators indicated they should not be used in fire situations. Because these elevators have not been designed for fire evacuation, they should not be used for fire evacuation. However, the idea of using elevators for fire evacuation has gained considerable attention. The Federal Aviation Administration (FAA) has sponsored a project to study the feasibility of elevator emergency evacuation at air traffic control towers. This paper describes this project including (1) a general discussion of elevator evacuation, (2) presentation of conceptual criteria for such elevator evacuation systems, and (3) application of that criteria to several ATCTs.

Global Navigation Systems

04,845
PB94-215712 PC A04/MF A01
National Inst. of Standards and Technology (PL), Boulder, CO. Time and Frequency Div.
Analytical Estimation of Carrier Multipath Bias on GPS Position Measurements.
Technical note.
C. M. Volk, and J. Levine. Apr 94, 67p, NIST/TN-1366.
Also available from Supt. of Docs. as SN003-003-03266-2. Prepared in cooperation with Joint Inst. for Lab. Astrophysics, Boulder, CO.

Keywords: *Global positioning system, *Multipath transmission, *Position finding, Phase measurement, Mathematical models, Error analysis, Degradation, Accuracy, Bias.

Multipath is one of the factors degrading the accuracy of position measurements obtained with the Global Positioning System (GPS). We investigate the effects of multipath on the carrier phase measurements and the resulting bias on relative GPS positions for observation times longer than several hours. We first model the phase error due to multipath from a single plane reflector in terms of satellite reflector geometry. The model is then employed to estimate upper limits of the multipath bias for general receiver environments. We also consider bias due to multipath from the flat ground, from nearby objects and from tilted ground, obtaining formulae for each situation that depend only on reflector characteristics and geometry. We find that the multipath phase error gives rise to vertical biases smaller than 2 mm and horizontal biases smaller than 1 mm if carrier-phase observations are averaged for at least several hours and if some basic precautions are taken regarding the placement of the receiving antenna.

Pipeline Transportation

04,846
PB94-161999 PC A05/MF A01
National Inst. of Standards and Technology (BFRL), Gaithersburg, MD.
Earthquake Resistant Construction of Gas and Liquid Fuel Pipeline Systems Serving, or Regulated By, the Federal Government.
Earthquake hazard reduction series no. 67.
F. Y. Yokel, and R. G. Mathey. Jul 92, 79p, NISTIR-4795, FEMA-233.
See also PB94-161817. Sponsored by Federal Emergency Management Agency, Washington, DC.

Keywords: *Pipelines, *Storage tanks, *Earthquake resistant structures, Seismic design, Design standards, Building codes, Piping systems, Pipe joints, Welded joints, Dynamic structural analysis, Natural gas distribution systems, Liquefied natural gas, Oil lines, Gas mains, Soil-Structure interactions, Earthquake engineering, Lifeline systems.

The vulnerability of gas and liquid fuel pipeline systems to damage in past earthquakes, as well as available standards and technologies that can protect these facilities against earthquake damage are reviewed. An overview is presented of measures taken by various Federal Agencies to protect pipeline systems under their jurisdiction against earthquake hazards. It is concluded that the overall performance of pipeline systems in past earthquakes was relatively good, however, older pipelines and above-ground storage tanks were damaged in many earthquakes. Standards and regulations for liquid fuel pipelines contain only general references to seismic loads. Standards and regulations for above-ground fuel storage tanks and for liquefied natural gas facilities contain explicit seismic design provisions. It is recommended that a guideline for earthquake resistant design of gas and liquid fuel pipeline systems be prepared for Federal Agencies to ensure a uniform approach to the protection of these systems.

04,847
PB96-147129 Not available NTIS
National Inst. of Standards and Technology (MSEL), Boulder, CO. Materials Reliability Div.
Gas-Coupled, Pulse-Echo Ultrasonic Crack Detection and Thickness Gaging.
Final rept.
C. M. Fortunko, R. E. Schramm, C. M. Teller, W. P. Dube, M. C. Renken, G. M. Light, and J. D. McColskey. 1995, 8p.
Pub. in Review of Progress in Quantitative Nondestructive Evaluation, Snowmass Village, CO., July 31-August 5, 1994, v14A p951-958 1995.

Keywords: *Nondestructive tests, *Crack detection, Reprints, *Thickness gages, Ultrasonic thickness gages, Gas-coupled, Pulse-echo.

Ultrasonic inspection is a standard method to assess the integrity of large-diameter oil pipelines. However, similar methods applied to natural-gas pipelines present a considerably greater challenge; gas is apoor coupling agent for the probing ultrasonic signals between the transducer and the pipe wall. Natural gas exhibits a very low specific acoustic impedance (300 Rayls for methane at atmospheric pressure) compared to oil (1.5 Mrayls and higher). Consequently, large ultrasonic-signal transmission losses occur at the transducer/gas and pipe-wall/gas interfaces. To circumvent this obstacle, past exploratory developments included the use of a liquid-filled wheel, electromagnetic- acoustic-transducer (EMAT), and liquid-slug technology. While prototypes of high-speed, in-line inspection systems employing such principles do exist, all exhibit serious operational shortcomings that prevent widespread commercial exploitation.

Railroad Transportation

04,848
PB94-152006 PC A11/MF A03
National Inst. of Standards and Technology (BFRL), Gaithersburg, MD. Fire Safety Engineering Div.
Fire Safety of Passenger Trains: A Review of Current Approaches and of New Concepts.
Technical note (Final).
R. D. Peacock, R. W. Bukowski, W. W. Jones, J. E. Brown, P. A. Reneke, and V. Babrauskas. Jan 94, 239p, NIST/TN-1406.
Also available from Supt. of Docs. as SN003-003-03246-8. Sponsored by Department of Transportation, Washington, DC.

Keywords: *Fire safety, *Trains, *Passengers, Smoke, Fire tests, Evacuating(Transportation), Rapid transit systems.

New alternative technologies have been developed which can be used to increase intercity passenger train operating speeds. These technologies include steel-wheel-on-rail and magnetic levitation (maglev) systems. Fire safety is an area of particular interest for these technologies, as well as for conventional intercity and commuter trains. While the historical fire record has been very good and few serious passenger train fires have occurred, minor incidents could develop into potential life-threatening events. The report presents a detailed comparison of the fire safety approaches used in the United States, France, and Germany. The strengths and weaknesses of current methods for measuring the fire performance of rail transportation systems are evaluated. An optimum systems approach to fire safety which addresses typical passenger train fire scenarios is analyzed and recommendations are presented to address the current state-of-the-art in materials testing.

04,849
PB95-140430 Not available NTIS
National Inst. of Standards and Technology (MSEL), Boulder, CO. Materials Reliability Div.
Ultrasonic Measurement of Residual Stress in Railroad Wheel Rims.
Final rept.
R. E. Schramm, A. V. Clark, and T. J. McGuire. 1992, 5p.
Sponsored by Federal Railroad Administration, Washington, DC.
Pub. in Proceedings of International Wheelset Congress (10th), Sydney, Australia, September 27-October 1, 1992, p151-155.

Keywords: *Nondestructive tests, *Ultrasonic flow detection, *Railroad trucks, *Stress measurement, *Wheels, Acoustic measurement, Accuracy, Signal processing, Ultrasonics, Transducers, Residual stress, Data analysis, Birefringence, Reprints.

This work discusses three possible acoustic measurement techniques to detect and quantify the stress railroad wheel rims. The goal is to develop instrumentation useful for nondestructive testing during field inspection for potentially dangerous conditions. In each case, the application of novel noncontact transducers (EMATs) takes advantage of minimal surface preparation and the elimination of fluid couplants. Each tech-

nique depends on the very precise (one part in 10(exp 4)) timing of signal arrival. Elastic changes caused by stress generate very small, but detectable velocity changes. However, other factors, notably changes in metallurgical texture, will similarly alter the velocity. Initial tests indicate the possibility of determining the size of this texture effect and reducing the uncertainty in measured stress to about 55 MPa or less. This accuracy would allow judgment on the safety of continued operation of a wheel. For one method, a birefringence approach, we have constructed a prototype that is now at a railroad research center. Ultrasonic data collected with this gear correlate well with those from destructive sawcutting for the four wheels we have examined so far. Work on the design and construction of transducers and data analysis continues.

04,850
PB95-162046 Not available NTIS
National Inst. of Standards and Technology (BFRL), Gaithersburg, MD. Fire Safety Engineering Div.
New Concepts for Fire Protection of Passenger Rail Transportation Vehicles.
Final rept.
R. D. Peacock, R. W. Bukowski, W. W. Jones, and P. A. Reneke. 1993, 10p.
Sponsored by John A. Volpe National Transportation Systems Center, Cambridge, MA.
Pub. in Proceedings of Fire and Materials, International Conference and Exhibition (2nd), Arlington, VA. September 23-24 1993 p171-180.

Keywords: *Rail transportation, *Fire safety, *Fire protection, Railroad passenger service, Railroad cars, Passenger compartments, Trains, Fire prevention, Fire hazards, Fire tests, Test methods, Smoke, Reprints.

Recent advances in guided ground transportation, fire test methods, and hazard analysis necessitate re-examination of requirements for fire safety. A comparison of the approaches used in the United States, Germany, and France is presented. With the strengths and weaknesses of current methods for measuring the fire performance of materials used in rail transit systems reviewed, a direction is suggested in which most fire science-oriented organizations in the world are clearly headed - fire hazard and fire risk assessment methods supported by measurement methods based on heat release rate.

04,851
PB95-162673 Not available NTIS
National Inst. of Standards and Technology (MSEL), Gaithersburg, MD. Materials Reliability Div.
Noncontact Ultrasonic Inspection of Train Rails for Stress.
Final rept.
R. E. Schramm, A. Van Clark, T. J. McGuire, P. T. Purtscher, B. J. Filla, and D. V. Mitrakovic. 1993, 10p.
Contract DTF53-91-X-0068
Sponsored by Federal Railroad Administration, Washington, DC.
Pub. in Proceedings of International Conference on Rail Quality and Maintenance for Modern Railway Operation, Delft, The Netherlands, June 1992, p99-108 1993.

Keywords: *Railroad tracks, *Acoustic measurement, *Nondestructive tests, Ultrasonic frequencies, Ultrasonic tests, Texture, Stresses, Stress analysis, Sound transducers, Reprints, EMAT.

The paper discusses acoustic techniques to quantify stress, the construction of transducers, and initial measurements on a short test section of railroad track. Our goal is to develop instrumentation useful for nondestructive testing during field inspection for potentially dangerous conditions, such as those generated by thermal stress. The application of unconventional noncontact transducers (EMATs) takes advantage of minimal surface preparation and the elimination of fluid couplants.

04,852
PB95-169199 Not available NTIS
National Inst. of Standards and Technology (MSEL), Boulder, CO. Materials Reliability Div.
Ultrasonic Measurement of Residual Stress in Cast Steel Railroad Wheels.
Final rept.
R. E. Schramm, A. V. Clark, and J. Szelazek. 1994, 6p.
Contract FRA-DTF53-91-X-0068
Sponsored by Federal Railroad Administration, Washington, DC.
Pub. in Proceedings of Pressure Vessels and Piping Conference, Minneapolis, MN., June 19-23, 1994, p157-162.

Keywords: *Residual stress, *Ultrasonic tests, *Railroad cars, *Wheels, Nondestructive tests, Transducers, Inspection, Steels, Transportation safety, Detection, Cracks, Defects, Reprints, *Cast steel railroad wheels.

Residual hoop stresses in the rims of railroad wheels may change from compressive to tensile during their lifetime, a potentially hazardous condition that could lead to wheel failure by cracking. The current U.S. regulation calls for the measurement of discoloration in the wheel plate indicating a history of heating that may lead to unsafe stress. Quantitative measurement by ultrasonic methods is an attractive alternative. Stress influences elastic parameters and causes small changes in sound velocity. We did an extensive series of measurements around the circumference of ten cast-steel wheels; two were as-made, while the others received induction heating at three different energy levels to generate stresses similar to those of in-service wheels. Two different ultrasonic instruments gave comparable results. Destructive evaluation of stress in three wheels by sawcutting showed a good correlation between flange-tip opening displacement and the ultrasonic measurements. This suggests a reliable method and a field-usable instrument for quantitative nondestructive inspection. This could contribute to the safety and dependability of freight rail systems, and reduce costs due to failures and the unnecessary replacement of good wheels.

04,853
PB96-102868 Not available NTIS
National Inst. of Standards and Technology (BFRL), Gaithersburg, MD. Fire Safety Engineering Div.
Concepts for Fire Protection of Passenger Rail Transportation Vehicles: Past, Present, and Future.
Final rept.
1995, 17p.
See also PB95-162046 and PB95-180774.
Pub. in Fire and Materials, v19 p71-87 1995.

Keywords: *Railroad passenger service, *Fire protection, *Risk assessment, *Safety engineering, Rail transportation, Passenger transportation, Fire safety, Transportation safety, Railroad cars, Trains, Fire prevention, Fire hazards, Reprints, Heat release rate.

Recent advances in passenger rail transportation, fire test methods, and hazard analysis necissitate re-examination of requirements for fire safety. The strengths and weaknesses of current methods for measuring the fire performance of rail transportation systems are evaluated. A systems approach to fire safety which addresses typical passenger train fire scenarios is analyzed. A rationale is presented for the direction in which most fire science-oriented organizations in the world are clearly headed - the use of fire hazard and fire risk assessment methods supported by measurement methods based on heat release rate.

04,854
PB96-106992 PC A04/MF A01
National Inst. of Standards and Technology (MSEL), Boulder, CO. Materials Reliability Div.
Residual Stress in Induction-Heated Railroad Wheels: Ultrasonic and Saw Cut Measurements. Report No. 28.
Rept. for 30 May 91-30 Sep 94.
R. E. Schramm, J. Szelazek, and A. V. Clark. May 95, 60p, NISTIR-5038.
Sponsored by Federal Railroad Administration, Washington, DC.

Keywords: *Railroad trains, *Wheels, *Nondestructive tests, Ultrasonic tests, Residual stress, Stress measurement, Mathematical models, Cross sections, Service life.

This is Report Number 28 in a series covering research performed by the National Institute of Standards and Technology for the Federal Railroad Administration. The report covers a project by the Materials Reliability Division to develop and test an ultrasonic system to measure residual stress in the rims of railroad wheels.

04,855
PB96-141114 Not available NTIS
National Inst. of Standards and Technology (MSEL), Boulder, CO. Materials Reliability Div.
Safety Assessment of Railroad Wheels by Residual Stress Measurements.
Final rept.
R. E. Schramm, A. V. Clark, and J. Szelazek. 1995, 12p.
Pub. in Proceedings of Society of Photo-Optical Instrumentation Engineers Conference on Nondestructive Evaluation of Aging Infrastructure, Oakland, CA., June 6-8, 1995, v2458 p97-108 1995.

Keywords: *Railroad trucks, *Wheels, *Stress analysis, *Detection, Defects, Inspection, Ultrasonic tests, Nondestructive tests, Residual stresses, Acoustic properties, Elastic properties, Railroad cars, Reprints, Electromagnetic acoustic transducers.

Residual stresses in railroad wheels may change from compressive to tensile; this change could lead to wheel failure. The current U.S. regulation calls for the measurement of discoloration indicating heating that may lead to unsafe stress. Quantitative measurement by ultrasonic methods is an attractive alternative, since stress causes small changes in sound velocity. We did an extensive series of measurements on ten cast-steel wheels. Two different ultrasonic instruments gave comparable results. Destructive evaluation of stress in three wheels showed a good correlation with the ultrasonic measurements.

04,856
PB96-141254 Not available NTIS
National Inst. of Standards and Technology (MSEL), Boulder, CO. Materials Reliability Div.
Safety Assessment of Railroad Wheels Through Roll-by Detection of Tread Cracks.
Final rept.
A. V. Clark, R. E. Schramm, S. R. Schaps, and B. J. Filla. 1995, 11p.
Pub. in Proceedings of Society of Photo-Optical Instrumentation Engineers Conference on Nondestructive Evaluation of Aging Railroads, Oakland, CA., June 6-8, 1995, p109-119.

Keywords: *Railroad trucks, *Wheels, *Cracks, *Detection, Defects, Inspection, Rolling stock, Ultrasonic tests, Nondestructive tests, Railroad cars, Reprints, Electromagnetic acoustic transducers.

A prototype system has been developed for roll-by inspection of cracks in the trends of freight car wheels. The system uses noncontacting electromagnetic-acoustic transducers (EMATs) which generate and receive surface waves propagating along the trend surface. If a defect is present it reflects an echo back to the EMAT. The EMAT itself consists of a coil and permanent magnet which are embedded in a 'rocking shoe'. The rocking shoe is suspended by a spring system in a recess machined into the outer surface of a rail plug. When the wheel is centerend over the shoe, it activates a trigger circuit which energizes the EMAT and causes propagation of the surface wave. The detected echoes are analyzed by a microprocessor which characterizes the wheel as being safe or unsafe. The crack detector system has been subjected to field testing using actual locomotive and rolling stock. It has been able to detect both artificial and real defects at roll-by speeds of 25 km/h (15 mph).

04,857
PB96-183199 PC A04/MF A01
National Inst. of Standards and Technology (MSEL), Boulder, CO. Materials Reliability Div.
Dynamometer-Induced Residual Stress in Railroad Wheels: Ultrasonic and Saw Cut Measurements. Report No. 30.
R. E. Schramm, J. Szelazek, and A. V. Clark. Mar 95, 44p, NISTIR-5043.
See also PB91-222653. Sponsored by Federal Railroad Administration, Washington, DC. Office of Research and Development.

Keywords: *Railroad trains, *Nondestructive tests, *Wheels, Rolling stock, Ultrasonic tests, Residual stress, Piezoelectric gages, Thermal stresses.

The effect of stress on elastic parameters causes a small change in sound wave velocity. This acoustoelastic effect is the basis for a method of nondestructive evaluation (NDE). The authors used two types of ultrasonic transducers, piezoelectric and electromagnetic, to measure both thickness-averaged and near-surface stresses in the rims of twenty unused, cast-steel railroad wheels. The manufacturer mounted these wheels on a unique dynamometer and induced thermal damage by dragging tread breaks to simulate in-service conditions that might generate tensile hoop

stress. After the authors' ultrasonic nondestructive tests, they cut eighteen wheels with a saw along a radius to measure flange tip opening and verify the stress state.

Road Transportation

04,858
PB94-177060 PC A10/MF A03
National Inst. of Standards and Technology (EEEL), Gaithersburg, MD. Electricity Div.
Advanced Components for Electric and Hybrid Electric Vehicles. Workshop Proceedings. Held in Gaithersburg, Maryland on October 27-28, 1993.
Special pub.
K. L. Stricklett, A. H. Cookson, R. W. Bartholomew, and T. Leedy. Mar 94, 217p, NIST/SP-860.
Also available from Supt. of Docs. as SN003-003-03253-1.

Keywords: *Hybrid electric-powered vehicles, *Electric-powered vehicles, *Meetings, Electric batteries, Standards, Electric propulsion, Energy storage, Energy conversion, Electrochemistry, Engine components, Automotive engineering.

This is a key period in the development of electric and hybrid electric vehicles. The landmark 1990 legislation in California requires that 2 percent of new automobiles be zero emission vehicles in 1998, rising to 10 percent in the year 2005. This can only be met by electric vehicles. The purpose of the workshop was to concentrate on the technologies to improve the design, performance, manufacturability, and economics of the critical components for the next generation of electric and hybrid electric vehicles for the year 2000 and beyond. The workshop began with invited speakers to cover the general topics of impact of the California legislation, Federal agency programs, development of standards, infrastructure needs, advanced battery development, and the imperatives for commercial success of electric and hybrid electric vehicles. Working sessions were five parallel meetings on Energy Conversion Systems, Energy Storage Systems, Electric Propulsion Systems, Controls and Instrumentation, and Ancillary Systems.

04,859
PB94-195914 PC A05/MF A01
National Inst. of Standards and Technology (MEL), Gaithersburg, MD. Robot Systems Div.
Recommendations on Selection of Vehicle-to-Roadside Communications Standards for Commercial Vehicle Operations.
H. Scott, K. Stouffer, and P. Rowe. Jun 94, 80p, NISTIR-5444.

Keywords: *Highway communication, *Standards, *Data transmission, *Commercial vehicles, Radio links, Communication systems, Transponders, Communication equipment, Communications networks, Automatic highways, Intelligent Vehicle Highway Systems.

The National Institute of Standards and Technology (NIST) Robot Systems Division is participating in a Federal Highway Administration (FHWA) program that is to lead to the recommendation of standards in Vehicle-to-Roadside Communications (VRC) equipment used in commercial vehicle operations (CVO). There is substantial motivation to develop these standards, both on the part of the government and the CVO community. A standardized VRC system will allow states to check credentials, weight, and safety parameters while commercial vehicles travel at highway speeds of up to 160 km/h. This will improve the current situation in which substantial time and productivity is lost while commercial vehicles stop and wait for inspections. More sophisticated systems may employ weigh-in-motion equipment, on-vehicle sensors to determine brake temperature and other parameters in real-time, and other subsystems (navigation, etc.) capable of generating relevant data. This communications link will serve an important role in passing data between various onboard intelligent control system computers and the roadside systems.

04,860
PB95-188827 PC A05/MF A01
National Inst. of Standards and Technology (MEL), Gaithersburg, MD. Intelligent Systems Div.
Vehicle-to-Roadside Communications for Commercial Vehicle Operations: Requirements and Approaches.
H. Scott, K. Stouffer, and P. Rowe. Feb 95, 88p, NISTIR-5593.
See also PB94-195914.

Keywords: *Highway communication, *Commercial vehicles, *Data transmission, Transponders, Standards, Communications networks, Communication systems, Automatic highways, Communication equipment, Radio links, Intelligent Vehicle Highway Systems.

The National Institute of Standards and Technology (NIST) Robot Systems Division is participating in a Federal Highway Administration (FHWA) program that is to lead to the recommendation of standards in Vehicle-to-Roadside Communications (VRC) equipment. A standardized VRC system will allow states to check credentials, weight, and safety parameters while commercial vehicles travel at highway speeds of up to 160 km/h. This will improve the current situation in which substantial time and productivity is lost while commercial vehicles stop and wait for inspections. More sophisticated systems may employ weight-in-motion equipment, on-vehicle sensors to determine brake temperature and other parameters in real-time, and other subsystems (navigation, etc.) capable of generating relevant data. This communications link will serve an important role in passing data between various onboard intelligent control system computers and the roadside systems. Numerous incompatible VRC designs and protocols exist, or are being developed. The deployment of incompatible systems will not result in transparent borders, where a truck can pass, for example, from one state to another without stopping. A standard is to be developed or chosen that will meet current and projected requirements, such as those of the Intelligent Vehicle Highway System (IVHS). NIST interacted with various users, VRC equipment manufacturers, IVHS planners, and other government agencies to determine the current and projected VRC requirements. Fifteen systems and six protocols were examined in this study.

04,861
PB95-197455 PC A03/MF A01
National Highway Traffic Safety Administration, Washington, DC. Traffic Safety Programs.
Model Minimum Performance Specifications for Lidar Speed Measurement Devices.
Technical rept. Apr 92-Dec 94 (Final).
J. Worthy, G. Lieberman, and B. Moran. Jan 95, 50p, DOT-HS-808 214.
Prepared in cooperation with National Inst. of Standards and Technology (EEEL), Gaithersburg, MD. Office of Law Enforcement Standards.

Keywords: *Specifications, *Optical radar, *Speed indicators, Speed limit effectiveness, Speed limits, Electronic monitoring systems, Traffic law enforcement, Laser applications, Traffic law violations, Highway safety, Velocity measurement, *LIDAR(Light Detection and Ranging).

This technical report provides an overview of the circumstances leading to a request from the International Association of Chiefs of Police to the National Highway Traffic Safety Administration (NHTSA) for the development of performance specifications for LIDAR (LIght Detection And Ranging) aka Laser, devices used in speed limit enforcement. Chapter I provides an overview and description of the use of lidar speed measurement devices in speed limit enforcement. This chapter also contains NHTSA's recommendations concerning the use of lidar in speed limit enforcement and for the training of law enforcement officers using these devices. Chapter II contains the model minimum performance specifications for the lidar along with the protocol for use in the laboratory and field testing of these devices to determine their compliance with the model performance specifications.

Transportation Safety

04,862
PB94-194065 PC A03/MF A01
National Inst. of Standards and Technology (BFRL), Gaithersburg, MD.
Risk Analysis for the Fire Safety of Airline Passengers.
R. L. Smith. Jun 94, 40p, NISTIR-5441.
Contract DTFA03-92-Z-00018
Sponsored by Federal Aviation Administration Technical Center, Atlantic City, NJ.

Keywords: *Fire safety, *Airlines, Passengers, Aircraft fires, Software, Risk analysis, Decision theory, Water.

The purpose of this report is to describe the National Institute of Standards and Technology's work to date relating to the general methodology being developed for the project Risk Analysis for the Fire Safety of Airline Passengers and the software being used to facilitate this methodology. The approach selected involved the use of influence diagrams. Therefore, a brief discussion of influence diagrams is given. The status of their application to the water mist system for passenger planes is given and the overall approach to carrying out the project is described. An example is included that shows how the process works, but the case is fictional, not intended to be realistic.

04,863
PB95-180774 Not available NTIS
National Inst. of Standards and Technology (BFRL), Gaithersburg, MD. Fire Safety Engineering Div.
New Concepts for Fire Protection of Passenger Rail Transportation Vehicles. (NIST Reprint).
Final rept.
R. D. Peacock, R. W. Bukowski, W. W. Jones, and P. A. Reneke. 1994, 10p.
See also PB95-162046.
Pub. in Proceedings of International Symposium on Fire Safety Science (4th), Ottawa, Ontario, Canada, June 13-17, 1994, p1007-1016.

Keywords: *Fire safety, *Rail transportation, *Risk assessment, *Transportation safety, Fires, Railroad cars, Test methods, Standards, Burning rate, Smoke, Combustion, Reprints, *Heat release rate.

Recent advances in guided group transportation, fire test methods, and hazard analysis necessitate re-examination of requirements for fire safety. Several studies have indicated nearly random ability of current tests to predict actual fire behavior. A comparison of the approaches used in the United States, Germany, and France is presented. With the strengths and weaknesses of current methods for measuring the fire performance of materials used in rail transit systems reviewed, a direction is suggested in which most fire science-oriented organizations in the world are clearly headed--fire hazard and fire risk assessment methods supported by measurement methods based on heat release rate.

URBAN & REGIONAL TECHNOLOGY & DEVELOPMENT

General

04,864
AD-A297 420/2 PC A06/MF A02
National Inst. of Standards and Technology, Gaithersburg, MD.
Properties of Working Fluids for Thermoacoustic Refrigerators.
Annual rept. 1 Oct 94-30 Sep 95.
M. R. Moldover, and K. A. Gillis. 1 Aug 95, 108p.
Contract N00014-93-F-0101

Keywords: *Acoustic data, *Refrigerants, *Refrigeration systems, *Thermophysical properties, Computer programs, Density, Temperature, Vapor phases, Gas dynamics, Thermal conductivity, Pressure, Fluids, Helium, Viscosity, Acoustic velocity, Enthalpy, Xenon, Entropy, Prandtl number, Viscometers, *Thermoacoustics, Nobleg computer program.

The objective of this project is to provide thermophysical property data for candidate working

General

fluids in a form suitable for optimizing the design of thermoacoustic refrigerators. The data will be provided in a computer program that calculates the properties of the most promising gas mixtures. This package will consist of currently available data from the literature (provided that it is of sufficient quality) and our own measurements (when insufficient literature data exist). The properties provided are viscosity, thermal conductivity, Prandtl number, density, speed-of-sound, specific heat, enthalpy, and entropy for temperatures between -20 and 30 C and pressures up to 20 bars. We will also explore methods of varying the composition of the working fluid to maintain a constant speed of sound over the operating range of the refrigerator. (MM).

04,865
FIPS PUB 55-3 PC E04
National Inst. of Standards and Technology (CSL), Gaithersburg, MD.
Guideline: Codes for Named Populated Places, Primary County Divisions, and Other Locational Entities of the United States, Puerto Rico, and the Outlying Areas. Category: Data Standards and Guidelines. Subcategory: Representations and Codes.
Federal information processing standards.
28 Dec 94, 30p.
Supersedes FIPS PUB 55-2.
Three ring vinyl binder also available, North American Continent price $7.00; all others write for quote.

Keywords: *Geocoding, *Census tracts, *Classification, *Geography, Counties, Cities, Urban areas, Municipalities, Communities, Airports, National parks, Military facilities, Data files, Data processing, United States, Federal Information Processing Standards, Data standards and guidelines, Representations and codes, Populated places, Data elements.

The publication, which supersedes FIPS PUB 55-2 and 55DC-4, provides a 2-character FIPS State code and a 5-character FIPS numeric code to uniquely identify each entity contained in a list of names of incorporated places, other communities and settlements, primary county divisions (such as townships, New England towns, and census county divisions), American Indian and Alaska Native areas, airports, military bases, national parks, post offices, and other locational entities (except natural or physical features). A 2-character class code distinguishes the different types of geographic entities. The purpose of the codes is to promote the interchange of formatted, machine-sensible data.

04,866
FIPS PUB 55-DC3 PC E99
National Inst. of Standards and Technology, Gaithersburg, MD.
Guideline: Codes for Named Populatd Places, Primary County Divisions, and Other Locational Entities of the United States, Puerto Rico, and the Outlying Areas. Category: Data Standards and Guidelines; Subcategory: Representation and Codes.
Federal information processing standards.
28 Dec 94, 3976p.
Supersedes FIPS PUB 55-2.
Three ring vinyl binder also available; North American Continent price $7.00; all others write for quote.

Keywords: *Geocoding, *Census tracts, *Classification, *Geography, Counties, Cities, Urban areas, Municipalities, Communities, Airports, National parks, Military facilities, Data files, Data processing, United States, Federal Information Processing Standards, Data standards and guidelines, Representations and codes, Populated places, Data elements.

The publication, which supersedes FIPS PUB 55-2 and 55DC-4, provides a 2-character FIPS state code and a 5-character FIPS numeric code to uniquely identify each entity contained in a list of names of incorporated places, other communities and settlements, primary county divisions (such as townships, New England towns, and census county divisions), American Indian and Alaska Native areas, airports, military bases, national parks, post offices, and other locational entities (except natural or physical features).

Fire Services, Law Enforcement, & Criminal Justice

04,867
PB95-151379 Not available NTIS
National Inst. of Standards and Technology (CAML), Gaithersburg, MD.
Evaluating Investments in Law Enforcement Equipment: An Annotated Bibliography.
Final rept.
S. F. Weber, B. C. Lippiatt, and K. S. Johnson. 1989, 27p.
Pub. in National Institute of Justice Report 900-89, 27p 1989.

Keywords: *Bibliographies, *Protective equipment, *Police vehicles, *Law enforcement, *Investments, Ammunition, Weapons, Police patrol cars, Operations research, Information systems, Cost benefit analysis, Economic analysis, Reprints, Police equipment.

The report is a guide to the literature and annotated bibliography on evaluating investments in law enforcement equipment. Each entry includes the complete citation, an abstract with key words, and in most cases, information on availability. The search strategy is documented and a subject index and lists of references by author and by subject area are included. The main categories are: (1) evaluation methods; (2) police vehicles; (3) police armament; (4) Automatic Vehicle Monitoring (AVM) systems; and (5) police information systems. All 43 included publications both address economic issues such as costs or benefits and are relevant to current decisions on procuring police equipment. The search focused on three primary sources: (1) the NCJRS (National Criminal Justice Reference Service) database; (2) the Criminal Justice Periodical Index (CJPI); and (3) the NTIS (National Technical Information Service) database.

04,868
PB95-162913 Not available NTIS
National Inst. of Standards and Technology (NEL), Gaithersburg, MD. Fire Science and Engineering Div.
Exposure: An Expert System Fire Code.
Final rept.
R. L. Smith. 1991, 15p.
Pub. in Fire Technology 27, n2 p145-159 May 91.

Keywords: *Fire codes, *Artificial intelligence, *Building codes, Fire spread, Computer programs, Exposure, Cost effectiveness, Walls, Fire safety, Reprints, *Building fires, *Expert systems, Combustibles.

The report addresses the issue of developing an expert or knowledge-based system that deals with the problem of preventing the spread of fire between buildings. A knowledge-based program, EXPOSURE, has been developed that facilitates using more appropriate technology, expanding the problem domain, and providing cost-effective solutions. EXPOSURE can solve the problem of the prevention of the spread of fire between buildings for the case when the exposed building has combustible walls. The use of the expert system EXPOSURE and NFPA 80A produce significantly different recommended minimum separation between buildings. In one case the separation required by NFPA 80A was more than five times greater than what EXPOSURE recommended. The program demonstrates that significant cost savings in achieving the desired level of fire safety and in assuring the levels of safety can be obtained by use of expert system fire codes.

04,869
PB95-162939 Not available NTIS
National Inst. of Standards and Technology (BFRL), Gaithersburg, MD. Building and Fire Research Lab. Office.
Forum for International Cooperation on Fire Research.
Final rept.
J. E. Snell. 1993, 9p.
Pub. in Proceedings of Nordic Fire Safety Engineering Symposium, Development and Verification of Tools for Performance Codes, Espoo, Finland, August 30-September 1, 1993, 9p.

Keywords: *Fire research, *International cooperation, *Meetings, Fire safety engineering, Norway, Sweden, Finland, Reprints, *Nordic countries, FORUM research group.

The paper describes the Forum for International Cooperation on Fire Research (FORUM) and its rule in the Nordic Fire Safety Engineering Symposium. The FORUM is an informal group of individuals who direct fire research programs and laboratories. This group shares a common commitment to the advance of fire safety engineering through cooperation in research and its application. The paper suggests actions needed to accelerate the advance of fire safety engineering.

04,870
PB95-162947 Not available NTIS
National Inst. of Standards and Technology (NEL), Gaithersburg, MD. Center for Fire Research.
Fresh Look at Strategies for Fire Safety.
Final rept.
J. E. Snell. 1990, 10p.
Pub. in Proceedings of Interflam '90 Conference, Canterbury, England, September 3-6, 1990, p305-314.

Keywords: *Fire research, *Technology innovation, *Fire safety, Cost effectiveness, Fire losses, Fire codes, International cooperation, Reprints, Fire research strategies.

Recently, in the U.S.A., fire deaths and injuries have plateaued (and may even be increasing) and the costs of fire safety to society have been increasing and in most cases well ahead of inflation. The paper presents a preliminary analysis of this situation from the perspective of the potential contribution of fire research. It points to the need for major technical innovations in five areas to provide the basis for legitimizing fire prevention technology, or what we have termed the technologies for assured fire safety. These technologies may complement and strengthen the traditional fire safety strategies, further reducing the losses to fire and the economic burdens of fire on society.

04,871
PB96-154570 PC A03/MF A01
National Inst. of Standards and Technology (BFRL), Gaithersburg, MD. Office of Applied Economics.
AutoBid 2.0: The Microcomputer System for Police Patrol Vehicle Selection.
S. F. Weber. Feb 96, 12p, NISTIR-5787.
Sponsored by National Inst. of Justice, Washington, DC.

Keywords: *Police patrol cars, *Fleet management, *Acquisition, *Decision support systems, Selection, Ranking, Ratings, Factor analysis, Cost benefit analysis, Performance evaluation, Procurement, Decision making, Optimization, Police vehicles, User manuals(Computer programs), AutoBid computer program, Police equipment, Multiattribute analysis.

This report is the user manual for a microcomputer system designed to help police fleet administrators select the patrol vehicle that is best suited to their needs. The system is called AutoBid and uses vehicle performance test data for police patrol package models published annually by the Michigan State Police. The system offers two vehicle selection methods: performance-based and value-based. Performance selection is based on both vehicle test scores alone. It ranks vehicles by their overall test performance independent of cost. Value selection is based on both vehicle cost and test scores. It identifies which vehicle is the 'Best Buy' in terms of the lowest cost for equivalent test performance and ranks the vehicles by the bid price adjusted for performance. Either or both of these methods may be used for a given fleet acqusition decision.

04,872
PB96-178918 PC A05/MF A01
National Inst. of Standards and Technology (EEEL), Gaithersburg, MD. Office of Law Enforcement Standards.
Directory of Law Enforcement and Criminal Justice Associations and Research Centers.
Special pub.
S. Lyles, M. Leach, and R. Joel. Mar 96, 65p, NIST/SP-480/20-ED-1996.
Supersedes PB86-213089. Also available from Supt. of Docs. as SN003-003-03403-7.

Keywords: *Directories, *Law enforcement, *Organizations, United States, Criminal justice.

This is a directory of organizations that are active in one or more areas of the criminal justice system, including law enforcement, courts, corrections and rehabilitation. The directory lists national organizations primarily, but also includes regional organizations and local organizations of special interest as well as international organizations which have a significant number of American members, a U.S. chapter or subcommit-

tee, or are doing work applicable to law enforcement in this country. The types of national law enforcement and criminal justice organizations listed in this directory are limited by the criterion that they be nonprofit. Included in this category are professional and volunteer social action associations, research centers (usually connected with a university), and government agencies. Strictly social or fraternal organizations are not listed.

Urban Administration & Planning

04,873
FIPS PUB 8-6 PC E09
National Inst. of Standards and Technology (CSL), Gaithersburg, MD.
Metropolitan Areas (Including MSAs, CMSAs, PMASs, and NECMAs). Category: Data Standards and Guidelines; Subcategory: Representations and Codes.
Mar 95, 133p.
Supersedes FIPS PUB 8-5. Also available from Supt. of Docs.

Keywords: *Metropolitan areas, *Geocoding, *Classification, *Geography, Metropolitan statistical areas, Standard Metropolitan Statistical Areas, New England, Cities, Counties, Urban areas, States(United States), Federal Information Processing Standards, Data standards and guidelines, Representation and codes, Consolidated Metropolitan Statistical Areas, Primary Metropolitan Statistical Areas, Data elements.

The standard specifies titles, components, and identification codes for the Metropolitan Areas (MAs) of the United States and Puerto Rico, including units called Metropolitan Statistical Areas (MSAs), Consolidated Metropolitan Statistical Areas (CMSAs), and Primary Metropolitan Statistical Areas (PMSAs), and related units called New England County Metropolitan Areas (NECMAs). The general concept underlying Metropolitan Areas is that of a core are containing a large population nucleus together with adjacent communities having a high degree of economic and social integration with that core. The revision incorporates minor editorial changes and technical changes that have been issued in change notices and supersedes FIPS PUB 8-5 in its entirety.

04,874
PB95-503280 Diskette $59.00
National Inst. of Standards and Technology, Gaithersburg, MD.
FIPS PUB 8-6, Metropolitan Areas (for Microcomputers).
Data file.
May 95, 1 diskette.
This product contains text only. Customers must provide their own search and retrieval software.

The datafile is on one 3 1/2 inch DOS diskette, 1.44M high density. File format: WordPerfect 5.1. Also available in paper copy, order number FIPS PUB 8-6.

Keywords: *Data file, *Metropolitan areas, *Geocoding, *Classification, *Geography, Metropolitan statistical areas, Statistical Metropolitan Statistical Areas, New England, Cities, Countries, Urban areas, States(United States), Diskettes, Federal Information Processing Standards, Data standards and guidelines, Representation and codes, Consolidated Metropolitan Statistical Areas, Primary Metropolitan Statistical Areas, Data elements.

This standard specifies titles, components, and identification codes for the Metropolitan Areas (MAs) of the United States and Puerto Rico, including units called Metropolitan Statistical Areas (MSAs), Consolidated Metropolitan Statistical Areas (CMSAs), and Primary Metropolitan Statistical Areas (PMSAs), and related units called New England County Metropolitan Areas (NECMAs). The general concept underlying MAs is that of a core area containing a large population nucleus together with adjacent communities having a high degree of economic and social integration with that core. This revision incorporates technical changes which reflect revised definitions by the Office of Management and Budget.

PERSONAL AUTHOR INDEX

SAMPLE ENTRY

SMITH, R. L.
Performance Parameters of Fire Detection Systems
PB94-194339 *00,123*

Author name(s)
Title
NTIS order number *Abstract number*

AAMODT, R. L.
External Gamma-ray Counting of Selected Tissues from a Thorotrast Patient.
PB96-160254 *03,637*

ABBOTT, P. J.
Comments on the Stability of Bayard-Alpert Ionization Gages.
PB96-103080 *02,673*

Commercial Helium Permeation Leak Standards: Their Properties and Reliability.
PB97-111413 *04,146*

Influence of the Filament Potential Wave Form on the Sensitivity of Glass-Envelope Bayard-Alpert Gages.
PB95-175014 *02,657*

Long-Term Stability of Bayard-Alpert Gauge Performance: Results Obtained from Repeated Calibrations against the National Institute of Standards and Technology Primary Vacuum Standard.
PB96-123567 *02,676*

ABDEL REHIM, F.
Thin Dyed-Plastic Dosimeter for Large Radiation Doses.
PB95-107363 *03,872*

ABOLA, E. E.
Protein Data Bank: Current Status and Future Challenges.
PB97-109060 *00,517*

ABRAHAM, B.
Taguchi's Parameter Design: A Panel Discussion.
PB96-111802 *03,445*

ABRAHAMS, S. C.
Statistical Descriptors in Crystallography. 2. Report of a Working Group on Expression of Uncertainty in Measurement.
PB96-146824 *04,764*

ABRAMOWITZ, S.
Conformational Alterations of Bovine Insulin Adsorbed on a Silver Electrode.
PB96-161773 *00,510*

Thermodynamic Properties of Gas Phase Species of Importance to Ozone Depletion.
PB94-198215 *00,126*

ABRAMS, M.
Proceedings of the Workshop on the Federal Criteria for Information Technology Security. Held in Ellicot City, Maryland on June 2-3, 1993.
PB94-162583 *01,575*

ABRAMS, M. D.
Head Start on Assurance: Proceedings of an Invitational Workshop on Information Technology (IT) Assurance and Trustworthiness. Held in Williamsburg, Virginia on March 21-23, 1994.
PB94-215746 *01,586*

ACET, M.
Polarization Analysis of the Magnetic Excitations in Fe65Ni35 Invar.
PB95-150082 *04,558*

ACQUISTA, N.
Laser-Produced and Tokamak Spectra of Lithiumlike Iron, Fe(23+).
PB95-180857 *04,314*

ADAIR, D.
Electro-Optical Sensor for Surface Displacement Measurements of Compliant Coatings.
PB94-198223 *02,123*

ADAMS, J.
Electric-Field Strengths Measured Near Personal Transceivers.
PB94-172020 *01,564*

ADAMS, J. W.
Aperture Excitation of Electrically Large, Lossy Cavities.
PB94-145711 *00,029*

Characterization of Unknown Linear Systems Based on Measured CW Amplitude.
PB95-161485 *01,897*

ADAMS, V. H.
Natural Convection from an Array of Electronic Packages Mounted on a Horizontal Board in a Narrow Aspect Ratio Enclosure.
PB96-164017 *02,087*

ADAMUTI-TRACHE, M.
Segmental Concentration Profiles of End-Tethered Polymers with Excluded-Volume and Surface Interactions.
PB97-119002 *00,654*

ADVANI, S. G.
Interaction between Micro and Macroscopic Flow in RTM Preforms.
PB95-162012 *03,159*

AEPPLI, G.
Isolated Spin Pairs and Two-Dimensional Magnetism in SrCr(sub 9p)Ga(sub 12-9p)O19.
PB97-112387 *04,154*

AFEEFY, H. Y.
Alcohol Solutions of Triphenyl-Tetrazolium Chloride as High-Dose Radiochromic Dosimeters.
PB96-135249 *03,716*

AGHAJANIAN, J.
Genetically Engineered Pore as a Metal Ion Biosensor.
PB96-161658 *03,551*

AGOSTINI, P.
Intensity-Dependent Scattering Rings in High Order Above-Threshold Ionization.
PB96-110739 *04,032*

AGREN, J.
Extrapolation of the Heat Capacity in Liquid and Amorphous Phases.
PB97-111421 *04,147*

AHMED, G. N.
Calculating Flame Spread on Horizontal and Vertical Surfaces.
PB94-187283 *00,335*

AIZED, D.
Comparing the Accuracy of Critical-Current Measurements Using the Voltage-Current Simulator.
PB96-119219 *02,227*

AKE, T. B.
First Results from the Goddard High-Resolution Spectrograph: The Chromosphere of Tauri.
PB94-199528 *00,054*

AKMAN, S.
Modification of DNA Bases in Chromatin of Intact Target Human Cells by Activated Human Polymorphonuclear Leukocytes.
PB94-199833 *03,526*

AKMAN, S. A.

Copper Ion-Mediated Modification of Bases in DNA in Vitro by Benzoyl Peroxide.
PB94-198231 *03,645*

Formation of DNA-Protein Cross-Links in Cultured Mammalian Cells Upon Treatment with Iron Ions.
PB96-137724 *03,651*

AKSAY, I. A.

High Resolution Inelastic Neutron Scattering Study of Phonon Self-Energy Effects in YBCO.
PB95-180881 *04,688*

q Dependence of Self-Energy Effects of the Plane Oxygen Vibration in YBa2Cu3O7.
PB96-138516 *01,096*

AL-NAAFA, M. A.

Brownian Diffusion of Hard Spheres at Finite Concentrations.
PB95-164307 *00,975*

AL-SHEIKHLY, M.

Alcohol Solutions of Triphenyl-Tetrazolium Chloride as High-Dose Radiochromic Dosimeters.
PB96-135249 *03,716*

Anionic Triphenylmethane Dye Solutions for Low-Dose Food Irradiation Dosimetry.
PB96-135173 *03,715*

Novel Radiochromic Films for Clinical Dosimetry.
PB97-119259 *03,641*

Polymerization Initiation by N-p-Tolylglycine: Free-Radical Reactions Studied by Pulse and Steady-State Radiolysis.
PB95-180014 *01,269*

Radiochromic Solid-State Polymerization Reaction.
PB95-180683 *01,271*

Radiochromic Solid-State Polymerization Reaction.
PB96-180146 *01,290*

ALBERS, J.

Exact Recursion Relation Solution for the Steady-State Surface Temperature of a General Multilayer Structure.
PB96-102017 *02,376*

Exact Solution of the Steady-State Surface Temperature for a General Multilayer Structure.
PB95-152773 *02,337*

JEDEC 'TCR' Interlaboratory Experiment: Lessons Learned.
PB95-203188 *02,371*

Semiconductor Measurement Technology: HOTPAC. Programs for Thermal Analysis Including Version 3.0 of the TXYZ Program, TXYZ30, and the Thermal MultiLayer Program, TML.
PB95-260766 *02,374*

ALBERS, J. C.

Santa Ana Fire Department Experiment at 1315 South Bristol, July 14, 1994.
PB95-188868 *00,389*

Santa Ana Fire Department Experiment at 1315 South Bristol, July 14, 1994. (Reprint).
PB96-102934 *00,207*

Santa Ana Fire Department Experiments at South Bristol Street.
PB96-154810 *00,305*

ALBERTY, R. A.

Calorimetric Determination of the Standard Transformed Enthalpy of a Biochemical Reaction at Specified PH and pMg.
PB94-198249 *03,454*

ALBRIGHT, B. J.

Core Potentials for Quasi-One-Electron Systems.
PB95-202214 *03,970*

ALBUS, C.

Proceedings of the Annual Manufacturing Technology Conference (2nd): Toward a Common Agenda. Held in Gaithersburg, Maryland on April 18-20, 1995.
PB96-112693 *02,887*

Publications of the Manufacturing Engineering Laboratory Covering the Period January 1989-September 1992.
PB94-165966 *02,750*

ALBUS, C. F.

Automated Manufacturing Research Facility 1994 Annual Report.
PB95-209854 *00,015*

Proceedings of the Manufacturing Technology Needs and Issues: Establishing National Priorities and Strategies Conference. Held in Gaithersburg, Maryland on April 26-28, 1994.
PB95-206181 *02,930*

ALBUS, J. S.

Hierarchical Interaction between Sensory Processing and World Modeling in Intelligent Systems.
PB94-198256 *01,580*

Intelligent Control for Multiple Autonomous Undersea Vehicles.
PB94-211877 *03,747*

NIST Support to the Next Generation Controller Program: 1991 Final Technical Report.
PB94-163490 *02,808*

Overview of NASREM: The NASA/NBS Standard Reference Model for Telerobot Control System Architecture.
PB94-194560 *04,831*

Real-Time Vision for Autonomous and Teleoperated Control of Unmanned Vehicles.
PB94-211885 *03,701*

Real-Time Vision for Unmanned Vehicles.
PB94-211893 *03,702*

Reference Model Architecture for Intelligent Systems Design.
PB95-143137 *01,789*

Role of World Modeling and Value Judgment in Perception.
PB94-198264 *01,581*

Theory of Intelligent Systems.
PB94-198272 *01,582*

Toward a Reference Model Architecture for Real-Time Intelligent Control Systems (ARTICS).
PB94-172046 *02,932*

ALCOCK, C. B.

Thermodynamic Properties of the Group IIA Elements.
PB94-160983 *00,730*

ALDERMAN, D. F.

Airborne Asbestos Analysis: National Voluntary Laboratory Accreditation Program.
PB96-147392 *02,566*

National Voluntary Laboratory Accreditation Program: Bulk Asbestos Analysis.
PB95-138129 *02,541*

National Voluntary Laboratory Accreditation Program (NVLAP): Fasteners and Metals.
PB97-114185 *02,881*

ALEXEFF, I.

Observations of Partial Discharges in Hexane Under High Magnification.
PB95-163127 *01,900*

ALFASSI, Z. B.

Oxidation of Ferrous and Ferrocyanide Ions by Peroxyl Radicals.
PB97-122402 *01,191*

Temperature Dependence of the Rate Constants for Reaction of Dihalide and Azide Radicals with Inorganic Reductants.
PB95-162756 *00,964*

Temperature Dependence of the Rate Constants for Reaction of Inorganic Radicals with Organic Reductants.
PB94-198280 *00,783*

ALGEO, M. E. A.

Process for Selecting Standard Reference Algorithms for Evaluating Coordinate Measurement Software.
PB94-173754 *02,629*

State-of-the-Art Survey of Methodologies for Representing Manufacturing Process Capabilities.
PB94-187655 *02,812*

ALIBE, B.

Algebraic Approximation of Attractors for Galloping Oscillators.
PB95-162897 *04,820*

Chaotic Motions of Coupled Galloping Oscillators and Their Modeling as Diffusion Progresses.
PB96-122718 *04,823*

Foias-Temam Approximations of Attractors for Galloping Oscillators.
PB94-198298 *04,817*

ALKAN DONMEZ, M.

Real Time Compensation for Tool Form Errors in Turning Using Computer Vision.
PB95-107231 *02,945*

ALLAN, D. W.

Confidence on the Second Difference Estimation of Frequency Drift.
PB95-151460 *01,532*

Precision Oscillators: Dependence of Frequency on Temperature, Humidity and Pressure.
PB94-198306 *02,031*

Smart Clock: A New Time.
PB95-151445 *01,530*

ALLEN, A. J.

Analysis of Small-Angle Scattering Data Dominated by Multiple Scattering for Systems Containing Eccentrically Shaped Particles or Pores.
PB96-160411 *03,075*

Anisotropy of the Surfaces of Pores in Plasma Sprayed Alumina Deposits.
PB96-123211 *03,126*

ALLEN, L. P.

Effect of Anneal Temperature on Si/Buried Oxide Interface Roughness on SIMOX.
PB96-112206 *02,382*

ALLEN, O. E.

Time-Domain Antenna Characterizations.
PB95-152781 *02,003*

ALLEN, R.

Resolution of DNA in the Presence of Mobility Modifying Polar and Nonpolar Compounds by Discontinuous Electrophoresis on Rehydratable Polyacrylamide Gels.
PB95-152799 *00,590*

ALLEN, R. A.

Application of the Modified Voltage-Dividing Potentiometer to Overlay Metrology in a CMOS/Bulk Process.
PB94-181997 *02,302*

Comparisons of Measured Linewidths of Sub-Micrometer Lines Using Optical, Electrical, and SEM Metrologies.
PB95-152807 *02,338*

Electrical Test Structure for Improved Measurement of Feature Placement and Overlay in Integrated Circuit Fabrication Processes.
PB95-164273 *02,355*

Electrical Test Structure for Overlay Metrology Referenced to Absolute Length Standards.
PB95-152278 *02,336*

Electrical Test Structures Replicated in Silicon-on-Insulator Material.
PB97-111827 *02,454*

Enhanced Voltage-Dividing Potentiometer for High-Precision Feature Placement Metrology.
PB96-164025 *02,428*

Hybrid Optical-Electrical Overlay Test Structure.
PB96-204136 *02,450*

Measurement of Patterned Film Linewidth for Interconnect Characterization.
PB96-148168 *02,420*

Microelectronic Test Structures for Feature Placement and Electrical Linewidth Metrology.
PB95-180568 *02,367*

Microelectronic Test Structures for Overlay Metrology.
PB96-164249 *02,430*

New Test Structure for Nanometer-Level Overlay and Feature-Placement Metrology.
PB95-175345 *02,363*

Test Structures for the In-Plane Locations of Projected Features with Nanometer-Level Accuracy Traceable to a Coordinate Measurement System.
PB94-200565 *02,313*

ALLEN, S. M.

Electronic Structure and Phase Equilibria in Ternary Substitutional Alloys.
PB97-119366 *03,378*

ALLGOOD, C.

Hair Analysis for Drugs of Abuse: Evaluation of Analytical Methods, Environmental Issues, and Development of Reference Materials.
PB95-176269 *03,501*

ALLGOOD, C. C.

Interlaboratory Comparison Studies on the Analysis of Hair for Drugs of Abuse.
PB95-176251 *03,500*

ALLISON, W.

Variation in Magnetic Properties of Cu/Fcc (001) Sandwich Structures.
PB95-141164 *04,555*

ALPERT, B. K.

Hybrid Gauss-Trapezoidal Quadrature Rules.
PB96-193750 *03,422*

Integral Occurring in Coherence Theory.
PB95-203550 *04,324*

Video Microscopy Applied to Optical Fiber Geometry Measurements.
PB95-173068 *04,295*

ALPERT, R. L.

Prediction of Fire Dynamics.
PB94-193620 *00,336*

ALSHEH, D.

Degradation of Powder Epoxy Coated Panels Immersed in a Saturated Calcium Hydroxide Solution Containing Sodium Chloride.
PB96-101050 *01,344*

ALSTRIN, A. L.

Direct Detection of Atomic Arsenic Desorption from Si(100).
PB95-202230 *01,024*

In-situ Monitoring of Molecular Beam Epitaxial Growth Using Single Photon Ionization.
PB95-202222 *01,023*

Laser Gas Ionization Technique Monitors MEB Crystal Growth.
PB96-112172 *01,076*

Laser-Induced Desorption of In and Ga from Si(100) and Adsorbate Enhanced Surface Damage.
PB95-203311 *01,050*

Laser Vacuum Ultraviolet Single Photon Ionization Probing of III-V Semiconductor Growth.
PB95-202370 *04,691*

Pulsed Laser Irradiation at 532 nm of In and Ga Adsorbed on Si(100): Desorption, Incorporation, and Damage.
PB95-203329 *01,051*

Single-Photon Ionization and Detection of Ga, In, and As(sub n) Species in GaAs Growth.
PB95-152815 *00,591*

Single Photon Ionization, Laser Optical Probe Technique for Semiconductor Growth.
PB95-202776 *01,032*

Single Photon Laser Ionization as an In-situ Diagnostic for MBE growth.
PB96-102025 *01,059*

Single-Photon Laser Ionization Time-of-Flight Mass Spectroscopy Detection in Molecular-Beam Epitaxy: Application to As4, As2, and Ga.
PB95-203337 *01,052*

Vibrational Distributions of As2 in the Cracking of As4 on Si(100) and Si(111).
PB94-198314 00,784

ALTAFIM, R. A. C.

Electrohydrodynamic Instability and Electrical Discharge Initiation in Hexane.
PB96-186119 02,244

ALTMAN, S.

Tert-Butyl Hydroperoxide-Mediated DNA Base Damage in Cultured Mammalian Cells.
PB94-182003 03,644

ALTMAN, S. A.

Formation of DNA-Protein Cross-Links in Cultured Mammalian Cells Upon Treatment with Iron Ions.
PB96-137724 03,651

ALVAREZ, R.

Recently Developed NIST Food Related Standard Reference Materials.
PB94-198322 00,035

Standard Reference Materials for Dioxins and Other Environmental Pollutants.
PB94-198330 02,518

ALVORD, D. M.

CFAST Output Comparison Method and Its Use in Comparing Different CFAST Versions.
PB96-109541 00,401

Feasibility and Design Considerations of Emergency Evacuation by Elevators.
PB94-163441 00,287

AMAR, A.

Application of Single Electron Tunneling: Precision Capacitance Ratio Measurements.
PB96-102157 04,703

AMATO, A.

Dynamics of Mu(+) in Sc and ScHx.
PB96-180021 04,112

AMBUEL, L. M.

Proceedings of the Workshop on the Federal Criteria for Information Technology Security. Held in Ellicot City, Maryland on June 2-3, 1993.
PB94-162583 01,575

AMIRTHARAJ, P. M.

Buffer Layer Modulation-Doped Field-Effect-Transistor Interactions in the Al0.33Ga0.67As/GaAs Superlattice System.
PB96-102876 02,380

Comparison of Techniques for Nondestructive Composition Measurements in CdZnTe Substrates.
PB96-103098 02,703

Double Modulation and Selective Excitation Photoreflectance for Characterizing Highly Luminescent Semiconductor Structures and Samples with Poor Surface Morphology.
PB97-111439 02,452

Double-Modulation and Selective Excitation Photoreflectance for Wafer-Level Characterization of Quantum-Well Laser Structures.
PB96-167325 04,372

High-Accuracy Principal-Angle Scanning Spectroscopic Ellipsometry of Semiconductor Interfaces.
PB96-163787 02,427

Interface Roughness of Short-Period AlAs/GaAs Superlattices Studied by Spectroscopic Ellipsometry.
PB95-107215 02,137

Interface Sharpness during the Initial Stages of Growth of Thin, Short-Period III-V Superlattices.
PB95-108783 02,139

Interface Sharpness in Low-Order III-V Superlattices.
PB95-108775 02,138

Spectroscopic Ellipsometry Determination of the Properties of the Thin Underlying Strained Si Layer and the Roughness at SiO2/Si Interface.
PB95-150157 04,560

Use of Pressure for Quantum-Well Band-Structure Characterization.
PB96-164058 04,779

AMMERLAAN, M. J. J.

Loss-Free Counting at IRI and NIST.
PB96-167119 04,105

AMMON, H. L.

Crystal Structure of Calcium Adipate Monohydrate.
PB94-216579 00,153

Crystal Structure of Decacalcium Tetrapotassium Hexakis (Pyrophosphate) Nonahydrate.
PB96-141064 01,099

ANANDA, M. V.

Residual Error Compensation of a Vision-Based Coordinate Measuring Machine.
PB96-161617 04,091

ANASTASIADIS, S. H.

Morphology of Symmetric Diblock Copolymers as Revealed by Neutron Reflectivity.
PB95-140075 01,234

Temperature Dependence of the Morphology of Thin Diblock Copolymer Films as Revealed by Neutron Reflectivity.
PB94-172756 01,199

ANDERSEN, N.

Can Quantum Mechanical Description of Electron-Sodium Collisions Be Considered Complete. Present Status and Future Prospects for 3s <-> 3p Transitions.
PB94-185014 00,768

ANDERSON, A. C.

Use of Ion Scattering Spectroscopy to Monitor the Nb Target Nitridation during Reactive Sputtering.
PB94-172525 00,761

ANDERSON, D. B.

Evaluation of Corrosion Data: A Review.
PB94-198348 03,187

ANDERSON, D. L.

Effects of Target Shape and Neutron Scattering on Element Sensitivities for Neutron-Capture Prompt Gamma-ray Activation Analysis.
PB94-216157 00,558

Neutron Capture Prompt Gamma-Ray Activation Analysis at the NIST Cold Neutron Research Facility.
PB94-213394 00,556

Use of Neutron Beams for Chemical Analysis at NIST.
PB97-112437 00,652

ANDERSON, D. M.

Diffuse-Interface Description of Fluid Systems.
PB96-210711 01,170

ANDERSON, E.

Performance of HUD-Affiliated Properties during the January 17, 1994 Northridge Earthquake.
PB95-174488 00,443

Thermodynamics of Enzyme-Catalyzed Reactions: Part 1. Oxidoreductases.
PB94-162252 00,737

ANDERSON, E. D.

Stranding Experiments on Double Hull Tanker Structures.
PB96-123112 03,749

ANDERSON, E. H.

Room-Temperature Thermal Conductivity of Expanded Polystyrene Board for a Standard Reference Material.
PB96-193693 00,412

ANDERSON, H. M.

Dusty Plasma Studies in the Gaseous Electronics Conference Reference Cell.
PB96-113410 02,396

Gaseous Electronics Conference Radio-Frequency Reference Cell: A Defined Parallel-Plate Radio-Frequency System for Experimental and Theoretical Studies of Plasma-Processing Discharges.
PB94-172327 04,404

ANDERSON, I. S.

Characterization of the Structure of TbD2.25 at 70 K by Neutron Powder Diffraction.
PB96-160528 01,130

Characterization of the Vibrational Dynamics in the Octahedral Sublattices of LaD2.25 and LaH2.25.
PB96-123724 01,091

Dynamics of Mu(+) in Sc and ScHx.
PB96-180021 04,112

Local-Mode Dynamics in YH2 and YD2 by Isotope-Dilution Neutron Spectroscopy.
PB95-181012 01,017

Neutron-Powder-Diffraction Study of the Long-Range Order in the Octahedral Sublattice of LaD2.25.
PB96-141155 04,753

Neutron Spectroscopic Comparison of beta-Phase Rare Earth Hydrides.
PB96-160742 01,134

Neutron Spectroscopic Comparison of Rare-Earth/Hydrogen alpha-Phase Systems.
PB95-163523 00,970

Neutron Spectroscopic Evidence of Concentration-Dependent Hydrogen Ordering in the Octahedral Sublattice of beta-TbH2+x.
PB95-181020 01,018

Vibrations of Hydrogen and Deuterium in Solid Solution with Lutetium.
PB95-181038 01,019

ANDERSON, M. H.

Behavior of Atoms in a Compressed Magneto-Optical Trap.
PB95-203105 03,999

Reduction of Light-Assisted Collisional Loss Rate from a Low-Pressure Vapor-Cell Trap.
PB95-202248 03,971

Stable, Tightly Confining Magnetic Trap for Evaporative Cooling of Neutral Atoms.
PB96-200720 04,126

ANDERSON, P.

Fracture in Multilayers.
PB96-163613 02,988

ANDERSON, P. M.

Nonlocal Effects of Existing Dislocations on Crack-Tip Emission and Cleavage.
PB96-161807 03,367

ANDERSON, R. C.

Product Realization Process Modeling: A Study of Requirements, Methods and Research Issues.
PB96-147962 02,836

ANDERSON, T. J.

Assessment of the Al-Sb System.
PB94-200474 03,329

ANDREEV, A. V.

Magnetic Properties of Single-Crystalline UCu3Al2.
PB95-180717 04,686

ANDREWS, A. P.

Small Angle Neutron Scattering Studies of Structural Characteristics of Argarose Gels.
PB96-112305 03,475

ANDREWS, M.

Histopathology, Blood Chemistry, and Physiological Status of Normal and Moribund Striped Bass ('Morone saxatilis') Involved in Summer Mortality ('Die-Off') in the Sacramento-San Joaquin Delta of California.
PB94-198157 00,034

ANDRULIS, C.

Deuterium in the Local Interstellar Medium: Its Cosmological Significance.
PB95-202842 00,081

Redshifts in Stellar Transition Regions.
PB96-123310 00,104

Relationship between Radiative and Magnetic Fluxes for Three Active Solar-Type Dwarfs.
PB96-119540 00,097

Transition Regions of Capella.
PB96-123336 00,105

Transition Regions of Capella (1995).
PB96-176714 00,108

ANDRUS, R. D.

Ground Improvement Techniques for Liquefaction Remediation Near Existing Lifelines.
PB96-128111 01,350

ANGELINI, P.

Matrix Grain Bridging Contribution to the Toughness of Whisker Reinforced Ceramics.
PB94-198645 03,134

ANGELINO, G.

Report of the Refrigeration, Air Conditioning and Heat Pumps Technical Options Committee.
PB96-176755 03,293

ANICICH, V. G.

Evaluated Bimolecular Ion-Molecule Gas Phase Kinetics of Positive Ions for Use in Modeling Planetary Atmospheres, Cometary Comae, and Interstellar Clouds.
PB94-168598 00,753

ANKNER, J. F.

Antiferromagnetic Interlayer Correlations in Annealed Ni80Fe20/Ag Multilayers.
PB97-122220 03,109

Combined Low- and High-Angle X-Ray Structural Refinement of a Co/Pt(111) Multilayer Exhibiting Perpendicular Magnetic Anisotropy.
PB94-198355 04,457

Compatibilization of Polymer Blends by Complexation. 2. Kinetics of Interfacial Mixing.
PB97-111900 01,295

Diffraction of Neutron Standing Waves in Thin Films with Resonance Enhancement.
PB97-113278 04,164

Extending the Angular Range of Neutron Reflectivity Measurements from Planar Lipid Bilayers: Applications to a Model Biological Membrane.
PB96-122569 03,476

Magnetic Dead Layer in Fe/Si Multilayer: Profile Refinement of Polarized Neutron Reflectivity Data.
PB94-198363 04,458

Magnetic Structure Determination for Annealed Ni80Fe20/Ag Multilayers Using Polarized-Neutron Reflectivity.
PB96-176615 03,739

Neutron Reflectivity Study of the Density Profile of a Model End-Grafted Polymer Brush: Influence of Solvent Quality.
PB95-202735 01,274

Supermirror Transmission Polarizers for Neutrons.
PB94-216215 03,866

ANNE, A.

Oxidation of 10-Methylacridan, a Synthetic Analogue of NADH and Deprotonation of Its Cation Radical. Convergent Application of Laser Flash Photolysis and Direct and Redox Catalyzed Electrochemistry to the Kinetics of Deprotonation of the Cation Radical.
PB94-198371 00,785

ANTIOCHOS, S.

Sleuthing the Dynamo: HST/FOS Observations of UV Emissions of Solar-Type Stars in Young Clusters.
PB96-122817 00,098

ANTIOCHOS, S. K.

Far-Ultraviolet Flare on a Pleiades G Dwarf.
PB96-102033 00,086

ANTONISHEK, J. K.

Operating Principles of the SBus MultiKron Interface Board.
PB95-231783 01,630

Using S-Check, Alpha Release 1.0.
PB96-165964 01,767

ANTONISHEK, T. A.

North American ISDN Users' Forum Agreements on Integrated Services Digital Network.
PB94-162559 01,466

ANTONUCCI, J.
Ring-Opening Dental Resin Systems Based on Cyclic Acetals.
PB95-162251 *00,162*

ANTONUCCI, J. M.
Bioactive Polymeric Dental Materials Based on Amorphous Calcium Phosphate.
PB96-147012 *03,572*

Dental Materials.
PB94-172871 *00,142*

Effects of Surface-Active Resins on Dentin/Composite Bonds.
PB95-140448 *00,156*

Evaluation of Methylene Lactone Monomers in Dental Resins.
PB95-164661 *00,164*

Facile Synthesis of Novel Fluorinated Multifunctional Acrylates.
PB94-198389 *01,207*

Formation of Hydroxyapatite in a Polymeric Calcium Phosphate Cement.
PB95-180642 *00,173*

Polymeric Calcium Phosphate Cements Derived from Poly(methyl vinyl ether-maleic acid).
PB96-164264 *00,180*

Polymeric Calcium Phosphate Composites with Remineralization Potential.
PB96-155544 *03,575*

Properties and Interactions of Oral Structures and Restorative Materials. Annual Report for Period October 1, 1990 to September 30, 1991.
PB94-160843 *03,558*

Remineralizing Dental Composites Based on Amorphous Calcium Phosphate.
PB96-147020 *03,573*

ANUTA, M. A.
Basic Linear Algebra Operations in SLI Arithmetic.
PB96-165931 *03,421*

MasPar MP-1 as a Computer Arithmetic Laboratory.
PB95-189437 *01,627*

MasPar MP-1 as a Computer Arithmetic Laboratory.
PB96-179155 *01,617*

APPEL, N.
Group 1 for the Process Engineering Data STEP Application Protocol.
PB97-116073 *02,797*

ARAGON, A. S.
Measurements of the Viscosities of Saturated and Compressed Liquid 1,1,1,2-Tetrafluoroethane (R134a), 2,2-Dichloro-1,1,1-Trifluoroethane (R123) and 1,1-Dichloro-1-Fluoroethane (R141b).
PB95-175386 *03,273*

ARAGON, B. P.
Inductively Coupled Plasma Source for the Gaseous Electronics Conference RF Reference Cell.
PB96-113394 *02,394*

ARANGO, I.
Energy-Based Method for Liquefaction Potential Evaluation. Phase 1. Feasibility Study.
PB96-214747 *03,691*

ARBON, R. E.
Calibration and Performance of GafChromic DM-100 Radiochromic Dosemeters.
PB97-119291 *00,703*

ARCHER, D. G.
Enthalpy Increment Measurements from 4.5 K to 350 K and the Thermodynamic Properties of the Titanium Silicide Ti5Si3(cr).
PB96-204037 *00,679*

Enthalpy Increment Measurements from 4.5 to 318 K for Bismuth(cr). Thermodynamic Properties from 0 K to the Melting Point.
PB96-204011 *01,166*

Enthalpy Increment Measurements from 4.5 to 350 K and the Thermodynamic Properties of Titanium Disilicide(cr) to 1700 K.
PB96-204029 *00,678*

Isopiestic Investigation of the Osmotic and Activity Coefficients of Aqueous NaBr and the Solubility of NaBr2H2O(cr) at 298.15 K: Thermodynamic Properties of the NaBr + H2O System over Wide Ranges of Temperature and Pressure.
PB97-110365 *01,175*

Thermodynamic Properties of Synthetic Otavite, CdCO3(cr): Enthalpy Increment Measurements from 4.5 K to 350 K.
PB97-111447 *00,680*

Thermodynamic Properties of Synthetic Sapphire (alpha-Al2O3), Standard Reference Material 720 and the Effect of Temperature-Scale Differences on Thermodynamic Properties.
PB94-168564 *00,750*

ARD, C. K.
Comparison of Techniques for Nondestructive Composition Measurements in CdZnTe Substrates.
PB96-103098 *02,703*

ARDOUIN, B.
International Marine-Atmospheric (222)Rn Measurement Intercomparison in Bermuda. Part 2. Results for the Participating Laboratories.
PB96-175682 *00,115*

ARIF, M.
Multi-Stage, Position Stabilized Vibration Isolation System for Neutron Interferometry.
PB95-175022 *03,955*

Precision Comparison of the Lattice Parameters of Silicon Monocrystals.
PB94-169745 *04,438*

ARKIN, E. M.
Point Probe Decision Trees for Geometric Concept Classes.
PB96-160817 *01,612*

ARNAUD, D.
Report of the Refrigeration, Air Conditioning and Heat Pumps Technical Options Committee.
PB96-176755 *03,293*

ARNDT, T.
Harmonic and Static Susceptibilities of YBa2Cu3O7.
PB95-161139 *04,599*

ARNOLD, F. E.
Evidence of Crosslinking in Methyl Pendent PBZT Fiber.
PB97-112486 *03,393*

ARONOFF, R.
Analysis of ANSI ASC X12 and UN/EDIFACT Electronic Data Interchange (EDI) Standards.
PB95-220554 *01,729*

ARP, U.
Measuring Nondipolar Asymmetries of Photoelectron Angular Distributions.
PB97-122493 *01,193*

ARTYMOWICZ, D.
Incorporation of Gold into YBa2Cu3O7: Structure and Tc Enhancement.
PB94-200276 *04,481*

ARVAY, E.
dc Method for the Absolute Determination of Conductivities of the Primary Standard KCl Solutions from 0C to 50C.
PB94-219342 *02,644*

ASAOKA, K.
Behavior of a Calcium Phosphate Cement in Simulated Blood Plasma In vitro.
PB95-168712 *00,165*

Effect of Transformation of Alloy on Transient and Residual Stresses in a Porcelain-Metal Strip.
PB94-198397 *00,143*

Evaluation of Fracture Toughness and Residual Stress in Dental Porcelain by Indentation-Microfracture Method.
PB95-125613 *00,154*

Evaluation of Fracture Toughness and Residual Stress in Dental Porcelain by Indentation-Microfracture Method.
PB95-152831 *00,159*

Influence of Tempering Method on Residual Stress in Dental Porcelain.
PB94-172012 *00,138*

Properties and Interactions of Oral Structures and Restorative Materials. Annual Report for Period October 1, 1990 to September 30, 1991.
PB94-160843 *03,558*

ASCARRUNZ, F.
Frequency Synthesis and Metrology at 10(-17) and Beyond.
PB97-113187 *02,101*

ASCARRUNZ, F. G.
Effect of Harmonic Distortion on Phase Errors in Frequency Distribution and Synthesis.
PB96-200779 *01,563*

ASCARUNZ, F. G.
Investigations of AM and PM Noise in X-Band Devices.
PB95-180022 *02,062*

ASHE, M. J.
Surface Roughness of Glass-Ceramic Insert. Composite Restorations: Assessing Several Polishing Techniques.
PB97-119010 *03,583*

ASHFOLD, M. N. R.
Photodissociation of Ammonia at 193.3nm: Rovibrational State Distribution of the NH2(A(2)A1) Fragment.
PB95-151775 *00,937*

Resonance Enhanced Multiphoton Ionization Spectroscopy of the PF Radical.
PB97-119119 *00,702*

ASHLEY, K.
Lead Abatement in Buildings and Related Structures.
PB94-172038 *03,601*

ASHWORTH, S.
High-Efficiency, High-Power Difference-Frequency Generation of 0.9-1.5 mu m Light in BBO.
PB95-202255 *04,317*

High-Resolution Infrared Spectroscopy of DF Trimer: A Cyclic Ground State Structure and DF Stretch Induced Intramolecular Vibrational Coupling.
PB95-150678 *00,920*

ASHWORTH, S. H.
Stabilization and Precise Calibration of a Continuous-Wave Difference Frequency Spectrometer by Use of a Simple Transfer Cavity.
PB95-162350 *04,276*

ASMAIL, C.
Rayleigh Scattering Limits for Low-Level Bidirectional Reflectance Distribution Function Measurements.
PB95-180030 *04,307*

ASPECT, A.
Frequency-Stabilized LNA Laser at 1.083 mum: Application to the Manipulation of Helium 4 Atoms.
PB95-176186 *04,304*

ASSAEL, M. J.
Standard Reference Data for the Thermal Conductivity of Water.
PB96-145875 *01,111*

Status of the Round Robin on the Transport Properties of R134a.
PB96-167218 *01,152*

Transient Methods for Thermal Conductivity.
PB94-198405 *04,197*

ASTUMIAN, R. D.
Electropermeabilization of Cell Membranes: Effect of the Resting Membrane Potential.
PB95-163291 *03,537*

Energy Transduction between a Concentration Gradient and an Alternating Electric Field.
PB94-216363 *03,461*

Imposed Oscillations of Kinetic Barriers Can Cause an Enzyme to Drive a Chemical Reaction Away from Equilibrium.
PB96-161625 *01,137*

Michaelis-Menten Equation for an Enzyme in an Oscillating Electric Field.
PB95-140489 *00,906*

Quadratic Response of a Chemical Reaction to External Oscillations.
PB96-161633 *01,138*

ATALLA, R. H.
Solid State (13)C NMR and Raman Studies of Cellulose Triacetate: Oligomers, Polymorphism, and Inferences about Chain Polarity.
PB96-176532 *01,289*

ATHA, D.
Physicochemical Characterization of Low Molecular Weight Heparin.
PB96-112040 *03,474*

ATHA, D. H.
Physical Characterization of Herparin by Light Scattering.
PB96-119383 *03,598*

Structural Analysis of Heparin by Raman Spectroscopy.
PB96-167226 *03,480*

Thermodynamic Analysis of Heparin Binding to Human Antithrombin.
PB94-199593 *03,455*

ATZMONY, U.
Magnetic and Structural Properties of Electrodeposited Copper-Nickel Microlayered Alloys.
PB94-213121 *04,512*

AUCIELLO, O.
Growth of Epitaxial KNbO3 Thin Films.
PB96-135181 *02,409*

AUSLOOS, P. J.
Ionization Energy of Sulfur Pentafluoride and the Sulfur Pentafluoride-Fluorine Atom Bond Dissociation Energy.
PB95-162814 *00,966*

AUST, J. A.
Distributed Feedback Lasers in Rare-Earth-Doped Phosphate Glass.
PB96-123773 *04,740*

Linewidth Narrowing in an Imbalanced Y-Branch Waveguide Laser.
PB95-140844 *04,258*

Nd:LiTaO3 Waveguide Laser.
PB95-140851 *04,259*

Passively Q-Switched Nd-Doped Waveguide Laser.
PB95-180048 *04,308*

Rare-Earth-Doped Waveguide Devices: The Potential for Compact Blue-Green Lasers.
PB95-140836 *04,257*

AUSTIN, M.
Thermal Expansion of an SiC Particle-Reinforced Aluminum Composite.
PB94-213204 *03,144*

AUSTIN, M. A.
Contributions of Out-of-Plane Material to a Scanned-Beam Laminography Image.
PB96-111786 *02,704*

AUSTIN, M. W.
Evaluation and Qualification Standards for an X-Ray Laminography System.
PB94-172954 *02,029*

X-Ray Image Quality Indicator Designed for Easy Alignment.
PB95-164455 *02,907*

AUTERI, F. P.
Research and Development Activities in Electron Paramagnetic Resonance Dosimetry.
PB96-141288 *03,635*

AUZERAIS, F.
Transport and Diffusion in Three-Dimensional Composite Media.
PB95-176129 *04,668*

AVEDISIAN, C. T.
Analysis of Droplet Arrival Statistics in a Pressure-Atomized Spray Flame.
PB97-112270 *01,352*

Combustion of Methanol and Methanol/Dodecanol Spray Flames.
PB95-108544 *02,478*

Effect of Dodecanol Content on the Combustion of Methanol Spray Flames.
PB95-176020 *01,389*

Role of Combustion on Droplet Transport in Pressure-Atomized Spray Flames.
PB96-204433 *01,434*

Study of Droplet Transport in Alcohol-Based Spray Flames Using Phase/Doppler Interferometry.
PB95-108551 *02,479*

AVERITT, R. D.
Photoluminescence Spectra of Epitaxial Single Crystal C60.
PB96-141205 *04,754*

AVGOLOUPIS, S.
Rotational Modulation and Flares on RS Canum Venaticorum and BY Draconis Stars. XVI. IUE Spectroscopy and VLA Observations of C1182(=V 1005 Orionis) in October 1983.
PB94-185626 *00,050*

AVILA, M. J.
Experimental Validation of Radiopharmaceutical Absorbed Dose to Mineralized Bone Tissue.
PB94-199668 *03,617*

Radiation Doses.
PB94-199676 *03,618*

AVRAMOV, I. D.
Surface Transverse Wave Oscillators with Extremely Low Thermal Noise Floors.
PB96-186010 *01,967*

AVRAMOV, S.
Automatic Calibration of Inductive Voltage Dividers for the NASA Zeno Experiment.
PB95-152849 *02,041*

Automatic Inductive Voltage Divider Bridge Operates from 10 Hz to 100 kHz.
PB94-198413 *02,032*

Inductive Voltage Divider Calibration for the NASA Flight Experiment.
PB95-152856 *02,042*

AVRAMOV-ZAMUROVIC, S.
Binary versus Decade Inductive Voltage Divider Comparison and Error Decomposition.
PB96-112263 *02,071*

Exploring the Low-Frequency Performance of Thermal Converters Using Circuit Models and a Digitally Synthesized Source.
PB97-112551 *02,848*

Low Voltage Standards in the 10 Hz to 1 MHz Range.
PB97-112569 *02,100*

Proposed Tests to Evaluate the Frequency-Dependent Capacitor Ratio for Single Electron Tunneling Experiment.
PB97-111454 *01,982*

AVRIN, W. F.
24 GHz Josephson Array Voltage Standard.
PB94-211588 *02,033*

AXELBAUM, R. L.
In-situ Studies of a Novel Sodium Flame Process for Synthesis of Fine Particles.
PB97-113047 *00,681*

Optical and Modeling Studies of Sodium/Halide Reactions for the Formation of Titanium and Boron Nanoparticles.
PB97-113054 *00,682*

AXLEY, J. W.
New Mass Transport Elements and Components for the NIST IAQ Model.
PB95-255899 *02,558*

AYRES, R. L.
NIST-NRL Free-Electron Laser Facility.
PB94-212511 *04,237*

AYRES, T.
Sleuthing the Dynamo: HST/FOS Observations of UV Emissions of Solar-Type Stars in Young Clusters.
PB96-122817 *00,098*

AYRES, T. R.
Deuterium and the Local Interstellar Medium: Properties for the Procyon and Capella Lines of Sight.
PB96-200639 *00,111*

Distant Future of Solar Activity: A Case Study of Beta Hydri. 3. Transition Region, Corona, and Stellar Wind.
PB94-185220 *00,049*

Distant Future of Solar Activity: A Case Study of beta Hydri. 3. Transition Region, Corona, and Stellar Wind.
PB95-153441 *00,074*

Far-Ultraviolet Flare on a Pleiades G Dwarf.
PB96-102033 *00,086*

Goddard High-Resolution Spectrograph Observations of the Local Interstellar Medium and the Deuterium/Hydrogen Ratio along the Line of Sight Toward Capella.
PB94-213444 *00,066*

Hydrogen Lyman-alpha Emission of Capella.
PB95-202263 *00,075*

Relationship between Radiative and Magnetic Fluxes for Three Active Solar-Type Dwarfs.
PB96-119540 *00,097*

Riass Coronathon: Joint X-ray and Ultraviolet Observations of Normal F-K Stars.
PB96-200217 *00,109*

Transition Regions of Capella.
PB96-123336 *00,105*

Transition Regions of Capella (1995).
PB96-176714 *00,108*

AZIZ, M. J.
Disorder Trapping in Ni2TiAl.
PB94-198942 *03,322*

AZIZ, R. A.
Ab initio Calculations for Helium: A Standard for Transport Property Measurements.
PB96-102041 *01,060*

AZUMA, Y.
Evolution of X-ray Resonance Raman Scattering into X-ray Fluorescence from the Excitation of Xenon Near the L3 Edge.
PB96-102751 *04,025*

High-Energy Behavior of the Double Photoionization of Helium from 2 to 12 keV.
PB94-213279 *03,860*

BA, W. Z.
Thin Dyed-Plastic Dosimeter for Large Radiation Doses.
PB95-107363 *03,872*

BABA, T.
High-Temperature Laser-Pulse Thermal Diffusivity Apparatus.
PB94-185147 *02,631*

Thermal Diffusivity of POCO AXM-5Q1 Graphite in the Range 1500 to 2500 K Measured by a Laser-Pulse Technique.
PB94-185022 *03,013*

BABCOCK, S. E.
Electromagnetic Coupling Character of (001) Twist Boundaries in Sintered Bi2Sr2CaCu2O8+x Bicrystals.
PB96-176573 *01,963*

Weak-Link-Free Behavior of High Angle YBa2Cu3O7-x Grain Boundaries in High Magnetic Fields.
PB94-198421 *04,459*

BABECKI, M. B. G.
Hair Testing for Drugs of Abuse: International Research on Standards and Technology.
PB96-120555 *03,504*

BABRAUSKAS, V.
Developing Rational Performance-Based Fire Safety Requirements in Model Building Codes.
PB95-175220 *00,200*

Effective Measurement Techniques for Heat, Smoke, and Toxic Fire Gases.
PB94-198439 *01,369*

Effects of Specimen Edge Conditions on Heat Release Rate.
PB95-152864 *00,375*

Fire Safety of Passenger Trains: A Review of Current Approaches and of New Concepts.
PB94-152006 *04,848*

Modern Test Methods for Flammability.
PB94-198447 *01,370*

Standardization of Formats and Presentation of Fire Data - The FDMS.
PB94-198462 *01,371*

Toxicity, Fire Hazard and Upholstered Furniture.
PB94-198454 *00,289*

BACH, B. W.
New cw CO2 Laser Lines: The 9-mu m Hot Band.
PB95-168548 *04,281*

BACH, H.
Polarization Analysis of the Magnetic Excitations in Fe65Ni35 Invar.
PB95-150082 *04,558*

Temperature Dependence of the Magnetic Excitations in Ordered and Disordered Fe72Pt28.
PB95-150223 *04,563*

BACH, K. G.
New cw CO2 Laser Lines: The 9-mu m Hot Band.
PB95-168548 *04,281*

BACHEM, E.
Extension of Heterodyne Frequency Measurements on OCS to 87 THz (2900 cm(-1)).
PB94-200680 *00,811*

BACKES, P. G.
Unified Telerobotic Architecture Project (UTAP) Standard Interface Environment (SIE), May 1995.
PB95-242350 *02,938*

BACON, D.
Crystal Packing Interactions of Two Different Crystal Forms of Bovine Ribonuclease A.
PB95-152823 *00,943*

BACON, M. C.
Nutritional Status and Growth in Juvenile Rheumatoid Arthritis.
PB94-198470 *03,515*

BADNELL, N. R.
Dielectronic Capture Processes in the Electron-Impact Ionization of Sc(2+).
PB95-203113 *04,000*

BADZIAN, A.
Analysis of Boron in CVD Diamond Surfaces Using Neutron Depth Profiling.
PB94-213089 *04,511*

BADZIAN, T.
Analysis of Boron in CVD Diamond Surfaces Using Neutron Depth Profiling.
PB94-213089 *04,511*

BAECHTEL, F. S.
Interlaboratory Comparison of Autoradiographic DNA Profiling Measurements. 1. Data and Summary Statistics.
PB95-175923 *03,542*

BAGCHI, S.
Mechanism of Defect Formation in Low-Dose Oxygen Implanted Silicon-on-Insulator Material.
PB97-111462 *02,453*

BAGG, T. C.
Dilemma-Preservation versus Access.
PB94-198488 *02,711*

BAGWILL, R.
Security in Open Systems.
PB95-105383 *01,473*

BAGWILL, R. H.
Electronic Implementors' Workshop.
PB95-210936 *01,484*

Sharing Information via the Internet: An Infoserver Case Study.
PB96-131511 *01,493*

BAHEL, A.
Energy Dependence of Collision Characteristics in Molecule-Surface Collisions.
PB94-198504 *00,786*

BAHN, W. L.
Electromechanical properties of superconductors for DOE fusion applications.
DE95015476 *04,432*

Electromechanical Properties of Superconductors for DOE Fusion Applications.
PB94-139672 *02,250*

BAHR, R.
Laser-Produced and Tokamak Spectra of Lithiumlike Iron, Fe(23+).
PB95-180857 *04,314*

BAKER, E. F.
Application of ODF to the Rietveld Profile Refinement of Polycrystalline Solid.
PB95-202388 *03,401*

BAKER, E. L.
Microstructure Study of Molybdenum Liners by Neutron Diffraction.
PB95-202396 *03,756*

Texture Study of Two Molybdenum Shaped Charge Liners by Neutron Diffraction.
PB94-200177 *03,754*

BAKER-JARVIS, J.
Analysis of an Open-Ended Coaxial Probe with Lift-Off for Nondestructive Testing.
PB96-135116 *01,940*

Applicability of Effective Medium Theory to Ferroelectric/Ferrimagnetic Composites with Composition and Frequency-Dependent Complex Permittivities and Permeabilities.
PB96-157854 *01,945*

Dielectric and Magnetic Measurements from -50C to 200C and in the Frequency Band 50 MHz to 2 GHz.
PB96-191382 *02,245*

Distribution of Dielectric Relaxation Times and the Moment Problem.
PB96-112032 *04,727*

Effective Medium Theory for Ferrite-Loaded Materials.
PB95-154662 *01,893*

Preparation, Crystal Structure, Dielectric Properties, and Magnetic Behavior of Ba2Fe2Ti4O13.
PB96-186176 *01,162*

Transmission/Reflection and Short-Circuit Line Methods for Measuring Permittivity and Permeability.
PB94-165537 *02,211*

BAKER-JARVIS, J. R.
Dielectric Measurements on Printed-Wiring and Circuit Boards, Thin Films, and Substrates: An Overview.
PB96-147038 *02,236*

Open-Ended Coaxial Probes for Nondestructive Testing of Substrates and Circuit Boards.
PB96-122825 *02,078*

BAKHSHAI, A.
Incorporation of Gold into YBa2Cu3O7: Structure and Tc Enhancement.
PB94-200276 *04,481*

BALASUBRAMANIAN, R.
Comparison of Techniques for Nondestructive Composition Measurements in CdZnTe Substrates.
PB96-103098 *02,703*

BALASUBRAMANIAN, V.
Energy Dependence of Collision Characteristics in Molecule-Surface Collisions.
PB94-198504 *00,786*

BALDONI, J. G.
Tensile Creep of Whisker Reinforced Silicon Nitride.
PB94-211984 *03,142*

BALDWIN, J. R.
Standard Reference Materials: Glass Filters as a Standard Reference Material for Spectrophotometry - Selection, Preparation, Certification, and Use of SRM 930 and SRM 1930.
PB94-188844 *00,536*

BALIZER, E.
Hysteresis Measurements of Remanent Polarization and Coercive Field in Polymers.
PB94-199767 *04,475*

BALLINGER, R. G.
Charpy Impact Test as an Evaluation of 4 K Fracture Toughness.
PB96-190194 *03,219*

BALLSCHMITER, K.
Comparison of Methods for Gas Chromatographic Determination of PCBs and Chlorinated Pesticides in Marine Reference Materials.
PB95-140091 *02,584*

BALSARA, N. P.
Thermodynamic Interactions and Correlations in Mixtures of Two Homopolymers and a Block Copolymers by Small Angle Neutron Scattering.
PB95-152872 *01,247*

Thermodynamic Interactions in Model Polyolefin Blends Obtained by Small-Angle Neutron Scattering.
PB94-198496 *01,208*

BALTATU, M. E.
Viscosity of Defined and Undefined Hydrocarbon Liquids Calculated Using an Extended Corresponding-States Model.
PB96-167234 *02,498*

BALTZER, P.
Inner-Valence States CO(+) between 22 eV and 46 eV Studied by High Resolution Photoelectron Spectroscopy and ab Initio CI Calculations.
PB95-180055 *03,961*

BALZAR, D.
Accurate Modeling of Size and Strain Broadening in the Rietveld Refinement: The 'Double-Voigt' Approach.
PB96-200225 *00,664*

Crystal Structure and Compressibility of 3:2 Mullite.
PB95-175030 *03,682*

Enhanced Flux Pinning via Chemical Substitution in Bulk Superconducting T1-2212.
PB95-169033 *04,647*

Microstrains and Domain Sizes in Bi-Cu-O Superconductors: An X-Ray Diffraction Peak-Broadening Study.
PB94-198520 *04,461*

Profile Fitting of X-Ray Diffraction Lines and Fourier Analysis of Broadening.
PB94-198512 *04,460*

Residual Stresses in Aluminum-Mullite (alpha-Alumina) Composites.
PB95-152880 *03,155*

Voigt-Function Modeling in Fourier Analysis of Size- and Strain-Broadened X-Ray Diffraction Peaks.
PB94-198538 *04,462*

BAN, Y. B.
Neutron Scattering Study of Shear Induced Turbidity in Polystyrene/Dioctyl Phthalate Solutions at High Shear Rates.
PB94-172624 *01,197*

Neutron Scattering Study of Shear Induced Turbidity in Polystyrene Dissolved in Dioctyl Phthalate.
PB95-161865 *01,256*

BAND, A.
Closed Loop Controller for Electron-Beam Evaporators.
PB97-111470 *04,393*

BAND, Y. B.
Density Matrix Calculation of Population Transfer between Vibrational Levels of Na2 by Stimulated Raman Scattering with Temporally Shifted Laser Beams.
PB94-198546 *00,787*

Excitons in Complex Quantum Nanostructures.
PB97-118343 *01,184*

BANDY, H. T.
Compensation of Errors Detected by Process-Intermittent Gauging.
PB97-110472 *02,846*

Data Management for Error Compensation and Process Control.
PB97-110480 *02,847*

PIECS: A Software Program for Machine Tool Process-Intermittent Error Compensation.
PB96-165980 *02,842*

BANG, C. A.
Thermal Isolation of High-Temperature Superconducting Thin Films Using Silicon Wafer Bonding and Micromachining.
PB96-135017 *02,408*

BANNISTER, M.
Collisions of Electrons with Highly-Charged Ions.
PB96-200340 *04,791*

BANNISTER, M. E.
Absolute Cross Sections for Electron-Impact Single Ionization of Si(+) and Si(2+).
PB95-202529 *03,982*

Backscattering in Electron-Impact Excitation of Multiply Charged Ions.
PB94-185345 *03,799*

Evidence for Significant Backscattering in Near-Threshold Electron-Impact Excitation of Ar(7+)(3s yields 3p).
PB95-126405 *03,883*

Merged-Beams Energy-Loss Technique for Electron-Ion Excitation: Absolute Total Cross Sections for O(5+) (2s yields 2p).
PB96-102058 *04,017*

Resonance Structure and Absolute Cross Sections in Near-Threshold Electron-Impact Excitation of the 4s(2) (1)S yields 4s4p (3)P Intercombination Transition in Kr(6+).
PB95-202271 *03,972*

BARBEE, T. W.
Experimental Constraints on Some Mechanisms for High-Temperature Superconductivity.
PB94-198553 *04,463*

XUV Characterization Comparison of Mo/Si Multilayer Coatings.
PB95-164000 *04,278*

BARBERA, A. J.
Continuous Mining Machine Control Using the Real-Time Control System.
PB94-203528 *03,700*

BARCELO, M.
Effect of Formulation Changes on the Response to Ionizing Radiation of Radiochromic Dye Films.
PB97-119028 *04,171*

BARCO, M. T.
Wear of Human Enamel against a Commercial Castable Ceramic Restorative Material.
PB95-161972 *00,161*

BARD, A.
Microlithography by Using Neutral Metastable Atoms and Self-Assembled Monolayers.
PB96-190038 *02,441*

BARILO, S. N.
Magnetic Structure and Spin Dynamics of the Pr and Cu in Pr2CuO4.
PB96-111836 *04,036*

BARKER, E.
EDI and EFT Security Standards.
PB96-122833 *01,605*

BARKER, J. G.
Instrumental Smearing Effects in Radially Symmetric Small-Angle Neutron Scattering by Numerical and Analytical Methods.
PB96-160429 *02,984*

Small Angle Neutrons Scattering from Nanocrystalline Palladium as a Function of Annealing.
PB95-176103 *03,354*

BARKLEY, J.
Distributed Communication Methods and Role-Based Access Control for Use in Health Care Applications.
PB96-183165 *01,508*

Security in Open Systems.
PB95-105383 *01,473*

BARKLEY, J. F.
Comparing Remote Procedure Calls: Open Network Computing, Distributed Computing Environment and International Organization for Standardization.
PB95-194205 *01,724*

BARKMEYER, E.
Control Entity Interface Specification.
PB94-191715 *02,815*

BARKMEYER, E. J.
Requisite Elements, Rationale, and Technology Overview for the Systems Intergration for Manufacturing Applications (SIMA) Program. Background Study.
PB96-112685 *02,831*

BARMAK, K.
Effect of Microstructure on Phase Formation in the Reaction of Nb/Al Multilayer Thin Films.
PB95-168415 *03,352*

First Phase Formation Kinetics in the Reaction of Nb/Al.
PB95-168456 *03,353*

Thin Film Reaction Kinetics of Niobium/Aluminum Multilayers.
PB95-175295 *04,651*

BARNARD, J. A.
Size and Self-Field Effects in Giant Magnetoresistive Thin-Film Devices.
PB95-180188 *04,674*

BARNEA, G.
Study of Multiple Scattering Background in Compton Scatter Imaging.
PB96-112222 *04,425*

BARNES, C. S.
Binary Decision Clustering for Neural Network Based Optical Character Recognition.
PB95-171971 *01,848*

Binary Decision Clustering for Neural-Network-Based Optical Character Recognition.
PB96-186184 *01,857*

Face Recognition Technology for Law Enforcement Applications.
PB94-207768 *01,837*

BARNES, F.
Dielectric Properties of Thin Film SrTiO3 Grown on LaAlO3 with YBa2Cu3O7-x Electodes.
PB95-181160 *02,267*

BARNES, G.
Critical Current and Normal Resistance of High-Tc Step-Edge SNS Junctions.
PB96-111752 *04,724*

BARNES, J.
Precision Oscillators: Dependence of Frequency on Temperature, Humidity and Pressure.
PB94-198306 *02,031*

BARNES, J. D.
Synthesis of Hybrid Organic-Inorganic Materials from Interpenetrating Polymer Network Chemistry.
PB96-180054 *02,994*

BARNES, K. A.
Flow-Induced Structure in Polymers: Chapter 16. Shear-Induced Changes in the Order-Disorder Transition Temperature and the Morphology of a Triblock Copolymer.
PB96-123237 *03,127*

Shear-Excited Morphological States in a Triblock Copolymer.
PB94-172392 *01,196*

Shear-Induced Martensitic-Like Transformation in a Block Copolymer Melt.
PB96-119508 *01,277*

BARNES, P. Y.
45 deg/0 deg Reflectance Factors of Pressed Polytetrafluoroethylene (PTFE) Powder.
PB95-260758 *04,328*

BARNETT, J. P.
Using Emulator/Testers for Commissioning EMCS Software, Operator Training, Algorithm Development, and Tuning Local Control Loops.
PB94-212735 *00,245*

BAROGHEL-BOUNY, V.
Modelling Drying Shrinkage of Cement Paste and Mortar. Part 1. Structural Models from Angstroms to Millimeters.
PB96-135132 *03,074*

BAROUCH, E.
Numerical Simulation of Submicron Photolithographic Processing.
PB94-198561 *02,310*

BARR, R. M.
Regulation of Lithium and Boron Levels in Normal Human Blood: Environmental and Genetic Considerations.
PB94-198579 *03,491*

BARTHOLOMEUSZ, M. F.
Experimental Assessment of Crack-Tip Dislocation Emission Models for an Al67Cr8Ti25 Intermetallic Alloy.
PB96-204466 *03,377*

BARTHOLOMEW, R. W.
Advanced Components for Electric and Hybrid Electric Vehicles. Workshop Proceedings. Held in Gaithersburg, Maryland on October 27-28, 1993.
PB94-177060 *04,858*

BARTLETT, R. J.
Vibronic Coupling and Other Many-Body Effects in the 4sigmag(-1) Photoionization Channel of CO2.
PB95-162509 *00,962*

BARTSCHAT, K.
Can Quantum Mechanical Description of Electron-Sodium Collisions Be Considered Complete. Present Status and Future Prospects for 3s <-> 3p Transitions.
PB94-185014 *00,768*

Characteristics of Light Emission After Low-Energy Electron Impact Excitation of Caesium Atoms.
PB94-198587 *03,806*

Charge Cloud Distribution of Heavy Atoms After Excitation by Polarized Electrons.
PB95-203147 *04,001*

Connection between Superelastic and Inelastic Electron-Atom Collisions Involving Polarized Collision Partners.
PB95-202297 *03,974*

Core Potentials for Quasi-One-Electron Systems.
PB95-202214 *03,970*

Low-Energy-Electron Collisions with Sodium: Elastic and Inelastic Scattering from the Ground State.
PB96-103106 *04,030*

Low-Energy Electron Scattering from Caesium Atoms: Comparison of a Semirelativistic Breit-Pauli and a Full Relativistic Direc Treatment.
PB94-185030 *00,769*

Polarization of Light Emitted After Positron Impact Excitation of Alkali Atoms.
PB94-199734 03,816

Relativistic Effects in Spin-Polarization Parameters for Low-Energy Electron-Cs Scattering.
PB95-150868 03,901

Short-Range Correlation and Relaxation Effects on the (6p(2))(1)SO Autoionizing State of Atomic Barium.
PB95-202289 03,973

BARYSCHPOLEC, S. W.

Radiation Process Data: Collection, Analysis, and Interpretation.
PB95-162632 03,628

BASCH, H.

Strong Hydrogen Bond in the Formic Acid-Formate Anion System.
PB94-198595 00,788

Structure of Glycine-Water H-Bonded Complexes.
PB94-198603 00,789

BASKO, M. M.

Physics and Prospects of Inertial Confinement Fusion.
PB94-185048 04,405

BASRI, G.

Sleuthing the Dynamo: HST/FOS Observations of UV Emissions of Solar-Type Stars in Young Clusters.
PB96-122817 00,098

BASRI, G. S.

Far-Ultraviolet Flare on a Pleiades G Dwarf.
PB96-102033 00,086

BASSHAM, L. E.

Precise Identification of Computer Viruses.
PB96-160825 01,613

Security Considerations for SQL-Based Implementations of STEP.
PB94-139649 02,766

BASTIAN, M. J.

Laser-Induced Fluorescence Measurements of Rotationally Resolved Velocity Distributions for CO(+) Drifted in He.
PB94-213139 00,848

BASTIAN, T. S.

Class of Radio-Emitting Magnetic B Stars and a Wind-Fed Magnetosphere Model.
PB94-213451 00,067

Radio Emission from Chemically Peculiar Stars.
PB94-213469 00,068

BASTIE, J.

Comparison of Regular Transmittance Scales of Four National Standardizing Laboratories.
PB94-211232 04,233

BATES, F. S.

Grazing Incidence Prompt Gamma Emissions and Resonance-Enhanced Neutron Standing Waves in a Thin-Film.
PB95-150470 03,892

BATRA, P.

Optical Density Measurements of Laser Eye Protection Materials.
PB96-190301 00,190

BAUER, B.

Relaxation After a Temperature Jump Within the One Phase Region of a Polymer Mixture.
PB97-112494 03,394

BAUER, B. J.

Cylinder Wipe Air-Drying Intaglio Ink Vehicles for U.S. Currency Inks.
PB94-160801 03,115

Electron Beam Crosslinking of Poly(vinylmethyl ether).
PB94-185550 01,205

Grafted Interpenetrating Polymer Networks.
PB94-185055 01,200

Slow Dynamics of Segregation in Hydrogen-Bonded Polymer Blends.
PB96-123591 01,281

Synthesis of Hybrid Organic-Inorganic Materials from Interpenetrating Polymer Network Chemistry.
PB96-180054 02,994

BAUM, H.

Dispersion and Deposition of Smoke Plumes Generated in Massive Fires.
PB95-126066 02,540

Ignition and Subsequent Transition to Flame Spread in a Microgravity Environment.
N96-15584/1 04,828

Smoke Emission from Burning Crude Oil.
PB96-122890 01,407

BAUM, H. R.

Application of Boundary Element Methods to a Transient Axis-Symmetric Heat Conduction Problem.
PB94-212693 01,375

Gravity-Current Transport in Building Fires.
PB96-147046 01,415

Heat Transfer in an Intumescent Material Using a Three-Dimensional Lagrangian Model.
PB96-164066 00,408

Ignition and Subsequent Flame Spread Over a Thin Cellulosic Material.
PB96-160270 04,836

Ignition and Transition to Flame Spread Over a Thermally Thin Cellulosic Sheet in a Microgravity Environment.
PB96-160288 04,837

In situ Burning of Oil Spills: Mesoscale Experiments and Analysis.
PB95-163747 02,587

Large Eddy Simulations of Smoke Movement in Three Dimensions.
PB96-190012 01,426

Mathematical Modeling and Computer Simulation of Fire Phenomena.
PB95-180063 00,384

Numerical Simulation of Rapid Combustion in an Underground Enclosure.
PB96-183132 01,424

Transition from Localized Ignition to Flame Spread Over a Thin Cellulosic Material in Microgravity.
PB96-155809 04,835

Transport by Gravity Currents in Building Fires.
PB97-119325 01,441

BAUM, M. S.

Federal Certification Authority Liability and Policy: Law and Policy of Certificate-Based Public Key and Digital Signatures.
PB94-191202 01,578

BAUMERT, T.

Femtosecond Time-Resolved Molecular Multiphoton Ionization: The Na2 System.
PB95-202305 03,975

Femtosecond Time-Resolved Wave Packet Motion in Molecular Multiphoton Ionization and Fragmentation.
PB94-198611 00,790

BAUMONT, F.

Preliminary Comparison of Time Transfers via LASSO, GPS and Two-Way Satellite.
PB95-151098 01,529

BAUR, W. H.

Neutron Powder Diffraction Study of a Na, Cs-Rho Zeolite.
PB94-198629 00,791

BAUSUM, H. T.

Determination of 3-Quinuclidinyl Benzilate (Qnb) and Its Major Metabolites in Urine by Isotope Dilution Gas Chromatography Mass Spectrometry.
PB94-199379 03,492

BAYLEY, H.

Genetically Engineered Pore as a Metal Ion Biosensor.
PB96-161658 03,551

Genetically Engineered Pores as Metal Ion Biosensors.
PB96-167408 03,553

Genetically Engineered Pores for New Materials.
PB96-161641 03,550

Pore-Forming Protein with a Metal-Actuated Switch.
PB96-176557 03,554

BEACH, R. S.

Enhanced Curie Temperatures and Magnetoelastic Domains in Dy/Lu Super Lattices and Films.
PB94-172665 04,443

BEAHN, T. J.

Magneto-Optic Magnetic Field Sensor with 1.4pT/square root of 1(Hz) Minimum Detectable Field at 1 kHz.
PB94-199551 02,125

BEALE, P. D.

Bias Current Dependent Resistance Peaks in NiFe/Ag Giant Magnetoresistance Multilayers.
PB97-112346 04,153

BEALL, J.

Dielectric Properties of Thin Film SrTiO3 Grown on LaAlO3 with YBa2Cu3O7-x Electodes.
PB95-181160 02,267

BEALL, J. A.

Characterization of a Tunable Thin Film Microwave YBa2Cu3O7-x/SrTiO3 Coplanar Capacitor.
PB95-175527 02,264

Critical Current Behavior of Ag-Coated YBa2Cu3O7-x Thin Films.
PB95-141016 04,549

Ferroelectric Thin Film Characterization Using Superconducting Microstrip Resonators.
PB96-102389 02,270

High Critical Temperature Superconductor Tunneling Spectroscopy Using Squeezable Electron Tunneling Junctions.
PB95-163721 04,627

Increased Transition Temperature in In situ Coevaporated YBa2Cu3O7-delta Thin Films by Low Temperature Post-Annealing.
PB95-180071 04,672

Magnetic Field Dependence of the Critical Current Anisotropy in Normal Metal-YBa2Cu3O7-delta Thin Film Bilayers.
PB95-141024 04,550

Microwave Properties of Voltage-Tunable YBa2Cu3O7-delta/SrTiO3 Coplanar Waveguide Transmission Lines.
PB96-141262 02,235

Tunable High Temperature Superconductor Microstrip Resonators.
PB95-168423 02,048

BEAN, J. W.

Optical Performance of Commercial Windows.
PB95-208757 00,392

BEAN, V. E.

Development of the NIST Transient Pressure and Temperature Calibration Facility.
PB96-160833 00,626

Executive Summary: Proceedings of the Workshop on the Measurement of Transient Pressure and Temperature.
PB96-160841 02,679

NIST Measurement Services: NIST Pressure Calibration Service.
PB94-164043 02,892

Pressure Measurements with the Mercury Melting Line Referred to ITS-90.
PB96-161005 01,136

BEARDEN, D. W.

Influence of Surface Interaction and Chain Stiffness on Polymer-Induced Entropic Forces and the Dimensions of Confined Polymers.
PB94-185469 01,203

BEARY, E. S.

Comparative Strategies for Correction of Interferences in Isotope Dilution Mass Spectrometric Determination of Vanadium.
PB94-185261 00,531

BEATON, S. P.

Determination of the Molecular Parameters of NiH in Its (2)Delta Ground State by Laser Magnetic Resonance.
PB95-107116 00,869

High-Order Harmonic Mixing with GaAs Schottky Diodes.
PB95-108585 01,528

Rotational Spectroscopy of the CoH Radical in Its Ground (3)Phi State by Far-Infrared Laser Magnetic Resonance: Determination of Molecular Parameters.
PB95-175048 00,992

Rotational Spectrum of Copper Hydride Using Tunable Far Infrared Radiation.
PB94-198637 00,792

BEAUCHAMP, C. R.

Electrochemical Synthesis of Metal and Intermetallic Composites.
AD-A294 088/0 03,304

BEAVER, E. A.

Observations of 3C 273 with the Goddard High Resolution Spectrograph on the Hubble Space Telescope.
PB95-202321 00,076

BEAZLEY, W. G.

Framework for Information Technology Integration in Process Plant and Related Industries.
PB94-219086 02,772

BECHER, P. F.

Matrix Grain Bridging Contribution to the Toughness of Whisker Reinforced Ceramics.
PB94-198645 03,134

BECHIS, D. J.

Display-Measurement Round-Robin.
PB96-119227 02,186

Survey of the Components of Display-Measurement Standards.
PB96-122528 02,188

Survey of the Components of Display-Measurement Standards.
PB97-122394 02,209

BECK, C. M.

Classical Analysis: A Look at the Past, Present, and Future.
PB94-185063 00,528

Preparation and Certification of a Rhodium Standard Reference Material Solution.
PB94-185071 00,529

Thermodynamic Properties of Silicides. 5. Standard Molar Enthalpy of Formation at the Temperature 298.15 K of Trimolybdenum Monosilicide Mo3Si Determined by Fluorine-Combustion Calorimetry.
PB97-119358 01,190

BECK, D. R.

Hyperfine-Structure Studies of Zr II: Experimental and Relativistic Configuration-Interaction Results.
PB95-203824 04,011

BECK, H.

Influence of Deposition Parameters on Properties of Laser Ablated YBa2Cu3O7-Delta Films.
PB95-140539 04,544

BECK, R.

Infrared and Microwave Spectroscopy of the Argon - Propyne Dimer.
PB94-198892 00,794

BECK TAN, N. C.

Advances in the Measurement of Polymer CTE: Micrometer- to Atomic-Scale Measurements.
PB96-180229 03,390

BECKER, D. A.

Certifying the Chemical Composition of a Biological Material: A Case Study.
PB96-164272 00,636

Determination of 21 Elements by INAA for Certification of SRM 1570a, Spinach.
PB96-167242 *00,698*

New NIST Rapid Pneumatic Tube System.
PB96-167259 *03,738*

Recent Developments in NIST Botanical SRMs.
PB96-167267 *03,489*

Resolution of Discrepant Analytical Data in the Certification of Platinum in Two Automobile Catalyst SRMs.
PB96-167283 *00,638*

Results of the ASTM Nuclear Methods Intercomparison on NIST Apple and Peach Leaves Standard Reference Materials.
PB97-119036 *03,490*

Role of Certified Reference Materials in Trace Analysis Quality Assurance.
PB97-110019 *00,650*

Unique Quality Assurance Aspects of INAA for Reference Material Homogeneity and Certification.
PB96-200811 *00,699*

BECKER, P. R.

Alaska Marine Mammal Tissue Archival Project: Specimen Inventory.
PB95-171344 *02,589*

Concentrations of Chlorinated Hydrocarbons, Heavy Metals and Other Elements in Tissues Banked by the Alaska Marine Mammal Tissue Archival Project.
PB95-209870 *02,590*

Determination of Inorganic Constituents in Marine Mammal Tissues.
PB95-152047 *00,589*

Determination of PCBs and Chlorinated Hydrocarbons in Marine Mammal Tissues.
PB95-162640 *03,744*

Relationship of Silver with Selenium and Mercury in the Liver of Two Species of Toothed Whales (Odontocetes).
PB96-167275 *02,596*

Trace Element Concentrations in Cetacean Liver Tissues Archived in the National Marine Mammal Tissue Bank.
PB96-167127 *02,595*

BECKER, R. H.

Discovery of an X-Ray Selected, Radio-Loud Quasar at z=3.9.
PB94-198652 *00,052*

New High-Redshift Damped Lyman-alpha Absorption Systems and the Redshift Evolution of Damped Absorbers.
PB95-203501 *00,083*

BECKERLEY, J. G.

Preliminary List of References Containing Compilations of Data on Properties of Materials.
AD-A302 670/5 *03,243*

Preliminary Subject and Authors Index to Compilations of Data on Properties of Materials.
AD-A302 669/7 *03,242*

BEECH, F.

Neutron Powder Diffraction Study of the Structures of La1.9Ca1.1Cu2O6 and La1.9Sr1.1Cu2O6+Delta.
PB95-140042 *04,538*

BEERS, J.

Verification of Revised Water Vapour Correction to the Index of Refraction of Air.
PB96-161666 *02,680*

BEERS, J. S.

Evolution of Automatic Line Scale Measurement at the National Institute of Standards and Technology.
PB95-108809 *02,897*

Gage Block Handbook.
PB95-251716 *02,667*

Measuring Long Gage Blocks with the NIST Line Scale Interferometer.
PB95-242400 *02,665*

BEESABATHINA, D. P.

Characterization of the ZnSe/GaAs Interface Layer by TEM and Spectroscopic Ellipsometry.
PB95-175360 *04,655*

BEGLEY, E. F.

Database Development and Management (Project A.2.2): The Annual Report for 1992-1993.
PB97-110290 *03,098*

Guide to Locating and Accessing Computerized Numeric Materials Databases.
PB96-204045 *03,007*

Multimedia Tutorial on Phase Equilibria Diagrams.
PB96-200829 *03,088*

Structural Ceramics Database. Topical Report, June 1989-May 1991.
PB95-203758 *03,060*

BEHLKE, M. K.

Investigations of Sulfur Interferences in the Extraction of Methylmercury from Marine Tissues.
PB96-190020 *03,482*

BEHRENS, H.

Data Import and Validation in the Inorganic Crystal Structure Database.
PB97-109201 *04,809*

BEICHL, I.

Data-Parallel Algorithm for Three-Dimensional Delaunay Triangulation and Its Implementation.
PB95-163309 *01,714*

Faster BKL Monte Carlo Simulations.
PB95-136370 *01,706*

Faster Monte Carlo Simulations.
PB96-102074 *04,018*

Heap of Data.
PB97-111488 *03,424*

Making Connections.
PB97-119044 *01,785*

Self-Avoiding Surfaces, Topology, and Lattice Animals.
PB95-150512 *04,571*

Submissions to a Planned Encyclopedia of Operations Research on Computational Geometry and the Voronoi/Delaunay Construct.
PB94-152709 *03,425*

Tree-Lookup for Partial Sums Or: How Can I Find This Stuff Quickly.
PB96-179411 *01,770*

BEICHL, I. M.

Computing S(alpha) Using Symbolic Monte Carlo.
PB94-198660 *03,410*

Parallel Monte Carlo Simulation of MBE Growth.
PB96-122841 *02,406*

BELIC, D. S.

Merged-Beams Energy-Loss Technique for Electron-Ion Excitation: Absolute Total Cross Sections for O(5+) (2s yields 2p).
PB96-102058 *04,017*

BELL, B.

Exploring the Low-Frequency Performance of Thermal Converters Using Circuit Models and a Digitally Synthesized Source.
PB97-112551 *02,848*

BELL, D.

Thermodynamics of Enzyme-Catalyzed Reactions: Part 1. Oxidoreductases.
PB94-162252 *00,737*

BELL, E. W.

Absolute Cross-Section Measurements for Electron-Impact Ionization of C1(+1).
PB94-199841 *03,818*

Absolute Cross-Section Measurements for Electron-Impact Single Ionization of Se(+) and Te(+).
PB95-202503 *03,980*

Absolute Cross Sections for Electron-Impact Single Ionization of Si(+) and Si(2+).
PB95-202529 *03,982*

Backscattering in Electron-Impact Excitation of Multiply Charged Ions.
PB94-185345 *03,799*

Beam Line for Highly Charged Ions.
PB97-111256 *04,143*

Crossed-Beams Measurements of Absolute Cross Sections for Electron Impact Ionization of S(+).
PB95-202511 *03,981*

Electron-Impact Ionization of In(+) and Xe(+).
PB94-185089 *00,770*

Electron-Impact Ionization of In(+) and Xe(+).
PB95-152906 *03,918*

Evidence for Significant Backscattering in Near-Threshold Electron-Impact Excitation of Ar(7+)(3s yields 3p).
PB95-126405 *03,883*

Merged-Beams Energy-Loss Technique for Electron-Ion Excitation: Absolute Total Cross Sections for O(5+) (2s yields 2p).
PB96-102058 *04,017*

BELLAMA, J. M.

L-threo-beta-Hydroxyhistidine, an Unprecedented Iron(III) Ion-Binding Amino Acid in a Pyoverdine-type Siderophore from Pseudomonas fluorescens 244.
PB94-211620 *00,553*

Potentiometric Enzyme-Amplified Flow Injection Analysis Detection System: Behavior of Free and Liposome-Released Peroxidase.
PB95-151833 *03,534*

Total Surface Areas of Group IVA Organometallic Compounds: Predictors of Toxicity to Algae and Bacteria.
PB94-211331 *00,814*

BELLISSENT, R.

Inelastic Neutron Scattering Measurements of Phonons in Icosahedral Al-Li-Cu.
PB95-126215 *04,532*

Neutron Scattering Structural Study of AlCuFe Quasicrystals Using Double Isotopic Substitution.
PB94-200458 *04,485*

RDFs and Fe-Fe Pair Correlations in an AlCuFe Icosahedral Alloy by Double Isotopic Substitution.
PB94-172129 *04,439*

BELMONT, G.

Effect of Formulation Changes on the Response to Ionizing Radiation of Radiochromic Dye Films.
PB97-119028 *04,171*

BELOV, S. P.

Tunneling-Rotation Spectrum of the Hydrogen Fluoride Dimer.
PB94-198678 *00,793*

BELTRACCHI, L.

Analysis of Standards for the Assurance of High Integrity Software.
PB96-161351 *03,735*

Control and Instrumentation: Standards for High-Integrity Software.
PB96-161369 *03,736*

Proceedings of the Digital Systems Reliability and Nuclear Safety Workshop. Held in Rockville, Maryland on September 13-14, 1993.
NUREG/CP-0136 *03,728*

Standards for High Integrity Software.
PB96-161385 *01,764*

BENCK, E. C.

Optical and Mass Spectrometric Investigations of Ions and Neutral Species in SF6 Radio-Frequency Discharges.
PB97-111918 *01,985*

BENDEC, F.

Ultrasonic Spectroscopy of Metallic Spheres Using Electromagnetic-Acoustic Transduction.
PB94-212537 *04,185*

BENDER, P.

Low-Frequency, Active Vibration Isolation System.
PB95-203303 *02,710*

Slant Path Atmospheric Refraction Calibrator: An Instrument to Measure the Microwave Propagation Delays Induced by Atmospheric Water Vapor.
PB95-151270 *01,476*

BENDER, P. L.

Integrated Laser Doppler Method for Measuring Planetary Gravity Fields.
PB94-198686 *03,681*

Lunar Laser Ranging: A Continuing Legacy of the Apollo Program.
PB95-202495 *03,683*

BENDERSKY, L. A.

Coherent Precipitates in the BCC/Orthorhombic Two Phase Field of the Ti-Al-Nb System.
PB94-198694 *03,317*

Crystallographic Characterization of Some Intermetallic Compounds in the Al-Cr System.
PB94-198702 *03,318*

Disorder Trapping in Ni2TiAl.
PB94-198942 *03,322*

Ordered omega-Derivatives in a Ti-37.5Al-2ONb at% Alloy.
PB94-211091 *03,331*

Transformation of BCC and B2 High Temperature Phases to HCP and Orthorhombic Structures in the Ti-Al-Nb System. Part 1. Microstructural Predictions Based on a Subgroup Relation between Phases.
PB96-169065 *03,370*

Transformation of BCC and B2 High Temperature Phases to HCP and Orthorhombic Structures in the Ti-Al-Nb System. Part 2. Experimental TEM Study of Microstructures.
PB96-169073 *03,371*

BENECKE, J. D.

Application of the Modified Voltage-Dividing Potentiometer to Overlay Metrology in a CMOS/Bulk Process.
PB94-181997 *02,302*

BENEDETTO, J. M.

Microstructure and Ferroelectric Properties of Lead Zirconate-Titanate Films Produced by Laser Evaporation.
PB94-199148 *04,470*

BENGTSSON, L.

Laser Ablation of Thin Films as a Free Atom Source for Pulsed RIMS.
PB94-198710 *00,540*

BENITEZ, E. L.

Soft-X-ray Damage to p-terphenyl Coatings for Detectors.
PB96-159611 *04,364*

BENNAHMIAS, M.

Crystal Structure and Magnetic Ordering of the Rare-Earth and Cu Moments in RBa2Cu2NbO8(R=Nd,Pr).
PB95-140554 *04,546*

BENNDORF, C.

Role of Adsorbed Alkalis in Desorption Induced by Electronic Transitions.
PB94-172574 *00,762*

BENNER, B. A.

Certification of Polycyclic Aromatic Hydrocarbons in a Marine Sediment Standard Reference Material.
PB96-111778 *02,592*

Certification of Standard Reference Material (SRM) 1941a, Organics in Marine Sediment.
PB96-123690 *02,593*

Distinguishing the Contributions of Residential Wood Combustion and Mobile Source Emissions Using Relative Concentrations of Dimethylphenanthrene Isomers.
PB96-135124 *02,563*

Ground-Based Smoke Sampling Techniques Training Course and Collaborative Local Smoke Sampling in Saudi Arabia.
PB94-143542 *02,532*

Standard Reference Materials for the Determination of Polycyclic Aromatic Hydrocarbons in Environmental Samples - Current Activities.
PB95-151668 *00,586*

BENNETT, G. E.

Time and Frequency: Bibliography of NIST Publications, March 1995.
PB95-220463 *01,548*

BENNETT, H. S.

Can Displays Deliver a Full Measure: Manufacturing.
PB96-111935 *02,185*

Effects of Heavy Doping on Numerical Simulations of Gallium Arsenide Bipolar Transistors.
PB95-150975 *02,334*

Majority and Minority Electron and Hole Mobilities in Heavily Doped Gallium Aluminum Arsenide.
PB97-118335 *04,814*

Majority and Minority Mobilities in Heavily Doped Silicon for Device Simulations.
PB94-198728 *02,311*

Making Displays Deliver a Full Measure.
PB96-122411 *01,490*

Physics for Device Simulations and Its Verification by Measurements.
PB95-141172 *02,327*

Physics for Device Simulations and Its Verification by Measurements.
PB95-152914 *02,339*

BENNETT, J.

Integration of Scanning Tunneling Microscope Nanolithography and Electronics Device Processing.
PB95-153359 *02,341*

Relative Sensitivity Factors and Useful Yields for a Microfocused Gallium Ion Beam and Time-of-Flight Secondary Ion Mass Spectrometer.
PB94-198736 *00,541*

BENNETT, K. W.

Microstructure and Ferroelectric Properties of Lead Zirconate-Titanate Films Produced by Laser Evaporation.
PB94-199148 *04,470*

BENNETT, L. H.

Determination of Thermoactivation Parameters of Vortex Mobility in YBa2Cu3O7 Using Only Magnetic Measurements.
PB95-163499 *04,624*

Effect of Sm2BaCuO5 on the Properties of Sintered (Bulk) YBa2Cu3O6+x.
PB96-119441 *04,733*

Experimental Verification of a Vector Preisach Model.
PB95-163564 *04,626*

Langevin Approach to Hysteresis and Barkhausen Modeling in Steel.
PB94-185675 *03,206*

Magnetic and Structural Properties of Electrodeposited Copper-Nickel Microlayered Alloys.
PB94-213121 *04,512*

Magnetocaloric Effect in Nanocomposites.
PB95-162798 *04,618*

Magnetocaloric Effect in Rapidly Solidified Nd-Fe-Al-B Materials.
PB94-185667 *04,451*

Meissner, Shielding, and Flux Loss Behavior in Single-Crystal YBa2Cu3O6+x.
PB94-198744 *04,464*

Monte Carlo and Mean-Field Calculations of the Magnetocaloric Effect of Ferromagnetically Interacting Clusters.
PB94-172087 *03,201*

Nanocomposite Magnetic Materials
PB95-162780 *04,617*

Temperature Dependence of Vortex Twin Boundary Interaction in Yttrium Barium Copper Oxide (YBa2Cu3O6+x).
PB95-162442 *04,613*

BENNETT, P. S.

New Surface-Active Comonomer for Adhesive Bonding.
PB96-204052 *03,579*

BENNETT, W. R.

Concurrent Enhancement of Kerr Rotation and Antiferromagnetic Coupling in Epitaxial Fe/Cu/Fe Structures.
PB94-198769 *04,466*

Magnetic Properties of Pd/Co Multilayers.
PB94-198751 *04,465*

BENNISON, S. J.

Fabrication of Flaw-Tolerant Aluminum-Titanate-Reinforced Alumina.
PB95-162533 *03,161*

Flaw-Insensitive Ceramics.
PB97-110027 *03,095*

Flaw-Tolerance and Crack-Resistance Properties of Alumina-Aluminum Titanate Composites with Tailored Microstructures.
PB97-110324 *03,101*

Loading Device for Fracture Testing of Compact Tension Specimens in the Scanning Electron Microscope.
PB95-162434 *02,652*

Model for Toughness Curves in Two-Phase Ceramics. 1. Basic Fracture Mechanics.
PB96-180088 *03,085*

Model for Toughness Curves in Two-Phase Ceramics. 2. Microstructural Variables.
PB96-163795 *03,078*

Objective Evaluation of Short-Crack Toughness Curves Using Indentation Flaws: Case Study on Alumina-Based Ceramics.
PB96-179429 *03,079*

BENOIT, H.

Neutron Scattering by Multiblock Copolymers of Structure (A-B)N-A.
PB94-211547 *01,219*

BENSEN, D.

Commentary on 'Optimization of Experimental Parameters for the EPR Detection of the Cellulosic Radical in Irradiated Foodstuffs'.
PB96-164124 *00,043*

BENSEN, D. L.

Investigation of Applicability of Alanine and Radiochromic Detectors to Dosimetry of Proton Clinical Beams.
PB96-146782 *03,636*

BENT, B. E.

Silicon Surface Chemistry by IR Spectroscopy in the Mid- to Far-IR Region: H2O and Ethanol on Si(100).
PB96-138565 *01,097*

BENTZ, D.

Development of a Method for Measuring Water-Stripping Resistance of Asphalt/Siliceous Aggregate Mixtures.
PB96-197249 *01,348*

Development of a Method for Measuring Water-Stripping Resistance of Asphalt/Siliceous Aggregate Mixtures.
PB96-202296 *01,329*

Digitized Simulation of Mercury Intrusion Porosimetry.
PB94-172236 *01,304*

Percolation and Pore Structure in Mortars and Concrete.
PB95-150439 *00,370*

BENTZ, D. P.

Application of Digital-Image-Based Models to Microstructure, Transport Properties, and Degradation of Cement-Based Materials.
PB96-156161 *00,406*

Calculation of the Thermal Conductivity and Gas Permeability in a Uniaxial Bundle of Fibers.
PB95-180931 *03,058*

Cellular Automaton Simulations of Cement Hydration and Microstructure Development.
PB95-175055 *01,320*

Computer Simulation of the Diffusivity of Cement-Based Materials.
PB95-125985 *00,362*

Computer Simulations of Binder Removal from 2-D and 3-D Model Particulate Bodies.
PB97-121339 *00,418*

Cross-Property Relations and Permeability Estimation in Model Porous Media.
PB95-150280 *04,205*

Diffusion Studies in a Digital-Image-Based Cement Paste Microstructural Model.
PB94-198801 *01,312*

Digital Simulation of the Aggregate-Cement Paste Interfacial Zone in Concrete.
PB95-125993 *00,363*

Digitized Direct Simulation Model of the Microstructural Development of Cement Paste.
PB94-198777 *01,309*

Digitized Simulation Model for Microstructural Development.
PB94-198785 *01,310*

Evolution of Porosity and Calcium Hydroxide in Laboratory Concretes Containing Silica Fume.
PB95-175063 *01,321*

Fundamental Computer Simulation Models for Cement-Based Materials.
PB95-126009 *00,364*

Hydraulic Radius and Transport in Reconstructed Model Three-Dimensional Porous Media.
PB96-123419 *00,403*

Interfacial Transport in Porous Media: Application to dc Electrical Conductivity of Mortars.
PB96-146816 *01,326*

Modelling Drying Shrinkage of Cement Paste and Mortar. Part 1. Structural Models from Angstroms to Millimeters.
PB96-135132 *03,074*

Modelling the Leaching of Calcium Hydroxide from Cement Paste: Effects on Pore Space Percolation and Diffusivity.
PB94-198793 *01,311*

Multi-Scale Picture of Concrete and Its Transport Properties: Introduction for Non-Cement Researchers.
PB97-115802 *03,107*

Survey of Recent Cementitious Materials Research in Western Europe.
PB94-218583 *00,353*

Transport and Diffusion in Three-Dimensional Composite Media.
PB95-176129 *04,668*

Unreacted Cement Content in Macro-Defect-Free Composites: Impact on Processing-Structure-Property Relations.
PB96-141270 *03,174*

Water Permeability and Chloride Ion Diffusion in Portland Cement Mortars: Relationship to Sand Content and Critical Pore Diameter.
PB96-148036 *03,193*

BENZ, S. P.

Characterization of the Emission from 2D Array Josephson Oscillators.
PB95-175121 *02,054*

Design of High-Frequency, High-Power Oscillators Using Josephson-Junction Arrays.
PB96-200258 *02,094*

Direct Observation of Vortex Dynamics in Two-Dimensional Josephson-Junction Arrays.
PB96-102223 *02,067*

Emission Linewidth Measurements of Two-Dimensional Array Josephson Oscillators.
PB95-175139 *02,055*

Experimental Results on Single Flux Quantum Logic.
PB95-175071 *02,053*

Frequency Dependence of the Emission from 2D Array Josephson Oscillators.
PB95-175147 *02,056*

High-Frequency Oscillators Using Phase-Locked Arrays of Josephson Junctions.
PB96-135157 *02,080*

High Power Generation with Distributed Josephson-Junction Arrays.
PB97-111520 *02,099*

High-Power, High-Frequency Oscillators Using Distributed Josephson-Junction Arrays.
PB96-200266 *02,095*

Intrinsic Stress in DC Sputtered Niobium.
PB94-199031 *04,468*

Large-Amplitude Shapiro Steps and Self-Field Effects in High-Tc Josephson Weak Links.
PB95-180410 *04,682*

Metallic-Barrier Junctions for Programmable Josephson Voltage Standards.
PB96-200134 *02,089*

Novel Vortex Dynamics in Two-Dimensional Josephson Arrays.
PB96-200167 *02,091*

Observation of Vortex Dynamics in Two-Dimensional Josephson-Junction Arrays.
PB95-168811 *02,050*

Phase-Locked Oscillator Optimization for Arrays of Josephson Junctions.
PB95-169314 *02,052*

Pulse-Driven Programmable Josephson Voltage Standard.
PB97-111496 *04,148*

Resonances in Two-Dimensional Array Oscillator Circuits.
PB96-102082 *02,066*

Stable Phase Locking in a Two-Cell Ladder Array of Josephson Junctions.
PB96-111679 *04,722*

Stacked Series Arrays of High-Tc Trilayer Josephson Junctions.
PB96-102272 *04,705*

Step-Edge and Stacked-Heterostructure High-Tc Josephson Junctions for Voltage-Standard Arrays.
PB96-102066 *04,702*

Superconducting Integrated Circuit Fabrication with Low Temperature ECR-Based PECVD SiO2 Dielectric Films.
PB96-103015 *04,719*

Superconductor- Normal-Superconductor Junctions for Digital/Analog Converters.
PB96-200233 *02,092*

Superconductor- Normal-Superconductor Junctions for Programmable Voltage Standards.
PB96-200241 *02,093*

SUSAN: SUperconducting Systems ANalysis by Low Temperature Scanning Electron Microscopy (LTSEM).
PB96-112065 *04,728*

BEREZANSKY, P. A.

Low Electrolytic Conductivity Standards.
PB96-122098 *01,081*

BERG, R. F.

Flow of Microemulsions through Microscopic Pores.
PB95-140463 *00,905*

Hydrodynamic Similarity in an Oscillating-Body Viscometer.
PB96-122429 *01,082*

Internal Waves in Xenon Near the Critical Point.
PB97-111504 *04,221*

Milliwatt Mixer for Small Fluid Samples.
PB94-198819 *02,634*

Temperature and Frequency Dependence of Anelasticity in a Nickel Oscillator.
PB96-137732 *03,689*

Thermal Equilibration Near the Critical Point: Effects Due to Three Dimensions and Gravity.
PB95-152922 *03,919*

BERGER, J. R.

Influence of Specimen Absorbed Energy in LOX Mechanical-Impact Tests.
PB95-107355 *03,341*

BERGER, P. W.
General Types of Information Services.
PB96-147053 *02,735*

BERGERHOFF, G.
Evaluation of Crystallographic Data with the Program DIAMOND.
PB97-109045 *00,649*

BERGGREN, K. K.
Microlithography by Using Neutral Metastable Atoms and Self-Assembled Monolayers.
PB96-190038 *02,441*

BERGMANN, D. J.
Environmental Aspects of Halon Replacements: Considerations for Advanced Agents and the Ozone Depletion Potential of CF3I.
PB97-122261 *03,301*

BERGQUIST, J. C.
High-Resolution Atomic Spectroscopy of Laser-Cooled Ions.
PB95-169330 *03,953*

Interference in the Resonance Fluorescence of Two Trapped Atoms.
PB95-168514 *03,948*

Laser Cooling of Trapped Ions.
PB95-168746 *03,950*

Light Scattered from Two Atoms.
PB95-168753 *04,286*

Precise Spectroscopy for Fundamental Physics.
PB96-112164 *04,040*

Progress on a Cryogenic Linear Trap for (199)Hg(+) Ions.
PB95-180790 *03,965*

Quantum Measurements of Trapped Ions.
PB95-161147 *03,928*

Quantum Projection Noise: Population Fluctuations in Two-Level Systems.
PB94-212271 *03,850*

Recent Experiments on Trapped Ions at the National Institute of Standards and Technology.
PB95-169322 *03,952*

Trapped Ions and Laser Cooling 4: Selected Publications of the Ion Storage Group of the Time and Frequency Division, NIST, Boulder, Colorado.
PB96-172358 *04,108*

BERGREN, N. F.
Magnetic Measurement of Transport Critical Current Density of Granular Superconductors.
PB95-126199 *04,531*

BERGTOLD, D. S.
Standard Reference Materials (SRM's) for Measuring Genetic Damage.
PB94-198827 *03,516*

BERK, N. F.
Analysis of SANS from Controlled Pore Glasses.
PB94-198843 *03,035*

Analysis of Small-Angle Scattering Data Dominated by Multiple Scattering for Systems Containing Eccentrically Shaped Particles or Pores.
PB96-160411 *03,075*

Characterization of Chemically Modified Pore Surfaces by Small Angle Neutron Scattering.
PB95-126181 *00,898*

Neutron Spectroscopic Comparison of Rare-Earth/Hydrogen alpha-Phase Systems.
PB95-163523 *00,970*

Scattering Properties of the Leveled-Wave Model of Random Morphologies.
PB94-198835 *03,807*

Structure of a Triglyceride Microemulsion: A Small Angle Neutron Scattering Study.
PB96-112255 *01,077*

BERKOWITZ, J. B.
High Temperature.
PB94-211737 *03,844*

BERKOWITZ, S. J.
Coexistence of Grains with Differing Orthorhombicity in High Quality YBa2Cu3O7-delta Thin Films.
PB96-135033 *04,742*

Controlling the Critical Current Density of High-Temperature SNS Josephson Junctions.
PB96-200712 *04,794*

Increased Transition Temperature in In situ Coevaporated YBa2Cu3O7-delta Thin Films by Low Temperature Post-Annealing.
PB95-180071 *04,672*

Temperature Dependence and Magnetic Field Modulation of Critical Currents in Step-Edge SNS YBCO/Au Junctions.
PB96-111745 *04,723*

Thermal Noise in High-Temperature Superconducting-Normal-Superconducting Step-Edge Josephson Junctions.
PB95-175089 *04,650*

BERLINER, R.
Structures of Sodium Metal.
PB94-198850 *03,319*

BERLINSKY, Y.
Effect of Liftoff on Accuracu of Phase Velocity Measurements Made with Electromagnetic-Acoustic Transducers.
PB96-186044 *02,280*

Methods to Improve the Accuracy of On-Line Ultrasonic Measurement of Steel Sheet Formability.
PB96-186051 *02,281*

BERMAN, H. M.
Nucleic Acid Database: Present and Future.
PB97-109078 *00,518*

BERN, H. A.
Histopathology, Blood Chemistry, and Physiological Status of Normal and Moribund Striped Bass ('Morone saxatilis') Involved in Summer Mortality ('Die-Off') in the Sacramento-San Joaquin Delta of California.
PB94-198157 *00,034*

BERNAL, J.
Growth Surface for the Slopes at the Boundary of a Polygon.
PB94-152725 *03,408*

Inserting Line Segments into Triangulations and Tetrahedralizations.
PB95-198933 *03,415*

Probabilistic Computation of Poiseuille Flow Velocity Fields.
PB96-102520 *04,209*

Submissions to a Planned Encyclopedia of Operations Research on Computational Geometry and the Voronoi/Delaunay Construct.
PB94-152709 *03,425*

BERNDT, C. C.
Anisotropy of the Surfaces of Pores in Plasma Sprayed Alumina Deposits.
PB96-123211 *03,126*

BERNDT, M.
Evaluation of Crystallographic Data with the Program DIAMOND.
PB97-109045 *00,649*

BERNING, D. W.
Double-Modulation and Selective Excitation Photoreflectance for Wafer-Level Characterization of Quantum-Well Laser Structures.
PB96-167325 *04,372*

BERNSTEIN, B.
Non-Equilibrium Thermodynamic Theory of Viscoplastic Materials.
PB94-198868 *04,467*

Nonequilibrium Thermodynamic Theory of Viscoplastic Materials.
PB96-111661 *04,034*

PC-Based Prototype Expert System for Data Management and Analysis of Creep and Fatigue of Selected Materials at Elevated Temperatures.
PB94-172251 *03,202*

BERRAH, N.
High-Energy Behavior of the Double Photoionization of Helium from 2 to 12 keV.
PB94-213279 *03,860*

BERRY, A. K.
Transition Metal Implants in In0.53GA0.47As.
PB95-126389 *04,534*

BERRY, H. G.
High-Energy Behavior of the Double Photoionization of Helium from 2 to 12 keV.
PB94-213279 *03,860*

BERRY, R. J.
Halon Thermochemistry: 'Ab Initio' Calculations of the Enthalpies of Formation of Fluoromethanes.
PB96-175740 *03,289*

BERRY, S. D.
Structural and Magnetic Ordering in Iron Oxide/Nickel Oxide Multilayers by X-ray and Neutron Diffraction (Invited).
PB94-172558 *04,442*

BERTNESS, K. A.
In situ Observation of Surface Morphology of InP Grown on Singular and Vicinal (001) Substrates.
PB95-168431 *04,636*

BERTOCCI, U.
Evaluation of the Electrochemical Behavior of Ductile Nickel Aluminide and Nickel in a pH 7.9 Solution. Technical Report Number 3, April-June 1991.
DE94017351 *03,307*

Evaluation of the Environmentally Induced Fracture Resistance of Ductile Nickel Aluminide. Technical Report Number 1, Final report. October-December 1990.
DE94017331 *03,306*

Modeling Polarization Curves and Impedance Spectra for Simple Electrode Systems.
PB94-198876 *03,188*

BERUBE, J.
Compatibility Analysis of the ANSI and ISO IRDS Services Interfaces.
PB94-163474 *01,805*

BERUFF, R. B.
Test of Newton's Inverse Square Law of Gravitation Using the 300-m Tower at Erie, Colorado.
PB95-202446 *03,978*

BESSON, R.
New Model of 1/F Noise in Baw Quartz Resonators.
PB96-112248 *02,383*

BEVERIDGE, T. J.
Characterization of the Binding of Gallium, Platinum, and Uranium to Pseudomonas Fluorescens by Small-Angle X-ray Scattering and Transmission Electron Microscopy.
PB94-172509 *03,453*

BEZNUKHOV, S.
Genetically Engineered Pores for New Materials.
PB96-161641 *03,550*

BEZRUKOV, S. M.
Current Fluctuations Reveal Protonation Dynamics and Number of Ionizable Residues in the alpha-Toxin Channel.
PB96-161732 *03,588*

Current Noise Reveals Protonation Kinetics and Number of Ionizable Sites in an Open Protein Ion Channel.
PB96-161674 *04,092*

Noise Analysis of Ionization Kinetics in a Protein Ion Channel.
PB96-161682 *04,093*

Protonation Dynamics in an Ion Channel Pore.
PB96-161757 *03,589*

Protonation Dynamics of the alpha-Toxin Ion Channel from Spectral Analysis of pH-Dependent Current Fluctuations.
PB96-161740 *03,652*

BHADURI, S.
Report of the Refrigeration, Air Conditioning and Heat Pumps Technical Options Committee.
PB96-176755 *03,293*

BIANCANIELLO, F.
Parametric Investigation of Metal Powder Atomization Using Laser Diffraction.
PB95-108577 *03,342*

BIANCANIELLO, F. S.
Beneficial Effects of Nitrogen Atomization on an Austenitic Stainless Steel.
PB94-212396 *03,209*

Development of Adaptive Control Strategies for Inert Gas Atomization.
PB95-162335 *02,823*

Effect of Backfill and Atomizing Gas on the Powder Porosity and Mechanical Properties of 304L Stainless Steel.
PB94-185394 *03,205*

Effects of Elastic Stress on Phase Equilibrium in the Ni-V System.
PB94-172707 *03,313*

Intelligent Control of an Inert Gas Atomization Process.
PB95-141057 *03,344*

Optimization of Inert Gas Atomization.
PB95-107405 *01,377*

Ordered omega-Derivatives in a Ti-37.5Al-2ONb at% Alloy.
PB94-211091 *03,331*

Process Modeling and Control of Inert Gas Atomization.
PB95-162343 *02,824*

BICKHAM, D.
Biological Macromolecular Crystallization Database: A Tool for Developing Crystallization Strategies.
PB95-126157 *00,897*

BIEDENHARN, L. C.
Comprehensive Theory of Nuclear Effects on the Intrinsic Sticking Probability. 1.
PB94-200623 *03,832*

Comprehensive Theory of Nuclear Effects on the Intrinsic Sticking Probability. 2.
PB94-200631 *03,833*

BIEGEL, J.
Modeling Detector Response for Neutron Depth Profiling.
PB96-157813 *04,066*

BIENENSTOCK, A.
Real-Time Small-Angle X-Ray Scattering Study of the Early Stage of Phase Separation in the SiO2-BaO-K20 System.
PB95-163069 *03,052*

BIENIAWSKI, A.
How-To Suggestions for Implementing Executive Order 12941 on Seismic Safety of Existing Federal Buildings, A Handbook.
PB96-131552 *00,461*

ICSSC Guidance on Implementing Executive Order 12941 on Seismic Safety of Existing Federally Owned or Leased Buildings.
PB96-128103 *00,459*

Performance of Federal Buildings in the January 17, 1994 Northridge Earthquake.
PB95-231775 *00,453*

BIENIOK, A.
Neutron Powder Diffraction Study of a Na, Cs-Rho Zeolite.
PB94-198629 *00,791*

BIERBAUM, V. M.
Kinetics and Dynamics of Vibrationally State Resolved Ion-Molecule Reactions: (14)N2(+)(v=1 and 2) and (15)N2(+)(v=0,1 and 2) with (14)N2.
PB96-102348 *04,023*

Laser-Induced Fluorescence Measurements of Rotationally Resolved Velocity Distributions for CO(+) Drifted in He.
PB94-213139 *00,848*

Selected Ion Flow Tube-Laser Induced Fluorescence Instrument for Vibrationally State-Specific Ion-Molecule Reactions.
PB94-185444 *00,774*

BINKLEY, D.
Slicing in the Presence of Parameter Aliasing.
PB96-160858 *01,755*

BINKLEY, D. W.
Application of the Pointer State Subgraph to Static Program Slicing.
PB96-167838 *01,768*

C++ in Safety Critical Systems.
PB96-154588 *01,750*

Unravel: A CASE Tool to Assist Evaluation of High Integrity Software. Volume 1. Requirements and Design.
PB95-267886 *01,736*

Unravel: A CASE Tool to Assist Evaluation of High Integrity Software. Volume 2. User Manual.
PB95-267894 *01,737*

BIR, N.
Rapid Method for the Isolation of Genomic DNA from 'Aspergillus fumigatus'.
PB96-147061 *03,488*

BIRBER, R.
Effect of Cross-Links on the Miscibility of a Deuterated Polybutadiene and Protonated Polybutadiene Blend.
PB94-212438 *01,225*

BIRMINGHAM, B. W.
Design and Construction of a Liquid Hydrogen Temperature Refrigeration System.
AD-A286 618/4 *02,619*

Helium Refrigeration and Liquefaction Using a Liquid Hydrogen Refrigerator for Precooling.
AD-A286 683/8 *02,749*

BIRNBAUM, D.
Location of a (1)A(sub g) State in Bithiophene.
PB95-202313 *01,025*

BIRNBAUM, G.
Collision-Induced Emission in the Fundamental Vibration-Rotation Band of H2.
PB94-199445 *03,811*

Intelligent Processing of Materials, Technical Activities 1994 (NAS-NRC Assessment Panel, April 6-7, 1995).
PB96-115050 *03,359*

Memory Function Approach to the Shape of Pressure Broadened Molecular Bands.
PB95-152930 *00,944*

BISS, B.
Response Comparison of Electret Ion Chambers, LiF TLD, and HPIC.
PB96-190103 *02,578*

BISWAS, P.
In situ Characterization of Vapor Phase Growth of Iron Oxide-Silica Nanocomposites: Part 1. 2-D Planar Laser-Induced Fluorescence and Mie Imaging.
PB97-112478 *03,185*

BIVENS, D. B.
Role of Refrigerant Mixtures as Alternatives to CFCs.
PB94-199775 *03,252*

BLAAUW, M.
Local Area Networks in NAA: Advantages and Pitfalls.
PB94-172095 *00,527*

BLACK, D. R.
Diffraction Imaging of Polycrystalline Materials.
PB94-198884 *02,971*

Evolution of the Pore Size Distribution in Final-Stage Sintering of Alumina Measured by Small-Angle X-ray Scattering. (Reannouncement with New Availability Information).
AD-A249 178/5 *03,023*

Structures of Vapor-Deposited Yttria and Zirconia Thin Films.
PB94-216025 *03,041*

BLACKBURN, D. L.
Natural Convection from an Array of Electronic Packages Mounted on a Horizontal Board in a Narrow Aspect Ratio Enclosure.
PB96-164017 *02,087*

Simulating the Dynamic Electro Thermal Behavior of Power Electronic Circuits and Systems.
PB95-161014 *02,345*

Status and Trends in Power Semiconductor Devices.
PB95-175097 *02,361*

Thermal Component Models for Electro-Thermal Network Simulation.
PB95-161022 *02,346*

BLAIR, J. J.
Uncertainties of Frequency Response Estimates Derived from Responses to Uncertain Step-Like Inputs.
PB97-111843 *01,984*

BLAIR, W. P.
Rapid Decline in the Optical Emission from SN 1957D in M83.
PB94-216033 *00,070*

BLAIR, W. R.
Certification of the Standard Reference Material 1473a, a Low Density Polyethylene Resin.
PB96-128251 *01,282*

Cylinder Wipe Air-Drying Intaglio Ink Vehicles for U.S. Currency Inks.
PB94-160801 *03,115*

Preparation and Monitoring of Lead Acetate Containing Drinking Water Solutions for Toxicity Studies.
PB94-193885 *00,538*

BLAKE, R. L.
Design and Characterization of X-Ray Multilayer Analyzers for the 50 - 1000 eV Region.
PB94-211851 *03,848*

BLAKE, T. A.
Infrared and Microwave Spectroscopy of the Argon - Propyne Dimer.
PB94-198892 *00,794*

BLALOCK, T. V.
Observations of Partial Discharges in Hexane Under High Magnification.
PB95-163127 *01,900*

BLANCA ROS, M.
X-ray Observation of Electroclinic Layer Constriction and Rearrangement in a Chiral Smectic-A Liquid Crystal.
PB96-141080 *01,100*

BLANPIED, W. A.
Thermal Conductivity of Metals and Alloys at Low Temperatures. A Review of the Literature.
AD-A279 180/4 *03,302*

BLASCHKO, O.
Neutron Spectroscopic Comparison of Rare-Earth/Hydrogen alpha-Phase Systems.
PB95-163523 *00,970*

Vibrations of Hydrogen and Deuterium in Solid Solution with Lutetium.
PB95-181038 *01,019*

BLAU, M.
Cold Neutron Gain Calculations for the NBSR Using MCNP.
PB95-163978 *03,731*

Nuclear Heat Load Calculations for the NBSR Cold Neutron Source Using MCNP.
PB95-152955 *03,730*

BLENDELL, J. E.
Effect of Sm2BaCuO5 on the Properties of Sintered (Bulk) YBa2Cu3O6+x.
PB96-119441 *04,733*

Stability and Surface Energies of Wetted Grain Boundaries in Aluminum Oxide.
PB95-202750 *03,059*

Texture Measurement of Sintered Alumina Using the March-Dollase Function.
PB96-179494 *04,784*

BLESSING, G. V.
Design, Construction and Application of a Large Aperture Lens-Less Line-Focus PVDF Transducer.
PB97-122584 *02,765*

Dynamic Shear Modulus Measurements with Four Independent Techniques in Nickel-Based Alloys.
PB94-198900 *03,320*

Material Characterization By a Time-Resolved and Polarization-Sensitive Ultrasonic Technique.
PB97-122576 *02,764*

NIST Calibration of ASTM E127-Type Ultrasonic Reference Blocks.
PB94-191640 *02,702*

Transient Analysis of a Line-Focus Transducer Probing a Liquid/Solid Interface.
PB97-118681 *02,763*

Ultrasonic Measurement of Sheet Anisotropy and Formability.
PB95-153235 *03,213*

Ultrasonic Measurements of Surface Roughness.
PB94-172137 *04,181*

Ultrasonic NDE of Sprayed Ceramic Coatings.
PB96-201157 *02,761*

BLETZINGER, P.
Gaseous Electronics Conference Radio-Frequency Reference Cell: A Defined Parallel-Plate Radio-Frequency System for Experimental and Theoretical Studies of Plasma-Processing Discharges.
PB94-172327 *04,404*

BLOCK, S.
1,4-Dinitrocubane and Cubane under High Pressure.
PB95-108437 *03,755*

BLOMQUIST, B. W.
International Marine-Atmospheric (222)Rn Measurement Intercomparison in Bermuda. Part 2. Results for the Participating Laboratories.
PB96-175682 *00,115*

BLOMQUIST, D. S.
Quality in Automated Manufacturing.
PB96-160437 *02,839*

BLOOM, H. M.
Formulation of Position on U.S. Standards Role in Enterprise Integration.
PB95-105052 *02,773*

Technical Program Description Systems Integration for Manufacturing (SIMA).
PB94-213758 *02,819*

Technical Program of the Factory Automation Systems Division 1993.
PB94-160819 *02,805*

BLUE, J. L.
Effect of Training Dynamics on Neural Network Performance.
PB95-267845 *01,852*

Faster BKL Monte Carlo Simulations.
PB95-136370 *01,706*

Faster Monte Carlo Simulations.
PB96-102074 *04,018*

Improving Neural Network Performance for Character and Fingerprint Classification by Altering Network Dynamics.
PB95-267803 *01,851*

Improving Neural Network Performance for Character and Fingerprint Classification by Altering Network Dynamics.
PB96-123195 *01,856*

Micromagnetic Structure of Domains in Co/Pt Multilayers. 1. Investigations of Wall Structure.
PB95-162111 *04,610*

NIST Form-Based Handprint Recognition System.
PB94-217106 *01,838*

Parallel Monte Carlo Simulation of MBE Growth.
PB96-122841 *02,406*

Trace Detection in Conducting Solids Using Laser-Induced Fluorescence in a Cathodic Sputtering Cell.
PB95-163424 *00,598*

BLUM, K.
Charge Cloud Distribution of Heavy Atoms After Excitation by Polarized Electrons.
PB95-203147 *04,001*

BLUMBERG, R. L.
Catastrophic Failures Propagate Field of Fracture Mechanics.
PB96-135140 *03,217*

BLUNDELL, S. A.
Evaluation of Two-Photon Exchange Graphs for Highly-Charged Heliumlike Ions.
PB94-198918 *03,808*

BOATNER, L. A.
Anomalous Dispersion and Thermal Expansion in Lightly-Doped KTa1-xNbxO3.
PB95-152302 *04,585*

BOCHMANN, G. V.
Open Issues in OSI Protocol Development and Conformance Testing.
PB96-122908 *01,818*

BODARKY, S.
Guide to Configuration Management and the Revision Control System for Testbed Users.
PB94-150919 *01,678*

BODE, M.
Epitaxial Growth and Characterization of the Ordered Vacancy Compound CuIn3Se5 on GaAs (100) Fabricated by Molecular Beam Epitaxy.
PB95-180725 *04,687*

BOETTINGER, W. J.
Coherent Precipitates in the BCC/Orthorhombic Two Phase Field of the Ti-Al-Nb System.
PB94-198694 *03,317*

Disorder Trapping in Ni2TiAl.
PB94-198942 *03,322*

Lubrication Theory for Reactive Spreading of a Thin Drop.
PB95-189460 *02,865*

Lubrication Theory for Reactive Spreading of a Thin Drop.
PB96-123427 *04,214*

Ordered omega-Derivatives in a Ti-37.5Al-2ONb at% Alloy.
PB94-211091 *03,331*

Phase-Field Model for Solidification of a Eutectic Alloy.
PB95-147914 *03,345*

Thermodynamic Calculation of the Ternary Ti-Al-Nb System.
PB94-212636 *03,336*

Thermodynamic Constraints on Non-Equilibrium Solidification of Ordered Intermetallic Compounds.
PB94-198934 *03,321*

Transformation of BCC and B2 High Temperature Phases to HCP and Orthorhombic Structures in the Ti-Al-Nb System. Part 1. Microstructural Predictions Based on a Subgroup Relation between Phases.
PB96-169065 *03,370*

Transformation of BCC and B2 High Temperature Phases to HCP and Orthorhombic Structures in the Ti-Al-Nb System. Part 2. Experimental TEM Study of Microstructures.
PB96-169073 *03,371*

BOGGESS, A.
Observations of 3C 273 with the Goddard High Resolution Spectrograph on the Hubble Space Telescope.
PB95-202321 *00,076*

BOGGS, P. T.
Algorithmic Enhancements to the Method of Centers for Linear Programming Problems.
PB94-198959 *03,426*

Convergence Properties of a Class of Rank-Two Updates. (NIST Reprint).
PB95-180097 *03,430*

Guidelines for Reporting Results of Computational Experiments. Report of the Ad hoc Committee.
PB94-212347 *03,427*

Interior-Point Method for Linear and Quadratic Programming Problems. (NIST Reprint).
PB95-180089 03,429

BOGGS, S. A.

Transient Errors in a Precision Resistive Divider.
PB97-111512 01,983

BOISVERT, R. F.

Boundary Integral Method for the Simulation of Two-Dimensional Particle Coarsening.
PB94-216744 03,411

Portable Vectorized Software for Bessel Function Evaluation.
PB94-198975 01,690

Software Libraries, Numerical and Statistical.
PB94-198967 01,689

Virtual Software Repository System.
PB94-198983 01,691

BOITEUX, S.

Substrate Specificity of the Escherichia coli Endonuclease III: Excision of Thymine- and Cytosine-Derived Lesions in DNA Produced by Radiation-Generated Free Radicals.
PB95-153425 03,535

BOLAND, T.

Asynchronous Transfer Mode Procurement and Usage Guide.
PB95-174967 01,481

Data Communications Strategy.
PB96-167846 02,738

ISDN LAN Bridging.
PB95-154696 01,477

BOLGER, J. A.

Time-Resolved Measurements of the Polarization State of Four-Wave Mixing Signals from GaAs Multiple Quantum Wells.
PB96-201058 04,796

BOLLINGER, J.

Electrostatic Modes of Ion-Trap Plasmas.
PB95-152963 03,920

Experimental Results on Normal Modes in Cold, Pure Ion Plasmas.
PB95-175105 03,956

BOLLINGER, J. J.

Electrostatic Modes as a Diagnostic in Penning-Trap Experiments.
PB95-176244 03,959

High-Resolution Atomic Spectroscopy of Laser-Cooled Ions.
PB95-169330 03,953

Interference in the Resonance Fluorescence of Two Trapped Atoms.
PB95-168514 03,948

Laser-Cooled Positron Source.
PB95-169348 03,954

Laser Cooling of Trapped Ions.
PB95-168746 03,950

Light Scattered from Two Atoms.
PB95-168753 04,286

Liquid and Solid Atomic Ion Plasmas.
PB94-198991 03,809

Non-Neutral Ion Plasmas and Crystals, Laser Cooling, and Atomic Clocks.
PB95-175113 03,957

Precise Spectroscopy for Fundamental Physics.
PB96-112164 04,040

Quantum Measurements of Trapped Ions.
PB95-161147 03,928

Quantum Projection Noise: Population Fluctuations in Two-Level Systems.
PB94-212271 03,850

Recent Experiments on Trapped Ions at the National Institute of Standards and Technology.
PB95-169322 03,952

Spin Squeezing and Reduced Quantum Noise in Spectroscopy.
PB95-151635 03,912

Squeezed Atomic States and Projection Noise in Spectroscopy.
PB95-176293 03,960

Trapped Ions and Laser Cooling 4: Selected Publications of the Ion Storage Group of the Time and Frequency Division, NIST, Boulder, Colorado.
PB96-172358 04,108

BOLLONG, A. B.

Comparison of Techniques for Nondestructive Composition Measurements in CdZnTe Substrates.
PB96-103098 02,703

BOND, L. J.

Absorption of Sound in Gases between 10 and 25 MHz: Argon.
PB94-199015 04,183

Absorption of Ultrasonic Waves in Air at High Frequencies (10-20 MHz).
PB94-199007 04,182

Interaction of Rayleigh Waves with a Rib Attached to a Plate.
PB94-199023 04,184

Sensor System for Intelligent Processing of Hot-Rolled Steel.
PB96-186069 03,373

Ultrasonic Technique for Sizing Voids Using Area Functions.
PB95-151916 02,904

BONNELL, D. W.

High Temperature.
PB94-211737 03,844

Recent Experimental and Modeling Developments in High Temperature Thermochemistry.
PB94-172343 00,759

BONOWITZ, D.

Survey of Steel Moment-Resisting Frame Buildings Affected by the 1994 Northridge Earthquake.
PB95-211918 00,451

BOOI, A. A. P.

High Power Generation with Distributed Josephson-Junction Arrays.
PB97-111520 02,099

BOOI, P. A. A.

Characterization of the Emission from 2D Array Josephson Oscillators.
PB95-175121 02,054

Design of High-Frequency, High-Power Oscillators Using Josephson-Junction Arrays.
PB96-200258 02,094

Direct Observation of Vortex Dynamics in Two-Dimensional Josephson-Junction Arrays.
PB96-102223 02,067

Emission Linewidth Measurements of Two-Dimensional Array Josephson Oscillators.
PB95-175139 02,055

Frequency Dependence of the Emission from 2D Array Josephson Oscillators.
PB95-175147 02,056

High-Frequency Oscillators Using Phase-Locked Arrays of Josephson Junctions.
PB96-135157 02,080

High-Power, High-Frequency Oscillators Using Distributed Josephson-Junction Arrays.
PB96-200266 02,095

Intrinsic Stress in DC Sputtered Niobium.
PB94-199031 04,468

Novel Vortex Dynamics in Two-Dimensional Josephson Arrays.
PB96-200167 02,091

Observation of Vortex Dynamics in Two-Dimensional Josephson-Junction Arrays.
PB95-168811 02,050

Phase-Locked Oscillator Optimization for Arrays of Josephson Junctions.
PB95-169314 02,052

Resonances in Two-Dimensional Array Oscillator Circuits.
PB96-102082 02,066

Superconducting Integrated Circuit Fabrication with Low Temperature ECR-Based PECVD SiO2 Dielectric Films.
PB96-103015 04,719

SUSAN: SUperconducting Systems ANalysis by Low Temperature Scanning Electron Microscopy (LTSEM).
PB96-112065 04,728

BOOKBINDER, J.

Sleuthing the Dynamo: HST/FOS Observations of UV Emissions of Solar-Type Stars in Young Clusters.
PB96-122817 00,098

BOOKBINDER, J. A.

Far-Ultraviolet Flare on a Pleiades G Dwarf.
PB96-102033 00,086

Four Years of Monitoring alpha Orionis with the VLA: Where Have All the Flares Gone.
PB94-185212 00,048

Search for Radio Emission from the 'Non-Magnetic' Chemically Peculiar Stars.
PB96-102249 00,087

BORCHARDT, B.

Displacement Method for Machine Geometry Calibration.
PB95-152088 02,946

Estimation of Measurement Uncertainty of Small Circular Features Measured by CMMs.
PB95-267928 02,918

Interim Testing Artifact (ITA): A Performance Evaluation System for Coordinate Measuring Machines (CMMs). User Manual.
PB95-210589 02,914

NIST SRM 9983 High-Rigidity Ball-Bar Stand. User Manual.
PB95-255840 02,669

Some Considerations for Interim Testing of Coordinate Measuring Machine Performance Using a Specific Artifact.
PB95-108858 02,898

BORCHARDT, B. R.

User's Guide to NIST SRM 2084: CMM Probe Performance Standard.
PB94-206109 02,709

BORCHERDT, L.

Critical Current and Normal Resistance of High-Tc Step-Edge SNS Junctions.
PB96-111752 04,724

BORCHERDT, L. J.

High-Tc Superconducting Antenna-Coupled Microbolometer on Silicon.
PB95-169124 02,166

BORCHERS, J.

Magnetoelasticity in Rare-Earth Multilayers and Films.
PB94-211356 04,495

BORCHERS, J. A.

Combined Low- and High-Angle X-Ray Structural Refinement of a Co/Pt(111) Multilayer Exhibiting Perpendicular Magnetic Anisotropy.
PB94-198355 04,457

Comment on 'Phase Transitions in Antiferromagnetic Superlattices'.
PB95-152971 04,587

Magnetic Rare Earth Artificial Metallic Superlattices.
PB95-162293 04,611

Magnetic Structure Determination for Annealed Ni80Fe20/Ag Multilayers Using Polarized-Neutron Reflectivity.
PB96-176615 03,739

Structural and Magnetic Ordering in Iron Oxide/Nickel Oxide Multilayers by X-ray and Neutron Diffraction (Invited).
PB94-172558 04,442

Unconventional Ferromagnetic Transition in La(sub 1-x)Ca(sub x)MnO3.
PB97-112429 04,156

BOREHERS, J. A.

Enhanced Curie Temperatures and Magnetoelastic Domains in Dy/Lu Super Lattices and Films.
PB94-172665 04,443

BORST, P.

beta-D-Glucosyl-Hydroxymethyluracil: A Novel Modified Base Present in the DNA of the Parastic Protozoan T. brucei.
PB94-172319 03,524

BORSUK, G.

Beyond the Technology Roadmaps: An Assessment of Electronic Materials Research and Development.
PB96-165998 01,961

BORTFELD, D. P.

Display-Measurement Round-Robin.
PB96-119227 02,186

BORTHWICK, P.

Suppression of Ignition Over a Heated Metal Surface.
PB96-176425 03,291

BORYSOW, J.

N2(a'(sup 1)Sigma(sub g)(sup +)) Metastable Collisional Destruction and Rotational Excitation Transfer by N2.
PB95-151395 00,933

BOSE, J.

Error Protecting Characteristics of CDMA and Impacts on Speech.
PB96-122452 01,491

BOUDREAUX, J. C.

Optoelectronics and Optomechanics Manufacturing: An ATP Focused Program Development. Workshop Proceedings. Held in Gaithersburg, Maryland on February 15, 1995.
PB97-104186 02,204

BOUR, D. P.

Double Modulation and Selective Excitation Photoreflectance for Characterizing Highly Luminescent Semiconductor Structures and Samples with Poor Surface Morphology.
PB97-111439 02,452

BOWDEN, E. F.

Characterization of Cytochrome c/Alkanethiolate Structures Prepared by Self-Assembly on Gold.
PB95-164638 00,987

BOWEN, D. K.

Comparison of Techniques for Nondestructive Composition Measurements in CdZnTe Substrates.
PB96-103098 02,703

BOWEN, E. D.

Micromachined Coplanar Waveguides in CMOS Technology.
PB97-119283 02,456

BOWEN, H. J.

Effects of Calcium Phosphate Solutions on Dentin Permeability.
PB95-151080 00,157

BOWEN, K. O.

Statistical Quality Control Technology in Japan.
PB94-199064 02,708

BOWEN, R. L.

Adhesion of Composites to Dentin and Enamel.
PB94-199049 00,144

Development of an Adhesive Bonding System.
PB94-199056 00,145

New Surface-Active Comonomer for Adhesive Bonding.
PB96-204052 03,579

Physical and Chemical Properties of Resin-Reinforced Calcium Phosphate Cements.
PB95-180212 00,171

Polymerization Initiation by N-p-Tolylglycine: Free-Radical Reactions Studied by Pulse and Steady-State Radiolysis.
PB95-180014 01,269

BOWERS, G.
Frozen Human Serum Reference Material for Standardization of Sodium and Potassium Measurements in Serum or Plasma by Ion-Selective Electrode Analyzers.
PB94-185337 *00,532*

BOWERS, G. N.
History of NIST's Contributions to Development of Standard Reference Materials and Reference and Definitive Methods for Clinical Chemistry.
PB96-119706 *03,503*

BOWERS, W. J.
Development of the NIST Transient Pressure and Temperature Calibration Facility.
PB96-160833 *00,626*

Simultaneous Forward-Backward Raman Scattering Studies of D2 Broadened by D2, He, and Ar.
PB95-162459 *00,961*

BOWMAN, K. J.
Texture Measurement of Sintered Alumina Using the March-Dollase Function.
PB96-179494 *04,784*

BOWMAN, W. A.
Study of Laser Resonance Ionization Mass Spectrometry Using a Glow Discharge Source.
DE94018566 *03,308*

Study of Laser Resonance Ionization Mass Spectrometry Using a Glow Discharge Source.
PB96-123203 *03,360*

BOX, G.
Taguchi's Parameter Design: A Panel Discussion.
PB96-111802 *03,445*

BOYD, C. F.
Fire Protection Foam Behavior in a Radiative Environment.
PB97-116131 *00,237*

BOYER, C. I.
Minimum Mass Flux Requirements to Suppress Burning Surfaces with Water Sprays.
PB96-183181 *01,425*

BOYES, S. J.
Interatomic Potential of Argon.
PB95-141180 *00,912*

Interatomic Potential of Argon.
PB95-152989 *00,945*

Vapor Pressures and Gas-Phase PVT Data for 1-Chloro-1,2,2,2-Tetrafluoroethane (R124).
PB95-175154 *03,271*

Vapour Pressures and Gas-Phase (p, rho n, T) Values for CF3CHF2(R125).
PB96-102090 *04,019*

BOYKO, K. C.
Experimental Investigation of the Validity of TDDB Voltage Acceleration Models.
PB94-185949 *02,304*

Field and Temperature Acceleration of Time-Dependent Dielectric Breakdown in Intrinsic Thin SiO2.
PB94-185956 *02,305*

BOYNTON, P.
Perception of Clamp Noise in Television Receivers.
PB96-119433 *01,489*

BOYNTON, P. A.
Display-Measurement Round-Robin.
PB96-119227 *02,186*

Interface-Filter Characterization of Spectraradiometers and Colorimeters.
PB97-122212 *04,399*

Survey of the Components of Display-Measurement Standards.
PB96-122528 *02,188*

Survey of the Components of Display-Measurement Standards.
PB97-122394 *02,209*

BOZIN, J.
Excitation of Balmer Lines in Low-Current Discharges of Hydrogen and Deuterium.
PB95-150546 *03,893*

BOZOVIC, I.
Stacked Series Arrays of High-Tc Trilayer Josephson Junctions.
PB96-102272 *04,705*

Step-Edge and Stacked-Heterostructure High-Tc Josephson Junctions for Voltage-Standard Arrays.
PB96-102066 *04,702*

BRABERS, J. H. V. J.
Magnetic Properties of Single-Crystalline UCu3Al2.
PB95-180717 *04,686*

BRACHA, E.
Channel Coding for Code Excited Linear Prediction (CELP) Encoded Speech in Mobile Radio Applications.
PB95-143178 *01,475*

BRADFORD, A. G.
Metrology for Electromagnetic Technology: A Bibliography of NIST Publications.
PB97-116057 *04,396*

Metrology for Electromagnetic Technology: A Bibliography of NIST Publications, September 1995.
PB96-128269 *01,938*

BRADLEY, P.
Energy Flows in an Orifice Pulse Tube Refrigerator.
PB95-169082 *02,752*

Graded and Nongraded Regenerator Performance.
PB95-169090 *02,753*

BRADY, K.
Distributed Communication Methods and Role-Based Access Control for Use in Health Care Applications.
PB96-183165 *01,508*

BRADY, K. G.
Conformance Testing and Specification Management.
PB97-113781 *02,849*

User's Guide for the PHIGS Validation Tests (Version 2.1).
PB94-165206 *01,682*

BRAKE, M. L.
Gaseous Electronics Conference Radio-Frequency Reference Cell: A Defined Parallel-Plate Radio-Frequency System for Experimental and Theoretical Studies of Plasma-Processing Discharges.
PB94-172327 *04,404*

Reactive Ion Etching in the Gaseous Electronics Conference RF Reference Cell.
PB96-113402 *02,395*

BRAND, P. C.
Determination of the Residual Stresses Near the Ends of Skip Welds Using Neutron Diffraction and X-ray Diffraction Procedures.
PB95-253589 *02,868*

BRANDENBURG, K.
Evaluation of Crystallographic Data with the Program DIAMOND.
PB97-109045 *00,649*

BRANDT, J. C.
Observations of 3C 273 with the Goddard High Resolution Spectrograph on the Hubble Space Telescope.
PB95-202321 *00,076*

Observing Stellar Coronae with the Goddard High Resolution Spectrograph. I. The dMe Star AU Microscopii.
PB96-102777 *00,092*

BRANECKY, R. J.
Evaluation of Wear Resistant Ceramic Valve Seats in Gas-Fueled Power Generation Engines. Topical Report, December 1991-April 1994.
PB95-200218 *02,466*

BRANSFORD, J. W.
Recommended Changes in ASTM Test Methods D2512-82 and G86-84 for Oxygen-Compatibility Mechanical Impact Tests on Metals.
PB94-216694 *03,338*

BRANSTAD, D.
Introduction to Secure Telephone Terminals.
PB97-110498 *01,512*

BRANSTAD, D. K.
Report of the NIST Workshop on Digital Signature Certificate Management. Held on December 10-11, 1992.
PB94-135001 *01,574*

Report of the NIST Workshop on Key Escrow Encryption. Held in Gaithersburg, Maryland on June 8-10, 1994.
PB94-209459 *01,584*

Response to Comments on the NIST Proposed Digital Signature Standard.
PB96-161815 *01,615*

BRAUN, E.
Early Detection of Room Fires Through Acoustic Emission. (NIST Reprint).
PB95-180311 *00,298*

Fire Performance of an Interstitial Space Construction System.
PB95-188918 *00,390*

Further Development of the N-Gas Mathematical Model: An Approach for Predicting the Toxic Potency of Complex Combustion Mixtures.
PB96-123260 *03,650*

New Approach for Reducing the Toxicity of the Combustion Products from Flexible Polyurethane Foam.
PB96-123625 *01,411*

Quantifying the Ignition Propensity of Cigarettes.
PB96-155411 *00,306*

Relating Bench-Scale and Full-Scale Toxicity Data.
PB95-125977 *00,361*

BRAUN, L. M.
Model for Toughness Curves in Two-Phase Ceramics. 1. Basic Fracture Mechanics.
PB96-180088 *03,085*

Model for Toughness Curves in Two-Phase Ceramics. 2. Microstructural Variables.
PB96-163795 *03,078*

Need for Advanced Characterization Techniques in Product Manufacturing: A Case Study on Ceramic Matrix Composites.
PB96-204060 *03,089*

Objective Evaluation of Short-Crack Toughness Curves Using Indentation Flaws: Case Study on Alumina-Based Ceramics.
PB96-179429 *03,079*

BRAUN, R. J.
Anisotropy of Interfaces in an Ordered Alloy: A Multiple-Order-Parameter Model.
PB96-131594 *04,741*

Asymptotic Behavior of Modulated Taylor-Couette Flows with a Crystalline Inner Cylinder.
PB94-199072 *04,469*

Lubrication Theory for Reactive Spreading of a Thin Drop.
PB95-189460 *02,865*

Lubrication Theory for Reactive Spreading of a Thin Drop.
PB96-123427 *04,214*

BRAUN, W.
Reaction Rate Determinations of Vinyl Radical Reactions with Vinyl, Methyl, and Hydrogen Atoms.
PB94-211398 *00,815*

BRAXENTHALER, M.
Positive and Negative Cooperativities at Subsequent Steps of Oxygenation Regulate the Allosteric Behavior of Multistate Sebacylhemoglobin.
PB97-119374 *03,486*

BRAY, S. L.
Critical-Current Degradation in Nb3 Al Wires Due to Axial and Transverse Stress.
PB95-202784 *02,226*

Effect of Magnetic Field Orientation on the Critical Current of HTS Conductor and Coils.
PB96-141189 *02,956*

Electromechanical properties of superconductors for DOE fusion applications.
DE95015476 *04,432*

Electromechanical Properties of Superconductors for DOE Fusion Applications.
PB94-139672 *02,250*

Improved Uniaxial Strain Tolerance of the Critical Current Measured in Ag-Sheathed Bi2Sr2Ca1Cu2O8+x Superconductors.
PB95-153565 *04,594*

Quench Energy and Fatigue Degradation Properties of Cu- and Al/Cu-Stablized Nb-Ti Epoxy-Impregnated Superconductor Coils.
PB96-141213 *04,755*

Transverse stress effect on the critical current of internal tin and bronze process Nb(sub 3)Sn superconductors.
DE95016659 *04,434*

BREEN, J. J.
Application of a Novel Slurry Furnace AAS Protocol for Rapid Assessment of Lead Environmental Contamination.
PB96-112354 *02,526*

BREESE, R. S.
Investigation of the Thermal Stability and Char-Forming Tendency of Cross-linked Poly(methyl methacrylate).
PB94-213501 *03,380*

BREHOB, E.
Turbulent Upward Flame Spread on a Vertical Wall under External Radiation.
PB94-207388 *00,341*

BREITENBERG, M.
Electrical Product Requirements (Especially Quality Requirements) in the United States.
PB96-119235 *01,929*

Questions and Answers on Quality, the ISO 9000 Standard Series, Quality System Registration, and Related Issues. More Questions and Answers on the ISO 9000 Standard Series and Related Issues.
PB95-103461 *00,495*

Survey on the Implementation of ISO/IEC Guide 25 by National Laboratory Accreditation Programs.
PB94-210150 *00,479*

BREUER, E.
In vitro Inhibition of Membrane-Mediated Calcification by Novel Phosphonates.
PB96-201140 *03,595*

BREWCZYK, M.
Appearance Intensities for Multiply Charged Ions in a Strong Laser Field.
PB96-160445 *04,089*

BREWER, P. D.
Effects of Aluminum Oxalate/Glycine Pretreatment Solutions on Dentin Permeability.
PB95-164505 *03,565*

BREWER, W. D.
Precision Nuclear Orientation Measurements for Determining Mixed Magnetic Dipole/Electric Quadrupole Hyperfine Interactions.
PB94-199080 *03,810*

BRIBER, R. M.
Electron Beam Crosslinking of Poly(vinylmethyl ether).
PB94-185550 *01,205*

Grafted Interpenetrating Polymer Networks.
PB94-185055 *01,200*

BRICKENKAMP, C. S.
Checking the Net Contents of Packaged Goods as Adopted by the 79th National Conference on Weights and Measures, 1994, Third Edition, Supplement 4.
PB95-182226 *00,484*

Method of Sale for CNG Paves Way to Greater Public Acceptance.
PB95-168449 *02,489*

Report of the National Conference on Weight and Measures (78th). Held in Kansas City, MO. on July 18-22, 1993.
PB94-138989 *02,623*

Report of the National Conference on Weights and Measures (79th). Held in San Diego, California on July 17-21, 1994.
PB95-169819 *02,656*

BRIDGES, J. M.

Development and Calibration of UV/VUV Radiometric Sources.
PB94-199098 *04,229*

Irradiances of Spectral Lines in Mercury Pencil Lamps
PB96-176466 *04,375*

BRIESMEISTER, J.

Neutron Leakage Benchmark for Criticality Safety Research.
PB95-126132 *03,723*

BRIGGS, M. E.

Susceptibility Critical Exponent for a Nonaqueous Ionic Binary Mixture Near a Consolute Point.
PB95-152112 *00,938*

BRIGHAM-BURKE, M.

Phospholipid/Alkanethiol Bilayers for Cell-Surface Receptor Studies by Surface Plasmon Resonance.
PB96-102900 *03,472*

BRIGHT, D.

Fabrication of Platinum-Gold Alloys in Pre-Hispanic South America: Issues of Temperature and Microstructure Control.
PB94-211646 *03,333*

BRIGHT, D. S.

Compositional Mapping of the Microstructure of Materials.
PB95-107199 *00,565*

Concentration Histogram Imaging: A Scatter Diagram Technique for Viewing Two or Three Related Images.
PB94-199114 *00,542*

Object Finder for Digital Images Based on Multiple Thresholds, Connectivity, and Internal Structures.
PB94-199106 *01,833*

Study of Diffusion Zones with Electron Microprobe Compositional Mapping.
PB94-216348 *00,559*

BRILL, W. J.

Learning to Change: Opportunities to Improve the Performance of Smaller Manufacturers.
PB94-166212 *00,010*

BRILLIANT, N. A.

Video Microscopy Applied to Optical Fiber Geometry Measurements.
PB95-173068 *04,295*

BRINCKMAN, F. E.

Atmospheric and Marine Trace Chemistry: Interfacial Biomediation and Monitoring.
PB94-199122 *03,752*

Bioleaching of Cobalt from Smelter Wastes by 'Thiobacillus ferrooxidans'.
PB95-140968 *02,582*

Total Surface Areas of Group IVA Organometallic Compounds: Predictors of Toxicity to Algae and Bacteria.
PB94-211331 *00,814*

BROADHURST, M. G.

Spatial Dependence of Electrical Fields Due to Space Charges in Films of Organic Dielectrics Used for Insulation of Power Cables.
PB94-199130 *02,214*

BROBERG, J. B.

NIST-NRL Free-Electron Laser Facility.
PB94-212511 *04,237*

BROCHERS, J. A.

Antiferromagnetic Interlayer Correlations in Annealed Ni80Fe20/Ag Multilayers.
PB97-122220 *03,109*

BROCK, C. P.

Investigations of the Systematics of Crystal Packing Using the Cambridge Structural Database.
PB97-109144 *00,519*

BROCKER, C. W.

Design of a High-Flux Backscattering Spectrometer for Ultra-High Resolution Inelastic Neutron Measurements.
PB96-179577 *02,992*

BRODY, P. S.

Microstructure and Ferroelectric Properties of Lead Zirconate-Titanate Films Produced by Laser Evaporation.
PB94-199148 *04,470*

BROHOLM, C.

Isolated Spin Pairs and Two-Dimensional Magnetism in SrCr(sub 9p)Ga(sub 12-9p)O19.
PB97-112387 *04,154*

BROMAGE, G.

First Results from a Coordinated ROSAT, IUE, and VLA Study of RS CVn Systems.
PB94-213477 *00,069*

BROMAGE, G. E.

Rotational Modulation and Flares on RS Canum Venaticorum and BY Draconis Stars. XVIII. Coordinated VLA, ROSAT, and IUE Observations of RS CVn Binaries.
PB96-102322 *00,089*

Volume-Limited ROSAT Survey of Extreme Ultraviolet Emission from all Nondegenerate Stars within 10 Parsecs.
PB96-103189 *00,093*

BROMBACHER, W. G.

Methods of Measuring Humidity and Testing Hygrometers.
AD-A278 851/1 *00,123*

BROMBACKER, W. G.

Guide to Instrumentation Literature.
AD-A280 278/3 *02,617*

BROOKS, D. B.

Physical Properties of Some Purified Aliphatic Hydrocarbons.
AD-A297 265/1 *00,657*

BROSIUS, J. W.

Observing Stellar Coronae with the Goddard High Resolution Spectrograph. I. The dMe Star AU Microscopii.
PB96-102777 *00,092*

BROWN, A.

Deuterium and the Local Interstellar Medium: Properties for the Procyon and Capella Lines of Sight.
PB96-200639 *00,111*

Deuterium in the Local Interstellar Medium: Its Cosmological Significance.
PB95-202842 *00,081*

Dynamic Phenomena on the RS Canum Venaticorum Binary II Pegasi in August 1989. 1. Observational Data.
PB94-211067 *00,056*

Far-Ultraviolet Flare on a Pleiades G Dwarf.
PB96-102033 *00,086*

First Results from a Coordinated ROSAT, IUE, and VLA Study of RS CVn Systems.
PB94-213477 *00,069*

First Results from the Goddard High-Resolution Spectrograph: The Chromosphere of Tauri.
PB94-199528 *00,054*

GHRS Observations of Cool, Low-Gravity Stars. 1. The Far-Ultraviolet Spectrum of alpha Orions (M2 Iab).
PB96-112016 *00,094*

Goddard High-Resolution Spectrograph Observations of the Local Interstellar Medium and the Deuterium/Hydrogen Ratio along the Line of Sight Toward Capella.
PB94-213444 *00,066*

High Sensitivity Survey of Radio Continuum Emission in Herbig Ae/Be Stars.
PB94-185915 *00,051*

Hydrogen Lyman-alpha Emission of Capella.
PB95-202263 *00,075*

Next Generation Computer Resources: Reference Model for Project Support Environments (Version 2.0).
PB94-143401 *01,677*

Observing Stellar Coronae with the Goddard High Resolution Spectrograph. I. The dMe Star AU Microscopii.
PB96-102777 *00,092*

Riass Coronathon: Joint X-ray and Ultraviolet Observations of Normal F-K Stars.
PB96-200217 *00,109*

Rotational Modulation and Flares on RS Canum Venaticorum and BY Draconis Stars. XVIII. Coordinated VLA, ROSAT, and IUE Observations of RS CVn Binaries.
PB96-102322 *00,089*

Sleuthing the Dynamo: HST/FOS Observations of UV Emissions of Solar-Type Stars in Young Clusters.
PB96-122817 *00,098*

Transition Regions of Capella.
PB96-123336 *00,105*

Transition Regions of Capella (1995).
PB96-176714 *00,108*

Volume-Limited ROSAT Survey of Extreme Ultraviolet Emission from all Nondegenerate Stars within 10 Parsecs.
PB96-103189 *00,093*

BROWN, C. L.

Histopathology, Blood Chemistry, and Physiological Status of Normal and Moribund Striped Bass ('Morone saxatilis') Involved in Summer Mortality ('Die-Off') in the Sacramento-San Joaquin Delta of California.
PB94-198157 *00,034*

BROWN, C. M.

Observation and Visible and uv Magnetic Dipole Transitions in Highly Charged Xenon and Barium.
PB96-138441 *04,056*

Polarization Measurements on a Magnetic Quadrupole Line in Ne-Like Barium.
PB97-113104 *04,161*

BROWN, D. E.

Multi-Stage, Position Stabilized Vibration Isolation System for Neutron Interferometry.
PB95-175022 *03,955*

BROWN, D. M.

Boron-Implanted 6H-SiC Diodes.
PB96-159678 *04,081*

BROWN, D. R.

External Gamma-ray Counting of Selected Tissues from a Thorotrast Patient.
PB96-160254 *03,637*

Germanium Detector Optimization of MDA for Efficiency vs. Low Intrinsic Background.
PB94-199155 *00,543*

BROWN, G. A.

Electron and Hole Trapping in Irradiated SIMOX, ZMR and BESOI Buried Oxides.
PB96-160320 *01,956*

BROWN, H. J.

Aging Effects on XRF Measurements of Solder Coatings.
PB95-140927 *03,123*

BROWN, I. D.

CIF Crystallographic Information File: A Standard for Crystallographic Data Interchange.
PB97-109169 *04,805*

BROWN, J.

Bacteriorhodopsin Immobilized in Sol-Gel Glass.
PB95-151429 *03,532*

BROWN, J. E.

Computer-Aided Molecular Design of Fire Resistant Aircraft Materials.
PB96-160601 *00,025*

Fire Safety of Passenger Trains: A Review of Current Approaches and of New Concepts.
PB94-152006 *04,848*

Gas Phase Oxygen Effect on Chain Scission and Monomer Content in Bulk Poly(methyl methacrylate) Degraded by External Thermal Radiation.
PB96-204078 *01,293*

Investigation into the Flammability Properties of Honeycomb Composites.
PB95-143293 *03,152*

Investigation of the Thermal Stability and Char-Forming Tendency of Cross-linked Poly(methyl methacrylate).
PB94-213501 *03,380*

New Generation of Fire Resistant Polymers. Part 1. Computer-Aided Molecular Design.
PB96-160593 *01,419*

BROWN, J. M.

Atomic Iron in Its (5)D Ground State: A Direct Measurement of the J = 0 inverted arrow 1 and J = 1 inverted arrow 2 Fine-Structure Intervals (1.2).
PB96-141221 *04,756*

Atomic Sulfur: Frequency Measurement of the J=0 inversely maps 1 Fine-Structure Transition at 56.3 Microns by Laser Magnetic Resonance.
PB95-180105 *01,007*

Detection of OH+ in Its a(1)Delta State by Far Infrared Laser Magnetic Resonance.
PB95-181087 *01,021*

Determination of the Molecular Parameters of NiH in Its (2)Delta Ground State by Laser Magnetic Resonance.
PB95-107116 *00,869*

Fine-Structure Intervals of (14)N(+) By Far-Infrared Laser Magnetic Resonance.
PB95-175162 *00,993*

Laser Magnetic-Resonance Measurement of the (3)P1 - (3)P2 Fine-Structure Splittings in (17)O and (18)O.
PB95-175170 *00,994*

Measurement of the J=2 less than 1 Fine-Structure Interval for (28)Si and (29)Si in the Ground (3)P State.
PB94-185097 *00,771*

Rotational Spectroscopy of the CoH Radical in Its Ground (3)Phi State by Far-Infrared Laser Magnetic Resonance: Determination of Molecular Parameters.
PB95-175048 *00,992*

BROWN, L.

Laser Ablation of Thin Films as a Free Atom Source for Pulsed RIMS.
PB94-198710 *00,540*

BROWN, M. A.

Economic, Energy, and Environmental Impacts of the Energy-Related Inventions Program.
DE94-017162 *00,008*

BROWN, P. F.

Design Engineering Research at NIST.
PB95-267860 *02,784*

BROWN, R.

Laboratory Accreditation for Testing Energy Efficient Lighting.
PB96-122932 *00,270*

BROWN, R. S.

Diagnosis and Treatment of an Oral Base-Metal Contact Lesion Following Negative Dermatologic Patch Tests.
PB95-180626 *00,172*

BROWN, T. J.

Liquid Chromatographic Determination of Carotenoids in Human Serum Using an Engineered C30 and a C18 Stationary Phase.
PB97-119333 *03,512*

BROWN, W. E.

Critical Evaluation of the Purification of Biominerals by Hypochlorite Treatment.
PB95-150959 *00,186*

Crystal Structure of Dicalcium Potassium Trihydrogen Bis(pyrophosphate) Trihydrate.
PB94-216561 *00,152*

Octacalcium Phosphate Carboxylates IV. Kinetics of Formation and Solubility of Octacalcium Phosphate Succinate.
PB94-185600 *00,776*

Octacalcium Phosphate Carboxylates. 1. Preparation and Identification.
PB95-161535 00,660

Octacalcium Phosphate Carboxylates. 2. Characterization and Structural Consideration.
PB95-161543 00,955

Octacalcium Phosphate Carboxylates. 5. Incorporation of Excess Succinate and Ammonium Ions in the Octacalcium Phosphate Succinate Structure.
PB95-168894 00,166

Octacalcium Phosphate. 3. Infrared and Raman Vibrational Spectra.
PB94-172244 00,756

Periapical Tissue Reactions to a Calcium Phosphate Cement in the Teeth of Monkeys.
PB94-212008 00,149

Physicochemical Properties of Calcific Deposits Isolated from Porcine Bioprosthetic Heart Valves Removed from Patients Following 2-13 Years Function.
PB94-172863 00,184

Procedure for the Study of Acidic Calcium Phosphate Precursor Phases in Enamel Mineral Formation.
PB95-164448 03,564

Selective Inhibition of Crystal Growth on Octacalcium Phosphate and Nonstoichiometric Hydroxyapatite by Pyrophosphate at Physiological Concentration.
PB94-211257 00,147

BROWNING, D. F.

PC-Based Spinning Rotor Gage Controller.
PB95-175832 02,609

BROWNING, M.

Status of Electrocomposites.
PB94-212453 03,143

BROWNING, V.

Optical Conductivity of Single Crystals of Ba1-xMxBiO3(M=K, Rb, x=0.04, 0.37).
PB94-185329 04,447

BRUCE, S.

Optical Metrology and More. Programs and Services of the Radiometric Physics Division, Physics Laboratory.
PB94-191707 04,228

BRUCE, S. S.

Assessing the Credibility of the Calorific Content of Muncipal Solid Waste.
PB94-199882 02,581

Developing Quality System Documentation Based on ANSI/NCSL Z540-1-1994: The Optical Technology Division's Effort.
PB96-202122 01,869

NIST High Accuracy Scale for Absolute Spectral Response from 406 nm to 920 nm.
PB96-179122 01,865

BRUCK, E.

Magnetic Properties of Single-Crystalline UCu3Al2.
PB95-180717 04,686

BRUENING, R. J.

Overview of Radiometric Program of the NIST Thermal Imaging Laboratory.
PB94-199163 04,230

BRUNO, T. J.

Applications of the Vortex Tube in Chemical Analysis.
PB94-199171 00,544

Applications of the Vortex Tube in Chemical Analysis. Part 2. Applications.
PB96-112107 00,615

Chromatographic Cryofocusing and Cryotrapping with the Vortex Tube.
PB95-180113 00,604

Constituents and Physical Properties of the C6+ Fraction of Natural Gas. Topical Report, April-June 1994.
PB95-136644 02,483

Fugacity Coefficients of Hydrogen in (Hydrogen + Butane).
PB95-175212 02,491

High-Pressure Equilibrium Cell for Solubility Measurements in Supercritical Fluids.
PB95-175634 00,998

Measurement of Diffusion in Fluid Systems: Applications to the Supercritical Fluid Region.
PB95-175188 02,490

Measurement of Diffusion in Supercritical Fluid Systems: A Review.
PB94-199189 00,795

Permeation Tube Approach to Long-Term Use of Automatic Sampler Retention Index Standards.
PB96-167291 00,639

Process Gas Chromatography Detector for Hydrocarbons Based on Catalytic Cracking.
PB95-141099 02,485

Refractive Indices of Fluids Related to Alternative Refrigerants.
PB94-219375 03,260

Retention of Halocarbons on a Hexafluoropropylene Epoxide Modified Graphitized Carbon Black. Part 1. Methane-Based Compounds.
PB95-175196 03,272

Retention of Halocarbons on a Hexafluoropropylene Epoxide-Modified Graphitized Carbon Black. 3. Ethene-Based Compounds.
PB96-167309 03,286

Retention of Halocarbons on a Hexafluoropropylene Epoxide-Modified Graphitized Carbon Black. 4. Propane-Based Compounds.
PB96-164033 03,284

Simple and Efficient Low-Temperature Sample Cell for Infrared Spectrophotometry.
PB94-199197 00,545

Simple and Efficient Methane-Marker Devices for Chromatographic Samples.
PB96-164041 00,635

Simple, Inexpensive Apparatus for Sample Concentration.
PB94-199205 00,546

Solubilities of Copper(II) and Chromium(III) beta-Diketonates in Supercritical Carbon Dioxide.
PB96-164215 01,147

Solubility Measurement by Direct Injection of Supercritical-Fluid Solutions into a HPLC System.
PB95-175626 00,997

Summary of the Patent Literature of Supercritical Fluid Technology.
PB94-199213 00,502

Supercritical Fluid Extraction of Biological Products.
PB95-175204 00,040

Thermophysical Properties of Fluids for the Gas Industry.
PB96-122437 02,494

Thermophysical Properties of Fluids for the Gas Industry. Final Report, February 1, 1988-August 31, 1993.
PB94-146677 02,472

Thermophysical Property Data for Supercritical Fluid Extraction Design.
PB94-199221 00,668

BRUSCHKE, M. V.

Report on the Workshop on Manufacturing Polymer Composites by Liquid Molding. Held in Gaithersburg, Maryland on September 20-22, 1993.
PB94-160066 03,131

BRUSH, L. N.

Laser Melting of Thin Silicon Films.
PB94-199239 04,471

BRUSIL, P.

Integrated Network Management.
PB94-199247 01,583

BRUST, J.

Excitation Transfer in Barium by Collisions with Noble Gases.
PB96-200274 01,163

BRYANT, G. W.

Excitons in Complex Quantum Nanostructures.
PB97-118343 01,184

Quantum Dots in Quantum Well Structures.
PB97-118350 01,185

Theory for Quantum-Dot Quantum Wells: Pair Correlation and Internal Quantum Confinement in Nanoheterostructures.
PB96-179445 02,437

BRYDEN, W.

Incorporation of Gold into YBa2Cu3O7: Structure and Tc Enhancement.
PB94-200276 04,481

BRYNER, N. P.

Carbon Monoxide Production in Compartment Fires: Reduced-Scale Enclosure Test Facility.
PB95-231700 01,394

Ground-Based Smoke Sampling Techniques Training Course and Collaborative Local Smoke Sampling in Saudi Arabia.
PB94-143542 02,532

Radiometric Model of the Transmission Cell-Reciprocal Nephelometer.
PB95-150132 00,124

Scaling Compartment Fires: Reduced- and Full-Scale Enclosure Burns.
PB96-175708 00,224

BUCCI, E.

Positive and Negative Cooperativities at Subsequent Steps of Oxygenation Regulate the Allosteric Behavior of Multistate Sebacylhemoglobin.
PB97-119374 03,486

BUCHNEV, L. M.

Precision High Temperature Blackbodies.
PB95-140059 03,885

BUCKLEY, T. J.

All-Metal Collection System for Preparative-Scale Gas Chromatography: Purification of Low-Boiling-Point Compounds.
PB96-123435 00,619

Assessing the Credibility of the Calorific Content of Muncipal Solid Waste.
PB94-199882 02,581

Calculation of Higher Heating Values of Biomass Materials and Waste Components from Elemental Analyses.
PB94-199254 02,474

Ionization Energies, Appearance Energies and Thermochemistry of CF2O and FCO.
PB97-111538 01,179

Sulfur Dioxide Capture in the Combustion of Mixtures of Lime, Refuse-Derived Fuel, and Coal.
PB94-155587 02,534

Temperature Dependence of the Gas and Liquid Phase Ultraviolet Absorption Cross Sections of HCFC-123 (CF3CHCl2) and HCFC-142b (CH3CF2Cl).
PB96-201033 03,298

BUDNICK, J. I.

Soft-X-ray-Emission Investigation of Cobalt Implanted Silicon Crystals.
PB96-157912 04,069

Soft-X-ray-Emission Studies of Bulk Fe3Si, FeSi, and FeSi2, and Implanted Iron Silicides.
PB96-157938 04,071

BUDOWLE, B.

Resolution of DNA in the Presence of Mobility Modifying Polar and Nonpolar Compounds by Discontinuous Electrophoresis on Rehydratable Polyacrylamide Gels.
PB95-152799 00,590

BUFFA, G.

Self Broadening in the nu1 Band of NH3.
PB94-216371 00,857

BUHLER, B.

Femtosecond Time-Resolved Wave Packet Motion in Molecular Multiphoton Ionization and Fragmentation.
PB94-198611 00,790

BUIE, E. A.

Usability Engineering: Industry-Government Collaboration for System Effectiveness and Efficiency.
PB97-122287 01,514

BUIE, M. J.

Reactive Ion Etching in the Gaseous Electronics Conference RF Reference Cell.
PB96-113402 02,395

BUKOWSKI, R. W.

Analysis of the Happyland Social Club Fire with HAZARD I.
PB94-199270 00,193

Developing Rational Performance-Based Fire Safety Requirements in Model Building Codes.
PB95-175220 00,200

Earthquake and Fire in Japan: When the Threat Became a Reality.
PB95-175238 00,201

Field Modeling: Simulating the Effect of Sloped Beamed Ceilings on Detector and Sprinkler Response.
PB96-122866 01,406

Fire Codes for Global Practice.
PB96-102108 00,205

Fire Protection Engineering Tools. Simple Tools: The Equations.
PB96-156179 00,221

Fire Safety Engineering in the Pursuit of Performance-Based Codes: Collected Papers.
PB97-114482 00,235

Fire Safety of Passenger Trains: A Review of Current Approaches and of New Concepts.
PB94-152006 04,848

How to Evaluate Alternative Designs Based on Fire Modeling.
PB96-102116 00,206

New Concepts for Fire Protection of Passenger Rail Transportation Vehicles.
PB95-162046 04,850

New Concepts for Fire Protection of Passenger Rail Transportation Vehicles. (NIST Reprint).
PB95-180774 04,863

Predicting the Fire Performance of Buildings: Establishing Appropriate Calculation Methods for Regulatory Applications.
PB96-141239 00,316

Protecting Your Family from Fire.
PB96-156187 00,307

Review of Internatioanl Fire Risk Predictions Methods.
PB96-156195 00,222

Studies Assess Performance of Residential Detectors.
PB94-199262 00,290

Verification of a Model of Fire and Smoke Transport.
PB95-108718 00,357

BULJAN, S. T.

Tensile Creep of Whisker Reinforced Silicon Nitride.
PB94-211984 03,142

BULLIS, W. M.

Business and Manufacturing Motivations for the Developing of Analytical Technology and Metrology for Semiconductors.
PB96-161948 04,778

Optical Characterization of Materials and Devices for the Semiconductor Industry: Trends and Needs.
PB96-167192 02,431

Semiconductor Measurement Technology: Survey of Optical Characterization Methods for Materials, Processing, and Manufacturing in the Semiconductor Industry.
PB96-154596 02,706

BUMA, W. J.

Lowest Excited Singlet State of Isolated 1-phenyl-1,3-butadiene and 1-phenyl-1,3,5-hexatriene.
PB95-202339 01,026

BUNCH, W. R.

AMRF Composite Fabrication Workstation.
PB94-172681 *02,810*

BUNTIN, S. A.

Laser-Induced Desorption of NO from Si(111): Effects of Coverage on NO Vibrational Populations.
PB95-162319 *00,959*

Photodecomposition Dynamics of Mo(CO)6/Si(111) 7x7: CO Internal State and Translational Energy Distributions--Translation.
PB94-199288 *00,687*

Photodecomposition of Mo(CO)6/Si(111) 7x7: CO State-Resolved Evidence for Excited State Relaxation and Quenching.
PB95-180154 *01,009*

Photodesorption Dynamics of CO from Si(111): The Role of Surface Defects.
PB96-111646 *03,066*

BUR, A. J.

Fluorescence Anisotropy Measurements on a Polymer Melt as a Function of Applied Shear Stress.
PB94-199296 *01,209*

In-Line Optical Monitoring of Injection Molding.
PB94-185105 *01,201*

Observations of Shear Induced Molecular Orientation in a Polymer Melt Using Fluorescence Anisotropy Measurements.
PB94-199304 *01,210*

Observations of Shear Stress and Molecular Orientation Using Fluorescence Anisotropy Measurements.
PB94-199312 *01,211*

BURCH, D.

Parametric Study of Wall Moisture Contents Using a Revised Variable Indoor Relative Humidity Version of the 'Moist' Transient Heat and Moisture Transfer Model.
PB97-122535 *00,419*

BURCH, D. M.

Analysis of Moisture Accumulation in a Wood-Frame Wall Subjected to Winter Climate.
PB94-199320 *00,338*

Controlling Moisture in the Walls of Manufactured Housing.
PB95-105136 *00,355*

Empirical Validation of a Transient Computer Model for Combined Heat and Moisture Transfer.
PB97-111991 *00,416*

Experimental Verification of a Moisture and Heat Transfer Model in the Hygroscopic Regime.
PB97-111546 *00,309*

Heat and Moisture Transfer in Wood-Based Wall Construction: Measured versus Predicted.
PB95-200655 *00,391*

Manufactured Housing Walls That Provide Satisfactory Moisture Performance in All Climates.
PB95-178885 *00,383*

Mathematical Analysis of Practices to Control Moisture in the Roof Cavities of Manufactured Houses.
PB97-106843 *00,278*

Water-Vapor Measurements of Low-Slope Roofing Materials.
PB95-251617 *00,399*

BURDETTE, H. E.

Diffraction Imaging of Polycrystalline Materials.
PB94-198884 *02,971*

High-Temperature Furnace for In situ Small-Angle Neutron Scattering during Ceramic Processing.
PB96-148127 *03,743*

BURGES, C. J. C.

Second Census Optical Character Recognition Systems Conference.
PB94-188711 *01,832*

BURGESS, D.

Fluorinated Hydrocarbon Flame Suppression Chemistry.
PB94-185113 *01,362*

Gas Phase Reactions Relevant to Chemical Vapor Deposition: Numerical Modeling.
PB94-199346 *03,117*

Incinerability of Perchloroethylene and Chlorobenzene.
PB95-163457 *01,388*

Thin Film Thermocouples for Measurement of Wall Temperatures in Internal Combustion Engines.
PB94-172103 *01,449*

BURGESS, D. B.

Gas Phase Reactions Relevant to Chemical Vapor Deposition: Optical Diagnostics.
PB94-199338 *03,116*

BURGESS, D. R. F.

Halon Thermochemistry: 'Ab Initio' Calculations of the Enthalpies of Formation of Fluoromethanes.
PB96-175740 *03,289*

Thermochemical and Chemical Kinetic Data for Fluorinated Hydrocarbons.
PB95-260618 *01,056*

UV-Photopatterning of Alkylthiolate Monolayers Self-Assembled on Gold and Silver.
PB95-150751 *00,924*

BURK, B.

Scanning Tunneling Microscopy of the Charge-Density-Wave Structure in 1T-TaS2.
PB95-180980 *04,689*

BURKE, R. W.

Standard Reference Materials: Glass Filters as a Standard Reference Material for Spectrophotometry - Selection, Preparation, Certification, and Use of SRM 930 and SRM 1930.
PB94-188844 *00,536*

BURKETT, W.

Group 1 for the Plant Spatial Configuration STEP Application Protocol.
PB96-165402 *02,789*

BURKHOLDER, J. B.

Infrared Spectrum of OClO in the 2000/cm(-1) Region: The 2(nu sub 1) and (nu sub 1 + nu sub 3) Bands.
PB95-141032 *00,908*

Intensities and Dipole Moment Derivatives of the Fundamental Bands of (35)ClO2 and an Intensity Analysis of the nu1 Band.
PB95-141040 *00,909*

BURLINSKA, G.

Research and Development Activities in Electron Paramagnetic Resonance Dosimetry.
PB96-141288 *03,635*

BURNETT, J. H.

Double-Modulation and Selective Excitation Photoreflectance for Wafer-Level Characterization of Quantum-Well Laser Structures.
PB96-167325 *04,372*

Use of Pressure for Quantum-Well Band-Structure Characterization.
PB96-164058 *04,779*

BURNETT, K.

Numerical Solution of the Nonlinear Schroedinger Equation for Small Samples of Trapped Neutral Atoms.
PB95-202578 *03,985*

Properties of a Bose-Einstein Condensate in an Anisotropic Harmonic Potential.
PB96-204144 *04,133*

BURNS, G. W.

Assessment of Uncertainties of Thermocouple Calibrations at NIST.
PB94-152691 *03,782*

BUROW, M.

Determination of Inorganic Constituents in Marine Mammal Tissues.
PB95-152047 *00,589*

Development of Frozen Whale Blubber and Liver Reference Materials for the Measurement of Organic and Inorganic Contaminants.
PB95-151676 *00,587*

BURR, C. R.

Structural and Magnetic Properties of CuCl2 Graphite Intercalation Compounds.
PB96-119748 *03,020*

BURR, W. E.

Comparison of FDDI Asynchronous Mode and DQDB Queue Arbitrated Mode Data Transmission for Metropolitan Area Network Applications.
PB96-160452 *01,498*

NIST Workshop on the Computer Interface to Flat Panel Displays. Held in San Jose, California on January 13-14, 1994.
PB95-136388 *01,625*

Planning for the Fiber Distributed Data Interface (FDDI).
PB94-135761 *01,621*

Public Key Infrastructure Invitational Workshop. Held in McLean, Virginia on September 28, 1995.
PB96-166004 *01,616*

BURRAHM, R. W.

Evaluation of Wear Resistant Ceramic Valve Seats in Gas-Fueled Power Generation Engines. Topical Report, December 1991-April 1994.
PB95-200218 *02,466*

BURRIS, S. B.

Proficiency Tests for the NIST Airborne Asbestos Program - 1991.
PB94-193828 *00,537*

Proficiency Tests for the NIST Airborne Asbestos Program - 1992.
PB94-194362 *00,539*

BURRISS, W. L.

Cryogenic Materials Data Handbook.
AD-A286 675/4 *03,303*

BURROUGHS, C. J.

Automated Josephson Integrated Circuit Test System.
PB95-175246 *02,057*

Experimental Results on Single Flux Quantum Logic.
PB95-175071 *02,053*

Josephson D/A Converter with Fundamental Accuracy.
PB96-148044 *02,418*

Performance and Reliability of NIST 10-V Josephson Arrays.
PB96-148051 *02,419*

Superconducting Integrated Circuit Fabrication with Low Temperature ECR-Based PECVD SiO2 Dielectric Films.
PB96-103015 *04,719*

BURROUGHTS, C. J.

Optimization of ECR-Based PECVD Oxide Films for Superconducting Integrated Circuit Fabrication.
PB95-169165 *02,051*

BURROWS, J. H.

Information Technology Standards in a Changing World: The Rose of the Users.
PB96-160866 *02,737*

BURTON, B. P.

Ca4Bi6O13: A Compound Containing an Unusually Low Bismuth Coordination Number and Short Bi Bi Contacts.
PB95-141131 *00,911*

LMTO/CVM and LAPW/CVM Calculations of the Nickel Aluminide/Nickel Titanium Pseudobinary Phase Diagram.
PB94-199353 *03,323*

Ordered omega-Derivatives in a Ti-37.5Al-2ONb at% Alloy.
PB94-211091 *03,331*

Phase Equilibria in the Systems CaO-CuO and CaO-Bi2O3.
PB95-140570 *03,048*

BURTON, R.

Real Time Compensation for Tool Form Errors in Turning Using Computer Vision.
PB95-107231 *02,945*

BUSATTO, G.

Experimental Study of Reverse-Bias Failure Mechanisms in Bipolar Mode JFET (BMFET).
PB95-152997 *02,340*

BUSCHE, R. M.

Opportunities for Innovation: Biotechnology.
PB94-157831 *00,009*

BUSCHOW, K. H. J.

Crystallographic and Magnetic Properties of UAuSn.
PB95-140521 *04,543*

Incommensurate Magnetic Order in UPtGe.
PB95-140513 *04,542*

Magnetic Properties of Single-Crystalline UCu3Al2.
PB95-180717 *04,686*

BUSH, M. T.

Effect of CF3H and CF3Br on Laminar Diffusion Flames in Normal and Microgravity.
PB96-161831 *01,420*

Effect of CF3H and CF3Br on Laminar Diffusion Flames in Normal and Microgravity.
PB96-161849 *01,421*

BUSHBY, S. T.

Testing Conformance and Interoperability of BACnet (Trade Name) Building Automation Products.
PB97-111553 *00,310*

BUSSIBA, A.

Charpy Specimen Tests at 4 K.
PB96-190335 *03,002*

BUTCHER, K.

Checking the Net Contents of Packaged Goods as Adopted by the 79th National Conference on Weights and Measures, 1994, Third Edition, Supplement 4.
PB95-182226 *00,484*

BUTCHER, K. S.

Uniform Laws and Regulations in the Areas of Legal Metrology and Motor Fuel Quality as Adopted by the 80th National Conference on Weights and Measures 1995. 1996 Edition.
PB96-172309 *02,927*

Uniform Laws and Regulations in the Areas of Legal Metrology and Motor Fuel Quality, 1994 as Adopted by the 79th National Conference on Weights and Measures 1994.
PB95-174470 *02,909*

BUTCHER, T. G.

NIST Handbook 44, 1994: Specifications, Tolerances and Other Technical Requirements for Weighing and Measuring Devices as Adopted by the 78th National Conference on Weights and Measures 1993.
PB94-136009 *02,888*

NIST Handbook 44, 1995: Specifications, Tolerances and Other Technical Requirements for Weighing and Measuring Devices as Adopted by the 79th National Conference on Weights and Measures 1994.
PB95-146379 *02,903*

NIST Handbook 44, 1996: Specifications, Tolerances, and Other Technical Requirements for Weighing and Measuring Devices as Adopted by the 80th National Conference on Weights and Measures, 1995.
PB96-166616 *02,926*

BUTLER, B. D.

Dynamic Scaling in an Aggregating 2D Lennard-Jones System.
PB96-167317 *04,106*

BUTLER, C. J.

Dynamic Phenomena on the RS Canum Venaticorum Binary II Pegasi in August 1989. 1. Observational Data.
PB94-211067 *00,056*

BUTLER, E. P.

Determination of Fiber-Matrix Interfacial Properties of Importance to Ceramic Composite Toughening.
PB95-125811 *03,149*

Interface Properties for Ceramic Composites from a Single Fiber Pull-Out Test.
PB94-199361 *03,135*

Micro-Mechanical Aspects of Asperity-Controlled Friction in Fiber-Toughened Ceramic Composites.
PB94-199536 *03,136*

BUTLER, J. J.

Calibration in the Earth Observing System (EOS) Project. Part 2. Implementation.
PB97-112213 *04,842*

Organization and Implementation of Calibration in the EOS Project. Part 1.
PB96-179437 *04,841*

BUTLER, K. M.

Heat Transfer in an Intumescent Material Using a Three-Dimensional Lagrangian Model.
PB96-164066 *00,408*

BUTLER, T. A.

Preparation and Certification of a Rhodium Standard Reference Material Solution.
PB94-185071 *00,529*

BUTTERBAUGH, J. W.

Gaseous Electronics Conference Radio-Frequency Reference Cell: A Defined Parallel-Plate Radio-Frequency System for Experimental and Theoretical Studies of Plasma-Processing Discharges.
PB94-172327 *04,404*

BUXTON, G. V.

Critical Review of Rate Constants for Reactions of Transients from Metal Ions and Metal Complexes in Aqueous Solution.
PB96-145859 *01,109*

BYRAM, S. K.

Using NIST Crystal Data within Siemens Software for Four-Circle and SMART CCD Diffractometers.
PB97-109110 *04,803*

BYRD, E.

Degradation of Powder Epoxy Coated Panels Immersed in a Saturated Calcium Hydroxide Solution Containing Sodium Chloride.
PB96-101050 *01,344*

Development of a Method for Measuring Water-Stripping Resistance of Asphalt/Siliceous Aggregate Mixtures.
PB96-197249 *01,348*

Development of a Method for Measuring Water-Stripping Resistance of Asphalt/Siliceous Aggregate Mixtures.
PB96-202296 *01,329*

Development of a Test Method for Leaching of Lead from Lead-Based Paints Through Encapsulants.
PB96-154984 *03,128*

Materials-Science Based Approach to Phenol Emissions from a Flooring Material in an Office Building.
PB97-118749 *02,572*

Source of Phenol Emissions Affecting the Indoor Air of an Office Building.
PB94-154382 *03,600*

BYRD, G. D.

Determination of 3-Quinuclidinyl Benzilate (Qnb) and Its Major Metabolites in Urine by Isotope Dilution Gas Chromatography Mass Spectrometry.
PB94-199379 *03,492*

BYRNE, J.

Preparation and Characterization of (6)LiF and (10)B Reference Deposits for the Measurement of the Neutron Lifetime.
PB95-108692 *03,874*

Problems Related to the Determination of Mass Densities of Evaporated Reference Deposits.
PB95-163226 *03,941*

BYRNE, P. B.

Dynamic Phenomena on the RS Canum Venaticorum Binary II Pegasi in August 1989. 1. Observational Data.
PB94-211067 *00,056*

Observing Stellar Coronae with the Goddard High Resolution Spectrograph. I. The dMe Star AU Microscopii.
PB96-102777 *00,092*

Rotational Modulation and Flares on RS Canum Venaticorum and BY Draconis Stars. XVI. IUE Spectroscopy and VLA Observations of C1182(=V 1005 Orionis) in October 1983.
PB94-185626 *00,050*

CABEZAS, H.

Statistical Thermodynamics of Phase Separation and Ion Partitioning in Aqueous Two-Phase Systems.
PB94-199387 *01,212*

CABLE, J. S.

One Gigarad Passivating Nitrided Oxides for 100% Internal Quantum Efficiency Silicon Photodiodes.
PB94-185485 *02,119*

CABRERA, B.

Hot-Electron Microcalorimeter for X-ray Detection Using a Superconducting Transition Edge Sensor with Electrothermal Feedback.
PB96-200399 *04,792*

Noise Reduction in Low-Frequency SQUID Measurements with Laser-Driven Switching.
PB96-135165 *02,081*

Self-Biasing Cryogenic Particle Detector Utilizing Electrothermal Feedback and a SQUID Readout.
PB96-102538 *04,712*

Trapped Vortices in a Superconducting Microbridge.
PB95-141149 *04,554*

CACCIUTTOLO, M. A.

Formation of DNA-Protein Cross-Links in Cultured Mammalian Cells Upon Treatment with Iron Ions.
PB96-137724 *03,651*

CACIARI, M.

Retention of Halocarbons on a Hexafluoropropylene Epoxide Modified Graphitized Carbon Black. Part 1. Methane-Based Compounds.
PB95-175196 *03,272*

Retention of Halocarbons on a Hexafluoropropylene Epoxide-Modified Graphitized Carbon Black. 3. Ethene-Based Compounds.
PB96-167309 *03,286*

Retention of Halocarbons on a Hexafluoropropylene Epoxide-Modified Graphitized Carbon Black. 4. Propane-Based Compounds.
PB96-164033 *03,284*

CAGAN, J.

HVAC CAD Layout Tools: A Case Study of University/Industry Collaboration.
PB97-112221 *00,281*

CAGE, M. E.

Anomalous Behavior of a Quantized Hall Plateau in a High-Mobility Si Metal-Oxide-Semiconductor Field-Effect Transistor.
PB95-164174 *02,354*

Design Challenges in a Commercial Quantum Hall Effect-Based Resistance Standard.
PB95-171419 *02,263*

Evidence That Voltage Rather Than Resistance is Quantized in Breakdown of the Quantum Hall Effect.
PB96-179163 *01,868*

Potential and Current Distributions Calculated Across a Quantum Hall Effect Sample at Low and High Currents.
PB96-122106 *04,045*

Precision Tests of a Quantum Hall Effect Device DC Equivalent Circuit Using Double-Series and Triple-Series Connections.
PB96-159256 *01,953*

Quantized Dissipation of the Quantum Hall Effect at High Currents.
PB94-199395 *04,472*

Sources of Uncertainty in a DVM-Based Measurement System for a Quantized Hall Resistance Standard.
PB94-219334 *01,884*

Spectroscopic Study of Quantized Breakdown Voltage States of the Quantum Hall Effect.
PB96-113584 *04,730*

Using Quantized Breakdown Voltage Signals to Determine the Maximum Electric Fields in a Quantum Hall Effect Sample.
PB95-261947 *02,375*

CAHN, J. W.

Anisotropy of Interfaces in an Ordered Alloy: A Multiple-Order-Parameter Model.
PB96-131594 *04,741*

Evolution Equations for Phase Separation and Ordering in Binary Alloys.
PB96-119243 *02,979*

Exponentially Rapid Coarsening and Buckling in Coherently Self-Stressed Thin Plates.
PB95-202347 *04,821*

Linking Anisotropic Sharp and Diffuse Surface Motion Laws via Gradient Flows.
PB95-203378 *04,698*

Microstructural Evolution in Two-Dimensional Two-Phase Polycrystals.
PB94-211992 *04,498*

Modeling the Evolution of Structure in Unstable Solid Solution Phases by Diffusional Mechanisms.
PB94-199403 *03,324*

Neutron Scattering Structural Study of AlCuFe Quasicrystals Using Double Isotopic Substitution.
PB94-200458 *04,485*

Numerical Simulation of Submicron Photolithographic Processing.
PB94-198561 *02,310*

RDFs and Fe-Fe Pair Correlations in an AlCuFe Icosahedral Alloy by Double Isotopic Substitution.
PB94-172129 *04,439*

Singularities in Minimum Surface Energy Problems and Their Influence in Surface Motion.
PB94-199411 *04,473*

Stability, Microstructural Evolution, Grain Growth, and Coarsening in a Two-Dimensional Two-Phase Microstructure.
PB94-199429 *03,325*

CAI, H.

Deformation and Fracture of Mica-Containing Glass-Ceramics in Hertzian Contacts.
PB96-179452 *03,080*

Flaw Tolerance and Toughness Curves in Two-Phase Particulate Composites: SiC/Glass System.
PB96-179460 *03,081*

Indentation Fatigue: A Simple Cyclic Hertzian Test for Measuring Damage Accumulation in Polycrystalline Ceramics.
PB96-180013 *03,084*

Model for Microcrack Initiation and Propagation beneath Hertzian Contacts in Polycrystalline Ceramics.
PB96-163704 *03,077*

CAI, X. Y.

Electromagnetic Coupling Character of (001) Twist Boundaries in Sintered Bi2Sr2CaCu2O8+x Bicrystals.
PB96-176573 *01,963*

Weak-Link-Free Behavior of High Angle YBa2Cu3O7-x Grain Boundaries in High Magnetic Fields.
PB94-198421 *04,459*

CAILLAULT, J. P.

IUE Observations of Solar-Type Stars in the Pleiades and the Hyades.
PB94-199437 *00,053*

CAIRELLI, S. G.

Documentation for Immediately Dangerous to Life or Health Concentrations (IDLHs).
PB94-195047 *03,602*

CAKIROGLU, F.

Comparisons of Some NIST Fixed-Point Cells with Similar Cells of Other Standards Laboratories.
PB97-119242 *00,655*

CALCOTT, T. A.

Improved Reflectometry Facility at the National Institute of Standards and Technology.
PB96-160338 *04,087*

New NIST/ARPA National Soft X-ray Reflectometry Facility.
PB96-158092 *04,080*

CALEDONIA, G. E.

Collision-Induced Emission in the Fundamental Vibration-Rotation Band of H2.
PB94-199445 *03,811*

CALHOUN, J. M.

Assay of the Eluent from the Alumina-Based Tungsten-188-Rhenium-188 Generator.
PB94-200482 *03,829*

Liquid-Scintillation Counting Techniques for the Standardization of Radionuclides Used in Therapy.
PB97-110084 *03,709*

Radioassays of Yttrium-90 Used in Nuclear Medicine.
PB97-110100 *03,522*

Review of the USCEA/NIST Measurement Assurance Program for the Nuclear Power Industry.
PB95-126272 *03,712*

System for Intercomparing Standard Solutions of Beta-Particle Emitting Radionuclides.
PB96-159637 *03,707*

CALLAHAN, A. P.

Assay of the Eluent from the Alumina-Based Tungsten-188-Rhenium-188 Generator.
PB94-200482 *03,829*

CALLCOTT, T. A.

Al L2,3 Core Excitons in AlxGa1-x as Studied by Soft-X-ray Reflection and Emission.
PB96-157839 *04,067*

Barium Contributions to the Valence Electronic Structure of YBa2Cu3O7-delta, PrBa2Cu3O7-delta, and Other Barium-Containing Compounds.
PB96-158019 *04,076*

Charge-Transfer-Induced Multiplet Structure in the N4,5O2,3 Soft-X-ray Emission Spectrum of Lanthanum.
PB96-163746 *04,102*

Cooper M(sub II,III) X-ray-Emission Spectra of Copper Oxides and the Bismuth Cuprate Superconductor.
PB96-158027 *04,077*

Intermediate Coupling in L2-L3 Core Excitons of MgO, Al2O3, and SiO2.
PB96-158043 *04,079*

Laser-Synchrotron Hybrid Experiments: A Photon to Tickle, A Photon to Poke.
PB96-157847 *03,704*

Local Partial Densities of States in Ni and Co Silicides Studied by Soft X-Ray Emission Spectroscopy.
PB94-212412 *04,504*

Phonon Relaxation in Soft-X-ray Emission of Insulators.
PB96-160296 *04,085*

Simple Variable Line Space Grating Monochromator for Synchrotron Light Source Beamlines.
PB96-156203 *04,065*

Soft-X-ray-Emission Investigation of Cobalt Implanted Silicon Crystals.
PB96-157912 *04,069*

Soft-X-ray-Emission Spectra of Solid Kr and Xe.
PB96-157920 *04,070*

Soft-X-ray-Emission Studies of Bulk Fe3Si, FeSi, and FeSi2, and Implanted Iron Silicides.
PB96-157938 *04,071*

CALM, J. M.

Report of the Refrigeration, Air Conditioning and Heat Pumps Technical Options Committee.
PB96-176755 *03,293*

CALSOU, P.
Modification of Deoxyribose-Phosphate Residues by Extracts of Ataxia Telangiectasia Cells.
PB94-212602 *03,458*

CALVANO, N. J.
Study to Determine the Most Important Parameters for Evaluating the Resistance of Soft Body Armor to Penetration by Edged Weapons.
PB94-158573 *03,757*

CALVAYRAC, Y.
Neutron Scattering Structural Study of AlCuFe Quasicrystals Using Double Isotopic Substitution.
PB94-200458 *04,485*

RDFs and Fe-Fe Pair Correlations in an AlCuFe Icosahedral Alloy by Double Isotopic Substitution.
PB94-172129 *04,439*

CAMELL, D.
Standard Source Method for Reducing Antenna Factor Errors in Shielded Room Measurements.
PB96-183157 *02,013*

CAMELL, D. G.
Assessment of Data by a Second-Order Transfer Function.
PB95-182390 *03,760*

Data Evaluation of a Linear System by a Second-Order Transfer Function.
PB96-200282 *01,970*

Measurements of Shielding Effectiveness and Cavity Characteristics of Airplanes.
PB94-210051 *00,030*

Radiated Emissions and Immunity of Microstrip Transmission Lines: Theory and Measurements.
PB96-162649 *02,238*

TEM/Reverberating Chamber Electromagnetic Radiation Test Facility at Rome Laboratory.
PB96-155023 *03,675*

CAMERON, J. M.
Churchill Eisenhart, 1913-1994.
PB96-137740 *03,447*

CAMPANA, C. F.
Using NIST Crystal Data within Siemens Software for Four-Circle and SMART CCD Diffractometers.
PB97-109110 *04,803*

CAMPBELL, D.
Effect of Three Sterilization Techniques on Finger Pluggers.
PB94-216090 *00,150*

CAMPBELL, E. J.
Experimental Studies of Line Shapes from a Balle-Flygare Spectrometer.
PB94-199452 *00,796*

CAMPISI, G. J.
Electron and Hole Trapping in Irradiated SIMOX, ZMR and BESOI Buried Oxides.
PB96-160320 *01,956*

CAMUS, P. P.
Performance of a Reflectron Energy Compensating Mirror.
PB94-199460 *00,547*

CAMUS, T. A.
Calculating Time-to-Contact Using Real-Time Quantized Optical Flow.
PB95-210522 *01,604*

CANALES, N.
Planar Near-Field Measurements and Microwave Holography for Measuring Aperture Distribution on a 60 GHz Active Array Antenna.
PB96-167366 *03,762*

CANDELA, G. T.
Bringing Natural Language Information Retrieval Out of the Closet.
PB94-172335 *02,720*

Comparison of FFT Fingerprint Filtering Methods for Neural Network Classification.
PB95-136362 *01,840*

NIST Form-Based Handprint Recognition System.
PB94-217106 *01,838*

PCASYS: A Pattern-Level Classification Automation System for Fingerprints.
PB95-267936 *01,853*

CANEAU, C.
Range Statistics and Rutherford Backscattering Studies on Fe-Implanted In0.53Ga0.47As.
PB95-126397 *04,535*

CANFIELD, L. R.
One Gigarad Passivating Nitrided Oxides for 100% Internal Quantum Efficiency Silicon Photodiodes.
PB94-185485 *02,119*

Silicon Photodiodes Optimized for EUV and Soft X-Ray Regions.
PB94-199478 *02,124*

Stable Silicon Photodiodes for Absolute Intensity Measurements in the VUV and Soft X-ray Regions.
PB97-110175 *04,135*

CANTILLO, A.
National Status and Trends Program Specimen Bank: Sampling Protocols, Analytical Methods, Results, and Archive Samples.
PB97-119226 *02,598*

CAO, G.
Magnetic Ordering of the Cu Spins in PrBa2Cu3O6+x.
PB95-140547 *04,545*

CAO, L. X.
Determination of Surface Roughness from Scattered Light.
PB94-216520 *04,243*

CAPPARELLI, R.
Displacement Method for Machine Geometry Calibration.
PB95-152088 *02,946*

CAPPELLETTI, R. L.
Phase Transitions in Solid C70: Supercooling, Metastable Phases, and Impurity Effect.
PB95-150090 *00,914*

Rotational Dynamics of Solid C70: A Neutron-Scattering Study.
PB94-172178 *00,755*

Rotational Dynamics of Solid C70: A Neutron-Scattering Study.
PB95-153219 *00,949*

CAPPONI, J. J.
Crystal Structure of Pb2Sr2YCu3O8+delta with delta=1.32, 1.46, 1.61, 1.71, by Powder Neutron Diffraction.
PB94-216314 *04,518*

CARASSO, A. S.
Image Restoration and Diffusion Processes.
PB95-153003 *01,843*

Infinite Divisibility and the Identification of Singular Waveforms.
PB94-172111 *02,701*

Overcoming Hoelder Continuity in Ill-Posed Continuation Problems.
PB95-202354 *03,416*

Slow Evolution from the Boundary: A New Stabilizing Constraint in Ill-Posed Continuation Problems.
PB96-122858 *03,418*

Slowly Divergent Space Marching Schemes in the Inverse Heat Conduction Problem.
PB94-199486 *03,812*

CAREY, C. M.
Cyclic Polyamine Ionophore for Use in a Dibasic Phosphate-Selective Electrode.
PB95-180121 *01,008*

Distribution of Fluoride in Saliva and Plaque Fluid After a 0.048 mol/L NaF Rinse.
PB95-151205 *03,561*

Intensive Swimming: Can It Affect Your Patients' Smiles.
PB96-123666 *03,570*

CARINO, N.
Northridge Earthquake, 1994. Performance of Structures, Lifelines and Fire Protection Systems.
PB94-161114 *00,421*

Northridge Earthquake 1994: Performance of Structures, Lifelines, and Fire Protection Systems.
PB94-207461 *04,825*

Performance of HUD-Affiliated Properties during the January 17, 1994 Northridge Earthquake.
PB95-174488 *00,443*

CARINO, N. J.
Detection of Voids in Grouted Ducts Using the Impact-Echo Method.
PB94-185121 *01,306*

Effects of Testing Variables on the Measured Compressive Strength of High-Strength (90 MPa) Concrete.
PB95-179040 *00,445*

Effects of Testing Variables on the Strength of High-Strength (90 Mpa) Concrete Cylinders.
PB96-112198 *00,456*

High-Performance Concrete: Research Needs to Enhance Its Use.
PB95-180147 *01,322*

Maturity Functions for Concrete Made with Various Cements and Admixtures.
PB94-199502 *01,314*

Maturity Method.
PB94-199494 *01,313*

Nondestructive Testing of Concrete: History and Challenges.
PB95-180139 *00,385*

Prediction of Cracking in Reinforced Concrete Structures.
PB95-220448 *03,725*

Prediction of Potential Concrete Strength at Later Ages.
PB96-112180 *01,324*

Recent Development in Nondestructive Testing of Concrete.
PB96-122445 *01,325*

Shear Design of High-Strength Concrete Beams: A Review of the State-of-the-Art.
PB96-214713 *01,330*

CARLSON, A. D.
Intermediate Structure in the Neutron-Induced Fission Cross Section of 236U.
PB94-185741 *03,802*

Measurements of the (235)U(n,f) Cross Section in the 3 to 30 MeV Neutron Energy Region.
PB97-119051 *04,172*

Measurements of the (237)Np(n,f) Cross Section.
PB97-119069 *04,173*

Neutron Standard Cross Sections in Reactor Physics: Need and Status.
PB94-199510 *03,813*

CARLSON, N. M.
Ultrasonic Sensing of GMAW: Laser/EMAT Defect Detection System.
PB96-186028 *02,878*

CARLSSON, A.
Lattice Imperfections Studied by Use of Lattice Green's Functions.
PB95-150850 *04,576*

CARLSSON, A. E.
Dislocation Core-Core Interaction and Peierls Stress in a Model Hexagonal Lattice.
PB96-162003 *04,101*

CARMICAL, J. R.
Novel DNA N-Glycosylase Activity of E. coli T4 Endonuclease V That Excises 4,6-Diamino-5-Formamidopyrimidine from DNA, a UV-Radiation- and Hydroxyl Radical-Induced Product of Adenine.
PB96-160478 *03,549*

CARNAHAN, L.
Security in Open Systems.
PB95-105383 *01,473*

CARNAHAN, L. J.
Guideline for the Analysis of Local Area Network Security. Category: Computer Security; Subcategory: Risk Analysis and Contingency Planning.
FIPS PUB 191 *01,799*

Keeping Your Site Comfortably Secure: An Introduction to Internet Firewalls.
PB95-182275 *02,730*

CARNEY, D.
Next Generation Computer Resources: Reference Model for Project Support Environments (Version 2.0).
PB94-143401 *01,677*

CARO, T.
Evaluation of Survey Procedures for Determining Occupant Load Factors in Contemporary Office Buildings.
PB97-116222 *00,238*

CARO, T. C.
Survey of Fuel Loads in Contemporary Office Buildings.
PB97-114235 *00,233*

CAROSELLA, C. A.
Effect of Beam Voltage on the Properties of Aluminum Nitride Prepared by Ion Beam Assisted Deposition.
PB97-118616 *01,995*

CARPENTER, J. A.
Dielectric Properties Measurements and Data.
PB94-172186 *01,876*

Measurements of Properties of Materials in Electronic Packaging.
PB96-200837 *01,973*

NIST/NCMS Program on Electronic Packaging: First Update.
PB96-204086 *03,008*

Overview of U.S. Government Advanced Packaging Programs.
PB96-200845 *02,443*

Photonic Materials: A Report on the Results of a Workshop. Held in Gaithersburg, Maryland on August 26-27, 1992, Volume 1.
PB94-152733 *02,114*

CARPENTER, K. G.
First Results from the Goddard High-Resolution Spectrograph: The Chromosphere of Tauri.
PB94-199528 *00,054*

GHRS Observations of Cool, Low-Gravity Stars. 1. The Far-Ultraviolet Spectrum of alpha Orions (M2 Iab).
PB96-112016 *00,094*

Observations of 3C 273 with the Goddard High Resolution Spectrograph on the Hubble Space Telescope.
PB95-202321 *00,076*

Observing Stellar Coronae with the Goddard High Resolution Spectrograph. I. The dMe Star AU Microscopii.
PB96-102777 *00,092*

CARR, G. L.
Laser-Synchrotron Hybrid Experiments: A Photon to Tickle, A Photon to Poke.
PB96-157847 *03,704*

CARR, P. J.
Validation Testing System Requirements. National PDES Testbed Report Series.
PB94-163482 *02,771*

CARROLL, L.
Two New Probes for a Coordinate Measuring Machine.
PB95-163093 *02,653*

CARTER, W.
Effect of Axial Strain on the Critical Current of Ag-Sheathed Bi-Based Superconductors in Magnetic Fields Up to 25 T.
PB94-211315 *04,493*

CARTER, W. C.
Determination of Fiber-Matrix Interfacial Properties of Importance to Ceramic Composite Toughening.
PB95-125811 *03,149*

Micro-Mechanical Aspects of Asperity-Controlled Friction in Fiber-Toughened Ceramic Composites.
PB94-199536 03,136

Transient Subcritical Crack-Growth Behavior in Transformation-Toughened Ceramics.
PB94-200656 03,038

CARTWRIGHT, A. N.

Interdigitated Stacked P-I-N Multiple Quantum Well Modulator.
PB97-112296 02,455

Scaling of the Nonlinear Optical Cross Sections of GaAs-AlGaAs Multiple Quantum-Well Hetero n-i-p-i's.
PB96-102793 02,183

CARVER, G. P.

Federal Metric Progress in 1993.
PB94-196029 02,600

Metric for Success.
PB94-187630 02,633

Metric Path to Global Markets and New Jobs: A Question-and-Answer and Thematic Discussion.
PB94-206307 02,601

Metrication.
PB94-172079 03,676

METRICATION: An Economic Wake-Up Call for Surveyors and Mappers.
PB96-159629 03,680

Program of the Manufacturing Engineering Laboratory, 1995. Infrastructural Technology, Measurements, and Standards for the U.S. Manufacturing Industries.
PB95-188835 02,754

CASASSA, M. P.

Fragment Energy and Vector Correlations in the Overtone-Pumped Dissociation of HN3X(1)A'.
PB94-199908 00,802

Fragment State Correlations in the Dissociation of NO.HF(v=1).
PB95-164430 00,982

Product Kinetic Energies, Correlations, and Scattering Anisotropy in the Bimolecular Reactor O((1)D)+H2O yields 2OH.
PB94-212792 00,838

Product State Correlations in the Reaction of O((1)D) and H2O in Bimolecular Collisions and in O3.H2O Clusters--Translation.
PB95-153011 00,946

Vibrational Predissociation Dynamics of Overtone-Excited HN3.
PB95-125720 00,691

CASELLA, R. C.

Roles of Local Classical Acceleration and Spatial Separation in the Neutral Particle Analogs of the Aharonov-Bohm Phases.
PB95-202362 03,976

CASEY, S. M.

Laser Vacuum Ultraviolet Single Photon Ionization Probing of III-V Semiconductor Growth.
PB95-202370 04,691

Single Photon Ionization, Laser Optical Probe Technique for Semiconductor Growth.
PB95-202776 01,032

CASHMAN, J. R.

Histopathology, Blood Chemistry, and Physiological Status of Normal and Moribund Striped Bass ('Morone saxatilis') Involved in Summer Mortality ('Die-Off') in the Sacramento-San Joaquin Delta of California.
PB94-198157 00,034

CASKEY, G.

Interim Testing Artifact (ITA): A Performance Evaluation System for Coordinate Measuring Machines (CMMs). User Manual.
PB95-210589 02,914

NIST SRM 9983 High-Rigidity Ball-Bar Stand. User Manual.
PB95-255840 02,669

Two New Probes for a Coordinate Measuring Machine.
PB95-163093 02,653

CASKEY, G. W.

User's Guide to NIST SRM 2084: CMM Probe Performance Standard.
PB94-206109 02,709

CASS, G. R.

Sources of Urban Contemporary Carbon Aerosol.
PB95-175659 02,551

CASSEL, K. W.

Gravity-Current Transport in Building Fires.
PB96-147046 01,415

Transport by Gravity Currents in Building Fires.
PB97-119325 01,441

CASSIDY, M. M.

Field Evaluation of the System for Calibration of the Marshall Compaction Hammer.
PB95-190674 01,323

System for Calibration of the Marshall Compaction Hammer.
PB94-145661 01,303

CASTLES, S.

Hot-Electron Microcalorimeters for X-ray and Phonon Detection.
PB95-168993 04,644

CASWELL, R. S.

Measurement of Absorbed Dose of Neutrons, and of Mixtures of Neutrons and gamma rays.
AD-A286 647/3 03,710

Microdosimetry and Cellular Radiation Effects of Radon Progency in Human Bronchial Airways.
PB95-152344 03,625

Monte Carlo and Analytic Methods in the Transport of Electrons, Neutrons, and Alpha Particles.
PB96-111612 04,033

Neutron Energy Deposition on the Nanometer Scale.
PB95-152260 03,624

Neutron Measurement Intercomparisons Sponsored by CCEMRI, Section 3 (Neutron Measurements).
PB94-199916 03,819

Radon in the Lung.
PB97-110035 03,638

Systematics of Alpha-Particle Energy Spectra and Lineal Energy (Y) Spectra for Radon Daughters.
PB94-185139 03,615

CATICHA, A.

Diffraction of X-rays at the Far Tails of the Bragg Peaks.
PB94-199924 04,476

CATRON, B. A.

Generic Manufacturing Controllers.
PB94-199940 02,818

Implementing a Transition Manager in the AMRF Cell Controller.
PB94-199932 02,817

CAVA, R. J.

Crystal Structure of Pb2Sr2YCu3O8+delta with delta=1.32, 1.46, 1.61, 1.71, by Powder Neutron Diffraction.
PB94-216314 04,518

Neutron Powder Diffraction Study of the Crystal Structure of YSr2AlCu2O7.
PB94-212073 04,499

Neutron Powder Diffraction Study of the Structures of La1.9Ca1.1Cu2O6 and La1.9Sr1.1Cu2O6+Delta.
PB95-140042 04,538

Observation of Oscillatory Magnetic Order in the Antiferromagnetic Superconductor HoNi2B2C.
PB95-180303 04,679

CAVALLI, A. R.

Formal Methods in Conformance Testing: Result and Perspectives.
PB95-153029 01,710

CAVANAGH, R. R.

Characterization of the Interaction of Hydrogen with Iridium Clusters in Zeolites by Inelastic Neutron Scattering Spectroscopy.
PB95-180741 01,013

Dynamics of Nonthermal Reactions: Femtosecond Surface Chemistry.
PB94-199965 00,688

Hot Carrier Excitation of Adlayers: Time-Resolved Measurement of Adsorbate-Lattice Coupling.
PB94-172285 00,758

Laser-Induced Desorption of NO from Si(111): Effects of Coverage on NO Vibrational Populations.
PB95-162319 00,959

Neutron and Raman Spectroscopies of 134 and 134a Hydrofluorocarbons Encaged in Na-X Zeolite.
PB96-186168 03,001

Photodecomposition Dynamics of Mo(CO)6/Si(111) 7x7: CO Internal State and Translational Energy Distributions--Translation.
PB94-199288 00,687

Photodecomposition of Mo(CO)6/Si(111) 7x7: CO State-Resolved Evidence for Excited State Relaxation and Quenching.
PB95-180154 01,009

Photodesorption Dynamics of CO from Si(111): The Role of Surface Defects.
PB96-111646 03,066

Picosecond Measurement of Substrate-to-Adsorbate Energy Transfer: The Frustrated Translation of CO/Pt(111)--Translation.
PB95-126041 00,895

Time-Resolved Measurements of Energy Transfer at Surfaces.
PB95-141198 00,913

Time-Resolved Measurements of Energy Transfer at Surfaces.
PB95-153037 00,947

Time-Resolved Probes of Surface Dynamics.
PB94-199957 00,803

Ultrafast Time-Resolved Infrared Probing of Energy Transfer at Surfaces.
PB96-123443 00,620

Vibrational Relaxation Measurements of Carbon Monoxide on Metal Clusters.
PB94-211810 00,820

CAVCEY, K. H.

Crosstalk between Microstrip Transmission Lines.
PB94-135639 02,210

Crosstalk between Microstrip Transmission Lines. (NIST Reprint).
PB95-180337 02,225

Radiated Emissions and Immunity of Microstrip Transmission Lines: Theory and Measurements.
PB96-162649 02,238

CAVICCHI, R.

Reactivity of Pd and Sn Adsorbates on Plasma and Thermally Oxidized SnO2(110).
PB94-199973 00,804

CAVICCHI, R. E.

Tin Oxide Gas Sensor Fabricated Using CMOS Micro-Hotplates and In-situ Processing.
PB95-150603 00,580

CELEBI, M.

Comparison of Responses of a Select Number of Buildings to the 10/17/1989 Loma Prieta (California) Earthquake and Low-Level Amplitude Test Results.
PB96-159645 00,467

Dynamic Characteristics of Five Tall Buildings during Strong and Low-Amplitude Motions.
PB94-199981 00,427

Response of Buildings to Ambient Vibration and the Loma Prieta Earthquake: A Comparison.
PB96-119607 00,457

CELOTTA, R. J.

Atomic Manipulation of Polarizable Atoms by Electric Field Directional Diffusion.
PB95-150587 04,572

Determination of Complex Scattering Amplitudes in Low-Energy Elastic Electron-Sodium Scattering.
PB94-216652 03,869

Electron-atom collision studies using optically state selected beams. Progress report, May 15, 1987--May 14, 1988.
DE95004446 03,776

Electron-atom collision studies using optically state selected beams. Progress report, May 15, 1988--May 14, 1991.
DE95004447 03,777

Influence of Cr Growth on Exchange Coupling in Fe/Cr/Fe(100).
PB95-150181 04,562

Influence of Thickness Fluctuations on Exchange Coupling in Fe/Cr/Fe Structures.
PB96-135371 04,745

Laser-Focused Atomic Deposition.
PB95-161618 04,604

Laser Focused Atomic Deposition.
PB95-180659 04,685

Magnetic Moments in Cr Thin Films on Fe(100).
PB95-108429 04,525

Manipulation of Adsorbed Atoms and Creation of New Structures on Room-Temperature Surfaces with a Scanning Tunneling Microscope.
PB95-151536 04,578

Nanofabrication of a Two-Dimensional Array Using Laser-Focused Atomic Deposition.
PB96-119417 04,732

Nanostructure Fabrication via Direct Writing with Atoms Focused in Laser Fields.
PB95-150272 04,564

Nanostructure Fabrication via Laser-Focused Atomic Deposition (Invited).
PB96-204094 04,132

Oscillatory Exchange Coupling in Fe/Au/Fe(100).
PB95-150371 04,569

Scanning Tunneling Microscopy Study of the Growth of Cr/Fe(001): Correlation with Exchange Coupling of Magnetic Layers.
PB95-150330 04,568

SEMPA Studies of Exchange Coupling in Magnetic Multilayers.
PB96-164074 04,780

SEMPA Studies of Oscillatory Exchange Coupling.
PB95-163556 04,625

Spin-Resolved Elastic Scattering of Electrons from Sodium.
PB95-161774 03,933

Surface Magnetic Microstructural Analysis Using Scanning Electron Microscopy with Polarization Analysis (SEMPA).
PB95-162657 03,938

Tunneling Spectroscopy of bcc(001) Surface States.
PB96-155585 04,775

Using Atom Optics to Fabricate Nanostructures.
PB96-141247 04,757

CELOTTA, R. L.

Uncertainty Intervals for Polarized Beam Scattering Asymmetry Statistics.
PB94-200342 03,825

CENTENO, L.

Compositional Analysis of Beneficiated Fly Ashes.
PB95-220497 00,397

CEREMUGA, J.

Influence of Films' Thickness and Air Gaps in Surface Impedance Measurements of High Temperature Superconductors Using the Dielectric Resonator Technique.
PB96-157862 01,946

CERNY, E. H.

Trace Elements Associated with Proteins. Neutron Activation Analysis Combined with Biological Isolation Techniques.
PB95-163101 00,597

CERNYAR, E. W.
Importance of Unraveling Memory Propagation Effects in Interpreting Data on Partial Discharge Statistics.
PB95-163572 *01,901*

CESSNA, J.
Assay of the Eluent from the Alumina-Based Tungsten-188-Rhenium-188 Generator.
PB94-200482 *03,829*

International Radon-in-Air Measurement Intercomparison Using a New Transfer Standard.
PB96-159751 *03,708*

Liquid-Scintillation Counting Techniques for the Standardization of Radionuclides Used in Therapy.
PB97-110084 *03,709*

Standardization and Decay Scheme of Rhenium-186.
PB94-200490 *03,830*

CESSNA, J. T.
Radioassays of Yttrium-90 Used in Nuclear Medicine.
PB97-110100 *03,522*

System for Intercomparing Standard Solutions of Beta-Particle Emitting Radionuclides.
PB96-159637 *03,707*

CEZAIRLIYAN, A.
Dynamic Measurements of Thermophysical Properties of Metals and Alloys at High Temperatures by Subsecond Pulse Heating Techniques.
N94-25124/6 *03,309*

Dynamic Technique for Measuring Normal Spectral Emissivity of Electrically Conducting Solids at High Temperatures with a High-Speed Spatial Scanning Pyrometer.
PB95-153045 *03,921*

High-Speed Spatial Scanning Pyrometer.
PB94-200003 *02,636*

High-Temperature Laser-Pulse Thermal Diffusivity Apparatus.
PB94-185147 *02,631*

Issues in High-Speed Pyrometry.
PB97-118368 *02,693*

Measurement of Surface Tension of Tantalum by a Dynamic Technique in a Microgravity Environment.
PB95-161667 *03,932*

Measurement of the Heat of Fusion of Tungsten by a Microsecond-Resolution Transient Technique.
PB94-216686 *03,400*

Measurements of Thermophysical Properties of Nickel Near Its Melting Temperature by a Microsecond-Resolution Transient Technique.
PB96-102579 *04,210*

Millisecond-Resolution Pulse Heating System for Specific-Heat Measurements at High Temperatures.
PB94-199999 *02,635*

Radiance Temperature (in the Wavelength Range 519-906 nm) of Tungsten at Its Melting Point by a Pulse-Heating Technique.
PB94-172590 *03,397*

Radiance Temperatures at 1500 nm of Niobium and Molybdenum at Their Melting Points by a Pulse-Heating Technique.
PB97-118699 *04,167*

Radiance Temperatures (in the Wavelength Range 523-907 nm) of Group IV B Transition Metals Titanium, Zirconium, and Hafnium at Their Melting Points by a Pulse-Heating Technique.
PB96-102207 *03,356*

Radiance Temperatures (in the Wavelength Range 523-907 nm) of Group IVB Transition Metals Titanium, Zirconium, and Hafnium at Their Melting Points by a Pulse-Heating Technique.
PB96-135025 *02,677*

Simultaneous Measurement of Normal Spectral Emissivity by Spectral Radiometry and Laser Polarimetry at High Temperatures in Pulse-Heating Experiments: Application to Molybdenum and Tungsten.
PB97-118376 *02,694*

Thermal Diffusivity of POCO AXM-5Q1 Graphite in the Range 1500 to 2500 K Measured by a Laser-Pulse Technique.
PB94-185022 *03,013*

Wavelength Dependence of Normal Spectral Emissivity of High-Temperature Metals at Their Melting Point.
PB94-200011 *03,398*

CHABAL, Y. J.
Silicon Surface Chemistry by IR Spectroscopy in the Mid- to Far-IR Region: H2O and Ethanol on Si(100).
PB96-138565 *01,097*

CHABAN, E. E.
Silicon Surface Chemistry by IR Spectroscopy in the Mid- to Far-IR Region: H2O and Ethanol on Si(100).
PB96-138565 *01,097*

CHACON, L.
Effect of Sm2BaCuO5 on the Properties of Sintered (Bulk) YBa2Cu3O6+x.
PB96-119441 *04,733*

CHACONAS, G.
Measuring the Stability of Three Copper Alloys.
PB94-199866 *03,326*

CHACONAS, K.
Three Dimensional Position Determination from Motion.
PB95-107108 *01,788*

CHAKARIAN, V.
Influence of Coadsorbed Potassium on the Electron-Stimulated Desorption of F(+), F(-), and F(*) from PF3 on Ru(0001).
PB96-157946 *04,072*

CHAKOUMAKOS, B. C.
Preparation, Crystal Structure, Dielectric Properties, and Magnetic Behavior of Ba2Fe2Ti4O13.
PB96-186176 *01,162*

CHAKRABARTI, C.
VLSI Architectures for Template Matching and Block Matching.
PB94-200029 *01,834*

CHALKLEY, M. W.
Publication and Presentation Abstracts, 1993. (Published by Paffenbarger Research Center and Center of Excellence for Materials Science Research).
PB95-153052 *03,562*

Publication and Presentation Abstracts, 1994.
PB96-176623 *03,577*

Publication and Presentation Abstracts, 1995.
PB96-164082 *03,576*

Publication and Presentation Abstracts, 1996.
PB97-122238 *03,585*

Publications and Presentation Abstracts, 1995. (Published by Paffenbarger Research Center and Center of Excellence for Materials Science Research).
PB96-119250 *03,568*

CHAMBERS, G. P.
Pure Element Sputtering Yield Data: Appendix 4.
PB94-200037 *00,805*

CHAN, H. M.
Flaw-Tolerance and Crack-Resistance Properties of Alumina-Aluminum Titanate Composites with Tailored Microstructures.
PB97-110324 *03,101*

Interface Properties for Ceramic Composites from a Single Fiber Pull-Out Test.
PB94-199361 *03,135*

CHAN, W. R.
Experimental and Numerical Studies on Two-Dimensional Gravity Currents in a Horizontal Channel.
PB94-165941 *01,359*

CHANDLER-HOROWITZ, D.
Characterization of the ZnSe/GaAs Interface Layer by TEM and Spectroscopic Ellipsometry.
PB95-175360 *04,655*

Comparison of Techniques for Nondestructive Composition Measurements in CdZnTe Substrates.
PB96-103098 *02,703*

Determination of the Optical Constants of ZnSe Films by Spectroscopic Ellipsometry.
PB95-175378 *04,656*

Double Modulation and Selective Excitation Photoreflectance for Characterizing Highly Luminescent Semiconductor Structures and Samples with Poor Surface Morphology.
PB97-111439 *02,452*

Double-Modulation and Selective Excitation Photoreflectance for Wafer-Level Characterization of Quantum-Well Laser Structures.
PB96-167325 *04,372*

High-Accuracy Principal-Angle Scanning Spectroscopic Ellipsometry of Semiconductor Interfaces.
PB96-163787 *02,427*

Interface Roughness-Induced Changes in the Near-E(sub 0) Spectroscopic Behavior of Short-Period AlAs/GaAs Superlattices.
PB94-185154 *02,118*

Optical Conductivity of Single Crystals of Ba1-xMxBiO3(M=K, Rb, x=0.04, 0.37).
PB94-185329 *04,447*

Spectroscopic Ellipsometry Determination of the Properties of the Thin Underlying Strained Si Layer and the Roughness at SiO2/Si Interface.
PB95-150157 *04,560*

CHANDRASEKHARAIAH, M. S.
Disilicides of Tungsten, Molybdenum, Tantalum, Titanium, Cobalt, and Nickel, and Platinum Monosilicide: A Survey of Their Thermodynamic Properties.
PB94-168580 *00,752*

CHANG, K. J.
Electronic Correlations and Satellites in Superconducting Oxides.
PB94-200045 *04,477*

CHANG, R. F.
High-Speed Spatial Scanning Pyrometer.
PB94-200003 *02,636*

High-Temperature High-Pressure Oscillating Tube Densimeter.
PB96-146618 *01,123*

CHANG, S.
Security in Open Systems.
PB95-105383 *01,473*

CHANG, S. J.
Preliminary Functional Specifications of a Prototype Electronic Research Notebook for NIST.
PB94-207750 *00,012*

CHANG, S. S.
Effect of Curing History on Ultimate Glass Transition Temperature and Network Structure of Crosslinking Polymers.
PB94-200052 *01,214*

CHANG, Y.
Introduction to Traffic Management for Broadband ISDN.
PB94-142494 *01,464*

CHANG, Y. A.
Thermodynamic Assessment and Calculation of the Ti-Al System.
PB94-212644 *03,337*

CHANG, Y. M.
NIST Capacitance Measurement Assurance Program (MAP).
PB94-200060 *02,254*

NIST Measurement Assurance Program for Capacitance Standards at 1 kHz.
PB96-172333 *02,276*

CHANTLER, C. T.
Energy Dependences of Absorption in Beryllium Windows and Argon Gas.
PB96-102124 *04,020*

Flat and Curved Crystal Spectrography for Mammographic X-ray Sources.
PB97-122246 *03,642*

Improvements in Computation of Form Factors.
PB94-200078 *03,820*

Photographic Response to X-Ray Irradiation. 1. Estimation of the Photographic Error Statistic and Development of Analytic Density-Intensity Equations.
PB94-200086 *03,821*

Photographic Response to X-Ray Irradiation. 2. Correlated Models.
PB94-200094 *03,822*

Photographic Response to X-Ray Irradiation. 3. Photographic Linearization of Beam-Foil Spectra.
PB94-200102 *03,823*

Polarization Measurements on a Magnetic Quadrupole Line in Ne-Like Barium.
PB97-113104 *04,161*

Systematic Correction in Bragg X-ray Diffraction of Flat and Curved Crystals.
PB97-112239 *04,152*

Theoretical Form Factor, Attenuation and Scattering Tabulation for Z=1-92 from E=1-10 eV to E=0.4-1.0 MeV.
PB96-145594 *01,104*

CHAPARALA, P.
Assessing MOS Gate Oxide Reliability on Wafer Level with Ramped/Constant Voltage and Current Stress.
PB96-180112 *04,115*

Characterization of Time-Dependent Dielectric Breakdown in Intrinsic Thin SiO2.
PB97-122527 *02,458*

Electric Field Dependent Dielectric Breakdown of Intrinsic SiO2 Films Under Dynamic Stress.
PB96-204102 *02,449*

Experimental Investigation of the Validity of TDDB Voltage Acceleration Models.
PB94-185949 *02,304*

Field and Temperature Acceleration of Time-Dependent Dielectric Breakdown in Intrinsic Thin SiO2.
PB94-185956 *02,305*

High Temperature Reliability of Thin Film SiO2.
PB95-150348 *02,333*

New Oxide Degradation Mechanism for Stresses in the Fowler-Nordheim Tunneling Regime.
PB96-200985 *04,128*

New Physics-Based Model for Time-Dependent- Dielectric-Breakdown.
PB96-186093 *02,440*

New Physics-Based Model for Time-Dependent- Dielectric-Breakdown.
PB96-201132 *02,448*

TDDB Characterization of Thin SiO2 Films with Bimodal Failure Populations.
PB96-102926 *02,381*

Time-Dependent Dielectric Breakdown of Intrinsic SiO2 Films under Dynamic Stress.
PB96-179478 *02,438*

CHAPMAN, J. B.
Framework for Information Technology Integration in Process Plant and Related Industries.
PB94-219086 *02,772*

CHAPMAN, J. N.
Micromagnetic Structure of Domains in Co/Pt Multilayers. 1. Investigations of Wall Structure.
PB95-162111 *04,610*

CHAPMAN, R. E.
Benefits and Costs of Research: A Case Study of the Fire Safety Evaluation System.
PB96-202288 *00,232*

Benefits and Costs of Research: Two Case Studies in Building Technology.
PB96-202221 *00,230*

CHAPMAN, W. B.
State-Resolved Rotational Energy Transfer in Open Shell Collisions: Cl((2)P3/2)+HCl.
PB96-176607 *01,157*

CHAR, K.

Evidence for Parallel Junctions Within High-Tc Grain-Boundary Junctions.
PB95-175410 *04,657*

Half-Integral Constant Voltage Steps in High-Tc Grain Boundary Junctions.
PB94-211216 *04,489*

CHASE, M. W.

NIST Standard Reference Data Products Catalog, 1994.
PB94-151842 *00,727*

Numeric Data Distribution: The Vital Role of Data Exchange in Today's World.
N95-15937/2 *02,622*

Thermodynamic Properties of Gas Phase Species of Importance to Ozone Depletion.
PB94-198215 *00,126*

Thermodynamic Properties of the Group IIA Elements.
PB94-160983 *00,730*

CHASE, S. C.

Representing Designs with Logic Formulations of Spatial Relations.
PB97-111561 *02,792*

Using Logic to Specify Shapes and Spatial Relations in Design Grammars.
PB97-111579 *02,793*

CHATTOPADHYAY, T.

Magnetic Structure and Spin Dynamics of the Pr and Cu in Pr2CuO4.
PB96-111836 *04,036*

Temperature Dependence of the Magnetic Excitations in Ordered and Disordered Fe72Pt28.
PB95-150223 *04,563*

CHATTORAJ, D.

Deletion Analysis of the Mini-P1 Plasmid Origin of Replication and the Role of E.coli DnaA Protein.
PB95-163911 *03,539*

CHATTPADHYAY, T.

Dispersions of Magnetic Excitations of the Pr Ions in Pr2CuO4.
PB94-173044 *04,444*

CHAUDHURI, D. K.

Tribological Behavior of 440/Diamond-Like-Carbon Film Couples.
PB96-119714 *03,019*

Tribometer for Measurements in Hostile Environments.
PB95-180949 *02,967*

Wear Mechanism Maps of 440C Martensitic Stainless Steel.
PB96-111810 *04,834*

CHAUDURI, D. K.

Friction and Oxidative Wear of 440C Ball Bearing Steels Under High Load and Extreme Bulk Temperatures.
PB95-175253 *03,215*

CHEETHAM, A. K.

Determination of Complex Structures from Powder Diffraction Data: The Crystal Structure of La3Ti5Al15O37.
PB95-202966 *01,038*

CHEIM, L. A. V.

Correlations between Electrical and Acoustic Detection of Partial Discharge in Liquids and Implications for Continuous Data Recording.
PB96-204490 *02,248*

CHELLAPPA, R.

Face Recognition Technology for Law Enforcement Applications.
PB94-207768 *01,837*

General Motion Model and Spatio-Temporal Filters for Computing Optical Flow.
PB95-171096 *01,847*

Human and Machine Recognition of Faces: A Survey.
PB96-111687 *01,854*

Image Gradient Evolution: A Visual Cue for Danger.
PB96-154562 *02,939*

Motion-Model-Based Boundary Extraction.
PB95-189502 *01,849*

Reliable Optical Flow Algorithm Using 3-D Hermite Polynomials.
PB94-145620 *01,829*

CHELTON, D. B.

Design and Construction of a Liquid Hydrogen Temperature Refrigeration System.
AD-A286 618/4 *02,619*

CHEN, C. F.

Cavitation Damage During Flexural Creep of SiAlON-YAG Ceramics.
PB94-200110 *03,036*

CHEN, D. H.

Anomalous Dispersion and Thermal Expansion in Lightly-Doped KTa1-xNbxO3.
PB95-152302 *04,585*

CHEN, D. X.

Effects of Critical Current Density, Equilibrium Magnetization and Surface Barrier on Magnetization of High Temperature Superconductors.
PB94-185162 *04,446*

Effects of Critical Current Density, Equilibrium Magnetization and Surface Barrier on Magnetization of High Temperature Superconductors.
PB95-153060 *04,588*

Surface Barrier and Lower Critical Field in YBa2Cu3O7-delta Superconductors.
PB94-200128 *04,478*

CHEN, H.

Neutron Focusing Lens Using Polycapillary Fibers.
PB95-141206 *03,889*

Neutron Focusing Lens Using Polycapillary Fibers.
PB95-153078 *03,922*

Reference Relations for the Evaluation of the Materials Properties of Orthorhombic YBa2Cu3Ox Superconductors.
PB96-176763 *04,782*

CHEN, H. M.

Beamcon III, a Linearity Measurement Instrument for Optical Detectors.
PB96-113576 *04,337*

CHEN, L. T.

Determination of Sulfur in Fossil Fuels by Isotope Dilution Thermal Ionization Mass Spectrometry.
PB96-141379 *02,495*

CHEN, M. C.

Characterization of Liquid-Phase Epitaxially Grown HgCdTe Films by Magnetoresistance Measurements.
PB96-123617 *04,738*

Characterization of LPE HgCdTe Film by Magnetoresistance.
PB96-157961 *02,197*

Electrical Characterization of Liquid-Phase Epitaxially Grown Single-Crystal Films of Mercury Cadmium Telluride by Variable-Magnetic-Field Hall Measurements.
PB95-175782 *02,177*

CHEN-MAYER, H.

Use of Neutron Beams for Chemical Analysis at NIST.
PB97-112437 *00,652*

CHEN, S.

SPC Artifact for Automated Solder Joint Inspection.
PB96-161716 *04,095*

CHEN, W.

Densification of Nano-Size Powders. 1994 Report.
DE94013486 *03,027*

Equipment for Investigation of Cryogenic Compaction of Nanosize Silicon Nitride Powders. 1993 Report.
DE94013593 *03,028*

CHEN, Y.

Localization Model of Rubber Elasticity: Comparison with Torsional Data for Natural Rubber Networks in the Dry State.
PB95-107033 *03,195*

CHEN, Y. D.

Anionic Triphenylmethane Dye Solutions for Low-Dose Food Irradiation Dosimetry.
PB96-135173 *03,715*

CHEN, Y. M.

Fracture Mechanics Analysis of Near-Surface Cracks.
PB94-172400 *03,230*

Hybrid Method for Determining Material Properties from Instrumented Micro-Indentation Experiments.
PB95-152229 *03,348*

CHEN, Y. T.

Dynamic Shear Modulus Measurements with Four Independent Techniques in Nickel-Based Alloys.
PB94-198900 *03,320*

CHENG, G. W.

Facile Synthesis of Novel Fluorinated Multifunctional Acrylates.
PB94-198389 *01,207*

CHENG, H. S.

Mechano-Chemical Model: Reaction Temperatures in a Concentrated Contact.
PB96-119466 *03,227*

CHENG, Y.

Prediction of Strengthening Due to V Additions in Direct-Cooled Ferrite-Pearlite Forging Steels.
PB96-190251 *03,220*

CHENG, Y. W.

Hot-Deformation Apparatus for Thermomechanical Processing Simulation.
PB94-200136 *03,207*

Microstructure and Tensile Properties of Microalloyed Steel Forgings.
PB94-172715 *03,204*

Prediction of the Strength Properties for Plain-Carbon and Vanadium Micro-Alloyed Ferrite-Pearlite Steel.
PB96-123393 *03,216*

CHEOK, G.

Performance of HUD-Affiliated Properties during the January 17, 1994 Northridge Earthquake.
PB95-174488 *00,443*

CHEOK, G. S.

Model Precast Concrete Beam-to-Column Connections Subject to Cyclic Loading.
PB95-153094 *00,438*

Partially Prestressed and Debonded Precast Concrete Beam-Column Joints.
PB95-153102 *00,439*

Performance of 1/3-Scale Model Precast Concrete Beam-Column Connections Subjected to Cyclic Inelastic Loads. Report No. 4.
PB95-179024 *00,444*

Seismic Performance Behavior of Precast Concrete Beam-Column Joints.
PB95-153110 *00,440*

Simplified Design Procedure for Hybrid Precast Concrete Connections.
PB96-154836 *00,405*

Strengthening Methodology for Lightly Reinforced Concrete Frames: Recommended Design Guidelines for Strengthening with Infill Walls.
PB95-260725 *00,454*

CHEONG, H. M.

Use of Pressure for Quantum-Well Band-Structure Characterization.
PB96-164058 *04,779*

CHERBAUCICH, C.

Approach to Setting Performance Requirements for Automated Evaluation of the Parameters of High-Voltage Impulses.
PB94-185634 *01,878*

CHEREPKOV, N. A.

Resonant Two-Color Detachment of H(-) with Excitation of H(n=2).
PB95-202552 *03,984*

CHERNIAVSKY, J. C.

High Integrity Software Standards Activities at NIST.
PB96-112214 *01,744*

Report of a Workshop on the Assurance of High Integrity Software.
PB96-161377 *01,763*

CHERNOV, A. A.

Convection and Morphological Stability During Directional Solidification.
N95-14548/8 *03,310*

CHERRY, S. M.

Summaries of Center for Fire Research In-House Projects and Grants: 1990.
PB94-160876 *00,286*

CHESLER, R.

Liposome-Based Flow-Injection Immunoassay for Determining Theophylline in Serum.
PB94-213493 *03,494*

CHESLER, S. N.

Standard Reference Materials for the Determination of Polycyclic Aromatic Hydrocarbons in Environmental Samples - Current Activities.
PB95-151668 *00,586*

Supercritical Fluid Extraction-Immunoassay for the Rapid Screening of Cocaine in Hair.
PB96-167168 *00,637*

CHESTER, M.

X-Ray Photoelectron and Auger Electron Spectroscopy Study of Ultraviolet/Ozone Oxidized P2S5/(NH4)2S Treated GaAs(100) Surfaces.
PB94-200144 *04,479*

CHESTER, M. J.

Grazing Angle X-Ray Photoemission System for Depth-Dependent Analysis.
PB95-161154 *04,600*

Grazing-Incidence X-Ray Photoelectron Spectroscopy: A Novel Approach to Thin Film Characterization.
PB95-153128 *04,589*

Grazing Incidence X-ray Photoemission and Its Implementation on Synchrotron Light Source X-ray Beamlines.
PB95-175766 *01,001*

Grazing-Incidence X-Ray Photoemission Spectroscopy Investigation of Oxidized GaAs(100): A Novel Approach to Nondestructive Depth Profiling.
PB94-200151 *04,480*

CHEUNG, S. K.

Interdigitated Stacked P-I-N Multiple Quantum Well Modulator.
PB97-112296 *02,455*

CHEYNET, B.

Extrapolation of the Heat Capacity in Liquid and Amorphous Phases.
PB97-111421 *04,147*

CHI, P. H.

Transition Metal Implants in In0.53GA0.47As.
PB95-126389 *04,534*

CHIANG, C. H.

Absorption of Sound in Gases between 10 and 25 MHz: Argon.
PB94-199015 *04,183*

Absorption of Ultrasonic Waves in Air at High Frequencies (10-20 MHz).
PB94-199007 *04,182*

CHIANG, C. K.

Effect of Sm2BaCuO5 on the Properties of Sintered (Bulk) YBa2Cu3O6+x.
PB96-119441 *04,733*

Efficient Experiment to Study Superconducting Ceramics.
PB94-212578 *04,505*

Microstructure and Ferroelectric Properties of Lead Zirconate-Titanate Films Produced by Laser Evaporation.
PB94-199148 *04,470*

Reactive Coevaporation of DyBaCuO Superconducting Films: The Segregation of Bulk Impurities on Annealed MgO(100) Substrates.
PB95-164562 *04,635*

X-Ray Characterization of the Crystallization Process of High-Tc Superconducting Oxides in the Sr-Bi-Pb-Ca-Cu-O System.
PB95-151700 *04,579*

CHIANG, M. Y.

Properties and Interactions of Oral Structures and Restorative Materials. Annual Report for Period October 1, 1990 to September 30, 1991.
PB94-160843 *03,558*

CHIANG, M. Y. M.

Hygrothermal Effects on the Performance of Polymers and Polymeric Composites: A Workshop Report. Held in Gaithersburg, Maryland on September 21-22, 1995.
PB96-183207 *03,180*

CHIEH, K.

24 GHz Josephson Array Voltage Standard.
PB94-211588 *02,033*

CHIEN, C. L.

Domain Structures in Magnetoresistive Granular Metals.
PB96-141346 *04,760*

Incorporation of Gold into YBa2Cu3O7: Structure and Tc Enhancement.
PB94-200276 *04,481*

Unexpected Effects of Gold on the Structure, Superconductivity, and Normal State of YBa2Cu3O7.
PB94-200284 *04,482*

CHILD, M. S.

Rotational-RKR Inversion of Intermolecular Stretching Potentials: Extension to Linear Hydrogen Bonded Complexes.
PB95-203014 *01,041*

CHILDERS, C. B.

AC-DC Difference Characteristics of High-Voltage Thermal Converters.
PB96-148093 *02,083*

Frequency Extension of the NIST AC-DC Difference Calibration Service for Current.
PB95-161253 *01,895*

High-Current Thin Film Multijunction Thermal Converters and Multi-Converter Modules.
PB97-112379 *01,989*

CHIN, J. W.

Materials Aspects of Fiber-Reinforced Polymer Composites in Infrastructure.
PB96-210695 *03,184*

CHIOU, T. T.

Gas Absorption during Ion-Irradiation of a Polymer Target.
PB96-161864 *04,099*

CHIRICO, R. D.

Thermodynamic Properties of Alkenes (Mono-Olefins Larger Than C4).
PB94-162237 *00,735*

CHMAISSEM, O.

Crystal Structure of Pb2Sr2YCu3O8+delta with delta=1.32, 1.46, 1.61, 1.71, by Powder Neutron Diffraction.
PB94-216314 *04,518*

CHOCK, P. B.

Electropermeabilization of Cell Membranes: Effect of the Resting Membrane Potential.
PB95-163291 *03,537*

CHOI, B.

Distributed Architecture for Standards Processing.
PB96-164181 *00,276*

CHOI, C. S.

Application of ODF to the Rietveld Profile Refinement of Polycrystalline Solid.
PB95-202388 *03,401*

Methyl Torsional Levels of Solid Acetonitrile (CH3CN): A Neutron Scattering Study.
PB95-151015 *00,926*

Microstructure Study of Molybdenum Liners by Neutron Diffraction.
PB95-202396 *03,756*

Neutron Diffraction Texture Study of Deformed Uranium Plates.
PB97-111587 *03,010*

Texture Study of Two Molybdenum Shaped Charge Liners by Neutron Diffraction.
PB94-200177 *03,754*

Textures of Tantalum Metal Sheets by Neutron Diffraction.
PB94-200169 *03,399*

CHOI, M.

Simultaneous Optical Measurement of Soot Volume Fraction, Temperature, and CO2 in Heptane Pool Fire.
PB96-102132 *01,397*

CHONG, R. A.

Viscosity of Defined and Undefined Hydrocarbon Liquids Calculated Using an Extended Corresponding-States Model.
PB96-167234 *02,498*

CHOO, R. T. C.

Mathematical Models of Transport Phenomena Associated with Arc-Welding Processes: A Survey.
PB96-135058 *02,870*

CHOQUETTE, S.

Planar Waveguide Optical Sensors.
PB94-200185 *03,586*

CHOQUETTE, S. J.

Embossable Grating Couplers for Planar Waveguide Optical Sensors.
PB96-190277 *00,641*

Instrument for Evaluating Phase Behavior of Mixtures for Supercritical Fluid Experiments.
PB95-180758 *00,606*

CHOU, C. C.

Improved Molecular Constants and Frequencies for the CO2 Laser from New High-J Regular and Hot-Band Frequency Measurements.
PB95-180634 *04,312*

New cw CO2 Laser Lines: The 9-mu m Hot Band.
PB95-168548 *04,281*

CHOU, H.

Anomalous Dispersion and Thermal Expansion in Lightly-Doped KTa1-xNbxO3.
PB95-152302 *04,585*

CHOU, Y.

Chip Morphology, Tool Wear and Cutting Mechanics in Finish Hard Turning.
PB97-112247 *03,106*

CHOUDHARY, L.

Copolymerization of N-Phenyl Maleimide and gamma-Methacryloxypropyl Trimethoxysilane.
PB95-153144 *01,248*

Thermal Behavior of 4-Maleimidophenyl Glycidyl Ether Resins.
PB95-153151 *01,249*

Thermal Behaviour of Methyl Methacrylate and N-Phenyl Maleimide Copolymers.
PB95-152237 *01,246*

CHOUDHARY, V.

Copolymerization of N-Phenyl Maleimide and gamma-Methacryloxypropyl Trimethoxysilane.
PB95-153144 *01,248*

Thermal Behavior of 4-Maleimidophenyl Glycidyl Ether Resins.
PB95-153151 *01,249*

CHOW, A. F.

Growth of Epitaxial KNbO3 Thin Films.
PB96-135181 *02,409*

CHOW, H. M.

Grain Alignment and Transport Properties of Bi2Sr2CaCu2O8 Grown by Laser Heated Float Zone Method.
PB95-161451 *04,602*

CHOW, L. C.

Behavior of a Calcium Phosphate Cement in Simulated Blood Plasma In vitro.
PB95-168712 *00,165*

Calcium Phosphate Cements.
PB97-111595 *03,580*

Dental Materials.
PB94-172871 *00,142*

Deposition of Loosely Bound and Firmly Bound Fluorides on Tooth Enamel by an Acidic Gel Containing Fluorosilicate and Monocalcium Phosphate Monohydrate.
PB95-150710 *03,559*

Effects on Whole Saliva of Chewing Gums Containing Calcium Phosphates.
PB95-153169 *03,563*

Formation of Hydroxyapatite in a Polymeric Calcium Phosphate Cement.
PB95-180642 *00,173*

Formation of Hydroxyapatite in Cement Systems.
PB95-175261 *00,170*

Periapical Tissue Reactions to a Calcium Phosphate Cement in the Teeth of Monkeys.
PB94-212008 *00,149*

Physical and Chemical Properties of Resin-Reinforced Calcium Phosphate Cements.
PB95-180212 *00,171*

Polymeric Calcium Phosphate Cements Derived from Poly(methyl vinyl ether-maleic acid).
PB96-164264 *00,180*

Procedure for the Study of Acidic Calcium Phosphate Precursor Phases in Enamel Mineral Formation.
PB95-164448 *03,564*

Properties and Mechanisms of Fast-Setting Calcium Phosphate Cements.
PB96-123229 *00,178*

Reinforcement of Cancellous Bone Screws with Calcium Phosphate Cement.
PB96-158001 *00,179*

Remineralization of Root Lesions with Concentrated Calcium and Phosphate Solutions.
PB96-102140 *03,567*

CHOW, P. C.

Epitaxial Integration of Single Crystal C60.
PB95-153490 *04,592*

CHOW, T. H.

Effect of Ethanol on the Solubility of Hydroxyapatite in the System Ca(OH)2-H3PO4-H2O at 25C and 33C.
PB95-169231 *00,169*

Effects on Whole Saliva of Chewing Gums Containing Calcium Phosphates.
PB95-153169 *03,563*

CHRISTENSEN, D. H.

Characterization of Vertical-Cavity Semiconductor Structures.
PB94-200193 *02,126*

Comparative Photoluminescence Measurement and Simulation of Vertical-Cavity Semiconductor Laser Structures.
PB95-169173 *02,169*

Correlation of Optical, X-ray, and Electron Microscopy Measurements of Semiconductor Multilayer Structures.
PB95-175279 *02,174*

Cross-Sectional Photoluminescence and Its Application to Buried-Layer Semiconductor Structures.
PB96-141106 *02,415*

Determination of the Complex Refractive Index of Individual Quantum Wells from Distributed Reflectance.
PB95-175642 *02,176*

Measurement and Simulation of Photoluminescence Spectra from Vertical-Cavity Quantum-Well Laser Structures.
PB95-169181 *02,170*

Vertical-Cavity Optoelectronic Structures: CAD, Growth, and Structural Characterization.
PB95-153177 *02,148*

Vertical-Cavity Semiconductor Lasers: Structural Characterization, CAD, and DFB Structures.
PB95-153193 *02,150*

Vertical-Cavity Semiconductor Structures: Materials Characterization.
PB95-153185 *02,149*

CHRISTENSEN, R. G.

Certification of Morphine and Codeine in a Human Urine Standard Reference Material.
PB95-176160 *03,499*

Certification of Phencyclidine in Lyophilized Human Urine Reference Materials.
PB96-160692 *03,508*

Determination of Oltipraz in Serum by High-Performanace Liquid Chromatography with Optical Absorbance and Mass Spectrometric Detection.
PB94-200201 *03,493*

Flow Immunoassay Using Solid-Phase Entrapment.
PB96-200951 *00,642*

Instrument for Evaluating Phase Behavior of Mixtures for Supercritical Fluid Experiments.
PB95-180758 *00,606*

NIST Reference Materials to Support Accuracy in Drug Testing.
PB96-123807 *03,505*

Preliminary Investigation of Oleoresin Capsicum.
PB96-179486 *03,520*

CHRISTIDES, C.

Neutron-Scattering Study of C60(n-) (n=3,6) Librations in Alkali-Metal Fullerides.
PB94-200219 *00,806*

Rotational Dynamics of C60 in Na2RbC60.
PB95-153201 *00,948*

Rotational Dynamics of Solid C70: A Neutron-Scattering Study.
PB94-172178 *00,755*

Rotational Dynamics of Solid C70: A Neutron-Scattering Study.
PB95-153219 *00,949*

CHRISTMAN, S.

Silicon Surface Chemistry by IR Spectroscopy in the Mid- to Far-IR Region: H2O and Ethanol on Si(100).
PB96-138565 *01,097*

CHRISTOPHOROU, L. G.

Dependence of the Thermal Electron Attachment Rate Constant in Gases and Liquids on the Energy Position of the Electron Attaching State.
PB97-122253 *01,996*

Electron Attachment to Excited Molecules(1).
PB96-122809 *01,087*

Fundamental Processes in Gas Discharges.
PB96-123450 *01,089*

Gaseous Dielectrics Research: Possible SF6 Substitutes.
PB96-119268 *02,228*

SF6 Insulation: Possible Greenhouse Problems and Solutions.
PB95-251625 *02,269*

SF6/N2 Mixtures: Basic and High-Voltage-Insulation Properties.
PB96-123468 *02,230*

CHRISTOU, C. A.

Novel Radiochromic Films for Clinical Dosimetry.
PB97-119259 *03,641*

CHU, C. W.

Crystal Structure of Annealed and As-Prepared HgBa2CaCu2O6+delta Superconductors.
PB95-161105 *03,927*

Oxygen Dependance of the Crystal Structure of HgBa2CuO4+ and Its Relation to Superconductivity.
PB96-102512 *04,711*

CHU, F. Y.

Decomposition of SF6 and Production of S2F10 in Power Arcs.
PB96-122619 *01,084*

Investigation of S2F10 Production and Mitigation in Compressed SF6-Insulated Power Systems.
PB94-212388 *02,467*

Investigation of S2F10 Production and Mitigation in Compressed SF6- Insulated Power Systems.
PB96-155528 *02,468*

CHU, J. L.

Asymmetric Tip Morphology of Creep Microcracks Growing Along Bimaterial Interfaces.
PB94-200243 *03,138*

Diffusive Crack Growth at a Bimaterial Interface.
PB96-204110 *03,090*

CHU, P. M.

Photodecomposition of Mo(CO)6/Si(111) 7x7: CO State-Resolved Evidence for Excited State Relaxation and Quenching.
PB95-180154 *01,009*

Photodesorption Dynamics of CO from Si(111): The Role of Surface Defects.
PB96-111646 *03,066*

CHUANG, T. J.

Analysis of Creep in a Si-SiC C-Ring by Finite Element Method.
PB94-200268 *03,037*

Application of a Simple Technique for Estimating Errors of Finite-Element Solutions Using a General-Purpose Code.
PB94-200250 *04,818*

Asymmetric Tip Morphology of Creep Microcracks Growing Along Bimaterial Interfaces.
PB94-200243 *03,138*

Cavitation Damage During Flexural Creep of SiAlON-YAG Ceramics.
PB94-200110 *03,036*

Crack Growth Resistance of Strain-Softening Materials under Flexural Loading.
PB94-200227 *02,972*

Creep and Creep Rupture of Structural Ceramics.
PB96-204524 *03,093*

Diffusive Crack Growth at a Bimaterial Interface.
PB96-204110 *03,090*

Generic Model for Creep Rupture Lifetime Estimation on Fibrous Ceramic Composites.
PB94-200235 *03,137*

Life Prediction of a Continuous Fiber Reinforced Ceramic Composite Under Creep Conditions.
PB96-204128 *03,091*

CHUGG, B.

Self-Biasing Cryogenic Particle Detector Utilizing Electrothermal Feedback and a SQUID Readout.
PB96-102538 *04,712*

CHUN, S. W.

Vapor-Liquid Equilibria of Mixtures of Propane and Isomeric Hexanes.
PB95-175287 *00,995*

CHUNG, R.

January 17, 1995 Hyogoken-Nanbu (Kobe) Earthquake. Performance of Structures, Lifelines and Fire Protection Systems. Executive Summary and Paper.
PB97-104160 *00,475*

Performance of HUD-Affiliated Properties during the January 17, 1994 Northridge Earthquake.
PB95-174488 *00,443*

CHUNG, R. M.

Ground Improvement Techniques for Liquefaction Remediation Near Existing Lifelines.
PB96-128111 *01,350*

Method of Estimating the Parameters of Tuned Mass Dampers for Seismic Applications.
PB96-167820 *00,473*

Northridge Earthquake, 1994. Performance of Structures, Lifelines and Fire Protection Systems.
PB94-161114 *00,421*

Northridge Earthquake 1994: Performance of Structures, Lifelines, and Fire Protection Systems.
PB94-207461 *04,825*

Post-Earthquake Fire and Lifelines Workshop. Held in Long Beach, California on January 30-31, 1995. Proceedings.
PB96-117916 *00,209*

Proceedings of a Workshop on Developing and Adopting Seismic Design and Construction Standards for Lifelines. Held in Denver, Colorado on September 25-27, 1991.
PB97-115794 *01,302*

CHUNG, Y. S.

Collisions of Electrons with Highly-Charged Ions.
PB96-200340 *04,791*

CHURCH, D. A.

Beam Line for Highly Charged Ions.
PB97-111256 *04,143*

CHURNEY, K. L.

Assessing the Credibility of the Calorific Content of Muncipal Solid Waste.
PB94-199882 *02,581*

Sulfur Dioxide Capture in the Combustion of Mixtures of Lime, Refuse-Derived Fuel, and Coal.
PB94-155587 *02,534*

CICHY, M. A.

Neutron-Scattering Study of Librations and Intramolecular Phonons in Rb2.6K0.4C60.
PB95-162269 *00,958*

CIEPLAK, M. Z.

Incorporation of Gold into YBa2Cu3O7: Structure and Tc Enhancement.
PB94-200276 *04,481*

Unexpected Effects of Gold on the Structure, Superconductivity, and Normal State of YBa2Cu3O7.
PB94-200284 *04,482*

CIGLER, J. L.

National Voluntary Laboratory Accreditation Program: Procedures and General Requirements.
PB94-178225 *02,630*

CIMA, M. J.

Effects of Substrate Surface Steps on the Microstructure of Epitaxial Ba2YCu3O7-x Thin Films on (001) LaAlO3.
PB96-148184 *04,774*

Epitaxial Nucleation and Growth of Chemically Derived Ba2YCu3O7-x Thin Films on (001) SrTiO3.
PB96-190186 *04,787*

Grain Alignment and Transport Properties of Bi2Sr2CaCu2O8 Grown by Laser Heated Float Zone Method.
PB95-161451 *04,602*

CINCOTTA, A.

Distributed Communication Methods and Role-Based Access Control for Use in Health Care Applications.
PB96-183165 *01,508*

CIRAC, J. I.

Phase Shifts and Intensity Dependence in Frequency-Modulation Spectroscopy.
PB96-103205 *01,071*

CIVIS, S.

Perpendicular C-H Stretching Band nu9/nu13 and the Torsional Potential of Dimethylacetylene.
PB97-122451 *01,192*

CLAGUE, F. R.

Calibration Service for Coaxial Reference Standards for Microwave Power.
PB96-162722 *01,958*

Coaxial Reference Standard for Microwave Power.
PB94-193786 *01,880*

Developing a NIST Coaxial Microwave Power Standard at 1 mW.
PB95-202412 *01,914*

Method to Determine the Calorimetric Equivalence Correction for a Coaxial Microwave Microcalorimeter.
PB95-202404 *01,913*

New Coaxial Microwave Microcalorimeter Evaluation Technique.
PB95-153227 *01,892*

NIST Model PM2 Power Measurement System for 1 mW at 1 GHz.
PB94-135803 *02,018*

CLAIRON, A.

Atoms in Optical Molasses.
PB95-108874 *03,875*

Atoms in Optical Molasses: Applications to Frequency Standards.
PB95-108882 *03,876*

Optical Molasses: Cold Atoms for Precision Measurements.
PB95-108890 *03,877*

Optical Molasses: The Coldest Atoms Ever.
PB95-108908 *03,878*

CLARK, A. F.

Accuracy Comparisons of Josephson Array Systems.
PB95-164687 *02,047*

Application of Single Electron Tunneling: Precision Capacitance Ratio Measurements.
PB96-102157 *04,703*

Cryogenic Precision Capacitance Bridge Using a Single Electron Tunneling Electrometer.
PB95-126074 *04,529*

Cryogenic Precision Capacitance Bridge Using a Single Electron Tunneling Electrometer.
PB95-152310 *02,040*

Cryogenic Precision Capacitance Bridge Using a Single Electron Tunneling Electrometer.
PB96-112271 *02,072*

Evidence for Parallel Junctions Within High-Tc Grain-Boundary Junctions.
PB95-175410 *04,657*

From Superconductivity to Supernovae: The Ginzburg Symposium. Report on the Symposium Held in Honor of Vitaly L. Ginzburg. Held in Gaithersburg, Maryland on May 22, 1992
PB95-171963 *04,649*

Half-Integral Constant Voltage Steps in High-Tc Grain Boundary Junctions.
PB94-211216 *04,489*

Noise Characteristics Below 1 Hz of Zener Diode-Based Voltage Reference.
PB96-123476 *04,049*

Physical Basis for Half-Integral Shapiro Steps in a DC SQUID.
PB96-102264 *04,704*

Proposed Tests to Evaluate the Frequency-Dependent Capacitor Ratio for Single Electron Tunneling Experiment.
PB97-111454 *01,982*

Results of Capacitance Ratio Measurements for the Single Electron Pump-Capacitor Charging Experiment.
PB97-113286 *04,813*

Superconducting Energy Gap of Bulk UBe13.
PB95-150116 *04,559*

CLARK, A. M.

Coexistence of Grains with Differing Orthorhombicity in High Quality YBa2Cu3O7-delta Thin Films.
PB96-135033 *04,742*

CLARK, A. V.

Application of Electromagnetic-Acoustic Transducers for Nondestructive Evaluation of Stresses in Steel Bridge Structures.
PB96-167978 *01,301*

Determination of Sheet Steel Formability Using Wide Band Electromagnetic-Acoustic Transducers.
PB96-186036 *02,279*

Dynamometer-Induced Residual Stress in Railroad Wheels: Ultrasonic and Saw Cut Measurements. Report No. 30.
PB96-183199 *04,857*

Effect of Liftoff on Accuracu of Phase Velocity Measurements Made with Electromagnetic-Acoustic Transducers.
PB96-186044 *02,280*

Methods to Improve the Accuracy of On-Line Ultrasonic Measurement of Steel Sheet Formability.
PB96-186051 *02,281*

Residual Stress in Induction-Heated Railroad Wheels: Ultrasonic and Saw Cut Measurements. Report No. 28.
PB96-106992 *04,854*

Safety Assessment of Railroad Wheels by Residual Stress Measurements.
PB96-141114 *04,855*

Safety Assessment of Railroad Wheels Through Roll-by Detection of Tread Cracks.
PB96-141254 *04,856*

Sensor System for Intelligent Processing of Hot-Rolled Steel.
PB96-186069 *03,373*

Ultrasonic Measurement of Residual Stress in Cast Steel Railroad Wheels.
PB95-169199 *04,852*

Ultrasonic Measurement of Residual Stress in Railroad Wheel Rims.
PB95-140430 *04,849*

Ultrasonic Measurement of Sheet Anisotropy and Formability.
PB95-153235 *03,213*

Ultrasonic Methods.
PB96-190327 *02,707*

Well-Shielded EMAT for On-Line Ultrasonic Monitoring of GMA Welding.
PB96-186077 *02,879*

CLARK, C.

Influence of Coadsorbed Potassium on the Electron-Stimulated Desorption of F(+), F(-), and F(*) from PF3 on Ru(0001).
PB96-157946 *04,072*

CLARK, C. W.

Appearance Intensities for Multiply Charged Ions in a Strong Laser Field.
PB96-160445 *04,089*

Charge-Transfer-Induced Multiplet Structure in the N4,5O2,3 Soft-X-ray Emission Spectrum of Lanthanum.
PB96-163746 *04,102*

Perturbative Calculation of the AC Stark Effect by the Complex Rotation Method.
PB95-141123 *04,260*

Population Trapping in Short-Pulse Multiphoton Ionization.
PB96-164140 *04,371*

Properties of a Bose-Einstein Condensate in an Anisotropic Harmonic Potential.
PB96-204144 *04,133*

CLARK, D. D.

Neutron Capture Prompt Gamma-Ray Activation Analysis at the NIST Cold Neutron Research Facility.
PB94-213394 *00,556*

CLARK, F. E.

Intercomparison of Internal Proportional Gas Counting of (85)Kr and (3)H.
PB94-185576 *03,800*

CLARK, N. A.
Dielectric Spectroscopic Determination of Temperature Behavior of Electroclinic Parameters in the Liquid Crystal W317.
PB96-140397 *01,098*

Shear-Induced Melting of Two-Dimensional Solids.
PB96-112057 *01,075*

Studies of the Higher Order Smectic Phase of the Large Electroclinic Effect Material W317.
PB95-151601 *00,935*

X-ray Observation of Electroclinic Layer Constriction and Rearrangement in a Chiral Smectic-A Liquid Crystal.
PB96-141080 *01,100*

CLARK, R.
HVAC CAD Layout Tools: A Case Study of University/Industry Collaboration.
PB97-112221 *00,281*

CLARK, R. A.
Characterization of Cytochrome c/Alkanethiolate Structures Prepared by Self-Assembly on Gold.
PB95-164638 *00,987*

CLARK, S. N.
APDE Demonstration System Architecture. National PDES Testbed Report Series.
PB94-154325 *02,767*

Object-Oriented Tel/Tk Binding for Interpreted Control of the NIST EXPRESS Toolkit in the NIST STEP Application Protocol Development Environment.
PB96-141049 *02,785*

CLARKE, I.
Effect of Semiconductor Laser Characteristics on Optical Fiber Sensor Performance.
PB95-169132 *02,167*

CLARKE, I. G.
Polarization Insensitive 3x3 Sagnac Current Sensor Using Polarizing Spun High-Birefringence Fiber.
PB96-119276 *02,187*

Standard Polarization Components: Progress Toward an Optical Retardance Standard.
PB96-119672 *04,342*

CLARKE, J.
Fabrication Issues in Optimizing YBa2Cu3O7-x Flux Transformers for Low l/f Noise.
PB95-175857 *02,059*

Low Noise YBa2Cu3O7-x-SrTiO3-YBa2Cu3O7-x Mulitlayers for Improved Superconducting Magnetometers.
PB96-138417 *04,747*

Scanning Tunneling Microscopy of the Charge-Density-Wave Structure in 1T-TaS2.
PB95-180980 *04,689*

CLARKE, R. M.
Regulation of Lithium and Boron Levels in Normal Human Blood: Environmental and Genetic Considerations.
PB94-198579 *03,491*

CLARKE, S. M.
Structure and Rheology of Hard-Sphere Systems.
PB96-167333 *00,662*

CLARKE, W. B.
Determination of Boron and Lithium in Diverse Biological Matrices Using Neutron Activation - Mass Spectrometry (NA-MS).
PB94-212289 *00,554*

Regulation of Lithium and Boron Levels in Normal Human Blood: Environmental and Genetic Considerations.
PB94-198579 *03,491*

CLAVAGUERA-MORA, M. T.
Extrapolation of the Heat Capacity in Liquid and Amorphous Phases.
PB97-111421 *04,147*

CLAY, D. T.
In-situ Fume Particle Size and Number Density Measurements from a Synthetic Smelt.
PB94-212040 *03,334*

CLEARY, T. G.
Effect of Fuel Tank Rupture Mode on the Ignitability of Expelled Fuel.
PB97-110043 *01,444*

Effects of Sample Mounting on Flammability Properties of Intumescent Polymers.
PB96-159777 *03,389*

Flammability Characterization with the Lift Apparatus and the Cone Calorimeter.
PB97-110050 *01,435*

Flow of Alternative Agents in Piping.
PB95-202420 *00,022*

Generation and Characterization of Acetylene Smokes.
PB94-200292 *01,372*

Heat Flux from Flames to Vertical Surfaces.
PB97-110357 *01,438*

Influence of Ignition Source on the Flaming Fire Hazard of Upholstered Furniture. (NIST Reprint).
PB95-180162 *00,297*

Letter Report on Flame Spread Testing of a Composite Material.
PB97-110068 *01,436*

Ultrafine Combustion Aerosol Generator.
PB94-200300 *01,373*

CLEMENTS, A.
Preliminary Comparison of Time Transfers via LASSO, GPS and Two-Way Satellite.
PB95-151098 *01,529*

CLEVELAND, W. G.
Evolution of a Turbulent Boundary Layer Induced by a Three-Dimensional Roughness Element.
PB94-212818 *04,200*

CLICKNER, C. C.
Evidence for Tunneling and Magnetic Scatttering at 'In situ' YBCO/Noble-Metal Interfaces.
PB96-141098 *04,752*

In situ Noble Metal YBa2Cu3O7 Thin-Film Contacts.
PB94-211323 *04,494*

Insulating Boundary Layer and Magnetic Scattering in YBa2Cu3O7-delta/Ag Interfaces Over a Contact Resistivity Range of 10(-8) - 10(-3) Omega cm(2).
PB95-169157 *04,648*

Oxygen Annealing of Ex-situ YBCO/Ag Thin-Film Interfaces.
PB96-141312 *04,758*

CLIFTON, C. L.
Electron Transfer Reaction Rates and Equilibria of the Carbonate and Sulfate Radical Anions.
PB94-212180 *00,829*

Kinetics of the Reaction of the Sulfate Radical with the Oxalate Anion.
PB97-119127 *01,186*

Kinetics of the Self-Reaction of Hydroxymethylperoxyl Radicals.
PB94-212164 *00,827*

Temperature Dependence of the Rate Constants for Reactions of the Sulfate Radical, SO4-, with Anions.
PB94-212172 *00,828*

CLIFTON, J.
Optimization of Highway Concrete Technology.
PB94-182995 *01,333*

Warping of Terrace Pavers at the U.S. Capitol Building.
PB96-193651 *00,411*

CLIFTON, J. R.
4SIGHT Manual: A Computer Program for Modelling Degradation of Underground Low Level Waste Concrete Vaults.
PB95-231593 *03,726*

Corrosion Resistant Epoxy-Coated Reinforcing Steel.
PB94-185618 *01,307*

Diagnosis of Causes of Concrete Deterioration in the MLP-7A Parking Garage.
PB95-143095 *01,318*

Expansion of Cementitious Materials Exposed to Sulfate Solutions.
PB94-185782 *02,577*

High-Performance Concrete: Research Needs to Enhance Its Use.
PB95-180147 *01,322*

Highway Concrete (HWYCON) Expert System User Reference and Enhancement Guide.
PB94-215670 *01,316*

Long-Term Performance of Engineered Concrete Barriers.
PB95-260816 *03,727*

Microstructural Features of Some Low Water/Solids, Silica Fume Mortars Cured at Different Temperatures.
PB94-160777 *00,330*

Prediction of Cracking in Reinforced Concrete Structures.
PB95-220448 *03,725*

Sulfate Attack of Cementitious Materials: Volumetric Relations and Expansions.
PB94-187317 *03,232*

CLINE, J.
Disorder Trapping in Ni2TiAl.
PB94-198942 *03,322*

CLINE, J. P.
Ceramic Characterization.
DE94013170 *03,026*

Characterization of Phase and Surface Composition of Silicon Carbide Platelets.
PB94-216264 *03,043*

Epitaxial Growth of BaTiO3 Thin Films at 600C by Metalorganic Chemical Vapor Deposition.
PB96-122510 *03,071*

Introduction of a NIST Instrument Sensitivity Standard Reference Material for X-Ray Powder Diffraction.
PB94-200318 *00,807*

Texture Measurement of Sintered Alumina Using the March-Dollase Function.
PB96-179494 *04,784*

CLOTHIER, R.
Multi-Stage, Position Stabilized Vibration Isolation System for Neutron Interferometry.
PB95-175022 *03,955*

CLOUGH, R. B.
Investigation into a Practical Grain Growth Model for Hot Isostatic Pressing.
PB95-151684 *03,347*

Micromechanics of Densification and Distortion.
PB94-200326 *03,327*

CLOWNEY, L.
Nucleic Acid Database: Present and Future.
PB97-109078 *00,518*

CLUTTER, L. K.
Reactor Radiation Technical Activities, 1995.
PB96-193644 *03,741*

COAKLEY, K.
Certification of Phencyclidine in Lyophilized Human Urine Reference Materials.
PB96-160692 *03,508*

Stochastic Modeling of a New Spectrometer.
PB96-157870 *04,068*

COAKLEY, K. J.
Analysis of Scattering Asymmetry Statistics When Background Corrected Counts Are Negative.
PB94-200334 *03,824*

Effect of Splitting on Estimation of Emission Rate Profiles from Neutron Depth Profiling Spectra.
PB95-152245 *03,916*

Modeling Detector Response for Neutron Depth Profiling.
PB96-157813 *04,066*

Uncertainty Intervals for Polarized Beam Scattering Asymmetry Statistics.
PB94-200342 *03,825*

COCHRAN, J. F.
Brillouin Light Scattering Intensities for Thin Magnetic Films with Large Perpendicular Anisotropies.
PB94-211174 *04,488*

COFER, S.
Hierarchical Ada Robot Programming System (HARPS): A Complete and Working Telerobot Control System Based on the NASREM Model.
PB94-213162 *02,934*

COFFEN, L.
Approach to Setting Performance Requirements for Automated Evaluation of the Parameters of High-Voltage Impulses.
PB94-185634 *01,878*

COFFEY, K. R.
Antiferromagnetic Interlayer Correlations in Annealed Ni80Fe20/Ag Multilayers.
PB97-122220 *03,109*

Effect of Microstructure on Phase Formation in the Reaction of Nb/Al Multilayer Thin Films.
PB95-168415 *03,352*

First Phase Formation Kinetics in the Reaction of Nb/Al.
PB95-168456 *03,353*

Magnetic Structure Determination for Annealed Ni80Fe20/Ag Multilayers Using Polarized-Neutron Reflectivity.
PB96-176615 *03,739*

Thin Film Reaction Kinetics of Niobium/Aluminum, Multilayers.
PB95-175295 *04,651*

COFFEY, M. W.
Aspects of a Deformable Superconductor Model for the Vortex Mass.
PB95-175303 *04,652*

Deformable Superconductor Model for the Fluxon Mass.
PB95-175311 *04,653*

High-Frequency Linear Response of Anisotropic Type-II Superconductors in the Mixed State.
PB94-200359 *04,483*

Microwave Properties of YBa2Cu3O7-x Films at 35 GHz from Magnetotransmission and Magnetoreflection Measurements.
PB95-168977 *04,643*

Nonlinear Response of Type-II Superconductors in the Mixed State in Slab Geometry.
PB94-200367 *04,484*

Self-Reciprocal Fourier Functions.
PB96-200852 *01,974*

Transverse Thermomagnetic Effects in the Mixed State and Lower Critical Field of High-Tc Superconductors.
PB95-153250 *04,590*

COFFEY, S.
Frozen Orbits for Satellites Close to an Earth-Like Planet.
PB96-102165 *04,839*

COHEN, E. R.
How Accurate Are the Josephson and Quantum Hall Effects and QED.
PB95-163283 *03,942*

COHEN, M.
Percolation and Pore Structure in Mortars and Concrete.
PB95-150439 *00,370*

COHEN, M. E.
Error Propagation Biases in the Calculation of Indentation Fracture Toughness for Ceramics.
PB94-172434 *03,032*

COHEN, M. L.
Anharmonic Phonons and the Isotope Effect in Superconductivity.
PB94-200557 *04,486*

Electronic Correlations and Satellites in Superconducting Oxides.
PB94-200045 04,477

Experimental Constraints on Some Mechanisms for High-Temperature Superconductivity.
PB94-198553 04,463

Total-Dielectric-Function Approach to Electron and Phonon Response in Solids.
PB96-102884 01,067

COHEN, R.

Role of R22 in Refrigerating and Air Conditioning Equipment.
PB94-199783 03,253

COHEN-TANNOUDJI, C. N.

New Mechanisms for Laser Cooling.
PB95-153268 03,923

COHEN, Y.

Effect of Hydrodynamic Interactions on a Terminally Anchored Bead-Rod Model Chain.
PB95-141156 01,237

Methods to Improve the Accuracy of On-Line Ultrasonic Measurement of Steel Sheet Formability.
PB96-186051 02,281

Response of a Terminally Anchored Polymer Chain to Simple Shear Flow.
PB95-108668 01,233

COHN, S. M.

Economic, Energy, and Environmental Impacts of the Energy-Related Inventions Program.
DE94-017162 00,008

COHN, T. B.

International Green Building Conference and Exposition (2nd). Held in Big Sky, Montana on August 13-15, 1995.
PB95-253605 02,525

COLBERT, J.

What Is a 'Standard Reference Material' - What Is Any Reference Material.
PB96-186135 03,000

COLBERT, J. C.

Assessing the Credibility of the Calorific Content of Muncipal Solid Waste.
PB94-199882 02,581

Standard Reference Materials: Glass Filters as a Standard Reference Material for Spectrophotometry - Selection, Preparation, Certification, and Use of SRM 930 and SRM 1930.
PB94-188844 00,536

COLE, B. F.

Insulating Nanoparticles on YBa2Cu3O7-delta Thin Films Revealed by Comparison of Atomic Force and Scanning Tunneling Microscopy.
PB95-150843 04,575

COLE, K. D.

Determination of Total Protein Adsorbed on Solid (Membrane) Surface by a Hydrolysis Technique: Single Protein Adsorption.
PB96-167093 03,552

Phase Composition, Viscosities, and Densities for Aqueous Two-Phase Systems Composed of Polyethylene Glycol and Various Salts at 25C.
PB95-164596 00,986

Salt-PEG Two-Phase Aqueous Systems to Purify Proteins and Nucleic Acid Mixtures.
PB94-200375 03,527

COLEMAN, T.

Checking the Net Contents of Packaged Goods as Adopted by the 79th National Conference on Weights and Measures, 1994, Third Edition, Supplement 4.
PB95-182226 00,484

COLLE, R.

36Cl/Cl Accelerator-Mass-Spectrometry Standards: Verification of Their Serial-Dilution-Solution Preparations by Radioactivity Measurements.
PB94-140563 00,524

63Ni Half-Life: A New Experimental Determination and Critical Review.
PB97-111603 00,700

Alpha-Particle and Electron Capture Decay of (209)Po.
PB96-186085 04,119

Calibration of Electret-Based Integral Radon Monitors Using NIST Polyethylene-Encapsulated (226)Ra/(222)Rn Emanation (PERE) Standards.
PB96-159223 01,950

International Marine-Atmospheric (222)Rn Measurement Intercomparison in Bermuda. Part 1. NIST Calibration and Methodology for Standardized Sample Additions.
PB96-175674 00,114

International Marine-Atmospheric (222)Rn Measurement Intercomparison in Bermuda. Part 2. Results for the Participating Laboratories.
PB96-175682 00,115

International Radon-in-Air Measurement Intercomparison Using a New Transfer Standard.
PB96-159751 03,708

Long-Term Stability of Carrier-Free Polonium Solution Standards.
PB94-185170 00,685

Nickel-63 Standardization: 1968-1995.
PB97-111819 00,701

COLLICA, L. A.

ISDN Conformance Testing.
PB95-163176 01,478

ISDN Conformance Testing Guidelines: Guidelines for Implementors of ISDN Customer Premises Equipment to Conform to Both National ISDN-1 and North American ISDN Users' Forum Layer 3 Basic Rate Interface Basic Call Control Abstract Test Suites.
PB94-219094 01,471

COLLINS, B. L.

Consensus Process in Standards Development.
PB96-179502 00,136

Helping to Reduce Technical Barriers to Trade.
PB96-190046 00,491

Papers Presentations Shine.
PB94-200383 00,244

Performance of Compact Fluorescent Lamps at Different Ambient Temperatures.
PB95-175329 00,258

Post-Occupancy Evaluation of the Forrestal Building.
PB97-111298 00,280

Psychological Aspects of Lighting: A Review of the Work of CIE TC 3.16.
PB94-172160 00,241

Psychological Aspects of Lighting: A Review of the Work of CIE TC 3.16.
PB95-153276 00,254

COLLINS, J.

Positive and Negative Cooperativities at Subsequent Steps of Oxygenation Regulate the Allosteric Behavior of Multistate Sebacylhemoglobin.
PB97-119374 03,486

COLOMBINI, M.

Extending the Angular Range of Neutron Reflectivity Measurements from Planar Lipid Bilayers: Applications to a Model Biological Membrane.
PB96-122569 03,476

COLOMBO, L.

Characterization of Liquid-Phase Epitaxially Grown HgCdTe Films by Magnetoresistance Measurements.
PB96-123617 04,738

Characterization of LPE HgCdTe Film by Magnetoresistance.
PB96-157961 02,197

Electrical Characterization of Liquid-Phase Epitaxially Grown Single-Crystal Films of Mercury Cadmium Telluride by Variable-Magnetic-Field Hall Measurements.
PB95-175782 02,177

COLTON, R. J.

Summary Report: Workshop on Industrial Applications of Scanned Probe Microscopy (2nd). A Workshop Co-Sponsored by NIST, SEMATECH, ASTM E42.14, and the American Vacuum Society. Held in Gaithersburg, Maryland on May 2-3, 1995.
PB96-131602 00,509

Workshop Summary Report: Industrial Applications of Scanned Probe Microscopy. A Workshop Co-sponsored by NIST, SEMATECH, ASTM, E42.14, and the American Vacuum Society. Held in Gaithersburg, Maryland on March 24-25, 1994.
PB95-170387 00,506

COLWELL, J. H.

Development of a Temperature Scale below 0.5 K.
PB95-125639 03,879

Systematic Studies of the Effect of a Bandpass Filter on a Josephson-Junction Noise Thermometer.
PB95-162970 03,939

Systematic Studies of the Effect of a Post-Detection Filter on a Josephson-Junction Noise Thermometer.
PB95-162988 03,940

COMAS, J.

Influence of Lattice Mismatch on Indium Phosphide Based High Electron Mobility Transistor (HEMT) Structures Observed in High Resolution Monochromatic Synchrotron X-Radiation Diffraction Imaging.
PB95-164679 02,357

Interface Roughness, Composition, and Alloying of Low-Order AlAs/GaAs Superlattices Studies by X-ray Diffraction.
PB96-160262 02,983

Interface Sharpness during the Initial Stages of Growth of Thin, Short-Period III-V Superlattices.
PB95-108783 02,139

Interface Sharpness in Low-Order III-V Superlattices.
PB95-108775 02,138

Scaling of the Nonlinear Optical Cross Sections of GaAs-AlGaAs Multiple Quantum-Well Hetero n-i-p-i's.
PB96-102793 02,183

COMPOS, R.

Tribological Behavior of 440/Diamond-Like-Carbon Film Couples.
PB96-119714 03,019

Tribometer for Measurements in Hostile Environments.
PB95-180949 02,967

Wear Mechanism Maps of 440C Martensitic Stainless Steel.
PB96-111810 04,834

COMPOSTO, R. J.

Gas Absorption during Ion-Irradiation of a Polymer Target.
PB96-161864 04,099

CONE, E. J.

Hair Testing for Drugs of Abuse: International Research on Standards and Technology.
PB96-120555 03,504

CONLEY, J. F.

Electron Traps, Structural Change, and Hydrogen Related SIMOX Defects.
PB94-200391 02,312

Evidence for a Deep Electron Trap and Charge Compensation in Separation by Implanted Oxygen Oxides.
PB95-175337 02,362

CONNELL, P. S.

Environmental Aspects of Halon Replacements: Considerations for Advanced Agents and the Ozone Depletion Potential of CF3I.
PB97-122261 03,301

COOK, G. R.

Algebraic Approximation of Attractors for Galloping Oscillators.
PB95-162897 04,820

Chaotic Motions of Coupled Galloping Oscillators and Their Modeling as Diffusion Progresses.
PB96-122718 04,823

Experimental and Numerical Chaos in Continuous Systems: Two Case Studies.
PB96-156146 00,219

Foias-Temam Approximations of Attractors for Galloping Oscillators.
PB94-198298 04,817

COOK, J. C.

Analysis of the Effectiveness of Oscillating Radial Collimators in Neutron Scattering Applications.
PB95-152252 03,917

COOK, L.

Single-Photon Ionization and Detection of Ga, In, and As(sub n) Species in GaAs Growth.
PB95-152815 00,591

COOK, L. P.

Crystal Chemistry and Phase Equilibrium Studies of the BaO(BaCO3)-R2O3-CuO Systems. 5. Melting Relations in Ba2(Y,Nd,Eu)Cu3O6+x.
PB95-151718 04,580

Microstructure and Ferroelectric Properties of Lead Zirconate-Titanate Films Produced by Laser Evaporation.
PB94-199148 04,470

X-Ray Characterization of the Crystallization Process of High-Tc Superconducting Oxides in the Sr-Bi-Pb-Ca-Cu-O System.
PB95-151700 04,579

COOKSON, A. H.

Advanced Components for Electric and Hybrid Electric Vehicles. Workshop Proceedings. Held in Gaithersburg, Maryland on October 27-28, 1993.
PB94-177060 04,858

President's Column 'Editorial'.
PB96-164090 02,239

President's Column for Dielectrics and Electrical Insulation Society Newsletter.
PB94-200409 01,882

COOKSY, A. L.

Fine-Structure Intervals of (14)N(+) By Far-Infrared Laser Magnetic Resonance.
PB95-175162 00,993

COOLEY, L. D.

Crossover in the Pinning Mechanism of Anisotropic Fluxon Cores.
PB95-180170 04,673

Pinch Effect in Commensurate Vortex-Pin Lattices.
PB96-147079 01,125

Temperature and Field Dependence of Flux Pinning in NbTi with Aritificial Pinning Centers.
PB96-112024 04,726

COOMBS, D.

Real-Time Obstacle Avoidance Using Central Flow Divergence and Peripheral Flow.
PB95-198677 02,937

COOPER, J.

Attempts at Extending the Unified Theory to Include Many-Body Effects.
PB94-212719 04,408

Collisional Energy Transfer between Excited-State Strontium and Noble-Gas Atoms.
PB95-202958 03,995

Cone Emission from Laser-Pumped Two-Level Atoms. 1. Quantum Theory of Resonant Light Propagation.
PB95-203584 04,325

Cone Emission from Laser-Pumped Two-Level Atoms. 2. Analytical Model Studies.
PB95-203592 04,326

Energy-Pooling Collisions in Barium.
PB95-203030 03,997

Failures of the Four-Wave Mixing Model for Cone Emission.
PB95-202636 04,318

Suppression of Ionization in One- and Two-Dimensional Model Calculations.
PB95-203600 04,009

COOPER, J. D.
Northridge Earthquake 1994: Performance of Structures, Lifelines, and Fire Protection Systems.
PB94-207461 *04,825*

COOPER, J. P.
Learning to Change: Opportunities to Improve the Performance of Smaller Manufacturers.
PB94-166212 *00,010*

COOPER, J. W.
Autoionizing Resonances in Electric Fields.
PB94-212727 *03,853*

COOPER, L. Y.
Calculating Combined Buoyancy- and Pressure-Driven Flow Through a Shallow, Horizontal, Circular Vent; Application to Problem of Steady Burning in a Ceiling-Vented Enclosure.
PB96-164108 *00,409*

Combined Buoyancy- and Pressure-Driven Flow Through a Shallow, Horizontal, Circular Vent.
PB94-210077 *00,344*

Combined Buoyancy and Pressure-Driven Flow Through a Shallow, Horizontal, Circular Vent.
PB96-164116 *00,410*

Fire-Plume-Generated Ceiling Jet Characteristics and Convective Heat Transfer to Ceiling and Wall Surfaces in a Two-Layer Fire Environment: Uniform Temperature Ceiling and Walls.
PB95-164711 *00,382*

Generation Rate and Distribution of Products of Combustion in Two-Layer Fire Environments: A Model and Applications.
PB96-102173 *01,398*

Interaction of an Isolated Sprinkler Spray and a Two-Layer Compartment Fire Environment. Phenomena and Model Simulations.
PB97-110076 *01,437*

Methodology for Developing and Implementing Alternative Temperature-Time Curves for Testing the Fire Resistance of Barriers for Nuclear Power Plant Applications.
PB96-193784 *03,742*

Simulating Smoke Movement through Long Vertical Shafts in Zone-Type Compartment Fire Models.
PB95-143152 *00,368*

Some Factors Affecting Design of a Furniture Calorimeter Hood and Exhaust.
PB94-139193 *00,285*

Some Factors Affecting the Design of a Calorimeter Hood and Exhaust.
PB96-102181 *00,302*

VENTCF2: An Algorithm and Associated FORTRAN 77 Subroutine for Calculating Flow through a Horizontal Ceiling/Floor Vent in a Zone-Type Compartment Fire Model.
PB94-210127 *00,345*

COPLEN, T. B.
New IUPAC Guidelines for the Reporting of Stable Hydrogen, Carbon, and Oxygen Isotope-Ratio Data. Letter to the Editor.
PB95-261962 *01,058*

COPLEY, J. R. D.
Acceptance Diagram Analysis of the Performance of Multidisk Neutron Velocity Selectors.
PB94-200417 *03,826*

Acceptance Diagram Analysis of the Performance of Vertically Curved Neutron Monochromators.
PB94-200425 *03,827*

Analysis of the Effectiveness of Oscillating Radial Collimators in Neutron Scattering Applications.
PB95-152252 *03,917*

Discontinuous Volume Change at the Orientational-Ordering Transition in Solid C60.
PB94-211828 *00,821*

Energy Distributions of Neutrons Scattered from Solid C60 by the Beryllium Detector Method.
PB96-176631 *03,740*

Inelastic Neutron Scattering Studies of Rotational Excitations and the Orientational Potential in C60 and A3C60 Compounds.
PB94-172673 *00,763*

Joy of Acceptance Diagrams.
PB94-200433 *03,828*

Neutron and X-Ray Scattering Cross Sections of Orientationally Disordered Soild C60.
PB95-153300 *00,951*

Neutron-Scattering Study of C60(n-) (n=3,6) Librations in Alkali-Metal Fullerides.
PB94-200219 *00,806*

Neutron-Scattering Study of Librations and Intramolecular Phonons in Rb2.6K0.4C60.
PB95-162269 *00,958*

Orientational Fluctuations, Diffuse Scattering, and Orientational Order in Solid C60.
PB97-119275 *04,176*

Rotational Dynamics of C60 in Na2RbC60.
PB95-153201 *00,948*

Rotational Dynamics of Solid C70: A Neutron-Scattering Study.
PB94-172178 *00,755*

Rotational Dynamics of Solid C70: A Neutron-Scattering Study.
PB95-153219 *00,949*

Scattering and Absorption Effects in Neutron Beam Activation Analysis Experiments.
PB94-216140 *00,557*

Simulations of Neutron Focusing with Curved Mirrors.
PB96-176649 *02,200*

Structure and Dynamics of Buckyballs.
PB95-153292 *00,950*

Structures of Sodium Metal.
PB94-198850 *03,319*

Supermirror Transmission Polarizers for Neutrons.
PB94-216215 *03,866*

Transmission Properties of Short Curved Neutron Guides. Part 1. Acceptance Diagram Analysis and Calculations.
PB96-102199 *04,021*

X-ray Powder Diffraction from Carbon Nanotubes and Nanoparticles.
PB96-102975 *03,064*

CORBIN, D. R.
Neutron and Raman Spectroscopies of 134 and 134a Hydrofluorocarbons Encaged in Na-X Zeolite.
PB96-186168 *03,001*

CORDARA, F.
Precision Oscillators: Dependence of Frequency on Temperature, Humidity and Pressure.
PB94-198306 *02,031*

CORDTS, B. F.
Effect of Annealing Ambient on the Removal of Oxide Precipitates in High-Dose Oxygen Implanted Silicon.
PB95-164356 *02,356*

CORIELL, S. R.
Asymptotic Behavior of Modulated Taylor-Couette Flows with a Crystalline Inner Cylinder.
PB94-199072 *04,469*

Convection and Morphological Stability During Directional Solidification.
N95-14548/8 *03,310*

Convective Stability in the Rayleigh-Benard and Directional Solidification Problems: High-Frequency Gravity Modulation.
PB95-181145 *04,208*

Effect of Modulated Taylor-Couette Flows on Crystal-Melt Interfaces: Theory and Initial Experiments.
PB94-216736 *04,521*

Effects of Crystalline Anisotropy and Buoyancy-Driven Convection on Morphological Stability.
PB94-200441 *03,328*

Laser Melting of Thin Silicon Films.
PB94-199239 *04,471*

Morphological Stability.
PB95-153318 *04,591*

Rayleigh Instability for a Cylindrical Crystal-Melt Interface.
PB95-180667 *01,010*

Stagnant Film Model of the Effect of Natural Convection on the Dendrite Operating State.
PB96-146832 *04,765*

CORMIER, A.
Frozen Human Serum Reference Material for Standardization of Sodium and Potassium Measurements in Serum or Plasma by Ion-Selective Electrode Analyzers.
PB94-185337 *00,532*

CORNELL, E. A.
Behavior of Atoms in a Compressed Magneto-Optical Trap.
PB95-203105 *03,999*

Comment on <<A Dynamic Electric Trap for Ground-State Atoms>>.
PB96-200290 *04,123*

Gravitational Sisyphus Cooling of (87)Rb in a Magnetic Trap.
PB96-200704 *04,379*

Reduction of Light-Assisted Collisional Loss Rate from a Low-Pressure Vapor-Cell Trap.
PB95-202248 *03,971*

Stable, Tightly Confining Magnetic Trap for Evaporative Cooling of Neutral Atoms.
PB96-200720 *04,126*

CORNIER-QUIQUANDON, M.
Neutron Scattering Structural Study of AlCuFe Quasicrystals Using Double Isotopic Substitution.
PB94-200458 *04,485*

CORRUCCINI, R. J.
Reference Tables for Thermocouples.
AD-A279 948/4 *02,614*

COSANDEY, F.
Imaging of Fine Porosity in a Colloidal Silica: Potassium Silicate Gel by Defocus Contrast Microscopy.
PB94-212750 *03,039*

COTELL, C. M.
Interface Sharpness during the Initial Stages of Growth of Thin, Short-Period III-V Superlattices.
PB95-108783 *02,139*

COTSORADIS, C.
NIST Handbook 44, 1996: Specifications, Tolerances, and Other Technical Requirements for Weighing and Measuring Devices as Adopted by the 80th National Conference on Weights and Measures, 1995.
PB96-166616 *02,926*

COTTS, E. J.
Enthalpy Increment Measurements from 4.5 K to 350 K and the Thermodynamic Properties of the Titanium Silicide Ti5Si3(cr).
PB96-204037 *00,679*

Enthalpy Increment Measurements from 4.5 to 350 K and the Thermodynamic Properties of Titanium Disilicide(cr) to 1700 K.
PB96-204029 *00,678*

COUDERT, L. H.
2-Tunneling Path Internal-Axis-Method-Like Treatment of the Microwave Spectrum of Divinyl Ether.
PB94-200466 *00,808*

COUGHANOWR, C. A.
Assessment of the Al-Sb System.
PB94-200474 *03,329*

COURMONT, S.
Diffusion of Water along 'Closed' Mica Interfaces.
PB96-180039 *02,993*

Pressurized Internal Lenticular Cracks at Healed Mica Interfaces.
PB96-180252 *02,997*

COURSEY, B. M.
Assay of the Eluent from the Alumina-Based Tungsten-188-Rhenium-188 Generator.
PB94-200482 *03,829*

Dose Mapping of Radioactive Hot Particles Using Radiochromic Film.
PB95-162954 *03,714*

Experimental Validation of Radiopharmaceutical Absorbed Dose to Mineralized Bone Tissue.
PB94-199668 *03,617*

Investigation of Applicability of Alanine and Radiochromic Detectors to Dosimetry of Proton Clinical Beams.
PB96-146782 *03,636*

Liquid-Scintillation Counting Techniques for the Standardization of Radionuclides Used in Therapy.
PB97-110084 *03,709*

Needs for Brachytherapy Source Calibrations in the United States.
PB97-110092 *03,521*

Overview of a Radiation Accident at an Industrial Accelerator Facility.
PB97-122485 *02,612*

Radiation Accident at an Industrial Accelerator Facility.
PB95-140117 *02,575*

Radiation Doses.
PB94-199676 *03,618*

Radioassays of Yttrium-90 Used in Nuclear Medicine.
PB97-110100 *03,522*

Role of the Office of Radiation Measurement in Quality Assurance.
PB94-212255 *00,689*

Standardization and Decay Scheme of Rhenium-186.
PB94-200490 *03,830*

System for Intercomparing Standard Solutions of Beta-Particle Emitting Radionuclides.
PB96-159637 *03,707*

COURSOL, N.
Intercomparison of Internal Proportional Gas Counting of (85)Kr and (3)H.
PB94-185576 *03,800*

COUSTEL, N.
Discontinuous Volume Change at the Orientational-Ordering Transition in Solid C60.
PB94-211828 *00,821*

COVENEY, P. V.
Cellular Automaton Simulations of Cement Hydration and Microstructure Development.
PB95-175055 *01,320*

COVERDALE, R. T.
Calculation of the Thermal Conductivity and Gas Permeability in a Uniaxial Bundle of Fibers.
PB95-180931 *03,058*

COWAN, P.
Lattice Position of Si in GaAs Determined by X-Ray Standing Wave Measurements.
PB95-164406 *04,632*

COWAN, P. L.
Anisotropy of Polarized X-ray Emission from Atoms and Molecules.
PB95-163002 *04,621*

Evolution of X-ray Resonance Raman Scattering into X-ray Fluorescence from the Excitation of Xenon Near the L3 Edge.
PB96-102751 *04,025*

Polarized X-Ray Emission Spectroscopy.
PB94-213360 *03,862*

COWLEY, R. A.
Observation of Two Length Scales Above (T sub N) in a Holmium Thin Film.
PB97-111942 *04,151*

COX, D. E.
Discontinuous Volume Change at the Orientational-Ordering Transition in Solid C60.
PB94-211828 *00,821*

COX, D. M.
Discontinuous Volume Change at the Orientational-Ordering Transition in Solid C60.
PB94-211828 *00,821*

COX, S. D.
Inelastic Neutron Scattering Studies of Nonlinear Optical Materials: p-Nitroaniline Adsorbed in ALPO-5.
PB95-107223 *00,874*

COXON, B.
L-threo-beta-Hydroxyhistidine, an Unprecedented Iron(III) Ion-Binding Amino Acid in a Pyoverdine-type Siderophore from Pseudomonas fluorescens 244.
PB94-211620 *00,553*

Physicochemical Characterization of Low Molecular Weight Heparin.
PB96-112040 *03,474*

Two-Dimensional POMMIE Carbon-Proton Chemical Shift Correlated (13)C NMR Spectrum Editing.
PB94-200508 *00,809*

COYNE, J. J.
Microdosimetry and Cellular Radiation Effects of Radon Progency in Human Bronchial Airways.
PB95-152344 *03,625*

Neutron Energy Deposition on the Nanometer Scale.
PB95-152260 *03,624*

Systematics of Alpha-Particle Energy Spectra and Lineal Energy (Y) Spectra for Radon Daughters.
PB94-185139 *03,615*

CRAFT, N.
Development of Engineered Stationary Phases for the Separation of Carotenoid Isomers.
PB95-150249 *00,578*

Nutritional Status and Growth in Juvenile Rheumatoid Arthritis.
PB94-198470 *03,515*

CRAFT, N. E.
Carotenoid Reversed-Phase High-Performance Liquid Chromatography Methods: Reference Compendium.
PB94-200516 *00,549*

Device for Subambient Temperature Control in Liquid Chromatography.
PB95-140604 *00,573*

High-Performance Liquid Chromatography of Phytoplankton Pigments Using a Polymeric Reversed-Phase C18 Column.
PB95-151130 *00,583*

Individual Carotenoid Content of SRM 1548 Total Diet and Influence of Storage Temperature, Lyophilization, and Irradiation on Dietary Carotenoids.
PB94-200524 *00,033*

Liquid Chromatographic Method for the Determination of Carotenoids, Retinoids, and Tocopherols in Human Serum and in Food.
PB95-153599 *00,593*

CRAFTON, H. C.
Physical Properties of Some Purified Aliphatic Hydrocarbons.
AD-A297 265/1 *00,657*

CRAIG, D.
Guidelines for the Development of Mapping Tables.
PB96-154539 *02,786*

CRAIG, R. M.
Interlaboratory Comparison of Polarization-Holding Parameter Measurements on High-Birefringence Optical Fiber.
PB95-168464 *04,280*

CRAIN, P.
beta-D-Glucosyl-Hydroxymethyluracil: A Novel Modified Base Present in the DNA of the Parastic Protozoan T. brucei.
PB94-172319 *03,524*

CRANKSHAW, O. S.
Proficiency Tests for the NIST Airborne Asbestos Program, 1993.
PB96-106463 *00,610*

CRANMER, D. C.
Assessment of Testing Methodology for Ceramic Matrix Composites.
PB94-200532 *03,139*

Moisture and Water-Induced Crack Growth in Optical Materials.
PB95-153334 *04,267*

Perspective on Fiber Coating Technology.
PB94-200540 *03,118*

Tensile Creep Testing of Structural Ceramics.
PB97-110464 *03,105*

Transient Creep Behaviour of Hot Isostatically Pressed Silicon Nitride.
PB96-180278 *03,086*

CRASEMANN, B.
Atomic, Molecular, and Optical Physics with X-rays.
PB94-213378 *03,863*

CRAWFORD-BROWN, D. J.
Microdosimetry and Cellular Radiation Effects of Radon Progency in Human Bronchial Airways.
PB95-152344 *03,625*

CRAWFORD, M. K.
Neutron and Raman Spectroscopies of 134 and 134a Hydrofluorocarbons Encaged in Na-X Zeolite.
PB96-186168 *03,001*

CRAWFORD, M. L.
Alternative EMC Compliance Test Facilities.
PB96-200324 *02,247*

Aperture Coupling to a Coaxial Air Line: Theory and Experiment.
PB94-211968 *02,216*

Aperture Excitation of Electrically Large, Lossy Cavities.
PB94-145711 *00,029*

Aperture Excitation of Electrically Large, Lossy Cavities.
PB95-175675 *00,031*

Band-Limited, White Gaussian Noise Excitation for Reverberation Chambers and Applications to Radiated Susceptibility Testing.
PB96-165410 *01,960*

Measurements of Shielding Effectiveness and Cavity Characteristics of Airplanes.
PB94-210051 *00,030*

TEM/Reverberating Chamber Electromagnetic Radiation Test Facility at Rome Laboratory.
PB96-155023 *03,675*

CRAWFORD, T. M.
Observation of the Transverse Second Harmonic Magneto-Optic Kerr Effect from Ni81Fe19 Thin Film Structures.
PB96-200332 *01,971*

CREECY, R.
Second Census Optical Character Recognition Systems Conference.
PB94-188711 *01,832*

CREEGAN, K. M.
Discontinuous Volume Change at the Orientational-Ordering Transition in Solid C60.
PB94-211828 *00,821*

CRESPI, V. H.
Anharmonic Phonons and the Isotope Effect in Superconductivity.
PB94-200557 *04,486*

CRESSWELL, M. W.
Application of the Modified Voltage-Dividing Potentiometer to Overlay Metrology in a CMOS/Bulk Process.
PB94-181997 *02,302*

Design Guide for CMOS-On-SIMOX. Test Chips NIST3 and NIST4.
PB94-163458 *02,297*

Electrical Test Structure for Overlay Metrology Referenced to Absolute Length Standards.
PB95-152278 *02,336*

Electrical Test Structures Replicated in Silicon-on-Insulator Material.
PB97-111827 *02,454*

Enhanced Voltage-Dividing Potentiometer for High-Precision Feature Placement Metrology.
PB96-164025 *02,428*

Hybrid Optical-Electrical Overlay Test Structure.
PB96-204136 *02,450*

Measurement of Patterned Film Linewidth for Interconnect Characterization.
PB96-148168 *02,420*

Metrology Standards for Advanced Semiconductor Lithography Referenced to Atomic Spacings and Geometry.
PB96-160718 *02,424*

Microelectronic Test Structures for Feature Placement and Electrical Linewidth Metrology.
PB95-180568 *02,367*

Microelectronic Test Structures for Overlay Metrology.
PB96-164249 *02,430*

New Test Structure for Nanometer-Level Overlay and Feature-Placement Metrology.
PB95-175345 *02,363*

Test Structures for the In-Plane Locations of Projected Features with Nanometer-Level Accuracy Traceable to a Coordinate Measurement System.
PB94-200565 *02,313*

CRISCO, J. J.
Reinforcement of Cancellous Bone Screws with Calcium Phosphate Cement.
PB96-158001 *00,179*

CRISSMAN, J. M.
Performance of Plastic Packaging for Hazardous Materials Transportation. Part 1. Mechanical Properties.
AD-A301 258/0 *02,580*

CROARKIN, M. C.
Cryogenic Blackbody Calibrations at the National Institute of Standards and Technology Low Background Infrared Calibration Facility.
PB94-169802 *02,117*

Measurement and Uncertainty of a Calibration Standard for the Scanning Electron Microscope.
PB94-219250 *00,560*

CROCHIERE, S. M.
Characterization of Vertical-Cavity Semiconductor Structures.
PB94-200193 *02,126*

Vertical-Cavity Optoelectronic Structures: CAD, Growth, and Structural Characterization.
PB95-153177 *02,148*

Vertical-Cavity Semiconductor Lasers: Structural Characterization, CAD, and DFB Structures.
PB95-153193 *02,150*

CROMAR, M.
High Critical Temperature Superconductor Tunneling Spectroscopy Using Squeezable Electron Tunneling Junctions.
PB95-163721 *04,627*

CROMAR, M. W.
Critical Current Behavior of Ag-Coated YBa2Cu3O7-x Thin Films.
PB95-141016 *04,549*

Optimization of ECR-Based PECVD Oxide Films for Superconducting Integrated Circuit Fabrication.
PB95-169165 *02,051*

Superconducting Integrated Circuit Fabrication with Low Temperature ECR-Based PECVD SiO2 Dielectric Films.
PB96-103015 *04,719*

CROMER, C.
Method of Realizing Spectral Irradiance Based on an Absolute Cryogenic Radiometer.
PB95-161204 *04,270*

CROMER, C. L.
Absolute Response Calibration of a Transfer Standard Cryogenic Bolometer.
PB96-147103 *04,358*

Comparison of Filter Radiometer Spectral Responsivity with the NIST Spectral-Irradiance and Illuminance Scales.
PB97-113161 *04,162*

Detector-Based Candela Scale and Related Photometric Calibration Procedures at NIST.
PB95-161949 *04,273*

Improved Dose Metrology in Optical Lithography.
PB96-179510 *02,439*

Mode-Locked Lasers for High-Accuracy Radiometry.
PB96-204201 *04,134*

National Institute of Standards and Technology High-Accuracy Cryogenic Radiometer.
PB96-179585 *04,378*

NIST Detector-Based Luminous Intensity Scale.
PB96-179114 *01,864*

NIST High Accuracy Scale for Absolute Spectral Response from 406 nm to 920 nm.
PB96-179122 *01,865*

Realization of a Scale of Absolute Spectral Response Using the NIST High Accuracy Cryogenic Radiometer.
PB97-118640 *04,397*

CROMPTON, R. W.
Analyses of Recent Experimental and Theoretical Determinations of e-H2 Vibrational Excitation Cross Sections: Assessing a Long-Standing Controversy.
PB95-202438 *03,977*

CROS, D.
Measurements of Permittivity and the Dielectric Loss Tangent of Low Loss Dielectric Materials with a Dielectric Resonator Operating on the Higher Order Te(sub 0 gamma delta) Modes.
PB96-111869 *02,273*

CROSBY, F. J.
Modulation of Fossil Fuel Production by Global Temperature Variations, 2.
PB94-146636 *02,533*

CROSS, R. W.
Effects of Critical Current Density, Equilibrium Magnetization and Surface Barrier on Magnetization of High Temperature Superconductors.
PB94-185162 *04,446*

Effects of Critical Current Density, Equilibrium Magnetization and Surface Barrier on Magnetization of High Temperature Superconductors.
PB95-153060 *04,588*

Magnetic Measurement of Transport Critical Current Density of Granular Superconductors.
PB95-126199 *04,531*

Magnetoresistance of Thin-Film NiFe Devices Exhibiting Single-Domain Behavior.
PB96-147087 *04,766*

Micromagnetic Scanning Microprobe System.
PB95-176178 *02,224*

Models of Granualr Giant Magnetoresistance Multilayer Thin Films.
PB96-190228 *01,968*

Offset Susceptibility of Superconductors.
PB94-212263 *04,503*

Simulating Device Size Effects on Magnetization Pinning Mechanisms in Spin Valves.
PB97-112593 *04,158*

Size and Self-Field Effects in Giant Magnetoresistive Thin-Film Devices.
PB95-180188 *04,674*

Size Effects and Giant Magnetoresistance in Unannealed NiFe/Ag Multilayer Stripes.
PB97-111306 *04,145*

Size Effects in Submicron NiFe/Ag GMR Devices.
PB96-155510 *02,237*

Surface Barrier and Lower Critical Field in YBa2Cu3O7-delta Superconductors.
PB94-200128 *04,478*

CROUCH, A. E.

Assessment of Technology for Detection of Stress Corrosion Cracking in Gas Pipelines. Final Report, July 1993-March 1994.
PB94-206646 *02,475*

CROVETTO, R.

Standard States, Reference States and Finite-Concentration Effects in Near-Critical Mixtures with Applications to Aqueous Solutions.
PB95-164349 *00,979*

Thermodynamic Behavior of the CO2-H2O System from 400 to 1000 K, up to 100 MPa and 30% Mole Fraction of CO2.
PB94-162245 *00,736*

CROW, J. E.

Magnetic Ordering of the Cu Spins in PrBa2Cu3O6+x.
PB95-140547 *04,545*

CROWDER, J. M.

Visual Measurement Technique for Analysis of Nucleate Flow Boiling.
PB95-143301 *03,262*

CRUPE, W. E.

Application of the Electronic Balance in High Precision Pycnometry.
PB94-187564 *00,534*

CRUZ, J. Y.

Test of Newton's Inverse Square Law of Gravitation Using the 300-m Tower at Erie, Colorado.
PB95-202446 *03,978*

Validation of the Inverse Square Law of Gravitation Using the Tower at Erie, Colorado, USA.
PB95-164646 *03,947*

CUGINI, J.

Common Criteria: On the Road to International Harmonization.
PB96-123484 *01,606*

Functional Security Criteria for Distributed Systems.
PB96-123492 *01,607*

CUGINI, J. A.

Proceedings of the Workshop on the Federal Criteria for Information Technology Security. Held in Ellicot City, Maryland on June 2-3, 1993.
PB94-162583 *01,575*

CUGINI, J. V.

Graphical Conceptual Navigation as a Presentation Technique for a Graphics Standard.
PB94-200573 *01,692*

User's Guide for the PHIGS Validation Tests (Version 2.1).
PB94-165206 *01,682*

CUI, J. P.

Homogeneous Gas Phase Decyclization of Tetralin and Benzocyclobutene.
PB95-151049 *00,928*

Rate Constants for Hydrogem Atom Attack on Some Chlorinated Benzenes at High Temperature.
PB94-200581 *00,810*

CUI, S. T.

Conditions for Existence of a Reentrant Solid Phase in a Sheared Atomic Fluid.
PB94-211380 *04,198*

CULLIN, D.

Bacteriorhodopsin Immobilized in Sol-Gel Glass.
PB95-151429 *03,532*

CULLIN, D. W.

Holographic Properties of Triton X-100-Treated Bacteriorhodopsin Embedded in Gelatin Films.
PB96-119284 *03,761*

Optical Properties of Triton X-100-Treated Purple Membranes Embedded in Gelatin Films.
PB96-123500 *03,546*

CUNNINGHAM, C. E.

Noise Reduction in Low-Frequency SQUID Measurements with Laser-Driven Switching.
PB96-135165 *02,081*

Trapped Vortices in a Superconducting Microbridge.
PB95-141149 *04,554*

CUNNINGHAM, D.

Abstract and Index Collection in the Research Information Center of the National Institute of Standards and Technology.
PB94-152204 *02,744*

Abstract and Index Collection in the Research Information Center of the National Institute of Standards and Technology.
PB95-232633 *02,741*

Databases Available in the Research Information Center of the National Institute of Standards and Technology.
PB95-128641 *02,724*

Databases Available in the Research Information Center of the National Institute of Standards and Technology (December 1995).
PB96-139407 *02,734*

CUNNINGHAM, M.

Parametric Study of Wall Moisture Contents Using a Revised Variable Indoor Relative Humidity Version of the 'Moist' Transient Heat and Moisture Transfer Model.
PB97-122535 *00,419*

CURRIE, L. A.

Comparative Study of Fe-C Bead and Graphite Target Performance with the National Ocean Sciences AMS (NOSAMS) Facility Recombinator Ion Source.
PB95-175790 *00,693*

Distinguishing the Contributions of Residential Wood Combustion and Mobile Source Emissions Using Relative Concentrations of Dimethylphenanthrene Isomers.
PB96-135124 *02,563*

Importance of Chemometrics in Biomedical Measurements.
PB94-200599 *00,550*

Interlaboratory Comparison of Autoradiographic DNA Profiling Measurements. 1. Data and Summary Statistics.
PB95-175923 *03,542*

Interlaboratory Comparison of Autoradiographic DNA Profiling Measurements. 2. Measurement Uncertainty and Its Propagation.
PB96-112123 *03,545*

Metrological Measurement Accuracy: Discussion of 'Measurement Error Models' by Leon Jay Gleser.
PB94-200607 *00,551*

Radiocarbon Measurements of Atmospheric Volatile Organic Compounds: Quantifying the Biogenic Contribution.
PB97-122352 *02,574*

Sources of Urban Contemporary Carbon Aerosol.
PB95-175659 *02,551*

CURTISS, L. A.

Thermodynamics of (Germanium + Selenium): A Review and Critical Assessment.
PB97-112536 *01,182*

CUTHILL, B.

Defining Environment Integration Requirements.
PB96-131545 *02,733*

Information Technology Engineering and Measurement Model: Adding Lane Markings to the Information Superhighway.
PB95-143145 *01,474*

Making Sense of Software Engineering Environment Framework Standards.
PB95-105037 *01,701*

CUTHILL, B. B.

Guide to Software Engineering Environment Assessment and Evaluation.
PB94-140167 *01,676*

Proceedings of the Digital Systems Reliability and Nuclear Safety Workshop. Held in Rockville, Maryland on September 13-14, 1993.
NUREG/CP-0136 *03,728*

Reference Information for the Software Verification and Validation Process.
PB96-188164 *01,773*

Using a Multi-Layered Approach to Representing Tort Law Cases for Case-Based Reasoning.
PB96-160874 *00,135*

CUTLER, R. I.

NIST-NRL Free-Electron Laser Facility.
PB94-212511 *04,237*

CUTRO, J. A.

Increased Pinning Energies and Critical Current Densities in Heavy-Ion-Irradiated Bi2Sr2CaCu2O8 Single Crystals.
PB95-175352 *04,654*

CYPHER, D.

Error Protecting Characteristics of CDMA and Impacts on Speech.
PB96-122452 *01,491*

Framework for National Information Infrastructure Services.
PB95-103719 *02,723*

Provision of Isochronous Service on IEEE 802.6.
PB96-160635 *01,501*

Standardization for ATM and Related B-ISDN Technologies.
PB96-160460 *01,499*

D'ORAZIO, P.

Frozen Human Serum Reference Material for Standardization of Sodium and Potassium Measurements in Serum or Plasma by Ion-Selective Electrode Analyzers.
PB94-185337 *00,532*

DA SILVA, T. A.

Angular Variation of the Personal Dose Equivalent, Hp(0.07), for Beta Radiation and Nearly Monoenergetic Electron Beams: Preliminary Results.
PB95-168472 *03,630*

DABROWSKI, C.

Context Analysis of the Network Management Domain. Conducted as Part of the Domain Analysis Case Study.
PB94-142528 *01,465*

Domain Analysis of the Alarm Surveillance Domain. Version 1.0. Conducted as Part of the Domain Analysis Case Study Project.
PB95-136339 *01,705*

Glossary of Software Reuse Terms.
PB95-178992 *01,720*

DABROWSKI, C. E.

Application of Expert System to Select Data Sources from Chemical Information Databases.
PB95-125654 *00,505*

DADMUN, M. D.

Neutron Scattering Study of the Orientation of a Liquid Crystalline Polymer by Shear Flow.
PB95-180196 *01,270*

Phase Behavior of a Hydrogen Bonding Molecular Composite.
PB94-185188 *01,202*

DAGALAKIS, N.

NIST Support to the Next Generation Controller Program: 1991 Final Technical Report.
PB94-163490 *02,808*

DAGATA, J. A.

Integration of Scanning Tunneling Microscope Nanolithography and Electronics Device Processing.
PB95-153359 *02,341*

Junction Locations by Scanning Tunneling Microscopy: In-Air-Ambient Investigation of Passivated GaAs pn Junctions.
PB94-185964 *02,306*

Scanning Tunneling Microscopy and Fabrication of Nanometer Scale Structures at the Liquid-Gold Interface.
PB95-140414 *00,904*

Summary Report: Workshop on Industrial Applications of Scanned Probe Microscopy (2nd). A Workshop Co-Sponsored by NIST, SEMATECH, ASTM E42.14, and the American Vacuum Society. Held in Gaithersburg, Maryland on May 2-3, 1995.
PB96-131602 *00,509*

Workshop Summary Report: Industrial Applications of Scanned Probe Microscopy. A Workshop Co-sponsored by NIST, SEMATECH, ASTM, E42.14, and the American Vacuum Society. Held in Gaithersburg, Maryland on March 24-25, 1994.
PB95-170387 *00,506*

X-Ray Photoelectron and Auger Electron Spectroscopy Study of Ultraviolet/Ozone Oxidized P2S5/(NH4)2S Treated GaAs(100) Surfaces.
PB94-200144 *04,479*

DAHMANI, R.

Characterization of the ZnSe/GaAs Interface Layer by TEM and Spectroscopic Ellipsometry.
PB95-175360 *04,655*

Determination of the Optical Constants of ZnSe Films by Spectroscopic Ellipsometry.
PB95-175378 *04,656*

DAI, Z.

Mixing and Radiation Properties of Buoyant Luminous Flame Environments.
PB96-202254 *01,432*

Mixing and Radiation Properties of Buoyant Turbulent Diffusion Flames.
PB95-242327 *01,396*

Radiation and Mixing Properties of Buoyant Turbulent Diffusion Flames.
PB94-165974 *01,360*

DALBERTH, M. J.

Alignment Probing of Rydberg States by Stimulated Emission.
PB96-200316 *04,124*

Initial and Final Orbital Alignment Probing of the Fine-Structure-Changing Collisions among the Ca (4s)(1)(4p)(1), (3)PJ States with He: Determination of Coherence and Conventional Cross-Sections.
PB95-203279 *04,004*

Orbital Alignment and Vector Correlations in Inelastic Atomic Collisions.
PB96-122742 *04,047*

DALGARNO, A.

Papers on the Symposium on Collision Phenomena in Astrophysics, Geophysics, and Masers.
AD-A280 291/6 *00,047*

DALIBARD, J.

Atoms in Optical Molasses.
PB95-108874 *03,875*

Atoms in Optical Molasses: Applications to Frequency Standards.
PB95-108882 *03,876*

Optical Molasses: Cold Atoms for Precision Measurements.
PB95-108890 *03,877*

Optical Molasses: The Coldest Atoms Ever.
PB95-108908 *03,878*

sigma+-sigma- Optical Molasses in a Longitudinal Magnetic Field.
PB95-161840 *03,934*

DALLY, J. W.

Fracture Mechanics Analysis of Near-Surface Cracks.
PB94-172400 *03,230*

Hybrid Method for Determining Material Properties from Instrumented Micro-Indentation Experiments.
PB95-152229 *03,348*

Theory of Electron Beam Moire.
PB96-175690 *04,373*

DALVIE, M.

Gaseous Electronics Conference Radio-Frequency Reference Cell: A Defined Parallel-Plate Radio-Frequency System for Experimental and Theoretical Studies of Plasma-Processing Discharges.
PB94-172327 *04,404*

DAMAVARAPU, R.

1,4-Dinitrocubane and Cubane under High Pressure.
PB95-108437 *03,755*

DAMAZO, B.
Open Architectures for Machine Control.
PB94-135621 *02,942*

DANG, T. D.
Evidence of Crosslinking in Methyl Pendent PBZT Fiber.
PB97-112486 *03,393*

DANG, T. T.
International Marine-Atmospheric (222)Rn Measurement Intercomparison in Bermuda. Part 2. Results for the Participating Laboratories.
PB96-175682 *00,115*

DANIEL, E.
Absolute Cross-Section Measurements for Electron-Impact Ionization of C1(+1).
PB94-199841 *03,818*

DANIEL, R. G.
Environmental Aspects of Halon Replacements: Considerations for Advanced Agents and the Ozone Depletion Potential of CF3I.
PB97-122261 *03,301*

DANIELSON, B. L.
Low-Coherence Interferometric Measurement of Group Transit Times in Precision Optical Fibre Delay Lines.
PB95-168480 *02,158*

DANIELSON, P.
Transverse stress effect on the critical current of internal tin and bronze process Nb(sub 3)Sn superconductors.
DE95016659 *04,434*

DANOS, M.
Accuracy-Weighted Variational Principle for Degenerate Continuum States.
PB94-200615 *03,831*

Comprehensive Theory of Nuclear Effects on the Intrinsic Sticking Probability. 1.
PB94-200623 *03,832*

Comprehensive Theory of Nuclear Effects on the Intrinsic Sticking Probability. 2.
PB94-200631 *03,833*

Strangeness Flow Difference in Nuclear Collisions at 15A and 200A GeV.
PB96-119631 *04,042*

DANTSKER, E.
Fabrication Issues in Optimizing YBa2Cu3O7-x Flux Transformers for Low I/f Noise.
PB95-175857 *02,059*

Low Noise YBa2Cu3O7-x-SrTiO3-YBa2Cu3O7-x Mulitlayers for Improved Superconducting Magnetometers.
PB96-138417 *04,747*

DAOU, J. N.
Neutron Spectroscopic Comparison of Rare-Earth/Hydrogen alpha-Phase Systems.
PB95-163523 *00,970*

DAPKUNAS, J. S.
Densification of Nano-Size Powders. 1994 Report.
DE94013486 *03,027*

DAPKUNAS, S. J.
Ceramics Technical Activities, 1995.
PB96-193677 *03,087*

Characterization and Processing of Spray-Dried Zirconia Powders for Plasma Spray Application.
PB97-111231 *04,419*

Corrosion Characteristics of Silicon Carbide and Silicon Nitride.
PB96-169081 *03,372*

Equipment for Investigation of Cryogenic Compaction of Nanosize Silicon Nitride Powders. 1993 Report.
DE94013593 *03,028*

Guide to Locating and Accessing Computerized Numeric Materials Databases.
PB96-204045 *03,007*

Measurement Methods and Standards for Processing and Application of Thermal Barrier Coatings.
N95-26123/6 *01,447*

NMR Characterization of Injection-Moulded Alumina Green Compacts. Part 2. T2-Weighted Proton Imaging.
PB96-201181 *01,165*

Review of Corrosion Behavior of Ceramic Heat Exchanger Materals: Corrosion Characteristics of Silicon Carbide and Silicon Nitride. Final Report, September 11, 1992--March 11, 1993.
DE93041307 *03,228*

DARIEL, M. P.
Ambient Temperature Synthesis of Bulk Intermetallics.
PB95-169074 *00,168*

Magnetic and Structural Properties of Electrodeposited Copper-Nickel Microlayered Alloys.
PB94-213121 *04,512*

DARK, M. L.
Soft-X-ray Damage to p-terphenyl Coatings for Detectors.
PB96-159611 *04,364*

DARTER, M.
Optimization of Highway Concrete Technology.
PB94-182995 *01,333*

DAS, A.
Thermodynamic and Thermophysical Properties of Organic Nitrogen Compounds. Part II. 1- and 2-Butanamine, 2-Methyl-1-Propanamine, 2-Methyl-2-Propanamine, Pyrrole, 1-, 2-, and 3-Methylpyrrole, Pyridine, 2-, 3-, and 4-Methylpyridine, Pyrrolidine, Piperidine, Indole, Quinoline, Isoquinoline, Acridine, Carbazole, Phenanthridine, 1- and 2-Naphthalenamine, and 9-Methylcarbazole.
PB94-162294 *00,741*

DAS SARMA, S.
Correction to the Decay Rate of Nonequilibrium Carrier Distributions Due to Scattering-in Processes.
PB94-185840 *04,452*

DASTIDAR, P.
HVAC CAD Layout Tools: A Case Study of University/Industry Collaboration.
PB97-112221 *00,281*

DATLA, R. U.
Cryogenic Blackbody Calibrations at the National Institute of Standards and Technology Low Background Infrared Calibration Facility.
PB94-169802 *02,117*

Development of Neutral-Density Infrared Filters Using Metallic Thin Films.
PB96-180286 *02,998*

Metrology Issues in Terahertz Physics and Technology.
PB96-128277 *01,939*

Standard Reference Materials: Polystyrene Films for Calibrating the Wavelength Scale of Infrared Spectrophotometers - SRM 1921.
PB95-226866 *03,386*

Thermal Modeling of Absolute Cryogenic Radiometers.
PB95-181236 *04,316*

DATTA, D.
Hyperfine-Structure Studies of Zr II: Experimental and Relativistic Configuration-Interaction Results.
PB95-203824 *04,011*

DATTA, S.
Cast-Iron Elastic Constants: Effect of Graphite Aspect Ratio.
PB94-213212 *03,211*

Elastic Properties of Al2O3/Al Composites: Measurements and Modeling.
PB95-161378 *03,157*

Elastic Properties of Uniaxial-Fiber Reinforced Composites: General Features.
PB94-200649 *03,140*

DAUSKARDT, R. H.
Transient Subcritical Crack-Growth Behavior in Transformation-Toughened Ceramics.
PB94-200656 *03,038*

DAVID, W. I. F.
Structure and Dynamics of Buckyballs.
PB95-153292 *00,950*

DAVIDSON, E. R.
Vibrations of S1((1)B2u) p-Difluorobenzene - d4. S1-S0 Fluorescence Spectroscopy and ab Initio Calculations.
PB95-202586 *01,028*

DAVIDSON, M. P.
Numerical Reference Models for Optical Metrology Simulation.
PB97-111330 *04,392*

DAVIES, A.
Tunneling Spectroscopy of bcc(001) Surface States.
PB96-155585 *04,775*

DAVIES, K.
Use of Ionospheric Data in GPS Time Transfer.
PB95-163853 *01,540*

DAVIES, M.
Effects of Spindle Dynamic Characteristics on Hard Turning.
PB96-122981 *02,699*

DAVIES, M. A.
Chip Morphology, Tool Wear and Cutting Mechanics in Finish Hard Turning.
PB97-112247 *03,106*

DAVIS, D. D.
Calibration of GPS Equipment in Japan.
PB95-151452 *01,531*

High Resolution Time Interval Counter.
PB96-138607 *01,495*

Smart Clock: A New Time.
PB95-151445 *01,530*

DAVIS, G.
Standards Development in North America for Performance of Whole Buildings and Facilities.
PB94-185196 *00,312*

DAVIS, G. T.
Advances in the Measurement of Polymer CTE: Micrometer- to Atomic-Scale Measurements.
PB96-180229 *03,390*

Electronics Packaging Materials Research at NIST.
PB96-122692 *02,405*

Piezoelectric and Pyroelectric Polymers.
PB95-153367 *01,250*

Thermal Stability of Internal Electric Field and Polarization Distribution in Blend of Polyvinylidene Fluoride and Polymethylmethacrylate.
PB95-151072 *01,240*

DAVIS, M. W.
Room-Temperature Thermal Conductivity of Expanded Polystyrene Board for a Standard Reference Material.
PB96-193693 *00,412*

DAVIS, R. S.
Determining the Magnetic Properties of 1 kg Mass Standards.
PB95-261905 *04,016*

Mass and Density Determinations.
PB94-200672 *00,504*

Report of Density Intercomparisons Undertaken by the Working Group on Density of the CCM.
PB94-200664 *00,503*

DAVIS, S.
Pairwise and Nonpairwise Additive Forces in Weakly Bound Complexes: High Resolution Infrared Spectroscopy of ArnDF (n=1,2,3).
PB96-200357 *04,125*

DAVIS, S. H.
Effects of Elastic Stress on the Stability of a Solid-Liquid Interface.
PB95-163028 *03,350*

DAVIS, W.
Analysis of High Bay Hangar Facilities for Detector Sensitivity and Placement.
PB96-190210 *01,429*

DAVIS, W. D.
Field Modeling: Simulating the Effect of Sloped Beamed Ceilings on Detector and Sprinkler Response.
PB96-122866 *01,406*

NASA Fire Detector Study.
PB96-183108 *01,423*

Use of Computer Models to Predict Temperature and Smoke Movement in High Bay Spaces.
PB94-145976 *00,191*

DAWBER, P.
Preparation and Characterization of (6)LiF and (10)B Reference Deposits for the Measurement of the Neutron Lifetime.
PB95-108692 *03,874*

Problems Related to the Determination of Mass Densities of Evaporated Reference Deposits.
PB95-163226 *03,941*

DAX, A.
Extension of Heterodyne Frequency Measurements on OCS to 87 THz (2900 cm(-1)).
PB94-200680 *00,811*

Sub-Doppler Frequency Measurements on OCS at 87 Thz (3.4 micrometers) with the CO Overtone Laser: Considerations and Details.
PB95-128633 *04,255*

Sub-Doppler Frequency Measurements on OCS at 87 THz (3.4 mu m) with the CO Overtone Laser.
PB96-102215 *04,330*

DAY, G. W.
Effect of Semiconductor Laser Characteristics on Optical Fiber Sensor Performance.
PB95-169132 *02,167*

Faraday Effect Current Sensor with Improved Sensitivity-Bandwidth Product.
PB95-203154 *02,180*

Faraday Effect Current Sensors.
PB94-200698 *02,127*

Faraday Effect Sensors: A Review of Recent Progress.
PB94-200706 *02,128*

Faraday Effect Sensors for Magnet Field and Electric Current.
PB96-119664 *04,736*

Fundamentals and Problems of Fiber Current Sensors.
PB97-111835 *02,205*

High Frequency Magnetic Field Sensors Based on the Faraday Effect in Garnet Thick Films.
PB96-190384 *02,282*

Improved Annealing Technique for Optical Fiber.
PB96-119680 *04,343*

Interlaboratory Comparison of Polarization-Holding Parameter Measurements on High-Birefringence Optical Fiber.
PB95-168464 *04,280*

Magneto-Optic Magnetic Field Sensor with 1.4pT/square root of 1(Hz) Minimum Detectable Field at 1 kHz.
PB94-199551 *02,125*

Magneto-Optic Magnetic Field Sensors Based on Uniaxial Iron Garnet Films in Optical Waveguide Geometry.
PB95-153409 *02,152*

Magneto-Optic Magnetic Field Sensors Based on Uniaxial Iron Garnet Films in Optical Waveguide Geometry.
PB95-168498 *02,159*

Magnetooptic Effects.
PB96-119292 *04,338*

Novel Bulk Iron Garnets for Magneto-Optic Magnetic Field Sensing.
PB95-180204 *04,675*

Optical Fiber Sensors: Accelerating Applications in Navy Ships.
PB94-186848 *02,632*

Optoelectronics at NIST.
PB96-200860 *02,202*

Polarization Dependence of Response Functions in 3x3 Sagnac Optical Fiber Current Sensors.
PB95-162426 *02,154*

Polarization Dependence of Response Functions in 3x3 Sagnac Optical Fiber Current Sensors.
PB96-122684 *02,189*

Polarization Insensitive 3x3 Sagnac Current Sensor Using Polarizing Spun High-Birefringence Fiber.
PB96-119276 *02,187*

Self-Calibrating Fiber Optic Sensors: Potential Design Methods.
PB95-169298 *02,172*

Self Calibrating Fiber Optic Sensors: Potential Design Methods.
PB95-169306 *02,173*

Standard Polarization Components: Progress Toward an Optical Retardance Standard.
PB96-119672 *04,342*

Studies of the Higher Order Smectic Phase of the Large Electroclinic Effect Material W317.
PB95-151601 *00,935*

Submicroampere-Per-Root-Hertz Current Sensor Based on the Faraday Effect in Ga: YIG.
PB95-162467 *02,155*

Technical Digest: Symposium on Optical Fiber Measurements (8th), 1994. Held in Boulder, Colorado on September 13-15, 1994.
PB94-207636 *04,231*

Technical Digest: Symposium on Optical Fiber Measurements (9th), 1996. Held in Boulder, Colorado on October 1-3, 1996.
PB97-108583 *04,383*

Wideband Current and Magnetic Field Sensors Based on Iron Garnets.
PB96-200878 *01,975*

DAY, J. M.

Internal Droplet Circulation Induced by Surface-Driven Rotation.
PB97-119267 *02,500*

DAY, P.

Crystal Structure and Magnetic Properties of CuGeO3.
PB95-180287 *04,678*

Lattice Dynamics of Ba1-xKxBiO3.
PB96-102421 *04,706*

Lattice Dynamics of Semiconducting, Metallic, and Superconducting Ba1-xKxBiO3 Studied by Inelastic Neutron Scattering.
PB96-102447 *04,708*

Structure and Conductivity of Layered Oxides (Ba,Sr)n+1(Sn,Sb)nO3n+1.
PB96-102439 *04,707*

DAYAL, V.

Dynamic Shear Modulus Measurements with Four Independent Techniques in Nickel-Based Alloys.
PB94-198900 *03,320*

DAYHOFF, R. E.

Prototyping a Graphical User Interface for DHCP.
PB96-160544 *02,599*

DAYWITT, W. C.

Single-Port Technique for Adaptor Efficiency Evaluation.
PB96-176441 *02,088*

DE BEER, A.

beta-D-Glucosyl-Hydroxymethyluracil: A Novel Modified Base Present in the DNA of the Parastic Protozoan T. brucei.
PB94-172319 *03,524*

DE BIEVRE, P.

New Values for Silicon Reference Materials, Certified for Isotope Abundance Ratios. Letter to the Editor.
PB94-219268 *00,863*

DE BOER, F. R.

Magnetic Properties of Single-Crystalline UCu3Al2.
PB95-180717 *04,686*

DE HAAN, G.

Perception of Clamp Noise in Television Receivers.
PB96-119433 *01,489*

DE LUCA, N. P.

Milliwatt Mixer for Small Fluid Samples.
PB94-198819 *02,634*

DE LUCIA, F. C.

Millimeter- and Submillimeter-Wave Spectrum of trans-Ethyl Alcohol.
PB96-145578 *01,102*

DE MARCHI, A.

New 5 and 10 MHz High Isolation Distribution Amplifier.
PB96-190202 *01,510*

DE NATALE, P.

Rotational Far Infrared Spectrum of (13)CO.
PB95-152187 *00,941*

DE OBALDIA, E.

Increased Transition Temperature in In situ Coevaporated YBa2Cu3O7-delta Thin Films by Low Temperature Post-Annealing.
PB95-180071 *04,672*

DE OBALDIA, E. I.

Coexistence of Grains with Differing Orthorhombicity in High Quality YBa2Cu3O7-delta Thin Films.
PB96-135033 *04,742*

DE RIS, J.

Prediction of Fire Dynamics.
PB94-193620 *00,336*

DE ROOS, J. L.

Principle of Congruence and Its Application to Compressible States.
PB96-102892 *01,068*

DE SWAAN ARONS, J.

Principle of Congruence and Its Application to Compressible States.
PB96-102892 *01,068*

DE VIVIE-RIEDLE, R.

Three-Vector Correlation Study of Orientation and Coherence Effects in Na(3p, (2)P1/2 inversely maps (2)P3/2)+He: Semiclassical and Quantum Calculations.
PB95-202453 *03,979*

DE VREEDE, J.

Intercomparison of Thermal Converters at NIM, NIST, PTB, SIRI and VSL from 10 to 100 MHz.
PB94-172459 *02,027*

DE VREEDE, J. P. M.

Intercomparison of NIST, NPL, PTB, and VSL Thermal Voltage Converters from 100 kHz to 1 MHz.
PB94-172442 *02,026*

DEAL, S.

Evaluating Small Board and Care Homes: Sprinklered vs. Nonsprinklered Fire Protection.
PB94-206356 *00,195*

Santa Ana Fire Department Experiment at 1315 South Bristol, July 14, 1994.
PB95-188868 *00,389*

Santa Ana Fire Department Experiment at 1315 South Bristol, July 14, 1994. (Reprint).
PB96-102934 *00,207*

DEAL, S. P.

Numerical Simulation of Rapid Combustion in an Underground Enclosure.
PB96-183132 *01,424*

DEAN, B. E.

Correlation of HgCdTe Epilayer Defects with Underlying Substrate Defects by Synchrotron X-Ray Topography.
PB94-200714 *02,129*

DEAN, J. W.

Design and Construction of a Liquid Hydrogen Temperature Refrigeration System.
AD-A286 618/4 *02,619*

Helium Refrigeration and Liquefaction Using a Liquid Hydrogen Refrigerator for Precooling.
AD-A286 683/8 *02,749*

Tabulation of the Thermodynamic Properties of Normal Hydrogen from Low Temperatures to 300K and from 1 to 100 Atmospheres.
AD-A279 951/8 *00,713*

DEARDEN, D. V.

New Rydberg States of Aluminum Monofluoride Observed by Resonance-Enhanced Multiphoton Ionization Spectroscopy.
PB94-199544 *00,797*

DEASY, J. O.

Extrapolation Chamber Measurements on (90)Sr + (90)Y Beta-Particle Ophthalmic Applicator Dose Rates.
PB95-153375 *03,626*

DEBENHAM, P. H.

NIST-NRL Free-Electron Laser Facility.
PB94-212511 *04,237*

DEBIEVRE, P.

Reference Materials by Isotope Dilution Mass Spectrometry.
PB95-153383 *00,592*

DECKMAN, D. E.

Measuring Matching Wear Scars on Balls and Flats.
PB95-151528 *03,153*

DEETER, M. N.

Domain Effects in Faraday Effect Sensors Based on Iron Garnets.
PB95-202461 *02,268*

Faraday Effect Current Sensor with Improved Sensitivity-Bandwidth Product.
PB95-203154 *02,180*

Faraday Effect Current Sensors.
PB94-200698 *02,127*

Faraday Effect Sensors: A Review of Recent Progress.
PB94-200706 *02,128*

Faraday Effect Sensors for Magnet Field and Electric Current.
PB96-119664 *04,736*

Fiber-Optic Faraday-Effect Magnetic-Field Sensor Based on Flux Concentrators.
PB96-200308 *02,201*

High Frequency Magnetic Field Sensors Based on the Faraday Effect in Garnet Thick Films.
PB96-190384 *02,282*

High Speed, High Sensitivity Magnetic Field Sensors Based on the Faraday Effect in Iron Garnets.
PB95-153391 *02,151*

Magneto-Optic Magnetic Field Sensor with 1.4pT/square root of 1(Hz) Minimum Detectable Field at 1 kHz.
PB94-199551 *02,125*

Magneto-Optic Magnetic Field Sensors Based on Uniaxial Iron Garnet Films in Optical Waveguide Geometry.
PB95-153409 *02,152*

Magneto-Optic Magnetic Field Sensors Based on Uniaxial Iron Garnet Films in Optical Waveguide Geometry.
PB95-168498 *02,159*

Magnetooptic Effects.
PB96-119292 *04,338*

Novel Bulk Iron Garnets for Magneto-Optic Magnetic Field Sensing.
PB95-180204 *04,675*

Submicroampere-Per-Root-Hertz Current Sensor Based on the Faraday Effect in Ga: YIG.
PB95-162467 *02,155*

Wideband Current and Magnetic Field Sensors Based on Iron Garnets.
PB96-200878 *01,975*

DEFIBAUGH, D. E.

Vapor Pressure of 1,1,1,2,2-Pentafluoropropane.
PB97-113237 *00,684*

DEFIBAUGH, D. R.

Compressed Liquid Densities, Saturated Liquid Densities, and Vapor Pressures of 1,1-Difluoroethane.
PB97-110118 *01,173*

Interaction Coefficients for 15 Mixtures of Flammable and Non-Flammable Components.
PB96-146626 *03,281*

Thermodynamic Properties of CF3-CHF-CHF2, 1,1,1,2,3,3-Hexafluoropropane.
PB97-118384 *03,299*

Thermodynamic Properties of CHF2-CF2-CHF, 1,1,2,2,3-Pentafluoropropane.
PB97-118392 *03,300*

Thermodynamic Properties of CHF2-O-CHF2,Bis(difluoromethyl) Ether.
PB94-199569 *00,798*

Thermodynamic Properties of Difluoromethane.
PB94-185204 *00,772*

Vapor Pressure of Pentafluorodimethyl Ether.
PB96-201199 *00,677*

Vapor Pressure of 1,1-dichloro-2,2,2-trifluoroethane (R123).
PB95-126231 *00,899*

Virial Coefficients of Five Binary Mixtures of Fluorinated Methanes and Ethanes.
PB96-156054 *01,128*

Viscosity of 1,1,1,2,3,3-Hexafluoropropane and 1,1,1,3,3,3-Hexafluoropropane at Saturated-Liquid Conditions from 262 K to 353 K.
PB96-176680 *03,292*

DEGROOT, D. C.

High-Speed Interconnection Characterization Using Time Domain Network Analysis.
PB96-148176 *04,061*

Microwave Properties of Voltage-Tunable YBa2Cu3O7-delta/SrTiO3 Coplanar Waveguide Transmission Lines.
PB96-141262 *02,235*

Optimizing Time-Domain Network Analysis.
PB96-157821 *02,085*

DEHMER, J. L.

High Resolution Angle Resolved Photoelectron Spectroscopy Study of N2.
PB95-151494 *03,907*

Inner-Valence States CO(+) between 22 eV and 46 eV Studied by High Resolution Photoelectron Spectroscopy and ab Initio CI Calculations.
PB95-180055 *03,961*

Photoelectron Study of Electronic Autoionization in Rotationally Cooled N2: The n=6 Member of the Hopfield Series.
PB95-163531 *00,971*

Shape-Resonance-Enhanced Continuum-Continuum Coupling in Photoionization of CO2.
PB95-164471 *00,983*

Vibrational Autoionization in H2: Vibrational Branching Ratios and Photoelectron Angular Distributions Near the v(+)=3 Threshold.
PB94-199577 *00,799*

Vibrationally Resolved Photoelectron Angular Distributions and Branching Ratios for the Carbon Dioxide Molecule in the Wavelength Region 685-795 Angstrom.
PB96-201207 *04,131*

Vibronic Coupling and Other Many-Body Effects in the 4sigmag(-1) Photoionization Channel of CO2.
PB95-162509 *00,962*

DEHMER, P. M.

Vibrational Autoionization in H2: Vibrational Branching Ratios and Photoelectron Angular Distributions Near the v(+)=3 Threshold.
PB94-199577 *00,799*

Vibrationally Resolved Photoelectron Angular Distributions and Branching Ratios for the Carbon Dioxide Molecule in the Wavelength Region 685-795 Angstrom.
PB96-201207 *04,131*

DEILAMIAN, K.

Isotope Shifts and Hyperfine Splittings of the 398.8-nm Yb I Line.
PB94-199585 *03,814*

Search for Small Violations of the Symmetrization Postulate in an Excited State of Helium.
PB96-123518 *04,050*

DEISSLER, A.

Liquid Chromatographic Determination of Polycyclic Aromatic Hydrocarbon Isomers of Molecular Weight 278 and 302 in Environmental Standard Reference Materials.
PB95-164042 *02,523*

DEITERS, U. K.

Application of the Taylor Dispersion Method in Supercritical Fluids.
PB95-164323 *00,977*

DELAETER, J. R.

Reference Materials by Isotope Dilution Mass Spectrometry.
PB95-153383 *00,592*

DELANEY, H. D.

Stacking the Cards in Europe: One Company's Story.
PB97-110126 *00,493*

DELAUDER, S.

Thermodynamic Analysis of Heparin Binding to Human Antithrombin.
PB94-199593 *03,455*

DELAUTER, L.

Fire Performance of an Interstitial Space Construction System.
PB95-188918 *00,390*

DELLA TORRE, E.

Experimental Verification of a Vector Preisach Model.
PB95-163564 *04,626*

DELOZANNE, A. L.

Vortex Images in Thin Films of YBa2Cu3O(sub 7-x) and Bi2Sr2Ca1Cu2O(sub 8+x) Obtained by Low-Temperature Magnetic Force Microscopy.
PB97-119408 *04,815*

DEMATTEIS, R.

Comparisons of Some NIST Fixed-Point Cells with Similar Cells of Other Standards Laboratories.
PB97-119242 *00,655*

DEMIRALP, R.

Certification of Standard Reference Material (SRM) 1941a, Organics in Marine Sediment.
PB96-123690 *02,593*

Concentrations of Chlorinated Hydrocarbons, Heavy Metals and Other Elements in Tissues Banked by the Alaska Marine Mammal Tissue Archival Project.
PB95-209870 *02,590*

Determination of Inorganic Constituents in Marine Mammal Tissues.
PB95-152047 *00,589*

Development of Frozen Whale Blubber and Liver Reference Materials for the Measurement of Organic and Inorganic Contaminants.
PB95-151676 *00,587*

Relationship of Silver with Selenium and Mercury in the Liver of Two Species of Toothed Whales (Odontocetes).
PB96-167275 *02,596*

Trace Element Concentrations in Cetacean Liver Tissues Archived in the National Marine Mammal Tissue Bank.
PB96-167127 *02,595*

DEMPSEY, R.

First Results from a Coordinated ROSAT, IUE, and VLA Study of RS CVn Systems.
PB94-213477 *00,069*

DEMPSEY, R. C.

Riass Coronathon: Joint X-ray and Ultraviolet Observations of Normal F-K Stars.
PB96-200217 *00,109*

ROSAT All-Sky Survey of Active Binary Coronae. 1. Quiescent Fluxes for the RS Canum Venaticorum Systems.
PB95-202479 *00,077*

ROSAT All-Sky Survey of Active Binary Coronae. 2. Coronal Temperatures of the RS Canum Venaticorum Systems.
PB94-199601 *00,055*

Rotational Modulation and Flares on RS Canum Venaticorum and BY Draconis Stars. XVIII. Coordinated VLA, ROSAT, and IUE Observations of RS CVn Binaries.
PB96-102322 *00,089*

DENENBERG, R.

Z39.50 Implementation Experiences.
PB96-114939 *01,816*

DENG, N.

Energy-Based Method for Liquefaction Potential Evaluation. Phase 1. Feasibility Study.
PB96-214747 *03,691*

DENNIS, T. J. S.

Rotational Dynamics of Solid C70: A Neutron-Scattering Study.
PB94-172178 *00,755*

Rotational Dynamics of Solid C70: A Neutron-Scattering Study.
PB95-153219 *00,949*

DENNO, P.

Dynamic Objects and Meta-Level Programming of an EXPRESS Language Environment.
PB96-190053 *01,774*

DENNO, P. O.

Aspects of a Product Model Supporting Apparel Virtual Enterprises.
PB96-183231 *02,790*

DEPAOLA, B. D.

Merged-Beams Energy-Loss Technique for Electron-Ion Excitation: Absolute Total Cross Sections for O(5+) (2s yields 2p).
PB96-102058 *04,017*

DEPONDT, P.

Maximum Entropy as a Tool for the Determination of the C-Axis Profile of Layered Compounds.
PB94-199619 *00,800*

DEPRIT, A.

Complete Reduction of the Euler-Poinsot Problem.
PB94-172152 *03,788*

Frozen Orbits for Satellites Close to an Earth-Like Planet.
PB96-102165 *04,839*

DEPRIT, E.

Frozen Orbits for Satellites Close to an Earth-Like Planet.
PB96-102165 *04,839*

DEREGGI, A.

Effect of DC Tests on Induced Space Charge.
PB94-172350 *02,212*

DEREGGI, A. S.

Hysteresis Measurements of Remanent Polarization and Coercive Field in Polymers.
PB94-199767 *04,475*

Spatial Dependence of Electrical Fields Due to Space Charges in Films of Organic Dielectrics Used for Insulation of Power Cables.
PB94-199130 *02,214*

Thermal Pulse Study of the Polarization Distributions Produced in Polyvinylidene Fluoride by Corona Poling at Constant Current.
PB94-172293 *01,195*

Thermal Stability of Internal Electric Field and Polarization Distribution in Blend of Polyvinylidene Fluoride and Polymethylmethacrylate.
PB95-151072 *01,240*

DERKSON, G.

Effects of Calcium Phosphate Solutions on Dentin Permeability.
PB95-151080 *00,157*

DERR, L. S.

Bibliography of the NIST Optoelectronics Division.
PB96-128210 *02,193*

DESAI, P. G.

Unreacted Cement Content in Macro-Defect-Free Composites: Impact on Processing-Structure-Property Relations.
PB96-141270 *03,174*

DESCHAMPS, M. F.

Approach to Setting Performance Requirements for Automated Evaluation of the Parameters of High-Voltage Impulses.
PB94-185634 *01,878*

DESJARLAIS, A. O.

Water-Vapor Measurements of Low-Slope Roofing Materials.
PB95-251617 *00,399*

DESLATTES, R. D.

Crystal Diffraction Spectrometry for Accurate, Non-Invasive kV/Spectral Measurement for Improvement of Mammographic Image Quality.
AD-A297 943/3 *00,721*

Early History and Future Outlook for the X-ray Crystal Density Method.
PB95-202487 *04,692*

Electron-Ion-X-ray Spectrometer System.
PB95-176137 *03,958*

Evolution of X-ray Resonance Raman Scattering into X-ray Fluorescence from the Excitation of Xenon Near the L3 Edge.
PB96-102751 *04,025*

Experimental Aspects and Z-Dependent Systematics in One- and Two-Electron Ions and Single Vacancy Systems.
PB94-199627 *03,815*

Flat and Curved Crystal Spectrography for Mammographic X-ray Sources.
PB97-122246 *03,642*

Noninvasive High-Voltage Measurement in Mammography by Crystal Diffraction Spectroscopy.
PB95-153417 *00,160*

Polarization Measurements on a Magnetic Quadrupole Line in Ne-Like Barium.
PB97-113104 *04,161*

Polarized X-Ray Emission Spectroscopy.
PB94-213360 *03,862*

Precision Comparison of the Lattice Parameters of Silicon Monocrystals.
PB94-169745 *04,438*

Production and Characterization of Ion Beam Sputtered Multilayers.
PB95-162053 *03,936*

Status of a Silicon Lattice Measurement and Dissemination Exercise.
PB94-199635 *04,474*

Systematic Correction in Bragg X-ray Diffraction of Flat and Curved Crystals.
PB97-112239 *04,152*

Upgraded Facility for Multilayer Mirror Characterization at NIST.
PB96-160387 *04,367*

DESROSIERS, M.

Commentary on 'Optimization of Experimental Parameters for the EPR Detection of the Cellulosic Radical in Irradiated Foodstuffs'.
PB96-164124 *00,043*

DESROSIERS, M. F.

Complex Time Dependence of the EPR Signal of Irradiated L-alpha-alanine.
PB97-122436 *04,180*

Dosimetry Systems for Radiation Processing.
PB96-135280 *03,717*

EPR Bone Dosimetry: A New Approach to Spectral Deconvolution Problems.
PB94-199643 *03,616*

EPR Dosimetry of Cortical Bone and Tooth Enamel Irradiated with X and Gamma Rays: Study of Energy Dependence.
PB97-110373 *03,639*

ESR-Based Analysis in Radiation Processing.
PB95-161634 *03,931*

Estimation of the Absorbed Dose in Radiation-Processed Food. 1. Test of the EPR Response Function by a Linear Regression Analysis.
PB94-199718 *00,039*

Estimation of the Absorbed Dose in Radiation-Processed Food. 2. Test of the EPR Response Function by an Exponential Fitting Analysis.
PB94-199650 *00,036*

Estimation of the Absorbed Dose in Radiation-Processed Food. 3. The Effect of Time of Evaluation on the Accuracy of the Estimate.
PB94-199684 *00,037*

Estimation of the Absorbed Dose in Radiation-Processed Food. 4. EPR Measurements on Eggshell.
PB94-199692 *00,038*

Experimental assessment of absorbed dose to mineralized bone tissue from internal emitters: An electron paramagnetic resonance study.
DE96007979 *03,614*

Experimental Validation of Radiopharmaceutical Absorbed Dose to Mineralized Bone Tissue.
PB94-199668 *03,617*

Inter-Laboratory Trials of the EPR Method for the Detection of Irradiated Meats Containing Bone.
PB96-161690 *00,042*

Investigation of Applicability of Alanine and Radiochromic Detectors to Dosimetry of Proton Clinical Beams.
PB96-146782 *03,636*

New EPR Dosimeter Based on Polyvinylalcohol.
PB94-199700 *03,619*

Orientation Effects on ESR Analysis of Alanine-Polymer Dosimeters.
PB96-146725 *03,720*

Overview of a Radiation Accident at an Industrial Accelerator Facility.
PB97-122485 *02,612*

Radiation Accident at an Industrial Accelerator Facility.
PB95-140117 *02,575*

Radiation Doses.
PB94-199676 *03,618*

Research and Development Activities in Electron Paramagnetic Resonance Dosimetry.
PB96-141288 *03,635*

Unusual Spin-Trap Chemistry for the Reaction of Hydroxyl Radical with the Carcinogen N-Nitrosodimethylamine.
PB95-151643 *00,692*

DESSENS, J.

Intercomparison of NIST, NPL, PTB, and VSL Thermal Voltage Converters from 100 kHz to 1 MHz.
PB94-172442 *02,026*

DETERS, T. M.

Atomic Branching Ratio Data for Carbon-Like Ions.
PB94-212842 *03,855*

Atomic Branching Ratio Data for Oxygen-Like Species.
PB95-180436 *03,963*

DETWEILER, R. J.

Water Permeability and Chloride Ion Diffusion in Portland Cement Mortars: Relationship to Sand Content and Critical Pore Diameter.
PB96-148036 *03,193*

DEVANEY, J. E.

Experience with MPI: 'Converting Pvmmake to Mpimake under LAM' and 'MPI and Parallel Genetic Programming'.
PB96-141296 *01,748*

DEVOE, J. R.

Establishing Quality Measurements for Inorganic Analysis of Biomaterials.
PB94-199726 *00,548*

DEVORET, M. H.

Even-Odd Asymmetry of a Superconductor Revealed by the Coulomb Blockade of Andreev Reflection.
PB95-153540 *04,593*

Observation of Hot-Electron Shot Noise in a Metallic Resistor.
PB97-112007 *01,988*

DEVRIES, K. M.

Polarization of Light Emitted After Positron Impact Excitation of Alkali Atoms.
PB94-199734 *03,816*

DEWEESE, M. E.

Metrology for Electromagnetic Technology: A Bibliography of NIST Publications.
PB94-159761 *02,116*

DEWEY, M. S.

Current Results and Future Prospects for a Neutron Lifetime Determination Using Trapped Protons.
PB94-199742 *03,817*

Mass Assay and Uniformity Test of Boron Targets by Neutron Beam Methods.
PB97-119085 *04,175*

Measurement of the Neutron Lifetime.
PB96-161708 *04,094*

DEWIT, R.

Fracture Behavior of Large-Scale Thin-Sheet Aluminum Alloy.
N95-19494/0 *03,311*

Fracture Testing of Large-Scale Thin-Sheet Aluminum Alloy.
AD-A306 625/5 *03,305*

Fracture Testing of Large-Scale Thin-Sheet Aluminum Alloy.
PB95-242368 *00,024*

DEXTER, A. L.

Use of Building Emulators to Evaluate the Performance of Building Energy Management Systems.
PB96-111901 *00,269*

DEYST, J. P.

Bounds on Frequency Response Estimates Derived from Uncertain Step Response Data.
PB96-122874 *03,419*

Bounds on Least-Squares Four-Parameter Sine-Fit Errors Due to Harmonic Distortion and Noise.
PB96-141304 *01,609*

Uncertainties of Frequency Response Estimates Derived from Responses to Uncertain Step-Like Inputs.
PB97-111843 *01,984*

Wideband Sampling Voltmeter.
PB97-113039 *01,990*

DEZSI, G.

High Accuracy Measurement of Aperture Area Relative to a Standard Known Aperture.
PB95-261954 *01,919*

Method of Realizing Spectral Irradiance Based on an Absolute Cryogenic Radiometer.
PB95-161204 *04,270*

DHAR, S.

Procedure for Product Data Exchange Using STEP Developed in the AutoSTEP Pilot.
PB96-183058 *02,843*

DI MARZIO, E. A.

Glass Temperature of Polymer Blends: Comparison of Both the Free Volume and the Entropy Predictions with Data.
PB95-140190 *01,236*

Mixing Plate-Like and Rod-Like Molecules with Solvent: A Test of Flory-Huggins Lattice Statistics.
PB96-126206 *03,173*

DI MARZO, M.

Application of Boundary Element Methods to a Transient Axis-Symmetric Heat Conduction Problem.
PB94-212693 *01,375*

Fire Protection Foam Behavior in a Radiative Environment.
PB97-116131 *00,237*

Sparse Water Sprays in Fire Protection.
PB96-202304 *01,433*

Transient Cooling of a Hot Surface by Droplets Evaporation.
PB94-156957 *03,783*

Transient Cooling of a Hot Surface by Droplets Evaporation.
PB95-143194 *03,890*

Water Droplet Evaporation from Radiantly Heated Solids.
PB95-217147 *00,394*

DIAMOND, S.

Interaction between Naphthalene Sulfonate and Silica Fume in Portland Cement Pastes.
PB94-199759 *01,315*

DIAMONDSTONE, B. I.

CSTL Technical Activities 1991.
PB94-160769 *00,728*

DIANOUX, A. J.

Inelastic-Neutron-Scattering Studies of Poly(p-phenylene vinylene).
PB95-180766 *01,014*

DIAZ, C.

Algorithm Testing and Evaluation Program for Coordinate Measuring Systems: Long Range Plan.
PB95-231833 *02,915*

Algorithm Testing and Evaluation Program for Coordinate Measuring Systems: Testing Methods.
PB95-251658 *02,666*

Concept for an Algorithm Testing and Evaluation Program at NIST.
PB94-163029 *02,890*

Process for Selecting Standard Reference Algorithms for Evaluating Coordinate Measurement Software.
PB94-173754 *02,629*

DICK, C. E.

Calibration of High-Energy Electron Beams by Use of Graphite Calorimeters.
PB95-161113 *04,598*

Electron and Proton Dosimetry with Custom-Developed Radiochromic Dye Films.
PB95-151106 *03,713*

Image Information Transfer Properties of X-Ray Intensifying Screens in the Energy Range from 17 to 320 keV.
PB95-126173 *00,155*

Investigation of Applicability of Alanine and Radiochromic Detectors to Dosimetry of Proton Clinical Beams.
PB96-146782 *03,636*

Overview of a Radiation Accident at an Industrial Accelerator Facility.
PB97-122485 *02,612*

Radiation Accident at an Industrial Accelerator Facility.
PB95-140117 *02,575*

Research and Development Activities in Electron Paramagnetic Resonance Dosimetry.
PB96-141288 *03,635*

Study of Multiple Scattering Background in Compton Scatter Imaging.
PB96-112222 *04,425*

DICKENS, B.

Cylinder Wipe Air-Drying Intaglio Ink Vehicles for U.S. Currency Inks.
PB94-160801 *03,115*

Effect of DC Tests on Induced Space Charge.
PB94-172350 *02,212*

Grafted Interpenetrating Polymer Networks.
PB94-185055 *01,200*

Hysteresis Measurements of Remanent Polarization and Coercive Field in Polymers.
PB94-199767 *04,475*

Modified Surface-Active Monomers for Adhesive Bonding to Dentin.
PB95-151163 *00,158*

NIR-Spectroscopic Investigation of Water Sorption Characteristics of Dental Resins and Composites.
PB95-151171 *00,189*

NIST/NCMS Program on Electronic Packaging: First Update.
PB96-204086 *03,008*

Physical and Chemical Properties of Resin-Reinforced Calcium Phosphate Cements.
PB95-180212 *00,171*

Preparation and Characterization of Cyclopolymerizable Resin Formulations.
PB96-146840 *01,285*

Spatial Dependence of Electrical Fields Due to Space Charges in Films of Organic Dielectrics Used for Insulation of Power Cables.
PB94-199130 *02,214*

DICKENS, J. K.

Measurement of the (10)B(n, alpha1gamma)(7)Li Cross Section in the 0.3 to 4 MeV Neutron Energy Interval.
PB96-161799 *04,098*

DICKENS, S. V.

Effect of Two Initiator/Stabilizer Concentrations in a Metal Primer on Bond Strengths of a Composite to a Base Metal Alloy.
PB94-172723 *00,141*

DICKENS-VENZ, S.

Physical and Chemical Properties of Resin-Reinforced Calcium Phosphate Cements.
PB95-180212 *00,171*

DICKEY, J. O.

Lunar Laser Ranging: A Continuing Legacy of the Apollo Program.
PB95-202495 *03,683*

DIDION, D. A.

Causes of the Apparent Heat Transfer Degradation for Refrigerant Mixtures.
PB94-212701 *03,259*

Role of R22 in Refrigerating and Air Conditioning Equipment.
PB94-199783 *03,253*

Role of Refrigerant Mixtures as Alternatives to CFCs.
PB94-199775 *03,252*

Study of Heat Pump Performance Using Mixtures of R32/R134a and R32/R125/R134a as 'Drop-In' Working Fluids for R22 with and Without a Liquid-Suction Heat Exchanger.
PB94-218559 *02,503*

Study to Determine the Existence of an Azeotropic R-22 'Drop-In' Substitute.
PB96-167812 *02,568*

DIEBOLD, A. C.

Business and Manufacturing Motivations for the Developing of Analytical Technology and Metrology for Semiconductors.
PB96-161948 *04,778*

Characterization of Two-Dimensional Dopant Profiles: Status and Review.
PB96-119300 *02,400*

Characterization of Two-Dimensional Dopant Profiles: Status and Review.
PB97-110134 *02,451*

Summary Report: Workshop on Industrial Applications of Scanned Probe Microscopy (2nd). A Workshop Co-Sponsored by NIST, SEMATECH, ASTM E42.14, and the American Vacuum Society. Held in Gaithersburg, Maryland on May 2-3, 1995.
PB96-131602 *00,509*

Workshop Summary Report: Industrial Applications of Scanned Probe Microscopy. A Workshop Co-sponsored by NIST, SEMATECH, ASTM, E42.14, and the American Vacuum Society. Held in Gaithersburg, Maryland on March 24-25, 1994.
PB95-170387 *00,506*

DIERCKS, G.

Novel Bulk Iron Garnets for Magneto-Optic Magnetic Field Sensing.
PB95-180204 *04,675*

DIETENBERGER, M. A.

Calculating Flame Spread on Horizontal and Vertical Surfaces.
PB94-187283 *00,335*

DIETRICH, D. D.

Photographic Response to X-Ray Irradiation. 3. Photographic Linearization of Beam-Foil Spectra.
PB94-200102 *03,823*

DIETRICH, H.

Lattice Position of Si in GaAs Determined by X-Ray Standing Wave Measurements.
PB95-164406 *04,632*

DIETRICH, H. B.

Range Statistics and Rutherford Backscattering Studies on Fe-Implanted In0.53Ga0.47As.
PB95-126397 *04,535*

Transition Metal Implants in In0.53GA0.47As.
PB95-126389 *04,534*

DIKKERS, R. D.

Proceedings of a Workshop on Developing and Adopting Seismic Design and Construction Standards for Lifelines. Held in Denver, Colorado on September 25-27, 1991.
PB97-115794 *01,302*

DILL, J.

Crystal Packing Interactions of Two Different Crystal Forms of Bovine Ribonuclease A.
PB95-152823 *00,943*

DILLER, D. E.

Measurements of the Viscosities of Saturated and Compressed Fluid 1-chloro-1,2,2,2-tetrafluoroethane (R124) and Pentafluoroethane (R125) at Temperatures between 120 and 420 K.
PB94-199791 *03,254*

Measurements of the Viscosities of Saturated and Compressed Liquid 1,1,1,2-Tetrafluoroethane (R134a), 2,2-Dichloro-1,1,1-Trifluoroethane (R123) and 1,1-Dichloro-1-Fluoroethane (R141b).
PB95-175386 *03,273*

DIMARZIO, E. A.

Peeling a Polymer from a Surface or from a Line.
PB94-199809 *01,213*

DIMAURO, L. F.

Intensity-Dependent Scattering Rings in High Order Above-Threshold Ionization.
PB96-110739 *04,032*

DIMITRIOU, P.

Controlled Nucleation in Aerosol Reactors for Supression of Agglomerate Formation.
PB95-151973 *00,672*

DIMMICK, D. L.

Evaluating Form Designs for Optical Character Recognition.
PB94-168044 *01,830*

NIST Form-Based Handprint Recognition System.
PB94-217106 *01,838*

DINKEL, C.

Telecommunications Security Guidelines for Telecommunications Management Network. Computer Security.
PB96-139415 *01,496*

DINSE, K. P.

High-Resolution Optical Multiplex Spectroscopy.
PB95-203543 *04,323*

DIPLAS, A.

Deuterium and the Local Interstellar Medium: Properties for the Procyon and Capella Lines of Sight.
PB96-200639 *00,111*

Deuterium in the Local Interstellar Medium: Its Cosmological Significance.
PB95-202842 *00,081*

Goddard High-Resolution Spectrograph Observations of the Local Interstellar Medium and the Deuterium/Hydrogen Ratio along the Line of Sight Toward Capella.
PB94-213444 *00,066*

DISDAROGLU, M.

Commentary: The Measurement of Oxidative Damage to DNA by HPLC and GC/MS Techniques.
PB96-200894 *03,484*

DITMARS, D. A.

Calibration Standards for Differential Scanning Calorimetry. 1. Zinc Absolute Calorimetric Measurement of Enthalpy of Fusion and Temperature of Fusion HM.
PB94-199817 *00,801*

DITTMANN, S.

Measurement Comparability, Traceability, and Measurement Assurance Programs.
PB97-111850 *02,692*

DIWAN, B.

Nickel(II)-Mediated Oxidative DNA Base Damage in Renal and Hepatic Chromatin of Pregnant Rats and Their Fetuses. Possible Relevance to Carcinogenesis.
PB94-212628 *03,646*

Oxidative DNA Base Damage in Renal, Hepatic, and Pulmonary Chromatin of Rats After Intraperitoneal Injection of Cobalt (II) Acetate.
PB95-150025 *03,647*

DIXON, R. N.

Resonance Enhanced Multiphoton Ionization Spectroscopy of the SnF Radical.
PB97-111223 *01,176*

DIXSON, R.

Increasing the Value of Atomic Force Microscopy Process Metrology Using a High-Accuracy Scanner, Tip Characterization, and Morphological Image Analysis.
PB96-190293 *02,758*

Progress Toward Accurate Metrology Using Atomic Force Microscopy.
PB96-146774 *02,417*

DIZDAROGLU, M.

beta-D-Glucosyl-Hydroxymethyluracil: A Novel Modified Base Present in the DNA of the Parastic Protozoan T. brucei.
PB94-172319 *03,524*

Copper Ion-Mediated Modification of Bases in DNA in Vitro by Benzoyl Peroxide.
PB94-198231 *03,645*

DNA Base Damage Generated In vivo in Hepatic Chromatin of Mice upon Whole Body y-Irradiation.
PB95-161741 *03,627*

DNA Base Damage in Lymphocytes of Cancer Patients Undergoing Radiation Therapy.
PB97-122444 *03,643*

DNA Base Modifications in Renal Chromatin of Wistar Rats Treated with a Renal Carcinogen, Ferric Nitrilotriacetate.
PB95-150363 *03,648*

DNA Damage and DNA Sequence Retrieval from Ancient Tissues.
PB97-111983 *03,556*

Formation of DNA-Protein Cross-Links in Cultured Mammalian Cells Upon Treatment with Iron Ions.
PB96-137724 *03,651*

Ionizing Radiation Causes Greater DNA Base Damage in Radiation-Sensitive Mutant M10 Cells That in Parent Mouse Lymphoma L5178Y Cells.
PB95-175915 *03,632*

Modification of DNA Bases in Chromatin of Intact Target Human Cells by Activated Human Polymorphonuclear Leukocytes.
PB94-199833 *03,526*

Nickel(II)-Mediated Oxidative DNA Base Damage in Renal and Hepatic Chromatin of Pregnant Rats and Their Fetuses. Possible Relevance to Carcinogenesis.
PB94-212628 *03,646*

Novel Activities of Human Uracil DNA N-glycosylase for Cytosine-Derived Products of Oxidative DNA Damage.
PB96-164132 *03,479*

Novel Activity of E. coli uracil DNA N-glycosylase Excision of Isodialuric Acid (5,6-dihydroxyuracil), a Major Product of Oxidative DNA Damage, from DNA.
PB96-110747 *03,543*

Novel DNA N-Glycosylase Activity of E. coli T4 Endonuclease V That Excises 4,6-Diamino-5-Formamidopyrimidine from DNA, a UV-Radiation- and Hydroxyl Radical-Induced Product of Adenine.
PB96-160478 *03,549*

Oxidative Damage to DNA in Mammalian Chromatin.
PB94-199825 *03,525*

Oxidative DNA Base Damage in Renal, Hepatic, and Pulmonary Chromatin of Rats After Intraperitoneal Injection of Cobalt (II) Acetate.
PB95-150025 *03,647*

Quantitative Determination of Oxidative Base Damage in DNA by Stable Isotope-Dilution Mass Spectrometry.
PB96-200886 *03,483*

Repair of Products of Oxidative DNA Base Damage in Human Cells.
PB96-190129 *03,555*

Substrate Specificity of the Escherichia coli Endonuclease III: Excision of Thymine- and Cytosine-Derived Lesions in DNA Produced by Radiation-Generated Free Radicals.
PB95-153425 *03,535*

Tert-Butyl Hydroperoxide-Mediated DNA Base Damage in Cultured Mammalian Cells.
PB94-182003 *03,644*

Treatment of Wistar Rats with a Renal Carcinogen, Ferric Nitrilotriacetate, Causes DNA-Protein Cross-Linking between Thymine and Tyrosine in Their Renal Chromatin.
PB96-112115 *03,649*

DIZDAROGLU, M. M.

Chemical Determination of Oxidative DNA Damage by Gas Chromatography-Mass Spectrometry.
PB95-175394 *03,540*

DJURIC, N.

Absolute Cross-Section Measurements for Electron-Impact Ionization of C1(+1).
PB94-199841 *03,818*

Absolute Cross-Section Measurements for Electron-Impact Single Ionization of Se(+) and Te(+).
PB95-202503 *03,980*

Absolute Cross Sections for Electron-Impact Single Ionization of Si(+) and Si(2+).
PB95-202529 *03,982*

Collisions of Electrons with Highly-Charged Ions.
PB96-200340 *04,791*

Crossed-Beams Measurements of Absolute Cross Sections for Electron Impact Ionization of S(+).
PB95-202511 *03,981*

Electron-Impact Ionization of In(+) and Xe(+).
PB94-185089 *00,770*

Electron-Impact Ionization of In(+) and Xe(+).
PB95-152906 *03,918*

DJUROVIC, S.

Hydrogen Balmer Alpha Line Shapes for Hydrogen-Argon Mixtures in a Low-Pressure rf Discharge.
PB95-153433 *03,924*

Ion Kinetic-Energy Distributions and Balmer-alpha (Halpha) Excitation in Ar-H2 Radio-Frequency Discharges.
PB96-102959 *04,029*

DMITRIEV, I. A.

Precision High Temperature Blackbodies.
PB95-140059 *03,885*

DOBBYN, R.

High Resolution Hard X-Ray Microscope.
PB94-213055 *03,856*

DOBBYN, R. C.

Correlation of HgCdTe Epilayer Defects with Underlying Substrate Defects by Synchrotron X-Ray Topography.
PB94-200714 *02,129*

DOBISZ, E.

Lattice Position of Si in GaAs Determined by X-Ray Standing Wave Measurements.
PB95-164406 *04,632*

DOBISZ, E. A.

Integration of Scanning Tunneling Microscope Nanolithography and Electronics Device Processing.
PB95-153359 *02,341*

DOBLECKI, W.

Effect of Three Sterilization Techniques on Finger Pluggers.
PB94-216090 *00,150*

DOBROW, R. P.

Move-to-Root Rule for Self-Organizing Trees with Markov Dependent Requests.
PB96-179528 *03,431*

DOBRY, R.

Functional Security Criteria for Distributed Systems.
PB96-123492 *01,607*

DODD, R. J.

Properties of a Bose-Einstein Condensate in an Anisotropic Harmonic Potential.
PB96-204144 *04,133*

DODERER, T.

Direct Observation of Vortex Dynamics in Two-Dimensional Josephson-Junction Arrays.
PB96-102223 *02,067*

Frequency Dependence of the Emission from 2D Array Josephson Oscillators.
PB95-175147 *02,056*

Novel Vortex Dynamics in Two-Dimensional Josephson Arrays.
PB96-200167 *02,091*

Observation of Vortex Dynamics in Two-Dimensional Josephson-Junction Arrays.
PB95-168811 *02,050*

SUSAN: SUperconducting Systems ANalysis by Low Temperature Scanning Electron Microscopy (LTSEM).
PB96-112065 *04,728*

DOETSCH, P.

Novel Activity of E. coli uracil DNA N-glycosylase Excision of Isodialuric Acid (5,6-dihydroxyuracil), a Major Product of Oxidative DNA Damage, from DNA.
PB96-110747 *03,543*

DOGAN, F.

High Resolution Inelastic Neutron Scattering Study of Phonon Self-Energy Effects in YBCO.
PB95-180881 *04,688*

q Dependence of Self-Energy Effects of the Plane Oxygen Vibration in YBa2Cu3O7.
PB96-138516 *01,096*

DOIRON, D. T.

Length Metrology of Complimentary Small Plastic Rulers.
PB96-161724 *04,096*

DOIRON, T.

Gage Block Handbook.
PB95-251716 *02,667*

Gage Block Standards, Measurement Capabilities and Laboratory Accreditation.
PB96-163621 *02,757*

Measuring the Stability of Three Copper Alloys.
PB94-199866 *03,326*

Residual Error Compensation of a Vision-Based Coordinate Measuring Machine.
PB96-161617 *04,091*

SPC Artifact for Automated Solder Joint Inspection.
PB96-161716 *04,095*

Verification of Revised Water Vapour Correction to the Index of Refraction of Air.
PB96-161666 *02,680*

DOIRON, T. D.

Computer Vision Based Tool Setting Station.
PB94-199858 *02,944*

Length Metrology of Complimentary Small Plastic Rulers.
PB96-161724 *04,096*

DOLEV, A.

NIST High-Accuracy Sampling Wattmeter.
PB97-108575 *02,689*

DOLS, W. S.

Air Change Effectiveness Measurements in Two Modern Office Buildings.
PB94-185766 *00,243*

Environmental Evaluation of a New Federal Office Building.
PB94-199874 *02,538*

Field Measurements of Ventilation and Ventilation Effectiveness in an Office/Library Building.
PB95-108833 *00,247*

Indoor Air Quality Commissioning of a New Office Building.
PB95-182309 *00,262*

Indoor Air Quality Commissioning of a New Office Building.
PB97-110142 *00,279*

Measurements of Outdoor Air Distribution in an Office Building.
PB95-210944 *00,264*

Study of Ventilation and Carbon Dioxide in an Office Building.
PB95-150140 *02,542*

Ventilation Effectiveness Measurements in Two Modern Office Buildings.
PB95-176012 *02,553*

DOMALSKI, E. S.

Assessing the Credibility of the Calorific Content of Muncipal Solid Waste.
PB94-199882 *02,581*

Conference Report: Calorimetry Conference (50th).
PB97-122279 *03,722*

Estimation of the Heat Capacities of Organic Liquids as a Function of Temperature Using Group Additivity. I. Hydrocarbon Compounds.
PB94-162278 *00,739*

Estimation of the Heat Capacities of Organic Liquids as a Function of Temperature Using Group Additivity. II. Compounds of Carbon, Hydrogen, Halogens, Nitrogen, Oxygen, and Sulfur.
PB94-162286 *00,740*

Estimation of the Thermodynamic Properties of C-H-N-O-S-Halogen Compounds at 298.15 K.
PB94-162328 *00,744*

DOMANSKI, P. A.

Intracycle Evaporative Cooling in a Vapor Compression Cycle.
PB97-116107 *02,762*

Simplified Cycle Simulation Model for the Performance Rating of Refrigerants and Refrigerant Mixtures.
PB94-199890 *03,255*

Theoretical Evaluation of the Vapor Compression Cycle with a Liquid-Line/Suction-Line Heat Exchanger, Economizer, and Ejector.
PB95-216917 *02,607*

DOMEN, S. R.

Problem of Convection in the Water Absorbed Dose Calorimeter.
PB97-110159 *03,523*

Sealed Water Calorimeter for Measuring Absorbed Dose.
PB94-219227 *03,517*

DOMICH, P. D.

Algorithmic Enhancements to the Method of Centers for Linear Programming Problems.
PB94-198959 ***03,426***

Analysis of an Open-Ended Coaxial Probe with Lift-Off for Nondestructive Testing.
PB96-135116 ***01,940***

Interior-Point Method for Linear and Quadratic Programming Problems. (NIST Reprint).
PB95-180089 ***03,429***

DONAHUE, D. J.

Radiocarbon Measurements of Atmospheric Volatile Organic Compounds: Quantifying the Biogenic Contribution.
PB97-122352 *02,574*

DONALDSON, J. R.

Algorithmic Enhancements to the Method of Centers for Linear Programming Problems.
PB94-198959 *03,426*

DONG, Q. Y.

Al L2,3 Core Excitons in AlxGa1-x as Studied by Soft-X-ray Reflection and Emission.
PB96-157839 *04,067*

Barium Contributions to the Valence Electronic Structure of YBa2Cu3O7-delta, PrBa2Cu3O7-delta, and Other Barium-Containing Compounds.
PB96-158019 *04,076*

Charge-Transfer-Induced Multiplet Structure in the N4,5O2,3 Soft-X-ray Emission Spectrum of Lanthanum.
PB96-163746 *04,102*

Cooper M(sub II,III) X-ray-Emission Spectra of Copper Oxides and the Bismuth Cuprate Superconductor.
PB96-158027 *04,077*

Intermediate Coupling in L2-L3 Core Excitons of MgO, Al2O3, and SiO2.
PB96-158043 *04,079*

Laser-Synchrotron Hybrid Experiments: A Photon to Tickle, A Photon to Poke.
PB96-157847 *03,704*

Local Partial Densities of States in Ni and Co Silicides Studied by Soft X-Ray Emission Spectroscopy.
PB94-212412 *04,504*

Phonon Relaxation in Soft-X-ray Emission of Insulators.
PB96-160296 *04,085*

Simple Variable Line Space Grating Monochromator for Synchrotron Light Source Beamlines.
PB96-156203 *04,065*

Soft-X-ray-Emission Investigation of Cobalt Implanted Silicon Crystals.
PB96-157912 *04,069*

Soft-X-ray-Emission Spectra of Solid Kr and Xe.
PB96-157920 *04,070*

Soft-X-ray-Emission Studies of Bulk Fe3Si, FeSi, and FeSi2, and Implanted Iron Silicides.
PB96-157938 *04,071*

DONG, X.

Mechanism of Mild to Severe Wear Transition in Alpha-Alumina.
PB94-212354 *03,233*

Tribological Characteristics of Alpha-Alumina at Elevated Temperatures.
PB94-211018 *02,963*

DONGARRA, J.

IML++ v.1.2 Iterative Methods Library Reference Guide.
PB96-195219 *01,776*

DONMEZ, A.

Displacement Method for Machine Geometry Calibration.
PB95-152088 *02,946*

Effects of Spindle Dynamic Characteristics on Hard Turning.
PB96-122981 *02,699*

DONMEZ, M. A.

Development of a New Quality Control Strategy for Automated Manufacturing.
PB96-160486 *02,840*

Evaluation of a Tapered Roller Bearing Spindle for High-Precision Hard Turning Applications.
PB96-160494 *02,700*

Integrated Inspection System for Improved Machine Performance.
PB96-160569 *02,959*

Prediction of Geometric-Thermal Machine Tool Errors by Artificial Neural Networks.
PB94-186673 *02,943*

DOOM, S. S.

Proficiency Tests for the NIST Airborne Asbestos Program - 1991.
PB94-193828 *00,537*

DOORN, S. S.

Proficiency Tests for the NIST Airborne Asbestos Program, 1990.
PB94-188836 *00,535*

Proficiency Tests for the NIST Airborne Asbestos Program - 1992.
PB94-194362 *00,539*

DORKO, W. D.

NIST Traceable Reference Material Program for Gas Standards: Standard Reference Materials.
PB96-210786 *00,644*

Standards for Atmospheric Measurements.
PB95-163622 *02,547*

DOROFEEVA, O. V.

Ideal Gas Thermodynamic Properties of Sulphur Heterocyclic Compounds.
PB96-145867 *01,110*

DOROSHOW, J.

Modification of DNA Bases in Chromatin of Intact Target Human Cells by Activated Human Polymorphonuclear Leukocytes.
PB94-199833 *03,526*

DOROSHOW, J. H.

Copper Ion-Mediated Modification of Bases in DNA in Vitro by Benzoyl Peroxide.
PB94-198231 *03,645*

DOSCHEK, G.

Sleuthing the Dynamo: HST/FOS Observations of UV Emissions of Solar-Type Stars in Young Clusters.
PB96-122817 *00,098*

DOSCHEK, G. A.

Far-Ultraviolet Flare on a Pleiades G Dwarf.
PB96-102033 *00,086*

DOU, S. X.

Critical Current Density, Irreversibility Line, and Flux Creep Activation Energy in Silver-Sheathed Bi2Sr2Ca2Cu2Ox Superconducting Tapes.
PB95-162749 *04,616*

DOUGHERTY, T. P.

Bimolecular Interactions in (Et)3SiOH:Base:CCl4 Hydrogen-Bonded Solutions Studied by Deactivation of the Free OH-Stretch Vibration.
PB97-118657 *04,166*

DOUGHTY, D. A.

Plasma Chemistry in Disilane Discharges.
PB94-211075 *02,514*

Plasma Chemistry in Silane/Germane and Disilane/Germane Mixtures.
PB95-202537 *01,027*

DOUGLAS, J.

Book Review: Aspects and Applications of the Random Walk.
PB96-123534 *04,215*

Book Review: Statistical Physics of Macromolecules.
PB96-123526 *01,280*

Dynamic Light-Scattering Study of a Diluted Polymer Blend Near Its Critical Point.
PB95-151890 *01,245*

Generalized Stokes-Einstein Equation for Spherical Particle Suspensions.
PB95-202743 *01,031*

How Far Is Far from Critical Point in Polymer Blends. Lattice Cluster Theory Computations for Structured Monomer, Compressible Systems.
PB94-211141 *01,217*

Non-Perturbative Relation between the Mutual Diffusion Coefficient, Suspension Viscosity, and Osmotic Compressibility: Application to Concentrated Protein Solutions.
PB96-102355 *01,062*

Thermodynamic Properties of Dilute and Semidilute Solutions of Regular Star Polymers.
PB96-146808 *01,284*

DOUGLAS, J. F.

Competition between Hydrodynamic Screening ('Draining') and Excluded Volume Interactions in an Isolated Polymer Chain.
PB95-175402 *01,265*

Dimensional Crossover in the Phase Separation Kinetics of Thin Polymer Blend Films.
PB97-113088 *03,395*

Effect of Swelling on the Elasticity of Rubber: Localization Model Description.
PB94-211034 *01,216*

Electrostatic Rigidity of Polyelectrolytes from Reparametrization Invariance.
PB96-180062 *04,113*

Examination of the l/d Expansion Method from Exact Enumeration for a Self-Interacting Self-Avoiding Walk.
PB95-175733 *01,266*

Geometrical Percolation Threshold of Overlapping Ellipsoids.
PB96-102397 *03,167*

Hydrodynamic Friction of Arbitrarily Shaped Brownian Particles.
PB97-110191 *04,136*

Hypercubic Lattice SAW Exponents nu and gamma : 3.99 Dimensions Revisited.
PB94-211026 *01,215*

Influence of Shear on the Ordering Temperature of a Triblock Copolymer Melt.
PB96-163753 *01,288*

Influence of Surface Interaction and Chain Stiffness on Polymer-Induced Entropic Forces and the Dimensions of Confined Polymers.
PB94-185469 *01,203*

Intrinsic Conductivity of Objects Having Arbitrary Shape and Conductivity.
PB97-111934 *04,150*

Intrinsic Viscosity and the Polarizability of Particles Having a Wide Range of Shapes.
PB96-119318 *03,170*

Localization Model of Rubber Elasticity: Comparison with Torsional Data for Natural Rubber Networks in the Dry State.
PB95-107033 *03,195*

Modification of the Phase Stability of Polymer Blends by Diblock Copolymer Additivies.
PB96-123542 *03,172*

Neutron Reflectivity Study of the Density Profile of a Model End-Grafted Polymer Brush: Influence of Solvent Quality.
PB95-202735 *01,274*

Neutron Scattering Study of Shear Induced Turbidity in Polystyrene/Dioctyl Phthalate Solutions at High Shear Rates.
PB94-172624 *01,197*

Neutron Scattering Study of Shear Induced Turbidity in Polystyrene Dissolved in Dioctyl Phthalate.
PB95-161865 *01,256*

Phase Separation in Thin Film Polymer Blends With and Without Block Copolymer Additives.
PB96-204482 *01,294*

Probabilistic Computation of Poiseuille Flow Velocity Fields.
PB96-102520 *04,209*

Response to 'Draining in Dilute Polymer Solutions and Renormalization'.
PB96-146667 *01,283*

Segmental Concentration Profiles of End-Tethered Polymers with Excluded-Volume and Surface Interactions.
PB97-119002 *00,654*

Self-Avoiding-Walk Contacts and Random-Walk Self-Intersections in Variable Dimensionality.
PB96-102231 *01,276*

Shear-Induced Changes in the Order-Disorder Transition Temperature and the Morphology of a Triblock Copolymer.
PB97-118772 *03,130*

Shear Suppression of Critical Fluctuations in a Diluted Polymer Blend.
PB96-204458 *04,418*

Swelling and Growth of Polymers, Membranes and Sponges.
PB97-118400 *03,396*

Topological Influences on Polymer Adsorption and Desorption Dynamics.
PB94-212479 *01,227*

DOUMAS, B. T.

Molar Absorptivities of Bilirubin (NIST SRM 916A) and Its Neutral and Alkaline Azopigments.
PB94-211042 *03,456*

DOWNEY, E.

Boron-Implanted 6H-SiC Diodes.
PB96-159678 *04,081*

DOWNEY, L. L.

Design and Development of an Information Retrieval System for the EAMATE Data. Volume 2 of 2. Appendices.
PB94-168390 *00,487*

Usability Engineering: Industry-Government Collaboration for System Effectiveness and Efficiency.
PB97-122287 *01,514*

DOWNING, R. G.

Analysis of Boron in CVD Diamond Surfaces Using Neutron Depth Profiling.
PB94-213089 *04,511*

Determination of Boron and Lithium in Diverse Biological Matrices Using Neutron Activation - Mass Spectrometry (NA-MS).
PB94-212289 *00,554*

Measurement of Boron at Silicon Wafer Surfaces by Neutron Depth Profiling.
PB94-211059 *04,487*

Modeling Detector Response for Neutron Depth Profiling.
PB96-157813 *04,066*

Regulation of Lithium and Boron Levels in Normal Human Blood: Environmental and Genetic Considerations.
PB94-198579 *03,491*

Use of Neutron Beams for Chemical Analysis at NIST.
PB97-112437 *00,652*

DOYLE, J. G.

Dynamic Phenomena on the RS Canum Venaticorum Binary II Pegasi in August 1989. 1. Observational Data.
PB94-211067 *00,056*

Rotational Modulation and Flares on RS Canum Venaticorum and BY Draconis Stars. XVI. IUE Spectroscopy and VLA Observations of C1182(=V 1005 Orionis) in October 1983.
PB94-185626 *00,050*

DOYLE, J. R.

Plasma Chemistry in Disilane Discharges.
PB94-211075 *02,514*

Plasma Chemistry in Silane/Germane and Disilane/Germane Mixtures.
PB95-202537 *01,027*

DRABECK, L. M.

Increased Transition Temperature in In situ Coevaporated YBa2Cu3O7-delta Thin Films by Low Temperature Post-Annealing.
PB95-180071 *04,672*

DRAGOO, A. L.

Analysis of Physical Properties of Ceramic Powders in an International Interlaboratory Comparison Program.
PB95-161501 *03,050*

Ceramic Characterization.
DE94013170 *03,026*

DRAGOSET, R. A.

Atomic Manipulation of Polarizable Atoms by Electric Field Directional Diffusion.
PB95-150587 *04,572*

Homoepitaxial Growth of Iron and a Real Space View of Reflection-High-Energy-Electron Diffraction.
PB94-173069 *04,445*

Manipulation of Adsorbed Atoms and Creation of New Structures on Room-Temperature Surfaces with a Scanning Tunneling Microscope.
PB95-151536 *04,578*

DRAKE, S. A.

Class of Radio-Emitting Magnetic B Stars and a Wind-Fed Magnetosphere Model.
PB94-213451 *00,067*

Efficient Way of Identifying New Active Stars: A VLA Survey of X-ray Selected Active Stellar Candidates.
PB96-122882 *00,099*

Four Years of Monitoring alpha Orionis with the VLA: Where Have All the Flares Gone.
PB94-185212 *00,048*

Radio Continuum and X-Ray Properties of the Coronae of RS Canum Venaticorum and Related Active Binary Systems.
PB94-211083 *00,057*

Radio Emission from Chemically Peculiar Stars.
PB94-213469 *00,068*

Search for Radio Emission from the 'Non-Magnetic' Chemically Peculiar Stars.
PB96-102249 *00,087*

X-ray Emission from Chemically Peculiar Stars.
PB96-102256 *00,088*

DRAPELA, T. J.

Optical Fiber, Fiber Coating, and Connector Ferrule Geometry: Results of Interlaboratory Measurement Comparisons.
PB96-154422 *04,360*

DRAVID, V. P.

Suitability of Metalorganic Chemical Vapor Deposition-Derived PrGaO3 Films as Buffer Layers for YBa2Cu3O7-x Pulsed Laser Deposition.
PB95-168670 *04,640*

DRAVINS, D.

Distant Future of Solar Activity: A Case Study of Beta Hydri. 3. Transition Region, Corona, and Stellar Wind.
PB94-185220 *00,049*

Distant Future of Solar Activity: A Case Study of beta Hydri. 3. Transition Region, Corona, and Stellar Wind.
PB95-153441 *00,074*

DRAY, J. F.

Formal Specification and Verification of Control Software for Cryptographic Equipment.
PB94-213030 *01,585*

Guideline for the Use of Advanced Authentication Technology Alternatives. Category: Computer Security. Subcategory: Access Control.
FIPS PUB 190 *01,798*

DRAYER, D. E.

Compilation of the Physical Equilibria and Related Properties of the Hydrogen-Carbon Monoxide System.
AD-A286 603/6 *00,716*

DRESCHER-KRASICKA, E.

Leady Axisymmetric Modes in Infinite Clad Rods. Part 1.
PB95-162905 *04,187*

DREWS, A. R.

Preparation and Crystal Structure of Sr5TiNb4O17.
PB96-167341 *04,107*

DREXLER, E. S.

Aluminum-Lithium Alloys: Evaluation of Fracture Toughness by Two Test Standards, ASTM Method E 813 and E 1304.
PB96-190236 *03,374*

Light-Weight Alloys for Aerospace Applications II.
PB96-190244 *03,375*

DRIESSEN, J. P. J.

Alignment Probing of Rydberg States by Stimulated Emission.
PB96-200316 *04,124*

Initial and Final Orbital Alignment Probing of the Fine-Structure-Changing Collisions among the Ca (4s)(1)(4p)(1), (3)PJ States with He: Determination of Coherence and Conventional Cross-Sections.
PB95-203279 *04,004*

Laser Preparation and Probing of Initial and Final Orbital Alignment in Collision-Induced Energy Transfer Ca(4s5p,(1)P1) + He yields Ca(4s5p,(3)P2) + He.
PB95-203261 *04,003*

n-Vector Correlations in Collision Dynamics with Atomic Orbital Alignment: The Importance of Coherence Denoting Azimuthal Structure for n (greater than or equal to) 3.
PB95-202545 *03,983*

Three-Vector Correlation Study of Orientation and Coherence Effects in Na(3p, (2)P1/2 inversely maps (2)P3/2)+He: Semiclassical and Quantum Calculations.
PB95-202453 *03,979*

Three-Vector Correlation Theory for Orientation/Alignment Studies in Atomic and Molecular Collisions.
PB94-211109 *03,834*

DROUIN, N.

Computing Effects and Error for Large Synthetic Perturbation Screenings.
PB94-139623 *01,675*

DROUIN, N. V.

Using S-Check, Alpha Release 1.0.
PB96-165964 *01,767*

DRULLINGER, R. E.

Diode-Laser Pumped, Rubidium Cell Frequency Standards.
PB95-163218 *01,538*

Error Analysis of the NIST Optically Pumped Primary Frequency Standard.
PB95-153482 *01,535*

Hybrid Digital/Analog Servo for the NIST-7 Frequency Standard.
PB95-180618 *01,544*

Improved Rubidium Frequency Standards Using Diode Lasers with AM and FM Noise Control.
PB95-176152 *04,303*

Microwave Leakage as a Source of Frequency Error and Long-Term Instability in Cesium Atomic-Beam Frequency Standards.
PB95-180501 *01,541*

NIST Optically Pumped Cesium Frequency Standard.
PB94-211117 *03,835*

NIST-7, the New US Primary Frequency Standard.
PB95-153458 *01,534*

Reducing the Effect of Local Oscillator Phase Noise on the Frequency Stability of Passive Frequency Standards.
PB95-180972 *01,545*

Ultra-High Stability Synthesizer for Diode Laser Pumped Rubidium.
PB94-216066 *01,527*

Velocity Distribution of Atomic Beams by Gated Optical Pumping.
PB95-180519 *01,542*

DU, N. Y.

Resonant Two-Color Detachment of H(-) with Excitation of H(n=2).
PB95-202552 *03,984*

DU, R.

Magnetic Rare Earth Artificial Metallic Superlattices.
PB95-162293 *04,611*

Magnetoelasticity in Rare-Earth Multilayers and Films.
PB94-211356 *04,495*

DUAN, H. M.

Asymmetry between Flux Penetration and Flux Expulsion in Tl-2212 Superconductors.
PB95-125647 *04,527*

DUAN, S. L.

Correlations of Modulation Noise with Magnetic Microstructure and Intergranular Interactions for CoCrTa and CoNi Thin Film Media.
PB94-212768 *04,509*

DUBE, W. P.

Gas-Coupled, Pulse-Echo Ultrasonic Crack Detection and Thickness Gaging.
PB96-147129 *04,847*

DUBEY, I. P.

Energy Dependence of Collision Characteristics in Molecule-Surface Collisions.
PB94-198504 *00,786*

DUBIN, D.

Electrostatic Modes of Ion-Trap Plasmas.
PB95-152963 *03,920*

DUBIN, D. H. E.

Non-Neutral Ion Plasmas and Crystals, Laser Cooling, and Atomic Clocks.
PB95-175113 *03,957*

DUBS, R. L.

Intersystem Crossing in Collisions of Aligned Ca(4s5p (1)P) + He: A Half Collision Analysis Using Multichannel Quantum Defect Theory.
PB94-211133 *00,813*

Multichannel Quantum Defect Half Collision Analysis of K2 Photodissociation Through the B1Pi(sub u) State.
PB94-211125 *00,812*

DUDOWICZ, J.

How Far Is Far from Critical Point in Polymer Blends. Lattice Cluster Theory Computations for Structured Monomer, Compressible Systems.
PB94-211141 *01,217*

Modification of the Phase Stability of Polymer Blends by Diblock Copolymer Additivies.
PB96-123542 *03,172*

DUEWER, D. L.

Intercomparison of DNA Sizing Ladders in Electrophoretic Separation Matrices and Their Potential for Accurate Typing of the D1S80 Locus.
PB96-200928 *03,485*

Interlaboratory Comparison of Autoradiographic DNA Profiling Measurements. 1. Data and Summary Statistics.
PB95-175923 *03,542*

Interlaboratory Comparison of Autoradiographic DNA Profiling Measurements. 2. Measurement Uncertainty and Its Propagation.
PB96-112123 *03,545*

Measurement of Ascorbic Acid in Human Plasma and Serum: Stability, Intralaboratory Repeatability, and Interlaboratory Reproducibility.
PB97-112445 *03,511*

Population Distributions and Intralaboratory Reproducibility for Fat-Soluble Vitamin-Related Compounds in Human Serum.
PB96-155536 *00,624*

DUFAUX, D. P.

In-situ Studies of a Novel Sodium Flame Process for Synthesis of Fine Particles.
PB97-113047 *00,681*

Optical and Modeling Studies of Sodium/Halide Reactions for the Formation of Titanium and Boron Nanoparticles.
PB97-113054 *00,682*

DUFFEY, M. R.

Product Realization Process Modeling: A Study of Requirements, Methods and Research Issues.
PB96-147962 *02,836*

DUNCAN, W. M.

Comparison of Techniques for Nondestructive Composition Measurements in CdZnTe Substrates.
PB96-103098 *02,703*

Optical Characterization in Microelectronics Manufacturing.
PB95-169397 *02,358*

DUNGAN, D. F.

Applicability of Effective Medium Theory to Ferroelectric/Ferrimagnetic Composites with Composition and Frequency-Dependent Complex Permittivities and Permeabilities.
PB96-157854 *01,945*

DUNN, G. H.

Absolute Cross-Section Measurements for Electron-Impact Ionization of C1(+1).
PB94-199841 *03,818*

Absolute Cross-Section Measurements for Electron-Impact Single Ionization of Se(+) and Te(+).
PB95-202503 *03,980*

Absolute Cross Sections for Electron-Impact Single Ionization of Si(+) and Si(2+).
PB95-202529 *03,982*

Backscattering in Electron-Impact Excitation of Multiply Charged Ions.
PB94-185345 *03,799*

Collisions of Electrons with Highly-Charged Ions.
PB96-200340 *04,791*

Crossed-Beams Measurements of Absolute Cross Sections for Electron Impact Ionization of S(+).
PB95-202511 *03,981*

Dielectronic Capture Processes in the Electron-Impact Ionization of Sc(2+).
PB95-203113 *04,000*

Early Dielectronic Recombination Measurements: Singly Charged Ions.
PB94-211158 *03,836*

Electron-Impact Excitation of Si(3+)(3S yields 3P) Using a Merged-Beam Electron-Energy-Loss Technique.
PB95-151239 *03,904*

Electron-Impact Ionization of In(+) and Xe(+).
PB94-185089 *00,770*

Electron-Impact Ionization of In(+) and Xe(+).
PB95-152906 *03,918*

Electron-Ion Collisions in the Plasma Edge.
PB96-111885 *04,037*

Evidence for Significant Backscattering in Near-Threshold Electron-Impact Excitation of Ar(7+)(3s yields 3p).
PB95-126405 *03,883*

Merged-Beams Energy-Loss Technique for Electron-Ion Excitation: Absolute Total Cross Sections for O(5+) (2s yields 2p).
PB96-102058 *04,017*

Resonance Structure and Absolute Cross Sections in Near-Threshold Electron-Impact Excitation of the 4s(2) (1)S yields 4s4p (3)P Intercombination Transition in Kr(6+).
PB95-202271 *03,972*

Superconducting Resonator and a Cryogenic GaAs Field-Effect Transistor Amplifier as a Single-Ion Detection System.
PB95-202727 *03,990*

DUNN, M.

Void Shape in Sintered Titanium.
PB96-141023 *02,705*

DUNN, M. L.

Estimation of the Orientation Distribution of Short-Fiber Composites Using Ultrasonic Velocities.
PB96-176656 *03,178*

DUNSMUIR, J.

Transport and Diffusion in Three-Dimensional Composite Media.
PB95-176129 *04,668*

DURA, J. A.

Buffer Layer Modulation-Doped Field-Effect-Transistor Interactions in the Al0.33Ga0.67As/GaAs Superlattice System.
PB96-102876 *02,380*

Diffraction of Neutron Standing Waves in Thin Films with Resonance Enhancement.
PB97-113278 *04,164*

Epitaxial Growth of Sb/GaSb Structures: An Example of V/III-V Heteroepitaxy.
PB95-202560 *04,693*

Epitaxial Integration of Single Crystal C60.
PB95-153490 *04,592*

In-situ Neutron Reflectivity of MBE Grown and Chemically Processed Surfaces and Interfaces.
PB96-146634 *02,416*

Photoluminescence Spectra of Epitaxial Single Crystal C60.
PB96-141205 04,754

X-ray Reflectivity Determination of Interface Roughness Correlated with Transport Properties of (AlGa)As/GaAs High Electron Mobility Transistor Devices.
PB97-111868 04,149

DURAN, R.

Using Torsional Dilatometry to Measure the Effects of Deformations on Physical Aging.
PB95-140901 03,384

DURAN, R. S.

Aging in Glasses Subjected to Large Stresses and Deformations.
PB95-107041 03,235

Torsional Dilatometer for Volume Change Measurements on Deformed Glasses: Instrument Description and Measurements on Equilibrated Glasses.
PB94-211166 03,379

Volume Recovery in Epoxy Glasses Subjected to Torsional Deformations: The Question of Rejuvenation.
PB95-140018 03,382

DURST, R.

Liposome-Based Flow-Injection Immunoassay for Determining Theophylline in Serum.
PB94-213493 03,494

DURST, R. A.

Planar Waveguide Optical Sensors.
PB94-200185 03,586

Potentiometric Enzyme-Amplified Flow Injection Analysis Detection System: Behavior of Free and Liposome-Released Peroxidase.
PB95-151833 03,534

DUTCHER, J. R.

Brillouin Light Scattering Intensities for Thin Magnetic Films with Large Perpendicular Anisotropies.
PB94-211174 04,488

DUTHINH, D.

Shear Design of High-Strength Concrete Beams: A Review of the State-of-the-Art.
PB96-214713 01,330

DUTTA, P.

Investigation of Oil and Gas Well Fires and Flares.
PB94-193976 03,695

DUVALL, K. C.

Role of the Office of Radiation Measurement in Quality Assurance.
PB94-212255 00,689

DYUKOVA, T. V.

Holographic Properties of Triton X-100-Treated Bacteriorhodopsin Embedded in Gelatin Films.
PB96-119284 03,761

Optical Properties of Triton X-100-Treated Purple Membranes Embedded in Gelatin Films.
PB96-123500 03,546

Retinal-Protein Complexes as Optoelectronic Components.
PB95-150397 02,146

DZIERZEGA, K.

Time-Resolved Balmer-Alpha Emission from Fast Hydrogen Atoms in Low Pressure, Radio-Frequency Discharges in Hydrogen.
PB96-102942 04,028

DZIUBA, R. F.

Automated Resistance Measurements at NIST.
PB96-119326 02,274

High-Temperature Superconductor Cryogenic Current Comparator.
PB96-119334 02,074

Loading Effects in Resistance Scaling.
PB97-111884 02,285

Low Thermal Guarded Scanner for High Resistance Measurement Systems.
PB97-112452 02,288

NIST Comparison of the Quantized Hall Resistance and the Realization of the SI Ohm Through the Calculable Capacitor.
PB97-119184 02,291

NIST Comparison of the Quantized Hall Resistance and the Realization of the SI Ohm Through the Calculable Capacitor. Conference Proceedings, June 17-20, 1996.
PB97-119192 02,292

Pressure Dependencies of Standard Resistors.
PB95-153516 02,257

Resistors.
PB97-111876 02,284

DZUBA, V. A.

Fine Structure of Negative Ions of Alkaline-Earth-Metal Atoms.
PB94-211182 03,837

EAGAR, T.

In-Space Welding: Visions and Realities.
PB95-163234 04,830

EANES, E. D.

Behavior of a Calcium Phosphate Cement in Simulated Blood Plasma In vitro.
PB95-168712 00,165

Bioactive Polymeric Dental Materials Based on Amorphous Calcium Phosphate.
PB96-147012 03,572

Calcium Phosphate Precipitation in Liposomal Suspensions.
PB94-172145 03,452

Critical Evaluation of the Purification of Biominerals by Hypochlorite Treatment.
PB95-150959 00,186

Dynamics of Calcium Phosphate Precipitation.
PB96-147095 03,574

Effect of Supersaturation on Apatite Crystal Formation in Aqueous Solutions at Physiologic pH and Temperature.
PB96-135215 03,571

Effect of 1-Hydroxyethylidene-1,1-Bisphosphonate on Membrane-Mediated Calcium Phosphate Formation in Model Liposomal Suspensions.
PB95-169223 03,469

In vitro Inhibition of Membrane-Mediated Calcification by Novel Phosphonates.
PB96-201140 03,595

Membrane-Mediated Precipitation of Calcium Phosphate in Model Liposomes with Matrix Vesicle-Like Lipid Composition.
PB95-164547 03,468

Mixed Phospholipid Liposome Calcification.
PB94-211190 03,457

Polymeric Calcium Phosphate Composites with Remineralization Potential.
PB96-155544 03,575

Proteoglycan Inhibition of Calcium Phosphate Precipitation in Liposomal Suspensions.
PB94-211208 00,658

Remineralizing Dental Composites Based on Amorphous Calcium Phosphate.
PB96-147020 03,573

EARLY, E. A.

Evidence for Parallel Junctions Within High-Tc Grain-Boundary Junctions.
PB95-175410 04,657

Half-Integral Constant Voltage Steps in High-Tc Grain Boundary Junctions.
PB94-211216 04,489

Irradiance of Horizontal Quartz-Halogen Standard Lamps.
PB96-179130 01,866

Physical Basis for Half-Integral Shapiro Steps in a DC SQUID.
PB96-102264 04,704

Report on USDA Ultraviolet Spectroradiometers.
PB96-214648 00,125

Voltage Ratio Measurements of a Zener Reference Using a Digital Voltmeter.
PB95-164695 01,906

EARLY, G.

Relationship of Silver with Selenium and Mercury in the Liver of Two Species of Toothed Whales (Odontocetes).
PB96-167275 02,596

EASTERLING, R. G.

Agile Manufacturing from a Statistical Perspective.
PB96-109525 02,886

EATON, P. E.

Neutron Scattering Study of the Lattice Modes of Solid Cubane.
PB96-147152 01,126

EBBERTS, D. F.

Room Temperature Thermal Conductivity of Fumed-Silica Insulation for a Standard Reference Material.
PB95-152039 00,374

EBBESEN, T. W.

Rotational Dynamics of C60 in Na2RbC60.
PB95-153201 00,948

EBBETS, D. C.

First Results from the Goddard High-Resolution Spectrograph: The Chromosphere of Tauri.
PB94-199528 00,054

Observations of 3C 273 with the Goddard High Resolution Spectrograph on the Hubble Space Telescope.
PB95-202321 00,076

EBERHARDT, K. R.

Combining Data from Independent Chemical Analysis Methods.
PB95-140141 00,572

Constant-Width Calibration Intervals for Linear Regression.
PB95-153524 03,439

Quantifying the Ignition Propensity of Cigarettes.
PB96-155411 00,306

EBNER, S. C.

Update on the Low Background IR Calibration Facility at the National Institute of Standards and Technology.
PB94-211224 04,232

EBRAHEEM, S.

Thin Dyed-Plastic Dosimeter for Large Radiation Doses.
PB95-107363 03,872

EBRAHIM EID, S. E.

Radiation-Chemical Reaction of 2,3,5-Triphenyl-Tetrazolium Chloride in Liquid and Solid State.
PB96-146733 01,124

EBY, R. K.

Application of Thermal Analysis Techniques to the Characterization of EPDM Roofing Membrane Materials.
PB95-125845 00,359

Use of Thermal Mechanical Analysis to Characterize Ethylene-Propylene-Diene Terpolymer (EPDM) Roofing Membrane Materials.
PB95-125852 00,360

ECKERLE, K.

Standards for Corrected Fluorescence Spectra.
PB95-150835 00,581

ECKERLE, K. E.

Comparison of Regular Transmittance Scales of Four National Standardizing Laboratories.
PB94-211232 04,233

ECKSTEIN, J. N.

Stacked Series Arrays of High-Tc Trilayer Josephson Junctions.
PB96-102272 04,705

Step-Edge and Stacked-Heterostructure High-Tc Josephson Junctions for Voltage-Standard Arrays.
PB96-102066 04,702

Vortex Images in Thin Films of YBa2Cu3O(sub 7-x) and Bi2Sr2Ca1Cu2O(sub 8+x) Obtained by Low-Temperature Magnetic Force Microscopy.
PB97-119408 04,815

ECONOMOU, D. J.

Two-Dimensional Self-Consistent Radio Frequency Plasma Simulations Relevant to the Gaseous Electronics Conference RF Reference Cell.
PB96-113436 02,398

EDDY, C. R.

Effect of Beam Voltage on the Properties of Aluminum Nitride Prepared by Ion Beam Assisted Deposition.
PB97-118616 01,995

EDERER, D. L.

Al L2,3 Core Excitons in AlxGa1-x as Studied by Soft-X-ray Reflection and Emission.
PB96-157839 04,067

Charge-Transfer-Induced Multiplet Structure in the N4,5O2,3 Soft-X-ray Emission Spectrum of Lanthanum.
PB96-163746 04,102

Cooper M(sub II,III) X-ray-Emission Spectra of Copper Oxides and the Bismuth Cuprate Superconductor.
PB96-158027 04,077

Intermediate Coupling in L2-L3 Core Excitons of MgO, Al2O3, and SiO2.
PB96-158043 04,079

Laser-Synchrotron Hybrid Experiments: A Photon to Tickle, A Photon to Poke.
PB96-157847 03,704

Local Partial Densities of States in Ni and Co Silicides Studied by Soft X-Ray Emission Spectroscopy.
PB94-212412 04,504

NIST Metrology for Soft X-ray Multilayer Optics.
PB96-160379 04,088

Phonon Relaxation in Soft-X-ray Emission of Insulators.
PB96-160296 04,085

Simple Variable Line Space Grating Monochromator for Synchrotron Light Source Beamlines.
PB96-156203 04,065

Soft-X-ray-Emission Investigation of Cobalt Implanted Silicon Crystals.
PB96-157912 04,069

Soft-X-ray-Emission Spectra of Solid Kr and Xe.
PB96-157920 04,070

Soft-X-ray-Emission Studies of Bulk Fe3Si, FeSi, and FeSi2, and Implanted Iron Silicides.
PB96-157938 04,071

Upgraded Facility for Multilayer Mirror Characterization at NIST.
PB96-160387 04,367

EDERER, T. A.

Barium Contributions to the Valence Electronic Structure of YBa2Cu3O7-delta, PrBa2Cu3O7-delta, and Other Barium-Containing Compounds.
PB96-158019 04,076

EDGAR, J. H.

Effect of Beam Voltage on the Properties of Aluminum Nitride Prepared by Ion Beam Assisted Deposition.
PB97-118616 01,995

EDGERLY, D. E.

Opportunities for Innovation: Optoelectronics.
PB96-118039 01,928

Opportunities for Innovation: Pollution Prevention.
PB95-147146 02,520

Opportunities for Innovation: Software for Manufacturing.
PB95-155578 02,851

EDWARDS, J.

Non-Perturbative Relation between the Mutual Diffusion Coefficient, Suspension Viscosity, and Osmotic Compressibility: Application to Concentrated Protein Solutions.
PB96-102355 01,062

EDWARDS, M.

Population Trapping in Short-Pulse Multiphoton Ionization.
PB96-164140 04,371

Properties of a Bose-Einstein Condensate in an Anisotropic Harmonic Potential.
PB96-204144 04,133

EDWARDS, M. A.

Numerical Solution of the Nonlinear Schroedinger Equation for Small Samples of Trapped Neutral Atoms.
PB95-202578 03,985

EDWARDS, W. E.

Physicochemical Characterization of Natural and Bioprosthetic Heart Valve Calcific Deposits: Implications for Prevention.
PB96-156039 00,187

EGELHOFF, W. F.

Brillouin Light Scattering Intensities for Thin Magnetic Films with Large Perpendicular Anisotropies.
PB94-211174 04,488

Concurrent Enhancement of Kerr Rotation and Antiferromagnetic Coupling in Epitaxial Fe/Cu/Fe Structures.
PB94-198769 04,466

Semiclassical Explanation of the Generalized Ramsauer-Townsend Minima in Electron-Atom Scattering.
PB95-153532 03,925

Spot-Profile-Analyzing LEED Study of the Epitaxial Growth of Fe, Co, and Cu on Cu(100).
PB95-150165 04,561

Variation in Magnetic Properties of Cu/Fcc (001) Sandwich Structures.
PB95-141164 04,555

X-ray Photoelectron and Auger Electron Forward Scattering: A Structural Diagnostic for Epitaxial Thin Films.
PB95-180220 04,676

EGGERS, D. F.

Infrared and Microwave Spectroscopy of the Argon - Propyne Dimer.
PB94-198892 00,794

EHARA, K.

Experimental Optimization of Peak Shape with Application to Aerosol Generation.
PB94-185535 00,501

Stochastic Modeling of a New Spectrometer.
PB96-157870 04,068

EHLEN, M. A.

Economics of New-Technology Materials: A Case Study of FRP Bridge Decking.
PB96-202353 01,349

EHRLICH, C.

Working Conference on Global Growth of Technology: Is America Prepared. Held in Gaithersburg, Maryland on December 7, 1995.
PB96-210059 00,018

EHRLICH, C. D.

Intercomparison between NPL (India) and NIST (USA) Pressure Standards in the Hydraulic Pressure Region Up to 26 MPa.
PB96-113543 04,211

Intercomparison of the Effective Areas of a Pneumatic Piston Gauge Determined by Different Techniques.
PB94-212370 02,640

Look at Uncertainties over Twenty Decades of Pressure Measurement.
PB95-168506 02,655

Operational Mode and Gas Species Effects on Rotational Drag in Pneumatic Dead Weight Pressure Gages.
PB95-140182 00,903

EHRLICH, M.

Comparison of NIST and ISO Filtered Bremsstrahlung Calibration Beams.
PB95-180956 03,967

Interpreting the Readings of Multi-Element Personnel Dosimeters in Terms of the Personal Dose Equivalent.
PB95-175428 03,631

EHRSTEIN, J. R.

Development of a Standard Reference Material for Measurement of Interstitial Oxygen Concentration in Semiconductor Silicon by Infrared Absorption.
PB96-122668 02,404

Methodology for the Certification of Reference Specimens for Determination of Oxygen Concentration in Semiconductor Silicon by Infrared Spectrophotometry.
PB96-155478 02,421

EICHHORN, R. M.

Spatial Dependence of Electrical Fields Due to Space Charges in Films of Organic Dielectrics Used for Insulation of Power Cables.
PB94-199130 02,214

EICHMANN, U.

Interference in the Resonance Fluorescence of Two Trapped Atoms.
PB95-168514 03,948

Light Scattered from Two Atoms.
PB95-168753 04,286

EICHMILLER, F.

Diagnosis and Treatment of an Oral Base-Metal Contact Lesion Following Negative Dermatologic Patch Tests.
PB95-180626 00,172

Effect of Two Initiator/Stabilizer Concentrations in a Metal Primer on Bond Strengths of a Composite to a Base Metal Alloy.
PB94-172723 00,141

Effects of Aluminum Oxalate/Glycine Pretreatment Solutions on Dentin Permeability.
PB95-164505 03,565

EICHMILLER, F. C.

Clinical Perspective on Dentin Adhesives.
PB94-211240 00,146

Dental Applications of Ceramics.
PB96-122940 00,177

Dental Materials.
PB94-172871 00,142

Effect of Three Sterilization Techniques on Finger Pluggers.
PB94-216090 00,150

Effects of Surface-Active Resins on Dentin/Composite Bonds.
PB95-140448 00,156

New Method for Shielding Electron Beams Used for Head and Neck Cancer Treatment.
PB94-211430 03,621

New Surface-Active Comonomer for Adhesive Bonding.
PB96-204052 03,579

Posterior Restorative Materials Research.
PB97-118624 03,582

Reduction of Marginal Gaps in Composite Restorations by Use of Glass-Ceramic Inserts.
PB96-102405 00,174

Surface Roughness of Glass-Ceramic Insert. Composite Restorations: Assessing Several Polishing Techniques.
PB97-119010 03,583

Tapered Cross-Pin Attachments for Fixed Bridges.
PB94-185238 00,185

Wear of Enamel against Glass-Ceramic, Porcelain, and Amalgam.
PB96-179593 03,082

EICHORN, B.

Substitution-Induced Midgap States in the Mixed Oxides RxBa1-ChiTiO3-Delta, with R=Y, La, and Nd.
PB95-140505 04,541

EIDELMAN, N.

In vitro Inhibition of Membrane-Mediated Calcification by Novel Phosphonates.
PB96-201140 03,595

Selective Inhibition of Crystal Growth on Octacalcium Phosphate and Nonstoichiometric Hydroxyapatite by Pyrophosphate at Physiological Concentration.
PB94-211257 00,147

EILES, M. T.

Even-Odd Asymmetry of a Superconductor Revealed by the Coulomb Blockade of Andreev Reflection.
PB95-153540 04,593

EILES, T. M.

Combined Josephson and Charging Behavior of the Supercurrent in the Superconducting Single-Electron Transistor.
PB95-168522 04,637

Electronic Microrefrigerator Based on a Normal-Insulator-Superconductor Tunnel Junction.
PB96-102827 04,718

Noise in the Coulomb Blockade Electrometer.
PB95-176327 04,670

Thermal Enhancement of Cotunneling in Ultra-Small Tunnel Junctions.
PB95-175436 04,658

EINSTEIN, T. L.

Self-Avoiding Surfaces, Topology, and Lattice Animals.
PB95-150512 04,571

EISENHAUER, C. M.

DETAN 95: Computer Code for Calculating Spectrum-Averaged Cross Sections and Detector Responses in Neutron Spectra.
PB95-242384 04,014

Neutron Leakage Benchmark for Criticality Safety Research.
PB95-126132 03,723

Slab Transmission and Reflection for Point Source and Point Detector.
PB94-211265 03,838

EISENHOWER, E.

Role of the Office of Radiation Measurement in Quality Assurance.
PB94-212255 00,689

EISENHOWER, E. H.

National Quality Assurance Program for Personnel Radiation Dosimetry: A Case History.
PB94-211273 03,620

EITZEN, D. G.

Ultrasonic Measurements of Surface Roughness.
PB94-172137 04,181

EKBERG, J. O.

Spectrum and Energy Levels of Five-Times-Ionized Niobium (Nb VI).
PB94-185246 04,226

EKIN, J. W.

Critical-Current Degradation in Nb3 Al Wires Due to Axial and Transverse Stress.
PB95-202784 02,226

Critical Magnetic-Field Angle for High-Field Current Transport in YBa2Cu3O7 at 76 K.
PB94-211281 04,490

Effect of Axial Strain on the Critical Current of Ag-Sheathed Bi-Based Superconductors in Magnetic Fields Up to 25 T.
PB94-211315 04,493

Effect of Magnetic Field Orientation on the Critical Current of HTS Conductor and Coils.
PB96-141189 02,956

Electromechanical properties of superconductors for DOE fusion applications.
DE95015476 04,432

Electromechanical Properties of Superconductors for DOE Fusion Applications.
PB94-139672 02,250

Evidence for Tunneling and Magnetic Scatttering at 'In situ' YBCO/Noble-Metal Interfaces.
PB96-141098 04,752

Growth of Laser Ablated YBa2Cu3O7-delta Films as Examined by Rheed and Scanning Tunneling Microscopy.
PB95-162541 04,614

Improved Uniaxial Strain Tolerance of the Critical Current Measured in Ag-Sheathed Bi2Sr2Ca1Cu2O8+x Superconductors.
PB95-153565 04,594

In situ Noble Metal YBa2Cu3O7 Thin-Film Contacts.
PB94-211323 04,494

Insulating Boundary Layer and Magnetic Scattering in YBa2Cu3O7-delta/Ag Interfaces Over a Contact Resistivity Range of 10(-8) - 10(-3) Omega cm(2).
PB95-169157 04,648

Oxygen Annealing of Ex-situ YBCO/Ag Thin-Film Interfaces.
PB96-141312 04,758

Preparation of Low Resistivity Contacts for High-Tc Superconductors.
PB95-153557 02,258

Quench Energy and Fatigue Degradation Properties of Cu- and Al/Cu-Stablized Nb-Ti Epoxy-Impregnated Superconductor Coils.
PB96-141213 04,755

Superconducting Materials: Specification.
PB94-211299 04,491

Surface Degradation of Superconducting YBa2Cu3O7-delta Thin Films.
PB95-176095 04,667

Transport Critical Current of Aligned Polycrystalline Yttrium Barium Copper Oxide (YBa2Cu3O7-delta).
PB94-211307 04,492

Transverse stress effect on the critical current of internal tin and bronze process Nb(sub 3)Sn superconductors.
DE95016659 04,434

VAMAS interlaboratory comparisons of critical current vs. strain in Nb(sub 3)Sn.
DE95016656 04,433

EKSTRAND, J.

Distribution of Fluoride in Saliva and Plaque Fluid After a 0.048 mol/L NaF Rinse.
PB95-151205 03,561

EL-ASSY, N. B.

Alcohol Solutions of Triphenyl-Tetrazolium Chloride as High-Dose Radiochromic Dosimeters.
PB96-135249 03,716

Anionic Triphenylmethane Dye Solutions for Low-Dose Food Irradiation Dosimetry.
PB96-135173 03,715

EL-GHOR, M.

Defect of Thermal Ramping and Annealing Conditions on Defect Formation in Oxygen Implanted Silicon-On-Insulator Material.
PB94-212966 02,318

EL-GHOR, M. K.

Effect of Intermediate Thermal Processing on Microstructural Changes of Oxygen Implanted Silicon-on-Insulator Material.
PB96-160213 02,982

ELAM, W.

Surface Geometry of BaO on W(100): A Surface-Extended X-Ray-Absorption Fine-Structure Study.
PB95-164414 00,980

ELIASON, L.

Rechargeable Batteries for Personal/Portable.
PB96-164231 02,459

ELIPE, A.

Complete Reduction of the Euler-Poinsot Problem.
PB94-172152 03,788

ELKIND, J. L.

Investigation of Mercury Interstitials in Hg(1-x)CdxTe Alloys Using Resonant Impact-Ionization Spectroscopy.
PB94-213485 02,133

RII Spectroscopy of Trap Levels in Bulk and LPE Hg1-xCdxTe.
PB96-160247 04,084

ELLENWOOD, C. H.

Application of the Modified Voltage-Dividing Potentiometer to Overlay Metrology in a CMOS/Bulk Process.
PB94-181997 02,302

Design Guide for CMOS-On-SIMOX. Test Chips NIST3 and NIST4.
PB94-163458 *02,297*

Electrical Test Structure for Overlay Metrology Referenced to Absolute Length Standards.
PB95-152278 *02,336*

Enhanced Voltage-Dividing Potentiometer for High-Precision Feature Placement Metrology.
PB96-164025 *02,428*

New Test Structure for Nanometer-Level Overlay and Feature-Placement Metrology.
PB95-175345 *02,363*

Test Structures for the In-Plane Locations of Projected Features with Nanometer-Level Accuracy Traceable to a Coordinate Measurement System.
PB94-200565 *02,313*

ELLERBE, P.

Certification of Phencyclidine in Lyophilized Human Urine Reference Materials.
PB96-160692 *03,508*

Determination of Amphetamine and Methamphetamine in a Lyophilized Human Urine Reference Material.
PB95-175444 *03,597*

Isotope Dilution Mass Spectrometry as a Candidate Definitive Method for Determining Total Glycerides and Triglycerides in Serum.
PB96-102280 *03,519*

NIST Reference Materials to Support Accuracy in Drug Testing.
PB96-123807 *03,505*

ELLINGSEN, R.

High-Resolution Diode-Laser Spectroscopy of Calcium.
PB95-181244 *03,969*

ELLIOTT, D. S.

Phase Shifts and Intensity Dependence in Frequency-Modulation Spectroscopy.
PB96-103205 *01,071*

ELLSWORTH, J.

Correlation of HgCdTe Epilayer Defects with Underlying Substrate Defects by Synchrotron X-Ray Topography.
PB94-200714 *02,129*

ELMAN, B.

Use of Pressure for Quantum-Well Band-Structure Characterization.
PB96-164058 *04,779*

ELMQUIST, R. E.

High-Temperature Superconductor Cryogenic Current Comparator.
PB96-119334 *02,074*

Leakage Current Detection in Cryogenic Current Comparator Bridges.
PB94-172228 *02,024*

Loading Effects in Resistance Scaling.
PB97-111884 *02,285*

NIST Comparison of the Quantized Hall Resistance and the Realization of the SI Ohm Through the Calculable Capacitor.
PB97-119184 *02,291*

NIST Comparison of the Quantized Hall Resistance and the Realization of the SI Ohm Through the Calculable Capacitor. Conference Proceedings, June 17-20, 1996.
PB97-119192 *02,292*

Precision Tests of a Quantum Hall Effect Device DC Equivalent Circuit Using Double-Series and Triple-Series Connections.
PB96-159256 *01,953*

Progress on the Quantized Hall Resistance Recommended Intrinsic/Derived Standards Practice.
PB96-122460 *02,403*

Spectroscopic Study of Quantized Breakdown Voltage States of the Quantum Hall Effect.
PB96-113584 *04,730*

ELSTON, H. J.

Vibrations of S1((1)B2u) p-Difluorobenzene - d4. S1-S0 Fluorescence Spectroscopy and ab Initio Calculations.
PB95-202586 *01,028*

ELTA, M. E.

Gaseous Electronics Conference Radio-Frequency Reference Cell: A Defined Parallel-Plate Radio-Frequency System for Experimental and Theoretical Studies of Plasma-Processing Discharges.
PB94-172327 *04,404*

ELY, J. F.

Equation of State Formulation of the Thermodynamic Properties of R134a (1,1,1,2-Tetrafluoroethane).
PB94-212081 *03,256*

New Data and Correlations for the Custody Transfer of Natural Gas Liquids.
PB96-176664 *02,499*

Prediction of the Thermal Conductivity of Refrigerants and Refrigerant Mixtures.
PB94-212107 *03,258*

Prediction of Viscosity of Refrigerants and Refrigerant Mixtures.
PB94-212099 *03,257*

Predictive Extended Corresponding States Model for Pure and Mixed Refrigerants Including an Equation of State for R134a.
PB95-175717 *03,275*

Thermodynamic Properties of the Methane-Ethane System.
PB95-125779 *00,891*

EMBREE, E.

Degradation of Powder Epoxy Coated Panels Immersed in a Saturated Calcium Hydroxide Solution Containing Sodium Chloride.
PB96-101050 *01,344*

Non-Osmotic, Defect-Controlled Cathodic Disbondment of a Coating from a Steel Substrate.
PB94-216447 *03,120*

Performance of Tape-Bonded Seams of EPDM Membranes: Comparison of the Peel Creep-Rupture Response of Tape-Bonded and Liquid-Adhesive-Bonded Seams.
PB96-183249 *03,012*

EMENHISER, C.

Isolation and Structural Elucidation of the Predominant Geometrical Isomers of alpha-Carotene.
PB96-190061 *00,640*

EMMERICH, S. J.

Application of a Multizone Airflow and Contaminant Dispersal Model to Indoor Air Quality Control in Residential Buildings.
PB95-180238 *02,555*

Effectiveness of a Heat Recovery Ventilator, an Outdoor Air Intake Damper and an Electrostatic Particulate Filter at Controlling Indoor Air Quality in Residential Buildings.
PB96-146642 *02,564*

Indoor Air Quality Impacts of Residential HVAC Systems Phase II.B Report: IAQ Control Retrofit Simulations and Analysis.
PB96-106877 *02,559*

Indoor Air Quality Impacts of Residential HVAC Systems, Phase 1 Report: Computer Simulation Plan.
PB95-135596 *00,249*

Indoor Air Quality Impacts of Residential HVAC Systems. Phase 2.A Report: Baseline and Preliminary Simulations.
PB95-178893 *02,554*

Multizone Modeling of Three Residential Indoor Air Quality Control Options.
PB96-146659 *02,565*

Multizone Modeling of Three Residential Indoor Air Quality Control Options.
PB96-165782 *02,567*

Workplan to Analyze the Energy Impacts of Envelope Airtightness in Office Buildings.
PB96-154463 *00,273*

ENDOH, Y.

High-Energy Phonon Dispersion in La1.85Sr0.15CuO4.
PB96-138458 *04,748*

ENG, G.

Microbial Degradation of Polysulfides and Insights into Their Possible Occurrence in Coal.
PB95-163374 *02,488*

Total Surface Areas of Group IVA Organometallic Compounds: Predictors of Toxicity to Algae and Bacteria.
PB94-211331 *00,814*

ENGEN, G. F.

Terminal Invariant Description of Amplifier Noise.
PB95-153573 *02,043*

ENGLAND, C. D.

Magnetic Properties of Pd/Co Multilayers.
PB94-198751 *04,465*

ENGLEMAN, R.

Measurements of the Resonance Lines of (6)Li and (7)Li by Doppler-Free Frequency-Modulation Spectroscopy.
PB96-180211 *04,118*

ENGLERT, G.

Isolation and Structural Elucidation of the Predominant Geometrical Isomers of alpha-Carotene.
PB96-190061 *00,640*

ENO, L.

Laser Preparation and Probing of Initial and Final Orbital Alignment in Collision-Induced Energy Transfer Ca(4s5p,(1)P1) + He yields Ca(4s5p,(3)P2) + He.
PB95-203261 *04,003*

Three-Vector Correlation Theory for Orientation/Alignment Studies in Atomic and Molecular Collisions.
PB94-211109 *03,834*

ENSHER, J. R.

Behavior of Atoms in a Compressed Magneto-Optical Trap.
PB95-203105 *03,999*

Reduction of Light-Assisted Collisional Loss Rate from a Low-Pressure Vapor-Cell Trap.
PB95-202248 *03,971*

Stable, Tightly Confining Magnetic Trap for Evaporative Cooling of Neutral Atoms.
PB96-200720 *04,126*

EPLER, K. S.

Liquid Chromatographic Method for the Determination of Carotenoids, Retinoids, and Tocopherols in Human Serum and in Food.
PB95-153599 *00,593*

Liquid Chromatography: Laser-Enhanced Ionization Spectrometry for the Speciation of Organolead Compounds.
PB94-185253 *00,530*

EPPELDAUER, G.

Absolute Response Calibration of a Transfer Standard Cryogenic Bolometer.
PB96-147103 *04,358*

Detector-Based Candela Scale and Related Photometric Calibration Procedures at NIST.
PB95-161949 *04,273*

Longterm Changes of Silicon Photodiodes and Their Use for Photometric Standardization.
PB94-211349 *04,234*

Method of Realizing Spectral Irradiance Based on an Absolute Cryogenic Radiometer.
PB95-161204 *04,270*

NIST Detector-Based Luminous Intensity Scale.
PB96-179114 *01,864*

EPSTEIN, M. S.

Application of a Novel Slurry Furnace AAS Protocol for Rapid Assessment of Lead Environmental Contamination.
PB96-112354 *02,526*

Spectral Interference in the Determination of Arsenic in High-Purity Lead and Lead-Base Alloys Using Electrothermal Atomic Absorption Spectrometry and Zeeman-Effect Background Correction.
PB96-112099 *00,614*

ERICKSON, A.

2D-Scanning Capacitance Microscopy Measurements of Cross-Sectioned VLSI Teststructures.
PB96-163779 *04,104*

ERWIN, R. W.

Antiferromagnetic Interlayer Correlations in Annealed Ni80Fe20/Ag Multilayers.
PB97-122220 *03,109*

Comment on 'Phase Transitions in Antiferromagnetic Superlattices'.
PB95-152971 *04,587*

Enhanced Curie Temperatures and Magnetoelastic Domains in Dy/Lu Super Lattices and Films.
PB94-172665 *04,443*

Magnetic Rare Earth Artificial Metallic Superlattices.
PB95-162293 *04,611*

Magnetoelasticity in Rare-Earth Multilayers and Films.
PB94-211356 *04,495*

Normal Modes and Structure Factor for a Canted Spin System: The Generalized Villain Model.
PB95-140067 *04,539*

Unconventional Ferromagnetic Transition in La(sub 1-x)Ca(sub x)MnO3.
PB97-112429 *04,156*

ESCALANTE, E.

Corrosion Resistance of Materials for Renovation of the United States Botanic Garden Conservatory.
PB94-154390 *00,032*

Evidence of Film-Induced Cleavage by Electrodeposited Rhodium.
PB95-162327 *03,191*

ESCRIBANO, R.

Infrared Spectrum of OClO in the 2000/cm(-1) Region: The 2(nu sub 1) and (nu sub 1 + nu sub 3) Bands.
PB95-141032 *00,908*

Intensities and Dipole Moment Derivatives of the Fundamental Bands of (35)ClO2 and an Intensity Analysis of the nu1 Band.
PB95-141040 *00,909*

ESPINA, P. I.

Development of Adaptive Control Strategies for Inert Gas Atomization.
PB95-162335 *02,823*

Intelligent Control of an Inert Gas Atomization Process.
PB95-141057 *03,344*

Optimization of Inert Gas Atomization.
PB95-107405 *01,377*

Process Modeling and Control of Inert Gas Atomization.
PB95-162343 *02,824*

ESTLER, W. T.

Advanced Angle Metrology System.
PB94-211364 *02,637*

Estimation of Measurement Uncertainty of Small Circular Features Measured by CMMs.
PB95-267928 *02,918*

Upgraded Facility for Multilayer Mirror Characterization at NIST.
PB96-160387 *04,367*

ETEMAD, S.

Laser-Synchrotron Hybrid Experiments: A Photon to Tickle, A Photon to Poke.
PB96-157847 *03,704*

ETZ, E. S.

Complementary Molecular Information on Phthalocyanine Compounds Derived from Laser Microprobe Mass Spectrometry and Micro-Raman Spectroscopy.
PB94-172269 *00,757*

Raman and Fluorescence Spectra Observed in Laser Microprobe Measurements of Several Compositions in the Ln-Ba-Cu-O System.
PB94-172210 *04,440*

EUGEN, G. F.

Multi-State Two-Port: An Alternative Transfer Standard.
PB95-168530 *02,049*

EVANS, C. J.

Chemical Aspects of Tool Wear in Single Point Diamond Turning.
PB97-112601 *03,021*

Chip Morphology, Tool Wear and Cutting Mechanics in Finish Hard Turning.
PB97-112247 03,106

Compensation for Errors Introduced by Nonzero Fringe Densities in Phase-Measuring Interferometers.
PB97-110506 04,386

Damage Processes in Ceramics Resulting from Diamond Tool Indentation and Scratching in Various Environments.
PB96-102983 03,065

Fabrication of Optics by Diamond Turning.
PB96-111695 02,954

Japan Technology Program Assessment: Precision Engineering/Precision Optics in Japan.
PB95-171112 02,884

Rapid Post-Polishing of Diamond-Turned Optics.
PB95-175949 04,301

Test of a Slow Off-Axis Parabola at Its Center of Curvature.
PB96-138482 04,352

Test Optics Error Removal.
PB96-179536 04,377

Upgraded Facility for Multilayer Mirror Characterization at NIST.
PB96-160387 04,367

Visualization of Surface Figure by the Use of Zernike Polynomials.
PB96-137757 04,351

EVANS, D.

Smoke Emission from Burning Crude Oil.
PB96-122890 01,407

EVANS, D. D.

Application of Boundary Element Methods to a Transient Axis-Symmetric Heat Conduction Problem.
PB94-212693 01,375

Development of Hazard Assessment and Suppression Technology for Oil and Gas Well Blowout and Diverter Fires.
PB96-122965 01,408

Flame Heights and Heat Release Rates of 1991 Kuwait Oil Field Fires.
PB96-119342 01,404

In situ Burning of Oil Spills: Mesoscale Experiments and Analysis.
PB95-163747 02,587

Large Fire Experiments for Fire Model Evaluations.
PB96-190079 01,427

Smoke Plume Trajectory from In situ Burning of Crude Oil in Alaska: Field Experiments.
PB96-131560 02,594

Suppression Research: Strategies.
PB94-211372 00,346

EVANS, D. J.

Conditions for Existence of a Reentrant Solid Phase in a Sheared Atomic Fluid.
PB94-211380 04,198

Dynamic Scaling in an Aggregating 2D Lennard-Jones System.
PB96-167317 04,106

Simulation and SANS Studies of Gelation Under Shear.
PB96-167176 01,150

Testing the Sensitivity of Accelerometers Using Mechanical Shock Pulses Under NIST Special Publication 250 Test No. 24040S.
PB96-179544 02,683

EVANS, J.

Overview of U.S. Government Advanced Packaging Programs.
PB96-200845 02,443

EVANS, J. D.

Exact Series Solution to the Epstein-Hubbell Generalized Elliptic Type Integral Using Complex Variable Residue Theory.
PB97-110167 03,423

EVANS, R. D.

NIST/NCMS Program on Electronic Packaging: First Update.
PB96-204086 03,008

EVENSEN, K. M.

30 THz Mixing Experiments on High Temperature Superconducting Josephson Junctions.
PB96-102462 04,709

EVENSON, K.

Absolute Frequency Measurements of Methanol from 1.5 to 6.5 THz.
PB95-175881 04,300

EVENSON, K. M.

Atomic Iron in Its (5)D Ground State: A Direct Measurement of the J = 0 inverted arrow 1 and J = 1 inverted arrow 2 Fine-Structure Intervals (1.2).
PB96-141221 04,756

Atomic Oxygen Fine Structure Splittings with Tunable Far Infrared Spectroscopy.
PB95-152203 03,915

Atomic Sulfur: Frequency Measurement of the J=0 inversely maps 1 Fine-Structure Transition at 56.3 Microns by Laser Magnetic Resonance.
PB95-180105 01,007

Detection of OH+ in Its a(1)Delta State by Far Infrared Laser Magnetic Resonance.
PB95-181087 01,021

Determination of the Molecular Parameters of NiH in Its (2)Delta Ground State by Laser Magnetic Resonance.
PB95-107116 00,869

Far Infrared Laser Frequencies of CH3OD and N2H4.
PB96-119623 04,341

Far Infrared Laser Frequencies of (13)CD3OH.
PB95-169363 04,292

Improved Molecular Constants and Frequencies for the CO2 Laser from New High-J Regular and Hot-Band Frequency Measurements.
PB95-180634 04,312

Laboratory Measurements for the Astrophysical Identification of MgH.
PB95-152195 00,073

Laser Magnetic-Resonance Measurement of the (3)P1 - (3)P2 Fine-Structure Splittings in (17)O and (18)O.
PB95-175170 00,994

Measurement of the J=2 less than 1 Fine-Structure Interval for (28)Si and (29)Si in the Ground (3)P State.
PB94-185097 00,771

New cw CO2 Laser Lines: The 9-mu m Hot Band.
PB95-168548 04,281

Pure Rotational Spectra of CuH and CuD in Their Ground States Measured by Tunable Far-Infrared Spectroscopy.
PB95-176194 01,005

Rotational Far Infrared Spectrum of (13)CO.
PB95-152187 00,941

Rotational Spectroscopy of the CoH Radical in Its Ground (3)Phi State by Far-Infrared Laser Magnetic Resonance: Determination of Molecular Parameters.
PB95-175048 00,992

Rotational Spectrum of Copper Hydride Using Tunable Far Infrared Radiation.
PB94-198637 00,792

Rotational Spectrum of OH in the v=0-3 Levels of Its Ground State.
PB95-176202 01,006

EVERHART, K.

Computer Security Training and Awareness Course Compendium.
PB95-130985 01,589

EVERITT, B.

Enhanced Curie Temperatures and Magnetoelastic Domains in Dy/Lu Super Lattices and Films.
PB94-172665 04,443

EWRIN, R. W.

Structural and Magnetic Ordering in Iron Oxide/Nickel Oxide Multilayers by X-ray and Neutron Diffraction (Invited).
PB94-172558 04,442

EYGENRAAM, M.

Decomposition of SF6 and Production of S2F10 in Power Arcs.
PB96-122619 01,084

EYKENS, R.

Preparation and Characterization of (6)LiF and (10)B Reference Deposits for the Measurement of the Neutron Lifetime.
PB95-108692 03,874

Problems Related to the Determination of Mass Densities of Evaporated Reference Deposits.
PB95-163226 03,941

EYLEM, C.

Substitution-Induced Midgap States in the Mixed Oxides RxBa1-ChiTiO3-Delta, with R=Y, La, and Nd.
PB95-140505 04,541

FACTOR, B. J.

Dielectric Behavior of a Polycarbonate/Polyester Mixture Upon Transesterification.
PB96-179551 04,785

FAETH, G. M.

Mixing and Radiation Properties of Buoyant Luminous Flame Environments.
PB96-202254 01,432

Mixing and Radiation Properties of Buoyant Turbulent Diffusion Flames.
PB95-242327 01,396

Radiation and Mixing Properties of Buoyant Turbulent Diffusion Flames.
PB94-165974 01,360

FAHR, A.

Deuterium Isotope Effect in Vinyl Radical Combination/ Dispropor tionationReactions.
PB96-204151 01,167

Experimental Determination of the Rate Constant for the Reaction of C2H3 with H2 and Implications for the Partitioning of Hydrocarbons in Atmospheres of the Outer Planets.
PB97-122295 00,112

Reaction Rate Determinations of Vinyl Radical Reactions with Vinyl, Methyl, and Hydrogen Atoms.
PB94-211398 00,815

Temperature Dependence of the Gas and Liquid Phase Ultraviolet Absorption Cross Sections of HCFC-123 (CF3CHCl2) and HCFC-142b (CH3CF2Cl).
PB96-201033 03,298

Temperature Dependence of the Ultraviolet Absorption Cross Section of CF3I.
PB96-204169 01,168

Temperature Dependent Ultraviolet Absorption Cross Sections of Propylene, Methylacetylene and Vinylacetylene.
PB96-204177 01,169

UV Absorption Cross Sections of Methylchloroform: Temperature-Dependent Gas and Liquid Phase Measurements.
PB96-201041 00,643

FAHY, R. F.

Enhancement of EXIT89 and Analysis of World Trade Center Data.
PB96-202247 00,231

FAIRBANK, W. M.

Anomalous Odd- to Even-Mass Isotope Ratios in Resonance Ionization with Broad-Band Lasers.
PB94-211406 03,839

FAIRCHILD, C. O.

Technologic Papers of the Bureau of Standards: Number 170. Pyrometric Practice.
AD-A279 282/8 03,766

FAIT, J.

Using NIST Crystal Data within Siemens Software for Four-Circle and SMART CCD Diffractometers.
PB97-109110 04,803

FALCO, C. M.

Interfaces in Mo/Si Multilayers.
PB96-160668 02,423

Magnetic Properties of Pd/Co Multilayers.
PB94-198751 04,465

FALICOV, L. M.

Effects of Interfacial Roughness on the Magnetoresistance of Magnetic Metallic Multilayers.
PB95-150017 04,556

FALLER, J.

Low-Frequency, Active Vibration Isolation System.
PB95-203303 02,710

Validation of the Inverse Square Law of Gravitation Using the Tower at Erie, Colorado, USA
PB95-164646 03,947

FALLER, J. E.

Calibration of a Superconducting Gravimeter Using Absolute Gravity Measurements.
PB95-202651 03,684

Continuous Gravity Observations Using Joint Institute for Laboratory Astrophysics Absolute Gravimeters.
PB95-203048 03,685

Earth-Based Gravitational Experiments.
PB94-211414 03,840

Intracomparison Tests of the FG5 Absolute Gravity Meters.
PB96-102991 03,688

Lunar Laser Ranging: A Continuing Legacy of the Apollo Program.
PB95-202495 03,683

Test of Newton's Inverse Square Law of Gravitation Using the 300-m Tower at Erie, Colorado.
PB95-202446 03,978

FANCONI, B. M.

Monitoring Polymer Cure by Fluorescence Recovery After Photobleaching.
PB94-211422 01,218

Polymers Technical Activities 1994. NAC-NRC Assessment Panel, April 6-7, 1995.
PB95-209896 01,275

Polymers Technical Activities, 1995.
PB96-193719 01,291

Review of Cure Monitoring Techniques for On-Line Process Control.
PB94-216728 03,145

FANG, J. B.

Computer Simulations of Airflow and Radon Transport in Four Large Buildings.
PB95-220422 02,557

CONTAM88 Building Input Files for Multi-Zone Airflow and Contaminant Dispersal Modeling.
PB94-194388 02,537

FANNEY, A. H.

Experimental Verification of a Moisture and Heat Transfer Model in the Hygroscopic Regime.
PB97-111546 00,309

Heat and Moisture Transfer in Wood-Based Wall Construction: Measured versus Predicted.
PB95-200655 00,391

International Green Building Conference and Exposition (2nd). Held in Big Sky, Montana on August 13-15, 1995.
PB95-253605 02,525

International Green Building Conference and Exposition (3rd). Held in San Diego, California on November 17-19, 1996. (Reannouncement with new abstract).
PB97-121826 02,531

Test Procedures for Advanced Insulation Panels.
PB97-111892 00,415

U.S. Green Building Conference, 1994.
PB94-206364 02,519

PERSONAL AUTHOR INDEX

FARABAUGH, E. N.

Lineshape Analysis of the Raman Spectrum of Diamond Films Grown by Hot-Filament and Microwave-Plasma Chemical-Vapor Deposition.
PB95-162392 *03,016*

Structures of Vapor-Deposited Yttria and Zirconia Thin Films.
PB94-216025 *03,041*

Studies of Defects in Diamond Films and Particles by Raman and Luminescence Spectroscopies.
PB95-162400 *03,017*

Surface Roughness Evaluation of Diamond Films Grown on Substrates with a High Density of Nucleation Sites.
PB95-162418 *03,018*

FARAH, O. G.

Framework for National Information Infrastructure Services.
PB95-103719 *02,723*

FARAHANI, M.

New Method for Shielding Electron Beams Used for Head and Neck Cancer Treatment.
PB94-211430 *03,621*

New Surface-Active Comonomer for Adhesive Bonding.
PB96-204052 *03,579*

Polymerization Initiation by N-p-Tolylglycine: Free-Radical Reactions Studied by Pulse and Steady-State Radiolysis.
PB95-180014 *01,269*

FARRELL, J. T.

High-Resolution Infrared Overtone Spectroscopy of ArHF via Nd:YAG/Dye Laser Difference Frequency Generation.
PB94-211448 *00,816*

High-Resolution Infrared Overtone Spectroscopy of N2-HF: Vibrational Red Shifts and Predissociation Rate as a Function of HF Stretching Quanta.
PB96-102298 *01,061*

High-Resolution Infrared Spectroscopy of DF Trimer: A Cyclic Ground State Structure and DF Stretch Induced Intramolecular Vibrational Coupling.
PB95-150678 *00,920*

Pairwise and Nonpairwise Additive Forces in Weakly Bound Complexes: High Resolution Infrared Spectroscopy of ArnDF (n=1,2,3).
PB96-200357 *04,125*

Slit Jet Infrared Spectroscopy of Hydrogen Bonded N2HF Isotopomers: Rotational Rydberg-Klein-Rees Analysis and H/D Dependent Vibrational Predissociation Rates.
PB95-161873 *00,956*

Stabilization and Precise Calibration of a Continuous-Wave Difference Frequency Spectrometer by Use of a Simple Transfer Cavity.
PB95-162350 *04,276*

FARROW, R. F. C.

Combined Low- and High-Angle X-Ray Structural Refinement of a Co/Pt(111) Multilayer Exhibiting Perpendicular Magnetic Anisotropy.
PB94-198355 *04,457*

FARROW, R. L.

Measurement of the Self Broadening of the H2Q(0-5) Raman Transitions from 295 to 1000 K.
PB95-108627 *00,884*

FARVARDIN, N.

Channel Coding for Code Excited Linear Prediction (CELP) Encoded Speech in Mobile Radio Applications.
PB95-143178 *01,475*

FASSETT, J.

Working Conference on Global Growth of Technology: Is America Prepared. Held in Gaithersburg, Maryland on December 7, 1995.
PB96-210059 *00,018*

FASSETT, J. D.

Comparative Strategies for Correction of Interferences in Isotope Dilution Mass Spectrometric Determination of Vanadium.
PB94-185261 *00,531*

Isotopic and Nuclear Analytical Techniques in Biological Systems: A Critical Study. 10. Elemental Isotopic Dilution Analysis with Radioactive and Stable Isotopes (Technical Report).
PB96-164157 *00,696*

Study of Laser Resonance Ionization Mass Spectrometry Using a Glow Discharge Source.
DE94018566 *03,308*

Study of Laser Resonance Ionization Mass Spectrometry Using a Glow Discharge Source.
PB96-123203 *03,360*

Traceability to the Mole: A New Initiative by CIPM.
PB95-180246 *00,605*

FAUST, B.

Interim Testing Artifact (ITA): A Performance Evaluation System for Coordinate Measuring Machines (CMMs). User Manual.
PB95-210589 *02,914*

FAVREAU, J. P.

Federal Implementaion Guideline for Eletronic Data Interchange. ASC X12 003050 Transaction Set 865 Purchase Order Change Acknowledgement/Request - Seller Initiated. Implementation Convention.
PB96-172549 *01,825*

Federal Implementation Guideline for Electronic Data Interchange: ASC X12 003040 Transaction Set 838 Trading Partner Profile (Confirmation of Vendor Registration). Implementation Convention.
PB96-111190 *01,813*

Federal Implementation Guideline for Electronic Data Interchange: ASC X12 003040 Transaction Set 838 Trading Partner Profile (Vendor Registration), Implementation Convention.
PB96-112651 *03,674*

Federal Implementation Guideline for Electronic Data Interchange: ASC X12 003050 Transaction Set 836 Procurement Notices. Implementation Convention.
PB96-178892 *01,827*

Federal Implementation Guideline for Electronic Data Interchange. ASC X12 003050 Transaction Set 840 Request for Quotation. Implementation Convention.
PB96-172531 *01,824*

Federal Implementation Guideline for Electronic Data Interchange. ASC X12 003050 Transaction Set 843 Response to Request for Quotation. Implementation Convention.
PB96-168984 *01,822*

Federal Implementation Guideline for Electronic Data Interchange. ASC X12 003050 Transaction Set 850 Award Instrument. Implementation Convention.
PB96-114913 *01,814*

Federal Implementation Guideline for Electronic Data Interchange. ASC X12 003050 Transaction Set 855 Purchase Order Acknowledgment: Implementation Convention.
PB96-172374 *01,823*

Federal Implementation Guideline for Electronic Data Interchange. ASC X12 003050 Transaction Set 860 Modifications to Award Instrument. Implementation Convention.
PB96-114921 *01,815*

Five Q's (Cues) of the U.S. GOSIP Testing Program.
PB96-175716 *01,826*

Formal Methods in Conformance Testing: Result and Perspectives.
PB95-153029 *01,710*

Formal Multi-Layer Test Methodology and Its Application to OSI.
PB94-172194 *02,718*

Industry/Government Open Systems Specification Testing Framework. Version 1.0.
PB94-219110 *01,809*

ISO/IEC Workshop on Worldwide Recognition of OSI Test Results Regional Progress - North America.
PB94-172202 *02,719*

Lessons from the Establishment of the U.S. GOSIP Testing Program.
PB96-119359 *01,817*

National Voluntary Laboratory Accreditation Program. GOSIP: Government Open Systems Interconnection Profile.
PB95-267993 *01,486*

Open Issues in OSI Protocol Development and Conformance Testing.
PB96-122908 *01,818*

U.S. GOSIP Testing Program.
PB94-211455 *01,807*

FAWZY, W. M.

P-Type Doubling in the Infrared Spectrum of NO-HF.
PB94-211463 *00,817*

FAZIO, K.

Thermodynamics of Enzyme-Catalyzed Reactions: Part 1. Oxidoreductases.
PB94-162252 *00,737*

FEDOR, L. S.

Dual-Frequency Millimeter-Wave Radiometer Antenna for Airborne Remote Sensing of Atmosphere and Ocean.
PB96-112289 *02,009*

Dual Frequency mm-Wave Radiometer Antenna for Airborne Remote Sensing of Atmosphere and Ocean.
PB95-180378 *02,006*

FEENEY, A. B.

APDE Demonstration System Architecture. National PDES Testbed Report Series.
PB94-154325 *02,767*

Challenges to the National Information Infrastructure: The Barriers to Product Data Sharing. National PDES Testbed Report Series.
PB95-136347 *02,776*

Guidelines for the Development of Mapping Tables.
PB96-154539 *02,786*

Issues and Recommendations for a STEP Application Protocol Framework. National PDES Testbed.
PB94-160868 *02,770*

FEINSTEIN, J.

Higher-Order Approximations in Ionospheric Wave-Propagation.
AD-A292 471/0 *04,420*

FELCHER, G. P.

Neutron Scattering Studies of Surfaces and Interfaces.
PB94-216207 *04,517*

FELDER, R. J.

Increased Pinning Energies and Critical Current Densities in Heavy-Ion-Irradiated Bi2Sr2CaCu2O8 Single Crystals.
PB95-175352 *04,654*

FELDMAN, A.

Analysis of Thermal Wave Propagation in Diamond Films.
PB94-211471 *03,014*

Applications of Diamond Films and Related Materials: International Conference (3rd). Held in Gaithersburg, Maryland on August 21-24, 1995. Supplement to NIST Special Publication 885.
PB95-256053 *03,063*

Lineshape Analysis of the Raman Spectrum of Diamond Films Grown by Hot-Filament and Microwave-Plasma Chemical-Vapor Deposition.
PB95-162392 *03,016*

Proceedings of the Applied Diamond Conference 1995: Applications of Diamond Films and Related Materials International Conference (3rd). Held in Gaithersburg, Maryland, on August 21-24, 1995.
PB95-255204 *04,701*

Structures of Vapor-Deposited Yttria and Zirconia Thin Films.
PB94-216025 *03,041*

Studies of Defects in Diamond Films and Particles by Raman and Luminescence Spectroscopies.
PB95-162400 *03,017*

Surface Roughness Evaluation of Diamond Films Grown on Substrates with a High Density of Nucleation Sites.
PB95-162418 *03,018*

Thermal Wave Propagation in Diamond Films.
PB94-211489 *03,015*

Workshop on Characterizing Diamond Films (3rd). Held in Gaithersburg, Maryland on February 23-24, 1994.
PB94-187663 *04,456*

Workshop on Characterizing Diamond Films (4th). Held in Gaithersburg, Maryland on March 4-5, 1996.
PB96-183090 *04,786*

FELDMAN, U.

Magnetic Dipole Line from U LXXI Ground-Term Levels Predicted at 3200 Angstroms.
PB94-211497 *04,407*

Observation and Visible and uv Magnetic Dipole Transitions in Highly Charged Xenon and Barium.
PB96-138441 *04,056*

FELL, N. F.

Embossable Grating Couplers for Planar Waveguide Optical Sensors.
PB96-190277 *00,641*

FELLER, I.

Learning to Change: Opportunities to Improve the Performance of Smaller Manufacturers.
PB94-166212 *00,010*

FELTON, C. M.

High Spectral Purity X-Band Source.
PB95-163713 *02,045*

FENG, D.

dc Method for the Absolute Determination of Conductivities of the Primary Standard KCl Solutions from 0C to 50C.
PB94-219342 *02,644*

FENG, L.

Addition of M and L-Series Lines to NIST Algorithm for Calculation of X-Ray Tube Output Spectral Distributions.
PB95-108742 *00,569*

FENG, S. C.

Dimensional Inspection Planning Based on Product Data Standards.
PB95-175451 *02,910*

Machining Process Planning Activity Model for Systems Integration.
PB96-165428 *02,841*

U.S. Navy Coordinate Measuring Machines: A Study of Needs.
PB94-162831 *02,807*

FENG, Y.

Compatibilization of Polymer Blends by Complexation. 2. Kinetics of Interfacial Mixing.
PB97-111900 *01,295*

Structural Stabilization of Phase Separating PC/Polyester Blends through Interfacial Modification by Transesterification Reaction.
PB95-150454 *01,239*

FENGHOUR, A.

Viscosity of Ammonia.
PB96-145933 *01,117*

FENIMORE, C.

Can Displays Deliver a Full Measure: Manufacturing.
PB96-111935 *02,185*

Digital Techniques in HV Tests - Summary of 1989 Panel Session.
PB94-216702 *02,035*

Distributions of Measurement Error for Three-Axis Magnetic Field Meters during Measurements Near Appliances.
PB96-180153 *02,110*

Making Displays Deliver a Full Measure.
PB96-122411 *01,490*

National Information Infrastructure and Advanced Digital Video.
PB96-119367 *01,488*

Nonlinear Color Transformations in Real Time Using a Video Supercomputer.
PB96-123021 *02,191*

Observations of Partial Discharges in Hexane Under High Magnification.
PB95-163127 01,900

Report on the Workshop on Advanced Digital Video in the National Information Infrastructure. Held in Washington, D.C. on May 10-11, 1994.
PB95-103677 01,472

Summary Report on the Workshop on Advanced Digital Video in the National Information Infrastructure.
PB96-141320 01,497

Three-Axis Coil Probe Dimensions and Uncertainties during Measurement of Magnetic Fields from Appliances.
PB94-219359 01,885

FERAUDY, D.

Preliminary Comparison of Time Transfers via LASSO, GPS and Two-Way Satellite.
PB95-151098 01,529

FEREK, R. J.

Smoke Plume Trajectory from In situ Burning of Crude Oil: Field Experiments.
PB96-200993 02,597

FERNANDES, G.

Comparison of POSIX Open System Environment (OSE) and Open Distributed Processing (ODP) Reference Models.
PB96-131495 01,820

Distributed Systems: Survey of Open Management Approaches.
PB96-128202 01,746

FERNANDEZ, D. P.

Database for the Static Dielectric Constant of Water and Steam.
PB96-145586 01,103

Measurements of the Relative Permittivity of Liquid Water at Frequencies in the Range of 0.1 to 10 kHz and at Temperatures between 273.1 and 373.2 K at Ambient Pressure.
PB96-119375 01,078

Static Dielectric Constant of Water and Steam.
PB96-123559 01,090

FERNANDEZ, J. E.

Polarization Effects on Multiple Scattering Gamma Transport.
PB95-153615 03,926

FERNANDEZ-PELLO, A. C.

Fire Propagation in Concurrent Flows.
PB94-193844 01,365

FERRARIS, C. F.

Alkali-Silica Reaction and High Performance Concrete.
PB96-131537 01,345

Guide to a Format for Data on Chemical Admixtures in a Materials Property Database.
PB96-165394 01,327

Guide to a Format for Data on Chemical Admixtures in a Materials Property Database. (Reannouncement with new abstract).
PB96-186192 01,328

Measurement of Rheological Properties of High Performance Concrete: State of the Art Report.
PB96-202338 00,414

Testing of Selected Self-Leveling Compounds for Floors.
PB95-220455 00,395

Warping of Terrace Pavers at the U.S. Capitol Building.
PB96-193651 00,411

FERRE, E. S.

Investigations of AM and PM Noise in X-Band Devices.
PB95-180022 02,062

FERRE-PIKAL, E. S.

Design Criteria for BJT Amplifiers with Low l/f AM and PM Noise.
PB96-200365 02,442

Origin of l/f PM and AM Noise in Bipolar Junction Transistor Amplifiers.
PB96-200787 02,096

Reducing the 1/f AM and PM Noise in Electronics for Precision Frequency Metrology.
PB97-113195 02,102

FERRELL, R. A.

Electric Field Effects on a Near-Critical Fluid in Microgravity.
PB96-161880 04,217

FERRETT, T. A.

High Resolution Angle Resolved Photoelectron Spectroscopy Study of N2.
PB95-151494 03,907

Photoionization of Small Molecules Using Synchrotron Radiation.
PB94-211505 03,841

Vibronic Coupling and Other Many-Body Effects in the 4sigmag(-1) Photoionization Channel of CO2.
PB95-162509 00,962

FETTERS, L. J.

Neutron Reflectivity of End-Grafted Polymers: Concentration and Solvent Quality Dependence in Equilibrium Conditions.
PB94-185758 01,206

Neutron Reflectivity Study of the Density Profile of a Model End-Grafted Polymer Brush: Influence of Solvent Quality.
PB95-202735 01,274

Thermodynamic Interactions in Model Polyolefin Blends Obtained by Small-Angle Neutron Scattering.
PB94-198496 01,208

FEYERHERM, R.

Dynamics of Mu(+) in Sc and ScHx.
PB96-180021 04,112

FIALA, J. C.

Visual Pursuit Systems.
PB95-143285 01,841

FICK, S. E.

NIST Power Reference Source.
PB94-211513 00,148

Ultrasound Power Measurement Techniques at NIST.
PB96-179569 02,684

FICKETT, F. R.

Cryogenic Properties of Silver.
PB94-203593 03,330

Improved Eddy-Current Decay Method for Resistivity Characterization.
PB95-180451 02,265

Low-Temperature Properties of Silver.
PB96-126198 03,361

Roles of Copper in Applied Superconductivity.
PB94-211521 02,255

FIELD, B.

Report on the Workshop on Advanced Digital Video in the National Information Infrastructure. Held in Washington, D.C. on May 10-11, 1994.
PB95-103677 01,472

Summary Report on the Workshop on Advanced Digital Video in the National Information Infrastructure.
PB96-141320 01,497

FIELD, B. F.

Can Displays Deliver a Full Measure: Manufacturing.
PB96-111935 02,185

Making Displays Deliver a Full Measure.
PB96-122411 01,490

Nonlinear Color Transformations in Real Time Using a Video Supercomputer.
PB96-123021 02,191

Perception of Clamp Noise in Television Receivers.
PB96-119433 01,489

Specification for Interoperability between Ballistic Imaging Systems. Part 1. Cartridge Cases.
PB96-195524 01,860

FIELD, J.

One-Electron Oxidation of Metalloporphycenes as Studied by Radiolytic Methods.
PB97-111967 01,179

FIELDS, A. B.

Fracture of Silicon Nitride and Silicon Carbide at Elevated Temperatures.
PB96-180260 03,179

FIELDS, R.

Void Shape in Sintered Titanium
PB96-141023 02,705

FIELDS, R. J.

Effect of Backfill and Atomizing Gas on the Powder Porosity and Mechanical Properties of 304L Stainless Steel.
PB94-185394 03,205

Fracture Behavior of Large-Scale Thin-Sheet Aluminum Alloy.
N95-19494/0 03,311

Fracture Testing of Large-Scale Thin-Sheet Aluminum Alloy.
AD-A306 625/5 03,305

Fracture Testing of Large-Scale Thin-Sheet Aluminum Alloy.
PB95-242368 00,024

FILIPPELLI, A. R.

Comments on the Stability of Bayard-Alpert Ionization Gages.
PB96-103080 02,673

FILLA, B. J.

Noncontact Ultrasonic Inspection of Train Rails for Stress.
PB95-162673 04,851

Safety Assessment of Railroad Wheels Through Roll-by Detection of Tread Cracks.
PB96-141254 04,856

Sensor System for Intelligent Processing of Hot-Rolled Steel.
PB96-186069 03,373

FILLIBEN, J. J.

Factors Significant to Precracking of Fracture Specimens.
PB96-109558 03,358

FILLIPPELLI, A. R.

Influence of Envelopes Geometry on the Sensitivity of 'Nude' Ionization Gauges.
PB97-119077 04,174

Long-Term Stability of Bayard-Alpert Gauge Performance: Results Obtained from Repeated Calibrations against the National Institute of Standards and Technology Primary Vacuum Standard.
PB96-123567 02,676

FILLMORE, C. L.

High Temperature Reactions of Uranium Dioxide with Various Metal Oxides.
AD-A286 648/1 00,717

FILOR, D.

Enthalpy Increment Measurements from 4.5 K to 350 K and the Thermodynamic Properties of the Titanium Silicide Ti5Si3(cr).
PB96-204037 00,679

FINE, J.

Pure Element Sputtering Yield Data: Appendix 4.
PB94-200037 00,805

FINK, J. L.

Analysis of Failed Dry Pipe Fire Suppression System Couplings from the Filene Center at Wolf Trap Farm Park for the Performing Arts.
PB94-164407 00,331

Comparison of the Corrosion Rates of FeAl, Fe(sub 3)Al and Steel in Distilled Water and 0.5 M Sodium Chloride. Technical Report Number 2, January--March 1991.
DE94017332 03,186

Evaluation of the Environmentally Induced Fracture Resistance of Ductile Nickel Aluminide. Technical Report Number 1, Final report. October-December 1990.
DE94017331 03,306

Evidence of Film-Induced Cleavage by Electrodeposited Rhodium.
PB95-162327 03,191

FINK, S. E.

Transient Analysis of a Line-Focus Transducer Probing a Liquid/Solid Interface.
PB97-118681 02,763

FINKELSTEIN, R.

Robotics Application to Highway Transportation. Volume 2. Literature Search.
PB95-170551 01,337

FINNEMORE, D. K.

Effect of Axial Strain on the Critical Current of Ag-Sheathed Bi-Based Superconductors in Magnetic Fields Up to 25 T.
PB94-211315 04,493

Improved Uniaxial Strain Tolerance of the Critical Current Measured in Ag-Sheathed Bi2Sr2Ca1Cu2O8+x Superconductors.
PB95-153565 04,594

Thermally Activated Hopping of a Single Abrikosov Vortex.
PB95-140810 04,548

FIOCK, E. F.

Bibliography of Books and Published Reports on Gas Turbines, Jet Propulsion, and Rocket Power Plants.
AD-A278 138/3 01,445

Bibliography of Books and Published Reports on Gas Turbines, Jet Propulsion, and Rocket Power Plants, January 1950 through December 1953.
AD-A278 213/4 01,446

FIREBAUGH, S. L.

Measurement of S2OF10, and S2O2F10 Production Rates from Spark and Negative Glow Corona Discharge in SF6/O2 Gas Mixtures.
PB96-123740 01,093

FISCHER, J. E.

Discontinuous Volume Change at the Orientational-Ordering Transition in Solid C60.
PB94-211828 00,821

Inelastic-Neutron-Scattering Studies of Poly(p-phenylene vinylene).
PB95-180766 01,014

Neutron-Scattering Study of Librations and Intramolecular Phonons in Rb2.6K0.4C60.
PB95-162269 00,958

Phase Transitions in Solid C70: Supercooling, Metastable Phases, and Impurity Effect.
PB95-150090 00,914

FISH, G.

Polarization Analysis of the Magnetic Excitations in Invar and Non-Invar Amorphous Alloys.
PB94-216116 04,516

FISHER, G.

Open System Environment Procurement.
N94-36858/6 02,716

FISHER, G. E.

Application Portability Profile (APP): The U.S. Government's Open System Environment Profile Version 3.0.
PB96-158712 01,753

CSL View of Applications Portability, Scalability, and Interoperability.
PB97-122303 01,787

Guide on Open System Environment (OSE) Procurements.
PB95-169496 01,626

FISHER, J. L.

Assessment of Technology for Detection of Stress Corrosion Cracking in Gas Pipelines. Final Report, July 1993-March 1994.
PB94-206646 02,475

FISHER, W. M.

Benchmarks for the Evaluation of Speech Recognizers.
PB94-211539 01,566

FITTING, D. W.

Appropriate Ultrasonic System Components for NDE of Thick Polymer Composites.
PB95-125696 03,148

Composite Materials for Offshore Operations: Proceedings of the International Workshop (1st). Held in Houston, Texas on October 26-28, 1993.
PB96-109509 *03,169*

Hemispherical Test Fixture for Measuring the Wavefields Generated in an Anisotropic Solid.
PB96-190087 *03,181*

High-Sensitivity Acoustic Emission Sensor/Preamplifier Subsystems.
PB95-125704 *02,900*

Selection of Appropriate Ultrasonic System Components for NDE of Thick Polymer-Composites.
PB94-185279 *03,133*

FITZPATRICK, G. J.

Active High Voltage Divider with 20-PPM Uncertainty.
PB97-119317 *02,104*

Approach to Setting Performance Requirements for Automated Evaluation of the Parameters of High-Voltage Impulses.
PB94-185634 *01,878*

Comparative Measurements of High-Voltage Impulses Using a Kerr Cell and a Resistor Divider.
PB94-172582 *02,028*

Investigation of the Effects of Aging on the Calibration of a Kerr-Cell Measuring System for High Voltage Impulses.
PB94-172384 *02,025*

Optical Current Transducer for Calibration Studies.
PB94-185907 *02,121*

Transient Errors in a Precision Resistive Divider.
PB97-111512 *01,983*

FLACH, D. R.

Custom Integrated Circuit Comparator for High-Performance Sampling Applications.
PB94-213147 *02,320*

FLACK, H. D.

Statistical Descriptors in Crystallography. 2. Report of a Working Group on Expression of Uncertainty in Measurement.
PB96-146824 *04,764*

World Wide Web for Crystallography.
PB97-109219 *04,810*

FLAHAVIN, E.

Multi-Agency Certification and Accreditation (C and A) Process: A Worked Example.
PB95-171955 *01,601*

FLAHAVIN, E. C.

TMACH Experiment Phase 1. Preliminary Developmental Evaluation.
PB96-195318 *01,618*

FLAHAVIN, E. E.

Concept Paper: An Overview of the Proposed Trust Technology Assessment Program.
PB96-160882 *01,614*

Guidance to Federal Agencies on the Use of Trusted Systems.
PB95-163440 *01,597*

FLAITZ, C. M.

Diagnosis and Treatment of an Oral Base-Metal Contact Lesion Following Negative Dermatologic Patch Tests.
PB95-180626 *00,172*

FLAMBAUM, V. V.

Fine Structure of Negative Ions of Alkaline-Earth-Metal Atoms.
PB94-211182 *03,837*

Hole Dispersion and Enhancement of Antiferromagnetic Interaction of Localized Spins in High-Tc Superconductors.
PB95-202602 *04,694*

Long-Range Parity-Nonconserving Interaction.
PB95-202594 *03,986*

FLANIGAN, L.

In-Space Welding: Visions and Realities.
PB95-163234 *04,830*

FLATER, D.

Coping with Different Retrieval Methods in Next Generation Networks.
PB95-168555 *02,726*

FLAUD, J. M.

Reanalysis of the (010), (020), (100), and (001) Rotational Levels of (32)S(16)O2.
PB95-125621 *00,887*

FLEISCHMANN, C. M.

Backdraft Phenomena.
PB94-193927 *01,366*

FLEMING, R. F.

Dead Time, Pileup, and Accurate Gamma-Ray Spectrometry.
PB96-167101 *00,697*

FLEMING, T.

First Results from a Coordinated ROSAT, IUE, and VLA Study of RS CVn Systems.
PB94-213477 *00,069*

FLEMING, T. A.

Riass Coronathon: Joint X-ray and Ultraviolet Observations of Normal F-K Stars.
PB96-200217 *00,109*

ROSAT All-Sky Survey of Active Binary Coronae. 1. Quiescent Fluxes for the RS Canum Venaticorum Systems.
PB95-202479 *00,077*

ROSAT All-Sky Survey of Active Binary Coronae. 2. Coronal Temperatures of the RS Canum Venaticorum Systems.
PB94-199601 *00,055*

FLETCHER, R. A.

Complementary Molecular Information on Phthalocyanine Compounds Derived from Laser Microprobe Mass Spectrometry and Micro-Raman Spectroscopy.
PB94-172269 *00,757*

Generation and Characterization of Acetylene Smokes.
PB94-200292 *01,372*

Measurement of the Uniformity of Particle Deposition of Filter Cassette Sampling in a Low Velocity Wind Tunnel.
PB95-163754 *02,549*

Ultrafine Combustion Aerosol Generator.
PB94-200300 *01,373*

FLICEK, P. R.

Core Potentials for Quasi-One-Electron Systems.
PB95-202214 *03,970*

FLIK, M. I.

Thermal Isolation of High-Temperature Superconducting Thin Films Using Silicon Wafer Bonding and Micromachining.
PB96-135017 *02,408*

FLORKOWSKI, D. R.

Four Years of Monitoring alpha Orionis with the VLA: Where Have All the Flares Gone.
PB94-185212 *00,048*

FLORSCH, N.

Calibration of a Superconducting Gravimeter Using Absolute Gravity Measurements.
PB95-202651 *03,684*

FLORUSSE, L. J.

Principle of Congruence and Its Application to Compressible States.
PB96-102892 *01,068*

FLOWERS, G.

Inexpensive Laser Cooling and Trapping Experiment for Undergraduate Laboratories.
PB96-140371 *04,353*

FLOYD, F. L.

Methodologies for Predicting the Service Lives of Coating Systems.
PB95-146387 *03,124*

FLUCK, E.

Inorganic Crystal Structure Database (ICSD) and Standardized Data and Crystal Chemical Characterization of Inorganic Structure Types (TYPIX): Two Tools for Inorganic Chemists and Crystallographers.
PB97-109037 *00,648*

FLURY, B. D.

Representing a Large Collection of Curves: A Case for Principal Points.
PB95-152286 *03,438*

FLYNN, C. P.

Diffraction of Neutron Standing Waves in Thin Films with Resonance Enhancement.
PB97-113278 *04,164*

Enhanced Curie Temperatures and Magnetoelastic Domains in Dy/Lu Super Lattices and Films.
PB94-172665 *04,443*

Magnetic Rare Earth Artificial Metallic Superlattices.
PB95-162293 *04,611*

Magnetoelasticity in Rare-Earth Multilayers and Films.
PB94-211356 *04,495*

FLYNN, G. W.

Silicon Surface Chemistry by IR Spectroscopy in the Mid- to Far-IR Region: H2O and Ethanol on Si(100).
PB96-138565 *01,097*

FLYNN, K. M.

Localization Model of Rubber Elasticity: Comparison with Torsional Data for Natural Rubber Networks in the Dry State.
PB95-107033 *03,195*

FLYNN, T. M.

Bibliography of the Physical Equilibria and Related Properties of Some Cryogenic Systems.
AD-A281 167/7 *03,769*

Compilation of the Physical Equilibria and Related Properties of the Hydrogen-Carbon Monoxide System.
AD-A286 603/6 *00,716*

FOECKE, T.

Fracture Testing of Large-Scale Thin-Sheet Aluminum Alloy.
AD-A306 625/5 *03,305*

Fracture Testing of Large-Scale Thin-Sheet Aluminum Alloy.
PB95-242368 *00,024*

FOEST, R.

Optical and Mass Spectrometric Investigations of Ions and Neutral Species in SF6 Radio-Frequency Discharges.
PB97-111918 *01,985*

FOGLE, W. E.

Development of a Temperature Scale below 0.5 K.
PB95-125639 *03,879*

Systematic Studies of the Effect of a Bandpass Filter on a Josephson-Junction Noise Thermometer.
PB95-162970 *03,939*

Systematic Studies of the Effect of a Post-Detection Filter on a Josephson-Junction Noise Thermometer.
PB95-162988 *03,940*

FOKSINSKI, M.

DNA Base Damage in Lymphocytes of Cancer Patients Undergoing Radiation Therapy.
PB97-122444 *03,643*

FOLDEAKI, M.

Asymmetry between Flux Penetration and Flux Expulsion in Tl-2212 Superconductors.
PB95-125647 *04,527*

Enhanced Flux Pinning via Chemical Substitution in Bulk Superconducting T1-2212.
PB95-169033 *04,647*

Magnetic Susceptibility of Pr2-xCexCuO4 Monocrystals and Polycrystals.
PB95-180253 *04,677*

FOLEY, G. M.

High-Speed Spatial Scanning Pyrometer.
PB94-200003 *02,636*

FOLEY, J. T.

Theoretical Analysis of the Coherence-Induced Spectral Shift Experiments of Kandpal, Vaishya, and Joshi.
PB94-219383 *00,561*

FOLEY, R. P.

Prediction of Strengthening Due to V Additions in Direct-Cooled Ferrite-Pearlite Forging Steels.
PB96-190251 *03,220*

Prediction of the Strength Properties for Plain-Carbon and Vanadium Micro-Alloyed Ferrite-Pearlite Steel.
PB96-123393 *03,216*

FOLMAR, L. C.

Histopathology, Blood Chemistry, and Physiological Status of Normal and Moribund Striped Bass ('Morone saxatilis') Involved in Summer Mortality ('Die-Off') in the Sacramento-San Joaquin Delta of California.
PB94-198157 *00,034*

FONER, S.

Effect of Microstructure on Phase Formation in the Reaction of Nb/Al Multilayer Thin Films.
PB95-168415 *03,352*

First Phase Formation Kinetics in the Reaction of Nb/Al.
PB95-168456 *03,353*

Thin Film Reaction Kinetics of Niobium/Aluminum Multilayers.
PB95-175295 *04,651*

FONG, E.

Interoperability Experiments with CORBA and Persistent Object Base Systems.
PB96-183140 *01,772*

Preliminary Functional Specifications of a Prototype Electronic Research Notebook for NIST.
PB94-207750 *00,012*

Report on Application Integration Architectures (AIA) Workshop. Held in Dallas, Texas on February 8-12, 1993.
PB94-142536 *01,803*

FONG, E. N.

Application of Expert System to Select Data Sources from Chemical Information Databases.
PB95-125654 *00,505*

Persistent Object Base System Testing and Evaluation.
PB95-220588 *01,730*

FONG, J. T.

Application of a Simple Technique for Estimating Errors of Finite-Element Solutions Using a General-Purpose Code.
PB94-200250 *04,818*

Non-Equilibrium Thermodynamic Theory of Viscoplastic Materials.
PB94-198868 *04,467*

Nonequilibrium Thermodynamic Theory of Viscoplastic Materials.
PB96-111661 *04,034*

PC-Based Prototype Expert System for Data Management and Analysis of Creep and Fatigue of Selected Materials at Elevated Temperatures.
PB94-172251 *03,202*

FOOTE, P. D.

Technologic Papers of the Bureau of Standards: Number 170. Pyrometric Practice.
AD-A279 282/8 *03,766*

FORAND, J. L.

Merged-Beams Energy-Loss Technique for Electron-Ion Excitation: Absolute Total Cross Sections for O(5+) (2s yields 2p).
PB96-102058 *04,017*

FORMAN, P. R.

Polarization Dependence of Response Functions in 3x3 Sagnac Optical Fiber Current Sensors.
PB95-162426 *02,154*

Polarization Dependence of Response Functions in 3x3 Sagnac Optical Fiber Current Sensors.
PB96-122684 *02,189*

FORNEY, D.

Infrared and Near-Infrared Spectra of HCC and DCC Trapped in Solid Neon.
AD-A295 578/9 *03,773*

Mid- and Near-Infrared Spectra of Water and Water Dimer Isolated in Solid Neon.
PB95-125662 *00,888*

Vibrational Spectra of Molecular Ions Isolated in Solid Neon: HCCH+ and HCC-. (Reannouncement with New Availability Information).
AD-A253 551/6 *00,707*

Vibrational Spectra of Molecular Ions Isolated in Solid Neon. X. H2O(+), HDO(+), and D2O(+).
PB95-125670 *00,889*

Vibrational Spectra of Molecular Ions Isolated in Solid Neon. XI. NO2(+), NO2(-), and NO3(-).
PB95-125688 *00,890*

Vibrational Spectra of Molecular Ions Isolated in Solid Neon. 11. NO2(+), NO2(-), and NO3(-).
AD-A275 828/2 *00,708*

FORNEY, G. P.

Analyzing and Exploiting Numerical Characteristics of Zone Fire Models.
PB96-102314 *01,400*

Computing Radiative Heat Transfer Occurring in a Zone Fire Model.
PB96-102306 *01,399*

Computing the Effect of Sprinkler Sprays on Fire Induced Gas Flow.
PB96-147111 *00,404*

Field Modeling: Simulating the Effect of Sloped Beamed Ceilings on Detector and Sprinkler Response.
PB96-122866 *01,406*

Improvement in Predicting Smoke Movement in Compartmented Structures.
PB94-172418 *00,332*

Pressure Equations in Zone-Fire Modeling.
PB96-102967 *00,208*

FORTUNKO, C.

Artificial Crack in Steel: An Ultrasonic-Resonance-Spectroscopy and Modeling Study.
PB96-141395 *03,241*

Compressibility of Polycrystal and Monocrystal Copper: Acoustic-Resonance Spectroscopy.
PB96-164223 *02,990*

Elastic Constants and Internal Friction of Polycrystalline Copper.
PB96-141015 *03,364*

Orthotropic Elastic Constants of a Boron-Aluminum Fiber-Reinforced Composite: An Acoustic-Resonance-Spectroscopy Study.
PB96-200175 *03,182*

Ultrasonic-Resonance Spectroscopy of Bulk and Layered Solids.
PB96-141338 *04,759*

FORTUNKO, C. M.

Absorption of Sound in Gases between 10 and 25 MHz: Argon.
PB94-199015 *04,183*

Absorption of Ultrasonic Waves in Air at High Frequencies (10-20 MHz).
PB94-199007 *04,182*

Appropriate Ultrasonic System Components for NDE of Thick Polymer Composites.
PB95-125696 *03,148*

Assessment of Technology for Detection of Stress Corrosion Cracking in Gas Pipelines. Final Report, July 1993-March 1994.
PB94-206646 *02,475*

Determination of Sheet Steel Formability Using Wide Band Electromagnetic-Acoustic Transducers.
PB96-186036 *02,279*

Examination of Objects Made of Wood Using Air-Coupled Ultrasound.
PB95-125712 *03,404*

Gas-Coupled, Pulse-Echo Ultrasonic Crack Detection and Thickness Gaging.
PB96-147129 *04,847*

Hemispherical Test Fixture for Measuring the Wavefields Generated in an Anisotropic Solid.
PB96-190087 *03,181*

High-Sensitivity Acoustic Emission Sensor/Preamplifier Subsystems.
PB95-125704 *02,900*

Selection of Appropriate Ultrasonic System Components for NDE of Thick Polymer-Composites.
PB94-185279 *03,133*

Well-Shielded EMAT for On-Line Ultrasonic Monitoring of GMA Welding.
PB96-186077 *02,879*

FOSSUM, B. M.

Learning to Change: Opportunities to Improve the Performance of Smaller Manufacturers.
PB94-166212 *00,010*

FOSTER, N.

Development of the National Marine Mammal Tissue Bank.
PB95-161402 *02,586*

FOTI, J.

Preliminary Functional Specifications of a Prototype Electronic Research Notebook for NIST.
PB94-207750 *00,012*

FOTIADAS, L.

Lattice Position of Si in GaAs Determined by X-Ray Standing Wave Measurements.
PB95-164406 *04,632*

FOUQUET, Y.

Hardware Measurement Techniques for High-Speed Networks.
PB96-160551 *01,500*

FOWELL, A. J.

Fire Hazard Model Developments and Research Efforts at NIST.
PB96-159652 *00,407*

International Organization for Standardization: Current Activities in Fire Safety Engineering.
PB96-159660 *00,223*

National Planning for Construction and Building R and D.
PB96-137104 *00,324*

Program of the Subcommittee on Construction and Building.
PB94-193646 *00,319*

Program of the Subcommittee on Construction and Building (July 1994).
PB95-122537 *00,321*

Rationale and Preliminary Plan for Federal Research for Construction and Building.
PB95-154704 *00,322*

White Papers Prepared for the White House: Construction Industry Workshop on National Construction Goals. Held on December 14-16, 1994.
PB95-216891 *01,299*

FOWLER, B. O.

Composition and Solubility Product of a Synthetic Calcium Hydroxyapatite.
PB96-180104 *02,995*

Crystal Structure of Calcium Succinate Monohydrate.
PB95-168928 *00,167*

Octacalcium Phosphate Carboxylates IV. Kinetics of Formation and Solubility of Octacalcium Phosphate Succinate.
PB94-185600 *00,776*

Octacalcium Phosphate Carboxylates. 1. Preparation and Identification.
PB95-161535 *00,660*

Octacalcium Phosphate Carboxylates. 2. Characterization and Structural Consideration.
PB95-161543 *00,955*

Octacalcium Phosphate Carboxylates. 5. Incorporation of Excess Succinate and Ammonium Ions in the Octacalcium Phosphate Succinate Structure.
PB95-168894 *00,166*

Octacalcium Phosphate. 3. Infrared and Raman Vibrational Spectra.
PB94-172244 *00,756*

FOWLER, J.

Method of Realizing Spectral Irradiance Based on an Absolute Cryogenic Radiometer.
PB95-161204 *04,270*

FOWLER, J. B.

High Accuracy Measurement of Aperture Area Relative to a Standard Known Aperture.
PB95-261954 *01,919*

Third Generation Water Bath Based Blackbody Source.
PB96-122148 *04,046*

FOWLER, J. E.

Systems Integration for Manufacturing Applications Program 1995 Annual Report.
PB96-193735 *02,844*

Variant Design for Mechanical Artifacts-A State of the Art Survey.
PB94-154358 *02,768*

FOX, D.

Dynamic Phenomena on the RS Canum Venaticorum Binary II Pegasi in August 1989. 1. Observational Data.
PB94-211067 *00,056*

First Results from a Coordinated ROSAT, IUE, and VLA Study of RS CVn Systems.
PB94-213477 *00,069*

FOX, D. C.

Rotational Modulation and Flares on RS Canum Venaticorum and BY Draconis Stars. XVIII. Coordinated VLA, ROSAT, and IUE Observations of RS CVn Binaries.
PB96-102322 *00,089*

FOX, R. W.

Diode Laser as a Spectroscopic Tool.
PB95-175485 *00,600*

High-Resolution Diode-Laser Spectroscopy of Calcium.
PB95-181244 *03,969*

High-Sensitivity Spectroscopy with Diode Lasers.
PB95-175477 *04,297*

Optical Probing of Cold Trapped Atoms.
PB95-175469 *04,296*

Precise Optical Frequency References and Difference Frequency Measurements with Diode Lasers.
PB95-176228 *04,305*

FOY, B. R.

Fragment Energy and Vector Correlations in the Overtone-Pumped Dissociation of HN3X(1)A'.
PB94-199908 *00,802*

Vibrational Predissociation Dynamics of Overtone-Excited HN3.
PB95-125720 *00,691*

FRAGA, M. M. F. R.

Excitation of Balmer Lines in Low-Current Discharges of Hydrogen and Deuterium.
PB95-150546 *03,893*

FRAIME, L.

Proceedings of the Workshop on the Federal Criteria for Information Technology Security. Held in Ellicot City, Maryland on June 2-3, 1993.
PB94-162583 *01,575*

FRAKER, A. C.

Dental Materials.
PB94-172871 *00,142*

Information Retrieval Using Key Words and a Structured Review.
PB95-161121 *03,724*

FRALEY, K. L.

Advanced Mass Calibration and Measurement Assurance Program for State Calibration Laboratories.
PB95-253571 *02,492*

FRANASZEK, M.

Fluctuations in Probability Distribution on Chaotic Attractors.
PB96-102330 *04,022*

FRANCHUK, C. A.

Economic, Energy, and Environmental Impacts of the Energy-Related Inventions Program.
DE94-017162 *00,008*

FRANCIS, M. H.

Comparison of k-Correction and Taylor-Series Correction for Probe-Position Errors in Planar Near-Field Scanning.
PB96-147137 *02,012*

Comparison of Ultralow-Sidelobe-Antenna Far-Field Patterns Using the Planar-Near-Field Method and the Far-Field Method.
PB96-200373 *02,015*

Dual-Frequency Millimeter-Wave Radiometer Antenna for Airborne Remote Sensing of Atmosphere and Ocean.
PB96-112289 *02,009*

Dual Frequency mm-Wave Radiometer Antenna for Airborne Remote Sensing of Atmosphere and Ocean.
PB95-180378 *02,006*

Planar Near-Field Measurements of Low-Sidelobe Antennas.
PB94-219235 *02,001*

Proposed Analysis of RCS Measurement Uncertainty.
PB95-203568 *01,871*

FRANCONI, B.

Binder Characterization and Evaluation by Nuclear Magnetic Resonance Spectroscopy.
PB94-193471 *01,334*

FRANK, D. E.

Preliminary Investigation of Oleoresin Capsicum.
PB96-179486 *03,520*

FRANK, H.

Report on the Workshop on Advanced Digital Video in the National Information Infrastructure. Held in Washington, D.C. on May 10-11, 1994.
PB95-103677 *01,472*

Summary Report on the Workshop on Advanced Digital Video in the National Information Infrastructure.
PB96-141320 *01,497*

FRANKLIN, W. A.

Modification of Deoxyribose-Phosphate Residues by Extracts of Ataxia Telangiectasia Cells.
PB94-212602 *03,458*

FRANZ, J.

Harmonic and Static Susceptibilities of YBa2Cu3O7.
PB95-161139 *04,599*

FRANZEN, D. L.

Accurate Characterization of High Speed Photodectors.
PB95-153763 *02,153*

High-Sensitivity Optical Sampling Using an Erbium-Doped Fiber Laser Strobe.
PB95-176111 *04,302*

Lightwave Standards Development at NIST.
PB95-168563 *01,480*

Metrology Applications of Mode-Locked Erbium Fiber Lasers.
PB95-140158 *04,256*

Millimeter-Resolution Optical Time-Domain Reflectometry Using a Four-Wave Mixing Sampling Gate.
PB96-122700 *02,190*

Optical Fiber, Fiber Coating, and Connector Ferrule Geometry: Results of Interlaboratory Measurement Comparisons.
PB96-154422 *04,360*

Optical Sampling Using Nondegenerate Four-Wave Mixing in a Semiconductor Laser Amplifier.
PB96-122502 *02,076*

Optical Sampling Using Nondegenerate Four-Wave Mixing in a Semiconductor Laser Amplifier.
PB96-123609 *04,348*

Precise Laser-Based Measurements of Zero-Dispersion Wavelength in Single-Mode Fibers.
PB96-201124 *01,511*

Technical Digest: Symposium on Optical Fiber Measurements (8th), 1994. Held in Boulder, Colorado on September 13-15, 1994.
PB94-207636 *04,231*

Technical Digest: Symposium on Optical Fiber Measurements (9th), 1996. Held in Boulder, Colorado on October 1-3, 1996.
PB97-108583 *04,383*

FRASER, G. T.

Infrared Spectra of van der Waals Complexes of Importance in Planetary Atmospheres.
PB95-125738 *00,071*

Microwave and Submillimeter Spectroscopy of Ar-NH3 States Correlating with Ar+NH3(j=1, k=1).
PB95-152211 *00,942*

Microwave Spectrum and Structure of CH3NO2-H20.
AD-A296 377/5 *00,719*

Molecular-Beam Optothermal Spectrum of the OH Stretching Band of Methanol.
PB94-212826 *00,839*

P-Type Doubling in the Infrared Spectrum of NO-HF.
PB94-211463 *00,817*

Rotational Spectra of CH3CCH-NH3, NCCCH-NH3, and NCCCH-OH2.
PB97-118798 *04,170*

FRATELLO, V.

Magneto-Optic Magnetic Field Sensors Based on Uniaxial Iron Garnet Films in Optical Waveguide Geometry.
PB95-153409 *02,152*

FRATELLO, V. J.

High Frequency Magnetic Field Sensors Based on the Faraday Effect in Garnet Thick Films.
PB96-190384 *02,282*

Magneto-Optic Magnetic Field Sensors Based on Uniaxial Iron Garnet Films in Optical Waveguide Geometry.
PB95-168498 *02,159*

FRECHETTE, M. F.

Investigation of S2F10 Production and Mitigation in Compressed SF6- Insulated Power Systems.
PB96-155528 *02,468*

FRECHETTE, S.

NIST SIMA Interactive Management Workshop. Held in Fort Belvoir, Virginia on November 14-16, 1994.
PB96-154877 *02,838*

Open Architectures for Machine Control.
PB94-135621 *02,942*

FRECHETTE, S. P.

Interoperability Requirements for CAD Data Transfer in the AutoSTEP Project.
PB97-114268 *02,796*

FREDERICK, N.

Distributed measurements of tracer response on packed bed flows using a fiberoptic probe array. Final report.
DE95013079 *00,667*

FREDERICK, N. V.

Development of a Dual-Sinker Densimeter for High-Accuracy Fluid P-V-T Measurements.
PB95-168951 *03,267*

Development of a Dual-Sinker Densimeter for High-Accuracy Fluid P-V-T Measurements. Appendix A.
DE93019682 *02,620*

Speed-of-Sound Measurements in Liquid and Gaseous Air.
PB95-151957 *04,186*

FREDERIKSE, H. P. R.

Analysis of Thermal Wave Propagation in Diamond Films.
PB94-211471 *03,014*

Thermal Wave Propagation in Diamond Films.
PB94-211489 *03,015*

FREE, G. M.

Measurements of the Characteristic Impedance of Coaxial Air Line Standards.
PB95-168787 *02,221*

FREED, K.

How Far Is Far from Critical Point in Polymer Blends. Lattice Cluster Theory Computations for Structured Monomer, Compressible Systems.
PB94-211141 *01,217*

FREED, K. F.

Competition between Hydrodynamic Screening ('Draining') and Excluded Volume Interactions in an Isolated Polymer Chain.
PB95-175402 *01,265*

Examination of the l/d Expansion Method from Exact Enumeration for a Self-Interacting Self-Avoiding Walk.
PB95-175733 *01,266*

Hypercubic Lattice SAW Exponents nu and gamma : 3.99 Dimensions Revisited.
PB94-211026 *01,215*

Modification of the Phase Stability of Polymer Blends by Diblock Copolymer Additivies.
PB96-123542 *03,172*

Response to 'Draining in Dilute Polymer Solutions and Renormalization'.
PB96-146667 *01,283*

FREEMAN, J. J.

Standard of Attenuation for Microwave Measurements.
AD-A297 905/2 *01,517*

FREIMAN, S. W.

Ceramics Technical Activities, 1995.
PB96-193677 *03,087*

Electric Field Effects on Crack Growth in a Lead Magnesium Niobate.
PB95-107322 *03,339*

Environmentally Enhanced Fracture of Ceramics.
PB95-125746 *03,046*

Moisture and Water-Induced Crack Growth in Optical Materials.
PB95-153334 *04,267*

Molecular Orbital Calculations of Bond Rupture in Brittle Solids.
PB95-164059 *00,973*

Molecular Orbital Study of Water Enhanced Crack Growth Process.
PB95-164067 *03,240*

Photonic Materials: A Report on the Results of a Workshop. Held in Gaithersburg, Maryland on August 26-27, 1992, Volume 1.
PB94-152733 *02,114*

X-Ray Characterization of the Crystallization Process of High-Tc Superconducting Oxides in the Sr-Bi-Pb-Ca-Cu-O System.
PB95-151700 *04,579*

FRENCH, J. D.

Creep Rupture of MoSi2/SiCp Composites.
PB95-152294 *03,154*

Sources of Strain-Measurement Error in Flag-Based Extensometry.
PB97-118731 *03,108*

FRENKEL, A.

Broadband High-Optical-Density Filters in the Infrared.
PB95-180261 *04,309*

Filter Transmittance Measurements in the Infrared.
PB94-140589 *04,224*

Thermal and Nonequilibrium Responses of Superconductors for Radiation Detectors.
PB95-164232 *02,156*

FRENKEL, M.

Thermodynamic and Thermophysical Properties of Organic Nitrogen Compounds. Part II. 1- and 2-Butanamine, 2-Methyl-1-Propanamine, 2-Methyl-2-Propanamine, Pyrrole, 1-, 2-, and 3-Methylpyrrole, Pyridine, 2-, 3-, and 4-Methylpyridine, Pyrrolidine, Piperidine, Indole, Quinoline, Isoquinoline, Acridine, Carbazole, Phenanthridine, 1- and 2-Naphthalenamine, and 9-Methylcarbazole.
PB94-162294 *00,741*

FREY, M.

Deterministic and Stochastic Chaos.
PB96-156138 *00,218*

Melnikov Function and Homoclinic Chaos Induced by Weak Perturbations.
PB95-180923 *03,414*

Necessary Condition for Homoclinic Chaos Induces by Additive Noise.
PB96-155775 *04,063*

Noise-Induced Chaos and Phase Space Flux.
PB95-125761 *03,433*

Noise-Induced Transitions to Chaos.
PB96-156120 *00,217*

Noise Modeling and Reliability of Behavior Prediction for Multi-Stable Hydroelastic Systems.
PB96-111943 *04,822*

Spectrum of the Stochastically Forced Duffing-Holmes Oscillator.
PB96-155767 *00,216*

Transitions to Chaos Induced by Additive and Multiplicative Noise.
PB96-155759 *03,750*

FREY, M. R.

Capacity of the Lp Norm-Constrained Poisson Channel.
PB95-125753 *01,515*

FREYER, G. J.

Band-Limited, White Gaussian Noise Excitation for Reverberation Chambers and Applications to Radiated Susceptibility Testing.
PB96-165410 *01,960*

FRIDAY, D. S.

NIST and the Navy: Past, Present and Future.
PB96-119649 *03,655*

FRIEDMAN, C.

Reinforcement of Cancellous Bone Screws with Calcium Phosphate Cement.
PB96-158001 *00,179*

FRIEDMAN, D. J.

Surface Topography and Ordering-Variant Segregation in GaInP2.
PB95-153649 *04,595*

FRIEND, D. G.

Calculation of Enthalpy and Entropy Differences of Near-Critical Binary Mixtures with the Modified Leung-Griffiths Model.
PB95-108635 *00,885*

Composition Dependence of a Field Variable Along the Binary Fluid Mixture Critical Locus.
PB95-176038 *01,003*

Critical Lines for Type-III Aqueous Mixtures by Generalized Corresponding-States Models.
PB96-102371 *01,063*

Prediction of the Thermal Conductivity of Refrigerants and Refrigerant Mixtures.
PB94-212107 *03,258*

Reference Data for the Thermophysical Properties of Cryogenic Fluids.
PB95-168688 *03,263*

Thermodynamic Properties of the Methane-Ethane System.
PB95-125779 *00,891*

Thermophysical Property Computer Packages from NIST.
PB95-125787 *04,203*

Thermophysical Property Standard Reference Data from NIST.
PB96-167358 *01,153*

FRIEND, J. P.

International Marine-Atmospheric (222)Rn Measurement Intercomparison in Bermuda. Part 2. Results for the Participating Laboratories.
PB96-175682 *00,115*

FROHNSDORFF, G.

Suggestions for a Logically-Consistent Structure for Service Life Prediction Standards.
PB95-125795 *00,358*

FROHNSDORFF, G. J. C.

Performance Approach to the Development of Criteria for Low-Sloped Roof Membranes.
PB94-160751 *00,329*

FRONCZEK, F. R.

X-Ray-Diffraction Study of a Thermomechanically Detwinned Single Crystal of YBa2Cu3O6+x.
PB95-151726 *04,581*

FRONCZEK, L. J.

Portsmouth Fastener Manufacturing Workstation. User's Manual.
PB95-147922 *02,860*

FRONTICELLI, C.

Positive and Negative Cooperativities at Subsequent Steps of Oxygenation Regulate the Allosteric Behavior of Multistate Sebacylhemoglobin.
PB97-119374 *03,486*

FROST, M. J.

Kinetics and Dynamics of Vibrationally State Resolved Ion-Molecule Reactions: (14)N2(+)(v=1 and 2) and (15)N2(+)(v=0,1 and 2) with (14)N2.
PB96-102348 *04,023*

Selected Ion Flow Tube-Laser Induced Fluorescence Instrument for Vibrationally State-Specific Ion-Molecule Reactions.
PB94-185444 *00,774*

FRYBERGER, T.

Fundamental Studies of Gas Sensor Response Mechanisms: Palladium on SnO2(110).
PB95-162731 *00,963*

FRYBERGER, T. B.

Conductance Response of Pd/SnO2(110) Model Gas Sensors to H2 and O2.
PB95-125803 *00,892*

FU, J.

Junction Locations by Scanning Tunneling Microscopy: In-Air-Ambient Investigation of Passivated GaAs pn Junctions.
PB94-185964 *02,306*

Measurement and Uncertainty of a Calibration Standard for the Scanning Electron Microscope.
PB94-219250 *00,560*

FUCHS, P. A.

Application of Electromagnetic-Acoustic Transducers for Nondestructive Evaluation of Stresses in Steel Bridge Structures.
PB96-167978 *01,301*

FUERST, C. D.

Magnetocaloric Effect in Rapidly Solidified Nd-Fe-Al-B Materials.
PB94-185667 *04,451*

FUHR, J. R.

Atomic Branching Ratio Data for Carbon-Like Ions.
PB94-212842 *03,855*

Atomic Branching Ratio Data for Nitrogen-Like Species.
PB96-190152 *04,122*

Atomic Branching Ratio Data for Oxygen-Like Species.
PB95-180436 *03,963*

Spectroscopic Data Tables for Highly-Ionized Atoms.
PB95-151585 *03,910*

FUJII, K.

Measurement and Reduction of Alignment Errors of the NIST Watt Experiment.
PB97-111959 *01,987*

New Refractometer by Combining a Variable Length Vacuum Cell and a Double-Pass Michelson Interferometer.
PB97-111926 *01,986*

NIST Watt Balance: Progress Toward Monitoring the Kilogram.
PB97-113062 *01,991*

FULCRAND, H.
Oxidation of Caffeic Acid and Related Hydroxycinnamic Acids.
PB97-111975 *00,651*

FULLER, E. R.
Ceramic Characterization.
DE94013170 *03,026*

Crystal Chemistry and Phase Equilibria Studies of the BaO(BaCO3)-R2O3-CuO Systems. 4. Crystal Chemistry and Subsolidus Phase Relationship Studies of the CuO-Rich Region of the Ternary Diagrams, R=Lanthanides.
PB95-151759 *00,936*

Crystal Chemistry and Phase Equilibrium Studies of the BaO(BaCO3)-R2O3-CuO Systems. 5. Melting Relations in Ba2(Y,Nd,Eu)Cu3O6+x.
PB95-151718 *04,580*

Determination of Fiber-Matrix Interfacial Properties of Importance to Ceramic Composite Toughening.
PB95-125811 *03,149*

Efficient Experiment to Study Superconducting Ceramics.
PB94-212578 *04,505*

Interface Properties for Ceramic Composites from a Single Fiber Pull-Out Test.
PB94-199361 *03,135*

Matrix Grain Bridging Contribution to the Toughness of Whisker Reinforced Ceramics.
PB94-198645 *03,134*

Micro-Mechanical Aspects of Asperity-Controlled Friction in Fiber-Toughened Ceramic Composites.
PB94-199536 *03,136*

FULLER, S. K.
Benefits and Costs of Research: Two Case Studies in Building Technology.
PB96-202221 *00,230*

Life-Cycle Costing Manual for the Federal Energy Management Program. 1995 Edition.
PB96-172317 *02,511*

Life-Cycle Costing Workshop for Energy Conservation in Buildings: Student Manual.
PB95-175006 *00,257*

FURDYNA, J. K.
Microwave Properties of YBa2Cu3O7-x Films at 35 GHz from Magnetotransmission and Magnetoreflection Measurements.
PB95-168977 *04,643*

FURLANI, C. M.
National PDES Testbed: An Overview.
PB95-125829 *02,775*

FURUKAWA, G. T.
Preliminary Results of a Comparison of Water Triple-Point Cells Prepared by Different Methods.
PB96-161344 *00,634*

FURUTA, R.
Important Papers in the History of Document Preparation Systems: Basic Sources.
PB95-125837 *02,712*

G'SELL, C.
Influence of Physical Aging on the Yield Response of Model DGEBA + Poly(propylene oxide) Epoxy Glasses.
PB95-126363 *03,381*

GADALLA, N. A. M.
Thermodynamic and Thermophysical Properties of Organic Nitrogen Compounds. Part II. 1- and 2-Butanamine, 2-Methyl-1-Propanamine, 2-Methyl-2-Propanamine, Pyrrole, 1-, 2-, and 3-Methylpyrrole, Pyridine, 2-, 3-, and 4-Methylpyridine, Pyrrolidine, Piperidine, Indole, Quinoline, Isoquinoline, Acridine, Carbazole, Phenanthridine, 1- and 2-Naphthalenamine, and 9-Methylcarbazole.
PB94-162294 *00,741*

GADDY, G. D.
Application of Thermal Analysis Techniques to the Characterization of EPDM Roofing Membrane Materials.
PB95-125845 *00,359*

Use of Thermal Mechanical Analysis to Characterize Ethylene-Propylene-Diene Terpolymer (EPDM) Roofing Membrane Materials.
PB95-125852 *00,360*

GADZUK, J. W.
Energy Dependence of Collision Characteristics in Molecule-Surface Collisions.
PB94-198504 *00,786*

Single-Atom Point Source for Electrons: Field-Emission Resonance Tunneling in Scanning Tunneling Microscopy.
PB95-125860 *00,893*

GAGNEPAIN, J. J.
Aging, Warm-Up Time and Retrace; Important Characteristics of Standard Frequency Generators.
PB96-103122 *04,031*

Environmental Sensitivities of Quartz Oscillators.
PB96-103148 *02,271*

New Model of 1/F Noise in Baw Quartz Resonators.
PB96-112248 *02,383*

GAIGALAS, A.
Conformational Alterations of Bovine Insulin Adsorbed on a Silver Electrode.
PB96-161773 *00,510*

Physicochemical Characterization of Low Molecular Weight Heparin.
PB96-112040 *03,474*

GAIGALAS, A. K.
Aggregation Kinetics of Colloidal Particles Destabilized by Enzymes.
PB95-125878 *00,894*

Method for the Assay of Hydrolytic Enzymes Using Dynamic Light Scattering.
PB95-151411 *03,531*

Non-Perturbative Relation between the Mutual Diffusion Coefficient, Suspension Viscosity, and Osmotic Compressibility: Application to Concentrated Protein Solutions.
PB96-102355 *01,062*

Physical Characterization of Herparin by Light Scattering.
PB96-119383 *03,598*

Structural Analysis of Heparin by Raman Spectroscopy.
PB96-167226 *03,480*

GAIGNEBET, J.
Preliminary Comparison of Time Transfers via LASSO, GPS and Two-Way Satellite.
PB95-151098 *01,529*

GAITAN, M.
CMOS Circuit Design for Controlling Temperature in Micromachined Devices.
PB96-156088 *02,196*

Efficient Method to Compute the Maximum Transient Drain Current Overshoot in Silicon on Insulator Devices.
PB94-172483 *02,300*

High-Level CAD Melds Micromachined Devices with Foundries.
PB94-216413 *02,321*

Interaction of Stoichiometry, Mechanical Stress, and Interface Trap Density in LPCVD Si-rich SiNx-Si Structures.
PB95-176301 *02,366*

MEMS in Standard CMOS VLSI Technology.
PB96-102363 *02,377*

Micromachined Coplanar Waveguides in CMOS Technology.
PB97-119283 *02,456*

Micromachined Display Output for a Cellular Neural Network.
PB96-156070 *02,422*

Multijunction Thermal Converters by Commercial CMOS Fabrication.
PB95-153664 *02,343*

Performance of Commercial CMOS Foundry-Compatible Multijunction Thermal Converters.
PB95-153656 *02,342*

Realizing Suspended Structures on Chips Fabricated by CMOS Foundry Processes Through the MOSIS Service.
PB94-193984 *01,881*

Test Structures for Determining Design Rules for Microelectromechanical-Based Sensors and Actuators.
PB95-150488 *02,105*

Tin Oxide Gas Sensor Fabricated Using CMOS Micro-Hotplates and In-situ Processing.
PB95-150603 *00,580*

GALAMBOS, J.
Extreme Value Theory and Applications: Proceedings of the Conference on Extreme Value Theory and Applications, Volume 3. Held in Gaithersburg, Maryland in May 1993.
PB95-104956 *03,432*

GALLAGHER, A.
Associative Ionization in Collisions of Slowed and Trapped Sodium.
PB95-125886 *03,880*

Atom Cooling and Trapping, and Collisions of Trapped Atoms.
PB96-122916 *04,048*

Atomic-scale characterization of hydrogenated amorphous-silicon films and devices. Annual subcontract report, 14 February 1994--14 April 1995.
DE95009287 *02,294*

Collisional Energy Transfer between Excited-State Strontium and Noble-Gas Atoms.
PB95-202958 *03,995*

Construction of Silicon Nanocolumns with the Scanning Tunneling Microscope.
PB95-203063 *04,696*

Deposition Rates in Direct Current Diode Sputtering.
PB95-203345 *04,697*

Energy-Pooling Collisions in Barium.
PB95-203030 *03,997*

Failures of the Four-Wave Mixing Model for Cone Emission.
PB95-202636 *04,318*

Nanoscale Study of the As-Grown Hydrogenated Amorphous Silicon Surface.
PB95-150595 *04,573*

Oscillator Strengths and Radiative Branching Ratios in Atomic Sr.
PB95-203493 *04,008*

Plasma Chemistry in Disilane Discharges.
PB94-211075 *02,514*

Plasma Chemistry in Silane/Germane and Disilane/Germane Mixtures.
PB95-202537 *01,027*

Threshold Electron Excitation of Na.
PB95-202917 *03,994*

GALLAGHER, A. C.
Excitation Transfer in Barium by Collisions with Noble Gases.
PB96-200274 *01,163*

Growth and Nucleation of Hydrogenated Amorphous Silicon on Silicon (100) Surfaces.
PB96-176516 *02,991*

Nanoscale Study of the Hydrogenated Amorphous Silicon Surface.
PB96-103056 *04,720*

GALLAGHER, J. G.
REFPROP Refrigerant Properties Database: Capabilities, Limitations, and Future Directions.
PB96-167150 *01,149*

GALLAGHER, J. S.
Critical Lines for Type-III Aqueous Mixtures by Generalized Corresponding-States Models.
PB96-102371 *01,063*

Formulation of the Refractive Index of Water and Steam.
PB95-140133 *00,900*

Standard States, Reference States and Finite-Concentration Effects in Near-Critical Mixtures with Applications to Aqueous Solutions.
PB95-164349 *00,979*

Thermodynamic Behavior of the CO2-H2O System from 400 to 1000 K, up to 100 MPa and 30% Mole Fraction of CO2.
PB94-162245 *00,736*

Thermophysical Property Computer Packages from NIST.
PB95-125787 *04,203*

GALLAGHER, J. W.
Journal of Physical and Chemical Reference Data, Volume 22, No. 1, January/February 1993.
PB94-160975 *00,729*

Journal of Physical and Chemical Reference Data, Volume 22, No. 2, March/April 1993.
PB94-162211 *00,733*

Journal of Physical and Chemical Reference Data, Volume 22, No. 3, May/June 1993.
PB94-162260 *00,738*

Journal of Physical and Chemical Reference Data, Volume 22, No. 4, July/August 1993.
PB94-162310 *00,743*

Journal of Physical and Chemical Reference Data, Volume 22, No. 5, September/October 1993.
PB94-162336 *00,745*

Journal of Physical and Chemical Reference Data, Volume 22, No. 6, November/December 1993.
PB94-168556 *00,749*

Journal of Physical and Chemical Reference Data, Volume 24, No. 1, January/February 1995.
PB96-145560 *01,101*

Journal of Physical and Chemical Reference Data, Volume 24, No. 2, March/April 1995.
PB96-145818 *01,105*

Journal of Physical and Chemical Reference Data, Volume 24, No. 3, May/June 1995.
PB96-145842 *01,108*

Journal of Physical and Chemical Reference Data, Volume 24, No. 4, July/August 1995.
PB96-145883 *01,112*

Journal of Physical and Chemical Reference Data, Volume 24, No. 5, September/October 1995.
PB96-145925 *01,116*

Journal of Physical and Chemical Reference Data, Volume 24, No. 6, November/December 1995.
PB96-145966 *01,120*

GALLAGHER, K. B.
Assessing Functional Diversity by Program Slicing.
PB96-160890 *03,734*

Software Safety and Program Slicing.
PB95-125894 *01,703*

Unravel: A CASE Tool to Assist Evaluation of High Integrity Software. Volume 1. Requirements and Design.
PB95-267886 *01,736*

Unravel: A CASE Tool to Assist Evaluation of High Integrity Software. Volume 2. User Manual.
PB95-267894 *01,737*

GALLAGHER, L.
Database Management Standards: Status and Applicability.
PB96-122924 *01,819*

GALLAGHER, L. J.
Object SQL: Language Extensions for Object Data Management.
PB95-125902 *01,704*

GALLAGHER, M. D.
Annealing of Bragg Gratings in Hydrogen-Loaded Optical Fiber.
PB96-155437 *04,361*

GALLAGHER, P. D.
Diffraction of Neutron Standing Waves in Thin Films with Resonance Enhancement.
PB97-113278 *04,164*

Grazing Incidence Prompt Gamma Emissions and Resonance-Enhanced Neutron Standing Waves in a Thin-Film.
PB95-150470 *03,892*

Observed Frustration in Confined Block Copolymers.
PB95-150033 *01,238*

GALLAS, M. R.

Bulk Modulus and Young's Modulus of Nanocrystalline gamma-Alumina.
PB96-204185 *03,092*

Fabrication of Transparent gamma-Al2O3 from Nanosize Particles.
PB95-175493 *03,054*

GALLAWA, R. L.

Accuracy of Eigenvalues: A Comparison of Two Methods.
PB95-126249 *03,413*

Anharmonic Oscillator Analysis Using Modified Airy Functions.
PB94-185311 *03,798*

Approximate Solution to the Scalar Wave Equation for Optical Waveguides.
PB95-126256 *04,254*

Bending-Induced Loss in Dual-Mode Rectangular Waveguides.
PB95-168795 *04,288*

Bending-Induced Phase Shifts in Dual-Mode Planar Optical Waveguides.
PB95-161329 *04,271*

Bent Rectangular Core Waveguides: An Accurate Perturbation Approach.
PB95-168803 *04,289*

Calculated Fiber Attenuation: A General Method Yielding Stationary Values.
PB95-175501 *04,298*

Complex Propagation Constants for Nonuniform Optical Waveguides: Calculations.
PB95-125910 *04,249*

Fiber Spot Size: A Simple Method of Calculation.
PB95-125936 *04,250*

Fibre Splice Loss: A Simple Method of Calculation.
PB95-175519 *04,299*

Improved Variational Analysis of Inhomogeneous Optical Waveguides Using Airy Functions.
PB95-168639 *04,285*

International Intercomparison of Detector Responsivity at 1300 and 1550 nm.
PB95-125928 *02,140*

International Intercomparison of Detector Responsivity at 1300 and 1550 nm.
PB95-126017 *02,141*

LP11-Mode Leakage Loss in Coated Depressed Clad Fibers.
PB95-141115 *02,145*

Modal Characteristics of Bent Dual Mode Planar Optical Waveguide.
PB95-180485 *04,311*

Modal Properties of Circular and Noncircular Optical Waveguides.
PB95-125944 *04,251*

Mode Coupling and Loss on Tapered Optical Waveguides.
PB95-168571 *04,282*

Modified Airy Function Method for the Analysis of Tunneling Problems in Optical Waveguides and Quantum Well Structures.
PB94-185824 *02,120*

Symbolic Programming with Series Expansions: Applications to Optical Waveguides.
PB95-168589 *04,283*

Vector and Quasi-Vector Solutions for Optical Waveguide Modes Using Efficient Galerkin's Method with Hermite-Gauss Basis Functions.
PB96-141197 *04,357*

GALLER, M. A.

Computer Simulations of Binder Removal from 2-D and 3-D Model Particulate Bodies.
PB97-121339 *00,418*

GALOWIN, L.

Laboratory Accreditation for Testing Energy Efficient Lighting.
PB96-122932 *00,270*

Proceedings of the Open Forum on Laboratory Accreditation at the National Institute of Standards and Technology, October 13, 1995.
PB96-210141 *02,686*

GALOWIN, L. S.

Efficiency of Electric Motors. National Voluntary Lab. Accreditation Program (NVLAP).
PB96-111174 *02,107*

National Voluntary Laboratory Accreditation Program: Carpet and Carpet Cushion.
PB95-155560 *00,295*

National Voluntary Laboratory Accreditation Program: Energy Efficient Lighting Products.
PB94-219060 *02,642*

National Voluntary Laboratory Accreditation Program (NVLAP): Wood Based Products.
PB95-170429 *03,405*

Water Efficient Plumbing Fixtures through Standards and Test Methods.
PB95-125951 *00,248*

GALT, D.

Characterization of a Tunable Thin Film Microwave YBa2Cu3O7-x/SrTiO3 Coplanar Capacitor.
PB95-175527 *02,264*

Dielectric Properties of Thin Film SrTiO3 Grown on LaAlO3 with YBa2Cu3O7-x Electodes.
PB95-181160 *02,267*

Ferroelectric Thin Film Characterization Using Superconducting Microstrip Resonators.
PB96-102389 *02,270*

Tunable High Temperature Superconductor Microstrip Resonators.
PB95-168423 *02,048*

GALVAO, G. P.

Far Infrared Laser Frequencies of CH3OD and N2H4.
PB96-119623 *04,341*

Far Infrared Laser Frequencies of (13)CD3OH.
PB95-169363 *04,292*

GAMMON, R. W.

Binary versus Decade Inductive Voltage Divider Comparison and Error Decomposition.
PB96-112263 *02,071*

Inductive Voltage Divider Calibration for the NASA Flight Experiment.
PB95-152856 *02,042*

Susceptibility Critical Exponent for a Nonaqueous Ionic Binary Mixture Near a Consolute Point.
PB95-152112 *00,938*

GANGOPADHYAY, A.

Control of Friction and Wear of Alpha-Alumina with a Composite Solid-Lubricant Coating.
PB95-125969 *03,225*

GANGULI, B.

Kinetics and Mechanism of the Collision-Activated Dissociation of the Acetone Cation.
PB94-216462 *00,859*

GANN, R.

Agent Screening for Halon 1301 Aviation Replacement.
PB96-159710 *03,282*

GANN, R. G.

Effect of Fuel Tank Rupture Mode on the Ignitability of Expelled Fuel.
PB97-110043 *01,444*

Evaluation of Alternative In-Flight Fire Suppressants for Full-Scale Testing in Simulated Aircraft Engine Nacelles and Dry Bays.
PB94-203403 *00,023*

Fire Suppression System Performance of Alternative Agents in Aircraft Engine and Dry Bay Laboratory Simulations. SP890: Volume 1.
PB96-117775 *03,277*

Fire Suppression System Performance of Alternative Agents in Aircraft Engine and Dry Bay Laboratory Simulations. SP 890: Volume 2.
PB96-117783 *03,278*

Flame Retardants - Overview.
PB94-185287 *01,363*

Innovation in the Japanese Construction Industry: A 1995 Appraisal.
PB96-177373 *00,225*

Materials and Fire Threat.
PB97-122311 *01,442*

NIST Research on Less-Flammable Materials.
PB97-118632 *01,439*

Quantifying the Ignition Propensity of Cigarettes.
PB96-155411 *00,306*

Relating Bench-Scale and Full-Scale Toxicity Data.
PB95-125977 *00,361*

GAO, B.

Variationally Stable Treatment of Two- and Three-Photon Detachment of H(-) Including Electron-Correlation Effects.
PB95-202867 *03,992*

GARBOCZI, E.

Digitized Simulation of Mercury Intrusion Porosimetry.
PB94-172236 *01,304*

Percolation and Pore Structure in Mortars and Concrete.
PB95-150439 *00,370*

GARBOCZI, E. J.

Application of Digital-Image-Based Models to Microstructure, Transport Properties, and Degradation of Cement-Based Materials.
PB96-156161 *00,406*

Cellular Automaton Simulations of Cement Hydration and Microstructure Development.
PB95-175055 *01,320*

Computer Simulation of the Diffusivity of Cement-Based Materials.
PB95-125985 *00,362*

Cross-Property Relations and Permeability Estimation in Model Porous Media.
PB95-150280 *04,205*

Diffusion Studies in a Digital-Image-Based Cement Paste Microstructural Model.
PB94-198801 *01,312*

Digital Simulation of the Aggregate-Cement Paste Interfacial Zone in Concrete.
PB95-125993 *00,363*

Digitized Direct Simulation Model of the Microstructural Development of Cement Paste.
PB94-198777 *01,309*

Digitized Simulation Model for Microstructural Development.
PB94-198785 *01,310*

Elastic Properties of Central-Force Networks with Bond-Length Mismatch.
PB95-163366 *04,623*

Fundamental Computer Simulation Models for Cement-Based Materials.
PB95-126009 *00,364*

Geometrical Percolation Threshold of Overlapping Ellipsoids.
PB96-102397 *03,167*

Interfacial Transport in Porous Media: Application to dc Electrical Conductivity of Mortars.
PB96-146816 *01,326*

Intrinsic Conductivity of Objects Having Arbitrary Shape and Conductivity.
PB97-111934 *04,150*

Intrinsic Viscosity and the Polarizability of Particles Having a Wide Range of Shapes.
PB96-119318 *03,170*

Modelling Drying Shrinkage of Cement Paste and Mortar. Part 1. Structural Models from Angstroms to Millimeters.
PB96-135132 *03,074*

Modelling the Leaching of Calcium Hydroxide from Cement Paste: Effects on Pore Space Percolation and Diffusivity.
PB94-198793 *01,311*

Multi-Scale Picture of Concrete and Its Transport Properties: Introduction for Non-Cement Researchers.
PB97-115802 *03,107*

Water Permeability and Chloride Ion Diffusion in Portland Cement Mortars: Relationship to Sand Content and Critical Pore Diameter.
PB96-148036 *03,193*

GARCIA-TORANO, E.

Standardization and Decay Scheme of Rhenium-186.
PB94-200490 *03,830*

GARDENER, J. L.

International Intercomparison of Detector Responsivity at 1300 and 1550 nm.
PB95-125928 *02,140*

International Intercomparison of Detector Responsivity at 1300 and 1550 nm.
PB95-126017 *02,141*

GARGUILO, J. J.

Guidelines for the Evaluation of Electronic Data Interchange Products.
PB96-172325 *01,506*

GARMER, D.

Active Site Ionicity and the Mechanism of Carbonic Anhydrase.
PB94-212974 *00,843*

GARRETSON, S. P.

Learning to Change: Opportunities to Improve the Performance of Smaller Manufacturers.
PB94-166212 *00,010*

GARRETT, J. H.

Development of Computer-Based Models of Standards and Attendant Knowledge-Base and Procedural Systems.
PB96-155783 *00,464*

Distributed Architecture for Standards Processing.
PB96-164181 *00,276*

GARRIS, M. D.

Analysis of a Biologically Motivated Neural Network for Character Recognition.
PB94-172277 *00,182*

Component-Based Handprint Segmentation Using Adaptive Writing Style Model.
PB96-193669 *01,859*

Evaluating Form Designs for Optical Character Recognition.
PB94-168044 *01,830*

Generalized Form Registration Using Structure-Based Techniques.
PB96-191374 *01,858*

Method and Evaluation of Character Stroke Preservation on Handprint Recognition.
PB95-251724 *01,850*

NIST Form-Based Handprint Recognition System.
PB94-217106 *01,838*

Self-Organizing Neural Network Character Recognition on a Massively Parallel Computer.
PB95-163994 *01,845*

Self-Organizing Neural Network Character Recognition Using Adaptive Filtering and Feature Extraction.
PB96-119797 *01,855*

Unconstrained Handprint Recognition Using a Limited Lexicon.
PB94-168051 *01,831*

GARSCADDEN, A.

Gaseous Electronics Conference Radio-Frequency Reference Cell: A Defined Parallel-Plate Radio-Frequency Sys-

tem for Experimental and Theoretical Studies of Plasma-Processing Discharges.
PB94-172327 04,404

GARSON, L. R.

Electronic Publishing and the Journals of the American Chemical Society.
PB97-109185 04,807

GARVEY, M.

Precision Oscillators: Dependence of Frequency on Temperature, Humidity and Pressure.
PB94-198306 02,031

GARY, D.

Rotational Modulation and Flares on RS Canum Venaticorum and BY Draconis Stars. XVI. IUE Spectroscopy and VLA Observations of C1182(=V 1005 Orionis) in October 1983.
PB94-185626 00,050

GARY, J.

Accurate Computations of Radar Cross Sections of Simple Objects.
PB96-138474 04,426

Graded and Nongraded Regenerator Performance.
PB95-169090 02,753

GARY, J. M.

Technique to Evaluate Benchmarks: A Case Study Using the Livermore Loops.
PB95-151320 04,577

GASS, S. I.

Development and Validation of Multicriteria Ratings: A Case Study.
PB95-126025 00,004

GATES, B. C.

Characterization of the Interaction of Hydrogen with Iridium Clusters in Zeolites by Inelastic Neutron Scattering Spectroscopy.
PB95-180741 01,013

GATES, R. S.

Boundary Lubrication of Silicon Nitride.
PB95-213583 03,226

Silicon Nitride Boundary Lubrication: Effect of Oxygenates.
PB96-111711 03,068

Silicon Nitride Boundary Lubrication: Lubrication Mechanism of Alcohols.
PB96-111703 03,067

GAVIN, R. J.

Portsmouth Fastener Manufacturing Workstation. User's Manual.
PB95-147922 02,860

GAVRIN, A.

Domain Structures in Magnetoresistive Granular Metals.
PB96-141346 04,760

Nanostructure Fabrication via Direct Writing with Atoms Focused in Laser Fields.
PB95-150272 04,564

GAYLE, F. W.

Inelastic Neutron Scattering Measurements of Phonons in Icosahedral Al-Li-Cu.
PB95-126215 04,532

Nature of (001) Tilt Grain Boundaries in YBa2Cu3O6+x.
PB95-126033 04,528

Temperature Dependence of Vortex Twin Boundary Interaction in Yttrium Barium Copper Oxide (YBa2Cu3O6+x).
PB95-162442 04,613

X-Ray-Diffraction Study of a Thermomechanically Detwinned Single Crystal of YBa2Cu3O6+x.
PB95-151726 04,581

GAYLEY, K.

Goddard High-Resolution Spectrograph Observations of the Local Interstellar Medium and the Deuterium/Hydrogen Ratio along the Line of Sight Toward Capella.
PB94-213444 00,066

GAYLEY, K. G.

Hydrogen Lyman-alpha Emission of Capella.
PB95-202263 00,075

GEBASE, L.

Analyzing Electronic Commerce.
PB94-219102 00,480

GEBBIE, K. B.

Physics Laboratory Technical Activities, 1993.
PB94-176088 03,796

GEHRING, P. M.

Anomalous Dispersion and Thermal Expansion in Lightly-Doped KTa1-xNbxO3.
PB95-152302 04,585

Antiferromagnetic Interlayer Correlations in Annealed Ni80Fe20/Ag Multilayers.
PB97-122220 03,109

Design of a High-Flux Backscattering Spectrometer for Ultra-High Resolution Inelastic Neutron Measurements.
PB96-179577 02,992

High-Energy Phonon Dispersion in La1.85Sr0.15CuO4.
PB96-138458 04,748

Low-Frequency Excitations of Oriented DNA.
PB96-137799 03,548

Magnetic Structure Determination for Annealed Ni80Fe20/Ag Multilayers Using Polarized-Neutron Reflectivity.
PB96-176615 03,739

Neutron-Scattering Studies of the Two Magnetic Correlation Lengths in Terbium.
PB95-152328 04,586

Neutron Scattering Study of the Lattice Modes of Solid Cubane.
PB96-147152 01,126

Observation of Two Length Scales Above (T sub N) in a Holmium Thin Film.
PB97-111942 04,151

Origin of the Second Length Scale Above the Magnetic Spiral Phase of Tb.
PB95-153698 04,596

GEIST, J.

NIST Form-Based Handprint Recognition System.
PB94-217106 01,838

Second Census Optical Character Recognition Systems Conference.
PB94-188711 01,832

GELBIN, A.

Nucleic Acid Database: Present and Future.
PB97-109078 00,518

GENIS, A.

Effect of Anneal Temperature on Si/Buried Oxide Interface Roughness on SIMOX.
PB96-112206 02,382

GENTILE, T. R.

Absolute Response Calibration of a Transfer Standard Cryogenic Bolometer.
PB96-147103 04,358

Mode-Locked Lasers for High-Accuracy Radiometry.
PB96-204201 04,134

National Institute of Standards and Technology High-Accuracy Cryogenic Radiometer.
PB96-179585 04,378

Realization of a Scale of Absolute Spectral Response Using the NIST High Accuracy Cryogenic Radiometer.
PB97-118640 04,397

GENTRY, J. W.

Generation and Characterization of Acetylene Smokes.
PB94-200292 01,372

Measurement of the Uniformity of Particle Deposition of Filter Cassette Sampling in a Low Velocity Wind Tunnel.
PB95-163754 02,549

Ultrafine Combustion Aerosol Generator.
PB94-200300 01,373

GEORG, E.

Report on the Workshop on Advanced Digital Video in the National Information Infrastructure. Held in Washington, D.C. on May 10-11, 1994.
PB95-103677 01,472

Summary Report on the Workshop on Advanced Digital Video in the National Information Infrastructure.
PB96-141320 01,497

GEORGE, L. A.

Dental Applications of Ceramics.
PB96-122940 00,177

Dental Materials.
PB94-172871 00,142

Paffenbarger Research Center: The Cutting Edge of Dental Science.
PB94-216355 00,151

Reduction of Marginal Gaps in Composite Restorations by Use of Glass-Ceramic Inserts.
PB96-102405 00,174

Surface Roughness of Glass-Ceramic Insert. Composite Restorations: Assessing Several Polishing Techniques.
PB97-119010 03,583

Wear of Enamel against Glass-Ceramic, Porcelain, and Amalgam.
PB96-179593 03,082

GEORGE, T.

Optically Stabilized Tunable Diode-Laser System for Saturation Spectroscopy.
PB96-102819 04,717

GERARDO, J. B.

Gaseous Electronics Conference Radio-Frequency Reference Cell: A Defined Parallel-Plate Radio-Frequency System for Experimental and Theoretical Studies of Plasma-Processing Discharges.
PB94-172327 04,404

GERBER, G.

Femtosecond Time-Resolved Molecular Multiphoton Ionization: The Na2 System.
PB95-202305 03,975

Femtosecond Time-Resolved Wave Packet Motion in Molecular Multiphoton Ionization and Fragmentation.
PB94-198611 00,790

Photoelectron Spectroscopy of Negatively Charged Bismuth Clusters: Bi(-)2, Bi(-)3, and Bi(-)4.
PB95-108494 00,880

Photoelectron Spectroscopy of Small Antimony Cluster Anions: Sb(-), Sb2(-), Sb3(-), and Sb4(-).
PB95-203139 01,045

GERHARDT, R.

Imaging of Fine Porosity in a Colloidal Silica: Potassium Silicate Gel by Defocus Contrast Microscopy.
PB94-212750 03,039

GERHARDT, R. A.

Small-Angle Neutron Scattering Characterization of Processing/Microstructure Relationships in the Sintering of Crystalline and Glassy Ceramics. (Reannouncement with New Availability Information).
AD-A249 510/9 03,025

GERMER, T. A.

Hot Carrier Excitation of Adlayers: Time-Resolved Measurement of Adsorbate-Lattice Coupling.
PB94-172285 00,758

Picosecond Measurement of Substrate-to-Adsorbate Energy Transfer: The Frustrated Translation of CO/Pt(111)--Translation.
PB95-126041 00,895

Specular and Diffuse Reflection Measurements of Electronic Displays.
PB97-119200 02,208

Ultrafast Time-Resolved Infrared Probing of Energy Transfer at Surfaces.
PB96-123443 00,620

GERZ, C.

Frequency-Stabilized LNA Laser at 1.083 mum: Application to the Manipulation of Helium 4 Atoms.
PB95-176186 04,304

Temperature of Optical Molasses for Two Different Atomic Angular Momenta.
PB95-126058 03,881

GETTINGS, R. J.

Tensile Creep of Silicide Composites.
PB96-200803 03,183

GEYER, R. G.

Analysis of an Open-Ended Coaxial Probe with Lift-Off for Nondestructive Testing.
PB96-135116 01,940

Applicability of Effective Medium Theory to Ferroelectric/Ferrimagnetic Composites with Composition and Frequency-Dependent Complex Permittivities and Permeabilities.
PB96-157854 01,945

Dielectric Properties of Materials at Cryogenic Temperatures and Microwave Frequencies.
PB95-202610 02,369

Dielectric Properties of Single Crystals of Al2O3, LaAlO3, SrTiO3, and MgO at Cryogenic Temperatures.
PB95-180477 02,266

Effective Medium Theory for Ferrite-Loaded Materials.
PB95-154662 01,893

Influence of Films' Thickness and Air Gaps in Surface Impedance Measurements of High Temperature Superconductors Using the Dielectric Resonator Technique.
PB96-157862 01,946

Measurements of Permittivity and the Dielectric Loss Tangent of Low Loss Dielectric Materials with a Dielectric Resonator Operating on the Higher Order Te(sub 0 gamma delta) Modes.
PB96-111869 02,273

Microwave Dielectric Properties of Anisotropic Materials at Cryogenic Temperatures.
PB96-137765 02,412

NIST 60-Millimeter Diameter Cylindrical Cavity Resonator: Performance Evaluation for Permittivity Measurements.
PB94-151776 02,251

Preparation, Crystal Structure, Dielectric Properties, and Magnetic Behavior of Ba2Fe2Ti4O13.
PB96-186176 01,162

Transmission/Reflection and Short-Circuit Line Methods for Measuring Permittivity and Permeability.
PB94-165537 02,211

GHATAK, A. K.

Accuracy of Eigenvalues: A Comparison of Two Methods.
PB95-126249 03,413

Anharmonic Oscillator Analysis Using Modified Airy Functions.
PB94-185311 03,798

Approximate Solution to the Scalar Wave Equation for Optical Waveguides.
PB95-126256 04,254

Calculated Fiber Attenuation: A General Method Yielding Stationary Values.
PB95-175501 04,298

Fiber Spot Size: A Simple Method of Calculation.
PB95-125936 04,250

Improved Variational Analysis of Inhomogeneous Optical Waveguides Using Airy Functions.
PB95-168639 04,285

Modal Properties of Circular and Noncircular Optical Waveguides.
PB95-125944 04,251

Modified Airy Function Method for the Analysis of Tunneling Problems in Optical Waveguides and Quantum Well Structures.
PB94-185824 02,120

GHEZZO, M.

Boron-Implanted 6H-SiC Diodes.
PB96-159678 04,081

GHONIEM, A.
Smoke Emission from Burning Crude Oil.
PB96-122890 *01,407*

GHONIEM, A. F.
Computational Model for the Rise and Dispersion of Wind-Blown, Buoyancy-Driven Plumes. Part 2. Linearly Stratified Atmosphere.
PB94-143427 *00,119*

Dispersion and Deposition of Smoke Plumes Generated in Massive Fires.
PB95-126066 *02,540*

GHOSH, R. N.
Cryogenic Precision Capacitance Bridge Using a Single Electron Tunneling Electrometer.
PB95-126074 *04,529*

Cryogenic Precision Capacitance Bridge Using a Single Electron Tunneling Electrometer.
PB95-152310 *02,040*

Cryogenic Precision Capacitance Bridge Using a Single Electron Tunneling Electrometer.
PB96-112271 *02,072*

GHOSHTAGORE, R. N.
Electrical Test Structures Replicated in Silicon-on-Insulator Material.
PB97-111827 *02,454*

Measurement of Patterned Film Linewidth for Interconnect Characterization.
PB96-148168 *02,420*

GIACOMETTI, J. A.
Thermal Pulse Study of the Polarization Distributions Produced in Polyvinylidene Fluoride by Corona Poling at Constant Current.
PB94-172293 *01,195*

GIAMPAPA, M. S.
Relationship between Radiative and Magnetic Fluxes for Three Active Solar-Type Dwarfs.
PB96-119540 *00,097*

GIARRATANO, P. J.
Experimental plan to determine the performance of the Oak Ridge National Laboratory Cold Neutron Moderator. Final report, September 1, 1993--November 30, 1993.
DE95011352 *03,778*

GIBBS, D.
Observation of Two Length Scales Above (T sub N) in a Holmium Thin Film.
PB97-111942 *04,151*

GIBSON, C.
Intercomparison of the ITS-90 Radiance Temperature Scales of the National Physical Laboratory (U.K.) and the National Institute of Standards and Technology.
PB96-113550 *02,674*

GIBSON, C. E.
Results of a NIST/VNIIOFI Comparison of Spectral-Radiance Measurements.
PB97-113021 *04,159*

GIBSON, D. M.
Rotational Modulation and Flares on RS Canum Venaticorum and BY Draconis Stars. XVI. IUE Spectroscopy and VLA Observations of C1182(=V 1005 Orionis) in October 1983.
PB94-185626 *00,050*

GIBSON, K. A.
Bibliography of the NIST Electromagnetic Fields Division Publications.
PB94-165990 *01,875*

Bibliography of the NIST Electromagnetic Fields Division Publications.
PB95-135562 *01,886*

GIER, T. E.
Structural and Chemical Investigations of Na3(ABO4)3.4H2O-Type Sodalite Phases.
PB95-180733 *01,012*

Tetrahedral-Framework Lithium Zinc Phosphate Phases: Location of Light-Atom Positions in LiZnPO4 H2O by Powder Neutron Diffraction and Structure Determination of LiZnPO4 by ab Initio Methods.
PB96-160510 *01,129*

GIFFORD, A.
Photodetector Frequency Response Measurements at NIST, US, and NPL, UK: Preliminary Results of a Standards Laboratory Comparison.
PB95-175592 *02,175*

GIFFORD, A. D.
Comparison of Photodiode Frequency Response Measurements to 40 GHz between NPL and NIST.
PB96-111992 *04,038*

GILBERT, D. M.
Study of Federal Agency Needs for Information Technology Security.
PB94-193653 *01,579*

GILBERT, M.
Group 1 for the Process Engineering Data STEP Application Protocol.
PB97-116073 *02,797*

GILBERT, S.
Comparison of UV Photosensitivity and Fluorescence during Fiber Grating Formation.
PB96-155445 *04,362*

Inexpensive Laser Cooling and Trapping Experiment for Undergraduate Laboratories.
PB96-140371 *04,353*

GILBERT, S. L.
Annealing of Bragg Gratings in Hydrogen-Loaded Optical Fiber.
PB96-155437 *04,361*

Bragg Gratings in Optical Fibers Produced by a Continuous-Wave Ultraviolet Source.
PB95-162020 *04,274*

Comparison of UV-Induced Fluorescence and Bragg Grating Growth in Optical Fiber.
PB95-168597 *04,284*

Decay of Bragg Gratings in Hydrogen-Loaded Optical Fibers.
PB96-122643 *04,345*

Decrease of Fluorescence in Optical Fiber during Exposure to Pulsed or Continuous-Wave Ultraviolet Light.
PB95-203071 *04,320*

Electronically Tunable Fiber Laser for Optical Pumping of (3)He and (4)He.
PB96-201165 *04,381*

Frequency Stabilization of a Fiber Laser to Rubidium: A High-Accuracy 1.53 mu m Wavelength Standard.
PB95-126082 *04,252*

Growth Characteristics of Fiber Gratings.
PB96-122957 *04,346*

Growth of Bragg Gratings Produced by Continuous-Wave Ultraviolet Light in Optical Fiber.
PB95-162038 *04,275*

High-Resolution Spectroscopy of Laser-Cooled Rubidium in a Vapor-Cell Trap.
PB95-153714 *04,268*

Laser Cooling and Trapping for the Masses.
PB95-126090 *04,253*

Liquid and Solid Atomic Ion Plasmas.
PB94-198991 *03,809*

Optical Probing of Cold Trapped Atoms.
PB95-175469 *04,296*

GILES, N. C.
Comparison of Techniques for Nondestructive Composition Measurements in CdZnTe Substrates.
PB96-103098 *02,703*

GILLASPY, J. D.
Beam Line for Highly Charged Ions.
PB97-111256 *04,143*

Isotope Shifts and Hyperfine Splittings of the 398.8-nm Yb I Line.
PB94-199585 *03,814*

Microlithography by Using Neutral Metastable Atoms and Self-Assembled Monolayers.
PB96-190038 *02,441*

Observation and Visible and uv Magnetic Dipole Transitions in Highly Charged Xenon and Barium.
PB96-138441 *04,056*

Polarization Measurements on a Magnetic Quadrupole Line in Ne-Like Barium.
PB97-113104 *04,161*

Search for Small Violations of the Symmetrization Postulate in an Excited State of Helium.
PB96-123518 *04,050*

Visible and UV Light from Highly Charged Ions: Exotic Matter Advancing Technology.
PB96-119391 *04,414*

GILLEN, G.
Image Depth Profiling SIMS: An Evaluation for the Analysis of Light Element Diffusion in YBa2Cu3O7-x Single Crystal Superconductors.
PB95-126116 *04,530*

Molecular Ion Imaging and Dynamic Secondary Ion Mass Spectrometry of Organic Compounds.
PB95-126124 *00,571*

Use of Kinetic Energy Distributions to Determine the Relative Contributions of Gas Phase and Surface Fragmentation in KeV Ion Sputtering of a Quaternary Ammonium Salt.
PB95-126108 *00,570*

GILLEN, J. G.
Epitaxial Growth of BaTiO3 Thin Films at 600C by Metalorganic Chemical Vapor Deposition.
PB96-122510 *03,071*

UV-Photopatterning of Alkylthiolate Monolayers Self-Assembled on Gold and Silver.
PB95-150751 *00,924*

GILLESPIE, A.
Measurement and Reduction of Alignment Errors of the NIST Watt Experiment.
PB97-111959 *01,987*

NIST Watt Balance: Progress Toward Monitoring the Kilogram.
PB97-113062 *01,991*

NIST Watt Experiment: Monitoring the Kilogram.
PB97-122329 *01,997*

GILLIAM, D.
Preparation and Characterization of (6)LiF and (10)B Reference Deposits for the Measurement of the Neutron Lifetime.
PB95-108692 *03,874*

GILLIAM, D. M.
Mass Assay and Uniformity Test of Boron Targets by Neutron Beam Methods.
PB97-119085 *04,175*

Measurement of the Neutron Lifetime.
PB96-161708 *04,094*

Neutron Leakage Benchmark for Criticality Safety Research.
PB95-126132 *03,723*

Problems Related to the Determination of Mass Densities of Evaporated Reference Deposits.
PB95-163226 *03,941*

GILLIAND, G. L.
Crystal Packing Interactions of Two Different Crystal Forms of Bovine Ribonuclease A.
PB95-152823 *00,943*

GILLIES, C. W.
Rotational Spectrum and Structure of a Weakly Bound Complex of Ketene and Acetylene.
PB95-126140 *00,896*

GILLIES, J. Z.
Rotational Spectrum and Structure of a Weakly Bound Complex of Ketene and Acetylene.
PB95-126140 *00,896*

GILLIGAN, J. M.
High-Resolution Atomic Spectroscopy of Laser-Cooled Ions.
PB95-169330 *03,953*

Interference in the Resonance Fluorescence of Two Trapped Atoms.
PB95-168514 *03,948*

Light Scattered from Two Atoms.
PB95-168753 *04,286*

Precise Spectroscopy for Fundamental Physics.
PB96-112164 *04,040*

Quantum Measurements of Trapped Ions.
PB95-161147 *03,928*

Quantum Projection Noise: Population Fluctuations in Two-Level Systems.
PB94-212271 *03,850*

Recent Experiments on Trapped Ions at the National Institute of Standards and Technology.
PB95-169322 *03,952*

Using Archie to Find Files on the INTERNET.
PB95-168605 *02,727*

GILLILAND, D.
Catalogue of Electromagnetic Environment Measurements, 30-300 Hz.
PB96-155452 *01,943*

Condensed Catalogue of Electromagnetic Environment Measurements, 30 - 300 Hz.
PB95-162210 *01,899*

GILLILAND, G.
Positive and Negative Cooperativities at Subsequent Steps of Oxygenation Regulate the Allosteric Behavior of Multistate Sebacylhemoglobin.
PB97-119374 *03,486*

GILLILAND, G. L.
Biological Macromolecular Crystallization Database: A Tool for Developing Crystallization Strategies.
PB95-126157 *00,897*

Biological Macromolecule Crystallization Database and NASA Protein Crystal Growth Archive.
PB97-109136 *01,171*

GILLILAND, R. J.
Observations of 3C 273 with the Goddard High Resolution Spectrograph on the Hubble Space Telescope.
PB95-202321 *00,076*

GILLIS, K. A.
All-Metal Collection System for Preparative-Scale Gas Chromatography: Purification of Low-Boiling-Point Compounds.
PB96-123435 *00,619*

Greenspan Acoustic Viscometer for Gases.
PB96-204417 *04,220*

Properties of Working Fluids for Thermoacoustic Refrigerators.
AD-A297 420/2 *04,864*

Thermodynamic Properties of CF3-CHF-CHF2, 1,1,1,2,3,3-Hexafluoropropane.
PB97-118384 *03,299*

Thermodynamic Properties of CHF2-CF2-CHF, 1,1,2,2,3-Pentafluoropropane.
PB97-118392 *03,300*

Thermodynamic Properties of CHF2-O-CHF2,Bis(difluoromethyl) Ether.
PB94-199569 *00,798*

Thermodynamic Properties of Two Gaseous Halogenated Ethers from Speed-of-Sound Measurements: Difluoromethoxy-Difluoromethane and 2-Difluoromethoxy-1,1,1-Trifluoroethane.
PB96-102413 *04,189*

GILLS, T. E.
Certification, Development and Use of Standard Reference Materials.
PB95-107272 *00,567*

Certifying the Chemical Composition of a Biological Material: A Case Study.
PB96-164272 *00,636*

Recent Developments in NIST Botanical SRMs.
PB96-167267 *03,489*

GILSINN, D. E.

Comparison of Finite Element and Analytic Calculations of the Resonant Modes and Frequencies of a Thick Shell Sphere.
PB94-160785 *02,626*

Compensation of Errors Detected by Process-Intermittent Gauging.
PB97-110472 *02,846*

Constructing Invariant Tori for Two Weakly Coupled van der Pol Oscillators.
PB95-126165 *03,412*

Data Management for Error Compensation and Process Control.
PB97-110480 *02,847*

PIECS: A Software Program for Machine Tool Process-Intermittent Error Compensation.
PB96-165980 *02,842*

Prediction of Geometric-Thermal Machine Tool Errors by Artificial Neural Networks.
PB94-186673 *02,943*

GINGOLD, D.

Diffusion Studies in a Digital-Image-Based Cement Paste Microstructural Model.
PB94-198801 *01,312*

GINLEY, R. A.

NIST 30 MHz Linear Measurement System.
PB94-169752 *02,020*

GINZBURG, A.

Image Information Transfer Properties of X-Ray Intensifying Screens in the Energy Range from 17 to 320 keV.
PB95-126173 *00,155*

Study of Multiple Scattering Background in Compton Scatter Imaging.
PB96-112222 *04,425*

GINZBURG, V. L.

From Superconductivity to Supernovae: The Ginzburg Symposium. Report on the Symposium Held in Honor of Vitaly L. Ginzburg. Held in Gaithersburg, Maryland on May 22, 1992.
PB95-171963 *04,649*

GIRARD, J. E.

Comparison of Selectivities for PCBs in Gas Chromatography for a Series of Cyanobiphenyl Stationary Phases.
PB96-119458 *00,618*

Enhanced Detection of PCR Products Through Use of TOTO and YOYO Intercalating Dyes with Laser Induced Fluorescence - Capillary Electrophoresis.
PB95-164653 *00,599*

Quantitative Analysis of Selected PCB Congeners in Marine Matrix Reference Materials Using a Novel Cyanobiphenyl Stationary Phase.
PB96-111737 *02,591*

GIVEN, J. A.

Critical Behavior of Ionic Fluids.
PB95-164331 *00,978*

Critical Lines for Type-III Aqueous Mixtures by Generalized Corresponding-States Models.
PB96-102371 *01,063*

GJERTSON, W.

Catalogue of Electromagnetic Environment Measurements, 30-300 Hz.
PB96-155452 *01,943*

Condensed Catalogue of Electromagnetic Environment Measurements, 30 - 300 Hz.
PB95-162210 *01,899*

GLADHILL, R. L.

Program Handbook: Requirements for Obtaining NIST Approval/Recognition of a Laboratory Accreditation Body Under P.L. 101-592. The Fastener Quality Act.
PB94-210143 *02,859*

GLASER, M. A.

Shear-Induced Melting of Two-Dimensional Solids.
PB96-112057 *01,075*

GLASER, S. D.

Estimation of System Damping at the Lotung Site by Application of System Identification.
PB96-214697 *01,351*

Preliminary Processing of the Lotung LSST Data.
PB96-165972 *03,690*

GLAZE, D. J.

Error Analysis of the NIST Optically Pumped Primary Frequency Standard.
PB95-153482 *01,535*

NIST Optically Pumped Cesium Frequency Standard.
PB94-211117 *03,835*

NIST-7, the New US Primary Frequency Standard.
PB95-153458 *01,534*

GLAZIER, S. A.

Amperometric Flow-Injection Analysis Biosensor for Glucose Based on Graphite Paste Modified with Tetracyanoquinodimethane.
PB95-161980 *03,498*

Autofluorescence Detection of 'Escherichia coli' on Silver Membrane Filters.
PB96-163639 *03,590*

Bacterial Enumeration in Storage Water.
PB96-163647 *03,591*

Feasibility of Fluorescence Detection of Tetracycline in Media Mixtures Employing a Fiber Optic Probe.
PB96-163654 *00,511*

Fluorescence Measurements of Tetracycline in High Cell Mass for Fermentation Monitoring.
PB95-175709 *00,601*

In situ Fluorescence Cell Mass Measurements of 'Saccharomyces cerevisiae' Using Cellular Tryptophan.
PB96-135041 *03,547*

Novel Amperometric Immunosensor for Procainamide Employing Light Activated Labels.
PB96-163662 *00,512*

Optical Control of Enzymatic Conversion of Sucrose to Glucose by Bacteriorhodopsin Incorporated into Self-Assembled Phosphatidylcholine Vesicles.
PB96-123344 *03,477*

GLEITER, H.

Inelastic Neutron Scattering Study of Hydrogen in Nanocrystalline Pd.
PB96-146857 *03,366*

Vibrational Excitations and the Position of Hydrogen in Nanocrystalline Palladium.
PB96-111828 *04,035*

GLENN, K. R.

RDI-SIM ECMA Inter-Domain Routing Protocol Simulation Tool.
PB94-172301 *01,683*

GLENZER, S.

Investigation of LS Coupling in Boronlike Ions.
PB94-185295 *03,797*

GLICKSMAN, M. E.

Asymptotic Behavior of Modulated Taylor-Couette Flows with a Crystalline Inner Cylinder.
PB94-199072 *04,469*

Effect of Modulated Taylor-Couette Flows on Crystal-Melt Interfaces: Theory and Initial Experiments.
PB94-216736 *04,521*

GLIGOR, V.

Functional Security Criteria for Distributed Systems.
PB96-123492 *01,607*

Proceedings of the Workshop on the Federal Criteria for Information Technology Security. Held in Ellicot City, Maryland on June 2-3, 1993.
PB94-162583 *01,575*

GLINKA, C. J.

Analysis of SANS from Controlled Pore Glasses.
PB94-198843 *03,035*

Characterization of Chemically Modified Pore Surfaces by Small Angle Neutron Scattering.
PB95-126181 *00,898*

Small Angle Neutron Scattering Study of the Structure and Formation of MCM-41 Mesoporous Molecular Sieves.
PB97-122337 *03,110*

Small Angle Neutron Scattering Study of the Structure and Formation of Ordered Mesopores in Silica.
PB96-111919 *03,069*

GLOTZER, S. C.

Mixing Plate-Like and Rod-Like Molecules with Solvent: A Test of Flory-Huggins Lattice Statistics.
PB96-126206 *03,173*

GLOVER, M.

Suppression of Elevated Temperature Hydraulic Fluid and JP-8 Spray Flames.
PB95-181095 *00,021*

GMURCZYK, G.

Effectiveness of Halon Alternatives in Suppressing Dynamic Combustion Process.
PB96-175732 *03,288*

Inhibition of Premixed Methane-Air Flames by Iron Pentacarbonyl.
PB96-163712 *00,513*

Interaction of HFC-125, FC-218 and CF3I with High Speed Combustion Waves.
PB96-176417 *03,290*

Parametric Study of Hydrogen Fluoride Formation in Suppressed Fires.
PB96-163720 *00,514*

Suppression Effectiveness of Extinguishing Agents under Highly Dynamic Conditions.
PB95-180279 *00,020*

Suppression of High-Speed C2H4/Air Flames with C1-Halocarbons.
PB96-175724 *03,287*

Suppression of High Speed Turbulent Flames in a Detonation/Deflagration Tube.
PB95-231817 *01,395*

GOCKENBACH, E.

Digital Techniques in HV Tests - Summary of 1989 Panel Session.
PB94-216702 *02,035*

GODART, C.

Neutron Scattering Study of Antiferromagnetic Order in the Magnetic Superconductors RNi2B2C.
PB97-112411 *04,812*

GODEFROID, M.

Fundamental Torsion Band in Acetaldehyde.
PB94-212834 *00,840*

GOEHNER, R. P.

Phase Identification in a Scanning Electron Microscope Using Backscattered Electron Kikuchi Patterns.
PB97-109128 *04,804*

GOFORTH, T. L.

Low-Energy-Electron Collisions with Sodium: Elastic and Inelastic Scattering from the Ground State.
PB96-103106 *04,030*

GOLAND, A. N.

Anisotropy of the Surfaces of Pores in Plasma Sprayed Alumina Deposits.
PB96-123211 *03,126*

GOLAS, D. B.

Assay of the Eluent from the Alumina-Based Tungsten-188-Rhenium-188 Generator.
PB94-200482 *03,829*

Liquid-Scintillation Counting Techniques for the Standardization of Radionuclides Used in Therapy.
PB97-110084 *03,709*

Review of the USCEA/NIST Measurement Assurance Program for the Nuclear Power Industry.
PB95-126272 *03,712*

Standardization and Decay Scheme of Rhenium-186.
PB94-200490 *03,830*

USCEA/NIST Measurement Assurance Programs for the Radiopharmaceutical and Nuclear Power Industries.
PB97-110514 *03,721*

GOLDBERG, R. N.

Apparent Molar Heat Capacities and Apparent Molar Volumes of Aqueous Glucose at Temperatures from 298.15 K to 327.01 K.
PB94-212800 *03,459*

Application of Thermodynamics to Biotechnology.
PB95-150793 *03,529*

Calorimetric Determination of the Standard Transformed Enthalpy of a Biochemical Reaction at Specified PH and pMg.
PB94-198249 *03,454*

Conference Report: Calorimetry Conference (50th).
PB97-122279 *03,722*

Equilibrium and Calorimetric Investigation of the Hydrolysis of L-Tryptophan to (Indole + Pyruvate + Ammonia).
PB95-163317 *00,661*

Thermochemistry of the Hydrolysis of L-arginine to (L-citrulline + Ammonia) and of the Hydrolysis of L-arginine to (L-ornithine + Urea).
PB95-150801 *03,463*

Thermochemistry of the Reactions between Adenosine, Adenosine 5'-monophosphate, Inosine, and Inosine 5'-monophosphate; the Conversion of L-histidine to (Urocanic Acid+Ammonia).
PB94-213113 *03,460*

Thermodynamic and NMR Study of the Interactions of Cyclodextrins with Cyclohexane Derivatives.
PB94-185816 *00,781*

Thermodynamic Study of the Reactions of Cyclodextrins with Primary and Secondary Aliphatic Alcohols, with D- and L-Phenylalanine, and with L-Phenylalanineamide.
PB95-180873 *01,016*

Thermodynamics of Enzyme-Catalyzed Reactions: Part 1. Oxidoreductases.
PB94-162252 *00,737*

Thermodynamics of Enzyme-Catalyzed Reactions. Part 4. Lyases.
PB96-145941 *01,118*

Thermodynamics of Enzyme-Catalyzed Reactions. Part 5. Isomerases and Ligases.
PB96-145974 *01,121*

Thermodynamics of the Hydrolysis of N-Acetyl-L-phenylalanine Ethyl Ester in Water and in Organic Solvents.
PB95-203386 *01,053*

Thermodynamics of the Hydrolysis of Penicillin G and Ampicillin.
PB94-172467 *03,596*

Thermodynamics of the Hydrolysis of 3,4,5-Trihydroxybenzoic Acid Propyl Ester (n-Propylgallate) to 3,4,5-Trihydroxybenzoic Acid (Gallic Acid) and Propan-I-ol in Aqueous Media and in Toluene.
PB96-186143 *01,160*

GOLDEN, D. M.

International Conference on Chemical Kinetics (2nd). Held in Gaithersburg, Maryland on July 24-27, 1989.
PB94-211901 *00,822*

GOLDFARB, L.

Preferential In-Plane Rotational Excitation of H2O (001) by Translational-to-Vibrational Transfer from 2.2 eV H Atoms.
PB95-202875 *01,035*

GOLDFARB, R. B.

Alternating-Field Susceptometry and Magnetic Susceptibility of Supercondoctors. Presented at Office of Naval Research

Workshop on Magnetic Susceptibility of Superconductors and Other Spin Systems. Held in Berkeley Springs, West Virginia on 20 May 1991.
PB94-145984 *04,435*

Alternating-Field Susceptometry and Magnetic Susceptibility of Superconductors.
PB95-168613 *04,638*

Harmonic and Static Susceptibilities of YBa2Cu3O7.
PB95-161139 *04,599*

Magnetic Characteristics and Measurements of Filamentary Nb-Ti Wire for the Superconducting Super Collider.
DE94005988 *03,775*

Magnetic Measurement of Transport Critical Current Density of Granular Superconductors.
PB95-126199 *04,531*

Offset Susceptibility of Superconductors.
PB94-212263 *04,503*

Panel Discussion on Units in Magnetism.
PB96-137773 *04,746*

Preparation, Crystal Structure, Dielectric Properties, and Magnetic Behavior of Ba2Fe2Ti4O13.
PB96-186176 *01,162*

Reduction of Interfilament Contact Loss in Nb3Sn Superconductor Wires.
PB95-175535 *02,223*

Surface Barrier and Lower Critical Field in YBa2Cu3O7-delta Superconductors.
PB94-200128 *04,478*

Volume Magnetic Hysteresis Loss of Nb3Sn Superconductors as a Function of Wire Length.
PB95-153722 *04,597*

GOLDFIELD, E. M.

Quantum Dynamics of Renner-Teller Vibronic Coupling: The Predissociation HCO.
PB94-185303 *00,773*

GOLDFINE, A.

Compatibility Analysis of the ANSI and ISO IRDS Services Interfaces.
PB94-163474 *01,805*

Information Resource Dictionary System (IRDS): A Status Report.
PB95-126207 *01,810*

GOLDING, T. D.

Epitaxial Growth of Sb/GaSb Structures: An Example of V/III-V Heteroepitaxy.
PB95-202560 *04,693*

GOLDMAN, A. I.

Inelastic Neutron Scattering Measurements of Phonons in Icosahedral Al-Li-Cu.
PB95-126215 *04,532*

GOLDSTEIN, R. E.

Nonlinear Dynamics of Stiff Polymers.
PB96-122478 *01,278*

GOLMIE, N.

NIST ATM Network Simulator: Operation and Programming, Version 1.0.
PB96-106851 *01,487*

GOLOMB, G.

In vitro Inhibition of Membrane-Mediated Calcification by Novel Phosphonates.
PB96-201140 *03,595*

GOMAA, H.

Knowledge-Based Approach for Automating a Design Method for Concurrent and Real-Time Systems.
PB97-112502 *01,780*

GOMMERS-AMPT, J.

beta-D-Glucosyl-Hydroxymethyluracil: A Novel Modified Base Present in the DNA of the Parastic Protozoan T. brucei.
PB94-172319 *03,524*

GONZALEZ, E. J.

Low temperature fabrication from nano-size ceramic powders.
DE95013505 *03,029*

GONZALEZ, J. A.

Center for Electronics and Electrical Engineering Technical Progress Bulletin Covering Center Programs, October to December, with 1991 CEEE Events Calendar.
PB94-159787 *02,296*

Electronics and Electrical Engineering Laboratory Technical Progress Bulletin Covering Laboratory Programs, January to March 1991, with 1991 EEEL Events Calendar.
PB94-145968 *02,113*

Electronics and Electrical Engineering Laboratory Technical Progress Bulletin Covering Laboratory Programs, January to March 1992, with 1992/1993 EEEL Events Calendar.
PB95-210480 *01,917*

GOODMAN, A. A.

Magnetic Fields in Star-Forming Regions: Observations.
PB96-123005 *00,100*

GOODMAN, L. J.

Needs for Brachytherapy Source Calibrations in the United States.
PB97-110092 *03,521*

GOODRICH, L. F.

Anomalous Switching Phenomenon in Critical-Current Measurements When Using Conductive Mandrels.
PB96-137781 *02,233*

Comparing the Accuracy of Critical-Current Measurements Using the Voltage-Current Simulator.
PB96-119219 *02,227*

Critical Current Behavior of Ag-Coated YBa2Cu3O7-x Thin Films.
PB95-141016 *04,549*

Critical Current Density, Irreversibility Line, and Flux Creep Activation Energy in Silver-Sheathed Bi2Sr2Ca2Cu2Ox Superconducting Tapes.
PB95-162749 *04,616*

First VAMAS USA Interlaboratory Comparison of High Temperature Superconductor Critical Current Measurements.
PB96-147178 *04,768*

High Current Pressure Contacts to Ag Pads on Thin Film Superconductors.
PB95-168621 *04,639*

II-3: Critical Current Measurement Methods: Quantitative Evaluation.
PB96-147160 *04,767*

II-5: Thermal Contraction of Materials Used in Nb3Sn Critical Current Measurements.
PB96-147186 *04,769*

Influence of Deposition Parameters on Properties of Laser Ablated YBa2Cu3O7-Delta Films.
PB95-140539 *04,544*

Magnetic Field Dependence of the Critical Current Anisotropy in Normal Metal-YBa2Cu3O7-delta Thin Film Bilayers.
PB95-141024 *04,550*

Magnetic Flux Pinning in Epitaxial YBa2Cu3O7-delta Thin Films.
PB96-200746 *04,795*

Magnetic Measurement of Transport Critical Current Density of Granular Superconductors.
PB95-126199 *04,531*

n-Value and Second Derivative of the Superconductor Voltage-Current Characteristic.
PB95-126223 *04,533*

Simple and Repeatable Technique for Measuring the Critical Current of Nb3Sn Wires.
PB96-119409 *02,229*

Standard Reference Devices for High Temperature Superconductor Critical Current Measurements.
PB95-175543 *04,659*

Superconductor Critical Current Standards for Fusion Applications. Final Progress Report, October 1993-July 1994.
PB95-169538 *02,222*

USA Interlaboratory Comparison of Superconductor Simulator Critical Current Measurements.
PB96-147194 *04,770*

V-6: Effects of Temperature Variation.
PB96-148143 *04,772*

VAMAS Intercomparison of Critical Current Measurements on NB3Sn Superconductors: A Summary Report.
PB96-119763 *04,043*

GOODRICH, M. T.

Point Probe Decision Trees for Geometric Concept Classes.
PB96-160817 *01,612*

GOODWIN, A. R. H.

Database for the Static Dielectric Constant of Water and Steam.
PB96-145586 *01,103*

Dielectric Studies of Fluids with Reentrant Resonators.
PB95-153730 *00,952*

Dielectric Studies of Fluids with Reentrant Resonators. Appendix B.
DE93019683 *03,244*

Ebulliometric Measurement of the Vapor Pressure of Difluoromethane.
PB95-151361 *00,931*

Measurements of the Relative Permittivity of Liquid Water at Frequencies in the Range of 0.1 to 10 kHz and at Temperatures between 273.1 and 373.2 K at Ambient Pressure.
PB96-119375 *01,078*

Static Dielectric Constant of Water and Steam.
PB96-123559 *01,090*

Vapor Pressure of 1,1-dichloro-2,2,2-trifluoroethane (R123).
PB95-126231 *00,899*

GOODWIN, T. J.

Crystal Structure and Magnetic Ordering of the Rare-Earth and Cu Moments in RBa2Cu2NbO8(R=Nd,Pr).
PB95-140554 *04,546*

GOR'KOV, L. P.

From Superconductivity to Supernovae: The Ginzburg Symposium. Report on the Symposium Held in Honor of Vitaly L. Ginzburg. Held in Gaithersburg, Maryland on May 22, 1992.
PB95-171963 *04,649*

GORCZYCA, T. W.

Dielectronic Capture Processes in the Electron-Impact Ionization of Sc(2+).
PB95-203113 *04,000*

GORDON, G. E.

Effects of Target Shape and Neutron Scattering on Element Sensitivities for Neutron-Capture Prompt Gamma-ray Activation Analysis.
PB94-216157 *00,558*

Trace Elements Associated with Proteins. Neutron Activation Analysis Combined with Biological Isolation Techniques.
PB95-163101 *00,597*

GORE, J.

Estimate of Flame Radiance via a Single Location Measurement in Liquid Pool Flames.
PB94-211596 *02,476*

Measurement of Radiative Feedback to the Fuel Surface of a Pool Fire.
PB94-211604 *02,477*

GORE, J. P.

Development of Hazard Assessment and Suppression Technology for Oil and Gas Well Blowout and Diverter Fires.
PB96-122965 *01,408*

Investigation of Oil and Gas Well Fires and Flares.
PB94-193976 *03,695*

Structure and Radiation Properties of Pool Fires.
PB94-193802 *02,473*

GOTT, J. E.

Analysis of High Bay Hangar Facilities for Detector Sensitivity and Placement.
PB96-190210 *01,429*

GOTTSCHO, R. A.

Gaseous Electronics Conference Radio-Frequency Reference Cell: A Defined Parallel-Plate Radio-Frequency System for Experimental and Theoretical Studies of Plasma-Processing Discharges.
PB94-172327 *04,404*

GOUESBET, G.

Forward Scattering of a Gaussian Beam by a Nonabsorbing Sphere.
PB97-112288 *04,395*

Generalized Optical Theorem for On-Axis Gaussian Beams.
PB97-122345 *04,177*

GOUGH, S. R.

CRYSTMET: The NRCC Metals Crystallographic Data File.
PB97-109029 *04,799*

GOULD, H.

Long-Lived Structures in Fragile Glass-Forming Liquids.
PB96-119565 *04,212*

GOULD, P.

Ultracold Collisions: Associative Ionization in a Laser Trap.
PB94-213238 *03,859*

GOULD, P. L.

Heterodyne Measurement of the Fluorescence Spectrum of Optical Molasses.
PB95-108411 *03,873*

Laser Modification of Ultracold Collisions: Experiment.
PB96-157987 *04,075*

Localization of Atoms in a Three-Dimensional Standing Wave.
PB95-163887 *03,944*

GOVINDAN, T. R.

One-Dimensional Modeling Studies of the Gaseous Electronics Conference RF Reference Cell.
PB96-113428 *02,397*

GOYAL, I. C.

Accuracy of Eigenvalues: A Comparison of Two Methods.
PB95-126249 *03,413*

Anharmonic Oscillator Analysis Using Modified Airy Functions.
PB94-185311 *03,798*

Approximate Solution to the Scalar Wave Equation for Optical Waveguides.
PB95-126256 *04,254*

Calculated Fiber Attenuation: A General Method Yielding Stationary Values.
PB95-175501 *04,298*

Fiber Spot Size: A Simple Method of Calculation.
PB95-125936 *04,250*

Improved Variational Analysis of Inhomogeneous Optical Waveguides Using Airy Functions.
PB95-168639 *04,285*

LP11-Mode Leakage Loss in Coated Depressed Clad Fibers.
PB95-141115 *02,145*

Modal Characteristics of Bent Dual Mode Planar Optical Waveguide.
PB95-180485 *04,311*

Modal Properties of Circular and Noncircular Optical Waveguides.
PB95-125944 *04,251*

Modified Airy Function Method for the Analysis of Tunneling Problems in Optical Waveguides and Quantum Well Structures.
PB94-185824 *02,120*

Vector and Quasi-Vector Solutions for Optical Waveguide Modes Using Efficient Galerkin's Method with Hermite-Gauss Basis Functions.
PB96-141197 *04,357*

GRABBE, A.

Adhesion, Contact Electrification, and Acid-Base Properties of Surfaces.
PB96-204425 *03,693*

Contact Electrification Induced by Monolayer Modification of a Surface and Relation to Acid-Base Interactions.
PB94-185378 03,034

GRACIA-SALCEDO, C.

Reaction Sensitivities of Al-Li Alloys and Alloy 2219 in Mechanical-Impact Tests.
PB94-172764 03,314

GRADY, W. M.

Surging the Upside-Down House: Measurements and Modeling Results.
PB96-180138 02,243

GRAEBNER, J. E.

Workshop on Characterizing Diamond Films (4th). Held in Gaithersburg, Maryland on March 4-5, 1996.
PB96-183090 04,786

GRAESSLEY, W. W.

Thermodynamic Interactions in Model Polyolefin Blends Obtained by Small-Angle Neutron Scattering.
PB94-198496 01,208

GRAETTINGER, T. M.

Growth of Epitaxial KNbO3 Thin Films.
PB96-135181 02,409

GRAHAM, J. R.

Unravel: A CASE Tool to Assist Evaluation of High Integrity Software. Volume 1. Requirements and Design.
PB95-267886 01,736

Unravel: A CASE Tool to Assist Evaluation of High Integrity Software. Volume 2. User Manual.
PB95-267894 01,737

GRAM, D. M.

Evaluation of the Electrochemical Behavior of Ductile Nickel Aluminide and Nickel in a pH 7.9 Solution. Technical Report Number 3, April-June 1991.
DE94017351 03,307

GRANICK, S.

Topological Influences on Polymer Adsorption and Desorption Dynamics.
PB94-212479 01,227

GRANTHAM, R. E.

Standard of Attenuation for Microwave Measurements.
AD-A297 905/2 01,517

GRANVEAUD, M.

Aging, Warm-Up Time and Retrace; Important Characteristics of Standard Frequency Generators.
PB96-103122 04,031

Preliminary Comparison of Time Transfers via LASSO, GPS and Two-Way Satellite.
PB95-151098 01,529

GRATIAS, D.

Neutron Scattering Structural Study of AlCuFe Quasicrystals Using Double Isotopic Substitution.
PB94-200458 04,485

RDFs and Fe-Fe Pair Correlations in an AlCuFe Icosahedral Alloy by Double Isotopic Substitution.
PB94-172129 04,439

GRAU MALONDA, A.

Standardization and Decay Scheme of Rhenium-186.
PB94-200490 03,830

GRAVES, D. B.

Gaseous Electronics Conference Radio-Frequency Reference Cell: A Defined Parallel-Plate Radio-Frequency System for Experimental and Theoretical Studies of Plasma-Processing Discharges.
PB94-172327 04,404

GRAVES, R. S.

Comparison of Heat-Flow-Meter Tests from Four Laboratories.
PB95-126264 00,365

GRAY, B. J.

Electronic Implementors' Workshop.
PB95-210936 01,484

GRAY, D. H.

Review of the USCEA/NIST Measurement Assurance Program for the Nuclear Power Industry.
PB95-126272 03,712

Standardization and Decay Scheme of Rhenium-186.
PB94-200490 03,830

GRAY, M.

Fokker-Planck Description of Multivalent Interactions.
PB95-108478 00,879

GRAY, M. M.

National Voluntary Laboratory Accreditation Program: POSIX. Portable Operating System Interface.
PB95-189478 02,661

Testers Open Dialogue at Inaugural NIST Workshop.
PB95-175550 01,718

GRAY, S. K.

Quantum Dynamics of Renner-Teller Vibronic Coupling: The Predissociation HCO.
PB94-185303 00,773

GRAYBEAL, J. M.

Effects of Anneal Time and Cooling Rate on the Formation and Texture of Bi2Sr2CaCu2O8 Films.
PB95-161600 04,603

Grain Alignment and Transport Properties of Bi2Sr2CaCu2O8 Grown by Laser Heated Float Zone Method.
PB95-161451 04,602

GREEN, J. W.

Corrected Optical Pyrometer Readings.
AD-A279 949/2 02,615

GREEN, M.

Crystal Structure and Magnetic Properties of CuGeO3.
PB95-180287 04,678

GREEN, M. A.

Lattice Dynamics of Ba1-xKxBiO3.
PB96-102421 04,706

Lattice Dynamics of Semiconducting, Metallic, and Superconducting Ba1-xKxBiO3 Studied by Inelastic Neutron Scattering.
PB96-102447 04,708

Structure and Conductivity of Layered Oxides (Ba,Sr)n+1(Sn,Sb)nO3n+1.
PB96-102439 04,707

GREEN, T.

Hierarchical Ada Robot Programming System (HARPS): A Complete and Working Telerobot Control System Based on the NASREM Model.
PB94-213162 02,934

GREENBAUM, A.

Laplace's Equation and the Dirichlet-Neumann Map in Multiply Connected Domains. (NIST Reprint).
PB95-180295 03,962

GREENBERG, K. E.

Gaseous Electronics Conference Radio-Frequency Reference Cell: A Defined Parallel-Plate Radio-Frequency System for Experimental and Theoretical Studies of Plasma-Processing Discharges.
PB94-172327 04,404

Gaseous Electronics Conference RF Reference Cell: An Introduction.
PB96-113329 02,387

Inductively Coupled Plasma Source for the Gaseous Electronics Conference RF Reference Cell.
PB96-113394 02,394

Optical Diagnostics in the Gaseous Electronics Conference Reference Cell.
PB96-113352 02,390

GREENBERG, N.

Frozen Human Serum Reference Material for Standardization of Sodium and Potassium Measurements in Serum or Plasma by Ion-Selective Electrode Analyzers.
PB94-185337 00,532

GREENBERG, R.

Development of Frozen Whale Blubber and Liver Reference Materials for the Measurement of Organic and Inorganic Contaminants.
PB95-151676 00,587

GREENBERG, R. R.

Certification of Standard Reference Material (SRM) 1941a, Organics in Marine Sediment.
PB96-123690 02,593

Concentrations of Chlorinated Hydrocarbons, Heavy Metals and Other Elements in Tissues Banked by the Alaska Marine Mammal Tissue Archival Project.
PB95-209870 02,590

Dissolution Problems with Botanical Reference Materials.
PB95-126280 03,487

External Gamma-ray Counting of Selected Tissues from a Thorotrast Patient.
PB96-160254 03,637

Measuring Hydrogen by Cold-Neutron Prompt-Gamma Activation Analysis.
PB96-111877 00,612

Neutron Capture Prompt Gamma-Ray Activation Analysis at the NIST Cold Neutron Research Facility.
PB94-213394 00,556

New NIST Rapid Pneumatic Tube System.
PB96-167259 03,738

Trace Element Concentrations in Cetacean Liver Tissues Archived in the National Marine Mammal Tissue Bank.
PB96-167127 02,595

Use of Neutron Beams for Chemical Analysis at NIST.
PB97-112437 00,652

GREENE, C. H.

Oscillator Strengths and Radiative Branching Ratios in Atomic Sr.
PB95-203493 04,008

Short-Range Correlation and Relaxation Effects on the (6p(2))(1)SO Autoionizing State of Atomic Barium.
PB95-202289 03,973

GREENE, G. C.

Supermirror Transmission Polarizers for Neutrons.
PB94-216215 03,866

GREENE, G. L.

Elastic Deformation of a Monolithic Perfect Crystal Interferometer: Implications for Gravitational Phase Shift Experiments.
PB94-213154 03,858

Mass Assay and Uniformity Test of Boron Targets by Neutron Beam Methods.
PB97-119085 04,175

Measurement of the Neutron Lifetime.
PB96-161708 04,094

Multi-Stage, Position Stabilized Vibration Isolation System for Neutron Interferometry.
PB95-175022 03,955

Some Aspects of Fundamental Neutron Physics.
PB95-126298 03,882

GREENGARD, L.

Laplace's Equation and the Dirichlet-Neumann Map in Multiply Connected Domains. (NIST Reprint).
PB95-180295 03,962

GREENHALL, C. A.

Confidence on the Modified Allan Variance and the Time Variance.
PB96-190376 01,557

GREENSPAN, L.

Evaluation of a Tapered Roller Bearing Spindle for High-Precision Hard Turning Applications.
PB96-160494 02,700

GREGORY, D. C.

Electron-Impact Excitation of Si(3+)(3S yields 3P) Using a Merged-Beam Electron-Energy-Loss Technique.
PB95-151239 03,904

Merged-Beams Energy-Loss Technique for Electron-Ion Excitation: Absolute Total Cross Sections for O(5+) (2s yields 2p).
PB96-102058 04,017

GREHAN, G.

Elastic Scattering from Spheres under Non Plane-Wave Illumination.
PB96-163688 04,370

Forward Scattering of a Gaussian Beam by a Nonabsorbing Sphere.
PB97-112288 04,395

Generalized Optical Theorem for On-Axis Gaussian Beams.
PB97-122345 04,177

GREY, C. P.

Neutron and Raman Spectroscopies of 134 and 134a Hydrofluorocarbons Encaged in Na-X Zeolite.
PB96-186168 03,001

GRIBAKIN, G. F.

Fine Structure of Negative Ions of Alkaline-Earth-Metal Atoms.
PB94-211182 03,837

GRIESMEYER, J. M.

Integrating Automated Systems with Modular Architecture.
PB95-150231 00,577

GRIFFIN, D. C.

Absolute Cross Sections for Electron-Impact Single Ionization of Si(+) and Si(2+).
PB95-202529 03,982

Dielectronic Capture Processes in the Electron-Impact Ionization of Sc(2+).
PB95-203113 04,000

GRIFFIN, G. D.

Investigation of S2F10 Production and Mitigation in Compressed SF6-Insulated Power Systems.
PB94-212388 02,467

Investigation of S2F10 Production and Mitigation in Compressed SF6- Insulated Power Systems.
PB96-155528 02,468

GRIGEREIT, T. E.

Observation of Oscillatory Magnetic Order in the Antiferromagnetic Superconductor HoNi2B2C.
PB95-180303 04,679

Vortex Dynamics and Melting in Niobium.
PB96-112362 02,073

GRIGORIU, M.

Necessary Condition for Homoclinic Chaos Induces by Additive Noise.
PB96-155775 04,063

Non-Gaussian Noise Effects on Reliability of Multistable Systems.
PB96-122726 04,213

GRILLY, E. R.

Pressure-Volume-Temperature Relations in Liquid and Solid Tritium.
PB94-140571 00,726

GRIMES, T. L.

NIST Handbook 44, 1996: Specifications, Tolerances, and Other Technical Requirements for Weighing and Measuring Devices as Adopted by the 80th National Conference on Weights and Measures, 1995.
PB96-166616 02,926

Uniform Laws and Regulations in the Areas of Legal Metrology and Motor Fuel Quality as Adopted by the 80th National Conference on Weights and Measures 1995. 1996 Edition.
PB96-172309 02,927

GRIMM, H.

Low-Frequency Excitations of Oriented DNA.
PB96-137799 03,548

GRIMM, K. R.

Comparison of Ultralow-Sidelobe-Antenna Far-Field Patterns Using the Planar-Near-Field Method and the Far-Field Method.
PB96-200373 02,015

Planar Near-Field Measurements of Low-Sidelobe Antennas.
PB94-219235 *02,001*

GRINBERG, Y.

Ultrasonic Method for Reconstructing the Two-Dimensional Liquid-Solid Interface in Solidifying Bodies.
PB95-161782 *03,349*

GRISHCHUK, L. P.

Quantum Mechanics of a Solid-State Bar Gravitational Antenna.
PB95-202628 *03,987*

GRISHIN, A. M.

Novel YBa2Cu3O7-x and YBa2Cu3O7-x/Y4Ba3O9 Multilayer Films by Bias-Masked 'On-Axis' Magnetron Sputtering.
PB95-181186 *04,690*

Pinch Effect in Commensurate Vortex-Pin Lattices.
PB96-147079 *01,125*

GRITZO, L.

Materials and Fire Threat.
PB97-122311 *01,442*

GRODKOWSKI, J.

One-Electron Oxidation of Metalloporphycenes as Studied by Radiolytic Methods.
PB97-111967 *01,179*

GRODSTEIN, G. W.

X-ray Attenuation Coefficients from 10 Kev to 100 Mev.
AD-A278 139/1 *03,765*

X-Ray Attenuation Coefficients from 10 KEV to 100 MEV.
AD-A280 290/8 *03,768*

GROH, R. J.

New Surface-Active Comonomer for Adhesive Bonding.
PB96-204052 *03,579*

GRONER, N. E.

Feasibility and Design Considerations of Emergency Evacuation by Elevators.
PB94-163441 *00,287*

Feasibility of Fire Evacuation by Elevators at FAA Control Towers.
PB94-213857 *04,844*

Human Factors Considerations for the Potential Use of Elevators for Fire Evacuation of FAA Air Traffic Control Towers.
PB94-217163 *01,300*

GROSS, J.

Performance of HUD-Affiliated Properties during the January 17, 1994 Northridge Earthquake.
PB95-174488 *00,443*

GROSS, J. G.

Growing Significance of CIB.
PB95-126306 *00,314*

Standards Development in North America for Performance of Whole Buildings and Facilities.
PB94-185196 *00,312*

GROSS, J. L.

Ashland Tank Collapse Investigation.
PB95-126314 *02,481*

Ashland Tank-Collapse Investigation: Closure by Authors.
PB95-126322 *02,482*

Extreme Wind Estimates by the Conditional Mean Exceedance Procedure.
PB95-220471 *00,120*

Extreme Winds Estimation by 'Peaks Over Threshold' and Epochal Methods.
PB96-159686 *00,468*

Modeling of Extreme Loading by 'Peaks Over Threshold' Methods.
PB96-159694 *00,469*

Survey of Steel Moment-Resisting Frame Buildings Affected by the 1994 Northridge Earthquake.
PB95-211918 *00,451*

Workgroup Summary Report: Plastic Hinge-Based Techniques for Advanced Analysis.
PB96-159702 *00,470*

GROSSER, M.

Femtosecond Time-Resolved Molecular Multiphoton Ionization: The Na2 System.
PB95-202305 *03,975*

Femtosecond Time-Resolved Wave Packet Motion in Molecular Multiphoton Ionization and Fragmentation.
PB94-198611 *00,790*

GROSSHANDLER, W.

Acoustic Emission of Structural Materials Exposed to Open Flames.
PB95-164810 *00,296*

Agent Screening for Halon 1301 Aviation Replacement.
PB96-159710 *03,282*

Assessing Halon Alternatives for Aircraft Engine Nacelle Fire Suppression.
PB96-102454 *01,401*

Assessment of Technologies for Advanced Fire Detection.
PB95-126330 *00,294*

Early Detection of Room Fires Through Acoustic Emission. (NIST Reprint).
PB95-180311 *00,298*

Lean flammability limit as a fundamental refrigerant property. Phase 1, Interim technical report, 1 October 1994--31 March 1995.
DE95011238 *03,248*

Protection of Data Processing Equipment with Fine Water Sprays.
PB95-174975 *02,610*

Suppression Effectiveness of Extinguishing Agents under Highly Dynamic Conditions.
PB95-180279 *00,020*

Suppression of Elevated Temperature Hydraulic Fluid and JP-8 Spray Flames.
PB95-181095 *00,021*

Suppression of High-Speed C2H4/Air Flames with C1-Halocarbons.
PB96-175724 *03,287*

Turbulent Spray Burner for Assessing Halon Alternative Fire Suppressants.
PB95-153748 *01,385*

Validation of a Turbulent Spray Flame Facility for the Assessment of Halon Alternatives.
PB96-159728 *03,283*

GROSSHANDLER, W. L.

Effectiveness of Halon Alternatives in Suppressing Dynamic Combustion Process.
PB96-175732 *03,288*

Evaluation of Alternative In-Flight Fire Suppressants for Full-Scale Testing in Simulated Aircraft Engine Nacelles and Dry Bays.
PB94-203403 *00,023*

Flow of Alternative Agents in Piping.
PB95-202420 *00,022*

Interaction of HFC-125, FC-218 and CF3I with High Speed Combustion Waves.
PB96-176417 *03,290*

Minimum Mass Flux Requirements to Suppress Burning Surfaces with Water Sprays.
PB96-183181 *01,425*

Proceedings of the 1995 Workshop on Fire Detector Research. Held on February 6-7, 1995.
PB95-270062 *02,611*

Review of Measurements and Candidate Signatures for Early Fire Detection.
PB95-189452 *00,300*

Solid Propellant Gas Generators: Proceedings of the 1995 Workshop. Held in Gaithersburg, Maryland on June 28-29, 1995.
PB96-131479 *01,412*

Suppression of High Speed Turbulent Flames in a Detonation/Deflagration Tube.
PB95-231817 *01,395*

GROSSMAN

High-Tc Superconducting Antenna-Coupled Microbolometer on Silicon.
PB95-169124 *02,166*

GROSSMAN, E.

Metrology Issues in Terahertz Physics and Technology.
PB96-128277 *01,939*

GROSSMAN, E. N.

30 THz Mixing Experiments on High Temperature Superconducting Josephson Junctions.
PB96-102462 *04,709*

Antenna-Coupled High-Tc Air-Bridge Microbolometer on Silicon.
PB95-180899 *04,315*

Extended CO(7 yields 6) Emission from Warm Gas in Orion.
PB96-102504 *00,090*

Far-Infrared Kinetic Inductance Detector.
PB95-126348 *02,142*

Heterodyne Mixing and Direct Detection in High Temperature Josephson Junctions.
PB96-147202 *01,565*

High Temperature Superconductor-Normal Metal-Superconductor Josephson Junctions with High Characteristic Voltages.
PB95-176079 *04,666*

Microwave Noise in High-Tc Josephson Junctions.
PB96-148010 *04,771*

Niobium Microbolometers for Far-Infrared Detection.
PB96-111729 *02,184*

Optical Performance of Photoinductive Mixers at Terahertz Frequencies.
PB95-168662 *02,161*

Partially Coherent Transmittance of Dielectric Lamellae.
PB96-148028 *04,359*

Superconducting Kinetic Inductance Radiometer.
PB95-140083 *02,144*

Terahertz Detectors Based on Superconducting Kinetic Inductance.
PB95-168647 *02,160*

Terahertz Shapiro Steps in High Temperature SNS Josephson Junctions.
PB95-169140 *02,168*

GROSVENOR, J.

Applicability of Effective Medium Theory to Ferroelectric/Ferrimagnetic Composites with Composition and Frequency-Dependent Complex Permittivities and Permeabilities.
PB96-157854 *01,945*

GROSVENOR, J. H.

Dielectric and Magnetic Measurements from -50C to 200C and in the Frequency Band 50 MHz to 2 GHz.
PB96-191382 *02,245*

Transmission/Reflection and Short-Circuit Line Methods for Measuring Permittivity and Permeability.
PB94-165537 *02,211*

GROTE, M. D.

Display-Measurement Round-Robin.
PB96-119227 *02,186*

Survey of the Components of Display-Measurement Standards.
PB96-122528 *02,188*

Survey of the Components of Display-Measurement Standards.
PB97-122394 *02,209*

GROTHER, P. J.

Binary Decision Clustering for Neural Network Based Optical Character Recognition.
PB95-171971 *01,848*

Binary Decision Clustering for Neural-Network-Based Optical Character Recognition.
PB96-186184 *01,857*

Comparison of FFT Fingerprint Filtering Methods for Neural Network Classification.
PB95-136362 *01,840*

Generalized Form Registration Using Structure-Based Techniques.
PB96-191374 *01,858*

NIST Form-Based Handprint Recognition System.
PB94-217106 *01,838*

PCASYS: A Pattern-Level Classification Automation System for Fingerprints.
PB95-267936 *01,853*

Second Census Optical Character Recognition Systems Conference.
PB94-188711 *01,832*

GRUBBS, W. T.

Bimolecular Interactions in (Et)3SiOH:Base:CCl4 Hydrogen-Bonded Solutions Studied by Deactivation of the Free OH-Stretch Vibration.
PB97-118657 *04,166*

GRUDLER, P.

Preliminary Comparison of Time Transfers via LASSO, GPS and Two-Way Satellite.
PB95-151098 *01,529*

GRUNINGER, S. E.

Procedure for the Study of Acidic Calcium Phosphate Precursor Phases in Enamel Mineral Formation.
PB95-164448 *03,564*

GRUSHKO, B.

Effect of Mn Content on the Microstructure of Al-Mn Alloys Electrodeposited at 150C.
PB95-126355 *03,343*

GRYCZYNSKI, Z.

Positive and Negative Cooperativities at Subsequent Steps of Oxygenation Regulate the Allosteric Behavior of Multistate Sebacylhemoglobin.
PB97-119374 *03,486*

GUANG-QIU, T.

Wide Band Active Current Transformer and Shunt.
PB95-126371 *02,036*

GUEGUETCHKERI, M.

New Method for the Detection and Measurement of Polyaromatic Carcinogens and Related Compounds by DNA Intercalation.
PB96-167382 *03,481*

Supported Phospholipid/Alkanthiol Biomimetic Membranes: Insulating Properties.
PB95-180782 *03,470*

GUELACHVILI, G.

Reanalysis of the (010), (020), (100), and (001) Rotational Levels of (32)S(16)O2.
PB95-125621 *00,887*

GUELLATI, S.

Atoms in Optical Molasses.
PB95-108874 *03,875*

Atoms in Optical Molasses: Applications to Frequency Standards.
PB95-108882 *03,876*

Optical Molasses: Cold Atoms for Precision Measurements.
PB95-108890 *03,877*

Optical Molasses: The Coldest Atoms Ever.
PB95-108908 *03,878*

GUENTHER, F. R.

Integrating Automated Systems with Modular Architecture.
PB95-150231 *00,577*

Materials-Science Based Approach to Phenol Emissions from a Flooring Material in an Office Building.
PB97-118749 *02,572*

NIST Traceable Reference Material Program for Gas Standards: Standard Reference Materials.
PB96-210786 *00,644*

Source of Phenol Emissions Affecting the Indoor Air of an Office Building.
PB94-154382 03,600

GUERRIERI, J.

Planar Near-Field Measurements and Microwave Holography for Measuring Aperture Distribution on a 60 GHz Active Array Antenna.
PB96-167366 03,762

GUERRIERI, J. R.

New Extrapolation/Spherical/Cylindrical Measurement Facility at the National Institute of Standards and Technology.
PB95-153755 02,004

GUHA, S.

Optical Conductivity of Single Crystals of Ba1-xMxBiO3(M=K, Rb, x=0.04, 0.37).
PB94-185329 04,447

GUIBERTEAU, F.

Effect of Grain Size on Hertzian Contact Damage in Alumina.
PB96-179601 03,083

Indentation Fatigue: A Simple Cyclic Hertzian Test for Measuring Damage Accumulation in Polycrystalline Ceramics.
PB96-180013 03,084

Model for Microcrack Initiation and Propagation beneath Hertzian Contacts in Polycrystalline Ceramics.
PB96-163704 03,077

GUILLOT, B.

Dipole Moments in Rare Gas Interactions.
PB94-212982 00,844

GULDI, D. M.

One-Electron Oxidation of Metalloporphycenes as Studied by Radiolytic Methods.
PB97-111967 01,179

GULLIKSON, E. M.

Design and Characterization of X-Ray Multilayer Analyzers for the 50 - 1000 eV Region.
PB94-211851 03,848

Stable Silicon Photodiodes for Absolute Intensity Measurements in the VUV and Soft X-ray Regions.
PB97-110175 04,135

GULWADI, S. M.

Range Statistics and Rutherford Backscattering Studies on Fe-Implanted In0.53Ga0.47As.
PB95-126397 04,535

Transition Metal Implants in In0.53GA0.47As.
PB95-126389 04,534

GUNARATNA, P.

Frozen Human Serum Reference Material for Standardization of Sodium and Potassium Measurements in Serum or Plasma by Ion-Selective Electrode Analyzers.
PB94-185337 00,532

GUNTHER, E.

Intercomparison of Internal Proportional Gas Counting of (85)Kr and (3)H.
PB94-185576 03,800

GUO, X. Q.

Absolute Cross Sections for Electron-Impact Single Ionization of Si(+) and Si(2+).
PB95-202529 03,982

Backscattering in Electron-Impact Excitation of Multiply Charged Ions.
PB94-185345 03,799

Evidence for Significant Backscattering in Near-Threshold Electron-Impact Excitation of Ar(7+)(3s yields 3p).
PB95-126405 03,883

Merged-Beams Energy-Loss Technique for Electron-Ion Excitation: Absolute Total Cross Sections for O(5+) (2s yields 2p).
PB96-102058 04,017

Resonance Structure and Absolute Cross Sections in Near-Threshold Electron-Impact Excitation of the 4s(2) (1)S yields 4s4p (3)P Intercombination Transition in Kr(6+).
PB95-202271 03,972

GUO, Y. C.

Critical Current Density, Irreversibility Line, and Flux Creep Activation Energy in Silver-Sheathed Bi2Sr2Ca2Cu2Ox Superconducting Tapes.
PB95-162749 04,616

GUPTA, A.

New Method for the Detection and Measurement of Polyaromatic Carcinogens and Related Compounds by DNA Intercalation.
PB96-167382 03,481

GUPTA, A. K.

Analysis of Droplet Arrival Statistics in a Pressure-Atomized Spray Flame.
PB97-112270 01,352

Combustion of Methanol and Methanol/Dodecanol Spray Flames.
PB95-108544 02,478

Effect of Dodecanol Content on the Combustion of Methanol Spray Flames.
PB95-176020 01,389

Role of Combustion on Droplet Transport in Pressure-Atomized Spray Flames.
PB96-204433 01,434

Structure of a Swirl-Stabilized Kerosene Spray Flame.
PB95-108569 02,480

Study of Droplet Transport in Alcohol-Based Spray Flames Using Phase/Doppler Interferometry.
PB95-108551 02,479

GUPTA, D.

Standard Reference Materials: Polystyrene Films for Calibrating the Wavelength Scale of Infrared Spectrophotometers - SRM 1921.
PB95-226866 03,386

GUPTA, L. C.

Neutron Scattering Study of Antiferromagnetic Order in the Magnetic Superconductors RNi2B2C.
PB97-112411 04,812

GUPTA, R.

Laser Focused Atomic Deposition.
PB95-180659 04,685

Nanofabrication of a Two-Dimensional Array Using Laser-Focused Atomic Deposition.
PB96-119417 04,732

Nanostructure Fabrication via Laser-Focused Atomic Deposition (Invited).
PB96-204094 04,132

Using Atom Optics to Fabricate Nanostructures.
PB96-141247 04,757

GUREVICH, A.

Crossover in the Pinning Mechanism of Anisotropic Fluxon Cores.
PB95-180170 04,673

GURLEY, D.

Extending the Angular Range of Neutron Reflectivity Measurements from Planar Lipid Bilayers: Applications to a Model Biological Membrane.
PB96-122569 03,476

GURNELL, A. W.

Hybrid Optical-Electrical Overlay Test Structure.
PB96-204136 02,450

GURVICH, L. V.

Ideal Gas Thermodynamic Properties of Sulphur Heterocyclic Compounds.
PB96-145867 01,110

GUTHRIE, W.

Advances in the Measurement of Polymer CTE: Micrometer- to Atomic-Scale Measurements.
PB96-180229 03,390

GUTHRIE, W. F.

Effects of Testing Variables on the Measured Compressive Strength of High-Strength (90 MPa) Concrete.
PB95-179040 00,445

Effects of Testing Variables on the Strength of High-Strength (90 Mpa) Concrete Cylinders.
PB96-112198 00,456

Hybrid Optical-Electrical Overlay Test Structure.
PB96-204136 02,450

Study on the Reuse of Plastic Concrete Using Extended Set-Retarding Admixtures.
PB96-122130 00,402

GUTMAN, D.

Kinetics of the Reaction of CCl3-Br-2 and the Thermochemistry of CCl3 Radical and Cation.
PB94-212115 00,824

GUTMAN, G.

Influence of Electrical Isolation on the Structure and Reflectivity of Multilayer Coatings Deposited on Dielectric Substrates.
PB96-159736 04,365

New Method for Achieving Accurate Thickness Control for Uniform and Graded Multilayer Coatings on Large Flat Substrates.
PB96-159744 04,366

GUTTMAN, B.

Computer Security: An Introduction to Computer Security The NIST Handbook.
PB96-131610 01,608

Computer Security: Generally Accepted Principles and Practices for Securing Information Technology Systems.
PB97-110811 01,619

Security Program Management.
PB96-156112 01,610

GUTTMAN, C. M.

Certification of the Standard Reference Material 1473a, a Low Density Polyethylene Resin.
PB96-128251 01,282

Determination of the Weight Average Molecular Weight of Two Poly(Ethylene Oxides), SRM 1923 and SRM 1924.
PB94-217031 01,230

Peeling a Polymer from a Surface or from a Line.
PB94-199809 01,213

Performance of Plastic Packaging for Hazardous Materials Transportation. Part 1. Mechanical Properties.
AD-A301 258/0 02,580

Recertification of the Standard Reference Material 1475A, a Linear Polyethylene Resin.
PB94-161932 02,628

GYGAX, F. N.

Dynamics of Mu(+) in Sc and ScHx.
PB96-180021 04,112

GYORGY, E. M.

High Frequency Magnetic Field Sensors Based on the Faraday Effect in Garnet Thick Films.
PB96-190384 02,282

Increased Pinning Energies and Critical Current Densities in Heavy-Ion-Irradiated Bi2Sr2CaCu2O8 Single Crystals.
PB95-175352 04,654

HAASS, M.

Improved Reflectometry Facility at the National Institute of Standards and Technology.
PB96-160338 04,087

New NIST/ARPA National Soft X-ray Reflectometry Facility.
PB96-158092 04,080

HABRAM, M.

Hair Analysis for Drugs of Abuse: Evaluation of Analytical Methods, Environmental Issues, and Development of Reference Materials.
PB95-176269 03,501

HACK, K.

Extrapolation of the Heat Capacity in Liquid and Amorphous Phases.
PB97-111421 04,147

HACKENBERGER, L. B.

Effect of Stoichiometry on the Phases Present in Boron Nitride Thin Films.
PB96-102470 04,710

HACKLEY, V. A.

Effects of Soxhlet Extraction on the Surface Oxide Layer of Silicon Nitride Powders.
PB95-175584 03,057

Electroacoustic Characterization of Particle Size and Zeta Potential in Moderately Concentrated Suspensions.
PB96-119425 01,079

Electrokinetic Sonic Analysis of Silicon Nitride Suspensions.
PB96-123575 03,073

Polyelectrolytes as Dispersants in Colloidal Processing of Silicon Nitride Ceramics.
PB95-175568 03,055

Standard Reference Material for the Measurement of Particle Mobility by Electrophoretic Light Scattering.
PB96-102488 00,609

Surface Chemical Interactions of Si3N4 with Polyelectrolyte Deflocculants.
PB95-175576 03,056

Surface Chemistry of Silicon Nitride Powder in the Presence of Dissolved Ions.
PB96-111760 01,073

HACKMAN, C.

Confidence on the Three-Point Estimator of Frequency Drift.
PB95-163838 01,539

HADDAD, J. W.

Comparing the Accuracy of Critical-Current Measurements Using the Voltage-Current Simulator.
PB96-119219 02,227

HADDON, R. C.

Neutron-Scattering Study of C60(n-) (n=3,6) Librations in Alkali-Metal Fullerides.
PB94-200219 00,806

HADJICHRISTIDIS, N.

Thermodynamic Interactions in Model Polyolefin Blends Obtained by Small-Angle Neutron Scattering.
PB94-198496 01,208

HADZIIOANNOU, G.

Neutron Scattering by Multiblock Copolymers of Structure (A-B)N-A.
PB94-211547 01,219

HAEGEL, N. M.

Band-to-Band Photoluminescence and Luminescence Excitation in Extremely Heavily Carbon-Doped Epitaxial GaAs.
PB95-150413 04,570

HAGER, G. D.

Efficient Br(*) Laser Pumped by Frequency-Doubled Nd: YAG and Electronic-to-Vibrational Transfer-Pumped CO2 and HCN Lasers.
PB95-108684 04,248

HAGER, J. P.

Vapor Transport in Materials and Process Chemistry.
PB94-211745 00,669

HAGWOOD, C.

Exits in Multistable Systems Excited by Coin-Toss Square-Wave Dichotomous Noise: A Chaotic Dynamics Approach.
PB96-160650 04,824

Extreme Value Theory and Applications: Proceedings of the Conference on Extreme Value Theory and Applications, Volume 3. Held in Gaithersburg, Maryland in May 1993.
PB95-104956 03,432

Stochastic Modeling of a New Spectrometer.
PB96-157870 04,068

HAHN, M. H.

Line-Heat-Source Guarded-Hot-Plate Apparatus.
PB97-118996 00,417

HAHN, T. D.

Atomic Transition Probability Ratios between Some Ar I 4s-4p and 4s-5p Transitions.
PB94-211554 03,842

Ion Broadening Parameters for Several Argon and Carbon Lines.
PB94-211562 *03,843*

HAILER, A. W.

Proteoglycan Inhibition of Calcium Phosphate Precipitation in Liposomal Suspensions.
PB94-211208 *00,658*

HAIR, D.

Dynamic Light-Scattering Study of a Diluted Polymer Blend Near Its Critical Point.
PB95-151890 *01,245*

HAIR, D. W.

Crossover to Strong Shear in a Low-Molecular-Weight Critical Polymer Blend.
PB94-211976 *01,222*

HAKIM, E. B.

Overview of U.S. Government Advanced Packaging Programs.
PB96-200845 *02,443*

HALAMICKOVA, P.

Water Permeability and Chloride Ion Diffusion in Portland Cement Mortars: Relationship to Sand Content and Critical Pore Diameter.
PB96-148036 *03,193*

HALAS, N. J.

Epitaxial Integration of Single Crystal C60.
PB95-153490 *04,592*

Photoluminescence Spectra of Epitaxial Single Crystal C60.
PB96-141205 *04,754*

HALE, P. D.

Accurate Characterization of High Speed Photodectors.
PB95-153763 *02,153*

Comparison of Photodiode Frequency Response Measurements to 40 GHz between NPL and NIST.
PB96-111992 *04,038*

High-Sensitivity Optical Sampling Using an Erbium-Doped Fiber Laser Strobe.
PB95-176111 *04,302*

Metrology Applications of Mode-Locked Erbium Fiber Lasers.
PB95-140158 *04,256*

Optical Fiber Geometry: Accurate Measurement of Cladding Diameter.
PB95-151940 *04,266*

Photodetector Frequency Response Measurements at NIST, US, and NPL, UK: Preliminary Results of a Standards Laboratory Comparison.
PB95-175592 *02,175*

Standard Polarization Components: Progress Toward an Optical Retardance Standard.
PB96-119672 *04,342*

HALL, D. E.

Intelligent Processing of Materials, Technical Activities 1994 (NAS-NRC Assessment Panel, April 6-7, 1995).
PB96-115050 *03,359*

HALL, H. G.

Learning to Change: Opportunities to Improve the Performance of Smaller Manufacturers.
PB94-166212 *00,010*

HALL, J.

Atomic Beam Splitters and Mirrors by Adiabatic Passage in Multilevel Systems.
PB94-216439 *03,867*

HALL, J. L.

Delivering the Same Optical Frequency at Two Places: Accurate Cancellation of Phase Noise Introduced by an Optical Fiber or Other Time-Varying Path.
PB96-102736 *04,332*

Dreams About the Next Generation of Super-Stable Lasers.
PB94-211570 *04,235*

Frequency-Stabilized Lasers: A Driving Force for New Spectroscopies.
PB96-135199 *04,350*

Frequency Stabilized Lasers: A Parochial Review.
PB95-153771 *04,269*

High-Resolution Optical Multiplex Spectroscopy.
PB95-203543 *04,323*

Improved Hyperfine Measurements of the Na NP Excited State Through Frequency-Controlled Dopplerless Spectroscopy in a Zeeman Magneto-Optic Laser Trap.
PB95-203840 *04,012*

Introduction to Phase-Stable Optical Sources.
PB96-122973 *04,347*

Low-Noise High-Speed Diode Laser Current Controller.
PB95-202826 *02,178*

Phase Shifts and Intensity Dependence in Frequency-Modulation Spectroscopy.
PB96-103205 *01,071*

Stabilization of Optical Phase/Frequency of a Laser System: Application to a Commercial Dye Laser with an External Stabilizer.
PB95-203832 *04,327*

HALL, W.

National Voluntary Laboratory Accreditation Program: Energy Efficient Lighting Products.
PB94-219060 *02,642*

HALL, W. A.

Efficiency of Electric Motors. National Voluntary Lab. Accreditation Program (NVLAP).
PB96-111174 *02,107*

National Voluntary Laboratory Accreditation Program: Carpet and Carpet Cushion.
PB95-155560 *00,295*

National Voluntary Laboratory Accreditation Program (NVLAP): Wood Based Products.
PB95-170429 *03,405*

HALLER, W.

Analysis of SANS from Controlled Pore Glasses.
PB94-198843 *03,035*

Real-Time Small-Angle X-Ray Scattering Study of the Early Stage of Phase Separation in the SiO2-BaO-K20 System.
PB95-163069 *03,052*

HALLETT, B.

Comparison of Magnetic Fields of Thin-Film Heads and Their Corresponding Bit Patterns Using Magnetic Force Microscopy.
PB95-180907 *03,763*

HALLIWELL, B.

Commentary: The Measurement of Oxidative Damage to DNA by HPLC and GC/MS Techniques.
PB96-200894 *03,484*

HALLOCK, R. B.

X-Ray Powder Diffraction Data for BaCu(C2O4)2.6H2O.
PB95-151767 *04,583*

HALPERN, C.

Bibliography of Books and Published Reports on Gas Turbines, Jet Propulsion, and Rocket Power Plants.
AD-A278 138/3 *01,445*

Bibliography of Books and Published Reports on Gas Turbines, Jet Propulsion, and Rocket Power Plants, January 1950 through December 1953.
AD-A278 213/4 *01,446*

HAMANN, W. F.

Self Calibrating Fiber Optic Sensors: Potential Design Methods.
PB95-169306 *02,173*

HAMBRIGHT, P.

Metalloporphyrin Sensitized Photooxidation of Water to Oxygen on the Surface of Colloidal Iridium Oxides - Photochemical and Pulse Radiolytic Studies.
PB95-107082 *00,868*

One-Electron Oxidation of Nickel Porphyrins. Effect of Structure and Medium on Formation of Nickel(III) Porphyrin or Nickel(II) Porphyrin pi-Radical Cation.
PB95-107058 *00,865*

Site of One-Electron Reduction of Ni(II) Porphyrins. Formation of Ni(I) Porphyrin of Ni(II) Porphyrin pi-Radical Anion.
PB95-107066 *00,866*

HAMEL, J. F.

Supercritical Fluid Extraction of Biological Products.
PB95-175204 *00,040*

HAMILTON, B. E.

Learning to Change: Opportunities to Improve the Performance of Smaller Manufacturers.
PB94-166212 *00,010*

HAMILTON, C. A.

24 GHz Josephson Array Voltage Standard.
PB94-211588 *02,033*

Automated Josephson Integrated Circuit Test System.
PB95-175246 *02,057*

Experimental Results on Single Flux Quantum Logic.
PB95-175071 *02,053*

Josephson D/A Converter with Fundamental Accuracy.
PB96-148044 *02,418*

Josephson Voltage Standard Based on Single-Flux-Quantum Voltage Multipliers.
PB95-175600 *02,058*

Performance and Reliability of NIST 10-V Josephson Arrays.
PB96-148051 *02,419*

Pulse-Driven Programmable Josephson Voltage Standard.
PB97-111496 *04,148*

Voltage-Standard Devices.
PB96-102496 *01,920*

HAMINS, A.

Agent Screening for Halon 1301 Aviation Replacement.
PB96-159710 *03,282*

Combustion of a Polymer (PMMA) Sphere in Microgravity.
N96-15569/2 *01,354*

Estimate of Flame Radiance via a Single Location Measurement in Liquid Pool Flames.
PB94-211596 *02,476*

Estimate of the Effect of Scale on Radiative Heat Loss Fraction and Combustion Efficiency.
PB95-150447 *02,486*

Measurement of Radiative Feedback to the Fuel Surface of a Pool Fire.
PB94-211604 *02,477*

Simultaneous Optical Measurement of Soot Volume Fraction, Temperature, and CO2 in Heptane Pool Fire.
PB96-102132 *01,397*

Suppression of Ignition Over a Heated Metal Surface.
PB96-176425 *03,291*

HAMMER, L. H.

Display-Measurement Round-Robin.
PB96-119227 *02,186*

HAMMOND, B.

Second Census Optical Character Recognition Systems Conference.
PB94-188711 *01,832*

HAMSTAD, M. A.

High-Sensitivity Acoustic Emission Sensor/Preamplifier Subsystems.
PB95-125704 *02,900*

HAN, B.

Suitability of Metalorganic Chemical Vapor Deposition-Derived PrGaO3 Films as Buffer Layers for YBa2Cu3O7-x Pulsed Laser Deposition.
PB95-168670 *04,640*

HAN, C.

Dynamic Light-Scattering Study of a Diluted Polymer Blend Near Its Critical Point.
PB95-151890 *01,245*

Molecular Weight Dependence of the Lamellar Domain Spacing of ABC Triblock Copolymers and Their Chain Conformation in Lamellar Domains.
PB95-161691 *01,254*

Relaxation After a Temperature Jump Within the One Phase Region of a Polymer Mixture.
PB97-112494 *03,394*

HAN, C. C.

Anisotropic Phase Separation Kinetics in a Polymer Blend Solution Following Cessation of Shear Studied by Light Scattering.
PB95-151247 *01,241*

Compatibilization of Polymer Blends by Complexation. 2. Kinetics of Interfacial Mixing.
PB97-111900 *01,295*

Crossover to Strong Shear in a Low-Molecular-Weight Critical Polymer Blend.
PB94-211976 *01,222*

Dielectric Behavior of a Polycarbonate/Polyester Mi ure Upon Transesterification.
PB96-179551 *04,785*

Dimensional Crossover in the Phase Separation Kinetics of Thin Polymer Blend Films.
PB97-113088 *03,395*

Effect of Cross-Links on the Miscibility of a Deuterated Polybutadiene and Protonated Polybutadiene Blend.
PB94-212438 *01,225*

Flow-Induced Structure in Polymers: Chapter 16. Shear-Induced Changes in the Order-Disorder Transition Temperature and the Morphology of a Triblock Copolymer.
PB96-123237 *03,127*

Flow-Induced Structure in Polymers. Chapter 17. Phase-Separation Kinetics of a Polymer Blend Solution Studied by a Two-Step Shear Quench.
PB96-123377 *03,388*

Influence of Shear on the Ordering Temperature of a Triblock Copolymer Melt.
PB96-163753 *01,288*

Inversion of the Phase Diagram from UCST to LCST in Deuterated Polybutadiene and Protonated Polybutadiene Blends.
PB94-212446 *01,226*

Lattice Model of a Hydrogen-Bonded Polymer Blend.
PB97-112262 *03,391*

Light-Scattering Studies on Phase Separation in a Binary Blend with Addition of Diblock Copolymers.
PB96-146865 *01,286*

Localization of a Homopolymer Dissolved in a Lamellar Structure of a Block Copolymer Studied by Small-Angle Neutron Scattering.
PB95-161592 *01,253*

Microstructure Effect on the Phase Behavior of Blends of Deuterated Polybutadiene and Protonated Polyisopene.
PB97-113146 *01,296*

Morphology and Phase Separation Kinetics of a Compatibilized Blend.
PB97-119135 *01,297*

Neutron Scattering by Multiblock Copolymers of Structure (A-B)N-A.
PB94-211547 *01,219*

Neutron Scattering Study of Shear Induced Turbidity in Polystyrene/Dioctyl Phthalate Solutions at High Shear Rates.
PB94-172624 *01,197*

Neutron Scattering Study of Shear Induced Turbidity in Polystyrene Dissolved in Dioctyl Phthalate.
PB95-161865 *01,256*

Neutron Scattering Study of the Orientation of a Liquid Crystalline Polymer by Shear Flow.
PB95-180196 *01,270*

Phase Behavior of a Hydrogen Bonding Molecular Composite.
PB94-185188 *01,202*

Phase Separation in Thin Film Polymer Blends With and Without Block Copolymer Additives.
PB96-204482 *01,294*

Preparation of 2-Dimensional Ultra Thin Polystyrene Film by Water Casting Method.
PB95-162806 04,619

SANS Studies of Space-Time Organization of Structure in Polymer Blends.
PB95-153789 01,251

Shear Dependence of Critical Fluctuations in Binary Polymer Mixtures by Small Angle Neutron Scattering.
PB94-211612 01,220

Shear-Excited Morphological States in a Triblock Copolymer.
PB94-172392 01,196

Shear-Induced Changes in the Order-Disorder Transition Temperature and the Morphology of a Triblock Copolymer.
PB97-118772 03,130

Shear-Induced Martensitic-Like Transformation in a Block Copolymer Melt.
PB96-119508 01,277

Shear-Induced Mixing in Polymer Blends.
PB96-148085 01,287

Shear Suppression of Critical Fluctuations in a Diluted Polymer Blend.
PB96-204458 04,418

Slow Dynamics of Segregation in Hydrogen-Bonded Polymer Blends.
PB96-123591 01,281

Small Angle Neutron Scattering Study on Poly(N-Isopropyl Acrylamide) Gels Near Their Volume-Phase Transition Temperature.
PB95-164380 01,263

Small-Angle Neutron Scattering Study on Weakly Charged Temperature Sensitive Polymer Gels.
PB95-164398 01,264

Small-Angle X-Ray and Neutron Scattering Study of Block Copolymer/Homopolymer Mixtures.
PB94-211729 01,221

Structural Stabilization of Phase Separating PC/Polyester Blends through Interfacial Modification by Transesterification Reaction.
PB95-150454 01,239

Thermodynamic Interactions and Correlations in Mixtures of Two Homopolymers and a Block Copolymers by Small Angle Neutron Scattering.
PB95-152872 01,247

Thermodynamic Interactions in Model Polyolefin Blends Obtained by Small-Angle Neutron Scattering.
PB94-198496 01,208

Time Dependent Small Angle Neutron Scattering Behavior in Triblock Copolymers Under Steady Shear.
PB94-172632 01,198

Time-Resolved Small-Angle Neutron Scattering Study of Spinodal Decomposition in Deuterated and Protonated Polybutadiene Blends. 1. Effect of Initial Thermal Fluctuations.
PB95-161196 01,252

HANCOCK, D. K.

L-threo-beta-Hydroxyhistidine, an Unprecedented Iron(III) Ion-Binding Amino Acid in a Pyoverdine-type Siderophore from Pseudomonas fluorescens 244.
PB94-211620 00,553

HANDEL, P. H.

New Model of 1/F Noise in Baw Quartz Resonators.
PB96-112248 02,383

HANDWERKER, C.

Energy and Migration of Grain Boundaries in Polycrystals.
PB94-211638 03,332

Fabrication of Platinum-Gold Alloys in Pre-Hispanic South America: Issues of Temperature and Microstructure Control.
PB94-211646 03,333

HANDWERKER, C. A.

Determination of the Prior-Austenitic Grain Size of Selected Steels Using a Molten Glass Etch.
PB94-211927 03,208

Electronics Packaging Materials Research at NIST.
PB96-122692 02,405

Stability and Surface Energies of Wetted Grain Boundaries in Aluminum Oxide.
PB95-202750 03,059

Study of Diffusion Zones with Electron Microprobe Compositional Mapping.
PB94-216348 00,559

Texture Measurement of Sintered Alumina Using the March-Dollase Function.
PB96-179494 04,784

HANIQUE, E.

Approach to Setting Performance Requirements for Automated Evaluation of the Parameters of High-Voltage Impulses.
PB94-185634 01,878

HANLEY, H. J. M.

Conditions for Existence of a Reentrant Solid Phase in a Sheared Atomic Fluid.
PB94-211380 04,198

Contrast Matched Studies of a Sheared Binary Colloidal Suspension.
PB95-150561 00,918

Density Dependence of Fluid Properties and Non-Newtonian Flows: The Weisenberg Effect.
PB96-161898 01,140

Dynamic Scaling in an Aggregating 2D Lennard-Jones System.
PB96-167317 04,106

Partial Scattered Intensities from a Binary Suspension of Polystyrene and Silica.
PB95-175618 00,996

Shear-Induced Melting of Two-Dimensional Solids.
PB96-112057 01,075

Simulation and SANS Studies of Gelation Under Shear.
PB96-167176 01,150

Small-Angle Neutron Scattering (SANS) Study of Worm-Like Micelles Under Shear.
PB96-176698 04,111

Small Angle Neutron Scattering Study of a Clay Suspension Under Shear.
PB96-167374 00,663

Small-Angle Neutron-Scattering Study of Dense Sheared Silica Gels.
PB96-167184 01,151

Structure and Rheology of Hard-Sphere Systems.
PB96-167333 00,662

HANLEY, J. M.

Non-Newtonian Flow between Concentric Cylinders Calculated from Thermophysical Properties Obtained from Simulations.
PB96-163761 04,103

HANSEN, B. N.

High-Pressure Equilibrium Cell for Solubility Measurements in Supercritical Fluids.
PB95-175634 00,998

Refractive Indices of Fluids Related to Alternative Refrigerants.
PB94-219375 03,260

Solubilities of Copper(II) and Chromium(III) beta-Diketonates in Supercritical Carbon Dioxide.
PB96-164215 01,147

Solubility Measurement by Direct Injection of Supercritical-Fluid Solutions into a HPLC System.
PB95-175626 00,997

HANSEN, D.

Dynamic Scaling in an Aggregating 2D Lennard-Jones System.
PB96-167317 04,106

Simulation and SANS Studies of Gelation Under Shear.
PB96-167176 01,150

HANSEN, H. J.

Comparison of Finite Element and Analytic Calculations of the Resonant Modes and Frequencies of a Thick Shell Sphere.
PB94-160785 02,626

HANSFORD, W.

Realizing Suspended Structures on Chips Fabricated by CMOS Foundry Processes Through the MOSIS Service.
PB94-193984 01,881

HANSMA, P. K.

Scanning Tunneling Microscopy and Fabrication of Nanometer Scale Structures at the Liquid-Gold Interface.
PB95-140414 00,904

HANSON, A. L.

Polarization Effects on Multiple Scattering Gamma Transport.
PB95-153615 03,926

HANSON, D. W.

Satellite Two-Way Time Transfer: Fundamentals and Recent Progress.
PB95-161089 01,536

HANSON, W.

Precision Oscillators: Dependence of Frequency on Temperature, Humidity and Pressure.
PB94-198306 02,031

Preliminary Comparison of Time Transfers via LASSO, GPS and Two-Way Satellite.
PB95-151098 01,529

HANSSEN, L. M.

Development of Neutral-Density Infrared Filters Using Metallic Thin Films.
PB96-180286 02,998

Standard Reference Materials: Polystyrene Films for Calibrating the Wavelength Scale of Infrared Spectrophotometers - SRM 1921.
PB95-226866 03,386

HAO, H.

Electric Field Effects on a Near-Critical Fluid in Microgravity.
PB96-161880 04,217

HAPIOT, P.

Changes in the Redox State of Iridium Oxide Clusters and Their Relation to Catalytic Water Oxidation: Radiolytic and Electrochemical Studies.
PB95-107017 00,864

Oxidation of Caffeic Acid and Related Hydroxycinnamic Acids.
PB97-111975 00,651

Oxidation of 10-Methylacridan, a Synthetic Analogue of NADH and Deprotonation of Its Cation Radical. Convergent Application of Laser Flash Photolysis and Direct and Redox Catalyzed Electrochemistry to the Kinetics of Deprotonation of the Cation Radical.
PB94-198371 00,785

HARARY, H.

Integration of Scanning Tunneling Microscope Nanolithography and Electronics Device Processing.
PB95-153359 02,341

Polyethylene Crystallized from an Entangled Solution Observed by Scanning Tunneling Microscopy.
PB95-107389 01,232

HARARY, H. H.

Scanning Tunneling Microscopy and Fabrication of Nanometer Scale Structures at the Liquid-Gold Interface.
PB95-140414 00,904

U.S. Navy Coordinate Measuring Machines: A Study of Needs.
PB94-162831 02,807

HARCHENKO, C. D.

Results of a NIST/VNIIOFI Comparison of Spectral-Radiance Measurements.
PB97-113021 04,159

HARDING, L. B.

Quantum Dynamics of Renner-Teller Vibronic Coupling: The Predissociation HCO.
PB94-185303 00,773

HARDIS, J. E.

Detector-Based Candela Scale and Related Photometric Calibration Procedures at NIST.
PB95-161949 04,273

High Resolution Angle Resolved Photoelectron Spectroscopy Study of N2.
PB95-151494 03,907

Improving Color Measurements of Displays.
PB96-204441 02,203

National Institute of Standards and Technology High-Accuracy Cryogenic Radiometer.
PB96-179585 04,378

NIST Detector-Based Luminous Intensity Scale.
PB96-179114 01,864

Vibrationally Resolved Photoelectron Angular Distributions and Branching Ratios for the Carbon Dioxide Molecule in the Wavelength Region 685-795 Angstrom.
PB96-201207 04,131

Vibronic Coupling and Other Many-Body Effects in the 4sigmag(-1) Photoionization Channel of CO2.
PB95-162509 00,962

HARDY, S. C.

Metallurgy Technical Activities 1994 (NAS-NRC Assessment Panel, April 6-7, 1995).
PB96-136981 02,981

Metallurgy. Technical Activities, 1995.
PB96-195284 03,003

HAREWOOD, P. M.

Estimation of the Absorbed Dose in Radiation-Processed Food. 4. EPR Measurements on Eggshell.
PB94-199692 00,038

HARGIS, P. J.

Gaseous Electronics Conference Radio-Frequency Reference Cell: A Defined Parallel-Plate Radio-Frequency System for Experimental and Theoretical Studies of Plasma-Processing Discharges.
PB94-172327 04,404

HARLOW, R. L.

Troublesome Crystal Structures: Prevention, Detection, and Resolution.
PB97-109151 01,172

HARMAN, D.

Lab Report Special Section: Natural Language Processing and Information Retrieval Group Information Access and User Interfaces Division, National Institute of Standards and Technology.
PB97-118665 02,742

Panel: Building and Using Test Collections.
PB97-118673 02,743

HARMAN, D. K.

Bringing Natural Language Information Retrieval Out of the Closet.
PB94-172335 02,720

Overview of the Text REtrieval Conference (3rd) (TREC-3). Held in Gaithersburg, Maryland on November 2-4, 1994.
PB95-216883 01,728

Second Text REtrieval Conference (TREC-2). Held in Gaithersburg, Maryland on August 31-September 2, 1993.
PB94-178407 01,686

Text REtrieval Conference (4th) (TREC-4). Held in Gaithersburg, Maryland on November 1-3, 1995.
PB97-121636 01,786

HARMAN, G. G.

Semiconductor Measurement Technology: Improved Characterization and Evaluation Measurements for HgCdTe Detector Materials, Processes, and Devices Used on the GOES and TIROS Satellites.
PB94-188810 02,122

Wire Bond Testing.
PB94-211653 02,314

Wire Bonding to Multichip Modules and Other Soft Substrates.
PB96-123583 02,079

Wire Bonding to Multichip Modules and Other Soft Substrates
PB96-135207 02,082

HARMOUCHE, M. R.

Dynamic Shear Modulus Measurements with Four Independent Techniques in Nickel-Based Alloys.
PB94-198900 03,320

HARNE, D.

Fracture Behavior of Large-Scale Thin-Sheet Aluminum Alloy.
N95-19494/0 03,311

HARNE, D. E.

Fracture Testing of Large-Scale Thin-Sheet Aluminum Alloy.
AD-A306 625/5 03,305

Fracture Testing of Large-Scale Thin-Sheet Aluminum Alloy.
PB95-242368 00,024

HARPER, K.

Effects of Spindle Dynamic Characteristics on Hard Turning.
PB96-122981 02,699

Evaluation of a Tapered Roller Bearing Spindle for High-Precision Hard Turning Applications.
PB96-160494 02,700

HARRIMAN, A.

Metalloporphyrin Sensitized Photooxidation of Water to Oxygen on the Surface of Colloidal Iridium Oxides - Photochemical and Pulse Radiolytic Studies.
PB95-107082 00,868

Radiation Chemistry of Cyanine Dyes: Oxidation and Reduction of Merocyanine 540.
PB94-211661 00,818

Reduction of Dinitrogen to Ammonia in Aqueous Solution Mediated by Colloidal Metals.
PB95-107074 00,867

Site of One-Electron Reduction of Ni(II) Porphyrins. Formation of Ni(I) Porphyrin of Ni(II) Porphyrin pi-Radical Anion.
PB95-107066 00,866

HARRIMAN, P.

Changes in the Redox State of Iridium Oxide Clusters and Their Relation to Catalytic Water Oxidation: Radiolytic and Electrochemical Studies.
PB95-107017 00,864

HARRINGTON, J. E.

Greatly Enhanced Soot Scattering in Flickering Ch4/Air Diffusion Flames.
PB94-172988 01,361

Laser Imaging of Chemistry-Flowfield Interactions: Enhanced Soot Formation in Time-Varying Diffusion Flames.
PB94-185352 01,364

Laser-Induced Fluorescence Measurements of Formaldehyde in a Methane/Air Diffusion Flame.
PB94-211679 01,374

Measurement of CO Pressures in the Ultrahigh Vacuum Regime Using Resonance-Enhanced Multiphoton-Ionization Time-of-Flight Mass Spectroscopy.
PB94-216041 03,864

Quantitative Measurements of Enhanced Soot Production in a Flickering Methane/Air Diffusion Flame.
PB95-203246 01,393

HARRIS, D. R.

Journal of Research of the National Institute of Standards and Technology. March/April 1994. Volume 99, Number 2.
PB94-219219 02,000

Journal of Research of the National Institute of Standards and Technology. May/June 1994. Volume 99, Number 3.
PB94-219326 02,643

Journal of Research of the National Institute of Standards and Technology, September-October 1993. Volume 98, Number 5.
PB96-134954 03,362

HARRIS, G. L.

Advanced Mass Calibration and Measurement Assurance Program for State Calibration Laboratories.
PB95-253571 02,492

Ensuring Accuracy and Traceability of Weighing Instruments.
PB94-211687 02,638

Evaluation and Accreditation of State Calibration Laboratories.
PB97-110183 00,486

Specifications and Tolerances for Reference Standards and Field Standard Weights and Measures. 2. Specifications and Tolerances for Field Standard Measuring Flasks.
PB96-178926 02,682

State Weights and Measures Laboratories: Program Handbook.
PB96-214705 02,687

State Weights and Measures Laboratories: State Standards Program Description and Directory. 1994 Edition.
PB94-207727 02,895

HARRIS, J. R.

De Facto Microzonation through the Use of Soils Factors in Design Triggers.
PB96-141148 00,462

HARRIS, R. H.

New Approach for Reducing the Toxicity of the Combustion Products from Flexible Polyurethane Foam.
PB96-123625 01,411

Quantifying the Ignition Propensity of Cigarettes.
PB96-155411 00,306

HARRISON, J. C.

Test of Newton's Inverse Square Law of Gravitation Using the 300-m Tower at Erie, Colorado.
PB95-202446 03,978

Validation of the Inverse Square Law of Gravitation Using the Tower at Erie, Colorado, USA.
PB95-164646 03,947

HARRISON, T. R.

Technologic Papers of the Bureau of Standards: Number 170. Pyrometric Practice.
AD-A279 282/8 03,766

HARRISON, W. T. A.

Crystal Structure of a New Sodium Zinc Arsenate Phase Solved by 'Simulated Annealing'.
PB95-107124 00,870

Structural and Chemical Investigations of Na3(ABO4)3.4H2O-Type Sodalite Phases.
PB95-180733 01,012

Tetrahedral-Framework Lithium Zinc Phosphate Phases: Location of Light-Atom Positions in LiZnPO4 H2O by Powder Neutron Diffraction and Structure Determination of LiZnPO4 by ab Initio Methods.
PB96-160510 01,129

HART, R. C.

Failures of the Four-Wave Mixing Model for Cone Emission.
PB95-202636 04,318

HARTMAN, A. W.

Geometric Characterization of Rockwell Diamond Indenters.
PB95-203287 02,950

Microform Calibrations in Surface Metrology.
PB95-203295 02,951

Particle Size Standards and Their Certification at NIST.
PB94-211695 02,639

HARTSON, H. R.

Usability Engineering: Industry-Government Collaboration for System Effectiveness and Efficiency.
PB97-122287 01,514

HARVATH, J. J.

In situ Fluorescence Cell Mass Measurements of 'Saccharomyces cerevisiae' Using Cellular Tryptophan.
PB96-135041 03,547

HARVEY, A. H.

Standard States, Reference States and Finite-Concentration Effects in Near-Critical Mixtures with Applications to Aqueous Solutions.
PB95-164349 00,979

Supercritical Solubility of Solids from Near-Critical Dilute-Mixture Theory.
PB94-211703 00,819

HARVEY, T.

High Critical Temperature Superconductor Tunneling Spectroscopy Using Squeezable Electron Tunneling Junctions.
PB95-163721 04,627

HARVEY, T. E.

Critical Current and Normal Resistance of High-Tc Step-Edge SNS Junctions.
PB96-111752 04,724

Critical Current Behavior of Ag-Coated YBa2Cu3O7-x Thin Films.
PB95-141016 04,549

Ferroelectric Thin Film Characterization Using Superconducting Microstrip Resonators.
PB96-102389 02,270

High-Tc Multilayer Step-Edge Josephson Junctions and SQUIDs.
PB96-200183 04,790

Mutual Phase Locking in Systems of High-Tc Superconductor-Normal Metal-Superconductor Junctions.
PB96-135348 04,744

Phase Locking in Two-Junction Systems of High-Temperature Superconductor-Normal Metal-Superconductor Junctions.
PB95-176053 02,060

YBa2Cu3O7-x to Si Interconnection for Hybrid Superconductor/Semiconductor Integration.
PB94-211711 02,315

HASCALL, V. C.

Proteoglycan Inhibition of Calcium Phosphate Precipitation in Liposomal Suspensions.
PB94-211208 00,658

HASEGAWA, H.

Effect of Cross-Links on the Miscibility of a Deuterated Polybutadiene and Protonated Polybutadiene Blend.
PB94-212438 01,225

Inversion of the Phase Diagram from UCST to LCST in Deuterated Polybutadiene and Protonated Polybutadiene Blends.
PB94-212446 01,226

SANS Studies of Space-Time Organization of Structure in Polymer Blends.
PB95-153789 01,251

Small-Angle X-Ray and Neutron Scattering Study of Block Copolymer/Homopolymer Mixtures.
PB94-211729 01,221

Time-Resolved Small-Angle Neutron Scattering Study of Spinodal Decomposition in Deuterated and Protonated Polybutadiene Blends. 1. Effect of Initial Thermal Fluctuations.
PB95-161196 01,252

HASHIMOTO, T.

Effect of Cross-Links on the Miscibility of a Deuterated Polybutadiene and Protonated Polybutadiene Blend.
PB94-212438 01,225

Inversion of the Phase Diagram from UCST to LCST in Deuterated Polybutadiene and Protonated Polybutadiene Blends.
PB94-212446 01,226

SANS Studies of Space-Time Organization of Structure in Polymer Blends.
PB95-153789 01,251

Small-Angle X-Ray and Neutron Scattering Study of Block Copolymer/Homopolymer Mixtures.
PB94-211729 01,221

Time-Resolved Small-Angle Neutron Scattering Study of Spinodal Decomposition in Deuterated and Protonated Polybutadiene Blends. 1. Effect of Initial Thermal Fluctuations.
PB95-161196 01,252

HASTIE, J. W.

High Temperature.
PB94-211737 03,844

Recent Experimental and Modeling Developments in High Temperature Thermochemistry.
PB94-172343 00,759

Vapor Transport in Materials and Process Chemistry.
PB94-211745 00,669

HATAT, J. L.

Preliminary Comparison of Time Transfers via LASSO, GPS and Two-Way Satellite.
PB95-151098 01,529

HATCH, C. R.

Network Brokers Handbook: An Entrepreneurial Guide to Cooperative Strategies for Manufacturing Competitiveness.
PB95-219325 00,490

HATFIELD, M. O.

Band-Limited, White Gaussian Noise Excitation for Reverberation Chambers and Applications to Radiated Susceptibility Testing.
PB96-165410 01,960

HATTORI, K.

Direct Dispersion Measurement of Highly-Erbium-Doped Optical Amplifiers Using a Low Coherence Reflectometer Coupled with Dispersive Fourier Spectroscopy.
PB95-150702 04,263

HAUSNER, H.

Analysis of Physical Properties of Ceramic Powders in an International Interlaboratory Comparison Program.
PB95-161501 03,050

HAVES, P.

Reproducibility of Tests on Energy Management and Control Systems Using Building Emulators.
PB95-175980 00,260

Use of Building Emulators to Evaluate the Performance of Building Energy Management Systems.
PB96-111901 00,269

HAYDEN, J. S.

Glasses for Waveguide Lasers.
PB96-111950 04,335

Integrated Optic Laser Emitting at 905, 1057, 1356 nm.
PB94-216298 02,136

Integrated Optic Laser Emitting at 906, 1057, and 1358 nm.
PB94-216280 02,135

HAYDEN, L. A.

Accuracy and Repeatability in Time Domain Network Analysis.
PB95-202644 02,064

Accuracy in Time Domain Transmission Line Measurements.
PB96-148069 04,060

Time Domain Network Analysis Using the Multiline TRL Calibration.
PB95-202925 02,065

HAYES, M. A.

High Resolution Angle Resolved Photoelectron Spectroscopy Study of N2.
PB95-151494 03,907

Inner-Valence States CO(+) between 22 eV and 46 eV Studied by High Resolution Photoelectron Spectroscopy and ab Initio CI Calculations.
PB95-180055 03,961

Photoelectron Study of Electronic Autoionization in Rotationally Cooled N2: The n=6 Member of the Hopfield Series.
PB95-163531 00,971

Shape-Resonance-Enhanced Continuum-Continuum Coupling in Photoionization of CO2.
PB95-164471 00,983

Vibrational Autoionization in H2: Vibrational Branching Ratios and Photoelectron Angular Distributions Near the v(+)=3 Threshold.
PB94-199577 00,799

Vibrationally Resolved Photoelectron Angular Distributions and Branching Ratios for the Carbon Dioxide Molecule in the Wavelength Region 685-795 Angstrom.
PB96-201207 04,131

HAYES, P.

Superconducting Resonator and a Cryogenic GaAs Field-Effect Transistor Amplifier as a Single-Ion Detection System.
PB95-202727 03,990

HAYNES, G. A.

Flame Heights and Heat Release Rates of 1991 Kuwait Oil Field Fires.
PB96-119342 01,404

HAYNES, W. M.

Isochoric (p-p-T) Measurements on Liquid and Gaseous Air from 67 to 400 K at Pressures to 35 MPa.
PB96-167390 01,154

New Data and Correlations for the Custody Transfer of Natural Gas Liquids.
PB96-176664 02,499

Reference Data for the Thermophysical Properties of Cryogenic Fluids.
PB95-168688 03,263

Thermophysical Properties of Fluids for the Gas Industry.
PB96-122437 02,494

Thermophysical Properties of Fluids for the Gas Industry. Final Report, February 1, 1988-August 31, 1993.
PB94-146677 02,472

Thermophysical properties of HCFC alternatives. Quarterly report, April 1--June 30, 1995.
DE96010579 03,250

Thermophysical properties of HCFC alternatives. Quarterly report, October 1--December 31, 1995.
DE96010433 03,249

Thermophysical properties of HCFC alternatives. Quarterly report, 1 July 1994--30 September 1994.
DE95002261 03,247

Thermophysical Properties of HFC-143a and HFC-152a. Quarterly Report, 1 July 1993--30 September 1993.
DE94004236 03,245

HAYS, M. J.

Certification of Polycyclic Aromatic Hydrocarbons in a Marine Sediment Standard Reference Material.
PB96-111778 02,592

Certification of Standard Reference Material (SRM) 1941a, Organics in Marine Sediment.
PB96-123690 02,593

HAYWARD, E.

Drill-Hearn-Gerasimov Sum Rule.
PB94-211752 03,845

Polarizability of the Nucleon.
PB94-211760 03,846

HAZEN, D. A.

Dual-Frequency Millimeter-Wave Radiometer Antenna for Airborne Remote Sensing of Atmosphere and Ocean.
PB96-112289 02,009

Dual Frequency mm-Wave Radiometer Antenna for Airborne Remote Sensing of Atmosphere and Ocean.
PB95-180378 02,006

HE, C.

Effect of Microstructure on the Wear Transition of Zirconia-Toughened Alumina.
PB94-211778 03,141

Wear Transitions in Monolithic Alumina and Zirconia-Alumina Composites.
PB96-103163 03,168

HE, Y. Z.

Rate Constants for Hydrogem Atom Attack on Some Chlorinated Benzenes at High Temperature.
PB94-200581 00,810

HEALD, A. L.

Learning to Change: Opportunities to Improve the Performance of Smaller Manufacturers.
PB94-166212 00,010

HEALD, P. R.

Droplet Transfer Modes for a MIL 100S-1 GMAW Electrode.
PB95-209300 02,867

Mapping the Droplet Transfer Modes for an ER100S-1 GMAW Electrode.
PB96-190095 03,295

HEAP, S. R.

Goddard High-Resolution Spectrograph Observations of the Local Interstellar Medium and the Deuterium/Hydrogen Ratio along the Line of Sight Toward Capella.
PB94-213444 00,066

Observations of 3C 273 with the Goddard High Resolution Spectrograph on the Hubble Space Telescope.
PB95-202321 00,076

HEARING, E. D.

Estimation of the Thermodynamic Properties of C-H-N-O-S-Halogen Compounds at 298.15 K.
PB94-162328 00,744

HEATHER, R.

Hyperfine Effects and Associative Ionization of Ultracold Sodium.
PB95-151221 03,903

Laser Assisted Collisions at Ultracold Temperatures.
PB95-161220 03,929

Theory of Atomic Collisions at Ultracold Temperatures.
PB94-212560 03,851

HEATHER, R. W.

Asymptotic Wave Function Splitting Procedure for Propagating Spatially Extended Wave Functions: Application to Intense Field Photodissociation of H2(+).
PB94-211786 03,847

HEATON, H. T.

Role of the Office of Radiation Measurement in Quality Assurance.
PB94-212255 00,689

HEAVNER, T.

Superconducting Resonator and a Cryogenic GaAs Field-Effect Transistor Amplifier as a Single-Ion Detection System.
PB95-202727 03,990

HEBNER, G. A.

Gaseous Electronics Conference Radio-Frequency Reference Cell: A Defined Parallel-Plate Radio-Frequency System for Experimental and Theoretical Studies of Plasma-Processing Discharges.
PB94-172327 04,404

Inductively Coupled Plasma Source for the Gaseous Electronics Conference RF Reference Cell.
PB96-113394 02,394

Optical Diagnostics in the Gaseous Electronics Conference Reference Cell.
PB96-113352 02,390

HEBNER, R.

Transfer of Technology from Defense to Civilian Sectors.
PB94-185360 00,011

HEBNER, R. E.

Directions in MEMS Research Application Development.
PB95-153797 02,106

Metrology Requirements of Future Space Power Systems.
PB95-140984 04,840

HECKERT, N. A.

Assessment of 'Peaks Over Threshold' Methods for Estimating Extreme Value Distribution Tails.
PB95-161360 00,441

Estimates of Hurricane Wind Speeds by the 'Peaks Over Threshold' Method.
PB96-162540 00,471

Extreme Wind Distribution Tails: A 'Peaks Over Threshold' Approach.
PB95-219416 00,127

Extreme Wind Estimates by the Conditional Mean Exceedance Procedure.
PB95-220471 00,120

Extreme Winds Estimation by 'Peaks Over Threshold' and Epochal Methods.
PB96-159686 00,468

Graphical Analysis of the CCRL Portland Cement Proficiency Sample Database (Samples 1-72). (Part 1. Univariant Analysis of Portland Cement).
PB94-196557 01,308

Modeling of Extreme Loading by 'Peaks Over Threshold' Methods.
PB96-159694 00,469

HEFNER, A. R.

Electro-Thermal Simulation of an IGBT PWM Inverter.
PB94-185592 02,303

Investigation of the Drive Circuit Requirements for the Power Insulated Gate Bipolar Transistor (IGBT).
PB94-211794 02,316

Modeling Buffer Layer IGBT's for Circuit Simulation.
PB96-164173 02,429

Modeling Buffer Layer IGBTs for Circuit Simulation.
PB95-153805 02,344

Simulating the Dynamic Electro Thermal Behavior of Power Electronic Circuits and Systems.
PB95-161014 02,345

Thermal Component Models for Electro-Thermal Network Simulation.
PB95-161022 02,346

HEID, C.

Hydrogen in YBa2Cu3Ox: A Neutron Spectroscopy and a Nuclear Magnetic Resonance Study.
PB95-161279 04,601

HEIDENREICH, J. E.

Gaseous Electronics Conference Radio-Frequency Reference Cell: A Defined Parallel-Plate Radio-Frequency System for Experimental and Theoretical Studies of Plasma-Processing Discharges.
PB94-172327 04,404

HEILES, C.

Interstellar Disk-Halo Connection in Galaxies: Review of Observational Aspects.
PB94-211802 00,058

Magnetic Fields in Star-Forming Regions: Observations.
PB96-123005 00,100

HEILWEIL, E. J.

Bimolecular Interactions in (Et)3SiOH:Base:CCl4 Hydrogen-Bonded Solutions Studied by Deactivation of the Free OH-Stretch Vibration.
PB97-118657 04,166

Hot Carrier Excitation of Adlayers: Time-Resolved Measurement of Adsorbate-Lattice Coupling.
PB94-172285 00,758

Picosecond Measurement of Substrate-to-Adsorbate Energy Transfer: The Frustrated Translation of CO/Pt(111)--Translation.
PB95-126041 00,895

Time-Resolved Measurements of Energy Transfer at Surfaces.
PB95-141198 00,913

Time-Resolved Measurements of Energy Transfer at Surfaces.
PB95-153037 00,947

Time-Resolved Probes of Surface Dynamics.
PB94-199957 00,803

Vibrational Relaxation Measurements of Carbon Monoxide on Metal Clusters.
PB94-211810 00,820

HEIMAN, N.

Correlations of Modulation Noise with Magnetic Microstructure and Intergranular Interactions for CoCrTa and CoNi Thin Film Media.
PB94-212768 04,509

HEINEY, P. A.

Discontinuous Volume Change at the Orientational-Ordering Transition in Solid C60.
PB94-211828 00,821

Phase Transitions in Solid C70: Supercooling, Metastable Phases, and Impurity Effect.
PB95-150090 00,914

HEINZ, T. F.

Dynamics of Nonthermal Reactions: Femtosecond Surface Chemistry.
PB94-199965 00,688

HEINZEN, D.

Electrostatic Modes of Ion-Trap Plasmas.
PB95-152963 03,920

Experimental Results on Normal Modes in Cold, Pure Ion Plasmas.
PB95-175105 03,956

HEINZEN, D. J.

Liquid and Solid Atomic Ion Plasmas.
PB94-198991 03,809

Precise Spectroscopy for Fundamental Physics.
PB96-112164 04,040

Quantum-Limited Cooling and Detection of Radio-Frequency Oscillations by Laser-Cooled Ions.
PB96-112073 04,039

Quantum Measurements of Trapped Ions.
PB95-161147 03,928

Quantum Projection Noise: Population Fluctuations in Two-Level Systems.
PB94-212271 03,850

Recent Experiments on Trapped Ions at the National Institute of Standards and Technology.
PB95-169322 03,952

Spin Squeezing and Reduced Quantum Noise in Spectroscopy.
PB95-151635 03,912

Squeezed Atomic States and Projection Noise in Spectroscopy.
PB95-176293 03,960

HELFAND, D. J.

Discovery of an X-Ray Selected, Radio-Loud Quasar at z=3.9.
PB94-198652 00,052

HELG, A. G.

Microlithography by Using Neutral Metastable Atoms and Self-Assembled Monolayers.
PB96-190038 02,441

HELGESEN, G.

Observation of Two Length Scales Above (T sub N) in a Holmium Thin Film.
PB97-111942 04,151

HELGESON, H. C.

Summary of the Apparent Standard Partial Molal Gibbs Free Energies of Formation of Aqueous Species, Minerals, and Gases at Pressures 1 to 5000 Bars and Temperatures 25 to 1000C.
PB96-145891 01,113

HELLWIG, H.

Differences in Competitive Strategies between the United States and Japan.
PB94-211836 00,013

Importance of Measurement in Technology-Based Competition.
PB94-211844 02,929

HELMAN, W. P.

Quantum Yields for the Photosensitized Formation of the Lowest Electronically Excited Singlet State of Molecular Oxygen in Solution.
PB94-161007 00,732

Rate Constants for the Decay and Reactions of the Lowest Electronically Excited Singlet State of Molecular Oxygen in Solution. An Expanded and Revised Compilation.
PB96-145826 01,106

HELMERSON, K.
Hyperfine Effects and Associative Ionization of Ultracold Sodium
PB95-151221 *03,903*

HEMPELMANN, R.
Low-Energy Vibrations and Octahedral Site Occupation in Nb95V5H(D)y.
PB96-160734 *01,133*

HENINS, A.
Evolution of X-ray Resonance Raman Scattering into X-ray Fluorescence from the Excitation of Xenon Near the L3 Edge.
PB96-102751 *04,025*

Flat and Curved Crystal Spectrography for Mammographic X-ray Sources.
PB97-122246 *03,642*

Noninvasive High-Voltage Measurement in Mammography by Crystal Diffraction Spectroscopy.
PB95-153417 *00,160*

Precision Comparison of the Lattice Parameters of Silicon Monocrystals.
PB94-169745 *04,438*

HENKE, B. L.
Design and Characterization of X-Ray Multilayer Analyzers for the 50 - 1000 eV Region.
PB94-211851 *03,848*

HENNION, B.
High-Energy Phonon Dispersion in La1.85Sr0.15CuO4.
PB96-138458 *04,748*

HENS, K. F.
NMR Characterization of Injection-Moulded Alumina Green Compacts. Part 2. T2-Weighted Proton Imaging.
PB96-201181 *01,165*

HERBST, E.
Millimeter- and Submillimeter-Wave Spectrum of trans-Ethyl Alcohol.
PB96-145578 *01,102*

HERBST, J. F.
Magnetocaloric Effect in Rapidly Solidified Nd-Fe-Al-B Materials.
PB94-185667 *04,451*

HEREMANS, C.
Fast-Ion Conducting Y2(ZryTi1-y)2O7 Pyrochlores: Neutron Rietveld Analysis of Disorder Induced by Zr Substitution.
PB96-156104 *04,776*

Fast-Ion Conduction and Disorder in Cation and Anion Arrays in Y2(ZryTi(1-y))2O7 Pyrochlores Induced by Zr Substitution: A Neutron Rietveld Analysis.
PB94-211869 *04,496*

HERMAN, H.
Anisotropy of the Surfaces of Pores in Plasma Sprayed Alumina Deposits.
PB96-123211 *03,126*

HERMAN, M.
Fundamental Torsion Band in Acetaldehyde.
PB94-212834 *00,840*

General Motion Model and Spatio-Temporal Filters for Computing Optical Flow.
PB95-171096 *01,847*

Image Gradient Evolution: A Visual Cue for Danger.
PB96-154562 *02,939*

Integrated Mobile Robot System for Testing Vision Algorithms.
PB95-164133 *02,936*

Integrated Vision Touch-Probe System for Dimensional Inspection Tasks.
PB95-255832 *02,917*

Intelligent Control for Multiple Autonomous Undersea Vehicles.
PB94-211877 *03,747*

Motion-Model-Based Boundary Extraction.
PB95-189502 *01,849*

Real Time Differential Range Estimation Based on Time-Space Imagery Using PIPE.
PB95-161808 *01,844*

Real-Time Implementation of a Differential Range Finder.
PB95-108650 *01,839*

Real-Time Obstacle Avoidance Using Central Flow Divergence and Peripheral Flow.
PB95-198677 *02,937*

Real-Time Vision for Autonomous and Teleoperated Control of Unmanned Vehicles.
PB94-211885 *03,701*

Real-Time Vision for Unmanned Vehicles.
PB94-211893 *03,702*

Reliable Optical Flow Algorithm Using 3-D Hermite Polynomials.
PB94-145620 *01,829*

Unified Approach to Camera Fixation and Vision-Based Road Following.
PB95-162244 *01,594*

Visual Road Following without 3-D Reconstruction.
PB95-161030 *01,591*

HERMAN, S.
Perception of Clamp Noise in Television Receivers.
PB96-119433 *01,489*

HERMANN, A.
Low-Temperature Elastic Constants of Y1Ba2Cu3O7.
PB95-168837 *04,642*

HERMANN, A. M.
Asymmetry between Flux Penetration and Flux Expulsion in Tl-2212 Superconductors.
PB95-125647 *04,527*

Enhanced Flux Pinning via Chemical Substitution in Bulk Superconducting T1-2212.
PB95-169033 *04,647*

HERNDAY, P. R.
Anomalous Relation between Time and Frequency Domain PMD Measurements.
PB97-119390 *04,398*

HERRON, J. T.
International Conference on Chemical Kinetics (2nd). Held in Gaithersburg, Maryland on July 24-27, 1989.
PB94-211901 *00,822*

Plasma Chemical Model for Decomposition of SF6 in a Negative Glow Corona Discharge.
PB95-181053 *01,020*

Progress in the Development of a Chemical Kinetic Database for Combustion Chemistry.
PB95-151056 *01,384*

HERTZ, H. S.
CSTL Technical Activities 1991.
PB94-160769 *00,728*

HERTZ, J.
Extrapolation of the Heat Capacity in Liquid and Amorphous Phases.
PB97-111421 *04,147*

HESS, K. R.
Study of Laser Resonance Ionization Mass Spectrometry Using a Glow Discharge Source.
DE94018566 *03,308*

Study of Laser Resonance Ionization Mass Spectrometry Using a Glow Discharge Source.
PB96-123203 *03,360*

HESS, V.
Beyond the Technology Roadmaps: An Assessment of Electronic Materials Research and Development.
PB96-165998 *01,961*

HESSEL, M. M.
Conceptual Design Plan for the National Advanced Manufacturing Testbed.
PB95-231866 *02,828*

HESSEN, B.
Isolated Spin Pairs and Two-Dimensional Magnetism in SrCr(sub 9p)Ga(sub 12-9p)O19.
PB97-112387 *04,154*

HEYES, D.
Structure and Rheology of Hard-Sphere Systems.
PB96-167333 *00,662*

HEYLIGER, P.
Artificial Crack in Steel: An Ultrasonic-Resonance-Spectroscopy and Modeling Study.
PB96-141395 *03,241*

Compressibility of Polycrystal and Monocrystal Copper: Acoustic-Resonance Spectroscopy.
PB96-164223 *02,990*

Elastic Constants and Internal Friction of Polycrystalline Copper.
PB96-141015 *03,364*

Orthotropic Elastic Constants of a Boron-Aluminum Fiber-Reinforced Composite: An Acoustic-Resonance-Spectroscopy Study.
PB96-200175 *03,182*

Ultrasonic-Resonance Spectroscopy of Bulk and Layered Solids.
PB96-141338 *04,759*

HEYLIGER, P. R.
Elastic Constants of Isotropic Cylinders Using Resonant Ultrasound.
PB94-211919 *04,497*

HIAI, H.
Treatment of Wistar Rats with a Renal Carcinogen, Ferric Nitrilotriacetate, Causes DNA-Protein Cross-Linking between Thymine and Tyrosine in Their Renal Chromatin.
PB96-112115 *03,649*

HICHO, G. E.
Determination of the Prior-Austenitic Grain Size of Selected Steels Using a Molten Glass Etch.
PB94-211927 *03,208*

Determination of the Residual Stresses Near the Ends of Skip Welds Using Neutron Diffraction and X-ray Diffraction Procedures.
PB95-253589 *02,868*

Effect of Backfill and Atomizing Gas on the Powder Porosity and Mechanical Properties of 304L Stainless Steel.
PB94-185394 *03,205*

HICKERNELL, R.
Direct Dispersion Measurement of Highly-Erbium-Doped Optical Amplifiers Using a Low Coherence Reflectometer Coupled with Dispersive Fourier Spectroscopy.
PB95-150702 *04,263*

HICKERNELL, R. K.
Characterization of Vertical-Cavity Semiconductor Structures.
PB94-200193 *02,126*

Comparative Photoluminescence Measurement and Simulation of Vertical-Cavity Semiconductor Laser Structures.
PB95-169173 *02,169*

Correlation of Optical, X-ray, and Electron Microscopy Measurements of Semiconductor Multilayer Structures.
PB95-175279 *02,174*

Determination of the Complex Refractive Index of Individual Quantum Wells from Distributed Reflectance.
PB95-175642 *02,176*

Measurement and Simulation of Photoluminescence Spectra from Vertical-Cavity Quantum-Well Laser Structures.
PB95-169181 *02,170*

Optical Fiber Sensors: Accelerating Applications in Navy Ships.
PB94-186848 *02,632*

Pump-Induced Dispersion of Erbium-Doped Fiber Measured by Fourier-Transform Spectroscopy.
PB94-211935 *04,236*

Technical Digest: Symposium on Optical Fiber Measurements (8th), 1994. Held in Boulder, Colorado on September 13-15, 1994.
PB94-207636 *04,231*

Vertical-Cavity Optoelectronic Structures: CAD, Growth, and Structural Characterization.
PB95-153177 *02,148*

Vertical-Cavity Semiconductor Lasers: Structural Characterization, CAD, and DFB Structures.
PB95-153193 *02,150*

Vertical-Cavity Semiconductor Structures: Materials Characterization.
PB95-153185 *02,149*

HIDAKA, Y.
Magnetic Susceptibility of Pr2-xCexCuO4 Monocrystals and Polycrystals.
PB95-180253 *04,677*

HIDNERT, P.
Density of Solids and Liquids.
AD-A278 517/8 *00,711*

HIGGINS, J. B.
Small Angle Neutron Scattering Study of the Structure and Formation of MCM-41 Mesoporous Molecular Sieves.
PB97-122337 *03,110*

HIGGINS, K.
Rechargeable Batteries for Personal/Portable.
PB96-164231 *02,459*

HIGHT WALKER, A. R.
Rotational Spectra of CH3CCH-NH3, NCCCH-NH3, and NCCCH-OH2.
PB97-118798 *04,170*

HILDEMANN, L. M.
Sources of Urban Contemporary Carbon Aerosol.
PB95-175659 *02,551*

HILL, D. A.
Aperture Coupling to a Coaxial Air Line: Theory and Experiment.
PB94-211968 *02,216*

Aperture Excitation of Electrically Large, Lossy Cavities.
PB94-145711 *00,029*

Aperture Excitation of Electrically Large, Lossy Cavities.
PB95-175675 *00,031*

Bistatic Scattering of Absorbing Materials from 30 to 1000 MHz.
PB95-150934 *01,891*

Crosstalk between Microstrip Transmission Lines.
PB94-135639 *02,210*

Crosstalk between Microstrip Transmission Lines. (NIST Reprint).
PB95-180337 *02,225*

Currents Induced on Multiconductor Transmission Lines by Radiation and Injection.
PB94-211943 *02,215*

Electric Dipole Excitation of a Long Conductor in a Lossy Medium.
PB96-146675 *04,058*

Electromagnetic Scattering by a Periodic Surface with a Wedge Profile.
PB94-211950 *04,421*

Electromagnetic Shielding Characterization of Gaskets.
PB95-198917 *01,911*

Electronic Mode Stirring for Reverberation Chambers.
PB95-180329 *01,908*

Gradiometer Antennas for Detection of Long Subsurface Conductors.
PB95-175667 *01,862*

Measurements of Shielding Effectiveness and Cavity Characteristics of Airplanes.
PB94-210051 *00,030*

Radiated Emissions and Immunity of Microstrip Transmission Lines: Theory and Measurements.
PB96-162649 *02,238*

Spatial Correlation Function for Fields in a Reverberation Chamber.
PB96-148077 *04,427*

Time-Domain Antenna Characterizations.
PB95-152781 02,003

HILL, J. R.

Correlation of Optical, X-ray, and Electron Microscopy Measurements of Semiconductor Multilayer Structures.
PB95-175279 02,174

Vertical-Cavity Semiconductor Lasers: Structural Characterization, CAD, and DFB Structures.
PB95-153193 02,150

Vertical-Cavity Semiconductor Structures: Materials Characterization.
PB95-153185 02,149

HILL, M.

Crystal Chemistry and Phase Equilibrium Studies of the BaO(BaCO3)-R2O3-CuO Systems. 5. Melting Relations in Ba2(Y,Nd,Eu)Cu3O6+x.
PB95-151718 04,580

HILL, M. D.

Effect of Sm2BaCuO5 on the Properties of Sintered (Bulk) YBa2Cu3O6+x.
PB96-119441 04,733

Efficient Experiment to Study Superconducting Ceramics.
PB94-212578 04,505

X-Ray Characterization of the Crystallization Process of High-Tc Superconducting Oxides in the Sr-Bi-Pb-Ca-Cu-O System.
PB95-151700 04,579

HILL, N. W.

Intermediate Structure in the Neutron-Induced Fission Cross Section of 236U.
PB94-185741 03,802

Measurements of the (235)U(n,f) Cross Section in the 3 to 30 MeV Neutron Energy Region.
PB97-119051 04,172

Measurements of the (237)Np(n,f) Cross Section.
PB97-119069 04,173

HILL, S. D.

Test Procedures for Advanced Insulation Panels.
PB97-111892 00,415

HILL, S. M.

Full-Scale Room Fire Experiments Conducted at the University of Maryland.
PB97-116081 00,236

HILL, T. A.

Application of the Modified Voltage-Dividing Potentiometer to Overlay Metrology in a CMOS/Bulk Process.
PB94-181997 02,302

HILL, W. T.

Precision Lifetime Measurements of Cs 6p (2)P1/2 and 6p (2)P3/2 Levels by Single-Photon Counting.
PB95-203816 04,010

HILLERY, B. R.

Comparison of Selectivities for PCBs in Gas Chromatography for a Series of Cyanobiphenyl Stationary Phases.
PB96-119458 00,618

Quantitative Analysis of Selected PCB Congeners in Marine Matrix Reference Materials Using a Novel Cyanobiphenyl Stationary Phase.
PB96-111737 02,591

HILLS, C. R.

Interfaces in Mo/Si Multilayers.
PB96-160668 02,423

HILPERT, G.

Rotational Spectra of CH3CCH-NH3, NCCCH-NH3, and NCCCH-OH2.
PB97-118798 04,170

HILS, D.

Dreams About the Next Generation of Super-Stable Lasers.
PB94-211570 04,235

HILT, R. L.

Intracomparison Tests of the FG5 Absolute Gravity Meters.
PB96-102991 03,688

HILTON, G. C.

Hot-Electron Microcalorimeter for X-ray Detection Using a Superconducting Transition Edge Sensor with Electrothermal Feedback.
PB96-200399 04,792

HINDERER, J.

Calibration of a Superconducting Gravimeter Using Absolute Gravity Measurements.
PB95-202651 03,684

HINKEN, J. H.

Dielectric Properties of Single Crystals of Al2O3, LaAlO3, SrTiO3, and MgO at Cryogenic Temperatures.
PB95-180477 02,266

HIROSAWA, I.

Rotational Dynamics of C60 in Na2RbC60.
PB95-153201 00,948

HIROTA, K.

Neutron-Scattering Studies of the Two Magnetic Correlation Lengths in Terbium.
PB95-152328 04,586

Origin of the Second Length Scale Above the Magnetic Spiral Phase of Tb.
PB95-153698 04,596

HIRSCHMUGL, C. J.

Laser-Synchrotron Hybrid Experiments: A Photon to Tickle, A Photon to Poke.
PB96-157847 03,704

HISSONG, D. W.

Critical Properties and Vapor-Liquid Equilibria of the Binary System Propane + Neopentane.
PB95-175683 00,999

HIXENBAUGH, G. W.

Science, Technology, and Competitiveness: Retrospective on a Symposium in Celebration of NIST's 90th Anniversary and the 25th Anniversary of the Gaithersburg Laboratories, November 14-15, 1991.
PB97-121610 02,696

HO, J.

Photoelectron Spectroscopy of Negatively Charged Bismuth Clusters: Bi(-)2, Bi(-)3, and Bi(-)4.
PB95-108494 00,880

Photoelectron Spectroscopy of Small Antimony Cluster Anions: Sb(-), Sb2(-), Sb3(-), and Sb4(-).
PB95-203139 01,045

HOBBIE, E. K.

Crossover to Strong Shear in a Low-Molecular-Weight Critical Polymer Blend.
PB94-211976 01,222

Lattice Model of a Hydrogen-Bonded Polymer Blend.
PB97-112262 03,391

Shear-Induced Mixing in Polymer Blends.
PB96-148085 01,287

Shear Suppression of Critical Fluctuations in a Diluted Polymer Blend.
PB96-204458 04,418

Slow Dynamics of Segregation in Hydrogen-Bonded Polymer Blends.
PB96-123591 01,281

HOBBS, T.

Response Comparison of Electret Ion Chambers, LiF TLD, and HPIC.
PB96-190103 02,578

HOBISH, M. K.

Metrology Issues in Terahertz Physics and Technology.
PB96-128277 01,939

HOCHGREB, S.

Effect of CF3H and CF3Br on Laminar Diffusion Flames in Normal and Microgravity.
PB96-161831 01,420

Effect of CF3H and CF3Br on Laminar Diffusion Flames in Normal and Microgravity.
PB96-161849 01,421

HOCKEN, R.

Displacement Method for Machine Geometry Calibration.
PB95-152088 02,946

HOCKEY, B.

Fabrication of Transparent gamma-Al2O3 from Nanosize Particles.
PB95-175493 03,054

Low temperature fabrication from nano-size ceramic powders.
DE95013505 03,029

HOCKEY, B. J.

Cavitation Contributes Substantially to Tensile Creep in Silicon Nitride.
PB96-122577 03,171

Cavity Evolution during Tensil Creep of Si3N4.
PB96-204193 03,376

Creep and Creep Rupture of Structural Ceramics.
PB96-204524 03,093

Fracture of Silicon Nitride and Silicon Carbide at Elevated Temperatures.
PB96-180260 03,179

High Temperature Degradation of Structural Composites.
PB94-172848 03,132

Stability and Surface Energies of Wetted Grain Boundaries in Aluminum Oxide.
PB95-202750 03,059

Tensile Creep of Whisker Reinforced Silicon Nitride.
PB94-211984 03,142

Transient Creep Behaviour of Hot Isostatically Pressed Silicon Nitride.
PB96-180278 03,086

Wear Transitions in Monolithic Alumina and Zirconia-Alumina Composites.
PB96-103163 03,168

HODAPP, T.

Temperature of Optical Molasses for Two Different Atomic Angular Momenta.
PB95-126058 03,881

HODGE, P. A.

International Marine-Atmospheric (222)Rn Measurement Intercomparison in Bermuda. Part 1. NIST Calibration and Methodology for Standardized Sample Additions.
PB96-175674 00,114

International Radon-in-Air Measurement Intercomparison Using a New Transfer Standard.
PB96-159751 03,708

Measurement and Calibration of Large-Area Alpha-Particle Sources at NIST.
PB94-172855 03,791

HODGES, J. T.

Analysis of Droplet Arrival Statistics in a Pressure-Atomized Spray Flame.
PB97-112270 01,352

Effect of Finite Beam Width on Elastic Light Scattering from Droplets.
PB96-163670 01,144

Elastic Scattering from Spheres under Non Plane-Wave Illumination.
PB96-163688 04,370

Forward Scattering of a Gaussian Beam by a Nonabsorbing Sphere.
PB97-112288 04,395

Generalized Optical Theorem for On-Axis Gaussian Beams.
PB97-122345 04,177

Internal Droplet Circulation Induced by Surface-Driven Rotation.
PB97-119267 02,500

Laser Bandwidth Effects in Quantitative Cavity Ring-Down Spectroscopy.
PB97-112254 04,394

Role of Combustion on Droplet Transport in Pressure-Atomized Spray Flames.
PB96-204433 01,434

HODGES, R.

Report on Application Integration Architectures (AIA) Workshop. Held in Dallas, Texas on February 8-12, 1993.
PB94-142536 01,803

HODGKIN, S. T.

Volume-Limited ROSAT Survey of Extreme Ultraviolet Emission from all Nondegenerate Stars within 10 Parsecs.
PB96-103189 00,093

HOEFT, J.

Rayleigh Scattering Limits for Low-Level Bidirectional Reflectance Distribution Function Measurements.
PB95-180030 04,307

HOEFT, S.

Complementary Molecular Information on Phthalocyanine Compounds Derived from Laser Microprobe Mass Spectrometry and Micro-Raman Spectroscopy.
PB94-172269 00,757

HOFFMAN, D.

SUSAN: SUperconducting Systems ANalysis by Low Temperature Scanning Electron Microscopy (LTSEM).
PB96-112065 04,728

HOFFMAN, D. M.

ISDN Conformance Testing Guidelines: Guidelines for Implementors of ISDN Customer Premises Equipment to Conform to Both National ISDN-1 and North American ISDN Users' Forum Layer 3 Basic Rate Interface Basic Call Control Abstract Test Suites.
PB94-219094 01,471

HOFFMAN, J.

Comparison of Ultralow-Sidelobe-Antenna Far-Field Patterns Using the Planar-Near-Field Method and the Far-Field Method.
PB96-200373 02,015

Planar Near-Field Measurements of Low-Sidelobe Antennas.
PB94-219235 02,001

HOFFMANN, D.

Frequency Dependence of the Emission from 2D Array Josephson Oscillators.
PB95-175147 02,056

Observation of Vortex Dynamics in Two-Dimensional Josephson-Junction Arrays.
PB95-168811 02,050

HOFFMANN, H.

Micromagnetic Structure of Domains in Co/Pt Multilayers. 1. Investigations of Wall Structure.
PB95-162111 04,610

HOFMANN, G.

Dielectronic Capture Processes in the Electron-Impact Ionization of Sc(2+).
PB95-203113 04,000

HOFMANN, W.

Microdosimetry and Cellular Radiation Effects of Radon Progency in Human Bronchial Airways.
PB95-152344 03,625

HOFSASS, H. C.

Modeling Detector Response for Neutron Depth Profiling.
PB96-157813 04,066

HOGAN, S. R.

Design of Technically Complex Facilities.
PB97-119101 02,695

HOLCOMB, C. D.

Coexisting Densities, Vapor Pressures and Critical Densities of Refrigerants R-32 and R-152a, at 300 - 385 K.
PB95-175691 03,274

New Data and Correlations for the Custody Transfer of Natural Gas Liquids.
PB96-176664 02,499

HOLLAND, J. Z.
Rare-Earth Isotopes as Tracers of Particulate Emissions: An Urban Scale Test.
PB94-161635 *02,535*

HOLLAND, L. A.
dc Method for the Absolute Determination of Conductivities of the Primary Standard KCl Solutions from 0C to 50C.
PB94-219342 *02,644*

HOLLAND, O. W.
Range Statistics and Rutherford Backscattering Studies on Fe-Implanted In0.53Ga0.47As.
PB95-126397 *04,535*

HOLLBERG, L.
Diode Laser as a Spectroscopic Tool.
PB95-175485 *00,600*

Frequency-Stabilized LNA Laser at 1.083 mum: Application to the Manipulation of Helium 4 Atoms.
PB95-176186 *04,304*

High-Resolution Diode-Laser Spectroscopy of Calcium.
PB95-181244 *03,969*

Optical Probing of Cold Trapped Atoms.
PB95-175469 *04,296*

Precise Optical Frequency References and Difference Frequency Measurements with Diode Lasers.
PB95-176228 *04,305*

Sub-Doppler Frequency Measurements on OCS at 87 Thz (3.4 micrometers) with the CO Overtone Laser: Considerations and Details.
PB95-128633 *04,255*

Sub-Doppler Frequency Measurements on OCS at 87 THz (3.4 mu m) with the CO Overtone Laser.
PB96-102215 *04,330*

HOLLBERG, L. W.
High-Sensitivity Spectroscopy with Diode Lasers.
PB95-175477 *04,297*

HOLLERBACH, U.
Numerical Simulation of Submicron Photolithographic Processing.
PB94-198561 *02,310*

HOLLY, S.
Workshop on Characterizing Diamond Films (3rd). Held in Gaithersburg, Maryland on February 23-24, 1994.
PB94-187663 *04,456*

HOLM, E. A.
Microstructural Evolution in Two-Dimensional Two-Phase Polycrystals.
PB94-211992 *04,498*

HOLMES, W. T.
Evaluation and Strengthening Guidelines for Federal Buildings: Assessment of Current Federal Agency Evaluation Programs and Rehabilitation Criteria and Development of Typical Costs for Seismic Rehabilitation.
PB94-181856 *00,425*

Evaluation and Strengthening Guidelines for Federal Buildings: Identification of Current Federal Agency Programs.
PB94-176278 *00,424*

HOLWITT, E.
Standard Reference Materials (SRM's) for Measuring Genetic Damage.
PB94-198827 *03,516*

HOMMA, H.
Magnetic Dead Layer in Fe/Si Multilayer: Profile Refinement of Polarized Neutron Reflectivity Data.
PB94-198363 *04,458*

HONG, C. Y.
Periapical Tissue Reactions to a Calcium Phosphate Cement in the Teeth of Monkeys.
PB94-212008 *00,149*

HONG, T.
Real-Time Implementation of a Differential Range Finder.
PB95-108650 *01,839*

Real-Time Obstacle Avoidance Using Central Flow Divergence and Peripheral Flow.
PB95-198677 *02,937*

HONG, T. H.
General Motion Model and Spatio-Temporal Filters for Computing Optical Flow.
PB95-171096 *01,847*

Image Gradient Evolution: A Visual Cue for Danger.
PB96-154562 *02,939*

Integrated Vision Touch-Probe System for Dimensional Inspection Tasks.
PB95-255832 *02,917*

Intelligent Control for Multiple Autonomous Undersea Vehicles.
PB94-211877 *03,747*

Motion-Model-Based Boundary Extraction.
PB95-189502 *01,849*

Real Time Differential Range Estimation Based on Time-Space Imagery Using PIPE.
PB95-161808 *01,844*

Real-Time Vision for Autonomous and Teleoperated Control of Unmanned Vehicles.
PB94-211885 *03,701*

Real-Time Vision for Unmanned Vehicles.
PB94-211893 *03,702*

Reliable Optical Flow Algorithm Using 3-D Hermite Polynomials.
PB94-145620 *01,829*

HONG, W. P.
Range Statistics and Rutherford Backscattering Studies on Fe-Implanted In0.53Ga0.47As.
PB95-126397 *04,535*

HONG, Y. C.
Periapical Tissue Reactions to a Calcium Phosphate Cement in the Teeth of Monkeys.
PB94-212008 *00,149*

HONG, Z.
Associated Object Model for Distributed Systems.
PB94-212016 *01,694*

HOOD, R. Q.
Effects of Interfacial Roughness on the Magnetoresistance of Magnetic Metallic Multilayers.
PB95-150017 *04,556*

HOOKS, B. M.
Flaw Tolerance and Toughness Curves in Two-Phase Particulate Composites: SiC/Glass System.
PB96-179460 *03,081*

HOPE, G. A.
Thermodynamic Properties of Silicides. 5. Standard Molar Enthalpy of Formation at the Temperature 298.15 K of Trimolybdenum Monosilicide Mo3Si Determined by Fluorine-Combustion Calorimetry.
PB97-119358 *01,190*

HOPKINS, D.
Predicting the Ignition Time and Burning Rate of Thermoplastics in the Cone Calorimeter.
PB96-154794 *01,418*

HOPKINS, M. B.
Langmuir Probe Measurements in the Gaseous Electronics Conference RF Reference Cell.
PB96-113386 *02,393*

HOPP, T. H.
Performance Measures for Geometric Fitting in the NIST Algorithm Testing and Evaluation Program for Coordinate Measurement Systems.
PB96-122122 *01,745*

Representation of Axes for Geometric Fitting.
PB97-113799 *01,782*

Requisite Elements, Rationale, and Technology Overview for the Systems Intergration for Manufacturing Applications (SIMA) Program. Background Study.
PB96-112685 *02,831*

Sensitivity of Three-Point Circle Fitting.
PB95-136354 *02,901*

Statistical Quality Control Technology in Japan.
PB94-199064 *02,708*

User's Guide to 'SuperFit' Modeling Software for CMM Probe Lobing.
PB96-128236 *02,921*

HOPPES, D. D.
Assay of the Eluent from the Alumina-Based Tungsten-188-Rhenium-188 Generator.
PB94-200482 *03,829*

Needs for Brachytherapy Source Calibrations in the United States.
PB97-110092 *03,521*

New and Revised Half-Life Measurement Results.
PB96-160346 *00,695*

Standardization and Decay Scheme of Rhenium-186.
PB94-200490 *03,830*

HOR, C.
Lattice Position of Si in GaAs Determined by X-Ray Standing Wave Measurements.
PB95-164406 *04,632*

Surface Geometry of BaO on W(100): A Surface-Extended X-Ray-Absorption Fine-Structure Study.
PB95-164414 *00,980*

HORI, Y.
DNA Base Damage Generated In vivo in Hepatic Chromatin of Mice upon Whole Body y-Irradiation.
PB95-161741 *03,627*

HORIGUCHI, M.
Direct Dispersion Measurement of Highly-Erbium-Doped Optical Amplifiers Using a Low Coherence Reflectometer Coupled with Dispersive Fourier Spectroscopy.
PB95-150702 *04,263*

Pump-Induced Dispersion of Erbium-Doped Fiber Measured by Fourier-Transform Spectroscopy.
PB94-211935 *04,236*

HORLICK, J.
National Voluntary Laboratory Accreditation Program: Electromagnetic Compatibility and Telecommunications. FCC Methods.
PB95-242376 *02,664*

National Voluntary Laboratory Accreditation Program. GOSIP: Government Open Systems Interconnection Profile.
PB95-267993 *01,486*

National Voluntary Laboratory Accreditation Program: POSIX. Portable Operating System Interface.
PB95-189478 *02,661*

NVLAP Procedures U.S. Code of Federal Regulations. Title 15, Subtitle A, Chapter 2, Part 7. (Effective December 1984; Amended September 1990).
PB94-160850 *02,627*

HORN, R.
Diffusion of Water along 'Closed' Mica Interfaces.
PB96-180039 *02,993*

HORN, R. G.
Adhesion, Contact Electrification, and Acid-Base Properties of Surfaces.
PB96-204425 *03,693*

Contact Electrification Induced by Monolayer Modification of a Surface and Relation to Acid-Base Interactions.
PB94-185378 *03,034*

Pressurized Internal Lenticular Cracks at Healed Mica Interfaces.
PB96-180252 *02,997*

Surface Forces and Adhesion between Dissimilar Materials Measured in Various Environments.
PB94-172970 *03,033*

HORNER, G.
Epitaxial Growth and Characterization of the Ordered Vacancy Compound CuIn3Se5 on GaAs (100) Fabricated by Molecular Beam Epitaxy.
PB95-180725 *04,687*

HORNER, J. A.
Effects of Aluminum Oxalate/Glycine Pretreatment Solutions on Dentin Permeability.
PB95-164505 *03,565*

HORST, J. A.
Certainty Grid to Object Boundary Algorithm.
PB94-203510 *01,835*

Continuous Mining Machine Control Using the Real-Time Control System.
PB94-203528 *03,700*

Environment Simulation for a Continuous Mining Machine.
PB94-203536 *03,697*

Integration of Servo Control into a Large-Scale Control System Design: An Example from Coal Mining.
PB94-203429 *03,696*

HORVAI, G.
Flow Immunoassay Using Solid-Phase Entrapment.
PB96-200951 *00,642*

HORVATH, J. J.
Feasibility of Fluorescence Detection of Tetracycline in Media Mixtures Employing a Fiber Optic Probe.
PB96-163654 *00,511*

Fluorescence Measurements of Tetracycline in High Cell Mass for Fermentation Monitoring.
PB95-175709 *00,601*

In situ On-Line Optical Fiber Sensor for Fluorescence Monitoring in Bioreactors.
PB94-212024 *03,587*

New Method for the Detection and Measurement of Polyaromatic Carcinogens and Related Compounds by DNA Intercalation.
PB96-167382 *03,481*

HORWATH, R.
Gaseous Electronics Conference Radio-Frequency Reference Cell: A Defined Parallel-Plate Radio-Frequency System for Experimental and Theoretical Studies of Plasma-Processing Discharges.
PB94-172327 *04,404*

HOSKINS, J.
Deletion Analysis of the Mini-P1 Plasmid Origin of Replication and the Role of E.coli DnaA Protein.
PB95-163911 *03,539*

DnaJ, DnaK, and GrpE Heat Shock Proteins are Required in 'ori'P1 DNA Replication Solely at the RepA Monomerization Step.
PB97-119382 *03,557*

Function of DnaJ and DnaK as Chaperones in Origin-Specific DNA Binding by RepA.
PB95-151544 *03,533*

Mapping Domains in Proteins: Dissection and Expression of 'Escherichia coli' Adenylyl Cyclase.
PB96-155460 *03,478*

HOSS, M.
DNA Damage and DNA Sequence Retrieval from Ancient Tissues.
PB97-111983 *03,556*

HOSSAIN, T. Z.
Measurement of Boron at Silicon Wafer Surfaces by Neutron Depth Profiling.
PB94-211059 *04,487*

HOSSAIN, Z.
Neutron Scattering Study of Antiferromagnetic Order in the Magnetic Superconductors RNi2B2C.
PB97-112411 *04,812*

HOSSIAN, S. A.
Size and Self-Field Effects in Giant Magnetoresistive Thin-Film Devices.
PB95-180188 *04,674*

HOUCK, J.
Pressure Measurements with the Mercury Melting Line Referred to ITS-90.
PB96-161005 *01,136*

HOUCK, J. C.
Intercomparison between NPL (India) and NIST (USA) Pressure Standards in the Hydraulic Pressure Region Up to 26 MPa.
PB96-113543 *04,211*

Intercomparison of the Effective Areas of a Pneumatic Piston Gauge Determined by Different Techniques.
PB94-212370 *02,640*

HOUGEN, J. T.
Molecular-Beam Optothermal Spectrum of the OH Stretching Band of Methanol.
PB94-212826 *00,839*

P-Type Doubling in the Infrared Spectrum of NO-HF.
PB94-211463 *00,817*

Use of Extended Permutation-Inversion Groups in Constructing Hyperfine Hamiltonians for Symmetrical-Top Internal Rotor Molecules Like H3C-SiH3.
PB94-212032 *00,823*

HOUSE, J. M.
Optimal Control of Building and HVAC Systems.
PB96-141353 *00,272*

HOUSTON, J. M.
National Institute of Standards and Technology High-Accuracy Cryogenic Radiometer.
PB96-179585 *04,378*

Realization of a Scale of Absolute Spectral Response Using the NIST High Accuracy Cryogenic Radiometer.
PB97-118640 *04,397*

HOVEL, H. J.
Nano-Defects in Commercial Bonded SOI and SIMOX.
PB96-123674 *02,407*

HOWARD, F. L.
Physical Properties of Some Purified Aliphatic Hydrocarbons.
AD-A297 265/1 *00,657*

HOWARD, J. K.
Antiferromagnetic Interlayer Correlations in Annealed Ni80Fe20/Ag Multilayers.
PB97-122220 *03,109*

Magnetic Structure Determination for Annealed Ni80Fe20/Ag Multilayers Using Polarized-Neutron Reflectivity.
PB96-176615 *03,739*

HOWARD, L. P.
Force Calibrations in the Nanonewton Regime.
PB95-168696 *03,949*

HOWE, D.
Confidence on the Second Difference Estimation of Frequency Drift.
PB95-151460 *01,532*

HOWE, D. A.
Satellite Two-Way Time Transfer: Fundamentals and Recent Progress.
PB95-161089 *01,536*

Wavelet Analysis for Synchronization and Timekeeping.
PB96-200381 *01,558*

Wavelet Variance, Allan Variance, and Leakage.
PB96-190111 *01,509*

HOWE, J.
Resonance Enhanced Multiphoton Ionization Spectroscopy of the PF Radical.
PB97-119119 *00,702*

HOWE, J. E.
Extended CO(7 yields 6) Emission from Warm Gas in Orion.
PB96-102504 *00,090*

HOWELL, B.
Polyethylene Crystallized from an Entangled Solution Observed by Scanning Tunneling Microscopy.
PB95-107389 *01,232*

HOWLEY, J. B.
Isochoric (p-p-T) Measurements on Liquid and Gaseous Air from 67 to 400 K at Pressures to 35 MPa.
PB96-167390 *01,154*

Vapour Pressure Measurements on 1,1,1,2-Tetrafluoroethane (R134a) from 180 to 350 K.
PB95-168886 *03,265*

HOYT, C. C.
Update on the Low Background IR Calibration Facility at the National Institute of Standards and Technology.
PB94-211224 *04,232*

HOZUMI, N.
Effect of DC Tests on Induced Space Charge.
PB94-172350 *02,212*

HRILJAC, J. A.
Anomalous Dispersion and Thermal Expansion in Lightly-Doped KTa1-xNbxO3.
PB95-152302 *04,585*

HSIA, J.
Rayleigh Scattering Limits for Low-Level Bidirectional Reflectance Distribution Function Measurements.
PB95-180030 *04,307*

HSIA, J. J.
45 deg/0 deg Reflectance Factors of Pressed Polytetrafluoroethylene (PTFE) Powder.
PB95-260758 *04,328*

Standard Reference Materials: Polystyrene Films for Calibrating the Wavelength Scale of Infrared Spectrophotometers - SRM 1921.
PB95-226866 *03,386*

HSIAO-YU, C.
Variations in Size Measurements by Indicating Gaging Systems.
PB95-163614 *02,864*

HSIEH, S. H.
Nucleic Acid Database: Present and Future.
PB97-109078 *00,518*

HSIEH, T. J.
Reactive Coevaporation of DyBaCuO Superconducting Films: The Segregation of Bulk Impurities on Annealed MgO(100) Substrates.
PB95-164562 *04,635*

HSIN, Y. E.
Acid Gas Production in Inhibited Diffusion Flames.
PB95-180576 *01,390*

HSING, K.
Analysis of ANSI ASC X12 and UN/EDIFACT Electronic Data Interchange (EDI) Standards.
PB95-220554 *01,729*

HSLA, J. J.
NIST Response to the Fifth CORM Report on the Pressing Problems and Projected Needs in Optical Radiation Measurements.
PB94-188240 *04,227*

HSU, J. C. L.
In-situ Fume Particle Size and Number Density Measurements from a Synthetic Smelt.
PB94-212040 *03,334*

HSU, N. N.
Design, Construction and Application of a Large Aperture Lens-Less Line-Focus PVDF Transducer.
PB97-122584 *02,765*

Material Characterization By a Time-Resolved and Polarization-Sensitive Ultrasonic Technique.
PB97-122576 *02,764*

Transient Analysis of a Line-Focus Transducer Probing a Liquid/Solid Interface.
PB97-118681 *02,763*

HSU, S. M.
Analysis of Physical Properties of Ceramic Powders in an International Interlaboratory Comparison Program.
PB95-161501 *03,050*

Asperity-Asperity Contact Mechanisms Simulated by a Two-Ball Collision Apparatus.
PB95-164158 *02,966*

Boundary Lubrication of Silicon Nitride.
PB95-213583 *03,226*

Ceramic Powders Characterization: Results of an International Laboratory Study.
PB95-270039 *02,672*

Chemical Effect in Ceramics Grinding.
PB97-122592 *03,113*

Chemically Assisted Machining of Si3N4.
PB96-122999 *03,072*

Deposit Forming Tendencies of Diesel Engine Oils-Correlation between the Two-Peak Method and Engine Tests.
PB95-152138 *01,452*

Effect of Microstructure on the Wear Transition of Zirconia-Toughened Alumina.
PB94-211778 *03,141*

Evaluation of Wear Resistant Ceramic Valve Seats in Gas-Fueled Power Generation Engines. Topical Report, December 1991-April 1994.
PB95-200218 *02,466*

Glimpse of Materials Research in China: A Report from an Interagency Study Team on Materials Visiting China from June 19, 1995 to June 30, 1995.
PB96-112677 *02,978*

Mechano-Chemical Model: Reaction Temperatures in a Concentrated Contact.
PB96-119466 *03,227*

New Method to Evaluate Deposit Forming Tendencies of Liquid Lubricants by Differential Scanning Calorimetry.
PB95-152120 *01,451*

Silicon Nitride Boundary Lubrication: Effect of Oxygenates.
PB96-111711 *03,068*

Silicon Nitride Boundary Lubrication: Lubrication Mechanism of Alcohols.
PB96-111703 *03,067*

Tribochemical Reaction of Stearic Acid on Copper Surface Studied by Surface Enhanced Raman Spectroscopy.
PB94-212057 *02,964*

Tribological Characteristics of Alpha-Alumina at Elevated Temperatures.
PB94-211018 *02,963*

Variances in the Measurement of Ceramic Powder Properties.
PB97-110316 *03,100*

Wear Mechanism Maps of Ceramics.
PB94-172368 *03,229*

Wear Model for Alumina Sliding Wear.
PB95-163796 *03,239*

Wear Modeling of Si-Based Ceramics.
PB97-122501 *03,112*

Wear Transitions in Monolithic Alumina and Zirconia-Alumina Composites.
PB96-103163 *03,168*

HSY, C. J.
Chemically Assisted Machining of Si3N4.
PB96-122999 *03,072*

HU, B. Y. K.
Correction to the Decay Rate of Nonequilibrium Carrier Distributions Due to Scattering-in Processes.
PB94-185840 *04,452*

HU, J. T.
Structural Heterogeneity in Epoxies.
PB95-151866 *01,243*

HU, X. M.
High Resolution Angle Resolved Photoelectron Spectroscopy Study of N2.
PB95-151494 *03,907*

HU, Z. S.
Tribochemical Reaction of Stearic Acid on Copper Surface Studied by Surface Enhanced Raman Spectroscopy.
PB94-212057 *02,964*

HUANG, D.
Intercomparison of Thermal Converters at NIM, NIST, PTB, SIRI and VSL from 10 to 100 MHz.
PB94-172459 *02,027*

HUANG, D. X.
AC-DC Difference Characteristics of High-Voltage Thermal Converters.
PB96-148093 *02,083*

Development of Thin-Film Multijunction Thermal Converters at NIST.
PB97-112338 *02,286*

Integrated Thin-Film Micropotentiometers.
PB96-146709 *02,109*

Multijunction Thermal Converters by Commercial CMOS Fabrication.
PB95-153664 *02,343*

Performance of Commercial CMOS Foundry-Compatible Multijunction Thermal Converters.
PB95-153656 *02,342*

Performance of Multilayer Thin-Film Multijunction Thermal Converters.
PB96-148135 *02,084*

HUANG, H. M.
Certainty Grid to Object Boundary Algorithm.
PB94-203510 *01,835*

Hierarchical Real-Time Control System for Use with Coal Mining Automation.
PB94-212065 *03,698*

Operator Experience with a Hierarchical Real-Time Control System (RCS).
PB96-195516 *03,751*

Outline of a Multiple Dimensional Reference Model Architecture and a Knowledge Engineering Methodology for Intelligent Systems Control.
PB95-220414 *03,703*

Submarine Automation: Demonstration No. 5.
PB95-251633 *03,748*

Task Decomposition Methodology for the Design of a Coal Mining Automation Hierarchical Real-Time Control System.
PB94-185386 *03,694*

HUANG, P. H.
New Expressions of Uncertainties for Humidity Calibrations at the National Institute of Standards and Technology.
PB95-103826 *02,645*

HUANG, Q.
Characterization of the Structure of LaD2.50 by Neutron Powder Diffraction.
PB96-176797 *04,783*

Characterization of the Structure of TbD2.25 at 70 K by Neutron Powder Diffraction.
PB96-160528 *01,130*

Characterization of the Structure of YD3 by Neutron Powder Diffraction.
PB96-186150 *01,161*

Crystal Structure of Annealed and As-Prepared HgBa2CaCu2O6+delta Superconductors.
PB95-161105 *03,927*

Crystal Structure of Pb2Sr2YCu3O8+delta with delta=1.32, 1.46, 1.61, 1.71, by Powder Neutron Diffraction.
PB94-216314 *04,518*

Neutron Powder Diffraction Study of the Crystal Structure of YSr2AlCu2O7.
PB94-212073 *04,499*

Neutron-Powder-Diffraction Study of the Long-Range Order in the Octahedral Sublattice of LaD2.25.
PB96-141155 *04,753*

Neutron Powder Diffraction Study of the Nuclear and Magnetic Structures of the Oxygen-Deficient Perovskite YBaCuCoO5.
PB95-161097 *00,954*

Neutron Scattering Study of Antiferromagnetic Order in the Magnetic Superconductors RNi2B2C.
PB97-112411 *04,812*

Observation of Oscillatory Magnetic Order in the Antiferromagnetic Superconductor HoNi2B2C.
PB95-180303 *04,679*

Oxygen Dependance of the Crystal Structure of HgBa2CuO4+ and Its Relation to Superconductivity.
PB96-102512 *04,711*

Preparation, Crystal Structure, Dielectric Properties, and Magnetic Behavior of Ba2Fe2Ti4O13.
PB96-186176 *01,162*

Unconventional Ferromagnetic Transition in La(sub 1-x)Ca(sub x)MnO3.
PB97-112429 *04,156*

HUANG, X. R.

Interdigitated Stacked P-I-N Multiple Quantum Well Modulator.
PB97-112296 *02,455*

HUBBARD, J.

Determining Mobility from Homodyne ac Electrophoretic Light Scattering.
PB95-140497 *03,462*

Non-Perturbative Relation between the Mutual Diffusion Coefficient, Suspension Viscosity, and Osmotic Compressibility: Application to Concentrated Protein Solutions.
PB96-102355 *01,062*

HUBBARD, J. B.

Electrolytes Constrained on Fractal Structures: Debye-Huckel Theory.
PB97-110241 *01,174*

Fluctuation Dominated Recombination Kinetics with Traps.
PB95-107264 *00,875*

Fokker-Planck Description of Multivalent Interactions.
PB95-108478 *00,879*

Hydrodynamic Friction of Arbitrarily Shaped Brownian Particles.
PB97-110191 *04,136*

Physical Characterization of Herparin by Light Scattering.
PB96-119383 *03,598*

HUBBELL, J. H.

Bibliography of Photon Total Cross Section (Attenuation Coefficient) Measurements 10 eV to 13.5 GeV, 1907-1993.
PB94-193760 *03,804*

Experimentally Measured Total X-ray Attenuation Coefficients Extracted from Previously Unprocessed Documents Held by the NIST Photon and Charged Particle Data Center.
PB97-114474 *04,165*

Polarization Effects on Multiple Scattering Gamma Transport.
PB95-153615 *03,926*

Tables of X-ray Mass Attenuation Coefficients and Mass Energy-Absorption Coefficients 1 keV to 20 MeV for Elements Z = 1 to 92 and 48 Additional Substances of Dosimetric Interest.
PB95-220539 *04,013*

HUBER, M. E.

Noise Reduction in Low-Frequency SQUID Measurements with Laser-Driven Switching.
PB96-135165 *02,081*

Trapped Vortices in a Superconducting Microbridge.
PB95-141149 *04,554*

HUBER, M. L.

Equation of State Formulation of the Thermodynamic Properties of R134a (1,1,1,2-Tetrafluoroethane).
PB94-212081 *03,256*

Prediction of the Thermal Conductivity of Refrigerants and Refrigerant Mixtures.
PB94-212107 *03,258*

Prediction of Viscosity of Refrigerants and Refrigerant Mixtures.
PB94-212099 *03,257*

Predictive Extended Corresponding States Model for Pure and Mixed Refrigerants Including an Equation of State for R134a.
PB95-175717 *03,275*

REFPROP Refrigerant Properties Database: Capabilities, Limitations, and Future Directions.
PB96-167150 *01,149*

Thermodynamic Properties of R134a(1,1,1,2-Tetrafluoroethane).
PB95-168704 *00,988*

Thermophysical Property Computer Packages from NIST.
PB95-125787 *04,203*

Thermophysical Property Standard Reference Data from NIST.
PB96-167358 *01,153*

Viscosity of Defined and Undefined Hydrocarbon Liquids Calculated Using an Extended Corresponding-States Model.
PB96-167234 *02,498*

HUCKER, T.

Standardised Computer Data File Format for Storage, Transport, and Off-Line Processing of Partial Discharge Data.
PB96-122486 *01,930*

HUDGENS, J. W.

Electronic Spectra of CF2Cl and CFCl2 Radicals Observed by Resonance Enhanced Multiphoton Ionization.
PB95-151023 *00,927*

Experimental and Abinitio Studies of Electronic Structures of the CCl3 Radical and Cation.
PB94-212131 *00,826*

Kinetics of the Reaction of CCl3-Br-2 and the Thermochemistry of CCl3 Radical and Cation.
PB94-212115 *00,824*

Multiphoton Ionization of SiH3 and SiD3 Radicals: Electronic Spectra, Vibrational Analyses of the Ground and Rydberg States, and Ionization Potential.
PB94-212503 *00,837*

Multiphoton Ionization of SiH3 and SiD3 Radicals. 2. Three Photon Resonance-Enhanced Spectra Observed between 460 and 610 nm.
PB94-212487 *00,835*

New Electronic States of NH and ND Observed from 258 to 288 nm by Resonance Enhanced Multiphoton Ionization Spectroscopy.
PB94-212495 *00,836*

New Rydberg States of Aluminum Monofluoride Observed by Resonance-Enhanced Multiphoton Ionization Spectroscopy.
PB94-199544 *00,797*

Resonance Enhanced Multiphoton Ionization Detection of GeF and GeCl Radicals.
PB94-212123 *00,825*

Resonance Enhanced Multiphoton Ionization Spectroscopy of the PF Radical.
PB97-119119 *00,702*

Resonance Enhanced Multiphoton Ionization Spectroscopy of the SnF Radical.
PB97-111223 *01,176*

Resonance Enhanced Multiphoton Ionization Spectroscopy of 2-Butene-1-yl (C4H7) between 455-485 nm.
PB95-151031 *00,670*

HUDSON, L.

Crystal Diffraction Spectrometry for Accurate, Non-Invasive kV/Spectral Measurement for Improvement of Mammographic Image Quality.
AD-A297 943/3 *00,721*

HUDSON, L. T.

Flat and Curved Crystal Spectrography for Mammographic X-ray Sources.
PB97-122246 *03,642*

Photoelectron Spectroscopic Study of the Valence and Core-Level Electronic Structure of BaTiO3.
PB94-212149 *04,500*

Polarization Measurements on a Magnetic Quadrupole Line in Ne-Like Barium.
PB97-113104 *04,161*

Resonant-Photoemission Investigation of the Heusler Alloys Ni2MnSb and NiMnSb.
PB95-162384 *04,612*

Substitution-Induced Midgap States in the Mixed Oxides RxBa1-ChiTiO3-Delta, with R=Y, La, and Nd.
PB95-140505 *04,541*

Surface Core-Level Shifts of Barium Observed in Photoemission of Vacuum-Fractured BaTiO3 (100).
PB94-212156 *04,501*

HUEBENER, R. P.

Direct Observation of Vortex Dynamics in Two-Dimensional Josephson-Junction Arrays.
PB96-102223 *02,067*

Frequency Dependence of the Emission from 2D Array Josephson Oscillators.
PB95-175147 *02,056*

Novel Vortex Dynamics in Two-Dimensional Josephson Arrays.
PB96-200167 *02,091*

Observation of Vortex Dynamics in Two-Dimensional Josephson-Junction Arrays.
PB95-168811 *02,050*

SUSAN: SUperconducting Systems ANalysis by Low Temperature Scanning Electron Microscopy (LTSEM).
PB96-112065 *04,728*

HUERTA-GARNICA, M.

Comparison of Finite Element and Analytic Calculations of the Resonant Modes and Frequencies of a Thick Shell Sphere.
PB94-160785 *02,626*

HUHNERMANN, H.

Hyperfine Structure Investigations and Identification of New Energy Levels in the Ionic Spectrum of (147)Pm.
PB96-180203 *04,117*

HUIE, R. E.

Atmospheric Lifetimes of HFC-143a and HFC-245fa: Flash Photolysis Resonance Fluorescence Measurements of the OH Reaction Rate Constants.
PB97-112577 *00,118*

Atmospheric Reactivity of alpha-Methyl-Tetrahydrofuran.
PB95-163705 *02,548*

Electron Transfer Reaction Rates and Equilibria of the Carbonate and Sulfate Radical Anions.
PB94-212180 *00,829*

Environmental Aspects of Halon Replacements: Considerations for Advanced Agents and the Ozone Depletion Potential of CF3I.
PB97-122261 *03,301*

Experimental Determination of the Ionization Energy of IO(X(sup 2)II(sub 3/2)) and Estimations of Delta(sub f)H(sup deg)(sub 0)(IO(sup -)) and PA(IO).
PB96-146899 *00,694*

Ferric Ion Assisted Photooxidation of Halocetates.
PB97-112460 *00,521*

Free Radical Chemistry of the Atmospheric Aqueous Phase.
PB96-148101 *00,117*

Gas Phase Reactivity Study of OH Radicals with 1,1-Dichloroethene and cis-1,1-Dichloroethene and Trans-1,2-Dichloroethene over the Temperature Range 240-400 K.
PB95-152146 *00,939*

Ionization Energies, Appearance Energies and Thermochemistry of CF2O and FCO.
PB97-111538 *01,178*

Kinetics of the Reaction of the Sulfate Radical with the Oxalate Anion.
PB97-119127 *01,186*

Kinetics of the Self-Reaction of Hydroxymethylperoxyl Radicals.
PB94-212164 *00,827*

Oxidation of Ferrous and Ferrocyanide Ions by Peroxyl Radicals.
PB97-122402 *01,191*

Rate Constants for the Gas Phase Reactions of the OH Radical with CF3CF2CHCl2 (HCFC-225ca) and CF2ClCF2CHClF (HCFC-225cb).
PB95-152153 *00,940*

Reaction of Nitric Oxide with Organic Peroxyl Radicals.
PB95-141107 *00,910*

Reaction of NO with Superoxide.
PB94-212198 *00,830*

Solvent Effects in the Reactions of Peroxyl Radicals with Organic Reductants. Evidence for Proton Transfer Mediated Electron Transfer.
PB95-107157 *00,873*

Temperature Dependence of the Rate Constants for Reaction of Dihalide and Azide Radicals with Inorganic Reductants.
PB95-162756 *00,964*

Temperature Dependence of the Rate Constants for Reaction of Inorganic Radicals with Organic Reductants.
PB94-198280 *00,783*

Temperature Dependence of the Rate Constants for Reactions of the Carbonate Radical with Organic and Inorganic Reductants.
PB94-212206 *00,831*

Temperature Dependence of the Rate Constants for Reactions of the Sulfate Radical, SO4-, with Anions.
PB94-212172 *00,828*

Temperature Dependence of the Ultraviolet Absorption Cross Section of CF3I.
PB96-204169 *01,168*

HULL, J. J.

Second Census Optical Character Recognition Systems Conference.
PB94-188711 *01,832*

HUMMER, D. G.

Fast Computer Evaluation of Radiative Properties of Hydrogenic Systems.
PB95-150553 *03,894*

Opacity Project and the Practical Utilization of Atomic Data.
PB94-212214 *00,059*

Radiation-Driven Winds of Hot Luminous Stars X. The Determination of Stellar Masses Radii and Distances from Terminal Velocities and Mass-Loss Rates.
PB94-213022 *00,060*

Recombination Line Intensities for Hydrogenic Ions-III. Effects of Finite Optical Depth and Dust.
PB95-202677 *00,079*

Sobolev Approximation for Line Formation with Partial Frequency Redistribution.
PB95-202669 *00,078*

Stars, Atmospheres, Radiative Transfer.
PB96-119474 *00,095*

HUMPHREYS, D. A.

Comparison of Photodiode Frequency Response Measurements to 40 GHz between NPL and NIST.
PB96-111992 *04,038*

Photodetector Frequency Response Measurements at NIST, US, and NPL, UK: Preliminary Results of a Standards Laboratory Comparison.
PB95-175592 *02,175*

HUMPHREYS, J. C.

Calibration of High-Energy Electron Beams by Use of Graphite Calorimeters.
PB95-161113 *04,598*

Calorimeters for Calibration of High-Dose Dosimeters in High-Energy Electron Beams.
PB96-135272 *04,055*

Role of the Office of Radiation Measurement in Quality Assurance.
PB94-212255 *00,689*

HUNGATE, J.

Comparison of POSIX Open System Environment (OSE) and Open Distributed Processing (ODP) Reference Models.
PB96-131495 *01,820*

Distributed Systems: Survey of Open Management Approaches.
PB96-128202 01,746

Open System Environment Implementors Workshop (OIW); Standardization Role Defined.
PB96-180047 01,828

HUNSTON, D. L.

Micromechanics of Fracture in Rubber-Toughened Epoxies.
PB94-212222 03,011

Review of Cure Monitoring Techniques for On-Line Process Control.
PB94-216728 03,145

Structural Heterogeneity in Epoxies.
PB95-151866 01,243

Water Adsorption at a Polyimide/Silicon Wafer Interface.
PB96-103197 01,070

HUNT, F. Y.

Analytical Expressions for Barkhausen Jump Size Distributions.
PB95-180345 04,680

Monte Carlo Approach to the Approximation of Invariant Measures.
PB94-172053 03,409

Probabilistic Computation of Poiseuille Flow Velocity Fields.
PB96-102520 04,209

HUNTER, C. R.

Estimation of the Absorbed Dose in Radiation-Processed Food. 1. Test of the EPR Response Function by a Linear Regression Analysis.
PB94-199718 00,039

HUO, Q.

Small Angle Neutron Scattering Study of the Structure and Formation of MCM-41 Mesoporous Molecular Sieves.
PB97-122337 03,110

Small Angle Neutron Scattering Study of the Structure and Formation of Ordered Mesopores in Silica.
PB96-111919 03,069

HURLY, J. J.

Absence of Quantum-Mechanical Effects on the Mobility of Argon Ions in Helium Gas at 4.35 K.
PB97-122543 01,194

HURST, G. S.

Measurement of Absorbed Dose of Neutrons, and of Mixtures of Neutrons and gamma rays.
AD-A286 647/3 03,710

HURST, W. S.

Development of the NIST Transient Pressure and Temperature Calibration Facility.
PB96-160833 00,626

Q Branch Lineshape Functions for CARS Thermometry.
PB96-160643 01,132

Simultaneous Forward-Backward Raman Scattering Studies of D2 Broadened by D2, He, and Ar.
PB95-162459 00,961

HURWITZ, L. M.

Radiation Process Data: Collection, Analysis, and Interpretation.
PB95-162632 03,628

HUSK, D. E.

Soft-X-ray Damage to p-terphenyl Coatings for Detectors.
PB96-159611 04,364

HUTCHINGS, J. B.

Observations of 3C 273 with the Goddard High Resolution Spectrograph on the Hubble Space Telescope.
PB95-202321 00,076

HUTCHINSON, J. M. R.

Anomalous Odd- to Even-Mass Isotope Ratios in Resonance Ionization with Broad-Band Lasers.
PB94-211406 03,839

Atom-counting standards and Doppler-free resonance ionization mass spectroscopy. (Progress report).
DE94018562 00,723

Calibration of Electret-Based Integral Radon Monitors Using NIST Polyethylene-Encapsulated (226)Ra/(222)Rn Emanation (PERE) Standards.
PB96-159223 01,950

International Marine-Atmospheric (222)Rn Measurement Intercomparison in Bermuda. Part 1. NIST Calibration and Methodology for Standardized Sample Additions.
PB96-175674 00,114

International Marine-Atmospheric (222)Rn Measurement Intercomparison in Bermuda. Part 2. Results for the Participating Laboratories.
PB96-175682 00,115

International Radon-in-Air Measurement Intercomparison Using a New Transfer Standard.
PB96-159751 03,708

Measurement and Calibration of Large-Area Alpha-Particle Sources at NIST.
PB94-172855 03,791

Study of Laser Resonance Ionization Mass Spectrometry Using a Glow Discharge Source.
DE94018566 03,308

Study of Laser Resonance Ionization Mass Spectrometry Using a Glow Discharge Source.
PB96-123203 03,360

HUTSON, J. M.

Signatures of Large Amplitude Motion in a Weakly Bound Complex: High-Resolution IR Spectroscopy and Quantum Calculations for HeCO2.
PB95-203485 01,054

Spectroscopic Puzzle in ArHF Solved: The Test of a New Potential.
PB94-216058 00,850

Vibrational Dependence of the Anisotropic Intermolecular Potential of Ar-HCl.
PB95-202685 01,029

Vibrational Dependence of the Anisotropic Intermolecular Potential of Ar-HF.
PB95-202693 01,030

HUTTER, A. R.

International Marine-Atmospheric (222)Rn Measurement Intercomparison in Bermuda. Part 2. Results for the Participating Laboratories.
PB96-175682 00,115

HUTTER, E.

Use of Building Emulators to Evaluate the Performance of Building Energy Management Systems.
PB96-111901 00,269

HUTTON, D. R.

Estimation of the Absorbed Dose in Radiation-Processed Food. 1. Test of the EPR Response Function by a Linear Regression Analysis.
PB94-199718 00,039

HUZAREWICZ, S.

Flame Synthesis of High Tc Superconductors.
PB95-151981 00,659

Parametric Investigation of Metal Powder Atomization Using Laser Diffraction.
PB95-108577 03,342

HWANG, C. S.

Epitaxial Growth of BaTiO3 Thin Films at 600C by Metalorganic Chemical Vapor Deposition.
PB96-122510 03,071

HWANG, H. H.

Evidence for Inelastic Processes for N(+)3 and N(+)4 from Ion Energy Distributions in He/N2 Radio Frequency Glow Discharges.
PB96-146683 04,059

HWANG, I. S.

Charpy Impact Test as an Evaluation of 4 K Fracture Toughness.
PB96-190194 03,219

Fatigue Crack Thresholds of a Nickel-Iron Alloy for Superconductor Sheaths at 4 K.
PB96-190343 03,223

HWANG, J. T.

Existence and Nonexistence Theorems of Finite Diameter Sequential Confidence Regions for Errors-in-Variables Models.
PB95-180352 03,441

HWANG, M. S.

Application of the Electronic Balance in High Precision Pycnometry.
PB94-187564 00,534

Determination of Density of Mass Standards: Requirement and Method.
PB94-163078 03,787

Electronic Balance and Some Gravimetric Applications. (The Density of Solids and Liquids, Pycnometry and Mass).
PB94-163052 03,785

HWANG, N. M.

Phase Equilibria in the Systems CaO-CuO and CaO-Bi2O3.
PB95-140570 03,048

X-Ray Characterization of the Crystallization Process of High-Tc Superconducting Oxides in the Sr-Bi-Pb-Ca-Cu-O System.
PB95-151700 04,579

HYATT, J. A.

Solid State (13)C NMR and Raman Studies of Cellulose Triacetate: Oligomers, Polymorphism, and Inferences about Chain Polarity.
PB96-176532 01,289

HYER, C. W.

Directory of U.S. Private Sector Product Certification Programs.
PB96-215074 02,688

HYLTON, T. L.

Antiferromagnetic Interlayer Correlations in Annealed Ni80Fe20/Ag Multilayers.
PB97-122220 03,109

Magnetic Structure Determination for Annealed Ni80Fe20/Ag Multilayers Using Polarized-Neutron Reflectivity.
PB96-176615 03,739

HYUN, O. B.

Experimental Aspects of Flux Expulsion in Type-II Superconductors.
PB95-175725 04,660

Flux Expulsion at Intermediate Fields in Type-II Superconductors.
PB94-212230 04,502

IACONIS, C.

High-Efficiency, High-Power Difference-Frequency Generation of 0.9-1.5 mu m Light in BBO.
PB95-202255 04,317

IDRISS, I. M.

Assessment of Site Response Analysis Procedures.
PB95-210928 00,450

IGA, I.

Shape-Resonance-Enhanced Continuum-Continuum Coupling in Photoionization of CO2.
PB95-164471 00,983

ILAVSKY, J.

Anisotropy of the Surfaces of Pores in Plasma Sprayed Alumina Deposits.
PB96-123211 03,126

IMAE, M.

Use of Ionospheric Data in GPS Time Transfer.
PB95-163853 01,540

IMHOFF, J.

Radiation-Driven Winds of Hot Luminous Stars X. The Determination of Stellar Masses Radii and Distances from Terminal Velocities and Mass-Loss Rates.
PB94-213022 00,060

INAM, A.

Laser-Synchrotron Hybrid Experiments: A Photon to Tickle, A Photon to Poke.
PB96-157847 03,704

INCE, A. T.

Comparisons of Some NIST Fixed-Point Cells with Similar Cells of Other Standards Laboratories.
PB97-119242 00,655

INDELICATO, P.

Electron Screening Correction to the Self Energy in High-Z Atoms.
PB94-172376 03,789

K alpha Transitions in Few-Electron Ions and in Atoms.
PB94-212248 03,849

Magnetic Dipole Line from U LXXI Ground-Term Levels Predicted at 3200 Angstroms.
PB94-211497 04,407

INGHAM, H.

Process Gas Chromatography Detector for Hydrocarbons Based on Catalytic Cracking.
PB95-141099 02,485

INGUSCIO, M.

Rotational Far Infrared Spectrum of (13)CO.
PB95-152187 00,941

INN, K. G. W.

Atom-counting standards and Doppler-free resonance ionization mass spectroscopy. (Progress report).
DE94018562 00,723

External Gamma-ray Counting of Selected Tissues from a Thorotrast Patient.
PB96-160254 03,637

Intercomparison Study of (237)Np Determination in Artificial Urine Samples.
PB96-102645 03,633

Pilot Studies for Improving Sampling Protocols.
PB97-118715 02,530

Role of the Office of Radiation Measurement in Quality Assurance.
PB94-212255 00,689

Summary of the Proceedings of the Workshop on Standard Phantoms for In-vivo Radioactivity Measurement.
PB94-212933 03,622

INTERRANTE, C. G.

Factors Significant to Precracking of Fracture Specimens.
PB96-109558 03,358

Information Retrieval Using Key Words and a Structured Review.
PB95-161121 03,724

IPPOLITO, L.

Assessing Functional Diversity by Program Slicing.
PB96-160890 03,734

IPPOLITO, L. M.

Analysis of Selected Software Safety Standards.
PB95-151262 01,708

Analysis of Standards for the Assurance of High Integrity Software.
PB96-161351 03,735

Control and Instrumentation: Standards for High-Integrity Software.
PB96-161369 03,736

Framework for the Development and Assurance of High Integrity Software.
PB95-173084 01,716

Proceedings of the Digital Systems Reliability and Nuclear Safety Workshop. Held in Rockville, Maryland on September 13-14, 1993.
NUREG/CP-0136 03,728

Reference Information for the Software Verification and Validation Process.
PB96-188164 01,773

Study on Hazard Analysis in High Integrity Software Standards and Guidelines.
PB95-198727 01,725

IRIKURA, K. K.

Matrix Isolation Study of the Interaction of Excited Neon Atoms with BCl3: Infrared Spectra of BCl(sub 3, sup +), BCl(sub 2, sup +), and BCl(sub 3, sup -).
PB97-119143 01,187

IRWIN, K. D.

Hot-Electron Microcalorimeter for X-ray Detection Using a Superconducting Transition Edge Sensor with Electrothermal Feedback.
PB96-200399 *04,792*

Self-Biasing Cryogenic Particle Detector Utilizing Electrothermal Feedback and a SQUID Readout.
PB96-102538 *04,712*

ISAACS, W. A.

Modified Effective Range Theory as an Alternative to Low-Energy Close-Coupling Calculations.
PB95-202701 *03,988*

ISAACSON, M.

NIST Metrology for Soft X-ray Multilayer Optics.
PB96-160379 *04,088*

ISHIBASHI, T.

Effects of Heavy Doping on Numerical Simulations of Gallium Arsenide Bipolar Transistors.
PB95-150975 *02,334*

ISHIDA, H.

Upward Flame Spread along the Vertical Corner Walls (October 1993).
PB94-206299 *00,340*

ISHIDA, T.

Harmonic and Static Susceptibilities of YBa2Cu3O7.
PB95-161139 *04,599*

Offset Susceptibility of Superconductors.
PB94-212263 *04,503*

ISHIKAWA, K.

Behavior of a Calcium Phosphate Cement in Simulated Blood Plasma In vitro.
PB95-168712 *00,165*

Effect of Supersaturation on Apatite Crystal Formation in Aqueous Solutions at Physiologic pH and Temperature.
PB96-135215 *03,571*

Formation of Hydroxyapatite in Cement Systems.
PB95-175261 *00,170*

Properties and Mechanisms of Fast-Setting Calcium Phosphate Cements.
PB96-123229 *00,178*

ISHIKAWA, Y.

Behavior of a Calcium Phosphate Cement in Simulated Blood Plasma In vitro.
PB95-168712 *00,165*

Properties and Mechanisms of Fast-Setting Calcium Phosphate Cements.
PB96-123229 *00,178*

ISHINABE, T.

Examination of the l/d Expansion Method from Exact Enumeration for a Self-Interacting Self-Avoiding Walk.
PB95-175733 *01,266*

Hypercubic Lattice SAW Exponents nu and gamma : 3.99 Dimensions Revisited.
PB94-211026 *01,215*

Self-Avoiding-Walk Contacts and Random-Walk Self-Intersections in Variable Dimensionality.
PB96-102231 *01,276*

ITANO, W.

Electrostatic Modes of Ion-Trap Plasmas.
PB95-152963 *03,920*

Obtaining and Installing a Public Domain TEX.
PB95-175741 *01,719*

ITANO, W. M.

Accurate Measurement of Time.
PB96-119482 *01,552*

Atomic Clock.
PB96-119490 *01,553*

Experimental Results on Normal Modes in Cold, Pure Ion Plasmas.
PB95-175105 *03,956*

Getting Started on Mosaic.
PB95-180360 *01,721*

High-Resolution Atomic Spectroscopy of Laser-Cooled Ions.
PB95-169330 *03,953*

Interference in the Resonance Fluorescence of Two Trapped Atoms.
PB95-168514 *03,948*

Laser Cooling of Trapped Ions.
PB95-168746 *03,950*

Light Scattered from Two Atoms.
PB95-168753 *04,286*

Liquid and Solid Atomic Ion Plasmas.
PB94-198991 *03,809*

Precise Spectroscopy for Fundamental Physics.
PB96-112164 *04,040*

Progress on a Cryogenic Linear Trap for (199)Hg(+) Ions.
PB95-180790 *03,965*

Quantum Measurements of Trapped Ions.
PB95-161147 *03,928*

Quantum Projection Noise: Population Fluctuations in Two-Level Systems.
PB94-212271 *03,850*

Recent Experiments on Trapped Ions at the National Institute of Standards and Technology.
PB95-169322 *03,952*

Retrieving Articles from the Internet (without a UNIX Workstation). Part 1. File Formats and Software Tools.
PB95-168720 *02,728*

Retrieving Articles from the Internet (without a UNIX Workstation). Part 2. An Example.
PB95-168738 *02,729*

Spin Squeezing and Reduced Quantum Noise in Spectroscopy.
PB95-151635 *03,912*

Squeezed Atomic States and Projection Noise in Spectroscopy.
PB95-176293 *03,960*

Trapped Ions and Laser Cooling 4: Selected Publications of the Ion Storage Group of the Time and Frequency Division, NIST, Boulder, Colorado.
PB96-172358 *04,108*

ITKIN, V.

Thermodynamic Properties of the Group IIA Elements.
PB94-160983 *00,730*

ITOH, K.

Reduction of Interfilament Contact Loss in Nb3Sn Superconductor Wires.
PB95-175535 *02,223*

IULIANO, M. J.

Overview of the Manufacturing Engineering Toolkit Prototype.
PB96-128228 *02,833*

IVES, L. K.

Abrasive Wear by Diesel Engine Coal-Fuel and Related Particles.
PB95-104915 *01,450*

Generation and Characterization of Acetylene Smokes.
PB94-200292 *01,372*

Ultrafine Combustion Aerosol Generator.
PB94-200300 *01,373*

IYENGAR, G. V.

Determination of Boron and Lithium in Diverse Biological Matrices Using Neutron Activation - Mass Spectrometry (NA-MS).
PB94-212289 *00,554*

Mixed Diet Reference Materials for Nutrient Analysis of Foods: Preparation of SRM-1548 Total Diet.
PB95-151692 *03,593*

IYENGAR, V. G.

External Gamma-ray Counting of Selected Tissues from a Thorotrast Patient.
PB96-160254 *03,637*

IYER, H. K.

Moments of the Quartic Assignment Statistic with an Application to Multiple Regression.
PB95-181103 *03,442*

Technique to Evaluate Benchmarks: A Case Study Using the Livermore Loops.
PB95-151320 *04,577*

Tolerance Intervals for the Distribution of True Values in the Presence of Measurement Errors.
PB95-150405 *03,434*

IYER, S.

1,4-Dinitrocubane and Cubane under High Pressure.
PB95-108437 *03,755*

IZWORSKI, N.

Methods to Improve the Accuracy of On-Line Ultrasonic Measurement of Steel Sheet Formability.
PB96-186051 *02,281*

JABBOUR, Z. J.

Nanofabrication of a Two-Dimensional Array Using Laser-Focused Atomic Deposition.
PB96-119417 *04,732*

JABLONSKI, A.

Elastic-Electron-Scattering Effects on Angular Distributions in X-ray Photoelectron Spectroscopy.
PB95-175758 *01,000*

Formalism and Parameters for Quantitative Surface Analysis by Auger Electron Spectroscopy and X-Ray Photoelectron Spectroscopy.
PB94-212297 *00,832*

JACH, T.

Grazing Angle X-Ray Photoemission System for Depth-Dependent Analysis.
PB95-161154 *04,600*

Grazing-Incidence X-Ray Photoelectron Spectroscopy: A Novel Approach to Thin Film Characterization.
PB95-153128 *04,589*

Grazing Incidence X-ray Photoemission and Its Implementation on Synchrotron Light Source X-ray Beamlines.
PB95-175766 *01,001*

Grazing-Incidence X-Ray Photoemission Spectroscopy Investigation of Oxidized GaAs(100): A Novel Approach to Nondestructive Depth Profiling.
PB94-200151 *04,480*

Polarized X-Ray Emission Spectroscopy.
PB94-213360 *03,862*

X-Ray Photoelectron and Auger Electron Spectroscopy Study of Ultraviolet/Ozone Oxidized P2S5/(NH4)2S Treated GaAs(100) Surfaces.
PB94-200144 *04,479*

JACKSON, C. L.

Anomalous Freezing and Melting of Solvent Crystals in Swollen Gels of Natural Rubber.
PB94-212321 *01,223*

Flow-Induced Structure in Polymers: Chapter 16. Shear-Induced Changes in the Order-Disorder Transition Temperature and the Morphology of a Triblock Copolymer.
PB96-123237 *03,127*

Glass Transition of Organic Liquids Confined to Small Pores.
PB94-212305 *00,833*

Influence of Shear on the Ordering Temperature of a Triblock Copolymer Melt.
PB96-163753 *01,288*

Melting Behavior of Organic Materials Confined in Porous Solids.
PB94-212313 *00,834*

Morphology and Phase Separation Kinetics of a Compatibilized Blend.
PB97-119135 *01,297*

Polymer Liquid Crystalline Materials.
PB94-212339 *01,224*

Shear-Excited Morphological States in a Triblock Copolymer.
PB94-172392 *01,196*

Shear-Induced Changes in the Order-Disorder Transition Temperature and the Morphology of a Triblock Copolymer.
PB97-118772 *03,130*

Shear-Induced Martensitic-Like Transformation in a Block Copolymer Melt.
PB96-119508 *01,277*

Synthesis of Hybrid Organic-Inorganic Materials from Interpenetrating Polymer Network Chemistry.
PB96-180054 *02,994*

Vitrification and Crystallization of Organic Liquids Confined to Nanoscale Pores.
PB97-112304 *03,392*

JACKSON, J.

Scattered Fractions of Dose from 18 and 25 MV X-ray Radiotherapy Linear Accelerators.
PB96-186101 *04,120*

JACKSON, J. K.

Characterization of Modified FEL Quartz-Halogen Lamps for Photometric Standards.
PB97-112544 *00,282*

JACKSON, M.

Acoustic Emission of Structural Materials Exposed to Open Flames.
PB95-164810 *00,296*

JACKSON, M. A.

Comparison of Fire Sprinkler Piping Materials: Steel, Copper, Chlorinated Polyvinyl Chloride and Polybutylene, in Residential and Light Hazard Installations.
PB95-182267 *00,299*

JACKSON, R. H. F.

Guidelines for Reporting Results of Computational Experiments. Report of the Ad hoc Committee.
PB94-212347 *03,427*

JACOB, I.

Brillouin Light Scattering Intensities for Thin Magnetic Films with Large Perpendicular Anisotropies.
PB94-211174 *04,488*

Variation in Magnetic Properties of Cu/Fcc (001) Sandwich Structures.
PB95-141164 *04,555*

JACOBI, A. M.

Visual Measurement Technique for Analysis of Nucleate Flow Boiling.
PB95-143301 *03,262*

JACOBS, G.

Effect of Anneal Temperature on Si/Buried Oxide Interface Roughness on SIMOX.
PB96-112206 *02,382*

JACOBS, R. B.

Survey of the Literature on Heat Transfer from Solid Surfaces to Cryogenic Fluids.
AD-A286 680/4 *04,193*

JACOBSON, A. D.

Overview of a Radiation Accident at an Industrial Accelerator Facility.
PB97-122485 *02,612*

Radiation Accident at an Industrial Accelerator Facility.
PB95-140117 *02,575*

JACOBSON, A. J.

Powder Neutron Diffraction Investigation of Structure and Cation Ordering in Ba2+xBi2-xO6-y.
PB95-180865 *01,015*

JACOBSON, M. D.

Dual-Frequency Millimeter-Wave Radiometer Antenna for Airborne Remote Sensing of Atmosphere and Ocean.
PB96-112289 *02,009*

Dual Frequency mm-Wave Radiometer Antenna for Airborne Remote Sensing of Atmosphere and Ocean.
PB95-180378 *02,006*

JACOFF, A.

World Model Registration for Effective Off-Line Programming of Robots.
PB94-173010 *02,933*

JACOX, M. B.

Spectroscopic Study of Reaction Intermediates and Mechanisms in Nitramine Decomposition and Combustion.
AD-A296 061/5 *03,774*

JACOX, M. E.

Infrared and Near-Infrared Spectra of HCC and DCC Trapped in Solid Neon.
AD-A295 578/9 *03,773*

Matrix Isolation Study of the Interaction of Excited Neon Atoms with BCl3: Infrared Spectra of BCl(sub 3, sup +), BCl(sub 2, sup +), and BCl(sub 3, sup -).
PB97-119143 *01,187*

Matrix Isolation Study of the Interaction of Excited Neon Atoms with O3: Infrared Spectrum of O((sub 3)(-)) and Evidence for the Stabilization of O2...O((sub 4)(+)).
PB97-112403 *04,155*

Mid- and Near-Infrared Spectra of Water and Water Dimer Isolated in Solid Neon.
PB95-125662 *00,888*

Production and Spectroscopy of Small Polyatomic Molecular Ions Isolated in Solid Neon. (Reannouncement with New Availability Information).
AD-A234 043/8 *00,704*

Vibrational Spectra of Molecular Ions Isolated in Solid Neon: HCCH+ and HCC-. (Reannouncement with New Availability Information).
AD-A253 551/6 *00,707*

Vibrational Spectra of Molecular Ions Isolated in Solid Neon. X. H2O(+), HDO(+), and D2O(+).
PB95-125670 *00,889*

Vibrational Spectra of Molecular Ions Isolated in Solid Neon. XI. NO2(+), NO2(-), and NO3(-).
PB95-125688 *00,890*

Vibrational Spectra of Molecular Ions Isolated in Solid Neon. 6. CO4(-). (Reannouncement with New Availability Information).
AD-A238 415/4 *00,705*

Vibrational Spectra of Molecular Ions Isolated in Solid Neon. 7. CO(+), C2O2(+), and C2O2(-). (Reannouncement with New Availability Information).
AD-A239 729/7 *00,706*

Vibrational Spectra of Molecular Ions Isolated in Solid Neon. 11. NO2(+), NO2(-), and NO3(-).
AD-A275 828/2 *00,708*

Vibrational Spectra of Molecular Ions Isolated in Solid Neon. 13. Ions Derived from HBr and HI.
PB97-119234 *01,188*

JAFARABAD, K. R.

Enzyme and Protein Mass Transfer Coefficient in Aqueous Two Phase Systems. 1. Spray Extraction Columns.
PB95-161162 *00,594*

JAFFE, D. T.

Extended CO(7 yields 6) Emission from Warm Gas in Orion.
PB96-102504 *00,090*

JAHANMIR, S.

Control of Friction and Wear of Alpha-Alumina with a Composite Solid-Lubricant Coating.
PB95-125969 *03,225*

Evaluation of Thermal Wave Imaging for Detection of Machining Damage in Ceramics.
PB95-220547 *03,062*

Fracture Mechanics Analysis of Near-Surface Cracks.
PB94-172400 *03,230*

Mechanism of Mild to Severe Wear Transition in Alpha-Alumina.
PB94-212354 *03,233*

Tribological Characteristics of Alpha-Alumina at Elevated Temperatures.
PB94-211018 *02,963*

Tribology Education: Present Status and Future Challenges.
PB94-212362 *02,965*

JAI, J.

Laser-Synchrotron Hybrid Experiments: A Photon to Tickle, A Photon to Poke.
PB96-157847 *03,704*

JAIN, A.

Slow-Electron Collisions with CO Molecules in an Exact-Exchange Plus Parameter-Free Polarization Model.
PB95-202719 *03,989*

JAIN, K. K.

Intercomparison between NPL (India) and NIST (USA) Pressure Standards in the Hydraulic Pressure Region Up to 26 MPa.
PB96-113543 *04,211*

Intercomparison of the Effective Areas of a Pneumatic Piston Gauge Determined by Different Techniques.
PB94-212370 *02,640*

JAIN, M. K.

Characterization of Phase and Surface Composition of Silicon Carbide Platelets.
PB94-216264 *03,043*

JAJA, J.

Using Synthetic-Perturbation Techniques for Tuning Shared Memory Programs (Extended Abstract).
PB94-172657 *01,685*

Using Synthetic Perturbations and Statistical Screening to Assay Shared-Memory Programs.
PB96-103031 *01,740*

VLSI Architectures for Template Matching and Block Matching.
PB94-200029 *01,834*

JAMES, D. R.

Investigation of S2F10 Production and Mitigation in Compressed SF6-Insulated Power Systems.
PB94-212388 *02,467*

Investigation of S2F10 Production and Mitigation in Compressed SF6- Insulated Power Systems.
PB96-155528 *02,468*

JANET, S.

Second Census Optical Character Recognition Systems Conference.
PB94-188711 *01,832*

JANET, S. A.

NIST Form-Based Handprint Recognition System.
PB94-217106 *01,838*

JANEZIC, M. D.

Analysis of an Open-Ended Coaxial Probe with Lift-Off for Nondestructive Testing.
PB96-135116 *01,940*

Distribution of Dielectric Relaxation Times and the Moment Problem.
PB96-112032 *04,727*

NIST 60-Millimeter Diameter Cylindrical Cavity Resonator: Performance Evaluation for Permittivity Measurements.
PB94-151776 *02,251*

Open-Ended Coaxial Probes for Nondestructive Testing of Substrates and Circuit Boards.
PB96-122825 *02,078*

Transmission/Reflection and Short-Circuit Line Methods for Measuring Permittivity and Permeability.
PB94-165537 *02,211*

JANIK, D.

Intercomparison of Thermal Converters at NIM, NIST, PTB, SIRI and VSL from 10 to 100 MHz.
PB94-172459 *02,027*

JANOWSKI, G. M.

Beneficial Effects of Nitrogen Atomization on an Austenitic Stainless Steel.
PB94-212396 *03,209*

Effect of Backfill and Atomizing Gas on the Powder Porosity and Mechanical Properties of 304L Stainless Steel.
PB94-185394 *03,205*

JANSEN, W.

Framework for National Information Infrastructure Services.
PB95-103719 *02,723*

JANSEN, W. A.

Conformance Assessment of Transport Layer Security Implementations.
PB94-164373 *01,576*

Conformance Testing of a Lower Layer Security Protocol.
PB94-185402 *01,577*

SDNS Security Management.
PB95-161170 *01,592*

Taxonomy for Security Standards.
PB95-180386 *01,602*

JANSSENS, M.

Rate of Heat Release of Wood Products.
PB94-212404 *03,403*

Standardization of Formats and Presentation of Fire Data - The FDMS.
PB94-198462 *01,371*

JANZEN, A. R.

Ab initio Calculations for Helium: A Standard for Transport Property Measurements.
PB96-102041 *01,060*

JARGON, J. A.

30 MHz Comparison Receiver.
PB96-200407 *01,972*

Coaxial Line-Reflect-Match Calibration.
PB96-200118 *02,246*

Electrical Measurements of Microwave Flip-Chip Interconnections.
PB96-176748 *02,436*

High-Speed Interconnection Characterization Using Time Domain Network Analysis.
PB96-148176 *04,061*

Microwave Characterization of Flip-Chip MMIC Components.
PB96-176722 *02,434*

Microwave Characterization of Flip-Chip MMIC Interconnections.
PB96-176730 *02,435*

NIST 30 MHz Linear Measurement System.
PB94-169752 *02,020*

Revised Uncertainty Analysis for the NIST 30-MHz Attenuation Calibration System.
PB95-168761 *01,907*

Time Domain Network Analysis Using the Multiline TRL Calibration.
PB95-202925 *02,065*

Two-Tier Multiline TRL for Calibration of Low-Cost Network Analyzers.
PB96-157888 *01,947*

JARRETT, D. G.

Automated Guarded Bridge for Calibration of Multimegohm Standard Resistors.
PB97-119150 *02,289*

Automatic Inductive Voltage Divider Bridge Operates from 10 Hz to 100 kHz.
PB94-198413 *02,032*

Constant Temperature and Humidity Chamber for Standard Resistors.
PB96-122494 *02,275*

Low Thermal Guarded Scanner for High Resistance Measurement Systems.
PB97-112452 *02,288*

Resistance Measurements from 10 M Omega to 1 T Omega at NIST.
PB97-119168 *02,290*

JARUGA, P.

DNA Base Damage in Lymphocytes of Cancer Patients Undergoing Radiation Therapy.
PB97-122444 *03,643*

DNA Damage and DNA Sequence Retrieval from Ancient Tissues.
PB97-111983 *03,556*

Novel Activities of Human Uracil DNA N-glycosylase for Cytosine-Derived Products of Oxidative DNA Damage.
PB96-164132 *03,479*

Repair of Products of Oxidative DNA Base Damage in Human Cells.
PB96-190129 *03,555*

JASON, N. H.

BFRL Fire Publications, 1993.
PB94-164191 *00,192*

Building and Fire Research Laboratory Publications, 1993.
PB95-143202 *00,369*

Building and Fire Research Laboratory Publications, 1994.
PB95-226684 *00,398*

Evolution of a United States Information System.
PB96-157896 *02,713*

FIREDOC Users Manual, 3rd Edition.
PB95-128674 *01,378*

In Situ Burning Oil Spill Workshop Proceedings. Held in Orlando, Florida on January 26-28, 1994.
PB95-104907 *02,583*

Information Resources for the Fire Community.
PB96-148119 *00,211*

Information Transfer in the 21st Century.
PB96-157904 *02,714*

Locating Fire Engineering Information.
PB95-161188 *00,198*

Locating Fire Information.
PB96-190137 *00,227*

Post-Earthquake Fire and Lifelines Workshop. Held in Long Beach, California on January 30-31, 1995. Proceedings.
PB96-117916 *00,209*

Publications 1995: NIST Building and Fire Research Laboratory.
PB96-183074 *00,226*

Summaries of BFRL Fire Research In-House Projects and Grants, 1994.
PB95-130845 *00,366*

JASSIE, L.

Hydrolysis of Proteins by Microwave Energy.
PB94-216322 *03,528*

JEANNERET, B.

In situ Noble Metal YBa2Cu3O7 Thin-Film Contacts.
PB94-211323 *04,494*

YBa2Cu3O7-x to Si Interconnection for Hybrid Superconductor/Semiconductor Integration.
PB94-211711 *02,315*

JEFFERSON, D. K.

Ada Compiler Validation Summary Report: Certificate Number 940902S1.11376. UNISYS Corporation IntegrAda for Windows NT, Version 1.0. Intel Deskside Server for Intel Pentium 60 MHz =>. Intel Deskside Server with Intel Pentium 60 MHz.
AD-A288 572/1 *01,659*

Ada Compiler Validation Summary Report: Certificate Number 940902S1.11377 UNISYS Corporation. IntegrAda for Windows NT, Version 1.0. Intel Deskside Server with Intel 80486DX266 => Intel Deskside Server with Intel 80486DX266.
AD-A288 571/3 *01,658*

Impact of Computer-Aided Acquisition and Logistic Support (CALS) in the Application of Standards.
PB96-160908 *01,756*

JEFFERTS, S. R.

Origin of l/f PM and AM Noise in Bipolar Junction Transistor Amplifiers.
PB96-200787 *02,096*

Reducing the 1/f AM and PM Noise in Electronics for Precision Frequency Metrology.
PB97-113195 *02,102*

Superconducting Resonator and a Cryogenic GaAs Field-Effect Transistor Amplifier as a Single-Ion Detection System.
PB95-202727 *03,990*

JEFFERY, A.

Conversion of a 2-Terminal-Pair Bridge to a 4-Terminal-Pair Bridge for Increased Range and Precision in Impedance Measurements.
PB97-119176 *02,103*

NIST Comparison of the Quantized Hall Resistance and the Realization of the SI Ohm Through the Calculable Capacitor.
PB97-119184 *02,291*

NIST Comparison of the Quantized Hall Resistance and the Realization of the SI Ohm Through the Calculable Capacitor. Conference Proceedings, June 17-20, 1996.
PB97-119192 *02,292*

Precision Tests of a Quantum Hall Effect Device DC Equivalent Circuit Using Double-Series and Triple-Series Connections.
PB96-159256 *01,953*

Proposed Tests to Evaluate the Frequency-Dependent Capacitor Ratio for Single Electron Tunneling Experiment.
PB97-111454 *01,982*

JELENKOVIC, B.

Atomic-scale characterization of hydrogenated amorphous-silicon films and devices. Annual subcontract report, 14 February 1994--14 April 1995.
DE95009287 *02,294*

JELENKOVIC, B. M.

Excitation of Balmer Lines in Low-Current Discharges of Hydrogen and Deuterium.
PB95-150546 *03,893*

JEMIAN, P. R.

Evolution of the Pore Size Distribution in Final-Stage Sintering of Alumina Measured by Small-Angle X-ray Scattering (Reannouncement with New Availability Information).
AD-A249 178/5 *03,023*

JENKINS, R.

Introduction of a NIST Instrument Sensitivity Standard Reference Material for X-Ray Powder Diffraction.
PB94-200318 *00,807*

Powder Diffraction File: Past, Present, and Future.
PB97-109086 *04,800*

JENNINGS, D. A.

Laboratory Measurements for the Astrophysical Identification of MgH.
PB95-152195 *00,073*

JENNINGS, H.

Calculation of the Thermal Conductivity and Gas Permeability in a Uniaxial Bundle of Fibers.
PB95-180931 *03,058*

JENNINGS, H. M.

Diffusion Studies in a Digital-Image-Based Cement Paste Microstructural Model.
PB94-198801 *01,312*

Modelling Drying Shrinkage of Cement Paste and Mortar. Part 1. Structural Models from Angstroms to Millimeters.
PB96-135132 *03,074*

JENNINGS, P. W.

Binder Characterization and Evaluation by Nuclear Magnetic Resonance Spectroscopy.
PB94-193471 *01,334*

JENSEN, H. D.

Accuracy of the Electron Pump.
PB96-135223 *04,743*

Metrological Accuracy of the Electron Pump.
PB95-168910 *03,951*

Performance of the Electron Pump with Stray Capacitances.
PB96-200902 *01,976*

Testing for Metrological Accuracy of the Electron Pump.
PB95-175873 *04,663*

Thermal Enhancement of Cotunneling in Ultra-Small Tunnel Junctions.
PB95-175436 *04,658*

JESPERSEN, J.

Preliminary Comparison of Time Transfers via LASSO, GPS and Two-Way Satellite.
PB95-151098 *01,529*

JESPERSEN, J. L.

Satellite Two-Way Time Transfer: Fundamentals and Recent Progress.
PB95-161089 *01,536*

JESSEN, P.

Temperature of Optical Molasses for Two Different Atomic Angular Momenta.
PB95-126058 *03,881*

Ultracold Collisions: Associative Ionization in a Laser Trap.
PB94-213238 *03,859*

JESSEN, P. S.

Laser Modification of Ultracold Collisions: Experiment.
PB96-157987 *04,075*

Measurements of Fluorescence from Cold Atoms: Localization in Three-Dimensional Standing Waves.
PB95-163879 *03,943*

JESSUP, R. S.

Precise Measurement of Heat of Combustion with a Bomb Calorimeter.
AD-A286 701/8 *03,770*

JEWETT, K. L.

Preparation and Monitoring of Lead Acetate Containing Drinking Water Solutions for Toxicity Studies.
PB94-193885 *00,538*

JI, X.

Positive and Negative Cooperativities at Subsequent Steps of Oxygenation Regulate the Allosteric Behavior of Multistate Sebacylhemoglobin.
PB97-119374 *03,486*

JIA, J.

Improved Reflectometry Facility at the National Institute of Standards and Technology.
PB96-160338 *04,087*

New NIST/ARPA National Soft X-ray Reflectometry Facility.
PB96-158092 *04,080*

Phonon Relaxation in Soft-X-ray Emission of Insulators.
PB96-160296 *04,085*

JIA, J. J.

Al L2,3 Core Excitons in AlxGa1-x as Studied by Soft-X-ray Reflection and Emission.
PB96-157839 *04,067*

Barium Contributions to the Valence Electronic Structure of YBa2Cu3O7-delta, PrBa2Cu3O7-delta, and Other Barium-Containing Compounds.
PB96-158019 *04,076*

Charge-Transfer-Induced Multiplet Structure in the N4,5O2,3 Soft-X-ray Emission Spectrum of Lanthanum.
PB96-163746 *04,102*

Cooper M(sub II,III) X-ray-Emission Spectra of Copper Oxides and the Bismuth Cuprate Superconductor.
PB96-158027 *04,077*

Intermediate Coupling in L2-L3 Core Excitons of MgO, Al2O3, and SiO2.
PB96-158043 *04,079*

Local Partial Densities of States in Ni and Co Silicides Studied by Soft X-Ray Emission Spectroscopy.
PB94-212412 *04,504*

Simple Variable Line Space Grating Monochromator for Synchrotron Light Source Beamlines.
PB96-156203 *04,065*

Soft-X-ray-Emission Investigation of Cobalt Implanted Silicon Crystals.
PB96-157912 *04,069*

Soft-X-ray-Emission Spectra of Solid Kr and Xe.
PB96-157920 *04,070*

Soft-X-ray-Emission Studies of Bulk Fe3Si, FeSi, and FeSi2, and Implanted Iron Silicides.
PB96-157938 *04,071*

JIANG, X. P.

Grain Alignment and Transport Properties of Bi2Sr2CaCu2O8 Grown by Laser Heated Float Zone Method.
PB95-161451 *04,602*

JIGGETS, R.

Texture Measurement of Sintered Alumina Using the March-Dollase Function.
PB96-179494 *04,784*

JILANI, A.

Elastic Constants of Isotropic Cylinders Using Resonant Ultrasound.
PB94-211919 *04,497*

JIN, G. X.

Critical Scaling Laws and a Classical Equation of State.
PB95-169249 *00,990*

Global Thermodynamic Behavior of Fluid Mixtures in the Critical Region.
PB94-212420 *04,199*

JINNAI, H.

Effect of Cross-Links on the Miscibility of a Deuterated Polybutadiene and Protonated Polybutadiene Blend.
PB94-212438 *01,225*

Inversion of the Phase Diagram from UCST to LCST in Deuterated Polybutadiene and Protonated Polybutadiene Blends.
PB94-212446 *01,226*

SANS Studies of Space-Time Organization of Structure in Polymer Blends.
PB95-153789 *01,251*

Time-Resolved Small-Angle Neutron Scattering Study of Spinodal Decomposition in Deuterated and Protonated Polybutadiene Blends. 1. Effect of Initial Thermal Fluctuations.
PB95-161196 *01,252*

JINNO, M.

Millimeter-Resolution Optical Time-Domain Reflectometry Using a Four-Wave Mixing Sampling Gate.
PB96-122700 *02,190*

Optical Sampling Using Nondegenerate Four-Wave Mixing in a Semiconductor Laser Amplifier.
PB96-122502 *02,076*

Optical Sampling Using Nondegenerate Four-Wave Mixing in a Semiconductor Laser Amplifier.
PB96-123609 *04,348*

JOARDER, K.

New Method to Calculate Looming for Autonomous Obstacle Avoidance.
PB95-171435 *01,600*

JOB, V. A.

2nu9 Band of Propyne-d3.
PB95-164513 *00,985*

JOEL, R.

Directory of Law Enforcement and Criminal Justice Associations and Research Centers.
PB96-178918 *04,872*

JOHANSSON, M.

Critical Current Behavior of Ag-Coated YBa2Cu3O7-x Thin Films.
PB95-141016 *04,549*

JOHANSSON, M. E.

Effects of Etching on the Morphology and Surface Resistance of YBa2Cu3O7-delta Films.
PB96-135355 *02,410*

Magnetic Field Dependence of the Critical Current Anisotropy in Normal Metal-YBa2Cu3O7-delta Thin Film Bilayers.
PB95-141024 *04,550*

JOHNK, R.

Aperture Excitation of Electrically Large, Lossy Cavities.
PB95-175675 *00,031*

Crosstalk between Microstrip Transmission Lines. (NIST Reprint).
PB95-180337 *02,225*

JOHNK, R. T.

Alternative Contour Technique for the Efficient Computation of the Effective Length of an Antenna.
PB96-141361 *02,011*

Aperture Excitation of Electrically Large, Lossy Cavities.
PB94-145711 *00,029*

Crosstalk between Microstrip Transmission Lines.
PB94-135639 *02,210*

Measurements of Shielding Effectiveness and Cavity Characteristics of Airplanes.
PB94-210051 *00,030*

Rapid Evaluation of Mode-Stirred Chambers Using Impulsive Waveforms.
PB96-210026 *01,979*

Time-Domain Measurements of the Electromagnetic Backscatter of Pyramidal Absorbers and Metallic Plates.
PB94-185410 *01,877*

JOHNSON, A. L.

Structure of Molecules on Surfaces as Determined Using Electron-Stimulated Desorption.
PB94-216165 *00,852*

JOHNSON, B. C.

Calibration in the Earth Observing System (EOS) Project. Part 2. Implementation.
PB97-112213 *04,842*

Comparison of Filter Radiometer Spectral Responsivity with the NIST Spectral-Irradiance and Illuminance Scales.
PB97-113161 *04,162*

Intercomparison of the ITS-90 Radiance Temperature Scales of the National Physical Laboratory (U.K.) and the National Institute of Standards and Technology.
PB96-113550 *02,674*

Method of Realizing Spectral Irradiance Based on an Absolute Cryogenic Radiometer.
PB95-161204 *04,270*

NIST-NRL Free-Electron Laser Facility.
PB94-212511 *04,237*

NIST Thermal Infrared Transfer Standard Radiometer for the Earth Observing System (EOS) Program.
PB97-113013 *04,843*

Organization and Implementation of Calibration in the EOS Project. Part 1.
PB96-179437 *04,841*

Precision High Temperature Blackbodies.
PB95-140059 *03,885*

Realization of New NIST Radiation Temperature Scales for the 1000 K to 3000 K Region, Using Absolute Radiometric Techniques.
PB94-172905 *03,794*

JOHNSON, B. M.

High-Energy Behavior of the Double Photoionization of Helium from 2 to 12 keV.
PB94-213279 *03,860*

JOHNSON, C.

NIST SIMA Interactive Management Workshop. Held in Fort Belvoir, Virginia on November 14-16, 1994.
PB96-154877 *02,838*

JOHNSON, C. E.

Electrochemical Synthesis of Metal and Intermetallic Composites.
AD-A294 088/0 *03,304*

Status of Electrocomposites.
PB94-212453 *03,143*

JOHNSON, C. J.

Correlation of HgCdTe Epilayer Defects with Underlying Substrate Defects by Synchrotron X-Ray Topography.
PB94-200714 *02,129*

JOHNSON, D. L.

Calculation of the Thermal Conductivity and Gas Permeability in a Uniaxial Bundle of Fibers.
PB95-180931 *03,058*

JOHNSON, D. R.

Aid for Smaller Businesses.
PB94-212461 *00,492*

Montgomery Education Connection and Resource Education Awareness Partnership Making Connections between Local Schools and NIST Volunteers.
PB96-159769 *00,134*

JOHNSON, H. E.

Topological Influences on Polymer Adsorption and Desorption Dynamics.
PB94-212479 *01,227*

JOHNSON, J. A.

Ultrasonic Sensing of GMAW: Laser/EMAT Defect Detection System.
PB96-186028 *02,878*

JOHNSON, J. W.

Summary of the Apparent Standard Partial Molal Gibbs Free Energies of Formation of Aqueous Species, Minerals, and Gases at Pressures 1 to 5000 Bars and Temperatures 25 to 1000C.
PB96-145891 *01,113*

JOHNSON, K. S.

Evaluating Investments in Law Enforcement Equipment: An Annotated Bibliography.
PB95-151379 *04,867*

JOHNSON, L. A.

Ada Compiler Validation Summary Report: Certificate Number 940902S1.11376. UNISYS Corporation IntegrAda for Windows NT, Version 1.0. Intel Deskside Server for Intel Pentium 60 MHz =>. Intel Deskside Server with Intel Pentium 60 MHz.
AD-A288 572/1 *01,659*

Ada Compiler Validation Summary Report: Certificate Number 940902S1.11377 UNISYS Corporation. IntegrAda for Windows NT, Version 1.0. Intel Deskside Server with Intel 80486DX266 => Intel Deskside Server with Intel 80486DX266.
AD-A288 571/3 *01,658*

JOHNSON, R. D.

Electronic Spectra of CF2Cl and CFCl2 Radicals Observed by Resonance Enhanced Multiphoton Ionization.
PB95-151023 *00,927*

Experimental and Abinitio Studies of Electronic Structures of the CCl3 Radical and Cation.
PB94-212131 *00,826*

Ionization Energies, Appearance Energies and Thermochemistry of CF2O and FCO.
PB97-111538 *01,178*

Kinetics of the Reaction of CCl3-Br-2 and the Thermochemistry of CCl3 Radical and Cation.
PB94-212115 *00,824*

Multiphoton Ionization of SiH3 and SiD3 Radicals: Electronic Spectra, Vibrational Analyses of the Ground and Rydberg States, and Ionization Potential.
PB94-212503 *00,837*

Multiphoton Ionization of SiH3 and SiD3 Radicals. 2. Three Photon Resonance-Enhanced Spectra Observed between 460 and 610 nm.
PB94-212487 *00,835*

New Electronic States of NH and ND Observed from 258 to 288 nm by Resonance Enhanced Multiphoton Ionization Spectroscopy.
PB94-212495 *00,836*

New Rydberg States of Aluminum Monofluoride Observed by Resonance-Enhanced Multiphoton Ionization Spectroscopy.
PB94-199544 *00,797*

Resonance Enhanced Multiphoton Ionization Detection of GeF and GeCl Radicals.
PB94-212123 *00,825*

Resonance Enhanced Multiphoton Ionization Spectroscopy of the SnF Radical.
PB97-111223 *01,176*

Resonance Enhanced Multiphoton Ionization Spectroscopy of 2-Butene-1-yl (C4H7) between 455-485 nm.
PB95-151031 *00,670*

JOHNSON, R. G.

Hybrid Undulator for the NIST-NRL Free-Electron Laser.
PB94-212529 *04,238*

NIST-NRL Free-Electron Laser Facility.
PB94-212511 *04,237*

JOHNSON, S. D.

Simulation of C60 Through the Plastic Transition Temperatures.
PB96-102546 *04,713*

JOHNSON, W. C.

Morphological Development of Second-Phase Particles in Elastically-Stressed Solids.
PB95-181111 *03,355*

JOHNSON, W. L.

Ultrasonic Spectroscopy of Metallic Spheres Using Electromagnetic-Acoustic Transduction.
PB94-212537 *04,185*

JOHNSON, W. R.

Evaluation of Two-Photon Exchange Graphs for Highly-Charged Heliumlike Ions.
PB94-198918 *03,808*

JOHNSONBAUGH, D.

Characterization of the Binding of Gallium, Platinum, and Uranium to Pseudomonas Fluorescens by Small-Angle X-ray Scattering and Transmission Electron Microscopy.
PB94-172509 *03,453*

JOHNSONBAUGH, D. S.

Flow-Induced Structure in Polymers. Chapter 17. Phase-Separation Kinetics of a Polymer Blend Solution Studied by a Two-Step Shear Quench.
PB96-123377 *03,388*

JOHNSSON, E. L.

Carbon Monoxide Production in Compartment Fires: Reduced-Scale Enclosure Test Facility.
PB95-231700 *01,394*

Greatly Enhanced Soot Scattering in Flickering Ch4/Air Diffusion Flames.
PB94-172988 *01,361*

Scaling Compartment Fires: Reduced- and Full-Scale Enclosure Burns.
PB96-175708 *00,224*

Study of Technology for Detecting Pre-Ignition Conditions of Cooking-Related Fires Associated with Electric and Gas Ranges and Cooktops, Phase 1 Report.
PB96-128095 *00,303*

JOHNSTON, A. D.

Physical and Chemical Properties of Resin-Reinforced Calcium Phosphate Cements.
PB95-180212 *00,171*

JOKLIK, R. G.

Multiphoton Ionization Spectroscopy Measurements of Silicon Atoms during Vapor Phase Synthesis of Ceramic Particles.
PB95-151999 *03,913*

JONES, A.

Japan Technology Program Assessment. Simulation: State-of the-Art in Japan.
PB95-217097 *02,827*

JONES, C. A.

Dielectric Measurements on Printed-Wiring and Circuit Boards, Thin Films, and Substrates: An Overview.
PB96-147038 *02,236*

Substrate and Thin Film Measurements.
PB96-112297 *02,384*

JONES, C. G.

Characterization of a Health Physics Instrument Calibration Range.
PB95-164554 *03,629*

JONES, D.

Economic, Energy, and Environmental Impacts of the Energy-Related Inventions Program.
DE94-017162 *00,008*

JONES, F. E.

Examination of Parameters That Can Cause Error in Mass Determinations.
PB94-163037 *03,784*

Use of the Electronic Balance for Highly Accurate Direct Mass Measurements Without the Use of External Mass Standards.
PB94-187713 *03,803*

JONES, G. A.

Comparative Study of Fe-C Bead and Graphite Target Performance with the National Ocean Sciences AMS (NOSAMS) Facility Recombinator Ion Source.
PB95-175790 *00,693*

JONES, G. R.

Display-Measurement Round-Robin.
PB96-119227 *02,186*

Specular and Diffuse Reflection Measurements of Electronic Displays.
PB97-119200 *02,208*

Survey of the Components of Display-Measurement Standards.
PB96-122528 *02,188*

Survey of the Components of Display-Measurement Standards.
PB97-122394 *02,209*

JONES, K.

Temperature of Optical Molasses for Two Different Atomic Angular Momenta.
PB95-126058 *03,881*

JONES, K. M.

Measurement of the Atomic Na(3P) Lifetime and of Retardation in the Interaction between Two Atoms Bound in a Molecule.
PB97-122360 *04,178*

JONES, M. C.

Brownian Diffusion of Hard Spheres at Finite Concentrations.
PB95-164307 *00,975*

Distributed measurements of tracer response on packed bed flows using a fiberoptic probe array. Final report.
DE95013079 *00,667*

JONES, R. D.

Beam Analysis Round Robin.
PB94-212545 *04,239*

Error Propagation in Laser Beam Spatial Parameters.
PB95-180394 *04,310*

Laser-Beam Analysis Pinpoints Critical Parameters.
PB94-212552 *04,240*

Thermal Modeling and Analysis of Laser Calorimeters.
PB96-140405 *04,354*

Widths and Propagation of a Truncated Gaussian Beam.
PB95-168779 *04,287*

JONES, S.

Report on the NIST Low Accelerating Voltage SEM Magnification Standard Interlaboratory Study.
PB96-201074 *02,445*

JONES, S. N.

Electrical Method for Determining the Thickness of Metal Films and the Cross-Sectional Area of Metal Lines.
PB95-203170 *02,370*

Scanning Electron Microscope Magnification Calibration Interlaboratory Study.
PB96-201082 *01,164*

JONES, W. W.

Calculating Flame Spread on Horizontal and Vertical Surfaces.
PB94-187283 *00,335*

Fire Safety of Passenger Trains: A Review of Current Approaches and of New Concepts.
PB94-152006 *04,848*

Improvement in Predicting Smoke Movement in Compartmented Structures.
PB94-172418 *00,332*

New Concepts for Fire Protection of Passenger Rail Transportation Vehicles.
PB95-162046 *04,850*

New Concepts for Fire Protection of Passenger Rail Transportation Vehicles. (NIST Reprint).
PB95-180774 *04,863*

Verification of a Model of Fire and Smoke Transport.
PB95-108718 *00,357*

JONKER, B. T.

Characterization of the ZnSe/GaAs Interface Layer by TEM and Spectroscopic Ellipsometry.
PB95-175360 *04,655*

Determination of the Optical Constants of ZnSe Films by Spectroscopic Ellipsometry.
PB95-175378 *04,656*

JONNALAGADDA, S. V.

Thermodynamic Interactions and Correlations in Mixtures of Two Homopolymers and a Block Copolymers by Small Angle Neutron Scattering.
PB95-152872 *01,247*

JONSSON, L.

Large Local-Field Corrections in Optical Rotatory Power of Quartz and Selenium.
PB97-122378 *04,400*

JONSSON, P. G.

Mathematical Models of Transport Phenomena Associated with Arc-Welding Processes: A Survey.
PB96-135058 *02,870*

Power Characteristics in GMAW: Experimental and Numerical Investigation.
PB96-190145 *03,296*

JOSELL, D.

Interfacial Free Energies from Substrate Curvature Measurements of the Creep of Multilayer Thin Films.
PB94-185428 *04,448*

JOSEPHSON, E. S.

Estimation of the Absorbed Dose in Radiation-Processed Food. 4. EPR Measurements on Eggshell.
PB94-199692 *00,038*

JOSHI, A. A.

Fire Induced Thermal Fields in Window Glass I: Theory.
PB94-139722 *00,328*

JOSHI, C. H.

Comparing the Accuracy of Critical-Current Measurements Using the Voltage-Current Simulator.
PB96-119219 *02,227*

Effect of Magnetic Field Orientation on the Critical Current of HTS Conductor and Coils.
PB96-141189 *02,956*

JOSHI, J. B.

Continuous Counter-Current Two Phase Aqueous Extraction.
PB95-161212 *00,675*

Enzyme and Protein Mass Transfer Coefficient in Aqueous Two Phase Systems. 1. Spray Extraction Columns.
PB95-161162 *00,594*

Protein Extraction in a Spray Column Using a Polyethylene Glycol Maltodextrin Two-Phase Polymer System.
PB95-162228 *00,595*

Two Phase Aqueous Extraction: Rheological Properties of Dextran, Polyethylene Glycol, Bovine Serum Albumin and Their Mixtures.
PB95-161998 *00,676*

JOSHI, Y.
Natural Convection from an Array of Electronic Packages Mounted on a Horizontal Board in a Narrow Aspect Ratio Enclosure.
PB96-164017 *02,087*

JOSHI, Y. N.
Analysis of the (5d(2)+5d6s)-5d6p Transition Arrays of Os VII and Ir VIII, and the 6s (2)S-6p (2)P Transitions of Ir IX.
PB96-159264 *01,954*

Analysis of the 5s(2)5p(2)-(5s5p(3)+5s(2)5p5d+5s(2)5p6s) Transitions of Four-Times Ionized Xenon (Xe V).
PB95-150769 *03,900*

Spectrum and Energy Levels of Triply Ionized Barium (Ba IV).
PB95-140877 *03,888*

JOUBRAN, R.
Structure of a Triglyceride Microemulsion: A Small Angle Neutron Scattering Study.
PB96-112255 *01,077*

JOYCE, S. A.
Desorption Induced by Electronic Transitions.
PB94-216173 *00,853*

Influence of Coadsorbed Potassium on the Electron-Stimulated Desorption of F(+), F(-), and F(*) from PF3 on Ru(0001).
PB96-157946 *04,072*

Role of Adsorbed Alkalis in Desorption Induced by Electronic Transitions.
PB94-172574 *00,762*

Structure of Molecules on Surfaces as Determined Using Electron-Stimulated Desorption.
PB94-216165 *00,852*

JUBERTS, M.
Ground Vehicle Control at NIST: From Teleoperation to Autonomy.
N94-34037/9 *03,758*

JUDGE, P.
Transition Regions of Capella.
PB96-123336 *00,105*

Transition Regions of Capella (1995).
PB96-176714 *00,108*

JUDISH, R. M.
Multi-State Two-Port: An Alternative Transfer Standard.
PB95-168530 *02,049*

JUDY, D. C.
Electrical Breakdown in Transformer Oil in Large Gaps.
PB95-150579 *01,889*

JUHASZ, E.
dc Method for the Absolute Determination of Conductivities of the Primary Standard KCl Solutions from 0C to 50C.
PB94-219342 *02,644*

JULIENNE, P.
Ultracold Collisions: Associative Ionization in a Laser Trap.
PB94-213238 *03,859*

JULIENNE, P. S.
Density Matrix Calculation of Population Transfer between Vibrational Levels of Na2 by Stimulated Raman Scattering with Temporally Shifted Laser Beams.
PB94-198546 *00,787*

Excitons in Complex Quantum Nanostructures.
PB97-118343 *01,184*

Intersystem Crossing in Collisions of Aligned Ca(4s5p (1)P) + He: A Half Collision Analysis Using Multichannel Quantum Defect Theory.
PB94-211133 *00,813*

Laser Assisted Collisions at Ultracold Temperatures.
PB95-161220 *03,929*

Measurement of the Atomic Na(3P) Lifetime and of Retardation in the Interaction between Two Atoms Bound in a Molecule.
PB97-122360 *04,178*

Multichannel Quantum Defect Half Collision Analysis of K2 Photodissociation Through the B1Pi(sub u) State.
PB94-211125 *00,812*

Theory of Atomic Collisions at Ultracold Temperatures.
PB94-212560 *03,851*

JULL, A. J. T.
Radiocarbon Measurements of Atmospheric Volatile Organic Compounds: Quantifying the Biogenic Contribution.
PB97-122352 *02,574*

JULLIENNE, P.
Hyperfine Effects and Associative Ionization of Ultracold Sodium.
PB95-151221 *03,903*

JUN, J. S.
Metrology Standards for Advanced Semiconductor Lithography Referenced to Atomic Spacings and Geometry.
PB96-160718 *02,424*

JUNG, H. J.
Comparisons of Some NIST Fixed-Point Cells with Similar Cells of Other Standards Laboratories.
PB97-119242 *00,655*

Direct Comparison of Three PTB Silver Fixed-Point Cells with the NIST Silver Fixed-Point Cell.
PB96-161286 *00,628*

JUNGNER, P.
Delivering the Same Optical Frequency at Two Places: Accurate Cancellation of Phase Noise Introduced by an Optical Fiber or Other Time-Varying Path.
PB96-102736 *04,332*

JURA, M.
Observations of 3C 273 with the Goddard High Resolution Spectrograph on the Hubble Space Telescope.
PB95-202321 *00,076*

JUROSHEK, J.
Multi-State Two-Port: An Alternative Transfer Standard.
PB95-168530 *02,049*

JUROSHEK, J. R.
Measurements of the Characteristic Impedance of Coaxial Air Line Standards.
PB95-168787 *02,221*

KABIRI-BADR, M.
Statistical Thermodynamics of Phase Separation and Ion Partitioning in Aqueous Two-Phase Systems.
PB94-199387 *01,212*

KACKER, R.
Computing Effects and Error for Large Synthetic Perturbation Screenings.
PB94-139623 *01,675*

Scalability Test for Parallel Code.
PB96-146758 *01,749*

Simple Scalability Test for MIMD Code.
PB94-193638 *01,688*

Study on the Reuse of Plastic Concrete Using Extended Set-Retarding Admixtures.
PB96-122130 *00,402*

Synthetic-Perturbation Tuning of MIMD Programs.
PB94-185568 *01,687*

Time-Perturbation Tuning of MIMD Programs.
PB94-164399 *01,681*

Time-Perturbation Tuning of MIMD Programs.
PB94-172566 *01,684*

Using Synthetic-Perturbation Techniques for Tuning Shared Memory Programs (Extended Abstract).
PB94-172657 *01,685*

Using Synthetic Perturbations and Statistical Screening to Assay Shared-Memory Programs.
PB96-103031 *01,740*

KACKER, R. N.
Efficient Experiment to Study Superconducting Ceramics.
PB94-212578 *04,505*

Statistical Analysis of Parameters Affecting the Measurement of Particle-Size Distribution of Silicon Nitride Powders by Sedigraph (Trade Name).
PB94-216249 *03,042*

Statistical Quality Control Technology in Japan.
PB94-199064 *02,708*

Taguchi's Parameter Design: A Panel Discussion.
PB96-111802 *03,445*

KADUK, J. A.
Conventional and Eccentric Uses of Crystallographic Databases in Practical Materials Identification Problems.
PB97-109102 *04,802*

KAESER, R. S.
ITS-90 Calibration Facility.
PB96-160916 *00,627*

KAETZEL, L.
Optimization of Highway Concrete Technology.
PB94-182995 *01,333*

KAETZEL, L. J.
Highway Concrete (HWYCON) Expert System User Reference and Enhancement Guide.
PB94-215670 *01,316*

KAFAFI, S. A.
Carbon Acidities of Aromatic Compounds. 1. Effects of In-Ring Aza and External Electron-Withdrawing Groups.
PB94-216595 *00,860*

Experimental and Abinitio Studies of Electronic Structures of the CCl3 Radical and Cation.
PB94-212131 *00,826*

Thermal Decomposition of Hydroxy- and Methoxy-Substituted Anisoles.
PB94-173036 *00,767*

KAHN, A. H.
Development in the Theory and Analysis of Eddy Current Sensing of Velocity in Liquid Metals.
PB94-212586 *03,335*

KAHN, R.
Low-Frequency Excitations of Oriented DNA.
PB96-137799 *03,548*

KAISER, D. L.
Epitaxial Growth of BaTiO3 Thin Films at 600C by Metalorganic Chemical Vapor Deposition.
PB96-122510 *03,071*

Image Depth Profiling SIMS: An Evaluation for the Analysis of Light Element Diffusion in YBa2Cu3O7-x Single Crystal Superconductors.
PB95-126116 *04,530*

Meissner, Shielding, and Flux Loss Behavior in Single-Crystal YBa2Cu3O6+x.
PB94-198744 *04,464*

Nature of (001) Tilt Grain Boundaries in YBa2Cu3O6+x.
PB95-126033 *04,528*

Temperature Dependence of Vortex Twin Boundary Interaction in Yttrium Barium Copper Oxide (YBa2Cu3O6+x).
PB95-162442 *04,613*

Weak-Link-Free Behavior of High Angle YBa2Cu3O7-x Grain Boundaries in High Magnetic Fields.
PB94-198421 *04,459*

X-Ray-Diffraction Study of a Thermomechanically Detwinned Single Crystal of YBa2Cu3O6+x.
PB95-151726 *04,581*

KAISER, R.
Frequency-Stabilized LNA Laser at 1.083 mum: Application to the Manipulation of Helium 4 Atoms.
PB95-176186 *04,304*

KAJIYAMA, T.
Preparation of 2-Dimensional Ultra Thin Polystyrene Film by Water Casting Method.
PB95-162806 *04,619*

KALCEFF, M. A.
Deformation and Fracture of Mica-Containing Glass-Ceramics in Hertzian Contacts.
PB96-179452 *03,080*

KALKUR, T. S.
High Critical Temperature Superconductor Tunneling Spectroscopy Using Squeezable Electron Tunneling Junctions.
PB95-163721 *04,627*

Tunneling Measurement of the Zero-Bias Conductance Peak and the Bi-Sr-Ca-Cu-O Thin-Film Energy Gap.
PB95-163739 *04,628*

KAMAL, M. R.
Weatherability of Plastic Materials.
AD-A301 675/5 *02,968*

KAMITAKAHARA, W. A.
Discontinuous Volume Change at the Orientational-Ordering Transition in Solid C60.
PB94-211828 *00,821*

Energy Distributions of Neutrons Scattered from Solid C60 by the Beryllium Detector Method.
PB96-176631 *03,740*

Inelastic Neutron Scattering Studies of Rotational Excitations and the Orientational Potential in C60 and A3C60 Compounds.
PB94-172673 *00,763*

Neutron-Scattering Study of Librations and Intramolecular Phonons in Rb2.6K0.4C60.
PB95-162269 *00,958*

Neutron Scattering Study of the Lattice Modes of Solid Cubane.
PB96-147152 *01,126*

KANA, T. M.
High-Performance Liquid Chromatography of Phytoplankton Pigments Using a Polymeric Reversed-Phase C18 Column.
PB95-151130 *00,583*

KANDA, M.
Alternative Contour Technique for the Efficient Computation of the Effective Length of an Antenna.
PB96-141361 *02,011*

Aperture Coupling to a Coaxial Air Line: Theory and Experiment.
PB94-211968 *02,216*

Bistatic Scattering of Absorbing Materials from 30 to 1000 MHz.
PB95-150934 *01,891*

Methodology for Electromagnetic Interference Measurements.
PB96-200126 *02,014*

Optically Linked Three-Loop Antenna System for Determining the Radiation Characteristics of an Electrically Small Source.
PB95-161915 *02,005*

Optically Sensed EM-Field Probes for Pulsed Fields.
PB94-212594 *02,130*

Standard Antennas for Electromagnetic Interference Measurements and Methods to Calibrate Them.
PB96-102561 *02,007*

Standard Probes for Electromagnetic Field Measurements.
PB94-185436 *01,999*

Time-Domain Measurements of the Electromagnetic Backscatter of Pyramidal Absorbers and Metallic Plates.
PB94-185410 *01,877*

KANDHAL, P. S.
Precision of Marchall Stability and Flow Test Using 6-in. (152.4-mm) Diameter Specimens.
PB96-200910 *03,006*

KANG, Y. S.
CO2/CH4 Transport in Polyperfluorosulfonate Ionomers: Effects of Polar Solvents on Permeation and Solubility.
PB96-163803 *01,145*

KANTOROW, M.
Escherichis coli Cyclic AMP Receptor Protein Mutants Provide Evidence for Ligand Contacts Important in Activation.
PB96-201017 *03,592*

KAO, C. C.
Phonon Relaxation in Soft-X-ray Emission of Insulators.
PB96-160296 *04,085*

KAO, J. Y.

Evaluation of GSA Maintenance Practices of Large Centrifugal Chillers and Review of GSA Refrigerant Management Practices.
PB94-143344 *02,502*

Factors Affecting the Energy Consumption of Two Refrigerator-Freezers.
PB97-112312 *00,311*

Using Emulators to Evaluate the Performance of Building Energy Management Systems.
PB95-175774 *00,259*

KAPLAN, B.

SQA Standards and Total Quality Management.
PB96-111844 *01,743*

KAPLAN, C. R.

Computations of Enhanced Soot Production in Time-Varying CH4/Air Diffusion Flames.
PB97-119218 *01,440*

KARAKAYA, A.

Novel Activities of Human Uracil DNA N-glycosylase for Cytosine-Derived Products of Oxidative DNA Damage.
PB96-164132 *03,479*

KARAM, L. R.

Modification of Deoxyribose-Phosphate Residues by Extracts of Ataxia Telangiectasia Cells.
PB94-212602 *03,458*

Radon in the Lung.
PB97-110035 *03,638*

Systematics of Alpha-Particle Energy Spectra and Lineal Energy (Y) Spectra for Radon Daughters.
PB94-185139 *03,615*

KARASZ, F. A.

Inelastic-Neutron-Scattering Studies of Poly(p-phenylene vinylene).
PB95-180766 *01,014*

KAREN, P.

Neutron Powder Diffraction Study of the Nuclear and Magnetic Structures of the Oxygen-Deficient Perovskite YBaCuCoO5.
PB95-161097 *00,954*

KAREN, V. L.

Neutron Powder Diffraction Study of the Nuclear and Magnetic Structures of the Oxygen-Deficient Perovskite YBaCuCoO5.
PB95-161097 *00,954*

NIST Crystallographic Databases for Research and Analysis.
PB97-109094 *04,801*

Workshop Highlights.
PB97-109227 *04,811*

KARIM, A.

Compatibilization of Polymer Blends by Complexation. 2. Kinetics of Interfacial Mixing.
PB97-111900 *01,295*

Dimensional Crossover in the Phase Separation Kinetics of Thin Polymer Blend Films.
PB97-113088 *03,395*

Neutron Reflectivity Study of the Density Profile of a Model End-Grafted Polymer Brush: Influence of Solvent Quality.
PB95-202735 *01,274*

Phase Separation in Thin Film Polymer Blends With and Without Block Copolymer Additives.
PB96-204482 *01,294*

KARKI, S.

Reproducibility of Tests on Energy Management and Control Systems Using Building Emulators.
PB95-175980 *00,260*

KARLIN, B.

Lattice Position of Si in GaAs Determined by X-Ray Standing Wave Measurements.
PB95-164406 *04,632*

KARLIN, B. A.

Evolution of X-ray Resonance Raman Scattering into X-ray Fluorescence from the Excitation of Xenon Near the L3 Edge.
PB96-102751 *04,025*

KARLSSON, L.

Inner-Valence States CO(+) between 22 eV and 46 eV Studied by High Resolution Photoelectron Spectroscopy and ab Initio CI Calculations.
PB95-180055 *03,961*

KARR, P. R.

Penetration and Diffusion of Hard X-rays through Thick Barriers. III. Studies of Spectral Distributions.
AD-A292 502/2 *03,771*

KARTHA, V. B.

2nu9 Band of Propyne-d3.
PB95-164513 *00,985*

KARYAKIN, E. N.

Tunneling-Rotation Spectrum of the Hydrogen Fluoride Dimer.
PB94-198678 *00,793*

KASCHNITZ, E.

Measurements of Thermophysical Properties of Nickel Near Its Melting Temperature by a Microsecond-Resolution Transient Technique.
PB96-102579 *04,210*

Radiance Temperatures at 1500 nm of Niobium and Molybdenum at Their Melting Points by a Pulse-Heating Technique.
PB97-118699 *04,167*

KASHIWAGI, T.

Effects of Molecular Weight and Thermal Stability on Polymer Gasification.
PB94-212610 *01,228*

Effects of Sample Mounting on Flammability Properties of Intumescent Polymers.
PB96-159777 *03,389*

Estimate of Flame Radiance via a Single Location Measurement in Liquid Pool Flames.
PB94-211596 *02,476*

Estimate of the Effect of Scale on Radiative Heat Loss Fraction and Combustion Efficiency.
PB95-150447 *02,486*

Gas Phase Oxygen Effect on Chain Scission and Monomer Content in Bulk Poly(methyl methacrylate) Degraded by External Thermal Radiation.
PB96-204078 *01,293*

Heat Transfer in an Intumescent Material Using a Three-Dimensional Lagrangian Model.
PB96-164066 *00,408*

Ignition and Subsequent Flame Spread Over a Thin Cellulosic Material.
PB96-160270 *04,836*

Ignition and Subsequent Transition to Flame Spread in a Microgravity Environment.
N96-15584/1 *04,828*

Ignition and Transition to Flame Spread Over a Thermally Thin Cellulosic Sheet in a Microgravity Environment.
PB96-160288 *04,837*

Measurement of Radiative Feedback to the Fuel Surface of a Pool Fire.
PB94-211604 *02,477*

Polymer Combustion and Flammability: Role of the Condensed Phase.
PB96-123245 *01,279*

Simultaneous Optical Measurement of Soot Volume Fraction, Temperature, and CO2 in Heptane Pool Fire.
PB96-102132 *01,397*

Transition from Localized Ignition to Flame Spread Over a Thin Cellulosic Material in Microgravity.
PB96-155809 *04,835*

KASHIWAZAKI, S.

Orientation Effects on ESR Analysis of Alanine-Polymer Dosimeters.
PB96-146725 *03,720*

KASIANOWICZ, J.

Genetically Engineered Pores as Metal Ion Biosensors.
PB96-167408 *03,553*

Pore-Forming Protein with a Metal-Actuated Switch.
PB96-176557 *03,554*

KASIANOWICZ, J. J.

Current Fluctuations Reveal Protonation Dynamics and Number of Ionizable Residues in the alpha-Toxin Channel.
PB96-161732 *03,588*

Current Noise Reveals Protonation Kinetics and Number of Ionizable Sites in an Open Protein Ion Channel.
PB96-161674 *04,092*

Genetically Engineered Pore as a Metal Ion Biosensor.
PB96-161658 *03,551*

Genetically Engineered Pores for New Materials.
PB96-161641 *03,550*

Noise Analysis of Ionization Kinetics in a Protein Ion Channel.
PB96-161682 *04,093*

Protonation Dynamics in an Ion Channel Pore.
PB96-161757 *03,589*

Protonation Dynamics of the alpha-Toxin Ion Channel from Spectral Analysis of pH-Dependent Current Fluctuations.
PB96-161740 *03,652*

KASPRZAK, K.

Nickel(II)-Mediated Oxidative DNA Base Damage in Renal and Hepatic Chromatin of Pregnant Rats and Their Fetuses. Possible Relevance to Carcinogenesis.
PB94-212628 *03,646*

Oxidative DNA Base Damage in Renal, Hepatic, and Pulmonary Chromatin of Rats After Intraperitoneal Injection of Cobalt (II) Acetate.
PB95-150025 *03,647*

KASSOFF, J. M.

Appearance Potentials of Ions Produced by Electron-Impact Induced Dissociative Ionization of SF6, SF4, SF5Cl, S2F10, SO2, SO2F2, SOF2, and SOF4.
PB96-119730 *01,080*

KASTNER, J.

Temperature Dependence of the Magnetic Excitations in Ordered and Disordered Fe72Pt28.
PB95-150223 *04,563*

KATO, S.

Kinetics and Dynamics of Vibrationally State Resolved Ion-Molecule Reactions: (14)N2(+)(v=1 and 2) and (15)N2(+)(v=0,1 and 2) with (14)N2.
PB96-102348 *04,023*

Selected Ion Flow Tube-Laser Induced Fluorescence Instrument for Vibrationally State-Specific Ion-Molecule Reactions.
PB94-185444 *00,774*

KATTI, R.

Magnetic Force Microscopy Images of Magnetic Garnet with Thin-Film Magnetic Tip.
PB95-176210 *04,669*

KATTNER, U.

Extrapolation of the Heat Capacity in Liquid and Amorphous Phases.
PB97-111421 *04,147*

KATTNER, U. R.

Assessment of the Al-Sb System.
PB94-200474 *03,329*

Thermodynamic Assessment and Calculation of the Ti-Al System.
PB94-212644 *03,337*

Thermodynamic Calculation of the Ternary Ti-Al-Nb System.
PB94-212636 *03,336*

KATZ, S.

Glossary of Software Reuse Terms.
PB95-178992 *01,720*

KATZ, S. B.

Context Analysis of the Network Management Domain. Conducted as Part of the Domain Analysis Case Study.
PB94-142528 *01,465*

KAUFFMAN, D. A.

Determination of the Prior-Austenitic Grain Size of Selected Steels Using a Molten Glass Etch.
PB94-211927 *03,208*

KAUFMAN, V.

Analysis of the 5s(2)5p(2)-(5s5p(3)+5s(2)5p5d+5s(2)5p6s) Transitions of Four-Times Ionized Xenon (Xe V).
PB95-150769 *03,900*

Compilation of Energy Levels and Wavelengths for the Spectrum of Singly-Ionized Oxygen (O II).
PB94-162344 *00,746*

Improved Wavelengths for Prominent Lines of Cr XVI to Cr XXII.
PB95-150629 *03,895*

Observation of Pd-Like Resonance Lines Through Pt(32+) and Zn-Like Resonance Lines of Er(38+) and Hf(42+).
PB95-150637 *03,896*

Rb-Like Spectra: Pd X to Nd XXIV.
PB95-150645 *03,897*

Rh I Isoelectronic Sequence Observed from Er(23+) to Pt(33+).
PB95-150652 *03,898*

Spectra of Ag I Isoelectronic Sequence Observed from Er(21+) to Au(32+).
PB95-150660 *03,899*

Wavelengths and Energy Level Classifications for the Spectra of Sulfur (S I through S XVI).
PB94-162229 *00,734*

Wavelengths and Energy Levels of Neutral Kr(84) and Level Shifts in All Kr Even Isotopes.
PB94-140605 *03,780*

KAUTZ, R. L.

24 GHz Josephson Array Voltage Standard.
PB94-211588 *02,033*

Chaos in a Computer-Animated Pendulum.
PB94-212651 *03,852*

Design and Operation of Series-Array Josephson Voltage Standards.
PB94-185451 *02,030*

Effect of Thermal Noise on Shapiro Steps in High-Tc Josephson Weak Links.
PB94-212677 *04,506*

Josephson D/A Converter with Fundamental Accuracy.
PB96-148044 *02,418*

Large-Amplitude Shapiro Steps and Self-Field Effects in High-Tc Josephson Weak Links.
PB95-180410 *04,682*

Metallic-Barrier Junctions for Programmable Josephson Voltage Standards.
PB96-200134 *02,089*

Noise in the Coulomb Blockade Electrometer.
PB95-176327 *04,670*

Phase Locking in Two-Dimensional Arrays of Josephson Junctions: Effect of Critical-Current Nonuniformity.
PB96-102587 *04,714*

Proposed High-Accuracy Superconducting Power Meter for Millimeter Waves.
PB94-212669 *02,034*

Quasipotential and the Stability of Phase Lock in Nonhysteretic Josephson Junctions.
PB95-180402 *04,681*

Self-Heating in the Coulomb-Blockade Electrometer.
PB94-212685 *04,507*

Shapiro Steps in Large-Area Metallic-Barrier Josephson Junctions.
PB96-200142 *02,090*

Voltage Gain in the Single-Electron Transistor.
PB95-176335 *04,671*

KAVOOSI, F.
Application of Boundary Element Methods to a Transient Axis-Symmetric Heat Conduction Problem.
PB94-212693 *01,375*

KAWANISHI, S.
Multiwavelength Birefringent-Cavity Mode-Locked Fibre Laser.
PB95-150496 *04,262*

KAWI, S.
Characterization of the Interaction of Hydrogen with Iridium Clusters in Zeolites by Inelastic Neutron Scattering Spectroscopy.
PB95-180741 *01,013*

KAY, J. G.
International Marine-Atmospheric (222)Rn Measurement Intercomparison in Bermuda. Part 2. Results for the Participating Laboratories.
PB96-175682 *00,115*

KAY, W. B.
Critical Properties and Vapor-Liquid Equilibria of the Binary System Propane + Neopentane.
PB95-175683 *00,999*

Vapor-Liquid Equilibria of Mixtures of Propane and Isomeric Hexanes.
PB95-175287 *00,995*

KAZUMATA, Y.
Harmonic and Static Susceptibilities of YBa2Cu3O7.
PB95-161139 *04,599*

KEARNEY, P. A.
Interfaces in Mo/Si Multilayers.
PB96-160668 *02,423*

KECK, J.
Proposed International Interactive Courseware Standard.
PB96-123161 *00,137*

KEDER, N. L.
Structural and Chemical Investigations of Na3(ABO4)3.4H2O-Type Sodalite Phases.
PB95-180733 *01,012*

KEDZIERSKI, M. A.
Calorimetric and Visual Measurements of R123 Pool Boiling on Four Enhanced Surfaces.
PB96-128129 *04,053*

Causes of the Apparent Heat Transfer Degradation for Refrigerant Mixtures.
PB94-212701 *03,259*

Design and Machining of Copper Specimens with Micro Holes for Accurate Heat Transfer Measurements.
PB95-180428 *02,658*

Effect of Inclination on the Performance of a Compact Brazed Plate Condenser and Evaporator.
PB96-136973 *02,756*

Enhancement of R123 Pool Boiling by the Addition of N-Hexane.
PB96-165956 *02,605*

Simultaneous Visual and Calorimetric Measurements of R11, R123, and R123/Alkylbenzene Nucleate Flow Boiling.
PB94-172426 *03,251*

Single-Phase Heat Transfer and Pressure Drop Characteristics of an Integral-Spine-Fin Within an Annulus.
PB94-194073 *03,805*

Single-Phase Heat Transfer and Pressure Drop Characteristics of an Integral-Spine Fin Within an Annulus.
PB97-122386 *04,179*

Visual Measurement Technique for Analysis of Nucleate Flow Boiling.
PB95-143301 *03,262*

KEEM, J.
Influence of Electrical Isolation on the Structure and Reflectivity of Multilayer Coatings Deposited on Dielectric Substrates.
PB96-159736 *04,365*

New Method for Achieving Accurate Thickness Control for Uniform and Graded Multilayer Coatings on Large Flat Substrates.
PB96-159744 *04,366*

KEENY, S. M.
Properties and Interactions of Oral Structures and Restorative Materials. Annual Report for Period October 1, 1990 to September 30, 1991.
PB94-160843 *03,558*

KEERY, W. J.
Modification of a Commercial SEM with a Computer Controlled Cathode Stabilized Power Supply.
PB96-201066 *04,129*

Report on the NIST Low Accelerating Voltage SEM Magnification Standard Interlaboratory Study.
PB96-201074 *02,445*

Scanning Electron Microscope Magnification Calibration Interlaboratory Study.
PB96-201082 *01,164*

SEM Linewidth Metrology of X-ray Lithography Masks.
PB96-201108 *02,447*

X-ray Mask Metrology: The Development of Linewidth Standards for X-ray Lithography.
PB95-162129 *02,348*

KEIMER, B.
High Resolution Inelastic Neutron Scattering Study of Phonon Self-Energy Effects in YBCO.
PB95-180881 *04,688*

q Dependence of Self-Energy Effects of the Plane Oxygen Vibration in YBa2Cu3O7.
PB96-138516 *01,096*

KELLEHER, D. E.
Attempts at Extending the Unified Theory to Include Many-Body Effects.
PB94-212719 *04,408*

Autoionizing Resonances in Electric Fields.
PB94-212727 *03,853*

Filter Transmittance Measurements in the Infrared.
PB94-140589 *04,224*

Isotope Shifts and Hyperfine Splittings of the 398.8-nm Yb I Line.
PB94-199585 *03,814*

Search for Small Violations of the Symmetrization Postulate in an Excited State of Helium.
PB96-123518 *04,050*

KELLER, L.
Evaluation of a Tapered Roller Bearing Spindle for High-Precision Hard Turning Applications.
PB96-160494 *02,700*

KELLER, R. R.
Scanning Electron Microscopy Observations of Misfit Dislocations in Epitaxial In0.25Ga0.75As on GaAs(001).
PB96-200159 *03,004*

Tensile Deformation-Induced Microstructures in Free-Standing Copper Thin Films.
PB96-102595 *04,715*

KELLERMANN, K.
From Superconductivity to Supernovae: The Ginzburg Symposium. Report on the Symposium Held in Honor of Vitaly L. Ginzburg. Held in Gaithersburg, Maryland on May 22, 1992.
PB95-171963 *04,649*

KELLETT, B. J.
Dynamic Phenomena on the RS Canum Venaticorum Binary II Pegasi in August 1989. 1. Observational Data.
PB94-211067 *00,056*

Volume-Limited ROSAT Survey of Extreme Ultraviolet Emission from all Nondegenerate Stars within 10 Parsecs.
PB96-103189 *00,093*

KELLEY, E. F.
Can Displays Deliver a Full Measure: Manufacturing.
PB96-111935 *02,185*

Display-Measurement Round-Robin.
PB96-119227 *02,186*

Interface-Filter Characterization of Spectraradiometers and Colorimeters.
PB97-122212 *04,399*

Making Displays Deliver a Full Measure.
PB96-122411 *01,490*

Nonlinear Color Transformations in Real Time Using a Video Supercomputer.
PB96-123021 *02,191*

Observations of Partial Discharges in Hexane Under High Magnification.
PB95-163127 *01,900*

Specification for Interoperability between Ballistic Imaging Systems. Part 1. Cartridge Cases.
PB96-195524 *01,860*

Specular and Diffuse Reflection Measurements of Electronic Displays.
PB97-119200 *02,208*

Survey of the Components of Display-Measurement Standards.
PB96-122528 *02,188*

Survey of the Components of Display-Measurement Standards.
PB97-122394 *02,209*

KELLEY, M. H.
Determination of Complex Scattering Amplitudes in Low-Energy Elastic Electron-Sodium Scattering.
PB94-216652 *03,869*

Domain Structures in Magnetoresistive Granular Metals.
PB96-141346 *04,760*

Electron-atom collision studies using optically state selected beams. Progress report, May 15, 1987--May 14, 1988.
DE95004446 *03,776*

Electron-atom collision studies using optically state selected beams. Progress report, May 15, 1988--May 14, 1991.
DE95004447 *03,777*

Spin-Resolved Elastic Scattering of Electrons from Sodium.
PB95-161774 *03,933*

Uncertainty Intervals for Polarized Beam Scattering Asymmetry Statistics.
PB94-200342 *03,825*

KELLEY, R. J.
Electromagnetic Coupling Character of (001) Twist Boundaries in Sintered Bi2Sr2CaCu2O8+x Bicrystals.
PB96-176573 *01,963*

KELLOG, G. J.
Observed Frustration in Confined Block Copolymers.
PB95-150033 *01,238*

KELLY, G.
Use of Building Emulators to Evaluate the Performance of Building Energy Management Systems.
PB96-111901 *00,269*

KELLY, G. E.
Factors Affecting the Energy Consumption of Two Refrigerator-Freezers.
PB97-112312 *00,311*

Performance Testing of a Family of Type I Combination Appliance.
PB95-220521 *02,505*

Predicting the Energy Performance Ratings of a Family of Type I Combination Appliances.
PB95-105524 *02,504*

Using Emulator/Testers for Commissioning EMCS Software, Operator Training, Algorithm Development, and Tuning Local Control Loops.
PB94-212735 *00,245*

Using Emulators to Evaluate the Performance of Building Energy Management Systems.
PB95-175774 *00,259*

KELLY, J.
Statistical Analysis of Parameters Affecting the Measurement of Particle-Size Distribution of Silicon Nitride Powders by Sedigraph (Trade Name).
PB94-216249 *03,042*

KELLY, J. F.
Compositional Homogeneity in Processing Precursor Powders to the Ba2YCu3O7-x High Tc Superconductor.
PB94-212743 *04,508*

Effect of Sm2BaCuO5 on the Properties of Sintered (Bulk) YBa2Cu3O6+x.
PB96-119441 *04,733*

Interface Modification and Characterization of Silicon Carbide Platelets Coated with Alumina Particles.
PB95-108734 *03,121*

Loading Device for Fracture Testing of Compact Tension Specimens in the Scanning Electron Microscope.
PB95-162434 *02,652*

Study of the Hydroxycarbonate Precursor Route to the YBa2Cu3O7-x High Tc Superconductor.
PB95-140471 *04,540*

KELLY, J. R.
Dental Materials.
PB94-172871 *00,142*

Error Propagation Biases in the Calculation of Indentation Fracture Toughness for Ceramics.
PB94-172434 *03,032*

Evaluation of Fracture Toughness and Residual Stress in Dental Porcelain by Indentation-Microfracture Method.
PB95-125613 *00,154*

Evaluation of Fracture Toughness and Residual Stress in Dental Porcelain by Indentation-Microfracture Method.
PB95-152831 *00,159*

Failure of All-Ceramic Fixed Partial Dentures 'In vitro' and 'In vivo': Analysis and Modeling.
PB96-122536 *00,175*

In vitro Fracture Behavior of Ceramic and Metal-Ceramic Restorations.
PB96-119722 *03,569*

KELLY, R. M.
Chemical and Microbiological Problems Associated with Research on the Biodesulfurization of Coal.
PB95-140950 *02,484*

Microbial Degradation of Polysulfides and Insights into Their Possible Occurrence in Coal.
PB95-163374 *02,488*

KELLY, W. R.
Certification of Standard Reference Material (SRM) 1941a, Organics in Marine Sediment.
PB96-123690 *02,593*

Determination of Sulfur in Fossil Fuels by Isotope Dilution Thermal Ionization Mass Spectrometry.
PB96-141379 *02,495*

Rare-Earth Isotopes as Tracers of Particulate Emissions: An Urban Scale Test.
PB94-161635 *02,535*

KENDALL, K. N.
Report on the Workshop on Manufacturing Polymer Composites by Liquid Molding. Held in Gaithersburg, Maryland on September 20-22, 1993.
PB94-160066 *03,131*

KENNEDY, F. E.
Tribology Education: Present Status and Future Challenges.
PB94-212362 *02,965*

KENNEDY, J. J.
Correlation of HgCdTe Epilayer Defects with Underlying Substrate Defects by Synchrotron X-Ray Topography.
PB94-200714 *02,129*

KENSLER, T. W.
Copper Ion-Mediated Modification of Bases in DNA in Vitro by Benzoyl Peroxide.
PB94-198231 *03,645*

KENT, E.
Scale-Space-Based Visual-Motion-Cue for Autonomous Navigation.
PB96-183173 *02,940*

Study of Potential Applications of Automation and Robotics Technology in Construction, Maintenance and Operation of Highway Systems: A Final Report. Volume 1.
PB95-251682 01,341

Study of Potential Applications of Automation and Robotics Technology in Construction, Maintenance and Operation of Highway Systems: A Final Report. Volume 2.
PB95-255865 01,343

Study of Potential Applications of Automation and Robotics Technology in Construction, Maintenance and Operation of Highway Systems: A Final Report. Volume 3.
PB95-251690 01,342

KENT, E. W.

Robotics Application to Highway Transportation. Volume 1. Final Report.
PB95-203790 03,654

Robotics Application to Highway Transportation. Volume 2. Literature Search.
PB95-170551 01,337

Robotics Application to Highway Transportation. Volume 3. Proposed Research Topics and Cost/Benefit Evaluations by CERF.
PB95-171633 01,338

Robotics Application to Highway Transportation. Volume 4. Proposals for Potential Research.
PB95-193173 01,339

Study of Potential Applications of Automation and Robotics Technology in Construction, Maintenance and Operation of Highway Systems: A Final Report. Volume 4.
PB95-251641 01,340

Workshop on the Application of Virtual Reality to Manufacturing. Final Report. Held in Gaithersburg, Maryland on August 9, 1994.
PB95-173555 02,825

KERCH, H.

Imaging of Fine Porosity in a Colloidal Silica: Potassium Silicate Gel by Defocus Contrast Microscopy.
PB94-212750 03,039

KERCH, H. M.

High-Temperature Furnace for In situ Small-Angle Neutron Scattering during Ceramic Processing.
PB96-148127 03,743

KERNER, J.

Design and Characterization of X-Ray Multilayer Analyzers for the 50 - 1000 eV Region.
PB94-211851 03,848

Silicon Photodiodes Optimized for EUV and Soft X-Ray Regions.
PB94-199478 02,124

KERSTEL, E.

Sub-Doppler, Infrared Laser Spectroscopy of the Propyne 2nu1 Band: Evidence of z-Axis Coriolis Dominated Intramolecular State Mixing in the Acetylenic CH Stretch Overtone.
PB95-202941 01,037

KESSLER, E. G.

Precision Comparison of the Lattice Parameters of Silicon Monocrystals.
PB94-169745 04,438

Status of a Silicon Lattice Measurement and Dissemination Exercise.
PB94-199635 04,474

KESSNER, A.

Molar Absorptivities of Bilirubin (NIST SRM 916A) and Its Neutral and Alkaline Azopigments.
PB94-211042 03,456

KESTNER, R. N.

Test Optics Error Removal.
PB96-179536 04,377

KEY, T. S.

Surging the Upside-Down House: Looking into Upsetting Reference Voltages.
PB96-112313 02,385

KEYSER, P. T.

Test of Newton's Inverse Square Law of Gravitation Using the 300-m Tower at Erie, Colorado.
PB95-202446 03,978

KHAIKIN, G. I.

Oxidation of Ferrous and Ferrocyanide Ions by Peroxyl Radicals.
PB97-122402 01,191

KHAN. M. R.

Correlations of Modulation Noise with Magnetic Microstructure and Intergranular Interactions for CoCrTa and CoNi Thin Film Media.
PB94-212768 04,509

KHLEVNOY, B. B.

Results of a NIST/VNIIOFI Comparison of Spectral-Radiance Measurements.
PB97-113021 04,159

KHODAKOVSKII, I. L.

Thermodynamic Properties of the Aqueous Ions (2+ and 3+) of Iron and the Key Compounds of Iron.
PB96-145958 01,119

KHOLODENKO, A.

Generalized Stokes-Einstein Equation for Spherical Particle Suspensions.
PB95-202743 01,031

KHOLODENKO, A. L.

Electrostatic Rigidity of Polyelectrolytes from Reparametrization Invariance.
PB96-180062 04,113

Influence of Surface Interaction and Chain Stiffness on Polymer-Induced Entropic Forces and the Dimensions of Confined Polymers.
PB94-185469 01,203

KHORRAMSHAHGOL, R.

SQA Standards and Total Quality Management.
PB96-111844 01,743

KIBBLER, A. E.

Surface Topography and Ordering-Variant Segregation in GaInP2.
PB95-153649 04,595

KIDDER, C.

Transient Cooling of a Hot Surface by Droplets Evaporation.
PB94-156957 03,783

KIEF, M. T.

Spot-Profile-Analyzing LEED Study of the Epitaxial Growth of Fe, Co, and Cu on Cu(100).
PB95-150165 04,561

KIELY, A. B.

Model of an Optical Roughness-Measuring Instrument.
PB97-110209 04,384

KIKUCHI, H.

Properties and Interactions of Oral Structures and Restorative Materials. Annual Report for Period October 1, 1990 to September 30, 1991.
PB94-160843 03,558

KILE, L. L.

Programmable Guarded Coaxial Connector Panel.
PB96-122544 02,108

KILICCOTE, H.

Distributed Architecture for Standards Processing.
PB96-164181 00,276

KILMER, R. D.

AMRF Composite Fabrication Workstation.
PB94-172681 02,810

KIM, B. S.

Intracycle Evaporative Cooling in a Vapor Compression Cycle.
PB97-116107 02,762

KIM, D. Y.

Stability and Surface Energies of Wetted Grain Boundaries in Aluminum Oxide.
PB95-202750 03,059

KIM, G. J.

Combining Interactive Exploration and Optimization for Assembly Design.
PB97-112320 02,794

KIM, J. B.

RIS Measurement of AC Stark Shifts and Photoionization Cross Sections in Calcium.
PB96-157953 04,073

Verification of the Ponderomotive Approximation for the ac Stark Shift in Xe Rydberg Levels.
PB94-185709 03,801

KIM, J. H.

Causes of the Apparent Heat Transfer Degradation for Refrigerant Mixtures.
PB94-212701 03,259

KIM, J. S.

Characterization of Liquid-Phase Epitaxially Grown HgCdTe Films by Magnetoresistance Measurements.
PB96-123617 04,738

Characterization of LPE HgCdTe Film by Magnetoresistance.
PB96-157961 02,197

Electrical Characterization of Liquid-Phase Epitaxially Grown Single-Crystal Films of Mercury Cadmium Telluride by Variable-Magnetic-Field Hall Measurements.
PB95-175782 02,177

Electrical Characterization of Narrow Gap n-Type Bulk HgCdTe Single Crystals by Variable-Magnetic-Field Hall Measurements and Reduced-Conductivity-Tensor Analyses.
PB96-164199 01,146

Magneto-Transport Properties of HgCdTe.
PB95-175840 04,661

Multicarrier Characterization Method for Extracting Mobilities and Carrier Densities of Semiconductors from Variable Magnetic Field Measurements.
PB94-212776 02,317

KIM, M. S.

Single-Phase Heat Transfer and Pressure Drop Characteristics of an Integral-Spine-Fin Within an Annulus.
PB94-194073 03,805

Single-Phase Heat Transfer and Pressure Drop Characteristics of an Integral-Spine Fin Within an Annulus.
PB97-122386 04,179

Study to Determine the Existence of an Azeotropic R-22 'Drop-In' Substitute.
PB96-167812 02,568

KIM, M. W.

Small-Angle Neutron Scattering (SANS) Study of Worm-Like Micelles Under Shear.
PB96-176698 04,111

KIM, S.

Artificial Crack in Steel: An Ultrasonic-Resonance-Spectroscopy and Modeling Study.
PB96-141395 03,241

Compressibility of Polycrystal and Monocrystal Copper: Acoustic-Resonance Spectroscopy.
PB96-164223 02,990

Correlation between Tc and Elastic Constants of (La-M)2CuO4.
PB94-213220 04,514

Off-Diagonal Orthorhombic-Symmetry Elastic Constants.
PB95-202768 04,695

Void Shape in Sintered Titanium.
PB96-141023 02,705

KIM, S. Y.

Strategy to Support Multipoint Communication Service Over Native ATM Service.
PB96-176672 01,507

KIM, Y. K.

Investigation of LS Coupling in Boronlike Ions.
PB94-185295 03,797

Labeling Conventions in Isoelectronic Sequences - Reply.
PB95-162574 03,937

Low Magnetostriction in Annealed NiFe/Ag Giant Magnetoresistive Multilayers.
PB96-146691 04,762

Magnetoresistance of Thin-Film NiFe Devices Exhibiting Single-Domain Behavior.
PB96-147087 04,766

Magnetostriction and Giant Magnetoresistance in Annealed NiFe/Ag Multilayers.
PB96-102603 04,716

Modeling Effects of Temperature Annealing on Giant Magnetoresistive Response in Discontinuous Multilayer NiFe/Ag Films.
PB97-112585 04,157

Observation of the Transverse Second Harmonic Magneto-Optic Kerr Effect from Ni81Fe19 Thin Film Structures.
PB96-200332 01,971

Relativistic and Quantum Electrodynamic Effects in Highly-Charged Ions.
PB94-212784 03,854

Relativistic Modifications of Charge Expansion Theory.
PB96-123799 04,052

Simulating Device Size Effects on Magnetization Pinning Mechanisms in Spin Valves.
PB97-112593 04,158

KIMMINS, J.

Telecommunications Security Guidelines for Telecommunications Management Network. Computer Security.
PB96-139415 01,496

KINARD, J.

Performance of Commercial CMOS Foundry-Compatible Multijunction Thermal Converters.
PB95-153656 02,342

KINARD, J. R.

AC-DC Difference Characteristics of High-Voltage Thermal Converters.
PB96-148093 02,083

Development of Thin-Film Multijunction Thermal Converters at NIST.
PB97-112338 02,286

Empirical Linear Prediction Applied to a NIST Calibration Service.
PB97-112353 02,287

Frequency Extension of the NIST AC-DC Difference Calibration Service for Current.
PB95-161253 01,895

High-Current Thin Film Multijunction Thermal Converters and Multi-Converter Modules.
PB97-112379 01,989

Integrated Thin-Film Micropotentiometers.
PB96-146709 02,109

Intercomparison of NIST, NPL, PTB, and VSL Thermal Voltage Converters from 100 kHz to 1 MHz.
PB94-172442 02,026

Intercomparison of Thermal Converters at NIM, NIST, PTB, SIRI and VSL from 10 to 100 MHz.
PB94-172459 02,027

Multijunction Thermal Converters by Commercial CMOS Fabrication.
PB95-153664 02,343

Performance of Multilayer Thin-Film Multijunction Thermal Converters.
PB96-148135 02,084

KING, A. H.

Interaction between Dislocations and Intergranular Cracks.
PB95-152096 03,190

KING, D. I.

Publications of the National Institute of Standards and Technology 1992 Catalog.
PB95-200747 00,014

Publications of the National Institute of Standards and Technology 1993 Catalog.
PB96-183215 00,017

KING, D. S.
Dynamics of Nonthermal Reactions: Femtosecond Surface Chemistry.
PB94-199965 *00,688*
Fragment Energy and Vector Correlations in the Overtone-Pumped Dissociation of HN3X(1)A'.
PB94-199908 *00,802*
Fragment State Correlations in the Dissociation of NO.HF(v=1).
PB95-164430 *00,982*
Laser-Induced Desorption of NO from Si(111): Effects of Coverage on NO Vibrational Populations.
PB95-162319 *00,959*
Product Kinetic Energies, Correlations, and Scattering Anisotropy in the Bimolecular Reactor O((1)D)+H2O yields 2OH.
PB94-212792 *00,838*
Product State Correlations in the Reaction of O((1)D) and H2O in Bimolecular Collisions and in O3.H2O Clusters--Translation.
PB95-153011 *00,946*
Vibrational Predissociation Dynamics of Overtone-Excited HN3.
PB95-125720 *00,691*

KING, J. B.
Configuration-Dependent AC Stark Shifts in Calcium.
PB96-157995 *04,363*

KING, M.
Lean flammability limit as a fundamental refrigerant property. Phase 1, Interim technical report, 1 October 1994--31 March 1995.
DE95011238 *03,248*

KING, M. D.
Acid Gas Production in Inhibited Diffusion Flames.
PB95-180576 *01,390*

KINGON, A. I.
Growth of Epitaxial KNbO3 Thin Films.
PB96-135181 *02,409*

KINGSTON, H. M.
Dissolution Problems with Botanical Reference Materials.
PB95-126280 *03,487*
Hydrolysis of Proteins by Microwave Energy.
PB94-216322 *03,528*

KINNEY, A. L.
New High-Redshift Damped Lyman-alpha Absorption Systems and the Redshift Evolution of Damped Absorbers.
PB95-203501 *00,083*

KINNISON, D. E.
Environmental Aspects of Halon Replacements: Considerations for Advanced Agents and the Ozone Depletion Potential of CF3I.
PB97-122261 *03,301*

KINRA, V. K.
Dynamic Shear Modulus Measurements with Four Independent Techniques in Nickel-Based Alloys.
PB94-198900 *03,320*

KINSMAN, R.
Precision Oscillators: Dependence of Frequency on Temperature, Humidity and Pressure.
PB94-198306 *02,031*

KIRCHMANN, N.
SUSAN: SUperconducting Systems ANalysis by Low Temperature Scanning Electron Microscopy (LTSEM).
PB96-112065 *04,728*

KIRCHMAYR, H.
V-6: Effects of Temperature Variation.
PB96-148143 *04,772*

KIRKLAND, J.
Surface Geometry of BaO on W(100): A Surface-Extended X-Ray-Absorption Fine-Structure Study.
PB95-164414 *00,980*

KIRSCHENBAUM, L. S.
Bias Current Dependent Resistance Peaks in NiFe/Ag Giant Magnetoresistance Multilayers.
PB97-112346 *04,153*
Telegraph Noise in Silver-Permalloy Giant Magnetoresistance Test Structures.
PB96-146717 *04,763*

KISELEV, S. B.
Physical Limit to the Stability of Superheated and Stretched Water.
PB96-122551 *01,083*

KISER, C.
Accuracy Comparisons of Josephson Array Systems.
PB95-164687 *02,047*
Voltage Ratio Measurements of a Zener Reference Using a Digital Voltmeter.
PB95-164695 *01,906*

KISHORE, N.
Apparent Molar Heat Capacities and Apparent Molar Volumes of Aqueous Glucose at Temperatures from 298.15 K to 327.01 K.
PB94-212800 *03,459*
Thermochemistry of the Hydrolysis of L-arginine to (L-citrulline + Ammonia) and of the Hydrolysis of L-arginine to (L-ornithine + Urea).
PB95-150801 *03,463*
Thermodynamics of the Hydrolysis of Penicillin G and Ampicillin.
PB94-172467 *03,596*

KISLIUK, P.
Molecular Microwave Spectra Tables.
AD-A296 498/9 *00,720*

KITAGAWA, T.
Direct Dispersion Measurement of Highly-Erbium-Doped Optical Amplifiers Using a Low Coherence Reflectometer Coupled with Dispersive Fourier Spectroscopy.
PB95-150702 *04,263*

KITTEL, P.
Design Equations and Scaling Laws for Linear Compressors with Flexure Springs.
PB95-168902 *02,948*

KIYOTSUKURI, T.
Thermal Stability of Internal Electric Field and Polarization Distribution in Blend of Polyvinylidene Fluoride and Polymethylmethacrylate.
PB95-151072 *01,240*

KJEKSHUS, A.
Neutron Powder Diffraction Study of the Nuclear and Magnetic Structures of the Oxygen-Deficient Perovskite YBaCuCoO5.
PB95-161097 *00,954*

KLASK, U.
Application of the Taylor Dispersion Method in Supercritical Fluids.
PB95-164323 *00,977*

KLASSEN, M.
Estimate of Flame Radiance via a Single Location Measurement in Liquid Pool Flames.
PB94-211596 *02,476*
Measurement of Radiative Feedback to the Fuel Surface of a Pool Fire.
PB94-211604 *02,477*
Structure and Radiation Properties of Pool Fires.
PB94-193802 *02,473*

KLAUS, E. E.
Mechano-Chemical Model: Reaction Temperatures in a Concentrated Contact.
PB96-119466 *03,227*

KLAVINS, P.
Crystal Structure and Magnetic Ordering of the Rare-Earth and Cu Moments in RBa2Cu2NbO8(R=Nd,Pr).
PB95-140554 *04,546*

KLEAR, R. M.
Second Census Optical Character Recognition Systems Conference.
PB94-188711 *01,832*

KLEBANOFF, P. S.
Characteristics of Turbulence in a Boundary Layer with Zero Pressure Gradient.
AD-A278 249/8 *04,192*
Evolution of a Turbulent Boundary Layer Induced by a Three-Dimensional Roughness Element.
PB94-212818 *04,200*

KLEIBER, P. D.
Alignment Probing of Rydberg States by Stimulated Emission.
PB96-200316 *04,124*

KLEIN, C. A.
Workshop on Characterizing Diamond Films (3rd). Held in Gaithersburg, Maryland on February 23-24, 1994.
PB94-187663 *04,456*

KLEIN, M. L.
Molecular Dynamics Investigation of the Surface/Bulk Equilibrium in an Ethanol-Water Solution.
PB97-113112 *01,183*

KLEIN, R.
Reaction Rate Determinations of Vinyl Radical Reactions with Vinyl, Methyl, and Hydrogen Atoms.
PB94-211398 *00,815*

KLEIN, W.
Long-Lived Structures in Fragile Glass-Forming Liquids.
PB96-119565 *04,212*

KLEINER, I.
Fundamental Torsion Band in Acetaldehyde.
PB94-212834 *00,840*
Molecular-Beam Optothermal Spectrum of the OH Stretching Band of Methanol.
PB94-212826 *00,839*

KLEMM, R. B.
Experimental Determination of the Ionization Energy of IO(X(sup 2)II(sub 3/2)) and Estimations of Delta(sub f)H(sup deg)(sub 0)(IO(sup -)) and PA(IO).
PB96-146899 *00,694*
Ionization Energies, Appearance Energies and Thermochemistry of CF2O and FCO.
PB97-111538 *01,178*

KLEMPERER, W.
Microwave and Submillimeter Spectroscopy of Ar-NH3 States Correlating with Ar+NH3(j=1, k=1).
PB95-152211 *00,942*

KLEVNOY, B. B.
Precision High Temperature Blackbodies.
PB95-140059 *03,885*

KLEYN, M. F.
Cellular Automaton Simulations of Cement Hydration and Microstructure Development.
PB95-175055 *01,320*

KLIEGER, P.
Highway Concrete (HWYCON) Expert System User Reference and Enhancement Guide.
PB94-215670 *01,316*

KLINE, M. C.
Enhanced Detection of PCR Products Through Use of TOTO and YOYO Intercalating Dyes with Laser Induced Fluorescence - Capillary Electrophoresis.
PB95-164653 *00,599*
Intercomparison of DNA Sizing Ladders in Electrophoretic Separation Matrices and Their Potential for Accurate Typing of the D1S80 Locus.
PB96-200928 *03,485*
Overview of Reference Materials Prepared for Standardization of DNA Typing Procedures.
PB96-111653 *00,611*

KLINE, R. W.
Use of a Radiochromic Detector for the Determination of Stereotactic Radiosurgery Dose Characteristics.
PB94-185642 *03,514*

KLINE, S. W.
Group 1 for the Plant Spatial Configuration STEP Application Protocol.
PB96-165402 *02,789*
Group 1 for the Process Engineering Data STEP Application Protocol.
PB97-116073 *02,797*

KLINEDINST, D.
Sources of Urban Contemporary Carbon Aerosol.
PB95-175659 *02,551*

KLINEDINST, D. B.
Comparative Study of Fe-C Bead and Graphite Target Performance with the National Ocean Sciences AMS (NOSAMS) Facility Recombinator Ion Source.
PB95-175790 *00,693*
Distinguishing the Contributions of Residential Wood Combustion and Mobile Source Emissions Using Relative Concentrations of Dimethylphenanthrene Isomers.
PB96-135124 *02,563*

KLONZ, M.
Intercomparison of NIST, NPL, PTB, and VSL Thermal Voltage Converters from 100 kHz to 1 MHz.
PB94-172442 *02,026*

KLOPPING, F.
Intracomparison Tests of the FG5 Absolute Gravity Meters.
PB96-102991 *03,688*

KLOSE, J. Z.
Atomic Branching Ratio Data for Carbon-Like Ions.
PB94-212842 *03,855*
Atomic Branching Ratio Data for Nitrogen-Like Species.
PB96-190152 *04,122*
Atomic Branching Ratio Data for Oxygen-Like Species.
PB95-180436 *03,963*

KLOTE, J. H.
Feasibility and Design Considerations of Emergency Evacuation by Elevators.
PB94-163441 *00,287*
Feasibility of Fire Evacuation by Elevators at FAA Control Towers.
PB94-213857 *04,844*
Fire and Smoke Control: An Historical Perspective.
PB95-175808 *00,202*
Full Scale Smoke Control Tests at the Plaza Hotel Building.
PB94-212859 *00,347*
Method of Predicting Smoke Movement in Atria with Application to Smoke Management.
PB95-154746 *00,376*
Overview of Smoke Control Technology.
PB94-212867 *00,348*
Preview of ASHRAE's Revised Smoke Control Manual.
PB94-212875 *00,349*
Smoke Control Systems for Elevator Fire Evacuation.
PB94-212883 *00,291*

KLOUDA, G. A.
Comparative Study of Fe-C Bead and Graphite Target Performance with the National Ocean Sciences AMS (NOSAMS) Facility Recombinator Ion Source.
PB95-175790 *00,693*
Distinguishing the Contributions of Residential Wood Combustion and Mobile Source Emissions Using Relative Concentrations of Dimethylphenanthrene Isomers.
PB96-135124 *02,563*
Factorial Design Techniques Applied to Optimization of AMS Graphite Target Preparation.
PB95-151197 *00,584*
Radiocarbon Measurements of Atmospheric Volatile Organic Compounds: Quantifying the Biogenic Contribution.
PB97-122352 *02,574*

Sources of Urban Contemporary Carbon Aerosol.
PB95-175659 02,551

KLUKEN, A. O.

Cryogenic Toughness of Austenitic Stainless Steel Weld Metals: Effect of Inclusions.
PB95-161261 03,214

Effects of Copper, Nickel and Boron on Mechanical Properties of Low-Alloy Steel Weld Metals Deposited at High Heat Input.
PB96-135231 03,363

KNAB, L. I.

National Voluntary Laboratory Accreditation Program: Carpet and Carpet Cushion.
PB95-155560 00,295

National Voluntary Laboratory Accreditation Program (NVLAP): Commercial Products Testing.
PB95-267944 02,671

National Voluntary Laboratory Accreditation Program (NVLAP): Wood Based Products.
PB95-170429 03,405

National Voluntary Laboratory Accreditation Program: Thermal Insulation Materials.
PB95-267985 02,977

KNAPP, F. F.

Assay of the Eluent from the Alumina-Based Tungsten-188-Rhenium-188 Generator.
PB94-200482 03,829

KNAPPE, S.

Fabrication Issues in Optimizing YBa2Cu3O7-x Flux Transformers for Low l/f Noise.
PB95-175857 02,059

KNEELAND, D. R.

Real Time Monitoring of Electron Processors.
PB96-135306 03,719

KNELL, U.

Hydrogen in YBa2Cu3Ox: A Neutron Spectroscopy and a Nuclear Magnetic Resonance Study.
PB95-161279 04,601

Neutron-Spectroscopy Study of the Hydrogen Vibrations in Hydrogen-Doped YBa2Cu3Ox.
PB94-172475 04,441

KNIGHT, A. E. W.

High-Resolution Infrared Overtone Spectroscopy of ArHF via Nd:YAG/Dye Laser Difference Frequency Generation.
PB94-211448 00,816

KNIGHT, R. B. D.

Intercomparison of NIST, NPL, PTB, and VSL Thermal Voltage Converters from 100 kHz to 1 MHz.
PB94-172442 02,026

KNIO, O. M.

Dispersion and Deposition of Smoke Plumes Generated in Massive Fires.
PB95-126066 02,540

KNOLL, W.

Surface Plasmon Microscopy of Biotin-Streptavidin Binding Reactions on UV-Photopatterned Alkanethiol Self-Assembled Monolayers.
PB96-176771 01,158

KNUDSEN, F. P.

High Temperature Reactions of Uranium Dioxide with Various Metal Oxides.
AD-A286 648/1 00,717

KNUTILLA, A.

Unified Process Specification Language: Requirements for Modeling Process.
PB97-116123 02,850

KO, M.

Low Temperature H(sub 2)S Separation Using Membrane Reactor with Redox Catalyst.
DE94008991 02,471

KO, M. K.

Characterization of the Adsorption-Fouling Layer Using Globular Proteins on Ultrafiltration Membranes.
PB94-212909 00,842

Determination of Osmotic Pressure and Fouling Resistances and Their Effects on Performance of Ultrafiltration Membranes.
PB94-212891 00,841

Determination of Total Protein Adsorbed on Solid (Membrane) Surface by a Hydrolysis Technique: Single Protein Adsorption.
PB96-167093 03,552

KOBAYASHI, R.

Exponentially Rapid Coarsening and Buckling in Coherently Self-Stressed Thin Plates.
PB95-202347 04,821

KOCAOGLU, D. F.

Learning to Change: Opportunities to Improve the Performance of Smaller Manufacturers.
PB94-166212 00,010

KOCH, H.

Fabrication Issues in Optimizing YBa2Cu3O7-x Flux Transformers for Low l/f Noise.
PB95-175857 02,059

KOCH, J. A.

Optimization of ECR-Based PECVD Oxide Films for Superconducting Integrated Circuit Fabrication.
PB95-169165 02,051

Superconducting Integrated Circuit Fabrication with Low Temperature ECR-Based PECVD SiO2 Dielectric Films.
PB96-103015 04,719

KOCH, W.

Frozen Human Serum Reference Material for Standardization of Sodium and Potassium Measurements in Serum or Plasma by Ion-Selective Electrode Analyzers.
PB94-185337 00,532

KOCH, W. F.

Absolute Determination of Electrolytic Conductivity for Primary Standard KC1 Solutions from 0 to 50C.
PB94-172798 00,765

CSTL Technical Activities, 1995.
PB96-214630 00,647

dc Method for the Absolute Determination of Conductivities of the Primary Standard KCl Solutions from 0C to 50C.
PB94-219342 02,644

Development of a Standard Reference Material for ISE Measurements of Sodium and Potassium.
PB96-159785 03,507

Faraday Constant.
PB96-159793 01,955

Mass and Density Determinations.
PB94-200672 00,504

KOEDAM, J. C.

Molar Absorptivities of Bilirubin (NIST SRM 916A) and Its Neutral and Alkaline Azopigments.
PB94-211042 03,456

KOELLE, D.

Fabrication Issues in Optimizing YBa2Cu3O7-x Flux Transformers for Low l/f Noise.
PB95-175857 02,059

Low Noise YBa2Cu3O7-x-SrTiO3-YBa2Cu3O7-x Mulitlayers for Improved Superconducting Magnetometers.
PB96-138417 04,747

KOENIG, A.

NIST ATM Network Simulator: Operation and Programming, Version 1.0.
PB96-106851 01,487

KOENIG, J.

Examination Procedure Outlines: Keys to Solving the Handbook 44 Puzzle.
PB97-110217 02,690

KOENIG, J. A.

Uniform Laws and Regulations in the Areas of Legal Metrology and Motor Fuel Quality as Adopted by the 80th National Conference on Weights and Measures 1995. 1996 Edition.
PB96-172309 02,927

Uniform Laws and Regulations in the Areas of Legal Metrology and Motor Fuel Quality, 1994 as Adopted by the 79th National Conference on Weights and Measures 1994.
PB95-174470 02,909

KOEPKE, G.

Screened-Room Measurements on the NIST Spherical-Dipole Standard Radiator.
PB96-113568 01,926

Standard Source Method for Reducing Antenna Factor Errors in Shielded Room Measurements.
PB96-183157 02,013

KOEPKE, G. H.

Radiated Emissions and Immunity of Microstrip Transmission Lines: Theory and Measurements.
PB96-162649 02,238

KOEYLUE, U. O.

Mixing and Radiation Properties of Buoyant Turbulent Diffusion Flames.
PB95-242327 01,396

KOFFMAN, A. D.

Binary versus Decade Inductive Voltage Divider Comparison and Error Decomposition.
PB96-112263 02,071

Empirical Linear Prediction Applied to a NIST Calibration Service.
PB97-112353 02,287

Modeling and Test Point Selection for a Thermal Transfer Standard.
PB95-161287 01,896

NIST Strategies for Reducing Testing Requirements.
PB95-180444 01,909

KOGA, K.

Structural and Magnetic Properties of CuCl2 Graphite Intercalation Compounds.
PB96-119748 03,020

KOHL, M. L.

Measurement and Interpretation of Tidal Tilts in a Small Array.
PB96-102611 03,686

KOHLER, B.

Phase Shifts and Intensity Dependence in Frequency-Modulation Spectroscopy.
PB96-103205 01,071

KOHLER, B. E.

Location of a (1)A(sub g) State in Bithiophene.
PB95-202313 01,025

Lowest Excited Singlet State of Isolated 1-phenyl-1,3-butadiene and 1-phenyl-1,3,5-hexatriene.
PB95-202339 01,026

KOJIMA, H.

High-Energy Phonon Dispersion in La1.85Sr0.15CuO4.
PB96-138458 04,748

KOJIMA, T.

Investigation of Applicability of Alanine and Radiochromic Detectors to Dosimetry of Proton Clinical Beams.
PB96-146782 03,636

Orientation Effects on ESR Analysis of Alanine-Polymer Dosimeters.
PB96-146725 03,720

KOJIMA, T. M.

Resonance Structure and Absolute Cross Sections in Near-Threshold Electron-Impact Excitation of the 4s(2) (1)S yields 4s4p (3)P Intercombination Transition in Kr(6+).
PB95-202271 03,972

KOLASINSKI, K. W.

Dynamics of Hydrogen Interactions with Si(100) and Si(111) Surfaces.
PB96-159801 04,082

KOLESKE, D. D.

Temperature Dependence and Anharmonicity of Phonons on Ni(110) and Cu(110) Using Molecular Dynamics Simulations.
PB94-185477 04,449

KOMITOV, L.

Studies of the Higher Order Smectic Phase of the Large Electroclinic Effect Material W317.
PB95-151601 00,935

KONJEVIC, N.

New Critical Review of Experimental Stark Widths and Shifts.
PB94-172830 03,790

KOPANSKI, J. J.

Boron-Implanted 6H-SiC Diodes.
PB96-159678 04,081

Characterization of Two-Dimensional Dopant Profiles: Status and Review.
PB96-119300 02,400

Characterization of Two-Dimensional Dopant Profiles: Status and Review.
PB97-110134 02,451

Development and Characterization of Insulating Layers on Silicon Carbide: Annual Report for February 14, 1988 to February 14, 1989.
PB94-155579 02,295

High-Spatial-Resolution Resistivity Mapping Applied to Mercury Cadmium Telluride.
PB94-212917 02,131

Oxidation of SiC.
PB96-119516 02,401

Review of Semiconductor Microelectronic Test Structures with Applications to Infrared Detector Materials and Processes.
PB94-212925 02,132

Scanning Capacitance Microscopy Measurements and Modeling for Dopant Profiling of Silicon.
PB96-164207 04,781

Scanning Capacitance Microscopy Measurements and Modeling: Progress Towards Dopant Profiling of Silicon.
PB96-148150 04,773

Scanning Capacitance Microscopy Measurements and Modeling: Progress Towards Dopant Profiling of Silicon.
PB96-180070 01,964

Semiconductor Measurement Technology: Improved Characterization and Evaluation Measurements for HgCdTe Detector Materials, Processes, and Devices Used on the GOES and TIROS Satellites.
PB94-188810 02,122

KOPETKA, P.

Liquid-Hydrogen Cold Neutron Source for the NBSR.
PB95-151619 03,729

Thermal Hydraulic Tests of a Liquid Hydrogen Cold Neutron Source.
PB95-135570 03,884

KORDE, R.

One Gigarad Passivating Nitrided Oxides for 100% Internal Quantum Efficiency Silicon Photodiodes.
PB94-185485 02,119

Silicon Photodiodes Optimized for EUV and Soft X-Ray Regions.
PB94-199478 02,124

Stable Silicon Photodiodes for Absolute Intensity Measurements in the VUV and Soft X-ray Regions.
PB97-110175 04,135

KORMAN, C.

Efficient Method to Compute the Maximum Transient Drain Current Overshoot in Silicon on Insulator Devices.
PB94-172483 02,300

KORTE, B. J.

Laser-Induced Desorption of In and Ga from Si(100) and Adsorbate Enhanced Surface Damage.
PB95-203311 01,050

Pulsed Laser Irradiation at 532 nm of In and Ga Adsorbed on Si(100): Desorption, Incorporation, and Damage.
PB95-203329 01,051

KOS, A. B.

Dependence of Contrast on Probe/Sample Spacing with the Magneto-Optic Kerr-Effect Scanning Near-Field Optical Microscope (MOKE-SNOM).
PB96-138557 *04,750*

Improved Eddy-Current Decay Method for Resistivity Characterization.
PB95-180451 *02,265*

Micromagnetic Scanning Microprobe System.
PB95-176178 *02,224*

Offset Susceptibility of Superconductors.
PB94-212263 *04,503*

KOSEKI, H.

Airborne Smoke Sampling Package for Field Measurements of Fires.
PB95-150041 *01,381*

In situ Burning of Oil Spills: Mesoscale Experiments and Analysis.
PB95-163747 *02,587*

Smoke Emission from Burning Crude Oil.
PB96-122890 *01,407*

KOSOBUKIN, V. A.

Theory of the Magneto-Optic Kerr Effect in the Near Field.
PB96-141387 *04,761*

KOSTER, B.

Current Activities Within the National Biomonitoring Specimen Bank.
PB94-172806 *02,516*

Development of Frozen Whale Blubber and Liver Reference Materials for the Measurement of Organic and Inorganic Contaminants.
PB95-151676 *00,587*

National Status and Trends Program Specimen Bank: Sampling Protocols, Analytical Methods, Results, and Archive Samples.
PB97-119226 *02,598*

KOSTER, B. J.

Alaska Marine Mammal Tissue Archival Project: Specimen Inventory.
PB95-171344 *02,589*

Certification of Polychlorinated Biphenyl Congeners and Chlorinated Pesticides in a Whale Blubber Standard Reference Material.
PB96-103023 *03,745*

Concentrations of Chlorinated Hydrocarbons, Heavy Metals and Other Elements in Tissues Banked by the Alaska Marine Mammal Tissue Archival Project.
PB95-209870 *02,590*

Considerations in the Design of an Environmental Specimen Bank: Experiences of the National Biomonitoring Specimen Bank Program.
PB96-112370 *02,527*

Determination of Inorganic Constituents in Marine Mammal Tissues.
PB95-152047 *00,589*

Determination of PCBs and Chlorinated Hydrocarbons in Marine Mammal Tissues.
PB95-162640 *03,744*

Relationship of Silver with Selenium and Mercury in the Liver of Two Species of Toothed Whales (Odontocetes).
PB96-167275 *02,596*

Standard Reference Materials for the Determination of Polycyclic Aromatic Hydrocarbons in Environmental Samples - Current Activities.
PB95-151668 *00,586*

Trace Element Concentrations in Cetacean Liver Tissues Archived in the National Marine Mammal Tissue Bank.
PB96-167127 *02,595*

KOSTIJUCHENKO, V.

Investigation of Applicability of Alanine and Radiochromic Detectors to Dosimetry of Proton Clinical Beams.
PB96-146782 *03,636*

KOSTREVA, M. M.

Mathematical Modeling of Human Egress from Fires in Residential Buildings.
PB94-193778 *00,337*

Sensitivity Analysis for Mathematical Modeling of Fires in Residential Buildings.
PB96-154968 *00,215*

KOTELES, E. S.

Use of Pressure for Quantum-Well Band-Structure Characterization.
PB96-164058 *04,779*

KOTRAPPA, P.

Calibration of Electret-Based Integral Radon Monitors Using NIST Polyethylene-Encapsulated (226)Ra/(222)Rn Emanation (PERE) Standards.
PB96-159223 *01,950*

Response Comparison of Electret Ion Chambers, LiF TLD, and HPIC.
PB96-190103 *02,578*

KOTSUJI, H.

Molecular Weight Dependence of the Lamellar Domain Spacing of ABC Triblock Copolymers and Their Chain Conformation in Lamellar Domains.
PB95-161691 *01,254*

KOVAC, A.

Radiation-Chemical Reaction of 2,3,5-Triphenyl-Tetrazolium Chloride in Liquid and Solid State.
PB96-146733 *01,124*

KOVACS, A.

Alcohol Solutions of Triphenyl-Tetrazolium Chloride as High-Dose Radiochromic Dosimeters.
PB96-135249 *03,716*

Novel Radiochromic Films for Clinical Dosimetry.
PB97-119259 *03,641*

Oscillometric and Conductometric Analysis of Aqueous and Organic Dosimeter Solutions.
PB96-135256 *04,054*

Radiochromic Solid-State Polymerization Reaction.
PB95-180683 *01,271*

Radiochromic Solid-State Polymerization Reaction.
PB96-180146 *01,290*

KOVAL, C.

Gas Transport Properties of Solution-Cast Perfluorosulfonic Acid Ionomer Films Containing Ionic Surfactants.
PB95-175998 *01,267*

KOWALAK, J.

beta-D-Glucosyl-Hydroxymethyluracil: A Novel Modified Base Present in the DNA of the Parastic Protozoan T. brucei.
PB94-172319 *03,524*

KOYLU, U. U.

Radiation and Mixing Properties of Buoyant Turbulent Diffusion Flames.
PB94-165974 *01,360*

KOZIN, I. N.

Tunneling-Rotation Spectrum of the Hydrogen Fluoride Dimer.
PB94-198678 *00,793*

KRAFT, K. M.

Performance of Tape-Bonded Seams of EPDM Membranes: Comparison of the Peel Creep-Rupture Response of Tape-Bonded and Liquid-Adhesive-Bonded Seams.
PB96-183249 *03,012*

KRAJEWSKI, J. J.

Observation of Oscillatory Magnetic Order in the Antiferromagnetic Superconductor HoNi2B2C.
PB95-180303 *04,679*

KRAMAR, J. A.

Measurement of Patterned Film Linewidth for Interconnect Characterization.
PB96-148168 *02,420*

Metrology Standards for Advanced Semiconductor Lithography Referenced to Atomic Spacings and Geometry.
PB96-160718 *02,424*

KRAMER, C.

In situ Observation of Surface Morphology of InP Grown on Singular and Vicinal (001) Substrates.
PB95-168431 *04,636*

KRAMER, E. J.

Grazing Incidence Prompt Gamma Emissions and Resonance-Enhanced Neutron Standing Waves in a Thin-Film.
PB95-150470 *03,892*

KRAMER, G. H.

Summary of the Proceedings of the Workshop on Standard Phantoms for In-vivo Radioactivity Measurement.
PB94-212933 *03,622*

KRAMER, G. W.

Integrating Automated Systems with Modular Architecture.
PB95-150231 *00,577*

Minutes of the CAALS Workshop on modularity and communications standards.
DE95005780 *02,621*

KRAMER, T.

NIST Support to the Next Generation Controller Program: 1991 Final Technical Report.
PB94-163490 *02,808*

KRAMER, T. R.

Feasibility Study: Reference Architecture for Machine Control Systems Integration.
PB94-142791 *02,804*

Issues and Recommendations for a STEP Application Protocol Framework. National PDES Testbed.
PB94-160868 *02,770*

Issues Concerning Material Removal Shape Element Volumes (MRSEVs).
PB94-185493 *02,882*

Issues Concerning Material Removal Shape Element Volumes (MRSEVs).
PB95-210167 *02,885*

NIST RS274KT Interpreter.
PB96-147954 *02,835*

NIST RS274/NGC Interpreter Version 1.
PB94-187788 *02,814*

Reference Architecture for Machine Control Systems Integration: Interim Report.
PB95-144549 *02,820*

Structural EXPRESS Editor.
PB94-159795 *02,769*

KRANBUEHL, D. E.

Effects of Variable Excluded Volume on the Dimensions of Off-Lattice Polymer Chains.
PB94-212941 *01,229*

KRANZ, H. G.

Standardised Computer Data File Format for Storage, Transport, and Off-Line Processing of Partial Discharge Data.
PB96-122486 *01,930*

KRAUSE, R.

Fracture Mechanism Maps: Their Applicability to Silicon Nitride.
PB96-204532 *03,094*

High Temperature Structural Reliability of Silicon Nitride.
PB97-110456 *03,104*

Tensile Creep Testing of Structural Ceramics.
PB97-110464 *03,105*

KRAUSE, R. F.

Cavitation Contributes Substantially to Tensile Creep in Silicon Nitride.
PB96-122577 *03,171*

Flat and Rising R-Curves for Elliptical Surface Cracks from Indentation and Superposed Flexure.
PB95-161295 *03,156*

Observed and Theoretical Creep Rates for an Alumina Ceramic and a Silicon Nitride Ceramic in Flexure.
PB94-212958 *03,040*

Tensile Creep of a Silicon Nitride Ceramic.
PB95-161303 *03,049*

KRAUSE, S.

Defect Formation Mechanism Causing Increasing Defect Density during Decreasing Implant Dose in Low-Dose Simox.
PB96-119524 *02,402*

KRAUSE, S. J.

Defect of Thermal Ramping and Annealing Conditions on Defect Formation in Oxygen Implanted Silicon-On-Insulator Material.
PB94-212966 *02,318*

Defect Pair Formation by Implantation-Induced Stresses in High-Dose Oxygen Implanted Silicon-on-Insulator Material.
PB95-175824 *02,364*

Effect of Annealing Ambient on the Removal of Oxide Precipitates in High-Dose Oxygen Implanted Silicon.
PB95-164356 *02,356*

Effect of Single versus Multiple Implant Processing on Defect Types and Densities in SIMOX.
PB96-160353 *01,957*

Mechanism of Defect Formation in Low-Dose Oxygen Implanted Silicon-on-Insulator Material.
PB97-111462 *02,453*

Stacking Fault Pyramid Formation and Energetics in Silicon-on-Insulator Material Formed by Multiple Cycles of Oxygen Implantation and Annealing.
PB96-160221 *04,083*

KRAUSS, A.

Problem of Convection in the Water Absorbed Dose Calorimeter.
PB97-110159 *03,523*

KRAUSS, G.

Ductile Fracture and Tempered Martensite Embrittlement of 4140 Steel.
PB96-190285 *03,222*

Temperature-Induced Transition in Ductile Fracture Appearance of a Nitrogen-Strengthened Austenitic Stainless Steel.
PB96-190269 *03,221*

KRAUSS, M.

Active Site Ionicity and the Mechanism of Carbonic Anhydrase.
PB94-212974 *00,843*

Analysis of Protein Metal Binding Selectivity in a Cluster Model.
PB94-212990 *00,845*

Cs Cluster Binding to a GaAs Surface.
PB94-213006 *00,846*

Dipole Moments in Rare Gas Interactions.
PB94-212982 *00,844*

KRAUSS, S. J.

Effect of Intermediate Thermal Processing on Microstructural Changes of Oxygen Implanted Silicon-on-Insulator Material.
PB96-160213 *02,982*

KRAYER, W. R.

Gust Factors Applied to Hurricane Winds.
PB95-180469 *00,446*

KRECH, R. H.

Collision-Induced Emission in the Fundamental Vibration-Rotation Band of H2.
PB94-199445 *03,811*

KREIDER, K.

Iridium Oxide Thin-Film Stability in High-Temperature Corrosive Solutions.
PB94-213014 *03,234*

Laser Ablation of Thin Films as a Free Atom Source for Pulsed RIMS.
PB94-198710 *00,540*

Thin Film Thermocouples for Measurement of Wall Temperatures in Internal Combustion Engines.
PB94-172103 *01,449*

KREIDER, K. G.

High Temperature Silicide Thin-Film Thermocouples.
PB94-185501 *02,252*

NIST/NCMS Program on Electronic Packaging: First Update.
PB96-204086 *03,008*

Sputtered High Temperature Thin Film Thermocouples.
PB95-161311 *02,259*

Thin-Film Ruthenium Oxide - Iridium Oxide Thermocouples.
PB97-110225 *00,520*

Thin Film Thermocouple Research at NIST.
PB97-110233 *02,283*

Thin Film Transparent Thermocouples.
PB94-185519 *02,253*

KREMER, D.

Planar Near-Field Alignment.
PB94-172491 *01,998*

KREMER, D. P.

Dual-Frequency Millimeter-Wave Radiometer Antenna for Airborne Remote Sensing of Atmosphere and Ocean.
PB96-112289 *02,009*

Dual Frequency mm-Wave Radiometer Antenna for Airborne Remote Sensing of Atmosphere and Ocean.
PB95-180378 *02,006*

New Extrapolation/Spherical/Cylindrical Measurement Facility at the National Institute of Standards and Technology.
PB95-153755 *02,004*

KRESIN, V. Z.

From Superconductivity to Supernovae: The Ginzburg Symposium. Report on the Symposium Held in Honor of Vitaly L. Ginzburg. Held in Gaithersburg, Maryland on May 22, 1992.
PB95-171963 *04,649*

KRETCHMER, J.

Boron-Implanted 6H-SiC Diodes.
PB96-159678 *04,081*

KRISHNAMOORTI, R.

Thermodynamic Interactions and Correlations in Mixtures of Two Homopolymers and a Block Copolymers by Small Angle Neutron Scattering.
PB95-152872 *01,247*

Thermodynamic Interactions in Model Polyolefin Blends Obtained by Small-Angle Neutron Scattering.
PB94-198496 *01,208*

KRISHNAN, S.

Adaptive, Predictive 2-D Feature Tracking Algorithm for Finding the Focus of Expansion.
PB94-218575 *01,588*

Simultaneous Measurement of Normal Spectral Emissivity by Spectral Radiometry and Laser Polarimetry at High Temperatures in Pulse-Heating Experiments: Application to Molybdenum and Tungsten.
PB97-118376 *02,694*

KRISHNAN, S. K.

Mixing and Radiation Properties of Buoyant Luminous Flame Environments.
PB96-202254 *01,432*

KRISHNASASTRY, M.

Genetically Engineered Pore as a Metal Ion Biosensor.
PB96-161658 *03,551*

Genetically Engineered Pores as Metal Ion Biosensors.
PB96-167408 *03,553*

Genetically Engineered Pores for New Materials.
PB96-161641 *03,550*

Pore-Forming Protein with a Metal-Actuated Switch.
PB96-176557 *03,554*

KRIZ, R. D.

Generalized Plane Strain Analysis of a Bimaterial Composite Containing a Free Surface Normal to the Interface.
PB95-163341 *03,164*

KROKAN, H. E.

Novel Activities of Human Uracil DNA N-glycosylase for Cytosine-Derived Products of Oxidative DNA Damage.
PB96-164132 *03,479*

KROLL, M.

Liposome-Based Flow-Injection Immunoassay for Determining Theophylline in Serum.
PB94-213493 *03,494*

KRUEGER, S.

Anisotropy of the Surfaces of Pores in Plasma Sprayed Alumina Deposits.
PB96-123211 *03,126*

Characterization of the Binding of Gallium, Platinum, and Uranium to Pseudomonas Fluorescens by Small-Angle X-ray Scattering and Transmission Electron Microscopy.
PB94-172509 *03,453*

Characterization of the Densification of Alumina by Multiple Small-Angle Neutron Scattering. (Reannouncement with New Availability Information).
AD-A249 179/3 *03,024*

Effect of Green Density and the Role of Magnesium Oxide Additive on the Densification of Alumina Measured by Small-Angle Neutron Scattering. (Reannouncement with New Availability Information).
AD-A244 582/3 *03,022*

Evolution of the Pore Size Distribution in Final-Stage Sintering of Alumina Measured by Small-Angle X-ray Scattering. (Reannouncement with New Availability Information).
AD-A249 178/5 *03,023*

Extending the Angular Range of Neutron Reflectivity Measurements from Planar Lipid Bilayers: Applications to a Model Biological Membrane.
PB96-122569 *03,476*

Small-Angle Neutron Scattering Characterization of Processing/Microstructure Relationships in the Sintering of Crystalline and Glassy Ceramics. (Reannouncement with New Availability Information).
AD-A249 510/9 *03,025*

Small Angle Neutron Scattering Studies of Structural Characteristics of Argarose Gels.
PB96-112305 *03,475*

KRULLE, C. A.

SUSAN: SUperconducting Systems ANalysis by Low Temperature Scanning Electron Microscopy (LTSEM).
PB96-112065 *04,728*

KRUMRINE, J. R.

Comment On: Two-Photon Absorption Series of Calcium.
PB96-157979 *04,074*

KRUPKA, J.

Dielectric Properties of Single Crystals of Al2O3, LaAlO3, SrTiO3, and MgO at Cryogenic Temperatures.
PB95-180477 *02,266*

Influence of Films' Thickness and Air Gaps in Surface Impedance Measurements of High Temperature Superconductors Using the Dielectric Resonator Technique.
PB96-157862 *01,946*

Measurements of Permittivity and the Dielectric Loss Tangent of Low Loss Dielectric Materials with a Dielectric Resonator Operating on the Higher Order Te(sub 0 gamma delta) Modes.
PB96-111869 *02,273*

Microwave Dielectric Properties of Anisotropic Materials at Cryogenic Temperatures.
PB96-137765 *02,412*

KRUPNOV, A. F.

Tunneling-Rotation Spectrum of the Hydrogen Fluoride Dimer.
PB94-198678 *00,793*

KUANG, J.

Transient Errors in a Precision Resistive Divider.
PB97-111512 *01,983*

KUBIAK, G. D.

XUV Characterization Comparison of Mo/Si Multilayer Coatings.
PB95-164000 *04,278*

KUBOTA, T.

Experimental and Numerical Studies on Two-Dimensional Gravity Currents in a Horizontal Channel.
PB94-165941 *01,359*

KUDCHADKER, S.

Thermodynamic and Thermophysical Properties of Organic Nitrogen Compounds. Part II. 1- and 2-Butanamine, 2-Methyl-1-Propanamine, 2-Methyl-2-Propanamine, Pyrrole, 1-, 2-, and 3-Methylpyrrole, Pyridine, 2-, 3-, and 4-Methylpyridine, Pyrrolidine, Piperidine, Indole, Quinoline, Isoquinoline, Acridine, Carbazole, Phenanthridine, 1- and 2-Naphthalenamine, and 9-Methylcarbazole.
PB94-162294 *00,741*

KUDRITZKI, R. P.

Radiation-Driven Winds of Hot Luminous Stars X. The Determination of Stellar Masses Radii and Distances from Terminal Velocities and Mass-Loss Rates.
PB94-213022 *00,060*

KUFFEL, J.

Digital Techniques in HV Tests - Summary of 1989 Panel Session.
PB94-216702 *02,035*

KUHN, D. R.

Analysis of Selected Software Safety Standards.
PB95-151262 *01,708*

Analysis of Standards for the Assurance of High Integrity Software.
PB96-161351 *03,735*

Control and Instrumentation: Standards for High-Integrity Software.
PB96-161369 *03,736*

Formal Specification and Verification of Control Software for Cryptographic Equipment.
PB94-213030 *01,585*

High Integrity Software Standards Activities at NIST.
PB96-112214 *01,744*

IEEE's POSIX: Making Progress.
PB96-160924 *01,757*

Open Systems Software Standards in Concurrent Engineering.
PB96-160932 *01,758*

Predicate Differences and the Analysis of Dependencies in Formal Specifications.
PB96-160940 *01,759*

Report of a Workshop on the Assurance of High Integrity Software.
PB96-161377 *01,763*

Report on the Advanced Software Technology Workshop. Held on February 1, 1994.
PB95-136610 *01,707*

Technique for Analyzing the Effects of Changes in Formal Specifications.
PB96-160957 *01,760*

KUHN, M.

Dielectric Properties of Single Crystals of Al2O3, LaAlO3, SrTiO3, and MgO at Cryogenic Temperatures.
PB95-180477 *02,266*

KUHN, R.

Security in Open Systems.
PB95-105383 *01,473*

KULANDER, K. C.

Intensity-Dependent Scattering Rings in High Order Above-Threshold Ionization.
PB96-110739 *04,032*

KULKARNI, A. K.

Turbulent Upward Flame Spread on a Vertical Wall under External Radiation.
PB94-207388 *00,341*

KUMAR, A.

Bending-Induced Loss in Dual-Mode Rectangular Waveguides.
PB95-168795 *04,288*

Bending-Induced Phase Shifts in Dual-Mode Planar Optical Waveguides.
PB95-161329 *04,271*

Bent Rectangular Core Waveguides: An Accurate Perturbation Approach.
PB95-168803 *04,289*

Fibre Splice Loss: A Simple Method of Calculation.
PB95-175519 *04,299*

Modal Characteristics of Bent Dual Mode Planar Optical Waveguide.
PB95-180485 *04,311*

Mode Coupling and Loss on Tapered Optical Waveguides.
PB95-168571 *04,282*

Symbolic Programming with Series Expansions: Applications to Optical Waveguides.
PB95-168589 *04,283*

KUMAR, S.

Evidence of Crosslinking in Methyl Pendent PBZT Fiber.
PB97-112486 *03,393*

Provision of Isochronous Service on IEEE 802.6.
PB96-160635 *01,501*

KUMP, M.

Characterization of Two-Dimensional Dopant Profiles: Status and Review.
PB96-119300 *02,400*

KUMP, M. R.

Characterization of Two-Dimensional Dopant Profiles: Status and Review.
PB97-110134 *02,451*

KUNDU, M. R.

Observing Stellar Coronae with the Goddard High Resolution Spectrograph. I. The dMe Star AU Microscopii.
PB96-102777 *00,092*

KUNDUR, S. R.

Novel Active-Vision-Based Motion Cues for Local Navigation.
PB96-193727 *02,941*

Scale-Space-Based Visual-Motion-Cue for Autonomous Navigation.
PB96-183173 *02,940*

Texture-Independent Vision-Based Closed-Loop Fuzzy Controllers for Navigation Tasks.
PB95-220505 *00,183*

KUNKEL, G.

Controlling the Critical Current Density of High-Temperature SNS Josephson Junctions.
PB96-200712 *04,794*

Critical Current and Normal Resistance of High-Tc Step-Edge SNS Junctions.
PB96-111752 *04,724*

KUNNATH, S. K.

Enhancements to Program IDARC: Modeling Inelastic Behavior of Welded Connections in Steel Moment-Resisting Frames.
PB95-231601 *00,452*

KUNZ, A. K.

In-situ Monitoring of Molecular Beam Epitaxial Growth Using Single Photon Ionization.
PB95-202222 *01,023*

Laser Vacuum Ultraviolet Single Photon Ionization Probing of III-V Semiconductor Growth.
PB95-202370 *04,691*

Single Photon Ionization, Laser Optical Probe Technique for Semiconductor Growth.
PB95-202776 *01,032*

Single Photon Laser Ionization as an In-situ Diagnostic for MBE growth.
PB96-102025 *01,059*

KUNZE, H. J.
Investigation of LS Coupling in Boronlike Ions.
PB94-185295 *03,797*

KUO, S. C.
Experimental Determination of the Ionization Energy of IO(X(sup 2)II(sub 3/2)) and Estimations of Delta(sub f)H(sup deg)(sub 0)(IO(sup -)) and PA(IO).
PB96-146899 *00,694*

Ionization Energies, Appearance Energies and Thermochemistry of CF2O and FCO.
PB97-111538 *01,178*

KUPPUSAMY, P.
Research and Development Activities in Electron Paramagnetic Resonance Dosimetry.
PB96-141288 *03,635*

KURFESS, J. D.
From Superconductivity to Supernovae: The Ginzburg Symposium. Report on the Symposium Held in Honor of Vitaly L. Ginzburg. Held in Gaithersburg, Maryland on May 22, 1992.
PB95-171963 *04,649*

KURITSYN, Y. A.
High-Resolution Measurements of the nu2 and 2nu2-nu2 Bands of (34)S(16)O2.
PB94-216223 *00,855*

KURIYAMA, M.
Correlation of HgCdTe Epilayer Defects with Underlying Substrate Defects by Synchrotron X-Ray Topography.
PB94-200714 *02,129*

Diffraction Imaging of Polycrystalline Materials.
PB94-198884 *02,971*

High Resolution Hard X-Ray Microscope.
PB94-213055 *03,856*

Materials Science with SR Using X-Ray Imaging: Spatial-Resolution/Source Size.
PB94-213048 *04,510*

KURMOO, M.
Crystal Structure and Magnetic Properties of CuGeO3.
PB95-180287 *04,678*

KURODA, T.
Critical-Current Degradation in Nb3 Al Wires Due to Axial and Transverse Stress.
PB95-202784 *02,226*

KUROKAWA, H.
Small-Angle Neutron Scattering of Poly(vinyl alcohol) Gels.
PB95-164117 *01,260*

Small Angle Neutron Scattering Studies on Chain Asymmetry of Coextruded Poly(Vinyl Alcohol) Film.
PB95-164372 *01,262*

KURSTER, M.
Rotational Modulation and Flares on RS Canum Venaticorum and BY Draconis Stars. XVIII. Coordinated VLA, ROSAT, and IUE Observations of RS CVn Binaries.
PB96-102322 *00,089*

KURTZ, C. A.
Hyperfine-Structure Studies of Zr II: Experimental and Relativistic Configuration-Interaction Results.
PB95-203824 *04,011*

KURTZ, R. L.
Photoelectron Spectroscopic Study of the Valence and Core-Level Electronic Structure of BaTiO3.
PB94-212149 *04,500*

Resonant-Photoemission Investigation of the Heusler Alloys Ni2MnSb and NiMnSb.
PB95-162384 *04,612*

Surface Core-Level Shifts of Barium Observed in Photoemission of Vacuum-Fractured BaTiO3 (100).
PB94-212156 *04,501*

KURYLO, M. J.
Atmospheric Lifetimes of HFC-143a and HFC-245fa: Flash Photolysis Resonance Fluorescence Measurements of the OH Reaction Rate Constants.
PB97-112577 *00,118*

Atmospheric Reactivity of alpha-Methyl-Tetrahydrofuran.
PB95-163705 *02,548*

Gas Phase Reactivity Study of OH Radicals with 1,1-Dichloroethene and cis-1,1-Dichloroethene and Trans-1,2-Dichloroethene over the Temperature Range 240-400 K.
PB95-152146 *00,939*

Rate Constants for the Gas Phase Reactions of the OH Radical with CF3CF2CHCl2 (HCFC-225ca) and CF2ClCF2CHClF (HCFC-225cb).
PB95-152153 *00,940*

Temperature Dependence of the Gas and Liquid Phase Ultraviolet Absorption Cross Sections of HCFC-123 (CF3CHCl2) and HCFC-142b (CH3CF2Cl).
PB96-201033 *03,298*

UV Absorption Cross Sections of Methylchloroform: Temperature-Dependent Gas and Liquid Phase Measurements.
PB96-201041 *00,643*

KURZ, J.
Comparison of Methods for Gas Chromatographic Determination of PCBs and Chlorinated Pesticides in Marine Reference Materials.
PB95-140091 *02,584*

KURZBAN, S. A.
Computer Virus Attacks.
PB95-163655 *01,715*

KUS, D.
Frozen Human Serum Reference Material for Standardization of Sodium and Potassium Measurements in Serum or Plasma by Ion-Selective Electrode Analyzers.
PB94-185337 *00,532*

KUSHIDA, G.
Ignition and Transition to Flame Spread Over a Thermally Thin Cellulosic Sheet in a Microgravity Environment.
PB96-160288 *04,837*

KUSHNER, M. J.
Evidence for Inelastic Processes for N(+)3 and N(+)4 from Ion Energy Distributions in He/N2 Radio Frequency Glow Discharges.
PB96-146683 *04,059*

Gaseous Electronics Conference Radio-Frequency Reference Cell: A Defined Parallel-Plate Radio-Frequency System for Experimental and Theoretical Studies of Plasma-Processing Discharges.
PB94-172327 *04,404*

KUSTERS, J.
Precision Oscillators: Dependence of Frequency on Temperature, Humidity and Pressure.
PB94-198306 *02,031*

KUWAYAMA, N.
Influence of Tempering Method on Residual Stress in Dental Porcelain.
PB94-172012 *00,138*

KUYATT, C. E.
Guidelines for Evaluating and Expressing the Uncertainty of NIST Measurement Results. 1994 Edition.
PB95-143087 *02,649*

KUZIAK, R.
Prediction of Strengthening Due to V Additions in Direct-Cooled Ferrite-Pearlite Forging Steels.
PB96-190251 *03,220*

KWANSA, H.
Positive and Negative Cooperativities at Subsequent Steps of Oxygenation Regulate the Allosteric Behavior of Multistate Sebacylhemoglobin.
PB97-119374 *03,486*

KWEI, G. H.
Colossal Magnetoresistance without Mn(3+)/Mn(4-) Double Exchange in the Stoichiometric Pyrochlore Tl2Mn2O7.
PB97-113070 *04,160*

KWOK, S.
IRAS Spectroscopic Observations of Young Planetary Nebulae.
PB95-152070 *00,072*

LACEY, P. I.
Mechano-Chemical Model: Reaction Temperatures in a Concentrated Contact.
PB96-119466 *03,227*

Wear Mechanism Maps of Ceramics.
PB94-172368 *03,229*

Wear Transitions in Monolithic Alumina and Zirconia-Alumina Composites.
PB96-103163 *03,168*

LACHENMANN, S.
Frequency Dependence of the Emission from 2D Array Josephson Oscillators.
PB95-175147 *02,056*

SUSAN: SUperconducting Systems ANalysis by Low Temperature Scanning Electron Microscopy (LTSEM).
PB96-112065 *04,728*

LACHENMANN, S. G.
Direct Observation of Vortex Dynamics in Two-Dimensional Josephson-Junction Arrays.
PB96-102223 *02,067*

Novel Vortex Dynamics in Two-Dimensional Josephson Arrays.
PB96-200167 *02,091*

Observation of Vortex Dynamics in Two-Dimensional Josephson-Junction Arrays.
PB95-168811 *02,050*

LADBURY, J. M.
Rapid Evaluation of Mode-Stirred Chambers Using Impulsive Waveforms.
PB96-210026 *01,979*

LADNER, J.
Biological Macromolecule Crystallization Database and NASA Protein Crystal Growth Archive.
PB97-109136 *01,171*

LAESECKE, A.
Correlation of the Ideal Gas Properties of Five Aromatic Hydrocarbons.
PB95-175816 *01,002*

Measurements of the Viscosities of Saturated and Compressed Liquid 1,1,1,2-Tetrafluoroethane (R134a), 2,2-Dichloro-1,1,1-Trifluoroethane (R123) and 1,1-Dichloro-1-Fluoroethane (R141b).
PB95-175386 *03,273*

Polarized Transient Hot Wire Thermal Conductivity Measurements.
PB95-108817 *00,886*

Thermal Conductivity of R134a.
PB94-213063 *03,857*

Viscosity of 1,1,1,2,3,3-Hexafluoropropane and 1,1,1,3,3,3-Hexafluoropropane at Saturated-Liquid Conditions from 262 K to 353 K.
PB96-176680 *03,292*

LAFFERTY, W. J.
Infrared Spectra of van der Waals Complexes of Importance in Planetary Atmospheres.
PB95-125738 *00,071*

Infrared Spectrum of OClO in the 2000/cm(-1) Region: The 2(nu sub 1) and (nu sub 1 + nu sub 3) Bands.
PB95-141032 *00,908*

Intensities and Dipole Moment Derivatives of the Fundamental Bands of (35)ClO2 and an Intensity Analysis of the nu1 Band.
PB95-141040 *00,909*

Reanalysis of the (010), (020), (100), and (001) Rotational Levels of (32)S(16)O2.
PB95-125621 *00,887*

Spectroscopic Constants for the 2.5 and 3.0 micrometer Bands of Acetylene.
PB94-213071 *00,847*

Tunneling-Rotation Spectrum of the Hydrogen Fluoride Dimer.
PB94-198678 *00,793*

LAGALANTE, A. F.
High-Pressure Equilibrium Cell for Solubility Measurements in Supercritical Fluids.
PB95-175634 *00,998*

Solubilities of Copper(II) and Chromium(III) beta-Diketonates in Supercritical Carbon Dioxide.
PB96-164215 *01,147*

LAGERGREN, E.
Statistical Analysis of Parameters Affecting the Measurement of Particle-Size Distribution of Silicon Nitride Powders by Sedigraph (Trade Name).
PB94-216249 *03,042*

LAGERGREN, E. S.
Composition and Solubility Product of a Synthetic Calcium Hydroxyapatite.
PB96-180104 *02,995*

Effects of Testing Variables on the Strength of High-Strength (90 Mpa) Concrete Cylinders.
PB96-112198 *00,456*

LAI, J. S.
Cascading Surge-Protective Devices: Options for Effective Implementation.
PB94-216488 *02,464*

Coordinating Cascaded Surge Protection Devices: High-Low versus Low-High.
PB94-172061 *02,463*

Coordinating Cascaded Surge-Protective Devices: An Elusive Goal.
PB94-216496 *02,465*

LAKHTAKIA, A.
Two Numerical Techniques for Light Scattering by Dielectric Agglomerated Structures.
PB94-140597 *04,225*

LAMAZE, G. P.
Analysis of Boron in CVD Diamond Surfaces Using Neutron Depth Profiling.
PB94-213089 *04,511*

Effect of Stoichiometry on the Phases Present in Boron Nitride Thin Films.
PB96-102470 *04,710*

Mass Assay and Uniformity Test of Boron Targets by Neutron Beam Methods.
PB97-119085 *04,175*

Measurement of the (93)Nb(n,2n) (92m)Nb Cross Section in a (235)U Fission Spectrum.
PB95-163986 *03,945*

Modeling Detector Response for Neutron Depth Profiling.
PB96-157813 *04,066*

Use of Neutron Beams for Chemical Analysis at NIST.
PB97-112437 *00,652*

LAMBERTY, A.
Preparation and Characterization of (6)LiF and (10)B Reference Deposits for the Measurement of the Neutron Lifetime.
PB95-108692 *03,874*

LAMBOOY, P.
Grazing Incidence Prompt Gamma Emissions and Resonance-Enhanced Neutron Standing Waves in a Thin-Film.
PB95-150470 *03,892*

Observed Frustration in Confined Block Copolymers.
PB95-150033 *01,238*

LAMING, J. M.
Polarization Measurements on a Magnetic Quadrupole Line in Ne-Like Barium.
PB97-113104 *04,161*

LAMKIN, J. C.
Penetration and Diffusion of Hard X-rays through Thick Barriers. III. Studies of Spectral Distributions.
AD-A292 502/2 *03,771*

LAN, G.
Verification of the Ponderomotive Approximation for the ac Stark Shift in Xe Rydberg Levels.
PB94-185709 *03,801*

LANCASTER, R. A.
Electrical Characterization of Narrow Gap n-Type Bulk HgCdTe Single Crystals by Variable-Magnetic-Field Hall Measurements and Reduced-Conductivity-Tensor Analyses.
PB96-164199 *01,146*

LAND, J. L.
Interim Testing Artifact (ITA): A Performance Evaluation System for Coordinate Measuring Machines (CMMs). User Manual.
PB95-210589 *02,914*

LANDBERG, A. T.
Electronic Implementors' Workshop.
PB95-210936 *01,484*

LANDEE, C. P.
Quasielastic and Inelastic Neutron-Scattering Studies of ((CD3)3ND)FeCl3.2D2O: A One-Dimensional Ising Ferromagnet.
PB95-140562 *04,547*

LANDSMAN, W.
Goddard High-Resolution Spectrograph Observations of the Local Interstellar Medium and the Deuterium/Hydrogen Ratio along the Line of Sight Toward Capella.
PB94-213444 *00,066*

LANG, S. M.
High Temperature Reactions of Uranium Dioxide with Various Metal Oxides.
AD-A286 648/1 *00,717*

LANGER, S. A.
Nonlinear Dynamics of Stiff Polymers.
PB96-122478 *01,278*

LANGLAND, J.
Current Activities Within the National Biomonitoring Specimen Bank.
PB94-172806 *02,516*

LANGLAND, J. K.
New NIST Rapid Pneumatic Tube System.
PB96-167259 *03,738*

LAOR, U.
Influence of Lattice Mismatch on Indium Phosphide Based High Electron Mobility Transistor (HEMT) Structures Observed in High Resolution Monochromatic Synchrotron X-Radiation Diffraction Imaging.
PB95-164679 *02,357*

LARACUENTE, A.
Atomic-scale characterization of hydrogenated amorphous-silicon films and devices. Annual subcontract report, 14 February 1994--14 April 1995.
DE95009287 *02,294*

Growth and Nucleation of Hydrogenated Amorphous Silicon on Silicon (100) Surfaces.
PB96-176516 *02,991*

Nanoscale Study of the Hydrogenated Amorphous Silicon Surface.
PB96-103056 *04,720*

LARAMEE, S.
Analysis of High Bay Hangar Facilities for Detector Sensitivity and Placement.
PB96-190210 *01,429*

LARASON, T. C.
Developing Quality System Documentation Based on ANSI/NCSL Z540-1-1994: The Optical Technology Division's Effort.
PB96-202122 *01,869*

NIST Detector-Based Luminous Intensity Scale.
PB96-179114 *01,864*

NIST High Accuracy Scale for Absolute Spectral Response from 406 nm to 920 nm.
PB96-179122 *01,865*

LARBALESTIER, D. C.
Crossover in the Pinning Mechanism of Anisotropic Fluxon Cores.
PB95-180170 *04,673*

Electromagnetic Coupling Character of (001) Twist Boundaries in Sintered Bi2Sr2CaCu2O8+x Bicrystals.
PB96-176573 *01,963*

Weak-Link-Free Behavior of High Angle YBa2Cu3O7-x Grain Boundaries in High Magnetic Fields.
PB94-198421 *04,459*

LARRABEE, R. D.
Normal-Incidence Complex-Index Refractometry.
PB94-213097 *04,241*

Precision, Accuracy, Uncertainty and Traceability and Their Application to Submicrometer Dimensional Metrology.
PB94-213105 *02,319*

SEM Linewidth Metrology of X-ray Lithography Masks.
PB96-201108 *02,447*

X-ray Mask Metrology: The Development of Linewidth Standards for X-ray Lithography.
PB95-162129 *02,348*

LARSEN, B. H.
Stable Phase Locking in a Two-Cell Ladder Array of Josephson Junctions.
PB96-111679 *04,722*

LARSEN, E. D.
Ultrasonic Sensing of GMAW: Laser/EMAT Defect Detection System.
PB96-186028 *02,878*

LARSEN, N. W.
Second Census Optical Character Recognition Systems Conference.
PB94-188711 *01,832*

LARSEN, R. J.
International Marine-Atmospheric (222)Rn Measurement Intercomparison in Bermuda. Part 2. Results for the Participating Laboratories.
PB96-175682 *00,115*

LARSON, D. C.
Measurement of the (10)B(n, alpha1gamma)(7)Li Cross Section in the 0.3 to 4 MeV Neutron Energy Interval.
PB96-161799 *04,098*

LARSON, D. R.
Electrically Calibrated Pyroelectric Detector-Refinements for Improved Optical Power Measurements.
PB95-169066 *02,164*

Integrated Optical Polarization-Discriminating Receiver in Glass.
PB97-113179 *02,206*

Linewidth Narrowing in an Imbalanced Y-Branch Waveguide Laser.
PB95-140844 *04,258*

Nd:LiTaO3 Waveguide Laser.
PB95-140851 *04,259*

Rare-Earth-Doped Waveguide Devices: The Potential for Compact Blue-Green Lasers.
PB95-140836 *04,257*

Waveguide Polarizers Processed by Localized Plasma Etching.
PB95-169264 *02,171*

LARSON, J. W.
Thermochemistry of the Reactions between Adenosine, Adenosine 5'-monophosphate, Inosine, and Inosine 5'-monophosphate; the Conversion of L-histidine to (Urocanic Acid+Ammonia).
PB94-213113 *03,460*

LARSSON, M.
Inner-Valence States CO(+) between 22 eV and 46 eV Studied by High Resolution Photoelectron Spectroscopy and ab Initio CI Calculations.
PB95-180055 *03,961*

LAS, T.
Influence of Surface Charge on the Stochastic Behavior of Partial Discharge in Dielectrics.
PB96-122767 *01,931*

Modification of Cast Epoxy Resin Surfaces during Exposure to Partial Discharges.
PB96-122734 *01,086*

Nonstationary Behavior of Partial Discharge during Insulation Aging.
PB95-163580 *01,902*

Nonstationary Behaviour of Partial Discharge during Discharge Induced Ageing of Dielectrics.
PB96-103114 *01,922*

Partial Discharge: Induced Aging of Cast Epoxies and Related Nonstationary Behavior of the Discharge Statistics.
PB95-163598 *01,903*

LASCOLA, R.
High Resolution, Jet-Cooled Infrared Spectroscopy of (HCl)2: Analysis of nu1 and nu2 HCl Stretching Fundamentals, Interconversion Tunneling, and Mode-Specific Predissociation Lifetimes.
PB95-203196 *01,046*

Slit-Jet Near-Infrared Spectroscopy and Internal Rotor Dynamics of the ArH2O van der Waals Complex: An Angular Potential-Energy Surface for Internal H2O Rotation.
PB95-202792 *01,033*

Vibration, Rotation, and Parity Specific Predissociation Dynamics in Asymmetric OH Stretch Excited ArH2O: A Half Collision Study of Resonant V-V Energy Transfer in a Weakly Bound Complex.
PB95-107140 *00,872*

LASHMORE, D. S.
Ambient Temperature Synthesis of Bulk Intermetallics.
PB95-169074 *00,168*

Cracks and Dislocations in Face-Centered Cubic Metallic Multilayers.
PB96-163696 *02,989*

Electrochemical Synthesis of Metal and Intermetallic Composites.
AD-A294 088/0 *03,304*

Electrodeposited Cobalt-Tungsten as a Diffusion Barrier between Graphite Fibers and Nickel.
PB96-146881 *03,176*

Electrodeposition.
PB94-172517 *00,760*

Magnetic and Structural Properties of Electrodeposited Copper-Nickel Microlayered Alloys.
PB94-213121 *04,512*

LASHOF, T. W.
Precision Laboratory Standards of Mass and Laboratory Weights.
AD-A280 562/0 *02,618*

LASKOWSKI, S. J.
Electronic Access to Standards on the Information Highway.
PB96-131578 *01,494*

Usability Engineering: Industry-Government Collaboration for System Effectiveness and Efficiency.
PB97-122287 *01,514*

LASKY, J.
Nano-Defects in Commercial Bonded SOI and SIMOX.
PB96-123674 *02,407*

LATTIMER, B. Y.
Compartment Fire Combustion Dynamics. Annual Report, September 1, 1993-September 1, 1994.
PB95-217162 *00,203*

LATUSEK, J. P.
Evaluation of Wear Resistant Ceramic Valve Seats in Gas-Fueled Power Generation Engines. Topical Report, December 1991-April 1994.
PB95-200218 *02,466*

LAU, K.
Two New Probes for a Coordinate Measuring Machine.
PB95-163093 *02,653*

LAUBER, W.
Catalogue of Electromagnetic Environment Measurements, 30-300 Hz.
PB96-155452 *01,943*

Condensed Catalogue of Electromagnetic Environment Measurements, 30 - 300 Hz.
PB95-162210 *01,899*

LAUENSTEIN, C. P.
Laser-Induced Fluorescence Measurements of Rotationally Resolved Velocity Distributions for CO(+) Drifted in He.
PB94-213139 *00,848*

LAUENSTEIN, G.
National Status and Trends Program Specimen Bank: Sampling Protocols, Analytical Methods, Results, and Archive Samples.
PB97-119226 *02,598*

LAUENSTEIN, G. G.
Certification of Standard Reference Material (SRM) 1941a, Organics in Marine Sediment.
PB96-123690 *02,593*

LAUFER, A.
Reaction Rate Determinations of Vinyl Radical Reactions with Vinyl, Methyl, and Hydrogen Atoms.
PB94-211398 *00,815*

LAUFER, A. H.
Deuterium Isotope Effect in Vinyl Radical Combination/Dispropor tionationReactions.
PB96-204151 *01,167*

Experimental Determination of the Rate Constant for the Reaction of C2H3 with H2 and Implications for the Partitioning of Hydrocarbons in Atmospheres of the Outer Planets.
PB97-122295 *00,112*

LAUG, O. B.
100 A, 100 kHz Transconductance Amplifier.
PB96-200936 *02,098*

100 Ampere, 100 kHZ Transconductance Amplifier.
PB96-102629 *02,068*

Custom Integrated Circuit Comparator for High-Performance Sampling Applications.
PB94-213147 *02,320*

Wideband Sampling Voltmeter.
PB97-113039 *01,990*

LAURITZEN, J. I.
Reference Tables for Thermocouples.
AD-A279 948/4 *02,614*

LAUTER, H. J.
Hydrogen in YBa2Cu3Ox: A Neutron Spectroscopy and a Nuclear Magnetic Resonance Study.
PB95-161279 *04,601*

Neutron-Spectroscopy Study of the Hydrogen Vibrations in Hydrogen-Doped YBa2Cu3Ox.
PB94-172475 *04,441*

LAVAL, J.
Substrate Specificity of the Escherichia coli Endonuclease III: Excision of Thymine- and Cytosine-Derived Lesions in DNA Produced by Radiation-Generated Free Radicals.
PB95-153425 *03,535*

LAVILLA, R. E.
Polarized X-Ray Emission Spectroscopy.
PB94-213360 *03,862*

LAVINE, C. F.
Potential and Current Distributions Calculated Across a Quantum Hall Effect Sample at Low and High Currents.
PB96-122106 *04,045*

Spectroscopic Study of Quantized Breakdown Voltage States of the Quantum Hall Effect.
PB96-113584 *04,730*

Using Quantized Breakdown Voltage Signals to Determine the Maximum Electric Fields in a Quantum Hall Effect Sample.
PB95-261947 *02,375*

LAW, M.
Glossary of Software Reuse Terms.
PB95-178992 *01,720*

LAW, M. H.
Template-Driven Systems Development with IDEF: Enterprise Standards for Reuse.
PB96-160965 *02,788*

LAWN, B.
Friction Processes in Brittle Fracture.
PB96-161765 *03,076*

LAWN, B. R.
Correlations between Flaw Tolerance and Reliability in Zirconia.
PB96-161922 *02,986*

Deformation and Fracture of Mica-Containing Glass-Ceramics in Hertzian Contacts.
PB96-179452 *03,080*

Diffusion of Water along 'Closed' Mica Interfaces.
PB96-180039 *02,993*

Effect of Chemical Interaction on Barenblatt Crack Profiles in Brittle Solids.
PB96-180245 *02,996*

Effect of Grain Size on Hertzian Contact Damage in Alumina.
PB96-179601 *03,083*

Flaw-Insensitive Ceramics.
PB97-110027 *03,095*

Flaw Tolerance and Toughness Curves in Two-Phase Particulate Composites: SiC/Glass System.
PB96-179460 *03,081*

Indentation Fatigue: A Simple Cyclic Hertzian Test for Measuring Damage Accumulation in Polycrystalline Ceramics.
PB96-180013 *03,084*

Model for Microcrack Initiation and Propagation beneath Hertzian Contacts in Polycrystalline Ceramics.
PB96-163704 *03,077*

Model for Toughness Curves in Two-Phase Ceramics. 1. Basic Fracture Mechanics.
PB96-180088 *03,085*

Model for Toughness Curves in Two-Phase Ceramics. 2. Microstructural Variables.
PB96-163795 *03,078*

Objective Evaluation of Short-Crack Toughness Curves Using Indentation Flaws: Case Study on Alumina-Based Ceramics.
PB96-179429 *03,079*

Pressurized Internal Lenticular Cracks at Healed Mica Interfaces.
PB96-180252 *02,997*

LAWSON, A. C.
Crystallographic and Magnetic Properties of UAuSn.
PB95-140521 *04,543*

Incommensurate Magnetic Order in UPtGe.
PB95-140513 *04,542*

LAWSON, J.
Smoke Emission from Burning Crude Oil.
PB96-122890 *01,407*

LAWSON, J. R.
Airborne Smoke Sampling Package for Field Measurements of Fires.
PB95-150041 *01,381*

Fire Performance of an Interstitial Space Construction System.
PB95-188918 *00,390*

Quantifying the Ignition Propensity of Cigarettes.
PB96-155411 *00,306*

LAYER, H. P.
Elastic Deformation of a Monolithic Perfect Crystal Interferometer: Implications for Gravitational Phase Shift Experiments.
PB94-213154 *03,858*

LE, F. G.
EPR Dosimetry of Cortical Bone and Tooth Enamel Irradiated with X and Gamma Rays: Study of Energy Dependence.
PB97-110373 *03,639*

Estimation of the Absorbed Dose in Radiation-Processed Food. 3. The Effect of Time of Evaluation on the Accuracy of the Estimate.
PB94-199684 *00,037*

Estimation of the Absorbed Dose in Radiation-Processed Food. 4. EPR Measurements on Eggshell.
PB94-199692 *00,038*

Inter-Laboratory Trials of the EPR Method for the Detection of Irradiated Meats Containing Bone.
PB96-161690 *00,042*

LEACH, M.
Directory of Law Enforcement and Criminal Justice Associations and Research Centers.
PB96-178918 *04,872*

LEAKE, S.
Hierarchical Ada Robot Programming System (HARPS): A Complete and Working Telerobot Control System Based on the NASREM Model.
PB94-213162 *02,934*

LEBLANC, L.
Measured Stopping Powers of Hydrogen and Helium in Polystyrene Near Their Maximum Values.
PB96-112321 *04,729*

LEBRUN, T.
Electron-Ion-X-ray Spectrometer System.
PB95-176137 *03,958*

Evolution of X-ray Resonance Raman Scattering into X-ray Fluorescence from the Excitation of Xenon Near the L3 Edge.
PB96-102751 *04,025*

LEBURTON, J. P.
Determination of the Complex Refractive Index of Individual Quantum Wells from Distributed Reflectance.
PB95-175642 *02,176*

LECHNER, J.
Characteristics of Adhesive-Bonded Seams Sampled from EPDM Roof Membranes.
PB95-162491 *00,377*

Extreme Value Theory and Applications: Proceedings of the Conference on Extreme Value Theory and Applications, Volume 3. Held in Gaithersburg, Maryland in May 1993.
PB95-104956 *03,432*

LECHNER, J. A.
Assessment of 'Peaks Over Threshold' Methods for Estimating Extreme Value Distribution Tails.
PB95-161360 *00,441*

Degradation of Powder Epoxy Coated Panels Immersed in a Saturated Calcium Hydroxide Solution Containing Sodium Chloride.
PB96-101050 *01,344*

Extreme Wind Estimates by the Conditional Mean Exceedance Procedure.
PB95-220471 *00,120*

Extreme Winds Estimation by 'Peaks Over Threshold' and Epochal Methods.
PB96-159686 *00,468*

Modeling of Extreme Loading by 'Peaks Over Threshold' Methods.
PB96-159694 *00,469*

Recent Approaches to Extreme Value Estimation with Application to Wind Speeds. Part 1. The Pickands Method.
PB94-213170 *00,019*

LECHTMAN, H.
Fabrication of Platinum-Gold Alloys in Pre-Hispanic South America: Issues of Temperature and Microstructure Control.
PB94-211646 *03,333*

LECKRONE, D. S.
Observations of 3C 273 with the Goddard High Resolution Spectrograph on the Hubble Space Telescope.
PB95-202321 *00,076*

LEDBETTER, H.
Accurate Modeling of Size and Strain Broadening in the Rietveld Refinement: The 'Double-Voigt' Approach.
PB96-200225 *00,664*

Artificial Crack in Steel: An Ultrasonic-Resonance-Spectroscopy and Modeling Study.
PB96-141395 *03,241*

Asymmetry between Flux Penetration and Flux Expulsion in Tl-2212 Superconductors.
PB95-125647 *04,527*

Cast-Iron Elastic Constants: Effect of Graphite Aspect Ratio.
PB94-213212 *03,211*

Compressibility of Polycrystal and Monocrystal Copper: Acoustic-Resonance Spectroscopy.
PB96-164223 *02,990*

Correlation between Tc and Elastic Constants of (La-M)2CuO4.
PB94-213220 *04,514*

Crystal Structure and Compressibility of 3:2 Mullite.
PB95-175030 *03,682*

Dependence of Tc on Debye Temperature Theta(sub D) for Various Cuprates.
PB95-180493 *04,683*

Dynamics vs. Static Young's Moduli: A Case Study.
PB94-213188 *03,210*

Elastic Constants and Debye Temperature of Y1Ba2Cu3Ox: Effect of Oxygen Content.
PB94-213352 *04,515*

Elastic Constants and Internal Friction of Polycrystalline Copper.
PB96-141015 *03,364*

Elastic Constants and Microcracks in YBa2Cu3O7.
PB96-200761 *03,005*

Elastic Constants of a Material with Orthorhombic Symmetry: An Alternative Measurement Approach.
PB95-180527 *04,684*

Elastic Constants of Isotropic Cylinders Using Resonant Ultrasound.
PB94-211919 *04,497*

Elastic Constants of Polycrystalline Y1Ba2Cu3Ox.
PB94-213196 *04,513*

Elastic Properties of Al2O3/Al Composites: Measurements and Modeling.
PB95-161378 *03,157*

Elastic Properties of Uniaxial-Fiber Reinforced Composites: General Features.
PB94-200649 *03,140*

Enhanced Flux Pinning via Chemical Substitution in Bulk Superconducting T1-2212.
PB95-169033 *04,647*

Estimation of the Orientation Distribution of Short-Fiber Composites Using Ultrasonic Velocities.
PB96-176656 *03,178*

Low-Temperature Elastic Constants of Y1Ba2Cu3O7.
PB95-168837 *04,642*

Magnetic Susceptibility of Pr2-xCexCuO4 Monocrystals and Polycrystals.
PB95-180253 *04,677*

Microstrains and Domain Sizes in Bi-Cu-O Superconductors: An X-Ray Diffraction Peak-Broadening Study.
PB94-198520 *04,461*

Nitrogen Effect on Elastic Constants of f.c.c. Fe-18Cr-19Mn Alloys.
PB94-172541 *03,203*

Orthotropic Elastic Constants of a Boron-Aluminum Fiber-Reinforced Composite: An Acoustic-Resonance-Spectroscopy Study.
PB96-200175 *03,182*

Relationship between Bulk-Modulus Temperature Dependence and Thermal Expansivity.
PB95-168829 *04,641*

Residual Stresses in Aluminum-Mullite (alpha-Alumina) Composites.
PB95-152880 *03,155*

Thermal Expansion of an SiC Particle-Reinforced Aluminum Composite.
PB94-213204 *03,144*

Torsion Modulus and Internal Friction of a Fiber-Reinforced Composite.
PB96-112339 *03,070*

Ultrasonic-Resonance Spectroscopy of Bulk and Layered Solids.
PB96-141338 *04,759*

Void Shape in Sintered Titanium.
PB96-141023 *02,705*

Voigt-Function Modeling in Fourier Analysis of Size- and Strain-Broadened X-Ray Diffraction Peaks.
PB94-198538 *04,462*

LEDFORD, A. E.
Assessing the Credibility of the Calorific Content of Muncipal Solid Waste.
PB94-199882 *02,581*

LEE, A.
Aging in Glasses Subjected to Large Stresses and Deformations.
PB95-107041 *03,235*

Multi-Agency Certification and Accreditation (C and A) Process: A Worked Example.
PB95-171955 *01,601*

LEE, D. H.
High-Energy Behavior of the Double Photoionization of Helium from 2 to 12 keV.
PB94-213279 *03,860*

LEE, J. D.
Defect Formation Mechanism Causing Increasing Defect Density during Decreasing Implant Dose in Low-Dose Simox.
PB96-119524 *02,402*

Defect of Thermal Ramping and Annealing Conditions on Defect Formation in Oxygen Implanted Silicon-On-Insulator Material.
PB94-212966 *02,318*

Defect Pair Formation by Implantation-Induced Stresses in High-Dose Oxygen Implanted Silicon-on-Insulator Material.
PB95-175824 *02,364*

Effect of Intermediate Thermal Processing on Microstructural Changes of Oxygen Implanted Silicon-on-Insulator Material.
PB96-160213 *02,982*

Effect of Single versus Multiple Implant Processing on Defect Types and Densities in SIMOX.
PB96-160353 *01,957*

Mechanism of Defect Formation in Low-Dose Oxygen Implanted Silicon-on-Insulator Material.
PB97-111462 *02,453*

Stacking Fault Pyramid Formation and Energetics in Silicon-on-Insulator Material Formed by Multiple Cycles of Oxygen Implantation and Annealing.
PB96-160221 *04,083*

LEE, K.
Integration of Real-Time Process Planning for Small-Batch Flexible Manufacturing.
PB95-151908 *02,822*

LEE, K. B.
Portsmouth Fastener Manufacturing Workstation. User's Manual.
PB95-147922 *02,860*

LEE, K. C.
Bonding Wires to Quantized Hall Resistors.
PB96-102637 *01,921*

Design Challenges in a Commercial Quantum Hall Effect-Based Resistance Standard.
PB95-171419 *02,263*

Lithium-Drift Technique for Making Submicron Thick Silicon Membranes.
PB95-161386 *02,260*

Quantum Hall Effect-Based Resistance Standard: Capabilities and Implementation.
PB96-180096 *04,114*

Quantum Hall Effect-Based Resistance Standard (Quantum Hall Res).
PB96-200944 *04,127*

Sources of Uncertainty in a DVM-Based Measurement System for a Quantized Hall Resistance Standard.
PB94-219334 *01,884*

LEE, L. H.

Conversion of a 2-Terminal-Pair Bridge to a 4-Terminal-Pair Bridge for Increased Range and Precision in Impedance Measurements.
PB97-119176 *02,103*

NIST Comparison of the Quantized Hall Resistance and the Realization of the SI Ohm Through the Calculable Capacitor.
PB97-119184 *02,291*

NIST Comparison of the Quantized Hall Resistance and the Realization of the SI Ohm Through the Calculable Capacitor. Conference Proceedings, June 17-20, 1996.
PB97-119192 *02,292*

LEE, M. L.

Comparison of Selectivities for PCBs in Gas Chromatography for a Series of Cyanobiphenyl Stationary Phases.
PB96-119458 *00,618*

LEE, S.

Asymmetric Tip Morphology of Creep Microcracks Growing Along Bimaterial Interfaces.
PB94-200243 *03,138*

Diffusive Crack Growth at a Bimaterial Interface.
PB96-204110 *03,090*

Unified Telerobotic Architecture Project (UTAP) Standard Interface Environment (SIE), May 1995.
PB95-242350 *02,938*

LEE, S. C.

Intercomparison Study of (237)Np Determination in Artificial Urine Samples.
PB96-102645 *03,633*

LEE, S. H.

Electrolytes Constrained on Fractal Structures: Debye-Huckel Theory.
PB97-110241 *01,174*

Isolated Spin Pairs and Two-Dimensional Magnetism in SrCr(sub 9p)Ga(sub 12-9p)O19.
PB97-112387 *04,154*

LEE, S. W.

Wear Mechanism Maps of Ceramics.
PB94-172368 *03,229*

LEE, S. Y.

Correlations of Modulation Noise with Magnetic Microstructure and Intergranular Interactions for CoCrTa and CoNi Thin Film Media.
PB94-212768 *04,509*

LEE, V. J.

Portsmouth Fastener Manufacturing Workstation. User's Manual.
PB95-147922 *02,860*

LEE, W. D.

Hybrid Digital/Analog Servo for the NIST-7 Frequency Standard.
PB95-180618 *01,544*

Microwave Leakage as a Source of Frequency Error and Long-Term Instability in Cesium Atomic-Beam Frequency Standards.
PB95-180501 *01,541*

Velocity Distribution of Atomic Beams by Gated Optical Pumping.
PB95-180519 *01,542*

LEE, W. Y.

Fault Diagnosis of an Air-Handling Unit Using Artificial Neural Networks.
PB97-121321 *00,283*

LEE, Y. T.

Bibliography on Apparel Sizing and Related Issues.
PB94-161924 *02,806*

Extensions of the Prototype Application Protocol of Ready-to-Wear Apparel Pattern Making.
PB96-128194 *03,198*

LEE, Y. T. T.

Body Dimensions for Apparel.
PB94-187739 *02,813*

LEEDS, A. L.

Estimation of System Damping at the Lotung Site by Application of System Identification.
PB96-214697 *01,351*

Preliminary Processing of the Lotung LSST Data.
PB96-165972 *03,690*

LEEDY, T.

Advanced Components for Electric and Hybrid Electric Vehicles. Workshop Proceedings. Held in Gaithersburg, Maryland on October 27-28, 1993.
PB94-177060 *04,858*

LEGG, K. O.

Opportunities for Innovation: Advanced Surface Engineering.
PB94-176666 *02,697*

LEGOWIK, S. A.

Control System Architecture for a Remotely Operated Unmanned Land Vehicle.
PB95-163200 *03,759*

Ground Vehicle Control at NIST: From Teleoperation to Autonomy.
N94-34037/9 *03,758*

LEGROS, H.

Calibration of a Superconducting Gravimeter Using Absolute Gravity Measurements.
PB95-202651 *03,684*

LEHENY, R. F.

Beyond the Technology Roadmaps: An Assessment of Electronic Materials Research and Development.
PB96-165998 *01,961*

LEHMAN, J. H.

Electrically Calibrated Pyroelectric Detector-Refinements for Improved Optical Power Measurements.
PB95-169066 *02,164*

LEHMANN, K.

Approach to Setting Performance Requirements for Automated Evaluation of the Parameters of High-Voltage Impulses.
PB94-185634 *01,878*

LEHMANN, K. K.

Sub-Doppler, Infrared Laser Spectroscopy of the Propyne 2nu1 Band: Evidence of z-Axis Coriolis Dominated Intramolecular State Mixing in the Acetylenic CH Stretch Overtone.
PB95-202941 *01,037*

LEI, M.

Elastic Constants and Debye Temperature of Y1Ba2Cu3Ox: Effect of Oxygen Content.
PB94-213352 *04,515*

Elastic Constants of a Material with Orthorhombic Symmetry: An Alternative Measurement Approach.
PB95-180527 *04,684*

Elastic Properties of Uniaxial-Fiber Reinforced Composites: General Features.
PB94-200649 *03,140*

Low-Temperature Elastic Constants of Y1Ba2Cu3O7.
PB95-168837 *04,642*

Torsion Modulus and Internal Friction of a Fiber-Reinforced Composite.
PB96-112339 *03,070*

LEIGH, S.

Graphical Analysis of the CCRL Portland Cement Proficiency Sample Database (Samples 1-72). (Part 1. Univariant Analysis of Portland Cement).
PB94-196557 *01,308*

LEIGH, S. D.

Airborne Asbestos Method: Bootstrap Method for Determining the Uncertainty of Asbestos Concentration. Version 1.0.
PB96-214614 *00,646*

Interlaboratory Comparison of Autoradiographic DNA Profiling Measurements. 1. Data and Summary Statistics.
PB95-175923 *03,542*

Interlaboratory Comparison of Autoradiographic DNA Profiling Measurements. 2. Measurement Uncertainty and Its Propagation.
PB96-112123 *03,545*

Recent Approaches to Extreme Value Estimation with Application to Wind Speeds. Part 1. The Pickands Method.
PB94-213170 *00,019*

LEIGHT, W.

Proceedings of the Open Forum on Laboratory Accreditation at the National Institute of Standards and Technology, October 13, 1995.
PB96-210141 *02,686*

LEIGHT, W. G.

U.S. Government Accreditation and Conformity Assessment System Evaluation.
PB96-160239 *02,678*

LEISURE, R. G.

Elastic Constants of Isotropic Cylinders Using Resonant Ultrasound.
PB94-211919 *04,497*

LELENTAL, M.

Alternating-Field Susceptometry and Magnetic Susceptibility of Supercondoctors. Presented at Office of Naval Research Workshop on Magnetic Susceptibility of Superconductors and Other Spin Systems. Held in Berkeley Springs, West Virginia on 20 May 1991.
PB94-145984 *04,435*

Alternating-Field Susceptometry and Magnetic Susceptibility of Superconductors.
PB95-168613 *04,638*

LENAHAN, P. M.

Electron Traps, Structural Change, and Hydrogen Related SIMOX Defects.
PB94-200391 *02,312*

Evidence for a Deep Electron Trap and Charge Compensation in Separation by Implanted Oxygen Oxides.
PB95-175337 *02,362*

LENNON, E.

NIST POSIX Testing Program.
PB96-160973 *01,821*

LENNON, E. B.

Computer Systems Laboratory Annual Report, 1993.
PB94-162518 *01,622*

Computer Systems Laboratory Annual Report 1994.
PB95-209920 *01,629*

Computer Systems Laboratory Computing and Applied Mathematics Laboratory Technical Accomplishments, October 1994-March 1996.
PB96-193768 *01,638*

LEONE, S. R.

Alignment Probing of Rydberg States by Stimulated Emission.
PB96-200316 *04,124*

Charge Transfer and Collision-Induced Dissociation Reactions of CF(2+) and CF2(2+) with the Rare Gases at a Laboratory Collision Energy of 49 eV.
PB94-185584 *00,775*

Collision-Induced Neutral Loss Reactions of Molecular Dications.
PB94-185808 *00,780*

Direct Detection of Atomic Arsenic Desorption from Si(100).
PB95-202230 *01,024*

Efficient Br(*) Laser Pumped by Frequency-Doubled Nd: YAG and Electronic-to-Vibrational Transfer-Pumped CO2 and HCN Lasers.
PB95-108684 *04,248*

In-situ Monitoring of Molecular Beam Epitaxial Growth Using Single Photon Ionization.
PB95-202222 *01,023*

Initial and Final Orbital Alignment Probing of the Fine-Structure-Changing Collisions among the Ca (4s)(1)(4p)(1), (3)PJ States with He: Determination of Coherence and Conventional Cross-Sections.
PB95-203279 *04,004*

Investigating the 3.3 Micron Infrared Fluorescence from Naphthalene Following Ultraviolet Excitation.
N95-15839/0 *00,724*

Kinetic-Energy-Enhanced Neutral Etching.
PB96-200613 *00,665*

Kinetics and Dynamics of Vibrationally State Resolved Ion-Molecule Reactions: (14)N2(+)(v=1 and 2) and (15)N2(+)(v=0,1 and 2) with (14)N2.
PB96-102348 *04,023*

Kinetics of the Reaction C2H + O2 from 193 to 350 K Using Laser Flash Kinetic Infrared Absorption Spectroscopy.
PB95-203055 *01,043*

Laboratory Studies of Low-Temperature Reactions of C2H with C2H2 and Implications for Atmospheric Models of Titan.
PB95-108726 *00,690*

Laser Double Resonance Measurements of the Quenching Rates of Br((2)P1/2) with H20, D20, HDO, and O2.
PB95-150694 *00,921*

Laser Flash Photolysis, Time-Resolved Fourier Transform Infrared Emission Study of the Reaction Cl + C2H5 yields HCl(v) + C2H4.
PB95-203238 *01,049*

Laser Flash Photolysis/Time-Resolved FTIR Emission Study of a New Channel in the Reaction of CH3+O: Production of CO(v).
PB95-164281 *00,974*

Laser Gas Ionization Technique Monitors MEB Crystal Growth.
PB96-112172 *01,076*

Laser-Induced Desorption of In and Ga from Si(100) and Adsorbate Enhanced Surface Damage.
PB95-203311 *01,050*

Laser-Induced Fluorescence Measurements of Rotationally Resolved Velocity Distributions for CO(+) Drifted in He.
PB94-213139 *00,848*

Laser Preparation and Probing of Initial and Final Orbital Alignment in Collision-Induced Energy Transfer Ca(4s5p,(1)P1) + He yields Ca(4s5p,(3)P2) + He.
PB95-203261 *04,003*

Laser Vacuum Ultraviolet Single Photon Ionization Probing of III-V Semiconductor Growth.
PB95-202370 *04,691*

n-Vector Correlations in Collision Dynamics with Atomic Orbital Alignment: The Importance of Coherence Denoting Azimuthal Structure for n (greater than or equal to) 3.
PB95-202545 *03,983*

Orbital Alignment and Vector Correlations in Inelastic Atomic Collisions.
PB96-122742 *04,047*

Orbital Stereochemistry: Discovering the Symmetries of Collision Processes.
PB95-202800 *01,034*

Photodissociation of Ammonia at 193.3nm: Rovibrational State Distribution of the NH2(A(2)A1) Fragment.
PB95-151775 *00,937*

Precision Lifetime Measurements of Cs 6p (2)P1/2 and 6p (2)P3/2 Levels by Single-Photon Counting.
PB95-203816 *04,010*

Preferential In-Plane Rotational Excitation of H2O (001) by Translational-to-Vibrational Transfer from 2.2 eV H Atoms.
PB95-202875 *01,035*

Pulsed Laser Irradiation at 532 nm of In and Ga Adsorbed on Si(100): Desorption, Incorporation, and Damage.
PB95-203329 *01,051*

Pulsed Laser Photolysis Time-Resolved FT-IR Emission Studies of Molecular Dynamics.
PB95-203162 *04,002*

Selected Ion Flow Tube-Laser Induced Fluorescence Instrument for Vibrationally State-Specific Ion-Molecule Reactions.
PB94-185444 *00,774*

Single-Photon Ionization and Detection of Ga, In, and As(sub n) Species in GaAs Growth.
PB95-152815 *00,591*

Single Photon Ionization, Laser Optical Probe Technique for Semiconductor Growth.
PB95-202776 *01,032*

Single Photon Laser Ionization as an In-situ Diagnostic for MBE growth.
PB96-102025 *01,059*

Single-Photon Laser Ionization Time-of-Flight Mass Spectroscopy Detection in Molecular-Beam Epitaxy: Application to As4, As2, and Ga.
PB95-203337 *01,052*

Three-Vector Correlation Study of Orientation and Coherence Effects in Na(3p, (2)P1/2 inversely maps (2)P3/2)+He: Semiclassical and Quantum Calculations.
PB95-202453 *03,979*

Vibrational Distributions of As2 in the Cracking of As4 on Si(100) and Si(111).
PB94-198314 *00,784*

LEONG, S.

Computer-Aided Manufacturing Engineering Forum (1st). Technical Meeting Proceedings. Held in Gaithersburg, Maryland on March 21-22, 1995.
PB96-136965 *02,834*

Computer-Aided Manufacturing Engineering Forum (2nd). Technical Meeting Proceedings. Held in Gaithersburg, Maryland on August 22-23, 1995.
PB96-195334 *02,845*

LEONHARDT, R. W.

Deep-UV Excimer Laser Measurements at NIST.
PB96-141031 *04,355*

LEONOWICZ, M. E.

Small Angle Neutron Scattering Study of the Structure and Formation of MCM-41 Mesoporous Molecular Sieves.
PB97-122337 *03,110*

LEOPOLD, K. R.

Laboratory Measurements for the Astrophysical Identification of MgH.
PB95-152195 *00,073*

LEPEK, A.

Cross-Correlation Analysis Improves Time Domain Measurements.
PB95-180535 *01,543*

LERIDON, B.

Autocorrelation Functions from Optical Scattering for One-Dimensionally Rough Surfaces.
PB94-216538 *04,244*

LESAGE, R.

Physical Characterization of Herparin by Light Scattering.
PB96-119383 *03,598*

LETELLIER, C.

Generalized Optical Theorem for On-Axis Gaussian Beams.
PB97-122345 *04,177*

LETT, P.

Hyperfine Effects and Associative Ionization of Ultracold Sodium.
PB95-151221 *03,903*

Optical Molasses: The Coldest Atoms Ever.
PB95-108908 *03,878*

Ultracold Collisions: Associative Ionization in a Laser Trap.
PB94-213238 *03,859*

LETT, P. D.

Atoms in Optical Molasses.
PB95-108874 *03,875*

Atoms in Optical Molasses: Applications to Frequency Standards.
PB95-108882 *03,876*

Heterodyne Measurement of the Fluorescence Spectrum of Optical Molasses.
PB95-108411 *03,873*

Laser Cooling and the Recoil Limit.
PB97-111280 *04,391*

Laser Modification of Ultracold Collisions: Experiment.
PB96-157987 *04,075*

Localization of Atoms in a Three-Dimensional Standing Wave.
PB95-163887 *03,944*

Measurement of the Atomic Na(3P) Lifetime and of Retardation in the Interaction between Two Atoms Bound in a Molecule.
PB97-122360 *04,178*

Measurements of Fluorescence from Cold Atoms: Localization in Three-Dimensional Standing Waves.
PB95-163879 *03,943*

Optical Molasses: Cold Atoms for Precision Measurements.
PB95-108890 *03,877*

LETTIERI, T.

Optoelectronics and Optomechanics Manufacturing: An ATP Focused Program Development. Workshop Proceedings. Held in Gaithersburg, Maryland on February 15, 1995.
PB97-104186 *02,204*

LETTIERI, T. R.

Autocorrelation Functions from Optical Scattering for One-Dimensionally Rough Surfaces.
PB94-216538 *04,244*

Light Scattered by Coated Paper.
PB94-216546 *04,245*

Light Scattering by Sinusoidal Surfaces: Illumination Windows and Harmonics in Standards.
PB97-110548 *04,387*

Light Scattering from Glossy Coatings on Paper.
PB94-213246 *04,242*

Model of an Optical Roughness-Measuring Instrument.
PB97-110209 *04,384*

Optical Scattering from Moderately Rough Surfaces.
PB97-110415 *04,385*

Present and Future Standard Specimens for Surface Finish Metrology.
PB97-110423 *02,928*

Regimes of Surface Roughness Measurable with Light Scattering.
PB95-151213 *04,265*

Sinusoidal Surfaces as Standards for BRDF Instruments.
PB97-110597 *04,388*

LEVANDER, O. A.

Nutritional Status and Growth in Juvenile Rheumatoid Arthritis.
PB94-198470 *03,515*

LEVELT SENGERS, J. M. H.

Database for the Static Dielectric Constant of Water and Steam.
PB96-145586 *01,103*

Formulation of the Refractive Index of Water and Steam.
PB95-140133 *00,900*

Measurements of the Relative Permittivity of Liquid Water at Frequencies in the Range of 0.1 to 10 kHz and at Temperatures between 273.1 and 373.2 K at Ambient Pressure.
PB96-119375 *01,078*

Physical Limit to the Stability of Superheated and Stretched Water.
PB96-122551 *01,083*

Significant Contributions of IAPWS to the Power Industry, Science and Technology.
PB96-123252 *01,088*

Static Dielectric Constant of Water and Steam.
PB96-123559 *01,090*

Susceptibility Critical Exponent for a Nonaqueous Ionic Binary Mixture Near a Consolute Point.
PB95-152112 *00,938*

LEVENSON, M. S.

Performance Measures for Geometric Fitting in the NIST Algorithm Testing and Evaluation Program for Coordinate Measurement Systems.
PB96-122122 *01,745*

LEVIN, B. C.

Development of a New Small-Scale Smoke Toxicity Test Method and Its Comparison with Real-Scale Fire Tests.
PB94-213253 *00,350*

Further Development of the N-Gas Mathematical Model: An Approach for Predicting the Toxic Potency of Complex Combustion Mixtures.
PB96-123260 *03,650*

New Approach for Reducing the Toxicity of the Combustion Products from Flexible Polyurethane Foam.
PB96-123625 *01,411*

Relating Bench-Scale and Full-Scale Toxicity Data.
PB95-125977 *00,361*

LEVIN, B. M.

EXITT: A Simulation Model of Occupant Decisions and Actions in Residential Fires.
PB94-213261 *00,351*

Feasibility and Design Considerations of Emergency Evacuation by Elevators.
PB94-163441 *00,287*

Feasibility of Fire Evacuation by Elevators at FAA Control Towers.
PB94-213857 *04,844*

Human Factors Considerations for the Potential Use of Elevators for Fire Evacuation of FAA Air Traffic Control Towers.
PB94-217163 *01,300*

LEVIN, J. C.

Evolution of X-ray Resonance Raman Scattering into X-ray Fluorescence from the Excitation of Xenon Near the L3 Edge.
PB96-102751 *04,025*

High-Energy Behavior of the Double Photoionization of Helium from 2 to 12 keV.
PB94-213279 *03,860*

Noninvasive High-Voltage Measurement in Mammography by Crystal Diffraction Spectroscopy.
PB95-153417 *00,160*

LEVINE, J.

Analytical Estimation of Carrier Multipath Bias on GPS Position Measurements.
PB94-215712 *04,845*

Future of Time and Frequency Dissemination.
AD-P009 138/9 *01,520*

Future of Time and Frequency Dissemination.
N94-30684/2 *01,524*

Measurement and Interpretation of Tidal Tilts in a Small Array.
PB96-102611 *03,686*

Measurement Methods and Algorithms for Comparison of Local and Remote Clocks.
PB96-102652 *01,549*

Measurement of Very Low Frequency Vibrations.
PB96-102660 *03,687*

NIST Internet Time Service.
AD-P009 132/2 *01,519*

Smart Clock: A New Time.
PB95-151445 *01,530*

Time and Frequency Metrology.
PB96-190319 *01,556*

Time Generation and Distribution.
PB96-103049 *01,550*

Utc Dissemination to the Real-Time User.
N19960042622 *01,521*

LEVINE, J. P.

Measurement of Boron at Silicon Wafer Surfaces by Neutron Depth Profiling.
PB94-211059 *04,487*

LEVINE, Z. H.

Large Local-Field Corrections in Optical Rotatory Power of Quartz and Selenium.
PB97-122378 *04,400*

LEW, H. S.

Model Precast Concrete Beam-to-Column Connections Subject to Cyclic Loading.
PB95-153094 *00,438*

Northridge Earthquake, 1994. Performance of Structures, Lifelines and Fire Protection Systems.
PB94-161114 *00,421*

Northridge Earthquake 1994: Performance of Structures, Lifelines, and Fire Protection Systems.
PB94-207461 *04,825*

Partially Prestressed and Debonded Precast Concrete Beam-Column Joints.
PB95-153102 *00,439*

Proceedings of a Workshop on Developing and Adopting Seismic Design and Construction Standards for Lifelines. Held in Denver, Colorado on September 25-27, 1991.
PB97-115794 *01,302*

Seismic Performance Behavior of Precast Concrete Beam-Column Joints.
PB95-153110 *00,440*

Seismic Strengthening of Reinforced Concrete Frame Buildings.
PB95-108841 *00,430*

Strengthening Methodology for Lightly Reinforced Concrete Frames.
PB96-158050 *00,466*

Strengthening Methodology for Lightly Reinforced Concrete Frames-II. Recommended Calculation Techniques for the Design of Infill Walls.
PB94-187648 *00,426*

LEWENSTEIN, M.

Probing Bose-Einstein Condensed Atoms with Short Laser Pulses.
PB95-202818 *03,991*

LEWERENZ, M.

Infrared and Microwave Spectroscopy of the Argon Propyne Dimer.
PB94-198892 *00,794*

LEWETT, G. P.

Encouraging Environmentally-Aware Inventions.
PB95-161394 *02,521*

LEWIS, C. W.

Distinguishing the Contributions of Residential Wood Combustion and Mobile Source Emissions Using Relative Concentrations of Dimethylphenanthrene Isomers.
PB96-135124 *02,563*

Radiocarbon Measurements of Atmospheric Volatile Organic Compounds: Quantifying the Biogenic Contribution.
PB97-122352 *02,574*

LEWIS, D. F.

Novel Radiochromic Films for Clinical Dosimetry.
PB97-119259 *03,641*

Radiochromic Solid-State Polymerization Reaction.
PB95-180683 *01,271*

Radiochromic Solid-State Polymerization Reaction.
PB96-180146 *01,290*

LEWIS, E. L.

Astrophysical Aspects of Neutral Atom Line Broadening.
PB94-213287 *00,061*

LEWIS, J. A.

Computer Simulations of Binder Removal from 2-D and 3-D Model Particulate Bodies.
PB97-121339 *00,418*

Unreacted Cement Content in Macro-Defect-Free Composites: Impact on Processing-Structure-Property Relations.
PB96-141270 *03,174*

LEWIS, M. A.
Cryogenic Flow Calibration in NIST.
PB96-161930 *01,143*
Flow Conditioner Tests for Three Orifice Flowmeter Sizes.
PB95-105540 *04,201*
Thermal Hydraulic Tests of a Liquid Hydrogen Cold Neutron Source.
PB95-135570 *03,884*
Uncertainty Analysis of the NIST Nitrogen Flow Facility.
PB95-128906 *02,608*
Vortex Shedding Flowmeters for SSME Ducts.
PB95-169215 *01,453*

LEWIS, R. L.
Polarimetric Calibration of Reciprocal-Antenna Radars.
PB95-216925 *01,872*
Polarimetric Calibration of Reciprocal-Antenna Radars.
PB96-200696 *02,016*
Proposed Analysis of RCS Measurement Uncertainty.
PB95-203568 *01,871*
RangeCAD and the NIST RCS Uncertainty Analysis.
PB94-218591 *01,870*
Spherical-Wave Source-Scattering Matrix Analysis of Antennas and Antenna-Antenna Interactions.
PB96-111166 *02,008*

LEWIS, S.
Proposed International Interactive Courseware Standard.
PB96-123161 *00,137*

LEWIS, S. P.
Total-Dielectric-Function Approach to Electron and Phonon Response in Solids.
PB96-102884 *01,067*

LEWIS, V. E.
Neutron Measurement Intercomparisons Sponsored by CCEMRI, Section 3 (Neutron Measurements).
PB94-199916 *03,819*

LEWITUS, A. J.
High-Performance Liquid Chromatography of Phytoplankton Pigments Using a Polymeric Reversed-Phase C18 Column.
PB95-151130 *00,583*

LGROSSHANDLER, W. L.
In Search of Alternative Fire Suppressants.
PB96-164165 *03,285*

LI, Q.
Configuration-Dependent AC Stark Shifts in Calcium.
PB96-157995 *04,363*
Effect of Axial Strain on the Critical Current of Ag-Sheathed Bi-Based Superconductors in Magnetic Fields Up to 25 T.
PB94-211315 *04,493*
RIS Studies of Autoionization in Calcium.
PB94-213295 *00,849*
Thermally Activated Hopping of a Single Abrikosov Vortex.
PB95-140810 *04,548*

LI, R. S.
Quadratic Response of a Chemical Reaction to External Oscillations.
PB96-161633 *01,138*

LI, S. H.
Effect of Three Sterilization Techniques on Finger Pluggers.
PB94-216090 *00,150*

LI, X.
Accurate Measurement of Optical Detector Nonlinearity.
PB95-203576 *02,181*
Automated Measurement of Nonlinearity of Optical Fiber Power Meters.
PB96-176540 *04,110*
Optical Detector Nonlinearity: A Comparison of Five Methods.
PB95-169355 *04,291*
Optical Detector Nonlinearity: Simulation.
PB96-165378 *02,199*
Optical Power Meter Calibration Using Tunable Laser Diodes.
PB95-169256 *04,290*
Spatial Uniformity of Optical Detector Responsivity.
PB95-168845 *02,162*

LI, Z. Y.
Field Dependence of the Magnetic Ordering of Cu in R2CuO4 (R = Nd, Sm).
PB95-164521 *04,633*
Observation of Noncollinear Magnetic Structure for the Cu Spins in Nd2CuO4-Type Systems.
PB95-164539 *04,634*

LIAO, Y.
Transient Cooling of a Hot Surface by Droplets Evaporation.
PB94-156957 *03,783*

LIBBRECHT, K. G.
Low-Noise High-Speed Diode Laser Current Controller.
PB95-202826 *02,178*

LIBES, D.
Concepts of the NIST EXPRESS Server.
PB95-180543 *02,781*
Debugger for Tcl Applications.
PB94-213303 *01,695*
Handling Passwords with Security and Reliability in Background Processes.
PB95-180550 *01,722*
Kibitz-Connecting Multiple Interactive Programs Together.
PB94-213311 *01,696*
Object-Oriented Tel/Tk Binding for Interpreted Control of the NIST EXPRESS Toolkit in the NIST STEP Application Protocol Development Environment.
PB96-141049 *02,785*
Ouch Those Programs are Painful.
PB96-102678 *01,739*
Using Expect to Automate System Administration Tasks.
PB94-213329 *01,697*

LIBURDY, K.
Testers Open Dialogue at Inaugural NIST Workshop.
PB95-175550 *01,718*

LICHT, S. J.
High Frequency Magnetic Field Sensors Based on the Faraday Effect in Garnet Thick Films.
PB96-190384 *02,282*

LICHTENWALNER, D. J.
Growth of Epitaxial KNbO3 Thin Films.
PB96-135181 *02,409*
Use of Ion Scattering Spectroscopy to Monitor the Nb Target Nitridation during Reactive Sputtering.
PB94-172525 *00,761*

LIDE, D. R.
Molecular Spectroscopy.
PB94-213337 *03,861*

LIDGARD, A.
Annealing of Bragg Gratings in Hydrogen-Loaded Optical Fiber.
PB96-155437 *04,361*
Decrease of Fluorescence in Optical Fiber during Exposure to Pulsed or Continuous-Wave Ultraviolet Light.
PB95-203071 *04,320*

LIEBERMAN, A. G.
Rechargeable Batteries for Personal/Portable.
PB96-164231 *02,459*

LIEBERMAN, G.
Model Minimum Performance Specifications for Lidar Speed Measurement Devices.
PB95-197455 *04,861*

LIEBERMAN, R. A.
High Frequency Magnetic Field Sensors Based on the Faraday Effect in Garnet Thick Films.
PB96-190384 *02,282*

LIEBMAN, J. F.
Experimental Determination of the Ionization Energy of IO(X(sup 2)II(sub 3/2)) and Estimations of Delta(sub f)H(sup deg)(sub 0)(IO(sup -)) and PA(IO).
PB96-146899 *00,694*

LIFSCHITZ, M.
How Far Is Far from Critical Point in Polymer Blends. Lattice Cluster Theory Computations for Structured Monomer, Compressible Systems.
PB94-211141 *01,217*

LIFSHITZ, A.
Shock Tube Techniques in Chemical Kinetics.
PB95-163465 *00,968*

LIGGETT, W.
Developing Measurement for Experimentation.
PB97-118707 *03,450*
Discussion: Statistical Signal Processing of Quasiperiodicities.
PB96-119532 *00,096*
Replicate Measurements for Data Quality and Environmental Modeling.
PB94-172533 *02,515*
Scientific Protocols in Statistical Standards for Environmental Studies.
PB94-185527 *02,517*

LIGGETT, W. S.
Experimental Optimization of Peak Shape with Application to Aerosol Generation.
PB94-185535 *00,501*
Materials-Science Based Approach to Phenol Emissions from a Flooring Material in an Office Building.
PB97-118749 *02,572*
Pilot Studies for Improving Sampling Protocols.
PB97-118715 *02,530*
Source of Phenol Emissions Affecting the Indoor Air of an Office Building.
PB94-154382 *03,600*

LIGHT, G. M.
Assessment of Technology for Detection of Stress Corrosion Cracking in Gas Pipelines. Final Report, July 1993-March 1994.
PB94-206646 *02,475*
Gas-Coupled, Pulse-Echo Ultrasonic Crack Detection and Thickness Gaging.
PB96-147129 *04,847*

LILLESTOLEN, T.
Development of Frozen Whale Blubber and Liver Reference Materials for the Measurement of Organic and Inorganic Contaminants.
PB95-151676 *00,587*
Development of the National Marine Mammal Tissue Bank.
PB95-161402 *02,586*

LILLY, W. D.
Behavior of Charring Materials in Simulated Fire Environments.
PB94-196045 *01,368*

LIN, C.
Diffusion of Cations Beneath Organic Coatings on Steel Substrate.
PB94-215704 *03,119*
Effect of Ethanol on the Solubility of Hydroxyapatite in the System Ca(OH)2-H3PO4-H2O at 25C and 33C.
PB95-169231 *00,169*
In situ Measurements of Chloride Ion and Corrosion Potential at the Coating/Metal Interface.
PB95-140893 *03,122*
Relation between AC Impedance Data and Degradation of Coated Steel. 1. Effects of Surface Roughness and Contamination on the Corrosion Behavior of Epoxy Coated Steel.
PB94-213345 *03,189*

LIN, C. C.
Thermodynamic Interactions and Correlations in Mixtures of Two Homopolymers and a Block Copolymers by Small Angle Neutron Scattering.
PB95-152872 *01,247*

LIN, H. B.
Photonic Band-Structure Effects for Low-Index-Contrast Two-Dimensional Lattices in the Near Infrared.
PB97-122469 *04,401*

LIN, I. H.
Fracture in Multilayers.
PB96-163613 *02,988*

LIN, J. C.
Thermodynamic Assessment and Calculation of the Ti-Al System.
PB94-212644 *03,337*

LIN, J. H.
Comparisons of Some NIST Fixed-Point Cells with Similar Cells of Other Standards Laboratories.
PB97-119242 *00,655*

LIN, K. F.
Fluorescence Monitoring of Polarity Change and Gelation during Epoxy Cure.
PB94-185543 *01,204*

LIN, M. Y.
Small-Angle Neutron Scattering (SANS) Study of Worm-Like Micelles Under Shear.
PB96-176698 *04,111*

LIN, S.
Elastic Constants and Debye Temperature of Y1Ba2Cu3Ox: Effect of Oxygen Content.
PB94-213352 *04,515*
Nitrogen Effect on Elastic Constants of f.c.c. Fe-18Cr-19Mn Alloys.
PB94-172541 *03,203*

LIN, Z.
Tert-Butyl Hydroperoxide-Mediated DNA Base Damage in Cultured Mammalian Cells.
PB94-182003 *03,644*

LIN, Z. C.
Rare-Earth Isotopes as Tracers of Particulate Emissions: An Urban Scale Test.
PB94-161635 *02,535*

LIN, Z. Y.
Phonon Density of States in R2CuO4 and Superconducting R1.85Ce0.15CuO4 (R = Nd, Pr).
PB95-150686 *04,574*

LIND, D. M.
Structural and Magnetic Ordering in Iron Oxide/Nickel Oxide Multilayers by X-ray and Neutron Diffraction (Invited).
PB94-172558 *04,442*

LINDAHL, T.
Modification of Deoxyribose-Phosphate Residues by Extracts of Ataxia Telangiectasia Cells.
PB94-212602 *03,458*

LINDE, P.
Distant Future of Solar Activity: A Case Study of Beta Hydri. 3. Transition Region, Corona, and Stellar Wind.
PB94-185220 *00,049*
Distant Future of Solar Activity: A Case Study of beta Hydri. 3. Transition Region, Corona, and Stellar Wind.
PB95-153441 *00,074*

LINDEMAN, T. G.
Slit Jet Infrared Spectroscopy of Hydrogen Bonded N2HF Isotopomers: Rotational Rydberg-Klein-Rees Analysis and H/D Dependent Vibrational Predissociation Rates.
PB95-161873 *00,956*

LINDLE, D. W.
Anisotropy of Polarized X-ray Emission from Atoms and Molecules.
PB95-163002 *04,621*
Atomic, Molecular, and Optical Physics with X-rays.
PB94-213378 *03,863*
High-Energy Behavior of the Double Photoionization of Helium from 2 to 12 keV.
PB94-213279 *03,860*

Polarized X-Ray Emission Spectroscopy.
PB94-213360 *03,862*

LINDLER, D. J.

Observations of 3C 273 with the Goddard High Resolution Spectrograph on the Hubble Space Telescope.
PB95-202321 *00,076*

LINDNER, P.

Partial Scattered Intensities from a Binary Suspension of Polystyrene and Silica.
PB95-175618 *00,996*

LINDSAY, C. G.

Multimedia Tutorial on Phase Equilibria Diagrams.
PB96-200829 *03,088*

LINDSTROM, E. R.

National Voluntary Laboratory Accreditation Program: Electromagnetic Compatibility and Telecommunications. FCC Methods.
PB95-242376 *02,664*

NIST-NRL Free-Electron Laser Facility.
PB94-212511 *04,237*

LINDSTROM, R. M.

Analytical Applications of Guided Neutron Beams.
PB96-112347 *04,041*

Cold Neutron Prompt Gamma Activation Analysis at NIST: A Progress Report.
PB95-175964 *00,602*

Dead Time, Pileup, and Accurate Gamma-Ray Spectrometry.
PB96-167101 *00,697*

Determination of Hydrogen in Titanium Alloy Jet Engine Compressor Blades by Cold Neutron Capture Prompt Gamma-ray Activation Analysis.
PB95-175956 *01,448*

Effects of Target Shape and Neutron Scattering on Element Sensitivities for Neutron-Capture Prompt Gamma-ray Activation Analysis.
PB94-216157 *00,558*

Grazing Incidence Prompt Gamma Emissions and Resonance-Enhanced Neutron Standing Waves in a Thin-Film.
PB95-150470 *03,892*

High-Sensitivity Determination of Iodine Isotopic Ratios by Thermal and Fast Neutron Activation.
PB94-213386 *00,555*

Inelastic Neutron Scattering Studies of Rotational Excitations and the Orientational Potential in C60 and A3C60 Compounds.
PB94-172673 *00,763*

Local Area Networks in NAA: Advantages and Pitfalls.
PB94-172095 *00,527*

Loss-Free Counting at IRI and NIST.
PB96-167119 *04,105*

Measuring Hydrogen by Cold-Neutron Prompt-Gamma Activation Analysis.
PB96-111877 *00,612*

Neutron Capture Prompt Gamma-Ray Activation Analysis at the NIST Cold Neutron Research Facility.
PB94-213394 *00,556*

New NIST Rapid Pneumatic Tube System.
PB96-167259 *03,738*

SUM and MEAN: Standard Programs for Activation Analysis.
PB96-112149 *00,617*

Use of Neutron Beams for Chemical Analysis at NIST.
PB97-112437 *00,652*

LINEBERGER, W. C.

Photoelectron Spectroscopy of Negatively Charged Bismuth Clusters: Bi(-)2, Bi(-)3, and Bi(-)4.
PB95-108494 *00,880*

Photoelectron Spectroscopy of Small Antimony Cluster Anions: Sb(-), Sb2(-), Sb3(-), and Sb4(-).
PB95-203139 *01,045*

LINHOLM, L. W.

Application of the Modified Voltage-Dividing Potentiometer to Overlay Metrology in a CMOS/Bulk Process.
PB94-181997 *02,302*

Comparisons of Measured Linewidths of Sub-Micrometer Lines Using Optical, Electrical, and SEM Metrologies.
PB95-152807 *02,338*

Design Guide for CMOS-On-SIMOX. Test Chips NIST3 and NIST4.
PB94-163458 *02,297*

Electrical Test Structure for Overlay Metrology Referenced to Absolute Length Standards.
PB95-152278 *02,336*

Electrical Test Structures Replicated in Silicon-on-Insulator Material.
PB97-111827 *02,454*

Enhanced Voltage-Dividing Potentiometer for High-Precision Feature Placement Metrology.
PB96-164025 *02,428*

Hybrid Optical-Electrical Overlay Test Structure.
PB96-204136 *02,450*

Measurement of Patterned Film Linewidth for Interconnect Characterization.
PB96-141168 *02,420*

Metrology Standards for Advanced Semiconductor Lithography Referenced to Atomic Spacings and Geometry.
PB96-160718 *02,424*

Microelectronic Test Structures for Feature Placement and Electrical Linewidth Metrology.
PB95-180568 *02,367*

Microelectronic Test Structures for Overlay Metrology.
PB96-164249 *02,430*

New Test Structure for Nanometer-Level Overlay and Feature-Placement Metrology.
PB95-175345 *02,363*

Test Structures for Determining Design Rules for Microelectromechanical-Based Sensors and Actuators.
PB95-150488 *02,105*

Test Structures for the In-Plane Locations of Projected Features with Nanometer-Level Accuracy Traceable to a Coordinate Measurement System.
PB94-200565 *02,313*

LINK, A. N.

Evaluation of the Economic Impacts Associated with the NIST Power and Energy Calibration Services.
PB95-188850 *02,461*

LINKS, J. M.

EPR Dosimetry of Cortical Bone and Tooth Enamel Irradiated with X and Gamma Rays: Study of Energy Dependence.
PB97-110373 *03,639*

Exposure-to-Absorbed-Dose Conversion for Human Adult Cortical Bone.
PB97-110381 *03,640*

LINN, R. J.

Conformance Testing for OSI Protocols.
PB96-102686 *01,631*

Copyright and Information Services in the Context of the National Research and Education Network.
PB96-160536 *02,736*

Formal Multi-Layer Test Methodology and Its Application to OSI.
PB94-172194 *02,718*

Using Technology to Manage and Protect Intellectual Property.
PB97-112395 *01,513*

LINNARTZ, H.

Microwave and Submillimeter Spectroscopy of Ar-NH3 States Correlating with Ar+NH3(j=1, k=1).
PB95-152211 *00,942*

LINSKY, J.

High Sensitivity Survey of Radio Continuum Emission in Herbig Ae/Be Stars.
PB94-185915 *00,051*

Sleuthing the Dynamo: HST/FOS Observations of UV Emissions of Solar-Type Stars in Young Clusters.
PB96-122817 *00,098*

LINSKY, J. E.

Dynamic Phenomena on the RS Canum Venaticorum Binary II Pegasi in August 1989. 1. Observational Data.
PB94-211067 *00,056*

LINSKY, J. L.

Accurate Measurements of the Local Deuterium Abundance from HST Spectra.
PB96-200621 *00,110*

Atomic Data Needed for Far Ultraviolet Astronomy with HUT and FUSE.
PB94-213402 *00,062*

Class of Radio-Emitting Magnetic B Stars and a Wind-Fed Magnetosphere Model.
PB94-213451 *00,067*

Deuterium and the Local Interstellar Medium: Properties for the Procyon and Capella Lines of Sight.
PB96-200639 *00,111*

Deuterium in the Local Interstellar Medium: Its Cosmological Significance.
PB95-202842 *00,081*

Developments in Stellar Coronae.
PB96-176706 *00,107*

Distant Future of Solar Activity: A Case Study of Beta Hydri. 3. Transition Region, Corona, and Stellar Wind.
PB94-185220 *00,049*

Distant Future of Solar Activity: A Case Study of beta Hydri. 3. Transition Region, Corona, and Stellar Wind.
PB95-153441 *00,074*

Efficient Way of Identifying New Active Stars: A VLA Survey of X-ray Selected Active Stellar Candidates.
PB96-122882 *00,099*

Far-Ultraviolet Flare on a Pleiades G Dwarf.
PB96-102033 *00,086*

First Results from a Coordinated ROSAT, IUE, and VLA Study of RS CVn Systems.
PB94-213477 *00,069*

First Results from the Goddard High-Resolution Spectrograph: The Chromosphere of Tauri.
PB94-199528 *00,054*

Four Years of Monitoring alpha Orionis with the VLA: Where Have All the Flares Gone.
PB94-185212 *00,048*

FUSE: The Far Ultraviolet Spectrograph Explorer.
PB94-213410 *00,063*

GHRS Observations of Cool, Low-Gravity Stars. 1. The Far-Ultraviolet Spectrum of alpha Orions (M2 Iab).
PB96-112016 *00,094*

Goddard High Resolution Spectrograph: Instrument, Goals, and Science Results.
PB96-123278 *00,044*

Goddard High-Resolution Spectrograph Observations of the Local Interstellar Medium and the Deuterium/Hydrogen Ratio along the Line of Sight Toward Capella.
PB94-213444 *00,066*

High Velocity Plasm in the Transition Region of Au Mic: A Stellar Analog of Solar Explosive Events.
PB96-123294 *00,102*

High-Velocity Plasma in the Transition Region of AU Microscopii: Evidence for Magnetic Reconnection and Saturated Heating during Quiescent and Flaring Conditions.
PB96-102694 *00,091*

Hydrogen Lyman-alpha Emission of Capella.
PB95-202263 *00,075*

IUE Observations of Solar-Type Stars in the Pleiades and the Hyades.
PB94-199437 *00,053*

Observations of 3C 273 with the Goddard High Resolution Spectrograph on the Hubble Space Telescope.
PB95-202321 *00,076*

Observing Stellar Coronae with the Goddard High Resolution Spectrograph. I. The dMe Star AU Microscopii.
PB96-102777 *00,092*

Peeking Through the Picket Fence: What Astrophysical Surprises May Be Present in the 100-1200 Angstrom Region.
PB95-202859 *00,082*

Radio and X-ray Emissions from Chemically Peculiar B- and A-Type Stars: Observations and a Model.
PB96-123302 *00,103*

Radio Continuum and X-Ray Properties of the Coronae of RS Canum Venaticorum and Related Active Binary Systems.
PB94-211083 *00,057*

Radio Emission from Chemically Peculiar Stars.
PB94-213469 *00,068*

Recalibration for the Final Archive of the International Ultraviolet Explorer (IUE) Satellite.
PB96-135264 *00,106*

Redshifts in Stellar Transition Regions.
PB96-123310 *00,104*

Relationship between Radiative and Magnetic Fluxes for Three Active Solar-Type Dwarfs.
PB96-119540 *00,097*

Riass Coronathon: Joint X-ray and Ultraviolet Observations of Normal F-K Stars.
PB96-200217 *00,109*

ROSAT All-Sky Survey of Active Binary Coronae. 1. Quiescent Fluxes for the RS Canum Venaticorum Systems.
PB95-202479 *00,077*

ROSAT All-Sky Survey of Active Binary Coronae. 2. Coronal Temperatures of the RS Canum Venaticorum Systems.
PB94-199601 *00,055*

Rotational Modulation and Flares on RS Canum Venaticorum and BY Draconis Stars. XVI. IUE Spectroscopy and VLA Observations of C1182(=V 1005 Orionis) in October 1983.
PB94-185626 *00,050*

Rotational Modulation and Flares on RS Canum Venaticorum and BY Draconis Stars. XVIII. Coordinated VLA, ROSAT, and IUE Observations of RS CVn Binaries.
PB96-102322 *00,089*

Scientific Rationale and Present Implementation Strategy for the Far Ultraviolet Spectrograph Explorer (FUSE).
PB96-123328 *00,045*

Search for Radio Emission from the 'Non-Magnetic' Chemically Peculiar Stars.
PB96-102249 *00,087*

Stellar Coronal Structures.
PB95-202834 *00,080*

Transition Regions of Capella.
PB96-123336 *00,105*

Transition Regions of Capella (1995).
PB96-176714 *00,108*

A-type and Chemically Peculiar Stars.
PB96-123286 *00,101*

Ultraviolet Observations of Stellar Coronae: Early Results from HST.
PB94-213428 *00,064*

Volume-Limited ROSAT Survey of Extreme Ultraviolet Emission from all Nondegenerate Stars within 10 Parsecs.
PB96-103189 *00,093*

X-ray Emission from Chemically Peculiar Stars.
PB96-102256 *00,088*

X-rays from Stellar Flares.
PB94-213436 *00,065*

LINTERIS, G.

Acid Gas Production in Inhibited Diffusion Flames.
PB95-180576 *01,390*

Parametric Study of Hydrogen Fluoride Formation in Suppressed Fires.
PB96-163720 *00,514*

LINTERIS, G. T.

Asymptotic and Numerical Analysis of a Premixed Laminar Nitrogen Dioxide-Hydrogen Flame.
PB96-164256 *01,422*

Burning Rate of Premixed Methane-Air Flames Inhibited by Fluorinated Hydrocarbons.
PB95-180584 *01,391*

Effect of CF3H and CF3Br on Laminar Diffusion Flames in Normal and Microgravity.
PB96-161831 *01,420*

Effect of CF3H and CF3Br on Laminar Diffusion Flames in Normal and Microgravity.
PB96-161849 *01,421*

Experimental and Numerical Burning Rates of Premixed Methane-Air Inhibited by Fluoromethanes.
PB95-180592 *01,392*

Inhibition of Premixed Methane-Air Flames by Halon Alternatives.
PB96-146741 *01,414*

Inhibition of Premixed Methane-Air Flames by Iron Pentacarbonyl.
PB96-163712 *00,513*

LINZ, A.

Scalability Test for Parallel Code.
PB96-146758 *01,749*

LIPE, T. E.

AC-DC Difference Characteristics of High-Voltage Thermal Converters.
PB96-148093 *02,083*

Development of Thin-Film Multijunction Thermal Converters at NIST.
PB97-112338 *02,286*

Empirical Linear Prediction Applied to a NIST Calibration Service.
PB97-112353 *02,287*

Frequency Extension of the NIST AC-DC Difference Calibration Service for Current.
PB95-161253 *01,895*

High-Current Thin Film Multijunction Thermal Converters and Multi-Converter Modules.
PB97-112379 *01,989*

LIPNICK, R. N.

Nutritional Status and Growth in Juvenile Rheumatoid Arthritis.
PB94-198470 *03,515*

LIPPIATT, B. C.

Evaluating Investments in Law Enforcement Equipment: An Annotated Bibliography.
PB95-151379 *04,867*

LISOWSKI, P. W.

Intermediate Structure in the Neutron-Induced Fission Cross Section of 236U.
PB94-185741 *03,802*

Measurements of the (235)U(n,f) Cross Section in the 3 to 30 MeV Neutron Energy Region.
PB97-119051 *04,172*

Measurements of the (237)Np(n,f) Cross Section.
PB97-119069 *04,173*

LITTLE, W. A.

From Superconductivity to Supernovae: The Ginzburg Symposium. Report on the Symposium Held in Honor of Vitaly L. Ginzburg. Held in Gaithersburg, Maryland on May 22, 1992.
PB95-171963 *04,649*

LITTLER, C. L.

Heavily Accumulated Surfaces of Mercury Cadmium Telluride Detectors: Theory and Experiment.
PB94-216074 *02,134*

Investigation of Mercury Interstitials in Hg(1-x)CdxTe Alloys Using Resonant Impact-Ionization Spectroscopy.
PB94-213485 *02,133*

RII Spectroscopy of Trap Levels in Bulk and LPE Hg1-xCdxTe.
PB96-160247 *04,084*

LITTRELL, K.

Multi-Stage, Position Stabilized Vibration Isolation System for Neutron Interferometry.
PB95-175022 *03,955*

LIU, A.

Acid Gas Production in Inhibited Diffusion Flames.
PB95-180576 *01,390*

LIU, C.

Variationally Stable Treatment of Two- and Three-Photon Detachment of H(-) Including Electron-Correlation Effects.
PB95-202867 *03,992*

LIU, D. W.

Preparation and Characterization of Cyclopolymerizable Resin Formulations.
PB96-146840 *01,285*

LIU, H.

Existence and Nonexistence Theorems of Finite Diameter Sequential Confidence Regions for Errors-in-Variables Models.
PB95-180352 *03,441*

General Motion Model and Spatio-Temporal Filters for Computing Optical Flow.
PB95-171096 *01,847*

General Motion Model and Spatio-Temporal Filters for 3-D Motion Interpretations.
PB96-210703 *01,861*

Image Gradient Evolution: A Visual Cue for Danger.
PB96-154562 *02,939*

Motion-Model-Based Boundary Extraction.
PB95-189502 *01,849*

Reliable Optical Flow Algorithm Using 3-D Hermite Polynomials.
PB94-145620 *01,829*

LIU, H. K.

Critical Current Density, Irreversibility Line, and Flux Creep Activation Energy in Silver-Sheathed Bi2Sr2Ca2Cu2Ox Superconducting Tapes.
PB95-162749 *04,616*

Interlaboratory Comparison of Autoradiographic DNA Profiling Measurements. 1. Data and Summary Statistics.
PB95-175923 *03,542*

Interlaboratory Comparison of Autoradiographic DNA Profiling Measurements. 2. Measurement Uncertainty and Its Propagation.
PB96-112123 *03,545*

LIU, L.

Observations of 3C 273 with the Goddard High Resolution Spectrograph on the Hubble Space Telescope.
PB95-202321 *00,076*

LIU, R.

Atmospheric Reactivity of alpha-Methyl-Tetrahydrofuran.
PB95-163705 *02,548*

Gas Phase Reactivity Study of OH Radicals with 1,1-Dichloroethene and cis-1,1-Dichloroethene and Trans-1,2-Dichloroethene over the Temperature Range 240-400 K.
PB95-152146 *00,939*

Rate Constants for the Gas Phase Reactions of the OH Radical with CF3CF2CHCl2 (HCFC-225ca) and CF2ClCF2CHClF (HCFC-225cb).
PB95-152153 *00,940*

LIU, S.

Droplet Transfer Modes for a MIL 100S-1 GMAW Electrode.
PB95-209300 *02,867*

Mapping the Droplet Transfer Modes for an ER100S-1 GMAW Electrode.
PB96-190095 *03,295*

LIU, S. T.

Performance Testing of a Family of Type I Combination Appliance.
PB95-220521 *02,505*

Predicting the Energy Performance Ratings of a Family of Type I Combination Appliances.
PB95-105524 *02,504*

LIU, W.

Tensile Creep of Whisker Reinforced Silicon Nitride.
PB94-211984 *03,142*

LIU, X.

Electron Beam Crosslinking of Poly(vinylmethyl ether).
PB94-185550 *01,205*

LIU, Y.

Comparisons of Some NIST Fixed-Point Cells with Similar Cells of Other Standards Laboratories.
PB97-119242 *00,655*

LIVIGNI, D.

Spatial Uniformity of Optical Detector Responsivity.
PB95-168845 *02,162*

LIVIGNI, D. J.

Thermal Modeling and Analysis of Laser Calorimeters.
PB96-140405 *04,354*

LIVINGSTON, C. A.

Intrinsic Stress in DC Sputtered Niobium.
PB94-199031 *04,468*

LLOYD, R. S.

Novel DNA N-Glycosylase Activity of E. coli T4 Endonuclease V That Excises 4,6-Diamino-5-Formamidopyrimidine from DNA, a UV-Radiation- and Hydroxyl Radical-Induced Product of Adenine.
PB96-160478 *03,549*

LOBB, C. J.

Application of Single Electron Tunneling: Precision Capacitance Ratio Measurements.
PB96-102157 *04,703*

Diffusion Studies in a Digital-Image-Based Cement Paste Microstructural Model.
PB94-198801 *01,312*

Physical Basis for Half-Integral Shapiro Steps in a DC SQUID.
PB96-102264 *04,704*

LOBO, C.

Study on the Reuse of Plastic Concrete Using Extended Set-Retarding Admixtures.
PB96-122130 *00,402*

LOCASCIO-BROWN, L.

Flow Immunoassay Using Solid-Phase Entrapment.
PB96-200951 *00,642*

Liposome-Based Flow-Injection Immunoassay for Determining Theophylline in Serum.
PB94-213493 *03,494*

Planar Waveguide Optical Sensors.
PB94-200185 *03,586*

LOEVINGER, R.

Needs for Brachytherapy Source Calibrations in the United States.
PB97-110092 *03,521*

LOEZOS, J. M.

Magnetic Dielectric Oxides: Subsolidus Phase Relations in the BaO: Fe2O3: TiO2 System.
PB96-176524 *01,156*

LOGSDON, B. W.

Membrane Gas Separation for a Fluidized-Bed Incinerator.
PB95-169041 *02,550*

LOH, H. T.

Concurrent Flow Flame Spread Study.
PB94-156866 *01,356*

LOHSE, D. J.

Thermodynamic Interactions in Model Polyolefin Blends Obtained by Small-Angle Neutron Scattering.
PB94-198496 *01,208*

LOMAKIN, S. M.

Investigation of the Thermal Stability and Char-Forming Tendency of Cross-linked Poly(methyl methacrylate).
PB94-213501 *03,380*

LOMBARDI, M.

Introduction to Frequency Calibration. Part 1.
PB96-200654 *01,560*

Preliminary Comparison of Time Transfers via LASSO, GPS and Two-Way Satellite.
PB95-151098 *01,529*

Using LORAN-C Broadcasts for Automated Frequency Calibrations.
PB94-216017 *01,526*

LOMBARDI, M. A.

High Resolution Time Interval Counter.
PB96-138607 *01,495*

How to Get NIST-Traceable Time on Your Computer.
PB96-200647 *01,559*

Keeping Time on Your PC.
PB95-161410 *01,537*

NIST Frequency Measurement Service.
PB96-200662 *01,561*

Satellite Two-Way Time Transfer: Fundamentals and Recent Progress.
PB95-161089 *01,536*

LONBERGER, S. T.

Reference Tables for Thermocouples.
AD-A279 948/4 *02,614*

LONG, F. G.

PC-Based Spinning Rotor Gage Controller.
PB95-175832 *02,609*

LONG, G. G.

Anisotropy of the Surfaces of Pores in Plasma Sprayed Alumina Deposits.
PB96-123211 *03,126*

Cavitation Contributes Substantially to Tensile Creep in Silicon Nitride.
PB96-122577 *03,171*

Cavity Evolution during Tensil Creep of Si3N4.
PB96-204193 *03,376*

Characterization of the Densification of Alumina by Multiple Small-Angle Neutron Scattering. (Reannouncement with New Availability Information).
AD-A249 179/3 *03,024*

Effect of Green Density and the Role of Magnesium Oxide Additive on the Densification of Alumina Measured by Small-Angle Neutron Scattering. (Reannouncement with New Availability Information).
AD-A244 582/3 *03,022*

Evolution of the Pore Size Distribution in Final-Stage Sintering of Alumina Measured by Small-Angle X-ray Scattering. (Reannouncement with New Availability Information).
AD-A249 178/5 *03,023*

High-Temperature Furnace for In situ Small-Angle Neutron Scattering during Ceramic Processing.
PB96-148127 *03,743*

Small-Angle Neutron Scattering Characterization of Processing/Microstructure Relationships in the Sintering of Crystalline and Glassy Ceramics. (Reannouncement with New Availability Information).
AD-A249 510/9 *03,025*

Structures of Vapor-Deposited Yttria and Zirconia Thin Films.
PB94-216025 *03,041*

LONG, K. S.

Rapid Decline in the Optical Emission from SN 1957D in M83.
PB94-216033 *00,070*

LONG, T.

Certification of Phencyclidine in Lyophilized Human Urine Reference Materials.
PB96-160692 *03,508*

Determination of Amphetamine and Methamphetamine in a Lyophilized Human Urine Reference Material.
PB95-175444 *03,597*

LOONEY, J. P.

Decoupling in the Line Mixing of Acetylene Infrared Q Branches.
PB95-108452 *00,877*

Influence of the Filament Potential Wave Form on the Sensitivity of Glass-Envelope Bayard-Alpert Gages.
PB95-175014 *02,657*

Laser Bandwidth Effects in Quantitative Cavity Ring-Down Spectroscopy.
PB97-112254 *04,394*

Laser Photoionization Measurements of Pressure in Vacuum.
PB95-180600 *03,964*

Measurement of CO Pressures in the Ultrahigh Vacuum Regime Using Resonance-Enhanced Multiphoton-Ionization Time-of-Flight Mass Spectroscopy.
PB94-216041 *03,864*

PC-Based Spinning Rotor Gage Controller.
PB95-175832 *02,609*

Simultaneous Forward-Backward Raman Scattering Studies of D2 Broadened by D2, He, and Ar.
PB95-162459 *00,961*

LOONG, C. K.

Phonon Density of States in R2CuO4 and Superconducting R1.85Ce0.15CuO4 (R = Nd, Pr).
PB95-150686 *04,574*

LOPES, V. C.

Comparison of Techniques for Nondestructive Composition Measurements in CdZnTe Substrates.
PB96-103098 *02,703*

LORENTZ, S. R.

Determination of Complex Scattering Amplitudes in Low-Energy Elastic Electron-Sodium Scattering.
PB94-216652 *03,869*

Spin-Resolved Elastic Scattering of Electrons from Sodium.
PB95-161774 *03,933*

Thermal Modeling of Absolute Cryogenic Radiometers.
PB95-181236 *04,316*

LORENZEN, T. J.

Taguchi's Parameter Design: A Panel Discussion.
PB96-111802 *03,445*

LOS ARCOS, J. M.

Standardization and Decay Scheme of Rhenium-186.
PB94-200490 *03,830*

LOUGHRY, T. A.

Band-Limited, White Gaussian Noise Excitation for Reverberation Chambers and Applications to Radiated Susceptibility Testing.
PB96-165410 *01,960*

LOVAS, F. J.

Experimental Studies of Line Shapes from a Balle-Flygare Spectrometer.
PB94-199452 *00,796*

Infrared and Microwave Spectroscopy of the Argon - Propyne Dimer.
PB94-198892 *00,794*

Microwave Spectra of van der Waals Complexes of Importance in Planetary Atmospheres.
PB95-150611 *00,919*

Microwave Spectrum and Structure of CH2O-H2O.
PB97-118723 *04,168*

Microwave Spectrum and Structure of CH3NO2-H2O.
AD-A296 377/5 *00,719*

Rotational Spectrum and Structure of a Weakly Bound Complex of Ketene and Acetylene.
PB95-126140 *00,896*

Thermal Decomposition Pathways in Nitramine Propellants.
AD-A295 896/5 *03,753*

LOVEJOY, C. M.

High Resolution, Jet-Cooled Infrared Spectroscopy of (HCl)2: Analysis of nu1 and nu2 HCl Stretching Fundamentals, Interconversion Tunneling, and Mode-Specific Predissociation Lifetimes.
PB95-203196 *01,046*

Laser Double Resonance Measurements of the Quenching Rates of Br((2)P1/2) with H20, D20, HDO, and O2.
PB95-150694 *00,921*

Preferential In-Plane Rotational Excitation of H2O (001) by Translational-to-Vibrational Transfer from 2.2 eV H Atoms.
PB95-202875 *01,035*

Rigid Bender Analysis of van der Waals Complexes: The Intermolecular Bending Potential of a Hydrogen Bond.
PB95-203022 *01,042*

Slit Jet Infrared Spectroscopy of Hydrogen Bonded N2HF Isotopomers: Rotational Rydberg-Klein-Rees Analysis and H/D Dependent Vibrational Predissociation Rates.
PB95-161873 *00,956*

Spectroscopic Puzzle in ArHF Solved: The Test of a New Potential.
PB94-216058 *00,850*

LOVELY, P. S.

Optical Fiber Sensors: Accelerating Applications in Navy Ships.
PB94-186848 *02,632*

LOVETT, C. D.

Machine Performance Standard Provides Opportunity to Improve Quality and Productivity.
PB96-154521 *02,837*

Standards Promote Credibility and Technology Transfer: The Need for Greater Industry Support of Technical Committees.
PB97-116206 *02,961*

LOW, S. R.

Fracture Behavior of Large-Scale Thin-Sheet Aluminum Alloy.
N95-19494/0 *03,311*

Fracture Testing of Large-Scale Thin-Sheet Aluminum Alloy.
AD-A306 625/5 *03,305*

Fracture Testing of Large-Scale Thin-Sheet Aluminum Alloy.
PB95-242368 *00,024*

Review and Upgrading of Military Fastener Test Standard MIL-STD-1312.
PB95-154720 *02,947*

LOWE, D.

Analysis of High Bay Hangar Facilities for Detector Sensitivity and Placement.
PB96-190210 *01,429*

Assessing Halon Alternatives for Aircraft Engine Nacelle Fire Suppression.
PB96-102454 *01,401*

Protection of Data Processing Equipment with Fine Water Sprays.
PB95-174975 *02,610*

Suppression Effectiveness of Extinguishing Agents under Highly Dynamic Conditions.
PB95-180279 *00,020*

Turbulent Spray Burner for Assessing Halon Alternative Fire Suppressants.
PB95-153748 *01,385*

Validation of a Turbulent Spray Flame Facility for the Assessment of Halon Alternatives.
PB96-159728 *03,283*

LOWE, J.

Ultra-High Stability Synthesizer for Diode Laser Pumped Rubidium.
PB94-216066 *01,527*

Ultralinear Small-Angle Phase Modulator.
PB95-168852 *02,261*

LOWE, J. L.

Error Analysis of the NIST Optically Pumped Primary Frequency Standard.
PB95-153482 *01,535*

NIST Optically Pumped Cesium Frequency Standard.
PB94-211117 *03,835*

LOWE, J. P.

Diode-Laser Pumped, Rubidium Cell Frequency Standards.
PB95-163218 *01,538*

Hybrid Digital/Analog Servo for the NIST-7 Frequency Standard.
PB95-180618 *01,544*

Microwave Leakage as a Source of Frequency Error and Long-Term Instability in Cesium Atomic-Beam Frequency Standards.
PB95-180501 *01,541*

NIST-7, the New US Primary Frequency Standard.
PB95-153458 *01,534*

Reducing the Effect of Local Oscillator Phase Noise on the Frequency Stability of Passive Frequency Standards.
PB95-180972 *01,545*

LOWNEY, J. R.

Band-to-Band Photoluminescence and Luminescence Excitation in Extremely Heavily Carbon-Doped Epitaxial GaAs.
PB95-150413 *04,570*

Characterization of Interface Defects in Oxygen-Implanted Silicon Films.
PB94-216629 *02,322*

Effects of Heavy Doping on Numerical Simulations of Gallium Arsenide Bipolar Transistors.
PB95-150975 *02,334*

Heavily Accumulated Surfaces of Mercury Cadmium Telluride Detectors: Theory and Experiment.
PB94-216074 *02,134*

Hg1-xCdxTe Characterization Measurements: Current Practice and Future Needs.
PB95-164299 *02,157*

High-Spatial-Resolution Resistivity Mapping Applied to Mercury Cadmium Telluride.
PB94-212917 *02,131*

Investigation of Mercury Interstitials in Hg(1-x)CdxTe Alloys Using Resonant Impact-Ionization Spectroscopy.
PB94-213485 *02,133*

Junction Locations by Scanning Tunneling Microscopy: In-Air-Ambient Investigation of Passivated GaAs pn Junctions.
PB94-185964 *02,306*

Magneto-Transport Properties of HgCdTe.
PB95-175840 *04,661*

Majority and Minority Mobilities in Heavily Doped Silicon for Device Simulations.
PB94-198728 *02,311*

Model for Determining the Density and Mobility of Carriers in Thin Semiconducting Layers with Only Two Contacts.
PB96-102702 *02,378*

MONSEL-II: Monte Carlo Simulation of SEM Signals for Linewidth Metrology.
PB96-102710 *02,379*

Monte Carlo Model for SEM Linewidth Metrology.
PB95-150058 *02,331*

Monte Carlo Simulation of Scanning Electron Microscope Signals.
PB96-200969 *02,444*

Physics for Device Simulations and Its Verification by Measurements.
PB95-141172 *02,327*

Physics for Device Simulations and Its Verification by Measurements.
PB95-152914 *02,339*

RII Spectroscopy of Trap Levels in Bulk and LPE Hg1-xCdxTe.
PB96-160247 *04,084*

Scanning Capacitance Microscopy Measurements and Modeling for Dopant Profiling of Silicon.
PB96-164207 *04,781*

Scanning Capacitance Microscopy Measurements and Modeling: Progress Towards Dopant Profiling of Silicon.
PB96-148150 *04,773*

Scanning Capacitance Microscopy Measurements and Modeling: Progress Towards Dopant Profiling of Silicon.
PB96-180070 *01,964*

SEM Linewidth Metrology of X-ray Lithography Masks.
PB96-201108 *02,447*

Semiconductor Measurement Technology: Improved Characterization and Evaluation Measurements for HgCdTe Detector Materials, Processes, and Devices Used on the GOES and TIROS Satellites.
PB94-188810 *02,122*

Transverse Magnetoresistance: A Novel Two-Terminal Method for Measuring the Carrier Density and Mobility of a Semiconductor Layer.
PB95-150066 *02,332*

Use of Monte Carlo Modeling for Interpreting Scanning Electron Microscope Linewidth Measurements.
PB96-137807 *02,413*

User's Manual for the Program MONSEL-1: Monte Carlo Simulation of SEM Signals for Linewidth Metrology.
PB95-111522 *02,325*

X-ray Mask Metrology: The Development of Linewidth Standards for X-ray Lithography.
PB95-162129 *02,348*

LOWRY, R. E.

Fluorescence Anisotropy Measurements on a Polymer Melt as a Function of Applied Shear Stress.
PB94-199296 *01,209*

Observations of Shear Induced Molecular Orientation in a Polymer Melt Using Fluorescence Anisotropy Measurements.
PB94-199304 *01,210*

Observations of Shear Stress and Molecular Orientation Using Fluorescence Anisotropy Measurements.
PB94-199312 *01,211*

LOZEV, M. G.

Application of Electromagnetic-Acoustic Transducers for Nondestructive Evaluation of Stresses in Steel Bridge Structures.
PB96-167978 *01,301*

Determination of Sheet Steel Formability Using Wide Band Electromagnetic-Acoustic Transducers.
PB96-186036 *02,279*

Sensor System for Intelligent Processing of Hot-Rolled Steel.
PB96-186069 *03,373*

LOZIER, D. W.

Basic Linear Algebra Operations in SLI Arithmetic.
PB96-165931 *03,421*

Error-Bounding in Level-Index Computer Arithmetic.
PB96-109582 *01,742*

MasPar MP-1 as a Computer Arithmetic Laboratory.
PB95-189437 *01,627*

MasPar MP-1 as a Computer Arithmetic Laboratory.
PB96-179155 *01,617*

Numerical Evaluation of Special Functions.
PB96-119557 *03,417*

Parallel and Serial Implementations of SLI Arithmetic.
PB95-242335 *01,732*

Review of Mathematical Function Library for Microsoft-FORTRAN, John Wiley and Sons, 1989.
PB94-160793 *01,679*

Software Needs in Special Functions.
PB95-105045 *01,702*

Software Needs in Special Functions.
PB96-200977 *01,778*

Underflow-Induced Graphics Failure Solved by SLI Arithmetic.
PB95-161444 *01,712*

LU, B.

Displacement Method for Machine Geometry Calibration.
PB95-152088 *02,946*

LU, G.

Workshop on Characterizing Diamond Films (3rd). Held in Gaithersburg, Maryland on February 23-24, 1994.
PB94-187663 *04,456*

LU, W. Y.

Ultrasonic Methods.
PB96-190327 *02,707*

LUBELL, J.
Application Protocol Information Base World Wide Web Gateway.
PB96-202320 *02,791*

SC4 Short Names Registry.
PB97-122410 *02,799*

SGML Environment for STEP.
PB95-143103 *02,778*

LUCAS, J. M.
Taguchi's Parameter Design: A Panel Discussion.
PB96-111802 *03,445*

LUCATORTO, T.
Soft X-ray Reflectometry Program at the National Institute of Standards and Technology.
PB96-160395 *04,368*

LUCATORTO, T. B.
Comment On: Two-Photon Absorption Series of Calcium.
PB96-157979 *04,074*

Configuration-Dependent AC Stark Shifts in Calcium.
PB96-157995 *04,363*

Improved Dose Metrology in Optical Lithography.
PB96-179510 *02,439*

Improved Reflectometry Facility at the National Institute of Standards and Technology.
PB96-160338 *04,087*

Laser Ablation of Thin Films as a Free Atom Source for Pulsed RIMS.
PB94-198710 *00,540*

Measurement of CO Pressures in the Ultrahigh Vacuum Regime Using Resonance-Enhanced Multiphoton-Ionization Time-of-Flight Mass Spectroscopy.
PB94-216041 *03,864*

New NIST/ARPA National Soft X-ray Reflectometry Facility.
PB96-158092 *04,080*

NIST Metrology for Soft X-ray Multilayer Optics.
PB96-160379 *04,088*

RIS Measurement of AC Stark Shifts and Photoionization Cross Sections in Calcium.
PB96-157953 *04,073*

RIS Studies of Autoionization in Calcium.
PB94-213295 *00,849*

Study of Laser Resonance Ionization Mass Spectrometry Using a Glow Discharge Source.
DE94018566 *03,308*

Study of Laser Resonance Ionization Mass Spectrometry Using a Glow Discharge Source.
PB96-123203 *03,360*

Upgraded Facility for Multilayer Mirror Characterization at NIST.
PB96-160387 *04,367*

Verification of the Ponderomotive Approximation for the ac Stark Shift in Xe Rydberg Levels.
PB94-185709 *03,801*

LUCE, M.
NIST SIMA Interactive Management Workshop. Held in Fort Belvoir, Virginia on November 14-16, 1994.
PB96-154877 *02,838*

LUCE, M. E.
Systems Integration for Manufacturing Applications Program 1995 Annual Report.
PB96-193735 *02,844*

LUCEY, G.
Evaluation and Qualification Standards for an X-Ray Laminography System.
PB94-172954 *02,029*

LUCK, R.
Real Time Differential Range Estimation Based on Time-Space Imagery Using PIPE.
PB95-161808 *01,844*

LUDWIG, B.
Isolation and Structural Elucidation of the Predominant Geometrical Isomers of alpha-Carotene.
PB96-190061 *00,640*

LUDWIG, F.
Fabrication Issues in Optimizing YBa2Cu3O7-x Flux Transformers for Low l/f Noise.
PB95-175857 *02,059*

Low Noise YBa2Cu3O7-x-SrTiO3-YBa2Cu3O7-x Mulitlayers for Improved Superconducting Magnetometers.
PB96-138417 *04,747*

LUDWIG, H. R.
Documentation for Immediately Dangerous to Life or Health Concentrations (IDLHs).
PB94-195047 *03,602*

LUDWIG, K. F.
Coexistence of Grains with Differing Orthorhombicity in High Quality YBa2Cu3O7-delta Thin Films.
PB96-135033 *04,742*

Increased Transition Temperature in In situ Coevaporated YBa2Cu3O7-delta Thin Films by Low Temperature Post-Annealing.
PB95-180071 *04,672*

LUECKE, W.
Cavity Evolution during Tensil Creep of Si3N4.
PB96-204193 *03,376*

LUECKE, W. E.
Cavitation Contributes Substantially to Tensile Creep in Silicon Nitride.
PB96-122577 *03,171*

Sources of Strain-Measurement Error in Flag-Based Extensometry.
PB97-118731 *03,108*

Tension/Compression Creep Asymmetry in Si3N4.
PB97-110258 *03,096*

LUGEZ, C. L.
Matrix Isolation Study of the Interaction of Excited Neon Atoms with O3: Infrared Spectrum of O((sub 3)(-)) and Evidence for the Stabilization of O2...O((sub 4)(+)).
PB97-112403 *04,155*

Microwave Spectrum and Structure of CH2O-H2O.
PB97-118723 *04,168*

Vibrational Spectra of Molecular Ions Isolated in Solid Neon. 13. Ions Derived from HBr and HI.
PB97-119234 *01,188*

LUJAN, A.
Gaseous Electronics Conference Radio-Frequency Reference Cell: A Defined Parallel-Plate Radio-Frequency System for Experimental and Theoretical Studies of Plasma-Processing Discharges.
PB94-172327 *04,404*

LUKASHEV, E. P.
Bacteriorhodopsin Retains Its Light-Induced Proton-Pumping Function After Being Heated to 140C.
PB96-102728 *03,471*

Rapid pH Change Due to Bacteriorhodopsin Measured with a Tin-Oxide Electrode.
PB96-112081 *03,544*

LUM, L. S. H.
Ceramic Powders Characterization: Results of an International Laboratory Study.
PB95-270039 *02,672*

Characterization of Phase and Surface Composition of Silicon Carbide Platelets.
PB94-216264 *03,043*

Statistical Analysis of Parameters Affecting the Measurement of Particle-Size Distribution of Silicon Nitride Powders by Sedigraph (Trade Name).
PB94-216249 *03,042*

LUMIA, R.
Evolution of the Flight Telerobotic Servicer.
PB94-216082 *04,832*

Overview of NASREM: The NASA/NBS Standard Reference Model for Telerobot Control System Architecture.
PB94-194560 *04,831*

Unified Telerobotic Architecture Project (UTAP) Standard Interface Environment (SIE), May 1995.
PB95-242350 *02,938*

World Model Registration for Effective Off-Line Programming of Robots.
PB94-173010 *02,933*

LUMPKIN, J.
Tert-Butyl Hydroperoxide-Mediated DNA Base Damage in Cultured Mammalian Cells.
PB94-182003 *03,644*

LUMSDAINE, A.
IML++ v.1.2 Iterative Methods Library Reference Guide.
PB96-195219 *01,776*

SparseLib++ v. 1.5 Sparse Matrix Class Library. Reference Guide.
PB96-193636 *01,775*

LUNDEGARD, R. J.
Statistical Quality Control Technology in Japan.
PB94-199064 *02,708*

LUNDQVIST, M.
Inner-Valence States CO(+) between 22 eV and 46 eV Studied by High Resolution Photoelectron Spectroscopy and ab Initio CI Calculations.
PB95-180055 *03,961*

LUO, J.
Grain Alignment and Transport Properties of Bi2Sr2CaCu2O8 Grown by Laser Heated Float Zone Method.
PB95-161451 *04,602*

LUPER, W. D.
Effect of Three Sterilization Techniques on Finger Pluggers.
PB94-216090 *00,150*

LUPO, J.
Real Time Differential Range Estimation Based on Time-Space Imagery Using PIPE.
PB95-161808 *01,844*

Real-Time Implementation of a Differential Range Finder.
PB95-108650 *01,839*

LUTGEN, C. L.
Electromechanical properties of superconductors for DOE fusion applications.
DE95015476 *04,432*

Electromechanical Properties of Superconductors for DOE Fusion Applications.
PB94-139672 *02,250*

LUTTERMOSER, D. G.
Peeking Through the Picket Fence: What Astrophysical Surprises May Be Present in the 100-1200 Angstrom Region.
PB95-202859 *00,082*

LUTZ, G. J.
High-Sensitivity Determination of Iodine Isotopic Ratios by Thermal and Fast Neutron Activation.
PB94-213386 *00,555*

LYELL, M. J.
Internal Waves in Xenon Near the Critical Point.
PB97-111504 *04,221*

LYKE, J.
Overview of U.S. Government Advanced Packaging Programs.
PB96-200845 *02,443*

LYLE, J. R.
Application of the Pointer State Subgraph to Static Program Slicing.
PB96-167838 *01,768*

Assessing Functional Diversity by Program Slicing.
PB96-160890 *03,734*

Program Slicing.
PB96-160981 *01,761*

Software Safety and Program Slicing.
PB95-125894 *01,703*

Unravel: A CASE Tool to Assist Evaluation of High Integrity Software. Volume 1. Requirements and Design.
PB95-267886 *01,736*

Unravel: A CASE Tool to Assist Evaluation of High Integrity Software. Volume 2. User Manual.
PB95-267894 *01,737*

LYLES, S.
Directory of Law Enforcement and Criminal Justice Associations and Research Centers.
PB96-178918 *04,872*

LYMBEROPOULOS, D. P.
Two-Dimensional Self-Consistent Radio Frequency Plasma Simulations Relevant to the Gaseous Electronics Conference RF Reference Cell.
PB96-113436 *02,398*

LYNCH, J. J.
Modified Leung-Griffiths Model of Vapor-Liquid Equilibrium: Extended Scaling and Binary Mixtures of Dissimilar Fluids.
PB94-216108 *00,851*

Nonlinear Correlation of High-Pressure Vapor-Liquid Equilibrium Data for Ethylene + n-Butane Showing Inconsistencies in Experimental Compositions.
PB96-161906 *01,141*

LYNCH, T. P.
External Gamma-ray Counting of Selected Tissues from a Thorotrast Patient.
PB96-160254 *03,637*

LYNN, J. E.
Intermediate Structure in the Neutron-Induced Fission Cross Section of 236U.
PB94-185741 *03,802*

LYNN, J. W.
Analytic Calculation of Polarized Neutron Reflectivity from Superconductors.
PB95-164224 *04,629*

Coupled-Bilayer Two-Dimensional Magnetic Order of the Dy Ions in Dy2Ba4Cu7O15.
PB95-152104 *04,584*

Crystal Structure and Magnetic Ordering of the Rare-Earth and Cu Moments in RBa2Cu2NbO8(R=Nd,Pr).
PB95-140554 *04,546*

Crystal Structure of Annealed and As-Prepared HgBa2CaCu2O6+delta Superconductors.
PB95-161105 *03,927*

Crystallographic and Magnetic Properties of UAuSn.
PB95-140521 *04,543*

Dispersions of Magnetic Excitations of the Pr Ions in Pr2CuO4.
PB94-173044 *04,444*

Field Dependence of the Magnetic Ordering of Cu in R2CuO4 (R = Nd, Sm).
PB95-164521 *04,633*

Incommensurate Magnetic Order in UPtGe.
PB95-140513 *04,542*

Magnetic Neutron Scattering (Invited).
PB95-150074 *04,557*

Magnetic Ordering of the Cu Spins in PrBa2Cu3O6+x.
PB95-140547 *04,545*

Magnetic Properties of Single-Crystalline UCu3Al2.
PB95-180717 *04,686*

Magnetic Structure and Spin Dynamics of the Pr and Cu in Pr2CuO4.
PB96-111836 *04,036*

Neutron Powder Diffraction Study of the Nuclear and Magnetic Structures of the Oxygen-Deficient Perovskite YBaCuCoO5.
PB95-161097 *00,954*

Neutron Scattering Study of Antiferromagnetic Order in the Magnetic Superconductors RNi2B2C.
PB97-112411 *04,812*

New Exact Solution of the One-Dimensional Schrodinger Equation and Its Application to Polarized Neutron Reflectometry.
PB95-161832 *04,609*

Observation of Noncollinear Magnetic Structure for the Cu Spins in Nd2CuO4-Type Systems.
PB95-164539 04,634

Observation of Oscillatory Magnetic Order in the Antiferromagnetic Superconductor HoNi2B2C.
PB95-180303 04,679

Oxygen Dependance of the Crystal Structure of HgBa2CuO4+ and Its Relation to Superconductivity.
PB96-102512 04,711

Phonon Density of States in R2CuO4 and Superconducting R1.85Ce0.15CuO4 (R = Nd, Pr).
PB95-150686 04,574

Polarization Analysis of the Magnetic Excitations in Fe65Ni35 Invar.
PB95-150082 04,558

Polarization Analysis of the Magnetic Excitations in Invar and Non-Invar Amorphous Alloys.
PB94-216116 04,516

Quasielastic and Inelastic Neutron-Scattering Studies of ((CD3)3ND)FeCl3.2D2O: A One-Dimensional Ising Ferromagnet.
PB95-140562 04,547

Temperature Dependence of the Magnetic Excitations in Ordered and Disordered Fe72Pt28.
PB95-150223 04,563

Unconventional Ferromagnetic Transition in La(sub 1-x)Ca(sub x)MnO3.
PB97-112429 04,156

Vortex Dynamics and Melting in Niobium.
PB96-112362 02,073

LYON, G.

Computing Effects and Error for Large Synthetic Perturbation Screenings.
PB94-139623 01,675

Scalability Test for Parallel Code.
PB96-146758 01,749

Simple Scalability Test for MIMD Code.
PB94-193638 01,688

Synthetic-Perturbation Tuning of MIMD Programs.
PB94-185568 01,687

Time-Perturbation Tuning of MIMD Programs.
PB94-164399 01,681

Time-Perturbation Tuning of MIMD Programs.
PB94-172566 01,684

Using Synthetic-Perturbation Techniques for Tuning Shared Memory Programs (Extended Abstract).
PB94-172657 01,685

Using Synthetic Perturbations and Statistical Screening to Assay Shared-Memory Programs.
PB96-103031 01,740

LYON, R.

Materials and Fire Threat.
PB97-122311 01,442

LYONS, K. W.

Design Engineering Research at NIST.
PB95-267860 02,784

Product Realization Process Modeling: A Study of Requirements, Methods and Research Issues.
PB96-147962 02,836

LYONS, R. M.

Bibliography of the NIST Electromagnetic Fields Division Publications.
PB94-165990 01,875

Bibliography of the NIST Electromagnetic Fields Division Publications.
PB95-135562 01,886

Bibliography of the NIST Electromagnetic Fields Division Publications.
PB96-210778 01,980

LYZAK, W. A.

Diagnosis and Treatment of an Oral Base-Metal Contact Lesion Following Negative Dermatologic Patch Tests.
PB95-180626 00,172

MA, D. I.

Interaction of Stoichiometry, Mechanical Stress, and Interface Trap Density in LPCVD Si-rich SiNx-Si Structures.
PB95-176301 02,366

MA, L. M.

Mechanical Properties and Warm Prestress of Ultra-Low Carbon Steel at 4 K.
PB96-190350 03,224

MA, L. S.

Delivering the Same Optical Frequency at Two Places: Accurate Cancellation of Phase Noise Introduced by an Optical Fiber or Other Time-Varying Path.
PB96-102736 04,332

MA, M. T.

Aperture Excitation of Electrically Large, Lossy Cavities.
PB94-145711 00,029

Aperture Excitation of Electrically Large, Lossy Cavities.
PB95-175675 00,031

Assessment of Data by a Second-Order Transfer Function.
PB95-182390 03,760

Characterization of Unknown Linear Systems Based on Measured CW Amplitude.
PB95-161485 01,897

Data Evaluation of a Linear System by a Second-Order Transfer Function.
PB96-200282 01,970

MACADAM, K. B.

Alignment in Two-Step Pulsed Laser Excitation of Rydberg Levels in Light Atoms: The Example of Sodium.
PB95-202883 03,993

Low-Energy-Electron Collisions with Sodium: Elastic and Inelastic Scattering from the Ground State.
PB96-103106 04,030

Narrow-Band Tunable Diode Laser System with Grating Feedback, and a Saturated Absorption Spectrometer for Cs and Rb.
PB95-202891 04,319

MACCREHAN, W. A.

Determination of Vitamin K1 in Serum Using Catalytic-Reduction Liquid Chromatography with Fluorescence Detection.
PB96-138425 03,506

Separation and Identification of Organic Gunshot and Explosive Constituents by Micellar Electrokinetic Capillary Electrophoresis.
PB95-107249 00,566

MACDONALD, M. A.

Electron-Ion-X-ray Spectrometer System.
PB95-176137 03,958

Evolution of X-ray Resonance Raman Scattering into X-ray Fluorescence from the Excitation of Xenon Near the L3 Edge.
PB96-102751 04,025

MACDONALD, M. E.

Niobium Microbolometers for Far-Infrared Detection.
PB96-111729 02,184

MACDONALD, R. A.

Analytical Method for Determining Thermal Conductivity from Dynamic Experiments.
PB96-102744 04,024

Analytical Method of Determining the Heat Capacity at High Temperatures from the Surface Temperature of a Cooling Sphere.
PB94-216124 03,865

MACHIN, G.

Intercomparison of the ITS-90 Radiance Temperature Scales of the National Physical Laboratory (U.K.) and the National Institute of Standards and Technology.
PB96-113550 02,674

MACKAY, D. R.

Performance Standards: The Pro's and Con's.
PB94-216132 02,896

MACKAY, J.

Taguchi's Parameter Design: A Panel Discussion.
PB96-111802 03,445

MACKEY, E.

Development of Frozen Whale Blubber and Liver Reference Materials for the Measurement of Organic and Inorganic Contaminants.
PB95-151676 00,587

MACKEY, E. A.

Analytical Applications of Guided Neutron Beams.
PB96-112347 04,041

Concentrations of Chlorinated Hydrocarbons, Heavy Metals and Other Elements in Tissues Banked by the Alaska Marine Mammal Tissue Archival Project.
PB95-209870 02,590

Effects of Target Shape and Neutron Scattering on Element Sensitivities for Neutron-Capture Prompt Gamma-ray Activation Analysis.
PB94-216157 00,558

Effects of Target Temperature on Analytical Sensitivities of Cold-Neutron Capture Prompt gamma-ray Activation Analysis.
PB96-112131 00,616

Neutron Capture Prompt Gamma-Ray Activation Analysis at the NIST Cold Neutron Research Facility.
PB94-213394 00,556

Neutron Scattering by Hydrogen in Cold Neutron Prompt Gamma-Activation Analysis.
PB95-175972 00,603

Relationship of Silver with Selenium and Mercury in the Liver of Two Species of Toothed Whales (Odontocetes).
PB96-167275 02,596

Scattering and Absorption Effects in Neutron Beam Activation Analysis Experiments.
PB94-216140 00,557

Trace Element Concentrations in Cetacean Liver Tissues Archived in the National Marine Mammal Tissue Bank.
PB96-167127 02,595

Use of Neutron Beams for Chemical Analysis at NIST.
PB97-112437 00,652

MACKIE, N.

High-Sensitivity Spectroscopy with Diode Lasers.
PB95-175477 04,297

MACREYNOLDS, K.

Planar Near-Field Measurements and Microwave Holography for Measuring Aperture Distribution on a 60 GHz Active Array Antenna.
PB96-167366 03,762

MACURDY, L. B.

Precision Laboratory Standards of Mass and Laboratory Weights.
AD-A280 562/0 02,618

MADEY, T. E.

Desorption Induced by Electronic Transitions.
PB94-216173 00,853

Influence of Coadsorbed Potassium on the Electron-Stimulated Desorption of F(+), F(-), and F(*) from PF3 on Ru(0001).
PB96-157946 04,072

Role of Adsorbed Alkalis in Desorption Induced by Electronic Transitions.
PB94-172574 00,762

Structure of Molecules on Surfaces as Determined Using Electron-Stimulated Desorption.
PB94-216165 00,852

MADIGAN, B.

Through-the-Arc Sensing for Measuring Gas Metal Arc Weld Quality in Real Time.
PB95-164463 02,908

MADIGAN, R. B.

Computers in Welding: A Primer.
PB95-162863 02,862

Contact Tube Wear Detection in Gas Metal Arc Welding.
PB96-135330 02,872

Control of Gas-Metal-Arc Welding Using Arc-Light Sensing.
PB96-131461 02,869

Droplet Transfer Modes for a MIL 100S-1 GMAW Electrode.
PB95-209300 02,867

Electrode Extension Model for Gas Metal Arc Welding.
PB96-135074 02,871

Mapping the Droplet Transfer Modes for an ER100S-1 GMAW Electrode.
PB96-190095 03,295

Power Characteristics in GMAW: Experimental and Numerical Investigation.
PB96-190145 03,296

Sensing Droplet Detachment and Electrode Extension for Control of Gas Metal Arc Welding.
PB96-190160 0^ 297

Through-the-Arc Sensing for Monitoring Arc Welding.
PB94-185899 02,858

Through-the-Arc Sensing for Real-Time Measurement of Gas Metal Arc Weld Quality.
PB95-162871 02,863

MADIGOSKY, W. M.

Electro-Optical Sensor for Surface Displacement Measurements of Compliant Coatings.
PB94-198223 02,123

MADISON, D. H.

Connection between Superelastic and Inelastic Electron-Atom Collisions Involving Polarized Collision Partners.
PB95-202297 03,974

MADRZYKOWSKI, D.

Evaluation of Sprinkler Activation Prediction Methods.
PB96-141056 00,304

Fire Service and Fire Sciences: A Winning Combination.
PB95-150264 01,383

Flame Heights and Heat Release Rates of 1991 Kuwait Oil Field Fires.
PB96-119342 01,404

In situ Burning of Oil Spills: Mesoscale Experiments and Analysis.
PB95-163747 02,587

Office Work Station Heat Release Rate Study: Full Scale versus Bench Scale.
PB96-190178 01,428

Sprinkler Fire Suppression Algorithm.
PB94-216181 00,293

MADSEN, W. B.

Dual-Frequency Millimeter-Wave Radiometer Antenna for Airborne Remote Sensing of Atmosphere and Ocean.
PB96-112289 02,009

Dual Frequency mm-Wave Radiometer Antenna for Airborne Remote Sensing of Atmosphere and Ocean.
PB95-180378 02,006

MAGEE, J. W.

High-Temperature Adiabatic Calorimeter for Constant-Volume Heat Capacity Measurements of Compressed Gases and Liquids.
PB95-168860 00,989

Isochoric (p-p-T) Measurements on Liquid and Gaseous Air from 67 to 400 K at Pressures to 35 MPa.
PB96-167390 01,154

Measurements of Molar Heat Capacity at Constant Volume (Cv) for 1,1,1,2-Tetrafluoroethane (R134a).
PB95-168878 03,264

Molar Heat Capacity at Constant Volume for Air from 67 to 300 K at Pressures to 35 MPa.
PB96-163738 00,515

Molar Heat Capacity at Constant Volume for (xCO2 + (1-x)C2H6) from 220 to 340 K at Pressures to 35 MPa.
PB96-167135 01,148

New Data and Correlations for the Custody Transfer of Natural Gas Liquids.
PB96-176664 02,499

Thermophysical Properties of CO2 and CO2-Rich Mixtures.
PB94-216199 00,854

Vapour Pressure Measurements on 1,1,1,2-Tetrafluoroethane (R134a) from 180 to 350 K.
PB95-168886 03,265

MAGYAR, J.

High-Sensitivity Spectroscopy with Diode Lasers.
PB95-175477 04,297

MAIENSCHEIN, F. C.

Measurement of Absorbed Dose of Neutrons, and of Mixtures of Neutrons and gamma rays.
AD-A286 647/3 03,710

MAITZ, A. H.

Use of a Radiochromic Detector for the Determination of Stereotactic Radiosurgery Dose Characteristics.
PB94-185642 03,514

MAJKRZAK, C. F.

Antiferromagnetic Interlayer Correlations in Annealed Ni80Fe20/Ag Multilayers.
PB97-122220 03,109

Extending the Angular Range of Neutron Reflectivity Measurements from Planar Lipid Bilayers: Applications to a Model Biological Membrane.
PB96-122569 03,476

In-situ Neutron Reflectivity of MBE Grown and Chemically Processed Surfaces and Interfaces.
PB96-146634 02,416

Magnetic Dead Layer in Fe/Si Multilayer: Profile Refinement of Polarized Neutron Reflectivity Data.
PB94-198363 04,458

Magnetic Structure Determination for Annealed Ni80Fe20/Ag Multilayers Using Polarized-Neutron Reflectivity.
PB96-176615 03,739

Morphology of Symmetric Diblock Copolymers as Revealed by Neutron Reflectivity.
PB95-140075 01,234

Neutron Reflectometry Studies of Surface Oxidation.
PB95-150421 00,917

Neutron Scattering Studies of Surfaces and Interfaces.
PB94-216207 04,517

Neutron-Scattering Studies of the Two Magnetic Correlation Lengths in Terbium.
PB95-152328 04,586

Observation of Two Length Scales Above (T sub N) in a Holmium Thin Film.
PB97-111942 04,151

Origin of the Second Length Scale Above the Magnetic Spiral Phase of Tb.
PB95-153698 04,596

Supermirror Transmission Polarizers for Neutrons.
PB94-216215 03,866

Temperature Dependence of the Morphology of Thin Diblock Copolymer Films as Revealed by Neutron Reflectivity.
PB94-172756 01,199

MAJKRZAK, C. J.

Water Adsorption at a Polyimide/Silicon Wafer Interface.
PB96-103197 01,070

MAJURSKI, W.

Framework for National Information Infrastructure Services.
PB95-103719 02,723

MAJURSKI, W. J.

Open Systems Software Standards in Concurrent Engineering.
PB96-160932 01,758

Prototyping a Graphical User Interface for DHCP.
PB96-160544 02,599

MAKEPEACE, J. L.

Intercomparison of Internal Proportional Gas Counting of (85)Kr and (3)H.
PB94-185576 03,800

MAKI, A. G.

FTS Infrared Measurements of the Rotational and Vibrational Spectrum of LiH and LiD.
PB94-216231 00,856

High-Resolution Measurements of the nu2 and 2nu2-nu2 Bands of (34)S(16)O2.
PB94-216223 00,855

Improved Molecular Constants and Frequencies for the CO2 Laser from New High-J Regular and Hot-Band Frequency Measurements.
PB95-180634 04,312

Sub-Doppler Frequency Measurements on OCS at 87 Thz (3.4 micrometers) with the CO Overtone Laser: Considerations and Details.
PB95-128633 04,255

Sub-Doppler Frequency Measurements on OCS at 87 THz (3.4 mu m) with the CO Overtone Laser.
PB96-102215 04,330

MAKINEN, J.

Calibration of a Superconducting Gravimeter Using Absolute Gravity Measurements.
PB95-202651 03,684

Test of Newton's Inverse Square Law of Gravitation Using the 300-m Tower at Erie, Colorado.
PB95-202446 03,978

MALDONADO, E.

Investigation of Mercury Interstitials in Hg(1-x)CdxTe Alloys Using Resonant Impact-Ionization Spectroscopy.
PB94-213485 02,133

MALENFANT, A.

Frozen Human Serum Reference Material for Standardization of Sodium and Potassium Measurements in Serum or Plasma by Ion-Selective Electrode Analyzers.
PB94-185337 00,532

MALEWSKI, R.

Digital Techniques in HV Tests - Summary of 1989 Panel Session.
PB94-216702 02,035

MALGHAN, S. G.

Analysis of Physical Properties of Ceramic Powders in an International Interlaboratory Comparison Program.
PB95-161501 03,050

Ceramic Powders Characterization: Results of an International Laboratory Study.
PB95-270039 02,672

Characterization and Processing of Spray-Dried Zirconia Powders for Plasma Spray Application.
PB97-111231 04,419

Characterization of Phase and Surface Composition of Silicon Carbide Platelets.
PB94-216264 03,043

Coating of Fibers by Colloidal Techniques in Ceramic Composites.
PB94-216256 03,196

Densification of Nano-Size Powders. 1994 Report.
DE94013486 03,027

Deposition of Colloidal Sintering-Aid Particles on Silicon Nitride.
PB94-216272 03,044

Effects of Soxhlet Extraction on the Surface Oxide Layer of Silicon Nitride Powders.
PB95-175584 03,057

Electroacoustic Characterization of Particle Size and Zeta Potential in Moderately Concentrated Suspensions.
PB96-119425 01,079

Electroacoustics for Characterization of Particulates and Suspensions. Proceedings of a Workshop. Held in Gaithersburg, Maryland on February 3-4, 1993.
PB94-112695 00,725

Electrokinetic Sonic Analysis of Silicon Nitride Suspensions.
PB96-123575 03,073

Equipment for Investigation of Cryogenic Compaction of Nanosize Silicon Nitride Powders. 1993 Report.
DE94013593 03,028

Interface Modification and Characterization of Silicon Carbide Platelets Coated with Alumina Particles.
PB95-108734 03,121

NMR Characterization of Injection-Moulded Alumina Green Compacts. Part 2. T2-Weighted Proton Imaging.
PB96-201181 01,165

Polyelectrolytes as Dispersants in Colloidal Processing of Silicon Nitride Ceramics.
PB95-175568 03,055

Standard Reference Material for the Measurement of Particle Mobility by Electrophoretic Light Scattering.
PB96-102488 00,609

Statistical Analysis of Parameters Affecting the Measurement of Particle-Size Distribution of Silicon Nitride Powders by Sedigraph (Trade Name).
PB94-216249 03,042

Surface Chemical Interactions of Si3N4 with Polyelectrolyte Deflocculants.
PB95-175576 03,056

Surface Chemistry of Silicon Nitride Powder in the Presence of Dissolved Ions.
PB96-111760 01,073

Variances in the Measurement of Ceramic Powder Properties.
PB97-110316 03,100

MALIK, A.

Comparison of Selectivities for PCBs in Gas Chromatography for a Series of Cyanobiphenyl Stationary Phases.
PB96-119458 00,618

MALLARD, G.

Progress in the Development of a Chemical Kinetic Database for Combustion Chemistry.
PB95-151056 01,384

MALLEY, J. O.

Evaluation and Strengthening Guidelines for Federal Buildings: Identification of Current Federal Agency Programs.
PB94-176278 00,424

MALONE, K.

Using Secondary Ion Mass Spectrometry (SIMS) to Characterize Optical Waveguide Materials.
PB96-119599 04,340

MALONE, K. J.

Distributed Feedback Lasers in Rare-Earth-Doped Phosphate Glass.
PB96-123773 04,740

Glasses for Waveguide Lasers.
PB96-111950 04,335

Integrated Optic Laser Emitting at 905, 1057, 1356 nm.
PB94-216298 02,136

Integrated Optic Laser Emitting at 906, 1057, and 1358 nm.
PB94-216280 02,135

Integrated-Optical Devices in Rare-Earth-Doped Glass.
PB95-202909 02,179

Linewidth Narrowing in an Imbalanced Y-Branch Waveguide Laser.
PB95-140844 04,258

Nd:LiTaO3 Waveguide Laser.
PB95-140851 04,259

Passively Q-Switched Nd-Doped Waveguide Laser.
PB95-180048 04,308

Rare-Earth-Doped Waveguide Devices: The Potential for Compact Blue-Green Lasers.
PB95-140836 04,257

MALONE, W.

Determination of Oltipraz in Serum by High-Performanace Liquid Chromatography with Optical Absorbance and Mass Spectrometric Detection.
PB94-200201 03,493

MALONEY, D. L.

Prototyping a Graphical User Interface for DHCP.
PB96-160544 02,599

MALSHE, A. P.

Workshop on Characterizing Diamond Films (4th). Held in Gaithersburg, Maryland on March 4-5, 1996.
PB96-183090 04,786

MAMILETI, L.

Optical Fiber Geometry by Gray-Scale Analysis with Robust Regression.
PB95-161519 04,272

MANDEL, J.

Models and Interactions.
PB94-216306 02,641

MANDELKERN, L.

SANS Study of the Plastic Deformation Mechanism in Polyethylene.
PB95-151841 01,242

MANGAMELLI, A.

Chemical Aspects of Tool Wear in Single Point Diamond Turning.
PB97-112601 03,021

MANGIN, J. F.

Preliminary Comparison of Time Transfers via LASSO, GPS and Two-Way Satellite.
PB95-151098 01,529

MANGUM, B. W.

Comparisons of Some NIST Fixed-Point Cells with Similar Cells of Other Standards Laboratories.
PB97-119242 00,655

Current Status and Trends in Temperature Measurements at NIST, Cooperative Projects and New Mutual Agreement between NIST and IMGC.
PB97-110266 02,691

Direct Comparison of Three PTB Silver Fixed-Point Cells with the NIST Silver Fixed-Point Cell.
PB96-161286 00,628

Investigation of High-Temperature Platinum Resistance Thermometers at Temperatures Up to 962C, and, in Some Cases, 1064C.
PB96-161294 00,629

NIST Measurement Assurance of SPRT Calibrations on the ITS-90: A Quantitative Approach.
PB96-161336 00,633

Practical Applications of the ITS-90: Inherent Uncertainties.
PB95-161527 03,930

Preliminary Results of a Comparison of Water Triple-Point Cells Prepared by Different Methods.
PB96-161344 00,634

Reproducibility of the Temperature of the Ice Point in Routine Measurements.
PB95-255923 04,015

MANGUM, J. G.

Extended CO(7 yields 6) Emission from Warm Gas in Orion.
PB96-102504 00,090

MANHEIMER, M.

Magneto-Optic Magnetic Field Sensor with 1.4pT/square root of 1(Hz) Minimum Detectable Field at 1 kHz.
PB94-199551 02,125

MANKIEWICH, P. M.

Coexistence of Grains with Differing Orthorhombicity in High Quality YBa2Cu3O7-delta Thin Films.
PB96-135033 04,742

Increased Transition Temperature in In situ Coevaporated YBa2Cu3O7-delta Thin Films by Low Temperature Post-Annealing.
PB95-180071 04,672

Thermal Noise in High-Temperature Superconducting-Normal-Superconducting Step-Edge Josephson Junctions.
PB95-175089 04,650

MANN, D. B.

Helium Refrigeration and Liquefaction Using a Liquid Hydrogen Refrigerator for Precooling.
AD-A286 683/8 02,749

MANN, W. B.
NBS/NIST Peltier-Effect Microcalorimeter: A Four-Decade Review.
PB96-102769 *01,064*

MANNEY, C. H.
High-Resolution Atomic Spectroscopy of Laser-Cooled Ions.
PB95-169330 *03,953*
Recent Experiments on Trapped Ions at the National Institute of Standards and Technology.
PB95-169322 *03,952*

MANNING, J. R.
Electronics Packaging Materials Research at NIST.
PB96-122692 *02,405*
NIST/NCMS Program on Electronic Packaging: First Update.
PB96-204086 *03,008*

MANNING, M.
Charge Transfer and Collision-Induced Dissociation Reactions of CF(2+) and CF2(2+) with the Rare Gases at a Laboratory Collision Energy of 49 eV.
PB94-185584 *00,775*
Collision-Induced Neutral Loss Reactions of Molecular Dications.
PB94-185808 *00,780*

MANNING, N. O.
Protein Data Bank: Current Status and Future Challenges.
PB97-109060 *00,517*

MANOHAR, S.
Turbulent Upward Flame Spread on a Vertical Wall under External Radiation.
PB94-207388 *00,341*

MANSOOR, A.
Surging the Upside-Down House: Measurements and Modeling Results.
PB96-180138 *02,243*

MANSURIPUR, M.
Micromagnetic Structure of Domains in Co/Pt Multilayers. 1. Investigations of Wall Structure.
PB95-162111 *04,610*

MANTESE, J.
Effective Medium Theory for Ferrite-Loaded Materials.
PB95-154662 *01,893*

MANTESE, J. V.
Applicability of Effective Medium Theory to Ferroelectric/Ferrimagnetic Composites with Composition and Frequency-Dependent Complex Permittivities and Permeabilities.
PB96-157854 *01,945*

MANTL, S.
Silicon Surface Chemistry by IR Spectroscopy in the Mid- to Far-IR Region: H2O and Ethanol on Si(100).
PB96-138565 *01,097*

MANTOOTH, H. A.
Electro-Thermal Simulation of an IGBT PWM Inverter.
PB94-185592 *02,303*

MAO, G.
Inelastic-Neutron-Scattering Studies of Poly(p-phenylene vinylene).
PB95-180766 *01,014*

MARAN, S. P.
Observations of 3C 273 with the Goddard High Resolution Spectrograph on the Hubble Space Telescope
PB95-202321 *00,076*
Observing Stellar Coronae with the Goddard High Resolution Spectrograph. I. The dMe Star AU Microscopii.
PB96-102777 *00,092*

MARCARINO, P.
Comparisons of Some NIST Fixed-Point Cells with Similar Cells of Other Standards Laboratories.
PB97-119242 *00,655*

MARCHIANDO, J. F.
Application of the Collocation Method in Three Dimensions to a Model Semiconductor Problem.
PB97-122428 *02,457*
Scanning Capacitance Microscopy Measurements and Modeling for Dopant Profiling of Silicon.
PB96-164207 *04,781*
Scanning Capacitance Microscopy Measurements and Modeling: Progress Towards Dopant Profiling of Silicon.
PB96-148150 *04,773*
Scanning Capacitance Microscopy Measurements and Modeling: Progress Towards Dopant Profiling of Silicon.
PB96-180070 *01,964*
Using Collocation in Three Dimensions and Solving a Model Semiconductor Problem.
PB96-159249 *01,952*

MAREZIO, M.
Crystal Structure of Pb2Sr2YCu3O8+delta with delta=1.32, 1.46, 1.61, 1.71, by Powder Neutron Diffraction.
PB94-216314 *04,518*

MARGOLESE, D.
Small Angle Neutron Scattering Study of the Structure and Formation of MCM-41 Mesoporous Molecular Sieves.
PB97-122337 *03,110*

MARGOLESE, D. I.
Small Angle Neutron Scattering Study of the Structure and Formation of Ordered Mesopores in Silica.
PB96-111919 *03,069*

MARGOLIS, S.
Nutritional Status and Growth in Juvenile Rheumatoid Arthritis.
PB94-198470 *03,515*

MARGOLIS, S. A.
Amperometric Measurement of Moisture in Transformer Oil Using Karl Fischer Reagents.
PB96-146766 *00,623*
Ascorbic and Dehydroascorbic Acids Measured in Plasma Preserved with Dithiothreitol or Metaphorphoric Acid.
PB94-216330 *03,495*
Hydrolysis of Proteins by Microwave Energy.
PB94-216322 *03,528*
Measurement of Ascorbic Acid in Human Plasma and Serum: Stability, Intralaboratory Repeatability, and Interlaboratory Reproducibility.
PB97-112445 *03,511*
Thermochemistry of the Hydrolysis of L-arginine to (L-citrulline + Ammonia) and of the Hydrolysis of L-arginine to (L-ornithine + Urea).
PB95-150801 *03,463*

MARGRAVE, J. L.
Corrected Optical Pyrometer Readings.
AD-A279 949/2 *02,615*
Disilicides of Tungsten, Molybdenum, Tantalum, Titanium, Cobalt, and Nickel, and Platinum Monosilicide: A Survey of Their Thermodynamic Properties.
PB94-168580 *00,752*

MARINENKO, R.
Fabrication of Platinum-Gold Alloys in Pre-Hispanic South America: Issues of Temperature and Microstructure Control.
PB94-211646 *03,333*

MARINENKO, R. B.
Apparent Bias in the X-Ray Fluorescence Determination of Titanium in Selected NIST SRM Low Alloy Steels.
PB95-108759 *03,212*
Compositional Mapping of the Microstructure of Materials.
PB95-107199 *00,565*
Design of a Protocol for an Electron Probe Microanalyzer k-Value Round Robin.
PB95-107181 *00,564*
Epitaxial Growth of BaTiO3 Thin Films at 600C by Metalorganic Chemical Vapor Deposition.
PB96-122510 *03,071*
Study of Diffusion Zones with Electron Microprobe Compositional Mapping.
PB94-216348 *00,559*

MARINKOVIC, B.
Threshold Electron Excitation of Na.
PB95-202917 *03,994*

MARJENHOFF, W. A.
Adhesion of Composites to Dentin and Enamel.
PB94-199049 *00,144*
Development of an Adhesive Bonding System.
PB94-199056 *00,145*
Paffenbarger Research Center: The Cutting Edge of Dental Science.
PB94-216355 *00,151*
Posterior Restorative Materials Research.
PB97-118624 *03,582*
Publication and Presentation Abstracts, 1993. (Published by Paffenbarger Research Center and Center of Excellence for Materials Science Research).
PB95-153052 *03,562*
Publication and Presentation Abstracts, 1994.
PB96-176623 *03,577*
Publication and Presentation Abstracts, 1995.
PB96-164082 *03,576*
Publication and Presentation Abstracts, 1996.
PB97-122238 *03,585*
Publications and Presentation Abstracts, 1995. (Published by Paffenbarger Research Center and Center of Excellence for Materials Science Research).
PB96-119250 *03,568*

MARKIN, V. S.
Energy Transduction between a Concentration Gradient and an Alternating Electric Field.
PB94-216363 *03,461*

MARKO, P.
Characterization of the Adsorption-Fouling Layer Using Globular Proteins on Ultrafiltration Membranes.
PB94-212909 *00,842*

MARKOV, V. N.
Self Broadening in the nu1 Band of NH3.
PB94-216371 *00,857*

MARKOVIC, M.
Composition and Solubility Product of a Synthetic Calcium Hydroxyapatite.
PB96-180104 *02,995*
Crystal Structure of Calcium Succinate Monohydrate.
PB95-168928 *00,167*
Octacalcium Phosphate Carboxylates IV. Kinetics of Formation and Solubility of Octacalcium Phosphate Succinate.
PB94-185600 *00,776*
Octacalcium Phosphate Carboxylates. 1. Preparation and Identification.
PB95-161535 *00,660*
Octacalcium Phosphate Carboxylates. 2. Characterization and Structural Consideration.
PB95-161543 *00,955*
Octacalcium Phosphate Carboxylates. 5. Incorporation of Excess Succinate and Ammonium Ions in the Octacalcium Phosphate Succinate Structure.
PB95-168894 *00,166*
Octacalcium Phosphate. 3. Infrared and Raman Vibrational Spectra.
PB94-172244 *00,756*

MARKOVITS, G.
Learning to Change: Opportunities to Improve the Performance of Smaller Manufacturers.
PB94-166212 *00,010*

MARKOVITZ, P.
Guidelines for the Evaluation of Electronic Data Interchange Products.
PB96-172325 *01,506*
Security in Open Systems.
PB95-105383 *01,473*

MARKS, R. B.
Accuracy and Repeatability in Time Domain Network Analysis.
PB95-202644 *02,064*
Accuracy in Time Domain Transmission Line Measurements.
PB96-148069 *04,060*
Accurate Electrical Characterization of High-Speed Interconnections.
PB96-167143 *02,240*
Accurate Experimental Characterization of Interconnects: A Discussion of 'Experimental Electrical Characterization of Interconnects and Discontinuities in High-Speed Digital Systems'.
PB94-216389 *02,217*
Accurate Transmission Line Characterization.
PB95-151593 *02,220*
Calibrating On-Wafer Probes to the Probe Tips.
PB95-163945 *02,352*
Coaxial Line-Reflect-Match Calibration.
PB96-200118 *02,246*
Comments on 'Conversions between S, Z, Y, h, ABCD, and T Parameters Which Are Valid for Complex Source and Load Impedances'.
PB96-102785 *02,069*
Comments on 'Protecting EFIE-Based Scattering Computations from Effects of Internal Resonances'.
PB95-161568 *01,898*
Compensation for Substrate Permittivity in Probe-Tip Calibration.
PB95-203519 *01,915*
Electrical Measurements of Microwave Flip-Chip Interconnections.
PB96-176748 *02,436*
High-Speed Interconnection Characterization Using Time Domain Network Analysis.
PB96-148176 *04,061*
Interconnection Transmission Line Parameter Characterization.
PB94-216397 *02,218*
LRM Probe-Tip Calibrations Using Nonideal Standards.
PB96-135389 *02,411*
LRM Probe-Tip Calibrations with Imperfect Resistors and Lossy Lines.
PB95-163952 *02,353*
Microwave Characterization of Flip-Chip MMIC Components.
PB96-176722 *02,434*
Microwave Characterization of Flip-Chip MMIC Interconnections.
PB96-176730 *02,435*
Microwave Characterization of Printed Circuit Transmission Lines.
PB96-122585 *02,077*
Microwave Properties of Voltage-Tunable YBa2Cu3O7-delta/SrTiO3 Coplanar Waveguide Transmission Lines.
PB96-141262 *02,235*
On-Wafer Impedance Measurement on Lossy Substrates.
PB95-176285 *02,365*
Optimizing Time-Domain Network Analysis.
PB96-157821 *02,085*
Reciprocity Relations in Waveguide Junctions.
PB94-172814 *02,213*
Time Domain Network Analysis Using the Multiline TRL Calibration.
PB95-202925 *02,065*
Two-Tier Multiline TRL for Calibration of Low-Cost Network Analyzers.
PB96-157888 *01,947*
Verification of Commercial Probe-Tip Calibrations.
PB95-161576 *02,347*

Verification of Scattering Parameter Measurements.
PB95-163960 01,904

MARKS, R. F.

Combined Low- and High-Angle X-Ray Structural Refinement of a Co/Pt(111) Multilayer Exhibiting Perpendicular Magnetic Anisotropy.
PB94-198355 04,457

MARKS, T. J.

Suitability of Metalorganic Chemical Vapor Deposition-Derived PrGaO3 Films as Buffer Layers for YBa2Cu3O7-x Pulsed Laser Deposition.
PB95-168670 04,640

MARLOW, A.

Apparent Bias in the X-Ray Fluorescence Determination of Titanium in Selected NIST SRM Low Alloy Steels.
PB95-108759 03,212

MARQUARDT, E.

Design Equations and Scaling Laws for Linear Compressors with Flexure Springs.
PB95-168902 02,948

MARQUARDT, J.

High-Sensitivity Spectroscopy with Diode Lasers.
PB95-175477 04,297

MARQUARDT, J. H.

Optical Probing of Cold Trapped Atoms.
PB95-175469 04,296

MARR, G. V.

High Resolution Angle Resolved Photoelectron Spectroscopy Study of N2.
PB95-151494 03,907

MARSCHALL, E.

Comparison of Elastic and Plastic Contact Models for the Prediction of Thermal Contact Conductance.
PB95-161659 04,605

MARSH, K. N.

Thermodynamic and Thermophysical Properties of Organic Nitrogen Compounds. Part II. 1- and 2-Butanamine, 2-Methyl-1-Propanamine, 2-Methyl-2-Propanamine, Pyrrole, 1-, 2-, and 3-Methylpyrrole, Pyridine, 2-, 3-, and 4-Methylpyridine, Pyrrolidine, Piperidine, Indole, Quinoline, Isoquinoline, Acridine, Carbazole, Phenanthridine, 1- and 2-Naphthalenamine, and 9-Methylcarbazole.
PB94-162294 00,741

MARSHAK, H.

Precision Nuclear Orientation Measurements for Determining Mixed Magnetic Dipole/Electric Quadrupole Hyperfine Interactions.
PB94-199080 03,810

MARSHALL, H. E.

Economic Methods and Risk Analysis Techniques for Evaluating Building Investments: A Survey.
PB96-122593 00,323

Economics of New-Technology Materials: A Case Study of FRP Bridge Decking.
PB96-202353 01,349

Least-Cost Energy Decisions for Buildings: Part 2. Uncertainty and Risk Video Training Workbook.
PB94-165982 00,240

Least-Cost Energy Decisions for Buildings. Part 3. Choosing Economic Evaluation Methods. Video Training Workbook.
PB95-253597 00,265

Multiattribute Decision Analysis Method for Evaluating Buildings and Building Systems.
PB96-158670 00,325

Standards in Building Economics: Why We Need Them and How to Write Them.
PB94-216405 00,320

MARSHALL, J.

Realizing Suspended Structures on Chips Fabricated by CMOS Foundry Processes Through the MOSIS Service.
PB94-193984 01,881

MARSHALL, J. A.

Low Thermal Guarded Scanner for High Resistance Measurement Systems.
PB97-112452 02,288

MARSHALL, J. C.

Color Supplement to NIST Special Publication 400-93: Semiconductor Measurement Technology: Design and Testing Guides for the CMOS and Lateral Bipolar-on-SOI Test Library.
PB94-164316 02,298

Design Guide for CMOS-On-SIMOX. Test Chips NIST3 and NIST4.
PB94-163458 02,297

High-Level CAD Melds Micromachined Devices with Foundries.
PB94-216413 02,321

Semiconductor Measurement Technology: Design and Testing Guides for the CMOS and Lateral Bipolar-on-SOI Test Library.
PB94-178019 02,301

MARSHALL, R.

Some Notable Hurricanes Revisited.
PB96-122601 00,458

MARSHALL, R. D.

Comparison of Responses of a Select Number of Buildings to the 10/17/1989 Loma Prieta (California) Earthquake and Low-Level Amplitude Test Results.
PB96-159645 00,467

Dynamic Characteristics of Five Tall Buildings during Strong and Low-Amplitude Motions.
PB94-199981 00,427

Gust Factors Applied to Hurricane Winds.
PB95-180469 00,446

Lessons Learned by a Wing Engineer.
PB94-216421 00,429

Manufactured Homes: Probability of Failure and the Need for Better Windstorm Protection through Improved Anchoring Systems.
PB95-143129 00,432

Proceedings: Workshop on Research Needs in Wind Engineering. Held in Gaithersburg, Maryland on September 12-13, 1994.
PB95-189528 00,448

Recommended Performance-Based Criteria for the Design of Manufactured Home Foundation Systems to Resist Wind and Seismic Loads.
PB96-128285 00,460

Response of Buildings to Ambient Vibration and the Loma Prieta Earthquake: A Comparison.
PB96-119607 00,457

Wind Load Provisions of the Manufactured Home Construction and Safety Standards: A Review and Recommendations for Improvement.
PB94-206125 00,428

MARSHALL, T. A.

Low Thermal Guarded Scanner for High Resistance Measurement Systems.
PB97-112452 02,288

MARSHALL, W. J.

Colossal Magnetoresistance without Mn(3+)/Mn(4-) Double Exchange in the Stoichiometric Pyrochlore Tl2Mn2O7.
PB97-113070 04,160

MARTE, P.

Atomic Beam Splitters and Mirrors by Adiabatic Passage in Multilevel Systems.
PB94-216439 03,867

MARTENS, J. S.

Effects of Etching on the Morphology and Surface Resistance of YBa2Cu3O7-delta Films.
PB96-135355 02,410

MARTIN, A.

Assessing MOS Gate Oxide Reliability on Wafer Level with Ramped/Constant Voltage and Current Stress.
PB96-180112 04,115

New Oxide Degradation Mechanism for Stresses in the Fowler-Nordheim Tunneling Regime.
PB96-200985 04,128

MARTIN-CASALLO, M. T.

Standardization and Decay Scheme of Rhenium-186.
PB94-200490 03,830

MARTIN, J.

Non-Osmotic, Defect-Controlled Cathodic Disbondment of a Coating from a Steel Substrate.
PB94-216447 03,120

MARTIN, J. W.

Degradation of Powder Epoxy Coated Panels Immersed in a Saturated Calcium Hydroxide Solution Containing Sodium Chloride.
PB96-101050 01,344

Materials-Science Based Approach to Phenol Emissions from a Flooring Material in an Office Building.
PB97-118749 02,572

Methodologies for Predicting the Service Lives of Coating Systems.
PB95-146387 03,124

Performance Approach to the Development of Criteria for Low-Sloped Roof Membranes.
PB94-160751 00,329

Sorption of Moisture on Epoxy and Alkyd Free Films and Coated Steel Panels.
PB95-162475 03,192

Source of Phenol Emissions Affecting the Indoor Air of an Office Building.
PB94-154382 03,600

MARTIN, P.

Intercomparison of NIST, NPL, PTB, and VSL Thermal Voltage Converters from 100 kHz to 1 MHz.
PB94-172442 02,026

MARTIN, P. R.

National Voluntary Laboratory Accreditation Program Acoustical Testing Services.
PB95-182234 04,188

National Voluntary Laboratory Accreditation Program: Construction Materials Testing.
PB95-155552 01,319

National Voluntary Laboratory Accreditation Program: Ionizing Radiation Dosimetry.
PB95-128658 03,623

MARTIN, R. J.

Perspective on Software Engineering Standards.
PB95-171377 01,811

MARTIN, W. C.

Compilation of Energy Levels and Wavelengths for the Spectrum of Singly-Ionized Oxygen (O II).
PB94-162344 00,746

Designations of ds(2)p Energy Levels in Neutral Zirconium, Hafnium, and Rutherfordium (Z=104).
PB96-180120 04,116

Spectroscopic Data Tables for Highly-Ionized Atoms.
PB95-151585 03,910

Wavelengths and Energy Level Classifications for the Spectra of Sulfur (S I through S XVI).
PB94-162229 00,734

MARTINEZ, R. I.

Kinetics and Mechanism of the Collision-Activated Dissociation of the Acetone Cation.
PB94-216462 00,859

Precision and Accuracy in Tandem Mass Spectrometry Measurements: A Kinetics-Based Protocol for Instrument-Independent Measurements of Collision-Activated Dissociation in RF-Only Quadrupoles.
PB94-216454 00,858

MARTINIS, J. M.

Accuracy of the Electron Pump.
PB96-135223 04,743

Combined Josephson and Charging Behavior of the Supercurrent in the Superconducting Single-Electron Transistor.
PB95-168522 04,637

Electronic Microrefrigerator Based on a Normal-Insulator-Superconductor Tunnel Junction.
PB96-102827 04,718

Even-Odd Asymmetry of a Superconductor Revealed by the Coulomb Blockade of Andreev Reflection.
PB95-153540 04,593

Hot-Electron Microcalorimeter for X-ray Detection Using a Superconducting Transition Edge Sensor with Electrothermal Feedback.
PB96-200399 04,792

Hot-Electron Microcalorimeters as High-Resolution X-ray Detectors.
PB96-123641 04,739

Hot-Electron Microcalorimeters for X-ray and Phonon Detection.
PB95-168993 04,644

Hot-Electron-Microcalorimeters with 0.25 mm(2) Area.
PB96-200670 04,793

Measurement of the Weak-Localization Complex Conductivity at 1 Ghz in Disordered Ag Wires.
PB96-117239 04,731

Metrological Accuracy of the Electron Pump.
PB95-168910 03,951

Noise in the Coulomb Blockade Electrometer.
PB95-176327 04,670

Novel Hot-Electron Microbolometer.
PB96-201025 01,977

Observation of Hot-Electron Shot Noise in a Metallic Resistor.
PB97-112007 01,988

Performance of the Electron Pump with Stray Capacitances.
PB96-200902 01,976

Self-Biasing Cryogenic Particle Detector Utilizing Electrothermal Feedback and a SQUID Readout.
PB96-102538 04,712

Self-Heating in the Coulomb-Blockade Electrometer.
PB94-212685 04,507

Series Array of DC SQUIDs.
PB95-163861 02,046

Testing for Metrological Accuracy of the Electron Pump.
PB95-175873 04,663

Thermal Enhancement of Cotunneling in Ultra-Small Tunnel Junctions.
PB95-175436 04,658

Two-Stage Integrated SQUID Amplifier with Series Array Output.
PB95-176277 02,061

Ultrasensitive-Hot-Electron Microbolometer.
PB95-168985 02,163

Voltage Gain in the Single-Electron Transistor.
PB95-176335 04,671

MARTIRE, D. E.

Separation and Identification of Organic Gunshot and Explosive Constituents by Micellar Electrokinetic Capillary Electrophoresis.
PB95-107249 00,566

MARTYNOVA, L.

Flow Immunoassay Using Solid-Phase Entrapment.
PB96-200951 00,642

MARTYS, N.

Calculation of the Thermal Conductivity and Gas Permeability in a Uniaxial Bundle of Fibers.
PB95-180931 03,058

Cross-Property Relations and Permeability Estimation in Model Porous Media.
PB95-150280 04,205

Transport and Diffusion in Three-Dimensional Composite Media.
PB95-176129 04,668

MARTYS, N. S.

Application of Digital-Image-Based Models to Microstructure, Transport Properties, and Degradation of Cement-Based Materials.
PB96-156161 00,406

Hydraulic Radius and Transport in Reconstructed Model Three-Dimensional Porous Media.
PB96-123419 *00,403*

Survey of Concrete Transport Properties and Their Measurement.
PB95-220489 *00,396*

MARTZLOFF, F. D.

Cascading Surge-Protective Devices: Options for Effective Implementation.
PB94-216488 *02,464*

Classified Bibliography: Insulation Condition Monitoring Methods, 1989-1995.
PB96-131586 *02,232*

Coordinating Cascaded Surge Protection Devices: High-Low versus Low-High.
PB94-172061 *02,463*

Coordinating Cascaded Surge-Protective Devices: An Elusive Goal.
PB94-216496 *02,465*

Guarding Against Transients.
PB94-216470 *01,623*

Important Link in Entire-House Protection: Surge Reference Equalizers.
PB94-216504 *02,219*

Keeping Up with the Reality of Today's Surge Environment.
PB96-123633 *02,231*

Surging the Upside-Down House: Looking into Upsetting Reference Voltages.
PB96-112313 *02,385*

Surging the Upside-Down House: Measurements and Modeling Results.
PB96-180138 *02,243*

Technical Impact of the NIST Calibration Service for Electrical Power and Energy.
PB96-147913 *02,462*

MARUTHAMUTHU, P.

Ferric Ion Assisted Photooxidation of Halocetates.
PB97-112460 *00,521*

Solvent Effects in the Reactions of Peroxyl Radicals with Organic Reductants. Evidence for Proton Transfer Mediated Electron Transfer.
PB95-107157 *00,873*

MARX, E.

Alternative Single Integral Equation for Scattering by a Dielectric.
PB94-216512 *04,422*

Autocorrelation Functions from Optical Scattering for One-Dimensionally Rough Surfaces.
PB94-216538 *04,244*

Causality and Maxwell's Equations.
PB97-110522 *04,429*

Determination of Surface Roughness from Scattered Light.
PB94-216520 *04,243*

Electromagnetic Scattering from a Dielectric Wedge and the Single Hypersingular Integral Equation
PB97-110530 *04,430*

Hypersingular Single Integral Equation and the Dielectric Wedge.
PB97-110274 *04,428*

Light Scattered by Coated Paper.
PB94-216546 *04,245*

Light Scattering by Sinusoidal Surfaces: Illumination Windows and Harmonics in Standards.
PB97-110548 *04,387*

Light Scattering from Glossy Coatings on Paper.
PB94-213246 *04,242*

Numerical Evaluation of Hypersingular Integrals for Scattering by a Dielectric Wedge.
PB97-110555 *02,017*

Numerical Reference Models for Optical Metrology Simulation.
PB97-111330 *04,392*

Optical Scattering from Moderately Rough Surfaces.
PB97-110415 *04,385*

Point Charges, Radiation Reaction, and Quantum Mechanics.
PB97-110563 *04,139*

Positronium in Relativistic Quantum Mechanics.
PB97-110571 *04,140*

Present and Future Standard Specimens for Surface Finish Metrology.
PB97-110423 *02,928*

Regimes of Surface Roughness Measurable with Light Scattering.
PB95-151213 *04,265*

Relativistic Quantum Mechanics of Interacting Particles.
PB97-110589 *04,141*

SEM Linewidth Metrology of X-ray Lithography Masks.
PB96-201108 *02,447*

Sinusoidal Surfaces as Standards for BRDF Instruments.
PB97-110597 *04,388*

Spinor Equations in Relativistic Quantum Mechanics.
PB97-110605 *04,142*

User's Manual for the Program MONSEL-1: Monte Carlo Simulation of SEM Signals for Linewidth Metrology.
PB95-111522 *02,325*

Windowing Effects on Light Scattering by Sinusoidal Surfaces.
PB97-111215 *04,389*

X-ray Mask Metrology: The Development of Linewidth Standards for X-ray Lithography.
PB95-162129 *02,348*

MARYOTT, A. A.

Table of Dielectric Constants of Pure Liquids.
AD-A278 956/8 *00,712*

MASCHHOFF, B.

Influence of Coadsorbed Potassium on the Electron-Stimulated Desorption of F(+), F(-), and F(*) from PF3 on Ru(0001).
PB96-157946 *04,072*

MASON, J.

Low-Frequency, Active Vibration Isolation System.
PB95-203303 *02,710*

MASON, J. L.

Cryogenic Materials Data Handbook.
AD-A286 675/4 *03,303*

MASTERS, L.

Suggestions for a Logically-Consistent Structure for Service Life Prediction Standards.
PB95-125795 *00,358*

MASTERS, L. W.

Performance Approach to the Development of Criteria for Low-Sloped Roof Membranes.
PB94-160751 *00,329*

Technical Program of the Factory Automation Systems Division 1993.
PB94-160819 *02,805*

MASTERSON, K. D.

Optically Sensed EM-Field Probes for Pulsed Fields.
PB94-212594 *02,130*

MASTOWSKI, J.

Suppression of Ionization in One- and Two-Dimensional Model Calculations.
PB95-203600 *04,009*

MASUDA-JINDO, K.

Atomic Theory of Fracture of Brittle Materials: Application to Covalent Semiconductors.
PB94-216553 *04,519*

MASZARA, W. P.

Electron and Hole Trapping in Irradiated SIMOX, ZMR and BESOI Buried Oxides.
PB96-160320 *01,956*

MATAR, O.

Viscosity of the Saturated Liquid Phase of Six Halogenated Compounds and Three Mixtures.
PB95-162368 *00,960*

MATERSON, K. D.

Optically Linked Three-Loop Antenna System for Determining the Radiation Characteristics of an Electrically Small Source.
PB95-161915 *02,005*

MATHENY, A.

Enhanced Curie Temperatures and Magnetoelastic Domains in Dy/Lu Super Lattices and Films.
PB94-172665 *04,443*

MATHEW, M.

Crystal Structure of a New Monoclinic Form of Potassium Dihydrogen Phosphate Containing Orthophosphacidium Ion, (H4PO4)(sup+1).
PB96-111794 *04,725*

Crystal Structure of Calcium Adipate Monohydrate.
PB94-216579 *00,153*

Crystal Structure of Calcium Glutarate Monohydrate.
PB96-111893 *01,074*

Crystal Structure of Calcium Succinate Monohydrate.
PB95-168928 *00,167*

Crystal Structure of Decacalcium Tetrapotassium Hexakis (Pyrophosphate) Nonahydrate.
PB96-141064 *01,099*

Crystal Structure of Dicalcium Potassium Trihydrogen Bis(pyrophosphate) Trihydrate.
PB94-216561 *00,152*

MATHEWSON, A.

Assessing MOS Gate Oxide Reliability on Wafer Level with Ramped/Constant Voltage and Current Stress.
PB96-180112 *04,115*

New Oxide Degradation Mechanism for Stresses in the Fowler-Nordheim Tunneling Regime.
PB96-200985 *04,128*

MATHEY, R. G.

Corrosion Resistant Epoxy-Coated Reinforcing Steel.
PB94-185618 *01,307*

Earthquake Resistant Construction of Gas and Liquid Fuel Pipeline Systems Serving, or Regulated By, the Federal Government.
PB94-161999 *04,846*

MATHIOUDAKIS, M.

Rotational Modulation and Flares on RS Canum Venaticorum and BY Draconis Stars. XVI. IUE Spectroscopy and VLA Observations of C1182(=V 1005 Orionis) in October 1983.
PB94-185626 *00,050*

MATLOCK, D.

Ultrasonic Measurement of Sheet Anisotropy and Formability.
PB95-153235 *03,213*

MATLOCK, D. K.

Ductile Fracture and Tempered Martensite Embrittlement of 4140 Steel.
PB96-190285 *03,222*

Temperature-Induced Transition in Ductile Fracture Appearance of a Nitrogen-Strengthened Austenitic Stainless Steel.
PB96-190269 *03,221*

MATSKO, M. J.

Second Census Optical Character Recognition Systems Conference.
PB94-188711 *01,832*

MATSON, D. W.

Magnetometer Calibration Services.
PB97-113252 *01,993*

MATSUBUCHI, K.

In-Space Welding: Visions and Realities.
PB95-163234 *04,830*

MATSUDA, M.

High-Energy Phonon Dispersion in La1.85Sr0.15CuO4.
PB96-138458 *04,748*

MATSUMOTO, Y.

Evaluation of a Tapered Roller Bearing Spindle for High-Precision Hard Turning Applications.
PB96-160494 *02,700*

MATSUSHIMA, F.

Absolute Frequency Measurements of Methanol from 1.5 to 6.5 THz.
PB95-175881 *04,300*

Atomic Oxygen Fine Structure Splittings with Tunable Far Infrared Spectroscopy.
PB95-152203 *03,915*

MATSUSHITA, Y.

Localization of a Homopolymer Dissolved in a Lamellar Structure of a Block Copolymer Studied by Small-Angle Neutron Scattering.
PB95-161592 *01,253*

Molecular Weight Dependence of the Lamellar Domain Spacing of ABC Triblock Copolymers and Their Chain Conformation in Lamellar Domains.
PB95-161691 *01,254*

MATSUYA, S.

Formation of Hydroxyapatite in a Polymeric Calcium Phosphate Cement.
PB95-180642 *00,173*

Polymeric Calcium Phosphate Cements Derived from Poly(methyl vinyl ether-maleic acid).
PB96-164264 *00,180*

MATSUYA, Y.

Formation of Hydroxyapatite in a Polymeric Calcium Phosphate Cement.
PB95-180642 *00,173*

Polymeric Calcium Phosphate Cements Derived from Poly(methyl vinyl ether-maleic acid).
PB96-164264 *00,180*

Properties and Interactions of Oral Structures and Restorative Materials. Annual Report for Period October 1, 1990 to September 30, 1991.
PB94-160843 *03,558*

MATTHEWS, M. D.

Rapid Hot Pressing of Ultra-Fine PSZ Powders.
PB94-216587 *03,045*

MATTHIESEN, M. M.

Effects of Anneal Time and Cooling Rate on the Formation and Texture of Bi2Sr2CaCu2O8 Films.
PB95-161600 *04,603*

MATTINGLY, G. E.

Effects of Pipe Elbows and Tube Bundles on Selected Types of Flowmeters.
PB96-160999 *01,135*

Flowmeter Installation Effects Due to a Generic Header.
PB96-210893 *02,606*

Laser Doppler Velocimeter Studies of the Pipeflow Produced by a Generic Header.
PB95-226916 *02,602*

Summary Report of NIST's Industry-Government Consortium Research Program on Flowmeter Installation Effects: The 45 Degree Elbow.
PB95-143061 *04,204*

Summary Report of NIST's Industry-Government Consortium Research Program on Flowmeter Installation Effects with Emphasis on the Research Period, January-September 1991: The Reducer.
PB94-160736 *04,196*

MATTIS, R. L.

NIST/NCMS Program on Electronic Packaging: First Update.
PB96-204086 *03,008*

MATUSHIMA, F.

Far Infrared Laser Frequencies of CH3OD and N2H4.
PB96-119623 *04,341*

MAUER, F. A.

Ultrasonic Method for Reconstructing the Two-Dimensional Liquid-Solid Interface in Solidifying Bodies.
PB95-161782 *03,349*

MAUREY, J. R.

Certification of the Standard Reference Material 1473a, a Low Density Polyethylene Resin.
PB96-128251 *01,282*

Determination of the Weight Average Molecular Weight of Two Poly(Ethylene Oxides), SRM 1923 and SRM 1924.
PB94-217031 *01,230*

Recertification of the Standard Reference Material 1475A, a Linear Polyethylene Resin.
PB94-161932 *02,628*

MAUTNER, M.

Carbon Acidities of Aromatic Compounds. 1. Effects of In-Ring Aza and External Electron-Withdrawing Groups.
PB94-216595 *00,860*

MAVRIDIS, L. N.

Rotational Modulation and Flares on RS Canum Venaticorum and BY Draconis Stars. XVI. IUE Spectroscopy and VLA Observations of C1182(=V 1005 Orionis) in October 1983.
PB94-185626 *00,050*

MAVRODINEANU, R.

Standard Reference Materials: Glass Filters as a Standard Reference Material for Spectrophotometry - Selection, Preparation, Certification, and Use of SRM 930 and SRM 1930.
PB94-188844 *00,536*

MAXIMON, L. C.

Theoretical Aspects of Tagged Photon Facilities.
PB94-216611 *03,868*

MAY, A. D.

Simultaneous Forward-Backward Raman Scattering Studies of D2 Broadened by D2, He, and Ar.
PB95-162459 *00,961*

MAY, W. B.

Using Emulators to Evaluate the Performance of Building Energy Management Systems.
PB95-175774 *00,259*

MAY, W. E.

Determination of Polycyclic Aromatic Hydrocarbons by Liquid Chromatography.
PB95-151650 *00,585*

Standard Reference Materials for the Determination of Polycyclic Aromatic Hydrocarbons in Environmental Samples - Current Activities.
PB95-151668 *00,586*

MAYER, F.

Proceedings of the Workshop on the Federal Criteria for Information Technology Security. Held in Ellicot City, Maryland on June 2-3, 1993.
PB94-162583 *01,575*

MAYER, R.

Anisotropy of Polarized X-ray Emission from Atoms and Molecules.
PB95-163002 *04,621*

MAYERGOYZ, I.

Efficient Method to Compute the Maximum Transient Drain Current Overshoot in Silicon on Insulator Devices.
PB94-172483 *02,300*

MAYES, A. M.

Observed Frustration in Confined Block Copolymers.
PB95-150033 *01,238*

MAYFIELD, T.

Functional Security Criteria for Distributed Systems.
PB96-123492 *01,607*

Proceedings of the Workshop on the Federal Criteria for Information Technology Security. Held in Ellicot City, Maryland on June 2-3, 1993.
PB94-162583 *01,575*

MAYO, S.

Characterization of Interface Defects in Oxygen-Implanted Silicon Films.
PB94-216629 *02,322*

Charge Trapping and Breakdown Mechanism in SIMOX.
PB94-216637 *02,323*

Electrical Characterization of Integrated Circuit Metal Line Thickness.
PB96-138433 *02,414*

Electrical Method for Determining the Thickness of Metal Films and the Cross-Sectional Area of Metal Lines.
PB95-203170 *02,370*

Hg1-xCdxTe Characterization Measurements: Current Practice and Future Needs.
PB95-164299 *02,157*

Measurement of Patterned Film Linewidth for Interconnect Characterization.
PB96-148168 *02,420*

MAYS, C. W.

External Gamma-ray Counting of Selected Tissues from a Thorotrast Patient.
PB96-160254 *03,637*

MAYS, J. W.

Flow-Induced Structure in Polymers: Chapter 16. Shear-Induced Changes in the Order-Disorder Transition Temperature and the Morphology of a Triblock Copolymer.
PB96-123237 *03,127*

Influence of Shear on the Ordering Temperature of a Triblock Copolymer Melt.
PB96-163753 *01,288*

Shear-Excited Morphological States in a Triblock Copolymer.
PB94-172392 *01,196*

Shear-Induced Changes in the Order-Disorder Transition Temperature and the Morphology of a Triblock Copolymer.
PB97-118772 *03,130*

Shear-Induced Martensitic-Like Transformation in a Block Copolymer Melt.
PB96-119508 *01,277*

Time Dependent Small Angle Neutron Scattering Behavior in Triblock Copolymers Under Steady Shear.
PB94-172632 *01,198*

MCBRIDE, J.

Approach to Setting Performance Requirements for Automated Evaluation of the Parameters of High-Voltage Impulses.
PB94-185634 *01,878*

MCCABE, R. M.

NIST-Coordinated Standard for Fingerprint Data Interchange.
PB94-216645 *01,808*

Specification for Interoperability between Ballistic Imaging Systems. Part 1. Cartridge Cases.
PB96-195524 *01,860*

MCCABE, T. J.

Structured Testing: A Testing Methodology Using the Cyclomatic Complexity Metric.
PB97-114169 *01,784*

MCCALLEN, C. L.

Correlations between Flaw Tolerance and Reliability in Zirconia.
PB96-161922 *02,986*

MCCALLUM, D. S.

Scaling of the Nonlinear Optical Cross Sections of GaAs-AlGaAs Multiple Quantum-Well Hetero n-i-p-i's.
PB96-102793 *02,183*

MCCARTNEY, R.

Using a Multi-Layered Approach to Representing Tort Law Cases for Case-Based Reasoning.
PB96-160874 *00,135*

MCCAULEY, J. P.

Discontinuous Volume Change at the Orientational-Ordering Transition in Solid C60.
PB94-211828 *00,821*

MCCELLAND, J. J.

Uncertainty Intervals for Polarized Beam Scattering Asymmetry Statistics.
PB94-200342 *03,825*

MCCLELLAND, J. J.

Atom-Optical Properties of a Standing-Wave Light Field.
PB96-141072 *04,356*

Determination of Complex Scattering Amplitudes in Low-Energy Elastic Electron-Sodium Scattering.
PB94-216652 *03,869*

Laser-Focused Atomic Deposition.
PB95-161618 *04,604*

Laser Focused Atomic Deposition.
PB95-180659 *04,685*

Laser Focusing of Atoms: A Particle Optics Approach.
PB94-216660 *03,870*

Microlithography by Using Neutral Metastable Atoms and Self-Assembled Monolayers.
PB96-190038 *02,441*

Nanofabrication of a Two-Dimensional Array Using Laser-Focused Atomic Deposition.
PB96-119417 *04,732*

Nanostructure Fabrication via Direct Writing with Atoms Focused in Laser Fields.
PB95-150272 *04,564*

Nanostructure Fabrication via Laser-Focused Atomic Deposition (Invited).
PB96-204094 *04,132*

Simple, Compact, High-Purity Cr Evaporator for Ultrahigh Vacuum.
PB94-216678 *04,520*

Spin-Resolved Elastic Scattering of Electrons from Sodium.
PB95-161774 *03,933*

Using Atom Optics to Fabricate Nanostructures.
PB96-141247 *04,757*

MCCLELLAND, M. R.

Research and Development Activities in Electron Paramagnetic Resonance Dosimetry.
PB96-141288 *03,635*

MCCLOREY, M. J.

Microwave Properties of YBa2Cu3O7-x Films at 35 GHz from Magnetotransmission and Magnetoreflection Measurements.
PB95-168977 *04,643*

MCCLURE, J. L.

Measurement of the Heat of Fusion of Tungsten by a Microsecond-Resolution Transient Technique.
PB94-216686 *03,400*

Measurements of Thermophysical Properties of Nickel Near Its Melting Temperature by a Microsecond-Resolution Transient Technique.
PB96-102579 *04,210*

Radiance Temperatures (in the Wavelength Range 523-907 nm) of Group IV B Transition Metals Titanium, Zirconium, and Hafnium at Their Melting Points by a Pulse-Heating Technique.
PB96-102207 *03,356*

Radiance Temperatures (in the Wavelength Range 523-907 nm) of Group IVB Transition Metals Titanium, Zirconium, and Hafnium at Their Melting Points by a Pulse-Heating Technique.
PB96-135025 *02,677*

Simultaneous Measurement of Normal Spectral Emissivity by Spectral Radiometry and Laser Polarimetry at High Temperatures in Pulse-Heating Experiments: Application to Molybdenum and Tungsten.
PB97-118376 *02,694*

MCCOLLUM, M. J.

Correlation of Optical, X-ray, and Electron Microscopy Measurements of Semiconductor Multilayer Structures.
PB95-175279 *02,174*

MCCOLSKEY, G. W.

Recommended Changes in ASTM Test Methods D2512-82 and G86-84 for Oxygen-Compatibility Mechanical Impact Tests on Metals.
PB94-216694 *03,338*

MCCOLSKEY, J. D.

Absorption of Sound in Gases between 10 and 25 MHz: Argon.
PB94-199015 *04,183*

Aluminum-Lithium Alloys: Evaluation of Fracture Toughness by Two Test Standards, ASTM Method E 813 and E 1304.
PB96-190236 *03,374*

Composite Struts for SMES Plants.
PB95-155586 *02,507*

Gas-Coupled, Pulse-Echo Ultrasonic Crack Detection and Thickness Gaging.
PB96-147129 *04,847*

Influence of Specimen Absorbed Energy in LOX Mechanical-Impact Tests.
PB95-107355 *03,341*

Macro- and Microreactions in Mechanical-Impact Tests of Aluminum Alloys.
PB95-107348 *03,340*

Reaction Sensitivities of Al-Li Alloys and Alloy 2219 in Mechanical-Impact Tests.
PB94-172764 *03,314*

MCCOMB, R. B.

Molar Absorptivities of Bilirubin (NIST SRM 916A) and Its Neutral and Alkaline Azopigments.
PB94-211042 *03,456*

MCCOMB, T. R.

Approach to Setting Performance Requirements for Automated Evaluation of the Parameters of High-Voltage Impulses.
PB94-185634 *01,878*

Comparative Measurements of High-Voltage Impulses Using a Kerr Cell and a Resistor Divider.
PB94-172582 *02,028*

Digital Techniques in HV Tests - Summary of 1989 Panel Session.
PB94-216702 *02,035*

Investigation of the Effects of Aging on the Calibration of a Kerr-Cell Measuring System for High Voltage Impulses.
PB94-172384 *02,025*

MCCORMICK, M. J.

Lake Erie Water Temperature Data, Put-in-Bay, Ohio, 1918-1992.
PB96-202452 *03,692*

MCCOWAN, C. N.

Cryogenic Toughness of Austenitic Stainless Steel Weld Metals: Effect of Inclusions.
PB95-161261 *03,214*

Macro- and Microreactions in Mechanical-Impact Tests of Aluminum Alloys.
PB95-107348 *03,340*

Welding for Cryogenic Service.
PB95-162889 *02,852*

MCCOY, W.

Associated Object Model for Distributed Systems.
PB94-212016 *01,694*

Framework for National Information Infrastructure Services.
PB95-103719 *02,723*

Open Systems Software Standards in Concurrent Engineering.
PB96-160932 *01,758*

MCCRARY, V. R.

Optoelectronics and Optomechanics Manufacturing: An ATP Focused Program Development. Workshop Proceedings. Held in Gaithersburg, Maryland on February 15, 1995.
PB97-104186 *02,204*

MCCREA, S. P.

Bibliography of Computer Security Glossaries.
PB94-216710 *01,587*

MCCULLOUGH, E. C.

Use of a Radiochromic Detector for the Determination of Stereotactic Radiosurgery Dose Characteristics.
PB94-185642 *03,514*

MCCURLEY, M. F.

Optical Biosensor Using a Fluorescent, Swelling Sensing Element.
PB95-175899 *03,541*

Optical Control of Enzymatic Conversion of Sucrose to Glucose by Bacteriorhodopsin Incorporated into Self-Assembled Phosphatidylcholine Vesicles.
PB96-123344 *03,477*

MCDEVITT, S. C.

Correlation of HgCdTe Epilayer Defects with Underlying Substrate Defects by Synchrotron X-Ray Topography.
PB94-200714 *02,129*

MCDONALD, D. G.

Far-Infrared Kinetic Inductance Detector.
PB95-126348 *02,142*

Optical Performance of Photoinductive Mixers at Terahertz Frequencies.
PB95-168662 *02,161*

Partially Coherent Transmittance of Dielectric Lamellae.
PB96-148028 *04,359*

Proposed High-Accuracy Superconducting Power Meter for Millimeter Waves.
PB94-212669 *02,034*

Superconducting Kinetic Inductance Radiometer.
PB95-140083 *02,144*

Terahertz Detectors Based on Superconducting Kinetic Inductance.
PB95-168647 *02,160*

MCDONALD, R. C.

Business and Manufacturing Motivations for the Developing of Analytical Technology and Metrology for Semiconductors.
PB96-161948 *04,778*

MCDONOUGH, W.

Micromechanics of Fracture in Rubber-Toughened Epoxies.
PB94-212222 *03,011*

MCDONOUGH, W. G.

Review of Cure Monitoring Techniques for On-Line Process Control.
PB94-216728 *03,145*

MCEACHRAN, R. P.

Polarization of Light Emitted After Positron Impact Excitation of Alkali Atoms.
PB94-199734 *03,816*

MCELROY, D. L.

Comparison of Heat-Flow-Meter Tests from Four Laboratories.
PB95-126264 *00,365*

MCELROY, J.

Smoke Plume Trajectory from In situ Burning of Crude Oil in Alaska: Field Experiments.
PB96-131560 *02,594*

MCFADDEN, G. B.

Anisotropy of Interfaces in an Ordered Alloy: A Multiple-Order-Parameter Model.
PB96-131594 *04,741*

Asymptotic Behavior of Modulated Taylor-Couette Flows with a Crystalline Inner Cylinder.
PB94-199072 *04,469*

Boundary Integral Method for the Simulation of Two-Dimensional Particle Coarsening.
PB94-216744 *03,411*

Convection and Morphological Stability During Directional Solidification.
N95-14548/8 *03,310*

Convective Stability in the Rayleigh-Benard and Directional Solidification Problems: High-Frequency Gravity Modulation.
PB95-181145 *04,208*

Diffuse-Interface Description of Fluid Systems.
PB96-210711 *01,170*

Effect of Modulated Taylor-Couette Flows on Crystal-Melt Interfaces: Theory and Initial Experiments.
PB94-216736 *04,521*

Effects of Crystalline Anisotropy and Buoyancy-Driven Convection on Morphological Stability.
PB94-200441 *03,328*

Effects of Elastic Stress on the Stability of a Solid-Liquid Interface.
PB95-163028 *03,350*

Internal Waves in Xenon Near the Critical Point.
PB97-111504 *04,221*

Laplace's Equation and the Dirichlet-Neumann Map in Multiply Connected Domains. (NIST Reprint).
PB95-180295 *03,962*

Laser Melting of Thin Silicon Films.
PB94-199239 *04,471*

Lubrication Theory for Reactive Spreading of a Thin Drop.
PB95-189460 *02,865*

Lubrication Theory for Reactive Spreading of a Thin Drop.
PB96-123427 *04,214*

Morphological Development of Second-Phase Particles in Elastically-Stressed Solids.
PB95-181111 *03,355*

Morphological Stability.
PB95-153318 *04,591*

Notion of a xi-Vector and a Stress Tensor for a General Class of Anisotropic Diffuse Interface Models.
PB96-193776 *04,788*

Phase-Field Model for Solidification of a Eutectic Alloy.
PB95-147914 *03,345*

Rayleigh Instability for a Cylindrical Crystal-Melt Interface.
PB95-180667 *01,010*

Stagnant Film Model of the Effect of Natural Convection on the Dendrite Operating State.
PB96-146832 *04,765*

xi-Vector Formulation of Anisotropic Phase-Field Models: 3-D Asymptotics.
PB95-136628 *04,536*

Xi-Vector Formulation of Anisotropic Phase-Field Models: 3-D Asymptotics.
PB97-122550 *04,816*

MCGARAGHAN, S.

Summary of Federal Construction and Building R and D in 1994.
PB97-114250 *00,234*

MCGHIE, A. R.

Phase Transitions in Solid C70: Supercooling, Metastable Phases, and Impurity Effect.
PB95-150090 *00,914*

MCGINNIES, R. T.

X-Ray Attenuation Coefficients from 10 kev to 100 Mev.
AD-A279 289/3 *03,767*

MCGLAUFLIN, M. L.

Chemical Aspects of Tool Wear in Single Point Diamond Turning.
PB97-112601 *03,021*

MCGRATTAN, K.

Ignition and Subsequent Transition to Flame Spread in a Microgravity Environment.
N96-15584/1 *04,828*

MCGRATTAN, K. B.

Computing the Effect of Sprinkler Sprays on Fire Induced Gas Flow.
PB96-147111 *00,404*

Gravity-Current Transport in Building Fires.
PB96-147046 *01,415*

Ignition and Transition to Flame Spread Over a Thermally Thin Cellulosic Sheet in a Microgravity Environment.
PB96-160288 *04,837*

In situ Burning of Oil Spills: Mesoscale Experiments and Analysis.
PB95-163747 *02,587*

Large Eddy Simulations of Smoke Movement in Three Dimensions.
PB96-190012 *01,426*

Mathematical Modeling and Computer Simulation of Fire Phenomena.
PB95-180063 *00,384*

Numerical Simulation of Rapid Combustion in an Underground Enclosure.
PB96-183132 *01,424*

Smoke Plume Trajectory from In situ Burning of Crude Oil: Field Experiments.
PB96-200993 *02,597*

Smoke Plume Trajectory from In situ Burning of Crude Oil in Alaska: Field Experiments.
PB96-131560 *02,594*

Transition from Localized Ignition to Flame Spread Over a Thin Cellulosic Material in Microgravity.
PB96-155809 *04,835*

Transport by Gravity Currents in Building Fires.
PB97-119325 *01,441*

MCGUCKIN, R. S.

Diagnosis and Treatment of an Oral Base-Metal Contact Lesion Following Negative Dermatologic Patch Tests.
PB95-180626 *00,172*

MCGUIRE, E. G.

SQA Standards and Total Quality Management.
PB96-111844 *01,743*

MCGUIRE, T. J.

Noncontact Ultrasonic Inspection of Train Rails for Stress.
PB95-162673 *04,851*

Ultrasonic Measurement of Residual Stress in Railroad Wheel Rims.
PB95-140430 *04,849*

MCHENRY, H. I.

Hot-Deformation Apparatus for Thermomechanical Processing Simulation.
PB94-200136 *03,207*

Materials Reliability. Technical Activities, 1995.
PB96-183082 *02,999*

MCHUGH, M. P.

Test of Newton's Inverse Square Law of Gravitation Using the 300-m Tower at Erie, Colorado.
PB95-202446 *03,978*

MCILRATH, T. J.

Configuration-Dependent AC Stark Shifts in Calcium.
PB96-157995 *04,363*

RIS Measurement of AC Stark Shifts and Photoionization Cross Sections in Calcium.
PB96-157953 *04,073*

RIS Studies of Autoionization in Calcium.
PB94-213295 *00,849*

Verification of the Ponderomotive Approximation for the ac Stark Shift in Xe Rydberg Levels.
PB94-185709 *03,801*

MCILROY, A.

High-Resolution Infrared Overtone Spectroscopy of ArHF via Nd:YAG/Dye Laser Difference Frequency Generation.
PB94-211448 *00,816*

High-Resolution IR Laser-Driven Vibrational Dynamics in Supersonic Jets: Weakly Bound Complexes and Intramolecular Energy Flow.
PB94-216751 *00,862*

Intermolecular HF Motion in Ar(sub n)HF Micromatrices (n=1,2,3,4,): Classical and Quantum Calculations on a Pairwise Additive Potential Surface.
PB95-107025 *03,871*

Large Amplitude Skeletal Isomerization as a Promoter of Intramolecular Vibrational Relaxation in CH Stretch Excited Hydrocarbons.
PB95-202933 *01,036*

Sub-Doppler, Infrared Laser Spectroscopy of the Propyne 2nu1 Band: Evidence of z-Axis Coriolis Dominated Intramolecular State Mixing in the Acetylenic CH Stretch Overtone.
PB95-202941 *01,037*

MCINERNEY, M.

Condensed Catalogue of Electromagnetic Environment Measurements, 30 - 300 Hz.
PB95-162210 *01,899*

MCINERNEY, W.

Catalogue of Electromagnetic Environment Measurements, 30-300 Hz.
PB96-155452 *01,943*

MCINTOSH, M.

Sinusoidal Surfaces as Standards for BRDF Instruments.
PB97-110597 *04,388*

MCINTYRE, P. C.

Effects of Substrate Surface Steps on the Microstructure of Epitaxial Ba2YCu3O7-x Thin Films on (001) LaAlO3.
PB96-148184 *04,774*

Epitaxial Nucleation and Growth of Chemically Derived Ba2YCu3O7-x Thin Films on (001) SrTiO3.
PB96-190186 *04,787*

MCKEE, C. F.

Magnetic Fields in Star-Forming Regions: Observations.
PB96-123005 *00,100*

MCKELLAR, A. R. W.

Fundamental Torsion Band in Acetaldehyde.
PB94-212834 *00,840*

MCKENNA, G.

Using Torsional Dilatometry to Measure the Effects of Deformations on Physical Aging.
PB95-140901 *03,384*

MCKENNA, G. B.

Aging in Glasses Subjected to Large Stresses and Deformations.
PB95-107041 *03,235*

Anomalous Freezing and Melting of Solvent Crystals in Swollen Gels of Natural Rubber.
PB94-212321 *01,223*

Effect of Swelling on the Elasticity of Rubber: Localization Model Description.
PB94-211034 *01,216*

Glass Transition of Organic Liquids Confined to Small Pores.
PB94-212305 *00,833*

Hygrothermal Effects on the Performance of Polymers and Polymeric Composites: A Workshop Report. Held in Gaithersburg, Maryland on September 21-22, 1995.
PB96-183207 *03,180*

Influence of Physical Aging on the Yield Response of Model DGEBA + Poly(propylene oxide) Epoxy Glasses.
PB95-126363 *03,381*

Localization Model of Rubber Elasticity: Comparison with Torsional Data for Natural Rubber Networks in the Dry State.
PB95-107033 *03,195*

Melting Behavior of Organic Materials Confined in Porous Solids.
PB94-212313 *00,834*

Physics Required for Prediction of Long Term Performance of Polymers and Their Composites.
PB94-219243 *03,146*

Torsional Dilatometer for Volume Change Measurements on Deformed Glasses: Instrument Description and Measurements on Equilibrated Glasses.
PB94-211166 *03,379*

Torsional Relaxation and Volume Response during Physical Aging in Epoxy Glasses Subjected to Large Torsional Deformations.
PB95-140026 *03,383*

Vitrification and Crystallization of Organic Liquids Confined to Nanoscale Pores.
PB97-112304 *03,392*

Volume Recovery in Epoxy Glasses Subjected to Torsional Deformations: The Question of Rejuvenation.
PB95-140018 *03,382*

MCKENNEY, K.

Deletion Analysis of the Mini-P1 Plasmid Origin of Replication and the Role of E.coli DnaA Protein.
PB95-163911 *03,539*

DnaJ, DnaK, and GrpE Heat Shock Proteins are Required in 'ori'P1 DNA Replication Solely at the RepA Monomerization Step.
PB97-119382 *03,557*

Escherichis coli Cyclic AMP Receptor Protein Mutants Provide Evidence for Ligand Contacts Important in Activation.
PB96-201017 *03,592*

Function of DnaJ and DnaK as Chaperones in Origin-Specific DNA Binding by RepA.
PB95-151544 *03,533*

Mapping Domains in Proteins: Dissection and Expression of 'Escherichia coli' Adenylyl Cyclase.
PB96-155460 *03,478*

Small genomes: New initiatives in mapping and sequencing. Workshop summary report.
DE96014476 *03,451*

MCKINNEY, J. E.

Wear of Human Enamel against a Commercial Castable Ceramic Restorative Material.
PB95-161972 *00,161*

MCKITTERICK, J. B.

Electron and Hole Trapping in Irradiated SIMOX, ZMR and BESOI Buried Oxides.
PB96-160320 *01,956*

MCKNIGHT, M.

Relation between AC Impedance Data and Degradation of Coated Steel. 1. Effects of Surface Roughness and Contamination on the Corrosion Behavior of Epoxy Coated Steel.
PB94-213345 *03,189*

MCKNIGHT, M. E.

Development of a Test Method for Leaching of Lead from Lead-Based Paints Through Encapsulants.
PB96-154984 *03,128*

Lead Abatement in Buildings and Related Structures.
PB94-172038 *03,601*

MCLAUGHLIN, W. L.

Alcohol Solutions of Triphenyl-Tetrazolium Chloride as High-Dose Radiochromic Dosimeters.
PB96-135249 *03,716*

Anionic Triphenylmethane Dye Solutions for Low-Dose Food Irradiation Dosimetry.
PB96-135173 *03,715*

Calibration and Performance of GafChromic DM-100 Radiochromic Dosemeters.
PB97-119291 *00,703*

Calibration of Dosimeters for the Cryogenic Irradiation of Composite Materials Using an Electron Beam.
PB95-180964 *03,968*

Calibration of High-Energy Electron Beams by Use of Graphite Calorimeters.
PB95-161113 *04,598*

Calorimeters for Calibration of High-Dose Dosimeters in High-Energy Electron Beams.
PB96-135272 *04,055*

Colour Centres in LiF for Measurement of Absorbed Doses Up to 100 MGy.
PB97-118756 *04,169*

Dosimetry Systems for Radiation Processing.
PB96-135280 *03,717*

Effect of Formulation Changes on the Response to Ionizing Radiation of Radiochromic Dye Films.
PB97-119028 *04,171*

Electron and Proton Dosimetry with Custom-Developed Radiochromic Dye Films.
PB95-151106 *03,713*

ESR-Based Analysis in Radiation Processing.
PB95-161634 *03,931*

Food Irradiation Dosimetry.
PB95-180675 *00,041*

Inter-Laboratory Trials of the EPR Method for the Detection of Irradiated Meats Containing Bone.
PB96-161690 *00,042*

Investigation of Applicability of Alanine and Radiochromic Detectors to Dosimetry of Proton Clinical Beams.
PB96-146782 *03,636*

Measurement of Radial Dose Distributions Around Small Beta Particle Emitters Using High Resolution Radiochromic Foil Dosimetry.
PB95-164604 *03,518*

Needs for Brachytherapy Source Calibrations in the United States.
PB97-110092 *03,521*

New EPR Dosimeter Based on Polyvinylalcohol.
PB94-199700 *03,619*

New Method for Shielding Electron Beams Used for Head and Neck Cancer Treatment.
PB94-211430 *03,621*

Novel Radiochromic Films for Clinical Dosimetry.
PB97-119259 *03,641*

Orientation Effects on ESR Analysis of Alanine-Polymer Dosimeters.
PB96-146725 *03,720*

Oscillometric and Conductometric Analysis of Aqueous and Organic Dosimeter Solutions.
PB96-135256 *04,054*

Overview of a Radiation Accident at an Industrial Accelerator Facility.
PB97-122485 *02,612*

Radiation Accident at an Industrial Accelerator Facility.
PB95-140117 *02,575*

Radiation-Chemical Reaction of 2,3,5-Triphenyl-Tetrazolium Chloride in Liquid and Solid State.
PB96-146733 *01,124*

Radiation Process Data: Collection, Analysis, and Interpretation.
PB95-162632 *03,628*

Radiochromic Solid-State Polymerization Reaction.
PB95-180683 *01,271*

Radiochromic Solid-State Polymerization Reaction.
PB96-180146 *01,290*

Real Time Monitoring of Electron Processors.
PB96-135306 *03,719*

Research and Development Activities in Electron Paramagnetic Resonance Dosimetry.
PB96-141288 *03,635*

Temperature and Relative Humidity Dependence of Radiochromic Film Dosimeter Response to Gamma and Electron Radiation.
PB96-135298 *03,718*

Thin Dyed-Plastic Dosimeter for Large Radiation Doses.
PB95-107363 *03,872*

Use of a Radiochromic Detector for the Determination of Stereotactic Radiosurgery Dose Characteristics.
PB94-185642 *03,514*

MCLAY, M.

Validation Testing System Requirements. National PDES Testbed Report Series.
PB94-163482 *02,771*

MCLEAN, C. R.

Using Grafcet to Design Generic Controllers.
PB95-150827 *02,821*

MCLINDEN, M.

Need for, and Availability of, Working Fluid Property Data: Results from Annexes XIII and XVIII.
PB95-168969 *03,268*

MCLINDEN, M. O.

Annex 18: An International Study of Refrigerant Properties.
PB95-168936 *03,266*

Development of a Dual-Sinker Densimeter for High-Accuracy Fluid P-V-T Measurements.
PB95-168951 *03,267*

Development of a Dual-Sinker Densimeter for High-Accuracy Fluid P-V-T Measurements. Appendix A.
DE93019682 *02,620*

International Standard Equation of State for the Thermodynamic Properties of Refrigerant 123 (2,2-Dichloro- 1,1,1-Trifluoroethane).
PB96-176805 *03,294*

Physical Properties of Alternatives to the Fully Halogenated Chlorofluorocarbons.
PB96-119573 *03,279*

REFPROP Refrigerant Properties Database: Capabilities, Limitations, and Future Directions.
PB96-167150 *01,149*

Report of the Refrigeration, Air Conditioning and Heat Pumps Technical Options Committee.
PB96-176755 *03,293*

Simplified Cycle Simulation Model for the Performance Rating of Refrigerants and Refrigerant Mixtures.
PB94-199890 *03,255*

Thermodynamic Properties of R134a(1,1,1,2-Tetrafluoroethane).
PB95-168704 *00,988*

MCMAHON, B.

Role of Journals in Maintaining Data Integrity: Checking of Crystal Structure Data in 'Acta Crystallographica'.
PB97-109177 *04,806*

MCMICHAEL, R. D.

Analytical Expressions for Barkhausen Jump Size Distributions.
PB95-180345 *04,680*

Enhanced Magnetocaloric Effect in Gd3Ga5-xFexO12.
PB94-185659 *04,450*

Langevin Approach to Hysteresis and Barkhausen Modeling in Steel.
PB94-185675 *03,206*

Magnetocaloric Effect in Rapidly Solidified Nd-Fe-Al-B Materials.
PB94-185667 *04,451*

Method for Determining Both Magnetostriction and Elastic Modulus by Ferromagnetic Resonance.
PB95-150108 *02,974*

Monte Carlo and Mean-Field Calculations of the Magnetocaloric Effect of Ferromagnetically Interacting Clusters.
PB94-172087 *03,201*

MCMILLAN, C. S.

X-Ray Diffraction from Anodic TiO2 Films: In situ and Ex situ Comparison of the Ti(0001) Face.
PB94-185972 *00,782*

MCMILLIN, B. K.

In situ Characterization of Vapor Phase Growth of Iron Oxide-Silica Nanocomposites: Part 1. 2-D Planar Laser-Induced Fluorescence and Mie Imaging.
PB97-112478 *03,185*

MCMORROW, D. F.

Observation of Two Length Scales Above (T sub N) in a Holmium Thin Film.
PB97-111942 *04,151*

MCMULLEN, W. E.

Segmental Concentration Profiles of End-Tethered Polymers with Excluded-Volume and Surface Interactions.
PB97-119002 *00,654*

MCMURDIE, H. F.

Improved Crystallographic Data for Aluminum Niobate (AlNbO4).
PB95-107306 *04,523*

Powder X-ray Diffraction Data for Ca2Bi2O5 and C4Bi6O13.
PB96-161278 *04,777*

MCNAMARA, P. D.

Correlations between Flaw Tolerance and Reliability in Zirconia.
PB96-161922 *02,986*

MCNICHOL, A. P.

Comparative Study of Fe-C Bead and Graphite Target Performance with the National Ocean Sciences AMS (NOSAMS) Facility Recombinator Ion Source.
PB95-175790 *00,693*

MCWAID, T.

Progress Toward Accurate Metrology Using Atomic Force Microscopy.
PB96-146774 *02,417*

MCWAID, T. H.

Comparison of Elastic and Plastic Contact Models for the Prediction of Thermal Contact Conductance.
PB95-161659 *04,605*

Development of a Calibrated Atomic Force Microscope.
PB94-185683 *02,894*

Increasing the Value of Atomic Force Microscopy Process Metrology Using a High-Accuracy Scanner, Tip Characterization, and Morphological Image Analysis.
PB96-190293 *02,758*

MCWILLIAMS, F. F.

Dose Mapping of Radioactive Hot Particles Using Radiochromic Film.
PB95-162954 *03,714*

MEASE, N. E.

Electro-Optical Sensor for Surface Displacement Measurements of Compliant Coatings.
PB94-198223 *02,123*

MECHELS, S. E.

Optical Fiber Geometry: Accurate Measurement of Cladding Diameter.
PB95-151940 *04,266*

Precise Laser-Based Measurements of Zero-Dispersion Wavelength in Single-Mode Fibers.
PB96-201124 *01,511*

MECHOLSKY, J. J.

Study of Diffusion Zones with Electron Microprobe Compositional Mapping.
PB94-216348 *00,559*

MEDENDORP, N.

Texture Measurement of Sintered Alumina Using the March-Dollase Function.
PB96-179494 *04,784*

MEDINA, L. T.

First VAMAS USA Interlaboratory Comparison of High Temperature Superconductor Critical Current Measurements.
PB96-147178 *04,768*

USA Interlaboratory Comparison of Superconductor Simulator Critical Current Measurements.
PB96-147194 *04,770*

MEE, R. W.

Constant-Width Calibration Intervals for Linear Regression.
PB95-153524 *03,439*

MEERTS, W. L.

Microwave and Submillimeter Spectroscopy of Ar-NH3 States Correlating with Ar+NH3(j=1, k=1).
PB95-152211 *00,942*

Use of Extended Permutation-Inversion Groups in Constructing Hyperfine Hamiltonians for Symmetrical-Top Internal Rotor Molecules Like H3C-SiH3.
PB94-212032 *00,823*

MEGARIDIS, C. M.

Internal Droplet Circulation Induced by Surface-Driven Rotation.
PB97-119267 *02,500*

MEGENS, H. J. L.

Magneto-Optical Trapping of Metastable Xenon: Isotope-Shift Measurements.
PB95-151254 *03,905*

MEGGERS, K.

Measurements of the (237)Np(n,f) Cross Section.
PB97-119069 *04,173*

MEGGERS, W. F.
Arc Spectra of Gallium, Indium, and Thallium.
AD-A295 411/3 *00,718*

MEHL, J. B.
Greenspan Acoustic Viscometer for Gases.
PB96-204417 *04,220*

MEHTA, V. R.
Evidence of Crosslinking in Methyl Pendent PBZT Fiber.
PB97-112486 *03,393*

MEIERS, J. C.
Surface Roughness of Glass-Ceramic Insert. Composite Restorations: Assessing Several Polishing Techniques.
PB97-119010 *03,583*

MEIGS, B. M.
Voluntary Product Standard PS 1-95 Construction and Industrial Plywood.
PB96-178900 *03,406*

MEIJER, P. H. E.
Effect of Electrode-Polymer Interfacial Layers on Polymer Conduction. Part 2. Device Summary.
PB95-151155 *02,335*

Simulation of C60 Through the Plastic Transition Temperatures.
PB96-102546 *04,713*

MEIRON, D. I.
Boundary Integral Method for the Simulation of Two-Dimensional Particle Coarsening.
PB94-216744 *03,411*

MEKHONTSEV, S. N.
Results of a NIST/VNIIOFI Comparison of Spectral-Radiance Measurements.
PB97-113021 *04,159*

MEL'CUK, A. I.
Long-Lived Structures in Fragile Glass-Forming Liquids.
PB96-119565 *04,212*

MELMED, A. J.
Performance of a Reflectron Energy Compensating Mirror.
PB94-199460 *00,547*

MELROSE, J.
Structure and Rheology of Hard-Sphere Systems.
PB96-167333 *00,662*

MELROY, O. R.
X-Ray Diffraction from Anodic TiO2 Films: In situ and Ex situ Comparison of the Ti(0001) Face.
PB94-185972 *00,782*

MELVILLE, R. S.
History of NIST's Contributions to Development of Standard Reference Materials and Reference and Definitive Methods for Clinical Chemistry.
PB96-119706 *03,503*

MENACHE, M. G.
Microdosimetry and Cellular Radiation Effects of Radon Progency in Human Bronchial Airways.
PB95-152344 *03,625*

MENG, R. L.
Crystal Structure of Annealed and As-Prepared HgBa2CaCu2O6+delta Superconductors.
PB95-161105 *03,927*

MENG, W. G.
Experimental Assessment of Crack-Tip Dislocation Emission Models for an Al67Cr8Ti25 Intermetallic Alloy.
PB96-204466 *03,377*

MEOT-NER, M.
Proton Affinity Ladders from Variable-Temperature Equilibrium Measurements. 1. A Re-Evaluation of the Upper Proton Affinity Range.
PB94-216603 *00,861*

MERKLE, G.
Relaxation After a Temperature Jump Within the One Phase Region of a Polymer Mixture.
PB97-112494 *03,394*

Slow Dynamics of Segregation in Hydrogen-Bonded Polymer Blends.
PB96-123591 *01,281*

MERMELSTEIN, L. E.
Reinforcement of Cancellous Bone Screws with Calcium Phosphate Cement.
PB96-158001 *00,179*

MESSICK, C.
Assessing MOS Gate Oxide Reliability on Wafer Level with Ramped/Constant Voltage and Current Stress.
PB96-180112 *04,115*

Electric Field Dependent Dielectric Breakdown of Intrinsic SiO2 Films Under Dynamic Stress.
PB96-204102 *02,449*

Experimental Investigation of the Validity of TDDB Voltage Acceleration Models.
PB94-185949 *02,304*

Field and Temperature Acceleration of Time-Dependent Dielectric Breakdown in Intrinsic Thin SiO2.
PB94-185956 *02,305*

High Temperature Reliability of Thin Film SiO2.
PB95-150348 *02,333*

New Physics-Based Model for Time-Dependent- Dielectric-Breakdown.
PB96-186093 *02,440*

New Physics-Based Model for Time-Dependent- Dielectric-Breakdown.
PB96-201132 *02,448*

Time-Dependent Dielectric Breakdown of Intrinsic SiO2 Films under Dynamic Stress.
PB96-179478 *02,438*

MESSIER, R.
Effect of Stoichiometry on the Phases Present in Boron Nitride Thin Films.
PB96-102470 *04,710*

MESSINA, C. A.
Information Retrieval Using Key Words and a Structured Review.
PB95-161121 *03,724*

MESSMAN, J. D.
Standard Reference Materials: Glass Filters as a Standard Reference Material for Spectrophotometry - Selection, Preparation, Certification, and Use of SRM 930 and SRM 1930.
PB94-188844 *00,536*

MEYER, E. S.
Observation and Visible and uv Magnetic Dipole Transitions in Highly Charged Xenon and Barium.
PB96-138441 *04,056*

Polarization Measurements on a Magnetic Quadrupole Line in Ne-Like Barium.
PB97-113104 *04,161*

MEYER, J. D.
Joint DoD/NIST Workshop on International Manufacturing Systems Research and Development. Held in Rockville, Maryland on November 3-5, 1992. Proceedings.
PB96-109491 *02,931*

Proceedings of the Manufacturing Technology Needs and Issues: Establishing National Priorities and Strategies Conference. Held in Gaithersburg, Maryland on April 26-28, 1994.
PB95-206181 *02,930*

MEYER, J. L.
Selective Inhibition of Crystal Growth on Octacalcium Phosphate and Nonstoichiometric Hydroxyapatite by Pyrophosphate at Physiological Concentration.
PB94-211257 *00,147*

MEYER, W.
Bonding in Doubly Charged Diatomics.
PB95-164315 *00,976*

MEYYAPPAN, M.
One-Dimensional Modeling Studies of the Gaseous Electronics Conference RF Reference Cell.
PB96-113428 *02,397*

MICHAEL, J. R.
Phase Identification in a Scanning Electron Microscope Using Backscattered Electron Kikuchi Patterns.
PB97-109128 *04,804*

MICHALOSKI, J.
Configuration and Performance Evaluation of a Real-Time Robot Control System: A Skeleton Approach.
PB95-163895 *01,598*

Enhanced Machine Controller Architecture Overview.
PB94-142460 *02,802*

NIST Support to the Next Generation Controller Program: 1991 Final Technical Report.
PB94-163490 *02,808*

Reference Architecture for Machine Control Systems Integration: Interim Report.
PB95-144549 *02,820*

Unified Telerobotic Architecture Project (UTAP) Standard Interface Environment (SIE), May 1995.
PB95-242350 *02,938*

MICHALOSKI, J. L.
NIST RS274/NGC Interpreter Version 1.
PB94-187788 *02,814*

MICHEL, K. H.
Neutron and X-Ray Scattering Cross Sections of Orientationally Disordered Soild C60.
PB95-153300 *00,951*

Orientational Fluctuations, Diffuse Scattering, and Orientational Order in Solid C60.
PB97-119275 *04,176*

MICHELI, A. L.
Applicability of Effective Medium Theory to Ferroelectric/Ferrimagnetic Composites with Composition and Frequency-Dependent Complex Permittivities and Permeabilities.
PB96-157854 *01,945*

MIDURA, R. J.
Proteoglycan Inhibition of Calcium Phosphate Precipitation in Liposomal Suspensions.
PB94-211208 *00,658*

MIELENZ, K. D.
Comments on the Paper 'Wolf Shifts and Their Physical Interpretation under Laboratory Conditions'.
PB94-219391 *04,246*

Realization of New NIST Radiation Temperature Scales for the 1000 K to 3000 K Region, Using Absolute Radiometric Techniques.
PB94-172905 *03,794*

Reply to Professor Wolf's Comments on My Paper on Wolf Shifts.
PB94-219409 *04,247*

Results of a NIST/VNIIOFI Comparison of Spectral-Radiance Measurements.
PB97-113021 *04,159*

MIES, F. H.
Intersystem Crossing in Collisions of Aligned Ca(4s5p (1)P) + He: A Half Collision Analysis Using Multichannel Quantum Defect Theory.
PB94-211133 *00,813*

MIGDALL, A. L.
Absolute Response Calibration of a Transfer Standard Cryogenic Bolometer.
PB96-147103 *04,358*

Filter Transmittance Measurements in the Infrared.
PB94-140589 *04,224*

MIGHELL, A.
Workshop Highlights.
PB97-109227 *04,811*

MIGHELL, A. D.
Neutron Powder Diffraction Study of the Nuclear and Magnetic Structures of the Oxygen-Deficient Perovskite YBaCuCoO5.
PB95-161097 *00,954*

NIST Crystallographic Databases for Research and Analysis.
PB97-109094 *04,801*

MIILLER, A. P.
Dynamic Technique for Measuring Normal Spectral Emissivity of Electrically Conducting Solids at High Temperatures with a High-Speed Spatial Scanning Pyrometer.
PB95-153045 *03,921*

High-Speed Spatial Scanning Pyrometer.
PB94-200003 *02,636*

Measurement of Surface Tension of Tantalum by a Dynamic Technique in a Microgravity Environment.
PB95-161667 *03,932*

Radiance Temperature (in the Wavelength Range 519-906 nm) of Tungsten at Its Melting Point by a Pulse-Heating Technique.
PB94-172590 *03,397*

Radiance Temperatures (in the Wavelength Range 523-907 nm) of Group IVB Transition Metals Titanium, Zirconium, and Hafnium at Their Melting Points by a Pulse-Heating Technique.
PB96-135025 *02,677*

Wavelength Dependence of Normal Spectral Emissivity of High-Temperature Metals at Their Melting Point.
PB94-200011 *03,398*

MIKLICH, A. H.
Fabrication Issues in Optimizing YBa2Cu3O7-x Flux Transformers for Low I/f Noise.
PB95-175857 *02,059*

Low Noise YBa2Cu3O7-x-SrTiO3-YBa2Cu3O7-x Mulitlayers for Improved Superconducting Magnetometers.
PB96-138417 *04,747*

MILANOVIC, V.
Micromachined Coplanar Waveguides in CMOS Technology.
PB97-119283 *02,456*

MILDNER, D. F. R.
Neutron Focusing Lens Using Polycapillary Fibers.
PB95-141206 *03,889*

Neutron Focusing Lens Using Polycapillary Fibers.
PB95-153078 *03,922*

Use of Neutron Beams for Chemical Analysis at NIST.
PB97-112437 *00,652*

MILES, K.
Glossary of Software Reuse Terms.
PB95-178992 *01,720*

MILIAN BON, S.
Novel Bulk Iron Garnets for Magneto-Optic Magnetic Field Sensing.
PB95-180204 *04,675*

MILKE, J. A.
Evaluation of Survey Procedures for Determining Occupant Load Factors in Contemporary Office Buildings.
PB97-116222 *00,238*

Full-Scale Room Fire Experiments Conducted at the University of Maryland.
PB97-116081 *00,236*

Survey of Fuel Loads in Contemporary Office Buildings.
PB97-114235 *00,233*

MILLAT, J.
Viscosity of Ammonia.
PB96-145933 *01,117*

MILLER, A.
Novel Radiochromic Films for Clinical Dosimetry.
PB97-119259 *03,641*

Oscillometric and Conductometric Analysis of Aqueous and Organic Dosimeter Solutions.
PB96-135256 *04,054*

Radiation-Chemical Reaction of 2,3,5-Triphenyl-Tetrazolium Chloride in Liquid and Solid State.
PB96-146733 *01,124*

Temperature and Relative Humidity Dependence of Radiochromic Film Dosimeter Response to Gamma and Electron Radiation.
PB96-135298 *03,718*

MILLER, A. P.

Radiance Temperatures (in the Wavelength Range 523-907 nm) of Group IV B Transition Metals Titanium, Zirconium, and Hafnium at Their Melting Points by a Pulse-Heating Technique.
PB96-102207 *03,356*

MILLER, B. R.

Expression Formatter for MACSYMA.
PB95-267829 *01,735*

MILLER, C. A.

Self-Calibrating Fiber Optic Sensors: Potential Design Methods.
PB95-169298 *02,172*

Self Calibrating Fiber Optic Sensors: Potential Design Methods.
PB95-169306 *02,173*

MILLER, D. A.

Collisional Energy Transfer between Excited-State Strontium and Noble-Gas Atoms.
PB95-202958 *03,995*

MILLER, H. C.

Efficient Br(*) Laser Pumped by Frequency-Doubled Nd: YAG and Electronic-to-Vibrational Transfer-Pumped CO2 and HCN Lasers.
PB95-108684 *04,248*

MILLER, J. H.

Comparison of Experimental and Computed Species Concentration and Temperature Profiles in Laminar, Two-Dimensional Methane/Air Diffusion Flames.
PB95-140919 *01,379*

MILLER, P. A.

Gaseous Electronics Conference Radio-Frequency Reference Cell: A Defined Parallel-Plate Radio-Frequency System for Experimental and Theoretical Studies of Plasma-Processing Discharges.
PB94-172327 *04,404*

Inductively Coupled Plasma Source for the Gaseous Electronics Conference RF Reference Cell.
PB96-113394 *02,394*

Reactive Ion Etching in the Gaseous Electronics Conference RF Reference Cell.
PB96-113402 *02,395*

MILLER, R.

Frozen Human Serum Reference Material for Standardization of Sodium and Potassium Measurements in Serum or Plasma by Ion-Selective Electrode Analyzers.
PB94-185337 *00,532*

MILLER, R. D.

High-Energy Behavior of the Double Photoionization of Helium from 2 to 12 keV.
PB94-213279 *03,860*

MILLER, R. G.

Comparison of Heat-Flow-Meter Tests from Four Laboratories.
PB95-126264 *00,365*

MILLER, T. A.

Improved Uniaxial Strain Tolerance of the Critical Current Measured in Ag-Sheathed Bi2Sr2Ca1Cu2O8+x Superconductors.
PB95-153565 *04,594*

MILLER, W. M.

Experimental Investigation of the Validity of TDDB Voltage Acceleration Models.
PB94-185949 *02,304*

Field and Temperature Acceleration of Time-Dependent Dielectric Breakdown in Intrinsic Thin SiO2.
PB94-185956 *02,305*

MILLER, W. R.

Interface Roughness, Composition, and Alloying of Low-Order AlAs/GaAs Superlattices Studies by X-ray Diffraction.
PB96-160262 *02,983*

NIST Traceable Reference Material Program for Gas Standards: Standard Reference Materials.
PB96-210786 *00,644*

Stability of Compressed Gas Mixtures Containing Low Level Volatile Organic Compounds in Aluminum Cylinders.
PB96-111968 *00,613*

MILLS, K. L.

Experimental Evaluation of Specification Techniques for Improving Functional Testing.
PB96-201009 *01,779*

Knowledge-Based Approach for Automating a Design Method for Concurrent and Real-Time Systems.
PB97-112502 *01,780*

U.S. GOSIP Testing Program.
PB94-211455 *01,807*

MILNER, S. T.

Neutron Reflectivity of End-Grafted Polymers: Concentration and Solvent Quality Dependence in Equilibrium Conditions.
PB94-185758 *01,206*

MILOSAVLJEVIC, I.

Behavior of Charring Materials in Simulated Fire Environments.
PB94-196045 *01,368*

MINCHER, B. J.

Calibration and Performance of GafChromic DM-100 Radiochromic Dosemeters.
PB97-119291 *00,703*

MINK, A.

Hardware Measurement Techniques for High-Speed Networks.
PB96-160551 *01,500*

Operating Principles of MultiKron II Performance Instrumentation for MIMD Computers.
PB95-189486 *01,628*

Operating Principles of MultiKron Virtual Counter Performance Instrumentation for MIMD Computers.
PB96-131529 *01,632*

Operating Principles of the SBus MultiKron Interface Board.
PB95-231783 *01,630*

MINOR, D.

Evolution of the Pore Size Distribution in Final-Stage Sintering of Alumina Measured by Small-Angle X-ray Scattering. (Reannouncement with New Availability Information).
AD-A249 178/5 *03,023*

MINOR, D. B.

Coating of Fibers by Colloidal Techniques in Ceramic Composites.
PB94-216256 *03,196*

MIRZADEH, S.

Assay of the Eluent from the Alumina-Based Tungsten-188-Rhenium-188 Generator.
PB94-200482 *03,829*

MISAKIAN, M.

Distributions of Measurement Error for Three-Axis Magnetic Field Meters during Measurements Near Appliances.
PB96-180153 *02,110*

ELF Electric and Magnetic Field Measurement Methods.
PB95-161675 *04,423*

Three-Axis Coil Probe Dimensions and Uncertainties during Measurement of Magnetic Fields from Appliances.
PB94-219359 *01,885*

MISRA, D. N.

Adsorption of Low-Molecular-Weight Sodium Polyacrylate on Hydroxyapatite.
PB94-172608 *00,139*

Adsorption of Polyacrylic Acids and Their Sodium Salts on Hydroxyapatite: Effect of Relative Molar Mass.
PB97-112510 *03,581*

Adsorption of Potassium N-phenylglycinate on Hydroxyapatite: Role of Solvents and Ionic Charge.
PB96-180161 *01,159*

Interaction of Chlorhexidine Digluconate with and Adsorption of Chlorhexidine on Hydroxyapatite.
PB95-175907 *03,566*

Interaction of Citric Acid with Hydroxyapatite: Surface Exchange of Ions and Precipitation of Calcium Citrate.
PB97-119309 *03,584*

Interaction of Some Coupling Agents and Organic Compounds with Hydroxyapatite: Hydrogen Bonding, Adsorption and Adhesion.
PB94-172616 *00,140*

MISRA, M.

Nickel(II)-Mediated Oxidative DNA Base Damage in Renal and Hepatic Chromatin of Pregnant Rats and Their Fetuses. Possible Relevance to Carcinogenesis.
PB94-212628 *03,646*

MISSEN, N.

Phase Locking in Two-Junction Systems of High-Temperature Superconductor-Normal Metal-Superconductor Junctions.
PB95-176053 *02,060*

MISSERT, N.

Critical Current and Normal Resistance of High-Tc Step-Edge SNS Junctions.
PB96-111752 *04,724*

High-Tc Multilayer Step-Edge Josephson Junctions and SQUIDs.
PB96-200183 *04,790*

Insulating Nanoparticles on YBa2Cu3O7-delta Thin Films Revealed by Comparison of Atomic Force and Scanning Tunneling Microscopy.
PB95-150843 *04,575*

Mutual Phase Locking in Systems of High-Tc Superconductor-Normal Metal-Superconductor Junctions.
PB96-135348 *04,744*

Observation of Insulating Nanoparticles on YBCO Thin-Films by Atomic Force Microscopy.
PB95-163358 *04,622*

Temperature Dependence and Magnetic Field Modulation of Critical Currents in Step-Edge SNS YBCO/Au Junctions.
PB96-111745 *04,723*

MISSERT, N. A.

Thermal Noise in High-Temperature Superconducting-Normal-Superconducting Step-Edge Josephson Junctions.
PB95-175089 *04,650*

MITCHELL, J. S. B.

Point Probe Decision Trees for Geometric Concept Classes.
PB96-160817 *01,612*

MITCHELL, M. J.

Capabilities for Product Data Exchange.
PB97-118764 *02,798*

Challenges to the National Information Infrastructure: The Barriers to Product Data Sharing. National PDES Testbed Report Series.
PB95-136347 *02,776*

Initial NIST Testing Policy for STEP: Beta Testing Program for AP 203 Implementations. National PDES Testbed Report Series.
PB95-154688 *02,779*

MITCHELL, P. J.

Structure and Rheology of Hard-Sphere Systems.
PB96-167333 *00,662*

MITLER, H. E.

Algorithm to Describe the Spread of a Wall Fire under a Ceiling.
PB95-182259 *00,261*

Comparison of Wall-Fire Behavior With and Without a Ceiling.
PB94-207404 *00,342*

Heights of Wall-Fire Flames.
PB96-148192 *00,212*

MITRAKOVIC, D. V.

Methods to Improve the Accuracy of On-Line Ultrasonic Measurement of Steel Sheet Formability.
PB96-186051 *02,281*

Noncontact Ultrasonic Inspection of Train Rails for Stress.
PB95-162673 *04,851*

MITTAL, J. P.

Fluoride Elimination Upon Reaction of Pentafluoroaniline with e (sub eq')(sup -), H, and OH Radicals in Aqueous Solution.
PB97-111314 *01,177*

MIYANO, K. E.

Barium Contributions to the Valence Electronic Structure of YBa2Cu3O7-delta, PrBa2Cu3O7-delta, and Other Barium-Containing Compounds.
PB96-158019 *04,076*

Phonon Relaxation in Soft-X-ray Emission of Insulators.
PB96-160296 *04,085*

MIZE, J. H.

Learning to Change: Opportunities to Improve the Performance of Smaller Manufacturers.
PB94-166212 *00,010*

MIZIOLEK, A. W.

Environmental Aspects of Halon Replacements: Considerations for Advanced Agents and the Ozone Depletion Potential of CF3I.
PB97-122261 *03,301*

MIZUKI, J.

Rotational Dynamics of C60 in Na2RbC60.
PB95-153201 *00,948*

MIZUMACHI, H.

Micromechanics of Fracture in Rubber-Toughened Epoxies.
PB94-212222 *03,011*

MOCK, J. L.

Gaseous Electronics Conference Radio-Frequency Reference Cell: A Defined Parallel-Plate Radio-Frequency System for Experimental and Theoretical Studies of Plasma-Processing Discharges.
PB94-172327 *04,404*

MODELSKI, J.

Influence of Films' Thickness and Air Gaps in Surface Impedance Measurements of High Temperature Superconductors Using the Dielectric Resonator Technique.
PB96-157862 *01,946*

MOEN, W. E.

Z39.50 Implementation Experiences.
PB96-114939 *01,816*

MOERMAN, R.

Coexistence of Grains with Differing Orthorhombicity in High Quality YBa2Cu3O7-delta Thin Films.
PB96-135033 *04,742*

Magnetic Flux Pinning in Epitaxial YBa2Cu3O7-delta Thin Films.
PB96-200746 *04,795*

MOFFAT, T.

Electrochemical Synthesis of Metal and Intermetallic Composites.
AD-A294 088/0 *03,304*

MOGI, Y.

Localization of a Homopolymer Dissolved in a Lamellar Structure of a Block Copolymer Studied by Small-Angle Neutron Scattering.
PB95-161592 *01,253*

Molecular Weight Dependence of the Lamellar Domain Spacing of ABC Triblock Copolymers and Their Chain Conformation in Lamellar Domains.
PB95-161691 *01,254*

MOHN, H.

Phase Transitions in Solid C70: Supercooling, Metastable Phases, and Impurity Effect.
PB95-150090 *00,914*

MOHR, D. L.

Hybrid Undulator for the NIST-NRL Free-Electron Laser.
PB94-212529 *04,238*

NIST-NRL Free-Electron Laser Facility.
PB94-212511 *04,237*

MOHR, P. J.

Electron Screening Correction to the Self Energy in High-Z Atoms.
PB94-172376 *03,789*

Evaluation of Two-Photon Exchange Graphs for Highly-Charged Heliumlike Ions.
PB94-198918 *03,808*

MOHRAZ, B.

Method of Estimating the Parameters of Tuned Mass Dampers for Seismic Applications.
PB96-167820 *00,473*

Modified Optimal Algorithm for Active Structural Control.
PB96-165949 *00,472*

Post-Earthquake Fire and Lifelines Workshop. Held in Long Beach, California on January 30-31, 1995. Proceedings.
PB96-117916 *00,209*

Proceedings of a Workshop on Developing and Adopting Seismic Design and Construction Standards for Lifelines. Held in Denver, Colorado on September 25-27, 1991.
PB97-115794 *01,302*

MOIROUX, J.

Oxidation of 10-Methylacridan, a Synthetic Analogue of NADH and Deprotonation of Its Cation Radical. Convergent Application of Laser Flash Photolysis and Direct and Redox Catalyzed Electrochemistry to the Kinetics of Deprotonation of the Cation Radical.
PB94-198371 *00,785*

MOISEEVA, N. P.

Investigation of High-Temperature Platinum Resistance Thermometers at Temperatures Up to 962C, and, in Some Cases, 1064C.
PB96-161294 *00,629*

MOLDOVER, M. R.

Ab initio Calculations for Helium: A Standard for Transport Property Measurements.
PB96-102041 *01,060*

Dielectric Studies of Fluids with Reentrant Resonators.
PB95-153730 *00,952*

Dielectric Studies of Fluids with Reentrant Resonators. Appendix B.
DE93019683 *03,244*

Electric Field Effects on a Near-Critical Fluid in Microgravity.
PB96-161880 *04,217*

Greenspan Acoustic Viscometer for Gases.
PB96-204417 *04,220*

High-Temperature High-Pressure Oscillating Tube Densimeter.
PB96-146618 *01,123*

Properties of Working Fluids for Thermoacoustic Refrigerators.
AD-A297 420/2 *04,864*

Structure of the Vapor-Liquid Interface Near the Critical Point
PB95-140174 *00,902*

Thermodynamic Properties of CF3-CHF-CHF2, 1,1,1,2,3,3-Hexafluoropropane.
PB97-118384 *03,299*

Thermodynamic Properties of CHF2-CF2-CHF, 1,1,2,2,3-Pentafluoropropane.
PB97-118392 *03,300*

Thermodynamic Properties of CHF2-O-CHF2,Bis(difluoromethyl) Ether.
PB94-199569 *00,798*

MOLINAR, G. F.

Pressure Measurements with the Mercury Melting Line Referred to ITS-90.
PB96-161005 *01,136*

MOLINE, J.

Electronic Access: Blueprint for the National Archives and Records Administration.
PB95-219218 *02,731*

User Profile for Researchers Studying Objects: Implications for Computer Systems.
PB94-188463 *00,133*

User Study: Informational Needs of Remote National Archives and Records Administration Customers.
PB95-154738 *02,725*

Virtual Environments for Health Care. A White Paper for the Advanced Technology Program (ATP), the National Institute of Standards and Technology.
PB96-147814 *03,594*

MOLMER, K.

Temperature of Optical Molasses for Two Different Atomic Angular Momenta.
PB95-126058 *03,881*

MONCARZ, H. T.

Automated Optical Roughness Inspection.
PB95-152179 *02,905*

Information Technologies Make Business Sense for the Custom Therapeutic Footwear Industry.
PB95-251708 *02,829*

Program Requirements to Advance the Technology of Custom Footwear Manufacturing.
PB95-147906 *02,883*

Visualization Applications for Manufacturing: A State-of-the-Art Survey. Final Report.
PB94-194552 *02,816*

MONDAIN-MONVAL, P.

Open Issues in OSI Protocol Development and Conformance Testing.
PB96-122908 *01,818*

MONKS, P. S.

Experimental Determination of the Ionization Energy of IO(X(sup 2)Ii(sub 3/2)) and Estimations of Delta(sub f)H(sup deg)(sub 0)(IO(sup -)) and PA(IO).
PB96-146899 *00,694*

Experimental Determination of the Rate Constant for the Reaction of C2H3 with H2 and Implications for the Partitioning of Hydrocarbons in Atmospheres of the Outer Planets.
PB97-122295 *00,112*

MONROE, C. R.

Trapped Ions and Laser Cooling 4: Selected Publications of the Ion Storage Group of the Time and Frequency Division, NIST, Boulder, Colorado.
PB96-172358 *04,108*

MONSINGNORI-FOSSI, B.

Distant Future of Solar Activity: A Case Study of Beta Hydri. 3. Transition Region, Corona, and Stellar Wind.
PB94-185220 *00,049*

Distant Future of Solar Activity: A Case Study of beta Hydri. 3. Transition Region, Corona, and Stellar Wind.
PB95-153441 *00,074*

MONTESALVO, M.

Estimation of the Absorbed Dose in Radiation-Processed Food. 4. EPR Measurements on Eggshell.
PB94-199692 *00,038*

MONTGOMERY, D.

NIST Cooperative Laboratory for OSI Routing Technology.
DE94015308 *01,791*

MONTI, C. L.

National Voluntary Laboratory Accreditation Program 1995 Directory.
PB95-174454 *00,483*

MONTRESS, G. K.

Surface Transverse Wave Oscillators with Extremely Low Thermal Noise Floors.
PB96-186010 *01,967*

MOODY, J. R.

Development of the Ion Exchange-Gravimetric Method for Sodium in Serum as a Definitive Method.
PB96-179148 *01,867*

MOON, B. M.

Novel YBa2Cu3O7-x and YBa2Cu3O7-x/Y4Ba3O9 Multilayer Films by Bias-Masked 'On-Axis' Magnetron Sputtering.
PB95-181186 *04,690*

MOORE, C. E.

Atomic Energy Levels As Derived from the Analyses of Optical Spectra. Volume 1. Section 1. The Spectra of Hydrogen, Deuterium, Helium, Lithium Beryllium, Boron, Carbon, Nitrogen, Oxygen, and Fluorine.
AD-A278 130/0 *03,764*

Atomic Energy Levels. As Derived From the Analyses of Optical Spectra. Volume 3.
AD-A280 279/1 *00,714*

Ultraviolet Multiplet Table.
AD-A278 446/0 *00,710*

Ultraviolet Multiplet Table. Finding List for Spectra of the Elements Molybdenum to Lanthanum (Z = 42 to 57); Hafnium to Radium (Z = 72 to 88).
AD-A278 131/8 *00,709*

MOORE, F.

Electrostatic Modes of Ion-Trap Plasmas.
PB95-152963 *03,920*

Experimental Results on Normal Modes in Cold, Pure Ion Plasmas.
PB95-175105 *03,956*

Lattice Position of Si in GaAs Determined by X-Ray Standing Wave Measurements.
PB95-164406 *04,632*

MOORE, F. L.

Electrostatic Modes as a Diagnostic in Penning-Trap Experiments.
PB95-176244 *03,959*

High-Order Multipole Excitation of a Bound Electron.
PB96-119789 *04,044*

High-Resolution Atomic Spectroscopy of Laser-Cooled Ions.
PB95-169330 *03,953*

Precise Spectroscopy for Fundamental Physics.
PB96-112164 *04,040*

Quantum Measurements of Trapped Ions.
PB95-161147 *03,928*

Quantum Projection Noise: Population Fluctuations in Two-Level Systems.
PB94-212271 *03,850*

Recent Experiments on Trapped Ions at the National Institute of Standards and Technology.
PB95-169322 *03,952*

Spin Squeezing and Reduced Quantum Noise in Spectroscopy.
PB95-151635 *03,912*

MOORE, J.

Escherichis coli Cyclic AMP Receptor Protein Mutants Provide Evidence for Ligand Contacts Important in Activation.
PB96-201017 *03,592*

MOORE, J. H.

Associative Electron Attachment to S2F10, S2OF10, and S2O2F10.
PB95-140992 *00,907*

Electron Scattering and Dissociative Attachment by SF6 and Its Electrical-Discharge By-Products.
PB95-151288 *02,256*

MOORE, L. J.

Comparative Strategies for Correction of Interferences in Isotope Dilution Mass Spectrometric Determination of Vanadium.
PB94-185261 *00,531*

MOPSIK, F. I.

Advances in the Measurement of Polymer CTE: Micrometer- to Atomic-Scale Measurements.
PB96-180229 *03,390*

Dielectric Behavior of a Polycarbonate/Polyester Mixture Upon Transesterification.
PB96-179551 *04,785*

Electronics Packaging Materials Research at NIST.
PB96-122692 *02,405*

Review of Cure Monitoring Techniques for On-Line Process Control.
PB94-216728 *03,145*

MORAN, B.

Model Minimum Performance Specifications for Lidar Speed Measurement Devices.
PB95-197455 *04,861*

MORDFIN, L.

Fracture Behavior of Large-Scale Thin-Sheet Aluminum Alloy.
N95-19494/0 *03,311*

MOREA, G. F.

Operating Procedures and Life Cycle Documentation for the Initial Graphics Exchange Specification.
PB95-242285 *02,782*

MORELAND, J.

Comparison of Magnetic Fields of Thin-Film Heads and Their Corresponding Bit Patterns Using Magnetic Force Microscopy.
PB95-180907 *03,763*

Critical Current Behavior of Ag-Coated YBa2Cu3O7-x Thin Films.
PB95-141016 *04,549*

dc Magnetic Force Microscopy Imaging of Thin-Film Recording Head.
PB95-176061 *04,665*

Development of Highly Conductive Cantilevers for Atomic Force Microscopy Point Contact Measurements.
PB96-138573 *04,751*

Epitaxial Growth and Characterization of the Ordered Vacancy Compound CuIn3Se5 on GaAs (100) Fabricated by Molecular Beam Epitaxy.
PB95-180725 *04,687*

Flexible-Diaphragm Force Microscope.
PB95-180915 *03,966*

Growth of Laser Ablated YBa2Cu3O7-delta Films as Examined by Rheed and Scanning Tunneling Microscopy.
PB95-162541 *04,614*

High Critical Temperature Superconductor Tunneling Spectroscopy Using Squeezable Electron Tunneling Junctions.
PB95-163721 *04,627*

In situ Observation of Surface Morphology of InP Grown on Singular and Vicinal (001) Substrates.
PB95-168431 *04,636*

Influence of Deposition Parameters on Properties of Laser Ablated YBa2Cu3O7-Delta Films.
PB95-140539 *04,544*

Insulating Nanoparticles on YBa2Cu3O7-delta Thin Films Revealed by Comparison of Atomic Force and Scanning Tunneling Microscopy.
PB95-150843 *04,575*

Magnetic Force Microscopy Images of Magnetic Garnet with Thin-Film Magnetic Tip.
PB95-176210 *04,669*

Magnetic Force Microscopy of Flux in Superconductors.
PB95-161733 *04,608*

Novel YBa2Cu3O7-x and YBa2Cu3O7-x/Y4Ba3O9 Multilayer Films by Bias-Masked 'On-Axis' Magnetron Sputtering.
PB95-181186 *04,690*

Observation of Insulating Nanoparticles on YBCO Thin-Films by Atomic Force Microscopy.
PB95-163358 *04,622*

Recent Results in Magnetic Force Microscopy.
PB96-103130 *04,721*

Superconducting Energy Gap of Bulk UBe13.
PB95-150116 *04,559*

Surface Modification of YBa2Cu3O7-delta Thin Films Using the Scanning Tunneling Microscope: Five Methods.
PB95-203394 *04,699*

Surface Topography and Ordering-Variant Segregation in GaInP2.
PB95-153649 *04,595*

Tunneling Measurement of the Zero-Bias Conductance Peak and the Bi-Sr-Ca-Cu-O Thin-Film Energy Gap.
PB95-163739 *04,628*

Tunneling Spectroscopy of Thallium-Based High-Temperature Superconductors.
PB95-161709 *04,606*

Tunneling Stabilized Magnetic-Force Microscopy.
PB95-161717 *04,607*

YBa2Cu3O7-x to Si Interconnection for Hybrid Superconductor/Semiconductor Integration.
PB94-211711 02,315

MORGAN, C. A.

Beam Line for Highly Charged Ions.
PB97-111256 04,143

Observation and Visible and uv Magnetic Dipole Transitions in Highly Charged Xenon and Barium.
PB96-138441 04,056

MORGAN, G. L.

Intermediate Structure in the Neutron-Induced Fission Cross Section of 236U.
PB94-185741 03,802

Measurements of the (237)Np(n,f) Cross Section.
PB97-119069 04,173

MORGAN, N.

Planar Resistors for Probe Station Calibration.
PB95-163697 02,351

MORGAN, T. J.

Wear Mechanism Maps of 440C Martensitic Stainless Steel.
PB96-111810 04,834

MORI, K.

Molecular Weight Dependence of the Lamellar Domain Spacing of ABC Triblock Copolymers and Their Chain Conformation in Lamellar Domains.
PB95-161691 01,254

MORI, T.

DNA Base Damage Generated In vivo in Hepatic Chromatin of Mice upon Whole Body y-Irradiation.
PB95-161741 03,627

DNA Base Modifications in Renal Chromatin of Wistar Rats Treated with a Renal Carcinogen, Ferric Nitrilotriacetate.
PB95-150363 03,648

Ionizing Radiation Causes Greater DNA Base Damage in Radiation-Sensitive Mutant M10 Cells That in Parent Mouse Lymphoma L5178Y Cells.
PB95-175915 03,632

Treatment of Wistar Rats with a Renal Carcinogen, Ferric Nitrilotriacetate, Causes DNA-Protein Cross-Linking between Thymine and Tyrosine in Their Renal Chromatin.
PB96-112115 03,649

MORNIS, M.

Through-the-Arc Sensing for Measuring Gas Metal Arc Weld Quality in Real Time.
PB95-164463 02,908

MORNIS, M. A.

Contact Tube Wear Detection in Gas Metal Arc Welding.
PB96-135330 02,872

Through-the-Arc Sensing for Monitoring Arc Welding.
PB94-185899 02,858

Through-the-Arc Sensing for Real-Time Measurement of Gas Metal Arc Weld Quality.
PB95-162871 02,863

MORRA, M. M.

Charpy Impact Test as an Evaluation of 4 K Fracture Toughness.
PB96-190194 03,219

MORRIS, D. E.

Coupled-Bilayer Two-Dimensional Magnetic Order of the Dy Ions in Dy2Ba4Cu7O15.
PB95-152104 04,584

MORRIS, K. C.

Structural EXPRESS Editor.
PB94-159795 02,769

Validation Testing System Requirements. National PDES Testbed Report Series.
PB94-163482 02,771

MORRIS, P. A.

Growth of Epitaxial KNbO3 Thin Films.
PB96-135181 02,409

MORRIS, R. E.

Determination of Complex Structures from Powder Diffraction Data: The Crystal Structure of La3Ti5Al15O37.
PB95-202966 01,038

MORRIS, S. C.

Enhanced Detection of PCR Products Through Use of TOTO and YOYO Intercalating Dyes with Laser Induced Fluorescence - Capillary Electrophoresis.
PB95-164653 00,599

MORRIS, S. L.

Observations of 3C 273 with the Goddard High Resolution Spectrograph on the Hubble Space Telescope.
PB95-202321 00,076

MORRISON, F. A.

Flow-Induced Structure in Polymers: Chapter 16. Shear-Induced Changes in the Order-Disorder Transition Temperature and the Morphology of a Triblock Copolymer.
PB96-123237 03,127

Influence of Shear on the Ordering Temperature of a Triblock Copolymer Melt.
PB96-163753 01,288

Shear-Excited Morphological States in a Triblock Copolymer.
PB94-172392 01,196

Shear-Induced Changes in the Order-Disorder Transition Temperature and the Morphology of a Triblock Copolymer.
PB97-118772 03,130

Shear-Induced Martensitic-Like Transformation in a Block Copolymer Melt.
PB96-119508 01,277

Time Dependent Small Angle Neutron Scattering Behavior in Triblock Copolymers Under Steady Shear.
PB94-172632 01,198

MORRISON, G.

Compressed Liquid Densities, Saturated Liquid Densities, and Vapor Pressures of 1,1-Difluoroethane.
PB97-110118 01,173

Interaction Coefficients for 15 Mixtures of Flammable and Non-Flammable Components.
PB96-146626 03,281

REFPROP Refrigerant Properties Database: Capabilities, Limitations, and Future Directions.
PB96-167150 01,149

Shape of the Temperature-Entropy Saturation Boundary.
PB96-135066 02,506

Study to Determine the Existence of an Azeotropic R-22 'Drop-In' Substitute.
PB96-167812 02,568

Thermodynamic Properties of CHF2-O-CHF2,Bis(difluoromethyl) Ether.
PB94-199569 00,798

Thermodynamic Properties of Difluoromethane.
PB94-185204 00,772

Vapor Pressure of 1,1-dichloro-2,2,2-trifluoroethane (R123).
PB95-126231 00,899

MORRISON, H. D.

Decomposition of SF6 and Production of S2F10 in Power Arcs.
PB96-122619 01,084

Investigation of S2F10 Production and Mitigation in Compressed SF6-Insulated Power Systems.
PB94-212388 02,467

Investigation of S2F10 Production and Mitigation in Compressed SF6- Insulated Power Systems.
PB96-155528 02,468

MORRISON, J. F.

Instrument for Evaluating Phase Behavior of Mixtures for Supercritical Fluid Experiments.
PB95-180758 00,606

Supercritical Fluid Extraction-Immunoassay for the Rapid Screening of Cocaine in Hair.
PB96-167168 00,637

MORRISON, M. A.

Alignment in Two-Step Pulsed Laser Excitation of Rydberg Levels in Light Atoms: The Example of Sodium.
PB95-202883 03,993

Analyses of Recent Experimental and Theoretical Determinations of e-H2 Vibrational Excitation Cross Sections: Assessing a Long-Standing Controversy.
PB95-202438 03,977

Importance of Bound-Free Correlation Effects for Vibrational Excitation of Molecules by Electron Impact: A Sensitivity Analysis.
PB95-202974 03,996

Low-Energy-Electron Collisions with Sodium: Elastic and Inelastic Scattering from the Ground State.
PB96-103106 04,030

Modified Effective Range Theory as an Alternative to Low-Energy Close-Coupling Calculations.
PB95-202701 03,988

MOSER, E. K.

Microwave Properties of YBa2Cu3O7-x Films at 35 GHz from Magnetotransmission and Magnetoreflection Measurements.
PB95-168977 04,643

MOSER, M.

Laser-Induced Fluorescence Measurements of OH. Concentrations in the Oxidation Region of Laminar, Hydrocarbon Diffusion Flames.
PB95-162160 01,387

Laser-Induced Fluorescence Measurements of OH in Laminar Diffusion Flames in the Presence of Soot Particles.
PB96-123120 01,409

MOSS, D. B.

Acceleration of Intramolecular Vibrational Redistribution by methyl Internal Rotation. A Chemical Timing Study of p-fluorotoluene and p-fluorotoluene-d3.
PB95-202982 01,039

MOSS, S. C.

Epitaxial Growth of Sb/GaSb Structures: An Example of V/III-V Heteroepitaxy.
PB95-202560 04,693

Epitaxial Integration of Single Crystal C60.
PB95-153490 04,592

MOSS, W. F.

Analyzing and Exploiting Numerical Characteristics of Zone Fire Models.
PB96-102314 01,400

Numerical Analysis Support for Compartment Fire Modeling and Incorporation of Heat Conduction into a Zone Fire Model.
PB94-156965 01,357

MOSSMAN, K. L.

External Gamma-ray Counting of Selected Tissues from a Thorotrast Patient.
PB96-160254 03,637

MOSTOWSKI, J.

Cone Emission from Laser-Pumped Two-Level Atoms. 1. Quantum Theory of Resonant Light Propagation.
PB95-203584 04,325

Cone Emission from Laser-Pumped Two-Level Atoms. 2. Analytical Model Studies.
PB95-203592 04,326

MOU, J.

Integrated Inspection System for Improved Machine Performance.
PB96-160569 02,959

MOUDDEN, A. H.

High-Energy Phonon Dispersion in La1.85Sr0.15CuO4.
PB96-138458 04,748

MOUDDEN, H.

Inelastic Neutron Scattering Measurements of Phonons in Icosahedral Al-Li-Cu.
PB95-126215 04,532

MOULD, J.

Numerical Reference Models for Optical Metrology Simulation.
PB97-111330 04,392

MOULT, J.

Crystal Packing Interactions of Two Different Crystal Forms of Bovine Ribonuclease A.
PB95-152823 00,943

Positive and Negative Cooperativities at Subsequent Steps of Oxygenation Regulate the Allosteric Behavior of Multistate Sebacylhemoglobin.
PB97-119374 03,486

MOUNT, D.

Point Probe Decision Trees for Geometric Concept Classes.
PB96-160817 01,612

MOUNTAIN, R. D.

Activated Dynamics, Loss of Ergodicity, and Transport in Supercooled Liquids.
PB95-150819 00,925

Collection of Results for the SPC/E Water Model.
PB96-147889 01,127

Comparison of a Fixed-Charge and a Polarizable Water Model.
PB96-111620 01,072

Length Scales for Fragile Glass-Forming Liquids.
PB96-102801 01,065

Long-Lived Structures in Fragile Glass-Forming Liquids.
PB96-119565 04,212

Neighbor Tables for Molecular Dynamics Simulations.
PB95-171948 00,991

Quantitative Measure of Efficiency of Monte Carlo Simulations.
PB95-180691 01,011

Simulation of C60 Through the Plastic Transition Temperatures.
PB96-102546 04,713

Simulation Studies of Supercooled and Glass Forming Liquids.
PB96-122627 01,085

Simulations of Glass Forming Liquids: What Has Been Learned.
PB95-150124 00,915

MOWRER, F. W.

Development of the Fire Data Management System.
PB94-206091 00,339

Post-Earthquake Fire and Lifelines Workshop. Held in Long Beach, California on January 30-31, 1995. Proceedings.
PB96-117916 00,209

MOYNIHAN, S.

Metrology for Electromagnetic Technology: A Bibliography of NIST Publications.
PB94-159761 02,116

MOZER, B.

Neutron Scattering Structural Study of AlCuFe Quasicrystals Using Double Isotopic Substitution.
PB94-200458 04,485

RDFs and Fe-Fe Pair Correlations in an AlCuFe Icosahedral Alloy by Double Isotopic Substitution.
PB94-172129 04,439

MUDD, J. L.

Interlaboratory Comparison of Autoradiographic DNA Profiling Measurements. 1. Data and Summary Statistics.
PB95-175923 03,542

Interlaboratory Comparison of Autoradiographic DNA Profiling Measurements. 2. Measurement Uncertainty and Its Propagation.
PB96-112123 03,545

MUELLER, D.

Surface Geometry of BaO on W(100): A Surface-Extended X-Ray-Absorption Fine-Structure Study.
PB95-164414 00,980

MUELLER, D. L.

Intermediate Coupling in L2-L3 Core Excitons of MgO, Al2O3, and SiO2.
PB96-158043 04,079

MUELLER, D. R.

Barium Contributions to the Valence Electronic Structure of YBa2Cu3O7-delta, PrBa2Cu3O7-delta, and Other Barium-Containing Compounds.
PB96-158019 *04,076*

Charge-Transfer-Induced Multiplet Structure in the N4,5O2,3 Soft-X-ray Emission Spectrum of Lanthanum.
PB96-163746 *04,102*

Cooper M(sub II,III) X-ray-Emission Spectra of Copper Oxides and the Bismuth Cuprate Superconductor.
PB96-158027 *04,077*

Laser-Synchrotron Hybrid Experiments: A Photon to Tickle, A Photon to Poke.
PB96-157847 *03,704*

Local Partial Densities of States in Ni and Co Silicides Studied by Soft X-Ray Emission Spectroscopy.
PB94-212412 *04,504*

Phonon Relaxation in Soft-X-ray Emission of Insulators.
PB96-160296 *04,085*

Simple Variable Line Space Grating Monochromator for Synchrotron Light Source Beamlines.
PB96-156203 *04,065*

Soft-X-ray-Emission Investigation of Cobalt Implanted Silicon Crystals.
PB96-157912 *04,069*

Soft-X-ray-Emission Spectra of Solid Kr and Xe.
PB96-157920 *04,070*

Soft-X-ray-Emission Studies of Bulk Fe3Si, FeSi, and FeSi2, and Implanted Iron Silicides.
PB96-157938 *04,071*

MUELLER, W. H.

Phase Transitions in Solid C70: Supercooling, Metastable Phases, and Impurity Effect.
PB95-150090 *00,914*

MUIR, D. C. G.

Concentrations of Chlorinated Hydrocarbons, Heavy Metals and Other Elements in Tissues Banked by the Alaska Marine Mammal Tissue Archival Project.
PB95-209870 *02,590*

MULAZZANI, Q. G.

Critical Review of Rate Constants for Reactions of Transients from Metal Ions and Metal Complexes in Aqueous Solution.
PB96-145859 *01,109*

MULEV, Y.

Database for the Static Dielectric Constant of Water and Steam.
PB96-145586 *01,103*

Static Dielectric Constant of Water and Steam.
PB96-123559 *01,090*

MULHOLLAND, G.

Smoke Emission from Burning Crude Oil.
PB96-122890 *01,407*

Working Conference on Global Growth of Technology: Is America Prepared. Held in Gaithersburg, Maryland on December 7, 1995.
PB96-210059 *00,018*

MULHOLLAND, G. W.

Airborne Smoke Sampling Package for Field Measurements of Fires.
PB95-150041 *01,381*

Generation and Characterization of Acetylene Smokes.
PB94-200292 *01,372*

Global Climatic Effects of Aerosols: The AAAR Symposium.
PB95-108791 *00,122*

Radiometric Model of the Transmission Cell-Reciprocal Nephelometer.
PB95-150132 *00,124*

Two Numerical Techniques for Light Scattering by Dielectric Agglomerated Structures.
PB94-140597 *04,225*

Ultrafine Combustion Aerosol Generator.
PB94-200300 *01,373*

MULLEN, J. L.

Electrochemical Synthesis of Metal and Intermetallic Composites.
AD-A294 088/0 *03,304*

MULLER, A.

Dielectronic Capture Processes in the Electron-Impact Ionization of Sc(2+).
PB95-203113 *04,000*

Merged-Beams Energy-Loss Technique for Electron-Ion Excitation: Absolute Total Cross Sections for O(5+) (2s yields 2p).
PB96-102058 *04,017*

MULLINGS, G. M.

Effects of Testing Variables on the Strength of High-Strength (90 Mpa) Concrete Cylinders.
PB96-112198 *00,456*

MULROY, W. J.

Study to Determine the Existence of an Azeotropic R-22 'Drop-In' Substitute.
PB96-167812 *02,568*

MULVENNA, G.

IGOSS-Industry/Government Open Systems Specification.
PB94-207453 *01,806*

MULVENNA, J.

Data Communications Strategy.
PB96-167846 *02,738*

MUNRO, R. G.

Ceramic Powders Characterization: Results of an International Laboratory Study.
PB95-270039 *02,672*

Characterizing Materials Properties for Ceramic Matrix Composites.
PB97-110282 *03,097*

Corrosion Characteristics of Silicon Carbide and Silicon Nitride.
PB96-169081 *03,372*

Database Development and Management (Project A.2.2): The Annual Report for 1992-1993.
PB97-110290 *03,098*

Reference Relations for the Evaluation of the Materials Properties of Orthorhombic YBa2Cu3Ox Superconductors.
PB96-176763 *04,782*

Review of Corrosion Behavior of Ceramic Heat Exchanger Materals: Corrosion Characteristics of Silicon Carbide and Silicon Nitride. Final Report, September 11, 1992--March 11, 1993.
DE93041307 *03,228*

Role of Corrosion in a Material Selector Expert System for Advanced Structural Ceramics.
PB97-110308 *03,099*

Structural Ceramics Database. Topical Report, June 1989-May 1991.
PB95-203758 *03,060*

Variances in the Measurement of Ceramic Powder Properties.
PB97-110316 *03,100*

Wear Model for Alumina Sliding Wear.
PB95-163796 *03,239*

MURAKAWA, M.

Applications of Diamond Films and Related Materials: International Conference (3rd). Held in Gaithersburg, Maryland on August 21-24, 1995. Supplement to NIST Special Publication 885.
PB95-256053 *03,063*

Proceedings of the Applied Diamond Conference 1995: Applications of Diamond Films and Related Materials International Conference (3rd). Held in Gaithersburg, Maryland, on August 21-24, 1995.
PB95-255204 *04,701*

MURALIDHAR, K.

Rapid Method for the Isolation of Genomic DNA from 'Aspergillus fumigatus'.
PB96-147061 *03,488*

MURE, T.

Characterization of the Interaction of Hydrogen with Iridium Clusters in Zeolites by Inelastic Neutron Scattering Spectroscopy.
PB95-180741 *01,013*

MURPHY, D. W.

Neutron-Scattering Study of C60(n-) (n=3,6) Librations in Alkali-Metal Fullerides.
PB94-200219 *00,806*

MURPHY, E.

TDDB Characterization of Thin SiO2 Films with Bimodal Failure Populations.
PB96-102926 *02,381*

MURPHY, K.

Control System Architecture for a Remotely Operated Unmanned Land Vehicle.
PB95-163200 *03,759*

MURPHY, K. E.

Determination of Sulfur in Fossil Fuels by Isotope Dilution Thermal Ionization Mass Spectrometry.
PB96-141379 *02,495*

MURPHY, K. N.

Ground Vehicle Control at NIST: From Teleoperation to Autonomy.
N94-34037/9 *03,758*

MURPHY, R. J.

Arc Spectra of Gallium, Indium, and Thallium.
AD-A295 411/3 *00,718*

MURRAY, A.

Examination of Objects Made of Wood Using Air-Coupled Ultrasound.
PB95-125712 *03,404*

MURRAY, B. T.

Asymptotic Behavior of Modulated Taylor-Couette Flows with a Crystalline Inner Cylinder.
PB94-199072 *04,469*

Computation of Dendrites Using a Phase Field Model.
PB94-160744 *04,436*

Convection and Morphological Stability During Directional Solidification.
N95-14548/8 *03,310*

Convective Stability in the Rayleigh-Benard and Directional Solidification Problems: High-Frequency Gravity Modulation.
PB95-181145 *04,208*

Effect of Modulated Taylor-Couette Flows on Crystal-Melt Interfaces: Theory and Initial Experiments.
PB94-216736 *04,521*

Lubrication Theory for Reactive Spreading of a Thin Drop.
PB95-189460 *02,865*

Lubrication Theory for Reactive Spreading of a Thin Drop.
PB96-123427 *04,214*

Rayleigh Instability for a Cylindrical Crystal-Melt Interface.
PB95-180667 *01,010*

MURTHY, N. S.

Hydration in Semicrystalline Polymers: Small-Angle Neutron Scattering Studies of the Effect of Drawing in Nylon-6 Fibers.
PB95-202990 *03,385*

MURTZ, M.

Extension of Heterodyne Frequency Measurements on OCS to 87 THz (2900 cm(-1)).
PB94-200680 *00,811*

Optically Stabilized Tunable Diode-Laser System for Saturation Spectroscopy.
PB96-102819 *04,717*

Stabilization of 3.3 and 5.1 m Lead-Salt Diode Lasers by Optical Feedback.
PB95-180709 *04,313*

MUSGROVE, A.

Comment On: Two-Photon Absorption Series of Calcium.
PB96-157979 *04,074*

Compilation of Energy Levels and Wavelengths for the Spectrum of Singly-Ionized Oxygen (O II).
PB94-162344 *00,746*

Energy Levels of Germanium, Ge I through Ge XXXII.
PB94-162351 *00,747*

Energy Levels of Zinc, Zn I through Zn XXX.
PB96-145982 *01,122*

Spectroscopic Data Tables for Highly-Ionized Atoms.
PB95-151585 *03,910*

MUSIELOK, J.

Atomic Transition Probabilities and Tests of the Spectroscopic Coupling Scheme for N I.
PB96-138466 *04,057*

Investigation of LS Coupling in Boronlike Ions.
PB94-185295 *03,797*

MUTH, L. A.

Accurate Computations of Radar Cross Sections of Simple Objects.
PB96-138474 *04,426*

General Order 'N' Analytic Correction of Probe-Position Errors in Planar Near-Field Measurements.
PB96-200688 *01,562*

Polarimetric Calibration of Reciprocal-Antenna Radars.
PB95-216925 *01,872*

Polarimetric Calibration of Reciprocal-Antenna Radars.
PB96-200696 *02,016*

Proposed Analysis of RCS Measurement Uncertainty.
PB95-203568 *01,871*

RangeCAD and the NIST RCS Uncertainty Analysis.
PB94-218591 *01,870*

MUTHUKUMAR, M.

Flow-Induced Structure in Polymers: Chapter 16. Shear-Induced Changes in the Order-Disorder Transition Temperature and the Morphology of a Triblock Copolymer.
PB96-123237 *03,127*

Influence of Shear on the Ordering Temperature of a Triblock Copolymer Melt.
PB96-163753 *01,288*

Shear-Excited Morphological States in a Triblock Copolymer.
PB94-172392 *01,196*

Shear-Induced Changes in the Order-Disorder Transition Temperature and the Morphology of a Triblock Copolymer.
PB97-118772 *03,130*

Time Dependent Small Angle Neutron Scattering Behavior in Triblock Copolymers Under Steady Shear.
PB94-172632 *01,198*

MUZNY, C. D.

Simulation and SANS Studies of Gelation Under Shear.
PB96-167176 *01,150*

Small-Angle Neutron-Scattering Study of Dense Sheared Silica Gels.
PB96-167184 *01,151*

MYATT, C. J.

Gravitational Sisyphus Cooling of (87)Rb in a Magnetic Trap.
PB96-200704 *04,379*

MYERS, R. H.

Taguchi's Parameter Design: A Panel Discussion.
PB96-111802 *03,445*

MYKLEBUST, R. L.

Airborne Asbestos Method: Bootstrap Method for Determining the Uncertainty of Asbestos Concentration. Version 1.0.
PB96-214614 *00,646*

Compositional Mapping of the Microstructure of Materials.
PB95-107199 *00,565*

Monte Carlo Electron Trajectory Simulation of X-Ray Emission from Films Supported on Substrates.
PB95-107207 *04,522*

NABINGER, S. J.

Air Change Effectiveness Measurements in Two Modern Office Buildings.
PB94-185766 *00,243*

Development and Application of an Indoor Air Quality Commissioning Program in a New Office Building.
PB96-155601 00,275

Environmental Evaluation of a New Federal Office Building.
PB94-199874 02,538

Indoor Air Quality Commissioning of a New Office Building.
PB95-182309 00,262

Indoor Air Quality Commissioning of a New Office Building.
PB97-110142 00,279

Measurements of Indoor Pollutant Emissions from EPA Phase II Wood Stoves.
PB95-198735 02,556

Study of Ventilation and Carbon Dioxide in an Office Building.
PB95-150140 02,542

Ventilation Effectiveness Measurements in Two Modern Office Buildings.
PB95-176012 02,553

NABLO, S. V.

Real Time Monitoring of Electron Processors.
PB96-135306 03,719

NACHT, G. G.

Operating Principles of the SBus MultiKron Interface Board.
PB95-231783 01,630

NACLERIO, N. J.

Overview of U.S. Government Advanced Packaging Programs.
PB96-200845 02,443

NADLER, W.

International Marine-Atmospheric (222)Rn Measurement Intercomparison in Bermuda. Part 2. Results for the Participating Laboratories.
PB96-175682 00,115

NAGARAJAN, R.

Neutron Scattering Study of Antiferromagnetic Order in the Magnetic Superconductors RNi2B2C.
PB97-112411 04,812

NAGASAKA, Y.

Standard Reference Data for the Thermal Conductivity of Water.
PB96-145875 01,111

Status of the Round Robin on the Transport Properties of R134a.
PB96-167218 01,152

NAGASHIMA, A.

Standard Reference Data for the Thermal Conductivity of Water.
PB96-145875 01,111

NAGI, M.

Optimization of Highway Concrete Technology.
PB94-182995 01,333

NAGUSRINIVAS, N.

Effect of DC Tests on Induced Space Charge.
PB94-172350 02,212

NAGY, V. Y.

Complex Time Dependence of the EPR Signal of Irradiated L-alpha-alanine.
PB97-122436 04,180

NAHOR, G. S.

Changes in the Redox State of Iridium Oxide Clusters and Their Relation to Catalytic Water Oxidation: Radiolytic and Electrochemical Studies.
PB95-107017 00,864

Metalloporphyrin Sensitized Photooxidation of Water to Oxygen on the Surface of Colloidal Iridium Oxides - Photochemical and Pulse Radiolytic Studies.
PB95-107082 00,868

One-Electron Oxidation of Nickel Porphyrins. Effect of Structure and Medium on Formation of Nickel(III) Porphyrin or Nickel(II) Porphyrin pi-Radical Cation.
PB95-107058 00,865

Reduction of Dinitrogen to Ammonia in Aqueous Solution Mediated by Colloidal Metals.
PB95-107074 00,867

Site of One-Electron Reduction of Ni(II) Porphyrins. Formation of Ni(I) Porphyrin of Ni(II) Porphyrin pi-Radical Anion.
PB95-107066 00,866

NAHUM, M.

Electronic Microrefrigerator Based on a Normal-Insulator-Superconductor Tunnel Junction.
PB96-102827 04,718

Hot-Electron Microcalorimeters as High-Resolution X-ray Detectors.
PB96-123641 04,739

Hot-Electron Microcalorimeters for X-ray and Phonon Detection.
PB95-168993 04,644

Metrological Accuracy of the Electron Pump.
PB95-168910 03,951

Novel Hot-Electron Microbolometer.
PB96-201025 01,977

Testing for Metrological Accuracy of the Electron Pump.
PB95-175873 04,663

Ultrasensitive-Hot-Electron Microbolometer.
PB95-168985 02,163

NAIR, R.

Turbulent Upward Flame Spread on a Vertical Wall under External Radiation.
PB94-207388 00,341

NAJARRO, F.

Radiation-Driven Winds of Hot Luminous Stars X. The Determination of Stellar Masses Radii and Distances from Terminal Velocities and Mass-Loss Rates.
PB94-213022 00,060

NAKABE, K.

Ignition and Subsequent Flame Spread Over a Thin Cellulosic Material.
PB96-160270 04,836

Ignition and Transition to Flame Spread Over a Thermally Thin Cellulosic Sheet in a Microgravity Environment.
PB96-160288 04,837

Transition from Localized Ignition to Flame Spread Over a Thin Cellulosic Material in Microgravity.
PB96-155809 04,835

NAKAGAKI, T.

Spectral Data and Grotrian Diagrams for Highly Ionized Chromium, Cr V through Cr XXIV.
PB94-162369 00,748

NAKAI, Y.

Spectral Data and Grotrian Diagrams for Highly Ionized Chromium, Cr V through Cr XXIV.
PB94-162369 00,748

NAKAJIMA, H.

Charpy Impact Test as an Evaluation of 4 K Fracture Toughness.
PB96-190194 03,219

NAKAKI, S. D.

Simplified Design Procedure for Hybrid Precast Concrete Connections.
PB96-154836 00,405

NAKANTANI, A. I.

Flow-Induced Structure in Polymer. Chapter 1. An Introduction to Flow-Induced Structures in Polymers.
PB96-123369 03,387

NAKASSIS, A.

Security in Open Systems.
PB95-105383 01,473

NAKATANI, A.

Dynamic Light-Scattering Study of a Diluted Polymer Blend Near Its Critical Point.
PB95-151890 01,245

NAKATANI, A. I.

Anisotropic Phase Separation Kinetics in a Polymer Blend Solution Following Cessation of Shear Studied by Light Scattering.
PB95-151247 01,241

Crossover to Strong Shear in a Low-Molecular-Weight Critical Polymer Blend.
PB94-211976 01,222

Flow-Induced Structure in Polymers: Chapter 16. Shear-Induced Changes in the Order-Disorder Transition Temperature and the Morphology of a Triblock Copolymer.
PB96-123237 03,127

Flow-Induced Structure in Polymers. Chapter 17. Phase-Separation Kinetics of a Polymer Blend Solution Studied by a Two-Step Shear Quench.
PB96-123377 03,388

Influence of Shear on the Ordering Temperature of a Triblock Copolymer Melt.
PB96-163753 01,288

Neutron Scattering Study of Shear Induced Turbidity in Polystyrene/Dioctyl Phthalate Solutions at High Shear Rates.
PB94-172624 01,197

Neutron Scattering Study of Shear Induced Turbidity in Polystyrene Dissolved in Dioctyl Phthalate.
PB95-161865 01,256

SANS and LS Studies of Polymer Mixtures Under Shear Flow.
PB95-107090 01,231

Shear Dependence of Critical Fluctuations in Binary Polymer Mixtures by Small Angle Neutron Scattering.
PB94-211612 01,220

Shear-Excited Morphological States in a Triblock Copolymer.
PB94-172392 01,196

Shear-Induced Changes in the Order-Disorder Transition Temperature and the Morphology of a Triblock Copolymer.
PB97-118772 03,130

Shear-Induced Martensitic-Like Transformation in a Block Copolymer Melt.
PB96-119508 01,277

Shear-Induced Mixing in Polymer Blends.
PB96-148085 01,287

Shear Suppression of Critical Fluctuations in a Diluted Polymer Blend.
PB96-204458 04,418

Synthesis of Hybrid Organic-Inorganic Materials from Interpenetrating Polymer Network Chemistry.
PB96-180054 02,994

Time Dependent Small Angle Neutron Scattering Behavior in Triblock Copolymers Under Steady Shear.
PB94-172632 01,198

NAKOTTE, H.

Crystallographic and Magnetic Properties of UAuSn.
PB95-140521 04,543

Magnetic Properties of Single-Crystalline UCu3Al2.
PB95-180717 04,686

NAM, S. W.

Self-Biasing Cryogenic Particle Detector Utilizing Electrothermal Feedback and a SQUID Readout.
PB96-102538 04,712

NAMAVAR, F.

Soft-X-ray-Emission Investigation of Cobalt Implanted Silicon Crystals.
PB96-157912 04,069

NANCOLLAS, G. H.

Influence of Natural and Synthetic Inhibitors on the Crystallization of Calcium Oxalate Hydrates.
PB95-150967 03,560

NARAYAN, A.

Density Dependence of Fluid Properties and Non-Newtonian Flows: The Weisenberg Effect.
PB96-161898 01,140

NARAYAN, A. P.

Non-Newtonian Flow between Concentric Cylinders Calculated from Thermophysical Properties Obtained from Simulations.
PB96-163761 04,103

NASH, S. G.

Guidelines for Reporting Results of Computational Experiments. Report of the Ad hoc Committee.
PB94-212347 03,427

NASHMAN, M.

Ground Vehicle Control at NIST: From Teleoperation to Autonomy.
N94-34037/9 03,758

Integrated Vision Touch-Probe System for Dimensional Inspection Tasks.
PB95-255832 02,917

Real-Time Obstacle Avoidance Using Central Flow Divergence and Peripheral Flow.
PB95-198677 02,937

Three Dimensional Position Determination from Motion.
PB95-107108 01,788

Visual Road Following without 3-D Reconstruction.
PB95-161030 01,591

NASSIMBENE, R.

Distributed measurements of tracer response on packed bed flows using a fiberoptic probe array. Final report.
DE95013079 00,667

NASSIMBENE, R. D.

Characterization of the Adsorption-Fouling Layer Using Globular Proteins on Ultrafiltration Membranes.
PB94-212909 00,842

NATER, R.

Determination of Density of Mass Standards: Requirement and Method.
PB94-163078 03,787

NAVARRO, M.

Further Development of the N-Gas Mathematical Model: An Approach for Predicting the Toxic Potency of Complex Combustion Mixtures.
PB96-123260 03,650

NAVON, E.

Study of Multiple Scattering Background in Compton Scatter Imaging.
PB96-112222 04,425

NAYAK, A.

Temperature Dependent Ultraviolet Absorption Cross Sections of Propylene, Methylacetylene and Vinylacetylene.
PB96-204177 01,169

NAYAK, A. K.

Temperature Dependence of the Gas and Liquid Phase Ultraviolet Absorption Cross Sections of HCFC-123 (CF3CHCl2) and HCFC-142b (CH3CF2Cl).
PB96-201033 03,298

Temperature Dependence of the Ultraviolet Absorption Cross Section of CF3I.
PB96-204169 01,168

UV Absorption Cross Sections of Methylchloroform: Temperature-Dependent Gas and Liquid Phase Measurements.
PB96-201041 00,643

NAZARIO, N. A.

Addressing U.S. Government Security Requirements for OSI.
PB96-160577 01,611

General Procedures for Registering Computer Security Objects.
PB94-134897 01,573

NEDZELNITSKY, V.

Complicated Cases and Shielded Rooms: Audiometric Booths Shielded to Attenuate Electromagnetic Interference.
PB96-180179 02,278

Determination of Acoustic Center Correction for Type LS2aP Condensor Microphones.
PB96-204508 04,190

NEFF, J. E.

Dynamic Phenomena on the RS Canum Venaticorum Binary II Pegasi in August 1989. 1. Observational Data.
PB94-211067 00,056

First Results from a Coordinated ROSAT, IUE, and VLA Study of RS CVn Systems.
PB94-213477 *00,069*

Rotational Modulation and Flares on RS Canum Venaticorum and BY Draconis Stars. XVIII. Coordinated VLA, ROSAT, and IUE Observations of RS CVn Binaries.
PB96-102322 *00,089*

NEGIZ, A.

Stochastic Modeling of a New Spectrometer.
PB96-157870 *04,068*

NELDER, J. A.

Taguchi's Parameter Design: A Panel Discussion.
PB96-111802 *03,445*

NELIS, T.

Atomic Oxygen Fine Structure Splittings with Tunable Far Infrared Spectroscopy.
PB95-152203 *03,915*

Determination of the Molecular Parameters of NiH in Its (2)Delta Ground State by Laser Magnetic Resonance.
PB95-107116 *00,869*

NELSON, A. J.

Enhanced Flux Pinning via Chemical Substitution in Bulk Superconducting T1-2212.
PB95-169033 *04,647*

Epitaxial Growth and Characterization of the Ordered Vacancy Compound CuIn3Se5 on GaAs (100) Fabricated by Molecular Beam Epitaxy.
PB95-180725 *04,687*

NELSON, C. W.

Design Criteria for BJT Amplifiers with Low l/f AM and PM Noise.
PB96-200365 *02,442*

Frequency Synthesis and Metrology at 10(-17) and Beyond.
PB97-113187 *02,101*

New 5 and 10 MHz High Isolation Distribution Amplifier.
PB96-190202 *01,510*

Relationship of AM to PM Noise in Selected RF Oscillators.
PB95-169009 *02,262*

NELSON, D. D.

Microwave and Submillimeter Spectroscopy of Ar-NH3 States Correlating with Ar+NH3(j=1, k=1).
PB95-152211 *00,942*

Slit-Jet Near-Infrared Diode Laser Spectroscopy of (DCl)2: nu1, nu2 DCl Stretching Fundamentals, Tunneling Dynamics, and the Influence of Large Amplitude 'Geared' Intermolecular Rotation.
PB95-203204 *01,047*

NELSON, H. E.

Fire Growth Analysis of the Fire of March 20, 1990, Pulaski Building, 20 Massachusetts Avenue, N.W., Washington, DC.
PB94-205952 *00,194*

FPETOOL: Fire Protection Tools for Hazard Estimation. An Overview of Features.
PB95-140885 *00,367*

NELSON, L. M.

Frequency Synthesis and Metrology at 10(-17) and Beyond.
PB97-113187 *02,101*

Relationship of AM to PM Noise in Selected RF Oscillators.
PB95-169009 *02,262*

NELSON, R. D.

Learning to Change: Opportunities to Improve the Performance of Smaller Manufacturers.
PB94-166212 *00,010*

NEMETH, D. T.

Fabrication Issues in Optimizing YBa2Cu3O7-x Flux Transformers for Low l/f Noise.
PB95-175857 *02,059*

Low Noise YBa2Cu3O7-x-SrTiO3-YBa2Cu3O7-x Mulitlayers for Improved Superconducting Magnetometers.
PB96-138417 *04,747*

NEMIROVSKY, A.

Hypercubic Lattice SAW Exponents nu and gamma : 3.99 Dimensions Revisited.
PB94-211026 *01,215*

NEMIROVSKY, A. M.

Examination of the l/d Expansion Method from Exact Enumeration for a Self-Interacting Self-Avoiding Walk.
PB95-175733 *01,266*

NENOFF, T. M.

Crystal Structure of a New Sodium Zinc Arsenate Phase Solved by 'Simulated Annealing'.
PB95-107124 *00,870*

Structural and Chemical Investigations of Na3(ABO4)3.4H2O-Type Sodalite Phases.
PB95-180733 *01,012*

NESBITT, D. J.

Collisional Alignment of CO2 Rotational Angular Momentum States in a Supersonic Expansion.
PB96-103171 *01,069*

High-Resolution, Direct Infrared Laser Absorption Spectroscopy in Slit Supersonic Jets: Intermolecular Forces and Unimolecular Vibrational Dynamics in Clusters.
PB95-203006 *01,040*

High-Resolution Infrared Overtone Spectroscopy of ArHF via Nd:YAG/Dye Laser Difference Frequency Generation.
PB94-211448 *00,816*

High-Resolution Infrared Overtone Spectroscopy of N2-HF: Vibrational Red Shifts and Predissociation Rate as a Function of HF Stretching Quanta.
PB96-102298 *01,061*

High-Resolution Infrared Spectroscopy of DF Trimer: A Cyclic Ground State Structure and DF Stretch Induced Intramolecular Vibrational Coupling.
PB95-150678 *00,920*

High-Resolution IR Laser-Driven Vibrational Dynamics in Supersonic Jets: Weakly Bound Complexes and Intramolecular Energy Flow.
PB94-216751 *00,862*

High Resolution IR Studies of Polymolecular Clusters: Micromatrices and Unimolecular Ring Opening.
PB94-185691 *00,777*

High Resolution, Jet-Cooled Infrared Spectroscopy of (HCl)2: Analysis of nu1 and nu2 HCl Stretching Fundamentals, Interconversion Tunneling, and Mode-Specific Predissociation Lifetimes.
PB95-203196 *01,046*

High Resolution Near Infrared Spectroscopy of HCl-DCl and DCl-HCl: Relative Binding Energies, Isomer Interconversion Rates, and Mode Specific Vibrational Predissociation.
PB95-203212 *01,048*

Intermolecular HF Motion in Ar(sub n)HF Micromatrices (n=1,2,3,4,): Classical and Quantum Calculations on a Pairwise Additive Potential Surface.
PB95-107025 *03,871*

Large Amplitude Skeletal Isomerization as a Promoter of Intramolecular Vibrational Relaxation in CH Stretch Excited Hydrocarbons.
PB95-202933 *01,036*

Mode Specific Vibrational Predissociation Dynamics in Fragile Molecules.
PB95-107132 *00,871*

Pairwise and Nonpairwise Additive Forces in Weakly Bound Complexes: High Resolution Infrared Spectroscopy of ArnDF (n=1,2,3).
PB96-200357 *04,125*

Photodissociation Dynamics in Quantum State-Selected Clusters: A Test of the One-Atom Cage Effect in Ar-H2O.
PB95-203121 *01,044*

Potential Surfaces and Dynamics of Weakly Bound Trimers: Perspectives from High Resolution IR Spectroscopy.
PB96-176508 *01,155*

Probing Potential-Energy Surfaces via High-Resolution IR Laser Spectroscopy.
PB96-102835 *01,066*

Rigid Bender Analysis of van der Waals Complexes: The Intermolecular Bending Potential of a Hydrogen Bond.
PB95-203022 *01,042*

Rotational-RKR Inversion of Intermolecular Stretching Potentials: Extension to Linear Hydrogen Bonded Complexes.
PB95-203014 *01,041*

Signatures of Large Amplitude Motion in a Weakly Bound Complex: High-Resolution IR Spectroscopy and Quantum Calculations for HeCO2.
PB95-203485 *01,054*

Slit Jet Infrared Spectroscopy of Hydrogen Bonded N2HF Isotopomers: Rotational Rydberg-Klein-Rees Analysis and H/D Dependent Vibrational Predissociation Rates.
PB95-161873 *00,956*

Slit-Jet Near-Infrared Diode Laser Spectroscopy of (DCl)2: nu1, nu2 DCl Stretching Fundamentals, Tunneling Dynamics, and the Influence of Large Amplitude 'Geared' Intermolecular Rotation.
PB95-203204 *01,047*

Slit-Jet Near-Infrared Spectroscopy and Internal Rotor Dynamics of the ArH2O van der Waals Complex: An Angular Potential-Energy Surface for Internal H2O Rotation.
PB95-202792 *01,033*

Spectroscopic Puzzle in ArHF Solved: The Test of a New Potential.
PB94-216058 *00,850*

Stabilization and Precise Calibration of a Continuous-Wave Difference Frequency Spectrometer by Use of a Simple Transfer Cavity.
PB95-162350 *04,276*

State-Resolved Rotational Energy Transfer in Open Shell Collisions: Cl((2)P3/2)+HCl.
PB96-176607 *01,157*

Sub-Doppler, Infrared Laser Spectroscopy of the Propyne 2nu1 Band: Evidence of z-Axis Coriolis Dominated Intramolecular State Mixing in the Acetylenic CH Stretch Overtone.
PB95-202941 *01,037*

Vibration, Rotation, and Parity Specific Predissociation Dynamics in Asymmetric OH Stretch Excited ArH2O: A Half Collision Study of Resonant V-V Energy Transfer in a Weakly Bound Complex.
PB95-107140 *00,872*

NETA, P.

Changes in the Redox State of Iridium Oxide Clusters and Their Relation to Catalytic Water Oxidation: Radiolytic and Electrochemical Studies.
PB95-107017 *00,864*

Electron Transfer Reaction Rates and Equilibria of the Carbonate and Sulfate Radical Anions.
PB94-212180 *00,829*

Fluoride Elimination Upon Reaction of Pentafluoroaniline with e (sub eq')(sup -), H, and OH Radicals in Aqueous Solution.
PB97-111314 *01,177*

Iodine Atoms and Iodomethane Radical Cations: Their Formation in the Pulse Radiolysis of Iodomethane in Organic Solvents, Their Complexes, and Their Reactivity with Organic Reductants.
PB95-162764 *00,965*

Metalloporphyrin Sensitized Photooxidation of Water to Oxygen on the Surface of Colloidal Iridium Oxides - Photochemical and Pulse Radiolytic Studies.
PB95-107082 *00,868*

One-Electron Oxidation of Metalloporphycenes as Studied by Radiolytic Methods.
PB97-111967 *01,179*

One-Electron Oxidation of Nickel Porphyrins. Effect of Structure and Medium on Formation of Nickel(III) Porphyrin or Nickel(II) Porphyrin pi-Radical Cation.
PB95-107058 *00,865*

Oxidation of Caffeic Acid and Related Hydroxycinnamic Acids.
PB97-111975 *00,651*

Oxidation of Ferrous and Ferrocyanide Ions by Peroxyl Radicals.
PB97-122402 *01,191*

Oxidation of 10-Methylacridan, a Synthetic Analogue of NADH and Deprotonation of Its Cation Radical. Convergent Application of Laser Flash Photolysis and Direct and Redox Catalyzed Electrochemistry to the Kinetics of Deprotonation of the Cation Radical.
PB94-198371 *00,785*

Radiation Chemistry of Cyanine Dyes: Oxidation and Reduction of Merocyanine 540.
PB94-211661 *00,818*

Reduction of Dinitrogen to Ammonia in Aqueous Solution Mediated by Colloidal Metals.
PB95-107074 *00,867*

Site of One-Electron Reduction of Ni(II) Porphyrins. Formation of Ni(I) Porphyrin of Ni(II) Porphyrin pi-Radical Anion.
PB95-107066 *00,866*

Solvent Effects in the Reactions of Peroxyl Radicals with Organic Reductants. Evidence for Proton Transfer Mediated Electron Transfer.
PB95-107157 *00,873*

Temperature Dependence of the Rate Constants for Reaction of Dihalide and Azide Radicals with Inorganic Reductants.
PB95-162756 *00,964*

Temperature Dependence of the Rate Constants for Reaction of Inorganic Radicals with Organic Reductants.
PB94-198280 *00,783*

Temperature Dependence of the Rate Constants for Reactions of the Carbonate Radical with Organic and Inorganic Reductants.
PB94-212206 *00,831*

NETTLETON, D. H.

International Intercomparison of Detector Responsivity at 1300 and 1550 nm.
PB95-125928 *02,140*

International Intercomparison of Detector Responsivity at 1300 and 1550 nm.
PB95-126017 *02,141*

NEUBAUER, G.

2D-Scanning Capacitance Microscopy Measurements of Cross-Sectioned VLSI Teststructures.
PB96-163779 *04,104*

NEUDECK, A.

Oxidation of Caffeic Acid and Related Hydroxycinnamic Acids.
PB97-111975 *00,651*

NEUGEBAUER, G. T.

Correlation of HgCdTe Epilayer Defects with Underlying Substrate Defects by Synchrotron X-Ray Topography.
PB94-200714 *02,129*

NEUMAN, D. A.

Neutron Scattering Study of the Lattice Modes of Solid Cubane.
PB96-147152 *01,126*

NEUMAN, J. A.

Energy-Pooling Collisions in Barium.
PB95-203030 *03,997*

NEUMANN, D. A.

Design of a High-Flux Backscattering Spectrometer for Ultra-High Resolution Inelastic Neutron Measurements.
PB96-179577 *02,992*

Discontinuous Volume Change at the Orientational-Ordering Transition in Solid C60.
PB94-211828 *00,821*

Energy Distributions of Neutrons Scattered from Solid C60 by the Beryllium Detector Method.
PB96-176631 *03,740*

Inelastic Neutron Scattering Studies of Rotational Excitations and the Orientational Potential in C60 and A3C60 Compounds.
PB94-172673 *00,763*

Lattice Dynamics of Ba1-xKxBiO3.
PB96-102421 *04,706*

Lattice Dynamics of Semiconducting, Metallic, and Superconducting Ba1-xKxBiO3 Studied by Inelastic Neutron Scattering.
PB96-102447 04,708

Maximum Entropy as a Tool for the Determination of the C-Axis Profile of Layered Compounds.
PB94-199619 00,800

Methyl Torsional Levels of Solid Acetonitrile (CH3CN): A Neutron Scattering Study.
PB95-151015 00,926

Neutron-Scattering Study of C60(n-) (n=3,6) Librations in Alkali-Metal Fullerides.
PB94-200219 00,806

Neutron-Scattering Study of Librations and Intramolecular Phonons in Rb2.6K0.4C60.
PB95-162269 00,958

Phase Transitions in Solid C70: Supercooling, Metastable Phases, and Impurity Effect.
PB95-150090 00,914

Phonon Density of States in R2CuO4 and Superconducting R1.85Ce0.15CuO4 (R = Nd, Pr).
PB95-150686 04,574

Rotational Dynamics of C60 in Na2RbC60.
PB95-153201 00,948

Rotational Dynamics of Solid C70: A Neutron-Scattering Study.
PB94-172178 00,755

Rotational Dynamics of Solid C70: A Neutron-Scattering Study.
PB95-153219 00,949

Structure and Dynamics of Buckyballs.
PB95-153292 00,950

X-ray Powder Diffraction from Carbon Nanotubes and Nanoparticles.
PB96-102975 03,064

NEUMAYER, D. A.

Suitability of Metalorganic Chemical Vapor Deposition-Derived PrGaO3 Films as Buffer Layers for YBa2Cu3O7-x Pulsed Laser Deposition.
PB95-168670 04,640

NEUSSER, H. J.

Doppler-Free Spectroscopy of Large Polyatomic Molecules and van der Waals Complexes.
PB96-119581 04,339

Frequency Shifting of Pulsed Narrow-Band Laser Light in a Multipass Raman Cell.
PB95-203352 04,321

Van der Waals Bond Lengths and Electronic Spectral Shifts of the Benzene-Kr and Benzene-Xe Complexes.
PB95-151387 00,932

NEWBURY, D.

Fabrication of Platinum-Gold Alloys in Pre-Hispanic South America: Issues of Temperature and Microstructure Control.
PB94-211646 03,333

NEWBURY, D. E.

Compositional Mapping of the Microstructure of Materials.
PB95-107199 00,565

Concentration Histogram Imaging: A Scatter Diagram Technique for Viewing Two or Three Related Images.
PB94-199114 00,542

Design of a Protocol for an Electron Probe Microanalyzer k-Value Round Robin.
PB95-107181 00,564

Electron Probe X-Ray Microanalysis.
PB95-107165 00,562

Microanalysis to Nanoanalysis: Measuring Composition at High Spatial Resolution.
PB95-107173 00,563

Monte Carlo Electron Trajectory Simulation of X-Ray Emission from Films Supported on Substrates.
PB95-107207 04,522

NEWBURY, N. R.

Gravitational Sisyphus Cooling of (87)Rb in a Magnetic Trap.
PB96-200704 04,379

NEWELL, A.

Planar Near-Field Alignment.
PB94-172491 01,998

NEWELL, A. C.

Comparison of Ultralow-Sidelobe-Antenna Far-Field Patterns Using the Planar-Near-Field Method and the Far-Field Method.
PB96-200373 02,015

Planar Near-Field Measurements of Low-Sidelobe Antennas.
PB94-219235 02,001

NEWELL, B. L.

Fabrication Issues for the Prototype National Institute of Standards and Technology SRM 2090A Scanning Electron Microscope Magnification Calibration Standard.
PB96-160585 01,131

NEWELL, D.

Low-Frequency, Active Vibration Isolation System.
PB95-203303 02,710

Measurement and Reduction of Alignment Errors of the NIST Watt Experiment.
PB97-111959 01,987

NIST Watt Balance: Progress Toward Monitoring the Kilogram.
PB97-113062 01,991

NEWELL, K.

National Type Evaluation Program: Index of Device Evaluations by Company. NCWM Publication 5 Part A (Second Edition).
PB94-160835 02,889

NEWHALL

Lunar Laser Ranging: A Continuing Legacy of the Apollo Program.
PB95-202495 03,683

NEWSAM, J. M.

Crystal Structure of a New Sodium Zinc Arsenate Phase Solved by 'Simulated Annealing'.
PB95-107124 00,870

NEWTON, J.

Application of Metadata Standards.
PB96-180187 01,771

NEWTON, J. J.

Standards and Linkages: What Data Sharing Needs.
PB95-161881 01,713

NG, B.

Hybrid Undulator for the NIST-NRL Free-Electron Laser.
PB94-212529 04,238

NGUYEN, N. V.

Characterization of the ZnSe/GaAs Interface Layer by TEM and Spectroscopic Ellipsometry.
PB95-175360 04,655

Determination of the Optical Constants of ZnSe Films by Spectroscopic Ellipsometry.
PB95-175378 04,656

High-Accuracy Principal-Angle Scanning Spectroscopic Ellipsometry of Semiconductor Interfaces.
PB96-163787 02,427

Interface Roughness-Induced Changes in the Near-E(sub 0) Spectroscopic Behavior of Short-Period AlAs/GaAs Superlattices.
PB94-185154 02,118

Interface Roughness of Short-Period AlAs/GaAs Superlattices Studied by Spectroscopic Ellipsometry.
PB95-107215 02,137

Interface Sharpness during the Initial Stages of Growth of Thin, Short-Period III-V Superlattices.
PB95-108783 02,139

Interface Sharpness in Low-Order III-V Superlattices.
PB95-108775 02,138

Spectroscopic Ellipsometry Determination of the Properties of the Thin Underlying Strained Si Layer and the Roughness at SiO2/Si Interface.
PB95-150157 04,560

NGUYEN, T.

Degradation of Powder Epoxy Coated Panels Immersed in a Saturated Calcium Hydroxide Solution Containing Sodium Chloride.
PB96-101050 01,344

Development of a Method for Measuring Water-Stripping Resistance of Asphalt/Siliceous Aggregate Mixtures.
PB96-197249 01,348

Development of a Method for Measuring Water-Stripping Resistance of Asphalt/Siliceous Aggregate Mixtures.
PB96-202296 01,329

Development of a Test Method for Leaching of Lead from Lead-Based Paints Through Encapsulants.
PB96-154984 03,128

Diffusion of Cations Beneath Organic Coatings on Steel Substrate.
PB94-215704 03,119

Effect of Environmentally Exposures on the Properties of Polyisocyanurate Foam Insulation: Thermal Conductivity Measurements.
PB95-181210 00,388

Effects of Humidity and Elevated Temperature on the Density and Thermal Conductivity of a Rigid Polyisocyanurate Foam.
PB95-152021 00,373

Effects of Humidity and Elevated Temperature on the Density and Thermal Conductivity of a Rigid Polyisocyanurate Foam Co-Blown with CCl3F and CO2.
PB95-150462 00,371

In situ Measurements of Chloride Ion and Corrosion Potential at the Coating/Metal Interface.
PB95-140893 03,122

Materials-Science Based Approach to Phenol Emissions from a Flooring Material in an Office Building.
PB97-118749 02,572

Relation between AC Impedance Data and Degradation of Coated Steel. 1. Effects of Surface Roughness and Contamination on the Corrosion Behavior of Epoxy Coated Steel.
PB94-213345 03,189

Source of Phenol Emissions Affecting the Indoor Air of an Office Building.
PB94-154382 03,600

NICHIPOROV, D.

Investigation of Applicability of Alanine and Radiochromic Detectors to Dosimetry of Proton Clinical Beams.
PB96-146782 03,636

NICOL, J.

Inelastic Neutron Scattering Studies of Nonlinear Optical Materials: p-Nitroaniline Adsorbed in ALPO-5.
PB95-107223 00,874

NICOL, J. M.

Characterization of the Interaction of Hydrogen with Iridium Clusters in Zeolites by Inelastic Neutron Scattering Spectroscopy.
PB95-180741 01,013

Crystal Structure of a New Sodium Zinc Arsenate Phase Solved by 'Simulated Annealing'.
PB95-107124 00,870

Neutron and Raman Spectroscopies of 134 and 134a Hydrofluorocarbons Encaged in Na-X Zeolite.
PB96-186168 03,001

Powder Neutron Diffraction Investigation of Structure and Cation Ordering in Ba2+xBi2-xO6-y.
PB95-180865 01,015

Small Angle Neutron Scattering Study of the Structure and Formation of MCM-41 Mesoporous Molecular Sieves.
PB97-122337 03,110

Small Angle Neutron Scattering Study of the Structure and Formation of Ordered Mesopores in Silica.
PB96-111919 03,069

Structural and Chemical Investigations of Na3(ABO4)3.4H2O-Type Sodalite Phases.
PB95-180733 01,012

Tetrahedral-Framework Lithium Zinc Phosphate Phases: Location of Light-Atom Positions in LiZnPO4 H2O by Powder Neutron Diffraction and Structure Determination of LiZnPO4 by ab Initio Methods.
PB96-160510 01,129

NIEBAUER, T. M.

Continuous Gravity Observations Using Joint Institute for Laboratory Astrophysics Absolute Gravimeters.
PB95-203048 03,685

Intracomparison Tests of the FG5 Absolute Gravity Meters.
PB96-102991 03,688

Test of Newton's Inverse Square Law of Gravitation Using the 300-m Tower at Erie, Colorado.
PB95-202446 03,978

NIELSEN, L.

Precision Comparison of the Lattice Parameters of Silicon Monocrystals.
PB94-169745 04,438

NIEMEYER, J.

SUSAN: SUperconducting Systems ANalysis by Low Temperature Scanning Electron Microscopy (LTSEM).
PB96-112065 04,728

NIESEN, V. G.

Coexisting Densities, Vapor Pressures and Critical Densities of Refrigerants R-32 and R-152a, at 300 - 385 K.
PB95-175691 03,274

Experimental Method for Obtaining Critical Densities of Binary Mixtures: Application to Ethane + n-Butane.
PB95-151148 00,930

NIETO DE CASTRO, C. A.

Polarized Transient Hot Wire Thermal Conductivity Measurements.
PB95-108817 00,886

Standard Reference Data for the Thermal Conductivity of Water.
PB96-145875 01,111

Status of the Round Robin on the Transport Properties of R134a.
PB96-167218 01,152

Supercritical Fluid Extraction of Biological Products.
PB95-175204 00,040

Thermal Conductivity of R134a.
PB94-213063 03,857

Transient Methods for Thermal Conductivity.
PB94-198405 04,197

NIGHTINGALE, J. S.

Lessons from the Establishment of the U.S. GOSIP Testing Program.
PB96-119359 01,817

U.S. GOSIP Testing Program.
PB94-211455 01,807

NIGHTINGALE, S.

Formal Multi-Layer Test Methodology and Its Application to OSI.
PB94-172194 02,718

National Voluntary Laboratory Accreditation Program. GOSIP: Government Open Systems Interconnection Profile.
PB95-267993 01,486

NIMIS, R.

Northridge Earthquake 1994: Performance of Structures, Lifelines, and Fire Protection Systems.
PB94-207461 04,825

NISHIOKA, R. S.

Histopathology, Blood Chemistry, and Physiological Status of Normal and Moribund Striped Bass ('Morone saxatilis') Involved in Summer Mortality ('Die-Off') in the Sacramento-San Joaquin Delta of California.
PB94-198157 00,034

NOBEL, G.

Real Time Compensation for Tool Form Errors in Turning Using Computer Vision.
PB95-107231 02,945

NOBLE, R.
Gas Transport Properties of Solution-Cast Perfluorosulfonic Acid Ionomer Films Containing Ionic Surfactants.
PB95-175998 *01,267*

NOCHOLS-BOHLIN, J.
Recalibration for the Final Archive of the International Ultraviolet Explorer (IUE) Satellite.
PB96-135264 *00,106*

NODA, I.
Localization of a Homopolymer Dissolved in a Lamellar Structure of a Block Copolymer Studied by Small-Angle Neutron Scattering.
PB95-161592 *01,253*

Molecular Weight Dependence of the Lamellar Domain Spacing of ABC Triblock Copolymers and Their Chain Conformation in Lamellar Domains.
PB95-161691 *01,254*

NOESTERER, M.
Microdosimetry and Cellular Radiation Effects of Radon Progency in Human Bronchial Airways.
PB95-152344 *03,625*

NOMURA, S.
Small Angle Neutron Scattering Studies on Chain Asymmetry of Coextruded Poly(Vinyl Alcohol) Film.
PB95-164372 *01,262*

NORCROSS, D. W.
Angle-Differential and Momentum-Transfer Cross Sections for Low-Energy Electron-Cs Scattering.
PB95-203402 *04,005*

Characteristics of Light Emission After Low-Energy Electron Impact Excitation of Caesium Atoms.
PB94-198587 *03,806*

High-Precision Calculations of Cross Sections for Low-Energy Electron Scattering by Ground and Excited State of Sodium.
PB95-152161 *03,914*

Low-Energy-Electron Collisions with Sodium: Elastic and Inelastic Scattering from the Ground State.
PB96-103106 *04,030*

Relativistic Effects in Spin-Polarization Parameters for Low-Energy Electron-Cs Scattering.
PB95-150868 *03,901*

Relativistic R-Matrix Calculations for Electron - Alkali-Metal-Atom Scattering: Cs as a Test Case.
PB95-203410 *04,006*

Slow-Electron Collisions with CO Molecules in an Exact-Exchange Plus Parameter-Free Polarization Model.
PB95-202719 *03,989*

NORCROSS, R. J.
AMRF Composite Fabrication Workstation.
PB94-172681 *02,810*

NORDLANDER, P.
Influence of Coadsorbed Potassium on the Electron-Stimulated Desorption of F(+), F(-), and F(*) from PF3 on Ru(0001).
PB96-157946 *04,072*

Photoluminescence Spectra of Epitaxial Single Crystal C60.
PB96-141205 *04,754*

NORMAN, B. R.
High-Sensitivity Determination of Iodine Isotopic Ratios by Thermal and Fast Neutron Activation.
PB94-213386 *00,555*

NORMAN, G. R.
Regulation of Lithium and Boron Levels in Normal Human Blood: Environmental and Genetic Considerations.
PB94-198579 *03,491*

NORRIS, G. A.
Multiattribute Decision Analysis Method for Evaluating Buildings and Building Systems.
PB96-158670 *00,325*

NORRIS, J. A.
Apparent Bias in the X-Ray Fluorescence Determination of Titanium in Selected NIST SRM Low Alloy Steels.
PB95-108759 *03,212*

NORTH, S.
Oxidative DNA Base Damage in Renal, Hepatic, and Pulmonary Chromatin of Rats After Intraperitoneal Injection of Cobalt (II) Acetate.
PB95-150025 *03,647*

NORTHROP, D. M.
Separation and Identification of Organic Gunshot and Explosive Constituents by Micellar Electrokinetic Capillary Electrophoresis.
PB95-107249 *00,566*

NORTON, M.
Optical Conductivity of Single Crystals of Ba1-xMxBiO3(M=K, Rb, x=0.04, 0.37).
PB94-185329 *04,447*

NORTON, P. W.
Comparison of Techniques for Nondestructive Composition Measurements in CdZnTe Substrates.
PB96-103098 *02,703*

NORTON, S.
Analysis of Thermal Wave Propagation in Diamond Films.
PB94-211471 *03,014*

Thermal Wave Propagation in Diamond Films.
PB94-211489 *03,015*

NORTON, S. J.
Reconstructing Stratified Fluid Flow from Reciprocal Scattering Measurements.
PB95-107256 *04,202*

Ultrasonic Method for Reconstructing the Two-Dimensional Liquid-Solid Interface in Solidifying Bodies.
PB95-161782 *03,349*

Ultrasonic Spectroscopy of Metallic Spheres Using Electromagnetic-Acoustic Transduction.
PB94-212537 *04,185*

NORTON, T. S.
Comparison of Experimental and Computed Species Concentration and Temperature Profiles in Laminar, Two-Dimensional Methane/Air Diffusion Flames.
PB95-140919 *01,379*

NOSSAL, R.
Small Angle Neutron Scattering Studies of Structural Characteristics of Argarose Gels.
PB96-112305 *03,475*

NOTARIANNI, K.
Protection of Data Processing Equipment with Fine Water Sprays.
PB95-174975 *02,610*

NOTARIANNI, K. A.
Analysis of High Bay Hangar Facilities for Detector Sensitivity and Placement.
PB96-190210 *01,429*

Comparison of Fire Sprinkler Piping Materials: Steel, Copper, Chlorinated Polyvinyl Chloride and Polybutylene, in Residential and Light Hazard Installations.
PB95-182267 *00,299*

Measurement of Room Conditions and Response of Sprinklers and Smoke Detectors during a Simulated Two-Bed Hospital Patient Room Fire.
PB94-213717 *00,292*

NASA Fire Detector Study.
PB96-183108 *01,423*

Use of Computer Models to Predict Temperature and Smoke Movement in High Bay Spaces.
PB94-145976 *00,191*

Water Mist Fire Suppression Workshop Summary.
PB95-161907 *02,853*

NOVAK, S. W.
Using Secondary Ion Mass Spectrometry (SIMS) to Characterize Optical Waveguide Materials.
PB96-119599 *04,340*

NOVICK, A.
Diode-Laser Pumped, Rubidium Cell Frequency Standards.
PB95-163218 *01,538*

Reducing the Effect of Local Oscillator Phase Noise on the Frequency Stability of Passive Frequency Standards.
PB95-180972 *01,545*

NOVICK-COHEN, A.
Evolution Equations for Phase Separation and Ordering in Binary Alloys.
PB96-119243 *02,979*

NOVOTNY, D.
Realizing Suspended Structures on Chips Fabricated by CMOS Foundry Processes Through the MOSIS Service.
PB94-193984 *01,881*

NOVOTNY, D. B.
Development and Characterization of Insulating Layers on Silicon Carbide: Annual Report for February 14, 1988 to February 14, 1989.
PB94-155579 *02,295*

Development of Thin-Film Multijunction Thermal Converters at NIST.
PB97-112338 *02,286*

High-Current Thin Film Multijunction Thermal Converters and Multi-Converter Modules.
PB97-112379 *01,989*

High-Spatial-Resolution Resistivity Mapping Applied to Mercury Cadmium Telluride.
PB94-212917 *02,131*

Integrated Thin-Film Micropotentiometers.
PB96-146709 *02,109*

Performance of Multilayer Thin-Film Multijunction Thermal Converters.
PB96-148135 *02,084*

NOVOTNY, D. R.
Optically Linked Three-Loop Antenna System for Determining the Radiation Characteristics of an Electrically Small Source.
PB95-161915 *02,005*

NOZAKI, H.
Elastic Constants and Microcracks in YBa2Cu3O7.
PB96-200761 *03,005*

NUBBEMEYER, H. G.
Comparisons of Some NIST Fixed-Point Cells with Similar Cells of Other Standards Laboratories.
PB97-119242 *00,655*

Direct Comparison of Three PTB Silver Fixed-Point Cells with the NIST Silver Fixed-Point Cell.
PB96-161286 *00,628*

NUNEZ, V.
Crystallographic and Magnetic Properties of UAuSn.
PB95-140521 *04,543*

Supermirror Transmission Polarizers for Neutrons.
PB94-216215 *03,866*

NUSGENS, P.
Use of Building Emulators to Evaluate the Performance of Building Energy Management Systems.
PB96-111901 *00,269*

NUSS, J. M.
Lowest Excited Singlet State of Isolated 1-phenyl-1,3-butadiene and 1-phenyl-1,3,5-hexatriene.
PB95-202339 *01,026*

NYBERG, G. L.
Spot-Profile-Analyzing LEED Study of the Epitaxial Growth of Fe, Co, and Cu on Cu(100).
PB95-150165 *04,561*

NYDEN, M.
Agent Screening for Halon 1301 Aviation Replacement.
PB96-159710 *03,282*

NYDEN, M. R.
Computer-Aided Molecular Design of Fire Resistant Aircraft Materials.
PB96-160601 *00,025*

Halon Thermochemistry: 'Ab Initio' Calculations of the Enthalpies of Formation of Fluoromethanes.
PB96-175740 *03,289*

Investigation into the Flammability Properties of Honeycomb Composites.
PB95-143293 *03,152*

Investigation of the Thermal Stability and Char-Forming Tendency of Cross-linked Poly(methyl methacrylate).
PB94-213501 *03,380*

New Generation of Fire Resistant Polymers. Part 1. Computer-Aided Molecular Design.
PB96-160593 *01,419*

Tomographic Reconstruction of the Moments of Local Probability Density Functions in Turbulent Flow Fields.
PB96-180195 *04,219*

O'BRIAN, T.
RIS Measurements of the AC Stark Shift.
PB96-158035 *04,078*

O'BRIAN, T. R.
Configuration-Dependent AC Stark Shifts in Calcium.
PB96-157995 *04,363*

Improved Dose Metrology in Optical Lithography.
PB96-179510 *02,439*

Measurement of CO Pressures in the Ultrahigh Vacuum Regime Using Resonance-Enhanced Multiphoton-Ionization Time-of-Flight Mass Spectroscopy.
PB94-216041 *03,864*

RIS Measurement of AC Stark Shifts and Photoionization Cross Sections in Calcium.
PB96-157953 *04,073*

Verification of the Ponderomotive Approximation for the ac Stark Shift in Xe Rydberg Levels.
PB94-185709 *03,801*

O'BRIEN, W. L.
Al L2,3 Core Excitons in AlxGa1-x as Studied by Soft-X-ray Reflection and Emission.
PB96-157839 *04,067*

Barium Contributions to the Valence Electronic Structure of YBa2Cu3O7-delta, PrBa2Cu3O7-delta, and Other Barium-Containing Compounds.
PB96-158019 *04,076*

Charge-Transfer-Induced Multiplet Structure in the N4,5O2,3 Soft-X-ray Emission Spectrum of Lanthanum.
PB96-163746 *04,102*

Cooper M(sub II,III) X-ray-Emission Spectra of Copper Oxides and the Bismuth Cuprate Superconductor.
PB96-158027 *04,077*

Intermediate Coupling in L2-L3 Core Excitons of MgO, Al2O3, and SiO2.
PB96-158043 *04,079*

Laser-Synchrotron Hybrid Experiments: A Photon to Tickle, A Photon to Poke.
PB96-157847 *03,704*

Local Partial Densities of States in Ni and Co Silicides Studied by Soft X-Ray Emission Spectroscopy.
PB94-212412 *04,504*

Phonon Relaxation in Soft-X-ray Emission of Insulators.
PB96-160296 *04,085*

Simple Variable Line Space Grating Monochromator for Synchrotron Light Source Beamlines.
PB96-156203 *04,065*

Soft-X-ray-Emission Investigation of Cobalt Implanted Silicon Crystals.
PB96-157912 *04,069*

Soft-X-ray-Emission Spectra of Solid Kr and Xe.
PB96-157920 *04,070*

Soft-X-ray-Emission Studies of Bulk Fe3Si, FeSi, and FeSi2, and Implanted Iron Silicides.
PB96-157938 *04,071*

O'CONNELL, K.
Frozen Human Serum Reference Material for Standardization of Sodium and Potassium Measurements in Serum or Plasma by ion-Selective Electrode Analyzers.
PB94-185337 *00,532*

O'CONNOR, C. L.

NIST Reactor: Summary of Activities October 1992 through September 1993.
PB94-161502 *04,437*

NIST Reactor: Summary of Activities, October 1993 through September 1994.
PB95-220430 *04,700*

O'FARRELL, T. J.

Effect of Ethanol on the Solubility of Dicalcium Phosphate Dihydrate in the System Ca(OH)2-H3PO4-H2O at 37C.
PB95-163507 *00,163*

O'HARE, P. A. G.

Conference Report: Calorimetry Conference (50th).
PB97-122279 *03,722*

Disilicides of Tungsten, Molybdenum, Tantalum, Titanium, Cobalt, and Nickel, and Platinum Monosilicide: A Survey of Their Thermodynamic Properties.
PB94-168580 *00,752*

Thermochemical Studies of Inorganic Chalocogenides by Fluorine-Combustion Calorimetry: Binary Compounds of Germanium and Silicon with Sulfur, Selenium and Tellurium.
PB97-112528 *01,181*

Thermodynamic Properties of Gaseous Silicon Monotelluride and the Bond Dissociation Enthalpy D(sub m)(SiTe) at T approaches 0.
PB94-168572 *00,751*

Thermodynamic Properties of Silicides. 5. Standard Molar Enthalpy of Formation at the Temperature 298.15 K of Trimolybdenum Monosilicide Mo3Si Determined by Fluorine-Combustion Calorimetry.
PB97-119358 *01,190*

Thermodynamics of (Germanium + Selenium): A Review and Critical Assessment.
PB97-112536 *01,182*

O'HAVER, T. C.

Liquid Chromatography: Laser-Enhanced Ionization Spectrometry for the Speciation of Organolead Compounds.
PB94-185253 *00,530*

O'MALLEY, M. L.

Increased Transition Temperature in In situ Coevaporated YBa2Cu3O7-delta Thin Films by Low Temperature Post-Annealing.
PB95-180071 *04,672*

O'REILLY, J. W.

Magnetic Ordering of the Cu Spins in PrBa2Cu3O6+x.
PB95-140547 *04,545*

O'SHANNESSY, D. J.

Phospholipid/Alkanethiol Bilayers for Cell-Surface Receptor Studies by Surface Plasmon Resonance.
PB96-102900 *03,472*

O'SULLIVAN, P.

Assessing MOS Gate Oxide Reliability on Wafer Level with Ramped/Constant Voltage and Current Stress.
PB96-180112 *04,115*

New Oxide Degradation Mechanism for Stresses in the Fowler-Nordheim Tunneling Regime.
PB96-200985 *04,128*

OAKLEY, E.

Enthalpy Increment Measurements from 4.5 K to 350 K and the Thermodynamic Properties of the Titanium Silicide Ti5Si3(cr).
PB96-204037 *00,679*

OAKLEY, L.

Materials-Science Based Approach to Phenol Emissions from a Flooring Material in an Office Building.
PB97-118749 *02,572*

Source of Phenol Emissions Affecting the Indoor Air of an Office Building.
PB94-154382 *03,600*

OAKLEY, L. M.

Certification of Polychlorinated Biphenyl Congeners and Chlorinated Pesticides in a Whale Blubber Standard Reference Material.
PB96-103023 *03,745*

OATES, C. W.

High-Resolution Optical Multiplex Spectroscopy.
PB95-203543 *04,323*

Improved Hyperfine Measurements of the Na NP Excited State Through Frequency-Controlled Dopplerless Spectroscopy in a Zeeman Magneto-Optic Laser Trap.
PB95-203840 *04,012*

OBERLE, R. R.

Magnetic and Structural Properties of Electrodeposited Copper-Nickel Microlayered Alloys.
PB94-213121 *04,512*

OBERNDORF, P.

Next Generation Computer Resources: Reference Model for Project Support Environments (Version 2.0).
PB94-143401 *01,677*

OELKERS, E. H.

Summary of the Apparent Standard Partial Molal Gibbs Free Energies of Formation of Aqueous Species, Minerals, and Gases at Pressures 1 to 5000 Bars and Temperatures 25 to 1000C.
PB96-145891 *01,113*

OGBURN, F.

Aging Effects on XRF Measurements of Solder Coatings.
PB95-140927 *03,123*

OHLEMILLER, T.

One- and Two-Sided Burning of Thermally Thin Materials.
PB95-140935 *03,151*

OHLEMILLER, T. J.

Behavior of Mock-Ups in the California Technical Bulletin 133 Test Protocol: Fabric and Barrier Effects.
PB95-231585 *00,301*

Effect of Suppressants on Metal Fires.
PB96-109574 *01,402*

Examination of the Correlation between Cone Calorimeter Data and Full-Scale Furniture Mock-Up Fires.
PB96-148200 *01,417*

Influence of Ignition Source on the Flaming Fire Hazard of Upholstered Furniture. (NIST Reprint).
PB95-180162 *00,297*

Low Heat-Flux Measurements: Some Precautions.
PB96-201116 *02,685*

Quantifying the Ignition Propensity of Cigarettes.
PB96-155411 *00,306*

OHNO, Y.

Characterization of Modified FEL Quartz-Halogen Lamps for Photometric Standards.
PB97-112544 *00,282*

Detector-Based Candela Scale and Related Photometric Calibration Procedures at NIST.
PB95-161949 *04,273*

Integrating Sphere Simulation: Application to Total Flux Scale Realization.
PB95-150173 *04,261*

Intercomparison of Photometric Units Maintained at NIST (USA) and PTB (Germany), 1993.
PB95-261913 *04,329*

Interface-Filter Characterization of Spectraradiometers and Colorimeters.
PB97-122212 *04,399*

New Method for Realizing a Luminous Flux Scale Using an Integrating Sphere with an External Source.
PB96-102843 *04,333*

NIST Detector-Based Luminous Intensity Scale.
PB96-179114 *01,864*

Realization of NIST 1995 Luminous Flux Scale Using the Integrating Sphere Method.
PB96-176433 *04,374*

OISHI, Y.

Preparation of 2-Dimensional Ultra Thin Polystyrene Film by Water Casting Method.
PB95-162806 *04,619*

OKAMOTO, P.

Optimization of Highway Concrete Technology.
PB94-182995 *01,333*

OKAMOTO, T.

Standardised Computer Data File Format for Storage, Transport, and Off-Line Processing of Partial Discharge Data.
PB96-122486 *01,930*

OKAYASU, S.

Harmonic and Static Susceptibilities of YBa2Cu3O7.
PB95-161139 *04,599*

OKAZAKI, K.

Spectral Data for Highly Ionized Krypton, Kr V through Kr XXXVI.
PB96-145917 *01,115*

OKORODUDU, A.

Frozen Human Serum Reference Material for Standardization of Sodium and Potassium Measurements in Serum or Plasma by Ion-Selective Electrode Analyzers.
PB94-185337 *00,532*

OLDEHOEFT, A. E.

Assessment of the DOD Goal Security Architecture (DGSA) for Non-Military Use.
PB95-189510 *03,653*

Report of the NIST Workshop on Key Escrow Encryption. Held in Gaithersburg, Maryland on June 8-10, 1994.
PB94-209459 *01,584*

OLDHAM, N.

Exploring the Low-Frequency Performance of Thermal Converters Using Circuit Models and a Digitally Synthesized Source.
PB97-112551 *02,848*

OLDHAM, N. M.

Automatic Calibration of Inductive Voltage Dividers for the NASA Zeno Experiment.
PB95-152849 *02,041*

Automatic Inductive Voltage Divider Bridge Operates from 10 Hz to 100 kHz.
PB94-198413 *02,032*

Binary versus Decade Inductive Voltage Divider Comparison and Error Decomposition.
PB96-112263 *02,071*

DC-MHz Wattmeter Based on RMS Voltage Measurements.
PB97-113211 *01,992*

Digital Impedance Bridge.
PB96-103155 *02,272*

Inductive Voltage Divider Calibration for the NASA Flight Experiment.
PB95-152856 *02,042*

Low Voltage Standards in the 10 Hz to 1 MHz Range.
PB97-112569 *02,100*

Overview of Bioelectrical Impedance Analyzers
PB96-122635 *00,176*

Overview of Bioelectrical Impedance Analyzers.
PB97-118780 *00,181*

OLINGER, T. M.

CCD Mosaic Images of the Supernova Remnant 3C 400.2.
PB95-203527 *00,084*

OLINSKI, R.

DNA Base Damage in Lymphocytes of Cancer Patients Undergoing Radiation Therapy.
PB97-122444 *03,643*

Modification of DNA Bases in Chromatin of Intact Target Human Cells by Activated Human Polymorphonuclear Leukocytes.
PB94-199833 *03,526*

Nickel(II)-Mediated Oxidative DNA Base Damage in Renal and Hepatic Chromatin of Pregnant Rats and Their Fetuses. Possible Relevance to Carcinogenesis.
PB94-212628 *03,646*

OLK, C. H.

X-ray Powder Diffraction from Carbon Nanotubes and Nanoparticles.
PB96-102975 *03,064*

OLSEN, K.

Impact of the FCC's Open Network Architecture on NS/NP Telecommunications Security.
PB95-189445 *01,483*

Introduction to the P1003.1g and CPI-C Network Application Programming Interfaces.
PB95-231726 *01,731*

Security in Open Systems.
PB95-105383 *01,473*

OLSEN, P. T.

Measurement and Reduction of Alignment Errors of the NIST Watt Experiment.
PB97-111959 *01,987*

Methods for Aligning the NIST Watt-Balance.
PB96-123153 *01,934*

NIST Watt Balance: Progress Toward Monitoring the Kilogram.
PB97-113062 *01,991*

OLSON, D. A.

Heat Transfer in Thin, Compact Heat Exchangers with Circular, Rectangular, or Pin-Fin Flow Passages.
PB95-140943 *02,751*

Thermal Hydraulic Tests of a Liquid Hydrogen Cold Neutron Source.
PB95-135570 *03,884*

OLSON, G. J.

Atmospheric and Marine Trace Chemistry: Interfacial Biomediation and Monitoring.
PB94-199122 *03,752*

Bioleaching of Cobalt from Smelter Wastes by 'Thiobacillus ferrooxidans'.
PB95-140968 *02,582*

Characterization of the Binding of Gallium, Platinum, and Uranium to Pseudomonas Fluorescens by Small-Angle X-ray Scattering and Transmission Electron Microscopy.
PB94-172509 *03,453*

Chemical and Microbiological Problems Associated with Research on the Biodesulfurization of Coal.
PB95-140950 *02,484*

Microbial Degradation of Polysulfides and Insights into Their Possible Occurrence in Coal.
PB95-163374 *02,488*

Total Surface Areas of Group IVA Organometallic Compounds: Predictors of Toxicity to Algae and Bacteria.
PB94-211331 *00,814*

OLSON, J. M.

In situ Observation of Surface Morphology of InP Grown on Singular and Vicinal (001) Substrates.
PB95-168431 *04,636*

Surface Topography and Ordering-Variant Segregation in GaInP2.
PB95-153649 *04,595*

OLSON, W. B.

2nu9 Band of Propyne-d3.
PB95-164513 *00,985*

FTS Infrared Measurements of the Rotational and Vibrational Spectrum of LiH and LiD.
PB94-216231 *00,856*

OLSSON, M.

Comparison of the Liquid Chromatographic Behavior of Selected Steroid Isomers Using Different Reversed-Phase Materials and Mobile Phase Compositions.
PB95-140976 *00,574*

Modification of Deoxyribose-Phosphate Residues by Extracts of Ataxia Telangiectasia Cells.
PB94-212602 *03,458*

OLTHOFF, J. K.

Appearance Potentials of Ions Produced by Electron-Impact Induced Dissociative Ionization of SF6, SF4, SF5Cl, S2F10, SO2, SO2F2, SOF2, and SOF4.
PB96-119730 *01,080*

Associative Electron Attachment to S2F10, S2OF10, and S2O2F10.
PB95-140992 *00,907*

Decomposition of Sulfur Hexafluoride by X-rays.
PB96-135314 *01,095*

Effect of Electrode Material on Measured Ion Energy Distributions in Radio-Frequency Discharges.
PB96-102850 *04,026*

Electrical Sensors for Monitoring rf Plasma Sheaths.
PB95-162962 *04,412*

Electron Scattering and Dissociative Attachment by SF6 and Its Electrical-Discharge By-Products.
PB95-151288 *02,256*

Evidence for Inelastic Processes for N(+)3 and N(+)4 from Ion Energy Distributions in He/N2 Radio Frequency Glow Discharges.
PB96-146683 *04,059*

Fundamental Processes in Gas Discharges.
PB96-123450 *01,089*

Gaseous Electronics Conference Radio-Frequency Reference Cell: A Defined Parallel-Plate Radio-Frequency System for Experimental and Theoretical Studies of Plasma-Processing Discharges.
PB94-172327 *04,404*

Gaseous Electronics Conference RF Reference Cell: An Introduction.
PB96-113329 *02,387*

Influence of Electrode Material on Measured Ion Kinetic-Energy Distributions in Radio-Frequency Discharges.
PB96-123179 *01,935*

Investigation of S2F10 Production and Mitigation in Compressed SF6-Insulated Power Systems.
PB94-212388 *02,467*

Investigation of S2F10 Production and Mitigation in Compressed SF6- Insulated Power Systems.
PB96-155528 *02,468*

Ion Kinetic-Energy Distributions and Balmer-alpha (Halpha) Excitation in Ar-H2 Radio-Frequency Discharges.
PB96-102959 *04,029*

Ion Kinetic-Energy Distributions in Argon rf Glow Discharges.
PB95-141008 *04,409*

Ion Kinetics and Symmetric Charge-Transfer Collisions in Low-Current, Diffuse (Townsend) Discharges in Argon and Nitrogen.
PB96-123658 *04,051*

Kinetic Energy Distribution of Ions Produced from Townsend Discharges in Neon and Argon.
PB96-111927 *04,413*

Kinetic Energy Distributions of H(+), H2(+), and H3(+) from a Diffuse Townsend Discharge in H2 at High E/N.
PB96-123351 *04,415*

Kinetic-Energy Distributions of Ions Sampled from Argon Plasmas in a Parallel-Plate, Radio-Frequency Reference Call.
PB95-161964 *03,935*

Kinetic-Energy Distributions of Ions Sampled from Radio-Frequency Discharges in Helium, Nitrogen, and Oxygen.
PB96-123732 *01,092*

Kinetic-Energy Distributions of K(+) in Argon and Neon in Uniform Electric Fields.
PB95-151122 *03,902*

Measurement of S2OF10, and S2O2F10 Production Rates from Spark and Negative Glow Corona Discharge in SF6/O2 Gas Mixtures.
PB96-123740 *01,093*

Metrology Requirements of Future Space Power Systems.
PB95-140984 *04,840*

Optical and Mass Spectrometric Investigations of Ions and Neutral Species in SF6 Radio-Frequency Discharges.
PB97-111918 *01,985*

Procedure for Measuring Trace Quantities of S2F10, S2OF10, and S2O2F10 in SF6 Using a Gas Chromatograph-Mass Spectrometer.
PB96-119755 *02,513*

Studies of Ion Kinetic-Energy Distributions in the Gaseous Electronics Conference RF Reference Cell.
PB96-113360 *02,391*

Time-Resolved Balmer-Alpha Emission from Fast Hydrogen Atoms in Low Pressure, Radio-Frequency Discharges in Hydrogen.
PB96-102942 *04,028*

Use of an Ion Energy Analyzer: Mass Spectrometer to Measure Ion Kinetic-Energy Distributions from RF Discharges in Argon-Helium Gas Mixtures.
PB94-185717 *04,406*

OLVER, F. W. J.

Numerical Evaluation of Special Functions.
PB96-119557 *03,417*

Review of Mathematical Function Library for Microsoft-FORTRAN, John Wiley and Sons, 1989.
PB94-160793 *01,679*

OMIDVAR, O. M.

Effect of Training Dynamics on Neural Network Performance.
PB95-267845 *01,852*

Improving Neural Network Performance for Character and Fingerprint Classification by Altering Network Dynamics.
PB95-267803 *01,851*

Improving Neural Network Performance for Character and Fingerprint Classification by Altering Network Dynamics.
PB96-123195 *01,856*

OMORI, A.

Effects of Molecular Weight and Thermal Stability on Polymer Gasification.
PB94-212610 *01,228*

OMRON, R. M.

Rotational Spectra of CH3CCH-NH3, NCCCH-NH3, and NCCCH-OH2.
PB97-118798 *04,170*

ONDOV, J. M.

Rare-Earth Isotopes as Tracers of Particulate Emissions: An Urban Scale Test.
PB94-161635 *02,535*

ONDREJKA, A.

Time-Domain Measurements of the Electromagnetic Backscatter of Pyramidal Absorbers and Metallic Plates.
PB94-185410 *01,877*

ONDREJKA, A. R.

Aperture Excitation of Electrically Large, Lossy Cavities.
PB94-145711 *00,029*

Aperture Excitation of Electrically Large, Lossy Cavities.
PB95-175675 *00,031*

Bistatic Scattering of Absorbing Materials from 30 to 1000 MHz.
PB95-150934 *01,891*

Measurements of Shielding Effectiveness and Cavity Characteristics of Airplanes.
PB94-210051 *00,030*

Rapid Evaluation of Mode-Stirred Chambers Using Impulsive Waveforms.
PB96-210026 *01,979*

Time-Domain Antenna Characterizations.
PB95-152781 *02,003*

ONEIL, S.

Bonding in Doubly Charged Diatomics.
PB95-164315 *00,976*

ONO, R. H.

Characterization of a Tunable Thin Film Microwave YBa2Cu3O7-x/SrTiO3 Coplanar Capacitor.
PB95-175527 *02,264*

Coexistence of Grains with Differing Orthorhombicity in High Quality YBa2Cu3O7-delta Thin Films.
PB96-135033 *04,742*

Controlling the Critical Current Density of High-Temperature SNS Josephson Junctions.
PB96-200712 *04,794*

Critical Current and Normal Resistance of High-Tc Step-Edge SNS Junctions.
PB96-111752 *04,724*

Critical Current Behavior of Ag-Coated YBa2Cu3O7-x Thin Films.
PB95-141016 *04,549*

Effect of Thermal Noise on Shapiro Steps in High-Tc Josephson Weak Links.
PB94-212677 *04,506*

High Critical Temperature Superconductor Tunneling Spectroscopy Using Squeezable Electron Tunneling Junctions.
PB95-163721 *04,627*

High-Tc Multilayer Step-Edge Josephson Junctions and SQUIDs.
PB96-200183 *04,790*

High Temperature Superconductor-Normal Metal-Superconductor Josephson Junctions with High Characteristic Voltages.
PB95-176079 *04,666*

Increased Transition Temperature in In situ Coevaporated YBa2Cu3O7-delta Thin Films by Low Temperature Post-Annealing.
PB95-180071 *04,672*

Magnetic Field Dependence of the Critical Current Anisotropy in Normal Metal-YBa2Cu3O7-delta Thin Film Bilayers.
PB95-141024 *04,550*

Mutual Phase Locking in Systems of High-Tc Superconductor-Normal Metal-Superconductor Junctions.
PB96-135348 *04,744*

Phase Locking in Two-Junction Systems of High-Temperature Superconductor-Normal Metal-Superconductor Junctions.
PB95-176053 *02,060*

Stacked Series Arrays of High-Tc Trilayer Josephson Junctions.
PB96-102272 *04,705*

Step-Edge and Stacked-Heterostructure High-Tc Josephson Junctions for Voltage-Standard Arrays.
PB96-102066 *04,702*

Temperature Dependence and Magnetic Field Modulation of Critical Currents in Step-Edge SNS YBCO/Au Junctions.
PB96-111745 *04,723*

Thermal Noise in High-Temperature Superconducting-Normal-Superconducting Step-Edge Josephson Junctions.
PB95-175089 *04,650*

Tunable High Temperature Superconductor Microstrip Resonators.
PB95-168423 *02,048*

Tunneling Measurement of the Zero-Bias Conductance Peak and the Bi-Sr-Ca-Cu-O Thin-Film Energy Gap.
PB95-163739 *04,628*

YBa2Cu3O7-x to Si Interconnection for Hybrid Superconductor/Semiconductor Integration.
PB94-211711 *02,315*

ONYSHCZAK, R.

Standardization of Testing Methods for Optical Disk Media Characteristics and Related Activities at NIST.
PB95-108486 *01,624*

OP DE BEEK, S. S.

Alignment Probing of Rydberg States by Stimulated Emission.
PB96-200316 *04,124*

OPANSKY, B. J.

Kinetics of the Reaction C2H + O2 from 193 to 350 K Using Laser Flash Kinetic Infrared Absorption Spectroscopy.
PB95-203055 *01,043*

Laboratory Studies of Low-Temperature Reactions of C2H with C2H2 and Implications for Atmospheric Models of Titan.
PB95-108726 *00,690*

Laser Double Resonance Measurements of the Quenching Rates of Br((2)P1/2) with H20, D20, HDO, and O2.
PB95-150694 *00,921*

OPPERMANN, H.

Metrology and Regional Trade Pacts.
PB96-155429 *02,923*

OPPERMANN, H. V.

NIST Handbook 44, 1994: Specifications, Tolerances and Other Technical Requirements for Weighing and Measuring Devices as Adopted by the 78th National Conference on Weights and Measures 1993.
PB94-136009 *02,888*

NIST Handbook 44, 1995: Specifications, Tolerances and Other Technical Requirements for Weighing and Measuring Devices as Adopted by the 79th National Conference on Weights and Measures 1994.
PB95-146379 *02,903*

OREN, A. L.

Design and Characterization of X-Ray Multilayer Analyzers for the 50 - 1000 eV Region.
PB94-211851 *03,848*

ORKIN, V. L.

Atmospheric Lifetimes of HFC-143a and HFC-245fa: Flash Photolysis Resonance Fluorescence Measurements of the OH Reaction Rate Constants.
PB97-112577 *00,118*

ORLANDINI, E.

Self-Avoiding Surfaces, Topology, and Lattice Animals.
PB95-150512 *04,571*

ORLANDO, T. P.

Effects of Anneal Time and Cooling Rate on the Formation and Texture of Bi2Sr2CaCu2O8 Films.
PB95-161600 *04,603*

Grain Alignment and Transport Properties of Bi2Sr2CaCu2O8 Grown by Laser Heated Float Zone Method.
PB95-161451 *04,602*

Increased Pinning Energies and Critical Current Densities in Heavy-Ion-Irradiated Bi2Sr2CaCu2O8 Single Crystals.
PB95-175352 *04,654*

OROSZ, J.

Application of ODF to the Rietveld Profile Refinement of Polycrystalline Solid.
PB95-202388 *03,401*

Microstructure Study of Molybdenum Liners by Neutron Diffraction.
PB95-202396 *03,756*

Texture Study of Two Molybdenum Shaped Charge Liners by Neutron Diffraction.
PB94-200177 *03,754*

Textures of Tantalum Metal Sheets by Neutron Diffraction.
PB94-200169 *03,399*

ORSZAG, S. A.

Numerical Simulation of Submicron Photolithographic Processing.
PB94-198561 *02,310*

ORTIGOSO, J.

Infrared Spectrum of OClO in the 2000/cm(-1) Region: The 2(nu sub 1) and (nu sub 1 + nu sub 3) Bands.
PB95-141032 *00,908*

Intensities and Dipole Moment Derivatives of the Fundamental Bands of (35)ClO2 and an Intensity Analysis of the nu1 Band.
PB95-141040 *00,909*

ORTS, W. J.

Hydration in Semicrystalline Polymers: Small-Angle Neutron Scattering Studies of the Effect of Drawing in Nylon-6 Fibers.
PB95-202990 *03,385*

Water Adsorption at a Polyimide/Silicon Wafer Interface.
PB96-103197 01,070

OSBURN, J. E.

LMTO/CVM and LAPW/CVM Calculations of the Nickel Aluminide/Nickel Titanium Pseudobinary Phase Diagram.
PB94-199353 03,323

OSELLA, S. A.

Development of Adaptive Control Strategies for Inert Gas Atomization.
PB95-162335 02,823

Expert Control System Shell Version 1.0 User's Guide.
PB95-198859 01,790

Intelligent Control of an Inert Gas Atomization Process.
PB95-141057 03,344

Process Modeling and Control of Inert Gas Atomization.
PB95-162343 02,824

OSTADAN, F.

Energy-Based Method for Liquefaction Potential Evaluation. Phase 1. Feasibility Study.
PB96-214747 03,691

OSTAPCZUK, P.

Determination of Inorganic Constituents in Marine Mammal Tissues.
PB95-152047 00,589

Development of Frozen Whale Blubber and Liver Reference Materials for the Measurement of Organic and Inorganic Contaminants.
PB95-151676 00,587

OSTERTAG, C.

Tensile Creep of Silicide Composites.
PB96-200803 03,183

OSTERTAG, C. P.

Coating of Fibers by Colloidal Techniques in Ceramic Composites.
PB94-216256 03,196

OSTROM, R. M.

Construction of Silicon Nanocolumns with the Scanning Tunneling Microscope.
PB95-203063 04,696

Nanoscale Study of the As-Grown Hydrogenated Amorphous Silicon Surface.
PB95-150595 04,573

OTI, J.

Experimental Verification of a Vector Preisach Model.
PB95-163564 04,626

OTI, J. O.

Experimental Verification of a Micromagnetic Model of Dual-Layer Magnetic Films.
PB95-141081 04,553

Magnetic and Magnetoresistive Properties of Inhomogeneous Magnetic Dual-Layer Films.
PB95-169025 04,646

Magnetoresistance of Thin-Film NiFe Devices Exhibiting Single-Domain Behavior.
PB96-147087 04,766

Micromagnetic Model of Dual-Layer Magnetic-Recording Thin Films.
PB95-141065 04,551

Micromagnetic Simulations of Tunneling Stabilized Magnetic Force Microscopy.
PB95-141073 04,552

Modeling Effects of Temperature Annealing on Giant Magnetoresistive Response in Discontinuous Multilayer NiFe/Ag Films.
PB97-112585 04,157

Models of Granualr Giant Magnetoresistance Multilayer Thin Films.
PB96-190228 01,968

Numerical Micromagnetic Techniques and Their Applications to Magnetic Force Microscopy Calculations.
PB95-175931 04,664

Proposed Antiferromagnetically Coupled Dual-Layer Magnetic Force Microscope Tips.
PB95-169017 04,645

Simulating Device Size Effects on Magnetization Pinning Mechanisms in Spin Valves.
PB97-112593 04,158

Size Effects and Giant Magnetoresistance in Unannealed NiFe/Ag Multilayer Stripes.
PB97-111306 04,145

Size Effects in Submicron NiFe/Ag GMR Devices.
PB96-155510 02,237

OTTEWILL, R. H.

Structure and Rheology of Hard-Sphere Systems.
PB96-167333 00,662

OTTO, R.

Hyperfine Structure Investigations and Identification of New Energy Levels in the Ionic Spectrum of (147)Pm.
PB96-180203 04,117

OTTO, S.

Electronic Access: Blueprint for the National Archives and Records Administration.
PB95-219218 02,731

User Study: Informational Needs of Remote National Archives and Records Administration Customers.
PB95-154738 02,725

OUELLETTE, M. J.

Performance of Compact Fluorescent Lamps at Different Ambient Temperatures.
PB95-175329 00,258

OUTCALT, S. L.

Coexisting Densities, Vapor Pressures and Critical Densities of Refrigerants R-32 and R-152a, at 300 - 385 K.
PB95-175691 03,274

Fugacity Coefficients of Hydrogen in (Hydrogen + Butane).
PB95-175212 02,491

Process Gas Chromatography Detector for Hydrocarbons Based on Catalytic Cracking.
PB95-141099 02,485

OUYANG, R.

Displacement Method for Machine Geometry Calibration.
PB95-152088 02,946

OVER, P.

Z39.50 Implementation Experiences.
PB96-114939 01,816

OVERETT, T.

Calibration of Dosimeters for the Cryogenic Irradiation of Composite Materials Using an Electron Beam.
PB95-180964 03,968

OVERMAN, J.

National Center for Standards and Certification Information: Service and Programs.
N95-15938/0 02,717

OVERMAN, J. R.

GATT Standards Code Activities of the National Institute of Standards and Technology 1994.
PB96-106935 00,497

TBT Agreement Activities of the National Institute of Standards and Technology, 1995.
PB97-104178 00,499

OVERZET, L. J.

Microwave Diagnostic Results from the Gaseous Electronics Conference RF Reference Cell.
PB96-113378 02,392

OWEN, J. C.

Application of the Modified Voltage-Dividing Potentiometer to Overlay Metrology in a CMOS/Bulk Process.
PB94-181997 02,302

Comparisons of Measured Linewidths of Sub-Micrometer Lines Using Optical, Electrical, and SEM Metrologies.
PB95-152807 02,338

OWEN, J. J.

Determination of Complex Structures from Powder Diffraction Data: The Crystal Structure of La3Ti5Al15O37.
PB95-202966 01,038

OZERY, N.

Visual-Motion Fixation Invariant.
PB94-206281 01,836

OZIER, I.

Use of Extended Permutation-Inversion Groups in Constructing Hyperfine Hamiltonians for Symmetrical-Top Internal Rotor Molecules Like H3C-SiH3.
PB94-212032 00,823

PAABO, M.

Further Development of the N-Gas Mathematical Model: An Approach for Predicting the Toxic Potency of Complex Combustion Mixtures.
PB96-123260 03,650

New Approach for Reducing the Toxicity of the Combustion Products from Flexible Polyurethane Foam.
PB96-123625 01,411

PAABO, S.

DNA Damage and DNA Sequence Retrieval from Ancient Tissues.
PB97-111983 03,556

PACE, M. O.

Observations of Partial Discharges in Hexane Under High Magnification.
PB95-163127 01,900

PADMAJA, S.

Reaction of Nitric Oxide with Organic Peroxyl Radicals.
PB95-141107 00,910

Reaction of NO with Superoxide.
PB94-212198 00,830

PADTURE, N. P.

Effect of Grain Size on Hertzian Contact Damage in Alumina.
PB96-179601 03,083

Flaw-Insensitive Ceramics.
PB97-110027 03,095

Flaw-Tolerance and Crack-Resistance Properties of Alumina-Aluminum Titanate Composites with Tailored Microstructures.
PB97-110324 03,101

Flaw Tolerance and Toughness Curves in Two-Phase Particulate Composites: SiC/Glass System.
PB96-179460 03,081

In situ-Toughened Silicon Carbide.
PB97-110332 03,102

Indentation Fatigue: A Simple Cyclic Hertzian Test for Measuring Damage Accumulation in Polycrystalline Ceramics.
PB96-180013 03,084

Model for Microcrack Initiation and Propagation beneath Hertzian Contacts in Polycrystalline Ceramics.
PB96-163704 03,077

Model for Toughness Curves in Two-Phase Ceramics. 1. Basic Fracture Mechanics.
PB96-180088 03,085

Model for Toughness Curves in Two-Phase Ceramics. 2. Microstructural Variables.
PB96-163795 03,078

Postfailure Subsidiary Cracking from Indentation Flaws in Brittle Materials.
PB97-110340 03,103

PAGANO, I.

First Results from a Coordinated ROSAT, IUE, and VLA Study of RS CVn Systems.
PB94-213477 00,069

Rotational Modulation and Flares on RS Canum Venaticorum and BY Draconis Stars. XVIII. Coordinated VLA, ROSAT, and IUE Observations of RS CVn Binaries.
PB96-102322 00,089

PAGE, R. A.

Characterization of the Densification of Alumina by Multiple Small-Angle Neutron Scattering. (Reannouncement with New Availability Information).
AD-A249 179/3 03,024

Effect of Green Density and the Role of Magnesium Oxide Additive on the Densification of Alumina Measured by Small-Angle Neutron Scattering. (Reannouncement with New Availability Information).
AD-A244 582/3 03,022

Small-Angle Neutron Scattering Characterization of Processing/Microstructure Relationships in the Sintering of Crystalline and Glassy Ceramics. (Reannouncement with New Availability Information).
AD-A249 510/9 03,025

PAGE, S. H.

Instrument for Evaluating Phase Behavior of Mixtures for Supercritical Fluid Experiments.
PB95-180758 00,606

Selectivity Trends in Packed Column Supercritical Fluid Chromatography with C18 Stationary Phases.
PB96-138581 00,622

PAGEL, C.

Overview of U.S. Government Advanced Packaging Programs.
PB96-200845 02,443

PAGNI, P. J.

Fire Induced Thermal Fields in Window Glass I: Theory.
PB94-139722 00,328

PAINTER, R. B.

Modification of Deoxyribose-Phosphate Residues by Extracts of Ataxia Telangiectasia Cells.
PB94-212602 03,458

PAL, B. P.

LP11-Mode Leakage Loss in Coated Depressed Clad Fibers.
PB95-141115 02,145

PALAVRA, A. M. F.

Supercritical Fluid Extraction of Biological Products.
PB95-175204 00,040

PALIWAL, A.

Rapid Method for the Isolation of Genomic DNA from 'Aspergillus fumigatus'.
PB96-147061 03,488

PALM, E. C.

Laser-Focused Atomic Deposition.
PB95-161618 04,604

Nanostructure Fabrication via Direct Writing with Atoms Focused in Laser Fields.
PB95-150272 04,564

PALMER, D.

Overview of U.S. Government Advanced Packaging Programs.
PB96-200845 02,443

PALMER, D. S.

Wear of Human Enamel against a Commercial Castable Ceramic Restorative Material.
PB95-161972 00,161

PALMER, M. E.

Group 1 for the Plant Spatial Configuration STEP Application Protocol.
PB96-165402 02,789

Group 1 for the Process Engineering Data STEP Application Protocol.
PB97-116073 02,797

Issues and Recommendations for a STEP Application Protocol Framework. National PDES Testbed.
PB94-160868 02,770

PAN, C.

Angular Distributions for Near-Threshold (e,2e) Processes for Li and Mg.
PB94-185725 00,778

Relative Photoionization and Photodetachment Cross Sections for Particular Fine-Structure Transitions with Application to Cl 3s-subshell Photoionization.
PB95-203097 03,998

PAN, L.

Perturbative Calculation of the AC Stark Effect by the Complex Rotation Method.
PB95-141123 *04,260*

PANDEY, P. C.

Amperometric Flow-Injection Analysis Biosensor for Glucose Based on Graphite Paste Modified with Tetracyanoquinodimethane.
PB95-161980 *03,498*

Application of Photochemical Reaction in Electrochemical Detection of DNA Intercalation.
PB94-185733 *00,686*

Detection of Aromatic Compounds Based on DNA Intercalation Using an Evanescent Wave Biosensor.
PB96-111976 *03,473*

Thermodynamics of the Hydrolysis of N-Acetyl-L-phenylalanine Ethyl Ester in Water and in Organic Solvents.
PB95-203386 *01,053*

PANDIT, A.

Two Phase Aqueous Extraction: Rheological Properties of Dextran, Polyethylene Glycol, Bovine Serum Albumin and Their Mixtures.
PB95-161998 *00,676*

PAO, C. K.

Electrical Measurements of Microwave Flip-Chip Interconnections.
PB96-176748 *02,436*

Microwave Characterization of Flip-Chip MMIC Components.
PB96-176722 *02,434*

Microwave Characterization of Flip-Chip MMIC Interconnections.
PB96-176730 *02,435*

PAPANEK, P.

Inelastic-Neutron-Scattering Studies of Poly(p-phenylene vinylene).
PB95-180766 *01,014*

PAPANYAN, V. O.

Photoluminescence Spectra of Epitaxial Single Crystal C60.
PB96-141205 *04,754*

PAPILLO, M.

Report on the Workshop on Advanced Digital Video in the National Information Infrastructure. Held in Washington, D.C. on May 10-11, 1994.
PB95-103677 *01,472*

Summary Report on the Workshop on Advanced Digital Video in the National Information Infrastructure.
PB96-141320 *01,497*

PARAMESWARAN, M.

High-Level CAD Melds Micromachined Devices with Foundries.
PB94-216413 *02,321*

PARANTHAMAN, M.

Asymmetry between Flux Penetration and Flux Expulsion in Tl-2212 Superconductors.
PB95-125647 *04,527*

Enhanced Flux Pinning via Chemical Substitution in Bulk Superconducting T1-2212.
PB95-169033 *04,647*

PARDAVI-HORVATH, M.

Experimental Verification of a Vector Preisach Model.
PB95-163564 *04,626*

PARETZKIN, B.

Crystal Chemistry and Phase Equilibria Studies of the BaO(BaCO3)-R2O3-CuO Systems. 4. Crystal Chemistry and Subsolidus Phase Relationship Studies of the CuO-Rich Region of the Ternary Diagrams, R=Lanthanides.
PB95-151759 *00,936*

Crystal Chemistry and Phase Equilibrium Studies of the BaO(BaCO3)-R2O3-CuO Systems. 5. Melting Relations in Ba2(Y,Nd,Eu)Cu3O6+x.
PB95-151718 *04,580*

Crystal Chemistry and Phase Equilibrium Studies of the BaO-R2O3-CuO Systems. 2. X-Ray Characterization and Standard Patterns of BaR2CuO4, R=Lanthanides.
PB95-151734 *04,582*

PARISE, J. B.

Ca4Bi6O13: A Compound Containing an Unusually Low Bismuth Coordination Number and Short Bi Bi Contacts.
PB95-141131 *00,911*

PARK, C.

Fault Diagnosis of an Air-Handling Unit Using Artificial Neural Networks.
PB97-121321 *00,283*

Reproducibility of Tests on Energy Management and Control Systems Using Building Emulators.
PB95-175980 *00,260*

Using Emulator/Testers for Commissioning EMCS Software, Operator Training, Algorithm Development, and Tuning Local Control Loops.
PB94-212735 *00,245*

Using Emulators to Evaluate the Performance of Building Energy Management Systems.
PB95-175774 *00,259*

PARK, G. S.

Noise Reduction in Low-Frequency SQUID Measurements with Laser-Driven Switching.
PB96-135165 *02,081*

Trapped Vortices in a Superconducting Microbridge.
PB95-141149 *04,554*

PARK, J. C.

Defect Formation Mechanism Causing Increasing Defect Density during Decreasing Implant Dose in Low-Dose Simox.
PB96-119524 *02,402*

Defect of Thermal Ramping and Annealing Conditions on Defect Formation in Oxygen Implanted Silicon-On-Insulator Material.
PB94-212966 *02,318*

Defect Pair Formation by Implantation-Induced Stresses in High-Dose Oxygen Implanted Silicon-on-Insulator Material.
PB95-175824 *02,364*

Effect of Intermediate Thermal Processing on Microstructural Changes of Oxygen Implanted Silicon-on-Insulator Material.
PB96-160213 *02,982*

Effect of Single versus Multiple Implant Processing on Defect Types and Densities in SIMOX.
PB96-160353 *01,957*

Stacking Fault Pyramid Formation and Energetics in Silicon-on-Insulator Material Formed by Multiple Cycles of Oxygen Implantation and Annealing.
PB96-160221 *04,083*

PARK, S. G.

Self-Biasing Cryogenic Particle Detector Utilizing Electrothermal Feedback and a SQUID Readout.
PB96-102538 *04,712*

PARKER, A. J.

Characterization of Polyquinoline Blends Using Small Angle Scattering.
PB95-164125 *01,261*

Characterization of Polyquinoline Block Copolymer Using Small Angle Scattering.
PB95-151882 *01,244*

PARKER, F.

Precision of Marchall Stability and Flow Test Using 6-in. (152.4-mm) Diameter Specimens.
PB96-200910 *03,006*

PARKER, K.

New Method for Achieving Accurate Thickness Control for Uniform and Graded Multilayer Coatings on Large Flat Substrates.
PB96-159744 *04,366*

PARKER, M. A.

Antiferromagnetic Interlayer Correlations in Annealed Ni80Fe20/Ag Multilayers.
PB97-122220 *03,109*

Magnetic Structure Determination for Annealed Ni80Fe20/Ag Multilayers Using Polarized-Neutron Reflectivity.
PB96-176615 *03,739*

PARKER, M. E.

Exploring the Low-Frequency Performance of Thermal Converters Using Circuit Models and a Digitally Synthesized Source.
PB97-112551 *02,848*

Low Voltage Standards in the 10 Hz to 1 MHz Range.
PB97-112569 *02,100*

PARKER, M. R.

Size and Self-Field Effects in Giant Magnetoresistive Thin-Film Devices.
PB95-180188 *04,674*

PARKER, T. E.

Surface Transverse Wave Oscillators with Extremely Low Thermal Noise Floors.
PB96-186010 *01,967*

PARKER, V. B.

Thermodynamic Properties of the Aqueous Ba(sup 2+) Ion and the Key Compounds of Barium.
PB96-145834 *01,107*

Thermodynamic Properties of the Aqueous Ions (2+ and 3+) of Iron and the Key Compounds of Iron.
PB96-145958 *01,119*

PARKER, W. E.

Intermediate Structure in the Neutron-Induced Fission Cross Section of 236U.
PB94-185741 *03,802*

Measurements of the (237)Np(n,f) Cross Section.
PB97-119069 *04,173*

PARKER, W. J.

Effects of Specimen Edge Conditions on Heat Release Rate.
PB95-152864 *00,375*

PARKS, C.

Operating Procedures and Life Cycle Documentation for the Initial Graphics Exchange Specification.
PB95-242285 *02,782*

PARKS, E. J.

Bioleaching of Cobalt from Smelter Wastes by 'Thiobacillus ferrooxidans'.
PB95-140968 *02,582*

PARKS, J. E.

Anomalous Odd- to Even-Mass Isotope Ratios in Resonance Ionization with Broad-Band Lasers.
PB94-211406 *03,839*

PARKS, N. J.

Experimental Validation of Radiopharmaceutical Absorbed Dose to Mineralized Bone Tissue.
PB94-199668 *03,617*

Radiation Doses.
PB94-199676 *03,618*

PARKS, R. E.

Rapid Post-Polishing of Diamond-Turned Optics.
PB95-175949 *04,301*

Test of a Slow Off-Axis Parabola at Its Center of Curvature.
PB96-138482 *04,352*

Visualization of Surface Figure by the Use of Zernike Polynomials.
PB96-137757 *04,351*

PARMENTER, C. S.

Acceleration of Intramolecular Vibrational Redistribution by methyl Internal Rotation. A Chemical Timing Study of p-fluorotoluene and p-fluorotoluene-d3.
PB95-202982 *01,039*

Vibrational Energy Transfer in S1 p-Difluorobenzene. A Comparison of Low and Room Temperature Collisions.
PB95-108619 *00,883*

Vibrations of S1((1)B2u) p-Difluorobenzene - d4. S1-S0 Fluorescence Spectroscopy and ab Initio Calculations.
PB95-202586 *01,028*

PARNAS, R. S.

Comparison of the Unidirectional and Radial In-Plane Flow of Fluids Through Woven Composite Reinforcements.
PB95-162004 *02,698*

Effect of Heterogeneous Porous Media on Mold Filling in Resin Transfer Molding.
PB95-108676 *03,197*

Effect of Hydrodynamic Interactions on a Terminally Anchored Bead-Rod Model Chain.
PB95-141156 *01,237*

Interaction between Micro and Macroscopic Flow in RTM Preforms.
PB95-162012 *03,159*

Report on the Workshop on Manufacturing Polymer Composites by Liquid Molding. Held in Gaithersburg, Maryland on September 20-22, 1993.
PB94-160066 *03,131*

Response of a Terminally Anchored Polymer Chain to Simple Shear Flow.
PB95-108668 *01,233*

PARR, A.

Rayleigh Scattering Limits for Low-Level Bidirectional Reflectance Distribution Function Measurements.
PB95-180030 *04,307*

PARR, A. C.

Cryogenic Blackbody Calibrations at the National Institute of Standards and Technology Low Background Infrared Calibration Facility.
PB94-169802 *02,117*

High Resolution Angle Resolved Photoelectron Spectroscopy Study of N2.
PB95-151494 *03,907*

Inner-Valence States CO(+) between 22 eV and 46 eV Studied by High Resolution Photoelectron Spectroscopy and ab Initio CI Calculations.
PB95-180055 *03,961*

National Institute of Standards and Technology High-Accuracy Cryogenic Radiometer.
PB96-179585 *04,378*

National Measurement System for Radiometry, Photometry, and Pyrometry Base Upon Absolute Detectors.
PB97-108559 *04,382*

NIST Detector-Based Luminous Intensity Scale.
PB96-179114 *01,864*

NIST Response to the Fifth CORM Report on the Pressing Problems and Projected Needs in Optical Radiation Measurements.
PB94-188240 *04,227*

Photoelectron Study of Electronic Autoionization in Rotationally Cooled N2: The n=6 Member of the Hopfield Series.
PB95-163531 *00,971*

Photoionization of Small Molecules Using Synchrotron Radiation.
PB94-211505 *03,841*

Shape-Resonance-Enhanced Continuum-Continuum Coupling in Photoionization of CO2.
PB95-164471 *00,983*

Update on the Low Background IR Calibration Facility at the National Institute of Standards and Technology.
PB94-211224 *04,232*

Vibrational Autoionization in H2: Vibrational Branching Ratios and Photoelectron Angular Distributions Near the v(+)=3 Threshold.
PB94-199577 *00,799*

Vibrationally Resolved Photoelectron Angular Distributions and Branching Ratios for the Carbon Dioxide Molecule in the Wavelength Region 685-795 Angstrom.
PB96-201207 *04,131*

Vibronic Coupling and Other Many-Body Effects in the 4sigmag(-1) Photoionization Channel of CO2.
PB95-162509 *00,962*

PARRIS, N.
Structure of a Triglyceride Microemulsion: A Small Angle Neutron Scattering Study.
PB96-112255 *01,077*

PARRIS, R.
Comparison of Methods for Gas Chromatographic Determination of PCBs and Chlorinated Pesticides in Marine Reference Materials.
PB95-140091 *02,584*

PARRIS, R. M.
NIST Standard Reference Materials (SRMs) for Polychlorinated Biphenyl (PCB) Determinations and Their Applicability to Toxaphene Measurements.
PB95-140109 *02,585*

Standard Reference Materials for the Determination of Polycyclic Aromatic Hydrocarbons in Environmental Samples - Current Activities.
PB95-151668 *00,586*

PARRY, E. E.
Dental Materials.
PB94-172871 *00,142*

Tapered Cross-Pin Attachments for Fixed Bridges.
PB94-185238 *00,185*

PARSONS, C. A.
Characterization of Vertical-Cavity Semiconductor Structures.
PB94-200193 *02,126*

Vertical-Cavity Optoelectronic Structures: CAD, Growth, and Structural Characterization.
PB95-153177 *02,148*

Vertical-Cavity Semiconductor Lasers: Structural Characterization, CAD, and DFB Structures.
PB95-153193 *02,150*

PASHLEY, D. H.
Effects of Aluminum Oxalate/Glycine Pretreatment Solutions on Dentin Permeability.
PB95-164505 *03,565*

Effects of Calcium Phosphate Solutions on Dentin Permeability.
PB95-151080 *00,157*

PASSOW, M. L.
Gaseous Electronics Conference Radio-Frequency Reference Cell: A Defined Parallel-Plate Radio-Frequency System for Experimental and Theoretical Studies of Plasma-Processing Discharges.
PB94-172327 *04,404*

PASTEL, R. L.
Efficient Br(*) Laser Pumped by Frequency-Doubled Nd: YAG and Electronic-to-Vibrational Transfer-Pumped CO2 and HCN Lasers.
PB95-108684 *04,248*

PASTUREL, A.
LMTO/CVM and LAPW/CVM Calculations of the Nickel Aluminide/Nickel Titanium Pseudobinary Phase Diagram.
PB94-199353 *03,323*

PATE, B. H.
Sub-Doppler, Infrared Laser Spectroscopy of the Propyne 2nu1 Band: Evidence of z-Axis Coriolis Dominated Intramolecular State Mixing in the Acetylenic CH Stretch Overtone.
PB95-202941 *01,037*

PATIL, T. A.
Continuous Counter-Current Two Phase Aqueous Extraction.
PB95-161212 *00,675*

PATRICK, H.
Annealing of Bragg Gratings in Hydrogen-Loaded Optical Fiber.
PB96-155437 *04,361*

Bragg Gratings in Optical Fibers Produced by a Continuous-Wave Ultraviolet Source.
PB95-162020 *04,274*

Comparison of UV-Induced Fluorescence and Bragg Grating Growth in Optical Fiber.
PB95-168597 *04,284*

Comparison of UV Photosensitivity and Fluorescence during Fiber Grating Formation.
PB96-155445 *04,362*

Decay of Bragg Gratings in Hydrogen-Loaded Optical Fibers.
PB96-122643 *04,345*

Decrease of Fluorescence in Optical Fiber during Exposure to Pulsed or Continuous-Wave Ultraviolet Light.
PB95-203071 *04,320*

Electronically Tunable Fiber Laser for Optical Pumping of (3)He and (4)He.
PB96-201165 *04,381*

Growth Characteristics of Fiber Gratings.
PB96-122957 *04,346*

Growth of Bragg Gratings Produced by Continuous-Wave Ultraviolet Light in Optical Fiber.
PB95-162038 *04,275*

PATTEN, K. O.
Environmental Aspects of Halon Replacements: Considerations for Advanced Agents and the Ozone Depletion Potential of CF3I.
PB97-122261 *03,301*

PAUL, A. E.
Time-Resolved Measurements of the Polarization State of Four-Wave Mixing Signals from GaAs Multiple Quantum Wells.
PB96-201058 *04,796*

PAUL, E.
Chemical Aspects of Tool Wear in Single Point Diamond Turning.
PB97-112601 *03,021*

PAUL, R. L.
Analytical Applications of Guided Neutron Beams.
PB96-112347 *04,041*

Cold Neutron Prompt Gamma Activation Analysis at NIST: A Progress Report.
PB95-175964 *00,602*

Determination of Hydrogen in Titanium Alloy Jet Engine Compressor Blades by Cold Neutron Capture Prompt Gamma-ray Activation Analysis.
PB95-175956 *01,448*

Grazing Incidence Prompt Gamma Emissions and Resonance-Enhanced Neutron Standing Waves in a Thin-Film.
PB95-150470 *03,892*

Inelastic Neutron Scattering Studies of Rotational Excitations and the Orientational Potential in C60 and A3C60 Compounds.
PB94-172673 *00,763*

Measuring Hydrogen by Cold-Neutron Prompt-Gamma Activation Analysis.
PB96-111877 *00,612*

Neutron Scattering by Hydrogen in Cold Neutron Prompt Gamma-Activation Analysis.
PB95-175972 *00,603*

Use of Neutron Beams for Chemical Analysis at NIST.
PB97-112437 *00,652*

PAUL, W.
Use of Pressure for Quantum-Well Band-Structure Characterization.
PB96-164058 *04,779*

PAULDRACH, A. W. A.
Radiation-Driven Winds of Hot Luminous Stars X. The Determination of Stellar Masses Radii and Distances from Terminal Velocities and Mass-Loss Rates.
PB94-213022 *00,060*

PAULE, R.
Frozen Human Serum Reference Material for Standardization of Sodium and Potassium Measurements in Serum or Plasma by Ion-Selective Electrode Analyzers.
PB94-185337 *00,532*

PAULE, R. C.
Ascorbic and Dehydroascorbic Acids Measured in Plasma Preserved with Dithiothreitol or Metaphorphoric Acid.
PB94-216330 *03,495*

Assessing the Credibility of the Calorific Content of Muncipal Solid Waste.
PB94-199882 *02,581*

Certification of Morphine and Codeine in a Human Urine Standard Reference Material.
PB95-176160 *03,499*

Determination of 3-Quinuclidinyl Benzilate (Qnb) and Its Major Metabolites in Urine by Isotope Dilution Gas Chromatography Mass Spectrometry.
PB94-199379 *03,492*

Development of a Standard Reference Material for ISE Measurements of Sodium and Potassium.
PB96-159785 *03,507*

Molar Absorptivities of Bilirubin (NIST SRM 916A) and Its Neutral and Alkaline Azopigments.
PB94-211042 *03,456*

PAULSEN, P. J.
Determination of Sulfur in Fossil Fuels by Isotope Dilution Thermal Ionization Mass Spectrometry.
PB96-141379 *02,495*

Rare-Earth Isotopes as Tracers of Particulate Emissions: An Urban Scale Test.
PB94-161635 *02,535*

PAULTER, N. G.
Casual Regularizing Deconvolution Filter for Optimal Waveform Reconstruction.
PB95-203089 *01,603*

Electro-Optic-Based RMS Voltage Measurement Technique.
PB96-138490 *02,194*

PAUWELS, J.
Preparation and Characterization of (6)LiF and (10)B Reference Deposits for the Measurement of the Neutron Lifetime.
PB95-108692 *03,874*

Problems Related to the Determination of Mass Densities of Evaporated Reference Deposits.
PB95-163226 *03,941*

PAVONE, F. S.
Rotational Far Infrared Spectrum of (13)CO.
PB95-152187 *00,941*

PAWLAK, C. G.
Survey of Standards for the U.S. Fiber/Textile/Apparel Industry.
PB96-193792 *03,199*

PAYNE, B. F.
Vibration Laboratory Automation at NIST with Personal Computers.
PB95-108700 *02,648*

PEACOCK, R. D.
Fire Safety of Passenger Trains: A Review of Current Approaches and of New Concepts.
PB94-152006 *04,848*

New Concepts for Fire Protection of Passenger Rail Transportation Vehicles.
PB95-162046 *04,850*

New Concepts for Fire Protection of Passenger Rail Transportation Vehicles. (NIST Reprint).
PB95-180774 *04,863*

Standardization of Formats and Presentation of Fire Data - The FDMS.
PB94-198462 *01,371*

Verification of a Model of Fire and Smoke Transport.
PB95-108718 *00,357*

PEARSON, J.
Resonance Enhanced Multiphoton Ionization Spectroscopy of the SnF Radical.
PB97-111223 *01,176*

PEARSON, J. C.
Millimeter- and Submillimeter-Wave Spectrum of trans-Ethyl Alcohol.
PB96-145578 *01,102*

PECHENIK, A.
Densification of Nano-Size Powders. 1994 Report.
DE94013486 *03,027*

Equipment for Investigation of Cryogenic Compaction of Nanosize Silicon Nitride Powders. 1993 Report.
DE94013593 *03,028*

Fabrication of Transparent gamma-Al2O3 from Nanosize Particles.
PB95-175493 *03,054*

Rapid Hot Pressing of Ultra-Fine PSZ Powders.
PB94-216587 *03,045*

PECK, W. F.
Observation of Oscillatory Magnetic Order in the Antiferromagnetic Superconductor HoNi2B2C.
PB95-180303 *04,679*

PECKER, C.
Papers on the Symposium on Collision Phenomena in Astrophysics, Geophysics, and Masers.
AD-A280 291/6 *00,047*

PECKERAR, M. C.
Interaction of Stoichiometry, Mechanical Stress, and Interface Trap Density in LPCVD Si-rich SiNx-Si Structures.
PB95-176301 *02,366*

PEDERSEN, J. O. P.
Kinetics of the Reaction C2H + O2 from 193 to 350 K Using Laser Flash Kinetic Infrared Absorption Spectroscopy.
PB95-203055 *01,043*

Laboratory Studies of Low-Temperature Reactions of C2H with C2H2 and Implications for Atmospheric Models of Titan.
PB95-108726 *00,690*

PEDERSEN, J. S.
Instrumental Smearing Effects in Radially Symmetric Small-Angle Neutron Scattering by Numerical and Analytical Methods.
PB96-160429 *02,984*

PEDULLA, J.
Production and Characterization of Ion Beam Sputtered Multilayers.
PB95-162053 *03,936*

PEEBLES, D.
Optical Conductivity of Single Crystals of Ba1-xMxBiO3(M=K, Rb, x=0.04, 0.37).
PB94-185329 *04,447*

PEFFER, E. L.
Density of Solids and Liquids.
AD-A278 517/8 *00,711*

PEI, K.
Artificial Crack in Steel: An Ultrasonic-Resonance-Spectroscopy and Modeling Study.
PB96-141395 *03,241*

PEI, P.
Characterization and Processing of Spray-Dried Zirconia Powders for Plasma Spray Application.
PB97-111231 *04,419*

Deposit Forming Tendencies of Diesel Engine Oils-Correlation between the Two-Peak Method and Engine Tests.
PB95-152138 *01,452*

New Method to Evaluate Deposit Forming Tendencies of Liquid Lubricants by Differential Scanning Calorimetry.
PB95-152120 *01,451*

PEI, P. T.
Interface Modification and Characterization of Silicon Carbide Platelets Coated with Alumina Particles.
PB95-108734 *03,121*

PEIFER, D. J.
Ada Compiler Validation Summary Report: Certificate Number 940902S1.11377 UNISYS Corporation. IntegrAda for

Windows NT, Version 1.0. Intel Deskside Server with Intel 80486DX266 => Intel Deskside Server with Intel 80486DX266.
AD-A288 571/3 *01,658*

PEIFFER, D. G.

Compatibilization of Polymer Blends by Complexation. 2. Kinetics of Interfacial Mixing.
PB97-111900 *01,295*

Small-Angle Neutron Scattering (SANS) Study of Worm-Like Micelles Under Shear.
PB96-176698 *04,111*

PEISER, H. S.

New Values for Silicon Reference Materials, Certified for Isotope Abundance Ratios. Letter to the Editor.
PB94-219268 *00,863*

Reference Materials by Isotope Dilution Mass Spectrometry.
PB95-153383 *00,592*

PEITSMAN, H. C.

Reproducibility of Tests on Energy Management and Control Systems Using Building Emulators.
PB95-175980 *00,260*

PELLA, P. A.

Addition of M and L-Series Lines to NIST Algorithm for Calculation of X-Ray Tube Output Spectral Distributions.
PB95-108742 *00,569*

Apparent Bias in the X-Ray Fluorescence Determination of Titanium in Selected NIST SRM Low Alloy Steels.
PB95-108759 *03,212*

Secondary Target X-Ray Excitation for In vivo Measurement of Lead in Bone.
PB95-108767 *03,496*

PELLEGRINO, J.

CO2/CH4 Transport in Polyperfluorosulfonate Ionomers: Effects of Polar Solvents on Permeation and Solubility.
PB96-163803 *01,145*

Determination of Total Protein Adsorbed on Solid (Membrane) Surface by a Hydrolysis Technique: Single Protein Adsorption.
PB96-167093 *03,552*

Gas Transport Properties of Solution-Cast Perfluorosulfonic Acid Ionomer Films Containing Ionic Surfactants.
PB95-175998 *01,267*

Interface Sharpness in Low-Order III-V Superlattices.
PB95-108775 *02,138*

PELLEGRINO, J. C.

Mesoscopic Conductance Fluctuations in Large Devices.
PB96-119656 *04,735*

PELLEGRINO, J. G.

Buffer Layer Modulation-Doped Field-Effect-Transistor Interactions in the Al0.33Ga0.67As/GaAs Superlattice System.
PB96-102876 *02,380*

Characterization of Vertical-Cavity Semiconductor Structures.
PB94-200193 *02,126*

Comparative Photoluminescence Measurement and Simulation of Vertical-Cavity Semiconductor Laser Structures.
PB95-169173 *02,169*

Correlation of Optical, X-ray, and Electron Microscopy Measurements of Semiconductor Multilayer Structures.
PB95-175279 *02,174*

Determination of the Complex Refractive Index of Individual Quantum Wells from Distributed Reflectance.
PB95-175642 *02,176*

Double-Modulation and Selective Excitation Photoreflectance for Wafer-Level Characterization of Quantum-Well Laser Structures.
PB96-167325 *04,372*

High-Accuracy Principal-Angle Scanning Spectroscopic Ellipsometry of Semiconductor Interfaces.
PB96-163787 *02,427*

Interface Roughness, Composition, and Alloying of Low-Order AlAs/GaAs Superlattices Studies by X-ray Diffraction.
PB96-160262 *02,983*

Interface Roughness-Induced Changes in the Near-E(sub 0) Spectroscopic Behavior of Short-Period AlAs/GaAs Superlattices.
PB94-185154 *02,118*

Interface Roughness of Short-Period AlAs/GaAs Superlattices Studied by Spectroscopic Ellipsometry.
PB95-107215 *02,137*

Interface Sharpness during the Initial Stages of Growth of Thin, Short-Period III-V Superlattices.
PB95-108783 *02,139*

Novel Magnetic Field Characterization Techniques for Compound Semiconductor Materials and Devices.
PB96-176458 *02,433*

Quantum Conductance Fluctuations in the Larger-Size-Scale Regime.
PB97-111264 *04,144*

Scaling of the Nonlinear Optical Cross Sections of GaAs-AlGaAs Multiple Quantum-Well Hetero n-i-p-i's.
PB96-102793 *02,183*

Spectroscopic Ellipsometry Determination of the Properties of the Thin Underlying Strained Si Layer and the Roughness at SiO2/Si Interface.
PB95-150157 *04,560*

Time-Resolved Measurements of the Polarization State of Four-Wave Mixing Signals from GaAs Multiple Quantum Wells.
PB96-201058 *04,796*

Vertical-Cavity Optoelectronic Structures: CAD, Growth, and Structural Characterization.
PB95-153177 *02,148*

Vertical-Cavity Semiconductor Lasers: Structural Characterization, CAD, and DFB Structures.
PB95-153193 *02,150*

Vertical-Cavity Semiconductor Structures: Materials Characterization.
PB95-153185 *02,149*

X-ray Reflectivity Determination of Interface Roughness Correlated with Transport Properties of (AlGa)As/GaAs High Electron Mobility Transistor Devices.
PB97-111868 *04,149*

PELLEGRINO, J. J.

Characterization of the Adsorption-Fouling Layer Using Globular Proteins on Ultrafiltration Membranes.
PB94-212909 *00,842*

Determination of Osmotic Pressure and Fouling Resistances and Their Effects on Performance of Ultrafiltration Membranes.
PB94-212891 *00,841*

Low Temperature H(sub 2)S Separation Using Membrane Reactor with Redox Catalyst.
DE94008991 *02,471*

Membrane Gas Separation for a Fluidized-Bed Incinerator.
PB95-169041 *02,550*

PELLEU, G. B.

Wear of Human Enamel against a Commercial Castable Ceramic Restorative Material.
PB95-161972 *00,161*

PENDER, J.

Gaseous Electronics Conference Radio-Frequency Reference Cell: A Defined Parallel-Plate Radio-Frequency System for Experimental and Theoretical Studies of Plasma-Processing Discharges.
PB94-172327 *04,404*

PENDER, J. T. P.

Reactive Ion Etching in the Gaseous Electronics Conference RF Reference Cell.
PB96-113402 *02,395*

PENFOLD, J.

Variation in Magnetic Properties of Cu/Fcc (001) Sandwich Structures.
PB95-141164 *04,555*

PENG, J. L.

Field Dependence of the Magnetic Ordering of Cu in R2CuO4 (R = Nd, Sm).
PB95-164521 *04,633*

Magnetic Structure and Spin Dynamics of the Pr and Cu in Pr2CuO4.
PB96-111836 *04,036*

Observation of Noncollinear Magnetic Structure for the Cu Spins in Nd2CuO4-Type Systems.
PB95-164539 *04,634*

Phonon Density of States in R2CuO4 and Superconducting R1.85Ce0.15CuO4 (R = Nd, Pr).
PB95-150686 *04,574*

PENN, D. R.

Anharmonic Phonons and the Isotope Effect in Superconductivity.
PB94-200557 *04,486*

Calculations of Electron Inelastic Mean Free Paths (IMFPs). 4. Evaluation of Calculated IMFPs and of the Predictive IMFP Formula TPP-2 for Electron Energies between 50 and 2000 eV.
PB95-150728 *00,922*

Calculations of Electron Inelastic Mean Free Paths. 5. Data for 14 Organic Compounds over the 50-2000 eV Range.
PB95-150355 *00,916*

Effects of Interfacial Roughness on the Magnetoresistance of Magnetic Metallic Multilayers.
PB95-150017 *04,556*

Electronic Correlations and Satellites in Superconducting Oxides.
PB94-200045 *04,477*

Experimental Constraints on Some Mechanisms for High-Temperature Superconductivity.
PB94-198553 *04,463*

Total-Dielectric-Function Approach to Electron and Phonon Response in Solids.
PB96-102884 *01,067*

Use of Sum Rules on the Energy-Loss Function for the Evaluation of Experimental Optical Data.
PB95-150736 *04,264*

PENN, S. M.

Laser-Induced Fluorescence Measurements of Rotationally Resolved Velocity Distributions for CO(+) Drifted in He.
PB94-213139 *00,848*

PENNER, J. E.

Global Climatic Effects of Aerosols: The AAAR Symposium.
PB95-108791 *00,122*

PENNER, S.

Hybrid Undulator for the NIST-NRL Free-Electron Laser.
PB94-212529 *04,238*

NIST-NRL Free-Electron Laser Facility.
PB94-212511 *04,237*

PENONCELLO, S. G.

Static Dielectric Constant of Water and Steam.
PB96-123559 *01,090*

PENUMATCHU, D.

New Method for the Detection and Measurement of Polyaromatic Carcinogens and Related Compounds by DNA Intercalation.
PB96-167382 *03,481*

PENZES, W. B.

Electrical Test Structure for Overlay Metrology Referenced to Absolute Length Standards.
PB95-152278 *02,336*

Evolution of Automatic Line Scale Measurement at the National Institute of Standards and Technology.
PB95-108809 *02,897*

Metrology Standards for Advanced Semiconductor Lithography Referenced to Atomic Spacings and Geometry.
PB96-160718 *02,424*

New Test Structure for Nanometer-Level Overlay and Feature-Placement Metrology.
PB95-175345 *02,363*

Test Structures for the In-Plane Locations of Projected Features with Nanometer-Level Accuracy Traceable to a Coordinate Measurement System.
PB94-200565 *02,313*

PEPPIN, R. J.

National Voluntary Laboratory Accreditation Program Acoustical Testing Services.
PB95-182234 *04,188*

PERAHIA, D.

Neutron Reflectivity of End-Grafted Polymers: Concentration and Solvent Quality Dependence in Equilibrium Conditions.
PB94-185758 *01,206*

PERCIVAL, D. B.

Wavelet Analysis for Synchronization and Timekeeping.
PB96-200381 *01,558*

Wavelet Variance, Allan Variance, and Leakage.
PB96-190111 *01,509*

PEREIRA, N. R.

Electrical Breakdown in Transformer Oil in Large Gaps.
PB95-150579 *01,889*

PERERA, S.

Broadband Mismatch Error in Noise Measurement Systems.
PB95-162061 *02,044*

PEREZ, J. M.

Deposit Forming Tendencies of Diesel Engine Oils-Correlation between the Two-Peak Method and Engine Tests.
PB95-152138 *01,452*

New Method to Evaluate Deposit Forming Tendencies of Liquid Lubricants by Differential Scanning Calorimetry.
PB95-152120 *01,451*

PERKINS, R. A.

Measurement of the Thermal Properties of Electrically Conducting Fluids Using Coated Transient Hot Wires.
DE94017816 *00,722*

Measurement of the Thermal Properties of Electrically Conducting Fluids Using Coated Transient Hot Wires.
PB95-169058 *03,269*

Polarized Transient Hot Wire Thermal Conductivity Measurements.
PB95-108817 *00,886*

Status of the Round Robin on the Transport Properties of R134a.
PB96-167218 *01,152*

Thermal Conductivity of R134a.
PB94-213063 *03,857*

Two Phase Aqueous Extraction: Rheological Properties of Dextran, Polyethylene Glycol, Bovine Serum Albumin and Their Mixtures.
PB95-161998 *00,676*

PERKOWITZ, S.

Optical Characterization in Microelectronics Manufacturing.
PB95-169397 *02,358*

Optical Characterization of Materials and Devices for the Semiconductor Industry: Trends and Needs.
PB96-167192 *02,431*

Semiconductor Measurement Technology: Survey of Optical Characterization Methods for Materials, Processing, and Manufacturing in the Semiconductor Industry.
PB96-154596 *02,706*

PERNAMBUCO-WISE, P.

Magnetic Ordering of the Cu Spins in PrBa2Cu3O6+x.
PB95-140547 *04,545*

PERRIN, A.

Reanalysis of the (010), (020), (100), and (001) Rotational Levels of (32)S(16)O2.
PB95-125621 *00,887*

PERRING, T. G.

Isolated Spin Pairs and Two-Dimensional Magnetism in SrCr(sub 9p)Ga(sub 12-9p)O19.
PB97-112387 *04,154*

PERRY, B. W.

Molar Absorptivities of Bilirubin (NIST SRM 916A) and Its Neutral and Alkaline Azopigments.
PB94-211042 *03,456*

PERSILY, A.
Ventilation Rates in Office Buildings.
PB95-108825 *02,539*

PERSILY, A. K.
Air Change Effectiveness Measurements in Two Modern Office Buildings.
PB94-185766 *00,243*

Application of a Multizone Airflow and Contaminant Dispersal Model to Indoor Air Quality Control in Residential Buildings.
PB95-180238 *02,555*

Assessing Ventilation Effectiveness in Mechanically Ventilated Office Buildings.
PB95-162079 *00,255*

Carbon Monoxide Dispersion in Residential Buildings: Literature Review and Technical Analysis.
PB97-114227 *02,571*

Computer Simulations of Airflow and Radon Transport in Four Large Buildings.
PB95-220422 *02,557*

CONTAM88 Building Input Files for Multi-Zone Airflow and Contaminant Dispersal Modeling.
PB94-194388 *02,537*

Development and Application of an Indoor Air Quality Commissioning Program in a New Office Building.
PB96-155601 *00,275*

Effectiveness of a Heat Recovery Ventilator, an Outdoor Air Intake Damper and an Electrostatic Particulate Filter at Controlling Indoor Air Quality in Residential Buildings.
PB96-146642 *02,564*

Environmental Evaluation of a New Federal Office Building.
PB94-199874 *02,538*

Field Measurements of Ventilation and Ventilation Effectiveness in an Office/Library Building.
PB95-108833 *00,247*

Improving the Evaluation of Building Ventilation.
PB96-138508 *00,271*

Indoor Air Quality Commissioning of a New Office Building.
PB95-182309 *00,262*

Indoor Air Quality Commissioning of a New Office Building.
PB97-110142 *00,279*

Indoor Air Quality Impacts of Residential HVAC Systems Phase II.B Report: IAQ Control Retrofit Simulations and Analysis.
PB96-106877 *02,559*

Indoor Air Quality Impacts of Residential HVAC Systems, Phase 1 Report: Computer Simulation Plan.
PB95-135596 *00,249*

Indoor Air Quality Impacts of Residential HVAC Systems. Phase 2.A Report: Baseline and Preliminary Simulations.
PB95-178893 *02,554*

Issues in the Field Measurement of VOC Emission Rates.
PB97-118806 *02,573*

Limits of CO2 Monitoring in Determining Ventilation Rates.
PB95-176004 *02,552*

Manual for Ventilation Assessment in Mechanically Ventilated Commercial Buildings.
PB94-145653 *00,239*

Materials-Science Based Approach to Phenol Emissions from a Flooring Material in an Office Building.
PB97-118749 *02,572*

Measurements of Indoor Pollutant Emissions from EPA Phase II Wood Stoves.
PB95-198735 *02,556*

Measurements of Outdoor Air Distribution in an Office Building.
PB95-210944 *00,264*

Modeling Radon Transport in Multistory Residential Buildings.
PB95-162087 *00,256*

Multizone Modeling of Three Residential Indoor Air Quality Control Options.
PB96-146659 *02,565*

Multizone Modeling of Three Residential Indoor Air Quality Control Options.
PB96-165782 *02,567*

Relationship between Indoor Air Quality and Carbon Dioxide.
PB97-111249 *02,569*

Study of Ventilation and Carbon Dioxide in an Office Building.
PB95-150140 *02,542*

Study of Ventilation Measurement in an Office Building.
PB96-155593 *00,274*

Ventilation, Carbon Dioxide and ASHRAE Standard 62-1989.
PB95-162095 *02,544*

Ventilation Effectiveness Measurements in Two Modern Office Buildings.
PB95-176012 *02,553*

Workplan to Analyze the Energy Impacts of Envelope Airtightness in Office Buildings.
PB96-154463 *00,273*

PERSILY, A. P.
Few Caveats on Carbon Dioxide Monitoring.
PB96-122650 *02,562*

PERSON, D. C.
Magnetic Properties of Pd/Co Multilayers.
PB94-198751 *04,465*

PESHKIN, D.
Optimization of Highway Concrete Technology.
PB94-182995 *01,333*

PETERS, C. J.
Principle of Congruence and Its Application to Compressible States.
PB96-102892 *01,068*

PETERSEN, S. R.
BLCC: The NIST 'Building Life-Cycle Cost' Program, Version 4.21, User's Guide and Reference Manual.
PB95-190682 *00,263*

EMISS: A Program for Estimating Local Air Pollution Emission Factors Related to Energy Use in Buildings: User's Guide and Reference Manual.
PB96-109566 *02,560*

Energy Price Indices and Discount Factors for Life-Cycle Cost Analysis 1995. Annual Supplement to NIST Handbook 135 and NBS Special Publication 709. (Revised).
PB95-105011 *02,509*

Energy Price Indices and Discount Factors for Life-Cycle Cost Analysis 1996. Annual Supplement to NIST Handbook 135 and NBS Special Publication 709. (Revised).
PB96-162441 *02,510*

Energy Price Indices and Discount Factors for Life-Cycle Cost Analysis 1997. Annual Supplement to NIST Handbook 135 and NBS Special Publication 709. (Revised).
PB96-210745 *02,512*

Energy Prices and Discount Factors for Life-Cycle Cost Analysis 1994. Annual Supplement to NIST Handbook 135 and NBS Special Publication 709.
PB94-206018 *02,508*

Life-Cycle Costing Manual for the Federal Energy Management Program. 1995 Edition.
PB96-172317 *02,511*

Life-Cycle Costing Workshop for Energy Conservation in Buildings: Student Manual.
PB95-175006 *00,257*

Present Worth Factors for Life-Cycle Cost Studies in the Department of Defense (1995).
PB95-105029 *03,664*

Present Worth Factors for Life-Cycle Cost Studies in the Department of Defense (1996).
PB96-106869 *03,673*

PETERSON, M. B.
Wear of Selected Materials and Composites Sliding against MoS2 Films.
PB94-172749 *03,231*

PETERSON, S. M.
Measurements of the Viscosities of Saturated and Compressed Fluid 1-chloro-1,2,2,2-tetrafluoroethane (R124) and Pentafluoroethane (R125) at Temperatures between 120 and 420 K.
PB94-199791 *03,254*

PETERSONS, O.
Active High Voltage Divider with 20-PPM Uncertainty.
PB97-119317 *02,104*

PETIETTE-HALL, C. L.
Microwave Properties of YBa2Cu3O7-x Films at 35 GHz from Magnetotransmission and Magnetoreflection Measurements.
PB95-168977 *04,643*

PETIT, G.
Comparison of GPS Broadcast and DMA Precise Ephemerides.
AD-P009 114/0 *01,518*

Comparison of GPS Broadcast and DMA Precise Ephemerides.
N94-30660/2 *01,523*

PETRELLA, E. C.
Phospholipid/Alkanethiol Bilayers for Cell-Surface Receptor Studies by Surface Plasmon Resonance.
PB96-102900 *03,472*

PETRICH, W.
Behavior of Atoms in a Compressed Magneto-Optical Trap.
PB95-203105 *03,999*

Reduction of Light-Assisted Collisional Loss Rate from a Low-Pressure Vapor-Cell Trap.
PB95-202248 *03,971*

Stable, Tightly Confining Magnetic Trap for Evaporative Cooling of Neutral Atoms.
PB96-200720 *04,126*

PETRILLO, K.
Nano-Defects in Commercial Bonded SOI and SIMOX.
PB96-123674 *02,407*

PETROVIC, J. J.
Creep Rupture of MoSi2/SiCp Composites.
PB95-152294 *03,154*

Tensile Creep of Silicide Composites.
PB96-200803 *03,183*

PETROVIC, Z. L.
Excitation of Balmer Lines in Low-Current Discharges of Hydrogen and Deuterium.
PB95-150546 *03,893*

PETTIT, K.
Enhanced Curie Temperatures and Magnetoelastic Domains in Dy/Lu Super Lattices and Films.
PB94-172665 *04,443*

PFEIFER, M. J.
Effects of Elastic Stress on Phase Equilibrium in the Ni-V System.
PB94-172707 *03,313*

PFEIFFER, E. R.
Comparisons of Some NIST Fixed-Point Cells with Similar Cells of Other Standards Laboratories.
PB97-119242 *00,655*

Practical Applications of the ITS-90: Inherent Uncertainties.
PB95-161527 *03,930*

PFUFF, M.
Potential Drop in the Center-Cracked Panel with Asymmetric Crack Extension.
PB95-107330 *04,819*

PHADKE, M. S.
Taguchi's Parameter Design: A Panel Discussion.
PB96-111802 *03,445*

PHALIPPOU, M.
Formal Methods in Conformance Testing: Result and Perspectives.
PB95-153029 *01,710*

PHAN, L.
Performance of HUD-Affiliated Properties during the January 17, 1994 Northridge Earthquake.
PB95-174488 *00,443*

PHAN, L. T.
Comparison of Responses of a Select Number of Buildings to the 10/17/1989 Loma Prieta (California) Earthquake and Low-Level Amplitude Test Results.
PB96-159645 *00,467*

Dynamic Characteristics of Five Tall Buildings during Strong and Low-Amplitude Motions.
PB94-199981 *00,427*

Response of Buildings to Ambient Vibration and the Loma Prieta Earthquake: A Comparison.
PB96-119607 *00,457*

Seismic Instrumentation of Existing Buildings.
PB94-159779 *00,420*

Seismic Strengthening of Reinforced Concrete Frame Buildings.
PB95-108841 *00,430*

State of the Art Report on Seismic Design Requirements for Nonstructural Building Components.
PB96-193800 *00,308*

Strengthening Methodology for Lightly Reinforced Concrete Frames.
PB96-158050 *00,466*

Strengthening Methodology for Lightly Reinforced Concrete Frames-II. Recommended Calculation Techniques for the Design of Infill Walls.
PB94-187648 *00,426*

Strengthening Methodology for Lightly Reinforced Concrete Frames: Recommended Design Guidelines for Strengthening with Infill Walls.
PB95-260725 *00,454*

PHANEUF, R. A.
Absolute Cross Sections for Electron-Impact Single Ionization of Si(+) and Si(2+).
PB95-202529 *03,982*

Backscattering in Electron-Impact Excitation of Multiply Charged Ions.
PB94-185345 *03,799*

Electron-Impact Excitation of Si(3+)(3S yields 3P) Using a Merged-Beam Electron-Energy-Loss Technique.
PB95-151239 *03,904*

Evidence for Significant Backscattering in Near-Threshold Electron-Impact Excitation of Ar(7+)(3s yields 3p).
PB95-126405 *03,883*

Merged-Beams Energy-Loss Technique for Electron-Ion Excitation: Absolute Total Cross Sections for O(5+) (2s yields 2p).
PB96-102058 *04,017*

PHELAN, F. R.
Analysis of Transverse Flow in Aligned Fibrous Porous Media.
PB96-167200 *03,177*

Effect of Heterogeneous Porous Media on Mold Filling in Resin Transfer Molding.
PB95-108676 *03,197*

PHELAN, R. J.
Electrically Calibrated Pyroelectric Detector-Refinements for Improved Optical Power Measurements.
PB95-169066 *02,164*

PHELPS, A. V.
N2(a'(sup 1)Sigma(sub g)(sup +)) Metastable Collisional Destruction and Rotational Excitation Transfer by N2.
PB95-151395 *00,933*

PHELPS, J. M.
Guidelines for Refractive Index Measurements of Asbestos.
PB95-151189 *02,543*

Proficiency Tests for the NIST Airborne Asbestos Program, 1990.
PB94-188836 *00,535*

Scanning Electron Microscopy Observations of Misfit Dislocations in Epitaxial In0.25Ga0.75As on GaAs(001).
PB96-200159 *03,004*

Tensile Deformation-Induced Microstructures in Free-Standing Copper Thin Films.
PB96-102595 *04,715*

PHILLIPS, L.

SGML Environment for STEP.
PB95-143103 *02,778*

PHILLIPS, L. C.

Development in the Theory and Analysis of Eddy Current Sensing of Velocity in Liquid Metals.
PB94-212586 *03,335*

PHILLIPS, M. P.

Stranding Experiments on Double Hull Tanker Structures.
PB96-123112 *03,749*

PHILLIPS, S.

Automated Inspection: The Integration of National Standards and Commercial Products at NIST.
PB95-163077 *02,906*

Two New Probes for a Coordinate Measuring Machine.
PB95-163093 *02,653*

PHILLIPS, S. D.

Development of an Automated Part Inspection System Using the DMIS Standard.
PB95-108866 *02,899*

Estimation of Measurement Uncertainty of Small Circular Features Measured by CMMs.
PB95-267928 *02,918*

Interim Testing Artifact (ITA): A Performance Evaluation System for Coordinate Measuring Machines (CMMs). User Manual.
PB95-210589 *02,914*

NIST SRM 9983 High-Rigidity Ball-Bar Stand. User Manual.
PB95-255840 *02,669*

Some Considerations for Interim Testing of Coordinate Measuring Machine Performance Using a Specific Artifact.
PB95-108858 *02,898*

User's Guide to NIST SRM 2084: CMM Probe Performance Standard.
PB94-206109 *02,709*

PHILLIPS, W.

Hyperfine Effects and Associative Ionization of Ultracold Sodium.
PB95-151221 *03,903*

Optical Molasses: The Coldest Atoms Ever.
PB95-108908 *03,878*

Temperature of Optical Molasses for Two Different Atomic Angular Momenta.
PB95-126058 *03,881*

Ultracold Collisions: Associative Ionization in a Laser Trap.
PB94-213238 *03,859*

PHILLIPS, W. D.

Atoms in Optical Molasses.
PB95-108874 *03,875*

Atoms in Optical Molasses: Applications to Frequency Standards.
PB95-108882 *03,876*

Heterodyne Measurement of the Fluorescence Spectrum of Optical Molasses.
PB95-108411 *03,873*

Laser-Cooled Neutral Atom Frequency Standards.
PB96-160312 *04,086*

Laser Cooling.
PB95-151502 *03,908*

Laser Cooling and the Recoil Limit.
PB97-111280 *04,391*

Laser Modification of Ultracold Collisions: Experiment.
PB96-157987 *04,075*

Localization of Atoms in a Three-Dimensional Standing Wave.
PB95-163887 *03,944*

Measurement of the Atomic Na(3P) Lifetime and of Retardation in the Interaction between Two Atoms Bound in a Molecule.
PB97-122360 *04,178*

Measurements of Fluorescence from Cold Atoms: Localization in Three-Dimensional Standing Waves.
PB95-163879 *03,943*

Microlithography by Using Neutral Metastable Atoms and Self-Assembled Monolayers.
PB96-190038 *02,441*

New Mechanisms for Laser Cooling.
PB95-153268 *03,923*

Optical Molasses: Cold Atoms for Precision Measurements.
PB95-108890 *03,877*

sigma+-sigma- Optical Molasses in a Longitudinal Magnetic Field.
PB95-161840 *03,934*

PHINNEY, C. S.

Analysis by a Combination of Gas Chromatography and Tandem Mass Spectrometry: Development of Quantitative Tandem-in-Time Ion Trap Mass Spectrometry: Isotope Dilution Quantification of 11-Nor-Delta-9-Tetrahydro cannabinol-9-Carboxylic Acid.
PB96-117221 *02,561*

NIST Reference Materials to Support Accuracy in Drug Testing.
PB96-123807 *03,505*

PHIPPS, K. O.

Surging the Upside-Down House: Measurements and Modeling Results.
PB96-180138 *02,243*

PI, J. I.

Realizing Suspended Structures on Chips Fabricated by CMOS Foundry Processes Through the MOSIS Service.
PB94-193984 *01,881*

PIATKO, C. D.

Point Probe Decision Trees for Geometric Concept Classes.
PB96-160817 *01,612*

PICARD, A.

Measurement and Reduction of Alignment Errors of the NIST Watt Experiment.
PB97-111959 *01,987*

NIST Watt Balance: Progress Toward Monitoring the Kilogram.
PB97-113062 *01,991*

PICOLO, J. L.

Intercomparison of Internal Proportional Gas Counting of (85)Kr and (3)H.
PB94-185576 *03,800*

PIELERT, J. H.

Graphical Analysis of the CCRL Portland Cement Proficiency Sample Database (Samples 1-72). (Part 1. Univariant Analysis of Portland Cement).
PB94-196557 *01,308*

Proficiency Testing as a Component of Quality Assurance in Construction Materials Laboratories.
PB94-185774 *00,334*

PIEPER, J.

Contrast Matched Studies of a Sheared Binary Colloidal Suspension.
PB95-150561 *00,918*

PIEPER, J. B.

Measurement of the Weak-Localization Complex Conductivity at 1 Ghz in Disordered Ag Wires.
PB96-117239 *04,731*

PIERCE, D. T.

Coarsening of Unstable Surface Features during Fe(001) Homoepitaxy.
PB96-186127 *04,121*

Growth of Iron on Iron Whiskers.
PB95-150322 *04,567*

Homoepitaxial Growth of Iron and a Real Space View of Reflection-High-Energy-Electron Diffraction.
PB94-173069 *04,445*

Influence of Cr Growth on Exchange Coupling in Fe/Cr/Fe(100).
PB95-150181 *04,562*

Influence of Thickness Fluctuations on Exchange Coupling in Fe/Cr/Fe Structures.
PB96-135371 *04,745*

Magnetic Moments in Cr Thin Films on Fe(100).
PB95-108429 *04,525*

Oscillatory Exchange Coupling in Fe/Au/Fe(100).
PB95-150371 *04,569*

Scaling of Diffusion-Mediated Island Growth in Iron-on-Iron Homoepitaxy.
PB94-185923 *04,455*

Scanning Tunneling Microscopy Study of the Growth of Cr/Fe(001): Correlation with Exchange Coupling of Magnetic Layers.
PB95-150330 *04,568*

SEMPA Studies of Exchange Coupling in Magnetic Multilayers.
PB96-164074 *04,780*

SEMPA Studies of Oscillatory Exchange Coupling.
PB95-163556 *04,625*

Simple, Compact, High-Purity Cr Evaporator for Ultrahigh Vacuum.
PB94-216678 *04,520*

Surface Magnetic Microstructural Analysis Using Scanning Electron Microscopy with Polarization Analysis (SEMPA).
PB95-162657 *03,938*

Tunneling Spectroscopy of bcc(001) Surface States.
PB96-155585 *04,775*

PIERMARINI, G.

Densification of Nano-Size Powders. 1994 Report.
DE94013486 *03,027*

PIERMARINI, G. J.

1,4-Dinitrocubane and Cubane under High Pressure.
PB95-108437 *03,755*

Alvin Van Valkenburg and the Diamond Anvil Cell.
PB96-204474 *04,797*

Bulk Modulus and Young's Modulus of Nanocrystalline gamma-Alumina.
PB96-204185 *03,092*

Equipment for Investigation of Cryogenic Compaction of Nanosize Silicon Nitride Powders. 1993 Report.
DE94013593 *03,028*

Fabrication of Transparent gamma-Al2O3 from Nanosize Particles.
PB95-175493 *03,054*

Low temperature fabrication from nano-size ceramic powders.
DE95013505 *03,029*

NIST/NCMS Program on Electronic Packaging: First Update.
PB96-204086 *03,008*

PIKIN, A. I.

Beam Line for Highly Charged Ions.
PB97-111256 *04,143*

PILIONE, L.

Analysis of Boron in CVD Diamond Surfaces Using Neutron Depth Profiling.
PB94-213089 *04,511*

PILIONE, L. J.

Effect of Stoichiometry on the Phases Present in Boron Nitride Thin Films.
PB96-102470 *04,710*

PINA, C.

Realizing Suspended Structures on Chips Fabricated by CMOS Foundry Processes Through the MOSIS Service.
PB94-193984 *01,881*

PINDZOLA, M. S.

Absolute Cross Sections for Electron-Impact Single Ionization of Si(+) and Si(2+).
PB95-202529 *03,982*

Dielectronic Capture Processes in the Electron-Impact Ionization of Sc(2+).
PB95-203113 *04,000*

PINE, A. S.

Decoupling in the Line Mixing of Acetylene Infrared Q Branches.
PB95-108452 *00,877*

Infrared Spectra of van der Waals Complexes of Importance in Planetary Atmospheres.
PB95-125738 *00,071*

Molecular-Beam Optothermal Spectrum of the OH Stretching Band of Methanol.
PB94-212826 *00,839*

P-Type Doubling in the Infrared Spectrum of NO-HF.
PB94-211463 *00,817*

Perpendicular C-H Stretching Band nu9/nu13 and the Torsional Potential of Dimethylacetylene.
PB97-122451 *01,192*

Self Broadening in the nu1 Band of NH3.
PB94-216371 *00,857*

Self-, N2- and Ar-Broadening and Line Mixing in HCN and C2H2.
PB95-108445 *00,876*

Spectroscopic Constants for the 2.5 and 3.0 micrometer Bands of Acetylene.
PB94-213071 *00,847*

PINEO, V. C.

Comparison of Meteor Activity with Occurrence of Sporadic E Reflections.
AD-A292 039/5 *00,116*

PINKASI, M.

Planar Near-Field Alignment.
PB94-172491 *01,998*

PINNINGTON, E. H.

Analysis of the 5s(2)5p(2)-(5s5p(3)+5s(2)5p5d+5s(2)5p6s) Transitions of Four-Times Ionized Xenon (Xe V).
PB95-150769 *03,900*

PINSKY, D. A.

SPC Artifact for Automated Solder Joint Inspection.
PB96-161716 *04,095*

PINSON, J.

Oxidation of Caffeic Acid and Related Hydroxycinnamic Acids.
PB97-111975 *00,651*

PIPPENGER, P. M.

Epitaxial Integration of Single Crystal C60.
PB95-153490 *04,592*

Photoluminescence Spectra of Epitaxial Single Crystal C60.
PB96-141205 *04,754*

PISCEVIC, D.

Surface Plasmon Microscopy of Biotin-Streptavidin Binding Reactions on UV-Photopatterned Alkanethiol Self-Assembled Monolayers.
PB96-176771 *01,158*

PITCHURE, D.

Ultrasonic Method for Reconstructing the Two-Dimensional Liquid-Solid Interface in Solidifying Bodies.
PB95-161782 *03,349*

PITTS, W.

Agent Screening for Halon 1301 Aviation Replacement.
PB96-159710 *03,282*

Global Density Effects on the Self-Preservation Behavior of Turbulent Free Jets.
PB95-162301 *04,207*

PITTS, W. M.

Application of Thermodynamic and Detailed Chemical Kinetic Modeling to Understanding Combustion Product Generation in Enclosure Fires.
PB96-135322 *01,413*

Carbon Monoxide Production in Compartment Fires: Reduced-Scale Enclosure Test Facility.
PB95-231700 01,394

Chemical Stability of Upper-Layer Fire Gases.
PB96-123385 01,410

Evaluation of Alternative In-Flight Fire Suppressants for Full-Scale Testing in Simulated Aircraft Engine Nacelles and Dry Bays.
PB94-203403 00,023

Experimental Study of the Stabilization Region of Lifted Turbulent-Jet Diffusion Flames.
PB96-122676 01,405

Global Equivalence Ratio Concept and the Formation Mechanisms of Carbon Monoxide in Enclosure Fires.
PB96-146790 00,210

Global Equivalence Ratio Concept and the Prediction of Carbon Monoxide Formation in Enclosure Fires.
PB94-207511 00,313

Greatly Enhanced Soot Scattering in Flickering Ch4/Air Diffusion Flames.
PB94-172988 01,361

Reactivity of Product Gases Generated in Idealized Enclosure Fire Environments.
PB95-161790 01,386

Scaling Compartment Fires: Reduced- and Full-Scale Enclosure Burns.
PB96-175708 00,224

PLANT, A.

Liposome-Based Flow-Injection Immunoassay for Determining Theophylline in Serum.
PB94-213493 03,494

PLANT, A. L.

Fokker-Planck Description of Multivalent Interactions.
PB95-108478 00,879

Phospholipid/Alkanethiol Bilayers for Cell-Surface Receptor Studies by Surface Plasmon Resonance.
PB96-102900 03,472

Self-Assembled Phospholipid/Alkanethiol Biomimetic Bilayers on Gold.
PB95-108460 00,878

Supported Phospholipid/Alkanthiol Biomimetic Membranes: Insulating Properties.
PB95-180782 03,470

PLESS, R.

Ultrasonic Spectroscopy of Metallic Spheres Using Electromagnetic-Acoustic Transduction.
PB94-212537 04,185

PLIVA, J.

Perpendicular C-H Stretching Band nu9/nu13 and the Torsional Potential of Dimethylacetylene.
PB97-122451 01,192

PLOESSL, R.

Micromagnetic Structure of Domains in Co/Pt Multilayers. 1. Investigations of Wall Structure.
PB95-162111 04,610

PLOTT, M.

Evaluation and Qualification Standards for an X-Ray Laminography System.
PB94-172954 02,029

SPC Artifact for Automated Solder Joint Inspection.
PB96-161716 04,095

PLUMB, O. A.

Development of an Economical Video Based Fire Detection and Location System.
PB96-193743 00,228

PLUSQUELLIC, D.

Photodissociation Dynamics in Quantum State-Selected Clusters: A Test of the One-Atom Cage Effect in Ar-H2O.
PB95-203121 01,044

POCHAN, P. D.

Inductively Coupled Plasma Source for the Gaseous Electronics Conference RF Reference Cell.
PB96-113394 02,394

Reactive Ion Etching in the Gaseous Electronics Conference RF Reference Cell.
PB96-113402 02,395

PODIO, F. L.

NIST Program for Investigating Error Reporting Capabilities of Optical Disk Drives.
PB96-160627 01,635

Optical Storage Media Data Integrity Studies.
N95-24130/3 01,620

Research on Methods for Determining Optical Disk Media Life Expectancy Estimates.
PB96-160304 01,633

Standardization of Testing Methods for Optical Disk Media Characteristics and Related Activities at NIST.
PB95-108486 01,624

Status of Emerging Standards for Removable Computer Storage Media and Related Contributions of NIST.
PB96-160619 01,634

POITZSCH, M. E.

Progress on a Cryogenic Linear Trap for (199)Hg(+) Ions.
PB95-180790 03,965

POKHODUN, A. I.

Investigation of High-Temperature Platinum Resistance Thermometers at Temperatures Up to 962C, and, in Some Cases, 1064C.
PB96-161294 00,629

POKROVSKII, V. A.

Summary of the Apparent Standard Partial Molal Gibbs Free Energies of Formation of Aqueous Species, Minerals, and Gases at Pressures 1 to 5000 Bars and Temperatures 25 to 1000C.
PB96-145891 01,113

POLAK, M. J.

Display-Measurement Round-Robin.
PB96-119227 02,186

POLAK, M. L.

Photoelectron Spectroscopy of Negatively Charged Bismuth Clusters: Bi(-)2, Bi(-)3, and Bi(-)4.
PB95-108494 00,880

Photoelectron Spectroscopy of Small Antimony Cluster Anions: Sb(-), Sb2(-), Sb3(-), and Sb4(-).
PB95-203139 01,045

POLAKOS, P. A.

Increased Transition Temperature in in situ Coevaporated YBa2Cu3O7-delta Thin Films by Low Temperature Post-Annealing.
PB95-180071 04,672

POLAND, C. D.

Evaluation and Strengthening Guidelines for Federal Buildings: Assessment of Current Federal Agency Evaluation Programs and Rehabilitation Criteria and Development of Typical Costs for Seismic Rehabilitation.
PB94-181856 00,425

Evaluation and Strengthening Guidelines for Federal Buildings: Identification of Current Federal Agency Programs.
PB94-176278 00,424

POLAND, D. E.

Corrected Optical Pyrometer Readings.
AD-A279 949/2 02,615

POLIAN, G.

International Marine-Atmospheric (222)Rn Measurement Intercomparison in Bermuda. Part 2. Results for the Participating Laboratories.
PB96-175682 00,115

POLK, M. B.

Evidence of Crosslinking in Methyl Pendent PBZT Fiber.
PB97-112486 03,393

POLK, W. T.

Precise Identification of Computer Viruses.
PB96-160825 01,613

Security Considerations for SQL-Based Implementations of STEP.
PB94-139649 02,766

POLLAND, J. F.

Analysis of Autocorrelations in Dynamic Processes.
PB95-181228 02,826

POLVANI, R. S.

Chemical Aspects of Tool Wear in Single Point Diamond Turning.
PB97-112601 03,021

POLYANSKY, O. L.

Tunneling-Rotation Spectrum of the Hydrogen Fluoride Dimer.
PB94-198678 00,793

POMMERSHEIM, J.

Diffusion of Cations Beneath Organic Coatings on Steel Substrate.
PB94-215704 03,119

POMMERSHEIM, J. M.

Long-Term Performance of Engineered Concrete Barriers.
PB95-260816 03,727

Sulfate Attack of Cementitious Materials: Volumetric Relations and Expansions.
PB94-187317 03,232

POMMERSHEIM, J. R.

Expansion of Cementitious Materials Exposed to Sulfate Solutions.
PB94-185782 02,577

POMPE, R.

Analysis of Physical Properties of Ceramic Powders in an International Interlaboratory Comparison Program.
PB95-161501 03,050

POOLE, J.

Distributed Communication Methods and Role-Based Access Control for Use in Health Care Applications.
PB96-183165 01,508

Method to Determine a Basis Set of Paths to Perform Program Testing.
PB96-131503 01,747

POOLE, J. P.

Unravel: A CASE Tool to Assist Evaluation of High Integrity Software. Volume 1. Requirements and Design.
PB95-267886 01,736

Unravel: A CASE Tool to Assist Evaluation of High Integrity Software. Volume 2. User Manual.
PB95-267894 01,737

POPEL, R.

SUSAN: SUperconducting Systems ANalysis by Low Temperature Scanning Electron Microscopy (LTSEM).
PB96-112065 04,728

POPESCU, G.

Scattered Fractions of Dose from 18 and 25 MV X-ray Radiotherapy Linear Accelerators.
PB96-186101 04,120

PORTIER, R. W.

Fire Data Management System, FDMS 2.0, Technical Documentation.
PB94-164019 01,358

POSTEK, M. T.

Critical Issues in Scanning Electron Microscope Metrology.
PB95-169405 02,359

Fabrication Issues for the Prototype National Institute of Standards and Technology SRM 2090A Scanning Electron Microscope Magnification Calibration Standard.
PB96-160585 01,131

Modification of a Commercial SEM with a Computer Controlled Cathode Stabilized Power Supply.
PB96-201066 04,129

Monte Carlo Model for SEM Linewidth Metrology.
PB95-150058 02,331

Precision, Accuracy, Uncertainty and Traceability and Their Application to Submicrometer Dimensional Metrology.
PB94-213105 02,319

Report on the NIST Low Accelerating Voltage SEM Magnification Standard Interlaboratory Study.
PB96-201074 02,445

Scanning Electron Microscope Magnification Calibration Interlaboratory Study.
PB96-201082 01,164

Scanning Electron Microscope Metrology.
PB96-201090 02,446

SEM Linewidth Metrology of X-ray Lithography Masks.
PB96-201108 02,447

X-ray Mask Metrology: The Development of Linewidth Standards for X-ray Lithography.
PB95-162129 02,348

POTTMEYER, J.

Framework for National Information Infrastructure Services.
PB95-103719 02,723

POTZICK, J.

Comparisons of Measured Linewidths of Sub-Micrometer Lines Using Optical, Electrical, and SEM Metrologies.
PB95-152807 02,338

Metrology Model for Submicrometer Dimensional Measurements.
PB95-108502 02,647

Practical Photomask Linewidth Measurements.
PB95-108510 02,324

POTZICK, J. E.

Accuracy in Integrated Circuit Dimensional Measurements.
PB95-180808 02,368

Improving Photomask Linewidth Measurement Accuracy via Emulated Stepper Aerial Image Measurement.
PB95-180816 02,911

POWELL, C. J.

Activities of ISO Technical Committee 201 on Surface Chemical Analysis.
PB95-180824 00,607

Activities of the ASTM Committee E-42 on Surface Analysis.
PB95-108528 00,881

Calculations of Electron Inelastic Mean Free Paths (IMFPs). 4. Evaluation of Calculated IMFPs and of the Predictive IMFP Formula TPP-2 for Electron Energies between 50 and 2000 eV.
PB95-150728 00,922

Calculations of Electron Inelastic Mean Free Paths. 5. Data for 14 Organic Compounds over the 50-2000 eV Range.
PB95-150355 00,916

Compositional Analyses of Surfaces and Thin Films by Electron and Ion Spectroscopies.
PB94-185790 00,779

Elastic-Electron-Scattering Effects on Angular Distributions in X-ray Photoelectron Spectroscopy.
PB95-175758 01,000

Energy Calibration of X-ray Photoelectron Spectrometers: Results of an Interlaboratory Comparison to Evaluate a Proposed Calibration Procedure.
PB96-102918 04,027

Formalism and Parameters for Quantitative Surface Analysis by Auger Electron Spectroscopy and X-Ray Photoelectron Spectroscopy.
PB94-212297 00,832

Formation of Technical Committee 201 on Surface Chemical Analysis by the International Organization for Standardization.
PB95-108536 00,568

Inelastic Interactions of Electrons with Surfaces: Application to Auger-Electron Spectroscopy and X-ray Photoelectron Spectroscopy.
PB94-172699 00,764

Use of Sum Rules on the Energy-Loss Function for the Evaluation of Experimental Optical Data.
PB95-150736 04,264

POWELL, R. L.

Thermal Conductivity of Metals and Alloys at Low Temperatures. A Review of the Literature.
AD-A279 180/4 03,302

POWELL, R. M.

Electronics and Electrical Engineering Laboratory: 1994 Strategic Plan. Supporting Technology for U.S. Competitiveness in Electronics.
PB94-161320 *01,874*

POWELL, S.

Guidelines for Reporting Results of Computational Experiments. Report of the Ad hoc Committee.
PB94-212347 *03,427*

POZO, R.

IML++ v.1.2 Iterative Methods Library Reference Guide.
PB96-195219 *01,776*

MV++ v. 1.5a Matrix/Vector Class Reference Guide.
PB96-195326 *01,777*

Performance Characteristics of Fast Elliptic Solvers on Parallel Platforms.
PB95-180832 *01,723*

SparseLib++ v. 1.5 Sparse Matrix Class Library. Reference Guide.
PB96-193636 *01,775*

PRASK, H. J.

Determination of the Residual Stresses Near the Ends of Skip Welds Using Neutron Diffraction and X-ray Diffraction Procedures.
PB95-253589 *02,868*

Neutron Techniques in Materials Science and Related Disciplines.
PB96-119698 *02,980*

Texture Study of Two Molybdenum Shaped Charge Liners by Neutron Diffraction.
PB94-200177 *03,754*

Textures of Tantalum Metal Sheets by Neutron Diffraction.
PB94-200169 *03,399*

PRASSIDES, K.

Lattice Dynamics of Ba1-xKxBiO3.
PB96-102421 *04,706*

Lattice Dynamics of Semiconducting, Metallic, and Superconducting Ba1-xKxBiO3 Studied by Inelastic Neutron Scattering.
PB96-102447 *04,708*

Neutron-Scattering Study of C60(n-) (n=3,6) Librations in Alkali-Metal Fullerides.
PB94-200219 *00,806*

Rotational Dynamics of C60 in Na2RbC60.
PB95-153201 *00,948*

Rotational Dynamics of Solid C70: A Neutron-Scattering Study.
PB94-172178 *00,755*

Rotational Dynamics of Solid C70: A Neutron-Scattering Study.
PB95-153219 *00,949*

Structure and Conductivity of Layered Oxides (Ba,Sr)n+1(Sn,Sb)nO3n+1.
PB96-102439 *04,707*

PRATHER, J. L.

Atomic Energy Levels in Crystals.
AD-A280 150/4 *04,431*

PRATT, K. W.

Automated, High-Precision Coulometric Titrimetry. Part 1. Engineering and Implementation.
PB95-150199 *00,575*

Automated, High Precision Coulometric Titrimetry. Part 2. Strong and Weak Acids and Bases.
PB95-150207 *00,576*

Dissolution Problems with Botanical Reference Materials.
PB95-126280 *03,487*

PRATT, M. J.

Product Models and Virtual Prototypes in Mechanical Engineering.
PB95-253563 *02,783*

Requisite Elements, Rationale, and Technology Overview for the Systems Intergration for Manufacturing Applications (SIMA) Program. Background Study.
PB96-112685 *02,831*

PREISEGGER, E.

Report of the Refrigeration, Air Conditioning and Heat Pumps Technical Options Committee.
PB96-176755 *03,293*

PREMACHANDRAN, R.

Surface Chemical Interactions of Si3N4 with Polyelectrolyte Deflocculants.
PB95-175576 *03,056*

PREMACHANDRAN, R. S.

Electrokinetic Sonic Analysis of Silicon Nitride Suspensions.
PB96-123575 *03,073*

Standard Reference Material for the Measurement of Particle Mobility by Electrophoretic Light Scattering.
PB96-102488 *00,609*

PRENDERGAST, J.

TDDB Characterization of Thin SiO2 Films with Bimodal Failure Populations.
PB96-102926 *02,381*

PRENTISS, M.

Microlithography by Using Neutral Metastable Atoms and Self-Assembled Monolayers.
PB96-190038 *02,441*

PRESSER, C.

Analysis of Droplet Arrival Statistics in a Pressure-Atomized Spray Flame.
PB97-112270 *01,352*

Assessing Halon Alternatives for Aircraft Engine Nacelle Fire Suppression.
PB96-102454 *01,401*

Combustion of Methanol and Methanol/Dodecanol Spray Flames.
PB95-108544 *02,478*

Effect of Dodecanol Content on the Combustion of Methanol Spray Flames.
PB95-176020 *01,389*

Effect of Finite Beam Width on Elastic Light Scattering from Droplets.
PB96-163670 *01,144*

Effectiveness of Halon Alternatives in Suppressing Dynamic Combustion Process.
PB96-175732 *03,288*

Elastic Scattering from Spheres under Non Plane-Wave Illumination.
PB96-163688 *04,370*

Forward Scattering of a Gaussian Beam by a Nonabsorbing Sphere.
PB97-112288 *04,395*

In-situ Fume Particle Size and Number Density Measurements from a Synthetic Smelt.
PB94-212040 *03,334*

Internal Droplet Circulation Induced by Surface-Driven Rotation.
PB97-119267 *02,500*

Parametric Investigation of Metal Powder Atomization Using Laser Diffraction.
PB95-108577 *03,342*

Role of Combustion on Droplet Transport in Pressure-Atomized Spray Flames.
PB96-204433 *01,434*

Structure of a Swirl-Stabilized Kerosene Spray Flame.
PB95-108569 *02,480*

Study of Droplet Transport in Alcohol-Based Spray Flames Using Phase/Doppler Interferometry.
PB95-108551 *02,479*

Suppression of Elevated Temperature Hydraulic Fluid and JP-8 Spray Flames.
PB95-181095 *00,021*

Suppression of Ignition Over a Heated Metal Surface.
PB96-176425 *03,291*

Turbulent Spray Burner for Assessing Halon Alternative Fire Suppressants.
PB95-153748 *01,385*

Validation of a Turbulent Spray Flame Facility for the Assessment of Halon Alternatives.
PB96-159728 *03,283*

PRESSESKY, J. L.

Correlations of Modulation Noise with Magnetic Microstructure and Intergranular Interactions for CoCrTa and CoNi Thin Film Media.
PB94-212768 *04,509*

PREVEDELLI, M.

High-Order Harmonic Mixing with GaAs Schottky Diodes.
PB95-108585 *01,528*

Rotational Far Infrared Spectrum of (13)CO.
PB95-152187 *00,941*

PRIBANIC, J. A.

Binder Characterization and Evaluation by Nuclear Magnetic Resonance Spectroscopy.
PB94-193471 *01,334*

PRICE, J.

Dielectric Properties of Thin Film SrTiO3 Grown on LaAlO3 with YBa2Cu3O7-x Electodes.
PB95-181160 *02,267*

PRICE, J. C.

Characterization of a Tunable Thin Film Microwave YBa2Cu3O7-x/SrTiO3 Coplanar Capacitor.
PB95-175527 *02,264*

Ferroelectric Thin Film Characterization Using Superconducting Microstrip Resonators.
PB96-102389 *02,270*

Measurement of the Weak-Localization Complex Conductivity at 1 Ghz in Disordered Ag Wires.
PB96-117239 *04,731*

Tunable High Temperature Superconductor Microstrip Resonators.
PB95-168423 *02,048*

PRICE, S. D.

Charge Transfer and Collision-Induced Dissociation Reactions of CF(2+) and CF2(2+) with the Rare Gases at a Laboratory Collision Energy of 49 eV.
PB94-185584 *00,775*

Collision-Induced Neutral Loss Reactions of Molecular Dications.
PB94-185808 *00,780*

Precision Lifetime Measurements of Cs 6p (2)P1/2 and 6p (2)P3/2 Levels by Single-Photon Counting.
PB95-203816 *04,010*

PRILUSKY, J.

Protein Data Bank: Current Status and Future Challenges.
PB97-109060 *00,517*

PRINCE, E.

Construction of Maximum-Entropy Density Maps, and Their Use in Phase Determination and Extension.
PB95-108593 *00,882*

Fast-Ion Conducting Y2(ZryTi1-y)2O7 Pyrochlores: Neutron Rietveld Analysis of Disorder Induced by Zr Substitution.
PB96-156104 *04,776*

Fast-Ion Conduction and Disorder in Cation and Anion Arrays in Y2(ZryTi(1-y))2O7 Pyrochlores Induced by Zr Substitution: A Neutron Rietveld Analysis.
PB94-211869 *04,496*

Mathematical Aspects of Rietveld Refinement.
PB95-108601 *04,526*

Neutron Powder Diffraction Study of a Na, Cs-Rho Zeolite.
PB94-198629 *00,791*

Rietveld Analysis of NaxWO3+x/2.yH2O, Which Has the Hexagonal Tungsten Bronze Structure.
PB95-107371 *04,524*

Statistical Descriptors in Crystallography. 2. Report of a Working Group on Expression of Uncertainty in Measurement.
PB96-146824 *04,764*

PRITZKER, R. A.

Learning to Change: Opportunities to Improve the Performance of Smaller Manufacturers.
PB94-166212 *00,010*

PROCHOROV, A. V.

Precision High Temperature Blackbodies.
PB95-140059 *03,885*

PROCTOR, F.

NIST RS274KT Interpreter.
PB96-147954 *02,835*

NIST Support to the Next Generation Controller Program: 1991 Final Technical Report.
PB94-163490 *02,808*

PROCTOR, F. M.

Enhanced Machine Controller Architecture Overview.
PB94-142460 *02,802*

NIST RS274/NGC Interpreter Version 1.
PB94-187788 *02,814*

Open Architectures for Machine Control.
PB94-135621 *02,942*

PROKES, K.

Magnetic Properties of Single-Crystalline UCu3Al2.
PB95-180717 *04,686*

PROVENCHER, D.

Evaluation and Strengthening Guidelines for Federal Buildings: Identification of Current Federal Agency Programs.
PB94-176278 *00,424*

PROVENCHER, D. L.

Evaluation and Strengthening Guidelines for Federal Buildings: Assessment of Current Federal Agency Evaluation Programs and Rehabilitation Criteria and Development of Typical Costs for Seismic Rehabilitation.
PB94-181856 *00,425*

PRUSS, A.

International Equations for the Saturation Properties of Ordinary Water Substance. Revised According to the International Temperature Scale of 1990. Addendum to Journal of Physical and Chemical Reference Data 16, 893 (1987).
PB94-162302 *00,742*

PUCIC, S. P.

Derivation of the System Equation for Null-Balanced Total-Power Radiometer System NCS1.
PB94-169786 *02,022*

Diffusion of Copper into Gold Plating.
PB95-162152 *00,957*

Evaluation of Uncertainties of the Null-Balanced Total-Power Radiometer System NCS1.
PB94-169794 *02,023*

Null-Balanced Total-Power Radiometer System NCS1.
PB94-169778 *02,021*

Single-Port Technique for Adaptor Efficiency Evaluation.
PB96-176441 *02,088*

Uncertainties of the NIST Coaxial Noise Calibration System.
PB96-111984 *02,070*

PUGH, E. N.

Metallurgy Technical Activities 1994 (NAS-NRC Assessment Panel, April 6-7, 1995).
PB96-136981 *02,981*

Metallurgy. Technical Activities, 1995.
PB96-195284 *03,003*

PUHL, J. M.

Calibration of High-Energy Electron Beams by Use of Graphite Calorimeters.
PB95-161113 *04,598*

Investigation of Applicability of Alanine and Radiochromic Detectors to Dosimetry of Proton Clinical Beams.
PB96-146782 *03,636*

New EPR Dosimeter Based on Polyvinylalcohol.
PB94-199700 *03,619*

Novel Radiochromic Films for Clinical Dosimetry.
PB97-119259 *03,641*

Overview of a Radiation Accident at an Industrial Accelerator Facility.
PB97-122485 *02,612*

Radiation Accident at an Industrial Accelerator Facility.
PB95-140117 02,575

Temperature and Relative Humidity Dependence of Radiochromic Film Dosimeter Response to Gamma and Electron Radiation.
PB96-135298 03,718

PULS, J.

Radiation-Driven Winds of Hot Luminous Stars X. The Determination of Stellar Masses Radii and Distances from Terminal Velocities and Mass-Loss Rates.
PB94-213022 00,060

PUPPO, E.

Data-Parallel Algorithm for Three-Dimensional Delaunay Triangulation and Its Implementation.
PB95-163309 01,714

PURI, K. D.

Thermodynamics of the Binding of Galactopyranoside Derivatives to the Basic Lectin from Winged Bean (Psophocarpus Tetrogonolobus).
PB95-162715 03,465

PURI, R.

Laser-Induced Fluorescence Measurements of OH. Concentrations in the Oxidation Region of Laminar, Hydrocarbon Diffusion Flames.
PB95-162160 01,387

Laser-Induced Fluorescence Measurements of OH in Laminar Diffusion Flames in the Presence of Soot Particles.
PB96-123120 01,409

Oxidation of Soot and Carbon Monoxide in Hydrocarbon Diffusion Flames.
PB95-150215 01,382

PURSELL, C. J.

Vibrational Energy Transfer in S1 p-Difluorobenzene. A Comparison of Low and Room Temperature Collisions.
PB95-108619 00,883

PURTSCHER, P. T.

Aluminum-Lithium Alloys: Evaluation of Fracture Toughness by Two Test Standards, ASTM Method E 813 and E 1304.
PB96-190236 03,374

Ductile Fracture and Tempered Martensite Embrittlement of 4140 Steel.
PB96-190285 03,222

Light-Weight Alloys for Aerospace Applications II.
PB96-190244 03,375

Microstructure and Tensile Properties of Microalloyed Steel Forgings.
PB94-172715 03,204

Noncontact Ultrasonic Inspection of Train Rails for Stress.
PB95-162673 04,851

Prediction of Strengthening Due to V Additions in Direct-Cooled Ferrite-Pearlite Forging Steels.
PB96-190251 03,220

Prediction of the Strength Properties for Plain-Carbon and Vanadium Micro-Alloyed Ferrite-Pearlite Steel.
PB96-123393 03,216

Temperature-Induced Transition in Ductile Fracture Appearance of a Nitrogen-Strengthened Austenitic Stainless Steel.
PB96-190269 03,221

PURWANTO, A.

Magnetic Properties of Single-Crystalline UCu3Al2.
PB95-180717 04,686

PUTORTI, A. D.

In situ Burning of Oil Spills: Mesoscale Experiments and Analysis.
PB95-163747 02,587

Santa Ana Fire Department Experiment at 1315 South Bristol, July 14, 1994.
PB95-188868 00,389

Santa Ana Fire Department Experiment at 1315 South Bristol, July 14, 1994. (Reprint).
PB96-102934 00,207

Santa Ana Fire Department Experiments at South Bristol Street.
PB96-154810 00,305

Smoke Plume Trajectory from In situ Burning of Crude Oil in Alaska: Field Experiments.
PB96-131560 02,594

PYE, J. P.

Volume-Limited ROSAT Survey of Extreme Ultraviolet Emission from all Nondegenerate Stars within 10 Parsecs.
PB96-103189 00,093

PYKA, N.

Inelastic Neutron Scattering Measurements of Phonons in Icosahedral Al-Li-Cu.
PB95-126215 04,532

QADRI, S. B.

Buffer Layer Modulation-Doped Field-Effect-Transistor Interactions in the Al0.33Ga0.67As/GaAs Superlattice System.
PB96-102876 02,380

Interface Roughness-Induced Changes in the Near-E(sub 0) Spectroscopic Behavior of Short-Period AlAs/GaAs Superlattices.
PB94-185154 02,118

Interface Roughness of Short-Period AlAs/GaAs Superlattices Studied by Spectroscopic Ellipsometry.
PB95-107215 02,137

Interface Sharpness during the Initial Stages of Growth of Thin, Short-Period III-V Superlattices.
PB95-108783 02,139

Interface Sharpness in Low-Order III-V Superlattices.
PB95-108775 02,138

QIAN, C.

Turbulent Flame Spread on Vertical Corner Walls.
PB96-114764 01,403

Upward Flame Spread along the Vertical Corner Walls (October 1993).
PB94-206299 00,340

QIAN, X.

Comparison of FDDI Asynchronous Mode and DQDB Queue Arbitrated Mode Data Transmission for Metropolitan Area Network Applications.
PB96-160452 01,498

Provision of Isochronous Service on IEEE 802.6.
PB96-160635 01,501

QIU, Y.

Structural Stabilization of Phase Separating PC/Polyester Blends through Interfacial Modification by Transesterification Reaction.
PB95-150454 01,239

QUANG, E.

Neutron Leakage Benchmark for Criticality Safety Research.
PB95-126132 03,723

QUEEN, Y. H.

Advanced Angle Metrology System.
PB94-211364 02,637

Tilt Effects in Optical Angle Measurements.
PB95-169389 04,294

QUENARD, D. A.

Modelling Drying Shrinkage of Cement Paste and Mortar. Part 1. Structural Models from Angstroms to Millimeters.
PB96-135132 03,074

QUENTER, D.

SUSAN: SUperconducting Systems ANalysis by Low Temperature Scanning Electron Microscopy (LTSEM).
PB96-112065 04,728

QUINN, G.

Fracture Toughness of Advanced Ceramics at Room Temperature: A Vamas Round-Robin.
PB95-162194 03,160

QUINN, G. D.

Fracture Mechanism Maps: Their Applicability to Silicon Nitride.
PB96-204532 03,094

High Temperature Structural Reliability of Silicon Nitride.
PB97-110456 03,104

Room-Temperature Flexure Fixture for Advanced Ceramics.
PB95-210498 03,061

QUINN, T.

Through-the-Arc Sensing for Measuring Gas Metal Arc Weld Quality in Real Time.
PB95-164463 02,908

QUINN, T. P.

Computers in Welding: A Primer.
PB95-162863 02,862

Contact Tube Wear Detection in Gas Metal Arc Welding.
PB96-135330 02,872

Control of Gas-Metal-Arc Welding Using Arc-Light Sensing.
PB96-131461 02,869

Electrode Extension Model for Gas Metal Arc Welding.
PB96-135074 02,871

Mathematical Models of Transport Phenomena Associated with Arc-Welding Processes: A Survey.
PB96-135058 02,870

Power Characteristics in GMAW: Experimental and Numerical Investigation.
PB96-190145 03,296

Sensing Droplet Detachment and Electrode Extension for Control of Gas Metal Arc Welding.
PB96-190160 03,297

Through-the-Arc Sensing for Monitoring Arc Welding.
PB94-185899 02,858

Through-the-Arc Sensing for Real-Time Measurement of Gas Metal Arc Weld Quality.
PB95-162871 02,863

QUINTERO, R.

NIST Support to the Next Generation Controller Program: 1991 Final Technical Report.
PB94-163490 02,808

Overview of NASREM: The NASA/NBS Standard Reference Model for Telerobot Control System Architecture.
PB94-194560 04,831

Reference Architecture for Machine Control Systems Integration: Interim Report.
PB95-144549 02,820

Submarine Automation: Demonstration No. 5.
PB95-251633 03,748

Task Decomposition Methodology for the Design of a Coal Mining Automation Hierarchical Real-Time Control System.
PB94-185386 03,694

Toward a Reference Model Architecture for Real-Time Intelligent Control Systems (ARTICS).
PB94-172046 02,932

QUINTIERE, J. G.

Fire Growth Models for Materials.
PB94-195856 01,367

Heat Flux from Flames to Vertical Surfaces.
PB97-110357 01,438

Wall Flame Heights with External Radiation.
PB95-163481 00,380

RABAGO, R.

Gas Transport Properties of Solution-Cast Perfluorosulfonic Acid Ionomer Films Containing Ionic Surfactants.
PB95-175998 01,267

RABY, T. M.

Reactor Radiation Technical Activities, 1994. NAS-NRC Assessment Panel, April 6-7, 1995.
PB95-209888 03,732

RADACK, S. M.

Computer Systems Laboratory Annual Report, 1993.
PB94-162518 01,622

Computer Systems Laboratory Annual Report 1994.
PB95-209920 01,629

Conference Report: International Conference on the Application of Standards for Open Systems (6th).
PB96-161211 01,762

Federal Government and Information Technology Standards: Building the National Information Infrastructure.
PB95-180840 01,812

GOSIP Testing Program.
PB96-161229 01,504

Guidance of the Legality of Keystroke Monitoring.
PB96-161237 00,005

Industry/Government Open Systems Specification: The Development of GOSIP Version 3.
PB96-161245 01,505

Information Technology Standards in Federal Acquisitions.
PB96-161252 01,636

Using Information Technology Standards in Federal Acquisitions.
PB96-161260 01,637

RADEBAUGH, R.

Building a Better Crycooler.
PB96-119615 04,734

Design Equations and Scaling Laws for Linear Compressors with Flexure Springs.
PB95-168902 02,948

Energy Flows in an Orifice Pulse Tube Refrigerator.
PB95-169082 02,752

Graded and Nongraded Regenerator Performance.
PB95-169090 02,753

Resistance Thermometers with Fast Response for Use in Rapidly Oscillating Gas Flows.
PB95-107298 03,261

Thermal Anemonetry for Mass Flow Measurement in Oscillating Cryogenic Gas Flows.
PB96-176789 04,218

RADERMACHER, K.

Silicon Surface Chemistry by IR Spectroscopy in the Mid- to Far-IR Region: H2O and Ethanol on Si(100).
PB96-138565 01,097

RADFORD, H. E.

Far Infrared Laser Frequencies of CH3OD and N2H4.
PB96-119623 04,341

RADOUSKY, H. B.

Crystal Structure and Magnetic Ordering of the Rare-Earth and Cu Moments in RBa2Cu2NbO8(R=Nd,Pr).
PB95-140554 04,546

RADOVANOV, S.

Ion Kinetic-Energy Distributions in Argon rf Glow Discharges.
PB95-141008 04,409

RADOVANOV, S. B.

Dusty Plasma Studies in the Gaseous Electronics Conference Reference Cell.
PB96-113410 02,396

Effect of Electrode Material on Measured Ion Energy Distributions in Radio-Frequency Discharges.
PB96-102850 04,026

Evidence for Inelastic Processes for N(+)3 and N(+)4 from Ion Energy Distributions in He/N2 Radio Frequency Glow Discharges.
PB96-146683 04,059

Influence of Electrode Material on Measured Ion Kinetic-Energy Distributions in Radio-Frequency Discharges.
PB96-123179 01,935

Ion Kinetic-Energy Distributions and Balmer-alpha (Halpha) Excitation in Ar-H2 Radio-Frequency Discharges.
PB96-102959 04,029

Ion Kinetics and Symmetric Charge-Transfer Collisions in Low-Current, Diffuse (Townsend) Discharges in Argon and Nitrogen.
PB96-123658 04,051

Kinetic Energy Distribution of Ions Produced from Townsend Discharges in Neon and Argon.
PB96-111927 04,413

Kinetic-Energy Distributions of Ions Sampled from Argon Plasmas in a Parallel-Plate, Radio-Frequency Reference Cell.
PB95-161964 *03,935*

Studies of Ion Kinetic-Energy Distributions in the Gaseous Electronics Conference RF Reference Cell.
PB96-113360 *02,391*

Time-Resolved Balmer-Alpha Emission from Fast Hydrogen Atoms in Low Pressure, Radio-Frequency Discharges in Hydrogen.
PB96-102942 *04,028*

Use of an Ion Energy Analyzer: Mass Spectrometer to Measure Ion Kinetic-Energy Distributions from RF Discharges in Argon-Helium Gas Mixtures.
PB94-185717 *04,406*

RADZIEMSKI, L. J.

Measurements of the Resonance Lines of (6)Li and (7)Li by Doppler-Free Frequency-Modulation Spectroscopy.
PB96-180211 *04,118*

RAEKER, A.

Charge Cloud Distribution of Heavy Atoms After Excitation by Polarized Electrons.
PB95-203147 *04,001*

RAFELSKI, J.

Strangeness Flow Difference in Nuclear Collisions at 15A and 200A GeV.
PB96-119631 *04,042*

RAGHAV RAO, K. S. M. S.

Protein Extraction in a Spray Column Using a Polyethylene Glycol Maltodextrin Two-Phase Polymer System.
PB95-162228 *00,595*

RAGHAVA RAO, K. S. M. S.

Continuous Counter-Current Two Phase Aqueous Extraction.
PB95-161212 *00,675*

RAGHAVACHARI, K.

Silicon Surface Chemistry by IR Spectroscopy in the Mid- to Far-IR Region: H2O and Ethanol on Si(100).
PB96-138565 *01,097*

RAHN, L. A.

Measurement of the Self Broadening of the H2Q(0-5) Raman Transitions from 295 to 1000 K.
PB95-108627 *00,884*

RAI, R. S.

Characterization of Vertical-Cavity Semiconductor Structures.
PB94-200193 *02,126*

Correlation of Optical, X-ray, and Electron Microscopy Measurements of Semiconductor Multilayer Structures.
PB95-175279 *02,174*

Vertical-Cavity Optoelectronic Structures: CAD, Growth, and Structural Characterization.
PB95-153177 *02,148*

Vertical-Cavity Semiconductor Lasers: Structural Characterization, CAD, and DFB Structures.
PB95-153193 *02,150*

RAINWATER, J. C.

Calculation of Enthalpy and Entropy Differences of Near-Critical Binary Mixtures with the Modified Leung-Griffiths Model.
PB95-108635 *00,885*

Composition Dependence of a Field Variable Along the Binary Fluid Mixture Critical Locus.
PB95-176038 *01,003*

Critical Properties and Vapor-Liquid Equilibria of the Binary System Propane + Neopentane.
PB95-175683 *00,999*

Density Dependence of Fluid Properties and Non-Newtonian Flows: The Weisenberg Effect.
PB96-161898 *01,140*

Equilibrium Pair Distribution Function of a Gas: Aspects Associated with the Presence of Bound States.
PB95-176046 *01,004*

Experimental Method for Obtaining Critical Densities of Binary Mixtures: Application to Ethane + n-Butane.
PB95-151148 *00,930*

Modified Leung-Griffiths Model of Vapor-Liquid Equilibrium: Extended Scaling and Binary Mixtures of Dissimilar Fluids.
PB94-216108 *00,851*

Non-Newtonian Flow between Concentric Cylinders Calculated from Thermophysical Properties Obtained from Simulations.
PB96-163761 *04,103*

Nonlinear Correlation of High-Pressure Vapor-Liquid Equilibrium Data for Ethylene + n-Butane Showing Inconsistencies in Experimental Compositions.
PB96-161906 *01,141*

Quantum Collisional Transfer Contributions to the Density Dependence of Gaseous Viscosity.
PB96-161914 *01,142*

Vapor-Liquid Equilibria of Mixtures of Propane and Isomeric Hexanes.
PB95-175287 *00,995*

Vapor-Liquid Equilibria of Ternary Mixtures in the Critical Region on Paths of Constant Temperature and Overall Composition.
PB96-161856 *01,139*

RAITEN, D. J.

Nutritional Status and Growth in Juvenile Rheumatoid Arthritis.
PB94-198470 *03,515*

RAIZEN, M. G.

High-Resolution Atomic Spectroscopy of Laser-Cooled Ions.
PB95-169330 *03,953*

Interference in the Resonance Fluorescence of Two Trapped Atoms.
PB95-168514 *03,948*

Light Scattered from Two Atoms.
PB95-168753 *04,286*

Precise Spectroscopy for Fundamental Physics.
PB96-112164 *04,040*

Quantum Measurements of Trapped Ions.
PB95-161147 *03,928*

Quantum Projection Noise: Population Fluctuations in Two-Level Systems.
PB94-212271 *03,850*

Recent Experiments on Trapped Ions at the National Institute of Standards and Technology.
PB95-169322 *03,952*

RAJA, J.

Dimensional Characterization of Small Bores: A Survey.
PB95-162202 *02,651*

Residual Error Compensation of a Vision-Based Coordinate Measuring Machine.
PB96-161617 *04,091*

RAJAPPAN, G.

2nu9 Band of Propyne-d3.
PB95-164513 *00,985*

RAKOSKI, B.

Standard Source Method for Reducing Antenna Factor Errors in Shielded Room Measurements.
PB96-183157 *02,013*

RAMAN, R.

NMR Characterization of Injection-Moulded Alumina Green Compacts. Part 2. T2-Weighted Proton Imaging.
PB96-201181 *01,165*

RAMATY, R.

From Superconductivity to Supernovae: The Ginzburg Symposium. Report on the Symposium Held in Honor of Vitaly L. Ginzburg. Held in Gaithersburg, Maryland on May 22, 1992.
PB95-171963 *04,649*

RAMAYYA, V. V.

Electronic Access to Standards on the Information Highway.
PB96-131578 *01,494*

RAMBOZ, J. D.

Technical Impact of the NIST Calibration Service for Electrical Power and Energy.
PB96-147913 *02,462*

RAMIRES, M. L. V.

Standard Reference Data for the Thermal Conductivity of Water.
PB96-145875 *01,111*

RAMIREZ, A. P.

Colossal Magnetoresistance without Mn(3+)/Mn(4-) Double Exchange in the Stoichiometric Pyrochlore Tl2Mn2O7.
PB97-113070 *04,160*

RAMLI, E.

Small Angle Neutron Scattering Study of the Structure and Formation of MCM-41 Mesoporous Molecular Sieves.
PB97-122337 *03,110*

Small Angle Neutron Scattering Study of the Structure and Formation of Ordered Mesopores in Silica.
PB96-111919 *03,069*

RAMON, J. T.

Crystallographic Characterization of Some Intermetallic Compounds in the Al-Cr System.
PB94-198702 *03,318*

RAMOS, B. L.

Embossable Grating Couplers for Planar Waveguide Optical Sensors.
PB96-190277 *00,641*

RAMOS, R. A.

Long-Lived Structures in Fragile Glass-Forming Liquids.
PB96-119565 *04,212*

RAMSEY, J.

High-Spatial-Resolution Resistivity Mapping Applied to Mercury Cadmium Telluride.
PB94-212917 *02,131*

RAMSEY, L.

Sleuthing the Dynamo: HST/FOS Observations of UV Emissions of Solar-Type Stars in Young Clusters.
PB96-122817 *00,098*

RAMSEY, L. W.

Far-Ultraviolet Flare on a Pleiades G Dwarf.
PB96-102033 *00,086*

RAMSEY, N. F.

Accurate Measurement of Time.
PB96-119482 *01,552*

RANCOURT, C. F.

Opportunities for Innovation: Advanced Manufacturing Technology.
PB94-100278 *02,801*

RANDA, J.

Catalogue of Electromagnetic Environment Measurements, 30-300 Hz.
PB96-155452 *01,943*

Condensed Catalogue of Electromagnetic Environment Measurements, 30 - 300 Hz.
PB95-162210 *01,899*

Correction Factor for Nonplanar Incident Field in Monopole Calibrations.
PB95-108643 *02,002*

Low-Frequency Model for Radio-Frequency Absorbers.
PB95-261939 *04,424*

Screened-Room Measurements on the NIST Spherical-Dipole Standard Radiator.
PB96-113568 *01,926*

RANDALL, C. E.

Observations of 3C 273 with the Goddard High Resolution Spectrograph on the Hubble Space Telescope.
PB95-202321 *00,076*

RANDERS-EICHHORN, L.

Formation of DNA-Protein Cross-Links in Cultured Mammalian Cells Upon Treatment with Iron Ions.
PB96-137724 *03,651*

RANDERS, L.

Tert-Butyl Hydroperoxide-Mediated DNA Base Damage in Cultured Mammalian Cells.
PB94-182003 *03,644*

RANDOVANOV, S. B.

Kinetic-Energy Distributions of Ions Sampled from Radio-Frequency Discharges in Helium, Nitrogen, and Oxygen.
PB96-123732 *01,092*

RANGACHAR, R.

Real Time Differential Range Estimation Based on Time-Space Imagery Using PIPE.
PB95-161808 *01,844*

Real-Time Implementation of a Differential Range Finder.
PB95-108650 *01,839*

RANSOM, M.

Security in Open Systems.
PB95-105383 *01,473*

RAO, G.

Formation of DNA-Protein Cross-Links in Cultured Mammalian Cells Upon Treatment with Iron Ions.
PB96-137724 *03,651*

Tert-Butyl Hydroperoxide-Mediated DNA Base Damage in Cultured Mammalian Cells.
PB94-182003 *03,644*

RAO, K. V.

Novel YBa2Cu3O7-x and YBa2Cu3O7-x/Y4Ba3O9 Multilayer Films by Bias-Masked 'On-Axis' Magnetron Sputtering.
PB95-181186 *04,690*

RAO, M. V.

Range Statistics and Rutherford Backscattering Studies on Fe-Implanted In0.53Ga0.47As.
PB95-126397 *04,535*

Transition Metal Implants in In0.53GA0.47As.
PB95-126389 *04,534*

RAO, M. V. V. S.

Kinetic Energy Distribution of Ions Produced from Townsend Discharges in Neon and Argon.
PB96-111927 *04,413*

Kinetic Energy Distributions of H(+), H2(+), and H3(+) from a Diffuse Townsend Discharge in H2 at High E/N.
PB96-123351 *04,415*

RAPPAPORT, A. G.

Studies of the Higher Order Smectic Phase of the Large Electroclinic Effect Material W317.
PB95-151601 *00,935*

X-ray Observation of Electroclinic Layer Constriction and Rearrangement in a Chiral Smectic-A Liquid Crystal.
PB96-141080 *01,100*

RARD, J. A.

Isopiestic Investigation of the Osmotic and Activity Coefficients of Aqueous NaBr and the Solubility of NaBr2H2O(cr) at 298.15 K: Thermodynamic Properties of the NaBr + H2O System over Wide Ranges of Temperature and Pressure.
PB97-110365 *01,175*

RASAIAH, J. C.

Fluctuation Dominated Recombination Kinetics with Traps.
PB95-107264 *00,875*

RASBERRY, S. D.

Certification, Development and Use of Standard Reference Materials.
PB95-107272 *00,567*

Should NIST Accredit U.S. Calibration Laboratories.
PB95-107280 *02,646*

RASMUSSEN, R. A.

Radiocarbon Measurements of Atmospheric Volatile Organic Compounds: Quantifying the Biogenic Contribution.
PB97-122352 *02,574*

RATLIFF, L. P.

Beam Line for Highly Charged Ions.
PB97-111256 *04,143*

RATZKER, M.

Ambient Temperature Synthesis of Bulk Intermetallics.
PB95-169074 *00,168*

RAUFASTE, N. J.

Project Summaries 1994: NIST Building and Fire Research Laboratory.
PB94-207495 *00,343*

Project Summaries 1995: NIST Building and Fire Research Laboratory.
PB95-270047 *00,400*

Wind and Seismic Effects: Proceedings of the Joint Meeting of the U.S.-Japan Cooperative Program in Natural Resources Panel on Wind and Seismic Effects (28th). Held in Gaithersburg, Maryland on May 14-17, 1996.
PB97-104376 *00,476*

Wind and Seismic Effects. Proceedings of the U.S.-Japan Cooperative Program in Natural Resources Panel on Wind and Seismic Effects (26th). Held in Gaithersburg, Maryland on May 17-20, 1994.
PB95-147385 *00,433*

RAVIV, D.

Adaptive, Predictive 2-D Feature Tracking Algorithm for Finding the Focus of Expansion.
PB94-218575 *01,588*

Integrated Mobile Robot System for Testing Vision Algorithms.
PB95-164133 *02,936*

New Method to Calculate Looming for Autonomous Obstacle Avoidance.
PB95-171435 *01,600*

Novel Active-Vision-Based Motion Cues for Local Navigation.
PB96-193727 *02,941*

Reconstruction during Camera Fixation.
PB95-162236 *01,593*

Scale-Space-Based Visual-Motion-Cue for Autonomous Navigation.
PB96-183173 *02,940*

Texture-Independent Vision-Based Closed-Loop Fuzzy Controllers for Navigation Tasks.
PB95-220505 *00,183*

Unified Approach to Camera Fixation and Vision-Based Road Following.
PB95-162244 *01,594*

Visual-Motion Fixation Invariant.
PB94-206281 *01,836*

Visual Road Following without 3-D Reconstruction.
PB95-161030 *01,591*

RAWLINS, W.

Energy Flows in an Orifice Pulse Tube Refrigerator.
PB95-169082 *02,752*

Graded and Nongraded Regenerator Performance.
PB95-169090 *02,753*

Resistance Thermometers with Fast Response for Use in Rapidly Oscillating Gas Flows.
PB95-107298 *03,261*

Thermal Anemonetry for Mass Flow Measurement in Oscillating Cryogenic Gas Flows.
PB96-176789 *04,218*

RAWN, C. J.

Ca1-xCuO2, a NaCuO2-Type Related Structure.
PB95-162822 *04,620*

Ca4Bi6O13: A Compound Containing an Unusually Low Bismuth Coordination Number and Short Bi Bi Contacts.
PB95-141131 *00,911*

Improved Crystallographic Data for Aluminum Niobate (AlNbO4).
PB95-107306 *04,523*

Phase Equilibria in the Systems CaO-CuO and CaO-Bi2O3.
PB95-140570 *03,048*

Powder X-ray Diffraction Data for Ca2Bi2O5 and C4Bi6O13.
PB96-161278 *04,777*

RAY, S.

Control Entity Interface Specification.
PB94-191715 *02,815*

Unified Process Specification Language: Requirements for Modeling Process.
PB97-116123 *02,850*

RAY, S. R.

Production Management Information Model for Discrete Manufacturing.
PB96-112008 *02,830*

Reference Architecture for Machine Control Systems Integration: Interim Report.
PB95-144549 *02,820*

Summary and Notes of the Joint ISO/IGES/PDES Organization Technical Committee Meeting. Held in Albuquerque, New Mexico on October 15-20, 1989.
PB95-107314 *02,774*

RAYNES, A. S.

Electric Field Effects on Crack Growth in a Lead Magnesium Niobate.
PB95-107322 *03,339*

Moisture and Water-Induced Crack Growth in Optical Materials.
PB95-153334 *04,267*

RAZYNSKA, A.

Positive and Negative Cooperativities at Subsequent Steps of Oxygenation Regulate the Allosteric Behavior of Multistate Sebacylhemoglobin.
PB97-119374 *03,486*

READ, D. T.

Electronics Packaging Materials Research at NIST.
PB96-122692 *02,405*

NIST/NCMS Program on Electronic Packaging: First Update.
PB96-204086 *03,008*

Potential Drop in the Center-Cracked Panel with Asymmetric Crack Extension.
PB95-107330 *04,819*

Tensile Deformation-Induced Microstructures in Free-Standing Copper Thin Films.
PB96-102595 *04,715*

Theory of Electron Beam Moire.
PB96-175690 *04,373*

READ, M. E.

Apparel Manufacturing Glossary for Application Protocol Development.
PB95-198750 *02,755*

READER, J.

Hyperfine Structure Investigations and Identification of New Energy Levels in the Ionic Spectrum of (147)Pm.
PB96-180203 *04,117*

Irradiances of Spectral Lines in Mercury Pencil Lamps.
PB96-176466 *04,375*

Laser-Produced and Tokamak Spectra of Lithiumlike Iron, Fe(23+).
PB95-180857 *04,314*

Measurements of quantum electrodynamic sensitive transitions in Na-like and Cu-like ions: Final report, 1 October 1993--29 September 1994.
DE95011593 *04,403*

Spectrum and Energy Levels of Five-Times-Ionized Niobium (Nb VI).
PB94-185246 *04,226*

Spectrum and Energy Levels of Triply Ionized Barium (Ba IV).
PB95-140877 *03,888*

Wavelengths and Isotope Shifts for Lines of Astrophysical Interest in the Spectrum of Doubly Ionized Mercury (Hg III).
PB95-140869 *03,887*

Wavelengths of Spectral Lines in Mercury Pencil Lamps.
PB96-176474 *04,376*

READEY, M. J.

Correlations between Flaw Tolerance and Reliability in Zirconia.
PB96-161922 *02,986*

REBBERT, R. E.

Standard Reference Materials for the Determination of Polycyclic Aromatic Hydrocarbons in Environmental Samples - Current Activities.
PB95-151668 *00,586*

REBULDELA, G.

Intercomparison of Thermal Converters at NIM, NIST, PTB, SIRI and VSL from 10 to 100 MHz.
PB94-172459 *02,027*

REDDY, P.

Glucose Permease of Bacillus Subtilis Is a Single Polypeptide Chain That Functions to Energize the Sucrose Permease.
PB95-163192 *03,466*

Mapping Domains in Proteins: Dissection and Expression of 'Escherichia coli' Adenylyl Cyclase.
PB96-155460 *03,478*

Rapid Method for the Isolation of Genomic DNA from 'Aspergillus fumigatus'.
PB96-147061 *03,488*

REDMAN, J. W.

Intercomparison of DNA Sizing Ladders in Electrophoretic Separation Matrices and Their Potential for Accurate Typing of the D1S80 Locus.
PB96-200928 *03,485*

REED, B.

Ring-Opening Dental Resin Systems Based on Cyclic Acetals.
PB95-162251 *00,162*

REED, K. A.

Development of Computer-Based Models of Standards and Attendant Knowledge-Base and Procedural Systems.
PB96-155783 *00,464*

Distributed Architecture for Standards Processing.
PB96-164181 *00,276*

REED, R. P.

Composite Struts for SMES Plants.
PB95-155586 *02,507*

Influence of Specimen Absorbed Energy in LOX Mechanical-Impact Tests.
PB95-107355 *03,341*

Macro- and Microreactions in Mechanical-Impact Tests of Aluminum Alloys.
PB95-107348 *03,340*

Mechanical Properties and Warm Prestress of Ultra-Low Carbon Steel at 4 K.
PB96-190350 *03,224*

Reaction Sensitivities of Al-Li Alloys and Alloy 2219 in Mechanical-Impact Tests.
PB94-172764 *03,314*

Recommended Changes in ASTM Test Methods D2512-82 and G86-84 for Oxygen-Compatibility Mechanical Impact Tests on Metals.
PB94-216694 *03,338*

Temperature Increases in Aluminum Alloys during Mechanical-Impact Tests for Oxygen Compatibility.
PB94-172962 *03,316*

REED, W. P.

Reference Materials by Isotope Dilution Mass Spectrometry.
PB95-153383 *00,592*

REEDER, D.

Resolution of DNA in the Presence of Mobility Modifying Polar and Nonpolar Compounds by Discontinuous Electrophoresis on Rehydratable Polyacrylamide Gels.
PB95-152799 *00,590*

REEDER, D. J.

Enhanced Detection of PCR Products Through Use of TOTO and YOYO Intercalating Dyes with Laser Induced Fluorescence - Capillary Electrophoresis.
PB95-164653 *00,599*

Intercomparison of DNA Sizing Ladders in Electrophoretic Separation Matrices and Their Potential for Accurate Typing of the D1S80 Locus.
PB96-200928 *03,485*

Interlaboratory Comparison of Autoradiographic DNA Profiling Measurements. 1. Data and Summary Statistics.
PB95-175923 *03,542*

Interlaboratory Comparison of Autoradiographic DNA Profiling Measurements. 2. Measurement Uncertainty and Its Propagation.
PB96-112123 *03,545*

L-threo-beta-Hydroxyhistidine, an Unprecedented Iron(III) Ion-Binding Amino Acid in a Pyoverdine-type Siderophore from Pseudomonas fluorescens 244.
PB94-211620 *00,553*

Overview of Reference Materials Prepared for Standardization of DNA Typing Procedures.
PB96-111653 *00,611*

REES, J. A.

Kinetic-Energy Distributions of Ions Sampled from Argon Plasmas in a Parallel-Plate, Radio-Frequency Reference Cell.
PB95-161964 *03,935*

Use of an Ion Energy Analyzer: Mass Spectrometer to Measure Ion Kinetic-Energy Distributions from RF Discharges in Argon-Helium Gas Mixtures.
PB94-185717 *04,406*

REEVE, G. R.

NIST and the Navy: Past, Present and Future.
PB96-119649 *03,655*

REHM, R.

Dispersion and Deposition of Smoke Plumes Generated in Massive Fires.
PB95-126066 *02,540*

REHM, R. G.

Gravity-Current Transport in Building Fires.
PB96-147046 *01,415*

In situ Burning of Oil Spills: Mesoscale Experiments and Analysis.
PB95-163747 *02,587*

Internal Waves in Xenon Near the Critical Point.
PB97-111504 *04,221*

Large Eddy Simulations of Smoke Movement in Three Dimensions.
PB96-190012 *01,426*

Mathematical Modeling and Computer Simulation of Fire Phenomena.
PB95-180063 *00,384*

Pressure Equations in Zone-Fire Modeling.
PB96-102967 *00,208*

Transport by Gravity Currents in Building Fires.
PB97-119325 *01,441*

REID, E.

Operating Procedures and Life Cycle Documentation for the Initial Graphics Exchange Specification.
PB95-242285 *02,782*

REIFER, D. J.

Ada Compiler Validation Summary Report: Certificate Number 940902S1.11376. UNISYS Corporation IntegrAda for Windows NT, Version 1.0. Intel Deskside Server for Intel Pentium 60 MHz =>. Intel Deskside Server with Intel Pentium 60 MHz.
AD-A288 572/1 *01,659*

REILLY, M. L.

Assessing the Credibility of the Calorific Content of Muncipal Solid Waste.
PB94-199882 *02,581*

REINE, M. B.

Electrical Characterization of Narrow Gap n-Type Bulk HgCdTe Single Crystals by Variable-Magnetic-Field Hall Measurements and Reduced-Conductivity-Tensor Analyses.
PB96-164199 *01,146*

REINS, J. L.

Supercritical Fluid Extraction-Immunoassay for the Rapid Screening of Cocaine in Hair.
PB96-167168 *00,637*

REINTSEMA, C.
High Critical Temperature Superconductor Tunneling Spectroscopy Using Squeezable Electron Tunneling Junctions.
PB95-163721 *04,627*

REINTSEMA, C. D.
Controlling the Critical Current Density of High-Temperature SNS Josephson Junctions.
PB96-200712 *04,794*

Critical Current and Normal Resistance of High-Tc Step-Edge SNS Junctions.
PB96-111752 *04,724*

Critical Current Behavior of Ag-Coated YBa2Cu3O7-x Thin Films.
PB95-141016 *04,549*

Effect of Thermal Noise on Shapiro Steps in High-Tc Josephson Weak Links.
PB94-212677 *04,506*

High-Tc Multilayer Step-Edge Josephson Junctions and SQUIDs.
PB96-200183 *04,790*

Large-Amplitude Shapiro Steps and Self-Field Effects in High-Tc Josephson Weak Links.
PB95-180410 *04,682*

Mutual Phase Locking in Systems of High-Tc Superconductor-Normal Metal-Superconductor Junctions.
PB96-135348 *04,744*

Phase Locking in Two-Junction Systems of High-Temperature Superconductor-Normal Metal-Superconductor Junctions.
PB95-176053 *02,060*

Step-Edge and Stacked-Heterostructure High-Tc Josephson Junctions for Voltage-Standard Arrays.
PB96-102066 *04,702*

Temperature Dependence and Magnetic Field Modulation of Critical Currents in Step-Edge SNS YBCO/Au Junctions.
PB96-111745 *04,723*

REINTSEMA, C. R.
Magnetic Field Dependence of the Critical Current Anisotropy in Normal Metal-YBa2Cu3O7-delta Thin Film Bilayers.
PB95-141024 *04,550*

REIPA, V.
Conformational Alterations of Bovine Insulin Adsorbed on a Silver Electrode.
PB96-161773 *00,510*

Non-Perturbative Relation between the Mutual Diffusion Coefficient, Suspension Viscosity, and Osmotic Compressibility: Application to Concentrated Protein Solutions.
PB96-102355 *01,062*

Physicochemical Characterization of Low Molecular Weight Heparin.
PB96-112040 *03,474*

Structural Analysis of Heparin by Raman Spectroscopy.
PB96-167226 *03,480*

REIPURTH, B.
G203.2-12.3: A New Optical Supernova Remnant in Orion.
PB95-203535 *00,085*

REIS, K. P.
Powder Neutron Diffraction Investigation of Structure and Cation Ordering in Ba2+xBi2-xO6-y.
PB95-180865 *01,015*

Rietveld Analysis of NaxWO3+x/2.yH2O, Which Has the Hexagonal Tungsten Bronze Structure.
PB95-107371 *04,524*

REITMEIER, G.
Report on the Workshop on Advanced Digital Video in the National Information Infrastructure. Held in Washington, D.C. on May 10-11, 1994.
PB95-103677 *01,472*

Summary Report on the Workshop on Advanced Digital Video in the National Information Infrastructure.
PB96-141320 *01,497*

REIZER, J.
Glucose Permease of Bacillus Subtilis Is a Single Polypeptide Chain That Functions to Energize the Sucrose Permease.
PB95-163192 *03,466*

REKHARSKY, M. V.
Thermodynamic and NMR Study of the Interactions of Cyclodextrins with Cyclohexane Derivatives.
PB94-185816 *00,781*

Thermodynamic Study of the Reactions of Cyclodextrins with Primary and Secondary Aliphatic Alcohols, with D- and L-Phenylalanine, and with L-Phenylalanineamide.
PB95-180873 *01,016*

Thermodynamics of the Hydrolysis of N-Acetyl-L-phenylalanine Ethyl Ester in Water and in Organic Solvents.
PB95-203386 *01,053*

Thermodynamics of the Hydrolysis of 3,4,5-Trihydroxybenzoic Acid Propyl Ester (n-Propylgallate) to 3,4,5-Trihydroxybenzoic Acid (Gallic Acid) and Propan-I-ol in Aqueous Media and in Toluene.
PB96-186143 *01,160*

REMACLE, J.
Tert-Butyl Hydroperoxide-Mediated DNA Base Damage in Cultured Mammalian Cells.
PB94-182003 *03,644*

REMINGTON, K. A.
IML++ v.1.2 Iterative Methods Library Reference Guide.
PB96-195219 *01,776*

SparseLib++ v. 1.5 Sparse Matrix Class Library. Reference Guide.
PB96-193636 *01,775*

REN, Z. B.
Improved Annealing Technique for Optical Fiber.
PB96-119680 *04,343*

RENEKE, P. A.
Fire Safety of Passenger Trains: A Review of Current Approaches and of New Concepts.
PB94-152006 *04,848*

New Concepts for Fire Protection of Passenger Rail Transportation Vehicles.
PB95-162046 *04,850*

New Concepts for Fire Protection of Passenger Rail Transportation Vehicles. (NIST Reprint).
PB95-180774 *04,863*

RENEKER, D. H.
Polyethylene Crystallized from an Entangled Solution Observed by Scanning Tunneling Microscopy.
PB95-107389 *01,232*

RENKEN, M. C.
Determination of Sheet Steel Formability Using Wide Band Electromagnetic-Acoustic Transducers.
PB96-186036 *02,279*

Examination of Objects Made of Wood Using Air-Coupled Ultrasound.
PB95-125712 *03,404*

Gas-Coupled, Pulse-Echo Ultrasonic Crack Detection and Thickness Gaging.
PB96-147129 *04,847*

RENNEX, B.
Standard Reference Materials: Certification of a Standard Reference Material for the Determination of Interstitial Oxygen Concentration in Semiconductor Silicon by Infrared Spectrophotometry.
PB95-125076 *02,326*

RENNEX, B. G.
Development of a Standard Reference Material for Measurement of Interstitial Oxygen Concentration in Semiconductor Silicon by Infrared Absorption.
PB96-122668 *02,404*

Methodology for the Certification of Reference Specimens for Determination of Oxygen Concentration in Semiconductor Silicon by Infrared Spectrophotometry.
PB96-155478 *02,421*

RENNIE, A. R.
Structure and Rheology of Hard-Sphere Systems.
PB96-167333 *00,662*

RENO, R. C.
Ultrasonic Measurement of Sheet Anisotropy and Formability.
PB95-153235 *03,213*

RENSBERGER, R. A.
Standards Setting in the European Union: Standards Organization and Officials in EU Standards Activities.
PB96-115019 *02,919*

REPJAR, A.
Planar Near-Field Alignment.
PB94-172491 *01,998*

RESNICK, R.
Two New Probes for a Coordinate Measuring Machine.
PB95-163093 *02,653*

RESSLER, S.
Applying Virtual Environments to Manufacturing.
PB94-142502 *02,803*

Approaches Using Virtual Environments with Mosaic.
PB95-169108 *01,599*

RETTIG, J. B.
Accuracy and Repeatability in Time Domain Network Analysis.
PB95-202644 *02,064*

REYMANN, D.
Accuracy Comparisons of Josephson Array Systems.
PB95-164687 *02,047*

REZNIK, D.
High Resolution Inelastic Neutron Scattering Study of Phonon Self-Energy Effects in YBCO.
PB95-180881 *04,688*

Inelastic Neutron Scattering Studies of Rotational Excitations and the Orientational Potential in C60 and A3C60 Compounds.
PB94-172673 *00,763*

Neutron-Scattering Study of Librations and Intramolecular Phonons in Rb2.6K0.4C60.
PB95-162269 *00,958*

q Dependence of Self-Energy Effects of the Plane Oxygen Vibration in YBa2Cu3O7.
PB96-138516 *01,096*

X-ray Powder Diffraction from Carbon Nanotubes and Nanoparticles.
PB96-102975 *03,064*

RHINE, W. E.
X-Ray Powder Diffraction Data for BaCu(C2O4)2.6H2O.
PB95-151767 *04,583*

RHODERICK, G. C.
Development of a Gas Standard Reference Material Co taining Eighteen Volatile Organic Compounds.
PB95-162277 *02,545*

Development of Gas Standards from Solid 1,4-dichlorobenzene.
PB96-155486 *02,496*

Measurement of Atmospheric Methyl Bromide Using Gravimetric Gas Standards.
PB96-155494 *02,497*

NIST Traceable Reference Material Program for Gas Standards: Standard Reference Materials.
PB96-210786 *00,644*

Radiocarbon Measurements of Atmospheric Volatile Organic Compounds: Quantifying the Biogenic Contribution.
PB97-122352 *02,574*

Stability/Instability of Gas Mixtures Containing 1,3-Butadiene in Treated Aluminum Gas Cylinders.
PB95-162285 *02,546*

Stability of Compressed Gas Mixtures Containing Low Level Volatile Organic Compounds in Aluminum Cylinders.
PB96-111968 *00,613*

RHODES, B.
Fire Growth Models for Materials.
PB94-195856 *01,367*

RHODES, B. T.
Burning Rate and Flame Heat Flux For PMMA in the Cone Calorimeter.
PB95-216990 *00,393*

RHODES, T. R.
Report on the Advanced Software Technology Workshop. Held on February 1, 1994.
PB95-136610 *01,707*

RHORER, R. L.
Fabrication of Optics by Diamond Turning.
PB96-111695 *02,954*

RHYNE, J. J.
Enhanced Curie Temperatures and Magnetoelastic Domains in Dy/Lu Super Lattices and Films.
PB94-172665 *04,443*

Incorporation of Gold into YBa2Cu3O7: Structure and Tc Enhancement.
PB94-200276 *04,481*

Magnetic Rare Earth Artificial Metallic Superlattices.
PB95-162293 *04,611*

Magnetoelasticity in Rare-Earth Multilayers and Films.
PB94-211356 *04,495*

Unexpected Effects of Gold on the Structure, Superconductivity, and Normal State of YBa2Cu3O7.
PB94-200284 *04,482*

RIBOT, J. J.
Approach to Setting Performance Requirements for Automated Evaluation of the Parameters of High-Voltage Impulses.
PB94-185634 *01,878*

RICCI, A.
Reactive Ion Etching in the Gaseous Electronics Conference RF Reference Cell.
PB96-113402 *02,395*

RICE, J.
Nickel(II)-Mediated Oxidative DNA Base Damage in Renal and Hepatic Chromatin of Pregnant Rats and Their Fetuses. Possible Relevance to Carcinogenesis.
PB94-212628 *03,646*

Oxidative DNA Base Damage in Renal, Hepatic, and Pulmonary Chromatin of Rats After Intraperitoneal Injection of Cobalt (II) Acetate.
PB95-150025 *03,647*

RICE, J. P.
Antenna-Coupled High-Tc Air-Bridge Microbolometer on Silicon.
PB95-180899 *04,315*

High-Tc Superconducting Antenna-Coupled Microbolometer on Silicon.
PB95-169124 *02,166*

Kinetic-Inductance Infrared Detector Based on an Antenna-Coupled High-Tc SQUID.
PB95-169116 *02,165*

Liquid-Nitrogen-Cooled High Tc Electrical Substitution Radiometer as a Broadband IR Transfer Standard.
PB96-158704 *02,198*

NIST Thermal Infrared Transfer Standard Radiometer for the Earth Observing System (EOS) Program.
PB97-113013 *04,843*

Thermal Isolation of High-Temperature Superconducting Thin Films Using Silicon Wafer Bonding and Micromachining.
PB96-135017 *02,408*

RICE, P.
Comparison of Magnetic Fields of Thin-Film Heads and Their Corresponding Bit Patterns Using Magnetic Force Microscopy.
PB95-180907 *03,763*

dc Magnetic Force Microscopy Imaging of Thin-Film Recording Head.
PB95-176061 04,665

Flexible-Diaphragm Force Microscope.
PB95-180915 03,966

Magnetic Force Microscopy Images of Magnetic Garnet with Thin-Film Magnetic Tip.
PB95-176210 04,669

Magnetic Force Microscopy of Flux in Superconductors.
PB95-161733 04,608

Micromagnetic Simulations of Tunneling Stabilized Magnetic Force Microscopy.
PB95-141073 04,552

Proposed Antiferromagnetically Coupled Dual-Layer Magnetic Force Microscope Tips.
PB95-169017 04,645

Recent Results in Magnetic Force Microscopy.
PB96-103130 04,721

RICHARDS, C.

Global Density Effects on the Self-Preservation Behavior of Turbulent Free Jets.
PB95-162301 04,207

RICHARDS, C. D.

Experimental Study of the Stabilization Region of Lifted Turbulent-Jet Diffusion Flames.
PB96-122676 01,405

RICHARDS, N. D.

Effect of Two Initiator/Stabilizer Concentrations in a Metal Primer on Bond Strengths of a Composite to a Base Metal Alloy.
PB94-172723 00,141

Reduction of Marginal Gaps in Composite Restorations by Use of Glass-Ceramic Inserts.
PB96-102405 00,174

RICHARDS, R. F.

Development of an Economical Video Based Fire Detection and Location System.
PB96-193743 00,228

Measurements of Moisture Diffusivity for Porous Building Materials.
PB95-107397 00,356

RICHARDS, R. J.

Survey of the Literature on Heat Transfer from Solid Surfaces to Cryogenic Fluids.
AD-A286 680/4 04,193

RICHIE, K. L.

Overview of Reference Materials Prepared for Standardization of DNA Typing Procedures.
PB96-111653 00,611

RICHMAN, S.

Low-Frequency, Active Vibration Isolation System.
PB95-203303 02,710

RICHMOND, H. M.

NVLAP Procedures U.S. Code of Federal Regulations. Title 15, Subtitle A, Chapter 2, Part 7. (Effective December 1984; Amended September 1990).
PB94-160850 02,627

Proficiency Tests for the NIST Airborne Asbestos Program, 1993.
PB96-106463 00,610

RICHOU, B.

Measurements of the Resonance Lines of (6)Li and (7)Li by Doppler-Free Frequency-Modulation Spectroscopy.
PB96-180211 04,118

RICHTER, C. A.

Buffer Layer Modulation-Doped Field-Effect-Transistor Interactions in the Al0.33Ga0.67As/GaAs Superlattice System.
PB96-102876 02,380

Mesoscopic Conductance Fluctuations in Large Devices.
PB96-119656 04,735

Novel Magnetic Field Characterization Techniques for Compound Semiconductor Materials and Devices.
PB96-176458 02,433

Quantum Conductance Fluctuations in the Larger-Size-Scale Regime.
PB97-111264 04,144

X-ray Reflectivity Determination of Interface Roughness Correlated with Transport Properties of (AlGa)As/GaAs High Electron Mobility Transistor Devices.
PB97-111868 04,149

RICHTER, D.

Low-Energy Vibrations and Octahedral Site Occupation in Nb95V5H(D)y.
PB96-160734 01,133

RICHTER, L. J.

Laser-Induced Desorption of NO from Si(111): Effects of Coverage on NO Vibrational Populations.
PB95-162319 00,959

Photodecomposition Dynamics of Mo(CO)6/Si(111) 7x7: CO Internal State and Translational Energy Distributions--Translation.
PB94-199288 00,687

Photodecomposition of Mo(CO)6/Si(111) 7x7: CO State-Resolved Evidence for Excited State Relaxation and Quenching.
PB95-180154 01,009

Photodesorption Dynamics of CO from Si(111): The Role of Surface Defects.
PB96-111646 03,066

RICHTER, R.

Federal Labs Have Key Role in Metrication.
PB96-123401 02,920

RICKER, R. E.

Analysis of Failed Dry Pipe Fire Suppression System Couplings from the Filene Center at Wolf Trap Farm Park for the Performing Arts.
PB94-164407 00,331

Characterization of the Hydrogen Induced Cold Cracking Susceptibility at Simulated Weld Zones in HSLA-100 Steel.
AD-A279 759/5 03,200

Characterization of the Hydrogen Induced Cold Cracking Susceptibility at Simulated Weld Zones in HSLA-100 Steel.
PB94-174505 03,746

Comparison of the Corrosion Rates of FeAl, Fe(sub 3)Al and Steel in Distilled Water and 0.5 M Sodium Chloride. Technical Report Number 2, January--March 1991.
DE94017332 03,186

Corrosion Resistance of Materials for Renovation of the United States Botanic Garden Conservatory.
PB94-154390 00,032

Evaluation of the Electrochemical Behavior of Ductile Nickel Aluminide and Nickel in a pH 7.9 Solution. Technical Report Number 3, April-June 1991.
DE94017351 03,307

Evaluation of the Environmentally Induced Fracture Resistance of Ductile Nickel Aluminide. Technical Report Number 1, Final report. October-December 1990.
DE94017331 03,306

Evidence of Film-Induced Cleavage by Electrodeposited Rhodium.
PB95-162327 03,191

Modeling Polarization Curves and Impedance Spectra for Simple Electrode Systems.
PB94-198876 03,188

RICKLEFS, R. L.

Lunar Laser Ranging: A Continuing Legacy of the Apollo Program.
PB95-202495 03,683

RIDDER, S. D.

Beneficial Effects of Nitrogen Atomization on an Austenitic Stainless Steel.
PB94-212396 03,209

Development of Adaptive Control Strategies for Inert Gas Atomization.
PB95-162335 02,823

Effect of Backfill and Atomizing Gas on the Powder Porosity and Mechanical Properties of 304L Stainless Steel.
PB94-185394 03,205

Intelligent Control of an Inert Gas Atomization Process.
PB95-141057 03,344

Optimization of Inert Gas Atomization.
PB95-107405 01,377

Parametric Investigation of Metal Powder Atomization Using Laser Diffraction.
PB95-108577 03,342

Process Modeling and Control of Inert Gas Atomization.
PB95-162343 02,824

RIDDLE, B. F.

Aperture Excitation of Electrically Large, Lossy Cavities.
PB94-145711 00,029

Aperture Excitation of Electrically Large, Lossy Cavities.
PB95-175675 00,031

TEM/Reverberating Chamber Electromagnetic Radiation Test Facility at Rome Laboratory.
PB96-155023 03,675

RIEDLE, E.

Doppler-Free Spectroscopy of Large Polyatomic Molecules and van der Waals Complexes.
PB96-119581 04,339

Frequency Shifting of Pulsed Narrow-Band Laser Light in a Multipass Raman Cell.
PB95-203352 04,321

High-Efficiency, High-Power Difference-Frequency Generation of 0.9-1.5 mu m Light in BBO.
PB95-202255 04,317

Stabilization and Precise Calibration of a Continuous-Wave Difference Frequency Spectrometer by Use of a Simple Transfer Cavity.
PB95-162350 04,276

Van der Waals Bond Lengths and Electronic Spectral Shifts of the Benzene-Kr and Benzene-Xe Complexes.
PB95-151387 00,932

RIES, J. G.

Lunar Laser Ranging: A Continuing Legacy of the Apollo Program.
PB95-202495 03,683

RIGGAN, W. B.

Cyclic Polyamine Ionophore for Use in a Dibasic Phosphate-Selective Electrode.
PB95-180121 01,008

RIGGS, C.

Oxidative DNA Base Damage in Renal, Hepatic, and Pulmonary Chromatin of Rats After Intraperitoneal Injection of Cobalt (II) Acetate.
PB95-150025 03,647

RIGHINI, F.

Issues in High-Speed Pyrometry.
PB97-118368 02,693

Wavelength Dependence of Normal Spectral Emissivity of High-Temperature Metals at Their Melting Point.
PB94-200011 03,398

RILEY, M. E.

Gaseous Electronics Conference Radio-Frequency Reference Cell: A Defined Parallel-Plate Radio-Frequency System for Experimental and Theoretical Studies of Plasma-Processing Discharges.
PB94-172327 04,404

RILEY, W. J.

Aging, Warm-Up Time and Retrace; Important Characteristics of Standard Frequency Generators.
PB96-103122 04,031

RIMINGTON, P. D.

Learning to Change: Opportunities to Improve the Performance of Smaller Manufacturers.
PB94-166212 00,010

RINAUDOT, G. R.

Requisite Elements, Rationale, and Technology Overview for the Systems Intergration for Manufacturing Applications (SIMA) Program. Background Study.
PB96-112685 02,831

STEP On-Line Information Service (SOLIS). The IGES/PDES Organization.
PB95-137790 02,777

Summary and Notes of the Joint ISO/IGES/PDES Organization Technical Committee Meeting, Held in Albuquerque, New Mexico on October 15-20, 1989.
PB95-107314 02,774

RINKINEN, W.

Assessing Halon Alternatives for Aircraft Engine Nacelle Fire Suppression.
PB96-102454 01,401

Protection of Data Processing Equipment with Fine Water Sprays.
PB95-174975 02,610

Suppression of Elevated Temperature Hydraulic Fluid and JP-8 Spray Flames.
PB95-181095 00,021

Turbulent Spray Burner for Assessing Halon Alternative Fire Suppressants.
PB95-153748 01,385

RINN, K.

Merged-Beams Energy-Loss Technique for Electron-Ion Excitation: Absolute Total Cross Sections for O(5+) (2s yields 2p).
PB96-102058 04,017

RIPPEY, W.

Integrated Vision Touch-Probe System for Dimensional Inspection Tasks.
PB95-255832 02,917

RIPPEY, W. G.

Proceedings of NIST Workshop: Industry Needs in Welding Research and Standards Development. Held on August 15-16, 1995.
PB96-183124 02,877

Reference Architecture for Machine Control Systems Integration: Interim Report.
PB95-144549 02,820

RIPPLE, D.

Assessment of Uncertainties of Thermocouple Calibrations at NIST.
PB94-152691 03,782

Flow of Microemulsions through Microscopic Pores.
PB95-140463 00,905

Viscosity of the Saturated Liquid Phase of Six Halogenated Compounds and Three Mixtures.
PB95-162368 00,960

RITCHIE, R. O.

Transient Subcritical Crack-Growth Behavior in Transformation-Toughened Ceramics.
PB94-200656 03,038

RITLEY, K.

Diffraction of Neutron Standing Waves in Thin Films with Resonance Enhancement.
PB97-113278 04,164

RITTER, J. J.

Ca1-xCuO2, a NaCuO2-Type Related Structure.
PB95-162822 04,620

Compositional Homogeneity in Processing Precursor Powders to the Ba2YCu3O7-x High Tc Superconductor.
PB94-212743 04,508

Effect of Sm2BaCuO5 on the Properties of Sintered (Bulk) YBa2Cu3O6+x.
PB96-119441 04,733

Enhanced Magnetocaloric Effect in Gd3Ga5-xFexO12.
PB94-185659 04,450

Phase Equilibria in the Systems CaO-CuO and CaO-Bi2O3.
PB95-140570 03,048

Study of the Hydroxycarbonate Precursor Route to the YBa2Cu3O7-x High Tc Superconductor.
PB95-140471 04,540

RIZZI, G.
Approach to Setting Performance Requirements for Automated Evaluation of the Parameters of High-Voltage Impulses.
PB94-185634 *01,878*

ROACH, R. K.
Computer Systems Laboratory Annual Report, 1993.
PB94-162518 *01,622*

Computer Systems Laboratory Annual Report 1994.
PB95-209920 *01,629*

ROADARMEL, G.
Fire Performance of an Interstitial Space Construction System.
PB95-188918 *00,390*

ROBACK, E.
Data Encryption Standard.
PB95-162376 *01,595*

Security Program Management.
PB96-156112 *01,610*

ROBACK, E. A.
Computer Security: An Introduction to Computer Security. The NIST Handbook.
PB96-131610 *01,608*

ROBB, F.
Small genomes: New initiatives in mapping and sequencing. Workshop summary report.
DE96014476 *03,451*

ROBERTS, D. E.
Tensile Creep of Silicide Composites.
PB96-200803 *03,183*

ROBERTS, J. R.
Gaseous Electronics Conference Radio-Frequency Reference Cell: A Defined Parallel-Plate Radio-Frequency System for Experimental and Theoretical Studies of Plasma-Processing Discharges.
PB94-172327 *04,404*

Hydrogen Balmer Alpha Line Shapes for Hydrogen-Argon Mixtures in a Low-Pressure rf Discharge.
PB95-153433 *03,924*

Observation and Visible and uv Magnetic Dipole Transitions in Highly Charged Xenon and Barium.
PB96-138441 *04,056*

Optical and Mass Spectrometric Investigations of Ions and Neutral Species in SF6 Radio-Frequency Discharges.
PB97-111918 *01,985*

Optical Emission Spectroscopy on the Gaseous Electronics Conference RF Reference Cell.
PB96-113345 *02,389*

Polarization Measurements on a Magnetic Quadrupole Line in Ne-Like Barium.
PB97-113104 *04,161*

Time-Resolved Balmer-Alpha Emission from Fast Hydrogen Atoms in Low Pressure, Radio-Frequency Discharges in Hydrogen.
PB96-102942 *04,028*

ROBERTS, J. W.
NIST Workshop on the Computer Interface to Flat Panel Displays. Held in San Jose, California on January 13-14, 1994.
PB95-136388 *01,625*

ROBERTS, K.
Application Profile for ISDN.
PB95-163689 *01,479*

North American Agreements on ISDN.
PB96-160775 *01,503*

ROBERTSON, A. F.
Low Heat-Flux Measurements: Some Precautions.
PB96-201116 *02,685*

ROBERTSON, B.
Bacteriorhodopsin Immobilized in Sol-Gel Glass.
PB95-151429 *03,532*

Bacteriorhodopsin Retains Its Light-Induced Proton-Pumping Function After Being Heated to 140C.
PB96-102728 *03,471*

Determining Mobility from Homodyne ac Electrophoretic Light Scattering.
PB95-140497 *03,462*

Energy Transduction between a Concentration Gradient and an Alternating Electric Field.
PB94-216363 *03,461*

Imposed Oscillations of Kinetic Barriers Can Cause an Enzyme to Drive a Chemical Reaction Away from Equilibrium.
PB96-161625 *01,137*

Michaelis-Menten Equation for an Enzyme in an Oscillating Electric Field.
PB95-140489 *00,906*

Nonequilibrium Statistical Mechanics.
PB96-161781 *04,097*

Quadratic Response of a Chemical Reaction to External Oscillations.
PB96-161633 *01,138*

Rapid pH Change Due to Bacteriorhodopsin Measured with a Tin-Oxide Electrode.
PB96-112081 *03,544*

ROBEY, S. W.
Photoelectron Spectroscopic Study of the Valence and Core-Level Electronic Structure of BaTiO3.
PB94-212149 *04,500*

Reactive Coevaporation of DyBaCuO Superconducting Films: The Segregation of Bulk Impurities on Annealed MgO(100) Substrates.
PB95-164562 *04,635*

Resonant-Photoemission Investigation of the Heusler Alloys Ni2MnSb and NiMnSb.
PB95-162384 *04,612*

Substitution-Induced Midgap States in the Mixed Oxides RxBa1-ChiTiO3-Delta, with R=Y, La, and Nd.
PB95-140505 *04,541*

Surface Core-Level Shifts of Barium Observed in Photoemission of Vacuum-Fractured BaTiO3 (100).
PB94-212156 *04,501*

ROBIN HUTCHINSON, J. M.
Intercomparison Study of (237)Np Determination in Artificial Urine Samples.
PB96-102645 *03,633*

ROBINS, J. R.
Investigation of S2F10 Production and Mitigation in Compressed SF6-Insulated Power Systems.
PB94-212388 *02,467*

ROBINS, L. H.
Lineshape Analysis of the Raman Spectrum of Diamond Films Grown by Hot-Filament and Microwave-Plasma Chemical-Vapor Deposition.
PB95-162392 *03,016*

Studies of Defects in Diamond Films and Particles by Raman and Luminescence Spectroscopies.
PB95-162400 *03,017*

Surface Roughness Evaluation of Diamond Films Grown on Substraies with a High Density of Nucleation Sites.
PB95-162418 *03,018*

ROBINSON, H. G.
High-Sensitivity Spectroscopy with Diode Lasers.
PB95-175477 *04,297*

Optical Probing of Cold Trapped Atoms.
PB95-175469 *04,296*

Precise Optical Frequency References and Difference Frequency Measurements with Diode Lasers.
PB95-176228 *04,305*

ROBINSON, L. R.
One-Electron Oxidation of Nickel Porphyrins. Effect of Structure and Medium on Formation of Nickel(III) Porphyrin or Nickel(II) Porphyrin pi-Radical Cation.
PB95-107058 *00,865*

Site of One-Electron Reduction of Ni(II) Porphyrins. Formation of Ni(I) Porphyrin of Ni(II) Porphyrin pi-Radical Anion.
PB95-107066 *00,866*

ROBINSON, R.
Atomic Oxygen Fine Structure Splittings with Tunable Far Infrared Spectroscopy.
PB95-152203 *03,915*

ROBINSON, R. A.
Crystallographic and Magnetic Properties of UAuSn.
PB95-140521 *04,543*

Incommensurate Magnetic Order in UPtGe.
PB95-140513 *04,542*

Magnetic Properties of Single-Crystalline UCu3Al2.
PB95-180717 *04,686*

ROBINSON, R. D.
First Results from the Goddard High-Resolution Spectrograph: The Chromosphere of Tauri.
PB94-199528 *00,054*

GHRS Observations of Cool, Low-Gravity Stars. 1. The Far-Ultraviolet Spectrum of alpha Orions (M2 Iab).
PB96-112016 *00,094*

Observations of 3C 273 with the Goddard High Resolution Spectrograph on the Hubble Space Telescope.
PB95-202321 *00,076*

Observing Stellar Coronae with the Goddard High Resolution Spectrograph. I. The dMe Star AU Microscopii.
PB96-102777 *00,092*

ROBY, R. J.
Compartment Fire Combustion Dynamics. Annual Report, September 1, 1993-September 1, 1994.
PB95-217162 *00,203*

Dynamics, Transport and Chemical Kinetics of Compartment Fire Exhaust Gases.
PB96-195508 *00,229*

ROCHFORD, K. B.
Effect of Semiconductor Laser Characteristics on Optical Fiber Sensor Performance.
PB95-169132 *02,167*

Faraday Effect Current Sensor with Improved Sensitivity-Bandwidth Product.
PB95-203154 *02,180*

Faraday Effect Sensors for Magnet Field and Electric Current.
PB96-119664 *04,736*

Fundamentals and Problems of Fiber Current Sensors.
PB97-111835 *02,205*

Magneto-Optic Rotation Sensor Using a Laser Diode as Both Source and Detector.
PB97-111272 *04,390*

Polarization Dependence of Response Functions in 3x3 Sagnac Optical Fiber Current Sensors.
PB95-162426 *02,154*

Polarization Dependence of Response Functions in 3x3 Sagnac Optical Fiber Current Sensors.
PB96-122684 *02,189*

Polarization Insensitive 3x3 Sagnac Current Sensor Using Polarizing Spun High-Birefringence Fiber.
PB96-119276 *02,187*

Simultaneous Laser-Diode Emission and Detection for Fiber-Optic Sensor Applications.
PB96-155502 *04,062*

Standard Polarization Components: Progress Toward an Optical Retardance Standard.
PB96-119672 *04,342*

Wideband Current and Magnetic Field Sensors Based on Iron Garnets.
PB96-200878 *01,975*

ROCKWELL, R. J.
Optical Density Measurements of Laser Eye Protection Materials.
PB96-190301 *00,190*

ROD, B. J.
Microstructure and Ferroelectric Properties of Lead Zirconate-Titanate Films Produced by Laser Evaporation.
PB94-199148 *04,470*

RODD, J. L.
Stranding Experiments on Double Hull Tanker Structures.
PB96-123112 *03,749*

RODE, C.
Empirical Validation of a Transient Computer Model for Combined Heat and Moisture Transfer.
PB97-111991 *00,416*

RODEL, J.
Loading Device for Fracture Testing of Compact Tension Specimens in the Scanning Electron Microscope.
PB95-162434 *02,652*

RODENBUSH, A. J.
Effect of Magnetic Field Orientation on the Critical Current of HTS Conductor and Coils.
PB96-141189 *02,956*

RODER, H. M.
Transient Methods for Thermal Conductivity.
PB94-198405 *0, 197*

RODGERS, A. S.
Thermodynamic and Thermophysical Properties of Organic Nitrogen Compounds. Part II. 1- and 2-Butanamine, 2-Methyl-1-Propanamine, 2-Methyl-2-Propanamine, Pyrrole, 1-, 2-, and 3-Methylpyrrole, Pyridine, 2-, 3-, and 4-Methylpyridine, Pyrrolidine, Piperidine, Indole, Quinoline, Isoquinoline, Acridine, Carbazole, Phenanthridine, 1- and 2-Naphthalenamine, and 9-Methylcarbazole.
PB94-162294 *00,741*

RODGERS, J. E.
Scattered Fractions of Dose from 18 and 25 MV X-ray Radiotherapy Linear Accelerators.
PB96-186101 *04,120*

RODGERS, J. R.
CRYSTMET: The NRCC Metals Crystallographic Data File.
PB97-109029 *04,799*

RODONO, M.
First Results from a Coordinated ROSAT, IUE, and VLA Study of RS CVn Systems.
PB94-213477 *00,069*

Rotational Modulation and Flares on RS Canum Venaticorum and BY Draconis Stars. XVI. IUE Spectroscopy and VLA Observations of C1182(=V 1005 Orionis) in October 1983.
PB94-185626 *00,050*

Rotational Modulation and Flares on RS Canum Venaticorum and BY Draconis Stars. XVIII. Coordinated VLA, ROSAT, and IUE Observations of RS CVn Binaries.
PB96-102322 *00,089*

ROGERS, C. T.
Bias Current Dependent Resistance Peaks in NiFe/Ag Giant Magnetoresistance Multilayers.
PB97-112346 *04,153*

Observation of the Transverse Second Harmonic Magneto-Optic Kerr Effect from Ni81Fe19 Thin Film Structures.
PB96-200332 *01,971*

Telegraph Noise in Silver-Permalloy Giant Magnetoresistance Test Structures.
PB96-146717 *04,763*

ROGERS, J. E.
Interior-Point Method for Linear and Quadratic Programming Problems. (NIST Reprint).
PB95-180089 *03,429*

ROGERS, S. A.
Pulsed Laser Photolysis Time-Resolved FT-IR Emission Studies of Molecular Dynamics.
PB95-203162 *04,002*

ROHRBAUGH, J. M.
Electronics and Electrical Engineering Laboratory Technical Progress Bulletin Covering Laboratory Programs, April to June 1994 with 1994/1995 EEEL Events Calendar.
PB95-143186 *02,329*

Electronics and Electrical Engineering Laboratory Technical Progress Bulletin Covering Laboratory Programs, April to June 1995 with 1995 EEEL Events Calendar.
PB96-106455 *01,923*

Electronics and Electrical Engineering Laboratory Technical Progress Bulletin Covering Laboratory Programs, April to June 1996 with 1996-1998 EEEL Events Calendar.
PB97-113880 01,994

Electronics and Electrical Engineering Laboratory Technical Progress Bulletin Covering Laboratory Programs, January to March 1994 with 1994/1995 EEEL Events Calendar.
PB94-193810 02,308

Electronics and Electrical Engineering Laboratory Technical Progress Bulletin Covering Laboratory Programs, January to March 1996, with 1996 EEEL Events Calendar.
PB96-191390 01,969

Electronics and Electrical Engineering Laboratory Technical Progress Bulletin Covering Laboratory Programs, July to September 1993 with 1994 EEEL Events Calendar.
PB94-194354 02,309

Electronics and Electrical Engineering Laboratory Technical Progress Bulletin Covering Laboratory Programs, July to September 1994 with 1994/1995 EEEL Events Calendar.
PB95-170395 02,360

Electronics and Electrical Engineering Laboratory Technical Progress Bulletin Covering Laboratory Programs, July to September 1995 with 1996 EEEL Events Calendar.
PB96-147905 01,942

Electronics and Electrical Engineering Laboratory Technical Progress Bulletin Covering Laboratory Programs, October to December 1992, with 1992/1993 EEEL Events Calendar.
PB94-165958 02,299

Electronics and Electrical Engineering Laboratory Technical Progress Bulletin Covering Laboratory Programs, October to December 1994 with 1995 EEEL Events Calendar.
PB95-208724 02,372

Electronics and Electrical Engineering Laboratory Technical Progress Bulletin Covering Laboratory Programs, October to December 1995 with 1996 EEEL Events Calendar.
PB96-183116 01,966

Electronics and Electrical Engineering Laboratory Technical Progress Bulletin Covering Programs, October to December 1993, with 1994/1995 EEEL Events Calendar.
PB94-154341 02,115

Electronics and Electrical Engineering Laboratory Technical Publication Announcements Covering Laboratory Programs, April to June 1995 with 1995 EEEL Events Calendar.
PB96-137187 01,941

Electronics and Electrical Engineering Laboratory Technical Publication Announcements Covering Laboratory Programs, January to March 1994 with 1994/1995 EEEL Events Calendar.
PB94-213774 01,883

Electronics and Electrical Engineering Laboratory Technical Publication Announcements Covering Laboratory Programs, January to March 1995 with 1995 EEEl Events Calendar.
PB95-242277 02,373

Electronics and Electrical Engineering Laboratory Technical Publication Announcements Covering Laboratory Programs, January to March 1996, with 1996 EEEL Events Calendar.
PB96-214622 01,981

Electronics and Electrical Engineering Laboratory Technical Publication Announcements Covering Laboratory Programs, July to September 1994 with 1995 EEEL Events Calendar.
PB95-198925 01,912

Electronics and Electrical Engineering Laboratory Technical Publication Announcements Covering Laboratory Programs, July to September 1995 with 1996 EEEL Events Calendar.
PB96-183066 01,965

Electronics and Electrical Engineering Laboratory Technical Publication Announcements Covering Laboratory Programs, October to December 1993 with 1994/1995 EEEL Events Calendar.
PB94-193752 02,307

Electronics and Electrical Engineering Laboratory Technical Publication Announcements Covering Laboratory Programs, October to December 1994 with 1995 EEEL Events Calendar.
PB95-231841 01,918

Electronics and Electrical Engineering Laboratory Technical Publication Announcements Covering Laboratory Programs, October to December 1995, with 1996 EEEL Events Calendar.
PB96-202346 01,978

ROITBURD, A.

Temperature Dependence of Vortex Twin Boundary Interaction in Yttrium Barium Copper Oxide (YBa2Cu3O6+x).
PB95-162442 04,613

ROITMAN, P.

Characterization of Interface Defects in Oxygen-Implanted Silicon Films.
PB94-216629 02,322

Charge Trapping and Breakdown Mechanism in SIMOX.
PB94-216637 02,323

Defect Formation Mechanism Causing Increasing Defect Density during Decreasing Implant Dose in Low-Dose Simox.
PB96-119524 02,402

Defect of Thermal Ramping and Annealing Conditions on Defect Formation in Oxygen Implanted Silicon-On-Insulator Material.
PB94-212966 02,318

Defect Pair Formation by Implantation-Induced Stresses in High-Dose Oxygen Implanted Silicon-on-Insulator Material.
PB95-175824 02,364

Design Guide for CMOS-On-SIMOX. Test Chips NIST3 and NIST4.
PB94-163458 02,297

Effect of Annealing Ambient on the Removal of Oxide Precipitates in High-Dose Oxygen Implanted Silicon.
PB95-164356 02,356

Effect of Intermediate Thermal Processing on Microstructural Changes of Oxygen Implanted Silicon-on-Insulator Material.
PB96-160213 02,982

Effect of Single versus Multiple Implant Processing on Defect Types and Densities in SIMOX.
PB96-160353 01,957

Electron and Hole Trapping in Irradiated SIMOX, ZMR and BESOI Buried Oxides.
PB96-160320 01,956

Electron Traps, Structural Change, and Hydrogen Related SIMOX Defects.
PB94-200391 02,312

Evidence for a Deep Electron Trap and Charge Compensation in Separation by Implanted Oxygen Oxides.
PB95-175337 02,362

Mechanism of Defect Formation in Low-Dose Oxygen Implanted Silicon-on-Insulator Material.
PB97-111462 02,453

Nano-Defects in Commercial Bonded SOI and SIMOX.
PB96-123674 02,407

Stacking Fault Pyramid Formation and Energetics in Silicon-on-Insulator Material Formed by Multiple Cycles of Oxygen Implantation and Annealing.
PB96-160221 04,083

ROLANDO, C.

Oxidation of Caffeic Acid and Related Hydroxycinnamic Acids.
PB97-111975 00,651

ROLSTON, S.

Hyperfine Effects and Associative Ionization of Ultracold Sodium.
PB95-151221 03,903

Optical Molasses: The Coldest Atoms Ever.
PB95-108908 03,878

Ultracold Collisions: Associative Ionization in a Laser Trap.
PB94-213238 03,859

ROLSTON, S. L.

Atoms in Optical Molasses.
PB95-108874 03,875

Atoms in Optical Molasses: Applications to Frequency Standards.
PB95-108882 03,876

Heterodyne Measurement of the Fluorescence Spectrum of Optical Molasses.
PB95-108411 03,873

Laser-Cooled Neutral Atom Frequency Standards.
PB96-160312 04,086

Laser Cooling and the Recoil Limit.
PB97-111280 04,391

Laser Modification of Ultracold Collisions: Experiment.
PB96-157987 04,075

Localization of Atoms in a Three-Dimensional Standing Wave.
PB95-163887 03,944

Magneto-Optical Trapping of Metastable Xenon: Isotope-Shift Measurements.
PB95-151254 03,905

Measurements of Fluorescence from Cold Atoms: Localization in Three-Dimensional Standing Waves.
PB95-163879 03,943

Microlithography by Using Neutral Metastable Atoms and Self-Assembled Monolayers.
PB96-190038 02,441

Optical Molasses: Cold Atoms for Precision Measurements.
PB95-108890 03,877

sigma+-sigma- Optical Molasses in a Longitudinal Magnetic Field.
PB95-161840 03,934

ROMAN, P.

Precision Nuclear Orientation Measurements for Determining Mixed Magnetic Dipole/Electric Quadrupole Hyperfine Interactions.
PB94-199080 03,810

ROMANKIW, L.

Magnetic and Structural Properties of Electrodeposited Copper-Nickel Microlayered Alloys.
PB94-213121 04,512

ROMANOVSKY, A.

Precise Optical Frequency References and Difference Frequency Measurements with Diode Lasers.
PB95-176228 04,305

RONNING, C.

Modeling Detector Response for Neutron Depth Profiling.
PB96-157813 04,066

ROOK, H. L.

Materials Science and Engineering Laboratory Annual Report, 1993. NAS-NRC Assessment Panel, April 21-22, 1994.
PB94-162534 02,969

Materials Science and Engineering Laboratory Annual Report, 1995. Technical Activities.
PB96-214754 03,009

ROOS, C.

Parametric Study of Wall Moisture Contents Using a Revised Variable Indoor Relative Humidity Version of the 'Moist' Transient Heat and Moisture Transfer Model.
PB97-122535 00,419

ROOS, M.

Problem of Convection in the Water Absorbed Dose Calorimeter.
PB97-110159 03,523

ROOVERS, J.

Thermodynamic Properties of Dilute and Semidilute Solutions of Regular Star Polymers.
PB96-146808 01,284

RORRER, D. E.

Videoconferencing Procurement and Usage Guide.
PB94-217023 01,470

ROSASCO, G. J.

Development of the NIST Transient Pressure and Temperature Calibration Facility.
PB96-160833 00,626

Executive Summary: Proceedings of the Workshop on the Measurement of Transient Pressure and Temperature.
PB96-160841 02,679

Measurement of the Self Broadening of the H2Q(0-5) Raman Transitions from 295 to 1000 K.
PB95-108627 00,884

Q Branch Lineshape Functions for CARS Thermometry.
PB96-160643 01,132

Simultaneous Forward-Backward Raman Scattering Studies of D2 Broadened by D2, He, and Ar.
PB95-162459 00,961

ROSE, A. H.

Effect of Semiconductor Laser Characteristics on Optical Fiber Sensor Performance.
PB95-169132 02,167

Faraday Effect Current Sensor with Improved Sensitivity-Bandwidth Product.
PB95-203154 02,180

Faraday Effect Current Sensors.
PB94-200698 02,127

Faraday Effect Sensors: A Review of Recent Progress.
PB94-200706 02,128

Faraday Effect Sensors for Magnet Field and Electric Current.
PB96-119664 04,736

Fundamentals and Problems of Fiber Current Sensors.
PB97-111835 02,205

Improved Annealing Technique for Optical Fiber.
PB96-119680 04,343

Magneto-Optic Rotation Sensor Using a Laser Diode as Both Source and Detector.
PB97-111272 04,390

Magnetooptic Effects.
PB96-119292 04,338

Optical Current Transducer for Calibration Studies.
PB94-185907 02,121

Polarization Insensitive 3x3 Sagnac Current Sensor Using Polarizing Spun High-Birefringence Fiber.
PB96-119276 02,187

Self-Calibrated Intelligent Optical Sensors and Systems.
PB96-200738 04,380

Self-Calibrating Fiber Optic Sensors: Potential Design Methods.
PB95-169298 02,172

Self Calibrating Fiber Optic Sensors: Potential Design Methods.
PB95-169306 02,173

Simultaneous Laser-Diode Emission and Detection for Fiber-Optic Sensor Applications.
PB96-155502 04,062

Standard Polarization Components: Progress Toward an Optical Retardance Standard.
PB96-119672 04,342

Submicroampere-Per-Root-Hertz Current Sensor Based on the Faraday Effect in Ga: YIG.
PB95-162467 02,155

Wideband Current and Magnetic Field Sensors Based on Iron Garnets.
PB96-200878 01,975

ROSE, C.

Planar Near-Field Alignment.
PB94-172491 01,998

ROSE, J.

Two New Probes for a Coordinate Measuring Machine.
PB95-163093 02,653

ROSE, J. E.

NIST-NRL Free-Electron Laser Facility.
PB94-212511 04,237

ROSE, J. L.

In-Line Optical Monitoring of Injection Molding.
PB94-185105 01,201

ROSE, K. J.
Intensive Swimming: Can It Affect Your Patients' Smiles.
PB96-123666 *03,570*

ROSEN, B.
Preliminary Functional Specifications of a Prototype Electronic Research Notebook for NIST.
PB94-207750 *00,012*

ROSEN, H. N.
Sorption of Moisture on Epoxy and Alkyd Free Films and Coated Steel Panels.
PB95-162475 *03,192*

ROSENBERG, A.
Photonic Band-Structure Effects for Low-Index-Contrast Two-Dimensional Lattices in the Near Infrared.
PB97-122469 *04,401*

ROSENBLATT, J. R.
Churchill Eisenhart, 1913-1994.
PB96-137740 *03,447*

ROSENFELD, A. H.
National Planning for Construction and Building R and D.
PB96-137104 *00,324*

Program of the Subcommittee on Construction and Building.
PB94-193646 *00,319*

Program of the Subcommittee on Construction and Building (July 1994).
PB95-122537 *00,321*

Rationale and Preliminary Plan for Federal Research for Construction and Building.
PB95-154704 *00,322*

ROSENFELD, D. A.
Procedure for Product Data Exchange Using STEP Developed in the AutoSTEP Pilot.
PB96-183058 *02,843*

Reference Manual for the Algorithm Testing System Version 2.0.
PB96-128244 *02,922*

User's Guide for the Algorithm Testing System Version 2.0.
PB95-251666 *02,916*

ROSENTHAL, L. S.
Computer Graphics Metafile (CGM): Procedures for NIST CGM Validation Test Service.
PB94-161809 *01,804*

Initial Graphics Exchange Specification (IGES): Procedures for the NIST IGES Validation Test Service.
PB95-171427 *02,780*

STandard for the Exchange of Product Model Data (STEP): Procedures for NIST STEP Validation.
PB96-154976 *02,787*

ROSENTHAL, P. A.
Critical Current and Normal Resistance of High-Tc Step-Edge SNS Junctions.
PB96-111752 *04,724*

High Temperature Superconductor-Normal Metal-Superconductor Josephson Junctions with High Characteristic Voltages.
PB95-176079 *04,666*

Terahertz Shapiro Steps in High Temperature SNS Josephson Junctions.
PB95-169140 *02,168*

Thermal Noise in High-Temperature Superconducting-Normal-Superconducting Step-Edge Josephson Junctions.
PB95-175089 *04,650*

ROSHKO, A.
Coexistence of Grains with Differing Orthorhombicity in High Quality YBa2Cu3O7-delta Thin Films.
PB96-135033 *04,742*

Correlation between Tc and Elastic Constants of (La-M)2CuO4.
PB94-213220 *04,514*

Critical Current Behavior of Ag-Coated YBa2Cu3O7-x Thin Films.
PB95-141016 *04,549*

Distributed Feedback Lasers in Rare-Earth-Doped Phosphate Glass.
PB96-123773 *04,740*

Effects of Etching on the Morphology and Surface Resistance of YBa2Cu3O7-delta Films.
PB96-135355 *02,410*

Effects of Substrate Surface Steps on the Microstructure of Epitaxial Ba2YCu3O7-x Thin Films on (001) LaAlO3.
PB96-148184 *04,774*

Epitaxial Nucleation and Growth of Chemically Derived Ba2YCu3O7-x Thin Films on (001) SrTiO3.
PB96-190186 *04,787*

Growth of Epitaxial KNbO3 Thin Films.
PB96-135181 *02,409*

Growth of Laser Ablated YBa2Cu3O7-delta Films as Examined by Rheed and Scanning Tunneling Microscopy.
PB95-162541 *04,614*

High Current Pressure Contacts to Ag Pads on Thin Film Superconductors.
PB95-168621 *04,639*

Influence of Deposition Parameters on Properties of Laser Ablated YBa2Cu3O7-Delta Films.
PB95-140539 *04,544*

Magnetic Flux Pinning in Epitaxial YBa2Cu3O7-delta Thin Films.
PB96-200746 *04,795*

Nd:LiTaO3 Waveguide Laser.
PB95-140851 *04,259*

Passively Q-Switched Nd-Doped Waveguide Laser.
PB95-180048 *04,308*

Size Effects and Giant Magnetoresistance in Unannealed NiFe/Ag Multilayer Stripes.
PB97-111306 *04,145*

Surface Degradation of Superconducting YBa2Cu3O7-delta Thin Films.
PB95-176095 *04,667*

Surface Modification of YBa2Cu3O7-delta Thin Films Using the Scanning Tunneling Microscope: Five Methods.
PB95-203394 *04,699*

ROSOV, N.
Crystal Structure and Magnetic Ordering of the Rare-Earth and Cu Moments in RBa2Cu2NbO8(R=Nd,Pr).
PB95-140554 *04,546*

Determination of Anomalous Superexchange in MnCl2 and Its Graphite Intercalation Compound.
PB97-122568 *00,666*

Magnetic Ordering of the Cu Spins in PrBa2Cu3O6+x.
PB95-140547 *04,545*

Neutron Powder Diffraction Study of the Nuclear and Magnetic Structures of the Oxygen-Deficient Perovskite YBaCuCoO5.
PB95-161097 *00,954*

Polarization Analysis of the Magnetic Excitations in Fe65Ni35 Invar.
PB95-150082 *04,558*

Polarization Analysis of the Magnetic Excitations in Invar and Non-Invar Amorphous Alloys.
PB94-216116 *04,516*

Quasielastic and Inelastic Neutron-Scattering Studies of ((CD3)3ND)FeCl3.2D2O: A One-Dimensional Ising Ferromagnet.
PB95-140562 *04,547*

Structural and Magnetic Properties of CuCl2 Graphite Intercalation Compounds.
PB96-119748 *03,020*

Temperature Dependence of the Magnetic Excitations in Ordered and Disordered Fe72Pt28.
PB95-150223 *04,563*

Vortex Dynamics and Melting in Niobium.
PB96-112362 *02,073*

ROSS, A. B.
Critical Review of Rate Constants for Reactions of Transients from Metal Ions and Metal Complexes in Aqueous Solution.
PB96-145859 *01,109*

Quantum Yields for the Photosensitized Formation of the Lowest Electronically Excited Singlet State of Molecular Oxygen in Solution.
PB94-161007 *00,732*

Rate Constants for the Decay and Reactions of the Lowest Electronically Excited Singlet State of Molecular Oxygen in Solution. An Expanded and Revised Compilation.
PB96-145826 *01,106*

ROSS, G. G.
Measured Stopping Powers of Hydrogen and Helium in Polystyrene Near Their Maximum Values.
PB96-112321 *04,729*

ROSS, J.
Quadratic Response of a Chemical Reaction to External Oscillations.
PB96-161633 *01,138*

ROSSEINSKY, M. J.
Neutron-Scattering Study of C60(n-) (n=3,6) Librations in Alkali-Metal Fullerides.
PB94-200219 *00,806*

ROSSI, H. H.
Measurement of Absorbed Dose of Neutrons, and of Mixtures of Neutrons and gamma rays.
AD-A286 647/3 *03,710*

ROSSITER, W.
Characteristics of Adhesive-Bonded Seams Sampled from EPDM Roof Membranes.
PB95-162491 *00,377*

Laboratory Accreditation for Testing Energy Efficient Lighting.
PB96-122932 *00,270*

ROSSITER, W. J.
Application of Thermal Analysis Techniques to the Characterization of EPDM Roofing Membrane Materials.
PB95-125845 *00,359*

Effects of Adhesive Thickness, Open Time, and Surface Cleanness on the Peel Strength of Adhesive-Bonded Seams of EPDM Rubber Roofing Membrane.
PB95-151338 *00,372*

Efficiency of Electric Motors. National Voluntary Lab. Accreditation Program (NVLAP).
PB96-111174 *02,107*

National Voluntary Laboratory Accreditation Program: Carpet and Carpet Cushion.
PB95-155560 *00,295*

National Voluntary Laboratory Accreditation Program: Energy Efficient Lighting Products.
PB94-219060 *02,642*

National Voluntary Laboratory Accreditation Program (NVLAP): Wood Based Products.
PB95-170429 *03,405*

Performance Approach to the Development of Criteria for Low-Sloped Roof Membranes.
PB94-160751 *00,329*

Performance of Tape-Bonded Seams of EPDM Membranes: Comparison of the Peel Creep-Rupture Response of Tape-Bonded and Liquid-Adhesive-Bonded Seams.
PB96-183249 *03,012*

Pulse-Echo Ultrasonic Evaluation of the Integrity of Seams of Single-Ply Roof Membranes.
PB95-163804 *00,381*

Use of Thermal Mechanical Analysis to Characterize Ethylene-Propylene-Diene Terpolymer (EPDM) Roofing Membrane Materials.
PB95-125852 *00,360*

ROSSO, A.
Wavelength Dependence of Normal Spectral Emissivity of High-Temperature Metals at Their Melting Point.
PB94-200011 *03,398*

ROSSO, C.
X-ray Emission from Chemically Peculiar Stars.
PB96-102256 *00,088*

ROSTAMI, K. M.
Continuous Counter-Current Two Phase Aqueous Extraction.
PB95-161212 *00,675*

ROTH, R. S.
Ca1-xCuO2, a NaCuO2-Type Related Structure.
PB95-162822 *04,620*

Ca4Bi6O13: A Compound Containing an Unusually Low Bismuth Coordination Number and Short Bi Bi Contacts.
PB95-141131 *00,911*

Crystallographic Characterization of Some Intermetallic Compounds in the Al-Cr System.
PB94-198702 *03,318*

High Temperature Reactions of Uranium Dioxide with Various Metal Oxides.
AD-A286 648/1 *00,717*

Improved Crystallographic Data for Aluminum Niobate (AlNbO4).
PB95-107306 *04,523*

Magnetic Dielectric Oxides: Subsolidus Phase Relations in the BaO: Fe2O3: TiO2 System.
PB96-176524 *01,156*

Phase Equilibria in the Systems CaO-CuO and CaO-Bi2O3.
PB95-140570 *03,048*

Powder X-ray Diffraction Data for Ca2Bi2O5 and C4Bi6O13.
PB96-161278 *04,777*

Preparation and Crystal Structure of Sr5TiNb4O17.
PB96-167341 *04,107*

Preparation, Crystal Structure, Dielectric Properties, and Magnetic Behavior of Ba2Fe2Ti4O13.
PB96-186176 *01,162*

ROTH, S. C.
Fluorescence Anisotropy Measurements on a Polymer Melt as a Function of Applied Shear Stress.
PB94-199296 *01,209*

Hysteresis Measurements of Remanent Polarization and Coercive Field in Polymers.
PB94-199767 *04,475*

Observations of Shear Induced Molecular Orientation in a Polymer Melt Using Fluorescence Anisotropy Measurements.
PB94-199304 *01,210*

Observations of Shear Stress and Molecular Orientation Using Fluorescence Anisotropy Measurements.
PB94-199312 *01,211*

ROTHFLEISCH, P. I.
Simple Method of Composition Shifting with a Distillation Column for a Heat Pump Employing a Zeotropic Refrigerant Mixture.
PB95-255824 *02,603*

Study of Heat Pump Performance Using Mixtures of R32/R134a and R32/R125/R134a as 'Drop-In' Working Fluids for R22 with and Without a Liquid-Suction Heat Exchanger.
PB94-218559 *02,503*

ROTHLEDER, J.
Mass Unit Disseminated to Surrogated Laboratories Using the NIST Portable Mass Calibration Package.
PB94-142486 *03,781*

ROTHMAN, J. B.
Gas Absorption during Ion-Irradiation of a Polymer Target.
PB96-161864 *04,099*

ROTTER, L. D.
Epitaxial Growth of BaTiO3 Thin Films at 600C by Metalorganic Chemical Vapor Deposition.
PB96-122510 *03,071*

ROUGHANI, B.
Buffer Layer Modulation-Doped Field-Effect-Transistor Interactions in the Al0.33Ga0.67As/GaAs Superlattice System.
PB96-102876 *02,380*

ROUSE, W. B.
Learning to Change: Opportunities to Improve the Performance of Smaller Manufacturers.
PB94-166212 *00,010*

ROUSH, M.
Electric Field Dependent Dielectric Breakdown of Intrinsic SiO2 Films Under Dynamic Stress.
PB96-204102 *02,449*

Time-Dependent Dielectric Breakdown of Intrinsic SiO2 Films under Dynamic Stress.
PB96-179478 *02,438*

ROWAN, W. L.
Improved Wavelengths for Prominent Lines of Cr XVI to Cr XXII.
PB95-150629 *03,895*

Improved Wavelengths for Prominent Lines of Fe XX to Fe XXIII.
PB96-111638 *04,334*

Observation of Pd-Like Resonance Lines Through Pt(32+) and Zn-Like Resonance Lines of Er(38+) and Hf(42+).
PB95-150637 *03,896*

Rb-Like Spectra: Pd X to Nd XXIV.
PB95-150645 *03,897*

Rh I Isoelectronic Sequence Observed from Er(23+) to Pt(33+).
PB95-150652 *03,898*

Spectra of Ag I Isoelectronic Sequence Observed from Er(21+) to Au(32+).
PB95-150660 *03,899*

ROWE, J. E.
Local Partial Densities of States in Ni and Co Silicides Studied by Soft X-Ray Emission Spectroscopy.
PB94-212412 *04,504*

ROWE, J. M.
Cold Neutron Gain Calculations for the NBSR Using MCNP.
PB95-163978 *03,731*

Liquid-Hydrogen Cold Neutron Source for the NBSR.
PB95-151619 *03,729*

Neutron Techniques in Materials Science and Related Disciplines.
PB96-119698 *02,980*

Nuclear Heat Load Calculations for the NBSR Cold Neutron Source Using MCNP.
PB95-152955 *03,730*

Reactor Radiation Technical Activities, 1994. NAS-NRC Assessment Panel, April 6-7, 1995.
PB95-209888 *03,732*

Thermal Hydraulic Tests of a Liquid Hydrogen Cold Neutron Source.
PB95-135570 *03,884*

ROWE, P.
Recommendations on Selection of Vehicle-to-Roadside Communications Standards for Commercial Vehicle Operations.
PB94-195914 *04,859*

Vehicle-to-Roadside Communications for Commercial Vehicle Operations: Requirements and Approaches.
PB95-188827 *04,860*

ROWE, P. S.
Sources of Uncertainty in a DVM-Based Measurement System for a Quantized Hall Resistance Standard.
PB94-219334 *01,884*

ROY, P.
Vibronic Coupling and Other Many-Body Effects in the 4sigmag(-1) Photoionization Channel of CO2.
PB95-162509 *00,962*

ROY, S.
Anharmonic Oscillator Analysis Using Modified Airy Functions.
PB94-185311 *03,798*

Small-Angle Neutron Scattering of Poly(vinyl alcohol) Gels.
PB95-164117 *01,260*

Small Angle Neutron Scattering Studies on Chain Asymmetry of Coextruded Poly(Vinyl Alcohol) Film.
PB95-164372 *01,262*

ROYTBURD, A.
Coherent Precipitates in the BCC/Orthorhombic Two Phase Field of the Ti-Al-Nb System.
PB94-198694 *03,317*

Transformation of BCC and B2 High Temperature Phases to HCP and Orthorhombic Structures in the Ti-Al-Nb System. Part 1. Microstructural Predictions Based on a Subgroup Relation between Phases.
PB96-169065 *03,370*

ROYTBURD, A. L.
Determination of Thermoactivation Parameters of Vortex Mobility in YBa2Cu3O7 Using Only Magnetic Measurements.
PB95-163499 *04,624*

ROZSA, K.
Deposition Rates in Direct Current Diode Sputtering.
PB95-203345 *04,697*

RUBENSSON, J. E.
Intermediate Coupling in L2-L3 Core Excitons of MgO, Al2O3, and SiO2.
PB96-158043 *04,079*

Laser-Synchrotron Hybrid Experiments: A Photon to Tickle, A Photon to Poke.
PB96-157847 *03,704*

Local Partial Densities of States in Ni and Co Silicides Studied by Soft X-Ray Emission Spectroscopy.
PB94-212412 *04,504*

Soft-X-ray-Emission Investigation of Cobalt Implanted Silicon Crystals.
PB96-157912 *04,069*

Soft-X-ray-Emission Spectra of Solid Kr and Xe.
PB96-157920 *04,070*

RUBIN, R. J.
Fluctuation Dominated Recombination Kinetics with Traps.
PB95-107264 *00,875*

RUDDER, F. F.
Geometric Characterization of Rockwell Diamond Indenters.
PB95-203287 *02,950*

Microform Calibration Uncertainties of Rockwell Diamond Indenters.
PB96-122114 *03,280*

Microform Calibrations in Surface Metrology.
PB95-203295 *02,951*

Post-Process Control of Machine Tools.
PB95-203451 *02,952*

Static Structural Analysis of a Reconfigurable Rigid Platform Supported by Elastic Legs.
PB97-113898 *02,960*

Stylus Technique for the Direct Verification of Rockwell Diamond Intenders.
PB96-155569 *02,958*

RUDELL, M.
Liposome-Based Flow-Injection Immunoassay for Determining Theophylline in Serum.
PB94-213493 *03,494*

RUDMAN, D. A.
30 THz Mixing Experiments on High Temperature Superconducting Josephson Junctions.
PB96-102462 *04,709*

Antenna-Coupled High-Tc Air-Bridge Microbolometer on Silicon.
PB95-180899 *04,315*

Coexistence of Grains with Differing Orthorhombicity in High Quality YBa2Cu3O7-delta Thin Films.
PB96-135033 *04,742*

Critical Current and Normal Resistance of High-Tc Step-Edge SNS Junctions.
PB96-111752 *04,724*

Effect of Microstructure on Phase Formation in the Reaction of Nb/Al Multilayer Thin Films.
PB95-168415 *03,352*

Effects of Anneal Time and Cooling Rate on the Formation and Texture of Bi2Sr2CaCu2O8 Films.
PB95-161600 *04,603*

First Phase Formation Kinetics in the Reaction of Nb/Al.
PB95-168456 *03,353*

Grain Alignment and Transport Properties of Bi2Sr2CaCu2O8 Grown by Laser Heated Float Zone Method.
PB95-161451 *04,602*

Growth of Laser Ablated YBa2Cu3O7-delta Films as Examined by Rheed and Scanning Tunneling Microscopy.
PB95-162541 *04,614*

High-Tc Superconducting Antenna-Coupled Microbolometer on Silicon.
PB95-169124 *02,166*

Increased Pinning Energies and Critical Current Densities in Heavy-Ion-Irradiated Bi2Sr2CaCu2O8 Single Crystals.
PB95-175352 *04,654*

Increased Transition Temperature in In situ Coevaporated YBa2Cu3O7-delta Thin Films by Low Temperature Post-Annealing.
PB95-180071 *04,672*

Influence of Deposition Parameters on Properties of Laser Ablated YBa2Cu3O7-Delta Films.
PB95-140539 *04,544*

Insulating Nanoparticles on YBa2Cu3O7-delta Thin Films Revealed by Comparison of Atomic Force and Scanning Tunneling Microscopy.
PB95-150843 *04,575*

Magnetic Flux Pinning in Epitaxial YBa2Cu3O7-delta Thin Films.
PB96-200746 *04,795*

Microwave Noise in High-Tc Josephson Junctions.
PB96-148010 *04,771*

Microwave Properties of Voltage-Tunable YBa2Cu3O7-delta/SrTiO3 Coplanar Waveguide Transmission Lines.
PB96-141262 *02,235*

Observation of Insulating Nanoparticles on YBCO Thin-Films by Atomic Force Microscopy.
PB95-163358 *04,622*

Suitability of Metalorganic Chemical Vapor Deposition-Derived PrGaO3 Films as Buffer Layers for YBa2Cu3O7-x Pulsed Laser Deposition.
PB95-168670 *04,640*

Temperature Dependence and Magnetic Field Modulation of Critical Currents in Step-Edge SNS YBCO/Au Junctions.
PB96-111745 *04,723*

Thermal Isolation of High-Temperature Superconducting Thin Films Using Silicon Wafer Bonding and Micromachining.
PB96-135017 *02,408*

Thin Film Reaction Kinetics of Niobium/Aluminum Multilayers.
PB95-175295 *04,651*

Use of Ion Scattering Spectroscopy to Monitor the Nb Target Nitridation during Reactive Sputtering.
PB94-172525 *00,761*

Vortex Images in Thin Films of YBa2Cu3O(sub 7-x) and Bi2Sr2Ca1Cu2O(sub 8+x) Obtained by Low-Temperature Magnetic Force Microscopy.
PB97-119408 *04,815*

YBa2Cu3O7-x to Si Interconnection for Hybrid Superconductor/Semiconductor Integration.
PB94-211711 *02,315*

RUFF, A. W.
Considerations on Data Requirements for Tribological Modeling.
PB94-172731 *02,962*

Critical Factors in Non-Lubricated, Non-Abrasive Wear Testing.
PB95-140588 *03,236*

Damage Processes in Ceramics Resulting from Diamond Tool Indentation and Scratching in Various Environments.
PB96-102983 *03,065*

Hybrid Method for Determining Material Properties from Instrumented Micro-Indentation Experiments.
PB95-152229 *03,348*

Modified Surface Layers and Coatings.
PB95-176087 *03,125*

Nanoindentation and Instrumented Scratching Measurements on Hard Coatings.
PB97-122477 *03,111*

Tribological Data: Needs and Opportunities.
PB95-140596 *03,237*

Wear of Selected Materials and Composites Sliding against MoS2 Films.
PB94-172749 *03,231*

RUHL, M. K.
Findings and Recommendations from a Software Reengineering Case Study.
PB96-155791 *01,752*

RULE, D. L.
Thermal Conductivity of Polypyromellitimide Film with Alumina Filler Particles from 4.2 to 300 K.
PB96-200753 *01,292*

RUMBLE, J.
Access Paths for Materials Databases: Approaches for Large Databases and Systems.
PB95-162525 *02,975*

RUNKLES, R.
Laboratory Accreditation for Testing Energy Efficient Lighting.
PB96-122932 *00,270*

RUNYAN, J. L.
Fabrication of Flaw-Tolerant Aluminum-Titanate-Reinforced Alumina.
PB95-162533 *03,161*

Flaw-Insensitive Ceramics.
PB97-110027 *03,095*

Model for Toughness Curves in Two-Phase Ceramics. 2. Microstructural Variables.
PB96-163795 *03,078*

RUPP, N. W.
Dental Materials.
PB94-172871 *00,142*

RUPPRECHT, A.
Low-Frequency Excitations of Oriented DNA.
PB96-137799 *03,548*

RUPRECHT, P. A.
Properties of a Bose-Einstein Condensate in an Anisotropic Harmonic Potential.
PB96-204144 *04,133*

RUSBY, R. L.
Intercomparison of the ITS-90 Radiance Temperature Scales of the National Physical Laboratory (U.K.) and the National Institute of Standards and Technology.
PB96-113550 *02,674*

RUSH, J. J.
Characterization of the Structure of LaD2.50 by Neutron Powder Diffraction.
PB96-176797 *04,783*

Characterization of the Structure of TbD2.25 at 70 K by Neutron Powder Diffraction.
PB96-160528 *01,130*

Characterization of the Structure of YD3 by Neutron Powder Diffraction.
PB96-186150 *01,161*

Characterization of the Vibrational Dynamics in the Octahedral Sublattices of LaD2.25 and LaH2.25.
PB96-123724 *01,091*

Hydrogen in YBa2Cu3Ox: A Neutron Spectroscopy and a Nuclear Magnetic Resonance Study.
PB95-161279 *04,601*

Inelastic Neutron Scattering Studies of Nonlinear Optical Materials: p-Nitroaniline Adsorbed in ALPO-5.
PB95-107223 *00,874*

Inelastic Neutron Scattering Studies of Rotational Excitations and the Orientational Potential in C60 and A3C60 Compounds.
PB94-172673 *00,763*

Local-Mode Dynamics in YH2 and YD2 by Isotope-Dilution Neutron Spectroscopy.
PB95-181012 *01,017*

Low-Energy Vibrations and Octahedral Site Occupation in Nb95V5H(D)y.
PB96-160734 *01,133*

Neutron and Raman Spectroscopies of 134 and 134a Hydrofluorocarbons Encaged in Na-X Zeolite.
PB96-186168 *03,001*

Neutron-Powder-Diffraction Study of the Long-Range Order in the Octahedral Sublattice of LaD2.25.
PB96-141155 *04,753*

Neutron-Scattering Study of C60(n-) (n=3,6) Librations in Alkali-Metal Fullerides.
PB94-200219 *00,806*

Neutron Scattering Study of the Lattice Modes of Solid Cubane.
PB96-147152 *01,126*

Neutron Spectroscopic Comparison of beta-Phase Rare Earth Hydrides.
PB96-160742 *01,134*

Neutron Spectroscopic Comparison of Rare-Earth/Hydrogen alpha-Phase Systems.
PB95-163523 *00,970*

Neutron Spectroscopic Evidence of Concentration-Dependent Hydrogen Ordering in the Octahedral Sublattice of beta-TbH2+x.
PB95-181020 *01,018*

Neutron-Spectroscopy Study of the Hydrogen Vibrations in Hydrogen-Doped YBa2Cu3Ox.
PB94-172475 *04,441*

Phonon Density of States in R2CuO4 and Superconducting R1.85Ce0.15CuO4 (R = Nd, Pr).
PB95-150686 *04,574*

Vibrations of Hydrogen and Deuterium in Solid Solution with Lutetium.
PB95-181038 *01,019*

RUSHMEIER, H.

Simultaneous Optical Measurement of Soot Volume Fraction, Temperature, and CO2 in Heptane Pool Fire.
PB96-102132 *01,397*

RUSSEK, S.

Proposed Antiferromagnetically Coupled Dual-Layer Magnetic Force Microscope Tips.
PB95-169017 *04,645*

RUSSEK, S. E.

Bias Current Dependent Resistance Peaks in NiFe/Ag Giant Magnetoresistance Multilayers.
PB97-112346 *04,153*

Effects of Etching on the Morphology and Surface Resistance of YBa2Cu3O7-delta Films.
PB96-135355 *02,410*

Evidence for Tunneling and Magnetic Scatttering at 'In situ' YBCO/Noble-Metal Interfaces.
PB96-141098 *04,752*

Experimental Verification of a Micromagnetic Model of Dual-Layer Magnetic Films.
PB95-141081 *04,553*

Growth of Laser Ablated YBa2Cu3O7-delta Films as Examined by Rheed and Scanning Tunneling Microscopy.
PB95-162541 *04,614*

In situ Noble Metal YBa2Cu3O7 Thin-Film Contacts.
PB94-211323 *04,494*

Insulating Boundary Layer and Magnetic Scattering in YBa2Cu3O7-delta/Ag Interfaces Over a Contact Resistivity Range of 10(-8) - 10(-3) Omega cm(2).
PB95-169157 *04,648*

Low Magnetostriction in Annealed NiFe/Ag Giant Magnetoresistive Multilayers.
PB96-146691 *04,762*

Magnetic and Magnetoresistive Properties of Inhomogeneous Magnetic Dual-Layer Films.
PB95-169025 *04,646*

Magnetoresistance of Thin-Film NiFe Devices Exhibiting Single-Domain Behavior.
PB96-147087 *04,766*

Models of Granualr Giant Magnetoresistance Multilayer Thin Films.
PB96-190228 *01,968*

Oxygen Annealing of Ex-situ YBCO/Ag Thin-Film Interfaces.
PB96-141312 *04,758*

Simulating Device Size Effects on Magnetization Pinning Mechanisms in Spin Valves.
PB97-112593 *04,158*

Size and Self-Field Effects in Giant Magnetoresistive Thin-Film Devices.
PB95-180188 *04,674*

Size Effects and Giant Magnetoresistance in Unannealed NiFe/Ag Multilayer Stripes.
PB97-111306 *04,145*

Size Effects in Submicron NiFe/Ag GMR Devices.
PB96-155510 *02,237*

Surface Degradation of Superconducting YBa2Cu3O7-delta Thin Films.
PB95-176095 *04,667*

Telegraph Noise in Silver-Permalloy Giant Magnetoresistance Test Structures.
PB96-146717 *04,763*

RUSSELL, C. S.

Standard Generalized Markup Language Test Suite Evaluation Report.
PB96-154992 *01,751*

RUSSELL, D. L. F.

Publications of the Intelligent Systems Division (Previously Robot Systems Division) Covering the Period January 1971-April 1994.
PB94-217098 *02,935*

RUSSELL, J. B.

Measurement of Boron at Silicon Wafer Surfaces by Neutron Depth Profiling.
PB94-211059 *04,487*

RUSSELL, R.

Unified Telerobotic Architecture Project (UTAP) Standard Interface Environment (SIE), May 1995.
PB95-242350 *02,938*

RUSSELL, T. J.

Beyond the Technology Roadmaps: An Assessment of Electronic Materials Research and Development.
PB96-165998 *01,961*

RUSSELL, T. P.

Grazing Incidence Prompt Gamma Emissions and Resonance-Enhanced Neutron Standing Waves in a Thin-Film.
PB95-150470 *03,892*

Morphology of Symmetric Diblock Copolymers as Revealed by Neutron Reflectivity.
PB95-140075 *01,234*

Observed Frustration in Confined Block Copolymers.
PB95-150033 *01,238*

Temperature Dependence of the Morphology of Thin Diblock Copolymer Films as Revealed by Neutron Reflectivity.
PB94-172756 *01,199*

RUST, B. W.

Modulation of Fossil Fuel Production by Global Temperature Variations, 2.
PB94-146636 *02,533*

RUSYN, T.

New Extrapolation/Spherical/Cylindrical Measurement Facility at the National Institute of Standards and Technology.
PB95-153755 *02,004*

RUZICKA, V.

Estimation of the Heat Capacities of Organic Liquids as a Function of Temperature Using Group Additivity. I. Hydrocarbon Compounds.
PB94-162278 *00,739*

Estimation of the Heat Capacities of Organic Liquids as a Function of Temperature Using Group Additivity. II. Compounds of Carbon, Hydrogen, Halogens, Nitrogen, Oxygen, and Sulfur.
PB94-162286 *00,740*

RYAN, H. M.

Ultrasonic Measurements of Surface Roughness.
PB94-172137 *04,181*

RYBICKI, G. B.

Sobolev Approximation for Line Formation with Partial Frequency Redistribution.
PB95-202669 *00,078*

RYTZ, D.

Anomalous Dispersion and Thermal Expansion in Lightly-Doped KTa1-xNbxO3.
PB95-152302 *04,585*

RZAZEWSKI, K.

Appearance Intensities for Multiply Charged Ions in a Strong Laser Field.
PB96-160445 *04,089*

SAAR, S. H.

Relationship between Radiative and Magnetic Fluxes for Three Active Solar-Type Dwarfs.
PB96-119540 *00,097*

SABATINI, R. L.

Transverse stress effect on the critical current of internal tin and bronze process Nb(sub 3)Sn superconductors.
DE95016659 *04,434*

SABELLA, M. S.

Enthalpy Increment Measurements from 4.5 to 350 K and the Thermodynamic Properties of Titanium Disilicide(cr) to 1700 K.
PB96-204029 *00,678*

SACCHET, L. L.

Electronics and Electrical Engineering Laboratory: 1996 Program Plan. Supporting Technology for U.S. Competitiveness in Electronics.
PB96-175237 *01,962*

SACKS, J.

Taguchi's Parameter Design: A Panel Discussion.
PB96-111802 *03,445*

SADANA, D. K.

Nano-Defects in Commercial Bonded SOI and SIMOX.
PB96-123674 *02,407*

SADEK, F.

Method of Estimating the Parameters of Tuned Mass Dampers for Seismic Applications.
PB96-167820 *00,473*

Modified Optimal Algorithm for Active Structural Control.
PB96-165949 *00,472*

SADIQ, T. A. K.

Interaction between Micro and Macroscopic Flow in RTM Preforms.
PB95-162012 *03,159*

SAGERGREN, E. S.

Efficient Experiment to Study Superconducting Ceramics.
PB94-212578 *04,505*

SAIER, M. H.

Glucose Permease of Bacillus Subtilis Is a Single Polypeptide Chain That Functions to Energize the Sucrose Permease.
PB95-163192 *03,466*

SAITO, K.

Upward Flame Spread along the Vertical Corner Walls (October 1993).
PB94-206299 *00,340*

SAKAI, C. K.

Bioleaching of Cobalt from Smelter Wastes by 'Thiobacillus ferrooxidans'.
PB95-140968 *02,582*

SALAH, L. M.

Reanalysis of the (010), (020), (100), and (001) Rotational Levels of (32)S(16)O2.
PB95-125621 *00,887*

SALAMANCA-RIBA, L.

Characterization of the ZnSe/GaAs Interface Layer by TEM and Spectroscopic Ellipsometry.
PB95-175360 *04,655*

Determination of the Optical Constants of ZnSe Films by Spectroscopic Ellipsometry.
PB95-175378 *04,656*

SALAMON, M. B.

Enhanced Curie Temperatures and Magnetoelastic Domains in Dy/Lu Super Lattices and Films.
PB94-172665 *04,443*

Magnetic Rare Earth Artificial Metallic Superlattices.
PB95-162293 *04,611*

Magnetoelasticity in Rare-Earth Multilayers and Films.
PB94-211356 *04,495*

SALAMON, W.

Distributed Communication Methods and Role-Based Access Control for Use in Health Care Applications.
PB96-183165 *01,508*

SALAMON, W. J.

Object-Oriented Technology Research Areas.
PB95-199329 *01,726*

Quality Characteristics and Metrics for Reusable Software (Preliminary Report).
PB94-203437 *01,693*

SALEM, A. J.

Comparison of the Unidirectional and Radial In-Plane Flow of Fluids Through Woven Composite Reinforcements.
PB95-162004 *02,698*

Interaction between Micro and Macroscopic Flow in RTM Preforms.
PB95-162012 *03,159*

Report on the Workshop on Manufacturing Polymer Composites by Liquid Molding. Held in Gaithersburg, Maryland on September 20-22, 1993.
PB94-160066 *03,131*

SALIT, M. L.

Fourier Transform Atomic Emission Studies Using a Glow Discharge as the Emission Source.
PB94-185980 *00,533*

Integrating Automated Systems with Modular Architecture.
PB95-150231 *00,577*

Preparation and Certification of a Rhodium Standard Reference Material Solution.
PB94-185071 *00,529*

Wavelengths of Spectral Lines in Mercury Pencil Lamps.
PB96-176474 *04,376*

SALOMAN, E. B.

Autoionizing Resonances in Electric Fields.
PB94-212727 *03,853*

Interfaces in Mo/Si Multilayers.
PB96-160668 *02,423*

Labeling Conventions in Isoelectronic Sequences - Reply.
PB95-162574 *03,937*

National Institute of Standards and Technology Resonance Ionization Spectroscopy/Resonance Ionization Mass Spectroscopy Data Service.
PB94-172897 *03,793*

Resonance Ionization Spectroscopy/Resonance Ionization Mass Spectrometry Data Service. V-Data Sheets for Ga, Mn, Sc, and Tl.
PB96-158068 *00,625*

RIS Studies of Autoionization in Calcium.
PB94-213295 00,849

SALOMON, C.

Atoms in Optical Molasses.
PB95-108874 03,875

Atoms in Optical Molasses: Applications to Frequency Standards.
PB95-108882 03,876

Frequency-Stabilized LNA Laser at 1.083 mum: Application to the Manipulation of Helium 4 Atoms.
PB95-176186 04,304

Optical Molasses: Cold Atoms for Precision Measurements.
PB95-108890 03,877

Optical Molasses: The Coldest Atoms Ever.
PB95-108908 03,878

SALSBURY, J. G.

Development of an Automated Part Inspection System Using the DMIS Standard.
PB95-108866 02,899

SALTMAN, R. G.

Good Security Practices for Electronic Commerce, Including Electronic Data Interchange.
PB94-139045 01,463

Planning the Infrastructure for Global Electronic Commerce.
PB94-185832 00,494

SALZBORN, E.

Dielectronic Capture Processes in the Electron-Impact Ionization of Sc(2+).
PB95-203113 04,000

SAMI, S.

Nutritional Status and Growth in Juvenile Rheumatoid Arthritis.
PB94-198470 03,515

SAMOTYJ, M.

Important Link in Entire-House Protection: Surge Reference Equalizers.
PB94-216504 02,219

SAMS, R. L.

Radiocarbon Measurements of Atmospheric Volatile Organic Compounds: Quantifying the Biogenic Contribution.
PB97-122352 02,574

SAMUELSON, S.

Novel Bulk Iron Garnets for Magneto-Optic Magnetic Field Sensing.
PB95-180204 04,675

SANBORN, B. A.

Correction to the Decay Rate of Nonequilibrium Carrier Distributions Due to Scattering-in Processes.
PB94-185840 04,452

Cryogenic Precision Capacitance Bridge Using a Single Electron Tunneling Electrometer.
PB96-112271 02,072

Electron-electron Interactions, Coupled-Plasmon-Phonon Modes, and Mobility in n-Type GaAs.
PB96-138524 04,749

Nonequilibrium Total-Dielectric-Function Approach to the Electron Boltzmann Equation for Inelastic Scattering in Doped Polar Semiconductors.
PB96-138532 04,416

SANCHEZ, A.

Effects of Critical Current Density, Equilibrium Magnetization and Surface Barrier on Magnetization of High Temperature Superconductors.
PB94-185162 04,446

Effects of Critical Current Density, Equilibrium Magnetization and Surface Barrier on Magnetization of High Temperature Superconductors.
PB95-153060 04,588

Surface Barrier and Lower Critical Field in YBa2Cu3O7-delta Superconductors.
PB94-200128 04,478

SANDER, L.

Comparison of the Liquid Chromatographic Behavior of Selected Steroid Isomers Using Different Reversed-Phase Materials and Mobile Phase Compositions.
PB95-140976 00,574

Development of Engineered Stationary Phases for the Separation of Carotenoid Isomers.
PB95-150249 00,578

SANDER, L. C.

Analysis of SANS from Controlled Pore Glasses.
PB94-198843 03,035

Certification of Morphine and Codeine in a Human Urine Standard Reference Material.
PB95-176160 03,499

Characterization of Chemically Modified Pore Surfaces by Small Angle Neutron Scattering.
PB95-126181 00,898

Determination of Polycyclic Aromatic Hydrocarbons by Liquid Chromatography.
PB95-151650 00,585

Determination of 3-Quinuclidinyl Benzilate (Qnb) and Its Major Metabolites in Urine by Isotope Dilution Gas Chromatography Mass Spectrometry.
PB94-199379 03,492

Device for Subambient Temperature Control in Liquid Chromatography.
PB95-140604 00,573

Influence of Stationary Phase Chemistry on Shape Recognition in Liquid Chromatography.
PB96-123682 00,621

Isolation and Structural Elucidation of the Predominant Geometrical Isomers of alpha-Carotene.
PB96-190061 00,640

Liquid Chromatographic Determination of Carotenoids in Human Serum Using an Engineered C30 and a C18 Stationary Phase.
PB97-119333 03,512

Liquid Chromatographic Determination of Polycyclic Aromatic Hydrocarbon Isomers of Molecular Weight 278 and 302 in Environmental Standard Reference Materials.
PB95-164042 02,523

NIST Reference Materials to Support Accuracy in Drug Testing.
PB96-123807 03,505

Selectivity Trends in Packed Column Supercritical Fluid Chromatography with C18 Stationary Phases.
PB96-138581 00,622

Shape Selectivity Assessment of Stationary Phases in Gas Chromatography.
PB95-150256 00,579

Shape Selectivity in Reversed-Phase Liquid Chromatography for the Separation of Planar and Non-Planar Solutes.
PB95-162608 00,596

Standard Reference Materials for the Determination of Polycyclic Aromatic Hydrocarbons in Environmental Samples - Current Activities.
PB95-151668 00,586

Use of a Naphthylethylcarbamoylated- beta-Cyclodextrin Chiral Stationary Phase for the Separation of Drug Enantiomers and Related Compounds by Sub- and Supercritical Fluid Chromatography.
PB97-113260 00,653

SANDERS, J. A.

Ductile Fracture and Tempered Martensite Embrittlement of 4140 Steel.
PB96-190285 03,222

SANDERS, P. A.

Post-Occupancy Evaluation of the Forrestal Building.
PB97-111298 00,280

SANDERS, P. G.

Small Angle Neutrons Scattering from Nanocrystalline Palladium as a Function of Annealing.
PB95-176103 03,354

SANDERS, R. E.

Fire Service and Fire Sciences: A Winning Combination.
PB95-150264 01,383

SANDERS, S.

Insulating Nanoparticles on YBa2Cu3O7-delta Thin Films Revealed by Comparison of Atomic Force and Scanning Tunneling Microscopy.
PB95-150843 04,575

SANDERS, S. A.

NIST Serial Holdings, 1994.
PB94-178068 02,745

NIST Serial Holdings, 1995.
PB95-188926 02,746

NIST Serial Holdings, 1996.
PB96-172523 02,748

SANDERS, S. C.

Bias Current Dependent Resistance Peaks in NiFe/Ag Giant Magnetoresistance Multilayers.
PB97-112346 04,153

Effects of Etching on the Morphology and Surface Resistance of YBa2Cu3O7-delta Films.
PB96-135355 02,410

Evidence for Tunneling and Magnetic Scatttering at 'In situ' YBCO/Noble-Metal Interfaces.
PB96-141098 04,752

Growth of Laser Ablated YBa2Cu3O7-delta Films as Examined by Rheed and Scanning Tunneling Microscopy.
PB95-162541 04,614

Insulating Boundary Layer and Magnetic Scattering in YBa2Cu3O7-delta/Ag Interfaces Over a Contact Resistivity Range of 10(-8) - 10(-3) Omega cm(2).
PB95-169157 04,648

Low Magnetostriction in Annealed NiFe/Ag Giant Magnetoresistive Multilayers.
PB96-146691 04,762

Magnetic and Magnetoresistive Properties of Inhomogeneous Magnetic Dual-Layer Films.
PB95-169025 04,646

Magnetostriction and Giant Magnetoresistance in Annealed NiFe/Ag Multilayers.
PB96-102603 04,716

Models of Granualr Giant Magnetoresistance Multilayer Thin Films.
PB96-190228 01,968

Observation of Insulating Nanoparticles on YBCO Thin-Films by Atomic Force Microscopy.
PB95-163358 04,622

Oxygen Annealing of Ex-situ YBCO/Ag Thin-Film Interfaces.
PB96-141312 04,758

Size and Self-Field Effects in Giant Magnetoresistive Thin-Film Devices.
PB95-180188 04,674

Size Effects and Giant Magnetoresistance in Unannealed NiFe/Ag Multilayer Stripes.
PB97-111306 04,145

Size Effects in Submicron NiFe/Ag GMR Devices.
PB96-155510 02,237

Surface Degradation of Superconducting YBa2Cu3O7-delta Thin Films.
PB95-176095 04,667

Telegraph Noise in Silver-Permalloy Giant Magnetoresistance Test Structures.
PB96-146717 04,763

Thermally Activated Hopping of a Single Abrikosov Vortex.
PB95-140810 04,548

SANDLIN, A. C.

Surface Energy Reduction in Fibrous Monotectic Structures.
PB95-140828 03,150

SANFORD, N. A.

Distributed Feedback Lasers in Rare-Earth-Doped Phosphate Glass.
PB96-123773 04,740

Glasses for Waveguide Lasers.
PB96-111950 04,335

Integrated Optic Laser Emitting at 905, 1057, 1356 nm.
PB94-216298 02,136

Integrated Optic Laser Emitting at 906, 1057, and 1358 nm.
PB94-216280 02,135

Linewidth Narrowing in an Imbalanced Y-Branch Waveguide Laser.
PB95-140844 04,258

Nd:LiTaO3 Waveguide Laser.
PB95-140851 04,259

Passively Q-Switched Nd-Doped Waveguide Laser.
PB95-180048 04,308

Rare-Earth-Doped Waveguide Devices: The Potential for Compact Blue-Green Lasers.
PB95-140836 04,257

SANGRAS, R.

Mixing and Radiation Properties of Buoyant Luminous Flame Environments.
PB96-202254 01,432

SANSALONE, M.

Detection of Voids in Grouted Ducts Using the Impact-Echo Method.
PB94-185121 01,306

SANSONETTI, C. J.

Irradiances of Spectral Lines in Mercury Pencil Lamps.
PB96-176466 04,375

Measurements of the Resonance Lines of (6)Li and (7)Li by Doppler-Free Frequency-Modulation Spectroscopy.
PB96-180211 04,118

Spectrum and Energy Levels of Triply Ionized Barium (Ba IV).
PB95-140877 03,888

Wavelengths and Isotope Shifts for Lines of Astrophysical Interest in the Spectrum of Doubly Ionized Mercury (Hg III).
PB95-140869 03,887

Wavelengths of Spectral Lines in Mercury Pencil Lamps.
PB96-176474 04,376

SANTORE, M.

Using Torsional Dilatometry to Measure the Effects of Deformations on Physical Aging.
PB95-140901 03,384

SANTORE, M. M.

Aging in Glasses Subjected to Large Stresses and Deformations.
PB95-107041 03,235

Torsional Relaxation and Volume Response during Physical Aging in Epoxy Glasses Subjected to Large Torsional Deformations.
PB95-140026 03,383

Volume Recovery in Epoxy Glasses Subjected to Torsional Deformations: The Question of Rejuvenation.
PB95-140018 03,382

SANTORO, A.

Crystal Structure of Pb2Sr2YCu3O8+delta with delta=1.32, 1.46, 1.61, 1.71, by Powder Neutron Diffraction.
PB94-216314 04,518

Defective Structures of Barium Yttrium Copper Oxide (Ba2YCu3Ox) and Ba2YCu3-yMyOz (M=Fe, Co, Al, Ga, ..).
PB95-140034 04,537

Description of Layered Structures: Applications to High Tc Superconductors.
PB95-162624 04,615

Neutron Powder Diffraction Study of the Crystal Structure of YSr2AlCu2O7.
PB94-212073 04,499

Neutron Powder Diffraction Study of the Nuclear and Magnetic Structures of the Oxygen-Deficient Perovskite YBaCuCoO5.
PB95-161097 00,954

Neutron Powder Diffraction Study of the Structures of La1.9Ca1.1Cu2O6 and La1.9Sr1.1Cu2O6+Delta.
PB95-140042 04,538

Observation of Oscillatory Magnetic Order in the Antiferromagnetic Superconductor HoNi2B2C.
PB95-180303 04,679

Preparation, Crystal Structure, Dielectric Properties, and Magnetic Behavior of Ba2Fe2Ti4O13.
PB96-186176 01,162

Unconventional Ferromagnetic Transition in La(sub 1-x)Ca(sub x)MnO3.
PB97-112429 04,156

SANTORO, R. J.

Fundamental Mechanisms for CO and Soot Formation.
PB95-143160 01,380

Laser-Induced Fluorescence Measurements of OH. Concentrations in the Oxidation Region of Laminar, Hydrocarbon Diffusion Flames.
PB95-162160 01,387

Laser-Induced Fluorescence Measurements of OH in Laminar Diffusion Flames in the Presence of Soot Particles.
PB96-123120 01,409

Oxidation of Soot and Carbon Monoxide in Hydrocarbon Diffusion Flames.
PB95-150215 01,382

SAPAK, D. L.

Integrated Optic Laser Emitting at 905, 1057, 1356 nm.
PB94-216298 02,136

SAPIRSTEIN, J.

Evaluation of Two-Photon Exchange Graphs for Highly-Charged Heliumlike Ions.
PB94-198918 03,808

SAPRITSKY, V.

Comparison of Regular Transmittance Scales of Four National Standardizing Laboratories.
PB94-211232 04,233

Method of Realizing Spectral Irradiance Based on an Absolute Cryogenic Radiometer.
PB95-161204 04,270

Realization of New NIST Radiation Temperature Scales for the 1000 K to 3000 K Region, Using Absolute Radiometric Techniques.
PB94-172905 03,794

SAPRITSKY, V. I.

Precision High Temperature Blackbodies.
PB95-140059 03,885

Results of a NIST/VNIIOFI Comparison of Spectral-Radiance Measurements.
PB97-113021 04,159

SARUWATARI, M.

Multiwavelength Birefringent-Cavity Mode-Locked Fibre Laser.
PB95-150496 04,262

SASAGAWA, G. S.

Intracomparison Tests of the FG5 Absolute Gravity Meters.
PB96-102991 03,688

SASLOW, W. M.

Normal Modes and Structure Factor for a Canted Spin System: The Generalized Villain Model.
PB95-140067 04,539

SASSI, M. P.

Precise Optical Frequency References and Difference Frequency Measurements with Diode Lasers.
PB95-176228 04,305

SASTRY, K. V. L. N.

Millimeter- and Submillimeter-Wave Spectrum of trans-Ethyl Alcohol.
PB96-145578 01,102

SATHYAMURTHY, N.

Energy Dependence of Collision Characteristics in Molecule-Surface Collisions.
PB94-198504 00,786

SATIJA, S. K.

Diffraction of Neutron Standing Waves in Thin Films with Resonance Enhancement.
PB97-113278 04,164

Grazing Incidence Prompt Gamma Emissions and Resonance-Enhanced Neutron Standing Waves in a Thin-Film.
PB95-150470 03,892

Morphology of Symmetric Diblock Copolymers as Revealed by Neutron Reflectivity.
PB95-140075 01,234

Neutron Reflectivity of End-Grafted Polymers: Concentration and Solvent Quality Dependence in Equilibrium Conditions.
PB94-185758 01,206

Neutron Reflectivity Study of the Density Profile of a Model End-Grafted Polymer Brush: Influence of Solvent Quality.
PB95-202735 01,274

Observed Frustration in Confined Block Copolymers.
PB95-150033 01,238

Temperature Dependence of the Morphology of Thin Diblock Copolymer Films as Revealed by Neutron Reflectivity.
PB94-172756 01,199

SAUDER, D. A.

Challenges to the National Information Infrastructure: The Barriers to Product Data Sharing. National PDES Testbed Report Series.
PB95-136347 02,776

Structural EXPRESS Editor.
PB94-159795 02,769

SAUDER, D. G.

Product Kinetic Energies, Correlations, and Scattering Anisotropy in the Bimolecular Reactor O((1)D)+H2O yields 2OH.
PB94-212792 00,838

Product State Correlations in the Reaction of O((1)D) and H2O in Bimolecular Collisions and in O3.H2O Clusters--Translation.
PB95-153011 00,946

SAUERS, I.

Associative Electron Attachment to S2F10, S2OF10, and S2O2F10.
PB95-140992 00,907

Decomposition of SF6 and Production of S2F10 in Power Arcs.
PB96-122619 01,084

Investigation of S2F10 Production and Mitigation in Compressed SF6-Insulated Power Systems.
PB94-212388 02,467

Investigation of S2F10 Production and Mitigation in Compressed SF6- Insulated Power Systems.
PB96-155528 02,468

Measurement of S2OF10, and S2O2F10 Production Rates from Spark and Negative Glow Corona Discharge in SF6/O2 Gas Mixtures.
PB96-123740 01,093

SAUERWEIN, J. C.

NIST Standard Reference Data Products Catalog, 1994.
PB94-151842 00,727

NIST Standard Reference Data Products Catalog, 1995-96. Achieve with Standard Reference Data.
PB95-260808 01,057

SAUERWEIN, T.

Hierarchical Ada Robot Programming System (HARPS): A Complete and Working Telerobot Control System Based on the NASREM Model.
PB94-213162 02,934

SAUNDERS, B. V.

Boundary Conforming Grid Generation System for Interface Tracking.
PB94-158268 03,312

Boundary Conforming Grid Generation System for Interface Tracking.
PB96-103007 03,357

Portable Vectorized Software for Bessel Function Evaluation.
PB94-198975 01,690

SAUNDERS, C. A.

Manufactured Housing Walls That Provide Satisfactory Moisture Performance in All Climates.
PB95-178885 00,383

Test Procedures for Advanced Insulation Panels.
PB97-111892 00,415

SAUNDERS, M. H.

International Challenges in Defining the Public and Private Interest in Standards.
PB96-160361 00,498

ISO Environmental Management Standardization Efforts.
PB95-220513 02,524

ISO Environmental Management Standardization Efforts.
PB96-158662 02,528

SAUNDERS, R.

Method of Realizing Spectral Irradiance Based on an Absolute Cryogenic Radiometer.
PB95-161204 04,270

SAUNDERS, R. D.

Comparison of Filter Radiometer Spectral Responsivity with the NIST Spectral-Irradiance and Illuminance Scales.
PB97-113161 04,162

Precision High Temperature Blackbodies.
PB95-140059 03,885

Realization of New NIST Radiation Temperature Scales for the 1000 K to 3000 K Region, Using Absolute Radiometric Techniques.
PB94-172905 03,794

Results of a NIST/VNIIOFI Comparison of Spectral-Radiance Measurements.
PB97-113021 04,159

SAUNDERS, S. C.

Methodologies for Predicting the Service Lives of Coating Systems.
PB95-146387 03,124

SAUTER, G.

Intercomparison of Photometric Units Maintained at NIST (USA) and PTB (Germany), 1993.
PB95-261913 04,329

SAUVAGEAU, J. E.

Far-Infrared Kinetic Inductance Detector.
PB95-126348 02,142

Optical Performance of Photoinductive Mixers at Terahertz Frequencies.
PB95-168662 02,161

Optimization of ECR-Based PECVD Oxide Films for Superconducting Integrated Circuit Fabrication.
PB95-169165 02,051

Superconducting Integrated Circuit Fabrication with Low Temperature ECR-Based PECVD SiO2 Dielectric Films.
PB96-103015 04,719

Superconducting Kinetic Inductance Radiometer.
PB95-140083 02,144

Terahertz Detectors Based on Superconducting Kinetic Inductance.
PB95-168647 02,160

SAUVAJOL, J. L.

Inelastic-Neutron-Scattering Studies of Poly(p-phenylene vinylene).
PB95-180766 01,014

SAVAGE, B.

Deuterium in the Local Interstellar Medium: Its Cosmological Significance.
PB95-202842 00,081

SAVAGE, B. D.

Deuterium and the Local Interstellar Medium: Properties for the Procyon and Capella Lines of Sight.
PB96-200639 00,111

Goddard High-Resolution Spectrograph Observations of the Local Interstellar Medium and the Deuterium/Hydrogen Ratio along the Line of Sight Toward Capella.
PB94-213444 00,066

Observations of 3C 273 with the Goddard High Resolution Spectrograph on the Hubble Space Telescope.
PB95-202321 00,076

SAVAGE, D. A.

System for Calibration of the Marshall Compaction Hammer.
PB94-145661 01,303

SAVEANT, J. M.

Oxidation of 10-Methylacridan, a Synthetic Analogue of NADH and Deprotonation of Its Cation Radical. Convergent Application of Laser Flash Photolysis and Direct and Redox Catalyzed Electrochemistry to the Kinetics of Deprotonation of the Cation Radical.
PB94-198371 00,785

SAWANO, K.

Determination of Thermoactivation Parameters of Vortex Mobility in YBa2Cu3O7 Using Only Magnetic Measurements.
PB95-163499 04,624

SAWANT, S. B.

Continuous Counter-Current Two Phase Aqueous Extraction.
PB95-161212 00,675

Enzyme and Protein Mass Transfer Coefficient in Aqueous Two Phase Systems. 1. Spray Extraction Columns.
PB95-161162 00,594

Protein Extraction in a Spray Column Using a Polyethylene Glycol Maltodextrin Two-Phase Polymer System.
PB95-162228 00,595

Two Phase Aqueous Extraction: Rheological Properties of Dextran, Polyethylene Glycol, Bovine Serum Albumin and Their Mixtures.
PB95-161998 00,676

SAWIN, H. H.

Gaseous Electronics Conference Radio-Frequency Reference Cell: A Defined Parallel-Plate Radio-Frequency System for Experimental and Theoretical Studies of Plasma-Processing Discharges.
PB94-172327 04,404

SAWYER, D.

Interim Testing Artifact (ITA): A Performance Evaluation System for Coordinate Measuring Machines (CMMs). User Manual.
PB95-210589 02,914

NIST SRM 9983 High-Rigidity Ball-Bar Stand. User Manual.
PB95-255840 02,669

SAWYER, D. S.

User's Guide to NIST SRM 2084: CMM Probe Performance Standard.
PB94-206109 02,709

SAYEG, J. A.

Measurement of Absorbed Dose of Neutrons, and of Mixtures of Neutrons and gamma rays.
AD-A286 647/3 03,710

Use of a Radiochromic Detector for the Determination of Stereotactic Radiosurgery Dose Characteristics.
PB94-185642 03,514

SAYLOR, M. C.

ESR-Based Analysis in Radiation Processing.
PB95-161634 03,931

Radiation Process Data: Collection, Analysis, and Interpretation.
PB95-162632 03,628

SCACE, B. R.

Geometric Characterization of Rockwell Diamond Indenters.
PB95-203287 02,950

Microform Calibrations in Surface Metrology.
PB95-203295 02,951

Post-Process Control of Machine Tools.
PB95-203451 02,952

Present and Future Standard Specimens for Surface Finish Metrology.
PB97-110423 02,928

SCACE, R. I.

Development of a Standard Reference Material for Measurement of Interstitial Oxygen Concentration in Semiconductor Silicon by Infrared Absorption.
PB96-122668 *02,404*

Methodology for the Certification of Reference Specimens for Determination of Oxygen Concentration in Semiconductor Silicon by Infrared Spectrophotometry.
PB96-155478 *02,421*

SCANNELL, M. J.

Dose Mapping of Radioactive Hot Particles Using Radiochromic Film.
PB95-162954 *03,714*

SCAWTHORN, C.

Earthquake and Fire in Japan: When the Threat Became a Reality.
PB95-175238 *00,201*

SCHAAFSMA, D. T.

Comparative Photoluminescence Measurement and Simulation of Vertical-Cavity Semiconductor Laser Structures.
PB95-169173 *02,169*

Correlation of Optical, X-ray, and Electron Microscopy Measurements of Semiconductor Multilayer Structures.
PB95-175279 *02,174*

Cross-Sectional Photoluminescence and Its Application to Buried-Layer Semiconductor Structures.
PB96-141106 *02,415*

Measurement and Simulation of Photoluminescence Spectra from Vertical-Cavity Quantum-Well Laser Structures.
PB95-169181 *02,170*

Vertical-Cavity Semiconductor Lasers: Structural Characterization, CAD, and DFB Structures.
PB95-153193 *02,150*

Vertical-Cavity Semiconductor Structures: Materials Characterization.
PB95-153185 *02,149*

SCHABANEL, N.

Basic Linear Algebra Operations in SLI Arithmetic.
PB96-165931 *03,421*

SCHAEFER, M.

Optically Stabilized Tunable Diode-Laser System for Saturation Spectroscopy.
PB96-102819 *04,717*

Stabilization of 3.3 and 5.1 m Lead-Salt Diode Lasers by Optical Feedback.
PB95-180709 *04,313*

SCHAEFER, R. J.

Computation of Dendrites Using a Phase Field Model.
PB94-160744 *04,436*

Intelligent Processing of Hot Isostatic Pressing.
PB94-172913 *03,315*

Micromechanics of Densification and Distortion.
PB94-200326 *03,327*

Surface Energy Reduction in Fibrous Monotectic Structures.
PB95-140828 *03,150*

SCHAFER, K. J.

Intensity-Dependent Scattering Rings in High Order Above-Threshold Ionization.
PB96-110739 *04,032*

SCHAFFER, R.

History of NIST's Contributions to Development of Standard Reference Materials and Reference and Definitive Methods for Clinical Chemistry.
PB96-119706 *03,503*

SCHAFFT, H. A.

Electrical Characterization of Integrated Circuit Metal Line Thickness.
PB96-138433 *02,414*

Electrical Method for Determining the Thickness of Metal Films and the Cross-Sectional Area of Metal Lines.
PB95-203170 *02,370*

JEDEC 'TCR' Interlaboratory Experiment: Lessons Learned.
PB95-203188 *02,371*

Measurement of Patterned Film Linewidth for Interconnect Characterization.
PB96-148168 *02,420*

SCHANTZ, M.

Comparison of Methods for Gas Chromatographic Determination of PCBs and Chlorinated Pesticides in Marine Reference Materials.
PB95-140091 *02,584*

Development of Frozen Whale Blubber and Liver Reference Materials for the Measurement of Organic and Inorganic Contaminants.
PB95-151676 *00,587*

National Status and Trends Program Specimen Bank: Sampling Protocols, Analytical Methods, Results, and Archive Samples.
PB97-119226 *02,598*

SCHANTZ, M. M.

Certification of Polychlorinated Biphenyl Congeners and Chlorinated Pesticides in a Whale Blubber Standard Reference Material.
PB96-103023 *03,745*

Certification of Polycyclic Aromatic Hydrocarbons in a Marine Sediment Standard Reference Material.
PB96-111778 *02,592*

Certification of Standard Reference Material (SRM) 1941a, Organics in Marine Sediment.
PB96-123690 *02,593*

Comparison of Selectivities for PCBs in Gas Chromatography for a Series of Cyanobiphenyl Stationary Phases.
PB96-119458 *00,618*

Concentrations of Chlorinated Hydrocarbons, Heavy Metals and Other Elements in Tissues Banked by the Alaska Marine Mammal Tissue Archival Project.
PB95-209870 *02,590*

Determination of PCBs and Chlorinated Hydrocarbons in Marine Mammal Tissues.
PB95-162640 *03,744*

Investigations of Sulfur Interferences in the Extraction of Methylmercury from Marine Tissues.
PB96-190020 *03,482*

NIST Standard Reference Materials (SRMs) for Polychlorinated Biphenyl (PCB) Determinations and Their Applicability to Toxaphene Measurements.
PB95-140109 *02,585*

Quantitative Analysis of Selected PCB Congeners in Marine Matrix Reference Materials Using a Novel Cyanobiphenyl Stationary Phase.
PB96-111737 *02,591*

Standard Reference Materials for the Determination of Polycyclic Aromatic Hydrocarbons in Environmental Samples - Current Activities.
PB95-151668 *00,586*

Thermodynamics of the Hydrolysis of N-Acetyl-L-phenylalanine Ethyl Ester in Water and in Organic Solvents.
PB95-203386 *01,053*

Thermodynamics of the Hydrolysis of 3,4,5-Trihydroxybenzoic Acid Propyl Ester (n-Propylgallate) to 3,4,5-Trihydroxybenzoic Acid (Gallic Acid) and Propan-I-ol in Aqueous Media and in Toluene.
PB96-186143 *01,160*

SCHAPPACHER, J. B.

Line-Reflect-Match Calibrations with Nonideal Microstrip Standards.
PB96-176599 *02,242*

SCHAPS, S. R.

Determination of Sheet Steel Formability Using Wide Band Electromagnetic-Acoustic Transducers.
PB96-186036 *02,279*

Methods to Improve the Accuracy of On-Line Ultrasonic Measurement of Steel Sheet Formability.
PB96-186051 *02,281*

Safety Assessment of Railroad Wheels Through Roll-by Detection of Tread Cracks.
PB96-141254 *04,856*

Well-Shielded EMAT for On-Line Ultrasonic Monitoring of GMA Welding.
PB96-186077 *02,879*

SCHAUER, D. A.

EPR Dosimetry of Cortical Bone and Tooth Enamel Irradiated with X and Gamma Rays: Study of Energy Dependence.
PB97-110373 *03,639*

Experimental Validation of Radiopharmaceutical Absorbed Dose to Mineralized Bone Tissue.
PB94-199668 *03,617*

Exposure-to-Absorbed-Dose Conversion for Human Adult Cortical Bone.
PB97-110381 *03,640*

Overview of a Radiation Accident at an Industrial Accelerator Facility.
PB97-122485 *02,612*

Radiation Accident at an Industrial Accelerator Facility.
PB95-140117 *02,575*

SCHAUER, W.

Harmonic and Static Susceptibilities of YBa2Cu3O7.
PB95-161139 *04,599*

SCHEFER, J.

Characterization of the Structure of TbD2.25 at 70 K by Neutron Powder Diffraction.
PB96-160528 *01,130*

Neutron-Powder-Diffraction Study of the Long-Range Order in the Octahedral Sublattice of LaD2.25.
PB96-141155 *04,753*

SCHEIFLER, R. W.

X Window System, Version 11, Release 5.
PB96-169099 *01,769*

SCHEINFEIN, M. R.

Correlations of Modulation Noise with Magnetic Microstructure and Intergranular Interactions for CoCrTa and CoNi Thin Film Media.
PB94-212768 *04,509*

Laser Focusing of Atoms: A Particle Optics Approach.
PB94-216660 *03,870*

Micromagnetic Structure of Domains in Co/Pt Multilayers. 1. Investigations of Wall Structure.
PB95-162111 *04,610*

Surface Magnetic Microstructural Analysis Using Scanning Electron Microscopy with Polarization Analysis (SEMPA).
PB95-162657 *03,938*

SCHEN, M.

Advances in the Measurement of Polymer CTE: Micrometer- to Atomic-Scale Measurements.
PB96-180229 *03,390*

SCHEN, M. A.

Beyond the Technology Roadmaps: An Assessment of Electronic Materials Research and Development.
PB96-165998 *01,961*

Electronics Packaging Materials Research at NIST.
PB96-122692 *02,405*

Metrology and Data for Microelectronic Packaging and Interconnection: Results of a Joint Workshop on Materials Metrology and Data for Commercial Electrical and Optical Packaging and Interconnection Technologies. Held in Gaithersburg, Maryland on May 5-6, 1994. Volume 1. Results.
PB95-143111 *02,328*

Metrology and Data for Microelectronic Packaging and Interconnection: Results of a Joint Workshop on Materials Metrology and Data for Commercial Electrical and Optical Packaging and Interconnection Technologies. Held in Gaithersburg, Maryland on May 5-6, 1994. Volume 2. Presentation Material.
PB95-143327 *02,330*

Novel Polydiacetylenes Derived from Liquid Crystalline Monomers.
PB95-140125 *01,235*

SCHENCK, A.

Dynamics of Mu(+) in Sc and ScHx.
PB96-180021 *04,112*

SCHENCK, P. K.

Microstructure and Ferroelectric Properties of Lead Zirconate-Titanate Films Produced by Laser Evaporation.
PB94-199148 *04,470*

SCHIEBENER, P.

Formulation of the Refractive Index of Water and Steam.
PB95-140133 *00,900*

SCHIESSL, U.

Stabilization of 3.3 and 5.1 m Lead-Salt Diode Lasers by Optical Feedback.
PB95-180709 *04,313*

SCHILLER, S.

Combining Data from Independent Chemical Analysis Methods.
PB95-140141 *00,572*

SCHILLER, S. B.

Certification of Polychlorinated Biphenyl Congeners and Chlorinated Pesticides in a Whale Blubber Standard Reference Material.
PB96-103023 *03,745*

Certification of Polycyclic Aromatic Hydrocarbons in a Marine Sediment Standard Reference Material.
PB96-111778 *02,592*

Certification of Standard Reference Material (SRM) 1941a, Organics in Marine Sediment.
PB96-123690 *02,593*

Introduction of a NIST Instrument Sensitivity Standard Reference Material for X-Ray Powder Diffraction.
PB94-200318 *00,807*

Preparation and Monitoring of Lead Acetate Containing Drinking Water Solutions for Toxicity Studies.
PB94-193885 *00,538*

Standard Reference Material for the Measurement of Particle Mobility by Electrophoretic Light Scattering.
PB96-102488 *00,609*

Statistical Aspects of the Certification of Chemical Batch SRMs. Standard Reference Materials.
PB96-210877 *00,645*

SCHIMA, F. J.

Alpha-Particle and Electron Capture Decay of (209)Po.
PB96-186085 *04,119*

Assay of the Eluent from the Alumina-Based Tungsten-188-Rhenium-188 Generator.
PB94-200482 *03,829*

External Gamma-ray Counting of Selected Tissues from a Thorotrast Patient.
PB96-160254 *03,637*

Liquid-Scintillation Counting Techniques for the Standardization of Radionuclides Used in Therapy.
PB97-110084 *03,709*

New and Revised Half-Life Measurement Results.
PB96-160346 *00,695*

Standardization and Decay Scheme of Rhenium-186.
PB94-200490 *03,830*

Study of Laser Resonance Ionization Mass Spectrometry Using a Glow Discharge Source.
DE94018566 *03,308*

Study of Laser Resonance Ionization Mass Spectrometry Using a Glow Discharge Source.
PB96-123203 *03,360*

SCHINKE, R.

Nonadiabatic Effects in the Photoassociation of H2S.
PB95-151437 *00,934*

SCHLAG, E. W.

Doppler-Free Spectroscopy of Large Polyatomic Molecules and van der Waals Complexes.
PB96-119581 *04,339*

Van der Waals Bond Lengths and Electronic Spectral Shifts of the Benzene-Kr and Benzene-Xe Complexes.
PB95-151387 *00,932*

SCHLAGER, J. B.

High-Sensitivity Optical Sampling Using an Erbium-Doped Fiber Laser Strobe.
PB95-176111 *04,302*

Metrology Applications of Mode-Locked Erbium Fiber Lasers.
PB95-140158 *04,256*

Millimeter-Resolution Optical Time-Domain Reflectometry Using a Four-Wave Mixing Sampling Gate.
PB96-122700 *02,190*

Multiwavelength Birefringent-Cavity Mode-Locked Fibre Laser.
PB95-150496 *04,262*

Optical Sampling Using Nondegenerate Four-Wave Mixing in a Semiconductor Laser Amplifier.
PB96-122502 *02,076*

Optical Sampling Using Nondegenerate Four-Wave Mixing in a Semiconductor Laser Amplifier.
PB96-123609 *04,348*

Precise Laser-Based Measurements of Zero-Dispersion Wavelength in Single-Mode Fibers.
PB96-201124 *01,511*

SCHLENOFF, C.

Unified Process Specification Language: Requirements for Modeling Process.
PB97-116123 *02,850*

SCHLENOFF, C. I.

World Wide Web and Mosaic: User's Guide.
PB94-207354 *02,722*

SCHLUND, B.

New Physics-Based Model for Time-Dependent- Dielectric-Breakdown.
PB96-186093 *02,440*

New Physics-Based Model for Time-Dependent- Dielectric-Breakdown.
PB96-201132 *02,448*

SCHMIDT, J.

Frequency Dependence of the Emission from 2D Array Josephson Oscillators.
PB95-175147 *02,056*

SUSAN: SUperconducting Systems ANalysis by Low Temperature Scanning Electron Microscopy (LTSEM).
PB96-112065 *04,728*

SCHMIDT, J. W.

Near Critical Fluid Interfaces: A Comparison of Theory and Experiment.
PB95-140166 *00,901*

Operational Mode and Gas Species Effects on Rotational Drag in Pneumatic Dead Weight Pressure Gages.
PB95-140182 *00,903*

Structure of the Vapor-Liquid Interface Near the Critical Point.
PB95-140174 *00,902*

Thermodynamic Properties of CF3-CHF-CHF2, 1,1,1,2,3,3-Hexafluoropropane.
PB97-118384 *03,299*

Thermodynamic Properties of CHF2-CF2-CHF, 1,1,2,2,3-Pentafluoropropane.
PB97-118392 *03,300*

Thermodynamic Properties of CHF2-O-CHF2,Bis(difluoromethyl) Ether.
PB94-199569 *00,798*

SCHMIDT, M. A.

Thermal Isolation of High-Temperature Superconducting Thin Films Using Silicon Wafer Bonding and Micromachining.
PB96-135017 *02,408*

SCHMIDT, V.

Vibronic Coupling and Other Many-Body Effects in the 4sigmag(-1) Photoionization Channel of CO2.
PB95-162509 *00,962*

SCHMITT, C.

First Results from a Coordinated ROSAT, IUE, and VLA Study of RS CVn Systems.
PB94-213477 *00,069*

SCHMITT, J. H. M. M.

First Results from a Coordinated ROSAT, IUE, and VLA Study of RS CVn Systems.
PB94-213477 *00,069*

ROSAT All-Sky Survey of Active Binary Coronae. 1. Quiescent Fluxes for the RS Canum Venaticorum Systems.
PB95-202479 *00,077*

ROSAT All-Sky Survey of Active Binary Coronae. 2. Coronal Temperatures of the RS Canum Venaticorum Systems.
PB94-199601 *00,055*

Rotational Modulation and Flares on RS Canum Venaticorum and BY Draconis Stars. XVIII. Coordinated VLA, ROSAT, and IUE Observations of RS CVn Binaries.
PB96-102322 *00,089*

X-ray Emission from Chemically Peculiar Stars.
PB96-102256 *00,088*

SCHNATTERLY, S. E.

Soft-X-ray Damage to p-terphenyl Coatings for Detectors.
PB96-159611 *04,364*

SCHNEEMAN, R.

Framework for National Information Infrastructure Services.
PB95-103719 *02,723*

SCHNEEMAN, R. D.

Distributed Supercomputing Software: Experiences with the Parallel Virtual Machine - PVM.
PB94-163086 *01,680*

Porting Multimedia Applications to the Open System Environment.
PB94-172921 *02,721*

SCHNEEMEYER, L. F.

Increased Pinning Energies and Critical Current Densities in Heavy-Ion-Irradiated Bi2Sr2CaCu2O8 Single Crystals.
PB95-175352 *04,654*

SCHNEIDER, G. M.

Application of the Taylor Dispersion Method in Supercritical Fluids.
PB95-164323 *00,977*

SCHNEIDER, H. A.

Glass Temperature of Polymer Blends: Comparison of Both the Free Volume and the Entropy Predictions with Data.
PB95-140190 *01,236*

SCHNEIDER, J. A.

Computer Graphics Metafile (CGM): Procedures for NIST CGM Validation Test Service.
PB94-161809 *01,804*

Initial Graphics Exchange Specification (IGES): Procedures for the NIST IGES Validation Test Service.
PB95-171427 *02,780*

SCHNEIDER, M.

Extension of Heterodyne Frequency Measurements on OCS to 87 THz (2900 cm(-1)).
PB94-200680 *00,811*

Shape Selectivity Assessment of Stationary Phases in Gas Chromatography.
PB95-150256 *00,579*

Stabilization of 3.3 and 5.1 m Lead-Salt Diode Lasers by Optical Feedback.
PB95-180709 *04,313*

SCHNEIDER, R. J.

Comparative Study of Fe-C Bead and Graphite Target Performance with the National Ocean Sciences AMS (NOSAMS) Facility Recombinator Ion Source.
PB95-175790 *00,693*

SCHNEIDER, S.

Classification of Advanced Technical Ceramics.
N94-35335/6 *03,030*

New Materials, Advanced Ceramics and Standards.
PB95-140208 *03,047*

SCHNEIDERMAN, H.

Ground Vehicle Control at NIST: From Teleoperation to Autonomy.
N94-34037/9 *03,758*

Visual Road Following without 3-D Reconstruction.
PB95-161030 *01,591*

SCHNEIR, J.

Development of a Calibrated Atomic Force Microscope.
PB94-185683 *02,894*

Increasing the Value of Atomic Force Microscopy Process Metrology Using a High-Accuracy Scanner, Tip Characterization, and Morphological Image Analysis.
PB96-190293 *02,758*

Integration of Scanning Tunneling Microscope Nanolithography and Electronics Device Processing.
PB95-153359 *02,341*

Polyethylene Crystallized from an Entangled Solution Observed by Scanning Tunneling Microscopy.
PB95-107389 *01,232*

Progress Toward Accurate Metrology Using Atomic Force Microscopy.
PB96-146774 *02,417*

Scanning Tunneling Microscopy and Fabrication of Nanometer Scale Structures at the Liquid-Gold Interface.
PB95-140414 *00,904*

SCHOEN, F. J.

Physicochemical Characterization of Natural and Bioprosthetic Heart Valve Calcific Deposits: Implications for Prevention.
PB96-156039 *00,187*

Physicochemical Properties of Calcific Deposits Isolated from Porcine Bioprosthetic Heart Valves Removed from Patients Following 2-13 Years Function.
PB94-172863 *00,184*

SCHOLTEN, R. E.

Determination of Complex Scattering Amplitudes in Low-Energy Elastic Electron-Sodium Scattering.
PB94-216652 *03,869*

Laser-Focused Atomic Deposition.
PB95-161618 *04,604*

Laser Focused Atomic Deposition.
PB95-180659 *04,685*

Nanostructure Fabrication via Direct Writing with Atoms Focused in Laser Fields.
PB95-150272 *04,564*

Nanostructure Fabrication via Laser-Focused Atomic Deposition (Invited).
PB96-204094 *04,132*

Simple, Compact, High-Purity Cr Evaporator for Ultrahigh Vacuum.
PB94-216678 *04,520*

Spin-Resolved Elastic Scattering of Electrons from Sodium.
PB95-161774 *03,933*

Using Atom Optics to Fabricate Nanostructures.
PB96-141247 *04,757*

SCHON, K.

Digital Techniques in HV Tests - Summary of 1989 Panel Session.
PB94-216702 *02,035*

SCHONBERGER, E.

Determination of Vitamin K1 in Serum Using Catalytic-Reduction Liquid Chromatography with Fluorescence Detection.
PB96-138425 *03,506*

SCHOONOVER, R. M.

Application of the Electronic Balance in High Precision Pycnometry.
PB94-187564 *00,534*

Determination of Density of Mass Standards: Requirement and Method.
PB94-163078 *03,787*

Electronic Balance and Some Gravimetric Applications. (The Density of Solids and Liquids, Pycnometry and Mass).
PB94-163052 *03,785*

Examination of Parameters That Can Cause Error in Mass Determinations.
PB94-163037 *03,784*

Mass Unit Disseminated to Surrogated Laboratories Using the NIST Portable Mass Calibration Package.
PB94-142486 *03,781*

Piggyback Balance Experiment: An Illustration of Archimedes' Principles and Newton's Third Law.
PB94-163060 *03,786*

Use of the Electronic Balance for Highly Accurate Direct Mass Measurements Without the Use of External Mass Standards.
PB94-187713 *03,803*

SCHRACK, R. A.

Measurement of the (10)B(n, alpha1gamma)(7)Li Cross Section in the 0.3 to 4 MeV Neutron Energy Interval.
PB96-161799 *04,098*

Measurement of the (235)U(n,f) Reaction from Thermal to 1 keV.
PB95-140422 *03,886*

SCHRAMM, R. E.

Dynamometer-Induced Residual Stress in Railroad Wheels: Ultrasonic and Saw Cut Measurements. Report No. 30.
PB96-183199 *04,857*

Gas-Coupled, Pulse-Echo Ultrasonic Crack Detection and Thickness Gaging.
PB96-147129 *04,847*

Noncontact Ultrasonic Inspection of Train Rails for Stress.
PB95-162673 *04,851*

Residual Stress in Induction-Heated Railroad Wheels: Ultrasonic and Saw Cut Measurements. Report No. 28.
PB96-106992 *04,854*

Safety Assessment of Railroad Wheels by Residual Stress Measurements.
PB96-141114 *04,855*

Safety Assessment of Railroad Wheels Through Roll-by Detection of Tread Cracks.
PB96-141254 *04,856*

Ultrasonic Measurement of Residual Stress in Cast Steel Railroad Wheels.
PB95-169199 *04,852*

Ultrasonic Measurement of Residual Stress in Railroad Wheel Rims.
PB95-140430 *04,849*

SCHRANK, H. E.

Comparison of Ultralow-Sidelobe-Antenna Far-Field Patterns Using the Planar-Near-Field Method and the Far-Field Method.
PB96-200373 *02,015*

Planar Near-Field Measurements of Low-Sidelobe Antennas.
PB94-219235 *02,001*

SCHROEDER, L. W.

Crystal Structure of Dicalcium Potassium Trihydrogen Bis(pyrophosphate) Trihydrate.
PB94-216561 *00,152*

SCHROEDER, T. D.

Raman and Fluorescence Spectra Observed in Laser Microprobe Measurements of Several Compositions in the Ln-Ba-Cu-O System.
PB94-172210 *04,440*

SCHUBAUER, G. B.

Air Flow in the Boundary Layer of an Elliptic Cylinder.
AD-A297 391/5 *04,194*

SCHUDER, M. D.

High Resolution, Jet-Cooled Infrared Spectroscopy of (HCl)2: Analysis of nu1 and nu2 HCl Stretching Fundamentals, Interconversion Tunneling, and Mode-Specific Predissociation Lifetimes.
PB95-203196 *01,046*

High Resolution Near Infrared Spectroscopy of HCl-DCl and DCl-HCl: Relative Binding Energies, Isomer Interconversion Rates, and Mode Specific Vibrational Predissociation.
PB95-203212 *01,048*

Slit-Jet Near-Infrared Diode Laser Spectroscopy of (DCl)2: nu1, nu2 DCl Stretching Fundamentals, Tunneling Dynamics, and the Influence of Large Amplitude 'Geared' Intermolecular Rotation.
PB95-203204 01,047

SCHULTZ, A. E.

Performance of HUD-Affiliated Properties during the January 17, 1994 Northridge Earthquake.
PB95-174488 00,443

SCHULZ, F.

Open System Environment (OSE): Architectural Framework for Information Infrastructure.
PB96-146360 00,002

Open System Environments.
N94-36857/8 01,674

Open Systems Software Standards in Concurrent Engineering.
PB96-160932 01,758

SCHULZE, D. W.

Interfaces in Mo/Si Multilayers.
PB96-160668 02,423

SCHUMACHER, G. E.

Effects of Surface-Active Resins on Dentin/Composite Bonds.
PB95-140448 00,156

SCHUSTER, C. E.

Electrical Test Structure for Improved Measurement of Feature Placement and Overlay in Integrated Circuit Fabrication Processes.
PB95-164273 02,355

Review of Semiconductor Microelectronic Test Structures with Applications to Infrared Detector Materials and Processes.
PB94-212925 02,132

Semiconductor Measurement Technology: Test Structure Implementation Document: DC Parametric Test Structures and Test Methods for Monolithic Microwave Integrated Circuits (MMICs).
PB96-117692 02,399

SCHUTTE, C. L.

Environmental Durability of Glass-Fiber Composites.
PB95-203220 03,166

SCHWARTZ, L. H.

Glimpse of Materials Research in China: A Report from an Interagency Study Team on Materials Visiting China from June 19, 1995 to June 30, 1995.
PB96-112677 02,978

Industry and Government-Laboratory Cooperative R and D: An Idea Whose Time Has Come.
PB94-172939 02,970

Materials Science and Engineering Laboratory Annual Report, 1993. NAS-NRC Assessment Panel, April 21-22, 1994.
PB94-162534 02,969

Materials Science and Engineering Laboratory Annual Report, 1994. NAS-NRC Assessment Panel, April 6-7, 1995.
PB95-196697 02,976

Materials Science and Engineering Laboratory Annual Report, 1995. Technical Activities.
PB96-214754 03,009

Nondestructive Evaluation and Materials Processing.
PB95-140455 02,902

Recent VAMAS Activity in Ceramics.
PB95-162681 03,051

SCHWARTZ, L. M.

Cross-Property Relations and Permeability Estimation in Model Porous Media.
PB95-150280 04,205

Interfacial Transport in Porous Media: Application to dc Electrical Conductivity of Mortars.
PB96-146816 01,326

Transport and Diffusion in Three-Dimensional Composite Media.
PB95-176129 04,668

SCHWARTZ, M.

Halon Thermochemistry: 'Ab Initio' Calculations of the Enthalpies of Formation of Fluoromethanes.
PB96-175740 03,289

SCHWARTZ, S. J.

Isolation and Structural Elucidation of the Predominant Geometrical Isomers of alpha-Carotene.
PB96-190061 00,640

SCHWARZ, F. P.

Biological Thermodynamic Data for the Calibration of Differential Scanning Calorimeters: Dynamic Temperature Data on the Gel to Liquid Crystal Phase Transition of Dialkylphosphatidylcholine in Water Suspensions.
PB95-162707 03,464

Thermodynamic Analysis of Heparin Binding to Human Antithrombin.
PB94-199593 03,455

Thermodynamic and NMR Study of the Interactions of Cyclodextrins with Cyclohexane Derivatives.
PB94-185816 00,781

Thermodynamic Study of the Reactions of Cyclodextrins with Primary and Secondary Aliphatic Alcohols, with D- and L-Phenylalanine, and with L-Phenylalanineamide.
PB95-180873 01,016

Thermodynamics of the Binding of Galactopyranoside Derivatives to the Basic Lectin from Winged Bean (Psophocarpus Tetrogonolobus).
PB95-162715 03,465

SCHWARZACHER, W.

Concurrent Enhancement of Kerr Rotation and Antiferromagnetic Coupling in Epitaxial Fe/Cu/Fe Structures.
PB94-198769 04,466

Variation in Magnetic Properties of Cu/Fcc (001) Sandwich Structures.
PB95-141164 04,555

SCHWARZBEK, S. M.

Microwave Properties of YBa2Cu3O7-x Films at 35 GHz from Magnetotransmission and Magnetoreflection Measurements.
PB95-168977 04,643

SCHWARZENBACH, D.

Statistical Descriptors in Crystallography. 2. Report of a Working Group on Expression of Uncertainty in Measurement.
PB96-146824 04,764

SCHWENDIMAN, G. L.

Calibration and Performance of GafChromic DM-100 Radiochromic Dosemeters.
PB97-119291 00,703

SCIRE, F. E.

Metrology Standards for Advanced Semiconductor Lithography Referenced to Atomic Spacings and Geometry.
PB96-160718 02,424

SCOLES, G.

Sub-Doppler, Infrared Laser Spectroscopy of the Propyne 2nu1 Band: Evidence of z-Axis Coriolis Dominated Intramolecular State Mixing in the Acetylenic CH Stretch Overtone.
PB95-202941 01,037

SCOTT, H.

Recommendations on Selection of Vehicle-to-Roadside Communications Standards for Commercial Vehicle Operations.
PB94-195914 04,859

Vehicle-to-Roadside Communications for Commercial Vehicle Operations: Requirements and Approaches.
PB95-188827 04,860

SCOTT, H. A.

Control System Architecture for a Remotely Operated Unmanned Land Vehicle.
PB95-163200 03,759

Ground Vehicle Control at NIST: From Teleoperation to Autonomy.
N94-34037/9 03,758

Vehicle-Command Center Communications in a Robotic Vehicle System.
PB95-162723 03,665

SCOTT, J. L.

Comparing NIST-B 50 mm Orifice Meter Gas Data to the ANSI Equation.
PB95-169207 02,949

Cryogenic Flow Calibration in NIST.
PB96-161930 01,143

Flow Conditioner Tests for Three Orifice Flowmeter Sizes.
PB95-105540 04,201

Uncertainty Analysis of the NIST Nitrogen Flow Facility.
PB95-128906 02,608

SCOTT, R.

Preparation and Characterization of (6)LiF and (10)B Reference Deposits for the Measurement of the Neutron Lifetime.
PB95-108692 03,874

SCOTT, R. D.

Problems Related to the Determination of Mass Densities of Evaporated Reference Deposits.
PB95-163226 03,941

SCOTT, T. R.

Accurate Measurement of Optical Detector Nonlinearity.
PB95-203576 02,181

Automated Measurement of Nonlinearity of Optical Fiber Power Meters.
PB96-176540 04,110

Beam Analysis Round Robin.
PB94-212545 04,239

Deep-UV Excimer Laser Measurements at NIST.
PB96-141031 04,355

Error Propagation in Laser Beam Spatial Parameters.
PB95-180394 04,310

Laser-Beam Analysis Pinpoints Critical Parameters.
PB94-212552 04,240

Optical Density Measurements of Laser Eye Protection Materials.
PB96-190301 00,190

Optical Detector Nonlinearity: A Comparison of Five Methods.
PB95-169355 04,291

Optical Detector Nonlinearity: Simulation.
PB96-165378 02,199

Optical Power Meter Calibration Using Tunable Laser Diodes.
PB95-169256 04,290

Thermal Modeling and Analysis of Laser Calorimeters.
PB96-140405 04,354

Widths and Propagation of a Truncated Gaussian Beam.
PB95-168779 04,287

SCROGER, M. G.

Assessment of Uncertainties of Thermocouple Calibrations at NIST.
PB94-152691 03,782

SEAKINS, P. W.

Kinetics of the Reaction C2H + O2 from 193 to 350 K Using Laser Flash Kinetic Infrared Absorption Spectroscopy.
PB95-203055 01,043

Laser Flash Photolysis, Time-Resolved Fourier Transform Infrared Emission Study of the Reaction Cl + C2H5 yields HCl(v) + C2H4.
PB95-203238 01,049

Laser Flash Photolysis/Time-Resolved FTIR Emission Study of a New Channel in the Reaction of CH3+O: Production of CO(v).
PB95-164281 00,974

SEARS, T. J.

Far Infrared Laser Frequencies of CH3OD and N2H4.
PB96-119623 04,341

SEATON, M. J.

Papers on the Symposium on Collision Phenomena in Astrophysics, Geophysics, and Masers.
AD-A280 291/6 00,047

SECHOVSKY, V.

Magnetic Properties of Single-Crystalline UCu3Al2.
PB95-180717 04,686

SEESTROM, S. J.

Measurements of the (237)Np(n,f) Cross Section.
PB97-119069 04,173

SEETULA, J. A.

Kinetics of the Reaction of CCl3-Br-2 and the Thermochemistry of CCl3 Radical and Cation.
PB94-212115 00,824

SEILA, R. L.

Radiocarbon Measurements of Atmospheric Volatile Organic Compounds: Quantifying the Biogenic Contribution.
PB97-122352 02,574

SEILER, D. G.

Business and Manufacturing Motivations for the Developing of Analytical Technology and Metrology for Semiconductors.
PB96-161948 04,778

Characterization of Liquid-Phase Epitaxially Grown HgCdTe Films by Magnetoresistance Measurements.
PB96-123617 04,738

Characterization of LPE HgCdTe Film by Magnetoresistance.
PB96-157961 02,197

Characterization of Two-Dimensional Dopant Profiles: Status and Review.
PB96-119300 02,400

Characterization of Two-Dimensional Dopant Profiles: Status and Review.
PB97-110134 02,451

Electrical Characterization of Liquid-Phase Epitaxially Grown Single-Crystal Films of Mercury Cadmium Telluride by Variable-Magnetic-Field Hall Measurements.
PB95-175782 02,177

Electrical Characterization of Narrow Gap n-Type Bulk HgCdTe Single Crystals by Variable-Magnetic-Field Hall Measurements and Reduced-Conductivity-Tensor Analyses.
PB96-164199 01,146

Heavily Accumulated Surfaces of Mercury Cadmium Telluride Detectors: Theory and Experiment.
PB94-216074 02,134

Hg1-xCdxTe Characterization Measurements: Current Practice and Future Needs.
PB95-164299 02,157

High-Spatial-Resolution Resistivity Mapping Applied to Mercury Cadmium Telluride.
PB94-212917 02,131

Interface Roughness of Short-Period AlAs/GaAs Superlattices Studied by Spectroscopic Ellipsometry.
PB95-107215 02,137

Investigation of Mercury Interstitials in Hg(1-x)CdxTe Alloys Using Resonant Impact-Ionization Spectroscopy.
PB94-213485 02,133

Magneto-Transport Properties of HgCdTe.
PB95-175840 04,661

Mesoscopic Conductance Fluctuations in Large Devices.
PB96-119656 04,735

Multicarrier Characterization Method for Extracting Mobilities and Carrier Densities of Semiconductors from Variable Magnetic Field Measurements.
PB94-212776 02,317

Novel Magnetic Field Characterization Techniques for Compound Semiconductor Materials and Devices.
PB96-176458 02,433

Optical Characterization in Microelectronics Manufacturing.
PB95-169397 02,358

Optical Characterization of Materials and Devices for the Semiconductor Industry: Trends and Needs.
PB96-167192 02,431

Quantum Conductance Fluctuations in the Larger-Size-Scale Regime.
PB97-111264 04,144

RII Spectroscopy of Trap Levels in Bulk and LPE Hg1-xCdxTe.
PB96-160247 04,084

Semiconductor Measurement Technology: Improved Characterization and Evaluation Measurements for HgCdTe Detector Materials, Processes, and Devices Used on the GOES and TIROS Satellites.
PB94-188810 02,122

Semiconductor Measurement Technology: Survey of Optical Characterization Methods for Materials, Processing, and Manufacturing in the Semiconductor Industry.
PB96-154596 02,706

Transverse Magnetoresistance: A Novel Two-Terminal Method for Measuring the Carrier Density and Mobility of a Semiconductor Layer.
PB95-150066 02,332

SEILER, J.

Characteristics of Adhesive-Bonded Seams Sampled from EPDM Roof Membranes.
PB95-162491 00,377

Degradation of Powder Epoxy Coated Panels Immersed in a Saturated Calcium Hydroxide Solution Containing Sodium Chloride.
PB96-101050 01,344

Development of a Method for Measuring Water-Stripping Resistance of Asphalt/Siliceous Aggregate Mixtures.
PB96-197249 01,348

Development of a Method for Measuring Water-Stripping Resistance of Asphalt/Siliceous Aggregate Mixtures.
PB96-202296 01,329

SEILER, J. F.

Performance of Tape-Bonded Seams of EPDM Membranes: Comparison of the Peel Creep-Rupture Response of Tape-Bonded and Liquid-Adhesive-Bonded Seams.
PB96-183249 03,012

SEKERKA, R. F.

Effects of Crystalline Anisotropy and Buoyancy-Driven Convection on Morphological Stability.
PB94-200441 03,328

Stagnant Film Model of the Effect of Natural Convection on the Dendrite Operating State.
PB96-146832 04,765

SELIM, M. S.

Brownian Diffusion of Hard Spheres at Finite Concentrations.
PB95-164307 00,975

SELLECK, M. E.

Asymptotic Behavior of Modulated Taylor-Couette Flows with a Crystalline Inner Cylinder.
PB94-199072 04,469

Effect of Modulated Taylor-Couette Flows on Crystal-Melt Interfaces: Theory and Initial Experiments.
PB94-216736 04,521

SELLIN, I. A.

High-Energy Behavior of the Double Photoionization of Helium from 2 to 12 keV.
PB94-213279 03,860

SELTZER, S. M.

Calculation of Photon Mass Energy-Transfer and Mass Energy-Absorption Coefficients.
PB97-110399 04,137

Electron-Photon Monte Carlo Calculations: The ETRAN Code.
PB97-110407 04,138

Electron transport calculations with biomedical and environmental applications. Final report, December 23, 1992--January 31, 1994.
DE95007065 03,613

EPR Dosimetry of Cortical Bone and Tooth Enamel Irradiated with X and Gamma Rays: Study of Energy Dependence.
PB97-110373 03,639

Exposure-to-Absorbed-Dose Conversion for Human Adult Cortical Bone.
PB97-110381 03,640

Monte Carlo and Analytic Methods in the Transport of Electrons, Neutrons, and Alpha Particles.
PB96-111612 04,033

Pattern-Recognition Analysis of Low-Resolution X-Ray Fluorescence Spectra.
PB95-151924 00,588

Study of Multiple Scattering Background in Compton Scatter Imaging.
PB96-112222 04,425

Tables of X-ray Mass Attenuation Coefficients and Mass Energy-Absorption Coefficients 1 keV to 20 MeV for Elements Z = 1 to 92 and 48 Additional Substances of Dosimetric Interest.
PB95-220539 04,013

Tomographic Decoding Algorithm for a Nonoverlapping Redundant Array.
PB95-151932 01,842

Updated Calculations for Routine Space-Shielding Radiation Dose Estimates: SHIELDOSE-2.
PB95-171039 04,838

SELWYN, G.

Gaseous Electronics Conference Radio-Frequency Reference Cell: A Defined Parallel-Plate Radio-Frequency System for Experimental and Theoretical Studies of Plasma-Processing Discharges.
PB94-172327 04,404

SEMANCIK, S.

Conductance Response of Pd/SnO2(110) Model Gas Sensors to H2 and O2.
PB95-125803 00,892

Fundamental Studies of Gas Sensor Response Mechanisms: Palladium on SnO2(110).
PB95-162731 00,963

NIST Workshop on Gas Sensors: Strategies for Future Technologies. Proceedings of a Workshop. Held in Gaithersburg, Maryland on September 8-9, 1993.
PB95-210225 00,507

Reactivity of Pd and Sn Adsorbates on Plasma and Thermally Oxidized SnO2(110).
PB94-199973 00,804

Tin Oxide Gas Sensor Fabricated Using CMOS Micro-Hotplates and In-situ Processing.
PB95-150603 00,580

SEMERJIAN, H. G.

Combustion of Methanol and Methanol/Dodecanol Spray Flames.
PB95-108544 02,478

CSTL Technical Activities, 1994.
PB95-242319 00,608

CSTL Technical Activities, 1995.
PB96-214630 00,647

Effect of Dodecanol Content on the Combustion of Methanol Spray Flames.
PB95-176020 01,389

Elastic Scattering from Spheres under Non Plane-Wave Illumination.
PB96-163688 04,370

Experimental and Numerical Studies of Refractory Particle Formation in Flames: Application to Silica Growth.
PB95-152005 00,673

Parametric Investigation of Metal Powder Atomization Using Laser Diffraction.
PB95-108577 03,342

Simulation of Ceramic Particle Formation: Comparison with In-situ Measurements.
PB95-152013 00,674

Structure of a Swirl-Stabilized Kerosene Spray Flame.
PB95-108569 02,480

Study of Droplet Transport in Alcohol-Based Spray Flames Using Phase/Doppler Interferometry.
PB95-108551 02,479

SENEHI, M. K.

Control Entity Interface Specification.
PB94-191715 02,815

Feasibility Study: Reference Architecture for Machine Control Systems Integration.
PB94-142791 02,804

Reference Architecture for Machine Control Systems Integration: Interim Report.
PB95-144549 02,820

SENEKOWITSCH, J.

Bonding in Doubly Charged Diatomics.
PB95-164315 00,976

SENGERS, J. M. H.

Principle of Congruence and Its Application to Compressible States.
PB96-102892 01,068

SENGERS, J. M. H. L.

Application of the Taylor Dispersion Method in Supercritical Fluids.
PB95-164323 00,977

Critical Behavior of Ionic Fluids.
PB95-164331 00,978

Critical Lines for Type-III Aqueous Mixtures by Generalized Corresponding-States Models.
PB96-102371 01,063

Standard States, Reference States and Finite-Concentration Effects in Near-Critical Mixtures with Applications to Aqueous Solutions.
PB95-164349 00,979

Thermodynamic Behavior of the CO2-H2O System from 400 to 1000 K, up to 100 MPa and 30% Mole Fraction of CO2.
PB94-162245 00,736

SENGERS, J. V.

Critical Scaling Laws and a Classical Equation of State.
PB95-169249 00,990

Global Thermodynamic Behavior of Fluid Mixtures in the Critical Region.
PB94-212420 04,199

SENGUPTA, S.

Critical Current Density, Irreversibility Line, and Flux Creep Activation Energy in Silver-Sheathed Bi2Sr2Ca2Cu2Ox Superconducting Tapes.
PB95-162749 04,616

SEPICH, J. L.

Correlation of HgCdTe Epilayer Defects with Underlying Substrate Defects by Synchrotron X-Ray Topography.
PB94-200714 02,129

SERAPHIN, S.

Effect of Annealing Ambient on the Removal of Oxide Precipitates in High-Dose Oxygen Implanted Silicon.
PB95-164356 02,356

SERPA, F. G.

Observation and Visible and uv Magnetic Dipole Transitions in Highly Charged Xenon and Barium.
PB96-138441 04,056

SESHADRI, K.

Chemical Inhibition of Methane-Air Diffusion Flame.
PB96-195532 01,431

SETTLE-RASKIN, A. D.

National Semiconductor Metrology Program, Project Portfolio FY 1996.
PB96-195268 04,789

SHADDIX, C. R.

Computations of Enhanced Soot Production in Time-Varying CH4/Air Diffusion Flames.
PB97-119218 01,440

Laser Imaging of Chemistry-Flowfield Interactions: Enhanced Soot Formation in Time-Varying Diffusion Flames.
PB94-185352 01,364

Quantitative Measurements of Enhanced Soot Production in a Flickering Methane/Air Diffusion Flame.
PB95-203246 01,393

SHAFFNER, T. J.

Business and Manufacturing Motivations for the Developing of Analytical Technology and Metrology for Semiconductors.
PB96-161948 04,778

SHALER, T. A.

Lowest Excited Singlet State of Isolated 1-phenyl-1,3-butadiene and 1-phenyl-1,3,5-hexatriene.
PB95-202339 01,026

SHANNON, R. D.

Neutron Powder Diffraction Study of a Na, Cs-Rho Zeolite.
PB94-198629 00,791

SHAO, L.

Test of a Slow Off-Axis Parabola at Its Center of Curvature.
PB96-138482 04,352

SHAPIRO, S. M.

Anomalous Dispersion and Thermal Expansion in Lightly-Doped KTa1-xNbxO3.
PB95-152302 04,585

Low-Frequency Excitations of Oriented DNA.
PB96-137799 03,548

SHAPOVAL, V. I.

Precision High Temperature Blackbodies.
PB95-140059 03,885

SHARMA, J. K. N.

Intercomparison between NPL (India) and NIST (USA) Pressure Standards in the Hydraulic Pressure Region Up to 26 MPa.
PB96-113543 04,211

Intercomparison of the Effective Areas of a Pneumatic Piston Gauge Determined by Different Techniques.
PB94-212370 02,640

SHARPLESS, K.

Development of Engineered Stationary Phases for the Separation of Carotenoid Isomers.
PB95-150249 00,578

SHARPLESS, K. E.

Liquid Chromatographic Determination of Carotenoids in Human Serum Using an Engineered C30 and a C18 Stationary Phase.
PB97-119333 03,512

Methods for Analysis of Cancer Chemopreventive Agents in Human Serum.
PB95-200648 03,502

SHARPLESS, K. S.

Measurements of Indoor Pollutant Emissions from EPA Phase II Wood Stoves.
PB95-198735 02,556

Population Distributions and Intralaboratory Reproducibility for Fat-Soluble Vitamin-Related Compounds in Human Serum.
PB96-155536 00,624

SHASTRY, V.

Nonlocal Effects of Existing Dislocations on Crack-Tip Emission and Cleavage.
PB96-161807 03,367

SHATTIL, S.

Comparison of GPS Broadcast and DMA Precise Ephemerides.
AD-P009 114/0 01,518

Comparison of GPS Broadcast and DMA Precise Ephemerides.
N94-30660/2 01,523

SHAW, M. T.

Polymer Liquid Crystalline Materials.
PB94-212339 01,224

SHAW, P. S.

Measuring Nondipolar Asymmetries of Photoelectron Angular Distributions.
PB97-122493 01,193

SHECHTMAN, D.
Crystallographic Characterization of Some Intermetallic Compounds in the Al-Cr System.
PB94-198702 *03,318*

SHEEHAN, M. E.
Influence of Natural and Synthetic Inhibitors on the Crystallization of Calcium Oxalate Hydrates.
PB95-150967 *03,560*

SHELTON, D. B.
Helium Refrigeration and Liquefaction Using a Liquid Hydrogen Refrigerator for Precooling.
AD-A286 683/8 *02,749*

SHELTON, R. N.
Crystal Structure and Magnetic Ordering of the Rare-Earth and Cu Moments in RBa2Cu2NbO8(R=Nd,Pr).
PB95-140554 *04,546*

SHELUS, P. J.
Lunar Laser Ranging: A Continuing Legacy of the Apollo Program.
PB95-202495 *03,683*

SHEN, M. C.
Evaluation of Wear Resistant Ceramic Valve Seats in Gas-Fueled Power Generation Engines. Topical Report, December 1991-April 1994.
PB95-200218 *02,466*

Mechano-Chemical Model: Reaction Temperatures in a Concentrated Contact.
PB96-119466 *03,227*

Wear Modeling of Si-Based Ceramics.
PB97-122501 *03,112*

SHENG, Z.
Low-Temperature Elastic Constants of Y1Ba2Cu3O7.
PB95-168837 *04,642*

SHENKER, H.
Reference Tables for Thermocouples.
AD-A279 948/4 *02,614*

SHENTON, H. W.
Draft Guideline for Testing and Evaluation of Seismic Isolation Systems.
PB94-172947 *00,423*

Draft Guidelines for Pre-Qualification and Prototype Testing of Seismic Isolation Systems.
PB94-161940 *01,331*

Draft Guidelines for Quality Control Testing of Elastomeric Seismic Isolation Systems.
PB94-161734 *00,422*

Draft Guidelines for Quality Control Testing of Sliding Seismic Isolation Systems.
PB94-161957 *01,332*

Field Evaluation of the System for Calibration of the Marshall Compaction Hammer.
PB95-190674 *01,323*

Guidelines for Pre-Qualification, Prototype and Quality Control Testing of Seismic Isolation Systems.
PB96-193685 *01,347*

Performance of HUD-Affiliated Properties during the January 17, 1994 Northridge Earthquake.
PB95-174488 *00,443*

Summary and Results of the NIST Workshop on Proposed Guidelines for Testing and Evaluation of Seismic Isolation Systems. Held in San Francisco, California on July 25, 1994.
PB96-154901 *00,463*

System for Calibration of the Marshall Compaction Hammer.
PB94-145661 *01,303*

SHERN, R. J.
Effects on Whole Saliva of Chewing Gums Containing Calcium Phosphates.
PB95-153169 *03,563*

SHERWOOD, G. V.
Dimensional Characterization of Precision Coaxial Transmission Line Standards.
PB96-176482 *02,241*

SHI, D.
Critical Current Density, Irreversibility Line, and Flux Creep Activation Energy in Silver-Sheathed Bi2Sr2Ca2Cu2Ox Superconducting Tapes.
PB95-162749 *04,616*

SHIBATANI, T.
Thermochemistry of the Hydrolysis of L-arginine to (L-citrulline + Ammonia) and of the Hydrolysis of L-arginine to (L-ornithine + Urea).
PB95-150801 *03,463*

SHIBAYAMA, M.
Small Angle Neutron Scattering Studies on Chain Asymmetry of Coextruded Poly(Vinyl Alcohol) Film.
PB95-164372 *01,262*

Small Angle Neutron Scattering Study on Poly(N-Isopropyl Acrylamide) Gels Near Their Volume-Phase Transition Temperature.
PB95-164380 *01,263*

Small-Angle Neutron Scattering Study on Weakly Charged Temperature Sensitive Polymer Gels.
PB95-164398 *01,264*

SHIELDS, J.
One- and Two-Sided Burning of Thermally Thin Materials.
PB95-140935 *03,151*

SHIELDS, J. Q.
Conversion of a 2-Terminal-Pair Bridge to a 4-Terminal-Pair Bridge for Increased Range and Precision in Impedance Measurements.
PB97-119176 *02,103*

NIST Comparison of the Quantized Hall Resistance and the Realization of the SI Ohm Through the Calculable Capacitor.
PB97-119184 *02,291*

NIST Comparison of the Quantized Hall Resistance and the Realization of the SI Ohm Through the Calculable Capacitor. Conference Proceedings, June 17-20, 1996.
PB97-119192 *02,292*

SHIELDS, J. R.
Behavior of Mock-Ups in the California Technical Bulletin 133 Test Protocol: Fabric and Barrier Effects.
PB95-231585 *00,301*

Effect of Suppressants on Metal Fires.
PB96-109574 *01,402*

SHIH, A.
Lattice Position of Si in GaAs Determined by X-Ray Standing Wave Measurements.
PB95-164406 *04,632*

Surface Geometry of BaO on W(100): A Surface-Extended X-Ray-Absorption Fine-Structure Study.
PB95-164414 *00,980*

SHIH, C. K.
Summary Report: Workshop on Industrial Applications of Scanned Probe Microscopy (2nd). A Workshop Co-Sponsored by NIST, SEMATECH, ASTM E42.14, and the American Vacuum Society. Held in Gaithersburg, Maryland on May 2-3, 1995.
PB96-131602 *00,509*

Workshop Summary Report: Industrial Applications of Scanned Probe Microscopy. A Workshop Co-sponsored by NIST, SEMATECH, ASTM, E42.14, and the American Vacuum Society. Held in Gaithersburg, Maryland on March 24-25, 1994.
PB95-170387 *00,506*

SHIMIZU, M.
Pump-Induced Dispersion of Erbium-Doped Fiber Measured by Fourier-Transform Spectroscopy.
PB94-211935 *04,236*

SHIMIZU, R.
Activities of ISO Technical Committee 201 on Surface Chemical Analysis.
PB95-180824 *00,607*

Formation of Technical Committee 201 on Surface Chemical Analysis by the International Organization for Standardization.
PB95-108536 *00,568*

SHIN, H.
Damage Processes in Ceramics Resulting from Diamond Tool Indentation and Scratching in Various Environments.
PB96-102983 *03,065*

SHINDO, Y.
Elastic Constants and Microcracks in YBa2Cu3O7.
PB96-200761 *03,005*

SHINN, N. D.
Observation of a Stable Methoxy Intermediate on Cr(110).
PB95-164422 *00,981*

SHIRAI, T.
Spectral Data and Grotrian Diagrams for Highly Ionized Chromium, Cr V through Cr XXIV.
PB94-162369 *00,748*

Spectral Data for Highly Ionized Krypton, Kr V through Kr XXXVI.
PB96-145917 *01,115*

SHIRANE, G.
High-Energy Phonon Dispersion in La1.85Sr0.15CuO4.
PB96-138458 *04,748*

Neutron-Scattering Studies of the Two Magnetic Correlation Lengths in Terbium.
PB95-152328 *04,586*

Origin of the Second Length Scale Above the Magnetic Spiral Phase of Tb.
PB95-153698 *04,596*

SHIRLEY, E. L.
Photonic Band-Structure Effects for Low-Index-Contrast Two-Dimensional Lattices in the Near Infrared.
PB97-122469 *04,401*

Self-Consistent 'GW' and Higher-Order Calculations of Electron States in Metals.
PB97-119341 *01,189*

SHIRLEY, J.
NIST-7, the New US Primary Frequency Standard.
PB95-153458 *01,534*

SHIRLEY, J. H.
Error Analysis of the NIST Optically Pumped Primary Frequency Standard.
PB95-153482 *01,535*

Microwave Leakage as a Source of Frequency Error and Long-Term Instability in Cesium Atomic-Beam Frequency Standards.
PB95-180501 *01,541*

NIST Optically Pumped Cesium Frequency Standard.
PB94-211117 *03,835*

Velocity Distribution of Atomic Beams by Gated Optical Pumping.
PB95-180519 *01,542*

SHOBE, J.
Scattered Fractions of Dose from 18 and 25 MV X-ray Radiotherapy Linear Accelerators.
PB96-186101 *04,120*

SHOCK, E. L.
Summary of the Apparent Standard Partial Molal Gibbs Free Energies of Formation of Aqueous Species, Minerals, and Gases at Pressures 1 to 5000 Bars and Temperatures 25 to 1000C.
PB96-145891 *01,113*

SHOEMAKER, A. C.
Taguchi's Parameter Design: A Panel Discussion.
PB96-111802 *03,445*

SHORE, S. N.
Goddard High-Resolution Spectrograph Observations of the Local Interstellar Medium and the Deuterium/Hydrogen Ratio along the Line of Sight Toward Capella.
PB94-213444 *00,066*

Observations of 3C 273 with the Goddard High Resolution Spectrograph on the Hubble Space Telescope.
PB95-202321 *00,076*

Observing Stellar Coronae with the Goddard High Resolution Spectrograph. I. The dMe Star AU Microscopii.
PB96-102777 *00,092*

SHORTER, J. H.
Fragment State Correlations in the Dissociation of NO.HF(v=1).
PB95-164430 *00,982*

SHOUTE, L. C. T.
Fluoride Elimination Upon Reaction of Pentafluoroaniline with e (sub eq')(sup -), H, and OH Radicals in Aqueous Solution.
PB97-111314 *01,177*

Iodine Atoms and Iodomethane Radical Cations: Their Formation in the Pulse Radiolysis of Iodomethane in Organic Solvents, Their Complexes, and Their Reactivity with Organic Reductants.
PB95-162764 *00,965*

Reduction of Dinitrogen to Ammonia in Aqueous Solution Mediated by Colloidal Metals.
PB95-107074 *00,867*

Temperature Dependence of the Rate Constants for Reaction of Dihalide and Azide Radicals with Inorganic Reductants.
PB95-162756 *00,964*

Temperature Dependence of the Rate Constants for Reaction of Inorganic Radicals with Organic Reductants.
PB94-198280 *00,783*

Temperature Dependence of the Rate Constants for Reactions of the Carbonate Radical with Organic and Inorganic Reductants.
PB94-212206 *00,831*

SHUH, D. K.
Influence of Coadsorbed Potassium on the Electron-Stimulated Desorption of F(+), F(-), and F(*) from PF3 on Ru(0001).
PB96-157946 *04,072*

SHUKER, R.
Laser-Synchrotron Hybrid Experiments: A Photon to Tickle, A Photon to Poke.
PB96-157847 *03,704*

SHULL, K.
Neutron Scattering by Multiblock Copolymers of Structure (A-B)N-A.
PB94-211547 *01,219*

SHULL, R. D.
Enhanced Magnetocaloric Effect in Gd3Ga5-xFexO12.
PB94-185659 *04,450*

Magnetocaloric Effect in Nanocomposites.
PB95-162798 *04,618*

Magnetocaloric Effect in Rapidly Solidified Nd-Fe-Al-B Materials.
PB94-185667 *04,451*

Magnetocaloric Effect of Ferromagnetic Particles.
PB94-185857 *04,453*

Monte Carlo and Mean-Field Calculations of the Magnetocaloric Effect of Ferromagnetically Interacting Clusters.
PB94-172087 *03,201*

Nanocomposite Magnetic Materials.
PB95-162780 *04,617*

NIST Workshop on Nanostructured Material (1st): Report of an Industrial Workshop Conducted by the National Institute of Standards and Technology. Held in Gaithersburg, Maryland on May 14-15, 1992.
PB94-218567 *02,973*

Viewpoint: Nanocrystalline and Nanophase Materials.
PB94-185865 *04,454*

SHULTZ, A. E.
NIST Research Program on the Seismic Resistance of Partially-Grouted Masonry Shear Walls.
PB94-219052 *00,354*

SHUTO, K.
Preparation of 2-Dimensional Ultra Thin Polystyrene Film by Water Casting Method.
PB95-162806 *04,619*

SHY, J. T.

Improved Molecular Constants and Frequencies for the CO2 Laser from New High-J Regular and Hot-Band Frequency Measurements.
PB95-180634 *04,312*

SIBENER, S. J.

Precision Lifetime Measurements of Cs 6p (2)P1/2 and 6p (2)P3/2 Levels by Single-Photon Counting.
PB95-203816 *04,010*

Temperature Dependence and Anharmonicity of Phonons on Ni(110) and Cu(110) Using Molecular Dynamics Simulations.
PB94-185477 *04,449*

SICARRDI, M.

New 5 and 10 MHz High Isolation Distribution Amplifier.
PB96-190202 *01,510*

SIECK, B. A.

Deposition of Loosely Bound and Firmly Bound Fluorides on Tooth Enamel by an Acidic Gel Containing Fluorosilicate and Monocalcium Phosphate Monohydrate.
PB95-150710 *03,559*

Effects on Whole Saliva of Chewing Gums Containing Calcium Phosphates.
PB95-153169 *03,563*

SIECK, L. W.

Ionization Energy of Sulfur Pentafluoride and the Sulfur Pentafluoride-Fluorine Atom Bond Dissociation Energy.
PB95-162814 *00,966*

Proton Affinity Ladders from Variable-Temperature Equilibrium Measurements. 1. A Re-Evaluation of the Upper Proton Affinity Range.
PB94-216603 *00,861*

SIEGAL, W. O.

Atmospheric Reactivity of alpha-Methyl-Tetrahydrofuran.
PB95-163705 *02,548*

SIEGEL, R. W.

Small Angle Neutrons Scattering from Nanocrystalline Palladium as a Function of Annealing.
PB95-176103 *03,354*

SIEGRIST, T.

Ca1-xCuO2, a NaCuO2-Type Related Structure.
PB95-162822 *04,620*

SIEGWARTH, J. D.

Experimental plan to determine the performance of the Oak Ridge National Laboratory Cold Neutron Moderator. Final report, September 1, 1993--November 30, 1993.
DE95011352 *03,778*

Friction and Oxidative Wear of 440C Ball Bearing Steels Under High Load and Extreme Bulk Temperatures.
PB95-175253 *03,215*

SSME LOX Duct Flowmeter Design and Test Results.
PB96-161955 *04,826*

Thermal Hydraulic Tests of a Liquid Hydrogen Cold Neutron Source.
PB95-135570 *03,884*

Tribometer for Measurements in Hostile Environments.
PB95-180949 *02,967*

Vortex Shedding Flowmeters for SSME Ducts.
PB95-169215 *01,453*

SIES, R.

Manager's Guide for Monitoring Data Integrity in Financial Systems.
PB96-165915 *00,003*

SIES, R. F.

Self Monitoring Accounting Systems.
PB95-216602 *00,007*

SIEVERS, R. E.

High-Pressure Equilibrium Cell for Solubility Measurements in Supercritical Fluids.
PB95-175634 *00,998*

Solubilities of Copper(II) and Chromium(III) beta-Diketonates in Supercritical Carbon Dioxide.
PB96-164215 *01,147*

SIEW, C.

Procedure for the Study of Acidic Calcium Phosphate Precursor Phases in Enamel Mineral Formation.
PB95-164448 *03,564*

SIEWERT, T.

In-Space Welding: Visions and Realities.
PB95-163234 *04,830*

International Institute of Welding: Report on 1992 Actions.
PB94-185873 *02,856*

International Institute of Welding: Report on 1995 Actions.
PB96-158076 *02,874*

Through-the-Arc Sensing for Measuring Gas Metal Arc Weld Quality in Real Time.
PB95-164463 *02,908*

SIEWERT, T. A.

Computers in Welding: A Primer.
PB95-162863 *02,862*

Contact Tube Wear Detection in Gas Metal Arc Welding.
PB96-135330 *02,872*

Contributions of Out-of-Plane Material to a Scanned-Beam Laminography Image.
PB96-111786 *02,704*

Control of Gas-Metal-Arc Welding Using Arc-Light Sensing.
PB96-131461 *02,869*

Cryogenic Toughness of Austenitic Stainless Steel Weld Metals: Effect of Inclusions.
PB95-161261 *03,214*

Droplet Transfer Modes for a MIL 100S-1 GMAW Electrode.
PB95-209300 *02,867*

Effect of Charpy V-Notch Striker Radii on the Absorbed Energy.
PB96-141122 *03,365*

Effects of Copper, Nickel and Boron on Mechanical Properties of Low-Alloy Steel Weld Metals Deposited at High Heat Input.
PB96-135231 *03,363*

Electrode Extension Model for Gas Metal Arc Welding.
PB96-135074 *02,871*

Evaluation and Qualification Standards for an X-Ray Laminography System.
PB94-172954 *02,029*

IIW Commission V Quality Control and Quality Assurance of Welded Products Annual Report 1994/95.
PB95-198743 *02,866*

IIW Commission V Quality Control and Quality Assurance of Welded Products, Annual Report 1995/96.
PB96-191366 *02,880*

International Institute of Welding: Report on 1993 Actions.
PB94-185881 *02,857*

Mapping the Droplet Transfer Modes for an ER100S-1 GMAW Electrode.
PB96-190095 *03,295*

Materials Reliability. Technical Activities, 1995.
PB96-183082 *02,999*

Report on 1994 Actions of the International Institute of Welding.
PB96-138540 *02,873*

Sensing Droplet Detachment and Electrode Extension for Control of Gas Metal Arc Welding.
PB96-190160 *03,297*

Status Report: AWS Standards for Identifying Arc Welds (A91.1) and Recording Weld Data (A9.2).
PB95-162855 *02,861*

Through-the-Arc Sensing for Monitoring Arc Welding.
PB94-185899 *02,858*

Through-the-Arc Sensing for Real-Time Measurement of Gas Metal Arc Weld Quality.
PB95-162871 *02,863*

Welding for Cryogenic Service.
PB95-162889 *02,852*

What's Available in Welding Software.
PB96-158084 *02,875*

X-Ray Image Quality Indicator Designed for Easy Alignment.
PB95-164455 *02,907*

SIGGEL, M. R. F.

Inner-Valence States CO(+) between 22 eV and 46 eV Studied by High Resolution Photoelectron Spectroscopy and ab Initio CI Calculations.
PB95-180055 *03,961*

Photoelectron Study of Electronic Autoionization in Rotationally Cooled N2: The n=6 Member of the Hopfield Series.
PB95-163531 *00,971*

Shape-Resonance-Enhanced Continuum-Continuum Coupling in Photoionization of CO2.
PB95-164471 *00,983*

Vibrational Autoionization in H2: Vibrational Branching Ratios and Photoelectron Angular Distributions Near the v(+)=3 Threshold.
PB94-199577 *00,799*

Vibrationally Resolved Photoelectron Angular Distributions and Branching Ratios for the Carbon Dioxide Molecule in the Wavelength Region 685-795 Angstrom.
PB96-201207 *04,131*

SIJELMASSI, R.

PET and DINGO Tools for Deriving Distributed Implementations from Estelle.
PB95-203253 *01,727*

SIKDAR, S. K.

Continuous Counter-Current Two Phase Aqueous Extraction.
PB95-161212 *00,675*

Enzyme and Protein Mass Transfer Coefficient in Aqueous Two Phase Systems. 1. Spray Extraction Columns.
PB95-161162 *00,594*

Protein Extraction in a Spray Column Using a Polyethylene Glycol Maltodextrin Two-Phase Polymer System.
PB95-162228 *00,595*

Two Phase Aqueous Extraction: Rheological Properties of Dextran, Polyethylene Glycol, Bovine Serum Albumin and Their Mixtures.
PB95-161998 *00,676*

SILBERSTEIN, S.

Proficiency Tests for the NIST Airborne Asbestos Program, 1993.
PB96-106463 *00,610*

SILVA, A. M.

Design of a High-Pressure Ebulliometer, with Vapor-Liquid Equilibrium Results for the Systems CHF2Cl + CF3-CH3 and CF3-CH2F + CH2F2.
PB97-113229 *04,163*

Ebulliometers for Measuring the Thermodynamic Properties of Fluids and Fluid Mixtures.
DE94017817 *04,195*

Ebulliometric Measurement of the Vapor Pressure of 1-Chloro-1,1-Difluoroethane and 1,1-Difluoroethane.
PB95-164489 *00,984*

Measurements of the Vapor Pressures of Difluoromethane, 1-Chloro-1,2,2,2-Tetrafluoroethane, and Pentafluoroethane.
PB95-169272 *03,270*

SILVA, T.

Magnetoresistance of Thin-Film NiFe Devices Exhibiting Single-Domain Behavior.
PB96-147087 *04,766*

SILVA, T. J.

Dependence of Contrast on Probe/Sample Spacing with the Magneto-Optic Kerr-Effect Scanning Near-Field Optical Microscope (MOKE-SNOM).
PB96-138557 *04,750*

Observation of the Transverse Second Harmonic Magneto-Optic Kerr Effect from Ni81Fe19 Thin Film Structures.
PB96-200332 *01,971*

SILVER, J. D.

Photographic Response to X-Ray Irradiation. 3. Photographic Linearization of Beam-Foil Spectra.
PB94-200102 *03,823*

SILVER, R. M.

Junction Locations by Scanning Tunneling Microscopy: In-Air-Ambient Investigation of Passivated GaAs pn Junctions.
PB94-185964 *02,306*

SIMAKHODSKIY, I.

Mapping Integration Definition for Information Modeling (IDEF1X) Model into CASE Data Interchange Format (CDIF) Transfer File.
PB95-154670 *01,711*

SIMAKHODSKIY, I. V.

Mapping Integration Definition for Function Modeling (IDEFO) Model into CASE Data Interchange Format (CDIF) Transfer File.
PB96-109533 *01,741*

SIMIC, M. G.

Standard Reference Materials (SRM's) for Measuring Genetic Damage.
PB94-198827 *03,516*

SIMIU, E.

Algebraic Approximation of Attractors for Galloping Oscillators.
PB95-162897 *04,820*

Assessment of 'Peaks Over Threshold' Methods for Estimating Extreme Value Distribution Tails.
PB95-161360 *00,441*

Chaotic Motions of Coupled Galloping Oscillators and Their Modeling as Diffusion Progresses.
PB96-122718 *04,823*

Deterministic and Stochastic Chaos.
PB96-156138 *00,218*

Development of Computer-Based Models of Standards and Attendant Knowledge-Base and Procedural Systems.
PB96-155783 *00,464*

Estimates of Hurricane Wind Speeds by the 'Peaks Over Threshold' Method.
PB96-162540 *00,471*

Exits in Multistable Systems Excited by Coin-Toss Square-Wave Dichotomous Noise: A Chaotic Dynamics Approach.
PB96-160650 *04,824*

Experimental and Numerical Chaos in Continuous Systems: Two Case Studies.
PB96-156146 *00,219*

Extreme Value Theory and Applications: Proceedings of the Conference on Extreme Value Theory and Applications, Volume 3. Held in Gaithersburg, Maryland in May 1993.
PB95-104956 *03,432*

Extreme Wind Distribution Tails: A 'Peaks Over Threshold' Approach.
PB95-219416 *00,127*

Extreme Wind Estimates by the Conditional Mean Exceedance Procedure.
PB95-220471 *00,120*

Extreme Winds Estimation by 'Peaks Over Threshold' and Epochal Methods.
PB96-159686 *00,468*

Foias-Temam Approximations of Attractors for Galloping Oscillators.
PB94-198298 *04,817*

Melnikov Function and Homoclinic Chaos Induced by Weak Perturbations.
PB95-180923 *03,414*

Modeling of Extreme Loading by 'Peaks Over Threshold' Methods.
PB96-159694 *00,469*

Necessary Condition for Homoclinic Chaos Induces by Additive Noise.
PB96-155775 *04,063*

Noise-Induced Chaos and Phase Space Flux.
PB95-125761 03,433

Noise-Induced Transitions to Chaos.
PB96-156120 00,217

Noise Modeling and Reliability of Behavior Prediction for Multi-Stable Hydroelastic Systems.
PB96-111943 04,822

Non-Gaussian Noise Effects on Reliability of Multistable Systems.
PB96-122726 04,213

Recent Approaches to Extreme Value Estimation with Application to Wind Speeds. Part 1. The Pickands Method.
PB94-213170 00,019

Spectrum of the Stochastically Forced Duffing-Holmes Oscillator.
PB96-155767 00,216

Transitions to Chaos Induced by Additive and Multiplicative Noise.
PB96-155759 03,750

SIMMON, E.

Active High Voltage Divider with 20-PPM Uncertainty.
PB97-119317 02,104

SIMMON, E. D.

Optical Current Transducer for Calibration Studies.
PB94-185907 02,121

SIMMONDS, M. B.

24 GHz Josephson Array Voltage Standard.
PB94-211588 02,033

SIMMONS, A.

High-Spatial-Resolution Resistivity Mapping Applied to Mercury Cadmium Telluride.
PB94-212917 02,131

SIMMONS, J. A.

Leady Axisymmetric Modes in Infinite Clad Rods. Part 1.
PB95-162905 04,187

SIMMONS, J. D.

Should NIST Accredit U.S. Calibration Laboratories.
PB95-107280 02,646

SIMON, H.

Beyond the Technology Roadmaps: An Assessment of Electronic Materials Research and Development.
PB96-165998 01,961

SIMON, L. N.

U.S. Green Building Conference, 1994.
PB94-206364 02,519

SIMON, N. J.

Cryogenic Properties of Inorganic Insulation Materials for ITER Magnets: A Review.
PB95-198768 03,706

Influence of Specimen Absorbed Energy in LOX Mechanical-Impact Tests.
PB95-107355 03,341

Irradiation Damage in Inorganic Insulation Materials for ITER Magnets: A Review.
PB95-147351 03,705

Macro- and Microreactions in Mechanical-Impact Tests of Aluminum Alloys.
PB95-107348 03,340

Reaction Sensitivities of Al-Li Alloys and Alloy 2219 in Mechanical-Impact Tests.
PB94-172764 03,314

Recommended Changes in ASTM Test Methods D2512-82 and G86-84 for Oxygen-Compatibility Mechanical Impact Tests on Metals.
PB94-216694 03,338

Temperature Increases in Aluminum Alloys during Mechanical-Impact Tests for Oxygen Compatibility.
PB94-172962 03,316

SIMON, T.

Distant Future of Solar Activity: A Case Study of Beta Hydri. 3. Transition Region, Corona, and Stellar Wind.
PB94-185220 00,049

Distant Future of Solar Activity: A Case Study of beta Hydri. 3. Transition Region, Corona, and Stellar Wind.
PB95-153441 00,074

Efficient Way of Identifying New Active Stars: A VLA Survey of X-ray Selected Active Stellar Candidates.
PB96-122882 00,099

Far-Ultraviolet Flare on a Pleiades G Dwarf.
PB96-102033 00,086

Four Years of Monitoring alpha Orionis with the VLA: Where Have All the Flares Gone.
PB94-185212 00,048

Radio Continuum and X-Ray Properties of the Coronae of RS Canum Venaticorum and Related Active Binary Systems.
PB94-211083 00,057

Sleuthing the Dynamo: HST/FOS Observations of UV Emissions of Solar-Type Stars in Young Clusters.
PB96-122817 00,098

SIMONI, F. V.

Effect of Two Initiator/Stabilizer Concentrations in a Metal Primer on Bond Strengths of a Composite to a Base Metal Alloy.
PB94-172723 00,141

SIMONS, D.

Relative Sensitivity Factors and Useful Yields for a Microfocused Gallium Ion Beam and Time-of-Flight Secondary Ion Mass Spectrometer.
PB94-198736 00,541

SIMONS, D. S.

Effect of Annealing Ambient on the Removal of Oxide Precipitates in High-Dose Oxygen Implanted Silicon.
PB95-164356 02,356

Molecular Ion Imaging and Dynamic Secondary Ion Mass Spectrometry of Organic Compounds.
PB95-126124 00,571

Range Statistics and Rutherford Backscattering Studies on Fe-Implanted In0.53Ga0.47As.
PB95-126397 04,535

Transition Metal Implants in In0.53GA0.47As.
PB95-126389 04,534

SIMONS, G. R.

Opportunities for Innovation: Advanced Manufacturing Technology.
PB94-100278 02,801

SIMPSON, J. A.

Metrology.
PB95-164497 03,946

SIMPSON, M. D.

Effects of Aluminum Oxalate/Glycine Pretreatment Solutions on Dentin Permeability.
PB95-164505 03,565

SINGER, A. T.

Interim Testing Artifact (ITA): A Performance Evaluation System for Coordinate Measuring Machines (CMMs). User Manual.
PB95-210589 02,914

SINGH, K.

2nu9 Band of Propyne-d3.
PB95-164513 00,985

SINGH, S.

Resonance Fluorescence with Squeezed-Light Excitation.
PB95-203469 04,322

SINHA, K.

Epitaxial Growth and Characterization of the Ordered Vacancy Compound CuIn3Se5 on GaAs (100) Fabricated by Molecular Beam Epitaxy.
PB95-180725 04,687

SINHA, S. K.

Neutron Reflectivity of End-Grafted Polymers: Concentration and Solvent Quality Dependence in Equilibrium Conditions.
PB94-185758 01,206

Neutron Scattering Study of Antiferromagnetic Order in the Magnetic Superconductors RNi2B2C.
PB97-112411 04,812

Small-Angle Neutron Scattering (SANS) Study of Worm-Like Micelles Under Shear.
PB96-176698 04,111

SIROHEY, S.

Human and Machine Recognition of Faces: A Survey.
PB96-111687 01,854

SIROHEY, S. A.

Face Recognition Technology for Law Enforcement Applications.
PB94-207768 01,837

SIVAKUMAR, A.

Deposition of Colloidal Sintering-Aid Particles on Silicon Nitride.
PB94-216272 03,044

SIVATHANU, Y. R.

Exits in Multistable Systems Excited by Coin-Toss Square-Wave Dichotomous Noise: A Chaotic Dynamics Approach.
PB96-160650 04,824

Investigation of Oil and Gas Well Fires and Flares.
PB94-193976 03,695

Tomographic Reconstruction of the Moments of Local Probability Density Functions in Turbulent Flow Fields.
PB96-180195 04,219

SJOLIN, L.

Crystal Packing Interactions of Two Different Crystal Forms of Bovine Ribonuclease A.
PB95-152823 00,943

SKAMSER, D. J.

Calculation of the Thermal Conductivity and Gas Permeability in a Uniaxial Bundle of Fibers.
PB95-180931 03,058

SKANTHAKUMAR, S.

Field Dependence of the Magnetic Ordering of Cu in R2CuO4 (R = Nd, Sm).
PB95-164521 04,633

Observation of Noncollinear Magnetic Structure for the Cu Spins in Nd2CuO4-Type Systems.
PB95-164539 04,634

SKEELS, J.

Group 1 for the Plant Spatial Configuration STEP Application Protocol.
PB96-165402 02,789

SKIENA, S. S.

Point Probe Decision Trees for Geometric Concept Classes.
PB96-160817 01,612

SKINNER, S. L.

High Sensitivity Survey of Radio Continuum Emission in Herbig Ae/Be Stars.
PB94-185915 00,051

SKOCPOL, W. J.

Coexistence of Grains with Differing Orthorhombicity in High Quality YBa2Cu3O7-delta Thin Films.
PB96-135033 04,742

Increased Transition Temperature in In situ Coevaporated YBa2Cu3O7-delta Thin Films by Low Temperature Post-Annealing.
PB95-180071 04,672

Thermal Noise in High-Temperature Superconducting-Normal-Superconducting Step-Edge Josephson Junctions.
PB95-175089 04,650

SKOWYRA, D.

DnaJ, DnaK, and GrpE Heat Shock Proteins are Required in 'ori'P1 DNA Replication Solely at the RepA Monomerization Step.
PB97-119382 03,557

SKRTIC, D.

Bioactive Polymeric Dental Materials Based on Amorphous Calcium Phosphate.
PB96-147012 03,572

Effect of 1-Hydroxyethylidene-1,1-Bisphosphonate on Membrane-Mediated Calcium Phosphate Formation in Model Liposomal Suspensions.
PB95-169223 03,469

In vitro Inhibition of Membrane-Mediated Calcification by Novel Phosphonates.
PB96-201140 03,595

Membrane-Mediated Precipitation of Calcium Phosphate in Model Liposomes with Matrix Vesicle-Like Lipid Composition.
PB95-164547 03,468

Polymeric Calcium Phosphate Composites with Remineralization Potential.
PB96-155544 03,575

Remineralizing Dental Composites Based on Amorphous Calcium Phosphate.
PB96-147020 03,573

SLABACK, L. A.

Characterization of a Health Physics Instrument Calibration Range.
PB95-164554 03,629

Germanium Detector Optimization of MDA for Efficiency vs. Low Intrinsic Background.
PB94-199155 00,543

SLABACK, L. S.

External Gamma-ray Counting of Selected Tissues from a Thorotrast Patient.
PB96-160254 03,637

SLAUGHTER, J. M.

Interfaces in Mo/Si Multilayers.
PB96-160668 02,423

SLEIGHT, A. W.

Colossal Magnetoresistance without Mn(3+)/Mn(4-) Double Exchange in the Stoichiometric Pyrochlore Tl2Mn2O7.
PB97-113070 04,160

SLEZSAK, I.

Oscillometric and Conductometric Analysis of Aqueous and Organic Dosimeter Solutions.
PB96-135256 04,054

SLIFKA, A. J.

Friction and Oxidative Wear of 440C Ball Bearing Steels Under High Load and Extreme Bulk Temperatures.
PB95-175253 03,215

Tribological Behavior of 440/Diamond-Like-Carbon Film Couples.
PB96-119714 03,019

Tribometer for Measurements in Hostile Environments.
PB95-180949 02,967

Wear Mechanism Maps of 440C Martensitic Stainless Steel.
PB96-111810 04,834

SLOTWINSKI, J. A.

NIST Calibration of ASTM E127-Type Ultrasonic Reference Blocks.
PB94-191640 02,702

Ultrasonic Measurements of Surface Roughness.
PB94-172137 04,181

Ultrasonic NDE of Sprayed Ceramic Coatings.
PB96-201157 02,761

SLOWIKOWSKA, H.

Modification of Cast Epoxy Resin Surfaces during Exposure to Partial Discharges.
PB96-122734 01,086

SLOWIKOWSKI, J.

Modification of Cast Epoxy Resin Surfaces during Exposure to Partial Discharges.
PB96-122734 01,086

SLUPPHAUG, G.

Novel Activities of Human Uracil DNA N-glycosylase for Cytosine-Derived Products of Oxidative DNA Damage.
PB96-164132 03,479

SMALL, J. A.

Addition of M and L-Series Lines to NIST Algorithm for Calculation of X-Ray Tube Output Spectral Distributions.
PB95-108742 00,569

SMATHERS, D.
Transverse stress effect on the critical current of internal tin and bronze process Nb(sub 3)Sn superconductors.
DE95016659 *04,434*

SMID, M. E.
Response to Comments on the NIST Proposed Digital Signature Standard.
PB96-161815 *01,615*

SMILGYS, R. V.
Laser Gas Ionization Technique Monitors MEB Crystal Growth.
PB96-112172 *01,076*

Reactive Coevaporation of DyBaCuO Superconducting Films: The Segregation of Bulk Impurities on Annealed MgO(100) Substrates.
PB95-164562 *04,635*

Single-Photon Laser Ionization Time-of-Flight Mass Spectroscopy Detection in Molecular-Beam Epitaxy: Application to As4, As2, and Ga.
PB95-203337 *01,052*

Vibrational Distributions of As2 in the Cracking of As4 on Si(100) and Si(111).
PB94-198314 *00,784*

SMIRL, A. L.
Interdigitated Stacked P-I-N Multiple Quantum Well Modulator.
PB97-112296 *02,455*

Scaling of the Nonlinear Optical Cross Sections of GaAs-AlGaAs Multiple Quantum-Well Hetero n-i-p-i's.
PB96-102793 *02,183*

Time-Resolved Measurements of the Polarization State of Four-Wave Mixing Signals from GaAs Multiple Quantum Wells.
PB96-201058 *04,796*

SMITH, A. B.
Discontinuous Volume Change at the Orientational-Ordering Transition in Solid C60.
PB94-211828 *00,821*

Neutron-Scattering Study of Librations and Intramolecular Phonons in Rb2.6K0.4C60.
PB95-162269 *00,958*

SMITH, A. C. H.
Backscattering in Electron-Impact Excitation of Multiply Charged Ions.
PB94-185345 *03,799*

Collisions of Electrons with Highly-Charged Ions.
PB96-200340 *04,791*

Electron-Impact Excitation of Si(3+)(3S yields 3P) Using a Merged-Beam Electron-Energy-Loss Technique.
PB95-151239 *03,904*

Evidence for Significant Backscattering in Near-Threshold Electron-Impact Excitation of Ar(7+)(3s yields 3p).
PB95-126405 *03,883*

Merged-Beams Energy-Loss Technique for Electron-Ion Excitation: Absolute Total Cross Sections for O(5+) (2s yields 2p).
PB96-102058 *04,017*

SMITH, A. J.
Bibliography of the NIST Optoelectronics Division.
PB96-128210 *02,193*

Bibliography of the NIST Optoelectronics Division.
PB97-116040 *02,207*

Metrology for Electromagnetic Technology: A Bibliography of NIST Publications.
PB95-135588 *02,143*

SMITH, A. M.
Observations of 3C 273 with the Goddard High Resolution Spectrograph on the Hubble Space Telescope.
PB95-202321 *00,076*

SMITH, B. M.
ISO TC 184/SC4 Reference Manual.
PB95-242293 *02,663*

SMITH, C.
Electronic Balance and Some Gravimetric Applications. (The Density of Solids and Liquids, Pycnometry and Mass).
PB94-163052 *03,785*

SMITH, C. J.
Initial and Final Orbital Alignment Probing of the Fine-Structure-Changing Collisions among the Ca (4s)(1)(4p)(1), (3)PJ States with He: Determination of Coherence and Conventional Cross-Sections.
PB95-203279 *04,004*

Laser Preparation and Probing of Initial and Final Orbital Alignment in Collision-Induced Energy Transfer Ca(4s5p,(1)P1) + He yields Ca(4s5p,(3)P2) + He.
PB95-203261 *04,003*

Orbital Alignment and Vector Correlations in Inelastic Atomic Collisions.
PB96-122742 *04,047*

SMITH, D. K.
Powder Diffraction File: Past, Present, and Future.
PB97-109086 *04,800*

SMITH, D. R.
Cryogenic Properties of Silver.
PB94-203593 *03,330*

Low-Temperature Properties of Silver.
PB96-126198 *03,361*

Thermal Conductivity of Polypyromellitimide Film with Alumina Filler Particles from 4.2 to 300 K.
PB96-200753 *01,292*

SMITH, D. T.
Adhesion, Contact Electrification, and Acid-Base Properties of Surfaces.
PB96-204425 *03,693*

Conference Proceedings: International Workshop on Instrumented Indentation. Held in San Diego, California on April 22-23, 1995.
PB96-158688 *01,948*

Contact Electrification Induced by Monolayer Modification of a Surface and Relation to Acid-Base Interactions.
PB94-185378 *03,034*

Effect of Beam Voltage on the Properties of Aluminum Nitride Prepared by Ion Beam Assisted Deposition.
PB97-118616 *01,995*

Measuring Contact Charge Transfer at Interfaces: A New Experimental Technique.
PB95-164570 *03,053*

Surface Forces and Adhesion between Dissimilar Materials Measured in Various Environments.
PB94-172970 *03,033*

SMITH, E. R.
Table of Dielectric Constants of Pure Liquids.
AD-A278 956/8 *00,712*

SMITH, H. G.
Structures of Sodium Metal.
PB94-198850 *03,319*

SMITH, J. F.
Guide to Instrumentation Literature.
AD-A280 278/3 *02,617*

SMITH, J. H.
Ashland Tank Collapse Investigation.
PB95-126314 *02,481*

Ashland Tank-Collapse Investigation: Closure by Authors.
PB95-126322 *02,482*

Geometric Characterization of Rockwell Diamond Indenters.
PB95-203287 *02,950*

Metrology Approach to Unifying Rockwell C Hardness Scales.
PB96-155551 *02,957*

Microform Calibration Uncertainties of Rockwell Diamond Indenters.
PB96-122114 *03,280*

Microform Calibrations in Surface Metrology.
PB95-203295 *02,951*

Stylus Technique for the Direct Verification of Rockwell Diamond Intenders.
PB96-155569 *02,958*

SMITH, J. L.
Superconducting Energy Gap of Bulk UBe13.
PB95-150116 *04,559*

SMITH, K.
Optimization of Highway Concrete Technology.
PB94-182995 *01,333*

SMITH, L. C.
Determination of the Prior-Austenitic Grain Size of Selected Steels Using a Molten Glass Etch.
PB94-211927 *03,208*

SMITH, L. E.
Polymers Technical Activities 1994. NAC-NRC Assessment Panel, April 6-7, 1995.
PB95-209896 *01,275*

Polymers Technical Activities, 1995.
PB96-193719 *01,291*

SMITH, M.
Computer-Aided Manufacturing Engineering Forum (1st). Technical Meeting Proceedings. Held in Gaithersburg, Maryland on March 21-22, 1995.
PB96-136965 *02,834*

Computer-Aided Manufacturing Engineering Forum (2nd). Technical Meeting Proceedings. Held in Gaithersburg, Maryland on August 22-23, 1995.
PB96-195334 *02,845*

Critical Current Density, Irreversibility Line, and Flux Creep Activation Energy in Silver-Sheathed Bi2Sr2Ca2Cu2Ox Superconducting Tapes.
PB95-162749 *04,616*

SMITH, M. V.
Determination of the Transmittance Uniformity of Optical Filter Standard Reference Materials.
PB95-261921 *02,182*

Standard Reference Materials: Glass Filters as a Standard Reference Material for Spectrophotometry - Selection, Preparation, Certification, and Use of SRM 930 and SRM 1930.
PB94-188844 *00,536*

SMITH, R.
Effects of Copper, Nickel and Boron on Mechanical Properties of Low-Alloy Steel Weld Metals Deposited at High Heat Input.
PB96-135231 *03,363*

Standard Source Method for Reducing Antenna Factor Errors in Shielded Room Measurements.
PB96-183157 *02,013*

SMITH, R. L.
Exposure: An Expert System Fire Code.
PB95-162913 *04,868*

Performance Parameters of Fire Detection Systems.
PB94-194339 *00,288*

Risk Analysis for the Fire Safety of Airline Passengers.
PB94-194065 *04,862*

SMITH, R. W.
Federal Basis for Weights and Measures: A Historical Review of Federal Legislative Effort, Statutes, and Administrative Action in the Field of Weights and Measures in the United States.
AD-A280 086/0 *02,616*

SMITH, S. B.
Annual Conference on Fire Research: Book of Abstracts, October 17-20, 1994.
PB95-104964 *01,376*

SMITH, S. M.
Application of a Novel Slurry Furnace AAS Protocol for Rapid Assessment of Lead Environmental Contamination.
PB96-112354 *02,526*

SMITH, T. B.
In vitro Fracture Behavior of Ceramic and Metal-Ceramic Restorations.
PB96-119722 *03,569*

SMITH, T. F.
Optimal Control of Building and HVAC Systems.
PB96-141353 *00,272*

SMOOKE, M. D.
Comparison of Experimental and Computed Species Concentration and Temperature Profiles in Laminar, Two-Dimensional Methane/Air Diffusion Flames.
PB95-140919 *01,379*

SMYRL, W. H.
X-Ray Diffraction from Anodic TiO2 Films: In situ and Ex situ Comparison of the Ti(0001) Face.
PB94-185972 *00,782*

SMYTH, D. C.
Laser-Induced Fluorescence Measurements of Formaldehyde in a Methane/Air Diffusion Flame.
PB94-211679 *01,374*

SMYTH, K. C.
Comparison of Experimental and Computed Species Concentration and Temperature Profiles in Laminar, Two-Dimensional Methane/Air Diffusion Flames.
PB95-140919 *01,379*

Computations of Enhanced Soot Production in Time-Varying CH4/Air Diffusion Flames.
PB97-119218 *01,440*

Gordon Research Conference on the Physics and Chemistry of Laser Diagnostics in Combustion Held in Plymouth, New Hampshire on 12-16 July 1993.
AD-A274 609/7 *01,353*

Greatly Enhanced Soot Scattering in Flickering Ch4/Air Diffusion Flames.
PB94-172988 *01,361*

Laser Imaging of Chemistry-Flowfield Interactions: Enhanced Soot Formation in Time-Varying Diffusion Flames.
PB94-185352 *01,364*

Laser-Induced Fluorescence Measurements of OH. Concentrations in the Oxidation Region of Laminar, Hydrocarbon Diffusion Flames.
PB95-162160 *01,387*

Laser-Induced Fluorescence Measurements of OH in Laminar Diffusion Flames in the Presence of Soot Particles.
PB96-123120 *01,409*

Measurement of CO Pressures in the Ultrahigh Vacuum Regime Using Resonance-Enhanced Multiphoton-Ionization Time-of-Flight Mass Spectroscopy.
PB94-216041 *03,864*

NO Production and Destruction in a Methane/Air Diffusion Flame.
PB97-122519 *01,443*

Optical Measurements of Atomic Hydrogen, Hydroxyl, and Carbon Monoxide in Hydrocarbon Diffusion Flames.
PB95-150900 *02,487*

Oxidation of Soot and Carbon Monoxide in Hydrocarbon Diffusion Flames.
PB95-150215 *01,382*

Quantitative Measurements of Enhanced Soot Production in a Flickering Methane/Air Diffusion Flame.
PB95-203246 *01,393*

Simultaneous Forward-Backward Raman Scattering Studies of D2 Broadened by D2, He, and Ar.
PB95-162459 *00,961*

SMYTHE, R.
Precision Oscillators: Dependence of Frequency on Temperature, Humidity and Pressure.
PB94-198306 *02,031*

SNEH, O.
High-Resolution Infrared Overtone Spectroscopy of ArHF via Nd:YAG/Dye Laser Difference Frequency Generation.
PB94-211448 *00,816*

High-Resolution Infrared Overtone Spectroscopy of N2-HF: Vibrational Red Shifts and Predissociation Rate as a Function of HF Stretching Quanta.
PB96-102298 *01,061*

SNELICK, R.

Synthetic-Perturbation Tuning of MIMD Programs.
PB94-185568 *01,687*

Time-Perturbation Tuning of MIMD Programs.
PB94-164399 *01,681*

Time-Perturbation Tuning of MIMD Programs.
PB94-172566 *01,684*

Using Synthetic-Perturbation Techniques for Tuning Shared Memory Programs (Extended Abstract).
PB94-172657 *01,685*

Using Synthetic Perturbations and Statistical Screening to Assay Shared-Memory Programs.
PB96-103031 *01,740*

SNELICK, R. D.

Using S-Check, Alpha Release 1.0.
PB96-165964 *01,767*

SNELL, J. E.

Elements of a Framework for Fire Safety Engineering.
PB96-151402 *00,214*

Fire Hazard and Risk: Evaluating Alternative Technologies.
PB94-173077 *00,242*

Fire Safety Engineering Research in the United States.
PB96-151394 *00,213*

Forum for International Cooperation on Fire Research.
PB95-162939 *04,869*

Fresh Look at Strategies for Fire Safety.
PB95-162947 *04,870*

Internationalization of Fire Safety Engineering Research and Strategy.
PB96-156153 *00,220*

Quantitative Evaluation of Building Fire Safety: New Tools for Assessing Fire and Building Code Provisions.
PB95-164588 *00,199*

SNIDER, R. F.

Equilibrium Pair Distribution Function of a Gas: Aspects Associated with the Presence of Bound States.
PB95-176046 *01,004*

SNIEGOSKI, L.

Hair Analysis for Drugs of Abuse: Evaluation of Analytical Methods, Environmental Issues, and Development of Reference Materials.
PB95-176269 *03,501*

SNIEGOSKI, L. T.

Determination of 3-Quinuclidinyl Benzilate (Qnb) and Its Major Metabolites in Urine by Isotope Dilution Gas Chromatography Mass Spectrometry.
PB94-199379 *03,492*

Interlaboratory Comparison Studies on the Analysis of Hair for Drugs of Abuse.
PB95-176251 *03,500*

Interlaboratory Studies on the Analysis of Hair for Drugs of Abuse: Results from the Fifth Exercise.
PB97-110449 *03,509*

Interlaboratory Studies on the Analysis of Hair for Drugs of Abuse: Results from the Fourth Exercise.
PB97-111322 *03,510*

Isotope Dilution Mass Spectrometry as a Candidate Definitive Method for Determining Total Glycerides and Triglycerides in Serum.
PB96-102280 *03,519*

NIST Reference Materials to Support Accuracy in Drug Testing.
PB96-123807 *03,505*

SNIEGOWSKI, J. J.

Electrical Test Structures Replicated in Silicon-on-Insulator Material.
PB97-111827 *02,454*

SNOOTS, P.

Interim Testing Artifact (ITA): A Performance Evaluation System for Coordinate Measuring Machines (CMMs). User Manual.
PB95-210589 *02,914*

Measuring the Stability of Three Copper Alloys.
PB94-199866 *03,326*

NIST SRM 9983 High-Rigidity Ball-Bar Stand. User Manual.
PB95-255840 *02,669*

SNOW, M.

Observations of 3C 273 with the Goddard High Resolution Spectrograph on the Hubble Space Telescope.
PB95-202321 *00,076*

SNOW, W. M.

Measurement of the Neutron Lifetime.
PB96-161708 *04,094*

SNYDER, K.

Highway Concrete (HWYCON) Expert System User Reference and Enhancement Guide.
PB94-215670 *01,316*

Long-Term Performance of Engineered Concrete Barriers.
PB95-260816 *03,727*

Percolation and Pore Structure in Mortars and Concrete.
PB95-150439 *00,370*

SNYDER, K. A.

4SIGHT Manual: A Computer Program for Modelling Degradation of Underground Low Level Waste Concrete Vaults.
PB95-231593 *03,726*

Geometrical Percolation Threshold of Overlapping Ellipsoids.
PB96-102397 *03,167*

SNYDER, S. M.

Phase Composition, Viscosities, and Densities for Aqueous Two-Phase Systems Composed of Polyethylene Glycol and Various Salts at 25C.
PB95-164596 *00,986*

SOARES, C. G.

Angular Variation of the Personal Dose Equivalent, Hp(0.07), for Beta Radiation and Nearly Monoenergetic Electron Beams: Preliminary Results.
PB95-168472 *03,630*

Comparison of NIST and ISO Filtered Bremsstrahlung Calibration Beams.
PB95-180956 *03,967*

Comparison of NIST and Manufacturer Calibrations of (90)Sr+(90)Y Ophthalmic Applicators.
PB96-123708 *03,634*

Dose Mapping of Radioactive Hot Particles Using Radiochromic Film.
PB95-162954 *03,714*

Extrapolation Chamber Measurements on (90)Sr + (90)Y Beta-Particle Ophthalmic Applicator Dose Rates.
PB95-153375 *03,626*

Measurement of Radial Dose Distributions Around Small Beta Particle Emitters Using High Resolution Radiochromic Foil Dosimetry.
PB95-164604 *03,518*

Needs for Brachytherapy Source Calibrations in the United States.
PB97-110092 *03,521*

Secondary Target X-Ray Excitation for In vivo Measurement of Lead in Bone.
PB95-108767 *03,496*

Use of a Radiochromic Detector for the Determination of Stereotactic Radiosurgery Dose Characteristics.
PB94-185642 *03,514*

SOARES, J. H.

Individual Carotenoid Content of SRM 1548 Total Diet and Influence of Storage Temperature, Lyophilization, and Irradiation on Dietary Carotenoids.
PB94-200524 *00,033*

SOBOLEWSKI, M. A.

Current and Voltage Measurements in the Gaseous Electronics Conference RF Reference Cell.
PB96-113337 *02,388*

Electrical Characteristics of Argon Radio Frequency Glow Discharges in an Asymmetric Cell.
PB96-176490 *04,109*

Electrical Characterization of Radio-Frequency Discharges in the Gaseous Electronics Conference Reference Cell.
PB95-164612 *01,905*

Electrical Measurements for Monitoring and Control of rf Plasma Processing.
PB96-161963 *04,369*

Electrical Sensors for Monitoring rf Plasma Sheaths.
PB95-162962 *04,412*

Gaseous Electronics Conference Radio-Frequency Reference Cell: A Defined Parallel-Plate Radio-Frequency System for Experimental and Theoretical Studies of Plasma-Processing Discharges.
PB94-172327 *04,404*

SOK, J.

Thermally Activated Hopping of a Single Abrikosov Vortex.
PB95-140810 *04,548*

SOLOMON, O. M.

Bounds on Least-Squares Four-Parameter Sine-Fit Errors Due to Harmonic Distortion and Noise.
PB96-141304 *01,609*

SOLT, G.

Dynamics of Mu(+) in Sc and ScHx.
PB96-180021 *04,112*

SOMASUNDARAN, P.

Deposition of Colloidal Sintering-Aid Particles on Silicon Nitride.
PB94-216272 *03,044*

SOMERS, T. A.

Room Temperature Thermal Conductivity of Fumed-Silica Insulation for a Standard Reference Material.
PB95-152039 *00,374*

SOMMER, F.

Extrapolation of the Heat Capacity in Liquid and Amorphous Phases.
PB97-111421 *04,147*

SONG, D.

Application of Single Electron Tunneling: Precision Capacitance Ratio Measurements.
PB96-102157 *04,703*

SONG, J. F.

Autocorrelation Functions from Optical Scattering for One-Dimensionally Rough Surfaces.
PB94-216538 *04,244*

Geometric Characterization of Rockwell Diamond Indenters.
PB95-203287 *02,950*

Light Scattered by Coated Paper.
PB94-216546 *04,245*

Light Scattering from Glossy Coatings on Paper.
PB94-213246 *04,242*

Metrology Approach to Unifying Rockwell C Hardness Scales.
PB96-155551 *02,957*

Microform Calibration Uncertainties of Rockwell Diamond Indenters.
PB96-122114 *03,280*

Microform Calibrations in Surface Metrology.
PB95-203295 *02,951*

Present and Future Standard Specimens for Surface Finish Metrology.
PB97-110423 *02,928*

Stylus Flight in Surface Profiling.
PB96-123138 *02,675*

Stylus Technique for the Direct Verification of Rockwell Diamond Intenders.
PB96-155569 *02,958*

Surface Texture.
PB95-164620 *03,351*

SONG, K.

Lowest Excited Singlet State of Isolated 1-phenyl-1,3-butadiene and 1-phenyl-1,3,5-hexatriene.
PB95-202339 *01,026*

SONG, S.

Characterization of Cytochrome c/Alkanethiolate Structures Prepared by Self-Assembly on Gold.
PB95-164638 *00,987*

SONG, X. N.

Heavily Accumulated Surfaces of Mercury Cadmium Telluride Detectors: Theory and Experiment.
PB94-216074 *02,134*

Investigation of Mercury Interstitials in Hg(1-x)CdxTe Alloys Using Resonant Impact-Ionization Spectroscopy.
PB94-213485 *02,133*

RII Spectroscopy of Trap Levels in Bulk and LPE Hg1-xCdxTe.
PB96-160247 *04,084*

SONIKER, J.

Reactive Ion Etching in the Gaseous Electronics Conference RF Reference Cell.
PB96-113402 *02,395*

SONNENFELD, R.

Scanning Tunneling Microscopy and Fabrication of Nanometer Scale Structures at the Liquid-Gold Interface.
PB95-140414 *00,904*

SOODPRASERT, T.

Interpreting the Readings of Multi-Element Personnel Dosimeters in Terms of the Personal Dose Equivalent.
PB95-175428 *03,631*

SOONS, H. A.

Precision in Machining: Research Challenges.
PB95-242301 *02,953*

SORA, I. N.

Neutron Powder Diffraction Study of the Nuclear and Magnetic Structures of the Oxygen-Deficient Perovskite YBaCuCoO5.
PB95-161097 *00,954*

SORATHIA, U.

Materials and Fire Threat.
PB97-122311 *01,442*

SORENSEN, C. M.

Post-Flame Soot.
PB96-193701 *01,430*

SORENSEN, J. A.

Failure of All-Ceramic Fixed Partial Dentures 'In vitro' and 'In vivo': Analysis and Modeling.
PB96-122536 *00,175*

SOUDERS, T. M.

Bounds on Frequency Response Estimates Derived from Uncertain Step Response Data.
PB96-122874 *03,419*

Bounds on Least-Squares Four-Parameter Sine-Fit Errors Due to Harmonic Distortion and Noise.
PB96-141304 *01,609*

Compensation of Markov Estimator Errors in Time-Jittered Sampling of Nonmonotonic Signals.
PB95-150983 *01,590*

Custom Integrated Circuit Comparator for High-Performance Sampling Applications.
PB94-213147 *02,320*

Developing Linear Error Models for Analog Devices.
PB95-150520 *02,037*

Empirical Linear Prediction Applied to a NIST Calibration Service.
PB97-112353 *02,287*

NIST Strategies for Reducing Testing Requirements.
PB95-180444 *01,909*

Uncertainties of Frequency Response Estimates Derived from Responses to Uncertain Step-Like Inputs.
PB97-111843 *01,984*

Wideband Sampling Voltmeter.
PB97-113039 *01,990*

SOULAGES, J.

Evaluation and Strengthening Guidelines for Federal Buildings: Identification of Current Federal Agency Programs.
PB94-176278 *00,424*

SOULAGES, J. R.

Evaluation and Strengthening Guidelines for Federal Buildings: Assessment of Current Federal Agency Evaluation Programs and Rehabilitation Criteria and Development of Typical Costs for Seismic Rehabilitation.
PB94-181856 *00,425*

SOULEN, R. J.

Application of Single Electron Tunneling: Precision Capacitance Ratio Measurements.
PB96-102157 *04,703*

Cryogenic Precision Capacitance Bridge Using a Single Electron Tunneling Electrometer.
PB95-126074 *04,529*

Cryogenic Precision Capacitance Bridge Using a Single Electron Tunneling Electrometer.
PB95-152310 *02,040*

Development of a Temperature Scale below 0.5 K.
PB95-125639 *03,879*

Superconducting Energy Gap of Bulk UBe13.
PB95-150116 *04,559*

Systematic Studies of the Effect of a Bandpass Filter on a Josephson-Junction Noise Thermometer.
PB95-162970 *03,939*

Systematic Studies of the Effect of a Post-Detection Filter on a Josephson-Junction Noise Thermometer.
PB95-162988 *03,940*

SOUTHWORTH, S.

Lattice Position of Si in GaAs Determined by X-Ray Standing Wave Measurements.
PB95-164406 *04,632*

SOUTHWORTH, S. H.

Anisotropy of Polarized X-ray Emission from Atoms and Molecules.
PB95-163002 *04,621*

Electron-Ion-X-ray Spectrometer System.
PB95-176137 *03,958*

Evolution of X-ray Resonance Raman Scattering into X-ray Fluorescence from the Excitation of Xenon Near the L3 Edge.
PB96-102751 *04,025*

High Resolution Angle Resolved Photoelectron Spectroscopy Study of N2.
PB95-151494 *03,907*

Measuring Nondipolar Asymmetries of Photoelectron Angular Distributions.
PB97-122493 *01,193*

Resonance and Threshold Effects in Polarized X-Ray Emission from Atoms and Molecules.
PB95-150298 *03,891*

Vibronic Coupling and Other Many-Body Effects in the 4sigmag(-1) Photoionization Channel of CO2.
PB95-162509 *00,962*

SPAAR, M. T.

Anomalous Odd- to Even-Mass Isotope Ratios in Resonance Ionization with Broad-Band Lasers.
PB94-211406 *03,839*

SPAIN, E. M.

Alignment Probing of Rydberg States by Stimulated Emission.
PB96-200316 *04,124*

Initial and Final Orbital Alignment Probing of the Fine-Structure-Changing Collisions among the Ca (4s)(1)(4p)(1), (3)PJ States with He: Determination of Coherence and Conventional Cross-Sections.
PB95-203279 *04,004*

Orbital Alignment and Vector Correlations in Inelastic Atomic Collisions.
PB96-122742 *04,047*

SPAL, R.

High Resolution Hard X-Ray Microscope.
PB94-213055 *03,856*

SPAL, R. D.

Diffraction Imaging of Polycrystalline Materials.
PB94-198884 *02,971*

Effect of a Crystal Monochromator on the Local Angular Divergence of an X-Ray Beam.
PB95-150306 *04,565*

Structures of Vapor-Deposited Yttria and Zirconia Thin Films.
PB94-216025 *03,041*

SPANGLER, C. J.

In situ Fluorescence Cell Mass Measurements of 'Saccharomyces cerevisiae' Using Cellular Tryptophan.
PB96-135041 *03,547*

In situ On-Line Optical Fiber Sensor for Fluorescence Monitoring in Bioreactors.
PB94-212024 *03,587*

SPARKS, L. L.

Cryogenics.
PB95-164703 *02,654*

Thermal Conductivity of Polypyromellitimide Film with Alumina Filler Particles from 4.2 to 300 K.
PB96-200753 *01,292*

SPARKS, R. A.

Using NIST Crystal Data within Siemens Software for Four-Circle and SMART CCD Diffractometers.
PB97-109110 *04,803*

SPEAKE, C.

Validation of the Inverse Square Law of Gravitation Using the Tower at Erie, Colorado, USA.
PB95-164646 *03,947*

SPEAKE, C. C.

Test of Newton's Inverse Square Law of Gravitation Using the 300-m Tower at Erie, Colorado.
PB95-202446 *03,978*

SPELIOTIS, D. E.

Correlations of Modulation Noise with Magnetic Microstructure and Intergranular Interactions for CoCrTa and CoNi Thin Film Media.
PB94-212768 *04,509*

SPELLERBERG, P. A.

Precision of Marchall Stability and Flow Test Using 6-in. (152.4-mm) Diameter Specimens.
PB96-200910 *03,006*

System for Calibration of the Marshall Compaction Hammer.
PB94-145661 *01,303*

SPENCER, B. J.

Effects of Elastic Stress on the Stability of a Solid-Liquid Interface.
PB95-163028 *03,350*

SPENCER, L. V.

Further Calculations of X-ray Diffusion in an Infinite Medium.
AD-A295 314/9 *03,772*

Polarization Effects on Multiple Scattering Gamma Transport.
PB95-153615 *03,926*

SPENCER, W.

Characteristics of Adhesive-Bonded Seams Sampled from EPDM Roof Membranes.
PB95-162491 *00,377*

SPERHAC, J. M.

Signatures of Large Amplitude Motion in a Weakly Bound Complex: High-Resolution IR Spectroscopy and Quantum Calculations for HeCO2.
PB95-203485 *01,054*

SPETZLER, R. C.

Analysis of the Happyland Social Club Fire with HAZARD I.
PB94-199270 *00,193*

SPIEGEL, V.

Neutron Leakage Benchmark for Criticality Safety Research.
PB95-126132 *03,723*

SPINDEL, A.

Calibration of Dosimeters for the Cryogenic Irradiation of Composite Materials Using an Electron Beam.
PB95-180964 *03,968*

SPLETT, J. D.

Developing a NIST Coaxial Microwave Power Standard at 1 mW.
PB95-202412 *01,914*

Outlier-Resistant Methods for Estimation and Model Fitting.
PB95-203436 *03,444*

Proposed Changes to Charpy V-Notch Machine Certification Requirements.
PB96-135363 *02,955*

SPLICHAL, M. P.

Gaseous Electronics Conference Radio-Frequency Reference Cell: A Defined Parallel-Plate Radio-Frequency System for Experimental and Theoretical Studies of Plasma-Processing Discharges.
PB94-172327 *04,404*

SPOMER, R. L.

Magnetic Characteristics and Measurements of Filamentary Nb-Ti Wire for the Superconducting Super Collider.
DE94005988 *03,775*

SPOTZ, M. S.

Calculation of the Thermal Conductivity and Gas Permeability in a Uniaxial Bundle of Fibers.
PB95-180931 *03,058*

SPRANGLE, P.

NIST-NRL Free-Electron Laser Facility.
PB94-212511 *04,237*

SPRING, C. B.

Graphical Analysis of the CCRL Portland Cement Proficiency Sample Database (Samples 1-72). (Part 1. Univariant Analysis of Portland Cement).
PB94-196557 *01,308*

SPRING, J. D.

Electronic Publishing and the Journals of the American Chemical Society.
PB97-109185 *04,807*

SPRINGMANN, J. L.

Virtual Software Repository System.
PB94-198983 *01,691*

SPROUL, W. D.

Opportunities for Innovation: Advanced Surface Engineering.
PB94-176666 *02,697*

SRDANOV, V. I.

Structural and Chemical Investigations of Na3(ABO4)3.4H2O-Type Sodalite Phases.
PB95-180733 *01,012*

SRINIVASAN, K.

Electrophoretic Separations of Polymerase Chain Reaction: Amplified DNA Fragments in DNA Typing Using a Capillary Electrophoresis-Lased Induced Fluorescence System.
PB95-163036 *03,536*

Enhanced Detection of PCR Products Through Use of TOTO and YOYO Intercalating Dyes with Laser Induced Fluorescence - Capillary Electrophoresis.
PB95-164653 *00,599*

SRIVASTAVA, A. N.

Anomalous Switching Phenomenon in Critical-Current Measurements When Using Conductive Mandrels.
PB96-137781 *02,233*

Comparing the Accuracy of Critical-Current Measurements Using the Voltage-Current Simulator.
PB96-119219 *02,227*

First VAMAS USA Interlaboratory Comparison of High Temperature Superconductor Critical Current Measurements.
PB96-147178 *04,768*

High Current Pressure Contacts to Ag Pads on Thin Film Superconductors.
PB95-168621 *04,639*

II-3: Critical Current Measurement Methods: Quantitative Evaluation.
PB96-147160 *04,767*

II-5: Thermal Contraction of Materials Used in Nb3Sn Critical Current Measurements.
PB96-147186 *04,769*

n-Value and Second Derivative of the Superconductor Voltage-Current Characteristic.
PB95-126223 *04,533*

Simple and Repeatable Technique for Measuring the Critical Current of Nb3Sn Wires.
PB96-119409 *02,229*

Standard Reference Devices for High Temperature Superconductor Critical Current Measurements.
PB95-175543 *04,659*

Superconductor Critical Current Standards for Fusion Applications. Final Progress Report, October 1993-July 1994.
PB95-169538 *02,222*

USA Interlaboratory Comparison of Superconductor Simulator Critical Current Measurements.
PB96-147194 *04,770*

SROLOVITZ, D. J.

Microstructural Evolution in Two-Dimensional Two-Phase Polycrystals.
PB94-211992 *04,498*

ST. PIERRE, J. A.

Conformance Testing and Specification Management.
PB97-113781 *02,849*

Roadmap for the Computer Integrated Manufacturing (CIM) Application Framework.
PB96-122759 *02,832*

STACEY, G. J.

Extended CO(7 yields 6) Emission from Warm Gas in Orion.
PB96-102504 *00,090*

STACKHOUSE, W.

Report on the Workshop on Advanced Digital Video in the National Information Infrastructure. Held in Washington, D.C. on May 10-11, 1994.
PB95-103677 *01,472*

Summary Report on the Workshop on Advanced Digital Video in the National Information Infrastructure.
PB96-141320 *01,497*

STAEMMLER, V.

Nonadiabatic Effects in the Photoassociation of H2S.
PB95-151437 *00,934*

STAFFORD, G. R.

Effect of Mn Content on the Microstructure of Al-Mn Alloys Electrodeposited at 150C.
PB95-126355 *03,343*

STAHLBUSH, R. E.

Electron and Hole Trapping in Irradiated SIMOX, ZMR and BESOI Buried Oxides.
PB96-160320 *01,956*

STAHLHOFEN, A.

Comprehensive Theory of Nuclear Effects on the Intrinsic Sticking Probability. 1.
PB94-200623 *03,832*

Comprehensive Theory of Nuclear Effects on the Intrinsic Sticking Probability. 2.
PB94-200631 *03,833*

STAIJA, S. K.

Extending the Angular Range of Neutron Reflectivity Measurements from Planar Lipid Bilayers: Applications to a Model Biological Membrane.
PB96-122569 *03,476*

STAKER, M.

Neutron Diffraction Texture Study of Deformed Uranium Plates.
PB97-111587 *03,010*

STALICK, J.

Crystal Structure and Magnetic Properties of CuGeO3.
PB95-180287 *04,678*

STALICK, J. K.

Determination of Complex Structures from Powder Diffraction Data: The Crystal Structure of La3Ti5Al15O37.
PB95-202966 *01,038*

Fast-Ion Conducting Y2(ZryTi1-y)2O7 Pyrochlores: Neutron Rietveld Analysis of Disorder Induced by Zr Substitution.
PB96-156104 *04,776*

Fast-Ion Conduction and Disorder in Cation and Anion Arrays in Y2(ZryTi(1-y))2O7 Pyrochlores Induced by Zr Substitution: A Neutron Rietveld Analysis.
PB94-211869 *04,496*

Incorporation of Gold into YBa2Cu3O7: Structure and Tc Enhancement.
PB94-200276 *04,481*

Structure and Conductivity of Layered Oxides (Ba,Sr)n+1(Sn,Sb)nO3n+1.
PB96-102439 *04,707*

Unexpected Effects of Gold on the Structure, Superconductivity, and Normal State of YBa2Cu3O7.
PB94-200284 *04,482*

STAMPF, D. R.

Protein Data Bank: Current Status and Future Challenges.
PB97-109060 *00,517*

STANSBURY, J.

Ring-Opening Dental Resin Systems Based on Cyclic Acetals.
PB95-162251 *00,162*

STANSBURY, J. W.

Dental Materials.
PB94-172871 *00,142*

Evaluation of Methylene Lactone Monomers in Dental Resins.
PB95-164661 *00,164*

Facile Synthesis of Novel Fluorinated Multifunctional Acrylates.
PB94-198389 *01,207*

Preparation and Characterization of Cyclopolymerizable Resin Formulations.
PB96-146840 *01,285*

Properties and Interactions of Oral Structures and Restorative Materials. Annual Report for Period October 1, 1990 to September 30, 1991.
PB94-160843 *03,558*

Ring-Opening Polymerication of a 2-Methylene Spiro Orthocarbonate Bearing a Pendant Methacrylate Group.
PB95-176145 *01,268*

Synthesis and Polymerization of Difunctional and Multifunctional Monomers Capable of Cyclopolymerization.
PB95-163044 *01,257*

STARACE, A. F.

Angular Distributions for Near-Threshold (e,2e) Processes for Li and Mg.
PB94-185725 *00,778*

Relative Photoionization and Photodetachment Cross Sections for Particular Fine-Structure Transitions with Application to Cl 3s-subshell Photoionization.
PB95-203097 *03,998*

Resonant Two-Color Detachment of H(-) with Excitation of H(n=2).
PB95-202552 *03,984*

Short-Pulse Detachment of H(-) in the Presence of a Static Electric Field.
PB95-203477 *04,007*

Variationally Stable Treatment of Two- and Three-Photon Detachment of H(-) Including Electron-Correlation Effects.
PB95-202867 *03,992*

STARNER, K. K.

Proficiency Tests for the NIST Airborne Asbestos Program, 1990.
PB94-188836 *00,535*

STARZYK, J. A.

Diakoptic and Large Change Sensitivity Analysis.
PB95-150538 *02,038*

STASSIS, C.

Inelastic Neutron Scattering Measurements of Phonons in Icosahedral Al-Li-Cu.
PB95-126215 *04,532*

STAUDENMANN, J. L.

Energy Dependences of Absorption in Beryllium Windows and Argon Gas.
PB96-102124 *04,020*

STAUFFER, A. D.

Polarization of Light Emitted After Positron Impact Excitation of Alkali Atoms.
PB94-199734 *03,816*

STAUFFER, J.

Sleuthing the Dynamo: HST/FOS Observations of UV Emissions of Solar-Type Stars in Young Clusters.
PB96-122817 *00,098*

STAUFFER, J. R.

Far-Ultraviolet Flare on a Pleiades G Dwarf.
PB96-102033 *00,086*

STAUFFER, T. C.

Critical Current Behavior of Ag-Coated YBa2Cu3O7-x Thin Films.
PB95-141016 *04,549*

First VAMAS USA Interlaboratory Comparison of High Temperature Superconductor Critical Current Measurements.
PB96-147178 *04,768*

High Current Pressure Contacts to Ag Pads on Thin Film Superconductors.
PB95-168621 *04,639*

Standard Reference Devices for High Temperature Superconductor Critical Current Measurements.
PB95-175543 *04,659*

Superconductor Critical Current Standards for Fusion Applications. Final Progress Report, October 1993-July 1994.
PB95-169538 *02,222*

USA Interlaboratory Comparison of Superconductor Simulator Critical Current Measurements.
PB96-147194 *04,770*

STEBBINS, R.

Low-Frequency, Active Vibration Isolation System.
PB95-203303 *02,710*

STECKLER, K. D.

Comparison of Wall-Fire Behavior With and Without a Ceiling.
PB94-207404 *00,342*

Methodology for Developing and Implementing Alternative Temperature-Time Curves for Testing the Fire Resistance of Barriers for Nuclear Power Plant Applications.
PB96-193784 *03,742*

STEEL, E.

Measurement of the Uniformity of Particle Deposition of Filter Cassette Sampling in a Low Velocity Wind Tunnel.
PB95-163754 *02,549*

STEEL, E. B.

Airborne Asbestos Analysis: National Voluntary Laboratory Accreditation Program.
PB96-147392 *02,566*

Airborne Asbestos Method: Bootstrap Method for Determining the Uncertainty of Asbestos Concentration. Version 1.0.
PB96-214614 *00,646*

Airborne Asbestos Method: Standard Practice for Recording Transmission Electron Microscopy Data for the Analysis of Asbestos Collected onto Filters. Version 1.0.
PB94-210168 *00,552*

Airborne Asbestos Method: Standard Test Method for High Precision Counting of Asbestos Collected on Filters. Version 1.0.
PB94-163003 *00,525*

Airborne Asbestos Method: Standard Test Method for Verified Analysis of Asbestos by Transmission Electron Microscopy. Version 2.0.
PB94-163045 *00,526*

Guidelines for Refractive Index Measurements of Asbestos.
PB95-151189 *02,543*

Monte Carlo Electron Trajectory Simulation of X-Ray Emission from Films Supported on Substrates.
PB95-107207 *04,522*

National Voluntary Laboratory Accreditation Program: Bulk Asbestos Analysis.
PB95-138129 *02,541*

Proficiency Tests for the NIST Airborne Asbestos Program, 1990.
PB94-188836 *00,535*

Proficiency Tests for the NIST Airborne Asbestos Program - 1991.
PB94-193828 *00,537*

Proficiency Tests for the NIST Airborne Asbestos Program - 1992.
PB94-194362 *00,539*

Proficiency Tests for the NIST Airborne Asbestos Program, 1993.
PB96-106463 *00,610*

STEELE, R. D.

Unified Telerobotic Architecture Project (UTAP) Standard Interface Environment (SIE), May 1995.
PB95-242350 *02,938*

STEELE, W. V.

Thermodynamic Properties of Alkenes (Mono-Olefins Larger Than C4).
PB94-162237 *00,735*

STEENKEN, S.

Solvent Effects in the Reactions of Peroxyl Radicals with Organic Reductants. Evidence for Proton Transfer Mediated Electron Transfer.
PB95-107157 *00,873*

STEFFENS, K. L.

In-situ Studies of a Novel Sodium Flame Process for Synthesis of Fine Particles.
PB97-113047 *00,681*

Optical and Modeling Studies of Sodium/Halide Reactions for the Formation of Titanium and Boron Nanoparticles.
PB97-113054 *00,682*

STEHLE, S.

SUSAN: SUperconducting Systems ANalysis by Low Temperature Scanning Electron Microscopy (LTSEM).
PB96-112065 *04,728*

STEIN, R. S.

Small-Angle Neutron Scattering of Poly(vinyl alcohol) Gels.
PB95-164117 *01,260*

Small Angle Neutron Scattering Studies on Chain Asymmetry of Coextruded Poly(Vinyl Alcohol) Film.
PB95-164372 *01,262*

STEIN, S. E.

Diamond and Graphite Precursors: Comments.
PB95-163051 *00,967*

International Conference on Chemical Kinetics (2nd). Held in Gaithersburg, Maryland on July 24-27, 1989.
PB94-211901 *00,822*

Thermal Decomposition of Hydroxy- and Methoxy-Substituted Anisoles.
PB94-173036 *00,767*

STEINBACH, A.

Narrow-Band Tunable Diode Laser System with Grating Feedback, and a Saturated Absorption Spectrometer for Cs and Rb.
PB95-202891 *04,319*

STEINBACH, A. H.

Observation of Hot-Electron Shot Noise in a Metallic Resistor.
PB97-112007 *01,988*

STEINER, B.

Influence of Lattice Mismatch on Indium Phosphide Based High Electron Mobility Transistor (HEMT) Structures Observed in High Resolution Monochromatic Synchrotron X-Radiation Diffraction Imaging.
PB95-164679 *02,357*

Recent VAMAS Activity in Ceramics.
PB95-162681 *03,051*

STEINER, R.

Measurement and Reduction of Alignment Errors of the NIST Watt Experiment.
PB97-111959 *01,987*

Methods for Aligning the NIST Watt-Balance.
PB96-123153 *01,934*

NIST Watt Balance: Progress Toward Monitoring the Kilogram.
PB97-113062 *01,991*

STEINER, R. L.

Accuracy Comparisons of Josephson Array Systems.
PB95-164687 *02,047*

Evidence for Parallel Junctions Within High-Tc Grain-Boundary Junctions.
PB95-175410 *04,657*

New Refractometer by Combining a Variable Length Vacuum Cell and a Double-Pass Michelson Interferometer.
PB97-111926 *01,986*

Noise Characteristics Below 1 Hz of Zener Diode-Based Voltage Reference.
PB96-123476 *04,049*

Voltage Ratio Measurements of a Zener Reference Using a Digital Voltmeter.
PB95-164695 *01,906*

STEINER, T. W.

Comparison of Techniques for Nondestructive Composition Measurements in CdZnTe Substrates.
PB96-103098 *02,703*

STELLA, A. L.

Self-Avoiding Surfaces, Topology, and Lattice Animals.
PB95-150512 *04,571*

STENBAKKEN, G.

Measurement and Reduction of Alignment Errors of the NIST Watt Experiment.
PB97-111959 *01,987*

NIST Watt Balance: Progress Toward Monitoring the Kilogram.
PB97-113062 *01,991*

STENBAKKEN, G. N.

Binary versus Decade Inductive Voltage Divider Comparison and Error Decomposition.
PB96-112263 *02,071*

Developing Linear Error Models for Analog Devices.
PB95-150520 *02,037*

Diakoptic and Large Change Sensitivity Analysis.
PB95-150538 *02,038*

Effects of Nonmedel Errors on Model-Based Testing.
PB96-155577 *03,420*

Effects of Nonmodel Errors on Model-Based Testing.
PB96-123146 *02,604*

Empirical Linear Prediction Applied to a NIST Calibration Service.
PB97-112353 *02,287*

Methods for Aligning the NIST Watt-Balance.
PB96-123153 *01,934*

NIST High-Accuracy Sampling Wattmeter.
PB97-108575 *02,689*

NIST Strategies for Reducing Testing Requirements.
PB95-180444 *01,909*

STENCEL, R. E.

Four Years of Monitoring alpha Orionis with the VLA: Where Have All the Flares Gone.
PB94-185212 *00,048*

STENKE, M.

Dielectronic Capture Processes in the Electron-Impact Ionization of Sc(2+).
PB95-203113 *04,000*

STEPHENS, E. F.

Electronically Tunable Fiber Laser for Optical Pumping of (3)He and (4)He.
PB96-201165 *04,381*

STEPHENS, P. W.

Phase Transitions in Solid C70: Supercooling, Metastable Phases, and Impurity Effect.
PB95-150090 *00,914*

STEPHENSON, G. B.

Real-Time Small-Angle X-Ray Scattering Study of the Early Stage of Phase Separation in the SiO2-BaO-K20 System.
PB95-163069 *03,052*

STEPHENSON, J. C.

Dynamics of Nonthermal Reactions: Femtosecond Surface Chemistry.
PB94-199965 *00,688*

Fragment Energy and Vector Correlations in the Overtone-Pumped Dissociation of HN3X(1)A'.
PB94-199908 *00,802*

Hot Carrier Excitation of Adlayers: Time-Resolved Measurement of Adsorbate-Lattice Coupling.
PB94-172285 *00,758*

Picosecond Measurement of Substrate-to-Adsorbate Energy Transfer: The Frustrated Translation of CO/Pt(111)--Translation.
PB95-126041 *00,895*

Time-Resolved Measurements of Energy Transfer at Surfaces.
PB95-141198 *00,913*

Time-Resolved Measurements of Energy Transfer at Surfaces.
PB95-153037 *00,947*

Time-Resolved Probes of Surface Dynamics.
PB94-199957 *00,803*

Ultrafast Time-Resolved Infrared Probing of Energy Transfer at Surfaces.
PB96-123443 *00,620*

Vibrational Predissociation Dynamics of Overtone-Excited HN3.
PB95-125720 *00,691*

Vibrational Relaxation Measurements of Carbon Monoxide on Metal Clusters.
PB94-211810 *00,820*

STEPHENSON, M.

TDDB Characterization of Thin SiO2 Films with Bimodal Failure Populations.
PB96-102926 *02,381*

STERN, R.

Sleuthing the Dynamo: HST/FOS Observations of UV Emissions of Solar-Type Stars in Young Clusters.
PB96-122817 *00,098*

STERN, R. A.

Far-Ultraviolet Flare on a Pleiades G Dwarf.
PB96-102033 *00,086*

STEVENS, R. K.

Distinguishing the Contributions of Residential Wood Combustion and Mobile Source Emissions Using Relative Concentrations of Dimethylphenanthrene Isomers.
PB96-135124 *02,563*

Radiocarbon Measurements of Atmospheric Volatile Organic Compounds: Quantifying the Biogenic Contribution.
PB97-122352 *02,574*

STEVENS, W. J.

Analysis of Protein Metal Binding Selectivity in a Cluster Model.
PB94-212990 *00,845*

Cs Cluster Binding to a GaAs Surface.
PB94-213006 *00,846*

Strong Hydrogen Bond in the Formic Acid-Formate Anion System.
PB94-198595 *00,788*

Structure of Glycine-Water H-Bonded Complexes.
PB94-198603 *00,789*

STEWARD, W. G.

Survey of the Literature on Heat Transfer from Solid Surfaces to Cryogenic Fluids.
AD-A286 680/4 *04,193*

STEWART, H. D.

Application of the Modified Voltage-Dividing Potentiometer to Overlay Metrology in a CMOS/Bulk Process.
PB94-181997 *02,302*

STEWART, R. T.

High Sensitivity Survey of Radio Continuum Emission in Herbig Ae/Be Stars.
PB94-185915 *00,051*

STEWART, S. L.

Conformance Testing and Specification Management.
PB97-113781 *02,849*

Roadmap for the Computer Integrated Manufacturing (CIM) Application Framework.
PB96-122759 *02,832*

STIEF, L. J.

Experimental Determination of the Ionization Energy of IO(X(sup 2)II(sub 3/2)) and Estimations of Delta(sub f)H(sup deg)(sub 0)(IO(sup -)) and PA(IO).
PB96-146899 *00,694*

Experimental Determination of the Rate Constant for the Reaction of C2H3 with H2 and Implications for the Partitioning of Hydrocarbons in Atmospheres of the Outer Planets.
PB97-122295 *00,112*

STIEFEL, S. W.

Implementation of the Fastener Quality Act.
PB96-160676 *02,876*

STIEG, M.

24 GHz Josephson Array Voltage Standard.
PB94-211588 *02,033*

STIEREN, D. C.

Automated Inspection: The Integration of National Standards and Commercial Products at NIST.
PB95-163077 *02,906*

Automated Manufacturing Research Facility 1994 Annual Report.
PB95-209854 *00,015*

Development of an Automated Part Inspection System Using the DMIS Standard.
PB95-108866 *02,899*

U.S. Navy Coordinate Measuring Machines: A Study of Needs.
PB94-162831 *02,807*

STILES, M. D.

Coarsening of Unstable Surface Features during Fe(001) Homoepitaxy.
PB96-186127 *04,121*

Exchange Coupling in Magnetic Heterostructures.
PB95-150314 *04,566*

Spin-Dependent Interface Transmission and Reflection in Magnetic Multilayers (Invited).
PB96-201173 *04,130*

STILLE, J. K.

Characterization of Polyquinoline Blends Using Small Angle Scattering.
PB95-164125 *01,261*

Characterization of Polyquinoline Block Copolymer Using Small Angle Scattering.
PB95-151882 *01,244*

STILLMAN, S. E.

Enthalpy Increment Measurements from 4.5 to 350 K and the Thermodynamic Properties of Titanium Disilicide(cr) to 1700 K.
PB96-204029 *00,678*

STINSON, F.

Further Calculations of X-ray Diffusion in an Infinite Medium.
AD-A295 314/9 *03,772*

STOCK, K. D.

International Intercomparison of Detector Responsivity at 1300 and 1550 nm.
PB95-125928 *02,140*

International Intercomparison of Detector Responsivity at 1300 and 1550 nm.
PB95-126017 *02,141*

STOCKBAUER, R. L.

Photoelectron Spectroscopic Study of the Valence and Core-Level Electronic Structure of BaTiO3.
PB94-212149 *04,500*

Surface Core-Level Shifts of Barium Observed in Photoemission of Vacuum-Fractured BaTiO3 (100).
PB94-212156 *04,501*

STOJANOVIC, V.

Excitation of Balmer Lines in Low-Current Discharges of Hydrogen and Deuterium.
PB95-150546 *03,893*

STOKESBERRY, D.

ISDN in North America.
PB96-160767 *01,502*

STOKESBERRY, D. P.

Application Software Interface: ISDN Services for an Open Systems Environment.
PB96-131487 *01,492*

Integrated Network Management.
PB94-199247 *01,583*

North American ISDN Users' Forum Agreements on Integrated Services Digital Network.
PB94-162559 *01,466*

STOKIC, Z.

Excitation of Balmer Lines in Low-Current Discharges of Hydrogen and Deuterium.
PB95-150546 *03,893*

STONE, C. A.

Neutron Capture Prompt Gamma-Ray Activation Analysis at the NIST Cold Neutron Research Facility.
PB94-213394 *00,556*

STONE, J.

Two New Probes for a Coordinate Measuring Machine.
PB95-163093 *02,653*

STONE, S.

National Status and Trends Program Specimen Bank: Sampling Protocols, Analytical Methods, Results, and Archive Samples.
PB97-119226 *02,598*

STONE, S. F.

Trace Elements Associated with Proteins. Neutron Activation Analysis Combined with Biological Isolation Techniques.
PB95-163101 *00,597*

STONE, W. C.

Evaluating the Seismic Performance of Lightly-Reinforced Circular Concrete Bridge Columns.
PB95-163259 *01,335*

Jacket Thickness Requirements for Seismic Retrofitting of Circular Bridge Columns.
PB95-163267 *01,336*

NIST Construction Automation Program Report No. 2. Proceedings of the NIST Construction Automation Workshop. Held in Gaithersburg, Maryland on March 30-31, 1995.
PB96-202239 *00,413*

Partially Prestressed and Debonded Precast Concrete Beam-Column Joints.
PB95-153102 *00,439*

Performance of 1/3-Scale Model Precast Concrete Beam-Column Connections Subjected to Cyclic Inelastic Loads. Report No. 4.
PB95-179024 *00,444*

Seismic Performance Behavior of Precast Concrete Beam-Column Joints.
PB95-153110 *00,440*

Seismic Performance of Circular Bridge Columns Designed in Accordance with AASHTO/CALTRANS Standards.
PB96-146352 *01,346*

Simplified Design Procedure for Hybrid Precast Concrete Connections.
PB96-154836 *00,405*

STOREY, P. J.

Fast Computer Evaluation of Radiative Properties of Hydrogenic Systems.
PB95-150553 *03,894*

Recombination Line Intensities for Hydrogenic Ions-III. Effects of Finite Optical Depth and Dust.
PB95-202677 *00,079*

STOTT, H. L.

Modeling and Test Point Selection for a Thermal Transfer Standard.
PB95-161287 *01,896*

STOUDT, M. R.

Analysis of Failed Dry Pipe Fire Suppression System Couplings from the Filene Center at Wolf Trap Farm Park for the Performing Arts.
PB94-164407 *00,331*

Characterization of the Hydrogen Induced Cold Cracking Susceptibility at Simulated Weld Zones in HSLA-100 Steel.
AD-A279 759/5 *03,200*

Characterization of the Hydrogen Induced Cold Cracking Susceptibility at Simulated Weld Zones in HSLA-100 Steel.
PB94-174505 *03,746*

Evaluation of the Environmentally Induced Fracture Resistance of Ductile Nickel Aluminide. Technical Report Number 1, Final report. October-December 1990.
DE94017331 *03,306*

Loading Device for Fracture Testing of Compact Tension Specimens in the Scanning Electron Microscope.
PB95-162434 *02,652*

STOUFFER, K.

Recommendations on Selection of Vehicle-to-Roadside Communications Standards for Commercial Vehicle Operations.
PB94-195914 *04,859*

Vehicle-to-Roadside Communications for Commercial Vehicle Operations: Requirements and Approaches.
PB95-188827 *04,860*

STOUP, J.

Measuring the Stability of Three Copper Alloys.
PB94-199866 *03,326*

STOVEL, L.

Z39.50 Implementation Experiences.
PB96-114939 *01,816*

STRANG, A.

Variations in Size Measurements by Indicating Gaging Systems.
PB95-163614 *02,864*

STRATY, G. C.

Conditions for Existence of a Reentrant Solid Phase in a Sheared Atomic Fluid.
PB94-211380 *04,198*

Contrast Matched Studies of a Sheared Binary Colloidal Suspension.
PB95-150561 *00,918*

Partial Scattered Intensities from a Binary Suspension of Polystyrene and Silica.
PB95-175618 *00,996*

Simulation and SANS Studies of Gelation Under Shear.
PB96-167176 *01,150*

Small-Angle Neutron Scattering (SANS) Study of Worm-Like Micelles Under Shear.
PB96-176698 *04,111*

Small Angle Neutron Scattering Study of a Clay Suspension Under Shear.
PB96-167374 *00,663*

Small-Angle Neutron-Scattering Study of Dense Sheared Silica Gels.
PB96-167184 01,151

Structure and Rheology of Hard-Sphere Systems.
PB96-167333 00,662

STRAUB, J.

Formulation of the Refractive Index of Water and Steam.
PB95-140133 00,900

STRAUSSER, B.

PET and DINGO Tools for Deriving Distributed Implementations from Estelle.
PB95-203253 01,727

STRAWBRIDGE, M. L.

Virtual Software Repository System.
PB94-198983 01,691

STRICKLETT, K. L.

Advanced Components for Electric and Hybrid Electric Vehicles. Workshop Proceedings. Held in Gaithersburg, Maryland on October 27-28, 1993.
PB94-177060 04,858

Appearance Potentials of Ions Produced by Electron-Impact Induced Dissociative Ionization of SF6, SF4, SF5Cl, S2F10, SO2, SO2F2, SOF2, and SOF4.
PB96-119730 01,080

Associative Electron Attachment to S2F10, S2OF10, and S2O2F10.
PB95-140992 00,907

Correlations between Electrical and Acoustic Detection of Partial Discharge in Liquids and Implications for Continuous Data Recording.
PB96-204490 02,248

Electrical Breakdown in Transformer Oil in Large Gaps.
PB95-150579 01,889

Electrohydrodynamic Instability and Electrical Discharge Initiation in Hexane.
PB96-186119 02,244

Investigation of S2F10 Production and Mitigation in Compressed SF6-Insulated Power Systems.
PB94-212388 02,467

Investigation of S2F10 Production and Mitigation in Compressed SF6- Insulated Power Systems.
PB96-155528 02,468

Observations of Partial Discharges in Hexane Under High Magnification.
PB95-163127 01,900

Procedure for Measuring Trace Quantities of S2F10, S2OF10, and S2O2F10 in SF6 Using a Gas Chromatograph-Mass Spectrometer.
PB96-119755 02,513

Refraction of Light by Graded Birefringent Media.
PB96-123716 02,192

STROBRIDGE, T. R.

Helium Refrigeration and Liquefaction Using a Liquid Hydrogen Refrigerator for Precooling.
AD-A286 683/8 02,749

STROM, K.

Status of the Round Robin on the Transport Properties of R134a.
PB96-167218 01,152

STRONGIN, R. M.

Neutron-Scattering Study of Librations and Intramolecular Phonons in Rb2.6K0.4C60.
PB95-162269 00,958

STROSCIO, J. A.

Atomic Manipulation of Polarizable Atoms by Electric Field Directional Diffusion.
PB95-150587 04,572

Closed Loop Controller for Electron-Beam Evaporators.
PB97-111470 04,393

Coarsening of Unstable Surface Features during Fe(001) Homoepitaxy.
PB96-186127 04,121

Growth of Iron on Iron Whiskers.
PB95-150322 04,567

Homoepitaxial Growth of Iron and a Real Space View of Reflection-High-Energy-Electron Diffraction.
PB94-173069 04,445

Influence of Cr Growth on Exchange Coupling in Fe/Cr/Fe(100).
PB95-150181 04,562

Influence of Thickness Fluctuations on Exchange Coupling in Fe/Cr/Fe Structures.
PB96-135371 04,745

Manipulation of Adsorbed Atoms and Creation of New Structures on Room-Temperature Surfaces with a Scanning Tunneling Microscope.
PB95-151536 04,578

Scaling of Diffusion-Mediated Island Growth in Iron-on-Iron Homoepitaxy.
PB94-185923 04,455

Scanning Tunneling Microscopy Study of the Growth of Cr/Fe(001): Correlation with Exchange Coupling of Magnetic Layers.
PB95-150330 04,568

SEMPA Studies of Oscillatory Exchange Coupling.
PB95-163556 04,625

Tunneling Spectroscopy of bcc(001) Surface States.
PB96-155585 04,775

STROUSE, G. F.

Assessment of Uncertainties of Calibration of Resistance Thermometers at the National Institute of Standards and Technology.
PB94-142478 02,624

Comparisons of Some NIST Fixed-Point Cells with Similar Cells of Other Standards Laboratories.
PB97-119242 00,655

Direct Comparison of Three PTB Silver Fixed-Point Cells with the NIST Silver Fixed-Point Cell.
PB96-161286 00,628

Investigation of High-Temperature Platinum Resistance Thermometers at Temperatures Up to 962C, and, in Some Cases, 1064C.
PB96-161294 00,629

Investigation of the ITS-90 Subrange Inconsistencies for 25.5 Omega SPRTs.
PB96-161302 00,630

ITS-90 Calibration Facility.
PB96-160916 00,627

NIST Assessment of ITS-90 Non-Uniqueness for 25.5 Ohm SPRTs at Gallium, Indium and Cadmium Fixed Points.
PB96-161310 00,631

NIST Implementation and Realization of the ITS-90 Over the Range 83 K to 1235 K: Reproducibility, Stability, and Uncertainties.
PB96-161328 00,632

NIST Measurement Assurance of SPRT Calibrations on the ITS-90: A Quantitative Approach.
PB96-161336 00,633

Practical Applications of the ITS-90: Inherent Uncertainties.
PB95-161527 03,930

Preliminary Results of a Comparison of Water Triple-Point Cells Prepared by Different Methods.
PB96-161344 00,634

Standard Reference Material 1744: Aluminum Freezing-Point Standard.
PB95-251732 01,055

STRUBLE, L.

Interaction between Naphthalene Sulfonate and Silica Fume in Portland Cement Pastes.
PB94-199759 01,315

STRUBLE, L. J.

Rheology of Fresh Cement Paste.
PB95-163150 00,378

STRUCK, L. M.

Silicon Surface Chemistry by IR Spectroscopy in the Mid- to Far-IR Region: H2O and Ethanol on Si(100).
PB96-138565 01,097

STRUPP, P. G.

Direct Detection of Atomic Arsenic Desorption from Si(100).
PB95-202230 01,024

Laser Gas Ionization Technique Monitors MEB Crystal Growth.
PB96-112172 01,076

Laser-Induced Desorption of In and Ga from Si(100) and Adsorbate Enhanced Surface Damage.
PB95-203311 01,050

Pulsed Laser Irradiation at 532 nm of In and Ga Adsorbed on Si(100): Desorption, Incorporation, and Damage.
PB95-203329 01,051

Single-Photon Ionization and Detection of Ga, In, and As(sub n) Species in GaAs Growth.
PB95-152815 00,591

Single Photon Laser Ionization as an In-situ Diagnostic for MBE growth.
PB96-102025 01,059

Single-Photon Laser Ionization Time-of-Flight Mass Spectroscopy Detection in Molecular-Beam Epitaxy: Application to As4, As2, and Ga.
PB95-203337 01,052

Vibrational Distributions of As2 in the Cracking of As4 on Si(100) and Si(111).
PB94-198314 00,784

STUART DOLS, W.

Development and Application of an Indoor Air Quality Commissioning Program in a New Office Building.
PB96-155601 00,275

Study of Ventilation Measurement in an Office Building.
PB96-155593 00,274

STUART, J. W.

Sliding Vane Flow Conditioner Tests in a 100 Diameter Long 10 inch Natural Gas Orifice Meter at Pacific Gas and Electric. Topical Report, 1990-1992.
PB95-256335 02,493

STUBENRAUCH, C. F.

Development of Near-Field Test Procedures for Communication Satellite Antennas.
PB96-135082 02,010

STUCKY, G. D.

Crystal Structure of a New Sodium Zinc Arsenate Phase Solved by 'Simulated Annealing'.
PB95-107124 00,870

Inelastic Neutron Scattering Studies of Nonlinear Optical Materials: p-Nitroaniline Adsorbed in ALPO-5.
PB95-107223 00,874

Small Angle Neutron Scattering Study of the Structure and Formation of MCM-41 Mesoporous Molecular Sieves.
PB97-122337 03,110

Small Angle Neutron Scattering Study of the Structure and Formation of Ordered Mesopores in Silica.
PB96-111919 03,069

Structural and Chemical Investigations of Na3(ABO4)3.4H2O-Type Sodalite Phases.
PB95-180733 01,012

Tetrahedral-Framework Lithium Zinc Phosphate Phases: Location of Light-Atom Positions in LiZnPO4 H2O by Powder Neutron Diffraction and Structure Determination of LiZnPO4 by ab Initio Methods.
PB96-160510 01,129

STUHR, U.

Inelastic Neutron Scattering Study of Hydrogen in Nanocrystalline Pd.
PB96-146857 03,366

Vibrational Excitations and the Position of Hydrogen in Nanocrystalline Palladium.
PB96-111828 04,035

STULL, D. M.

Membrane Gas Separation for a Fluidized-Bed Incinerator.
PB95-169041 02,550

STUTZIN, G. C.

Deposition Rates in Direct Current Diode Sputtering.
PB95-203345 04,697

Nanoscale Study of the As-Grown Hydrogenated Amorphous Silicon Surface.
PB95-150595 04,573

STUTZMAN, P.

Characteristics of Adhesive-Bonded Seams Sampled from EPDM Roof Membranes.
PB95-162491 00,377

Warping of Terrace Pavers at the U.S. Capitol Building.
PB96-193651 00,411

STUTZMAN, P. E.

Cellular Automaton Simulations of Cement Hydration and Microstructure Development.
PB95-175055 01,320

Cement and Concrete Characterization by Scanning Electron Microscopy.
PB95-163168 00,379

Compositional Analysis of Beneficiated Fly Ashes.
PB95-220497 00,397

Diagnosis of Causes of Concrete Deterioration in the MLP-7A Parking Garage.
PB95-143095 01,318

Evolution of Porosity and Calcium Hydroxide in Laboratory Concretes Containing Silica Fume.
PB95-175063 01,321

Microstructural Features of Some Low Water/Solids, Silica Fume Mortars Cured at Different Temperatures.
PB94-160777 00,330

Quantitative Phase Abundance Analysis of Three Cement Clinker Reference Materials by Scanning Electron Microscopy.
PB94-173051 00,333

Quantitative X-Ray Powder Diffraction Methods for Clinker and Cement.
PB95-143079 01,317

Serial Sectioning of Hardened Cement Paste for Scanning Electron Microscopy.
PB94-172640 01,305

STWALLEY, W. C.

Spectroscopy and Structure of the Lithium Hydride Diatomic Molecules and Ions.
PB94-160991 00,731

SU, D.

Introduction to Traffic Management for Broadband ISDN.
PB94-142494 01,464

NIST ATM Network Simulator: Operation and Programming, Version 1.0.
PB96-106851 01,487

SU, D. H.

ISDN Conformance Testing.
PB95-163176 01,478

SU, R.

In-Space Welding: Visions and Realities.
PB95-163234 04,830

SUBRAMANIAN, M. A.

Colossal Magnetoresistance without Mn(3+)/Mn(4-) Double Exchange in the Stoichiometric Pyrochlore Tl2Mn2O7.
PB97-113070 04,160

SUDAREV, K. A.

Precision High Temperature Blackbodies.
PB95-140059 03,885

Results of a NIST/VNIIOFI Comparison of Spectral-Radiance Measurements.
PB97-113021 04,159

SUEHLE, J.

Assessing MOS Gate Oxide Reliability on Wafer Level with Ramped/Constant Voltage and Current Stress.
PB96-180112 04,115

Multijunction Thermal Converters by Commercial CMOS Fabrication.
PB95-153664 02,343

New Physics-Based Model for Time-Dependent- Dielectric-Breakdown.
PB96-186093 02,440

SUEHLE, J. S.

Characterization of Time-Dependent Dielectric Breakdown in Intrinsic Thin SiO2.
PB97-122527 02,458

Charge Trapping and Breakdown Mechanism in SIMOX.
PB94-216637 02,323

Electric Field Dependent Dielectric Breakdown of Intrinsic SiO2 Films Under Dynamic Stress.
PB96-204102 02,449

Electrical Method for Determining the Thickness of Metal Films and the Cross-Sectional Area of Metal Lines.
PB95-203170 02,370

Experimental Investigation of the Validity of TDDB Voltage Acceleration Models.
PB94-185949 02,304

Field and Temperature Acceleration of Time-Dependent Dielectric Breakdown in Intrinsic Thin SiO2.
PB94-185956 02,305

High Temperature Reliability of Thin Film SiO2.
PB95-150348 02,333

Interaction of Stoichiometry, Mechanical Stress, and Interface Trap Density in LPCVD Si-rich SiNx-Si Structures.
PB95-176301 02,366

JEDEC 'TCR' Interlaboratory Experiment: Lessons Learned.
PB95-203188 02,371

New Oxide Degradation Mechanism for Stresses in the Fowler-Nordheim Tunneling Regime.
PB96-200985 04,128

New Physics-Based Model for Time-Dependent- Dielectric-Breakdown.
PB96-201132 02,448

Reproducibility of JEDEC Standard Current and Voltage Ramp Test Procedures for Thin-Dielectric Breakdown Characterization.
PB94-185931 01,879

TDDB Characterization of Thin SiO2 Films with Bimodal Failure Populations.
PB96-102926 02,381

Time-Dependent Dielectric Breakdown of Intrinsic SiO2 Films under Dynamic Stress.
PB96-179478 02,438

Tin Oxide Gas Sensor Fabricated Using CMOS Micro-Hotplates and In-situ Processing.
PB95-150603 00,580

SUENRAM, R. D.

Microwave Spectra of van der Waals Complexes of Importance in Planetary Atmospheres.
PB95-150611 00,919

Microwave Spectrum and Structure of CH3NO2-H20.
AD-A296 377/5 00,719

Rotational Spectra of CH3CCH-NH3, NCCCH-NH3, and NCCCH-OH2.
PB97-118798 04,170

Rotational Spectrum and Structure of a Weakly Bound Complex of Ketene and Acetylene.
PB95-126140 00,896

Thermal Decomposition Pathways in Nitramine Propellants.
AD-A295 896/5 03,753

Tunneling-Rotation Spectrum of the Hydrogen Fluoride Dimer.
PB94-198678 00,793

SUGAR, J.

Analysis of the (5d(2)+5d6s)-5d6p Transition Arrays of Os VII and Ir VIII, and the 6s (2)S-6p (2)P Transitions of Ir IX.
PB96-159264 01,954

Analysis of the 5s(2)5p(2)-(5s5p(3)+5s(2)5p5d+5s(2)5p6s) Transitions of Four-Times Ionized Xenon (Xe V).
PB95-150769 03,900

Designations of ds(2)p Energy Levels in Neutral Zirconium, Hafnium, and Rutherfordium (Z=104).
PB96-180120 04,116

Energy Levels of Germanium, Ge I through Ge XXXII.
PB94-162351 00,747

Energy Levels of Zinc, Zn I through Zn XXX.
PB96-145982 01,122

Improved Wavelengths for Prominent Lines of Cr XVI to Cr XXII.
PB95-150629 03,895

Improved Wavelengths for Prominent Lines of Fe XX to Fe XXIII.
PB96-111638 04,334

Laser-Produced and Tokamak Spectra of Lithiumlike Iron, Fe(23+).
PB95-180857 04,314

Magnetic Dipole Line from U LXXI Ground-Term Levels Predicted at 3200 Angstroms.
PB94-211497 04,407

Observation and Visible and uv Magnetic Dipole Transitions in Highly Charged Xenon and Barium.
PB96-138441 04,056

Observation of Pd-Like Resonance Lines Through Pt(32+) and Zn-Like Resonance Lines of Er(38+) and Hf(42+).
PB95-150637 03,896

Rb-Like Spectra: Pd X to Nd XXIV.
PB95-150645 03,897

Rh I Isoelectronic Sequence Observed from Er(23+) to Pt(33+).
PB95-150652 03,898

Spectra of Ag I Isoelectronic Sequence Observed from Er(21+) to Au(32+).
PB95-150660 03,899

Spectral Data and Grotrian Diagrams for Highly Ionized Chromium, Cr V through Cr XXIV.
PB94-162369 00,748

Spectral Data for Highly Ionized Krypton, Kr V through Kr XXXVI.
PB96-145917 01,115

Spectroscopic Data Tables for Highly-Ionized Atoms.
PB95-151585 03,910

SUHM, M. A.

High-Resolution Infrared Spectroscopy of DF Trimer: A Cyclic Ground State Structure and DF Stretch Induced Intramolecular Vibrational Coupling.
PB95-150678 00,920

Potential Surfaces and Dynamics of Weakly Bound Trimers: Perspectives from High Resolution IR Spectroscopy.
PB96-176508 01,155

SUI, P. C.

Evaluation of Wear Resistant Ceramic Valve Seats in Gas-Fueled Power Generation Engines. Topical Report, December 1991-April 1994.
PB95-200218 02,466

SUKHDEV, R.

Modified Airy Function Method for the Analysis of Tunneling Problems in Optical Waveguides and Quantum Well Structures.
PB94-185824 02,120

SULLIVAN, D. B.

Time and Frequency: Bibliography of NIST Publications, March 1995.
PB95-220463 01,548

Time and Frequency Metrology.
PB96-190319 01,556

Time and Frequency Technology at NIST.
N94-30641/2 01,522

Time Generation and Distribution.
PB96-103049 01,550

SULLIVAN, F.

Computing S(alpha) Using Symbolic Monte Carlo.
PB94-198660 03,410

Data-Parallel Algorithm for Three-Dimensional Delaunay Triangulation and Its Implementation.
PB95-163309 01,714

Faster BKL Monte Carlo Simulations.
PB95-136370 01,706

Faster Monte Carlo Simulations.
PB96-102074 04,018

Heap of Data.
PB97-111488 03,424

Making Connections.
PB97-119044 01,785

Measuring Performance of Parallel Computers. Final Report.
DE94014586 01,665

Measuring Performance of Parallel Computers. Progress Report, 1989.
DE94014587 01,666

Self-Avoiding Surfaces, Topology, and Lattice Animals.
PB95-150512 04,571

Submissions to a Planned Encyclopedia of Operations Research on Computational Geometry and the Voronoi/ Delaunay Construct.
PB94-152709 03,425

Tree-Lookup for Partial Sums Or: How Can I Find This Stuff Quickly.
PB96-179411 01,770

SULLIVAN, P. J.

Visualization of Surface Figure by the Use of Zernike Polynomials.
PB96-137757 04,351

SUMARLIN, I. W.

Dispersions of Magnetic Excitations of the Pr Ions in Pr2CuO4.
PB94-173044 04,444

Magnetic Structure and Spin Dynamics of the Pr and Cu in Pr2CuO4.
PB96-111836 04,036

Phonon Density of States in R2CuO4 and Superconducting R1.85Ce0.15CuO4 (R = Nd, Pr).
PB95-150686 04,574

SUNG, L.

Dimensional Crossover in the Phase Separation Kinetics of Thin Polymer Blend Films.
PB97-113088 03,395

Light-Scattering Studies on Phase Separation in a Binary Blend with Addition of Diblock Copolymers.
PB96-146865 01,286

Morphology and Phase Separation Kinetics of a Compatibilized Blend.
PB97-119135 01,297

Phase Separation in Thin Film Polymer Blends With and Without Block Copolymer Additives.
PB96-204482 01,294

SUNG, P.

Effect of Ethanol on the Solubility of Hydroxyapatite in the System Ca(OH)2-H3PO4-H2O at 25C and 33C.
PB95-169231 00,169

SUNSHINE, S. A.

Neutron Powder Diffraction Study of the Crystal Structure of YSr2AlCu2O7.
PB94-212073 04,499

SUNUNU, C.

Refraction of Light by Graded Birefringent Media.
PB96-123716 02,192

SUPERCYNSKI, M. J.

Quench Energy and Fatigue Degradation Properties of Cu- and Al/Cu-Stablized Nb-Ti Epoxy-Impregnated Superconductor Coils.
PB96-141213 04,755

SURETTE, J.

Electronics and Electrical Engineering Laboratory 1995 Technical Accomplishments: Advancing Metrology for Electrotechnology to Support the U.S. Economy.
PB96-164520 01,959

SURETTE, J. M.

Electronics and Electrical Engineering Laboratory 1994 Program Plan: Supporting Technology for U.S. Competitiveness in Electronics.
PB94-126901 01,873

SUROLIA, A.

Thermodynamics of the Binding of Galactopyranoside Derivatives to the Basic Lectin from Winged Bean (Psophocarpus Tetrogonolobus).
PB95-162715 03,465

SUROWIEC, R.

Kinetic-Energy Distributions of Ions Sampled from Argon Plasmas in a Parallel-Plate, Radio-Frequency Reference Cell.
PB95-161964 03,935

SURYAN, M. M.

Thermal Decomposition of Hydroxy- and Methoxy-Substituted Anisoles.
PB94-173036 00,767

SUSHKOV, D. P.

Fine Structure of Negative Ions of Alkaline-Earth-Metal Atoms.
PB94-211182 03,837

SUSHKOV, O. P.

Hole Dispersion and Enhancement of Antiferromagnetic Interaction of Localized Spins in High-Tc Superconductors.
PB95-202602 04,694

SUSSMAN, J. L.

Protein Data Bank: Current Status and Future Challenges.
PB97-109060 00,517

SUSSMANN, R.

Frequency Shifting of Pulsed Narrow-Band Laser Light in a Multipass Raman Cell.
PB95-203352 04,321

SUTRINA, S. L.

Glucose Permease of Bacillus Subtilis Is a Single Polypeptide Chain That Functions to Energize the Sucrose Permease.
PB95-163192 03,466

SUTTON, D. D.

NIST 30 MHz Linear Measurement System.
PB94-169752 02,020

SUUBERG, E. M.

Behavior of Charring Materials in Simulated Fire Environments.
PB94-196045 01,368

SUYDAM, R.

Relationship of Silver with Selenium and Mercury in the Liver of Two Species of Toothed Whales (Odontocetes).
PB96-167275 02,596

SUZUKI, I. S.

Determination of Anomalous Superexchange in MnCl2 and Its Graphite Intercalation Compound.
PB97-122568 00,666

Structural and Magnetic Properties of CuCl2 Graphite Intercalation Compounds.
PB96-119748 03,020

SUZUKI, M.

Determination of Anomalous Superexchange in MnCl2 and Its Graphite Intercalation Compound.
PB97-122568 00,666

Structural and Magnetic Properties of CuCl2 Graphite Intercalation Compounds.
PB96-119748 03,020

SVENSSON, L. A.

Crystal Packing Interactions of Two Different Crystal Forms of Bovine Ribonuclease A.
PB95-152823 00,943

SVERJENSKY, D. A.

Summary of the Apparent Standard Partial Molal Gibbs Free Energies of Formation of Aqueous Species, Minerals,

and Gases at Pressures 1 to 5000 Bars and Temperatures 25 to 1000C.
PB96-145891 *01,113*

SVINCEK, P. R.

International Green Building Conference and Exposition (3rd). Held in San Diego, California on November 17-19, 1996. (Reannouncement with new abstract).
PB97-121826 *02,531*

SWAFFIELD, J. A.

Water Efficient Plumbing Fixtures through Standards and Test Methods.
PB95-125951 *00,248*

SWANSON, M.

Computer Security: Generally Accepted Principles and Practices for Securing Information Technology Systems.
PB97-110811 *01,619*

SWARTZ, S.

Phase Shifts and Intensity Dependence in Frequency-Modulation Spectroscopy.
PB96-103205 *01,071*

SWARTZENDRUBER, L.

Magnetic and Structural Properties of Electrodeposited Copper-Nickel Microlayered Alloys.
PB94-213121 *04,512*

SWARTZENDRUBER, L. J.

Determination of Thermoactivation Parameters of Vortex Mobility in YBa2Cu3O7 Using Only Magnetic Measurements.
PB95-163499 *04,624*

Experimental Verification of a Vector Preisach Model.
PB95-163564 *04,626*

Langevin Approach to Hysteresis and Barkhausen Modeling in Steel.
PB94-185675 *03,206*

Magnetocaloric Effect in Nanocomposites.
PB95-162798 *04,618*

Meissner, Shielding, and Flux Loss Behavior in Single-Crystal YBa2Cu3O6+x.
PB94-198744 *04,464*

Monte Carlo and Mean-Field Calculations of the Magnetocaloric Effect of Ferromagnetically Interacting Clusters.
PB94-172087 *03,201*

Temperature Dependence of Vortex Twin Boundary Interaction in Yttrium Barium Copper Oxide (YBa2Cu3O6+x).
PB95-162442 *04,613*

SWENSON, D. R.

Merged-Beams Energy-Loss Technique for Electron-Ion Excitation: Absolute Total Cross Sections for O(5+) (2s yields 2p).
PB96-102058 *04,017*

SWIDERSKY, P.

Application of the Taylor Dispersion Method in Supercritical Fluids.
PB95-164323 *00,977*

SWIFT, R. P.

Infrared and Microwave Spectroscopy of the Argon - Propyne Dimer.
PB94-198892 *00,794*

SWYDEN, T. A.

Planar Lenses for Field-Emitter Arrays.
PB96-103064 *02,112*

SWYT, D. A.

Design, Specification and Tolerancing of Micrometer-Tolerance Assemblies.
PB95-209862 *02,913*

Investing in Education to Meet a National Need for a Technical-Professional Workforce in a Post-Industrial Economy.
PB94-173028 *00,132*

New Concepts of Precision Dimensional Measurement for Modern Manufacturing.
PB96-160684 *02,924*

Uncertainties in Dimensional Measurements Made at Nonstandard Temperatures.
PB94-169760 *02,893*

SYLLAIOS, A. J.

Comparison of Techniques for Nondestructive Composition Measurements in CdZnTe Substrates.
PB96-103098 *02,703*

SZABO, S.

Control System Architecture for a Remotely Operated Unmanned Land Vehicle.
PB95-163200 *03,759*

Ground Vehicle Control at NIST: From Teleoperation to Autonomy.
N94-34037/9 *03,758*

SZEKELY, C.

Diode-Laser Pumped, Rubidium Cell Frequency Standards.
PB95-163218 *01,538*

Improved Rubidium Frequency Standards Using Diode Lasers with AM and FM Noise Control.
PB95-176152 *04,303*

Reducing the Effect of Local Oscillator Phase Noise on the Frequency Stability of Passive Frequency Standards.
PB95-180972 *01,545*

SZEKELY, J.

Mathematical Models of Transport Phenomena Associated with Arc-Welding Processes: A Survey.
PB96-135058 *02,870*

Power Characteristics in GMAW: Experimental and Numerical Investigation.
PB96-190145 *03,296*

SZELAZEK, J.

Dynamometer-Induced Residual Stress in Railroad Wheels: Ultrasonic and Saw Cut Measurements. Report No. 30.
PB96-183199 *04,857*

Residual Stress in Induction-Heated Railroad Wheels: Ultrasonic and Saw Cut Measurements. Report No. 28.
PB96-106992 *04,854*

Safety Assessment of Railroad Wheels by Residual Stress Measurements.
PB96-141114 *04,855*

Ultrasonic Measurement of Residual Stress in Cast Steel Railroad Wheels.
PB95-169199 *04,852*

SZLAG, D. C.

Phase Composition, Viscosities, and Densities for Aqueous Two-Phase Systems Composed of Polyethylene Glycol and Various Salts at 25C.
PB95-164596 *00,986*

Statistical Thermodynamics of Phase Separation and Ion Partitioning in Aqueous Two-Phase Systems.
PB94-199387 *01,212*

SZLAG, D. S.

Protein Extraction in a Spray Column Using a Polyethylene Glycol Maltodextrin Two-Phase Polymer System.
PB95-162228 *00,595*

SZYKMAN, S.

Combining Interactive Exploration and Optimization for Assembly Design.
PB97-112320 *02,794*

HVAC CAD Layout Tools: A Case Study of University/Industry Collaboration.
PB97-112221 *00,281*

Improving the Design Process by Predicting Downstream Values of Design Attributes.
PB97-113096 *02,795*

TAATJES, C. A.

Laser Double Resonance Measurements of the Quenching Rates of Br((2)P1/2) with H20, D20, HDO, and O2.
PB95-150694 *00,921*

TACHIBANA, H.

Orientation Effects on ESR Analysis of Alanine-Polymer Dosimeters.
PB96-146725 *03,720*

TACHIKAWA

VAMAS Intercomparison of Critical Current Measurements on NB3Sn Superconductors: A Summary Report.
PB96-119763 *04,043*

TACKE, M.

Stabilization of 3.3 and 5.1 m Lead-Salt Diode Lasers by Optical Feedback.
PB95-180709 *04,313*

TAGUCHI, S.

Taguchi's Parameter Design: A Panel Discussion.
PB96-111802 *03,445*

TAGZIRIA, H.

Preparation and Characterization of (6)LiF and (10)B Reference Deposits for the Measurement of the Neutron Lifetime.
PB95-108692 *03,874*

Problems Related to the Determination of Mass Densities of Evaporated Reference Deposits.
PB95-163226 *03,941*

TAI, G.

Efficient Method to Compute the Maximum Transient Drain Current Overshoot in Silicon on Insulator Devices.
PB94-172483 *02,300*

TAI, S. S. C.

Certification of Morphine and Codeine in a Human Urine Standard Reference Material.
PB95-176160 *03,499*

Certification of Phencyclidine in Lyophilized Human Urine Reference Materials.
PB96-160692 *03,508*

NIST Reference Materials to Support Accuracy in Drug Testing.
PB96-123807 *03,505*

TAKACS, E.

Observation and Visible and uv Magnetic Dipole Transitions in Highly Charged Xenon and Barium.
PB96-138441 *04,056*

Polarization Measurements on a Magnetic Quadrupole Line in Ne-Like Barium.
PB97-113104 *04,161*

TAKADA, K.

Direct Dispersion Measurement of Highly-Erbium-Doped Optical Amplifiers Using a Low Coherence Reflectometer Coupled with Dispersive Fourier Spectroscopy.
PB95-150702 *04,263*

Pump-Induced Dispersion of Erbium-Doped Fiber Measured by Fourier-Transform Spectroscopy.
PB94-211935 *04,236*

TAKAGI, K. K.

Effects on Whole Saliva of Chewing Gums Containing Calcium Phosphates.
PB95-153169 *03,563*

TAKAGI, S.

Behavior of a Calcium Phosphate Cement in Simulated Blood Plasma In vitro.
PB95-168712 *00,165*

Calcium Phosphate Cements.
PB97-111595 *03,580*

Crystal Structure of Calcium Adipate Monohydrate.
PB94-216579 *00,153*

Crystal Structure of Calcium Glutarate Monohydrate.
PB96-111893 *01,074*

Crystal Structure of Calcium Succinate Monohydrate.
PB95-168928 *00,167*

Deposition of Loosely Bound and Firmly Bound Fluorides on Tooth Enamel by an Acidic Gel Containing Fluorosilicate and Monocalcium Phosphate Monohydrate.
PB95-150710 *03,559*

Effects on Whole Saliva of Chewing Gums Containing Calcium Phosphates.
PB95-153169 *03,563*

Formation of Hydroxyapatite in a Polymeric Calcium Phosphate Cement.
PB95-180642 *00,173*

Formation of Hydroxyapatite in Cement Systems.
PB95-175261 *00,170*

Physical and Chemical Properties of Resin-Reinforced Calcium Phosphate Cements.
PB95-180212 *00,171*

Polymeric Calcium Phosphate Cements Derived from Poly(methyl vinyl ether-maleic acid).
PB96-164264 *00,180*

Properties and Mechanisms of Fast-Setting Calcium Phosphate Cements.
PB96-123229 *00,178*

Remineralization of Root Lesions with Concentrated Calcium and Phosphate Solutions.
PB96-102140 *03,567*

TAKARA, H.

Multiwavelength Birefringent-Cavity Mode-Locked Fibre Laser.
PB95-150496 *04,262*

TAMIR, D.

In-Space Welding: Visions and Realities.
PB95-163234 *04,830*

TAMURA, D.

Planar Near-Field Measurements and Microwave Holography for Measuring Aperture Distribution on a 60 GHz Active Array Antenna.
PB96-167366 *03,762*

TAMURA, G. T.

Smoke Control Systems for Elevator Fire Evacuation.
PB94-212883 *00,291*

TAN, Z.

Soft-X-ray-Emission Investigation of Cobalt Implanted Silicon Crystals.
PB96-157912 *04,069*

Soft-X-ray-Emission Studies of Bulk Fe3Si, FeSi, and FeSi2, and Implanted Iron Silicides.
PB96-157938 *04,071*

TANAKA, D. K.

Structures of Vapor-Deposited Yttria and Zirconia Thin Films.
PB94-216025 *03,041*

TANAKA, H.

Small-Angle X-Ray and Neutron Scattering Study of Block Copolymer/Homopolymer Mixtures.
PB94-213729 *01,221*

TANAKA, I.

High-Energy Phonon Dispersion in La1.85Sr0.15CuO4.
PB96-138458 *04,748*

TANAKA, J.

Effect of DC Tests on Induced Space Charge.
PB94-172350 *02,212*

TANAKA, M.

Thermodynamic and NMR Study of the Interactions of Cyclodextrins with Cyclohexane Derivatives.
PB94-185816 *00,781*

TANAKA, R.

Orientation Effects on ESR Analysis of Alanine-Polymer Dosimeters.
PB96-146725 *03,720*

TANAKA, T.

Small Angle Neutron Scattering Study on Poly(N-Isopropyl Acrylamide) Gels Near Their Volume-Phase Transition Temperature.
PB95-164380 *01,263*

Small-Angle Neutron Scattering Study on Weakly Charged Temperature Sensitive Polymer Gels.
PB95-164398 *01,264*

TANENBAUM, D.
Atomic-scale characterization of hydrogenated amorphous-silicon films and devices. Annual subcontract report, 14 February 1994--14 April 1995.
DE95009287 *02,294*

TANENBAUM, D. M.
Construction of Silicon Nanocolumns with the Scanning Tunneling Microscope.
PB95-203063 *04,696*

Growth and Nucleation of Hydrogenated Amorphous Silicon on Silicon (100) Surfaces.
PB96-176516 *02,991*

Nanoscale Study of the As-Grown Hydrogenated Amorphous Silicon Surface.
PB95-150595 *04,573*

Nanoscale Study of the Hydrogenated Amorphous Silicon Surface.
PB96-103056 *04,720*

TANG, C. M.
NIST-NRL Free-Electron Laser Facility.
PB94-212511 *04,237*

Planar Lenses for Field-Emitter Arrays.
PB96-103064 *02,112*

TANG, D.
Interlaboratory Comparison of Polarization-Holding Parameter Measurements on High-Birefringence Optical Fiber.
PB95-168464 *04,280*

TANG, H. C.
Thermal Modeling of Absolute Cryogenic Radiometers.
PB95-181236 *04,316*

TANG, J.
Neutron Leakage Benchmark for Criticality Safety Research.
PB95-126132 *03,723*

Properties and Interactions of Oral Structures and Restorative Materials. Annual Report for Period October 1, 1990 to September 30, 1991.
PB94-160843 *03,558*

TANG, J. T.
Application of a Simple Technique for Estimating Errors of Finite-Element Solutions Using a General-Purpose Code.
PB94-200250 *04,818*

TANG, S.
Global Thermodynamic Behavior of Fluid Mixtures in the Critical Region.
PB94-212420 *04,199*

TANG, W.
Neutron Scattering by Multiblock Copolymers of Structure (A-B)N-A.
PB94-211547 *01,219*

TANIGAK, K.
Rotational Dynamics of C60 in Na2RbC60.
PB95-153201 *00,948*

TANK, R. C.
Maturity Functions for Concrete Made with Various Cements and Admixtures.
PB94-199502 *01,314*

TANNER, A. B.
Measurement and Determination of Radon Source Potential: A Literature Review.
PB94-165602 *02,576*

TANNER, B. K.
Comparison of Techniques for Nondestructive Composition Measurements in CdZnTe Substrates.
PB96-103098 *02,703*

TANNER, C.
Optical Molasses: The Coldest Atoms Ever.
PB95-108908 *03,878*

TANNER, C. E.
Atoms in Optical Molasses.
PB95-108874 *03,875*

Atoms in Optical Molasses: Applications to Frequency Standards.
PB95-108882 *03,876*

Heterodyne Measurement of the Fluorescence Spectrum of Optical Molasses.
PB95-108411 *03,873*

Localization of Atoms in a Three-Dimensional Standing Wave.
PB95-163887 *03,944*

Measurements of Fluorescence from Cold Atoms: Localization in Three-Dimensional Standing Waves.
PB95-163879 *03,943*

Optical Molasses: Cold Atoms for Precision Measurements.
PB95-108890 *03,877*

Precision Lifetime Measurements of Cs 6p (2)P1/2 and 6p (2)P3/2 Levels by Single-Photon Counting.
PB95-203816 *04,010*

TANNER, D. B.
Laser-Synchrotron Hybrid Experiments: A Photon to Tickle, A Photon to Poke.
PB96-157847 *03,704*

TANNER, J. T.
Mixed Diet Reference Materials for Nutrient Analysis of Foods: Preparation of SRM-1548 Total Diet.
PB95-151692 *03,593*

TANUMA, S.
Calculations of Electron Inelastic Mean Free Paths (IMFPs). 4. Evaluation of Calculated IMFPs and of the Predictive IMFP Formula TPP-2 for Electron Energies between 50 and 2000 eV.
PB95-150728 *00,922*

Calculations of Electron Inelastic Mean Free Paths. 5. Data for 14 Organic Compounds over the 50-2000 eV Range.
PB95-150355 *00,916*

Use of Sum Rules on the Energy-Loss Function for the Evaluation of Experimental Optical Data.
PB95-150736 *04,264*

TAO, H. S.
Influence of Coadsorbed Potassium on the Electron-Stimulated Desorption of F(+), F(-), and F(*) from PF3 on Ru(0001).
PB96-157946 *04,072*

TAREK, M.
Molecular Dynamics Investigation of the Surface/Bulk Equilibrium in an Ethanol-Water Solution.
PB97-113112 *01,183*

TARLOV, M. J.
Characterization of Cytochrome c/Alkanethiolate Structures Prepared by Self-Assembly on Gold.
PB95-164638 *00,987*

Silver Metalization of Octadecanethiol Monolayers Self-Assembled on Gold.
PB95-150744 *00,923*

Surface Plasmon Microscopy of Biotin-Streptavidin Binding Reactions on UV-Photopatterned Alkanethiol Self-Assembled Monolayers.
PB96-176771 *01,158*

UV-Photopatterning of Alkylthiolate Monolayers Self-Assembled on Gold and Silver.
PB95-150751 *00,924*

TARNOFF, N.
NIST Support to the Next Generation Controller Program: 1991 Final Technical Report.
PB94-163490 *02,808*

World Model Registration for Effective Off-Line Programming of Robots.
PB94-173010 *02,933*

TARPEY, T.
Principal Points and Self-Consistent Points of Symmetric Multivariate Distributions.
PB96-135090 *03,446*

Representing a Large Collection of Curves: A Case for Principal Points.
PB95-152286 *03,438*

Two Principal Points of Symmetric, Strongly Unimodal Distributions.
PB95-203360 *03,443*

TARRINI, O.
Self Broadening in the nu1 Band of NH3.
PB94-216371 *00,857*

TARRIO, C.
Improved Reflectometry Facility at the National Institute of Standards and Technology.
PB96-160338 *04,087*

Influence of Electrical Isolation on the Structure and Reflectivity of Multilayer Coatings Deposited on Dielectric Substrates.
PB96-159736 *04,365*

New Method for Achieving Accurate Thickness Control for Uniform and Graded Multilayer Coatings on Large Flat Substrates.
PB96-159744 *04,366*

New NIST/ARPA National Soft X-ray Reflectometry Facility.
PB96-158092 *04,080*

Soft-X-ray Damage to p-terphenyl Coatings for Detectors.
PB96-159611 *04,364*

Soft X-ray Reflectometry Program at the National Institute of Standards and Technology.
PB96-160395 *04,368*

TARTARINI, P.
Transient Cooling of a Hot Surface by Droplets Evaporation.
PB94-156957 *03,783*

TASSEY, G.
Functions of Technology Infrastructure in a Competitive Economy.
PB94-173002 *00,478*

TAUHEED, A.
Analysis of the 5s(2)5p(2)-(5s5p(3)+5s(2)5p5d+5s(2)5p6s) Transitions of Four-Times Ionized Xenon (Xe V).
PB95-150769 *03,900*

Spectrum and Energy Levels of Triply Ionized Barium (Ba IV).
PB95-140877 *03,888*

TAY, S. P.
Structural and Magnetic Ordering in Iron Oxide/Nickel Oxide Multilayers by X-ray and Neutron Diffraction (Invited).
PB94-172558 *04,442*

TAYLOR, A.
Isolated Spin Pairs and Two-Dimensional Magnetism in SrCr(sub 9p)Ga(sub 12-9p)O19.
PB97-112387 *04,154*

Performance of HUD-Affiliated Properties during the January 17, 1994 Northridge Earthquake.
PB95-174488 *00,443*

TAYLOR, A. W.
Evaluating the Seismic Performance of Lightly-Reinforced Circular Concrete Bridge Columns.
PB95-163259 *01,335*

Jacket Thickness Requirements for Seismic Retrofitting of Circular Bridge Columns.
PB95-163267 *01,336*

Method of Estimating the Parameters of Tuned Mass Dampers for Seismic Applications.
PB96-167820 *00,473*

Northridge Earthquake, 1994. Performance of Structures, Lifelines and Fire Protection Systems.
PB94-161114 *00,421*

Northridge Earthquake 1994: Performance of Structures, Lifelines, and Fire Protection Systems.
PB94-207461 *04,825*

Report of a Workshop on Requalification of Tubular Steel Joints in Offshore Structures. Held in Houston, Texas on September 5-6, 1995.
PB96-210760 *03,699*

Seismic Performance of Circular Bridge Columns Designed in Accordance with AASHTO/CALTRANS Standards.
PB96-146352 *01,346*

State of the Art Report on Seismic Design Requirements for Nonstructural Building Components.
PB96-193800 *00,308*

TAYLOR, B. N.
Fine-Structure Constant.
PB94-172996 *03,795*

Guide for the Use of the International System of Units (SI).
PB95-226692 *02,747*

Guidelines for Evaluating and Expressing the Uncertainty of NIST Measurement Results. 1994 Edition.
PB95-143087 *02,649*

How Accurate Are the Josephson and Quantum Hall Effects and QED.
PB95-163283 *03,942*

Journal of Research of the National Institute of Standards and Technology. March/April 1994. Volume 99, Number 2.
PB94-219219 *02,000*

Journal of Research of the National Institute of Standards and Technology. May/June 1994. Volume 99, Number 3.
PB94-219326 *02,643*

Journal of Research of the National Institute of Standards and Technology, September-October 1993. Volume 98, Number 5.
PB96-134954 *03,362*

New International Representations of the Volt and Ohm Effective January 1, 1990.
PB95-150777 *01,890*

Report on the Meeting of the CCU (10th) (of the International Committee of Weights and Measures). Held on July 10-11, 1990.
PB94-172889 *03,792*

TAYLOR, J.
Electronic Balance and Some Gravimetric Applications. (The Density of Solids and Liquids, Pycnometry and Mass).
PB94-163052 *03,785*

Interaction of Rayleigh Waves with a Rib Attached to a Plate.
PB94-199023 *04,184*

TAYLOR, J. E.
Linking Anisotropic Sharp and Diffuse Surface Motion Laws via Gradient Flows.
PB95-203378 *04,698*

Mass Unit Disseminated to Surrogated Laboratories Using the NIST Portable Mass Calibration Package.
PB94-142486 *03,781*

TAYLOR, J. S.
Visualization of Surface Figure by the Use of Zernike Polynomials.
PB96-137757 *04,351*

TAYLOR, K. T.
Perturbative Calculation of the AC Stark Effect by the Complex Rotation Method.
PB95-141123 *04,260*

TAYLOR, L. S.
X-ray Protection Design.
AD-A279 181/2 *03,606*

TAYLOR, M. L.
Nutritional Status and Growth in Juvenile Rheumatoid Arthritis.
PB94-198470 *03,515*

TAYLOR, P. L.
Scattered Fractions of Dose from 18 and 25 MV X-ray Radiotherapy Linear Accelerators.
PB96-186101 *04,120*

TAYLOR, R.
High-Temperature Laser-Pulse Thermal Diffusivity Apparatus.
PB94-185147 *02,631*

TAYLOR, R. L.
Collision-Induced Emission in the Fundamental Vibration-Rotation Band of H2.
PB94-199445 *03,811*

TEAGUE, E. C.

Comparison of Finite Element and Analytic Calculations of the Resonant Modes and Frequencies of a Thick Shell Sphere.
PB94-160785 *02,626*

Electrical Test Structure for Overlay Metrology Referenced to Absolute Length Standards.
PB95-152278 *02,336*

Force Calibrations in the Nanonewton Regime.
PB95-168696 *03,949*

Generating and Measuring Displacements Up to 0.1 m to an Accuracy of 0.1 nm: Is It Possible.
PB96-160700 *04,090*

Measurement of Patterned Film Linewidth for Interconnect Characterization.
PB96-148168 *02,420*

Metrology Standards for Advanced Semiconductor Lithography Referenced to Atomic Spacings and Geometry.
PB96-160718 *02,424*

Nanometrology.
PB96-160726 *02,425*

New Test Structure for Nanometer-Level Overlay and Feature-Placement Metrology.
PB95-175345 *02,363*

Scanned Probe Microscopies: Opportunities and Issues in Metrology.
PB96-160783 *02,426*

Test Structures for the In-Plane Locations of Projected Features with Nanometer-Level Accuracy Traceable to a Coordinate Measurement System.
PB94-200565 *02,313*

TEBBUTT, J.

Guidelines for the Evaluation of X.500 Directory Products.
PB95-231908 *02,732*

Impact of the FCC's Open Network Architecture on NS/NP Telecommunications Security.
PB95-189445 *01,483*

X.500 Directory Schema Design Handbook.
PB96-183041 *02,739*

TEKLE, E.

Electropermeabilization of Cell Membranes: Effect of the Resting Membrane Potential.
PB95-163291 *03,537*

TELLER, C. M.

Assessment of Technology for Detection of Stress Corrosion Cracking in Gas Pipelines. Final Report, July 1993-March 1994.
PB94-206646 *02,475*

Gas-Coupled, Pulse-Echo Ultrasonic Crack Detection and Thickness Gaging.
PB96-147129 *04,847*

TEMPLE, D.

Photoelectron Spectroscopic Study of the Valence and Core-Level Electronic Structure of BaTiO3.
PB94-212149 *04,500*

Surface Core-Level Shifts of Barium Observed in Photoemission of Vacuum-Fractured BaTiO3 (100).
PB94-212156 *04,501*

TENBRINK, J.

Effect of Axial Strain on the Critical Current of Ag-Sheathed Bi-Based Superconductors in Magnetic Fields Up to 25 T.
PB94-211315 *04,493*

Improved Uniaxial Strain Tolerance of the Critical Current Measured in Ag-Sheathed Bi2Sr2Ca1Cu2O8+x Superconductors.
PB95-153565 *04,594*

TENG, Y. A.

Data-Parallel Algorithm for Three-Dimensional Delaunay Triangulation and Its Implementation.
PB95-163309 *01,714*

Parallel Monte Carlo Simulation of MBE Growth.
PB96-122841 *02,406*

TENNYSON, E. J.

In situ Burning of Oil Spills: Mesoscale Experiments and Analysis.
PB95-163747 *02,587*

TENWOLDE, A.

Controlling Moisture in the Walls of Manufactured Housing.
PB95-105136 *00,355*

Manufactured Housing Walls That Provide Satisfactory Moisture Performance in All Climates.
PB95-178885 *00,383*

TER MEER, H. U.

Phase Transitions in Solid C70: Supercooling, Metastable Phases, and Impurity Effect.
PB95-150090 *00,914*

TERLIZZI, C. P.

Performance Testing of a Family of Type I Combination Appliance.
PB95-220521 *02,505*

TERRANOVA, P.

Dynamic Shear Modulus Measurements with Four Independent Techniques in Nickel-Based Alloys.
PB94-198900 *03,320*

TESI, M. C.

Self-Avoiding Surfaces, Topology, and Lattice Animals.
PB95-150512 *04,571*

TESK, J.

Influence of Tempering Method on Residual Stress in Dental Porcelain.
PB94-172012 *00,138*

TESK, J. A.

Dental Materials.
PB94-172871 *00,142*

Effect of Transformation of Alloy on Transient and Residual Stresses in a Porcelain-Metal Strip.
PB94-198397 *00,143*

Error Propagation Biases in the Calculation of Indentation Fracture Toughness for Ceramics.
PB94-172434 *03,032*

Evaluation of Fracture Toughness and Residual Stress in Dental Porcelain by Indentation-Microfracture Method.
PB95-125613 *00,154*

Evaluation of Fracture Toughness and Residual Stress in Dental Porcelain by Indentation-Microfracture Method.
PB95-152831 *00,159*

Failure of All-Ceramic Fixed Partial Dentures 'In vitro' and 'In vivo': Analysis and Modeling.
PB96-122536 *00,175*

In vitro Fracture Behavior of Ceramic and Metal-Ceramic Restorations.
PB96-119722 *03,569*

International Standards and Reference Materials.
PB97-113120 *00,188*

Properties and Interactions of Oral Structures and Restorative Materials. Annual Report for Period October 1, 1990 to September 30, 1991.
PB94-160843 *03,558*

What Is a 'Standard Reference Material' - What Is Any Reference Material.
PB96-186135 *03,000*

TESORIERO, R.

Measurement of Process Complexity.
PB97-113138 *01,781*

TEW, W. L.

Assessment of Uncertainties of Calibration of Resistance Thermometers at the National Institute of Standards and Technology.
PB94-142478 *02,624*

Flux-Locked Current Source Reference.
PB95-150785 *02,039*

TEWARI, Y. B.

Apparent Molar Heat Capacities and Apparent Molar Volumes of Aqueous Glucose at Temperatures from 298.15 K to 327.01 K.
PB94-212800 *03,459*

Application of Thermodynamics to Biotechnology.
PB95-150793 *03,529*

Equilibrium and Calorimetric Investigation of the Hydrolysis of L-Tryptophan to (Indole + Pyruvate + Ammonia).
PB95-163317 *00,661*

Thermochemistry of the Hydrolysis of L-arginine to (L-citrulline + Ammonia) and of the Hydrolysis of L-arginine to (L-ornithine + Urea).
PB95-150801 *03,463*

Thermochemistry of the Reactions between Adenosine, Adenosine 5'-monophosphate, Inosine, and Inosine 5'-monophosphate; the Conversion of L-histidine to (Urocanic Acid+Ammonia).
PB94-213113 *03,460*

Thermodynamic and NMR Study of the Interactions of Cyclodextrins with Cyclohexane Derivatives.
PB94-185816 *00,781*

Thermodynamic Study of the Reactions of Cyclodextrins with Primary and Secondary Aliphatic Alcohols, with D- and L-Phenylalanine, and with L-Phenylalanineamide.
PB95-180873 *01,016*

Thermodynamics of Enzyme-Catalyzed Reactions: Part 1. Oxidoreductases.
PB94-162252 *00,737*

Thermodynamics of Enzyme-Catalyzed Reactions. Part 4. Lyases.
PB96-145941 *01,118*

Thermodynamics of Enzyme-Catalyzed Reactions. Part 5. Isomerases and Ligases.
PB96-145974 *01,121*

Thermodynamics of the Hydrolysis of N-Acetyl-L-phenylalanine Ethyl Ester in Water and in Organic Solvents.
PB95-203386 *01,053*

Thermodynamics of the Hydrolysis of Penicillin G and Ampicillin.
PB94-172467 *03,596*

Thermodynamics of the Hydrolysis of 3,4,5-Trihydroxybenzoic Acid Propyl Ester (n-Propylgallate) to 3,4,5-Trihydroxybenzoic Acid (Gallic Acid) and Propan-I-ol in Aqueous Media and in Toluene.
PB96-186143 *01,160*

TEWARY, V.

Lattice Imperfections Studied by Use of Lattice Green's Functions.
PB95-150850 *04,576*

TEWARY, V. K.

Atomic Theory of Fracture of Brittle Materials: Application to Covalent Semiconductors.
PB94-216553 *04,519*

Elastic Green's Function for a Bimaterial Composite Solid Containing a Free Surface Normal to the Interface.
PB95-163325 *03,162*

Generalized Plane Strain Analysis of a Bimaterial Composite Containing a Free Surface Normal to the Interface.
PB95-163341 *03,164*

Green's Function for Generalized Hilbert Problem for Cracks and Free Surfaces in Composite Materials.
PB95-163333 *03,163*

Lattice Statics of Interfaces and Interfacial Cracks in Bimaterial Solids.
PB96-161823 *02,985*

THALWEISER, R.

Femtosecond Time-Resolved Molecular Multiphoton Ionization: The Na2 System.
PB95-202305 *03,975*

Femtosecond Time-Resolved Wave Packet Motion in Molecular Multiphoton Ionization and Fragmentation.
PB94-198611 *00,790*

THEIN, M.

Intercomparison Study of (237)Np Determination in Artificial Urine Samples.
PB96-102645 *03,633*

THEN, S. S.

Loss-Free Counting at IRI and NIST.
PB96-167119 *04,105*

THEODOSIOU, C. E.

Oscillator Strengths and Radiative Branching Ratios in Atomic Sr.
PB95-203493 *04,008*

THIRUMALAI, D.

Activated Dynamics, Loss of Ergodicity, and Transport in Supercooled Liquids.
PB95-150819 *00,925*

Quantitative Measure of Efficiency of Monte Carlo Simulations.
PB95-180691 *01,011*

THODE, W. F.

Proposed International Interactive Courseware Standard.
PB96-123161 *00,137*

THOMAS, B. H.

Generic Manufacturing Controllers.
PB94-199940 *02,818*

Using Grafcet to Design Generic Controllers.
PB95-150827 *02,821*

THOMAS, B. N.

Studies of the Higher Order Smectic Phase of the Large Electroclinic Effect Material W317.
PB95-151601 *00,935*

X-ray Observation of Electroclinic Layer Constriction and Rearrangement in a Chiral Smectic-A Liquid Crystal.
PB96-141080 *01,100*

THOMAS, C.

Implementation of a Standard Format for GPS Common View Data.
N95-32323/4 *03,779*

Implementation of a Standard Format for GPS Common View Data.
PB96-176581 *01,555*

Use of Ionospheric Data in GPS Time Transfer.
PB95-163853 *01,540*

THOMAS, C. L.

Fluorescence Anisotropy Measurements on a Polymer Melt as a Function of Applied Shear Stress.
PB94-199296 *01,209*

In-Line Optical Monitoring of Injection Molding.
PB94-185105 *01,201*

Observations of Shear Induced Molecular Orientation in a Polymer Melt Using Fluorescence Anisotropy Measurements.
PB94-199304 *01,210*

Observations of Shear Stress and Molecular Orientation Using Fluorescence Anisotropy Measurements.
PB94-199312 *01,211*

THOMAS, J. B.

Methods for Analysis of Cancer Chemopreventive Agents in Human Serum.
PB95-200648 *03,502*

THOMAS, J. L.

Precision Resistors and Their Measurement.
AD-A284 623/6 *02,249*

THOMAS, J. W. L.

36Cl/Cl Accelerator-Mass-Spectrometry Standards: Verification of Their Serial-Dilution-Solution Preparations by Radioactivity Measurements.
PB94-140563 *00,524*

THOMAS, K. M.

Hybrid Undulator for the NIST-NRL Free-Electron Laser.
PB94-212529 *04,238*

THOMAS, R. N.

Aerodynamic Phenomena in Stellar Atmospheres - A Bibliography.
AD-A278 521/0 *00,046*

THOMAS, W. C.

Analysis of Moisture Accumulation in a Wood-Frame Wall Subjected to Winter Climate.
PB94-199320 *00,338*

THOMPSON, A.

Beamcon III, a Linearity Measurement Instrument for Optical Detectors.
PB96-113576 *04,337*

Improved Automated Current Control for Standard Lamps.
PB94-219367 *00,246*

Irradiance of Horizontal Quartz-Halogen Standard Lamps.
PB96-179130 *01,866*

Report on USDA Ultraviolet Spectroradiometers.
PB96-214648 *00,125*

Standards for Corrected Fluorescence Spectra.
PB95-150835 *00,581*

THOMPSON, A. N.

Metalloporphyrin Sensitized Photooxidation of Water to Oxygen on the Surface of Colloidal Iridium Oxides - Photochemical and Pulse Radiolytic Studies.
PB95-107082 *00,868*

THOMPSON, C.

Report on Application Integration Architectures (AIA) Workshop. Held in Dallas, Texas on February 8-12, 1993.
PB94-142536 *01,803*

THOMPSON, C. A.

Alternating-Field Susceptometry and Magnetic Susceptibility of Supercondoctors. Presented at Office of Naval Research Workshop on Magnetic Susceptibility of Superconductors and Other Spin Systems. Held in Berkeley Springs, West Virginia on 20 May 1991.
PB94-145984 *04,435*

Apparatus for Resistance Measurement of Short, Small-Diameter Conductors.
PB96-141130 *04,417*

Micromagnetic Scanning Microprobe System.
PB95-176178 *02,224*

THOMPSON, G.

FTS Infrared Measurements of the Rotational and Vibrational Spectrum of LiH and LiD.
PB94-216231 *00,856*

THOMPSON, J. S.

Backscattering in Electron-Impact Excitation of Multiply Charged Ions.
PB94-185345 *03,799*

Electron-Impact Excitation of Si(3+)(3S yields 3P) Using a Merged-Beam Electron-Energy-Loss Technique.
PB95-151239 *03,904*

Evidence for Significant Backscattering in Near-Threshold Electron-Impact Excitation of Ar(7+)(3s yields 3p).
PB95-126405 *03,883*

Merged-Beams Energy-Loss Technique for Electron-Ion Excitation: Absolute Total Cross Sections for O(5+) (2s yields 2p).
PB96-102058 *04,017*

THOMPSON, R.

Fracture in Multilayers.
PB96-163613 *02,988*

THOMPSON, R. B.

Ultrasonic Measurement of Sheet Anisotropy and Formability.
PB95-153235 *03,213*

Ultrasonic Methods.
PB96-190327 *02,707*

THOMPSON, W. E.

Infrared and Near-Infrared Spectra of HCC and DCC Trapped in Solid Neon.
AD-A295 578/9 *03,773*

Matrix Isolation Study of the Interaction of Excited Neon Atoms with BCl3: Infrared Spectra of BCl(sub 3, sup +), BCl(sub 2, sup +), and BCl(sub 3, sup -).
PB97-119143 *01,187*

Matrix Isolation Study of the Interaction of Excited Neon Atoms with O3: Infrared Spectrum of O((sub 3)(-)) and Evidence for the Stabilization of O2...O((sub 4)(+)).
PB97-112403 *04,155*

Mid- and Near-Infrared Spectra of Water and Water Dimer Isolated in Solid Neon.
PB95-125662 *00,888*

Production and Spectroscopy of Small Polyatomic Molecular Ions Isolated in Solid Neon. (Reannouncement with New Availability Information).
AD-A234 043/8 *00,704*

Vibrational Spectra of Molecular Ions Isolated in Solid Neon: HCCH+ and HCC-. (Reannouncement with New Availability Information).
AD-A253 551/6 *00,707*

Vibrational Spectra of Molecular Ions Isolated in Solid Neon. X. H2O(+), HDO(+), and D2O(+).
PB95-125670 *00,889*

Vibrational Spectra of Molecular Ions Isolated in Solid Neon. XI. NO2(+), NO2(-), and NO3(-).
PB95-125688 *00,890*

Vibrational Spectra of Molecular Ions Isolated in Solid Neon. 6. CO4(-). (Reannouncement with New Availability Information).
AD-A238 415/4 *00,705*

Vibrational Spectra of Molecular Ions Isolated in Solid Neon. 7. CO(+), C2O2(+), and C2O2(-). (Reannouncement with New Availability Information).
AD-A239 729/7 *00,706*

Vibrational Spectra of Molecular Ions Isolated in Solid Neon. 11. NO2(+), NO2(-), and NO3(-).
AD-A275 828/2 *00,708*

Vibrational Spectra of Molecular Ions Isolated in Solid Neon. 13. Ions Derived from HBr and HI.
PB97-119234 *01,188*

THOMSON, R.

Atomic Theory of Fracture of Brittle Materials: Application to Covalent Semiconductors.
PB94-216553 *04,519*

Cracks and Dislocations in Face-Centered Cubic Metallic Multilayers.
PB96-163696 *02,989*

Dislocation Core-Core Interaction and Peierls Stress in a Model Hexagonal Lattice.
PB96-162003 *04,101*

Dislocation Emission at Ledges on Cracks.
PB95-164240 *04,630*

Fundamentals of Fracture: A 1993 Prologue, and Other Comments.
PB96-161971 *03,218*

Interaction between Dislocations and Intergranular Cracks.
PB95-152096 *03,190*

Interfacial Crack in a Two-Dimensional Hexagonal Lattice.
PB96-161989 *04,100*

Lattice Imperfections Studied by Use of Lattice Green's Functions.
PB95-150850 *04,576*

Lattice Statics of Interfaces and Interfacial Cracks in Bimaterial Solids.
PB96-161823 *02,985*

Nonlocal Effects of Existing Dislocations on Crack-Tip Emission and Cleavage.
PB96-161807 *03,367*

Shielding of Cracks in a Plastically Polarizable Material.
PB95-164257 *04,631*

Whither Computational Materials Science. Some Thoughts from the Mechanical Properties Front.
PB96-161997 *02,987*

THOMSON, R. E.

Development of Highly Conductive Cantilevers for Atomic Force Microscopy Point Contact Measurements.
PB96-138573 *04,751*

Fabrication Issues in Optimizing YBa2Cu3O7-x Flux Transformers for Low I/f Noise.
PB95-175857 *02,059*

Insulating Nanoparticles on YBa2Cu3O7-delta Thin Films Revealed by Comparison of Atomic Force and Scanning Tunneling Microscopy.
PB95-150843 *04,575*

Low Noise YBa2Cu3O7-x-SrTiO3-YBa2Cu3O7-x Mulitlayers for Improved Superconducting Magnetometers.
PB96-138417 *04,747*

Observation of Insulating Nanoparticles on YBCO Thin-Films by Atomic Force Microscopy.
PB95-163358 *04,622*

Scanning Tunneling Microscopy of the Charge-Density-Wave Structure in 1T-TaS2.
PB95-180980 *04,689*

Surface Modification of YBa2Cu3O7-delta Thin Films Using the Scanning Tunneling Microscope: Five Methods.
PB95-203394 *04,699*

Temperature Dependence and Magnetic Field Modulation of Critical Currents in Step-Edge SNS YBCO/Au Junctions.
PB96-111745 *04,723*

THORNE, B. B.

Airborne Asbestos Method: Bootstrap Method for Determining the Uncertainty of Asbestos Concentration. Version 1.0.
PB96-214614 *00,646*

THORPE, M. F.

Elastic Properties of Central-Force Networks with Bond-Length Mismatch.
PB95-163366 *04,623*

THORPE, M. R.

Geometrical Percolation Threshold of Overlapping Ellipsoids.
PB96-102397 *03,167*

THUDIUM, R. N.

Microstructure Effect on the Phase Behavior of Blends of Deuterated Polybutadiene and Protonated Polyisopene.
PB97-113146 *01,296*

THUMM, U.

Angle-Differential and Momentum-Transfer Cross Sections for Low-Energy Electron-Cs Scattering.
PB95-203402 *04,005*

Characteristics of Light Emission After Low-Energy Electron Impact Excitation of Caesium Atoms.
PB94-198587 *03,806*

Relativistic Effects in Spin-Polarization Parameters for Low-Energy Electron-Cs Scattering.
PB95-150868 *03,901*

Relativistic R-Matrix Calculations for Electron - Alkali-Metal-Atom Scattering: Cs as a Test Case.
PB95-203410 *04,006*

THURBER, W. R.

Heavily Accumulated Surfaces of Mercury Cadmium Telluride Detectors: Theory and Experiment.
PB94-216074 *02,134*

Novel Magnetic Field Characterization Techniques for Compound Semiconductor Materials and Devices.
PB96-176458 *02,433*

Semiconductor Measurement Technology: Improved Characterization and Evaluation Measurements for HgCdTe Detector Materials, Processes, and Devices Used on the GOES and TIROS Satellites.
PB94-188810 *02,122*

Transverse Magnetoresistance: A Novel Two-Terminal Method for Measuring the Carrier Density and Mobility of a Semiconductor Layer.
PB95-150066 *02,332*

THURGATE, S.

Grazing-Incidence X-Ray Photoemission Spectroscopy Investigation of Oxidized GaAs(100): A Novel Approach to Nondestructive Depth Profiling.
PB94-200151 *04,480*

THURGATE, S. M.

Grazing Angle X-Ray Photoemission System for Depth-Dependent Analysis.
PB95-161154 *04,600*

Grazing Incidence X-ray Photoemission and Its Implementation on Synchrotron Light Source X-ray Beamlines.
PB95-175766 *01,001*

TIDSTROM, K. D.

Evolution of a Turbulent Boundary Layer Induced by a Three-Dimensional Roughness Element.
PB94-212818 *04,200*

TIERNEY, E. J.

Total Surface Areas of Group IVA Organometallic Compounds: Predictors of Toxicity to Algae and Bacteria.
PB94-211331 *00,814*

TIESINGA, E.

Measurement of the Atomic Na(3P) Lifetime and of Retardation in the Interaction between Two Atoms Bound in a Molecule.
PB97-122360 *04,178*

TIETZ, L. A.

Fiber Coating Diameter: Toward a Glass Artifact Standard.
PB96-140389 *02,234*

TILFORD, C. R.

Characteristics of Partial Pressure Analyzers.
PB95-150876 *00,582*

Comments on the Stability of Bayard-Alpert Ionization Gages.
PB96-103080 *02,673*

Measurement of Very-Low Partial Pressures.
PB95-180998 *02,659*

Partial Pressure Analysis in Space Testing.
N95-14084/4 *04,827*

Partial Pressure Analysis in Space Testing.
PB96-103072 *04,829*

PC-Based Spinning Rotor Gage Controller.
PB95-175832 *02,609*

Process Monitoring with Residual Gas Analyzers (RGAs): Limiting Factors.
PB95-181004 *02,660*

Vacuum Gauges and Partial Pressure Analyzers.
PB95-150884 *02,650*

TILLNER-ROTH, R.

Report of the Refrigeration, Air Conditioning and Heat Pumps Technical Options Committee.
PB96-176755 *03,293*

TILSTRA, L.

Microbial Degradation of Polysulfides and Insights into Their Possible Occurrence in Coal.
PB95-163374 *02,488*

TIMMER, C. A.

Merged-Beams Energy-Loss Technique for Electron-Ion Excitation: Absolute Total Cross Sections for O(5+) (2s yields 2p).
PB96-102058 *04,017*

TIMMERHAUS, K.

Energy Flows in an Orifice Pulse Tube Refrigerator.
PB95-169082 *02,752*

TIMMERHAUS, K. D.

Graded and Nongraded Regenerator Performance.
PB95-169090 *02,753*

Resistance Thermometers with Fast Response for Use in Rapidly Oscillating Gas Flows.
PB95-107298 *03,261*

Thermal Anemonetry for Mass Flow Measurement in Oscillating Cryogenic Gas Flows.
PB96-176789 *04,218*

TIMONEN, R. S.

Kinetics of the Reaction of CCl3-Br-2 and the Thermochemistry of CCl3 Radical and Cation.
PB94-212115 *00,824*

TING, A. C.

Planar Lenses for Field-Emitter Arrays.
PB96-103064 *02,112*

TINKER, S.

Transient Cooling of a Hot Surface by Droplets Evaporation.
PB95-143194 *03,890*

Water Droplet Evaporation from Radiantly Heated Solids.
PB95-217147 00,394

TINO, G. M.

High-Resolution Diode-Laser Spectroscopy of Calcium.
PB95-181244 03,969

TINSCHERT, K.

Dielectronic Capture Processes in the Electron-Impact Ionization of Sc(2+).
PB95-203113 04,000

TIRUMALAI, V. C.

Solid State (13)C NMR and Raman Studies of Cellulose Triacetate: Oligomers, Polymorphism, and Inferences about Chain Polarity.
PB96-176532 01,289

TISON, S. A.

Commercial Helium Permeation Leak Standards: Their Properties and Reliability.
PB97-111413 04,146

Critical Evaluation of Thermal Mass Flow Meters.
PB97-113153 00,683

Experimental Data and Theoretical Modeling of Gas Flows Through Metal Capillary Leaks.
PB95-150892 04,206

Improved Gas Flow Measurements for Next-Generation Processes.
PB96-156013 04,216

TJOSSEM, P. J. H.

Optical Measurements of Atomic Hydrogen, Hydroxyl, and Carbon Monoxide in Hydrocarbon Diffusion Flames.
PB95-150900 02,487

TOBIAS, D. J.

Molecular Dynamics Investigation of the Surface/Bulk Equilibrium in an Ethanol-Water Solution.
PB97-113112 01,183

TOBIN, S. P.

Comparison of Techniques for Nondestructive Composition Measurements in CdZnTe Substrates.
PB96-103098 02,703

TOBLER, R. L.

Charpy Impact Test as an Evaluation of 4 K Fracture Toughness.
PB96-190194 03,219

Charpy Specimen Tests at 4 K.
PB96-190335 03,002

Fatigue Crack Thresholds of a Nickel-Iron Alloy for Superconductor Sheaths at 4 K.
PB96-190343 03,223

Mechanical Properties and Warm Prestress of Ultra-Low Carbon Steel at 4 K.
PB96-190350 03,224

TOBY, B. H.

Colossal Magnetoresistance without Mn(3+)/Mn(4-) Double Exchange in the Stoichiometric Pyrochlore Tl2Mn2O7.
PB97-113070 04,160

TODD, D.

De Facto Microzonation through the Use of Soils Factors in Design Triggers.
PB96-141148 00,462

Evaluation and Retrofit Standards for Existing Federally Owned and Leased Buildings.
PB95-150918 00,434

Executive Order 12941. Seismic Safety of Existing Federally Owned or Leased Buildings: It's History, Content and Objectives.
PB96-156021 00,465

How-To Suggestions for Implementing Executive Order 12941 on Seismic Safety of Existing Federal Buildings, A Handbook.
PB96-131552 00,461

ICSSC Guidance on Implementing Executive Order 12941 on Seismic Safety of Existing Federally Owned or Leased Buildings.
PB96-128103 00,459

Northridge Earthquake, 1994. Performance of Structures, Lifelines and Fire Protection Systems.
PB94-161114 00,421

Northridge Earthquake 1994: Performance of Structures, Lifelines, and Fire Protection Systems.
PB94-207461 04,825

Performance of Federal Buildings in the January 17, 1994 Northridge Earthquake.
PB95-231775 00,453

Performance of HUD-Affiliated Properties during the January 17, 1994 Northridge Earthquake.
PB95-174488 00,443

Some Basics on Who's Who and What's What in Seismic Safety.
PB95-150926 00,435

World of Building Codes.
PB95-203428 00,449

TODD, D. R.

Seismic Safety of Federal Buildings. Initial Program: How Much Will It Cost.
PB95-182291 00,447

Seismic Strengthening of Reinforced Concrete Frame Buildings.
PB95-108841 00,430

Standards of Seismic Safety for Existing Federally Owned or Leased Buildings and Commentary.
PB95-130209 00,431

Strengthening Methodology for Lightly Reinforced Concrete Frames.
PB96-158050 00,466

Strengthening Methodology for Lightly Reinforced Concrete Frames-II. Recommended Calculation Techniques for the Design of Infill Walls.
PB94-187648 00,426

Strengthening Methodology for Lightly Reinforced Concrete Frames: Recommended Design Guidelines for Strengthening with Infill Walls.
PB95-260725 00,454

TODD, F. G.

Vibrations of S1((1)B2u) p-Difluorobenzene - d4. S1-S0 Fluorescence Spectroscopy and ab Initio Calculations.
PB95-202586 01,028

TODD, J. H.

Measurement of the (10)B(n, alpha1gamma)(7)Li Cross Section in the 0.3 to 4 MeV Neutron Energy Interval.
PB96-161799 04,098

TODD, P.

Gravity Dependent Processes and Intracellular Motion.
PB95-163382 03,538

TOFANI, S.

Bistatic Scattering of Absorbing Materials from 30 to 1000 MHz.
PB95-150934 01,891

Time-Domain Measurements of the Electromagnetic Backscatter of Pyramidal Absorbers and Metallic Plates.
PB94-185410 01,877

TOLLE, J. W.

Convergence Properties of a Class of Rank-Two Updates. (NIST Reprint).
PB95-180097 03,430

TOM, H.

Geographic Information Systems Standards: A Federal Perspective.
PB95-163390 03,678

Spatial Information and Technology Standards Evolving.
PB96-135108 03,679

Standards: A Cardinal Direction for Geographic Information Systems.
PB95-150942 03,677

TOMASCH, W. J.

Microwave Properties of YBa2Cu3O7-x Films at 35 GHz from Magnetotransmission and Magnetoreflection Measurements.
PB95-168977 04,643

TOMASZKIEWICZ, I.

Thermodynamic Properties of Silicides. 5. Standard Molar Enthalpy of Formation at the Temperature 298.15 K of Trimolybdenum Monosilicide Mo3Si Determined by Fluorine-Combustion Calorimetry.
PB97-119358 01,190

TOMAZIC, B. B.

Critical Evaluation of the Purification of Biominerals by Hypochlorite Treatment.
PB95-150959 00,186

Influence of Natural and Synthetic Inhibitors on the Crystallization of Calcium Oxalate Hydrates.
PB95-150967 03,560

Physicochemical Characterization of Natural and Bioprosthetic Heart Valve Calcific Deposits: Implications for Prevention.
PB96-156039 00,187

Physicochemical Properties of Calcific Deposits Isolated from Porcine Bioprosthetic Heart Valves Removed from Patients Following 2-13 Years Function.
PB94-172863 00,184

TOMEK, A.

dc Method for the Absolute Determination of Conductivities of the Primary Standard KCl Solutions from 0C to 50C.
PB94-219342 02,644

TOMIZAWA, M.

Effects of Heavy Doping on Numerical Simulations of Gallium Arsenide Bipolar Transistors.
PB95-150975 02,334

TONER, M.

Crystal Packing Interactions of Two Different Crystal Forms of Bovine Ribonuclease A.
PB95-152823 00,943

TONEY, M. F.

X-Ray Diffraction from Anodic TiO2 Films: In situ and Ex situ Comparison of the Ti(0001) Face.
PB94-185972 00,782

TONG, G.

Compensation of Markov Estimator Errors in Time-Jittered Sampling of Nonmonotonic Signals.
PB95-150983 01,590

TONUCCI, R. J.

Photonic Band-Structure Effects for Low-Index-Contrast Two-Dimensional Lattices in the Near Infrared.
PB97-122469 04,401

TOPOROWSKI, P. M.

Thermodynamic Properties of Dilute and Semidilute Solutions of Regular Star Polymers.
PB96-146808 01,284

TORARDI, C. C.

Ca4Bi6O13: A Compound Containing an Unusually Low Bismuth Coordination Number and Short Bi Bi Contacts.
PB95-141131 00,911

TORCZYNSKI, J. R.

Gaseous Electronics Conference Radio-Frequency Reference Cell: A Defined Parallel-Plate Radio-Frequency System for Experimental and Theoretical Studies of Plasma-Processing Discharges.
PB94-172327 04,404

TORIKAI, N.

Localization of a Homopolymer Dissolved in a Lamellar Structure of a Block Copolymer Studied by Small-Angle Neutron Scattering.
PB95-161592 01,253

TORQUATO, S.

Cross-Property Relations and Permeability Estimation in Model Porous Media.
PB95-150280 04,205

Transport and Diffusion in Three-Dimensional Composite Media.
PB95-176129 04,668

TORRE, J. M.

Preliminary Comparison of Time Transfers via LASSO, GPS and Two-Way Satellite.
PB95-151098 01,529

TORRENCE, S. R.

Development and Validation of Multicriteria Ratings: A Case Study.
PB95-126025 00,004

TORTONESE, M.

Vortex Images in Thin Films of YBa2Cu3O(sub 7-x) and Bi2Sr2Ca1Cu2O(sub 8+x) Obtained by Low-Temperature Magnetic Force Microscopy.
PB97-119408 04,815

TOSSELL, J. A.

Associative Electron Attachment to S2F10, S2OF10, and S2O2F10.
PB95-140992 00,907

TOTH, P.

Proceedings of the Workshop on the Federal Criteria for Information Technology Security. Held in Ellicot City, Maryland on June 2-3, 1993.
PB94-162583 01,575

Proceedings Report of the International Invitation Workshop on Development Assurance. Held in Ellicott City, Maryland on June 16-17, 1994.
PB95-189494 02,912

TOTH, P. R.

Concept Paper: An Overview of the Proposed Trust Technology Assessment Program.
PB96-160882 01,614

Head Start on Assurance: Proceedings of an Invitational Workshop on Information Technology (IT) Assurance and Trustworthiness. Held in Williamsburg, Virginia on March 21-23, 1994.
PB94-215746 01,586

TOTH, R. B.

Standards Activities of Organizations in the United States.
PB97-124135 00,006

TOULOUSE, J.

Anomalous Dispersion and Thermal Expansion in Lightly-Doped KTa1-xNbxO3.
PB95-152302 04,585

TOURDE, R.

Preliminary Comparison of Time Transfers via LASSO, GPS and Two-Way Satellite.
PB95-151098 01,529

TOWER, J. P.

Comparison of Techniques for Nondestructive Composition Measurements in CdZnTe Substrates.
PB96-103098 02,703

TOWNES, C. H.

Molecular Microwave Spectra Tables.
AD-A296 498/9 00,720

TOYOKUNI, S.

DNA Base Modifications in Renal Chromatin of Wistar Rats Treated with a Renal Carcinogen, Ferric Nitrilotriacetate.
PB95-150363 03,648

Treatment of Wistar Rats with a Renal Carcinogen, Ferric Nitrilotriacetate, Causes DNA-Protein Cross-Linking between Thymine and Tyrosine in Their Renal Chromatin.
PB96-112115 03,649

TRABELSI, A.

Planar Near-Field Alignment.
PB94-172491 01,998

TRACY, J.

Response Comparison of Electret Ion Chambers, LiF TLD, and HPIC.
PB96-190103 02,578

TRACY, J. W.

External Gamma-ray Counting of Selected Tissues from a Thorotrast Patient.
PB96-160254 03,637

TRAFTON, L. M.

Observations of 3C 273 with the Goddard High Resolution Spectrograph on the Hubble Space Telescope.
PB95-202321 00,076

TRAHEY, N. M.
NIST Standard Reference Materials (Trade Name) Catalog 1995-1996.
PB95-232518 *00,508*

TRAIBER, A. J. S.
Electronic Structure and Phase Equilibria in Ternary Substitutional Alloys.
PB97-119366 *03,378*

TRAIL, W. K.
Importance of Bound-Free Correlation Effects for Vibrational Excitation of Molecules by Electron Impact: A Sensitivity Analysis.
PB95-202974 *03,996*

Low-Energy-Electron Collisions with Sodium: Elastic and Inelastic Scattering from the Ground State.
PB96-103106 *04,030*

TRAUGOTT, A. E.
U.S. Green Building Conference, 1994.
PB94-206364 *02,519*

TRAVIS, J.
Laser Ablation of Thin Films as a Free Atom Source for Pulsed RIMS.
PB94-198710 *00,540*

TRAVIS, J. C.
Determination of the Transmittance Uniformity of Optical Filter Standard Reference Materials.
PB95-261921 *02,182*

Fourier Transform Atomic Emission Studies Using a Glow Discharge as the Emission Source.
PB94-185980 *00,533*

Standard Reference Materials: Glass Filters as a Standard Reference Material for Spectrophotometry - Selection, Preparation, Certification, and Use of SRM 930 and SRM 1930.
PB94-188844 *00,536*

Trace Detection in Conducting Solids Using Laser-Induced Fluorescence in a Cathodic Sputtering Cell.
PB95-163424 *00,598*

TREADO, S. J.
Lighting and HVAC.
PB95-150991 *00,250*

NIST Lighting and HVAC Interaction Test Facility.
PB95-151007 *00,251*

Optical Performance of Commercial Windows.
PB95-208757 *00,392*

Performance of Compact Fluorescent Lamps at Different Ambient Temperatures.
PB95-175329 *00,258*

TREE, D. R.
Role of R22 in Refrigerating and Air Conditioning Equipment.
PB94-199783 *03,253*

TRELA, W. J.
Vibronic Coupling and Other Many-Body Effects in the 4sigmag(-1) Photoionization Channel of CO2.
PB95-162509 *00,962*

TRETYAKOV, M. Y.
Tunneling-Rotation Spectrum of the Hydrogen Fluoride Dimer.
PB94-198678 *00,793*

TREVINO, S. F.
Maximum Entropy as a Tool for the Determination of the C-Axis Profile of Layered Compounds.
PB94-199619 *00,800*

Methyl Torsional Levels of Solid Acetonitrile (CH3CN): A Neutron Scattering Study.
PB95-151015 *00,926*

Structure of a Triglyceride Microemulsion: A Small Angle Neutron Scattering Study.
PB96-112255 *01,077*

TRIPP, G. A.
Surface Roughness of Glass-Ceramic Insert. Composite Restorations: Assessing Several Polishing Techniques.
PB97-119010 *03,583*

TRIVISONNO, J.
Structures of Sodium Metal.
PB94-198850 *03,319*

TROCCOLO, P.
Comparisons of Measured Linewidths of Sub-Micrometer Lines Using Optical, Electrical, and SEM Metrologies.
PB95-152807 *02,338*

TROTT, K. A.
Effects of Etching on the Morphology and Surface Resistance of YBa2Cu3O7-delta Films.
PB96-135355 *02,410*

TROY, E. F.
Computer Security Management and Planning in the U.S. Federal Government.
PB95-163432 *01,596*

Guidance to Federal Agencies on the Use of Trusted Systems.
PB95-163440 *01,597*

TROY, G.
Proceedings of the Workshop on the Federal Criteria for Information Technology Security. Held in Ellicot City, Maryland on June 2-3, 1993.
PB94-162583 *01,575*

TRUETT, L.
Burning Rate of Premixed Methane-Air Flames Inhibited by Fluorinated Hydrocarbons.
PB95-180584 *01,391*

Experimental and Numerical Burning Rates of Premixed Methane-Air Inhibited by Fluoromethanes.
PB95-180592 *01,392*

Inhibition of Premixed Methane-Air Flames by Halon Alternatives.
PB96-146741 *01,414*

TRUS, S.
Analyzing Electronic Commerce.
PB94-219102 *00,480*

TSAI, B.
Resonance Enhanced Multiphoton Ionization Detection of GeF and GeCl Radicals.
PB94-212123 *00,825*

TSAI, B. K.
Comparison of Filter Radiometer Spectral Responsivity with the NIST Spectral-Irradiance and Illuminance Scales.
PB97-113161 *04,162*

TSAI, B. P.
Electronic Spectra of CF2Cl and CFCl2 Radicals Observed by Resonance Enhanced Multiphoton Ionization.
PB95-151023 *00,927*

Experimental and Abinitio Studies of Electronic Structures of the CCl3 Radical and Cation.
PB94-212131 *00,826*

Multiphoton Ionization of SiH3 and SiD3 Radicals: Electronic Spectra, Vibrational Analyses of the Ground and Rydberg States, and Ionization Potential.
PB94-212503 *00,837*

Resonance Enhanced Multiphoton Ionization Spectroscopy of 2-Butene-1-yl (C4H7) between 455-485 nm.
PB95-151031 *00,670*

TSAI, T. M.
Certainty Grid to Object Boundary Algorithm.
PB94-203510 *01,835*

TSAI, V. W.
Increasing the Value of Atomic Force Microscopy Process Metrology Using a High-Accuracy Scanner, Tip Characterization, and Morphological Image Analysis.
PB96-190293 *02,758*

Progress Toward Accurate Metrology Using Atomic Force Microscopy.
PB96-146774 *02,417*

TSANG, J. W.
Characterization of Polyquinoline Blends Using Small Angle Scattering.
PB95-164125 *01,261*

Characterization of Polyquinoline Block Copolymer Using Small Angle Scattering.
PB95-151882 *01,244*

TSANG, W.
Fluorinated Hydrocarbon Flame Suppression Chemistry.
PB94-185113 *01,362*

Homogeneous Gas Phase Decyclization of Tetralin and Benzocyclobutene.
PB95-151049 *00,928*

Hydrogen Atom Attack on Perchloroethylene.
PB95-163473 *00,969*

Incinerability of Perchloroethylene and Chlorobenzene.
PB95-163457 *01,388*

International Conference on Chemical Kinetics (2nd), Held in Gaithersburg, Maryland on July 24-27, 1989.
PB94-211901 *00,822*

Mechanism and Rate Constants for the Reactions of Hydrogen Atoms with Isobutene at High Temperatures.
PB95-151064 *00,929*

Progress in the Development of a Chemical Kinetic Database for Combustion Chemistry.
PB95-151056 *01,384*

Rate Constants for Hydrogem Atom Attack on Some Chlorinated Benzenes at High Temperature.
PB94-200581 *00,810*

Shock Tube Techniques in Chemical Kinetics.
PB95-163465 *00,968*

Thermochemical and Chemical Kinetic Data for Fluorinated Hydrocarbons.
PB95-260618 *01,056*

TSAO, W.
Non-Osmotic, Defect-Controlled Cathodic Disbondment of a Coating from a Steel Substrate.
PB94-216447 *03,120*

TSENG, L. K.
Mixing and Radiation Properties of Buoyant Turbulent Diffusion Flames.
PB95-242327 *01,396*

Radiation and Mixing Properties of Buoyant Turbulent Diffusion Flames.
PB94-165974 *01,360*

TSENG, S. H.
Infrared and Microwave Spectroscopy of the Argon - Propyne Dimer.
PB94-198892 *00,794*

TSENG, W.
Influence of Lattice Mismatch on Indium Phosphide Based High Electron Mobility Transistor (HEMT) Structures Observed in High Resolution Monochromatic Synchrotron X-Radiation Diffraction Imaging.
PB95-164679 *02,357*

Integration of Scanning Tunneling Microscope Nanolithography and Electronics Device Processing.
PB95-153359 *02,341*

TSENG, W. F.
Interdigitated Stacked P-I-N Multiple Quantum Well Modulator.
PB97-112296 *02,455*

Junction Locations by Scanning Tunneling Microscopy: In-Air-Ambient Investigation of Passivated GaAs pn Junctions.
PB94-185964 *02,306*

Multicarrier Characterization Method for Extracting Mobilities and Carrier Densities of Semiconductors from Variable Magnetic Field Measurements.
PB94-212776 *02,317*

Novel Magnetic Field Characterization Techniques for Compound Semiconductor Materials and Devices.
PB96-176458 *02,433*

Scaling of the Nonlinear Optical Cross Sections of GaAs-AlGaAs Multiple Quantum-Well Hetero n-i-p-i's.
PB96-102793 *02,183*

Vertical-Cavity Optoelectronic Structures: CAD, Growth, and Structural Characterization.
PB95-153177 *02,148*

Vertical-Cavity Semiconductor Structures: Materials Characterization.
PB95-153185 *02,149*

TSONG, T. Y.
Energy Transduction between a Concentration Gradient and an Alternating Electric Field.
PB94-216363 *03,461*

TSONGAS, G.
Parametric Study of Wall Moisture Contents Using a Revised Variable Indoor Relative Humidity Version of the 'Moist' Transient Heat and Moisture Transfer Model.
PB97-122535 *00,419*

TSONGAS, G. A.
Mathematical Analysis of Practices to Control Moisture in the Roof Cavities of Manufactured Houses.
PB97-106843 *00,278*

TSUI, K. L.
Taguchi's Parameter Design: A Panel Discussion.
PB96-111802 *03,445*

TSUJI, H.
Charpy Impact Test as an Evaluation of 4 K Fracture Toughness.
PB96-190194 *03,219*

TSUTSUMI, N.
Thermal Stability of Internal Electric Field and Polarization Distribution in Blend of Polyvinylidene Fluoride and Polymethylmethacrylate.
PB95-151072 *01,240*

TSVETKOV, F.
Small Angle Neutron Scattering Study of a Clay Suspension Under Shear.
PB96-167374 *00,663*

TU, K. M.
Wall Flame Heights with External Radiation.
PB95-163481 *00,380*

TUNG, M.
Biological Macromolecule Crystallization Database and NASA Protein Crystal Growth Archive.
PB97-109136 *01,171*

TUNG, M. S.
Composition and Solubility Product of a Synthetic Calcium Hydroxyapatite.
PB96-180104 *02,995*

Effect of Ethanol on the Solubility of Dicalcium Phosphate Dihydrate in the System Ca(OH)2-H3PO4-H2O at 37C.
PB95-163507 *00,163*

Effect of Ethanol on the Solubility of Hydroxyapatite in the System Ca(OH)2-H3PO4-H2O at 25C and 33C.
PB95-169231 *00,169*

Effect of Supersaturation on Apatite Crystal Formation in Aqueous Solutions at Physiologic pH and Temperature.
PB96-135215 *03,571*

Effects of Calcium Phosphate Solutions on Dentin Permeability.
PB95-151080 *00,157*

TUPPER, M. L.
Calibration of Dosimeters for the Cryogenic Irradiation of Composite Materials Using an Electron Beam.
PB95-180964 *03,968*

TURCHI, P. E. A.
Electronic Structure and Phase Equilibria in Ternary Substitutional Alloys.
PB97-119366 *03,378*

TURCHINSKAYA, M. J.
Determination of Thermoactivation Parameters of Vortex Mobility in YBa2Cu3O7 Using Only Magnetic Measurements.
PB95-163499 *04,624*

TURGEL, R. S.
10 kV DC Resistive Divider Calibration.
PB95-198685 *02,063*

TURK, G. C.
Diode Laser as a Spectroscopic Tool.
PB95-175485 *00,600*

Liquid Chromatography: Laser-Enhanced Ionization Spectrometry for the Speciation of Organolead Compounds.
PB94-185253 *00,530*

Spectral Interference in the Determination of Arsenic in High-Purity Lead and Lead-Base Alloys Using Electrothermal Atomic Absorption Spectrometry and Zeeman-Effect Background Correction.
PB96-112099 *00,614*

Trace Detection in Conducting Solids Using Laser-Induced Fluorescence in a Cathodic Sputtering Cell.
PB95-163424 *00,598*

TURNER, A. H.
Report of the National Conference on Weight and Measures (78th). Held in Kansas City, MO. on July 18-22, 1993.
PB94-138989 *02,623*

Report of the National Conference on Weights and Measures (79th). Held in San Diego, California on July 17-21, 1994.
PB95-169819 *02,656*

Report of the National Conference on Weights and Measures (80th) as Adopted by the 80th National Conference on Weights and Measures, 1995. Held in Portland, Maine on July 16-20, 1995.
PB96-165840 *02,681*

TURNER, P. R.
Basic Linear Algebra Operations in SLI Arithmetic.
PB96-165931 *03,421*

Error-Bounding in Level-Index Computer Arithmetic.
PB96-109582 *01,742*

MasPar MP-1 as a Computer Arithmetic Laboratory.
PB95-189437 *01,627*

MasPar MP-1 as a Computer Arithmetic Laboratory.
PB96-179155 *01,617*

Parallel and Serial Implementations of SLI Arithmetic.
PB95-242335 *01,732*

TURNER, S.
Airborne Asbestos Analysis: National Voluntary Laboratory Accreditation Program.
PB96-147392 *02,566*

Airborne Asbestos Method: Bootstrap Method for Determining the Uncertainty of Asbestos Concentration. Version 1.0.
PB96-214614 *00,646*

Airborne Asbestos Method: Standard Practice for Recording Transmission Electron Microscopy Data for the Analysis of Asbestos Collected onto Filters. Version 1.0.
PB94-210168 *00,552*

Airborne Asbestos Method: Standard Test Method for High Precision Counting of Asbestos Collected on Filters. Version 1.0.
PB94-163003 *00,525*

Airborne Asbestos Method: Standard Test Method for Verified Analysis of Asbestos by Transmission Electron Microscopy. Version 2.0.
PB94-163045 *00,526*

Proficiency Tests for the NIST Airborne Asbestos Program, 1990.
PB94-188836 *00,535*

Proficiency Tests for the NIST Airborne Asbestos Program - 1991.
PB94-193828 *00,537*

Proficiency Tests for the NIST Airborne Asbestos Program - 1992.
PB94-194362 *00,539*

Proficiency Tests for the NIST Airborne Asbestos Program, 1993.
PB96-106463 *00,610*

TURNER, T. R.
Gaseous Electronics Conference Radio-Frequency Reference Cell: A Defined Parallel-Plate Radio-Frequency System for Experimental and Theoretical Studies of Plasma-Processing Discharges.
PB94-172327 *04,404*

TWILLEY, W. H.
Effects of Specimen Edge Conditions on Heat Release Rate.
PB95-152864 *00,375*

In situ Burning of Oil Spills: Mesoscale Experiments and Analysis.
PB95-163747 *02,587*

Santa Ana Fire Department Experiment at 1315 South Bristol, July 14, 1994.
PB95-188868 *00,389*

Santa Ana Fire Department Experiment at 1315 South Bristol, July 14, 1994. (Reprint).
PB96-102934 *00,207*

Santa Ana Fire Department Experiments at South Bristol Street.
PB96-154810 *00,305*

Smoke Plume Trajectory from In situ Burning of Crude Oil in Alaska: Field Experiments.
PB96-131560 *02,594*

TYLER, J. E.
Models, Managing Models, Quality Models: An Example of Quality Management.
PB94-163466 *02,891*

TYREE, V.
Realizing Suspended Structures on Chips Fabricated by CMOS Foundry Processes Through the MOSIS Service.
PB94-193984 *01,881*

TZENG, Y.
Applications of Diamond Films and Related Materials: International Conference (3rd). Held in Gaithersburg, Maryland on August 21-24, 1995. Supplement to NIST Special Publication 885.
PB95-256053 *03,063*

Proceedings of the Applied Diamond Conference 1995: Applications of Diamond Films and Related Materials International Conference (3rd). Held in Gaithersburg, Maryland, on August 21-24, 1995.
PB95-255204 *04,701*

UDEN, P. C.
Investigations of Sulfur Interferences in the Extraction of Methylmercury from Marine Tissues.
PB96-190020 *03,482*

UDOVIC, T. J.
Characterization of the Interaction of Hydrogen with Iridium Clusters in Zeolites by Inelastic Neutron Scattering Spectroscopy.
PB95-180741 *01,013*

Characterization of the Structure of LaD2.50 by Neutron Powder Diffraction.
PB96-176797 *04,783*

Characterization of the Structure of TbD2.25 at 70 K by Neutron Powder Diffraction.
PB96-160528 *01,130*

Characterization of the Structure of YD3 by Neutron Powder Diffraction.
PB96-186150 *01,161*

Characterization of the Vibrational Dynamics in the Octahedral Sublattices of LaD2.25 and LaH2.25.
PB96-123724 *01,091*

Dynamics of Mu(+) in Sc and ScHx.
PB96-180021 *04,112*

Hydrogen in YBa2Cu3Ox: A Neutron Spectroscopy and a Nuclear Magnetic Resonance Study.
PB95-161279 *04,601*

Inelastic Neutron Scattering Studies of Nonlinear Optical Materials: p-Nitroaniline Adsorbed in ALPO-5.
PB95-107223 *00,874*

Inelastic Neutron Scattering Study of Hydrogen in Nanocrystalline Pd.
PB96-146857 *03,366*

Local-Mode Dynamics in YH2 and YD2 by Isotope-Dilution Neutron Spectroscopy.
PB95-181012 *01,017*

Low-Energy Vibrations and Octahedral Site Occupation in Nb95V5H(D)y.
PB96-160734 *01,133*

Neutron and Raman Spectroscopies of 134 and 134a Hydrofluorocarbons Encaged in Na-X Zeolite.
PB96-186168 *03,001*

Neutron-Powder-Diffraction Study of the Long-Range Order in the Octahedral Sublattice of LaD2.25.
PB96-141155 *04,753*

Neutron Spectroscopic Comparison of beta-Phase Rare Earth Hydrides.
PB96-160742 *01,134*

Neutron Spectroscopic Comparison of Rare-Earth/Hydrogen alpha-Phase Systems.
PB95-163523 *00,970*

Neutron Spectroscopic Evidence of Concentration-Dependent Hydrogen Ordering in the Octahedral Sublattice of beta-TbH2+x.
PB95-181020 *01,018*

Neutron-Spectroscopy Study of the Hydrogen Vibrations in Hydrogen-Doped YBa2Cu3Ox.
PB94-172475 *04,441*

Vibrational Excitations and the Position of Hydrogen in Nanocrystalline Palladium.
PB96-111828 *04,035*

Vibrations of Hydrogen and Deuterium in Solid Solution with Lutetium.
PB95-181038 *01,019*

UEDA, K.
Photoelectron Study of Electronic Autoionization in Rotationally Cooled N2: The n=6 Member of the Hopfield Series.
PB95-163531 *00,971*

UEDA, Y.
Thermal Stability of Internal Electric Field and Polarization Distribution in Blend of Polyvinylidene Fluoride and Polymethylmethacrylate.
PB95-151072 *01,240*

UGIANSKY, G. M.
Report of the National Conference on Weights and Measures (80th) as Adopted by the 80th National Conference on Weights and Measures, 1995. Held in Portland, Maine on July 16-20, 1995.
PB96-165840 *02,681*

UHRICH, P.
Preliminary Comparison of Time Transfers via LASSO, GPS and Two-Way Satellite.
PB95-151098 *01,529*

ULBRECHT, J. J.
Metrology.
PB96-160759 *02,925*

ULLMANN, J. L.
Measurements of the (235)U(n,f) Cross Section in the 3 to 30 MeV Neutron Energy Region.
PB97-119051 *04,172*

ULYANOV, A.
Comparison of Regular Transmittance Scales of Four National Standardizing Laboratories.
PB94-211232 *04,233*

UNGER, R.
Positive and Negative Cooperativities at Subsequent Steps of Oxygenation Regulate the Allosteric Behavior of Multistate Sebacylhemoglobin.
PB97-119374 *03,486*

UNGURIS, J.
Influence of Cr Growth on Exchange Coupling in Fe/Cr/Fe(100).
PB95-150181 *04,562*

Influence of Thickness Fluctuations on Exchange Coupling in Fe/Cr/Fe Structures.
PB96-135371 *04,745*

Magnetic Moments in Cr Thin Films on Fe(100).
PB95-108429 *04,525*

Oscillatory Exchange Coupling in Fe/Au/Fe(100).
PB95-150371 *04,569*

Scanning Tunneling Microscopy Study of the Growth of Cr/Fe(001): Correlation with Exchange Coupling of Magnetic Layers.
PB95-150330 *04,568*

SEMPA Studies of Exchange Coupling in Magnetic Multilayers.
PB96-164074 *04,780*

SEMPA Studies of Oscillatory Exchange Coupling.
PB95-163556 *04,625*

Simple, Compact, High-Purity Cr Evaporator for Ultrahigh Vacuum.
PB94-216678 *04,520*

Surface Magnetic Microstructural Analysis Using Scanning Electron Microscopy with Polarization Analysis (SEMPA).
PB95-162657 *03,938*

UNTERWEGER, M. P.
Assay of the Eluent from the Alumina-Based Tungsten-188-Rhenium-188 Generator.
PB94-200482 *03,829*

Intercomparison of Internal Proportional Gas Counting of (85)Kr and (3)H.
PB94-185576 *03,800*

International Marine-Atmospheric (222)Rn Measurement Intercomparison in Bermuda. Part 1. NIST Calibration and Methodology for Standardized Sample Additions.
PB96-175674 *00,114*

International Marine-Atmospheric (222)Rn Measurement Intercomparison in Bermuda. Part 2. Results for the Participating Laboratories.
PB96-175682 *00,115*

Liquid-Scintillation Counting Techniques for the Standardization of Radionuclides Used in Therapy.
PB97-110084 *03,709*

Measurement and Calibration of Large-Area Alpha-Particle Sources at NIST.
PB94-172855 *03,791*

NBS/NIST Peltier-Effect Microcalorimeter: A Four-Decade Review.
PB96-102769 *01,064*

New and Revised Half-Life Measurement Results.
PB96-160346 *00,695*

Standardization and Decay Scheme of Rhenium-186.
PB94-200490 *03,830*

URBAN, W.
Extension of Heterodyne Frequency Measurements on OCS to 87 THz (2900 cm(-1)).
PB94-200680 *00,811*

Optically Stabilized Tunable Diode-Laser System for Saturation Spectroscopy.
PB96-102819 *04,717*

Stabilization of 3.3 and 5.1 m Lead-Salt Diode Lasers by Optical Feedback.
PB95-180709 *04,313*

Sub-Doppler Frequency Measurements on OCS at 87 Thz (3.4 micrometers) with the CO Overtone Laser: Considerations and Details.
PB95-128633 *04,255*

Sub-Doppler Frequency Measurements on OCS at 87 THz (3.4 mu m) with the CO Overtone Laser.
PB96-102215 *04,330*

URIBE, R. M.
Effect of Formulation Changes on the Response to Ionizing Radiation of Radiochromic Dye Films.
PB97-119028 *04,171*

Electron and Proton Dosimetry with Custom-Developed Radiochromic Dye Films.
PB95-151106 *03,713*

USHA SARMA, P.

Rapid Method for the Isolation of Genomic DNA from 'Aspergillus fumigatus'.
PB96-147061 *03,488*

UTHE, E. E.

Smoke Plume Trajectory from In situ Burning of Crude Oil: Field Experiments.
PB96-200993 *02,597*

VADER, H. L.

Molar Absorptivities of Bilirubin (NIST SRM 916A) and Its Neutral and Alkaline Azopigments.
PB94-211042 *03,456*

VAESSEN, P.

Approach to Setting Performance Requirements for Automated Evaluation of the Parameters of High-Voltage Impulses.
PB94-185634 *01,878*

VAEZI-NEJAD, H.

Use of Building Emulators to Evaluate the Performance of Building Energy Management Systems.
PB96-111901 *00,269*

VAJDA, F.

Experimental Verification of a Vector Preisach Model.
PB95-163564 *04,626*

VAJDA, J. N.

Vibrations of Hydrogen and Deuterium in Solid Solution with Lutetium.
PB95-181038 *01,019*

VAJDA, P.

Neutron Spectroscopic Comparison of Rare-Earth/Hydrogen alpha-Phase Systems.
PB95-163523 *00,970*

VALE, L.

Coexistence of Grains with Differing Orthorhombicity in High Quality YBa2Cu3O7-delta Thin Films.
PB96-135033 *04,742*

VALE, L. R.

30 THz Mixing Experiments on High Temperature Superconducting Josephson Junctions.
PB96-102462 *04,709*

Controlling the Critical Current Density of High-Temperature SNS Josephson Junctions.
PB96-200712 *04,794*

Critical Current and Normal Resistance of High-Tc Step-Edge SNS Junctions.
PB96-111752 *04,724*

Heterodyne Mixing and Direct Detection in High Temperature Josephson Junctions.
PB96-147202 *01,565*

High Current Pressure Contacts to Ag Pads on Thin Film Superconductors.
PB95-168621 *04,639*

High Temperature Superconductor-Normal Metal-Superconductor Josephson Junctions with High Characteristic Voltages.
PB95-176079 *04,666*

Increased Transition Temperature in In situ Coevaporated YBa2Cu3O7-delta Thin Films by Low Temperature Post-Annealing.
PB95-180071 *04,672*

Influence of Deposition Parameters on Properties of Laser Ablated YBa2Cu3O7-Delta Films.
PB95-140539 *04,544*

Magnetic Flux Pinning in Epitaxial YBa2Cu3O7-delta Thin Films.
PB96-200746 *04,795*

Microwave Noise in High-Tc Josephson Junctions.
PB96-148010 *04,771*

Mutual Phase Locking in Systems of High-Tc Superconductor-Normal Metal-Superconductor Junctions.
PB96-135348 *04,744*

Phase Locking in Two-Junction Systems of High-Temperature Superconductor-Normal Metal-Superconductor Junctions.
PB95-176053 *02,060*

Temperature Dependence and Magnetic Field Modulation of Critical Currents in Step-Edge SNS YBCO/Au Junctions.
PB96-111745 *04,723*

Thermal Noise in High-Temperature Superconducting-Normal-Superconducting Step-Edge Josephson Junctions.
PB95-175089 *04,650*

VALENCIA-RODRIGUEZ, J.

Comparisons of Some NIST Fixed-Point Cells with Similar Cells of Other Standards Laboratories.
PB97-119242 *00,655*

VALKIERS, S.

New Values for Silicon Reference Materials, Certified for Isotope Abundance Ratios. Letter to the Editor.
PB94-219268 *00,863*

VALLIKUL, P.

Tomographic Reconstruction of the Moments of Local Probability Density Functions in Turbulent Flow Fields.
PB96-180195 *04,219*

VAMAN, D.

Comparison of FDDI Asynchronous Mode and DQDB Queue Arbitrated Mode Data Transmission for Metropolitan Area Network Applications.
PB96-160452 *01,498*

Error Protecting Characteristics of CDMA and Impacts on Speech.
PB96-122452 *01,491*

Provision of Isochronous Service on IEEE 802.6.
PB96-160635 *01,501*

VAMLING, L.

Need for, and Availability of, Working Fluid Property Data: Results from Annexes XIII and XVIII.
PB95-168969 *03,268*

VAN BRUNT, R. J.

Appearance Potentials of Ions Produced by Electron-Impact Induced Dissociative Ionization of SF6, SF4, SF5Cl, S2F10, SO2, SO2F2, SOF2, and SOF4.
PB96-119730 *01,080*

Associative Electron Attachment to S2F10, S2OF10, and S2O2F10.
PB95-140992 *00,907*

Behavior of Surface Partial Discharge on Aluminum Oxide Dielectrics.
PB96-123781 *01,937*

Continuous Recording and Stochastic Analysis of PD.
PB96-112156 *01,925*

Correlations between Electrical and Acoustic Detection of Partial Discharge in Liquids and Implications for Continuous Data Recording.
PB96-204490 *02,248*

Decomposition of SF6 and Production of S2F10 in Power Arcs.
PB96-122619 *01,084*

Decomposition of Sulfur Hexafluoride by X-rays.
PB96-135314 *01,095*

Effect of Electrode Material on Measured Ion Energy Distributions in Radio-Frequency Discharges.
PB96-102850 *04,026*

Electron Scattering and Dissociative Attachment by SF6 and Its Electrical-Discharge By-Products.
PB95-151288 *02,256*

Evidence for Inelastic Processes for N(+)3 and N(+)4 from Ion Energy Distributions in He/N2 Radio Frequency Glow Discharges.
PB96-146683 *04,059*

Fundamental Processes in Gas Discharges.
PB96-123450 *01,089*

Gaseous Dielectrics Research: Possible SF6 Substitutes.
PB96-119268 *02,228*

Gaseous Electronics Conference Radio-Frequency Reference Cell: A Defined Parallel-Plate Radio-Frequency System for Experimental and Theoretical Studies of Plasma-Processing Discharges.
PB94-172327 *04,404*

Importance of Unraveling Memory Propagation Effects in Interpreting Data on Partial Discharge Statistics.
PB95-163572 *01,901*

Influence of Electrode Material on Measured Ion Kinetic-Energy Distributions in Radio-Frequency Discharges.
PB96-123179 *01,935*

Influence of Surface Charge on the Stochastic Behavior of Partial Discharge in Dielectrics.
PB96-122767 *01,931*

Investigation of S2F10 Production and Mitigation in Compressed SF6-Insulated Power Systems.
PB94-212388 *02,467*

Investigation of S2F10 Production and Mitigation in Compressed SF6- Insulated Power Systems.
PB96-155528 *02,468*

Ion Kinetic-Energy Distributions and Balmer-alpha (Halpha) Excitation in Ar-H2 Radio-Frequency Discharges.
PB96-102959 *04,029*

Ion Kinetic-Energy Distributions in Argon rf Glow Discharges.
PB95-141008 *04,409*

Ion Kinetics and Symmetric Charge-Transfer Collisions in Low-Current, Diffuse (Townsend) Discharges in Argon and Nitrogen.
PB96-123658 *04,051*

Kinetic Energy Distribution of Ions Produced from Townsend Discharges in Neon and Argon.
PB96-111927 *04,413*

Kinetic Energy Distributions of H(+), H2(+), and H3(+) from a Diffuse Townsend Discharge in H2 at High E/N.
PB96-123351 *04,415*

Kinetic-Energy Distributions of Ions Sampled from Argon Plasmas in a Parallel-Plate, Radio-Frequency Reference Call.
PB95-161964 *03,935*

Kinetic-Energy Distributions of Ions Sampled from Radio-Frequency Discharges in Helium, Nitrogen, and Oxygen.
PB96-123732 *01,092*

Kinetic-Energy Distributions of K(+) in Argon and Neon in Uniform Electric Fields.
PB95-151122 *03,902*

Measurement of S2OF10, and S2O2F10 Production Rates from Spark and Negative Glow Corona Discharge in SF6/O2 Gas Mixtures.
PB96-123740 *01,093*

Modification of Cast Epoxy Resin Surfaces during Exposure to Partial Discharges.
PB96-122734 *01,086*

Nonstationary Behavior of Partial Discharge during Insulation Aging.
PB95-163580 *01,902*

Nonstationary Behaviour of Partial Discharge during Discharge Induced Ageing of Dielectrics.
PB96-103114 *01,922*

Optical and Mass Spectrometric Investigations of Ions and Neutral Species in SF6 Radio-Frequency Discharges.
PB97-111918 *01,985*

Partial Discharge: Induced Aging of Cast Epoxies and Related Nonstationary Behavior of the Discharge Statistics.
PB95-163598 *01,903*

Physics and Chemistry of Partial Discharge and Corona: Recent Advances and Future Challenges.
PB95-181046 *01,910*

Physics and Chemistry of Partial Discharge and Corona - Recent Advances and Future Challenges.
PB96-123757 *01,936*

Plasma Chemical Model for Decomposition of SF6 in a Negative Glow Corona Discharge.
PB95-181053 *01,020*

Procedure for Measuring Trace Quantities of S2F10, S2OF10, and S2O2F10 in SF6 Using a Gas Chromatograph-Mass Spectrometer.
PB96-119755 *02,513*

Recent Developments at NIST on Optical Current Sensors and Partial Discharge Diagnostics.
PB95-151114 *02,147*

SF6 Insulation: Possible Greenhouse Problems and Solutions.
PB95-251625 *02,269*

SF6/N2 Mixtures: Basic and High-Voltage-Insulation Properties.
PB96-123468 *02,230*

Studies of Ion Kinetic-Energy Distributions in the Gaseous Electronics Conference RF Reference Cell.
PB96-113360 *02,391*

Use of an Ion Energy Analyzer: Mass Spectrometer to Measure Ion Kinetic-Energy Distributions from RF Discharges in Argon-Helium Gas Mixtures.
PB94-185717 *04,406*

VAN CLARK, A.

Noncontact Ultrasonic Inspection of Train Rails for Stress.
PB95-162673 *04,851*

Ultrasonic Sensing of GMAW: Laser/EMAT Defect Detection System.
PB96-186028 *02,878*

VAN DE ZANDE, R.

Standards Setting in the European Union: Standards Organization and Officials in EU Standards Activities.
PB96-115019 *02,919*

VAN DEGRIFT, C.

Report on the Workshop on Advanced Digital Video in the National Information Infrastructure. Held in Washington, D.C. on May 10-11, 1994.
PB95-103677 *01,472*

Summary Report on the Workshop on Advanced Digital Video in the National Information Infrastructure.
PB96-141320 *01,497*

VAN DEGRIFT, C. T.

Anomalous Behavior of a Quantized Hall Plateau in a High-Mobility Si Metal-Oxide-Semiconductor Field-Effect Transistor.
PB95-164174 *02,354*

VAN DER PYL, L. M.

Guide to Instrumentation Literature.
AD-A280 278/3 *02,617*

VAN DER SLUIS, L.

Digital Techniques in HV Tests - Summary of 1989 Panel Session.
PB94-216702 *02,035*

VAN DER ZIEL, J. P.

Fabrication Issues for the Prototype National Institute of Standards and Technology SRM 2090A Scanning Electron Microscope Magnification Calibration Standard.
PB96-160585 *01,131*

VAN DOVER, R. B.

Increased Pinning Energies and Critical Current Densities in Heavy-Ion-Irradiated Bi2Sr2CaCu2O8 Single Crystals.
PB95-175352 *04,654*

VAN GESTEL, J.

Preparation and Characterization of (6)LiF and (10)B Reference Deposits for the Measurement of the Neutron Lifetime.
PB95-108692 *03,874*

Problems Related to the Determination of Mass Densities of Evaporated Reference Deposits.
PB95-163226 *03,941*

VAN HET HOF, G. J.

Analysis of the (5d(2)+5d6s)-5d6p Transition Arrays of Os VII and Ir VIII, and the 6s (2)S-6p (2)P Transitions of Ir IX.
PB96-159264 *01,954*

VAN HEUKELEM, L.

High-Performance Liquid Chromatography of Phytoplankton Pigments Using a Polymeric Reversed-Phase C18 Column.
PB95-151130 *00,583*

VAN LEEUWEN, F.
beta-D-Glucosyl-Hydroxymethyluracil: A Novel Modified Base Present in the DNA of the Parastic Protozoan T. brucei.
PB94-172319 *03,524*

VAN PELT, A.
Critical Scaling Laws and a Classical Equation of State.
PB95-169249 *00,990*

VAN POOLEN, L. J.
Coexisting Densities, Vapor Pressures and Critical Densities of Refrigerants R-32 and R-152a, at 300 - 385 K.
PB95-175691 *03,274*

Experimental Method for Obtaining Critical Densities of Binary Mixtures: Application to Ethane + n-Butane.
PB95-151148 *00,930*

Vapor-Liquid Equilibria of Ternary Mixtures in the Critical Region on Paths of Constant Temperature and Overall Composition.
PB96-161856 *01,139*

VAN ROGGEN, A.
Effect of Electrode-Polymer Interfacial Layers on Polymer Conduction. Part 2. Device Summary.
PB95-151155 *02,335*

VAN ZANTEN, J. H.
Influence of an Impenetrable Interface on a Polymer Glass-Transition Temperature.
PB96-146873 *03,175*

Terminally Anchored Chain Interphases: The Effect of Multicomponent, Polydisperse Solvents on Their Equilibrium Properties.
PB95-181079 *01,273*

Terminally Anchored Chain Interphases: Their Chromatographic Properties.
PB95-181061 *01,272*

Zimm Plot and Its Analogs as Indicators of Vesicle and Micelle Size Polydispersity.
PB96-123765 *01,094*

VAN ZEE, R. D.
Laser Bandwidth Effects in Quantitative Cavity Ring-Down Spectroscopy.
PB97-112254 *04,394*

VANBRONKHORST, D. A.
Workplan to Analyze the Energy Impacts of Envelope Airtightness in Office Buildings.
PB96-154463 *00,273*

VANBRUNT, R. J.
Performance Evaluation of a New Digital Partial Discharge Recording and Analysis System.
PB95-150389 *01,888*

VANDER SANDE, J. B.
Effects of Anneal Time and Cooling Rate on the Formation and Texture of Bi2Sr2CaCu2O8 Films.
PB95-161600 *04,603*

VANDERAH, T. A.
Magnetic Dielectric Oxides: Subsolidus Phase Relations in the BaO: Fe2O3: TiO2 System.
PB96-176524 *01,156*

Preparation and Crystal Structure of Sr5TiNb4O17.
PB96-167341 *04,107*

Preparation, Crystal Structure, Dielectric Properties, and Magnetic Behavior of Ba2Fe2Ti4O13.
PB96-186176 *01,162*

VANDERHART, D. L.
Binder Characterization and Evaluation by Nuclear Magnetic Resonance Spectroscopy.
PB94-193471 *01,334*

Evidence of Crosslinking in Methyl Pendent PBZT Fiber.
PB97-112486 *03,393*

Solid State (13)C NMR and Raman Studies of Cellulose Triacetate: Oligomers, Polymorphism, and Inferences about Chain Polarity.
PB96-176532 *01,289*

VANDERWEGE, B. A.
Effect of CF3H and CF3Br on Laminar Diffusion Flames in Normal and Microgravity.
PB96-161831 *01,420*

Effect of CF3H and CF3Br on Laminar Diffusion Flames in Normal and Microgravity.
PB96-161849 *01,421*

VANDERZWAAG, D.
Escherichis coli Cyclic AMP Receptor Protein Mutants Provide Evidence for Ligand Contacts Important in Activation.
PB96-201017 *03,592*

VANDSBURGER, U.
Compartment Fire Combustion Dynamics. Annual Report, September 1, 1993-September 1, 1994.
PB95-217162 *00,203*

Dynamics, Transport and Chemical Kinetics of Compartment Fire Exhaust Gases.
PB96-195508 *00,229*

VANGEL, M. G.
Anova Estimates of Variance Components for a Class of Mixed Models.
PB96-141163 *03,448*

One-Sided beta-Content Tolerance Intervals for Mixed Models.
PB96-141171 *03,449*

Performance of Tape-Bonded Seams of EPDM Membranes: Comparison of the Peel Creep-Rupture Response of Tape-Bonded and Liquid-Adhesive-Bonded Seams.
PB96-183249 *03,012*

VANIER, J.
Aging, Warm-Up Time and Retrace; Important Characteristics of Standard Frequency Generators.
PB96-103122 *04,031*

VANMEURS, D. P.
Neutron Scattering Study of the Lattice Modes of Solid Cubane.
PB96-147152 *01,126*

VANSTEENKISTE, N.
Frequency-Stabilized LNA Laser at 1.083 mum: Application to the Manipulation of Helium 4 Atoms.
PB95-176186 *04,304*

VANZURA, E. J.
NIST 60-Millimeter Diameter Cylindrical Cavity Resonator: Performance Evaluation for Permittivity Measurements.
PB94-151776 *02,251*

VARBERG, T. D.
Detection of OH+ in Its a(1)Delta State by Far Infrared Laser Magnetic Resonance.
PB95-181087 *01,021*

Laser Spectroscopy of Carbon Monoxide: A Frequency Reference for the Far Infrared.
PB95-163606 *04,277*

Pure Rotational Spectra of CuH and CuD in Their Ground States Measured by Tunable Far-Infrared Spectroscopy.
PB95-176194 *01,005*

Rotational Spectrum of OH in the v=0-3 Levels of Its Ground State.
PB95-176202 *01,006*

VARGAS-ABURTO, C.
Electron and Proton Dosimetry with Custom-Developed Radiochromic Dye Films.
PB95-151106 *03,713*

VARMA, D. S.
Copolymerization of N-Phenyl Maleimide and gamma-Methacryloxypropyl Trimethoxysilane.
PB95-153144 *01,248*

Thermal Behavior of 4-Maleimidophenyl Glycidyl Ether Resins.
PB95-153151 *01,249*

Thermal Behaviour of Methyl Methacrylate and N-Phenyl Maleimide Copolymers.
PB95-152237 *01,246*

VARMA, I. K.
Copolymerization of N-Phenyl Maleimide and gamma-Methacryloxypropyl Trimethoxysilane.
PB95-153144 *01,248*

Thermal Behavior of 4-Maleimidophenyl Glycidyl Ether Resins.
PB95-153151 *01,249*

Thermal Behaviour of Methyl Methacrylate and N-Phenyl Maleimide Copolymers.
PB95-152237 *01,246*

VARVOGLIS, P.
Rotational Modulation and Flares on RS Canum Venaticorum and BY Draconis Stars. XVI. IUE Spectroscopy and VLA Observations of C1182(=V 1005 Orionis) in October 1983.
PB94-185626 *00,050*

VASCONCELLOS, E. C. C.
Far Infrared Laser Frequencies of (13)CD3OH.
PB95-169363 *04,292*

VASILIU-DOLOC, L.
High-Energy Phonon Dispersion in La1.85Sr0.15CuO4.
PB96-138458 *04,748*

VAUDIN, M.
Characterization of Phase and Surface Composition of Silicon Carbide Platelets.
PB94-216264 *03,043*

VAUDIN, M. D.
Ceramic Characterization.
DE94013170 *03,026*

Electromagnetic Coupling Character of (001) Twist Boundaries in Sintered Bi2Sr2CaCu2O8+x Bicrystals.
PB96-176573 *01,963*

Epitaxial Growth of BaTiO3 Thin Films at 600C by Metalorganic Chemical Vapor Deposition.
PB96-122510 *03,071*

Experimental Assessment of Crack-Tip Dislocation Emission Models for an Al67Cr8Ti25 Intermetallic Alloy.
PB96-204466 *03,377*

Texture Measurement of Sintered Alumina Using the March-Dollase Function.
PB96-179494 *04,784*

VAUGHAN, G. B. M.
Discontinuous Volume Change at the Orientational-Ordering Transition in Solid C60.
PB94-211828 *00,821*

VAYSHENKER, I.
Accurate Measurement of Optical Detector Nonlinearity.
PB95-203576 *02,181*

Automated Measurement of Nonlinearity of Optical Fiber Power Meters.
PB96-176540 *04,110*

Optical Detector Nonlinearity: A Comparison of Five Methods.
PB95-169355 *04,291*

Optical Detector Nonlinearity: Simulation.
PB96-165378 *02,199*

Optical Power Meter Calibration Using Tunable Laser Diodes.
PB95-169256 *04,290*

VAZQUEZ, I.
Suppression of Elevated Temperature Hydraulic Fluid and JP-8 Spray Flames.
PB95-181095 *00,021*

VEALE, A.
Rotational Modulation and Flares on RS Canum Venaticorum and BY Draconis Stars. XVIII. Coordinated VLA, ROSAT, and IUE Observations of RS CVn Binaries.
PB96-102322 *00,089*

VEALE, R.
Dimensional Characterization of Small Bores: A Survey.
PB95-162202 *02,651*

Displacement Method for Machine Geometry Calibration.
PB95-152088 *02,946*

Variations in Size Measurements by Indicating Gaging Systems.
PB95-163614 *02,864*

VEALE, R. C.
U.S. Navy Coordinate Measuring Machines: A Study of Needs.
PB94-162831 *02,807*

VEASEY, D. L.
Distributed Feedback Lasers in Rare-Earth-Doped Phosphate Glass.
PB96-123773 *04,740*

Glasses for Waveguide Lasers.
PB96-111950 *04,335*

Integrated Optical Polarization-Discriminating Receiver in Glass.
PB97-113179 *02,206*

Passively Q-Switched Nd-Doped Waveguide Laser.
PB95-180048 *04,308*

Waveguide Polarizers Processed by Localized Plasma Etching.
PB95-169264 *02,171*

VECCHIA, D. F.
Moments of the Quartic Assignment Statistic with an Application to Multiple Regression.
PB95-181103 *03,442*

Optical Fiber Geometry by Gray-Scale Analysis with Robust Regression.
PB95-161519 *04,272*

Outlier-Resistant Methods for Estimation and Model Fitting.
PB95-203436 *03,444*

VEERAPANDIAN, B.
Crystal Packing Interactions of Two Different Crystal Forms of Bovine Ribonuclease A.
PB95-152823 *00,943*

VEIGL, I.
Waveguide Polarizers Processed by Localized Plasma Etching.
PB95-169264 *02,171*

VEILLET, C.
Lunar Laser Ranging: A Continuing Legacy of the Apollo Program.
PB95-202495 *03,683*

Preliminary Comparison of Time Transfers via LASSO, GPS and Two-Way Satellite.
PB95-151098 *01,529*

VEIRS, D. K.
Transient Subcritical Crack-Growth Behavior in Transformation-Toughened Ceramics.
PB94-200656 *03,038*

VELAPOLDI, R. A.
Standards for Atmospheric Measurements.
PB95-163622 *02,547*

VELICHANSKY, V. L.
High-Resolution Diode-Laser Spectroscopy of Calcium.
PB95-181244 *03,969*

VENABLES, D.
Defect Pair Formation by Implantation-Induced Stresses in High-Dose Oxygen Implanted Silicon-on-Insulator Material.
PB95-175824 *02,364*

Effect of Single versus Multiple Implant Processing on Defect Types and Densities in SIMOX.
PB96-160353 *01,957*

Stacking Fault Pyramid Formation and Energetics in Silicon-on-Insulator Material Formed by Multiple Cycles of Oxygen Implantation and Annealing.
PB96-160221 *04,083*

VENKATESWARLU, P.
Fluoride Analytical Methods.
PB96-180237 *03,578*

VENTURELLI, J.
Regulation of Lithium and Boron Levels in Normal Human Blood: Environmental and Genetic Considerations.
PB94-198579 *03,491*

VENZ, S.
Modified Surface-Active Monomers for Adhesive Bonding to Dentin.
PB95-151163 *00,158*

NIR-Spectroscopic Investigation of Water Sorption Characteristics of Dental Resins and Composites.
PB95-151171 *00,189*

VERDEYEN, J. T.
Gaseous Electronics Conference Radio-Frequency Reference Cell: A Defined Parallel-Plate Radio-Frequency System for Experimental and Theoretical Studies of Plasma-Processing Discharges.
PB94-172327 *04,404*

VERDIER, P. H.
Effects of Variable Excluded Volume on the Dimensions of Off-Lattice Polymer Chains.
PB94-212941 *01,229*

VERDONK, J.
Problems Related to the Determination of Mass Densities of Evaporated Reference Deposits.
PB95-163226 *03,941*

VERES, G.
Atomic Transition Probabilities and Tests of the Spectroscopic Coupling Scheme for N I.
PB96-138466 *04,057*

VERKOUTEREN, J.
National Voluntary Laboratory Accreditation Program: Bulk Asbestos Analysis.
PB95-138129 *02,541*

VERKOUTEREN, J. R.
Guidelines for Refractive Index Measurements of Asbestos.
PB95-151189 *02,543*

VERKOUTEREN, R. M.
Comparative Study of Fe-C Bead and Graphite Target Performance with the National Ocean Sciences AMS (NOSAMS) Facility Recombinator Ion Source.
PB95-175790 *00,693*

Factorial Design Techniques Applied to Optimization of AMS Graphite Target Preparation.
PB95-151197 *00,584*

VESOVIC, V.
Viscosity of Ammonia.
PB96-145933 *01,117*

VEST, R. E.
Stable Silicon Photodiodes for Absolute Intensity Measurements in the VUV and Soft X-ray Regions.
PB97-110175 *04,135*

VETTER, T. W.
Development of the Ion Exchange-Gravimetric Method for Sodium in Serum as a Definitive Method.
PB96-179148 *01,867*

VETTORI, R. L.
Sprinkler Fire Suppression Algorithm.
PB94-216181 *00,293*

VIADAR, A. E.
X-ray Mask Metrology: The Development of Linewidth Standards for X-ray Lithography.
PB95-162129 *02,348*

VIEHLAND, L. A.
Absence of Quantum-Mechanical Effects on the Mobility of Argon Ions in Helium Gas at 4.35 K.
PB97-122543 *01,194*

VIG, J. R.
Fundamental Limits on the Frequency Stabilities of Crystal Oscillators.
PB96-176565 *02,277*

VIGLIANTE, A.
Epitaxial Growth of Sb/GaSb Structures: An Example of V/III-V Heteroepitaxy.
PB95-202560 *04,693*

Observation of Two Length Scales Above (T sub N) in a Holmium Thin Film.
PB97-111942 *04,151*

VIGLIOTTI, D. P.
Effect of Charpy V-Notch Striker Radii on the Absorbed Energy.
PB96-141122 *03,365*

VIGUE, J.
Laser Assisted Collisions at Ultracold Temperatures.
PB95-161220 *03,929*

Theory of Atomic Collisions at Ultracold Temperatures.
PB94-212560 *03,851*

VILGIS, T. A.
Electrostatic Rigidity of Polyelectrolytes from Reparametrization Invariance.
PB96-180062 *04,113*

VILHU, O.
IUE Observations of Solar-Type Stars in the Pleiades and the Hyades.
PB94-199437 *00,053*

VILLA, K.
Influence of Ignition Source on the Flaming Fire Hazard of Upholstered Furniture. (NIST Reprint).
PB95-180162 *00,297*

VILLA, K. M.
Quantifying the Ignition Propensity of Cigarettes.
PB96-155411 *00,306*

VILLAGRAN, E. S.
Standardization of Testing Methods for Optical Disk Media Characteristics and Related Activities at NIST.
PB95-108486 *01,624*

VILLARRUBIA, J. S.
Electrical Test Structures Replicated in Silicon-on-Insulator Material.
PB97-111827 *02,454*

Increasing the Value of Atomic Force Microscopy Process Metrology Using a High-Accuracy Scanner, Tip Characterization, and Morphological Image Analysis.
PB96-190293 *02,758*

Metrology Standards for Advanced Semiconductor Lithography Referenced to Atomic Spacings and Geometry.
PB96-160718 *02,424*

Morphological Estimation of Tip Geometry for Scanned Probe Microscopy.
PB95-203444 *02,662*

Progress Toward Accurate Metrology Using Atomic Force Microscopy.
PB96-146774 *02,417*

Scanned Probe Microscope Tip Characterization Without Calibrated Tip Characterizers.
PB96-190368 *02,759*

VILLARS, P.
CRYSTMET: The NRCC Metals Crystallographic Data File.
PB97-109029 *04,799*

VINCENT, D. H.
Cold Neutron Prompt Gamma Activation Analysis at NIST: A Progress Report.
PB95-175964 *00,602*

Measuring Hydrogen by Cold-Neutron Prompt-Gamma Activation Analysis.
PB96-111877 *00,612*

Neutron Capture Prompt Gamma-Ray Activation Analysis at the NIST Cold Neutron Research Facility.
PB94-213394 *00,556*

VINING, G. G.
Taguchi's Parameter Design: A Panel Discussion.
PB96-111802 *03,445*

VINK, K. L. J.
Molar Absorptivities of Bilirubin (NIST SRM 916A) and Its Neutral and Alkaline Azopigments.
PB94-211042 *03,456*

VIRSHUP, G. F.
Stacked Series Arrays of High-Tc Trilayer Josephson Junctions.
PB96-102272 *04,705*

Step-Edge and Stacked-Heterostructure High-Tc Josephson Junctions for Voltage-Standard Arrays.
PB96-102066 *04,702*

VISCIDI, R. P.
Trace Elements Associated with Proteins. Neutron Activation Analysis Combined with Biological Isolation Techniques.
PB95-163101 *00,597*

VLADAR, A. E.
Modification of a Commercial SEM with a Computer Controlled Cathode Stabilized Power Supply.
PB96-201066 *04,129*

Monte Carlo Model for SEM Linewidth Metrology.
PB95-150058 *02,331*

Report on the NIST Low Accelerating Voltage SEM Magnification Standard Interlaboratory Study.
PB96-201074 *02,445*

Scanning Electron Microscope Magnification Calibration Interlaboratory Study.
PB96-201082 *01,164*

SEM Linewidth Metrology of X-ray Lithography Masks.
PB96-201108 *02,447*

VLASOV, L. V.
Precision High Temperature Blackbodies.
PB95-140059 *03,885*

VLIEGENTHART, J.
beta-D-Glucosyl-Hydroxymethyluracil: A Novel Modified Base Present in the DNA of the Parastic Protozoan T. brucei.
PB94-172319 *03,524*

VOCCIO, J. P.
Effect of Magnetic Field Orientation on the Critical Current of HTS Conductor and Coils.
PB96-141189 *02,956*

VOCKE, R. D.
Certification of Standard Reference Material (SRM) 1941a, Organics in Marine Sediment.
PB96-123690 *02,593*

Determination of Sulfur in Fossil Fuels by Isotope Dilution Thermal Ionization Mass Spectrometry.
PB96-141379 *02,495*

VOGEL, E.
One-Electron Oxidation of Metalloporphycenes as Studied by Radiolytic Methods.
PB97-111967 *01,179*

Status of the Round Robin on the Transport Properties of R134a.
PB96-167218 *01,152*

Viscosity of Ammonia.
PB96-145933 *01,117*

VOGEL, G.
Fluoride Analytical Methods.
PB96-180237 *03,578*

VOGEL, G. L.
Distribution of Fluoride in Saliva and Plaque Fluid After a 0.048 mol/L NaF Rinse.
PB95-151205 *03,561*

VOGL, T. P.
Second Census Optical Character Recognition Systems Conference.
PB94-188711 *01,832*

VOLK, C. M.
Analytical Estimation of Carrier Multipath Bias on GPS Position Measurements.
PB94-215712 *04,845*

VOLK, S. R.
Application of the Modified Voltage-Dividing Potentiometer to Overlay Metrology in a CMOS/Bulk Process.
PB94-181997 *02,302*

VON GLAHN, P.
Behavior of Surface Partial Discharge on Aluminum Oxide Dielectrics.
PB96-123781 *01,937*

Comment and Discussion on Digital Processing of PD Pulses.
PB96-122775 *01,932*

Continuous Recording and Stochastic Analysis of PD.
PB96-112156 *01,925*

Correlations between Electrical and Acoustic Detection of Partial Discharge in Liquids and Implications for Continuous Data Recording.
PB96-204490 *02,248*

Importance of Unraveling Memory Propagation Effects in Interpreting Data on Partial Discharge Statistics.
PB95-163572 *01,901*

Influence of Surface Charge on the Stochastic Behavior of Partial Discharge in Dielectrics.
PB96-122767 *01,931*

Nonstationary Behavior of Partial Discharge during Insulation Aging.
PB95-163580 *01,902*

Nonstationary Behaviour of Partial Discharge during Discharge Induced Ageing of Dielectrics.
PB96-103114 *01,922*

Partial Discharge: Induced Aging of Cast Epoxies and Related Nonstationary Behavior of the Discharge Statistics.
PB95-163598 *01,903*

Performance Evaluation of a New Digital Partial Discharge Recording and Analysis System.
PB95-150389 *01,888*

Standardised Computer Data File Format for Storage, Transport, and Off-Line Processing of Partial Discharge Data.
PB96-122486 *01,930*

VONREDEN, K. F.
Comparative Study of Fe-C Bead and Graphite Target Performance with the National Ocean Sciences AMS (NOSAMS) Facility Recombinator Ion Source.
PB95-175790 *00,693*

VOORHEES, P. W.
Boundary Integral Method for the Simulation of Two-Dimensional Particle Coarsening.
PB94-216744 *03,411*

Effects of Elastic Stress on Phase Equilibrium in the Ni-V System.
PB94-172707 *03,313*

Effects of Elastic Stress on the Stability of a Solid-Liquid Interface.
PB95-163028 *03,350*

Morphological Development of Second-Phase Particles in Elastically-Stressed Solids.
PB95-181111 *03,355*

VORBURGER, T.
Determination of Surface Roughness from Scattered Light.
PB94-216520 *04,243*

Proposed Coating Technology Consortium. (National Coil Coaters Association Fall Conference). Held in Rosemont, Illinois in September 1992.
PB97-110431 *03,129*

VORBURGER, T. V.
Autocorrelation Functions from Optical Scattering for One-Dimensionally Rough Surfaces.
PB94-216538 *04,244*

Automated Optical Roughness Inspection.
PB95-152179 *02,905*

Geometric Characterization of Rockwell Diamond Indenters.
PB95-203287 *02,950*

Light Scattered by Coated Paper.
PB94-216546 04,245

Light Scattering by Sinusoidal Surfaces: Illumination Windows and Harmonics in Standards.
PB97-110548 04,387

Light Scattering from Glossy Coatings on Paper.
PB94-213246 04,242

Measurement and Uncertainty of a Calibration Standard for the Scanning Electron Microscope.
PB94-219250 00,560

Metrology Approach to Unifying Rockwell C Hardness Scales.
PB96-155551 02,957

Microform Calibration Uncertainties of Rockwell Diamond Indenters.
PB96-122114 03,280

Microform Calibrations in Surface Metrology.
PB95-203295 02,951

Model of an Optical Roughness-Measuring Instrument.
PB97-110209 04,384

Optical Scattering from Moderately Rough Surfaces.
PB97-110415 04,385

Post-Process Control of Machine Tools.
PB95-203451 02,952

Present and Future Standard Specimens for Surface Finish Metrology.
PB97-110423 02,928

Regimes of Surface Roughness Measurable with Light Scattering.
PB95-151213 04,265

Sinusoidal Surfaces as Standards for BRDF Instruments.
PB97-110597 04,388

Stylus Flight in Surface Profiling.
PB96-123138 02,675

Stylus Technique for the Direct Verification of Rockwell Diamond Intenders.
PB96-155569 02,958

Surface Texture.
PB95-164620 03,351

Upgraded Facility for Multilayer Mirror Characterization at NIST.
PB96-160387 04,367

Windowing Effects on Light Scattering by Sinusoidal Surfaces.
PB97-111215 04,389

VORIS, P. G.

Coaxial Reference Standard for Microwave Power.
PB94-193786 01,880

VOTAVA, O.

High-Efficiency, High-Power Difference-Frequency Generation of 0.9-1.5 mu m Light in BBO.
PB95-202255 04,317

Photodissociation Dynamics in Quantum State-Selected Clusters: A Test of the One-Atom Cage Effect in Ar-H2O.
PB95-203121 01,044

VSEVOLODOV, N. N.

Holographic Properties of Triton X-100-Treated Bacteriorhodopsin Embedded in Gelatin Films.
PB96-119284 03,761

Optical Properties of Triton X-100-Treated Purple Membranes Embedded in Gelatin Films.
PB96-123500 03,546

Retinal-Protein Complexes as Optoelectronic Components.
PB95-150397 02,146

VYAS, R.

Resonance Fluorescence with Squeezed-Light Excitation.
PB95-203469 04,322

VYDYANATH, H. R.

Correlation of HgCdTe Epilayer Defects with Underlying Substrate Defects by Synchrotron X-Ray Topography.
PB94-200714 02,129

WACK, J.

Security in Open Systems.
PB95-105383 01,473

WACK, J. P.

Computer Virus Attacks.
PB95-163655 01,715

Keeping Your Site Comfortably Secure: An Introduction to Internet Firewalls.
PB95-182275 02,730

WADA, H.

Critical-Current Degradation in Nb3 Al Wires Due to Axial and Transverse Stress.
PB95-202784 02,226

n-Value and Second Derivative of the Superconductor Voltage-Current Characteristic.
PB95-126223 04,533

VAMAS Intercomparison of Critical Current Measurements on NB3Sn Superconductors: A Summary Report.
PB96-119763 04,043

WADAS, A.

dc Magnetic Force Microscopy Imaging of Thin-Film Recording Head.
PB95-176061 04,665

Magnetic Force Microscopy Images of Magnetic Garnet with Thin-Film Magnetic Tip.
PB95-176210 04,669

Magnetic Force Microscopy of Flux in Superconductors.
PB95-161733 04,608

Recent Results in Magnetic Force Microscopy.
PB96-103130 04,721

WADLEY, H. N. G.

Leady Axisymmetric Modes in Infinite Clad Rods. Part 1.
PB95-162905 04,187

Ultrasonic Method for Reconstructing the Two-Dimensional Liquid-Solid Interface in Solidifying Bodies.
PB95-161782 03,349

WAGNER, R. P.

Determination of Acoustic Center Correction for Type LS2aP Condensor Microphones.
PB96-204508 04,190

WAGNER, W.

International Equations for the Saturation Properties of Ordinary Water Substance. Revised According to the International Temperature Scale of 1990. Addendum to Journal of Physical and Chemical Reference Data 16, 893 (1987).
PB94-162302 00,742

WAGSHUL, M.

Hyperfine Effects and Associative Ionization of Ultracold Sodium.
PB95-151221 03,903

WAHL, D. C.

Standards and Linkages: What Data Sharing Needs.
PB95-161881 01,713

WAHLGREN, G. M.

First Results from the Goddard High-Resolution Spectrograph: The Chromosphere of Tauri.
PB94-199528 00,054

GHRS Observations of Cool, Low-Gravity Stars. 1. The Far-Ultraviolet Spectrum of alpha Orions (M2 Iab).
PB96-112016 00,094

WAHLIN, E. K.

Electron-Impact Excitation of Si(3+)(3S yields 3P) Using a Merged-Beam Electron-Energy-Loss Technique.
PB95-151239 03,904

Merged-Beams Energy-Loss Technique for Electron-Ion Excitation: Absolute Total Cross Sections for O(5+) (2s yields 2p).
PB96-102058 04,017

WAIT, D. F.

Comparison of Three Techniques for the Precision Measurement of Amplifier Noise.
PB95-163663 02,349

Measurement Accuracies for Various Techniques for Measuring Amplifier Noise.
PB95-163671 02,350

Radiometer Equation for Noise Comparison Radiometers.
PB96-140363 02,195

Relative Accuracy of Isolated and Unisolated Noise Comparison Radiometers.
PB96-111851 01,924

Terminal Invariant Description of Amplifier Noise.
PB95-153573 02,043

WAKEHAM, W. A.

Standard Reference Data for the Thermal Conductivity of Water.
PB96-145875 01,111

Status of the Round Robin on the Transport Properties of R134a.
PB96-167218 01,152

Transient Methods for Thermal Conductivity.
PB94-198405 04,197

Viscosity of Ammonia.
PB96-145933 01,117

WAKID, S.

Application Profile for ISDN.
PB95-163689 01,479

Comparison of FDDI Asynchronous Mode and DQDB Queue Arbitrated Mode Data Transmission for Metropolitan Area Network Applications.
PB96-160452 01,498

Error Protecting Characteristics of CDMA and Impacts on Speech.
PB96-122452 01,491

Hardware Measurement Techniques for High-Speed Networks.
PB96-160551 01,500

Introduction to Traffic Management for Broadband ISDN.
PB94-142494 01,464

ISDN in North America.
PB96-160767 01,502

Provision of Isochronous Service on IEEE 802.6.
PB96-160635 01,501

Standardization for ATM and Related B-ISDN Technologies.
PB96-160460 01,499

WAKID, S. A.

North American Agreements on ISDN.
PB96-160775 01,503

WALBA, D. M.

Studies of the Higher Order Smectic Phase of the Large Electroclinic Effect Material W317.
PB95-151601 00,935

X-ray Observation of Electroclinic Layer Constriction and Rearrangement in a Chiral Smectic-A Liquid Crystal.
PB96-141080 01,100

WALCH, M.

Bacteriorhodopsin Immobilized in Sol-Gel Glass.
PB95-151429 03,532

WALDOW, D. A.

Anisotropic Phase Separation Kinetics in a Polymer Blend Solution Following Cessation of Shear Studied by Light Scattering.
PB95-151247 01,241

WALHOUT, M.

Improved Dose Metrology in Optical Lithography.
PB96-179510 02,439

Magneto-Optical Trapping of Metastable Xenon: Isotope-Shift Measurements.
PB95-151254 03,905

sigma+-sigma- Optical Molasses in a Longitudinal Magnetic Field.
PB95-161840 03,934

WALKER, B.

Genetically Engineered Pore as a Metal Ion Biosensor.
PB96-161658 03,551

Genetically Engineered Pores as Metal Ion Biosensors.
PB96-167408 03,553

Genetically Engineered Pores for New Materials.
PB96-161641 03,550

Intensity-Dependent Scattering Rings in High Order Above-Threshold Ionization.
PB96-110739 04,032

Pore-Forming Protein with a Metal-Actuated Switch.
PB96-176557 03,554

WALKER, D. K.

Planar Resistors for Probe Station Calibration.
PB95-163697 02,351

Proposed High-Accuracy Superconducting Power Meter for Millimeter Waves.
PB94-212669 02,034

WALKER, J. A.

Hydrogen Atom Attack on Perchloroethylene.
PB95-163473 00,969

Mechanism and Rate Constants for the Reactions of Hydrogen Atoms with Isobutene at High Temperatures.
PB95-151064 00,929

WALKER, J. H.

Improved Automated Current Control for Standard Lamps.
PB94-219367 00,246

WALKER, M. D.

Noninvasive High-Voltage Measurement in Mammography by Crystal Diffraction Spectroscopy.
PB95-153417 00,160

Role of the Office of Radiation Measurement in Quality Assurance.
PB94-212255 00,689

WALKER, M. L.

Alcohol Solutions of Triphenyl-Tetrazolium Chloride as High-Dose Radiochromic Dosimeters.
PB96-135249 03,716

Anionic Triphenylmethane Dye Solutions for Low-Dose Food Irradiation Dosimetry.
PB96-135173 03,715

Calibration of High-Energy Electron Beams by Use of Graphite Calorimeters.
PB95-161113 04,598

Calorimeters for Calibration of High-Dose Dosimeters in High-Energy Electron Beams.
PB96-135272 04,055

Electron and Proton Dosimetry with Custom-Developed Radiochromic Dye Films.
PB95-151106 03,713

WALL, W. F.

Extended CO(7 yields 6) Emission from Warm Gas in Orion.
PB96-102504 00,090

WALLACE, D.

Assessing Functional Diversity by Program Slicing.
PB96-160890 03,734

SQA and TQM in Software Quality Improvement.
PB96-160791 01,754

WALLACE, D. R.

Analysis of Selected Software Safety Standards.
PB95-151262 01,708

Analysis of Standards for the Assurance of High Integrity Software.
PB96-161351 03,735

Center for High Integrity Software System Assurance: Initial Goals and Activities.
PB95-251674 01,734

Control and Instrumentation: Standards for High-Integrity Software.
PB96-161369 03,736

Experimental Models for Software Diagnosis.
PB97-113906 01,783

Framework for the Development and Assurance of High Integrity Software.
PB95-173084 01,716

High Integrity Software Standards Activities at NIST.
PB96-112214 01,744

Object-Oriented Technology Research Areas.
PB95-199329 01,726

Perspective on Software Engineering Standards.
PB95-171377 01,811

Proceedings of the Digital Systems Reliability and Nuclear Safety Workshop. Held in Rockville, Maryland on September 13-14, 1993.
NUREG/CP-0136 03,728

Quality Characteristics and Metrics for Reusable Software (Preliminary Report).
PB94-203437 01,693

Reference Information for the Software Verification and Validation Process.
PB96-188164 01,773

Report of a Workshop on the Assurance of High Integrity Software.
PB96-161377 01,763

Report on the Advanced Software Technology Workshop. Held on February 1, 1994.
PB95-136610 01,707

SQA Standards and Total Quality Management.
PB96-111844 01,743

Standards for High Integrity Software.
PB96-161385 01,764

Structured Testing: A Testing Methodology Using the Cyclomatic Complexity Metric.
PB97-114169 01,784

Study on Hazard Analysis in High Integrity Software Standards and Guidelines.
PB95-198727 01,725

Unravel: A CASE Tool to Assist Evaluation of High Integrity Software. Volume 1. Requirements and Design.
PB95-267886 01,736

Unravel: A CASE Tool to Assist Evaluation of High Integrity Software. Volume 2. User Manual.
PB95-267894 01,737

Verification and Validation.
PB96-161393 01,765

Verification and Validation of Reengineered Software.
PB96-161401 01,766

WALLACE, E. K.

Control Entity Interface Specification.
PB94-191715 02,815

WALLACE, J.

Cooper M(sub II,III) X-ray-Emission Spectra of Copper Oxides and the Bismuth Cuprate Superconductor.
PB96-158027 04,077

WALLACE, J. S.

Barium Contributions to the Valence Electronic Structure of YBa2Cu3O7-delta, PrBa2Cu3O7-delta, and Other Barium-Containing Compounds.
PB96-158019 04,076

Effect of Microstructure on the Wear Transition of Zirconia-Toughened Alumina.
PB94-211778 03,141

Image Depth Profiling SIMS: An Evaluation for the Analysis of Light Element Diffusion in YBa2Cu3O7-x Single Crystal Superconductors.
PB95-126116 04,530

WALLACE, M. A.

Videoconferencing Procurement and Usage Guide.
PB94-217023 01,470

WALLACE, S.

Control Entity Interface Specification.
PB94-191715 02,815

Production Management Information Model for Discrete Manufacturing.
PB96-112008 02,830

Reference Architecture for Machine Control Systems Integration: Interim Report.
PB95-144549 02,820

WALLACE, W. E.

Advances in the Measurement of Polymer CTE: Micrometer- to Atomic-Scale Measurements.
PB96-180229 03,390

Electronics Packaging Materials Research at NIST.
PB96-122692 02,405

Gas Absorption during Ion-Irradiation of a Polymer Target.
PB96-161864 04,099

Influence of an Impenetrable Interface on a Polymer Glass-Transition Temperature.
PB96-146873 03,175

Measured Stopping Powers of Hydrogen and Helium in Polystyrene Near Their Maximum Values.
PB96-112321 04,729

Novel Method for Determining Thin Film Density by Energy-Dispersive X-ray Reflectivity.
PB96-122783 04,737

WALLINDER, F.

Distant Future of Solar Activity: A Case Study of Beta Hydri. 3. Transition Region, Corona, and Stellar Wind.
PB94-185220 00,049

Distant Future of Solar Activity: A Case Study of beta Hydri. 3. Transition Region, Corona, and Stellar Wind.
PB95-153441 00,074

WALLINGTON, T. J.

Atmospheric Reactivity of alpha-Methyl-Tetrahydrofuran.
PB95-163705 02,548

WALLQVIST, A.

Collection of Results for the SPC/E Water Model.
PB96-147889 01,127

WALLS, F. L.

Aging, Warm-Up Time and Retrace; Important Characteristics of Standard Frequency Generators.
PB96-103122 04,031

Confidence on the Modified Allan Variance and the Time Variance.
PB96-190376 01,557

Cross-Correlation Analysis Improves Time Domain Measurements.
PB95-180535 01,543

Design Criteria for BJT Amplifiers with Low I/f AM and PM Noise.
PB96-200365 02,442

Diode-Laser Pumped, Rubidium Cell Frequency Standards.
PB95-163218 01,538

Effect of Harmonic Distortion on Phase Errors in Frequency Distribution and Synthesis.
PB96-200779 01,563

Environmental Sensitivities of Quartz Oscillators.
PB96-103148 02,271

Frequency Synthesis and Metrology at 10(-17) and Beyond.
PB97-113187 02,101

Fundamental Limits on the Frequency Stabilities of Crystal Oscillators.
PB96-176565 02,277

High-Order Harmonic Mixing with GaAs Schottky Diodes.
PB95-108585 01,528

High Spectral Purity X-Band Source.
PB95-163713 02,045

Hybrid Digital/Analog Servo for the NIST-7 Frequency Standard.
PB95-180618 01,544

Investigations of AM and PM Noise in X-Band Devices.
PB95-180022 02,062

Local Oscillator Requirements and Strategies for the Next Generation of High-Stability Frequency Standards.
PB96-112230 01,551

New Model of 1/F Noise in Baw Quartz Resonators.
PB96-112248 02,383

New 5 and 10 MHz High Isolation Distribution Amplifier.
PB96-190202 01,510

Origin of I/f PM and AM Noise in Bipolar Junction Transistor Amplifiers.
PB96-200787 02,096

Practical Standards for PM and AM Noise at 5, 10 and 100 MHz.
PB95-181129 01,546

Precision Oscillators: Dependence of Frequency on Temperature, Humidity and Pressure.
PB94-198306 02,031

Quest to Understand and Reduce I/f Noise in Amplifiers and Baw Quartz Oscillators.
PB96-200795 02,097

Reducing Errors, Complexity, and Measurement Time of PM Noise Measurements.
PB96-119771 02,075

Reducing the Effect of Local Oscillator Phase Noise on the Frequency Stability of Passive Frequency Standards.
PB95-180972 01,545

Reducing the 1/f AM and PM Noise in Electronics for Precision Frequency Metrology.
PB97-113195 02,102

Relationship of AM to PM Noise in Selected RF Oscillators.
PB95-169009 02,262

Secondary Standard for PM and AM Noise at 5, 10, and 100 MHz.
PB96-123187 01,554

Surface Transverse Wave Oscillators with Extremely Low Thermal Noise Floors.
PB96-186010 01,967

Ultra-High Stability Synthesizer for Diode Laser Pumped Rubidium.
PB94-216066 01,527

Ultralinear Small-Angle Phase Modulator.
PB95-168852 02,261

WALSH, T.

High Critical Temperature Superconductor Tunneling Spectroscopy Using Squeezable Electron Tunneling Junctions.
PB95-163721 04,627

Tunneling Measurement of the Zero-Bias Conductance Peak and the Bi-Sr-Ca-Cu-O Thin-Film Energy Gap.
PB95-163739 04,628

WALTER, F.

Sleuthing the Dynamo: HST/FOS Observations of UV Emissions of Solar-Type Stars in Young Clusters.
PB96-122817 00,098

WALTER, F. M.

Far-Ultraviolet Flare on a Pleiades G Dwarf.
PB96-102033 00,086

First Results from the Goddard High-Resolution Spectrograph: The Chromosphere of Tauri.
PB94-199528 00,054

Observations of 3C 273 with the Goddard High Resolution Spectrograph on the Hubble Space Telescope.
PB95-202321 00,076

WALTER, S.

Slant Path Atmospheric Refraction Calibrator: An Instrument to Measure the Microwave Propagation Delays Induced by Atmospheric Water Vapor.
PB95-151270 01,476

WALTER, T.

Confidence on the Modified Allan Variance and the Time Variance.
PB96-190376 01,557

WALTERS, C. R.

VAMAS Intercomparison of Critical Current Measurements on NB3Sn Superconductors: A Summary Report.
PB96-119763 04,043

WALTERS, D.

Telecommunications Security Guidelines for Telecommunications Management Network. Computer Security.
PB96-139415 01,496

WALTERS, J.

NIST List of Publications, LP 103, March 1996. National Semiconductor Metrology Program.
PB96-175856 02,432

WALTMAN, D. J.

Quench Energy and Fatigue Degradation Properties of Cu- and Al/Cu-Stablized Nb-Ti Epoxy-Impregnated Superconductor Coils.
PB96-141213 04,755

WALTMAN, S.

Precise Optical Frequency References and Difference Frequency Measurements with Diode Lasers.
PB95-176228 04,305

WALTON, G. N.

Application of a Multizone Airflow and Contaminant Dispersal Model to Indoor Air Quality Control in Residential Buildings.
PB95-180238 02,555

Computer Programs for Simulation of Lighting/HVAC Interactions.
PB94-140407 02,501

CONTAM93 User Manual.
PB94-164381 02,536

CONTAM94: A Multizone Airflow and Contaminant Dispersal Model with a Graphic User Interface.
PB97-113203 02,570

Mathematical Analysis of Practices to Control Moisture in the Roof Cavities of Manufactured Houses.
PB97-106843 00,278

WALTON, W.

Smoke Emission from Burning Crude Oil.
PB96-122890 01,407

WALTON, W. D.

In situ Burning of Oil Spills: Mesoscale Experiments.
PB94-142973 01,355

In situ Burning of Oil Spills: Mesoscale Experiments and Analysis.
PB95-163747 02,587

Northridge Earthquake, 1994. Performance of Structures, Lifelines and Fire Protection Systems.
PB94-161114 00,421

Northridge Earthquake 1994: Performance of Structures, Lifelines, and Fire Protection Systems.
PB94-207461 04,825

Post-Earthquake Fire and Lifelines Workshop. Held in Long Beach, California on January 30-31, 1995. Proceedings.
PB96-117916 00,209

Santa Ana Fire Department Experiment at 1315 South Bristol, July 14, 1994.
PB95-188868 00,389

Santa Ana Fire Department Experiment at 1315 South Bristol, July 14, 1994. (Reprint).
PB96-102934 00,207

Santa Ana Fire Department Experiments at South Bristol Street.
PB96-154810 00,305

Smoke Plume Trajectory from In situ Burning of Crude Oil in Alaska: Field Experiments.
PB96-131560 02,594

WALTRIP, B. C.

Automatic Inductive Voltage Divider Bridge Operates from 10 Hz to 100 kHz.
PB94-198413 02,032

DC-MHz Wattmeter Based on RMS Voltage Measurements.
PB97-113211 01,992

Digital Impedance Bridge.
PB96-103155 02,272

Low Voltage Standards in the 10 Hz to 1 MHz Range.
PB97-112569 02,100

Wideband Sampling Voltmeter.
PB97-113039 01,990

WAN, H. X.

Electron Scattering and Dissociative Attachment by SF6 and Its Electrical-Discharge By-Products.
PB95-151288 02,256

WAN, K. T.

Diffusion of Water along 'Closed' Mica Interfaces.
PB96-180039 02,993

Effect of Chemical Interaction on Barenblatt Crack Profiles in Brittle Solids.
PB96-180245 02,996

Pressurized Internal Lenticular Cracks at Healed Mica Interfaces.
PB96-180252 02,997

WANG, C. C.

Measurement of the Uniformity of Particle Deposition of Filter Cassette Sampling in a Low Velocity Wind Tunnel.
PB95-163754 02,549

WANG, C. L.

Elastic Constants of Isotropic Cylinders Using Resonant Ultrasound.
PB94-211919 04,497

WANG, C. M.

Approximate Confidence Intervals on Linear Combinations of Expected Mean Squares.
PB95-151296 03,435

Approximate Confidence Intervals on Positive Linear Combinations of Expected Mean Squares.
PB95-151304 03,436

Ranges of Confidence Coefficients for Confiedence Intervals on Variance Components.
PB95-151312 03,437

Tolerance Intervals for the Distribution of True Values in the Presence of Measurement Errors.
PB95-150405 03,434

WANG, C. M. J.

Optical Fiber Geometry by Gray-Scale Analysis with Robust Regression.
PB95-161519 04,272

WANG, D.

Gas Transport Properties of Solution-Cast Perfluorosulfonic Acid Ionomer Films Containing Ionic Surfactants.
PB95-175998 01,267

WANG, F. W.

Applications of Fluorescence Spectroscopy in Polymer Science and Technology.
PB95-163770 01,258

Copolymerization of N-Phenyl Maleimide and gamma-Methacryloxypropyl Trimethoxysilane.
PB95-153144 01,248

Fluorescence Anisotropy Measurements on a Polymer Melt as a Function of Applied Shear Stress.
PB94-199296 01,209

Fluorescence Monitoring of Polarity Change and Gelation during Epoxy Cure.
PB94-185543 01,204

In-Line Optical Monitoring of Injection Molding.
PB94-185105 01,201

Observations of Shear Induced Molecular Orientation in a Polymer Melt Using Fluorescence Anisotropy Measurements.
PB94-199304 01,210

Observations of Shear Stress and Molecular Orientation Using Fluorescence Anisotropy Measurements.
PB94-199312 01,211

Preparation and Monitoring of Lead Acetate Containing Drinking Water Solutions for Toxicity Studies.
PB94-193885 00,538

Thermal Behavior of 4-Maleimidophenyl Glycidyl Ether Resins.
PB95-153151 01,249

Thermal Behaviour of Methyl Methacrylate and N-Phenyl Maleimide Copolymers.
PB95-152237 01,246

WANG, H. P.

Interaction between Micro and Macroscopic Flow in RTM Preforms.
PB95-162012 03,159

WANG, J.

Determination of the Complex Refractive Index of Individual Quantum Wells from Distributed Reflectance.
PB95-175642 02,176

WANG, J. C.

Chemically Assisted Machining of Si3N4.
PB96-122999 03,072

WANG, J. C. M.

Proposed Changes to Charpy V-Notch Machine Certification Requirements.
PB96-135363 02,955

Technique to Evaluate Benchmarks: A Case Study Using the Livermore Loops.
PB95-151320 04,577

WANG, J. L.

Electromagnetic Coupling Character of (001) Twist Boundaries in Sintered Bi2Sr2CaCu2O8+x Bicrystals.
PB96-176573 01,963

WANG, J. T.

Periapical Tissue Reactions to a Calcium Phosphate Cement in the Teeth of Monkeys.
PB94-212008 00,149

WANG, L.

Band-to-Band Photoluminescence and Luminescence Excitation in Extremely Heavily Carbon-Doped Epitaxial GaAs.
PB95-150413 04,570

Standard Reference Materials: Polystyrene Films for Calibrating the Wavelength Scale of Infrared Spectrophotometers - SRM 1921.
PB95-226866 03,386

WANG, M.

Theoretical Analysis of the Coherence-Induced Spectral Shift Experiments of Kandpal, Vaishya, and Joshi.
PB94-219383 00,561

WANG, P.

Threshold Electron Excitation of Na.
PB95-202917 03,994

WANG, P. S.

Characterization of Phase and Surface Composition of Silicon Carbide Platelets.
PB94-216264 03,043

Coating of Fibers by Colloidal Techniques in Ceramic Composites.
PB94-216256 03,196

Deposition of Colloidal Sintering-Aid Particles on Silicon Nitride.
PB94-216272 03,044

Effects of Soxhlet Extraction on the Surface Oxide Layer of Silicon Nitride Powders.
PB95-175584 03,057

NMR Characterization of Injection-Moulded Alumina Green Compacts. Part 2. T2-Weighted Proton Imaging.
PB96-201181 01,165

Tribochemical Reaction of Stearic Acid on Copper Surface Studied by Surface Enhanced Raman Spectroscopy.
PB94-212057 02,964

WANG, Q.

Short-Pulse Detachment of H(-) in the Presence of a Static Electric Field.
PB95-203477 04,007

User's Guide for the PHIGS Validation Tests (Version 2.1).
PB94-165206 01,682

WANG, S.

Reproducibility of Tests on Energy Management and Control Systems Using Building Emulators.
PB95-175980 00,260

Use of Building Emulators to Evaluate the Performance of Building Energy Management Systems.
PB96-111901 00,269

WANG, S. S.

Composite Materials for Offshore Operations: Proceedings of the International Workshop (1st). Held in Houston, Texas on October 26-28, 1993.
PB96-109509 03,169

WANG, S. Y.

L-threo-beta-Hydroxyhistidine, an Unprecedented Iron(III) Ion-Binding Amino Acid in a Pyoverdine-type Siderophore from Pseudomonas fluorescens 244.
PB94-211620 00,553

WANG, Y. S.

Effect of Microstructure on the Wear Transition of Zirconia-Toughened Alumina.
PB94-211778 03,141

Wear Mechanism Maps of Ceramics.
PB94-172368 03,229

Wear Model for Alumina Sliding Wear.
PB95-163796 03,239

Wear Transitions in Monolithic Alumina and Zirconia-Alumina Composites.
PB96-103163 03,168

WANG, Z.

Critical Current Density, Irreversibility Line, and Flux Creep Activation Energy in Silver-Sheathed Bi2Sr2Ca2Cu2Ox Superconducting Tapes.
PB95-162749 04,616

WANG, Z. D.

Analysis of Creep in a Si-SiC C-Ring by Finite Element Method.
PB94-200268 03,037

WANG, Z. L.

Epitaxial Growth of BaTiO3 Thin Films at 600C by Metalorganic Chemical Vapor Deposition.
PB96-122510 03,071

WANNBERG, B.

Inner-Valence States CO(+) between 22 eV and 46 eV Studied by High Resolution Photoelectron Spectroscopy and ab Initio CI Calculations.
PB95-180055 03,961

WARBURTON, W. K.

Real-Time Small-Angle X-Ray Scattering Study of the Early Stage of Phase Separation in the SiO2-BaO-K20 System.
PB95-163069 03,052

WARD, B.

Digital Techniques in HV Tests - Summary of 1989 Panel Session.
PB94-216702 02,035

WARD, D.

Interim Testing Artifact (ITA): A Performance Evaluation System for Coordinate Measuring Machines (CMMs). User Manual.
PB95-210589 02,914

NIST SRM 9983 High-Rigidity Ball-Bar Stand. User Manual.
PB95-255840 02,669

WARD, D. B.

Intercomparison between NPL (India) and NIST (USA) Pressure Standards in the Hydraulic Pressure Region Up to 26 MPa.
PB96-113543 04,211

WARD, D. E.

User's Guide to NIST SRM 2084: CMM Probe Performance Standard.
PB94-206109 02,709

WARD, R. C.

Variation in Magnetic Properties of Cu/Fcc (001) Sandwich Structures.
PB95-141164 04,555

WARD, R. C. C.

Observation of Two Length Scales Above (T sub N) in a Holmium Thin Film.
PB97-111942 04,151

WARDLE, C. E.

SQA and TQM in Software Quality Improvement.
PB96-160791 01,754

SQA Standards and Total Quality Management.
PB96-111844 01,743

WARNAR, C. A.

X.500 Directory Schema Design Handbook.
PB96-183041 02,739

WARSHAW, S. I.

International Challenges in Defining the Public and Private Interest in Standards.
PB96-160361 00,498

WASKIEWICZ, W. K.

XUV Characterization Comparison of Mo/Si Multilayer Coatings.
PB95-164000 04,278

WASSERMANN, E. F.

Temperature Dependence of the Magnetic Excitations in Ordered and Disordered Fe72Pt28.
PB95-150223 04,563

WASSON, O. A.

Measurement of the (10)B(n, alpha1gamma)(7)Li Cross Section in the 0.3 to 4 MeV Neutron Energy Interval.
PB96-161799 04,098

Measurements of the (235)U(n,f) Cross Section in the 3 to 30 MeV Neutron Energy Region.
PB97-119051 04,172

WASZCZAK, J. V.

Increased Pinning Energies and Critical Current Densities in Heavy-Ion-Irradiated Bi2Sr2CaCu2O8 Single Crystals.
PB95-175352 04,654

WATANABE, H.

Effects of Adhesive Thickness, Open Time, and Surface Cleanness on the Peel Strength of Adhesive-Bonded Seams of EPDM Rubber Roofing Membrane.
PB95-151338 00,372

Pulse-Echo Ultrasonic Evaluation of the Integrity of Seams of Single-Ply Roof Membranes.
PB95-163804 00,381

WATANABE, K.

Report of the Refrigeration, Air Conditioning and Heat Pumps Technical Options Committee.
PB96-176755 03,293

WATERSTRAT, R. M.

Electronic Structure and Phase Equilibria in Ternary Substitutional Alloys.
PB97-119366 03,378

New Alloys Show Extraordinary Resistance to Fracture and Wear.
PB95-151346 03,346

WATERSTRAT, R. W.

Dental Materials.
PB94-172871 00,142

WATKINS, J.

Domain Analysis of the Alarm Surveillance Domain. Version 1.0. Conducted as Part of the Domain Analysis Case Study Project.
PB95-136339 01,705

WATKINS, S. F.

X-Ray-Diffraction Study of a Thermomechanically Detwinned Single Crystal of YBa2Cu3O6+x.
PB95-151726 04,581

WATSON, A. H.

Structured Testing: A Testing Methodology Using the Cyclomatic Complexity Metric.
PB97-114169 01,784

WATSON, C. I.

Comparison of FFT Fingerprint Filtering Methods for Neural Network Classification.
PB95-136362 *01,840*

PCASYS: A Pattern-Level Classification Automation System for Fingerprints.
PB95-267936 *01,853*

WATSON, D. G.

Cambridge Structural Database (CSD): Current Activities and Future Plans.
PB97-109052 *00,516*

How the Cambridge Crystallographic Data Centre Obtains Its Information.
PB97-109193 *04,808*

WATSON, J. T. R.

Viscosity of Ammonia.
PB96-145933 *01,117*

WATSON, R. E.

Monte Carlo and Mean-Field Calculations of the Magnetocaloric Effect of Ferromagnetically Interacting Clusters.
PB94-172087 *03,201*

WATTERS, R. L.

Dissolution Problems with Botanical Reference Materials.
PB95-126280 *03,487*

Preparation and Certification of a Rhodium Standard Reference Material Solution.
PB94-185071 *00,529*

Trace Detection in Conducting Solids Using Laser-Induced Fluorescence in a Cathodic Sputtering Cell.
PB95-163424 *00,598*

Traceability to the Mole: A New Initiative by CIPM.
PB95-180246 *00,605*

WATTS, L.

Low Temperature H(sub 2)S Separation Using Membrane Reactor with Redox Catalyst.
DE94008991 *02,471*

WATTS, R.

Atoms in Optical Molasses.
PB95-108874 *03,875*

Influence of Electrical Isolation on the Structure and Reflectivity of Multilayer Coatings Deposited on Dielectric Substrates.
PB96-159736 *04,365*

New Method for Achieving Accurate Thickness Control for Uniform and Graded Multilayer Coatings on Large Flat Substrates.
PB96-159744 *04,366*

Optical Molasses: The Coldest Atoms Ever.
PB95-108908 *03,878*

Soft X-ray Reflectometry Program at the National Institute of Standards and Technology.
PB96-160395 *04,368*

WATTS, R. N.

Atoms in Optical Molasses: Applications to Frequency Standards.
PB95-108882 *03,876*

Heterodyne Measurement of the Fluorescence Spectrum of Optical Molasses.
PB95-108411 *03,873*

Improved Reflectometry Facility at the National Institute of Standards and Technology.
PB96-160338 *04,087*

Interfaces in Mo/Si Multilayers.
PB96-160668 *02,423*

Localization of Atoms in a Three-Dimensional Standing Wave.
PB95-163887 *03,944*

Measurements of Fluorescence from Cold Atoms: Localization in Three-Dimensional Standing Waves.
PB95-163879 *03,943*

New NIST/ARPA National Soft X-ray Reflectometry Facility.
PB96-158092 *04,080*

NIST Metrology for Soft X-ray Multilayer Optics.
PB96-160379 *04,088*

Optical Molasses: Cold Atoms for Precision Measurements.
PB95-108890 *03,877*

Simple Variable Line Space Grating Monochromator for Synchrotron Light Source Beamlines.
PB96-156203 *04,065*

Upgraded Facility for Multilayer Mirror Characterization at NIST.
PB96-160387 *04,367*

XUV Characterization Comparison of Mo/Si Multilayer Coatings.
PB95-164000 *04,278*

WATTS, R. O.

Infrared and Microwave Spectroscopy of the Argon - Propyne Dimer.
PB94-198892 *00,794*

WAVERING, A. J.

Visual Pursuit Systems.
PB95-143285 *01,841*

WEAVER, J. T.

Needs for Brachytherapy Source Calibrations in the United States.
PB97-110092 *03,521*

WEBER, A.

2nu9 Band of Propyne-d3.
PB95-164513 *00,985*

Molecular Spectroscopy.
PB94-213337 *03,861*

WEBER, L. A.

Criteria for Establishing Accurate Vapor Pressure Curves.
PB95-163812 *00,972*

Design of a High-Pressure Ebulliometer, with Vapor-Liquid Equilibrium Results for the Systems CHF2Cl + CF3-CH3 and CF3-CH2F + CH2F2.
PB97-113229 *04,163*

Ebulliometers for Measuring the Thermodynamic Properties of Fluids and Fluid Mixtures.
DE94017817 *04,195*

Ebulliometric Measurement of the Vapor Pressure of Difluoromethane.
PB95-151361 *00,931*

Ebulliometric Measurement of the Vapor Pressure of 1-Chloro-1,1-Difluoroethane and 1,1-Difluoroethane.
PB95-164489 *00,984*

Estimating the Virial Coefficients of Small Polar Molecules.
PB95-176236 *03,276*

Measurements of the Vapor Pressures of Difluoromethane, 1-Chloro-1,2,2,2-Tetrafluoroethane, and Pentafluoroethane.
PB95-169272 *03,270*

Measurements of the Virial Coefficients and Equation of State of the Carbon Dioxide + Ethane System in the Supercritical Region.
PB95-151353 *03,906*

Model for Calculating Virial Coefficients of Natural Gas Hydrocarbons with Impurities.
PB96-156047 *04,064*

Thermodynamic Properties of CF3-CHF-CHF2, 1,1,1,2,3,3-Hexafluoropropane.
PB97-118384 *03,299*

Thermodynamic Properties of CHF2-CF2-CHF, 1,1,2,2,3-Pentafluoropropane.
PB97-118392 *03,300*

Thermodynamic Properties of Difluoromethane.
PB94-185204 *00,772*

Vapor Pressure of Pentafluorodimethyl Ether.
PB96-201199 *00,677*

Vapor Pressure of 1,1,1,2,2-Pentafluoropropane.
PB97-113237 *00,684*

Vapor Pressure of 1,1-dichloro-2,2,2-trifluoroethane (R123).
PB95-126231 *00,899*

Vapor Pressures and Gas-Phase PVT Data for 1-Chloro-1,2,2,2-Tetrafluoroethane (R124).
PB95-175154 *03,271*

Vapour Pressures and Gas-Phase (p, rho n, T) Values for CF3CHF2(R125).
PB96-102090 *04,019*

Virial Coefficients of Five Binary Mixtures of Fluorinated Methanes and Ethanes.
PB96-156054 *01,128*

WEBER, S. F.

AutoBid 2.0: The Microcomputer System for Police Patrol Vehicle Selection.
PB96-154570 *04,871*

Benefits and Costs of Research: A Case Study of the Fire Safety Evaluation System.
PB96-202288 *00,232*

Evaluating Investments in Law Enforcement Equipment: An Annotated Bibliography.
PB95-151379 *04,867*

WEBER, T.

Doppler-Free Spectroscopy of Large Polyatomic Molecules and van der Waals Complexes.
PB96-119581 *04,339*

Frequency Shifting of Pulsed Narrow-Band Laser Light in a Multipass Raman Cell.
PB95-203352 *04,321*

Van der Waals Bond Lengths and Electronic Spectral Shifts of the Benzene-Kr and Benzene-Xe Complexes.
PB95-151387 *00,932*

WEDDING, A. B.

N2(a'(sup 1)Sigma(sub g)(sup +)) Metastable Collisional Destruction and Rotational Excitation Transfer by N2.
PB95-151395 *00,933*

WEERTMAN, J. R.

Small Angle Neutrons Scattering from Nanocrystalline Palladium as a Function of Annealing.
PB95-176103 *03,354*

WEETALL, H.

Bacteriorhodopsin Immobilized in Sol-Gel Glass.
PB95-151429 *03,532*

WEETALL, H. H.

Affinity Chromatography on Inorganic Support Materials.
PB95-163820 *03,467*

Aggregation Kinetics of Colloidal Particles Destabilized by Enzymes.
PB95-125878 *00,894*

Amperometric Flow-Injection Analysis Biosensor for Glucose Based on Graphite Paste Modified with Tetracyanoquinodimethane.
PB95-161980 *03,498*

Application of Photochemical Reaction in Electrochemical Detection of DNA Intercalation.
PB94-185733 *00,686*

Autofluorescence Detection of 'Escherichia coli' on Silver Membrane Filters.
PB96-163639 *03,590*

Bacterial Enumeration in Storage Water.
PB96-163647 *03,591*

Detection of Aromatic Compounds Based on DNA Intercalation Using an Evanescent Wave Biosensor.
PB96-111976 *03,473*

Method for the Assay of Hydrolytic Enzymes Using Dynamic Light Scattering.
PB95-151411 *03,531*

New Method for the Detection and Measurement of Polyaromatic Carcinogens and Related Compounds by DNA Intercalation.
PB96-167382 *03,481*

Novel Amperometric Immunosensor for Procainamide Employing Light Activated Labels.
PB96-163662 *00,512*

Optical Properties of Triton X-100-Treated Purple Membranes Embedded in Gelatin Films.
PB96-123500 *03,546*

Preparation of Immobilized Proteins Covalently Coupled Through Silane Coupling Agents to Inorganic Supports.
PB95-151403 *03,530*

WEI, L.

Evaluation of Thermal Wave Imaging for Detection of Machining Damage in Ceramics.
PB95-220547 *03,062*

Thermal Wave NDE of Advanced Materials Using Mirage Effect Detection.
PB96-204516 *04,191*

WEI, R.

Tribological Behavior of 440/Diamond-Like-Carbon Film Couples.
PB96-119714 *03,019*

WEIDA, M. J.

Collisional Alignment of CO2 Rotational Angular Momentum States in a Supersonic Expansion.
PB96-103171 *01,069*

Signatures of Large Amplitude Motion in a Weakly Bound Complex: High-Resolution IR Spectroscopy and Quantum Calculations for HeCO2.
PB95-203485 *01,054*

WEIDE, K.

Nonadiabatic Effects in the Photoassociation of H2S.
PB95-151437 *00,934*

WEIDENHEIMER, D. M.

Electrical Breakdown in Transformer Oil in Large Gaps.
PB95-150579 *01,889*

WEIDER, T.

Shear-Induced Melting of Two-Dimensional Solids.
PB96-112057 *01,075*

WEIDMAN, M. P.

Direct Comparison Transfer of Microwave Power Sensor Calibrations.
PB96-158654 *02,086*

WEIL, C. M.

Electromagnetic Properties of Materials: The NIST Metrology Program.
PB96-122791 *01,933*

NIST Metrology Program on Electromagnetic Characterization of Materials.
PB96-156062 *01,944*

WEIMER, C.

Experimental Results on Normal Modes in Cold, Pure Ion Plasmas.
PB95-175105 *03,956*

WEIMER, C. S.

Diode Laser as a Spectroscopic Tool.
PB95-175485 *00,600*

Electrostatic Modes as a Diagnostic in Penning-Trap Experiments.
PB95-176244 *03,959*

High-Order Multipole Excitation of a Bound Electron.
PB96-119789 *04,044*

High-Resolution Atomic Spectroscopy of Laser-Cooled Ions.
PB95-169330 *03,953*

High-Resolution Diode-Laser Spectroscopy of Calcium.
PB95-181244 *03,969*

Laser-Cooled Positron Source.
PB95-169348 *03,954*

Recent Experiments on Trapped Ions at the National Institute of Standards and Technology.
PB95-169322 *03,952*

WEISS, A. W.

Relativistic Modifications of Charge Expansion Theory.
PB96-123799 *04,052*

WEISS, M.

Use of Ionospheric Data in GPS Time Transfer.
PB95-163853 *01,540*

WEISS, M. A.

Calibration of GPS Equipment in Japan.
PB95-151452 *01,531*

Comparison of GPS Broadcast and DMA Precise Ephemerides.
AD-P009 114/0 *01,518*

Comparison of GPS Broadcast and DMA Precise Ephemerides.
N94-30660/2 *01,523*

Confidence on the Modified Allan Variance and the Time Variance.
PB96-190376 *01,557*

Confidence on the Second Difference Estimation of Frequency Drift.
PB95-151460 *01,532*

Confidence on the Three-Point Estimator of Frequency Drift.
PB95-163838 *01,539*

Implementation of a Standard Format for GPS Common View Data.
N95-32323/4 *03,779*

Implementation of a Standard Format for GPS Common View Data.
PB96-176581 *01,555*

Promise into Practice: Implementing TA2 on Real Clocks at NIST.
PB95-151478 *01,533*

Sifting Through Nine Years of NIST Clock Data with TA2.
PB95-181137 *01,547*

Smart Clock: A New Time.
PB95-151445 *01,530*

Time Scale Algorithm for Post-Processing: AT1 Plus Frequency Variance.
PB94-172772 *01,525*

WEISS, P.

Report of the Refrigeration, Air Conditioning and Heat Pumps Technical Options Committee.
PB96-176755 *03,293*

WEISS, R. A.

Compatibilization of Polymer Blends by Complexation. 2. Kinetics of Interfacial Mixing.
PB97-111900 *01,295*

WEISS, V.

Femtosecond Time-Resolved Wave Packet Motion in Molecular Multiphoton Ionization and Fragmentation.
PB94-198611 *00,790*

WEISSBECKER, B.

Dielectronic Capture Processes in the Electron-Impact Ionization of Sc(2+).
PB95-203113 *04,000*

WEISSER, P.

HVAC CAD Layout Tools: A Case Study of University/Industry Collaboration.
PB97-112221 *00,281*

WEISSERT, T.

Promise into Practice: Implementing TA2 on Real Clocks at NIST.
PB95-151478 *01,533*

Time Scale Algorithm for Post-Processing: AT1 Plus Frequency Variance.
PB94-172772 *01,525*

Use of Ionospheric Data in GPS Time Transfer.
PB95-163853 *01,540*

WEISSERT, T. P.

Sifting Through Nine Years of NIST Clock Data with TA2.
PB95-181137 *01,547*

WEISSHAAR, A.

Fibre Splice Loss: A Simple Method of Calculation.
PB95-175519 *04,299*

Mode Coupling and Loss on Tapered Optical Waveguides.
PB95-168571 *04,282*

Symbolic Programming with Series Expansions: Applications to Optical Waveguides.
PB95-168589 *04,283*

Vector and Quasi-Vector Solutions for Optical Waveguide Modes Using Efficient Galerkin's Method with Hermite-Gauss Basis Functions.
PB96-141197 *04,357*

WEISSMULLER, J.

Inelastic Neutron Scattering Study of Hydrogen in Nanocrystalline Pd.
PB96-146857 *03,366*

Vibrational Excitations and the Position of Hydrogen in Nanocrystalline Palladium.
PB96-111828 *04,035*

WELCH, B.

Pressure Measurements with the Mercury Melting Line Referred to ITS-90.
PB96-161005 *01,136*

WELCH, B. E.

Operational Mode and Gas Species Effects on Rotational Drag in Pneumatic Dead Weight Pressure Gages.
PB95-140182 *00,903*

WELCH, M.

How to Verify Reference Materials.
PB95-151486 *03,497*

WELCH, M. J.

Analysis by a Combination of Gas Chromatography and Tandem Mass Spectrometry: Development of Quantitative Tandem-in-Time Ion Trap Mass Spectrometry: Isotope Dilution Quantification of 11-Nor-Delta-9-Tetrahydro cannabinol-9-Carboxylic Acid.
PB96-117221 *02,561*

Certification of Morphine and Codeine in a Human Urine Standard Reference Material.
PB95-176160 *03,499*

Certification of Phencyclidine in Lyophilized Human Urine Reference Materials.
PB96-160692 *03,508*

Determination of Amphetamine and Methamphetamine in a Lyophilized Human Urine Reference Material.
PB95-175444 *03,597*

Hair Analysis for Drugs of Abuse: Evaluation of Analytical Methods, Environmental Issues, and Development of Reference Materials.
PB95-176269 *03,501*

Hair Testing for Drugs of Abuse: International Research on Standards and Technology.
PB96-120555 *03,504*

Interlaboratory Comparison Studies on the Analysis of Hair for Drugs of Abuse.
PB95-176251 *03,500*

Interlaboratory Studies on the Analysis of Hair for Drugs of Abuse: Results from the Fifth Exercise.
PB97-110449 *03,509*

Interlaboratory Studies on the Analysis of Hair for Drugs of Abuse: Results from the Fourth Exercise.
PB97-111322 *03,510*

Isotope Dilution Mass Spectrometry as a Candidate Definitive Method for Determining Total Glycerides and Triglycerides in Serum.
PB96-102280 *03,519*

NIST Reference Materials to Support Accuracy in Drug Testing.
PB96-123807 *03,505*

WELCH, W. J.

Taguchi's Parameter Design: A Panel Discussion.
PB96-111802 *03,445*

WELLINGTON, J. D.

ISO TC 184/SC4 Reference Manual.
PB95-242293 *02,663*

WELLS, J.

Precise Optical Frequency References and Difference Frequency Measurements with Diode Lasers.
PB95-176228 *04,305*

WELLS, J. S.

Extension of Heterodyne Frequency Measurements on OCS to 87 THz (2900 cm(-1)).
PB94-200680 *00,811*

Optically Stabilized Tunable Diode-Laser System for Saturation Spectroscopy.
PB96-102819 *04,717*

Stabilization of 3.3 and 5.1 m Lead-Salt Diode Lasers by Optical Feedback.
PB95-180709 *04,313*

Sub-Doppler Frequency Measurements on OCS at 87 Thz (3.4 micrometers) with the CO Overtone Laser: Considerations and Details.
PB95-128633 *04,255*

Sub-Doppler Frequency Measurements on OCS at 87 THz (3.4 mu m) with the CO Overtone Laser.
PB96-102215 *04,330*

WELLS, M. R.

Observation of Two Length Scales Above (T sub N) in a Holmium Thin Film.
PB97-111942 *04,151*

WELLSTOOD, F. C.

Application of Single Electron Tunneling: Precision Capacitance Ratio Measurements.
PB96-102157 *04,703*

WELSCH, L. A.

Proposed International Interactive Courseware Standard.
PB96-123161 *00,137*

WELTY, R. P.

Self-Biasing Cryogenic Particle Detector Utilizing Electrothermal Feedback and a SQUID Readout.
PB96-102538 *04,712*

Series Array of DC SQUIDs.
PB95-163861 *02,046*

Two-Stage Integrated SQUID Amplifier with Series Array Output.
PB95-176277 *02,061*

WEN, C. P.

Electrical Measurements of Microwave Flip-Chip Interconnections.
PB96-176748 *02,436*

Microwave Characterization of Flip-Chip MMIC Components.
PB96-176722 *02,434*

Microwave Characterization of Flip-Chip MMIC Interconnections.
PB96-176730 *02,435*

WERIJ, H. G. C.

Oscillator Strengths and Radiative Branching Ratios in Atomic Sr.
PB95-203493 *04,008*

WERT, J. A.

Experimental Assessment of Crack-Tip Dislocation Emission Models for an Al67Cr8Ti25 Intermetallic Alloy.
PB96-204466 *03,377*

WERTZ, K. H.

Retention of Halocarbons on a Hexafluoropropylene Epoxide-Modified Graphitized Carbon Black. 4. Propane-Based Compounds.
PB96-164033 *03,284*

WEST, J. A.

Disorder Trapping in Ni2TiAl.
PB94-198942 *03,322*

WEST, J. B.

High Resolution Angle Resolved Photoelectron Spectroscopy Study of N2.
PB95-151494 *03,907*

Inner-Valence States CO(+) between 22 eV and 46 eV Studied by High Resolution Photoelectron Spectroscopy and ab Initio CI Calculations.
PB95-180055 *03,961*

Photoelectron Study of Electronic Autoionization in Rotationally Cooled N2: The n=6 Member of the Hopfield Series.
PB95-163531 *00,971*

Shape-Resonance-Enhanced Continuum-Continuum Coupling in Photoionization of CO2.
PB95-164471 *00,983*

Vibrational Autoionization in H2: Vibrational Branching Ratios and Photoelectron Angular Distributions Near the v(+)=3 Threshold.
PB94-199577 *00,799*

Vibrationally Resolved Photoelectron Angular Distributions and Branching Ratios for the Carbon Dioxide Molecule in the Wavelength Region 685-795 Angstrom.
PB96-201207 *04,131*

WESTBROOK, C.

Atoms in Optical Molasses.
PB95-108874 *03,875*

Optical Molasses: The Coldest Atoms Ever.
PB95-108908 *03,878*

Temperature of Optical Molasses for Two Different Atomic Angular Momenta.
PB95-126058 *03,881*

Ultracold Collisions: Associative Ionization in a Laser Trap.
PB94-213238 *03,859*

WESTBROOK, C. I.

Atoms in Optical Molasses: Applications to Frequency Standards.
PB95-108882 *03,876*

Heterodyne Measurement of the Fluorescence Spectrum of Optical Molasses.
PB95-108411 *03,873*

Laser Cooling.
PB95-151502 *03,908*

Laser Modification of Ultracold Collisions: Experiment.
PB96-157987 *04,075*

Localization of Atoms in a Three-Dimensional Standing Wave.
PB95-163887 *03,944*

Measurements of Fluorescence from Cold Atoms: Localization in Three-Dimensional Standing Waves.
PB95-163879 *03,943*

Optical Molasses: Cold Atoms for Precision Measurements.
PB95-108890 *03,877*

WESTBROOK, J.

Nucleic Acid Database: Present and Future.
PB97-109078 *00,518*

WESTERBEKE, S. A.

CCD Mosaic Images of the Supernova Remnant 3C 400.2.
PB95-203527 *00,084*

WESTERN, C. M.

Resonance Enhanced Multiphoton Ionization Spectroscopy of the PF Radical.
PB97-119119 *00,702*

WESTMORELAND, P. R.

Fluorinated Hydrocarbon Flame Suppression Chemistry.
PB94-185113 *01,362*

Thermochemical and Chemical Kinetic Data for Fluorinated Hydrocarbons.
PB95-260618 *01,056*

WEXLER, A.

Low-Temperature Performance of Radiosonde Electric Hygrometer Elements.
AD-A295 319/8 *00,121*

Methods of Measuring Humidity and Testing Hygrometers.
AD-A278 851/1 *00,123*

WEYMANN, R. J.

Observations of 3C 273 with the Goddard High Resolution Spectrograph on the Hubble Space Telescope.
PB95-202321 *00,076*

WHALEN, J. J.

Documentation for Immediately Dangerous to Life or Health Concentrations (IDLHs).
PB94-195047 *03,602*

WHALEN, T.
Estimates of Hurricane Wind Speeds by the 'Peaks Over Threshold' Method.
PB96-162540 *00,471*

WHALEN, T. M.
Dynamics of Multi-DOF Stochastic Nonlinear Systems.
PB97-113245 *00,477*

Probabilistic Estimates of Design Load Factors for Wind-Sensitive Structures Using the 'Peaks Over Threshold' Approach.
PB96-183223 *00,474*

WHANGBO, M. H.
Ca4Bi6O13: A Compound Containing an Unusually Low Bismuth Coordination Number and Short Bi Bi Contacts.
PB95-141131 *00,911*

WHEATLEY, T.
Configuration and Performance Evaluation of a Real-Time Robot Control System: A Skeleton Approach.
PB95-163895 *01,598*

WHEATLEY, T. E.
Mapping Processes to Processors for Space-Based Robot Systems.
PB95-151510 *04,833*

Unified Telerobotic Architecture Project (UTAP) Standard Interface Environment (SIE), May 1995.
PB95-242350 *02,938*

WHEELER, A. A.
Anisotropy of Interfaces in an Ordered Alloy: A Multiple-Order-Parameter Model.
PB96-131594 *04,741*

Computation of Dendrites Using a Phase Field Model.
PB94-160744 *04,436*

Convective Stability in the Rayleigh-Benard and Directional Solidification Problems: High-Frequency Gravity Modulation.
PB95-181145 *04,208*

Notion of a xi-Vector and a Stress Tensor for a General Class of Anisotropic Diffuse Interface Models.
PB96-193776 *04,788*

Phase-Field Model for Solidification of a Eutectic Alloy.
PB95-147914 *03,345*

xi-Vector Formulation of Anisotropic Phase-Field Models: 3-D Asymptotics.
PB95-136628 *04,536*

Xi-Vector Formulation of Anisotropic Phase-Field Models: 3-D Asymptotics.
PB97-122550 *04,816*

WHEELER, D. J.
Procedure for Measuring Trace Quantities of S2F10, S2OF10, and S2O2F10 in SF6 Using a Gas Chromatograph-Mass Spectrometer.
PB96-119755 *02,513*

WHEELER, N. S.
Electrodeposited Cobalt-Tungsten as a Diffusion Barrier between Graphite Fibers and Nickel.
PB96-146881 *03,176*

Microstructural Characterization of Cobalt-Tungsten Coated Graphite Fibers.
PB96-159231 *01,951*

WHETSTONE, J. R.
Electrical Measurements for Monitoring and Control of rf Plasma Processing.
PB96-161963 *04,369*

Gaseous Electronics Conference Radio-Frequency Reference Cell: A Defined Parallel-Plate Radio-Frequency System for Experimental and Theoretical Studies of Plasma-Processing Discharges.
PB94-172327 *04,404*

New Expressions of Uncertainties for Humidity Calibrations at the National Institute of Standards and Technology.
PB95-103826 *02,645*

WHIPPLE, A. L.
Lunar Laser Ranging: A Continuing Legacy of the Apollo Program.
PB95-202495 *03,683*

WHITE, A. E.
Increased Pinning Energies and Critical Current Densities in Heavy-Ion-Irradiated Bi2Sr2CaCu2O8 Single Crystals.
PB95-175352 *04,654*

Silicon Surface Chemistry by IR Spectroscopy in the Mid- to Far-IR Region: H2O and Ethanol on Si(100).
PB96-138565 *01,097*

WHITE, E.
Determination of 3-Quinuclidinyl Benzilate (Qnb) and Its Major Metabolites in Urine by Isotope Dilution Gas Chromatography Mass Spectrometry.
PB94-199379 *03,492*

WHITE, G.
Transient Cooling of a Hot Surface by Droplets Evaporation.
PB95-143194 *03,890*

WHITE, G. S.
Electric Field Effects on Crack Growth in a Lead Magnesium Niobate.
PB95-107322 *03,339*

Moisture and Water-Induced Crack Growth in Optical Materials.
PB95-153334 *04,267*

Molecular Orbital Calculations of Bond Rupture in Brittle Solids.
PB95-164059 *00,973*

Molecular Orbital Study of Water Enhanced Crack Growth Process.
PB95-164067 *03,240*

Thermal Wave NDE of Advanced Materials Using Mirage Effect Detection.
PB96-204516 *04,191*

WHITE, N. E.
Efficient Way of Identifying New Active Stars: A VLA Survey of X-ray Selected Active Stellar Candidates.
PB96-122882 *00,099*

WHITE, P. H.
Nutritional Status and Growth in Juvenile Rheumatoid Arthritis.
PB94-198470 *03,515*

WHITE, R. L.
Discovery of an X-Ray Selected, Radio-Loud Quasar at z=3.9.
PB94-198652 *00,052*

New High-Redshift Damped Lyman-alpha Absorption Systems and the Redshift Evolution of Damped Absorbers.
PB95-203501 *00,083*

WHITE, S.
Observing Stellar Coronae with the Goddard High Resolution Spectrograph. I. The dMe Star AU Microscopii.
PB96-102777 *00,092*

WHITE, V. E.
L-threo-beta-Hydroxyhistidine, an Unprecedented Iron(III) Ion-Binding Amino Acid in a Pyoverdine-type Siderophore from Pseudomonas fluorescens 244.
PB94-211620 *00,553*

WHITE, V. R.
National Voluntary Laboratory Accreditation Program: Procedures and General Requirements.
PB94-178225 *02,630*

National Voluntary Laboratory Accreditation Program 1994 Directory.
PB94-178969 *00,482*

National Voluntary Laboratory Accreditation Program 1995 Directory.
PB95-174454 *00,483*

National Voluntary Laboratory Accreditation Program 1996 Directory.
PB96-162714 *00,485*

WHITENTON, E. P.
Measuring Matching Wear Scars on Balls and Flats.
PB95-151528 *03,153*

Surface Roughness Evaluation of Diamond Films Grown on Substrates with a High Density of Nucleation Sites.
PB95-162418 *03,018*

WHITESEL, H. K.
Optical Fiber Sensors: Accelerating Applications in Navy Ships.
PB94-186848 *02,632*

Self-Calibrating Fiber Optic Sensors: Potential Design Methods.
PB95-169298 *02,172*

Self Calibrating Fiber Optic Sensors: Potential Design Methods.
PB95-169306 *02,173*

WHITESIDES, G. M.
Microlithography by Using Neutral Metastable Atoms and Self-Assembled Monolayers.
PB96-190038 *02,441*

WHITING, D.
Optimization of Highway Concrete Technology.
PB94-182995 *01,333*

WHITMAN, L. J.
Atomic Manipulation of Polarizable Atoms by Electric Field Directional Diffusion.
PB95-150587 *04,572*

Manipulation of Adsorbed Atoms and Creation of New Structures on Room-Temperature Surfaces with a Scanning Tunneling Microscope.
PB95-151536 *04,578*

WHITTAKER, H. L.
Calibration of Dosimeters for the Cryogenic Irradiation of Composite Materials Using an Electron Beam.
PB95-180964 *03,968*

WHITTAKER, J. K.
NIST-NRL Free-Electron Laser Facility.
PB94-212511 *04,237*

WHITTEN, B. L.
High-Precision Calculations of Cross Sections for Low-Energy Electron Scattering by Ground and Excited State of Sodium.
PB95-152161 *03,914*

Low-Energy-Electron Collisions with Sodium: Elastic and Inelastic Scattering from the Ground State.
PB96-103106 *04,030*

WHITTER, K. M.
International Green Building Conference and Exposition (2nd). Held in Big Sky, Montana on August 13-15, 1995.
PB95-253605 *02,525*

U.S. Green Building Conference, 1994.
PB94-206364 *02,519*

WHITTINGHAM, M. S.
Rietveld Analysis of NaxWO3+x/2.yH2O, Which Has the Hexagonal Tungsten Bronze Structure.
PB95-107371 *04,524*

WHITTLESTONE, S.
International Marine-Atmospheric (222)Rn Measurement Intercomparison in Bermuda. Part 2. Results for the Participating Laboratories.
PB96-175682 *00,115*

WIANT, J. R.
Lunar Laser Ranging: A Continuing Legacy of the Apollo Program.
PB95-202495 *03,683*

WICKNER, S.
Deletion Analysis of the Mini-P1 Plasmid Origin of Replication and the Role of E.coli DnaA Protein.
PB95-163911 *03,539*

DnaJ, DnaK, and GrpE Heat Shock Proteins are Required in 'ori'P1 DNA Replication Solely at the RepA Monomerization Step.
PB97-119382 *03,557*

Function of DnaJ and DnaK as Chaperones in Origin-Specific DNA Binding by RepA.
PB95-151544 *03,533*

WIEDENMANN, E.
Femtosecond Time-Resolved Wave Packet Motion in Molecular Multiphoton Ionization and Fragmentation.
PB94-198611 *00,790*

WIEDERHORN, S. M.
Cavitation Contributes Substantially to Tensile Creep in Silicon Nitride.
PB96-122577 *03,171*

Cavitation Damage During Flexural Creep of SiAlON-YAG Ceramics.
PB94-200110 *03,036*

Cavity Evolution during Tensil Creep of Si3N4.
PB96-204193 *03,376*

Creep and Creep Rupture of Ceramic Matrix Composites.
PB95-163929 *03,165*

Creep and Creep Rupture of Structural Ceramics.
PB96-204524 *03,093*

Creep Rupture of MoSi2/SiCp Composites.
PB95-152294 *03,154*

Fracture Mechanism Maps: Their Applicability to Silicon Nitride.
PB96-204532 *03,094*

Fracture of Silicon Nitride and Silicon Carbide at Elevated Temperatures.
PB96-180260 *03,179*

High Temperature Degradation of Structural Composites.
PB94-172848 *03,132*

High Temperature Structural Reliability of Silicon Nitride.
PB97-110456 *03,104*

Stability and Surface Energies of Wetted Grain Boundaries in Aluminum Oxide.
PB95-202750 *03,059*

Tensile Creep of a Silicon Nitride Ceramic.
PB95-161303 *03,049*

Tensile Creep of Silicide Composites.
PB96-200803 *03,183*

Tensile Creep of Whisker Reinforced Silicon Nitride.
PB94-211984 *03,142*

Tensile Creep Testing of Structural Ceramics.
PB97-110464 *03,105*

Tension/Compression Creep Asymmetry in Si3N4.
PB97-110258 *03,096*

Transient Creep Behaviour of Hot Isostatically Pressed Silicon Nitride.
PB96-180278 *03,086*

WIEJACZKA, J. A.
Anomalous Switching Phenomenon in Critical-Current Measurements When Using Conductive Mandrels.
PB96-137781 *02,233*

First VAMAS USA Interlaboratory Comparison of High Temperature Superconductor Critical Current Measurements.
PB96-147178 *04,768*

Superconductor Critical Current Standards for Fusion Applications. Final Progress Report, October 1993-July 1994.
PB95-169538 *02,222*

USA Interlaboratory Comparison of Superconductor Simulator Critical Current Measurements.
PB96-147194 *04,770*

WIEMAN, C.
Inexpensive Laser Cooling and Trapping Experiment for Undergraduate Laboratories.
PB96-140371 *04,353*

Narrow-Band Tunable Diode Laser System with Grating Feedback, and a Saturated Absorption Spectrometer for Cs and Rb.
PB95-202891 *04,319*

WIEMAN, C. E.
Gravitational Sisyphus Cooling of (87)Rb in a Magnetic Trap.
PB96-200704 *04,379*

Laser Cooling and Trapping for the Masses.
PB95-126090 04,253

Precision Lifetime Measurements of Cs 6p (2)P1/2 and 6p (2)P3/2 Levels by Single-Photon Counting.
PB95-203816 04,010

WIESE, W. L.

Atomic Branching Ratio Data for Carbon-Like Ions.
PB94-212842 03,855

Atomic Branching Ratio Data for Nitrogen-Like Species.
PB96-190152 04,122

Atomic Branching Ratio Data for Oxygen-Like Species.
PB95-180436 03,963

Atomic Transition Probabilities and Tests of the Spectroscopic Coupling Scheme for N I.
PB96-138466 04,057

Atomic Transition Probability Ratios between Some Ar I 4s-4p and 4s-5p Transitions.
PB94-211554 03,842

Comprehensive Spectroscopic Data Tabulations and Progress in the Compilation of Atomic Transition Probabilities.
PB95-151551 03,909

Investigation of LS Coupling in Boronlike Ions.
PB94-185295 03,797

New Critical Review of Experimental Stark Widths and Shifts.
PB94-172830 03,790

Spectral Data and Grotrian Diagrams for Highly Ionized Chromium, Cr V through Cr XXIV.
PB94-162369 00,748

Spectroscopic Data for Fusion Edge Plasmas.
PB95-151569 04,410

Spectroscopic Data Tables for Highly-Ionized Atoms.
PB95-151585 03,910

Spectroscopic Diagnostics of Low Temperature Plasmas: Techniques and Required Data.
PB95-151577 04,411

WIESENFELD, K.

Phase-Locked Oscillator Optimization for Arrays of Josephson Junctions.
PB95-169314 02,052

WIESLER, D. G.

Determination of Anomalous Superexchange in MnCl2 and Its Graphite Intercalation Compound.
PB97-122568 00,666

Neutron Reflectivity of End-Grafted Polymers: Concentration and Solvent Quality Dependence in Equilibrium Conditions.
PB94-185758 01,206

Neutron Reflectometry Studies of Surface Oxidation.
PB95-150421 00,917

Structural and Magnetic Properties of CuCl2 Graphite Intercalation Compounds.
PB96-119748 03,020

X-Ray Diffraction from Anodic TiO2 Films: In situ and Ex situ Comparison of the Ti(0001) Face.
PB94-185972 00,782

WIETING, T.

Optical Conductivity of Single Crystals of Ba1-xMxBiO3(M=K, Rb, x=0.04, 0.37).
PB94-185329 04,447

WIGHT, S. A.

Environmental Scanning Electron Microscope Imaging Examples Related to Particle Analysis.
PB94-172822 00,766

Rare-Earth Isotopes as Tracers of Particulate Emissions: An Urban Scale Test.
PB94-161635 02,535

WIGNALL, G. D.

SANS Study of the Plastic Deformation Mechanism in Polyethylene.
PB95-151841 01,242

WILBUR, J. L.

Microlithography by Using Neutral Metastable Atoms and Self-Assembled Monolayers.
PB96-190038 02,441

WILBUR, P.

Tribological Behavior of 440/Diamond-Like-Carbon Film Couples.
PB96-119714 03,019

WILHOIT, R. C.

Thermodynamic and Thermophysical Properties of Organic Nitrogen Compounds. Part II. 1- and 2-Butanamine, 2-Methyl-1-Propanamine, 2-Methyl-2-Propanamine, Pyrrole, 1-, 2-, and 3-Methylpyrrole, Pyridine, 2-, 3-, and 4-Methylpyridine, Pyrrolidine, Piperidine, Indole, Quinoline, Isoquinoline, Acridine, Carbazole, Phenanthridine, 1- and 2-Naphthalenamine, and 9-Methylcarbazole.
PB94-162294 00,741

WILKERSON, T.

Collision-Induced Emission in the Fundamental Vibration-Rotation Band of H2.
PB94-199445 03,811

WILKIN, N. D.

NIST-NRL Free-Electron Laser Facility.
PB94-212511 04,237

WILKINS, J. W.

Large Local-Field Corrections in Optical Rotatory Power of Quartz and Selenium.
PB97-122378 04,400

WILKINSON, F.

Quantum Yields for the Photosensitized Formation of the Lowest Electronically Excited Singlet State of Molecular Oxygen in Solution.
PB94-161007 00,732

Rate Constants for the Decay and Reactions of the Lowest Electronically Excited Singlet State of Molecular Oxygen in Solution. An Expanded and Revised Compilation.
PB96-145826 01,106

WILKINSON, R. A.

Analysis of a Biologically Motivated Neural Network for Character Recognition.
PB94-172277 00,182

Electric Field Effects on a Near-Critical Fluid in Microgravity.
PB96-161880 04,217

PCASYS: A Pattern-Level Classification Automation System for Fingerprints.
PB95-267936 01,853

Second Census Optical Character Recognition Systems Conference.
PB94-188711 01,832

Self-Organizing Neural Network Character Recognition on a Massively Parallel Computer.
PB95-163994 01,845

Self-Organizing Neural Network Character Recognition Using Adaptive Filtering and Feature Extraction.
PB96-119797 01,855

WILLIAMS, C. J.

Measurement of the Atomic Na(3P) Lifetime and of Retardation in the Interaction between Two Atoms Bound in a Molecule.
PB97-122360 04,178

WILLIAMS, D.

Proposed High-Accuracy Superconducting Power Meter for Millimeter Waves.
PB94-212669 02,034

WILLIAMS, D. F.

Accurate Electrical Characterization of High-Speed Interconnections.
PB96-167143 02,240

Accurate Experimental Characterization of Interconnects: A Discussion of 'Experimental Electrical Characterization of Interconnects and Discontinuities in High-Speed Digital Systems'.
PB94-216389 02,217

Accurate Transmission Line Characterization.
PB95-151593 02,220

Calibrating On-Wafer Probes to the Probe Tips.
PB95-163945 02,352

Coaxial Line-Reflect-Match Calibration.
PB96-200118 02,246

Comments on 'Conversions between S, Z, Y, h, ABCD, and T Parameters Which Are Valid for Complex Source and Load Impedances'.
PB96-102785 02,069

Compensation for Substrate Permittivity in Probe-Tip Calibration.
PB95-203519 01,915

Interconnection Transmission Line Parameter Characterization.
PB94-216397 02,218

Line-Reflect-Match Calibrations with Nonideal Microstrip Standards.
PB96-176599 02,242

LRM Probe-Tip Calibrations Using Nonideal Standards.
PB96-135389 02,411

LRM Probe-Tip Calibrations with Imperfect Resistors and Lossy Lines.
PB95-163952 02,353

Microwave Characterization of Printed Circuit Transmission Lines.
PB96-122585 02,077

On-Wafer Impedance Measurement on Lossy Substrates.
PB95-176285 02,365

Planar Resistors for Probe Station Calibration.
PB95-163697 02,351

Reciprocity Relations in Waveguide Junctions.
PB94-172814 02,213

Verification of Commercial Probe-Tip Calibrations.
PB95-161576 02,347

Verification of Scattering Parameter Measurements.
PB95-163960 01,904

WILLIAMS, D. H.

Fiber Coating Diameter: Toward a Glass Artifact Standard.
PB96-140389 02,234

WILLIAMS, E.

Measurement and Reduction of Alignment Errors of the NIST Watt Experiment.
PB97-111959 01,987

NIST Watt Balance: Progress Toward Monitoring the Kilogram.
PB97-113062 01,991

WILLIAMS, E. R.

Application of Single Electron Tunneling: Precision Capacitance Ratio Measurements.
PB96-102157 04,703

Cryogenic Precision Capacitance Bridge Using a Single Electron Tunneling Electrometer.
PB95-126074 04,529

Cryogenic Precision Capacitance Bridge Using a Single Electron Tunneling Electrometer.
PB95-152310 02,040

Cryogenic Precision Capacitance Bridge Using a Single Electron Tunneling Electrometer.
PB96-112271 02,072

Flux-Locked Current Source Reference.
PB95-150785 02,039

Magnetometer Calibration Services.
PB97-113252 01,993

Methods for Aligning the NIST Watt-Balance.
PB96-123153 01,934

New Refractometer by Combining a Variable Length Vacuum Cell and a Double-Pass Michelson Interferometer.
PB97-111926 01,986

Results of Capacitance Ratio Measurements for the Single Electron Pump-Capacitor Charging Experiment.
PB97-113286 04,813

WILLIAMS, F.

Time Domain Network Analysis Using the Multiline TRL Calibration.
PB95-202925 02,065

WILLIAMS, F. A.

Asymptotic and Numerical Analysis of a Premixed Laminar Nitrogen Dioxide-Hydrogen Flame.
PB96-164256 01,422

WILLIAMS, G. P.

Laser-Synchrotron Hybrid Experiments: A Photon to Tickle, A Photon to Poke.
PB96-157847 03,704

Silicon Surface Chemistry by IR Spectroscopy in the Mid- to Far-IR Region: H2O and Ethanol on Si(100).
PB96-138565 01,097

WILLIAMS, J.

Thermodynamic Analysis of Heparin Binding to Human Antithrombin.
PB94-199593 03,455

WILLIAMS, J. G.

Lunar Laser Ranging: A Continuing Legacy of the Apollo Program.
PB95-202495 03,683

WILLIAMS, J. J. M.

Quasielastic and Inelastic Neutron-Scattering Studies of ((CD3)3ND)FeCl3.2D2O: A One-Dimensional Ising Ferromagnet.
PB95-140562 04,547

WILLIAMS, K. L.

Selectivity Trends in Packed Column Supercritical Fluid Chromatography with C18 Stationary Phases.
PB96-138581 00,622

Use of a Naphthylethylcarbamoylated- beta-Cyclodextrin Chiral Stationary Phase for the Separation of Drug Enantiomers and Related Compounds by Sub- and Supercritical Fluid Chromatography.
PB97-113260 00,653

WILLIAMS, P.

Molecular Ion Imaging and Dynamic Secondary Ion Mass Spectrometry of Organic Compounds.
PB95-126124 00,571

WILLIAMS, P. A.

Anomalous Relation between Time and Frequency Domain PMD Measurements.
PB97-119390 04,398

Dielectric Spectroscopic Determination of Temperature Behavior of Electroclinic Parameters in the Liquid Crystal W317.
PB96-140397 01,098

Standard Polarization Components: Progress Toward an Optical Retardance Standard.
PB96-119672 04,342

Studies of the Higher Order Smectic Phase of the Large Electroclinic Effect Material W317.
PB95-151601 00,935

Technical Digest: Symposium on Optical Fiber Measurements (9th), 1996. Held in Boulder, Colorado on October 1-3, 1996.
PB97-108583 04,383

X-ray Observation of Electroclinic Layer Constriction and Rearrangement in a Chiral Smectic-A Liquid Crystal.
PB96-141080 01,100

WILLIAMS, R. C.

Static Dielectric Constant of Water and Steam.
PB96-123559 01,090

WILLIAMS, R. E.

Cold Neutron Gain Calculations for the NBSR Using MCNP.
PB95-163978 03,731

Liquid-Hydrogen Cold Neutron Source for the NBSR.
PB95-151619 03,729

MCNP Model of the National Bureau of Standards Reactor (NBSR) Core.
PB96-138599 *03,733*

Nuclear Heat Load Calculations for the NBSR Cold Neutron Source Using MCNP.
PB95-152955 *03,730*

Thermal Hydraulic Tests of a Liquid Hydrogen Cold Neutron Source.
PB95-135570 *03,884*

Upgrade and Modernization Projects at the NBSR.
PB96-161872 *03,737*

WILLIAMS, R. M.

Investigating the 3.3 Micron Infrared Fluorescence from Naphthalene Following Ultraviolet Excitation.
N95-15839/0 *00,724*

WILLIAMSON, C. K.

Environmental Aspects of Halon Replacements: Considerations for Advanced Agents and the Ozone Depletion Potential of CF3I.
PB97-122261 *03,301*

WILLIAMSON, M. P.

NIST Workshop on the Computer Interface to Flat Panel Displays. Held in San Jose, California on January 13-14, 1994.
PB95-136388 *01,625*

WILLIAMSON, T. G.

Measurement of the (93)Nb(n,2n) (92m)Nb Cross Section in a (235)U Fission Spectrum.
PB95-163986 *03,945*

WILLIS, R. F.

Variation in Magnetic Properties of Cu/Fcc (001) Sandwich Structures.
PB95-141164 *04,555*

WILLMAN, N.

Design and Development of an Information Retrieval System for the EAMATE Data. Volume 2 of 2. Appendices.
PB94-168390 *00,487*

WILLMAN, N. E.

Prototype Information Retrieval System to Perform a Best-Match Search for Names.
PB95-181152 *02,740*

WILSON, A. J. C.

Statistical Descriptors in Crystallography. 2. Report of a Working Group on Expression of Uncertainty in Measurement.
PB96-146824 *04,764*

WILSON, C. L.

Analysis of a Biologically Motivated Neural Network for Character Recognition.
PB94-172277 *00,182*

Binary Decision Clustering for Neural Network Based Optical Character Recognition.
PB95-171971 *01,848*

Binary Decision Clustering for Neural-Network-Based Optical Character Recognition.
PB96-186184 *01,857*

Effect of Training Dynamics on Neural Network Performance.
PB95-267845 *01,852*

Face Recognition Technology for Law Enforcement Applications.
PB94-207768 *01,837*

Human and Machine Recognition of Faces: A Survey.
PB96-111687 *01,854*

Improving Neural Network Performance for Character and Fingerprint Classification by Altering Network Dynamics.
PB95-267803 *01,851*

Improving Neural Network Performance for Character and Fingerprint Classification by Altering Network Dynamics.
PB96-123195 *01,856*

NIST Form-Based Handprint Recognition System.
PB94-217106 *01,838*

PCASYS: A Pattern-Level Classification Automation System for Fingerprints.
PB95-267936 *01,853*

Second Census Optical Character Recognition Systems Conference.
PB94-188711 *01,832*

Self-Organizing Neural Network Character Recognition on a Massively Parallel Computer.
PB95-163994 *01,845*

Self-Organizing Neural Network Character Recognition Using Adaptive Filtering and Feature Extraction.
PB96-119797 *01,855*

WILSON, C. R.

Economic, Energy, and Environmental Impacts of the Energy-Related Inventions Program.
DE94-017162 *00,008*

WILSON, G. L.

Estimation of the Absorbed Dose in Radiation-Processed Food. 1. Test of the EPR Response Function by a Linear Regression Analysis.
PB94-199718 *00,039*

WILSON, M. A.

Hybrid Undulator for the NIST-NRL Free-Electron Laser.
PB94-212529 *04,238*

NIST-NRL Free-Electron Laser Facility.
PB94-212511 *04,237*

WILSON, M. R.

Time Dependent Vector Dynamic Programming Algorithm for the Path Planning Problem.
PB94-215688 *03,428*

WILSON, R. B.

SGML Parser Validation Procedures.
PB95-174959 *01,717*

WINCHESTER, M. R.

Fourier Transform Atomic Emission Studies Using a Glow Discharge as the Emission Source.
PB94-185980 *00,533*

WINCHESTER, N. K.

Determination of the Transmittance Uniformity of Optical Filter Standard Reference Materials.
PB95-261921 *02,182*

WINDORBSKA, W.

DNA Base Damage in Lymphocytes of Cancer Patients Undergoing Radiation Therapy.
PB97-122444 *03,643*

WINDSOR, E. S.

Airborne Asbestos Method: Standard Practice for Recording Transmission Electron Microscopy Data for the Analysis of Asbestos Collected onto Filters. Version 1.0.
PB94-210168 *00,552*

Proficiency Tests for the NIST Airborne Asbestos Program, 1990.
PB94-188836 *00,535*

WINDT, D. L.

XUV Characterization Comparison of Mo/Si Multilayer Coatings.
PB95-164000 *04,278*

WINEBURG, J. P.

Methodologies for Predicting the Service Lives of Coating Systems.
PB95-146387 *03,124*

WINELAND, D.

Electrostatic Modes of Ion-Trap Plasmas.
PB95-152963 *03,920*

Experimental Results on Normal Modes in Cold, Pure Ion Plasmas.
PB95-175105 *03,956*

WINELAND, D. J.

Electrostatic Modes as a Diagnostic in Penning-Trap Experiments.
PB95-176244 *03,959*

High-Order Multipole Excitation of a Bound Electron.
PB96-119789 *04,044*

High-Resolution Atomic Spectroscopy of Laser-Cooled Ions.
PB95-169330 *03,953*

Interference in the Resonance Fluorescence of Two Trapped Atoms.
PB95-168514 *03,948*

Laser-Cooled Positron Source.
PB95-169348 *03,954*

Laser Cooling of Trapped Ions.
PB95-168746 *03,950*

Light Scattered from Two Atoms.
PB95-168753 *04,286*

Liquid and Solid Atomic Ion Plasmas.
PB94-198991 *03,809*

Non-Neutral Ion Plasmas and Crystals, Laser Cooling, and Atomic Clocks.
PB95-175113 *03,957*

Precise Spectroscopy for Fundamental Physics.
PB96-112164 *04,040*

Progress on a Cryogenic Linear Trap for (199)Hg(+) Ions.
PB95-180790 *03,965*

Quantum-Limited Cooling and Detection of Radio-Frequency Oscillations by Laser-Cooled Ions.
PB96-112073 *04,039*

Quantum Measurements of Trapped Ions.
PB95-161147 *03,928*

Quantum Projection Noise: Population Fluctuations in Two-Level Systems.
PB94-212271 *03,850*

Recent Experiments on Trapped Ions at the National Institute of Standards and Technology.
PB95-169322 *03,952*

Spin Squeezing and Reduced Quantum Noise in Spectroscopy.
PB95-151635 *03,912*

Squeezed Atomic States and Projection Noise in Spectroscopy.
PB95-176293 *03,960*

Trapped Atoms and Laser Cooling.
PB95-151627 *03,911*

Trapped Ions and Laser Cooling 4: Selected Publications of the Ion Storage Group of the Time and Frequency Division, NIST, Boulder, Colorado.
PB96-172358 *04,108*

WINK, D. A.

Unusual Spin-Trap Chemistry for the Reaction of Hydroxyl Radical with the Carcinogen N-Nitrosodimethylamine.
PB95-151643 *00,692*

WINKLER, P. F.

CCD Mosaic Images of the Supernova Remnant 3C 400.2.
PB95-203527 *00,084*

G203.2-12.3: A New Optical Supernova Remnant in Orion.
PB95-203535 *00,085*

Rapid Decline in the Optical Emission from SN 1957D in M83.
PB94-216033 *00,070*

WINNEWISSER, M.

Millimeter- and Submillimeter-Wave Spectrum of trans-Ethyl Alcohol.
PB96-145578 *01,102*

WINOKUR, M. J.

Inelastic-Neutron-Scattering Studies of Poly(p-phenylene vinylene).
PB95-180766 *01,014*

WINSLOW, D.

Percolation and Pore Structure in Mortars and Concrete.
PB95-150439 *00,370*

WINTENBURG, A. L.

Observations of Partial Discharges in Hexane Under High Magnification.
PB95-163127 *01,900*

WINTERS, M. P.

High-Resolution Optical Multiplex Spectroscopy.
PB95-203543 *04,323*

WIPF, H.

Hydrogen in YBa2Cu3Ox: A Neutron Spectroscopy and a Nuclear Magnetic Resonance Study.
PB95-161279 *04,601*

Inelastic Neutron Scattering Study of Hydrogen in Nanocrystalline Pd.
PB96-146857 *03,366*

Neutron-Spectroscopy Study of the Hydrogen Vibrations in Hydrogen-Doped YBa2Cu3Ox.
PB94-172475 *04,441*

Vibrational Excitations and the Position of Hydrogen in Nanocrystalline Palladium.
PB96-111828 *04,035*

WIPF, S. L.

Temperature and Field Dependence of Flux Pinning in NbTi with Aritificial Pinning Centers.
PB96-112024 *04,726*

WISE, G.

Analysis of Transverse Flow in Aligned Fibrous Porous Media.
PB96-167200 *03,177*

WISE, J. A.

Assessment of Uncertainties of Liquid-in-Glass Thermometer Calibrations at the National Institute of Standards and Technology.
PB94-142510 *02,625*

WISE, S.

Comparison of Methods for Gas Chromatographic Determination of PCBs and Chlorinated Pesticides in Marine Reference Materials.
PB95-140091 *02,584*

Comparison of the Liquid Chromatographic Behavior of Selected Steroid Isomers Using Different Reversed-Phase Materials and Mobile Phase Compositions.
PB95-140976 *00,574*

Development of Engineered Stationary Phases for the Separation of Carotenoid Isomers.
PB95-150249 *00,578*

Development of Frozen Whale Blubber and Liver Reference Materials for the Measurement of Organic and Inorganic Contaminants.
PB95-151676 *00,587*

Development of the National Marine Mammal Tissue Bank.
PB95-161402 *02,586*

National Status and Trends Program Specimen Bank: Sampling Protocols, Analytical Methods, Results, and Archive Samples.
PB97-119226 *02,598*

WISE, S. A.

Alaska Marine Mammal Tissue Archival Project: Specimen Inventory.
PB95-171344 *02,589*

Certification of Polychlorinated Biphenyl Congeners and Chlorinated Pesticides in a Whale Blubber Standard Reference Material.
PB96-103023 *03,745*

Certification of Polycyclic Aromatic Hydrocarbons in a Marine Sediment Standard Reference Material.
PB96-111778 *02,592*

Certification of Standard Reference Material (SRM) 1941a, Organics in Marine Sediment.
PB96-123690 *02,593*

Characterization of Chemically Modified Pore Surfaces by Small Angle Neutron Scattering.
PB95-126181 *00,898*

Comparison of Selectivities for PCBs in Gas Chromatography for a Series of Cyanobiphenyl Stationary Phases.
PB96-119458 *00,618*

Concentrations of Chlorinated Hydrocarbons, Heavy Metals and Other Elements in Tissues Banked by the Alaska Marine Mammal Tissue Archival Project.
PB95-209870 *02,590*

Considerations in the Design of an Environmental Specimen Bank: Experiences of the National Biomonitoring Specimen Bank Program.
PB96-112370 *02,527*

Current Activities Within the National Biomonitoring Specimen Bank.
PB94-172806 *02,516*

Determination of Inorganic Constituents in Marine Mammal Tissues.
PB95-152047 *00,589*

Determination of PCBs and Chlorinated Hydrocarbons in Marine Mammal Tissues.
PB95-162640 *03,744*

Determination of Polycyclic Aromatic Hydrocarbons by Liquid Chromatography.
PB95-151650 *00,585*

Distinguishing the Contributions of Residential Wood Combustion and Mobile Source Emissions Using Relative Concentrations of Dimethylphenanthrene Isomers.
PB96-135124 *02,563*

Individual Carotenoid Content of SRM 1548 Total Diet and Influence of Storage Temperature, Lyophilization, and Irradiation on Dietary Carotenoids.
PB94-200524 *00,033*

Influence of Stationary Phase Chemistry on Shape Recognition in Liquid Chromatography.
PB96-123682 *00,621*

Liquid Chromatographic Determination of Carotenoids in Human Serum Using an Engineered C30 and a C18 Stationary Phase.
PB97-119333 *03,512*

Liquid Chromatographic Determination of Polycyclic Aromatic Hydrocarbon Isomers of Molecular Weight 278 and 302 in Environmental Standard Reference Materials.
PB95-164042 *02,523*

Measurements of Indoor Pollutant Emissions from EPA Phase II Wood Stoves.
PB95-198735 *02,556*

NIST Standard Reference Materials (SRMs) for Polychlorinated Biphenyl (PCB) Determinations and Their Applicability to Toxaphene Measurements.
PB95-140109 *02,585*

Quality Assurance of Contaminant Measurements in Marine Mammal Tissues.
PB95-164034 *02,588*

Quantitative Analysis of Selected PCB Congeners in Marine Matrix Reference Materials Using a Novel Cyanobiphenyl Stationary Phase.
PB96-111737 *02,591*

Relationship of Silver with Selenium and Mercury in the Liver of Two Species of Toothed Whales (Odontocetes).
PB96-167275 *02,596*

Selectivity Trends in Packed Column Supercritical Fluid Chromatography with C18 Stationary Phases.
PB96-138581 *00,622*

Shape Selectivity Assessment of Stationary Phases in Gas Chromatography.
PB95-150256 *00,579*

Shape Selectivity in Reversed-Phase Liquid Chromatography for the Separation of Planar and Non-Planar Solutes.
PB95-162608 *00,596*

Standard Reference Materials for the Determination of Polycyclic Aromatic Hydrocarbons in Environmental Samples - Current Activities.
PB95-151668 *00,586*

Standard Reference Materials for the Determination of Trace Organic Constituents in Environmental Samples.
PB95-164026 *02,522*

Trace Element Concentrations in Cetacean Liver Tissues Archived in the National Marine Mammal Tissue Bank.
PB96-167127 *02,595*

Use of a Naphthylethylcarbamoylated- beta-Cyclodextrin Chiral Stationary Phase for the Separation of Drug Enantiomers and Related Compounds by Sub- and Supercritical Fluid Chromatography.
PB97-113260 *00,653*

WITCZAK, S. C.

Interaction of Stoichiometry, Mechanical Stress, and Interface Trap Density in LPCVD Si-rich SiNx-Si Structures.
PB95-176301 *02,366*

WITT, T. J.

Accuracy Comparisons of Josephson Array Systems.
PB95-164687 *02,047*

WITTE, A.

Magneto-Optical Trapping of Metastable Xenon: Isotope-Shift Measurements.
PB95-151254 *03,905*

WITTMAN, R. C.

Vector Theory of Diffraction by a Single-Mode Fiber: Application to Mode-Field Diameter Measurements.
PB95-164182 *04,279*

WITTMANN, R. C.

Integral Occurring in Coherence Theory.
PB95-203550 *04,324*

Polarimetric Calibration of Reciprocal-Antenna Radars.
PB95-216925 *01,872*

Polarimetric Calibration of Reciprocal-Antenna Radars.
PB96-200696 *02,016*

Proposed Analysis of RCS Measurement Uncertainty.
PB95-203568 *01,871*

RangeCAD and the NIST RCS Uncertainty Analysis.
PB94-218591 *01,870*

WITZGALL, C.

Algorithmic Enhancements to the Method of Centers for Linear Programming Problems.
PB94-198959 *03,426*

Interior-Point Method for Linear and Quadratic Programming Problems. (NIST Reprint).
PB95-180089 *03,429*

Submissions to a Planned Encyclopedia of Operations Research on Computational Geometry and the Voronoi/ Delaunay Construct.
PB94-152709 *03,425*

WLASSICH, J. J.

Investigation into a Practical Grain Growth Model for Hot Isostatic Pressing.
PB95-151684 *03,347*

WLODAWER, A.

Crystal Packing Interactions of Two Different Crystal Forms of Bovine Ribonuclease A.
PB95-152823 *00,943*

WOJCIK, G. L.

Numerical Reference Models for Optical Metrology Simulation.
PB97-111330 *04,392*

WOJNAROVITS, L.

Alcohol Solutions of Triphenyl-Tetrazolium Chloride as High-Dose Radiochromic Dosimeters.
PB96-135249 *03,716*

Novel Radiochromic Films for Clinical Dosimetry.
PB97-119259 *03,641*

Radiation-Chemical Reaction of 2,3,5-Triphenyl-Tetrazolium Chloride in Liquid and Solid State.
PB96-146733 *01,124*

Radiochromic Solid-State Polymerization Reaction.
PB95-180683 *01,271*

Radiochromic Solid-State Polymerization Reaction.
PB96-180146 *01,290*

WOLCOTT, D.

Multi-Agency Certification and Accreditation (C and A) Process: A Worked Example.
PB95-171955 *01,601*

WOLF, W. R.

Mixed Diet Reference Materials for Nutrient Analysis of Foods: Preparation of SRM-1548 Total Diet.
PB95-151692 *03,593*

WOLFE, J.

Distributed measurements of tracer response on packed bed flows using a fiberoptic probe array. Final report.
DE95013079 *00,667*

WOLFE, R.

High Frequency Magnetic Field Sensors Based on the Faraday Effect in Garnet Thick Films.
PB96-190384 *02,282*

Magneto-Optic Magnetic Field Sensors Based on Uniaxial Iron Garnet Films in Optical Waveguide Geometry.
PB95-153409 *02,152*

Magneto-Optic Magnetic Field Sensors Based on Uniaxial Iron Garnet Films in Optical Waveguide Geometry.
PB95-168498 *02,159*

WOLFENDEN, A.

Dynamic Shear Modulus Measurements with Four Independent Techniques in Nickel-Based Alloys.
PB94-198900 *03,320*

WOLTZ, L. A.

Ion Broadening Parameters for Several Argon and Carbon Lines.
PB94-211562 *03,843*

WOMELDORF, C.

Acid Gas Production in Inhibited Diffusion Flames.
PB95-180576 *01,390*

Lean flammability limit as a fundamental refrigerant property. Phase 1, Interim technical report, 1 October 1994--31 March 1995.
DE95011238 *03,248*

WONG-NG, W.

Crystal Chemistry and Phase Equilibria Studies of the BaO(BaCO3)-R2O3-CuO Systems. 4. Crystal Chemistry and Subsolidus Phase Relationship Studies of the CuO-Rich Region of the Ternary Diagrams, R=Lanthanides.
PB95-151759 *00,936*

Crystal Chemistry and Phase Equilibrium Studies of the BaO(BaCO3)-R2O3-CuO Systems. 5. Melting Relations in Ba2(Y,Nd,Eu)Cu3O6+x.
PB95-151718 *04,580*

Crystal Chemistry and Phase Equilibrium Studies of the BaO-R2O3-CuO Systems. 2. X-Ray Characterization and Standard Patterns of BaR2CuO4, R=Lanthanides.
PB95-151734 *04,582*

Crystal Structure of a New Monoclinic Form of Potassium Dihydrogen Phosphate Containing Orthophosphacidium Ion, (H4PO4)(sup+1).
PB96-111794 *04,725*

Efficient Experiment to Study Superconducting Ceramics.
PB94-212578 *04,505*

Microstructure and Ferroelectric Properties of Lead Zirconate-Titanate Films Produced by Laser Evaporation.
PB94-199148 *04,470*

Molecular Orbital Calculations of Bond Rupture in Brittle Solids.
PB95-164059 *00,973*

Molecular Orbital Study of Water Enhanced Crack Growth Process.
PB95-164067 *03,240*

Preparation and Crystal Structure of Sr5TiNb4O17.
PB96-167341 *04,107*

Preparation, Crystal Structure, Dielectric Properties, and Magnetic Behavior of Ba2Fe2Ti4O13.
PB96-186176 *01,162*

Raman and Fluorescence Spectra Observed in Laser Microprobe Measurements of Several Compositions in the Ln-Ba-Cu-O System.
PB94-172210 *04,440*

X-Ray Characterization of the Crystallization Process of High-Tc Superconducting Oxides in the Sr-Bi-Pb-Ca-Cu-O System.
PB95-151700 *04,579*

X-Ray-Diffraction Study of a Thermomechanically Detwinned Single Crystal of YBa2Cu3O6+x.
PB95-151726 *04,581*

X-Ray Powder Diffraction Data for BaCu(C2O4)2.6H2O.
PB95-151767 *04,583*

WOOD, B. E.

Deuterium and the Local Interstellar Medium: Properties for the Procyon and Capella Lines of Sight.
PB96-200639 *00,111*

High Velocity Plasm in the Transition Region of Au Mic: A Stellar Analog of Solar Explosive Events.
PB96-123294 *00,102*

High-Velocity Plasma in the Transition Region of AU Microscopii: Evidence for Magnetic Reconnection and Saturated Heating during Quiescent and Flaring Conditions.
PB96-102694 *00,091*

Redshifts in Stellar Transition Regions.
PB96-123310 *00,104*

Transition Regions of Capella.
PB96-123336 *00,105*

Transition Regions of Capella (1995).
PB96-176714 *00,108*

Volume-Limited ROSAT Survey of Extreme Ultraviolet Emission from all Nondegenerate Stars within 10 Parsecs.
PB96-103189 *00,093*

WOOD, G. H.

CRYSTMET: The NRCC Metals Crystallographic Data File.
PB97-109029 *04,799*

WOOD, J.

Influence of Electrical Isolation on the Structure and Reflectivity of Multilayer Coatings Deposited on Dielectric Substrates.
PB96-159736 *04,365*

WOOD, J. L.

New Method for Achieving Accurate Thickness Control for Uniform and Graded Multilayer Coatings on Large Flat Substrates.
PB96-159744 *04,366*

WOOD, L. J.

Preparation and Certification of a Rhodium Standard Reference Material Solution.
PB94-185071 *00,529*

WOOD, M. A.

Refractive Indices of Fluids Related to Alternative Refrigerants.
PB94-219375 *03,260*

WOODBRIDGE, E. L.

Laser Flash Photolysis, Time-Resolved Fourier Transform Infrared Emission Study of the Reaction Cl + C2H5 yields HCl(v) + C2H4.
PB95-203238 *01,049*

Photodissociation of Ammonia at 193.3nm: Rovibrational State Distribution of the NH2(A(2)A1) Fragment.
PB95-151775 *00,937*

WOODGATE, B. E.

Observing Stellar Coronae with the Goddard High Resolution Spectrograph. I. The dMe Star AU Microscopii.
PB96-102777 *00,092*

WOOLLEY, C.

Shape Selectivity Assessment of Stationary Phases in Gas Chromatography.
PB95-150256 *00,579*

WORTHEY, J. A.

Lighting Quality and Light Source Size.
PB95-151783 *00,252*

Lighting Research and Theory Can Create Business Prospects.
PB95-151791 *00,253*

Physics-Based Vision: Principles and Practice, Shape Recovery (Book Review).
PB95-164075 *01,846*

Spectrally Smooth Reflectances That Match.
PB95-176319 04,306

WORTHINGTON, J. L.

Design and Machining of Copper Specimens with Micro Holes for Accurate Heat Transfer Measurements.
PB95-180428 02,658

WORTHY, J.

Model Minimum Performance Specifications for Lidar Speed Measurement Devices.
PB95-197455 04,861

WRIGHT, J.

Polymer Composites Workshop. Held in Winona, Minnesota on April 29-30, 1992 (Video).
PB94-780129 03,147

WRIGHT, R. N.

Ashland Tank Collapse Investigation.
PB95-126314 02,481

Ashland Tank-Collapse Investigation: Closure by Authors.
PB95-126322 02,482

Implementation of Executive Order 12699: Seismic Safety of Federal and Federally Assisted or Regulated New Building Construction.
PB95-151809 00,436

Infratechnologies: Tools for Innovation.
PB94-185998 00,317

Lessons from the Loma Prieta Earthquake.
PB95-164091 00,442

National Planning for Construction and Building R and D.
PB96-137104 00,324

Proceedings of a Workshop on Developing and Adopting Seismic Design and Construction Standards for Lifelines. Held in Denver, Colorado on September 25-27, 1991.
PB97-115794 01,302

Program of the Subcommittee on Construction and Building.
PB94-193646 00,319

Program of the Subcommittee on Construction and Building (July 1994).
PB95-122537 00,321

Rationale and Preliminary Plan for Federal Research for Construction and Building.
PB95-154704 00,322

Status of Construction and Construction Technologies.
PB94-186004 00,318

Structural Analysis in Context.
PB95-151817 00,437

Think Metric.
PB95-151825 01,298

WU, A.

Use of a Radiochromic Detector for the Determination of Stereotactic Radiosurgery Dose Characteristics.
PB94-185642 03,514

WU, C. F.

Taguchi's Parameter Design: A Panel Discussion.
PB96-111802 03,445

WU, D.

Analysis of Creep in a Si-SiC C-Ring by Finite Element Method.
PB94-200268 03,037

WU, D. I.

Aperture Coupling to a Coaxial Air Line: Theory and Experiment.
PB94-211968 02,216

WU, H.

Dielectric Properties of Thin Film SrTiO3 Grown on LaAlO3 with YBa2Cu3O7-x Electodes.
PB95-181160 02,267

WU, J. S.

Mixing and Radiation Properties of Buoyant Luminous Flame Environments.
PB96-202254 01,432

WU, T. G.

Potentiometric Enzyme-Amplified Flow Injection Analysis Detection System: Behavior of Free and Liposome-Released Peroxidase.
PB95-151833 03,534

WU, W.

Advances in the Measurement of Polymer CTE: Micrometer- to Atomic-Scale Measurements.
PB96-180229 03,390

SANS Study of the Plastic Deformation Mechanism in Polyethylene.
PB95-151841 01,242

Small-Angle Neutron Scattering of Poly(vinyl alcohol) Gels.
PB95-164117 01,260

WU, W. L.

Characterization of Molecular Network of Thermosets Using Neutron Scattering.
PB95-164109 01,259

Characterization of Polyquinoline Blends Using Small Angle Scattering.
PB95-164125 01,261

Characterization of Polyquinoline Block Copolymer Using Small Angle Scattering.
PB95-151882 01,244

Elastic Scattering of Polymer Networks.
PB95-161816 01,255

Electronics Packaging Materials Research at NIST.
PB96-122692 02,405

Influence of an Impenetrable Interface on a Polymer Glass-Transition Temperature.
PB96-146873 03,175

Novel Method for Determining Thin Film Density by Energy-Dispersive X-ray Reflectivity.
PB96-122783 04,737

Small Angle Neutron Scattering Studies on Chain Asymmetry of Coextruded Poly(Vinyl Alcohol) Film.
PB95-164372 01,262

Structural Heterogeneity in Epoxies.
PB95-151866 01,243

Thermoacoustic Technique for Determining the Interface and/or Interply Strength in Polymeric Composites.
PB95-161824 03,158

Water Adsorption at a Polyimide/Silicon Wafer Interface.
PB96-103197 01,070

Water Adsorption at Polymer/Silicon Wafer Interfaces.
PB95-181178 01,022

WU, Y.

Precision of Marchall Stability and Flow Test Using 6-in. (152.4-mm) Diameter Specimens.
PB96-200910 03,006

WU, Y. C.

Absolute Determination of Electrolytic Conductivity for Primary Standard KC1 Solutions from 0 to 50C.
PB94-172798 00,765

dc Method for the Absolute Determination of Conductivities of the Primary Standard KCl Solutions from 0C to 50C.
PB94-219342 02,644

Low Electrolytic Conductivity Standards.
PB96-122098 01,081

WUEBBLES, D. J.

Environmental Aspects of Halon Replacements: Considerations for Advanced Agents and the Ozone Depletion Potential of CF3I.
PB97-122261 03,301

WUENSCH, B. J.

Fast-Ion Conducting Y2(ZryTi1-y)2O7 Pyrochlores: Neutron Rietveld Analysis of Disorder Induced by Zr Substitution.
PB96-156104 04,776

Fast-Ion Conduction and Disorder in Cation and Anion Arrays in Y2(ZryTi(1-y))2O7 Pyrochlores Induced by Zr Substitution: A Neutron Rietveld Analysis.
PB94-211869 04,496

WYART, J. F.

Analysis of the (5d(2)+5d6s)-5d6p Transition Arrays of Os VII and Ir VIII, and the 6s (2)S-6p (2)P Transitions of Ir IX.
PB96-159264 01,954

Hyperfine Structure Investigations and Identification of New Energy Levels in the Ionic Spectrum of (147)Pm.
PB96-180203 04,117

WYCKOFF, H. O.

X-ray Protection Design.
AD-A279 181/2 03,606

WYSS, J. C.

Self-Calibrated Intelligent Optical Sensors and Systems.
PB96-200738 04,380

XIA, H. R.

Phase Shifts and Intensity Dependence in Frequency-Modulation Spectroscopy.
PB96-103205 01,071

XIANG, D.

Design, Construction and Application of a Large Aperture Lens-Less Line-Focus PVDF Transducer.
PB97-122584 02,765

Material Characterization By a Time-Resolved and Polarization-Sensitive Ultrasonic Technique.
PB97-122576 02,764

Transient Analysis of a Line-Focus Transducer Probing a Liquid/Solid Interface.
PB97-118681 02,763

XIAO, G.

Incorporation of Gold into YBa2Cu3O7: Structure and Tc Enhancement.
PB94-200276 04,481

Unexpected Effects of Gold on the Structure, Superconductivity, and Normal State of YBa2Cu3O7.
PB94-200284 04,482

XIAO, J. Q.

Domain Structures in Magnetoresistive Granular Metals.
PB96-141346 04,760

XIAO, Q. F.

Neutron Focusing Lens Using Polycapillary Fibers.
PB95-141206 03,889

Neutron Focusing Lens Using Polycapillary Fibers.
PB95-153078 03,922

XIE, Y.

Elastic Constants of a Material with Orthorhombic Symmetry: An Alternative Measurement Approach.
PB95-180527 04,684

XIN, J.

Internal Droplet Circulation Induced by Surface-Driven Rotation.
PB97-119267 02,500

XIONG, Q.

Oxygen Dependance of the Crystal Structure of HgBa2CuO4+ and Its Relation to Superconductivity.
PB96-102512 04,711

XIONG, X.

Comparative Strategies for Correction of Interferences in Isotope Dilution Mass Spectrometric Determination of Vanadium.
PB94-185261 00,531

Configuration-Dependent AC Stark Shifts in Calcium.
PB96-157995 04,363

RIS Measurement of AC Stark Shifts and Photoionization Cross Sections in Calcium.
PB96-157953 04,073

Study of Laser Resonance Ionization Mass Spectrometry Using a Glow Discharge Source.
DE94018566 03,308

Study of Laser Resonance Ionization Mass Spectrometry Using a Glow Discharge Source.
PB96-123203 03,360

XIONG, X. Z.

Epitaxial Integration of Single Crystal C60.
PB95-153490 04,592

XIU-YE, X.

Wide Band Active Current Transformer and Shunt.
PB95-126371 02,036

XU, H. H. K.

Evaluation of Thermal Wave Imaging for Detection of Machining Damage in Ceramics.
PB95-220547 03,062

XU, J. H.

Novel YBa2Cu3O7-x and YBa2Cu3O7-x/Y4Ba3O9 Multilayer Films by Bias-Masked 'On-Axis' Magnetron Sputtering.
PB95-181186 04,690

XU, Y.

Comparison of Finite Element and Analytic Calculations of the Resonant Modes and Frequencies of a Thick Shell Sphere.
PB94-160785 02,626

XU, Z.

Characterization of the Interaction of Hydrogen with Iridium Clusters in Zeolites by Inelastic Neutron Scattering Spectroscopy.
PB95-180741 01,013

YACZKO, D.

Commentary on 'Optimization of Experimental Parameters for the EPR Detection of the Cellulosic Radical in Irradiated Foodstuffs'.
PB96-164124 00,043

YACZKO, D. M.

Research and Development Activities in Electron Paramagnetic Resonance Dosimetry.
PB96-141288 03,635

YAJIMA, H.

Dynamic Light-Scattering Study of a Diluted Polymer Blend Near Its Critical Point.
PB95-151890 01,245

Shear Suppression of Critical Fluctuations in a Diluted Polymer Blend.
PB96-204458 04,418

YAKALI, H. H.

Integrated Mobile Robot System for Testing Vision Algorithms.
PB95-164133 02,936

YAMADA, M.

Direct Dispersion Measurement of Highly-Erbium-Doped Optical Amplifiers Using a Low Coherence Reflectometer Coupled with Dispersive Fourier Spectroscopy.
PB95-150702 04,263

Pump-Induced Dispersion of Erbium-Doped Fiber Measured by Fourier-Transform Spectroscopy.
PB94-211935 04,236

YAMASHITA, H.

Ignition and Transition to Flame Spread Over a Thermally Thin Cellulosic Sheet in a Microgravity Environment.
PB96-160288 04,837

Observations of Partial Discharges in Hexane Under High Magnification.
PB95-163127 01,900

YAMASHOJI, Y.

Thermodynamic and NMR Study of the Interactions of Cyclodextrins with Cyclohexane Derivatives.
PB94-185816 00,781

YANCEY, C. W. C.

Hollow Clay Tile Prism Tests for Martin Marietta Energy Systems: Task 2 Testing.
PB94-217486 00,352

Performance of HUD-Affiliated Properties during the January 17, 1994 Northridge Earthquake.
PB95-174488 00,443

YANEY, D. S.

National Semiconductor Metrology Program, Project Portfolio FY 1996.
PB96-195268 04,789

YANG, A.
Beyond the Technology Roadmaps: An Assessment of Electronic Materials Research and Development.
PB96-165998 *01,961*

YANG, A. J. M.
Mixing Plate-Like and Rod-Like Molecules with Solvent: A Test of Flory-Huggins Lattice Statistics.
PB96-126206 *03,173*

YANG, B.
Intensity-Dependent Scattering Rings in High Order Above-Threshold Ionization.
PB96-110739 *04,032*

YANG, C.
Integration of Real-Time Process Planning for Small-Batch Flexible Manufacturing.
PB95-151908 *02,822*

Open Architectures for Machine Control.
PB94-135621 *02,942*

YANG, D.
Interoperability Experiments with CORBA and Persistent Object Base Systems.
PB96-183140 *01,772*

YANG, J.
Agent Screening for Halon 1301 Aviation Replacement.
PB96-159710 *03,282*

Ultrasonic Technique for Sizing Voids Using Area Functions.
PB95-151916 *02,904*

YANG, J. C.
Combustion of a Polymer (PMMA) Sphere in Microgravity.
N96-15569/2 *01,354*

Estimate of the Effect of Scale on Radiative Heat Loss Fraction and Combustion Efficiency.
PB95-150447 *02,486*

Flow of Alternative Agents in Piping.
PB95-202420 *00,022*

Minimum Mass Flux Requirements to Suppress Burning Surfaces with Water Sprays.
PB96-183181 *01,425*

Solid Propellant Gas Generators: Proceedings of the 1995 Workshop. Held in Gaithersburg, Maryland on June 28-29, 1995.
PB96-131479 *01,412*

YANG, S.
Accurate Measurement of Optical Detector Nonlinearity.
PB95-203576 *02,181*

Automated Measurement of Nonlinearity of Optical Fiber Power Meters.
PB96-176540 *04,110*

Optical Detector Nonlinearity: A Comparison of Five Methods.
PB95-169355 *04,291*

Optical Detector Nonlinearity: Simulation.
PB96-165378 *02,199*

YANIV, S. L.
Precision in Machining: Research Challenges.
PB95-242301 *02,953*

YAP, W.
Supported Phospholipid/Alkanthiol Biomimetic Membranes: Insulating Properties.
PB95-180782 *03,470*

YAP, W. T.
Thermodynamics of the Hydrolysis of Penicillin G and Ampicillin.
PB94-172467 *03,596*

YARBROUGH, D. W.
Comparison of Heat-Flow-Meter Tests from Four Laboratories.
PB95-126264 *00,365*

YARBROUGH, W. A.
Applications of Diamond Films and Related Materials: International Conference (3rd). Held in Gaithersburg, Maryland on August 21-24, 1995. Supplement to NIST Special Publication 885.
PB95-256053 *03,063*

Proceedings of the Applied Diamond Conference 1995: Applications of Diamond Films and Related Materials International Conference (3rd). Held in Gaithersburg, Maryland, on August 21-24, 1995.
PB95-255204 *04,701*

YARMOFF, J. A.
Desorption Induced by Electronic Transitions.
PB94-216173 *00,853*

Influence of Coadsorbed Potassium on the Electron-Stimulated Desorption of F(+), F(-), and F(*) from PF3 on Ru(0001).
PB96-157946 *04,072*

YE, J.
Delivering the Same Optical Frequency at Two Places: Accurate Cancellation of Phase Noise Introduced by an Optical Fiber or Other Time-Varying Path.
PB96-102736 *04,332*

YECKLEY, R.
Transient Creep Behaviour of Hot Isostatically Pressed Silicon Nitride.
PB96-180278 *03,086*

YEE, K. W.
Post-Process Control of Machine Tools.
PB95-203451 *02,952*

YEH, T. I.
Comparisons of Some NIST Fixed-Point Cells with Similar Cells of Other Standards Laboratories.
PB97-119242 *00,655*

YEH, T. T.
Effects of Pipe Elbows and Tube Bundles on Selected Types of Flowmeters.
PB96-160999 *01,135*

Flowmeter Installation Effects Due to a Generic Header.
PB96-210893 *02,606*

Laser Doppler Velocimeter Studies of the Pipeflow Produced by a Generic Header.
PB95-226916 *02,602*

Summary Report of NIST's Industry-Government Consortium Research Program on Flowmeter Installation Effects: The 45 Degree Elbow.
PB95-143061 *04,204*

Summary Report of NIST's Industry-Government Consortium Research Program on Flowmeter Installation Effects with Emphasis on the Research Period, January-September 1991: The Reducer.
PB94-160736 *04,196*

YENTIS, R.
Micromachined Display Output for a Cellular Neural Network.
PB96-156070 *02,422*

YESHA, Y.
Channel Coding for Code Excited Linear Prediction (CELP) Encoded Speech in Mobile Radio Applications.
PB95-143178 *01,475*

Coping with Different Retrieval Methods in Next Generation Networks.
PB95-168555 *02,726*

YIN, L. I.
Pattern-Recognition Analysis of Low-Resolution X-Ray Fluorescence Spectra.
PB95-151924 *00,588*

Tomographic Decoding Algorithm for a Nonoverlapping Redundant Array.
PB95-151932 *01,842*

YING, T. N.
Asperity-Asperity Contact Mechanisms Simulated by a Two-Ball Collision Apparatus.
PB95-164158 *02,966*

Chemical Effect in Ceramics Grinding.
PB97-122592 *03,113*

YODER, C. F.
Lunar Laser Ranging: A Continuing Legacy of the Apollo Program.
PB95-202495 *03,683*

YOKEL, F. Y.
Earthquake Resistant Construction of Electric Transmission and Telecommunication Facilities Serving the Federal Government Report.
PB94-161817 *02,460*

Earthquake Resistant Construction of Gas and Liquid Fuel Pipeline Systems Serving, or Regulated By, the Federal Government.
PB94-161999 *04,846*

Recommended Performance-Based Criteria for the Design of Manufactured Home Foundation Systems to Resist Wind and Seismic Loads.
PB96-128285 *00,460*

YOLKEN, H. T.
Intelligent Processing of Materials.
PB94-172780 *02,811*

YOON, H.
Structural Stabilization of Phase Separating PC/Polyester Blends through Interfacial Modification by Transesterification Reaction.
PB95-150454 *01,239*

YOSHIDA, K.
Charpy Impact Test as an Evaluation of 4 K Fracture Toughness.
PB96-190194 *03,219*

YOSHIHIRO, K.
Anomalous Behavior of a Quantized Hall Plateau in a High-Mobility Si Metal-Oxide-Semiconductor Field-Effect Transistor.
PB95-164174 *02,354*

YOSHIKAWA, M.
Applications of Diamond Films and Related Materials: International Conference (3rd). Held in Gaithersburg, Maryland on August 21-24, 1995. Supplement to NIST Special Publication 885.
PB95-256053 *03,063*

Proceedings of the Applied Diamond Conference 1995: Applications of Diamond Films and Related Materials International Conference (3rd). Held in Gaithersburg, Maryland, on August 21-24, 1995.
PB95-255204 *04,701*

YOU, L.
Collisional Energy Transfer between Excited-State Strontium and Noble-Gas Atoms.
PB95-202958 *03,995*

Cone Emission from Laser-Pumped Two-Level Atoms. 1. Quantum Theory of Resonant Light Propagation.
PB95-203584 *04,325*

Cone Emission from Laser-Pumped Two-Level Atoms. 2. Analytical Model Studies.
PB95-203592 *04,326*

Failures of the Four-Wave Mixing Model for Cone Emission.
PB95-202636 *04,318*

Probing Bose-Einstein Condensed Atoms with Short Laser Pulses.
PB95-202818 *03,991*

Suppression of Ionization in One- and Two-Dimensional Model Calculations.
PB95-203600 *04,009*

YOUNG, G.
Histopathology, Blood Chemistry, and Physiological Status of Normal and Moribund Striped Bass ('Morone saxatilis') Involved in Summer Mortality ('Die-Off') in the Sacramento-San Joaquin Delta of California.
PB94-198157 *00,034*

YOUNG, K.
Submarine Automation: Demonstration No. 5.
PB95-251633 *03,748*

YOUNG, L.
Hyperfine-Structure Studies of Zr II: Experimental and Relativistic Configuration-Interaction Results.
PB95-203824 *04,011*

Precision Lifetime Measurements of Cs 6p (2)P1/2 and 6p (2)P3/2 Levels by Single-Photon Counting.
PB95-203816 *04,010*

YOUNG, M.
Fiber Coating Diameter: Toward a Glass Artifact Standard.
PB96-140389 *02,234*

Optical Fiber, Fiber Coating, and Connector Ferrule Geometry: Results of Interlaboratory Measurement Comparisons.
PB96-154422 *04,360*

Optical Fiber Geometry: Accurate Measurement of Cladding Diameter.
PB95-151940 *04,266*

Optical Fiber Geometry by Gray-Scale Analysis with Robust Regression.
PB95-161519 *04,272*

Standard Reference Materials for Optical Fibers and Connectors.
PB96-119805 *04,344*

Vector Theory of Diffraction by a Single-Mode Fiber: Application to Mode-Field Diameter Measurements.
PB95-164182 *04,279*

Video Microscopy Applied to Optical Fiber Geometry Measurements.
PB95-173068 *04,295*

YOUNGER, F. C.
Hybrid Undulator for the NIST-NRL Free-Electron Laser.
PB94-212529 *04,238*

YOUNGLOVE, B. A.
International Standard Equation of State for the Thermodynamic Properties of Refrigerant 123 (2,2-Dichloro- 1,1,1-Trifluoroethane).
PB96-176805 *03,294*

Speed-of-Sound Measurements in Liquid and Gaseous Air.
PB95-151957 *04,186*

YOUSSEF, N. F. G.
Survey of Steel Moment-Resisting Frame Buildings Affected by the 1994 Northridge Earthquake.
PB95-211918 *00,451*

YU, D.
Anomalous Behavior of a Quantized Hall Plateau in a High-Mobility Si Metal-Oxide-Semiconductor Field-Effect Transistor.
PB95-164174 *02,354*

YU, L. J.
Spectral Interference in the Determination of Arsenic in High-Purity Lead and Lead-Base Alloys Using Electrothermal Atomic Absorption Spectrometry and Zeeman-Effect Background Correction.
PB96-112099 *00,614*

Trace Detection in Conducting Solids Using Laser-Induced Fluorescence in a Cathodic Sputtering Cell.
PB95-163424 *00,598*

YU, T.
Optimization of Highway Concrete Technology.
PB94-182995 *01,333*

YU, Z.
Heavily Accumulated Surfaces of Mercury Cadmium Telluride Detectors: Theory and Experiment.
PB94-216074 *02,134*

Investigation of Mercury Interstitials in Hg(1-x)CdxTe Alloys Using Resonant Impact-Ionization Spectroscopy.
PB94-213485 *02,133*

RII Spectroscopy of Trap Levels in Bulk and LPE Hg1-xCdxTe.
PB96-160247 *04,084*

YUAN, C. W.
Vortex Images in Thin Films of YBa2Cu3O(sub 7-x) and Bi2Sr2Ca1Cu2O(sub 8+x) Obtained by Low-Temperature Magnetic Force Microscopy.
PB97-119408 *04,815*

YUST, M.
Thin Film Thermocouples for Measurement of Wall Temperatures in Internal Combustion Engines.
PB94-172103 *01,449*

YUYAMA, M.
n-Value and Second Derivative of the Superconductor Voltage-Current Characteristic.
PB95-126223 *04,533*

ZACHARIAH, M.
Agent Screening for Halon 1301 Aviation Replacement.
PB96-159710 *03,282*

ZACHARIAH, M. R.
Controlled Nucleation in Aerosol Reactors for Supression of Agglomerate Formation.
PB95-151973 *00,672*

Experimental and Numerical Studies of Refractory Particle Formation in Flames: Application to Silica Growth.
PB95-152005 *00,673*

Flame Synthesis of High Tc Superconductors.
PB95-151981 *00,659*

Fluorinated Hydrocarbon Flame Suppression Chemistry.
PB94-185113 *01,362*

Gas Phase Reactions Relevant to Chemical Vapor Deposition: Numerical Modeling.
PB94-199346 *03,117*

Halon Thermochemistry: 'Ab Initio' Calculations of the Enthalpies of Formation of Fluoromethanes.
PB96-175740 *03,289*

In situ Characterization of Vapor Phase Growth of Iron Oxide-Silica Nanocomposites: Part 1. 2-D Planar Laser-Induced Fluorescence and Mie Imaging.
PB97-112478 *03,185*

In-situ Studies of a Novel Sodium Flame Process for Synthesis of Fine Particles.
PB97-113047 *00,681*

Modeling Ceramic Sub-Micron Particle Formation from the Vapor Using Detailed Chemical Kinetics: Comparison with In-situ Laser Diagnostics.
PB95-151965 *00,671*

Multiphoton Ionization Spectroscopy Measurements of Silicon Atoms during Vapor Phase Synthesis of Ceramic Particles.
PB95-151999 *03,913*

Optical and Modeling Studies of Sodium/Halide Reactions for the Formation of Titanium and Boron Nanoparticles.
PB97-113054 *00,682*

Simulation of Ceramic Particle Formation: Comparison with In-situ Measurements.
PB95-152013 *00,674*

Thermochemical and Chemical Kinetic Data for Fluorinated Hydrocarbons.
PB95-260618 *01,056*

ZAENGL, W.
Approach to Setting Performance Requirements for Automated Evaluation of the Parameters of High-Voltage Impulses.
PB94-185634 *01,878*

ZAGHLOUL, M.
High-Level CAD Melds Micromachined Devices with Foundries.
PB94-216413 *02,321*

Realizing Suspended Structures on Chips Fabricated by CMOS Foundry Processes Through the MOSIS Service.
PB94-193984 *01,881*

ZAGHLOUL, M. E.
Color Supplement to NIST Special Publication 400-93: Semiconductor Measurement Technology: Design and Testing Guides for the CMOS and Lateral Bipolar-on-SOI Test Library.
PB94-164316 *02,298*

Design Guide for CMOS-On-SIMOX. Test Chips NIST3 and NIST4.
PB94-163458 *02,297*

Micromachined Coplanar Waveguides in CMOS Technology.
PB97-119283 *02,456*

Micromachined Display Output for a Cellular Neural Network.
PB96-156070 *02,422*

Semiconductor Measurement Technology: Design and Testing Guides for the CMOS and Lateral Bipolar-on-SOI Test Library.
PB94-178019 *02,301*

Test Structures for Determining Design Rules for Microelectromechanical-Based Sensors and Actuators.
PB95-150488 *02,105*

ZAGLOUL, M. E.
CMOS Circuit Design for Controlling Temperature in Micromachined Devices.
PB96-156088 *02,196*

ZAIDI, M. K.
Calibration and Performance of GafChromic DM-100 Radiochromic Dosemeters.
PB97-119291 *00,703*

ZAJCHOWSKI, P. H.
Characterization and Processing of Spray-Dried Zirconia Powders for Plasma Spray Application.
PB97-111231 *04,419*

ZANDER, M.
Optical Detector Nonlinearity: Simulation.
PB96-165378 *02,199*

ZANGWILL, A.
Coarsening of Unstable Surface Features during Fe(001) Homoepitaxy.
PB96-186127 *04,121*

ZAPAS, L. J.
Performance of Plastic Packaging for Hazardous Materials Transportation. Part 1. Mechanical Properties.
AD-A301 258/0 *02,580*

ZARDECKI, C.
Nucleic Acid Database: Present and Future.
PB97-109078 *00,518*

ZAREMBA, C. M.
Structural and Chemical Investigations of Na3(ABO4)3.4H2O-Type Sodalite Phases.
PB95-180733 *01,012*

ZARR, R. R.
Comparison of Heat-Flow-Meter Tests from Four Laboratories.
PB95-126264 *00,365*

Control Stability of a Heat-Flow-Meter Appartus.
PB95-181194 *00,386*

Effect of Environmentally Exposures on the Properties of Polyisocyanurate Foam Insulation: Thermal Conductivity Measurements.
PB95-181210 *00,388*

Effects of Humidity and Elevated Temperature on the Density and Thermal Conductivity of a Rigid Polyisocyanurate Foam.
PB95-152021 *00,373*

Effects of Humidity and Elevated Temperature on the Density and Thermal Conductivity of a Rigid Polyisocyanurate Foam Co-Blown with CCl3F and CO2.
PB95-150462 *00,371*

Experimental Verification of a Moisture and Heat Transfer Model in the Hygroscopic Regime.
PB97-111546 *00,309*

Heat and Moisture Transfer in Wood-Based Wall Construction: Measured versus Predicted.
PB95-200655 *00,391*

Intra-Laboratory Comparison of a Line-Heat-Source Guarded Hot Plate and Heat-Flow-Meter Apparatus.
PB95-181202 *00,387*

Line-Heat-Source Guarded-Hot-Plate Apparatus.
PB97-118996 *00,417*

Room-Temperature Thermal Conductivity of Expanded Polystyrene Board for a Standard Reference Material.
PB96-193693 *00,412*

Room Temperature Thermal Conductivity of Fumed-Silica Insulation for a Standard Reference Material.
PB95-152039 *00,374*

ZASTAWNY, T.
Novel Activity of E. coli uracil DNA N-glycosylase Excision of Isodialuric Acid (5,6-dihydroxyuracil), a Major Product of Oxidative DNA Damage, from DNA.
PB96-110747 *03,543*

Oxidative DNA Base Damage in Renal, Hepatic, and Pulmonary Chromatin of Rats After Intraperitoneal Injection of Cobalt (II) Acetate.
PB95-150025 *03,647*

Tert-Butyl Hydroperoxide-Mediated DNA Base Damage in Cultured Mammalian Cells.
PB94-182003 *03,644*

ZASTAWNY, T. H.
DNA Base Damage in Lymphocytes of Cancer Patients Undergoing Radiation Therapy.
PB97-122444 *03,643*

DNA Damage and DNA Sequence Retrieval from Ancient Tissues.
PB97-111983 *03,556*

Formation of DNA-Protein Cross-Links in Cultured Mammalian Cells Upon Treatment with Iron Ions.
PB96-137724 *03,651*

Novel DNA N-Glycosylase Activity of E. coli T4 Endonuclease V That Excises 4,6-Diamino-5-Formamidopyrimidine from DNA, a UV-Radiation- and Hydroxyl Radical-Induced Product of Adenine.
PB96-160478 *03,549*

ZAVADA, J. M.
Using Secondary Ion Mass Spectrometry (SIMS) to Characterize Optical Waveguide Materials.
PB96-119599 *04,340*

ZEISLER, R.
Certifying the Chemical Composition of a Biological Material: A Case Study.
PB96-164272 *00,636*

Current Activities Within the National Biomonitoring Specimen Bank.
PB94-172806 *02,516*

Determination of Inorganic Constituents in Marine Mammal Tissues.
PB95-152047 *00,589*

National Status and Trends Program Specimen Bank: Sampling Protocols, Analytical Methods, Results, and Archive Samples.
PB97-119226 *02,598*

Neutron Capture Prompt Gamma-Ray Activation Analysis at the NIST Cold Neutron Research Facility.
PB94-213394 *00,556*

Trace Elements Associated with Proteins. Neutron Activation Analysis Combined with Biological Isolation Techniques.
PB95-163101 *00,597*

ZEISSLER, C. J.
Environmental Scanning Electron Microscope Imaging Examples Related to Particle Analysis.
PB94-172822 *00,766*

ZELKOWITZ, M.
Center for High Integrity Software System Assurance: Initial Goals and Activities.
PB95-251674 *01,734*

Defining Environment Integration Requirements.
PB96-131545 *02,733*

Information Technology Engineering and Measurement Model: Adding Lane Markings to the Information Superhighway.
PB95-143145 *01,474*

Next Generation Computer Resources: Reference Model for Project Support Environments (Version 2.0).
PB94-143401 *01,677*

ZELKOWITZ, M. V.
Experimental Models for Software Diagnosis.
PB97-113906 *01,783*

Measurement of Process Complexity.
PB97-113138 *01,781*

Use of an Environment Classification Model.
PB95-152062 *01,709*

ZEMKE, W. T.
Spectroscopy and Structure of the Lithium Hydride Diatomic Molecules and Ions.
PB94-160991 *00,731*

ZENNER, G. P.
Measurement of Boron at Silicon Wafer Surfaces by Neutron Depth Profiling.
PB94-211059 *04,487*

ZETTL, A.
Scanning Tunneling Microscopy of the Charge-Density-Wave Structure in 1T-TaS2.
PB95-180980 *04,689*

ZHANG, C. Y.
IRAS Spectroscopic Observations of Young Planetary Nebulae.
PB95-152070 *00,072*

ZHANG, D.
Effects of Etching on the Morphology and Surface Resistance of YBa2Cu3O7-delta Films.
PB96-135355 *02,410*

ZHANG, G.
Displacement Method for Machine Geometry Calibration.
PB95-152088 *02,946*

ZHANG, H.
Analytic Calculation of Polarized Neutron Reflectivity from Superconductors.
PB95-164224 *04,629*

Coupled-Bilayer Two-Dimensional Magnetic Order of the Dy Ions in Dy2Ba4Cu7O15.
PB95-152104 *04,584*

Diffraction of Neutron Standing Waves in Thin Films with Resonance Enhancement.
PB97-113278 *04,164*

Grazing Incidence Prompt Gamma Emissions and Resonance-Enhanced Neutron Standing Waves in a Thin-Film.
PB95-150470 *03,892*

Interaction between Dislocations and Intergranular Cracks.
PB95-152096 *03,190*

New Exact Solution of the One-Dimensional Schrodinger Equation and Its Application to Polarized Neutron Reflectometry.
PB95-161832 *04,609*

Suitability of Metalorganic Chemical Vapor Deposition-Derived PrGaO3 Films as Buffer Layers for YBa2Cu3O7-x Pulsed Laser Deposition.
PB95-168670 *04,640*

ZHANG, K. C.
Susceptibility Critical Exponent for a Nonaqueous Ionic Binary Mixture Near a Consolute Point.
PB95-152112 *00,938*

ZHANG, L. W.
Visual Measurement Technique for Analysis of Nucleate Flow Boiling.
PB95-143301 *03,262*

ZHANG, N. F.
Analysis of Autocorrelations in Dynamic Processes.
PB95-181228 *02,826*

ZHANG, V. S.
High Resolution Time Interval Counter.
PB96-138607 *01,495*

ZHANG, X.
Computational Model for the Rise and Dispersion of Wind-Blown, Buoyancy-Driven Plumes. Part 2. Linearly Stratified Atmosphere.
PB94-143427 *00,119*

Dispersion and Deposition of Smoke Plumes Generated in Massive Fires.
PB95-126066 02,540

ZHANG, Y.

Deposit Forming Tendencies of Diesel Engine Oils-Correlation between the Two-Peak Method and Engine Tests.
PB95-152138 01,452

New Method to Evaluate Deposit Forming Tendencies of Liquid Lubricants by Differential Scanning Calorimetry.
PB95-152120 01,451

ZHANG, Y. X.

Digital Techniques in HV Tests - Summary of 1989 Panel Session.
PB94-216702 02,035

ZHANG, Z.

Atmospheric Reactivity of alpha-Methyl-Tetrahydrofuran.
PB95-163705 02,548

Diffusion of Cations Beneath Organic Coatings on Steel Substrate.
PB94-215704 03,119

Experimental Determination of the Ionization Energy of IO(X(sup 2)II(sub 3/2)) and Estimations of Delta(sub f)H(sup deg)(sub 0)(IO(sup -)) and PA(IO).
PB96-146899 00,694

Gas Phase Reactivity Study of OH Radicals with 1,1-Dichloroethene and cis-1,1-Dichloroethene and Trans-1,2-Dichloroethene over the Temperature Range 240-400 K.
PB95-152146 00,939

Ionization Energies, Appearance Energies and Thermochemistry of CF2O and FCO.
PB97-111538 01,178

Rate Constants for the Gas Phase Reactions of the OH Radical with CF3CF2CHCl2 (HCFC-225ca) and CF2ClCF2CHClF (HCFC-225cb).
PB95-152153 00,940

Structures of Vapor-Deposited Yttria and Zirconia Thin Films.
PB94-216025 03,041

ZHANG, Z. M.

Broadband High-Optical-Density Filters in the Infrared.
PB95-180261 04,309

Development of Neutral-Density Infrared Filters Using Metallic Thin Films.
PB96-180286 02,998

Liquid-Nitrogen-Cooled High Tc Electrical Substitution Radiometer as a Broadband IR Transfer Standard.
PB96-158704 02,198

Thermal and Nonequilibrium Responses of Superconductors for Radiation Detectors.
PB95-164232 02,156

Thermal Modeling and Analysis of Laser Calorimeters.
PB96-140405 04,354

Thermal Modeling of Absolute Cryogenic Radiometers.
PB95-181236 04,316

ZHAO, Q.

Comparisons of Some NIST Fixed-Point Cells with Similar Cells of Other Standards Laboratories.
PB97-119242 00,655

ZHAO, Z. Q.

State-Resolved Rotational Energy Transfer in Open Shell Collisions: Cl((2)P3/2)+HCl.
PB96-176607 01,157

ZHEN, Z.

Intercomparison of Thermal Converters at NIM, NIST, PTB, SIRI and VSL from 10 to 100 MHz.
PB94-172459 02,027

ZHENG, G. G.

Novel YBa2Cu3O7-x and YBa2Cu3O7-x/Y4Ba3O9 Multilayer Films by Bias-Masked 'On-Axis' Magnetron Sputtering.
PB95-181186 04,690

ZHENG, Q.

Physical Limit to the Stability of Superheated and Stretched Water.
PB96-122551 01,083

ZHENG, Z.

Vortex Images in Thin Films of YBa2Cu3O(sub 7-x) and Bi2Sr2Ca1Cu2O(sub 8+x) Obtained by Low-Temperature Magnetic Force Microscopy.
PB97-119408 04,815

ZHIGUNOV, D. I.

Magnetic Structure and Spin Dynamics of the Pr and Cu in Pr2CuO4.
PB96-111836 04,036

ZHOU, H. L.

High-Precision Calculations of Cross Sections for Low-Energy Electron Scattering by Ground and Excited State of Sodium.
PB95-152161 03,914

Low-Energy-Electron Collisions with Sodium: Elastic and Inelastic Scattering from the Ground State.
PB96-103106 04,030

ZHOU, S.

Lattice Imperfections Studied by Use of Lattice Green's Functions.
PB95-150850 04,576

ZHOU, S. J.

Dislocation Core-Core Interaction and Peierls Stress in a Model Hexagonal Lattice.
PB96-162003 04,101

Dislocation Emission at Ledges on Cracks.
PB95-164240 04,630

Interfacial Crack in a Two-Dimensional Hexagonal Lattice.
PB96-161989 04,100

Shielding of Cracks in a Plastically Polarizable Material.
PB95-164257 04,631

ZHU, J.

Fluctuation Dominated Recombination Kinetics with Traps.
PB95-107264 00,875

ZHU, J. G.

Surface Topography and Ordering-Variant Segregation in GaInP2.
PB95-153649 04,595

ZHU, M.

Dreams About the Next Generation of Super-Stable Lasers.
PB94-211570 04,235

Improved Hyperfine Measurements of the Na NP Excited State Through Frequency-Controlled Dopplerless Spectroscopy in a Zeeman Magneto-Optic Laser Trap.
PB95-203840 04,012

Introduction to Phase-Stable Optical Sources.
PB96-122973 04,347

Stabilization of Optical Phase/Frequency of a Laser System: Application to a Commercial Dye Laser with an External Stabilizer.
PB95-203832 04,327

ZIBROV, A. S.

High-Resolution Diode-Laser Spectroscopy of Calcium.
PB95-181244 03,969

High-Sensitivity Spectroscopy with Diode Lasers.
PB95-175477 04,297

ZIEGLER, R. G.

Ascorbic and Dehydroascorbic Acids Measured in Plasma Preserved with Dithiothreitol or Metaphorphoric Acid.
PB94-216330 03,495

Liquid Chromatographic Method for the Determination of Carotenoids, Retinoids, and Tocopherols in Human Serum and in Food.
PB95-153599 00,593

ZIMMERLI, G.

Electric Field Effects on a Near-Critical Fluid in Microgravity.
PB96-161880 04,217

Noise in the Coulomb Blockade Electrometer.
PB95-176327 04,670

Self-Heating in the Coulomb-Blockade Electrometer.
PB94-212685 04,507

Thermal Enhancement of Cotunneling in Ultra-Small Tunnel Junctions.
PB95-175436 04,658

Voltage Gain in the Single-Electron Transistor.
PB95-176335 04,671

ZIMMERMAN, B. E.

63Ni Half-Life: A New Experimental Determination and Critical Review.
PB97-111603 00,700

Nickel-63 Standardization: 1968-1995.
PB97-111819 00,701

ZIMMERMAN, J.

Residual Error Compensation of a Vision-Based Coordinate Measuring Machine.
PB96-161617 04,091

ZIMMERMAN, J. H.

Automated Optical Roughness Inspection.
PB95-152179 02,905

ZIMMERMAN, N. M.

Application of Single Electron Tunneling: Precision Capacitance Ratio Measurements.
PB96-102157 04,703

Capacitors with Very Low Loss: Cryogenic Vacuum-Gap Capacitors.
PB97-122600 02,293

Proposed Tests to Evaluate the Frequency-Dependent Capacitor Ratio for Single Electron Tunneling Experiment.
PB97-111454 01,982

Results of Capacitance Ratio Measurements for the Single Electron Pump-Capacitor Charging Experiment.
PB97-113286 04,813

ZINCKE, C.

CMOS Circuit Design for Controlling Temperature in Micromachined Devices.
PB96-156088 02,196

Micromachined Display Output for a Cellular Neural Network.
PB96-156070 02,422

Test Structures for Determining Design Rules for Microelectromechanical-Based Sensors and Actuators.
PB95-150488 02,105

ZINK, L.

Absolute Frequency Measurements of Methanol from 1.5 to 6.5 THz.
PB95-175881 04,300

ZINK, L. R.

30 THz Mixing Experiments on High Temperature Superconducting Josephson Junctions.
PB96-102462 04,709

Atomic Oxygen Fine Structure Splittings with Tunable Far Infrared Spectroscopy.
PB95-152203 03,915

Atomic Sulfur: Frequency Measurement of the J=0 inversely maps 1 Fine-Structure Transition at 56.3 Microns by Laser Magnetic Resonance.
PB95-180105 01,007

Far Infrared Laser Frequencies of CH3OD and N2H4.
PB96-119623 04,341

Far Infrared Laser Frequencies of (13)CD3OH.
PB95-169363 04,292

Improved Molecular Constants and Frequencies for the CO2 Laser from New High-J Regular and Hot-Band Frequency Measurements.
PB95-180634 04,312

Laboratory Measurements for the Astrophysical Identification of MgH.
PB95-152195 00,073

Laser Magnetic-Resonance Measurement of the (3)P1 - (3)P2 Fine-Structure Splittings in (17)O and (18)O.
PB95-175170 00,994

Measurement of the J=2 less than 1 Fine-Structure Interval for (28)Si and (29)Si in the Ground (3)P State.
PB94-185097 00,771

Rotational Far Infrared Spectrum of (13)CO.
PB95-152187 00,941

ZINK, S.

Investigation of Applicability of Alanine and Radiochromic Detectors to Dosimetry of Proton Clinical Beams.
PB96-146782 03,636

ZOBOV, N.

Microwave Spectrum and Structure of CH3NO2-H20.
AD-A296 377/5 00,719

ZOBOV, N. F.

Tunneling-Rotation Spectrum of the Hydrogen Fluoride Dimer.
PB94-198678 00,793

ZOLLER, P.

Atomic Beam Splitters and Mirrors by Adiabatic Passage in Multilevel Systems.
PB94-216439 03,867

Phase Shifts and Intensity Dependence in Frequency-Modulation Spectroscopy.
PB96-103205 01,071

ZUKOSKI, E. E.

Experimental and Numerical Studies on Two-Dimensional Gravity Currents in a Horizontal Channel.
PB94-165941 01,359

Review of Flows Driven By Natural Convection in Adiabatic Shafts.
PB96-147897 01,416

ZULFUGARZADE, E. E.

Proceedings of the Meeting of the Intergovernmental U.S.-Russian Business Development Committee's Standard Working Group (4th). Held in New York City, New York on March 27-29, 1995 and in Northbrook, Illinois on March 30-31, 1995.
PB95-255881 00,496

ZWART, E.

Microwave and Submillimeter Spectroscopy of Ar-NH3 States Correlating with Ar+NH3(j=1, k=1).
PB95-152211 00,942

ZWEIBEL, E. G.

Magnetic Fields in Star-Forming Regions: Observations.
PB96-123005 00,100

ZWEIDINGER, R. B.

Distinguishing the Contributions of Residential Wood Combustion and Mobile Source Emissions Using Relative Concentrations of Dimethylphenanthrene Isomers.
PB96-135124 02,563

ZWEIER, J.

Research and Development Activities in Electron Paramagnetic Resonance Dosimetry.
PB96-141288 03,635

ZWINKELS, J.

Comparison of Regular Transmittance Scales of Four National Standardizing Laboratories.
PB94-211232 04,233

ZYWOCINSKI, A.

Thermodynamics of (Germanium + Selenium): A Review and Critical Assessment.
PB97-112536 01,182

KEYWORD INDEX

SAMPLE ENTRY

FIRE DETECTORS
Performance Parameters of Fire Detection Systems
PB94-194339 *00,123*

Keyword term
Title
NTIS order number *Abstract number*

1,1,1,2,3,3-HEXAFLUOROPROPANE
Dielectric Studies of Fluids with Reentrant Resonators.
PB95-153730 *00,952*

1,1,1,2-TETRAFLUOROETHANE
Viscosity of the Saturated Liquid Phase of Six Halogenated Compounds and Three Mixtures.
PB95-162368 *00,960*

Thermodynamic Properties of R134a(1,1,1,2-Tetrafluoroethane).
PB95-168704 *00,988*

Measurements of Molar Heat Capacity at Constant Volume (Cv) for 1,1,1,2-Tetrafluoroethane (R134a).
PB95-168878 *03,264*

Vapour Pressure Measurements on 1,1,1,2-Tetrafluoroethane (R134a) from 180 to 350 K.
PB95-168886 *03,265*

1,3-BUTADIENE
Stability/Instability of Gas Mixtures Containing 1,3-Butadiene in Treated Aluminum Gas Cylinders.
PB95-162285 *02,546*

1-CHLORO-1
Polarized Transient Hot Wire Thermal Conductivity Measurements.
PB95-108817 *00,886*

1-CHLORO-1,2,2,2-TETRAFLUOROETHANE
Viscosity of the Saturated Liquid Phase of Six Halogenated Compounds and Three Mixtures.
PB95-162368 *00,960*

10-METHYLACRIDAN
Oxidation of 10-Methylacridan, a Synthetic Analogue of NADH and Deprotonation of Its Cation Radical. Convergent Application of Laser Flash Photolysis and Direct and Redox Catalyzed Electrochemistry to the Kinetics of Deprotonation of the Cation Radical.
PB94-198371 *00,785*

2-DIFLUOROMETHOXY-1,1,1-TRIFLUOROETHANE
Viscosity of the Saturated Liquid Phase of Six Halogenated Compounds and Three Mixtures.
PB95-162368 *00,960*

2-METHYLPROPENE
Mechanism and Rate Constants for the Reactions of Hydrogen Atoms with Isobutene at High Temperatures.
PB95-151064 *00,929*

2D ARRAYS
SUSAN: SUperconducting Systems ANalysis by Low Temperature Scanning Electron Microscopy (LTSEM).
PB96-112065 *04,728*

High-Frequency Oscillators Using Phase-Locked Arrays of Josephson Junctions.
PB96-135157 *02,080*

3-QUINUCLIDINOL
Determination of 3-Quinuclidinyl Benzilate (Qnb) and Its Major Metabolites in Urine by Isotope Dilution Gas Chromatography Mass Spectrometry.
PB94-199379 *03,492*

3C 273 RADIO SOURCE
Observations of 3C 273 with the Goddard High Resolution Spectrograph on the Hubble Space Telescope.
PB95-202321 *00,076*

A STARS
A-type and Chemically Peculiar Stars.
PB96-123286 *00,101*

Radio and X-ray Emissions from Chemically Peculiar B- and A-Type Stars: Observations and a Model.
PB96-123302 *00,103*

AAMACS SYSTEM
Advanced Angle Metrology System.
PB94-211364 *02,637*

AB INITIO CALCULATION
Ab initio Calculations for Helium: A Standard for Transport Property Measurements.
PB96-102041 *01,060*

ABRASION
Abrasive Wear by Diesel Engine Coal-Fuel and Related Particles.
PB95-104915 *01,450*

ABRIKOSOV VORTICES
Thermally Activated Hopping of a Single Abrikosov Vortex.
PB95-140810 *04,548*

ABSOLUTE GRAVITY
Intracomparison Tests of the FG5 Absolute Gravity Meters.
PB96-102991 *03,688*

ABSOLUTE SPECTRAL RESPONSE
NIST High Accuracy Scale for Absolute Spectral Response from 406 nm to 920 nm.
PB96-179122 *01,865*

Developing Quality System Documentation Based on ANSI/NCSL Z540-1-1994: The Optical Technology Division's Effort.
PB96-202122 *01,869*

ABSORBATES
Ultrafast Time-Resolved Infrared Probing of Energy Transfer at Surfaces.
PB96-123443 *00,620*

ABSORBED DOSE
Problem of Convection in the Water Absorbed Dose Calorimeter.
PB97-110159 *03,523*

ABSORBERS (EQUIPMENT)
Low-Frequency Model for Radio-Frequency Absorbers.
PB95-261939 *04,424*

ABSORBERS (MATERIALS)
Bistatic Scattering of Absorbing Materials from 30 to 1000 MHz.
PB95-150934 *01,891*

ABSORPTANCE
Optical Performance of Commercial Windows.
PB95-208757 *00,392*

ABSORPTION
NIR-Spectroscopic Investigation of Water Sorption Characteristics of Dental Resins and Composites.
PB95-151171 *00,189*

Energy Dependences of Absorption in Beryllium Windows and Argon Gas.
PB96-102124 *04,020*

ABSORPTION CROSS SECTIONS
Scaling of the Nonlinear Optical Cross Sections of GaAs-AlGaAs Multiple Quantum-Well Hetero n-i-p-i's.
PB96-102793 *02,183*

Temperature Dependence of the Gas and Liquid Phase Ultraviolet Absorption Cross Sections of HCFC-123 (CF3CHCl2) and HCFC-142b (CH3CF2Cl).
PB96-201033 *03,298*

Temperature Dependent Ultraviolet Absorption Cross Sections of Propylene, Methylacetylene and Vinylacetylene.
PB96-204177 *01,169*

ABSORPTION SPECTRA
Memory Function Approach to the Shape of Pressure Broadened Molecular Bands.
PB95-152930 *00,944*

Intermediate Coupling in L2-L3 Core Excitons of MgO, Al2O3, and SiO2.
PB96-158043 04,079

ABSORPTION SPECTROMETRY
Spectral Interference in the Determination of Arsenic in High-Purity Lead and Lead-Base Alloys Using Electrothermal Atomic Absorption Spectrometry and Zeeman-Effect Background Correction.
PB96-112099 00,614

ABSORPTION SPECTROSCOPY
Application of a Novel Slurry Furnace AAS Protocol for Rapid Assessment of Lead Environmental Contamination.
PB96-112354 02,526

ABSORPTIVITY
Molar Absorptivities of Bilirubin (NIST SRM 916A) and Its Neutral and Alkaline Azopigments.
PB94-211042 03,456

ABSTRACTS
Abstract and Index Collection in the Research Information Center of the National Institute of Standards and Technology.
PB94-152204 02,744

Annual Conference on Fire Research: Book of Abstracts, October 17-20, 1994.
PB95-104964 01,376

Publication and Presentation Abstracts, 1993. (Published by Paffenbarger Research Center and Center of Excellence for Materials Science Research).
PB95-153052 03,562

Abstract and Index Collection in the Research Information Center of the National Institute of Standards and Technology.
PB95-232633 02,741

Publications and Presentation Abstracts, 1995. (Published by Paffenbarger Research Center and Center of Excellence for Materials Science Research).
PB96-119250 03,568

Publication and Presentation Abstracts, 1995.
PB96-164082 03,576

Publication and Presentation Abstracts, 1994.
PB96-176623 03,577

Publication and Presentation Abstracts, 1996.
PB97-122238 03,585

ABUNDANCE
New IUPAC Guidelines for the Reporting of Stable Hydrogen, Carbon, and Oxygen Isotope-Ratio Data. Letter to the Editor.
PB95-261962 01,058

Accurate Measurements of the Local Deuterium Abundance from HST Spectra.
PB96-200621 00,110

AC STARK EFFECT
Configuration-Dependent AC Stark Shifts in Calcium.
PB96-157995 04,363

AC STARK SHIFT
RIS Measurements of the AC Stark Shift.
PB96-158035 04,078

AC STARK SHIFTS
RIS Measurement of AC Stark Shifts and Photoionization Cross Sections in Calcium.
PB96-157953 04,073

ACCELERATED LIFE TESTS
Macro- and Microreactions in Mechanical-Impact Tests of Aluminum Alloys.
PB95-107348 03,340

ACCELERATED TESTING
Assessing MOS Gate Oxide Reliability on Wafer Level with Ramped/Constant Voltage and Current Stress.
PB96-180112 04,115

ACCELERATING VOLTAGE
Modification of a Commercial SEM with a Computer Controlled Cathode Stabilized Power Supply.
PB96-201066 04,129

ACCELERATOR FACILITIES
Overview of a Radiation Accident at an Industrial Accelerator Facility.
PB97-122485 02,612

ACCELERATOR MASS SPECTROMETRY
Factorial Design Techniques Applied to Optimization of AMS Graphite Target Preparation.
PB95-151197 00,584

Comparative Study of Fe-C Bead and Graphite Target Performance with the National Ocean Sciences AMS (NOSAMS) Facility Recombinator Ion Source.
PB95-175790 00,693

ACCELERATOR MASS SPECTROSCOPY
36Cl/Cl Accelerator-Mass-Spectrometry Standards: Verification of Their Serial-Dilution-Solution Preparations by Radioactivity Measurements.
PB94-140563 00,524

ACCELEROMETERS
Testing the Sensitivity of Accelerometers Using Mechanical Shock Pulses Under NIST Special Publication 250 Test No. 24040S.
PB96-179544 02,683

ACCEPTANCE DIAGRAMS
Joy of Acceptance Diagrams.
PB94-200433 03,828

Transmission Properties of Short Curved Neutron Guides. Part 1. Acceptance Diagram Analysis and Calculations.
PB96-102199 04,021

ACCESS CONTROL
Computer Security Management and Planning in the U.S. Federal Government.
PB95-163432 01,596

Guidance to Federal Agencies on the Use of Trusted Systems.
PB95-163440 01,597

Functional Security Criteria for Distributed Systems.
PB96-123492 01,607

Distributed Communication Methods and Role-Based Access Control for Use in Health Care Applications.
PB96-183165 01,508

TMACH Experiment Phase 1. Preliminary Developmental Evaluation.
PB96-195318 01,618

ACCESS TO INFORMATION
Global Information Infrastructure: Agenda for Cooperation.
PB95-178604 01,482

ACCESSIBILITY
Electronic Access to Standards on the Information Highway.
PB96-131578 01,494

ACCIDENT INVESTIGATIONS
Ashland Tank Collapse Investigation.
PB95-126314 02,481

Ashland Tank-Collapse Investigation: Closure by Authors.
PB95-126322 02,482

Radiation Accident at an Industrial Accelerator Facility.
PB95-140117 02,575

Overview of a Radiation Accident at an Industrial Accelerator Facility.
PB97-122485 02,612

ACCOUNTING
Manager's Guide for Monitoring Data Integrity in Financial Systems.
PB96-165915 00,003

ACCREDITATION
NVLAP Procedures U.S. Code of Federal Regulations. Title 15, Subtitle A, Chapter 2, Part 7. (Effective December 1984; Amended September 1990).
PB94-160850 02,627

Program Handbook: Requirements for Obtaining NIST Approval/Recognition of a Laboratory Accreditation Body Under P.L. 101-592. The Fastener Quality Act.
PB94-210143 02,859

Survey on the Implementation of ISO/IEC Guide 25 by National Laboratory Accreditation Programs.
PB94-210150 00,479

National Voluntary Laboratory Accreditation Program: Energy Efficient Lighting Products.
PB94-219060 02,642

Should NIST Accredit U.S. Calibration Laboratories.
PB95-107280 02,646

National Voluntary Laboratory Accreditation Program (NVLAP): Commercial Products Testing.
PB95-267944 02,671

Laboratory Accreditation for Testing Energy Efficient Lighting.
PB96-122932 00,270

Proceedings of the Open Forum on Laboratory Accreditation at the National Institute of Standards and Technology, October 13, 1995.
PB96-210141 02,686

State Weights and Measures Laboratories: Program Handbook.
PB96-214705 02,687

ACCURACY
Numeric Data Distribution: The Vital Role of Data Exchange in Today's World.
N95-15937/2 02,622

Utc Dissemination to the Real-Time User.
N19960042622 01,521

Detector-Based Candela Scale and Related Photometric Calibration Procedures at NIST.
PB95-161949 04,273

Estimation of Measurement Uncertainty of Small Circular Features Measured by CMMs.
PB95-267928 02,918

Error-Bounding in Level-Index Computer Arithmetic.
PB96-109582 01,742

Progress Toward Accurate Metrology Using Atomic Force Microscopy.
PB96-146774 02,417

New Concepts of Precision Dimensional Measurement for Modern Manufacturing.
PB96-160684 02,924

NIST Frequency Measurement Service.
PB96-200662 01,561

ACETALDEHYDE
Fundamental Torsion Band in Acetaldehyde.
PB94-212834 00,840

ACETALS
Ring-Opening Dental Resin Systems Based on Cyclic Acetals.
PB95-162251 00,162

ACETONE CATIONS
Kinetics and Mechanism of the Collision-Activated Dissociation of the Acetone Cation.
PB94-216462 00,859

ACETONITRILE
Methyl Torsional Levels of Solid Acetonitrile (CH3CN): A Neutron Scattering Study.
PB95-151015 00,926

ACETYLENE
Spectroscopic Constants for the 2.5 and 3.0 micrometer Bands of Acetylene.
PB94-213071 00,847

Self-, N2- and Ar-Broadening and Line Mixing in HCN and C2H2.
PB95-108445 00,876

Decoupling in the Line Mixing of Acetylene Infrared Q Branches.
PB95-108452 00,877

Laboratory Studies of Low-Temperature Reactions of C2H with C2H2 and Implications for Atmospheric Models of Titan.
PB95-108726 00,690

Novel Polydiacetylenes Derived from Liquid Crystalline Monomers.
PB95-140125 01,235

ACETYLENE COMPLEXES
Rotational Spectrum and Structure of a Weakly Bound Complex of Ketene and Acetylene.
PB95-126140 00,896

ACETYLENE RADICALS
Kinetics of the Reaction C2H + O2 from 193 to 350 K Using Laser Flash Kinetic Infrared Absorption Spectroscopy.
PB95-203055 01,043

ACETYLENES
Vibrational Spectra of Molecular Ions Isolated in Solid Neon: HCCH+ and HCC-. (Reannouncement with New Availability Information).
AD-A253 551/6 00,707

ACID-BASE EQUILIBRIUM
Contact Electrification Induced by Monolayer Modification of a Surface and Relation to Acid-Base Interactions.
PB94-185378 03,034

ACID BONDED REACTION CEMENTS
Development of an Adhesive Bonding System.
PB94-199056 00,145

Polymeric Calcium Phosphate Cements Derived from Poly(methyl vinyl ether-maleic acid).
PB96-164264 00,180

ACID GAS PRODUCTION
Acid Gas Production in Inhibited Diffusion Flames.
PB95-180576 01,390

ACIDIFICATION
Procedure for the Study of Acidic Calcium Phosphate Precursor Phases in Enamel Mineral Formation.
PB95-164448 03,564

ACIDITY
Carbon Acidities of Aromatic Compounds. 1. Effects of In-Ring Aza and External Electron-Withdrawing Groups.
PB94-216595 00,860

ACOUSTIC ABSORPTION
Absorption of Ultrasonic Waves in Air at High Frequencies (10-20 MHz).
PB94-199007 04,182

Absorption of Sound in Gases between 10 and 25 MHz: Argon.
PB94-199015 04,183

ACOUSTIC DATA
Properties of Working Fluids for Thermoacoustic Refrigerators.
AD-A297 420/2 04,864

ACOUSTIC DETECTION
Correlations between Electrical and Acoustic Detection of Partial Discharge in Liquids and Implications for Continuous Data Recording.
PB96-204490 02,248

ACOUSTIC EMISSION
High-Sensitivity Acoustic Emission Sensor/Preamplifier Subsystems.
PB95-125704 02,900

Thermoacoustic Technique for Determining the Interface and/or Interply Strength in Polymeric Composites.
PB95-161824 03,158

Acoustic Emission of Structural Materials Exposed to Open Flames.
PB95-164810 00,296

ACOUSTIC EMISSIONS
Interaction of Rayleigh Waves with a Rib Attached to a Plate.
PB94-199023 04,184

Early Detection of Room Fires Through Acoustic Emission. (NIST Reprint).
PB95-180311 00,298

ACOUSTIC MEASUREMENT
Noncontact Ultrasonic Inspection of Train Rails for Stress.
PB95-162673 04,851

National Voluntary Laboratory Accreditation Program Acoustical Testing Services.
PB95-182234 04,188

ACOUSTIC MEASUREMENTS
Speed-of-Sound Measurements in Liquid and Gaseous Air.
PB95-151957 *04,186*

ACOUSTIC RESONATORS
Speed-of-Sound Measurements in Liquid and Gaseous Air.
PB95-151957 *04,186*

ACOUSTIC SCATTERING
Reconstructing Stratified Fluid Flow from Reciprocal Scattering Measurements.
PB95-107256 *04,202*

ACOUSTIC TESTING
National Voluntary Laboratory Accreditation Program Acoustical Testing Services.
PB95-182234 *04,188*

ACOUSTIC VELOCITY
Speed-of-Sound Measurements in Liquid and Gaseous Air.
PB95-151957 *04,186*

Thermodynamic Properties of Two Gaseous Halogenated Ethers from Speed-of-Sound Measurements: Difluoromethoxy-Difluoromethane and 2-Difluoromethoxy-1,1,1-Trifluoroethane.
PB96-102413 *04,189*

ACOUSTICAL INSTRUMENTS
Determination of Acoustic Center Correction for Type LS2aP Condensor Microphones.
PB96-204508 *04,190*

ACOUSTICS
Determination of Sheet Steel Formability Using Wide Band Electromagnetic-Acoustic Transducers.
PB96-186036 *02,279*

Effect of Liftoff on Accuracu of Phase Velocity Measurements Made with Electromagnetic-Acoustic Transducers.
PB96-186044 *02,280*

Sensor System for Intelligent Processing of Hot-Rolled Steel.
PB96-186069 *03,373*

Well-Shielded EMAT for On-Line Ultrasonic Monitoring of GMA Welding.
PB96-186077 *02,879*

ACOUSTICS & SOUND
Electroacoustics for Characterization of Particulates and Suspensions. Proceedings of a Workshop. Held in Gaithersburg, Maryland on February 3-4, 1993.
PB94-112695 *00,725*

Absorption of Sound in Gases between 10 and 25 MHz: Argon.
PB94-199015 *04,183*

Interaction of Rayleigh Waves with a Rib Attached to a Plate.
PB94-199023 *04,184*

Benchmarks for the Evaluation of Speech Recognizers.
PB94-211539 *01,566*

Elastic Constants of Isotropic Cylinders Using Resonant Ultrasound.
PB94-211919 *04,497*

Examination of Objects Made of Wood Using Air-Coupled Ultrasound.
PB95-125712 *03,404*

Ultrasonic Measurement of Sheet Anisotropy and Formability.
PB95-153235 *03,213*

Electroacoustic Characterization of Particle Size and Zeta Potential in Moderately Concentrated Suspensions.
PB96-119425 *01,079*

Electrokinetic Sonic Analysis of Silicon Nitride Suspensions.
PB96-123575 *03,073*

Band-Limited, White Gaussian Noise Excitation for Reverberation Chambers and Applications to Radiated Susceptibility Testing.
PB96-165410 *01,960*

Ultrasound Power Measurement Techniques at NIST.
PB96-179569 *02,684*

Ultrasonic NDE of Sprayed Ceramic Coatings.
PB96-201157 *02,761*

Determination of Acoustic Center Correction for Type LS2aP Condensor Microphones.
PB96-204508 *04,190*

Transient Analysis of a Line-Focus Transducer Probing a Liquid/Solid Interface.
PB97-118681 *02,763*

Material Characterization By a Time-Resolved and Polarization-Sensitive Ultrasonic Technique.
PB97-122576 *02,764*

ACQUISITION
AutoBid 2.0: The Microcomputer System for Police Patrol Vehicle Selection.
PB96-154570 *04,871*

ACQUISITIONS
Federal Implementation Guideline for Electronic Data Interchange: ASC X12 003040 Transaction Set 838 Trading Partner Profile (Vendor Registration), Implementation Convention.
PB96-112651 *03,674*

ACRONYMS
Some Basics on Who's Who and What's What in Seismic Safety.
PB95-150926 *00,435*

ACRYLATE
Synthesis of Hybrid Organic-Inorganic Materials from Interpenetrating Polymer Network Chemistry.
PB96-180054 *02,994*

ACRYLATES
Facile Synthesis of Novel Fluorinated Multifunctional Acrylates.
PB94-198389 *01,207*

ACRYLIC RESINS
Preparation and Characterization of Cyclopolymerizable Resin Formulations.
PB96-146840 *01,285*

ACRYLONITRILE POLYMERS
Acrylonitrile-Butadiene-Styrene (ABS) Plastic Drain, Waste, and Vent Pipe and Fittings.
AD-A310 724/0 *00,327*

ACTIS DATA BASE
Tribological Data: Needs and Opportunities.
PB95-140596 *03,237*

ACTIVATION
Evaluation of Sprinkler Activation Prediction Methods.
PB96-141056 *00,304*

ACTIVATION ANALYSIS
Local Area Networks in NAA: Advantages and Pitfalls.
PB94-172095 *00,527*

High-Sensitivity Determination of Iodine Isotopic Ratios by Thermal and Fast Neutron Activation.
PB94-213386 *00,555*

Neutron Capture Prompt Gamma-Ray Activation Analysis at the NIST Cold Neutron Research Facility.
PB94-213394 *00,556*

Scattering and Absorption Effects in Neutron Beam Activation Analysis Experiments.
PB94-216140 *00,557*

Effects of Target Shape and Neutron Scattering on Element Sensitivities for Neutron-Capture Prompt Gamma-ray Activation Analysis.
PB94-216157 *00,558*

Cold Neutron Prompt Gamma Activation Analysis at NIST: A Progress Report.
PB95-175964 *00,602*

Neutron Scattering by Hydrogen in Cold Neutron Prompt Gamma-Activation Analysis.
PB95-175972 *00,603*

Measuring Hydrogen by Cold-Neutron Prompt-Gamma Activation Analysis.
PB96-111877 *00,612*

Effects of Target Temperature on Analytical Sensitivities of Cold-Neutron Capture Prompt gamma-ray Activation Analysis.
PB96-112131 *00,616*

SUM and MEAN: Standard Programs for Activation Analysis.
PB96-112149 *00,617*

ACTIVE CONTROL
Modified Optimal Algorithm for Active Structural Control.
PB96-165949 *00,472*

ACTIVE SITE IONICITY
Active Site Ionicity and the Mechanism of Carbonic Anhydrase.
PB94-212974 *00,843*

ACTIVITY COEFFICIENT
Model for Calculating Virial Coefficients of Natural Gas Hydrocarbons with Impurities.
PB96-156047 *04,064*

ACUTE EXPOSURE
Documentation for Immediately Dangerous to Life or Health Concentrations (IDLHs).
PB94-195047 *03,602*

ADA PROGRAMMING LANGUAGE
Ada Compiler Validation Summary Report: Certificate Number: 931029S1.11330, Digital Equipment Corporation, DEC Ada for DEC OSF/1 AXP Systems, Version 3.1, DEC 3000 Model 400 AXP Workstation, DEC 3000 Model 400 AXP Workstation.
AD-A274 872/1 *01,639*

Ada Compiler Validation Summary Report: Certificate Number: 931217S1.11336 Control Data Systems, Inc. NOS/VE Ada, Version 1.4 Cyber 180-930-31 => Cyber 180-930-31.
AD-A275 977/7 *01,640*

Ada Compiler Validation Summary Report. Certificate Number: 931119S1.11332, DDC-I, Inc. DACS MIPS R3000 Bare Ada Cross Compiler System, Version 4.7.1 Sun SPARCstation IPX => DACS Sun SPARC/SunOS to MIPS R3000 Bare Instruction Set Architecture Simulator, Version 4.7.1.
AD-A276 181/5 *01,641*

Ada Compiler Validation Summary Report: Certificate Number: 931119S1.11331 DDC-I, Inc. DACS Sun SPARC/SunOS to 80386 PM Bare Ada Cross Compiler System, Version 4.6.4 Sun Sparcstation 1+ => Bare Board iSBC 386/116.
AD-A276 283/9 *01,642*

Ada Compiler Validation Summary Report. Certificate Number: 930927S1.11328 Green Hills Software C Ada, Version 1.1 ZENY 386 => ZENY 386.
AD-A277 981/7 *01,643*

Ada Compiler Validation Summary Report: Certificate Number: 940325S1.11348 DDC-I, DACS Sun SPARC/Solaris to 80386 PM Bare Ada Cross Compiler System, Version 4.6.4 Sun SPARCclassic => Intel iSBC 386/116 (Bare Machine).
AD-A279 642/3 *01,644*

Ada Compiler Validation Summary Report: Certificate Number: 940325S1.11341 DDC-I, DACS Sun SPARC/SunOS to 80186 Bare Ada Cross Compiler System, Version 4.6.4 Sun SPARCstation IPX => Intel iSBC 186/100 (Bare Machine).
AD-A279 643/1 *01,645*

Ada Compiler Validation Summary Report: Certificate Number: 940325S1.11349 DDC-I, DACS Sun SPARC/Solaris to 80386 PM Bare Ada Cross Compiler System with Rate Monotonic Scheduling, Version 4.6.4 Sun SPARCclassic => Intel iSBC 386/116 (Bare Machine).
AD-A279 644/9 *01,646*

Ada Compiler Validation Summary Report: Certificate Number: 940325S1.11354 DDC-I, DACS Sun SPARC/Solaris Native Ada Compiler System, Version 4.6.2 Sun SPARCclassic => Sun SPARCclassic.
AD-A279 645/6 *01,647*

Ada Compiler Validation Summary Report: Certificate Number: 940325S1.11346 DDC-I, DACS Sun SPARC/SunOS to 680x0 Bare Ada Cross Compiler System (BASIC MODE), Version 4.6.9 Sun SPARCstation IPX => Lynwood j435TU (68030) (Bare Machine).
AD-A279 646/4 *01,648*

Ada Compiler Validation Summary Report: Certificate Number: 940325S1.11343 DDC-I, DACS Sun SPARC/Solaris to 80186 Bare Ada Cross Compiler System, Version 4.6.4 Sun SPARCclassic => Intel iSBC 186/100 (Bare Machine).
AD-A279 757/9 *01,649*

Ada Compiler Validation Summary Report: Certificate Number: 940325S1.11344 DDC-I, DACS Sun SPARC/Solaris to 80186 Bare Ada Cross Compiler System with Rate Monotonic Scheduling, Version 4.6.4 Sun SPARCclassic => Intel iSBC 186/100 (Bare Machine).
AD-A279 758/7 *01,650*

Ada Compiler Validation Summary Report: Certificate Number: 940325S1.11347 DDC-I, DACS Sun SPARC/SunOS to 680x0 Bare Ada Cross Compiler System (SECURE MODE), Version 4.6.9 Sun SPARCstation IPX => Lynwood j435TU (68030) (Bare Machine).
AD-A279 778/5 *01,651*

Ada Compiler Validation Summary Report: Certificate Number: 940325S1.11342 DDC-I, DACS Sun SPARC/SunOS to 80186 Bare Ada Cross Compiler System with Rate Monotonic Scheduling Version 4.6.4 Sun SPARCstation IPX => Intel iSBC 186/100 (Bare Machine).
AD-A279 779/3 *01,652*

Ada Compiler Validation Summary Report: Certificate Number: 940325S1.11351 DDC-I, DACS Sun SPARC/SunOS to Pentium PM Bare Ada Cross Compiler System with Rate Monotonic Scheduling, Version 4.6.4 Sun SPARCstation IPX => Intel Pentium (operated as Bare Machine) based in Xpress Desktop (Intel product number: XBASE6E4F-B).
AD-A279 804/9 *01,653*

Ada Compiler Validation Summary Report: Certificate Number: 940325S1.11353 DDC-I, DACS Sun SPARC/Solaris to Pentium PM Bare Ada Cross Compiler System with Rate Monotonic Scheduling, Version 4.6.4 Sun SPARCclassic => Intel Pentium (operated as Bare Machine) based in Xpress Desktop (Intel product number: XBASE6E4F-B).
AD-A279 805/6 *01,654*

Ada Compiler Validation Summary Report: Certificate Number: 940325S1.11350 DDC-I, DACS Sun SPARC/SunOS to Pentium PM Bare Ada Cross Compiler System, Version 4.6.4 Sun SPARCstation IPX => Intel Pentium (Operated as Bare Machine) Based in Xpress Desktop (Intel Product Number: XBASE6E4F-B).
AD-A279 864/3 *01,655*

Ada Compiler Validation Summary Report: Certificate Number 940325S1.11345 DDC-I. DACS Sun SPARC/SunOS to 680x0 Bare Ada Cross Compiler System, Version 4.6.9 Sun SPARCstation IPX => Motorola MVME143 68030/68882 (Bare Machine).
AD-A280 145/4 *01,656*

Ada Compiler Validation Summary Report: Certificate Number: 940325S1.11352 DDC-I DACS Sun SPARC/Solaries to Pentium PM Bare Ada Cross Compiler System, Version 4.6.4 Sun SPARCclassic => Intel Pentium (Operated as Bare Machine) Based in Xpress Desktop (Intel Product Number: XBASE6E4F-B).
AD-A280 295/7 *01,657*

Ada Compiler Validation Summary Report: Certificate Number 940902S1.11377 UNISYS Corporation. IntegrAda for Windows NT, Version 1.0. Intel Deskside Server with Intel 80486DX266 => Intel Deskside Server with Intel 80486DX266.
AD-A288 571/3 *01,658*

Ada Compiler Validation Summary Report: Certificate Number 940902S1.11376. UNISYS Corporation IntegrAda for Windows NT, Version 1.0. Intel Deskside Server for Intel Pentium 60 MHz =>. Intel Deskside Server with Intel Pentium 60 MHz.
AD-A288 572/1 *01,659*

Ada Compiler Validation Summary Report: Certificate Number 94101251.11379 TISOFT, Inc. Green Hills Optimizing Ada Compileer, Version 1.8.7 with PATCK ID 1 COMPAQ ProLiiant 2000 Model 55/66 => COMPAQ ProLiant 2000 Model 5/66.
AD-A288 573/9 *01,660*

Ada Complier Validation Summary Report: Certificate Number: 940929S1.11378. Digital Equipment Corporation DEC Ada for DEC OSF/1 AXP Systems, Version 3.2; DEC 3000 Model 400 AXP Workstation => DEC 3000 Model 400 AXP Workstation.
AD-A288 574/7 *01,661*

Ada Compiler Validation Summary Report. Certificate Number 941117S1.11380. Electronic Data Systems Corp. Compiler: OC Systems Legacy Ada/370, Release 1.4.1 (without optimization).
AD-A289 895/5 *01,662*

ADA Compiler Validation Summary Report, VC Number 950303S1.11381. Digital Equipment Corporation - Compiler Name: DEC Ada for OpenVMS Alpha Systems, Version 3.2.
AD-A293 709/2 *01,663*

Ada Compiler Validation Summary Report, VC No. 950609S1.11390 Digital Equipment Corporation - Compiler Name: DEC Ada Version 3.2 for OpenVMS VAX Systems.
AD-A296 794/1 *01,664*

ADA; Category: Software Standard; Subcategory: Programming Language.
FIPS PUB 119-1 *01,667*

Validated Products List (Cobol, Fortran, ADA, Pascal, MUMPS, SQL).
PB94-937300 *01,700*

Validated Products List (Cobol, Fortran, ADA, Pascal, MUMPS, SQL).
PB95-937300 *01,738*

ADAPTERS

Single-Port Technique for Adaptor Efficiency Evaluation.
PB96-176441 *02,088*

ADENOSINE MONOPHOSPHATES

Thermochemistry of the Reactions between Adenosine, Adenosine 5'-monophosphate, Inosine, and Inosine 5'-monophosphate; the Conversion of L-histidine to (Urocanic Acid+Ammonia).
PB94-213113 *03,460*

ADHESION

Interaction of Some Coupling Agents and Organic Compounds with Hydroxyapatite: Hydrogen Bonding, Adsorption and Adhesion.
PB94-172616 *00,140*

Surface Forces and Adhesion between Dissimilar Materials Measured in Various Environments.
PB94-172970 *03,033*

Peeling a Polymer from a Surface or from a Line.
PB94-199809 *01,213*

Effects of Adhesive Thickness, Open Time, and Surface Cleanness on the Peel Strength of Adhesive-Bonded Seams of EPDM Rubber Roofing Membrane.
PB95-151338 *00,372*

Diffusion of Water along 'Closed' Mica Interfaces.
PB96-180039 *02,993*

Pressurized Internal Lenticular Cracks at Healed Mica Interfaces.
PB96-180252 *02,997*

Adhesion, Contact Electrification, and Acid-Base Properties of Surfaces.
PB96-204425 *03,693*

ADHESIVE BONDING

Clinical Perspective on Dentin Adhesives.
PB94-211240 *00,146*

Micromechanics of Fracture in Rubber-Toughened Epoxies.
PB94-212222 *03,011*

Modified Surface-Active Monomers for Adhesive Bonding to Dentin.
PB95-151163 *00,158*

Characteristics of Adhesive-Bonded Seams Sampled from EPDM Roof Membranes.
PB95-162491 *00,377*

Pulse-Echo Ultrasonic Evaluation of the Integrity of Seams of Single-Ply Roof Membranes.
PB95-163804 *00,381*

Polymerization Initiation by N-p-Tolylglycine: Free-Radical Reactions Studied by Pulse and Steady-State Radiolysis.
PB95-180014 *01,269*

New Surface-Active Comonomer for Adhesive Bonding.
PB96-204052 *03,579*

ADHESIVE TAPES

Performance of Tape-Bonded Seams of EPDM Membranes: Comparison of the Peel Creep-Rupture Response of Tape-Bonded and Liquid-Adhesive-Bonded Seams.
PB96-183249 *03,012*

ADHESIVES

Adhesion of Composites to Dentin and Enamel.
PB94-199049 *00,144*

Development of an Adhesive Bonding System.
PB94-199056 *00,145*

Modified Surface-Active Monomers for Adhesive Bonding to Dentin.
PB95-151163 *00,158*

ADIABATIC CALORIMETERS

High-Temperature Adiabatic Calorimeter for Constant-Volume Heat Capacity Measurements of Compressed Gases and Liquids.
PB95-168860 *00,989*

ADIABATIC CONDITIONS

Review of Flows Driven By Natural Convection in Adiabatic Shafts.
PB96-147897 *01,416*

ADMIXTURES

Interaction between Naphthalene Sulfonate and Silica Fume in Portland Cement Pastes.
PB94-199759 *01,315*

Study on the Reuse of Plastic Concrete Using Extended Set-Retarding Admixtures.
PB96-122130 *00,402*

Guide to a Format for Data on Chemical Admixtures in a Materials Property Database.
PB96-165394 *01,327*

Guide to a Format for Data on Chemical Admixtures in a Materials Property Database. (Reannouncement with new abstract).
PB96-186192 *01,328*

ADSORBATES

Vibrational Relaxation Measurements of Carbon Monoxide on Metal Clusters.
PB94-211810 *00,820*

Picosecond Measurement of Substrate-to-Adsorbate Energy Transfer: The Frustrated Translation of CO/Pt(111)--Translation.
PB95-126041 *00,895*

Time-Resolved Measurements of Energy Transfer at Surfaces.
PB95-141198 *00,913*

Time-Resolved Measurements of Energy Transfer at Surfaces.
PB95-153037 *00,947*

ADSORPTION

Adsorption of Low-Molecular-Weight Sodium Polyacrylate on Hydroxyapatite.
PB94-172608 *00,139*

Interaction of Some Coupling Agents and Organic Compounds with Hydroxyapatite: Hydrogen Bonding, Adsorption and Adhesion.
PB94-172616 *00,140*

Topological Influences on Polymer Adsorption and Desorption Dynamics.
PB94-212479 *01,227*

Characterization of the Adsorption-Fouling Layer Using Globular Proteins on Ultrafiltration Membranes.
PB94-212909 *00,842*

Characterization of Cytochrome c/Alkanethiolate Structures Prepared by Self-Assembly on Gold.
PB95-164638 *00,987*

Interaction of Chlorhexidine Digluconate with and Adsorption of Chlorhexidine on Hydroxyapatite.
PB95-175907 *03,566*

Water Adsorption at Polymer/Silicon Wafer Interfaces.
PB95-181178 *01,022*

Determination of Total Protein Adsorbed on Solid (Membrane) Surface by a Hydrolysis Technique: Single Protein Adsorption.
PB96-167093 *03,552*

Adsorption of Potassium N-phenylglycinate on Hydroxyapatite: Role of Solvents and Ionic Charge.
PB96-180161 *01,159*

ADV (ADVANCED DIGITAL VIDEO)

Report on the Workshop on Advanced Digital Video in the National Information Infrastructure. Held in Washington, D.C. on May 10-11, 1994.
PB95-103677 *01,472*

ADVANCED DIGITAL VIDEO

Report on the Workshop on Advanced Digital Video in the National Information Infrastructure. Held in Washington, D.C. on May 10-11, 1994.
PB95-103677 *01,472*

ADVANCED MATERIALS

NIST Workshop on Nanostructured Material (1st): Report of an Industrial Workshop Conducted by the National Institute of Standards and Technology. Held in Gaithersburg, Maryland on May 14-15, 1992.
PB94-218567 *02,973*

Control of Friction and Wear of Alpha-Alumina with a Composite Solid-Lubricant Coating.
PB95-125969 *03,225*

New Materials, Advanced Ceramics and Standards.
PB95-140208 *03,047*

Recent VAMAS Activity in Ceramics.
PB95-162681 *03,051*

Structural Ceramics Database. Topical Report, June 1989-May 1991.
PB95-203758 *03,060*

Room-Temperature Flexure Fixture for Advanced Ceramics.
PB95-210498 *03,061*

ADVANCED TECHNOLOGY

Opportunities for Innovation: Advanced Surface Engineering.
PB94-176666 *02,697*

ADVANCED TECHNOLOGY LABORATORY

Design of Technically Complex Facilities.
PB97-119101 *02,695*

AERODYNAMICS

Aerodynamic Phenomena in Stellar Atmospheres - A Bibliography.
AD-A278 521/0 *00,046*

AEROSOL GENERATORS

Experimental Optimization of Peak Shape with Application to Aerosol Generation.
PB94-185535 *00,501*

Ultrafine Combustion Aerosol Generator.
PB94-200300 *01,373*

AEROSOL SPECTROMETERS

Stochastic Modeling of a New Spectrometer.
PB96-157870 *04,068*

AEROSOLS

Global Climatic Effects of Aerosols: The AAAR Symposium.
PB95-108791 *00,122*

Radiometric Model of the Transmission Cell-Reciprocal Nephelometer.
PB95-150132 *00,124*

Controlled Nucleation in Aerosol Reactors for Supression of Agglomerate Formation.
PB95-151973 *00,672*

Measurement of the Uniformity of Particle Deposition of Filter Cassette Sampling in a Low Velocity Wind Tunnel.
PB95-163754 *02,549*

Sources of Urban Contemporary Carbon Aerosol.
PB95-175659 *02,551*

AEROSPACE

Light-Weight Alloys for Aerospace Applications II.
PB96-190244 *03,375*

AEROSPACE ENVIRONMENTS

In-Space Welding: Visions and Realities.
PB95-163234 *04,830*

AEROSPACE VEHICLES

Combustion of a Polymer (PMMA) Sphere in Microgravity.
N96-15569/2 *01,354*

AFFINITY CHROMATOGRAPHY

Affinity Chromatography on Inorganic Support Materials.
PB95-163820 *03,467*

AGAROSE

Small Angle Neutron Scattering Studies of Structural Characteristics of Argarose Gels.
PB96-112305 *03,475*

AGGLOMERATION

Controlled Nucleation in Aerosol Reactors for Supression of Agglomerate Formation.
PB95-151973 *00,672*

AGGREGATES

Digital Simulation of the Aggregate-Cement Paste Interfacial Zone in Concrete.
PB95-125993 *00,363*

AGING (MATERIALS)

Aging in Glasses Subjected to Large Stresses and Deformations.
PB95-107041 *03,235*

Suggestions for a Logically-Consistent Structure for Service Life Prediction Standards.
PB95-125795 *00,358*

Aging Effects on XRF Measurements of Solder Coatings.
PB95-140927 *03,123*

Nonstationary Behavior of Partial Discharge during Insulation Aging.
PB95-163580 *01,902*

Partial Discharge: Induced Aging of Cast Epoxies and Related Nonstationary Behavior of the Discharge Statistics.
PB95-163598 *01,903*

Effect of Environmentally Exposures on the Properties of Polyisocyanurate Foam Insulation: Thermal Conductivity Measurements.
PB95-181210 *00,388*

Nonstationary Behaviour of Partial Discharge during Discharge Induced Ageing of Dielectrics.
PB96-103114 *01,922*

AGING TESTS (MATERIALS)

Influence of Physical Aging on the Yield Response of Model DGEBA + Poly(propylene oxide) Epoxy Glasses.
PB95-126363 *03,381*

Volume Recovery in Epoxy Glasses Subjected to Torsional Deformations: The Question of Rejuvenation.
PB95-140018 *03,382*

Torsional Relaxation and Volume Response during Physical Aging in Epoxy Glasses Subjected to Large Torsional Deformations.
PB95-140026 *03,383*

Using Torsional Dilatometry to Measure the Effects of Deformations on Physical Aging.
PB95-140901 *03,384*

Research on Methods for Determining Optical Disk Media Life Expectancy Estimates.
PB96-160304 *01,633*

AGREEMENTS

Consensus Process in Standards Development.
PB96-179502 *00,136*

AHARONOV-BOHM EFFECT

Roles of Local Classical Acceleration and Spatial Separation in the Neutral Particle Analogs of the Aharonov-Bohm Phases.
PB95-202362 *03,976*

AIR
Absorption of Ultrasonic Waves in Air at High Frequencies (10-20 MHz).
PB94-199007 *04,182*

Speed-of-Sound Measurements in Liquid and Gaseous Air.
PB95-151957 *04,186*

Molar Heat Capacity at Constant Volume for Air from 67 to 300 K at Pressures to 35 MPa.
PB96-163738 *00,515*

AIR CHANGE EFFECTIVENESS
Air Change Effectiveness Measurements in Two Modern Office Buildings.
PB94-185766 *00,243*

AIR CIRCULATION
Assessing Ventilation Effectiveness in Mechanically Ventilated Office Buildings.
PB95-162079 *00,255*

Measurements of Outdoor Air Distribution in an Office Building.
PB95-210944 *00,264*

Improving the Evaluation of Building Ventilation.
PB96-138508 *00,271*

AIR CONDITIONING
Theoretical Evaluation of the Vapor Compression Cycle with a Liquid-Line/Suction-Line Heat Exchanger, Economizer, and Ejector.
PB95-216917 *02,607*

AIR CONDITIONING EQUIPMENT
Role of R22 in Refrigerating and Air Conditioning Equipment.
PB94-199783 *03,253*

Simple Method of Composition Shifting with a Distillation Column for a Heat Pump Employing a Zeotropic Refrigerant Mixture.
PB95-255824 *02,603*

AIR FLOW
Air Flow in the Boundary Layer of an Elliptic Cylinder.
AD-A297 391/5 *04,194*

CONTAM93 User Manual.
PB94-164381 *02,536*

CONTAM88 Building Input Files for Multi-Zone Airflow and Contaminant Dispersal Modeling.
PB94-194388 *02,537*

Combined Buoyancy- and Pressure-Driven Flow Through a Shallow, Horizontal, Circular Vent.
PB94-210077 *00,344*

Field Measurements of Ventilation and Ventilation Effectiveness in an Office/Library Building.
PB95-108833 *00,247*

Simulating Smoke Movement through Long Vertical Shafts in Zone-Type Compartment Fire Models.
PB95-143152 *00,368*

Method of Predicting Smoke Movement in Atria with Application to Smoke Management.
PB95-154746 *00,376*

Fire and Smoke Control: An Historical Perspective.
PB95-175808 *00,202*

Application of a Multizone Airflow and Contaminant Dispersal Model to Indoor Air Quality Control in Residential Buildings.
PB95-180238 *02,555*

Computer Simulations of Airflow and Radon Transport in Four Large Buildings.
PB95-220422 *02,557*

New Mass Transport Elements and Components for the NIST IAQ Model.
PB95-255899 *02,558*

Indoor Air Quality Impacts of Residential HVAC Systems Phase II.B Report: IAQ Control Retrofit Simulations and Analysis.
PB96-106877 *02,559*

Study of Ventilation Measurement in an Office Building.
PB96-155593 *00,274*

Calculating Combined Buoyancy- and Pressure-Driven Flow Through a Shallow, Horizontal, Circular Vent; Application to Problem of Steady Burning in a Ceiling-Vented Enclosure.
PB96-164108 *00,409*

Combined Buoyancy and Pressure-Driven Flow Through a Shallow, Horizontal, Circular Vent.
PB96-164116 *00,410*

NASA Fire Detector Study.
PB96-183108 *01,423*

CONTAM94: A Multizone Airflow and Contaminant Dispersal Model with a Graphic User Interface.
PB97-113203 *02,570*

AIR FORCE TRAINING
Robotics Application to Highway Transportation. Volume 1. Final Report.
PB95-203790 *03,654*

AIR INFILTRATION
Ventilation Effectiveness Measurements in Two Modern Office Buildings.
PB95-176012 *02,553*

AIR POLLUTION
Modulation of Fossil Fuel Production by Global Temperature Variations, 2.
PB94-146636 *02,533*

Rare-Earth Isotopes as Tracers of Particulate Emissions: An Urban Scale Test.
PB94-161635 *02,535*

Global Climatic Effects of Aerosols: The AAAR Symposium.
PB95-108791 *00,122*

Atmospheric Reactivity of alpha-Methyl-Tetrahydrofuran.
PB95-163705 *02,548*

Airborne Asbestos Analysis: National Voluntary Laboratory Accreditation Program.
PB96-147392 *02,566*

AIR POLLUTION ABATEMENT
Simultaneous Visual and Calorimetric Measurements of R11, R123, and R123/Alkylbenzene Nucleate Flow Boiling.
PB94-172426 *03,251*

Chemical and Microbiological Problems Associated with Research on the Biodesulfurization of Coal.
PB95-140950 *02,484*

Microbial Degradation of Polysulfides and Insights into Their Possible Occurrence in Coal.
PB95-163374 *02,488*

AIR POLLUTION CONTROL
Sulfur Dioxide Capture in the Combustion of Mixtures of Lime, Refuse-Derived Fuel, and Coal.
PB94-155587 *02,534*

Membrane Gas Separation for a Fluidized-Bed Incinerator.
PB95-169041 *02,550*

Multizone Modeling of Three Residential Indoor Air Quality Control Options.
PB96-146659 *02,565*

AIR POLLUTION DETECTION
Proficiency Tests for the NIST Airborne Asbestos Program, 1990.
PB94-188836 *00,535*

Proficiency Tests for the NIST Airborne Asbestos Program - 1991.
PB94-193828 *00,537*

Proficiency Tests for the NIST Airborne Asbestos Program - 1992.
PB94-194362 *00,539*

AIR POLLUTION DISPERSION
New Mass Transport Elements and Components for the NIST IAQ Model.
PB95-255899 *02,558*

Carbon Monoxide Dispersion in Residential Buildings: Literature Review and Technical Analysis.
PB97-114227 *02,571*

AIR POLLUTION MONITORING
Environmental Evaluation of a New Federal Office Building.
PB94-199874 *02,538*

Limits of CO2 Monitoring in Determining Ventilation Rates.
PB95-176004 *02,552*

Indoor Air Quality Impacts of Residential HVAC Systems. Phase 2.A Report: Baseline and Preliminary Simulations.
PB95-178893 *02,554*

NIST Workshop on Gas Sensors: Strategies for Future Technologies. Proceedings of a Workshop. Held in Gaithersburg, Maryland on September 8-9, 1993.
PB95-210225 *00,507*

Indoor Air Quality Impacts of Residential HVAC Systems Phase II.B Report: IAQ Control Retrofit Simulations and Analysis.
PB96-106877 *02,559*

EMISS: A Program for Estimating Local Air Pollution Emission Factors Related to Energy Use in Buildings: User's Guide and Reference Manual.
PB96-109566 *02,560*

Few Caveats on Carbon Dioxide Monitoring.
PB96-122650 *02,562*

Relationship between Indoor Air Quality and Carbon Dioxide.
PB97-111249 *02,569*

Issues in the Field Measurement of VOC Emission Rates.
PB97-118806 *02,573*

AIR POLLUTION SAMPLING
Ground-Based Smoke Sampling Techniques Training Course and Collaborative Local Smoke Sampling in Saudi Arabia.
PB94-143542 *02,532*

Standards for Atmospheric Measurements.
PB95-163622 *02,547*

Measurement of the Uniformity of Particle Deposition of Filter Cassette Sampling in a Low Velocity Wind Tunnel.
PB95-163754 *02,549*

Measurements of Indoor Pollutant Emissions from EPA Phase II Wood Stoves.
PB95-198735 *02,556*

Radiocarbon Measurements of Atmospheric Volatile Organic Compounds: Quantifying the Biogenic Contribution.
PB97-122352 *02,574*

AIR POLLUTION SOURCES
Measurement and Determination of Radon Source Potential: A Literature Review.
PB94-165602 *02,576*

Sources of Urban Contemporary Carbon Aerosol.
PB95-175659 *02,551*

Distinguishing the Contributions of Residential Wood Combustion and Mobile Source Emissions Using Relative Concentrations of Dimethylphenanthrene Isomers.
PB96-135124 *02,563*

AIR QUALITY
Manual for Ventilation Assessment in Mechanically Ventilated Commercial Buildings.
PB94-145653 *00,239*

Environmental Evaluation of a New Federal Office Building.
PB94-199874 *02,538*

Ventilation Rates in Office Buildings.
PB95-108825 *02,539*

Application of a Multizone Airflow and Contaminant Dispersal Model to Indoor Air Quality Control in Residential Buildings.
PB95-180238 *02,555*

AIR QUALITY STANDARDS
Ventilation, Carbon Dioxide and ASHRAE Standard 62-1989.
PB95-162095 *02,544*

AIR SAMPLING
International Radon-in-Air Measurement Intercomparison Using a New Transfer Standard.
PB96-159751 *03,708*

AIR TIGHTNESS
Workplan to Analyze the Energy Impacts of Envelope Airtightness in Office Buildings.
PB96-154463 *00,273*

AIR TRAFFIC CONTROL
Feasibility of Fire Evacuation by Elevators at FAA Control Towers.
PB94-213857 *04,844*

AIR-WATER INTERFACES
Atmospheric and Marine Trace Chemistry: Interfacial Biomediation and Monitoring.
PB94-199122 *03,752*

AIRBORNE EQUIPMENT
Airborne Smoke Sampling Package for Field Measurements of Fires.
PB95-150041 *01,381*

Dual-Frequency Millimeter-Wave Radiometer Antenna for Airborne Remote Sensing of Atmosphere and Ocean.
PB96-112289 *02,009*

AIRCRAFT
Fracture Testing of Large-Scale Thin-Sheet Aluminum Alloy.
PB95-242368 *00,024*

AIRCRAFT CONSTRUCTION MATERIALS
Investigation into the Flammability Properties of Honeycomb Composites.
PB95-143293 *03,152*

Computer-Aided Molecular Design of Fire Resistant Aircraft Materials.
PB96-160601 *00,025*

AIRCRAFT ELECTRONICS
Aperture Excitation of Electrically Large, Lossy Cavities.
PB94-145711 *00,029*

AIRCRAFT ENGINES
Fire Suppression System Performance of Alternative Agents in Aircraft Engine and Dry Bay Laboratory Simulations. SP890: Volume 1.
PB96-117775 *03,277*

Fire Suppression System Performance of Alternative Agents in Aircraft Engine and Dry Bay Laboratory Simulations. SP 890: Volume 2.
PB96-117783 *03,278*

AIRCRAFT FIRE
Materials and Fire Threat.
PB97-122311 *01,442*

AIRCRAFT FIRES
Evaluation of Alternative In-Flight Fire Suppressants for Full-Scale Testing in Simulated Aircraft Engine Nacelles and Dry Bays.
PB94-203403 *00,023*

Investigation into the Flammability Properties of Honeycomb Composites.
PB95-143293 *03,152*

Turbulent Spray Burner for Assessing Halon Alternative Fire Suppressants.
PB95-153748 *01,385*

Suppression Effectiveness of Extinguishing Agents under Highly Dynamic Conditions.
PB95-180279 *00,020*

Suppression of Elevated Temperature Hydraulic Fluid and JP-8 Spray Flames.
PB95-181095 *00,021*

Flow of Alternative Agents in Piping.
PB95-202420 *00,022*

Assessing Halon Alternatives for Aircraft Engine Nacelle Fire Suppression.
PB96-102454 *01,401*

Agent Screening for Halon 1301 Aviation Replacement.
PB96-159710 *03,282*

Validation of a Turbulent Spray Flame Facility for the Assessment of Halon Alternatives.
PB96-159728 *03,283*

In Search of Alternative Fire Suppressants.
PB96-164165 03,285

Effectiveness of Halon Alternatives in Suppressing Dynamic Combustion Process.
PB96-175732 03,288

Interaction of HFC-125, FC-218 and CF3I with High Speed Combustion Waves.
PB96-176417 03,290

AIRLINES
Risk Analysis for the Fire Safety of Airline Passengers.
PB94-194065 04,862

AIRPORT TOWERS
Feasibility of Fire Evacuation by Elevators at FAA Control Towers.
PB94-213857 04,844

Human Factors Considerations for the Potential Use of Elevators for Fire Evacuation of FAA Air Traffic Control Towers.
PB94-217163 01,300

ALANINE
Research and Development Activities in Electron Paramagnetic Resonance Dosimetry.
PB96-141288 03,635

Orientation Effects on ESR Analysis of Alanine-Polymer Dosimeters.
PB96-146725 03,720

Investigation of Applicability of Alanine and Radiochromic Detectors to Dosimetry of Proton Clinical Beams.
PB96-146782 03,636

Complex Time Dependence of the EPR Signal of Irradiated L-alpha-alanine.
PB97-122436 04,180

ALCOHOL FUELS
Study of Droplet Transport in Alcohol-Based Spray Flames Using Phase/Doppler Interferometry.
PB95-108551 02,479

ALCOHOLS
Thermodynamic Study of the Reactions of Cyclodextrins with Primary and Secondary Aliphatic Alcohols, with D- and L-Phenylalanine, and with L-Phenylalanineamide.
PB95-180873 01,016

Silicon Nitride Boundary Lubrication: Lubrication Mechanism of Alcohols.
PB96-111703 03,067

ALGAE
Total Surface Areas of Group IVA Organometallic Compounds: Predictors of Toxicity to Algae and Bacteria.
PB94-211331 00,814

ALGORITHMS
Secure Hash Standard. Category: Computer Security.
FIPS PUB 180-1 01,568

Calculating Flame Spread on Horizontal and Vertical Surfaces.
PB94-187283 00,335

VENTCF2: An Algorithm and Associated FORTRAN 77 Subroutine for Calculating Flow through a Horizontal Ceiling/Floor Vent in a Zone-Type Compartment Fire Model.
PB94-210127 00,345

Sprinkler Fire Suppression Algorithm.
PB94-216181 00,293

Algorithm to Describe the Spread of a Wall Fire under a Ceiling.
PB95-182259 00,261

Computing Radiative Heat Transfer Occurring in a Zone Fire Model.
PB96-102306 01,399

Analyzing and Exploiting Numerical Characteristics of Zone Fire Models.
PB96-102314 01,400

Measurement Methods and Algorithms for Comparison of Local and Remote Clocks.
PB96-102652 01,549

Performance Measures for Geometric Fitting in the NIST Algorithm Testing and Evaluation Program for Coordinate Measurement Systems.
PB96-122122 01,745

Modified Optimal Algorithm for Active Structural Control.
PB96-165949 00,472

IML++ v.1.2 Iterative Methods Library Reference Guide.
PB96-195219 01,776

Representation of Axes for Geometric Fitting.
PB97-113799 01,782

ALIGNMENT
Electrical Test Structure for Improved Measurement of Feature Placement and Overlay in Integrated Circuit Fabrication Processes.
PB95-164273 02,355

Collisional Alignment of CO2 Rotational Angular Momentum States in a Supersonic Expansion.
PB96-103171 01,069

Microelectronic Test Structures for Overlay Metrology.
PB96-164249 02,430

ALIPHATIC HYDROCARBONS
Physical Properties of Some Purified Aliphatic Hydrocarbons.
AD-A297 265/1 00,657

ALKALI AGGREGATE REACTIONS
Alkali-Silica Reaction and High Performance Concrete.
PB96-131537 01,345

ALKALI METALS
Role of Adsorbed Alkalis in Desorption Induced by Electronic Transitions.
PB94-172574 00,762

Polarization of Light Emitted After Positron Impact Excitation of Alkali Atoms.
PB94-199734 03,816

Atomic Manipulation of Polarizable Atoms by Electric Field Directional Diffusion.
PB95-150587 04,572

Relativistic R-Matrix Calculations for Electron - Alkali-Metal-Atom Scattering: Cs as a Test Case.
PB95-203410 04,006

ALKANE THIOLATES
Characterization of Cytochrome c/Alkanethiolate Structures Prepared by Self-Assembly on Gold.
PB95-164638 00,987

ALKANES
Calculation of Enthalpy and Entropy Differences of Near-Critical Binary Mixtures with the Modified Leung-Griffiths Model.
PB95-108635 00,885

ALKANETHIOL MONOLAYERS
Supported Phospholipid/Alkanthiol Biomimetic Membranes: Insulating Properties.
PB95-180782 03,470

Phospholipid/Alkanethiol Bilayers for Cell-Surface Receptor Studies by Surface Plasmon Resonance.
PB96-102900 03,472

ALKANETHIOLS
Self-Assembled Phospholipid/Alkanethiol Biomimetic Bilayers on Gold.
PB95-108460 00,878

ALKYD RESINS
Cylinder Wipe Air-Drying Intaglio Ink Vehicles for U.S. Currency Inks.
PB94-160801 03,115

ALKYLTHIOLATES
UV-Photopatterning of Alkylthiolate Monolayers Self-Assembled on Gold and Silver.
PB95-150751 00,924

ALLAN VARIANCE
Cross-Correlation Analysis Improves Time Domain Measurements.
PB95-180535 01,543

Confidence on the Modified Allan Variance and the Time Variance.
PB96-190376 01,557

ALLERGIC DISEASES
Diagnosis and Treatment of an Oral Base-Metal Contact Lesion Following Negative Dermatologic Patch Tests.
PB95-180626 00,172

ALLOSTERIC EFFECTORS
Positive and Negative Cooperativities at Subsequent Steps of Oxygenation Regulate the Allosteric Behavior of Multistate Sebacylhemoglobin.
PB97-119374 03,486

ALLOYING
Prediction of the Strength Properties for Plain-Carbon and Vanadium Micro-Alloyed Ferrite-Pearlite Steel.
PB96-123393 03,216

ALLOYS
Thermal Conductivity of Metals and Alloys at Low Temperatures. A Review of the Literature.
AD-A279 180/4 03,302

Effect of Two Initiator/Stabilizer Concentrations in a Metal Primer on Bond Strengths of a Composite to a Base Metal Alloy.
PB94-172723 00,141

Characterization of the Hydrogen Induced Cold Cracking Susceptibility at Simulated Weld Zones in HSLA-100 Steel.
PB94-174505 03,746

Effect of Transformation of Alloy on Transient and Residual Stresses in a Porcelain-Metal Strip.
PB94-198397 00,143

Comparison of Techniques for Nondestructive Composition Measurements in CdZnTe Substrates.
PB96-103098 02,703

Evolution Equations for Phase Separation and Ordering in Binary Alloys.
PB96-119243 02,979

Anisotropy of Interfaces in an Ordered Alloy: A Multiple-Order-Parameter Model.
PB96-131594 04,741

Characterization of the Structure of YD3 by Neutron Powder Diffraction.
PB96-186150 01,161

Charpy Impact Test as an Evaluation of 4 K Fracture Toughness.
PB96-190194 03,219

ALPHA ORIONIS STAR
Four Years of Monitoring alpha Orionis with the VLA: Where Have All the Flares Gone.
PB94-185212 00,048

GHRS Observations of Cool, Low-Gravity Stars. 1. The Far-Ultraviolet Spectrum of alpha Orions (M2 Iab).
PB96-112016 00,094

ALPHA PARTICLES
Systematics of Alpha-Particle Energy Spectra and Lineal Energy (Y) Spectra for Radon Daughters.
PB94-185139 03,615

Monte Carlo and Analytic Methods in the Transport of Electrons, Neutrons, and Alpha Particles.
PB96-111612 04,033

ALPHA SOURCES
Measurement and Calibration of Large-Area Alpha-Particle Sources at NIST.
PB94-172855 03,791

ALPHA TOXIN
Protonation Dynamics in an Ion Channel Pore.
PB96-161757 03,589

ALTERNATING CURRENT
AC-DC Difference Characteristics of High-Voltage Thermal Converters.
PB96-148093 02,083

ALTERNATING ELECTRIC FIELDS
Energy Transduction between a Concentration Gradient and an Alternating Electric Field.
PB94-216363 03,461

ALTERNATIVE REFRIGERANTS
Permeation Tube Approach to Long-Term Use of Automatic Sampler Retention Index Standards.
PB96-167291 00,639

ALTERNATIVES
Inhibition of Premixed Methane-Air Flames by Halon Alternatives.
PB96-146741 01,414

In Search of Alternative Fire Suppressants.
PB96-164165 03,285

ALUMINA
Objective Evaluation of Short-Crack Toughness Curves Using Indentation Flaws: Case Study on Alumina-Based Ceramics.
PB96-179429 03,079

Texture Measurement of Sintered Alumina Using the March-Dollase Function.
PB96-179494 04,784

Effect of Grain Size on Hertzian Contact Damage in Alumina.
PB96-179601 03,083

Indentation Fatigue: A Simple Cyclic Hertzian Test for Measuring Damage Accumulation in Polycrystalline Ceramics.
PB96-180013 03,084

Flaw-Tolerance and Crack-Resistance Properties of Alumina-Aluminum Titanate Composites with Tailored Microstructures.
PB97-110324 03,101

ALUMINIUM ALLOYS
Evaluation of the Environmentally Induced Fracture Resistance of Ductile Nickel Aluminide. Technical Report Number 1, Final report. October-December 1990.
DE94017331 03,306

Comparison of the Corrosion Rates of FeAl, Fe(sub 3)Al and Steel in Distilled Water and 0.5 M Sodium Chloride. Technical Report Number 2, January--March 1991.
DE94017332 03,186

Evaluation of the Electrochemical Behavior of Ductile Nickel Aluminide and Nickel in a pH 7.9 Solution. Technical Report Number 3, April-June 1991.
DE94017351 03,307

ALUMINIUM BASE ALLOYS
Study of Laser Resonance Ionization Mass Spectrometry Using a Glow Discharge Source.
DE94018566 03,308

ALUMINIUM OXIDES
Densification of Nano-Size Powders. 1994 Report.
DE94013486 03,027

Low temperature fabrication from nano-size ceramic powders.
DE95013505 03,029

ALUMINUM
Cryogenic Materials Data Handbook.
AD-A286 675/4 03,303

Use of Sum Rules on the Energy-Loss Function for the Evaluation of Experimental Optical Data.
PB95-150736 04,264

Ultrasonic Method for Reconstructing the Two-Dimensional Liquid-Solid Interface in Solidifying Bodies.
PB95-161782 03,349

Effect of Microstructure on Phase Formation in the Reaction of Nb/Al Multilayer Thin Films.
PB95-168415 03,352

Standard Reference Material 1744: Aluminum Freezing-Point Standard.
PB95-251732 01,055

Factors Significant to Precracking of Fracture Specimens.
PB96-109558 03,358

Electrical Characterization of Integrated Circuit Metal Line Thickness.
PB96-138433 02,414

ALUMINUM ALLOYS
Electrochemical Synthesis of Metal and Intermetallic Composites.
AD-A294 088/0 03,304

Fracture Testing of Large-Scale Thin-Sheet Aluminum Alloy.
AD-A306 625/5 *03,305*

Fracture Behavior of Large-Scale Thin-Sheet Aluminum Alloy.
N95-19494/0 *03,311*

Temperature Increases in Aluminum Alloys during Mechanical-Impact Tests for Oxygen Compatibility.
PB94-172962 *03,316*

Thermodynamic Calculation of the Ternary Ti-Al-Nb System.
PB94-212636 *03,336*

Thermodynamic Assessment and Calculation of the Ti-Al System.
PB94-212644 *03,337*

Recommended Changes in ASTM Test Methods D2512-82 and G86-84 for Oxygen-Compatibility Mechanical Impact Tests on Metals.
PB94-216694 *03,338*

Macro- and Microreactions in Mechanical-Impact Tests of Aluminum Alloys.
PB95-107348 *03,340*

Influence of Specimen Absorbed Energy in LOX Mechanical-Impact Tests.
PB95-107355 *03,341*

Residual Stresses in Aluminum-Mullite (alpha-Alumina) Composites.
PB95-152880 *03,155*

Thin Film Reaction Kinetics of Niobium/Aluminum Multilayers.
PB95-175295 *04,651*

Fracture Testing of Large-Scale Thin-Sheet Aluminum Alloy.
PB95-242368 *00,024*

Journal of Research of the National Institute of Standards and Technology, September/October 1993. Volume 98, Number 5.
PB96-169057 *03,368*

Light-Weight Alloys for Aerospace Applications II.
PB96-190244 *03,375*

ALUMINUM ANTIMONY ALLOYS
Assessment of the Al-Sb System.
PB94-200474 *03,329*

ALUMINUM BASE ALLOYS
Study of Laser Resonance Ionization Mass Spectrometry Using a Glow Discharge Source.
PB96-123203 *03,360*

ALUMINUM FLUORIDES
New Rydberg States of Aluminum Monofluoride Observed by Resonance-Enhanced Multiphoton Ionization Spectroscopy.
PB94-199544 *00,797*

ALUMINUM GALLIUM ARSENIDE
Al L2,3 Core Excitons in AlxGa1-x as Studied by Soft-X-ray Reflection and Emission.
PB96-157839 *04,067*

X-ray Reflectivity Determination of Interface Roughness Correlated with Transport Properties of (AlGa)As/GaAs High Electron Mobility Transistor Devices.
PB97-111868 *04,149*

ALUMINUM GALLIUM ARSENIDES
Time-Resolved Measurements of the Polarization State of Four-Wave Mixing Signals from GaAs Multiple Quantum Wells.
PB96-201058 *04,796*

ALUMINUM GAS CYLINDERS
Stability/Instability of Gas Mixtures Containing 1,3-Butadiene in Treated Aluminum Gas Cylinders.
PB95-162285 *02,546*

ALUMINUM GRAPHITE COMPOSITES
Thermal Expansion of an SiC Particle-Reinforced Aluminum Composite.
PB94-213204 *03,144*

ALUMINUM INTERMETALLICS
Coherent Precipitates in the BCC/Orthorhombic Two Phase Field of the Ti-Al-Nb System.
PB94-198694 *03,317*

Crystallographic Characterization of Some Intermetallic Compounds in the Al-Cr System.
PB94-198702 *03,318*

ALUMINUM-LITHIUM ALLOYS
Reaction Sensitivities of Al-Li Alloys and Alloy 2219 in Mechanical-Impact Tests.
PB94-172764 *03,314*

Aluminum-Lithium Alloys: Evaluation of Fracture Toughness by Two Test Standards, ASTM Method E 813 and E 1304.
PB96-190236 *03,374*

ALUMINUM MANGANESE ALLOYS
Effect of Mn Content on the Microstructure of Al-Mn Alloys Electrodeposited at 150C.
PB95-126355 *03,343*

ALUMINUM MONOFLUORIDE
New Rydberg States of Aluminum Monofluoride Observed by Resonance-Enhanced Multiphoton Ionization Spectroscopy.
PB94-199544 *00,797*

ALUMINUM NIOBATES
Improved Crystallographic Data for Aluminum Niobate (AlNbO4).
PB95-107306 *04,523*

ALUMINUM NITRIDE
Effect of Beam Voltage on the Properties of Aluminum Nitride Prepared by Ion Beam Assisted Deposition.
PB97-118616 *01,995*

ALUMINUM OXALATE
Effects of Aluminum Oxalate/Glycine Pretreatment Solutions on Dentin Permeability.
PB95-164505 *03,565*

ALUMINUM OXIDE
Characterization of the Densification of Alumina by Multiple Small-Angle Neutron Scattering. (Reannouncement with New Availability Information).
AD-A249 179/3 *03,024*

Tribological Characteristics of Alpha-Alumina at Elevated Temperatures.
PB94-211018 *02,963*

Effect of Microstructure on the Wear Transition of Zirconia-Toughened Alumina.
PB94-211778 *03,141*

Mechanism of Mild to Severe Wear Transition in Alpha-Alumina.
PB94-212354 *03,233*

Observed and Theoretical Creep Rates for an Alumina Ceramic and a Silicon Nitride Ceramic in Flexure.
PB94-212958 *03,040*

Interface Modification and Characterization of Silicon Carbide Platelets Coated with Alumina Particles.
PB95-108734 *03,121*

Control of Friction and Wear of Alpha-Alumina with a Composite Solid-Lubricant Coating.
PB95-125969 *03,225*

Fabrication of Flaw-Tolerant Aluminum-Titanate-Reinforced Alumina.
PB95-162533 *03,161*

Wear Model for Alumina Sliding Wear.
PB95-163796 *03,239*

Dielectric Properties of Single Crystals of Al2O3, LaAlO3, SrTiO3, and MgO at Cryogenic Temperatures.
PB95-180477 *02,266*

Stability and Surface Energies of Wetted Grain Boundaries in Aluminum Oxide.
PB95-202750 *03,059*

Wear Transitions in Monolithic Alumina and Zirconia-Alumina Composites.
PB96-103163 *03,168*

ALUMINUM OXIDES
Effect of Green Density and the Role of Magnesium Oxide Additive on the Densification of Alumina Measured by Small-Angle Neutron Scattering. (Reannouncement with New Availability Information).
AD-A244 582/3 *03,022*

Evolution of the Pore Size Distribution in Final-Stage Sintering of Alumina Measured by Small-Angle X-ray Scattering. (Reannouncement with New Availability Information).
AD-A249 178/5 *03,023*

Measuring Matching Wear Scars on Balls and Flats.
PB95-151528 *03,153*

Residual Stresses in Aluminum-Mullite (alpha-Alumina) Composites.
PB95-152880 *03,155*

Flat and Rising R-Curves for Elliptical Surface Cracks from Indentation and Superposed Flexure.
PB95-161295 *03,156*

Fabrication of Transparent gamma-Al2O3 from Nanosize Particles.
PB95-175493 *03,054*

ALUMINUM TITANATE
Flaw-Tolerance and Crack-Resistance Properties of Alumina-Aluminum Titanate Composites with Tailored Microstructures.
PB97-110324 *03,101*

ALUMINUM TITANATES
Fabrication of Flaw-Tolerant Aluminum-Titanate-Reinforced Alumina.
PB95-162533 *03,161*

AMALGAM
Wear of Enamel against Glass-Ceramic, Porcelain, and Amalgam.
PB96-179593 *03,082*

AMBIENT TEMPERATURE
Ambient Temperature Synthesis of Bulk Intermetallics.
PB95-169074 *00,168*

AMERICAN ASSOCIATION OF AEROSOL RESEARCH
Global Climatic Effects of Aerosols: The AAAR Symposium.
PB95-108791 *00,122*

AMINE/N-NITROSODIMETHYL
Unusual Spin-Trap Chemistry for the Reaction of Hydroxyl Radical with the Carcinogen N-Nitrosodimethylamine.
PB95-151643 *00,692*

AMINES
New Surface-Active Comonomer for Adhesive Bonding.
PB96-204052 *03,579*

AMINO ACIDS
L-threo-beta-Hydroxyhistidine, an Unprecedented Iron(III) Ion-Binding Amino Acid in a Pyoverdine-type Siderophore from Pseudomonas fluorescens 244.
PB94-211620 *00,553*

Protonation Dynamics of the alpha-Toxin Ion Channel from Spectral Analysis of pH-Dependent Current Fluctuations.
PB96-161740 *03,652*

AMMONIA
Self Broadening in the nu1 Band of NH3.
PB94-216371 *00,857*

Photodissociation of Ammonia at 193.3nm: Rovibrational State Distribution of the NH2(A(2)A1) Fragment.
PB95-151775 *00,937*

Equilibrium and Calorimetric Investigation of the Hydrolysis of L-Tryptophan to (Indole + Pyruvate + Ammonia).
PB95-163317 *00,661*

Viscosity of Ammonia.
PB96-145933 *01,117*

AMMONIA COMPLEXES
Microwave and Submillimeter Spectroscopy of Ar-NH3 States Correlating with Ar+NH3(j=1, k=1).
PB95-152211 *00,942*

AMMONIA RADICALS
Photodissociation of Ammonia at 193.3nm: Rovibrational State Distribution of the NH2(A(2)A1) Fragment.
PB95-151775 *00,937*

AMMONIUM COMPOUNDS
Use of Kinetic Energy Distributions to Determine the Relative Contributions of Gas Phase and Surface Fragmentation in KeV Ion Sputtering of a Quaternary Ammonium Salt.
PB95-126108 *00,570*

AMMONIUM IONS
Planar Waveguide Optical Sensors.
PB94-200185 *03,586*

AMORPHOUS FERROMAGNETS
Polarization Analysis of the Magnetic Excitations in Invar and Non-Invar Amorphous Alloys.
PB94-216116 *04,516*

AMORPHOUS SILICON
Plasma Chemistry in Disilane Discharges.
PB94-211075 *02,514*

Nanoscale Study of the As-Grown Hydrogenated Amorphous Silicon Surface.
PB95-150595 *04,573*

AMORPHOUSE PHASES
Extrapolation of the Heat Capacity in Liquid and Amorphous Phases.
PB97-111421 *04,147*

AMPEROMETRIC
Novel Amperometric Immunosensor for Procainamide Employing Light Activated Labels.
PB96-163662 *00,512*

AMPERTURE AMPLITUDE DISTRIBUTION
Planar Near-Field Measurements and Microwave Holography for Measuring Aperture Distribution on a 60 GHz Active Array Antenna.
PB96-167366 *03,762*

AMPHETAMINE
Determination of Amphetamine and Methamphetamine in a Lyophilized Human Urine Reference Material.
PB95-175444 *03,597*

AMPICILLIN
Thermodynamics of the Hydrolysis of Penicillin G and Ampicillin.
PB94-172467 *03,596*

AMPLIFIER DESIGN
New 5 and 10 MHz High Isolation Distribution Amplifier.
PB96-190202 *01,510*

AMPLIFIER NOISE
Terminal Invariant Description of Amplifier Noise.
PB95-153573 *02,043*

Comparison of Three Techniques for the Precision Measurement of Amplifier Noise.
PB95-163663 *02,349*

Measurement Accuracies for Various Techniques for Measuring Amplifier Noise.
PB95-163671 *02,350*

AMPLIFIERS
Design Criteria for BJT Amplifiers with Low l/f AM and PM Noise.
PB96-200365 *02,442*

Frequency Synthesis and Metrology at 10(-17) and Beyond.
PB97-113187 *02,101*

AMPLITUDE MODULATION
Investigations of AM and PM Noise in X-Band Devices.
PB95-180022 *02,062*

Practical Standards for PM and AM Noise at 5, 10 and 100 MHz.
PB95-181129 *01,546*

Secondary Standard for PM and AM Noise at 5, 10, and 100 MHz.
PB96-123187 *01,554*

Origin of l/f PM and AM Noise in Bipolar Junction Transistor Amplifiers.
PB96-200787 *02,096*

Reducing the 1/f AM and PM Noise in Electronics for Precision Frequency Metrology.
PB97-113195 *02,102*

ANALINES
Inelastic Neutron Scattering Studies of Nonlinear Optical Materials: p-Nitroaniline Adsorbed in ALPO-5.
PB95-107223 *00,874*

ANALOG CIRCUITS
Developing Linear Error Models for Analog Devices.
PB95-150520 *02,037*

Diakoptic and Large Change Sensitivity Analysis.
PB95-150538 *02,038*

ANALOG TO DIGITAL CONVERTERS
Developing Linear Error Models for Analog Devices.
PB95-150520 *02,037*

ANALYSIS OF VARIANCE
Anova Estimates of Variance Components for a Class of Mixed Models.
PB96-141163 *03,448*

ANALYTICAL CHEMISTRY
Airborne Asbestos Method: Standard Test Method for High Precision Counting of Asbestos Collected on Filters. Version 1.0.
PB94-163003 *00,525*

Airborne Asbestos Method: Standard Test Method for Verified Analysis of Asbestos by Transmission Electron Microscopy. Version 2.0.
PB94-163045 *00,526*

Raman and Fluorescence Spectra Observed in Laser Microprobe Measurements of Several Compositions in the Ln-Ba-Cu-O System.
PB94-172210 *04,440*

Radiance Temperature (in the Wavelength Range 519-906 nm) of Tungsten at Its Melting Point by a Pulse-Heating Technique.
PB94-172590 *03,397*

Absolute Determination of Electrolytic Conductivity for Primary Standard KC1 Solutions from 0 to 50C.
PB94-172798 *00,765*

Classical Analysis: A Look at the Past, Present, and Future.
PB94-185063 *00,528*

Long-Term Stability of Carrier-Free Polonium Solution Standards.
PB94-185170 *00,685*

Liquid Chromatography: Laser-Enhanced Ionization Spectrometry for the Speciation of Organolead Compounds.
PB94-185253 *00,530*

Comparative Strategies for Correction of Interferences in Isotope Dilution Mass Spectrometric Determination of Vanadium.
PB94-185261 *00,531*

Relative Sensitivity Factors and Useful Yields for a Microfocused Gallium Ion Beam and Time-of-Flight Secondary Ion Mass Spectrometer.
PB94-198736 *00,541*

Object Finder for Digital Images Based on Multiple Thresholds, Connectivity, and Internal Structures.
PB94-199106 *01,833*

Concentration Histogram Imaging: A Scatter Diagram Technique for Viewing Two or Three Related Images.
PB94-199114 *00,542*

Atmospheric and Marine Trace Chemistry: Interfacial Biomediation and Monitoring.
PB94-199122 *03,752*

Determination of 3-Quinuclidinyl Benzilate (Qnb) and Its Major Metabolites in Urine by Isotope Dilution Gas Chromatography Mass Spectrometry.
PB94-199379 *03,492*

Thermodynamic Analysis of Heparin Binding to Human Antithrombin.
PB94-199593 *03,455*

Establishing Quality Measurements for Inorganic Analysis of Biomaterials.
PB94-199726 *00,548*

Determination of Oltipraz in Serum by High-Performanace Liquid Chromatography with Optical Absorbance and Mass Spectrometric Detection.
PB94-200201 *03,493*

Importance of Chemometrics in Biomedical Measurements.
PB94-200599 *00,550*

Metrological Measurement Accuracy: Discussion of 'Measurement Error Models' by Leon Jay Gleser.
PB94-200607 *00,551*

Airborne Asbestos Method: Standard Practice for Recording Transmission Electron Microscopy Data for the Analysis of Asbestos Collected onto Filters. Version 1.0.
PB94-210168 *00,552*

Determination of Boron and Lithium in Diverse Biological Matrices Using Neutron Activation - Mass Spectrometry (NA-MS).
PB94-212289 *00,554*

Spectroscopic Constants for the 2.5 and 3.0 micrometer Bands of Acetylene.
PB94-213071 *00,847*

Measurement of CO Pressures in the Ultrahigh Vacuum Regime Using Resonance-Enhanced Multiphoton-Ionization Time-of-Flight Mass Spectroscopy.
PB94-216041 *03,864*

Effects of Target Shape and Neutron Scattering on Element Sensitivities for Neutron-Capture Prompt Gamma-ray Activation Analysis.
PB94-216157 *00,558*

Study of Diffusion Zones with Electron Microprobe Compositional Mapping.
PB94-216348 *00,559*

Electron Probe X-Ray Microanalysis.
PB95-107165 *00,562*

Microanalysis to Nanoanalysis: Measuring Composition at High Spatial Resolution.
PB95-107173 *00,563*

Design of a Protocol for an Electron Probe Microanalyzer k-Value Round Robin.
PB95-107181 *00,564*

Compositional Mapping of the Microstructure of Materials.
PB95-107199 *00,565*

Separation and Identification of Organic Gunshot and Explosive Constituents by Micellar Electrokinetic Capillary Electrophoresis.
PB95-107249 *00,566*

Secondary Target X-Ray Excitation for In vivo Measurement of Lead in Bone.
PB95-108767 *03,496*

Image Depth Profiling SIMS: An Evaluation for the Analysis of Light Element Diffusion in YBa2Cu3O7-x Single Crystal Superconductors.
PB95-126116 *04,530*

Molecular Ion Imaging and Dynamic Secondary Ion Mass Spectrometry of Organic Compounds.
PB95-126124 *00,571*

Transition Metal Implants in In0.53GA0.47As.
PB95-126389 *04,534*

Range Statistics and Rutherford Backscattering Studies on Fe-Implanted In0.53Ga0.47As.
PB95-126397 *04,535*

Device for Subambient Temperature Control in Liquid Chromatography.
PB95-140604 *00,573*

Comparison of the Liquid Chromatographic Behavior of Selected Steroid Isomers Using Different Reversed-Phase Materials and Mobile Phase Compositions.
PB95-140976 *00,574*

Automated, High-Precision Coulometric Titrimetry. Part 1. Engineering and Implementation.
PB95-150199 *00,575*

Automated, High Precision Coulometric Titrimetry. Part 2. Strong and Weak Acids and Bases.
PB95-150207 *00,576*

Integrating Automated Systems with Modular Architecture.
PB95-150231 *00,577*

Development of Engineered Stationary Phases for the Separation of Carotenoid Isomers.
PB95-150249 *00,578*

Shape Selectivity Assessment of Stationary Phases in Gas Chromatography.
PB95-150256 *00,579*

Guidelines for Refractive Index Measurements of Asbestos.
PB95-151189 *02,543*

Factorial Design Techniques Applied to Optimization of AMS Graphite Target Preparation.
PB95-151197 *00,584*

Comprehensive Spectroscopic Data Tabulations and Progress in the Compilation of Atomic Transition Probabilities.
PB95-151551 *03,909*

Determination of Polycyclic Aromatic Hydrocarbons by Liquid Chromatography.
PB95-151650 *00,585*

Potentiometric Enzyme-Amplified Flow Injection Analysis Detection System: Behavior of Free and Liposome-Released Peroxidase.
PB95-151833 *03,534*

New Method to Evaluate Deposit Forming Tendencies of Liquid Lubricants by Differential Scanning Calorimetry.
PB95-152120 *01,451*

Development of a Gas Standard Reference Material Containing Eighteen Volatile Organic Compounds.
PB95-162277 *02,545*

Stability/Instability of Gas Mixtures Containing 1,3-Butadiene in Treated Aluminum Gas Cylinders.
PB95-162285 *02,546*

Shape Selectivity in Reversed-Phase Liquid Chromatography for the Separation of Planar and Non-Planar Solutes.
PB95-162608 *00,596*

Trace Elements Associated with Proteins. Neutron Activation Analysis Combined with Biological Isolation Techniques.
PB95-163101 *00,597*

Trace Detection in Conducting Solids Using Laser-Induced Fluorescence in a Cathodic Sputtering Cell.
PB95-163424 *00,598*

Measurement of the Uniformity of Particle Deposition of Filter Cassette Sampling in a Low Velocity Wind Tunnel.
PB95-163754 *02,549*

Applications of Fluorescence Spectroscopy in Polymer Science and Technology.
PB95-163770 *01,258*

Localization of Atoms in a Three-Dimensional Standing Wave.
PB95-163887 *03,944*

Comparative Study of Fe-C Bead and Graphite Target Performance with the National Ocean Sciences AMS (NOSAMS) Facility Recombinator Ion Source.
PB95-175790 *00,693*

Determination of Hydrogen in Titanium Alloy Jet Engine Compressor Blades by Cold Neutron Capture Prompt Gamma-ray Activation Analysis.
PB95-175956 *01,448*

Interlaboratory Comparison Studies on the Analysis of Hair for Drugs of Abuse.
PB95-176251 *03,500*

Cyclic Polyamine Ionophore for Use in a Dibasic Phosphate-Selective Electrode.
PB95-180121 *01,008*

Instrument for Evaluating Phase Behavior of Mixtures for Supercritical Fluid Experiments.
PB95-180758 *00,606*

Methods for Analysis of Cancer Chemopreventive Agents in Human Serum.
PB95-200648 *03,502*

Concentrations of Chlorinated Hydrocarbons, Heavy Metals and Other Elements in Tissues Banked by the Alaska Marine Mammal Tissue Archival Project.
PB95-209870 *02,590*

Isotope Dilution Mass Spectrometry as a Candidate Definitive Method for Determining Total Glycerides and Triglycerides in Serum.
PB96-102280 *03,519*

Intercomparison Study of (237)Np Determination in Artificial Urine Samples.
PB96-102645 *03,633*

Partial Pressure Analysis in Space Testing.
PB96-103072 *04,829*

Proficiency Tests for the NIST Airborne Asbestos Program, 1993.
PB96-106463 *00,610*

Quantitative Analysis of Selected PCB Congeners in Marine Matrix Reference Materials Using a Novel Cyanobiphenyl Stationary Phase.
PB96-111737 *02,591*

Stability of Compressed Gas Mixtures Containing Low Level Volatile Organic Compounds in Aluminum Cylinders.
PB96-111968 *00,613*

Spectral Interference in the Determination of Arsenic in High-Purity Lead and Lead-Base Alloys Using Electrothermal Atomic Absorption Spectrometry and Zeeman-Effect Background Correction.
PB96-112099 *00,614*

SUM and MEAN: Standard Programs for Activation Analysis.
PB96-112149 *00,617*

Application of a Novel Slurry Furnace AAS Protocol for Rapid Assessment of Lead Environmental Contamination.
PB96-112354 *02,526*

Analysis by a Combination of Gas Chromatography and Tandem Mass Spectrometry: Development of Quantitative Tandem-in-Time Ion Trap Mass Spectrometry: Isotope Dilution Quantification of 11-Nor-Delta-9-Tetrahydro cannabinol-9-Carboxylic Acid.
PB96-117221 *02,561*

Comparison of Selectivities for PCBs in Gas Chromatography for a Series of Cyanobiphenyl Stationary Phases.
PB96-119458 *00,618*

Hair Testing for Drugs of Abuse: International Research on Standards and Technology.
PB96-120555 *03,504*

Low Electrolytic Conductivity Standards.
PB96-122098 *01,081*

Influence of Stationary Phase Chemistry on Shape Recognition in Liquid Chromatography.
PB96-123682 *00,621*

Determination of Vitamin K1 in Serum Using Catalytic-Reduction Liquid Chromatography with Fluorescence Detection.
PB96-138425 *03,506*

Selectivity Trends in Packed Column Supercritical Fluid Chromatography with C18 Stationary Phases.
PB96-138581 *00,622*

Determination of Sulfur in Fossil Fuels by Isotope Dilution Thermal Ionization Mass Spectrometry.
PB96-141379 *02,495*

Amperometric Measurement of Moisture in Transformer Oil Using Karl Fischer Reagents.
PB96-146766 *00,623*

Development of Gas Standards from Solid 1,4-dichlorobenzene.
PB96-155486 *02,496*

Measurement of Atmospheric Methyl Bromide Using Gravimetric Gas Standards.
PB96-155494 *02,497*

Population Distributions and Intralaboratory Reproducibility for Fat-Soluble Vitamin-Related Compounds in Human Serum.
PB96-155536 *00,624*

Resonance Ionization Spectroscopy/Resonance Ionization Mass Spectrometry Data Service. V-Data Sheets for Ga, Mn, Sc, and Tl.
PB96-158068 *00,625*

Isotopic and Nuclear Analytical Techniques in Biological Systems: A Critical Study. 10. Elemental Isotopic Dilution Analysis with Radioactive and Stable Isotopes (Technical Report).
PB96-164157 *00,696*

Certifying the Chemical Composition of a Biological Material: A Case Study.
PB96-164272 *00,636*

Dead Time, Pileup, and Accurate Gamma-Ray Spectrometry.
PB96-167101 *00,697*

Loss-Free Counting at IRI and NIST.
PB96-167119 *04,105*

Trace Element Concentrations in Cetacean Liver Tissues Archived in the National Marine Mammal Tissue Bank.
PB96-167127 *02,595*

Supercritical Fluid Extraction-Immunoassay for the Rapid Screening of Cocaine in Hair.
PB96-167168 *00,637*

New NIST Rapid Pneumatic Tube System.
PB96-167259 *03,738*

Development of the Ion Exchange-Gravimetric Method for Sodium in Serum as a Definitive Method.
PB96-179148 *01,867*

Preliminary Investigation of Oleoresin Capsicum.
PB96-179486 *03,520*

Fluoride Analytical Methods.
PB96-180237 *03,578*

Isolation and Structural Elucidation of the Predominant Geometrical Isomers of alpha-Carotene.
PB96-190061 *00,640*

Role of Certified Reference Materials in Trace Analysis Quality Assurance.
PB97-110019 *00,650*

Interlaboratory Studies on the Analysis of Hair for Drugs of Abuse: Results from the Fourth Exercise.
PB97-111322 *03,510*

Use of Neutron Beams for Chemical Analysis at NIST.
PB97-112437 *00,652*

Measurement of Ascorbic Acid in Human Plasma and Serum: Stability, Intralaboratory Repeatability, and Interlaboratory Reproducibility.
PB97-112445 *03,511*

CONTAM94: A Multizone Airflow and Contaminant Dispersal Model with a Graphic User Interface.
PB97-113203 *02,570*

Liquid Chromatographic Determination of Carotenoids in Human Serum Using an Engineered C30 and a C18 Stationary Phase.
PB97-119333 *03,512*

Radiocarbon Measurements of Atmospheric Volatile Organic Compounds: Quantifying the Biogenic Contribution.
PB97-122352 *02,574*

ANALYTICAL METHODS

Certification of Polycyclic Aromatic Hydrocarbons in a Marine Sediment Standard Reference Material.
PB96-111778 *02,592*

Application of a Novel Slurry Furnace AAS Protocol for Rapid Assessment of Lead Environmental Contamination.
PB96-112354 *02,526*

ANALYTICAL TECHNIQUES

Classical Analysis: A Look at the Past, Present, and Future.
PB94-185063 *00,528*

Dissolution Problems with Botanical Reference Materials.
PB95-126280 *03,487*

Results of the ASTM Nuclear Methods Intercomparison on NIST Apple and Peach Leaves Standard Reference Materials.
PB97-119036 *03,490*

ANALYZERS

Design and Characterization of X-Ray Multilayer Analyzers for the 50 - 1000 eV Region.
PB94-211851 *03,848*

ANATOMIC MODELS

Summary of the Proceedings of the Workshop on Standard Phantoms for In-vivo Radioactivity Measurement.
PB94-212933 *03,622*

ANELASTICITY

Temperature and Frequency Dependence of Anelasticity in a Nickel Oscillator.
PB96-137732 *03,689*

ANEMOMETERS

Thermal Anemonetry for Mass Flow Measurement in Oscillating Cryogenic Gas Flows.
PB96-176789 *04,218*

ANGLE MEASUREMENT

Advanced Angle Metrology System.
PB94-211364 *02,637*

ANGLES (GEOMETRY)

Tilt Effects in Optical Angle Measurements.
PB95-169389 *04,294*

ANGULAR DISTRIBUTIONS

Measuring Nondipolar Asymmetries of Photoelectron Angular Distributions.
PB97-122493 *01,193*

ANGULAR MOMENTUM

Collisional Alignment of CO2 Rotational Angular Momentum States in a Supersonic Expansion.
PB96-103171 *01,069*

ANHARMONIC OSCILLATORS

Anharmonic Oscillator Analysis Using Modified Airy Functions.
PB94-185311 *03,798*

ANIMAL FEED

Individual Carotenoid Content of SRM 1548 Total Diet and Influence of Storage Temperature, Lyophilization, and Irradiation on Dietary Carotenoids.
PB94-200524 *00,033*

ANIMAL HUSBANDRY

Preparation and Monitoring of Lead Acetate Containing Drinking Water Solutions for Toxicity Studies.
PB94-193885 *00,538*

ANIMAL PHYSIOLOGY

Histopathology, Blood Chemistry, and Physiological Status of Normal and Moribund Striped Bass ('Morone saxatilis') Involved in Summer Mortality ('Die-Off') in the Sacramento-San Joaquin Delta of California.
PB94-198157 *00,034*

ANIMAL TISSUES

Development of Frozen Whale Blubber and Liver Reference Materials for the Measurement of Organic and Inorganic Contaminants.
PB95-151676 *00,587*

Determination of Inorganic Constituents in Marine Mammal Tissues.
PB95-152047 *00,589*

Development of the National Marine Mammal Tissue Bank.
PB95-161402 *02,586*

Quality Assurance of Contaminant Measurements in Marine Mammal Tissues.
PB95-164034 *02,588*

Alaska Marine Mammal Tissue Archival Project: Specimen Inventory.
PB95-171344 *02,589*

Concentrations of Chlorinated Hydrocarbons, Heavy Metals and Other Elements in Tissues Banked by the Alaska Marine Mammal Tissue Archival Project.
PB95-209870 *02,590*

Certification of Polychlorinated Biphenyl Congeners and Chlorinated Pesticides in a Whale Blubber Standard Reference Material.
PB96-103023 *03,745*

National Status and Trends Program Specimen Bank: Sampling Protocols, Analytical Methods, Results, and Archive Samples.
PB97-119226 *02,598*

ANIONS

Vibrational Spectra of Molecular Ions Isolated in Solid Neon. 11. NO2(+), NO2(-), and NO3(-).
AD-A275 828/2 *00,708*

Temperature Dependence of the Rate Constants for Reactions of the Sulfate Radical, SO4-, with Anions.
PB94-212172 *00,828*

Temperature Dependence of the Rate Constants for Reactions of the Carbonate Radical with Organic and Inorganic Reductants.
PB94-212206 *00,831*

ANISOLE

Thermal Decomposition of Hydroxy- and Methoxy-Substituted Anisoles.
PB94-173036 *00,767*

ANISOTROPHY

Ultrasonic Measurement of Sheet Anisotropy and Formability.
PB95-153235 *03,213*

ANISOTROPIC MATERIALS

Microwave Dielectric Properties of Anisotropic Materials at Cryogenic Temperatures.
PB96-137765 *02,412*

ANISOTROPY

Convection and Morphological Stability During Directional Solidification.
N95-14548/8 *03,310*

Anisotropic Phase Separation Kinetics in a Polymer Blend Solution Following Cessation of Shear Studied by Light Scattering.
PB95-151247 *01,241*

Anisotropy of Polarized X-ray Emission from Atoms and Molecules.
PB95-163002 *04,621*

ANISTROPY

Fluorescence Anisotropy Measurements on a Polymer Melt as a Function of Applied Shear Stress.
PB94-199296 *01,209*

Hemispherical Test Fixture for Measuring the Wavefields Generated in an Anisotropic Solid.
PB96-190087 *03,181*

Notion of a xi-Vector and a Stress Tensor for a General Class of Anisotropic Diffuse Interface Models.
PB96-193776 *04,78E*

ANNEALING

Magnetostriction and Giant Magnetoresistance in Annealed NiFe/Ag Multilayers.
PB96-102603 *04,716*

Low Magnetostriction in Annealed NiFe/Ag Giant Magnetoresistive Multilayers.
PB96-146691 *04,762*

Annealing of Bragg Gratings in Hydrogen-Loaded Optical Fiber.
PB96-155437 *04,361*

Effect of Intermediate Thermal Processing on Microstructural Changes of Oxygen Implanted Silicon-on-Insulator Material.
PB96-160213 *02,982*

Antiferromagnetic Interlayer Correlations in Annealed Ni80Fe20/Ag Multilayers.
PB97-122220 *03,109*

ANNELING

Oxygen Annealing of Ex-situ YBCO/Ag Thin-Film Interfaces.
PB96-141312 *04,758*

ANNULAR FLOW

Single-Phase Heat Transfer and Pressure Drop Characteristics of an Integral-Spine-Fin Within an Annulus.
PB94-194073 *03,805*

Single-Phase Heat Transfer and Pressure Drop Characteristics of an Integral-Spine Fin Within an Annulus.
PB97-122386 *04,179*

ANOMALOUS DISPERSIONS

Theoretical Form Factor, Attenuation and Scattering Tabulation for Z=1-92 from E=1-10 eV to E=0.4-1.0 MeV.
PB96-145594 *01,104*

ANSI/ASHRAE STANDARD 124-1991

Predicting the Energy Performance Ratings of a Family of Type I Combination Appliances.
PB95-105524 *02,504*

ANTENNA ARRAYS

Optically Linked Three-Loop Antenna System for Determining the Radiation Characteristics of an Electrically Small Source.
PB95-161915 *02,005*

ANTENNA MEASUREMENTS

Planar Near-Field Alignment.
PB94-172491 *01,998*

New Extrapolation/Spherical/Cylindrical Measurement Facility at the National Institute of Standards and Technology.
PB95-153755 *02,004*

ANTENNA RADIATION PATTERNS

Correction Factor for Nonplanar Incident Field in Monopole Calibrations.
PB95-108643 *02,002*

ANTENNAS

Standard Probes for Electromagnetic Field Measurements.
PB94-185436 *01,999*

Planar Near-Field Measurements of Low-Sidelobe Antennas.
PB94-219235 *02,001*

Dual Frequency mm-Wave Radiometer Antenna for Airborne Remote Sensing of Atmosphere and Ocean.
PB95-180378 *02,006*

Standard Antennas for Electromagnetic Interference Measurements and Methods to Calibrate Them.
PB96-102561 *02,007*

Dual-Frequency Millimeter-Wave Radiometer Antenna for Airborne Remote Sensing of Atmosphere and Ocean.
PB96-112289 *02,009*

Comparison of k-Correction and Taylor-Series Correction for Probe-Position Errors in Planar Near-Field Scanning.
PB96-147137 *02,012*

Standard Source Method for Reducing Antenna Factor Errors in Shielded Room Measurements.
PB96-183157 *02,013*

Methodology for Electromagnetic Interference Measurements.
PB96-200126 *02,014*

Comparison of Ultralow-Sidelobe-Antenna Far-Field Patterns Using the Planar-Near-Field Method and the Far-Field Method.
PB96-200373 *02,015*

General Order 'N' Analytic Correction of Probe-Position Errors in Planar Near-Field Measurements.
PB96-200688 *01,562*

Novel Hot-Electron Microbolometer.
PB96-201025 *01,977*

ANTHROPOMETRY

Bibliography on Apparel Sizing and Related Issues.
PB94-161924 *02,806*

Body Dimensions for Apparel.
PB94-187739 *02,813*

ANTIFERROMAGNETIC COUPLING

Magnetic Structure Determination for Annealed Ni80Fe20/Ag Multilayers Using Polarized-Neutron Reflectivity.
PB96-176615 *03,739*

ANTIFERROMAGNETIC MATERIALS

Comment on 'Phase Transitions in Antiferromagnetic Superlattices'.
PB95-152971 *04,587*

ANTIFERROMAGNETICS

Antiferromagnetic Interlayer Correlations in Annealed Ni80Fe20/Ag Multilayers.
PB97-122220 *03,109*

ANTIFERROMAGNETISM

Concurrent Enhancement of Kerr Rotation and Antiferromagnetic Coupling in Epitaxial Fe/Cu/Fe Structures.
PB94-198769 *04,466*

ANTIMONY
Epitaxial Growth of Sb/GaSb Structures: An Example of V/III-V Heteroepitaxy.
PB95-202560 *04,693*

ANTIMONY CLUSTERS
Photoelectron Spectroscopy of Small Antimony Cluster Anions: Sb(-), Sb2(-), Sb3(-), and Sb4(-).
PB95-203139 *01,045*

ANTITHROMBIN III
Thermodynamic Analysis of Heparin Binding to Human Antithrombin.
PB94-199593 *03,455*

ANTIVIRAL AGENTS
Radiation Chemistry of Cyanine Dyes: Oxidation and Reduction of Merocyanine 540.
PB94-211661 *00,818*

APATITE/HYDROXY
Effect of Ethanol on the Solubility of Hydroxyapatite in the System Ca(OH)2-H3PO4-H2O at 25C and 33C.
PB95-169231 *00,169*

APATITES
Effect of Supersaturation on Apatite Crystal Formation in Aqueous Solutions at Physiologic pH and Temperature.
PB96-135215 *03,571*

APDE (APPLICATION PROTOCOL DEVELOPMENT ENVIRONMENT)
APDE Demonstration System Architecture. National PDES Testbed Report Series.
PB94-154325 *02,767*

APERTURES
Aperture Excitation of Electrically Large, Lossy Cavities.
PB94-145711 *00,029*

Aperture Excitation of Electrically Large, Lossy Cavities.
PB95-175675 *00,031*

High Accuracy Measurement of Aperture Area Relative to a Standard Known Aperture.
PB95-261954 *01,919*

Third Generation Water Bath Based Blackbody Source.
PB96-122148 *04,046*

APPAREL CLOTHING
Survey of Standards for the U.S. Fiber/Textile/Apparel Industry.
PB96-193792 *03,199*

APPEARANCE POTENTIAL
Appearance Potentials of Ions Produced by Electron-Impact Induced Dissociative Ionization of SF6, SF4, SF5Cl, S2F10, SO2, SO2F2, SOF2, and SOF4.
PB96-119730 *01,080*

APPLICATION PORTABILITY PROFILE
Application Portability Profile (APP): The U.S. Government's Open System Environment Profile Version 3.0.
PB96-158712 *01,753*

APPLICATION PROGRAMS (COMPUTERS)
User Interface Component of the Applications Portability Profile Category: Software Standard; Subcategory: Application Program Interface.
FIPS PUB 158-1 *01,793*

APPLICATION PROTOCOLS
APDE Demonstration System Architecture. National PDES Testbed Report Series.
PB94-154325 *02,767*

Extensions of the Prototype Application Protocol of Ready-to-Wear Apparel Pattern Making.
PB96-128194 *03,198*

APPLICATION SPECIFIC INTEGRATED CIRCUITS
Custom Integrated Circuit Comparator for High-Performance Sampling Applications.
PB94-213147 *02,320*

APPLICATIONS PROGRAMS (COMPUTERS)
Open System Environments.
N94-36857/8 *01,674*

Associated Object Model for Distributed Systems.
PB94-212016 *01,694*

Security in Open Systems.
PB95-105383 *01,473*

APPLIED MATHEMATICS
Computer Systems Laboratory Computing and Applied Mathematics Laboratory Technical Accomplishments, October 1994-March 1996.
PB96-193768 *01,638*

APPROXIMATION
Higher-Order Approximations in Ionospheric Wave-Propagation.
AD-A292 471/0 *04,420*

APS (APPLICATION PROTOCOLS)
Issues and Recommendations for a STEP Application Protocol Framework. National PDES Testbed.
PB94-160868 *02,770*

AQEOUS SPECIES
Summary of the Apparent Standard Partial Molal Gibbs Free Energies of Formation of Aqueous Species, Minerals, and Gases at Pressures 1 to 5000 Bars and Temperatures 25 to 1000C.
PB96-145891 *01,113*

AQUEOUS ELECTROLYTES
Absolute Determination of Electrolytic Conductivity for Primary Standard KC1 Solutions from 0 to 50C.
PB94-172798 *00,765*

AQUEOUS IRON
Thermodynamic Properties of the Aqueous Ions (2+ and 3+) of Iron and the Key Compounds of Iron.
PB96-145958 *01,119*

AQUEOUS PHASE
Free Radical Chemistry of the Atmospheric Aqueous Phase.
PB96-148101 *00,117*

AQUEOUS SOLUTIONS
Apparent Molar Heat Capacities and Apparent Molar Volumes of Aqueous Glucose at Temperatures from 298.15 K to 327.01 K.
PB94-212800 *03,459*

Two Phase Aqueous Extraction: Rheological Properties of Dextran, Polyethylene Glycol, Bovine Serum Albumin and Their Mixtures.
PB95-161998 *00,676*

Standard States, Reference States and Finite-Concentration Effects in Near-Critical Mixtures with Applications to Aqueous Solutions.
PB95-164349 *00,979*

Critical Lines for Type-III Aqueous Mixtures by Generalized Corresponding-States Models.
PB96-102371 *01,063*

Significant Contributions of IAPWS to the Power Industry, Science and Technology.
PB96-123252 *01,088*

Critical Review of Rate Constants for Reactions of Transients from Metal Ions and Metal Complexes in Aqueous Solution.
PB96-145859 *01,109*

System for Intercomparing Standard Solutions of Beta-Particle Emitting Radionuclides.
PB96-159637 *03,707*

ARC DISCHARGES
Decomposition of SF6 and Production of S2F10 in Power Arcs.
PB96-122619 *01,084*

ARC MODELS
Mathematical Models of Transport Phenomena Associated with Arc-Welding Processes: A Survey.
PB96-135058 *02,870*

ARC SPECTRA
Arc Spectra of Gallium, Indium, and Thallium.
AD-A295 411/3 *00,718*

ARC WELDING
Status Report: AWS Standards for Identifying Arc Welds (A91.1) and Recording Weld Data (A9.2).
PB95-162855 *02,861*

Through-the-Arc Sensing for Measuring Gas Metal Arc Weld Quality in Real Time.
PB95-164463 *02,908*

ARCHIE
Using Archie to Find Files on the INTERNET.
PB95-168605 *02,727*

ARCHITECTURE (COMPUTERS)
Overview of NASREM: The NASA/NBS Standard Reference Model for Telerobot Control System Architecture.
PB94-194560 *04,831*

AREA
High Accuracy Measurement of Aperture Area Relative to a Standard Known Aperture.
PB95-261954 *01,919*

ARGININE
Thermochemistry of the Hydrolysis of L-arginine to (L-citrulline + Ammonia) and of the Hydrolysis of L-arginine to (L-ornithine + Urea).
PB95-150801 *03,463*

ARGON
Measurement of the Thermal Properties of Electrically Conducting Fluids Using Coated Transient Hot Wires.
DE94017816 *00,722*

Absorption of Sound in Gases between 10 and 25 MHz: Argon.
PB94-199015 *04,183*

Atomic Transition Probability Ratios between Some Ar I 4s-4p and 4s-5p Transitions.
PB94-211554 *03,842*

Ion Broadening Parameters for Several Argon and Carbon Lines.
PB94-211562 *03,843*

Intermolecular HF Motion in Ar(sub n)HF Micromatrices (n=1,2,3,4,): Classical and Quantum Calculations on a Pairwise Additive Potential Surface.
PB95-107025 *03,871*

Vibration, Rotation, and Parity Specific Predissociation Dynamics in Asymmetric OH Stretch Excited ArH2O: A Half Collision Study of Resonant V-V Energy Transfer in a Weakly Bound Complex.
PB95-107140 *00,872*

Interatomic Potential of Argon.
PB95-141180 *00,912*

Interatomic Potential of Argon.
PB95-152989 *00,945*

Electrical Sensors for Monitoring rf Plasma Sheaths.
PB95-162962 *04,412*

Energy Dependences of Absorption in Beryllium Windows and Argon Gas.
PB96-102124 *04,020*

Ion Kinetics and Symmetric Charge-Transfer Collisions in Low-Current, Diffuse (Townsend) Discharges in Argon and Nitrogen.
PB96-123658 *04,051*

Absence of Quantum-Mechanical Effects on the Mobility of Argon Ions in Helium Gas at 4.35 K.
PB97-122543 *01,194*

ARGON COMPLEXES
Infrared and Microwave Spectroscopy of the Argon - Propyne Dimer.
PB94-198892 *00,794*

High-Resolution Infrared Overtone Spectroscopy of ArHF via Nd:YAG/Dye Laser Difference Frequency Generation.
PB94-211448 *00,816*

Spectroscopic Puzzle in ArHF Solved: The Test of a New Potential.
PB94-216058 *00,850*

Microwave and Submillimeter Spectroscopy of Ar-NH3 States Correlating with Ar+NH3(j=1, k=1).
PB95-152211 *00,942*

Vibrational Dependence of the Anisotropic Intermolecular Potential of Ar-HCl.
PB95-202685 *01,029*

Vibrational Dependence of the Anisotropic Intermolecular Potential of Ar-HF.
PB95-202693 *01,030*

Slit-Jet Near-Infrared Spectroscopy and Internal Rotor Dynamics of the ArH2O van der Waals Complex: An Angular Potential-Energy Surface for Internal H2O Rotation.
PB95-202792 *01,033*

Photodissociation Dynamics in Quantum State-Selected Clusters: A Test of the One-Atom Cage Effect in Ar-H2O.
PB95-203121 *01,044*

ARGON HYDRIDES
Ion Kinetic-Energy Distributions in Argon rf Glow Discharges.
PB95-141008 *04,409*

ARGON IONS
Determination of Atomic Data Pertinent to the Fusion Energy Program. Progress Report for FY 92.
DE94004400 *04,402*

Backscattering in Electron-Impact Excitation of Multiply Charged Ions.
PB94-185345 *03,799*

Use of an Ion Energy Analyzer: Mass Spectrometer to Measure Ion Kinetic-Energy Distributions from RF Discharges in Argon-Helium Gas Mixtures.
PB94-185717 *04,406*

Evidence for Significant Backscattering in Near-Threshold Electron-Impact Excitation of Ar(7+)(3s yields 3p).
PB95-126405 *03,883*

Ion Kinetic-Energy Distributions in Argon rf Glow Discharges.
PB95-141008 *04,409*

Kinetic-Energy Distributions of Ions Sampled from Argon Plasmas in a Parallel-Plate, Radio-Frequency Reference Call.
PB95-161964 *03,935*

Ion Kinetic-Energy Distributions and Balmer-alpha (Halpha) Excitation in Ar-H2 Radio-Frequency Discharges.
PB96-102959 *04,029*

ARGON PLASMA
Electrical Characterization of Radio-Frequency Discharges in the Gaseous Electronics Conference Reference Call.
PB95-164612 *01,905*

ARITHMETIC UNITS
MasPar MP-1 as a Computer Arithmetic Laboratory.
PB95-189437 *01,627*

AROMATIC COMPOUNDS
Detection of Aromatic Compounds Based on DNA Intercalation Using an Evanescent Wave Biosensor.
PB96-111976 *03,473*

AROMATIC POLYCYCLIC HYDROCARBONS
Shape Selectivity in Reversed-Phase Liquid Chromatography for the Separation of Planar and Non-Planar Solutes.
PB95-162608 *00,596*

ARRAYS
Step-Edge and Stacked-Heterostructure High-Tc Josephson Junctions for Voltage-Standard Arrays.
PB96-102066 *04,702*

Direct Observation of Vortex Dynamics in Two-Dimensional Josephson-Junction Arrays.
PB96-102223 *02,067*

Stable Phase Locking in a Two-Cell Ladder Array of Josephson Junctions.
PB96-111679 *04,722*

Performance and Reliability of NIST 10-V Josephson Arrays.
PB96-148051 *02,419*

Novel Vortex Dynamics in Two-Dimensional Josephson Arrays.
PB96-200167 *02,091*

Superconductor- Normal-Superconductor Junctions for Programmable Voltage Standards.
PB96-200241 *02,093*

Design of High-Frequency, High-Power Oscillators Using Josephson-Junction Arrays.
PB96-200258 02,094

High-Power, High-Frequency Oscillators Using Distributed Josephson-Junction Arrays.
PB96-200266 02,095

High Power Generation with Distributed Josephson-Junction Arrays.
PB97-111520 02,099

ARSENIC

Vibrational Distributions of As2 in the Cracking of As4 on Si(100) and Si(111).
PB94-198314 00,784

Single-Photon Ionization and Detection of Ga, In, and As(sub n) Species in GaAs Growth.
PB95-152815 00,591

In-situ Monitoring of Molecular Beam Epitaxial Growth Using Single Photon Ionization.
PB95-202222 01,023

Direct Detection of Atomic Arsenic Desorption from Si(100).
PB95-202230 01,024

Single-Photon Laser Ionization Time-of-Flight Mass Spectroscopy Detection in Molecular-Beam Epitaxy: Application to As4, As2, and Ga.
PB95-203337 01,052

ARTIFICIAL INTELLIGENCE

Intelligent Processing of Materials, Technical Activities 1993 (NAS-NRC Assessment Panel, April 21-22, 1994).
PB94-164183 02,809

Hierarchical Interaction between Sensory Processing and World Modeling in Intelligent Systems.
PB94-198256 01,580

Role of World Modeling and Value Judgment in Perception.
PB94-198264 01,581

Theory of Intelligent Systems.
PB94-198272 01,582

Intelligent Control for Multiple Autonomous Undersea Vehicles.
PB94-211877 03,747

Publications of the Intelligent Systems Division (Previously Robot Systems Division) Covering the Period January 1971-April 1994.
PB94-217098 02,935

Intelligent Control of an Inert Gas Atomization Process.
PB95-141057 03,344

Reference Model Architecture for Intelligent Systems Design.
PB95-143137 01,789

Exposure: An Expert System Fire Code.
PB95-162913 04,868

Unified Telerobotic Architecture Project (UTAP) Standard Interface Environment (SIE), May 1995.
PB95-242350 02,938

Intelligent Processing of Materials, Technical Activities 1994 (NAS-NRC Assessment Panel, April 6-7, 1995).
PB96-115050 03,359

ARTIFICIAL MEMBRANES

Determination of Osmotic Pressure and Fouling Resistances and Their Effects on Performance of Ultrafiltration Membranes.
PB94-212891 00,841

Characterization of the Adsorption-Fouling Layer Using Globular Proteins on Ultrafiltration Membranes.
PB94-212909 00,842

Supported Phospholipid/Alkanthiol Biomimetic Membranes: Insulating Properties.
PB95-180782 03,470

Phospholipid/Alkanethiol Bilayers for Cell-Surface Receptor Studies by Surface Plasmon Resonance.
PB96-102900 03,472

ARTIFICIAL SATELLITES

Frozen Orbits for Satellites Close to an Earth-Like Planet.
PB96-102165 04,839

ARTIFICIAL SUPERLATTICES

Magnetic Rare Earth Artificial Metallic Superlattices.
PB95-162293 04,611

ARYL ETHERS

Thermal Decomposition of Hydroxy- and Methoxy-Substituted Anisoles.
PB94-173036 00,767

ASBESTOS

Airborne Asbestos Method: Standard Test Method for High Precision Counting of Asbestos Collected on Filters. Version 1.0.
PB94-163003 00,525

Airborne Asbestos Method: Standard Test Method for Verified Analysis of Asbestos by Transmission Electron Microscopy. Version 2.0.
PB94-163045 00,526

Proficiency Tests for the NIST Airborne Asbestos Program, 1990.
PB94-188836 00,535

Proficiency Tests for the NIST Airborne Asbestos Program - 1991.
PB94-193828 00,537

Proficiency Tests for the NIST Airborne Asbestos Program - 1992.
PB94-194362 00,539

Airborne Asbestos Method: Standard Practice for Recording Transmission Electron Microscopy Data for the Analysis of Asbestos Collected onto Filters. Version 1.0.
PB94-210168 00,552

National Voluntary Laboratory Accreditation Program: Bulk Asbestos Analysis.
PB95-138129 02,541

Guidelines for Refractive Index Measurements of Asbestos.
PB95-151189 02,543

Proficiency Tests for the NIST Airborne Asbestos Program, 1993.
PB96-106463 00,610

Airborne Asbestos Analysis: National Voluntary Laboratory Accreditation Program.
PB96-147392 02,566

Airborne Asbestos Method: Bootstrap Method for Determining the Uncertainty of Asbestos Concentration. Version 1.0.
PB96-214614 00,646

ASCORBIC ACID

Temperature Dependence of the Rate Constants for Reaction of Inorganic Radicals with Organic Reductants.
PB94-198280 00,783

Ascorbic and Dehydroascorbic Acids Measured in Plasma Preserved with Dithiothreitol or Metaphorphoric Acid.
PB94-216330 03,495

Measurement of Ascorbic Acid in Human Plasma and Serum: Stability, Intralaboratory Repeatability, and Interlaboratory Reproducibility.
PB97-112445 03,511

ASHRAE STANDARD 62-1989

Ventilation, Carbon Dioxide and ASHRAE Standard 62-1989.
PB95-162095 02,544

ASPERGILLUS FUMIGATUS

Rapid Method for the Isolation of Genomic DNA from 'Aspergillus fumigatus'.
PB96-147061 03,488

ASPERITY

Asperity-Asperity Contact Mechanisms Simulated by a Two-Ball Collision Apparatus.
PB95-164158 02,966

ASPHALT PAVEMENTS

Development of a Method for Measuring Water-Stripping Resistance of Asphalt/Siliceous Aggregate Mixtures.
PB96-202296 01,329

ASSIGNMENT MODELS

Moments of the Quartic Assignment Statistic with an Application to Multiple Regression.
PB95-181103 03,442

ASSOCIATIVE IONIZATION

Ultracold Collisions: Associative Ionization in a Laser Trap.
PB94-213238 03,859

ASTM STP 1199

Introduction to ASTM 1199 'Wear Test Selection for Design and Application'.
PB95-162517 03,238

ASTRONOMICAL SATELLITES

FUSE: The Far Ultraviolet Spectrograph Explorer.
PB94-213410 00,063

ASTROPHYSICS

Papers on the Symposium on Collision Phenomena in Astrophysics, Geophysics, and Masers.
AD-A280 291/6 00,047

ASYMMETRY PARAMETERS

Vibrationally Resolved Photoelectron Angular Distributions and Branching Ratios for the Carbon Dioxide Molecule in the Wavelength Region 685-795 Angstrom.
PB96-201207 04,131

ASYNCHRONOUS TRANSFER MODE

Asynchronous Transfer Mode Procurement and Usage Guide.
PB95-174967 01,481

NIST ATM Network Simulator: Operation and Programming, Version 1.0.
PB96-106851 01,487

Strategy to Support Multipoint Communication Service Over Native ATM Service.
PB96-176672 01,507

ATAXIA TELANGIECTASIA

Modification of Deoxyribose-Phosphate Residues by Extracts of Ataxia Telangiectasia Cells.
PB94-212602 03,458

ATM (ASYNCHRONOUS TRANSFER MODE)

Asynchronous Transfer Mode Procurement and Usage Guide.
PB95-174967 01,481

NIST ATM Network Simulator: Operation and Programming, Version 1.0.
PB96-106851 01,487

Strategy to Support Multipoint Communication Service Over Native ATM Service.
PB96-176672 01,507

ATMOSPHERIC CHEMISTRY

Thermodynamic Properties of Gas Phase Species of Importance to Ozone Depletion.
PB94-198215 00,126

Atmospheric Reactivity of alpha-Methyl-Tetrahydrofuran.
PB95-163705 02,548

Atmospheric Lifetimes of HFC-143a and HFC-245fa: Flash Photolysis Resonance Fluorescence Measurements of the OH Reaction Rate Constants.
PB97-112577 00,118

Kinetics of the Reaction of the Sulfate Radical with the Oxalate Anion.
PB97-119127 01,186

ATMOSPHERIC DIFFUSION

Smoke Plume Trajectory from In situ Burning of Crude Oil: Field Experiments.
PB96-200993 02,597

ATMOSPHERIC SCATTERING

Radiometric Model of the Transmission Cell-Reciprocal Nephelometer.
PB95-150132 00,124

ATMOSPHERIC TEMPERATURE

Modulation of Fossil Fuel Production by Global Temperature Variations, 2.
PB94-146636 02,533

ATOM-ATOM COLLISIONS

Intersystem Crossing in Collisions of Aligned Ca(4s5p (1)P) + He: A Half Collision Analysis Using Multichannel Quantum Defect Theory.
PB94-211133 00,813

Astrophysical Aspects of Neutral Atom Line Broadening.
PB94-213287 00,061

Associative Ionization in Collisions of Slowed and Trapped Sodium.
PB95-125886 03,880

Hydrogen Balmer Alpha Line Shapes for Hydrogen-Argon Mixtures in a Low-Pressure rf Discharge.
PB95-153433 03,924

Three-Vector Correlation Study of Orientation and Coherence Effects in Na(3p, (2)P1/2 inversely maps (2)P3/2)+He: Semiclassical and Quantum Calculations.
PB95-202453 03,979

Laser Preparation and Probing of Initial and Final Orbital Alignment in Collision-Induced Energy Transfer Ca(4s5p,(1)P1) + He yields Ca(4s5p,(3)P2) + He.
PB95-203261 04,003

Initial and Final Orbital Alignment Probing of the Fine-Structure-Changing Collisions among the Ca (4s)(1)(4p)(1), (3)PJ States with He: Determination of Coherence and Conventional Cross-Sections.
PB95-203279 04,004

ATOM COOLING

sigma+-sigma- Optical Molasses in a Longitudinal Magnetic Field.
PB95-161840 03,934

ATOM LITHOGRAPHY

Nanofabrication of a Two-Dimensional Array Using Laser-Focused Atomic Deposition.
PB96-119417 04,732

Microlithography by Using Neutral Metastable Atoms and Self-Assembled Monolayers.
PB96-190038 02,441

ATOM-MOLECULE COLLISIONS

Collision-Induced Emission in the Fundamental Vibration-Rotation Band of H2.
PB94-199445 03,811

Vibrational Energy Transfer in S1 p-Difluorobenzene. A Comparison of Low and Room Temperature Collisions.
PB95-108619 00,883

Preferential In-Plane Rotational Excitation of H2O (001) by Translational-to-Vibrational Transfer from 2.2 eV H Atoms.
PB95-202875 01,035

ATOM OPTICS

Laser-Focused Atomic Deposition.
PB95-161618 04,604

Using Atom Optics to Fabricate Nanostructures.
PB96-141247 04,757

ATOM PROBES

Performance of a Reflectron Energy Compensating Mirror.
PB94-199460 00,547

ATOM RADICAL REACTIONS

Laser Flash Photolysis, Time-Resolved Fourier Transform Infrared Emission Study of the Reaction Cl + C2H5 yields HCl(v) + C2H4.
PB95-203238 01,049

ATOM TRAPS

Localization of Atoms in a Three-Dimensional Standing Wave.
PB95-163887 03,944

Reduction of Light-Assisted Collisional Loss Rate from a Low-Pressure Vapor-Cell Trap.
PB95-202248 03,971

Numerical Solution of the Nonlinear Schroedinger Equation for Small Samples of Trapped Neutral Atoms.
PB95-202578 03,985

Probing Bose-Einstein Condensed Atoms with Short Laser Pulses.
PB95-202818 03,991

Behavior of Atoms in a Compressed Magneto-Optical Trap.
PB95-203105 *03,999*

Improved Hyperfine Measurements of the Na NP Excited State Through Frequency-Controlled Dopplerless Spectroscopy in a Zeeman Magneto-Optic Laser Trap.
PB95-203840 *04,012*

Comment on <<A Dynamic Electric Trap for Ground-State Atoms>>.
PB96-200290 *04,123*

ATOMIC ABSORPTION

Application of a Novel Slurry Furnace AAS Protocol for Rapid Assessment of Lead Environmental Contamination.
PB96-112354 *02,526*

ATOMIC BEAMS

Atomic Beam Splitters and Mirrors by Adiabatic Passage in Multilevel Systems.
PB94-216439 *03,867*

Laser Focusing of Atoms: A Particle Optics Approach.
PB94-216660 *03,870*

Velocity Distribution of Atomic Beams by Gated Optical Pumping.
PB95-180519 *01,542*

Nanofabrication of a Two-Dimensional Array Using Laser-Focused Atomic Deposition.
PB96-119417 *04,732*

ATOMIC CLOCKS

Utc Dissemination to the Real-Time User.
N19960042622 *01,521*

Confidence on the Three-Point Estimator of Frequency Drift.
PB95-163838 *01,539*

Non-Neutral Ion Plasmas and Crystals, Laser Cooling, and Atomic Clocks.
PB95-175113 *03,957*

Time and Frequency: Bibliography of NIST Publications, March 1995.
PB95-220463 *01,548*

Accurate Measurement of Time.
PB96-119482 *01,552*

Atomic Clock.
PB96-119490 *01,553*

ATOMIC CLUSTERS

Photoelectron Spectroscopy of Negatively Charged Bismuth Clusters: Bi(-)2, Bi(-)3, and Bi(-)4.
PB95-108494 *00,880*

Photoelectron Spectroscopy of Small Antimony Cluster Anions: Sb(-), Sb2(-), Sb3(-), and Sb4(-).
PB95-203139 *01,045*

ATOMIC COLLISIONS

Three-Vector Correlation Theory for Orientation/Alignment Studies in Atomic and Molecular Collisions.
PB94-211109 *03,834*

Intersystem Crossing in Collisions of Aligned Ca(4s5p (1)P) + He: A Half Collision Analysis Using Multichannel Quantum Defect Theory.
PB94-211133 *00,813*

Theory of Atomic Collisions at Ultracold Temperatures.
PB94-212560 *03,851*

Associative Ionization in Collisions of Slowed and Trapped Sodium.
PB95-125886 *03,880*

Hyperfine Effects and Associative Ionization of Ultracold Sodium.
PB95-151221 *03,903*

Laser Assisted Collisions at Ultracold Temperatures.
PB95-161220 *03,929*

Three-Vèctor Correlation Study of Orientation and Coherence Effects in Na(3p, (2)P1/2 inversely maps (2)P3/2)+He: Semiclassical and Quantum Calculations.
PB95-202453 *03,979*

n-Vector Correlations in Collision Dynamics with Atomic Orbital Alignment: The Importance of Coherence Denoting Azimuthal Structure for n (greater than or equal to) 3.
PB95-202545 *03,983*

Collisional Energy Transfer between Excited-State Strontium and Noble-Gas Atoms.
PB95-202958 *03,995*

Energy-Pooling Collisions in Barium.
PB95-203030 *03,997*

Laser Preparation and Probing of Initial and Final Orbital Alignment in Collision-Induced Energy Transfer Ca(4s5p,(1)P1) + He yields Ca(4s5p,(3)P2) + He.
PB95-203261 *04,003*

Initial and Final Orbital Alignment Probing of the Fine-Structure-Changing Collisions among the Ca (4s)(1)(4p)(1), (3)PJ States with He: Determination of Coherence and Conventional Cross-Sections.
PB95-203279 *04,004*

Orbital Alignment and Vector Correlations in Inelastic Atomic Collisions.
PB96-122742 *04,047*

Atom Cooling and Trapping, and Collisions of Trapped Atoms.
PB96-122916 *04,048*

Laser Modification of Ultracold Collisions: Experiment.
PB96-157987 *04,075*

ATOMIC DATA

Spectral Data for Highly Ionized Krypton, Kr V through Kr XXXVI.
PB96-145917 *01,115*

Resonance Ionization Spectroscopy/Resonance Ionization Mass Spectrometry Data Service. V-Data Sheets for Ga, Mn, Sc, and Tl.
PB96-158068 *00,625*

ATOMIC DEPOSITION

Nanostructure Fabrication via Laser-Focused Atomic Deposition (Invited).
PB96-204094 *04,132*

ATOMIC ENERGY LEVELS

Atomic Energy Levels As Derived from the Analyses of Optical Spectra. Volume 1. Section 1. The Spectra of Hydrogen, Deuterium, Helium, Lithium Beryllium, Boron, Carbon, Nitrogen, Oxygen, and Fluorine.
AD-A278 130/0 *03,764*

Atomic Energy Levels in Crystals.
AD-A280 150/4 *04,431*

Atomic Energy Levels. As Derived From the Analyses of Optical Spectra. Volume 3.
AD-A280 279/1 *00,714*

Wavelengths and Energy Levels of Neutral Kr(84) and Level Shifts in All Kr Even Isotopes.
PB94-140605 *03,780*

Energy Levels of Germanium, Ge I through Ge XXXII.
PB94-162351 *00,747*

Spectrum and Energy Levels of Five-Times-Ionized Niobium (Nb VI).
PB94-185246 *04,226*

Spectrum and Energy Levels of Triply Ionized Barium (Ba IV).
PB95-140877 *03,888*

Precision Lifetime Measurements of Cs 6p (2)P1/2 and 6p (2)P3/2 Levels by Single-Photon Counting.
PB95-203816 *04,010*

Designations of ds(2)p Energy Levels in Neutral Zirconium, Hafnium, and Rutherfordium (Z=104).
PB96-180120 *04,116*

ATOMIC FLUIDS

Conditions for Existence of a Reentrant Solid Phase in a Sheared Atomic Fluid.
PB94-211380 *04,198*

ATOMIC FORCE MICROSCOPES

Development of a Calibrated Atomic Force Microscope.
PB94-185683 *02,894*

Increasing the Value of Atomic Force Microscopy Process Metrology Using a High-Accuracy Scanner, Tip Characterization, and Morphological Image Analysis.
PB96-190293 *02,758*

Scanned Probe Microscope Tip Characterization Without Calibrated Tip Characterizers.
PB96-190368 *02,759*

ATOMIC FORCE MICROSCOPY

Force Calibrations in the Nanonewton Regime.
PB95-168696 *03,949*

Flexible-Diaphragm Force Microscope.
PB95-180915 *03,966*

Morphological Estimation of Tip Geometry for Scanned Probe Microscopy.
PB95-203444 *02,662*

Recent Results in Magnetic Force Microscopy.
PB96-103130 *04,721*

Effects of Etching on the Morphology and Surface Resistance of YBa2Cu3O7-delta Films.
PB96-135355 *02,410*

Development of Highly Conductive Cantilevers for Atomic Force Microscopy Point Contact Measurements.
PB96-138573 *04,751*

ATOMIC FOUNTAIN

Laser-Cooled Neutral Atom Frequency Standards.
PB96-160312 *04,086*

ATOMIC INTERACTIONS

Measurement of the Atomic Na(3P) Lifetime and of Retardation in the Interaction between Two Atoms Bound in a Molecule.
PB97-122360 *04,178*

ATOMIC IONS

Early Dielectronic Recombination Measurements: Singly Charged Ions.
PB94-211158 *03,836*

Bonding in Doubly Charged Diatomics.
PB95-164315 *00,976*

ATOMIC MANIPULATION

Nanostructure Fabrication via Direct Writing with Atoms Focused in Laser Fields.
PB95-150272 *04,564*

Atomic Manipulation of Polarizable Atoms by Electric Field Directional Diffusion.
PB95-150587 *04,572*

Manipulation of Adsorbed Atoms and Creation of New Structures on Room-Temperature Surfaces with a Scanning Tunneling Microscope.
PB95-151536 *04,578*

ATOMIC MASS

New Values for Silicon Reference Materials, Certified for Isotope Abundance Ratios. Letter to the Editor.
PB94-219268 *00,863*

ATOMIC & MOLECULAR STUDIES

Production and Spectroscopy of Small Polyatomic Molecular Ions Isolated in Solid Neon. (Reannouncement with New Availability Information).
AD-A234 043/8 *00,704*

Vibrational Spectra of Molecular Ions Isolated in Solid Neon. 6. CO4(-). (Reannouncement with New Availability Information).
AD-A238 415/4 *00,705*

Vibrational Spectra of Molecular Ions Isolated in Solid Neon. 7. CO(+), C2O2(+), and C2O2(-). (Reannouncement with New Availability Information).
AD-A239 729/7 *00,706*

Vibrational Spectra of Molecular Ions Isolated in Solid Neon: HCCH+ and HCC-. (Reannouncement with New Availability Information).
AD-A253 551/6 *00,707*

Vibrational Spectra of Molecular Ions Isolated in Solid Neon. 11. NO2(+), NO2(-), and NO3(-).
AD-A275 828/2 *00,708*

Atomic Energy Levels As Derived from the Analyses of Optical Spectra. Volume 1. Section 1. The Spectra of Hydrogen, Deuterium, Helium, Lithium Beryllium, Boron, Carbon, Nitrogen, Oxygen, and Fluorine.
AD-A278 130/0 *03,764*

Ultraviolet Multiplet Table. Finding List for Spectra of the Elements Molybdenum to Lanthanum (Z = 42 to 57); Hafnium to Radium (Z = 72 to 88).
AD-A278 131/8 *00,709*

Atomic Energy Levels in Crystals.
AD-A280 150/4 *04,431*

Arc Spectra of Gallium, Indium, and Thallium.
AD-A295 411/3 *00,718*

Infrared and Near-Infrared Spectra of HCC and DCC Trapped in Solid Neon.
AD-A295 578/9 *03,773*

Thermal Decomposition Pathways in Nitramine Propellants.
AD-A295 896/5 *03,753*

Spectroscopic Study of Reaction Intermediates and Mechanisms in Nitramine Decomposition and Combustion.
AD-A296 061/5 *03,774*

Microwave Spectrum and Structure of CH3NO2-H20.
AD-A296 377/5 *00,719*

Molecular Microwave Spectra Tables.
AD-A296 498/9 *00,720*

Physical Properties of Some Purified Aliphatic Hydrocarbons.
AD-A297 265/1 *00,657*

Determination of Atomic Data Pertinent to the Fusion Energy Program. Progress Report for FY 92.
DE94004400 *04,402*

Electron-atom collision studies using optically state selected beams. Progress report, May 15, 1987--May 14, 1988.
DE95004446 *03,776*

Electron-atom collision studies using optically state selected beams. Progress report, May 15, 1988--May 14, 1991.
DE95004447 *03,777*

Complementary Molecular Information on Phthalocyanine Compounds Derived from Laser Microprobe Mass Spectrometry and Micro-Raman Spectroscopy.
PB94-172269 *00,757*

Hot Carrier Excitation of Adlayers: Time-Resolved Measurement of Adsorbate-Lattice Coupling.
PB94-172285 *00,758*

Electron Screening Correction to the Self Energy in High-Z Atoms.
PB94-172376 *03,789*

Neutron-Spectroscopy Study of the Hydrogen Vibrations in Hydrogen-Doped YBa2Cu3Ox.
PB94-172475 *04,441*

Role of Adsorbed Alkalis in Desorption Induced by Electronic Transitions.
PB94-172574 *00,762*

Inelastic Neutron Scattering Studies of Rotational Excitations and the Orientational Potential in C60 and A3C60 Compounds.
PB94-172673 *00,763*

New Critical Review of Experimental Stark Widths and Shifts.
PB94-172830 *03,790*

National Institute of Standards and Technology Resonance Ionization Spectroscopy/Resonance Ionization Mass Spectroscopy Data Service.
PB94-172897 *03,793*

Homoepitaxial Growth of Iron and a Real Space View of Reflection-High-Energy-Electron Diffraction.
PB94-173069 *04,445*

Can Quantum Mechanical Description of Electron-Sodium Collisions Be Considered Complete. Present Status and Future Prospects for 3s <-> 3p Transitions.
PB94-185014 *00,768*

Low-Energy Electron Scattering from Caesium Atoms: Comparison of a Semirelativistic Breit-Pauli and a Full Relativistic Direc Treatment.
PB94-185030 *00,769*

Electron-Impact Ionization of In(+) and Xe(+).
PB94-185089 *00,770*

Measurement of the J=2 less than 1 Fine-Structure Interval for (28)Si and (29)Si in the Ground (3)P State.
PB94-185097 *00,771*

Spectrum and Energy Levels of Five-Times-Ionized Niobium (Nb VI).
PB94-185246 *04,226*

Investigation of LS Coupling in Boronlike Ions.
PB94-185295 *03,797*

Quantum Dynamics of Renner-Teller Vibronic Coupling: The Predissociation HCO.
PB94-185303 *00,773*

Optical Conductivity of Single Crystals of Ba1-xMxBiO3(M=K, Rb, x=0.04, 0.37).
PB94-185329 *04,447*

Backscattering in Electron-Impact Excitation of Multiply Charged Ions.
PB94-185345 *03,799*

Temperature Dependence and Anharmonicity of Phonons on Ni(110) and Cu(110) Using Molecular Dynamics Simulations.
PB94-185477 *04,449*

Charge Transfer and Collision-Induced Dissociation Reactions of CF(2+) and CF2(2+) with the Rare Gases at a Laboratory Collision Energy of 49 eV.
PB94-185584 *00,775*

High Resolution IR Studies of Polymolecular Clusters: Micromatrices and Unimolecular Ring Opening.
PB94-185691 *00,777*

Verification of the Ponderomotive Approximation for the ac Stark Shift in Xe Rydberg Levels.
PB94-185709 *03,801*

Angular Distributions for Near-Threshold (e,2e) Processes for Li and Mg.
PB94-185725 *00,778*

Collision-Induced Neutral Loss Reactions of Molecular Dications.
PB94-185808 *00,780*

Fourier Transform Atomic Emission Studies Using a Glow Discharge as the Emission Source.
PB94-185980 *00,533*

Oxidation of 10-Methylacridan, a Synthetic Analogue of NADH and Deprotonation of Its Cation Radical. Convergent Application of Laser Flash Photolysis and Direct and Redox Catalyzed Electrochemistry to the Kinetics of Deprotonation of the Cation Radical.
PB94-198371 *00,785*

Energy Dependence of Collision Characteristics in Molecule-Surface Collisions.
PB94-198504 *00,786*

Density Matrix Calculation of Population Transfer between Vibrational Levels of Na2 by Stimulated Raman Scattering with Temporally Shifted Laser Beams.
PB94-198546 *00,787*

Strong Hydrogen Bond in the Formic Acid-Formate Anion System.
PB94-198595 *00,788*

Structure of Glycine-Water H-Bonded Complexes.
PB94-198603 *00,789*

Rotational Spectrum of Copper Hydride Using Tunable Far Infrared Radiation.
PB94-198637 *00,792*

Tunneling-Rotation Spectrum of the Hydrogen Fluoride Dimer.
PB94-198678 *00,793*

Laser Ablation of Thin Films as a Free Atom Source for Pulsed RIMS.
PB94-198710 *00,540*

Scattering Properties of the Leveled-Wave Model of Random Morphologies.
PB94-198835 *03,807*

Infrared and Microwave Spectroscopy of the Argon - Propyne Dimer.
PB94-198892 *00,794*

Evaluation of Two-Photon Exchange Graphs for Highly-Charged Heliumlike Ions.
PB94-198918 *03,808*

Collision-Induced Emission in the Fundamental Vibration-Rotation Band of H2.
PB94-199445 *03,811*

New Rydberg States of Aluminum Monofluoride Observed by Resonance-Enhanced Multiphoton Ionization Spectroscopy.
PB94-199544 *00,797*

Vibrational Autoionization in H2: Vibrational Branching Ratios and Photoelectron Angular Distributions Near the v(+)=3 Threshold.
PB94-199577 *00,799*

Experimental Aspects and Z-Dependent Systematics in One- and Two-Electron Ions and Single Vacancy Systems.
PB94-199627 *03,815*

Status of a Silicon Lattice Measurement and Dissemination Exercise.
PB94-199635 *04,474*

Fragment Energy and Vector Correlations in the Overtone-Pumped Dissociation of HN3X(1)A'.
PB94-199908 *00,802*

2-Tunneling Path Internal-Axis-Method-Like Treatment of the Microwave Spectrum of Divinyl Ether.
PB94-200466 *00,808*

Two-Dimensional POMMIE Carbon-Proton Chemical Shift Correlated (13)C NMR Spectrum Editing.
PB94-200508 *00,809*

Anharmonic Phonons and the Isotope Effect in Superconductivity.
PB94-200557 *04,486*

Extension of Heterodyne Frequency Measurements on OCS to 87 THz (2900 cm(-1)).
PB94-200680 *00,811*

Multichannel Quantum Defect Half Collision Analysis of K2 Photodissociation Through the B1Pi(sub u) State.
PB94-211125 *00,812*

Intersystem Crossing in Collisions of Aligned Ca(4s5p (1)P) + He: A Half Collision Analysis Using Multichannel Quantum Defect Theory.
PB94-211133 *00,813*

Early Dielectronic Recombination Measurements: Singly Charged Ions.
PB94-211158 *03,836*

Brillouin Light Scattering Intensities for Thin Magnetic Films with Large Perpendicular Anisotropies.
PB94-211174 *04,488*

Reaction Rate Determinations of Vinyl Radical Reactions with Vinyl, Methyl, and Hydrogen Atoms.
PB94-211398 *00,815*

P-Type Doubling in the Infrared Spectrum of NO-HF.
PB94-211463 *00,817*

Magnetic Dipole Line from U LXXI Ground-Term Levels Predicted at 3200 Angstroms.
PB94-211497 *04,407*

Photoionization of Small Molecules Using Synchrotron Radiation.
PB94-211505 *03,841*

Atomic Transition Probability Ratios between Some Ar I 4s-4p and 4s-5p Transitions.
PB94-211554 *03,842*

Ion Broadening Parameters for Several Argon and Carbon Lines.
PB94-211562 *03,843*

Asymptotic Wave Function Splitting Procedure for Propagating Spatially Extended Wave Functions: Application to Intense Field Photodissociation of H2(+).
PB94-211786 *03,847*

Discontinuous Volume Change at the Orientational-Ordering Transition in Solid C60.
PB94-211828 *00,821*

Design and Characterization of X-Ray Multilayer Analyzers for the 50 - 1000 eV Region.
PB94-211851 *03,848*

Use of Extended Permutation-Inversion Groups in Constructing Hyperfine Hamiltonians for Symmetrical-Top Internal Rotor Molecules Like H3C-SiH3.
PB94-212032 *00,823*

Experimental and Abinitio Studies of Electronic Structures of the CCl3 Radical and Cation.
PB94-212131 *00,826*

Photoelectron Spectroscopic Study of the Valence and Core-Level Electronic Structure of BaTiO3.
PB94-212149 *04,500*

K alpha Transitions in Few-Electron Ions and in Atoms.
PB94-212248 *03,849*

Quantum Projection Noise: Population Fluctuations in Two-Level Systems.
PB94-212271 *03,850*

Multiphoton Ionization of SiH3 and SiD3 Radicals. 2. Three Photon Resonance-Enhanced Spectra Observed between 460 and 610 nm.
PB94-212487 *00,835*

New Electronic States of NH and ND Observed from 258 to 288 nm by Resonance Enhanced Multiphoton Ionization Spectroscopy.
PB94-212495 *00,836*

Multiphoton Ionization of SiH3 and SiD3 Radicals: Electronic Spectra, Vibrational Analyses of the Ground and Rydberg States, and Ionization Potential.
PB94-212503 *00,837*

Theory of Atomic Collisions at Ultracold Temperatures.
PB94-212560 *03,851*

Attempts at Extending the Unified Theory to Include Many-Body Effects.
PB94-212719 *04,408*

Autoionizing Resonances in Electric Fields.
PB94-212727 *03,853*

Relativistic and Quantum Electrodynamic Effects in Highly-Charged Ions.
PB94-212784 *03,854*

Product Kinetic Energies, Correlations, and Scattering Anisotropy in the Bimolecular Reactor O((1)D)+H2O yields 2OH.
PB94-212792 *00,838*

Molecular-Beam Optothermal Spectrum of the OH Stretching Band of Methanol.
PB94-212826 *00,839*

Fundamental Torsion Band in Acetaldehyde.
PB94-212834 *00,840*

Atomic Branching Ratio Data for Carbon-Like Ions.
PB94-212842 *03,855*

Active Site Ionicity and the Mechanism of Carbonic Anhydrase.
PB94-212974 *00,843*

Dipole Moments in Rare Gas Interactions.
PB94-212982 *00,844*

Ultracold Collisions: Associative Ionization in a Laser Trap.
PB94-213238 *03,859*

High-Energy Behavior of the Double Photoionization of Helium from 2 to 12 keV.
PB94-213279 *03,860*

RIS Studies of Autoionization in Calcium.
PB94-213295 *00,849*

Molecular Spectroscopy.
PB94-213337 *03,861*

Atomic, Molecular, and Optical Physics with X-rays.
PB94-213378 *03,863*

FTS Infrared Measurements of the Rotational and Vibrational Spectrum of LiH and LiD.
PB94-216231 *00,856*

Self Broadening in the nu1 Band of NH3.
PB94-216371 *00,857*

Kinetics and Mechanism of the Collision-Activated Dissociation of the Acetone Cation.
PB94-216462 *00,859*

Crystal Structure of Calcium Adipate Monohydrate.
PB94-216579 *00,153*

Proton Affinity Ladders from Variable-Temperature Equilibrium Measurements. 1. A Re-Evaluation of the Upper Proton Affinity Range.
PB94-216603 *00,861*

Determination of Complex Scattering Amplitudes in Low-Energy Elastic Electron-Sodium Scattering.
PB94-216652 *03,869*

Laser Focusing of Atoms: A Particle Optics Approach.
PB94-216660 *03,870*

One-Electron Oxidation of Nickel Porphyrins. Effect of Structure and Medium on Formation of Nickel(III) Porphyrin or Nickel(II) Porphyrin pi-Radical Cation.
PB95-107058 *00,865*

Site of One-Electron Reduction of Ni(II) Porphyrins. Formation of Ni(I) Porphyrin of Ni(II) Porphyrin pi-Radical Anion.
PB95-107066 *00,866*

Metalloporphyrin Sensitized Photooxidation of Water to Oxygen on the Surface of Colloidal Iridium Oxides - Photochemical and Pulse Radiolytic Studies.
PB95-107082 *00,868*

Determination of the Molecular Parameters of NiH in Its (2)Delta Ground State by Laser Magnetic Resonance.
PB95-107116 *00,869*

Mode Specific Vibrational Predissociation Dynamics in Fragile Molecules.
PB95-107132 *00,871*

Heterodyne Measurement of the Fluorescence Spectrum of Optical Molasses.
PB95-108411 *03,873*

Self-, N2- and Ar-Broadening and Line Mixing in HCN and C2H2.
PB95-108445 *00,876*

Decoupling in the Line Mixing of Acetylene Infrared Q Branches.
PB95-108452 *00,877*

Measurement of the Self Broadening of the H2Q(0-5) Raman Transitions from 295 to 1000 K.
PB95-108627 *00,884*

Addition of M and L-Series Lines to NIST Algorithm for Calculation of X-Ray Tube Output Spectral Distributions.
PB95-108742 *00,569*

Atoms in Optical Molasses.
PB95-108874 *03,875*

Atoms in Optical Molasses: Applications to Frequency Standards.
PB95-108882 *03,876*

Optical Molasses: Cold Atoms for Precision Measurements.
PB95-108890 *03,877*

Optical Molasses: The Coldest Atoms Ever.
PB95-108908 *03,878*

Reanalysis of the (010), (020), (100), and (001) Rotational Levels of (32)S(16)O2.
PB95-125621 *00,887*

Mid- and Near-Infrared Spectra of Water and Water Dimer Isolated in Solid Neon.
PB95-125662 *00,888*

Vibrational Spectra of Molecular Ions Isolated in Solid Neon. X. H2O(+), HDO(+), and D2O(+).
PB95-125670 *00,889*

Vibrational Spectra of Molecular Ions Isolated in Solid Neon. XI. NO2(+), NO2(-), and NO3(-).
PB95-125688 *00,890*

Infrared Spectra of van der Waals Complexes of Importance in Planetary Atmospheres.
PB95-125738 *00,071*

Single-Atom Point Source for Electrons: Field-Emission Resonance Tunneling in Scanning Tunneling Microscopy.
PB95-125860 *00,893*

Associative Ionization in Collisions of Slowed and Trapped Sodium.
PB95-125886 *03,880*

Temperature of Optical Molasses for Two Different Atomic Angular Momenta.
PB95-126058 *03,881*

Rotational Spectrum and Structure of a Weakly Bound Complex of Ketene and Acetylene.
PB95-126140 *00,896*

Wavelengths and Isotope Shifts for Lines of Astrophysical Interest in the Spectrum of Doubly Ionized Mercury (Hg III).
PB95-140869 *03,887*

Spectrum and Energy Levels of Triply Ionized Barium (Ba IV).
PB95-140877 *03,888*

Associative Electron Attachment to S2F10, S2OF10, and S2O2F10.
PB95-140992 *00,907*

Infrared Spectrum of OClO in the 2000/cm(-1) Region: The 2(nu sub 1) and (nu sub 1 + nu sub 3) Bands.
PB95-141032 *00,908*

Intensities and Dipole Moment Derivatives of the Fundamental Bands of (35)ClO2 and an Intensity Analysis of the nu1 Band.
PB95-141040 *00,909*

Perturbative Calculation of the AC Stark Effect by the Complex Rotation Method.
PB95-141123 *04,260*

Interatomic Potential of Argon.
PB95-141180 *00,912*

Resonance and Threshold Effects in Polarized X-Ray Emission from Atoms and Molecules.
PB95-150298 *03,891*

Self-Avoiding Surfaces, Topology, and Lattice Animals.
PB95-150512 *04,571*

Contrast Matched Studies of a Sheared Binary Colloidal Suspension.
PB95-150561 *00,918*

Atomic Manipulation of Polarizable Atoms by Electric Field Directional Diffusion.
PB95-150587 *04,572*

Microwave Spectra of van der Waals Complexes of Importance in Planetary Atmospheres.
PB95-150611 *00,919*

Improved Wavelengths for Prominent Lines of Cr XVI to Cr XXII.
PB95-150629 *03,895*

Observation of Pd-Like Resonance Lines Through Pt(32+) and Zn-Like Resonance Lines of Er(38+) and Hf(42+).
PB95-150637 *03,896*

Rb-Like Spectra: Pd X to Nd XXIV.
PB95-150645 *03,897*

Rh I Isoelectronic Sequence Observed from Er(23+) to Pt(33+).
PB95-150652 *03,898*

Spectra of Ag I Isoelectronic Sequence Observed from Er(21+) to Au(32+).
PB95-150660 *03,899*

High-Resolution Infrared Spectroscopy of DF Trimer: A Cyclic Ground State Structure and DF Stretch Induced Intramolecular Vibrational Coupling.
PB95-150678 *00,920*

Calculations of Electron Inelastic Mean Free Paths (IMFPs). 4. Evaluation of Calculated IMFPs and of the Predictive IMFP Formula TPP-2 for Electron Energies between 50 and 2000 eV.
PB95-150728 *00,922*

Analysis of the 5s(2)5p(2)-(5s5p(3)+5s(2)5p5d+5s(2)5p6s) Transitions of Four-Times Ionized Xenon (Xe V).
PB95-150769 *03,900*

Relativistic Effects in Spin-Polarization Parameters for Low-Energy Electron-Cs Scattering.
PB95-150868 *03,901*

Methyl Torsional Levels of Solid Acetonitrile (CH3CN): A Neutron Scattering Study.
PB95-151015 *00,926*

Electronic Spectra of CF2Cl and CFCl2 Radicals Observed by Resonance Enhanced Multiphoton Ionization.
PB95-151023 *00,927*

Homogeneous Gas Phase Decyclization of Tetralin and Benzocyclobutene.
PB95-151049 *00,928*

Hyperfine Effects and Associative Ionization of Ultracold Sodium.
PB95-151221 *03,903*

Magneto-Optical Trapping of Metastable Xenon: Isotope-Shift Measurements.
PB95-151254 *03,905*

High Resolution Angle Resolved Photoelectron Spectroscopy Study of N2.
PB95-151494 *03,907*

Spectroscopic Data for Fusion Edge Plasmas.
PB95-151569 *04,410*

Spectroscopic Diagnostics of Low Temperature Plasmas: Techniques and Required Data.
PB95-151577 *04,411*

Spectroscopic Data Tables for Highly-Ionized Atoms.
PB95-151585 *03,910*

Trapped Atoms and Laser Cooling.
PB95-151627 *03,911*

Spin Squeezing and Reduced Quantum Noise in Spectroscopy.
PB95-151635 *03,912*

Rotational Far Infrared Spectrum of (13)CO.
PB95-152187 *00,941*

Laboratory Measurements for the Astrophysical Identification of MgH.
PB95-152195 *00,073*

Atomic Oxygen Fine Structure Splittings with Tunable Far Infrared Spectroscopy.
PB95-152203 *03,915*

Microwave and Submillimeter Spectroscopy of Ar-NH3 States Correlating with Ar+NH3(j=1, k=1).
PB95-152211 *00,942*

Electron-Impact Ionization of In(+) and Xe(+).
PB95-152906 *03,918*

Memory Function Approach to the Shape of Pressure Broadened Molecular Bands.
PB95-152930 *00,944*

Interatomic Potential of Argon.
PB95-152989 *00,945*

Product State Correlations in the Reaction of O((1)D) and H2O in Bimolecular Collisions and in O3.H2O Clusters--Translation.
PB95-153011 *00,946*

Rotational Dynamics of C60 in Na2RbC60.
PB95-153201 *00,948*

Neutron and X-Ray Scattering Cross Sections of Orientationally Disordered Soild C60.
PB95-153300 *00,951*

Morphological Stability.
PB95-153318 *04,591*

Hydrogen Balmer Alpha Line Shapes for Hydrogen-Argon Mixtures in a Low-Pressure rf Discharge.
PB95-153433 *03,924*

Quantum Measurements of Trapped Ions.
PB95-161147 *03,928*

Laser Assisted Collisions at Ultracold Temperatures.
PB95-161220 *03,929*

Hydrogen in YBa2Cu3Ox: A Neutron Spectroscopy and a Nuclear Magnetic Resonance Study.
PB95-161279 *04,601*

Spin-Resolved Elastic Scattering of Electrons from Sodium.
PB95-161774 *03,933*

sigma+-sigma- Optical Molasses in a Longitudinal Magnetic Field.
PB95-161840 *03,934*

Slit Jet Infrared Spectroscopy of Hydrogen Bonded N2HF Isotopomers: Rotational Rydberg-Klein-Rees Analysis and H/D Dependent Vibrational Predissociation Rates.
PB95-161873 *00,956*

Laser-Induced Fluorescence Measurements of OH. Concentrations in the Oxidation Region of Laminar, Hydrocarbon Diffusion Flames.
PB95-162160 *01,387*

Neutron-Scattering Study of Librations and Intramolecular Phonons in Rb2.6K0.4C60.
PB95-162269 *00,958*

Resonant-Photoemission Investigation of the Heusler Alloys Ni2MnSb and NiMnSb.
PB95-162384 *04,612*

Simultaneous Forward-Backward Raman Scattering Studies of D2 Broadened by D2, He, and Ar.
PB95-162459 *00,961*

Labeling Conventions in Isoelectronic Sequences - Reply.
PB95-162574 *03,937*

Iodine Atoms and Iodomethane Radical Cations: Their Formation in the Pulse Radiolysis of Iodomethane in Organic Solvents, Their Complexes, and Their Reactivity with Organic Reductants.
PB95-162764 *00,965*

Ionization Energy of Sulfur Pentafluoride and the Sulfur Pentafluoride-Fluorine Atom Bond Dissociation Energy.
PB95-162814 *00,966*

Anisotropy of Polarized X-ray Emission from Atoms and Molecules.
PB95-163002 *04,621*

Photoelectron Study of Electronic Autoionization in Rotationally Cooled N2: The n=6 Member of the Hopfield Series.
PB95-163531 *00,971*

Laser Spectroscopy of Carbon Monoxide: A Frequency Reference for the Far Infrared.
PB95-163606 *04,277*

Measurements of Fluorescence from Cold Atoms: Localization in Three-Dimensional Standing Waves.
PB95-163879 *03,943*

XUV Characterization Comparison of Mo/Si Multilayer Coatings.
PB95-164000 *04,278*

Molecular Orbital Calculations of Bond Rupture in Brittle Solids.
PB95-164059 *00,973*

Lattice Position of Si in GaAs Determined by X-Ray Standing Wave Measurements.
PB95-164406 *04,632*

Surface Geometry of BaO on W(100): A Surface-Extended X-Ray-Absorption Fine-Structure Study.
PB95-164414 *00,980*

Fragment State Correlations in the Dissociation of NO.HF(v=1).
PB95-164430 *00,982*

Shape-Resonance-Enhanced Continuum-Continuum Coupling in Photoionization of CO2.
PB95-164471 *00,983*

2nu9 Band of Propyne-d3.
PB95-164513 *00,985*

Interference in the Resonance Fluorescence of Two Trapped Atoms.
PB95-168514 *03,948*

New cw CO2 Laser Lines: The 9-mu m Hot Band.
PB95-168548 *04,281*

Laser Cooling of Trapped Ions.
PB95-168746 *03,950*

Light Scattered from Two Atoms.
PB95-168753 *04,286*

Recent Experiments on Trapped Ions at the National Institute of Standards and Technology.
PB95-169322 *03,952*

High-Resolution Atomic Spectroscopy of Laser-Cooled Ions.
PB95-169330 *03,953*

Laser-Cooled Positron Source.
PB95-169348 *03,954*

Far Infrared Laser Frequencies of (13)CD3OH.
PB95-169363 *04,292*

Rotational Spectroscopy of the CoH Radical in Its Ground (3)Phi State by Far-Infrared Laser Magnetic Resonance: Determination of Molecular Parameters.
PB95-175048 *00,992*

Non-Neutral Ion Plasmas and Crystals, Laser Cooling, and Atomic Clocks.
PB95-175113 *03,957*

Fine-Structure Intervals of (14)N(+) By Far-Infrared Laser Magnetic Resonance.
PB95-175162 *00,993*

Laser Magnetic-Resonance Measurement of the (3)P1 - (3)P2 Fine-Structure Splittings in (17)O and (18)O.
PB95-175170 *00,994*

Optical Probing of Cold Trapped Atoms.
PB95-175469 *04,296*

Elastic-Electron-Scattering Effects on Angular Distributions in X-ray Photoelectron Spectroscopy.
PB95-175758 *01,000*

Absolute Frequency Measurements of Methanol from 1.5 to 6.5 THz.
PB95-175881 *04,300*

Frequency-Stabilized LNA Laser at 1.083 mum: Application to the Manipulation of Helium 4 Atoms.
PB95-176186 *04,304*

Pure Rotational Spectra of CuH and CuD in Their Ground States Measured by Tunable Far-Infrared Spectroscopy.
PB95-176194 *01,005*

Rotational Spectrum of OH in the v=0-3 Levels of Its Ground State.
PB95-176202 *01,006*

Squeezed Atomic States and Projection Noise in Spectroscopy.
PB95-176293 *03,960*

Inner-Valence States CO(+) between 22 eV and 46 eV Studied by High Resolution Photoelectron Spectroscopy and ab Initio CI Calculations.
PB95-180055 *03,961*

Atomic Sulfur: Frequency Measurement of the J=0 inversely maps 1 Fine-Structure Transition at 56.3 Microns by Laser Magnetic Resonance.
PB95-180105 *01,007*

Atomic Branching Ratio Data for Oxygen-Like Species.
PB95-180436 *03,963*

Microwave Leakage as a Source of Frequency Error and Long-Term Instability in Cesium Atomic-Beam Frequency Standards.
PB95-180501 *01,541*

Velocity Distribution of Atomic Beams by Gated Optical Pumping.
PB95-180519 *01,542*

Improved Molecular Constants and Frequencies for the CO2 Laser from New High-J Regular and Hot-Band Frequency Measurements.
PB95-180634 *04,312*

Laser Focused Atomic Deposition.
PB95-180659 *04,685*

Characterization of the Interaction of Hydrogen with Iridium Clusters in Zeolites by Inelastic Neutron Scattering Spectroscopy.
PB95-180741 *01,013*

Progress on a Cryogenic Linear Trap for (199)Hg(+) Ions.
PB95-180790 *03,965*

Laser-Produced and Tokamak Spectra of Lithiumlike Iron, Fe(23+).
PB95-180857 *04,314*

Neutron Spectroscopic Evidence of Concentration-Dependent Hydrogen Ordering in the Octahedral Sublattice of beta-TbH2+x.
PB95-181020 *01,018*

Vibrations of Hydrogen and Deuterium in Solid Solution with Lutetium.
PB95-181038 *01,019*

Detection of OH+ in Its a(1)Delta State by Far Infrared Laser Magnetic Resonance.
PB95-181087 *01,021*

Core Potentials for Quasi-One-Electron Systems.
PB95-202214 *03,970*

Reduction of Light-Assisted Collisional Loss Rate from a Low-Pressure Vapor-Cell Trap.
PB95-202248 *03,971*

High-Efficiency, High-Power Difference-Frequency Generation of 0.9-1.5 mu m Light in BBO.
PB95-202255 *04,317*

Hydrogen Lyman-alpha Emission of Capella.
PB95-202263 *00,075*

Resonance Structure and Absolute Cross Sections in Near-Threshold Electron-Impact Excitation of the 4s(2) (1)S yields 4s4p (3)P Intercombination Transition in Kr(6+).
PB95-202271 *03,972*

Short-Range Correlation and Relaxation Effects on the (6p(2))(1)SO Autoionizing State of Atomic Barium.
PB95-202289 *03,973*

Connection between Superelastic and Inelastic Electron-Atom Collisions Involving Polarized Collision Partners.
PB95-202297 *03,974*

Femtosecond Time-Resolved Molecular Multiphoton Ionization: The Na2 System.
PB95-202305 *03,975*

Location of a (1)A(sub g) State in Bithiophene.
PB95-202313 *01,025*

Observations of 3C 273 with the Goddard High Resolution Spectrograph on the Hubble Space Telescope.
PB95-202321 *00,076*

Lowest Excited Singlet State of Isolated 1-phenyl-1,3-butadiene and 1-phenyl-1,3,5-hexatriene.
PB95-202339 *01,026*

Analyses of Recent Experimental and Theoretical Determinations of e-H2 Vibrational Excitation Cross Sections: Assessing a Long-Standing Controversy.
PB95-202438 *03,977*

Test of Newton's Inverse Square Law of Gravitation Using the 300-m Tower at Erie, Colorado.
PB95-202446 *03,978*

Three-Vector Correlation Study of Orientation and Coherence Effects in Na(3p, (2)P1/2 inversely maps (2)P3/2)+He: Semiclassical and Quantum Calculations.
PB95-202453 *03,979*

ROSAT All-Sky Survey of Active Binary Coronae. 1. Quiescent Fluxes for the RS Canum Venaticorum Systems.
PB95-202479 *00,077*

Absolute Cross-Section Measurements for Electron-Impact Single Ionization of Se(+) and Te(+).
PB95-202503 *03,980*

Crossed-Beams Measurements of Absolute Cross Sections for Electron Impact Ionization of S(+).
PB95-202511 *03,981*

Absolute Cross Sections for Electron-Impact Single Ionization of Si(+) and Si(2+).
PB95-202529 *03,982*

Plasma Chemistry in Silane/Germane and Disilane/Germane Mixtures.
PB95-202537 *01,027*

n-Vector Correlations in Collision Dynamics with Atomic Orbital Alignment: The Importance of Coherence Denoting Azimuthal Structure for n (greater than or equal to) 3.
PB95-202545 *03,983*

Resonant Two-Color Detachment of H(-) with Excitation of H(n=2).
PB95-202552 *03,984*

Numerical Solution of the Nonlinear Schroedinger Equation for Small Samples of Trapped Neutral Atoms.
PB95-202578 *03,985*

Vibrations of S1((1)B2u) p-Difluorobenzene - d4. S1-S0 Fluorescence Spectroscopy and ab Initio Calculations.
PB95-202586 *01,028*

Long-Range Parity-Nonconserving Interaction.
PB95-202594 *03,986*

Hole Dispersion and Enhancement of Antiferromagnetic Interaction of Localized Spins in High-Tc Superconductors.
PB95-202602 *04,694*

Quantum Mechanics of a Solid-State Bar Gravitational Antenna.
PB95-202628 *03,987*

Failures of the Four-Wave Mixing Model for Cone Emission.
PB95-202636 *04,318*

Calibration of a Superconducting Gravimeter Using Absolute Gravity Measurements.
PB95-202651 *03,684*

Sobolev Approximation for Line Formation with Partial Frequency Redistribution.
PB95-202669 *00,078*

Recombination Line Intensities for Hydrogenic Ions-III. Effects of Finite Optical Depth and Dust.
PB95-202677 *00,079*

Vibrational Dependence of the Anisotropic Intermolecular Potential of Ar-HCl.
PB95-202685 *01,029*

Vibrational Dependence of the Anisotropic Intermolecular Potential of Ar-HF.
PB95-202693 *01,030*

Modified Effective Range Theory as an Alternative to Low-Energy Close-Coupling Calculations.
PB95-202701 *03,988*

Slow-Electron Collisions with CO Molecules in an Exact-Exchange Plus Parameter-Free Polarization Model.
PB95-202719 *03,989*

Superconducting Resonator and a Cryogenic GaAs Field-Effect Transistor Amplifier as a Single-Ion Detection System.
PB95-202727 *03,990*

Slit-Jet Near-Infrared Spectroscopy and Internal Rotor Dynamics of the ArH2O van der Waals Complex: An Angular Potential-Energy Surface for Internal H2O Rotation.
PB95-202792 *01,033*

Orbital Stereochemistry: Discovering the Symmetries of Collision Processes.
PB95-202800 *01,034*

Probing Bose-Einstein Condensed Atoms with Short Laser Pulses.
PB95-202818 *03,991*

Deuterium in the Local Interstellar Medium: Its Cosmological Significance.
PB95-202842 *00,081*

Peeking Through the Picket Fence: What Astrophysical Surprises May Be Present in the 100-1200 Angstrom Region.
PB95-202859 *00,082*

Variationally Stable Treatment of Two- and Three-Photon Detachment of H(-) Including Electron-Correlation Effects.
PB95-202867 *03,992*

Preferential In-Plane Rotational Excitation of H2O (001) by Translational-to-Vibrational Transfer from 2.2 eV H Atoms.
PB95-202875 *01,035*

Alignment in Two-Step Pulsed Laser Excitation of Rydberg Levels in Light Atoms: The Example of Sodium.
PB95-202883 *03,993*

Narrow-Band Tunable Diode Laser System with Grating Feedback, and a Saturated Absorption Spectrometer for Cs and Rb.
PB95-202891 *04,319*

Threshold Electron Excitation of Na.
PB95-202917 *03,994*

Large Amplitude Skeletal Isomerization as a Promoter of Intramolecular Vibrational Relaxation in CH Stretch Excited Hydrocarbons.
PB95-202933 *01,036*

Sub-Doppler, Infrared Laser Spectroscopy of the Propyne 2nu1 Band: Evidence of z-Axis Coriolis Dominated Intramolecular State Mixing in the Acetylenic CH Stretch Overtone.
PB95-202941 *01,037*

Collisional Energy Transfer between Excited-State Strontium and Noble-Gas Atoms.
PB95-202958 *03,995*

Importance of Bound-Free Correlation Effects for Vibrational Excitation of Molecules by Electron Impact: A Sensitivity Analysis.
PB95-202974 *03,996*

Acceleration of Intramolecular Vibrational Redistribution by methyl Internal Rotation. A Chemical Timing Study of p-fluorotoluene and p-fluorotoluene-d3.
PB95-202982 *01,039*

High-Resolution, Direct Infrared Laser Absorption Spectroscopy in Slit Supersonic Jets: Intermolecular Forces and Unimolecular Vibrational Dynamics in Clusters.
PB95-203006 *01,040*

Rotational-RKR Inversion of Intermolecular Stretching Potentials: Extension to Linear Hydrogen Bonded Complexes.
PB95-203014 *01,041*

Rigid Bender Analysis of van der Waals Complexes: The Intermolecular Bending Potential of a Hydrogen Bond.
PB95-203022 *01,042*

Energy-Pooling Collisions in Barium.
PB95-203030 *03,997*

Continuous Gravity Observations Using Joint Institute for Laboratory Astrophysics Absolute Gravimeters.
PB95-203048 *03,685*

Kinetics of the Reaction C2H + O2 from 193 to 350 K Using Laser Flash Kinetic Infrared Absorption Spectroscopy.
PB95-203055 *01,043*

Construction of Silicon Nanocolumns with the Scanning Tunneling Microscope.
PB95-203063 *04,696*

Relative Photoionization and Photodetachment Cross Sections for Particular Fine-Structure Transitions with Application to Cl 3s-subshell Photoionization.
PB95-203097 *03,998*

Behavior of Atoms in a Compressed Magneto-Optical Trap.
PB95-203105 *03,999*

Dielectronic Capture Processes in the Electron-Impact Ionization of Sc(2+).
PB95-203113 *04,000*

Photodissociation Dynamics in Quantum State-Selected Clusters: A Test of the One-Atom Cage Effect in Ar-H2O.
PB95-203121 *01,044*

Photoelectron Spectroscopy of Small Antimony Cluster Anions: Sb(-), Sb2(-), Sb3(-), and Sb4(-).
PB95-203139 *01,045*

Charge Cloud Distribution of Heavy Atoms After Excitation by Polarized Electrons.
PB95-203147 *04,001*

Pulsed Laser Photolysis Time-Resolved FT-IR Emission Studies of Molecular Dynamics.
PB95-203162 *04,002*

High Resolution, Jet-Cooled Infrared Spectroscopy of (HCl)2: Analysis of nu1 and nu2 HCl Stretching Fundamentals, Interconversion Tunneling, and Mode-Specific Predissociation Lifetimes.
PB95-203196 *01,046*

Slit-Jet Near-Infrared Diode Laser Spectroscopy of (DCl)2: nu1, nu2 DCl Stretching Fundamentals, Tunneling Dynamics, and the Influence of Large Amplitude 'Geared' Intermolecular Rotation.
PB95-203204 *01,047*

High Resolution Near Infrared Spectroscopy of HCl-DCl and DCl-HCl: Relative Binding Energies, Isomer Interconversion Rates, and Mode Specific Vibrational Predissociation.
PB95-203212 *01,048*

Laser Flash Photolysis, Time-Resolved Fourier Transform Infrared Emission Study of the Reaction Cl + C2H5 yields HCl(v) + C2H4.
PB95-203238 *01,049*

Laser Preparation and Probing of Initial and Final Orbital Alignment in Collision-Induced Energy Transfer Ca(4s5p,(1)P1) + He yields Ca(4s5p,(3)P2) + He.
PB95-203261 *04,003*

Initial and Final Orbital Alignment Probing of the Fine-Structure-Changing Collisions among the Ca (4s)(1)(4p)(1), (3)PJ States with He: Determination of Coherence and Conventional Cross-Sections.
PB95-203279 *04,004*

Laser-Induced Desorption of In and Ga from Si(100) and Adsorbate Enhanced Surface Damage.
PB95-203311 *01,050*

Pulsed Laser Irradiation at 532 nm of In and Ga Adsorbed on Si(100): Desorption, Incorporation, and Damage.
PB95-203329 *01,051*

Single-Photon Laser Ionization Time-of-Flight Mass Spectroscopy Detection in Molecular-Beam Epitaxy: Application to As4, As2, and Ga.
PB95-203337 *01,052*

Deposition Rates in Direct Current Diode Sputtering.
PB95-203345 *04,697*

Frequency Shifting of Pulsed Narrow-Band Laser Light in a Multipass Raman Cell.
PB95-203352 *04,321*

Angle-Differential and Momentum-Transfer Cross Sections for Low-Energy Electron-Cs Scattering.
PB95-203402 *04,005*

Relativistic R-Matrix Calculations for Electron - Alkali-Metal-Atom Scattering: Cs as a Test Case.
PB95-203410 *04,006*

Resonance Fluorescence with Squeezed-Light Excitation.
PB95-203469 *04,322*

Short-Pulse Detachment of H(-) in the Presence of a Static Electric Field.
PB95-203477 *04,007*

Signatures of Large Amplitude Motion in a Weakly Bound Complex: High-Resolution IR Spectroscopy and Quantum Calculations for HeCO2.
PB95-203485 *01,054*

Oscillator Strengths and Radiative Branching Ratios in Atomic Sr.
PB95-203493 *04,008*

G203.2-12.3: A New Optical Supernova Remnant in Orion.
PB95-203535 *00,085*

High-Resolution Optical Multiplex Spectroscopy.
PB95-203543 *04,323*

Cone Emission from Laser-Pumped Two-Level Atoms. 1. Quantum Theory of Resonant Light Propagation.
PB95-203584 *04,325*

Cone Emission from Laser-Pumped Two-Level Atoms. 2. Analytical Model Studies.
PB95-203592 *04,326*

Suppression of Ionization in One- and Two-Dimensional Model Calculations.
PB95-203600 *04,009*

Precision Lifetime Measurements of Cs 6p (2)P1/2 and 6p (2)P3/2 Levels by Single-Photon Counting.
PB95-203816 *04,010*

Hyperfine-Structure Studies of Zr II: Experimental and Relativistic Configuration-Interaction Results.
PB95-203824 *04,011*

Stabilization of Optical Phase/Frequency of a Laser System: Application to a Commercial Dye Laser with an External Stabilizer.
PB95-203832 *04,327*

Tables of X-ray Mass Attenuation Coefficients and Mass Energy-Absorption Coefficients 1 keV to 20 MeV for Elements Z = 1 to 92 and 48 Additional Substances of Dosimetric Interest.
PB95-220539 *04,013*

New IUPAC Guidelines for the Reporting of Stable Hydrogen, Carbon, and Oxygen Isotope-Ratio Data. Letter to the Editor.
PB95-261962 *01,058*

Ab initio Calculations for Helium: A Standard for Transport Property Measurements.
PB96-102041 *01,060*

Merged-Beams Energy-Loss Technique for Electron-Ion Excitation: Absolute Total Cross Sections for O(5+) (2s yields 2p).
PB96-102058 *04,017*

Energy Dependences of Absorption in Beryllium Windows and Argon Gas.
PB96-102124 *04,020*

Sub-Doppler Frequency Measurements on OCS at 87 THz (3.4 mu m) with the CO Overtone Laser.
PB96-102215 *04,330*

High-Resolution Infrared Overtone Spectroscopy of N2-HF: Vibrational Red Shifts and Predissociation Rate as a Function of HF Stretching Quanta.
PB96-102298 *01,061*

Kinetics and Dynamics of Vibrationally State Resolved Ion-Molecule Reactions: (14)N2(+)(v=1 and 2) and (15)N2(+)(v=0,1 and 2) with (14)N2.
PB96-102348 *04,023*

Length Scales for Fragile Glass-Forming Liquids.
PB96-102801 *01,065*

Optically Stabilized Tunable Diode-Laser System for Saturation Spectroscopy.
PB96-102819 *04,717*

Probing Potential-Energy Surfaces via High-Resolution IR Laser Spectroscopy.
PB96-102835 *01,066*

Time-Resolved Balmer-Alpha Emission from Fast Hydrogen Atoms in Low Pressure, Radio-Frequency Discharges in Hydrogen.
PB96-102942 *04,028*

Low-Energy-Electron Collisions with Sodium: Elastic and Inelastic Scattering from the Ground State.
PB96-103106 *04,030*

Collisional Alignment of CO2 Rotational Angular Momentum States in a Supersonic Expansion.
PB96-103171 *01,069*

Improved Wavelengths for Prominent Lines of Fe XX to Fe XXIII.
PB96-111638 *04,334*

Vibrational Excitations and the Position of Hydrogen in Nanocrystalline Palladium.
PB96-111828 *04,035*

Electron-Ion Collisions in the Plasma Edge.
PB96-111885 *04,037*

Quantum-Limited Cooling and Detection of Radio-Frequency Oscillations by Laser-Cooled Ions.
PB96-112073 *04,039*

Precise Spectroscopy for Fundamental Physics.
PB96-112164 *04,040*

Visible and UV Light from Highly Charged Ions: Exotic Matter Advancing Technology.
PB96-119391 *04,414*

Nanofabrication of a Two-Dimensional Array Using Laser-Focused Atomic Deposition.
PB96-119417 *04,732*

Atomic Clock.
PB96-119490 *01,553*

Doppler-Free Spectroscopy of Large Polyatomic Molecules and van der Waals Complexes.
PB96-119581 *04,339*

Far Infrared Laser Frequencies of CH3OD and N2H4.
PB96-119623 *04,341*

High-Order Multipole Excitation of a Bound Electron.
PB96-119789 *04,044*

Orbital Alignment and Vector Correlations in Inelastic Atomic Collisions.
PB96-122742 *04,047*

Atom Cooling and Trapping, and Collisions of Trapped Atoms.
PB96-122916 *04,048*

Search for Small Violations of the Symmetrization Postulate in an Excited State of Helium.
PB96-123518 *04,050*

Relativistic Modifications of Charge Expansion Theory.
PB96-123799 *04,052*

Observation and Visible and uv Magnetic Dipole Transitions in Highly Charged Xenon and Barium.
PB96-138441 *04,056*

High-Energy Phonon Dispersion in La1.85Sr0.15CuO4.
PB96-138458 *04,748*

Atomic Transition Probabilities and Tests of the Spectroscopic Coupling Scheme for N I.
PB96-138466 *04,057*

q Dependence of Self-Energy Effects of the Plane Oxygen Vibration in YBa2Cu3O7.
PB96-138516 *01,096*

Inexpensive Laser Cooling and Trapping Experiment for Undergraduate Laboratories.
PB96-140371 *04,353*

Photoluminescence Spectra of Epitaxial Single Crystal C60.
PB96-141205 *04,754*

Atomic Iron in Its (5)D Ground State: A Direct Measurement of the J = 0 inverted arrow 1 and J = 1 inverted arrow 2 Fine-Structure Intervals (1.2).
PB96-141221 *04,756*

Using Atom Optics to Fabricate Nanostructures.
PB96-141247 *04,757*

Inelastic Neutron Scattering Study of Hydrogen in Nanocrystalline Pd.
PB96-146857 *03,366*

Fast-Ion Conducting Y2(ZryTi1-y)2O7 Pyrochlores: Neutron Rietveld Analysis of Disorder Induced by Zr Substitution.
PB96-156104 *04,776*

RIS Measurement of AC Stark Shifts and Photoionization Cross Sections in Calcium.
PB96-157953 *04,073*

Comment On: Two-Photon Absorption Series of Calcium.
PB96-157979 *04,074*

Configuration-Dependent AC Stark Shifts in Calcium.
PB96-157995 *04,363*

Barium Contributions to the Valence Electronic Structure of YBa2Cu3O7-delta, PrBa2Cu3O7-delta, and Other Barium-Containing Compounds.
PB96-158019 *04,076*

RIS Measurements of the AC Stark Shift.
PB96-158035 *04,078*

Analysis of the (5d(2)+5d6s)-5d6p Transition Arrays of Os VII and Ir VIII, and the 6s (2)S-6p (2)P Transitions of Ir IX.
PB96-159264 *01,954*

Appearance Intensities for Multiply Charged Ions in a Strong Laser Field.
PB96-160445 *04,089*

Low-Energy Vibrations and Octahedral Site Occupation in Nb95V5H(D)y.
PB96-160734 *01,133*

Dislocation Core-Core Interaction and Peierls Stress in a Model Hexagonal Lattice.
PB96-162003 *04,101*

Charge-Transfer-Induced Multiplet Structure in the N4,5O2,3 Soft-X-ray Emission Spectrum of Lanthanum.
PB96-163746 *04,102*

Population Trapping in Short-Pulse Multiphoton Ionization.
PB96-164140 *04,371*

Trapped Ions and Laser Cooling 4: Selected Publications of the Ion Storage Group of the Time and Frequency Division, NIST, Boulder, Colorado.
PB96-172358 *04,108*

Irradiances of Spectral Lines in Mercury Pencil Lamps.
PB96-176466 *04,375*

Wavelengths of Spectral Lines in Mercury Pencil Lamps.
PB96-176474 *04,376*

Potential Surfaces and Dynamics of Weakly Bound Trimers: Perspectives from High Resolution IR Spectroscopy.
PB96-176508 *01,155*

Electromagnetic Coupling Character of (001) Twist Boundaries in Sintered Bi2Sr2CaCu2O8+x Bicrystals.
PB96-176573 *01,963*

State-Resolved Rotational Energy Transfer in Open Shell Collisions: Cl((2)P3/2)+HCl.
PB96-176607 *01,157*

Energy Distributions of Neutrons Scattered from Solid C60 by the Beryllium Detector Method.
PB96-176631 *03,740*

Characterization of the Structure of LaD2.50 by Neutron Powder Diffraction.
PB96-176797 *04,783*

Theory for Quantum-Dot Quantum Wells: Pair Correlation and Internal Quantum Confinement in Nanoheterostructures.
PB96-179445 *02,437*

Dynamics of Mu(+) in Sc and ScHx.
PB96-180021 *04,112*

Synthesis of Hybrid Organic-Inorganic Materials from Interpenetrating Polymer Network Chemistry.
PB96-180054 *02,994*

Designations of ds(2)p Energy Levels in Neutral Zirconium, Hafnium, and Rutherfordium (Z=104).
PB96-180120 *04,116*

Hyperfine Structure Investigations and Identification of New Energy Levels in the Ionic Spectrum of (147)Pm.
PB96-180203 *04,117*

Measurements of the Resonance Lines of (6)Li and (7)Li by Doppler-Free Frequency-Modulation Spectroscopy.
PB96-180211 *04,118*

Neutron and Raman Spectroscopies of 134 and 134a Hydrofluorocarbons Encaged in Na-X Zeolite.
PB96-186168 *03,001*

Microlithography by Using Neutral Metastable Atoms and Self-Assembled Monolayers.
PB96-190038 *02,441*

Atomic Branching Ratio Data for Nitrogen-Like Species.
PB96-190152 *04,122*

Excitation Transfer in Barium by Collisions with Noble Gases.
PB96-200274 *01,163*

Comment on <<A Dynamic Electric Trap for Ground-State Atoms>>.
PB96-200290 *04,123*

Alignment Probing of Rydberg States by Stimulated Emission.
PB96-200316 *04,124*

Collisions of Electrons with Highly-Charged Ions.
PB96-200340 *04,791*

Pairwise and Nonpairwise Additive Forces in Weakly Bound Complexes: High Resolution Infrared Spectroscopy of ArnDF (n=1,2,3).
PB96-200357 *04,125*

Gravitational Sisyphus Cooling of (87)Rb in a Magnetic Trap.
PB96-200704 *04,379*

Stable, Tightly Confining Magnetic Trap for Evaporative Cooling of Neutral Atoms.
PB96-200720 *04,126*

UV Absorption Cross Sections of Methylchloroform: Temperature-Dependent Gas and Liquid Phase Measurements.
PB96-201041 *00,643*

Vibrationally Resolved Photoelectron Angular Distributions and Branching Ratios for the Carbon Dioxide Molecule in the Wavelength Region 685-795 Angstrom.
PB96-201207 *04,131*

Nanostructure Fabrication via Laser-Focused Atomic Deposition (Invited).
PB96-204094 *04,132*

Properties of a Bose-Einstein Condensate in an Anisotropic Harmonic Potential.
PB96-204144 *04,133*

Temperature Dependence of the Ultraviolet Absorption Cross Section of CF3I.
PB96-204169 *01,168*

Positronium in Relativistic Quantum Mechanics.
PB97-110571 *04,140*

Relativistic Quantum Mechanics of Interacting Particles.
PB97-110589 *04,141*

Beam Line for Highly Charged Ions.
PB97-111256 *04,143*

Systematic Correction in Bragg X-ray Diffraction of Flat and Curved Crystals.
PB97-112239 *04,152*

Matrix Isolation Study of the Interaction of Excited Neon Atoms with O3: Infrared Spectrum of O((sub 3)(-)) and Evidence for the Stabilization of O2...O((sub 4)(+)).
PB97-112403 *04,155*

Polarization Measurements on a Magnetic Quadrupole Line in Ne-Like Barium.
PB97-113104 *04,161*

Quantum Dots in Quantum Well Structures.
PB97-118350 *01,185*

Bimolecular Interactions in (Et)3SiOH:Base:CCl4 Hydrogen-Bonded Solutions Studied by Deactivation of the Free OH-Stretch Vibration.
PB97-118657 *04,166*

Microwave Spectrum and Structure of CH2O-H2O.
PB97-118723 *04,168*

Rotational Spectra of CH3CCH-NH3, NCCCH-NH3, and NCCCH-OH2.
PB97-118798 *04,170*

Resonance Enhanced Multiphoton Ionization Spectroscopy of the PF Radical.
PB97-119119 *00,702*

Matrix Isolation Study of the Interaction of Excited Neon Atoms with BCl3: Infrared Spectra of BCl(sub 3, sup +), BCl(sub 2, sup +), and BCl(sub 3, sup -).
PB97-119143 *01,187*

Vibrational Spectra of Molecular Ions Isolated in Solid Neon. 13. Ions Derived from HBr and HI.
PB97-119234 *01,188*

Self-Consistent 'GW' and Higher-Order Calculations of Electron States in Metals.
PB97-119341 *01,189*

Measurement of the Atomic Na(3P) Lifetime and of Retardation in the Interaction between Two Atoms Bound in a Molecule.
PB97-122360 *04,178*

Perpendicular C-H Stretching Band nu9/nu13 and the Torsional Potential of Dimethylacetylene.
PB97-122451 *01,192*

ATOMIC OPTICS

Atom-Optical Properties of a Standing-Wave Light Field.
PB96-141072 *04,356*

ATOMIC SPECTRA

Atomic Energy Levels As Derived from the Analyses of Optical Spectra. Volume 1. Section 1. The Spectra of Hydrogen, Deuterium, Helium, Lithium Beryllium, Boron, Carbon, Nitrogen, Oxygen, and Fluorine.
AD-A278 130/0 *03,764*

Atomic Energy Levels. As Derived From the Analyses of Optical Spectra. Volume 3.
AD-A280 279/1 *00,714*

Relativistic and Quantum Electrodynamic Effects in Highly-Charged Ions.
PB94-212784 *03,854*

High-Resolution Atomic Spectroscopy of Laser-Cooled Ions.
PB95-169330 *03,953*

Measurements of the Resonance Lines of (6)Li and (7)Li by Doppler-Free Frequency-Modulation Spectroscopy.
PB96-180211 *04,118*

ATOMIC SPECTROSCOPY

Atomic, Molecular, and Optical Physics with X-rays.
PB94-213378 *03,863*

Comprehensive Spectroscopic Data Tabulations and Progress in the Compilation of Atomic Transition Probabilities.
PB95-151551 *03,909*

Spectroscopic Data Tables for Highly-Ionized Atoms.
PB95-151585 *03,910*

Spin Squeezing and Reduced Quantum Noise in Spectroscopy.
PB95-151635 *03,912*

Trace Detection in Conducting Solids Using Laser-Induced Fluorescence in a Cathodic Sputtering Cell.
PB95-163424 *00,598*

Squeezed Atomic States and Projection Noise in Spectroscopy.
PB95-176293 *03,960*

Observation and Visible and uv Magnetic Dipole Transitions in Highly Charged Xenon and Barium.
PB96-138441 *04,056*

ATOMIC STRUCTURE

Relativistic and Quantum Electrodynamic Effects in Highly-Charged Ions.
PB94-212784 *03,854*

Core Potentials for Quasi-One-Electron Systems.
PB95-202214 *03,970*

Relativistic Modifications of Charge Expansion Theory.
PB96-123799 *04,052*

ATOMIC THEORY

Atomic Theory of Fracture of Brittle Materials: Application to Covalent Semiconductors.
PB94-216553 *04,519*

ATOMIC TRANSITION PROBABILITIES

Atomic Transition Probabilities and Tests of the Spectroscopic Coupling Scheme for N I.
PB96-138466 *04,057*

ATOMIC WEIGHTS

Atomic Weights of the Elements, 1993.
PB96-145909 *01,114*

ATOMISTIC CALCULATIONS

Dislocation Core-Core Interaction and Peierls Stress in a Model Hexagonal Lattice.
PB96-162003 *04,101*

ATOMIZATION

Beneficial Effects of Nitrogen Atomization on an Austenitic Stainless Steel.
PB94-212396 *03,209*

Optimization of Inert Gas Atomization.
PB95-107405 *01,377*

Study of Droplet Transport in Alcohol-Based Spray Flames Using Phase/Doppler Interferometry.
PB95-108551 *02,479*

Parametric Investigation of Metal Powder Atomization Using Laser Diffraction.
PB95-108577 *03,342*

Turbulent Spray Burner for Assessing Halon Alternative Fire Suppressants.
PB95-153748 *01,385*

ATOMIZERS

Development of Adaptive Control Strategies for Inert Gas Atomization.
PB95-162335 *02,823*

ATOMIZING

Process Modeling and Control of Inert Gas Atomization.
PB95-162343 *02,824*

ATOMS

Determination of Atomic Data Pertinent to the Fusion Energy Program. Progress Report for FY 92.
DE94004400 *04,402*

Atomic Branching Ratio Data for Nitrogen-Like Species.
PB96-190152 *04,122*

ATOMSPHERIC CHEMISTRY

Free Radical Chemistry of the Atmospheric Aqueous Phase.
PB96-148101 *00,117*

ATRIA

Method of Predicting Smoke Movement in Atria with Application to Smoke Management.
PB95-154746 *00,376*

ATTENUATION

Theoretical Form Factor, Attenuation and Scattering Tabulation for Z=1-92 from E=1-10 eV to E=0.4-1.0 MeV.
PB96-145594 *01,104*

ATTENUATION CALIBRATION SYSTEM

Revised Uncertainty Analysis for the NIST 30-MHz Attenuation Calibration System.
PB95-168761 *01,907*

30 MHz Comparison Receiver.
PB96-200407 *01,972*

AUDITING

Self Monitoring Accounting Systems.
PB95-216602 *00,007*

AUGER ELECTRON SPECTROSCOPY

Inelastic Interactions of Electrons with Surfaces: Application to Auger-Electron Spectroscopy and X-ray Photoelectron Spectroscopy.
PB94-172699 *00,764*

X-ray Photoelectron and Auger Electron Forward Scattering: A Structural Diagnostic for Epitaxial Thin Films.
PB95-180220 *04,676*

AUGMENTED REALITY

Virtual Environments for Health Care. A White Paper for the Advanced Technology Program (ATP), the National Institute of Standards and Technology.
PB96-147814 *03,594*

AUSTENITE

Charpy Impact Test as an Evaluation of 4 K Fracture Toughness.
PB96-190194 *03,219*

AUSTENITIC STAINLESS STEELS

Determination of the Prior-Austenitic Grain Size of Selected Steels Using a Molten Glass Etch.
PB94-211927 *03,208*

Beneficial Effects of Nitrogen Atomization on an Austenitic Stainless Steel.
PB94-212396 *03,209*

Dynamics vs. Static Young's Moduli: A Case Study.
PB94-213188 *03,210*

Cryogenic Toughness of Austenitic Stainless Steel Weld Metals: Effect of Inclusions.
PB95-161261 *03,214*

AUSTENITIC STEELS

Charpy Specimen Tests at 4 K.
PB96-190335 *03,002*

AUTENNAS

Spherical-Wave Source-Scattering Matrix Analysis of Antennas and Antenna-Antenna Interactions.
PB96-111166 *02,008*

AUTHENTICATION

Guideline for the Use of Advanced Authentication Technology Alternatives. Category: Computer Security. Subcategory: Access Control.
FIPS PUB 190 *01,798*

AUTOFLUORESCENCE

Autofluorescence Detection of 'Escherichia coli' on Silver Membrane Filters.
PB96-163639 *03,590*

AUTOIONIZATION

Autoionizing Resonances in Electric Fields.
PB94-212727 *03,853*

RIS Studies of Autoionization in Calcium.
PB94-213295 *00,849*

Photoelectron Study of Electronic Autoionization in Rotationally Cooled N2: The n=6 Member of the Hopfield Series.
PB95-163531 *00,971*

Short-Range Correlation and Relaxation Effects on the (6p(2))(1)SO Autoionizing State of Atomic Barium.
PB95-202289 *03,973*

AUTOMATED BRIDGE

Automated Guarded Bridge for Calibration of Multimegohm Standard Resistors.
PB97-119150 *02,289*

AUTOMATED INSPECTION

Automated Inspection: The Integration of National Standards and Commercial Products at NIST.
PB95-163077 *02,906*

AUTOMATED SYSTEMS

Programmable Guarded Coaxial Connector Panel.
PB96-122544 *02,108*

AUTOMATIC CONTROL

Automated, High-Precision Coulometric Titrimetry. Part 1. Engineering and Implementation.
PB95-150199 *00,575*

Automated, High Precision Coulometric Titrimetry. Part 2. Strong and Weak Acids and Bases.
PB95-150207 *00,576*

Integrating Automated Systems with Modular Architecture.
PB95-150231 *00,577*

Vehicle-Command Center Communications in a Robotic Vehicle System.
PB95-162723 *03,665*

Outline of a Multiple Dimensional Reference Model Architecture and a Knowledge Engineering Methodology for Intelligent Systems Control.
PB95-220414 *03,703*

AUTOMATIC & ROBOTICS

Open Architectures for Machine Control.
PB94-135621 *02,942*

Enhanced Machine Controller Architecture Overview.
PB94-142460 *02,802*

Feasibility Study: Reference Architecture for Machine Control Systems Integration.
PB94-142791 *02,804*

Reliable Optical Flow Algorithm Using 3-D Hermite Polynomials.
PB94-145620 *01,829*

APDE Demonstration System Architecture. National PDES Testbed Report Series.
PB94-154325 *02,767*

Variant Design for Mechanical Artifacts-A State of the Art Survey.
PB94-154358 *02,768*

Technical Program of the Factory Automation Systems Division 1993.
PB94-160819 *02,805*

U.S. Navy Coordinate Measuring Machines: A Study of Needs.
PB94-162831 *02,807*

Concept for an Algorithm Testing and Evaluation Program at NIST.
PB94-163029 *02,890*

NIST Support to the Next Generation Controller Program: 1991 Final Technical Report.
PB94-163490 *02,808*

Publications of the Manufacturing Engineering Laboratory Covering the Period January 1989-September 1992.
PB94-165966 *02,750*

Toward a Reference Model Architecture for Real-Time Intelligent Control Systems (ARTICS).
PB94-172046 *02,932*

Ultrasonic Measurements of Surface Roughness.
PB94-172137 *04,181*

AMRF Composite Fabrication Workstation.
PB94-172681 *02,810*

World Model Registration for Effective Off-Line Programming of Robots.
PB94-173010 *02,933*

Characterization of the Hydrogen Induced Cold Cracking Susceptibility at Simulated Weld Zones in HSLA-100 Steel.
PB94-174505 *03,746*

Task Decomposition Methodology for the Design of a Coal Mining Automation Hierarchical Real-Time Control System.
PB94-185386 *03,694*

Issues Concerning Material Removal Shape Element Volumes (MRSEVs).
PB94-185493 *02,882*

Development of a Calibrated Atomic Force Microscope.
PB94-185683 *02,894*

Prediction of Geometric-Thermal Machine Tool Errors by Artificial Neural Networks.
PB94-186673 *02,943*

State-of-the-Art Survey of Methodologies for Representing Manufacturing Process Capabilities.
PB94-187655 *02,812*

NIST RS274/NGC Interpreter Version 1.
PB94-187788 *02,814*

Control Entity Interface Specification.
PB94-191715 *02,815*

Overview of NASREM: The NASA/NBS Standard Reference Model for Telerobot Control System Architecture.
PB94-194560 *04,831*

Recommendations on Selection of Vehicle-to-Roadside Communications Standards for Commercial Vehicle Operations.
PB94-195914 *04,859*

Hierarchical Interaction between Sensory Processing and World Modeling in Intelligent Systems.
PB94-198256 *01,580*

Role of World Modeling and Value Judgment in Perception.
PB94-198264 *01,581*

Theory of Intelligent Systems.
PB94-198272 *01,582*

Computer Vision Based Tool Setting Station.
PB94-199858 *02,944*

Implementing a Transition Manager in the AMRF Cell Controller.
PB94-199932 *02,817*

Generic Manufacturing Controllers.
PB94-199940 *02,818*

Integration of Servo Control into a Large-Scale Control System Design: An Example from Coal Mining.
PB94-203429 *03,696*

Certainty Grid to Object Boundary Algorithm.
PB94-203510 *01,835*

Continuous Mining Machine Control Using the Real-Time Control System.
PB94-203528 *03,700*

Environment Simulation for a Continuous Mining Machine.
PB94-203536 *03,697*

Visual-Motion Fixation Invariant.
PB94-206281 *01,836*

Advanced Angle Metrology System.
PB94-211364 *02,637*

Intelligent Control for Multiple Autonomous Undersea Vehicles.
PB94-211877 *03,747*

Real-Time Vision for Autonomous and Teleoperated Control of Unmanned Vehicles.
PB94-211885 *03,701*

Real-Time Vision for Unmanned Vehicles.
PB94-211893 *03,702*

Hierarchical Real-Time Control System for Use with Coal Mining Automation.
PB94-212065 *03,698*

Hierarchical Ada Robot Programming System (HARPS): A Complete and Working Telerobot Control System Based on the NASREM Model.
PB94-213162 *02,934*

Technical Program Description Systems Integration for Manufacturing (SIMA).
PB94-213758 *02,819*

Evolution of the Flight Telerobotic Servicer.
PB94-216082 *04,832*

Publications of the Intelligent Systems Division (Previously Robot Systems Division) Covering the Period January 1971-April 1994.
PB94-217098 *02,935*

Adaptive, Predictive 2-D Feature Tracking Algorithm for Finding the Focus of Expansion.
PB94-218575 *01,588*

Three Dimensional Position Determination from Motion.
PB95-107108 *01,788*

Real Time Compensation for Tool Form Errors in Turning Using Computer Vision.
PB95-107231 *02,945*

Summary and Notes of the Joint ISO/IGES/PDES Organization Technical Committee Meeting. Held in Albuquerque, New Mexico on October 15-20, 1989.
PB95-107314 *02,774*

Real-Time Implementation of a Differential Range Finder.
PB95-108650 *01,839*

Evolution of Automatic Line Scale Measurement at the National Institute of Standards and Technology.
PB95-108809 *02,897*

Some Considerations for Interim Testing of Coordinate Measuring Machine Performance Using a Specific Artifact.
PB95-108858 *02,898*

National PDES Testbed: An Overview.
PB95-125829 *02,775*

STEP On-Line Information Service (SOLIS). The IGES/PDES Organization.
PB95-137790 *02,777*

SGML Environment for STEP.
PB95-143103 *02,778*

Reference Model Architecture for Intelligent Systems Design.
PB95-143137 *01,789*

Visual Pursuit Systems.
PB95-143285 *01,841*

Reference Architecture for Machine Control Systems Integration: Interim Report.
PB95-144549 *02,820*

Program Requirements to Advance the Technology of Custom Footwear Manufacturing.
PB95-147906 *02,883*

Portsmouth Fastener Manufacturing Workstation. User's Manual.
PB95-147922 *02,860*

Using Grafcet to Design Generic Controllers.
PB95-150827 *02,821*

Mapping Processes to Processors for Space-Based Robot Systems.
PB95-151510 *04,833*

Integration of Real-Time Process Planning for Small-Batch Flexible Manufacturing.
PB95-151908 *02,822*

Displacement Method for Machine Geometry Calibration.
PB95-152088 *02,946*

Automated Optical Roughness Inspection.
PB95-152179 *02,905*

Visual Road Following without 3-D Reconstruction.
PB95-161030 *01,591*

Real Time Differential Range Estimation Based on Time-Space Imagery Using PIPE.
PB95-161808 *01,844*

Reconstruction during Camera Fixation.
PB95-162236 *01,593*

Unified Approach to Camera Fixation and Vision-Based Road Following.
PB95-162244 *01,594*

Vehicle-Command Center Communications in a Robotic Vehicle System.
PB95-162723 *03,665*

Automated Inspection: The Integration of National Standards and Commercial Products at NIST.
PB95-163077 *02,906*

Two New Probes for a Coordinate Measuring Machine.
PB95-163093 *02,653*

Control System Architecture for a Remotely Operated Unmanned Land Vehicle.
PB95-163200 *03,759*

Variations in Size Measurements by Indicating Gaging Systems.
PB95-163614 *02,864*

Configuration and Performance Evaluation of a Real-Time Robot Control System: A Skeleton Approach.
PB95-163895 *01,598*

Integrated Mobile Robot System for Testing Vision Algorithms.
PB95-164133 *02,936*

Force Calibrations in the Nanonewton Regime.
PB95-168696 *03,949*

Workshop Summary Report: Industrial Applications of Scanned Probe Microscopy. A Workshop Co-sponsored by NIST, SEMATECH, ASTM, E42.14, and the American Vacuum Society. Held in Gaithersburg, Maryland on March 24-25, 1994.
PB95-170387 *00,506*

Robotics Application to Highway Transportation. Volume 2. Literature Search.
PB95-170551 *01,337*

New Method to Calculate Looming for Autonomous Obstacle Avoidance.
PB95-171435 *01,600*

Robotics Application to Highway Transportation. Volume 3. Proposed Research Topics and Cost/Benefit Evaluations by CERF.
PB95-171633 *01,338*

Workshop on the Application of Virtual Reality to Manufacturing. Final Report. Held in Gaithersburg, Maryland on August 9, 1994.
PB95-173555 *02,825*

Dimensional Inspection Planning Based on Product Data Standards.
PB95-175451 *02,910*

Accuracy in Integrated Circuit Dimensional Measurements.
PB95-180808 *02,368*

Vehicle-to-Roadside Communications for Commercial Vehicle Operations: Requirements and Approaches.
PB95-188827 *04,860*

Program of the Manufacturing Engineering Laboratory, 1995. Infrastructural Technology, Measurements, and Standards for the U.S. Manufacturing Industries.
PB95-188835 *02,754*

Motion-Model-Based Boundary Extraction.
PB95-189502 *01,849*

Robotics Application to Highway Transportation. Volume 4. Proposals for Potential Research.
PB95-193173 *01,339*

Real-Time Obstacle Avoidance Using Central Flow Divergence and Peripheral Flow.
PB95-198677 *02,937*

Expert Control System Shell Version 1.0 User's Guide.
PB95-198859 *01,790*

Post-Process Control of Machine Tools.
PB95-203451 *02,952*

Proceedings of the Manufacturing Technology Needs and Issues: Establishing National Priorities and Strategies Conference. Held in Gaithersburg, Maryland on April 26-28, 1994.
PB95-206181 *02,930*

Automated Manufacturing Research Facility 1994 Annual Report.
PB95-209854 *00,015*

Design, Specification and Tolerancing of Micrometer-Tolerance Assemblies.
PB95-209862 *02,913*

Issues Concerning Material Removal Shape Element Volumes (MRSEVs).
PB95-210167 *02,885*

Calculating Time-to-Contact Using Real-Time Quantized Optical Flow.
PB95-210522 *01,604*

Interim Testing Artifact (ITA): A Performance Evaluation System for Coordinate Measuring Machines (CMMs). User Manual.
PB95-210589 *02,914*

Japan Technology Program Assessment. Simulation: State-of the-Art in Japan.
PB95-217097 *02,827*

Outline of a Multiple Dimensional Reference Model Architecture and a Knowledge Engineering Methodology for Intelligent Systems Control.
PB95-220414 *03,703*

Texture-Independent Vision-Based Closed-Loop Fuzzy Controllers for Navigation Tasks.
PB95-220505 *00,183*

Algorithm Testing and Evaluation Program for Coordinate Measuring Systems: Long Range Plan.
PB95-231833 *02,915*

Conceptual Design Plan for the National Advanced Manufacturing Testbed.
PB95-231866 *02,828*

ISO TC 184/SC4 Reference Manual.
PB95-242293 *02,663*

Precision in Machining: Research Challenges.
PB95-242301 *02,953*

Unified Telerobotic Architecture Project (UTAP) Standard Interface Environment (SIE), May 1995.
PB95-242350 *02,938*

DETAN 95: Computer Code for Calculating Spectrum-Averaged Cross Sections and Detector Responses in Neutron Spectra.
PB95-242384 *04,014*

Measuring Long Gage Blocks with the NIST Line Scale Interferometer.
PB95-242400 *02,665*

Submarine Automation: Demonstration No. 5.
PB95-251633 *03,748*

Study of Potential Applications of Automation and Robotics Technology in Construction, Maintenance and Operation of Highway Systems: A Final Report. Volume 4.
PB95-251641 *01,340*

Algorithm Testing and Evaluation Program for Coordinate Measuring Systems: Testing Methods.
PB95-251658 *02,666*

User's Guide for the Algorithm Testing System Version 2.0.
PB95-251666 *02,916*

Study of Potential Applications of Automation and Robotics Technology in Construction, Maintenance and Operation of Highway Systems: A Final Report. Volume 1.
PB95-251682 *01,341*

Study of Potential Applications of Automation and Robotics Technology in Construction, Maintenance and Operation of Highway Systems: A Final Report. Volume 3.
PB95-251690 *01,342*

Information Technologies Make Business Sense for the Custom Therapeutic Footwear Industry.
PB95-251708 *02,829*

Gage Block Handbook.
PB95-251716 *02,667*

Product Models and Virtual Prototypes in Mechanical Engineering.
PB95-253563 *02,783*

Integrated Vision Touch-Probe System for Dimensional Inspection Tasks.
PB95-255832 *02,917*

Study of Potential Applications of Automation and Robotics Technology in Construction, Maintenance and Operation of Highway Systems: A Final Report. Volume 2.
PB95-255865 *01,343*

Design Engineering Research at NIST.
PB95-267860 *02,784*

Estimation of Measurement Uncertainty of Small Circular Features Measured by CMMs.
PB95-267928 *02,918*

Ouch Those Programs are Painful.
PB96-102678 *01,739*

Joint DoD/NIST Workshop on International Manufacturing Systems Research and Development. Held in Rockville, Maryland on November 3-5, 1992. Proceedings.
PB96-109491 *02,931*

Fabrication of Optics by Diamond Turning.
PB96-111695 *02,954*

Production Management Information Model for Discrete Manufacturing.
PB96-112008 *02,830*

Requisite Elements, Rationale, and Technology Overview for the Systems Intergration for Manufacturing Applications (SIMA) Program. Background Study.
PB96-112685 *02,831*

Proceedings of the Annual Manufacturing Technology Conference (2nd): Toward a Common Agenda. Held in Gaithersburg, Maryland on April 18-20, 1995.
PB96-112693 *02,887*

Microform Calibration Uncertainties of Rockwell Diamond Indenters.
PB96-122114 *03,280*

Roadmap for the Computer Integrated Manufacturing (CIM) Application Framework.
PB96-122759 *02,832*

Effects of Spindle Dynamic Characteristics on Hard Turning.
PB96-122981 *02,699*

Extensions of the Prototype Application Protocol of Ready-to-Wear Apparel Pattern Making.
PB96-128194 *03,198*

User's Guide to 'SuperFit' Modeling Software for CMM Probe Lobing.
PB96-128236 *02,921*

Reference Manual for the Algorithm Testing System Version 2.0.
PB96-128244 *02,922*

Summary Report: Workshop on Industrial Applications of Scanned Probe Microscopy (2nd). A Workshop Co-Sponsored by NIST, SEMATECH, ASTM E42.14, and the American Vacuum Society. Held in Gaithersburg, Maryland on May 2-3, 1995.
PB96-131602 *00,509*

Computer-Aided Manufacturing Engineering Forum (1st). Technical Meeting Proceedings. Held in Gaithersburg, Maryland on March 21-22, 1995.
PB96-136965 *02,834*

Visualization of Surface Figure by the Use of Zernike Polynomials.
PB96-137757 *04,351*

Object-Oriented Tel/Tk Binding for Interpreted Control of the NIST EXPRESS Toolkit in the NIST STEP Application Protocol Development Environment.
PB96-141049 *02,785*

Progress Toward Accurate Metrology Using Atomic Force Microscopy.
PB96-146774 *02,417*

NIST RS274KT Interpreter.
PB96-147954 *02,835*

Product Realization Process Modeling: A Study of Requirements, Methods and Research Issues.
PB96-147962 *02,836*

Machine Performance Standard Provides Opportunity to Improve Quality and Productivity.
PB96-154521 *02,837*

Guidelines for the Development of Mapping Tables.
PB96-154539 *02,786*

Image Gradient Evolution: A Visual Cue for Danger.
PB96-154562 *02,939*

NIST SIMA Interactive Management Workshop. Held in Fort Belvoir, Virginia on November 14-16, 1994.
PB96-154877 *02,838*

Stylus Technique for the Direct Verification of Rockwell Diamond Intenders.
PB96-155569 *02,958*

Quality in Automated Manufacturing.
PB96-160437 *02,839*

Development of a New Quality Control Strategy for Automated Manufacturing.
PB96-160486 *02,840*

Integrated Inspection System for Improved Machine Performance.
PB96-160569 *02,959*

Fabrication Issues for the Prototype National Institute of Standards and Technology SRM 2090A Scanning Electron Microscope Magnification Calibration Standard.
PB96-160585 *01,131*

Metrology Standards for Advanced Semiconductor Lithography Referenced to Atomic Spacings and Geometry.
PB96-160718 *02,424*

Residual Error Compensation of a Vision-Based Coordinate Measuring Machine.
PB96-161617 *04,091*

SPC Artifact for Automated Solder Joint Inspection.
PB96-161716 *04,095*

Machining Process Planning Activity Model for Systems Integration.
PB96-165428 *02,841*

PIECS: A Software Program for Machine Tool Process-Intermittent Error Compensation.
PB96-165980 *02,842*

Testing the Sensitivity of Accelerometers Using Mechanical Shock Pulses Under NIST Special Publication 250 Test No. 24040S.
PB96-179544 *02,683*

Procedure for Product Data Exchange Using STEP Developed in the AutoSTEP Pilot.
PB96-183058 *02,843*

Proceedings of NIST Workshop: Industry Needs in Welding Research and Standards Development. Held on August 15-16, 1995.
PB96-183124 *02,877*

Scale-Space-Based Visual-Motion-Cue for Autonomous Navigation.
PB96-183173 *02,940*

Aspects of a Product Model Supporting Apparel Virtual Enterprises.
PB96-183231 *02,790*

Dynamic Objects and Meta-Level Programming of an EXPRESS Language Environment.
PB96-190053 *01,774*

Increasing the Value of Atomic Force Microscopy Process Metrology Using a High-Accuracy Scanner, Tip Characterization, and Morphological Image Analysis.
PB96-190293 *02,758*

Scanned Probe Microscope Tip Characterization Without Calibrated Tip Characterizers.
PB96-190368 *02,759*

Novel Active-Vision-Based Motion Cues for Local Navigation.
PB96-193727 *02,941*

Systems Integration for Manufacturing Applications Program 1995 Annual Report.
PB96-193735 *02,844*

Survey of Standards for the U.S. Fiber/Textile/Apparel Industry.
PB96-193792 *03,199*

Computer-Aided Manufacturing Engineering Forum (2nd). Technical Meeting Proceedings. Held in Gaithersburg, Maryland on August 22-23, 1995.
PB96-195334 *02,845*

Operator Experience with a Hierarchical Real-Time Control System (RCS).
PB96-195516 *03,751*

Scanning Electron Microscope Magnification Calibration Interlaboratory Study.
PB96-201082 *01,164*

Application Protocol Information Base World Wide Web Gateway.
PB96-202320 *02,791*

General Motion Model and Spatio-Temporal Filters for 3-D Motion Interpretations.
PB96-210703 *01,861*

Optoelectronics and Optomechanics Manufacturing: An ATP Focused Program Development. Workshop Proceedings. Held in Gaithersburg, Maryland on February 15, 1995.
PB97-104186 *02,204*

Compensation of Errors Detected by Process-Intermittent Gauging.
PB97-110472 *02,846*

Compensation for Errors Introduced by Nonzero Fringe Densities in Phase-Measuring Interferometers.
PB97-110506 *04,386*

Representing Designs with Logic Formulations of Spatial Relations.
PB97-111561 *02,792*

Using Logic to Specify Shapes and Spatial Relations in Design Grammars.
PB97-111579 *02,793*

HVAC CAD Layout Tools: A Case Study of University/Industry Collaboration.
PB97-112221 *00,281*

Chip Morphology, Tool Wear and Cutting Mechanics in Finish Hard Turning.
PB97-112247 *03,106*

Combining Interactive Exploration and Optimization for Assembly Design.
PB97-112320 *02,794*

Chemical Aspects of Tool Wear in Single Point Diamond Turning.
PB97-112601 *03,021*

Improving the Design Process by Predicting Downstream Values of Design Attributes.
PB97-113096 *02,795*

Static Structural Analysis of a Reconfigurable Rigid Platform Supported by Elastic Legs.
PB97-113898 *02,960*

Interoperability Requirements for CAD Data Transfer in the AutoSTEP Project.
PB97-114268 *02,796*

Unified Process Specification Language: Requirements for Modeling Process.
PB97-116123 *02,850*

Capabilities for Product Data Exchange.
PB97-118764 *02,798*

SC4 Short Names Registry.
PB97-122410 *02,799*

Absence of Quantum-Mechanical Effects on the Mobility of Argon Ions in Helium Gas at 4.35 K.
PB97-122543 *01,194*

AUTOMATION

Technical Program of the Factory Automation Systems Division 1993.
PB94-160819 *02,805*

Hierarchical Real-Time Control System for Use with Coal Mining Automation.
PB94-212065 *03,698*

Publications of the Intelligent Systems Division (Previously Robot Systems Division) Covering the Period January 1971-April 1994.
PB94-217098 *02,935*

Framework for Information Technology Integration in Process Plant and Related Industries.
PB94-219086 *02,772*

CALS-Markup Requirements and Generic Style Specifications for Electronic Printed Output and Exchange of Text.
PB94-962200 *03,659*

Vibration Laboratory Automation at NIST with Personal Computers.
PB95-108700 *02,648*

Development of an Automated Part Inspection System Using the DMIS Standard.
PB95-108866 *02,899*

Testers Open Dialogue at Inaugural NIST Workshop.
PB95-175550 *01,718*

Post-Process Control of Machine Tools.
PB95-203451 *02,952*

Submarine Automation: Demonstration No. 5.
PB95-251633 *03,748*

Study of Potential Applications of Automation and Robotics Technology in Construction, Maintenance and Operation of Highway Systems: A Final Report. Volume 4.
PB95-251641 *01,340*

Study of Potential Applications of Automation and Robotics Technology in Construction, Maintenance and Operation of Highway Systems: A Final Report. Volume 1.
PB95-251682 *01,341*

Study of Potential Applications of Automation and Robotics Technology in Construction, Maintenance and Operation of Highway Systems: A Final Report. Volume 3.
PB95-251690 *01,342*

Study of Potential Applications of Automation and Robotics Technology in Construction, Maintenance and Operation of Highway Systems: A Final Report. Volume 2.
PB95-255865 *01,343*

PCASYS: A Pattern-Level Classification Automation System for Fingerprints.
PB95-267936 *01,853*

CALS-Markup Requirements and Generic Style Specifications for Electronic Printed Output and Exchange of Text.
PB95-962200 *03,668*

Automated Resistance Measurements at NIST.
PB96-119326 *02,274*

Quality in Automated Manufacturing.
PB96-160437 *02,839*

Development of a New Quality Control Strategy for Automated Manufacturing.
PB96-160486 *02,840*

Manager's Guide for Monitoring Data Integrity in Financial Systems.
PB96-165915 *00,003*

PIECS: A Software Program for Machine Tool Process-Intermittent Error Compensation.
PB96-165980 *02,842*

NIST Construction Automation Program Report No. 2. Proceedings of the NIST Construction Automation Workshop. Held in Gaithersburg, Maryland on March 30-31, 1995.
PB96-202239 *00,413*

Compensation of Errors Detected by Process-Intermittent Gauging.
PB97-110472 *02,846*

Data Management for Error Compensation and Process Control.
PB97-110480 *02,847*

Testing Conformance and Interoperability of BACnet (Trade Name) Building Automation Products.
PB97-111553 *00,310*

Resistors.
PB97-111876 *02,284*

AUTOMOBILE CATALYST

Resolution of Discrepant Analytical Data in the Certification of Platinum in Two Automobile Catalyst SRMs.
PB96-167283 *00,638*

AUTOMOTIVE ENGINEERING

Interoperability Requirements for CAD Data Transfer in the AutoSTEP Project.
PB97-114268 *02,796*

AUTOMOTIVE INDUSTRY

Procedure for Product Data Exchange Using STEP Developed in the AutoSTEP Pilot.
PB96-183058 *02,843*

AUTONOMOUS GALLOPING OSCILLATORS

Foias-Temam Approximations of Attractors for Galloping Oscillators.
PB94-198298 *04,817*

Algebraic Approximation of Attractors for Galloping Oscillators.
PB95-162897 *04,820*

AUTONOMOUS NAVIGATION

Ground Vehicle Control at NIST: From Teleoperation to Autonomy.
N94-34037/9 *03,758*

Intelligent Control for Multiple Autonomous Undersea Vehicles.
PB94-211877 *03,747*

Real-Time Vision for Autonomous and Teleoperated Control of Unmanned Vehicles.
PB94-211885 *03,701*

Real-Time Vision for Unmanned Vehicles.
PB94-211893 *03,702*

Visual Road Following without 3-D Reconstruction.
PB95-161030 *01,591*

Reconstruction during Camera Fixation.
PB95-162236 *01,593*

Unified Approach to Camera Fixation and Vision-Based Road Following.
PB95-162244 *01,594*

New Method to Calculate Looming for Autonomous Obstacle Avoidance.
PB95-171435 *01,600*

Outline of a Multiple Dimensional Reference Model Architecture and a Knowledge Engineering Methodology for Intelligent Systems Control.
PB95-220414 *03,703*

Texture-Independent Vision-Based Closed-Loop Fuzzy Controllers for Navigation Tasks.
PB95-220505 *00,183*

Scale-Space-Based Visual-Motion-Cue for Autonomous Navigation.
PB96-183173 *02,940*

Novel Active-Vision-Based Motion Cues for Local Navigation.
PB96-193727 *02,941*

AUTORADIOGRAPHY

Interlaboratory Comparison of Autoradiographic DNA Profiling Measurements. 1. Data and Summary Statistics.
PB95-175923 *03,542*

Interlaboratory Comparison of Autoradiographic DNA Profiling Measurements. 2. Measurement Uncertainty and Its Propagation.
PB96-112123 *03,545*

AUTOREGRESSIVE PROCESSES
Analysis of Autocorrelations in Dynamic Processes.
PB95-181228 *02,826*

AVALANCHE BREAKDOWN
Experimental Study of Reverse-Bias Failure Mechanisms in Bipolar Mode JFET (BMFET).
PB95-152997 *02,340*

AVIATION FUELS
Measurement of Diffusion in Supercritical Fluid Systems: A Review.
PB94-199189 *00,795*

Measurement of Diffusion in Fluid Systems: Applications to the Supercritical Fluid Region.
PB95-175188 *02,490*

AVIATION SAFETY
Suppression of High Speed Turbulent Flames in a Detonation/Deflagration Tube.
PB95-231817 *01,395*

AVIONICS
Measurements of Shielding Effectiveness and Cavity Characteristics of Airplanes.
PB94-210051 *00,030*

AXES OF ROTATION
Evaluation of a Tapered Roller Bearing Spindle for High-Precision Hard Turning Applications.
PB96-160494 *02,700*

AXIAL STRAIN
Effect of Axial Strain on the Critical Current of Ag-Sheathed Bi-Based Superconductors in Magnetic Fields Up to 25 T.
PB94-211315 *04,493*

AZEOTROPES
Role of Refrigerant Mixtures as Alternatives to CFCs.
PB94-199775 *03,252*

Study to Determine the Existence of an Azeotropic R-22 'Drop-In' Substitute.
PB96-167812 *02,568*

AZO COMPOUNDS
Molar Absorptivities of Bilirubin (NIST SRM 916A) and Its Neutral and Alkaline Azopigments.
PB94-211042 *03,456*

BACILLUS SUBTILIS
Glucose Permease of Bacillus Subtilis Is a Single Polypeptide Chain That Functions to Energize the Sucrose Permease.
PB95-163192 *03,466*

BACKDRAFT PHENOMENA
Backdraft Phenomena.
PB94-193927 *01,366*

BACKGROUND CURRENTS
Novel Amperometric Immunosensor for Procainamide Employing Light Activated Labels.
PB96-163662 *00,512*

BACKSCATTERING
Evidence for Significant Backscattering in Near-Threshold Electron-Impact Excitation of Ar(7+)(3s yields 3p).
PB95-126405 *03,883*

Measured Stopping Powers of Hydrogen and Helium in Polystyrene Near Their Maximum Values.
PB96-112321 *04,729*

BACKSCATTERING SPECTROMETERS
Design of a High-Flux Backscattering Spectrometer for Ultra-High Resolution Inelastic Neutron Measurements.
PB96-179577 *02,992*

BACTERIA
Total Surface Areas of Group IVA Organometallic Compounds: Predictors of Toxicity to Algae and Bacteria.
PB94-211331 *00,814*

Holographic Properties of Triton X-100-Treated Bacteriorhodopsin Embedded in Gelatin Films.
PB96-119284 *03,761*

Autofluorescence Detection of 'Escherichia coli' on Silver Membrane Filters.
PB96-163639 *03,590*

Bacterial Enumeration in Storage Water.
PB96-163647 *03,591*

BACTERIORHODOPSIN
Retinal-Protein Complexes as Optoelectronic Components.
PB95-150397 *02,146*

Bacteriorhodopsin Immobilized in Sol-Gel Glass.
PB95-151429 *03,532*

Bacteriorhodopsin Retains Its Light-Induced Proton-Pumping Function After Being Heated to 140C.
PB96-102728 *03,471*

Rapid pH Change Due to Bacteriorhodopsin Measured with a Tin-Oxide Electrode.
PB96-112081 *03,544*

Holographic Properties of Triton X-100-Treated Bacteriorhodopsin Embedded in Gelatin Films.
PB96-119284 *03,761*

Optical Properties of Triton X-100-Treated Purple Membranes Embedded in Gelatin Films.
PB96-123500 *03,546*

BALANCES
Precision Laboratory Standards of Mass and Laboratory Weights.
AD-A280 562/0 *02,618*

BALL-BAR STANDS
NIST SRM 9983 High-Rigidity Ball-Bar Stand. User Manual.
PB95-255840 *02,669*

BALLE-FLYGARE SPECTROMETERS
Experimental Studies of Line Shapes from a Balle-Flygare Spectrometer.
PB94-199452 *00,796*

BALMER LINES
Excitation of Balmer Lines in Low-Current Discharges of Hydrogen and Deuterium.
PB95-150546 *03,893*

Hydrogen Balmer Alpha Line Shapes for Hydrogen-Argon Mixtures in a Low-Pressure rf Discharge.
PB95-153433 *03,924*

BAND SIZE
Interlaboratory Comparison of Autoradiographic DNA Profiling Measurements. 2. Measurement Uncertainty and Its Propagation.
PB96-112123 *03,545*

BAND STRUCTURE OF SOLIDS
Band-to-Band Photoluminescence and Luminescence Excitation in Extremely Heavily Carbon-Doped Epitaxial GaAs.
PB95-150413 *04,570*

BAND THEORY
Substitution-Induced Midgap States in the Mixed Oxides RxBa1-ChiTiO3-Delta, with R=Y, La, and Nd.
PB95-140505 *04,541*

BANDPASS FILTERS
Systematic Studies of the Effect of a Bandpass Filter on a Josephson-Junction Noise Thermometer.
PB95-162970 *03,939*

BARIUM
Short-Range Correlation and Relaxation Effects on the (6p(2))(1)SO Autoionizing State of Atomic Barium.
PB95-202289 *03,973*

Energy-Pooling Collisions in Barium.
PB95-203030 *03,997*

Excitation Transfer in Barium by Collisions with Noble Gases.
PB96-200274 *01,163*

BARIUM BISMUTH OXIDES
Powder Neutron Diffraction Investigation of Structure and Cation Ordering in Ba2+xBi2-xO6-y.
PB95-180865 *01,015*

BARIUM BISMUTHATES
Powder Neutron Diffraction Investigation of Structure and Cation Ordering in Ba2+xBi2-xO6-y.
PB95-180865 *01,015*

BARIUM BORATES
High-Efficiency, High-Power Difference-Frequency Generation of 0.9-1.5 mu m Light in BBO.
PB95-202255 *04,317*

BARIUM COMPOUNDS
Epitaxial Growth of BaTiO3 Thin Films at 600C by Metalorganic Chemical Vapor Deposition.
PB96-122510 *03,071*

BARIUM COPPER OXALATES
X-Ray Powder Diffraction Data for BaCu(C2O4)2.6H2O.
PB95-151767 *04,583*

BARIUM IONS
Fine Structure of Negative Ions of Alkaline-Earth-Metal Atoms.
PB94-211182 *03,837*

Spectrum and Energy Levels of Triply Ionized Barium (Ba IV).
PB95-140877 *03,888*

Thermodynamic Properties of the Aqueous Ba(sup 2+) Ion and the Key Compounds of Barium.
PB96-145834 *01,107*

BARIUM IRON TITANATE
Preparation, Crystal Structure, Dielectric Properties, and Magnetic Behavior of Ba2Fe2Ti4O13.
PB96-186176 *01,162*

BARIUM OXIDES
Crystal Chemistry and Phase Equilibria Studies of the BaO(BaCO3)-R2O3-CuO Systems. 4. Crystal Chemistry and Subsolidus Phase Relationship Studies of the CuO-Rich Region of the Ternary Diagrams, R=Lanthanides.
PB95-151759 *00,936*

Surface Geometry of BaO on W(100): A Surface-Extended X-Ray-Absorption Fine-Structure Study.
PB95-164414 *00,980*

Magnetic Dielectric Oxides: Subsolidus Phase Relations in the BaO: Fe2O3: TiO2 System.
PB96-176524 *01,156*

BARIUM PARTIAL DENSITY
Barium Contributions to the Valence Electronic Structure of YBa2Cu3O7-delta, PrBa2Cu3O7-delta, and Other Barium-Containing Compounds.
PB96-158019 *04,076*

BARIUM TITANATES
Photoelectron Spectroscopic Study of the Valence and Core-Level Electronic Structure of BaTiO3.
PB94-212149 *04,500*

Surface Core-Level Shifts of Barium Observed in Photoemission of Vacuum-Fractured BaTiO3 (100).
PB94-212156 *04,501*

BARKHAUSEN EFFECT
Langevin Approach to Hysteresis and Barkhausen Modeling in Steel.
PB94-185675 *03,206*

Analytical Expressions for Barkhausen Jump Size Distributions.
PB95-180345 *04,680*

BARRIERS
Helping to Reduce Technical Barriers to Trade.
PB96-190046 *00,491*

Methodology for Developing and Implementing Alternative Temperature-Time Curves for Testing the Fire Resistance of Barriers for Nuclear Power Plant Applications.
PB96-193784 *03,742*

TBT Agreement Activities of the National Institute of Standards and Technology, 1995.
PB97-104178 *00,499*

Stacking the Cards in Europe: One Company's Story.
PB97-110126 *00,493*

BARS
Degradation of Powder Epoxy Coated Panels Immersed in a Saturated Calcium Hydroxide Solution Containing Sodium Chloride.
PB96-101050 *01,344*

BASE ISOLATION
Modified Optimal Algorithm for Active Structural Control.
PB96-165949 *00,472*

BASELINE MEASUREMENTS
Indoor Air Quality Impacts of Residential HVAC Systems. Phase 2.A Report: Baseline and Preliminary Simulations.
PB95-178893 *02,554*

BAYARD-ALPERT GAGES
Comments on the Stability of Bayard-Alpert Ionization Gages.
PB96-103080 *02,673*

BAYARD-ALPERT IONIZATION GAGES
Influence of the Filament Potential Wave Form on the Sensitivity of Glass-Envelope Bayard-Alpert Gages.
PB95-175014 *02,657*

Long-Term Stability of Bayard-Alpert Gauge Performance: Results Obtained from Repeated Calibrations against the National Institute of Standards and Technology Primary Vacuum Standard.
PB96-123567 *02,676*

BAYS (STRUCTURAL UNITS)
Use of Computer Models to Predict Temperature and Smoke Movement in High Bay Spaces.
PB94-145976 *00,191*

BCC LATTICES
Transformation of BCC and B2 High Temperature Phases to HCP and Orthorhombic Structures in the Ti-Al-Nb System. Part 1. Microstructural Predictions Based on a Subgroup Relation between Phases.
PB96-169065 *03,370*

Transformation of BCC and B2 High Temperature Phases to HCP and Orthorhombic Structures in the Ti-Al-Nb System. Part 2. Experimental TEM Study of Microstructures.
PB96-169073 *03,371*

BEAD-ROD MODEL
Effect of Hydrodynamic Interactions on a Terminally Anchored Bead-Rod Model Chain.
PB95-141156 *01,237*

BEAM ADDITION METHOD
Beamcon III, a Linearity Measurement Instrument for Optical Detectors.
PB96-113576 *04,337*

BEAM CALIBRATION
Calorimeters for Calibration of High-Dose Dosimeters in High-Energy Electron Beams.
PB96-135272 *04,055*

BEAM-COLUMN JOINTS
Model Precast Concrete Beam-to-Column Connections Subject to Cyclic Loading.
PB95-153094 *00,438*

Partially Prestressed and Debonded Precast Concrete Beam-Column Joints.
PB95-153102 *00,439*

Seismic Performance Behavior of Precast Concrete Beam-Column Joints.
PB95-153110 *00,440*

BEAM LINES
Beam Line for Highly Charged Ions.
PB97-111256 *04,143*

BEAM MIRRORS
Atomic Beam Splitters and Mirrors by Adiabatic Passage in Multilevel Systems.
PB94-216439 *03,867*

BEAM SPLITTERS
Atomic Beam Splitters and Mirrors by Adiabatic Passage in Multilevel Systems.
PB94-216439 *03,867*

BEAM VOLTAGE
Effect of Beam Voltage on the Properties of Aluminum Nitride Prepared by Ion Beam Assisted Deposition.
PB97-118616 *01,995*

BEAMS
Generalized Optical Theorem for On-Axis Gaussian Beams.
PB97-122345 *04,177*

BEAMS (RADIATION)
Merged-Beams Energy-Loss Technique for Electron-Ion Excitation: Absolute Total Cross Sections for O(5+) (2s yields 2p).
PB96-102058 *04,017*

Beamcon III, a Linearity Measurement Instrument for Optical Detectors.
PB96-113576 *04,337*

BEAMS (STRUCTURAL)
Model Precast Concrete Beam-to-Column Connections Subject to Cyclic Loading.
PB95-153094 *00,438*

Partially Prestressed and Debonded Precast Concrete Beam-Column Joints.
PB95-153102 *00,439*

Seismic Performance Behavior of Precast Concrete Beam-Column Joints.
PB95-153110 *00,440*

BEAMS (SUPPORTS)
Performance of 1/3-Scale Model Precast Concrete Beam-Column Connections Subjected to Cyclic Inelastic Loads. Report No. 4.
PB95-179024 *00,444*

Simplified Design Procedure for Hybrid Precast Concrete Connections.
PB96-154836 *00,405*

Shear Design of High-Strength Concrete Beams: A Review of the State-of-the-Art.
PB96-214713 *01,330*

BEAMSPLITTERS
Deep-UV Excimer Laser Measurements at NIST.
PB96-141031 *04,355*

BEANS
Thermodynamics of the Binding of Galactopyranoside Derivatives to the Basic Lectin from Winged Bean (Psophocarpus Tetrogonolobus).
PB95-162715 *03,465*

BEDS
Measurement of Room Conditions and Response of Sprinklers and Smoke Detectors during a Simulated Two-Bed Hospital Patient Room Fire.
PB94-213717 *00,292*

BENCH TESTS
Modern Test Methods for Flammability.
PB94-198447 *01,370*

BEND STICK MODELS
Effects of Variable Excluded Volume on the Dimensions of Off-Lattice Polymer Chains.
PB94-212941 *01,229*

BENDING
Bending-Induced Phase Shifts in Dual-Mode Planar Optical Waveguides.
PB95-161329 *04,271*

BENEFIT-COST ANALYSIS
Building Life Cycle Cost Computer Program (BLCC) Version 4.22-95 (for Microcomputers).
PB95-503397 *00,268*

Building Life Cycle Cost Computer Program (BLCC) Version 4.4-97 (for Microcomputers).
PB97-500342 *00,284*

BENZENE
Carbon Acidities of Aromatic Compounds. 1. Effects of In-Ring Aza and External Electron-Withdrawing Groups.
PB94-216595 *00,860*

Calculation of Enthalpy and Entropy Differences of Near-Critical Binary Mixtures with the Modified Leung-Griffiths Model.
PB95-108635 *00,885*

Correlation of the Ideal Gas Properties of Five Aromatic Hydrocarbons.
PB95-175816 *01,002*

Doppler-Free Spectroscopy of Large Polyatomic Molecules and van der Waals Complexes.
PB96-119581 *04,339*

BENZENE COMPLEXES
Van der Waals Bond Lengths and Electronic Spectral Shifts of the Benzene-Kr and Benzene-Xe Complexes.
PB95-151387 *00,932*

BENZILIC ACID
Determination of 3-Quinuclidinyl Benzilate (Qnb) and Its Major Metabolites in Urine by Isotope Dilution Gas Chromatography Mass Spectrometry.
PB94-199379 *03,492*

BENZOCYCLOBUTENE
Homogeneous Gas Phase Decyclization of Tetralin and Benzocyclobutene.
PB95-151049 *00,928*

BENZOIC ACIDS
Automated, High Precision Coulometric Titrimetry. Part 2. Strong and Weak Acids and Bases.
PB95-150207 *00,576*

BENZOYL PEROXIDE
Copper Ion-Mediated Modification of Bases in DNA in Vitro by Benzoyl Peroxide.
PB94-198231 *03,645*

BERYLLIUM
Energy Dependences of Absorption in Beryllium Windows and Argon Gas.
PB96-102124 *04,020*

BERYLLIUM IONS
Experimental Results on Normal Modes in Cold, Pure Ion Plasmas.
PB95-175105 *03,956*

Precise Spectroscopy for Fundamental Physics.
PB96-112164 *04,040*

BESSEL FUNCTIONS
Portable Vectorized Software for Bessel Function Evaluation.
PB94-198975 *01,690*

BETA DOSIMETRY
Extrapolation Chamber Measurements on (90)Sr + (90)Y Beta-Particle Ophthalmic Applicator Dose Rates.
PB95-153375 *03,626*

BETA HYDRI STAR
Distant Future of Solar Activity: A Case Study of Beta Hydri. 3. Transition Region, Corona, and Stellar Wind.
PB94-185220 *00,049*

BETA PARTICLES
Measurement of Radial Dose Distributions Around Small Beta Particle Emitters Using High Resolution Radiochromic Foil Dosimetry.
PB95-164604 *03,518*

Angular Variation of the Personal Dose Equivalent, Hp(0.07), for Beta Radiation and Nearly Monoenergetic Electron Beams: Preliminary Results.
PB95-168472 *03,630*

System for Intercomparing Standard Solutions of Beta-Particle Emitting Radionuclides.
PB96-159637 *03,707*

BETZ-QUARTZ
Wear of Enamel against Glass-Ceramic, Porcelain, and Amalgam.
PB96-179593 *03,082*

BIAS
Error Propagation Biases in the Calculation of Indentation Fracture Toughness for Ceramics.
PB94-172434 *03,032*

BIBLIOGRAPHIC DATABASES
Evolution of a United States Information System.
PB96-157896 *02,713*

BIBLIOGRAPHIES
Bibliography of Books and Published Reports on Gas Turbines, Jet Propulsion, and Rocket Power Plants.
AD-A278 138/3 *01,445*

Bibliography of Books and Published Reports on Gas Turbines, Jet Propulsion, and Rocket Power Plants, January 1950 through December 1953.
AD-A278 213/4 *01,446*

Aerodynamic Phenomena in Stellar Atmospheres - A Bibliography.
AD-A278 521/0 *00,046*

Survey of the Literature on Heat Transfer from Solid Surfaces to Cryogenic Fluids.
AD-A286 680/4 *04,193*

Preliminary List of References Containing Compilations of Data on Properties of Materials.
AD-A302 670/5 *03,243*

Metrology for Electromagnetic Technology: A Bibliography of NIST Publications.
PB94-159761 *02,116*

Bibliography on Apparel Sizing and Related Issues.
PB94-161924 *02,806*

BFRL Fire Publications, 1993.
PB94-164191 *00,192*

Publications of the Manufacturing Engineering Laboratory Covering the Period January 1989-September 1992.
PB94-165966 *02,750*

Bibliography of the NIST Electromagnetic Fields Division Publications.
PB94-165990 *01,875*

NIST Serial Holdings, 1994.
PB94-178068 *02,745*

Electronics and Electrical Engineering Laboratory Technical Publication Announcements Covering Laboratory Programs, October to December 1993 with 1994/1995 EEEL Events Calendar.
PB94-193752 *02,307*

Bibliography of Photon Total Cross Section (Attenuation Coefficient) Measurements 10 eV to 13.5 GeV, 1907-1993.
PB94-193760 *03,804*

Electronics and Electrical Engineering Laboratory Technical Progress Bulletin Covering Laboratory Programs, January to March 1994 with 1994/1995 EEEL Events Calendar.
PB94-193810 *02,308*

Electronics and Electrical Engineering Laboratory Technical Progress Bulletin Covering Laboratory Programs, July to September 1993 with 1994 EEEL Events Calendar.
PB94-194354 *02,309*

Electronics and Electrical Engineering Laboratory Technical Publication Announcements Covering Laboratory Programs, January to March 1994 with 1994/1995 EEEL Events Calendar.
PB94-213774 *01,883*

Bibliography of Computer Security Glossaries.
PB94-216710 *01,587*

Publications of the Intelligent Systems Division (Previously Robot Systems Division) Covering the Period January 1971-April 1994.
PB94-217098 *02,935*

Bibliography of the NIST Electromagnetic Fields Division Publications.
PB95-135562 *01,886*

Metrology for Electromagnetic Technology: A Bibliography of NIST Publications.
PB95-135588 *02,143*

Electronics and Electrical Engineering Laboratory Technical Progress Bulletin Covering Laboratory Programs, April to June 1994 with 1994/1995 EEEL Events Calendar.
PB95-143186 *02,329*

Building and Fire Research Laboratory Publications, 1993.
PB95-143202 *00,369*

Evaluating Investments in Law Enforcement Equipment: An Annotated Bibliography.
PB95-151379 *04,867*

Electronics and Electrical Engineering Laboratory Technical Progress Bulletin Covering Laboratory Programs, July to September 1994 with 1994/1995 EEEL Events Calendar.
PB95-170395 *02,360*

NIST Serial Holdings, 1995.
PB95-188926 *02,746*

Electronics and Electrical Engineering Laboratory Technical Publication Announcements Covering Laboratory Programs, July to September 1994 with 1995 EEEL Events Calendar.
PB95-198925 *01,912*

Publications of the National Institute of Standards and Technology 1992 Catalog.
PB95-200747 *00,014*

Building and Fire Research Laboratory Publications, 1994.
PB95-226684 *00,398*

Electronics and Electrical Engineering Laboratory Technical Publication Announcements Covering Laboratory Programs, January to March 1995 with 1995 EEEI Events Calendar.
PB95-242277 *02,373*

Bibliography of the NIST Optoelectronics Division.
PB96-128210 *02,193*

Metrology for Electromagnetic Technology: A Bibliography of NIST Publications, September 1995.
PB96-128269 *01,938*

Classified Bibliography: Insulation Condition Monitoring Methods, 1989-1995.
PB96-131586 *02,232*

Catalogue of Electromagnetic Environment Measurements, 30-300 Hz.
PB96-155452 *01,943*

Publications 1995: NIST Building and Fire Research Laboratory.
PB96-183074 *00,226*

Publications of the National Institute of Standards and Technology 1993 Catalog.
PB96-183215 *00,017*

Bibliography of the NIST Electromagnetic Fields Division Publications.
PB96-210778 *01,980*

Experimentally Measured Total X-ray Attenuation Coefficients Extracted from Previously Unprocessed Documents Held by the NIST Photon and Charged Particle Data Center.
PB97-114474 *04,165*

Bibliography of the NIST Optoelectronics Division.
PB97-116040 *02,207*

Metrology for Electromagnetic Technology: A Bibliography of NIST Publications.
PB97-116057 *04,396*

BICRYSTALS
Electromagnetic Coupling Character of (001) Twist Boundaries in Sintered Bi2Sr2CaCu2O8+x Bicrystals.
PB96-176573 *01,963*

BIDIRECTIONAL SCATTERING DISTRIBUTION FUNCTIONS
Rayleigh Scattering Limits for Low-Level Bidirectional Reflectance Distribution Function Measurements.
PB95-180030 *04,307*

BILIRUBIN
Molar Absorptivities of Bilirubin (NIST SRM 916A) and Its Neutral and Alkaline Azopigments.
PB94-211042 *03,456*

BIMATERIAL INTERFACE
Diffusive Crack Growth at a Bimaterial Interface.
PB96-204110 *03,090*

BIMATERIALS
Asymmetric Tip Morphology of Creep Microcracks Growing Along Bimaterial Interfaces.
PB94-200243 *03,138*

BIMOLECULAR REACTION
Bimolecular Interactions in (Et)3SiOH:Base:CCl4 Hydrogen-Bonded Solutions Studied by Deactivation of the Free OH-Stretch Vibration.
PB97-118657 *04,166*

BINARY ALLOY SYSTEMS
Thermodynamic Assessment and Calculation of the Ti-Al System.
PB94-212644 *03,337*

BINARY ALLOYS
Convection and Morphological Stability During Directional Solidification.
N95-14548/8 *03,310*

Effects of Crystalline Anisotropy and Buoyancy-Driven Convection on Morphological Stability.
PB94-200441 *03,328*

BINARY MIXTURES
Calculation of Enthalpy and Entropy Differences of Near-Critical Binary Mixtures with the Modified Leung-Griffiths Model.
PB95-108635 *00,885*

Thermodynamic Properties of the Methane-Ethane System.
PB95-125779 *00,891*

Experimental Method for Obtaining Critical Densities of Binary Mixtures: Application to Ethane + n-Butane.
PB95-151148 *00,930*

Measurements of the Virial Coefficients and Equation of State of the Carbon Dioxide + Ethane System in the Supercritical Region.
PB95-151353 *03,906*

Stability/Instability of Gas Mixtures Containing 1,3-Butadiene in Treated Aluminum Gas Cylinders.
PB95-162285 *02,546*

Viscosity of the Saturated Liquid Phase of Six Halogenated Compounds and Three Mixtures.
PB95-162368 *00,960*

Critical Properties and Vapor-Liquid Equilibria of the Binary System Propane + Neopentane.
PB95-175683 *00,999*

Critical Lines for Type-III Aqueous Mixtures by Generalized Corresponding-States Models.
PB96-102371 *01,063*

BINARY STARS
ROSAT All-Sky Survey of Active Binary Coronae. 2. Coronal Temperatures of the RS Canum Venaticorum Systems.
PB94-199601 *00,055*

Dynamic Phenomena on the RS Canum Venaticorum Binary II Pegasi in August 1989. 1. Observational Data.
PB94-211067 *00,056*

Radio Continuum and X-Ray Properties of the Coronae of RS Canum Venaticorum and Related Active Binary Systems.
PB94-211083 *00,057*

ROSAT All-Sky Survey of Active Binary Coronae. 1. Quiescent Fluxes for the RS Canum Venaticorum Systems.
PB95-202479 *00,077*

Rotational Modulation and Flares on RS Canum Venaticorum and BY Draconis Stars. XVIII. Coordinated VLA, ROSAT, and IUE Observations of RS CVn Binaries.
PB96-102322 *00,089*

Discussion: Statistical Signal Processing of Quasiperiodicities.
PB96-119532 *00,096*

Transition Regions of Capella.
PB96-123336 *00,105*

Transition Regions of Capella (1995).
PB96-176714 *00,108*

BINARY SYSTEM (MATERIALS)
Statistical Thermodynamics of Phase Separation and Ion Partitioning in Aqueous Two-Phase Systems.
PB94-199387 *01,212*

BINARY SYSTEMS (MATERIALS)
Shear Dependence of Critical Fluctuations in Binary Polymer Mixtures by Small Angle Neutron Scattering.
PB94-211612 *01,220*

Small-Angle X-Ray and Neutron Scattering Study of Block Copolymer/Homopolymer Mixtures.
PB94-211729 *01,221*

Generalized Plane Strain Analysis of a Bimaterial Composite Containing a Free Surface Normal to the Interface.
PB95-163341 *03,164*

Partial Scattered Intensities from a Binary Suspension of Polystyrene and Silica.
PB95-175618 *00,996*

BINDERS
Binder Characterization and Evaluation by Nuclear Magnetic Resonance Spectroscopy.
PB94-193471 *01,334*

Computer Simulations of Binder Removal from 2-D and 3-D Model Particulate Bodies.
PB97-121339 *00,418*

BINDING ENERGY
Thermal Decomposition of Hydroxy- and Methoxy-Substituted Anisoles.
PB94-173036 *00,767*

Energy Calibration of X-ray Photoelectron Spectrometers: Results of an Interlaboratory Comparison to Evaluate a Proposed Calibration Procedure.
PB96-102918 *04,027*

Theory for Quantum-Dot Quantum Wells: Pair Correlation and Internal Quantum Confinement in Nanoheterostructures.
PB96-179445 *02,437*

BINDING SITES
Characterization of the Binding of Gallium, Platinum, and Uranium to Pseudomonas Fluorescens by Small-Angle X-ray Scattering and Transmission Electron Microscopy.
PB94-172509 *03,453*

Fokker-Planck Description of Multivalent Interactions.
PB95-108478 *00,879*

BIOACCUMULATION
Current Activities Within the National Biomonitoring Specimen Bank.
PB94-172806 *02,516*

Determination of Inorganic Constituents in Marine Mammal Tissues.
PB95-152047 *00,589*

Development of the National Marine Mammal Tissue Bank.
PB95-161402 *02,586*

Quality Assurance of Contaminant Measurements in Marine Mammal Tissues.
PB95-164034 *02,588*

Certification of Polychlorinated Biphenyl Congeners and Chlorinated Pesticides in a Whale Blubber Standard Reference Material.
PB96-103023 *03,745*

Trace Element Concentrations in Cetacean Liver Tissues Archived in the National Marine Mammal Tissue Bank.
PB96-167127 *02,595*

Relationship of Silver with Selenium and Mercury in the Liver of Two Species of Toothed Whales (Odontocetes).
PB96-167275 *02,596*

BIOACTIVE MATERIALS
Bioactive Polymeric Dental Materials Based on Amorphous Calcium Phosphate.
PB96-147012 *03,572*

BIOASSAY
Alaska Marine Mammal Tissue Archival Project: Specimen Inventory.
PB95-171344 *02,589*

Concentrations of Chlorinated Hydrocarbons, Heavy Metals and Other Elements in Tissues Banked by the Alaska Marine Mammal Tissue Archival Project.
PB95-209870 *02,590*

Intercomparison Study of (237)Np Determination in Artificial Urine Samples.
PB96-102645 *03,633*

Considerations in the Design of an Environmental Specimen Bank: Experiences of the National Biomonitoring Specimen Bank Program.
PB96-112370 *02,527*

BIOCHEMISTRY
Affinity Chromatography on Inorganic Support Materials.
PB95-163820 *03,467*

BIOCOMPATIBILITY
Behavior of a Calcium Phosphate Cement in Simulated Blood Plasma In vitro.
PB95-168712 *00,165*

BIOCOMPATIBLE MATERIALS
Establishing Quality Measurements for Inorganic Analysis of Biomaterials.
PB94-199726 *00,548*

Periapical Tissue Reactions to a Calcium Phosphate Cement in the Teeth of Monkeys.
PB94-212008 *00,149*

Dental Applications of Ceramics.
PB96-122940 *00,177*

Posterior Restorative Materials Research.
PB97-118624 *03,582*

BIODETERIORATION
Microbial Degradation of Polysulfides and Insights into Their Possible Occurrence in Coal.
PB95-163374 *02,488*

BIOELECTRICAL IMPEDANCE ANALYZERS
Overview of Bioelectrical Impedance Analyzers.
PB96-122635 *00,176*

Overview of Bioelectrical Impedance Analyzers.
PB97-118780 *00,181*

BIOFOULING
Determination of Total Protein Adsorbed on Solid (Membrane) Surface by a Hydrolysis Technique: Single Protein Adsorption.
PB96-167093 *03,552*

BIOINSTRUMENTATION
Overview of Bioelectrical Impedance Analyzers.
PB96-122635 *00,176*

Overview of Bioelectrical Impedance Analyzers.
PB97-118780 *00,181*

BIOLOGICAL ACCUMULATION
Development of Frozen Whale Blubber and Liver Reference Materials for the Measurement of Organic and Inorganic Contaminants.
PB95-151676 *00,587*

Concentrations of Chlorinated Hydrocarbons, Heavy Metals and Other Elements in Tissues Banked by the Alaska Marine Mammal Tissue Archival Project.
PB95-209870 *02,590*

BIOLOGICAL EFFECTS
Periapical Tissue Reactions to a Calcium Phosphate Cement in the Teeth of Monkeys.
PB94-212008 *00,149*

BIOLOGICAL MACROMOLECULES
Biological Macromolecular Crystallization Database: A Tool for Developing Crystallization Strategies.
PB95-126157 *00,897*

Biological Macromolecule Crystallization Database and NASA Protein Crystal Growth Archive.
PB97-109136 *01,171*

BIOLOGICAL MATERIALS
Certifying the Chemical Composition of a Biological Material: A Case Study.
PB96-164272 *00,636*

BIOLOGICAL RADIATION EFFECTS
Systematics of Alpha-Particle Energy Spectra and Lineal Energy (Y) Spectra for Radon Daughters.
PB94-185139 *03,615*

Microdosimetry and Cellular Radiation Effects of Radon Progency in Human Bronchial Airways.
PB95-152344 *03,625*

BIOLOGICAL SYSTEMS
Isotopic and Nuclear Analytical Techniques in Biological Systems: A Critical Study. 10. Elemental Isotopic Dilution Analysis with Radioactive and Stable Isotopes (Technical Report).
PB96-164157 *00,696*

BIOLOGICAL TREATMENT
Chemical and Microbiological Problems Associated with Research on the Biodesulfurization of Coal.
PB95-140950 *02,484*

Bioleaching of Cobalt from Smelter Wastes by 'Thiobacillus ferrooxidans'.
PB95-140968 *02,582*

BIOMARKERS
Hair Analysis for Drugs of Abuse: Evaluation of Analytical Methods, Environmental Issues, and Development of Reference Materials.
PB95-176269 *03,501*

BIOMASS
Calculation of Higher Heating Values of Biomass Materials and Waste Components from Elemental Analyses.
PB94-199254 *02,474*

Radiocarbon Measurements of Atmospheric Volatile Organic Compounds: Quantifying the Biogenic Contribution.
PB97-122352 *02,574*

BIOMATERIALS
Reinforcement of Cancellous Bone Screws with Calcium Phosphate Cement.
PB96-158001 *00,179*

BIOMEDICAL MEASUREMENT
Prototyping a Graphical User Interface for DHCP.
PB96-160544 *02,599*

BIOMEDICAL MEASUREMENTS
Importance of Chemometrics in Biomedical Measurements.
PB94-200599 *00,550*

BIOMEDICAL RADIOGRAPHY
Image Information Transfer Properties of X-Ray Intensifying Screens in the Energy Range from 17 to 320 keV.
PB95-126173 *00,155*

BIOPRODUCTS
Supercritical Fluid Extraction of Biological Products.
PB95-175204 *00,040*

BIOREACTORS
In situ On-Line Optical Fiber Sensor for Fluorescence Monitoring in Bioreactors.
PB94-212024 *03,587*

In situ Fluorescence Cell Mass Measurements of 'Saccharomyces cerevisiae' Using Cellular Tryptophan.
PB96-135041 *03,547*

BIOSENSORS
Retinal-Protein Complexes as Optoelectronic Components.
PB95-150397 *02,146*

Amperometric Flow-Injection Analysis Biosensor for Glucose Based on Graphite Paste Modified with Tetracyanoquinodimethane.
PB95-161980 *03,498*

Detection of Aromatic Compounds Based on DNA Intercalation Using an Evanescent Wave Biosensor.
PB96-111976 *03,473*

Genetically Engineered Pore as a Metal Ion Biosensor.
PB96-161658 *03,551*

BIOTECHNOLOGY
Ionizing radiation-induced DNA damage and its repair in human cells. Progress report, (April 1, 1993--February 28, 1994).
DE94014709 *03,612*

Opportunities for Innovation: Biotechnology.
PB94-157831 *00,009*

beta-D-Glucosyl-Hydroxymethyluracil: A Novel Modified Base Present in the DNA of the Parastic Protozoan T. brucei.
PB94-172319 *03,524*

Current Activities Within the National Biomonitoring Specimen Bank.
PB94-172806 *02,516*

Opportunities for Innovation: Advanced Surface Engineering.
PB94-176666 *02,697*

Tert-Butyl Hydroperoxide-Mediated DNA Base Damage in Cultured Mammalian Cells.
PB94-182003 *03,644*

Application of Photochemical Reaction in Electrochemical Detection of DNA Intercalation.
PB94-185733 *00,686*

Copper Ion-Mediated Modification of Bases in DNA in Vitro by Benzoyl Peroxide.
PB94-198231 *03,645*

Calorimetric Determination of the Standard Transformed Enthalpy of a Biochemical Reaction at Specified PH and pMg.
PB94-198249 *03,454*

Regulation of Lithium and Boron Levels in Normal Human Blood: Environmental and Genetic Considerations.
PB94-198579 *03,491*

Standard Reference Materials (SRM's) for Measuring Genetic Damage.
PB94-198827 *03,516*

Oxidative Damage to DNA in Mammalian Chromatin.
PB94-199825 *03,525*

Modification of DNA Bases in Chromatin of Intact Target Human Cells by Activated Human Polymorphonuclear Leukocytes.
PB94-199833 *03,526*

Carotenoid Reversed-Phase High-Performance Liquid Chromatography Methods: Reference Compendium.
PB94-200516 *00,549*

Individual Carotenoid Content of SRM 1548 Total Diet and Influence of Storage Temperature, Lyophilization, and Irradiation on Dietary Carotenoids.
PB94-200524 *00,033*

Mixed Phospholipid Liposome Calcification.
PB94-211190 *03,457*

Proteoglycan Inhibition of Calcium Phosphate Precipitation in Liposomal Suspensions.
PB94-211208 *00,658*

Total Surface Areas of Group IVA Organometallic Compounds: Predictors of Toxicity to Algae and Bacteria.
PB94-211331 *00,814*

L-threo-beta-Hydroxyhistidine, an Unprecedented Iron(III) Ion-Binding Amino Acid in a Pyoverdine-type Siderophore from Pseudomonas fluorescens 244.
PB94-211620 *00,553*

In situ On-Line Optical Fiber Sensor for Fluorescence Monitoring in Bioreactors.
PB94-212024 *03,587*

Modification of Deoxyribose-Phosphate Residues by Extracts of Ataxia Telangiectasia Cells.
PB94-212602 *03,458*

Nickel(II)-Mediated Oxidative DNA Base Damage in Renal and Hepatic Chromatin of Pregnant Rats and Their Fetuses. Possible Relevance to Carcinogenesis.
PB94-212628 *03,646*

Analysis of Protein Metal Binding Selectivity in a Cluster Model.
PB94-212990 *00,845*

Liposome-Based Flow-Injection Immunoassay for Determining Theophylline in Serum.
PB94-213493 *03,494*

Hydrolysis of Proteins by Microwave Energy.
PB94-216322 *03,528*

Ascorbic and Dehydroascorbic Acids Measured in Plasma Preserved with Dithiothreitol or Metaphorphoric Acid.
PB94-216330 *03,495*

Energy Transduction between a Concentration Gradient and an Alternating Electric Field.
PB94-216363 *03,461*

Self-Assembled Phospholipid/Alkanethiol Biomimetic Bilayers on Gold.
PB95-108460 *00,878*

Fokker-Planck Description of Multivalent Interactions.
PB95-108478 *00,879*

Aggregation Kinetics of Colloidal Particles Destabilized by Enzymes.
PB95-125878 *00,894*

Biological Macromolecular Crystallization Database: A Tool for Developing Crystallization Strategies.
PB95-126157 *00,897*

Michaelis-Menten Equation for an Enzyme in an Oscillating Electric Field.
PB95-140489 *00,906*

Chemical and Microbiological Problems Associated with Research on the Biodesulfurization of Coal.
PB95-140950 *02,484*

Bioleaching of Cobalt from Smelter Wastes by 'Thiobacillus ferrooxidans'.
PB95-140968 *02,582*

Opportunities for Innovation: Pollution Prevention.
PB95-147146 *02,520*

Oxidative DNA Base Damage in Renal, Hepatic, and Pulmonary Chromatin of Rats After Intraperitoneal Injection of Cobalt (II) Acetate.
PB95-150025 *03,647*

DNA Base Modifications in Renal Chromatin of Wistar Rats Treated with a Renal Carcinogen, Ferric Nitrilotriacetate.
PB95-150363 *03,648*

Retinal-Protein Complexes as Optoelectronic Components.
PB95-150397 *02,146*

Application of Thermodynamics to Biotechnology.
PB95-150793 *03,529*

Critical Evaluation of the Purification of Biominerals by Hypochlorite Treatment.
PB95-150959 *00,186*

Influence of Natural and Synthetic Inhibitors on the Crystallization of Calcium Oxalate Hydrates.
PB95-150967 *03,560*

High-Performance Liquid Chromatography of Phytoplankton Pigments Using a Polymeric Reversed-Phase C18 Column.
PB95-151130 *00,583*

Preparation of Immobilized Proteins Covalently Coupled Through Silane Coupling Agents to Inorganic Supports.
PB95-151403 *03,530*

Method for the Assay of Hydrolytic Enzymes Using Dynamic Light Scattering.
PB95-151411 *03,531*

Bacteriorhodopsin Immobilized in Sol-Gel Glass.
PB95-151429 *03,532*

Function of DnaJ and DnaK as Chaperones in Origin-Specific DNA Binding by RepA.
PB95-151544 *03,533*

Development of Frozen Whale Blubber and Liver Reference Materials for the Measurement of Organic and Inorganic Contaminants.
PB95-151676 *00,587*

Determination of Inorganic Constituents in Marine Mammal Tissues.
PB95-152047 *00,589*

Resolution of DNA in the Presence of Mobility Modifying Polar and Nonpolar Compounds by Discontinuous Electrophoresis on Rehydratable Polyacrylamide Gels.
PB95-152799 *00,590*

Substrate Specificity of the Escherichia coli Endonuclease III: Excision of Thymine- and Cytosine-Derived Lesions in DNA Produced by Radiation-Generated Free Radicals.
PB95-153425 *03,535*

Liquid Chromatographic Method for the Determination of Carotenoids, Retinoids, and Tocopherols in Human Serum and in Food.
PB95-153599 *00,593*

Development of the National Marine Mammal Tissue Bank.
PB95-161402 *02,586*

DNA Base Damage Generated In vivo in Hepatic Chromatin of Mice upon Whole Body y-Irradiation.
PB95-161741 *03,627*

Amperometric Flow-Injection Analysis Biosensor for Glucose Based on Graphite Paste Modified with Tetracyanoquinodimethane.
PB95-161980 *03,498*

Determination of PCBs and Chlorinated Hydrocarbons in Marine Mammal Tissues.
PB95-162640 *03,744*

Biological Thermodynamic Data for the Calibration of Differential Scanning Calorimeters: Dynamic Temperature Data on the Gel to Liquid Crystal Phase Transition of Dialkylphosphatidylcholine in Water Suspensions.
PB95-162707 *03,464*

Thermodynamics of the Binding of Galactopyranoside Derivatives to the Basic Lectin from Winged Bean (Psophocarpus Tetrogonolobus).
PB95-162715 *03,465*

Electrophoretic Separations of Polymerase Chain Reaction: Amplified DNA Fragments in DNA Typing Using a Capillary Electrophoresis-Lased Induced Fluorescence System.
PB95-163036 *03,536*

Glucose Permease of Bacillus Subtilis Is a Single Polypeptide Chain That Functions to Energize the Sucrose Permease.
PB95-163192 *03,466*

Electropermeabilization of Cell Membranes: Effect of the Resting Membrane Potential.
PB95-163291 *03,537*

Microbial Degradation of Polysulfides and Insights into Their Possible Occurrence in Coal.
PB95-163374 *02,488*

Affinity Chromatography on Inorganic Support Materials.
PB95-163820 *03,467*

Deletion Analysis of the Mini-P1 Plasmid Origin of Replication and the Role of E.coli DnaA Protein.
PB95-163911 *03,539*

Membrane-Mediated Precipitation of Calcium Phosphate in Model Liposomes with Matrix Vesicle-Like Lipid Composition.
PB95-164547 *03,468*

Characterization of Cytochrome c/Alkanethiolate Structures Prepared by Self-Assembly on Gold.
PB95-164638 *00,987*

Enhanced Detection of PCR Products Through Use of TOTO and YOYO Intercalating Dyes with Laser Induced Fluorescence - Capillary Electrophoresis.
PB95-164653 *00,599*

Alaska Marine Mammal Tissue Archival Project: Specimen Inventory.
PB95-171344 *02,589*

Supercritical Fluid Extraction of Biological Products.
PB95-175204 *00,040*

Chemical Determination of Oxidative DNA Damage by Gas Chromatography-Mass Spectrometry.
PB95-175394 *03,540*

Determination of Amphetamine and Methamphetamine in a Lyophilized Human Urine Reference Material.
PB95-175444 *03,597*

Fluorescence Measurements of Tetracycline in High Cell Mass for Fermentation Monitoring.
PB95-175709 *00,601*

Optical Biosensor Using a Fluorescent, Swelling Sensing Element.
PB95-175899 *03,541*

Ionizing Radiation Causes Greater DNA Base Damage in Radiation-Sensitive Mutant M10 Cells That in Parent Mouse Lymphoma L5178Y Cells.
PB95-175915 *03,632*

Interlaboratory Comparison of Autoradiographic DNA Profiling Measurements. 1. Data and Summary Statistics.
PB95-175923 *03,542*

Hair Analysis for Drugs of Abuse: Evaluation of Analytical Methods, Environmental Issues, and Development of Reference Materials.
PB95-176269 *03,501*

Supported Phospholipid/Alkanthiol Biomimetic Membranes: Insulating Properties.
PB95-180782 *03,470*

Non-Perturbative Relation between the Mutual Diffusion Coefficient, Suspension Viscosity, and Osmotic Compressibility: Application to Concentrated Protein Solutions.
PB96-102355 *01,062*

Bacteriorhodopsin Retains Its Light-Induced Proton-Pumping Function After Being Heated to 140C.
PB96-102728 *03,471*

Phospholipid/Alkanethiol Bilayers for Cell-Surface Receptor Studies by Surface Plasmon Resonance.
PB96-102900 *03,472*

Novel Activity of E. coli uracil DNA N-glycosylase Excision of Isodialuric Acid (5,6-dihydroxyuracil), a Major Product of Oxidative DNA Damage, from DNA.
PB96-110747 *03,543*

Overview of Reference Materials Prepared for Standardization of DNA Typing Procedures.
PB96-111653 *00,611*

Detection of Aromatic Compounds Based on DNA Intercalation Using an Evanescent Wave Biosensor.
PB96-111976 *03,473*

Physicochemical Characterization of Low Molecular Weight Heparin.
PB96-112040 *03,474*

Rapid pH Change Due to Bacteriorhodopsin Measured with a Tin-Oxide Electrode.
PB96-112081 *03,544*

Treatment of Wistar Rats with a Renal Carcinogen, Ferric Nitrilotriacetate, Causes DNA-Protein Cross-Linking between Thymine and Tyrosine in Their Renal Chromatin.
PB96-112115 *03,649*

Interlaboratory Comparison of Autoradiographic DNA Profiling Measurements. 2. Measurement Uncertainty and Its Propagation.
PB96-112123 *03,545*

Considerations in the Design of an Environmental Specimen Bank: Experiences of the National Biomonitoring Specimen Bank Program.
PB96-112370 *02,527*

Holographic Properties of Triton X-100-Treated Bacteriorhodopsin Embedded in Gelatin Films.
PB96-119284 *03,761*

Physical Characterization of Herparin by Light Scattering.
PB96-119383 *03,598*

Optical Control of Enzymatic Conversion of Sucrose to Glucose by Bacteriorhodopsin Incorporated into Self-Assembled Phosphatidylcholine Vesicles.
PB96-123344 *03,477*

Optical Properties of Triton X-100-Treated Purple Membranes Embedded in Gelatin Films.
PB96-123500 *03,546*

In situ Fluorescence Cell Mass Measurements of 'Saccharomyces cerevisiae' Using Cellular Tryptophan.
PB96-135041 *03,547*

Formation of DNA-Protein Cross-Links in Cultured Mammalian Cells Upon Treatment with Iron Ions.
PB96-137724 *03,651*

Rapid Method for the Isolation of Genomic DNA from 'Aspergillus fumigatus'.
PB96-147061 *03,488*

Dynamics of Calcium Phosphate Precipitation.
PB96-147095 *03,574*

Mapping Domains in Proteins: Dissection and Expression of 'Escherichia coli' Adenylyl Cyclase.
PB96-155460 *03,478*

Novel DNA N-Glycosylase Activity of E. coli T4 Endonuclease V That Excises 4,6-Diamino-5-Formamidopyrimidine from DNA, a UV-Radiation- and Hydroxyl Radical-Induced Product of Adenine.
PB96-160478 *03,549*

Evaluation of a Tapered Roller Bearing Spindle for High-Precision Hard Turning Applications.
PB96-160494 *02,700*

Genetically Engineered Pores for New Materials.
PB96-161641 *03,550*

Genetically Engineered Pore as a Metal Ion Biosensor.
PB96-161658 *03,551*

Current Noise Reveals Protonation Kinetics and Number of Ionizable Sites in an Open Protein Ion Channel.
PB96-161674 *04,092*

Noise Analysis of Ionization Kinetics in a Protein Ion Channel.
PB96-161682 *04,093*

Current Fluctuations Reveal Protonation Dynamics and Number of Ionizable Residues in the alpha-Toxin Channel.
PB96-161732 *03,588*

Protonation Dynamics of the alpha-Toxin Ion Channel from Spectral Analysis of pH-Dependent Current Fluctuations.
PB96-161740 *03,652*

Protonation Dynamics in an Ion Channel Pore.
PB96-161757 *03,589*

Conformational Alterations of Bovine Insulin Adsorbed on a Silver Electrode.
PB96-161773 *00,510*

Autofluorescence Detection of 'Escherichia coli' on Silver Membrane Filters.
PB96-163639 *03,590*

Bacterial Enumeration in Storage Water.
PB96-163647 *03,591*

Feasibility of Fluorescence Detection of Tetracycline in Media Mixtures Employing a Fiber Optic Probe.
PB96-163654 *00,511*

Novel Amperometric Immunosensor for Procainamide Employing Light Activated Labels.
PB96-163662 *00,512*

Novel Activities of Human Uracil DNA N-glycosylase for Cytosine-Derived Products of Oxidative DNA Damage.
PB96-164132 *03,479*

Structural Analysis of Heparin by Raman Spectroscopy.
PB96-167226 *03,480*

Relationship of Silver with Selenium and Mercury in the Liver of Two Species of Toothed Whales (Odontocetes).
PB96-167275 *02,596*

New Method for the Detection and Measurement of Polyaromatic Carcinogens and Related Compounds by DNA Intercalation.
PB96-167382 *03,481*

Genetically Engineered Pores as Metal Ion Biosensors.
PB96-167408 *03,553*

Pore-Forming Protein with a Metal-Actuated Switch.
PB96-176557 *03,554*

Investigations of Sulfur Interferences in the Extraction of Methylmercury from Marine Tissues.
PB96-190020 *03,482*

Repair of Products of Oxidative DNA Base Damage in Human Cells.
PB96-190129 *03,555*

Quantitative Determination of Oxidative Base Damage in DNA by Stable Isotope-Dilution Mass Spectrometry.
PB96-200886 *03,483*

Commentary: The Measurement of Oxidative Damage to DNA by HPLC and GC/MS Techniques.
PB96-200894 *03,484*

Intercomparison of DNA Sizing Ladders in Electrophoretic Separation Matrices and Their Potential for Accurate Typing of the D1S80 Locus.
PB96-200928 *03,485*

Flow Immunoassay Using Solid-Phase Entrapment.
PB96-200951 *00,642*

Escherichis coli Cyclic AMP Receptor Protein Mutants Provide Evidence for Ligand Contacts Important in Activation.
PB96-201017 *03,592*

Interlaboratory Studies on the Analysis of Hair for Drugs of Abuse: Results from the Fifth Exercise.
PB97-110449 *03,509*

DNA Damage and DNA Sequence Retrieval from Ancient Tissues.
PB97-111983 *03,556*

Use of a Naphthylethylcarbamoylated- beta-Cyclodextrin Chiral Stationary Phase for the Separation of Drug Enantiomers and Related Compounds by Sub- and Supercritical Fluid Chromatography.
PB97-113260 *00,653*

National Status and Trends Program Specimen Bank: Sampling Protocols, Analytical Methods, Results, and Archive Samples.
PB97-119226 *02,598*

Positive and Negative Cooperativities at Subsequent Steps of Oxygenation Regulate the Allosteric Behavior of Multistate Sebacylhemoglobin.
PB97-119374 *03,486*

DnaJ, DnaK, and GrpE Heat Shock Proteins are Required in 'ori'P1 DNA Replication Solely at the RepA Monomerization Step.
PB97-119382 *03,557*

DNA Base Damage in Lymphocytes of Cancer Patients Undergoing Radiation Therapy.
PB97-122444 *03,643*

BIPOLAR TRANSISTORS

Investigation of the Drive Circuit Requirements for the Power Insulated Gate Bipolar Transistor (IGBT).
PB94-211794 *02,316*

Effects of Heavy Doping on Numerical Simulations of Gallium Arsenide Bipolar Transistors.
PB95-150975 *02,334*

Experimental Study of Reverse-Bias Failure Mechanisms in Bipolar Mode JFET (BMFET).
PB95-152997 *02,340*

Modeling Buffer Layer IGBTs for Circuit Simulation.
PB95-153805 *02,344*

Modeling Buffer Layer IGBT's for Circuit Simulation.
PB96-164173 *02,429*

Design Criteria for BJT Amplifiers with Low I/f AM and PM Noise.
PB96-200365 *02,442*

BIREFRINGENCE

Polarization Insensitive 3x3 Sagnac Current Sensor Using Polarizing Spun High-Birefringence Fiber.
PB96-119276 *02,187*

Standard Polarization Components: Progress Toward an Optical Retardance Standard.
PB96-119672 *04,342*

Improved Annealing Technique for Optical Fiber.
PB96-119680 *04,343*

BIREFRINGENT MEDIA

Refraction of Light by Graded Birefringent Media.
PB96-123716 *02,192*

BIS (DIFLUOROMETHYL)ETHER

Thermodynamic Properties of CHF2-O-CHF2,Bis(difluoromethyl) Ether.
PB94-199569 *00,798*

Viscosity of the Saturated Liquid Phase of Six Halogenated Compounds and Three Mixtures.
PB95-162368 *00,960*

BISMUTH

Enthalpy Increment Measurements from 4.5 to 318 K for Bismuth(cr). Thermodynamic Properties from 0 K to the Melting Point.
PB96-204011 *01,166*

BISMUTH CLUSTERS

Photoelectron Spectroscopy of Negatively Charged Bismuth Clusters: Bi(-)2, Bi(-)3, and Bi(-)4.
PB95-108494 *00,880*

BISMUTH LEAD STRONTIUM CALCIUM CUPRATES

X-Ray Characterization of the Crystallization Process of High-Tc Superconducting Oxides in the Sr-Bi-Pb-Ca-Cu-O System.
PB95-151700 *04,579*

BISMUTH OXIDES

Phase Equilibria in the Systems CaO-CuO and CaO-Bi2O3.
PB95-140570 *03,048*

BISMUTH STRONTIUM CALCIUM CUPRATES

Microstrains and Domain Sizes in Bi-Cu-O Superconductors: An X-Ray Diffraction Peak-Broadening Study.
PB94-198520 *04,461*

Effect of Axial Strain on the Critical Current of Ag-Sheathed Bi-Based Superconductors in Magnetic Fields Up to 25 T.
PB94-211315 *04,493*

Flux Expulsion at Intermediate Fields in Type-II Superconductors.
PB94-212230 *04,502*

Improved Uniaxial Strain Tolerance of the Critical Current Measured in Ag-Sheathed Bi2Sr2Ca1Cu2O8+x Superconductors.
PB95-153565 *04,594*

Grain Alignment and Transport Properties of Bi2Sr2CaCu2O8 Grown by Laser Heated Float Zone Method.
PB95-161451 *04,602*

Effects of Anneal Time and Cooling Rate on the Formation and Texture of Bi2Sr2CaCu2O8 Films.
PB95-161600 *04,603*

Tunneling Measurement of the Zero-Bias Conductance Peak and the Bi-Sr-Ca-Cu-O Thin-Film Energy Gap.
PB95-163739 *04,628*

Increased Pinning Energies and Critical Current Densities in Heavy-Ion-Irradiated Bi2Sr2CaCu2O8 Single Crystals.
PB95-175352 *04,654*

BISPHENOL-A

Effect of Curing History on Ultimate Glass Transition Temperature and Network Structure of Crosslinking Polymers.
PB94-200052 *01,214*

BISTATIC SCATTERING

Bistatic Scattering of Absorbing Materials from 30 to 1000 MHz.
PB95-150934 *01,891*

BITHIOPHENES

Location of a (1)A(sub g) State in Bithiophene.
PB95-202313 *01,025*

BITUMINOUS CONCRETES

Binder Characterization and Evaluation by Nuclear Magnetic Resonance Spectroscopy.
PB94-193471 *01,334*

Development of a Method for Measuring Water-Stripping Resistance of Asphalt/Siliceous Aggregate Mixtures.
PB96-197249 *01,348*

BIVARIATE DISTRIBUTIONS

Population Distributions and Intralaboratory Reproducibility for Fat-Soluble Vitamin-Related Compounds in Human Serum.
PB96-155536 *00,624*

BLACK BODY RADIATION

Activities of NIST (National Inst. Of Standards and Technology).
N94-23605/6 *04,222*

BLACK DETECTORS

Measurement of the (10)B(n, alpha1gamma)(7)Li Cross Section in the 0.3 to 4 MeV Neutron Energy Interval.
PB96-161799 *04,098*

BLACKBODY RADIATION

Cryogenic Blackbody Calibrations at the National Institute of Standards and Technology Low Background Infrared Calibration Facility.
PB94-169802 *02,117*

Precision High Temperature Blackbodies.
PB95-140059 *03,885*

Third Generation Water Bath Based Blackbody Source.
PB96-122148 *04,046*

BLCC COMPUTER PROGRAM

Life-Cycle Costing Workshop for Energy Conservation in Buildings: Student Manual.
PB95-175006 *00,257*

BLENDS

Glass Temperature of Polymer Blends: Comparison of Both the Free Volume and the Entropy Predictions with Data.
PB95-140190 *01,236*

BLIND RECONSTRUCTION

Scanned Probe Microscope Tip Characterization Without Calibrated Tip Characterizers.
PB96-190368 *02,759*

BLISTERING

Non-Osmotic, Defect-Controlled Cathodic Disbondment of a Coating from a Steel Substrate.
PB94-216447 *03,120*

Gas Absorption during Ion-Irradiation of a Polymer Target.
PB96-161864 *04,099*

BLOCK COPOLYMERS

Shear-Excited Morphological States in a Triblock Copolymer.
PB94-172392 *01,196*

Time Dependent Small Angle Neutron Scattering Behavior in Triblock Copolymers Under Steady Shear.
PB94-172632 *01,198*

Temperature Dependence of the Morphology of Thin Diblock Copolymer Films as Revealed by Neutron Reflectivity.
PB94-172756 *01,199*

Neutron Scattering by Multiblock Copolymers of Structure (A-B)N-A.
PB94-211547 *01,219*

Small-Angle X-Ray and Neutron Scattering Study of Block Copolymer/Homopolymer Mixtures.
PB94-211729 *01,221*

Morphology of Symmetric Diblock Copolymers as Revealed by Neutron Reflectivity.
PB95-140075 *01,234*

Observed Frustration in Confined Block Copolymers.
PB95-150033 *01,238*

Characterization of Polyquinoline Block Copolymer Using Small Angle Scattering.
PB95-151882 *01,244*

Localization of a Homopolymer Dissolved in a Lamellar Structure of a Block Copolymer Studied by Small-Angle Neutron Scattering.
PB95-161592 *01,253*

Molecular Weight Dependence of the Lamellar Domain Spacing of ABC Triblock Copolymers and Their Chain Conformation in Lamellar Domains.
PB95-161691 *01,254*

Influence of Shear on the Ordering Temperature of a Triblock Copolymer Melt.
PB96-163753 *01,288*

Morphology and Phase Separation Kinetics of a Compatibilized Blend.
PB97-119135 *01,297*

BLOCKS

VLSI Architectures for Template Matching and Block Matching.
PB94-200029 *01,834*

BLOOD

Development of a Standard Reference Material for ISE Measurements of Sodium and Potassium.
PB96-159785 *03,507*

BLOOD ANALYSIS

Frozen Human Serum Reference Material for Standardization of Sodium and Potassium Measurements in Serum or Plasma by Ion-Selective Electrode Analyzers.
PB94-185337 *00,532*

BLOOD CHEMICAL ANALYSIS
Histopathology, Blood Chemistry, and Physiological Status of Normal and Moribund Striped Bass ('Morone saxatilis') Involved in Summer Mortality ('Die-Off') in the Sacramento-San Joaquin Delta of California.
PB94-198157 *00,034*

Regulation of Lithium and Boron Levels in Normal Human Blood: Environmental and Genetic Considerations.
PB94-198579 *03,491*

Determination of Oltipraz in Serum by High-Performanace Liquid Chromatography with Optical Absorbance and Mass Spectrometric Detection.
PB94-200201 *03,493*

Liposome-Based Flow-Injection Immunoassay for Determining Theophylline in Serum.
PB94-213493 *03,494*

Ascorbic and Dehydroascorbic Acids Measured in Plasma Preserved with Dithiothreitol or Metaphorphoric Acid.
PB94-216330 *03,495*

Measurement of Ascorbic Acid in Human Plasma and Serum: Stability, Intralaboratory Repeatability, and Interlaboratory Reproducibility.
PB97-112445 *03,511*

BLOOD PRESERVATION
Ascorbic and Dehydroascorbic Acids Measured in Plasma Preserved with Dithiothreitol or Metaphorphoric Acid.
PB94-216330 *03,495*

BLOWOUTS
Development of Hazard Assessment and Suppression Technology for Oil and Gas Well Blowout and Diverter Fires.
PB96-122965 *01,408*

BLUBBER
Certification of Polychlorinated Biphenyl Congeners and Chlorinated Pesticides in a Whale Blubber Standard Reference Material.
PB96-103023 *03,745*

BLUE GREEN LASERS
Rare-Earth-Doped Waveguide Devices: The Potential for Compact Blue-Green Lasers.
PB95-140836 *04,257*

BODY ARMOR
Study to Determine the Most Important Parameters for Evaluating the Resistance of Soft Body Armor to Penetration by Edged Weapons.
PB94-158573 *03,757*

BODY COMPOSITION
Overview of Bioelectrical Impedance Analyzers.
PB96-122635 *00,176*

Overview of Bioelectrical Impedance Analyzers.
PB97-118780 *00,181*

BODY MEASUREMENT (BIOLOGY)
Body Dimensions for Apparel.
PB94-187739 *02,813*

BOILING POINTS
Ebulliometers for Measuring the Thermodynamic Properties of Fluids and Fluid Mixtures.
DE94017817 *04,195*

BOLOMETER MOUNTS
Coaxial Reference Standard for Microwave Power.
PB94-193786 *01,880*

BOLOMETERS
Thermal and Nonequilibrium Responses of Superconductors for Radiation Detectors.
PB95-164232 *02,156*

Terahertz Detectors Based on Superconducting Kinetic Inductance.
PB95-168647 *02,160*

Optical Performance of Photoinductive Mixers at Terahertz Frequencies.
PB95-168662 *02,161*

Ultrasensitive-Hot-Electron Microbolometer.
PB95-168985 *02,163*

High-Tc Superconducting Antenna-Coupled Microbolometer on Silicon.
PB95-169124 *02,166*

Antenna-Coupled High-Tc Air-Bridge Microbolometer on Silicon.
PB95-180899 *04,315*

Niobium Microbolometers for Far-Infrared Detection.
PB96-111729 *02,184*

Absolute Response Calibration of a Transfer Standard Cryogenic Bolometer.
PB96-147103 *04,358*

Novel Hot-Electron Microbolometer.
PB96-201025 *01,977*

BOLTZMANN EQUATION
Quantum Collisional Transfer Contributions to the Density Dependence of Gaseous Viscosity.
PB96-161914 *01,142*

BOMB CALORIMETER
Precise Measurement of Heat of Combustion with a Bomb Calorimeter.
AD-A286 701/8 *03,770*

BOND-LENGTH MISMATCH
Elastic Properties of Central-Force Networks with Bond-Length Mismatch.
PB95-163366 *04,623*

BONDED PHASE
Influence of Stationary Phase Chemistry on Shape Recognition in Liquid Chromatography.
PB96-123682 *00,621*

BONDING
Bonding Wires to Quantized Hall Resistors.
PB96-102637 *01,921*

BONE DISORDERS
In vitro Inhibition of Membrane-Mediated Calcification by Novel Phosphonates.
PB96-201140 *03,595*

BONE TISSUES
Experimental assessment of absorbed dose to mineralized bone tissue from internal emitters: An electron paramagnetic resonance study.
DE96007979 *03,614*

BONES
EPR Bone Dosimetry: A New Approach to Spectral Deconvolution Problems.
PB94-199643 *03,616*

Experimental Validation of Radiopharmaceutical Absorbed Dose to Mineralized Bone Tissue.
PB94-199668 *03,617*

Estimation of the Absorbed Dose in Radiation-Processed Food. 1. Test of the EPR Response Function by a Linear Regression Analysis.
PB94-199718 *00,039*

Secondary Target X-Ray Excitation for In vivo Measurement of Lead in Bone.
PB95-108767 *03,496*

Exposure-to-Absorbed-Dose Conversion for Human Adult Cortical Bone.
PB97-110381 *03,640*

BORON
Regulation of Lithium and Boron Levels in Normal Human Blood: Environmental and Genetic Considerations.
PB94-198579 *03,491*

Measurement of Boron at Silicon Wafer Surfaces by Neutron Depth Profiling.
PB94-211059 *04,487*

Determination of Boron and Lithium in Diverse Biological Matrices Using Neutron Activation - Mass Spectrometry (NA-MS).
PB94-212289 *00,554*

Analysis of Boron in CVD Diamond Surfaces Using Neutron Depth Profiling.
PB94-213089 *04,511*

Optical and Modeling Studies of Sodium/Halide Reactions for the Formation of Titanium and Boron Nanoparticles.
PB97-113054 *00,682*

BORON 10
Preparation and Characterization of (6)LiF and (10)B Reference Deposits for the Measurement of the Neutron Lifetime.
PB95-108692 *03,874*

BORON-LIKE IONS
Investigation of LS Coupling in Boronlike Ions.
PB94-185295 *03,797*

BORON NITRIDES
Effect of Stoichiometry on the Phases Present in Boron Nitride Thin Films.
PB96-102470 *04,710*

Chip Morphology, Tool Wear and Cutting Mechanics in Finish Hard Turning.
PB97-112247 *03,106*

BORON TARGETS
Mass Assay and Uniformity Test of Boron Targets by Neutron Beam Methods.
PB97-119085 *04,175*

BOSE CONDENSATION
Stable, Tightly Confining Magnetic Trap for Evaporative Cooling of Neutral Atoms.
PB96-200720 *04,126*

BOSE-EINSTEIN CONDENSATION
Properties of a Bose-Einstein Condensate in an Anisotropic Harmonic Potential.
PB96-204144 *04,133*

BOTANICAL REFERENCE MATERIAL
Determination of 21 Elements by INAA for Certification of SRM 1570a, Spinach.
PB96-167242 *00,698*

BOTANICAL REFERENCE MATERIALS
Recent Developments in NIST Botanical SRMs.
PB96-167267 *03,489*

BOTANY
Dissolution Problems with Botanical Reference Materials.
PB95-126280 *03,487*

Results of the ASTM Nuclear Methods Intercomparison on NIST Apple and Peach Leaves Standard Reference Materials.
PB97-119036 *03,490*

BOTTOM SEDIMENTS
Certification of Standard Reference Material (SRM) 1941a, Organics in Marine Sediment.
PB96-123690 *02,593*

BOUNDARY
Using Collocation in Three Dimensions and Solving a Model Semiconductor Problem.
PB96-159249 *01,952*

BOUNDARY CONDITIONS
Transport by Gravity Currents in Building Fires
PB97-119325 *01,441*

BOUNDARY ELEMENT METHOD
Application of Boundary Element Methods to a Transient Axis-Symmetric Heat Conduction Problem.
PB94-212693 *01,375*

BOUNDARY INTEGRAL METHOD
Boundary Integral Method for the Simulation of Two-Dimensional Particle Coarsening.
PB94-216744 *03,411*

BOUNDARY LAYER
Air Flow in the Boundary Layer of an Elliptic Cylinder.
AD-A297 391/5 *04,194*

BOUNDARY LAYER TRANSITION
Evolution of a Turbulent Boundary Layer Induced by a Three-Dimensional Roughness Element.
PB94-212818 *04,200*

BOUNDARY LUBRICATION
Boundary Lubrication of Silicon Nitride.
PB95-213583 *03,226*

Silicon Nitride Boundary Lubrication: Lubrication Mechanism of Alcohols.
PB96-111703 *03,067*

Silicon Nitride Boundary Lubrication: Effect of Oxygenates.
PB96-111711 *03,068*

Mechano-Chemical Model: Reaction Temperatures in a Concentrated Contact.
PB96-119466 *03,227*

BOUNDARY VALUE PROBLEMS
Slow Evolution from the Boundary: A New Stabilizing Constraint in Ill-Posed Continuation Problems.
PB96-122858 *03,418*

BOVINE SERUM ALBUMIN
Hydrolysis of Proteins by Microwave Energy.
PB94-216322 *03,528*

BRACHYTHERAPY
Needs for Brachytherapy Source Calibrations in the United States.
PB97-110092 *03,521*

BRAGG GRATINGS
Bragg Gratings in Optical Fibers Produced by a Continuous-Wave Ultraviolet Source.
PB95-162020 *04,274*

Growth of Bragg Gratings Produced by Continuous-Wave Ultraviolet Light in Optical Fiber.
PB95-162038 *04,275*

Comparison of UV-Induced Fluorescence and Bragg Grating Growth in Optical Fiber.
PB95-168597 *04,284*

Annealing of Bragg Gratings in Hydrogen-Loaded Optical Fiber.
PB96-155437 *04,361*

Comparison of UV Photosensitivity and Fluorescence during Fiber Grating Formation.
PB96-155445 *04,362*

BRAGG X-RAY DIFFRACTION
Systematic Correction in Bragg X-ray Diffraction of Flat and Curved Crystals.
PB97-112239 *04,152*

BRANCHING RATIO
Atomic Branching Ratio Data for Carbon-Like Ions.
PB94-212842 *03,855*

Atomic Branching Ratio Data for Oxygen-Like Species.
PB95-180436 *03,963*

Atomic Branching Ratio Data for Nitrogen-Like Species.
PB96-190152 *04,122*

BRANCHING RATIOS
Vibrationally Resolved Photoelectron Angular Distributions and Branching Ratios for the Carbon Dioxide Molecule in the Wavelength Region 685-795 Angstrom.
PB96-201207 *04,131*

BREAKDOWN
Evidence That Voltage Rather Than Resistance is Quantized in Breakdown of the Quantum Hall Effect.
PB96-179163 *01,868*

BREAKDOWN (ELECTRONIC THRESHOLD)
Charge Trapping and Breakdown Mechanism in SIMOX.
PB94-216637 *02,323*

Experimental Study of Reverse-Bias Failure Mechanisms in Bipolar Mode JFET (BMFET).
PB95-152997 *02,340*

BREMSSTRAHLUNG
Comparison of NIST and ISO Filtered Bremsstrahlung Calibration Beams.
PB95-180956 *03,967*

BRIDGE
ITS-90 Calibration Facility.
PB96-160916 *00,627*

BRIDGE DECKS
Corrosion Resistant Epoxy-Coated Reinforcing Steel.
PB94-185618 *01,307*

Economics of New-Technology Materials: A Case Study of FRP Bridge Decking.
PB96-202353 *01,349*

BRIDGE MAINTENANCE
Optimization of Highway Concrete Technology.
PB94-182995 *01,333*

BRIDGES
Conversion of a 2-Terminal-Pair Bridge to a 4-Terminal-Pair Bridge for Increased Range and Precision in Impedance Measurements.
PB97-119176 *02,103*

BRIDGES (STRUCTURES)
Draft Guidelines for Pre-Qualification and Prototype Testing of Seismic Isolation Systems.
PB94-161940 *01,331*

Draft Guidelines for Quality Control Testing of Sliding Seismic Isolation Systems.
PB94-161957 *01,332*

Evaluating the Seismic Performance of Lightly-Reinforced Circular Concrete Bridge Columns.
PB95-163259 *01,335*

Jacket Thickness Requirements for Seismic Retrofitting of Circular Bridge Columns.
PB95-163267 *01,336*

Seismic Performance of Circular Bridge Columns Designed in Accordance with AASHTO/CALTRANS Standards.
PB96-146352 *01,346*

Application of Electromagnetic-Acoustic Transducers for Nondestructive Evaluation of Stresses in Steel Bridge Structures.
PB96-167978 *01,301*

BRIDGING
ISDN LAN Bridging.
PB95-154696 *01,477*

BRIGHTNESS
Far-Ultraviolet Flare on a Pleiades G Dwarf.
PB96-102033 *00,086*

BRILLOUIN EFFECT
Brillouin Light Scattering Intensities for Thin Magnetic Films with Large Perpendicular Anisotropies.
PB94-211174 *04,488*

BRITTLE FRACTURING
Analysis of Failed Dry Pipe Fire Suppression System Couplings from the Filene Center at Wolf Trap Farm Park for the Performing Arts.
PB94-164407 *00,331*

Atomic Theory of Fracture of Brittle Materials: Application to Covalent Semiconductors.
PB94-216553 *04,519*

BRITTLE MATERIALS
Crack Growth Resistance of Strain-Softening Materials under Flexural Loading.
PB94-200227 *02,972*

Friction Processes in Brittle Fracture.
PB96-161765 *03,076*

BRITTLE SOLIDS
Effect of Chemical Interaction on Barenblatt Crack Profiles in Brittle Solids.
PB96-180245 *02,996*

BRITTLENESS
Ashland Tank Collapse Investigation.
PB95-126314 *02,481*

Ashland Tank-Collapse Investigation: Closure by Authors.
PB95-126322 *02,482*

Molecular Orbital Calculations of Bond Rupture in Brittle Solids.
PB95-164059 *00,973*

BROADBAND ANTENNAS
Time-Domain Antenna Characterizations.
PB95-152781 *02,003*

BROADBAND INTEGRATED SERVICES DIGITAL NETWORK
Introduction to Traffic Management for Broadband ISDN.
PB94-142494 *01,464*

BROMINE ATOMS
Laser Double Resonance Measurements of the Quenching Rates of Br((2)P1/2) with H20, D20, HDO, and O2.
PB95-150694 *00,921*

BROMINE LASERS
Efficient Br(*) Laser Pumped by Frequency-Doubled Nd:YAG and Electronic-to-Vibrational Transfer-Pumped CO2 and HCN Lasers.
PB95-108684 *04,248*

BRONCHI
Systematics of Alpha-Particle Energy Spectra and Lineal Energy (Y) Spectra for Radon Daughters.
PB94-185139 *03,615*

Microdosimetry and Cellular Radiation Effects of Radon Progency in Human Bronchial Airways.
PB95-152344 *03,625*

BROWNIAN MOTION
Hydrodynamic Friction of Arbitrarily Shaped Brownian Particles.
PB97-110191 *04,136*

BROWNIAN MOVEMENT
Brownian Diffusion of Hard Spheres at Finite Concentrations.
PB95-164307 *00,975*

BSCCO SUPERCONDUCTORS
Microstrains and Domain Sizes in Bi-Cu-O Superconductors: An X-Ray Diffraction Peak-Broadening Study.
PB94-198520 *04,461*

Effect of Axial Strain on the Critical Current of Ag-Sheathed Bi-Based Superconductors in Magnetic Fields Up to 25 T.
PB94-211315 *04,493*

Flux Expulsion at Intermediate Fields in Type-II Superconductors.
PB94-212230 *04,502*

X-Ray Characterization of the Crystallization Process of High-Tc Superconducting Oxides in the Sr-Bi-Pb-Ca-Cu-O System.
PB95-151700 *04,579*

Improved Uniaxial Strain Tolerance of the Critical Current Measured in Ag-Sheathed Bi2Sr2Ca1Cu2O8+x Superconductors.
PB95-153565 *04,594*

Grain Alignment and Transport Properties of Bi2Sr2CaCu2O8 Grown by Laser Heated Float Zone Method.
PB95-161451 *04,602*

Effects of Anneal Time and Cooling Rate on the Formation and Texture of Bi2Sr2CaCu2O8 Films.
PB95-161600 *04,603*

Tunneling Measurement of the Zero-Bias Conductance Peak and the Bi-Sr-Ca-Cu-O Thin-Film Energy Gap.
PB95-163739 *04,628*

Increased Pinning Energies and Critical Current Densities in Heavy-Ion-Irradiated Bi2Sr2CaCu2O8 Single Crystals.
PB95-175352 *04,654*

BSDF (BIDIRECTIONAL SCATTERING DISTRIBUTION FUNCTION)
Rayleigh Scattering Limits for Low-Level Bidirectional Reflectance Distribution Function Measurements.
PB95-180030 *04,307*

BUBBLE CHAMBERS
Design and Construction of a Liquid Hydrogen Temperature Refrigeration System.
AD-A286 618/4 *02,619*

BUBBLES
Heat Transfer in an Intumescent Material Using a Three-Dimensional Lagrangian Model.
PB96-164066 *00,408*

BUCKLED COLUMNS
Experimental and Numerical Chaos in Continuous Systems: Two Case Studies.
PB96-156146 *00,219*

BUCKLING
Exponentially Rapid Coarsening and Buckling in Coherently Self-Stressed Thin Plates.
PB95-202347 *04,821*

BUCKMINSTERFULLERENE
Inelastic Neutron Scattering Studies of Rotational Excitations and the Orientational Potential in C60 and A3C60 Compounds.
PB94-172673 *00,763*

Discontinuous Volume Change at the Orientational-Ordering Transition in Solid C60.
PB94-211828 *00,821*

Rotational Dynamics of C60 in Na2RbC60.
PB95-153201 *00,948*

Structure and Dynamics of Buckyballs.
PB95-153292 *00,950*

Neutron and X-Ray Scattering Cross Sections of Orientationally Disordered Soild C60.
PB95-153300 *00,951*

Epitaxial Integration of Single Crystal C60.
PB95-153490 *04,592*

BUILDING
Project Summaries 1995: NIST Building and Fire Research Laboratory.
PB95-270047 *00,400*

CFAST Output Comparison Method and Its Use in Comparing Different CFAST Versions.
PB96-109541 *00,401*

BUILDING CODES
Draft Guideline for Testing and Evaluation of Seismic Isolation Systems.
PB94-172947 *00,423*

Standards Development in North America for Performance of Whole Buildings and Facilities.
PB94-185196 *00,312*

Lessons Learned by a Wing Engineer.
PB94-216421 *00,429*

Water Efficient Plumbing Fixtures through Standards and Test Methods.
PB95-125951 *00,248*

Growing Significance of CIB.
PB95-126306 *00,314*

Evaluation and Retrofit Standards for Existing Federally Owned and Leased Buildings.
PB95-150918 *00,434*

Exposure: An Expert System Fire Code.
PB95-162913 *04,868*

Quantitative Evaluation of Building Fire Safety: New Tools for Assessing Fire and Building Code Provisions.
PB95-164588 *00,199*

Developing Rational Performance-Based Fire Safety Requirements in Model Building Codes.
PB95-175220 *00,200*

World of Building Codes.
PB95-203428 *00,449*

Comparison of the Seismic Provisions of Model Building Codes and Standards to the 1991 NEHRP Recommended Provisions.
PB95-231858 *00,315*

Fire Codes for Global Practice.
PB96-102108 *00,205*

Recommended Performance-Based Criteria for the Design of Manufactured Home Foundation Systems to Resist Wind and Seismic Loads.
PB96-128285 *00,460*

Summary and Results of the NIST Workshop on Proposed Guidelines for Testing and Evaluation of Seismic Isolation Systems. Held in San Francisco, California on July 25, 1994.
PB96-154901 *00,463*

State of the Art Report on Seismic Design Requirements for Nonstructural Building Components.
PB96-193800 *00,308*

Fire Safety Engineering in the Pursuit of Performance-Based Codes: Collected Papers.
PB97-114482 *00,235*

BUILDING DESIGN
Distributed Architecture for Standards Processing.
PB96-164181 *00,276*

BUILDING ENERGY MANAGEMENT SYSTEMS
Using Emulators to Evaluate the Performance of Building Energy Management Systems.
PB95-175774 *00,259*

Use of Building Emulators to Evaluate the Performance of Building Energy Management Systems.
PB96-111901 *00,269*

BUILDING FIRES
BFRL Fire Publications, 1993.
PB94-164191 *00,192*

Studies Assess Performance of Residential Detectors.
PB94-199262 *00,290*

Fire Growth Analysis of the Fire of March 20, 1990, Pulaski Building, 20 Massachusetts Avenue, N.W., Washington, DC.
PB94-205952 *00,194*

Overview of Smoke Control Technology.
PB94-212867 *00,348*

Preview of ASHRAE's Revised Smoke Control Manual.
PB94-212875 *00,349*

Development of a New Small-Scale Smoke Toxicity Test Method and Its Comparison with Real-Scale Fire Tests.
PB94-213253 *00,350*

Sprinkler Fire Suppression Algorithm.
PB94-216181 *00,293*

Simulating Smoke Movement through Long Vertical Shafts in Zone-Type Compartment Fire Models.
PB95-143152 *00,368*

Exposure: An Expert System Fire Code.
PB95-162913 *04,868*

BUILDING MATERIALS
Percolation and Pore Structure in Mortars and Concrete.
PB95-150439 *00,370*

National Planning for Construction and Building R and D.
PB96-137104 *00,324*

NIST Research on Less-Flammable Materials.
PB97-118632 *01,439*

BUILDING OPERATION AND MAINTENANCE
Standards Development in North America for Performance of Whole Buildings and Facilities.
PB94-185196 *00,312*

BUILDING TECHNOLOGY
Computer Programs for Simulation of Lighting/HVAC Interactions.
PB94-140407 *02,501*

Evaluation of GSA Maintenance Practices of Large Centrifugal Chillers and Review of GSA Refrigerant Management Practices.
PB94-143344 *02,502*

Manual for Ventilation Assessment in Mechanically Ventilated Commercial Buildings.
PB94-145653 *00,239*

System for Calibration of the Marshall Compaction Hammer.
PB94-145661 *01,303*

Source of Phenol Emissions Affecting the Indoor Air of an Office Building.
PB94-154382 *03,600*

Seismic Instrumentation of Existing Buildings.
PB94-159779 *00,420*

Performance Approach to the Development of Criteria for Low-Sloped Roof Membranes.
PB94-160751 *00,329*

Microstructural Features of Some Low Water/Solids, Silica Fume Mortars Cured at Different Temperatures.
PB94-160777 *00,330*

Northridge Earthquake, 1994. Performance of Structures, Lifelines and Fire Protection Systems.
PB94-161114 *00,421*

Draft Guidelines for Quality Control Testing of Elastomeric Seismic Isolation Systems.
PB94-161734 *00,422*

Earthquake Resistant Construction of Electric Transmission and Telecommunication Facilities Serving the Federal Government Report.
PB94-161817 *02,460*

Draft Guidelines for Pre-Qualification and Prototype Testing of Seismic Isolation Systems.
PB94-161940 *01,331*

Draft Guidelines for Quality Control Testing of Sliding Seismic Isolation Systems.
PB94-161957 *01,332*

CONTAM93 User Manual.
PB94-164381 *02,536*

Measurement and Determination of Radon Source Potential: A Literature Review.
PB94-165602 *02,576*

Least-Cost Energy Decisions for Buildings: Part 2. Uncertainty and Risk Video Training Workbook.
PB94-165982 *00,240*

Psychological Aspects of Lighting: A Review of the Work of CIE TC 3.16.
PB94-172160 *00,241*

Digitized Simulation of Mercury Intrusion Porosimetry.
PB94-172236 *01,304*

Simultaneous Visual and Calorimetric Measurements of R11, R123, and R123/Alkylbenzene Nucleate Flow Boiling.
PB94-172426 *03,251*

Serial Sectioning of Hardened Cement Paste for Scanning Electron Microscopy.
PB94-172640 *01,305*

Draft Guideline for Testing and Evaluation of Seismic Isolation Systems.
PB94-172947 *00,423*

Quantitative Phase Abundance Analysis of Three Cement Clinker Reference Materials by Scanning Electron Microscopy.
PB94-173051 *00,333*

Evaluation and Strengthening Guidelines for Federal Buildings: Identification of Current Federal Agency Programs.
PB94-176278 *00,424*

Evaluation and Strengthening Guidelines for Federal Buildings: Assessment of Current Federal Agency Evaluation Programs and Rehabilitation Criteria and Development of Typical Costs for Seismic Rehabilitation.
PB94-181856 *00,425*

Optimization of Highway Concrete Technology.
PB94-182995 *01,333*

Detection of Voids in Grouted Ducts Using the Impact-Echo Method.
PB94-185121 *01,306*

Standards Development in North America for Performance of Whole Buildings and Facilities.
PB94-185196 *00,312*

Corrosion Resistant Epoxy-Coated Reinforcing Steel.
PB94-185618 *01,307*

Air Change Effectiveness Measurements in Two Modern Office Buildings.
PB94-185766 *00,243*

Proficiency Testing as a Component of Quality Assurance in Construction Materials Laboratories.
PB94-185774 *00,334*

Expansion of Cementitious Materials Exposed to Sulfate Solutions.
PB94-185782 *02,577*

Infratechnologies: Tools for Innovation.
PB94-185998 *00,317*

Status of Construction and Construction Technologies.
PB94-186004 *00,318*

Sulfate Attack of Cementitious Materials: Volumetric Relations and Expansions.
PB94-187317 *03,232*

Strengthening Methodology for Lightly Reinforced Concrete Frames-II. Recommended Calculation Techniques for the Design of Infill Walls.
PB94-187648 *00,426*

Federal Certification Authority Liability and Policy: Law and Policy of Certificate-Based Public Key and Digital Signatures.
PB94-191202 *01,578*

Program of the Subcommittee on Construction and Building.
PB94-193646 *00,319*

Single-Phase Heat Transfer and Pressure Drop Characteristics of an Integral-Spine-Fin Within an Annulus.
PB94-194073 *03,805*

Graphical Analysis of the CCRL Portland Cement Proficiency Sample Database (Samples 1-72). (Part 1. Univariant Analysis of Portland Cement).
PB94-196557 *01,308*

Foias-Temam Approximations of Attractors for Galloping Oscillators.
PB94-198298 *04,817*

Digitized Direct Simulation Model of the Microstructural Development of Cement Paste.
PB94-198777 *01,309*

Digitized Simulation Model for Microstructural Development.
PB94-198785 *01,310*

Modelling the Leaching of Calcium Hydroxide from Cement Paste: Effects on Pore Space Percolation and Diffusivity.
PB94-198793 *01,311*

Diffusion Studies in a Digital-Image-Based Cement Paste Microstructural Model.
PB94-198801 *01,312*

Analysis of Moisture Accumulation in a Wood-Frame Wall Subjected to Winter Climate.
PB94-199320 *00,338*

Maturity Method.
PB94-199494 *01,313*

Maturity Functions for Concrete Made with Various Cements and Admixtures.
PB94-199502 *01,314*

Interaction between Naphthalene Sulfonate and Silica Fume in Portland Cement Pastes.
PB94-199759 *01,315*

Role of Refrigerant Mixtures as Alternatives to CFCs.
PB94-199775 *03,252*

Role of R22 in Refrigerating and Air Conditioning Equipment.
PB94-199783 *03,253*

Environmental Evaluation of a New Federal Office Building.
PB94-199874 *02,538*

Simplified Cycle Simulation Model for the Performance Rating of Refrigerants and Refrigerant Mixtures.
PB94-199890 *03,255*

Dynamic Characteristics of Five Tall Buildings during Strong and Low-Amplitude Motions.
PB94-199981 *00,427*

Papers Presentations Shine.
PB94-200383 *00,244*

Energy Prices and Discount Factors for Life-Cycle Cost Analysis 1994. Annual Supplement to NIST Handbook 135 and NBS Special Publication 709.
PB94-206018 *02,508*

Wind Load Provisions of the Manufactured Home Construction and Safety Standards: A Review and Recommendations for Improvement.
PB94-206125 *00,428*

U.S. Green Building Conference, 1994.
PB94-206364 *02,519*

Northridge Earthquake 1994: Performance of Structures, Lifelines, and Fire Protection Systems.
PB94-207461 *04,825*

Project Summaries 1994: NIST Building and Fire Research Laboratory.
PB94-207495 *00,343*

Causes of the Apparent Heat Transfer Degradation for Refrigerant Mixtures.
PB94-212701 *03,259*

Using Emulator/Testers for Commissioning EMCS Software, Operator Training, Algorithm Development, and Tuning Local Control Loops.
PB94-212735 *00,245*

Highway Concrete (HWYCON) Expert System User Reference and Enhancement Guide.
PB94-215670 *01,316*

Diffusion of Cations Beneath Organic Coatings on Steel Substrate.
PB94-215704 *03,119*

Standards in Building Economics: Why We Need Them and How to Write Them.
PB94-216405 *00,320*

Lessons Learned by a Wing Engineer.
PB94-216421 *00,429*

Hollow Clay Tile Prism Tests for Martin Marietta Energy Systems: Task 2 Testing.
PB94-217486 *00,352*

Study of Heat Pump Performance Using Mixtures of R32/R134a and R32/R125/R134a as 'Drop-In' Working Fluids for R22 with and Without a Liquid-Suction Heat Exchanger.
PB94-218559 *02,503*

Survey of Recent Cementitious Materials Research in Western Europe.
PB94-218583 *00,353*

NIST Research Program on the Seismic Resistance of Partially-Grouted Masonry Shear Walls.
PB94-219052 *00,354*

National Voluntary Laboratory Accreditation Program: Energy Efficient Lighting Products.
PB94-219060 *02,642*

Framework for Information Technology Integration in Process Plant and Related Industries.
PB94-219086 *02,772*

Energy Price Indices and Discount Factors for Life-Cycle Cost Analysis 1995. Annual Supplement to NIST Handbook 135 and NBS Special Publication 709. (Revised).
PB95-105011 *02,509*

Present Worth Factors for Life-Cycle Cost Studies in the Department of Defense (1995).
PB95-105029 *03,664*

Controlling Moisture in the Walls of Manufactured Housing.
PB95-105136 *00,355*

Measurements of Moisture Diffusivity for Porous Building Materials.
PB95-107397 *00,356*

Ventilation Rates in Office Buildings.
PB95-108825 *02,539*

Field Measurements of Ventilation and Ventilation Effectiveness in an Office/Library Building.
PB95-108833 *00,247*

Seismic Strengthening of Reinforced Concrete Frame Buildings.
PB95-108841 *00,430*

Application of Thermal Analysis Techniques to the Characterization of EPDM Roofing Membrane Materials.
PB95-125845 *00,359*

Use of Thermal Mechanical Analysis to Characterize Ethylene-Propylene-Diene Terpolymer (EPDM) Roofing Membrane Materials.
PB95-125852 *00,360*

Water Efficient Plumbing Fixtures through Standards and Test Methods.
PB95-125951 *00,248*

Computer Simulation of the Diffusivity of Cement-Based Materials.
PB95-125985 *00,362*

Digital Simulation of the Aggregate-Cement Paste Interfacial Zone in Concrete.
PB95-125993 *00,363*

Fundamental Computer Simulation Models for Cement-Based Materials.
PB95-126009 *00,364*

Comparison of Heat-Flow-Meter Tests from Four Laboratories.
PB95-126264 *00,365*

Growing Significance of CIB.
PB95-126306 *00,314*

Ashland Tank-Collapse Investigation: Closure by Authors.
PB95-126322 *02,482*

Standards of Seismic Safety for Existing Federally Owned or Leased Buildings and Commentary.
PB95-130209 *00,431*

Indoor Air Quality Impacts of Residential HVAC Systems, Phase 1 Report: Computer Simulation Plan.
PB95-135596 *00,249*

Quantitative X-Ray Powder Diffraction Methods for Clinker and Cement.
PB95-143079 *01,317*

Diagnosis of Causes of Concrete Deterioration in the MLP-7A Parking Garage.
PB95-143095 *01,318*

Manufactured Homes: Probability of Failure and the Need for Better Windstorm Protection through Improved Anchoring Systems.
PB95-143129 *00,432*

Visual Measurement Technique for Analysis of Nucleate Flow Boiling.
PB95-143301 *03,262*

Methodologies for Predicting the Service Lives of Coating Systems.
PB95-146387 *03,124*

Wind and Seismic Effects. Proceedings of the U.S.-Japan Cooperative Program in Natural Resources Panel on Wind and Seismic Effects (26th). Held in Gaithersburg, Maryland on May 17-20, 1994.
PB95-147385 *00,433*

Study of Ventilation and Carbon Dioxide in an Office Building.
PB95-150140 *02,542*

Cross-Property Relations and Permeability Estimation in Model Porous Media.
PB95-150280 *04,205*

Percolation and Pore Structure in Mortars and Concrete.
PB95-150439 *00,370*

Effects of Humidity and Elevated Temperature on the Density and Thermal Conductivity of a Rigid Polyisocyanurate Foam Co-Blown with CCl3F and CO2.
PB95-150462 *00,371*

Evaluation and Retrofit Standards for Existing Federally Owned and Leased Buildings.
PB95-150918 *00,434*

Some Basics on Who's Who and What's What in Seismic Safety.
PB95-150926 *00,435*

Lighting and HVAC.
PB95-150991 *00,250*

NIST Lighting and HVAC Interaction Test Facility.
PB95-151007 *00,251*

Recent Developments at NIST on Optical Current Sensors and Partial Discharge Diagnostics.
PB95-151114 *02,147*

Effects of Adhesive Thickness, Open Time, and Surface Cleanness on the Peel Strength of Adhesive-Bonded Seams of EPDM Rubber Roofing Membrane.
PB95-151338 *00,372*

Lighting Quality and Light Source Size.
PB95-151783 *00,252*

Lighting Research and Theory Can Create Business Prospects.
PB95-151791 *00,253*

Implementation of Executive Order 12699: Seismic Safety of Federal and Federally Assisted or Regulated New Building Construction.
PB95-151809 *00,436*

Structural Analysis in Context.
PB95-151817 *00,437*

Room Temperature Thermal Conductivity of Fumed-Silica Insulation for a Standard Reference Material.
PB95-152039 *00,374*

Partially Prestressed and Debonded Precast Concrete Beam-Column Joints.
PB95-153102 *00,439*

Seismic Performance Behavior of Precast Concrete Beam-Column Joints.
PB95-153110 *00,440*

Psychological Aspects of Lighting: A Review of the Work of CIE TC 3.16.
PB95-153276 *00,254*

Rationale and Preliminary Plan for Federal Research for Construction and Building.
PB95-154704 *00,322*

Assessing Ventilation Effectiveness in Mechanically Ventilated Office Buildings.
PB95-162079 *00,255*

Modeling Radon Transport in Multistory Residential Buildings.
PB95-162087 *00,256*

Ventilation, Carbon Dioxide and ASHRAE Standard 62-1989.
PB95-162095 *02,544*

Characteristics of Adhesive-Bonded Seams Sampled from EPDM Roof Membranes.
PB95-162491 *00,377*

Algebraic Approximation of Attractors for Galloping Oscillators.
PB95-162897 *04,820*

Rheology of Fresh Cement Paste.
PB95-163150 *00,378*

Cement and Concrete Characterization by Scanning Electron Microscopy.
PB95-163168 *00,379*

Evaluating the Seismic Performance of Lightly-Reinforced Circular Concrete Bridge Columns.
PB95-163259 *01,335*

Jacket Thickness Requirements for Seismic Retrofitting of Circular Bridge Columns.
PB95-163267 *01,336*

Pulse-Echo Ultrasonic Evaluation of the Integrity of Seams of Single-Ply Roof Membranes.
PB95-163804 *00,381*

Lessons from the Loma Prieta Earthquake.
PB95-164091 *00,442*

Fire-Plume-Generated Ceiling Jet Characteristics and Convective Heat Transfer to Ceiling and Wall Surfaces in a Two-Layer Fire Environment: Uniform Temperature Ceiling and Walls.
PB95-164711 *00,382*

Performance of HUD-Affiliated Properties during the January 17, 1994 Northridge Earthquake.
PB95-174488 *00,443*

Life-Cycle Costing Workshop for Energy Conservation in Buildings: Student Manual.
PB95-175006 *00,257*

Cellular Automaton Simulations of Cement Hydration and Microstructure Development.
PB95-175055 *01,320*

Evolution of Porosity and Calcium Hydroxide in Laboratory Concretes Containing Silica Fume.
PB95-175063 *01,321*

Earthquake and Fire in Japan: When the Threat Became a Reality.
PB95-175238 *00,201*

Performance of Compact Fluorescent Lamps at Different Ambient Temperatures.
PB95-175329 *00,258*

Using Emulators to Evaluate the Performance of Building Energy Management Systems.
PB95-175774 *00,259*

Reproducibility of Tests on Energy Management and Control Systems Using Building Emulators.
PB95-175980 *00,260*

Limits of CO2 Monitoring in Determining Ventilation Rates.
PB95-176004 *02,552*

Ventilation Effectiveness Measurements in Two Modern Office Buildings.
PB95-176012 *02,553*

Spectrally Smooth Reflectances That Match.
PB95-176319 *04,306*

Manufactured Housing Walls That Provide Satisfactory Moisture Performance in All Climates.
PB95-178885 *00,383*

Indoor Air Quality Impacts of Residential HVAC Systems. Phase 2.A Report: Baseline and Preliminary Simulations.
PB95-178893 *02,554*

Performance of 1/3-Scale Model Precast Concrete Beam-Column Connections Subjected to Cyclic Inelastic Loads. Report No. 4.
PB95-179024 *00,444*

Effects of Testing Variables on the Measured Compressive Strength of High-Strength (90 MPa) Concrete.
PB95-179040 *00,445*

Nondestructive Testing of Concrete: History and Challenges.
PB95-180139 *00,385*

High-Performance Concrete: Research Needs to Enhance Its Use.
PB95-180147 *01,322*

Application of a Multizone Airflow and Contaminant Dispersal Model to Indoor Air Quality Control in Residential Buildings.
PB95-180238 *02,555*

Gust Factors Applied to Hurricane Winds.
PB95-180469 *00,446*

Melnikov Function and Homoclinic Chaos Induced by Weak Perturbations.
PB95-180923 *03,414*

Control Stability of a Heat-Flow-Meter Appartus.
PB95-181194 *00,386*

Intra-Laboratory Comparison of a Line-Heat-Source Guarded Hot Plate and Heat-Flow-Meter Apparatus.
PB95-181202 *00,387*

Seismic Safety of Federal Buildings. Initial Program: How Much Will It Cost.
PB95-182291 *00,447*

Indoor Air Quality Commissioning of a New Office Building.
PB95-182309 *00,262*

Proceedings: Workshop on Research Needs in Wind Engineering. Held in Gaithersburg, Maryland on September 12-13, 1994.
PB95-189528 *00,448*

Field Evaluation of the System for Calibration of the Marshall Compaction Hammer.
PB95-190674 *01,323*

BLCC: The NIST 'Building Life-Cycle Cost' Program, Version 4.21. User's Guide and Reference Manual.
PB95-190682 *00,263*

Heat and Moisture Transfer in Wood-Based Wall Construction: Measured versus Predicted.
PB95-200655 *00,391*

Optical Performance of Commercial Windows.
PB95-208757 *00,392*

Measurements of Outdoor Air Distribution in an Office Building.
PB95-210944 *00,264*

Survey of Steel Moment-Resisting Frame Buildings Affected by the 1994 Northridge Earthquake.
PB95-211918 *00,451*

White Papers Prepared for the White House: Construction Industry Workshop on National Construction Goals. Held on December 14-16, 1994.
PB95-216891 *01,299*

Theoretical Evaluation of the Vapor Compression Cycle with a Liquid-Line/Suction-Line Heat Exchanger, Economizer, and Ejector.
PB95-216917 *02,607*

Extreme Wind Distribution Tails: A 'Peaks Over Threshold' Approach.
PB95-219416 *00,127*

Computer Simulations of Airflow and Radon Transport in Four Large Buildings.
PB95-220422 *02,557*

Prediction of Cracking in Reinforced Concrete Structures.
PB95-220448 *03,725*

Testing of Selected Self-Leveling Compounds for Floors.
PB95-220455 *00,395*

Extreme Wind Estimates by the Conditional Mean Exceedance Procedure.
PB95-220471 *00,120*

Survey of Concrete Transport Properties and Their Measurement.
PB95-220489 *00,396*

Compositional Analysis of Beneficiated Fly Ashes.
PB95-220497 *00,397*

Performance Testing of a Family of Type I Combination Appliance.
PB95-220521 *02,505*

4SIGHT Manual: A Computer Program for Modelling Degradation of Underground Low Level Waste Concrete Vaults.
PB95-231593 *03,726*

Enhancements to Program IDARC: Modeling Inelastic Behavior of Welded Connections in Steel Moment-Resisting Frames.
PB95-231601 *00,452*

Performance of Federal Buildings in the January 17, 1994 Northridge Earthquake.
PB95-231775 *00,453*

Comparison of the Seismic Provisions of Model Building Codes and Standards to the 1991 NEHRP Recommended Provisions.
PB95-231858 *00,315*

Water-Vapor Measurements of Low-Slope Roofing Materials.
PB95-251617 *00,399*

Least-Cost Energy Decisions for Buildings. Part 3. Choosing Economic Evaluation Methods. Video Training Workbook.
PB95-253597 *00,265*

International Green Building Conference and Exposition (2nd). Held in Big Sky, Montana on August 13-15, 1995.
PB95-253605 *02,525*

Simple Method of Composition Shifting with a Distillation Column for a Heat Pump Employing a Zeotropic Refrigerant Mixture.
PB95-255824 *02,603*

New Mass Transport Elements and Components for the NIST IAQ Model.
PB95-255899 *02,558*

Strengthening Methodology for Lightly Reinforced Concrete Frames: Recommended Design Guidelines for Strengthening with Infill Walls.
PB95-260725 *00,454*

Long-Term Performance of Engineered Concrete Barriers.
PB95-260816 *03,727*

National Construction Sector Goals: Industry Strategies for Implementation.
PB95-269817 *00,204*

Building Life Cycle Cost Computer Program (BLCC) Version 4.21-95 (for Microcomputers).
PB95-502779 *00,267*

Building Life Cycle Cost Computer Program (BLCC) Version 4.22-95 (for Microcomputers).
PB95-503397 *00,268*

Geometrical Percolation Threshold of Overlapping Ellipsoids.
PB96-102397 *03,167*

100 Ampere, 100 kHZ Transconductance Amplifier.
PB96-102629 *02,068*

Present Worth Factors for Life-Cycle Cost Studies in the Department of Defense (1996).
PB96-106869 *03,673*

Indoor Air Quality Impacts of Residential HVAC Systems Phase II.B Report: IAQ Control Retrofit Simulations and Analysis.
PB96-106877 *02,559*

Literature Review on Seismic Performance of Building Cladding Systems.
PB96-106901 *00,455*

EMISS: A Program for Estimating Local Air Pollution Emission Factors Related to Energy Use in Buildings: User's Guide and Reference Manual.
PB96-109566 *02,560*

Use of Building Emulators to Evaluate the Performance of Building Energy Management Systems.
PB96-111901 *00,269*

Noise Modeling and Reliability of Behavior Prediction for Multi-Stable Hydroelastic Systems.
PB96-111943 *04,822*

Prediction of Potential Concrete Strength at Later Ages.
PB96-112180 *01,324*

Effects of Testing Variables on the Strength of High-Strength (90 Mpa) Concrete Cylinders.
PB96-112198 *00,456*

Post-Earthquake Fire and Lifelines Workshop. Held in Long Beach, California on January 30-31, 1995. Proceedings.
PB96-117916 *00,209*

Response of Buildings to Ambient Vibration and the Loma Prieta Earthquake: A Comparison.
PB96-119607 *00,457*

Study on the Reuse of Plastic Concrete Using Extended Set-Retarding Admixtures.
PB96-122130 *00,402*

Recent Development in Nondestructive Testing of Concrete.
PB96-122445 *01,325*

Economic Methods and Risk Analysis Techniques for Evaluating Building Investments: A Survey.
PB96-122593 *00,323*

Chaotic Motions of Coupled Galloping Oscillators and Their Modeling as Diffusion Progresses.
PB96-122718 *04,823*

Non-Gaussian Noise Effects on Reliability of Multistable Systems.
PB96-122726 *04,213*

Stranding Experiments on Double Hull Tanker Structures.
PB96-123112 *03,749*

Hydraulic Radius and Transport in Reconstructed Model Three-Dimensional Porous Media.
PB96-123419 *00,403*

ICSSC Guidance on Implementing Executive Order 12941 on Seismic Safety of Existing Federally Owned or Leased Buildings.
PB96-128103 *00,459*

Ground Improvement Techniques for Liquefaction Remediation Near Existing Lifelines.
PB96-128111 *01,350*

Calorimetric and Visual Measurements of R123 Pool Boiling on Four Enhanced Surfaces.
PB96-128129 *04,053*

Recommended Performance-Based Criteria for the Design of Manufactured Home Foundation Systems to Resist Wind and Seismic Loads.
PB96-128285 *00,460*

Alkali-Silica Reaction and High Performance Concrete.
PB96-131537 *01,345*

How-To Suggestions for Implementing Executive Order 12941 on Seismic Safety of Existing Federal Buildings, A Handbook.
PB96-131552 *00,461*

Modelling Drying Shrinkage of Cement Paste and Mortar. Part 1. Structural Models from Angstroms to Millimeters.
PB96-135132 *03,074*

Effect of Inclination on the Performance of a Compact Brazed Plate Condenser and Evaporator.
PB96-136973 *02,756*

National Planning for Construction and Building R and D.
PB96-137104 *00,324*

Improving the Evaluation of Building Ventilation.
PB96-138508 *00,271*

De Facto Microzonation through the Use of Soils Factors in Design Triggers.
PB96-141148 *00,462*

Predicting the Fire Performance of Buildings: Establishing Appropriate Calculation Methods for Regulatory Applications.
PB96-141239 *00,316*

Unreacted Cement Content in Macro-Defect-Free Composites: Impact on Processing-Structure-Property Relations.
PB96-141270 *03,174*

Optimal Control of Building and HVAC Systems.
PB96-141353 *00,272*

Seismic Performance of Circular Bridge Columns Designed in Accordance with AASHTO/CALTRANS Standards.
PB96-146352 *01,346*

Effectiveness of a Heat Recovery Ventilator, an Outdoor Air Intake Damper and an Electrostatic Particulate Filter at Controlling Indoor Air Quality in Residential Buildings.
PB96-146642 *02,564*

Multizone Modeling of Three Residential Indoor Air Quality Control Options.
PB96-146659 *02,565*

Interfacial Transport in Porous Media: Application to dc Electrical Conductivity of Mortars.
PB96-146816 *01,326*

Water Permeability and Chloride Ion Diffusion in Portland Cement Mortars: Relationship to Sand Content and Critical Pore Diameter.
PB96-148036 *03,193*

Workplan to Analyze the Energy Impacts of Envelope Airtightness in Office Buildings.
PB96-154463 *00,273*

AutoBid 2.0: The Microcomputer System for Police Patrol Vehicle Selection.
PB96-154570 *04,871*

Simplified Design Procedure for Hybrid Precast Concrete Connections.
PB96-154836 *00,405*

Summary and Results of the NIST Workshop on Proposed Guidelines for Testing and Evaluation of Seismic Isolation Systems. Held in San Francisco, California on July 25, 1994.
PB96-154901 *00,463*

Sensitivity Analysis for Mathematical Modeling of Fires in Residential Buildings.
PB96-154968 *00,215*

Development of a Test Method for Leaching of Lead from Lead-Based Paints Through Encapsulants.
PB96-154984 *03,128*

Study of Ventilation Measurement in an Office Building.
PB96-155593 *00,274*

Development and Application of an Indoor Air Quality Commissioning Program in a New Office Building.
PB96-155601 *00,275*

Transitions to Chaos Induced by Additive and Multiplicative Noise.
PB96-155759 *03,750*

Spectrum of the Stochastically Forced Duffing-Holmes Oscillator.
PB96-155767 *00,216*

Necessary Condition for Homoclinic Chaos Induces by Additive Noise.
PB96-155775 *04,063*

Executive Order 12941. Seismic Safety of Existing Federally Owned or Leased Buildings: It's History, Content and Objectives.
PB96-156021 *00,465*

Noise-Induced Transitions to Chaos.
PB96-156120 *00,217*

Experimental and Numerical Chaos in Continuous Systems: Two Case Studies.
PB96-156146 *00,219*

Application of Digital-Image-Based Models to Microstructure, Transport Properties, and Degradation of Cement-Based Materials.
PB96-156161 *00,406*

Intermediate Coupling in L2-L3 Core Excitons of MgO, Al2O3, and SiO2.
PB96-158043 *04,079*

Strengthening Methodology for Lightly Reinforced Concrete Frames.
PB96-158050 *00,466*

Multiattribute Decision Analysis Method for Evaluating Buildings and Building Systems.
PB96-158670 *00,325*

Comparison of Responses of a Select Number of Buildings to the 10/17/1989 Loma Prieta (California) Earthquake and Low-Level Amplitude Test Results.
PB96-159645 *00,467*

Extreme Winds Estimation by 'Peaks Over Threshold' and Epochal Methods.
PB96-159686 *00,468*

Modeling of Extreme Loading by 'Peaks Over Threshold' Methods.
PB96-159694 *00,469*

Workgroup Summary Report: Plastic Hinge-Based Techniques for Advanced Analysis.
PB96-159702 *00,470*

Effects of Pipe Elbows and Tube Bundles on Selected Types of Flowmeters.
PB96-160999 *01,135*

Energy Price Indices and Discount Factors for Life-Cycle Cost Analysis 1996. Annual Supplement to NIST Handbook 135 and NBS Special Publication 709. (Revised).
PB96-162441 *02,510*

Estimates of Hurricane Wind Speeds by the 'Peaks Over Threshold' Method.
PB96-162540 *00,471*

Distributed Architecture for Standards Processing.
PB96-164181 *00,276*

Guide to a Format for Data on Chemical Admixtures in a Materials Property Database.
PB96-165394 *01,327*

Group 1 for the Plant Spatial Configuration STEP Application Protocol.
PB96-165402 *02,789*

Multizone Modeling of Three Residential Indoor Air Quality Control Options.
PB96-165782 *02,567*

Modified Optimal Algorithm for Active Structural Control.
PB96-165949 *00,472*

Enhancement of R123 Pool Boiling by the Addition of N-Hexane.
PB96-165956 *02,605*

Preliminary Processing of the Lotung LSST Data.
PB96-165972 *03,690*

Study to Determine the Existence of an Azeotropic R-22 'Drop-In' Substitute.
PB96-167812 *02,568*

Method of Estimating the Parameters of Tuned Mass Dampers for Seismic Applications.
PB96-167820 *00,473*

Life-Cycle Costing Manual for the Federal Energy Management Program. 1995 Edition.
PB96-172317 *02,511*

Innovation in the Japanese Construction Industry: A 1995 Appraisal.
PB96-177373 *00,225*

Probabilistic Estimates of Design Load Factors for Wind-Sensitive Structures Using the 'Peaks Over Threshold' Approach.
PB96-183223 *00,474*

Performance of Tape-Bonded Seams of EPDM Membranes: Comparison of the Peel Creep-Rupture Response of Tape-Bonded and Liquid-Adhesive-Bonded Seams.
PB96-183249 *03,012*

Guide to a Format for Data on Chemical Admixtures in a Materials Property Database. (Reannouncement with new abstract).
PB96-186192 *01,328*

Warping of Terrace Pavers at the U.S. Capitol Building.
PB96-193651 *00,411*

Guidelines for Pre-Qualification, Prototype and Quality Control Testing of Seismic Isolation Systems.
PB96-193685 *01,347*

State of the Art Report on Seismic Design Requirements for Nonstructural Building Components.
PB96-193800 *00,308*

Precision of Marchall Stability and Flow Test Using 6-in. (152.4-mm) Diameter Specimens.
PB96-200910 *03,006*

Benefits and Costs of Research: Two Case Studies in Building Technology.
PB96-202221 *00,230*

NIST Construction Automation Program Report No. 2. Proceedings of the NIST Construction Automation Workshop. Held in Gaithersburg, Maryland on March 30-31, 1995.
PB96-202239 *00,413*

Development of a Method for Measuring Water-Stripping Resistance of Asphalt/Siliceous Aggregate Mixtures.
PB96-202296 *01,329*

Measurement of Rheological Properties of High Performance Concrete: State of the Art Report.
PB96-202338 *00,414*

Economics of New-Technology Materials: A Case Study of FRP Bridge Decking.
PB96-202353 *01,349*

Materials Aspects of Fiber-Reinforced Polymer Composites in Infrastructure.
PB96-210695 *03,184*

Energy Price Indices and Discount Factors for Life-Cycle Cost Analysis 1997. Annual Supplement to NIST Handbook 135 and NBS Special Publication 709. (Revised).
PB96-210745 *02,512*

Report of a Workshop on Requalification of Tubular Steel Joints in Offshore Structures. Held in Houston, Texas on September 5-6, 1995.
PB96-210760 *03,699*

Estimation of System Damping at the Lotung Site by Application of System Identification.
PB96-214697 *01,351*

Shear Design of High-Strength Concrete Beams: A Review of the State-of-the-Art.
PB96-214713 *01,330*

Energy-Based Method for Liquefaction Potential Evaluation. Phase 1. Feasibility Study.
PB96-214747 *03,691*

January 17, 1995 Hyogoken-Nanbu (Kobe) Earthquake. Performance of Structures, Lifelines and Fire Protection Systems. Executive Summary and Paper.
PB97-104160 *00,475*

Wind and Seismic Effects: Proceedings of the Joint Meeting of the U.S.-Japan Cooperative Program in Natural Resources Panel on Wind and Seismic Effects (28th). Held in Gaithersburg, Maryland on May 14-17, 1996.
PB97-104376 *00,476*

Indoor Air Quality Commissioning of a New Office Building.
PB97-110142 *00,279*

Relationship between Indoor Air Quality and Carbon Dioxide.
PB97-111249 *02,569*

Post-Occupancy Evaluation of the Forrestal Building.
PB97-111298 *00,280*

Experimental Verification of a Moisture and Heat Transfer Model in the Hygroscopic Regime.
PB97-111546 *00,309*

Testing Conformance and Interoperability of BACnet (Trade Name) Building Automation Products.
PB97-111553 *00,310*

Test Procedures for Advanced Insulation Panels.
PB97-111892 *00,415*

Empirical Validation of a Transient Computer Model for Combined Heat and Moisture Transfer.
PB97-111991 *00,416*

Factors Affecting the Energy Consumption of Two Refrigerator-Freezers.
PB97-112312 *00,311*

Dynamics of Multi-DOF Stochastic Nonlinear Systems.
PB97-113245 *00,477*

Carbon Monoxide Dispersion in Residential Buildings: Literature Review and Technical Analysis.
PB97-114227 *02,571*

Summary of Federal Construction and Building R and D in 1994.
PB97-114250 *00,234*

Proceedings of a Workshop on Developing and Adopting Seismic Design and Construction Standards for Lifelines. Held in Denver, Colorado on September 25-27, 1991.
PB97-115794 *01,302*

Multi-Scale Picture of Concrete and Its Transport Properties: Introduction for Non-Cement Researchers.
PB97-115802 *03,107*

Group 1 for the Process Engineering Data STEP Application Protocol.
PB97-116073 *02,797*

Intracycle Evaporative Cooling in a Vapor Compression Cycle.
PB97-116107 *02,762*

Evaluation of Survey Procedures for Determining Occupant Load Factors in Contemporary Office Buildings.
PB97-116222 *00,238*

Materials-Science Based Approach to Phenol Emissions from a Flooring Material in an Office Building.
PB97-118749 *02,572*

Issues in the Field Measurement of VOC Emission Rates.
PB97-118806 *02,573*

Line-Heat-Source Guarded-Hot-Plate Apparatus.
PB97-118996 *00,417*

Design of Technically Complex Facilities.
PB97-119101 *02,695*

Fault Diagnosis of an Air-Handling Unit Using Artificial Neural Networks.
PB97-121321 *00,283*

Computer Simulations of Binder Removal from 2-D and 3-D Model Particulate Bodies.
PB97-121339 *00,418*

International Green Building Conference and Exposition (3rd). Held in San Diego, California on November 17-19, 1996. (Reannouncement with new abstract).
PB97-121826 *02,531*

Single-Phase Heat Transfer and Pressure Drop Characteristics of an Integral-Spine Fin Within an Annulus.
PB97-122386 *04,179*

Parametric Study of Wall Moisture Contents Using a Revised Variable Indoor Relative Humidity Version of the 'Moist' Transient Heat and Moisture Transfer Model.
PB97-122535 *00,419*

BUILDINGS
Computer Programs for Simulation of Lighting/HVAC Interactions.
PB94-140407 *02,501*

Draft Guidelines for Quality Control Testing of Elastomeric Seismic Isolation Systems.
PB94-161734 *00,422*

CONTAM93 User Manual.
PB94-164381 *02,536*

Least-Cost Energy Decisions for Buildings: Part 2. Uncertainty and Risk Video Training Workbook.
PB94-165982 *00,240*

Lead Abatement in Buildings and Related Structures.
PB94-172038 *03,601*

Psychological Aspects of Lighting: A Review of the Work of CIE TC 3.16.
PB94-172160 *00,241*

Improvement in Predicting Smoke Movement in Compartmented Structures.
PB94-172418 *00,332*

Fire Hazard and Risk: Evaluating Alternative Technologies.
PB94-173077 *00,242*

Prediction of Fire Dynamics.
PB94-193620 *00,336*

Performance Parameters of Fire Detection Systems.
PB94-194339 *00,288*

CONTAM88 Building Input Files for Multi-Zone Airflow and Contaminant Dispersal Modeling.
PB94-194388 *02,537*

Analysis of the Happyland Social Club Fire with HAZARD I.
PB94-199270 *00,193*

Dynamic Characteristics of Five Tall Buildings during Strong and Low-Amplitude Motions.
PB94-199981 *00,427*

Development of the Fire Data Management System.
PB94-206091 *00,339*

U.S. Green Building Conference, 1994.
PB94-206364 *02,519*

Project Summaries 1994: NIST Building and Fire Research Laboratory.
PB94-207495 *00,343*

Global Equivalence Ratio Concept and the Prediction of Carbon Monoxide Formation in Enclosure Fires.
PB94-207511 *00,313*

Using Emulator/Testers for Commissioning EMCS Software, Operator Training, Algorithm Development, and Tuning Local Control Loops.
PB94-212735 *00,245*

Full Scale Smoke Control Tests at the Plaza Hotel Building.
PB94-212859 *00,347*

Overview of Smoke Control Technology.
PB94-212867 *00,348*

Preview of ASHRAE's Revised Smoke Control Manual.
PB94-212875 *00,349*

Sprinkler Fire Suppression Algorithm.
PB94-216181 *00,293*

Standards in Building Economics: Why We Need Them and How to Write Them.
PB94-216405 *00,320*

HAZARD I Fire Hazard Assessment Method (Version 1.2) (for Microcomputers).
PB94-501988 *00,196*

HAZARD I Fire Hazard Assessment Method, Version 1.2 (Upgrade Package) (for Microcomputers).
PB94-501996 *00,197*

Relating Bench-Scale and Full-Scale Toxicity Data.
PB95-125977 *00,361*

Assessment of Technologies for Advanced Fire Detection.
PB95-126330 *00,294*

Summaries of BFRL Fire Research In-House Projects and Grants, 1994.
PB95-130845 *00,366*

FPETOOL: Fire Protection Tools for Hazard Estimation. An Overview of Features.
PB95-140885 *00,367*

Building and Fire Research Laboratory Publications, 1993.
PB95-143202 *00,369*

Rationale and Preliminary Plan for Federal Research for Construction and Building.
PB95-154704 *00,322*

Method of Predicting Smoke Movement in Atria with Application to Smoke Management.
PB95-154746 *00,376*

Gust Factors Applied to Hurricane Winds.
PB95-180469 *00,446*

Algorithm to Describe the Spread of a Wall Fire under a Ceiling.
PB95-182259 *00,261*

Comparison of Fire Sprinkler Piping Materials: Steel, Copper, Chlorinated Polyvinyl Chloride and Polybutylene, in Residential and Light Hazard Installations.
PB95-182267 *00,299*

BLCC: The NIST 'Building Life-Cycle Cost' Program, Version 4.21. User's Guide and Reference Manual.
PB95-190682 *00,263*

Survey of Steel Moment-Resisting Frame Buildings Affected by the 1994 Northridge Earthquake.
PB95-211918 *00,451*

Compartment Fire Combustion Dynamics. Annual Report, September 1, 1993-September 1, 1994.
PB95-217162 *00,203*

Building and Fire Research Laboratory Publications, 1994.
PB95-226684 *00,398*

Least-Cost Energy Decisions for Buildings. Part 3. Choosing Economic Evaluation Methods. Video Training Workbook.
PB95-253597 *00,265*

International Green Building Conference and Exposition (2nd). Held in Big Sky, Montana on August 13-15, 1995.
PB95-253605 *02,525*

Building Life Cycle Cost Computer Program (BLCC), Version 4.2-95 (for Microcomputers).
PB95-501953 *00,266*

Building Life Cycle Cost Computer Program (BLCC) Version 4.21-95 (for Microcomputers).
PB95-502779 *00,267*

Building Life Cycle Cost Computer Program (BLCC) Version 4.22-95 (for Microcomputers).
PB95-503397 *00,268*

How to Evaluate Alternative Designs Based on Fire Modeling.
PB96-102116 *00,206*

Literature Review on Seismic Performance of Building Cladding Systems.
PB96-106901 *00,455*

Economic Methods and Risk Analysis Techniques for Evaluating Building Investments: A Survey.
PB96-122593 *00,323*

Optimal Control of Building and HVAC Systems.
PB96-141353 *00,272*

Strengthening Methodology for Lightly Reinforced Concrete Frames.
PB96-158050 *00,466*

Multiattribute Decision Analysis Method for Evaluating Buildings and Building Systems.
PB96-158670 *00,325*

Comparison of Responses of a Select Number of Buildings to the 10/17/1989 Loma Prieta (California) Earthquake and Low-Level Amplitude Test Results.
PB96-159645 *00,467*

Benefits and Costs of Research: Two Case Studies in Building Technology.
PB96-202221 *00,230*

NIST Construction Automation Program Report No. 2. Proceedings of the NIST Construction Automation Workshop. Held in Gaithersburg, Maryland on March 30-31, 1995.
PB96-202239 *00,413*

Building Life Cycle Cost Computer Program (BLCC) Version 4.22-95 (for Micrcomputers).
PB96-502794 *00,277*

Testing Conformance and Interoperability of BACnet (Trade Name) Building Automation Products.
PB97-111553 *00,310*

International Green Building Conference and Exposition (3rd). Held in San Diego, California on November 17-19, 1996. (Reannouncement with new abstract).
PB97-121826 *02,531*

Building Life Cycle Cost Computer Program (BLCC) Version 4.4-97 (for Microcomputers).
PB97-500342 *00,284*

BULK MODULUS
Relationship between Bulk-Modulus Temperature Dependence and Thermal Expansivity.
PB95-168829 *04,641*

Compressibility of Polycrystal and Monocrystal Copper: Acoustic-Resonance Spectroscopy.
PB96-164223 *02,990*

Bulk Modulus and Young's Modulus of Nanocrystalline gamma-Alumina.
PB96-204185 *03,092*

BUOYANCY
Computational Model for the Rise and Dispersion of Wind-Blown, Buoyancy-Driven Plumes. Part 2. Linearly Stratified Atmosphere.
PB94-143427 *00,119*

Piggyback Balance Experiment: An Illustration of Archimedes' Principles and Newton's Third Law.
PB94-163060 *03,786*

Combined Buoyancy- and Pressure-Driven Flow Through a Shallow, Horizontal, Circular Vent.
PB94-210077 *00,344*

Simulating Smoke Movement through Long Vertical Shafts in Zone-Type Compartment Fire Models.
PB95-143152 *00,368*

Calculating Combined Buoyancy- and Pressure-Driven Flow Through a Shallow, Horizontal, Circular Vent; Application to Problem of Steady Burning in a Ceiling-Vented Enclosure.
PB96-164108 *00,409*

Combined Buoyancy and Pressure-Driven Flow Through a Shallow, Horizontal, Circular Vent.
PB96-164116 *00,410*

BUOYANT SMOKE PLUMES
Dispersion and Deposition of Smoke Plumes Generated in Massive Fires.
PB95-126066 *02,540*

BURIED OXIDES
Electron and Hole Trapping in Irradiated SIMOX, ZMR and BESOI Buried Oxides.
PB96-160320 *01,956*

BURNING RATE
Fire Growth Models for Materials.
PB94-195856 *01,367*

Comparison of Wall-Fire Behavior With and Without a Ceiling.
PB94-207404 *00,342*

In Situ Burning Oil Spill Workshop Proceedings. Held in Orlando, Florida on January 26-28, 1994.
PB95-104907 *02,583*

One- and Two-Sided Burning of Thermally Thin Materials.
PB95-140935 *03,151*

Estimate of the Effect of Scale on Radiative Heat Loss Fraction and Combustion Efficiency.
PB95-150447 *02,486*

Wall Flame Heights with External Radiation.
PB95-163481 *00,380*

In situ Burning of Oil Spills: Mesoscale Experiments and Analysis.
PB95-163747 *02,587*

Burning Rate of Premixed Methane-Air Flames Inhibited by Fluorinated Hydrocarbons.
PB95-180584 *01,391*

Experimental and Numerical Burning Rates of Premixed Methane-Air Inhibited by Fluoromethanes.
PB95-180592 *01,392*

Burning Rate and Flame Heat Flux For PMMA in the Cone Calorimeter.
PB95-216990 *00,393*

Turbulent Flame Spread on Vertical Corner Walls.
PB96-114764 *01,403*

Smoke Emission from Burning Crude Oil.
PB96-122890 *01,407*

Predicting the Ignition Time and Burning Rate of Thermoplastics in the Cone Calorimeter.
PB96-154794 *01,418*

Minimum Mass Flux Requirements to Suppress Burning Surfaces with Water Sprays.
PB96-183181 *01,425*

BUTADIENES
Acrylonitrile-Butadiene-Styrene (ABS) Plastic Drain, Waste, and Vent Pipe and Fittings.
AD-A310 724/0 *00,327*

Stability/Instability of Gas Mixtures Containing 1,3-Butadiene in Treated Aluminum Gas Cylinders.
PB95-162285 *02,546*

BUTANES
Modified Leung-Griffiths Model of Vapor-Liquid Equilibrium: Extended Scaling and Binary Mixtures of Dissimilar Fluids.
PB94-216108 *00,851*

Experimental Method for Obtaining Critical Densities of Binary Mixtures: Application to Ethane + n-Butane.
PB95-151148 *00,930*

Fugacity Coefficients of Hydrogen in (Hydrogen + Butane).
PB95-175212 *02,491*

BUTENES
Resonance Enhanced Multiphoton Ionization Spectroscopy of 2-Butene-1-yl (C4H7) between 455-485 nm.
PB95-151031 *00,670*

Mechanism and Rate Constants for the Reactions of Hydrogen Atoms with Isobutene at High Temperatures.
PB95-151064 *00,929*

Large Amplitude Skeletal Isomerization as a Promoter of Intramolecular Vibrational Relaxation in CH Stretch Excited Hydrocarbons.
PB95-202933 *01,036*

BYPASSES
Wide Band Active Current Transformer and Shunt.
PB95-126371 *02,036*

C++ (PROGRAMMING LANGUAGE)
C++ in Safety Critical Systems.
PB96-154588 *01,750*

CABLES
Classified Bibliography: Insulation Condition Monitoring Methods, 1989-1995.
PB96-131586 *02,232*

CADMIUM
NIOSH Comments to DOL on Risk Estimates from the Cadmium Cohort Study by L. Stayner, February 7, 1992.
PB95-267779 *03,604*

CAFFEIC ACID
Oxidation of Caffeic Acid and Related Hydroxycinnamic Acids.
PB97-111975 *00,651*

CALCIFICATION
Mixed Phospholipid Liposome Calcification.
PB94-211190 *03,457*

Effect of Supersaturation on Apatite Crystal Formation in Aqueous Solutions at Physiologic pH and Temperature.
PB96-135215 *03,571*

CALCIUM
RIS Studies of Autoionization in Calcium.
PB94-213295 *00,849*

High-Resolution Diode-Laser Spectroscopy of Calcium.
PB95-181244 *03,969*

n-Vector Correlations in Collision Dynamics with Atomic Orbital Alignment: The Importance of Coherence Denoting Azimuthal Structure for n (greater than or equal to) 3.
PB95-202545 *03,983*

Laser Preparation and Probing of Initial and Final Orbital Alignment in Collision-Induced Energy Transfer Ca(4s5p,(1)P1) + He yields Ca(4s5p,(3)P2) + He.
PB95-203261 *04,003*

Initial and Final Orbital Alignment Probing of the Fine-Structure-Changing Collisions among the Ca (4s)(1)(4p)(1), (3)PJ States with He: Determination of Coherence and Conventional Cross-Sections.
PB95-203279 *04,004*

Orbital Alignment and Vector Correlations in Inelastic Atomic Collisions.
PB96-122742 *04,047*

RIS Measurement of AC Stark Shifts and Photoionization Cross Sections in Calcium.
PB96-157953 *04,073*

Comment On: Two-Photon Absorption Series of Calcium.
PB96-157979 *04,074*

Configuration-Dependent AC Stark Shifts in Calcium.
PB96-157995 *04,363*

Alignment Probing of Rydberg States by Stimulated Emission.
PB96-200316 *04,124*

CALCIUM ADIPATE MONOHYDRATE
Crystal Structure of Calcium Adipate Monohydrate.
PB94-216579 *00,153*

CALCIUM BISMUTH OXIDES
Ca4Bi6O13: A Compound Containing an Unusually Low Bismuth Coordination Number and Short Bi Bi Contacts.
PB95-141131 *00,911*

CALCIUM BISMUTHATES
Phase Equilibria in the Systems CaO-CuO and CaO-Bi2O3.
PB95-140570 *03,048*

Ca4Bi6O13: A Compound Containing an Unusually Low Bismuth Coordination Number and Short Bi Bi Contacts.
PB95-141131 *00,911*

CALCIUM CITRATE
Interaction of Citric Acid with Hydroxyapatite: Surface Exchange of Ions and Precipitation of Calcium Citrate.
PB97-119309 *03,584*

CALCIUM DICARBOXYLATE
Crystal Structure of Calcium Adipate Monohydrate.
PB94-216579 *00,153*

CALCIUM GLUTARATE MONOHYDRATE
Crystal Structure of Calcium Glutarate Monohydrate.
PB96-111893 *01,074*

CALCIUM HYDROXIDES
Evolution of Porosity and Calcium Hydroxide in Laboratory Concretes Containing Silica Fume.
PB95-175063 *01,321*

CALCIUM HYDROXYAPATITE
Composition and Solubility Product of a Synthetic Calcium Hydroxyapatite.
PB96-180104 *02,995*

CALCIUM IONS
Fine Structure of Negative Ions of Alkaline-Earth-Metal Atoms.
PB94-211182 *03,837*

Analysis of Protein Metal Binding Selectivity in a Cluster Model.
PB94-212990 *00,845*

CALCIUM METABOLISM
In vitro Inhibition of Membrane-Mediated Calcification by Novel Phosphonates.
PB96-201140 *03,595*

CALCIUM OXALATE HYDRATE
Influence of Natural and Synthetic Inhibitors on the Crystallization of Calcium Oxalate Hydrates.
PB95-150967 *03,560*

CALCIUM OXIDES
Phase Equilibria in the Systems CaO-CuO and CaO-Bi2O3.
PB95-140570 *03,048*

CALCIUM PHOSPHATE
Behavior of a Calcium Phosphate Cement in Simulated Blood Plasma In vitro.
PB95-168712 *00,165*

Polymeric Calcium Phosphate Composites with Remineralization Potential.
PB96-155544 *03,575*

CALCIUM PHOSPHATE CEMENT
Reinforcement of Cancellous Bone Screws with Calcium Phosphate Cement.
PB96-158001 *00,179*

CALCIUM PHOSPHATE CEMENTS
Calcium Phosphate Cements.
PB97-111595 *03,580*

CALCIUM PHOSPHATES
Calcium Phosphate Precipitation in Liposomal Suspensions.
PB94-172145 *03,452*

Physicochemical Properties of Calcific Deposits Isolated from Porcine Bioprosthetic Heart Valves Removed from Patients Following 2-13 Years Function.
PB94-172863 *00,184*

Proteoglycan Inhibition of Calcium Phosphate Precipitation in Liposomal Suspensions.
PB94-211208 *00,658*

Selective Inhibition of Crystal Growth on Octacalcium Phosphate and Nonstoichiometric Hydroxyapatite by Pyrophosphate at Physiological Concentration.
PB94-211257 *00,147*

Periapical Tissue Reactions to a Calcium Phosphate Cement in the Teeth of Monkeys.
PB94-212008 *00,149*

Crystal Structure of Dicalcium Potassium Trihydrogen Bis(pyrophosphate) Trihydrate.
PB94-216561 *00,152*

Effects of Calcium Phosphate Solutions on Dentin Permeability.
PB95-151080 *00,157*

Effects on Whole Saliva of Chewing Gums Containing Calcium Phosphates.
PB95-153169 *03,563*

Effect of Ethanol on the Solubility of Dicalcium Phosphate Dihydrate in the System Ca(OH)2-H3PO4-H2O at 37C.
PB95-163507 *00,163*

Membrane-Mediated Precipitation of Calcium Phosphate in Model Liposomes with Matrix Vesicle-Like Lipid Composition.
PB95-164547 *03,468*

Effect of 1-Hydroxyethylidene-1,1-Bisphosphonate on Membrane-Mediated Calcium Phosphate Formation in Model Liposomal Suspensions.
PB95-169223 *03,469*

Physical and Chemical Properties of Resin-Reinforced Calcium Phosphate Cements.
PB95-180212 *00,171*

Formation of Hydroxyapatite in a Polymeric Calcium Phosphate Cement.
PB95-180642 *00,173*

Remineralization of Root Lesions with Concentrated Calcium and Phosphate Solutions.
PB96-102140 *03,567*

Properties and Mechanisms of Fast-Setting Calcium Phosphate Cements.
PB96-123229 *00,178*

Crystal Structure of Decacalcium Tetrapotassium Hexakis (Pyrophosphate) Nonahydrate.
PB96-141064 *01,099*

Bioactive Polymeric Dental Materials Based on Amorphous Calcium Phosphate.
PB96-147012 *03,572*

Remineralizing Dental Composites Based on Amorphous Calcium Phosphate.
PB96-147020 *03,573*

Dynamics of Calcium Phosphate Precipitation.
PB96-147095 *03,574*

Polymeric Calcium Phosphate Cements Derived from Poly(methyl vinyl ether-maleic acid).
PB96-164264 *00,180*

CALCIUM SILICATES
Modelling Drying Shrinkage of Cement Paste and Mortar. Part 1. Structural Models from Angstroms to Millimeters.
PB96-135132 *03,074*

CALCIUM SUCCINATE MONOHYDRATE
Crystal Structure of Calcium Succinate Monohydrate.
PB95-168928 *00,167*

CALCULABLE CAPACITORS
NIST Comparison of the Quantized Hall Resistance and the Realization of the SI Ohm Through the Calculable Capacitor.
PB97-119184 *02,291*

NIST Comparison of the Quantized Hall Resistance and the Realization of the SI Ohm Through the Calculable Capacitor. Conference Proceedings, June 17-20, 1996.
PB97-119192 *02,292*

CALCULATION METHODS
Halon Thermochemistry: 'Ab Initio' Calculations of the Enthalpies of Formation of Fluoromethanes.
PB96-175740 *03,289*

CALIBRATING
Activities of NIST (National Inst. Of Standards and Technology).
N94-23605/6 *04,222*

NIST Calibration of ASTM E127-Type Ultrasonic Reference Blocks.
PB94-191640 *02,702*

Role of the Office of Radiation Measurement in Quality Assurance.
PB94-212255 *00,689*

Journal of Research of the National Institute of Standards and Technology. May/June 1994. Volume 99, Number 3.
PB94-219326 *02,643*

Sources of Uncertainty in a DVM-Based Measurement System for a Quantized Hall Resistance Standard.
PB94-219334 *01,884*

Constant-Width Calibration Intervals for Linear Regression.
PB95-153524 *03,439*

Characterization of a Health Physics Instrument Calibration Range.
PB95-164554 *03,629*

Tilt Effects in Optical Angle Measurements.
PB95-169389 *04,294*

Field Evaluation of the System for Calibration of the Marshall Compaction Hammer.
PB95-190674 *01,323*

Gage Block Handbook.
PB95-251716 *02,667*

Advanced Mass Calibration and Measurement Assurance Program for State Calibration Laboratories.
PB95-253571 *02,492*

Radiometer Equation for Noise Comparison Radiometers.
PB96-140363 *02,195*

CALIBRATING STANDARDS
Overview of Reference Materials Prepared for Standardization of DNA Typing Procedures.
PB96-111653 *00,611*

CALIBRATION
Assessment of Uncertainties of Calibration of Resistance Thermometers at the National Institute of Standards and Technology.
PB94-142478 *02,624*

Mass Unit Disseminated to Surrogated Laboratories Using the NIST Portable Mass Calibration Package.
PB94-142486 *03,781*

Assessment of Uncertainties of Liquid-in-Glass Thermometer Calibrations at the National Institute of Standards and Technology.
PB94-142510 *02,625*

Assessment of Uncertainties of Thermocouple Calibrations at NIST.
PB94-152691 *03,782*

NIST Measurement Services: NIST Pressure Calibration Service.
PB94-164043 *02,892*

Null-Balanced Total-Power Radiometer System NCS1.
PB94-169778 *02,021*

Cryogenic Blackbody Calibrations at the National Institute of Standards and Technology Low Background Infrared Calibration Facility.
PB94-169802 *02,117*

Investigation of the Effects of Aging on the Calibration of a Kerr-Cell Measuring System for High Voltage Impulses.
PB94-172384 *02,025*

Measurement and Calibration of Large-Area Alpha-Particle Sources at NIST.
PB94-172855 *03,791*

Development and Calibration of UV/VUV Radiometric Sources.
PB94-199098 *04,229*

Update on the Low Background IR Calibration Facility at the National Institute of Standards and Technology.
PB94-211224 *04,232*

Using LORAN-C Broadcasts for Automated Frequency Calibrations.
PB94-216017 *01,526*

New Expressions of Uncertainties for Humidity Calibrations at the National Institute of Standards and Technology.
PB95-103826 *02,645*

Correction Factor for Nonplanar Incident Field in Monopole Calibrations.
PB95-108643 *02,002*

Smart Clock: A New Time.
PB95-151445 *01,530*

Calibration of GPS Equipment in Japan.
PB95-151452 *01,531*

Displacement Method for Machine Geometry Calibration.
PB95-152088 *02,946*

Automatic Calibration of Inductive Voltage Dividers for the NASA Zeno Experiment.
PB95-152849 *02,041*

Inductive Voltage Divider Calibration for the NASA Flight Experiment.
PB95-152856 *02,042*

Satellite Two-Way Time Transfer: Fundamentals and Recent Progress.
PB95-161089 *01,536*

Crystal Structure of Annealed and As-Prepared HgBa2CaCu2O6+delta Superconductors.
PB95-161105 *03,927*

Keeping Time on Your PC.
PB95-161410 *01,537*

Verification of Commercial Probe-Tip Calibrations.
PB95-161576 *02,347*

Detector-Based Candela Scale and Related Photometric Calibration Procedures at NIST.
PB95-161949 *04,273*

Stabilization and Precise Calibration of a Continuous-Wave Difference Frequency Spectrometer by Use of a Simple Transfer Cavity.
PB95-162350 *04,276*

Calibrating On-Wafer Probes to the Probe Tips.
PB95-163945 *02,352*

LRM Probe-Tip Calibrations with Imperfect Resistors and Lossy Lines.
PB95-163952 *02,353*

Verification of Scattering Parameter Measurements.
PB95-163960 *01,904*

Force Calibrations in the Nanonewton Regime.
PB95-168696 *03,949*

Optical Power Meter Calibration Using Tunable Laser Diodes.
PB95-169256 *04,290*

Self-Calibrating Fiber Optic Sensors: Potential Design Methods.
PB95-169298 *02,172*

Self Calibrating Fiber Optic Sensors: Potential Design Methods.
PB95-169306 *02,173*

Calibration of Dosimeters for the Cryogenic Irradiation of Composite Materials Using an Electron Beam.
PB95-180964 *03,968*

Control Stability of a Heat-Flow-Meter Appartus.
PB95-181194 *00,386*

Evaluation of the Economic Impacts Associated with the NIST Power and Energy Calibration Services.
PB95-188850 *02,461*

10 kV DC Resistive Divider Calibration.
PB95-198685 *02,063*

Calibration of a Superconducting Gravimeter Using Absolute Gravity Measurements.
PB95-202651 *03,684*

Time Domain Network Analysis Using the Multiline TRL Calibration.
PB95-202925 *02,065*

Geometric Characterization of Rockwell Diamond Indenters.
PB95-203287 *02,950*

Microform Calibrations in Surface Metrology.
PB95-203295 *02,951*

Energy Calibration of X-ray Photoelectron Spectrometers: Results of an Interlaboratory Comparison to Evaluate a Proposed Calibration Procedure.
PB96-102918 *04,027*

Intracomparison Tests of the FG5 Absolute Gravity Meters.
PB96-102991 *03,688*

Uncertainties of the NIST Coaxial Noise Calibration System.
PB96-111984 *02,070*

Automated Resistance Measurements at NIST.
PB96-119326 *02,274*

History of NIST's Contributions to Development of Standard Reference Materials and Reference and Definitive Methods for Clinical Chemistry.
PB96-119706 *03,503*

Noise Characteristics Below 1 Hz of Zener Diode-Based Voltage Reference.
PB96-123476 *04,049*

Long-Term Stability of Bayard-Alpert Gauge Performance: Results Obtained from Repeated Calibrations against the National Institute of Standards and Technology Primary Vacuum Standard.
PB96-123567 *02,676*

Comparison of NIST and Manufacturer Calibrations of (90)Sr+(90)Y Ophthalmic Applicators.
PB96-123708 *03,634*

Analysis of an Open-Ended Coaxial Probe with Lift-Off for Nondestructive Testing.
PB96-135116 *01,940*

Recalibration for the Final Archive of the International Ultraviolet Explorer (IUE) Satellite.
PB96-135264 *00,106*

Dosimetry Systems for Radiation Processing.
PB96-135280 *03,717*

LRM Probe-Tip Calibrations Using Nonideal Standards.
PB96-135389 *02,411*

Fiber Coating Diameter: Toward a Glass Artifact Standard.
PB96-140389 *02,234*

Dielectric Measurements on Printed-Wiring and Circuit Boards, Thin Films, and Substrates: An Overview.
PB96-147038 *02,236*

Absolute Response Calibration of a Transfer Standard Cryogenic Bolometer.
PB96-147103 *04,358*

Technical Impact of the NIST Calibration Service for Electrical Power and Energy.
PB96-147913 *02,462*

Metrology Approach to Unifying Rockwell C Hardness Scales.
PB96-155551 *02,957*

Stylus Technique for the Direct Verification of Rockwell Diamond Intenders.
PB96-155569 *02,958*

Direct Comparison Transfer of Microwave Power Sensor Calibrations.
PB96-158654 *02,086*

Development of the NIST Transient Pressure and Temperature Calibration Facility.
PB96-160833 *00,626*

Residual Error Compensation of a Vision-Based Coordinate Measuring Machine.
PB96-161617 *04,091*

NIST Measurement Assurance Program for Capacitance Standards at 1 kHz.
PB96-172333 *02,276*

Journal of Research of the National Institute of Standards and Technology, January/February 1996. Volume 101, Number 1.
PB96-175666 *00,113*

International Marine-Atmospheric (222)Rn Measurement Intercomparison in Bermuda. Part 1. NIST Calibration and Methodology for Standardized Sample Additions.
PB96-175674 *00,114*

Journal of Research of the National Institute of Standards and Technology, March/April 1996. Volume 101, Number 2.
PB96-177381 *01,863*

NIST Detector-Based Luminous Intensity Scale.
PB96-179114 *01,864*

Organization and Implementation of Calibration in the EOS Project. Part 1.
PB96-179437 *04,841*

Ultrasound Power Measurement Techniques at NIST.
PB96-179569 *02,684*

Standard Source Method for Reducing Antenna Factor Errors in Shielded Room Measurements.
PB96-183157 *02,013*

Time and Frequency Metrology.
PB96-190319 *01,556*

NIST Frequency Measurement Service.
PB96-200662 *01,561*

Self-Calibrated Intelligent Optical Sensors and Systems.
PB96-200738 *04,380*

Developing Quality System Documentation Based on ANSI/NCSL Z540-1-1994: The Optical Technology Division's Effort.
PB96-202122 *01,869*

Improving Color Measurements of Displays.
PB96-204441 *02,203*

Evaluation and Accreditation of State Calibration Laboratories.
PB97-110183 *00,486*

Electrical Test Structures Replicated in Silicon-on-Insulator Material.
PB97-111827 *02,454*

Resistors.
PB97-111876 *02,284*

Calibration in the Earth Observing System (EOS) Project. Part 2. Implementation.
PB97-112213 *04,842*

Empirical Linear Prediction Applied to a NIST Calibration Service.
PB97-112353 *02,287*

CALIBRATION LABORATORIES

Should NIST Accredit U.S. Calibration Laboratories.
PB95-107280 *02,646*

CALIBRATION STANDARDS

Improving measurement quality assurance for photon irradiations at Department of Energy facilities. Final technical report.
DE96010065 *03,711*

Recertification of the Standard Reference Material 1475A, a Linear Polyethylene Resin.
PB94-161932 *02,628*

Determination of the Weight Average Molecular Weight of Two Poly(Ethylene Oxides), SRM 1923 and SRM 1924.
PB94-217031 *01,230*

Measurement and Uncertainty of a Calibration Standard for the Scanning Electron Microscope.
PB94-219250 *00,560*

Stability/Instability of Gas Mixtures Containing 1,3-Butadiene in Treated Aluminum Gas Cylinders.
PB95-162285 *02,546*

Standard Reference Material 1744: Aluminum Freezing-Point Standard.
PB95-251732 *01,055*

Intercomparison of Photometric Units Maintained at NIST (USA) and PTB (Germany), 1993.
PB95-261913 *04,329*

Determination of the Transmittance Uniformity of Optical Filter Standard Reference Materials.
PB95-261921 *02,182*

Standard Reference Material for the Measurement of Particle Mobility by Electrophoretic Light Scattering.
PB96-102488 *00,609*

Journal of Research of the National Institute of Standards and Technology, September/October 1995. Volume 100, Number 5.
PB96-117767 *01,927*

Low Electrolytic Conductivity Standards.
PB96-122098 *01,081*

Microform Calibration Uncertainties of Rockwell Diamond Indenters.
PB96-122114 *03,280*

Performance Measures for Geometric Fitting in the NIST Algorithm Testing and Evaluation Program for Coordinate Measurement Systems.
PB96-122122 *01,745*

Development of a Standard Reference Material for Measurement of Interstitial Oxygen Concentration in Semiconductor Silicon by Infrared Absorption.
PB96-122668 *02,404*

Certification of the Standard Reference Material 1473a, a Low Density Polyethylene Resin.
PB96-128251 *01,282*

High-Speed Interconnection Characterization Using Time Domain Network Analysis.
PB96-148176 *04,061*

Liquid-Nitrogen-Cooled High Tc Electrical Substitution Radiometer as a Broadband IR Transfer Standard.
PB96-158704 *02,198*

Journal of Research of the National Institute of Standards and Technology, November/December 1995. Volume 100, Number 6.
PB96-159215 *01,949*

Calibration of Electret-Based Integral Radon Monitors Using NIST Polyethylene-Encapsulated (226)Ra/(222)Rn Emanation (PERE) Standards.
PB96-159223 *01,950*

Fabrication Issues for the Prototype National Institute of Standards and Technology SRM 2090A Scanning Electron Microscope Magnification Calibration Standard.
PB96-160585 *01,131*

Certification of Phencyclidine in Lyophilized Human Urine Reference Materials.
PB96-160692 *03,508*

Calibration Service for Coaxial Reference Standards for Microwave Power.
PB96-162722 *01,958*

Investigations of Sulfur Interferences in the Extraction of Methylmercury from Marine Tissues.
PB96-190020 *03,482*

Coaxial Line-Reflect-Match Calibration.
PB96-200118 *02,246*

How to Get NIST-Traceable Time on Your Computer.
PB96-200647 *01,559*

Introduction to Frequency Calibration. Part 1.
PB96-200654 *01,560*

Scanning Electron Microscope Magnification Calibration Interlaboratory Study.
PB96-201082 *01,164*

NIST Traceable Reference Material Program for Gas Standards: Standard Reference Materials.
PB96-210786 *00,644*

Statistical Aspects of the Certification of Chemical Batch SRMs. Standard Reference Materials.
PB96-210877 *00,645*

State Weights and Measures Laboratories: Program Handbook.
PB96-214705 *02,687*

63Ni Half-Life: A New Experimental Determination and Critical Review.
PB97-111603 *00,700*

Nickel-63 Standardization: 1968-1995.
PB97-111819 *00,701*

NIST Thermal Infrared Transfer Standard Radiometer for the Earth Observing System (EOS) Program.
PB97-113013 *04,843*

NIST Watt Experiment: Monitoring the Kilogram.
PB97-122329 *01,997*

CALIBRATIONS

Magnetometer Calibration Services.
PB97-113252 *01,993*

CALIFORNIA

Northridge Earthquake, 1994. Performance of Structures, Lifelines and Fire Protection Systems.
PB94-161114 *00,421*

CALIFORNIA TECHNICAL BULLETIN 133

Behavior of Mock-Ups in the California Technical Bulletin 133 Test Protocol: Fabric and Barrier Effects.
PB95-231585 *00,301*

CALORIFIC VALUE

Calculation of Higher Heating Values of Biomass Materials and Waste Components from Elemental Analyses.
PB94-199254 *02,474*

Assessing the Credibility of the Calorific Content of Muncipal Solid Waste.
PB94-199882 *02,581*

CALORIMETERS

Precise Measurement of Heat of Combustion with a Bomb Calorimeter.
AD-A286 701/8 *03,770*

Some Factors Affecting Design of a Furniture Calorimeter Hood and Exhaust.
PB94-139193 *00,285*

Journal of Research of the National Institute of Standards and Technology. March/April 1994. Volume 99, Number 2.
PB94-219219 *02,000*

Sealed Water Calorimeter for Measuring Absorbed Dose.
PB94-219227 03,517

Effects of Specimen Edge Conditions on Heat Release Rate.
PB95-152864 00,375

New Coaxial Microwave Microcalorimeter Evaluation Technique.
PB95-153227 01,892

Crystal Structure of Annealed and As-Prepared HgBa2CaCu2O6+delta Superconductors.
PB95-161105 03,927

High-Temperature Adiabatic Calorimeter for Constant-Volume Heat Capacity Measurements of Compressed Gases and Liquids.
PB95-168860 00,989

Hot-Electron Microcalorimeters for X-ray and Phonon Detection.
PB95-168993 04,644

Method to Determine the Calorimetric Equivalence Correction for a Coaxial Microwave Microcalorimeter.
PB95-202404 01,913

Burning Rate and Flame Heat Flux For PMMA in the Cone Calorimeter.
PB95-216990 00,393

Some Factors Affecting the Design of a Calorimeter Hood and Exhaust.
PB96-102181 00,302

NBS/NIST Peltier-Effect Microcalorimeter: A Four-Decade Review.
PB96-102769 01,064

Hot-Electron Microcalorimeters as High-Resolution X-ray Detectors.
PB96-123641 04,739

Calorimeters for Calibration of High-Dose Dosimeters in High-Energy Electron Beams.
PB96-135272 04,055

Thermal Modeling and Analysis of Laser Calorimeters.
PB96-140405 04,354

Deep-UV Excimer Laser Measurements at NIST.
PB96-141031 04,355

Examination of the Correlation between Cone Calorimeter Data and Full-Scale Furniture Mock-Up Fires.
PB96-148200 01,417

Molar Heat Capacity at Constant Volume for Air from 67 to 300 K at Pressures to 35 MPa.
PB96-163738 00,515

Molar Heat Capacity at Constant Volume for (xCO2 + (1-x)C2H6) from 220 to 340 K at Pressures to 35 MPa.
PB96-167135 01,148

Office Work Station Heat Release Rate Study: Full Scale versus Bench Scale.
PB96-190178 01,428

Hot-Electron Microcalorimeter for X-ray Detection Using a Superconducting Transition Edge Sensor with Electrothermal Feedback.
PB96-200399 04,792

Hot-Electron-Microcalorimeters with 0.25 mm(2) Area.
PB96-200670 04,793

Flammability Characterization with the Lift Apparatus and the Cone Calorimeter.
PB97-110050 01,435

Problem of Convection in the Water Absorbed Dose Calorimeter.
PB97-110159 03,523

CALORIMETRY

Equilibrium and Calorimetric Investigation of the Hydrolysis of L-Tryptophan to (Indole + Pyruvate + Ammonia).
PB95-163317 00,661

Thermodynamics of the Hydrolysis of 3,4,5-Trihydroxybenzoic Acid Propyl Ester (n-Propylgallate) to 3,4,5-Trihydroxybenzoic Acid (Gallic Acid) and Propan-I-ol in Aqueous Media and in Toluene.
PB96-186143 01,160

UV Absorption Cross Sections of Methylchloroform: Temperature-Dependent Gas and Liquid Phase Measurements.
PB96-201041 00,643

Conference Report: Calorimetry Conference (50th).
PB97-122279 03,722

CALS

Computer Graphics Metafile (CGM): Procedures for NIST CGM Validation Test Service.
PB94-161809 01,804

Initial Graphics Exchange Specification (IGES): Procedures for the NIST IGES Validation Test Service.
PB95-171427 02,780

CALS (COMPUTER-AIDED ACQUISITION AND LOGISTIC SUPPORT)

Impact of Computer-Aided Acquisition and Logistic Support (CALS) in the Application of Standards.
PB96-160908 01,756

CALS (COMPUTER-AIDED ACQUISITION AND LOGISTICS SUPPORT)

CALS-Automated Interchange of Technical Information.
PB94-962000 03,657

CALS-Digital Representation for Communication of Product Data: IGES Application Subsets.
PB94-962100 03,658

CALS-Markup Requirements and Generic Style Specifications for Electronic Printed Output and Exchange of Text.
PB94-962200 03,659

CALS-Raster Graphics Representation Binary Format Requirements.
PB94-962300 03,660

CALS-Digital Representation for Communication of Illustration Date: CGM Application Profile.
PB94-962400 03,661

CALS-Department of Defense Computer Aided Acquisition Logistic Support (CALS).
PB94-962500 03,662

CALS-Contractor Integrated Technical Information Service (CITIS), Functional Requirements.
PB94-962600 03,663

CALS (CONTINUOUS ACQUISITION AND LIFE-CYCLE SUPPORT)

CALS-Automated Interchange of Technical Information.
PB95-962000 03,666

CALS-Digital Representation for Communication of Product Data: IGES Application Subsets.
PB95-962100 03,667

CALS-Markup Requirements and Generic Style Specifications for Electronic Printed Output and Exchange of Text.
PB95-962200 03,668

CALS-Raster Graphics Representation Binary Format Requirements.
PB95-962300 03,669

CALS-Digital Representation for Communication of Illustration Date: CGM Application Profile.
PB95-962400 03,670

CALS-Department of Defense Computer Aided Acquisition Logistic Support (CALS).
PB95-962500 03,671

CALS-Contractor Integrated Technical Information Service (CITIS), Functional Requirements.
PB95-962600 03,672

CAMERA FIXATION

Reconstruction during Camera Fixation.
PB95-162236 01,593

Unified Approach to Camera Fixation and Vision-Based Road Following.
PB95-162244 01,594

CANCELLOUS BONE

Reinforcement of Cancellous Bone Screws with Calcium Phosphate Cement.
PB96-158001 00,179

CANDELA

NIST Detector-Based Luminous Intensity Scale.
PB96-179114 01,864

CANDELA SCALE

Detector-Based Candela Scale and Related Photometric Calibration Procedures at NIST.
PB95-161949 04,273

CANTILEVERS

Development of Highly Conductive Cantilevers for Atomic Force Microscopy Point Contact Measurements.
PB96-138573 04,751

CAPACITANCE

NIST Capacitance Measurement Assurance Program (MAP).
PB94-200060 02,254

Application of Single Electron Tunneling: Precision Capacitance Ratio Measurements.
PB96-102157 04,703

NIST Measurement Assurance Program for Capacitance Standards at 1 kHz.
PB96-172333 02,276

Results of Capacitance Ratio Measurements for the Single Electron Pump-Capacitor Charging Experiment.
PB97-113286 04,813

CAPACITANCE BRIDGES

Cryogenic Precision Capacitance Bridge Using a Single Electron Tunneling Electrometer.
PB95-126074 04,529

Cryogenic Precision Capacitance Bridge Using a Single Electron Tunneling Electrometer.
PB95-152310 02,040

Cryogenic Precision Capacitance Bridge Using a Single Electron Tunneling Electrometer.
PB96-112271 02,072

Database for the Static Dielectric Constant of Water and Steam.
PB96-145586 01,103

CAPACITANCE IMAGING

Scanning Capacitance Microscopy Measurements and Modeling: Progress Towards Dopant Profiling of Silicon.
PB96-180070 01,964

CAPACITOR RATIO

Proposed Tests to Evaluate the Frequency-Dependent Capacitor Ratio for Single Electron Tunneling Experiment.
PB97-111454 01,982

CAPACITORS

Development and Characterization of Insulating Layers on Silicon Carbide: Annual Report for February 14, 1988 to February 14, 1989.
PB94-155579 02,295

Capacitors with Very Low Loss: Cryogenic Vacuum-Gap Capacitors.
PB97-122600 02,293

CAPELLA STAR

Ultraviolet Observations of Stellar Coronae: Early Results from HST.
PB94-213428 00,064

Hydrogen Lyman-alpha Emission of Capella.
PB95-202263 00,075

Transition Regions of Capella.
PB96-123336 00,105

Transition Regions of Capella (1995).
PB96-176714 00,108

CAPILLARY ELECTROPHORESIS

Electrophoretic Separations of Polymerase Chain Reaction: Amplified DNA Fragments in DNA Typing Using a Capillary Electrophoresis-Lased Induced Fluorescence System.
PB95-163036 03,536

Enhanced Detection of PCR Products Through Use of TOTO and YOYO Intercalating Dyes with Laser Induced Fluorescence - Capillary Electrophoresis.
PB95-164653 00,599

CAPILLARY FLOW

Lubrication Theory for Reactive Spreading of a Thin Drop.
PB95-189460 02,865

CAPILLARY TUBES

Experimental Data and Theoretical Modeling of Gas Flows Through Metal Capillary Leaks.
PB95-150892 04,206

CARBON

Recommendations for the Disposal of Carbon-14 Wastes.
AD-A279 133/3 02,579

Ion Broadening Parameters for Several Argon and Carbon Lines.
PB94-211562 03,843

Carbon Acidities of Aromatic Compounds. 1. Effects of In-Ring Aza and External Electron-Withdrawing Groups.
PB94-216595 00,860

Microstructural Characterization of Cobalt-Tungsten Coated Graphite Fibers.
PB96-159231 01,951

CARBON 13

Two-Dimensional POMMIE Carbon-Proton Chemical Shift Correlated (13)C NMR Spectrum Editing.
PB94-200508 00,809

CARBON 14

Factorial Design Techniques Applied to Optimization of AMS Graphite Target Preparation.
PB95-151197 00,584

Radiocarbon Measurements of Atmospheric Volatile Organic Compounds: Quantifying the Biogenic Contribution.
PB97-122352 02,574

CARBON 14 TARGET

Comparative Study of Fe-C Bead and Graphite Target Performance with the National Ocean Sciences AMS (NOSAMS) Facility Recombinator Ion Source.
PB95-175790 00,693

CARBON 60

Simulation of C60 Through the Plastic Transition Temperatures.
PB96-102546 04,713

CARBON ACIDITY

Carbon Acidities of Aromatic Compounds. 1. Effects of In-Ring Aza and External Electron-Withdrawing Groups.
PB94-216595 00,860

CARBON DIOXIDE

Photoionization of Small Molecules Using Synchrotron Radiation.
PB94-211505 03,841

Modified Leung-Griffiths Model of Vapor-Liquid Equilibrium: Extended Scaling and Binary Mixtures of Dissimilar Fluids.
PB94-216108 00,851

Thermophysical Properties of CO2 and CO2-Rich Mixtures.
PB94-216199 00,854

Study of Ventilation and Carbon Dioxide in an Office Building.
PB95-150140 02,542

Measurements of the Virial Coefficients and Equation of State of the Carbon Dioxide + Ethane System in the Supercritical Region.
PB95-151353 03,906

Ventilation, Carbon Dioxide and ASHRAE Standard 62-1989.
PB95-162095 02,544

Vibronic Coupling and Other Many-Body Effects in the 4sigmag(-1) Photoionization Channel of CO2.
PB95-162509 00,962

Limits of CO2 Monitoring in Determining Ventilation Rates.
PB95-176004 02,552

Critical Lines for Type-III Aqueous Mixtures by Generalized Corresponding-States Models.
PB96-102371 01,063

Collisional Alignment of CO2 Rotational Angular Momentum States in a Supersonic Expansion.
PB96-103171 *01,069*

Few Caveats on Carbon Dioxide Monitoring.
PB96-122650 *02,562*

Solubilities of Copper(II) and Chromium(III) beta-Diketonates in Supercritical Carbon Dioxide.
PB96-164215 *01,147*

CARBON DIOXIDE COMPLEXES

Infrared Spectra of van der Waals Complexes of Importance in Planetary Atmospheres.
PB95-125738 *00,071*

Signatures of Large Amplitude Motion in a Weakly Bound Complex: High-Resolution IR Spectroscopy and Quantum Calculations for HeCO2.
PB95-203485 *01,054*

CARBON DIOXIDE LASERS

Efficient Br(*) Laser Pumped by Frequency-Doubled Nd: YAG and Electronic-to-Vibrational Transfer-Pumped CO2 and HCN Lasers.
PB95-108684 *04,248*

New cw CO2 Laser Lines: The 9-mu m Hot Band.
PB95-168548 *04,281*

Improved Molecular Constants and Frequencies for the CO2 Laser from New High-J Regular and Hot-Band Frequency Measurements.
PB95-180634 *04,312*

CARBON FLUORIDES

Charge Transfer and Collision-Induced Dissociation Reactions of CF(2+) and CF2(2+) with the Rare Gases at a Laboratory Collision Energy of 49 eV.
PB94-185584 *00,775*

Collision-Induced Neutral Loss Reactions of Molecular Dications.
PB94-185808 *00,780*

CARBON ISOTOPES

New IUPAC Guidelines for the Reporting of Stable Hydrogen, Carbon, and Oxygen Isotope-Ratio Data. Letter to the Editor.
PB95-261962 *01,058*

CARBON-LIKE IONS

Atomic Branching Ratio Data for Carbon-Like Ions.
PB94-212842 *03,855*

CARBON MONOXIDE

Vibrational Spectra of Molecular Ions Isolated in Solid Neon. 7. CO(+), C2O2(+), and C2O2(-). (Reannouncement with New Availability Information).
AD-A239 729/7 *00,706*

Compilation of the Physical Equilibria and Related Properties of the Hydrogen-Carbon Monoxide System.
AD-A286 603/6 *00,716*

Hot Carrier Excitation of Adlayers: Time-Resolved Measurement of Adsorbate-Lattice Coupling.
PB94-172285 *00,758*

Photodecomposition Dynamics of Mo(CO)6/Si(111) 7x7: CO Internal State and Translational Energy Distributions--Translation.
PB94-199288 *00,687*

Time-Resolved Probes of Surface Dynamics.
PB94-199957 *00,803*

Global Equivalence Ratio Concept and the Prediction of Carbon Monoxide Formation in Enclosure Fires.
PB94-207511 *00,313*

Photoionization of Small Molecules Using Synchrotron Radiation.
PB94-211505 *03,841*

Vibrational Relaxation Measurements of Carbon Monoxide on Metal Clusters.
PB94-211810 *00,820*

Laser-Induced Fluorescence Measurements of Rotationally Resolved Velocity Distributions for CO(+) Drifted in He.
PB94-213139 *00,848*

Measurement of CO Pressures in the Ultrahigh Vacuum Regime Using Resonance-Enhanced Multiphoton-Ionization Time-of-Flight Mass Spectroscopy.
PB94-216041 *03,864*

Picosecond Measurement of Substrate-to-Adsorbate Energy Transfer: The Frustrated Translation of CO/Pt(111)--Translation.
PB95-126041 *00,895*

Fundamental Mechanisms for CO and Soot Formation.
PB95-143160 *01,380*

Oxidation of Soot and Carbon Monoxide in Hydrocarbon Diffusion Flames.
PB95-150215 *01,382*

Optical Measurements of Atomic Hydrogen, Hydroxyl, and Carbon Monoxide in Hydrocarbon Diffusion Flames.
PB95-150900 *02,487*

Rotational Far Infrared Spectrum of (13)CO.
PB95-152187 *00,941*

Laser Spectroscopy of Carbon Monoxide: A Frequency Reference for the Far Infrared.
PB95-163606 *04,277*

Laser Flash Photolysis/Time-Resolved FTIR Emission Study of a New Channel in the Reaction of CH3+O: Production of CO(v).
PB95-164281 *00,974*

Shape-Resonance-Enhanced Continuum-Continuum Coupling in Photoionization of CO2.
PB95-164471 *00,983*

Inner-Valence States CO(+) between 22 eV and 46 eV Studied by High Resolution Photoelectron Spectroscopy and ab Initio CI Calculations.
PB95-180055 *03,961*

Slow-Electron Collisions with CO Molecules in an Exact-Exchange Plus Parameter-Free Polarization Model.
PB95-202719 *03,989*

Carbon Monoxide Production in Compartment Fires: Reduced-Scale Enclosure Test Facility.
PB95-231700 *01,394*

Photodesorption Dynamics of CO from Si(111): The Role of Surface Defects.
PB96-111646 *03,066*

Relationship between Indoor Air Quality and Carbon Dioxide.
PB97-111249 *02,569*

Carbon Monoxide Dispersion in Residential Buildings: Literature Review and Technical Analysis.
PB97-114227 *02,571*

CARBON OXYSULFIDE

Extension of Heterodyne Frequency Measurements on OCS to 87 THz (2900 cm(-1)).
PB94-200680 *00,811*

Sub-Doppler Frequency Measurements on OCS at 87 Thz (3.4 micrometers) with the CO Overtone Laser: Considerations and Details.
PB95-128633 *04,255*

CARBON STEELS

Comparison of the Corrosion Rates of FeAl, Fe(sub 3)Al and Steel in Distilled Water and 0.5 M Sodium Chloride. Technical Report Number 2, January--March 1991.
DE94017332 *03,186*

Characterization of the Hydrogen Induced Cold Cracking Susceptibility at Simulated Weld Zones in HSLA-100 Steel.
PB94-174505 *03,746*

Langevin Approach to Hysteresis and Barkhausen Modeling in Steel.
PB94-185675 *03,206*

CARBONACEOUS MATERIALS

Sources of Urban Contemporary Carbon Aerosol.
PB95-175659 *02,551*

CARBONATE RADICALS

Electron Transfer Reaction Rates and Equilibria of the Carbonate and Sulfate Radical Anions.
PB94-212180 *00,829*

Temperature Dependence of the Rate Constants for Reactions of the Carbonate Radical with Organic and Inorganic Reductants.
PB94-212206 *00,831*

CARBONATES

Temperature Dependence of the Rate Constants for Reactions of the Carbonate Radical with Organic and Inorganic Reductants.
PB94-212206 *00,831*

CARBONIC ANHYDRASE

Active Site Ionicity and the Mechanism of Carbonic Anhydrase.
PB94-212974 *00,843*

CARBONYL COMPOUNDS

Sub-Doppler Frequency Measurements on OCS at 87 THz (3.4 mu m) with the CO Overtone Laser.
PB96-102215 *04,330*

CARBONYL SULFIDE

Extension of Heterodyne Frequency Measurements on OCS to 87 THz (2900 cm(-1)).
PB94-200680 *00,811*

Sub-Doppler Frequency Measurements on OCS at 87 Thz (3.4 micrometers) with the CO Overtone Laser: Considerations and Details.
PB95-128633 *04,255*

CARCINOGENESIS

Novel Activity of E. coli uracil DNA N-glycosylase Excision of Isodialuric Acid (5,6-dihydroxyuracil), a Major Product of Oxidative DNA Damage, from DNA.
PB96-110747 *03,543*

CARCINOGENS

DNA Base Modifications in Renal Chromatin of Wistar Rats Treated with a Renal Carcinogen, Ferric Nitrilotriacetate.
PB95-150363 *03,648*

Treatment of Wistar Rats with a Renal Carcinogen, Ferric Nitrilotriacetate, Causes DNA-Protein Cross-Linking between Thymine and Tyrosine in Their Renal Chromatin.
PB96-112115 *03,649*

CAREER DEVELOPMENT

Robotics Application to Highway Transportation. Volume 1. Final Report.
PB95-203790 *03,654*

CAROTENE

Development of Engineered Stationary Phases for the Separation of Carotenoid Isomers.
PB95-150249 *00,578*

Isolation and Structural Elucidation of the Predominant Geometrical Isomers of alpha-Carotene.
PB96-190061 *00,640*

CAROTENOIDS

Carotenoid Reversed-Phase High-Performance Liquid Chromatography Methods: Reference Compendium.
PB94-200516 *00,549*

Individual Carotenoid Content of SRM 1548 Total Diet and Influence of Storage Temperature, Lyophilization, and Irradiation on Dietary Carotenoids.
PB94-200524 *00,033*

Liquid Chromatographic Method for the Determination of Carotenoids, Retinoids, and Tocopherols in Human Serum and in Food.
PB95-153599 *00,593*

Population Distributions and Intralaboratory Reproducibility for Fat-Soluble Vitamin-Related Compounds in Human Serum.
PB96-155536 *00,624*

CARPETS

National Voluntary Laboratory Accreditation Program: Carpet and Carpet Cushion.
PB95-155560 *00,295*

CARQUINEZ STRAIT

Histopathology, Blood Chemistry, and Physiological Status of Normal and Moribund Striped Bass ('Morone saxatilis') Involved in Summer Mortality ('Die-Off') in the Sacramento-San Joaquin Delta of California.
PB94-198157 *00,034*

CARRIER DENSITY

Multicarrier Characterization Method for Extracting Mobilities and Carrier Densities of Semiconductors from Variable Magnetic Field Measurements.
PB94-212776 *02,317*

Transverse Magnetoresistance: A Novel Two-Terminal Method for Measuring the Carrier Density and Mobility of a Semiconductor Layer.
PB95-150066 *02,332*

CARRIER MOBILITY

Multicarrier Characterization Method for Extracting Mobilities and Carrier Densities of Semiconductors from Variable Magnetic Field Measurements.
PB94-212776 *02,317*

Transverse Magnetoresistance: A Novel Two-Terminal Method for Measuring the Carrier Density and Mobility of a Semiconductor Layer.
PB95-150066 *02,332*

CARRIERS

Model for Determining the Density and Mobility of Carriers in Thin Semiconducting Layers with Only Two Contacts.
PB96-102702 *02,378*

CARTRIDGES (EXPLOSIVES)

Specification for Interoperability between Ballistic Imaging Systems. Part 1. Cartridge Cases.
PB96-195524 *01,860*

CARVON MONOXIDE

Chemical Stability of Upper-Layer Fire Gases.
PB96-123385 *01,410*

CAS (COMPUTER ALGEBRA SYSTEM)

Expression Formatter for MACSYMA.
PB95-267829 *01,735*

CASCADED ELEMENTS

Coordinating Cascaded Surge Protection Devices: High-Low versus Low-High.
PB94-172061 *02,463*

Cascading Surge-Protective Devices: Options for Effective Implementation.
PB94-216488 *02,464*

Coordinating Cascaded Surge-Protective Devices: An Elusive Goal.
PB94-216496 *02,465*

CASE-BASED REASONING

Using a Multi-Layered Approach to Representing Tort Law Cases for Case-Based Reasoning.
PB96-160874 *00,135*

CASE DATA INTERCHANGE FORMAT

Mapping Integration Definition for Information Modeling (IDEF1X) Model into CASE Data Interchange Format (CDIF) Transfer File.
PB95-154670 *01,711*

Mapping Integration Definition for Function Modeling (IDEFO) Model into CASE Data Interchange Format (CDIF) Transfer File.
PB96-109533 *01,741*

CAST IRON

Cast-Iron Elastic Constants: Effect of Graphite Aspect Ratio.
PB94-213212 *03,211*

CAST STEEL RAILROAD WHEELS

Ultrasonic Measurement of Residual Stress in Cast Steel Railroad Wheels.
PB95-169199 *04,852*

CATALOGS (DOCUMENTATION)

NIST Serial Holdings, 1994.
PB94-178068 *02,745*

NIST Serial Holdings, 1995.
PB95-188926 *02,746*

CATALOGS (PUBLICATIONS)

NIST Standard Reference Data Products Catalog, 1994.
PB94-151842 *00,727*

Condensed Catalogue of Electromagnetic Environment Measurements, 30 - 300 Hz.
PB95-162210 *01,899*

Publications of the National Institute of Standards and Technology 1992 Catalog.
PB95-200747 *00,014*

NIST Standard Reference Materials (Trade Name) Catalog 1995-1996.
PB95-232518 *00,508*

NIST Standard Reference Data Products Catalog, 1995-96. Achieve with Standard Reference Data.
PB95-260808 *01,057*

Publications of the National Institute of Standards and Technology 1993 Catalog.
PB96-183215 *00,017*

CATALYSTS

Changes in the Redox State of Iridium Oxide Clusters and Their Relation to Catalytic Water Oxidation: Radiolytic and Electrochemical Studies.
PB95-107017 *00,864*

CATALYTIC CRACKING

Process Gas Chromatography Detector for Hydrocarbons Based on Catalytic Cracking.
PB95-141099 *02,485*

CATHODE RAY TUBE SCREENS

Display-Measurement Round-Robin.
PB96-119227 *02,186*

CATHODE RAY TUBES

Improving Color Measurements of Displays.
PB96-204441 *02,203*

CATHODIC DISBONDMENT MODEL

Non-Osmotic, Defect-Controlled Cathodic Disbondment of a Coating from a Steel Substrate.
PB94-216447 *03,120*

CATIONS

Vibrational Spectra of Molecular Ions Isolated in Solid Neon. 11. NO2(+), NO2(-), and NO3(-).
AD-A275 828/2 *00,708*

Tetrahedral-Framework Lithium Zinc Phosphate Phases: Location of Light-Atom Positions in LiZnPO4 H2O by Powder Neutron Diffraction and Structure Determination of LiZnPO4 by ab Initio Methods.
PB96-160510 *01,129*

CAUSALITY

Causality and Maxwell's Equations.
PB97-110522 *04,429*

CAVITATION

Cavitation Damage During Flexural Creep of SiAlON-YAG Ceramics.
PB94-200110 *03,036*

Cavitation Contributes Substantially to Tensile Creep in Silicon Nitride.
PB96-122577 *03,171*

Tension/Compression Creep Asymmetry in Si3N4.
PB97-110258 *03,096*

CAVITIES

Dimensional Characterization of Small Bores: A Survey.
PB95-162202 *02,651*

Aperture Excitation of Electrically Large, Lossy Cavities.
PB95-175675 *00,031*

Cavity Evolution during Tensil Creep of Si3N4.
PB96-204193 *03,376*

CAVITY LINERS

Texture Study of Two Molybdenum Shaped Charge Liners by Neutron Diffraction.
PB94-200177 *03,754*

Microstructure Study of Molybdenum Liners by Neutron Diffraction.
PB95-202396 *03,756*

CAVITY Q

Aperture Excitation of Electrically Large, Lossy Cavities.
PB94-145711 *00,029*

CAVITY RESONATORS

NIST 60-Millimeter Diameter Cylindrical Cavity Resonator: Performance Evaluation for Permittivity Measurements.
PB94-151776 *02,251*

Dielectric Studies of Fluids with Reentrant Resonators.
PB95-153730 *00,952*

CAVITY RINGDOWN

Laser Bandwidth Effects in Quantitative Cavity Ring-Down Spectroscopy.
PB97-112254 *04,394*

CDIF (CASE DATA INTERCHANGE FORMAT)

Mapping Integration Definition for Information Modeling (IDEF1X) Model into CASE Data Interchange Format (CDIF) Transfer File.
PB95-154670 *01,711*

Mapping Integration Definition for Function Modeling (IDEFO) Model into CASE Data Interchange Format (CDIF) Transfer File.
PB96-109533 *01,741*

CEILING JETS

Prediction of Fire Dynamics.
PB94-193620 *00,336*

CEILINGS

Comparison of Wall-Fire Behavior With and Without a Ceiling.
PB94-207404 *00,342*

Field Modeling: Simulating the Effect of Sloped Beamed Ceilings on Detector and Sprinkler Response.
PB96-122866 *01,406*

State of the Art Report on Seismic Design Requirements for Nonstructural Building Components.
PB96-193800 *00,308*

CEILINGS (ARCHITECTURE)

Fire-Plume-Generated Ceiling Jet Characteristics and Convective Heat Transfer to Ceiling and Wall Surfaces in a Two-Layer Fire Environment: Uniform Temperature Ceiling and Walls.
PB95-164711 *00,382*

Algorithm to Describe the Spread of a Wall Fire under a Ceiling.
PB95-182259 *00,261*

CELL DAMAGE

Microdosimetry and Cellular Radiation Effects of Radon Progency in Human Bronchial Airways.
PB95-152344 *03,625*

Radon in the Lung.
PB97-110035 *03,638*

CELL MASS

In situ Fluorescence Cell Mass Measurements of 'Saccharomyces cerevisiae' Using Cellular Tryptophan.
PB96-135041 *03,547*

CELL MEMBRANE

Electropermeabilization of Cell Membranes: Effect of the Resting Membrane Potential.
PB95-163291 *03,537*

CELL MOVEMENT

Gravity Dependent Processes and Intracellular Motion.
PB95-163382 *03,538*

CELLS

Gaseous Electronics Conference RF Reference Cell: An Introduction.
PB96-113329 *02,387*

Current and Voltage Measurements in the Gaseous Electronics Conference RF Reference Cell.
PB96-113337 *02,388*

Optical Emission Spectroscopy on the Gaseous Electronics Conference RF Reference Cell.
PB96-113345 *02,389*

Optical Diagnostics in the Gaseous Electronics Conference Reference Cell.
PB96-113352 *02,390*

Studies of Ion Kinetic-Energy Distributions in the Gaseous Electronics Conference RF Reference Cell.
PB96-113360 *02,391*

Microwave Diagnostic Results from the Gaseous Electronics Conference RF Reference Cell.
PB96-113378 *02,392*

Langmuir Probe Measurements in the Gaseous Electronics Conference RF Reference Cell.
PB96-113386 *02,393*

Inductively Coupled Plasma Source for the Gaseous Electronics Conference RF Reference Cell.
PB96-113394 *02,394*

Reactive Ion Etching in the Gaseous Electronics Conference RF Reference Cell.
PB96-113402 *02,395*

Dusty Plasma Studies in the Gaseous Electronics Conference Reference Cell.
PB96-113410 *02,396*

One-Dimensional Modeling Studies of the Gaseous Electronics Conference RF Reference Cell.
PB96-113428 *02,397*

Two-Dimensional Self-Consistent Radio Frequency Plasma Simulations Relevant to the Gaseous Electronics Conference RF Reference Cell.
PB96-113436 *02,398*

CELLS (BIOLOGY)

Gravity Dependent Processes and Intracellular Motion.
PB95-163382 *03,538*

Fluorescence Measurements of Tetracycline in High Cell Mass for Fermentation Monitoring.
PB95-175709 *00,601*

Repair of Products of Oxidative DNA Base Damage in Human Cells.
PB96-190129 *03,555*

CELLULOSE

Behavior of Charring Materials in Simulated Fire Environments.
PB94-196045 *01,368*

Transition from Localized Ignition to Flame Spread Over a Thin Cellulosic Material in Microgravity.
PB96-155809 *04,835*

Ignition and Subsequent Flame Spread Over a Thin Cellulosic Material.
PB96-160270 *04,836*

Ignition and Transition to Flame Spread Over a Thermally Thin Cellulosic Sheet in a Microgravity Environment.
PB96-160288 *04,837*

CELLULOSE TRIACETATE

Solid State (13)C NMR and Raman Studies of Cellulose Triacetate: Oligomers, Polymorphism, and Inferences about Chain Polarity.
PB96-176532 *01,289*

CELP (CODE EXCITED LINEAR PREDICTION)

Channel Coding for Code Excited Linear Prediction (CELP) Encoded Speech in Mobile Radio Applications.
PB95-143178 *01,475*

CEMENT

Cellular Automaton Simulations of Cement Hydration and Microstructure Development.
PB95-175055 *01,320*

CEMENT PASTES

Serial Sectioning of Hardened Cement Paste for Scanning Electron Microscopy.
PB94-172640 *01,305*

CEMENT SYSTEMS

Formation of Hydroxyapatite in Cement Systems.
PB95-175261 *00,170*

CEMENTS

Digitized Simulation of Mercury Intrusion Porosimetry.
PB94-172236 *01,304*

Serial Sectioning of Hardened Cement Paste for Scanning Electron Microscopy.
PB94-172640 *01,305*

Quantitative Phase Abundance Analysis of Three Cement Clinker Reference Materials by Scanning Electron Microscopy.
PB94-173051 *00,333*

Expansion of Cementitious Materials Exposed to Sulfate Solutions.
PB94-185782 *02,577*

Sulfate Attack of Cementitious Materials: Volumetric Relations and Expansions.
PB94-187317 *03,232*

Digitized Direct Simulation Model of the Microstructural Development of Cement Paste.
PB94-198777 *01,309*

Digitized Simulation Model for Microstructural Development.
PB94-198785 *01,310*

Modelling the Leaching of Calcium Hydroxide from Cement Paste: Effects on Pore Space Percolation and Diffusivity.
PB94-198793 *01,311*

Diffusion Studies in a Digital-Image-Based Cement Paste Microstructural Model.
PB94-198801 *01,312*

Survey of Recent Cementitious Materials Research in Western Europe.
PB94-218583 *00,353*

Fundamental Computer Simulation Models for Cement-Based Materials.
PB95-126009 *00,364*

Rheology of Fresh Cement Paste.
PB95-163150 *00,378*

Unreacted Cement Content in Macro-Defect-Free Composites: Impact on Processing-Structure-Property Relations.
PB96-141270 *03,174*

Application of Digital-Image-Based Models to Microstructure, Transport Properties, and Degradation of Cement-Based Materials.
PB96-156161 *00,406*

Calcium Phosphate Cements.
PB97-111595 *03,580*

CENSUS TRACTS

Guideline: Codes for Named Populated Places, Primary County Divisions, and Other Locational Entities of the United States, Puerto Rico, and the Outlying Areas. Category: Data Standards and Guidelines. Subcategory: Representations and Codes.
FIPS PUB 55-3 *04,865*

Guideline: Codes for Named Populatd Places, Primary County Divisions, and Other Locational Entities of the United States, Puerto Rico, and the Outlying Areas. Category: Data Standards and Guidelines; Subcategory: Representation and Codes.
FIPS PUB 55-DC3 *04,866*

CENTER FOR HIGH INTEGRITY SOFTWARE SYSTEM ASSURANCE

Center for High Integrity Software System Assurance: Initial Goals and Activities.
PB95-251674 *01,734*

CENTRIFUGAL PUMPS

Evaluation of GSA Maintenance Practices of Large Centrifugal Chillers and Review of GSA Refrigerant Management Practices.
PB94-143344 *02,502*

CERAMIC COATINGS

Modified Surface Layers and Coatings.
PB95-176087 *03,125*

Ultrasonic NDE of Sprayed Ceramic Coatings.
PB96-201157 *02,761*

CERAMIC COMPOSITES

Coating of Fibers by Colloidal Techniques in Ceramic Composites.
PB94-216256 *03,196*

Determination of Fiber-Matrix Interfacial Properties of Importance to Ceramic Composite Toughening.
PB95-125811 *03,149*

Fabrication of Flaw-Tolerant Aluminum-Titanate-Reinforced Alumina.
PB95-162533 *03,161*

Diffusive Crack Growth at a Bimaterial Interface.
PB96-204110 *03,090*

CERAMIC FIBERS

Wear Mechanism Maps of Ceramics.
PB94-172368 *03,229*

Coating of Fibers by Colloidal Techniques in Ceramic Composites.
PB94-216256 *03,196*

Calculation of the Thermal Conductivity and Gas Permeability in a Uniaxial Bundle of Fibers.
PB95-180931 *03,058*

CERAMIC MATERIALS

Small-Angle Neutron Scattering Characterization of Processing/Microstructure Relationships in the Sintering of Crystalline and Glassy Ceramics. (Reannouncement with New Availability Information).
AD-A249 510/9 *03,025*

Standard Materials. A Descriptive List with Prices.
AD-A278 140/9 *00,500*

Environmentally Enhanced Fracture of Ceramics.
PB95-125746 *03,046*

Tensile Creep of a Silicon Nitride Ceramic.
PB95-161303 *03,049*

Damage Processes in Ceramics Resulting from Diamond Tool Indentation and Scratching in Various Environments.
PB96-102983 *03,065*

Fracture Mechanism Maps: Their Applicability to Silicon Nitride.
PB96-204532 *03,094*

CERAMIC MATRIX COMPOSITES

High Temperature Degradation of Structural Composites.
PB94-172848 *03,132*

Matrix Grain Bridging Contribution to the Toughness of Whisker Reinforced Ceramics.
PB94-198645 *03,134*

Interface Properties for Ceramic Composites from a Single Fiber Pull-Out Test.
PB94-199361 *03,135*

Micro-Mechanical Aspects of Asperity-Controlled Friction in Fiber-Toughened Ceramic Composites.
PB94-199536 *03,136*

Generic Model for Creep Rupture Lifetime Estimation on Fibrous Ceramic Composites.
PB94-200235 *03,137*

Assessment of Testing Methodology for Ceramic Matrix Composites.
PB94-200532 *03,139*

Effect of Microstructure on the Wear Transition of Zirconia-Toughened Alumina.
PB94-211778 *03,141*

Creep Rupture of MoSi2/SiCp Composites.
PB95-152294 *03,154*

Fracture Toughness of Advanced Ceramics at Room Temperature: A Vamas Round-Robin.
PB95-162194 *03,160*

Creep and Creep Rupture of Ceramic Matrix Composites.
PB95-163929 *03,165*

Fracture of Silicon Nitride and Silicon Carbide at Elevated Temperatures.
PB96-180260 *03,179*

CERAMIC POWDER

Variances in the Measurement of Ceramic Powder Properties.
PB97-110316 *03,100*

CERAMIC SLURRIES

NMR Characterization of Injection-Moulded Alumina Green Compacts. Part 2. T2-Weighted Proton Imaging.
PB96-201181 *01,165*

CERAMICS

Classification of Advanced Technical Ceramics.
N94-35335/6 *03,030*

Ceramics Technical Activities, 1993 (NAS-NRC Assessment Panel April 21-22, 1994).
PB94-162591 *03,031*

Fracture Mechanics Analysis of Near-Surface Cracks.
PB94-172400 *03,230*

Error Propagation Biases in the Calculation of Indentation Fracture Toughness for Ceramics.
PB94-172434 *03,032*

Cavitation Damage During Flexural Creep of SiAlON-YAG Ceramics.
PB94-200110 *03,036*

Transient Subcritical Crack-Growth Behavior in Transformation-Toughened Ceramics.
PB94-200656 *03,038*

Observed and Theoretical Creep Rates for an Alumina Ceramic and a Silicon Nitride Ceramic in Flexure.
PB94-212958 *03,040*

Control of Friction and Wear of Alpha-Alumina with a Composite Solid-Lubricant Coating.
PB95-125969 *03,225*

New Materials, Advanced Ceramics and Standards.
PB95-140208 *03,047*

Modeling Ceramic Sub-Micron Particle Formation from the Vapor Using Detailed Chemical Kinetics: Comparison with In-situ Laser Diagnostics.
PB95-151965 *00,671*

Multiphoton Ionization Spectroscopy Measurements of Silicon Atoms during Vapor Phase Synthesis of Ceramic Particles.
PB95-151999 *03,913*

Simulation of Ceramic Particle Formation: Comparison with In-situ Measurements.
PB95-152013 *00,674*

Analysis of Physical Properties of Ceramic Powders in an International Interlaboratory Comparison Program.
PB95-161501 *03,050*

Wear of Human Enamel against a Commercial Castable Ceramic Restorative Material.
PB95-161972 *00,161*

Recent VAMAS Activity in Ceramics.
PB95-162681 *03,051*

Measuring Contact Charge Transfer at Interfaces: A New Experimental Technique.
PB95-164570 *03,053*

Polyelectrolytes as Dispersants in Colloidal Processing of Silicon Nitride Ceramics.
PB95-175568 *03,055*

Evaluation of Wear Resistant Ceramic Valve Seats in Gas-Fueled Power Generation Engines. Topical Report, December 1991-April 1994.
PB95-200218 *02,466*

Structural Ceramics Database. Topical Report, June 1989-May 1991.
PB95-203758 *03,060*

Room-Temperature Flexure Fixture for Advanced Ceramics.
PB95-210498 *03,061*

Boundary Lubrication of Silicon Nitride.
PB95-213583 *03,226*

Evaluation of Thermal Wave Imaging for Detection of Machining Damage in Ceramics.
PB95-220547 *03,062*

Ceramic Powders Characterization: Results of an International Laboratory Study.
PB95-270039 *02,672*

Electroacoustic Characterization of Particle Size and Zeta Potential in Moderately Concentrated Suspensions.
PB96-119425 *01,079*

Chemically Assisted Machining of Si3N4.
PB96-122999 *03,072*

High-Temperature Furnace for In situ Small-Angle Neutron Scattering during Ceramic Processing.
PB96-148127 *03,743*

NIST Metrology Program on Electromagnetic Characterization of Materials.
PB96-156062 *01,944*

Model for Microcrack Initiation and Propagation beneath Hertzian Contacts in Polycrystalline Ceramics.
PB96-163704 *03,077*

Preparation and Crystal Structure of Sr5TiNb4O17.
PB96-167341 *04,107*

Reference Relations for the Evaluation of the Materials Properties of Orthorhombic YBa2Cu3Ox Superconductors.
PB96-176763 *04,782*

Indentation Fatigue: A Simple Cyclic Hertzian Test for Measuring Damage Accumulation in Polycrystalline Ceramics.
PB96-180013 *03,084*

Transient Creep Behaviour of Hot Isostatically Pressed Silicon Nitride.
PB96-180278 *03,086*

Ceramics Technical Activities, 1995.
PB96-193677 *03,087*

Need for Advanced Characterization Techniques in Product Manufacturing: A Case Study on Ceramic Matrix Composites.
PB96-204060 *03,089*

Life Prediction of a Continuous Fiber Reinforced Ceramic Composite Under Creep Conditions.
PB96-204128 *03,091*

Creep and Creep Rupture of Structural Ceramics.
PB96-204524 *03,093*

Flaw-Insensitive Ceramics.
PB97-110027 *03,095*

Characterizing Materials Properties for Ceramic Matrix Composites.
PB97-110282 *03,097*

Database Development and Management (Project A.2.2): The Annual Report for 1992-1993.
PB97-110290 *03,098*

Role of Corrosion in a Material Selector Expert System for Advanced Structural Ceramics.
PB97-110308 *03,099*

Postfailure Subsidiary Cracking from Indentation Flaws in Brittle Materials.
PB97-110340 *03,103*

High Temperature Structural Reliability of Silicon Nitride.
PB97-110456 *03,104*

Tensile Creep Testing of Structural Ceramics.
PB97-110464 *03,105*

Surface Roughness of Glass-Ceramic Insert. Composite Restorations: Assessing Several Polishing Techniques.
PB97-119010 *03,583*

Nanoindentation and Instrumented Scratching Measurements on Hard Coatings.
PB97-122477 *03,111*

Wear Modeling of Si-Based Ceramics.
PB97-122501 *03,112*

Chemical Effect in Ceramics Grinding.
PB97-122592 *03,113*

CERTAINTY GRID TO OBJECT BOUNDARY

Certainty Grid to Object Boundary Algorithm.
PB94-203510 *01,835*

CERTIFICATION

National Center for Standards and Certification Information: Service and Programs.
N95-15938/0 *02,717*

Recertification of the Standard Reference Material 1475A, a Linear Polyethylene Resin.
PB94-161932 *02,628*

National Voluntary Laboratory Accreditation Program: Bulk Asbestos Analysis.
PB95-138129 *02,541*

National Voluntary Laboratory Accreditation Program: Construction Materials Testing.
PB95-155552 *01,319*

National Voluntary Laboratory Accreditation Program: Carpet and Carpet Cushion.
PB95-155560 *00,295*

Standard Reference Materials for the Determination of Trace Organic Constituents in Environmental Samples.
PB95-164026 *02,522*

National Voluntary Laboratory Accreditation Program (NVLAP): Wood Based Products.
PB95-170429 *03,405*

National Voluntary Laboratory Accreditation Program: Electromagnetic Compatibility and Telecommunications. FCC Methods.
PB95-242376 *02,664*

Electrical Product Requirements (Especially Quality Requirements) in the United States.
PB96-119235 *01,929*

Certification of the Standard Reference Material 1473a, a Low Density Polyethylene Resin.
PB96-128251 *01,282*

U.S. Government Accreditation and Conformity Assessment System Evaluation.
PB96-160239 *02,678*

Statistical Aspects of the Certification of Chemical Batch SRMs. Standard Reference Materials.
PB96-210877 *00,645*

CERTIFICATION PROGRAMS

Proposed Changes to Charpy V-Notch Machine Certification Requirements.
PB96-135363 *02,955*

CERTIFIED REFERENCE MATERIAL

What Is a 'Standard Reference Material' - What Is Any Reference Material.
PB96-186135 *03,000*

CERTIFIED REFERENCE MATERIALS

Comparison of Methods for Gas Chromatographic Determination of PCBs and Chlorinated Pesticides in Marine Reference Materials.
PB95-140091 *02,584*

Role of Certified Reference Materials in Trace Analysis Quality Assurance.
PB97-110019 *00,650*

CESIUM

Low-Energy Electron Scattering from Caesium Atoms: Comparison of a Semirelativistic Breit-Pauli and a Full Relativistic Direc Treatment.
PB94-185030 *00,769*

Characteristics of Light Emission After Low-Energy Electron Impact Excitation of Caesium Atoms.
PB94-198587 *03,806*

Cs Cluster Binding to a GaAs Surface.
PB94-213006 *00,846*

Relativistic Effects in Spin-Polarization Parameters for Low-Energy Electron-Cs Scattering.
PB95-150868 *03,901*

Optical Probing of Cold Trapped Atoms.
PB95-175469 *04,296*

Angle-Differential and Momentum-Transfer Cross Sections for Low-Energy Electron-Cs Scattering.
PB95-203402 *04,005*

Relativistic R-Matrix Calculations for Electron - Alkali-Metal-Atom Scattering: Cs as a Test Case.
PB95-203410 *04,006*

Precision Lifetime Measurements of Cs 6p (2)P1/2 and 6p (2)P3/2 Levels by Single-Photon Counting.
PB95-203816 *04,010*

CESIUM 137

Protection Against Radiations from Radium, Cobalt-60, and Cesium-137.
AD-A279 261/2 *03,607*

Estimation of the Absorbed Dose in Radiation-Processed Food. 1. Test of the EPR Response Function by a Linear Regression Analysis.
PB94-199718 *00,039*

CESIUM FREQUENCY STANDARDS

NIST Optically Pumped Cesium Frequency Standard.
PB94-211117 *03,835*

NIST-7, the New US Primary Frequency Standard.
PB95-153458 *01,534*

Microwave Leakage as a Source of Frequency Error and Long-Term Instability in Cesium Atomic-Beam Frequency Standards.
PB95-180501 *01,541*

Velocity Distribution of Atomic Beams by Gated Optical Pumping.
PB95-180519 *01,542*

Hybrid Digital/Analog Servo for the NIST-7 Frequency Standard.
PB95-180618 *01,544*

CF3I

Temperature Dependence of the Ultraviolet Absorption Cross Section of CF3I.
PB96-204169 *01,168*

CGOB (CERTAINTY GRID TO OBJECT BOUNDARY)

Certainty Grid to Object Boundary Algorithm.
PB94-203510 *01,835*

CHAIN MOLECULES

Principle of Congruence and Its Application to Compressible States.
PB96-102892 *01,068*

CHAIN POLARITY

Solid State (13)C NMR and Raman Studies of Cellulose Triacetate: Oligomers, Polymorphism, and Inferences about Chain Polarity.
PB96-176532 *01,289*

CHAIN SCISSION

Gas Phase Oxygen Effect on Chain Scission and Monomer Content in Bulk Poly(methyl methacrylate) Degraded by External Thermal Radiation.
PB96-204078 *01,293*

CHAINS

Effect of Hydrodynamic Interactions on a Terminally Anchored Bead-Rod Model Chain.
PB95-141156 *01,237*

CHALCOGENIDES

Thermochemical Studies of Inorganic Chalcogenides by Fluorine-Combustion Calorimetry: Binary Compounds of Germanium and Silicon with Sulfur, Selenium and Tellurium.
PB97-112528 *01,181*

CHAMBERS

Spatial Correlation Function for Fields in a Reverberation Chamber.
PB96-148077 *04,427*

CHANGES

Operating Procedures and Life Cycle Documentation for the Initial Graphics Exchange Specification.
PB95-242285 *02,782*

CHANNEL CAPACITY

Capacity of the Lp Norm-Constrained Poisson Channel.
PB95-125753 *01,515*

CHANNEL FLOW

Heat Transfer in Thin, Compact Heat Exchangers with Circular, Rectangular, or Pin-Fin Flow Passages.
PB95-140943 *02,751*

CHANNELS (DATA TRANSMISSION)

Channel Coding for Code Excited Linear Prediction (CELP) Encoded Speech in Mobile Radio Applications.
PB95-143178 *01,475*

CHAOS

Chaos in a Computer-Animated Pendulum.
PB94-212651 *03,852*

Fluctuations in Probability Distribution on Chaotic Attractors.
PB96-102330 *04,022*

Chaotic Motions of Coupled Galloping Oscillators and Their Modeling as Diffusion Progresses.
PB96-122718 *04,823*

Non-Gaussian Noise Effects on Reliability of Multistable Systems.
PB96-122726 *04,213*

Transitions to Chaos Induced by Additive and Multiplicative Noise.
PB96-155759 *03,750*

Spectrum of the Stochastically Forced Duffing-Holmes Oscillator.
PB96-155767 *00,216*

Necessary Condition for Homoclinic Chaos Induces by Additive Noise.
PB96-155775 *04,063*

Noise-Induced Transitions to Chaos.
PB96-156120 *00,217*

Deterministic and Stochastic Chaos.
PB96-156138 *00,218*

Experimental and Numerical Chaos in Continuous Systems: Two Case Studies.
PB96-156146 *00,219*

CHARACTER RECOGNITION

Analysis of a Biologically Motivated Neural Network for Character Recognition.
PB94-172277 *00,182*

Self-Organizing Neural Network Character Recognition on a Massively Parallel Computer.
PB95-163994 *01,845*

Self-Organizing Neural Network Character Recognition Using Adaptive Filtering and Feature Extraction.
PB96-119797 *01,855*

CHARACTERISTIC IMPEDANCE

Measurements of the Characteristic Impedance of Coaxial Air Line Standards.
PB95-168787 *02,221*

Comments on 'Conversions between S, Z, Y, h, ABCD, and T Parameters Which Are Valid for Complex Source and Load Impedances'.
PB96-102785 *02,069*

CHARACTERIZATION

Characteristics of Adhesive-Bonded Seams Sampled from EPDM Roof Membranes.
PB95-162491 *00,377*

Cement and Concrete Characterization by Scanning Electron Microscopy.
PB95-163168 *00,379*

CHARGE CARRIERS

Correction to the Decay Rate of Nonequilibrium Carrier Distributions Due to Scattering-in Processes.
PB94-185840 *04,452*

CHARGE DISTRIBUTION

Influence of Surface Charge on the Stochastic Behavior of Partial Discharge in Dielectrics.
PB96-122767 *01,931*

CHARGE EXPANSION THEORY

Relativistic Modifications of Charge Expansion Theory.
PB96-123799 *04,052*

CHARGE TRANSFER

Charge Transfer and Collision-Induced Dissociation Reactions of CF(2+) and CF2(2+) with the Rare Gases at a Laboratory Collision Energy of 49 eV.
PB94-185584 *00,775*

Measuring Contact Charge Transfer at Interfaces: A New Experimental Technique.
PB95-164570 *03,053*

Kinetics and Dynamics of Vibrationally State Resolved Ion-Molecule Reactions: (14)N2(+)(v=1 and 2) and (15)N2(+)(v=0,1 and 2) with (14)N2.
PB96-102348 *04,023*

Kinetic Energy Distribution of Ions Produced from Townsend Discharges in Neon and Argon.
PB96-111927 *04,413*

Influence of Coadsorbed Potassium on the Electron-Stimulated Desorption of F(+), F(-), and F(*) from PF3 on Ru(0001).
PB96-157946 *04,072*

CHARGED IONS

Observation and Visible and uv Magnetic Dipole Transitions in Highly Charged Xenon and Barium.
PB96-138441 *04,056*

CHARGED PARTICLES

Visible and UV Light from Highly Charged Ions: Exotic Matter Advancing Technology.
PB96-119391 *04,414*

CHARPY V NOTCH MACHINES

Proposed Changes to Charpy V-Notch Machine Certification Requirements.
PB96-135363 *02,955*

CHARRING

Behavior of Charring Materials in Simulated Fire Environments.
PB94-196045 *01,368*

Investigation of the Thermal Stability and Char-Forming Tendency of Cross-linked Poly(methyl methacrylate).
PB94-213501 *03,380*

CHARTS

Cryogenic Properties of Silver.
PB94-203593 *03,330*

CHEMICAL AFFINITY

Imposed Oscillations of Kinetic Barriers Can Cause an Enzyme to Drive a Chemical Reaction Away from Equilibrium.
PB96-161625 *01,137*

CHEMICAL ANALYSIS

Airborne Asbestos Method: Standard Test Method for High Precision Counting of Asbestos Collected on Filters. Version 1.0.
PB94-163003 *00,525*

Airborne Asbestos Method: Standard Test Method for Verified Analysis of Asbestos by Transmission Electron Microscopy. Version 2.0.
PB94-163045 *00,526*

Classical Analysis: A Look at the Past, Present, and Future.
PB94-185063 *00,528*

Preparation and Certification of a Rhodium Standard Reference Material Solution.
PB94-185071 *00,529*

Proficiency Tests for the NIST Airborne Asbestos Program, 1990.
PB94-188836 *00,535*

Proficiency Tests for the NIST Airborne Asbestos Program - 1991.
PB94-193828 *00,537*

Proficiency Tests for the NIST Airborne Asbestos Program - 1992.
PB94-194362 *00,539*

Standard Reference Materials for Dioxins and Other Environmental Pollutants.
PB94-198330 *02,518*

Establishing Quality Measurements for Inorganic Analysis of Biomaterials.
PB94-199726 *00,548*

Carotenoid Reversed-Phase High-Performance Liquid Chromatography Methods: Reference Compendium.
PB94-200516 *00,549*

Airborne Asbestos Method: Standard Practice for Recording Transmission Electron Microscopy Data for the Analysis of Asbestos Collected onto Filters. Version 1.0.
PB94-210168 *00,552*

Determination of Boron and Lithium in Diverse Biological Matrices Using Neutron Activation - Mass Spectrometry (NA-MS).
PB94-212289 *00,554*

Certification, Development and Use of Standard Reference Materials.
PB95-107272 *00,567*

Formation of Technical Committee 201 on Surface Chemical Analysis by the International Organization for Standardization.
PB95-108536 *00,568*

Apparent Bias in the X-Ray Fluorescence Determination of Titanium in Selected NIST SRM Low Alloy Steels.
PB95-108759 *03,212*

Dissolution Problems with Botanical Reference Materials.
PB95-126280 *03,487*

Comparison of Methods for Gas Chromatographic Determination of PCBs and Chlorinated Pesticides in Marine Reference Materials.
PB95-140091 *02,584*

NIST Standard Reference Materials (SRMs) for Polychlorinated Biphenyl (PCB) Determinations and Their Applicability to Toxaphene Measurements.
PB95-140109 *02,585*

Combining Data from Independent Chemical Analysis Methods.
PB95-140141 *00,572*

Automated, High-Precision Coulometric Titrimetry. Part 1. Engineering and Implementation.
PB95-150199 *00,575*

Automated, High Precision Coulometric Titrimetry. Part 2. Strong and Weak Acids and Bases.
PB95-150207 *00,576*

Integrating Automated Systems with Modular Architecture.
PB95-150231 *00,577*

Standard Reference Materials for the Determination of Polycyclic Aromatic Hydrocarbons in Environmental Samples - Current Activities.
PB95-151668 *00,586*

Mixed Diet Reference Materials for Nutrient Analysis of Foods: Preparation of SRM-1548 Total Diet.
PB95-151692 *03,593*

Liquid Chromatographic Method for the Determination of Carotenoids, Retinoids, and Tocopherols in Human Serum and in Food.
PB95-153599 *00,593*

Octacalcium Phosphate Carboxylates. 1. Preparation and Identification.
PB95-161535 *00,660*

Trace Detection in Conducting Solids Using Laser-Induced Fluorescence in a Cathodic Sputtering Cell.
PB95-163424 *00,598*

Standards for Atmospheric Measurements.
PB95-163622 *02,547*

Standard Reference Materials for the Determination of Trace Organic Constituents in Environmental Samples.
PB95-164026 *02,522*

Quality Assurance of Contaminant Measurements in Marine Mammal Tissues.
PB95-164034 *02,588*

Enhanced Detection of PCR Products Through Use of TOTO and YOYO Intercalating Dyes with Laser Induced Fluorescence - Capillary Electrophoresis.
PB95-164653 *00,599*

Fluorescence Measurements of Tetracycline in High Cell Mass for Fermentation Monitoring.
PB95-175709 *00,601*

Certification of Morphine and Codeine in a Human Urine Standard Reference Material.
PB95-176160 *03,499*

Traceability to the Mole: A New Initiative by CIPM.
PB95-180246 *00,605*

Activities of ISO Technical Committee 201 on Surface Chemical Analysis.
PB95-180824 *00,607*

Concentrations of Chlorinated Hydrocarbons, Heavy Metals and Other Elements in Tissues Banked by the Alaska Marine Mammal Tissue Archival Project.
PB95-209870 *02,590*

Certification of Polycyclic Aromatic Hydrocarbons in a Marine Sediment Standard Reference Material.
PB96-111778 *02,592*

Application of a Novel Slurry Furnace AAS Protocol for Rapid Assessment of Lead Environmental Contamination.
PB96-112354 *02,526*

Certification of Standard Reference Material (SRM) 1941a, Organics in Marine Sediment.
PB96-123690 02,593

Airborne Asbestos Analysis: National Voluntary Laboratory Accreditation Program.
PB96-147392 02,566

Isotopic and Nuclear Analytical Techniques in Biological Systems: A Critical Study. 10. Elemental Isotopic Dilution Analysis with Radioactive and Stable Isotopes (Technical Report).
PB96-164157 00,696

Composition and Solubility Product of a Synthetic Calcium Hydroxyapatite.
PB96-180104 02,995

Statistical Aspects of the Certification of Chemical Batch SRMs. Standard Reference Materials.
PB96-210877 00,645

Airborne Asbestos Method: Bootstrap Method for Determining the Uncertainty of Asbestos Concentration. Version 1.0.
PB96-214614 00,646

Results of the ASTM Nuclear Methods Intercomparison on NIST Apple and Peach Leaves Standard Reference Materials.
PB97-119036 03,490

CHEMICAL ASSISTED MACHINING

Chemically Assisted Machining of Si3N4.
PB96-122999 03,072

CHEMICAL BONDS

Effect of Two Initiator/Stabilizer Concentrations in a Metal Primer on Bond Strengths of a Composite to a Base Metal Alloy.
PB94-172723 00,141

Effects of Surface-Active Resins on Dentin/Composite Bonds.
PB95-140448 00,156

Van der Waals Bond Lengths and Electronic Spectral Shifts of the Benzene-Kr and Benzene-Xe Complexes.
PB95-151387 00,932

Molecular Orbital Calculations of Bond Rupture in Brittle Solids.
PB95-164059 00,973

Bonding in Doubly Charged Diatomics.
PB95-164315 00,976

Neutron Scattering Study of the Lattice Modes of Solid Cubane.
PB96-147152 01,126

CHEMICAL COMPOSITION

Standard Materials. A Descriptive List with Prices.
AD-A278 140/9 00,500

Classification of Advanced Technical Ceramics.
N94-35335/6 03,030

Recently Developed NIST Food Related Standard Reference Materials.
PB94-198322 00,035

Constituents and Physical Properties of the C6+ Fraction of Natural Gas. Topical Report, April-June 1994.
PB95-136644 02,483

Grazing-Incidence X-Ray Photoelectron Spectroscopy: A Novel Approach to Thin Film Characterization.
PB95-153128 04,589

Determination of Sulfur in Fossil Fuels by Isotope Dilution Thermal Ionization Mass Spectrometry.
PB96-141379 02,495

Inorganic Crystal Structure Database (ICSD) and Standardized Data and Crystal Chemical Characterization of Inorganic Structure Types (TYPIX): Two Tools for Inorganic Chemists and Crystallographers.
PB97-109037 00,648

Evaluation of Crystallographic Data with the Program DIAMOND.
PB97-109045 00,649

CHEMICAL COMPOSITIONS

Certifying the Chemical Composition of a Biological Material: A Case Study.
PB96-164272 00,636

CHEMICAL COMPOUNDS

NIOSH Pocket Guide to Chemical Hazards.
PB95-100368 03,603

CHEMICAL DISSOCIATION

Fragment State Correlations in the Dissociation of NO.HF(v=1).
PB95-164430 00,982

CHEMICAL ENGINEERING

Application of Expert System to Select Data Sources from Chemical Information Databases.
PB95-125654 00,505

CHEMICAL EQUILIBRIUM

Compilation of the Physical Equilibria and Related Properties of the Hydrogen-Carbon Monoxide System.
AD-A286 603/6 00,716

Calorimetric Determination of the Standard Transformed Enthalpy of a Biochemical Reaction at Specified PH and pMg.
PB94-198249 03,454

Electron Transfer Reaction Rates and Equilibria of the Carbonate and Sulfate Radical Anions.
PB94-212180 00,829

Thermochemistry of the Reactions between Adenosine, Adenosine 5'-monophosphate, Inosine, and Inosine 5'-monophosphate; the Conversion of L-histidine to (Urocanic Acid+Ammonia).
PB94-213113 03,460

CHEMICAL EXPLOSIVES

Separation and Identification of Organic Gunshot and Explosive Constituents by Micellar Electrokinetic Capillary Electrophoresis.
PB95-107249 00,566

CHEMICAL INHIBITION

Effect of CF3H and CF3Br on Laminar Diffusion Flames in Normal and Microgravity.
PB96-161831 01,420

Effect of CF3H and CF3Br on Laminar Diffusion Flames in Normal and Microgravity.
PB96-161849 01,421

Inhibition of Premixed Methane-Air Flames by Iron Pentacarbonyl.
PB96-163712 00,513

Parametric Study of Hydrogen Fluoride Formation in Suppressed Fires.
PB96-163720 00,514

CHEMICAL INTERACTIONS

Effect of Chemical Interaction on Barenblatt Crack Profiles in Brittle Solids.
PB96-180245 02,996

CHEMICAL KINETICS

Rate Constants for the Decay and Reactions of the Lowest Electronically Excited Singlet State of Molecular Oxygen in Solution. An Expanded and Revised Compilation.
PB96-145826 01,106

Critical Review of Rate Constants for Reactions of Transients from Metal Ions and Metal Complexes in Aqueous Solution.
PB96-145859 01,109

Kinetics of the Reaction of the Sulfate Radical with the Oxalate Anion.
PB97-119127 01,186

CHEMICAL MODELS

Fokker-Planck Description of Multivalent Interactions.
PB95-108478 00,879

CHEMICAL PREPARATION

Octacalcium Phosphate Carboxylates. 1. Preparation and Identification.
PB95-161535 00,660

CHEMICAL PROPERTIES

Classification of Advanced Technical Ceramics.
N94-35335/6 03,030

Journal of Physical and Chemical Reference Data, Volume 22, No. 1, January/February 1993.
PB94-160975 00,729

Journal of Physical and Chemical Reference Data, Volume 22, No. 2, March/April 1993.
PB94-162211 00,733

Journal of Physical and Chemical Reference Data, Volume 22, No. 3, May/June 1993.
PB94-162260 00,738

Journal of Physical and Chemical Reference Data, Volume 22, No. 4, July/August 1993.
PB94-162310 00,743

Journal of Physical and Chemical Reference Data, Volume 22, No. 5, September/October 1993.
PB94-162336 00,745

Journal of Physical and Chemical Reference Data, Volume 22, No. 6, November/December 1993.
PB94-168556 00,749

Physicochemical Properties of Calcific Deposits Isolated from Porcine Bioprosthetic Heart Valves Removed from Patients Following 2-13 Years Function.
PB94-172863 00,184

Physical and Chemical Properties of Resin-Reinforced Calcium Phosphate Cements.
PB95-180212 00,171

Journal of Physical and Chemical Reference Data, Volume 24, No. 1, January/February 1995.
PB96-145560 01,101

Journal of Physical and Chemical Reference Data, Volume 24, No. 2, March/April 1995.
PB96-145818 01,105

Journal of Physical and Chemical Reference Data, Volume 24, No. 3, May/June 1995.
PB96-145842 01,108

Journal of Physical and Chemical Reference Data, Volume 24, No. 4, July/August 1995.
PB96-145883 01,112

Journal of Physical and Chemical Reference Data, Volume 24, No. 5, September/October 1995.
PB96-145925 01,116

Journal of Physical and Chemical Reference Data, Volume 24, No. 6, November/December 1995.
PB96-145966 01,120

Environmental Aspects of Halon Replacements: Considerations for Advanced Agents and the Ozone Depletion Potential of CF3I.
PB97-122261 03,301

CHEMICAL RADICALS

Temperature Dependence of the Rate Constants for Reaction of Inorganic Radicals with Organic Reductants.
PB94-198280 00,783

Oxidation of 10-Methylacridan, a Synthetic Analogue of NADH and Deprotonation of Its Cation Radical. Convergent Application of Laser Flash Photolysis and Direct and Redox Catalyzed Electrochemistry to the Kinetics of Deprotonation of the Cation Radical.
PB94-198371 00,785

Temperature Dependence of the Rate Constants for Reactions of the Sulfate Radical, SO4-, with Anions.
PB94-212172 00,828

Temperature Dependence of the Rate Constants for Reactions of the Carbonate Radical with Organic and Inorganic Reductants.
PB94-212206 00,831

Resonance Enhanced Multiphoton Ionization Spectroscopy of the SnF Radical.
PB97-111223 01,176

CHEMICAL REACTION KINETICS

Progress in the Development of a Chemical Kinetic Database for Combustion Chemistry.
PB95-151056 01,384

Atmospheric Lifetimes of HFC-143a and HFC-245fa: Flash Photolysis Resonance Fluorescence Measurements of the OH Reaction Rate Constants.
PB97-112577 00,118

CHEMICAL REACTION MECHANISMS

Fluorinated Hydrocarbon Flame Suppression Chemistry.
PB94-185113 01,362

Unusual Spin-Trap Chemistry for the Reaction of Hydroxyl Radical with the Carcinogen N-Nitrosodimethylamine.
PB95-151643 00,692

Polymerization Initiation by N-p-Tolylglycine: Free-Radical Reactions Studied by Pulse and Steady-State Radiolysis.
PB95-180014 01,269

CHEMICAL REACTIONS

Tables of Chemical Kinetics Homogeneous Reactions.
AD-A280 293/2 00,715

Facile Synthesis of Novel Fluorinated Multifunctional Acrylates.
PB94-198389 01,207

New Rydberg States of Aluminum Monofluoride Observed by Resonance-Enhanced Multiphoton Ionization Spectroscopy.
PB94-199544 00,797

Equilibrium and Calorimetric Investigation of the Hydrolysis of L-Tryptophan to (Indole + Pyruvate + Ammonia).
PB95-163317 00,661

Thermodynamic Study of the Reactions of Cyclodextrins with Primary and Secondary Aliphatic Alcohols, with D- and L-Phenylalanine, and with L-Phenylalanineamide.
PB95-180873 01,016

Quadratic Response of a Chemical Reaction to External Oscillations.
PB96-161633 01,138

Noise Analysis of Ionization Kinetics in a Protein Ion Channel.
PB96-161682 04,093

CHEMICAL REACTORS

Low Temperature H(sub 2)S Separation Using Membrane Reactor with Redox Catalyst.
DE94008991 02,471

Modeling Ceramic Sub-Micron Particle Formation from the Vapor Using Detailed Chemical Kinetics: Comparison with In-situ Laser Diagnostics.
PB95-151965 00,671

Optimization of ECR-Based PECVD Oxide Films for Superconducting Integrated Circuit Fabrication.
PB95-169165 02,051

CHEMICAL SCIENCE AND TECHNOLOGY LIBRARY

CSTL Technical Activities 1991.
PB94-160769 00,728

CSTL Technical Activities, 1993.
PB95-160602 00,953

CHEMICAL VAPOR DEPOSITION

Gas Phase Reactions Relevant to Chemical Vapor Deposition: Optical Diagnostics.
PB94-199338 03,116

Gas Phase Reactions Relevant to Chemical Vapor Deposition: Numerical Modeling.
PB94-199346 03,117

Modeling Ceramic Sub-Micron Particle Formation from the Vapor Using Detailed Chemical Kinetics: Comparison with In-situ Laser Diagnostics.
PB95-151965 00,671

Multiphoton Ionization Spectroscopy Measurements of Silicon Atoms during Vapor Phase Synthesis of Ceramic Particles.
PB95-151999 03,913

Lineshape Analysis of the Raman Spectrum of Diamond Films Grown by Hot-Filament and Microwave-Plasma Chemical-Vapor Deposition.
PB95-162392 03,016

Studies of Defects in Diamond Films and Particles by Raman and Luminescence Spectroscopies.
PB95-162400 03,017

Surface Roughness Evaluation of Diamond Films Grown on Substrates with a High Density of Nucleation Sites.
PB95-162418 03,018

Optimization of ECR-Based PECVD Oxide Films for Superconducting Integrated Circuit Fabrication.
PB95-169165 *02,051*

CHEMICALS
Standard Materials. A Descriptive List with Prices.
AD-A278 140/9 *00,500*

CHEMISTRY
CSTL Technical Activities 1991.
PB94-160769 *00,728*

CSTL Technical Activities, 1993.
PB95-160602 *00,953*

CSTL Technical Activities, 1994.
PB95-242319 *00,608*

CSTL Technical Activities, 1995.
PB96-214630 *00,647*

CHEMISTRY WORKCELL
Integrating Automated Systems with Modular Architecture.
PB95-150231 *00,577*

CHEMOMETRICS
Importance of Chemometrics in Biomedical Measurements.
PB94-200599 *00,550*

Metrological Measurement Accuracy: Discussion of 'Measurement Error Models' by Leon Jay Gleser.
PB94-200607 *00,551*

CHEMOPREVENTIVE AGENTS
Methods for Analysis of Cancer Chemopreventive Agents in Human Serum.
PB95-200648 *03,502*

Liquid Chromatographic Determination of Carotenoids in Human Serum Using an Engineered C30 and a C18 Stationary Phase.
PB97-119333 *03,512*

CHEWING GUM
Effects on Whole Saliva of Chewing Gums Containing Calcium Phosphates.
PB95-153169 *03,563*

CHINA
Glimpse of Materials Research in China: A Report from an Interagency Study Team on Materials Visiting China from June 19, 1995 to June 30, 1995.
PB96-112677 *02,978*

CHISSA (CENTER FOR HIGH INTEGRITY SOFTWARE SYSTEM ASSURANCE)
Center for High Integrity Software System Assurance: Initial Goals and Activities.
PB95-251674 *01,734*

CHLORHEXIDINE
Interaction of Chlorhexidine Digluconate with and Adsorption of Chlorhexidine on Hydroxyapatite.
PB95-175907 *03,566*

CHLORHEXIDINE DIGLUCONATE
Interaction of Chlorhexidine Digluconate with and Adsorption of Chlorhexidine on Hydroxyapatite.
PB95-175907 *03,566*

CHLORIDES
Computer Simulation of the Diffusivity of Cement-Based Materials.
PB95-125985 *00,362*

In situ Measurements of Chloride Ion and Corrosion Potential at the Coating/Metal Interface.
PB95-140893 *03,122*

CHLORINATED AROMATIC HYDROCARBONS
Determination of PCBs and Chlorinated Hydrocarbons in Marine Mammal Tissues.
PB95-162640 *03,744*

Comparison of Selectivities for PCBs in Gas Chromatography for a Series of Cyanobiphenyl Stationary Phases.
PB96-119458 *00,618*

CHLORINATED POLYVINYL CHLORIDE
Comparison of Fire Sprinkler Piping Materials: Steel, Copper, Chlorinated Polyvinyl Chloride and Polybutylene, in Residential and Light Hazard Installations.
PB95-182267 *00,299*

CHLORINE
Relative Photoionization and Photodetachment Cross Sections for Particular Fine-Structure Transitions with Application to Cl 3s-subshell Photoionization.
PB95-203097 *03,998*

Laser Flash Photolysis, Time-Resolved Fourier Transform Infrared Emission Study of the Reaction Cl + C2H5 yields HCl(v) + C2H4.
PB95-203238 *01,049*

State-Resolved Rotational Energy Transfer in Open Shell Collisions: Cl((2)P3/2)+HCl.
PB96-176607 *01,157*

CHLORINE 36
36Cl/Cl Accelerator-Mass-Spectrometry Standards: Verification of Their Serial-Dilution-Solution Preparations by Radioactivity Measurements.
PB94-140563 *00,524*

CHLORINE IONS
Absolute Cross-Section Measurements for Electron-Impact Ionization of C1(+1).
PB94-199841 *03,818*

CHLORINE OXIDES
Infrared Spectrum of OClO in the 2000/cm(-1) Region: The 2(nu sub 1) and (nu sub 1 + nu sub 3) Bands.
PB95-141032 *00,908*

Intensities and Dipole Moment Derivatives of the Fundamental Bands of (35)ClO2 and an Intensity Analysis of the nu1 Band.
PB95-141040 *00,909*

CHLOROBENZENE
Oscillometric and Conductometric Analysis of Aqueous and Organic Dosimeter Solutions.
PB96-135256 *04,054*

CHLOROBENZENES
Rate Constants for Hydrogem Atom Attack on Some Chlorinated Benzenes at High Temperature.
PB94-200581 *00,810*

Incinerability of Perchloroethylene and Chlorobenzene.
PB95-163457 *01,388*

CHLOROFLUOROCARBONS
Role of R22 in Refrigerating and Air Conditioning Equipment.
PB94-199783 *03,253*

Retention of Halocarbons on a Hexafluoropropylene Epoxide Modified Graphitized Carbon Black. Part 1. Methane-Based Compounds.
PB95-175196 *03,272*

Physical Properties of Alternatives to the Fully Halogenated Chlorofluorocarbons.
PB96-119573 *03,279*

Retention of Halocarbons on a Hexafluoropropylene Epoxide-Modified Graphitized Carbon Black. 4. Propane-Based Compounds.
PB96-164033 *03,284*

REFPROP Refrigerant Properties Database: Capabilities, Limitations, and Future Directions.
PB96-167150 *01,149*

Retention of Halocarbons on a Hexafluoropropylene Epoxide-Modified Graphitized Carbon Black. 3. Ethene-Based Compounds.
PB96-167309 *03,286*

CHLOROHYDROCARBONS
Gas Phase Reactivity Study of OH Radicals with 1,1-Dichloroethene and cis-1,1-Dichloroethene and Trans-1,2-Dichloroethene over the Temperature Range 240-400 K.
PB95-152146 *00,939*

CHOLESTEROL
Isotope Dilution Mass Spectrometry as a Candidate Definitive Method for Determining Total Glycerides and Triglycerides in Serum.
PB96-102280 *03,519*

CHRIAL RECOGNITION
Use of a Naphthylethylcarbamoylated- beta-Cyclodextrin Chiral Stationary Phase for the Separation of Drug Enantiomers and Related Compounds by Sub- and Supercritical Fluid Chromatography.
PB97-113260 *00,653*

CHROMATIN
Oxidative Damage to DNA in Mammalian Chromatin.
PB94-199825 *03,525*

Modification of DNA Bases in Chromatin of Intact Target Human Cells by Activated Human Polymorphonuclear Leukocytes.
PB94-199833 *03,526*

Nickel(II)-Mediated Oxidative DNA Base Damage in Renal and Hepatic Chromatin of Pregnant Rats and Their Fetuses. Possible Relevance to Carcinogenesis.
PB94-212628 *03,646*

Oxidative DNA Base Damage in Renal, Hepatic, and Pulmonary Chromatin of Rats After Intraperitoneal Injection of Cobalt (II) Acetate.
PB95-150025 *03,647*

DNA Base Modifications in Renal Chromatin of Wistar Rats Treated with a Renal Carcinogen, Ferric Nitrilotriacetate.
PB95-150363 *03,648*

DNA Base Damage Generated In vivo in Hepatic Chromatin of Mice upon Whole Body y-Irradiation.
PB95-161741 *03,627*

Treatment of Wistar Rats with a Renal Carcinogen, Ferric Nitrilotriacetate, Causes DNA-Protein Cross-Linking between Thymine and Tyrosine in Their Renal Chromatin.
PB96-112115 *03,649*

Formation of DNA-Protein Cross-Links in Cultured Mammalian Cells Upon Treatment with Iron Ions.
PB96-137724 *03,651*

CHROMATOGRAPHIC ANALYSIS
Liquid Chromatography: Laser-Enhanced Ionization Spectrometry for the Speciation of Organolead Compounds.
PB94-185253 *00,530*

Measurement of Diffusion in Supercritical Fluid Systems: A Review.
PB94-199189 *00,795*

Comparison of the Liquid Chromatographic Behavior of Selected Steroid Isomers Using Different Reversed-Phase Materials and Mobile Phase Compositions.
PB95-140976 *00,574*

Chromatographic Cryofocusing and Cryotrapping with the Vortex Tube.
PB95-180113 *00,604*

Terminally Anchored Chain Interphases: Their Chromatographic Properties.
PB95-181061 *01,272*

Permeation Tube Approach to Long-Term Use of Automatic Sampler Retention Index Standards.
PB96-167291 *00,639*

CHROMATOGRAPHY
Measurement of Diffusion in Fluid Systems: Applications to the Supercritical Fluid Region.
PB95-175188 *02,490*

Solubility Measurement by Direct Injection of Supercritical-Fluid Solutions into a HPLC System.
PB95-175626 *00,997*

Determination of Vitamin K1 in Serum Using Catalytic-Reduction Liquid Chromatography with Fluorescence Detection.
PB96-138425 *03,506*

Selectivity Trends in Packed Column Supercritical Fluid Chromatography with C18 Stationary Phases.
PB96-138581 *00,622*

Simple and Efficient Methane-Marker Devices for Chromatographic Samples.
PB96-164041 *00,635*

CHROMIUM
Simple, Compact, High-Purity Cr Evaporator for Ultrahigh Vacuum.
PB94-216678 *04,520*

Magnetic Moments in Cr Thin Films on Fe(100).
PB95-108429 *04,525*

Influence of Cr Growth on Exchange Coupling in Fe/Cr/Fe(100).
PB95-150181 *04,562*

Scanning Tunneling Microscopy Study of the Growth of Cr/Fe(001): Correlation with Exchange Coupling of Magnetic Layers.
PB95-150330 *04,568*

Nanofabrication of a Two-Dimensional Array Using Laser-Focused Atomic Deposition.
PB96-119417 *04,732*

Influence of Thickness Fluctuations on Exchange Coupling in Fe/Cr/Fe Structures.
PB96-135371 *04,745*

CHROMIUM INTERMETALLICS
Crystallographic Characterization of Some Intermetallic Compounds in the Al-Cr System.
PB94-198702 *03,318*

CHROMIUM IONS
Improved Wavelengths for Prominent Lines of Cr XVI to Cr XXII.
PB95-150629 *03,895*

CHROMOSPHERES
High-Velocity Plasma in the Transition Region of AU Microscopii: Evidence for Magnetic Reconnection and Saturated Heating during Quiescent and Flaring Conditions.
PB96-102694 *00,091*

CHURCHILL EISENHART
Churchill Eisenhart, 1913-1994.
PB96-137740 *03,447*

CIGARETTES
Quantifying the Ignition Propensity of Cigarettes.
PB96-155411 *00,306*

CIM (COMPUTER INTEGRATED MANUFACTURING)
Roadmap for the Computer Integrated Manufacturing (CIM) Application Framework.
PB96-122759 *02,832*

CIRCUIT ANALYSIS
Diakoptic and Large Change Sensitivity Analysis.
PB95-150538 *02,038*

CIRCUIT BOARDS
Evaluation and Qualification Standards for an X-Ray Laminography System.
PB94-172954 *02,029*

Operating Principles of the SBus MultiKron Interface Board.
PB95-231783 *01,630*

Open-Ended Coaxial Probes for Nondestructive Testing of Substrates and Circuit Boards.
PB96-122825 *02,078*

Operating Principles of MultiKron Virtual Counter Performance Instrumentation for MIMD Computers.
PB96-131529 *01,632*

CIRCUIT BREAKERS
Investigation of S2F10 Production and Mitigation in Compressed SF6-Insulated Power Systems.
PB94-212388 *02,467*

CIRCUIT DESIGN
CMOS Circuit Design for Controlling Temperature in Micromachined Devices.
PB96-156088 *02,196*

CIRCUIT INTERCONNECTIONS
YBa2Cu3O7-x to Si Interconnection for Hybrid Superconductor/Semiconductor Integration.
PB94-211711 *02,315*

Accurate Experimental Characterization of Interconnects: A Discussion of 'Experimental Electrical Characterization of Interconnects and Discontinuities in High-Speed Digital Systems'.
PB94-216389 *02,217*

Interconnection Transmission Line Parameter Characterization.
PB94-216397 *02,218*

Metrology and Data for Microelectronic Packaging and Interconnection: Results of a Joint Workshop on Materials

Metrology and Data for Commercial Electrical and Optical Packaging and Interconnection Technologies. Held in Gaithersburg, Maryland on May 5-6, 1994. Volume 1. Results.
PB95-143111 *02,328*

Metrology and Data for Microelectronic Packaging and Interconnection: Results of a Joint Workshop on Materials Metrology and Data for Commercial Electrical and Optical Packaging and Interconnection Technologies. Held in Gaithersburg, Maryland on May 5-6, 1994. Volume 2. Presentation Material.
PB95-143327 *02,330*

Provision of Isochronous Service on IEEE 802.6.
PB96-160635 *01,501*

Accurate Electrical Characterization of High-Speed Interconnections.
PB96-167143 *02,240*

CIRCUIT PROTECTION
Coordinating Cascaded Surge Protection Devices: High-Low versus Low-High.
PB94-172061 *02,463*

Guarding Against Transients.
PB94-216470 *01,623*

Cascading Surge-Protective Devices: Options for Effective Implementation.
PB94-216488 *02,464*

Coordinating Cascaded Surge-Protective Devices: An Elusive Goal.
PB94-216496 *02,465*

Important Link in Entire-House Protection: Surge Reference Equalizers.
PB94-216504 *02,219*

Surging the Upside-Down House: Looking into Upsetting Reference Voltages.
PB96-112313 *02,385*

CIRCUIT SIMULATORS
Simulating the Dynamic Electro Thermal Behavior of Power Electronic Circuits and Systems.
PB95-161014 *02,345*

Thermal Component Models for Electro-Thermal Network Simulation.
PB95-161022 *02,346*

CIRCUIT TECHNOLOGY
Business and Manufacturing Motivations for the Developing of Analytical Technology and Metrology for Semiconductors.
PB96-161948 *04,778*

CIRCUIT TESTERS
Automated Josephson Integrated Circuit Test System.
PB95-175246 *02,057*

CIRCUITS
Handbook Preferred Circuits Navy Aeronautical Electronic Equipment. Supplement Number 3.
AD-A278 782/8 *00,026*

Handbook Preferred Circuits Navy Aeronautical Electronic Equipment. Supplement Number 2.
AD-A278 783/6 *00,027*

Handbook Preferred Circuits Navy Aeronautical Electronic Equipment. Supplement Number 1.
AD-A278 784/4 *00,028*

Wide Band Active Current Transformer and Shunt.
PB95-126371 *02,036*

Precision Tests of a Quantum Hall Effect Device DC Equivalent Circuit Using Double-Series and Triple-Series Connections.
PB96-159256 *01,953*

CIRCULAR BRIDGE COLUMNS
Jacket Thickness Requirements for Seismic Retrofitting of Circular Bridge Columns.
PB95-163267 *01,336*

CITIS (CONTRACTOR INTEGRATED TECHNICAL INFORMATION SERVICE)
CALS-Contractor Integrated Technical Information Service (CITIS), Functional Requirements.
PB94-962600 *03,663*

CALS-Contractor Integrated Technical Information Service (CITIS), Functional Requirements.
PB95-962600 *03,672*

CITRIC ACID
Interaction of Citric Acid with Hydroxyapatite: Surface Exchange of Ions and Precipitation of Calcium Citrate.
PB97-119309 *03,584*

CIVIL ENGINEERING
Materials Aspects of Fiber-Reinforced Polymer Composites in Infrastructure.
PB96-210695 *03,184*

CLAD METALS
Leady Axisymmetric Modes in Infinite Clad Rods. Part 1.
PB95-162905 *04,187*

CLADDING
Literature Review on Seismic Performance of Building Cladding Systems.
PB96-106901 *00,455*

CLADDINGS
Optical Fiber Geometry: Accurate Measurement of Cladding Diameter.
PB95-151940 *04,266*

CLAMPING CIRCUITS
Perception of Clamp Noise in Television Receivers.
PB96-119433 *01,489*

CLAPEYRON EQUATION
Calculation of Enthalpy and Entropy Differences of Near-Critical Binary Mixtures with the Modified Leung-Griffiths Model.
PB95-108635 *00,885*

CLASSICAL ANALYSIS
Classical Analysis: A Look at the Past, Present, and Future.
PB94-185063 *00,528*

CLASSICAL LIMIT
Quantum Collisional Transfer Contributions to the Density Dependence of Gaseous Viscosity.
PB96-161914 *01,142*

CLASSIFICATION
Metropolitan Areas (Including MSAs, CMSAs, PMASs, and NECMAs). Category: Data Standards and Guidelines; Subcategory: Representations and Codes.
FIPS PUB 8-6 *04,873*

Countries, Dependencies, Areas of Special Sovereignty, and Their Principal Administrative Divisions. Category: Data Standards and Guidelines; Subcategory: Representation and Codes.
FIPS PUB 10-4 *00,128*

Guideline: Codes for Named Populated Places, Primary County Divisions, and Other Locational Entities of the United States, Puerto Rico, and the Outlying Areas. Category: Data Standards and Guidelines. Subcategory: Representations and Codes.
FIPS PUB 55-3 *04,865*

Guideline: Codes for Named Populatd Places, Primary County Divisions, and Other Locational Entities of the United States, Puerto Rico, and the Outlying Areas. Category: Data Standards and Guidelines; Subcategory: Representation and Codes.
FIPS PUB 55-DC3 *04,866*

FIPS PUB 8-6, Metropolitan Areas (for Microcomputers).
PB95-503280 *04,874*

Countries, Dependencies, Areas of Special Sovereignty, and Their Principal Administrative Divisions (for Microcomputers).
PB95-503504 *00,130*

CLASSIFICATIONS
Classification of Advanced Technical Ceramics.
N94-35335/6 *03,030*

New Materials, Advanced Ceramics and Standards.
PB95-140208 *03,047*

CLASSIFYING
Description of Layered Structures: Applications to High Tc Superconductors.
PB95-162624 *04,615*

CLAY
Small Angle Neutron Scattering Study of a Clay Suspension Under Shear.
PB96-167374 *00,663*

CLAYS
Hollow Clay Tile Prism Tests for Martin Marietta Energy Systems: Task 2 Testing.
PB94-217486 *00,352*

CLEANING
Effects of Soxhlet Extraction on the Surface Oxide Layer of Silicon Nitride Powders.
PB95-175584 *03,057*

CLEAVAGE
Evidence of Film-Induced Cleavage by Electrodeposited Rhodium.
PB95-162327 *03,191*

CLIMATIC CHANGES
Global Climatic Effects of Aerosols: The AAAR Symposium.
PB95-108791 *00,122*

CLINICAL CHEMISTRY
History of NIST's Contributions to Development of Standard Reference Materials and Reference and Definitive Methods for Clinical Chemistry.
PB96-119706 *03,503*

CLINKER
Quantitative X-Ray Powder Diffraction Methods for Clinker and Cement.
PB95-143079 *01,317*

CLOCK
Wavelet Variance, Allan Variance, and Leakage.
PB96-190111 *01,509*

CLOCKS
Time and Frequency Technology at NIST.
N94-30641/2 *01,522*

Future of Time and Frequency Dissemination.
N94-30684/2 *01,524*

Smart Clock: A New Time.
PB95-151445 *01,530*

Keeping Time on Your PC.
PB95-161410 *01,537*

Sifting Through Nine Years of NIST Clock Data with TA2.
PB95-181137 *01,547*

CLOSED LOOP CONTROLLERS
Closed Loop Controller for Electron-Beam Evaporators.
PB97-111470 *04,393*

CLOTHING
Bibliography on Apparel Sizing and Related Issues.
PB94-161924 *02,806*

CLOTHING INDUSTRY
Body Dimensions for Apparel.
PB94-187739 *02,813*

Apparel Manufacturing Glossary for Application Protocol Development.
PB95-198750 *02,755*

Extensions of the Prototype Application Protocol of Ready-to-Wear Apparel Pattern Making.
PB96-128194 *03,198*

Aspects of a Product Model Supporting Apparel Virtual Enterprises.
PB96-183231 *02,790*

Survey of Standards for the U.S. Fiber/Textile/Apparel Industry.
PB96-193792 *03,199*

CLUSTER ANALYSIS
Representing a Large Collection of Curves: A Case for Principal Points.
PB95-152286 *03,438*

CLUSTER MODELS
Active Site Ionicity and the Mechanism of Carbonic Anhydrase.
PB94-212974 *00,843*

CLUSTERS
Potential Surfaces and Dynamics of Weakly Bound Trimers: Perspectives from High Resolution IR Spectroscopy.
PB96-176508 *01,155*

CMM (COORDINATE MEASURING MACHINES)
Two New Probes for a Coordinate Measuring Machine.
PB95-163093 *02,653*

User's Guide to 'SuperFit' Modeling Software for CMM Probe Lobing.
PB96-128236 *02,921*

CMMS (COORDINATE MEASURING MACHINES)
Some Considerations for Interim Testing of Coordinate Measuring Machine Performance Using a Specific Artifact.
PB95-108858 *02,898*

Sensitivity of Three-Point Circle Fitting.
PB95-136354 *02,901*

NIST SRM 9983 High-Rigidity Ball-Bar Stand. User Manual.
PB95-255840 *02,669*

Estimation of Measurement Uncertainty of Small Circular Features Measured by CMMs.
PB95-267928 *02,918*

CMOS
Defect of Thermal Ramping and Annealing Conditions on Defect Formation in Oxygen Implanted Silicon-On-Insulator Material.
PB94-212966 *02,318*

High-Level CAD Melds Micromachined Devices with Foundries.
PB94-216413 *02,321*

MEMS in Standard CMOS VLSI Technology.
PB96-102363 *02,377*

Development of Thin-Film Multijunction Thermal Converters at NIST.
PB97-112338 *02,286*

Micromachined Coplanar Waveguides in CMOS Technology.
PB97-119283 *02,456*

CMS
Process for Selecting Standard Reference Algorithms for Evaluating Coordinate Measurement Software.
PB94-173754 *02,629*

COAL
Abrasive Wear by Diesel Engine Coal-Fuel and Related Particles.
PB95-104915 *01,450*

Chemical and Microbiological Problems Associated with Research on the Biodesulfurization of Coal.
PB95-140950 *02,484*

Microbial Degradation of Polysulfides and Insights into Their Possible Occurrence in Coal.
PB95-163374 *02,488*

COAL MINING
Task Decomposition Methodology for the Design of a Coal Mining Automation Hierarchical Real-Time Control System.
PB94-185386 *03,694*

Integration of Servo Control into a Large-Scale Control System Design: An Example from Coal Mining.
PB94-203429 *03,696*

Continuous Mining Machine Control Using the Real-Time Control System.
PB94-203528 *03,700*

Environment Simulation for a Continuous Mining Machine.
PB94-203536 *03,697*

Hierarchical Real-Time Control System for Use with Coal Mining Automation.
PB94-212065 *03,698*

COARSENESS
Exponentially Rapid Coarsening and Buckling in Coherently Self-Stressed Thin Plates.
PB95-202347 *04,821*

COATING PROCESSES
Opportunities for Innovation: Advanced Surface Engineering.
PB94-176666 *02,697*

Perspective on Fiber Coating Technology.
PB94-200540 *03,118*

Interface Modification and Characterization of Silicon Carbide Platelets Coated with Alumina Particles.
PB95-108734 *03,121*

Methodologies for Predicting the Service Lives of Coating Systems.
PB95-146387 *03,124*

UV-Photopatterning of Alkylthiolate Monolayers Self-Assembled on Gold and Silver.
PB95-150751 *00,924*

COATINGS
Light Scattering from Glossy Coatings on Paper.
PB94-213246 *04,242*

Non-Osmotic, Defect-Controlled Cathodic Disbondment of a Coating from a Steel Substrate.
PB94-216447 *03,120*

Light Scattered by Coated Paper.
PB94-216546 *04,245*

Tribological Behavior of 440/Diamond-Like-Carbon Film Couples.
PB96-119714 *03,019*

Proposed Coating Technology Consortium. (National Coil Coaters Association Fall Conference). Held in Rosemont, Illinois in September 1992.
PB97-110431 *03,129*

Nanoindentation and Instrumented Scratching Measurements on Hard Coatings.
PB97-122477 *03,111*

COAXIAL AIR LINES
Aperture Coupling to a Coaxial Air Line: Theory and Experiment.
PB94-211968 *02,216*

Measurements of the Characteristic Impedance of Coaxial Air Line Standards.
PB95-168787 *02,221*

COAXIAL CABLES
Programmable Guarded Coaxial Connector Panel.
PB96-122544 *02,108*

Open-Ended Coaxial Probes for Nondestructive Testing of Substrates and Circuit Boards.
PB96-122825 *02,078*

Dielectric Measurements on Printed-Wiring and Circuit Boards, Thin Films, and Substrates: An Overview.
PB96-147038 *02,236*

Dimensional Characterization of Precision Coaxial Transmission Line Standards.
PB96-176482 *02,241*

Coaxial Line-Reflect-Match Calibration.
PB96-200118 *02,246*

COAXIAL CONFIGURATIONS
Calibration Service for Coaxial Reference Standards for Microwave Power.
PB96-162722 *01,958*

COAXIAL PROBES
Analysis of an Open-Ended Coaxial Probe with Lift-Off for Nondestructive Testing.
PB96-135116 *01,940*

COBALT
Combined Low- and High-Angle X-Ray Structural Refinement of a Co/Pt(111) Multilayer Exhibiting Perpendicular Magnetic Anisotropy.
PB94-198355 *04,457*

Magnetic Properties of Pd/Co Multilayers.
PB94-198751 *04,465*

Bioleaching of Cobalt from Smelter Wastes by 'Thiobacillus ferrooxidans'.
PB95-140968 *02,582*

Spot-Profile-Analyzing LEED Study of the Epitaxial Growth of Fe, Co, and Cu on Cu(100).
PB95-150165 *04,561*

Microstructural Characterization of Cobalt-Tungsten Coated Graphite Fibers.
PB96-159231 *01,951*

COBALT 60
Protection Against Radiations from Radium, Cobalt-60, and Cesium-137.
AD-A279 261/2 *03,607*

Dose Mapping of Radioactive Hot Particles Using Radiochromic Film.
PB95-162954 *03,714*

COBALT ACETATE
Oxidative DNA Base Damage in Renal, Hepatic, and Pulmonary Chromatin of Rats After Intraperitoneal Injection of Cobalt (II) Acetate.
PB95-150025 *03,647*

COBALT ALLOYS
Correlations of Modulation Noise with Magnetic Microstructure and Intergranular Interactions for CoCrTa and CoNi Thin Film Media.
PB94-212768 *04,509*

COBALT BASE ALLOYS
Electrodeposited Cobalt-Tungsten as a Diffusion Barrier between Graphite Fibers and Nickel.
PB96-146881 *03,176*

COBALT HYDRIDES
Rotational Spectroscopy of the CoH Radical in Its Ground (3)Phi State by Far-Infrared Laser Magnetic Resonance: Determination of Molecular Parameters.
PB95-175048 *00,992*

COBALT SILICIDES
Local Partial Densities of States in Ni and Co Silicides Studied by Soft X-Ray Emission Spectroscopy.
PB94-212412 *04,504*

COBOL
COBOL. Category: Software Standard; Subcategory: Programming Language. Includes ANSI'S X3.23-1985, X3.23A-1989 and X3.23B-1993.
FIPS PUB 21-4 *01,670*

COBOL. Category: Software Standard; Subcategory: Programming Language. Part A.
FIPS PUB 21-4A *01,671*

COBOL. Category: Software Standard; Subcategory: Programming Language. Part B.
FIPS PUB 21-4B *01,672*

COBOL PROGRAMMING LANGUAGE
Validated Products List (Cobol, Fortran, ADA, Pascal, MUMPS, SQL).
PB94-937300 *01,700*

Validated Products List (Cobol, Fortran, ADA, Pascal, MUMPS, SQL).
PB95-937300 *01,738*

COCAINE
Supercritical Fluid Extraction-Immunoassay for the Rapid Screening of Cocaine in Hair.
PB96-167168 *00,637*

COCOMBUSTION
Sulfur Dioxide Capture in the Combustion of Mixtures of Lime, Refuse-Derived Fuel, and Coal.
PB94-155587 *02,534*

CODE DIVISION MULTIPLE ACCESS
Error Protecting Characteristics of CDMA and Impacts on Speech.
PB96-122452 *01,491*

CODE EXCITED LINEAR PREDICTION
Channel Coding for Code Excited Linear Prediction (CELP) Encoded Speech in Mobile Radio Applications.
PB95-143178 *01,475*

CODE SCALABILITY
Scalability Test for Parallel Code.
PB96-146758 *01,749*

CODEINE
Certification of Morphine and Codeine in a Human Urine Standard Reference Material.
PB95-176160 *03,499*

CODING
Channel Coding for Code Excited Linear Prediction (CELP) Encoded Speech in Mobile Radio Applications.
PB95-143178 *01,475*

COEFFICIENT OF FRICTION
Mechanism of Mild to Severe Wear Transition in Alpha-Alumina.
PB94-212354 *03,233*

COEFFICIENT OR THERMAL EXPANSION
Advances in the Measurement of Polymer CTE: Micrometer- to Atomic-Scale Measurements.
PB96-180229 *03,390*

COEXTRUDING
Small Angle Neutron Scattering Studies on Chain Asymmetry of Coextruded Poly(Vinyl Alcohol) Film.
PB95-164372 *01,262*

COHERENT INTERFACES
Cracks and Dislocations in Face-Centered Cubic Metallic Multilayers.
PB96-163696 *02,989*

COHERENT LIGHT
Integral Occurring in Coherence Theory.
PB95-203550 *04,324*

COILS
Quench Energy and Fatigue Degradation Properties of Cu- and Al/Cu-Stablized Nb-Ti Epoxy-Impregnated Superconductor Coils.
PB96-141213 *04,755*

COLD NEUTRON CAPTURE PROMPT GAMMA-RAY ACTIVATION ANALYSIS
Determination of Hydrogen in Titanium Alloy Jet Engine Compressor Blades by Cold Neutron Capture Prompt Gamma-ray Activation Analysis.
PB95-175956 *01,448*

COLD NEUTRONS
Thermal Hydraulic Tests of a Liquid Hydrogen Cold Neutron Source.
PB95-135570 *03,884*

Neutron Focusing Lens Using Polycapillary Fibers.
PB95-141206 *03,889*

Liquid-Hydrogen Cold Neutron Source for the NBSR.
PB95-151619 *03,729*

Neutron Focusing Lens Using Polycapillary Fibers.
PB95-153078 *03,922*

Cold Neutron Gain Calculations for the NBSR Using MCNP.
PB95-163978 *03,731*

Analytical Applications of Guided Neutron Beams.
PB96-112347 *04,041*

MCNP Model of the National Bureau of Standards Reactor (NBSR) Core.
PB96-138599 *03,733*

COLD PLASMAS
Spectroscopic Diagnostics of Low Temperature Plasmas: Techniques and Required Data.
PB95-151577 *04,411*

COLLECTION
NIST Serial Holdings, 1994.
PB94-178068 *02,745*

COLLECTION SYSTEMS
All-Metal Collection System for Preparative-Scale Gas Chromatography: Purification of Low-Boiling-Point Compounds.
PB96-123435 *00,619*

COLLIMATORS
Analysis of the Effectiveness of Oscillating Radial Collimators in Neutron Scattering Applications.
PB95-152252 *03,917*

Tilt Effects in Optical Angle Measurements.
PB95-169389 *04,294*

COLLISION
Alignment Probing of Rydberg States by Stimulated Emission.
PB96-200316 *04,124*

COLLISION AVOIDANCE
Image Gradient Evolution: A Visual Cue for Danger.
PB96-154562 *02,939*

Novel Active-Vision-Based Motion Cues for Local Navigation.
PB96-193727 *02,941*

COLLISIONS
State-Resolved Rotational Energy Transfer in Open Shell Collisions: Cl((2)P3/2)+HCl.
PB96-176607 *01,157*

COLLOCATION
Using Collocation in Three Dimensions and Solving a Model Semiconductor Problem.
PB96-159249 *01,952*

Application of the Collocation Method in Three Dimensions to a Model Semiconductor Problem.
PB97-122428 *02,457*

COLLOIDAL DISPERSION
Structure and Rheology of Hard-Sphere Systems.
PB96-167333 *00,662*

COLLOIDAL SUSPENSION
Non-Newtonian Flow between Concentric Cylinders Calculated from Thermophysical Properties Obtained from Simulations.
PB96-163761 *04,103*

COLLOIDAL SUSPENSIONS
Contrast Matched Studies of a Sheared Binary Colloidal Suspension.
PB95-150561 *00,918*

Partial Scattered Intensities from a Binary Suspension of Polystyrene and Silica.
PB95-175618 *00,996*

COLLOIDING
Polyelectrolytes as Dispersants in Colloidal Processing of Silicon Nitride Ceramics.
PB95-175568 *03,055*

Surface Chemical Interactions of Si3N4 with Polyelectrolyte Deflocculants.
PB95-175576 *03,056*

COLLOIDS
Electroacoustics for Characterization of Particulates and Suspensions. Proceedings of a Workshop. Held in Gaithersburg, Maryland on February 3-4, 1993.
PB94-112695 *00,725*

Deposition of Colloidal Sintering-Aid Particles on Silicon Nitride.
PB94-216272 *03,044*

Reduction of Dinitrogen to Ammonia in Aqueous Solution Mediated by Colloidal Metals.
PB95-107074 *00,867*

Aggregation Kinetics of Colloidal Particles Destabilized by Enzymes.
PB95-125878 *00,894*

Effects of Soxhlet Extraction on the Surface Oxide Layer of Silicon Nitride Powders.
PB95-175584 *03,057*

COLOR CODING
Nonlinear Color Transformations in Real Time Using a Video Supercomputer.
PB96-123021 *02,191*

COLOR TEMPERATURE
Irradiance of Horizontal Quartz-Halogen Standard Lamps.
PB96-179130 *01,866*

COLORIMETERS
Interface-Filter Characterization of Spectraradiometers and Colorimeters.
PB97-122212 *04,399*

COLORIMETRIC DOSEMETERS
Temperature and Relative Humidity Dependence of Radiochromic Film Dosimeter Response to Gamma and Electron Radiation.
PB96-135298 *03,718*

COLUMN BUCKLING
Dynamics of Multi-DOF Stochastic Nonlinear Systems.
PB97-113245 *00,477*

COLUMNS (PROCESS ENGINEERING)
Continuous Counter-Current Two Phase Aqueous Extraction.
PB95-161212 *00,675*

COLUMNS (SUPPORTS)
Model Precast Concrete Beam-to-Column Connections Subject to Cyclic Loading.
PB95-153094 *00,438*

Partially Prestressed and Debonded Precast Concrete Beam-Column Joints.
PB95-153102 *00,439*

Seismic Performance Behavior of Precast Concrete Beam-Column Joints.
PB95-153110 *00,440*

Evaluating the Seismic Performance of Lightly-Reinforced Circular Concrete Bridge Columns.
PB95-163259 *01,335*

COMBINATION APPLIANCES
Predicting the Energy Performance Ratings of a Family of Type I Combination Appliances.
PB95-105524 *02,504*

COMBUSTION
Gordon Research Conference on the Physics and Chemistry of Laser Diagnostics in Combustion Held in Plymouth, New Hampshire on 12-16 July 1993.
AD-A274 609/7 *01,353*

Spectroscopic Study of Reaction Intermediates and Mechanisms in Nitramine Decomposition and Combustion.
AD-A296 061/5 *03,774*

Combustion of a Polymer (PMMA) Sphere in Microgravity.
N96-15569/2 *01,354*

Summaries of Center for Fire Research In-House Projects and Grants: 1990.
PB94-160876 *00,286*

Combustion of Methanol and Methanol/Dodecanol Spray Flames.
PB95-108544 *02,478*

Effect of Dodecanol Content on the Combustion of Methanol Spray Flames.
PB95-176020 *01,389*

Polymer Combustion and Flammability: Role of the Condensed Phase.
PB96-123245 *01,279*

Further Development of the N-Gas Mathematical Model: An Approach for Predicting the Toxic Potency of Complex Combustion Mixtures.
PB96-123260 *03,650*

Numerical Simulation of Rapid Combustion in an Underground Enclosure.
PB96-183132 *01,424*

Analysis of Droplet Arrival Statistics in a Pressure-Atomized Spray Flame.
PB97-112270 *01,352*

COMBUSTION CHEMISTRY
Progress in the Development of a Chemical Kinetic Database for Combustion Chemistry.
PB95-151056 *01,384*

New Approach for Reducing the Toxicity of the Combustion Products from Flexible Polyurethane Foam.
PB96-123625 *01,411*

Asymptotic and Numerical Analysis of a Premixed Laminar Nitrogen Dioxide-Hydrogen Flame.
PB96-164256 *01,422*

Scaling Compartment Fires: Reduced- and Full-Scale Enclosure Burns.
PB96-175708 *00,224*

NO Production and Destruction in a Methane/Air Diffusion Flame.
PB97-122519 *01,443*

COMBUSTION EFFICIENCY
Estimate of the Effect of Scale on Radiative Heat Loss Fraction and Combustion Efficiency.
PB95-150447 *02,486*

COMBUSTION GASES
Reactivity of Product Gases Generated in Idealized Enclosure Fire Environments.
PB95-161790 *01,386*

COMBUSTION KINETICS
Fluorinated Hydrocarbon Flame Suppression Chemistry.
PB94-185113 *01,362*

Hydrogen Atom Attack on Perchloroethylene.
PB95-163473 *00,969*

Effect of Suppressants on Metal Fires.
PB96-109574 *01,402*

Smoke Emission from Burning Crude Oil.
PB96-122890 *01,407*

Inhibition of Premixed Methane-Air Flames by Halon Alternatives.
PB96-146741 *01,414*

Suppression of High-Speed C2H4/Air Flames with C1-Halocarbons.
PB96-175724 *03,287*

Effectiveness of Halon Alternatives in Suppressing Dynamic Combustion Process.
PB96-175732 *03,288*

Interaction of HFC-125, FC-218 and CF3I with High Speed Combustion Waves.
PB96-176417 *03,290*

Dynamics, Transport and Chemical Kinetics of Compartment Fire Exhaust Gases.
PB96-195508 *00,229*

Chemical Inhibition of Methane-Air Diffusion Flame.
PB96-195532 *01,431*

COMBUSTION PHYSICS
Prediction of Fire Dynamics.
PB94-193620 *00,336*

COMBUSTION PRODUCTS
Airborne Smoke Sampling Package for Field Measurements of Fires.
PB95-150041 *01,381*

Reactivity of Product Gases Generated in Idealized Enclosure Fire Environments.
PB95-161790 *01,386*

Acid Gas Production in Inhibited Diffusion Flames.
PB95-180576 *01,390*

Compartment Fire Combustion Dynamics. Annual Report, September 1, 1993-September 1, 1994.
PB95-217162 *00,203*

Carbon Monoxide Production in Compartment Fires: Reduced-Scale Enclosure Test Facility.
PB95-231700 *01,394*

Distinguishing the Contributions of Residential Wood Combustion and Mobile Source Emissions Using Relative Concentrations of Dimethylphenanthrene Isomers.
PB96-135124 *02,563*

Application of Thermodynamic and Detailed Chemical Kinetic Modeling to Understanding Combustion Product Generation in Enclosure Fires.
PB96-135322 *01,413*

Global Equivalence Ratio Concept and the Formation Mechanisms of Carbon Monoxide in Enclosure Fires.
PB96-146790 *00,210*

Scaling Compartment Fires: Reduced- and Full-Scale Enclosure Burns.
PB96-175708 *00,224*

Post-Flame Soot.
PB96-193701 *01,430*

Smoke Plume Trajectory from In situ Burning of Crude Oil: Field Experiments.
PB96-200993 *02,597*

COMMENSURATE LATTICES
Pinch Effect in Commensurate Vortex-Pin Lattices.
PB96-147079 *01,125*

COMMERCE
Analyzing Electronic Commerce.
PB94-219102 *00,480*

Guidelines for the Evaluation of Electronic Data Interchange Products.
PB96-172325 *01,506*

COMMERCIAL BUILDINGS
Performance Approach to the Development of Criteria for Low-Sloped Roof Membranes.
PB94-160751 *00,329*

Lighting and HVAC.
PB95-150991 *00,250*

Improving the Evaluation of Building Ventilation.
PB96-138508 *00,271*

COMMERCIAL DEVELOPMENT
Opportunities for Innovation: Biotechnology.
PB94-157831 *00,009*

COMMERCIAL SECTOR
Assessment of the DOD Goal Security Architecture (DGSA) for Non-Military Use.
PB95-189510 *03,653*

COMMERCIAL VEHICLES
Recommendations on Selection of Vehicle-to-Roadside Communications Standards for Commercial Vehicle Operations.
PB94-195914 *04,859*

Vehicle-to-Roadside Communications for Commercial Vehicle Operations: Requirements and Approaches.
PB95-188827 *04,860*

COMMERCIALIZATION
Water Mist Fire Suppression Workshop Summary.
PB95-161907 *02,853*

COMMODITIES
Checking the Net Contents of Packaged Goods as Adopted by the 79th National Conference on Weights and Measures, 1994, Third Edition, Supplement 4.
PB95-182226 *00,484*

COMMUNICATION CHANNELS
Capacity of the Lp Norm-Constrained Poisson Channel.
PB95-125753 *01,515*

COMMUNICATION EQUIPMENT
Ground Vehicle Control at NIST: From Teleoperation to Autonomy.
N94-34037/9 *03,758*

COMMUNICATION NETWORKS
Integrated Services Digital Network (ISDN); Category: Telecommunications Standard; Subcategory: Integrated Services Digital Network.
FIPS PUB 182 *01,460*

Putting the Information Infrastructure to Work: Report of the Information Infrastructure Task Force Committee on Applications and Technology.
N94-31228/7 *02,715*

Context Analysis of the Network Management Domain. Conducted as Part of the Domain Analysis Case Study.
PB94-142528 *01,465*

Supplement to Stable Implementation Agreements for Open Systems Interconnection Protocols. Version 3, September 1990. Change Page Index, Version 3, June 1990 (Stable) Change Pages Issued December 1990; Output from September 1990 OSI Workshop (NIST Special Publication 500-177).
PB94-164035 *01,467*

National Voluntary Laboratory Accreditation Program. GOSIP: Government Open Systems Interconnection Profile.
PB95-267993 *01,486*

NIST ATM Network Simulator: Operation and Programming, Version 1.0.
PB96-106851 *01,487*

Application Software Interface: ISDN Services for an Open Systems Environment.
PB96-131487 *01,492*

Provision of Isochronous Service on IEEE 802.6.
PB96-160635 *01,501*

ISDN in North America.
PB96-160767 *01,502*

North American Agreements on ISDN.
PB96-160775 *01,503*

COMMUNICATIONS NETWORKS
Introduction to Traffic Management for Broadband ISDN.
PB94-142494 *01,464*

Domain Analysis of the Alarm Surveillance Domain. Version 1.0. Conducted as Part of the Domain Analysis Case Study Project.
PB95-136339 *01,705*

COMMUNITIES
Codes for Named Populated Places, Primary County Divisions, and Other Locational Entities of the United States (FIPS PUB 55-3) (on Magnetic Tape).
PB95-502563 *00,129*

COMPACT HEAT EXCHANGERS
Heat Transfer in Thin, Compact Heat Exchangers with Circular, Rectangular, or Pin-Fin Flow Passages.
PB95-140943 *02,751*

COMPACTING
Rapid Hot Pressing of Ultra-Fine PSZ Powders.
PB94-216587 *03,045*

COMPACTORS
Field Evaluation of the System for Calibration of the Marshall Compaction Hammer.
PB95-190674 *01,323*

COMPARATOR CIRCUITS
Leakage Current Detection in Cryogenic Current Comparator Bridges.
PB94-172228 *02,024*

Custom Integrated Circuit Comparator for High-Performance Sampling Applications.
PB94-213147 *02,320*

COMPARATORS
NIST Comparison of the Quantized Hall Resistance and the Realization of the SI Ohm Through the Calculable Capacitor.
PB97-119184 *02,291*

NIST Comparison of the Quantized Hall Resistance and the Realization of the SI Ohm Through the Calculable Capacitor. Conference Proceedings, June 17-20, 1996.
PB97-119192 *02,292*

COMPARTMENT ANALYSIS
Computing Radiative Heat Transfer Occurring in a Zone Fire Model.
PB96-102306 *01,399*

Analyzing and Exploiting Numerical Characteristics of Zone Fire Models.
PB96-102314 *01,400*

COMPARTMENT FIRES
Improvement in Predicting Smoke Movement in Compartmented Structures.
PB94-172418 *00,332*

Calculating Flame Spread on Horizontal and Vertical Surfaces.
PB94-187283 *00,335*

Backdraft Phenomena.
PB94-193927 *01,366*

Combined Buoyancy- and Pressure-Driven Flow Through a Shallow, Horizontal, Circular Vent.
PB94-210077 *00,344*

VENTCF2: An Algorithm and Associated FORTRAN 77 Subroutine for Calculating Flow through a Horizontal Ceiling/Floor Vent in a Zone-Type Compartment Fire Model.
PB94-210127 *00,345*

Carbon Monoxide Production in Compartment Fires: Reduced-Scale Enclosure Test Facility.
PB95-231700 *01,394*

Scaling Compartment Fires: Reduced- and Full-Scale Enclosure Burns.
PB96-175708 *00,224*

Dynamics, Transport and Chemical Kinetics of Compartment Fire Exhaust Gases.
PB96-195508 *00,229*

COMPETITION

Status of Construction and Construction Technologies.
PB94-186004 *00,318*

Differences in Competitive Strategies between the United States and Japan.
PB94-211836 *00,013*

COMPETITIVENESS

Program of the Subcommittee on Construction and Building.
PB94-193646 *00,319*

Program of the Subcommittee on Construction and Building (July 1994).
PB95-122537 *00,321*

COMPILERS

Ada Compiler Validation Summary Report: Certificate Number: 931029S1.11330, Digital Equipment Corporation, DEC Ada for DEC OSF/1 AXP Systems, Version 3.1, DEC 3000 Model 400 AXP Workstation, DEC 3000 Model 400 AXP Workstation.
AD-A274 872/1 *01,639*

Ada Compiler Validation Summary Report: Certificate Number: 931217S1.11336 Control Data Systems, Inc. NOS/VE Ada, Version 1.4 Cyber 180-930-31 => Cyber 180-930-31.
AD-A275 977/7 *01,640*

Ada Compiler Validation Summary Report. Certificate Number: 931119S1.11332, DDC-I, Inc. DACS MIPS R3000 Bare Ada Cross Compiler System, Version 4.7.1 Sun SPARCstation IPX => DACS Sun SPARC/SunOS to MIPS R3000 Bare Instruction Set Architecture Simulator, Version 4.7.1.
AD-A276 181/5 *01,641*

Ada Compiler Validation Summary Report: Certificate Number: 931119S1.11331 DDC-I, Inc. DACS Sun SPARC/SunOS to 80386 PM Bare Ada Cross Compiler System, Version 4.6.4 Sun Sparcstation 1+ => Bare Board iSBC 386/116.
AD-A276 283/9 *01,642*

Ada Compiler Validation Summary Report. Certificate Number: 930927S1.11328 Green Hills Software C Ada, Version 1.1 ZENY 386 => ZENY 386.
AD-A277 981/7 *01,643*

Ada Compiler Validation Summary Report: Certificate Number: 940325S1.11348 DDC-I, DACS Sun SPARC/Solaris to 80386 PM Bare Ada Cross Compiler System, Version 4.6.4 Sun SPARCclassic => Intel iSBC 386/116 (Bare Machine).
AD-A279 642/3 *01,644*

Ada Compiler Validation Summary Report: Certificate Number: 940325S1.11341 DDC-I, DACS Sun SPARC/SunOS to 80186 Bare Ada Cross Compiler System, Version 4.6.4 Sun SPARCstation IPX => Intel iSBC 186/100 (Bare Machine).
AD-A279 643/1 *01,645*

Ada Compiler Validation Summary Report: Certificate Number: 940325S1.11349 DDC-I, DACS Sun SPARC/Solaris to 80386 PM Bare Ada Cross Compiler System with Rate Monotonic Scheduling, Version 4.6.4 Sun SPARCclassic => Intel iSBC 386/116 (Bare Machine).
AD-A279 644/9 *01,646*

Ada Compiler Validation Summary Report: Certificate Number: 940325S1.11354 DDC-I, DACS Sun SPARC/Solaris Native Ada Compiler System, Version 4.6.2 Sun SPARCclassic => Sun SPARCclassic.
AD-A279 645/6 *01,647*

Ada Compiler Validation Summary Report: Certificate Number: 940325S1.11346 DDC-I, DACS Sun SPARC/SunOS to 680x0 Bare Ada Cross Compiler System (BASIC MODE), Version 4.6.9 Sun SPARCstation IPX => Lynwood j435TU (68030) (Bare Machine).
AD-A279 646/4 *01,648*

Ada Compiler Validation Summary Report: Certificate Number: 940325S1.11343 DDC-I, DACS Sun SPARC/Solaris to 80186 Bare Ada Cross Compiler System, Version 4.6.4 Sun SPARCclassic => Intel iSBC 186/100 (Bare Machine).
AD-A279 757/9 *01,649*

Ada Compiler Validation Summary Report: Certificate Number: 940325S1.11344 DDC-I, DACS Sun SPARC/Solaris to 80186 Bare Ada Cross Compiler System with Rate Monotonic Scheduling, Version 4.6.4 Sun SPARCclassic => Intel iSBC 186/100 (Bare Machine).
AD-A279 758/7 *01,650*

Ada Compiler Validation Summary Report: Certificate Number: 940325S1.11347 DDC-I, DACS Sun SPARC/SunOS to 680x0 Bare Ada Cross Compiler System (SECURE MODE), Version 4.6.9 Sun SPARCstation IPX => Lynwood j435TU (68030) (Bare Machine).
AD-A279 778/5 *01,651*

Ada Compiler Validation Summary Report: Certificate Number: 940325S1.11342 DDC-I, DACS Sun SPARC/SunOS to 80186 Bare Ada Cross Compiler System with Rate Monotonic Scheduling Version 4.6.4 Sun SPARCstation IPX => Intel iSBC 186/100 (Bare Machine).
AD-A279 779/3 *01,652*

Ada Compiler Validation Summary Report: Certificate Number: 940325S1.11351 DDC-I, DACS Sun SPARC/SunOS to Pentium PM Bare Ada Cross Compiler System with Rate Monotonic Scheduling, Version 4.6.4 Sun SPARCstation IPX => Intel Pentium (operated as Bare Machine) based in Xpress Desktop (Intel product number: XBASE6E4F-B).
AD-A279 804/9 *01,653*

Ada Compiler Validation Summary Report: Certificate Number: 940325S1.11353 DDC-I, DACS Sun SPARC/Solaris to Pentium PM Bare Ada Cross Compiler System with Rate Monotonic Scheduling, Version 4.6.4 Sun SPARCclassic => Intel Pentium (operated as Bare Machine) based in Xpress Desktop (Intel product number: XBASE6E4F-B).
AD-A279 805/6 *01,654*

Ada Compiler Validation Summary Report: Certificate Number: 940325S1.11350 DDC-I, DACS Sun SPARC/SunOS to Pentium PM Bare Ada Cross Compiler System, Version 4.6.4 Sun SPARCstation IPX => Intel Pentium (Operated as Bare Machine) Based in Xpress Desktop (Intel Product Number: XBASE6E4F-B).
AD-A279 864/3 *01,655*

Ada Compiler Validation Summary Report: Certificate Number 940325S1.11345 DDC-I. DACS Sun SPARC/SunOS to 680x0 Bare Ada Cross Compiler System, Version 4.6.9 Sun SPARCstation IPX => Motorola MVME143 68030/68882 (Bare Machine).
AD-A280 145/4 *01,656*

Ada Compiler Validation Summary Report: Certificate Number: 940325S1.11352 DDC-I DACS Sun SPARC/Solaries to Pentium PM Bare Ada Cross Compiler System, Version 4.6.4 Sun SPARCclassic => Intel Pentium (Operated as Bare Machine) Based in Xpress Desktop (Intel Product Number: XBASE6E4F-B).
AD-A280 295/7 *01,657*

Ada Compiler Validation Summary Report: Certificate Number 940902S1.11377 UNISYS Corporation. IntegrAda for Windows NT, Version 1.0. Intel Deskside Server with Intel 80486DX266 => Intel Deskside Server with Intel 80486DX266.
AD-A288 571/3 *01,658*

Ada Compiler Validation Summary Report: Certificate Number 940902S1.11376. UNISYS Corporation IntegrAda for Windows NT, Version 1.0. Intel Deskside Server for Intel Pentium 60 MHz =>. Intel Deskside Server with Intel Pentium 60 MHz.
AD-A288 572/1 *01,659*

Ada Compiler Validation Summary Report: Certificate Number 94101251.11379 TISOFT, Inc. Green Hills Optimizing Ada Compileer, Version 1.8.7 with PATCK ID 1 COMPAQ ProLiiant 2000 Model 55/66 => COMPAQ ProLiant 2000 Model 5/66.
AD-A288 573/9 *01,660*

Ada Complier Validation Summary Report: Certificate Number: 940929S1.11378. Digital Equipment Corporation DEC Ada for DEC OSF/1 AXP Systems, Version 3.2; DEC 3000 Model 400 AXP Workstation => DEC 3000 Model 400 AXP Workstation.
AD-A288 574/7 *01,661*

Ada Compiler Validation Summary Report. Certificate Number 941117S1.11380. Electronic Data Systems Corp. Compiler: OC Systems Legacy Ada/370, Release 1.4.1 (without optimization).
AD-A289 805/5 *01,662*

ADA Compiler Validation Summary Report, VC Number 950303S1.11381. Digital Equipment Corporation - Compiler Name: DEC Ada for OpenVMS Alpha Systems, Version 3.2.
AD-A293 709/2 *01,663*

Ada Compiler Validation Summary Report, VC No. 950609S1.11390 Digital Equipment Corporation - Compiler Name: DEC Ada Version 3.2 for OpenVMS VAX Systems.
AD-A296 794/1 *01,664*

FORTRAN Compiler Validation System, Version 2.1.
PB94-500691 *01,698*

M (also known as MUMPS) Validation Test Suite, Version 8.3 (for Microcomputers).
PB94-502077 *01,699*

COMPLEX RESONANCE ENERGIES

Population Trapping in Short-Pulse Multiphoton Ionization.
PB96-164140 *04,371*

COMPLEX TIME DEPENDENCE

Complex Time Dependence of the EPR Signal of Irradiated L-alpha-alanine.
PB97-122436 *04,180*

COMPLEX VARIABLE

Exact Series Solution to the Epstein-Hubbell Generalized Elliptic Type Integral Using Complex Variable Residue Theory.
PB97-110167 *03,423*

COMPLEXES

High-Resolution IR Laser-Driven Vibrational Dynamics in Supersonic Jets: Weakly Bound Complexes and Intramolecular Energy Flow.
PB94-216751 *00,862*

Infrared Spectra of van der Waals Complexes of Importance in Planetary Atmospheres.
PB95-125738 *00,071*

Microwave Spectra of van der Waals Complexes of Importance in Planetary Atmospheres.
PB95-150611 *00,919*

COMPLEXITY

Measurement of Process Complexity.
PB97-113138 *01,781*

COMPOSITE FABRICATION

Report on the Workshop on Manufacturing Polymer Composites by Liquid Molding. Held in Gaithersburg, Maryland on September 20-22, 1993.
PB94-160066 *03,131*

COMPOSITE MATERIALS

Report on the Workshop on Manufacturing Polymer Composites by Liquid Molding. Held in Gaithersburg, Maryland on September 20-22, 1993.
PB94-160066 *03,131*

Effect of Two Initiator/Stabilizer Concentrations in a Metal Primer on Bond Strengths of a Composite to a Base Metal Alloy.
PB94-172723 *00,141*

Wear of Selected Materials and Composites Sliding against MoS2 Films.
PB94-172749 *03,231*

Intelligent Processing of Materials.
PB94-172780 *02,811*

Phase Behavior of a Hydrogen Bonding Molecular Composite.
PB94-185188 *01,202*

Effect of Transformation of Alloy on Transient and Residual Stresses in a Porcelain-Metal Strip.
PB94-198397 *00,143*

Asymmetric Tip Morphology of Creep Microcracks Growing Along Bimaterial Interfaces.
PB94-200243 *03,138*

Physics Required for Prediction of Long Term Performance of Polymers and Their Composites.
PB94-219243 *03,146*

Polymer Composites Workshop. Held in Winona, Minnesota on April 29-30, 1992 (Video).
PB94-780129 *03,147*

One- and Two-Sided Burning of Thermally Thin Materials.
PB95-140935 *03,151*

Investigation into the Flammability Properties of Honeycomb Composites.
PB95-143293 *03,152*

NIR-Spectroscopic Investigation of Water Sorption Characteristics of Dental Resins and Composites.
PB95-151171 *00,189*

Interaction between Micro and Macroscopic Flow in RTM Preforms.
PB95-162012 *03,159*

Nanocomposite Magnetic Materials.
PB95-162780 *04,617*

Elastic Green's Function for a Bimaterial Composite Solid Containing a Free Surface Normal to the Interface.
PB95-163325 *03,162*

Green's Function for Generalized Hilbert Problem for Cracks and Free Surfaces in Composite Materials.
PB95-163333 *03,163*

Generalized Plane Strain Analysis of a Bimaterial Composite Containing a Free Surface Normal to the Interface.
PB95-163341 *03,164*

Polymers Technical Activities 1994. NAC-NRC Assessment Panel, April 6-7, 1995.
PB95-209896 *01,275*

Geometrical Percolation Threshold of Overlapping Ellipsoids.
PB96-102397 *03,167*

Reduction of Marginal Gaps in Composite Restorations by Use of Glass-Ceramic Inserts.
PB96-102405 *00,174*

Wear Transitions in Monolithic Alumina and Zirconia-Alumina Composites.
PB96-103163 *03,168*

Composite Materials for Offshore Operations: Proceedings of the International Workshop (1st). Held in Houston, Texas on October 26-28, 1993.
PB96-109509 *03,169*

Intrinsic Viscosity and the Polarizability of Particles Having a Wide Range of Shapes.
PB96-119318 *03,170*

Modification of the Phase Stability of Polymer Blends by Diblock Copolymer Additivies.
PB96-123542 *03,172*

Hygrothermal Effects on the Performance of Polymers and Polymeric Composites: A Workshop Report. Held in Gaithersburg, Maryland on September 21-22, 1995.
PB96-183207 *03,180*

Polymers Technical Activities, 1995.
PB96-193719 *01,291*

Economics of New-Technology Materials: A Case Study of FRP Bridge Decking.
PB96-202353 *01,349*

COMPOSITE STRUCTURES

Composite Struts for SMES Plants.
PB95-155586 *02,507*

COMPOSITES

Ultrasonic-Resonance Spectroscopy of Bulk and Layered Solids.
PB96-141338 *04,759*

Electrodeposited Cobalt-Tungsten as a Diffusion Barrier between Graphite Fibers and Nickel.
PB96-146881 *03,176*

Applicability of Effective Medium Theory to Ferroelectric/Ferrimagnetic Composites with Composition and Frequency-Dependent Complex Permittivities and Permeabilities.
PB96-157854 *01,945*

Lattice Statics of Interfaces and Interfacial Cracks in Bimaterial Solids.
PB96-161823 *02,985*

Estimation of the Orientation Distribution of Short-Fiber Composites Using Ultrasonic Velocities.
PB96-176656 *03,178*

Flaw Tolerance and Toughness Curves in Two-Phase Particulate Composites: SiC/Glass System.
PB96-179460 *03,081*

Orthotropic Elastic Constants of a Boron-Aluminum Fiber-Reinforced Composite: An Acoustic-Resonance-Spectroscopy Study.
PB96-200175 *03,182*

Tensile Creep of Silicide Composites.
PB96-200803 *03,183*

Need for Advanced Characterization Techniques in Product Manufacturing: A Case Study on Ceramic Matrix Composites.
PB96-204060 *03,089*

Life Prediction of a Continuous Fiber Reinforced Ceramic Composite Under Creep Conditions.
PB96-204128 *03,091*

Letter Report on Flame Spread Testing of a Composite Material.
PB97-110068 *01,436*

Characterizing Materials Properties for Ceramic Matrix Composites.
PB97-110282 *03,097*

Surface Roughness of Glass-Ceramic Insert. Composite Restorations: Assessing Several Polishing Techniques.
PB97-119010 *03,583*

COMPOSITION (PROPERTY)

Compositional Homogeneity in Processing Precursor Powders to the Ba2YCu3O7-x High Tc Superconductor.
PB94-212743 *04,508*

COMPOSITIONAL MAPPING

Study of Diffusion Zones with Electron Microprobe Compositional Mapping.
PB94-216348 *00,559*

COMPOUND SEMICONDUCTORS

Development and Characterization of Insulating Layers on Silicon Carbide: Annual Report for February 14, 1988 to February 14, 1989.
PB94-155579 *02,295*

COMPRESSED GAS

Stability of Compressed Gas Mixtures Containing Low Level Volatile Organic Compounds in Aluminum Cylinders.
PB96-111968 *00,613*

COMPRESSED GASES

Method of Sale for CNG Paves Way to Greater Public Acceptance.
PB95-168449 *02,489*

COMPRESSIBILITY

Crystal Structure and Compressibility of 3:2 Mullite.
PB95-175030 *03,682*

Compressibility of Polycrystal and Monocrystal Copper: Acoustic-Resonance Spectroscopy.
PB96-164223 *02,990*

COMPRESSIBLE FLUIDS

Measurements of the Viscosities of Saturated and Compressed Fluid 1-chloro-1,2,2,2-tetrafluoroethane (R124) and Pentafluoroethane (R125) at Temperatures between 120 and 420 K.
PB94-199791 *03,254*

Measurements of the Viscosities of Saturated and Compressed Liquid 1,1,1,2-Tetrafluoroethane (R134a), 2,2-Dichloro-1,1,1-Trifluoroethane (R123) and 1,1-Dichloro-1-Fluoroethane (R141b).
PB95-175386 *03,273*

COMPRESSION

Shape of the Temperature-Entropy Saturation Boundary.
PB96-135066 *02,506*

COMPRESSIVE STRENGTH

Maturity Method.
PB94-199494 *01,313*

Maturity Functions for Concrete Made with Various Cements and Admixtures.
PB94-199502 *01,314*

Hollow Clay Tile Prism Tests for Martin Marietta Energy Systems: Task 2 Testing.
PB94-217486 *00,352*

Effects of Testing Variables on the Measured Compressive Strength of High-Strength (90 MPa) Concrete.
PB95-179040 *00,445*

Prediction of Potential Concrete Strength at Later Ages.
PB96-112180 *01,324*

Effects of Testing Variables on the Strength of High-Strength (90 Mpa) Concrete Cylinders.
PB96-112198 *00,456*

COMPRESSOR BLADES

Determination of Hydrogen in Titanium Alloy Jet Engine Compressor Blades by Cold Neutron Capture Prompt Gamma-ray Activation Analysis.
PB95-175956 *01,448*

COMPTON EFFECT

Study of Multiple Scattering Background in Compton Scatter Imaging.
PB96-112222 *04,425*

COMPTON SCATTERING

Penetration and Diffusion of Hard X-rays through Thick Barriers. III. Studies of Spectral Distributions.
AD-A292 502/2 *03,771*

COMPUTATION

Computing S(alpha) Using Symbolic Monte Carlo.
PB94-198660 *03,410*

Portable Vectorized Software for Bessel Function Evaluation.
PB94-198975 *01,690*

Software Needs in Special Functions.
PB95-105045 *01,702*

Leady Axisymmetric Modes in Infinite Clad Rods. Part 1.
PB95-162905 *04,187*

Performance Characteristics of Fast Elliptic Solvers on Parallel Platforms.
PB95-180832 *01,723*

Error-Bounding in Level-Index Computer Arithmetic.
PB96-109582 *01,742*

COMPUTATIONAL FLUID DYNAMICS

Experimental and Numerical Studies on Two-Dimensional Gravity Currents in a Horizontal Channel.
PB94-165941 *01,359*

Dispersion and Deposition of Smoke Plumes Generated in Massive Fires.
PB95-126066 *02,540*

Mathematical Modeling and Computer Simulation of Fire Phenomena.
PB95-180063 *00,384*

Book Review: Aspects and Applications of the Random Walk.
PB96-123534 *04,215*

Transport by Gravity Currents in Building Fires.
PB97-119325 *01,441*

COMPUTATIONAL GEOMETRY

Submissions to a Planned Encyclopedia of Operations Research on Computational Geometry and the Voronoi/Delaunay Construct.
PB94-152709 *03,425*

Growth Surface for the Slopes at the Boundary of a Polygon.
PB94-152725 *03,408*

Data-Parallel Algorithm for Three-Dimensional Delaunay Triangulation and Its Implementation.
PB95-163309 *01,714*

Inserting Line Segments into Triangulations and Tetrahedralizations.
PB95-198933 *03,415*

COMPUTATIONAL MATERIALS SCIENCE

Whither Computational Materials Science. Some Thoughts from the Mechanical Properties Front.
PB96-161997 *02,987*

COMPUTER-AIDED ACQUISITION AND LOGISTIC SUPPORT

Impact of Computer-Aided Acquisition and Logistic Support (CALS) in the Application of Standards.
PB96-160908 *01,756*

COMPUTER AIDED DESIGN

APDE Demonstration System Architecture. National PDES Testbed Report Series.
PB94-154325 *02,767*

Variant Design for Mechanical Artifacts-A State of the Art Survey.
PB94-154358 *02,768*

Design Guide for CMOS-On-SIMOX. Test Chips NIST3 and NIST4.
PB94-163458 *02,297*

Semiconductor Measurement Technology: Design and Testing Guides for the CMOS and Lateral Bipolar-on-SOI Test Library.
PB94-178019 *02,301*

High-Level CAD Melds Micromachined Devices with Foundries.
PB94-216413 *02,321*

CALS-Digital Representation for Communication of Product Data: IGES Application Subsets.
PB94-962100 *03,658*

CALS-Raster Graphics Representation Binary Format Requirements.
PB94-962300 *03,660*

CALS-Digital Representation for Communication of Illustration Date: CGM Application Profile.
PB94-962400 *03,661*

Summary and Notes of the Joint ISO/IGES/PDES Organization Technical Committee Meeting. Held in Albuquerque, New Mexico on October 15-20, 1989.
PB95-107314 *02,774*

National PDES Testbed: An Overview.
PB95-125829 *02,775*

Challenges to the National Information Infrastructure: The Barriers to Product Data Sharing. National PDES Testbed Report Series.
PB95-136347 *02,776*

Vertical-Cavity Semiconductor Lasers: Structural Characterization, CAD, and DFB Structures.
PB95-153193 *02,150*

CALS-Digital Representation for Communication of Product Data: IGES Application Subsets.
PB95-962100 *03,667*

CALS-Raster Graphics Representation Binary Format Requirements.
PB95-962300 *03,669*

CALS-Digital Representation for Communication of Illustration Date: CGM Application Profile.
PB95-962400 *03,670*

Characterization of Two-Dimensional Dopant Profiles: Status and Review.
PB96-119300 *02,400*

Extensions of the Prototype Application Protocol of Ready-to-Wear Apparel Pattern Making.
PB96-128194 *03,198*

Micromachined Display Output for a Cellular Neural Network.
PB96-156070 *02,422*

New Generation of Fire Resistant Polymers. Part 1. Computer-Aided Molecular Design.
PB96-160593 *01,419*

Computer-Aided Molecular Design of Fire Resistant Aircraft Materials.
PB96-160601 *00,025*

Distributed Architecture for Standards Processing.
PB96-164181 *00,276*

Group 1 for the Plant Spatial Configuration STEP Application Protocol.
PB96-165402 *02,789*

Aspects of a Product Model Supporting Apparel Virtual Enterprises.
PB96-183231 *02,790*

Characterization of Two-Dimensional Dopant Profiles: Status and Review.
PB97-110134 *02,451*

Representing Designs with Logic Formulations of Spatial Relations.
PB97-111561 *02,792*

Using Logic to Specify Shapes and Spatial Relations in Design Grammars.
PB97-111579 *02,793*

HVAC CAD Layout Tools: A Case Study of University/Industry Collaboration.
PB97-112221 *00,281*

Combining Interactive Exploration and Optimization for Assembly Design.
PB97-112320 *02,794*

Knowledge-Based Approach for Automating a Design Method for Concurrent and Real-Time Systems.
PB97-112502 *01,780*

Improving the Design Process by Predicting Downstream Values of Design Attributes.
PB97-113096 *02,795*

Interoperability Requirements for CAD Data Transfer in the AutoSTEP Project.
PB97-114268 *02,796*

Group 1 for the Process Engineering Data STEP Application Protocol.
PB97-116073 *02,797*

Capabilities for Product Data Exchange.
PB97-118764 *02,798*

COMPUTER AIDED LANGUAGE

Guidelines for the Development of Mapping Tables.
PB96-154539 *02,786*

COMPUTER AIDED MANUFACTURING

Integration Definition for Function Modeling (IDEF0); Category: Software Standard; Subcategory: Modeling Techniques.
FIPSPUB183 *02,800*

Enhanced Machine Controller Architecture Overview.
PB94-142460 *02,802*

Feasibility Study: Reference Architecture for Machine Control Systems Integration.
PB94-142791 *02,804*

APDE Demonstration System Architecture. National PDES Testbed Report Series.
PB94-154325 *02,767*

U.S. Navy Coordinate Measuring Machines: A Study of Needs.
PB94-162831 *02,807*

NIST Support to the Next Generation Controller Program: 1991 Final Technical Report.
PB94-163490 *02,808*

AMRF Composite Fabrication Workstation.
PB94-172681 *02,810*

Intelligent Processing of Materials.
PB94-172780 *02,811*

State-of-the-Art Survey of Methodologies for Representing Manufacturing Process Capabilities.
PB94-187655 *02,812*

NIST RS274/NGC Interpreter Version 1.
PB94-187788 *02,814*

Control Entity Interface Specification.
PB94-191715 *02,815*

Visualization Applications for Manufacturing: A State-of-the-Art Survey. Final Report.
PB94-194552 02,816

Implementing a Transition Manager in the AMRF Cell Controller.
PB94-199932 02,817

Generic Manufacturing Controllers.
PB94-199940 02,818

Technical Program Description Systems Integration for Manufacturing (SIMA).
PB94-213758 02,819

Summary and Notes of the Joint ISO/IGES/PDES Organization Technical Committee Meeting. Held in Albuquerque, New Mexico on October 15-20, 1989.
PB95-107314 02,774

National PDES Testbed: An Overview.
PB95-125829 02,775

Challenges to the National Information Infrastructure: The Barriers to Product Data Sharing. National PDES Testbed Report Series.
PB95-136347 02,776

Reference Architecture for Machine Control Systems Integration: Interim Report.
PB95-144549 02,820

Portsmouth Fastener Manufacturing Workstation. User's Manual.
PB95-147922 02,860

Using Grafcet to Design Generic Controllers.
PB95-150827 02,821

Integration of Real-Time Process Planning for Small-Batch Flexible Manufacturing.
PB95-151908 02,822

Automated Optical Roughness Inspection.
PB95-152179 02,905

Workshop on the Application of Virtual Reality to Manufacturing. Final Report. Held in Gaithersburg, Maryland on August 9, 1994.
PB95-173555 02,825

Automated Manufacturing Research Facility 1994 Annual Report.
PB95-209854 00,015

Information Technologies Make Business Sense for the Custom Therapeutic Footwear Industry.
PB95-251708 02,829

Production Management Information Model for Discrete Manufacturing.
PB96-112008 02,830

Requisite Elements, Rationale, and Technology Overview for the Systems Intergration for Manufacturing Applications (SIMA) Program. Background Study.
PB96-112685 02,831

Overview of the Manufacturing Engineering Toolkit Prototype.
PB96-128228 02,833

Computer-Aided Manufacturing Engineering Forum (1st). Technical Meeting Proceedings. Held in Gaithersburg, Maryland on March 21-22, 1995.
PB96-136965 02,834

NIST RS274KT Interpreter.
PB96-147954 02,835

Product Realization Process Modeling: A Study of Requirements, Methods and Research Issues.
PB96-147962 02,836

Machine Performance Standard Provides Opportunity to Improve Quality and Productivity.
PB96-154521 02,837

Guidelines for the Development of Mapping Tables.
PB96-154539 02,786

NIST SIMA Interactive Management Workshop. Held in Fort Belvoir, Virginia on November 14-16, 1994.
PB96-154877 02,838

Quality in Automated Manufacturing.
PB96-160437 02,839

Development of a New Quality Control Strategy for Automated Manufacturing.
PB96-160486 02,840

Group 1 for the Plant Spatial Configuration STEP Application Protocol.
PB96-165402 02,789

Procedure for Product Data Exchange Using STEP Developed in the AutoSTEP Pilot.
PB96-183058 02,843

Systems Integration for Manufacturing Applications Program 1995 Annual Report.
PB96-193735 02,844

Computer-Aided Manufacturing Engineering Forum (2nd). Technical Meeting Proceedings. Held in Gaithersburg, Maryland on August 22-23, 1995.
PB96-195334 02,845

Optoelectronics and Optomechanics Manufacturing: An ATP Focused Program Development. Workshop Proceedings. Held in Gaithersburg, Maryland on February 15, 1995.
PB97-104186 02,204

Interoperability Requirements for CAD Data Transfer in the AutoSTEP Project.
PB97-114268 02,796

Group 1 for the Process Engineering Data STEP Application Protocol.
PB97-116073 02,797

Unified Process Specification Language: Requirements for Modeling Process.
PB97-116123 02,850

Capabilities for Product Data Exchange.
PB97-118764 02,798

COMPUTER AIDED MAPPING

Geographic Information Systems Standards: A Federal Perspective.
PB95-163390 03,678

COMPUTER ALGEBRA SYSTEM

Expression Formatter for MACSYMA.
PB95-267829 01,735

COMPUTER APPLICATIONS

Benchmarks for the Evaluation of Speech Recognizers.
PB94-211539 01,566

Important Papers in the History of Document Preparation Systems: Basic Sources.
PB95-125837 02,712

Standards: A Cardinal Direction for Geographic Information Systems.
PB95-150942 03,677

Computers in Welding: A Primer.
PB95-162863 02,862

COMPUTER ARCHITECTURE

VLSI Architectures for Template Matching and Block Matching.
PB94-200029 01,834

COMPUTER ARITHMETIC

Journal of Research of the National Institute of Standards and Technology, March/April 1996. Volume 101, Number 2.
PB96-177381 01,863

COMPUTER ARITHMETICS

MasPar MP-1 as a Computer Arithmetic Laboratory.
PB96-179155 01,617

COMPUTER ASSISTED INSTRUCTION

Proposed International Interactive Courseware Standard.
PB96-123161 00,137

COMPUTER CIRCUITS

High-Temperature Superconductor Cryogenic Current Comparator.
PB96-119334 02,074

COMPUTER CODES

Experience with MPI: 'Converting Pvmmake to Mpimake under LAM' and 'MPI and Parallel Genetic Programming'.
PB96-141296 01,748

COMPUTER COMMUNICATIONS

Comparing Remote Procedure Calls: Open Network Computing, Distributed Computing Environment and International Organization for Standardization.
PB95-194205 01,724

Ouch Those Programs are Painful.
PB96-102678 01,739

Conformance Testing for OSI Protocols.
PB96-102686 01,631

Lessons from the Establishment of the U.S. GOSIP Testing Program.
PB96-119359 01,817

GOSIP Testing Program.
PB96-161229 01,504

COMPUTER GENERATED ENVIRONMENTS

Approaches Using Virtual Environments with Mosaic.
PB95-169108 01,599

COMPUTER GRAPHICS

Graphical Kernel System (GKS). Category: Software Standard. Subcategory: Graphics. International Standard: Information Technology; Computer Graphics; Graphical Kernel System (GKS) Language Bindings. Part 4: C.
FIPS PUB 120-1C 01,792

Open Document Architecture (ODA) Raster Document Application Profile (DAP). Category: Software Standard; Subcategory: Graphics.
FIPS PUB 194 01,669

Computer Graphics Metafile (CGM): Procedures for NIST CGM Validation Test Service.
PB94-161809 01,804

Visualization Applications for Manufacturing: A State-of-the-Art Survey. Final Report.
PB94-194552 02,816

Graphical Conceptual Navigation as a Presentation Technique for a Graphics Standard.
PB94-200573 01,692

CALS-Raster Graphics Representation Binary Format Requirements.
PB94-962300 03,660

CALS-Digital Representation for Communication of Illustration Date: CGM Application Profile.
PB94-962400 03,661

Underflow-Induced Graphics Failure Solved by SLI Arithmetic.
PB95-161444 01,712

CALS-Raster Graphics Representation Binary Format Requirements.
PB95-962300 03,669

CALS-Digital Representation for Communication of Illustration Date: CGM Application Profile.
PB95-962400 03,670

COMPUTER GRAPHICS METAFILE

Computer Graphics Metafile (CGM): Procedures for NIST CGM Validation Test Service.
PB94-161809 01,804

COMPUTER INFORMATION SECURITY

Standard Security Label for Information Transfer; Category: Computer Security; Subcategory: Security Labels.
FIPS PUB 188 01,571

Computer Security Management and Planning in the U.S. Federal Government.
PB95-163432 01,596

Guidance to Federal Agencies on the Use of Trusted Systems.
PB95-163440 01,597

Addressing U.S. Government Security Requirements for OSI.
PB96-160577 01,611

Concept Paper: An Overview of the Proposed Trust Technology Assessment Program.
PB96-160882 01,614

COMPUTER INTEGRATED MANUFACTURING

Roadmap for the Computer Integrated Manufacturing (CIM) Application Framework.
PB96-122759 02,832

COMPUTER INTERFACE

NIST Workshop on the Computer Interface to Flat Panel Displays. Held in San Jose, California on January 13-14, 1994.
PB95-136388 01,625

COMPUTER MEDIATED COMMUNICATION

Information Infrastructure: Reaching Society's Goals. A Report of the Information Infrastructure Task Force Committee on Applications and Technology.
ED-376 823 00,131

COMPUTER MODELS

CFAST Output Comparison Method and Its Use in Comparing Different CFAST Versions.
PB96-109541 00,401

Empirical Validation of a Transient Computer Model for Combined Heat and Moisture Transfer.
PB97-111991 00,416

COMPUTER NETWORKS

NIST Cooperative Laboratory for OSI Routing Technology.
DE94015308 01,791

Report of the Federal Internetworking Requirements Panel.
DE95017761 03,407

Putting the Information Infrastructure to Work: Report of the Information Infrastructure Task Force Committee on Applications and Technology.
N94-31228/7 02,715

Open System Environment Procurement.
N94-36858/6 02,716

Supplement to Stable Implementation Agreements for Open Systems Interconnection Protocols. Version 3, September 1990. Change Page Index, Version 3, June 1990 (Stable) Change Pages Issued December 1990; Output from September 1990 OSI Workshop (NIST Special Publication 500-177).
PB94-164035 01,467

Conformance Assessment of Transport Layer Security Implementations.
PB94-164373 01,576

Local Area Networks in NAA: Advantages and Pitfalls.
PB94-172095 00,527

Conformance Testing of a Lower Layer Security Protocol.
PB94-185402 01,577

Integrated Network Management.
PB94-199247 01,583

IGOSS-Industry/Government Open Systems Specification.
PB94-207453 01,806

Information Infrastructure: Reaching Society's Goals. Report of the Information Infrastructure Task Force Committee on Applications and Technology.
PB94-214756 01,469

Framework for National Information Infrastructure Services.
PB95-103719 02,723

SDNS Security Management.
PB95-161170 01,592

Coping with Different Retrieval Methods in Next Generation Networks.
PB95-168555 02,726

Retrieving Articles from the Internet (without a UNIX Workstation). Part 1. File Formats and Software Tools.
PB95-168720 02,728

Retrieving Articles from the Internet (without a UNIX Workstation). Part 2. An Example.
PB95-168738 02,729

Comparing Remote Procedure Calls: Open Network Computing, Distributed Computing Environment and International Organization for Standardization.
PB95-194205 01,724

Introduction to the P1003.1g and CPI-C Network Application Programming Interfaces.
PB95-231726 *01,731*

National Voluntary Laboratory Accreditation Program. GOSIP: Government Open Systems Interconnection Profile.
PB95-267993 *01,486*

Z39.50 Implementation Experiences.
PB96-114939 *01,816*

Open System Environment (OSE): Architectural Framework for Information Infrastructure.
PB96-146360 *00,002*

Evolution of a United States Information System.
PB96-157896 *02,713*

Comparison of FDDI Asynchronous Mode and DQDB Queue Arbitrated Mode Data Transmission for Metropolitan Area Network Applications.
PB96-160452 *01,498*

Standardization for ATM and Related B-ISDN Technologies.
PB96-160460 *01,499*

Data Communications Strategy.
PB96-167846 *02,738*

Federal Implementation Guideline for Electronic Data Interchange. ASC X12 003050 Transaction Set 840 Request for Quotation. Implementation Convention.
PB96-172531 *01,824*

Federal Implementaion Guideline for Eletronic Data Interchange. ASC X12 003050 Transaction Set 865 Purchase Order Change Acknowledgement/Request - Seller Initiated. Implementation Convention.
PB96-172549 *01,825*

Five Q's (Cues) of the U.S. GOSIP Testing Program.
PB96-175716 *01,826*

Open System Environment Implementors Workshop (OIW); Standardization Role Defined.
PB96-180047 *01,828*

Unpredictable Certainty. Information Infrastructure through 2000.
PB96-182266 *00,016*

COMPUTER PERFORMANCE EVALUATION

Hardware Measurement Techniques for High-Speed Networks.
PB96-160551 *01,500*

Report of a Workshop on the Assurance of High Integrity Software.
PB96-161377 *01,763*

Standards for High Integrity Software.
PB96-161385 *01,764*

Using S-Check, Alpha Release 1.0.
PB96-165964 *01,767*

COMPUTER PROGRAM

Algorithm Testing and Evaluation Program for Coordinate Measuring Systems: Long Range Plan.
PB95-231833 *02,915*

COMPUTER PROGRAM DOCUMENTATION

IML++ v.1.2 Iterative Methods Library Reference Guide.
PB96-195219 *01,776*

COMPUTER PROGRAM INTEGRITY

Concept for an Algorithm Testing and Evaluation Program at NIST.
PB94-163029 *02,890*

Study on Hazard Analysis in High Integrity Software Standards and Guidelines.
PB95-198727 *01,725*

SQA Standards and Total Quality Management.
PB96-111844 *01,743*

Slicing in the Presence of Parameter Aliasing.
PB96-160858 *01,755*

Analysis of Standards for the Assurance of High Integrity Software.
PB96-161351 *03,735*

COMPUTER PROGRAM MANAGEMENT

Reference Information for the Software Verification and Validation Process.
PB96-188164 *01,773*

COMPUTER PROGRAM PORTABILITY

Porting Multimedia Applications to the Open System Environment.
PB94-172921 *02,721*

Simple Scalability Test for MIMD Code.
PB94-193638 *01,688*

Application Portability Profile (APP): The U.S. Government's Open System Environment Profile Version 3.0.
PB96-158712 *01,753*

Open Systems Software Standards in Concurrent Engineering.
PB96-160932 *01,758*

NIST POSIX Testing Program.
PB96-160973 *01,821*

CSL View of Applications Portability, Scalability, and Interoperability.
PB97-122303 *01,787*

COMPUTER PROGRAM RELIABILITY

Software Safety and Program Slicing.
PB95-125894 *01,703*

Center for High Integrity Software System Assurance: Initial Goals and Activities.
PB95-251674 *01,734*

Unravel: A CASE Tool to Assist Evaluation of High Integrity Software. Volume 1. Requirements and Design.
PB95-267886 *01,736*

Unravel: A CASE Tool to Assist Evaluation of High Integrity Software. Volume 2. User Manual.
PB95-267894 *01,737*

COMPUTER PROGRAM VALIDATION

Experimental Models for Software Diagnosis.
PB97-113906 *01,783*

COMPUTER PROGRAM VERFICATION

Verification and Validation.
PB96-161393 *01,765*

COMPUTER PROGRAM VERIFICATION

User's Guide for the PHIGS Validation Tests (Version 2.1).
PB94-165206 *01,682*

Process for Selecting Standard Reference Algorithms for Evaluating Coordinate Measurement Software.
PB94-173754 *02,629*

Formal Specification and Verification of Control Software for Cryptographic Equipment.
PB94-213030 *01,585*

FORTRAN Compiler Validation System, Version 2.1.
PB94-500691 *01,698*

SGML Parser Validation Procedures.
PB95-174959 *01,717*

Testers Open Dialogue at Inaugural NIST Workshop.
PB95-175550 *01,718*

Algorithm Testing and Evaluation Program for Coordinate Measuring Systems: Testing Methods.
PB95-251658 *02,666*

User's Guide for the Algorithm Testing System Version 2.0.
PB95-251666 *02,916*

Method to Determine a Basis Set of Paths to Perform Program Testing.
PB96-131503 *01,747*

Standard Generalized Markup Language Test Suite Evaluation Report.
PB96-154992 *01,751*

IEEE's POSIX: Making Progress.
PB96-160924 *01,757*

Analysis of Standards for the Assurance of High Integrity Software.
PB96-161351 *03,735*

Verification and Validation of Reengineered Software.
PB96-161401 *01,766*

Reference Information for the Software Verification and Validation Process.
PB96-188164 *01,773*

COMPUTER PROGRAMMING

World Model Registration for Effective Off-Line Programming of Robots.
PB94-173010 *02,933*

Introduction to the P1003.1g and CPI-C Network Application Programming Interfaces.
PB95-231726 *01,731*

X Window System, Version 11, Release 5.
PB96-169099 *01,769*

Interoperability Experiments with CORBA and Persistent Object Base Systems.
PB96-183140 *01,772*

Experimental Evaluation of Specification Techniques for Improving Functional Testing.
PB96-201009 *01,779*

COMPUTER PROGRAMS

Semiconductor Measurement Technology: HOTPAC. Programs for Thermal Analysis Including Version 3.0 of the TXYZ Program, TXYZ30, and the Thermal MultiLayer Program, TML.
PB95-260766 *02,374*

Error-Bounding in Level-Index Computer Arithmetic.
PB96-109582 *01,742*

Federal Implementation Guideline for Electronic Data Interchange: ASC X12 003040 Transaction Set 838 Trading Partner Profile (Confirmation of Vendor Registration). Implementation Convention.
PB96-111190 *01,813*

SUM and MEAN: Standard Programs for Activation Analysis.
PB96-112149 *00,617*

Federal Implementation Guideline for Electronic Data Interchange: ASC X12 003040 Transaction Set 838 Trading Partner Profile (Vendor Registration), Implementation Convention.
PB96-112651 *03,674*

User's Guide to 'SuperFit' Modeling Software for CMM Probe Lobing.
PB96-128236 *02,921*

Fire Protection Engineering Tools. Simple Tools: The Equations.
PB96-156179 *00,221*

Prototyping a Graphical User Interface for DHCP.
PB96-160544 *02,599*

Application of the Pointer State Subgraph to Static Program Slicing.
PB96-167838 *01,768*

Structured Testing: A Testing Methodology Using the Cyclomatic Complexity Metric.
PB97-114169 *01,784*

COMPUTER SCIENCE & TECHNOLOGY

Ada Compiler Validation Summary Report: Certificate Number: 931029S1.11330, Digital Equipment Corporation, DEC Ada for DEC OSF/1 AXP Systems, Version 3.1, DEC 3000 Model 400 AXP Workstation, DEC 3000 Model 400 AXP Workstation.
AD-A274 872/1 *01,639*

Ada Compiler Validation Summary Report: Certificate Number: 931217S1.11336 Control Data Systems, Inc. NOS/VE Ada, Version 1.4 Cyber 180-930-31 => Cyber 180-930-31.
AD-A275 977/7 *01,640*

Ada Compiler Validation Summary Report. Certificate Number: 931119S1.11332, DDC-I, Inc. DACS MIPS R3000 Bare Ada Cross Compiler System, Version 4.7.1 Sun SPARCstation IPX => DACS Sun SPARC/SunOS to MIPS R3000 Bare Instruction Set Architecture Simulator, Version 4.7.1.
AD-A276 181/5 *01,641*

Ada Compiler Validation Summary Report: Certificate Number: 931119S1.11331 DDC-I, Inc. DACS Sun SPARC/SunOS to 80386 PM Bare Ada Cross Compiler System, Version 4.6.4 Sun Sparcstation 1+ => Bare Board iSBC 386/116.
AD-A276 283/9 *01,642*

Ada Compiler Validation Summary Report. Certificate Number: 930927S1.11328 Green Hills Software C Ada, Version 1.1 ZENY 386 => ZENY 386.
AD-A277 981/7 *01,643*

Ada Compiler Validation Summary Report: Certificate Number: 940325S1.11348 DDC-I, DACS Sun SPARC/Solaris to 80386 PM Bare Ada Cross Compiler System, Version 4.6.4 Sun SPARCclassic => Intel iSBC 386/116 (Bare Machine).
AD-A279 642/3 *01,644*

Ada Compiler Validation Summary Report: Certificate Number: 940325S1.11341 DDC-I, DACS Sun SPARC/SunOS to 80186 Bare Ada Cross Compiler System, Version 4.6.4 Sun SPARCstation IPX => Intel iSBC 186/100 (Bare Machine).
AD-A279 643/1 *01,645*

Ada Compiler Validation Summary Report: Certificate Number: 940325S1.11349 DDC-I, DACS Sun SPARC/Solaris to 80386 PM Bare Ada Cross Compiler System with Rate Monotonic Scheduling, Version 4.6.4 Sun SPARCclassic => Intel iSBC 386/116 (Bare Machine).
AD-A279 644/9 *01,646*

Ada Compiler Validation Summary Report: Certificate Number: 940325S1.11354 DDC-I, DACS Sun SPARC/Solaris Native Ada Compiler System, Version 4.6.2 Sun SPARCclassic => Sun SPARCclassic.
AD-A279 645/6 *01,647*

Ada Compiler Validation Summary Report: Certificate Number: 940325S1.11346 DDC-I, DACS Sun SPARC/SunOS to 680x0 Bare Ada Cross Compiler System (BASIC MODE), Version 4.6.9 Sun SPARCstation IPX => Lynwood j435TU (68030) (Bare Machine).
AD-A279 646/4 *01,648*

Ada Compiler Validation Summary Report: Certificate Number: 940325S1.11343 DDC-I, DACS Sun SPARC/Solaris to 80186 Bare Ada Cross Compiler System, Version 4.6.4 Sun SPARCclassic => Intel iSBC 186/100 (Bare Machine).
AD-A279 757/9 *01,649*

Ada Compiler Validation Summary Report: Certificate Number: 940325S1.11344 DDC-I, DACS Sun SPARC/Solaris to 80186 Bare Ada Cross Compiler System with Rate Monotonic Scheduling, Version 4.6.4 Sun SPARCclassic => Intel iSBC 186/100 (Bare Machine).
AD-A279 758/7 *01,650*

Ada Compiler Validation Summary Report: Certificate Number: 940325S1.11347 DDC-I, DACS Sun SPARC/SunOS to 680x0 Bare Ada Cross Compiler System (SECURE MODE), Version 4.6.9 Sun SPARCstation IPX => Lynwood j435TU (68030) (Bare Machine).
AD-A279 778/5 *01,651*

Ada Compiler Validation Summary Report: Certificate Number: 940325S1.11342 DDC-I, DACS Sun SPARC/SunOS to 80186 Bare Ada Cross Compiler System with Rate Monotonic Scheduling Version 4.6.4 Sun SPARCstation IPX => Intel iSBC 186/100 (Bare Machine).
AD-A279 779/3 *01,652*

Ada Compiler Validation Summary Report: Certificate Number: 940325S1.11351 DDC-I, DACS Sun SPARC/SunOS to Pentium PM Bare Ada Cross Compiler System with Rate Monotonic Scheduling, Version 4.6.4 Sun SPARCstation IPX => Intel Pentium (operated as Bare Machine) based in Xpress Desktop (Intel product number: XBASE6E4F-B).
AD-A279 804/9 *01,653*

Ada Compiler Validation Summary Report: Certificate Number: 940325S1.11353 DDC-I, DACS Sun SPARC/Solaris to Pentium PM Bare Ada Cross Compiler System with Rate Monotonic Scheduling, Version 4.6.4 Sun SPARCclassic => Intel Pentium (operated as Bare Machine) based in Xpress Desktop (Intel product number: XBASE6E4F-B).
AD-A279 805/6 *01,654*

Ada Compiler Validation Summary Report: Certificate Number: 940325S1.11350 DDC-I, DACS Sun SPARC/ SunOS to Pentium PM Bare Ada Cross Compiler System, Version 4.6.4 Sun SPARCstation IPX => Intel Pentium (Operated as Bare Machine) Based in Xpress Desktop (Intel Product Number: XBASE6E4F-B).
AD-A279 864/3 *01,655*

Ada Compiler Validation Summary Report: Certificate Number 940325S1.11345 DDC-I. DACS Sun SPARC/ SunOS to 680x0 Bare Ada Cross Compiler System, Version 4.6.9 Sun SPARCstation IPX => Motorola MVME143 68030/68882 (Bare Machine).
AD-A280 145/4 *01,656*

Ada Compiler Validation Summary Report: Certificate Number 940902S1.11377 UNISYS Corporation. IntegrAda for Windows NT, Version 1.0. Intel Deskside Server with Intel 80486DX266 => Intel Deskside Server with Intel 80486DX266.
AD-A288 571/3 *01,658*

Ada Compiler Validation Summary Report: Certificate Number 940902S1.11376. UNISYS Corporation IntegrAda for Windows NT, Version 1.0. Intel Deskside Server for Intel Pentium 60 MHz =>. Intel Deskside Server with Intel Pentium 60 MHz.
AD-A288 572/1 *01,659*

Ada Compiler Validation Summary Report: Certificate Number 94101251.11379 TISOFT, Inc. Green Hills Optimizing Ada Compileer, Version 1.8.7 with PATCK ID 1 COMPAQ ProLiiant 2000 Model 55/66 => COMPAQ ProLiant 2000 Model 5/66.
AD-A288 573/9 *01,660*

Ada Complier Validation Summary Report: Certificate Number: 940929S1.11378. Digital Equipment Corporation DEC Ada for DEC OSF/1 AXP Systems, Version 3.2; DEC 3000 Model 400 AXP Workstation => DEC 3000 Model 400 AXP Workstation.
AD-A288 574/7 *01,661*

Ada Compiler Validation Summary Report. Certificate Number 941117S1.11380. Electronic Data Systems Corp. Compiler: OC Systems Legacy Ada/370, Release 1.4.1 (without optimization).
AD-A289 895/5 *01,662*

ADA Compiler Validation Summary Report, VC Number 950303S1.11381. Digital Equipment Corporation - Compiler Name: DEC Ada for OpenVMS Alpha Systems, Version 3.2.
AD-A293 709/2 *01,663*

Ada Compiler Validation Summary Report, VC No. 950609S1.11390 Digital Equipment Corporation - Compiler Name: DEC Ada Version 3.2 for OpenVMS VAX Systems.
AD-A296 794/1 *01,664*

Report of the Federal Internetworking Requirements Panel.
DE95017761 *03,407*

Metropolitan Areas (Including MSAs, CMSAs, PMASs, and NECMAs). Category: Data Standards and Guidelines; Subcategory: Representations and Codes.
FIPS PUB 8-6 *04,873*

Countries, Dependencies, Areas of Special Sovereignty, and Their Principal Administrative Divisions. Category: Data Standards and Guidelines; Subcategory: Representation and Codes.
FIPS PUB 10-4 *00,128*

COBOL. Category: Software Standard; Subcategory: Programming Language. Includes ANSI'S X3.23-1985, X3.23A-1989 and X3.23B-1993.
FIPS PUB 21-4 *01,670*

COBOL. Category: Software Standard; Subcategory: Programming Language. Part A.
FIPS PUB 21-4A *01,671*

COBOL. Category: Software Standard; Subcategory: Programming Language. Part B.
FIPS PUB 21-4B *01,672*

Data Encryption Standard (DES); Category: Computer Security; Subcategory: Cryptography.
FIPS PUB 46-2 *01,572*

Guideline: Codes for Named Populated Places, Primary County Divisions, and Other Locational Entities of the United States, Puerto Rico, and the Outlying Areas. Category: Data Standards and Guidelines. Subcategory: Representations and Codes.
FIPS PUB 55-3 *04,865*

Graphical Kernel System (GKS). Category: Software Standard. Subcategory: Graphics. International Standard: Information Technology; Computer Graphics; Graphical Kernel System (GKS) Language Bindings. Part 4: C.
FIPS PUB 120-1C *01,792*

Security Requirements for Cryptographic Modules; Category: Computer Security; Subcategory: Cryptography.
FIPS PUB 140-1 *01,567*

User Interface Component of the Applications Portability Profile Category: Software Standard; Subcategory: Application Program Interface.
FIPS PUB 158-1 *01,793*

Spatial Data Transfer Standard (SDTS): Category: Software Standard; Subcategory: Information Interchange.
FIPS PUB 173-1 *01,794*

Spatial Data Transfer Standard (SDTS). Category: Software Standard; Subcategory: Information Interchange. (FIPS PUB 173-1A).
FIPS PUB 173-1A *01,795*

Spatial Data Transfer Standard (SDTS). Category: Software Standard; Subcategory: Information Interchange. (FIPS PUB 173-1B).
FIPS PUB 173-1B *01,796*

Secure Hash Standard. Category: Computer Security.
FIPS PUB 180-1 *01,568*

Integrated Services Digital Network (ISDN); Category: Telecommunications Standard; Subcategory: Integrated Services Digital Network.
FIPS PUB 182 *01,460*

Escrowed Encryption Standard (EES); Category: Computer Security; Subcategory: Cryptography.
FIPS PUB 185 *01,569*

Digital Signature Standard (DSS). Category: Computer Security; Subcategory: Cryptography.
FIPS PUB 186 *01,570*

Administration Standard for the Telecommunications Infrastructure of Federal Buildings. Category: Telecommunications Standard; Subcategory: Telecommunications Administration.
FIPS PUB 187 *01,461*

Standard Security Label for Information Transfer; Category: Computer Security; Subcategory: Security Labels.
FIPS PUB 188 *01,571*

Portable Operating System Interface (POSIX). Part 2. Shell and Utilities. Category: Software Standard; Subcategory: Operating Systems.
FIPS PUB 189 *01,797*

Guideline for the Use of Advanced Authentication Technology Alternatives. Category: Computer Security. Subcategory: Access Control.
FIPS PUB 190 *01,798*

Guideline for the Analysis of Local Area Network Security. Category: Computer Security; Subcategory: Risk Analysis and Contingency Planning.
FIPS PUB 191 *01,799*

Application Profile for the Government Information Locator Service (GILS). Category: Software Standard; Subcategory: Information Interchange.
FIPS PUB 192 *01,800*

SQL Environments. Category: Software Standard; Subcategory: Database.
FIPS PUB 193 *01,801*

Integration Definition for Function Modeling (IDEF0); Category: Software Standard; Subcategory: Modeling Techniques.
FIPSPUB183 *02,800*

Integration Definition for Information Modeling (IDEF1X); Category: Software Standard; Subcategory: Modeling Techniques.
FIPSPUB184 *01,673*

Optical Storage Media Data Integrity Studies.
N95-24130/3 *01,620*

Proceedings of the Digital Systems Reliability and Nuclear Safety Workshop. Held in Rockville, Maryland on September 13-14, 1993.
NUREG/CP-0136 *03,728*

Technology Trends in Telecommunications: An Overview.
PB94-123080 *01,462*

General Procedures for Registering Computer Security Objects.
PB94-134897 *01,573*

Report of the NIST Workshop on Digital Signature Certificate Management. Held on December 10-11, 1992.
PB94-135001 *01,574*

Planning for the Fiber Distributed Data Interface (FDDI).
PB94-135761 *01,621*

NIST Model PM2 Power Measurement System for 1 mW at 1 GHz.
PB94-135803 *02,018*

Good Security Practices for Electronic Commerce, Including Electronic Data Interchange.
PB94-139045 *01,463*

Security Considerations for SQL-Based Implementations of STEP.
PB94-139649 *02,766*

Guide to Software Engineering Environment Assessment and Evaluation.
PB94-140167 *01,676*

Introduction to Traffic Management for Broadband ISDN.
PB94-142494 *01,464*

Applying Virtual Environments to Manufacturing.
PB94-142502 *02,803*

Context Analysis of the Network Management Domain. Conducted as Part of the Domain Analysis Case Study.
PB94-142528 *01,465*

Report on Application Integration Architectures (AIA) Workshop. Held in Dallas, Texas on February 8-12, 1993.
PB94-142536 *01,803*

Next Generation Computer Resources: Reference Model for Project Support Environments (Version 2.0).
PB94-143401 *01,677*

Guide to Configuration Management and the Revision Control System for Testbed Users.
PB94-150919 *01,678*

Structural EXPRESS Editor.
PB94-159795 *02,769*

Issues and Recommendations for a STEP Application Protocol Framework. National PDES Testbed.
PB94-160868 *02,770*

Computer Graphics Metafile (CGM): Procedures for NIST CGM Validation Test Service.
PB94-161809 *01,804*

Computer Systems Laboratory Annual Report, 1993.
PB94-162518 *01,622*

North American ISDN Users' Forum Agreements on Integrated Services Digital Network.
PB94-162559 *01,466*

Proceedings of the Workshop on the Federal Criteria for Information Technology Security. Held in Ellicot City, Maryland on June 2-3, 1993.
PB94-162583 *01,575*

Distributed Supercomputing Software: Experiences with the Parallel Virtual Machine - PVM.
PB94-163086 *01,680*

Compatibility Analysis of the ANSI and ISO IRDS Services Interfaces.
PB94-163474 *01,805*

Validation Testing System Requirements. National PDES Testbed Report Series.
PB94-163482 *02,771*

Fire Data Management System, FDMS 2.0, Technical Documentation.
PB94-164019 *01,358*

Supplement to Stable Implementation Agreements for Open Systems Interconnection Protocols. Version 3, September 1990. Change Page Index, Version 3, June 1990 (Stable) Change Pages Issued December 1990; Output from September 1990 OSI Workshop (NIST Special Publication 500-177).
PB94-164035 *01,467*

Conformance Assessment of Transport Layer Security Implementations.
PB94-164373 *01,576*

Time-Perturbation Tuning of MIMD Programs.
PB94-164399 *01,681*

User's Guide for the PHIGS Validation Tests (Version 2.1).
PB94-165206 *01,682*

Evaluating Form Designs for Optical Character Recognition.
PB94-168044 *01,830*

Unconstrained Handprint Recognition Using a Limited Lexicon.
PB94-168051 *01,831*

Design and Development of an Information Retrieval System for the EAMATE Data. Volume 2 of 2. Appendices.
PB94-168390 *00,487*

Local Area Networks in NAA: Advantages and Pitfalls.
PB94-172095 *00,527*

Formal Multi-Layer Test Methodology and Its Application to OSI.
PB94-172194 *02,718*

ISO/IEC Workshop on Worldwide Recognition of OSI Test Results Regional Progress - North America.
PB94-172202 *02,719*

Analysis of a Biologically Motivated Neural Network for Character Recognition.
PB94-172277 *00,182*

RDI-SIM ECMA Inter-Domain Routing Protocol Simulation Tool.
PB94-172301 *01,683*

Bringing Natural Language Information Retrieval Out of the Closet.
PB94-172335 *02,720*

Time-Perturbation Tuning of MIMD Programs.
PB94-172566 *01,684*

Using Synthetic-Perturbation Techniques for Tuning Shared Memory Programs (Extended Abstract).
PB94-172657 *01,685*

Porting Multimedia Applications to the Open System Environment.
PB94-172921 *02,721*

Second Text REtrieval Conference (TREC-2). Held in Gaithersburg, Maryland on August 31-September 2, 1993.
PB94-178407 *01,686*

Conformance Testing of a Lower Layer Security Protocol.
PB94-185402 *01,577*

Synthetic-Perturbation Tuning of MIMD Programs.
PB94-185568 *01,687*

User Profile for Researchers Studying Objects: Implications for Computer Systems.
PB94-188463 *00,133*

Second Census Optical Character Recognition Systems Conference.
PB94-188711 *01,832*

Simple Scalability Test for MIMD Code.
PB94-193638 *01,688*

Study of Federal Agency Needs for Information Technology Security.
PB94-193653 *01,579*

Software Libraries, Numerical and Statistical.
PB94-198967 *01,689*

Virtual Software Repository System.
PB94-198983 *01,691*

Integrated Network Management.
PB94-199247 *01,583*

VLSI Architectures for Template Matching and Block Matching.
PB94-200029 *01,834*

Graphical Conceptual Navigation as a Presentation Technique for a Graphics Standard.
PB94-200573 *01,692*

Quality Characteristics and Metrics for Reusable Software (Preliminary Report).
PB94-203437 *01,693*

World Wide Web and Mosaic: User's Guide.
PB94-207354 *02,722*

IGOSS-Industry/Government Open Systems Specification.
PB94-207453 *01,806*

Preliminary Functional Specifications of a Prototype Electronic Research Notebook for NIST.
PB94-207750 *00,012*

Face Recognition Technology for Law Enforcement Applications.
PB94-207768 *01,837*

Report of the NIST Workshop on Key Escrow Encryption. Held in Gaithersburg, Maryland on June 8-10, 1994.
PB94-209459 *01,584*

U.S. GOSIP Testing Program.
PB94-211455 *01,807*

Associated Object Model for Distributed Systems.
PB94-212016 *01,694*

Formal Specification and Verification of Control Software for Cryptographic Equipment.
PB94-213030 *01,585*

Debugger for Tcl Applications.
PB94-213303 *01,695*

Kibitz-Connecting Multiple Interactive Programs Together.
PB94-213311 *01,696*

Using Expect to Automate System Administration Tasks.
PB94-213329 *01,697*

Time Dependent Vector Dynamic Programming Algorithm for the Path Planning Problem.
PB94-215688 *03,428*

Head Start on Assurance: Proceedings of an Invitational Workshop on Information Technology (IT) Assurance and Trustworthiness. Held in Williamsburg, Virginia on March 21-23, 1994.
PB94-215746 *01,586*

NIST-Coordinated Standard for Fingerprint Data Interchange.
PB94-216645 *01,808*

Bibliography of Computer Security Glossaries.
PB94-216710 *01,587*

NIST Form-Based Handprint Recognition System.
PB94-217106 *01,838*

ISDN Conformance Testing Guidelines: Guidelines for Implementors of ISDN Customer Premises Equipment to Conform to Both National ISDN-1 and North American ISDN Users' Forum Layer 3 Basic Rate Interface Basic Call Control Abstract Test Suites.
PB94-219094 *01,471*

Analyzing Electronic Commerce.
PB94-219102 *00,480*

Industry/Government Open Systems Specification Testing Framework. Version 1.0.
PB94-219110 *01,809*

FORTRAN Compiler Validation System, Version 2.1.
PB94-500691 *01,698*

Validated Products List (Cobol, Fortran, ADA, Pascal, MUMPS, SQL).
PB94-937300 *01,700*

CALS-Automated Interchange of Technical Information.
PB94-962000 *03,657*

CALS-Digital Representation for Communication of Product Data: IGES Application Subsets.
PB94-962100 *03,658*

CALS-Markup Requirements and Generic Style Specifications for Electronic Printed Output and Exchange of Text.
PB94-962200 *03,659*

CALS-Raster Graphics Representation Binary Format Requirements.
PB94-962300 *03,660*

CALS-Digital Representation for Communication of Illustration Date: CGM Application Profile.
PB94-962400 *03,661*

CALS-Department of Defense Computer Aided Acquisition Logistic Support (CALS).
PB94-962500 *03,662*

CALS-Contractor Integrated Technical Information Service (CITIS), Functional Requirements.
PB94-962600 *03,663*

Framework for National Information Infrastructure Services.
PB95-103719 *02,723*

Making Sense of Software Engineering Environment Framework Standards.
PB95-105037 *01,701*

Software Needs in Special Functions.
PB95-105045 *01,702*

Security in Open Systems.
PB95-105383 *01,473*

Standardization of Testing Methods for Optical Disk Media Characteristics and Related Activities at NIST.
PB95-108486 *01,624*

Application of Expert System to Select Data Sources from Chemical Information Databases.
PB95-125654 *00,505*

Important Papers in the History of Document Preparation Systems: Basic Sources.
PB95-125837 *02,712*

Software Safety and Program Slicing.
PB95-125894 *01,703*

Object SQL: Language Extensions for Object Data Management.
PB95-125902 *01,704*

Information Resource Dictionary System (IRDS): A Status Report.
PB95-126207 *01,810*

Computer Security Training and Awareness Course Compendium.
PB95-130985 *01,589*

Domain Analysis of the Alarm Surveillance Domain. Version 1.0. Conducted as Part of the Domain Analysis Case Study Project.
PB95-136339 *01,705*

Challenges to the National Information Infrastructure: The Barriers to Product Data Sharing. National PDES Testbed Report Series.
PB95-136347 *02,776*

Comparison of FFT Fingerprint Filtering Methods for Neural Network Classification.
PB95-136362 *01,840*

Faster BKL Monte Carlo Simulations.
PB95-136370 *01,706*

NIST Workshop on the Computer Interface to Flat Panel Displays. Held in San Jose, California on January 13-14, 1994.
PB95-136388 *01,625*

Report on the Advanced Software Technology Workshop. Held on February 1, 1994.
PB95-136610 *01,707*

Information Technology Engineering and Measurement Model: Adding Lane Markings to the Information Superhighway.
PB95-143145 *01,474*

Channel Coding for Code Excited Linear Prediction (CELP) Encoded Speech in Mobile Radio Applications.
PB95-143178 *01,475*

Standards: A Cardinal Direction for Geographic Information Systems.
PB95-150942 *03,677*

Analysis of Selected Software Safety Standards.
PB95-151262 *01,708*

Formal Methods in Conformance Testing: Result and Perspectives.
PB95-153029 *01,710*

Model Precast Concrete Beam-to-Column Connections Subject to Cyclic Loading.
PB95-153094 *00,438*

Mapping Integration Definition for Information Modeling (IDEF1X) Model into CASE Data Interchange Format (CDIF) Transfer File.
PB95-154670 *01,711*

Initial NIST Testing Policy for STEP: Beta Testing Program for AP 203 Implementations. National PDES Testbed Report Series.
PB95-154688 *02,779*

ISDN LAN Bridging.
PB95-154696 *01,477*

User Study: Informational Needs of Remote National Archives and Records Administration Customers.
PB95-154738 *02,725*

SDNS Security Management.
PB95-161170 *01,592*

Keeping Time on Your PC.
PB95-161410 *01,537*

Standards and Linkages: What Data Sharing Needs.
PB95-161881 *01,713*

Data Encryption Standard.
PB95-162376 *01,595*

Access Paths for Materials Databases: Approaches for Large Databases and Systems.
PB95-162525 *02,975*

ISDN Conformance Testing.
PB95-163176 *01,478*

Geographic Information Systems Standards: A Federal Perspective.
PB95-163390 *03,678*

Computer Security Management and Planning in the U.S. Federal Government.
PB95-163432 *01,596*

Guidance to Federal Agencies on the Use of Trusted Systems.
PB95-163440 *01,597*

Computer Virus Attacks.
PB95-163655 *01,715*

Application Profile for ISDN.
PB95-163689 *01,479*

Self-Organizing Neural Network Character Recognition on a Massively Parallel Computer.
PB95-163994 *01,845*

Coping with Different Retrieval Methods in Next Generation Networks.
PB95-168555 *02,726*

Using Archie to Find Files on the INTERNET.
PB95-168605 *02,727*

Approaches Using Virtual Environments with Mosaic.
PB95-169108 *01,599*

Guide on Open System Environment (OSE) Procurements.
PB95-169496 *01,626*

Perspective on Software Engineering Standards.
PB95-171377 *01,811*

Initial Graphics Exchange Specification (IGES): Procedures for the NIST IGES Validation Test Service.
PB95-171427 *02,780*

Binary Decision Clustering for Neural Network Based Optical Character Recognition.
PB95-171971 *01,848*

Framework for the Development and Assurance of High Integrity Software.
PB95-173084 *01,716*

SGML Parser Validation Procedures.
PB95-174959 *01,717*

Asynchronous Transfer Mode Procurement and Usage Guide.
PB95-174967 *01,481*

Testers Open Dialogue at Inaugural NIST Workshop.
PB95-175550 *01,718*

Obtaining and Installing a Public Domain TEX.
PB95-175741 *01,719*

Global Information Infrastructure: Agenda for Cooperation.
PB95-178604 *01,482*

Glossary of Software Reuse Terms.
PB95-178992 *01,720*

Taxonomy for Security Standards.
PB95-180386 *01,602*

Concepts of the NIST EXPRESS Server.
PB95-180543 *02,781*

Handling Passwords with Security and Reliability in Background Processes.
PB95-180550 *01,722*

Federal Government and Information Technology Standards: Building the National Information Infrastructure.
PB95-180840 *01,812*

Prototype Information Retrieval System to Perform a Best-Match Search for Names.
PB95-181152 *02,740*

Keeping Your Site Comfortably Secure: An Introduction to Internet Firewalls.
PB95-182275 *02,730*

Impact of the FCC's Open Network Architecture on NS/NP Telecommunications Security.
PB95-189445 *01,483*

Operating Principles of MultiKron II Performance Instrumentation for MIMD Computers.
PB95-189486 *01,628*

Proceedings Report of the International Invitation Workshop on Development Assurance. Held in Ellicott City, Maryland on June 16-17, 1994.
PB95-189494 *02,912*

Assessment of the DOD Goal Security Architecture (DGSA) for Non-Military Use.
PB95-189510 *03,653*

Comparing Remote Procedure Calls: Open Network Computing, Distributed Computing Environment and International Organization for Standardization.
PB95-194205 *01,724*

Study on Hazard Analysis in High Integrity Software Standards and Guidelines.
PB95-198727 *01,725*

Cryogenic Properties of Inorganic Insulation Materials for ITER Magnets: A Review.
PB95-198768 *03,706*

Object-Oriented Technology Research Areas.
PB95-199329 *01,726*

PET and DINGO Tools for Deriving Distributed Implementations from Estelle.
PB95-203253 *01,727*

World of Building Codes.
PB95-203428 *00,449*

Computer Systems Laboratory Annual Report 1994.
PB95-209920 *01,629*

Electronic Implementors' Workshop.
PB95-210936 *01,484*

Self Monitoring Accounting Systems.
PB95-216602 *00,007*

Overview of the Text REtrieval Conference (3rd) (TREC-3). Held in Gaithersburg, Maryland on November 2-4, 1994.
PB95-216883 *01,728*

Electronic Access: Blueprint for the National Archives and Records Administration.
PB95-219218 *02,731*

Analysis of ANSI ASC X12 and UN/EDIFACT Electronic Data Interchange (EDI) Standards.
PB95-220554 *01,729*

Persistent Object Base System Testing and Evaluation.
PB95-220588 *01,730*

Introduction to the P1003.1g and CPI-C Network Application Programming Interfaces.
PB95-231726 *01,731*

Operating Principles of the SBus MultiKron Interface Board.
PB95-231783 *01,630*

Standards Policy and Information Infrastructure.
PB95-231882 *01,485*

Guidelines for the Evaluation of X.500 Directory Products.
PB95-231908 *02,732*

Testability of Object-Oriented Systems.
PB95-242418 *01,733*

Center for High Integrity Software System Assurance: Initial Goals and Activities.
PB95-251674 *01,734*

Method and Evaluation of Character Stroke Preservation on Handprint Recognition.
PB95-251724 *01,850*

Improving Neural Network Performance for Character and Fingerprint Classification by Altering Network Dynamics.
PB95-267803 *01,851*

Effect of Training Dynamics on Neural Network Performance.
PB95-267845 *01,852*

Unravel: A CASE Tool to Assist Evaluation of High Integrity Software. Volume 1. Requirements and Design.
PB95-267886 *01,736*

Unravel: A CASE Tool to Assist Evaluation of High Integrity Software. Volume 2. User Manual.
PB95-267894 *01,737*

PCASYS: A Pattern-Level Classification Automation System for Fingerprints.
PB95-267936 *01,853*

Building Life Cycle Cost Computer Program (BLCC), Version 4.2-95 (for Microcomputers).
PB95-501953 *00,266*

Validated Products List (Cobol, Fortran, ADA, Pascal, MUMPS, SQL).
PB95-937300 *01,738*

CALS-Automated Interchange of Technical Information.
PB95-962000 *03,666*

CALS-Digital Representation for Communication of Product Data: IGES Application Subsets.
PB95-962100 *03,667*

CALS-Markup Requirements and Generic Style Specifications for Electronic Printed Output and Exchange of Text.
PB95-962200 *03,668*

CALS-Raster Graphics Representation Binary Format Requirements.
PB95-962300 *03,669*

CALS-Digital Representation for Communication of Illustration Date: CGM Application Profile.
PB95-962400 *03,670*

CALS-Department of Defense Computer Aided Acquisition Logistic Support (CALS).
PB95-962500 *03,671*

CALS-Contractor Integrated Technical Information Service (CITIS), Functional Requirements.
PB95-962600 *03,672*

Faster Monte Carlo Simulations.
PB96-102074 *04,018*

Using Synthetic Perturbations and Statistical Screening to Assay Shared-Memory Programs.
PB96-103031 *01,740*

NIST ATM Network Simulator: Operation and Programming, Version 1.0.
PB96-106851 *01,487*

Mapping Integration Definition for Function Modeling (IDEFO) Model into CASE Data Interchange Format (CDIF) Transfer File.
PB96-109533 *01,741*

Federal Implementation Guideline for Electronic Data Interchange: ASC X12 003040 Transaction Set 838 Trading Partner Profile (Confirmation of Vendor Registration). Implementation Convention.
PB96-111190 *01,813*

Human and Machine Recognition of Faces: A Survey.
PB96-111687 *01,854*

SQA Standards and Total Quality Management.
PB96-111844 *01,743*

High Integrity Software Standards Activities at NIST.
PB96-112214 *01,744*

Federal Implementation Guideline for Electronic Data Interchange: ASC X12 003040 Transaction Set 838 Trading Partner Profile (Vendor Registration), Implementation Convention.
PB96-112651 *03,674*

Federal Implementation Guideline for Electronic Data Interchange. ASC X12 003050 Transaction Set 850 Award Instrument. Implementation Convention.
PB96-114913 *01,814*

Federal Implementation Guideline for Electronic Data Interchange. ASC X12 003050 Transaction Set 860 Modifications to Award Instrument. Implementation Convention.
PB96-114921 *01,815*

Z39.50 Implementation Experiences.
PB96-114939 *01,816*

Lessons from the Establishment of the U.S. GOSIP Testing Program.
PB96-119359 *01,817*

Self-Organizing Neural Network Character Recognition Using Adaptive Filtering and Feature Extraction.
PB96-119797 *01,855*

Error Protecting Characteristics of CDMA and Impacts on Speech.
PB96-122452 *01,491*

EDI and EFT Security Standards.
PB96-122833 *01,605*

Open Issues in OSI Protocol Development and Conformance Testing.
PB96-122908 *01,818*

Database Management Standards: Status and Applicability.
PB96-122924 *01,819*

Nonlinear Color Transformations in Real Time Using a Video Supercomputer.
PB96-123021 *02,191*

Proposed International Interactive Courseware Standard.
PB96-123161 *00,137*

Improving Neural Network Performance for Character and Fingerprint Classification by Altering Network Dynamics.
PB96-123195 *01,856*

Common Criteria: On the Road to International Harmonization.
PB96-123484 *01,606*

Functional Security Criteria for Distributed Systems.
PB96-123492 *01,607*

Distributed Systems: Survey of Open Management Approaches.
PB96-128202 *01,746*

Overview of the Manufacturing Engineering Toolkit Prototype.
PB96-128228 *02,833*

Application Software Interface: ISDN Services for an Open Systems Environment.
PB96-131487 *01,492*

Comparison of POSIX Open System Environment (OSE) and Open Distributed Processing (ODP) Reference Models.
PB96-131495 *01,820*

Method to Determine a Basis Set of Paths to Perform Program Testing.
PB96-131503 *01,747*

Sharing Information via the Internet: An Infoserver Case Study.
PB96-131511 *01,493*

Operating Principles of MultiKron Virtual Counter Performance Instrumentation for MIMD Computers.
PB96-131529 *01,632*

Defining Environment Integration Requirements.
PB96-131545 *02,733*

Computer Security: An Introduction to Computer Security. The NIST Handbook.
PB96-131610 *01,608*

Spatial Information and Technology Standards Evolving.
PB96-135108 *03,679*

Telecommunications Security Guidelines for Telecommunications Management Network. Computer Security.
PB96-139415 *01,496*

Experience with MPI: 'Converting Pvmmake to Mpimake under LAM' and 'MPI and Parallel Genetic Programming'.
PB96-141296 *01,748*

Open System Environment (OSE): Architectural Framework for Information Infrastructure.
PB96-146360 *00,002*

Scalability Test for Parallel Code.
PB96-146758 *01,749*

Virtual Environments for Health Care. A White Paper for the Advanced Technology Program (ATP), the National Institute of Standards and Technology.
PB96-147814 *03,594*

C++ in Safety Critical Systems.
PB96-154588 *01,750*

STandard for the Exchange of Product Model Data (STEP): Procedures for NIST STEP Validation.
PB96-154976 *02,787*

Standard Generalized Markup Language Test Suite Evaluation Report.
PB96-154992 *01,751*

Development of Computer-Based Models of Standards and Attendant Knowledge-Base and Procedural Systems.
PB96-155783 *00,464*

Findings and Recommendations from a Software Reengineering Case Study.
PB96-155791 *01,752*

Security Program Management.
PB96-156112 *01,610*

Application Portability Profile (APP): The U.S. Government's Open System Environment Profile Version 3.0.
PB96-158712 *01,753*

Research on Methods for Determining Optical Disk Media Life Expectancy Estimates.
PB96-160304 *01,633*

Comparison of FDDI Asynchronous Mode and DQDB Queue Arbitrated Mode Data Transmission for Metropolitan Area Network Applications.
PB96-160452 *01,498*

Standardization for ATM and Related B-ISDN Technologies.
PB96-160460 *01,499*

Copyright and Information Services in the Context of the National Research and Education Network.
PB96-160536 *02,736*

Prototyping a Graphical User Interface for DHCP.
PB96-160544 *02,599*

Hardware Measurement Techniques for High-Speed Networks.
PB96-160551 *01,500*

Addressing U.S. Government Security Requirements for OSI.
PB96-160577 *01,611*

Status of Emerging Standards for Removable Computer Storage Media and Related Contributions of NIST.
PB96-160619 *01,634*

NIST Program for Investigating Error Reporting Capabilities of Optical Disk Drives.
PB96-160627 *01,635*

Provision of Isochronous Service on IEEE 802.6.
PB96-160635 *01,501*

ISDN in North America.
PB96-160767 *01,502*

North American Agreements on ISDN.
PB96-160775 *01,503*

SQA and TQM in Software Quality Improvement.
PB96-160791 *01,754*

Precise Identification of Computer Viruses.
PB96-160825 *01,613*

Slicing in the Presence of Parameter Aliasing.
PB96-160858 *01,755*

Information Technology Standards in a Changing World: The Rose of the Users.
PB96-160866 *02,737*

Using a Multi-Layered Approach to Representing Tort Law Cases for Case-Based Reasoning.
PB96-160874 *00,135*

Concept Paper: An Overview of the Proposed Trust Technology Assessment Program.
PB96-160882 *01,614*

Assessing Functional Diversity by Program Slicing.
PB96-160890 *03,734*

Impact of Computer-Aided Acquisition and Logistic Support (CALS) in the Application of Standards.
PB96-160908 *01,756*

IEEE's POSIX: Making Progress.
PB96-160924 *01,757*

Open Systems Software Standards in Concurrent Engineering.
PB96-160932 *01,758*

Predicate Differences and the Analysis of Dependencies in Formal Specifications.
PB96-160940 *01,759*

Technique for Analyzing the Effects of Changes in Formal Specifications.
PB96-160957 *01,760*

Template-Driven Systems Development with IDEF: Enterprise Standards for Reuse.
PB96-160965 *02,788*

NIST POSIX Testing Program.
PB96-160973 *01,821*

Program Slicing.
PB96-160981 *01,761*

Conference Report: International Conference on the Application of Standards for Open Systems (6th).
PB96-161211 *01,762*

GOSIP Testing Program.
PB96-161229 *01,504*

Guidance of the Legality of Keystroke Monitoring.
PB96-161237 *00,005*

Industry/Government Open Systems Specification: The Development of GOSIP Version 3.
PB96-161245 *01,505*

Information Technology Standards in Federal Acquisitions.
PB96-161252 *01,636*

Using Information Technology Standards in Federal Acquisitions.
PB96-161260 *01,637*

Analysis of Standards for the Assurance of High Integrity Software.
PB96-161351 *03,735*

Control and Instrumentation: Standards for High-Integrity Software.
PB96-161369 *03,736*

Report of a Workshop on the Assurance of High Integrity Software.
PB96-161377 *01,763*

Standards for High Integrity Software.
PB96-161385 *01,764*

Verification and Validation.
PB96-161393 *01,765*

Verification and Validation of Reengineered Software.
PB96-161401 *01,766*

Response to Comments on the NIST Proposed Digital Signature Standard.
PB96-161815 *01,615*

Manager's Guide for Monitoring Data Integrity in Financial Systems.
PB96-165915 *00,003*

Public Key Infrastructure Invitational Workshop. Held in McLean, Virginia on September 28, 1995.
PB96-166004 *01,616*

Application of the Pointer State Subgraph to Static Program Slicing.
PB96-167838 *01,768*

Data Communications Strategy.
PB96-167846 *02,738*

X Window System, Version 11, Release 5.
PB96-169099 *01,769*

Guidelines for the Evaluation of Electronic Data Interchange Products.
PB96-172325 *01,506*

Federal Implementation Guideline for Electronic Data Interchange. ASC X12 003050 Transaction Set 855 Purchase Order Acknowledgment: Implementation Convention.
PB96-172374 *01,823*

Federal Implementation Guideline for Electronic Data Interchange. ASC X12 003050 Transaction Set 840 Request for Quotation. Implementation Convention.
PB96-172531 *01,824*

Federal Implementaion Guideline for Eletronic Data Interchange. ASC X12 003050 Transaction Set 865 Purchase Order Change Acknowledgement/Request - Seller Initiated. Implementation Convention.
PB96-172549 *01,825*

Five Q's (Cues) of the U.S. GOSIP Testing Program.
PB96-175716 *01,826*

Strategy to Support Multipoint Communication Service Over Native ATM Service.
PB96-176672 *01,507*

Federal Implementation Guideline for Electronic Data Interchange: ASC X12 003050 Transaction Set 836 Procurement Notices. Implementation Convention.
PB96-178892 *01,827*

Deformation and Fracture of Mica-Containing Glass-Ceramics in Hertzian Contacts.
PB96-179452 *03,080*

Open System Environment Implementors Workshop (OIW); Standardization Role Defined.
PB96-180047 *01,828*

Application of Metadata Standards.
PB96-180187 *01,771*

X.500 Directory Schema Design Handbook.
PB96-183041 *02,739*

Interoperability Experiments with CORBA and Persistent Object Base Systems.
PB96-183140 *01,772*

Distributed Communication Methods and Role-Based Access Control for Use in Health Care Applications.
PB96-183165 *01,508*

Binary Decision Clustering for Neural-Network-Based Optical Character Recognition.
PB96-186184 *01,857*

Reference Information for the Software Verification and Validation Process.
PB96-188164 *01,773*

Generalized Form Registration Using Structure-Based Techniques.
PB96-191374 *01,858*

Component-Based Handprint Segmentation Using Adaptive Writing Style Model.
PB96-193669 *01,859*

Computer Systems Laboratory Computing and Applied Mathematics Laboratory Technical Accomplishments, October 1994-March 1996.
PB96-193768 *01,638*

TMACH Experiment Phase 1. Preliminary Developmental Evaluation.
PB96-195318 *01,618*

Experimental Evaluation of Specification Techniques for Improving Functional Testing.
PB96-201009 *01,779*

Guide to Locating and Accessing Computerized Numeric Materials Databases.
PB96-204045 *03,007*

Introduction to Secure Telephone Terminals.
PB97-110498 *01,512*

Computer Security: Generally Accepted Principles and Practices for Securing Information Technology Systems.
PB97-110811 *01,619*

Using Technology to Manage and Protect Intellectual Property.
PB97-112395 *01,513*

Knowledge-Based Approach for Automating a Design Method for Concurrent and Real-Time Systems.
PB97-112502 *01,780*

Measurement of Process Complexity.
PB97-113138 *01,781*

Experimental Models for Software Diagnosis.
PB97-113906 *01,783*

Structured Testing: A Testing Methodology Using the Cyclomatic Complexity Metric.
PB97-114169 *01,784*

Lab Report Special Section: Natural Language Processing and Information Retrieval Group Information Access and User Interfaces Division, National Institute of Standards and Technology.
PB97-118665 *02,742*

Panel: Building and Using Test Collections.
PB97-118673 *02,743*

Text REtrieval Conference (4th) (TREC-4). Held in Gaithersburg, Maryland on November 1-3, 1995.
PB97-121636 *01,786*

Usability Engineering: Industry-Government Collaboration for System Effectiveness and Efficiency.
PB97-122287 *01,514*

CSL View of Applications Portability, Scalability, and Interoperability.
PB97-122303 *01,787*

COMPUTER SECURITY

Security Requirements for Cryptographic Modules; Category: Computer Security; Subcategory: Cryptography.
FIPS PUB 140-1 *01,567*

Secure Hash Standard. Category: Computer Security.
FIPS PUB 180-1 *01,568*

Digital Signature Standard (DSS). Category: Computer Security; Subcategory: Cryptography.
FIPS PUB 186 *01,570*

Guideline for the Use of Advanced Authentication Technology Alternatives. Category: Computer Security. Subcategory: Access Control.
FIPS PUB 190 *01,798*

Guideline for the Analysis of Local Area Network Security. Category: Computer Security; Subcategory: Risk Analysis and Contingency Planning.
FIPS PUB 191 *01,799*

General Procedures for Registering Computer Security Objects.
PB94-134897 *01,573*

Report of the NIST Workshop on Digital Signature Certificate Management. Held on December 10-11, 1992.
PB94-135001 *01,574*

Security Considerations for SQL-Based Implementations of STEP.
PB94-139649 *02,766*

Proceedings of the Workshop on the Federal Criteria for Information Technology Security. Held in Ellicot City, Maryland on June 2-3, 1993.
PB94-162583 *01,575*

Conformance Assessment of Transport Layer Security Implementations.
PB94-164373 *01,576*

Conformance Testing of a Lower Layer Security Protocol.
PB94-185402 *01,577*

Federal Certification Authority Liability and Policy: Law and Policy of Certificate-Based Public Key and Digital Signatures.
PB94-191202 *01,578*

Head Start on Assurance: Proceedings of an Invitational Workshop on Information Technology (IT) Assurance and Trustworthiness. Held in Williamsburg, Virginia on March 21-23, 1994.
PB94-215746 *01,586*

Bibliography of Computer Security Glossaries.
PB94-216710 *01,587*

Security in Open Systems.
PB95-105383 *01,473*

Computer Security Training and Awareness Course Compendium.
PB95-130985 *01,589*

SDNS Security Management.
PB95-161170 *01,592*

Multi-Agency Certification and Accreditation (C and A) Process: A Worked Example.
PB95-171955 *01,601*

Taxonomy for Security Standards.
PB95-180386 *01,602*

Handling Passwords with Security and Reliability in Background Processes.
PB95-180550 *01,722*

Keeping Your Site Comfortably Secure: An Introduction to Internet Firewalls.
PB95-182275 *02,730*

Assessment of the DOD Goal Security Architecture (DGSA) for Non-Military Use.
PB95-189510 *03,653*

Computer Security: An Introduction to Computer Security. The NIST Handbook.
PB96-131610 *01,608*

Security Program Management.
PB96-156112 *01,610*

Response to Comments on the NIST Proposed Digital Signature Standard.
PB96-161815 *01,615*

Public Key Infrastructure Invitational Workshop. Held in McLean, Virginia on September 28, 1995.
PB96-166004 *01,616*

TMACH Experiment Phase 1. Preliminary Developmental Evaluation.
PB96-195318 *01,618*

Computer Security: Generally Accepted Principles and Practices for Securing Information Technology Systems.
PB97-110811 *01,619*

COMPUTER SIMULATION

Effect of Transformation of Alloy on Transient and Residual Stresses in a Porcelain-Metal Strip.
PB94-198397 *00,143*

COMPUTER SOFTWARE

Graphical Kernel System (GKS). Category: Software Standard. Subcategory: Graphics. International Standard: Information Technology; Computer Graphics; Graphical Kernel System (GKS) Language Bindings. Part 4: C.
FIPS PUB 120-1C *01,792*

Programmer's Hierarchical Interactive Graphics System (PHIGS). Category: Software Standard; Subcategory: Graphics.
FIPS PUB 153-1 *01,668*

Guide to Configuration Management and the Revision Control System for Testbed Users.
PB94-150919 *01,678*

Computer Systems Laboratory Annual Report, 1993.
PB94-162518 *01,622*

Distributed Supercomputing Software: Experiences with the Parallel Virtual Machine - PVM.
PB94-163086 *01,680*

Portable Vectorized Software for Bessel Function Evaluation.
PB94-198975 *01,690*

Virtual Software Repository System.
PB94-198983 *01,691*

Kibitz-Connecting Multiple Interactive Programs Together.
PB94-213311 *01,696*

Software Needs in Special Functions.
PB95-105045 *01,702*

Report on the Advanced Software Technology Workshop. Held on February 1, 1994.
PB95-136610 *01,707*

Analysis of Selected Software Safety Standards.
PB95-151262 *01,708*

Opportunities for Innovation: Software for Manufacturing.
PB95-155578 *02,851*

Obtaining and Installing a Public Domain TEX.
PB95-175741 *01,719*

Getting Started on Mosaic.
PB95-180360 *01,721*

Study on Hazard Analysis in High Integrity Software Standards and Guidelines.
PB95-198727 *01,725*

High Integrity Software Standards Activities at NIST.
PB96-112214 *01,744*

Z39.50 Implementation Experiences.
PB96-114939 *01,816*

Numerical Evaluation of Special Functions.
PB96-119557 *03,417*

Performance Measures for Geometric Fitting in the NIST Algorithm Testing and Evaluation Program for Coordinate Measurement Systems.
PB96-122122 *01,745*

What's Available in Welding Software.
PB96-158084 *02,875*

Predicate Differences and the Analysis of Dependencies in Formal Specifications.
PB96-160940 *01,759*

Technique for Analyzing the Effects of Changes in Formal Specifications.
PB96-160957 *01,760*

Software Needs in Special Functions.
PB96-200977 *01,778*

COMPUTER SOFTWARE MAINTENANCE

Findings and Recommendations from a Software Reengineering Case Study.
PB96-155791 *01,752*

Program Slicing.
PB96-160981 *01,761*

COMPUTER STORAGE DEVICES

Status of Emerging Standards for Removable Computer Storage Media and Related Contributions of NIST.
PB96-160619 *01,634*

COMPUTER SYSTEMS DESIGN

Information Technology Engineering and Measurement Model: Adding Lane Markings to the Information Superhighway.
PB95-143145 *01,474*

COMPUTER SYSTEMS HARDWARE

Operating Principles of the SBus MultiKron Interface Board.
PB95-231783 *01,630*

Operating Principles of MultiKron Virtual Counter Performance Instrumentation for MIMD Computers.
PB96-131529 *01,632*

COMPUTER SYSTEMS LABORATORY
Computer Systems Laboratory Annual Report, 1993.
PB94-162518 *01,622*

Computer Systems Laboratory Annual Report 1994.
PB95-209920 *01,629*

Computer Systems Laboratory Computing and Applied Mathematics Laboratory Technical Accomplishments, October 1994-March 1996.
PB96-193768 *01,638*

COMPUTER SYSTEMS PROGRAMS
Using Expect to Automate System Administration Tasks.
PB94-213329 *01,697*

Locating Fire Information.
PB96-190137 *00,227*

COMPUTER VIRUSES
Computer Virus Attacks.
PB95-163655 *01,715*

Precise Identification of Computer Viruses.
PB96-160825 *01,613*

COMPUTER VISION
Computer Vision Based Tool Setting Station.
PB94-199858 *02,944*

Visual-Motion Fixation Invariant.
PB94-206281 *01,836*

Real-Time Vision for Autonomous and Teleoperated Control of Unmanned Vehicles.
PB94-211885 *03,701*

Real-Time Vision for Unmanned Vehicles.
PB94-211893 *03,702*

Adaptive, Predictive 2-D Feature Tracking Algorithm for Finding the Focus of Expansion.
PB94-218575 *01,588*

Real Time Compensation for Tool Form Errors in Turning Using Computer Vision.
PB95-107231 *02,945*

Visual Pursuit Systems.
PB95-143285 *01,841*

Visual Road Following without 3-D Reconstruction.
PB95-161030 *01,591*

Reconstruction during Camera Fixation.
PB95-162236 *01,593*

Unified Approach to Camera Fixation and Vision-Based Road Following.
PB95-162244 *01,594*

Physics-Based Vision: Principles and Practice, Shape Recovery (Book Review).
PB95-164075 *01,846*

Integrated Mobile Robot System for Testing Vision Algorithms.
PB95-164133 *02,936*

Motion-Model-Based Boundary Extraction.
PB95-189502 *01,849*

Real-Time Obstacle Avoidance Using Central Flow Divergence and Peripheral Flow.
PB95-198677 *02,937*

Calculating Time-to-Contact Using Real-Time Quantized Optical Flow.
PB95-210522 *01,604*

Texture-Independent Vision-Based Closed-Loop Fuzzy Controllers for Navigation Tasks.
PB95-220505 *00,183*

Integrated Vision Touch-Probe System for Dimensional Inspection Tasks.
PB95-255832 *02,917*

Human and Machine Recognition of Faces: A Survey.
PB96-111687 *01,854*

Image Gradient Evolution: A Visual Cue for Danger.
PB96-154562 *02,939*

Point Probe Decision Trees for Geometric Concept Classes.
PB96-160817 *01,612*

Scale-Space-Based Visual-Motion-Cue for Autonomous Navigation.
PB96-183173 *02,940*

Novel Active-Vision-Based Motion Cues for Local Navigation.
PB96-193727 *02,941*

COMPUTERIZED CONTROL SYSTEMS
Overview of NASREM: The NASA/NBS Standard Reference Model for Telerobot Control System Architecture.
PB94-194560 *04,831*

COMPUTERIZED SIMULATION
Ignition and Subsequent Transition to Flame Spread in a Microgravity Environment.
N96-15584/1 *04,828*

Computer Programs for Simulation of Lighting/HVAC Interactions.
PB94-140407 *02,501*

Use of Computer Models to Predict Temperature and Smoke Movement in High Bay Spaces.
PB94-145976 *00,191*

Digitized Simulation of Mercury Intrusion Porosimetry.
PB94-172236 *01,304*

RDI-SIM ECMA Inter-Domain Routing Protocol Simulation Tool.
PB94-172301 *01,683*

Digitized Direct Simulation Model of the Microstructural Development of Cement Paste.
PB94-198777 *01,309*

Digitized Simulation Model for Microstructural Development.
PB94-198785 *01,310*

Diffusion Studies in a Digital-Image-Based Cement Paste Microstructural Model.
PB94-198801 *01,312*

Simplified Cycle Simulation Model for the Performance Rating of Refrigerants and Refrigerant Mixtures.
PB94-199890 *03,255*

EXITT: A Simulation Model of Occupant Decisions and Actions in Residential Fires.
PB94-213261 *00,351*

Computer Simulation of the Diffusivity of Cement-Based Materials.
PB95-125985 *00,362*

Digital Simulation of the Aggregate-Cement Paste Interfacial Zone in Concrete.
PB95-125993 *00,363*

Fundamental Computer Simulation Models for Cement-Based Materials.
PB95-126009 *00,364*

Indoor Air Quality Impacts of Residential HVAC Systems, Phase 1 Report: Computer Simulation Plan.
PB95-135596 *00,249*

Faster BKL Monte Carlo Simulations.
PB95-136370 *01,706*

Physics for Device Simulations and Its Verification by Measurements.
PB95-141172 *02,327*

Simulation of Ceramic Particle Formation: Comparison with In-situ Measurements.
PB95-152013 *00,674*

Physics for Device Simulations and Its Verification by Measurements.
PB95-152914 *02,339*

Incinerability of Perchloroethylene and Chlorobenzene.
PB95-163457 *01,388*

Neighbor Tables for Molecular Dynamics Simulations.
PB95-171948 *00,991*

Using Emulators to Evaluate the Performance of Building Energy Management Systems.
PB95-175774 *00,259*

Reproducibility of Tests on Energy Management and Control Systems Using Building Emulators.
PB95-175980 *00,260*

Application of a Multizone Airflow and Contaminant Dispersal Model to Indoor Air Quality Control in Residential Buildings.
PB95-180238 *02,555*

Computer Simulations of Airflow and Radon Transport in Four Large Buildings.
PB95-220422 *02,557*

Enhancements to Program IDARC: Modeling Inelastic Behavior of Welded Connections in Steel Moment-Resisting Frames.
PB95-231601 *00,452*

Length Scales for Fragile Glass-Forming Liquids.
PB96-102801 *01,065*

Use of Building Emulators to Evaluate the Performance of Building Energy Management Systems.
PB96-111901 *00,269*

Simulation Studies of Supercooled and Glass Forming Liquids.
PB96-122627 *01,085*

Fire Hazard Model Developments and Research Efforts at NIST.
PB96-159652 *00,407*

Large Eddy Simulations of Smoke Movement in Three Dimensions.
PB96-190012 *01,426*

COMPUTERS
Computer Systems Laboratory Annual Report, 1993.
PB94-162518 *01,622*

Guarding Against Transients.
PB94-216470 *01,623*

Mapping Processes to Processors for Space-Based Robot Systems.
PB95-151510 *04,833*

Computers in Welding: A Primer.
PB95-162863 *02,862*

Computer Systems Laboratory Annual Report 1994.
PB95-209920 *01,629*

Computer Systems Laboratory Computing and Applied Mathematics Laboratory Technical Accomplishments, October 1994-March 1996.
PB96-193768 *01,638*

How to Get NIST-Traceable Time on Your Computer.
PB96-200647 *01,559*

CONCENTRATING
Simple, Inexpensive Apparatus for Sample Concentration.
PB94-199205 *00,546*

CONCENTRATION (COMPOSITION)
Concentration Histogram Imaging: A Scatter Diagram Technique for Viewing Two or Three Related Images.
PB94-199114 *00,542*

Shear Dependence of Critical Fluctuations in Binary Polymer Mixtures by Small Angle Neutron Scattering.
PB94-211612 *01,220*

Comparison of Experimental and Computed Species Concentration and Temperature Profiles in Laminar, Two-Dimensional Methane/Air Diffusion Flames.
PB95-140919 *01,379*

Laser-Induced Fluorescence Measurements of OH. Concentrations in the Oxidation Region of Laminar, Hydrocarbon Diffusion Flames.
PB95-162160 *01,387*

Determination of Hydrogen in Titanium Alloy Jet Engine Compressor Blades by Cold Neutron Capture Prompt Gamma-ray Activation Analysis.
PB95-175956 *01,448*

CONCENTRATION HISTOGRAM IMAGING
Concentration Histogram Imaging: A Scatter Diagram Technique for Viewing Two or Three Related Images.
PB94-199114 *00,542*

CONCENTRATIONS (COMPOSITION)
Development of a Standard Reference Material for Measurement of Interstitial Oxygen Concentration in Semiconductor Silicon by Infrared Absorption.
PB96-122668 *02,404*

CONCEPTUAL NAVIGATION
Graphical Conceptual Navigation as a Presentation Technique for a Graphics Standard.
PB94-200573 *01,692*

CONCRETE
Cement and Concrete Characterization by Scanning Electron Microscopy.
PB95-163168 *00,379*

Evolution of Porosity and Calcium Hydroxide in Laboratory Concretes Containing Silica Fume.
PB95-175063 *01,321*

Prediction of Potential Concrete Strength at Later Ages.
PB96-112180 *01,324*

Recent Development in Nondestructive Testing of Concrete.
PB96-122445 *01,325*

CONCRETE CONSTRUCTION
Graphical Analysis of the CCRL Portland Cement Proficiency Sample Database (Samples 1-72). (Part 1. Univariant Analysis of Portland Cement).
PB94-196557 *01,308*

CONCRETE DURABILITY
Diagnosis of Causes of Concrete Deterioration in the MLP-7A Parking Garage.
PB95-143095 *01,318*

CONCRETE PAVEMENTS
Optimization of Highway Concrete Technology.
PB94-182995 *01,333*

CONCRETE STRUCTURES
Detection of Voids in Grouted Ducts Using the Impact-Echo Method.
PB94-185121 *01,306*

Evaluating the Seismic Performance of Lightly-Reinforced Circular Concrete Bridge Columns.
PB95-163259 *01,335*

Prediction of Cracking in Reinforced Concrete Structures.
PB95-220448 *03,725*

Shear Design of High-Strength Concrete Beams: A Review of the State-of-the-Art.
PB96-214713 *01,330*

CONCRETES
Expansion of Cementitious Materials Exposed to Sulfate Solutions.
PB94-185782 *02,577*

Sulfate Attack of Cementitious Materials: Volumetric Relations and Expansions.
PB94-187317 *03,232*

Maturity Method.
PB94-199494 *01,313*

Maturity Functions for Concrete Made with Various Cements and Admixtures.
PB94-199502 *01,314*

Highway Concrete (HWYCON) Expert System User Reference and Enhancement Guide.
PB94-215670 *01,316*

Survey of Recent Cementitious Materials Research in Western Europe.
PB94-218583 *00,353*

Digital Simulation of the Aggregate-Cement Paste Interfacial Zone in Concrete.
PB95-125993 *00,363*

Percolation and Pore Structure in Mortars and Concrete.
PB95-150439 *00,370*

Nondestructive Testing of Concrete: History and Challenges.
PB95-180139 *00,385*

High-Performance Concrete: Research Needs to Enhance Its Use.
PB95-180147 *01,322*

Survey of Concrete Transport Properties and Their Measurement.
PB95-220489 *00,396*

Compositional Analysis of Beneficiated Fly Ashes.
PB95-220497 *00,397*

4SIGHT Manual: A Computer Program for Modelling Degradation of Underground Low Level Waste Concrete Vaults.
PB95-231593 *03,726*

Long-Term Performance of Engineered Concrete Barriers.
PB95-260816 *03,727*

Alkali-Silica Reaction and High Performance Concrete.
PB96-131537 *01,345*

Measurement of Rheological Properties of High Performance Concrete: State of the Art Report.
PB96-202338 *00,414*

Multi-Scale Picture of Concrete and Its Transport Properties: Introduction for Non-Cement Researchers.
PB97-115802 *03,107*

CONCURRENT ENGINEERING

Impact of Computer-Aided Acquisition and Logistic Support (CALS) in the Application of Standards.
PB96-160908 *01,756*

Open Systems Software Standards in Concurrent Engineering.
PB96-160932 *01,758*

Knowledge-Based Approach for Automating a Design Method for Concurrent and Real-Time Systems.
PB97-112502 *01,780*

CONCURRENT FLOW

Fire Propagation in Concurrent Flows.
PB94-193844 *01,365*

CONDENSED MATTER PHYSICS

Neighbor Tables for Molecular Dynamics Simulations.
PB95-171948 *00,991*

CONDENSED PHASE

Polymer Combustion and Flammability: Role of the Condensed Phase.
PB96-123245 *01,279*

CONDUCTANCE

Mesoscopic Conductance Fluctuations in Large Devices.
PB96-119656 *04,735*

Evidence for Tunneling and Magnetic Scatttering at 'In situ' YBCO/Noble-Metal Interfaces.
PB96-141098 *04,752*

Quantum Conductance Fluctuations in the Larger-Size-Scale Regime.
PB97-111264 *04,144*

CONDUCTANCE FLUCTUATIONS

Protonation Dynamics of the alpha-Toxin Ion Channel from Spectral Analysis of pH-Dependent Current Fluctuations.
PB96-161740 *03,652*

CONDUCTION

Numerical Analysis Support for Compartment Fire Modeling and Incorporation of Heat Conduction into a Zone Fire Model.
PB94-156965 *01,357*

Slowly Divergent Space Marching Schemes in the Inverse Heat Conduction Problem.
PB94-199486 *03,812*

CONDUCTIVE HEAT TRANSFER

Application of Boundary Element Methods to a Transient Axis-Symmetric Heat Conduction Problem.
PB94-212693 *01,375*

CONDUCTIVITY

Absolute Determination of Electrolytic Conductivity for Primary Standard KC1 Solutions from 0 to 50C.
PB94-172798 *00,765*

dc Method for the Absolute Determination of Conductivities of the Primary Standard KCl Solutions from 0C to 50C.
PB94-219342 *02,644*

Low Electrolytic Conductivity Standards.
PB96-122098 *01,081*

Oscillometric and Conductometric Analysis of Aqueous and Organic Dosimeter Solutions.
PB96-135256 *04,054*

Intrinsic Conductivity of Objects Having Arbitrary Shape and Conductivity.
PB97-111934 *04,150*

CONDUCTORS

Apparatus for Resistance Measurement of Short, Small-Diameter Conductors.
PB96-141130 *04,417*

Electric Dipole Excitation of a Long Conductor in a Lossy Medium.
PB96-146675 *04,058*

CONE CALORIMETERS

Examination of the Correlation between Cone Calorimeter Data and Full-Scale Furniture Mock-Up Fires.
PB96-148200 *01,417*

Flammability Characterization with the Lift Apparatus and the Cone Calorimeter.
PB97-110050 *01,435*

CONE EMISSION

Failures of the Four-Wave Mixing Model for Cone Emission.
PB95-202636 *04,318*

Cone Emission from Laser-Pumped Two-Level Atoms. 1. Quantum Theory of Resonant Light Propagation.
PB95-203584 *04,325*

Cone Emission from Laser-Pumped Two-Level Atoms. 2. Analytical Model Studies.
PB95-203592 *04,326*

CONFIDENCE INTERVALS

Effects of Nonmodel Errors on Model-Based Testing.
PB96-123146 *02,604*

Effects of Nonmedel Errors on Model-Based Testing.
PB96-155577 *03,420*

CONFIDENCE LIMITS

Approximate Confidence Intervals on Linear Combinations of Expected Mean Squares.
PB95-151296 *03,435*

Approximate Confidence Intervals on Positive Linear Combinations of Expected Mean Squares.
PB95-151304 *03,436*

Ranges of Confidence Coefficients for Confiedence Intervals on Variance Components.
PB95-151312 *03,437*

One-Sided beta-Content Tolerance Intervals for Mixed Models.
PB96-141171 *03,449*

Confidence on the Modified Allan Variance and the Time Variance.
PB96-190376 *01,557*

CONFIGURATION MANAGEMENT

Guide to Configuration Management and the Revision Control System for Testbed Users.
PB94-150919 *01,678*

CONFINED SEMIFLEXIBLE POLYMERS

Influence of Surface Interaction and Chain Stiffness on Polymer-Induced Entropic Forces and the Dimensions of Confined Polymers.
PB94-185469 *01,203*

CONFORMANCE

Open Issues in OSI Protocol Development and Conformance Testing.
PB96-122908 *01,818*

CONFORMANCE TESTING

Formal Methods in Conformance Testing: Result and Perspectives.
PB95-153029 *01,710*

ISDN Conformance Testing.
PB95-163176 *01,478*

NIST POSIX Testing Program.
PB96-160973 *01,821*

Conformance Testing and Specification Management.
PB97-113781 *02,849*

CONFORMITY

Conformance Testing of a Lower Layer Security Protocol.
PB94-185402 *01,577*

CONFORMITY ASSESSMENTS

Stacking the Cards in Europe: One Company's Story.
PB97-110126 *00,493*

CONGRUENCE

Principle of Congruence and Its Application to Compressible States.
PB96-102892 *01,068*

CONNECTION MACHINE

Making Connections.
PB97-119044 *01,785*

CONNECTORS

Programmable Guarded Coaxial Connector Panel.
PB96-122544 *02,108*

CONSTANT POWER

CMOS Circuit Design for Controlling Temperature in Micromachined Devices.
PB96-156088 *02,196*

CONSTANT VOLUME HEAT CAPACITY

High-Temperature Adiabatic Calorimeter for Constant-Volume Heat Capacity Measurements of Compressed Gases and Liquids.
PB95-168860 *00,989*

CONSTRUCTION

Infratechnologies: Tools for Innovation.
PB94-185998 *00,317*

Program of the Subcommittee on Construction and Building.
PB94-193646 *00,319*

Program of the Subcommittee on Construction and Building (July 1994).
PB95-122537 *00,321*

Rationale and Preliminary Plan for Federal Research for Construction and Building.
PB95-154704 *00,322*

Literature Review on Seismic Performance of Building Cladding Systems.
PB96-106901 *00,455*

NIST Construction Automation Program Report No. 2. Proceedings of the NIST Construction Automation Workshop. Held in Gaithersburg, Maryland on March 30-31, 1995.
PB96-202239 *00,413*

Summary of Federal Construction and Building R and D in 1994.
PB97-114250 *00,234*

Line-Heat-Source Guarded-Hot-Plate Apparatus.
PB97-118996 *00,417*

CONSTRUCTION INDUSTRY

Status of Construction and Construction Technologies.
PB94-186004 *00,318*

White Papers Prepared for the White House: Construction Industry Workshop on National Construction Goals. Held on December 14-16, 1994.
PB95-216891 *01,299*

National Construction Sector Goals: Industry Strategies for Implementation.
PB95-269817 *00,204*

National Planning for Construction and Building R and D.
PB96-137104 *00,324*

Innovation in the Japanese Construction Industry: A 1995 Appraisal.
PB96-177373 *00,225*

CONSTRUCTION JOINTS

Performance of 1/3-Scale Model Precast Concrete Beam-Column Connections Subjected to Cyclic Inelastic Loads. Report No. 4.
PB95-179024 *00,444*

Simplified Design Procedure for Hybrid Precast Concrete Connections.
PB96-154836 *00,405*

Workgroup Summary Report: Plastic Hinge-Based Techniques for Advanced Analysis.
PB96-159702 *00,470*

CONSTRUCTION MANAGEMENT

Economic Methods and Risk Analysis Techniques for Evaluating Building Investments: A Survey.
PB96-122593 *00,323*

CONSTRUCTION MATERIALS

Proficiency Testing as a Component of Quality Assurance in Construction Materials Laboratories.
PB94-185774 *00,334*

Graphical Analysis of the CCRL Portland Cement Proficiency Sample Database (Samples 1-72). (Part 1. Univariant Analysis of Portland Cement).
PB94-196557 *01,308*

Controlling Moisture in the Walls of Manufactured Housing.
PB95-105136 *00,355*

Measurements of Moisture Diffusivity for Porous Building Materials.
PB95-107397 *00,356*

Suggestions for a Logically-Consistent Structure for Service Life Prediction Standards.
PB95-125795 *00,358*

Fundamental Computer Simulation Models for Cement-Based Materials.
PB95-126009 *00,364*

Effects of Specimen Edge Conditions on Heat Release Rate.
PB95-152864 *00,375*

National Voluntary Laboratory Accreditation Program: Construction Materials Testing.
PB95-155552 *01,319*

Acoustic Emission of Structural Materials Exposed to Open Flames.
PB95-164810 *00,296*

Manufactured Housing Walls That Provide Satisfactory Moisture Performance in All Climates.
PB95-178885 *00,383*

Testing of Selected Self-Leveling Compounds for Floors.
PB95-220455 *00,395*

Application of Digital-Image-Based Models to Microstructure, Transport Properties, and Degradation of Cement-Based Materials.
PB96-156161 *00,406*

CONSULTATIVE COMMITTEE ON UNITS

Report on the Meeting of the CCU (10th) (of the International Committee of Weights and Measures). Held on July 10-11, 1990.
PB94-172889 *03,792*

CONSUMER PRODUCTS

Directory of U.S. Private Sector Product Certification Programs.
PB96-215074 *02,688*

CONTACT CRACKS

Friction Processes in Brittle Fracture.
PB96-161765 *03,076*

CONTACT LINE

Lubrication Theory for Reactive Spreading of a Thin Drop.
PB96-123427 *04,214*

CONTACT MECHANICS

Mechano-Chemical Model: Reaction Temperatures in a Concentrated Contact.
PB96-119466 *03,227*

CONTACT MODELS

Comparison of Elastic and Plastic Contact Models for the Prediction of Thermal Contact Conductance.
PB95-161659 *04,605*

CONTACT RESISTANCE

Comparison of Elastic and Plastic Contact Models for the Prediction of Thermal Contact Conductance.
PB95-161659 *04,605*

High Current Pressure Contacts to Ag Pads on Thin Film Superconductors.
PB95-168621 *04,639*

Surface Degradation of Superconducting YBa2Cu3O7-delta Thin Films.
PB95-176095 *04,667*

Thermal Conductivity of Polypyromellitimide Film with Alumina Filler Particles from 4.2 to 300 K.
PB96-200753 *01,292*

CONTAM88 COMPUTER PROGRAM
CONTAM88 Building Input Files for Multi-Zone Airflow and Contaminant Dispersal Modeling.
PB94-194388 *02,537*

CONTAM93 COMPUTER PROGRAM
CONTAM93 User Manual.
PB94-164381 *02,536*

CONTAM93 MODEL
Application of a Multizone Airflow and Contaminant Dispersal Model to Indoor Air Quality Control in Residential Buildings.
PB95-180238 *02,555*

CONTAMINANT DISPERSAL MODELING
CONTAM88 Building Input Files for Multi-Zone Airflow and Contaminant Dispersal Modeling.
PB94-194388 *02,537*

CONTAMINANTS
CONTAM94: A Multizone Airflow and Contaminant Dispersal Model with a Graphic User Interface.
PB97-113203 *02,570*

CONTAMINATION
Partial Pressure Analysis in Space Testing.
N95-14084/4 *04,827*

Relation between AC Impedance Data and Degradation of Coated Steel. 1. Effects of Surface Roughness and Contamination on the Corrosion Behavior of Epoxy Coated Steel.
PB94-213345 *03,189*

CONTINUOUS MINERS
Integration of Servo Control into a Large-Scale Control System Design: An Example from Coal Mining.
PB94-203429 *03,696*

Continuous Mining Machine Control Using the Real-Time Control System.
PB94-203528 *03,700*

Environment Simulation for a Continuous Mining Machine.
PB94-203536 *03,697*

CONTINUOUS RECORDING
Correlations between Electrical and Acoustic Detection of Partial Discharge in Liquids and Implications for Continuous Data Recording.
PB96-204490 *02,248*

CONTINUOUS WAVE LASERS
Stabilization of Optical Phase/Frequency of a Laser System: Application to a Commercial Dye Laser with an External Stabilizer.
PB95-203832 *04,327*

CONTRACT MANAGEMENT
Federal Implementation Guideline for Electronic Data Interchange: ASC X12 003050 Transaction Set 836 Procurement Notices. Implementation Convention.
PB96-178892 *01,827*

CONTROL
Post-Process Control of Machine Tools.
PB95-203451 *02,952*

CONTROL SYSTEMS
Feasibility Study: Reference Architecture for Machine Control Systems Integration.
PB94-142791 *02,804*

Toward a Reference Model Architecture for Real-Time Intelligent Control Systems (ARTICS).
PB94-172046 *02,932*

Task Decomposition Methodology for the Design of a Coal Mining Automation Hierarchical Real-Time Control System.
PB94-185386 *03,694*

Control Entity Interface Specification.
PB94-191715 *02,815*

Hierarchical Real-Time Control System for Use with Coal Mining Automation.
PB94-212065 *03,698*

Using Emulator/Testers for Commissioning EMCS Software, Operator Training, Algorithm Development, and Tuning Local Control Loops.
PB94-212735 *00,245*

Hierarchical Ada Robot Programming System (HARPS): A Complete and Working Telerobot Control System Based on the NASREM Model.
PB94-213162 *02,934*

Three Dimensional Position Determination from Motion.
PB95-107108 *01,788*

Reference Architecture for Machine Control Systems Integration: Interim Report.
PB95-144549 *02,820*

Control System Architecture for a Remotely Operated Unmanned Land Vehicle.
PB95-163200 *03,759*

Reproducibility of Tests on Energy Management and Control Systems Using Building Emulators.
PB95-175980 *00,260*

CONTROL SYSTEMS DESIGN
Continuous Mining Machine Control Using the Real-Time Control System.
PB94-203528 *03,700*

Reference Model Architecture for Intelligent Systems Design.
PB95-143137 *01,789*

Expert Control System Shell Version 1.0 User's Guide.
PB95-198859 *01,790*

Testing Conformance and Interoperability of BACnet (Trade Name) Building Automation Products.
PB97-111553 *00,310*

CONTROLLED NUCLEATION
Controlled Nucleation in Aerosol Reactors for Supression of Agglomerate Formation.
PB95-151973 *00,672*

CONTROLLERS
Open Architectures for Machine Control.
PB94-135621 *02,942*

Enhanced Machine Controller Architecture Overview.
PB94-142460 *02,802*

NIST Support to the Next Generation Controller Program: 1991 Final Technical Report.
PB94-163490 *02,808*

Implementing a Transition Manager in the AMRF Cell Controller.
PB94-199932 *02,817*

Generic Manufacturing Controllers.
PB94-199940 *02,818*

Intelligent Control of an Inert Gas Atomization Process.
PB95-141057 *03,344*

Using Grafcet to Design Generic Controllers.
PB95-150827 *02,821*

Texture-Independent Vision-Based Closed-Loop Fuzzy Controllers for Navigation Tasks.
PB95-220505 *00,183*

Intelligent Processing of Materials, Technical Activities 1994 (NAS-NRC Assessment Panel, April 6-7, 1995).
PB96-115050 *03,359*

CONVECTION
Convection and Morphological Stability During Directional Solidification.
N95-14548/8 *03,310*

Large Eddy Simulations of Smoke Movement in Three Dimensions.
PB96-190012 *01,426*

Problem of Convection in the Water Absorbed Dose Calorimeter.
PB97-110159 *03,523*

CONVECTIVE FLOW
Mathematical Modeling and Computer Simulation of Fire Phenomena.
PB95-180063 *00,384*

CONVECTIVE HEAT TRANSFER
Fire-Plume-Generated Ceiling Jet Characteristics and Convective Heat Transfer to Ceiling and Wall Surfaces in a Two-Layer Fire Environment: Uniform Temperature Ceiling and Walls.
PB95-164711 *00,382*

CONVERGENCE
Convergence Properties of a Class of Rank-Two Updates. (NIST Reprint).
PB95-180097 *03,430*

Hybrid Gauss-Trapezoidal Quadrature Rules.
PB96-193750 *03,422*

CONVERSION TABLES
Guide for the Use of the International System of Units (SI).
PB95-226692 *02,747*

CONVERTERS
Josephson D/A Converter with Fundamental Accuracy.
PB96-148044 *02,418*

AC-DC Difference Characteristics of High-Voltage Thermal Converters.
PB96-148093 *02,083*

Performance of Multilayer Thin-Film Multijunction Thermal Converters.
PB96-148135 *02,084*

CONVOLUTION INTEGRALS
Data Evaluation of a Linear System by a Second-Order Transfer Function.
PB96-200282 *01,970*

COOKING DEVICES
Study of Technology for Detecting Pre-Ignition Conditions of Cooking-Related Fires Associated with Electric and Gas Ranges and Cooktops, Phase 1 Report.
PB96-128095 *00,303*

COOL STARS
GHRS Observations of Cool, Low-Gravity Stars. 1. The Far-Ultraviolet Spectrum of alpha Orions (M2 lab).
PB96-112016 *00,094*

COOLANTS
Chemical Effect in Ceramics Grinding.
PB97-122592 *03,113*

COOLING
Transient Cooling of a Hot Surface by Droplets Evaporation.
PB94-156957 *03,783*

COOLING SYSTEMS
Device for Subambient Temperature Control in Liquid Chromatography.
PB95-140604 *00,573*

Graded and Nongraded Regenerator Performance.
PB95-169090 *02,753*

Multizone Modeling of Three Residential Indoor Air Quality Control Options.
PB96-165782 *02,567*

COOPERATION
Industry and Government-Laboratory Cooperative R and D: An Idea Whose Time Has Come.
PB94-172939 *02,970*

COORDINATE MEASURING MACHINES
Comparison of Finite Element and Analytic Calculations of the Resonant Modes and Frequencies of a Thick Shell Sphere.
PB94-160785 *02,626*

U.S. Navy Coordinate Measuring Machines: A Study of Needs.
PB94-162831 *02,807*

User's Guide to NIST SRM 2084: CMM Probe Performance Standard.
PB94-206109 *02,709*

Some Considerations for Interim Testing of Coordinate Measuring Machine Performance Using a Specific Artifact.
PB95-108858 *02,898*

Sensitivity of Three-Point Circle Fitting.
PB95-136354 *02,901*

Displacement Method for Machine Geometry Calibration.
PB95-152088 *02,946*

Two New Probes for a Coordinate Measuring Machine.
PB95-163093 *02,653*

NIST SRM 9983 High-Rigidity Ball-Bar Stand. User Manual.
PB95-255840 *02,669*

Estimation of Measurement Uncertainty of Small Circular Features Measured by CMMs.
PB95-267928 *02,918*

User's Guide to 'SuperFit' Modeling Software for CMM Probe Lobing.
PB96-128236 *02,921*

COORDINATE MEASURING SYSTEMS
Process for Selecting Standard Reference Algorithms for Evaluating Coordinate Measurement Software.
PB94-173754 *02,629*

COPLANAR WAVEGUIDES
Microwave Properties of Voltage-Tunable YBa2Cu3O7-delta/SrTiO3 Coplanar Waveguide Transmission Lines.
PB96-141262 *02,235*

COPLANARITY
Micromachined Coplanar Waveguides in CMOS Technology.
PB97-119283 *02,456*

COPOLYMERIZATION
Copolymerization of N-Phenyl Maleimide and gamma-Methacryloxypropyl Trimethoxysilane.
PB95-153144 *01,248*

COPOLYMERS
Thermal Behaviour of Methyl Methacrylate and N-Phenyl Maleimide Copolymers.
PB95-152237 *01,246*

Thermodynamic Interactions and Correlations in Mixtures of Two Homopolymers and a Block Copolymers by Small Angle Neutron Scattering.
PB95-152872 *01,247*

Shear-Induced Martensitic-Like Transformation in a Block Copolymer Melt.
PB96-119508 *01,277*

Flow-Induced Structure in Polymers: Chapter 16. Shear-Induced Changes in the Order-Disorder Transition Temperature and the Morphology of a Triblock Copolymer.
PB96-123237 *03,127*

Light-Scattering Studies on Phase Separation in a Binary Blend with Addition of Diblock Copolymers.
PB96-146865 *01,286*

Shear-Induced Changes in the Order-Disorder Transition Temperature and the Morphology of a Triblock Copolymer.
PB97-118772 *03,130*

COPPER
Temperature Dependence and Anharmonicity of Phonons on Ni(110) and Cu(110) Using Molecular Dynamics Simulations.
PB94-185477 *04,449*

Copper Ion-Mediated Modification of Bases in DNA in Vitro by Benzoyl Peroxide.
PB94-198231 *03,645*

Concurrent Enhancement of Kerr Rotation and Antiferromagnetic Coupling in Epitaxial Fe/Cu/Fe Structures.
PB94-198769 *04,466*

Roles of Copper in Applied Superconductivity.
PB94-211521 *02,255*

Tribochemical Reaction of Stearic Acid on Copper Surface Studied by Surface Enhanced Raman Spectroscopy.
PB94-212057 *02,964*

Spot-Profile-Analyzing LEED Study of the Epitaxial Growth of Fe, Co, and Cu on Cu(100).
PB95-150165 *04,561*

Hybrid Method for Determining Material Properties from Instrumented Micro-Indentation Experiments.
PB95-152229 *03,348*

Design and Machining of Copper Specimens with Micro Holes for Accurate Heat Transfer Measurements.
PB95-180428 *02,658*

Comparison of Fire Sprinkler Piping Materials: Steel, Copper, Chlorinated Polyvinyl Chloride and Polybutylene, in Residential and Light Hazard Installations.
PB95-182267 *00,299*

Tensile Deformation-Induced Microstructures in Free-Standing Copper Thin Films.
PB96-102595 *04,715*

Magnetic Structure and Spin Dynamics of the Pr and Cu in Pr2CuO4.
PB96-111836 *04,036*

Elastic Constants and Internal Friction of Polycrystalline Copper.
PB96-141015 *03,364*

Solubilities of Copper(II) and Chromium(III) beta-Diketonates in Supercritical Carbon Dioxide.
PB96-164215 *01,147*

Compressibility of Polycrystal and Monocrystal Copper: Acoustic-Resonance Spectroscopy.
PB96-164223 *02,990*

COPPER ALLOYS

Study of Laser Resonance Ionization Mass Spectrometry Using a Glow Discharge Source.
DE94018566 *03,308*

Measuring the Stability of Three Copper Alloys.
PB94-199866 *03,326*

Roles of Copper in Applied Superconductivity.
PB94-211521 *02,255*

Diffusion of Copper into Gold Plating.
PB95-162152 *00,957*

Study of Laser Resonance Ionization Mass Spectrometry Using a Glow Discharge Source.
PB96-123203 *03,360*

COPPER BISMUTHATES

Phase Equilibria in the Systems CaO-CuO and CaO-Bi2O3.
PB95-140570 *03,048*

COPPER CHLORIDES

Structural and Magnetic Properties of CuCl2 Graphite Intercalation Compounds.
PB96-119748 *03,020*

COPPER DEUTERIDES

Pure Rotational Spectra of CuH and CuD in Their Ground States Measured by Tunable Far-Infrared Spectroscopy.
PB95-176194 *01,005*

COPPER GERMANATES

Crystal Structure and Magnetic Properties of CuGeO3.
PB95-180287 *04,678*

COPPER HYDRIDES

Rotational Spectrum of Copper Hydride Using Tunable Far Infrared Radiation.
PB94-198637 *00,792*

Pure Rotational Spectra of CuH and CuD in Their Ground States Measured by Tunable Far-Infrared Spectroscopy.
PB95-176194 *01,005*

COPPER INDIUM SELENIDES

Epitaxial Growth and Characterization of the Ordered Vacancy Compound CuIn3Se5 on GaAs (100) Fabricated by Molecular Beam Epitaxy.
PB95-180725 *04,687*

COPPER OXIDES

Phase Equilibria in the Systems CaO-CuO and CaO-Bi2O3.
PB95-140570 *03,048*

Crystal Chemistry and Phase Equilibria Studies of the BaO(BaCO3)-R2O3-CuO Systems. 4. Crystal Chemistry and Subsolidus Phase Relationship Studies of the CuO-Rich Region of the Ternary Diagrams, R=Lanthanides.
PB95-151759 *00,936*

COPYRIGHTS

Copyright and Information Services in the Context of the National Research and Education Network.
PB96-160536 *02,736*

CORM (COUNCIL FOR OPTICAL RADIATION MEASUREMENTS)

NIST Response to the Fifth CORM Report on the Pressing Problems and Projected Needs in Optical Radiation Measurements.
PB94-188240 *04,227*

CORONA DISCHARGE

Measurement of S2OF10, and S2O2F10 Production Rates from Spark and Negative Glow Corona Discharge in SF6/O2 Gas Mixtures.
PB96-123740 *01,093*

CORONA DISCHARGES

Plasma Chemical Model for Decomposition of SF6 in a Negative Glow Corona Discharge.
PB95-181053 *01,020*

CORRECTIONS

Large Local-Field Corrections in Optical Rotatory Power of Quartz and Selenium.
PB97-122378 *04,400*

CORRELATION FUNCTION

Nonequilibrium Statistical Mechanics.
PB96-161781 *04,097*

CORRESPONDING STATES

Viscosity of Defined and Undefined Hydrocarbon Liquids Calculated Using an Extended Corresponding-States Model.
PB96-167234 *02,498*

CORROSION

Volatile Corrosion Inhibitors.
AD-A310 087/2 *03,114*

Evaluation of Corrosion Data: A Review.
PB94-198348 *03,187*

Relation between AC Impedance Data and Degradation of Coated Steel. 1. Effects of Surface Roughness and Contamination on the Corrosion Behavior of Epoxy Coated Steel.
PB94-213345 *03,189*

In situ Measurements of Chloride Ion and Corrosion Potential at the Coating/Metal Interface.
PB95-140893 *03,122*

Journal of Research of the National Institute of Standards and Technology, July/August 1994. Volume 99, Number 4. Special Issue: Extreme Value Theory and Applications. Proceedings of the Conference on Extreme Value Theory and Applications, Volume 2. Held at Gaithersburg, Maryland, in May 1993.
PB95-160594 *03,440*

Sorption of Moisture on Epoxy and Alkyd Free Films and Coated Steel Panels.
PB95-162475 *03,192*

Degradation of Powder Epoxy Coated Panels Immersed in a Saturated Calcium Hydroxide Solution Containing Sodium Chloride.
PB96-101050 *01,344*

Journal of Research of the National Institute of Standards and Technology, September/October 1993. Volume 98, Number 5.
PB96-169057 *03,368*

Corrosion Characteristics of Silicon Carbide and Silicon Nitride.
PB96-169081 *03,372*

Role of Corrosion in a Material Selector Expert System for Advanced Structural Ceramics.
PB97-110308 *03,099*

CORROSION INHIBITION

Volatile Corrosion Inhibitors.
AD-A310 087/2 *03,114*

CORROSION MECHANISMS

Diffusion of Cations Beneath Organic Coatings on Steel Substrate.
PB94-215704 *03,119*

CORROSION POTENTIAL

In situ Measurements of Chloride Ion and Corrosion Potential at the Coating/Metal Interface.
PB95-140893 *03,122*

CORROSION RESISTANCE

Review of Corrosion Behavior of Ceramic Heat Exchanger Materals: Corrosion Characteristics of Silicon Carbide and Silicon Nitride. Final Report, September 11, 1992--March 11, 1993.
DE93041307 *03,228*

Corrosion Resistance of Materials for Renovation of the United States Botanic Garden Conservatory.
PB94-154390 *00,032*

Corrosion Resistant Epoxy-Coated Reinforcing Steel.
PB94-185618 *01,307*

CORROSION TESTS

Comparison of the Corrosion Rates of FeAl, Fe(sub 3)Al and Steel in Distilled Water and 0.5 M Sodium Chloride. Technical Report Number 2, January--March 1991.
DE94017332 *03,186*

CORROSIVE EFFECTS

Comparison of the Corrosion Rates of FeAl, Fe(sub 3)Al and Steel in Distilled Water and 0.5 M Sodium Chloride. Technical Report Number 2, January--March 1991.
DE94017332 *03,186*

CORTICAL BONE

EPR Dosimetry of Cortical Bone and Tooth Enamel Irradiated with X and Gamma Rays: Study of Energy Dependence.
PB97-110373 *03,639*

COSMIC DUST

IRAS Spectroscopic Observations of Young Planetary Nebulae.
PB95-152070 *00,072*

COST ANALYSIS

Energy Prices and Discount Factors for Life-Cycle Cost Analysis 1994. Annual Supplement to NIST Handbook 135 and NBS Special Publication 709.
PB94-206018 *02,508*

Energy Price Indices and Discount Factors for Life-Cycle Cost Analysis 1995. Annual Supplement to NIST Handbook 135 and NBS Special Publication 709. (Revised).
PB95-105011 *02,509*

Lighting and HVAC.
PB95-150991 *00,250*

Energy Price Indices and Discount Factors for Life-Cycle Cost Analysis 1996. Annual Supplement to NIST Handbook 135 and NBS Special Publication 709. (Revised).
PB96-162441 *02,510*

Economics of New-Technology Materials: A Case Study of FRP Bridge Decking.
PB96-202353 *01,349*

Energy Price Indices and Discount Factors for Life-Cycle Cost Analysis 1997. Annual Supplement to NIST Handbook 135 and NBS Special Publication 709. (Revised).
PB96-210745 *02,512*

COST BENEFIT ANALYSIS

Robotics Application to Highway Transportation. Volume 3. Proposed Research Topics and Cost/Benefit Evaluations by CERF.
PB95-171633 *01,338*

Least-Cost Energy Decisions for Buildings. Part 3. Choosing Economic Evaluation Methods. Video Training Workbook.
PB95-253597 *00,265*

Economic Methods and Risk Analysis Techniques for Evaluating Building Investments: A Survey.
PB96-122593 *00,323*

Multiattribute Decision Analysis Method for Evaluating Buildings and Building Systems.
PB96-158670 *00,325*

COST ESTIMATES

Seismic Safety of Federal Buildings. Initial Program: How Much Will It Cost.
PB95-182291 *00,447*

COUETTE FLOW

Non-Newtonian Flow between Concentric Cylinders Calculated from Thermophysical Properties Obtained from Simulations.
PB96-163761 *04,103*

COULOMB BLOCKADE

Effect in Environmental Noise on the Accuracy of Coulomb-Blockade Devices.
PB95-175865 *04,662*

COULOMB BLOCKADE ELECTROMETERS

Noise in the Coulomb Blockade Electrometer.
PB95-176327 *04,670*

COULOMETERS

Automated, High-Precision Coulometric Titrimetry. Part 1. Engineering and Implementation.
PB95-150199 *00,575*

Automated, High Precision Coulometric Titrimetry. Part 2. Strong and Weak Acids and Bases.
PB95-150207 *00,576*

COULOMN BLOCKAGE

Performance of the Electron Pump with Stray Capacitances.
PB96-200902 *01,976*

COUNSTRUCTION MATERIALS

Unreacted Cement Content in Macro-Defect-Free Composites: Impact on Processing-Structure-Property Relations.
PB96-141270 *03,174*

COUNTIES

Codes for Named Populated Places, Primary County Divisions, and Other Locational Entities of the United States (FIPS PUB 55-3) (on Magnetic Tape).
PB95-502563 *00,129*

COUNTING TECHNIQUES

Airborne Asbestos Method: Standard Test Method for High Precision Counting of Asbestos Collected on Filters. Version 1.0.
PB94-163003 *00,525*

CRABON MONOXIDE

Global Equivalence Ratio Concept and the Formation Mechanisms of Carbon Monoxide in Enclosure Fires.
PB96-146790 *00,210*

CRACK BRIDGING

Model for Toughness Curves in Two-Phase Ceramics. 1. Basic Fracture Mechanics.
PB96-180088 *03,085*

CRACK DETECTION

Gas-Coupled, Pulse-Echo Ultrasonic Crack Detection and Thickness Gaging.
PB96-147129 *04,847*

CRACK GROWTH

Diffusive Crack Growth at a Bimaterial Interface.
PB96-204110 *03,090*

Creep and Creep Rupture of Structural Ceramics.
PB96-204524 *03,093*

CRACK PROPAGATION

Fracture Mechanics Analysis of Near-Surface Cracks.
PB94-172400 *03,230*

Crack Growth Resistance of Strain-Softening Materials under Flexural Loading.
PB94-200227 *02,972*

Asymmetric Tip Morphology of Creep Microcracks Growing Along Bimaterial Interfaces.
PB94-200243 *03,138*

Transient Subcritical Crack-Growth Behavior in Transformation-Toughened Ceramics.
PB94-200656 *03,038*

Micromechanics of Fracture in Rubber-Toughened Epoxies.
PB94-212222 *03,011*

Electric Field Effects on Crack Growth in a Lead Magnesium Niobate.
PB95-107322 *03,339*

Potential Drop in the Center-Cracked Panel with Asymmetric Crack Extension.
PB95-107330 *04,819*

Lattice Imperfections Studied by Use of Lattice Green's Functions.
PB95-150850 *04,576*

Moisture and Water-Induced Crack Growth in Optical Materials.
PB95-153334 *04,267*

Molecular Orbital Study of Water Enhanced Crack Growth Process.
PB95-164067 *03,240*

Nonlocal Effects of Existing Dislocations on Crack-Tip Emission and Cleavage.
PB96-161807 *03,367*

Interfacial Crack in a Two-Dimensional Hexagonal Lattice.
PB96-161989 *04,100*

Model for Microcrack Initiation and Propagation beneath Hertzian Contacts in Polycrystalline Ceramics.
PB96-163704 *03,077*

CRACK RESISTANCE

Characterization of the Hydrogen Induced Cold Cracking Susceptibility at Simulated Weld Zones in HSLA-100 Steel.
PB94-174505 *03,746*

Flaw-Tolerance and Crack-Resistance Properties of Alumina-Aluminum Titanate Composites with Tailored Microstructures.
PB97-110324 *03,101*

CRACK TIPS

Dislocation Emission at Ledges on Cracks.
PB95-164240 *04,630*

Shielding of Cracks in a Plastically Polarizable Material.
PB95-164257 *04,631*

CRACKING

Postfailure Subsidiary Cracking from Indentation Flaws in Brittle Materials.
PB97-110340 *03,103*

CRACKING (FRACTURING)

Prediction of Cracking in Reinforced Concrete Structures.
PB95-220448 *03,725*

CRACKS

Characterization of the Hydrogen Induced Cold Cracking Susceptibility at Simulated Weld Zones in HSLA-100 Steel.
AD-A279 759/5 *03,200*

Fracture Behavior of Large-Scale Thin-Sheet Aluminum Alloy.
N95-19494/0 *03,311*

Safety Assessment of Railroad Wheels Through Roll-by Detection of Tread Cracks.
PB96-141254 *04,856*

Artificial Crack in Steel: An Ultrasonic-Resonance-Spectroscopy and Modeling Study.
PB96-141395 *03,241*

Diffusion of Water along 'Closed' Mica Interfaces.
PB96-180039 *02,993*

CRASH TESTS

Effect of Fuel Tank Rupture Mode on the Ignitability of Expelled Fuel.
PB97-110043 *01,444*

CREEP

Temperature and Frequency Dependence of Anelasticity in a Nickel Oscillator.
PB96-137732 *03,689*

Tensile Creep of Silicide Composites.
PB96-200803 *03,183*

Cavity Evolution during Tensil Creep of Si3N4.
PB96-204193 *03,376*

Creep and Creep Rupture of Structural Ceramics.
PB96-204524 *03,093*

Tension/Compression Creep Asymmetry in Si3N4.
PB97-110258 *03,096*

CREEP BUCKLING

Analysis of Creep in a Si-SiC C-Ring by Finite Element Method.
PB94-200268 *03,037*

CREEP PROPERTIES

PC-Based Prototype Expert System for Data Management and Analysis of Creep and Fatigue of Selected Materials at Elevated Temperatures.
PB94-172251 *03,202*

High Temperature Degradation of Structural Composites.
PB94-172848 *03,132*

Cavitation Damage During Flexural Creep of SiAlON-YAG Ceramics.
PB94-200110 *03,036*

CREEP RAPTURE STRENGTH

Generic Model for Creep Rupture Lifetime Estimation on Fibrous Ceramic Composites.
PB94-200235 *03,137*

CREEP RATE

Observed and Theoretical Creep Rates for an Alumina Ceramic and a Silicon Nitride Ceramic in Flexure.
PB94-212958 *03,040*

CREEP RUPTURE

Transient Creep Behaviour of Hot Isostatically Pressed Silicon Nitride.
PB96-180278 *03,086*

Life Prediction of a Continuous Fiber Reinforced Ceramic Composite Under Creep Conditions.
PB96-204128 *03,091*

CREEP RUPTURE STRENGTH

Creep Rupture of MoSi2/SiCp Composites.
PB95-152294 *03,154*

Creep and Creep Rupture of Ceramic Matrix Composites.
PB95-163929 *03,165*

CREEP TESTS

Tensile Creep Testing of Structural Ceramics.
PB97-110464 *03,105*

CRITICAL CURRENT

Critical Magnetic-Field Angle for High-Field Current Transport in YBa2Cu3O7 at 76 K.
PB94-211281 *04,490*

Transport Critical Current of Aligned Polycrystalline Yttrium Barium Copper Oxide (YBa2Cu3O7-delta).
PB94-211307 *04,492*

Effect of Axial Strain on the Critical Current of Ag-Sheathed Bi-Based Superconductors in Magnetic Fields Up to 25 T.
PB94-211315 *04,493*

Magnetic Measurement of Transport Critical Current Density of Granular Superconductors.
PB95-126199 *04,531*

Critical Current Behavior of Ag-Coated YBa2Cu3O7-x Thin Films.
PB95-141016 *04,549*

Magnetic Field Dependence of the Critical Current Anisotropy in Normal Metal-YBa2Cu3O7-delta Thin Film Bilayers.
PB95-141024 *04,550*

Grain Alignment and Transport Properties of Bi2Sr2CaCu2O8 Grown by Laser Heated Float Zone Method.
PB95-161451 *04,602*

Superconductor Critical Current Standards for Fusion Applications. Final Progress Report, October 1993-July 1994.
PB95-169538 *02,222*

Increased Pinning Energies and Critical Current Densities in Heavy-Ion-Irradiated Bi2Sr2CaCu2O8 Single Crystals.
PB95-175352 *04,654*

Standard Reference Devices for High Temperature Superconductor Critical Current Measurements.
PB95-175543 *04,659*

Critical-Current Degradation in Nb3 Al Wires Due to Axial and Transverse Stress.
PB95-202784 *02,226*

Temperature Dependence and Magnetic Field Modulation of Critical Currents in Step-Edge SNS YBCO/Au Junctions.
PB96-111745 *04,723*

Critical Current and Normal Resistance of High-Tc Step-Edge SNS Junctions.
PB96-111752 *04,724*

Comparing the Accuracy of Critical-Current Measurements Using the Voltage-Current Simulator.
PB96-119219 *02,227*

Simple and Repeatable Technique for Measuring the Critical Current of Nb3Sn Wires.
PB96-119409 *02,229*

Effect of Sm2BaCuO5 on the Properties of Sintered (Bulk) YBa2Cu3O6+x.
PB96-119441 *04,733*

VAMAS Intercomparison of Critical Current Measurements on NB3Sn Superconductors: A Summary Report.
PB96-119763 *04,043*

Anomalous Switching Phenomenon in Critical-Current Measurements When Using Conductive Mandrels.
PB96-137781 *02,233*

Effect of Magnetic Field Orientation on the Critical Current of HTS Conductor and Coils.
PB96-141189 *02,956*

II-3: Critical Current Measurement Methods: Quantitative Evaluation.
PB96-147160 *04,767*

First VAMAS USA Interlaboratory Comparison of High Temperature Superconductor Critical Current Measurements.
PB96-147178 *04,768*

II-5: Thermal Contraction of Materials Used in Nb3Sn Critical Current Measurements.
PB96-147186 *04,769*

USA Interlaboratory Comparison of Superconductor Simulator Critical Current Measurements.
PB96-147194 *04,770*

CRITICAL CURRENT DENSITY

Electromagnetic Coupling Character of (001) Twist Boundaries in Sintered Bi2Sr2CaCu2O8+x Bicrystals.
PB96-176573 *01,963*

CRITICAL DENSITY

Experimental Method for Obtaining Critical Densities of Binary Mixtures: Application to Ethane + n-Butane.
PB95-151148 *00,930*

CRITICAL FLOW

Electric Field Effects on a Near-Critical Fluid in Microgravity.
PB96-161880 *04,217*

CRITICAL LINES

Critical Lines for Type-III Aqueous Mixtures by Generalized Corresponding-States Models.
PB96-102371 *01,063*

CRITICAL POINT

Supercritical Solubility of Solids from Near-Critical Dilute-Mixture Theory.
PB94-211703 *00,819*

Global Thermodynamic Behavior of Fluid Mixtures in the Critical Region.
PB94-212420 *04,199*

Structure of the Vapor-Liquid Interface Near the Critical Point.
PB95-140174 *00,902*

Dynamic Light-Scattering Study of a Diluted Polymer Blend Near Its Critical Point.
PB95-151890 *01,245*

Thermal Equilibration Near the Critical Point: Effects Due to Three Dimensions and Gravity.
PB95-152922 *03,919*

Standard States, Reference States and Finite-Concentration Effects in Near-Critical Mixtures with Applications to Aqueous Solutions.
PB95-164349 *00,979*

Critical Scaling Laws and a Classical Equation of State.
PB95-169249 *00,990*

Coexisting Densities, Vapor Pressures and Critical Densities of Refrigerants R-32 and R-152a, at 300 - 385 K.
PB95-175691 *03,274*

Diffuse-Interface Description of Fluid Systems.
PB96-210711 *01,170*

CRITICAL POINTS

Internal Waves in Xenon Near the Critical Point.
PB97-111504 *04,221*

CRITICAL REGION

Vapor-Liquid Equilibria of Ternary Mixtures in the Critical Region on Paths of Constant Temperature and Overall Composition.
PB96-161856 *01,139*

Nonlinear Correlation of High-Pressure Vapor-Liquid Equilibrium Data for Ethylene + n-Butane Showing Inconsistencies in Experimental Compositions.
PB96-161906 *01,141*

CRITICAL STATE

Pinch Effect in Commensurate Vortex-Pin Lattices.
PB96-147079 *01,125*

CRITICAL TEMPERATURE

Dependence of Tc on Debye Temperature Theta(sub D) for Various Cuprates.
PB95-180493 *04,683*

CRITICALITY

Neutron Leakage Benchmark for Criticality Safety Research.
PB95-126132 *03,723*

CRITICALITY CALCULATIONS

MCNP Model of the National Bureau of Standards Reactor (NBSR) Core.
PB96-138599 *03,733*

CROSS SECTIONS

Low-Energy-Electron Collisions with Sodium: Elastic and Inelastic Scattering from the Ground State.
PB96-103106 *04,030*

CROSSLINKING

Electron Beam Crosslinking of Poly(vinylmethyl ether).
PB94-185550 *01,205*

Effect of Curing History on Ultimate Glass Transition Temperature and Network Structure of Crosslinking Polymers.
PB94-200052 *01,214*

Effect of Cross-Links on the Miscibility of a Deuterated Polybutadiene and Protonated Polybutadiene Blend.
PB94-212438 *01,225*

Localization Model of Rubber Elasticity: Comparison with Torsional Data for Natural Rubber Networks in the Dry State.
PB95-107033 *03,195*

Elastic Scattering of Polymer Networks.
PB95-161816 *01,255*

Formation of DNA-Protein Cross-Links in Cultured Mammalian Cells Upon Treatment with Iron Ions.
PB96-137724 *03,651*

Evidence of Crosslinking in Methyl Pendent PBZT Fiber.
PB97-112486 *03,393*

CROSSLINKING NETWORK

Effect of Curing History on Ultimate Glass Transition Temperature and Network Structure of Crosslinking Polymers.
PB94-200052 *01,214*

CROSSTALK

Crosstalk between Microstrip Transmission Lines.
PB94-135639 *02,210*

Crosstalk between Microstrip Transmission Lines. (NIST Reprint).
PB95-180337 *02,225*

CRYOCOOLERS

Building a Better Crycooler.
PB96-119615 *04,734*

CRYOELECTRONICS
Metrology for Electromagnetic Technology: A Bibliography of NIST Publications.
PB95-135588 *02,143*

CRYOFOCUSING
Chromatographic Cryofocusing and Cryotrapping with the Vortex Tube.
PB95-180113 *00,604*

CRYOGENIC COOLING
Resistance Thermometers with Fast Response for Use in Rapidly Oscillating Gas Flows.
PB95-107298 *03,261*

Chromatographic Cryofocusing and Cryotrapping with the Vortex Tube.
PB95-180113 *00,604*

CRYOGENIC CURRENT COMPARATORS
High-Temperature Superconductor Cryogenic Current Comparator.
PB96-119334 *02,074*

CRYOGENIC EQUIPMENT
Cryogenic Toughness of Austenitic Stainless Steel Weld Metals: Effect of Inclusions.
PB95-161261 *03,214*

CRYOGENIC FLUIDS
Reference Data for the Thermophysical Properties of Cryogenic Fluids.
PB95-168688 *03,263*

CRYOGENIC PROPELLANTS
Cryogenic Research and Development (Quarterly Report Number 1 for Period Ending September 30, 1960).
AD-A280 401/1 *01,456*

Cryogenic Research and Development (June 30, 1961).
AD-A280 679/2 *01,457*

CRYOGENIC PROPERTIES
Temperature-Induced Transition in Ductile Fracture Appearance of a Nitrogen-Strengthened Austenitic Stainless Steel.
PB96-190269 *03,221*

CRYOGENIC RADIOMETERS
Journal of Research of the National Institute of Standards and Technology, March/April 1996. Volume 101, Number 2.
PB96-177381 *01,863*

NIST High Accuracy Scale for Absolute Spectral Response from 406 nm to 920 nm.
PB96-179122 *01,865*

CRYOGENIC TEMPERATURE
Development of a Temperature Scale below 0.5 K.
PB95-125639 *03,879*

Cryogenics.
PB95-164703 *02,654*

CRYOGENIC TEST PROCEDURES
Charpy Specimen Tests at 4 K.
PB96-190335 *03,002*

CRYOGENICS
Cryogenic Research and Development (Quarterly Report Number 2 for Period Ending December 31, 1960).
AD-A280 398/9 *01,454*

Cryogenic Research and Development (Progress Report Number 4 for Period Ending December 31, 1961).
AD-A280 399/7 *01,455*

Cryogenic Research and Development (Quarterly Report Number 1 for Period Ending September 30, 1960).
AD-A280 401/1 *01,456*

Cryogenic Research and Development (June 30, 1961).
AD-A280 679/2 *01,457*

Bibliography of the Physical Equilibria and Related Properties of Some Cryogenic Systems.
AD-A281 167/7 *03,769*

Progress Report to National Aeronautics and Space Administration on Cryogenic Research and Development.
AD-A286 612/7 *01,458*

Cryogenic Materials Data Handbook.
AD-A286 675/4 *03,303*

Survey of the Literature on Heat Transfer from Solid Surfaces to Cryogenic Fluids.
AD-A286 680/4 *04,193*

Cryogenic Properties of Silver.
PB94-203593 *03,330*

Welding for Cryogenic Service.
PB95-162889 *02,852*

High-Temperature Superconductor Cryogenic Current Comparator.
PB96-119334 *02,074*

Building a Better Crycooler.
PB96-119615 *04,734*

Microwave Dielectric Properties of Anisotropic Materials at Cryogenic Temperatures.
PB96-137765 *02,412*

Cryogenic Flow Calibration in NIST.
PB96-161930 *01,143*

National Institute of Standards and Technology High-Accuracy Cryogenic Radiometer.
PB96-179585 *04,378*

Charpy Impact Test as an Evaluation of 4 K Fracture Toughness.
PB96-190194 *03,219*

Realization of a Scale of Absolute Spectral Response Using the NIST High Accuracy Cryogenic Radiometer.
PB97-118640 *04,397*

CRYOSCOPY
Anomalous Freezing and Melting of Solvent Crystals in Swollen Gels of Natural Rubber.
PB94-212321 *01,223*

CRYOTRAPPING
Chromatographic Cryofocusing and Cryotrapping with the Vortex Tube.
PB95-180113 *00,604*

CRYPTOGRAPHY
Security Requirements for Cryptographic Modules; Category: Computer Security; Subcategory: Cryptography.
FIPS PUB 140-1 *01,567*

Digital Signature Standard (DSS). Category: Computer Security; Subcategory: Cryptography.
FIPS PUB 186 *01,570*

Report of the NIST Workshop on Digital Signature Certificate Management. Held on December 10-11, 1992.
PB94-135001 *01,574*

Federal Certification Authority Liability and Policy: Law and Policy of Certificate-Based Public Key and Digital Signatures.
PB94-191202 *01,578*

Formal Specification and Verification of Control Software for Cryptographic Equipment.
PB94-213030 *01,585*

EDI and EFT Security Standards.
PB96-122833 *01,605*

Response to Comments on the NIST Proposed Digital Signature Standard.
PB96-161815 *01,615*

CRYPTOLOGY
Data Encryption Standard.
PB95-162376 *01,595*

CRYSTAL CHEMISTRY
Crystal Chemistry and Phase Equilibrium Studies of the BaO(BaCO3)-R2O3-CuO Systems. 5. Melting Relations in Ba2(Y,Nd,Eu)Cu3O6+x.
PB95-151718 *04,580*

Crystal Chemistry and Phase Equilibrium Studies of the BaO-R2O3-CuO Systems. 2. X-Ray Characterization and Standard Patterns of BaR2CuO4, R=Lanthanides.
PB95-151734 *04,582*

Crystal Chemistry and Phase Equilibria Studies of the BaO(BaCO3)-R2O3-CuO Systems. 4. Crystal Chemistry and Subsolidus Phase Relationship Studies of the CuO-Rich Region of the Ternary Diagrams, R=Lanthanides.
PB95-151759 *00,936*

CRYSTAL DEFECTS
Correlation of HgCdTe Epilayer Defects with Underlying Substrate Defects by Synchrotron X-Ray Topography.
PB94-200714 *02,129*

Defect of Thermal Ramping and Annealing Conditions on Defect Formation in Oxygen Implanted Silicon-On-Insulator Material.
PB94-212966 *02,318*

Characterization of Interface Defects in Oxygen-Implanted Silicon Films.
PB94-216629 *02,322*

Defective Structures of Barium Yttrium Copper Oxide (Ba2YCu3Ox) and Ba2YCu3-yMyOz (M=Fe, Co, Al, Ga, ..).
PB95-140034 *04,537*

Lattice Imperfections Studied by Use of Lattice Green's Functions.
PB95-150850 *04,576*

Lineshape Analysis of the Raman Spectrum of Diamond Films Grown by Hot-Filament and Microwave-Plasma Chemical-Vapor Deposition.
PB95-162392 *03,016*

Studies of Defects in Diamond Films and Particles by Raman and Luminescence Spectroscopies.
PB95-162400 *03,017*

Elastic Properties of Central-Force Networks with Bond-Length Mismatch.
PB95-163366 *04,623*

Influence of Lattice Mismatch on Indium Phosphide Based High Electron Mobility Transistor (HEMT) Structures Observed in High Resolution Monochromatic Synchrotron X-Radiation Diffraction Imaging.
PB95-164679 *02,357*

Small Angle Neutrons Scattering from Nanocrystalline Palladium as a Function of Annealing.
PB95-176103 *03,354*

Nano-Defects in Commercial Bonded SOI and SIMOX.
PB96-123674 *02,407*

CRYSTAL DISLOCATIONS
Defect Pair Formation by Implantation-Induced Stresses in High-Dose Oxygen Implanted Silicon-on-Insulator Material.
PB95-175824 *02,364*

CRYSTAL GROWTH
Computation of Dendrites Using a Phase Field Model.
PB94-160744 *04,436*

Asymptotic Behavior of Modulated Taylor-Couette Flows with a Crystalline Inner Cylinder.
PB94-199072 *04,469*

Selective Inhibition of Crystal Growth on Octacalcium Phosphate and Nonstoichiometric Hydroxyapatite by Pyrophosphate at Physiological Concentration.
PB94-211257 *00,147*

Microstructural Evolution in Two-Dimensional Two-Phase Polycrystals.
PB94-211992 *04,498*

Effect of Modulated Taylor-Couette Flows on Crystal-Melt Interfaces: Theory and Initial Experiments.
PB94-216736 *04,521*

Morphological Stability.
PB95-153318 *04,591*

Lineshape Analysis of the Raman Spectrum of Diamond Films Grown by Hot-Filament and Microwave-Plasma Chemical-Vapor Deposition.
PB95-162392 *03,016*

Studies of Defects in Diamond Films and Particles by Raman and Luminescence Spectroscopies.
PB95-162400 *03,017*

Surface Roughness Evaluation of Diamond Films Grown on Substrates with a High Density of Nucleation Sites.
PB95-162418 *03,018*

In-situ Monitoring of Molecular Beam Epitaxial Growth Using Single Photon Ionization.
PB95-202222 *01,023*

Single Photon Ionization, Laser Optical Probe Technique for Semiconductor Growth.
PB95-202776 *01,032*

Laser Gas Ionization Technique Monitors MEB Crystal Growth.
PB96-112172 *01,076*

Stagnant Film Model of the Effect of Natural Convection on the Dendrite Operating State.
PB96-146832 *04,765*

Powder X-ray Diffraction Data for Ca2Bi2O5 and C4Bi6O13.
PB96-161278 *04,777*

Preparation and Crystal Structure of Sr5TiNb4O17.
PB96-167341 *04,107*

CRYSTAL LATTICES
Status of a Silicon Lattice Measurement and Dissemination Exercise.
PB94-199635 *04,474*

Elastic Properties of Central-Force Networks with Bond-Length Mismatch.
PB95-163366 *04,623*

Lattice Dynamics of Ba1-xKxBiO3.
PB96-102421 *04,706*

Lattice Dynamics of Semiconducting, Metallic, and Superconducting Ba1-xKxBiO3 Studied by Inelastic Neutron Scattering.
PB96-102447 *04,708*

CRYSTAL-MELT INTERFACE
Effect of Modulated Taylor-Couette Flows on Crystal-Melt Interfaces: Theory and Initial Experiments.
PB94-216736 *04,521*

Effects of Elastic Stress on the Stability of a Solid-Liquid Interface.
PB95-163028 *03,350*

Rayleigh Instability for a Cylindrical Crystal-Melt Interface.
PB95-180667 *01,010*

CRYSTAL OSCILLATORS
Fundamental Limits on the Frequency Stabilities of Crystal Oscillators.
PB96-176565 *02,277*

CRYSTAL-PHASE TRANSFORMATION
Modeling the Evolution of Structure in Unstable Solid Solution Phases by Diffusional Mechanisms.
PB94-199403 *03,324*

CRYSTAL-PHASE TRANSFORMATIONS
Journal of Research of the National Institute of Standards and Technology, September/October 1993. Volume 98, Number 5.
PB96-169057 *03,368*

CRYSTAL SIZE
Effect of Supersaturation on Apatite Crystal Formation in Aqueous Solutions at Physiologic pH and Temperature.
PB96-135215 *03,571*

CRYSTAL STRUCTURE
Neutron Powder Diffraction Study of a Na, Cs-Rho Zeolite.
PB94-198629 *00,791*

Crystallographic Characterization of Some Intermetallic Compounds in the Al-Cr System.
PB94-198702 *03,318*

Neutron Scattering Structural Study of AlCuFe Quasicrystals Using Double Isotopic Substitution.
PB94-200458 *04,485*

Fast-Ion Conduction and Disorder in Cation and Anion Arrays in Y2(ZryTi(1-y))2O7 Pyrochlores Induced by Zr Substitution: A Neutron Rietveld Analysis.
PB94-211869 *04,496*

Neutron Powder Diffraction Study of the Crystal Structure of YSr2AlCu2O7.
PB94-212073 *04,499*

Structures of Vapor-Deposited Yttria and Zirconia Thin Films.
PB94-216025 *03,041*

Crystal Structure of Pb2Sr2YCu3O8+delta with delta=1.32, 1.46, 1.61, 1.71, by Powder Neutron Diffraction.
PB94-216314 04,518

Crystal Structure of Dicalcium Potassium Trihydrogen Bis(pyrophosphate) Trihydrate.
PB94-216561 00,152

Crystal Structure of Calcium Adipate Monohydrate.
PB94-216579 00,153

Crystal Structure of a New Sodium Zinc Arsenate Phase Solved by 'Simulated Annealing'.
PB95-107124 00,870

Rietveld Analysis of NaxWO3+x/2.yH2O, Which Has the Hexagonal Tungsten Bronze Structure.
PB95-107371 04,524

Neutron Powder Diffraction Study of the Structures of La1.9Ca1.1Cu2O6 and La1.9Sr1.1Cu2O6+Delta.
PB95-140042 04,538

Crystallographic and Magnetic Properties of UAuSn.
PB95-140521 04,543

Crystal Structure and Magnetic Ordering of the Rare-Earth and Cu Moments in RBa2Cu2NbO8(R=Nd,Pr).
PB95-140554 04,546

Ca4Bi6O13: A Compound Containing an Unusually Low Bismuth Coordination Number and Short Bi Bi Contacts.
PB95-141131 00,911

X-Ray-Diffraction Study of a Thermomechanically Detwinned Single Crystal of YBa2Cu3O6+x.
PB95-151726 04,581

Crystal Chemistry and Phase Equilibrium Studies of the BaO-R2O3-CuO Systems. 2. X-Ray Characterization and Standard Patterns of BaR2CuO4, R=Lanthanides.
PB95-151734 04,582

X-Ray Powder Diffraction Data for BaCu(C2O4)2.6H2O.
PB95-151767 04,583

Neutron Powder Diffraction Study of the Nuclear and Magnetic Structures of the Oxygen-Deficient Perovskite YBaCuCoO5.
PB95-161097 00,954

Calibration of High-Energy Electron Beams by Use of Graphite Calorimeters.
PB95-161113 04,598

Ca1-xCuO2, a NaCuO2-Type Related Structure.
PB95-162822 04,620

Octacalcium Phosphate Carboxylates. 5. Incorporation of Excess Succinate and Ammonium Ions in the Octacalcium Phosphate Succinate Structure.
PB95-168894 00,166

Crystal Structure of Calcium Succinate Monohydrate.
PB95-168928 00,167

Crystal Structure and Compressibility of 3:2 Mullite.
PB95-175030 03,682

Crystal Structure and Magnetic Properties of CuGeO3.
PB95-180287 04,678

Structural and Chemical Investigations of Na3(ABO4)3.4H2O-Type Sodalite Phases.
PB95-180733 01,012

Powder Neutron Diffraction Investigation of Structure and Cation Ordering in Ba2+xBi2-xO6-y.
PB95-180865 01,015

Early History and Future Outlook for the X-ray Crystal Density Method.
PB95-202487 04,692

Determination of Complex Structures from Powder Diffraction Data: The Crystal Structure of La3Ti5Al15O37.
PB95-202966 01,038

Structure and Conductivity of Layered Oxides (Ba,Sr)n+1(Sn,Sb)nO3n+1.
PB96-102439 04,707

Oxygen Dependance of the Crystal Structure of HgBa2CuO4+ and Its Relation to Superconductivity.
PB96-102512 04,711

Crystal Structure of a New Monoclinic Form of Potassium Dihydrogen Phosphate Containing Orthophosphacidium Ion, (H4PO4)(sup+1).
PB96-111794 04,725

Crystal Structure of Calcium Glutarate Monohydrate.
PB96-111893 01,074

Crystal Structure of Decacalcium Tetrapotassium Hexakis (Pyrophosphate) Nonahydrate.
PB96-141064 01,099

Neutron-Powder-Diffraction Study of the Long-Range Order in the Octahedral Sublattice of LaD2.25.
PB96-141155 04,753

Fast-Ion Conducting Y2(ZryTi1-y)2O7 Pyrochlores: Neutron Rietveld Analysis of Disorder Induced by Zr Substitution.
PB96-156104 04,776

Tetrahedral-Framework Lithium Zinc Phosphate Phases: Location of Light-Atom Positions in LiZnPO4 H2O by Powder Neutron Diffraction and Structure Determination of LiZnPO4 by ab Initio Methods.
PB96-160510 01,129

Characterization of the Structure of TbD2.25 at 70 K by Neutron Powder Diffraction.
PB96-160528 01,130

CRYSTALLINE CERAMICS

Small-Angle Neutron Scattering Characterization of Processing/Microstructure Relationships in the Sintering of Crystalline and Glassy Ceramics. (Reannouncement with New Availability Information).
AD-A249 510/9 03,025

CRYSTALLIZATION

Polyethylene Crystallized from an Entangled Solution Observed by Scanning Tunneling Microscopy.
PB95-107389 01,232

Biological Macromolecular Crystallization Database: A Tool for Developing Crystallization Strategies.
PB95-126157 00,897

Influence of Natural and Synthetic Inhibitors on the Crystallization of Calcium Oxalate Hydrates.
PB95-150967 03,560

X-Ray Characterization of the Crystallization Process of High-Tc Superconducting Oxides in the Sr-Bi-Pb-Ca-Cu-O System.
PB95-151700 04,579

CRYSTALLOGRAPHY

Statistical Descriptors in Crystallography. 2. Report of a Working Group on Expression of Uncertainty in Measurement.
PB96-146824 04,764

Journal of Research of the National Institute of Standards and Technology, May/June 1996. Volume 101, Number 3. Special Issue: NIST Workshop on Crystallographic Databases.
PB97-109011 04,798

CRYSTMET: The NRCC Metals Crystallographic Data File.
PB97-109029 04,799

Inorganic Crystal Structure Database (ICSD) and Standardized Data and Crystal Chemical Characterization of Inorganic Structure Types (TYPIX): Two Tools for Inorganic Chemists and Crystallographers.
PB97-109037 00,648

Evaluation of Crystallographic Data with the Program DIAMOND.
PB97-109045 00,649

Cambridge Structural Database (CSD): Current Activities and Future Plans.
PB97-109052 00,516

Protein Data Bank: Current Status and Future Challenges.
PB97-109060 00,517

Nucleic Acid Database: Present and Future.
PB97-109078 00,518

Powder Diffraction File: Past, Present, and Future.
PB97-109086 04,800

NIST Crystallographic Databases for Research and Analysis.
PB97-109094 04,801

Conventional and Eccentric Uses of Crystallographic Databases in Practical Materials Identification Problems.
PB97-109102 04,802

Using NIST Crystal Data within Siemens Software for Four-Circle and SMART CCD Diffractometers.
PB97-109110 04,803

Phase Identification in a Scanning Electron Microscope Using Backscattered Electron Kikuchi Patterns.
PB97-109128 04,804

Biological Macromolecule Crystallization Database and NASA Protein Crystal Growth Archive.
PB97-109136 01,171

Investigations of the Systematics of Crystal Packing Using the Cambridge Structural Database.
PB97-109144 00,519

Troublesome Crystal Structures: Prevention, Detection, and Resolution.
PB97-109151 01,172

CIF Crystallographic Information File: A Standard for Crystallographic Data Interchange.
PB97-109169 04,805

Role of Journals in Maintaining Data Integrity: Checking of Crystal Structure Data in 'Acta Crystallographica'.
PB97-109177 04,806

Electronic Publishing and the Journals of the American Chemical Society.
PB97-109185 04,807

How the Cambridge Crystallographic Data Centre Obtains Its Information.
PB97-109193 04,808

Data Import and Validation in the Inorganic Crystal Structure Database.
PB97-109201 04,809

World Wide Web for Crystallography.
PB97-109219 04,810

Workshop Highlights.
PB97-109227 04,811

CRYSTALS

Effect of Electrode-Polymer Interfacial Layers on Polymer Conduction. Part 2. Device Summary.
PB95-151155 02,335

Crystal Packing Interactions of Two Different Crystal Forms of Bovine Ribonuclease A.
PB95-152823 00,943

Dynamics of Mu(+) in Sc and ScHx.
PB96-180021 04,112

Systematic Correction in Bragg X-ray Diffraction of Flat and Curved Crystals.
PB97-112239 04,152

CSOR (COMPUTER SECURITY OBJECTS REGISTER)

General Procedures for Registering Computer Security Objects.
PB94-134897 01,573

CUBANE

1,4-Dinitrocubane and Cubane under High Pressure.
PB95-108437 03,755

CUBANE/DINITRO

1,4-Dinitrocubane and Cubane under High Pressure.
PB95-108437 03,755

CUBANES

Neutron Scattering Study of the Lattice Modes of Solid Cubane.
PB96-147152 01,126

CUPRIC OXIDE

Cooper M(sub II,III) X-ray-Emission Spectra of Copper Oxides and the Bismuth Cuprate Superconductor.
PB96-158027 04,077

CURIE TEMPERATURE

Monte Carlo and Mean-Field Calculations of the Magnetocaloric Effect of Ferromagnetically Interacting Clusters.
PB94-172087 03,201

CURING

Fluorescence Monitoring of Polarity Change and Gelation during Epoxy Cure.
PB94-185543 01,204

Digitized Direct Simulation Model of the Microstructural Development of Cement Paste.
PB94-198777 01,309

Digitized Simulation Model for Microstructural Development.
PB94-198785 01,310

Diffusion Studies in a Digital-Image-Based Cement Paste Microstructural Model.
PB94-198801 01,312

Maturity Method.
PB94-199494 01,313

Maturity Functions for Concrete Made with Various Cements and Admixtures.
PB94-199502 01,314

Interaction between Naphthalene Sulfonate and Silica Fume in Portland Cement Pastes.
PB94-199759 01,315

Effect of Curing History on Ultimate Glass Transition Temperature and Network Structure of Crosslinking Polymers.
PB94-200052 01,214

Monitoring Polymer Cure by Fluorescence Recovery After Photobleaching.
PB94-211422 01,218

Review of Cure Monitoring Techniques for On-Line Process Control.
PB94-216728 03,145

Structural Heterogeneity in Epoxies.
PB95-151866 01,243

Applications of Fluorescence Spectroscopy in Polymer Science and Technology.
PB95-163770 01,258

CURRENT

Electrical Characteristics of Argon Radio Frequency Glow Discharges in an Asymmetric Cell.
PB96-176490 04,109

CURRENT CONTROLLERS

Low-Noise High-Speed Diode Laser Current Controller.
PB95-202826 02,178

CURRENT CONVERTERS

High-Current Thin Film Multijunction Thermal Converters and Multi-Converter Modules.
PB97-112379 01,989

CURRENT DENSITY

Controlling the Critical Current Density of High-Temperature SNS Josephson Junctions.
PB96-200712 04,794

CURRENT SENSING

Improved Annealing Technique for Optical Fiber.
PB96-119680 04,343

CURRENT SENSORS

Optical Current Transducer for Calibration Studies.
PB94-185907 02,121

Faraday Effect Current Sensors.
PB94-200698 02,127

Faraday Effect Sensors: A Review of Recent Progress.
PB94-200706 02,128

CURRENT SOURCES

Flux-Locked Current Source Reference.
PB95-150785 02,039

CURRENTS

Bias Current Dependent Resistance Peaks in NiFe/Ag Giant Magnetoresistance Multilayers.
PB97-112346 04,153

CURRICULA

Computer Security Training and Awareness Course Compendium.
PB95-130985 01,589

CURVE FITTING
Sensitivity of Three-Point Circle Fitting.
PB95-136354 *02,901*

Outlier-Resistant Methods for Estimation and Model Fitting.
PB95-203436 *03,444*

CURVE MOTION
Nonlinear Dynamics of Stiff Polymers.
PB96-122478 *01,278*

CURVED GUIDE
Transmission Properties of Short Curved Neutron Guides. Part 1. Acceptance Diagram Analysis and Calculations.
PB96-102199 *04,021*

CYANINE DYES
Radiation Chemistry of Cyanine Dyes: Oxidation and Reduction of Merocyanine 540.
PB94-211661 *00,818*

CYANOACETYLENE
Rotational Spectra of CH3CCH-NH3, NCCCH-NH3, and NCCCH-OH2.
PB97-118798 *04,170*

CYANOBIPHENYL PHASES
Comparison of Selectivities for PCBs in Gas Chromatography for a Series of Cyanobiphenyl Stationary Phases.
PB96-119458 *00,618*

CYCLIC COMPOUNDS
Ring-Opening Dental Resin Systems Based on Cyclic Acetals.
PB95-162251 *00,162*

Synthesis and Polymerization of Difunctional and Multifunctional Monomers Capable of Cyclopolymerization.
PB95-163044 *01,257*

CYCLIC LOADS
Model Precast Concrete Beam-to-Column Connections Subject to Cyclic Loading.
PB95-153094 *00,438*

Partially Prestressed and Debonded Precast Concrete Beam-Column Joints.
PB95-153102 *00,439*

Seismic Performance Behavior of Precast Concrete Beam-Column Joints.
PB95-153110 *00,440*

Evaluating the Seismic Performance of Lightly-Reinforced Circular Concrete Bridge Columns.
PB95-163259 *01,335*

Performance of 1/3-Scale Model Precast Concrete Beam-Column Connections Subjected to Cyclic Inelastic Loads. Report No. 4.
PB95-179024 *00,444*

CYCLOBUTENE COMPOUNDS
Homogeneous Gas Phase Decyclization of Tetralin and Benzocyclobutene.
PB95-151049 *00,928*

CYCLODEXTRINS
Thermodynamic and NMR Study of the Interactions of Cyclodextrins with Cyclohexane Derivatives.
PB94-185816 *00,781*

Thermodynamic Study of the Reactions of Cyclodextrins with Primary and Secondary Aliphatic Alcohols, with D- and L-Phenylalanine, and with L-Phenylalanineamide.
PB95-180873 *01,016*

CYCLOHEXANOLS
Thermodynamic and NMR Study of the Interactions of Cyclodextrins with Cyclohexane Derivatives.
PB94-185816 *00,781*

CYLINDRICAL BODIES
Elastic Constants of Isotropic Cylinders Using Resonant Ultrasound.
PB94-211919 *04,497*

CYTOCHROME C
Characterization of Cytochrome c/Alkanethiolate Structures Prepared by Self-Assembly on Gold.
PB95-164638 *00,987*

CYTOSINE
Substrate Specificity of the Escherichia coli Endonuclease III: Excision of Thymine- and Cytosine-Derived Lesions in DNA Produced by Radiation-Generated Free Radicals.
PB95-153425 *03,535*

DAMAGE
Repair of Products of Oxidative DNA Base Damage in Human Cells.
PB96-190129 *03,555*

DAMAGE ACCUMULATION
Model for Toughness Curves in Two-Phase Ceramics. 2. Microstructural Variables.
PB96-163795 *03,078*

Effect of Grain Size on Hertzian Contact Damage in Alumina.
PB96-179601 *03,083*

Indentation Fatigue: A Simple Cyclic Hertzian Test for Measuring Damage Accumulation in Polycrystalline Ceramics.
PB96-180013 *03,084*

DAMAGE ASSESSMENT
Northridge Earthquake, 1994. Performance of Structures, Lifelines and Fire Protection Systems.
PB94-161114 *00,421*

Northridge Earthquake 1994: Performance of Structures, Lifelines, and Fire Protection Systems.
PB94-207461 *04,825*

Lessons Learned by a Wing Engineer.
PB94-216421 *00,429*

Performance of HUD-Affiliated Properties during the January 17, 1994 Northridge Earthquake.
PB95-174488 *00,443*

Evaluation of Thermal Wave Imaging for Detection of Machining Damage in Ceramics.
PB95-220547 *03,062*

Some Notable Hurricanes Revisited.
PB96-122601 *00,458*

Comparison of Responses of a Select Number of Buildings to the 10/17/1989 Loma Prieta (California) Earthquake and Low-Level Amplitude Test Results.
PB96-159645 *00,467*

January 17, 1995 Hyogoken-Nanbu (Kobe) Earthquake. Performance of Structures, Lifelines and Fire Protection Systems. Executive Summary and Paper.
PB97-104160 *00,475*

DAMPERS
Method of Estimating the Parameters of Tuned Mass Dampers for Seismic Applications.
PB96-167820 *00,473*

DATA ACCESS
Sharing Information via the Internet: An Infoserver Case Study.
PB96-131511 *01,493*

DATA ACQUISITION
Tabulation of Data on Receiving Tubes. Handbook 68.
AD-A285 495/8 *02,111*

User Study: Informational Needs of Remote National Archives and Records Administration Customers.
PB95-154738 *02,725*

DATA ANALYSIS
Concept for an Algorithm Testing and Evaluation Program at NIST.
PB94-163029 *02,890*

Analysis of Autocorrelations in Dynamic Processes.
PB95-181228 *02,826*

Algorithm Testing and Evaluation Program for Coordinate Measuring Systems: Long Range Plan.
PB95-231833 *02,915*

Reference Manual for the Algorithm Testing System Version 2.0.
PB96-128244 *02,922*

DATA BASE ADMINISTRATORS
Computer Security Management and Planning in the U.S. Federal Government.
PB95-163432 *01,596*

DATA BASE MANAGEMENT
Database Management Standards: Status and Applicability.
PB96-122924 *01,819*

Findings and Recommendations from a Software Reengineering Case Study.
PB96-155791 *01,752*

DATA BASE MANAGEMENT SYSTEMS
Technical Program of the Factory Automation Systems Division 1993.
PB94-160819 *02,805*

Standardization of Formats and Presentation of Fire Data - The FDMS.
PB94-198462 *01,371*

Development of the Fire Data Management System.
PB94-206091 *00,339*

Application of Expert System to Select Data Sources from Chemical Information Databases.
PB95-125654 *00,505*

DATA BASES
NIST Standard Reference Data Products Catalog, 1994.
PB94-151842 *00,727*

Fire Data Management System, FDMS 2.0, Technical Documentation.
PB94-164019 *01,358*

Considerations on Data Requirements for Tribological Modeling.
PB94-172731 *02,962*

National Institute of Standards and Technology Resonance Ionization Spectroscopy/Resonance Ionization Mass Spectroscopy Data Service.
PB94-172897 *03,793*

Thermophysical Property Computer Packages from NIST.
PB95-125787 *04,203*

Biological Macromolecular Crystallization Database: A Tool for Developing Crystallization Strategies.
PB95-126157 *00,897*

Databases Available in the Research Information Center of the National Institute of Standards and Technology.
PB95-128641 *02,724*

Tribological Data: Needs and Opportunities.
PB95-140596 *03,237*

Status Report: AWS Standards for Identifying Arc Welds (A91.1) and Recording Weld Data (A9.2).
PB95-162855 *02,861*

Structural Ceramics Database. Topical Report, June 1989-May 1991.
PB95-203758 *03,060*

NIST Standard Reference Data Products Catalog, 1995-96. Achieve with Standard Reference Data.
PB95-260808 *01,057*

Electron-Ion Collisions in the Plasma Edge.
PB96-111885 *04,037*

Databases Available in the Research Information Center of the National Institute of Standards and Technology (December 1995).
PB96-139407 *02,734*

Information Resources for the Fire Community.
PB96-148119 *00,211*

Guide to a Format for Data on Chemical Admixtures in a Materials Property Database.
PB96-165394 *01,327*

Guide to a Format for Data on Chemical Admixtures in a Materials Property Database. (Reannouncement with new abstract).
PB96-186192 *01,328*

Guide to Locating and Accessing Computerized Numeric Materials Databases.
PB96-204045 *03,007*

Database Development and Management (Project A.2.2): The Annual Report for 1992-1993.
PB97-110290 *03,098*

DATA COLLECTION
Panel: Building and Using Test Collections.
PB97-118673 *02,743*

DATA COLLECTIONS
Lake Erie Water Temperature Data, Put-in-Bay, Ohio, 1918-1992.
PB96-202452 *03,692*

DATA COMMUNICATION SYSTEMS
Data Communications Strategy.
PB96-167846 *02,738*

DATA DICTIONARIES
Information Resource Dictionary System (IRDS): A Status Report.
PB95-126207 *01,810*

DATA ELEMENTS
Application of Metadata Standards.
PB96-180187 *01,771*

DATA ENCRYPTION
Data Encryption Standard (DES); Category: Computer Security; Subcategory: Cryptography.
FIPS PUB 46-2 *01,572*

Escrowed Encryption Standard (EES); Category: Computer Security; Subcategory: Cryptography.
FIPS PUB 185 *01,569*

Report of the NIST Workshop on Key Escrow Encryption. Held in Gaithersburg, Maryland on June 8-10, 1994.
PB94-209459 *01,584*

Data Encryption Standard.
PB95-162376 *01,595*

EDI and EFT Security Standards.
PB96-122833 *01,605*

Introduction to Secure Telephone Terminals.
PB97-110498 *01,512*

DATA FILE
Codes for Named Populated Places, Primary County Divisions, and Other Locational Entities of the United States (FIPS PUB 55-3) (on Magnetic Tape).
PB95-502563 *00,129*

FIPS PUB 8-6, Metropolitan Areas (for Microcomputers).
PB95-503280 *04,874*

Countries, Dependencies, Areas of Special Sovereignty, and Their Principal Administrative Divisions (for Microcomputers).
PB95-503504 *00,130*

DATA FILES
Standardised Computer Data File Format for Storage, Transport, and Off-Line Processing of Partial Discharge Data.
PB96-122486 *01,930*

DATA FLOW ANALYSIS
Hardware Measurement Techniques for High-Speed Networks.
PB96-160551 *01,500*

DATA LINKS
Provision of Isochronous Service on IEEE 802.6.
PB96-160635 *01,501*

DATA MANAGEMENT
Compatibility Analysis of the ANSI and ISO IRDS Services Interfaces.
PB94-163474 *01,805*

PC-Based Prototype Expert System for Data Management and Analysis of Creep and Fatigue of Selected Materials at Elevated Temperatures.
PB94-172251 *03,202*

Analyzing Electronic Commerce.
PB94-219102 *00,480*

Object SQL: Language Extensions for Object Data Management.
PB95-125902 *01,704*

DATA MODELS
Integration Definition for Information Modeling (IDEF1X); Category: Software Standard; Subcategory: Modeling Techniques.
FIPSPUB184 *01,673*

DATA PROCESSING
ADA; Category: Software Standard; Subcategory: Programming Language.
FIPS PUB 119-1 *01,667*

SQL Environments. Category: Software Standard; Subcategory: Database.
FIPS PUB 193 *01,801*

Implementation of a Standard Format for GPS Common View Data.
N95-32323/4 *03,779*

Radiation Process Data: Collection, Analysis, and Interpretation.
PB95-162632 *03,628*

Application Profile for ISDN.
PB95-163689 *01,479*

Federal Implementation Guideline for Electronic Data Interchange. ASC X12 003050 Transaction Set 840 Request for Quotation. Implementation Convention.
PB96-172531 *01,824*

DATA PROCESSING EQUIPMENT
Protection of Data Processing Equipment with Fine Water Sprays.
PB95-174975 *02,610*

DATA PROCESSING SECURITY
Good Security Practices for Electronic Commerce, Including Electronic Data Interchange.
PB94-139045 *01,463*

Study of Federal Agency Needs for Information Technology Security.
PB94-193653 *01,579*

Report of the NIST Workshop on Key Escrow Encryption. Held in Gaithersburg, Maryland on June 8-10, 1994.
PB94-209459 *01,584*

Analysis of Selected Software Safety Standards.
PB95-151262 *01,708*

Keeping Your Site Comfortably Secure: An Introduction to Internet Firewalls.
PB95-182275 *02,730*

Common Criteria: On the Road to International Harmonization.
PB96-123484 *01,606*

Functional Security Criteria for Distributed Systems.
PB96-123492 *01,607*

DATA PROCESSING TERMINALS
Guidance of the Legality of Keystroke Monitoring.
PB96-161237 *00,005*

DATA QUALITY
Replicate Measurements for Data Quality and Environmental Modeling.
PB94-172533 *02,515*

DATA RETRIEVAL
Retrieving Articles from the Internet (without a UNIX Workstation). Part 1. File Formats and Software Tools.
PB95-168720 *02,728*

Retrieving Articles from the Internet (without a UNIX Workstation). Part 2. An Example.
PB95-168738 *02,729*

DATA SERVICE
Resonance Ionization Spectroscopy/Resonance Ionization Mass Spectrometry Data Service. V-Data Sheets for Ga, Mn, Sc, and Tl.
PB96-158068 *00,625*

DATA SHARING
Standards and Linkages: What Data Sharing Needs.
PB95-161881 *01,713*

DATA STORAGE
Optical Storage Media Data Integrity Studies.
N95-24130/3 *01,620*

Dilemma-Preservation versus Access.
PB94-198488 *02,711*

Preliminary Functional Specifications of a Prototype Electronic Research Notebook for NIST.
PB94-207750 *00,012*

Standardised Computer Data File Format for Storage, Transport, and Off-Line Processing of Partial Discharge Data.
PB96-122486 *01,930*

Status of Emerging Standards for Removable Computer Storage Media and Related Contributions of NIST.
PB96-160619 *01,634*

DATA STORAGE SYSTEMS
Recalibration for the Final Archive of the International Ultraviolet Explorer (IUE) Satellite.
PB96-135264 *00,106*

DATA STRUCTURES
Standards and Linkages: What Data Sharing Needs.
PB95-161881 *01,713*

Tree-Lookup for Partial Sums Or: How Can I Find This Stuff Quickly.
PB96-179411 *01,770*

Move-to-Root Rule for Self-Organizing Trees with Markov Dependent Requests.
PB96-179528 *03,431*

Component-Based Handprint Segmentation Using Adaptive Writing Style Model.
PB96-193669 *01,859*

Heap of Data.
PB97-111488 *03,424*

Making Connections.
PB97-119044 *01,785*

DATA TRANSFER (COMPUTERS)
Spatial Data Transfer Standard (SDTS): Category: Software Standard; Subcategory: Information Interchange.
FIPS PUB 173-1 *01,794*

Spatial Data Transfer Standard (SDTS). Category: Software Standard; Subcategory: Information Interchange. (FIPS PUB 173-1A).
FIPS PUB 173-1A *01,795*

Spatial Data Transfer Standard (SDTS). Category: Software Standard; Subcategory: Information Interchange. (FIPS PUB 173-1B).
FIPS PUB 173-1B *01,796*

Standardization of Formats and Presentation of Fire Data - The FDMS.
PB94-198462 *01,371*

NIST-Coordinated Standard for Fingerprint Data Interchange.
PB94-216645 *01,808*

National PDES Testbed: An Overview.
PB95-125829 *02,775*

Mapping Integration Definition for Information Modeling (IDEF1X) Model into CASE Data Interchange Format (CDIF) Transfer File.
PB95-154670 *01,711*

Using Archie to Find Files on the INTERNET.
PB95-168605 *02,727*

Mapping Integration Definition for Function Modeling (IDEFO) Model into CASE Data Interchange Format (CDIF) Transfer File.
PB96-109533 *01,741*

DATA TRANSMISSION
Recommendations on Selection of Vehicle-to-Roadside Communications Standards for Commercial Vehicle Operations.
PB94-195914 *04,859*

Vehicle-to-Roadside Communications for Commercial Vehicle Operations: Requirements and Approaches.
PB95-188827 *04,860*

Comparison of FDDI Asynchronous Mode and DQDB Queue Arbitrated Mode Data Transmission for Metropolitan Area Network Applications.
PB96-160452 *01,498*

Addressing U.S. Government Security Requirements for OSI.
PB96-160577 *01,611*

DATA TRANSMISSION SYSTEMS
NIST ATM Network Simulator: Operation and Programming, Version 1.0.
PB96-106851 *01,487*

DATA VALIDATION
How the Cambridge Crystallographic Data Centre Obtains Its Information.
PB97-109193 *04,808*

Data Import and Validation in the Inorganic Crystal Structure Database.
PB97-109201 *04,809*

DATABASES
Progress in the Development of a Chemical Kinetic Database for Combustion Chemistry.
PB95-151056 *01,384*

Information Retrieval Using Key Words and a Structured Review.
PB95-161121 *03,724*

Locating Fire Engineering Information.
PB95-161188 *00,198*

Access Paths for Materials Databases: Approaches for Large Databases and Systems.
PB95-162525 *02,975*

Database for the Static Dielectric Constant of Water and Steam.
PB96-145586 *01,103*

Locating Fire Information.
PB96-190137 *00,227*

Workshop Highlights.
PB97-109227 *04,811*

DAUGHTER PRODUCTS
Systematics of Alpha-Particle Energy Spectra and Lineal Energy (Y) Spectra for Radon Daughters.
PB94-185139 *03,615*

DAYLIGHT
Lighting Quality and Light Source Size.
PB95-151783 *00,252*

DAYLIGHTING
Papers Presentations Shine.
PB94-200383 *00,244*

DEBONDING
Determination of Fiber-Matrix Interfacial Properties of Importance to Ceramic Composite Toughening.
PB95-125811 *03,149*

DEBUGGING (COMPUTERS)
Debugger for Tcl Applications.
PB94-213303 *01,695*

Method to Determine a Basis Set of Paths to Perform Program Testing.
PB96-131503 *01,747*

Program Slicing.
PB96-160981 *01,761*

Using S-Check, Alpha Release 1.0.
PB96-165964 *01,767*

DEBYE-HUCKEL THEORY
Electrolytes Constrained on Fractal Structures: Debye-Huckel Theory.
PB97-110241 *01,174*

DEBYE TEMPERATURE
Dependence of Tc on Debye Temperature Theta(sub D) for Various Cuprates.
PB95-180493 *04,683*

DEC/MASPAR MP-1 COMPUTER SYSTEMS
MasPar MP-1 as a Computer Arithmetic Laboratory.
PB95-189437 *01,627*

DECISION MAKING
EXITT: A Simulation Model of Occupant Decisions and Actions in Residential Fires.
PB94-213261 *00,351*

DECISION SUPPORT SYSTEMS
AutoBid 2.0: The Microcomputer System for Police Patrol Vehicle Selection.
PB96-154570 *04,871*

DECISION TREE ANALYSIS
Point Probe Decision Trees for Geometric Concept Classes.
PB96-160817 *01,612*

DECOMPOSITION
Thermal Decomposition Pathways in Nitramine Propellants.
AD-A295 896/5 *03,753*

Spectroscopic Study of Reaction Intermediates and Mechanisms in Nitramine Decomposition and Combustion.
AD-A296 061/5 *03,774*

Decomposition of SF6 and Production of S2F10 in Power Arcs.
PB96-122619 *01,084*

DECOMPOSITION REACTIONS
Oxidation of 10-Methylacridan, a Synthetic Analogue of NADH and Deprotonation of Its Cation Radical. Convergent Application of Laser Flash Photolysis and Direct and Redox Catalyzed Electrochemistry to the Kinetics of Deprotonation of the Cation Radical.
PB94-198371 *00,785*

Mechanism and Rate Constants for the Reactions of Hydrogen Atoms with Isobutene at High Temperatures.
PB95-151064 *00,929*

Decomposition of Sulfur Hexafluoride by X-rays.
PB96-135314 *01,095*

DECYCLIZATION
Homogeneous Gas Phase Decyclization of Tetralin and Benzocyclobutene.
PB95-151049 *00,928*

DEFECT FORMATION
Mechanism of Defect Formation in Low-Dose Oxygen Implanted Silicon-on-Insulator Material.
PB97-111462 *02,453*

DEFECTS
Fabrication of Flaw-Tolerant Aluminum-Titanate-Reinforced Alumina.
PB95-162533 *03,161*

Defect Formation Mechanism Causing Increasing Defect Density during Decreasing Implant Dose in Low-Dose Simox.
PB96-119524 *02,402*

Nano-Defects in Commercial Bonded SOI and SIMOX.
PB96-123674 *02,407*

Classified Bibliography: Insulation Condition Monitoring Methods, 1989-1995.
PB96-131586 *02,232*

Ultrasonic Sensing of GMAW: Laser/EMAT Defect Detection System.
PB96-186028 *02,878*

DEFENSE INDUSTRY
Transfer of Technology from Defense to Civilian Sectors.
PB94-185360 *00,011*

DEFINITIVE METHOD
Development of the Ion Exchange-Gravimetric Method for Sodium in Serum as a Definitive Method.
PB96-179148 *01,867*

DEFLOCCULATING
Surface Chemical Interactions of Si3N4 with Polyelectrolyte Deflocculants.
PB95-175576 *03,056*

DEFORMATION
Volume Recovery in Epoxy Glasses Subjected to Torsional Deformations: The Question of Rejuvenation.
PB95-140018 *03,382*

Torsional Relaxation and Volume Response during Physical Aging in Epoxy Glasses Subjected to Large Torsional Deformations.
PB95-140026 *03,383*

Using Torsional Dilatometry to Measure the Effects of Deformations on Physical Aging.
PB95-140901 *03,384*

DEGENERATE STATES
Accuracy-Weighted Variational Principle for Degenerate Continuum States.
PB94-200615 *03,831*

DEGRADATION
Relation between AC Impedance Data and Degradation of Coated Steel. 1. Effects of Surface Roughness and Contamination on the Corrosion Behavior of Epoxy Coated Steel.
PB94-213345 *03,189*

DEGREES OF FREEDOM
Confidence on the Modified Allan Variance and the Time Variance.
PB96-190376 *01,557*

DEHYDROASCORBIC ACID
Ascorbic and Dehydroascorbic Acids Measured in Plasma Preserved with Dithiothreitol or Metaphorphoric Acid.
PB94-216330 *03,495*

DELAUNAY TRIANGULATION
Submissions to a Planned Encyclopedia of Operations Research on Computational Geometry and the Voronoi/Delaunay Construct.
PB94-152709 *03,425*

DELAY LINES
Low-Coherence Interferometric Measurement of Group Transit Times in Precision Optical Fibre Delay Lines.
PB95-168480 *02,158*

DELAY TIME
Use of Ionospheric Data in GPS Time Transfer.
PB95-163853 *01,540*

DEMONSTRATION PROJECTS
Submarine Automation: Demonstration No. 5.
PB95-251633 *03,748*

DENDRITIC CRYSTALS
Computation of Dendrites Using a Phase Field Model.
PB94-160744 *04,436*

Stagnant Film Model of the Effect of Natural Convection on the Dendrite Operating State.
PB96-146832 *04,765*

DENSIFICATION
Micromechanics of Densification and Distortion.
PB94-200326 *03,327*

Rapid Hot Pressing of Ultra-Fine PSZ Powders.
PB94-216587 *03,045*

DENSIMETERS
Development of a Dual-Sinker Densimeter for High-Accuracy Fluid P-V-T Measurements. Appendix A.
DE93019682 *02,620*

DENSITOMETERS
High-Temperature High-Pressure Oscillating Tube Densimeter.
PB96-146618 *01,123*

DENSITY
Density of Solids and Liquids.
AD-A278 517/8 *00,711*

DENSITY CORRECTION
Quantum Collisional Transfer Contributions to the Density Dependence of Gaseous Viscosity.
PB96-161914 *01,142*

DENSITY (MASS/VOLUME)
Neutron Reflectivity of End-Grafted Polymers: Concentration and Solvent Quality Dependence in Equilibrium Conditions.
PB94-185758 *01,206*

Apparent Molar Heat Capacities and Apparent Molar Volumes of Aqueous Glucose at Temperatures from 298.15 K to 327.01 K.
PB94-212800 *03,459*

Effects of Humidity and Elevated Temperature on the Density and Thermal Conductivity of a Rigid Polyisocyanurate Foam Co-Blown with CCl3F and CO2.
PB95-150462 *00,371*

Experimental Method for Obtaining Critical Densities of Binary Mixtures: Application to Ethane + n-Butane.
PB95-151148 *00,930*

Effects of Humidity and Elevated Temperature on the Density and Thermal Conductivity of a Rigid Polyisocyanurate Foam.
PB95-152021 *00,373*

Global Density Effects on the Self-Preservation Behavior of Turbulent Free Jets.
PB95-162301 *04,207*

Neutron Reflectivity Study of the Density Profile of a Model End-Grafted Polymer Brush: Influence of Solvent Quality.
PB95-202735 *01,274*

DENSITY MEASUREMENT
Electronic Balance and Some Gravimetric Applications. (The Density of Solids and Liquids, Pycnometry and Mass).
PB94-163052 *03,785*

Determination of Density of Mass Standards: Requirement and Method.
PB94-163078 *03,787*

Report of Density Intercomparisons Undertaken by the Working Group on Density of the CCM.
PB94-200664 *00,503*

Mass and Density Determinations.
PB94-200672 *00,504*

Lattice Dynamics of Ba1-xKxBiO3.
PB96-102421 *04,706*

DENSITY PROFILES
Internal Waves in Xenon Near the Critical Point.
PB97-111504 *04,221*

DENTAL
Fluoride Analytical Methods.
PB96-180237 *03,578*

DENTAL CEMENTS
Adsorption of Low-Molecular-Weight Sodium Polyacrylate on Hydroxyapatite.
PB94-172608 *00,139*

Behavior of a Calcium Phosphate Cement in Simulated Blood Plasma In vitro.
PB95-168712 *00,165*

Formation of Hydroxyapatite in Cement Systems.
PB95-175261 *00,170*

Physical and Chemical Properties of Resin-Reinforced Calcium Phosphate Cements.
PB95-180212 *00,171*

Formation of Hydroxyapatite in a Polymeric Calcium Phosphate Cement.
PB95-180642 *00,173*

Properties and Mechanisms of Fast-Setting Calcium Phosphate Cements.
PB96-123229 *00,178*

Bioactive Polymeric Dental Materials Based on Amorphous Calcium Phosphate.
PB96-147012 *03,572*

Remineralizing Dental Composites Based on Amorphous Calcium Phosphate.
PB96-147020 *03,573*

Dynamics of Calcium Phosphate Precipitation.
PB96-147095 *03,574*

DENTAL CERAMICS
In vitro Fracture Behavior of Ceramic and Metal-Ceramic Restorations.
PB96-119722 *03,569*

DENTAL ENAMEL
Deposition of Loosely Bound and Firmly Bound Fluorides on Tooth Enamel by an Acidic Gel Containing Fluorosilicate and Monocalcium Phosphate Monohydrate.
PB95-150710 *03,559*

Wear of Human Enamel against a Commercial Castable Ceramic Restorative Material.
PB95-161972 *00,161*

Procedure for the Study of Acidic Calcium Phosphate Precursor Phases in Enamel Mineral Formation.
PB95-164448 *03,564*

DENTAL MATERIALS
Properties and Interactions of Oral Structures and Restorative Materials. Annual Report for Period October 1, 1990 to September 30, 1991.
PB94-160843 *03,558*

Influence of Tempering Method on Residual Stress in Dental Porcelain.
PB94-172012 *00,138*

Interaction of Some Coupling Agents and Organic Compounds with Hydroxyapatite: Hydrogen Bonding, Adsorption and Adhesion.
PB94-172616 *00,140*

Effect of Two Initiator/Stabilizer Concentrations in a Metal Primer on Bond Strengths of a Composite to a Base Metal Alloy.
PB94-172723 *00,141*

Dental Materials.
PB94-172871 *00,142*

Effect of Transformation of Alloy on Transient and Residual Stresses in a Porcelain-Metal Strip.
PB94-198397 *00,143*

Adhesion of Composites to Dentin and Enamel.
PB94-199049 *00,144*

Development of an Adhesive Bonding System.
PB94-199056 *00,145*

Clinical Perspective on Dentin Adhesives.
PB94-211240 *00,146*

Periapical Tissue Reactions to a Calcium Phosphate Cement in the Teeth of Monkeys.
PB94-212008 *00,149*

Paffenbarger Research Center: The Cutting Edge of Dental Science.
PB94-216355 *00,151*

Evaluation of Fracture Toughness and Residual Stress in Dental Porcelain by Indentation-Microfracture Method.
PB95-125613 *00,154*

Effects of Surface-Active Resins on Dentin/Composite Bonds.
PB95-140448 *00,156*

Effects of Calcium Phosphate Solutions on Dentin Permeability.
PB95-151080 *00,157*

NIR-Spectroscopic Investigation of Water Sorption Characteristics of Dental Resins and Composites.
PB95-151171 *00,189*

Evaluation of Fracture Toughness and Residual Stress in Dental Porcelain by Indentation-Microfracture Method.
PB95-152831 *00,159*

Publication and Presentation Abstracts, 1993. (Published by Paffenbarger Research Center and Center of Excellence for Materials Science Research).
PB95-153052 *03,562*

Wear of Human Enamel against a Commercial Castable Ceramic Restorative Material.
PB95-161972 *00,161*

Ring-Opening Dental Resin Systems Based on Cyclic Acetals.
PB95-162251 *00,162*

Effect of Ethanol on the Solubility of Dicalcium Phosphate Dihydrate in the System Ca(OH)2-H3PO4-H2O at 37C.
PB95-163507 *00,163*

Evaluation of Methylene Lactone Monomers in Dental Resins.
PB95-164661 *00,164*

Octacalcium Phosphate Carboxylates. 5. Incorporation of Excess Succinate and Ammonium Ions in the Octacalcium Phosphate Succinate Structure.
PB95-168894 *00,166*

Crystal Structure of Calcium Succinate Monohydrate.
PB95-168928 *00,167*

Ambient Temperature Synthesis of Bulk Intermetallics.
PB95-169074 *00,168*

Effect of Ethanol on the Solubility of Hydroxyapatite in the System Ca(OH)2-H3PO4-H2O at 25C and 33C.
PB95-169231 *00,169*

Physical and Chemical Properties of Resin-Reinforced Calcium Phosphate Cements.
PB95-180212 *00,171*

Diagnosis and Treatment of an Oral Base-Metal Contact Lesion Following Negative Dermatologic Patch Tests.
PB95-180626 *00,172*

Polymers Technical Activities 1994. NAC-NRC Assessment Panel, April 6-7, 1995.
PB95-209896 *01,275*

Reduction of Marginal Gaps in Composite Restorations by Use of Glass-Ceramic Inserts.
PB96-102405 *00,174*

Publications and Presentation Abstracts, 1995. (Published by Paffenbarger Research Center and Center of Excellence for Materials Science Research).
PB96-119250 *03,568*

Failure of All-Ceramic Fixed Partial Dentures 'In vitro' and 'In vivo': Analysis and Modeling.
PB96-122536 *00,175*

Dental Applications of Ceramics.
PB96-122940 *00,177*

Preparation and Characterization of Cyclopolymerizable Resin Formulations.
PB96-146840 *01,285*

Publication and Presentation Abstracts, 1995.
PB96-164082 *03,576*

Polymeric Calcium Phosphate Cements Derived from Poly(methyl vinyl ether-maleic acid).
PB96-164264 *00,180*

Publication and Presentation Abstracts, 1994.
PB96-176623 *03,577*

Polymers Technical Activities, 1995.
PB96-193719 *01,291*

Posterior Restorative Materials Research.
PB97-118624 *03,582*

Publication and Presentation Abstracts, 1996.
PB97-122238 *03,585*

DENTAL PLAQUE
Distribution of Fluoride in Saliva and Plaque Fluid After a 0.048 mol/L NaF Rinse.
PB95-151205 *03,561*

DENTAL PROSTHESIS DESIGN
Tapered Cross-Pin Attachments for Fixed Bridges.
PB94-185238 *00,185*

DENTAL RESTORATION
Wear of Human Enamel against a Commercial Castable Ceramic Restorative Material.
PB95-161972 *00,161*

DENTAL TUBULES
Effects of Calcium Phosphate Solutions on Dentin Permeability.
PB95-151080 *00,157*

DENTERIDES
Characterization of the Vibrational Dynamics in the Octahedral Sublattices of LaD2.25 and LaH2.25.
PB96-123724 *01,091*

DENTIN
Adhesion of Composites to Dentin and Enamel.
PB94-199049 *00,144*

Effects of Surface-Active Resins on Dentin/Composite Bonds.
PB95-140448 *00,156*

Modified Surface-Active Monomers for Adhesive Bonding to Dentin.
PB95-151163 *00,158*

New Surface-Active Comonomer for Adhesive Bonding.
PB96-204052 *03,579*

DENTIN PERMEABILITY
Effects of Calcium Phosphate Solutions on Dentin Permeability.
PB95-151080 *00,157*

Effects of Aluminum Oxalate/Glycine Pretreatment Solutions on Dentin Permeability.
PB95-164505 *03,565*

DENTISTRY
Clinical Perspective on Dentin Adhesives.
PB94-211240 *00,146*

Paffenbarger Research Center: The Cutting Edge of Dental Science.
PB94-216355 *00,151*

Influence of Natural and Synthetic Inhibitors on the Crystallization of Calcium Oxalate Hydrates.
PB95-150967 *03,560*

Interaction of Chlorhexidine Digluconate with and Adsorption of Chlorhexidine on Hydroxyapatite.
PB95-175907 *03,566*

DEOXYRIBONUCLEIC ACID
Resolution of DNA in the Presence of Mobility Modifying Polar and Nonpolar Compounds by Discontinuous Electrophoresis on Rehydratable Polyacrylamide Gels.
PB95-152799 *00,590*

Repair of Products of Oxidative DNA Base Damage in Human Cells.
PB96-190129 *03,555*

DEOXYRIBONUCLEIC ACIDS
Function of DnaJ and DnaK as Chaperones in Origin-Specific DNA Binding by RepA.
PB95-151544 *03,533*

Substrate Specificity of the Escherichia coli Endonuclease III: Excision of Thymine- and Cytosine-Derived Lesions in DNA Produced by Radiation-Generated Free Radicals.
PB95-153425 *03,535*

Electrophoretic Separations of Polymerase Chain Reaction: Amplified DNA Fragments in DNA Typing Using a Capillary Electrophoresis-Lased Induced Fluorescence System.
PB95-163036 *03,536*

Interlaboratory Comparison of Autoradiographic DNA Profiling Measurements. 1. Data and Summary Statistics.
PB95-175923 *03,542*

Detection of Aromatic Compounds Based on DNA Intercalation Using an Evanescent Wave Biosensor.
PB96-111976 *03,473*

Interlaboratory Comparison of Autoradiographic DNA Profiling Measurements. 2. Measurement Uncertainty and Its Propagation.
PB96-112123 *03,545*

Rapid Method for the Isolation of Genomic DNA from 'Aspergillus fumigatus'.
PB96-147061 *03,488*

Novel DNA N-Glycosylase Activity of E. coli T4 Endonuclease V That Excises 4,6-Diamino-5-Formamidopyrimidine from DNA, a UV-Radiation- and Hydroxyl Radical-Induced Product of Adenine.
PB96-160478 *03,549*

Novel Activities of Human Uracil DNA N-glycosylase for Cytosine-Derived Products of Oxidative DNA Damage.
PB96-164132 *03,479*

New Method for the Detection and Measurement of Polyaromatic Carcinogens and Related Compounds by DNA Intercalation.
PB96-167382 *03,481*

DnaJ, DnaK, and GrpE Heat Shock Proteins are Required in 'ori'P1 DNA Replication Solely at the RepA Monomerization Step.
PB97-119382 *03,557*

DEOXYRIBOSE
Modification of Deoxyribose-Phosphate Residues by Extracts of Ataxia Telangiectasia Cells.
PB94-212602 *03,458*

DEPOLARIZATION
Polarimetric Calibration of Reciprocal-Antenna Radars.
PB96-200696 *02,016*

DEPOSITION
Perspective on Fiber Coating Technology.
PB94-200540 *03,118*

Coating of Fibers by Colloidal Techniques in Ceramic Composites.
PB94-216256 *03,196*

Deposition of Colloidal Sintering-Aid Particles on Silicon Nitride.
PB94-216272 *03,044*

Deposition of Loosely Bound and Firmly Bound Fluorides on Tooth Enamel by an Acidic Gel Containing Fluorosilicate and Monocalcium Phosphate Monohydrate.
PB95-150710 *03,559*

Nanofabrication of a Two-Dimensional Array Using Laser-Focused Atomic Deposition.
PB96-119417 *04,732*

New Method for Achieving Accurate Thickness Control for Uniform and Graded Multilayer Coatings on Large Flat Substrates.
PB96-159744 *04,366*

DEPOSITS
New Method to Evaluate Deposit Forming Tendencies of Liquid Lubricants by Differential Scanning Calorimetry.
PB95-152120 *01,451*

Deposit Forming Tendencies of Diesel Engine Oils-Correlation between the Two-Peak Method and Engine Tests.
PB95-152138 *01,452*

DEPROTEINATION
Critical Evaluation of the Purification of Biominerals by Hypochlorite Treatment.
PB95-150959 *00,186*

DESCRIBING FUNCTIONS
Electrode Extension Model for Gas Metal Arc Welding.
PB96-135074 *02,871*

DESIGN
Simple, Inexpensive Apparatus for Sample Concentration.
PB94-199205 *00,546*

Advanced Mass Calibration and Measurement Assurance Program for State Calibration Laboratories.
PB95-253571 *02,492*

Design Engineering Research at NIST.
PB95-267860 *02,784*

Line-Heat-Source Guarded-Hot-Plate Apparatus.
PB97-118996 *00,417*

DESIGN ANALYSIS
How to Evaluate Alternative Designs Based on Fire Modeling.
PB96-102116 *00,206*

DESIGN CRITERIA
Design Equations and Scaling Laws for Linear Compressors with Flexure Springs.
PB95-168902 *02,948*

Can Displays Deliver a Full Measure: Manufacturing.
PB96-111935 *02,185*

Recommended Performance-Based Criteria for the Design of Manufactured Home Foundation Systems to Resist Wind and Seismic Loads.
PB96-128285 *00,460*

Elements of a Framework for Fire Safety Engineering.
PB96-151402 *00,214*

Distributed Architecture for Standards Processing.
PB96-164181 *00,276*

Design of Technically Complex Facilities.
PB97-119101 *02,695*

DESIGN PROCESS
Improving the Design Process by Predicting Downstream Values of Design Attributes.
PB97-113096 *02,795*

DESIGN STANDARDS
Evaluation and Strengthening Guidelines for Federal Buildings: Assessment of Current Federal Agency Evaluation Programs and Rehabilitation Criteria and Development of Typical Costs for Seismic Rehabilitation.
PB94-181856 *00,425*

Evaluation and Retrofit Standards for Existing Federally Owned and Leased Buildings.
PB95-150918 *00,434*

Lessons from the Loma Prieta Earthquake.
PB95-164091 *00,442*

World of Building Codes.
PB95-203428 *00,449*

Fire Codes for Global Practice.
PB96-102108 *00,205*

ICSSC Guidance on Implementing Executive Order 12941 on Seismic Safety of Existing Federally Owned or Leased Buildings.
PB96-128103 *00,459*

Predicting the Fire Performance of Buildings: Establishing Appropriate Calculation Methods for Regulatory Applications.
PB96-141239 *00,316*

DESORPTION
Vibrational Distributions of As2 in the Cracking of As4 on Si(100) and Si(111).
PB94-198314 *00,784*

Topological Influences on Polymer Adsorption and Desorption Dynamics.
PB94-212479 *01,227*

Desorption Induced by Electronic Transitions.
PB94-216173 *00,853*

Laser-Induced Desorption of NO from Si(111): Effects of Coverage on NO Vibrational Populations.
PB95-162319 *00,959*

Direct Detection of Atomic Arsenic Desorption from Si(100).
PB95-202230 *01,024*

Photodesorption Dynamics of CO from Si(111): The Role of Surface Defects.
PB96-111646 *03,066*

DESULFURIZATION
Low Temperature H(sub 2)S Separation Using Membrane Reactor with Redox Catalyst.
DE94008991 *02,471*

Chemical and Microbiological Problems Associated with Research on the Biodesulfurization of Coal.
PB95-140950 *02,484*

DETAN 95 COMPUTER CODE
DETAN 95: Computer Code for Calculating Spectrum-Averaged Cross Sections and Detector Responses in Neutron Spectra.
PB95-242384 *04,014*

DETECTION
Hair Analysis for Drugs of Abuse: Evaluation of Analytical Methods, Environmental Issues, and Development of Reference Materials.
PB95-176269 *03,501*

NIST Reference Materials to Support Accuracy in Drug Testing.
PB96-123807 *03,505*

Safety Assessment of Railroad Wheels by Residual Stress Measurements.
PB96-141114 *04,855*

Safety Assessment of Railroad Wheels Through Roll-by Detection of Tread Cracks.
PB96-141254 *04,856*

Interlaboratory Studies on the Analysis of Hair for Drugs of Abuse: Results from the Fourth Exercise.
PB97-111322 *03,510*

DETECTOR RESPONSE
Modeling Detector Response for Neutron Depth Profiling.
PB96-157813 *04,066*

DETECTORS
Use of a Radiochromic Detector for the Determination of Stereotactic Radiosurgery Dose Characteristics.
PB94-185642 *03,514*

Germanium Detector Optimization of MDA for Efficiency vs. Low Intrinsic Background.
PB94-199155 *00,543*

Process Gas Chromatography Detector for Hydrocarbons Based on Catalytic Cracking.
PB95-141099 *02,485*

Simultaneous Laser-Diode Emission and Detection for Fiber-Optic Sensor Applications.
PB96-155502 *04,062*

Soft-X-ray Damage to p-terphenyl Coatings for Detectors.
PB96-159611 *04,364*

Magneto-Optic Rotation Sensor Using a Laser Diode as Both Source and Detector.
PB97-111272 *04,390*

Fundamentals and Problems of Fiber Current Sensors.
PB97-111835 *02,205*

DETERIORATION
Diagnosis of Causes of Concrete Deterioration in the MLP-7A Parking Garage.
PB95-143095 *01,318*

DEUTERIUM
Experimental plan to determine the performance of the Oak Ridge National Laboratory Cold Neutron Moderator. Final report, September 1, 1993--November 30, 1993.
DE95011352 *03,778*

Simultaneous Forward-Backward Raman Scattering Studies of D2 Broadened by D2, He, and Ar.
PB95-162459 *00,961*

Vibrations of Hydrogen and Deuterium in Solid Solution with Lutetium.
PB95-181038 *01,019*

Deuterium in the Local Interstellar Medium: Its Cosmological Significance.
PB95-202842 *00,081*

Accurate Measurements of the Local Deuterium Abundance from HST Spectra.
PB96-200621 *00,110*

Deuterium and the Local Interstellar Medium: Properties for the Procyon and Capella Lines of Sight.
PB96-200639 *00,111*

DEUTERIUM CHLORIDE COMPLEXES
Vibrational Dependence of the Anisotropic Intermolecular Potential of Ar-HCl.
PB95-202685 *01,029*

High Resolution Near Infrared Spectroscopy of HCl-DCl and DCl-HCl: Relative Binding Energies, Isomer Interconversion Rates, and Mode Specific Vibrational Predissociation.
PB95-203212 *01,048*

DEUTERIUM CHLORIDE DIMERS
Slit-Jet Near-Infrared Diode Laser Spectroscopy of (DCl)2: nu1, nu2 DCl Stretching Fundamentals, Tunneling Dynamics, and the Influence of Large Amplitude 'Geared' Intermolecular Rotation.
PB95-203204 *01,047*

DEUTERIUM FLUORIDE COMPLEXES
Slit Jet Infrared Spectroscopy of Hydrogen Bonded N2HF Isotopomers: Rotational Rydberg-Klein-Rees Analysis and H/D Dependent Vibrational Predissociation Rates.
PB95-161873 *00,956*

Vibrational Dependence of the Anisotropic Intermolecular Potential of Ar-HF.
PB95-202693 *01,030*

DEUTERIUM FLUORIDES
High-Resolution Infrared Spectroscopy of DF Trimer: A Cyclic Ground State Structure and DF Stretch Induced Intramolecular Vibrational Coupling.
PB95-150678 *00,920*

DEUTERIUM ISOTOPE EFFECTS
Protonation Dynamics of the alpha-Toxin Ion Channel from Spectral Analysis of pH-Dependent Current Fluctuations.
PB96-161740 *03,652*

DEUTERIUM PLASMA
Excitation of Balmer Lines in Low-Current Discharges of Hydrogen and Deuterium.
PB95-150546 *03,893*

DEVELOPMENTAL ASSURANCE
Proceedings Report of the International Invitation Workshop on Development Assurance. Held in Ellicott City, Maryland on June 16-17, 1994.
PB95-189494 *02,912*

DEVICE CHARACTERIZATION
Progress on the Quantized Hall Resistance Recommended Intrinsic/Derived Standards Practice.
PB96-122460 *02,403*

DEW BUBBLE CURVES
Vapor-Liquid Equilibria of Mixtures of Propane and Isomeric Hexanes.
PB95-175287 *00,995*

DEXTRAN
Two Phase Aqueous Extraction: Rheological Properties of Dextran, Polyethylene Glycol, Bovine Serum Albumin and Their Mixtures.
PB95-161998 *00,676*

DGSA (DOD GOAL SECURITY ARCHITECTURE)
Assessment of the DOD Goal Security Architecture (DGSA) for Non-Military Use.
PB95-189510 *03,653*

DIACETYLENES
Radiochromic Solid-State Polymerization Reaction.
PB96-180146 *01,290*

DIAGRAMS
Shape of the Temperature-Entropy Saturation Boundary.
PB96-135066 *02,506*

DIAMOND
Tribological Behavior of 440/Diamond-Like-Carbon Film Couples.
PB96-119714 *03,019*

DIAMOND ANVIL CELLS
Alvin Van Valkenburg and the Diamond Anvil Cell.
PB96-204474 *04,797*

DIAMOND FILMS
Workshop on Characterizing Diamond Films (3rd). Held in Gaithersburg, Maryland on February 23-24, 1994.
PB94-187663 *04,456*

Analysis of Thermal Wave Propagation in Diamond Films.
PB94-211471 *03,014*

Thermal Wave Propagation in Diamond Films.
PB94-211489 *03,015*

Analysis of Boron in CVD Diamond Surfaces Using Neutron Depth Profiling.
PB94-213089 *04,511*

Lineshape Analysis of the Raman Spectrum of Diamond Films Grown by Hot-Filament and Microwave-Plasma Chemical-Vapor Deposition.
PB95-162392 *03,016*

Studies of Defects in Diamond Films and Particles by Raman and Luminescence Spectroscopies.
PB95-162400 *03,017*

Surface Roughness Evaluation of Diamond Films Grown on Substrates with a High Density of Nucleation Sites.
PB95-162418 *03,018*

DIAMOND INDENTERS
Geometric Characterization of Rockwell Diamond Indenters.
PB95-203287 *02,950*

Metrology Approach to Unifying Rockwell C Hardness Scales.
PB96-155551 *02,957*

Stylus Technique for the Direct Verification of Rockwell Diamond Intenders.
PB96-155569 *02,958*

DIAMOND TURNING
Fabrication of Optics by Diamond Turning.
PB96-111695 *02,954*

DIAMONDS
Diamond and Graphite Precursors: Comments.
PB95-163051 *00,967*

Proceedings of the Applied Diamond Conference 1995: Applications of Diamond Films and Related Materials International Conference (3rd). Held in Gaithersburg, Maryland, on August 21-24, 1995.
PB95-255204 *04,701*

Applications of Diamond Films and Related Materials: International Conference (3rd). Held in Gaithersburg, Maryland on August 21-24, 1995. Supplement to NIST Special Publication 885.
PB95-256053 *03,063*

Damage Processes in Ceramics Resulting from Diamond Tool Indentation and Scratching in Various Environments.
PB96-102983 *03,065*

Fabrication of Optics by Diamond Turning.
PB96-111695 *02,954*

Workshop on Characterizing Diamond Films (4th). Held in Gaithersburg, Maryland on March 4-5, 1996.
PB96-183090 *04,786*

Chemical Aspects of Tool Wear in Single Point Diamond Turning.
PB97-112601 *03,021*

DIAPHRAGMS (MECHANICS)
Flexible-Diaphragm Force Microscope.
PB95-180915 *03,966*

DIAZINES
Carbon Acidities of Aromatic Compounds. 1. Effects of In-Ring Aza and External Electron-Withdrawing Groups.
PB94-216595 *00,860*

DIBLOCK COPOLYMER ADDITIVES
Modification of the Phase Stability of Polymer Blends by Diblock Copolymer Additivies.
PB96-123542 *03,172*

DICALCIUM PHOSPHATE DIHYDRATE
Effect of Ethanol on the Solubility of Dicalcium Phosphate Dihydrate in the System Ca(OH)2-H3PO4-H2O at 37C.
PB95-163507 *00,163*

DICTIONARIES
Compatibility Analysis of the ANSI and ISO IRDS Services Interfaces.
PB94-163474 *01,805*

Bibliography of Computer Security Glossaries.
PB94-216710 *01,587*

Glossary of Software Reuse Terms.
PB95-178992 *01,720*

Apparel Manufacturing Glossary for Application Protocol Development.
PB95-198750 *02,755*

DIELECTRIC BREAKDOWN
Reproducibility of JEDEC Standard Current and Voltage Ramp Test Procedures for Thin-Dielectric Breakdown Characterization.
PB94-185931 *01,879*

Experimental Investigation of the Validity of TDDB Voltage Acceleration Models.
PB94-185949 *02,304*

Field and Temperature Acceleration of Time-Dependent Dielectric Breakdown in Intrinsic Thin SiO2.
PB94-185956 *02,305*

Charge Trapping and Breakdown Mechanism in SIMOX.
PB94-216637 *02,323*

High Temperature Reliability of Thin Film SiO2.
PB95-150348 *02,333*

Electrical Breakdown in Transformer Oil in Large Gaps.
PB95-150579 *01,889*

Observations of Partial Discharges in Hexane Under High Magnification.
PB95-163127 *01,900*

TDDB Characterization of Thin SiO2 Films with Bimodal Failure Populations.
PB96-102926 *02,381*

Time-Dependent Dielectric Breakdown of Intrinsic SiO2 Films under Dynamic Stress.
PB96-179478 *02,438*

New Physics-Based Model for Time-Dependent- Dielectric-Breakdown.
PB96-201132 *02,448*

Electric Field Dependent Dielectric Breakdown of Intrinsic SiO2 Films Under Dynamic Stress.
PB96-204102 *02,449*

Characterization of Time-Dependent Dielectric Breakdown in Intrinsic Thin SiO2.
PB97-122527 *02,458*

DIELECTRIC CONSTANT
Preparation, Crystal Structure, Dielectric Properties, and Magnetic Behavior of Ba2Fe2Ti4O13.
PB96-186176 *01,162*

DIELECTRIC CONSTANTS
Analysis of an Open-Ended Coaxial Probe with Lift-Off for Nondestructive Testing.
PB96-135116 *01,940*

DIELECTRIC FILMS
Novel YBa2Cu3O7-x and YBa2Cu3O7-x/Y4Ba3O9 Multilayer Films by Bias-Masked 'On-Axis' Magnetron Sputtering.
PB95-181186 *04,690*

DIELECTRIC FUNCTIONS
Nonequilibrium Total-Dielectric-Function Approach to the Electron Boltzmann Equation for Inelastic Scattering in Doped Polar Semiconductors.
PB96-138532 *04,416*

DIELECTRIC MATERIALS
Nonstationary Behaviour of Partial Discharge during Discharge Induced Ageing of Dielectrics.
PB96-103114 *01,922*

DIELECTRIC MEASUREMENTS
Dielectric Properties Measurements and Data.
PB94-172186 *01,876*

DIELECTRIC PROPERTIES
Table of Dielectric Constants of Pure Liquids.
AD-A278 956/8 *00,712*

Dielectric Studies of Fluids with Reentrant Resonators. Appendix B.
DE93019683 *03,244*

Dielectric Studies of Fluids with Reentrant Resonators.
PB95-153730 *00,952*

Dielectric Properties of Single Crystals of Al2O3, LaAlO3, SrTiO3, and MgO at Cryogenic Temperatures.
PB95-180477 *02,266*

Dielectric Properties of Thin Film SrTiO3 Grown on LaAlO3 with YBa2Cu3O7-x Electodes.
PB95-181160 *02,267*

Measurements of the Relative Permittivity of Liquid Water at Frequencies in the Range of 0.1 to 10 kHz and at Temperatures between 273.1 and 373.2 K at Ambient Pressure.
PB96-119375 *01,078*

Static Dielectric Constant of Water and Steam.
PB96-123559 *01,090*

Dielectric and Magnetic Measurements from -50C to 200C and in the Frequency Band 50 MHz to 2 GHz.
PB96-191382 *02,245*

DIELECTRIC RELAXATION
Distribution of Dielectric Relaxation Times and the Moment Problem.
PB96-112032 *04,727*

DIELECTRIC RESONATORS
Measurements of Permittivity and the Dielectric Loss Tangent of Low Loss Dielectric Materials with a Dielectric Resonator Operating on the Higher Order Te(sub 0 gamma delta) Modes.
PB96-111869 *02,273*

Influence of Films' Thickness and Air Gaps in Surface Impedance Measurements of High Temperature Superconductors Using the Dielectric Resonator Technique.
PB96-157862 *01,946*

DIELECTRIC SPECTROSCOPY
Dielectric Behavior of a Polycarbonate/Polyester Mixture Upon Transesterification.
PB96-179551 *04,785*

DIELECTRIC WAVEGUIDES
Mode Coupling and Loss on Tapered Optical Waveguides.
PB95-168571 *04,282*

Bent Rectangular Core Waveguides: An Accurate Perturbation Approach.
PB95-168803 *04,289*

DIELECTRIC WEDGE
Hypersingular Single Integral Equation and the Dielectric Wedge.
PB97-110274 *04,428*

DIELECTRIC WEDGES
Numerical Evaluation of Hypersingular Integrals for Scattering by a Dielectric Wedge.
PB97-110555 *02,017*

DIELECTRICS
Spatial Dependence of Electrical Fields Due to Space Charges in Films of Organic Dielectrics Used for Insulation of Power Cables.
PB94-199130 *02,214*

Modification of Cast Epoxy Resin Surfaces during Exposure to Partial Discharges.
PB96-122734 *01,086*

Influence of Surface Charge on the Stochastic Behavior of Partial Discharge in Dielectrics.
PB96-122767 *01,931*

SF6/N2 Mixtures: Basic and High-Voltage-Insulation Properties.
PB96-123468 *02,230*

Behavior of Surface Partial Discharge on Aluminum Oxide Dielectrics.
PB96-123781 *01,937*

Partially Coherent Transmittance of Dielectric Lamellae.
PB96-148028 *04,359*

President's Column 'Editorial'.
PB96-164090 *02,239*

Electromagnetic Scattering from a Dielectric Wedge and the Single Hypersingular Integral Equation.
PB97-110530 *04,430*

DIELECTRICS AND ELECTRICAL INSULATION SOCIETY
President's Column for Dielectrics and Electrical Insulation Society Newsletter.
PB94-200409 *01,882*

DIELECTRONIC RECOMBINATION
Early Dielectronic Recombination Measurements: Singly Charged Ions.
PB94-211158 *03,836*

DIESEL ENGINES
Abrasive Wear by Diesel Engine Coal-Fuel and Related Particles.
PB95-104915 *01,450*

Deposit Forming Tendencies of Diesel Engine Oils-Correlation between the Two-Peak Method and Engine Tests.
PB95-152138 *01,452*

Evaluation of Wear Resistant Ceramic Valve Seats in Gas-Fueled Power Generation Engines. Topical Report, December 1991-April 1994.
PB95-200218 *02,466*

DIETS
Mixed Diet Reference Materials for Nutrient Analysis of Foods: Preparation of SRM-1548 Total Diet.
PB95-151692 *03,593*

DIFFERENCE FREQUENCY
Precise Optical Frequency References and Difference Frequency Measurements with Diode Lasers.
PB95-176228 *04,305*

DIFFERENTIAL EQUATIONS
Accuracy of Eigenvalues: A Comparison of Two Methods.
PB95-126249 *03,413*

DIFFERENTIAL RANGE
Real-Time Implementation of a Differential Range Finder.
PB95-108650 *01,839*

DIFFRACTION
Vector Theory of Diffraction by a Single-Mode Fiber: Application to Mode-Field Diameter Measurements.
PB95-164182 *04,279*

X-ray Powder Diffraction from Carbon Nanotubes and Nanoparticles.
PB96-102975 *03,064*

Antiferromagnetic Interlayer Correlations in Annealed Ni80Fe20/Ag Multilayers.
PB97-122220 *03,109*

DIFFRACTION ANALYSIS
Parametric Investigation of Metal Powder Atomization Using Laser Diffraction.
PB95-108577 *03,342*

DIFFRACTION IMAGING
Diffraction Imaging of Polycrystalline Materials.
PB94-198884 *02,971*

DIFFRACTOMETERS
Introduction of a NIST Instrument Sensitivity Standard Reference Material for X-Ray Powder Diffraction.
PB94-200318 *00,807*

DIFFUSE INTERFACE
Diffuse-Interface Description of Fluid Systems.
PB96-210711 *01,170*

DIFFUSE REFLECTION
Specular and Diffuse Reflection Measurements of Electronic Displays.
PB97-119200 *02,208*

DIFFUSE SCATTERING
Orientational Fluctuations, Diffuse Scattering, and Orientational Order in Solid C60.
PB97-119275 *04,176*

DIFFUSION
Further Calculations of X-ray Diffusion in an Infinite Medium.
AD-A295 314/9 *03,772*

Energy and Migration of Grain Boundaries in Polycrystals.
PB94-211638 *03,332*

Transport and Diffusion in Three-Dimensional Composite Media.
PB95-176129 *04,668*

Chaotic Motions of Coupled Galloping Oscillators and Their Modeling as Diffusion Progresses.
PB96-122718 *04,823*

Electrodeposited Cobalt-Tungsten as a Diffusion Barrier between Graphite Fibers and Nickel.
PB96-146881 *03,176*

DIFFUSION COEFFICIENT
Measurement of Diffusion in Supercritical Fluid Systems: A Review.
PB94-199189 *00,795*

Diffusion of Copper into Gold Plating.
PB95-162152 *00,957*

Brownian Diffusion of Hard Spheres at Finite Concentrations.
PB95-164307 *00,975*

Measurement of Diffusion in Fluid Systems: Applications to the Supercritical Fluid Region.
PB95-175188 *02,490*

Non-Perturbative Relation between the Mutual Diffusion Coefficient, Suspension Viscosity, and Osmotic Compressibility: Application to Concentrated Protein Solutions.
PB96-102355 *01,062*

DIFFUSION FLAMES
Greatly Enhanced Soot Scattering in Flickering Ch4/Air Diffusion Flames.
PB94-172988 *01,361*

Laser Imaging of Chemistry-Flowfield Interactions: Enhanced Soot Formation in Time-Varying Diffusion Flames.
PB94-185352 *01,364*

Investigation of Oil and Gas Well Fires and Flares.
PB94-193976 *03,695*

Generation and Characterization of Acetylene Smokes.
PB94-200292 *01,372*

Ultrafine Combustion Aerosol Generator.
PB94-200300 *01,373*

Laser-Induced Fluorescence Measurements of Formaldehyde in a Methane/Air Diffusion Flame.
PB94-211679 *01,374*

Comparison of Experimental and Computed Species Concentration and Temperature Profiles in Laminar, Two-Dimensional Methane/Air Diffusion Flames.
PB95-140919 *01,379*

Fundamental Mechanisms for CO and Soot Formation.
PB95-143160 *01,380*

Oxidation of Soot and Carbon Monoxide in Hydrocarbon Diffusion Flames.
PB95-150215 *01,382*

Optical Measurements of Atomic Hydrogen, Hydroxyl, and Carbon Monoxide in Hydrocarbon Diffusion Flames.
PB95-150900 *02,487*

Experimental and Numerical Studies of Refractory Particle Formation in Flames: Application to Silica Growth.
PB95-152005 *00,673*

Laser-Induced Fluorescence Measurements of OH. Concentrations in the Oxidation Region of Laminar, Hydrocarbon Diffusion Flames.
PB95-162160 *01,387*

Acid Gas Production in Inhibited Diffusion Flames.
PB95-180576 *01,390*

Burning Rate of Premixed Methane-Air Flames Inhibited by Fluorinated Hydrocarbons.
PB95-180584 *01,391*

Experimental and Numerical Burning Rates of Premixed Methane-Air Inhibited by Fluoromethanes.
PB95-180592 *01,392*

Quantitative Measurements of Enhanced Soot Production in a Flickering Methane/Air Diffusion Flame.
PB95-203246 *01,393*

Mixing and Radiation Properties of Buoyant Turbulent Diffusion Flames.
PB95-242327 *01,396*

Experimental Study of the Stabilization Region of Lifted Turbulent-Jet Diffusion Flames.
PB96-122676 *01,405*

Laser-Induced Fluorescence Measurements of OH in Laminar Diffusion Flames in the Presence of Soot Particles.
PB96-123120 *01,409*

Chemical Inhibition of Methane-Air Diffusion Flame.
PB96-195532 *01,431*

Mixing and Radiation Properties of Buoyant Luminous Flame Environments.
PB96-202254 *01,432*

Computations of Enhanced Soot Production in Time-Varying CH4/Air Diffusion Flames.
PB97-119218 *01,440*

NO Production and Destruction in a Methane/Air Diffusion Flame.
PB97-122519 *01,443*

DIFFUSION THEORY
Modeling the Evolution of Structure in Unstable Solid Solution Phases by Diffusional Mechanisms.
PB94-199403 *03,324*

DIFFUSION ZONES
Study of Diffusion Zones with Electron Microprobe Compositional Mapping.
PB94-216348 *00,559*

DIFFUSIVITY
Measurements of Moisture Diffusivity for Porous Building Materials.
PB95-107397 *00,356*

Computer Simulation of the Diffusivity of Cement-Based Materials.
PB95-125985 *00,362*

DIFLUOROBENZENE
Vibrational Energy Transfer in S1 p-Difluorobenzene. A Comparison of Low and Room Temperature Collisions.
PB95-108619 *00,883*

Vibrations of S1((1)B2u) p-Difluorobenzene - d4. S1-S0 Fluorescence Spectroscopy and ab Initio Calculations.
PB95-202586 *01,028*

DIFLUOROETHANE
Coexisting Densities, Vapor Pressures and Critical Densities of Refrigerants R-32 and R-152a, at 300 - 385 K.
PB95-175691 *03,274*

Compressed Liquid Densities, Saturated Liquid Densities, and Vapor Pressures of 1,1-Difluoroethane.
PB97-110118 *01,173*

DIFLUOROMETHANE
Ebulliometric Measurement of the Vapor Pressure of Difluoromethane.
PB95-151361 *00,931*

Viscosity of the Saturated Liquid Phase of Six Halogenated Compounds and Three Mixtures.
PB95-162368 *00,960*

Measurements of the Vapor Pressures of Difluoromethane, 1-Chloro-1,2,2,2-Tetrafluoroethane, and Pentafluoroethane.
PB95-169272 *03,270*

Coexisting Densities, Vapor Pressures and Critical Densities of Refrigerants R-32 and R-152a, at 300 - 385 K.
PB95-175691 *03,274*

DIGITAL COMMUNICATIONS
Integrated Services Digital Network (ISDN); Category: Telecommunications Standard; Subcategory: Integrated Services Digital Network.
FIPS PUB 182 *01,460*

DIGITAL DATA
Report on the Workshop on Advanced Digital Video in the National Information Infrastructure. Held in Washington, D.C. on May 10-11, 1994.
PB95-103677 *01,472*

National Information Infrastructure and Advanced Digital Video.
PB96-119367 *01,488*

Spatial Information and Technology Standards Evolving.
PB96-135108 *03,679*

Summary Report on the Workshop on Advanced Digital Video in the National Information Infrastructure.
PB96-141320 *01,497*

Status of Emerging Standards for Removable Computer Storage Media and Related Contributions of NIST.
PB96-160619 *01,634*

DIGITAL MULTIMETER
Quantum Hall Effect-Based Resistance Standard: Capabilities and Implementation.
PB96-180096 *04,114*

Quantum Hall Effect-Based Resistance Standard (Quantum Hall Res).
PB96-200944 *04,127*

DIGITAL RECORDING SYSTEMS
Performance Evaluation of a New Digital Partial Discharge Recording and Analysis System.
PB95-150389 *01,888*

Continuous Recording and Stochastic Analysis of PD.
PB96-112156 *01,925*

DIGITAL SIGNATURES
Digital Signature Standard (DSS). Category: Computer Security; Subcategory: Cryptography.
FIPS PUB 186 *01,570*

Report of the NIST Workshop on Digital Signature Certificate Management. Held on December 10-11, 1992.
PB94-135001 *01,574*

Response to Comments on the NIST Proposed Digital Signature Standard.
PB96-161815 *01,615*

Public Key Infrastructure Invitational Workshop. Held in McLean, Virginia on September 28, 1995.
PB96-166004 *01,616*

DIGITAL SYSTEMS
Proceedings of the Digital Systems Reliability and Nuclear Safety Workshop. Held in Rockville, Maryland on September 13-14, 1993.
NUREG/CP-0136 *03,728*

Digital Impedance Bridge.
PB96-103155 *02,272*

Comment and Discussion on Digital Processing of PD Pulses.
PB96-122775 *01,932*

DIGITAL TECHNIQUES
Digital Techniques in HV Tests - Summary of 1989 Panel Session.
PB94-216702 *02,035*

DILATOMETRY
Aging in Glasses Subjected to Large Stresses and Deformations.
PB95-107041 *03,235*

DILUTED BLENDS
Shear Suppression of Critical Fluctuations in a Diluted Polymer Blend.
PB96-204458 *04,418*

DIMENSIONAL MEASUREMENT
Numeric Data Distribution: The Vital Role of Data Exchange in Today's World.
N95-15937/2 *02,622*

U.S. Navy Coordinate Measuring Machines: A Study of Needs.
PB94-162831 *02,807*

Concept for an Algorithm Testing and Evaluation Program at NIST.
PB94-163029 *02,890*

Uncertainties in Dimensional Measurements Made at Nonstandard Temperatures.
PB94-169760 *02,893*

User's Guide to NIST SRM 2084: CMM Probe Performance Standard.
PB94-206109 *02,709*

Precision, Accuracy, Uncertainty and Traceability and Their Application to Submicrometer Dimensional Metrology.
PB94-213105 *02,319*

Metrology Model for Submicrometer Dimensional Measurements.
PB95-108502 *02,647*

Practical Photomask Linewidth Measurements.
PB95-108510 *02,324*

Evolution of Automatic Line Scale Measurement at the National Institute of Standards and Technology.
PB95-108809 *02,897*

Development of an Automated Part Inspection System Using the DMIS Standard.
PB95-108866 *02,899*

User's Manual for the Program MONSEL-1: Monte Carlo Simulation of SEM Signals for Linewidth Metrology.
PB95-111522 *02,325*

Monte Carlo Model for SEM Linewidth Metrology.
PB95-150058 *02,331*

Optical Fiber Geometry: Accurate Measurement of Cladding Diameter.
PB95-151940 *04,266*

Comparisons of Measured Linewidths of Sub-Micrometer Lines Using Optical, Electrical, and SEM Metrologies.
PB95-152807 *02,338*

X-ray Mask Metrology: The Development of Linewidth Standards for X-ray Lithography.
PB95-162129 *02,348*

Dimensional Characterization of Small Bores: A Survey.
PB95-162202 *02,651*

Automated Inspection: The Integration of National Standards and Commercial Products at NIST.
PB95-163077 ***02,906***

Variations in Size Measurements by Indicating Gaging Systems.
PB95-163614 ***02,864***

Dimensional Inspection Planning Based on Product Data Standards.
PB95-175451 ***02,910***

Accuracy in Integrated Circuit Dimensional Measurements.
PB95-180808 *02,368*

Improving Photomask Linewidth Measurement Accuracy via Emulated Stepper Aerial Image Measurement.
PB95-180816 *02,911*

Electrical Method for Determining the Thickness of Metal Films and the Cross-Sectional Area of Metal Lines.
PB95-203170 *02,370*

Interim Testing Artifact (ITA): A Performance Evaluation System for Coordinate Measuring Machines (CMMs). User Manual.
PB95-210589 *02,914*

Algorithm Testing and Evaluation Program for Coordinate Measuring Systems: Long Range Plan.
PB95-231833 *02,915*

Integrated Vision Touch-Probe System for Dimensional Inspection Tasks.
PB95-255832 *02,917*

Estimation of Measurement Uncertainty of Small Circular Features Measured by CMMs.
PB95-267928 *02,918*

MONSEL-II: Monte Carlo Simulation of SEM Signals for Linewidth Metrology.
PB96-102710 *02,379*

User's Guide to 'SuperFit' Modeling Software for CMM Probe Lobing.
PB96-128236 *02,921*

Reference Manual for the Algorithm Testing System Version 2.0.
PB96-128244 *02,922*

Quality in Automated Manufacturing.
PB96-160437 *02,839*

New Concepts of Precision Dimensional Measurement for Modern Manufacturing.
PB96-160684 *02,924*

Dimensional Characterization of Precision Coaxial Transmission Line Standards.
PB96-176482 *02,241*

Representation of Axes for Geometric Fitting.
PB97-113799 *01,782*

DIMENSIONAL MEASUREMENTS

Metrology and Regional Trade Pacts.
PB96-155429 *02,923*

Report on the NIST Low Accelerating Voltage SEM Magnification Standard Interlaboratory Study.
PB96-201074 *02,445*

DIMENSIONAL MEASURING INTERFACE STANDARD

Dimensional Inspection Planning Based on Product Data Standards.
PB95-175451 *02,910*

DIMENSIONAL METROLOGY

Residual Error Compensation of a Vision-Based Coordinate Measuring Machine.
PB96-161617 *04,091*

DIMENSIONAL STABILITY

Measuring the Stability of Three Copper Alloys.
PB94-199866 *03,326*

DIMERS

Equilibrium Pair Distribution Function of a Gas: Aspects Associated with the Presence of Bound States.
PB95-176046 *01,004*

DIMETHYLACETYLENE

Perpendicular C-H Stretching Band nu9/nu13 and the Torsional Potential of Dimethylacetylene.
PB97-122451 *01,192*

DIMETHYLPHENANTHRENES

Distinguishing the Contributions of Residential Wood Combustion and Mobile Source Emissions Using Relative Concentrations of Dimethylphenanthrene Isomers.
PB96-135124 *02,563*

DIOXINS

Standard Reference Materials for Dioxins and Other Environmental Pollutants.
PB94-198330 *02,518*

DIPOLE ANTENNAS

Alternative Contour Technique for the Efficient Computation of the Effective Length of an Antenna.
PB96-141361 *02,011*

DIPOLE MOMENT

Microwave Spectrum and Structure of CH2O-H2O.
PB97-118723 *04,168*

DIPOLE MOMENTS

Dipole Moments in Rare Gas Interactions.
PB94-212982 *00,844*

DIPOLES

Electric Dipole Excitation of a Long Conductor in a Lossy Medium.
PB96-146675 *04,058*

DIRECT CURRENT

Physical Basis for Half-Integral Shapiro Steps in a DC SQUID.
PB96-102264 *04,704*

Interfacial Transport in Porous Media: Application to dc Electrical Conductivity of Mortars.
PB96-146816 *01,326*

AC-DC Difference Characteristics of High-Voltage Thermal Converters.
PB96-148093 *02,083*

DIRECTIONAL SOLIDIFICATION

Effects of Crystalline Anisotropy and Buoyancy-Driven Convection on Morphological Stability.
PB94-200441 *03,328*

Convective Stability in the Rayleigh-Benard and Directional Solidification Problems: High-Frequency Gravity Modulation.
PB95-181145 *04,208*

DIRECTIONAL SOLIDIFICATION (CRYSTALS)

Convection and Morphological Stability During Directional Solidification.
N95-14548/8 *03,310*

Surface Energy Reduction in Fibrous Monotectic Structures.
PB95-140828 *03,150*

DIRECTIVITY

Radiated Emissions and Immunity of Microstrip Transmission Lines: Theory and Measurements.
PB96-162649 *02,238*

DIRECTORIES

National Voluntary Laboratory Accreditation Program 1994 Directory.
PB94-178969 *00,482*

State Weights and Measures Laboratories: State Standards Program Description and Directory. 1994 Edition.
PB94-207727 *02,895*

National Voluntary Laboratory Accreditation Program 1995 Directory.
PB95-174454 *00,483*

National Voluntary Laboratory Accreditation Program 1996 Directory.
PB96-162714 *00,485*

Directory of Law Enforcement and Criminal Justice Associations and Research Centers.
PB96-178918 *04,872*

X.500 Directory Schema Design Handbook.
PB96-183041 *02,739*

Directory of U.S. Private Sector Product Certification Programs.
PB96-215074 *02,688*

Standards Activities of Organizations in the United States.
PB97-124135 *00,006*

DISCHARGE

Ion Kinetics and Symmetric Charge-Transfer Collisions in Low-Current, Diffuse (Townsend) Discharges in Argon and Nitrogen.
PB96-123658 *04,051*

DISCHARGES

Fundamental Processes in Gas Discharges.
PB96-123450 *01,089*

Electrical Characteristics of Argon Radio Frequency Glow Discharges in an Asymmetric Cell.
PB96-176490 *04,109*

DISCOLORATION

Intensive Swimming: Can It Affect Your Patients' Smiles.
PB96-123666 *03,570*

DISK SOURCE

Exact Series Solution to the Epstein-Hubbell Generalized Elliptic Type Integral Using Complex Variable Residue Theory.
PB97-110167 *03,423*

DISLOCATION CORE

Dislocation Core-Core Interaction and Peierls Stress in a Model Hexagonal Lattice.
PB96-162003 *04,101*

DISLOCATION EMISSION

Cracks and Dislocations in Face-Centered Cubic Metallic Multilayers.
PB96-163696 *02,989*

Experimental Assessment of Crack-Tip Dislocation Emission Models for an Al67Cr8Ti25 Intermetallic Alloy.
PB96-204466 *03,377*

DISLOCATIONS

Dislocation Emission at Ledges on Cracks.
PB95-164240 *04,630*

Shielding of Cracks in a Plastically Polarizable Material.
PB95-164257 *04,631*

Scanning Electron Microscopy Observations of Misfit Dislocations in Epitaxial In0.25Ga0.75As on GaAs(001).
PB96-200159 *03,004*

DISLOCATIONS (MATERIALS)

Interaction between Dislocations and Intergranular Cracks.
PB95-152096 *03,190*

Nonlocal Effects of Existing Dislocations on Crack-Tip Emission and Cleavage.
PB96-161807 *03,367*

DISPERSANTS

Polyelectrolytes as Dispersants in Colloidal Processing of Silicon Nitride Ceramics.
PB95-175568 *03,055*

DISPERSIONS

Computational Model for the Rise and Dispersion of Wind-Blown, Buoyancy-Driven Plumes. Part 2. Linearly Stratified Atmosphere.
PB94-143427 *00,119*

Contrast Matched Studies of a Sheared Binary Colloidal Suspension.
PB95-150561 *00,918*

DISPLACEMENT

Generating and Measuring Displacements Up to 0.1 m to an Accuracy of 0.1 nm: Is It Possible.
PB96-160700 *04,090*

DISPLACEMENT MEASUREMENT

Electro-Optical Sensor for Surface Displacement Measurements of Compliant Coatings.
PB94-198223 *02,123*

Displacement Method for Machine Geometry Calibration.
PB95-152088 *02,946*

Integrated Inspection System for Improved Machine Performance.
PB96-160569 *02,959*

DISPLACEMENT REACTIONS

Rate Constants for Hydrogem Atom Attack on Some Chlorinated Benzenes at High Temperature.
PB94-200581 *00,810*

DISPLAY DEVICES

NIST Workshop on the Computer Interface to Flat Panel Displays. Held in San Jose, California on January 13-14, 1994.
PB95-136388 *01,625*

Can Displays Deliver a Full Measure: Manufacturing.
PB96-111935 *02,185*

Display-Measurement Round-Robin.
PB96-119227 *02,186*

Making Displays Deliver a Full Measure.
PB96-122411 *01,490*

Survey of the Components of Display-Measurement Standards.
PB96-122528 *02,188*

Micromachined Display Output for a Cellular Neural Network.
PB96-156070 *02,422*

Specular and Diffuse Reflection Measurements of Electronic Displays.
PB97-119200 *02,208*

Survey of the Components of Display-Measurement Standards.
PB97-122394 *02,209*

DISSIMILAR MATERIALS BONDING

Surface Forces and Adhesion between Dissimilar Materials Measured in Various Environments.
PB94-172970 *03,033*

DISSOCIATION

Fragment Energy and Vector Correlations in the Overtone-Pumped Dissociation of HN3X(1)A'.
PB94-199908 *00,802*

DISSOCIATIVE IONIZATION

Appearance Potentials of Ions Produced by Electron-Impact Induced Dissociative Ionization of SF6, SF4, SF5Cl, S2F10, SO2, SO2F2, SOF2, and SOF4.
PB96-119730 *01,080*

DISSOLVING

Dissolution Problems with Botanical Reference Materials.
PB95-126280 *03,487*

DISTILLATION EQUIPMENT

Development of Engineered Stationary Phases for the Separation of Carotenoid Isomers.
PB95-150249 *00,578*

Shape Selectivity Assessment of Stationary Phases in Gas Chromatography.
PB95-150256 *00,579*

DISTORTION

Micromechanics of Densification and Distortion.
PB94-200326 *03,327*

DISTRIBUTED AMPLIFIERS

New 5 and 10 MHz High Isolation Distribution Amplifier.
PB96-190202 *01,510*

DISTRIBUTED COMPUTER SYSTEMS

Distributed Supercomputing Software: Experiences with the Parallel Virtual Machine - PVM.
PB94-163086 *01,680*

Associated Object Model for Distributed Systems.
PB94-212016 *01,694*

PET and DINGO Tools for Deriving Distributed Implementations from Estelle.
PB95-203253 *01,727*

Distributed Systems: Survey of Open Management Approaches.
PB96-128202 *01,746*

DISTRIBUTED DATA BASES

Guidelines for the Evaluation of X.500 Directory Products.
PB95-231908 *02,732*

X.500 Directory Schema Design Handbook.
PB96-183041 *02,739*

DISTRIBUTED FEEDBACK LASERS

Vertical-Cavity Semiconductor Lasers: Structural Characterization, CAD, and DFB Structures.
PB95-153193 *02,150*

DISTRIBUTED PROCESSING

Open System Environments.
N94-36857/8 *01,674*

Introduction to the P1003.1g and CPI-C Network Application Programming Interfaces.
PB95-231726 *01,731*

Application Portability Profile (APP): The U.S. Government's Open System Environment Profile Version 3.0.
PB96-158712 *01,753*

DISTRIBUTION FUNCTIONS
Equilibrium Pair Distribution Function of a Gas: Aspects Associated with the Presence of Bound States.
PB95-176046 *01,004*

DISTRIBUTION MOMENTS
Moments of the Quartic Assignment Statistic with an Application to Multiple Regression.
PB95-181103 *03,442*

DITHIOTHREITOL
Ascorbic and Dehydroascorbic Acids Measured in Plasma Preserved with Dithiothreitol or Metaphorphoric Acid.
PB94-216330 *03,495*

DIVALENT CATIONS
Genetically Engineered Pore as a Metal Ion Biosensor
PB96-161658 *03,551*

DIVERSIFICATION
Technology Trends in Telecommunications: An Overview.
PB94-123080 *01,462*

DIVINYL ETHER
2-Tunneling Path Internal-Axis-Method-Like Treatment of the Microwave Spectrum of Divinyl Ether.
PB94-200466 *00,808*

DMIS (DIMENSIONAL MEASURING INTERFACE STANDARD)
Dimensional Inspection Planning Based on Product Data Standards.
PB95-175451 *02,910*

DNA
Novel Activity of E. coli uracil DNA N-glycosylase Excision of Isodialuric Acid (5,6-dihydroxyuracil), a Major Product of Oxidative DNA Damage, from DNA.
PB96-110747 *03,543*

Overview of Reference Materials Prepared for Standardization of DNA Typing Procedures.
PB96-111653 *00,611*

Low-Frequency Excitations of Oriented DNA.
PB96-137799 *03,548*

Quantitative Determination of Oxidative Base Damage in DNA by Stable Isotope-Dilution Mass Spectrometry.
PB96-200886 *03,483*

Commentary: The Measurement of Oxidative Damage to DNA by HPLC and GC/MS Techniques.
PB96-200894 *03,484*

Intercomparison of DNA Sizing Ladders in Electrophoretic Separation Matrices and Their Potential for Accurate Typing of the D1S80 Locus.
PB96-200928 *03,485*

DNA-BINDING PROTEINS
Function of DnaJ and DnaK as Chaperones in Origin-Specific DNA Binding by RepA.
PB95-151544 *03,533*

Formation of DNA-Protein Cross-Links in Cultured Mammalian Cells Upon Treatment with Iron Ions.
PB96-137724 *03,651*

DNA DAMAGE
Ionizing radiation-induced DNA damage and its repair in human cells. Progress report, (April 1, 1993--February 28, 1994).
DE94014709 *03,612*

Tert-Butyl Hydroperoxide-Mediated DNA Base Damage in Cultured Mammalian Cells.
PB94-182003 *03,644*

Application of Photochemical Reaction in Electrochemical Detection of DNA Intercalation.
PB94-185733 *00,686*

Copper Ion-Mediated Modification of Bases in DNA in Vitro by Benzoyl Peroxide.
PB94-198231 *03,645*

Standard Reference Materials (SRM's) for Measuring Genetic Damage.
PB94-198827 *03,516*

Oxidative Damage to DNA in Mammalian Chromatin.
PB94-199825 *03,525*

Modification of DNA Bases in Chromatin of Intact Target Human Cells by Activated Human Polymorphonuclear Leukocytes.
PB94-199833 *03,526*

Nickel(II)-Mediated Oxidative DNA Base Damage in Renal and Hepatic Chromatin of Pregnant Rats and Their Fetuses. Possible Relevance to Carcinogenesis.
PB94-212628 *03,646*

Oxidative DNA Base Damage in Renal, Hepatic, and Pulmonary Chromatin of Rats After Intraperitoneal Injection of Cobalt (II) Acetate.
PB95-150025 *03,647*

DNA Base Modifications in Renal Chromatin of Wistar Rats Treated with a Renal Carcinogen, Ferric Nitrilotriacetate.
PB95-150363 *03,648*

DNA Base Damage Generated In vivo in Hepatic Chromatin of Mice upon Whole Body y-Irradiation.
PB95-161741 *03,627*

Chemical Determination of Oxidative DNA Damage by Gas Chromatography-Mass Spectrometry.
PB95-175394 *03,540*

Ionizing Radiation Causes Greater DNA Base Damage in Radiation-Sensitive Mutant M10 Cells That in Parent Mouse Lymphoma L5178Y Cells.
PB95-175915 *03,632*

Treatment of Wistar Rats with a Renal Carcinogen, Ferric Nitrilotriacetate, Causes DNA-Protein Cross-Linking between Thymine and Tyrosine in Their Renal Chromatin.
PB96-112115 *03,649*

Novel Activities of Human Uracil DNA N-glycosylase for Cytosine-Derived Products of Oxidative DNA Damage.
PB96-164132 *03,479*

DNA Damage and DNA Sequence Retrieval from Ancient Tissues.
PB97-111983 *03,556*

DNA Base Damage in Lymphocytes of Cancer Patients Undergoing Radiation Therapy.
PB97-122444 *03,643*

DNA REPAIR
Ionizing radiation-induced DNA damage and its repair in human cells. Progress report, (April 1, 1993--February 28, 1994).
DE94014709 *03,612*

DNA SEQUENCING
Small genomes: New initiatives in mapping and sequencing. Workshop summary report.
DE96014476 *03,451*

DNAA PROTEINS
Deletion Analysis of the Mini-P1 Plasmid Origin of Replication and the Role of E.coli DnaA Protein.
PB95-163911 *03,539*

DOCUMENTS
Open Document Architecture (ODA) Raster Document Application Profile (DAP). Category: Software Standard; Subcategory: Graphics.
FIPS PUB 194 *01,669*

Important Papers in the History of Document Preparation Systems: Basic Sources.
PB95-125837 *02,712*

SGML Environment for STEP.
PB95-143103 *02,778*

NIST List of Publications, LP 103, March 1996. National Semiconductor Metrology Program.
PB96-175856 *02,432*

Application Protocol Information Base World Wide Web Gateway.
PB96-202320 *02,791*

Panel: Building and Using Test Collections.
PB97-118673 *02,743*

DOD GOAL SECURITY ARCHITECTURE
Assessment of the DOD Goal Security Architecture (DGSA) for Non-Military Use.
PB95-189510 *03,653*

DODECANOIC ACID
Effect of Dodecanol Content on the Combustion of Methanol Spray Flames.
PB95-176020 *01,389*

DODECANOL
Effect of Dodecanol Content on the Combustion of Methanol Spray Flames.
PB95-176020 *01,389*

DOMAIN ANALYSIS
Context Analysis of the Network Management Domain. Conducted as Part of the Domain Analysis Case Study.
PB94-142528 *01,465*

DOMAIN STRUCTURES
Transformation of BCC and B2 High Temperature Phases to HCP and Orthorhombic Structures in the Ti-Al-Nb System. Part 1. Microstructural Predictions Based on a Subgroup Relation between Phases.
PB96-169065 *03,370*

Transformation of BCC and B2 High Temperature Phases to HCP and Orthorhombic Structures in the Ti-Al-Nb System. Part 2. Experimental TEM Study of Microstructures.
PB96-169073 *03,371*

DOMAIN WALLS
Micromagnetic Structure of Domains in Co/Pt Multilayers. 1. Investigations of Wall Structure.
PB95-162111 *04,610*

DOMAINS
Mapping Domains in Proteins: Dissection and Expression of 'Escherichia coli' Adenylyl Cyclase.
PB96-155460 *03,478*

DOPED MATERIALS
Incorporation of Gold into YBa2Cu3O7: Structure and Tc Enhancement.
PB94-200276 *04,481*

Unexpected Effects of Gold on the Structure, Superconductivity, and Normal State of YBa2Cu3O7.
PB94-200284 *04,482*

DOPED POLAR SEMICONDUCTORS
Nonequilibrium Total-Dielectric-Function Approach to the Electron Boltzmann Equation for Inelastic Scattering in Doped Polar Semiconductors.
PB96-138532 *04,416*

DOPPLER BROADENED EMISSION
Time-Resolved Balmer-Alpha Emission from Fast Hydrogen Atoms in Low Pressure, Radio-Frequency Discharges in Hydrogen.
PB96-102942 *04,028*

DOPPLER-FREE SPECTROSCOPY
Doppler-Free Spectroscopy of Large Polyatomic Molecules and van der Waals Complexes.
PB96-119581 *04,339*

DOPPLER RADAR
Delivering the Same Optical Frequency at Two Places: Accurate Cancellation of Phase Noise Introduced by an Optical Fiber or Other Time-Varying Path.
PB96-102736 *04,332*

DOSE EQUIVALENTS
Interpreting the Readings of Multi-Element Personnel Dosimeters in Terms of the Personal Dose Equivalent.
PB95-175428 *03,631*

DOSE RESPONSE RELATIONSHIPS
Microdosimetry and Cellular Radiation Effects of Radon Progency in Human Bronchial Airways.
PB95-152344 *03,625*

Radon in the Lung.
PB97-110035 *03,638*

DOSEMETERS
Improving measurement quality assurance for photon irradiations at Department of Energy facilities. Final technical report.
DE96010065 *03,711*

Dosimetry Systems for Radiation Processing.
PB96-135280 *03,717*

Calibration and Performance of GafChromic DM-100 Radiochromic Dosemeters.
PB97-119291 *00,703*

DOSIMETERS
Thin Dyed-Plastic Dosimeter for Large Radiation Doses.
PB95-107363 *03,872*

Calibration of Dosimeters for the Cryogenic Irradiation of Composite Materials Using an Electron Beam.
PB95-180964 *03,968*

Real Time Monitoring of Electron Processors.
PB96-135306 *03,719*

Orientation Effects on ESR Analysis of Alanine-Polymer Dosimeters.
PB96-146725 *03,720*

Response Comparison of Electret Ion Chambers, LiF TLD, and HPIC.
PB96-190103 *02,578*

Colour Centres in LiF for Measurement of Absorbed Doses Up to 100 MGy.
PB97-118756 *04,169*

DOSIMETRY
EPR Bone Dosimetry: A New Approach to Spectral Deconvolution Problems.
PB94-199643 *03,616*

Estimation of the Absorbed Dose in Radiation-Processed Food. 2. Test of the EPR Response Function by an Exponential Fitting Analysis.
PB94-199650 *00,036*

Experimental Validation of Radiopharmaceutical Absorbed Dose to Mineralized Bone Tissue.
PB94-199668 *03,617*

Radiation Doses.
PB94-199676 *03,618*

Estimation of the Absorbed Dose in Radiation-Processed Food. 3. The Effect of Time of Evaluation on the Accuracy of the Estimate.
PB94-199684 *00,037*

Estimation of the Absorbed Dose in Radiation-Processed Food. 4. EPR Measurements on Eggshell.
PB94-199692 *00,038*

New EPR Dosimeter Based on Polyvinylalcohol.
PB94-199700 *03,619*

Estimation of the Absorbed Dose in Radiation-Processed Food. 1. Test of the EPR Response Function by a Linear Regression Analysis.
PB94-199718 *00,039*

National Quality Assurance Program for Personnel Radiation Dosimetry: A Case History.
PB94-211273 *03,620*

National Voluntary Laboratory Accreditation Program: Ionizing Radiation Dosimetry.
PB95-128658 *03,623*

ESR-Based Analysis in Radiation Processing.
PB95-161634 *03,931*

Radiation Process Data: Collection, Analysis, and Interpretation.
PB95-162632 *03,628*

Dose Mapping of Radioactive Hot Particles Using Radiochromic Film.
PB95-162954 *03,714*

Food Irradiation Dosimetry.
PB95-180675 *00,041*

Anionic Triphenylmethane Dye Solutions for Low-Dose Food Irradiation Dosimetry.
PB96-135173 *03,715*

Alcohol Solutions of Triphenyl-Tetrazolium Chloride as High-Dose Radiochromic Dosimeters.
PB96-135249 *03,716*

Oscillometric and Conductometric Analysis of Aqueous and Organic Dosimeter Solutions.
PB96-135256 *04,054*

Research and Development Activities in Electron Paramagnetic Resonance Dosimetry.
PB96-141288 *03,635*

Investigation of Applicability of Alanine and Radiochromic Detectors to Dosimetry of Proton Clinical Beams.
PB96-146782 *03,636*

Needs for Brachytherapy Source Calibrations in the United States.
PB97-110092 *03,521*

EPR Dosimetry of Cortical Bone and Tooth Enamel Irradiated with X and Gamma Rays: Study of Energy Dependence.
PB97-110373 *03,639*

Measurements of the (237)Np(n,f) Cross Section.
PB97-119069 *04,173*

Novel Radiochromic Films for Clinical Dosimetry.
PB97-119259 *03,641*

DOUBLE HULLS
Stranding Experiments on Double Hull Tanker Structures.
PB96-123112 *03,749*

DOUBLE-MODULATION
Double Modulation and Selective Excitation Photoreflectance for Characterizing Highly Luminescent Semiconductor Structures and Samples with Poor Surface Morphology.
PB97-111439 *02,452*

DRAINAGE
Polyvinyl Chloride (PVC) Plastic Drain, Waste, and Vent Pipe and Fittings.
AD-A310 426/2 *00,326*

Acrylonitrile-Butadiene-Styrene (ABS) Plastic Drain, Waste, and Vent Pipe and Fittings.
AD-A310 724/0 *00,327*

DRAWING
Hydration in Semicrystalline Polymers: Small-Angle Neutron Scattering Studies of the Effect of Drawing in Nylon-6 Fibers.
PB95-202990 *03,385*

DRILLING
Design and Machining of Copper Specimens with Micro Holes for Accurate Heat Transfer Measurements.
PB95-180428 *02,658*

DRINKING WATER
Preparation and Monitoring of Lead Acetate Containing Drinking Water Solutions for Toxicity Studies.
PB94-193885 *00,538*

DROPLET-SOLID INTERACTIONS
Transient Cooling of a Hot Surface by Droplets Evaporation.
PB94-156957 *03,783*

DROPLETS
Transient Cooling of a Hot Surface by Droplets Evaporation.
PB95-143194 *03,890*

Effect of Finite Beam Width on Elastic Light Scattering from Droplets.
PB96-163670 *01,144*

Internal Droplet Circulation Induced by Surface-Driven Rotation.
PB97-119267 *02,500*

DROPS
Lubrication Theory for Reactive Spreading of a Thin Drop.
PB95-189460 *02,865*

Droplet Transfer Modes for a MIL 100S-1 GMAW Electrode.
PB95-209300 *02,867*

Analysis of Droplet Arrival Statistics in a Pressure-Atomized Spray Flame.
PB97-112270 *01,352*

DROPS (LIQUIDS)
Water Droplet Evaporation from Radiantly Heated Solids.
PB95-217147 *00,394*

DRUG ABUSE
Interlaboratory Comparison Studies on the Analysis of Hair for Drugs of Abuse.
PB95-176251 *03,500*

NIST Reference Materials to Support Accuracy in Drug Testing.
PB96-123807 *03,505*

Certification of Phencyclidine in Lyophilized Human Urine Reference Materials.
PB96-160692 *03,508*

Interlaboratory Studies on the Analysis of Hair for Drugs of Abuse: Results from the Fifth Exercise.
PB97-110449 *03,509*

Interlaboratory Studies on the Analysis of Hair for Drugs of Abuse: Results from the Fourth Exercise.
PB97-111322 *03,510*

DRUG ANALYSIS
Analysis by a Combination of Gas Chromatography and Tandem Mass Spectrometry: Development of Quantitative Tandem-in-Time Ion Trap Mass Spectrometry: Isotope Dilution Quantification of 11-Nor-Delta-9-Tetrahydro cannabinol-9-Carboxylic Acid.
PB96-117221 *02,561*

DRUG USERS
Hair Analysis for Drugs of Abuse: Evaluation of Analytical Methods, Environmental Issues, and Development of Reference Materials.
PB95-176269 *03,501*

Hair Testing for Drugs of Abuse: International Research on Standards and Technology.
PB96-120555 *03,504*

DRY PROCESSES
Kinetic-Energy-Enhanced Neutral Etching.
PB96-200613 *00,665*

DRYING
Modelling Drying Shrinkage of Cement Paste and Mortar. Part 1. Structural Models from Angstroms to Millimeters.
PB96-135132 *03,074*

DRYING TECHNIQUES
Recent Developments in NIST Botanical SRMs.
PB96-167267 *03,489*

DUCTED ROCKET ENGINES
Vortex Shedding Flowmeters for SSME Ducts.
PB95-169215 *01,453*

DUCTILE BRITTLE TRANSITION
Nonlocal Effects of Existing Dislocations on Crack-Tip Emission and Cleavage.
PB96-161807 *03,367*

DUCTILE FRACTURE
Ductile Fracture and Tempered Martensite Embrittlement of 4140 Steel.
PB96-190285 *03,222*

DUFFING DIFFERENTIAL EQUATION
Melnikov Function and Homoclinic Chaos Induced by Weak Perturbations.
PB95-180923 *03,414*

DURABILITY
Evolution of Porosity and Calcium Hydroxide in Laboratory Concretes Containing Silica Fume.
PB95-175063 *01,321*

Environmental Durability of Glass-Fiber Composites.
PB95-203220 *03,166*

DWARF STARS
Far-Ultraviolet Flare on a Pleiades G Dwarf.
PB96-102033 *00,086*

Relationship between Radiative and Magnetic Fluxes for Three Active Solar-Type Dwarfs.
PB96-119540 *00,097*

DYE BLEACHING
Anionic Triphenylmethane Dye Solutions for Low-Dose Food Irradiation Dosimetry.
PB96-135173 *03,715*

DYE LASERS
Stabilization of Optical Phase/Frequency of a Laser System: Application to a Commercial Dye Laser with an External Stabilizer.
PB95-203832 *04,327*

DYES
Enhanced Detection of PCR Products Through Use of TOTO and YOYO Intercalating Dyes with Laser Induced Fluorescence - Capillary Electrophoresis.
PB95-164653 *00,599*

DYNAMIC MODULUS OF ELASTICITY
Dynamics vs. Static Young's Moduli: A Case Study.
PB94-213188 *03,210*

DYNAMIC PROGRAMMING
Time Dependent Vector Dynamic Programming Algorithm for the Path Planning Problem.
PB94-215688 *03,428*

DYNAMIC RANGE
Genetically Engineered Pores as Metal Ion Biosensors.
PB96-167408 *03,553*

DYNAMIC RESPONSE
Dynamic Characteristics of Five Tall Buildings during Strong and Low-Amplitude Motions.
PB94-199981 *00,427*

Response of a Terminally Anchored Polymer Chain to Simple Shear Flow.
PB95-108668 *01,233*

Response of Buildings to Ambient Vibration and the Loma Prieta Earthquake: A Comparison.
PB96-119607 *00,457*

Bounds on Frequency Response Estimates Derived from Uncertain Step Response Data.
PB96-122874 *03,419*

Comparison of Responses of a Select Number of Buildings to the 10/17/1989 Loma Prieta (California) Earthquake and Low-Level Amplitude Test Results.
PB96-159645 *00,467*

DYNAMIC SCALING
Growth and Nucleation of Hydrogenated Amorphous Silicon on Silicon (100) Surfaces.
PB96-176516 *02,991*

DYNAMIC STRUCTURAL ANALYSIS
Strengthening Methodology for Lightly Reinforced Concrete Frames-II. Recommended Calculation Techniques for the Design of Infill Walls.
PB94-187648 *00,426*

Wind and Seismic Effects. Proceedings of the U.S.-Japan Cooperative Program in Natural Resources Panel on Wind and Seismic Effects (26th). Held in Gaithersburg, Maryland on May 17-20, 1994.
PB95-147385 *00,433*

Seismic Performance of Circular Bridge Columns Designed in Accordance with AASHTO/CALTRANS Standards.
PB96-146352 *01,346*

Strengthening Methodology for Lightly Reinforced Concrete Frames.
PB96-158050 *00,466*

January 17, 1995 Hyogoken-Nanbu (Kobe) Earthquake. Performance of Structures, Lifelines and Fire Protection Systems. Executive Summary and Paper.
PB97-104160 *00,475*

Wind and Seismic Effects: Proceedings of the Joint Meeting of the U.S.-Japan Cooperative Program in Natural Resources Panel on Wind and Seismic Effects (28th). Held in Gaithersburg, Maryland on May 14-17, 1996.
PB97-104376 *00,476*

DYNAMICAL SYSTEMS
Noise-Induced Chaos and Phase Space Flux.
PB95-125761 *03,433*

Non-Gaussian Noise Effects on Reliability of Multistable Systems.
PB96-122726 *04,213*

DYNAMICS
Dynamic Light-Scattering Study of a Diluted Polymer Blend Near Its Critical Point.
PB95-151890 *01,245*

DYSPROSIUM
Enhanced Curie Temperatures and Magnetoelastic Domains in Dy/Lu Super Lattices and Films.
PB94-172665 *04,443*

Magnetoelasticity in Rare-Earth Multilayers and Films.
PB94-211356 *04,495*

DYSPROSIUM BARIUM CUPRATES
Coupled-Bilayer Two-Dimensional Magnetic Order of the Dy Ions in Dy2Ba4Cu7O15.
PB95-152104 *04,584*

Reactive Coevaporation of DyBaCuO Superconducting Films: The Segregation of Bulk Impurities on Annealed MgO(100) Substrates.
PB95-164562 *04,635*

DYSPROSIUM IONS
Coupled-Bilayer Two-Dimensional Magnetic Order of the Dy Ions in Dy2Ba4Cu7O15.
PB95-152104 *04,584*

E. COLI
Novel Activity of E. coli uracil DNA N-glycosylase Excision of Isodialuric Acid (5,6-dihydroxyuracil), a Major Product of Oxidative DNA Damage, from DNA.
PB96-110747 *03,543*

E134
Thermodynamic Properties of CHF2-O-CHF2,Bis(difluoromethyl) Ether.
PB94-199569 *00,798*

EAMATE SYSTEM
Design and Development of an Information Retrieval System for the EAMATE Data. Volume 2 of 2. Appendices.
PB94-168390 *00,487*

EARTH GRAVITATION
Integrated Laser Doppler Method for Measuring Planetary Gravity Fields.
PB94-198686 *03,681*

EARTH OBSERVING SYSTEM (EOS)
Activities of NIST (National Inst. Of Standards and Technology).
N94-23605/6 *04,222*

Calibration in the Earth Observing System (EOS) Project. Part 2. Implementation.
PB97-112213 *04,842*

NIST Thermal Infrared Transfer Standard Radiometer for the Earth Observing System (EOS) Program.
PB97-113013 *04,843*

EARTH TIDES
Measurement and Interpretation of Tidal Tilts in a Small Array.
PB96-102611 *03,686*

EARTHQUAKE DAMAGE
Evaluating the Seismic Performance of Lightly-Reinforced Circular Concrete Bridge Columns.
PB95-163259 *01,335*

Performance of HUD-Affiliated Properties during the January 17, 1994 Northridge Earthquake.
PB95-174488 *00,443*

Survey of Steel Moment-Resisting Frame Buildings Affected by the 1994 Northridge Earthquake.
PB95-211918 *00,451*

Performance of Federal Buildings in the January 17, 1994 Northridge Earthquake.
PB95-231775 *00,453*

Post-Earthquake Fire and Lifelines Workshop. Held in Long Beach, California on January 30-31, 1995. Proceedings.
PB96-117916 *00,209*

Comparison of Responses of a Select Number of Buildings to the 10/17/1989 Loma Prieta (California) Earthquake and Low-Level Amplitude Test Results.
PB96-159645 *00,467*

January 17, 1995 Hyogoken-Nanbu (Kobe) Earthquake. Performance of Structures, Lifelines and Fire Protection Systems. Executive Summary and Paper.
PB97-104160 *00,475*

EARTHQUAKE ENGINEERING
Seismic Instrumentation of Existing Buildings.
PB94-159779 *00,420*

Draft Guidelines for Quality Control Testing of Elastomeric Seismic Isolation Systems.
PB94-161734 *00,422*

Evaluation and Strengthening Guidelines for Federal Buildings: Identification of Current Federal Agency Programs.
PB94-176278 *00,424*

Evaluation and Strengthening Guidelines for Federal Buildings: Assessment of Current Federal Agency Evaluation Programs and Rehabilitation Criteria and Development of Typical Costs for Seismic Rehabilitation.
PB94-181856 *00,425*

Northridge Earthquake 1994: Performance of Structures, Lifelines, and Fire Protection Systems.
PB94-207461 *04,825*

Evaluation and Retrofit Standards for Existing Federally Owned and Leased Buildings.
PB95-150918 *00,434*

Some Basics on Who's Who and What's What in Seismic Safety.
PB95-150926 *00,435*

Implementation of Executive Order 12699: Seismic Safety of Federal and Federally Assisted or Regulated New Building Construction.
PB95-151809 *00,436*

Lessons from the Loma Prieta Earthquake.
PB95-164091 *00,442*

Seismic Safety of Federal Buildings. Initial Program: How Much Will It Cost.
PB95-182291 *00,447*

Enhancements to Program IDARC: Modeling Inelastic Behavior of Welded Connections in Steel Moment-Resisting Frames.
PB95-231601 *00,452*

How-To Suggestions for Implementing Executive Order 12941 on Seismic Safety of Existing Federal Buildings, A Handbook.
PB96-131552 *00,461*

Executive Order 12941. Seismic Safety of Existing Federally Owned or Leased Buildings: It's History, Content and Objectives.
PB96-156021 *00,465*

Preliminary Processing of the Lotung LSST Data.
PB96-165972 *03,690*

State of the Art Report on Seismic Design Requirements for Nonstructural Building Components.
PB96-193800 *00,308*

EARTHQUAKE RESISTANCE

Literature Review on Seismic Performance of Building Cladding Systems.
PB96-106901 *00,455*

Ground Improvement Techniques for Liquefaction Remediation Near Existing Lifelines.
PB96-128111 *01,350*

Proceedings of a Workshop on Developing and Adopting Seismic Design and Construction Standards for Lifelines. Held in Denver, Colorado on September 25-27, 1991.
PB97-115794 *01,302*

EARTHQUAKE RESISTANT STRUCTURES

Earthquake Resistant Construction of Electric Transmission and Telecommunication Facilities Serving the Federal Government Report.
PB94-161817 *02,460*

Draft Guidelines for Pre-Qualification and Prototype Testing of Seismic Isolation Systems.
PB94-161940 *01,331*

Draft Guidelines for Quality Control Testing of Sliding Seismic Isolation Systems.
PB94-161957 *01,332*

Earthquake Resistant Construction of Gas and Liquid Fuel Pipeline Systems Serving, or Regulated By, the Federal Government.
PB94-161999 *04,846*

Draft Guideline for Testing and Evaluation of Seismic Isolation Systems.
PB94-172947 *00,423*

Seismic Strengthening of Reinforced Concrete Frame Buildings.
PB95-108841 *00,430*

Jacket Thickness Requirements for Seismic Retrofitting of Circular Bridge Columns.
PB95-163267 *01,336*

Performance of 1/3-Scale Model Precast Concrete Beam-Column Connections Subjected to Cyclic Inelastic Loads. Report No. 4.
PB95-179024 *00,444*

World of Building Codes.
PB95-203428 *00,449*

Comparison of the Seismic Provisions of Model Building Codes and Standards to the 1991 NEHRP Recommended Provisions.
PB95-231858 *00,315*

ICSSC Guidance on Implementing Executive Order 12941 on Seismic Safety of Existing Federally Owned or Leased Buildings.
PB96-128103 *00,459*

Seismic Performance of Circular Bridge Columns Designed in Accordance with AASHTO/CALTRANS Standards.
PB96-146352 *01,346*

Simplified Design Procedure for Hybrid Precast Concrete Connections.
PB96-154836 *00,405*

Summary and Results of the NIST Workshop on Proposed Guidelines for Testing and Evaluation of Seismic Isolation Systems. Held in San Francisco, California on July 25, 1994.
PB96-154901 *00,463*

Guidelines for Pre-Qualification, Prototype and Quality Control Testing of Seismic Isolation Systems.
PB96-193685 *01,347*

EARTHQUAKES

Northridge Earthquake, 1994. Performance of Structures, Lifelines and Fire Protection Systems.
PB94-161114 *00,421*

Earthquake and Fire in Japan: When the Threat Became a Reality.
PB95-175238 *00,201*

Energy-Based Method for Liquefaction Potential Evaluation. Phase 1. Feasibility Study.
PB96-214747 *03,691*

EBULLIOMETERS

Design of a High-Pressure Ebulliometer, with Vapor-Liquid Equilibrium Results for the Systems CHF2Cl + CF3-CH3 and CF3-CH2F + CH2F2.
PB97-113229 *04,163*

EBULLIOMETRY

Model for Calculating Virial Coefficients of Natural Gas Hydrocarbons with Impurities.
PB96-156047 *04,064*

ECONOMIC ANALYSIS

Least-Cost Energy Decisions for Buildings: Part 2. Uncertainty and Risk Video Training Workbook.
PB94-165982 *00,240*

Standards in Building Economics: Why We Need Them and How to Write Them.
PB94-216405 *00,320*

ECONOMIC DEVELOPMENT

Aid for Smaller Businesses.
PB94-212461 *00,492*

ECONOMIC IMPACT

Economic, Energy, and Environmental Impacts of the Energy-Related Inventions Program.
DE94-017162 *00,008*

ECONOMIC IMPACTS

Evaluation of the Economic Impacts Associated with the NIST Power and Energy Calibration Services.
PB95-188850 *02,461*

ECONOMIC MODELS

Functions of Technology Infrastructure in a Competitive Economy.
PB94-173002 *00,478*

EDDY CURRENTS

Development in the Theory and Analysis of Eddy Current Sensing of Velocity in Liquid Metals.
PB94-212586 *03,335*

Improved Eddy-Current Decay Method for Resistivity Characterization.
PB95-180451 *02,265*

EDGE DETECTION

Monte Carlo Model for SEM Linewidth Metrology.
PB95-150058 *02,331*

Motion-Model-Based Boundary Extraction.
PB95-189502 *01,849*

EDGES

Effects of Specimen Edge Conditions on Heat Release Rate.
PB95-152864 *00,375*

EDI (ELECTRONIC DATA INTERCHANGE)

Federal Implementation Guideline for Electronic Data Interchange: ASC X12 003040 Transaction Set 838 Trading Partner Profile (Vendor Registration), Implementation Convention.
PB96-112651 *03,674*

Federal Implementation Guideline for Electronic Data Interchange. ASC X12 003050 Transaction Set 850 Award Instrument. Implementation Convention.
PB96-114913 *01,814*

Federal Implementation Guideline for Electronic Data Interchange. ASC X12 003050 Transaction Set 860 Modifications to Award Instrument. Implementation Convention.
PB96-114921 *01,815*

Federal Implementation Guideline for Electronic Data Interchange. ASC X12 003050 Transaction Set 843 Response to Request for Quotation. Implementation Convention.
PB96-168984 *01,822*

Guidelines for the Evaluation of Electronic Data Interchange Products.
PB96-172325 *01,506*

Federal Implementation Guideline for Electronic Data Interchange. ASC X12 003050 Transaction Set 855 Purchase Order Acknowledgment: Implementation Convention.
PB96-172374 *01,823*

Federal Implementaion Guideline for Eletronic Data Interchange. ASC X12 003050 Transaction Set 865 Purchase Order Change Acknowledgement/Request - Seller Initiated. Implementation Convention.
PB96-172549 *01,825*

EDITING

Operating Procedures and Life Cycle Documentation for the Initial Graphics Exchange Specification.
PB95-242285 *02,782*

EDITING ROUTINES

Structural EXPRESS Editor.
PB94-159795 *02,769*

EDLEN EQUATION

Verification of Revised Water Vapour Correction to the Index of Refraction of Air.
PB96-161666 *02,680*

EDUCATION

Investing in Education to Meet a National Need for a Technical-Professional Workforce in a Post-Industrial Economy.
PB94-173028 *00,132*

Tribology Education: Present Status and Future Challenges.
PB94-212362 *02,965*

Structural Analysis in Context.
PB95-151817 *00,437*

Consensus Process in Standards Development.
PB96-179502 *00,136*

EEL PROGRAM

National Voluntary Laboratory Accreditation Program: Energy Efficient Lighting Products.
PB94-219060 *02,642*

EFFECTIVE RANGE THEORY

Modified Effective Range Theory as an Alternative to Low-Energy Close-Coupling Calculations.
PB95-202701 *03,988*

EFFICIENCY

Usability Engineering: Industry-Government Collaboration for System Effectiveness and Efficiency.
PB97-122287 *01,514*

EGRESS

Mathematical Modeling of Human Egress from Fires in Residential Buildings.
PB94-193778 *00,337*

EIGENVALUES

Accuracy of Eigenvalues: A Comparison of Two Methods.
PB95-126249 *03,413*

EJECTORS

Theoretical Evaluation of the Vapor Compression Cycle with a Liquid-Line/Suction-Line Heat Exchanger, Economizer, and Ejector.
PB95-216917 *02,607*

ELASTIC CONSTANTS

Compressibility of Polycrystal and Monocrystal Copper: Acoustic-Resonance Spectroscopy.
PB96-164223 *02,990*

Orthotropic Elastic Constants of a Boron-Aluminum Fiber-Reinforced Composite: An Acoustic-Resonance-Spectroscopy Study.
PB96-200175 *03,182*

Elastic Constants and Microcracks in YBa2Cu3O7.
PB96-200761 *03,005*

ELASTIC MODULUS

Nanoindentation and Instrumented Scratching Measurements on Hard Coatings.
PB97-122477 *03,111*

ELASTIC PROPERTIES

Effects of Elastic Stress on Phase Equilibrium in the Ni-V System.
PB94-172707 *03,313*

Elastic Properties of Uniaxial-Fiber Reinforced Composites: General Features.
PB94-200649 *03,140*

Elastic Constants of Isotropic Cylinders Using Resonant Ultrasound.
PB94-211919 *04,497*

Elastic Constants of Polycrystalline Y1Ba2Cu3Ox.
PB94-213196 *04,513*

Cast-Iron Elastic Constants: Effect of Graphite Aspect Ratio.
PB94-213212 *03,211*

Elastic Constants and Debye Temperature of Y1Ba2Cu3Ox: Effect of Oxygen Content.
PB94-213352 *04,515*

Localization Model of Rubber Elasticity: Comparison with Torsional Data for Natural Rubber Networks in the Dry State.
PB95-107033 *03,195*

Elastic Properties of Al2O3/Al Composites: Measurements and Modeling.
PB95-161378 *03,157*

Elastic Properties of Central-Force Networks with Bond-Length Mismatch.
PB95-163366 *04,623*

Low-Temperature Elastic Constants of Y1Ba2Cu3O7.
PB95-168837 *04,642*

Elastic Constants of a Material with Orthorhombic Symmetry: An Alternative Measurement Approach.
PB95-180527 *04,684*

Off-Diagonal Orthorhombic-Symmetry Elastic Constants.
PB95-202768 04,695

Elastic Constants and Internal Friction of Polycrystalline Copper.
PB96-141015 03,364

ELASTIC SCATTERING
Low-Energy-Electron Collisions with Sodium: Elastic and Inelastic Scattering from the Ground State.
PB96-103106 04,030

Effect of Finite Beam Width on Elastic Light Scattering from Droplets.
PB96-163670 01,144

Elastic Scattering from Spheres under Non Plane-Wave Illumination.
PB96-163688 04,370

ELASTICITY
Nonequilibrium Thermodynamic Theory of Viscoplastic Materials.
PB96-111661 04,034

ELASTICITY THEORY
Whither Computational Materials Science. Some Thoughts from the Mechanical Properties Front.
PB96-161997 02,987

ELASTOMER BLENDS
Microstructure Effect on the Phase Behavior of Blends of Deuterated Polybutadiene and Protonated Polyisopene.
PB97-113146 01,296

ELASTOMERS
Synthesis of Thermally Stable Elastomers.
AD-A307 789/8 03,194

Effect of Swelling on the Elasticity of Rubber: Localization Model Description.
PB94-211034 01,216

Anomalous Freezing and Melting of Solvent Crystals in Swollen Gels of Natural Rubber.
PB94-212321 01,223

ELCETRON PARAMAGNETIC RESONANCE
Orientation Effects on ESR Analysis of Alanine-Polymer Dosimeters.
PB96-146725 03,720

ELECRON MICROSCOPY
SUSAN: SUperconducting Systems ANalysis by Low Temperature Scanning Electron Microscopy (LTSEM).
PB96-112065 04,728

ELECTRET
Calibration of Electret-Based Integral Radon Monitors Using NIST Polyethylene-Encapsulated (226)Ra/(222)Rn Emanation (PERE) Standards.
PB96-159223 01,950

ELECTRETS
Response Comparison of Electret Ion Chambers, LiF TLD, and HPIC.
PB96-190103 02,578

ELECTRIC APPLIANCES
Three-Axis Coil Probe Dimensions and Uncertainties during Measurement of Magnetic Fields from Appliances.
PB94-219359 01,885

Distributions of Measurement Error for Three-Axis Magnetic Field Meters during Measurements Near Appliances.
PB96-180153 02,110

ELECTRIC ARCS
Decomposition of SF6 and Production of S2F10 in Power Arcs.
PB96-122619 01,084

ELECTRIC BRIDGES
Digital Impedance Bridge.
PB96-103155 02,272

ELECTRIC CABLES
Effect of DC Tests on Induced Space Charge.
PB94-172350 02,212

ELECTRIC CHARGE
Measuring Contact Charge Transfer at Interfaces: A New Experimental Technique.
PB95-164570 03,053

Electric Dipole Excitation of a Long Conductor in a Lossy Medium.
PB96-146675 04,058

ELECTRIC CONDUCTIVITY
Critical Current and Normal Resistance of High-Tc Step-Edge SNS Junctions.
PB96-111752 04,724

ELECTRIC CONTACTS
Contact Electrification Induced by Monolayer Modification of a Surface and Relation to Acid-Base Interactions.
PB94-185378 03,034

In situ Noble Metal YBa2Cu3O7 Thin-Film Contacts.
PB94-211323 04,494

YBa2Cu3O7-x to Si Interconnection for Hybrid Superconductor/Semiconductor Integration.
PB94-211711 02,315

Preparation of Low Resistivity Contacts for High-Tc Superconductors.
PB95-153557 02,258

High Current Pressure Contacts to Ag Pads on Thin Film Superconductors.
PB95-168621 04,639

Oxygen Annealing of Ex-situ YBCO/Ag Thin-Film Interfaces.
PB96-141312 04,758

ELECTRIC CONVERTERS
Comments on 'Conversions between S, Z, Y, h, ABCD, and T Parameters Which Are Valid for Complex Source and Load Impedances'.
PB96-102785 02,069

ELECTRIC CURRENT
Optical Current Transducer for Calibration Studies.
PB94-185907 02,121

Faraday Effect Current Sensors.
PB94-200698 02,127

Faraday Effect Sensors: A Review of Recent Progress.
PB94-200706 02,128

Frequency Extension of the NIST AC-DC Difference Calibration Service for Current.
PB95-161253 01,895

Polarization Insensitive 3x3 Sagnac Current Sensor Using Polarizing Spun High-Birefringence Fiber.
PB96-119276 02,187

ELECTRIC CURRENT METERS
Recent Developments at NIST on Optical Current Sensors and Partial Discharge Diagnostics.
PB95-151114 02,147

ELECTRIC CURRENT SENSORS
Polarization Dependence of Response Functions in 3x3 Sagnac Optical Fiber Current Sensors.
PB95-162426 02,154

Submicroampere-Per-Root-Hertz Current Sensor Based on the Faraday Effect in Ga: YIG.
PB95-162467 02,155

Faraday Effect Current Sensor with Improved Sensitivity-Bandwidth Product.
PB95-203154 02,180

Faraday Effect Sensors for Magnet Field and Electric Current.
PB96-119664 04,736

Polarization Dependence of Response Functions in 3x3 Sagnac Optical Fiber Current Sensors.
PB96-122684 02,189

Fundamentals and Problems of Fiber Current Sensors.
PB97-111835 02,205

ELECTRIC DEVICES
Effect of Electrode-Polymer Interfacial Layers on Polymer Conduction. Part 2. Device Summary.
PB95-151155 02,335

ELECTRIC DISCHARGES
Electrical Breakdown in Transformer Oil in Large Gaps.
PB95-150579 01,889

Recent Developments at NIST on Optical Current Sensors and Partial Discharge Diagnostics.
PB95-151114 02,147

Electron Scattering and Dissociative Attachment by SF6 and Its Electrical-Discharge By-Products.
PB95-151288 02,256

Observations of Partial Discharges in Hexane Under High Magnification.
PB95-163127 01,900

Importance of Unraveling Memory Propagation Effects in Interpreting Data on Partial Discharge Statistics.
PB95-163572 01,901

Nonstationary Behavior of Partial Discharge during Insulation Aging.
PB95-163580 01,902

Partial Discharge: Induced Aging of Cast Epoxies and Related Nonstationary Behavior of the Discharge Statistics.
PB95-163598 01,903

Physics and Chemistry of Partial Discharge and Corona: Recent Advances and Future Challenges.
PB95-181046 01,910

Nonstationary Behaviour of Partial Discharge during Discharge Induced Ageing of Dielectrics.
PB96-103114 01,922

Physics and Chemistry of Partial Discharge and Corona - Recent Advances and Future Challenges.
PB96-123757 01,936

ELECTRIC FAULTS
Keeping Up with the Reality of Today's Surge Environment.
PB96-123633 02,231

ELECTRIC FIELDS
Electric-Field Strengths Measured Near Personal Transceivers.
PB94-172020 01,564

Spatial Dependence of Electrical Fields Due to Space Charges in Films of Organic Dielectrics Used for Insulation of Power Cables.
PB94-199130 02,214

Energy Transduction between a Concentration Gradient and an Alternating Electric Field.
PB94-216363 03,461

Electric Field Effects on Crack Growth in a Lead Magnesium Niobate.
PB95-107322 03,339

Michaelis-Menten Equation for an Enzyme in an Oscillating Electric Field.
PB95-140489 00,906

ELF Electric and Magnetic Field Measurement Methods.
PB95-161675 04,423

Using Quantized Breakdown Voltage Signals to Determine the Maximum Electric Fields in a Quantum Hall Effect Sample.
PB95-261947 02,375

Electric Field Effects on a Near-Critical Fluid in Microgravity.
PB96-161880 04,217

ELECTRIC GENERATORS
Evaluation of Wear Resistant Ceramic Valve Seats in Gas-Fueled Power Generation Engines. Topical Report, December 1991-April 1994.
PB95-200218 02,466

ELECTRIC MEASURING INSTRUMENTS
NIST 30 MHz Linear Measurement System.
PB94-169752 02,020

ELECTRIC MOTORS
Efficiency of Electric Motors. National Voluntary Lab. Accreditation Program (NVLAP).
PB96-111174 02,107

ELECTRIC POTENTIAL
Potential Drop in the Center-Cracked Panel with Asymmetric Crack Extension.
PB95-107330 04,819

Step-Edge and Stacked-Heterostructure High-Tc Josephson Junctions for Voltage-Standard Arrays.
PB96-102066 04,702

Spectroscopic Study of Quantized Breakdown Voltage States of the Quantum Hall Effect.
PB96-113584 04,730

ELECTRIC POWER
Evaluation of the Economic Impacts Associated with the NIST Power and Energy Calibration Services.
PB95-188850 02,461

ELECTRIC POWER DISTRIBUTION
Investigation of S2F10 Production and Mitigation in Compressed SF6-Insulated Power Systems.
PB94-212388 02,467

Investigation of S2F10 Production and Mitigation in Compressed SF6- Insulated Power Systems.
PB96-155528 02,468

ELECTRIC POWER GENERATION
Earthquake Resistant Construction of Electric Transmission and Telecommunication Facilities Serving the Federal Government Report.
PB94-161817 02,460

ELECTRIC POWER METERS
Technical Impact of the NIST Calibration Service for Electrical Power and Energy.
PB96-147913 02,462

ELECTRIC-POWERED VEHICLES
Advanced Components for Electric and Hybrid Electric Vehicles. Workshop Proceedings. Held in Gaithersburg, Maryland on October 27-28, 1993.
PB94-177060 04,858

ELECTRIC PROBES
Standard Probes for Electromagnetic Field Measurements.
PB94-185436 01,999

Verification of Commercial Probe-Tip Calibrations.
PB95-161576 02,347

Calibrating On-Wafer Probes to the Probe Tips.
PB95-163945 02,352

LRM Probe-Tip Calibrations with Imperfect Resistors and Lossy Lines.
PB95-163952 02,353

LRM Probe-Tip Calibrations Using Nonideal Standards.
PB96-135389 02,411

ELECTRIC PULSES
Comparative Measurements of High-Voltage Impulses Using a Kerr Cell and a Resistor Divider.
PB94-172582 02,028

ELECTRIC RESISTANCE HEATING
Calorimetric and Visual Measurements of R123 Pool Boiling on Four Enhanced Surfaces.
PB96-128129 04,053

ELECTRIC TERMINALS
Terminal Invariant Description of Amplifier Noise.
PB95-153573 02,043

ELECTRIC WIRE
Spatial Dependence of Electrical Fields Due to Space Charges in Films of Organic Dielectrics Used for Insulation of Power Cables.
PB94-199130 02,214

ELECTRICAL CIRCUITS
Precision Tests of a Quantum Hall Effect Device DC Equivalent Circuit Using Double-Series and Triple-Series Connections.
PB96-159256 01,953

ELECTRICAL DETECTION
Correlations between Electrical and Acoustic Detection of Partial Discharge in Liquids and Implications for Continuous Data Recording.
PB96-204490 02,248

ELECTRICAL ENGINEERING
Electronics and Electrical Engineering Laboratory Technical Progress Bulletin Covering Laboratory Programs,

October to December 1992, with 1992/1993 EEEL Events Calendar.
PB94-165958 *02,299*

Electronics and Electrical Engineering Laboratory Technical Progress Bulletin Covering Laboratory Programs, October to December 1994 with 1995 EEEL Events Calendar.
PB95-208724 *02,372*

Electronics and Electrical Engineering Laboratory Technical Progress Bulletin Covering Laboratory Programs, January to March 1992, with 1992/1993 EEEL Events Calendar.
PB95-210480 *01,917*

Electronics and Electrical Engineering Laboratory Technical Publication Announcements Covering Laboratory Programs, October to December 1994 with 1995 EEEL Events Calendar.
PB95-231841 *01,918*

Electronics and Electrical Engineering Laboratory Technical Progress Bulletin Covering Laboratory Programs, April to June 1995 with 1995 EEEL Events Calendar.
PB96-106455 *01,923*

Electronics and Electrical Engineering Laboratory Technical Publication Announcements Covering Laboratory Programs, April to June 1995 with 1995 EEEL Events Calendar.
PB96-137187 *01,941*

Electronics and Electrical Engineering Laboratory Technical Progress Bulletin Covering Laboratory Programs, July to September 1995 with 1996 EEEL Events Calendar.
PB96-147905 *01,942*

Electronics and Electrical Engineering Laboratory 1995 Technical Accomplishments: Advancing Metrology for Electrotechnology to Support the U.S. Economy.
PB96-164520 *01,959*

Electronics and Electrical Engineering Laboratory Technical Publication Announcements Covering Laboratory Programs, July to September 1995 with 1996 EEEL Events Calendar.
PB96-183066 *01,965*

Electronics and Electrical Engineering Laboratory Technical Progress Bulletin Covering Laboratory Programs, October to December 1995 with 1996 EEEL Events Calendar.
PB96-183116 *01,966*

Electronics and Electrical Engineering Laboratory Technical Progress Bulletin Covering Laboratory Programs, January to March 1996, with 1996 EEEL Events Calendar.
PB96-191390 *01,969*

Electronics and Electrical Engineering Laboratory Technical Publication Announcements Covering Laboratory Programs, October to December 1995, with 1996 EEEL Events Calendar.
PB96-202346 *01,978*

Electronics and Electrical Engineering Laboratory Technical Publication Announcements Covering Laboratory Programs, January to March 1996, with 1996 EEEL Events Calendar.
PB96-214622 *01,981*

Electronics and Electrical Engineering Laboratory Technical Progress Bulletin Covering Laboratory Programs, April to June 1996 with 1996-1998 EEEL Events Calendar.
PB97-113880 *01,994*

Bibliography of the NIST Optoelectronics Division.
PB97-116040 *02,207*

ELECTRICAL EQUIPMENT

Electrical Product Requirements (Especially Quality Requirements) in the United States.
PB96-119235 *01,929*

Surging the Upside-Down House: Measurements and Modeling Results.
PB96-180138 *02,243*

ELECTRICAL FAULTS

Using Quantized Breakdown Voltage Signals to Determine the Maximum Electric Fields in a Quantum Hall Effect Sample.
PB95-261947 *02,375*

Spectroscopic Study of Quantized Breakdown Voltage States of the Quantum Hall Effect.
PB96-113584 *04,730*

ELECTRICAL IMPEDANCE

On-Wafer Impedance Measurement on Lossy Substrates.
PB95-176285 *02,365*

Overview of Bioelectrical Impedance Analyzers.
PB96-122635 *00,176*

Overview of Bioelectrical Impedance Analyzers.
PB97-118780 *00,181*

ELECTRICAL INSULATION

Spatial Dependence of Electrical Fields Due to Space Charges in Films of Organic Dielectrics Used for Insulation of Power Cables.
PB94-199130 *02,214*

Irradiation Damage in Inorganic Insulation Materials for ITER Magnets: A Review.
PB95-147351 *03,705*

Performance Evaluation of a New Digital Partial Discharge Recording and Analysis System.
PB95-150389 *01,888*

Importance of Unraveling Memory Propagation Effects in Interpreting Data on Partial Discharge Statistics.
PB95-163572 *01,901*

Nonstationary Behavior of Partial Discharge during Insulation Aging.
PB95-163580 *01,902*

Partial Discharge: Induced Aging of Cast Epoxies and Related Nonstationary Behavior of the Discharge Statistics.
PB95-163598 *01,903*

Cryogenic Properties of Inorganic Insulation Materials for ITER Magnets: A Review.
PB95-198768 *03,706*

SF6 Insulation: Possible Greenhouse Problems and Solutions.
PB95-251625 *02,269*

Gaseous Dielectrics Research: Possible SF6 Substitutes.
PB96-119268 *02,228*

Modification of Cast Epoxy Resin Surfaces during Exposure to Partial Discharges.
PB96-122734 *01,086*

SF6/N2 Mixtures: Basic and High-Voltage-Insulation Properties.
PB96-123468 *02,230*

Classified Bibliography: Insulation Condition Monitoring Methods, 1989-1995.
PB96-131586 *02,232*

President's Column 'Editorial'.
PB96-164090 *02,239*

Adhesion, Contact Electrification, and Acid-Base Properties of Surfaces.
PB96-204425 *03,693*

ELECTRICAL MEASUREMENT

Electronics and Electrical Engineering Laboratory 1994 Program Plan: Supporting Technology for U.S. Competitiveness in Electronics.
PB94-126901 *01,873*

Center for Electronics and Electrical Engineering Technical Progress Bulletin Covering Center Programs, October to December, with 1991 CEEE Events Calendar.
PB94-159787 *02,296*

Electronics and Electrical Engineering Laboratory: 1994 Strategic Plan. Supporting Technology for U.S. Competitiveness in Electronics.
PB94-161320 *01,874*

Transmission/Reflection and Short-Circuit Line Methods for Measuring Permittivity and Permeability.
PB94-165537 *02,211*

Electric-Field Strengths Measured Near Personal Transceivers.
PB94-172020 *01,564*

Optical Current Transducer for Calibration Studies.
PB94-185907 *02,121*

Reproducibility of JEDEC Standard Current and Voltage Ramp Test Procedures for Thin-Dielectric Breakdown Characterization.
PB94-185931 *01,879*

Electronics and Electrical Engineering Laboratory Technical Publication Announcements Covering Laboratory Programs, October to December 1993 with 1994/1995 EEEL Events Calendar.
PB94-193752 *02,307*

Electronics and Electrical Engineering Laboratory Technical Progress Bulletin Covering Laboratory Programs, January to March 1994 with 1994/1995 EEEL Events Calendar.
PB94-193810 *02,308*

Electronics and Electrical Engineering Laboratory Technical Progress Bulletin Covering Laboratory Programs, July to September 1993 with 1994 EEEL Events Calendar.
PB94-194354 *02,309*

Electronics and Electrical Engineering Laboratory Technical Progress Bulletin Covering Laboratory Programs, April to June 1994 with 1994/1995 EEEL Events Calendar.
PB95-143186 *02,329*

Electronics and Electrical Engineering Laboratory 1995 Program Plan. Supporting Technology for U.S. Competitiveness in Electronics.
PB95-159885 *01,894*

Frequency Extension of the NIST AC-DC Difference Calibration Service for Current.
PB95-161253 *01,895*

Verification of Scattering Parameter Measurements.
PB95-163960 *01,904*

Through-the-Arc Sensing for Measuring Gas Metal Arc Weld Quality in Real Time.
PB95-164463 *02,908*

Accuracy Comparisons of Josephson Array Systems.
PB95-164687 *02,047*

Voltage Ratio Measurements of a Zener Reference Using a Digital Voltmeter.
PB95-164695 *01,906*

Superconductor Critical Current Standards for Fusion Applications. Final Progress Report, October 1993-July 1994.
PB95-169538 *02,222*

Electronics and Electrical Engineering Laboratory Technical Progress Bulletin Covering Laboratory Programs, July to September 1994 with 1994/1995 EEEL Events Calendar.
PB95-170395 *02,360*

Standard Reference Devices for High Temperature Superconductor Critical Current Measurements.
PB95-175543 *04,659*

Improved Eddy-Current Decay Method for Resistivity Characterization.
PB95-180451 *02,265*

Accuracy and Repeatability in Time Domain Network Analysis.
PB95-202644 *02,064*

Electronics and Electrical Engineering Laboratory Technical Publication Announcements Covering Laboratory Programs, January to March 1995 with 1995 EEEl Events Calendar.
PB95-242277 *02,373*

Voltage-Standard Devices.
PB96-102496 *01,920*

Electronics and Electrical Engineering Laboratory Technical Publication Announcements Covering Laboratory Programs, April to June 1995 with 1995 EEEL Events Calendar.
PB96-137187 *01,941*

Amperometric Measurement of Moisture in Transformer Oil Using Karl Fischer Reagents.
PB96-146766 *00,623*

Technical Impact of the NIST Calibration Service for Electrical Power and Energy.
PB96-147913 *02,462*

Electronics and Electrical Engineering Laboratory: 1996 Program Plan. Supporting Technology for U.S. Competitiveness in Electronics.
PB96-175237 *01,962*

Single-Port Technique for Adaptor Efficiency Evaluation.
PB96-176441 *02,088*

Dielectric and Magnetic Measurements from -50C to 200C and in the Frequency Band 50 MHz to 2 GHz.
PB96-191382 *02,245*

Electrical Test Structures Replicated in Silicon-on-Insulator Material.
PB97-111827 *02,454*

Loading Effects in Resistance Scaling.
PB97-111884 *02,285*

Measurement and Reduction of Alignment Errors of the NIST Watt Experiment.
PB97-111959 *01,987*

Low Thermal Guarded Scanner for High Resistance Measurement Systems.
PB97-112452 *02,288*

Exploring the Low-Frequency Performance of Thermal Converters Using Circuit Models and a Digitally Synthesized Source.
PB97-112551 *02,848*

Low Voltage Standards in the 10 Hz to 1 MHz Range.
PB97-112569 *02,100*

ELECTRICAL MEASUREMENTS

Electrical Measurements for Monitoring and Control of rf Plasma Processing.
PB96-161963 *04,369*

Coaxial Line-Reflect-Match Calibration.
PB96-200118 *02,246*

30 MHz Comparison Receiver.
PB96-200407 *01,972*

Conversion of a 2-Terminal-Pair Bridge to a 4-Terminal-Pair Bridge for Increased Range and Precision in Impedance Measurements.
PB97-119176 *02,103*

ELECTRICAL NETWORKS

Diakoptic and Large Change Sensitivity Analysis.
PB95-150538 *02,038*

Simulating the Dynamic Electro Thermal Behavior of Power Electronic Circuits and Systems.
PB95-161014 *02,345*

Thermal Component Models for Electro-Thermal Network Simulation.
PB95-161022 *02,346*

ELECTRICAL RESISTANCE

Pressure Dependencies of Standard Resistors.
PB95-153516 *02,257*

Anomalous Behavior of a Quantized Hall Plateau in a High-Mobility Si Metal-Oxide-Semiconductor Field-Effect Transistor.
PB95-164174 *02,354*

Design Challenges in a Commercial Quantum Hall Effect-Based Resistance Standard.
PB95-171419 *02,263*

Progress on the Quantized Hall Resistance Recommended Intrinsic/Derived Standards Practice.
PB96-122460 *02,403*

Loading Effects in Resistance Scaling.
PB97-111884 *02,285*

Low Thermal Guarded Scanner for High Resistance Measurement Systems.
PB97-112452 *02,288*

ELECTRICAL RESISTIVITY

High-Spatial-Resolution Resistivity Mapping Applied to Mercury Cadmium Telluride.
PB94-212917 *02,131*

Diffusion of Copper into Gold Plating.
PB95-162152 ,00,957

Improved Eddy-Current Decay Method for Resistivity Characterization.
PB95-180451 02,265

Apparatus for Resistance Measurement of Short, Small-Diameter Conductors.
PB96-141130 04,417

Interfacial Transport in Porous Media: Application to dc Electrical Conductivity of Mortars.
PB96-146816 01,326

Characterization of LPE HgCdTe Film by Magnetoresistance.
PB96-157961 02,197

ELECTRICAL SUBSTITUTION
National Institute of Standards and Technology High-Accuracy Cryogenic Radiometer.
PB96-179585 04,378

Realization of a Scale of Absolute Spectral Response Using the NIST High Accuracy Cryogenic Radiometer.
PB97-118640 04,397

ELECTRICAL SYSTEMS
Electronics and Electrical Engineering Laboratory Technical Publication Announcements Covering Laboratory Programs, October to December 1994 with 1995 EEEL Events Calendar.
PB95-231841 01,918

ELECTRICAL TRANSPORT
Evidence for Tunneling and Magnetic Scatttering at 'In situ' YBCO/Noble-Metal Interfaces.
PB96-141098 04,752

ELECTRICALLY CONDUCTING FLUIDS
Measurement of the Thermal Properties of Electrically Conducting Fluids Using Coated Transient Hot Wires.
PB95-169058 03,269

ELECTRICALLY ISOLATED
Influence of Electrical Isolation on the Structure and Reflectivity of Multilayer Coatings Deposited on Dielectric Substrates.
PB96-159736 04,365

ELECTRIFICATION
Contact Electrification Induced by Monolayer Modification of a Surface and Relation to Acid-Base Interactions.
PB94-185378 03,034

Adhesion, Contact Electrification, and Acid-Base Properties of Surfaces.
PB96-204425 03,693

ELECTRO DEPOSITED COATINGS
Chemical Aspects of Tool Wear in Single Point Diamond Turning.
PB97-112601 03,021

ELECTRO-OPTIC CRYSTALS
Electro-Optic-Based RMS Voltage Measurement Technique.
PB96-138490 02,194

ELECTROACOUSTIC WAVES
Electroacoustic Characterization of Particle Size and Zeta Potential in Moderately Concentrated Suspensions.
PB96-119425 01,079

ELECTROACOUSTICS
Electroacoustics for Characterization of Particulates and Suspensions. Proceedings of a Workshop. Held in Gaithersburg, Maryland on February 3-4, 1993.
PB94-112695 00,725

Electrokinetic Sonic Analysis of Silicon Nitride Suspensions.
PB96-123575 03,073

Complicated Cases and Shielded Rooms: Audiometric Booths Shielded to Attenuate Electromagnetic Interference.
PB96-180179 02,278

ELECTROCHEMICAL CELLS
Structural and Magnetic Properties of CuCl2 Graphite Intercalation Compounds.
PB96-119748 03,020

ELECTROCHEMICAL CORROSION
Modeling Polarization Curves and Impedance Spectra for Simple Electrode Systems.
PB94-198876 03,188

ELECTROCHEMICAL IMMUNOASSAYS
Novel Amperometric Immunosensor for Procainamide Employing Light Activated Labels.
PB96-163662 00,512

ELECTROCHEMISTRY
Electrochemical Synthesis of Metal and Intermetallic Composites.
AD-A294 088/0 03,304

Evaluation of the Electrochemical Behavior of Ductile Nickel Aluminide and Nickel in a pH 7.9 Solution. Technical Report Number 3, April-June 1991.
DE94017351 03,307

Application of Photochemical Reaction in Electrochemical Detection of DNA Intercalation.
PB94-185733 00,686

Status of Electrocomposites.
PB94-212453 03,143

Self-Assembled Phospholipid/Alkanethiol Biomimetic Bilayers on Gold.
PB95-108460 00,878

Lithium-Drift Technique for Making Submicron Thick Silicon Membranes.
PB95-161386 02,260

Faraday Constant.
PB96-159793 01,955

ELECTROCLINIC EFFECT
Studies of the Higher Order Smectic Phase of the Large Electroclinic Effect Material W317.
PB95-151601 00,935

Dielectric Spectroscopic Determination of Temperature Behavior of Electroclinic Parameters in the Liquid Crystal W317.
PB96-140397 01,098

X-ray Observation of Electroclinic Layer Constriction and Rearrangement in a Chiral Smectic-A Liquid Crystal.
PB96-141080 01,100

ELECTROCONFORMATIONAL COUPLING
Energy Transduction between a Concentration Gradient and an Alternating Electric Field.
PB94-216363 03,461

ELECTRODE EXTENSIONS
Electrode Extension Model for Gas Metal Arc Welding.
PB96-135074 02,871

ELECTRODE SURFACE EFFECTS
Optical and Mass Spectrometric Investigations of Ions and Neutral Species in SF6 Radio-Frequency Discharges.
PB97-111918 01,985

ELECTRODEPOSITED COATINGS
Magnetic and Structural Properties of Electrodeposited Copper-Nickel Microlayered Alloys.
PB94-213121 04,512

ELECTRODEPOSITION
Electrodeposition.
PB94-172517 00,760

Effect of Mn Content on the Microstructure of Al-Mn Alloys Electrodeposited at 150C.
PB95-126355 03,343

Evidence of Film-Induced Cleavage by Electrodeposited Rhodium.
PB95-162327 03,191

Nanocomposite Magnetic Materials.
PB95-162780 04,617

ELECTRODES
Modeling Polarization Curves and Impedance Spectra for Simple Electrode Systems.
PB94-198876 03,188

Effect of Electrode-Polymer Interfacial Layers on Polymer Conduction. Part 2. Device Summary.
PB95-151155 02,335

Effect of Electrode Material on Measured Ion Energy Distributions in Radio-Frequency Discharges.
PB96-102850 04,026

Rapid pH Change Due to Bacteriorhodopsin Measured with a Tin-Oxide Electrode.
PB96-112081 03,544

Conformational Alterations of Bovine Insulin Adsorbed on a Silver Electrode.
PB96-161773 00,510

Mapping the Droplet Transfer Modes for an ER100S-1 GMAW Electrode.
PB96-190095 03,295

Sensing Droplet Detachment and Electrode Extension for Control of Gas Metal Arc Welding.
PB96-190160 03,297

ELECTROHYDRODYNAMICS
Electrohydrodynamic Instability and Electrical Discharge Initiation in Hexane.
PB96-186119 02,244

ELECTROLYTE SOLUTIONS
Summary of the Apparent Standard Partial Molal Gibbs Free Energies of Formation of Aqueous Species, Minerals, and Gases at Pressures 1 to 5000 Bars and Temperatures 25 to 1000C.
PB96-145891 01,113

ELECTROLYTES
Critical Behavior of Ionic Fluids.
PB95-164331 00,978

Low Electrolytic Conductivity Standards.
PB96-122098 01,081

Electrolytes Constrained on Fractal Structures: Debye-Huckel Theory.
PB97-110241 01,174

ELECTROLYTIC POLARIZATION
Modeling Polarization Curves and Impedance Spectra for Simple Electrode Systems.
PB94-198876 03,188

ELECTROMAGNETIC ACOUSTIC TRANSDUCERS
Determination of Sheet Steel Formability Using Wide Band Electromagnetic-Acoustic Transducers.
PB96-186036 02,279

Effect of Liftoff on Accuracu of Phase Velocity Measurements Made with Electromagnetic-Acoustic Transducers.
PB96-186044 02,280

ELECTROMAGNETIC CAPABILITY
Alternative EMC Compliance Test Facilities.
PB96-200324 02,247

ELECTROMAGNETIC COMPATIBILITY
Surging the Upside-Down House: Measurements and Modeling Results.
PB96-180138 02,243

Rapid Evaluation of Mode-Stirred Chambers Using Impulsive Waveforms.
PB96-210026 01,979

ELECTROMAGNETIC COUPLING
Electromagnetic Coupling Character of (001) Twist Boundaries in Sintered Bi2Sr2CaCu2O8+x Bicrystals.
PB96-176573 01,963

ELECTROMAGNETIC EMISSIONS
Optically Linked Three-Loop Antenna System for Determining the Radiation Characteristics of an Electrically Small Source.
PB95-161915 02,005

ELECTROMAGNETIC ENVIRONMENTS
Condensed Catalogue of Electromagnetic Environment Measurements, 30 - 300 Hz.
PB95-162210 01,899

Catalogue of Electromagnetic Environment Measurements, 30-300 Hz.
PB96-155452 01,943

ELECTROMAGNETIC FIELDS
Bibliography of the NIST Electromagnetic Fields Division Publications.
PB94-165990 01,875

Bibliography of the NIST Electromagnetic Fields Division Publications.
PB95-135562 01,886

Electro-Optic-Based RMS Voltage Measurement Technique.
PB96-138490 02,194

Standard Source Method for Reducing Antenna Factor Errors in Shielded Room Measurements.
PB96-183157 02,013

Bibliography of the NIST Electromagnetic Fields Division Publications.
PB96-210778 01,980

Metrology for Electromagnetic Technology: A Bibliography of NIST Publications.
PB97-116057 04,396

ELECTROMAGNETIC FLOWMETERS
Development in the Theory and Analysis of Eddy Current Sensing of Velocity in Liquid Metals.
PB94-212586 03,335

ELECTROMAGNETIC INTERACTIONS
Relativistic Quantum Mechanics of Interacting Particles.
PB97-110589 04,141

ELECTROMAGNETIC INTERFERENCE
Aperture Excitation of Electrically Large, Lossy Cavities.
PB94-145711 00,029

Measurements of Shielding Effectiveness and Cavity Characteristics of Airplanes.
PB94-210051 00,030

Assessment of Data by a Second-Order Transfer Function.
PB95-182390 03,760

Electronics and Electrical Engineering Laboratory Technical Publication Announcements Covering Laboratory Programs, October to December 1994 with 1995 EEEL Events Calendar.
PB95-231841 01,918

Standard Antennas for Electromagnetic Interference Measurements and Methods to Calibrate Them.
PB96-102561 02,007

Screened-Room Measurements on the NIST Spherical-Dipole Standard Radiator.
PB96-113568 01,926

Methodology for Electromagnetic Interference Measurements.
PB96-200126 02,014

Data Evaluation of a Linear System by a Second-Order Transfer Function.
PB96-200282 01,970

ELECTROMAGNETIC MEASUREMENT
Measurements of Shielding Effectiveness and Cavity Characteristics of Airplanes.
PB94-210051 00,030

Gradiometer Antennas for Detection of Long Subsurface Conductors.
PB95-175667 01,862

ELECTROMAGNETIC METROLOGY
Table of Dielectric Constants of Pure Liquids.
AD-A278 956/8 00,712

Comparison of Meteor Activity with Occurrence of Sporadic E Reflections.
AD-A292 039/5 00,116

Higher-Order Approximations in Ionospheric Wave-Propagation.
AD-A292 471/0 04,420

Standard of Attenuation for Microwave Measurements.
AD-A297 905/2 01,517

Dielectric Studies of Fluids with Reentrant Resonators. Appendix B.
DE93019683 03,244

Crosstalk between Microstrip Transmission Lines.
PB94-135639 02,210

Aperture Excitation of Electrically Large, Lossy Cavities.
PB94-145711 00,029

NIST 60-Millimeter Diameter Cylindrical Cavity Resonator: Performance Evaluation for Permittivity Measurements.
PB94-151776 02,251

Submissions to a Planned Encyclopedia of Operations Research on Computational Geometry and the Voronoi/ Delaunay Construct.
PB94-152709 *03,425*

Metrology for Electromagnetic Technology: A Bibliography of NIST Publications.
PB94-159761 *02,116*

Transmission/Reflection and Short-Circuit Line Methods for Measuring Permittivity and Permeability.
PB94-165537 *02,211*

Bibliography of the NIST Electromagnetic Fields Division Publications.
PB94-165990 *01,875*

NIST 30 MHz Linear Measurement System.
PB94-169752 *02,020*

Null-Balanced Total-Power Radiometer System NCS1.
PB94-169778 *02,021*

Electric-Field Strengths Measured Near Personal Transceivers.
PB94-172020 *01,564*

Lead Abatement in Buildings and Related Structures.
PB94-172038 *03,601*

Leakage Current Detection in Cryogenic Current Comparator Bridges.
PB94-172228 *02,024*

Effect of DC Tests on Induced Space Charge.
PB94-172350 *02,212*

Investigation of the Effects of Aging on the Calibration of a Kerr-Cell Measuring System for High Voltage Impulses.
PB94-172384 *02,025*

Intercomparison of NIST, NPL, PTB, and VSL Thermal Voltage Converters from 100 kHz to 1 MHz.
PB94-172442 *02,026*

Intercomparison of Thermal Converters at NIM, NIST, PTB, SIRI and VSL from 10 to 100 MHz.
PB94-172459 *02,027*

Planar Near-Field Alignment.
PB94-172491 *01,998*

Comparative Measurements of High-Voltage Impulses Using a Kerr Cell and a Resistor Divider.
PB94-172582 *02,028*

Time Scale Algorithm for Post-Processing: AT1 Plus Frequency Variance.
PB94-172772 *01,525*

Reciprocity Relations in Waveguide Junctions.
PB94-172814 *02,213*

Advanced Components for Electric and Hybrid Electric Vehicles. Workshop Proceedings. Held in Gaithersburg, Maryland on October 27-28, 1993.
PB94-177060 *04,858*

Time-Domain Measurements of the Electromagnetic Backscatter of Pyramidal Absorbers and Metallic Plates.
PB94-185410 *01,877*

Standard Probes for Electromagnetic Field Measurements.
PB94-185436 *01,999*

Approach to Setting Performance Requirements for Automated Evaluation of the Parameters of High-Voltage Impulses.
PB94-185634 *01,878*

Coaxial Reference Standard for Microwave Power.
PB94-193786 *01,880*

Automatic Inductive Voltage Divider Bridge Operates from 10 Hz to 100 kHz.
PB94-198413 *02,032*

Spatial Dependence of Electrical Fields Due to Space Charges in Films of Organic Dielectrics Used for Insulation of Power Cables.
PB94-199130 *02,214*

Quantized Dissipation of the Quantum Hall Effect at High Currents.
PB94-199395 *04,472*

NIST Capacitance Measurement Assurance Program (MAP).
PB94-200060 *02,254*

Faraday Effect Current Sensors.
PB94-200698 *02,127*

Measurements of Shielding Effectiveness and Cavity Characteristics of Airplanes.
PB94-210051 *00,030*

Longterm Changes of Silicon Photodiodes and Their Use for Photometric Standardization.
PB94-211349 *04,234*

Currents Induced on Multiconductor Transmission Lines by Radiation and Injection.
PB94-211943 *02,215*

Electromagnetic Scattering by a Periodic Surface with a Wedge Profile.
PB94-211950 *04,421*

Ultrasonic Spectroscopy of Metallic Spheres Using Electromagnetic-Acoustic Transduction.
PB94-212537 *04,185*

Optically Sensed EM-Field Probes for Pulsed Fields.
PB94-212594 *02,130*

Accurate Experimental Characterization of Interconnects: A Discussion of 'Experimental Electrical Characterization of Interconnects and Discontinuities in High-Speed Digital Systems'.
PB94-216389 *02,217*

Interconnection Transmission Line Parameter Characterization.
PB94-216397 *02,218*

Cascading Surge-Protective Devices: Options for Effective Implementation.
PB94-216488 *02,464*

Coordinating Cascaded Surge-Protective Devices: An Elusive Goal.
PB94-216496 *02,465*

Important Link in Entire-House Protection: Surge Reference Equalizers.
PB94-216504 *02,219*

Theoretical Aspects of Tagged Photon Facilities.
PB94-216611 *03,868*

Digital Techniques in HV Tests - Summary of 1989 Panel Session.
PB94-216702 *02,035*

RangeCAD and the NIST RCS Uncertainty Analysis.
PB94-218591 *01,870*

Planar Near-Field Measurements of Low-Sidelobe Antennas.
PB94-219235 *02,001*

Three-Axis Coil Probe Dimensions and Uncertainties during Measurement of Magnetic Fields from Appliances.
PB94-219359 *01,885*

High-Order Harmonic Mixing with GaAs Schottky Diodes.
PB95-108585 *01,528*

Correction Factor for Nonplanar Incident Field in Monopole Calibrations.
PB95-108643 *02,002*

Vibrational Predissociation Dynamics of Overtone-Excited HN3.
PB95-125720 *00,691*

Sub-Doppler Frequency Measurements on OCS at 87 Thz (3.4 micrometers) with the CO Overtone Laser: Considerations and Details.
PB95-128633 *04,255*

Bibliography of the NIST Electromagnetic Fields Division Publications.
PB95-135562 *01,886*

Metrology for Electromagnetic Technology: A Bibliography of NIST Publications.
PB95-135588 *02,143*

Ion Kinetic-Energy Distributions in Argon rf Glow Discharges.
PB95-141008 *04,409*

LP11-Mode Leakage Loss in Coated Depressed Clad Fibers.
PB95-141115 *02,145*

Electronics and Electrical Engineering Laboratory Technical Progress Bulletin Covering Laboratory Programs, April to June 1994 with 1994/1995 EEEL Events Calendar.
PB95-143186 *02,329*

Superconducting Energy Gap of Bulk UBe13.
PB95-150116 *04,559*

Electrical Breakdown in Transformer Oil in Large Gaps.
PB95-150579 *01,889*

Flux-Locked Current Source Reference.
PB95-150785 *02,039*

Bistatic Scattering of Absorbing Materials from 30 to 1000 MHz.
PB95-150934 *01,891*

Preliminary Comparison of Time Transfers via LASSO, GPS and Two-Way Satellite.
PB95-151098 *01,529*

Accurate Transmission Line Characterization.
PB95-151593 *02,220*

Time-Domain Antenna Characterizations.
PB95-152781 *02,003*

Automatic Calibration of Inductive Voltage Dividers for the NASA Zeno Experiment.
PB95-152849 *02,041*

Inductive Voltage Divider Calibration for the NASA Flight Experiment.
PB95-152856 *02,042*

New Coaxial Microwave Microcalorimeter Evaluation Technique.
PB95-153227 *01,892*

Pressure Dependencies of Standard Resistors.
PB95-153516 *02,257*

Terminal Invariant Description of Amplifier Noise.
PB95-153573 *02,043*

Performance of Commercial CMOS Foundry-Compatible Multijunction Thermal Converters.
PB95-153656 *02,342*

New Extrapolation/Spherical/Cylindrical Measurement Facility at the National Institute of Standards and Technology.
PB95-153755 *02,004*

Effective Medium Theory for Ferrite-Loaded Materials.
PB95-154662 *01,893*

Simulating the Dynamic Electro Thermal Behavior of Power Electronic Circuits and Systems.
PB95-161014 *02,345*

Frequency Extension of the NIST AC-DC Difference Calibration Service for Current.
PB95-161253 *01,895*

Modeling and Test Point Selection for a Thermal Transfer Standard.
PB95-161287 *01,896*

Bending-Induced Phase Shifts in Dual-Mode Planar Optical Waveguides.
PB95-161329 *04,271*

Characterization of Unknown Linear Systems Based on Measured CW Amplitude.
PB95-161485 *01,897*

Comments on 'Protecting EFIE-Based Scattering Computations from Effects of Internal Resonances'.
PB95-161568 *01,898*

Verification of Commercial Probe-Tip Calibrations.
PB95-161576 *02,347*

ELF Electric and Magnetic Field Measurement Methods.
PB95-161675 *04,423*

Optically Linked Three-Loop Antenna System for Determining the Radiation Characteristics of an Electrically Small Source.
PB95-161915 *02,005*

Kinetic-Energy Distributions of Ions Sampled from Argon Plasmas in a Parallel-Plate, Radio-Frequency Reference Cell.
PB95-161964 *03,935*

Broadband Mismatch Error in Noise Measurement Systems.
PB95-162061 *02,044*

Diffusion of Copper into Gold Plating.
PB95-162152 *00,957*

Condensed Catalogue of Electromagnetic Environment Measurements, 30 - 300 Hz.
PB95-162210 *01,899*

Importance of Unraveling Memory Propagation Effects in Interpreting Data on Partial Discharge Statistics.
PB95-163572 *01,901*

Nonstationary Behavior of Partial Discharge during Insulation Aging.
PB95-163580 *01,902*

Comparison of Three Techniques for the Precision Measurement of Amplifier Noise.
PB95-163663 *02,349*

Measurement Accuracies for Various Techniques for Measuring Amplifier Noise.
PB95-163671 *02,350*

Planar Resistors for Probe Station Calibration.
PB95-163697 *02,351*

Use of Ionospheric Data in GPS Time Transfer.
PB95-163853 *01,540*

Calibrating On-Wafer Probes to the Probe Tips.
PB95-163945 *02,352*

LRM Probe-Tip Calibrations with Imperfect Resistors and Lossy Lines.
PB95-163952 *02,353*

Verification of Scattering Parameter Measurements.
PB95-163960 *01,904*

Electrical Characterization of Radio-Frequency Discharges in the Gaseous Electronics Conference Reference Cell.
PB95-164612 *01,905*

Voltage Ratio Measurements of a Zener Reference Using a Digital Voltmeter.
PB95-164695 *01,906*

Tunable High Temperature Superconductor Microstrip Resonators.
PB95-168423 *02,048*

Multi-State Two-Port: An Alternative Transfer Standard.
PB95-168530 *02,049*

Revised Uncertainty Analysis for the NIST 30-MHz Attenuation Calibration System.
PB95-168761 *01,907*

Measurements of the Characteristic Impedance of Coaxial Air Line Standards.
PB95-168787 *02,221*

Observation of Vortex Dynamics in Two-Dimensional Josephson-Junction Arrays.
PB95-168811 *02,050*

Relationship of AM to PM Noise in Selected RF Oscillators.
PB95-169009 *02,262*

Self Calibrating Fiber Optic Sensors: Potential Design Methods.
PB95-169306 *02,173*

Electronics and Electrical Engineering Laboratory Technical Progress Bulletin Covering Laboratory Programs, July to September 1994 with 1994/1995 EEEL Events Calendar.
PB95-170395 *02,360*

Gradiometer Antennas for Detection of Long Subsurface Conductors.
PB95-175667 *01,862*

Aperture Excitation of Electrically Large, Lossy Cavities.
PB95-175675 *00,031*

Phase Locking in Two-Junction Systems of High-Temperature Superconductor-Normal Metal-Superconductor Junctions.
PB95-176053 *02,060*

On-Wafer Impedance Measurement on Lossy Substrates.
PB95-176285 *02,365*

Electronic Mode Stirring for Reverberation Chambers.
PB95-180329 *01,908*

Crosstalk between Microstrip Transmission Lines. (NIST Reprint).
PB95-180337 *02,225*

Dual Frequency mm-Wave Radiometer Antenna for Airborne Remote Sensing of Atmosphere and Ocean.
PB95-180378 *02,006*

Large-Amplitude Shapiro Steps and Self-Field Effects in High-Tc Josephson Weak Links.
PB95-180410 *04,682*

Dielectric Properties of Single Crystals of Al2O3, LaAlO3, SrTiO3, and MgO at Cryogenic Temperatures.
PB95-180477 *02,266*

Physics and Chemistry of Partial Discharge and Corona: Recent Advances and Future Challenges.
PB95-181046 *01,910*

Practical Standards for PM and AM Noise at 5, 10 and 100 MHz.
PB95-181129 *01,546*

Assessment of Data by a Second-Order Transfer Function.
PB95-182390 *03,760*

Evaluation of the Economic Impacts Associated with the NIST Power and Energy Calibration Services.
PB95-188850 *02,461*

10 kV DC Resistive Divider Calibration.
PB95-198685 *02,063*

Electromagnetic Shielding Characterization of Gaskets.
PB95-198917 *01,911*

Electronics and Electrical Engineering Laboratory Technical Publication Announcements Covering Laboratory Programs, July to September 1994 with 1995 EEEL Events Calendar.
PB95-198925 *01,912*

Method to Determine the Calorimetric Equivalence Correction for a Coaxial Microwave Microcalorimeter.
PB95-202404 *01,913*

Developing a NIST Coaxial Microwave Power Standard at 1 mW.
PB95-202412 *01,914*

Dielectric Properties of Materials at Cryogenic Temperatures and Microwave Frequencies.
PB95-202610 *02,369*

Casual Regularizing Deconvolution Filter for Optimal Waveform Reconstruction.
PB95-203089 *01,603*

Integral Occurring in Coherence Theory.
PB95-203550 *04,324*

Proposed Analysis of RCS Measurement Uncertainty.
PB95-203568 *01,871*

Accurate Measurement of Optical Detector Nonlinearity.
PB95-203576 *02,181*

Droplet Transfer Modes for a MIL 100S-1 GMAW Electrode.
PB95-209300 *02,867*

Electronics and Electrical Engineering Laboratory Technical Progress Bulletin Covering Laboratory Programs, January to March 1992, with 1992/1993 EEEL Events Calendar.
PB95-210480 *01,917*

Polarimetric Calibration of Reciprocal-Antenna Radars.
PB95-216925 *01,872*

Electronics and Electrical Engineering Laboratory Technical Publication Announcements Covering Laboratory Programs, January to March 1995 with 1995 EEEl Events Calendar.
PB95-242277 *02,373*

SF6 Insulation: Possible Greenhouse Problems and Solutions.
PB95-251625 *02,269*

Low-Frequency Model for Radio-Frequency Absorbers.
PB95-261939 *04,424*

Using Quantized Breakdown Voltage Signals to Determine the Maximum Electric Fields in a Quantum Hall Effect Sample.
PB95-261947 *02,375*

Standard Antennas for Electromagnetic Interference Measurements and Methods to Calibrate Them.
PB96-102561 *02,007*

Comments on 'Conversions between S, Z, Y, h, ABCD, and T Parameters Which Are Valid for Complex Source and Load Impedances'.
PB96-102785 *02,069*

Effect of Electrode Material on Measured Ion Energy Distributions in Radio-Frequency Discharges.
PB96-102850 *04,026*

Ion Kinetic-Energy Distributions and Balmer-alpha (Halpha) Excitation in Ar-H2 Radio-Frequency Discharges.
PB96-102959 *04,029*

Time Generation and Distribution.
PB96-103049 *01,550*

Digital Impedance Bridge.
PB96-103155 *02,272*

Spherical-Wave Source-Scattering Matrix Analysis of Antennas and Antenna-Antenna Interactions.
PB96-111166 *02,008*

Relative Accuracy of Isolated and Unisolated Noise Comparison Radiometers.
PB96-111851 *01,924*

Measurements of Permittivity and the Dielectric Loss Tangent of Low Loss Dielectric Materials with a Dielectric Resonator Operating on the Higher Order Te(sub 0 gamma delta) Modes.
PB96-111869 *02,273*

Kinetic Energy Distribution of Ions Produced from Townsend Discharges in Neon and Argon.
PB96-111927 *04,413*

Uncertainties of the NIST Coaxial Noise Calibration System.
PB96-111984 *02,070*

Distribution of Dielectric Relaxation Times and the Moment Problem.
PB96-112032 *04,727*

Continuous Recording and Stochastic Analysis of PD.
PB96-112156 *01,925*

Binary versus Decade Inductive Voltage Divider Comparison and Error Decomposition.
PB96-112263 *02,071*

Surging the Upside-Down House: Looking into Upsetting Reference Voltages.
PB96-112313 *02,385*

Gaseous Electronics Conference RF Reference Cell: An Introduction.
PB96-113329 *02,387*

Studies of Ion Kinetic-Energy Distributions in the Gaseous Electronics Conference RF Reference Cell.
PB96-113360 *02,391*

Microwave Diagnostic Results from the Gaseous Electronics Conference RF Reference Cell.
PB96-113378 *02,392*

Two-Dimensional Self-Consistent Radio Frequency Plasma Simulations Relevant to the Gaseous Electronics Conference RF Reference Cell.
PB96-113436 *02,398*

Screened-Room Measurements on the NIST Spherical-Dipole Standard Radiator.
PB96-113568 *01,926*

Display-Measurement Round-Robin.
PB96-119227 *02,186*

Gaseous Dielectrics Research: Possible SF6 Substitutes.
PB96-119268 *02,228*

High-Temperature Superconductor Cryogenic Current Comparator.
PB96-119334 *02,074*

Perception of Clamp Noise in Television Receivers.
PB96-119433 *01,489*

Progress on the Quantized Hall Resistance Recommended Intrinsic/Derived Standards Practice.
PB96-122460 *02,403*

Standardised Computer Data File Format for Storage, Transport, and Off-Line Processing of Partial Discharge Data.
PB96-122486 *01,930*

Constant Temperature and Humidity Chamber for Standard Resistors.
PB96-122494 *02,275*

Programmable Guarded Coaxial Connector Panel.
PB96-122544 *02,108*

Microwave Characterization of Printed Circuit Transmission Lines.
PB96-122585 *02,077*

Modification of Cast Epoxy Resin Surfaces during Exposure to Partial Discharges.
PB96-122734 *01,086*

Influence of Surface Charge on the Stochastic Behavior of Partial Discharge in Dielectrics.
PB96-122767 *01,931*

Comment and Discussion on Digital Processing of PD Pulses.
PB96-122775 *01,932*

Electromagnetic Properties of Materials: The NIST Metrology Program.
PB96-122791 *01,933*

Open-Ended Coaxial Probes for Nondestructive Testing of Substrates and Circuit Boards.
PB96-122825 *02,078*

Bounds on Frequency Response Estimates Derived from Uncertain Step Response Data.
PB96-122874 *03,419*

Methods for Aligning the NIST Watt-Balance.
PB96-123153 *01,934*

Influence of Electrode Material on Measured Ion Kinetic-Energy Distributions in Radio-Frequency Discharges.
PB96-123179 *01,935*

Kinetic Energy Distributions of H(+), H2(+), and H3(+) from a Diffuse Townsend Discharge in H2 at High E/N.
PB96-123351 *04,415*

Fundamental Processes in Gas Discharges.
PB96-123450 *01,089*

Keeping Up with the Reality of Today's Surge Environment.
PB96-123633 *02,231*

Ion Kinetics and Symmetric Charge-Transfer Collisions in Low-Current, Diffuse (Townsend) Discharges in Argon and Nitrogen.
PB96-123658 *04,051*

Refraction of Light by Graded Birefringent Media.
PB96-123716 *02,192*

Kinetic-Energy Distributions of Ions Sampled from Radio-Frequency Discharges in Helium, Nitrogen, and Oxygen.
PB96-123732 *01,092*

Development of Near-Field Test Procedures for Communication Satellite Antennas.
PB96-135082 *02,010*

Analysis of an Open-Ended Coaxial Probe with Lift-Off for Nondestructive Testing.
PB96-135116 *01,940*

LRM Probe-Tip Calibrations Using Nonideal Standards.
PB96-135389 *02,411*

Electronics and Electrical Engineering Laboratory Technical Publication Announcements Covering Laboratory Programs, April to June 1995 with 1995 EEEL Events Calendar.
PB96-137187 *01,941*

Microwave Dielectric Properties of Anisotropic Materials at Cryogenic Temperatures.
PB96-137765 *02,412*

Accurate Computations of Radar Cross Sections of Simple Objects.
PB96-138474 *04,426*

Alternative Contour Technique for the Efficient Computation of the Effective Length of an Antenna.
PB96-141361 *02,011*

Electric Dipole Excitation of a Long Conductor in a Lossy Medium.
PB96-146675 *04,058*

Evidence for Inelastic Processes for N(+)3 and N(+)4 from Ion Energy Distributions in He/N2 Radio Frequency Glow Discharges.
PB96-146683 *04,059*

Comparison of k-Correction and Taylor-Series Correction for Probe-Position Errors in Planar Near-Field Scanning.
PB96-147137 *02,012*

Electronics and Electrical Engineering Laboratory Technical Progress Bulletin Covering Laboratory Programs, July to September 1995 with 1996 EEEL Events Calendar.
PB96-147905 *01,942*

Technical Impact of the NIST Calibration Service for Electrical Power and Energy.
PB96-147913 *02,462*

Partially Coherent Transmittance of Dielectric Lamellae.
PB96-148028 *04,359*

Accuracy in Time Domain Transmission Line Measurements.
PB96-148069 *04,060*

Spatial Correlation Function for Fields in a Reverberation Chamber.
PB96-148077 *04,427*

AC-DC Difference Characteristics of High-Voltage Thermal Converters.
PB96-148093 *02,083*

Performance of Multilayer Thin-Film Multijunction Thermal Converters.
PB96-148135 *02,084*

High-Speed Interconnection Characterization Using Time Domain Network Analysis.
PB96-148176 *04,061*

TEM/Reverberating Chamber Electromagnetic Radiation Test Facility at Rome Laboratory.
PB96-155023 *03,675*

Catalogue of Electromagnetic Environment Measurements, 30-300 Hz.
PB96-155452 *01,943*

Investigation of S2F10 Production and Mitigation in Compressed SF6- Insulated Power Systems.
PB96-155528 *02,468*

Precision Tests of a Quantum Hall Effect Device DC Equivalent Circuit Using Double-Series and Triple-Series Connections.
PB96-159256 *01,953*

Radiated Emissions and Immunity of Microstrip Transmission Lines: Theory and Measurements.
PB96-162649 *02,238*

Accurate Electrical Characterization of High-Speed Interconnections.
PB96-167143 *02,240*

Planar Near-Field Measurements and Microwave Holography for Measuring Aperture Distribution on a 60 GHz Active Array Antenna.
PB96-167366 *03,762*

NIST Measurement Assurance Program for Capacitance Standards at 1 kHz.
PB96-172333 *02,276*

Dimensional Characterization of Precision Coaxial Transmission Line Standards.
PB96-176482 *02,241*

Electrical Characteristics of Argon Radio Frequency Glow Discharges in an Asymmetric Cell.
PB96-176490 *04,109*

Implementation of a Standard Format for GPS Common View Data.
PB96-176581 01,555

Line-Reflect-Match Calibrations with Nonideal Microstrip Standards.
PB96-176599 02,242

Microwave Characterization of Flip-Chip MMIC Components.
PB96-176722 02,434

Evidence That Voltage Rather Than Resistance is Quantized in Breakdown of the Quantum Hall Effect.
PB96-179163 01,868

Surging the Upside-Down House: Measurements and Modeling Results.
PB96-180138 02,243

Complicated Cases and Shielded Rooms: Audiometric Booths Shielded to Attenuate Electromagnetic Interference.
PB96-180179 02,278

Electronics and Electrical Engineering Laboratory Technical Publication Announcements Covering Laboratory Programs, July to September 1995 with 1996 EEEL Events Calendar.
PB96-183066 01,965

Standard Source Method for Reducing Antenna Factor Errors in Shielded Room Measurements.
PB96-183157 02,013

Electrohydrodynamic Instability and Electrical Discharge Initiation in Hexane.
PB96-186119 02,244

Dielectric and Magnetic Measurements from -50C to 200C and in the Frequency Band 50 MHz to 2 GHz.
PB96-191382 02,245

Electronics and Electrical Engineering Laboratory Technical Progress Bulletin Covering Laboratory Programs, January to March 1996, with 1996 EEEL Events Calendar.
PB96-191390 01,969

Coaxial Line-Reflect-Match Calibration.
PB96-200118 02,246

Methodology for Electromagnetic Interference Measurements.
PB96-200126 02,014

Alternative EMC Compliance Test Facilities.
PB96-200324 02,247

Comparison of Ultralow-Sidelobe-Antenna Far-Field Patterns Using the Planar-Near-Field Method and the Far-Field Method.
PB96-200373 02,015

General Order 'N' Analytic Correction of Probe-Position Errors in Planar Near-Field Measurements.
PB96-200688 01,562

Polarimetric Calibration of Reciprocal-Antenna Radars.
PB96-200696 02,016

100 A, 100 kHz Transconductance Amplifier.
PB96-200936 02,098

Quantum Hall Effect-Based Resistance Standard (Quantum Hall Res).
PB96-200944 04,127

Electronics and Electrical Engineering Laboratory Technical Publication Announcements Covering Laboratory Programs, October to December 1995, with 1996 EEEL Events Calendar.
PB96-202346 01,978

Correlations between Electrical and Acoustic Detection of Partial Discharge in Liquids and Implications for Continuous Data Recording.
PB96-204490 02,248

Rapid Evaluation of Mode-Stirred Chambers Using Impulsive Waveforms.
PB96-210026 01,979

Bibliography of the NIST Electromagnetic Fields Division Publications.
PB96-210778 01,980

Electronics and Electrical Engineering Laboratory Technical Publication Announcements Covering Laboratory Programs, January to March 1996, with 1996 EEEL Events Calendar.
PB96-214622 01,981

NIST High-Accuracy Sampling Wattmeter.
PB97-108575 02,689

Causality and Maxwell's Equations.
PB97-110522 04,429

Point Charges, Radiation Reaction, and Quantum Mechanics.
PB97-110563 04,139

Quantum Conductance Fluctuations in the Larger-Size-Scale Regime.
PB97-111264 04,144

Proposed Tests to Evaluate the Frequency-Dependent Capacitor Ratio for Single Electron Tunneling Experiment.
PB97-111454 01,982

Uncertainties of Frequency Response Estimates Derived from Responses to Uncertain Step-Like Inputs.
PB97-111843 01,984

Resistors.
PB97-111876 02,284

Loading Effects in Resistance Scaling.
PB97-111884 02,285

Low Thermal Guarded Scanner for High Resistance Measurement Systems.
PB97-112452 02,288

Exploring the Low-Frequency Performance of Thermal Converters Using Circuit Models and a Digitally Synthesized Source.
PB97-112551 02,848

Low Voltage Standards in the 10 Hz to 1 MHz Range.
PB97-112569 02,100

Wideband Sampling Voltmeter.
PB97-113039 01,990

DC-MHz Wattmeter Based on RMS Voltage Measurements.
PB97-113211 01,992

Magnetometer Calibration Services.
PB97-113252 01,993

Results of Capacitance Ratio Measurements for the Single Electron Pump-Capacitor Charging Experiment.
PB97-113286 04,813

Electronics and Electrical Engineering Laboratory Technical Progress Bulletin Covering Laboratory Programs, April to June 1996 with 1996-1998 EEEL Events Calendar.
PB97-113880 01,994

Metrology for Electromagnetic Technology: A Bibliography of NIST Publications.
PB97-116057 04,396

Conversion of a 2-Terminal-Pair Bridge to a 4-Terminal-Pair Bridge for Increased Range and Precision in Impedance Measurements.
PB97-119176 02,103

NIST Comparison of the Quantized Hall Resistance and the Realization of the SI Ohm Through the Calculable Capacitor. Conference Proceedings, June 17-20, 1996.
PB97-119192 02,292

Active High Voltage Divider with 20-PPM Uncertainty.
PB97-119317 02,104

NIST Watt Experiment: Monitoring the Kilogram.
PB97-122329 01,997

ELECTROMAGNETIC NOISE

Terminal Invariant Description of Amplifier Noise.
PB95-153573 02,043

Relationship of AM to PM Noise in Selected RF Oscillators.
PB95-169009 02,262

Investigations of AM and PM Noise in X-Band Devices.
PB95-180022 02,062

Secondary Standard for PM and AM Noise at 5, 10, and 100 MHz.
PB96-123187 01,554

Origin of I/f PM and AM Noise in Bipolar Junction Transistor Amplifiers.
PB96-200787 02,096

Reducing the 1/f AM and PM Noise in Electronics for Precision Frequency Metrology.
PB97-113195 02,102

ELECTROMAGNETIC NOISE MEASUREMENT

Broadband Mismatch Error in Noise Measurement Systems.
PB95-162061 02,044

Comparison of Three Techniques for the Precision Measurement of Amplifier Noise.
PB95-163663 02,349

Measurement Accuracies for Various Techniques for Measuring Amplifier Noise.
PB95-163671 02,350

Radiometer Equation for Noise Comparison Radiometers.
PB96-140363 02,195

ELECTROMAGNETIC PROPERTIES

Substrate and Thin Film Measurements.
PB96-112297 02,384

Electromagnetic Properties of Materials: The NIST Metrology Program.
PB96-122791 01,933

NIST Metrology Program on Electromagnetic Characterization of Materials.
PB96-156062 01,944

ELECTROMAGNETIC SCATTERING

Time-Domain Measurements of the Electromagnetic Backscatter of Pyramidal Absorbers and Metallic Plates.
PB94-185410 01,877

Electromagnetic Scattering by a Periodic Surface with a Wedge Profile.
PB94-211950 04,421

Alternative Single Integral Equation for Scattering by a Dielectric.
PB94-216512 04,422

Comments on 'Protecting EFIE-Based Scattering Computations from Effects of Internal Resonances'.
PB95-161568 01,898

Study of Multiple Scattering Background in Compton Scatter Imaging.
PB96-112222 04,425

Hypersingular Single Integral Equation and the Dielectric Wedge.
PB97-110274 04,428

Causality and Maxwell's Equations.
PB97-110522 04,429

Electromagnetic Scattering from a Dielectric Wedge and the Single Hypersingular Integral Equation.
PB97-110530 04,430

Numerical Evaluation of Hypersingular Integrals for Scattering by a Dielectric Wedge.
PB97-110555 02,017

Sinusoidal Surfaces as Standards for BRDF Instruments.
PB97-110597 04,388

Numerical Reference Models for Optical Metrology Simulation.
PB97-111330 04,392

ELECTROMAGNETIC SHIELDING

Aperture Excitation of Electrically Large, Lossy Cavities.
PB94-145711 00,029

Measurements of Shielding Effectiveness and Cavity Characteristics of Airplanes.
PB94-210051 00,030

Aperture Coupling to a Coaxial Air Line: Theory and Experiment.
PB94-211968 02,216

Aperture Excitation of Electrically Large, Lossy Cavities.
PB95-175675 00,031

Electromagnetic Shielding Characterization of Gaskets.
PB95-198917 01,911

Band-Limited, White Gaussian Noise Excitation for Reverberation Chambers and Applications to Radiated Susceptibility Testing.
PB96-165410 01,960

Complicated Cases and Shielded Rooms: Audiometric Booths Shielded to Attenuate Electromagnetic Interference.
PB96-180179 02,278

ELECTROMAGNETIC SUSCEPTIBILITY

Band-Limited, White Gaussian Noise Excitation for Reverberation Chambers and Applications to Radiated Susceptibility Testing.
PB96-165410 01,960

ELECTROMAGNETIC TESTING

TEM/Reverberating Chamber Electromagnetic Radiation Test Facility at Rome Laboratory.
PB96-155023 03,675

ELECTROMAGNETIC THEORY

Effective Medium Theory for Ferrite-Loaded Materials.
PB95-154662 01,893

ELECTROMANGETIC ACOUSTIC TRANSDUCERS

Methods to Improve the Accuracy of On-Line Ultrasonic Measurement of Steel Sheet Formability.
PB96-186051 02,281

ELECTROMECHANICAL DEVICES

Test Structures for Determining Design Rules for Microelectromechanical-Based Sensors and Actuators.
PB95-150488 02,105

ELECTROMECHANICS

Electromechanical Properties of Superconductors for DOE Fusion Applications.
PB94-139672 02,250

ELECTROMETERS

Cryogenic Precision Capacitance Bridge Using a Single Electron Tunneling Electrometer.
PB95-126074 04,529

Noise in the Coulomb Blockade Electrometer.
PB95-176327 04,670

Cryogenic Precision Capacitance Bridge Using a Single Electron Tunneling Electrometer.
PB96-112271 02,072

ELECTRON-ATOM COLLISIONS

Determination of Atomic Data Pertinent to the Fusion Energy Program. Progress Report for FY 92.
DE94004400 04,402

Electron-atom collision studies using optically state selected beams. Progress report, May 15, 1987--May 14, 1988.
DE95004446 03,776

Electron-@tom collision studies using optically state selected beams. Progress report, May 15, 1988--May 14, 1991.
DE95004447 03,777

Can Quantum Mechanical Description of Electron-Sodium Collisions Be Considered Complete. Present Status and Future Prospects for 3s <-> 3p Transitions.
PB94-185014 00,768

Low-Energy Electron Scattering from Caesium Atoms: Comparison of a Semirelativistic Breit-Pauli and a Full Relativistic Direc Treatment.
PB94-185030 00,769

Angular Distributions for Near-Threshold (e,2e) Processes for Li and Mg.
PB94-185725 00,778

Characteristics of Light Emission After Low-Energy Electron Impact Excitation of Caesium Atoms.
PB94-198587 03,806

Determination of Complex Scattering Amplitudes in Low-Energy Elastic Electron-Sodium Scattering.
PB94-216652 03,869

Relativistic Effects in Spin-Polarization Parameters for Low-Energy Electron-Cs Scattering.
PB95-150868 03,901

High-Precision Calculations of Cross Sections for Low-Energy Electron Scattering by Ground and Excited State of Sodium.
PB95-152161 *03,914*

Semiclassical Explanation of the Generalized Ramsauer-Townsend Minima in Electron-Atom Scattering.
PB95-153532 *03,925*

Spin-Resolved Elastic Scattering of Electrons from Sodium.
PB95-161774 *03,933*

Connection between Superelastic and Inelastic Electron-Atom Collisions Involving Polarized Collision Partners.
PB95-202297 *03,974*

Threshold Electron Excitation of Na.
PB95-202917 *03,994*

Charge Cloud Distribution of Heavy Atoms After Excitation by Polarized Electrons.
PB95-203147 *04,001*

Angle-Differential and Momentum-Transfer Cross Sections for Low-Energy Electron-Cs Scattering.
PB95-203402 *04,005*

Relativistic R-Matrix Calculations for Electron - Alkali-Metal-Atom Scattering: Cs as a Test Case.
PB95-203410 *04,006*

Low-Energy-Electron Collisions with Sodium: Elastic and Inelastic Scattering from the Ground State.
PB96-103106 *04,030*

ELECTRON ATTACHMENT

Associative Electron Attachment to S2F10, S2OF10, and S2O2F10.
PB95-140992 *00,907*

Electron Attachment to Excited Molecules(1).
PB96-122809 *01,087*

Dependence of the Thermal Electron Attachment Rate Constant in Gases and Liquids on the Energy Position of the Electron Attaching State.
PB97-122253 *01,996*

ELECTRON-BEAM HEATING

Closed Loop Controller for Electron-Beam Evaporators.
PB97-111470 *04,393*

ELECTRON BEAM ION TRAP (EBIT)

Observation and Visible and uv Magnetic Dipole Transitions in Highly Charged Xenon and Barium.
PB96-138441 *04,056*

Polarization Measurements on a Magnetic Quadrupole Line in Ne-Like Barium.
PB97-113104 *04,161*

ELECTRON BEAMS

New Method for Shielding Electron Beams Used for Head and Neck Cancer Treatment.
PB94-211430 *03,621*

Crystal Structure of Annealed and As-Prepared HgBa2CaCu2O6+delta Superconductors.
PB95-161105 *03,927*

Angular Variation of the Personal Dose Equivalent, Hp(0.07), for Beta Radiation and Nearly Monoenergetic Electron Beams: Preliminary Results.
PB95-168472 *03,630*

Planar Lenses for Field-Emitter Arrays.
PB96-103064 *02,112*

Calorimeters for Calibration of High-Dose Dosimeters in High-Energy Electron Beams.
PB96-135272 *04,055*

Journal of Research of the National Institute of Standards and Technology, January/February 1996. Volume 101, Number 1.
PB96-175666 *00,113*

ELECTRON CAPTURE

Dielectronic Capture Processes in the Electron-Impact Ionization of Sc(2+).
PB95-203113 *04,000*

ELECTRON CAPTURE DECAY

Alpha-Particle and Electron Capture Decay of (209)Po.
PB96-186085 *04,119*

ELECTRON CHARGE

Cryogenic Precision Capacitance Bridge Using a Single Electron Tunneling Electrometer.
PB95-126074 *04,529*

ELECTRON CLOUDS

Electrostatic Modes as a Diagnostic in Penning-Trap Experiments.
PB95-176244 *03,959*

ELECTRON COLLISIONS

Calculations of Electron Inelastic Mean Free Paths. 5. Data for 14 Organic Compounds over the 50-2000 eV Range.
PB95-150355 *00,916*

Calculations of Electron Inelastic Mean Free Paths (IMFPs). 4. Evaluation of Calculated IMFPs and of the Predictive IMFP Formula TPP-2 for Electron Energies between 50 and 2000 eV.
PB95-150728 *00,922*

ELECTRON CONFIGURATION

Designations of ds(2)p Energy Levels in Neutral Zirconium, Hafnium, and Rutherfordium (Z=104).
PB96-180120 *04,116*

ELECTRON CORRELATION

Relativistic Modifications of Charge Expansion Theory.
PB96-123799 *04,052*

ELECTRON DENSITY

Cooper M(sub II,III) X-ray-Emission Spectra of Copper Oxides and the Bismuth Cuprate Superconductor.
PB96-158027 *04,077*

ELECTRON DENSITY (CONCENTRATION)

Construction of Maximum-Entropy Density Maps, and Their Use in Phase Determination and Extension.
PB95-108593 *00,882*

ELECTRON DETACHMENT

Resonant Two-Color Detachment of H(-) with Excitation of H(n=2).
PB95-202552 *03,984*

Short-Pulse Detachment of H(-) in the Presence of a Static Electric Field.
PB95-203477 *04,007*

ELECTRON DIFFUSION CONSTANT

Measurement of the Weak-Localization Complex Conductivity at 1 Ghz in Disordered Ag Wires.
PB96-117239 *04,731*

ELECTRON DOSIMETRY

Electron and Proton Dosimetry with Custom-Developed Radiochromic Dye Films.
PB95-151106 *03,713*

Calibration of Dosimeters for the Cryogenic Irradiation of Composite Materials Using an Electron Beam.
PB95-180964 *03,968*

ELECTRON-ELECTRON INTERACTIONS

Electron-electron Interactions, Coupled-Plasmon-Phonon Modes, and Mobility in n-Type GaAs.
PB96-138524 *04,749*

ELECTRON-ION COLLISIONS

Determination of Atomic Data Pertinent to the Fusion Energy Program. Progress Report for FY 92.
DE94004400 *04,402*

Electron-Impact Ionization of In(+) and Xe(+).
PB94-185089 *00,770*

Backscattering in Electron-Impact Excitation of Multiply Charged Ions.
PB94-185345 *03,799*

Absolute Cross-Section Measurements for Electron-Impact Ionization of C1(+1).
PB94-199841 *03,818*

Evidence for Significant Backscattering in Near-Threshold Electron-Impact Excitation of Ar(7+)(3s yields 3p).
PB95-126405 *03,883*

Electron-Impact Excitation of Si(3+)(3S yields 3P) Using a Merged-Beam Electron-Energy-Loss Technique.
PB95-151239 *03,904*

Electron-Impact Ionization of In(+) and Xe(+).
PB95-152906 *03,918*

Resonance Structure and Absolute Cross Sections in Near-Threshold Electron-Impact Excitation of the 4s(2)(1)S yields 4s4p (3)P Intercombination Transition in Kr(6+).
PB95-202271 *03,972*

Absolute Cross-Section Measurements for Electron-Impact Single Ionization of Se(+) and Te(+).
PB95-202503 *03,980*

Crossed-Beams Measurements of Absolute Cross Sections for Electron Impact Ionization of S(+).
PB95-202511 *03,981*

Absolute Cross Sections for Electron-Impact Single Ionization of Si(+) and Si(2+).
PB95-202529 *03,982*

Dielectronic Capture Processes in the Electron-Impact Ionization of Sc(2+).
PB95-203113 *04,000*

Electron-Ion Collisions in the Plasma Edge.
PB96-111885 *04,037*

Collisions of Electrons with Highly-Charged Ions.
PB96-200340 *04,791*

ELECTRON-ION COUPLING

Merged-Beams Energy-Loss Technique for Electron-Ion Excitation: Absolute Total Cross Sections for O(5+) (2s yields 2p).
PB96-102058 *04,017*

ELECTRON MICROPROBE ANALYSIS

Study of Diffusion Zones with Electron Microprobe Compositional Mapping.
PB94-216348 *00,559*

ELECTRON MICROSCOPES

Surface Magnetic Microstructural Analysis Using Scanning Electron Microscopy with Polarization Analysis (SEMPA).
PB95-162657 *03,938*

Fabrication Issues for the Prototype National Institute of Standards and Technology SRM 2090A Scanning Electron Microscope Magnification Calibration Standard.
PB96-160585 *01,131*

Scanning Electron Microscope Magnification Calibration Interlaboratory Study.
PB96-201082 *01,164*

ELECTRON MICROSCOPY

Characterization of the Binding of Gallium, Platinum, and Uranium to Pseudomonas Fluorescens by Small-Angle X-ray Scattering and Transmission Electron Microscopy.
PB94-172509 *03,453*

Domain Structures in Magnetoresistive Granular Metals.
PB96-141346 *04,760*

ELECTRON MOBILITY

Majority and Minority Mobilities in Heavily Doped Silicon for Device Simulations.
PB94-198728 *02,311*

Majority and Minority Electron and Hole Mobilities in Heavily Doped Gallium Aluminum Arsenide.
PB97-118335 *04,814*

ELECTRON-MOLECULE COLLISIONS

Associative Electron Attachment to S2F10, S2OF10, and S2O2F10.
PB95-140992 *00,907*

Electron Scattering and Dissociative Attachment by SF6 and Its Electrical-Discharge By-Products.
PB95-151288 *02,256*

Analyses of Recent Experimental and Theoretical Determinations of e-H2 Vibrational Excitation Cross Sections: Assessing a Long-Standing Controversy.
PB95-202438 *03,977*

Modified Effective Range Theory as an Alternative to Low-Energy Close-Coupling Calculations.
PB95-202701 *03,988*

Slow-Electron Collisions with CO Molecules in an Exact-Exchange Plus Parameter-Free Polarization Model.
PB95-202719 *03,989*

Importance of Bound-Free Correlation Effects for Vibrational Excitation of Molecules by Electron Impact: A Sensitivity Analysis.
PB95-202974 *03,996*

ELECTRON PARAMAGNETIC RESONANCE

Inter-Laboratory Trials of the EPR Method for the Detection of Irradiated Meats Containing Bone.
PB96-161690 *00,042*

ELECTRON PROBE MICROANALYSIS

Design of a Protocol for an Electron Probe Microanalyzer k-Value Round Robin.
PB95-107181 *00,564*

ELECTRON PROBES

Electron Probe X-Ray Microanalysis.
PB95-107165 *00,562*

ELECTRON PROCESSORS

Real Time Monitoring of Electron Processors.
PB96-135306 *03,719*

ELECTRON PUMPS

Metrological Accuracy of the Electron Pump.
PB95-168910 *03,951*

Testing for Metrological Accuracy of the Electron Pump.
PB95-175873 *04,663*

Accuracy of the Electron Pump.
PB96-135223 *04,743*

Performance of the Electron Pump with Stray Capacitances.
PB96-200902 *01,976*

ELECTRON SCATTERING

Inelastic Interactions of Electrons with Surfaces: Application to Auger-Electron Spectroscopy and X-ray Photoelectron Spectroscopy.
PB94-172699 *00,764*

Evidence for Significant Backscattering in Near-Threshold Electron-Impact Excitation of Ar(7+)(3s yields 3p).
PB95-126405 *03,883*

Calculations of Electron Inelastic Mean Free Paths. 5. Data for 14 Organic Compounds over the 50-2000 eV Range.
PB95-150355 *00,916*

Calculations of Electron Inelastic Mean Free Paths (IMFPs). 4. Evaluation of Calculated IMFPs and of the Predictive IMFP Formula TPP-2 for Electron Energies between 50 and 2000 eV.
PB95-150728 *00,922*

Relativistic Effects in Spin-Polarization Parameters for Low-Energy Electron-Cs Scattering.
PB95-150868 *03,901*

Electron Scattering and Dissociative Attachment by SF6 and Its Electrical-Discharge By-Products.
PB95-151288 *02,256*

High-Precision Calculations of Cross Sections for Low-Energy Electron Scattering by Ground and Excited State of Sodium.
PB95-152161 *03,914*

Elastic-Electron-Scattering Effects on Angular Distributions in X-ray Photoelectron Spectroscopy.
PB95-175758 *01,000*

Total-Dielectric-Function Approach to Electron and Phonon Response in Solids.
PB96-102884 *01,067*

Intensity-Dependent Scattering Rings in High Order Above-Threshold Ionization.
PB96-110739 *04,032*

Electron-electron Interactions, Coupled-Plasmon-Phonon Modes, and Mobility in n-Type GaAs.
PB96-138524 *04,749*

ELECTRON SCREENING

Electron Screening Correction to the Self Energy in High-Z Atoms.
PB94-172376 *03,789*

ELECTRON SPECTROMETERS
Electron-Ion-X-ray Spectrometer System.
PB95-176137 *03,958*

ELECTRON SPECTROSCOPY
Compositional Analyses of Surfaces and Thin Films by Electron and Ion Spectroscopies.
PB94-185790 *00,779*

ELECTRON SPIN POLARIZATION
Relativistic Effects in Spin-Polarization Parameters for Low-Energy Electron-Cs Scattering.
PB95-150868 *03,901*

ELECTRON SPIN RESONANCE
Experimental assessment of absorbed dose to mineralized bone tissue from internal emitters: An electron paramagnetic resonance study.
DE96007979 *03,614*

ESR-Based Analysis in Radiation Processing.
PB95-161634 *03,931*

ELECTRON STATES
Self-Consistent 'GW' and Higher-Order Calculations of Electron States in Metals.
PB97-119341 *01,189*

ELECTRON STRUCTURE
Soft-X-ray-Emission Spectra of Solid Kr and Xe.
PB96-157920 *04,070*

ELECTRON TEMPERATURE
Self-Heating in the Coulomb-Blockade Electrometer.
PB94-212685 *04,507*

ELECTRON TRANSFER
Electron Transfer Reaction Rates and Equilibria of the Carbonate and Sulfate Radical Anions.
PB94-212180 *00,829*

Solvent Effects in the Reactions of Peroxyl Radicals with Organic Reductants. Evidence for Proton Transfer Mediated Electron Transfer.
PB95-107157 *00,873*

ELECTRON TRANSITIONS
Resonance Enhanced Multiphoton Ionization Detection of GeF and GeCl Radicals.
PB94-212123 *00,825*

Experimental and Abinitio Studies of Electronic Structures of the CCl3 Radical and Cation.
PB94-212131 *00,826*

Multiphoton Ionization of SiH3 and SiD3 Radicals. 2. Three Photon Resonance-Enhanced Spectra Observed between 460 and 610 nm.
PB94-212487 *00,835*

New Electronic States of NH and ND Observed from 258 to 288 nm by Resonance Enhanced Multiphoton Ionization Spectroscopy.
PB94-212495 *00,836*

Multiphoton Ionization of SiH3 and SiD3 Radicals: Electronic Spectra, Vibrational Analyses of the Ground and Rydberg States, and Ionization Potential.
PB94-212503 *00,837*

ELECTRON TRANSPORT
Buffer Layer Modulation-Doped Field-Effect-Transistor Interactions in the Al0.33Ga0.67As/GaAs Superlattice System.
PB96-102876 *02,380*

ELECTRON TRAPS
Evidence for a Deep Electron Trap and Charge Compensation in Separation by Implanted Oxygen Oxides.
PB95-175337 *02,362*

Electron and Hole Trapping in Irradiated SIMOX, ZMR and BESOI Buried Oxides.
PB96-160320 *01,956*

ELECTRON TUNNELING
Modified Airy Function Method for the Analysis of Tunneling Problems in Optical Waveguides and Quantum Well Structures.
PB94-185824 *02,120*

Insulating Boundary Layer and Magnetic Scattering in YBa2Cu3O7-delta/Ag Interfaces Over a Contact Resistivity Range of 10(-8) - 10(-3) Omega cm(2).
PB95-169157 *04,648*

Thermal Enhancement of Cotunneling in Ultra-Small Tunnel Junctions.
PB95-175436 *04,658*

Application of Single Electron Tunneling: Precision Capacitance Ratio Measurements.
PB96-102157 *04,703*

Results of Capacitance Ratio Measurements for the Single Electron Pump-Capacitor Charging Experiment.
PB97-113286 *04,813*

ELECTRON TUNNELING SPECTROSCOPY
Tunneling Spectroscopy of Thallium-Based High-Temperature Superconductors.
PB95-161709 *04,606*

ELECTRON WITHDRAWING GROUPS
Carbon Acidities of Aromatic Compounds. 1. Effects of In-Ring Aza and External Electron-Withdrawing Groups.
PB94-216595 *00,860*

ELECTRONIC ACCESS PROJECT
Electronic Access: Blueprint for the National Archives and Records Administration.
PB95-219218 *02,731*

ELECTRONIC BALANCES
Electronic Balance and Some Gravimetric Applications. (The Density of Solids and Liquids, Pycnometry and Mass).
PB94-163052 *03,785*

ELECTRONIC BEAMS
Theory of Electron Beam Moire.
PB96-175690 *04,373*

ELECTRONIC CIRCUITS
Simulating the Dynamic Electro Thermal Behavior of Power Electronic Circuits and Systems.
PB95-161014 *02,345*

Thermal Component Models for Electro-Thermal Network Simulation.
PB95-161022 *02,346*

ELECTRONIC COMMERCE
Planning the Infrastructure for Global Electronic Commerce.
PB94-185832 *00,494*

Analyzing Electronic Commerce.
PB94-219102 *00,480*

ELECTRONIC DATA EXCHANGE
Guidelines for the Evaluation of Electronic Data Interchange Products.
PB96-172325 *01,506*

ELECTRONIC DATA INTERCHANGE
Federal Implementation Guideline for Electronic Data Interchange: ASC X12 003040 Transaction Set 838 Trading Partner Profile (Vendor Registration), Implementation Convention.
PB96-112651 *03,674*

Federal Implementation Guideline for Electronic Data Interchange. ASC X12 003050 Transaction Set 850 Award Instrument. Implementation Convention.
PB96-114913 *01,814*

Federal Implementation Guideline for Electronic Data Interchange. ASC X12 003050 Transaction Set 860 Modifications to Award Instrument. Implementation Convention.
PB96-114921 *01,815*

Federal Implementation Guideline for Electronic Data Interchange. ASC X12 003050 Transaction Set 843 Response to Request for Quotation. Implementation Convention.
PB96-168984 *01,822*

Federal Implementation Guideline for Electronic Data Interchange. ASC X12 003050 Transaction Set 855 Purchase Order Acknowledgment: Implementation Convention.
PB96-172374 *01,823*

Federal Implementation Guideline for Electronic Data Interchange. ASC X12 003050 Transaction Set 840 Request for Quotation. Implementation Convention.
PB96-172531 *01,824*

Federal Implementation Guideline for Electronic Data Interchange: ASC X12 003050 Transaction Set 836 Procurement Notices. Implementation Convention.
PB96-178892 *01,827*

ELECTRONIC EQUIPMENT
Handbook Preferred Circuits Navy Aeronautical Electronic Equipment. Supplement Number 3.
AD-A278 782/8 *00,026*

Handbook Preferred Circuits Navy Aeronautical Electronic Equipment. Supplement Number 2.
AD-A278 783/6 *00,027*

Handbook Preferred Circuits Navy Aeronautical Electronic Equipment. Supplement Number 1.
AD-A278 784/4 *00,028*

Application of the Electronic Balance in High Precision Pycnometry.
PB94-187564 *00,534*

Important Link in Entire-House Protection: Surge Reference Equalizers.
PB94-216504 *02,219*

NIST Strategies for Reducing Testing Requirements.
PB95-180444 *01,909*

Surging the Upside-Down House: Looking into Upsetting Reference Voltages.
PB96-112313 *02,385*

Beyond the Technology Roadmaps: An Assessment of Electronic Materials Research and Development.
PB96-165998 *01,961*

Empirical Linear Prediction Applied to a NIST Calibration Service.
PB97-112353 *02,287*

ELECTRONIC INDUSTRY
Electronics and Electrical Engineering Laboratory: 1996 Program Plan. Supporting Technology for U.S. Competitiveness in Electronics.
PB96-175237 *01,962*

ELECTRONIC MAIL
Good Security Practices for Electronic Commerce, Including Electronic Data Interchange.
PB94-139045 *01,463*

ELECTRONIC PACKAGING
Metrology and Data for Microelectronic Packaging and Interconnection: Results of a Joint Workshop on Materials Metrology and Data for Commercial Electrical and Optical Packaging and Interconnection Technologies. Held in Gaithersburg, Maryland on May 5-6, 1994. Volume 1. Results.
PB95-143111 *02,328*

Metrology and Data for Microelectronic Packaging and Interconnection: Results of a Joint Workshop on Materials Metrology and Data for Commercial Electrical and Optical Packaging and Interconnection Technologies. Held in Gaithersburg, Maryland on May 5-6, 1994. Volume 2. Presentation Material.
PB95-143327 *02,330*

Electronics Packaging Materials Research at NIST.
PB96-122692 *02,405*

Natural Convection from an Array of Electronic Packages Mounted on a Horizontal Board in a Narrow Aspect Ratio Enclosure.
PB96-164017 *02,087*

Measurements of Properties of Materials in Electronic Packaging.
PB96-200837 *01,973*

Overview of U.S. Government Advanced Packaging Programs.
PB96-200845 *02,443*

NIST/NCMS Program on Electronic Packaging: First Update.
PB96-204086 *03,008*

ELECTRONIC SECURITY
Computer Virus Attacks.
PB95-163655 *01,715*

EDI and EFT Security Standards.
PB96-122833 *01,605*

Computer Security: An Introduction to Computer Security. The NIST Handbook.
PB96-131610 *01,608*

Assessing Functional Diversity by Program Slicing.
PB96-160890 *03,734*

Predicate Differences and the Analysis of Dependencies in Formal Specifications.
PB96-160940 *01,759*

Technique for Analyzing the Effects of Changes in Formal Specifications.
PB96-160957 *01,760*

Information Technology Standards in Federal Acquisitions.
PB96-161252 *01,636*

Using Information Technology Standards in Federal Acquisitions.
PB96-161260 *01,637*

Control and Instrumentation: Standards for High-Integrity Software.
PB96-161369 *03,736*

ELECTRONIC SPECTRA
New Rydberg States of Aluminum Monofluoride Observed by Resonance-Enhanced Multiphoton Ionization Spectroscopy.
PB94-199544 *00,797*

Resonance Enhanced Multiphoton Ionization Detection of GeF and GeCl Radicals.
PB94-212123 *00,825*

Experimental and Abinitio Studies of Electronic Structures of the CCl3 Radical and Cation.
PB94-212131 *00,826*

Multiphoton Ionization of SiH3 and SiD3 Radicals. 2. Three Photon Resonance-Enhanced Spectra Observed between 460 and 610 nm.
PB94-212487 *00,835*

New Electronic States of NH and ND Observed from 258 to 288 nm by Resonance Enhanced Multiphoton Ionization Spectroscopy.
PB94-212495 *00,836*

Multiphoton Ionization of SiH3 and SiD3 Radicals: Electronic Spectra, Vibrational Analyses of the Ground and Rydberg States, and Ionization Potential.
PB94-212503 *00,837*

Electronic Spectra of CF2Cl and CFCl2 Radicals Observed by Resonance Enhanced Multiphoton Ionization.
PB95-151023 *00,927*

Resonance Enhanced Multiphoton Ionization Spectroscopy of 2-Butene-1-yl (C4H7) between 455-485 nm.
PB95-151031 *00,670*

ELECTRONIC STRUCTURE
Photoelectron Spectroscopic Study of the Valence and Core-Level Electronic Structure of BaTiO3.
PB94-212149 *04,500*

Substitution-Induced Midgap States in the Mixed Oxides RxBa1-ChiTiO3-Delta, with R=Y, La, and Nd.
PB95-140505 *04,541*

Resonant-Photoemission Investigation of the Heusler Alloys Ni2MnSb and NiMnSb.
PB95-162384 *04,612*

Soft-X-ray-Emission Studies of Bulk Fe3Si, FeSi, and FeSi2, and Implanted Iron Silicides.
PB96-157938 *04,071*

ELECTRONIC TECHNOLOGY
Handbook Preferred Circuits Navy Aeronautical Electronic Equipment. Supplement Number 3.
AD-A278 782/8 *00,026*

Handbook Preferred Circuits Navy Aeronautical Electronic Equipment. Supplement Number 2.
AD-A278 783/6 *00,027*

Handbook Preferred Circuits Navy Aeronautical Electronic Equipment. Supplement Number 1.
AD-A278 784/4 *00,028*

Atomic-scale characterization of hydrogenated amorphous-silicon films and devices. Annual subcontract report, 14 February 1994--14 April 1995.
DE95009287 *02,294*

Electronics and Electrical Engineering Laboratory 1994 Program Plan: Supporting Technology for U.S. Competitiveness in Electronics.
PB94-126901 *01,873*

Electronics and Electrical Engineering Laboratory Technical Progress Bulletin Covering Laboratory Programs, January to March 1991, with 1991 EEEL Events Calendar.
PB94-145968 *02,113*

Electronics and Electrical Engineering Laboratory Technical Progress Bulletin Covering Programs, October to December 1993, with 1994/1995 EEEL Events Calendar.
PB94-154341 *02,115*

Development and Characterization of Insulating Layers on Silicon Carbide: Annual Report for February 14, 1988 to February 14, 1989.
PB94-155579 *02,295*

Center for Electronics and Electrical Engineering Technical Progress Bulletin Covering Center Programs, October to December, with 1991 CEEE Events Calendar.
PB94-159787 *02,296*

Electronics and Electrical Engineering Laboratory: 1994 Strategic Plan. Supporting Technology for U.S. Competitiveness in Electronics.
PB94-161320 *01,874*

Design Guide for CMOS-On-SIMOX. Test Chips NIST3 and NIST4.
PB94-163458 *02,297*

Color Supplement to NIST Special Publication 400-93: Semiconductor Measurement Technology: Design and Testing Guides for the CMOS and Lateral Bipolar-on-SOI Test Library.
PB94-164316 *02,298*

Experimental and Numerical Studies on Two-Dimensional Gravity Currents in a Horizontal Channel.
PB94-165941 *01,359*

Electronics and Electrical Engineering Laboratory Technical Progress Bulletin Covering Laboratory Programs, October to December 1992, with 1992/1993 EEEL Events Calendar.
PB94-165958 *02,299*

Coordinating Cascaded Surge Protection Devices: High-Low versus Low-High.
PB94-172061 *02,463*

Gaseous Electronics Conference Radio-Frequency Reference Cell: A Defined Parallel-Plate Radio-Frequency System for Experimental and Theoretical Studies of Plasma-Processing Discharges.
PB94-172327 *04,404*

Efficient Method to Compute the Maximum Transient Drain Current Overshoot in Silicon on Insulator Devices.
PB94-172483 *02,300*

Semiconductor Measurement Technology: Design and Testing Guides for the CMOS and Lateral Bipolar-on-SOI Test Library.
PB94-178019 *02,301*

Application of the Modified Voltage-Dividing Potentiometer to Overlay Metrology in a CMOS/Bulk Process.
PB94-181997 *02,302*

Interface Roughness-Induced Changes in the Near-E(sub 0) Spectroscopic Behavior of Short-Period AlAs/GaAs Superlattices.
PB94-185154 *02,118*

Thin Film Transparent Thermocouples.
PB94-185519 *02,253*

Electro-Thermal Simulation of an IGBT PWM Inverter.
PB94-185592 *02,303*

Use of an Ion Energy Analyzer: Mass Spectrometer to Measure Ion Kinetic-Energy Distributions from RF Discharges in Argon-Helium Gas Mixtures.
PB94-185717 *04,406*

Planning the Infrastructure for Global Electronic Commerce.
PB94-185832 *00,494*

Correction to the Decay Rate of Nonequilibrium Carrier Distributions Due to Scattering-in Processes.
PB94-185840 *04,452*

Optical Current Transducer for Calibration Studies.
PB94-185907 *02,121*

Reproducibility of JEDEC Standard Current and Voltage Ramp Test Procedures for Thin-Dielectric Breakdown Characterization.
PB94-185931 *01,879*

Experimental Investigation of the Validity of TDDB Voltage Acceleration Models.
PB94-185949 *02,304*

Field and Temperature Acceleration of Time-Dependent Dielectric Breakdown in Intrinsic Thin SiO2.
PB94-185956 *02,305*

Junction Locations by Scanning Tunneling Microscopy: In-Air-Ambient Investigation of Passivated GaAs pn Junctions.
PB94-185964 *02,306*

Semiconductor Measurement Technology: Improved Characterization and Evaluation Measurements for HgCdTe Detector Materials, Processes, and Devices Used on the GOES and TIROS Satellites.
PB94-188810 *02,122*

Electronics and Electrical Engineering Laboratory Technical Publication Announcements Covering Laboratory Programs, October to December 1993 with 1994/1995 EEEL Events Calendar.
PB94-193752 *02,307*

Electronics and Electrical Engineering Laboratory Technical Progress Bulletin Covering Laboratory Programs, January to March 1994 with 1994/1995 EEEL Events Calendar.
PB94-193810 *02,308*

Realizing Suspended Structures on Chips Fabricated by CMOS Foundry Processes Through the MOSIS Service.
PB94-193984 *01,881*

Electronics and Electrical Engineering Laboratory Technical Progress Bulletin Covering Laboratory Programs, July to September 1993 with 1994 EEEL Events Calendar.
PB94-194354 *02,309*

Numerical Simulation of Submicron Photolithographic Processing.
PB94-198561 *02,310*

Majority and Minority Mobilities in Heavily Doped Silicon for Device Simulations.
PB94-198728 *02,311*

Electron Traps, Structural Change, and Hydrogen Related SIMOX Defects.
PB94-200391 *02,312*

President's Column for Dielectrics and Electrical Insulation Society Newsletter.
PB94-200409 *01,882*

Test Structures for the In-Plane Locations of Projected Features with Nanometer-Level Accuracy Traceable to a Coordinate Measurement System.
PB94-200565 *02,313*

Survey on the Implementation of ISO/IEC Guide 25 by National Laboratory Accreditation Programs.
PB94-210150 *00,479*

Half-Integral Constant Voltage Steps in High-Tc Grain Boundary Junctions.
PB94-211216 *04,489*

Investigation of the Drive Circuit Requirements for the Power Insulated Gate Bipolar Transistor (IGBT).
PB94-211794 *02,316*

Aperture Coupling to a Coaxial Air Line: Theory and Experiment.
PB94-211968 *02,216*

Investigation of S2F10 Production and Mitigation in Compressed SF6-Insulated Power Systems.
PB94-212388 *02,467*

Multicarrier Characterization Method for Extracting Mobilities and Carrier Densities of Semiconductors from Variable Magnetic Field Measurements.
PB94-212776 *02,317*

High-Spatial-Resolution Resistivity Mapping Applied to Mercury Cadmium Telluride.
PB94-212917 *02,131*

Review of Semiconductor Microelectronic Test Structures with Applications to Infrared Detector Materials and Processes.
PB94-212925 *02,132*

Defect of Thermal Ramping and Annealing Conditions on Defect Formation in Oxygen Implanted Silicon-On-Insulator Material.
PB94-212966 *02,318*

Precision, Accuracy, Uncertainty and Traceability and Their Application to Submicrometer Dimensional Metrology.
PB94-213105 *02,319*

Custom Integrated Circuit Comparator for High-Performance Sampling Applications.
PB94-213147 *02,320*

Investigation of Mercury Interstitials in Hg(1-x)CdxTe Alloys Using Resonant Impact-Ionization Spectroscopy.
PB94-213485 *02,133*

Electronics and Electrical Engineering Laboratory Technical Publication Announcements Covering Laboratory Programs, January to March 1994 with 1994/1995 EEEL Events Calendar.
PB94-213774 *01,883*

Heavily Accumulated Surfaces of Mercury Cadmium Telluride Detectors: Theory and Experiment.
PB94-216074 *02,134*

High-Level CAD Melds Micromachined Devices with Foundries.
PB94-216413 *02,321*

Guarding Against Transients.
PB94-216470 *01,623*

Characterization of Interface Defects in Oxygen-Implanted Silicon Films.
PB94-216629 *02,322*

Charge Trapping and Breakdown Mechanism in SIMOX.
PB94-216637 *02,323*

Sources of Uncertainty in a DVM-Based Measurement System for a Quantized Hall Resistance Standard.
PB94-219334 *01,884*

Report on the Workshop on Advanced Digital Video in the National Information Infrastructure. Held in Washington, D.C. on May 10-11, 1994.
PB95-103677 *01,472*

Interface Roughness of Short-Period AlAs/GaAs Superlattices Studied by Spectroscopic Ellipsometry.
PB95-107215 *02,137*

Metrology Model for Submicrometer Dimensional Measurements.
PB95-108502 *02,647*

Practical Photomask Linewidth Measurements.
PB95-108510 *02,324*

Interface Sharpness in Low-Order III-V Superlattices.
PB95-108775 *02,138*

Interface Sharpness during the Initial Stages of Growth of Thin, Short-Period III-V Superlattices.
PB95-108783 *02,139*

User's Manual for the Program MONSEL-1: Monte Carlo Simulation of SEM Signals for Linewidth Metrology.
PB95-111522 *02,325*

Far-Infrared Kinetic Inductance Detector.
PB95-126348 *02,142*

Wide Band Active Current Transformer and Shunt.
PB95-126371 *02,036*

Superconducting Kinetic Inductance Radiometer.
PB95-140083 *02,144*

Metrology Requirements of Future Space Power Systems.
PB95-140984 *04,840*

Physics for Device Simulations and Its Verification by Measurements.
PB95-141172 *02,327*

Metrology and Data for Microelectronic Packaging and Interconnection: Results of a Joint Workshop on Materials Metrology and Data for Commercial Electrical and Optical Packaging and Interconnection Technologies. Held in Gaithersburg, Maryland on May 5-6, 1994. Volume 1. Results.
PB95-143111 *02,328*

Metrology and Data for Microelectronic Packaging and Interconnection: Results of a Joint Workshop on Materials Metrology and Data for Commercial Electrical and Optical Packaging and Interconnection Technologies. Held in Gaithersburg, Maryland on May 5-6, 1994. Volume 2. Presentation Material.
PB95-143327 *02,330*

Electronics and Electrical Engineering Laboratory 1994 Technical Accomplishments Supporting Technology for U.S. Competitiveness in Electronics.
PB95-144309 *01,887*

Monte Carlo Model for SEM Linewidth Metrology.
PB95-150058 *02,331*

Transverse Magnetoresistance: A Novel Two-Terminal Method for Measuring the Carrier Density and Mobility of a Semiconductor Layer.
PB95-150066 *02,332*

Spectroscopic Ellipsometry Determination of the Properties of the Thin Underlying Strained Si Layer and the Roughness at SiO2/Si Interface.
PB95-150157 *04,560*

High Temperature Reliability of Thin Film SiO2.
PB95-150348 *02,333*

Performance Evaluation of a New Digital Partial Discharge Recording and Analysis System.
PB95-150389 *01,888*

Band-to-Band Photoluminescence and Luminescence Excitation in Extremely Heavily Carbon-Doped Epitaxial GaAs.
PB95-150413 *04,570*

Test Structures for Determining Design Rules for Microelectromechanical-Based Sensors and Actuators.
PB95-150488 *02,105*

Developing Linear Error Models for Analog Devices.
PB95-150520 *02,037*

Diakoptic and Large Change Sensitivity Analysis.
PB95-150538 *02,038*

Tin Oxide Gas Sensor Fabricated Using CMOS Micro-Hotplates and In-situ Processing.
PB95-150603 *00,580*

Effects of Heavy Doping on Numerical Simulations of Gallium Arsenide Bipolar Transistors.
PB95-150975 *02,334*

Compensation of Markov Estimator Errors in Time-Jittered Sampling of Nonmonotonic Signals.
PB95-150983 *01,590*

Kinetic-Energy Distributions of K(+) in Argon and Neon in Uniform Electric Fields.
PB95-151122 *03,902*

Effect of Electrode-Polymer Interfacial Layers on Polymer Conduction. Part 2. Device Summary.
PB95-151155 *02,335*

Electron Scattering and Dissociative Attachment by SF6 and Its Electrical-Discharge By-Products.
PB95-151288 *02,256*

Electrical Test Structure for Overlay Metrology Referenced to Absolute Length Standards.
PB95-152278 *02,336*

Cryogenic Precision Capacitance Bridge Using a Single Electron Tunneling Electrometer.
PB95-152310 *02,040*

Exact Solution of the Steady-State Surface Temperature for a General Multilayer Structure.
PB95-152773 *02,337*

Comparisons of Measured Linewidths of Sub-Micrometer Lines Using Optical, Electrical, and SEM Metrologies.
PB95-152807 *02,338*

Physics for Device Simulations and Its Verification by Measurements.
PB95-152914 *02,339*

Experimental Study of Reverse-Bias Failure Mechanisms in Bipolar Mode JFET (BMFET).
PB95-152997 *02,340*

Integration of Scanning Tunneling Microscope Nanolithography and Electronics Device Processing.
PB95-153359 *02,341*

Multijunction Thermal Converters by Commercial CMOS Fabrication.
PB95-153664 *02,343*

Directions in MEMS Research Application Development.
PB95-153797 *02,106*

Modeling Buffer Layer IGBTs for Circuit Simulation.
PB95-153805 *02,344*

Electronics and Electrical Engineering Laboratory 1995 Program Plan. Supporting Technology for U.S. Competitiveness in Electronics.
PB95-159885 *01,894*

Thermal Component Models for Electro-Thermal Network Simulation.
PB95-161022 *02,346*

Lithium-Drift Technique for Making Submicron Thick Silicon Membranes.
PB95-161386 *02,260*

X-ray Mask Metrology: The Development of Linewidth Standards for X-ray Lithography.
PB95-162129 *02,348*

Effects of Elastic Stress on the Stability of a Solid-Liquid Interface.
PB95-163028 *03,350*

Partial Discharge: Induced Aging of Cast Epoxies and Related Nonstationary Behavior of the Discharge Statistics.
PB95-163598 *01,903*

High Spectral Purity X-Band Source.
PB95-163713 *02,045*

Series Array of DC SQUIDs.
PB95-163861 *02,046*

Anomalous Behavior of a Quantized Hall Plateau in a High-Mobility Si Metal-Oxide-Semiconductor Field-Effect Transistor.
PB95-164174 *02,354*

Electrical Test Structure for Improved Measurement of Feature Placement and Overlay in Integrated Circuit Fabrication Processes.
PB95-164273 *02,355*

Hg1-xCdxTe Characterization Measurements: Current Practice and Future Needs.
PB95-164299 *02,157*

Effect of Annealing Ambient on the Removal of Oxide Precipitates in High-Dose Oxygen Implanted Silicon.
PB95-164356 *02,356*

Measuring Contact Charge Transfer at Interfaces: A New Experimental Technique.
PB95-164570 *03,053*

Accuracy Comparisons of Josephson Array Systems.
PB95-164687 *02,047*

Ultralinear Small-Angle Phase Modulator.
PB95-168852 *02,261*

Optical Characterization in Microelectronics Manufacturing.
PB95-169397 *02,358*

Design Challenges in a Commercial Quantum Hall Effect-Based Resistance Standard.
PB95-171419 *02,263*

From Superconductivity to Supernovae: The Ginzburg Symposium. Report on the Symposium Held in Honor of Vitaly L. Ginzburg. Held in Gaithersburg, Maryland on May 22, 1992.
PB95-171963 *04,649*

Status and Trends in Power Semiconductor Devices.
PB95-175097 *02,361*

Evidence for a Deep Electron Trap and Charge Compensation in Separation by Implanted Oxygen Oxides.
PB95-175337 *02,362*

New Test Structure for Nanometer-Level Overlay and Feature-Placement Metrology.
PB95-175345 *02,363*

Evidence for Parallel Junctions Within High-Tc Grain-Boundary Junctions.
PB95-175410 *04,657*

Electrical Characterization of Liquid-Phase Epitaxially Grown Single-Crystal Films of Mercury Cadmium Telluride by Variable-Magnetic-Field Hall Measurements.
PB95-175782 *02,177*

Defect Pair Formation by Implantation-Induced Stresses in High-Dose Oxygen Implanted Silicon-on-Insulator Material.
PB95-175824 *02,364*

Magneto-Transport Properties of HgCdTe.
PB95-175840 *04,661*

Fabrication Issues in Optimizing YBa2Cu3O7-x Flux Transformers for Low l/f Noise.
PB95-175857 *02,059*

Interaction of Stoichiometry, Mechanical Stress, and Interface Trap Density in LPCVD Si-rich SiNx-Si Structures.
PB95-176301 *02,366*

Voltage Gain in the Single-Electron Transistor.
PB95-176335 *04,671*

Design and Machining of Copper Specimens with Micro Holes for Accurate Heat Transfer Measurements.
PB95-180428 *02,658*

Microelectronic Test Structures for Feature Placement and Electrical Linewidth Metrology.
PB95-180568 *02,367*

Hybrid Digital/Analog Servo for the NIST-7 Frequency Standard.
PB95-180618 *01,544*

Plasma Chemical Model for Decomposition of SF6 in a Negative Glow Corona Discharge.
PB95-181053 *01,020*

Epitaxial Growth of Sb/GaSb Structures: An Example of V/III-V Heteroepitaxy.
PB95-202560 *04,693*

Accuracy and Repeatability in Time Domain Network Analysis.
PB95-202644 *02,064*

Time Domain Network Analysis Using the Multiline TRL Calibration.
PB95-202925 *02,065*

Electrical Method for Determining the Thickness of Metal Films and the Cross-Sectional Area of Metal Lines.
PB95-203170 *02,370*

JEDEC 'TCR' Interlaboratory Experiment: Lessons Learned.
PB95-203188 *02,371*

Compensation for Substrate Permittivity in Probe-Tip Calibration.
PB95-203519 *01,915*

Electronics and Electrical Engineering Laboratory Technical Progress Bulletin Covering Laboratory Programs, October to December 1994 with 1995 EEEL Events Calendar.
PB95-208724 *02,372*

Electronics and Electrical Engineering Laboratory Technical Publication Announcements Covering Laboratory Programs, October to December 1994 with 1995 EEEL Events Calendar.
PB95-231841 *01,918*

Operating Procedures and Life Cycle Documentation for the Initial Graphics Exchange Specification.
PB95-242285 *02,782*

Semiconductor Measurement Technology: HOTPAC. Programs for Thermal Analysis Including Version 3.0 of the TXYZ Program, TXYZ30, and the Thermal MultiLayer Program, TML.
PB95-260766 *02,374*

Application of Single Electron Tunneling: Precision Capacitance Ratio Measurements.
PB96-102157 *04,703*

Physical Basis for Half-Integral Shapiro Steps in a DC SQUID.
PB96-102264 *04,704*

MEMS in Standard CMOS VLSI Technology.
PB96-102363 *02,377*

Bonding Wires to Quantized Hall Resistors.
PB96-102637 *01,921*

Model for Determining the Density and Mobility of Carriers in Thin Semiconducting Layers with Only Two Contacts.
PB96-102702 *02,378*

MONSEL-II: Monte Carlo Simulation of SEM Signals for Linewidth Metrology.
PB96-102710 *02,379*

Scaling of the Nonlinear Optical Cross Sections of GaAs-AlGaAs Multiple Quantum-Well Hetero n-i-p-i's.
PB96-102793 *02,183*

Buffer Layer Modulation-Doped Field-Effect-Transistor Interactions in the Al0.33Ga0.67As/GaAs Superlattice System.
PB96-102876 *02,380*

TDDB Characterization of Thin SiO2 Films with Bimodal Failure Populations.
PB96-102926 *02,381*

Comparison of Techniques for Nondestructive Composition Measurements in CdZnTe Substrates.
PB96-103098 *02,703*

Nonstationary Behaviour of Partial Discharge during Discharge Induced Ageing of Dielectrics.
PB96-103114 *01,922*

Environmental Sensitivities of Quartz Oscillators.
PB96-103148 *02,271*

Electronics and Electrical Engineering Laboratory Technical Progress Bulletin Covering Laboratory Programs, April to June 1995 with 1995 EEEL Events Calendar.
PB96-106455 *01,923*

Can Displays Deliver a Full Measure: Manufacturing.
PB96-111935 *02,185*

Effect of Anneal Temperature on Si/Buried Oxide Interface Roughness on SIMOX.
PB96-112206 *02,382*

New Model of 1/F Noise in Baw Quartz Resonators.
PB96-112248 *02,383*

Cryogenic Precision Capacitance Bridge Using a Single Electron Tunneling Electrometer.
PB96-112271 *02,072*

Substrate and Thin Film Measurements.
PB96-112297 *02,384*

Semiconductor Measurement Technology: Test Structure Implementation Document: DC Parametric Test Structures and Test Methods for Monolithic Microwave Integrated Circuits (MMICs).
PB96-117692 *02,399*

Opportunities for Innovation: Optoelectronics.
PB96-118039 *01,928*

Characterization of Two-Dimensional Dopant Profiles: Status and Review.
PB96-119300 *02,400*

Automated Resistance Measurements at NIST.
PB96-119326 *02,274*

National Information Infrastructure and Advanced Digital Video.
PB96-119367 *01,488*

Oxidation of SiC.
PB96-119516 *02,401*

Defect Formation Mechanism Causing Increasing Defect Density during Decreasing Implant Dose in Low-Dose Simox.
PB96-119524 *02,402*

Mesoscopic Conductance Fluctuations in Large Devices.
PB96-119656 *04,735*

Appearance Potentials of Ions Produced by Electron-Impact Induced Dissociative Ionization of SF6, SF4, SF5Cl, S2F10, SO2, SO2F2, SOF2, and SOF4.
PB96-119730 *01,080*

Procedure for Measuring Trace Quantities of S2F10, S2OF10, and S2O2F10 in SF6 Using a Gas Chromatograph-Mass Spectrometer.
PB96-119755 *02,513*

Potential and Current Distributions Calculated Across a Quantum Hall Effect Sample at Low and High Currents.
PB96-122106 *04,045*

Making Displays Deliver a Full Measure.
PB96-122411 *01,490*

Survey of the Components of Display-Measurement Standards.
PB96-122528 *02,188*

Decomposition of SF6 and Production of S2F10 in Power Arcs.
PB96-122619 *01,084*

Overview of Bioelectrical Impedance Analyzers.
PB96-122635 *00,176*

Electron Attachment to Excited Molecules(1).
PB96-122809 *01,087*

SF6/N2 Mixtures: Basic and High-Voltage-Insulation Properties.
PB96-123468 *02,230*

Noise Characteristics Below 1 Hz of Zener Diode-Based Voltage Reference.
PB96-123476 *04,049*

Wire Bonding to Multichip Modules and Other Soft Substrates.
PB96-123583 *02,079*

Characterization of Liquid-Phase Epitaxially Grown HgCdTe Films by Magnetoresistance Measurements.
PB96-123617 *04,738*

Nano-Defects in Commercial Bonded SOI and SIMOX.
PB96-123674 *02,407*

Measurement of S2OF10, and S2O2F10 Production Rates from Spark and Negative Glow Corona Discharge in SF6/O2 Gas Mixtures.
PB96-123740 *01,093*

Physics and Chemistry of Partial Discharge and Corona - Recent Advances and Future Challenges.
PB96-123757 *01,936*

Behavior of Surface Partial Discharge on Aluminum Oxide Dielectrics.
PB96-123781 *01,937*

Classified Bibliography: Insulation Condition Monitoring Methods, 1989-1995.
PB96-131586 *02,232*

Wire Bonding to Multichip Modules and Other Soft Substrates.
PB96-135207 *02,082*

Decomposition of Sulfur Hexafluoride by X-rays.
PB96-135314 *01,095*

Use of Monte Carlo Modeling for Interpreting Scanning Electron Microscope Linewidth Measurements.
PB96-137807 *02,413*

Electrical Characterization of Integrated Circuit Metal Line Thickness.
PB96-138433 *02,414*

Electro-Optic-Based RMS Voltage Measurement Technique.
PB96-138490 *02,194*

Electron-electron Interactions, Coupled-Plasmon-Phonon Modes, and Mobility in n-Type GaAs.
PB96-138524 *04,749*

Nonequilibrium Total-Dielectric-Function Approach to the Electron Boltzmann Equation for Inelastic Scattering in Doped Polar Semiconductors.
PB96-138532 *04,416*

High Resolution Time Interval Counter.
PB96-138607 *01,495*

Bounds on Least-Squares Four-Parameter Sine-Fit Errors Due to Harmonic Distortion and Noise.
PB96-141304 *01,609*

Summary Report on the Workshop on Advanced Digital Video in the National Information Infrastructure.
PB96-141320 *01,497*

Integrated Thin-Film Micropotentiometers.
PB96-146709 *02,109*

Josephson D/A Converter with Fundamental Accuracy.
PB96-148044 *02,418*

Performance and Reliability of NIST 10-V Josephson Arrays.
PB96-148051 *02,419*

Scanning Capacitance Microscopy Measurements and Modeling: Progress Towards Dopant Profiling of Silicon.
PB96-148150 *04,773*

Measurement of Patterned Film Linewidth for Interconnect Characterization.
PB96-148168 *02,420*

Semiconductor Measurement Technology: Survey of Optical Characterization Methods for Materials, Processing, and Manufacturing in the Semiconductor Industry.
PB96-154596 *02,706*

Micromachined Display Output for a Cellular Neural Network.
PB96-156070 *02,422*

CMOS Circuit Design for Controlling Temperature in Micromachined Devices.
PB96-156088 *02,196*

Optimizing Time-Domain Network Analysis.
PB96-157821 *02,085*

Two-Tier Multiline TRL for Calibration of Low-Cost Network Analyzers.
PB96-157888 *01,947*

Characterization of LPE HgCdTe Film by Magnetoresistance.
PB96-157961 *02,197*

Using Collocation in Three Dimensions and Solving a Model Semiconductor Problem.
PB96-159249 *01,952*

Boron-Implanted 6H-SiC Diodes.
PB96-159678 *04,081*

Effect of Intermediate Thermal Processing on Microstructural Changes of Oxygen Implanted Silicon-on-Insulator Material.
PB96-160213 *02,982*

Stacking Fault Pyramid Formation and Energetics in Silicon-on-Insulator Material Formed by Multiple Cycles of Oxygen Implantation and Annealing.
PB96-160221 *04,083*

RII Spectroscopy of Trap Levels in Bulk and LPE Hg1-xCdxTe
PB96-160247 *04,084*

Interface Roughness, Composition, and Alloying of Low-Order AlAs/GaAs Superlattices Studies by X-ray Diffraction.
PB96-160262 *02,983*

Electron and Hole Trapping in Irradiated SIMOX, ZMR and BESOI Buried Oxides.
PB96-160320 *01,956*

Effect of Single versus Multiple Implant Processing on Defect Types and Densities in SIMOX.
PB96-160353 *01,957*

Business and Manufacturing Motivations for the Developing of Analytical Technology and Metrology for Semiconductors.
PB96-161948 *04,778*

Electrical Measurements for Monitoring and Control of rf Plasma Processing.
PB96-161963 *04,369*

2D-Scanning Capacitance Microscopy Measurements of Cross-Sectioned VLSI Teststructures.
PB96-163779 *04,104*

High-Accuracy Principal-Angle Scanning Spectroscopic Ellipsometry of Semiconductor Interfaces.
PB96-163787 *02,427*

Natural Convection from an Array of Electronic Packages Mounted on a Horizontal Board in a Narrow Aspect Ratio Enclosure.
PB96-164017 *02,087*

Enhanced Voltage-Dividing Potentiometer for High-Precision Feature Placement Metrology.
PB96-164025 *02,428*

Use of Pressure for Quantum-Well Band-Structure Characterization.
PB96-164058 *04,779*

President's Column 'Editorial'.
PB96-164090 *02,239*

Modeling Buffer Layer IGBT's for Circuit Simulation.
PB96-164173 *02,429*

Electrical Characterization of Narrow Gap n-Type Bulk HgCdTe Single Crystals by Variable-Magnetic-Field Hall Measurements and Reduced-Conductivity-Tensor Analyses.
PB96-164199 *01,146*

Scanning Capacitance Microscopy Measurements and Modeling for Dopant Profiling of Silicon.
PB96-164207 *04,781*

Microelectronic Test Structures for Overlay Metrology.
PB96-164249 *02,430*

Beyond the Technology Roadmaps: An Assessment of Electronic Materials Research and Development.
PB96-165998 *01,961*

Optical Characterization of Materials and Devices for the Semiconductor Industry: Trends and Needs.
PB96-167192 *02,431*

Double-Modulation and Selective Excitation Photoreflectance for Wafer-Level Characterization of Quantum-Well Laser Structures.
PB96-167325 *04,372*

Electronics and Electrical Engineering Laboratory: 1996 Program Plan. Supporting Technology for U.S. Competitiveness in Electronics.
PB96-175237 *01,962*

Theory of Electron Beam Moire.
PB96-175690 *04,373*

Single-Port Technique for Adaptor Efficiency Evaluation.
PB96-176441 *02,088*

Novel Magnetic Field Characterization Techniques for Compound Semiconductor Materials and Devices.
PB96-176458 *02,433*

Microwave Characterization of Flip-Chip MMIC Interconnections.
PB96-176730 *02,435*

Electrical Measurements of Microwave Flip-Chip Interconnections.
PB96-176748 *02,436*

Time-Dependent Dielectric Breakdown of Intrinsic SiO2 Films under Dynamic Stress.
PB96-179478 *02,438*

Scanning Capacitance Microscopy Measurements and Modeling: Progress Towards Dopant Profiling of Silicon.
PB96-180070 *01,964*

Quantum Hall Effect-Based Resistance Standard: Capabilities and Implementation.
PB96-180096 *04,114*

Assessing MOS Gate Oxide Reliability on Wafer Level with Ramped/Constant Voltage and Current Stress.
PB96-180112 *04,115*

Electronics and Electrical Engineering Laboratory Technical Progress Bulletin Covering Laboratory Programs, October to December 1995 with 1996 EEEL Events Calendar.
PB96-183116 *01,966*

Surface Transverse Wave Oscillators with Extremely Low Thermal Noise Floors.
PB96-186010 *01,967*

New Physics-Based Model for Time-Dependent- Dielectric-Breakdown.
PB96-186093 *02,440*

New 5 and 10 MHz High Isolation Distribution Amplifier.
PB96-190202 *01,510*

Charpy Specimen Tests at 4 K.
PB96-190335 *03,002*

National Semiconductor Metrology Program, Project Portfolio FY 1996.
PB96-195268 *04,789*

Specification for Interoperability between Ballistic Imaging Systems. Part 1. Cartridge Cases.
PB96-195524 *01,860*

Design Criteria for BJT Amplifiers with Low l/f AM and PM Noise.
PB96-200365 *02,442*

30 MHz Comparison Receiver.
PB96-200407 *01,972*

How to Get NIST-Traceable Time on Your Computer.
PB96-200647 *01,559*

Origin of l/f PM and AM Noise in Bipolar Junction Transistor Amplifiers.
PB96-200787 *02,096*

Quest to Understand and Reduce l/f Noise in Amplifiers and Baw Quartz Oscillators.
PB96-200795 *02,097*

Measurements of Properties of Materials in Electronic Packaging.
PB96-200837 *01,973*

Monte Carlo Simulation of Scanning Electron Microscope Signals.
PB96-200969 *02,444*

Software Needs in Special Functions.
PB96-200977 *01,778*

New Oxide Degradation Mechanism for Stresses in the Fowler-Nordheim Tunneling Regime.
PB96-200985 *04,128*

Time-Resolved Measurements of the Polarization State of Four-Wave Mixing Signals from GaAs Multiple Quantum Wells.
PB96-201058 *04,796*

Scanning Electron Microscope Metrology.
PB96-201090 *02,446*

SEM Linewidth Metrology of X-ray Lithography Masks.
PB96-201108 *02,447*

New Physics-Based Model for Time-Dependent- Dielectric-Breakdown.
PB96-201132 *02,448*

NIST/NCMS Program on Electronic Packaging: First Update.
PB96-204086 *03,008*

Electric Field Dependent Dielectric Breakdown of Intrinsic SiO2 Films Under Dynamic Stress.
PB96-204102 *02,449*

Hybrid Optical-Electrical Overlay Test Structure.
PB96-204136 *02,450*

Characterization of Two-Dimensional Dopant Profiles: Status and Review.
PB97-110134 *02,451*

Double Modulation and Selective Excitation Photoreflectance for Characterizing Highly Luminescent Semiconductor Structures and Samples with Poor Surface Morphology.
PB97-111439 *02,452*

Mechanism of Defect Formation in Low-Dose Oxygen Implanted Silicon-on-Insulator Material.
PB97-111462 *02,453*

Transient Errors in a Precision Resistive Divider.
PB97-111512 *01,983*

Electrical Test Structures Replicated in Silicon-on-Insulator Material.
PB97-111827 *02,454*

Optical and Mass Spectrometric Investigations of Ions and Neutral Species in SF6 Radio-Frequency Discharges.
PB97-111918 *01,985*

New Refractometer by Combining a Variable Length Vacuum Cell and a Double-Pass Michelson Interferometer.
PB97-111926 *01,986*

Measurement and Reduction of Alignment Errors of the NIST Watt Experiment.
PB97-111959 *01,987*

Interdigitated Stacked P-I-N Multiple Quantum Well Modulator.
PB97-112296 *02,455*

Development of Thin-Film Multijunction Thermal Converters at NIST.
PB97-112338 *02,286*

High-Current Thin Film Multijunction Thermal Converters and Multi-Converter Modules.
PB97-112379 *01,989*

NIST Watt Balance: Progress Toward Monitoring the Kilogram.
PB97-113062 *01,991*

Frequency Synthesis and Metrology at 10(-17) and Beyond.
PB97-113187 *02,101*

Conformance Testing and Specification Management.
PB97-113781 *02,849*

Majority and Minority Electron and Hole Mobilities in Heavily Doped Gallium Aluminum Arsenide.
PB97-118335 *04,814*

Automated Guarded Bridge for Calibration of Multimegohm Standard Resistors.
PB97-119150 *02,289*

Resistance Measurements from 10 M Omega to 1 T Omega at NIST.
PB97-119168 *02,290*

NIST Comparison of the Quantized Hall Resistance and the Realization of the SI Ohm Through the Calculable Capacitor.
PB97-119184 *02,291*

Specular and Diffuse Reflection Measurements of Electronic Displays.
PB97-119200 *02,208*

Interface-Filter Characterization of Spectraradiometers and Colorimeters.
PB97-122212 *04,399*

Dependence of the Thermal Electron Attachment Rate Constant in Gases and Liquids on the Energy Position of the Electron Attaching State.
PB97-122253 *01,996*

Survey of the Components of Display-Measurement Standards.
PB97-122394 *02,209*

Characterization of Time-Dependent Dielectric Breakdown in Intrinsic Thin SiO2.
PB97-122527 *02,458*

Capacitors with Very Low Loss: Cryogenic Vacuum-Gap Capacitors.
PB97-122600 *02,293*

ELECTRONIC WORKSHOPS

Electronic Implementors' Workshop.
PB95-210936 *01,484*

ELECTRONICS

Electronics and Electrical Engineering Laboratory Technical Progress Bulletin Covering Laboratory Programs, October to December 1992, with 1992/1993 EEEL Events Calendar.
PB94-165958 *02,299*

Electronics and Electrical Engineering Laboratory Technical Progress Bulletin Covering Laboratory Programs, January to March 1992, with 1992/1993 EEEL Events Calendar.
PB95-210480 *01,917*

Electronics and Electrical Engineering Laboratory Technical Publication Announcements Covering Laboratory

Programs, April to June 1995 with 1995 EEEL Events Calendar.
PB96-137187 01,941

Electronics and Electrical Engineering Laboratory: 1996 Program Plan. Supporting Technology for U.S. Competitiveness in Electronics.
PB96-175237 01,962

ELECTRONICS INDUSTRY

Electronics and Electrical Engineering Laboratory 1994 Program Plan: Supporting Technology for U.S. Competitiveness in Electronics.
PB94-126901 01,873

Electronics and Electrical Engineering Laboratory 1994 Technical Accomplishments Supporting Technology for U.S. Competitiveness in Electronics.
PB95-144309 01,887

Electronics and Electrical Engineering Laboratory 1995 Program Plan. Supporting Technology for U.S. Competitiveness in Electronics.
PB95-159885 01,894

ELECTRONS

Electron-Photon Monte Carlo Calculations: The ETRAN Code.
PB97-110407 04,138

ELECTROOPTICS

Opportunities for Innovation: Optoelectronics.
PB96-118039 01,928

Optoelectronics and Optomechanics Manufacturing: An ATP Focused Program Development. Workshop Proceedings. Held in Gaithersburg, Maryland on February 15, 1995.
PB97-104186 02,204

Bibliography of the NIST Optoelectronics Division.
PB97-116040 02,207

ELECTROPHORESIS

Separation and Identification of Organic Gunshot and Explosive Constituents by Micellar Electrokinetic Capillary Electrophoresis.
PB95-107249 00,566

Standard Reference Material for the Measurement of Particle Mobility by Electrophoretic Light Scattering.
PB96-102488 00,609

ELECTROPHORETIC MOBILITY

Determining Mobility from Homodyne ac Electrophoretic Light Scattering.
PB95-140497 03,462

ELECTROPLATING

Diffusion of Copper into Gold Plating.
PB95-162152 00,957

ELECTROSTATIC MODES

Electrostatic Modes as a Diagnostic in Penning-Trap Experiments.
PB95-176244 03,959

ELECTROSTRICTION

Electric Field Effects on a Near-Critical Fluid in Microgravity.
PB96-161880 04,217

ELEVATOR FIRES

Smoke Control Systems for Elevator Fire Evacuation.
PB94-212883 00,291

ELEVATORS (LIFTS)

Feasibility and Design Considerations of Emergency Evacuation by Elevators.
PB94-163441 00,287

Smoke Control Systems for Elevator Fire Evacuation.
PB94-212883 00,291

Human Factors Considerations for the Potential Use of Elevators for Fire Evacuation of FAA Air Traffic Control Towers.
PB94-217163 01,300

ELLIPSOIDAL MIRROR

Simulations of Neutron Focusing with Curved Mirrors.
PB96-176649 02,200

ELLIPSOMETRY

Structure of the Vapor-Liquid Interface Near the Critical Point.
PB95-140174 00,902

ELLIPTIC DIFFERENTIAL EQUATIONS

Performance Characteristics of Fast Elliptic Solvers on Parallel Platforms.
PB95-180832 01,723

ELLIPTIC-TYPE INTEGRAL

Exact Series Solution to the Epstein-Hubbell Generalized Elliptic Type Integral Using Complex Variable Residue Theory.
PB97-110167 03,423

ELLIPTICAL CONFIGURATION

Near Critical Fluid Interfaces: A Comparison of Theory and Experiment.
PB95-140166 00,901

ELLIPTICAL DISTRIBUTIONS

Principal Points and Self-Consistent Points of Symmetric Multivariate Distributions.
PB96-135090 03,446

EMATS

Well-Shielded EMAT for On-Line Ultrasonic Monitoring of GMA Welding.
PB96-186077 02,879

EMBOSSABLE GRATING

Embossable Grating Couplers for Planar Waveguide Optical Sensors.
PB96-190277 00,641

EMERGENCY PLANNING

Post-Earthquake Fire and Lifelines Workshop. Held in Long Beach, California on January 30-31, 1995. Proceedings.
PB96-117916 00,209

EMERGENCY PREPAREDNESS

Earthquake and Fire in Japan: When the Threat Became a Reality.
PB95-175238 00,201

Impact of the FCC's Open Network Architecture on NS/NP Telecommunications Security.
PB95-189445 01,483

EMISSION

Interaction between Dislocations and Intergranular Cracks.
PB95-152096 03,190

Dislocation Emission at Ledges on Cracks.
PB95-164240 04,630

Resonances in Two-Dimensional Array Oscillator Circuits.
PB96-102082 02,066

EMISSION FACTORS

EMISS: A Program for Estimating Local Air Pollution Emission Factors Related to Energy Use in Buildings: User's Guide and Reference Manual.
PB96-109566 02,560

EMISSION SPECTROSCOPY

Fourier Transform Atomic Emission Studies Using a Glow Discharge as the Emission Source.
PB94-185980 00,533

EMISSION SPECTRUM

Charge-Transfer-Induced Multiplet Structure in the N4,5O2,3 Soft-X-ray Emission Spectrum of Lanthanum.
PB96-163746 04,102

EMISSIONS

Distinguishing the Contributions of Residential Wood Combustion and Mobile Source Emissions Using Relative Concentrations of Dimethylphenanthrene Isomers.
PB96-135124 02,563

Issues in the Field Measurement of VOC Emission Rates.
PB97-118806 02,573

EMISSIVITY

Wavelength Dependence of Normal Spectral Emissivity of High-Temperature Metals at Their Melting Point.
PB94-200011 03,398

Radiance Temperatures (in the Wavelength Range 523-907 nm) of Group IV B Transition Metals Titanium, Zirconium, and Hafnium at Their Melting Points by a Pulse-Heating Technique.
PB96-102207 03,356

EMPIRICAL EQUATIONS

Correlation of the Ideal Gas Properties of Five Aromatic Hydrocarbons.
PB95-175816 01,002

ENAMELS

Adhesion of Composites to Dentin and Enamel.
PB94-199049 00,144

Remineralization of Root Lesions with Concentrated Calcium and Phosphate Solutions.
PB96-102140 03,567

Polymeric Calcium Phosphate Composites with Remineralization Potential.
PB96-155544 03,575

ENANTIOMERIC SEPARATION

Use of a Naphthylethylcarbamoylated- beta-Cyclodextrin Chiral Stationary Phase for the Separation of Drug Enantiomers and Related Compounds by Sub- and Supercritical Fluid Chromatography.
PB97-113260 00,653

ENCAPSULATION

Development of a Test Method for Leaching of Lead from Lead-Based Paints Through Encapsulants.
PB96-154984 03,128

ENCLOSURE FIRES

Reactivity of Product Gases Generated in Idealized Enclosure Fire Environments.
PB95-161790 01,386

Mathematical Modeling and Computer Simulation of Fire Phenomena.
PB95-180063 00,384

END EFFECTS

Optical Fiber Geometry by Gray-Scale Analysis with Robust Regression.
PB95-161519 04,272

END GRAFTED POLYMERS

Neutron Reflectivity of End-Grafted Polymers: Concentration and Solvent Quality Dependence in Equilibrium Conditions.
PB94-185758 01,206

Neutron Reflectivity Study of the Density Profile of a Model End-Grafted Polymer Brush: Influence of Solvent Quality.
PB95-202735 01,274

ENDONUCLEASE III

Substrate Specificity of the Escherichia coli Endonuclease III: Excision of Thymine- and Cytosine-Derived Lesions in DNA Produced by Radiation-Generated Free Radicals.
PB95-153425 03,535

ENERGY ABSORPTION

Influence of Specimen Absorbed Energy in LOX Mechanical-Impact Tests.
PB95-107355 03,341

Effect of Charpy V-Notch Striker Radii on the Absorbed Energy.
PB96-141122 03,365

Calculation of Photon Mass Energy-Transfer and Mass Energy-Absorption Coefficients.
PB97-110399 04,137

ENERGY CONSERVATION

Least-Cost Energy Decisions for Buildings: Part 2. Uncertainty and Risk Video Training Workbook.
PB94-165982 00,240

Papers Presentations Shine.
PB94-200383 00,244

Energy Prices and Discount Factors for Life-Cycle Cost Analysis 1994. Annual Supplement to NIST Handbook 135 and NBS Special Publication 709.
PB94-206018 02,508

Energy Price Indices and Discount Factors for Life-Cycle Cost Analysis 1995. Annual Supplement to NIST Handbook 135 and NBS Special Publication 709. (Revised).
PB95-105011 02,509

Life-Cycle Costing Workshop for Energy Conservation in Buildings: Student Manual.
PB95-175006 00,257

Building Life Cycle Cost Computer Program (BLCC), Version 4.2-95 (for Microcomputers).
PB95-501953 00,266

Building Life Cycle Cost Computer Program (BLCC) Version 4.21-95 (for Microcomputers).
PB95-502779 00,267

Building Life Cycle Cost Computer Program (BLCC) Version 4.22-95 (for Microcomputers).
PB95-503397 00,268

Energy Price Indices and Discount Factors for Life-Cycle Cost Analysis 1996. Annual Supplement to NIST Handbook 135 and NBS Special Publication 709. (Revised).
PB96-162441 02,510

Energy Price Indices and Discount Factors for Life-Cycle Cost Analysis 1997. Annual Supplement to NIST Handbook 135 and NBS Special Publication 709. (Revised).
PB96-210745 02,512

Building Life Cycle Cost Computer Program (BLCC) Version 4.22-95 (for Mircomputers).
PB96-502794 00,277

Building Life Cycle Cost Computer Program (BLCC) Version 4.4-97 (for Microcomputers).
PB97-500342 00,284

ENERGY CONSERVATION & PRODUCTION

Predicting the Energy Performance Ratings of a Family of Type I Combination Appliances.
PB95-105524 02,504

Composite Materials for Offshore Operations: Proceedings of the International Workshop (1st). Held in Houston, Texas on October 26-28, 1993.
PB96-109509 03,169

Efficiency of Electric Motors. National Voluntary Lab. Accreditation Program (NVLAP).
PB96-111174 02,107

Significant Contributions of IAPWS to the Power Industry, Science and Technology.
PB96-123252 01,088

Bibliography of the NIST Optoelectronics Division.
PB96-128210 02,193

Directory of U.S. Private Sector Product Certification Programs.
PB96-215074 02,688

ENERGY CONSUMPTION

Lighting and HVAC.
PB95-150991 00,250

Factors Affecting the Energy Consumption of Two Refrigerator-Freezers.
PB97-112312 00,311

ENERGY DEPENDENCE

Energy Dependences of Absorption in Beryllium Windows and Argon Gas.
PB96-102124 04,020

ENERGY DISSIPATION

Merged-Beams Energy-Loss Technique for Electron-Ion Excitation: Absolute Total Cross Sections for O(5+) (2s yields 2p).
PB96-102058 04,017

ENERGY EFFICIENCY

Papers Presentations Shine.
PB94-200383 00,244

National Voluntary Laboratory Accreditation Program: Energy Efficient Lighting Products.
PB94-219060 02,642

Predicting the Energy Performance Ratings of a Family of Type I Combination Appliances.
PB95-105524 02,504

BLCC: The NIST 'Building Life-Cycle Cost' Program, Version 4.21. User's Guide and Reference Manual.
PB95-190682 00,263

Least-Cost Energy Decisions for Buildings. Part 3. Choosing Economic Evaluation Methods. Video Training Workbook.
PB95-253597 00,265

Laboratory Accreditation for Testing Energy Efficient Lighting.
PB96-122932 00,270

International Green Building Conference and Exposition (3rd). Held in San Diego, California on November 17-19, 1996. (Reannouncement with new abstract).
PB97-121826 02,531

ENERGY EFFICIENT LIGHTING PROGRAM

National Voluntary Laboratory Accreditation Program: Energy Efficient Lighting Products.
PB94-219060 02,642

ENERGY FLOW

Energy Flows in an Orifice Pulse Tube Refrigerator.
PB95-169082 02,752

ENERGY GAP

Superconducting Energy Gap of Bulk UBe13.
PB95-150116 04,559

Tunneling Measurement of the Zero-Bias Conductance Peak and the Bi-Sr-Ca-Cu-O Thin-Film Energy Gap.
PB95-163739 04,628

ENERGY-LEVEL CALCULATIONS

Designations of ds(2)p Energy Levels in Neutral Zirconium, Hafnium, and Rutherfordium (Z=104).
PB96-180120 04,116

ENERGY LEVELS

Energy Levels of Zinc, Zn I through Zn XXX.
PB96-145982 01,122

Comment On: Two-Photon Absorption Series of Calcium.
PB96-157979 04,074

Analysis of the (5d(2)+5d6s)-5d6p Transition Arrays of Os VII and Ir VIII, and the 6s (2)S-6p (2)P Transitions of Ir IX.
PB96-159264 01,954

Hyperfine Structure Investigations and Identification of New Energy Levels in the Ionic Spectrum of (147)Pm.
PB96-180203 04,117

Quantum Dots in Quantum Well Structures.
PB97-118350 01,185

ENERGY LOSSES

Measured Stopping Powers of Hydrogen and Helium in Polystyrene Near Their Maximum Values.
PB96-112321 04,729

ENERGY MANAGEMENT

Using Emulator/Testers for Commissioning EMCS Software, Operator Training, Algorithm Development, and Tuning Local Control Loops.
PB94-212735 00,245

Life-Cycle Costing Manual for the Federal Energy Management Program. 1995 Edition.
PB96-172317 02,511

ENERGY MANAGEMENT SYSTEMS

Reproducibility of Tests on Energy Management and Control Systems Using Building Emulators.
PB95-175980 00,260

ENERGY POSITIONS

Dependence of the Thermal Electron Attachment Rate Constant in Gases and Liquids on the Energy Position of the Electron Attaching State.
PB97-122253 01,996

ENERGY RELATED INVENTIONS PROGRAM

Encouraging Environmentally-Aware Inventions.
PB95-161394 02,521

ENERGY SUPPLIES

Present Worth Factors for Life-Cycle Cost Studies in the Department of Defense (1995).
PB95-105029 03,664

Present Worth Factors for Life-Cycle Cost Studies in the Department of Defense (1996).
PB96-106869 03,673

ENERGY TRANSFER

Atom Cooling and Trapping, and Collisions of Trapped Atoms.
PB96-122916 04,048

Ultrafast Time-Resolved Infrared Probing of Energy Transfer at Surfaces.
PB96-123443 00,620

State-Resolved Rotational Energy Transfer in Open Shell Collisions: Cl((2)P3/2)+HCl.
PB96-176607 01,157

Excitation Transfer in Barium by Collisions with Noble Gases.
PB96-200274 01,163

Calculation of Photon Mass Energy-Transfer and Mass Energy-Absorption Coefficients.
PB97-110399 04,137

ENERGY USE

EMISS: A Program for Estimating Local Air Pollution Emission Factors Related to Energy Use in Buildings: User's Guide and Reference Manual.
PB96-109566 02,560

ENGINE TESTS

New Method to Evaluate Deposit Forming Tendencies of Liquid Lubricants by Differential Scanning Calorimetry.
PB95-152120 01,451

Deposit Forming Tendencies of Diesel Engine Oils-Correlation between the Two-Peak Method and Engine Tests.
PB95-152138 01,452

ENGINE VALVES

Evaluation of Wear Resistant Ceramic Valve Seats in Gas-Fueled Power Generation Engines. Topical Report, December 1991-April 1994.
PB95-200218 02,466

ENGINE WEAR

Evaluation of Wear Resistant Ceramic Valve Seats in Gas-Fueled Power Generation Engines. Topical Report, December 1991-April 1994.
PB95-200218 02,466

ENGINEERING/PRODUCT/INFORMATION STANDARDS

Federal Basis for Weights and Measures: A Historical Review of Federal Legislative Effort, Statutes, and Administrative Action in the Field of Weights and Measures in the United States.
AD-A280 086/0 02,616

National Type Evaluation Program: Index of Device Evaluations by Company. NCWM Publication 5 Part A (Second Edition).
PB94-160835 02,889

NVLAP Procedures U.S. Code of Federal Regulations. Title 15, Subtitle A, Chapter 2, Part 7. (Effective December 1984; Amended September 1990).
PB94-160850 02,627

Voluntary Product Standard PS 20-94. American Softwood Lumber Standard.
PB94-162500 03,402

Models, Managing Models, Quality Models: An Example of Quality Management.
PB94-163466 02,891

National Voluntary Laboratory Accreditation Program: Procedures and General Requirements.
PB94-178225 02,630

National Voluntary Laboratory Accreditation Program 1994 Directory.
PB94-178969 00,482

International Institute of Welding: Report on 1992 Actions.
PB94-185873 02,856

International Institute of Welding: Report on 1993 Actions.
PB94-185881 02,857

Precision Oscillators: Dependence of Frequency on Temperature, Humidity and Pressure.
PB94-198306 02,031

State Weights and Measures Laboratories: State Standards Program Description and Directory. 1994 Edition.
PB94-207727 02,895

Program Handbook: Requirements for Obtaining NIST Approval/Recognition of a Laboratory Accreditation Body Under P.L. 101-592. The Fastener Quality Act.
PB94-210143 02,859

Performance Standards: The Pro's and Con's.
PB94-216132 02,896

Formulation of Position on U.S. Standards Role in Enterprise Integration.
PB95-105052 02,773

Flow Conditioner Tests for Three Orifice Flowmeter Sizes.
PB95-105540 04,201

Should NIST Accredit U.S. Calibration Laboratories.
PB95-107280 02,646

National Voluntary Laboratory Accreditation Program: Ionizing Radiation Dosimetry.
PB95-128658 03,623

National Voluntary Laboratory Accreditation Program: Bulk Asbestos Analysis.
PB95-138129 02,541

NIST Handbook 44, 1995: Specifications, Tolerances and Other Technical Requirements for Weighing and Measuring Devices as Adopted by the 79th National Conference on Weights and Measures 1994.
PB95-146379 02,903

Review and Upgrading of Military Fastener Test Standard MIL-STD-1312.
PB95-154720 02,947

National Voluntary Laboratory Accreditation Program: Construction Materials Testing.
PB95-155552 01,319

National Voluntary Laboratory Accreditation Program: Carpet and Carpet Cushion.
PB95-155560 00,295

Status Report: AWS Standards for Identifying Arc Welds (A91.1) and Recording Weld Data (A9.2).
PB95-162855 02,861

Report of the National Conference on Weights and Measures (79th). Held in San Diego, California on July 17-21, 1994.
PB95-169819 02,656

National Voluntary Laboratory Accreditation Program (NVLAP): Wood Based Products.
PB95-170429 03,405

Multi-Agency Certification and Accreditation (C and A) Process: A Worked Example.
PB95-171955 01,601

National Voluntary Laboratory Accreditation Program 1995 Directory.
PB95-174454 00,483

Uniform Laws and Regulations in the Areas of Legal Metrology and Motor Fuel Quality, 1994 as Adopted by the 79th National Conference on Weights and Measures 1994.
PB95-174470 02,909

Checking the Net Contents of Packaged Goods as Adopted by the 79th National Conference on Weights and Measures, 1994, Third Edition, Supplement 4.
PB95-182226 00,484

National Voluntary Laboratory Accreditation Program Acoustical Testing Services.
PB95-182234 04,188

National Voluntary Laboratory Accreditation Program: POSIX. Portable Operating System Interface.
PB95-189478 02,661

Electronics and Electrical Engineering Laboratory Technical Progress Bulletin Covering Laboratory Programs, April to June 1991, with 1992 EEEL Events Calendar.
PB95-209821 01,916

ISO Environmental Management Standardization Efforts.
PB95-220513 02,524

National Voluntary Laboratory Accreditation Program: Electromagnetic Compatibility and Telecommunications. FCC Methods.
PB95-242376 02,664

Advanced Mass Calibration and Measurement Assurance Program for State Calibration Laboratories.
PB95-253571 02,492

Proceedings of the Meeting of the Intergovernmental U.S.-Russian Business Development Committee's Standard Working Group (4th). Held in New York City, New York on March 27-29, 1995 and in Northbrook, Illinois on March 30-31, 1995.
PB95-255881 00,496

National Voluntary Laboratory Accreditation Program (NVLAP): Commercial Products Testing.
PB95-267944 02,671

National Voluntary Laboratory Accreditation Program: Thermal Insulation Materials.
PB95-267985 02,977

National Voluntary Laboratory Accreditation Program. GOSIP: Government Open Systems Interconnection Profile.
PB95-267993 01,486

Aging, Warm-Up Time and Retrace; Important Characteristics of Standard Frequency Generators.
PB96-103122 04,031

GATT Standards Code Activities of the National Institute of Standards and Technology 1994.
PB96-106935 00,497

Standards Setting in the European Union: Standards Organization and Officials in EU Standards Activities.
PB96-115019 02,919

Electrical Product Requirements (Especially Quality Requirements) in the United States.
PB96-119235 01,929

Laboratory Accreditation for Testing Energy Efficient Lighting.
PB96-122932 00,270

Electronic Access to Standards on the Information Highway.
PB96-131578 01,494

ISO Environmental Management Standardization Efforts.
PB96-158662 02,528

International Organization for Standardization: Current Activities in Fire Safety Engineering.
PB96-159660 00,223

U.S. Government Accreditation and Conformity Assessment System Evaluation.
PB96-160239 02,678

International Challenges in Defining the Public and Private Interest in Standards.
PB96-160361 00,498

Implementation of the Fastener Quality Act.
PB96-160676 02,876

National Voluntary Laboratory Accreditation Program 1996 Directory.
PB96-162714 00,485

Report of the National Conference on Weights and Measures (80th) as Adopted by the 80th National Conference on Weights and Measures, 1995. Held in Portland, Maine on July 16-20, 1995.
PB96-165840 02,681

Uniform Laws and Regulations in the Areas of Legal Metrology and Motor Fuel Quality as Adopted by the 80th National Conference on Weights and Measures 1995. 1996 Edition.
PB96-172309 02,927

Voluntary Product Standard PS 1-95 Construction and Industrial Plywood.
PB96-178900 03,406

Specifications and Tolerances for Reference Standards and Field Standard Weights and Measures. 2. Specifications and Tolerances for Field Standard Measuring Flasks.
PB96-178926 02,682

Consensus Process in Standards Development.
PB96-179502 00,136

Helping to Reduce Technical Barriers to Trade.
PB96-190046 00,491

IIW Commission V Quality Control and Quality Assurance of Welded Products, Annual Report 1995/96.
PB96-191366 *02,880*

Proceedings of the Open Forum on Laboratory Accreditation at the National Institute of Standards and Technology, October 13, 1995.
PB96-210141 *02,686*

State Weights and Measures Laboratories: Program Handbook.
PB96-214705 *02,687*

TBT Agreement Activities of the National Institute of Standards and Technology, 1995.
PB97-104178 *00,499*

Evaluation and Accreditation of State Calibration Laboratories.
PB97-110183 *00,486*

Examination Procedure Outlines: Keys to Solving the Handbook 44 Puzzle.
PB97-110217 *02,690*

Measurement Comparability, Traceability, and Measurement Assurance Programs.
PB97-111850 *02,692*

National Voluntary Laboratory Accreditation Program (NVLAP): Fasteners and Metals.
PB97-114185 *02,881*

Standards Promote Credibility and Technology Transfer: The Need for Greater Industry Support of Technical Committees.
PB97-116206 *02,961*

Standards Activities of Organizations in the United States.
PB97-124135 *00,006*

ENTERPRISE INTEGRATION

Formulation of Position on U.S. Standards Role in Enterprise Integration.
PB95-105052 *02,773*

Defining Environment Integration Requirements.
PB96-131545 *02,733*

ENTHALPY

Tabulation of the Thermodynamic Properties of Normal Hydrogen from Low Temperatures to 300K and from 1 to 100 Atmospheres.
AD-A279 951/8 *00,713*

Calibration Standards for Differential Scanning Calorimetry. 1. Zinc Absolute Calorimetric Measurement of Enthalpy of Fusion and Temperature of Fusion HM.
PB94-199817 *00,801*

Calculation of Enthalpy and Entropy Differences of Near-Critical Binary Mixtures with the Modified Leung-Griffiths Model.
PB95-108635 *00,885*

Correlation of the Ideal Gas Properties of Five Aromatic Hydrocarbons.
PB95-175816 *01,002*

Thermodynamics of the Hydrolysis of 3,4,5-Trihydroxybenzoic Acid Propyl Ester (n-Propylgallate) to 3,4,5-Trihydroxybenzoic Acid (Gallic Acid) and Propan-I-ol in Aqueous Media and in Toluene.
PB96-186143 *01,160*

Thermodynamic Properties of Synthetic Otavite, CdCO3(cr): Enthalpy Increment Measurements from 4.5 K to 350 K.
PB97-111447 *00,680*

Thermochemical Studies of Inorganic Chalocogenides by Fluorine-Combustion Calorimetry: Binary Compounds of Germanium and Silicon with Sulfur, Selenium and Tellurium.
PB97-112528 *01,181*

ENTHALPY FLOW

Energy Flows in an Orifice Pulse Tube Refrigerator.
PB95-169082 *02,752*

ENTHALPY INCREMENTS

Thermodynamic Properties of Silicides. 5. Standard Molar Enthalpy of Formation at the Temperature 298.15 K of Trimolybdenum Monosilicide Mo3Si Determined by Fluorine-Combustion Calorimetry.
PB97-119358 *01,190*

ENTHALPY OF FORMATION

Halon Thermochemistry: 'Ab Initio' Calculations of the Enthalpies of Formation of Fluoromethanes.
PB96-175740 *03,289*

ENTREPRENEURSHIP

Network Brokers Handbook: An Entrepreneurial Guide to Cooperative Strategies for Manufacturing Competitiveness.
PB95-219325 *00,490*

ENTROPIC CASIMIN FORCES

Influence of Surface Interaction and Chain Stiffness on Polymer-Induced Entropic Forces and the Dimensions of Confined Polymers.
PB94-185469 *01,203*

ENTROPY

Tabulation of the Thermodynamic Properties of Normal Hydrogen from Low Temperatures to 300K and from 1 to 100 Atmospheres.
AD-A279 951/8 *00,713*

Influence of Surface Interaction and Chain Stiffness on Polymer-Induced Entropic Forces and the Dimensions of Confined Polymers.
PB94-185469 *01,203*

Calculation of Enthalpy and Entropy Differences of Near-Critical Binary Mixtures with the Modified Leung-Griffiths Model.
PB95-108635 *00,885*

Glass Temperature of Polymer Blends: Comparison of Both the Free Volume and the Entropy Predictions with Data.
PB95-140190 *01,236*

Correlation of the Ideal Gas Properties of Five Aromatic Hydrocarbons.
PB95-175816 *01,002*

Shape of the Temperature-Entropy Saturation Boundary.
PB96-135066 *02,506*

ENUMERATION

Examination of the l/d Expansion Method from Exact Enumeration for a Self-Interacting Self-Avoiding Walk.
PB95-175733 *01,266*

Self-Avoiding-Walk Contacts and Random-Walk Self-Intersections in Variable Dimensionality.
PB96-102231 *01,276*

ENVELOPES

Influence of Envelopes Geometry on the Sensitivity of 'Nude' Ionization Gauges.
PB97-119077 *04,174*

ENVIROMENTAL CHEMICAL SUBSTITUTES

Report of the Refrigeration, Air Conditioning and Heat Pumps Technical Options Committee.
PB96-176755 *03,293*

ENVIRONIMENTAL CHEMICAL SUBSTITUTES

Gaseous Dielectrics Research: Possible SF6 Substitutes.
PB96-119268 *02,228*

ENVIRONMENT EFFECTS

Dispersion and Deposition of Smoke Plumes Generated in Massive Fires.
PB95-126066 *02,540*

ENVIRONMENT SIMULATION

Approaches Using Virtual Environments with Mosaic.
PB95-169108 *01,599*

ENVIRONMENTAL CHARACTERIZATION

Suggestions for a Logically-Consistent Structure for Service Life Prediction Standards.
PB95-125795 *00,358*

ENVIRONMENTAL CHEMICAL AGENTS

Effectiveness of Halon Alternatives in Suppressing Dynamic Combustion Process.
PB96-175732 *03,288*

ENVIRONMENTAL CHEMICAL SUBSTITUTES

Simultaneous Visual and Calorimetric Measurements of R11, R123, and R123/Alkylbenzene Nucleate Flow Boiling.
PB94-172426 *03,251*

Annex 18: An International Study of Refrigerant Properties.
PB95-168936 *03,266*

Development of a Dual-Sinker Densimeter for High-Accuracy Fluid P-V-T Measurements.
PB95-168951 *03,267*

Assessing Halon Alternatives for Aircraft Engine Nacelle Fire Suppression.
PB96-102454 *01,401*

Fire Suppression System Performance of Alternative Agents in Aircraft Engine and Dry Bay Laboratory Simulations. SP890: Volume 1.
PB96-117775 *03,277*

Fire Suppression System Performance of Alternative Agents in Aircraft Engine and Dry Bay Laboratory Simulations. SP 890: Volume 2.
PB96-117783 *03,278*

Agent Screening for Halon 1301 Aviation Replacement.
PB96-159710 *03,282*

Validation of a Turbulent Spray Flame Facility for the Assessment of Halon Alternatives.
PB96-159728 *03,283*

Study to Determine the Existence of an Azeotropic R-22 'Drop-In' Substitute.
PB96-167812 *02,568*

Environmental Aspects of Halon Replacements: Considerations for Advanced Agents and the Ozone Depletion Potential of CF3I.
PB97-122261 *03,301*

ENVIRONMENTAL COMPENSATION

Verification of Revised Water Vapour Correction to the Index of Refraction of Air.
PB96-161666 *02,680*

ENVIRONMENTAL EFFECTS

Expansion of Cementitious Materials Exposed to Sulfate Solutions.
PB94-185782 *02,577*

Sulfate Attack of Cementitious Materials: Volumetric Relations and Expansions.
PB94-187317 *03,232*

Evaluation of Corrosion Data: A Review.
PB94-198348 *03,187*

Analysis of Moisture Accumulation in a Wood-Frame Wall Subjected to Winter Climate.
PB94-199320 *00,338*

Methodologies for Predicting the Service Lives of Coating Systems.
PB95-146387 *03,124*

Molecular Orbital Calculations of Bond Rupture in Brittle Solids.
PB95-164059 *00,973*

Molecular Orbital Study of Water Enhanced Crack Growth Process.
PB95-164067 *03,240*

Environmental Durability of Glass-Fiber Composites.
PB95-203220 *03,166*

Environmental Sensitivities of Quartz Oscillators.
PB96-103148 *02,271*

Temperature and Relative Humidity Dependence of Radiochromic Film Dosimeter Response to Gamma and Electron Radiation.
PB96-135298 *03,718*

ENVIRONMENTAL ENGINEERING

U.S. Green Building Conference, 1994.
PB94-206364 *02,519*

ENVIRONMENTAL HEALTH

Regulation of Lithium and Boron Levels in Normal Human Blood: Environmental and Genetic Considerations.
PB94-198579 *03,491*

ENVIRONMENTAL IMPACT ASSESSMENTS

Atmospheric and Marine Trace Chemistry: Interfacial Biomediation and Monitoring.
PB94-199122 *03,752*

ENVIRONMENTAL IMPACTS

Environmental Aspects of Halon Replacements: Considerations for Advanced Agents and the Ozone Depletion Potential of CF3I.
PB97-122261 *03,301*

ENVIRONMENTAL MONITORING

Environmental Scanning Electron Microscope Imaging Examples Related to Particle Analysis.
PB94-172822 *00,766*

Atmospheric and Marine Trace Chemistry: Interfacial Biomediation and Monitoring.
PB94-199122 *03,752*

Certification of Polycyclic Aromatic Hydrocarbons in a Marine Sediment Standard Reference Material.
PB96-111778 *02,592*

Considerations in the Design of an Environmental Specimen Bank: Experiences of the National Biomonitoring Specimen Bank Program.
PB96-112370 *02,527*

Response Comparison of Electret Ion Chambers, LiF TLD, and HPIC.
PB96-190103 *02,578*

National Status and Trends Program Specimen Bank: Sampling Protocols, Analytical Methods, Results, and Archive Samples.
PB97-119226 *02,598*

ENVIRONMENTAL POLLUTION

Standard Reference Materials for Dioxins and Other Environmental Pollutants.
PB94-198330 *02,518*

ENVIRONMENTAL PROTECTION

Encouraging Environmentally-Aware Inventions.
PB95-161394 *02,521*

ISO Environmental Management Standardization Efforts.
PB95-220513 *02,524*

ISO Environmental Management Standardization Efforts.
PB96-158662 *02,528*

India: Environmental Technologies Export Market Plan.
PB97-114359 *02,529*

ENVIRONMENTAL RESEARCH

Replicate Measurements for Data Quality and Environmental Modeling.
PB94-172533 *02,515*

Pilot Studies for Improving Sampling Protocols.
PB97-118715 *02,530*

ENVIRONMENTAL SAMPLES

Determination of Polycyclic Aromatic Hydrocarbons by Liquid Chromatography.
PB95-151650 *00,585*

Standard Reference Materials for the Determination of Polycyclic Aromatic Hydrocarbons in Environmental Samples - Current Activities.
PB95-151668 *00,586*

Standard Reference Materials for the Determination of Trace Organic Constituents in Environmental Samples.
PB95-164026 *02,522*

Liquid Chromatographic Determination of Polycyclic Aromatic Hydrocarbon Isomers of Molecular Weight 278 and 302 in Environmental Standard Reference Materials.
PB95-164042 *02,523*

ENVIRONMENTAL STUDIES: POLLUTION MEASUREMENT

Lean flammability limit as a fundamental refrigerant property. Phase 1, Interim technical report, 1 October 1994--31 March 1995.
DE95011238 *03,248*

Modulation of Fossil Fuel Production by Global Temperature Variations, 2.
PB94-146636 *02,533*

Rare-Earth Isotopes as Tracers of Particulate Emissions: An Urban Scale Test.
PB94-161635 *02,535*

Proficiency Tests for the NIST Airborne Asbestos Program, 1990.
PB94-188836 *00,535*

Proficiency Tests for the NIST Airborne Asbestos Program - 1991.
PB94-193828 00,537

Proficiency Tests for the NIST Airborne Asbestos Program - 1992.
PB94-194362 00,539

Dilemma-Preservation versus Access.
PB94-198488 02,711

Precision and Accuracy in Tandem Mass Spectrometry Measurements: A Kinetics-Based Protocol for Instrument-Independent Measurements of Collision-Activated Dissociation in RF-Only Quadrupoles.
PB94-216454 00,858

Use of an Environment Classification Model.
PB95-152062 01,709

Encouraging Environmentally-Aware Inventions.
PB95-161394 02,521

Atmospheric Reactivity of alpha-Methyl-Tetrahydrofuran.
PB95-163705 02,548

Quality Assurance of Contaminant Measurements in Marine Mammal Tissues.
PB95-164034 02,588

Sources of Urban Contemporary Carbon Aerosol.
PB95-175659 02,551

Effect of Environmentally Exposures on the Properties of Polyisocyanurate Foam Insulation: Thermal Conductivity Measurements.
PB95-181210 00,388

Measurements of Indoor Pollutant Emissions from EPA Phase II Wood Stoves.
PB95-198735 02,556

Environmental Durability of Glass-Fiber Composites.
PB95-203220 03,166

NIST Workshop on Gas Sensors: Strategies for Future Technologies. Proceedings of a Workshop. Held in Gaithersburg, Maryland on September 8-9, 1993.
PB95-210225 00,507

Few Caveats on Carbon Dioxide Monitoring.
PB96-122650 02,562

Distinguishing the Contributions of Residential Wood Combustion and Mobile Source Emissions Using Relative Concentrations of Dimethylphenanthrene Isomers.
PB96-135124 02,563

Free Radical Chemistry of the Atmospheric Aqueous Phase.
PB96-148101 00,117

Airborne Asbestos Method: Bootstrap Method for Determining the Uncertainty of Asbestos Concentration. Version 1.0.
PB96-214614 00,646

Proposed Coating Technology Consortium. (National Coil Coaters Association Fall Conference). Held in Rosemont, Illinois in September 1992.
PB97-110431 03,129

Environmental Aspects of Halon Replacements: Considerations for Advanced Agents and the Ozone Depletion Potential of CF3I.
PB97-122261 03,301

ENVIRONMENTAL SURVEYS

Scientific Protocols in Statistical Standards for Environmental Studies.
PB94-185527 02,517

NIST Standard Reference Materials (SRMs) for Polychlorinated Biphenyl (PCB) Determinations and Their Applicability to Toxaphene Measurements.
PB95-140109 02,585

Development and Application of an Indoor Air Quality Commissioning Program in a New Office Building.
PB96-155601 00,275

Indoor Air Quality Commissioning of a New Office Building.
PB97-110142 00,279

ENVIRONMENTS

Use of an Environment Classification Model.
PB95-152062 01,709

ENZYMATIC METHODS

Optical Control of Enzymatic Conversion of Sucrose to Glucose by Bacteriorhodopsin Incorporated into Self-Assembled Phosphatidylcholine Vesicles.
PB96-123344 03,477

ENZYME-CATALYZED REACTIONS

Thermodynamics of Enzyme-Catalyzed Reactions. Part 4. Lyases.
PB96-145941 01,118

ENZYME KINETICS

Imposed Oscillations of Kinetic Barriers Can Cause an Enzyme to Drive a Chemical Reaction Away from Equilibrium.
PB96-161625 01,137

Novel Activities of Human Uracil DNA N-glycosylase for Cytosine-Derived Products of Oxidative DNA Damage.
PB96-164132 03,479

ENZYMES

Aggregation Kinetics of Colloidal Particles Destabilized by Enzymes.
PB95-125878 00,894

Michaelis-Menten Equation for an Enzyme in an Oscillating Electric Field.
PB95-140489 00,906

Method for the Assay of Hydrolytic Enzymes Using Dynamic Light Scattering.
PB95-151411 03,531

Potentiometric Enzyme-Amplified Flow Injection Analysis Detection System: Behavior of Free and Liposome-Released Peroxidase.
PB95-151833 03,534

Enzyme and Protein Mass Transfer Coefficient in Aqueous Two Phase Systems. 1. Spray Extraction Columns.
PB95-161162 00,594

EPDM ROOF MEMBRANES

Characteristics of Adhesive-Bonded Seams Sampled from EPDM Roof Membranes.
PB95-162491 00,377

EPDM RUBBER ROOFING

Application of Thermal Analysis Techniques to the Characterization of EPDM Roofing Membrane Materials.
PB95-125845 00,359

Use of Thermal Mechanical Analysis to Characterize Ethylene-Propylene-Diene Terpolymer (EPDM) Roofing Membrane Materials.
PB95-125852 00,360

EPDM RUBBER ROOFING MEMBRANE

Effects of Adhesive Thickness, Open Time, and Surface Cleanness on the Peel Strength of Adhesive-Bonded Seams of EPDM Rubber Roofing Membrane.
PB95-151338 00,372

EPHEMERIDES

Comparison of GPS Broadcast and DMA Precise Ephemerides.
AD-P009 114/0 01,518

Comparison of GPS Broadcast and DMA Precise Ephemerides.
N94-30660/2 01,523

EPIC COMPUTER PROGRAM

Hybrid Method for Determining Material Properties from Instrumented Micro-Indentation Experiments.
PB95-152229 03,348

EPIFLUORESCENCE

Autofluorescence Detection of 'Escherichia coli' on Silver Membrane Filters.
PB96-163639 03,590

EPITAXIAL FILMS

Scanning Electron Microscopy Observations of Misfit Dislocations in Epitaxial In0.25Ga0.75As on GaAs(001).
PB96-200159 03,004

EPITAXIAL GROWTH

Homoepitaxial Growth of Iron and a Real Space View of Reflection-High-Energy-Electron Diffraction.
PB94-173069 04,445

Scaling of Diffusion-Mediated Island Growth in Iron-on-Iron Homoepitaxy.
PB94-185923 04,455

Spot-Profile-Analyzing LEED Study of the Epitaxial Growth of Fe, Co, and Cu on Cu(100).
PB95-150165 04,561

Influence of Cr Growth on Exchange Coupling in Fe/Cr/Fe(100).
PB95-150181 04,562

Growth of Iron on Iron Whiskers.
PB95-150322 04,567

Scanning Tunneling Microscopy Study of the Growth of Cr/Fe(001): Correlation with Exchange Coupling of Magnetic Layers.
PB95-150330 04,568

Oscillatory Exchange Coupling in Fe/Au/Fe(100).
PB95-150371 04,569

Epitaxial Integration of Single Crystal C60.
PB95-153490 04,592

X-ray Photoelectron and Auger Electron Forward Scattering: A Structural Diagnostic for Epitaxial Thin Films.
PB95-180220 04,676

Epitaxial Growth and Characterization of the Ordered Vacancy Compound CuIn3Se5 on GaAs (100) Fabricated by Molecular Beam Epitaxy.
PB95-180725 04,687

Laser Vacuum Ultraviolet Single Photon Ionization Probing of III-V Semiconductor Growth.
PB95-202370 04,691

Epitaxial Growth of Sb/GaSb Structures: An Example of V/III-V Heteroepitaxy.
PB95-202560 04,693

Epitaxial Growth of BaTiO3 Thin Films at 600C by Metalorganic Chemical Vapor Deposition.
PB96-122510 03,071

Growth of Epitaxial KNbO3 Thin Films.
PB96-135181 02,409

Photoluminescence Spectra of Epitaxial Single Crystal C60.
PB96-141205 04,754

Coarsening of Unstable Surface Features during Fe(001) Homoepitaxy.
PB96-186127 04,121

EPITAXY

Effects of Substrate Surface Steps on the Microstructure of Epitaxial Ba2YCu3O7-x Thin Films on (001) LaAlO3.
PB96-148184 04,774

Epitaxial Nucleation and Growth of Chemically Derived Ba2YCu3O7-x Thin Films on (001) SrTiO3.
PB96-190186 04,787

EPOXY COATINGS

Corrosion Resistant Epoxy-Coated Reinforcing Steel.
PB94-185618 01,307

Degradation of Powder Epoxy Coated Panels Immersed in a Saturated Calcium Hydroxide Solution Containing Sodium Chloride.
PB96-101050 01,344

EPOXY MATRIX COMPOSITES

Composite Struts for SMES Plants.
PB95-155586 02,507

Torsion Modulus and Internal Friction of a Fiber-Reinforced Composite.
PB96-112339 03,070

EPOXY RESINS

Fluorescence Monitoring of Polarity Change and Gelation during Epoxy Cure.
PB94-185543 01,204

Torsional Dilatometer for Volume Change Measurements on Deformed Glasses: Instrument Description and Measurements on Equilibrated Glasses.
PB94-211166 03,379

Micromechanics of Fracture in Rubber-Toughened Epoxies.
PB94-212222 03,011

Relation between AC Impedance Data and Degradation of Coated Steel. 1. Effects of Surface Roughness and Contamination on the Corrosion Behavior of Epoxy Coated Steel.
PB94-213345 03,189

Influence of Physical Aging on the Yield Response of Model DGEBA + Poly(propylene oxide) Epoxy Glasses.
PB95-126363 03,381

Volume Recovery in Epoxy Glasses Subjected to Torsional Deformations: The Question of Rejuvenation.
PB95-140018 03,382

Torsional Relaxation and Volume Response during Physical Aging in Epoxy Glasses Subjected to Large Torsional Deformations.
PB95-140026 03,383

Using Torsional Dilatometry to Measure the Effects of Deformations on Physical Aging.
PB95-140901 03,384

Structural Heterogeneity in Epoxies.
PB95-151866 01,243

Partial Discharge: Induced Aging of Cast Epoxies and Related Nonstationary Behavior of the Discharge Statistics.
PB95-163598 01,903

Applications of Fluorescence Spectroscopy in Polymer Science and Technology.
PB95-163770 01,258

Characterization of Molecular Network of Thermosets Using Neutron Scattering.
PB95-164109 01,259

Modification of Cast Epoxy Resin Surfaces during Exposure to Partial Discharges.
PB96-122734 01,086

EPR

Commentary on 'Optimization of Experimental Parameters for the EPR Detection of the Cellulosic Radical in Irradiated Foodstuffs'.
PB96-164124 00,043

EPR SIGNAL

Complex Time Dependence of the EPR Signal of Irradiated L-alpha-alanine.
PB97-122436 04,180

EQUATIONS OF STATE

Measurements of the Virial Coefficients and Equation of State of the Carbon Dioxide + Ethane System in the Supercritical Region.
PB95-151353 03,906

Critical Scaling Laws and a Classical Equation of State.
PB95-169249 00,990

Predictive Extended Corresponding States Model for Pure and Mixed Refrigerants Including an Equation of State for R134a.
PB95-175717 03,275

International Standard Equation of State for the Thermodynamic Properties of Refrigerant 123 (2,2-Dichloro-1,1,1-Trifluoroethane).
PB96-176805 03,294

EQUILIBRIUM

Thermodynamic and NMR Study of the Interactions of Cyclodextrins with Cyclohexane Derivatives.
PB94-185816 00,781

Equilibrium and Calorimetric Investigation of the Hydrolysis of L-Tryptophan to (Indole + Pyruvate + Ammonia).
PB95-163317 00,661

Terminally Anchored Chain Interphases: The Effect of Multicomponent, Polydisperse Solvents on Their Equilibrium Properties.
PB95-181079 01,273

EQUILIBRIUM CONSTANTS

Thermodynamics of the Hydrolysis of 3,4,5-Trihydroxybenzoic Acid Propyl Ester (n-Propylgallate) to

3,4,5-Trihydroxybenzoic Acid (Gallic Acid) and Propan-I-ol in Aqueous Media and in Toluene.
PB96-186143 01,160

EQUIPMENT AND SUPPLIES
Dental Materials.
PB94-172871 00,142

EQUIPMENT INTERFACES
NIST Cooperative Laboratory for OSI Routing Technology.
DE94015308 01,791

ERBIUM
Magnetoelasticity in Rare-Earth Multilayers and Films.
PB94-211356 04,495

ERBIUM GLASS LASERS
Frequency Stabilization of a Fiber Laser to Rubidium: A High-Accuracy 1.53 mu m Wavelength Standard.
PB95-126082 04,252

Metrology Applications of Mode-Locked Erbium Fiber Lasers.
PB95-140158 04,256

Multiwavelength Birefringent-Cavity Mode-Locked Fibre Laser.
PB95-150496 04,262

ERBIUM IONS
Observation of Pd-Like Resonance Lines Through Pt(32+) and Zn-Like Resonance Lines of Er(38+) and Hf(42+).
PB95-150637 03,896

Rh I Isoelectronic Sequence Observed from Er(23+) to Pt(33+).
PB95-150652 03,898

Spectra of Ag I Isoelectronic Sequence Observed from Er(21+) to Au(32+).
PB95-150660 03,899

ERROR ANALYSIS
Error Propagation Biases in the Calculation of Indentation Fracture Toughness for Ceramics.
PB94-172434 03,032

Application of a Simple Technique for Estimating Errors of Finite-Element Solutions Using a General-Purpose Code.
PB94-200250 04,818

RangeCAD and the NIST RCS Uncertainty Analysis.
PB94-218591 01,870

Use of Ionospheric Data in GPS Time Transfer.
PB95-163853 01,540

Software Needs in Special Functions.
PB96-200977 01,778

Troublesome Crystal Structures: Prevention, Detection, and Resolution.
PB97-109151 01,172

ERROR CORRECTING CODES
Optical Storage Media Data Integrity Studies.
N95-24130/3 01,620

ERROR CORRECTION CODES
Prediction of Geometric-Thermal Machine Tool Errors by Artificial Neural Networks.
PB94-186673 02,943

PIECS: A Software Program for Machine Tool Process-Intermittent Error Compensation.
PB96-165980 02,842

Compensation of Errors Detected by Process-Intermittent Gauging.
PB97-110472 02,846

Data Management for Error Compensation and Process Control.
PB97-110480 02,847

ERROR DETECTION CODES
NIST Program for Investigating Error Reporting Capabilities of Optical Disk Drives.
PB96-160627 01,635

ERRORS
Real Time Compensation for Tool Form Errors in Turning Using Computer Vision.
PB95-107231 02,945

ERRORS IN VARIABLES MODELS
Existence and Nonexistence Theorems of Finite Diameter Sequential Confidence Regions for Errors-in-Variables Models.
PB95-180352 03,441

ESCHERICHIA COLI
Substrate Specificity of the Escherichia coli Endonuclease III: Excision of Thymine- and Cytosine-Derived Lesions in DNA Produced by Radiation-Generated Free Radicals.
PB95-153425 03,535

Deletion Analysis of the Mini-P1 Plasmid Origin of Replication and the Role of E.coli DnaA Protein.
PB95-163911 03,539

ESR DOSIMETRY
ESR-Based Analysis in Radiation Processing.
PB95-161634 03,931

ESTELLE TRANSLATOR
PET and DINGO Tools for Deriving Distributed Implementations from Estelle.
PB95-203253 01,727

ESTERIFICATION
Structural Stabilization of Phase Separating PC/Polyester Blends through Interfacial Modification by Transesterification Reaction.
PB95-150454 01,239

ESTIMATING
Recent Approaches to Extreme Value Estimation with Application to Wind Speeds. Part 1. The Pickands Method.
PB94-213170 00,019

Outlier-Resistant Methods for Estimation and Model Fitting.
PB95-203436 03,444

Extreme Wind Estimates by the Conditional Mean Exceedance Procedure.
PB95-220471 00,120

Estimation of Measurement Uncertainty of Small Circular Features Measured by CMMs.
PB95-267928 02,918

ESTIMATION
Extreme Winds Estimation by 'Peaks Over Threshold' and Epochal Methods.
PB96-159686 00,468

Estimates of Hurricane Wind Speeds by the 'Peaks Over Threshold' Method.
PB96-162540 00,471

ETCHING
Kinetic-Energy-Enhanced Neutral Etching.
PB96-200613 00,665

ETHANE
Thermodynamic Properties of the Methane-Ethane System.
PB95-125779 00,891

Experimental Method for Obtaining Critical Densities of Binary Mixtures: Application to Ethane + n-Butane.
PB95-151148 00,930

Measurements of the Virial Coefficients and Equation of State of the Carbon Dioxide + Ethane System in the Supercritical Region.
PB95-151353 03,906

Vapor-Liquid Equilibria of Ternary Mixtures in the Critical Region on Paths of Constant Temperature and Overall Composition.
PB96-161856 01,139

ETHANE/CHLORO-TETRAFLUORO
Measurements of the Viscosities of Saturated and Compressed Fluid 1-chloro-1,2,2,2-tetrafluoroethane (R124) and Pentafluoroethane (R125) at Temperatures between 120 and 420 K.
PB94-199791 03,254

ETHANE/DICHLORO-DIFLUORO
Measurements of the Viscosities of Saturated and Compressed Liquid 1,1,1,2-Tetrafluoroethane (R134a), 2,2-Dichloro-1,1,1-Trifluoroethane (R123) and 1,1-Dichloro-1-Fluoroethane (R141b).
PB95-175386 03,273

ETHANE/DICHLORO-FLUORO
Measurements of the Viscosities of Saturated and Compressed Liquid 1,1,1,2-Tetrafluoroethane (R134a), 2,2-Dichloro-1,1,1-Trifluoroethane (R123) and 1,1-Dichloro-1-Fluoroethane (R141b).
PB95-175386 03,273

ETHANE/DICHLORO-TRIFLUORO
Vapor Pressure of 1,1-dichloro-2,2,2-trifluoroethane (R123).
PB95-126231 00,899

ETHANE/PENTAFLUORO
Measurements of the Viscosities of Saturated and Compressed Fluid 1-chloro-1,2,2,2-tetrafluoroethane (R124) and Pentafluoroethane (R125) at Temperatures between 120 and 420 K.
PB94-199791 03,254

ETHANE/TETRAFLUORO
Measurements of the Viscosities of Saturated and Compressed Liquid 1,1,1,2-Tetrafluoroethane (R134a), 2,2-Dichloro-1,1,1-Trifluoroethane (R123) and 1,1-Dichloro-1-Fluoroethane (R141b).
PB95-175386 03,273

ETHANOL
Effect of Ethanol on the Solubility of Dicalcium Phosphate Dihydrate in the System Ca(OH)2-H3PO4-H2O at 37C.
PB95-163507 00,163

Effect of Ethanol on the Solubility of Hydroxyapatite in the System Ca(OH)2-H3PO4-H2O at 25C and 33C.
PB95-169231 00,169

Millimeter- and Submillimeter-Wave Spectrum of trans-Ethyl Alcohol.
PB96-145578 01,102

ETHANOL MONOCHLOROBENZENE
Oscillometric and Conductometric Analysis of Aqueous and Organic Dosimeter Solutions.
PB96-135256 04,054

ETHANOL WATER SOLUTION
Molecular Dynamics Investigation of the Surface/Bulk Equilibrium in an Ethanol-Water Solution.
PB97-113112 01,183

ETHER/MALEIMIDOPHENYL GLYCIDYL
Thermal Behavior of 4-Maleimidophenyl Glycidyl Ether Resins.
PB95-153151 01,249

ETHERS
Thermodynamic Properties of CHF2-O-CHF2,Bis(difluoromethyl) Ether.
PB94-199569 00,798

2-Tunneling Path Internal-Axis-Method-Like Treatment of the Microwave Spectrum of Divinyl Ether.
PB94-200466 00,808

Thermodynamic Properties of Two Gaseous Halogenated Ethers from Speed-of-Sound Measurements: Difluoromethoxy-Difluoromethane and 2-Difluoromethoxy-1,1,1-Trifluoroethane.
PB96-102413 04,189

ETHYL RADICALS
Laser Flash Photolysis, Time-Resolved Fourier Transform Infrared Emission Study of the Reaction Cl + C2H5 yields HCl(v) + C2H4.
PB95-203238 01,049

ETHYLENE
Nonlinear Correlation of High-Pressure Vapor-Liquid Equilibrium Data for Ethylene + n-Butane Showing Inconsistencies in Experimental Compositions.
PB96-161906 01,141

ETHYLENE/DICHLORO
Gas Phase Reactivity Study of OH Radicals with 1,1-Dichloroethene and cis-1,1-Dichloroethene and Trans-1,2-Dichloroethene over the Temperature Range 240-400 K.
PB95-152146 00,939

ETHYLIDENE BISPHOSPHONATE/HYDROXY
Effect of 1-Hydroxyethylidene-1,1-Bisphosphonate on Membrane-Mediated Calcium Phosphate Formation in Model Liposomal Suspensions.
PB95-169223 03,469

ETRAN CODE
Electron-Photon Monte Carlo Calculations: The ETRAN Code.
PB97-110407 04,138

EULER-POINSOT PROBLEM
Complete Reduction of the Euler-Poinsot Problem.
PB94-172152 03,788

EUROPE
Aid for Smaller Businesses.
PB94-212461 00,492

EUROPEAN COMMUNITIES
TMACH Experiment Phase 1. Preliminary Developmental Evaluation.
PB96-195318 01,618

EUROPEAN UNION
Standards Setting in the European Union: Standards Organization and Officials in EU Standards Activities.
PB96-115019 02,919

EUTECTIC ALLOYS
Phase-Field Model for Solidification of a Eutectic Alloy.
PB95-147914 03,345

EVACUATING (TRANSPORTATION)
Feasibility and Design Considerations of Emergency Evacuation by Elevators.
PB94-163441 00,287

Feasibility of Fire Evacuation by Elevators at FAA Control Towers.
PB94-213857 04,844

EVACUATION
Smoke Control Systems for Elevator Fire Evacuation.
PB94-212883 00,291

EXITT: A Simulation Model of Occupant Decisions and Actions in Residential Fires.
PB94-213261 00,351

Human Factors Considerations for the Potential Use of Elevators for Fire Evacuation of FAA Air Traffic Control Towers.
PB94-217163 01,300

Enhancement of EXIT89 and Analysis of World Trade Center Data.
PB96-202247 00,231

EVALUATION
Guide to Software Engineering Environment Assessment and Evaluation.
PB94-140167 01,676

EVANESCENCE
Fugacity Coefficients of Hydrogen in (Hydrogen + Butane).
PB95-175212 02,491

EVAPORATIVE COOLING
Transient Cooling of a Hot Surface by Droplets Evaporation.
PB94-156957 03,783

Transient Cooling of a Hot Surface by Droplets Evaporation.
PB95-143194 03,890

Water Droplet Evaporation from Radiantly Heated Solids.
PB95-217147 00,394

Stable, Tightly Confining Magnetic Trap for Evaporative Cooling of Neutral Atoms.
PB96-200720 04,126

Sparse Water Sprays in Fire Protection.
PB96-202304 01,433

Intracycle Evaporative Cooling in a Vapor Compression Cycle.
PB97-116107 02,762

EVAPORATORS
Simple, Compact, High-Purity Cr Evaporator for Ultrahigh Vacuum.
PB94-216678 04,520

Closed Loop Controller for Electron-Beam Evaporators.
PB97-111470 04,393

EXAMINATION PROCEDURE OUTLINES (EPOS)
Examination Procedure Outlines: Keys to Solving the Handbook 44 Puzzle.
PB97-110217 *02,690*

EXCHANGE COUPLING
Influence of Thickness Fluctuations on Exchange Coupling in Fe/Cr/Fe Structures.
PB96-135371 *04,745*

SEMPA Studies of Exchange Coupling in Magnetic Multilayers.
PB96-164074 *04,780*

EXCHANGE INTERACTIONS
SEMPA Studies of Oscillatory Exchange Coupling.
PB95-163556 *04,625*

EXCITATION
Estimation of System Damping at the Lotung Site by Application of System Identification.
PB96-214697 *01,351*

EXCITATIONS
Low-Frequency Excitations of Oriented DNA.
PB96-137799 *03,548*

EXCITED STATES
Search for Small Violations of the Symmetrization Postulate in an Excited State of Helium.
PB96-123518 *04,050*

EXCITODION SPECTRA
Population Trapping in Short-Pulse Multiphoton Ionization.
PB96-164140 *04,371*

EXCITON
Intermediate Coupling in L2-L3 Core Excitons of MgO, Al2O3, and SiO2.
PB96-158043 *04,079*

EXCITONS
Excitons in Complex Quantum Nanostructures.
PB97-118343 *01,184*

EXCLUDED VOLUME
Segmental Concentration Profiles of End-Tethered Polymers with Excluded-Volume and Surface Interactions.
PB97-119002 *00,654*

EXIMER LASERS
Deep-UV Excimer Laser Measurements at NIST.
PB96-141031 *04,355*

EXIT89 COMPUTER MODEL
Enhancement of EXIT89 and Analysis of World Trade Center Data.
PB96-202247 *00,231*

EXOSKELETON
Robotics Application to Highway Transportation. Volume 2. Literature Search.
PB95-170551 *01,337*

EXOTOXINS
Genetically Engineered Pores for New Materials.
PB96-161641 *03,550*

EXPECT COMPUTER PROGRAM
Ouch Those Programs are Painful.
PB96-102678 *01,739*

EXPERIMENTAL DATA
Models and Interactions.
PB94-216306 *02,641*

EXPERIMENTAL DESIGN
Measuring the Stability of Three Copper Alloys.
PB94-199866 *03,326*

Introduction to ASTM 1199 'Wear Test Selection for Design and Application'.
PB95-162517 *03,238*

Taguchi's Parameter Design: A Panel Discussion.
PB96-111802 *03,445*

Developing Measurement for Experimentation.
PB97-118707 *03,450*

EXPERIMENTAL MECHANICS
Journal of Research of the National Institute of Standards and Technology, January/February 1996. Volume 101, Number 1.
PB96-175666 *00,113*

Theory of Electron Beam Moire.
PB96-175690 *04,373*

EXPERIMENTATION
Guidelines for Reporting Results of Computational Experiments. Report of the Ad hoc Committee.
PB94-212347 *03,427*

EXPERT PROGRAMMING LANGUAGE
Kibitz-Connecting Multiple Interactive Programs Together.
PB94-213311 *01,696*

EXPERT SYSTEMS
PC-Based Prototype Expert System for Data Management and Analysis of Creep and Fatigue of Selected Materials at Elevated Temperatures.
PB94-172251 *03,202*

Highway Concrete (HWYCON) Expert System User Reference and Enhancement Guide.
PB94-215670 *01,316*

Application of Expert System to Select Data Sources from Chemical Information Databases.
PB95-125654 *00,505*

Exposure: An Expert System Fire Code.
PB95-162913 *04,868*

Expert Control System Shell Version 1.0 User's Guide.
PB95-198859 *01,790*

EXPOSURE (PHYSIOLOGY)
Maximum Permissible Body Burdens and Maximum Permissible Concentrations of Radionuclides in Air and in Water for Occupational Exposure.
AD-A280 282/5 *03,610*

EXPRESS
Concepts of the NIST EXPRESS Server.
PB95-180543 *02,781*

EXPRESS LANGUAGE
Extensions of the Prototype Application Protocol of Ready-to-Wear Apparel Pattern Making.
PB96-128194 *03,198*

EXPRESS LANGUAGE ENVIRONMENT
Dynamic Objects and Meta-Level Programming of an EXPRESS Language Environment.
PB96-190053 *01,774*

EXPRESS MODELING LANGUAGE
Structural EXPRESS Editor.
PB94-159795 *02,769*

EXTENDED CORRESPONDING STATES
Thermodynamic Properties of the Methane-Ethane System.
PB95-125779 *00,891*

EXTENSOMETERS
Torsional Dilatometer for Volume Change Measurements on Deformed Glasses: Instrument Description and Measurements on Equilibrated Glasses.
PB94-211166 *03,379*

EXTENSOMETRY
Sources of Strain-Measurement Error in Flag-Based Extensometry.
PB97-118731 *03,108*

EXTINCTION TIME
Suppression Research: Strategies.
PB94-211372 *00,346*

EXTRACTION
Distributed measurements of tracer response on packed bed flows using a fiberoptic probe array. Final report.
DE95013079 *00,667*

Thermophysical Property Data for Supercritical Fluid Extraction Design.
PB94-199221 *00,668*

EXTRACTION COLUMNS
Continuous Counter-Current Two Phase Aqueous Extraction.
PB95-161212 *00,675*

EXTRACTIVE METALLURGY
Vapor Transport in Materials and Process Chemistry.
PB94-211745 *00,669*

EXTRACTORS
Influence of Envelopes Geometry on the Sensitivity of 'Nude' Ionization Gauges.
PB97-119077 *04,174*

EXTRAPOLATION CHAMBERS
Extrapolation Chamber Measurements on (90)Sr + (90)Y Beta-Particle Ophthalmic Applicator Dose Rates.
PB95-153375 *03,626*

EXTREME ULTRAVIOLET
Improved Reflectometry Facility at the National Institute of Standards and Technology.
PB96-160338 *04,087*

EXTREME ULTRAVIOLET RADIATION
Volume-Limited ROSAT Survey of Extreme Ultraviolet Emission from all Nondegenerate Stars within 10 Parsecs.
PB96-103189 *00,093*

EXTREME VALUE ESTIMATION
Recent Approaches to Extreme Value Estimation with Application to Wind Speeds. Part 1. The Pickands Method.
PB94-213170 *00,019*

EXTREME-VALUE PROBLEMS
Recent Approaches to Extreme Value Estimation with Application to Wind Speeds. Part 1. The Pickands Method.
PB94-213170 *00,019*

Journal of Research of the National Institute of Standards and Technology, July/August 1994. Volume 99, Number 4. Special Issue: Extreme Value Theory and Applications. Proceedings of the Conference on Extreme Value Theory and Applications, Volume 2. Held at Gaithersburg, Maryland, in May 1993.
PB95-160594 *03,440*

Assessment of 'Peaks Over Threshold' Methods for Estimating Extreme Value Distribution Tails.
PB95-161360 *00,441*

Extreme Wind Distribution Tails: A 'Peaks Over Threshold' Approach.
PB95-219416 *00,127*

Development of Computer-Based Models of Standards and Attendant Knowledge-Base and Procedural Systems.
PB96-155783 *00,464*

Extreme Winds Estimation by 'Peaks Over Threshold' and Epochal Methods.
PB96-159686 *00,468*

Modeling of Extreme Loading by 'Peaks Over Threshold' Methods.
PB96-159694 *00,469*

EXTREME VALUE THEORY
Extreme Value Theory and Applications: Proceedings of the Conference on Extreme Value Theory and Applications, Volume 3. Held in Gaithersburg, Maryland in May 1993.
PB95-104956 *03,432*

Journal of Research of the National Institute of Standards and Technology, July/August 1994. Volume 99, Number 4. Special Issue: Extreme Value Theory and Applications. Proceedings of the Conference on Extreme Value Theory and Applications, Volume 2. Held at Gaithersburg, Maryland, in May 1993.
PB95-160594 *03,440*

EXTREMELY HIGH FREQUENCIES
Comparison of k-Correction and Taylor-Series Correction for Probe-Position Errors in Planar Near-Field Scanning.
PB96-147137 *02,012*

EXTREMELY LOW FREQUENCIES
ELF Electric and Magnetic Field Measurement Methods.
PB95-161675 *04,423*

EXTREMELY LOW FREQUENCY
Condensed Catalogue of Electromagnetic Environment Measurements, 30 - 300 Hz.
PB95-162210 *01,899*

Catalogue of Electromagnetic Environment Measurements, 30-300 Hz.
PB96-155452 *01,943*

EXTREMUM VALUES
Heap of Data.
PB97-111488 *03,424*

EYE PIGMENTS
Retinal-Protein Complexes as Optoelectronic Components.
PB95-150397 *02,146*

EYE PROTEINS
Retinal-Protein Complexes as Optoelectronic Components.
PB95-150397 *02,146*

EYE SAFETY
Optical Density Measurements of Laser Eye Protection Materials.
PB96-190301 *00,190*

F STARS
IUE Observations of Solar-Type Stars in the Pleiades and the Hyades.
PB94-199437 *00,053*

FABRICATION
Fabrication of Flaw-Tolerant Aluminum-Titanate-Reinforced Alumina.
PB95-162533 *03,161*

MEMS in Standard CMOS VLSI Technology.
PB96-102363 *02,377*

Superconducting Integrated Circuit Fabrication with Low Temperature ECR-Based PECVD SiO2 Dielectric Films.
PB96-103015 *04,719*

Fabrication of Optics by Diamond Turning.
PB96-111695 *02,954*

FACE (ANATOMY)
Face Recognition Technology for Law Enforcement Applications.
PB94-207768 *01,837*

FACE CENTERED CUBIC LATTICES
Anisotropy of Interfaces in an Ordered Alloy: A Multiple-Order-Parameter Model.
PB96-131594 *04,741*

FACE RECOGNITION
Face Recognition Technology for Law Enforcement Applications.
PB94-207768 *01,837*

FACSIMILE TRANSMISSION
Procedures for Document Facsimile Transmission Issued by General Services Administration, April 14, 1982. Federal Standard 1063.
FIPS PUB 148 *01,516*

FACTOR ANALYSIS
Factorial Design Techniques Applied to Optimization of AMS Graphite Target Preparation.
PB95-151197 *00,584*

FAILURE
Fracture Behavior of Large-Scale Thin-Sheet Aluminum Alloy.
N95-19494/0 *03,311*

FAILURE ANALYSIS
Fracture Behavior of Large-Scale Thin-Sheet Aluminum Alloy.
N95-19494/0 *03,311*

Analysis of Failed Dry Pipe Fire Suppression System Couplings from the Filene Center at Wolf Trap Farm Park for the Performing Arts.
PB94-164407 *00,331*

Potential Drop in the Center-Cracked Panel with Asymmetric Crack Extension.
PB95-107330 *04,819*

Creep Rupture of MoSi2/SiCp Composites.
PB95-152294 *03,154*

Journal of Research of the National Institute of Standards and Technology, July/August 1994. Volume 99, Number

4. Special Issue: Extreme Value Theory and Applications. Proceedings of the Conference on Extreme Value Theory and Applications, Volume 2. Held at Gaithersburg, Maryland, in May 1993.
PB95-160594 *03,440*

Characteristics of Adhesive-Bonded Seams Sampled from EPDM Roof Membranes.
PB95-162491 *00,377*

Exponentially Rapid Coarsening and Buckling in Coherently Self-Stressed Thin Plates.
PB95-202347 *04,821*

Critical-Current Degradation in Nb3 Al Wires Due to Axial and Transverse Stress.
PB95-202784 *02,226*

Room-Temperature Flexure Fixture for Advanced Ceramics.
PB95-210498 *03,061*

Evaluation of Thermal Wave Imaging for Detection of Machining Damage in Ceramics.
PB95-220547 *03,062*

Fracture Testing of Large-Scale Thin-Sheet Aluminum Alloy.
PB95-242368 *00,024*

Failure of All-Ceramic Fixed Partial Dentures 'In vitro' and 'In vivo': Analysis and Modeling.
PB96-122536 *00,175*

Catastrophic Failures Propagate Field of Fracture Mechanics.
PB96-135140 *03,217*

Correlations between Flaw Tolerance and Reliability in Zirconia.
PB96-161922 *02,986*

Cracks and Dislocations in Face-Centered Cubic Metallic Multilayers.
PB96-163696 *02,989*

Model for Microcrack Initiation and Propagation beneath Hertzian Contacts in Polycrystalline Ceramics.
PB96-163704 *03,077*

Fracture of Silicon Nitride and Silicon Carbide at Elevated Temperatures.
PB96-180260 *03,179*

Diffusive Crack Growth at a Bimaterial Interface.
PB96-204110 *03,090*

Life Prediction of a Continuous Fiber Reinforced Ceramic Composite Under Creep Conditions.
PB96-204128 *03,091*

Postfailure Subsidiary Cracking from Indentation Flaws in Brittle Materials.
PB97-110340 *03,103*

FAILURE (MECHANICS)

Catastrophic Failures Propagate Field of Fracture Mechanics.
PB96-135140 *03,217*

FAILURE MODES

Evaluating the Seismic Performance of Lightly-Reinforced Circular Concrete Bridge Columns.
PB95-163259 *01,335*

FAR INFRARED RADIATION

Laser Spectroscopy of Carbon Monoxide: A Frequency Reference for the Far Infrared.
PB95-163606 *04,277*

Niobium Microbolometers for Far-Infrared Detection.
PB96-111729 *02,184*

FAR ULTRAVIOLET RADIATION

Bibliography of Photon Total Cross Section (Attenuation Coefficient) Measurements 10 eV to 13.5 GeV, 1907-1993.
PB94-193760 *03,804*

GHRS Observations of Cool, Low-Gravity Stars. 1. The Far-Ultraviolet Spectrum of alpha Orions (M2 Iab).
PB96-112016 *00,094*

FAR ULTRAVIOLET SPECTROGRAPH EXPLORER

Scientific Rationale and Present Implementation Strategy for the Far Ultraviolet Spectrograph Explorer (FUSE).
PB96-123328 *00,045*

FARADAY CONSTANT

Faraday Constant.
PB96-159793 *01,955*

FARADAY EFFECT

Submicroampere-Per-Root-Hertz Current Sensor Based on the Faraday Effect in Ga: YIG.
PB95-162467 *02,155*

Magnetooptic Effects.
PB96-119292 *04,338*

Faraday Effect Sensors for Magnet Field and Electric Current.
PB96-119664 *04,736*

Fiber-Optic Faraday-Effect Magnetic-Field Sensor Based on Flux Concentrators.
PB96-200308 *02,201*

Fundamentals and Problems of Fiber Current Sensors.
PB97-111835 *02,205*

FARMED STRUCTURES

Enhancements to Program IDARC: Modeling Inelastic Behavior of Welded Connections in Steel Moment-Resisting Frames.
PB95-231601 *00,452*

FAST FOURIER TRANSFORMATIONS

Comparison of FFT Fingerprint Filtering Methods for Neural Network Classification.
PB95-136362 *01,840*

FASTENERS

Program Handbook: Requirements for Obtaining NIST Approval/Recognition of a Laboratory Accreditation Body Under P.L. 101-592. The Fastener Quality Act.
PB94-210143 *02,859*

Portsmouth Fastener Manufacturing Workstation. User's Manual.
PB95-147922 *02,860*

Review and Upgrading of Military Fastener Test Standard MIL-STD-1312.
PB95-154720 *02,947*

National Voluntary Laboratory Accreditation Program (NVLAP): Fasteners and Metals.
PB97-114185 *02,881*

FASTNER QUALITY ACT

Implementation of the Fastener Quality Act.
PB96-160676 *02,876*

FATIGUE LIFE

Generic Model for Creep Rupture Lifetime Estimation on Fibrous Ceramic Composites.
PB94-200235 *03,137*

FATIGUE (MECHANICS)

PC-Based Prototype Expert System for Data Management and Analysis of Creep and Fatigue of Selected Materials at Elevated Temperatures.
PB94-172251 *03,202*

Transient Subcritical Crack-Growth Behavior in Transformation-Toughened Ceramics.
PB94-200656 *03,038*

FAULT DETECTION

Recent Developments at NIST on Optical Current Sensors and Partial Discharge Diagnostics.
PB95-151114 *02,147*

Fault Diagnosis of an Air-Handling Unit Using Artificial Neural Networks.
PB97-121321 *00,283*

FAULTS

Software Needs in Special Functions.
PB96-200977 *01,778*

FDDI

Planning for the Fiber Distributed Data Interface (FDDI).
PB94-135761 *01,621*

FDMS COMPUTER DATA BASE

Fire Data Management System, FDMS 2.0, Technical Documentation.
PB94-164019 *01,358*

FEATURE EXTRACTION

Object Finder for Digital Images Based on Multiple Thresholds, Connectivity, and Internal Structures.
PB94-199106 *01,833*

Self-Organizing Neural Network Character Recognition Using Adaptive Filtering and Feature Extraction.
PB96-119797 *01,855*

FEDERAL AGENCIES

Study of Federal Agency Needs for Information Technology Security.
PB94-193653 *01,579*

Guidance to Federal Agencies on the Use of Trusted Systems.
PB95-163440 *01,597*

Multi-Agency Certification and Accreditation (C and A) Process: A Worked Example.
PB95-171955 *01,601*

Federal Labs Have Key Role in Metrication.
PB96-123401 *02,920*

Security Program Management.
PB96-156112 *01,610*

TMACH Experiment Phase 1. Preliminary Developmental Evaluation.
PB96-195318 *01,618*

Science, Technology, and Competitiveness: Retrospective on a Symposium in Celebration of NIST's 90th Anniversary and the 25th Anniversary of the Gaithersburg Laboratories, November 14-15, 1991.
PB97-121610 *02,696*

FEDERAL BUILDING

Summary of Federal Construction and Building R and D in 1994.
PB97-114250 *00,234*

FEDERAL BUILDINGS

Seismic Instrumentation of Existing Buildings.
PB94-159779 *00,420*

Evaluation and Strengthening Guidelines for Federal Buildings: Identification of Current Federal Agency Programs.
PB94-176278 *00,424*

Evaluation and Strengthening Guidelines for Federal Buildings: Assessment of Current Federal Agency Evaluation Programs and Rehabilitation Criteria and Development of Typical Costs for Seismic Rehabilitation.
PB94-181856 *00,425*

Environmental Evaluation of a New Federal Office Building.
PB94-199874 *02,538*

Standards of Seismic Safety for Existing Federally Owned or Leased Buildings and Commentary.
PB95-130209 *00,431*

Evaluation and Retrofit Standards for Existing Federally Owned and Leased Buildings.
PB95-150918 *00,434*

Implementation of Executive Order 12699: Seismic Safety of Federal and Federally Assisted or Regulated New Building Construction.
PB95-151809 *00,436*

Life-Cycle Costing Workshop for Energy Conservation in Buildings: Student Manual.
PB95-175006 *00,257*

Seismic Safety of Federal Buildings. Initial Program: How Much Will It Cost.
PB95-182291 *00,447*

Performance of Federal Buildings in the January 17, 1994 Northridge Earthquake.
PB95-231775 *00,453*

ICSSC Guidance on Implementing Executive Order 12941 on Seismic Safety of Existing Federally Owned or Leased Buildings.
PB96-128103 *00,459*

How-To Suggestions for Implementing Executive Order 12941 on Seismic Safety of Existing Federal Buildings, A Handbook.
PB96-131552 *00,461*

Executive Order 12941. Seismic Safety of Existing Federally Owned or Leased Buildings: It's History, Content and Objectives.
PB96-156021 *00,465*

Life-Cycle Costing Manual for the Federal Energy Management Program. 1995 Edition.
PB96-172317 *02,511*

FEDERAL COMMUNICATIONS COMMISSION

National Voluntary Laboratory Accreditation Program: Electromagnetic Compatibility and Telecommunications. FCC Methods.
PB95-242376 *02,664*

FEDERAL CRITERIA

Proceedings of the Workshop on the Federal Criteria for Information Technology Security. Held in Ellicot City, Maryland on June 2-3, 1993.
PB94-162583 *01,575*

FEDERAL GOVERNMENT

Computer Security Management and Planning in the U.S. Federal Government.
PB95-163432 *01,596*

Addressing U.S. Government Security Requirements for OSI.
PB96-160577 *01,611*

Federal Implementation Guideline for Electronic Data Interchange: ASC X12 003050 Transaction Set 836 Procurement Notices. Implementation Convention.
PB96-178892 *01,827*

FEDERAL INFORMATION PROCESSING STANDARDS

Data Encryption Standard (DES); Category: Computer Security; Subcategory: Cryptography.
FIPS PUB 46-2 *01,572*

Graphical Kernel System (GKS). Category: Software Standard. Subcategory: Graphics. International Standard: Information Technology; Computer Graphics; Graphical Kernel System (GKS) Language Bindings. Part 4: C.
FIPS PUB 120-1C *01,792*

Security Requirements for Cryptographic Modules; Category: Computer Security; Subcategory: Cryptography.
FIPS PUB 140-1 *01,567*

Programmer's Hierarchical Interactive Graphics System (PHIGS). Category: Software Standard; Subcategory: Graphics.
FIPS PUB 153-1 *01,668*

User Interface Component of the Applications Portability Profile Category: Software Standard; Subcategory: Application Program Interface.
FIPS PUB 158-1 *01,793*

Spatial Data Transfer Standard (SDTS): Category: Software Standard; Subcategory: Information Interchange.
FIPS PUB 173-1 *01,794*

Spatial Data Transfer Standard (SDTS). Category: Software Standard; Subcategory: Information Interchange. (FIPS PUB 173-1A).
FIPS PUB 173-1A *01,795*

Spatial Data Transfer Standard (SDTS). Category: Software Standard; Subcategory: Information Interchange. (FIPS PUB 173-1B).
FIPS PUB 173-1B *01,796*

Secure Hash Standard. Category: Computer Security.
FIPS PUB 180-1 *01,568*

Escrowed Encryption Standard (EES); Category: Computer Security; Subcategory: Cryptography.
FIPS PUB 185 *01,569*

Administration Standard for the Telecommunications Infrastructure of Federal Buildings. Category: Telecommunications Standard; Subcategory: Telecommunications Administration.
FIPS PUB 187 *01,461*

Standard Security Label for Information Transfer; Category: Computer Security; Subcategory: Security Labels.
FIPS PUB 188 *01,571*

Portable Operating System Interface (POSIX). Part 2. Shell and Utilities. Category: Software Standard; Subcategory: Operating Systems.
FIPS PUB 189 *01,797*

Guideline for the Analysis of Local Area Network Security. Category: Computer Security; Subcategory: Risk Analysis and Contingency Planning.
FIPS PUB 191 *01,799*

Application Profile for the Government Information Locator Service (GILS). Category: Software Standard; Subcategory: Information Interchange.
FIPS PUB 192 *01,800*

SQL Environments. Category: Software Standard; Subcategory: Database.
FIPS PUB 193 *01,801*

Open Document Architecture (ODA) Raster Document Application Profile (DAP). Category: Software Standard; Subcategory: Graphics.
FIPS PUB 194 *01,669*

Federal Building Grounding and Bonding Requirements for Telecommunications. Category: Telecommunications Standard; Subcategory: Grounding and Bonding.
FIPS PUB 195 *01,802*

Validated Products List (Cobol, Fortran, ADA, Pascal, MUMPS, SQL).
PB94-937300 *01,700*

Codes for Named Populated Places, Primary County Divisions, and Other Locational Entities of the United States (FIPS PUB 55-3) (on Magnetic Tape).
PB95-502563 *00,129*

Validated Products List (Cobol, Fortran, ADA, Pascal, MUMPS, SQL).
PB95-937300 *01,738*

FEDERAL INFORMATION PROCESSING STANDARDS; CRYPTOGRAPHY

Guideline for the Use of Advanced Authentication Technology Alternatives. Category: Computer Security. Subcategory: Access Control.
FIPS PUB 190 *01,798*

FEDERAL LAW

1950 Supplement to Screw-Thread Standards for Federal Services. 1944.
AD-A280 223/9 *03,656*

FEEDBACK CONTROL

Control of Gas-Metal-Arc Welding Using Arc-Light Sensing.
PB96-131461 *02,869*

FERMENTATION

Feasibility of Fluorescence Detection of Tetracycline in Media Mixtures Employing a Fiber Optic Probe.
PB96-163654 *00,511*

FERRIC NITRILOTRIACETATE

DNA Base Modifications in Renal Chromatin of Wistar Rats Treated with a Renal Carcinogen, Ferric Nitrilotriacetate.
PB95-150363 *03,648*

Treatment of Wistar Rats with a Renal Carcinogen, Ferric Nitrilotriacetate, Causes DNA-Protein Cross-Linking between Thymine and Tyrosine in Their Renal Chromatin.
PB96-112115 *03,649*

FERRITE GARNETS

Magneto-Optic Magnetic Field Sensors Based on Uniaxial Iron Garnet Films in Optical Waveguide Geometry.
PB95-168498 *02,159*

Magnetic Force Microscopy Images of Magnetic Garnet with Thin-Film Magnetic Tip.
PB95-176210 *04,669*

Novel Bulk Iron Garnets for Magneto-Optic Magnetic Field Sensing.
PB95-180204 *04,675*

Domain Effects in Faraday Effect Sensors Based on Iron Garnets.
PB95-202461 *02,268*

FERRITES

Applicability of Effective Medium Theory to Ferroelectric/Ferrimagnetic Composites with Composition and Frequency-Dependent Complex Permittivities and Permeabilities.
PB96-157854 *01,945*

FERROCENES

High-Pressure Equilibrium Cell for Solubility Measurements in Supercritical Fluids.
PB95-175634 *00,998*

FERROELECTRIC MATERIALS

Hysteresis Measurements of Remanent Polarization and Coercive Field in Polymers.
PB94-199767 *04,475*

FERROELECTRICITY

Ferroelectric Thin Film Characterization Using Superconducting Microstrip Resonators.
PB96-102389 *02,270*

FERROMAGNETIC MATERIALS

Monte Carlo and Mean-Field Calculations of the Magnetocaloric Effect of Ferromagnetically Interacting Clusters.
PB94-172087 *03,201*

FERROMAGNETIC RESONANCE

Method for Determining Both Magnetostriction and Elastic Modulus by Ferromagnetic Resonance.
PB95-150108 *02,974*

FERROUS TRIMETHYLAMMONIUM CHLORIDE

Quasielastic and Inelastic Neutron-Scattering Studies of ((CD3)3ND)FeCl3.2D2O: A One-Dimensional Ising Ferromagnet.
PB95-140562 *04,547*

FIBER AMPLIFIERS

Pump-Induced Dispersion of Erbium-Doped Fiber Measured by Fourier-Transform Spectroscopy.
PB94-211935 *04,236*

FIBER ANNEALING

Improved Annealing Technique for Optical Fiber.
PB96-119680 *04,343*

FIBER COMPOSITES

Interface Properties for Ceramic Composites from a Single Fiber Pull-Out Test.
PB94-199361 *03,135*

Generic Model for Creep Rupture Lifetime Estimation on Fibrous Ceramic Composites.
PB94-200235 *03,137*

Elastic Properties of Uniaxial-Fiber Reinforced Composites: General Features.
PB94-200649 *03,140*

Determination of Fiber-Matrix Interfacial Properties of Importance to Ceramic Composite Toughening.
PB95-125811 *03,149*

Environmental Durability of Glass-Fiber Composites.
PB95-203220 *03,166*

Torsion Modulus and Internal Friction of a Fiber-Reinforced Composite.
PB96-112339 *03,070*

FIBER DISTRIBUTED DATA INTERFACE

Planning for the Fiber Distributed Data Interface (FDDI).
PB94-135761 *01,621*

FIBER GRATINGS

Growth Characteristics of Fiber Gratings.
PB96-122957 *04,346*

FIBER LASERS

Electronically Tunable Fiber Laser for Optical Pumping of (3)He and (4)He.
PB96-201165 *04,381*

FIBER OPTIC SENSORS

Faraday Effect Current Sensors.
PB94-200698 *02,127*

Faraday Effect Sensors: A Review of Recent Progress.
PB94-200706 *02,128*

Recent Developments at NIST on Optical Current Sensors and Partial Discharge Diagnostics.
PB95-151114 *02,147*

High Speed, High Sensitivity Magnetic Field Sensors Based on the Faraday Effect in Iron Garnets.
PB95-153391 *02,151*

Polarization Dependence of Response Functions in 3x3 Sagnac Optical Fiber Current Sensors.
PB95-162426 *02,154*

Effect of Semiconductor Laser Characteristics on Optical Fiber Sensor Performance.
PB95-169132 *02,167*

Self-Calibrating Fiber Optic Sensors: Potential Design Methods.
PB95-169298 *02,172*

Self Calibrating Fiber Optic Sensors: Potential Design Methods.
PB95-169306 *02,173*

Simultaneous Laser-Diode Emission and Detection for Fiber-Optic Sensor Applications.
PB96-155502 *04,062*

High Frequency Magnetic Field Sensors Based on the Faraday Effect in Garnet Thick Films.
PB96-190384 *02,282*

Magneto-Optic Rotation Sensor Using a Laser Diode as Both Source and Detector.
PB97-111272 *04,390*

FIBER OPTICS

Technical Digest: Symposium on Optical Fiber Measurements (8th), 1994. Held in Boulder, Colorado on September 13-15, 1994.
PB94-207636 *04,231*

Complex Propagation Constants for Nonuniform Optical Waveguides: Calculations.
PB95-125910 *04,249*

Fiber Spot Size: A Simple Method of Calculation.
PB95-125936 *04,250*

LP11-Mode Leakage Loss in Coated Depressed Clad Fibers.
PB95-141115 *02,145*

Opportunities for Innovation: Optoelectronics.
PB96-118039 *01,928*

Polarization Dependence of Response Functions in 3x3 Sagnac Optical Fiber Current Sensors.
PB96-122684 *02,189*

Growth Characteristics of Fiber Gratings.
PB96-122957 *04,346*

Fiber Coating Diameter: Toward a Glass Artifact Standard.
PB96-140389 *02,234*

Feasibility of Fluorescence Detection of Tetracycline in Media Mixtures Employing a Fiber Optic Probe.
PB96-163654 *00,511*

Automated Measurement of Nonlinearity of Optical Fiber Power Meters.
PB96-176540 *04,110*

Technical Digest: Symposium on Optical Fiber Measurements (9th), 1996. Held in Boulder, Colorado on October 1-3, 1996.
PB97-108583 *04,383*

Anomalous Relation between Time and Frequency Domain PMD Measurements.
PB97-119390 *04,398*

FIBER OPTICS TRANSMISSION LINES

Optical Fiber Sensors: Accelerating Applications in Navy Ships.
PB94-186848 *02,632*

FIBER REINFORCED COMPOSITES

AMRF Composite Fabrication Workstation.
PB94-172681 *02,810*

Friction Processes in Brittle Fracture.
PB96-161765 *03,076*

Estimation of the Orientation Distribution of Short-Fiber Composites Using Ultrasonic Velocities.
PB96-176656 *03,178*

FIBERBOARD

Wall Flame Heights with External Radiation.
PB95-163481 *00,380*

FIBERS

Fuzed-Quartz Fibers. A Survey of Properties, Applications and Production Methods.
AD-A286 620/0 *00,656*

Perspective on Fiber Coating Technology.
PB94-200540 *03,118*

Effect of Heterogeneous Porous Media on Mold Filling in Resin Transfer Molding.
PB95-108676 *03,197*

Video Microscopy Applied to Optical Fiber Geometry Measurements.
PB95-173068 *04,295*

Optical Fiber, Fiber Coating, and Connector Ferrule Geometry: Results of Interlaboratory Measurement Comparisons.
PB96-154422 *04,360*

Evidence of Crosslinking in Methyl Pendent PBZT Fiber.
PB97-112486 *03,393*

FIBROUS POROUS MEDIA

Analysis of Transverse Flow in Aligned Fibrous Porous Media.
PB96-167200 *03,177*

FIELD EFFECT TRANSISTORS

Efficient Method to Compute the Maximum Transient Drain Current Overshoot in Silicon on Insulator Devices.
PB94-172483 *02,300*

Experimental Study of Reverse-Bias Failure Mechanisms in Bipolar Mode JFET (BMFET).
PB95-152997 *02,340*

Anomalous Behavior of a Quantized Hall Plateau in a High-Mobility Si Metal-Oxide-Semiconductor Field-Effect Transistor.
PB95-164174 *02,354*

Buffer Layer Modulation-Doped Field-Effect-Transistor Interactions in the Al0.33Ga0.67As/GaAs Superlattice System.
PB96-102876 *02,380*

FIELD EMISSION

Planar Lenses for Field-Emitter Arrays.
PB96-103064 *02,112*

FIELD EMITTER ARRAYS

Planar Lenses for Field-Emitter Arrays.
PB96-103064 *02,112*

FIELD VARIABLES

Composition Dependence of a Field Variable Along the Binary Fluid Mixture Critical Locus.
PB95-176038 *01,003*

FILAMENTS

Influence of the Filament Potential Wave Form on the Sensitivity of Glass-Envelope Bayard-Alpert Gages.
PB95-175014 *02,657*

FILE FORMAT

Retrieving Articles from the Internet (without a UNIX Workstation). Part 1. File Formats and Software Tools.
PB95-168720 *02,728*

FILE TRANSFER PROTOCOL

Using Archie to Find Files on the INTERNET.
PB95-168605 *02,727*

FILM DOSIMETERS

Radiochromic Solid-State Polymerization Reaction.
PB96-180146 *01,290*

FILM DOSIMETRY

Thin Dyed-Plastic Dosimeter for Large Radiation Doses.
PB95-107363 *03,872*

Electron and Proton Dosimetry with Custom-Developed Radiochromic Dye Films.
PB95-151106 *03,713*

Effect of Formulation Changes on the Response to Ionizing Radiation of Radiochromic Dye Films.
PB97-119028 *04,171*

FILM RESISTORS

Characterization of Interface Defects in Oxygen-Implanted Silicon Films.
PB94-216629 *02,322*

Planar Resistors for Probe Station Calibration.
PB95-163697 02,351

FILM THICKNESS
Electrical Method for Determining the Thickness of Metal Films and the Cross-Sectional Area of Metal Lines.
PB95-203170 02,370

Electrical Characterization of Integrated Circuit Metal Line Thickness.
PB96-138433 02,414

FILMS
Wear of Selected Materials and Composites Sliding against MoS2 Films.
PB94-172749 03,231

Critical Current Density, Irreversibility Line, and Flux Creep Activation Energy in Silver-Sheathed Bi2Sr2Ca2Cu2Ox Superconducting Tapes.
PB95-162749 04,616

Nanoscale Study of the Hydrogenated Amorphous Silicon Surface.
PB96-103056 04,720

Characterization of Liquid-Phase Epitaxially Grown HgCdTe Films by Magnetoresistance Measurements.
PB96-123617 04,738

Stagnant Film Model of the Effect of Natural Convection on the Dendrite Operating State.
PB96-146832 04,765

Lattice Statics of Interfaces and Interfacial Cracks in Bimaterial Solids.
PB96-161823 02,985

Workshop on Characterizing Diamond Films (4th). Held in Gaithersburg, Maryland on March 4-5, 1996.
PB96-183090 04,786

FILTERS
Systematic Studies of the Effect of a Post-Detection Filter on a Josephson-Junction Noise Thermometer.
PB95-162988 03,940

Interface-Filter Characterization of Spectraradiometers and Colorimeters.
PB97-122212 04,399

FINANCE
Financing Tomorrow's Infrastructure: Challenges and Issues. Proceedings of a Colloquium. Held in Washington, DC. on October 20, 1995.
PB96-189444 00,481

FINANCIAL MANAGEMENT
Self Monitoring Accounting Systems.
PB95-216602 00,007

Manager's Guide for Monitoring Data Integrity in Financial Systems.
PB96-165915 00,003

FINDING LIST
Ultraviolet Multiplet Table. Finding List for Spectra of the Elements Molybdenum to Lanthanum (Z = 42 to 57); Hafnium to Radium (Z = 72 to 88).
AD-A278 131/8 00,709

Ultraviolet Multiplet Table.
AD-A278 446/0 00,710

FINE STRUCTURE
Fine Structure of Negative Ions of Alkaline-Earth-Metal Atoms.
PB94-211182 03,837

Atomic Oxygen Fine Structure Splittings with Tunable Far Infrared Spectroscopy.
PB95-152203 03,915

FINE STRUCTURE CONSTANT
Fine-Structure Constant.
PB94-172996 03,795

FINE WATER SPRAYS
Protection of Data Processing Equipment with Fine Water Sprays.
PB95-174975 02,610

FINGER PLUGGERS
Effect of Three Sterilization Techniques on Finger Pluggers.
PB94-216090 00,150

FINGERPRINT CLASSIFICATION
Comparison of FFT Fingerprint Filtering Methods for Neural Network Classification.
PB95-136362 01,840

Improving Neural Network Performance for Character and Fingerprint Classification by Altering Network Dynamics.
PB95-267803 01,851

PCASYS: A Pattern-Level Classification Automation System for Fingerprints.
PB95-267936 01,853

Improving Neural Network Performance for Character and Fingerprint Classification by Altering Network Dynamics.
PB96-123195 01,856

FINGERPRINTS
NIST-Coordinated Standard for Fingerprint Data Interchange.
PB94-216645 01,808

FINITE ELEMENT METHOD
Application of a Simple Technique for Estimating Errors of Finite-Element Solutions Using a General-Purpose Code.
PB94-200250 04,818

Analysis of Creep in a Si-SiC C-Ring by Finite Element Method.
PB94-200268 03,037

FINS
Single-Phase Heat Transfer and Pressure Drop Characteristics of an Integral-Spine-Fin Within an Annulus.
PB94-194073 03,805

Single-Phase Heat Transfer and Pressure Drop Characteristics of an Integral-Spine Fin Within an Annulus.
PB97-122386 04,179

FIPS PUB 180
Secure Hash Standard. Category: Computer Security.
FIPS PUB 180-1 01,568

FIRE ALARM SYSTEMS
Assessment of Technologies for Advanced Fire Detection.
PB95-126330 00,294

FIRE CODES
Exposure: An Expert System Fire Code.
PB95-162913 04,868

FIRE DATA MANAGEMENT SYSTEM
Fire Data Management System, FDMS 2.0, Technical Documentation.
PB94-164019 01,358

Standardization of Formats and Presentation of Fire Data - The FDMS.
PB94-198462 01,371

Development of the Fire Data Management System.
PB94-206091 00,339

FIRE DETECTION SYSTEMS
Proceedings of the 1995 Workshop on Fire Detector Research. Held on February 6-7, 1995.
PB95-270062 02,611

Development of an Economical Video Based Fire Detection and Location System.
PB96-193743 00,228

FIRE DETECTORS
Performance Parameters of Fire Detection Systems.
PB94-194339 00,288

Studies Assess Performance of Residential Detectors.
PB94-199262 00,290

Assessment of Technologies for Advanced Fire Detection.
PB95-126330 00,294

Acoustic Emission of Structural Materials Exposed to Open Flames.
PB95-164810 00,296

Early Detection of Room Fires Through Acoustic Emission. (NIST Reprint).
PB95-180311 00,298

Santa Ana Fire Department Experiment at 1315 South Bristol, July 14, 1994.
PB95-188868 00,389

Review of Measurements and Candidate Signatures for Early Fire Detection.
PB95-189452 00,300

Field Modeling: Simulating the Effect of Sloped Beamed Ceilings on Detector and Sprinkler Response.
PB96-122866 01,406

NASA Fire Detector Study.
PB96-183108 01,423

FIRE DYNAMICS
Prediction of Fire Dynamics.
PB94-193620 00,336

FIRE ESTINGUISHING AGENTS
Minimum Mass Flux Requirements to Suppress Burning Surfaces with Water Sprays.
PB96-183181 01,425

FIRE EXTINGUISHERS
Suppression Research: Strategies.
PB94-211372 00,346

FIRE EXTINGUISHING AGENTS
Water Mist Fire Suppression Workshop Summary.
PB95-161907 02,853

Suppression Effectiveness of Extinguishing Agents under Highly Dynamic Conditions.
PB95-180279 00,020

Burning Rate of Premixed Methane-Air Flames Inhibited by Fluorinated Hydrocarbons.
PB95-180584 01,391

Experimental and Numerical Burning Rates of Premixed Methane-Air Inhibited by Fluoromethanes.
PB95-180592 01,392

Suppression of Elevated Temperature Hydraulic Fluid and JP-8 Spray Flames.
PB95-181095 00,021

Flow of Alternative Agents in Piping.
PB95-202420 00,022

Suppression of High Speed Turbulent Flames in a Detonation/Deflagration Tube.
PB95-231817 01,395

Assessing Halon Alternatives for Aircraft Engine Nacelle Fire Suppression.
PB96-102454 01,401

Solid Propellant Gas Generators: Proceedings of the 1995 Workshop. Held in Gaithersburg, Maryland on June 28-29, 1995.
PB96-131479 01,412

Inhibition of Premixed Methane-Air Flames by Halon Alternatives.
PB96-146741 01,414

Agent Screening for Halon 1301 Aviation Replacement.
PB96-159710 03,282

Validation of a Turbulent Spray Flame Facility for the Assessment of Halon Alternatives.
PB96-159728 03,283

In Search of Alternative Fire Suppressants.
PB96-164165 03,285

Effectiveness of Halon Alternatives in Suppressing Dynamic Combustion Process.
PB96-175732 03,288

Interaction of HFC-125, FC-218 and CF3I with High Speed Combustion Waves.
PB96-176417 03,290

FIRE EXTINGUISHING AGENTS. FIRE SUPPRESSION
Acid Gas Production in Inhibited Diffusion Flames.
PB95-180576 01,390

FIRE FIGHTING
Fire Service and Fire Sciences: A Winning Combination.
PB95-150264 01,383

FIRE GASES
Effective Measurement Techniques for Heat, Smoke, and Toxic Fire Gases.
PB94-198439 01,369

Chemical Stability of Upper-Layer Fire Gases.
PB96-123385 01,410

FIRE HAZARDS
Fire Hazard and Risk: Evaluating Alternative Technologies.
PB94-173077 00,242

Modern Test Methods for Flammability.
PB94-198447 01,370

Toxicity, Fire Hazard and Upholstered Furniture.
PB94-198454 00,289

Analysis of the Happyland Social Club Fire with HAZARD I.
PB94-199270 00,193

Global Equivalence Ratio Concept and the Prediction of Carbon Monoxide Formation in Enclosure Fires.
PB94-207511 00,313

HAZARD I Fire Hazard Assessment Method (Version 1.2) (for Microcomputers).
PB94-501988 00,196

HAZARD I Fire Hazard Assessment Method, Version 1.2 (Upgrade Package) (for Microcomputers).
PB94-501996 00,197

Annual Conference on Fire Research: Book of Abstracts, October 17-20, 1994.
PB95-104964 01,376

FPETOOL: Fire Protection Tools for Hazard Estimation. An Overview of Features.
PB95-140885 00,367

Fire Service and Fire Sciences: A Winning Combination.
PB95-150264 01,383

Quantitative Evaluation of Building Fire Safety: New Tools for Assessing Fire and Building Code Provisions.
PB95-164588 00,199

Influence of Ignition Source on the Flaming Fire Hazard of Upholstered Furniture. (NIST Reprint).
PB95-180162 00,297

Post-Earthquake Fire and Lifelines Workshop. Held in Long Beach, California on January 30-31, 1995. Proceedings.
PB96-117916 00,209

Global Equivalence Ratio Concept and the Formation Mechanisms of Carbon Monoxide in Enclosure Fires.
PB96-146790 00,210

Quantifying the Ignition Propensity of Cigarettes.
PB96-155411 00,306

Review of Internatioanl Fire Risk Predictions Methods.
PB96-156195 00,222

Fire Hazard Model Developments and Research Efforts at NIST.
PB96-159652 00,407

FIRE MODELS
Calculating Flame Spread on Horizontal and Vertical Surfaces.
PB94-187283 00,335

Fire Growth Models for Materials.
PB94-195856 01,367

Behavior of Charring Materials in Simulated Fire Environments.
PB94-196045 01,368

Combined Buoyancy- and Pressure-Driven Flow Through a Shallow, Horizontal, Circular Vent.
PB94-210077 00,344

VENTCF2: An Algorithm and Associated FORTRAN 77 Subroutine for Calculating Flow through a Horizontal Ceiling/Floor Vent in a Zone-Type Compartment Fire Model.
PB94-210127 00,345

Verification of a Model of Fire and Smoke Transport.
PB95-108718 00,357

Method of Predicting Smoke Movement in Atria with Application to Smoke Management.
PB95-154746 00,376

Generation Rate and Distribution of Products of Combustion in Two-Layer Fire Environments: A Model and Applications.
PB96-102173 *01,398*

Computing Radiative Heat Transfer Occurring in a Zone Fire Model.
PB96-102306 *01,399*

Analyzing and Exploiting Numerical Characteristics of Zone Fire Models.
PB96-102314 *01,400*

Fire Hazard Model Developments and Research Efforts at NIST.
PB96-159652 *00,407*

Numerical Simulation of Rapid Combustion in an Underground Enclosure.
PB96-183132 *01,424*

FIRE PREVENTION

Fire and Smoke Control: An Historical Perspective.
PB95-175808 *00,202*

Transition from Localized Ignition to Flame Spread Over a Thin Cellulosic Material in Microgravity.
PB96-155809 *04,835*

Ignition and Subsequent Flame Spread Over a Thin Cellulosic Material.
PB96-160270 *04,836*

Ignition and Transition to Flame Spread Over a Thermally Thin Cellulosic Sheet in a Microgravity Environment.
PB96-160288 *04,837*

FIRE PROTECTION

VENTCF2: An Algorithm and Associated FORTRAN 77 Subroutine for Calculating Flow through a Horizontal Ceiling/Floor Vent in a Zone-Type Compartment Fire Model.
PB94-210127 *00,345*

Measurement of Room Conditions and Response of Sprinklers and Smoke Detectors during a Simulated Two-Bed Hospital Patient Room Fire.
PB94-213717 *00,292*

FPETOOL: Fire Protection Tools for Hazard Estimation. An Overview of Features.
PB95-140885 *00,367*

New Concepts for Fire Protection of Passenger Rail Transportation Vehicles.
PB95-162046 *04,850*

Protection of Data Processing Equipment with Fine Water Sprays.
PB95-174975 *02,610*

Santa Ana Fire Department Experiment at 1315 South Bristol, July 14, 1994.
PB95-188868 *00,389*

Review of Measurements and Candidate Signatures for Early Fire Detection.
PB95-189452 *00,300*

Concepts for Fire Protection of Passenger Rail Transportation Vehicles: Past, Present, and Future.
PB96-102868 *04,853*

Protecting Your Family from Fire.
PB96-156187 *00,307*

Methodology for Developing and Implementing Alternative Temperature-Time Curves for Testing the Fire Resistance of Barriers for Nuclear Power Plant Applications.
PB96-193784 *03,742*

Fire Protection Foam Behavior in a Radiative Environment.
PB97-116131 *00,237*

FIRE RESEARCH

Gordon Research Conference on the Physics and Chemistry of Laser Diagnostics in Combustion Held in Plymouth, New Hampshire on 12-16 July 1993.
AD-A274 609/7 *01,353*

Some Factors Affecting Design of a Furniture Calorimeter Hood and Exhaust.
PB94-139193 *00,285*

Fire Induced Thermal Fields in Window Glass I: Theory.
PB94-139722 *00,328*

Two Numerical Techniques for Light Scattering by Dielectric Agglomerated Structures.
PB94-140597 *04,225*

Computational Model for the Rise and Dispersion of Wind-Blown, Buoyancy-Driven Plumes. Part 2. Linearly Stratified Atmosphere.
PB94-143427 *00,119*

Ground-Based Smoke Sampling Techniques Training Course and Collaborative Local Smoke Sampling in Saudi Arabia.
PB94-143542 *02,532*

Use of Computer Models to Predict Temperature and Smoke Movement in High Bay Spaces.
PB94-145976 *00,191*

Fire Safety of Passenger Trains: A Review of Current Approaches and of New Concepts.
PB94-152006 *04,848*

Concurrent Flow Flame Spread Study.
PB94-156866 *01,356*

Transient Cooling of a Hot Surface by Droplets Evaporation.
PB94-156957 *03,783*

Numerical Analysis Support for Compartment Fire Modeling and Incorporation of Heat Conduction into a Zone Fire Model.
PB94-156965 *01,357*

Summaries of Center for Fire Research In-House Projects and Grants: 1990.
PB94-160876 *00,286*

Feasibility and Design Considerations of Emergency Evacuation by Elevators.
PB94-163441 *00,287*

BFRL Fire Publications, 1993.
PB94-164191 *00,192*

Radiation and Mixing Properties of Buoyant Turbulent Diffusion Flames.
PB94-165974 *01,360*

Improvement in Predicting Smoke Movement in Compartmented Structures.
PB94-172418 *00,332*

Greatly Enhanced Soot Scattering in Flickering Ch4/Air Diffusion Flames.
PB94-172988 *01,361*

Fire Hazard and Risk: Evaluating Alternative Technologies.
PB94-173077 *00,242*

Fluorinated Hydrocarbon Flame Suppression Chemistry.
PB94-185113 *01,362*

Flame Retardants - Overview.
PB94-185287 *01,363*

Laser Imaging of Chemistry-Flowfield Interactions: Enhanced Soot Formation in Time-Varying Diffusion Flames.
PB94-185352 *01,364*

Calculating Flame Spread on Horizontal and Vertical Surfaces.
PB94-187283 *00,335*

Prediction of Fire Dynamics.
PB94-193620 *00,336*

Mathematical Modeling of Human Egress from Fires in Residential Buildings.
PB94-193778 *00,337*

Structure and Radiation Properties of Pool Fires.
PB94-193802 *02,473*

Fire Propagation in Concurrent Flows.
PB94-193844 *01,365*

Backdraft Phenomena.
PB94-193927 *01,366*

Investigation of Oil and Gas Well Fires and Flares.
PB94-193976 *03,695*

Risk Analysis for the Fire Safety of Airline Passengers.
PB94-194065 *04,862*

Performance Parameters of Fire Detection Systems.
PB94-194339 *00,288*

CONTAM88 Building Input Files for Multi-Zone Airflow and Contaminant Dispersal Modeling.
PB94-194388 *02,537*

Fire Growth Models for Materials.
PB94-195856 *01,367*

Behavior of Charring Materials in Simulated Fire Environments.
PB94-196045 *01,368*

Effective Measurement Techniques for Heat, Smoke, and Toxic Fire Gases.
PB94-198439 *01,369*

Modern Test Methods for Flammability.
PB94-198447 *01,370*

Toxicity, Fire Hazard and Upholstered Furniture.
PB94-198454 *00,289*

Standardization of Formats and Presentation of Fire Data - The FDMS.
PB94-198462 *01,371*

Studies Assess Performance of Residential Detectors.
PB94-199262 *00,290*

Analysis of the Happyland Social Club Fire with HAZARD I.
PB94-199270 *00,193*

Generation and Characterization of Acetylene Smokes.
PB94-200292 *01,372*

Ultrafine Combustion Aerosol Generator.
PB94-200300 *01,373*

Evaluation of Alternative In-Flight Fire Suppressants for Full-Scale Testing in Simulated Aircraft Engine Nacelles and Dry Bays.
PB94-203403 *00,023*

Fire Growth Analysis of the Fire of March 20, 1990, Pulaski Building, 20 Massachusetts Avenue, N.W., Washington, DC.
PB94-205952 *00,194*

Development of the Fire Data Management System.
PB94-206091 *00,339*

Upward Flame Spread along the Vertical Corner Walls (October 1993).
PB94-206299 *00,340*

Evaluating Small Board and Care Homes: Sprinklered vs. Nonsprinklered Fire Protection.
PB94-206356 *00,195*

Turbulent Upward Flame Spread on a Vertical Wall under External Radiation.
PB94-207388 *00,341*

Comparison of Wall-Fire Behavior With and Without a Ceiling.
PB94-207404 *00,342*

Global Equivalence Ratio Concept and the Prediction of Carbon Monoxide Formation in Enclosure Fires.
PB94-207511 *00,313*

Combined Buoyancy- and Pressure-Driven Flow Through a Shallow, Horizontal, Circular Vent.
PB94-210077 *00,344*

VENTCF2: An Algorithm and Associated FORTRAN 77 Subroutine for Calculating Flow through a Horizontal Ceiling/Floor Vent in a Zone-Type Compartment Fire Model.
PB94-210127 *00,345*

Suppression Research: Strategies.
PB94-211372 *00,346*

Estimate of Flame Radiance via a Single Location Measurement in Liquid Pool Flames.
PB94-211596 *02,476*

Measurement of Radiative Feedback to the Fuel Surface of a Pool Fire.
PB94-211604 *02,477*

Laser-Induced Fluorescence Measurements of Formaldehyde in a Methane/Air Diffusion Flame.
PB94-211679 *01,374*

Rate of Heat Release of Wood Products.
PB94-212404 *03,403*

Effects of Molecular Weight and Thermal Stability on Polymer Gasification.
PB94-212610 *01,228*

Application of Boundary Element Methods to a Transient Axis-Symmetric Heat Conduction Problem.
PB94-212693 *01,375*

Full Scale Smoke Control Tests at the Plaza Hotel Building.
PB94-212859 *00,347*

Overview of Smoke Control Technology.
PB94-212867 *00,348*

Preview of ASHRAE's Revised Smoke Control Manual.
PB94-212875 *00,349*

Smoke Control Systems for Elevator Fire Evacuation.
PB94-212883 *00,291*

Development of a New Small-Scale Smoke Toxicity Test Method and Its Comparison with Real-Scale Fire Tests.
PB94-213253 *00,350*

EXITT: A Simulation Model of Occupant Decisions and Actions in Residential Fires.
PB94-213261 *00,351*

Investigation of the Thermal Stability and Char-Forming Tendency of Cross-linked Poly(methyl methacrylate).
PB94-213501 *03,380*

Measurement of Room Conditions and Response of Sprinklers and Smoke Detectors during a Simulated Two-Bed Hospital Patient Room Fire.
PB94-213717 *00,292*

Feasibility of Fire Evacuation by Elevators at FAA Control Towers.
PB94-213857 *04,844*

Sprinkler Fire Suppression Algorithm.
PB94-216181 *00,293*

Human Factors Considerations for the Potential Use of Elevators for Fire Evacuation of FAA Air Traffic Control Towers.
PB94-217163 *01,300*

In Situ Burning Oil Spill Workshop Proceedings. Held in Orlando, Florida on January 26-28, 1994.
PB95-104907 *02,583*

Annual Conference on Fire Research: Book of Abstracts, October 17-20, 1994.
PB95-104964 *01,376*

Study of Droplet Transport in Alcohol-Based Spray Flames Using Phase/Doppler Interferometry.
PB95-108551 *02,479*

Structure of a Swirl-Stabilized Kerosene Spray Flame.
PB95-108569 *02,480*

Verification of a Model of Fire and Smoke Transport.
PB95-108718 *00,357*

Global Climatic Effects of Aerosols: The AAAR Symposium.
PB95-108791 *00,122*

Suggestions for a Logically-Consistent Structure for Service Life Prediction Standards.
PB95-125795 *00,358*

Relating Bench-Scale and Full-Scale Toxicity Data.
PB95-125977 *00,361*

Dispersion and Deposition of Smoke Plumes Generated in Massive Fires.
PB95-126066 *02,540*

Assessment of Technologies for Advanced Fire Detection.
PB95-126330 *00,294*

Summaries of BFRL Fire Research In-House Projects and Grants, 1994.
PB95-130845 *00,366*

FPETOOL: Fire Protection Tools for Hazard Estimation. An Overview of Features.
PB95-140885 *00,367*

Comparison of Experimental and Computed Species Concentration and Temperature Profiles in Laminar, Two-Dimensional Methane/Air Diffusion Flames.
PB95-140919 *01,379*

One- and Two-Sided Burning of Thermally Thin Materials.
PB95-140935 *03,151*

Simulating Smoke Movement through Long Vertical Shafts in Zone-Type Compartment Fire Models.
PB95-143152 *00,368*

Transient Cooling of a Hot Surface by Droplets Evaporation.
PB95-143194 *03,890*

Building and Fire Research Laboratory Publications, 1993.
PB95-143202 *00,369*

Investigation into the Flammability Properties of Honeycomb Composites.
PB95-143293 *03,152*

Airborne Smoke Sampling Package for Field Measurements of Fires.
PB95-150041 *01,381*

Oxidation of Soot and Carbon Monoxide in Hydrocarbon Diffusion Flames.
PB95-150215 *01,382*

Fire Service and Fire Sciences: A Winning Combination.
PB95-150264 *01,383*

Estimate of the Effect of Scale on Radiative Heat Loss Fraction and Combustion Efficiency.
PB95-150447 *02,486*

Optical Measurements of Atomic Hydrogen, Hydroxyl, and Carbon Monoxide in Hydrocarbon Diffusion Flames.
PB95-150900 *02,487*

Approximate Confidence Intervals on Linear Combinations of Expected Mean Squares.
PB95-151296 *03,435*

Flame Synthesis of High Tc Superconductors.
PB95-151981 *00,659*

Effects of Specimen Edge Conditions on Heat Release Rate.
PB95-152864 *00,375*

Turbulent Spray Burner for Assessing Halon Alternative Fire Suppressants.
PB95-153748 *01,385*

Method of Predicting Smoke Movement in Atria with Application to Smoke Management.
PB95-154746 *00,376*

Locating Fire Engineering Information.
PB95-161188 *00,198*

Reactivity of Product Gases Generated in Idealized Enclosure Fire Environments.
PB95-161790 *01,386*

Water Mist Fire Suppression Workshop Summary.
PB95-161907 *02,853*

New Concepts for Fire Protection of Passenger Rail Transportation Vehicles.
PB95-162046 *04,850*

Global Density Effects on the Self-Preservation Behavior of Turbulent Free Jets.
PB95-162301 *04,207*

Exposure: An Expert System Fire Code.
PB95-162913 *04,868*

Forum for International Cooperation on Fire Research.
PB95-162939 *04,869*

Fresh Look at Strategies for Fire Safety.
PB95-162947 *04,870*

Wall Flame Heights with External Radiation.
PB95-163481 *00,380*

In situ Burning of Oil Spills: Mesoscale Experiments and Analysis.
PB95-163747 *02,587*

Quantitative Evaluation of Building Fire Safety: New Tools for Assessing Fire and Building Code Provisions.
PB95-164588 *00,199*

Acoustic Emission of Structural Materials Exposed to Open Flames.
PB95-164810 *00,296*

Protection of Data Processing Equipment with Fine Water Sprays.
PB95-174975 *02,610*

Developing Rational Performance-Based Fire Safety Requirements in Model Building Codes.
PB95-175220 *00,200*

Fire and Smoke Control: An Historical Perspective.
PB95-175808 *00,202*

Effect of Dodecanol Content on the Combustion of Methanol Spray Flames.
PB95-176020 *01,389*

Mathematical Modeling and Computer Simulation of Fire Phenomena.
PB95-180063 *00,384*

Influence of Ignition Source on the Flaming Fire Hazard of Upholstered Furniture. (NIST Reprint).
PB95-180162 *00,297*

Suppression Effectiveness of Extinguishing Agents under Highly Dynamic Conditions.
PB95-180279 *00,020*

Early Detection of Room Fires Through Acoustic Emission. (NIST Reprint).
PB95-180311 *00,298*

Acid Gas Production in Inhibited Diffusion Flames.
PB95-180576 *01,390*

Burning Rate of Premixed Methane-Air Flames Inhibited by Fluorinated Hydrocarbons.
PB95-180584 *01,391*

Experimental and Numerical Burning Rates of Premixed Methane-Air Inhibited by Fluoromethanes.
PB95-180592 *01,392*

New Concepts for Fire Protection of Passenger Rail Transportation Vehicles. (NIST Reprint).
PB95-180774 *04,863*

Suppression of Elevated Temperature Hydraulic Fluid and JP-8 Spray Flames.
PB95-181095 *00,021*

Algorithm to Describe the Spread of a Wall Fire under a Ceiling.
PB95-182259 *00,261*

Comparison of Fire Sprinkler Piping Materials: Steel, Copper, Chlorinated Polyvinyl Chloride and Polybutylene, in Residential and Light Hazard Installations.
PB95-182267 *00,299*

Santa Ana Fire Department Experiment at 1315 South Bristol, July 14, 1994.
PB95-188868 *00,389*

Fire Performance of an Interstitial Space Construction System.
PB95-188918 *00,390*

Review of Measurements and Candidate Signatures for Early Fire Detection.
PB95-189452 *00,300*

Flow of Alternative Agents in Piping.
PB95-202420 *00,022*

Quantitative Measurements of Enhanced Soot Production in a Flickering Methane/Air Diffusion Flame.
PB95-203246 *01,393*

Burning Rate and Flame Heat Flux For PMMA in the Cone Calorimeter.
PB95-216990 *00,393*

Compartment Fire Combustion Dynamics. Annual Report, September 1, 1993-September 1, 1994.
PB95-217162 *00,203*

Building and Fire Research Laboratory Publications, 1994.
PB95-226684 *00,398*

Behavior of Mock-Ups in the California Technical Bulletin 133 Test Protocol: Fabric and Barrier Effects.
PB95-231585 *00,301*

Carbon Monoxide Production in Compartment Fires: Reduced-Scale Enclosure Test Facility.
PB95-231700 *01,394*

Suppression of High Speed Turbulent Flames in a Detonation/Deflagration Tube.
PB95-231817 *01,395*

Mixing and Radiation Properties of Buoyant Turbulent Diffusion Flames.
PB95-242327 *01,396*

Proceedings of the 1995 Workshop on Fire Detector Research. Held on February 6-7, 1995.
PB95-270062 *02,611*

Fire Codes for Global Practice.
PB96-102108 *00,205*

How to Evaluate Alternative Designs Based on Fire Modeling.
PB96-102116 *00,206*

Simultaneous Optical Measurement of Soot Volume Fraction, Temperature, and CO2 in Heptane Pool Fire.
PB96-102132 *01,397*

Generation Rate and Distribution of Products of Combustion in Two-Layer Fire Environments: A Model and Applications.
PB96-102173 *01,398*

Some Factors Affecting the Design of a Calorimeter Hood and Exhaust.
PB96-102181 *00,302*

Computing Radiative Heat Transfer Occurring in a Zone Fire Model.
PB96-102306 *01,399*

Analyzing and Exploiting Numerical Characteristics of Zone Fire Models.
PB96-102314 *01,400*

Assessing Halon Alternatives for Aircraft Engine Nacelle Fire Suppression.
PB96-102454 *01,401*

Concepts for Fire Protection of Passenger Rail Transportation Vehicles: Past, Present, and Future.
PB96-102868 *04,853*

Santa Ana Fire Department Experiment at 1315 South Bristol, July 14, 1994. (Reprint).
PB96-102934 *00,207*

Pressure Equations in Zone-Fire Modeling.
PB96-102967 *00,208*

CFAST Output Comparison Method and Its Use in Comparing Different CFAST Versions.
PB96-109541 *00,401*

Effect of Suppressants on Metal Fires.
PB96-109574 *01,402*

Turbulent Flame Spread on Vertical Corner Walls.
PB96-114764 *01,403*

Fire Suppression System Performance of Alternative Agents in Aircraft Engine and Dry Bay Laboratory Simulations. SP890: Volume 1.
PB96-117775 *03,277*

Fire Suppression System Performance of Alternative Agents in Aircraft Engine and Dry Bay Laboratory Simulations. SP 890: Volume 2.
PB96-117783 *03,278*

Flame Heights and Heat Release Rates of 1991 Kuwait Oil Field Fires.
PB96-119342 *01,404*

Experimental Study of the Stabilization Region of Lifted Turbulent-Jet Diffusion Flames.
PB96-122676 *01,405*

Field Modeling: Simulating the Effect of Sloped Beamed Ceilings on Detector and Sprinkler Response.
PB96-122866 *01,406*

Smoke Emission from Burning Crude Oil.
PB96-122890 *01,407*

Development of Hazard Assessment and Suppression Technology for Oil and Gas Well Blowout and Diverter Fires.
PB96-122965 *01,408*

Laser-Induced Fluorescence Measurements of OH in Laminar Diffusion Flames in the Presence of Soot Particles.
PB96-123120 *01,409*

Polymer Combustion and Flammability: Role of the Condensed Phase.
PB96-123245 *01,279*

Further Development of the N-Gas Mathematical Model: An Approach for Predicting the Toxic Potency of Complex Combustion Mixtures.
PB96-123260 *03,650*

Chemical Stability of Upper-Layer Fire Gases.
PB96-123385 *01,410*

New Approach for Reducing the Toxicity of the Combustion Products from Flexible Polyurethane Foam.
PB96-123625 *01,411*

Solid Propellant Gas Generators: Proceedings of the 1995 Workshop. Held in Gaithersburg, Maryland on June 28-29, 1995.
PB96-131479 *01,412*

Smoke Plume Trajectory from In situ Burning of Crude Oil in Alaska: Field Experiments.
PB96-131560 *02,594*

Application of Thermodynamic and Detailed Chemical Kinetic Modeling to Understanding Combustion Product Generation in Enclosure Fires.
PB96-135322 *01,413*

Evaluation of Sprinkler Activation Prediction Methods.
PB96-141056 *00,304*

Inhibition of Premixed Methane-Air Flames by Halon Alternatives.
PB96-146741 *01,414*

Global Equivalence Ratio Concept and the Formation Mechanisms of Carbon Monoxide in Enclosure Fires.
PB96-146790 *00,210*

Gravity-Current Transport in Building Fires.
PB96-147046 *01,415*

Computing the Effect of Sprinkler Sprays on Fire Induced Gas Flow.
PB96-147111 *00,404*

Review of Flows Driven By Natural Convection in Adiabatic Shafts.
PB96-147897 *01,416*

Information Resources for the Fire Community.
PB96-148119 *00,211*

Heights of Wall-Fire Flames.
PB96-148192 *00,212*

Examination of the Correlation between Cone Calorimeter Data and Full-Scale Furniture Mock-Up Fires.
PB96-148200 *01,417*

Fire Safety Engineering Research in the United States.
PB96-151394 *00,213*

Elements of a Framework for Fire Safety Engineering.
PB96-151402 *00,214*

Predicting the Ignition Time and Burning Rate of Thermoplastics in the Cone Calorimeter.
PB96-154794 *01,418*

Santa Ana Fire Department Experiments at South Bristol Street.
PB96-154810 *00,305*

Quantifying the Ignition Propensity of Cigarettes.
PB96-155411 *00,306*

Transition from Localized Ignition to Flame Spread Over a Thin Cellulosic Material in Microgravity.
PB96-155809 *04,835*

Internationalization of Fire Safety Engineering Research and Strategy.
PB96-156153 *00,220*

Fire Protection Engineering Tools. Simple Tools: The Equations.
PB96-156179 *00,221*

Protecting Your Family from Fire.
PB96-156187 *00,307*

Review of Internatioanl Fire Risk Predictions Methods.
PB96-156195 *00,222*

Evolution of a United States Information System.
PB96-157896 *02,713*

Information Transfer in the 21st Century.
PB96-157904 02,714

Fire Hazard Model Developments and Research Efforts at NIST.
PB96-159652 00,407

Agent Screening for Halon 1301 Aviation Replacement.
PB96-159710 03,282

Validation of a Turbulent Spray Flame Facility for the Assessment of Halon Alternatives.
PB96-159728 03,283

Effects of Sample Mounting on Flammability Properties of Intumescent Polymers.
PB96-159777 03,389

Ignition and Subsequent Flame Spread Over a Thin Cellulosic Material.
PB96-160270 04,836

Ignition and Transition to Flame Spread Over a Thermally Thin Cellulosic Sheet in a Microgravity Environment.
PB96-160288 04,837

New Generation of Fire Resistant Polymers. Part 1. Computer-Aided Molecular Design.
PB96-160593 01,419

Computer-Aided Molecular Design of Fire Resistant Aircraft Materials.
PB96-160601 00,025

Effect of CF3H and CF3Br on Laminar Diffusion Flames in Normal and Microgravity.
PB96-161831 01,420

Effect of CF3H and CF3Br on Laminar Diffusion Flames in Normal and Microgravity.
PB96-161849 01,421

Inhibition of Premixed Methane-Air Flames by Iron Pentacarbonyl.
PB96-163712 00,513

Parametric Study of Hydrogen Fluoride Formation in Suppressed Fires.
PB96-163720 00,514

Heat Transfer in an Intumescent Material Using a Three-Dimensional Lagrangian Model.
PB96-164066 00,408

Calculating Combined Buoyancy- and Pressure-Driven Flow Through a Shallow, Horizontal, Circular Vent; Application to Problem of Steady Burning in a Ceiling-Vented Enclosure.
PB96-164108 00,409

Combined Buoyancy and Pressure-Driven Flow Through a Shallow, Horizontal, Circular Vent.
PB96-164116 00,410

In Search of Alternative Fire Suppressants.
PB96-164165 03,285

Asymptotic and Numerical Analysis of a Premixed Laminar Nitrogen Dioxide-Hydrogen Flame.
PB96-164256 01,422

Scaling Compartment Fires: Reduced- and Full-Scale Enclosure Burns.
PB96-175708 00,224

Suppression of High-Speed C2H4/Air Flames with C1-Halocarbons.
PB96-175724 03,287

Effectiveness of Halon Alternatives in Suppressing Dynamic Combustion Process.
PB96-175732 03,288

Interaction of HFC-125, FC-218 and CF3I with High Speed Combustion Waves.
PB96-176417 03,290

Suppression of Ignition Over a Heated Metal Surface.
PB96-176425 03,291

Publications 1995: NIST Building and Fire Research Laboratory.
PB96-183074 00,226

NASA Fire Detector Study.
PB96-183108 01,423

Numerical Simulation of Rapid Combustion in an Underground Enclosure.
PB96-183132 01,424

Minimum Mass Flux Requirements to Suppress Burning Surfaces with Water Sprays.
PB96-183181 01,425

Large Eddy Simulations of Smoke Movement in Three Dimensions.
PB96-190012 01,426

Large Fire Experiments for Fire Model Evaluations.
PB96-190079 01,427

Locating Fire Information.
PB96-190137 00,227

Office Work Station Heat Release Rate Study: Full Scale versus Bench Scale.
PB96-190178 01,428

Analysis of High Bay Hangar Facilities for Detector Sensitivity and Placement.
PB96-190210 01,429

Post-Flame Soot.
PB96-193701 01,430

Development of an Economical Video Based Fire Detection and Location System.
PB96-193743 00,228

Methodology for Developing and Implementing Alternative Temperature-Time Curves for Testing the Fire Resistance of Barriers for Nuclear Power Plant Applications.
PB96-193784 03,742

Dynamics, Transport and Chemical Kinetics of Compartment Fire Exhaust Gases.
PB96-195508 00,229

Chemical Inhibition of Methane-Air Diffusion Flame.
PB96-195532 01,431

Smoke Plume Trajectory from In situ Burning of Crude Oil: Field Experiments.
PB96-200993 02,597

Low Heat-Flux Measurements: Some Precautions.
PB96-201116 02,685

Enhancement of EXIT89 and Analysis of World Trade Center Data.
PB96-202247 00,231

Mixing and Radiation Properties of Buoyant Luminous Flame Environments.
PB96-202254 01,432

Benefits and Costs of Research: A Case Study of the Fire Safety Evaluation System.
PB96-202288 00,232

Sparse Water Sprays in Fire Protection.
PB96-202304 01,433

Gas Phase Oxygen Effect on Chain Scission and Monomer Content in Bulk Poly(methyl methacrylate) Degraded by External Thermal Radiation.
PB96-204078 01,293

Role of Combustion on Droplet Transport in Pressure-Atomized Spray Flames.
PB96-204433 01,434

Effect of Fuel Tank Rupture Mode on the Ignitability of Expelled Fuel.
PB97-110043 01,444

Flammability Characterization with the Lift Apparatus and the Cone Calorimeter.
PB97-110050 01,435

Letter Report on Flame Spread Testing of a Composite Material.
PB97-110068 01,436

Interaction of an Isolated Sprinkler Spray and a Two-Layer Compartment Fire Environment. Phenomena and Model Simulations.
PB97-110076 01,437

Heat Flux from Flames to Vertical Surfaces.
PB97-110357 01,438

Analysis of Droplet Arrival Statistics in a Pressure-Atomized Spray Flame.
PB97-112270 01,352

Survey of Fuel Loads in Contemporary Office Buildings.
PB97-114235 00,233

Fire Safety Engineering in the Pursuit of Performance-Based Codes: Collected Papers.
PB97-114482 00,235

Full-Scale Room Fire Experiments Conducted at the University of Maryland.
PB97-116081 00,236

Fire Protection Foam Behavior in a Radiative Environment.
PB97-116131 00,237

NIST Research on Less-Flammable Materials.
PB97-118632 01,439

Computations of Enhanced Soot Production in Time-Varying CH4/Air Diffusion Flames.
PB97-119218 01,440

Transport by Gravity Currents in Building Fires.
PB97-119325 01,441

Materials and Fire Threat.
PB97-122311 01,442

NO Production and Destruction in a Methane/Air Diffusion Flame.
PB97-122519 01,443

FIRE RESEARCH INFORMATION SERVICES

FIREDOC Users Manual, 3rd Edition.
PB95-128674 01,378

FIRE RESISTANT MATERIALS

Summaries of BFRL Fire Research In-House Projects and Grants, 1994.
PB95-130845 00,366

Effects of Sample Mounting on Flammability Properties of Intumescent Polymers.
PB96-159777 03,389

New Generation of Fire Resistant Polymers. Part 1. Computer-Aided Molecular Design.
PB96-160593 01,419

Computer-Aided Molecular Design of Fire Resistant Aircraft Materials.
PB96-160601 00,025

Materials and Fire Threat.
PB97-122311 01,442

FIRE SAFETY

Fire Safety of Passenger Trains: A Review of Current Approaches and of New Concepts.
PB94-152006 04,848

Mathematical Modeling of Human Egress from Fires in Residential Buildings.
PB94-193778 00,337

Risk Analysis for the Fire Safety of Airline Passengers.
PB94-194065 04,862

Studies Assess Performance of Residential Detectors.
PB94-199262 00,290

Evaluating Small Board and Care Homes: Sprinklered vs. Nonsprinklered Fire Protection.
PB94-206356 00,195

Overview of Smoke Control Technology.
PB94-212867 00,348

Preview of ASHRAE's Revised Smoke Control Manual.
PB94-212875 00,349

Smoke Control Systems for Elevator Fire Evacuation.
PB94-212883 00,291

Feasibility of Fire Evacuation by Elevators at FAA Control Towers.
PB94-213857 04,844

Human Factors Considerations for the Potential Use of Elevators for Fire Evacuation of FAA Air Traffic Control Towers.
PB94-217163 01,300

FIREDOC Users Manual, 3rd Edition.
PB95-128674 01,378

Summaries of BFRL Fire Research In-House Projects and Grants, 1994.
PB95-130845 00,366

FPETOOL: Fire Protection Tools for Hazard Estimation. An Overview of Features.
PB95-140885 00,367

New Concepts for Fire Protection of Passenger Rail Transportation Vehicles.
PB95-162046 04,850

Fresh Look at Strategies for Fire Safety.
PB95-162947 04,870

Developing Rational Performance-Based Fire Safety Requirements in Model Building Codes.
PB95-175220 00,200

New Concepts for Fire Protection of Passenger Rail Transportation Vehicles. (NIST Reprint).
PB95-180774 04,863

Fire Codes for Global Practice.
PB96-102108 00,205

How to Evaluate Alternative Designs Based on Fire Modeling.
PB96-102116 00,206

Predicting the Fire Performance of Buildings: Establishing Appropriate Calculation Methods for Regulatory Applications.
PB96-141239 00,316

Fire Safety Engineering Research in the United States.
PB96-151394 00,213

Elements of a Framework for Fire Safety Engineering.
PB96-151402 00,214

Internationalization of Fire Safety Engineering Research and Strategy.
PB96-156153 00,220

Fire Protection Engineering Tools. Simple Tools: The Equations.
PB96-156179 00,221

Protecting Your Family from Fire.
PB96-156187 00,307

International Organization for Standardization: Current Activities in Fire Safety Engineering.
PB96-159660 00,223

Enhancement of EXIT89 and Analysis of World Trade Center Data.
PB96-202247 00,231

Benefits and Costs of Research: A Case Study of the Fire Safety Evaluation System.
PB96-202288 00,232

Survey of Fuel Loads in Contemporary Office Buildings.
PB97-114235 00,233

Fire Safety Engineering in the Pursuit of Performance-Based Codes: Collected Papers.
PB97-114482 00,235

FIRE SUPPRESSANTS

Effect of Suppressants on Metal Fires.
PB96-109574 01,402

FIRE SUPPRESSION

Transient Cooling of a Hot Surface by Droplets Evaporation.
PB94-156957 03,783

Fluorinated Hydrocarbon Flame Suppression Chemistry.
PB94-185113 01,362

Evaluation of Alternative In-Flight Fire Suppressants for Full-Scale Testing in Simulated Aircraft Engine Nacelles and Dry Bays.
PB94-203403 00,023

Sprinkler Fire Suppression Algorithm.
PB94-216181 00,293

Annual Conference on Fire Research: Book of Abstracts, October 17-20, 1994.
PB95-104964 01,376

Summaries of BFRL Fire Research In-House Projects and Grants, 1994.
PB95-130845 00,366

Turbulent Spray Burner for Assessing Halon Alternative Fire Suppressants.
PB95-153748 *01,385*

Water Mist Fire Suppression Workshop Summary.
PB95-161907 *02,853*

Suppression Effectiveness of Extinguishing Agents under Highly Dynamic Conditions.
PB95-180279 *00,020*

Flow of Alternative Agents in Piping.
PB95-202420 *00,022*

Fire Suppression System Performance of Alternative Agents in Aircraft Engine and Dry Bay Laboratory Simulations. SP890: Volume 1.
PB96-117775 *03,277*

Fire Suppression System Performance of Alternative Agents in Aircraft Engine and Dry Bay Laboratory Simulations. SP 890: Volume 2.
PB96-117783 *03,278*

Development of Hazard Assessment and Suppression Technology for Oil and Gas Well Blowout and Diverter Fires.
PB96-122965 *01,408*

Computing the Effect of Sprinkler Sprays on Fire Induced Gas Flow.
PB96-147111 *00,404*

Suppression of High-Speed C2H4/Air Flames with C1-Halocarbons.
PB96-175724 *03,287*

Suppression of Ignition Over a Heated Metal Surface.
PB96-176425 *03,291*

Analysis of High Bay Hangar Facilities for Detector Sensitivity and Placement.
PB96-190210 *01,429*

FIRE TEST DATA

Standardization of Formats and Presentation of Fire Data - The FDMS.
PB94-198462 *01,371*

FIRE TESTS

Some Factors Affecting Design of a Furniture Calorimeter Hood and Exhaust.
PB94-139193 *00,285*

In situ Burning of Oil Spills: Mesoscale Experiments.
PB94-142973 *01,355*

Use of Computer Models to Predict Temperature and Smoke Movement in High Bay Spaces.
PB94-145976 *00,191*

Fire Data Management System, FDMS 2.0, Technical Documentation.
PB94-164019 *01,358*

BFRL Fire Publications, 1993.
PB94-164191 *00,192*

Experimental and Numerical Studies on Two-Dimensional Gravity Currents in a Horizontal Channel.
PB94-165941 *01,359*

Fire Propagation in Concurrent Flows.
PB94-193844 *01,365*

Development of the Fire Data Management System.
PB94-206091 *00,339*

Suppression Research: Strategies.
PB94-211372 *00,346*

Full Scale Smoke Control Tests at the Plaza Hotel Building.
PB94-212859 *00,347*

In Situ Burning Oil Spill Workshop Proceedings. Held in Orlando, Florida on January 26-28, 1994.
PB95-104907 *02,583*

One- and Two-Sided Burning of Thermally Thin Materials.
PB95-140935 *03,151*

Effects of Specimen Edge Conditions on Heat Release Rate.
PB95-152864 *00,375*

Wall Flame Heights with External Radiation.
PB95-163481 *00,380*

In situ Burning of Oil Spills: Mesoscale Experiments and Analysis.
PB95-163747 *02,587*

Acoustic Emission of Structural Materials Exposed to Open Flames.
PB95-164810 *00,296*

Santa Ana Fire Department Experiment at 1315 South Bristol, July 14, 1994.
PB95-188868 *00,389*

Fire Performance of an Interstitial Space Construction System.
PB95-188918 *00,390*

Carbon Monoxide Production in Compartment Fires: Reduced-Scale Enclosure Test Facility.
PB95-231700 *01,394*

Some Factors Affecting the Design of a Calorimeter Hood and Exhaust.
PB96-102181 *00,302*

Santa Ana Fire Department Experiment at 1315 South Bristol, July 14, 1994. (Reprint).
PB96-102934 *00,207*

Pressure Equations in Zone-Fire Modeling.
PB96-102967 *00,208*

Application of Thermodynamic and Detailed Chemical Kinetic Modeling to Understanding Combustion Product Generation in Enclosure Fires.
PB96-135322 *01,413*

Review of Flows Driven By Natural Convection in Adiabatic Shafts.
PB96-147897 *01,416*

Santa Ana Fire Department Experiments at South Bristol Street.
PB96-154810 *00,305*

Scaling Compartment Fires: Reduced- and Full-Scale Enclosure Burns.
PB96-175708 *00,224*

Mixing and Radiation Properties of Buoyant Luminous Flame Environments.
PB96-202254 *01,432*

Sparse Water Sprays in Fire Protection.
PB96-202304 *01,433*

Interaction of an Isolated Sprinkler Spray and a Two-Layer Compartment Fire Environment. Phenomena and Model Simulations.
PB97-110076 *01,437*

Full-Scale Room Fire Experiments Conducted at the University of Maryland.
PB97-116081 *00,236*

NIST Research on Less-Flammable Materials.
PB97-118632 *01,439*

FIREDOC COMPUTER PROGRAM

FIREDOC Users Manual, 3rd Edition.
PB95-128674 *01,378*

FIRES

Fire Induced Thermal Fields in Window Glass I: Theory.
PB94-139722 *00,328*

Ground-Based Smoke Sampling Techniques Training Course and Collaborative Local Smoke Sampling in Saudi Arabia.
PB94-143542 *02,532*

Numerical Analysis Support for Compartment Fire Modeling and Incorporation of Heat Conduction into a Zone Fire Model.
PB94-156965 *01,357*

Radiation and Mixing Properties of Buoyant Turbulent Diffusion Flames.
PB94-165974 *01,360*

Improvement in Predicting Smoke Movement in Compartmented Structures.
PB94-172418 *00,332*

Mathematical Modeling of Human Egress from Fires in Residential Buildings.
PB94-193778 *00,337*

Effective Measurement Techniques for Heat, Smoke, and Toxic Fire Gases.
PB94-198439 *01,369*

Standardization of Formats and Presentation of Fire Data - The FDMS.
PB94-198462 *01,371*

Fire Growth Analysis of the Fire of March 20, 1990, Pulaski Building, 20 Massachusetts Avenue, N.W., Washington, DC.
PB94-205952 *00,194*

Project Summaries 1994: NIST Building and Fire Research Laboratory.
PB94-207495 *00,343*

Rate of Heat Release of Wood Products.
PB94-212404 *03,403*

Verification of a Model of Fire and Smoke Transport.
PB95-108718 *00,357*

Relating Bench-Scale and Full-Scale Toxicity Data.
PB95-125977 *00,361*

Dispersion and Deposition of Smoke Plumes Generated in Massive Fires.
PB95-126066 *02,540*

Summaries of BFRL Fire Research In-House Projects and Grants, 1994.
PB95-130845 *00,366*

Building and Fire Research Laboratory Publications, 1993.
PB95-143202 *00,369*

Method of Predicting Smoke Movement in Atria with Application to Smoke Management.
PB95-154746 *00,376*

Fire-Plume-Generated Ceiling Jet Characteristics and Convective Heat Transfer to Ceiling and Wall Surfaces in a Two-Layer Fire Environment: Uniform Temperature Ceiling and Walls.
PB95-164711 *00,382*

Earthquake and Fire in Japan: When the Threat Became a Reality.
PB95-175238 *00,201*

Compartment Fire Combustion Dynamics. Annual Report, September 1, 1993-September 1, 1994.
PB95-217162 *00,203*

Building and Fire Research Laboratory Publications, 1994.
PB95-226684 *00,398*

Project Summaries 1995: NIST Building and Fire Research Laboratory.
PB95-270047 *00,400*

Simultaneous Optical Measurement of Soot Volume Fraction, Temperature, and CO2 in Heptane Pool Fire.
PB96-102132 *01,397*

CFAST Output Comparison Method and Its Use in Comparing Different CFAST Versions.
PB96-109541 *00,401*

Flame Heights and Heat Release Rates of 1991 Kuwait Oil Field Fires.
PB96-119342 *01,404*

Study of Technology for Detecting Pre-Ignition Conditions of Cooking-Related Fires Associated with Electric and Gas Ranges and Cooktops, Phase 1 Report.
PB96-128095 *00,303*

Gravity-Current Transport in Building Fires.
PB96-147046 *01,415*

Examination of the Correlation between Cone Calorimeter Data and Full-Scale Furniture Mock-Up Fires.
PB96-148200 *01,417*

Sensitivity Analysis for Mathematical Modeling of Fires in Residential Buildings.
PB96-154968 *00,215*

Ignition and Subsequent Flame Spread Over a Thin Cellulosic Material.
PB96-160270 *04,836*

Evaluation of Survey Procedures for Determining Occupant Load Factors in Contemporary Office Buildings.
PB97-116222 *00,238*

Transport by Gravity Currents in Building Fires.
PB97-119325 *01,441*

FISHER RENORMALIZATION

Shear Suppression of Critical Fluctuations in a Diluted Polymer Blend.
PB96-204458 *04,418*

FISSION CHAMBER

Measurements of the (235)U(n,f) Cross Section in the 3 to 30 MeV Neutron Energy Region.
PB97-119051 *04,172*

FISSION CROSS SECTION

Measurements of the (237)Np(n,f) Cross Section.
PB97-119069 *04,173*

FISSION CROSS SECTIONS

Intermediate Structure in the Neutron-Induced Fission Cross Section of 236U.
PB94-185741 *03,802*

Measurement of the (235)U(n,f) Reaction from Thermal to 1 keV.
PB95-140422 *03,886*

FITTING

User's Guide for the Algorithm Testing System Version 2.0.
PB95-251666 *02,916*

FITTINGS

Acrylonitrile-Butadiene-Styrene (ABS) Plastic Drain, Waste, and Vent Pipe and Fittings.
AD-A310 724/0 *00,327*

FIXED INVESTMENT

Investing in Education to Meet a National Need for a Technical-Professional Workforce in a Post-Industrial Economy.
PB94-173028 *00,132*

FIXED POINTS

NIST Assessment of ITS-90 Non-Uniqueness for 25.5 Ohm SPRTs at Gallium, Indium and Cadmium Fixed Points.
PB96-161310 *00,631*

NIST Implementation and Realization of the ITS-90 Over the Range 83 K to 1235 K: Reproducibility, Stability, and Uncertainties.
PB96-161328 *00,632*

NIST Measurement Assurance of SPRT Calibrations on the ITS-90: A Quantitative Approach.
PB96-161336 *00,633*

Preliminary Results of a Comparison of Water Triple-Point Cells Prepared by Different Methods.
PB96-161344 *00,634*

Comparisons of Some NIST Fixed-Point Cells with Similar Cells of Other Standards Laboratories.
PB97-119242 *00,655*

FIXTURES

Room-Temperature Flexure Fixture for Advanced Ceramics.
PB95-210498 *03,061*

FLAME CHEMISTRY

Effect of CF3H and CF3Br on Laminar Diffusion Flames in Normal and Microgravity.
PB96-161831 *01,420*

Effect of CF3H and CF3Br on Laminar Diffusion Flames in Normal and Microgravity.
PB96-161849 *01,421*

Inhibition of Premixed Methane-Air Flames by Iron Pentacarbonyl.
PB96-163712 *00,513*

Parametric Study of Hydrogen Fluoride Formation in Suppressed Fires.
PB96-163720 *00,514*

FLAME HEIGHT

Estimate of the Effect of Scale on Radiative Heat Loss Fraction and Combustion Efficiency.
PB95-150447 *02,486*

FLAME PROPAGATION
Ignition and Subsequent Transition to Flame Spread in a Microgravity Environment.
N96-15584/1 *04,828*

Concurrent Flow Flame Spread Study.
PB94-156866 *01,356*

Radiation and Mixing Properties of Buoyant Turbulent Diffusion Flames.
PB94-165974 *01,360*

Calculating Flame Spread on Horizontal and Vertical Surfaces.
PB94-187283 *00,335*

Fire Propagation in Concurrent Flows.
PB94-193844 *01,365*

Backdraft Phenomena.
PB94-193927 *01,366*

Upward Flame Spread along the Vertical Corner Walls (October 1993).
PB94-206299 *00,340*

Turbulent Upward Flame Spread on a Vertical Wall under External Radiation.
PB94-207388 *00,341*

Comparison of Wall-Fire Behavior With and Without a Ceiling.
PB94-207404 *00,342*

Combined Buoyancy- and Pressure-Driven Flow Through a Shallow, Horizontal, Circular Vent.
PB94-210077 *00,344*

VENTCF2: An Algorithm and Associated FORTRAN 77 Subroutine for Calculating Flow through a Horizontal Ceiling/Floor Vent in a Zone-Type Compartment Fire Model.
PB94-210127 *00,345*

Annual Conference on Fire Research: Book of Abstracts, October 17-20, 1994.
PB95-104964 *01,376*

Combustion of Methanol and Methanol/Dodecanol Spray Flames.
PB95-108544 *02,478*

Study of Droplet Transport in Alcohol-Based Spray Flames Using Phase/Doppler Interferometry.
PB95-108551 *02,479*

Algorithm to Describe the Spread of a Wall Fire under a Ceiling.
PB95-182259 *00,261*

Generation Rate and Distribution of Products of Combustion in Two-Layer Fire Environments: A Model and Applications.
PB96-102173 *01,398*

CFAST Output Comparison Method and Its Use in Comparing Different CFAST Versions.
PB96-109541 *00,401*

Flame Heights and Heat Release Rates of 1991 Kuwait Oil Field Fires.
PB96-119342 *01,404*

Review of Internatioanl Fire Risk Predictions Methods.
PB96-156195 *00,222*

Ignition and Subsequent Flame Spread Over a Thin Cellulosic Material.
PB96-160270 *04,836*

Calculating Combined Buoyancy- and Pressure-Driven Flow Through a Shallow, Horizontal, Circular Vent; Application to Problem of Steady Burning in a Ceiling-Vented Enclosure.
PB96-164108 *00,409*

Combined Buoyancy and Pressure-Driven Flow Through a Shallow, Horizontal, Circular Vent.
PB96-164116 *00,410*

Dynamics, Transport and Chemical Kinetics of Compartment Fire Exhaust Gases.
PB96-195508 *00,229*

FLAME RETARDANTS
Flame Retardants - Overview.
PB94-185287 *01,363*

FLAME SPREAD
Letter Report on Flame Spread Testing of a Composite Material.
PB97-110068 *01,436*

FLAME SPREADING
Turbulent Flame Spread on Vertical Corner Walls.
PB96-114764 *01,403*

FLAME SYNTHESIS
Flame Synthesis of High Tc Superconductors.
PB95-151981 *00,659*

FLAMES
Ignition and Subsequent Transition to Flame Spread in a Microgravity Environment.
N96-15584/1 *04,828*

Fluorinated Hydrocarbon Flame Suppression Chemistry.
PB94-185113 *01,362*

Estimate of Flame Radiance via a Single Location Measurement in Liquid Pool Flames.
PB94-211596 *02,476*

Structure of a Swirl-Stabilized Kerosene Spray Flame.
PB95-108569 *02,480*

Burning Rate and Flame Heat Flux For PMMA in the Cone Calorimeter.
PB95-216990 *00,393*

Heights of Wall-Fire Flames.
PB96-148192 *00,212*

Role of Combustion on Droplet Transport in Pressure-Atomized Spray Flames.
PB96-204433 *01,434*

Heat Flux from Flames to Vertical Surfaces.
PB97-110357 *01,438*

In-situ Studies of a Novel Sodium Flame Process for Synthesis of Fine Particles.
PB97-113047 *00,681*

FLAMMABILITY
Reaction Sensitivities of Al-Li Alloys and Alloy 2219 in Mechanical-Impact Tests.
PB94-172764 *03,314*

Modern Test Methods for Flammability.
PB94-198447 *01,370*

Recommended Changes in ASTM Test Methods D2512-82 and G86-84 for Oxygen-Compatibility Mechanical Impact Tests on Metals.
PB94-216694 *03,338*

One- and Two-Sided Burning of Thermally Thin Materials.
PB95-140935 *03,151*

Investigation into the Flammability Properties of Honeycomb Composites.
PB95-143293 *03,152*

Polymer Combustion and Flammability: Role of the Condensed Phase.
PB96-123245 *01,279*

Flammability Characterization with the Lift Apparatus and the Cone Calorimeter.
PB97-110050 *01,435*

NIST Research on Less-Flammable Materials.
PB97-118632 *01,439*

FLAMMABILITY TESTING
Behavior of Mock-Ups in the California Technical Bulletin 133 Test Protocol: Fabric and Barrier Effects.
PB95-231585 *00,301*

Predicting the Ignition Time and Burning Rate of Thermoplastics in the Cone Calorimeter.
PB96-154794 *01,418*

Quantifying the Ignition Propensity of Cigarettes.
PB96-155411 *00,306*

Effects of Sample Mounting on Flammability Properties of Intumescent Polymers.
PB96-159777 *03,389*

Computer-Aided Molecular Design of Fire Resistant Aircraft Materials.
PB96-160601 *00,025*

FLARE STARS
High-Velocity Plasma in the Transition Region of AU Microscopii: Evidence for Magnetic Reconnection and Saturated Heating during Quiescent and Flaring Conditions.
PB96-102694 *00,091*

FLASKS
Specifications and Tolerances for Reference Standards and Field Standard Weights and Measures. 2. Specifications and Tolerances for Field Standard Measuring Flasks.
PB96-178926 *02,682*

FLAT PANEL DISPLAYS
NIST Workshop on the Computer Interface to Flat Panel Displays. Held in San Jose, California on January 13-14, 1994.
PB95-136388 *01,625*

Survey of the Components of Display-Measurement Standards.
PB96-122528 *02,188*

FLAW INSENSITIVITY
Flaw-Insensitive Ceramics.
PB97-110027 *03,095*

FLAW TOLERANCE
Correlations between Flaw Tolerance and Reliability in Zirconia.
PB96-161922 *02,986*

Objective Evaluation of Short-Crack Toughness Curves Using Indentation Flaws: Case Study on Alumina-Based Ceramics.
PB96-179429 *03,079*

Flaw-Tolerance and Crack-Resistance Properties of Alumina-Aluminum Titanate Composites with Tailored Microstructures.
PB97-110324 *03,101*

FLAW TOLERANCES
Flaw Tolerance and Toughness Curves in Two-Phase Particulate Composites: SiC/Glass System.
PB96-179460 *03,081*

FLEET MANAGEMENT
AutoBid 2.0: The Microcomputer System for Police Patrol Vehicle Selection.
PB96-154570 *04,871*

FLEXIBLE PAVEMENTS
System for Calibration of the Marshall Compaction Hammer.
PB94-145661 *01,303*

Development of a Method for Measuring Water-Stripping Resistance of Asphalt/Siliceous Aggregate Mixtures.
PB96-197249 *01,348*

FLEXING
Observed and Theoretical Creep Rates for an Alumina Ceramic and a Silicon Nitride Ceramic in Flexure.
PB94-212958 *03,040*

Flat and Rising R-Curves for Elliptical Surface Cracks from Indentation and Superposed Flexure.
PB95-161295 *03,156*

FLEXURAL PROPERTIES
Crack Growth Resistance of Strain-Softening Materials under Flexural Loading.
PB94-200227 *02,972*

FLEXURAL SPRINGS
Design Equations and Scaling Laws for Linear Compressors with Flexure Springs.
PB95-168902 *02,948*

FLIGHT
Stylus Flight in Surface Profiling.
PB96-123138 *02,675*

FLIGHT TELEROBOTIC SERVICER
Evolution of the Flight Telerobotic Servicer.
PB94-216082 *04,832*

FLIP-CHIP TECHNOLOGY
Microwave Characterization of Flip-Chip MMIC Components.
PB96-176722 *02,434*

Microwave Characterization of Flip-Chip MMIC Interconnections.
PB96-176730 *02,435*

Electrical Measurements of Microwave Flip-Chip Interconnections.
PB96-176748 *02,436*

FLOATING POINT ARITHMETIC
Underflow-Induced Graphics Failure Solved by SLI Arithmetic.
PB95-161444 *01,712*

Parallel and Serial Implementations of SLI Arithmetic.
PB95-242335 *01,732*

FLOORS
Fire Performance of an Interstitial Space Construction System.
PB95-188918 *00,390*

Testing of Selected Self-Leveling Compounds for Floors.
PB95-220455 *00,395*

Materials-Science Based Approach to Phenol Emissions from a Flooring Material in an Office Building.
PB97-118749 *02,572*

FLOREFFE TERMINAL
Ashland Tank Collapse Investigation.
PB95-126314 *02,481*

Ashland Tank-Collapse Investigation: Closure by Authors.
PB95-126322 *02,482*

FLOW CALIBRATION
Cryogenic Flow Calibration in NIST.
PB96-161930 *01,143*

FLOW CHARACTERISTICS
Effect of Heterogeneous Porous Media on Mold Filling in Resin Transfer Molding.
PB95-108676 *03,197*

FLOW CONDITIONERS
Flow Conditioner Tests for Three Orifice Flowmeter Sizes.
PB95-105540 *04,201*

FLOW DISTORTION
Comparing NIST-B 50 mm Orifice Meter Gas Data to the ANSI Equation.
PB95-169207 *02,949*

FLOW DISTRIBUTION
Ignition and Subsequent Transition to Flame Spread in a Microgravity Environment.
N96-15584/1 *04,828*

Comparison of the Unidirectional and Radial In-Plane Flow of Fluids Through Woven Composite Reinforcements.
PB95-162004 *02,698*

Interaction between Micro and Macroscopic Flow in RTM Preforms.
PB95-162012 *03,159*

FLOW FIELDS
Laser Imaging of Chemistry-Flowfield Interactions: Enhanced Soot Formation in Time-Varying Diffusion Flames.
PB94-185352 *01,364*

Tomographic Reconstruction of the Moments of Local Probability Density Functions in Turbulent Flow Fields.
PB96-180195 *04,219*

FLOW GEOMETRY
Heat Transfer in Thin, Compact Heat Exchangers with Circular, Rectangular, or Pin-Fin Flow Passages.
PB95-140943 *02,751*

FLOW INDUCED STRUCTURES
Flow-Induced Structure in Polymer. Chapter 1. An Introduction to Flow-Induced Structures in Polymers.
PB96-123369 *03,387*

Flow-Induced Structure in Polymers. Chapter 17. Phase-Separation Kinetics of a Polymer Blend Solution Studied by a Two-Step Shear Quench.
PB96-123377 *03,388*

FLOW INJECTION
Flow Immunoassay Using Solid-Phase Entrapment.
PB96-200951 *00,642*

FLOW INJECTION ANALYSIS
Liposome-Based Flow-Injection Immunoassay for Determining Theophylline in Serum.
PB94-213493 *03,494*

Potentiometric Enzyme-Amplified Flow Injection Analysis Detection System: Behavior of Free and Liposome-Released Peroxidase.
PB95-151833 *03,534*

Amperometric Flow-Injection Analysis Biosensor for Glucose Based on Graphite Paste Modified with Tetracyanoquinodimethane.
PB95-161980 *03,498*

FLOW MEASUREMENT
Ventilation Rates in Office Buildings.
PB95-108825 *02,539*

Energy Flows in an Orifice Pulse Tube Refrigerator.
PB95-169082 *02,752*

Laser Doppler Velocimeter Studies of the Pipeflow Produced by a Generic Header.
PB95-226916 *02,602*

Sliding Vane Flow Conditioner Tests in a 100 Diameter Long 10 inch Natural Gas Orifice Meter at Pacific Gas and Electric. Topical Report, 1990-1992.
PB95-256335 *02,493*

FLOW METERS
Summary Report of NIST's Industry-Government Consortium Research Program on Flowmeter Installation Effects with Emphasis on the Research Period, January-September 1991: The Reducer.
PB94-160736 *04,196*

Summary Report of NIST's Industry-Government Consortium Research Program on Flowmeter Installation Effects: The 45 Degree Elbow.
PB95-143061 *04,204*

Laser Doppler Velocimeter Studies of the Pipeflow Produced by a Generic Header.
PB95-226916 *02,602*

Critical Evaluation of Thermal Mass Flow Meters.
PB97-113153 *00,683*

FLOW MODELS
Improvement in Predicting Smoke Movement in Compartmented Structures.
PB94-172418 *00,332*

Modeling Radon Transport in Multistory Residential Buildings.
PB95-162087 *00,256*

FLOW RATE
Experimental Data and Theoretical Modeling of Gas Flows Through Metal Capillary Leaks.
PB95-150892 *04,206*

FLOW VELOCITY
Backdraft Phenomena.
PB94-193927 *01,366*

FLOW VISUALIZATION
Visual Measurement Technique for Analysis of Nucleate Flow Boiling.
PB95-143301 *03,262*

FLOWGRAPHS
Method to Determine a Basis Set of Paths to Perform Program Testing.
PB96-131503 *01,747*

FLOWMETERS
Flow Conditioner Tests for Three Orifice Flowmeter Sizes.
PB95-105540 *04,201*

Comparing NIST-B 50 mm Orifice Meter Gas Data to the ANSI Equation.
PB95-169207 *02,949*

Effects of Pipe Elbows and Tube Bundles on Selected Types of Flowmeters.
PB96-160999 *01,135*

SSME LOX Duct Flowmeter Design and Test Results.
PB96-161955 *04,826*

Flowmeter Installation Effects Due to a Generic Header.
PB96-210893 *02,606*

FLUCTUATIONS
Fluctuation Dominated Recombination Kinetics with Traps.
PB95-107264 *00,875*

Mesoscopic Conductance Fluctuations in Large Devices.
PB96-119656 *04,735*

Quantum Conductance Fluctuations in the Larger-Size-Scale Regime.
PB97-111264 *04,144*

Orientational Fluctuations, Diffuse Scattering, and Orientational Order in Solid C60.
PB97-119275 *04,176*

FLUID FLOW
Reconstructing Stratified Fluid Flow from Reciprocal Scattering Measurements.
PB95-107256 *04,202*

Effect of Heterogeneous Porous Media on Mold Filling in Resin Transfer Molding.
PB95-108676 *03,197*

Comparison of the Unidirectional and Radial In-Plane Flow of Fluids Through Woven Composite Reinforcements.
PB95-162004 *02,698*

Flow of Alternative Agents in Piping.
PB95-202420 *00,022*

FLUID MIXERS
Milliwatt Mixer for Small Fluid Samples.
PB94-198819 *02,634*

FLUIDELASTICITY
Chaotic Motions of Coupled Galloping Oscillators and Their Modeling as Diffusion Progresses.
PB96-122718 *04,823*

FLUIDS
Survey of the Literature on Heat Transfer from Solid Surfaces to Cryogenic Fluids.
AD-A286 680/4 *04,193*

Ebulliometers for Measuring the Thermodynamic Properties of Fluids and Fluid Mixtures.
DE94017817 *04,195*

Thermophysical Properties of Fluids for the Gas Industry. Final Report, February 1, 1988-August 31, 1993.
PB94-146677 *02,472*

Transient Methods for Thermal Conductivity.
PB94-198405 *04,197*

Measurements of the Viscosities of Saturated and Compressed Fluid 1-chloro-1,2,2,2-tetrafluoroethane (R124) and Pentafluoroethane (R125) at Temperatures between 120 and 420 K.
PB94-199791 *03,254*

Global Thermodynamic Behavior of Fluid Mixtures in the Critical Region.
PB94-212420 *04,199*

Thermophysical Property Computer Packages from NIST.
PB95-125787 *04,203*

Thermophysical Properties of Fluids for the Gas Industry.
PB96-122437 *02,494*

FLUIDS: LIQUIDS/GASES/PLASMAS
Characteristics of Turbulence in a Boundary Layer with Zero Pressure Gradient.
AD-A278 249/8 *04,192*

Air Flow in the Boundary Layer of an Elliptic Cylinder.
AD-A297 391/5 *04,194*

Distributed measurements of tracer response on packed bed flows using a fiberoptic probe array. Final report.
DE95013079 *00,667*

Summary Report of NIST's Industry-Government Consortium Research Program on Flowmeter Installation Effects with Emphasis on the Research Period, January-September 1991: The Reducer.
PB94-160736 *04,196*

Transient Methods for Thermal Conductivity.
PB94-198405 *04,197*

Liquid and Solid Atomic Ion Plasmas.
PB94-198991 *03,809*

Absorption of Ultrasonic Waves in Air at High Frequencies (10-20 MHz).
PB94-199007 *04,182*

Asymptotic Behavior of Modulated Taylor-Couette Flows with a Crystalline Inner Cylinder.
PB94-199072 *04,469*

Summary of the Patent Literature of Supercritical Fluid Technology.
PB94-199213 *00,502*

Development in the Theory and Analysis of Eddy Current Sensing of Velocity in Liquid Metals.
PB94-212586 *03,335*

Evolution of a Turbulent Boundary Layer Induced by a Three-Dimensional Roughness Element.
PB94-212818 *04,200*

Reconstructing Stratified Fluid Flow from Reciprocal Scattering Measurements.
PB95-107256 *04,202*

Structure of the Vapor-Liquid Interface Near the Critical Point.
PB95-140174 *00,902*

Flow of Microemulsions through Microscopic Pores.
PB95-140463 *00,905*

Summary Report of NIST's Industry-Government Consortium Research Program on Flowmeter Installation Effects: The 45 Degree Elbow.
PB95-143061 *04,204*

Simulations of Glass Forming Liquids: What Has Been Learned.
PB95-150124 *00,915*

Experimental Data and Theoretical Modeling of Gas Flows Through Metal Capillary Leaks.
PB95-150892 *04,206*

Controlled Nucleation in Aerosol Reactors for Supression of Agglomerate Formation.
PB95-151973 *00,672*

Gas Phase Reactivity Study of OH Radicals with 1,1-Dichloroethene and cis-1,1-Dichloroethene and Trans-1,2-Dichloroethene over the Temperature Range 240-400 K.
PB95-152146 *00,939*

Electrostatic Modes of Ion-Trap Plasmas.
PB95-152963 *03,920*

Two Phase Aqueous Extraction: Rheological Properties of Dextran, Polyethylene Glycol, Bovine Serum Albumin and Their Mixtures.
PB95-161998 *00,676*

Comparison of the Unidirectional and Radial In-Plane Flow of Fluids Through Woven Composite Reinforcements.
PB95-162004 *02,698*

Critical Behavior of Ionic Fluids.
PB95-164331 *00,978*

First Phase Formation Kinetics in the Reaction of Nb/Al.
PB95-168456 *03,353*

Experimental Results on Normal Modes in Cold, Pure Ion Plasmas.
PB95-175105 *03,956*

Equilibrium Pair Distribution Function of a Gas: Aspects Associated with the Presence of Bound States.
PB95-176046 *01,004*

Electrostatic Modes as a Diagnostic in Penning-Trap Experiments.
PB95-176244 *03,959*

Convective Stability in the Rayleigh-Benard and Directional Solidification Problems: High-Frequency Gravity Modulation.
PB95-181145 *04,208*

Laser Doppler Velocimeter Studies of the Pipeflow Produced by a Generic Header.
PB95-226916 *02,602*

Sliding Vane Flow Conditioner Tests in a 100 Diameter Long 10 inch Natural Gas Orifice Meter at Pacific Gas and Electric. Topical Report, 1990-1992.
PB95-256335 *02,493*

Langmuir Probe Measurements in the Gaseous Electronics Conference RF Reference Cell.
PB96-113386 *02,393*

Inductively Coupled Plasma Source for the Gaseous Electronics Conference RF Reference Cell.
PB96-113394 *02,394*

Reactive Ion Etching in the Gaseous Electronics Conference RF Reference Cell.
PB96-113402 *02,395*

Dusty Plasma Studies in the Gaseous Electronics Conference Reference Cell.
PB96-113410 *02,396*

Measurements of the Relative Permittivity of Liquid Water at Frequencies in the Range of 0.1 to 10 kHz and at Temperatures between 273.1 and 373.2 K at Ambient Pressure.
PB96-119375 *01,078*

Improved Gas Flow Measurements for Next-Generation Processes.
PB96-156013 *04,216*

Analysis of Transverse Flow in Aligned Fibrous Porous Media.
PB96-167200 *03,177*

Greenspan Acoustic Viscometer for Gases.
PB96-204417 *04,220*

Diffuse-Interface Description of Fluid Systems.
PB96-210711 *01,170*

Flowmeter Installation Effects Due to a Generic Header.
PB96-210893 *02,606*

Commercial Helium Permeation Leak Standards: Their Properties and Reliability.
PB97-111413 *04,146*

Critical Evaluation of Thermal Mass Flow Meters.
PB97-113153 *00,683*

Internal Droplet Circulation Induced by Surface-Driven Rotation.
PB97-119267 *02,500*

FLUORESCENCE
Fluorescence Monitoring of Polarity Change and Gelation during Epoxy Cure.
PB94-185543 *01,204*

Comparison of UV-Induced Fluorescence and Bragg Grating Growth in Optical Fiber.
PB95-168597 *04,284*

Optical Biosensor Using a Fluorescent, Swelling Sensing Element.
PB95-175899 *03,541*

Decrease of Fluorescence in Optical Fiber during Exposure to Pulsed or Continuous-Wave Ultraviolet Light.
PB95-203071 *04,320*

In situ Fluorescence Cell Mass Measurements of 'Saccharomyces cerevisiae' Using Cellular Tryptophan.
PB96-135041 *03,547*

Comparison of UV Photosensitivity and Fluorescence during Fiber Grating Formation.
PB96-155445 *04,362*

Bacterial Enumeration in Storage Water.
PB96-163647 *03,591*

Feasibility of Fluorescence Detection of Tetracycline in Media Mixtures Employing a Fiber Optic Probe.
PB96-163654 *00,511*

New Method for the Detection and Measurement of Polyaromatic Carcinogens and Related Compounds by DNA Intercalation.
PB96-167382 *03,481*

In situ Characterization of Vapor Phase Growth of Iron Oxide-Silica Nanocomposites: Part 1. 2-D Planar Laser-Induced Fluorescence and Mie Imaging.
PB97-112478 *03,185*

FLUORESCENCE DETECTION
Determination of Vitamin K1 in Serum Using Catalytic-Reduction Liquid Chromatography with Fluorescence Detection.
PB96-138425 *03,506*

FLUORESCENCE RECOVERY AFTER PHOTOBLEACHING TECHNIQUE
Monitoring Polymer Cure by Fluorescence Recovery After Photobleaching.
PB94-211422 *01,218*

FLUORESCENCE SPECTROSCOPY
In situ On-Line Optical Fiber Sensor for Fluorescence Monitoring in Bioreactors.
PB94-212024 *03,587*

Standards for Corrected Fluorescence Spectra.
PB95-150835 *00,581*

Electrophoretic Separations of Polymerase Chain Reaction: Amplified DNA Fragments in DNA Typing Using a Capillary Electrophoresis-Lased Induced Fluorescence System.
PB95-163036 *03,536*

Enhanced Detection of PCR Products Through Use of TQTO and YOYO Intercalating Dyes with Laser Induced Fluorescence - Capillary Electrophoresis.
PB95-164653 *00,599*

Fluorescence Measurements of Tetracycline in High Cell Mass for Fermentation Monitoring.
PB95-175709 *00,601*

FLUORESCENCE STANDARDS
Standards for Corrected Fluorescence Spectra.
PB95-150835 *00,581*

FLUORESCENT DYES
Applications of Fluorescence Spectroscopy in Polymer Science and Technology.
PB95-163770 *01,258*

FLUORESCENT LAMPS
Performance of Compact Fluorescent Lamps at Different Ambient Temperatures.
PB95-175329 *00,258*

FLUORESCENT SCREENS
Image Information Transfer Properties of X-Ray Intensifying Screens in the Energy Range from 17 to 320 keV.
PB95-126173 *00,155*

FLUORIDE
Fluoride Analytical Methods.
PB96-180237 *03,578*

FLUORIDES
Deposition of Loosely Bound and Firmly Bound Fluorides on Tooth Enamel by an Acidic Gel Containing Fluorosilicate and Monocalcium Phosphate Monohydrate.
PB95-150710 *03,559*

Distribution of Fluoride in Saliva and Plaque Fluid After a 0.048 mol/L NaF Rinse.
PB95-151205 *03,561*

FLUORINATED ACRYLATES
Facile Synthesis of Novel Fluorinated Multifunctional Acrylates.
PB94-198389 *01,207*

FLUORINATED ALIPHATIC HYDROCARBONS
Measurement of the Thermal Properties of Electrically Conducting Fluids Using Coated Transient Hot Wires.
DE94017816 *00,722*

FLUORINATED CELIPHATIC HYDROCARBONS
Vapour Pressures and Gas-Phase (p, rho n, T) Values for CF3CHF2(R125).
PB96-102090 *04,019*

FLUORINATED HYDROCARBONS
Burning Rate of Premixed Methane-Air Flames Inhibited by Fluorinated Hydrocarbons.
PB95-180584 *01,391*

FLUORINATION
Thermochemical and Chemical Kinetic Data for Fluorinated Hydrocarbons.
PB95-260618 *01,056*

FLUORINE
Influence of Coadsorbed Potassium on the Electron-Stimulated Desorption of F(+), F(-), and F(*) from PF3 on Ru(0001).
PB96-157946 *04,072*

FLUORINE-COMBUSTION CALORIMETRY
Thermochemical Studies of Inorganic Chalocogenides by Fluorine-Combustion Calorimetry: Binary Compounds of Germanium and Silicon with Sulfur, Selenium and Tellurium.
PB97-112528 *01,181*

FLUORINE ORGANIC COMPOUNDS
Facile Synthesis of Novel Fluorinated Multifunctional Acrylates.
PB94-198389 *01,207*

Thermodynamic Properties of CHF2-O-CHF2,Bis(difluoromethyl) Ether.
PB94-199569 *00,798*

FLUOROALKANES
Electronic Spectra of CF2Cl and CFCl2 Radicals Observed by Resonance Enhanced Multiphoton Ionization.
PB95-151023 *00,927*

FLUOROCARBONS
Retention of Halocarbons on a Hexafluoropropylene Epoxide Modified Graphitized Carbon Black. Part 1. Methane-Based Compounds.
PB95-175196 *03,272*

Retention of Halocarbons on a Hexafluoropropylene Epoxide-Modified Graphitized Carbon Black. 4. Propane-Based Compounds.
PB96-164033 *03,284*

Retention of Halocarbons on a Hexafluoropropylene Epoxide-Modified Graphitized Carbon Black. 3. Ethene-Based Compounds.
PB96-167309 *03,286*

Halon Thermochemistry: 'Ab Initio' Calculations of the Enthalpies of Formation of Fluoromethanes.
PB96-175740 *03,289*

FLUOROHYDROCARBONS
Fluorinated Hydrocarbon Flame Suppression Chemistry.
PB94-185113 *01,362*

Thermodynamic Properties of Difluoromethane.
PB94-185204 *00,772*

Thermal Conductivity of R134a.
PB94-213063 *03,857*

Polarized Transient Hot Wire Thermal Conductivity Measurements.
PB95-108817 *00,886*

Ebulliometric Measurement of the Vapor Pressure of Difluoromethane.
PB95-151361 *00,931*

Dielectric Studies of Fluids with Reentrant Resonators.
PB95-153730 *00,952*

Viscosity of the Saturated Liquid Phase of Six Halogenated Compounds and Three Mixtures.
PB95-162368 *00,960*

Criteria for Establishing Accurate Vapor Pressure Curves.
PB95-163812 *00,972*

Ebulliometric Measurement of the Vapor Pressure of 1-Chloro-1,1-Difluoroethane and 1,1-Difluoroethane.
PB95-164489 *00,984*

Thermodynamic Properties of R134a(1,1,1,2-Tetrafluoroethane).
PB95-168704 *00,988*

Measurements of Molar Heat Capacity at Constant Volume (Cv) for 1,1,1,2-Tetrafluoroethane (R134a).
PB95-168878 *03,264*

Vapour Pressure Measurements on 1,1,1,2-Tetrafluoroethane (R134a) from 180 to 350 K.
PB95-168886 *03,265*

Annex 18: An International Study of Refrigerant Properties.
PB95-168936 *03,266*

Development of a Dual-Sinker Densimeter for High-Accuracy Fluid P-V-T Measurements.
PB95-168951 *03,267*

Measurement of the Thermal Properties of Electrically Conducting Fluids Using Coated Transient Hot Wires.
PB95-169058 *03,269*

Measurements of the Vapor Pressures of Difluoromethane, 1-Chloro-1,2,2,2-Tetrafluoroethane, and Pentafluoroethane.
PB95-169272 *03,270*

Vapor Pressures and Gas-Phase PVT Data for 1-Chloro-1,2,2,2-Tetrafluoroethane (R124).
PB95-175154 *03,271*

Predictive Extended Corresponding States Model for Pure and Mixed Refrigerants Including an Equation of State for R134a.
PB95-175717 *03,275*

FLUOROMETHANES
Experimental and Numerical Burning Rates of Premixed Methane-Air Inhibited by Fluoromethanes.
PB95-180592 *01,392*

FLUOROMETRY
Optical Biosensor Using a Fluorescent, Swelling Sensing Element.
PB95-175899 *03,541*

FLUOROTOLUENES
Acceleration of Intramolecular Vibrational Redistribution by methyl Internal Rotation. A Chemical Timing Study of p-fluorotoluene and p-fluorotoluene-d3.
PB95-202982 *01,039*

FLUX PINNING
Temperature Dependence of Vortex Twin Boundary Interaction in Yttrium Barium Copper Oxide (YBa2Cu3O6+x).
PB95-162442 *04,613*

Enhanced Flux Pinning via Chemical Substitution in Bulk Superconducting T1-2212.
PB95-169033 *04,647*

Increased Pinning Energies and Critical Current Densities in Heavy-Ion-Irradiated Bi2Sr2CaCu2O8 Single Crystals.
PB95-175352 *04,654*

Crossover in the Pinning Mechanism of Anisotropic Fluxon Cores.
PB95-180170 *04,673*

Temperature and Field Dependence of Flux Pinning in NbTi with Aritificial Pinning Centers.
PB96-112024 *04,726*

Magnetic Flux Pinning in Epitaxial YBa2Cu3O7-delta Thin Films.
PB96-200746 *04,795*

FLUX (RATE)
Single Photon Laser Ionization as an In-situ Diagnostic for MBE growth.
PB96-102025 *01,059*

FLUX TRANSFORMERS
Fabrication Issues in Optimizing YBa2Cu3O7-x Flux Transformers for Low I/f Noise.
PB95-175857 *02,059*

Low Noise YBa2Cu3O7-x-SrTiO3-YBa2Cu3O7-x Mulitlayers for Improved Superconducting Magnetometers.
PB96-138417 *04,747*

FLUX TRAPPING
Trapped Vortices in a Superconducting Microbridge.
PB95-141149 *04,554*

FLUX VORTICES
Trapped Vortices in a Superconducting Microbridge.
PB95-141149 *04,554*

FLUXON OSCILLATIONS
SUSAN: SUperconducting Systems ANalysis by Low Temperature Scanning Electron Microscopy (LTSEM).
PB96-112065 *04,728*

FLUXONS
Deformable Superconductor Model for the Fluxon Mass.
PB95-175311 *04,653*

FLY ASH
Compositional Analysis of Beneficiated Fly Ashes.
PB95-220497 *00,397*

FOAM
Fire Protection Foam Behavior in a Radiative Environment.
PB97-116131 *00,237*

FOAMS
Effects of Humidity and Elevated Temperature on the Density and Thermal Conductivity of a Rigid Polyisocyanurate Foam Co-Blown with CCl3F and CO2.
PB95-150462 *00,371*

FOCUSING
Laser Focusing of Atoms: A Particle Optics Approach.
PB94-216660 *03,870*

Neutron Focusing Lens Using Polycapillary Fibers.
PB95-141206 *03,889*

FOIAS-TEMAM APPROXIMATION
Foias-Temam Approximations of Attractors for Galloping Oscillators.
PB94-198298 *04,817*

FOIAS-TEMAN APPROXIMATION
Algebraic Approximation of Attractors for Galloping Oscillators.
PB95-162897 *04,820*

FOKKER-PLANCK DESCRIPTIONS
Fokker-Planck Description of Multivalent Interactions.
PB95-108478 *00,879*

FOOD
Inter-Laboratory Trials of the EPR Method for the Detection of Irradiated Meats Containing Bone.
PB96-161690 *00,042*

FOOD ANALYSIS
Recently Developed NIST Food Related Standard Reference Materials.
PB94-198322 *00,035*

Individual Carotenoid Content of SRM 1548 Total Diet and Influence of Storage Temperature, Lyophilization, and Irradiation on Dietary Carotenoids.
PB94-200524 *00,033*

Mixed Diet Reference Materials for Nutrient Analysis of Foods: Preparation of SRM-1548 Total Diet.
PB95-151692 *03,593*

Liquid Chromatographic Method for the Determination of Carotenoids, Retinoids, and Tocopherols in Human Serum and in Food.
PB95-153599 *00,593*

FOOD CONTAMINATION
Recently Developed NIST Food Related Standard Reference Materials.
PB94-198322 *00,035*

FOOD IRRADIATION
Food Irradiation Dosimetry.
PB95-180675 *00,041*

Anionic Triphenylmethane Dye Solutions for Low-Dose Food Irradiation Dosimetry.
PB96-135173 *03,715*

FOOD PROCESSING
Estimation of the Absorbed Dose in Radiation-Processed Food. 2. Test of the EPR Response Function by an Exponential Fitting Analysis.
PB94-199650 *00,036*

Estimation of the Absorbed Dose in Radiation-Processed Food. 3. The Effect of Time of Evaluation on the Accuracy of the Estimate.
PB94-199684 *00,037*

Estimation of the Absorbed Dose in Radiation-Processed Food. 4. EPR Measurements on Eggshell.
PB94-199692 *00,038*

Estimation of the Absorbed Dose in Radiation-Processed Food. 1. Test of the EPR Response Function by a Linear Regression Analysis.
PB94-199718 *00,039*

Commentary on 'Optimization of Experimental Parameters for the EPR Detection of the Cellulosic Radical in Irradiated Foodstuffs'.
PB96-164124 *00,043*

FOOD STORAGE

Individual Carotenoid Content of SRM 1548 Total Diet and Influence of Storage Temperature, Lyophilization, and Irradiation on Dietary Carotenoids.
PB94-200524 *00,033*

FOOTWEAR

Program Requirements to Advance the Technology of Custom Footwear Manufacturing.
PB95-147906 *02,883*

FOOTWEAR INDUSTRY

Information Technologies Make Business Sense for the Custom Therapeutic Footwear Industry.
PB95-251708 *02,829*

FORCE MEASUREMENT

Force Calibrations in the Nanonewton Regime.
PB95-168696 *03,949*

FOREIGN COUNTRIES

Countries, Dependencies, Areas of Special Sovereignty, and Their Principal Administrative Divisions. Category: Data Standards and Guidelines; Subcategory: Representation and Codes.
FIPS PUB 10-4 *00,128*

Countries, Dependencies, Areas of Special Sovereignty, and Their Principal Administrative Divisions (for Microcomputers).
PB95-503504 *00,130*

FOREIGN TECHNOLOGY

Statistical Quality Control Technology in Japan.
PB94-199064 *02,708*

Japan Technology Program Assessment. Simulation: State-of the-Art in Japan.
PB95-217097 *02,827*

Parallel and Serial Implementations of SLI Arithmetic.
PB95-242335 *01,732*

Optically Stabilized Tunable Diode-Laser System for Saturation Spectroscopy.
PB96-102819 *04,717*

Energy Calibration of X-ray Photoelectron Spectrometers: Results of an Interlaboratory Comparison to Evaluate a Proposed Calibration Procedure.
PB96-102918 *04,027*

Damage Processes in Ceramics Resulting from Diamond Tool Indentation and Scratching in Various Environments.
PB96-102983 *03,065*

Measurements of Permittivity and the Dielectric Loss Tangent of Low Loss Dielectric Materials with a Dielectric Resonator Operating on the Higher Order Te(sub 0 gamma delta) Modes.
PB96-111869 *02,273*

Measuring Hydrogen by Cold-Neutron Prompt-Gamma Activation Analysis.
PB96-111877 *00,612*

Crystal Structure of Calcium Glutarate Monohydrate.
PB96-111893 *01,074*

Stability of Compressed Gas Mixtures Containing Low Level Volatile Organic Compounds in Aluminum Cylinders.
PB96-111968 *00,613*

Temperature and Field Dependence of Flux Pinning in NbTi with Aritificial Pinning Centers.
PB96-112024 *04,726*

Effects of Target Temperature on Analytical Sensitivities of Cold-Neutron Capture Prompt gamma-ray Activation Analysis.
PB96-112131 *00,616*

Study of Multiple Scattering Background in Compton Scatter Imaging.
PB96-112222 *04,425*

Local Oscillator Requirements and Strategies for the Next Generation of High-Stability Frequency Standards.
PB96-112230 *01,551*

Analytical Applications of Guided Neutron Beams.
PB96-112347 *04,041*

Vortex Dynamics and Melting in Niobium.
PB96-112362 *02,073*

Glimpse of Materials Research in China: A Report from an Interagency Study Team on Materials Visiting China from June 19, 1995 to June 30, 1995.
PB96-112677 *02,978*

Improved Annealing Technique for Optical Fiber.
PB96-119680 *04,343*

Neutron Techniques in Materials Science and Related Disciplines.
PB96-119698 *02,980*

Atom Cooling and Trapping, and Collisions of Trapped Atoms.
PB96-122916 *04,048*

Introduction to Phase-Stable Optical Sources.
PB96-122973 *04,347*

Effects of Spindle Dynamic Characteristics on Hard Turning.
PB96-122981 *02,699*

Study of Laser Resonance Ionization Mass Spectrometry Using a Glow Discharge Source.
PB96-123203 *03,360*

Hydraulic Radius and Transport in Reconstructed Model Three-Dimensional Porous Media.
PB96-123419 *00,403*

Lubrication Theory for Reactive Spreading of a Thin Drop.
PB96-123427 *04,214*

Ultrafast Time-Resolved Infrared Probing of Energy Transfer at Surfaces.
PB96-123443 *00,620*

Fundamental Processes in Gas Discharges.
PB96-123450 *01,089*

Kinetic-Energy Distributions of Ions Sampled from Radio-Frequency Discharges in Helium, Nitrogen, and Oxygen.
PB96-123732 *01,092*

Measurement of S2OF10, and S2O2F10 Production Rates from Spark and Negative Glow Corona Discharge in SF6/O2 Gas Mixtures.
PB96-123740 *01,093*

Distributed Feedback Lasers in Rare-Earth-Doped Phosphate Glass.
PB96-123773 *04,740*

Anionic Triphenylmethane Dye Solutions for Low-Dose Food Irradiation Dosimetry.
PB96-135173 *03,715*

Alcohol Solutions of Triphenyl-Tetrazolium Chloride as High-Dose Radiochromic Dosimeters.
PB96-135249 *03,716*

Oscillometric and Conductometric Analysis of Aqueous and Organic Dosimeter Solutions.
PB96-135256 *04,054*

Calorimeters for Calibration of High-Dose Dosimeters in High-Energy Electron Beams.
PB96-135272 *04,055*

Real Time Monitoring of Electron Processors.
PB96-135306 *03,719*

Influence of Thickness Fluctuations on Exchange Coupling in Fe/Cr/Fe Structures.
PB96-135371 *04,745*

Fiber Coating Diameter: Toward a Glass Artifact Standard.
PB96-140389 *02,234*

Research and Development Activities in Electron Paramagnetic Resonance Dosimetry.
PB96-141288 *03,635*

Ultrasonic-Resonance Spectroscopy of Bulk and Layered Solids.
PB96-141338 *04,759*

Inelastic Neutron Scattering Study of Hydrogen in Nanocrystalline Pd.
PB96-146857 *03,366*

II-3: Critical Current Measurement Methods: Quantitative Evaluation.
PB96-147160 *04,767*

II-5: Thermal Contraction of Materials Used in Nb3Sn Critical Current Measurements.
PB96-147186 *04,769*

Development of Gas Standards from Solid 1,4-dichlorobenzene.
PB96-155486 *02,496*

Transitions to Chaos Induced by Additive and Multiplicative Noise.
PB96-155759 *03,750*

Spectrum of the Stochastically Forced Duffing-Holmes Oscillator.
PB96-155767 *00,216*

Necessary Condition for Homoclinic Chaos Induces by Additive Noise.
PB96-155775 *04,063*

Physicochemical Characterization of Natural and Bioprosthetic Heart Valve Calcific Deposits: Implications for Prevention.
PB96-156039 *00,187*

Model for Calculating Virial Coefficients of Natural Gas Hydrocarbons with Impurities.
PB96-156047 *04,064*

Deterministic and Stochastic Chaos.
PB96-156138 *00,218*

Application of Digital-Image-Based Models to Microstructure, Transport Properties, and Degradation of Cement-Based Materials.
PB96-156161 *00,406*

Modeling Detector Response for Neutron Depth Profiling.
PB96-157813 *04,066*

Influence of Films' Thickness and Air Gaps in Surface Impedance Measurements of High Temperature Superconductors Using the Dielectric Resonator Technique.
PB96-157862 *01,946*

Information Transfer in the 21st Century.
PB96-157904 *02,714*

Comment On: Two-Photon Absorption Series of Calcium.
PB96-157979 *04,074*

Resonance Ionization Spectroscopy/Resonance Ionization Mass Spectrometry Data Service. V-Data Sheets for Ga, Mn, Sc, and Tl.
PB96-158068 *00,625*

Faraday Constant.
PB96-159793 *01,955*

Dynamics of Hydrogen Interactions with Si(100) and Si(111) Surfaces.
PB96-159801 *04,082*

RII Spectroscopy of Trap Levels in Bulk and LPE Hg1-xCdxTe.
PB96-160247 *04,084*

Instrumental Smearing Effects in Radially Symmetric Small-Angle Neutron Scattering by Numerical and Analytical Methods.
PB96-160429 *02,984*

Novel DNA N-Glycosylase Activity of E. coli T4 Endonuclease V That Excises 4,6-Diamino-5-Formamidopyrimidine from DNA, a UV-Radiation- and Hydroxyl Radical-Induced Product of Adenine.
PB96-160478 *03,549*

Development of the NIST Transient Pressure and Temperature Calibration Facility.
PB96-160833 *00,626*

Effects of Pipe Elbows and Tube Bundles on Selected Types of Flowmeters.
PB96-160999 *01,135*

Pressure Measurements with the Mercury Melting Line Referred to ITS-90.
PB96-161005 *01,136*

Direct Comparison of Three PTB Silver Fixed-Point Cells with the NIST Silver Fixed-Point Cell.
PB96-161286 *00,628*

Investigation of the ITS-90 Subrange Inconsistencies for 25.5 Omega SPRTs.
PB96-161302 *00,630*

Verification of Revised Water Vapour Correction to the Index of Refraction of Air.
PB96-161666 *02,680*

Current Noise Reveals Protonation Kinetics and Number of Ionizable Sites in an Open Protein Ion Channel.
PB96-161674 *04,092*

Inter-Laboratory Trials of the EPR Method for the Detection of Irradiated Meats Containing Bone.
PB96-161690 *00,042*

Protonation Dynamics in an Ion Channel Pore.
PB96-161757 *03,589*

Friction Processes in Brittle Fracture.
PB96-161765 *03,076*

Nonequilibrium Statistical Mechanics.
PB96-161781 *04,097*

Measurement of the (10)B(n, alpha1gamma)(7)Li Cross Section in the 0.3 to 4 MeV Neutron Energy Interval.
PB96-161799 *04,098*

Gas Absorption during Ion-Irradiation of a Polymer Target.
PB96-161864 *04,099*

Fundamentals of Fracture: A 1993 Prologue, and Other Comments.
PB96-161971 *03,218*

Fracture in Multilayers.
PB96-163613 *02,988*

Autofluorescence Detection of 'Escherichia coli' on Silver Membrane Filters.
PB96-163639 *03,590*

Model for Microcrack Initiation and Propagation beneath Hertzian Contacts in Polycrystalline Ceramics.
PB96-163704 *03,077*

Non-Newtonian Flow between Concentric Cylinders Calculated from Thermophysical Properties Obtained from Simulations.
PB96-163761 *04,103*

Retention of Halocarbons on a Hexafluoropropylene Epoxide-Modified Graphitized Carbon Black. 4. Propane-Based Compounds.
PB96-164033 *03,284*

Commentary on 'Optimization of Experimental Parameters for the EPR Detection of the Cellulosic Radical in Irradiated Foodstuffs'.
PB96-164124 *00,043*

Isotopic and Nuclear Analytical Techniques in Biological Systems: A Critical Study. 10. Elemental Isotopic Dilution Analysis with Radioactive and Stable Isotopes (Technical Report).
PB96-164157 *00,696*

Certifying the Chemical Composition of a Biological Material: A Case Study.
PB96-164272 *00,636*

Dead Time, Pileup, and Accurate Gamma-Ray Spectrometry.
PB96-167101 *00,697*

Loss-Free Counting at IRI and NIST.
PB96-167119 *04,105*

Trace Element Concentrations in Cetacean Liver Tissues Archived in the National Marine Mammal Tissue Bank.
PB96-167127 *02,595*

Simulation and SANS Studies of Gelation Under Shear.
PB96-167176 *01,150*

Analysis of Transverse Flow in Aligned Fibrous Porous Media.
PB96-167200 *03,177*

Determination of 21 Elements by INAA for Certification of SRM 1570a, Spinach.
PB96-167242 *00,698*

New NIST Rapid Pneumatic Tube System.
PB96-167259 *03,738*

Recent Developments in NIST Botanical SRMs.
PB96-167267 *03,489*

Relationship of Silver with Selenium and Mercury in the Liver of Two Species of Toothed Whales (Odontocetes).
PB96-167275 *02,596*

Resolution of Discrepant Analytical Data in the Certification of Platinum in Two Automobile Catalyst SRMs.
PB96-167283 *00,638*

Retention of Halocarbons on a Hexafluoropropylene Epoxide-Modified Graphitized Carbon Black. 3. Ethene-Based Compounds.
PB96-167309 *03,286*

Structure and Rheology of Hard-Sphere Systems.
PB96-167333 *00,662*

Thermophysical Property Standard Reference Data from NIST.
PB96-167358 *01,153*

Novel Magnetic Field Characterization Techniques for Compound Semiconductor Materials and Devices.
PB96-176458 *02,433*

Energy Distributions of Neutrons Scattered from Solid C60 by the Beryllium Detector Method.
PB96-176631 *03,740*

Small-Angle Neutron Scattering (SANS) Study of Worm-Like Micelles Under Shear.
PB96-176698 *04,111*

Surface Plasmon Microscopy of Biotin-Streptavidin Binding Reactions on UV-Photopatterned Alkanethiol Self-Assembled Monolayers.
PB96-176771 *01,158*

Flaw Tolerance and Toughness Curves in Two-Phase Particulate Composites: SiC/Glass System.
PB96-179460 *03,081*

Adsorption of Potassium N-phenylglycinate on Hydroxyapatite: Role of Solvents and Ionic Charge.
PB96-180161 *01,159*

Fluoride Analytical Methods.
PB96-180237 *03,578*

Fracture of Silicon Nitride and Silicon Carbide at Elevated Temperatures.
PB96-180260 *03,179*

Alpha-Particle and Electron Capture Decay of (209)Po.
PB96-186085 *04,119*

Scattered Fractions of Dose from 18 and 25 MV X-ray Radiotherapy Linear Accelerators.
PB96-186101 *04,120*

Characterization of the Structure of YD3 by Neutron Powder Diffraction.
PB96-186150 *01,161*

Comment on <<A Dynamic Electric Trap for Ground-State Atoms>>.
PB96-200290 *04,123*

Collisions of Electrons with Highly-Charged Ions.
PB96-200340 *04,791*

Kinetic-Energy-Enhanced Neutral Etching.
PB96-200613 *00,665*

Thermal Conductivity of Polypyromellitimide Film with Alumina Filler Particles from 4.2 to 300 K.
PB96-200753 *01,292*

Quantitative Determination of Oxidative Base Damage in DNA by Stable Isotope-Dilution Mass Spectrometry.
PB96-200886 *03,483*

Commentary: The Measurement of Oxidative Damage to DNA by HPLC and GC/MS Techniques.
PB96-200894 *03,484*

UV Absorption Cross Sections of Methylchloroform: Temperature-Dependent Gas and Liquid Phase Measurements.
PB96-201041 *00,643*

Low Heat-Flux Measurements: Some Precautions.
PB96-201116 *02,685*

Gas Phase Oxygen Effect on Chain Scission and Monomer Content in Bulk Poly(methyl methacrylate) Degraded by External Thermal Radiation.
PB96-204078 *01,293*

Creep and Creep Rupture of Structural Ceramics.
PB96-204524 *03,093*

Role of Certified Reference Materials in Trace Analysis Quality Assurance.
PB97-110019 *00,650*

Interaction of an Isolated Sprinkler Spray and a Two-Layer Compartment Fire Environment. Phenomena and Model Simulations.
PB97-110076 *01,437*

Liquid-Scintillation Counting Techniques for the Standardization of Radionuclides Used in Therapy.
PB97-110084 *03,709*

Needs for Brachytherapy Source Calibrations in the United States.
PB97-110092 *03,521*

Radioassays of Yttrium-90 Used in Nuclear Medicine.
PB97-110100 *03,522*

Problem of Convection in the Water Absorbed Dose Calorimeter.
PB97-110159 *03,523*

Stable Silicon Photodiodes for Absolute Intensity Measurements in the VUV and Soft X-ray Regions.
PB97-110175 *04,135*

Tension/Compression Creep Asymmetry in Si3N4.
PB97-110258 *03,096*

Current Status and Trends in Temperature Measurements at NIST, Cooperative Projects and New Mutual Agreement between NIST and IMGC.
PB97-110266 *02,691*

Electron-Photon Monte Carlo Calculations: The ETRAN Code.
PB97-110407 *04,138*

Interlaboratory Studies on the Analysis of Hair for Drugs of Abuse: Results from the Fifth Exercise.
PB97-110449 *03,509*

High Temperature Structural Reliability of Silicon Nitride.
PB97-110456 *03,104*

Magneto-Optic Rotation Sensor Using a Laser Diode as Both Source and Detector.
PB97-111272 *04,390*

Proposed Tests to Evaluate the Frequency-Dependent Capacitor Ratio for Single Electron Tunneling Experiment.
PB97-111454 *01,982*

New Refractometer by Combining a Variable Length Vacuum Cell and a Double-Pass Michelson Interferometer.
PB97-111926 *01,986*

Observation of Two Length Scales Above (T sub N) in a Holmium Thin Film.
PB97-111942 *04,151*

DNA Damage and DNA Sequence Retrieval from Ancient Tissues.
PB97-111983 *03,556*

High-Current Thin Film Multijunction Thermal Converters and Multi-Converter Modules.
PB97-112379 *01,989*

Ferric Ion Assisted Photooxidation of Halocetates.
PB97-112460 *00,521*

Wideband Sampling Voltmeter.
PB97-113039 *01,990*

NIST Watt Balance: Progress Toward Monitoring the Kilogram.
PB97-113062 *01,991*

Molecular Dynamics Investigation of the Surface/Bulk Equilibrium in an Ethanol-Water Solution.
PB97-113112 *01,183*

Comparison of Filter Radiometer Spectral Responsivity with the NIST Spectral-Irradiance and Illuminance Scales.
PB97-113161 *04,162*

DC-MHz Wattmeter Based on RMS Voltage Measurements.
PB97-113211 *01,992*

Results of Capacitance Ratio Measurements for the Single Electron Pump-Capacitor Charging Experiment.
PB97-113286 *04,813*

Issues in High-Speed Pyrometry.
PB97-118368 *02,693*

Radiance Temperatures at 1500 nm of Niobium and Molybdenum at Their Melting Points by a Pulse-Heating Technique.
PB97-118699 *04,167*

Effect of Formulation Changes on the Response to Ionizing Radiation of Radiochromic Dye Films.
PB97-119028 *04,171*

Results of the ASTM Nuclear Methods Intercomparison on NIST Apple and Peach Leaves Standard Reference Materials.
PB97-119036 *03,490*

Measurements of the (235)U(n,f) Cross Section in the 3 to 30 MeV Neutron Energy Region.
PB97-119051 *04,172*

Automated Guarded Bridge for Calibration of Multimegohm Standard Resistors.
PB97-119150 *02,289*

Conversion of a 2-Terminal-Pair Bridge to a 4-Terminal-Pair Bridge for Increased Range and Precision in Impedance Measurements.
PB97-119176 *02,103*

Novel Radiochromic Films for Clinical Dosimetry.
PB97-119259 *03,641*

Orientational Fluctuations, Diffuse Scattering, and Orientational Order in Solid C60.
PB97-119275 *04,176*

Calibration and Performance of GafChromic DM-100 Radiochromic Dosemeters.
PB97-119291 *00,703*

Electronic Structure and Phase Equilibria in Ternary Substitutional Alloys.
PB97-119366 *03,378*

Anomalous Relation between Time and Frequency Domain PMD Measurements.
PB97-119390 *04,398*

Dependence of the Thermal Electron Attachment Rate Constant in Gases and Liquids on the Energy Position of the Electron Attaching State.
PB97-122253 *01,996*

Generalized Optical Theorem for On-Axis Gaussian Beams.
PB97-122345 *04,177*

Measurement of the Atomic Na(3P) Lifetime and of Retardation in the Interaction between Two Atoms Bound in a Molecule.
PB97-122360 *04,178*

Complex Time Dependence of the EPR Signal of Irradiated L-alpha-alanine.
PB97-122436 *04,180*

DNA Base Damage in Lymphocytes of Cancer Patients Undergoing Radiation Therapy.
PB97-122444 *03,643*

Wear Modeling of Si-Based Ceramics.
PB97-122501 *03,112*

Characterization of Time-Dependent Dielectric Breakdown in Intrinsic Thin SiO2.
PB97-122527 *02,458*

Xi-Vector Formulation of Anisotropic Phase-Field Models: 3-D Asymptotics.
PB97-122550 *04,816*

Chemical Effect in Ceramics Grinding.
PB97-122592 *03,113*

FOREIGN TECHNOLOOGY
Viscosity of Defined and Undefined Hydrocarbon Liquids Calculated Using an Extended Corresponding-States Model.
PB96-167234 *02,498*

FORENSIC SCIENCE
Separation and Identification of Organic Gunshot and Explosive Constituents by Micellar Electrokinetic Capillary Electrophoresis.
PB95-107249 *00,566*

FORENSIC SCIENCES
Face Recognition Technology for Law Enforcement Applications.
PB94-207768 *01,837*

FORENSICS
Specification for Interoperability between Ballistic Imaging Systems. Part 1. Cartridge Cases.
PB96-195524 *01,860*

FORGING
Microstructure and Tensile Properties of Microalloyed Steel Forgings.
PB94-172715 *03,204*

FORGING STEELS
Prediction of Strengthening Due to V Additions in Direct-Cooled Ferrite-Pearlite Forging Steels.
PB96-190251 *03,220*

FORIEGN TECHNOLOGY
SPC Artifact for Automated Solder Joint Inspection.
PB96-161716 *04,095*

FORM FACTORS
Improvements in Computation of Form Factors.
PB94-200078 *03,820*

FORM REMOVAL
Method and Evaluation of Character Stroke Preservation on Handprint Recognition.
PB95-251724 *01,850*

FORMABILITY
Ultrasonic Measurement of Sheet Anisotropy and Formability.
PB95-153235 *03,213*

Determination of Sheet Steel Formability Using Wide Band Electromagnetic-Acoustic Transducers.
PB96-186036 *02,279*

Methods to Improve the Accuracy of On-Line Ultrasonic Measurement of Steel Sheet Formability.
PB96-186051 *02,281*

FORMAL METHODS
Formal Methods in Conformance Testing: Result and Perspectives.
PB95-153029 *01,710*

FORMALDEHYDE
Laser-Induced Fluorescence Measurements of Formaldehyde in a Methane/Air Diffusion Flame.
PB94-211679 *01,374*

FORMALDEHYDE-WATER COMPLEX
Microwave Spectrum and Structure of CH2O-H2O.
PB97-118723 *04,168*

FORMAT
Expression Formatter for MACSYMA.
PB95-267829 *01,735*

Guide to a Format for Data on Chemical Admixtures in a Materials Property Database.
PB96-165394 *01,327*

Guide to a Format for Data on Chemical Admixtures in a Materials Property Database. (Reannouncement with new abstract).
PB96-186192 *01,328*

FORMATION ENTHALPY
UV Absorption Cross Sections of Methylchloroform: Temperature-Dependent Gas and Liquid Phase Measurements.
PB96-201041 *00,643*

FORMATS
Standardised Computer Data File Format for Storage, Transport, and Off-Line Processing of Partial Discharge Data.
PB96-122486 *01,930*

FORMIC ACID
Strong Hydrogen Bond in the Formic Acid-Formate Anion System.
PB94-198595 *00,788*

FORMS (PAPER)
Evaluating Form Designs for Optical Character Recognition.
PB94-168044 *01,830*

Generalized Form Registration Using Structure-Based Techniques.
PB96-191374 *01,858*

FORMYL RADICALS
Quantum Dynamics of Renner-Teller Vibronic Coupling: The Predissociation HCO.
PB94-185303 *00,773*

FORTRAN
Review of Mathematical Function Library for Microsoft-FORTRAN, John Wiley and Sons, 1989.
PB94-160793 *01,679*

FORTRAN PROGRAMMING LANGUAGE
FORTRAN Compiler Validation System, Version 2.1.
PB94-500691 *01,698*

Validated Products List (Cobol, Fortran, ADA, Pascal, MUMPS, SQL).
PB94-937300 *01,700*

Validated Products List (Cobol, Fortran, ADA, Pascal, MUMPS, SQL).
PB95-937300 *01,738*

FORWARD SCATTERING
X-ray Photoelectron and Auger Electron Forward Scattering: A Structural Diagnostic for Epitaxial Thin Films.
PB95-180220 *04,676*

FOSSIL FUELS
Modulation of Fossil Fuel Production by Global Temperature Variations, 2.
PB94-146636 *02,533*

Determination of Sulfur in Fossil Fuels by Isotope Dilution Thermal Ionization Mass Spectrometry.
PB96-141379 *02,495*

FOULING ORGANISMS
Determination of Total Protein Adsorbed on Solid (Membrane) Surface by a Hydrolysis Technique: Single Protein Adsorption.
PB96-167093 *03,552*

FOULING RESISTANCE
Determination of Osmotic Pressure and Fouling Resistances and Their Effects on Performance of Ultrafiltration Membranes.
PB94-212891 *00,841*

Characterization of the Adsorption-Fouling Layer Using Globular Proteins on Ultrafiltration Membranes.
PB94-212909 *00,842*

FOUNDATIONS
Static Structural Analysis of a Reconfigurable Rigid Platform Supported by Elastic Legs.
PB97-113898 *02,960*

FOUR-TERMINAL-PAIR-BRIDGE
NIST Comparison of the Quantized Hall Resistance and the Realization of the SI Ohm Through the Calculable Capacitor.
PB97-119184 *02,291*

FOURIER ANALYSIS
Exact Recursion Relation Solution for the Steady-State Surface Temperature of a General Multilayer Structure.
PB96-102017 *02,376*

FOURIER-TRANSFORM SPECTROSCOPY
Wavelengths of Spectral Lines in Mercury Pencil Lamps.
PB96-176474 *04,376*

FOURIER TRANSFORMATION
Standard Reference Materials: Polystyrene Films for Calibrating the Wavelength Scale of Infrared Spectrophotometers - SRM 1921.
PB95-226866 *03,386*

Self-Reciprocal Fourier Functions.
PB96-200852 *01,974*

FOWLER-NORDHEIM
New Oxide Degradation Mechanism for Stresses in the Fowler-Nordheim Tunneling Regime.
PB96-200985 *04,128*

FPETOOL COMPUTER PROGRAM
FPETOOL: Fire Protection Tools for Hazard Estimation. An Overview of Features.
PB95-140885 *00,367*

FRACTAL AGGREGATION
Dynamic Scaling in an Aggregating 2D Lennard-Jones System.
PB96-167317 *04,106*

FRACTAL STRUCTURES
Electrolytes Constrained on Fractal Structures: Debye-Huckel Theory.
PB97-110241 *01,174*

FRACTOGRAPHY
Loading Device for Fracture Testing of Compact Tension Specimens in the Scanning Electron Microscope.
PB95-162434 *02,652*

Ductile Fracture and Tempered Martensite Embrittlement of 4140 Steel.
PB96-190285 *03,222*

FRACTURE
Lattice Statics of Interfaces and Interfacial Cracks in Bimaterial Solids.
PB96-161823 *02,985*

FRACTURE (MATERIALS)
Fundamentals of Fracture: A 1993 Prologue, and Other Comments.
PB96-161971 *03,218*

FRACTURE (MECHANICS)
Fracture Testing of Large-Scale Thin-Sheet Aluminum Alloy.
AD-A306 625/5 *03,305*

Fracture Behavior of Large-Scale Thin-Sheet Aluminum Alloy.
N95-19494/0 *03,311*

Fracture Mechanics Analysis of Near-Surface Cracks.
PB94-172400 *03,230*

Error Propagation Biases in the Calculation of Indentation Fracture Toughness for Ceramics.
PB94-172434 *03,032*

Temperature Increases in Aluminum Alloys during Mechanical-Impact Tests for Oxygen Compatibility.
PB94-172962 *03,316*

Generic Model for Creep Rupture Lifetime Estimation on Fibrous Ceramic Composites.
PB94-200235 *03,137*

Application of a Simple Technique for Estimating Errors of Finite-Element Solutions Using a General-Purpose Code.
PB94-200250 *04,818*

Environmentally Enhanced Fracture of Ceramics.
PB95-125746 *03,046*

Prediction of the Strength Properties for Plain-Carbon and Vanadium Micro-Alloyed Ferrite-Pearlite Steel.
PB96-123393 *03,216*

Catastrophic Failures Propagate Field of Fracture Mechanics.
PB96-135140 *03,217*

Pressurized Internal Lenticular Cracks at Healed Mica Interfaces.
PB96-180252 *02,997*

Fracture of Silicon Nitride and Silicon Carbide at Elevated Temperatures.
PB96-180260 *03,179*

Fatigue Crack Thresholds of a Nickel-Iron Alloy for Superconductor Sheaths at 4 K.
PB96-190343 *03,223*

Fracture Mechanism Maps: Their Applicability to Silicon Nitride.
PB96-204532 *03,094*

FRACTURE MECHANICS MODEL
Model for Toughness Curves in Two-Phase Ceramics. 2. Microstructural Variables.
PB96-163795 *03,078*

Model for Toughness Curves in Two-Phase Ceramics. 1. Basic Fracture Mechanics.
PB96-180088 *03,085*

FRACTURE PROPERTIES
Evaluation of the Environmentally Induced Fracture Resistance of Ductile Nickel Aluminide. Technical Report Number 1, Final report. October-December 1990.
DE94017331 *03,306*

Charpy Impact Test as an Evaluation of 4 K Fracture Toughness.
PB96-190194 *03,219*

FRACTURE RESISTANCE
Effects of Copper, Nickel and Boron on Mechanical Properties of Low-Alloy Steel Weld Metals Deposited at High Heat Input.
PB96-135231 *03,363*

FRACTURE STRENGTH
Matrix Grain Bridging Contribution to the Toughness of Whisker Reinforced Ceramics.
PB94-190645 *03,134*

Potential Drop in the Center-Cracked Panel with Asymmetric Crack Extension.
PB95-107330 *04,819*

Evaluation of Fracture Toughness and Residual Stress in Dental Porcelain by Indentation-Microfracture Method.
PB95-125613 *00,154*

New Alloys Show Extraordinary Resistance to Fracture and Wear.
PB95-151346 *03,346*

Evaluation of Fracture Toughness and Residual Stress in Dental Porcelain by Indentation-Microfracture Method.
PB95-152831 *00,159*

Fracture Toughness of Advanced Ceramics at Room Temperature: A Vamas Round-Robin.
PB95-162194 *03,160*

Shielding of Cracks in a Plastically Polarizable Material.
PB95-164257 *04,631*

FRACTURE TESTS
Fracture Testing of Large-Scale Thin-Sheet Aluminum Alloy.
PB95-242368 *00,024*

Factors Significant to Precracking of Fracture Specimens.
PB96-109558 *03,358*

FRACTURE TOUGHNESS
Aluminum-Lithium Alloys: Evaluation of Fracture Toughness by Two Test Standards, ASTM Method E 813 and E 1304.
PB96-190236 *03,374*

Light-Weight Alloys for Aerospace Applications II.
PB96-190244 *03,375*

Charpy Specimen Tests at 4 K.
PB96-190335 *03,002*

Mechanical Properties and Warm Prestress of Ultra-Low Carbon Steel at 4 K.
PB96-190350 *03,224*

FRACTURES
Fracture in Multilayers.
PB96-163613 *02,988*

FRACTURES (MATERIALS)
Micromechanics of Fracture in Rubber-Toughened Epoxies.
PB94-212222 *03,011*

Ashland Tank Collapse Investigation.
PB95-126314 *02,481*

Ashland Tank-Collapse Investigation: Closure by Authors.
PB95-126322 *02,482*

FRACTURING
Fracture Behavior of Large-Scale Thin-Sheet Aluminum Alloy.
N95-19494/0 *03,311*

FRAGILE GLASS
Long-Lived Structures in Fragile Glass-Forming Liquids.
PB96-119565 *04,212*

FRAME STRUCTURES
Survey of Steel Moment-Resisting Frame Buildings Affected by the 1994 Northridge Earthquake.
PB95-211918 *00,451*

FRAMES
Strengthening Methodology for Lightly Reinforced Concrete Frames-II. Recommended Calculation Techniques for the Design of Infill Walls.
PB94-187648 *00,426*

Strengthening Methodology for Lightly Reinforced Concrete Frames: Recommended Design Guidelines for Strengthening with Infill Walls.
PB95-260725 *00,454*

Strengthening Methodology for Lightly Reinforced Concrete Frames.
PB96-158050 *00,466*

FREE ELECTRON LASERS
NIST-NRL Free-Electron Laser Facility.
PB94-212511 *04,237*

Hybrid Undulator for the NIST-NRL Free-Electron Laser.
PB94-212529 *04,238*

FREE ENERGY
Interfacial Free Energies from Substrate Curvature Measurements of the Creep of Multilayer Thin Films.
PB94-185428 *04,448*

Stability and Surface Energies of Wetted Grain Boundaries in Aluminum Oxide.
PB95-202750 *03,059*

FREE ENERGY TRANSDUCTION
Imposed Oscillations of Kinetic Barriers Can Cause an Enzyme to Drive a Chemical Reaction Away from Equilibrium.
PB96-161625 *01,137*

FREE JETS
Global Density Effects on the Self-Preservation Behavior of Turbulent Free Jets.
PB95-162301 *04,207*

FREE RADICALS
Reaction Rate Determinations of Vinyl Radical Reactions with Vinyl, Methyl, and Hydrogen Atoms.
PB94-211398 *00,815*

Kinetics of the Reaction of CCl3-Br-2 and the Thermochemistry of CCl3 Radical and Cation.
PB94-212115 *00,824*

Experimental and Abinitio Studies of Electronic Structures of the CCl3 Radical and Cation.
PB94-212131 *00,826*

Electron Transfer Reaction Rates and Equilibria of the Carbonate and Sulfate Radical Anions.
PB94-212180 *00,829*

Multiphoton Ionization of SiH3 and SiD3 Radicals. 2. Three Photon Resonance-Enhanced Spectra Observed between 460 and 610 nm.
PB94-212487 *00,835*

New Electronic States of NH and ND Observed from 258 to 288 nm by Resonance Enhanced Multiphoton Ionization Spectroscopy.
PB94-212495 *00,836*

Multiphoton Ionization of SiH3 and SiD3 Radicals: Electronic Spectra, Vibrational Analyses of the Ground and Rydberg States, and Ionization Potential.
PB94-212503 *00,837*

Electronic Spectra of CF2Cl and CFCl2 Radicals Observed by Resonance Enhanced Multiphoton Ionization.
PB95-151023 *00,927*

Resonance Enhanced Multiphoton Ionization Spectroscopy of 2-Butene-1-yl (C4H7) between 455-485 nm.
PB95-151031 *00,670*

Polymerization Initiation by N-p-Tolylglycine: Free-Radical Reactions Studied by Pulse and Steady-State Radiolysis.
PB95-180014 01,269

Free Radical Chemistry of the Atmospheric Aqueous Phase.
PB96-148101 00,117

FREE ROTORS
Perpendicular C-H Stretching Band nu9/nu13 and the Torsional Potential of Dimethylacetylene.
PB97-122451 01,192

FREEZERS
Factors Affecting the Energy Consumption of Two Refrigerator-Freezers.
PB97-112312 00,311

FREEZING
Anomalous Freezing and Melting of Solvent Crystals in Swollen Gels of Natural Rubber.
PB94-212321 01,223

FREEZING POINT
Direct Comparison of Three PTB Silver Fixed-Point Cells with the NIST Silver Fixed-Point Cell.
PB96-161286 00,628

FREEZING POINT DEPRESSION
Anomalous Freezing and Melting of Solvent Crystals in Swollen Gels of Natural Rubber.
PB94-212321 01,223

FREONS
Thermophysical Properties of HFC-143a and HFC-152a. Quarterly Report, 1 July 1993--30 September 1993.
DE94004236 03,245

FREQUENCIES
Improved Molecular Constants and Frequencies for the CO2 Laser from New High-J Regular and Hot-Band Frequency Measurements.
PB95-180634 04,312

FREQUENCY
Aging, Warm-Up Time and Retrace; Important Characteristics of Standard Frequency Generators.
PB96-103122 04,031

FREQUENCY DISTRIBUTION
Effect of Harmonic Distortion on Phase Errors in Frequency Distribution and Synthesis.
PB96-200779 01,563

FREQUENCY DRIFT
Confidence on the Three-Point Estimator of Frequency Drift.
PB95-163838 01,539

FREQUENCY MEASUREMENT
Extension of Heterodyne Frequency Measurements on OCS to 87 THz (2900 cm(-1)).
PB94-200680 00,811

Using LORAN-C Broadcasts for Automated Frequency Calibrations.
PB94-216017 01,526

Sub-Doppler Frequency Measurements on OCS at 87 Thz (3.4 micrometers) with the CO Overtone Laser: Considerations and Details.
PB95-128633 04,255

ELF Electric and Magnetic Field Measurement Methods.
PB95-161675 04,423

Absolute Frequency Measurements of Methanol from 1.5 to 6.5 THz.
PB95-175881 04,300

Precise Optical Frequency References and Difference Frequency Measurements with Diode Lasers.
PB95-176228 04,305

Sub-Doppler Frequency Measurements on OCS at 87 THz (3.4 mu m) with the CO Overtone Laser.
PB96-102215 04,330

Atomic Clock.
PB96-119490 01,553

Introduction to Frequency Calibration. Part 1.
PB96-200654 01,560

NIST Frequency Measurement Service.
PB96-200662 01,561

FREQUENCY MEASUREMENTS
Accurate Measurement of Time.
PB96-119482 01,552

FREQUENCY MULTIPLIERS
High-Order Harmonic Mixing with GaAs Schottky Diodes.
PB95-108585 01,528

FREQUENCY REFERENCES
High-Resolution Diode-Laser Spectroscopy of Calcium.
PB95-181244 03,969

FREQUENCY RESPONSE
Photodetector Frequency Response Measurements at NIST, US, and NPL, UK: Preliminary Results of a Standards Laboratory Comparison.
PB95-175592 02,175

Bounds on Frequency Response Estimates Derived from Uncertain Step Response Data.
PB96-122874 03,419

Uncertainties of Frequency Response Estimates Derived from Responses to Uncertain Step-Like Inputs.
PB97-111843 01,984

FREQUENCY RESPONSES
Comparison of Photodiode Frequency Response Measurements to 40 GHz between NPL and NIST.
PB96-111992 04,038

FREQUENCY SHIFT
Frequency Shifting of Pulsed Narrow-Band Laser Light in a Multipass Raman Cell.
PB95-203352 04,321

FREQUENCY STABILITY
Precision Oscillators: Dependence of Frequency on Temperature, Humidity and Pressure.
PB94-198306 02,031

Frequency Stabilization of a Fiber Laser to Rubidium: A High-Accuracy 1.53 mu m Wavelength Standard.
PB95-126082 04,252

Confidence on the Second Difference Estimation of Frequency Drift.
PB95-151460 01,532

Frequency Stabilized Lasers: A Parochial Review.
PB95-153771 04,269

Reducing the Effect of Local Oscillator Phase Noise on the Frequency Stability of Passive Frequency Standards.
PB95-180972 01,545

Local Oscillator Requirements and Strategies for the Next Generation of High-Stability Frequency Standards.
PB96-112230 01,551

Fundamental Limits on the Frequency Stabilities of Crystal Oscillators.
PB96-176565 02,277

FREQUENCY STANDARDS
Future of Time and Frequency Dissemination.
AD-P009 138/9 01,520

Time and Frequency Technology at NIST.
N94-30641/2 01,522

Future of Time and Frequency Dissemination.
N94-30684/2 01,524

Utc Dissemination to the Real-Time User.
N19960042622 01,521

NIST Optically Pumped Cesium Frequency Standard.
PB94-211117 03,835

Ultra-High Stability Synthesizer for Diode Laser Pumped Rubidium.
PB94-216066 01,527

Atoms in Optical Molasses: Applications to Frequency Standards.
PB95-108882 03,876

Frequency Stabilization of a Fiber Laser to Rubidium: A High-Accuracy 1.53 mu m Wavelength Standard.
PB95-126082 04,252

Confidence on the Second Difference Estimation of Frequency Drift.
PB95-151460 01,532

NIST-7, the New US Primary Frequency Standard.
PB95-153458 01,534

Error Analysis of the NIST Optically Pumped Primary Frequency Standard.
PB95-153482 01,535

Diode-Laser Pumped, Rubidium Cell Frequency Standards.
PB95-163218 01,538

Confidence on the Three-Point Estimator of Frequency Drift.
PB95-163838 01,539

Improved Rubidium Frequency Standards Using Diode Lasers with AM and FM Noise Control.
PB95-176152 04,303

Microwave Leakage as a Source of Frequency Error and Long-Term Instability in Cesium Atomic-Beam Frequency Standards.
PB95-180501 01,541

Velocity Distribution of Atomic Beams by Gated Optical Pumping.
PB95-180519 01,542

Hybrid Digital/Analog Servo for the NIST-7 Frequency Standard.
PB95-180618 01,544

Reducing the Effect of Local Oscillator Phase Noise on the Frequency Stability of Passive Frequency Standards.
PB95-180972 01,545

Time and Frequency: Bibliography of NIST Publications, March 1995.
PB95-220463 01,548

Time Generation and Distribution.
PB96-103049 01,550

Laser-Cooled Neutral Atom Frequency Standards.
PB96-160312 04,086

Time and Frequency Metrology.
PB96-190319 01,556

FREQUENCY SYNTHESIZERS
High Spectral Purity X-Band Source.
PB95-163713 02,045

Reducing Errors, Complexity, and Measurement Time of PM Noise Measurements.
PB96-119771 02,075

Effect of Harmonic Distortion on Phase Errors in Frequency Distribution and Synthesis.
PB96-200779 01,563

Frequency Synthesis and Metrology at 10(-17) and Beyond.
PB97-113187 02,101

Reducing the 1/f AM and PM Noise in Electronics for Precision Frequency Metrology.
PB97-113195 02,102

FRICTION
Micro-Mechanical Aspects of Asperity-Controlled Friction in Fiber-Toughened Ceramic Composites.
PB94-199536 03,136

Asperity-Asperity Contact Mechanisms Simulated by a Two-Ball Collision Apparatus.
PB95-164158 02,966

FRICTION FACTOR
Mechanism of Mild to Severe Wear Transition in Alpha-Alumina.
PB94-212354 03,233

FRICTION MEASUREMENT
Tribometer for Measurements in Hostile Environments.
PB95-180949 02,967

FRICTION REDUCTION
Control of Friction and Wear of Alpha-Alumina with a Composite Solid-Lubricant Coating.
PB95-125969 03,225

FTP (FILE TRANSFER PROTOCOL)
Using Archie to Find Files on the INTERNET.
PB95-168605 02,727

FTS (FLIGHT TELEROBOTIC SERVICER)
Evolution of the Flight Telerobotic Servicer.
PB94-216082 04,832

FUEL ADDITIVES
Atmospheric Reactivity of alpha-Methyl-Tetrahydrofuran.
PB95-163705 02,548

FUEL COMBUSTION
Estimate of the Effect of Scale on Radiative Heat Loss Fraction and Combustion Efficiency.
PB95-150447 02,486

FUEL SPRAYS
Analysis of Droplet Arrival Statistics in a Pressure-Atomized Spray Flame.
PB97-112270 01,352

FUEL TANKS
Effect of Fuel Tank Rupture Mode on the Ignitability of Expelled Fuel.
PB97-110043 01,444

FUELS
Structure and Radiation Properties of Pool Fires.
PB94-193802 02,473

Estimate of Flame Radiance via a Single Location Measurement in Liquid Pool Flames.
PB94-211596 02,476

Measurement of Radiative Feedback to the Fuel Surface of a Pool Fire.
PB94-211604 02,477

Large Fire Experiments for Fire Model Evaluations.
PB96-190079 01,427

FUGACITY
Fugacity Coefficients of Hydrogen in (Hydrogen + Butane).
PB95-175212 02,491

FUGACITY COEFFICIENTS
Fugacity Coefficients of Hydrogen in (Hydrogen + Butane).
PB95-175212 02,491

Estimating the Virial Coefficients of Small Polar Molecules.
PB95-176236 03,276

FULLERENES
Rotational Dynamics of Solid C70: A Neutron-Scattering Study.
PB94-172178 00,755

Inelastic Neutron Scattering Studies of Rotational Excitations and the Orientational Potential in C60 and A3C60 Compounds.
PB94-172673 00,763

Discontinuous Volume Change at the Orientational-Ordering Transition in Solid C60.
PB94-211828 00,821

Phase Transitions in Solid C70: Supercooling, Metastable Phases, and Impurity Effect.
PB95-150090 00,914

Rotational Dynamics of C60 in Na2RbC60.
PB95-153201 00,948

Rotational Dynamics of Solid C70: A Neutron-Scattering Study.
PB95-153219 00,949

Structure and Dynamics of Buckyballs.
PB95-153292 00,950

Neutron and X-Ray Scattering Cross Sections of Orientationally Disordered Soild C60.
PB95-153300 00,951

Epitaxial Integration of Single Crystal C60.
PB95-153490 04,592

Neutron-Scattering Study of Librations and Intramolecular Phonons in Rb2.6K0.4C60.
PB95-162269 00,958

FULLERENESS
Energy Distributions of Neutrons Scattered from Solid C60 by the Beryllium Detector Method.
PB96-176631 03,740

FULLERIDES
Neutron-Scattering Study of C60(n-) (n=3,6) Librations in Alkali-Metal Fullerides.
PB94-200219 *00,806*

FUNCTIONAL TESTING
Experimental Evaluation of Specification Techniques for Improving Functional Testing.
PB96-201009 *01,779*

FUNCTIONS (MATHEMATICS)
Numerical Evaluation of Special Functions.
PB96-119557 *03,417*

Polarization Dependence of Response Functions in 3x3 Sagnac Optical Fiber Current Sensors.
PB96-122684 *02,189*

FUNDAMENTAL CONSTANTS
Fine-Structure Constant.
PB94-172996 *03,795*

FURAN/METHYL-TETRAHYDRO
Atmospheric Reactivity of alpha-Methyl-Tetrahydrofuran.
PB95-163705 *02,548*

FURNACE
ITS-90 Calibration Facility.
PB96-160916 *00,627*

FURNANCES
High-Temperature Furnace for In situ Small-Angle Neutron Scattering during Ceramic Processing.
PB96-148127 *03,743*

FURNITURE
Some Factors Affecting Design of a Furniture Calorimeter Hood and Exhaust.
PB94-139193 *00,285*

Summaries of Center for Fire Research In-House Projects and Grants: 1990.
PB94-160876 *00,286*

Toxicity, Fire Hazard and Upholstered Furniture.
PB94-198454 *00,289*

Sprinkler Fire Suppression Algorithm.
PB94-216181 *00,293*

Summaries of BFRL Fire Research In-House Projects and Grants, 1994.
PB95-130845 *00,366*

Behavior of Mock-Ups in the California Technical Bulletin 133 Test Protocol: Fabric and Barrier Effects.
PB95-231585 *00,301*

Some Factors Affecting the Design of a Calorimeter Hood and Exhaust.
PB96-102181 *00,302*

Examination of the Correlation between Cone Calorimeter Data and Full-Scale Furniture Mock-Up Fires.
PB96-148200 *01,417*

NIST Research on Less-Flammable Materials.
PB97-118632 *01,439*

FUSE (FAR ULTRAVIOLET SPECTROGRAPH EXPLORER)
Scientific Rationale and Present Implementation Strategy for the Far Ultraviolet Spectrograph Explorer (FUSE).
PB96-123328 *00,045*

FUSE SATELLITE
FUSE: The Far Ultraviolet Spectrograph Explorer.
PB94-213410 *00,063*

FUSED SILICA
Fuzed-Quartz Fibers. A Survey of Properties, Applications and Production Methods.
AD-A286 620/0 *00,656*

FUSION (MELTING)
Calibration Standards for Differential Scanning Calorimetry. 1. Zinc Absolute Calorimetric Measurement of Enthalpy of Fusion and Temperature of Fusion HM.
PB94-199817 *00,801*

FUZZY LOGIC
Texture-Independent Vision-Based Closed-Loop Fuzzy Controllers for Navigation Tasks.
PB95-220505 *00,183*

G STARS
IUE Observations of Solar-Type Stars in the Pleiades and the Hyades.
PB94-199437 *00,053*

Far-Ultraviolet Flare on a Pleiades G Dwarf.
PB96-102033 *00,086*

GAAS/ALGAAS
Quantum Conductance Fluctuations in the Larger-Size-Scale Regime.
PB97-111264 *04,144*

GADOLINIUM GALLIUM FERRATES
Enhanced Magnetocaloric Effect in Gd3Ga5-xFexO12.
PB94-185659 *04,450*

Magnetocaloric Effect of Ferromagnetic Particles.
PB94-185857 *04,453*

GAGE BLOCKS
Gage Block Handbook.
PB95-251716 *02,667*

Gage Block Standards, Measurement Capabilities and Laboratory Accreditation.
PB96-163621 *02,757*

GALACTIC HALOS
Interstellar Disk-Halo Connection in Galaxies: Review of Observational Aspects.
PB94-211802 *00,058*

GALACTOPYRANOSIDE
Thermodynamics of the Binding of Galactopyranoside Derivatives to the Basic Lectin from Winged Bean (Psophocarpus Tetrogonolobus).
PB95-162715 *03,465*

GALERKIN METHOD
Alternative Contour Technique for the Efficient Computation of the Effective Length of an Antenna.
PB96-141361 *02,011*

GALLIUM
Arc Spectra of Gallium, Indium, and Thallium.
AD-A295 411/3 *00,718*

Characterization of the Binding of Gallium, Platinum, and Uranium to Pseudomonas Fluorescens by Small-Angle X-ray Scattering and Transmission Electron Microscopy.
PB94-172509 *03,453*

Single-Photon Ionization and Detection of Ga, In, and As(sub n) Species in GaAs Growth.
PB95-152815 *00,591*

In-situ Monitoring of Molecular Beam Epitaxial Growth Using Single Photon Ionization.
PB95-202222 *01,023*

Laser-Induced Desorption of In and Ga from Si(100) and Adsorbate Enhanced Surface Damage.
PB95-203311 *01,050*

Pulsed Laser Irradiation at 532 nm of In and Ga Adsorbed on Si(100): Desorption, Incorporation, and Damage.
PB95-203329 *01,051*

Single-Photon Laser Ionization Time-of-Flight Mass Spectroscopy Detection in Molecular-Beam Epitaxy: Application to As4, As2, and Ga.
PB95-203337 *01,052*

GALLIUM ANTIMONIDES
Epitaxial Growth of Sb/GaSb Structures: An Example of V/III-V Heteroepitaxy.
PB95-202560 *04,693*

GALLIUM ARSENIDE
X-ray Reflectivity Determination of Interface Roughness Correlated with Transport Properties of (AlGa)As/GaAs High Electron Mobility Transistor Devices.
PB97-111868 *04,149*

GALLIUM ARSENIDE TRANSISTORS
Effects of Heavy Doping on Numerical Simulations of Gallium Arsenide Bipolar Transistors.
PB95-150975 *02,334*

GALLIUM ARSENIDES
Junction Locations by Scanning Tunneling Microscopy: In-Air-Ambient Investigation of Passivated GaAs pn Junctions.
PB94-185964 *02,306*

X-Ray Photoelectron and Auger Electron Spectroscopy Study of Ultraviolet/Ozone Oxidized P2S5/(NH4)2S Treated GaAs(100) Surfaces.
PB94-200144 *04,479*

Grazing-Incidence X-Ray Photoemission Spectroscopy Investigation of Oxidized GaAs(100): A Novel Approach to Nondestructive Depth Profiling.
PB94-200151 *04,480*

Cs Cluster Binding to a GaAs Surface.
PB94-213006 *00,846*

Band-to-Band Photoluminescence and Luminescence Excitation in Extremely Heavily Carbon-Doped Epitaxial GaAs.
PB95-150413 *04,570*

Single-Photon Ionization and Detection of Ga, In, and As(sub n) Species in GaAs Growth.
PB95-152815 *00,591*

Grazing Angle X-Ray Photoemission System for Depth-Dependent Analysis.
PB95-161154 *04,600*

Lattice Position of Si in GaAs Determined by X-Ray Standing Wave Measurements.
PB95-164406 *04,632*

Characterization of the ZnSe/GaAs Interface Layer by TEM and Spectroscopic Ellipsometry.
PB95-175360 *04,655*

In-situ Monitoring of Molecular Beam Epitaxial Growth Using Single Photon Ionization.
PB95-202222 *01,023*

Laser Vacuum Ultraviolet Single Photon Ionization Probing of III-V Semiconductor Growth.
PB95-202370 *04,691*

Epitaxial Growth of Sb/GaSb Structures: An Example of V/III-V Heteroepitaxy.
PB95-202560 *04,693*

Single Photon Ionization, Laser Optical Probe Technique for Semiconductor Growth.
PB95-202776 *01,032*

Single-Photon Laser Ionization Time-of-Flight Mass Spectroscopy Detection in Molecular-Beam Epitaxy: Application to As4, As2, and Ga.
PB95-203337 *01,052*

Single Photon Laser Ionization as an In-situ Diagnostic for MBE growth.
PB96-102025 *01,059*

Time-Resolved Measurements of the Polarization State of Four-Wave Mixing Signals from GaAs Multiple Quantum Wells.
PB96-201058 *04,796*

Majority and Minority Electron and Hole Mobilities in Heavily Doped Gallium Aluminum Arsenide.
PB97-118335 *04,814*

GALLIUM INDIUM PHOSPHIDES
Surface Topography and Ordering-Variant Segregation in GaInP2.
PB95-153649 *04,595*

GALLIUM IONS
Relative Sensitivity Factors and Useful Yields for a Microfocused Gallium Ion Beam and Time-of-Flight Secondary Ion Mass Spectrometer.
PB94-198736 *00,541*

GALLOPING OSCILLATORS
Chaotic Motions of Coupled Galloping Oscillators and Their Modeling as Diffusion Progresses.
PB96-122718 *04,823*

GAMMA DOSIMETRY
Measurement of Absorbed Dose of Neutrons, and of Mixtures of Neutrons and gamma rays.
AD-A286 647/3 *03,710*

Thin Dyed-Plastic Dosimeter for Large Radiation Doses.
PB95-107363 *03,872*

GAMMA DRACONIS STAR
Ultraviolet Observations of Stellar Coronae: Early Results from HST.
PB94-213428 *00,064*

GAMMA RADIATION
Effect of Formulation Changes on the Response to Ionizing Radiation of Radiochromic Dye Films.
PB97-119028 *04,171*

GAMMA RAY ASTRONOMY
From Superconductivity to Supernovae: The Ginzburg Symposium. Report on the Symposium Held in Honor of Vitaly L. Ginzburg. Held in Gaithersburg, Maryland on May 22, 1992.
PB95-171963 *04,649*

GAMMA RAY SCATTERING
Polarization Effects on Multiple Scattering Gamma Transport.
PB95-153615 *03,926*

GAMMA RAY SPECTROMETRY
Dead Time, Pileup, and Accurate Gamma-Ray Spectrometry.
PB96-167101 *00,697*

GAMMA RAY SPECTROSCOPY
Local Area Networks in NAA: Advantages and Pitfalls.
PB94-172095 *00,527*

GAMMA RAYS
X-ray Attenuation Coefficients from 10 Kev to 100 Mev.
AD-A278 139/1 *03,765*

Penetration and Diffusion of Hard X-rays through Thick Barriers. III. Studies of Spectral Distributions.
AD-A292 502/2 *03,771*

Bibliography of Photon Total Cross Section (Attenuation Coefficient) Measurements 10 eV to 13.5 GeV, 1907-1993.
PB94-193760 *03,804*

DNA Base Damage Generated In vivo in Hepatic Chromatin of Mice upon Whole Body y-Irradiation.
PB95-161741 *03,627*

Tables of X-ray Mass Attenuation Coefficients and Mass Energy-Absorption Coefficients 1 keV to 20 MeV for Elements Z = 1 to 92 and 48 Additional Substances of Dosimetric Interest.
PB95-220539 *04,013*

Needs for Brachytherapy Source Calibrations in the United States.
PB97-110092 *03,521*

GAMMA SPECTROMETRY
Loss-Free Counting at IRI and NIST.
PB96-167119 *04,105*

GARNET FILMS
Micromagnetic Simulations of Tunneling Stabilized Magnetic Force Microscopy.
PB95-141073 *04,552*

GAS ABSORPTION
Gas Absorption during Ion-Irradiation of a Polymer Target.
PB96-161864 *04,099*

GAS ANALYSIS
Characteristics of Partial Pressure Analyzers.
PB95-150876 *00,582*

Vacuum Gauges and Partial Pressure Analyzers.
PB95-150884 *02,650*

Development of a Gas Standard Reference Material Containing Eighteen Volatile Organic Compounds.
PB95-162277 *02,545*

Process Monitoring with Residual Gas Analyzers (RGAs): Limiting Factors.
PB95-181004 *02,660*

NIST Traceable Reference Material Program for Gas Standards: Standard Reference Materials.
PB96-210786 *00,644*

GAS ATOMIZATION
Intelligent Control of an Inert Gas Atomization Process.
PB95-141057 *03,344*

Intelligent Processing of Materials, Technical Activities 1994 (NAS-NRC Assessment Panel, April 6-7, 1995).
PB96-115050 *03,359*

GAS CHROMATOGRAPHY
Comparison of Methods for Gas Chromatographic Determination of PCBs and Chlorinated Pesticides in Marine Reference Materials.
PB95-140091 *02,584*

Process Gas Chromatography Detector for Hydrocarbons Based on Catalytic Cracking.
PB95-141099 *02,485*

Shape Selectivity Assessment of Stationary Phases in Gas Chromatography.
PB95-150256 *00,579*

Comparison of Selectivities for PCBs in Gas Chromatography for a Series of Cyanobiphenyl Stationary Phases.
PB96-119458 *00,618*

All-Metal Collection System for Preparative-Scale Gas Chromatography: Purification of Low-Boiling-Point Compounds.
PB96-123435 *00,619*

Investigations of Sulfur Interferences in the Extraction of Methylmercury from Marine Tissues.
PB96-190020 *03,482*

GAS CHROMOTOGRAPHY
Procedure for Measuring Trace Quantities of S2F10, S2OF10, and S2O2F10 in SF6 Using a Gas Chromatograph-Mass Spectrometer.
PB96-119755 *02,513*

GAS CYLINDERS
Stability/Instability of Gas Mixtures Containing 1,3-Butadiene in Treated Aluminum Gas Cylinders.
PB95-162285 *02,546*

Stability of Compressed Gas Mixtures Containing Low Level Volatile Organic Compounds in Aluminum Cylinders.
PB96-111968 *00,613*

GAS DETECTORS
Conductance Response of Pd/SnO2(110) Model Gas Sensors to H2 and O2.
PB95-125803 *00,892*

Tin Oxide Gas Sensor Fabricated Using CMOS Micro-Hotplates and In-situ Processing.
PB95-150603 *00,580*

Fundamental Studies of Gas Sensor Response Mechanisms: Palladium on SnO2(110).
PB95-162731 *00,963*

NIST Workshop on Gas Sensors: Strategies for Future Technologies. Proceedings of a Workshop. Held in Gaithersburg, Maryland on September 8-9, 1993.
PB95-210225 *00,507*

GAS DISCHARGES
Excitation of Balmer Lines in Low-Current Discharges of Hydrogen and Deuterium.
PB95-150546 *03,893*

Kinetic-Energy Distributions of Ions Sampled from Argon Plasmas in a Parallel-Plate, Radio-Frequency Reference Call.
PB95-161964 *03,935*

Electrical Characterization of Radio-Frequency Discharges in the Gaseous Electronics Conference Reference Call.
PB95-164612 *01,905*

Ion Kinetic-Energy Distributions and Balmer-alpha (Halpha) Excitation in Ar-H2 Radio-Frequency Discharges.
PB96-102959 *04,029*

Kinetic Energy Distribution of Ions Produced from Townsend Discharges in Neon and Argon.
PB96-111927 *04,413*

Modification of Cast Epoxy Resin Surfaces during Exposure to Partial Discharges.
PB96-122734 *01,086*

Influence of Electrode Material on Measured Ion Kinetic-Energy Distributions in Radio-Frequency Discharges.
PB96-123179 *01,935*

Kinetic Energy Distributions of H(+), H2(+), and H3(+) from a Diffuse Townsend Discharge in H2 at High E/N.
PB96-123351 *04,415*

Fundamental Processes in Gas Discharges.
PB96-123450 *01,089*

Kinetic-Energy Distributions of Ions Sampled from Radio-Frequency Discharges in Helium, Nitrogen, and Oxygen.
PB96-123732 *01,092*

GAS DISSOCIATION
Associative Electron Attachment to S2F10, S2OF10, and S2O2F10.
PB95-140992 *00,907*

GAS DYNAMICS
Operational Mode and Gas Species Effects on Rotational Drag in Pneumatic Dead Weight Pressure Gages.
PB95-140182 *00,903*

GAS FLOW
Concurrent Flow Flame Spread Study.
PB94-156866 *01,356*

Experimental Data and Theoretical Modeling of Gas Flows Through Metal Capillary Leaks.
PB95-150892 *04,206*

Improved Gas Flow Measurements for Next-Generation Processes.
PB96-156013 *04,216*

GAS GENERATORS
Solid Propellant Gas Generators: Proceedings of the 1995 Workshop. Held in Gaithersburg, Maryland on June 28-29, 1995.
PB96-131479 *01,412*

GAS GIANT PLANETS
Experimental Determination of the Rate Constant for the Reaction of C2H3 with H2 and Implications for the Partitioning of Hydrocarbons in Atmospheres of the Outer Planets.
PB97-122295 *00,112*

GAS METAL ARC WELDING
Through-the-Arc Sensing for Real-Time Measurement of Gas Metal Arc Weld Quality.
PB95-162871 *02,863*

Through-the-Arc Sensing for Measuring Gas Metal Arc Weld Quality in Real Time.
PB95-164463 *02,908*

Droplet Transfer Modes for a MIL 100S-1 GMAW Electrode.
PB95-209300 *02,867*

Control of Gas-Metal-Arc Welding Using Arc-Light Sensing.
PB96-131461 *02,869*

Contact Tube Wear Detection in Gas Metal Arc Welding.
PB96-135330 *02,872*

Ultrasonic Sensing of GMAW: Laser/EMAT Defect Detection System.
PB96-186028 *02,878*

Mapping the Droplet Transfer Modes for an ER100S-1 GMAW Electrode.
PB96-190095 *03,295*

Power Characteristics in GMAW: Experimental and Numerical Investigation.
PB96-190145 *03,296*

Sensing Droplet Detachment and Electrode Extension for Control of Gas Metal Arc Welding.
PB96-190160 *03,297*

GAS PIPELINES
Low Temperature H(sub 2)S Separation Using Membrane Reactor with Redox Catalyst.
DE94008991 *02,471*

GAS PRESSURE
Partial Pressure Analysis in Space Testing.
N95-14084/4 *04,827*

GAS STANDARDS
Development of Gas Standards from Solid 1,4-dichlorobenzene.
PB96-155486 *02,496*

GAS TRANSPORT
Gas Transport Properties of Solution-Cast Perfluorosulfonic Acid Ionomer Films Containing Ionic Surfactants.
PB95-175998 *01,267*

GAS TURBINES
Bibliography of Books and Published Reports on Gas Turbines, Jet Propulsion, and Rocket Power Plants.
AD-A278 138/3 *01,445*

Bibliography of Books and Published Reports on Gas Turbines, Jet Propulsion, and Rocket Power Plants, January 1950 through December 1953.
AD-A278 213/4 *01,446*

GASEOUS
Studies of Ion Kinetic-Energy Distributions in the Gaseous Electronics Conference RF Reference Cell.
PB96-113360 *02,391*

GASEOUS ELECTRONICS
Journal of Research of the National Institute of Standards and Technology, July/August 1995. Volume 100, Number 4. Special Issue: The Gaseous Electronics Conference Radio-Frequency Reference Cell.
PB96-113311 *02,386*

Gaseous Electronics Conference RF Reference Cell: An Introduction.
PB96-113329 *02,387*

Current and Voltage Measurements in the Gaseous Electronics Conference RF Reference Cell.
PB96-113337 *02,388*

Optical Emission Spectroscopy on the Gaseous Electronics Conference RF Reference Cell.
PB96-113345 *02,389*

Microwave Diagnostic Results from the Gaseous Electronics Conference RF Reference Cell.
PB96-113378 *02,392*

Langmuir Probe Measurements in the Gaseous Electronics Conference RF Reference Cell.
PB96-113386 *02,393*

Inductively Coupled Plasma Source for the Gaseous Electronics Conference RF Reference Cell.
PB96-113394 *02,394*

Reactive Ion Etching in the Gaseous Electronics Conference RF Reference Cell.
PB96-113402 *02,395*

Dusty Plasma Studies in the Gaseous Electronics Conference Reference Cell.
PB96-113410 *02,396*

One-Dimensional Modeling Studies of the Gaseous Electronics Conference RF Reference Cell.
PB96-113428 *02,397*

Two-Dimensional Self-Consistent Radio Frequency Plasma Simulations Relevant to the Gaseous Electronics Conference RF Reference Cell.
PB96-113436 *02,398*

Electrical Measurements for Monitoring and Control of rf Plasma Processing.
PB96-161963 *04,369*

GASEOUS ELECTRONICS CONFERENCE
Electrical Characteristics of Argon Radio Frequency Glow Discharges in an Asymmetric Cell.
PB96-176490 *04,109*

GASES
Equilibrium Pair Distribution Function of a Gas: Aspects Associated with the Presence of Bound States.
PB95-176046 *01,004*

Vapour Pressures and Gas-Phase (p, rho n, T) Values for CF3CHF2(R125).
PB96-102090 *04,019*

Thermodynamic Properties of Two Gaseous Halogenated Ethers from Speed-of-Sound Measurements: Difluoromethoxy-Difluoromethane and 2-Difluoromethoxy-1,1,1-Trifluoroethane.
PB96-102413 *04,189*

Gaseous Electronics Conference RF Reference Cell: An Introduction.
PB96-113329 *02,387*

Current and Voltage Measurements in the Gaseous Electronics Conference RF Reference Cell.
PB96-113337 *02,388*

Optical Emission Spectroscopy on the Gaseous Electronics Conference RF Reference Cell.
PB96-113345 *02,389*

Optical Diagnostics in the Gaseous Electronics Conference Reference Cell.
PB96-113352 *02,390*

Studies of Ion Kinetic-Energy Distributions in the Gaseous Electronics Conference RF Reference Cell.
PB96-113360 *02,391*

Microwave Diagnostic Results from the Gaseous Electronics Conference RF Reference Cell.
PB96-113378 *02,392*

Langmuir Probe Measurements in the Gaseous Electronics Conference RF Reference Cell.
PB96-113386 *02,393*

Inductively Coupled Plasma Source for the Gaseous Electronics Conference RF Reference Cell.
PB96-113394 *02,394*

Reactive Ion Etching in the Gaseous Electronics Conference RF Reference Cell.
PB96-113402 *02,395*

Dusty Plasma Studies in the Gaseous Electronics Conference Reference Cell.
PB96-113410 *02,396*

One-Dimensional Modeling Studies of the Gaseous Electronics Conference RF Reference Cell.
PB96-113428 *02,397*

Two-Dimensional Self-Consistent Radio Frequency Plasma Simulations Relevant to the Gaseous Electronics Conference RF Reference Cell.
PB96-113436 *02,398*

GASIFICATION
Effects of Molecular Weight and Thermal Stability on Polymer Gasification.
PB94-212610 *01,228*

GASKETS
Electromagnetic Shielding Characterization of Gaskets.
PB95-198917 *01,911*

GASOLINE GALLON EQUIVALENT
Method of Sale for CNG Paves Way to Greater Public Acceptance.
PB95-168449 *02,489*

GAUSSIAN BEAM
Effect of Finite Beam Width on Elastic Light Scattering from Droplets.
PB96-163670 *01,144*

GAUSSIAN BEAMS
Forward Scattering of a Gaussian Beam by a Nonabsorbing Sphere.
PB97-112288 *04,395*

Generalized Optical Theorem for On-Axis Gaussian Beams.
PB97-122345 *04,177*

GAUSSIAN QUADRATURE
Hybrid Gauss-Trapezoidal Quadrature Rules.
PB96-193750 *03,422*

GE SEMICONDUCTOR DETECTORS
International Intercomparison of Detector Responsivity at 1300 and 1550 nm.
PB95-125928 *02,140*

International Intercomparison of Detector Responsivity at 1300 and 1550 nm.
PB95-126017 *02,141*

GELATINS
Holographic Properties of Triton X-100-Treated Bacteriorhodopsin Embedded in Gelatin Films.
PB96-119284 *03,761*

GELATION
Simulation and SANS Studies of Gelation Under Shear.
PB96-167176 *01,150*

GELATON
Dynamic Scaling in an Aggregating 2D Lennard-Jones System.
PB96-167317 *04,106*

GELETIN FILMS
Optical Properties of Triton X-100-Treated Purple Membranes Embedded in Gelatin Films.
PB96-123500 *03,546*

GELS
Imaging of Fine Porosity in a Colloidal Silica: Potassium Silicate Gel by Defocus Contrast Microscopy.
PB94-212750 *03,039*

Small-Angle Neutron Scattering of Poly(vinyl alcohol) Gels.
PB95-164117 *01,260*

Small Angle Neutron Scattering Study on Poly(N-Isopropyl Acrylamide) Gels Near Their Volume-Phase Transition Temperature.
PB95-164380 *01,263*

Small-Angle Neutron Scattering Study on Weakly Charged Temperature Sensitive Polymer Gels.
PB95-164398 *01,264*

Optical Biosensor Using a Fluorescent, Swelling Sensing Element.
PB95-175899 *03,541*

Small Angle Neutron Scattering Studies of Structural Characteristics of Argarose Gels.
PB96-112305 *03,475*

Small-Angle Neutron-Scattering Study of Dense Sheared Silica Gels.
PB96-167184 *01,151*

GENERAL INTEREST
Bibliography of Books and Published Reports on Gas Turbines, Jet Propulsion, and Rocket Power Plants.
AD-A278 138/3 *01,445*

Standard Materials. A Descriptive List with Prices.
AD-A278 140/9 *00,500*

Bibliography of Books and Published Reports on Gas Turbines, Jet Propulsion, and Rocket Power Plants, January 1950 through December 1953.
AD-A278 213/4 *01,446*

Screw-Thread Standards for Federal Services, 1957. Part 3.
AD-A279 121/8 *02,854*

Screw-Thread Standards for Federal Services, 1957. Part 1.
AD-A279 290/1 *02,855*

Characterization of the Hydrogen Induced Cold Cracking Susceptibility at Simulated Weld Zones in HSLA-100 Steel.
AD-A279 759/5 *03,200*

National Standard Petroleum Oil Tables.
AD-A279 952/6 *02,469*

Screw-Thread Standards for Federal Services, 1957. Handbook H28 (1957), Part 2. Revised.
AD-A280 082/9 *03,599*

1950 Supplement to Screw-Thread Standards for Federal Services. 1944.
AD-A280 223/9 *03,656*

Guide to Instrumentation Literature.
AD-A280 278/3 *02,617*

Atomic Energy Levels. As Derived From the Analyses of Optical Spectra. Volume 3.
AD-A280 279/1 *00,714*

Maximum Permissible Amounts of Radioisotopes in the Human Body and Maximum Permissible Concentrations in Air and Water.
AD-A280 281/7 *03,609*

Maximum Permissible Body Burdens and Maximum Permissible Concentrations of Radionuclides in Air and in Water for Occupational Exposure.
AD-A280 282/5 *03,610*

X-Ray Attenuation Coefficients from 10 KEV to 100 MEV.
AD-A280 290/8 *03,768*

Papers on the Symposium on Collision Phenomena in Astrophysics, Geophysics, and Masers.
AD-A280 291/6 *00,047*

Tables of Chemical Kinetics Homogeneous Reactions.
AD-A280 293/2 *00,715*

Ada Compiler Validation Summary Report: Certificate Number: 940325S1.11352 DDC-I DACS Sun SPARC/Solaries to Pentium PM Bare Ada Cross Compiler System, Version 4.6.4 Sun SPARCclassic => Intel Pentium (Operated as Bare Machine) Based in Xpress Desktop (Intel Product Number: XBASE6E4F-B).
AD-A280 295/7 *01,657*

Cryogenic Research and Development (Quarterly Report Number 2 for Period Ending December 31, 1960).
AD-A280 398/9 *01,454*

Cryogenic Research and Development (Progress Report Number 4 for Period Ending December 31, 1961).
AD-A280 399/7 *01,455*

Cryogenic Research and Development (Quarterly Report Number 1 for Period Ending September 30, 1960).
AD-A280 401/1 *01,456*

Precision Laboratory Standards of Mass and Laboratory Weights.
AD-A280 562/0 *02,618*

Cryogenic Research and Development (June 30, 1961).
AD-A280 679/2 *01,457*

Bibliography of the Physical Equilibria and Related Properties of Some Cryogenic Systems.
AD-A281 167/7 *03,769*

Precision Resistors and Their Measurement.
AD-A284 623/6 *02,249*

Tabulation of Data on Receiving Tubes. Handbook 68.
AD-A285 495/8 *02,111*

Compilation of the Physical Equilibria and Related Properties of the Hydrogen-Carbon Monoxide System.
AD-A286 603/6 *00,716*

Progress Report to National Aeronautics and Space Administration on Cryogenic Research and Development.
AD-A286 612/7 *01,458*

Design and Construction of a Liquid Hydrogen Temperature Refrigeration System.
AD-A286 618/4 *02,619*

Ionospheric Radio Propagation.
AD-A286 619/2 *01,459*

Fuzed-Quartz Fibers. A Survey of Properties, Applications and Production Methods.
AD-A286 620/0 *00,656*

Measurement of Absorbed Dose of Neutrons, and of Mixtures of Neutrons and gamma rays.
AD-A286 647/3 *03,710*

High Temperature Reactions of Uranium Dioxide with Various Metal Oxides.
AD-A286 648/1 *00,717*

Survey of the Literature on Heat Transfer from Solid Surfaces to Cryogenic Fluids.
AD-A286 680/4 *04,193*

Performance of Plastic Packaging for Hazardous Materials Transportation. Part 1. Mechanical Properties.
AD-A301 258/0 *02,580*

Weatherability of Plastic Materials.
AD-A301 675/5 *02,968*

Preliminary Subject and Authors Index to Compilations of Data on Properties of Materials.
AD-A302 669/7 *03,242*

Preliminary List of References Containing Compilations of Data on Properties of Materials.
AD-A302 670/5 *03,243*

Fracture Testing of Large-Scale Thin-Sheet Aluminum Alloy.
AD-A306 625/5 *03,305*

Synthesis of Thermally Stable Elastomers.
AD-A307 789/8 *03,194*

Volatile Corrosion Inhibitors.
AD-A310 087/2 *03,114*

Polyvinyl Chloride (PVC) Plastic Drain, Waste, and Vent Pipe and Fittings.
AD-A310 426/2 *00,326*

Acrylonitrile-Butadiene-Styrene (ABS) Plastic Drain, Waste, and Vent Pipe and Fittings.
AD-A310 724/0 *00,327*

Comparison of GPS Broadcast and DMA Precise Ephemerides.
AD-P009 114/0 *01,518*

NIST Internet Time Service.
AD-P009 132/2 *01,519*

Future of Time and Frequency Dissemination.
AD-P009 138/9 *01,520*

Economic, Energy, and Environmental Impacts of the Energy-Related Inventions Program.
DE94-017162 *00,008*

Ceramic Characterization.
DE94013170 *03,026*

Densification of Nano-Size Powders. 1994 Report.
DE94013486 *03,027*

Equipment for Investigation of Cryogenic Compaction of Nanosize Silicon Nitride Powders. 1993 Report.
DE94013593 *03,028*

Measuring Performance of Parallel Computers. Final Report.
DE94014586 *01,665*

Measuring Performance of Parallel Computers. Progress Report, 1989.
DE94014587 *01,666*

NIST Cooperative Laboratory for OSI Routing Technology.
DE94015308 *01,791*

Evaluation of the Environmentally Induced Fracture Resistance of Ductile Nickel Aluminide. Technical Report Number 1, Final report. October-December 1990.
DE94017331 *03,306*

Comparison of the Corrosion Rates of FeAl, Fe(sub 3)Al and Steel in Distilled Water and 0.5 M Sodium Chloride. Technical Report Number 2, January--March 1991.
DE94017332 *03,186*

Evaluation of the Electrochemical Behavior of Ductile Nickel Aluminide and Nickel in a pH 7.9 Solution. Technical Report Number 3, April-June 1991.
DE94017351 *03,307*

Development of Measurement Capabilities for the Thermophysical Properties of Energy-Related Fluids. Annual Report, December 1, 1993--November 30, 1994.
DE94017738 *03,246*

Measurement of the Thermal Properties of Electrically Conducting Fluids Using Coated Transient Hot Wires.
DE94017816 *00,722*

Ebulliometers for Measuring the Thermodynamic Properties of Fluids and Fluid Mixtures.
DE94017817 *04,195*

Improvement of Ultrasensitive Techniques Isotopic Biasing in the RIS Process Ionization Efficiencies and Selectivities.
DE94018563 *00,522*

I: Improvement of Resonance Ionization Spectroscopy (RIS) Techniques; II: Atomic Data for RIS; III: Standards for Ultratrace Analysis. Progress Report.
DE94018565 *00,523*

Study of Laser Resonance Ionization Mass Spectrometry Using a Glow Discharge Source.
DE94018566 *03,308*

Minutes of the CAALS Workshop on modularity and communications standards.
DE95005780 *02,621*

Experimental assessment of absorbed dose to mineralized bone tissue from internal emitters: An electron paramagnetic resonance study.
DE96007979 *03,614*

Improving measurement quality assurance for photon irradiations at Department of Energy facilities. Final technical report.
DE96010065 *03,711*

Thermophysical properties of HCFC alternatives. Quarterly report, October 1--December 31, 1995.
DE96010433 *03,249*

Thermophysical properties of HCFC alternatives. Quarterly report, April 1--June 30, 1995.
DE96010579 *03,250*

Small genomes: New initiatives in mapping and sequencing. Workshop summary report.
DE96014476 *03,451*

Information Infrastructure: Reaching Society's Goals. A Report of the Information Infrastructure Task Force Committee on Applications and Technology.
ED-376 823 *00,131*

Guideline: Codes for Named Populatd Places, Primary County Divisions, and Other Locational Entities of the United States, Puerto Rico, and the Outlying Areas. Category: Data Standards and Guidelines; Subcategory: Representation and Codes.
FIPS PUB 55-DC3 *04,866*

ADA; Category: Software Standard; Subcategory: Programming Language.
FIPS PUB 119-1 *01,667*

Procedures for Document Facsimile Transmission Issued by General Services Administration, April 14, 1982. Federal Standard 1063.
FIPS PUB 148 *01,516*

Programmer's Hierarchical Interactive Graphics System (PHIGS). Category: Software Standard; Subcategory: Graphics.
FIPS PUB 153-1 *01,668*

Open Document Architecture (ODA) Raster Document Application Profile (DAP). Category: Software Standard; Subcategory: Graphics.
FIPS PUB 194 *01,669*

Federal Building Grounding and Bonding Requirements for Telecommunications. Category: Telecommunications Standard; Subcategory: Grounding and Bonding.
FIPS PUB 195 *01,802*

Activities of NIST (National Inst. Of Standards and Technology).
N94-23605/6 *04,222*

Comparison of GPS Broadcast and DMA Precise Ephemerides.
N94-30660/2 *01,523*

Future of Time and Frequency Dissemination.
N94-30684/2 *01,524*

Putting the Information Infrastructure to Work: Report of the Information Infrastructure Task Force Committee on Applications and Technology.
N94-31228/7 *02,715*

Ground Vehicle Control at NIST: From Teleoperation to Autonomy.
N94-34037/9 *03,758*

Classification of Advanced Technical Ceramics.
N94-35335/6 *03,030*

Open System Environments.
N94-36857/8 *01,674*

Open System Environment Procurement.
N94-36858/6 *02,716*

Partial Pressure Analysis in Space Testing.
N95-14084/4 *04,827*

Convection and Morphological Stability During Directional Solidification.
N95-14548/8 *03,310*

Investigating the 3.3 Micron Infrared Fluorescence from Naphthalene Following Ultraviolet Excitation.
N95-15839/0 *00,724*

National Center for Standards and Certification Information: Service and Programs.
N95-15938/0 *02,717*

Combustion of a Polymer (PMMA) Sphere in Microgravity.
N96-15569/2 *01,354*

Ignition and Subsequent Transition to Flame Spread in a Microgravity Environment.
N96-15584/1 *04,828*

Utc Dissemination to the Real-Time User.
N19960042622 *01,521*

In situ Burning of Oil Spills: Mesoscale Experiments.
PB94-142973 *01,355*

Abstract and Index Collection in the Research Information Center of the National Institute of Standards and Technology.
PB94-152204 *02,744*

Study to Determine the Most Important Parameters for Evaluating the Resistance of Soft Body Armor to Penetration by Edged Weapons.
PB94-158573 *03,757*

Metrology for Electromagnetic Technology: A Bibliography of NIST Publications.
PB94-159761 *02,116*

Review of Mathematical Function Library for Microsoft-FORTRAN, John Wiley and Sons, 1989.
PB94-160793 *01,679*

Bibliography on Apparel Sizing and Related Issues.
PB94-161924 *02,806*

Earthquake Resistant Construction of Gas and Liquid Fuel Pipeline Systems Serving, or Regulated By, the Federal Government.
PB94-161999 *04,846*

Materials Science and Engineering Laboratory Annual Report, 1993. NAS-NRC Assessment Panel, April 21-22, 1994.
PB94-162534 *02,969*

Ceramics Technical Activities, 1993 (NAS-NRC Assessment Panel April 21-22, 1994).
PB94-162591 *03,031*

Putting the Information Infrastructure to Work: Report of the Information Infrastructure Task Force Committee on Applications and Technology.
PB94-163383 *00,001*

Intelligent Processing of Materials, Technical Activities 1993 (NAS-NRC Assessment Panel, April 21-22, 1994).
PB94-164183 *02,809*

Catalog of National ISDN Solutions for Selected NIUF Applications.
PB94-166006 *01,468*

Learning to Change: Opportunities to Improve the Performance of Smaller Manufacturers.
PB94-166212 *00,010*

Metrication.
PB94-172079 *03,676*

Industry and Government-Laboratory Cooperative R and D: An Idea Whose Time Has Come.
PB94-172939 *02,970*

Functions of Technology Infrastructure in a Competitive Economy.
PB94-173002 *00,478*

Investing in Education to Meet a National Need for a Technical-Professional Workforce in a Post-Industrial Economy.
PB94-173028 *00,132*

Physics Laboratory Technical Activities, 1993.
PB94-176088 *03,796*

NIST Serial Holdings, 1994.
PB94-178068 *02,745*

Four Years of Monitoring alpha Orionis with the VLA: Where Have All the Flares Gone.
PB94-185212 *00,048*

Distant Future of Solar Activity: A Case Study of Beta Hydri. 3. Transition Region, Corona, and Stellar Wind.
PB94-185220 *00,049*

Rotational Modulation and Flares on RS Canum Venaticorum and BY Draconis Stars. XVI. IUE Spectroscopy and VLA Observations of C1182(=V 1005 Orionis) in October 1983.
PB94-185626 *00,050*

High Sensitivity Survey of Radio Continuum Emission in Herbig Ae/Be Stars.
PB94-185915 *00,051*

Metric for Success.
PB94-187630 *02,633*

Body Dimensions for Apparel.
PB94-187739 *02,813*

Optical Metrology and More. Programs and Services of the Radiometric Physics Division, Physics Laboratory.
PB94-191707 *04,228*

Binder Characterization and Evaluation by Nuclear Magnetic Resonance Spectroscopy.
PB94-193471 *01,334*

Bibliography of Photon Total Cross Section (Attenuation Coefficient) Measurements 10 eV to 13.5 GeV, 1907-1993.
PB94-193760 *03,804*

Visualization Applications for Manufacturing: A State-of-the-Art Survey. Final Report.
PB94-194552 *02,816*

Federal Metric Progress in 1993.
PB94-196029 *02,600*

Histopathology, Blood Chemistry, and Physiological Status of Normal and Moribund Striped Bass ('Morone saxatilis') Involved in Summer Mortality ('Die-Off') in the Sacramento-San Joaquin Delta of California.
PB94-198157 *00,034*

First Results from the Goddard High-Resolution Spectrograph: The Chromosphere of Tauri.
PB94-199528 *00,054*

ROSAT All-Sky Survey of Active Binary Coronae. 2. Coronal Temperatures of the RS Canum Venaticorum Systems.
PB94-199601 *00,055*

Polarization of Light Emitted After Positron Impact Excitation of Alkali Atoms.
PB94-199734 *03,816*

Metric Path to Global Markets and New Jobs: A Question-and-Answer and Thematic Discussion.
PB94-206307 *02,601*

Assessment of Technology for Detection of Stress Corrosion Cracking in Gas Pipelines. Final Report, July 1993-March 1994.
PB94-206646 *02,475*

Dynamic Phenomena on the RS Canum Venaticorum Binary II Pegasi in August 1989. 1. Observational Data.
PB94-211067 *00,056*

Differences in Competitive Strategies between the United States and Japan.
PB94-211836 *00,013*

Importance of Measurement in Technology-Based Competition.
PB94-211844 *02,929*

Opacity Project and the Practical Utilization of Atomic Data.
PB94-212214 *00,059*

Aid for Smaller Businesses.
PB94-212461 *00,492*

Class of Radio-Emitting Magnetic B Stars and a Wind-Fed Magnetosphere Model.
PB94-213451 *00,067*

Information Infrastructure: Reaching Society's Goals. Report of the Information Infrastructure Task Force Committee on Applications and Technology.
PB94-214756 *01,469*

Videoconferencing Procurement and Usage Guide.
PB94-217023 *01,470*

HAZARD I Fire Hazard Assessment Method (Version 1.2) (for Microcomputers).
PB94-501988 *00,196*

HAZARD I Fire Hazard Assessment Method, Version 1.2 (Upgrade Package) (for Microcomputers).
PB94-501996 *00,197*

M (also known as MUMPS) Validation Test Suite, Version 8.3 (for Microcomputers).
PB94-502077 *01,699*

Polymer Composites Workshop. Held in Winona, Minnesota on April 29-30, 1992 (Video).
PB94-780129 *03,147*

Questions and Answers on Quality, the ISO 9000 Standard Series, Quality System Registration, and Related Issues. More Questions and Answers on the ISO 9000 Standard Series and Related Issues.
PB95-103461 *00,495*

NIST Industrial Impacts: A Sampling of Successful Partnerships.
PB95-111514 *00,488*

Program of the Subcommittee on Construction and Building (July 1994).
PB95-122537 *00,321*

Evidence for Significant Backscattering in Near-Threshold Electron-Impact Excitation of Ar(7+)(3s yields 3p).
PB95-126405 *03,883*

Databases Available in the Research Information Center of the National Institute of Standards and Technology.
PB95-128641 *02,724*

FIREDOC Users Manual, 3rd Edition.
PB95-128674 *01,378*

Constituents and Physical Properties of the C6+ Fraction of Natural Gas. Topical Report, April-June 1994.
PB95-136644 *02,483*

Evaluating Investments in Law Enforcement Equipment: An Annotated Bibliography.
PB95-151379 *04,867*

Promise into Practice: Implementing TA2 on Real Clocks at NIST.
PB95-151478 *01,533*

Think Metric.
PB95-151825 *01,298*

Transverse Thermomagnetic Effects in the Mixed State and Lower Critical Field of High-Tc Superconductors.
PB95-153250 *04,590*

Distant Future of Solar Activity: A Case Study of beta Hydri. 3. Transition Region, Corona, and Stellar Wind.
PB95-153441 *00,074*

Opportunities for Innovation: Software for Manufacturing.
PB95-155578 *02,851*

Information Retrieval Using Key Words and a Structured Review.
PB95-161121 *03,724*

Computers in Welding: A Primer.
PB95-162863 *02,862*

Gravity Dependent Processes and Intracellular Motion.
PB95-163382 *03,538*

Physics-Based Vision: Principles and Practice, Shape Recovery (Book Review).
PB95-164075 *01,846*

Method of Sale for CNG Paves Way to Greater Public Acceptance.
PB95-168449 *02,489*

Retrieving Articles from the Internet (without a UNIX Workstation). Part 1. File Formats and Software Tools.
PB95-168720 *02,728*

Retrieving Articles from the Internet (without a UNIX Workstation). Part 2. An Example.
PB95-168738 *02,729*

Getting Started on Mosaic.
PB95-180360 *01,721*

NIST Serial Holdings, 1995.
PB95-188926 *02,746*

Materials Science and Engineering Laboratory Annual Report, 1994. NAS-NRC Assessment Panel, April 6-7, 1995.
PB95-196697 *02,976*

Apparel Manufacturing Glossary for Application Protocol Development.
PB95-198750 *02,755*

Publications of the National Institute of Standards and Technology 1992 Catalog.
PB95-200747 *00,014*

CCD Mosaic Images of the Supernova Remnant 3C 400.2.
PB95-203527 *00,084*

Robotics Application to Highway Transportation. Volume 1. Final Report.
PB95-203790 *03,654*

NIST Industrial Impacts: A Sampling of Successful Partnerships (Revision, March 1995).
PB95-209193 *00,489*

Polymers Technical Activities 1994. NAC-NRC Assessment Panel, April 6-7, 1995.
PB95-209896 *01,275*

Assessment of Site Response Analysis Procedures.
PB95-210928 *00,450*

Water Droplet Evaporation from Radiantly Heated Solids.
PB95-217147 *00,394*

Abstract and Index Collection in the Research Information Center of the National Institute of Standards and Technology.
PB95-232633 *02,741*

CSTL Technical Activities, 1994.
PB95-242319 *00,608*

Materials Science and Engineering Laboratory Annual Report, December 1993.
PB95-254439 *02,668*

Project Summaries 1995: NIST Building and Fire Research Laboratory.
PB95-270047 *00,400*

Codes for Named Populated Places, Primary County Divisions, and Other Locational Entities of the United States (FIPS PUB 55-3) (on Magnetic Tape).
PB95-502563 *00,129*

FIPS PUB 8-6, Metropolitan Areas (for Microcomputers).
PB95-503280 *04,874*

Countries, Dependencies, Areas of Special Sovereignty, and Their Principal Administrative Divisions (for Microcomputers).
PB95-503504 *00,130*

Exact Recursion Relation Solution for the Steady-State Surface Temperature of a General Multilayer Structure.
PB96-102017 *02,376*

X-ray Emission from Chemically Peculiar Stars.
PB96-102256 *00,088*

Rotational Modulation and Flares on RS Canum Venaticorum and BY Draconis Stars. XVIII. Coordinated VLA, ROSAT, and IUE Observations of RS CVn Binaries.
PB96-102322 *00,089*

Thermodynamic Properties of Two Gaseous Halogenated Ethers from Speed-of-Sound Measurements: Difluoromethoxy-Difluoromethane and 2-Difluoromethoxy-1,1,1-Trifluoroethane.
PB96-102413 *04,189*

Effect of Stoichiometry on the Phases Present in Boron Nitride Thin Films.
PB96-102470 *04,710*

Extended CO(7 yields 6) Emission from Warm Gas in Orion.
PB96-102504 *00,090*

Measurement and Interpretation of Tidal Tilts in a Small Array.
PB96-102611 *03,686*

Intensity-Dependent Scattering Rings in High Order Above-Threshold Ionization.
PB96-110739 *04,032*

Monte Carlo and Analytic Methods in the Transport of Electrons, Neutrons, and Alpha Particles.
PB96-111612 04,033

Effects of Target Temperature on Analytical Sensitivities of Cold-Neutron Capture Prompt gamma-ray Activation Analysis.
PB96-112131 00,616

Glimpse of Materials Research in China: A Report from an Interagency Study Team on Materials Visiting China from June 19, 1995 to June 30, 1995.
PB96-112677 02,978

Intelligent Processing of Materials, Technical Activities 1994 (NAS-NRC Assessment Panel, April 6-7, 1995).
PB96-115050 03,359

NIST and the Navy: Past, Present and Future.
PB96-119649 03,655

VAMAS Intercomparison of Critical Current Measurements on NB3Sn Superconductors: A Summary Report.
PB96-119763 04,043

Some Notable Hurricanes Revisited.
PB96-122601 00,458

Magnetic Fields in Star-Forming Regions: Observations.
PB96-123005 00,100

Federal Labs Have Key Role in Metrication.
PB96-123401 02,920

Book Review: Statistical Physics of Macromolecules.
PB96-123526 01,280

Book Review: Aspects and Applications of the Random Walk.
PB96-123534 04,215

Journal of Research of the National Institute of Standards and Technology, September-October 1993. Volume 98, Number 5.
PB96-134954 03,362

Metallurgy Technical Activities 1994 (NAS-NRC Assessment Panel, April 6-7, 1995).
PB96-136981 02,981

Churchill Eisenhart, 1913-1994.
PB96-137740 03,447

Report on 1994 Actions of the International Institute of Welding.
PB96-138540 02,873

Databases Available in the Research Information Center of the National Institute of Standards and Technology (December 1995).
PB96-139407 02,734

Influence of an Impenetrable Interface on a Polymer Glass-Transition Temperature.
PB96-146873 03,175

General Types of Information Services.
PB96-147053 02,735

Airborne Asbestos Analysis: National Voluntary Laboratory Accreditation Program.
PB96-147392 02,566

Metrology and Regional Trade Pacts.
PB96-155429 02,923

Information Transfer in the 21st Century.
PB96-157904 02,714

What's Available in Welding Software.
PB96-158084 02,875

Conference Proceedings: International Workshop on Instrumented Indentation. Held in San Diego, California on April 22-23, 1995.
PB96-158688 01,948

METRICATION: An Economic Wake-Up Call for Surveyors and Mappers.
PB96-159629 03,680

Montgomery Education Connection and Resource Education Awareness Partnership Making Connections between Local Schools and NIST Volunteers.
PB96-159769 00,134

Metrology.
PB96-160759 02,925

Lattice Statics of Interfaces and Interfacial Cracks in Bimaterial Solids.
PB96-161823 02,985

Gage Block Standards, Measurement Capabilities and Laboratory Accreditation.
PB96-163621 02,757

Publication and Presentation Abstracts, 1995.
PB96-164082 03,576

Rechargeable Batteries for Personal/Portable.
PB96-164231 02,459

Electronics and Electrical Engineering Laboratory 1995 Technical Accomplishments: Advancing Metrology for Electrotechnology to Support the U.S. Economy.
PB96-164520 01,959

NIST Handbook 44, 1996: Specifications, Tolerances, and Other Technical Requirements for Weighing and Measuring Devices as Adopted by the 80th National Conference on Weights and Measures, 1995.
PB96-166616 02,926

Application of Electromagnetic-Acoustic Transducers for Nondestructive Evaluation of Stresses in Steel Bridge Structures.
PB96-167978 01,301

Federal Implementation Guideline for Electronic Data Interchange. ASC X12 003050 Transaction Set 843 Response to Request for Quotation. Implementation Convention.
PB96-168984 01,822

NIST Serial Holdings, 1996.
PB96-172523 02,748

NIST List of Publications, LP 103, March 1996. National Semiconductor Metrology Program.
PB96-175856 02,432

Automated Measurement of Nonlinearity of Optical Fiber Power Meters.
PB96-176540 04,110

Developments in Stellar Coronae.
PB96-176706 00,107

Directory of Law Enforcement and Criminal Justice Associations and Research Centers.
PB96-178918 04,872

Unpredictable Certainty. Information Infrastructure through 2000.
PB96-182266 00,016

Materials Reliability. Technical Activities, 1995.
PB96-183082 02,999

Publications of the National Institute of Standards and Technology 1993 Catalog.
PB96-183215 00,017

Financing Tomorrow's Infrastructure: Challenges and Issues. Proceedings of a Colloquium. Held in Washington, DC. on October 20, 1995.
PB96-189444 00,481

Reactor Radiation Technical Activities, 1995.
PB96-193644 03,741

Ceramics Technical Activities, 1995.
PB96-193677 03,087

Polymers Technical Activities, 1995.
PB96-193719 01,291

Program of the Manufacturing Engineering Laboratory, 1996. Infrastructural Technology, Measurements, and Standards for the U.S. Manufacturing Industries.
PB96-195276 02,760

Metallurgy. Technical Activities, 1995.
PB96-195284 03,003

Development of a Method for Measuring Water-Stripping Resistance of Asphalt/Siliceous Aggregate Mixtures.
PB96-197249 01,348

NIST Frequency Measurement Service.
PB96-200662 01,561

Overview of U.S. Government Advanced Packaging Programs.
PB96-200845 02,443

Modification of a Commercial SEM with a Computer Controlled Cathode Stabilized Power Supply.
PB96-201066 04,129

Lake Erie Water Temperature Data, Put-in-Bay, Ohio, 1918-1992.
PB96-202452 03,692

Improving Color Measurements of Displays.
PB96-204441 02,203

Working Conference on Global Growth of Technology: Is America Prepared. Held in Gaithersburg, Maryland on December 7, 1995.
PB96-210059 00,018

CSTL Technical Activities, 1995.
PB96-214630 00,647

Materials Science and Engineering Laboratory Annual Report, 1995. Technical Activities.
PB96-214754 03,009

Building Life Cycle Cost Computer Program (BLCC) Version 4.22-95 (for Micrcomputers).
PB96-502794 00,277

Stacking the Cards in Europe: One Company's Story.
PB97-110126 00,493

Sinusoidal Surfaces as Standards for BRDF Instruments.
PB97-110597 04,388

Extrapolation of the Heat Capacity in Liquid and Amorphous Phases.
PB97-111421 04,147

NIST Thermal Infrared Transfer Standard Radiometer for the Earth Observing System (EOS) Program.
PB97-113013 04,843

Design of a High-Pressure Ebulliometer, with Vapor-Liquid Equilibrium Results for the Systems CHF2Cl + CF3-CH3 and CF3-CH2F + CH2F2.
PB97-113229 04,163

India: Environmental Technologies Export Market Plan.
PB97-114359 02,529

Bibliography of the NIST Optoelectronics Division.
PB97-116040 02,207

Orientational Fluctuations, Diffuse Scattering, and Orientational Order in Solid C60.
PB97-119275 04,176

Science, Technology, and Competitiveness: Retrospective on a Symposium in Celebration of NIST's 90th Anniversary and the 25th Anniversary of the Gaithersburg Laboratories, November 14-15, 1991.
PB97-121610 02,696

Photonic Band-Structure Effects for Low-Index-Contrast Two-Dimensional Lattices in the Near Infrared.
PB97-122469 04,401

Chemical Effect in Ceramics Grinding.
PB97-122592 03,113

Building Life Cycle Cost Computer Program (BLCC) Version 4.4-97 (for Microcomputers).
PB97-500342 00,284

GENERAL THEORETICAL CHEMISTRY & PHYSICS

Aerodynamic Phenomena in Stellar Atmospheres - A Bibliography.
AD-A278 521/0 00,046

Atom-counting standards and Doppler-free resonance ionization mass spectroscopy. (Progress report).
DE94018562 00,723

Time and Frequency Technology at NIST.
N94-30641/2 01,522

Implementation of a Standard Format for GPS Common View Data.
N95-32323/4 03,779

CSTL Technical Activities 1991.
PB94-160769 00,728

Diffraction of X-rays at the Far Tails of the Bragg Peaks.
PB94-199924 04,476

High Temperature.
PB94-211737 03,844

Fluctuation Dominated Recombination Kinetics with Traps.
PB95-107264 00,875

CSTL Technical Activities, 1993.
PB95-160602 00,953

Elastic Scattering of Polymer Networks.
PB95-161816 01,255

Diamond and Graphite Precursors: Comments.
PB95-163051 00,967

Hydrogen Atom Attack on Perchloroethylene.
PB95-163473 00,969

Quasipotential and the Stability of Phase Lock in Nonhysteretic Josephson Junctions.
PB95-180402 04,681

Generalized Stokes-Einstein Equation for Spherical Particle Suspensions.
PB95-202743 01,031

Stellar Coronal Structures.
PB95-202834 00,080

New High-Redshift Damped Lyman-alpha Absorption Systems and the Redshift Evolution of Damped Absorbers.
PB95-203501 00,083

Far-Ultraviolet Flare on a Pleiades G Dwarf.
PB96-102033 00,086

Search for Radio Emission from the 'Non-Magnetic' Chemically Peculiar Stars.
PB96-102249 00,087

High-Velocity Plasma in the Transition Region of AU Microscopii: Evidence for Magnetic Reconnection and Saturated Heating during Quiescent and Flaring Conditions.
PB96-102694 00,091

Observing Stellar Coronae with the Goddard High Resolution Spectrograph. I. The dMe Star AU Microscopii.
PB96-102777 00,092

Volume-Limited ROSAT Survey of Extreme Ultraviolet Emission from all Nondegenerate Stars within 10 Parsecs.
PB96-103189 00,093

Spectroscopic Study of Quantized Breakdown Voltage States of the Quantum Hall Effect.
PB96-113584 04,730

Stars, Atmospheres, Radiative Transfer.
PB96-119474 00,095

Relationship between Radiative and Magnetic Fluxes for Three Active Solar-Type Dwarfs.
PB96-119540 00,097

Simulation Studies of Supercooled and Glass Forming Liquids.
PB96-122627 01,085

Sleuthing the Dynamo: HST/FOS Observations of UV Emissions of Solar-Type Stars in Young Clusters.
PB96-122817 00,098

Efficient Way of Identifying New Active Stars: A VLA Survey of X-ray Selected Active Stellar Candidates.
PB96-122882 00,099

High Velocity Plasm in the Transition Region of Au Mic: A Stellar Analog of Solar Explosive Events.
PB96-123294 00,102

Radio and X-ray Emissions from Chemically Peculiar B- and A-Type Stars: Observations and a Model.
PB96-123302 00,103

Redshifts in Stellar Transition Regions.
PB96-123310 00,104

Transition Regions of Capella.
PB96-123336 00,105

Mixing Plate-Like and Rod-Like Molecules with Solvent: A Test of Flory-Huggins Lattice Statistics.
PB96-126206 03,173

Imposed Oscillations of Kinetic Barriers Can Cause an Enzyme to Drive a Chemical Reaction Away from Equilibrium.
PB96-161625 01,137

Quadratic Response of a Chemical Reaction to External Oscillations.
PB96-161633 *01,138*

Verification of Revised Water Vapour Correction to the Index of Refraction of Air.
PB96-161666 *02,680*

Effect of Finite Beam Width on Elastic Light Scattering from Droplets.
PB96-163670 *01,144*

Transition Regions of Capella (1995).
PB96-176714 *00,108*

Riass Coronathon: Joint X-ray and Ultraviolet Observations of Normal F-K Stars.
PB96-200217 *00,109*

Accurate Measurements of the Local Deuterium Abundance from HST Spectra.
PB96-200621 *00,110*

Deuterium and the Local Interstellar Medium: Properties for the Procyon and Capella Lines of Sight.
PB96-200639 *00,111*

Electrolytes Constrained on Fractal Structures: Debye-Huckel Theory.
PB97-110241 *01,174*

Spinor Equations in Relativistic Quantum Mechanics.
PB97-110605 *04,142*

GENERALLY ACCEPTED PRINCIPLES AND PRACTICES

Computer Security: Generally Accepted Principles and Practices for Securing Information Technology Systems.
PB97-110811 *01,619*

GENETIC MAPPING

Small genomes: New initiatives in mapping and sequencing. Workshop summary report.
DE96014476 *03,451*

GENETICS

Regulation of Lithium and Boron Levels in Normal Human Blood: Environmental and Genetic Considerations.
PB94-198579 *03,491*

GEOCODING

Metropolitan Areas (Including MSAs, CMSAs, PMASs, and NECMAs). Category: Data Standards and Guidelines; Subcategory: Representations and Codes.
FIPS PUB 8-6 *04,873*

Countries, Dependencies, Areas of Special Sovereignty, and Their Principal Administrative Divisions. Category: Data Standards and Guidelines; Subcategory: Representation and Codes.
FIPS PUB 10-4 *00,128*

Guideline: Codes for Named Populated Places, Primary County Divisions, and Other Locational Entities of the United States, Puerto Rico, and the Outlying Areas. Category: Data Standards and Guidelines. Subcategory: Representations and Codes.
FIPS PUB 55-3 *04,865*

Guideline: Codes for Named Populated Places, Primary County Divisions, and Other Locational Entities of the United States, Puerto Rico, and the Outlying Areas. Category: Data Standards and Guidelines; Subcategory: Representation and Codes.
FIPS PUB 55-DC3 *04,866*

FIPS PUB 8-6, Metropolitan Areas (for Microcomputers).
PB95-503280 *04,874*

Countries, Dependencies, Areas of Special Sovereignty, and Their Principal Administrative Divisions (for Microcomputers).
PB95-503504 *00,130*

GEODYNAMICS

Lunar Laser Ranging: A Continuing Legacy of the Apollo Program.
PB95-202495 *03,683*

GEOGRAPHIC INFORMATION SYSTEMS

Standards: A Cardinal Direction for Geographic Information Systems.
PB95-150942 *03,677*

Geographic Information Systems Standards: A Federal Perspective.
PB95-163390 *03,678*

Spatial Information and Technology Standards Evolving.
PB96-135108 *03,679*

GEOGRAPHY

Metropolitan Areas (Including MSAs, CMSAs, PMASs, and NECMAs). Category: Data Standards and Guidelines; Subcategory: Representations and Codes.
FIPS PUB 8-6 *04,873*

Countries, Dependencies, Areas of Special Sovereignty, and Their Principal Administrative Divisions. Category: Data Standards and Guidelines; Subcategory: Representation and Codes.
FIPS PUB 10-4 *00,128*

Guideline: Codes for Named Populated Places, Primary County Divisions, and Other Locational Entities of the United States, Puerto Rico, and the Outlying Areas. Category: Data Standards and Guidelines. Subcategory: Representations and Codes.
FIPS PUB 55-3 *04,865*

Guideline: Codes for Named Populated Places, Primary County Divisions, and Other Locational Entities of the United States, Puerto Rico, and the Outlying Areas. Category: Data Standards and Guidelines; Subcategory: Representation and Codes.
FIPS PUB 55-DC3 *04,866*

FIPS PUB 8-6, Metropolitan Areas (for Microcomputers).
PB95-503280 *04,874*

Countries, Dependencies, Areas of Special Sovereignty, and Their Principal Administrative Divisions (for Microcomputers).
PB95-503504 *00,130*

GEOMETRIC ABBERATIONS

Compensation for Errors Introduced by Nonzero Fringe Densities in Phase-Measuring Interferometers.
PB97-110506 *04,386*

GEOMETRIC FITTING SOFTWARE

Representation of Axes for Geometric Fitting.
PB97-113799 *01,782*

GEOMETRICAL ABERRATIONS

Test Optics Error Removal.
PB96-179536 *04,377*

GEOMETRY

User's Guide for the Algorithm Testing System Version 2.0.
PB95-251666 *02,916*

Optical Fiber, Fiber Coating, and Connector Ferrule Geometry: Results of Interlaboratory Measurement Comparisons.
PB96-154422 *04,360*

Using Logic to Specify Shapes and Spatial Relations in Design Grammars.
PB97-111579 *02,793*

GERMANES

Plasma Chemistry in Silane/Germane and Disilane/Germane Mixtures.
PB95-202537 *01,027*

GERMANIUM

Energy Levels of Germanium, Ge I through Ge XXXII.
PB94-162351 *00,747*

Germanium Detector Optimization of MDA for Efficiency vs. Low Intrinsic Background.
PB94-199155 *00,543*

Resonance Enhanced Multiphoton Ionization Detection of GeF and GeCl Radicals.
PB94-212123 *00,825*

Thermodynamics of (Germanium + Selenium): A Review and Critical Assessment.
PB97-112536 *01,182*

GERMANIUM CHLORIDE RADICALS

Resonance Enhanced Multiphoton Ionization Detection of GeF and GeCl Radicals.
PB94-212123 *00,825*

GERMANIUM DETECTOR

Measurement of the (10)B(n, alpha1gamma)(7)Li Cross Section in the 0.3 to 4 MeV Neutron Energy Interval.
PB96-161799 *04,098*

GERMANIUM FLUORIDE RADICALS

Resonance Enhanced Multiphoton Ionization Detection of GeF and GeCl Radicals.
PB94-212123 *00,825*

GERMANY (UNIFIED)

Ceramic Powders Characterization: Results of an International Laboratory Study.
PB95-270039 *02,672*

GII (GLOBAL INFORMATION INFRASTRUCTURE)

Global Information Infrastructure: Agenda for Cooperation.
PB95-178604 *01,482*

GILS (GOVERNMENT INFORMATION LOCATOR SERVICE)

Application Profile for the Government Information Locator Service (GILS). Category: Software Standard; Subcategory: Information Interchange.
FIPS PUB 192 *01,800*

GINZBURG SYMPOSIUM

From Superconductivity to Supernovae: The Ginzburg Symposium. Report on the Symposium Held in Honor of Vitaly L. Ginzburg. Held in Gaithersburg, Maryland on May 22, 1992.
PB95-171963 *04,649*

GLASS

Fire Induced Thermal Fields in Window Glass I: Theory.
PB94-139722 *00,328*

Analysis of SANS from Controlled Pore Glasses.
PB94-198843 *03,035*

Glass Transition of Organic Liquids Confined to Small Pores.
PB94-212305 *00,833*

Melting Behavior of Organic Materials Confined in Porous Solids.
PB94-212313 *00,834*

Aging in Glasses Subjected to Large Stresses and Deformations.
PB95-107041 *03,235*

Environmentally Enhanced Fracture of Ceramics.
PB95-125746 *03,046*

Length Scales for Fragile Glass-Forming Liquids.
PB96-102801 *01,065*

Glasses for Waveguide Lasers.
PB96-111950 *04,335*

Long-Lived Structures in Fragile Glass-Forming Liquids.
PB96-119565 *04,212*

Simulation Studies of Supercooled and Glass Forming Liquids.
PB96-122627 *01,085*

Distributed Feedback Lasers in Rare-Earth-Doped Phosphate Glass.
PB96-123773 *04,740*

Integrated Optical Polarization-Discriminating Receiver in Glass.
PB97-113179 *02,206*

GLASS-CERAMIC

Wear of Enamel against Glass-Ceramic, Porcelain, and Amalgam.
PB96-179593 *03,082*

GLASS FIBER REINFORCED PLASTICS

Composite Struts for SMES Plants.
PB95-155586 *02,507*

Torsion Modulus and Internal Friction of a Fiber-Reinforced Composite.
PB96-112339 *03,070*

GLASS LASERS

Integrated Optic Laser Emitting at 906, 1057, and 1358 nm.
PB94-216280 *02,135*

Integrated Optic Laser Emitting at 905, 1057, 1356 nm.
PB94-216298 *02,136*

GLASS TRANSITION TEMPERATURE

Effect of Curing History on Ultimate Glass Transition Temperature and Network Structure of Crosslinking Polymers.
PB94-200052 *01,214*

Glass Transition of Organic Liquids Confined to Small Pores.
PB94-212305 *00,833*

Physics Required for Prediction of Long Term Performance of Polymers and Their Composites.
PB94-219243 *03,146*

Glass Temperature of Polymer Blends: Comparison of Both the Free Volume and the Entropy Predictions with Data.
PB95-140190 *01,236*

Influence of an Impenetrable Interface on a Polymer Glass-Transition Temperature.
PB96-146873 *03,175*

GLASSY SILICA

Small-Angle Neutron Scattering Characterization of Processing/Microstructure Relationships in the Sintering of Crystalline and Glassy Ceramics. (Reannouncement with New Availability Information).
AD-A249 510/9 *03,025*

GLOBAL ASPECTS

Global Climatic Effects of Aerosols: The AAAR Symposium.
PB95-108791 *00,122*

GLOBAL DENSITY RATIO

Global Density Effects on the Self-Preservation Behavior of Turbulent Free Jets.
PB95-162301 *04,207*

GLOBAL ECONOMY

Working Conference on Global Growth of Technology: Is America Prepared. Held in Gaithersburg, Maryland on December 7, 1995.
PB96-210059 *00,018*

GLOBAL EQUIVALENCE RATIO

Global Equivalence Ratio Concept and the Formation Mechanisms of Carbon Monoxide in Enclosure Fires.
PB96-146790 *00,210*

GLOBAL INFORMATION INFRASTRUCTURE

Global Information Infrastructure: Agenda for Cooperation.
PB95-178604 *01,482*

GLOBAL POSITIONING SYSTEM

Comparison of GPS Broadcast and DMA Precise Ephemerides.
N94-30660/2 *01,523*

Implementation of a Standard Format for GPS Common View Data.
N95-32323/4 *03,779*

Analytical Estimation of Carrier Multipath Bias on GPS Position Measurements.
PB94-215712 *04,845*

Preliminary Comparison of Time Transfers via LASSO, GPS and Two-Way Satellite.
PB95-151098 *01,529*

Calibration of GPS Equipment in Japan.
PB95-151452 *01,531*

Use of Ionospheric Data in GPS Time Transfer.
PB95-163853 *01,540*

Implementation of a Standard Format for GPS Common View Data.
PB96-176581 *01,555*

GLOW DISCHARGES

Gaseous Electronics Conference Radio-Frequency Reference Cell: A Defined Parallel-Plate Radio-Frequency System for Experimental and Theoretical Studies of Plasma-Processing Discharges.
PB94-172327 *04,404*

Fourier Transform Atomic Emission Studies Using a Glow Discharge as the Emission Source.
PB94-185980 *00,533*

Ion Kinetic-Energy Distributions in Argon rf Glow Discharges.
PB95-141008 04,409

Electrical Characterization of Radio-Frequency Discharges in the Gaseous Electronics Conference Reference Call.
PB95-164612 01,905

Plasma Chemical Model for Decomposition of SF6 in a Negative Glow Corona Discharge.
PB95-181053 01,020

Plasma Chemistry in Silane/Germane and Disilane/Germane Mixtures.
PB95-202537 01,027

Evidence for Inelastic Processes for N(+)3 and N(+)4 from Ion Energy Distributions in He/N2 Radio Frequency Glow Discharges.
PB96-146683 04,059

GLUCOSE

Apparent Molar Heat Capacities and Apparent Molar Volumes of Aqueous Glucose at Temperatures from 298.15 K to 327.01 K.
PB94-212800 03,459

Amperometric Flow-Injection Analysis Biosensor for Glucose Based on Graphite Paste Modified with Tetracyanoquinodimethane.
PB95-161980 03,498

GLUCOSE PERMEASE

Glucose Permease of Bacillus Subtilis Is a Single Polypeptide Chain That Functions to Energize the Sucrose Permease.
PB95-163192 03,466

GLYCEROL

Isotope Dilution Mass Spectrometry as a Candidate Definitive Method for Determining Total Glycerides and Triglycerides in Serum.
PB96-102280 03,519

GLYCIDYL ETHERS

Effect of Curing History on Ultimate Glass Transition Temperature and Network Structure of Crosslinking Polymers.
PB94-200052 01,214

GLYCINE

Structure of Glycine-Water H-Bonded Complexes.
PB94-198603 00,789

Effects of Aluminum Oxalate/Glycine Pretreatment Solutions on Dentin Permeability.
PB95-164505 03,565

GLYCINE-WATER COMPLEX

Structure of Glycine-Water H-Bonded Complexes.
PB94-198603 00,789

GMR

Size Effects in Submicron NiFe/Ag GMR Devices.
PB96-155510 02,237

GOALS

White Papers Prepared for the White House: Construction Industry Workshop on National Construction Goals. Held on December 14-16, 1994.
PB95-216891 01,299

GODDARD HIGH RESOLUTION SPECTROGRAPH

Goddard High Resolution Spectrograph: Instrument, Goals, and Science Results.
PB96-123278 00,044

GOES SATELLITES

Semiconductor Measurement Technology: Improved Characterization and Evaluation Measurements for HgCdTe Detector Materials, Processes, and Devices Used on the GOES and TIROS Satellites.
PB94-188810 02,122

GOLD

Incorporation of Gold into YBa2Cu3O7: Structure and Tc Enhancement.
PB94-200276 04,481

Unexpected Effects of Gold on the Structure, Superconductivity, and Normal State of YBa2Cu3O7.
PB94-200284 04,482

Self-Assembled Phospholipid/Alkanethiol Biomimetic Bilayers on Gold.
PB95-108460 00,878

Scanning Tunneling Microscopy and Fabrication of Nanometer Scale Structures at the Liquid-Gold Interface.
PB95-140414 00,904

Oscillatory Exchange Coupling in Fe/Au/Fe(100).
PB95-150371 04,569

Silver Metalization of Octadecanethiol Monolayers Self-Assembled on Gold.
PB95-150744 00,923

UV-Photopatterning of Alkylthiolate Monolayers Self-Assembled on Gold and Silver.
PB95-150751 00,924

Characterization of Cytochrome c/Alkanethiolate Structures Prepared by Self-Assembly on Gold.
PB95-164638 00,987

Collisions of Electrons with Highly-Charged Ions.
PB96-200340 04,791

GOLD ALLOYS

Fabrication of Platinum-Gold Alloys in Pre-Hispanic South America: Issues of Temperature and Microstructure Control.
PB94-211646 03,333

Diffusion of Copper into Gold Plating.
PB95-162152 00,957

GOLD IONS

Spectra of Ag I Isoelectronic Sequence Observed from Er(21+) to Au(32+).
PB95-150660 03,899

GOSIP (GOVERNMENT OPEN SYSTEMS INTERCONNECTION PROFILE)

U.S. GOSIP Testing Program.
PB94-211455 01,807

National Voluntary Laboratory Accreditation Program. GOSIP: Government Open Systems Interconnection Profile.
PB95-267993 01,486

Lessons from the Establishment of the U.S. GOSIP Testing Program.
PB96-119359 01,817

GOSIP Testing Program.
PB96-161229 01,504

Industry/Government Open Systems Specification: The Development of GOSIP Version 3.
PB96-161245 01,505

Five Q's (Cues) of the U.S. GOSIP Testing Program.
PB96-175716 01,826

GOVERNMENT/INDUSTRY RELATIONS

Transfer of Technology from Defense to Civilian Sectors.
PB94-185360 00,011

NIST Industrial Impacts: A Sampling of Successful Partnerships.
PB95-111514 00,488

NIST Industrial Impacts: A Sampling of Successful Partnerships (Revision, March 1995).
PB95-209193 00,489

Conceptual Design Plan for the National Advanced Manufacturing Testbed.
PB95-231866 02,828

National Planning for Construction and Building R and D.
PB96-137104 00,324

Industry/Government Open Systems Specification: The Development of GOSIP Version 3.
PB96-161245 01,505

GOVERNMENT INFORMATION LOCATOR SERVICE

Application Profile for the Government Information Locator Service (GILS). Category: Software Standard; Subcategory: Information Interchange.
FIPS PUB 192 01,800

GOVERNMENT OPEN SYSTEMS INTERCONNECTION PROFILE

U.S. GOSIP Testing Program.
PB94-211455 01,807

National Voluntary Laboratory Accreditation Program. GOSIP: Government Open Systems Interconnection Profile.
PB95-267993 01,486

Lessons from the Establishment of the U.S. GOSIP Testing Program.
PB96-119359 01,817

GOSIP Testing Program.
PB96-161229 01,504

Industry/Government Open Systems Specification: The Development of GOSIP Version 3.
PB96-161245 01,505

Five Q's (Cues) of the U.S. GOSIP Testing Program.
PB96-175716 01,826

GOVERNMENT POLICIES

Proceedings of the Manufacturing Technology Needs and Issues: Establishing National Priorities and Strategies Conference. Held in Gaithersburg, Maryland on April 26-28, 1994.
PB95-206181 02,930

Unpredictable Certainty. Information Infrastructure through 2000.
PB96-182266 00,016

GOVERNMENT PROCUREMENT

Open System Environment Procurement.
N94-36858/6 02,716

Guide on Open System Environment (OSE) Procurements.
PB95-169496 01,626

Information Technology Standards in Federal Acquisitions.
PB96-161252 01,636

Using Information Technology Standards in Federal Acquisitions.
PB96-161260 01,637

Federal Implementation Guideline for Electronic Data Interchange: ASC X12 003050 Transaction Set 836 Procurement Notices. Implementation Convention.
PB96-178892 01,827

GRADIOMETERS

Gradiometer Antennas for Detection of Long Subsurface Conductors.
PB95-175667 01,862

GRAFT POLYMERIZATION

Grafted Interpenetrating Polymer Networks.
PB94-185055 01,200

GRAFTED POLYMER LAYER

Segmental Concentration Profiles of End-Tethered Polymers with Excluded-Volume and Surface Interactions.
PB97-119002 00,654

GRAIN BOUNDARIES

Weak-Link-Free Behavior of High Angle YBa2Cu3O7-x Grain Boundaries in High Magnetic Fields.
PB94-198421 04,459

Energy and Migration of Grain Boundaries in Polycrystals.
PB94-211638 03,332

Examination of Objects Made of Wood Using Air-Coupled Ultrasound.
PB95-125712 03,404

Nature of (001) Tilt Grain Boundaries in YBa2Cu3O6+x.
PB95-126033 04,528

Small Angle Neutrons Scattering from Nanocrystalline Palladium as a Function of Annealing.
PB95-176103 03,354

Stability and Surface Energies of Wetted Grain Boundaries in Aluminum Oxide.
PB95-202750 03,059

Inelastic Neutron Scattering Study of Hydrogen in Nanocrystalline Pd.
PB96-146857 03,366

GRAIN CLUSTERS

Modeling Effects of Temperature Annealing on Giant Magnetoresistive Response in Discontinuous Multilayer NiFe/Ag Films.
PB97-112585 04,157

GRAIN GROWTH

Stability, Microstructural Evolution, Grain Growth, and Coarsening in a Two-Dimensional Two-Phase Microstructure.
PB94-199429 03,325

Investigation into a Practical Grain Growth Model for Hot Isostatic Pressing.
PB95-151684 03,347

GRAIN SIZE

Determination of the Prior-Austenitic Grain Size of Selected Steels Using a Molten Glass Etch.
PB94-211927 03,208

GRAIN STRUCTURE

Grain Alignment and Transport Properties of Bi2Sr2CaCu2O8 Grown by Laser Heated Float Zone Method.
PB95-161451 04,602

GRANULAR MATERIALS

Domain Structures in Magnetoresistive Granular Metals.
PB96-141346 04,760

GRAPHICAL USER INTERFACE

Prototyping a Graphical User Interface for DHCP.
PB96-160544 02,599

Automated Guarded Bridge for Calibration of Multimegohm Standard Resistors.
PB97-119150 02,289

GRAPHITE

Thermal Diffusivity of POCO AXM-5Q1 Graphite in the Range 1500 to 2500 K Measured by a Laser-Pulse Technique.
PB94-185022 03,013

Diamond and Graphite Precursors: Comments.
PB95-163051 00,967

Determination of Anomalous Superexchange in MnCl2 and Its Graphite Intercalation Compound.
PB97-122568 00,666

GRAPHITE CALORIMETERS

Crystal Structure of Annealed and As-Prepared HgBa2CaCu2O6+delta Superconductors.
PB95-161105 03,927

GRAPHITE COMPOSITES

Thermoacoustic Technique for Determining the Interface and/or Interply Strength in Polymeric Composites.
PB95-161824 03,158

GRAPHITE INTERCALATION COMPOUNDS

Structural and Magnetic Properties of CuCl2 Graphite Intercalation Compounds.
PB96-119748 03,020

GRATING

Distributed Feedback Lasers in Rare-Earth-Doped Phosphate Glass.
PB96-123773 04,740

GRATING COUPLING

Embossable Grating Couplers for Planar Waveguide Optical Sensors.
PB96-190277 00,641

GRATINGS

Growth Characteristics of Fiber Gratings.
PB96-122957 04,346

GRATINGS (SPECTRA)

Bragg Gratings in Optical Fibers Produced by a Continuous-Wave Ultraviolet Source.
PB95-162020 04,274

Growth of Bragg Gratings Produced by Continuous-Wave Ultraviolet Light in Optical Fiber.
PB95-162038 04,275

Decay of Bragg Gratings in Hydrogen-Loaded Optical Fibers.
PB96-122643 04,345

GRAVIMETERS

Calibration of a Superconducting Gravimeter Using Absolute Gravity Measurements.
PB95-202651 03,684

Continuous Gravity Observations Using Joint Institute for Laboratory Astrophysics Absolute Gravimeters.
PB95-203048 *03,685*

Intracomparison Tests of the FG5 Absolute Gravity Meters.
PB96-102991 *03,688*

GRAVIMETRIC STANDARDS
Measurement of Atmospheric Methyl Bromide Using Gravimetric Gas Standards.
PB96-155494 *02,497*

GRAVIMETRY
Journal of Research of the National Institute of Standards and Technology, March/April 1996. Volume 101, Number 2.
PB96-177381 *01,863*

Development of the Ion Exchange-Gravimetric Method for Sodium in Serum as a Definitive Method.
PB96-179148 *01,867*

GRAVITATION
Earth-Based Gravitational Experiments.
PB94-211414 *03,840*

Elastic Deformation of a Monolithic Perfect Crystal Interferometer: Implications for Gravitational Phase Shift Experiments.
PB94-213154 *03,858*

Validation of the Inverse Square Law of Gravitation Using the Tower at Erie, Colorado, USA.
PB95-164646 *03,947*

Test of Newton's Inverse Square Law of Gravitation Using the 300-m Tower at Erie, Colorado.
PB95-202446 *03,978*

GRAVITATIONAL EFFECTS
Ignition and Subsequent Transition to Flame Spread in a Microgravity Environment.
N96-15584/1 *04,828*

GRAVITATIONAL FIELDS
Integrated Laser Doppler Method for Measuring Planetary Gravity Fields.
PB94-198686 *03,681*

GRAVITATIONAL WAVE ANTENNAS
Quantum Mechanics of a Solid-State Bar Gravitational Antenna.
PB95-202628 *03,987*

GRAVITY
Gravity Dependent Processes and Intracellular Motion.
PB95-163382 *03,538*

Validation of the Inverse Square Law of Gravitation Using the Tower at Erie, Colorado, USA.
PB95-164646 *03,947*

Test of Newton's Inverse Square Law of Gravitation Using the 300-m Tower at Erie, Colorado.
PB95-202446 *03,978*

Continuous Gravity Observations Using Joint Institute for Laboratory Astrophysics Absolute Gravimeters.
PB95-203048 *03,685*

GRAVITY CURRENTS
Gravity-Current Transport in Building Fires.
PB96-147046 *01,415*

Transport by Gravity Currents in Building Fires.
PB97-119325 *01,441*

GREEN'S FUNCTION
Design, Construction and Application of a Large Aperture Lens-Less Line-Focus PVDF Transducer.
PB97-122584 *02,765*

GREEN'S FUNCTIONS
Fracture in Multilayers.
PB96-163613 *02,988*

GREENHOUSES
Corrosion Resistance of Materials for Renovation of the United States Botanic Garden Conservatory.
PB94-154390 *00,032*

GREENS FUNCTION
Lattice Imperfections Studied by Use of Lattice Green's Functions.
PB95-150850 *04,576*

Elastic Green's Function for a Bimaterial Composite Solid Containing a Free Surface Normal to the Interface.
PB95-163325 *03,162*

Green's Function for Generalized Hilbert Problem for Cracks and Free Surfaces in Composite Materials.
PB95-163333 *03,163*

GROUND BASED CONTROL
Ground Vehicle Control at NIST: From Teleoperation to Autonomy.
N94-34037/9 *03,758*

GROUND MOTION
Assessment of Site Response Analysis Procedures.
PB95-210928 *00,450*

Energy-Based Method for Liquefaction Potential Evaluation. Phase 1. Feasibility Study.
PB96-214747 *03,691*

GROUND STATIONS
Satellite Two-Way Time Transfer: Fundamentals and Recent Progress.
PB95-161089 *01,536*

GROUND VEHICLES
Vehicle-Command Center Communications in a Robotic Vehicle System.
PB95-162723 *03,665*

GROUNDINGS
Stranding Experiments on Double Hull Tanker Structures.
PB96-123112 *03,749*

GROWTH ABNORMALITIES
Nutritional Status and Growth in Juvenile Rheumatoid Arthritis.
PB94-198470 *03,515*

GUARDED HOT PLATE
Intra-Laboratory Comparison of a Line-Heat-Source Guarded Hot Plate and Heat-Flow-Meter Apparatus.
PB95-181202 *00,387*

Line-Heat-Source Guarded-Hot-Plate Apparatus.
PB97-118996 *00,417*

GUIDELINES
Guidelines for Reporting Results of Computational Experiments. Report of the Ad hoc Committee.
PB94-212347 *03,427*

Guidelines for Refractive Index Measurements of Asbestos.
PB95-151189 *02,543*

Telecommunications Security Guidelines for Telecommunications Management Network. Computer Security.
PB96-139415 *01,496*

GUIDES
Guide to Instrumentation Literature.
AD-A280 278/3 *02,617*

GUNS
Specification for Interoperability between Ballistic Imaging Systems. Part 1. Cartridge Cases.
PB96-195524 *01,860*

GUST FACTORS
Gust Factors Applied to Hurricane Winds.
PB95-180469 *00,446*

GUST LOADS
Gust Factors Applied to Hurricane Winds.
PB95-180469 *00,446*

HAFNIUM IONS
Observation of Pd-Like Resonance Lines Through Pt(32+) and Zn-Like Resonance Lines of Er(38+) and Hf(42+).
PB95-150637 *03,896*

Rh I Isoelectronic Sequence Observed from Er(23+) to Pt(33+).
PB95-150652 *03,898*

Spectra of Ag I Isoelectronic Sequence Observed from Er(21+) to Au(32+).
PB95-150660 *03,899*

HAFNIUM TO RADIUM
Ultraviolet Multiplet Table. Finding List for Spectra of the Elements Molybdenum to Lanthanum (Z = 42 to 57); Hafnium to Radium (Z = 72 to 88).
AD-A278 131/8 *00,709*

HAIR
Interlaboratory Comparison Studies on the Analysis of Hair for Drugs of Abuse.
PB95-176251 *03,500*

Hair Analysis for Drugs of Abuse: Evaluation of Analytical Methods, Environmental Issues, and Development of Reference Materials.
PB95-176269 *03,501*

Hair Testing for Drugs of Abuse: International Research on Standards and Technology.
PB96-120555 *03,504*

Supercritical Fluid Extraction-Immunoassay for the Rapid Screening of Cocaine in Hair.
PB96-167168 *00,637*

Interlaboratory Studies on the Analysis of Hair for Drugs of Abuse: Results from the Fifth Exercise.
PB97-110449 *03,509*

Interlaboratory Studies on the Analysis of Hair for Drugs of Abuse: Results from the Fourth Exercise.
PB97-111322 *03,510*

HALF-LIFE
New and Revised Half-Life Measurement Results.
PB96-160346 *00,695*

63Ni Half-Life: A New Experimental Determination and Critical Review.
PB97-111603 *00,700*

HALL EFFECT
Quantized Dissipation of the Quantum Hall Effect at High Currents.
PB94-199395 *04,472*

Using Quantized Breakdown Voltage Signals to Determine the Maximum Electric Fields in a Quantum Hall Effect Sample.
PB95-261947 *02,375*

Spectroscopic Study of Quantized Breakdown Voltage States of the Quantum Hall Effect.
PB96-113584 *04,730*

Potential and Current Distributions Calculated Across a Quantum Hall Effect Sample at Low and High Currents.
PB96-122106 *04,045*

Electrical Characterization of Narrow Gap n-Type Bulk HgCdTe Single Crystals by Variable-Magnetic-Field Hall Measurements and Reduced-Conductivity-Tensor Analyses.
PB96-164199 *01,146*

HALLUCINOGENS
Determination of 3-Quinuclidinyl Benzilate (Qnb) and Its Major Metabolites in Urine by Isotope Dilution Gas Chromatography Mass Spectrometry.
PB94-199379 *03,492*

HALOACETATES
Ferric Ion Assisted Photooxidation of Halocetates.
PB97-112460 *00,521*

HALOBACTERIUM
Bacteriorhodopsin Retains Its Light-Induced Proton-Pumping Function After Being Heated to 140C.
PB96-102728 *03,471*

HALOCARBONS
Retention of Halocarbons on a Hexafluoropropylene Epoxide Modified Graphitized Carbon Black. Part 1. Methane-Based Compounds.
PB95-175196 *03,272*

Retention of Halocarbons on a Hexafluoropropylene Epoxide-Modified Graphitized Carbon Black. 3. Ethene-Based Compounds.
PB96-167309 *03,286*

HALOGEN LAMPS
Characterization of Modified FEL Quartz-Halogen Lamps for Photometric Standards.
PB97-112544 *00,282*

HALOGENATED HYDROCARBONS
Suppression of High-Speed C2H4/Air Flames with C1-Halocarbons.
PB96-175724 *03,287*

Suppression of Ignition Over a Heated Metal Surface.
PB96-176425 *03,291*

HALOHYDROCARBONS
Thermochemical and Chemical Kinetic Data for Fluorinated Hydrocarbons.
PB95-260618 *01,056*

Thermodynamic Properties of Two Gaseous Halogenated Ethers from Speed-of-Sound Measurements: Difluoromethoxy-Difluoromethane and 2-Difluoromethoxy-1,1,1-Trifluoroethane.
PB96-102413 *04,189*

HALON 1301
Evaluation of Alternative In-Flight Fire Suppressants for Full-Scale Testing in Simulated Aircraft Engine Nacelles and Dry Bays.
PB94-203403 *00,023*

HALON ALTERNATIVES
Evaluation of Alternative In-Flight Fire Suppressants for Full-Scale Testing in Simulated Aircraft Engine Nacelles and Dry Bays.
PB94-203403 *00,023*

HALONS
Chemical Inhibition of Methane-Air Diffusion Flame.
PB96-195532 *01,431*

HANDBOOKS
Handbook Preferred Circuits Navy Aeronautical Electronic Equipment. Supplement Number 3.
AD-A278 782/8 *00,026*

Handbook Preferred Circuits Navy Aeronautical Electronic Equipment. Supplement Number 2.
AD-A278 783/6 *00,027*

Handbook Preferred Circuits Navy Aeronautical Electronic Equipment. Supplement Number 1.
AD-A278 784/4 *00,028*

Report of the International Commission on Radiological Units and Measurements (ICRU), 1956.
AD-A279 120/0 *03,513*

X-ray Protection.
AD-A279 132/5 *03,605*

NIST Handbook 44, 1994: Specifications, Tolerances and Other Technical Requirements for Weighing and Measuring Devices as Adopted by the 78th National Conference on Weights and Measures 1993.
PB94-136009 *02,888*

NIOSH Pocket Guide to Chemical Hazards.
PB95-100368 *03,603*

National Voluntary Laboratory Accreditation Program: Ionizing Radiation Dosimetry.
PB95-128658 *03,623*

NIST Handbook 44, 1995: Specifications, Tolerances and Other Technical Requirements for Weighing and Measuring Devices as Adopted by the 79th National Conference on Weights and Measures 1994.
PB95-146379 *02,903*

Uniform Laws and Regulations in the Areas of Legal Metrology and Motor Fuel Quality, 1994 as Adopted by the 79th National Conference on Weights and Measures 1994.
PB95-174470 *02,909*

National Voluntary Laboratory Accreditation Program: Electromagnetic Compatibility and Telecommunications. FCC Methods.
PB95-242376 *02,664*

Computer Security: An Introduction to Computer Security. The NIST Handbook.
PB96-131610 *01,608*

Airborne Asbestos Analysis: National Voluntary Laboratory Accreditation Program.
PB96-147392 *02,566*

NIST Handbook 44, 1996: Specifications, Tolerances, and Other Technical Requirements for Weighing and Measuring Devices as Adopted by the 80th National Conference on Weights and Measures, 1995.
PB96-166616 *02,926*

HANDPRINT

NIST Form-Based Handprint Recognition System.
PB94-217106 *01,838*

Component-Based Handprint Segmentation Using Adaptive Writing Style Model.
PB96-193669 *01,859*

HANDWRITING

Unconstrained Handprint Recognition Using a Limited Lexicon.
PB94-168051 *01,831*

Second Census Optical Character Recognition Systems Conference.
PB94-188711 *01,832*

NIST Form-Based Handprint Recognition System.
PB94-217106 *01,838*

Binary Decision Clustering for Neural Network Based Optical Character Recognition.
PB95-171971 *01,848*

Method and Evaluation of Character Stroke Preservation on Handprint Recognition.
PB95-251724 *01,850*

Binary Decision Clustering for Neural-Network-Based Optical Character Recognition.
PB96-186184 *01,857*

Generalized Form Registration Using Structure-Based Techniques.
PB96-191374 *01,858*

Component-Based Handprint Segmentation Using Adaptive Writing Style Model.
PB96-193669 *01,859*

HANGARS

Analysis of High Bay Hangar Facilities for Detector Sensitivity and Placement.
PB96-190210 *01,429*

HAPPYLAND SOCIAL CLUB FIRE

Analysis of the Happyland Social Club Fire with HAZARD I.
PB94-199270 *00,193*

HARD TURNING

Evaluation of a Tapered Roller Bearing Spindle for High-Precision Hard Turning Applications.
PB96-160494 *02,700*

HARMONIC DISTORTION

Effect of Harmonic Distortion on Phase Errors in Frequency Distribution and Synthesis.
PB96-200779 *01,563*

HARMONIC MIXING

High-Order Harmonic Mixing with GaAs Schottky Diodes.
PB95-108585 *01,528*

HASH ALGORITHM

Secure Hash Standard. Category: Computer Security.
FIPS PUB 180-1 *01,568*

HAZARD ASSESSMENT

HAZARD I Fire Hazard Assessment Method (Version 1.2) (for Microcomputers).
PB94-501988 *00,196*

HAZARD I Fire Hazard Assessment Method, Version 1.2 (Upgrade Package) (for Microcomputers).
PB94-501996 *00,197*

HAZARDOUS MATERIALS

Performance of Plastic Packaging for Hazardous Materials Transportation. Part 1. Mechanical Properties.
AD-A301 258/0 *02,580*

Calculation of Higher Heating Values of Biomass Materials and Waste Components from Elemental Analyses.
PB94-199254 *02,474*

Membrane Gas Separation for a Fluidized-Bed Incinerator.
PB95-169041 *02,550*

HAZARDOUS WASTES

Recommendations for the Disposal of Carbon-14 Wastes.
AD-A279 133/3 *02,579*

HAZARDS

Study on Hazard Analysis in High Integrity Software Standards and Guidelines.
PB95-198727 *01,725*

HCFC-123

Temperature Dependence of the Gas and Liquid Phase Ultraviolet Absorption Cross Sections of HCFC-123 (CF3CHCl2) and HCFC-142b (CH3CF2Cl).
PB96-201033 *03,298*

HCFC-142B

Temperature Dependence of the Gas and Liquid Phase Ultraviolet Absorption Cross Sections of HCFC-123 (CF3CHCl2) and HCFC-142b (CH3CF2Cl).
PB96-201033 *03,298*

HEAD AND NECK NEOPLASMS

New Method for Shielding Electron Beams Used for Head and Neck Cancer Treatment.
PB94-211430 *03,621*

HEADERS

Flowmeter Installation Effects Due to a Generic Header.
PB96-210893 *02,606*

HEALTH

Virtual Environments for Health Care. A White Paper for the Advanced Technology Program (ATP), the National Institute of Standards and Technology.
PB96-147814 *03,594*

HEALTH CARE

Distributed Communication Methods and Role-Based Access Control for Use in Health Care Applications.
PB96-183165 *01,508*

HEALTH HAZARDS

Lead Abatement in Buildings and Related Structures.
PB94-172038 *03,601*

NIOSH Pocket Guide to Chemical Hazards.
PB95-100368 *03,603*

HEALTH PHYSICS

Characterization of a Health Physics Instrument Calibration Range.
PB95-164554 *03,629*

External Gamma-ray Counting of Selected Tissues from a Thorotrast Patient.
PB96-160254 *03,637*

HEALTH & SAFETY

Crystal Diffraction Spectrometry for Accurate, Non-Invasive kV/Spectral Measurement for Improvement of Mammographic Image Quality.
AD-A297 943/3 *00,721*

Electron transport calculations with biomedical and environmental applications. Final report, December 23, 1992--January 31, 1994.
DE95007065 *03,613*

Properties and Interactions of Oral Structures and Restorative Materials. Annual Report for Period October 1, 1990 to September 30, 1991.
PB94-160843 *03,558*

Influence of Tempering Method on Residual Stress in Dental Porcelain.
PB94-172012 *00,138*

Calcium Phosphate Precipitation in Liposomal Suspensions.
PB94-172145 *03,452*

Octacalcium Phosphate. 3. Infrared and Raman Vibrational Spectra.
PB94-172244 *00,756*

Adsorption of Low-Molecular-Weight Sodium Polyacrylate on Hydroxyapatite.
PB94-172608 *00,139*

Interaction of Some Coupling Agents and Organic Compounds with Hydroxyapatite: Hydrogen Bonding, Adsorption and Adhesion.
PB94-172616 *00,140*

Effect of Two Initiator/Stabilizer Concentrations in a Metal Primer on Bond Strengths of a Composite to a Base Metal Alloy.
PB94-172723 *00,141*

Physicochemical Properties of Calcific Deposits Isolated from Porcine Bioprosthetic Heart Valves Removed from Patients Following 2-13 Years Function.
PB94-172863 *00,184*

Dental Materials.
PB94-172871 *00,142*

Tapered Cross-Pin Attachments for Fixed Bridges.
PB94-185238 *00,185*

Octacalcium Phosphate Carboxylates IV. Kinetics of Formation and Solubility of Octacalcium Phosphate Succinate.
PB94-185600 *00,776*

Preparation and Monitoring of Lead Acetate Containing Drinking Water Solutions for Toxicity Studies.
PB94-193885 *00,538*

Documentation for Immediately Dangerous to Life or Health Concentrations (IDLHs).
PB94-195047 *03,602*

Nutritional Status and Growth in Juvenile Rheumatoid Arthritis.
PB94-198470 *03,515*

Adhesion of Composites to Dentin and Enamel.
PB94-199049 *00,144*

Development of an Adhesive Bonding System.
PB94-199056 *00,145*

Clinical Perspective on Dentin Adhesives.
PB94-211240 *00,146*

Selective Inhibition of Crystal Growth on Octacalcium Phosphate and Nonstoichiometric Hydroxyapatite by Pyrophosphate at Physiological Concentration.
PB94-211257 *00,147*

New Method for Shielding Electron Beams Used for Head and Neck Cancer Treatment.
PB94-211430 *03,621*

Periapical Tissue Reactions to a Calcium Phosphate Cement in the Teeth of Monkeys.
PB94-212008 *00,149*

Effect of Three Sterilization Techniques on Finger Pluggers.
PB94-216090 *00,150*

Paffenbarger Research Center: The Cutting Edge of Dental Science.
PB94-216355 *00,151*

NIOSH Pocket Guide to Chemical Hazards.
PB95-100368 *03,603*

Evaluation of Fracture Toughness and Residual Stress in Dental Porcelain by Indentation-Microfracture Method.
PB95-125613 *00,154*

Image Information Transfer Properties of X-Ray Intensifying Screens in the Energy Range from 17 to 320 keV.
PB95-126173 *00,155*

Effects of Surface-Active Resins on Dentin/Composite Bonds.
PB95-140448 *00,156*

Deposition of Loosely Bound and Firmly Bound Fluorides on Tooth Enamel by an Acidic Gel Containing Fluorosilicate and Monocalcium Phosphate Monohydrate.
PB95-150710 *03,559*

Effects of Calcium Phosphate Solutions on Dentin Permeability.
PB95-151080 *00,157*

Modified Surface-Active Monomers for Adhesive Bonding to Dentin.
PB95-151163 *00,158*

NIR-Spectroscopic Investigation of Water Sorption Characteristics of Dental Resins and Composites.
PB95-151171 *00,189*

Distribution of Fluoride in Saliva and Plaque Fluid After a 0.048 mol/L NaF Rinse.
PB95-151205 *03,561*

Evaluation of Fracture Toughness and Residual Stress in Dental Porcelain by Indentation-Microfracture Method.
PB95-152831 *00,159*

Publication and Presentation Abstracts, 1993. (Published by Paffenbarger Research Center and Center of Excellence for Materials Science Research).
PB95-153052 *03,562*

Effects on Whole Saliva of Chewing Gums Containing Calcium Phosphates.
PB95-153169 *03,563*

Noninvasive High-Voltage Measurement in Mammography by Crystal Diffraction Spectroscopy.
PB95-153417 *00,160*

Octacalcium Phosphate Carboxylates. 1. Preparation and Identification.
PB95-161535 *00,660*

Octacalcium Phosphate Carboxylates. 2. Characterization and Structural Consideration.
PB95-161543 *00,955*

Wear of Human Enamel against a Commercial Castable Ceramic Restorative Material.
PB95-161972 *00,161*

Ring-Opening Dental Resin Systems Based on Cyclic Acetals.
PB95-162251 *00,162*

Effect of Ethanol on the Solubility of Dicalcium Phosphate Dihydrate in the System Ca(OH)2-H3PO4-H2O at 37C.
PB95-163507 *00,163*

Procedure for the Study of Acidic Calcium Phosphate Precursor Phases in Enamel Mineral Formation.
PB95-164448 *03,564*

Effects of Aluminum Oxalate/Glycine Pretreatment Solutions on Dentin Permeability.
PB95-164505 *03,565*

Evaluation of Methylene Lactone Monomers in Dental Resins.
PB95-164661 *00,164*

Behavior of a Calcium Phosphate Cement in Simulated Blood Plasma In vitro.
PB95-168712 *00,165*

Octacalcium Phosphate Carboxylates. 5. Incorporation of Excess Succinate and Ammonium Ions in the Octacalcium Phosphate Succinate Structure.
PB95-168894 *00,166*

Ambient Temperature Synthesis of Bulk Intermetallics.
PB95-169074 *00,168*

Effect of 1-Hydroxyethylidene-1,1-Bisphosphonate on Membrane-Mediated Calcium Phosphate Formation in Model Liposomal Suspensions.
PB95-169223 *03,469*

Effect of Ethanol on the Solubility of Hydroxyapatite in the System Ca(OH)2-H3PO4-H2O at 25C and 33C.
PB95-169231 *00,169*

Interaction of Chlorhexidine Digluconate with and Adsorption of Chlorhexidine on Hydroxyapatite.
PB95-175907 *03,566*

Ring-Opening Polymerication of a 2-Methylene Spiro Orthocarbonate Bearing a Pendant Methacrylate Group.
PB95-176145 *01,268*

Physical and Chemical Properties of Resin-Reinforced Calcium Phosphate Cements.
PB95-180212 *00,171*

Diagnosis and Treatment of an Oral Base-Metal Contact Lesion Following Negative Dermatologic Patch Tests.
PB95-180626 *00,172*

Formation of Hydroxyapatite in a Polymeric Calcium Phosphate Cement.
PB95-180642 *00,173*

NIOSH Comments to DOL on Risk Estimates from the Cadmium Cohort Study by L. Stayner, February 7, 1992.
PB95-267779 *03,604*

Remineralization of Root Lesions with Concentrated Calcium and Phosphate Solutions.
PB96-102140 03,567

Reduction of Marginal Gaps in Composite Restorations by Use of Glass-Ceramic Inserts.
PB96-102405 00,174

Crystal Structure of a New Monoclinic Form of Potassium Dihydrogen Phosphate Containing Orthophosphacidium Ion, (H4PO4)(sup+1).
PB96-111794 04,725

Publications and Presentation Abstracts, 1995. (Published by Paffenbarger Research Center and Center of Excellence for Materials Science Research).
PB96-119250 03,568

In vitro Fracture Behavior of Ceramic and Metal-Ceramic Restorations.
PB96-119722 03,569

Failure of All-Ceramic Fixed Partial Dentures 'In vitro' and 'In vivo': Analysis and Modeling.
PB96-122536 00,175

Dental Applications of Ceramics.
PB96-122940 00,177

Intensive Swimming: Can It Affect Your Patients' Smiles.
PB96-123666 03,570

Effect of Supersaturation on Apatite Crystal Formation in Aqueous Solutions at Physiologic pH and Temperature.
PB96-135215 03,571

Bioactive Polymeric Dental Materials Based on Amorphous Calcium Phosphate.
PB96-147012 03,572

Remineralizing Dental Composites Based on Amorphous Calcium Phosphate.
PB96-147020 03,573

Polymeric Calcium Phosphate Composites with Remineralization Potential.
PB96-155544 03,575

Physicochemical Characterization of Natural and Bioprosthetic Heart Valve Calcific Deposits: Implications for Prevention.
PB96-156039 00,187

Reinforcement of Cancellous Bone Screws with Calcium Phosphate Cement.
PB96-158001 00,179

Commentary on 'Optimization of Experimental Parameters for the EPR Detection of the Cellulosic Radical in Irradiated Foodstuffs'.
PB96-164124 00,043

Polymeric Calcium Phosphate Cements Derived from Poly(methyl vinyl ether-maleic acid).
PB96-164264 00,180

Publication and Presentation Abstracts, 1994.
PB96-176623 03,577

Wear of Enamel against Glass-Ceramic, Porcelain, and Amalgam.
PB96-179593 03,082

Composition and Solubility Product of a Synthetic Calcium Hydroxyapatite.
PB96-180104 02,995

Adsorption of Potassium N-phenylglycinate on Hydroxyapatite: Role of Solvents and Ionic Charge.
PB96-180161 01,159

In vitro Inhibition of Membrane-Mediated Calcification by Novel Phosphonates.
PB96-201140 03,595

New Surface-Active Comonomer for Adhesive Bonding.
PB96-204052 03,579

Calcium Phosphate Cements.
PB97-111595 03,580

Adsorption of Polyacrylic Acids and Their Sodium Salts on Hydroxyapatite: Effect of Relative Molar Mass.
PB97-112510 03,581

Posterior Restorative Materials Research.
PB97-118624 03,582

Overview of Bioelectrical Impedance Analyzers.
PB97-118780 00,181

Surface Roughness of Glass-Ceramic Insert. Composite Restorations: Assessing Several Polishing Techniques.
PB97-119010 03,583

Interaction of Citric Acid with Hydroxyapatite: Surface Exchange of Ions and Precipitation of Calcium Citrate.
PB97-119309 03,584

Publication and Presentation Abstracts, 1996.
PB97-122238 03,585

HEART VALVE PROSTHESIS

Physicochemical Properties of Calcific Deposits Isolated from Porcine Bioprosthetic Heart Valves Removed from Patients Following 2-13 Years Function.
PB94-172863 00,184

Critical Evaluation of the Purification of Biominerals by Hypochlorite Treatment.
PB95-150959 00,186

HEART VALVE PROTHESIS

Physicochemical Characterization of Natural and Bioprosthetic Heart Valve Calcific Deposits: Implications for Prevention.
PB96-156039 00,187

HEAT

Effective Measurement Techniques for Heat, Smoke, and Toxic Fire Gases.
PB94-198439 01,369

Effects of Copper, Nickel and Boron on Mechanical Properties of Low-Alloy Steel Weld Metals Deposited at High Heat Input.
PB96-135231 03,363

HEAT CAPACITIES

Thermodynamic Properties of Silicides. 5. Standard Molar Enthalpy of Formation at the Temperature 298.15 K of Trimolybdenum Monosilicide Mo3Si Determined by Fluorine-Combustion Calorimetry.
PB97-119358 01,190

HEAT CAPACITY

Molar Heat Capacity at Constant Volume for Air from 67 to 300 K at Pressures to 35 MPa.
PB96-163738 00,515

Molar Heat Capacity at Constant Volume for (xCO2 + (1-x)C2H6) from 220 to 340 K at Pressures to 35 MPa.
PB96-167135 01,148

Extrapolation of the Heat Capacity in Liquid and Amorphous Phases.
PB97-111421 04,147

HEAT DETECTORS

Studies Assess Performance of Residential Detectors.
PB94-199262 00,290

HEAT EXCHANGERS

Review of Corrosion Behavior of Ceramic Heat Exchanger Materals: Corrosion Characteristics of Silicon Carbide and Silicon Nitride. Final Report, September 11, 1992--March 11, 1993.
DE93041307 03,228

Theoretical Evaluation of the Vapor Compression Cycle with a Liquid-Line/Suction-Line Heat Exchanger, Economizer, and Ejector.
PB95-216917 02,607

Upgrade and Modernization Projects at the NBSR.
PB96-161872 03,737

HEAT EXCHANGES

Effect of Inclination on the Performance of a Compact Brazed Plate Condenser and Evaporator.
PB96-136973 02,756

HEAT FEEDBACK

Measurement of Radiative Feedback to the Fuel Surface of a Pool Fire.
PB94-211604 02,477

HEAT FLOWMETERS

Comparison of Heat-Flow-Meter Tests from Four Laboratories.
PB95-126264 00,365

HEAT FLUX

Ignition and Subsequent Transition to Flame Spread in a Microgravity Environment.
N96-15584/1 04,828

Effects of Specimen Edge Conditions on Heat Release Rate.
PB95-152864 00,375

Burning Rate and Flame Heat Flux For PMMA in the Cone Calorimeter.
PB95-216990 00,393

Heat Flux from Flames to Vertical Surfaces.
PB97-110357 01,438

HEAT FLUXES

Low Heat-Flux Measurements: Some Precautions.
PB96-201116 02,685

HEAT LOSS

Estimate of Flame Radiance via a Single Location Measurement in Liquid Pool Flames.
PB94-211596 02,476

Estimate of the Effect of Scale on Radiative Heat Loss Fraction and Combustion Efficiency.
PB95-150447 02,486

HEAT MEASUREMENT

Assessing the Credibility of the Calorific Content of Muncipal Solid Waste.
PB94-199882 02,581

Comparison of Heat-Flow-Meter Tests from Four Laboratories.
PB95-126264 00,365

Thermochemistry of the Hydrolysis of L-arginine to (L-citrulline + Ammonia) and of the Hydrolysis of L-arginine to (L-ornithine + Urea).
PB95-150801 03,463

Biological Thermodynamic Data for the Calibration of Differential Scanning Calorimeters: Dynamic Temperature Data on the Gel to Liquid Crystal Phase Transition of Dialkylphosphatidylcholine in Water Suspensions.
PB95-162707 03,464

Thermodynamics of the Binding of Galactopyranoside Derivatives to the Basic Lectin from Winged Bean (Psophocarpus Tetrogonolobus).
PB95-162715 03,465

HEAT METERS

Control Stability of a Heat-Flow-Meter Appartus.
PB95-181194 00,386

Intra-Laboratory Comparison of a Line-Heat-Source Guarded Hot Plate and Heat-Flow-Meter Apparatus.
PB95-181202 00,387

HEAT OF COMBUSTION

Precise Measurement of Heat of Combustion with a Bomb Calorimeter.
AD-A286 701/8 03,770

Assessing the Credibility of the Calorific Content of Muncipal Solid Waste.
PB94-199882 02,581

HEAT OF FUSION

Calibration Standards for Differential Scanning Calorimetry. 1. Zinc Absolute Calorimetric Measurement of Enthalpy of Fusion and Temperature of Fusion HM.
PB94-199817 00,801

Measurement of the Heat of Fusion of Tungsten by a Microsecond-Resolution Transient Technique.
PB94-216686 03,400

HEAT OF REACTION

Thermodynamic and NMR Study of the Interactions of Cyclodextrins with Cyclohexane Derivatives.
PB94-185816 00,781

Calorimetric Determination of the Standard Transformed Enthalpy of a Biochemical Reaction at Specified PH and pMg.
PB94-198249 03,454

HEAT PUMPS

Study of Heat Pump Performance Using Mixtures of R32/R134a and R32/R125/R134a as 'Drop-In' Working Fluids for R22 with and Without a Liquid-Suction Heat Exchanger.
PB94-218559 02,503

Simple Method of Composition Shifting with a Distillation Column for a Heat Pump Employing a Zeotropic Refrigerant Mixture.
PB95-255824 02,603

HVAC CAD Layout Tools: A Case Study of University/Industry Collaboration.
PB97-112221 00,281

HEAT RELEASE RATE

New Concepts for Fire Protection of Passenger Rail Transportation Vehicles. (NIST Reprint).
PB95-180774 04,863

Effects of Sample Mounting on Flammability Properties of Intumescent Polymers.
PB96-159777 03,389

HEAT SHOCK PROTEINS

DnaJ, DnaK, and GrpE Heat Shock Proteins are Required in 'ori'P1 DNA Replication Solely at the RepA Monomerization Step.
PB97-119382 03,557

HEAT-SHOCK PROTEINS 60

Function of DnaJ and DnaK as Chaperones in Origin-Specific DNA Binding by RepA.
PB95-151544 03,533

HEAT-SHOCK PROTEINS 70

Function of DnaJ and DnaK as Chaperones in Origin-Specific DNA Binding by RepA.
PB95-151544 03,533

HEAT TRANSFER

Survey of the Literature on Heat Transfer from Solid Surfaces to Cryogenic Fluids.
AD-A286 680/4 04,193

Single-Phase Heat Transfer and Pressure Drop Characteristics of an Integral-Spine-Fin Within an Annulus.
PB94-194073 03,805

Rate of Heat Release of Wood Products.
PB94-212404 03,403

Heat Transfer in Thin, Compact Heat Exchangers with Circular, Rectangular, or Pin-Fin Flow Passages.
PB95-140943 02,751

Heat and Moisture Transfer in Wood-Based Wall Construction: Measured versus Predicted.
PB95-200655 00,391

Calorimetric and Visual Measurements of R123 Pool Boiling on Four Enhanced Surfaces.
PB96-128129 04,053

Natural Convection from an Array of Electronic Packages Mounted on a Horizontal Board in a Narrow Aspect Ratio Enclosure.
PB96-164017 02,087

Experimental Verification of a Moisture and Heat Transfer Model in the Hygroscopic Regime.
PB97-111546 00,309

Test Procedures for Advanced Insulation Panels.
PB97-111892 00,415

Empirical Validation of a Transient Computer Model for Combined Heat and Moisture Transfer.
PB97-111991 00,416

Single-Phase Heat Transfer and Pressure Drop Characteristics of an Integral-Spine Fin Within an Annulus.
PB97-122386 04,179

HEAT TRANSFER COEFFICIENTS

Causes of the Apparent Heat Transfer Degradation for Refrigerant Mixtures.
PB94-212701 03,259

HEAT TRANSMISSION

Numerical Analysis Support for Compartment Fire Modeling and Incorporation of Heat Conduction into a Zone Fire Model.
PB94-156965 01,357

Behavior of Mock-Ups in the California Technical Bulletin 133 Test Protocol: Fabric and Barrier Effects.
PB95-231585 00,301

HEAT TREATMENT

Determination of the Prior-Austenitic Grain Size of Selected Steels Using a Molten Glass Etch.
PB94-211927 03,208

HEATING SYSTEMS
Multizone Modeling of Three Residential Indoor Air Quality Control Options.
PB96-165782 *02,567*

HEAVY METALS
Genetically Engineered Pore as a Metal Ion Biosensor.
PB96-161658 *03,551*

HELIUM
Helium Refrigeration and Liquefaction Using a Liquid Hydrogen Refrigerator for Precooling.
AD-A286 683/8 *02,749*

High-Energy Behavior of the Double Photoionization of Helium from 2 to 12 keV.
PB94-213279 *03,860*

Operational Mode and Gas Species Effects on Rotational Drag in Pneumatic Dead Weight Pressure Gages.
PB95-140182 *00,903*

Ab initio Calculations for Helium: A Standard for Transport Property Measurements.
PB96-102041 *01,060*

Search for Small Violations of the Symmetrization Postulate in an Excited State of Helium.
PB96-123518 *04,050*

Kinetic-Energy Distributions of Ions Sampled from Radio-Frequency Discharges in Helium, Nitrogen, and Oxygen.
PB96-123732 *01,092*

Electronically Tunable Fiber Laser for Optical Pumping of (3)He and (4)He.
PB96-201165 *04,381*

Commercial Helium Permeation Leak Standards: Their Properties and Reliability.
PB97-111413 *04,146*

Absence of Quantum-Mechanical Effects on the Mobility of Argon Ions in Helium Gas at 4.35 K.
PB97-122543 *01,194*

HELIUM COMPLEXES
Signatures of Large Amplitude Motion in a Weakly Bound Complex: High-Resolution IR Spectroscopy and Quantum Calculations for HeCO2.
PB95-203485 *01,054*

HELIUM IONS
Use of an Ion Energy Analyzer: Mass Spectrometer to Measure Ion Kinetic-Energy Distributions from RF Discharges in Argon-Helium Gas Mixtures.
PB94-185717 *04,406*

HELIUM-LIKE IONS
Evaluation of Two-Photon Exchange Graphs for Highly-Charged Heliumlike Ions.
PB94-198918 *03,808*

Experimental Aspects and Z-Dependent Systematics in One- and Two-Electron Ions and Single Vacancy Systems.
PB94-199627 *03,815*

HELIUM SPECTROSCOPY
Frequency-Stabilized LNA Laser at 1.083 mum: Application to the Manipulation of Helium 4 Atoms.
PB95-176186 *04,304*

HELMET MOUNTED DISPLAYS
NIST Construction Automation Program Report No. 2. Proceedings of the NIST Construction Automation Workshop. Held in Gaithersburg, Maryland on March 30-31, 1995.
PB96-202239 *00,413*

HELMHOLTZ RESONATORS
Greenspan Acoustic Viscometer for Gases.
PB96-204417 *04,220*

HEMOGLOBIN
Positive and Negative Cooperativities at Subsequent Steps of Oxygenation Regulate the Allosteric Behavior of Multistate Sebacylhemoglobin.
PB97-119374 *03,486*

HEMOLYSIN
Genetically Engineered Pores as Metal Ion Biosensors.
PB96-167408 *03,553*

HEMOLYSIS
Genetically Engineered Pores for New Materials.
PB96-161641 *03,550*

HENDERSON METHOD
Anova Estimates of Variance Components for a Class of Mixed Models.
PB96-141163 *03,448*

HEPARIN
Thermodynamic Analysis of Heparin Binding to Human Antithrombin.
PB94-199593 *03,455*

Physicochemical Characterization of Low Molecular Weight Heparin.
PB96-112040 *03,474*

Structural Analysis of Heparin by Raman Spectroscopy.
PB96-167226 *03,480*

HEPARINS
Physical Characterization of Herparin by Light Scattering.
PB96-119383 *03,598*

HEPTANE
Simultaneous Optical Measurement of Soot Volume Fraction, Temperature, and CO2 in Heptane Pool Fire.
PB96-102132 *01,397*

HERTZIAN CONTACT
Deformation and Fracture of Mica-Containing Glass-Ceramics in Hertzian Contacts.
PB96-179452 *03,080*

Effect of Grain Size on Hertzian Contact Damage in Alumina.
PB96-179601 *03,083*

HETERODYNE DETECTION
Heterodyne Mixing and Direct Detection in High Temperature Josephson Junctions.
PB96-147202 *01,565*

HETERODYNE MIXERS
Terahertz Detectors Based on Superconducting Kinetic Inductance.
PB95-168647 *02,160*

HETERODYNING
30 THz Mixing Experiments on High Temperature Superconducting Josephson Junctions.
PB96-102462 *04,709*

HETEROGENEITY
Structural Heterogeneity in Epoxies.
PB95-151866 *01,243*

HETEROJUNCTIONS
Scaling of the Nonlinear Optical Cross Sections of GaAs-AlGaAs Multiple Quantum-Well Hetero n-i-p-i's.
PB96-102793 *02,183*

HEURISTIC METHODS
Move-to-Root Rule for Self-Organizing Trees with Markov Dependent Requests.
PB96-179528 *03,431*

HEXACARBONYLMOLYBDENUM
Photodecomposition of Mo(CO)6/Si(111) 7x7: CO State-Resolved Evidence for Excited State Relaxation and Quenching.
PB95-180154 *01,009*

HEXAFLUOROPROPANE
Thermodynamic Properties of CF3-CHF-CHF2, 1,1,1,2,3,3-Hexafluoropropane.
PB97-118384 *03,299*

HEXANES
Observations of Partial Discharges in Hexane Under High Magnification.
PB95-163127 *01,900*

Vapor-Liquid Equilibria of Mixtures of Propane and Isomeric Hexanes.
PB95-175287 *00,995*

Electrohydrodynamic Instability and Electrical Discharge Initiation in Hexane.
PB96-186119 *02,244*

HFC-236EA
Thermodynamic Properties of CF3-CHF-CHF2, 1,1,1,2,3,3-Hexafluoropropane.
PB97-118384 *03,299*

HFC-245CA
Thermodynamic Properties of CHF2-CF2-CHF, 1,1,2,2,3-Pentafluoropropane.
PB97-118392 *03,300*

HIERARCHIES
Hierarchical Real-Time Control System for Use with Coal Mining Automation.
PB94-212065 *03,698*

HIGH ELECTRON MOBILITY TRANSISTORS
Multicarrier Characterization Method for Extracting Mobilities and Carrier Densities of Semiconductors from Variable Magnetic Field Measurements.
PB94-212776 *02,317*

Influence of Lattice Mismatch on Indium Phosphide Based High Electron Mobility Transistor (HEMT) Structures Observed in High Resolution Monochromatic Synchrotron X-Radiation Diffraction Imaging.
PB95-164679 *02,357*

HIGH INTEGRITY
High Integrity Software Standards Activities at NIST.
PB96-112214 *01,744*

Report of a Workshop on the Assurance of High Integrity Software.
PB96-161377 *01,763*

Standards for High Integrity Software.
PB96-161385 *01,764*

HIGH INTEGRITY SOFTWARE
C++ in Safety Critical Systems.
PB96-154588 *01,750*

HIGH LEVEL RADIOACTIVE WASTES
Information Retrieval Using Key Words and a Structured Review.
PB95-161121 *03,724*

HIGH-PERFORMANCE CONCRETES
High-Performance Concrete: Research Needs to Enhance Its Use.
PB95-180147 *01,322*

HIGH PRESSURE
Molar Heat Capacity at Constant Volume for (xCO2 + (1-x)C2H6) from 220 to 340 K at Pressures to 35 MPa.
PB96-167135 *01,148*

Isochoric (p-p-T) Measurements on Liquid and Gaseous Air from 67 to 400 K at Pressures to 35 MPa.
PB96-167390 *01,154*

Alvin Van Valkenburg and the Diamond Anvil Cell.
PB96-204474 *04,797*

HIGH PRESSURE CELLS
High-Pressure Equilibrium Cell for Solubility Measurements in Supercritical Fluids.
PB95-175634 *00,998*

HIGH PRESSURE TESTS
1,4-Dinitrocubane and Cubane under High Pressure.
PB95-108437 *03,755*

HIGH RESOLUTION
Intermolecular HF Motion in Ar(sub n)HF Micromatrices (n=1,2,3,4,): Classical and Quantum Calculations on a Pairwise Additive Potential Surface.
PB95-107025 *03,871*

Mode Specific Vibrational Predissociation Dynamics in Fragile Molecules.
PB95-107132 *00,871*

Vibration, Rotation, and Parity Specific Predissociation Dynamics in Asymmetric OH Stretch Excited ArH2O: A Half Collision Study of Resonant V-V Energy Transfer in a Weakly Bound Complex.
PB95-107140 *00,872*

Making Displays Deliver a Full Measure.
PB96-122411 *01,490*

Potential Surfaces and Dynamics of Weakly Bound Trimers: Perspectives from High Resolution IR Spectroscopy.
PB96-176508 *01,155*

HIGH-SPEED MEASUREMENTS
Simultaneous Measurement of Normal Spectral Emissivity by Spectral Radiometry and Laser Polarimetry at High Temperatures in Pulse-Heating Experiments: Application to Molybdenum and Tungsten.
PB97-118376 *02,694*

HIGH-SPEED TECHNIQUES
Issues in High-Speed Pyrometry.
PB97-118368 *02,693*

HIGH STRENGTH CONCRETE
Effects of Testing Variables on the Measured Compressive Strength of High-Strength (90 MPa) Concrete.
PB95-179040 *00,445*

Effects of Testing Variables on the Strength of High-Strength (90 Mpa) Concrete Cylinders.
PB96-112198 *00,456*

HIGH SULFUR COAL
Sulfur Dioxide Capture in the Combustion of Mixtures of Lime, Refuse-Derived Fuel, and Coal.
PB94-155587 *02,534*

HIGH-TC SUPERCONDUCTORS
Flame Synthesis of High Tc Superconductors.
PB95-151981 *00,659*

Effects of Critical Current Density, Equilibrium Magnetization and Surface Barrier on Magnetization of High Temperature Superconductors.
PB95-153060 *04,588*

Preparation of Low Resistivity Contacts for High-Tc Superconductors.
PB95-153557 *02,258*

Dependence of Tc on Debye Temperature Theta(sub D) for Various Cuprates.
PB95-180493 *04,683*

Hole Dispersion and Enhancement of Antiferromagnetic Interaction of Localized Spins in High-Tc Superconductors.
PB95-202602 *04,694*

Effect of Magnetic Field Orientation on the Critical Current of HTS Conductor and Coils.
PB96-141189 *02,956*

First VAMAS USA Interlaboratory Comparison of High Temperature Superconductor Critical Current Measurements.
PB96-147178 *04,768*

HIGH TEMPERATURE
PC-Based Prototype Expert System for Data Management and Analysis of Creep and Fatigue of Selected Materials at Elevated Temperatures.
PB94-172251 *03,202*

Rate Constants for Hydrogem Atom Attack on Some Chlorinated Benzenes at High Temperature.
PB94-200581 *00,810*

High Temperature.
PB94-211737 *03,844*

Measurement of Surface Tension of Tantalum by a Dynamic Technique in a Microgravity Environment.
PB95-161667 *03,932*

Critical Current and Normal Resistance of High-Tc Step-Edge SNS Junctions.
PB96-111752 *04,724*

High-Temperature Superconductor Cryogenic Current Comparator.
PB96-119334 *02,074*

HIGH TEMPERATURE ELECTRONICS
Boron-Implanted 6H-SiC Diodes.
PB96-159678 *04,081*

HIGH TEMPERATURE ENVIRONMENTS
Dynamic Measurements of Thermophysical Properties of Metals and Alloys at High Temperatures by Subsecond Pulse Heating Techniques.
N94-25124/6 *03,309*

HIGH TEMPERATURE SUPERCONDUCTING
Thermal Isolation of High-Temperature Superconducting Thin Films Using Silicon Wafer Bonding and Micromachining.
PB96-135017 *02,408*

HIGH TEMPERATURE SUPERCONDUCTOR
Growth of Laser Ablated YBa2Cu3O7-delta Films as Examined by Rheed and Scanning Tunneling Microscopy.
PB95-162541 *04,614*

HIGH TEMPERATURE SUPERCONDUCTORS
Effects of Critical Current Density, Equilibrium Magnetization and Surface Barrier on Magnetization of High Temperature Superconductors.
PB94-185162 *04,446*

Experimental Constraints on Some Mechanisms for High-Temperature Superconductivity.
PB94-198553 *04,463*

Anharmonic Phonons and the Isotope Effect in Superconductivity.
PB94-200557 *04,486*

YBa2Cu3O7-x to Si Interconnection for Hybrid Superconductor/Semiconductor Integration.
PB94-211711 *02,315*

Offset Susceptibility of Superconductors.
PB94-212263 *04,503*

Efficient Experiment to Study Superconducting Ceramics.
PB94-212578 *04,505*

Asymmetry between Flux Penetration and Flux Expulsion in Tl-2212 Superconductors.
PB95-125647 *04,527*

Magnetic Measurement of Transport Critical Current Density of Granular Superconductors.
PB95-126199 *04,531*

Insulating Nanoparticles on YBa2Cu3O7-delta Thin Films Revealed by Comparison of Atomic Force and Scanning Tunneling Microscopy.
PB95-150843 *04,575*

X-Ray Characterization of the Crystallization Process of High-Tc Superconducting Oxides in the Sr-Bi-Pb-Ca-Cu-O System.
PB95-151700 *04,579*

Crystal Chemistry and Phase Equilibrium Studies of the BaO(BaCO3)-R2O3-CuO Systems. 5. Melting Relations in Ba2(Y,Nd,Eu)Cu3O6+x.
PB95-151718 *04,580*

X-Ray-Diffraction Study of a Thermomechanically Detwinned Single Crystal of YBa2Cu3O6+x.
PB95-151726 *04,581*

Flame Synthesis of High Tc Superconductors.
PB95-151981 *00,659*

Coupled-Bilayer Two-Dimensional Magnetic Order of the Dy Ions in Dy2Ba4Cu7O15.
PB95-152104 *04,584*

Effects of Critical Current Density, Equilibrium Magnetization and Surface Barrier on Magnetization of High Temperature Superconductors.
PB95-153060 *04,588*

Transverse Thermomagnetic Effects in the Mixed State and Lower Critical Field of High-Tc Superconductors.
PB95-153250 *04,590*

Preparation of Low Resistivity Contacts for High-Tc Superconductors.
PB95-153557 *02,258*

Improved Uniaxial Strain Tolerance of the Critical Current Measured in Ag-Sheathed Bi2Sr2Ca1Cu2O8+x Superconductors.
PB95-153565 *04,594*

Calibration of High-Energy Electron Beams by Use of Graphite Calorimeters.
PB95-161113 *04,598*

Harmonic and Static Susceptibilities of YBa2Cu3O7.
PB95-161139 *04,599*

Hydrogen in YBa2Cu3Ox: A Neutron Spectroscopy and a Nuclear Magnetic Resonance Study.
PB95-161279 *04,601*

Grain Alignment and Transport Properties of Bi2Sr2CaCu2O8 Grown by Laser Heated Float Zone Method.
PB95-161451 *04,602*

Effects of Anneal Time and Cooling Rate on the Formation and Texture of Bi2Sr2CaCu2O8 Films.
PB95-161600 *04,603*

Tunneling Spectroscopy of Thallium-Based High-Temperature Superconductors.
PB95-161709 *04,606*

Temperature Dependence of Vortex Twin Boundary Interaction in Yttrium Barium Copper Oxide (YBa2Cu3O6+x).
PB95-162442 *04,613*

Observation of Insulating Nanoparticles on YBCO Thin-Films by Atomic Force Microscopy.
PB95-163358 *04,622*

Determination of Thermoactivation Parameters of Vortex Mobility in YBa2Cu3O7 Using Only Magnetic Measurements.
PB95-163499 *04,624*

High Critical Temperature Superconductor Tunneling Spectroscopy Using Squeezable Electron Tunneling Junctions.
PB95-163721 *04,627*

Tunneling Measurement of the Zero-Bias Conductance Peak and the Bi-Sr-Ca-Cu-O Thin-Film Energy Gap.
PB95-163739 *04,628*

Thermal and Nonequilibrium Responses of Superconductors for Radiation Detectors.
PB95-164232 *02,156*

High Current Pressure Contacts to Ag Pads on Thin Film Superconductors.
PB95-168621 *04,639*

From Superconductivity to Supernovae: The Ginzburg Symposium. Report on the Symposium Held in Honor of Vitaly L. Ginzburg. Held in Gaithersburg, Maryland on May 22, 1992.
PB95-171963 *04,649*

Standard Reference Devices for High Temperature Superconductor Critical Current Measurements.
PB95-175543 *04,659*

Mutual Phase Locking in Systems of High-Tc Superconductor-Normal Metal-Superconductor Junctions.
PB96-135348 *04,744*

Influence of Films' Thickness and Air Gaps in Surface Impedance Measurements of High Temperature Superconductors Using the Dielectric Resonator Technique.
PB96-157862 *01,946*

High-Tc Multilayer Step-Edge Josephson Junctions and SQUIDs.
PB96-200183 *04,790*

HIGH TEMPERATURE TESTS
Recent Experimental and Modeling Developments in High Temperature Thermochemistry.
PB94-172343 *00,759*

High-Temperature Laser-Pulse Thermal Diffusivity Apparatus.
PB94-185147 *02,631*

Millisecond-Resolution Pulse Heating System for Specific-Heat Measurements at High Temperatures.
PB94-199999 *02,635*

Effects of Humidity and Elevated Temperature on the Density and Thermal Conductivity of a Rigid Polyisocyanurate Foam Co-Blown with CCl3F and CO2.
PB95-150462 *00,371*

Effects of Humidity and Elevated Temperature on the Density and Thermal Conductivity of a Rigid Polyisocyanurate Foam.
PB95-152021 *00,373*

HIGH TEMPERATURE THERMOMETRY
Investigation of High-Temperature Platinum Resistance Thermometers at Temperatures Up to 962C, and, in Some Cases, 1064C.
PB96-161294 *00,629*

HIGH VOLTAGE
Investigation of the Effects of Aging on the Calibration of a Kerr-Cell Measuring System for High Voltage Impulses.
PB94-172384 *02,025*

Comparative Measurements of High-Voltage Impulses Using a Kerr Cell and a Resistor Divider.
PB94-172582 *02,028*

Approach to Setting Performance Requirements for Automated Evaluation of the Parameters of High-Voltage Impulses.
PB94-185634 *01,878*

Digital Techniques in HV Tests - Summary of 1989 Panel Session.
PB94-216702 *02,035*

HIGHLY CHARGED IONS
Beam Line for Highly Charged Ions.
PB97-111256 *04,143*

HIGHWAY COMMUNICATION
Recommendations on Selection of Vehicle-to-Roadside Communications Standards for Commercial Vehicle Operations.
PB94-195914 *04,859*

Vehicle-to-Roadside Communications for Commercial Vehicle Operations: Requirements and Approaches.
PB95-188827 *04,860*

HIGHWAY CONSTRUCTION
National Voluntary Laboratory Accreditation Program: Construction Materials Testing.
PB95-155552 *01,319*

Robotics Application to Highway Transportation. Volume 4. Proposals for Potential Research.
PB95-193173 *01,339*

Study of Potential Applications of Automation and Robotics Technology in Construction, Maintenance and Operation of Highway Systems: A Final Report. Volume 4.
PB95-251641 *01,340*

Study of Potential Applications of Automation and Robotics Technology in Construction, Maintenance and Operation of Highway Systems: A Final Report. Volume 1.
PB95-251682 *01,341*

Study of Potential Applications of Automation and Robotics Technology in Construction, Maintenance and Operation of Highway Systems: A Final Report. Volume 3.
PB95-251690 *01,342*

Study of Potential Applications of Automation and Robotics Technology in Construction, Maintenance and Operation of Highway Systems: A Final Report. Volume 2.
PB95-255865 *01,343*

HIGHWAY MAINTENANCE
Highway Concrete (HWYCON) Expert System User Reference and Enhancement Guide.
PB94-215670 *01,316*

Robotics Application to Highway Transportation. Volume 4. Proposals for Potential Research.
PB95-193173 *01,339*

Study of Potential Applications of Automation and Robotics Technology in Construction, Maintenance and Operation of Highway Systems: A Final Report. Volume 4.
PB95-251641 *01,340*

Study of Potential Applications of Automation and Robotics Technology in Construction, Maintenance and Operation of Highway Systems: A Final Report. Volume 1.
PB95-251682 *01,341*

Study of Potential Applications of Automation and Robotics Technology in Construction, Maintenance and Operation of Highway Systems: A Final Report. Volume 3.
PB95-251690 *01,342*

Study of Potential Applications of Automation and Robotics Technology in Construction, Maintenance and Operation of Highway Systems: A Final Report. Volume 2.
PB95-255865 *01,343*

HIGHWAY MANAGEMENT
Robotics Application to Highway Transportation. Volume 4. Proposals for Potential Research.
PB95-193173 *01,339*

HIGHWAY TRANSPORTATION
Robotics Application to Highway Transportation. Volume 2. Literature Search.
PB95-170551 *01,337*

Robotics Application to Highway Transportation. Volume 3. Proposed Research Topics and Cost/Benefit Evaluations by CERF.
PB95-171633 *01,338*

HIGHWAYS
Binder Characterization and Evaluation by Nuclear Magnetic Resonance Spectroscopy.
PB94-193471 *01,334*

HILBERT PROBLEMS
Green's Function for Generalized Hilbert Problem for Cracks and Free Surfaces in Composite Materials.
PB95-163333 *03,163*

HILSCH TUBES
Applications of the Vortex Tube in Chemical Analysis.
PB94-199171 *00,544*

Chromatographic Cryofocusing and Cryotrapping with the Vortex Tube.
PB95-180113 *00,604*

Applications of the Vortex Tube in Chemical Analysis. Part 2. Applications.
PB96-112107 *00,615*

HISTIDINE
Pore-Forming Protein with a Metal-Actuated Switch.
PB96-176557 *03,554*

HISTOGRAMS
Concentration Histogram Imaging: A Scatter Diagram Technique for Viewing Two or Three Related Images.
PB94-199114 *00,542*

HISTORICAL ASPECTS
Fire and Smoke Control: An Historical Perspective.
PB95-175808 *00,202*

HOLD-UP TIMES
Simple and Efficient Methane-Marker Devices for Chromatographic Samples.
PB96-164041 *00,635*

HOLE MOBILITY
Majority and Minority Mobilities in Heavily Doped Silicon for Device Simulations.
PB94-198728 *02,311*

Hole Dispersion and Enhancement of Antiferromagnetic Interaction of Localized Spins in High-Tc Superconductors.
PB95-202602 *04,694*

Majority and Minority Electron and Hole Mobilities in Heavily Doped Gallium Aluminum Arsenide.
PB97-118335 *04,814*

HOLES
Dimensional Characterization of Small Bores: A Survey.
PB95-162202 *02,651*

HOLLOW CLAY TILE PRISMS
Hollow Clay Tile Prism Tests for Martin Marietta Energy Systems: Task 2 Testing.
PB94-217486 *00,352*

HOLMIUM
Observation of Two Length Scales Above (T sub N) in a Holmium Thin Film.
PB97-111942 *04,151*

HOLMIUM NICKEL BORON CARBIDES
Observation of Oscillatory Magnetic Order in the Antiferromagnetic Superconductor HoNi2B2C.
PB95-180303 *04,679*

HOLOGRAPHIC SPECTROSCOPY
Holographic Properties of Triton X-100-Treated Bacteriorhodopsin Embedded in Gelatin Films.
PB96-119284 *03,761*

HOLOGRAPHY
Optical Properties of Triton X-100-Treated Purple Membranes Embedded in Gelatin Films.
PB96-123500 *03,546*

HOME FIRES
Influence of Ignition Source on the Flaming Fire Hazard of Upholstered Furniture. (NIST Reprint).
PB95-180162 *00,297*

HOMOGENEITY
Recent Developments in NIST Botanical SRMs.
PB96-167267 *03,489*

HOMOSCEDASTICITY
Developing Measurement for Experimentation.
PB97-118707 *03,450*

HONEYCOMB COMPOSITES
Investigation into the Flammability Properties of Honeycomb Composites.
PB95-143293 *03,152*

HOSPITAL FIRES
Measurement of Room Conditions and Response of Sprinklers and Smoke Detectors during a Simulated Two-Bed Hospital Patient Room Fire.
PB94-213717 *00,292*

HOT ELECTRONS
30 THz Mixing Experiments on High Temperature Superconducting Josephson Junctions.
PB96-102462 *04,709*

HOT ISOSTATIC PRESSING
Intelligent Processing of Hot Isostatic Pressing.
PB94-172913 *03,315*

Micromechanics of Densification and Distortion.
PB94-200326 *03,327*

Investigation into a Practical Grain Growth Model for Hot Isostatic Pressing.
PB95-151684 *03,347*

HOT MIX PAVING MIXTURES
System for Calibration of the Marshall Compaction Hammer.
PB94-145661 *01,303*

Field Evaluation of the System for Calibration of the Marshall Compaction Hammer.
PB95-190674 *01,323*

HOT PRESSING
Intelligent Processing of Hot Isostatic Pressing.
PB94-172913 *03,315*

Fracture Mechanism Maps: Their Applicability to Silicon Nitride.
PB96-204532 *03,094*

HOT STARS
Radiation-Driven Winds of Hot Luminous Stars X. The Determination of Stellar Masses Radii and Distances from Terminal Velocities and Mass-Loss Rates.
PB94-213022 *00,060*

HOT SURFACES
Transient Cooling of a Hot Surface by Droplets Evaporation.
PB95-143194 *03,890*

HOT WIRE
Transient Methods for Thermal Conductivity.
PB94-198405 *04,197*

HOT WORKING
Hot-Deformation Apparatus for Thermomechanical Processing Simulation.
PB94-200136 *03,207*

HOTEL FIRES
Full Scale Smoke Control Tests at the Plaza Hotel Building.
PB94-212859 *00,347*

HOUSING (DWELLINGS)
Controlling Moisture in the Walls of Manufactured Housing.
PB95-105136 *00,355*

Predicting the Energy Performance Ratings of a Family of Type I Combination Appliances.
PB95-105524 *02,504*

HPC (HIGH PERFORMANCE CONCRETE)
Microstructural Features of Some Low Water/Solids, Silica Fume Mortars Cured at Different Temperatures.
PB94-160777 *00,330*

HSLA-100 STEEL
Characterization of the Hydrogen Induced Cold Cracking Susceptibility at Simulated Weld Zones in HSLA-100 Steel.
AD-A279 759/5 *03,200*

HUMAN BEHAVIOR
Mathematical Modeling of Human Egress from Fires in Residential Buildings.
PB94-193778 *00,337*

Enhancement of EXIT89 and Analysis of World Trade Center Data.
PB96-202247 *00,231*

HUMAN BODY
Maximum Permissible Amounts of Radioisotopes in the Human Body and Maximum Permissible Concentrations in Air and Water.
AD-A280 281/7 *03,609*

Maximum Permissible Body Burdens and Maximum Permissible Concentrations of Radionuclides in Air and in Water for Occupational Exposure.
AD-A280 282/5 *03,610*

HUMAN FACTORS
Human Factors Considerations for the Potential Use of Elevators for Fire Evacuation of FAA Air Traffic Control Towers.
PB94-217163 *01,300*

HUMAN FACTORS ENGINEERING
Evaluating Form Designs for Optical Character Recognition.
PB94-168044 *01,830*

Psychological Aspects of Lighting: A Review of the Work of CIE TC 3.16.
PB94-172160 *00,241*

Workshop on the Application of Virtual Reality to Manufacturing. Final Report. Held in Gaithersburg, Maryland on August 9, 1994.
PB95-173555 *02,825*

HUMAN SERUM
Development of the Ion Exchange-Gravimetric Method for Sodium in Serum as a Definitive Method.
PB96-179148 *01,867*

HUMANITIES
User Profile for Researchers Studying Objects: Implications for Computer Systems.
PB94-188463 *00,133*

HUMANS
Human and Machine Recognition of Faces: A Survey.
PB96-111687 *01,854*

HUMIDITY
Methods of Measuring Humidity and Testing Hygrometers.
AD-A278 851/1 *00,123*

Effects of Humidity and Elevated Temperature on the Density and Thermal Conductivity of a Rigid Polyisocyanurate Foam Co-Blown with CCl3F and CO2.
PB95-150462 *00,371*

Effects of Humidity and Elevated Temperature on the Density and Thermal Conductivity of a Rigid Polyisocyanurate Foam.
PB95-152021 *00,373*

HUMIDITY MEASUREMENT
New Expressions of Uncertainties for Humidity Calibrations at the National Institute of Standards and Technology.
PB95-103826 *02,645*

HURRICANES
Gust Factors Applied to Hurricane Winds.
PB95-180469 *00,446*

Some Notable Hurricanes Revisited.
PB96-122601 *00,458*

Estimates of Hurricane Wind Speeds by the 'Peaks Over Threshold' Method.
PB96-162540 *00,471*

Probabilistic Estimates of Design Load Factors for Wind-Sensitive Structures Using the 'Peaks Over Threshold' Approach.
PB96-183223 *00,474*

HY-100 STEEL
Characterization of the Hydrogen Induced Cold Cracking Susceptibility at Simulated Weld Zones in HSLA-100 Steel.
AD-A279 759/5 *03,200*

HYADES CLUSTER
IUE Observations of Solar-Type Stars in the Pleiades and the Hyades.
PB94-199437 *00,053*

HYBRID ELECTRIC-POWERED VEHICLES
Advanced Components for Electric and Hybrid Electric Vehicles. Workshop Proceedings. Held in Gaithersburg, Maryland on October 27-28, 1993.
PB94-177060 *04,858*

HYBRID METHODS
Hybrid Method for Determining Material Properties from Instrumented Micro-Indentation Experiments.
PB95-152229 *03,348*

HYDRATES
Modelling Drying Shrinkage of Cement Paste and Mortar. Part 1. Structural Models from Angstroms to Millimeters.
PB96-135132 *03,074*

HYDRATION
Digitized Direct Simulation Model of the Microstructural Development of Cement Paste.
PB94-198777 *01,309*

Digitized Simulation Model for Microstructural Development.
PB94-198785 *01,310*

Modelling the Leaching of Calcium Hydroxide from Cement Paste: Effects on Pore Space Percolation and Diffusivity.
PB94-198793 *01,311*

Diffusion Studies in a Digital-Image-Based Cement Paste Microstructural Model.
PB94-198801 *01,312*

Survey of Recent Cementitious Materials Research in Western Europe.
PB94-218583 *00,353*

Resolution of DNA in the Presence of Mobility Modifying Polar and Nonpolar Compounds by Discontinuous Electrophoresis on Rehydratable Polyacrylamide Gels.
PB95-152799 *00,590*

Cellular Automaton Simulations of Cement Hydration and Microstructure Development.
PB95-175055 *01,320*

Hydration in Semicrystalline Polymers: Small-Angle Neutron Scattering Studies of the Effect of Drawing in Nylon-6 Fibers.
PB95-202990 *03,385*

HYDRAULIC FLUIDS
Suppression of Elevated Temperature Hydraulic Fluid and JP-8 Spray Flames.
PB95-181095 *00,021*

Intercomparison between NPL (India) and NIST (USA) Pressure Standards in the Hydraulic Pressure Region Up to 26 MPa.
PB96-113543 *04,211*

HYDRAULIC RADIUS
Hydraulic Radius and Transport in Reconstructed Model Three-Dimensional Porous Media.
PB96-123419 *00,403*

HYDRAZINE
Far Infrared Laser Frequencies of CH3OD and N2H4.
PB96-119623 *04,341*

HYDRAZINE TREATMENT
Critical Evaluation of the Purification of Biominerals by Hypochlorite Treatment.
PB95-150959 *00,186*

HYDRAZOIC ACID
Fragment Energy and Vector Correlations in the Overtone-Pumped Dissociation of HN3X(1)A'.
PB94-199908 *00,802*

HYDRIDES
Neutron Spectroscopic Comparison of beta-Phase Rare Earth Hydrides.
PB96-160742 *01,134*

HYDROAZOIC ACID
Vibrational Predissociation Dynamics of Overtone-Excited HN3.
PB95-125720 *00,691*

HYDROCARBON DETECTORS
Process Gas Chromatography Detector for Hydrocarbons Based on Catalytic Cracking.
PB95-141099 *02,485*

HYDROCARBONS
Standard Materials. A Descriptive List with Prices.
AD-A278 140/9 *00,500*

Process Gas Chromatography Detector for Hydrocarbons Based on Catalytic Cracking.
PB95-141099 *02,485*

Optical Measurements of Atomic Hydrogen, Hydroxyl, and Carbon Monoxide in Hydrocarbon Diffusion Flames.
PB95-150900 *02,487*

Large Fire Experiments for Fire Model Evaluations.
PB96-190079 *01,427*

Experimental Determination of the Rate Constant for the Reaction of C2H3 with H2 and Implications for the Partitioning of Hydrocarbons in Atmospheres of the Outer Planets.
PB97-122295 *00,112*

HYDROCHLORIC ACID
Automated, High Precision Coulometric Titrimetry. Part 2. Strong and Weak Acids and Bases.
PB95-150207 *00,576*

HYDROCHLOROFLUOROCARBONS
Rate Constants for the Gas Phase Reactions of the OH Radical with CF3CF2CHCl2 (HCFC-225ca) and CF2ClCF2CHClF (HCFC-225cb).
PB95-152153 *00,940*

Annex 18: An International Study of Refrigerant Properties.
PB95-168936 *03,266*

HYDRODYNAMIC FRICTION
Hydrodynamic Friction of Arbitrarily Shaped Brownian Particles.
PB97-110191 *04,136*

HYDRODYNAMIC INTERACTIONS
Effect of Hydrodynamic Interactions on a Terminally Anchored Bead-Rod Model Chain.
PB95-141156 *01,237*

HYDRODYNAMICS
Effect of Hydrodynamic Interactions on a Terminally Anchored Bead-Rod Model Chain.
PB95-141156 *01,237*

Competition between Hydrodynamic Screening ('Draining') and Excluded Volume Interactions in an Isolated Polymer Chain.
PB95-175402 *01,265*

Hydrodynamic Similarity in an Oscillating-Body Viscometer.
PB96-122429 *01,082*

Book Review: Aspects and Applications of the Random Walk.
PB96-123534 *04,215*

Response to 'Draining in Dilute Polymer Solutions and Renormalization'.
PB96-146667 *01,283*

HYDROELASTIC SYSTEMS
Noise Modeling and Reliability of Behavior Prediction for Multi-Stable Hydroelastic Systems.
PB96-111943 *04,822*

HYDROELASTICITY
Noise Modeling and Reliability of Behavior Prediction for Multi-Stable Hydroelastic Systems.
PB96-111943 *04,822*

HYDROFLUORIC ACID
High-Resolution Infrared Overtone Spectroscopy of N2-HF: Vibrational Red Shifts and Predissociation Rate as a Function of HF Stretching Quanta.
PB96-102298 *01,061*

HYDROFLUOROCARBON
Neutron and Raman Spectroscopies of 134 and 134a Hydrofluorocarbons Encaged in Na-X Zeolite.
PB96-186168 *03,001*

HYDROFLUOROCARBONS
Development of a Dual-Sinker Densimeter for High-Accuracy Fluid P-V-T Measurements.
PB95-168951 *03,267*

Atmospheric Lifetimes of HFC-143a and HFC-245fa: Flash Photolysis Resonance Fluorescence Measurements of the OH Reaction Rate Constants.
PB97-112577 *00,118*

HYDROFLURORCARBONS
Virial Coefficients of Five Binary Mixtures of Fluorinated Methanes and Ethanes.
PB96-156054 *01,128*

HYDROGEN
Tabulation of the Thermodynamic Properties of Normal Hydrogen from Low Temperatures to 300K and from 1 to 100 Atmospheres.
AD-A279 951/8 *00,713*

Compilation of the Physical Equilibria and Related Properties of the Hydrogen-Carbon Monoxide System.
AD-A286 603/6 *00,716*

Collision-Induced Emission in the Fundamental Vibration-Rotation Band of H2.
PB94-199445 *03,811*

Vibrational Autoionization in H2: Vibrational Branching Ratios and Photoelectron Angular Distributions Near the v(+)=3 Threshold.
PB94-199577 *00,799*

Rate Constants for Hydrogem Atom Attack on Some Chlorinated Benzenes at High Temperature.
PB94-200581 *00,810*

Measurement of the Self Broadening of the H2Q(0-5) Raman Transitions from 295 to 1000 K.
PB95-108627 *00,884*

Conductance Response of Pd/SnO2(110) Model Gas Sensors to H2 and O2.
PB95-125803 *00,892*

Operational Mode and Gas Species Effects on Rotational Drag in Pneumatic Dead Weight Pressure Gages.
PB95-140182 *00,903*

Optical Measurements of Atomic Hydrogen, Hydroxyl, and Carbon Monoxide in Hydrocarbon Diffusion Flames.
PB95-150900 *02,487*

Mechanism and Rate Constants for the Reactions of Hydrogen Atoms with Isobutene at High Temperatures.
PB95-151064 *00,929*

Simultaneous Forward-Backward Raman Scattering Studies of D2 Broadened by D2, He, and Ar.
PB95-162459 *00,961*

Hydrogen Atom Attack on Perchloroethylene.
PB95-163473 *00,969*

Fugacity Coefficients of Hydrogen in (Hydrogen + Butane).
PB95-175212 *02,491*

Neutron Scattering by Hydrogen in Cold Neutron Prompt Gamma-Activation Analysis.
PB95-175972 *00,603*

Characterization of the Interaction of Hydrogen with Iridium Clusters in Zeolites by Inelastic Neutron Scattering Spectroscopy.
PB95-180741 *01,013*

Vibrations of Hydrogen and Deuterium in Solid Solution with Lutetium.
PB95-181038 *01,019*

Analyses of Recent Experimental and Theoretical Determinations of e-H2 Vibrational Excitation Cross Sections: Assessing a Long-Standing Controversy.
PB95-202438 *03,977*

Recombination Line Intensities for Hydrogenic Ions-III. Effects of Finite Optical Depth and Dust.
PB95-202677 *00,079*

Modified Effective Range Theory as an Alternative to Low-Energy Close-Coupling Calculations.
PB95-202701 *03,988*

Deuterium in the Local Interstellar Medium: Its Cosmological Significance.
PB95-202842 *00,081*

Importance of Bound-Free Correlation Effects for Vibrational Excitation of Molecules by Electron Impact: A Sensitivity Analysis.
PB95-202974 *03,996*

Time-Resolved Balmer-Alpha Emission from Fast Hydrogen Atoms in Low Pressure, Radio-Frequency Discharges in Hydrogen.
PB96-102942 *04,028*

Measuring Hydrogen by Cold-Neutron Prompt-Gamma Activation Analysis.
PB96-111877 *00,612*

Decay of Bragg Gratings in Hydrogen-Loaded Optical Fibers.
PB96-122643 *04,345*

Asymptotic and Numerical Analysis of a Premixed Laminar Nitrogen Dioxide-Hydrogen Flame.
PB96-164256 *01,422*

HYDROGEN ABSORPTION
Vibrational Excitations and the Position of Hydrogen in Nanocrystalline Palladium.
PB96-111828 *04,035*

HYDROGEN ADDITIONS
Hydrogen in YBa2Cu3Ox: A Neutron Spectroscopy and a Nuclear Magnetic Resonance Study.
PB95-161279 *04,601*

HYDROGEN ATOMS
Rate Constants for Hydrogem Atom Attack on Some Chlorinated Benzenes at High Temperature.
PB94-200581 *00,810*

Perturbative Calculation of the AC Stark Effect by the Complex Rotation Method.
PB95-141123 *04,260*

Mechanism and Rate Constants for the Reactions of Hydrogen Atoms with Isobutene at High Temperatures.
PB95-151064 *00,929*

Hydrogen Atom Attack on Perchloroethylene.
PB95-163473 *00,969*

Vibrational Excitations and the Position of Hydrogen in Nanocrystalline Palladium.
PB96-111828 *04,035*

HYDROGEN BONDING
Interaction of Some Coupling Agents and Organic Compounds with Hydroxyapatite: Hydrogen Bonding, Adsorption and Adhesion.
PB94-172616 *00,140*

Lattice Model of a Hydrogen-Bonded Polymer Blend.
PB97-112262 *03,391*

Relaxation After a Temperature Jump Within the One Phase Region of a Polymer Mixture.
PB97-112494 *03,394*

Bimolecular Interactions in (Et)3SiOH:Base:CCl4 Hydrogen-Bonded Solutions Studied by Deactivation of the Free OH-Stretch Vibration.
PB97-118657 *04,166*

Rotational Spectra of CH3CCH-NH3, NCCCH-NH3, and NCCCH-OH2.
PB97-118798 *04,170*

HYDROGEN BONDS
Phase Behavior of a Hydrogen Bonding Molecular Composite.
PB94-185188 *01,202*

Strong Hydrogen Bond in the Formic Acid-Formate Anion System.
PB94-198595 *00,788*

Structure of Glycine-Water H-Bonded Complexes.
PB94-198603 *00,789*

P-Type Doubling in the Infrared Spectrum of NO-HF.
PB94-211463 *00,817*

Mode Specific Vibrational Predissociation Dynamics in Fragile Molecules.
PB95-107132 *00,871*

Rigid Bender Analysis of van der Waals Complexes: The Intermolecular Bending Potential of a Hydrogen Bond.
PB95-203022 *01,042*

Comparison of a Fixed-Charge and a Polarizable Water Model.
PB96-111620 *01,072*

State-Resolved Rotational Energy Transfer in Open Shell Collisions: Cl((2)P3/2)+HCl.
PB96-176607 *01,157*

HYDROGEN CHLORIDE
Slit-Jet Near-Infrared Diode Laser Spectroscopy of (DCl)2: nu1, nu2 DCl Stretching Fundamentals, Tunneling Dynamics, and the Influence of Large Amplitude 'Geared' Intermolecular Rotation.
PB95-203204 *01,047*

HYDROGEN CHLORIDE COMPLEXES
Vibrational Dependence of the Anisotropic Intermolecular Potential of Ar-HCl.
PB95-202685 *01,029*

High Resolution Near Infrared Spectroscopy of HCl-DCl and DCl-HCl: Relative Binding Energies, Isomer Interconversion Rates, and Mode Specific Vibrational Predissociation.
PB95-203212 *01,048*

HYDROGEN CHLORIDE DIMERS
High Resolution, Jet-Cooled Infrared Spectroscopy of (HCl)2: Analysis of nu1 and nu2 HCl Stretching Fundamentals, Interconversion Tunneling, and Mode-Specific Predissociation Lifetimes.
PB95-203196 *01,046*

HYDROGEN CYANIDE
Self-, N2- and Ar-Broadening and Line Mixing in HCN and C2H2.
PB95-108445 *00,876*

New Approach for Reducing the Toxicity of the Combustion Products from Flexible Polyurethane Foam.
PB96-123625 *01,411*

HYDROGEN CYANIDE LASERS
Efficient Br(*) Laser Pumped by Frequency-Doubled Nd:YAG and Electronic-to-Vibrational Transfer-Pumped CO2 and HCN Lasers.
PB95-108684 *04,248*

HYDROGEN EMBRITTLEMENT
Determination of Hydrogen in Titanium Alloy Jet Engine Compressor Blades by Cold Neutron Capture Prompt Gamma-ray Activation Analysis.
PB95-175956 *01,448*

HYDROGEN FLUORIDE
Tunneling-Rotation Spectrum of the Hydrogen Fluoride Dimer.
PB94-198678 *00,793*

P-Type Doubling in the Infrared Spectrum of NO-HF.
PB94-211463 *00,817*

Intermolecular HF Motion in Ar(sub n)HF Micromatrices (n=1,2,3,4,): Classical and Quantum Calculations on a Pairwise Additive Potential Surface.
PB95-107025 *03,871*

High-Resolution Infrared Spectroscopy of DF Trimer: A Cyclic Ground State Structure and DF Stretch Induced Intramolecular Vibrational Coupling.
PB95-150678 *00,920*

HYDROGEN FLUORIDE COMPLEXES
High-Resolution Infrared Overtone Spectroscopy of ArHF via Nd:YAG/Dye Laser Difference Frequency Generation.
PB94-211448 *00,816*

Spectroscopic Puzzle in ArHF Solved: The Test of a New Potential.
PB94-216058 *00,850*

Slit Jet Infrared Spectroscopy of Hydrogen Bonded N2HF Isotopomers: Rotational Rydberg-Klein-Rees Analysis and H/D Dependent Vibrational Predissociation Rates.
PB95-161873 *00,956*

Fragment State Correlations in the Dissociation of NO.HF(v=1).
PB95-164430 *00,982*

Vibrational Dependence of the Anisotropic Intermolecular Potential of Ar-HF.
PB95-202693 *01,030*

Rotational-RKR Inversion of Intermolecular Stretching Potentials: Extension to Linear Hydrogen Bonded Complexes.
PB95-203014 *01,041*

Rigid Bender Analysis of van der Waals Complexes: The Intermolecular Bending Potential of a Hydrogen Bond.
PB95-203022 *01,042*

HYDROGEN IONS
Resonant Two-Color Detachment of H(-) with Excitation of H(n=2).
PB95-202552 *03,984*

Variationally Stable Treatment of Two- and Three-Photon Detachment of H(-) Including Electron-Correlation Effects.
PB95-202867 *03,992*

Short-Pulse Detachment of H(-) in the Presence of a Static Electric Field.
PB95-203477 *04,007*

Kinetic Energy Distributions of H(+), H2(+), and H3(+) from a Diffuse Townsend Discharge in H2 at High E/N.
PB96-123351 *04,415*

HYDROGEN IONS 2 PLUS
Asymptotic Wave Function Splitting Procedure for Propagating Spatially Extended Wave Functions: Application to Intense Field Photodissociation of H2(+).
PB94-211786 *03,847*

HYDROGEN ISOTOPES
New IUPAC Guidelines for the Reporting of Stable Hydrogen, Carbon, and Oxygen Isotope-Ratio Data. Letter to the Editor.
PB95-261962 *01,058*

HYDROGEN-LIKE IONS
Experimental Aspects and Z-Dependent Systematics in One- and Two-Electron Ions and Single Vacancy Systems.
PB94-199627 *03,815*

Fast Computer Evaluation of Radiative Properties of Hydrogenic Systems.
PB95-150553 *03,894*

HYDROGEN ORDERING
Neutron Spectroscopic Evidence of Concentration-Dependent Hydrogen Ordering in the Octahedral Sublattice of beta-TbH2+x.
PB95-181020 *01,018*

HYDROGEN PLASMA
Attempts at Extending the Unified Theory to Include Many-Body Effects.
PB94-212719 *04,408*

Excitation of Balmer Lines in Low-Current Discharges of Hydrogen and Deuterium.
PB95-150546 *03,893*

Hydrogen Balmer Alpha Line Shapes for Hydrogen-Argon Mixtures in a Low-Pressure rf Discharge.
PB95-153433 *03,924*

HYDROGEN SULFIDE
Nonadiabatic Effects in the Photoassociation of H2S.
PB95-151437 *00,934*

HYDROGEN VIBRATIONS
Neutron-Spectroscopy Study of the Hydrogen Vibrations in Hydrogen-Doped YBa2Cu3Ox.
PB94-172475 *04,441*

HYDROLYSIS
Thermodynamics of the Hydrolysis of Penicillin G and Ampicillin.
PB94-172467 *03,596*

Hydrolysis of Proteins by Microwave Energy.
PB94-216322 *03,528*

Thermochemistry of the Hydrolysis of L-arginine to (L-citrulline + Ammonia) and of the Hydrolysis of L-arginine to (L-ornithine + Urea).
PB95-150801 *03,463*

Equilibrium and Calorimetric Investigation of the Hydrolysis of L-Tryptophan to (Indole + Pyruvate + Ammonia).
PB95-163317 *00,661*

Thermodynamics of the Hydrolysis of N-Acetyl-L-phenylalanine Ethyl Ester in Water and in Organic Solvents.
PB95-203386 *01,053*

HYDROXYANISOLES
Thermal Decomposition of Hydroxy- and Methoxy-Substituted Anisoles.
PB94-173036 *00,767*

HYDROXYAPATITE
Formation of Hydroxyapatite in Cement Systems.
PB95-175261 *00,170*

Adsorption of Potassium N-phenylglycinate on Hydroxyapatite: Role of Solvents and Ionic Charge.
PB96-180161 *01,159*

In vitro Inhibition of Membrane-Mediated Calcification by Novel Phosphonates.
PB96-201140 *03,595*

Interaction of Citric Acid with Hydroxyapatite: Surface Exchange of Ions and Precipitation of Calcium Citrate.
PB97-119309 *03,584*

HYDROXYAPATITES
Adsorption of Low-Molecular-Weight Sodium Polyacrylate on Hydroxyapatite.
PB94-172608 *00,139*

Interaction of Some Coupling Agents and Organic Compounds with Hydroxyapatite: Hydrogen Bonding, Adsorption and Adhesion.
PB94-172616 *00,140*

Interaction of Chlorhexidine Digluconate with and Adsorption of Chlorhexidine on Hydroxyapatite.
PB95-175907 *03,566*

Formation of Hydroxyapatite in a Polymeric Calcium Phosphate Cement.
PB95-180642 *00,173*

Adsorption of Polyacrylic Acids and Their Sodium Salts on Hydroxyapatite: Effect of Relative Molar Mass.
PB97-112510 *03,581*

HYDROXYL EMISSION
Rotational Spectrum of OH in the v=0-3 Levels of Its Ground State.
PB95-176202 *01,006*

HYDROXYL RADICAL
Commentary: The Measurement of Oxidative Damage to DNA by HPLC and GC/MS Techniques.
PB96-200894 *03,484*

HYDROXYL RADICALS
Product Kinetic Energies, Correlations, and Scattering Anisotropy in the Bimolecular Reactor O((1)D)+H2O yields 2OH.
PB94-212792 *00,838*

Optical Measurements of Atomic Hydrogen, Hydroxyl, and Carbon Monoxide in Hydrocarbon Diffusion Flames.
PB95-150900 *02,487*

Unusual Spin-Trap Chemistry for the Reaction of Hydroxyl Radical with the Carcinogen N-Nitrosodimethylamine.
PB95-151643 *00,692*

Gas Phase Reactivity Study of OH Radicals with 1,1-Dichloroethene and cis-1,1-Dichloroethene and Trans-1,2-Dichloroethene over the Temperature Range 240-400 K.
PB95-152146 *00,939*

Rate Constants for the Gas Phase Reactions of the OH Radical with CF3CF2CHCl2 (HCFC-225ca) and CF2ClCF2CHClF (HCFC-225cb).
PB95-152153 *00,940*

Rotational Spectrum of OH in the v=0-3 Levels of Its Ground State.
PB95-176202 *01,006*

Detection of OH+ in Its a(1)Delta State by Far Infrared Laser Magnetic Resonance.
PB95-181087 *01,021*

Laser-Induced Fluorescence Measurements of OH in Laminar Diffusion Flames in the Presence of Soot Particles.
PB96-123120 *01,409*

Atmospheric Lifetimes of HFC-143a and HFC-245fa: Flash Photolysis Resonance Fluorescence Measurements of the OH Reaction Rate Constants.
PB97-112577 *00,118*

HYDROXYMETHYL PEROXY RADICALS
Kinetics of the Self-Reaction of Hydroxymethylperoxyl Radicals.
PB94-212164 *00,827*

HYGROMETERS
Methods of Measuring Humidity and Testing Hygrometers.
AD-A278 851/1 *00,123*

Low-Temperature Performance of Radiosonde Electric Hygrometer Elements.
AD-A295 319/8 *00,121*

HYGROTHERMAL EFFECT
Hygrothermal Effects on the Performance of Polymers and Polymeric Composites: A Workshop Report. Held in Gaithersburg, Maryland on September 21-22, 1995.
PB96-183207 *03,180*

HYOGOKEN-NANBU EARTHQUAKE
January 17, 1995 Hyogoken-Nanbu (Kobe) Earthquake. Performance of Structures, Lifelines and Fire Protection Systems. Executive Summary and Paper.
PB97-104160 *00,475*

HYPERFINE STRUCTURE
Hyperfine-Structure Studies of Zr II: Experimental and Relativistic Configuration-Interaction Results.
PB95-203824 *04,011*

HYPERFINE STRUCTURES
Hyperfine Structure Investigations and Identification of New Energy Levels in the Ionic Spectrum of (147)Pm.
PB96-180203 *04,117*

HYPOCHLORITE TREATMENT
Critical Evaluation of the Purification of Biominerals by Hypochlorite Treatment.
PB95-150959 *00,186*

HYSTERESIS
Langevin Approach to Hysteresis and Barkhausen Modeling in Steel.
PB94-185675 *03,206*

Hysteresis Measurements of Remanent Polarization and Coercive Field in Polymers.
PB94-199767 *04,475*

HYSTERETIC FAILURE MODEL
Evaluating the Seismic Performance of Lightly-Reinforced Circular Concrete Bridge Columns.
PB95-163259 *01,335*

ICE POINT
Reproducibility of the Temperature of the Ice Point in Routine Measurements.
PB95-255923 *04,015*

IDEAL GAS
Correlation of the Ideal Gas Properties of Five Aromatic Hydrocarbons.
PB95-175816 *01,002*

IDEF0 (INTEGRATION DEFINITION FOR FUNCTION MODELING)
Integration Definition for Function Modeling (IDEF0); Category: Software Standard; Subcategory: Modeling Techniques.
FIPSPUB183 *02,800*

IDEF1X (INFORMATION DEFINITION FOR INFORMATION MODELING)
Integration Definition for Information Modeling (IDEF1X); Category: Software Standard; Subcategory: Modeling Techniques.
FIPSPUB184 *01,673*

IDEF1X (INTEGRATION DEFINITION FOR INFORMATION MODELING)
Mapping Integration Definition for Information Modeling (IDEF1X) Model into CASE Data Interchange Format (CDIF) Transfer File.
PB95-154670 *01,711*

IDEFO (INTEGRATION DEFINITION FOR FUNCTION MODELING)
Mapping Integration Definition for Function Modeling (IDEFO) Model into CASE Data Interchange Format (CDIF) Transfer File.
PB96-109533 *01,741*

IDENTIFICATION
Precise Identification of Computer Viruses
PB96-160825 *01,613*

Specification for Interoperability between Ballistic Imaging Systems. Part 1. Cartridge Cases.
PB96-195524 *01,860*

IDLH (IMMEDIATELY DANGEROUS TO LIFE OR HEALTH)
Documentation for Immediately Dangerous to Life or Health Concentrations (IDLHs).
PB94-195047 *03,602*

IGES (INITIAL GRAPHICS EXCHANGE SPECIFICATION)
CALS-Digital Representation for Communication of Product Data: IGES Application Subsets.
PB94-962100 *03,658*

Summary and Notes of the Joint ISO/IGES/PDES Organization Technical Committee Meeting. Held in Albuquerque, New Mexico on October 15-20, 1989.
PB95-107314 *02,774*

Initial Graphics Exchange Specification (IGES): Procedures for the NIST IGES Validation Test Service.
PB95-171427 *02,780*

Operating Procedures and Life Cycle Documentation for the Initial Graphics Exchange Specification.
PB95-242285 *02,782*

CALS-Digital Representation for Communication of Product Data: IGES Application Subsets.
PB95-962100 *03,667*

IGNITION
Ignition and Subsequent Transition to Flame Spread in a Microgravity Environment.
N96-15584/1 *04,828*

Influence of Ignition Source on the Flaming Fire Hazard of Upholstered Furniture. (NIST Reprint).
PB95-180162 *00,297*

Study of Technology for Detecting Pre-Ignition Conditions of Cooking-Related Fires Associated with Electric and Gas Ranges and Cooktops, Phase 1 Report.
PB96-128095 *00,303*

Quantifying the Ignition Propensity of Cigarettes.
PB96-155411 *00,306*

Transition from Localized Ignition to Flame Spread Over a Thin Cellulosic Material in Microgravity.
PB96-155809 *04,835*

Ignition and Subsequent Flame Spread Over a Thin Cellulosic Material.
PB96-160270 *04,836*

Ignition and Transition to Flame Spread Over a Thermally Thin Cellulosic Sheet in a Microgravity Environment.
PB96-160288 *04,837*

IGNITION TIME
Predicting the Ignition Time and Burning Rate of Thermoplastics in the Cone Calorimeter.
PB96-154794 *01,418*

IGOSS (INDUSTRY/GOVERNMENT OPEN SYSTEMS SPECIFICATION)
Industry/Government Open Systems Specification Testing Framework. Version 1.0.
PB94-219110 *01,809*

ILL-POSED CONTINUATION
Slow Evolution from the Boundary: A New Stabilizing Constraint in Ill-Posed Continuation Problems.
PB96-122858 *03,418*

IMAGE ANALYSIS
Reliable Optical Flow Algorithm Using 3-D Hermite Polynomials.
PB94-145620 *01,829*

Quantitative Phase Abundance Analysis of Three Cement Clinker Reference Materials by Scanning Electron Microscopy.
PB94-173051 *00,333*

Visual Measurement Technique for Analysis of Nucleate Flow Boiling.
PB95-143301 *03,262*

Optical Fiber Geometry by Gray-Scale Analysis with Robust Regression.
PB95-161519 *04,272*

IMAGE DEBLURRING
Overcoming Hoelder Continuity in Ill-Posed Continuation Problems.
PB95-202354 *03,416*

IMAGE DECODING
Tomographic Decoding Algorithm for a Nonoverlapping Redundant Array.
PB95-151932 *01,842*

IMAGE GRADIENT
Image Gradient Evolution: A Visual Cue for Danger.
PB96-154562 *02,939*

IMAGE MOTION ANALYSIS
General Motion Model and Spatio-Temporal Filters for Computing Optical Flow.
PB95-171096 *01,847*

General Motion Model and Spatio-Temporal Filters for 3-D Motion Interpretations.
PB96-210703 *01,861*

IMAGE MOTION COMPENSATION
General Motion Model and Spatio-Temporal Filters for 3-D Motion Interpretations.
PB96-210703 *01,861*

IMAGE PROCESSING
Object Finder for Digital Images Based on Multiple Thresholds, Connectivity, and Internal Structures.
PB94-199106 *01,833*

Concentration Histogram Imaging: A Scatter Diagram Technique for Viewing Two or Three Related Images.
PB94-199114 *00,542*

VLSI Architectures for Template Matching and Block Matching.
PB94-200029 *01,834*

Certainty Grid to Object Boundary Algorithm.
PB94-203510 *01,835*

Compositional Mapping of the Microstructure of Materials.
PB95-107199 *00,565*

Real Time Differential Range Estimation Based on Time-Space Imagery Using PIPE.
PB95-161808 *01,844*

X-Ray Image Quality Indicator Designed for Easy Alignment.
PB95-164455 *02,907*

Morphological Estimation of Tip Geometry for Scanned Probe Microscopy.
PB95-203444 *02,662*

National Information Infrastructure and Advanced Digital Video.
PB96-119367 *01,488*

Specification for Interoperability between Ballistic Imaging Systems. Part 1. Cartridge Cases.
PB96-195524 *01,860*

IMAGE QUALITY INDICATOR
X-Ray Image Quality Indicator Designed for Easy Alignment.
PB95-164455 *02,907*

IMAGE RECONSTRUCTION
Tomographic Decoding Algorithm for a Nonoverlapping Redundant Array.
PB95-151932 *01,842*

Image Restoration and Diffusion Processes.
PB95-153003 *01,843*

IMAGE REGISTRATION
Crystal Diffraction Spectrometry for Accurate, Non-Invasive kV/Spectral Measurement for Improvement of Mammographic Image Quality.
AD-A297 943/3 *00,721*

IMAGE RESOLUTION
Contributions of Out-of-Plane Material to a Scanned-Beam Laminography Image.
PB96-111786 *02,704*

IMAGE RESTORATION
Image Restoration and Diffusion Processes.
PB95-153003 *01,843*

IMAGES
Metrology Standards for Advanced Semiconductor Lithography Referenced to Atomic Spacings and Geometry.
PB96-160718 *02,424*

IMAGING TECHNIQUES
Diffraction Imaging of Polycrystalline Materials.
PB94-198884 *02,971*

Molecular Ion Imaging and Dynamic Secondary Ion Mass Spectrometry of Organic Compounds.
PB95-126124 *00,571*

dc Magnetic Force Microscopy Imaging of Thin-Film Recording Head.
PB95-176061 *04,665*

Magnetic Force Microscopy Images of Magnetic Garnet with Thin-Film Magnetic Tip.
PB95-176210 *04,669*

Evaluation of Thermal Wave Imaging for Detection of Machining Damage in Ceramics.
PB95-220547 *03,062*

IMIDOGEN RADICALS
New Electronic States of NH and ND Observed from 258 to 288 nm by Resonance Enhanced Multiphoton Ionization Spectroscopy.
PB94-212495 *00,836*

IMMEDIATELY DANGEROUS TO LIFE OR HEALTH
Documentation for Immediately Dangerous to Life or Health Concentrations (IDLHs).
PB94-195047 *03,602*

IMMERSION TEST (CORROSION)
Degradation of Powder Epoxy Coated Panels Immersed in a Saturated Calcium Hydroxide Solution Containing Sodium Chloride.
PB96-101050 *01,344*

IMMUNOASSAY
Liposome-Based Flow-Injection Immunoassay for Determining Theophylline in Serum.
PB94-213493 *03,494*

Flow Immunoassay Using Solid-Phase Entrapment.
PB96-200951 *00,642*

IMMUNOASSAYS
Novel Amperometric Immunosensor for Procainamide Employing Light Activated Labels.
PB96-163662 *00,512*

IMMUNOLOGIC DISEASES
Diagnosis and Treatment of an Oral Base-Metal Contact Lesion Following Negative Dermatologic Patch Tests.
PB95-180626 *00,172*

IMPACT-ECHO METHOD
Detection of Voids in Grouted Ducts Using the Impact-Echo Method.
PB94-185121 *01,306*

IMPACT TESTS
Reaction Sensitivities of Al-Li Alloys and Alloy 2219 in Mechanical-Impact Tests.
PB94-172764 *03,314*

Temperature Increases in Aluminum Alloys during Mechanical-Impact Tests for Oxygen Compatibility.
PB94-172962 *03,316*

Recommended Changes in ASTM Test Methods D2512-82 and G86-84 for Oxygen-Compatibility Mechanical Impact Tests on Metals.
PB94-216694 *03,338*

Macro- and Microreactions in Mechanical-Impact Tests of Aluminum Alloys.
PB95-107348 *03,340*

Influence of Specimen Absorbed Energy in LOX Mechanical-Impact Tests.
PB95-107355 *03,341*

Hybrid Method for Determining Material Properties from Instrumented Micro-Indentation Experiments.
PB95-152229 *03,348*

Factors Significant to Precracking of Fracture Specimens.
PB96-109558 *03,358*

Effect of Charpy V-Notch Striker Radii on the Absorbed Energy.
PB96-141122 *03,365*

Charpy Impact Test as an Evaluation of 4 K Fracture Toughness.
PB96-190194 *03,219*

IMPEDANCE
Modeling Polarization Curves and Impedance Spectra for Simple Electrode Systems.
PB94-198876 *03,188*

IMPEDANCE BRIDGES
Automatic Inductive Voltage Divider Bridge Operates from 10 Hz to 100 kHz.
PB94-198413 *02,032*

IMPEDANCE GENERATORS
Multi-State Two-Port: An Alternative Transfer Standard.
PB95-168530 *02,049*

IMPEDANCE MEASUREMENT
Measurements of the Characteristic Impedance of Coaxial Air Line Standards.
PB95-168787 *02,221*

On-Wafer Impedance Measurement on Lossy Substrates.
PB95-176285 *02,365*

IMPEDENCE MEASUREMENT
Digital Impedance Bridge.
PB96-103155 *02,272*

IMPLEMENTATION
Implementation of the Fastener Quality Act.
PB96-160676 *02,876*

IMPROVEMENTS
Testability of Object-Oriented Systems.
PB95-242418 *01,733*

IN-SITU COMBUSTION
In situ Burning of Oil Spills: Mesoscale Experiments.
PB94-142973 *01,355*

In Situ Burning Oil Spill Workshop Proceedings. Held in Orlando, Florida on January 26-28, 1994.
PB95-104907 *02,583*

In situ Burning of Oil Spills: Mesoscale Experiments and Analysis.
PB95-163747 *02,587*

Smoke Emission from Burning Crude Oil.
PB96-122890 *01,407*

Smoke Plume Trajectory from In situ Burning of Crude Oil in Alaska: Field Experiments.
PB96-131560 *02,594*

Smoke Plume Trajectory from In situ Burning of Crude Oil: Field Experiments.
PB96-200993 *02,597*

IN SITU MEASUREMENT
In situ Measurements of Chloride Ion and Corrosion Potential at the Coating/Metal Interface.
PB95-140893 *03,122*

IN VIVO ANALYSIS
Secondary Target X-Ray Excitation for In vivo Measurement of Lead in Bone.
PB95-108767 *03,496*

INCANDESCENT LAMPS
Characterization of Modified FEL Quartz-Halogen Lamps for Photometric Standards.
PB97-112544 *00,282*

INCINERATORS
Incinerability of Perchloroethylene and Chlorobenzene.
PB95-163457 *01,388*

Membrane Gas Separation for a Fluidized-Bed Incinerator.
PB95-169041 *02,550*

INCLUSIONS
Cryogenic Toughness of Austenitic Stainless Steel Weld Metals: Effect of Inclusions.
PB95-161261 *03,214*

INDENTATION
Hybrid Method for Determining Material Properties from Instrumented Micro-Indentation Experiments.
PB95-152229 *03,348*

Flat and Rising R-Curves for Elliptical Surface Cracks from Indentation and Superposed Flexure.
PB95-161295 *03,156*

Postfailure Subsidiary Cracking from Indentation Flaws in Brittle Materials.
PB97-110340 *03,103*

INDENTATION HARDNESS TESTS
Conference Proceedings: International Workshop on Instrumented Indentation. Held in San Diego, California on April 22-23, 1995.
PB96-158688 *01,948*

INDENTATION-MICROFRACTURE METHOD
Evaluation of Fracture Toughness and Residual Stress in Dental Porcelain by Indentation-Microfracture Method.
PB95-125613 *00,154*

Evaluation of Fracture Toughness and Residual Stress in Dental Porcelain by Indentation-Microfracture Method.
PB95-152831 *00,159*

INDENTATION STRENGTH
Objective Evaluation of Short-Crack Toughness Curves Using Indentation Flaws: Case Study on Alumina-Based Ceramics.
PB96-179429 *03,079*

INDEXES (DOCUMENTATION)
Abstract and Index Collection in the Research Information Center of the National Institute of Standards and Technology.
PB94-152204 *02,744*

Abstract and Index Collection in the Research Information Center of the National Institute of Standards and Technology.
PB95-232633 *02,741*

INDIA
India: Environmental Technologies Export Market Plan.
PB97-114359 *02,529*

INDIUM
Arc Spectra of Gallium, Indium, and Thallium.
AD-A295 411/3 *00,718*

Single-Photon Ionization and Detection of Ga, In, and As(sub n) Species in GaAs Growth.
PB95-152815 *00,591*

Laser-Induced Desorption of In and Ga from Si(100) and Adsorbate Enhanced Surface Damage.
PB95-203311 *01,050*

Pulsed Laser Irradiation at 532 nm of In and Ga Adsorbed on Si(100): Desorption, Incorporation, and Damage.
PB95-203329 *01,051*

INDIUM GALLIUM ARSENIDES
Transition Metal Implants in In0.53GA0.47As.
PB95-126389 *04,534*

Range Statistics and Rutherford Backscattering Studies on Fe-Implanted In0.53Ga0.47As.
PB95-126397 *04,535*

INDIUM IONS
Electron-Impact Ionization of In(+) and Xe(+).
PB94-185089 *00,770*

Electron-Impact Ionization of In(+) and Xe(+).
PB95-152906 *03,918*

INDIUM OXIDES
Thin Film Thermocouple Research at NIST.
PB97-110233 *02,283*

INDIUM PHOSPHIDES
In situ Observation of Surface Morphology of InP Grown on Singular and Vicinal (001) Substrates.
PB95-168431 *04,636*

INDOLES
Equilibrium and Calorimetric Investigation of the Hydrolysis of L-Tryptophan to (Indole + Pyruvate + Ammonia).
PB95-163317 *00,661*

INDOOR AIR POLLUTION
Source of Phenol Emissions Affecting the Indoor Air of an Office Building.
PB94-154382 *03,600*

CONTAM93 User Manual.
PB94-164381 *02,536*

Measurement and Determination of Radon Source Potential: A Literature Review.
PB94-165602 *02,576*

CONTAM88 Building Input Files for Multi-Zone Airflow and Contaminant Dispersal Modeling.
PB94-194388 *02,537*

Environmental Evaluation of a New Federal Office Building.
PB94-199874 *02,538*

Ventilation Rates in Office Buildings.
PB95-108825 *02,539*

Field Measurements of Ventilation and Ventilation Effectiveness in an Office/Library Building.
PB95-108833 *00,247*

Indoor Air Quality Impacts of Residential HVAC Systems, Phase 1 Report: Computer Simulation Plan.
PB95-135596 *00,249*

Limits of CO2 Monitoring in Determining Ventilation Rates.
PB95-176004 *02,552*

Ventilation Effectiveness Measurements in Two Modern Office Buildings.
PB95-176012 *02,553*

Indoor Air Quality Impacts of Residential HVAC Systems, Phase 2.A Report: Baseline and Preliminary Simulations.
PB95-178893 *02,554*

Application of a Multizone Airflow and Contaminant Dispersal Model to Indoor Air Quality Control in Residential Buildings.
PB95-180238 *02,555*

Measurements of Indoor Pollutant Emissions from EPA Phase II Wood Stoves.
PB95-198735 *02,556*

New Mass Transport Elements and Components for the NIST IAQ Model.
PB95-255899 *02,558*

Indoor Air Quality Impacts of Residential HVAC Systems Phase II.B Report: IAQ Control Retrofit Simulations and Analysis.
PB96-106877 *02,559*

Few Caveats on Carbon Dioxide Monitoring.
PB96-122650 *02,562*

Effectiveness of a Heat Recovery Ventilator, an Outdoor Air Intake Damper and an Electrostatic Particulate Filter at Controlling Indoor Air Quality in Residential Buildings.
PB96-146642 *02,564*

Multizone Modeling of Three Residential Indoor Air Quality Control Options.
PB96-146659 *02,565*

Relationship between Indoor Air Quality and Carbon Dioxide.
PB97-111249 *02,569*

CONTAM94: A Multizone Airflow and Contaminant Dispersal Model with a Graphic User Interface.
PB97-113203 *02,570*

Carbon Monoxide Dispersion in Residential Buildings: Literature Review and Technical Analysis.
PB97-114227 *02,571*

Materials-Science Based Approach to Phenol Emissions from a Flooring Material in an Office Building.
PB97-118749 *02,572*

Issues in the Field Measurement of VOC Emission Rates.
PB97-118806 02,573

INDOOR AIR QUALITY

Air Change Effectiveness Measurements in Two Modern Office Buildings.
PB94-185766 00,243

Study of Ventilation and Carbon Dioxide in an Office Building.
PB95-150140 02,542

Assessing Ventilation Effectiveness in Mechanically Ventilated Office Buildings.
PB95-162079 00,255

Ventilation, Carbon Dioxide and ASHRAE Standard 62-1989.
PB95-162095 02,544

Indoor Air Quality Commissioning of a New Office Building.
PB95-182309 00,262

Measurements of Outdoor Air Distribution in an Office Building.
PB95-210944 00,264

Computer Simulations of Airflow and Radon Transport in Four Large Buildings.
PB95-220422 02,557

Development and Application of an Indoor Air Quality Commissioning Program in a New Office Building.
PB96-155601 00,275

Multizone Modeling of Three Residential Indoor Air Quality Control Options.
PB96-165782 02,567

Indoor Air Quality Commissioning of a New Office Building.
PB97-110142 00,279

INDOOR ENVIRONMENTS

Parametric Study of Wall Moisture Contents Using a Revised Variable Indoor Relative Humidity Version of the 'Moist' Transient Heat and Moisture Transfer Model.
PB97-122535 00,419

INDUCED CURRENT

Currents Induced on Multiconductor Transmission Lines by Radiation and Injection.
PB94-211943 02,215

INDUSTRIAL BUILDINGS

Performance Approach to the Development of Criteria for Low-Sloped Roof Membranes.
PB94-160751 00,329

INDUSTRIAL MANAGEMENT

Agile Manufacturing from a Statistical Perspective.
PB96-109525 02,886

INDUSTRIAL MEDICINE

Radiation Accident at an Industrial Accelerator Facility.
PB95-140117 02,575

INDUSTRIAL PLANTS

Technical Program of the Factory Automation Systems Division 1993.
PB94-160819 02,805

Evaluation of Corrosion Data: A Review.
PB94-198348 03,187

Framework for Information Technology Integration in Process Plant and Related Industries.
PB94-219086 02,772

Summaries of BFRL Fire Research In-House Projects and Grants, 1994.
PB95-130845 00,366

Group 1 for the Plant Spatial Configuration STEP Application Protocol.
PB96-165402 02,789

INDUSTRIAL WASTES

Opportunities for Innovation: Pollution Prevention.
PB95-147146 02,520

INDUSTRIES

NIST Industrial Impacts: A Sampling of Successful Partnerships.
PB95-111514 00,488

Workshop Summary Report: Industrial Applications of Scanned Probe Microscopy. A Workshop Co-sponsored by NIST, SEMATECH, ASTM, E42.14, and the American Vacuum Society. Held in Gaithersburg, Maryland on March 24-25, 1994.
PB95-170387 00,506

NIST Industrial Impacts: A Sampling of Successful Partnerships (Revision, March 1995).
PB95-209193 00,489

Summary Report: Workshop on Industrial Applications of Scanned Probe Microscopy (2nd). A Workshop Co-Sponsored by NIST, SEMATECH, ASTM E42.14, and the American Vacuum Society. Held in Gaithersburg, Maryland on May 2-3, 1995.
PB96-131602 00,509

INDUSTRY/GOVERNMENT OPEN SYSTEMS SPECIFICATION

Industry/Government Open Systems Specification Testing Framework. Version 1.0.
PB94-219110 01,809

INELASTIC SCATTERING

Low-Energy-Electron Collisions with Sodium: Elastic and Inelastic Scattering from the Ground State.
PB96-103106 04,030

Orbital Alignment and Vector Correlations in Inelastic Atomic Collisions.
PB96-122742 04,047

INERTIAL CONFINEMENT FUSION

Physics and Prospects of Inertial Confinement Fusion.
PB94-185048 04,405

INERTIAL NAVIGATION

Ground Vehicle Control at NIST: From Teleoperation to Autonomy.
N94-34037/9 03,758

INFILLED WALLS

Strengthening Methodology for Lightly Reinforced Concrete Frames: Recommended Design Guidelines for Strengthening with Infill Walls.
PB95-260725 00,454

INFORMATION CAPACITY

Capacity of the Lp Norm-Constrained Poisson Channel.
PB95-125753 01,515

INFORMATION CENTERS

NIST Serial Holdings, 1994.
PB94-178068 02,745

Databases Available in the Research Information Center of the National Institute of Standards and Technology (December 1995).
PB96-139407 02,734

NIST Crystallographic Databases for Research and Analysis.
PB97-109094 04,801

INFORMATION DISSEMINATION

Numeric Data Distribution: The Vital Role of Data Exchange in Today's World.
N95-15937/2 02,622

National Center for Standards and Certification Information: Service and Programs.
N95-15938/0 02,717

Sharing Information via the Internet: An Infoserver Case Study.
PB96-131511 01,493

INFORMATION EXCHANGE

Federal Implementation Guideline for Electronic Data Interchange: ASC X12 003040 Transaction Set 838 Trading Partner Profile (Confirmation of Vendor Registration). Implementation Convention.
PB96-111190 01,813

Federal Implementation Guideline for Electronic Data Interchange: ASC X12 003040 Transaction Set 838 Trading Partner Profile (Vendor Registration), Implementation Convention.
PB96-112651 03,674

Procedure for Product Data Exchange Using STEP Developed in the AutoSTEP Pilot.
PB96-183058 02,843

INFORMATION HIGHWAYS

Electronic Access to Standards on the Information Highway.
PB96-131578 01,494

INFORMATION MANAGEMENT

Dilemma-Preservation versus Access.
PB94-198488 02,711

Preliminary Functional Specifications of a Prototype Electronic Research Notebook for NIST.
PB94-207750 00,012

INFORMATION PROCESSING

User Profile for Researchers Studying Objects: Implications for Computer Systems.
PB94-188463 00,133

Federal Government and Information Technology Standards: Building the National Information Infrastructure.
PB95-180840 01,812

INFORMATION RESOURCE DICTIONARY SYSTEM

Information Resource Dictionary System (IRDS): A Status Report.
PB95-126207 01,810

INFORMATION RESOURCES

Montgomery Education Connection and Resource Education Awareness Partnership Making Connections between Local Schools and NIST Volunteers.
PB96-159769 00,134

INFORMATION RETRIEVAL

Design and Development of an Information Retrieval System for the EAMATE Data. Volume 2 of 2. Appendices.
PB94-168390 00,487

Bringing Natural Language Information Retrieval Out of the Closet.
PB94-172335 02,720

Second Text REtrieval Conference (TREC-2). Held in Gaithersburg, Maryland on August 31-September 2, 1993.
PB94-178407 01,686

World Wide Web and Mosaic: User's Guide.
PB94-207354 02,722

FIREDOC Users Manual, 3rd Edition.
PB95-128674 01,378

Information Retrieval Using Key Words and a Structured Review.
PB95-161121 03,724

Access Paths for Materials Databases: Approaches for Large Databases and Systems.
PB95-162525 02,975

Coping with Different Retrieval Methods in Next Generation Networks.
PB95-168555 02,726

Retrieving Articles from the Internet (without a UNIX Workstation). Part 1. File Formats and Software Tools.
PB95-168720 02,728

Retrieving Articles from the Internet (without a UNIX Workstation). Part 2. An Example.
PB95-168738 02,729

Prototype Information Retrieval System to Perform a Best-Match Search for Names.
PB95-181152 02,740

Overview of the Text REtrieval Conference (3rd) (TREC-3). Held in Gaithersburg, Maryland on November 2-4, 1994.
PB95-216883 01,728

Electronic Access: Blueprint for the National Archives and Records Administration.
PB95-219218 02,731

Z39.50 Implementation Experiences.
PB96-114939 01,816

Information Resources for the Fire Community.
PB96-148119 00,211

Using a Multi-Layered Approach to Representing Tort Law Cases for Case-Based Reasoning.
PB96-160874 00,135

Lab Report Special Section: Natural Language Processing and Information Retrieval Group Information Access and User Interfaces Division, National Institute of Standards and Technology.
PB97-118665 02,742

Panel: Building and Using Test Collections.
PB97-118673 02,743

Text REtrieval Conference (4th) (TREC-4). Held in Gaithersburg, Maryland on November 1-3, 1995.
PB97-121636 01,786

INFORMATION SERVICES

Information Infrastructure: Reaching Society's Goals. Report of the Information Infrastructure Task Force Committee on Applications and Technology.
PB94-214756 01,469

CALS-Contractor Integrated Technical Information Service (CITIS), Functional Requirements.
PB94-962600 03,663

Databases Available in the Research Information Center of the National Institute of Standards and Technology.
PB95-128641 02,724

STEP On-Line Information Service (SOLIS). The IGES/PDES Organization.
PB95-137790 02,777

User Study: Informational Needs of Remote National Archives and Records Administration Customers.
PB95-154738 02,725

CALS-Contractor Integrated Technical Information Service (CITIS), Functional Requirements.
PB95-962600 03,672

National Information Infrastructure and Advanced Digital Video.
PB96-119367 01,488

General Types of Information Services.
PB96-147053 02,735

INFORMATION SOURCES

Retrieving Articles from the Internet (without a UNIX Workstation). Part 2. An Example.
PB95-168738 02,729

INFORMATION STORAGE

Electronic Access: Blueprint for the National Archives and Records Administration.
PB95-219218 02,731

INFORMATION SYSTEMS

Putting the Information Infrastructure to Work: Report of the Information Infrastructure Task Force Committee on Applications and Technology.
N94-31228/7 02,715

Open System Environments.
N94-36857/8 01,674

Open System Environment Procurement.
N94-36858/6 02,716

National Center for Standards and Certification Information: Service and Programs.
N95-15938/0 02,717

Putting the Information Infrastructure to Work: Report of the Information Infrastructure Task Force Committee on Applications and Technology.
PB94-163383 00,001

Development of the Fire Data Management System.
PB94-206091 00,339

World Wide Web and Mosaic: User's Guide.
PB94-207354 02,722

Highway Concrete (HWYCON) Expert System User Reference and Enhancement Guide.
PB94-215670 01,316

Report on the Workshop on Advanced Digital Video in the National Information Infrastructure. Held in Washington, D.C. on May 10-11, 1994.
PB95-103677 01,472

Application of Expert System to Select Data Sources from Chemical Information Databases.
PB95-125654 00,505

FIREDOC Users Manual, 3rd Edition.
PB95-128674 *01,378*

Tribological Data: Needs and Opportunities.
PB95-140596 *03,237*

Information Technology Engineering and Measurement Model: Adding Lane Markings to the Information Superhighway.
PB95-143145 *01,474*

Locating Fire Engineering Information.
PB95-161188 *00,198*

Global Information Infrastructure: Agenda for Cooperation.
PB95-178604 *01,482*

Prototype Information Retrieval System to Perform a Best-Match Search for Names.
PB95-181152 *02,740*

Structural Ceramics Database. Topical Report, June 1989-May 1991.
PB95-203758 *03,060*

Computer Systems Laboratory Annual Report 1994.
PB95-209920 *01,629*

Analysis of ANSI ASC X12 and UN/EDIFACT Electronic Data Interchange (EDI) Standards.
PB95-220554 *01,729*

Guidelines for the Evaluation of X.500 Directory Products.
PB95-231908 *02,732*

Federal Implementation Guideline for Electronic Data Interchange. ASC X12 003050 Transaction Set 850 Award Instrument. Implementation Convention.
PB96-114913 *01,814*

Federal Implementation Guideline for Electronic Data Interchange. ASC X12 003050 Transaction Set 860 Modifications to Award Instrument. Implementation Convention.
PB96-114921 *01,815*

Defining Environment Integration Requirements.
PB96-131545 *02,733*

Open System Environment (OSE): Architectural Framework for Information Infrastructure.
PB96-146360 *00,002*

Security Program Management.
PB96-156112 *01,610*

Federal Implementation Guideline for Electronic Data Interchange. ASC X12 003050 Transaction Set 843 Response to Request for Quotation. Implementation Convention.
PB96-168984 *01,822*

Guidelines for the Evaluation of Electronic Data Interchange Products.
PB96-172325 *01,506*

Federal Implementation Guideline for Electronic Data Interchange. ASC X12 003050 Transaction Set 855 Purchase Order Acknowledgment: Implementation Convention.
PB96-172374 *01,823*

Federal Implementaion Guideline for Eletronic Data Interchange. ASC X12 003050 Transaction Set 865 Purchase Order Change Acknowledgement/Request - Seller Initiated. Implementation Convention.
PB96-172549 *01,825*

X.500 Directory Schema Design Handbook.
PB96-183041 *02,739*

Computer Systems Laboratory Computing and Applied Mathematics Laboratory Technical Accomplishments, October 1994-March 1996.
PB96-193768 *01,638*

Journal of Research of the National Institute of Standards and Technology, May/June 1996. Volume 101, Number 3. Special Issue: NIST Workshop on Crystallographic Databases.
PB97-109011 *04,798*

CRYSTMET: The NRCC Metals Crystallographic Data File.
PB97-109029 *04,799*

Inorganic Crystal Structure Database (ICSD) and Standardized Data and Crystal Chemical Characterization of Inorganic Structure Types (TYPIX): Two Tools for Inorganic Chemists and Crystallographers.
PB97-109037 *00,648*

Evaluation of Crystallographic Data with the Program DIAMOND.
PB97-109045 *00,649*

Cambridge Structural Database (CSD): Current Activities and Future Plans.
PB97-109052 *00,516*

Protein Data Bank: Current Status and Future Challenges.
PB97-109060 *00,517*

Nucleic Acid Database: Present and Future.
PB97-109078 *00,518*

Powder Diffraction File: Past, Present, and Future.
PB97-109086 *04,800*

NIST Crystallographic Databases for Research and Analysis.
PB97-109094 *04,801*

Conventional and Eccentric Uses of Crystallographic Databases in Practical Materials Identification Problems.
PB97-109102 *04,802*

Using NIST Crystal Data within Siemens Software for Four-Circle and SMART CCD Diffractometers.
PB97-109110 *04,803*

Investigations of the Systematics of Crystal Packing Using the Cambridge Structural Database.
PB97-109144 *00,519*

Troublesome Crystal Structures: Prevention, Detection, and Resolution.
PB97-109151 *01,172*

CIF Crystallographic Information File: A Standard for Crystallographic Data Interchange.
PB97-109169 *04,805*

How the Cambridge Crystallographic Data Centre Obtains Its Information.
PB97-109193 *04,808*

Data Import and Validation in the Inorganic Crystal Structure Database.
PB97-109201 *04,809*

World Wide Web for Crystallography.
PB97-109219 *04,810*

Workshop Highlights.
PB97-109227 *04,811*

Experimental Models for Software Diagnosis.
PB97-113906 *01,783*

INFORMATION TECHNOLOGY

Report on Application Integration Architectures (AIA) Workshop. Held in Dallas, Texas on February 8-12, 1993.
PB94-142536 *01,803*

Study of Federal Agency Needs for Information Technology Security.
PB94-193653 *01,579*

Framework for National Information Infrastructure Services.
PB95-103719 *02,723*

Computer Systems Laboratory Annual Report 1994.
PB95-209920 *01,629*

Electronic Implementors' Workshop.
PB95-210936 *01,484*

Information Technologies Make Business Sense for the Custom Therapeutic Footwear Industry.
PB95-251708 *02,829*

Common Criteria: On the Road to International Harmonization.
PB96-123484 *01,606*

Functional Security Criteria for Distributed Systems.
PB96-123492 *01,607*

Information Technology Standards in a Changing World: The Rose of the Users.
PB96-160866 *02,737*

Concept Paper: An Overview of the Proposed Trust Technology Assessment Program.
PB96-160882 *01,614*

Information Technology Standards in Federal Acquisitions.
PB96-161252 *01,636*

Using Information Technology Standards in Federal Acquisitions.
PB96-161260 *01,637*

Computer Systems Laboratory Computing and Applied Mathematics Laboratory Technical Accomplishments, October 1994-March 1996.
PB96-193768 *01,638*

INFORMATION TRANSFER

Standards and Linkages: What Data Sharing Needs.
PB95-161881 *01,713*

Information Transfer in the 21st Century.
PB96-157904 *02,714*

INFRARED ABSORPTION

Laser-Synchrotron Hybrid Experiments: A Photon to Tickle, A Photon to Poke.
PB96-157847 *03,704*

INFRARED BOLOMETERS

Far-Infrared Kinetic Inductance Detector.
PB95-126348 *02,142*

Superconducting Kinetic Inductance Radiometer.
PB95-140083 *02,144*

INFRARED DETECTORS

Semiconductor Measurement Technology: Improved Characterization and Evaluation Measurements for HgCdTe Detector Materials, Processes, and Devices Used on the GOES and TIROS Satellites.
PB94-188810 *02,122*

Review of Semiconductor Microelectronic Test Structures with Applications to Infrared Detector Materials and Processes.
PB94-212925 *02,132*

Heavily Accumulated Surfaces of Mercury Cadmium Telluride Detectors: Theory and Experiment.
PB94-216074 *02,134*

International Intercomparison of Detector Responsivity at 1300 and 1550 nm.
PB95-125928 *02,140*

International Intercomparison of Detector Responsivity at 1300 and 1550 nm.
PB95-126017 *02,141*

Far-Infrared Kinetic Inductance Detector.
PB95-126348 *02,142*

Thermal and Nonequilibrium Responses of Superconductors for Radiation Detectors.
PB95-164232 *02,156*

Hg1-xCdxTe Characterization Measurements: Current Practice and Future Needs.
PB95-164299 *02,157*

Terahertz Detectors Based on Superconducting Kinetic Inductance.
PB95-168647 *02,160*

Optical Performance of Photoinductive Mixers at Terahertz Frequencies.
PB95-168662 *02,161*

Spatial Uniformity of Optical Detector Responsivity.
PB95-168845 *02,162*

Ultrasensitive-Hot-Electron Microbolometer.
PB95-168985 *02,163*

Kinetic-Inductance Infrared Detector Based on an Antenna-Coupled High-Tc SQUID.
PB95-169116 *02,165*

Optical Detector Nonlinearity: A Comparison of Five Methods.
PB95-169355 *04,291*

Optical Detector Nonlinearity: Simulation.
PB96-165378 *02,199*

Novel Hot-Electron Microbolometer.
PB96-201025 *01,977*

INFRARED FILTERS

Filter Transmittance Measurements in the Infrared.
PB94-140589 *04,224*

Broadband High-Optical-Density Filters in the Infrared.
PB95-180261 *04,309*

Development of Neutral-Density Infrared Filters Using Metallic Thin Films.
PB96-180286 *02,998*

INFRARED RADIOMETERS

Activities of NIST (National Inst. Of Standards and Technology).
N94-23605/6 *04,222*

Superconducting Kinetic Inductance Radiometer.
PB95-140083 *02,144*

Terahertz Detectors Based on Superconducting Kinetic Inductance.
PB95-168647 *02,160*

Thermal Modeling of Absolute Cryogenic Radiometers.
PB95-181236 *04,316*

Liquid-Nitrogen-Cooled High Tc Electrical Substitution Radiometer as a Broadband IR Transfer Standard.
PB96-158704 *02,198*

NIST Thermal Infrared Transfer Standard Radiometer for the Earth Observing System (EOS) Program.
PB97-113013 *04,843*

INFRARED REFLECTANCE

Optical Conductivity of Single Crystals of Ba1-xMxBiO3(M=K, Rb, x=0.04, 0.37).
PB94-185329 *04,447*

INFRARED SIGNATURES

Review of Measurements and Candidate Signatures for Early Fire Detection.
PB95-189452 *00,300*

INFRARED SOURCES

Update on the Low Background IR Calibration Facility at the National Institute of Standards and Technology.
PB94-211224 *04,232*

INFRARED SPECTRA

Vibrational Spectra of Molecular Ions Isolated in Solid Neon. 7. CO(+), C2O2(+), and C2O2(-). (Reannouncement with New Availability Information).
AD-A239 729/7 *00,706*

Vibrational Spectra of Molecular Ions Isolated in Solid Neon. 11. NO2(+), NO2(-), and NO3(-).
AD-A275 828/2 *00,708*

Arc Spectra of Gallium, Indium, and Thallium.
AD-A295 411/3 *00,718*

Infrared and Near-Infrared Spectra of HCC and DCC Trapped in Solid Neon.
AD-A295 578/9 *03,773*

Investigating the 3.3 Micron Infrared Fluorescence from Naphthalene Following Ultraviolet Excitation.
N95-15839/0 *00,724*

Measurement of the J=2 less than 1 Fine-Structure Interval for (28)Si and (29)Si in the Ground (3)P State.
PB94-185097 *00,771*

P-Type Doubling in the Infrared Spectrum of NO-HF.
PB94-211463 *00,817*

Mid- and Near-Infrared Spectra of Water and Water Dimer Isolated in Solid Neon.
PB95-125662 *00,888*

Infrared Spectra of van der Waals Complexes of Importance in Planetary Atmospheres.
PB95-125738 *00,071*

Infrared Spectrum of OClO in the 2000/cm(-1) Region: The 2(nu sub 1) and (nu sub 1 + nu sub 3) Bands.
PB95-141032 *00,908*

Intensities and Dipole Moment Derivatives of the Fundamental Bands of (35)ClO2 and an Intensity Analysis of the nu1 Band.
PB95-141040 *00,909*

Rotational Far Infrared Spectrum of (13)CO.
PB95-152187 00,941

2nu9 Band of Propyne-d3.
PB95-164513 00,985

New cw CO2 Laser Lines: The 9-mu m Hot Band.
PB95-168548 04,281

Absolute Frequency Measurements of Methanol from 1.5 to 6.5 THz.
PB95-175881 04,300

Pure Rotational Spectra of CuH and CuD in Their Ground States Measured by Tunable Far-Infrared Spectroscopy.
PB95-176194 01,005

Rotational Spectrum of OH in the v=0-3 Levels of Its Ground State.
PB95-176202 01,006

Atomic Sulfur: Frequency Measurement of the J=0 inversely maps 1 Fine-Structure Transition at 56.3 Microns by Laser Magnetic Resonance.
PB95-180105 01,007

INFRARED SPECTROMETRY

Ultrafast Time-Resolved Infrared Probing of Energy Transfer at Surfaces.
PB96-123443 00,620

INFRARED SPECTROPHOTOMETERS

Simple and Efficient Low-Temperature Sample Cell for Infrared Spectrophotometry.
PB94-199197 00,545

Standard Reference Materials: Polystyrene Films for Calibrating the Wavelength Scale of Infrared Spectrophotometers - SRM 1921.
PB95-226866 03,386

INFRARED SPECTROSCOPY

High-Resolution Infrared Overtone Spectroscopy of ArHF via Nd:YAG/Dye Laser Difference Frequency Generation.
PB94-211448 00,816

Mode Specific Vibrational Predissociation Dynamics in Fragile Molecules.
PB95-107132 00,871

Vibration, Rotation, and Parity Specific Predissociation Dynamics in Asymmetric OH Stretch Excited ArH2O: A Half Collision Study of Resonant V-V Energy Transfer in a Weakly Bound Complex.
PB95-107140 00,872

High-Resolution Infrared Spectroscopy of DF Trimer: A Cyclic Ground State Structure and DF Stretch Induced Intramolecular Vibrational Coupling.
PB95-150678 00,920

Slit Jet Infrared Spectroscopy of Hydrogen Bonded N2HF Isotopomers: Rotational Rydberg-Klein-Rees Analysis and H/D Dependent Vibrational Predissociation Rates.
PB95-161873 00,956

High-Resolution, Direct Infrared Laser Absorption Spectroscopy in Slit Supersonic Jets: Intermolecular Forces and Unimolecular Vibrational Dynamics in Clusters.
PB95-203006 01,040

High-Resolution Infrared Overtone Spectroscopy of N2-HF: Vibrational Red Shifts and Predissociation Rate as a Function of HF Stretching Quanta.
PB96-102298 01,061

Silicon Surface Chemistry by IR Spectroscopy in the Mid- to Far-IR Region: H2O and Ethanol on Si(100).
PB96-138565 01,097

INFRARED SPECTRUMS

Perpendicular C-H Stretching Band nu9/nu13 and the Torsional Potential of Dimethylacetylene.
PB97-122451 01,192

INFRASTRUCTURE

Functions of Technology Infrastructure in a Competitive Economy.
PB94-173002 00,478

Planning the Infrastructure for Global Electronic Commerce.
PB94-185832 00,494

Financing Tomorrow's Infrastructure: Challenges and Issues. Proceedings of a Colloquium. Held in Washington, DC. on October 20, 1995.
PB96-189444 00,481

INHIBITORS

Selective Inhibition of Crystal Growth on Octacalcium Phosphate and Nonstoichiometric Hydroxyapatite by Pyrophosphate at Physiological Concentration.
PB94-211257 00,147

INITIAL GRAPHICS EXCHANGE SPECIFICATION

Summary and Notes of the Joint ISO/IGES/PDES Organization Technical Committee Meeting. Held in Albuquerque, New Mexico on October 15-20, 1989.
PB95-107314 02,774

Initial Graphics Exchange Specification (IGES): Procedures for the NIST IGES Validation Test Service.
PB95-171427 02,780

Operating Procedures and Life Cycle Documentation for the Initial Graphics Exchange Specification.
PB95-242285 02,782

INJECTION MOLDING

In-Line Optical Monitoring of Injection Molding.
PB94-185105 01,201

INKS

Cylinder Wipe Air-Drying Intaglio Ink Vehicles for U.S. Currency Inks.
PB94-160801 03,115

INORGANIC COMPOUNDS

Establishing Quality Measurements for Inorganic Analysis of Biomaterials.
PB94-199726 00,548

Determination of Inorganic Constituents in Marine Mammal Tissues.
PB95-152047 00,589

Affinity Chromatography on Inorganic Support Materials.
PB95-163820 03,467

Characterization of the Structure of YD3 by Neutron Powder Diffraction.
PB96-186150 01,161

Inorganic Crystal Structure Database (ICSD) and Standardized Data and Crystal Chemical Characterization of Inorganic Structure Types (TYPIX): Two Tools for Inorganic Chemists and Crystallographers.
PB97-109037 00,648

Evaluation of Crystallographic Data with the Program DIAMOND.
PB97-109045 00,649

Data Import and Validation in the Inorganic Crystal Structure Database.
PB97-109201 04,809

INORGANIC SALTS

Phase Composition, Viscosities, and Densities for Aqueous Two-Phase Systems Composed of Polyethylene Glycol and Various Salts at 25C.
PB95-164596 00,986

INORGANIC SUPPORTS

Preparation of Immobilized Proteins Covalently Coupled Through Silane Coupling Agents to Inorganic Supports.
PB95-151403 03,530

INOSINE MONOPHOSPHATE

Thermochemistry of the Reactions between Adenosine, Adenosine 5'-monophosphate, Inosine, and Inosine 5'-monophosphate; the Conversion of L-histidine to (Urocanic Acid+Ammonia).
PB94-213113 03,460

INSERTS

Reduction of Marginal Gaps in Composite Restorations by Use of Glass-Ceramic Inserts.
PB96-102405 00,174

INSOLATORS

Phonon Relaxation in Soft-X-ray Emission of Insulators.
PB96-160296 04,085

INSPECTION

Development of an Automated Part Inspection System Using the DMIS Standard.
PB95-108866 02,899

Sensitivity of Three-Point Circle Fitting.
PB95-136354 02,901

Automated Optical Roughness Inspection.
PB95-152179 02,905

Dimensional Inspection Planning Based on Product Data Standards.
PB95-175451 02,910

Interim Testing Artifact (ITA): A Performance Evaluation System for Coordinate Measuring Machines (CMMs). User Manual.
PB95-210589 02,914

International Institute of Welding: Report on 1995 Actions.
PB96-158076 02,874

Integrated Inspection System for Improved Machine Performance.
PB96-160569 02,959

INSPECTIONS

SPC Artifact for Automated Solder Joint Inspection.
PB96-161716 04,095

INSTALLATION

Flowmeter Installation Effects Due to a Generic Header.
PB96-210893 02,606

INSTRUMENT ERRORS

Partial Pressure Analysis in Space Testing.
N95-14084/4 04,827

Test Optics Error Removal.
PB96-179536 04,377

Compensation for Errors Introduced by Nonzero Fringe Densities in Phase-Measuring Interferometers.
PB97-110506 04,386

INSTRUMENT SETTINGS

Optimizing Time-Domain Network Analysis.
PB96-157821 02,085

INSTRUMENTAL NEUTRON ACTIVATION ANALYSIS

Relationship of Silver with Selenium and Mercury in the Liver of Two Species of Toothed Whales (Odontocetes).
PB96-167275 02,596

Resolution of Discrepant Analytical Data in the Certification of Platinum in Two Automobile Catalyst SRMs.
PB96-167283 00,638

INSTRUMENTATION

Guide to Instrumentation Literature.
AD-A280 278/3 02,617

Instrument for Evaluating Phase Behavior of Mixtures for Supercritical Fluid Experiments.
PB95-180758 00,606

INSTRUMENTATION & EXPERIMENTAL METHODS

Development of a Dual-Sinker Densimeter for High-Accuracy Fluid P-V-T Measurements. Appendix A.
DE93019682 02,620

Low Temperature H(sub 2)S Separation Using Membrane Reactor with Redox Catalyst.
DE94008991 02,471

Thin Film Thermocouples for Measurement of Wall Temperatures in Internal Combustion Engines.
PB94-172103 01,449

Evaluation and Qualification Standards for an X-Ray Laminography System.
PB94-172954 02,029

Physics and Prospects of Inertial Confinement Fusion.
PB94-185048 04,405

High-Temperature Laser-Pulse Thermal Diffusivity Apparatus.
PB94-185147 02,631

Selection of Appropriate Ultrasonic System Components for NDE of Thick Polymer-Composites.
PB94-185279 03,133

Electro-Optical Sensor for Surface Displacement Measurements of Compliant Coatings.
PB94-198223 02,123

Voigt-Function Modeling in Fourier Analysis of Size- and Strain-Broadened X-Ray Diffraction Peaks.
PB94-198538 04,462

Milliwatt Mixer for Small Fluid Samples.
PB94-198819 02,634

Applications of the Vortex Tube in Chemical Analysis.
PB94-199171 00,544

Simple and Efficient Low-Temperature Sample Cell for Infrared Spectrophotometry.
PB94-199197 00,545

Simple, Inexpensive Apparatus for Sample Concentration.
PB94-199205 00,546

Experimental Studies of Line Shapes from a Balle-Flygare Spectrometer.
PB94-199452 00,796

Millisecond-Resolution Pulse Heating System for Specific-Heat Measurements at High Temperatures.
PB94-199999 02,635

High-Speed Spatial Scanning Pyrometer.
PB94-200003 02,636

Planar Waveguide Optical Sensors.
PB94-200185 03,586

Salt-PEG Two-Phase Aqueous Systems to Purify Proteins and Nucleic Acid Mixtures.
PB94-200375 03,527

Torsional Dilatometer for Volume Change Measurements on Deformed Glasses: Instrument Description and Measurements on Equilibrated Glasses.
PB94-211166 03,379

Update on the Low Background IR Calibration Facility at the National Institute of Standards and Technology.
PB94-211224 04,232

NIST Power Reference Source.
PB94-211513 00,148

Intercomparison of the Effective Areas of a Pneumatic Piston Gauge Determined by Different Techniques.
PB94-212370 02,640

Determination of Osmotic Pressure and Fouling Resistances and Their Effects on Performance of Ultrafiltration Membranes.
PB94-212891 00,841

Characterization of the Adsorption-Fouling Layer Using Globular Proteins on Ultrafiltration Membranes.
PB94-212909 00,842

High Resolution Hard X-Ray Microscope.
PB94-213055 03,856

Light Scattering from Glossy Coatings on Paper.
PB94-213246 04,242

Analytical Estimation of Carrier Multipath Bias on GPS Position Measurements.
PB94-215712 04,845

Ultra-High Stability Synthesizer for Diode Laser Pumped Rubidium.
PB94-216066 01,527

Determination of Surface Roughness from Scattered Light.
PB94-216520 04,243

Simple, Compact, High-Purity Cr Evaporator for Ultrahigh Vacuum.
PB94-216678 04,520

Improved Automated Current Control for Standard Lamps.
PB94-219367 00,246

Resistance Thermometers with Fast Response for Use in Rapidly Oscillating Gas Flows.
PB95-107298 03,261

Vibration Laboratory Automation at NIST with Personal Computers.
PB95-108700 02,648

Appropriate Ultrasonic System Components for NDE of Thick Polymer Composites.
PB95-125696 03,148

High-Sensitivity Acoustic Emission Sensor/Preamplifier Subsystems.
PB95-125704 02,900

Conductance Response of Pd/SnO2(110) Model Gas Sensors to H2 and O2.
PB95-125803 00,892

Uncertainty Analysis of the NIST Nitrogen Flow Facility.
PB95-128906 *02,608*

Thermal Hydraulic Tests of a Liquid Hydrogen Cold Neutron Source.
PB95-135570 *03,884*

Heat Transfer in Thin, Compact Heat Exchangers with Circular, Rectangular, or Pin-Fin Flow Passages.
PB95-140943 *02,751*

Intelligent Control of an Inert Gas Atomization Process.
PB95-141057 *03,344*

Process Gas Chromatography Detector for Hydrocarbons Based on Catalytic Cracking.
PB95-141099 *02,485*

Radiometric Model of the Transmission Cell-Reciprocal Nephelometer.
PB95-150132 *00,124*

Integrating Sphere Simulation: Application to Total Flux Scale Realization.
PB95-150173 *04,261*

Characteristics of Partial Pressure Analyzers.
PB95-150876 *00,582*

Experimental and Numerical Studies of Refractory Particle Formation in Flames: Application to Silica Growth.
PB95-152005 *00,673*

Simulation of Ceramic Particle Formation: Comparison with In-situ Measurements.
PB95-152013 *00,674*

Thermal Behaviour of Methyl Methacrylate and N-Phenyl Maleimide Copolymers.
PB95-152237 *01,246*

Dynamic Technique for Measuring Normal Spectral Emissivity of Electrically Conducting Solids at High Temperatures with a High-Speed Spatial Scanning Pyrometer.
PB95-153045 *03,921*

Grazing Angle X-Ray Photoemission System for Depth-Dependent Analysis.
PB95-161154 *04,600*

Enzyme and Protein Mass Transfer Coefficient in Aqueous Two Phase Systems. 1. Spray Extraction Columns.
PB95-161162 *00,594*

Continuous Counter-Current Two Phase Aqueous Extraction.
PB95-161212 *00,675*

Fracture Toughness of Advanced Ceramics at Room Temperature: A Vamas Round-Robin.
PB95-162194 *03,160*

Protein Extraction in a Spray Column Using a Polyethylene Glycol Maltodextrin Two-Phase Polymer System.
PB95-162228 *00,595*

Development of Adaptive Control Strategies for Inert Gas Atomization.
PB95-162335 *02,823*

Loading Device for Fracture Testing of Compact Tension Specimens in the Scanning Electron Microscope.
PB95-162434 *02,652*

Noncontact Ultrasonic Inspection of Train Rails for Stress.
PB95-162673 *04,851*

Preparation of 2-Dimensional Ultra Thin Polystyrene Film by Water Casting Method.
PB95-162806 *04,619*

Electrical Sensors for Monitoring rf Plasma Sheaths.
PB95-162962 *04,412*

Brownian Diffusion of Hard Spheres at Finite Concentrations.
PB95-164307 *00,975*

Through-the-Arc Sensing for Measuring Gas Metal Arc Weld Quality in Real Time.
PB95-164463 *02,908*

Cryogenics.
PB95-164703 *02,654*

Annex 18: An International Study of Refrigerant Properties.
PB95-168936 *03,266*

Proposed Antiferromagnetically Coupled Dual-Layer Magnetic Force Microscope Tips.
PB95-169017 *04,645*

Membrane Gas Separation for a Fluidized-Bed Incinerator.
PB95-169041 *02,550*

Energy Flows in an Orifice Pulse Tube Refrigerator.
PB95-169082 *02,752*

Graded and Nongraded Regenerator Performance.
PB95-169090 *02,753*

Optimization of ECR-Based PECVD Oxide Films for Superconducting Integrated Circuit Fabrication.
PB95-169165 *02,051*

Comparative Photoluminescence Measurement and Simulation of Vertical-Cavity Semiconductor Laser Structures.
PB95-169173 *02,169*

Measurement and Simulation of Photoluminescence Spectra from Vertical-Cavity Quantum-Well Laser Structures.
PB95-169181 *02,170*

Vortex Shedding Flowmeters for SSME Ducts.
PB95-169215 *01,453*

Phase-Locked Oscillator Optimization for Arrays of Josephson Junctions.
PB95-169314 *02,052*

Critical Issues in Scanning Electron Microscope Metrology.
PB95-169405 *02,359*

Video Microscopy Applied to Optical Fiber Geometry Measurements.
PB95-173068 *04,295*

Influence of the Filament Potential Wave Form on the Sensitivity of Glass-Envelope Bayard-Alpert Gages.
PB95-175014 *02,657*

Retention of Halocarbons on a Hexafluoropropylene Epoxide Modified Graphitized Carbon Black. Part 1. Methane-Based Compounds.
PB95-175196 *03,272*

Automated Josephson Integrated Circuit Test System.
PB95-175246 *02,057*

Friction and Oxidative Wear of 440C Ball Bearing Steels Under High Load and Extreme Bulk Temperatures.
PB95-175253 *03,215*

Formation of Hydroxyapatite in Cement Systems.
PB95-175261 *00,170*

Correlation of Optical, X-ray, and Electron Microscopy Measurements of Semiconductor Multilayer Structures.
PB95-175279 *02,174*

High-Pressure Equilibrium Cell for Solubility Measurements in Supercritical Fluids.
PB95-175634 *00,998*

Determination of the Complex Refractive Index of Individual Quantum Wells from Distributed Reflectance.
PB95-175642 *02,176*

PC-Based Spinning Rotor Gage Controller.
PB95-175832 *02,609*

Investigations of AM and PM Noise in X-Band Devices.
PB95-180022 *02,062*

Passively Q-Switched Nd-Doped Waveguide Laser.
PB95-180048 *04,308*

Chromatographic Cryofocusing and Cryotrapping with the Vortex Tube.
PB95-180113 *00,604*

Tribometer for Measurements in Hostile Environments.
PB95-180949 *02,967*

Reducing the Effect of Local Oscillator Phase Noise on the Frequency Stability of Passive Frequency Standards.
PB95-180972 *01,545*

Low-Noise High-Speed Diode Laser Current Controller.
PB95-202826 *02,178*

Decrease of Fluorescence in Optical Fiber during Exposure to Pulsed or Continuous-Wave Ultraviolet Light.
PB95-203071 *04,320*

Low-Frequency, Active Vibration Isolation System.
PB95-203303 *02,710*

Surface Modification of YBa2Cu3O7-delta Thin Films Using the Scanning Tunneling Microscope: Five Methods.
PB95-203394 *04,699*

Single Photon Laser Ionization as an In-situ Diagnostic for MBE growth.
PB96-102025 *01,059*

Resonances in Two-Dimensional Array Oscillator Circuits.
PB96-102082 *02,066*

Direct Observation of Vortex Dynamics in Two-Dimensional Josephson-Junction Arrays.
PB96-102223 *02,067*

Stacked Series Arrays of High-Tc Trilayer Josephson Junctions.
PB96-102272 *04,705*

Self-Biasing Cryogenic Particle Detector Utilizing Electrothermal Feedback and a SQUID Readout.
PB96-102538 *04,712*

Measurement of Very Low Frequency Vibrations.
PB96-102660 *03,687*

Electronic Microrefrigerator Based on a Normal-Insulator-Superconductor Tunnel Junction.
PB96-102827 *04,718*

New Method for Realizing a Luminous Flux Scale Using an Integrating Sphere with an External Source.
PB96-102843 *04,333*

Superconducting Integrated Circuit Fabrication with Low Temperature ECR-Based PECVD SiO2 Dielectric Films.
PB96-103015 *04,719*

Comments on the Stability of Bayard-Alpert Ionization Gages.
PB96-103080 *02,673*

Niobium Microbolometers for Far-Infrared Detection.
PB96-111729 *02,184*

Temperature Dependence and Magnetic Field Modulation of Critical Currents in Step-Edge SNS YBCO/Au Junctions.
PB96-111745 *04,723*

Critical Current and Normal Resistance of High-Tc Step-Edge SNS Junctions.
PB96-111752 *04,724*

GHRS Observations of Cool, Low-Gravity Stars. 1. The Far-Ultraviolet Spectrum of alpha Orions (M2 Iab).
PB96-112016 *00,094*

Applications of the Vortex Tube in Chemical Analysis. Part 2. Applications.
PB96-112107 *00,615*

Dual-Frequency Millimeter-Wave Radiometer Antenna for Airborne Remote Sensing of Atmosphere and Ocean.
PB96-112289 *02,009*

Measured Stopping Powers of Hydrogen and Helium in Polystyrene Near Their Maximum Values.
PB96-112321 *04,729*

Intercomparison between NPL (India) and NIST (USA) Pressure Standards in the Hydraulic Pressure Region Up to 26 MPa.
PB96-113543 *04,211*

Intercomparison of the ITS-90 Radiance Temperature Scales of the National Physical Laboratory (U.K.) and the National Institute of Standards and Technology.
PB96-113550 *02,674*

Beamcon III, a Linearity Measurement Instrument for Optical Detectors.
PB96-113576 *04,337*

Comparing the Accuracy of Critical-Current Measurements Using the Voltage-Current Simulator.
PB96-119219 *02,227*

Polarization Insensitive 3x3 Sagnac Current Sensor Using Polarizing Spun High-Birefringence Fiber.
PB96-119276 *02,187*

Simple and Repeatable Technique for Measuring the Critical Current of Nb3Sn Wires.
PB96-119409 *02,229*

Faraday Effect Sensors for Magnet Field and Electric Current.
PB96-119664 *04,736*

Standard Polarization Components: Progress Toward an Optical Retardance Standard.
PB96-119672 *04,342*

Improved Annealing Technique for Optical Fiber.
PB96-119680 *04,343*

Reducing Errors, Complexity, and Measurement Time of PM Noise Measurements.
PB96-119771 *02,075*

Standard Reference Materials for Optical Fibers and Connectors.
PB96-119805 *04,344*

Third Generation Water Bath Based Blackbody Source.
PB96-122148 *04,046*

Hydrodynamic Similarity in an Oscillating-Body Viscometer.
PB96-122429 *01,082*

Thermophysical Properties of Fluids for the Gas Industry.
PB96-122437 *02,494*

Polarization Dependence of Response Functions in 3x3 Sagnac Optical Fiber Current Sensors.
PB96-122684 *02,189*

Novel Method for Determining Thin Film Density by Energy-Dispersive X-ray Reflectivity.
PB96-122783 *04,737*

Secondary Standard for PM and AM Noise at 5, 10, and 100 MHz.
PB96-123187 *01,554*

Goddard High Resolution Spectrograph: Instrument, Goals, and Science Results.
PB96-123278 *00,044*

A-type and Chemically Peculiar Stars.
PB96-123286 *00,101*

Scientific Rationale and Present Implementation Strategy for the Far Ultraviolet Spectrograph Explorer (FUSE).
PB96-123328 *00,045*

Prediction of the Strength Properties for Plain-Carbon and Vanadium Micro-Alloyed Ferrite-Pearlite Steel.
PB96-123393 *03,216*

Modification of the Phase Stability of Polymer Blends by Diblock Copolymer Additivies.
PB96-123542 *03,172*

Hot-Electron Microcalorimeters as High-Resolution X-ray Detectors.
PB96-123641 *04,739*

Distributed Feedback Lasers in Rare-Earth-Doped Phosphate Glass.
PB96-123773 *04,740*

Control of Gas-Metal-Arc Welding Using Arc-Light Sensing.
PB96-131461 *02,869*

Electrode Extension Model for Gas Metal Arc Welding.
PB96-135074 *02,871*

High-Frequency Oscillators Using Phase-Locked Arrays of Josephson Junctions.
PB96-135157 *02,080*

Recalibration for the Final Archive of the International Ultraviolet Explorer (IUE) Satellite.
PB96-135264 *00,106*

Mutual Phase Locking in Systems of High-Tc Superconductor-Normal Metal-Superconductor Junctions.
PB96-135348 *04,744*

Temperature and Frequency Dependence of Anelasticity in a Nickel Oscillator.
PB96-137732 *03,689*

Anomalous Switching Phenomenon in Critical-Current Measurements When Using Conductive Mandrels.
PB96-137781 *02,233*

Low Noise YBa2Cu3O7-x-SrTiO3-YBa2Cu3O7-x Mulitlayers for Improved Superconducting Magnetometers.
PB96-138417 *04,747*

Dependence of Contrast on Probe/Sample Spacing with the Magneto-Optic Kerr-Effect Scanning Near-Field Optical Microscope (MOKE-SNOM).
PB96-138557 *04,750*

Development of Highly Conductive Cantilevers for Atomic Force Microscopy Point Contact Measurements.
PB96-138573 *04,751*

Radiometer Equation for Noise Comparison Radiometers.
PB96-140363 *02,195*

Cross-Sectional Photoluminescence and Its Application to Buried-Layer Semiconductor Structures.
PB96-141106 *02,415*

Safety Assessment of Railroad Wheels by Residual Stress Measurements.
PB96-141114 *04,855*

Effect of Charpy V-Notch Striker Radii on the Absorbed Energy.
PB96-141122 *03,365*

Safety Assessment of Railroad Wheels Through Roll-by Detection of Tread Cracks.
PB96-141254 *04,856*

Microwave Properties of Voltage-Tunable YBa2Cu3O7-delta/SrTiO3 Coplanar Waveguide Transmission Lines.
PB96-141262 *02,235*

High-Temperature High-Pressure Oscillating Tube Densimeter.
PB96-146618 *01,123*

Low Magnetostriction in Annealed NiFe/Ag Giant Magnetoresistive Multilayers.
PB96-146691 *04,762*

Telegraph Noise in Silver-Permalloy Giant Magnetoresistance Test Structures.
PB96-146717 *04,763*

Magnetoresistance of Thin-Film NiFe Devices Exhibiting Single-Domain Behavior.
PB96-147087 *04,766*

Gas-Coupled, Pulse-Echo Ultrasonic Crack Detection and Thickness Gaging.
PB96-147129 *04,847*

Simultaneous Laser-Diode Emission and Detection for Fiber-Optic Sensor Applications.
PB96-155502 *04,062*

Simple Variable Line Space Grating Monochromator for Synchrotron Light Source Beamlines.
PB96-156203 *04,065*

Laser-Synchrotron Hybrid Experiments: A Photon to Tickle, A Photon to Poke.
PB96-157847 *03,704*

Improved Reflectometry Facility at the National Institute of Standards and Technology.
PB96-160338 *04,087*

Cryogenic Flow Calibration in NIST.
PB96-161930 *01,143*

SSME LOX Duct Flowmeter Design and Test Results.
PB96-161955 *04,826*

Retention of Halocarbons on a Hexafluoropropylene Epoxide-Modified Graphitized Carbon Black. 4. Propane-Based Compounds.
PB96-164033 *03,284*

Simple and Efficient Methane-Marker Devices for Chromatographic Samples.
PB96-164041 *00,635*

Compressibility of Polycrystal and Monocrystal Copper: Acoustic-Resonance Spectroscopy.
PB96-164223 *02,990*

Determination of Total Protein Adsorbed on Solid (Membrane) Surface by a Hydrolysis Technique: Single Protein Adsorption.
PB96-167093 *03,552*

Permeation Tube Approach to Long-Term Use of Automatic Sampler Retention Index Standards.
PB96-167291 *00,639*

Structure and Rheology of Hard-Sphere Systems.
PB96-167333 *00,662*

Fundamental Limits on the Frequency Stabilities of Crystal Oscillators.
PB96-176565 *02,277*

Thermal Anemometry for Mass Flow Measurement in Oscillating Cryogenic Gas Flows.
PB96-176789 *04,218*

NIST Detector-Based Luminous Intensity Scale.
PB96-179114 *01,864*

Development of Neutral-Density Infrared Filters Using Metallic Thin Films.
PB96-180286 *02,998*

Dynamometer-Induced Residual Stress in Railroad Wheels: Ultrasonic and Saw Cut Measurements. Report No. 30.
PB96-183199 *04,857*

Sensor System for Intelligent Processing of Hot-Rolled Steel.
PB96-186069 *03,373*

Well-Shielded EMAT for On-Line Ultrasonic Monitoring of GMA Welding.
PB96-186077 *02,879*

Response Comparison of Electret Ion Chambers, LiF TLD, and HPIC.
PB96-190103 *02,578*

Epitaxial Nucleation and Growth of Chemically Derived Ba2YCu3O7-x Thin Films on (001) SrTiO3.
PB96-190186 *04,787*

Charpy Impact Test as an Evaluation of 4 K Fracture Toughness.
PB96-190194 *03,219*

Prediction of Strengthening Due to V Additions in Direct-Cooled Ferrite-Pearlite Forging Steels.
PB96-190251 *03,220*

Ultrasonic Methods.
PB96-190327 *02,707*

Scanning Electron Microscopy Observations of Misfit Dislocations in Epitaxial In0.25Ga0.75As on GaAs(001).
PB96-200159 *03,004*

Novel Vortex Dynamics in Two-Dimensional Josephson Arrays.
PB96-200167 *02,091*

Superconductor- Normal-Superconductor Junctions for Digital/Analog Converters.
PB96-200233 *02,092*

Superconductor- Normal-Superconductor Junctions for Programmable Voltage Standards.
PB96-200241 *02,093*

Design of High-Frequency, High-Power Oscillators Using Josephson-Junction Arrays.
PB96-200258 *02,094*

High-Power, High-Frequency Oscillators Using Distributed Josephson-Junction Arrays.
PB96-200266 *02,095*

Fiber-Optic Faraday-Effect Magnetic-Field Sensor Based on Flux Concentrators.
PB96-200308 *02,201*

Hot-Electron Microcalorimeter for X-ray Detection Using a Superconducting Transition Edge Sensor with Electrothermal Feedback.
PB96-200399 *04,792*

Hot-Electron-Microcalorimeters with 0.25 mm(2) Area.
PB96-200670 *04,793*

Controlling the Critical Current Density of High-Temperature SNS Josephson Junctions.
PB96-200712 *04,794*

Self-Calibrated Intelligent Optical Sensors and Systems.
PB96-200738 *04,380*

Effect of Harmonic Distortion on Phase Errors in Frequency Distribution and Synthesis.
PB96-200779 *01,563*

Precise Laser-Based Measurements of Zero-Dispersion Wavelength in Single-Mode Fibers.
PB96-201124 *01,511*

Electronically Tunable Fiber Laser for Optical Pumping of (3)He and (4)He.
PB96-201165 *04,381*

Report on USDA Ultraviolet Spectroradiometers.
PB96-214648 *00,125*

Thin Film Thermocouple Research at NIST.
PB97-110233 *02,283*

Magneto-Optic Rotation Sensor Using a Laser Diode as Both Source and Detector.
PB97-111272 *04,390*

Closed Loop Controller for Electron-Beam Evaporators.
PB97-111470 *04,393*

Pulse-Driven Programmable Josephson Voltage Standard.
PB97-111496 *04,148*

High Power Generation with Distributed Josephson-Junction Arrays
PB97-111520 *02,099*

Fundamentals and Problems of Fiber Current Sensors.
PB97-111835 *02,205*

Integrated Optical Polarization-Discriminating Receiver in Glass.
PB97-113179 *02,206*

Reducing the 1/f AM and PM Noise in Electronics for Precision Frequency Metrology.
PB97-113195 *02,102*

Micromachined Coplanar Waveguides in CMOS Technology.
PB97-119283 *02,456*

Anomalous Relation between Time and Frequency Domain PMD Measurements.
PB97-119390 *04,398*

Design, Construction and Application of a Large Aperture Lens-Less Line-Focus PVDF Transducer.
PB97-122584 *02,765*

INSTRUMENTS

Conference Proceedings: International Workshop on Instrumented Indentation. Held in San Diego, California on April 22-23, 1995.
PB96-158688 *01,948*

INSULATED GATE BIPOLAR TRANSISTORS

Investigation of the Drive Circuit Requirements for the Power Insulated Gate Bipolar Transistor (IGBT).
PB94-211794 *02,316*

Modeling Buffer Layer IGBTs for Circuit Simulation.
PB95-153805 *02,344*

Modeling Buffer Layer IGBT's for Circuit Simulation.
PB96-164173 *02,429*

INSULATING GAS

SF6 Insulation: Possible Greenhouse Problems and Solutions.
PB95-251625 *02,269*

INSULATING MATERIALS

National Voluntary Laboratory Accreditation Program: Thermal Insulation Materials.
PB95-267985 *02,977*

INSULATION

Investigation of S2F10 Production and Mitigation in Compressed SF6-Insulated Power Systems.
PB94-212388 *02,467*

Investigation of S2F10 Production and Mitigation in Compressed SF6- Insulated Power Systems.
PB96-155528 *02,468*

INSULIN

Conformational Alterations of Bovine Insulin Adsorbed on a Silver Electrode.
PB96-161773 *00,510*

INTAGLIO INK RESINS

Cylinder Wipe Air-Drying Intaglio Ink Vehicles for U.S. Currency Inks.
PB94-160801 *03,115*

INTEGRAL EQUATIONS

Alternative Single Integral Equation for Scattering by a Dielectric.
PB94-216512 *04,422*

Causality and Maxwell's Equations.
PB97-110522 *04,429*

INTEGRALS

Integral Occurring in Coherence Theory.
PB95-203550 *04,324*

INTEGRATED CIRCUITS

Design Guide for CMOS-On-SIMOX. Test Chips NIST3 and NIST4.
PB94-163458 *02,297*

Color Supplement to NIST Special Publication 400-93: Semiconductor Measurement Technology: Design and Testing Guides for the CMOS and Lateral Bipolar-on-SOI Test Library.
PB94-164316 *02,298*

Semiconductor Measurement Technology: Design and Testing Guides for the CMOS and Lateral Bipolar-on-SOI Test Library.
PB94-178019 *02,301*

Application of the Modified Voltage-Dividing Potentiometer to Overlay Metrology in a CMOS/Bulk Process.
PB94-181997 *02,302*

YBa2Cu3O7-x to Si Interconnection for Hybrid Superconductor/Semiconductor Integration.
PB94-211711 *02,315*

Precision, Accuracy, Uncertainty and Traceability and Their Application to Submicrometer Dimensional Metrology.
PB94-213105 *02,319*

Practical Photomask Linewidth Measurements.
PB95-108510 *02,324*

User's Manual for the Program MONSEL-1: Monte Carlo Simulation of SEM Signals for Linewidth Metrology.
PB95-111522 *02,325*

Metrology and Data for Microelectronic Packaging and Interconnection: Results of a Joint Workshop on Materials Metrology and Data for Commercial Electrical and Optical Packaging and Interconnection Technologies. Held in Gaithersburg, Maryland on May 5-6, 1994. Volume 2. Presentation Material.
PB95-143327 *02,330*

Monte Carlo Model for SEM Linewidth Metrology.
PB95-150058 *02,331*

Electrical Test Structure for Overlay Metrology Referenced to Absolute Length Standards.
PB95-152278 *02,336*

Comparisons of Measured Linewidths of Sub-Micrometer Lines Using Optical, Electrical, and SEM Metrologies.
PB95-152807 *02,338*

Integration of Scanning Tunneling Microscope Nanolithography and Electronics Device Processing.
PB95-153359 *02,341*

Verification of Commercial Probe-Tip Calibrations.
PB95-161576 *02,347*

X-ray Mask Metrology: The Development of Linewidth Standards for X-ray Lithography.
PB95-162129 *02,348*

Calibrating On-Wafer Probes to the Probe Tips.
PB95-163945 *02,352*

LRM Probe-Tip Calibrations with Imperfect Resistors and Lossy Lines.
PB95-163952 *02,353*

Electrical Test Structure for Improved Measurement of Feature Placement and Overlay in Integrated Circuit Fabrication Processes.
PB95-164273 *02,355*

Critical Issues in Scanning Electron Microscope Metrology.
PB95-169405 *02,359*

Automated Josephson Integrated Circuit Test System.
PB95-175246 *02,057*

Microelectronic Test Structures for Feature Placement and Electrical Linewidth Metrology.
PB95-180568 *02,367*

Accuracy in Integrated Circuit Dimensional Measurements.
PB95-180808 *02,368*

Electrical Method for Determining the Thickness of Metal Films and the Cross-Sectional Area of Metal Lines.
PB95-203170 *02,370*

JEDEC 'TCR' Interlaboratory Experiment: Lessons Learned.
PB95-203188 *02,371*

Semiconductor Measurement Technology: HOTPAC. Programs for Thermal Analysis Including Version 3.0 of the TXYZ Program, TXYZ30, and the Thermal MultiLayer Program, TML.
PB95-260766 *02,374*

MEMS in Standard CMOS VLSI Technology.
PB96-102363 *02,377*

MONSEL-II: Monte Carlo Simulation of SEM Signals for Linewidth Metrology.
PB96-102710 *02,379*

Superconducting Integrated Circuit Fabrication with Low Temperature ECR-Based PECVD SiO2 Dielectric Films.
PB96-103015 *04,719*

Semiconductor Measurement Technology: Test Structure Implementation Document: DC Parametric Test Structures and Test Methods for Monolithic Microwave Integrated Circuits (MMICs).
PB96-117692 *02,399*

LRM Probe-Tip Calibrations Using Nonideal Standards.
PB96-135389 *02,411*

Electrical Characterization of Integrated Circuit Metal Line Thickness.
PB96-138433 *02,414*

Measurement of Patterned Film Linewidth for Interconnect Characterization.
PB96-148168 *02,420*

Scanned Probe Microscopies: Opportunities and Issues in Metrology.
PB96-160783 *02,426*

Scanning Electron Microscope Metrology.
PB96-201090 *02,446*

INTEGRATED OPTICS

Integrated-Optical Devices in Rare-Earth-Doped Glass.
PB95-202909 *02,179*

INTEGRATED SERVICES DIGITAL NETWORK

Integrated Services Digital Network (ISDN); Category: Telecommunications Standard; Subcategory: Integrated Services Digital Network.
FIPS PUB 182 *01,460*

Introduction to Traffic Management for Broadband ISDN.
PB94-142494 *01,464*

North American ISDN Users' Forum Agreements on Integrated Services Digital Network.
PB94-162559 *01,466*

ISDN Conformance Testing Guidelines: Guidelines for Implementors of ISDN Customer Premises Equipment to Conform to Both National ISDN-1 and North American ISDN Users' Forum Layer 3 Basic Rate Interface Basic Call Control Abstract Test Suites.
PB94-219094 *01,471*

ISDN LAN Bridging.
PB95-154696 *01,477*

Application Profile for ISDN.
PB95-163689 *01,479*

Application Software Interface: ISDN Services for an Open Systems Environment.
PB96-131487 *01,492*

ISDN in North America.
PB96-160767 *01,502*

North American Agreements on ISDN.
PB96-160775 *01,503*

Journal of Research of the National Institute of Standards and Technology, September/October 1993. Volume 98, Number 5.
PB96-169057 *03,368*

INTEGRATED SERVICES DIGITAL NETWORKS

ISDN Conformance Testing.
PB95-163176 *01,478*

INTEGRATED SYSTEMS

Feasibility Study: Reference Architecture for Machine Control Systems Integration.
PB94-142791 *02,804*

Integrated Network Management.
PB94-199247 *01,583*

Technical Program Description Systems Integration for Manufacturing (SIMA).
PB94-213758 *02,819*

Reference Architecture for Machine Control Systems Integration: Interim Report.
PB95-144549 *02,820*

Automated Inspection: The Integration of National Standards and Commercial Products at NIST.
PB95-163077 *02,906*

Requisite Elements, Rationale, and Technology Overview for the Systems Intergration for Manufacturing Applications (SIMA) Program. Background Study.
PB96-112685 *02,831*

NIST SIMA Interactive Management Workshop. Held in Fort Belvoir, Virginia on November 14-16, 1994.
PB96-154877 *02,838*

Template-Driven Systems Development with IDEF: Enterprise Standards for Reuse.
PB96-160965 *02,788*

Systems Integration for Manufacturing Applications Program 1995 Annual Report.
PB96-193735 *02,844*

INTEGRATING SPHERES

Integrating Sphere Simulation: Application to Total Flux Scale Realization.
PB95-150173 *04,261*

INTEGRATION DEFINITION FOR FUNCTION MODELING

Mapping Integration Definition for Function Modeling (IDEFO) Model into CASE Data Interchange Format (CDIF) Transfer File.
PB96-109533 *01,741*

INTEGRATION DEFINITION FOR INFORMATION MODELING

Mapping Integration Definition for Information Modeling (IDEF1X) Model into CASE Data Interchange Format (CDIF) Transfer File.
PB95-154670 *01,711*

INTELLECTUAL PROPERTY

Standards Policy and Information Infrastructure.
PB95-231882 *01,485*

Using Technology to Manage and Protect Intellectual Property.
PB97-112395 *01,513*

INTELLIGENT PROCESSING

Intelligent Processing of Materials.
PB94-172780 *02,811*

Intelligent Processing of Hot Isostatic Pressing.
PB94-172913 *03,315*

Sensor System for Intelligent Processing of Hot-Rolled Steel.
PB96-186069 *03,373*

INTELLIGENT PROCESSING OF MATERIALS

Nondestructive Evaluation and Materials Processing.
PB95-140455 *02,902*

INTENSITY

Phase Shifts and Intensity Dependence in Frequency-Modulation Spectroscopy.
PB96-103205 *01,071*

INTERACTION COEFFICIENTS

Interaction Coefficients for 15 Mixtures of Flammable and Non-Flammable Components.
PB96-146626 *03,281*

INTERACTION PARAMETERS

Microstructure Effect on the Phase Behavior of Blends of Deuterated Polybutadiene and Protonated Polyisopene.
PB97-113146 *01,296*

INTERACTIVE GRAPHICS

Programmer's Hierarchical Interactive Graphics System (PHIGS). Category: Software Standard; Subcategory: Graphics.
FIPS PUB 153-1 *01,668*

User's Guide for the PHIGS Validation Tests (Version 2.1).
PB94-165206 *01,682*

Approaches Using Virtual Environments with Mosaic.
PB95-169108 *01,599*

INTERACTIVE SYSTEMS

Kibitz-Connecting Multiple Interactive Programs Together.
PB94-213311 *01,696*

Handling Passwords with Security and Reliability in Background Processes.
PB95-180550 *01,722*

Ouch Those Programs are Painful.
PB96-102678 *01,739*

INTERAGENCY COOPERATION

NIST and the Navy: Past, Present and Future.
PB96-119649 *03,655*

INTERAGENCY COORDINATION

Overview of U.S. Government Advanced Packaging Programs.
PB96-200845 *02,443*

INTERATOMIC POTENTIALS

Interatomic Potential of Argon.
PB95-141180 *00,912*

Interatomic Potential of Argon.
PB95-152989 *00,945*

INTERBAND ABSORPTION

Band-to-Band Photoluminescence and Luminescence Excitation in Extremely Heavily Carbon-Doped Epitaxial GaAs.
PB95-150413 *04,570*

INTERCALATING AGENTS

Application of Photochemical Reaction in Electrochemical Detection of DNA Intercalation.
PB94-185733 *00,686*

Enhanced Detection of PCR Products Through Use of TOTO and YOYO Intercalating Dyes with Laser Induced Fluorescence - Capillary Electrophoresis.
PB95-164653 *00,599*

INTERCALATION

Detection of Aromatic Compounds Based on DNA Intercalation Using an Evanescent Wave Biosensor.
PB96-111976 *03,473*

INTERCALATION COMPOUND

Determination of Anomalous Superexchange in MnCl2 and Its Graphite Intercalation Compound.
PB97-122568 *00,666*

INTERFACE CRACKS

Pressurized Internal Lenticular Cracks at Healed Mica Interfaces.
PB96-180252 *02,997*

INTERFACE FILTERS

Interface-Filter Characterization of Spectraradiometers and Colorimeters.
PB97-122212 *04,399*

INTERFACE ROUGHNESS

Interface Roughness-Induced Changes in the Near-E(sub 0) Spectroscopic Behavior of Short-Period AlAs/GaAs Superlattices.
PB94-185154 *02,118*

Effects of Interfacial Roughness on the Magnetoresistance of Magnetic Metallic Multilayers.
PB95-150017 *04,556*

Spectroscopic Ellipsometry Determination of the Properties of the Thin Underlying Strained Si Layer and the Roughness at SiO2/Si Interface.
PB95-150157 *04,560*

Interface Roughness, Composition, and Alloying of Low-Order AlAs/GaAs Superlattices Studies by X-ray Diffraction.
PB96-160262 *02,983*

INTERFACE STABILITY

Convection and Morphological Stability During Directional Solidification.
N95-14548/8 *03,310*

INTERFACE TRANSMISSION

Spin-Dependent Interface Transmission and Reflection in Magnetic Multilayers (Invited).
PB96-201173 *04,130*

INTERFACES

Control Entity Interface Specification.
PB94-191715 *02,815*

Interface Properties for Ceramic Composites from a Single Fiber Pull-Out Test.
PB94-199361 *03,135*

Asymmetric Tip Morphology of Creep Microcracks Growing Along Bimaterial Interfaces.
PB94-200243 *03,138*

Neutron Scattering Studies of Surfaces and Interfaces.
PB94-216207 *04,517*

Interface Roughness of Short-Period AlAs/GaAs Superlattices Studied by Spectroscopic Ellipsometry.
PB95-107215 *02,137*

Interface Modification and Characterization of Silicon Carbide Platelets Coated with Alumina Particles.
PB95-108734 *03,121*

Interface Sharpness in Low-Order III-V Superlattices.
PB95-108775 *02,138*

Interface Sharpness during the Initial Stages of Growth of Thin, Short-Period III-V Superlattices.
PB95-108783 *02,139*

Digital Simulation of the Aggregate-Cement Paste Interfacial Zone in Concrete.
PB95-125993 *00,363*

Near Critical Fluid Interfaces: A Comparison of Theory and Experiment.
PB95-140166 *00,901*

Structural Stabilization of Phase Separating PC/Polyester Blends through Interfacial Modification by Transesterification Reaction.
PB95-150454 *01,239*

Diffusion of Copper into Gold Plating.
PB95-162152 *00,957*

Characterization of the ZnSe/GaAs Interface Layer by TEM and Spectroscopic Ellipsometry.
PB95-175360 *04,655*

Terminally Anchored Chain Interphases: Their Chromatographic Properties.
PB95-181061 *01,272*

Terminally Anchored Chain Interphases: The Effect of Multicomponent, Polydisperse Solvents on Their Equilibrium Properties.
PB95-181079 *01,273*

Water Adsorption at Polymer/Silicon Wafer Interfaces.
PB95-181178 *01,022*

Water Adsorption at a Polyimide/Silicon Wafer Interface.
PB96-103197 *01,070*

Standardization for ATM and Related B-ISDN Technologies.
PB96-160460 *01,499*

Interfaces in Mo/Si Multilayers.
PB96-160668 *02,423*

NIST POSIX Testing Program.
PB96-160973 *01,821*

Fracture in Multilayers.
PB96-163613 *02,988*

Notion of a xi-Vector and a Stress Tensor for a General Class of Anisotropic Diffuse Interface Models.
PB96-193776 *04,788*

INTERFACIAL CRACK

Interfacial Crack in a Two-Dimensional Hexagonal Lattice.
PB96-161989 *04,100*

INTERFACIAL FRACTURE
Cracks and Dislocations in Face-Centered Cubic Metallic Multilayers.
PB96-163696 *02,989*

INTERFACIAL REACTIONS
Effect of Microstructure on Phase Formation in the Reaction of Nb/Al Multilayer Thin Films.
PB95-168415 *03,352*

First Phase Formation Kinetics in the Reaction of Nb/Al.
PB95-168456 *03,353*

INTERFACIAL TENSION
Measurement of Surface Tension of Tantalum by a Dynamic Technique in a Microgravity Environment.
PB95-161667 *03,932*

INTERFACIAL ZONE
Digital Simulation of the Aggregate-Cement Paste Interfacial Zone in Concrete.
PB95-125993 *00,363*

INTERFEROMETERS
Measuring Long Gage Blocks with the NIST Line Scale Interferometer.
PB95-242400 *02,665*

Visualization of Surface Figure by the Use of Zernike Polynomials.
PB96-137757 *04,351*

New Refractometer by Combining a Variable Length Vacuum Cell and a Double-Pass Michelson Interferometer.
PB97-111926 *01,986*

INTERGRANULAR CORROSION
Interaction between Dislocations and Intergranular Cracks.
PB95-152096 *03,190*

INTERIOR POINT METHODS
Interior-Point Method for Linear and Quadratic Programming Problems. (NIST Reprint).
PB95-180089 *03,429*

INTERLABORATORY COMPARISONS
Proficiency Testing as a Component of Quality Assurance in Construction Materials Laboratories.
PB94-185774 *00,334*

Analysis of Physical Properties of Ceramic Powders in an International Interlaboratory Comparison Program.
PB95-161501 *03,050*

Interlaboratory Comparison of Autoradiographic DNA Profiling Measurements. 1. Data and Summary Statistics.
PB95-175923 *03,542*

Interlaboratory Comparison Studies on the Analysis of Hair for Drugs of Abuse.
PB95-176251 *03,500*

Intercomparison of Photometric Units Maintained at NIST (USA) and PTB (Germany), 1993.
PB95-261913 *04,329*

Ceramic Powders Characterization: Results of an International Laboratory Study.
PB95-270039 *02,672*

Interlaboratory Comparison of Autoradiographic DNA Profiling Measurements. 2. Measurement Uncertainty and Its Propagation.
PB96-112123 *03,545*

Intercomparison of the ITS-90 Radiance Temperature Scales of the National Physical Laboratory (U.K.) and the National Institute of Standards and Technology.
PB96-113550 *02,674*

V-6: Effects of Temperature Variation.
PB96-148143 *04,772*

Optical Fiber, Fiber Coating, and Connector Ferrule Geometry: Results of Interlaboratory Measurement Comparisons.
PB96-154422 *04,360*

International Radon-in-Air Measurement Intercomparison Using a New Transfer Standard.
PB96-159751 *03,708*

Interlaboratory Studies on the Analysis of Hair for Drugs of Abuse: Results from the Fifth Exercise.
PB97-110449 *03,509*

Measurement Comparability, Traceability, and Measurement Assurance Programs.
PB97-111850 *02,692*

Comparisons of Some NIST Fixed-Point Cells with Similar Cells of Other Standards Laboratories.
PB97-119242 *00,655*

INTERLABORATORY TEST
Development of a Standard Reference Material for ISE Measurements of Sodium and Potassium.
PB96-159785 *03,507*

INTERLABORATORY TESTS
Gage Block Standards, Measurement Capabilities and Laboratory Accreditation.
PB96-163621 *02,757*

INTERMETALLIC ALLOYS
Experimental Assessment of Crack-Tip Dislocation Emission Models for an Al67Cr8Ti25 Intermetallic Alloy.
PB96-204466 *03,377*

INTERMETALLIC COMPOUNDS
Intelligent Processing of Hot Isostatic Pressing.
PB94-172913 *03,315*

Thermodynamic Constraints on Non-Equilibrium Solidification of Ordered Intermetallic Compounds.
PB94-198934 *03,321*

Ambient Temperature Synthesis of Bulk Intermetallics.
PB95-169074 *00,168*

INTERMETALLICS
Status of Electrocomposites.
PB94-212453 *03,143*

INTERMOLECULAR FORCES
Pairwise and Nonpairwise Additive Forces in Weakly Bound Complexes: High Resolution Infrared Spectroscopy of ArnDF (n=1,2,3).
PB96-200357 *04,125*

INTERMOLECULAR POTENTIALS
Vibrational Dependence of the Anisotropic Intermolecular Potential of Ar-HCl.
PB95-202685 *01,029*

Vibrational Dependence of the Anisotropic Intermolecular Potential of Ar-HF.
PB95-202693 *01,030*

INTERNAL COMBUSTION ENGINES
Thin Film Thermocouples for Measurement of Wall Temperatures in Internal Combustion Engines.
PB94-172103 *01,449*

INTERNAL CONVERSION COEFFICIENTS
Alpha-Particle and Electron Capture Decay of (209)Po.
PB96-186085 *04,119*

INTERNAL ELECTRIC FIELDS
Thermal Stability of Internal Electric Field and Polarization Distribution in Blend of Polyvinylidene Fluoride and Polymethylmethacrylate.
PB95-151072 *01,240*

INTERNAL STATE DISTRIBUTION
Dynamics of Hydrogen Interactions with Si(100) and Si(111) Surfaces.
PB96-159801 *04,082*

INTERNAL WAVES
Internal Waves in Xenon Near the Critical Point.
PB97-111504 *04,221*

INTERNATIONAL AGREEMENTS
International Challenges in Defining the Public and Private Interest in Standards.
PB96-160361 *00,498*

INTERNATIONAL COOPERATION
National Center for Standards and Certification Information: Service and Programs.
N95-15938/0 *02,717*

Utc Dissemination to the Real-Time User.
N19960042622 *01,521*

Forum for International Cooperation on Fire Research.
PB95-162939 *04,869*

INTERNATIONAL INSTITUTE OF WELDING
IIW Commission V Quality Control and Quality Assurance of Welded Products Annual Report 1994/95.
PB95-198743 *02,866*

INTERNATIONAL ORGANIZATION FOR STANDARDIZATION
Questions and Answers on Quality, the ISO 9000 Standard Series, Quality System Registration, and Related Issues. More Questions and Answers on the ISO 9000 Standard Series and Related Issues.
PB95-103461 *00,495*

INTERNATIONAL SYSTEM OF UNITS
Guide for the Use of the International System of Units (SI).
PB95-226692 *02,747*

INTERNATIONAL TEMPERATURE SCALE OF 1990
Practical Applications of the ITS-90: Inherent Uncertainties.
PB95-161527 *03,930*

Current Status and Trends in Temperature Measurements at NIST, Cooperative Projects and New Mutual Agreement between NIST and IMGC.
PB97-110266 *02,691*

INTERNATIONAL TRADE
Planning the Infrastructure for Global Electronic Commerce.
PB94-185832 *00,494*

Questions and Answers on Quality, the ISO 9000 Standard Series, Quality System Registration, and Related Issues. More Questions and Answers on the ISO 9000 Standard Series and Related Issues.
PB95-103461 *00,495*

GATT Standards Code Activities of the National Institute of Standards and Technology 1994.
PB96-106935 *00,497*

Federal Labs Have Key Role in Metrication.
PB96-123401 *02,920*

Metrology and Regional Trade Pacts.
PB96-155429 *02,923*

TBT Agreement Activities of the National Institute of Standards and Technology, 1995.
PB97-104178 *00,499*

INTERNET
Retrieving Articles from the Internet (without a UNIX Workstation). Part 1. File Formats and Software Tools.
PB95-168720 *02,728*

Retrieving Articles from the Internet (without a UNIX Workstation). Part 2. An Example.
PB95-168738 *02,729*

Keeping Your Site Comfortably Secure: An Introduction to Internet Firewalls.
PB95-182275 *02,730*

Sharing Information via the Internet: An Infoserver Case Study.
PB96-131511 *01,493*

World Wide Web for Crystallography.
PB97-109219 *04,810*

INTEROPERABILITY
Procedures for Document Facsimile Transmission Issued by General Services Administration, April 14, 1982. Federal Standard 1063.
FIPS PUB 148 *01,516*

Electronic Implementors' Workshop.
PB95-210936 *01,484*

Open Issues in OSI Protocol Development and Conformance Testing.
PB96-122908 *01,818*

Application Portability Profile (APP): The U.S. Government's Open System Environment Profile Version 3.0.
PB96-158712 *01,753*

Information Technology Standards in a Changing World: The Rose of the Users.
PB96-160866 *02,737*

Data Communications Strategy.
PB96-167846 *02,738*

Five Q's (Cues) of the U.S. GOSIP Testing Program.
PB96-175716 *01,826*

Open System Environment Implementors Workshop (OIW); Standardization Role Defined.
PB96-180047 *01,828*

CSL View of Applications Portability, Scalability, and Interoperability.
PB97-122303 *01,787*

INTERPENETRATING POLYMER NETWORK
Synthesis of Hybrid Organic-Inorganic Materials from Interpenetrating Polymer Network Chemistry.
PB96-180054 *02,994*

INTERPENETRATING POLYMER NETWORKS
Grafted Interpenetrating Polymer Networks.
PB94-185055 *01,200*

INTERPRETERS
NIST RS274/NGC Interpreter Version 1.
PB94-187788 *02,814*

NIST RS274KT Interpreter.
PB96-147954 *02,835*

INTERPROCESSOR COMMUNICATION
Kibitz-Connecting Multiple Interactive Programs Together.
PB94-213311 *01,696*

INTERSTELLAR GAS
Extended CO(7 yields 6) Emission from Warm Gas in Orion.
PB96-102504 *00,090*

INTERSTELLAR MATTER
Goddard High-Resolution Spectrograph Observations of the Local Interstellar Medium and the Deuterium/Hydrogen Ratio along the Line of Sight Toward Capella.
PB94-213444 *00,066*

IRAS Spectroscopic Observations of Young Planetary Nebulae.
PB95-152070 *00,072*

Deuterium in the Local Interstellar Medium: Its Cosmological Significance.
PB95-202842 *00,081*

Deuterium and the Local Interstellar Medium: Properties for the Procyon and Capella Lines of Sight.
PB96-200639 *00,111*

INTERSTITIAL SPACE CONSTRUCTION SYSTEMS
Fire Performance of an Interstitial Space Construction System.
PB95-188918 *00,390*

INTRINSIC CONDUCTIVITY
Intrinsic Conductivity of Objects Having Arbitrary Shape and Conductivity.
PB97-111934 *04,150*

INTUMESCENCE
Heat Transfer in an Intumescent Material Using a Three-Dimensional Lagrangian Model.
PB96-164066 *00,408*

INVAR
Polarization Analysis of the Magnetic Excitations in Invar and Non-Invar Amorphous Alloys.
PB94-216116 *04,516*

Polarization Analysis of the Magnetic Excitations in Fe65Ni35 Invar.
PB95-150082 *04,558*

INVARIANT MEASURES
Monte Carlo Approach to the Approximation of Invariant Measures.
PB94-172053 *03,409*

INVENTIONS
Economic, Energy, and Environmental Impacts of the Energy-Related Inventions Program.
DE94-017162 *00,008*

Encouraging Environmentally-Aware Inventions.
PB95-161394 *02,521*

INVERTERS
Electro-Thermal Simulation of an IGBT PWM Inverter.
PB94-185592 *02,303*

INVESTMENTS
Least-Cost Energy Decisions for Buildings: Part 2. Uncertainty and Risk Video Training Workbook.
PB94-165982 *00,240*

Evaluating Investments in Law Enforcement Equipment: An Annotated Bibliography.
PB95-151379 *04,867*

IODINE
Iodine Atoms and Iodomethane Radical Cations: Their Formation in the Pulse Radiolysis of Iodomethane in Organic Solvents, Their Complexes, and Their Reactivity with Organic Reductants.
PB95-162764 *00,965*

IODINE 127
High-Sensitivity Determination of Iodine Isotopic Ratios by Thermal and Fast Neutron Activation.
PB94-213386 *00,555*

IODINE 129
High-Sensitivity Determination of Iodine Isotopic Ratios by Thermal and Fast Neutron Activation.
PB94-213386 *00,555*

IODINE MONOXIDE
Absorption Cross Sections, Kinetics of Formation, and Self-Reaction of the IO Radical Produced via the Laser Photolysis of N2O/I2/N2 Mixtures.
PB97-112361 *01,180*

IODINE ORGANIC COMPOUNDS
Iodine Atoms and Iodomethane Radical Cations: Their Formation in the Pulse Radiolysis of Iodomethane in Organic Solvents, Their Complexes, and Their Reactivity with Organic Reductants.
PB95-162764 *00,965*

IODINE OXIDE
Experimental Determination of the Ionization Energy of IO(X(sup 2)II(sub 3/2)) and Estimations of Delta(sub f)H(sup deg)(sub 0)(IO(sup -)) and PA(IO).
PB96-146899 *00,694*

ION-ATOM COLLISIONS
Charge Transfer and Collision-Induced Dissociation Reactions of CF(2+) and CF2(2+) with the Rare Gases at a Laboratory Collision Energy of 49 eV.
PB94-185584 *00,775*

Collision-Induced Neutral Loss Reactions of Molecular Dications.
PB94-185808 *00,780*

Hydrogen Balmer Alpha Line Shapes for Hydrogen-Argon Mixtures in a Low-Pressure rf Discharge.
PB95-153433 *03,924*

Collisions of Electrons with Highly-Charged Ions.
PB96-200340 *04,791*

ION BEAM ASSISTED DEPOSITION
Effect of Beam Voltage on the Properties of Aluminum Nitride Prepared by Ion Beam Assisted Deposition.
PB97-118616 *01,995*

ION BEAM MODIFICATION
Gas Absorption during Ion-Irradiation of a Polymer Target.
PB96-161864 *04,099*

ION BEAMS
Growth of Epitaxial KNbO3 Thin Films.
PB96-135181 *02,409*

ION CHANNEL
Noise Analysis of Ionization Kinetics in a Protein Ion Channel.
PB96-161682 *04,093*

ION CHANNELS
Genetically Engineered Pores for New Materials.
PB96-161641 *03,550*

Current Fluctuations Reveal Protonation Dynamics and Number of Ionizable Residues in the alpha-Toxin Channel.
PB96-161732 *03,588*

Protonation Dynamics in an Ion Channel Pore.
PB96-161757 *03,589*

ION DETECTION
Superconducting Resonator and a Cryogenic GaAs Field-Effect Transistor Amplifier as a Single-Ion Detection System.
PB95-202727 *03,990*

ION DISTRIBUTION
Evidence for Inelastic Processes for N(+)3 and N(+)4 from Ion Energy Distributions in He/N2 Radio Frequency Glow Discharges.
PB96-146683 *04,059*

ION EXCHANGE RESINS
Tetrahedral-Framework Lithium Zinc Phosphate Phases: Location of Light-Atom Positions in LiZnPO4 H2O by Powder Neutron Diffraction and Structure Determination of LiZnPO4 by ab Initio Methods.
PB96-160510 *01,129*

ION FILMS
Variation in Magnetic Properties of Cu/Fcc (001) Sandwich Structures.
PB95-141164 *04,555*

ION IMAGING
Molecular Ion Imaging and Dynamic Secondary Ion Mass Spectrometry of Organic Compounds.
PB95-126124 *00,571*

ION IMPLANTATION
Transition Metal Implants in In0.53GA0.47As.
PB95-126389 *04,534*

Boron-Implanted 6H-SiC Diodes.
PB96-159678 *04,081*

ION IRRADIATION
Increased Pinning Energies and Critical Current Densities in Heavy-Ion-Irradiated Bi2Sr2CaCu2O8 Single Crystals.
PB95-175352 *04,654*

ION MOLECULE INTERACTIONS
Vibrational Spectra of Molecular Ions Isolated in Solid Neon. 7. CO(+), C2O2(+), and C2O2(-). (Reannouncement with New Availability Information).
AD-A239 729/7 *00,706*

Selected Ion Flow Tube-Laser Induced Fluorescence Instrument for Vibrationally State-Specific Ion-Molecule Reactions.
PB94-185444 *00,774*

ION OPTICS
Beam Line for Highly Charged Ions.
PB97-111256 *04,143*

ION PLASMAS
Liquid and Solid Atomic Ion Plasmas.
PB94-198991 *03,809*

ION SELECTIVE ELECTRODES
Development of a Standard Reference Material for ISE Measurements of Sodium and Potassium.
PB96-159785 *03,507*

ION SOURCES
Relative Sensitivity Factors and Useful Yields for a Microfocused Gallium Ion Beam and Time-of-Flight Secondary Ion Mass Spectrometer.
PB94-198736 *00,541*

ION SPECTROSCOPY
Compositional Analyses of Surfaces and Thin Films by Electron and Ion Spectroscopies.
PB94-185790 *00,779*

ION STORAGE
Quantum Projection Noise: Population Fluctuations in Two-Level Systems.
PB94-212271 *03,850*

Electrostatic Modes of Ion-Trap Plasmas.
PB95-152963 *03,920*

Quantum Measurements of Trapped Ions.
PB95-161147 *03,928*

Laser Cooling of Trapped Ions.
PB95-168746 *03,950*

Recent Experiments on Trapped Ions at the National Institute of Standards and Technology.
PB95-169322 *03,952*

High-Resolution Atomic Spectroscopy of Laser-Cooled Ions.
PB95-169330 *03,953*

Experimental Results on Normal Modes in Cold, Pure Ion Plasmas.
PB95-175105 *03,956*

Non-Neutral Ion Plasmas and Crystals, Laser Cooling, and Atomic Clocks.
PB95-175113 *03,957*

Progress on a Cryogenic Linear Trap for (199)Hg(+) Ions.
PB95-180790 *03,965*

Precise Spectroscopy for Fundamental Physics.
PB96-112164 *04,040*

Trapped Ions and Laser Cooling 4: Selected Publications of the Ion Storage Group of the Time and Frequency Division, NIST, Boulder, Colorado.
PB96-172358 *04,108*

ION TRANSPORT
Current Fluctuations Reveal Protonation Dynamics and Number of Ionizable Residues in the alpha-Toxin Channel.
PB96-161732 *03,588*

ION TRAPS
Progress on a Cryogenic Linear Trap for (199)Hg(+) Ions.
PB95-180790 *03,965*

Quantum-Limited Cooling and Detection of Radio-Frequency Oscillations by Laser-Cooled Ions.
PB96-112073 *04,039*

IONIC CONDUCTIVITY
Fast-Ion Conduction and Disorder in Cation and Anion Arrays in Y2(ZryTi(1-y))2O7 Pyrochlores Induced by Zr Substitution: A Neutron Rietveld Analysis.
PB94-211869 *04,496*

Fast-Ion Conducting Y2(ZryTi1-y)2O7 Pyrochlores: Neutron Rietveld Analysis of Disorder Induced by Zr Substitution.
PB96-156104 *04,776*

IONIZATION
Multiphoton Ionization Spectroscopy Measurements of Silicon Atoms during Vapor Phase Synthesis of Ceramic Particles.
PB95-151999 *03,913*

Current Noise Reveals Protonation Kinetics and Number of Ionizable Sites in an Open Protein Ion Channel.
PB96-161674 *04,092*

IONIZATION CHAMBERS
Mass Assay and Uniformity Test of Boron Targets by Neutron Beam Methods.
PB97-119085 *04,175*

IONIZATION ENERGY
Experimental Determination of the Ionization Energy of IO(X(sup 2)II(sub 3/2)) and Estimations of Delta(sub f)H(sup deg)(sub 0)(IO(sup -)) and PA(IO).
PB96-146899 *00,694*

Ionization Energies, Appearance Energies and Thermochemistry of CF2O and FCO.
PB97-111538 *01,178*

IONIZATION GAUGES
Influence of Envelopes Geometry on the Sensitivity of 'Nude' Ionization Gauges.
PB97-119077 *04,174*

IONIZATION POTENTIALS
Ionization Energy of Sulfur Pentafluoride and the Sulfur Pentafluoride-Fluorine Atom Bond Dissociation Energy.
PB95-162814 *00,966*

IONIZATION SPECTROSCOPY
Resonance Enhanced Multiphoton Ionization Spectroscopy of the PF Radical.
PB97-119119 *00,702*

IONIZATION SUPPRESSION
Suppression of Ionization in One- and Two-Dimensional Model Calculations.
PB95-203600 *04,009*

IONIZATION TRAILS
Comparison of Meteor Activity with Occurrence of Sporadic E Reflections.
AD-A292 039/5 *00,116*

IONIZING RADIATION
Permissible Dose from External Sources of Ionizing Radiation.
AD-A279 281/0 *03,608*

Ionizing radiation-induced DNA damage and its repair in human cells. Progress report, (April 1, 1993--February 28, 1994).
DE94014709 *03,612*

Estimation of the Absorbed Dose in Radiation-Processed Food. 2. Test of the EPR Response Function by an Exponential Fitting Analysis.
PB94-199650 *00,036*

Estimation of the Absorbed Dose in Radiation-Processed Food. 3. The Effect of Time of Evaluation on the Accuracy of the Estimate.
PB94-199684 *00,037*

Estimation of the Absorbed Dose in Radiation-Processed Food. 4. EPR Measurements on Eggshell.
PB94-199692 *00,038*

Role of the Office of Radiation Measurement in Quality Assurance.
PB94-212255 *00,689*

Substrate Specificity of the Escherichia coli Endonuclease III: Excision of Thymine- and Cytosine-Derived Lesions in DNA Produced by Radiation-Generated Free Radicals.
PB95-153425 *03,535*

Ionizing Radiation Causes Greater DNA Base Damage in Radiation-Sensitive Mutant M10 Cells That in Parent Mouse Lymphoma L5178Y Cells.
PB95-175915 *03,632*

IONIZING RADIATION DOSIMETRY
National Voluntary Laboratory Accreditation Program: Ionizing Radiation Dosimetry.
PB95-128658 *03,623*

IONOSPHERIC PROPAGATION
Ionospheric Radio Propagation.
AD-A286 619/2 *01,459*

Higher-Order Approximations in Ionospheric Wave-Propagation.
AD-A292 471/0 *04,420*

IONOSPHERICS
Use of Ionospheric Data in GPS Time Transfer.
PB95-163853 *01,540*

IONS
Determination of Atomic Data Pertinent to the Fusion Energy Program. Progress Report for FY 92.
DE94004400 *04,402*

Energy Levels of Germanium, Ge I through Ge XXXII.
PB94-162351 *00,747*

Calorimetric Determination of the Standard Transformed Enthalpy of a Biochemical Reaction at Specified PH and pMg.
PB94-198249 *03,454*

Octacalcium Phosphate Carboxylates. 5. Incorporation of Excess Succinate and Ammonium Ions in the Octacalcium Phosphate Succinate Structure.
PB95-168894 *00,166*

Kinetics and Dynamics of Vibrationally State Resolved Ion-Molecule Reactions: (14)N2(+)(v=1 and 2) and (15)N2(+)(v=0,1 and 2) with (14)N2.
PB96-102348 *04,023*

Effect of Electrode Material on Measured Ion Energy Distributions in Radio-Frequency Discharges.
PB96-102850 *04,026*

Visible and UV Light from Highly Charged Ions: Exotic Matter Advancing Technology.
PB96-119391 *04,414*

Observation and Visible and uv Magnetic Dipole Transitions in Highly Charged Xenon and Barium.
PB96-138441 *04,056*

IR LASER SPECTROSCOPY
Probing Potential-Energy Surfaces via High-Resolution IR Laser Spectroscopy.
PB96-102835 *01,066*

IRDS (INFORMATION RESOURCE DICTIONARY SYSTEM)
Information Resource Dictionary System (IRDS): A Status Report.
PB95-126207 *01,810*

IRIDIUM
Use of Sum Rules on the Energy-Loss Function for the Evaluation of Experimental Optical Data.
PB95-150736 *04,264*

Characterization of the Interaction of Hydrogen with Iridium Clusters in Zeolites by Inelastic Neutron Scattering Spectroscopy.
PB95-180741 *01,013*

Analysis of the (5d(2)+5d6s)-5d6p Transition Arrays of Os VII and Ir VIII, and the 6s (2)S-6p (2)P Transitions of Ir IX.
PB96-159264 *01,954*

IRIDIUM OXIDE
Thin-Film Ruthenium Oxide - Iridium Oxide Thermocouples.
PB97-110225 *00,520*

IRIDIUM OXIDES
Iridium Oxide Thin-Film Stability in High-Temperature Corrosive Solutions.
PB94-213014 *03,234*

Changes in the Redox State of Iridium Oxide Clusters and Their Relation to Catalytic Water Oxidation: Radiolytic and Electrochemical Studies.
PB95-107017 *00,864*

IRON
Homoepitaxial Growth of Iron and a Real Space View of Reflection-High-Energy-Electron Diffraction.
PB94-173069 *04,445*

Scaling of Diffusion-Mediated Island Growth in Iron-on-Iron Homoepitaxy.
PB94-185923 *04,455*

Magnetic Dead Layer in Fe/Si Multilayer: Profile Refinement of Polarized Neutron Reflectivity Data.
PB94-198363 *04,458*

Concurrent Enhancement of Kerr Rotation and Antiferromagnetic Coupling in Epitaxial Fe/Cu/Fe Structures.
PB94-198769 *04,466*

Spot-Profile-Analyzing LEED Study of the Epitaxial Growth of Fe, Co, and Cu on Cu(100).
PB95-150165 *04,561*

Influence of Cr Growth on Exchange Coupling in Fe/Cr/Fe(100).
PB95-150181 *04,562*

Growth of Iron on Iron Whiskers.
PB95-150322 *04,567*

Oscillatory Exchange Coupling in Fe/Au/Fe(100).
PB95-150371 *04,569*

Improved Wavelengths for Prominent Lines of Fe XX to Fe XXIII.
PB96-111638 *04,334*

Formation of DNA-Protein Cross-Links in Cultured Mammalian Cells Upon Treatment with Iron Ions.
PB96-137724 *03,651*

Atomic Iron in Its (5)D Ground State: A Direct Measurement of the J = 0 inverted arrow 1 and J = 1 inverted arrow 2 Fine-Structure Intervals (1.2).
PB96-141221 *04,756*

IRON ALLOY 18CR 19MN
Nitrogen Effect on Elastic Constants of f.c.c. Fe-18Cr-19Mn Alloys.
PB94-172541 *03,203*

IRON ALLOYS
Study of Laser Resonance Ionization Mass Spectrometry Using a Glow Discharge Source.
DE94018566 *03,308*

Temperature Dependence of the Magnetic Excitations in Ordered and Disordered Fe72Pt28.
PB95-150223 *04,563*

Study of Laser Resonance Ionization Mass Spectrometry Using a Glow Discharge Source.
PB96-123203 *03,360*

Electronic Structure and Phase Equilibria in Ternary Substitutional Alloys.
PB97-119366 *03,378*

IRON BASE ALLOYS
Comparison of the Corrosion Rates of FeAl, Fe(sub 3)Al and Steel in Distilled Water and 0.5 M Sodium Chloride. Technical Report Number 2, January--March 1991.
DE94017332 *03,186*

IRON COMPOUNDS
Thermodynamic Properties of the Aqueous Ions (2+ and 3+) of Iron and the Key Compounds of Iron.
PB96-145958 *01,119*

IRON GARNETS
Wideband Current and Magnetic Field Sensors Based on Iron Garnets.
PB96-200878 *01,975*

IRON IONS
Measurements of quantum electrodynamic sensitive transitions in Na-like and Cu-like ions: Final report, 1 October 1993--29 September 1994.
DE95011593 *04,403*

Laser-Produced and Tokamak Spectra of Lithiumlike Iron, Fe(23+).
PB95-180857 *04,314*

Oxidation of Ferrous and Ferrocyanide Ions by Peroxyl Radicals.
PB97-122402 *01,191*

IRON OXIDES
Structural and Magnetic Ordering in Iron Oxide/Nickel Oxide Multilayers by X-ray and Neutron Diffraction (Invited).
PB94-172558 *04,442*

IRON SILICIDES
Soft-X-ray-Emission Studies of Bulk Fe3Si, FeSi, and FeSi2, and Implanted Iron Silicides.
PB96-157938 *04,071*

IRRADIANCE MEASUREMENT
Method of Realizing Spectral Irradiance Based on an Absolute Cryogenic Radiometer.
PB95-161204 *04,270*

IRRADIANCES
Irradiances of Spectral Lines in Mercury Pencil Lamps.
PB96-176466 *04,375*

IRRADIATION
Research and Development Activities in Electron Paramagnetic Resonance Dosimetry.
PB96-141288 *03,635*

Radiated Emissions and Immunity of Microstrip Transmission Lines: Theory and Measurements.
PB96-162649 *02,238*

ISDN (INTEGRATED SERVICES DIGITAL NETWORK)
Catalog of National ISDN Solutions for Selected NIUF Applications.
PB94-166006 *01,468*

ISDN Conformance Testing Guidelines: Guidelines for Implementors of ISDN Customer Premises Equipment to Conform to Both National ISDN-1 and North American ISDN Users' Forum Layer 3 Basic Rate Interface Basic Call Control Abstract Test Suites.
PB94-219094 *01,471*

ISDN LAN Bridging.
PB95-154696 *01,477*

Application Profile for ISDN.
PB95-163689 *01,479*

Application Software Interface: ISDN Services for an Open Systems Environment.
PB96-131487 *01,492*

ISDN in North America.
PB96-160767 *01,502*

North American Agreements on ISDN.
PB96-160775 *01,503*

ISDN (INTEGRATED SERVICES DIGITAL NETWORKS)
ISDN Conformance Testing.
PB95-163176 *01,478*

ISO
ISO Environmental Management Standardization Efforts.
PB95-220513 *02,524*

Conformance Testing for OSI Protocols.
PB96-102686 *01,631*

ISO Environmental Management Standardization Efforts.
PB96-158662 *02,528*

ISO/IEC GUIDE 25
Survey on the Implementation of ISO/IEC Guide 25 by National Laboratory Accreditation Programs.
PB94-210150 *00,479*

ISO (INTERNATIONAL ORGANIZATION FOR STANDARDIZATION)
Questions and Answers on Quality, the ISO 9000 Standard Series, Quality System Registration, and Related Issues. More Questions and Answers on the ISO 9000 Standard Series and Related Issues.
PB95-103461 *00,495*

ISOBUTENE
Mechanism and Rate Constants for the Reactions of Hydrogen Atoms with Isobutene at High Temperatures.
PB95-151064 *00,929*

ISOCHORIC
Isochoric (p-p-T) Measurements on Liquid and Gaseous Air from 67 to 400 K at Pressures to 35 MPa.
PB96-167390 *01,154*

ISOELECTRONIC SEQUENCE
Labeling Conventions in Isoelectronic Sequences - Reply.
PB95-162574 *03,937*

ISOLATION AMPLIFIERS
New 5 and 10 MHz High Isolation Distribution Amplifier.
PB96-190202 *01,510*

ISOMERASES
Thermodynamics of Enzyme-Catalyzed Reactions. Part 5. Isomerases and Ligases.
PB96-145974 *01,121*

ISOMERIZATION
Development of Engineered Stationary Phases for the Separation of Carotenoid Isomers.
PB95-150249 *00,578*

ISOMERS
Comparison of the Liquid Chromatographic Behavior of Selected Steroid Isomers Using Different Reversed-Phase Materials and Mobile Phase Compositions.
PB95-140976 *00,574*

Isolation and Structural Elucidation of the Predominant Geometrical Isomers of alpha-Carotene.
PB96-190061 *00,640*

ISOTHERMS
Water-Vapor Measurements of Low-Slope Roofing Materials.
PB95-251617 *00,399*

ISOTOPE DILUTION
Isotope Dilution Mass Spectrometry as a Candidate Definitive Method for Determining Total Glycerides and Triglycerides in Serum.
PB96-102280 *03,519*

Isotopic and Nuclear Analytical Techniques in Biological Systems: A Critical Study. 10. Elemental Isotopic Dilution Analysis with Radioactive and Stable Isotopes (Technical Report).
PB96-164157 *00,696*

ISOTOPE DILUTION MASS SPECTROSCOPY
Comparative Strategies for Correction of Interferences in Isotope Dilution Mass Spectrometric Determination of Vanadium.
PB94-185261 *00,531*

ISOTOPE EFFECT
Wavelengths and Energy Levels of Neutral Kr(84) and Level Shifts in All Kr Even Isotopes.
PB94-140605 *03,780*

Isotope Shifts and Hyperfine Splittings of the 398.8-nm Yb I Line.
PB94-199585 *03,814*

Wavelengths and Isotope Shifts for Lines of Astrophysical Interest in the Spectrum of Doubly Ionized Mercury (Hg III).
PB95-140869 *03,887*

Magneto-Optical Trapping of Metastable Xenon: Isotope-Shift Measurements.
PB95-151254 *03,905*

Deuterium Isotope Effect in Vinyl Radical Combination/Dispropor tionationReactions.
PB96-204151 *01,167*

ISOTOPE EFFECTS
Laser Magnetic-Resonance Measurement of the (3)P1 - (3)P2 Fine-Structure Splittings in (17)O and (18)O.
PB95-175170 *00,994*

ISOTOPE RATIO
Deuterium in the Local Interstellar Medium: Its Cosmological Significance.
PB95-202842 *00,081*

New IUPAC Guidelines for the Reporting of Stable Hydrogen, Carbon, and Oxygen Isotope-Ratio Data. Letter to the Editor.
PB95-261962 *01,058*

ISOTOPE RATIOS
New Values for Silicon Reference Materials, Certified for Isotope Abundance Ratios. Letter to the Editor.
PB94-219268 *00,863*

ISOTOPE SHIFT
Measurements of the Resonance Lines of (6)Li and (7)Li by Doppler-Free Frequency-Modulation Spectroscopy.
PB96-180211 *04,118*

ISOTOPIC COMPOSITIONS
Atomic Weights of the Elements, 1993.
PB96-145909 *01,114*

ISOTOPIC LABELING
Rare-Earth Isotopes as Tracers of Particulate Emissions: An Urban Scale Test.
PB94-161635 *02,535*

ISOTOPOMERS
Slit Jet Infrared Spectroscopy of Hydrogen Bonded N2HF Isotopomers: Rotational Rydberg-Klein-Rees Analysis and H/D Dependent Vibrational Predissociation Rates.
PB95-161873 *00,956*

ISOTROPIC MEDIA
Elastic Constants of Isotropic Cylinders Using Resonant Ultrasound.
PB94-211919 *04,497*

IT(INFORMATION TECHNOLOGY)
Report on Application Integration Architectures (AIA) Workshop. Held in Dallas, Texas on February 8-12, 1993.
PB94-142536 *01,803*

Study of Federal Agency Needs for Information Technology Security.
PB94-193653 *01,579*

ITER TOKAMAK
Irradiation Damage in Inorganic Insulation Materials for ITER Magnets: A Review.
PB95-147351 *03,705*

Cryogenic Properties of Inorganic Insulation Materials for ITER Magnets: A Review.
PB95-198768 *03,706*

ITS-90
Practical Applications of the ITS-90: Inherent Uncertainties.
PB95-161527 *03,930*

IUE
Recalibration for the Final Archive of the International Ultraviolet Explorer (IUE) Satellite.
PB96-135264 *00,106*

IUPAC COMMISSION ON ATOMIC WEIGHTS
Atomic Weights of the Elements, 1993.
PB96-145909 *01,114*

JAPAN

Statistical Quality Control Technology in Japan.
PB94-199064 *02,708*

Differences in Competitive Strategies between the United States and Japan.
PB94-211836 *00,013*

Calibration of GPS Equipment in Japan.
PB95-151452 *01,531*

Japan Technology Program Assessment: Precision Engineering/Precision Optics in Japan.
PB95-171112 *02,884*

Earthquake and Fire in Japan: When the Threat Became a Reality.
PB95-175238 *00,201*

Japan Technology Program Assessment. Simulation: State-of the-Art in Japan.
PB95-217097 *02,827*

Innovation in the Japanese Construction Industry: A 1995 Appraisal.
PB96-177373 *00,225*

JET ENGINES

Bibliography of Books and Published Reports on Gas Turbines, Jet Propulsion, and Rocket Power Plants.
AD-A278 138/3 *01,445*

Bibliography of Books and Published Reports on Gas Turbines, Jet Propulsion, and Rocket Power Plants, January 1950 through December 1953.
AD-A278 213/4 *01,446*

Determination of Hydrogen in Titanium Alloy Jet Engine Compressor Blades by Cold Neutron Capture Prompt Gamma-ray Activation Analysis.
PB95-175956 *01,448*

JET FLOW

Experimental Study of the Stabilization Region of Lifted Turbulent-Jet Diffusion Flames.
PB96-122676 *01,405*

JET MIXING FLOW

Global Density Effects on the Self-Preservation Behavior of Turbulent Free Jets.
PB95-162301 *04,207*

JOB CREATION

Metric Path to Global Markets and New Jobs: A Question-and-Answer and Thematic Discussion.
PB94-206307 *02,601*

JOINTS (JUNCTIONS)

Model Precast Concrete Beam-to-Column Connections Subject to Cyclic Loading.
PB95-153094 *00,438*

Partially Prestressed and Debonded Precast Concrete Beam-Column Joints.
PB95-153102 *00,439*

Seismic Performance Behavior of Precast Concrete Beam-Column Joints.
PB95-153110 *00,440*

Report of a Workshop on Requalification of Tubular Steel Joints in Offshore Structures. Held in Houston, Texas on September 5-6, 1995.
PB96-210760 *03,699*

JOSEPHSON ARRAYS

Accuracy Comparisons of Josephson Array Systems.
PB95-164687 *02,047*

JOSEPHSON EFFECT

How Accurate Are the Josephson and Quantum Hall Effects and QED.
PB95-163283 *03,942*

JOSEPHSON JUNCTIONS

Effect of Thermal Noise on Shapiro Steps in High-Tc Josephson Weak Links.
PB94-212677 *04,506*

Combined Josephson and Charging Behavior of the Supercurrent in the Superconducting Single-Electron Transistor.
PB95-168522 *04,637*

Observation of Vortex Dynamics in Two-Dimensional Josephson-Junction Arrays.
PB95-168811 *02,050*

Terahertz Shapiro Steps in High Temperature SNS Josephson Junctions.
PB95-169140 *02,168*

Phase-Locked Oscillator Optimization for Arrays of Josephson Junctions.
PB95-169314 *02,052*

Thermal Noise in High-Temperature Superconducting-Normal-Superconducting Step-Edge Josephson Junctions.
PB95-175089 *04,650*

Characterization of the Emission from 2D Array Josephson Oscillators.
PB95-175121 *02,054*

Emission Linewidth Measurements of Two-Dimensional Array Josephson Oscillators.
PB95-175139 *02,055*

Frequency Dependence of the Emission from 2D Array Josephson Oscillators.
PB95-175147 *02,056*

Evidence for Parallel Junctions Within High-Tc Grain-Boundary Junctions.
PB95-175410 *04,657*

Josephson Voltage Standard Based on Single-Flux-Quantum Voltage Multipliers.
PB95-175600 *02,058*

Phase Locking in Two-Junction Systems of High-Temperature Superconductor-Normal Metal-Superconductor Junctions.
PB95-176053 *02,060*

High Temperature Superconductor-Normal Metal-Superconductor Josephson Junctions with High Characteristic Voltages.
PB95-176079 *04,666*

Quasipotential and the Stability of Phase Lock in Nonhysteretic Josephson Junctions.
PB95-180402 *04,681*

Large-Amplitude Shapiro Steps and Self-Field Effects in High-Tc Josephson Weak Links.
PB95-180410 *04,682*

Step-Edge and Stacked-Heterostructure High-Tc Josephson Junctions for Voltage-Standard Arrays.
PB96-102066 *04,702*

Resonances in Two-Dimensional Array Oscillator Circuits.
PB96-102082 *02,066*

Direct Observation of Vortex Dynamics in Two-Dimensional Josephson-Junction Arrays.
PB96-102223 *02,067*

Physical Basis for Half-Integral Shapiro Steps in a DC SQUID.
PB96-102264 *04,704*

Stacked Series Arrays of High-Tc Trilayer Josephson Junctions.
PB96-102272 *04,705*

30 THz Mixing Experiments on High Temperature Superconducting Josephson Junctions.
PB96-102462 *04,709*

Phase Locking in Two-Dimensional Arrays of Josephson Junctions: Effect of Critical-Current Nonuniformity.
PB96-102587 *04,714*

Superconducting Integrated Circuit Fabrication with Low Temperature ECR-Based PECVD SiO2 Dielectric Films.
PB96-103015 *04,719*

Stable Phase Locking in a Two-Cell Ladder Array of Josephson Junctions.
PB96-111679 *04,722*

Temperature Dependence and Magnetic Field Modulation of Critical Currents in Step-Edge SNS YBCO/Au Junctions.
PB96-111745 *04,723*

Critical Current and Normal Resistance of High-Tc Step-Edge SNS Junctions.
PB96-111752 *04,724*

SUSAN: SUperconducting Systems ANalysis by Low Temperature Scanning Electron Microscopy (LTSEM).
PB96-112065 *04,728*

High-Frequency Oscillators Using Phase-Locked Arrays of Josephson Junctions.
PB96-135157 *02,080*

Heterodyne Mixing and Direct Detection in High Temperature Josephson Junctions.
PB96-147202 *01,565*

Microwave Noise in High-Tc Josephson Junctions.
PB96-148010 *04,771*

Josephson D/A Converter with Fundamental Accuracy.
PB96-148044 *02,418*

Performance and Reliability of NIST 10-V Josephson Arrays.
PB96-148051 *02,419*

Metallic-Barrier Junctions for Programmable Josephson Voltage Standards.
PB96-200134 *02,089*

Shapiro Steps in Large-Area Metallic-Barrier Josephson Junctions.
PB96-200142 *02,090*

Novel Vortex Dynamics in Two-Dimensional Josephson Arrays.
PB96-200167 *02,091*

High-Tc Multilayer Step-Edge Josephson Junctions and SQUIDs.
PB96-200183 *04,790*

Superconductor- Normal-Superconductor Junctions for Digital/Analog Converters.
PB96-200233 *02,092*

Superconductor- Normal-Superconductor Junctions for Programmable Voltage Standards.
PB96-200241 *02,093*

Design of High-Frequency, High-Power Oscillators Using Josephson-Junction Arrays.
PB96-200258 *02,094*

High-Power, High-Frequency Oscillators Using Distributed Josephson-Junction Arrays.
PB96-200266 *02,095*

Controlling the Critical Current Density of High-Temperature SNS Josephson Junctions.
PB96-200712 *04,794*

Pulse-Driven Programmable Josephson Voltage Standard.
PB97-111496 *04,148*

High Power Generation with Distributed Josephson-Junction Arrays.
PB97-111520 *02,099*

JOSEPHSON OSCILLATORS

Phase-Locked Oscillator Optimization for Arrays of Josephson Junctions.
PB95-169314 *02,052*

Characterization of the Emission from 2D Array Josephson Oscillators.
PB95-175121 *02,054*

Emission Linewidth Measurements of Two-Dimensional Array Josephson Oscillators.
PB95-175139 *02,055*

Frequency Dependence of the Emission from 2D Array Josephson Oscillators.
PB95-175147 *02,056*

Design of High-Frequency, High-Power Oscillators Using Josephson-Junction Arrays.
PB96-200258 *02,094*

High-Power, High-Frequency Oscillators Using Distributed Josephson-Junction Arrays.
PB96-200266 *02,095*

High Power Generation with Distributed Josephson-Junction Arrays.
PB97-111520 *02,099*

JOURNALS

Role of Journals in Maintaining Data Integrity: Checking of Crystal Structure Data in 'Acta Crystallographica'.
PB97-109177 *04,806*

Electronic Publishing and the Journals of the American Chemical Society.
PB97-109185 *04,807*

How the Cambridge Crystallographic Data Centre Obtains Its Information.
PB97-109193 *04,808*

JP-8 JET FUEL

Suppression of Elevated Temperature Hydraulic Fluid and JP-8 Spray Flames.
PB95-181095 *00,021*

JUVENILE RHEUMATOID ARTHRITIS

Nutritional Status and Growth in Juvenile Rheumatoid Arthritis.
PB94-198470 *03,515*

K LINES

K alpha Transitions in Few-Electron Ions and in Atoms.
PB94-212248 *03,849*

K-VALUE

Design of a Protocol for an Electron Probe Microanalyzer k-Value Round Robin.
PB95-107181 *00,564*

KALMAN FILTERS

Comparison of GPS Broadcast and DMA Precise Ephemerides.
N94-30660/2 *01,523*

KEROSENE

Structure of a Swirl-Stabilized Kerosene Spray Flame.
PB95-108569 *02,480*

KERR CELLS

Investigation of the Effects of Aging on the Calibration of a Kerr-Cell Measuring System for High Voltage Impulses.
PB94-172384 *02,025*

KERR EFFECT

Observation of the Transverse Second Harmonic Magneto-Optic Kerr Effect from Ni81Fe19 Thin Film Structures.
PB96-200332 *01,971*

KERR MAGNETOOPTICAL EFFECT

Concurrent Enhancement of Kerr Rotation and Antiferromagnetic Coupling in Epitaxial Fe/Cu/Fe Structures.
PB94-198769 *04,466*

Magnetooptic Effects.
PB96-119292 *04,338*

KETENE COMPLEXES

Rotational Spectrum and Structure of a Weakly Bound Complex of Ketene and Acetylene.
PB95-126140 *00,896*

KEY ESCROW ENCRYPTION

Report of the NIST Workshop on Key Escrow Encryption. Held in Gaithersburg, Maryland on June 8-10, 1994.
PB94-209459 *01,584*

KEYBOARDS

Guidance of the Legality of Keystroke Monitoring.
PB96-161237 *00,005*

KIDNEY

Nickel(II)-Mediated Oxidative DNA Base Damage in Renal and Hepatic Chromatin of Pregnant Rats and Their Fetuses. Possible Relevance to Carcinogenesis.
PB94-212628 *03,646*

Oxidative DNA Base Damage in Renal, Hepatic, and Pulmonary Chromatin of Rats After Intraperitoneal Injection of Cobalt (II) Acetate.
PB95-150025 *03,647*

DNA Base Modifications in Renal Chromatin of Wistar Rats Treated with a Renal Carcinogen, Ferric Nitrilotriacetate.
PB95-150363 *03,648*

Treatment of Wistar Rats with a Renal Carcinogen, Ferric Nitrilotriacetate, Causes DNA-Protein Cross-Linking between Thymine and Tyrosine in Their Renal Chromatin.
PB96-112115 *03,649*

KILOGRAMS
NIST Watt Experiment: Monitoring the Kilogram.
PB97-122329 *01,997*

KINEMATIC VISCOSITY
Viscosity of the Saturated Liquid Phase of Six Halogenated Compounds and Three Mixtures.
PB95-162368 *00,960*

KINETIC ENERGY
Kinetic Energy Distribution of Ions Produced from Townsend Discharges in Neon and Argon.
PB96-111927 *04,413*

KINETICS
Fokker-Planck Description of Multivalent Interactions.
PB95-108478 *00,879*

Aggregation Kinetics of Colloidal Particles Destabilized by Enzymes.
PB95-125878 *00,894*

Anisotropic Phase Separation Kinetics in a Polymer Blend Solution Following Cessation of Shear Studied by Light Scattering.
PB95-151247 *01,241*

Current Noise Reveals Protonation Kinetics and Number of Ionizable Sites in an Open Protein Ion Channel.
PB96-161674 *04,092*

KNOWLEDGE-BASED SYSTEMS
Development of Computer-Based Models of Standards and Attendant Knowledge-Base and Procedural Systems.
PB96-155783 *00,464*

KRYPTON
Intensity-Dependent Scattering Rings in High Order Above-Threshold Ionization.
PB96-110739 *04,032*

Spectral Data for Highly Ionized Krypton, Kr V through Kr XXXVI.
PB96-145917 *01,115*

KRYPTON 84
Wavelengths and Energy Levels of Neutral Kr(84) and Level Shifts in All Kr Even Isotopes.
PB94-140605 *03,780*

KRYPTON 85
Intercomparison of Internal Proportional Gas Counting of (85)Kr and (3)H.
PB94-185576 *03,800*

KRYPTON COMPLEXES
Van der Waals Bond Lengths and Electronic Spectral Shifts of the Benzene-Kr and Benzene-Xe Complexes.
PB95-151387 *00,932*

KRYPTON IONS
Resonance Structure and Absolute Cross Sections in Near-Threshold Electron-Impact Excitation of the 4s(2) (1)S yields 4s4p (3)P Intercombination Transition in Kr(6+).
PB95-202271 *03,972*

L-S COUPLING
Investigation of LS Coupling in Boronlike Ions.
PB94-185295 *03,797*

L-THREO-BETA-HYDROXYHISTIDINE
L-threo-beta-Hydroxyhistidine, an Unprecedented Iron(III) Ion-Binding Amino Acid in a Pyoverdine-type Siderophore from Pseudomonas fluorescens 244.
PB94-211620 *00,553*

LABELLING COMPLIANCE
Inter-Laboratory Trials of the EPR Method for the Detection of Irradiated Meats Containing Bone.
PB96-161690 *00,042*

LABELS
Checking the Net Contents of Packaged Goods as Adopted by the 79th National Conference on Weights and Measures, 1994, Third Edition, Supplement 4.
PB95-182226 *00,484*

LABOR FORCE
Investing in Education to Meet a National Need for a Technical-Professional Workforce in a Post-Industrial Economy.
PB94-173028 *00,132*

LABORATORIES
NVLAP Procedures U.S. Code of Federal Regulations. Title 15, Subtitle A, Chapter 2, Part 7. (Effective December 1984; Amended September 1990).
PB94-160850 *02,627*

National Voluntary Laboratory Accreditation Program: Procedures and General Requirements.
PB94-178225 *02,630*

National Voluntary Laboratory Accreditation Program 1994 Directory.
PB94-178969 *00,482*

Proficiency Testing as a Component of Quality Assurance in Construction Materials Laboratories.
PB94-185774 *00,334*

State Weights and Measures Laboratories: State Standards Program Description and Directory. 1994 Edition.
PB94-207727 *02,895*

Program Handbook: Requirements for Obtaining NIST Approval/Recognition of a Laboratory Accreditation Body Under P.L. 101-592. The Fastener Quality Act.
PB94-210143 *02,859*

National Voluntary Laboratory Accreditation Program: Energy Efficient Lighting Products.
PB94-219060 *02,642*

Comparison of Heat-Flow-Meter Tests from Four Laboratories.
PB95-126264 *00,365*

National Voluntary Laboratory Accreditation Program: Ionizing Radiation Dosimetry.
PB95-128658 *03,623*

National Voluntary Laboratory Accreditation Program: Bulk Asbestos Analysis.
PB95-138129 *02,541*

National Voluntary Laboratory Accreditation Program: Construction Materials Testing.
PB95-155552 *01,319*

National Voluntary Laboratory Accreditation Program: Carpet and Carpet Cushion.
PB95-155560 *00,295*

National Voluntary Laboratory Accreditation Program (NVLAP): Wood Based Products.
PB95-170429 *03,405*

National Voluntary Laboratory Accreditation Program 1995 Directory.
PB95-174454 *00,483*

National Voluntary Laboratory Accreditation Program Acoustical Testing Services.
PB95-182234 *04,188*

National Voluntary Laboratory Accreditation Program: POSIX. Portable Operating System Interface.
PB95-189478 *02,661*

National Voluntary Laboratory Accreditation Program: Electromagnetic Compatibility and Telecommunications. FCC Methods.
PB95-242376 *02,664*

Materials Science and Engineering Laboratory Annual Report, December 1993.
PB95-254439 *02,668*

National Voluntary Laboratory Accreditation Program (NVLAP): Commercial Products Testing.
PB95-267944 *02,671*

National Voluntary Laboratory Accreditation Program: Thermal Insulation Materials.
PB95-267985 *02,977*

Proficiency Tests for the NIST Airborne Asbestos Program, 1993.
PB96-106463 *00,610*

Laboratory Accreditation for Testing Energy Efficient Lighting.
PB96-122932 *00,270*

Inexpensive Laser Cooling and Trapping Experiment for Undergraduate Laboratories.
PB96-140371 *04,353*

U.S. Government Accreditation and Conformity Assessment System Evaluation.
PB96-160239 *02,678*

National Voluntary Laboratory Accreditation Program 1996 Directory.
PB96-162714 *00,485*

State Weights and Measures Laboratories: Program Handbook.
PB96-214705 *02,687*

LABORATORY ACCREDITATION
Survey on the Implementation of ISO/IEC Guide 25 by National Laboratory Accreditation Programs.
PB94-210150 *00,479*

Should NIST Accredit U.S. Calibration Laboratories.
PB95-107280 *02,646*

Gage Block Standards, Measurement Capabilities and Laboratory Accreditation.
PB96-163621 *02,757*

Proceedings of the Open Forum on Laboratory Accreditation at the National Institute of Standards and Technology, October 13, 1995.
PB96-210141 *02,686*

Evaluation and Accreditation of State Calibration Laboratories.
PB97-110183 *00,486*

LABORATORY AUTOMATION
Integrating Automated Systems with Modular Architecture.
PB95-150231 *00,577*

LABORATORY EQUIPMENT
Precision Laboratory Standards of Mass and Laboratory Weights.
AD-A280 562/0 *02,618*

Electroacoustics for Characterization of Particulates and Suspensions. Proceedings of a Workshop. Held in Gaithersburg, Maryland on February 3-4, 1993.
PB94-112695 *00,725*

Simple, Inexpensive Apparatus for Sample Concentration.
PB94-199205 *00,546*

NIST Power Reference Source.
PB94-211513 *00,148*

Anisotropic Phase Separation Kinetics in a Polymer Blend Solution Following Cessation of Shear Studied by Light Scattering.
PB95-151247 *01,241*

Constant Temperature and Humidity Chamber for Standard Resistors.
PB96-122494 *02,275*

LAKE ERIE
Lake Erie Water Temperature Data, Put-in-Bay, Ohio, 1918-1992.
PB96-202452 *03,692*

LAMELLA
Partially Coherent Transmittance of Dielectric Lamellae.
PB96-148028 *04,359*

LAMINAR FLOW
Probabilistic Computation of Poiseuille Flow Velocity Fields.
PB96-102520 *04,209*

LAMINATED GLASS
Influence of Physical Aging on the Yield Response of Model DGEBA + Poly(propylene oxide) Epoxy Glasses.
PB95-126363 *03,381*

Volume Recovery in Epoxy Glasses Subjected to Torsional Deformations: The Question of Rejuvenation.
PB95-140018 *03,382*

Torsional Relaxation and Volume Response during Physical Aging in Epoxy Glasses Subjected to Large Torsional Deformations.
PB95-140026 *03,383*

Using Torsional Dilatometry to Measure the Effects of Deformations on Physical Aging.
PB95-140901 *03,384*

LAMINOGRAPHY
Evaluation and Qualification Standards for an X-Ray Laminography System.
PB94-172954 *02,029*

Contributions of Out-of-Plane Material to a Scanned-Beam Laminography Image.
PB96-111786 *02,704*

LAMP ORIENTATION
Irradiance of Horizontal Quartz-Halogen Standard Lamps.
PB96-179130 *01,866*

LAMPS
Improved Automated Current Control for Standard Lamps.
PB94-219367 *00,246*

LANDSAT SATELLITES
Organization and Implementation of Calibration in the EOS Project. Part 1.
PB96-179437 *04,841*

LANTHANUM
Charge-Transfer-Induced Multiplet Structure in the N4,5O2,3 Soft-X-ray Emission Spectrum of Lanthanum.
PB96-163746 *04,102*

LANTHANUM ALUMINATES
Dielectric Properties of Single Crystals of Al2O3, LaAlO3, SrTiO3, and MgO at Cryogenic Temperatures.
PB95-180477 *02,266*

LANTHANUM BARIUM CUPRATES
Correlation between Tc and Elastic Constants of (La-M)2CuO4.
PB94-213220 *04,514*

LANTHANUM BARIUM TITANATES
Substitution-Induced Midgap States in the Mixed Oxides RxBa1-ChiTiO3-Delta, with R=Y, La, and Nd.
PB95-140505 *04,541*

LANTHANUM CALCIUM CUPRATES
Correlation between Tc and Elastic Constants of (La-M)2CuO4.
PB94-213220 *04,514*

Neutron Powder Diffraction Study of the Structures of La1.9Ca1.1Cu2O6 and La1.9Sr1.1Cu2O6+Delta.
PB95-140042 *04,538*

LANTHANUM DEUTERIDE
Neutron-Powder-Diffraction Study of the Long-Range Order in the Octahedral Sublattice of LaD2.25.
PB96-141155 *04,753*

Characterization of the Structure of LaD2.50 by Neutron Powder Diffraction.
PB96-176797 *04,783*

LANTHANUM STRONTIUM CUPRATES
Electronic Correlations and Satellites in Superconducting Oxides.
PB94-200045 *04,477*

Correlation between Tc and Elastic Constants of (La-M)2CuO4.
PB94-213220 *04,514*

Neutron Powder Diffraction Study of the Structures of La1.9Ca1.1Cu2O6 and La1.9Sr1.1Cu2O6+Delta.
PB95-140042 *04,538*

LANTHANUM TITANIUM ALUMINATES
Determination of Complex Structures from Powder Diffraction Data: The Crystal Structure of La3Ti5Al15O37.
PB95-202966 *01,038*

LAPLACE EQUATION
Laplace's Equation and the Dirichlet-Neumann Map in Multiply Connected Domains. (NIST Reprint).
PB95-180295 *03,962*

Exact Recursion Relation Solution for the Steady-State Surface Temperature of a General Multilayer Structure.
PB96-102017 *02,376*

LARGE SCALE INTEGRATION
Defect Formation Mechanism Causing Increasing Defect Density during Decreasing Implant Dose in Low-Dose Simox.
PB96-119524 *02,402*

KEYWORD INDEX

LASER ABLATION
Influence of Deposition Parameters on Properties of Laser Ablated YBa2Cu3O7-Delta Films.
PB95-140539 *04,544*

LASER AMPLIFIERS
Optical Sampling Using Nondegenerate Four-Wave Mixing in a Semiconductor Laser Amplifier.
PB96-122502 *02,076*

Optical Sampling Using Nondegenerate Four-Wave Mixing in a Semiconductor Laser Amplifier.
PB96-123609 *04,348*

LASER ANNEALING
Improved Dose Metrology in Optical Lithography.
PB96-179510 *02,439*

LASER APPLICATIONS
Optically Stabilized Tunable Diode-Laser System for Saturation Spectroscopy.
PB96-102819 *04,717*

LASER BEAMS
Beam Analysis Round Robin.
PB94-212545 *04,239*

Laser-Beam Analysis Pinpoints Critical Parameters.
PB94-212552 *04,240*

Widths and Propagation of a Truncated Gaussian Beam.
PB95-168779 *04,287*

Error Propagation in Laser Beam Spatial Parameters.
PB95-180394 *04,310*

Characterization of a Clipped Gaussian Beam.
PB96-102553 *04,331*

LASER COOLING
Laser Cooling and Trapping for the Masses.
PB95-126090 *04,253*

Laser Cooling.
PB95-151502 *03,908*

Trapped Atoms and Laser Cooling.
PB95-151627 *03,911*

New Mechanisms for Laser Cooling.
PB95-153268 *03,923*

Laser Cooling of Trapped Ions.
PB95-168746 *03,950*

Quantum-Limited Cooling and Detection of Radio-Frequency Oscillations by Laser-Cooled Ions.
PB96-112073 *04,039*

Inexpensive Laser Cooling and Trapping Experiment for Undergraduate Laboratories.
PB96-140371 *04,353*

Laser Modification of Ultracold Collisions: Experiment.
PB96-157987 *04,075*

Laser-Cooled Neutral Atom Frequency Standards.
PB96-160312 *04,086*

Gravitational Sisyphus Cooling of (87)Rb in a Magnetic Trap.
PB96-200704 *04,379*

Properties of a Bose-Einstein Condensate in an Anisotropic Harmonic Potential.
PB96-204144 *04,133*

Laser Cooling and the Recoil Limit.
PB97-111280 *04,391*

LASER DEPOSITION
Laser-Focused Atomic Deposition.
PB95-161618 *04,604*

LASER DIAGNOSTICS
Modeling Ceramic Sub-Micron Particle Formation from the Vapor Using Detailed Chemical Kinetics: Comparison with In-situ Laser Diagnostics.
PB95-151965 *00,671*

LASER DIFFRACTION
Parametric Investigation of Metal Powder Atomization Using Laser Diffraction.
PB95-108577 *03,342*

LASER DIODES
Simultaneous Laser-Diode Emission and Detection for Fiber-Optic Sensor Applications.
PB96-155502 *04,062*

Magneto-Optic Rotation Sensor Using a Laser Diode as Both Source and Detector.
PB97-111272 *04,390*

LASER FOCUSING
Laser Focused Atomic Deposition.
PB95-180659 *04,685*

Nanostructure Fabrication via Laser-Focused Atomic Deposition (Invited).
PB96-204094 *04,132*

LASER HAZARDS
Optical Density Measurements of Laser Eye Protection Materials.
PB96-190301 *00,190*

LASER INDUCED DESORPTION
Laser-Induced Desorption of NO from Si(111): Effects of Coverage on NO Vibrational Populations.
PB95-162319 *00,959*

Laser-Induced Desorption of In and Ga from Si(100) and Adsorbate Enhanced Surface Damage.
PB95-203311 *01,050*

Pulsed Laser Irradiation at 532 nm of In and Ga Adsorbed on Si(100): Desorption, Incorporation, and Damage.
PB95-203329 *01,051*

LASER INDUCED FLUORESCENCE
Greatly Enhanced Soot Scattering in Flickering Ch4/Air Diffusion Flames.
PB94-172988 *01,361*

Laser Imaging of Chemistry-Flowfield Interactions: Enhanced Soot Formation in Time-Varying Diffusion Flames.
PB94-185352 *01,364*

Laser-Induced Fluorescence Measurements of Formaldehyde in a Methane/Air Diffusion Flame.
PB94-211679 *01,374*

Optical Measurements of Atomic Hydrogen, Hydroxyl, and Carbon Monoxide in Hydrocarbon Diffusion Flames.
PB95-150900 *02,487*

Laser-Induced Fluorescence Measurements of OH. Concentrations in the Oxidation Region of Laminar, Hydrocarbon Diffusion Flames.
PB95-162160 *01,387*

Trace Detection in Conducting Solids Using Laser-Induced Fluorescence in a Cathodic Sputtering Cell.
PB95-163424 *00,598*

LASER MAGNETIC RESONANCE
Determination of the Molecular Parameters of NiH in Its (2)Delta Ground State by Laser Magnetic Resonance.
PB95-107116 *00,869*

LASER MATERIALS
Vertical-Cavity Semiconductor Structures: Materials Characterization.
PB95-153185 *02,149*

LASER MODE LOCKING
Millimeter-Resolution Optical Time-Domain Reflectometry Using a Four-Wave Mixing Sampling Gate.
PB96-122700 *02,190*

LASER PHOTOIONIZATION
Laser Photoionization Measurements of Pressure in Vacuum.
PB95-180600 *03,964*

LASER PHOTOLYSIS
Absorption Cross Sections, Kinetics of Formation, and Self-Reaction of the IO Radical Produced via the Laser Photolysis of N2O/I2/N2 Mixtures.
PB97-112361 *01,180*

LASER POLARIMETRY
Simultaneous Measurement of Normal Spectral Emissivity by Spectral Radiometry and Laser Polarimetry at High Temperatures in Pulse-Heating Experiments: Application to Molybdenum and Tungsten.
PB97-118376 *02,694*

LASER-PRODUCED PLASMA
Measurements of quantum electrodynamic sensitive transitions in Na-like and Cu-like ions: Final report, 1 October 1993--29 September 1994.
DE95011593 *04,403*

LASER PULSE METHOD
Thermal Diffusivity of POCO AXM-5Q1 Graphite in the Range 1500 to 2500 K Measured by a Laser-Pulse Technique.
PB94-185022 *03,013*

High-Temperature Laser-Pulse Thermal Diffusivity Apparatus.
PB94-185147 *02,631*

LASER RADIATION
Far Infrared Laser Frequencies of (13)CD3OH.
PB95-169363 *04,292*

Frequency Shifting of Pulsed Narrow-Band Laser Light in a Multipass Raman Cell.
PB95-203352 *04,321*

Nanofabrication of a Two-Dimensional Array Using Laser-Focused Atomic Deposition.
PB96-119417 *04,732*

Thermal Modeling and Analysis of Laser Calorimeters.
PB96-140405 *04,354*

LASER RANGE FINDERS
Preliminary Comparison of Time Transfers via LASSO, GPS and Two-Way Satellite.
PB95-151098 *01,529*

LASER SCATTERING
In situ Characterization of Vapor Phase Growth of Iron Oxide-Silica Nanocomposites: Part 1. 2-D Planar Laser-Induced Fluorescence and Mie Imaging.
PB97-112478 *03,185*

LASER SPECTROSCOPY
Dreams About the Next Generation of Super-Stable Lasers.
PB94-211570 *04,235*

High-Resolution Spectroscopy of Laser-Cooled Rubidium in a Vapor-Cell Trap.
PB95-153714 *04,268*

Laser Spectroscopy of Carbon Monoxide: A Frequency Reference for the Far Infrared.
PB95-163606 *04,277*

High-Sensitivity Spectroscopy with Diode Lasers.
PB95-175477 *04,297*

Diode Laser as a Spectroscopic Tool.
PB95-175485 *00,600*

High-Resolution Diode-Laser Spectroscopy of Calcium.
PB95-181244 *03,969*

High-Resolution Optical Multiplex Spectroscopy.
PB95-203543 *04,323*

Doppler-Free Spectroscopy of Large Polyatomic Molecules and van der Waals Complexes.
PB96-119581 *04,339*

Search for Small Violations of the Symmetrization Postulate in an Excited State of Helium.
PB96-123518 *04,050*

Frequency-Stabilized Lasers: A Driving Force for New Spectroscopies.
PB96-135199 *04,350*

Comment On: Two-Photon Absorption Series of Calcium.
PB96-157979 *04,074*

Configuration-Dependent AC Stark Shifts in Calcium.
PB96-157995 *04,363*

Measurements of the Resonance Lines of (6)Li and (7)Li by Doppler-Free Frequency-Modulation Spectroscopy.
PB96-180211 *04,118*

Electronically Tunable Fiber Laser for Optical Pumping of (3)He and (4)He.
PB96-201165 *04,381*

LASER STABILITY
Dreams About the Next Generation of Super-Stable Lasers.
PB94-211570 *04,235*

Frequency Stabilized Lasers: A Parochial Review.
PB95-153771 *04,269*

Stabilization of 3.3 and 5.1 m Lead-Salt Diode Lasers by Optical Feedback.
PB95-180709 *04,313*

Stabilization of Optical Phase/Frequency of a Laser System: Application to a Commercial Dye Laser with an External Stabilizer.
PB95-203832 *04,327*

Frequency-Stabilized Lasers: A Driving Force for New Spectroscopies.
PB96-135199 *04,350*

LASER STRUCTURES
Double-Modulation and Selective Excitation Photoreflectance for Wafer-Level Characterization of Quantum-Well Laser Structures.
PB96-167325 *04,372*

LASER SYNCHROTRON COINCIDENCE
Laser-Synchrotron Hybrid Experiments: A Photon to Tickle, A Photon to Poke.
PB96-157847 *03,704*

LASER TRAPPING
Laser Cooling and Trapping for the Masses.
PB95-126090 *04,253*

Inexpensive Laser Cooling and Trapping Experiment for Undergraduate Laboratories.
PB96-140371 *04,353*

LASER TRIGGERED BREAKDOWN
Electrohydrodynamic Instability and Electrical Discharge Initiation in Hexane.
PB96-186119 *02,244*

LASERS
Sub-Doppler Frequency Measurements on OCS at 87 THz (3.4 mu m) with the CO Overtone Laser.
PB96-102215 *04,330*

Far Infrared Laser Frequencies of CH3OD and N2H4.
PB96-119623 *04,341*

Introduction to Phase-Stable Optical Sources.
PB96-122973 *04,347*

Distributed Feedback Lasers in Rare-Earth-Doped Phosphate Glass.
PB96-123773 *04,740*

Coexistence of Grains with Differing Orthorhombicity in High Quality YBa2Cu3O7-delta Thin Films.
PB96-135033 *04,742*

Heterodyne Mixing and Direct Detection in High Temperature Josephson Junctions.
PB96-147202 *01,565*

Optoelectronics at NIST.
PB96-200860 *02,202*

Mode-Locked Lasers for High-Accuracy Radiometry.
PB96-204201 *04,134*

Sinusoidal Surfaces as Standards for BRDF Instruments.
PB97-110597 *04,388*

Double Modulation and Selective Excitation Photoreflectance for Characterizing Highly Luminescent Semiconductor Structures and Samples with Poor Surface Morphology.
PB97-111439 *02,452*

Laser Bandwidth Effects in Quantitative Cavity Ring-Down Spectroscopy.
PB97-112254 *04,394*

LASERS & THEIR APPLICATIONS
Measurements of quantum electrodynamic sensitive transitions in Na-like and Cu-like ions: Final report, 1 October 1993--29 September 1994.
DE95011593 *04,403*

Thermal Diffusivity of POCO AXM-5Q1 Graphite in the Range 1500 to 2500 K Measured by a Laser-Pulse Technique.
PB94-185022 *03,013*

Selected Ion Flow Tube-Laser Induced Fluorescence Instrument for Vibrationally State-Specific Ion-Molecule Reactions.
PB94-185444 *00,774*

Magneto-Optic Magnetic Field Sensor with 1.4pT/square root of 1(Hz) Minimum Detectable Field at 1 kHz.
PB94-199551 02,125

Pump-Induced Dispersion of Erbium-Doped Fiber Measured by Fourier-Transform Spectroscopy.
PB94-211935 04,236

Beam Analysis Round Robin.
PB94-212545 04,239

Laser-Beam Analysis Pinpoints Critical Parameters.
PB94-212552 04,240

Integrated Optic Laser Emitting at 906, 1057, and 1358 nm.
PB94-216280 02,135

Integrated Optic Laser Emitting at 905, 1057, 1356 nm.
PB94-216298 02,136

Laser Cooling and Trapping for the Masses.
PB95-126090 04,253

Metrology Applications of Mode-Locked Erbium Fiber Lasers.
PB95-140158 04,256

Rare-Earth-Doped Waveguide Devices: The Potential for Compact Blue-Green Lasers.
PB95-140836 04,257

Linewidth Narrowing in an Imbalanced Y-Branch Waveguide Laser.
PB95-140844 04,258

Nd:LiTaO3 Waveguide Laser.
PB95-140851 04,259

Nanostructure Fabrication via Direct Writing with Atoms Focused in Laser Fields.
PB95-150272 04,564

Multiwavelength Birefringent-Cavity Mode-Locked Fibre Laser.
PB95-150496 04,262

Direct Dispersion Measurement of Highly-Erbium-Doped Optical Amplifiers Using a Low Coherence Reflectometer Coupled with Dispersive Fourier Spectroscopy.
PB95-150702 04,263

Laser Cooling.
PB95-151502 03,908

Multiphoton Ionization Spectroscopy Measurements of Silicon Atoms during Vapor Phase Synthesis of Ceramic Particles.
PB95-151999 03,913

Vertical-Cavity Optoelectronic Structures: CAD, Growth, and Structural Characterization.
PB95-153177 02,148

Vertical-Cavity Semiconductor Structures: Materials Characterization.
PB95-153185 02,149

Vertical-Cavity Semiconductor Lasers: Structural Characterization, CAD, and DFB Structures.
PB95-153193 02,150

New Mechanisms for Laser Cooling.
PB95-153268 03,923

High Speed, High Sensitivity Magnetic Field Sensors Based on the Faraday Effect in Iron Garnets.
PB95-153391 02,151

Magneto-Optic Magnetic Field Sensors Based on Uniaxial Iron Garnet Films in Optical Waveguide Geometry.
PB95-153409 02,152

High-Resolution Spectroscopy of Laser-Cooled Rubidium in a Vapor-Cell Trap.
PB95-153714 04,268

Accurate Characterization of High Speed Photodectors.
PB95-153763 02,153

Frequency Stabilized Lasers: A Parochial Review.
PB95-153771 04,269

Bragg Gratings in Optical Fibers Produced by a Continuous-Wave Ultraviolet Source.
PB95-162020 04,274

Growth of Bragg Gratings Produced by Continuous-Wave Ultraviolet Light in Optical Fiber.
PB95-162038 04,275

Stabilization and Precise Calibration of a Continuous-Wave Difference Frequency Spectrometer by Use of a Simple Transfer Cavity.
PB95-162350 04,276

Polarization Dependence of Response Functions in 3x3 Sagnac Optical Fiber Current Sensors.
PB95-162426 02,154

Vector Theory of Diffraction by a Single-Mode Fiber: Application to Mode-Field Diameter Measurements.
PB95-164182 04,279

In situ Observation of Surface Morphology of InP Grown on Singular and Vicinal (001) Substrates.
PB95-168431 04,636

Interlaboratory Comparison of Polarization-Holding Parameter Measurements on High-Birefringence Optical Fiber.
PB95-168464 04,280

Low-Coherence Interferometric Measurement of Group Transit Times in Precision Optical Fibre Delay Lines.
PB95-168480 02,158

Improved Variational Analysis of Inhomogeneous Optical Waveguides Using Airy Functions.
PB95-168639 04,285

Spatial Uniformity of Optical Detector Responsivity.
PB95-168845 02,162

Electrically Calibrated Pyroelectric Detector-Refinements for Improved Optical Power Measurements.
PB95-169066 02,164

Optical Power Meter Calibration Using Tunable Laser Diodes.
PB95-169256 04,290

Waveguide Polarizers Processed by Localized Plasma Etching.
PB95-169264 02,171

Self-Calibrating Fiber Optic Sensors: Potential Design Methods.
PB95-169298 02,172

High-Sensitivity Spectroscopy with Diode Lasers.
PB95-175477 04,297

Diode Laser as a Spectroscopic Tool.
PB95-175485 00,600

Calculated Fiber Attenuation: A General Method Yielding Stationary Values.
PB95-175501 04,298

High-Sensitivity Optical Sampling Using an Erbium-Doped Fiber Laser Strobe.
PB95-176111 04,302

Precise Optical Frequency References and Difference Frequency Measurements with Diode Lasers.
PB95-176228 04,305

Error Propagation in Laser Beam Spatial Parameters.
PB95-180394 04,310

Modal Characteristics of Bent Dual Mode Planar Optical Waveguide.
PB95-180485 04,311

Laser Photoionization Measurements of Pressure in Vacuum.
PB95-180600 03,964

Stabilization of 3.3 and 5.1 m Lead-Salt Diode Lasers by Optical Feedback.
PB95-180709 04,313

High-Resolution Diode-Laser Spectroscopy of Calcium.
PB95-181244 03,969

Model Minimum Performance Specifications for Lidar Speed Measurement Devices.
PB95-197455 04,861

Lunar Laser Ranging: A Continuing Legacy of the Apollo Program.
PB95-202495 03,683

Improved Hyperfine Measurements of the Na NP Excited State Through Frequency-Controlled Dopplerless Spectroscopy in a Zeeman Magneto-Optic Laser Trap.
PB95-203840 04,012

Delivering the Same Optical Frequency at Two Places: Accurate Cancellation of Phase Noise Introduced by an Optical Fiber or Other Time-Varying Path.
PB96-102736 04,332

Phase Shifts and Intensity Dependence in Frequency-Modulation Spectroscopy.
PB96-103205 01,071

Glasses for Waveguide Lasers.
PB96-111950 04,335

Laser Gas Ionization Technique Monitors MEB Crystal Growth.
PB96-112172 01,076

Introduction to Phase-Stable Optical Sources.
PB96-122973 04,347

Frequency-Stabilized Lasers: A Driving Force for New Spectroscopies.
PB96-135199 04,350

Laser Modification of Ultracold Collisions: Experiment.
PB96-157987 04,075

Optical Density Measurements of Laser Eye Protection Materials.
PB96-190301 00,190

Laser Cooling and the Recoil Limit.
PB97-111280 04,391

Laser Bandwidth Effects in Quantitative Cavity Ring-Down Spectroscopy.
PB97-112254 04,394

LATE STARS

Volume-Limited ROSAT Survey of Extreme Ultraviolet Emission from all Nondegenerate Stars within 10 Parsecs.
PB96-103189 00,093

Sleuthing the Dynamo: HST/FOS Observations of UV Emissions of Solar-Type Stars in Young Clusters.
PB96-122817 00,098

High Velocity Plasm in the Transition Region of Au Mic: A Stellar Analog of Solar Explosive Events.
PB96-123294 00,102

LATHES

Effects of Spindle Dynamic Characteristics on Hard Turning.
PB96-122981 02,699

LATTICE MISMATCH

Influence of Lattice Mismatch on Indium Phosphide Based High Electron Mobility Transistor (HEMT) Structures Observed in High Resolution Monochromatic Synchrotron X-Radiation Diffraction Imaging.
PB95-164679 02,357

LATTICE MODELS

Lattice Model of a Hydrogen-Bonded Polymer Blend.
PB97-112262 03,391

LATTICE PARAMETERS

Precision Comparison of the Lattice Parameters of Silicon Monocrystals.
PB94-169745 04,438

Improved Crystallographic Data for Aluminum Niobate (AlNbO4).
PB95-107306 04,523

LATTICE SITES

Lattice Position of Si in GaAs Determined by X-Ray Standing Wave Measurements.
PB95-164406 04,632

LATTICE STRAIN

Accurate Modeling of Size and Strain Broadening in the Rietveld Refinement: The 'Double-Voigt' Approach.
PB96-200225 00,664

LATTICES

Interfacial Crack in a Two-Dimensional Hexagonal Lattice.
PB96-161989 04,100

Dislocation Core-Core Interaction and Peierls Stress in a Model Hexagonal Lattice.
PB96-162003 04,101

Photonic Band-Structure Effects for Low-Index-Contrast Two-Dimensional Lattices in the Near Infrared.
PB97-122469 04,401

LAW ENFORCEMENT

Face Recognition Technology for Law Enforcement Applications.
PB94-207768 01,837

Evaluating Investments in Law Enforcement Equipment: An Annotated Bibliography.
PB95-151379 04,867

Directory of Law Enforcement and Criminal Justice Associations and Research Centers.
PB96-178918 04,872

LAW FREQUENCIES

Low-Frequency Model for Radio-Frequency Absorbers.
PB95-261939 04,424

LAW (JURISPRUDENCE)

Federal Certification Authority Liability and Policy: Law and Policy of Certificate-Based Public Key and Digital Signatures.
PB94-191202 01,578

Uniform Laws and Regulations in the Areas of Legal Metrology and Motor Fuel Quality as Adopted by the 80th National Conference on Weights and Measures 1995. 1996 Edition.
PB96-172309 02,927

LAYER CONSTRICTION

X-ray Observation of Electroclinic Layer Constriction and Rearrangement in a Chiral Smectic-A Liquid Crystal.
PB96-141080 01,100

LAYERED COMPOUNDS

Maximum Entropy as a Tool for the Determination of the C-Axis Profile of Layered Compounds.
PB94-199619 00,800

LAYERS

Contact Electrification Induced by Monolayer Modification of a Surface and Relation to Acid-Base Interactions.
PB94-185378 03,034

Modified Surface Layers and Coatings.
PB95-176087 03,125

LEACHING

Modelling the Leaching of Calcium Hydroxide from Cement Paste: Effects on Pore Space Percolation and Diffusivity.
PB94-198793 01,311

Bioleaching of Cobalt from Smelter Wastes by 'Thiobacillus ferrooxidans'.
PB95-140968 02,582

Development of a Test Method for Leaching of Lead from Lead-Based Paints Through Encapsulants.
PB96-154984 03,128

LEAD ACETATE

Preparation and Monitoring of Lead Acetate Containing Drinking Water Solutions for Toxicity Studies.
PB94-193885 00,538

LEAD COATINGS

Development of a Test Method for Leaching of Lead from Lead-Based Paints Through Encapsulants.
PB96-154984 03,128

LEAD COMPOUNDS

Liquid Chromatography: Laser-Enhanced Ionization Spectrometry for the Speciation of Organolead Compounds.
PB94-185253 00,530

Electric Field Effects on Crack Growth in a Lead Magnesium Niobate.
PB95-107322 03,339

LEAD INORGANIC COMPOUNDS

Preparation and Monitoring of Lead Acetate Containing Drinking Water Solutions for Toxicity Studies.
PB94-193885 00,538

LEAD (METAL)

Lead Abatement in Buildings and Related Structures.
PB94-172038 03,601

Secondary Target X-Ray Excitation for In vivo Measurement of Lead in Bone.
PB95-108767 *03,496*

Spectral Interference in the Determination of Arsenic in High-Purity Lead and Lead-Base Alloys Using Electrothermal Atomic Absorption Spectrometry and Zeeman-Effect Background Correction.
PB96-112099 *00,614*

Application of a Novel Slurry Furnace AAS Protocol for Rapid Assessment of Lead Environmental Contamination.
PB96-112354 *02,526*

Development of a Test Method for Leaching of Lead from Lead-Based Paints Through Encapsulants.
PB96-154984 *03,128*

LEAD POISONING
Lead Abatement in Buildings and Related Structures.
PB94-172038 *03,601*

LEAD SALT DIODE LASERS
Optically Stabilized Tunable Diode-Laser System for Saturation Spectroscopy.
PB96-102819 *04,717*

LEAD STRONTIUM YTTRIUM CUPRATES
Crystal Structure of Pb2Sr2YCu3O8+delta with delta=1.32, 1.46, 1.61, 1.71, by Powder Neutron Diffraction.
PB94-216314 *04,518*

LEAD ZIRCONATE TITANATES
Microstructure and Ferroelectric Properties of Lead Zirconate-Titanate Films Produced by Laser Evaporation.
PB94-199148 *04,470*

LEAK DETECTORS
Experimental Data and Theoretical Modeling of Gas Flows Through Metal Capillary Leaks.
PB95-150892 *04,206*

LEAKAGE CURRENT
Leakage Current Detection in Cryogenic Current Comparator Bridges.
PB94-172228 *02,024*

LEAST SQUARE FIT
Bounds on Least-Squares Four-Parameter Sine-Fit Errors Due to Harmonic Distortion and Noise.
PB96-141304 *01,609*

LEDGES
Dislocation Emission at Ledges on Cracks.
PB95-164240 *04,630*

LEGALITY
Guidance of the Legality of Keystroke Monitoring.
PB96-161237 *00,005*

LENGTH
Uncertainties in Dimensional Measurements Made at Nonstandard Temperatures.
PB94-169760 *02,893*

Metrology Model for Submicrometer Dimensional Measurements.
PB95-108502 *02,647*

Evolution of Automatic Line Scale Measurement at the National Institute of Standards and Technology.
PB95-108809 *02,897*

Alternative Contour Technique for the Efficient Computation of the Effective Length of an Antenna.
PB96-141361 *02,011*

LENNARD-JONES POTENTIAL
Long-Lived Structures in Fragile Glass-Forming Liquids.
PB96-119565 *04,212*

LENSES
Planar Lenses for Field-Emitter Arrays.
PB96-103064 *02,112*

LEUKOCYTES
Modification of DNA Bases in Chromatin of Intact Target Human Cells by Activated Human Polymorphonuclear Leukocytes.
PB94-199833 *03,526*

LEUNG-GRIFFITHS MODEL
Calculation of Enthalpy and Entropy Differences of Near-Critical Binary Mixtures with the Modified Leung-Griffiths Model.
PB95-108635 *00,885*

LEUNG-GRIFFITHS THEORY
Vapor-Liquid Equilibria of Mixtures of Propane and Isomeric Hexanes.
PB95-175287 *00,995*

Critical Properties and Vapor-Liquid Equilibria of the Binary System Propane + Neopentane.
PB95-175683 *00,999*

LIBRARIES
National Center for Standards and Certification Information: Service and Programs.
N95-15938/0 *02,717*

Field Measurements of Ventilation and Ventilation Effectiveness in an Office/Library Building.
PB95-108833 *00,247*

LIBRATIONAL MOTION
Intermolecular HF Motion in Ar(sub n)HF Micromatrices (n=1,2,3,4,): Classical and Quantum Calculations on a Pairwise Additive Potential Surface.
PB95-107025 *03,871*

LIDAR (LIGHT DETECTION AND RANGING)
Model Minimum Performance Specifications for Lidar Speed Measurement Devices.
PB95-197455 *04,861*

LIFE APPARATUS
Flammability Characterization with the Lift Apparatus and the Cone Calorimeter.
PB97-110050 *01,435*

LIFE CYCLE ANALYSIS
ISO Environmental Management Standardization Efforts.
PB95-220513 *02,524*

ISO Environmental Management Standardization Efforts.
PB96-158662 *02,528*

LIFE CYCLE COSTS
Energy Prices and Discount Factors for Life-Cycle Cost Analysis 1994. Annual Supplement to NIST Handbook 135 and NBS Special Publication 709.
PB94-206018 *02,508*

Energy Price Indices and Discount Factors for Life-Cycle Cost Analysis 1995. Annual Supplement to NIST Handbook 135 and NBS Special Publication 709. (Revised).
PB95-105011 *02,509*

Present Worth Factors for Life-Cycle Cost Studies in the Department of Defense (1995).
PB95-105029 *03,664*

Life-Cycle Costing Workshop for Energy Conservation in Buildings: Student Manual.
PB95-175006 *00,257*

BLCC: The NIST 'Building Life-Cycle Cost' Program, Version 4.21. User's Guide and Reference Manual.
PB95-190682 *00,263*

Building Life Cycle Cost Computer Program (BLCC), Version 4.2-95 (for Microcomputers).
PB95-501953 *00,266*

Building Life Cycle Cost Computer Program (BLCC) Version 4.21-95 (for Microcomputers).
PB95-502779 *00,267*

Building Life Cycle Cost Computer Program (BLCC) Version 4.22-95 (for Microcomputers).
PB95-503397 *00,268*

Present Worth Factors for Life-Cycle Cost Studies in the Department of Defense (1996).
PB96-106869 *03,673*

Economic Methods and Risk Analysis Techniques for Evaluating Building Investments: A Survey.
PB96-122593 *00,323*

Multiattribute Decision Analysis Method for Evaluating Buildings and Building Systems.
PB96-158670 *00,325*

Energy Price Indices and Discount Factors for Life-Cycle Cost Analysis 1996. Annual Supplement to NIST Handbook 135 and NBS Special Publication 709. (Revised).
PB96-162441 *02,510*

Life-Cycle Costing Manual for the Federal Energy Management Program. 1995 Edition.
PB96-172317 *02,511*

Energy Price Indices and Discount Factors for Life-Cycle Cost Analysis 1997. Annual Supplement to NIST Handbook 135 and NBS Special Publication 709. (Revised).
PB96-210745 *02,512*

Building Life Cycle Cost Computer Program (BLCC) Version 4.22-95 (for Micrcomputers).
PB96-502794 *00,277*

Building Life Cycle Cost Computer Program (BLCC) Version 4.4-97 (for Microcomputers).
PB97-500342 *00,284*

LIFE (DURABILITY)
Research on Methods for Determining Optical Disk Media Life Expectancy Estimates.
PB96-160304 *01,633*

LIFE TESTS
Methodologies for Predicting the Service Lives of Coating Systems.
PB95-146387 *03,124*

LIFELINE SYSTEMS
Ground Improvement Techniques for Liquefaction Remediation Near Existing Lifelines.
PB96-128111 *01,350*

LIFELINES
Proceedings of a Workshop on Developing and Adopting Seismic Design and Construction Standards for Lifelines. Held in Denver, Colorado on September 25-27, 1991.
PB97-115794 *01,302*

LIFETIMES
Measurement of the Atomic Na(3P) Lifetime and of Retardation in the Interaction between Two Atoms Bound in a Molecule.
PB97-122360 *04,178*

LIFT
Experimental Study of the Stabilization Region of Lifted Turbulent-Jet Diffusion Flames.
PB96-122676 *01,405*

LIGAND CONTACTS
Escherichis coli Cyclic AMP Receptor Protein Mutants Provide Evidence for Ligand Contacts Important in Activation.
PB96-201017 *03,592*

LIGAND ENVIRONMENT
Isolated Spin Pairs and Two-Dimensional Magnetism in SrCr(sub 9p)Ga(sub 12-9p)O19.
PB97-112387 *04,154*

LIGANDS
Affinity Chromatography on Inorganic Support Materials.
PB95-163820 *03,467*

LIGASES
Thermodynamics of Enzyme-Catalyzed Reactions. Part 5. Isomerases and Ligases.
PB96-145974 *01,121*

LIGHT AMPLIFIERS
Direct Dispersion Measurement of Highly-Erbium-Doped Optical Amplifiers Using a Low Coherence Reflectometer Coupled with Dispersive Fourier Spectroscopy.
PB95-150702 *04,263*

Millimeter-Resolution Optical Time-Domain Reflectometry Using a Four-Wave Mixing Sampling Gate.
PB96-122700 *02,190*

LIGHT REFRACTION
Refraction of Light by Graded Birefringent Media.
PB96-123716 *02,192*

LIGHT SCATTERING
Two Numerical Techniques for Light Scattering by Dielectric Agglomerated Structures.
PB94-140597 *04,225*

Brillouin Light Scattering Intensities for Thin Magnetic Films with Large Perpendicular Anisotropies.
PB94-211174 *04,488*

Light Scattering from Glossy Coatings on Paper.
PB94-213246 *04,242*

Determination of Surface Roughness from Scattered Light.
PB94-216520 *04,243*

Autocorrelation Functions from Optical Scattering for One-Dimensionally Rough Surfaces.
PB94-216538 *04,244*

Light Scattered by Coated Paper.
PB94-216546 *04,245*

SANS and LS Studies of Polymer Mixtures Under Shear Flow.
PB95-107090 *01,231*

Radiometric Model of the Transmission Cell-Reciprocal Nephelometer.
PB95-150132 *00,124*

Regimes of Surface Roughness Measurable with Light Scattering.
PB95-151213 *04,265*

Method for the Assay of Hydrolytic Enzymes Using Dynamic Light Scattering.
PB95-151411 *03,531*

Dynamic Light-Scattering Study of a Diluted Polymer Blend Near Its Critical Point.
PB95-151890 *01,245*

Light Scattered from Two Atoms.
PB95-168753 *04,286*

Rayleigh Scattering Limits for Low-Level Bidirectional Reflectance Distribution Function Measurements.
PB95-180030 *04,307*

Standard Reference Material for the Measurement of Particle Mobility by Electrophoretic Light Scattering.
PB96-102488 *00,609*

Physicochemical Characterization of Low Molecular Weight Heparin.
PB96-112040 *03,474*

Physical Characterization of Herparin by Light Scattering.
PB96-119383 *03,598*

Zimm Plot and Its Analogs as Indicators of Vesicle and Micelle Size Polydispersity.
PB96-123765 *01,094*

Dependence of Contrast on Probe/Sample Spacing with the Magneto-Optic Kerr-Effect Scanning Near-Field Optical Microscope (MOKE-SNOM).
PB96-138557 *04,750*

Elastic Scattering from Spheres under Non Plane-Wave Illumination.
PB96-163688 *04,370*

Model of an Optical Roughness-Measuring Instrument.
PB97-110209 *04,384*

Light Scattering by Sinusoidal Surfaces: Illumination Windows and Harmonics in Standards.
PB97-110548 *04,387*

Windowing Effects on Light Scattering by Sinusoidal Surfaces.
PB97-111215 *04,389*

Forward Scattering of a Gaussian Beam by a Nonabsorbing Sphere.
PB97-112288 *04,395*

LIGHT SOURCES
Lighting Quality and Light Source Size.
PB95-151783 *00,252*

LIGHTING EQUIPMENT
Psychological Aspects of Lighting: A Review of the Work of CIE TC 3.16.
PB95-153276 *00,254*

Laboratory Accreditation for Testing Energy Efficient Lighting.
PB96-122932 *00,270*

State of the Art Report on Seismic Design Requirements for Nonstructural Building Components.
PB96-193800 *00,308*

LIGHTING SYSTEMS
Computer Programs for Simulation of Lighting/HVAC Interactions.
PB94-140407 *02,501*

Psychological Aspects of Lighting: A Review of the Work of CIE TC 3.16.
PB94-172160 00,241

Papers Presentations Shine.
PB94-200383 00,244

Lighting and HVAC.
PB95-150991 00,250

NIST Lighting and HVAC Interaction Test Facility.
PB95-151007 00,251

Lighting Research and Theory Can Create Business Prospects.
PB95-151791 00,253

LIGHTWEIGHT CONCRETES
Testing of Selected Self-Leveling Compounds for Floors.
PB95-220455 00,395

LINE BROADENING
Profile Fitting of X-Ray Diffraction Lines and Fourier Analysis of Broadening.
PB94-198512 04,460

Ion Broadening Parameters for Several Argon and Carbon Lines.
PB94-211562 03,843

Astrophysical Aspects of Neutral Atom Line Broadening.
PB94-213287 00,061

LINE-FOCUS TRANSDUCER
Transient Analysis of a Line-Focus Transducer Probing a Liquid/Solid Interface.
PB97-118681 02,763

Material Characterization By a Time-Resolved and Polarization-Sensitive Ultrasonic Technique.
PB97-122576 02,764

LINE-FOCUS TRANSDUCERS
Design, Construction and Application of a Large Aperture Lens-Less Line-Focus PVDF Transducer.
PB97-122584 02,765

LINE HEAT SOURCES
Intra-Laboratory Comparison of a Line-Heat-Source Guarded Hot Plate and Heat-Flow-Meter Apparatus.
PB95-181202 00,387

Line-Heat-Source Guarded-Hot-Plate Apparatus.
PB97-118996 00,417

LINE NARROWING
Linewidth Narrowing in an Imbalanced Y-Branch Waveguide Laser.
PB95-140844 04,258

LINE OF SIGHT
Deuterium and the Local Interstellar Medium: Properties for the Procyon and Capella Lines of Sight.
PB96-200639 00,111

LINE REFLECT MATCH CALIBRATIONS
Line-Reflect-Match Calibrations with Nonideal Microstrip Standards.
PB96-176599 02,242

LINE SHAPE
Experimental Studies of Line Shapes from a Balle-Flygare Spectrometer.
PB94-199452 00,796

LINE SPECTRA
Improved Wavelengths for Prominent Lines of Fe XX to Fe XXIII.
PB96-111638 04,334

LINE WIDTH
Practical Photomask Linewidth Measurements.
PB95-108510 02,324

User's Manual for the Program MONSEL-1: Monte Carlo Simulation of SEM Signals for Linewidth Metrology.
PB95-111522 02,325

Linewidth Narrowing in an Imbalanced Y-Branch Waveguide Laser.
PB95-140844 04,258

Monte Carlo Model for SEM Linewidth Metrology.
PB95-150058 02,331

Comparisons of Measured Linewidths of Sub-Micrometer Lines Using Optical, Electrical, and SEM Metrologies.
PB95-152807 02,338

X-ray Mask Metrology: The Development of Linewidth Standards for X-ray Lithography.
PB95-162129 02,348

Microelectronic Test Structures for Feature Placement and Electrical Linewidth Metrology.
PB95-180568 02,367

Improving Photomask Linewidth Measurement Accuracy via Emulated Stepper Aerial Image Measurement.
PB95-180816 02,911

MONSEL-II: Monte Carlo Simulation of SEM Signals for Linewidth Metrology.
PB96-102710 02,379

Use of Monte Carlo Modeling for Interpreting Scanning Electron Microscope Linewidth Measurements.
PB96-137807 02,413

LINEAR ACCELERATOR SCATTER
Scattered Fractions of Dose from 18 and 25 MV X-ray Radiotherapy Linear Accelerators.
PB96-186101 04,120

LINEAR ALGEBRA
Basic Linear Algebra Operations in SLI Arithmetic.
PB96-165931 03,421

LINEAR PROGRAMMING
Algorithmic Enhancements to the Method of Centers for Linear Programming Problems.
PB94-198959 03,426

LINEAR REGRESSION
Constant-Width Calibration Intervals for Linear Regression.
PB95-153524 03,439

LINEAR SYSTEMS
Characterization of Unknown Linear Systems Based on Measured CW Amplitude.
PB95-161485 01,897

SparseLib++ v. 1.5 Sparse Matrix Class Library. Reference Guide.
PB96-193636 01,775

LINEARITY
Beamcon III, a Linearity Measurement Instrument for Optical Detectors.
PB96-113576 04,337

LINKAGES
Standards and Linkages: What Data Sharing Needs.
PB95-161881 01,713

LIPID BILAYERS
Self-Assembled Phospholipid/Alkanethiol Biomimetic Bilayers on Gold.
PB95-108460 00,878

Supported Phospholipid/Alkanthiol Biomimetic Membranes: Insulating Properties.
PB95-180782 03,470

Phospholipid/Alkanethiol Bilayers for Cell-Surface Receptor Studies by Surface Plasmon Resonance.
PB96-102900 03,472

LIPIDS
Biological Thermodynamic Data for the Calibration of Differential Scanning Calorimeters: Dynamic Temperature Data on the Gel to Liquid Crystal Phase Transition of Dialkylphosphatidylcholine in Water Suspensions.
PB95-162707 03,464

Extending the Angular Range of Neutron Reflectivity Measurements from Planar Lipid Bilayers: Applications to a Model Biological Membrane.
PB96-122569 03,476

LIPOSOMES
Calcium Phosphate Precipitation in Liposomal Suspensions.
PB94-172145 03,452

Mixed Phospholipid Liposome Calcification.
PB94-211190 03,457

Proteoglycan Inhibition of Calcium Phosphate Precipitation in Liposomal Suspensions.
PB94-211208 00,658

Liposome-Based Flow-Injection Immunoassay for Determining Theophylline in Serum.
PB94-213493 03,494

Potentiometric Enzyme-Amplified Flow Injection Analysis Detection System: Behavior of Free and Liposome-Released Peroxidase.
PB95-151833 03,534

Membrane-Mediated Precipitation of Calcium Phosphate in Model Liposomes with Matrix Vesicle-Like Lipid Composition.
PB95-164547 03,468

Effect of 1-Hydroxyethylidene-1,1-Bisphosphonate on Membrane-Mediated Calcium Phosphate Formation in Model Liposomal Suspensions.
PB95-169223 03,469

Zimm Plot and Its Analogs as Indicators of Vesicle and Micelle Size Polydispersity.
PB96-123765 01,094

LIQUEFACTION
Helium Refrigeration and Liquefaction Using a Liquid Hydrogen Refrigerator for Precooling.
AD-A286 683/8 02,749

Ground Improvement Techniques for Liquefaction Remediation Near Existing Lifelines.
PB96-128111 01,350

Energy-Based Method for Liquefaction Potential Evaluation. Phase 1. Feasibility Study.
PB96-214747 03,691

LIQUID ALLOYS
Dynamic Measurements of Thermophysical Properties of Metals and Alloys at High Temperatures by Subsecond Pulse Heating Techniques.
N94-25124/6 03,309

LIQUID CHROMATOGRAPHY
Liquid Chromatography: Laser-Enhanced Ionization Spectrometry for the Speciation of Organolead Compounds.
PB94-185253 00,530

Liquid Chromatographic Method for the Determination of Carotenoids, Retinoids, and Tocopherols in Human Serum and in Food.
PB95-153599 00,593

Shape Selectivity in Reversed-Phase Liquid Chromatography for the Separation of Planar and Non-Planar Solutes.
PB95-162608 00,596

Influence of Stationary Phase Chemistry on Shape Recognition in Liquid Chromatography.
PB96-123682 00,621

LIQUID CIRCULATION
Internal Droplet Circulation Induced by Surface-Driven Rotation.
PB97-119267 02,500

LIQUID COLUMN CHROMATOGRAPHY
Device for Subambient Temperature Control in Liquid Chromatography.
PB95-140604 00,573

Comparison of the Liquid Chromatographic Behavior of Selected Steroid Isomers Using Different Reversed-Phase Materials and Mobile Phase Compositions.
PB95-140976 00,574

Determination of Polycyclic Aromatic Hydrocarbons by Liquid Chromatography.
PB95-151650 00,585

Shape Selectivity in Reversed-Phase Liquid Chromatography for the Separation of Planar and Non-Planar Solutes.
PB95-162608 00,596

Liquid Chromatographic Determination of Polycyclic Aromatic Hydrocarbon Isomers of Molecular Weight 278 and 302 in Environmental Standard Reference Materials.
PB95-164042 02,523

LIQUID COMPOSITE MOLDING
Report on the Workshop on Manufacturing Polymer Composites by Liquid Molding. Held in Gaithersburg, Maryland on September 20-22, 1993.
PB94-160066 03,131

LIQUID CRYSTALLINE POLYMERS
Phase Behavior of a Hydrogen Bonding Molecular Composite.
PB94-185188 01,202

Neutron Scattering Study of the Orientation of a Liquid Crystalline Polymer by Shear Flow.
PB95-180196 01,270

LIQUID CRYSTALS
Polymer Liquid Crystalline Materials.
PB94-212339 01,224

Novel Polydiacetylenes Derived from Liquid Crystalline Monomers.
PB95-140125 01,235

Studies of the Higher Order Smectic Phase of the Large Electroclinic Effect Material W317.
PB95-151601 00,935

Dielectric Spectroscopic Determination of Temperature Behavior of Electroclinic Parameters in the Liquid Crystal W317.
PB96-140397 01,098

X-ray Observation of Electroclinic Layer Constriction and Rearrangement in a Chiral Smectic-A Liquid Crystal.
PB96-141080 01,100

LIQUID DENSITIES
Compressed Liquid Densities, Saturated Liquid Densities, and Vapor Pressures of 1,1-Difluoroethane.
PB97-110118 01,173

LIQUID FUELS
Development of Measurement Capabilities for the Thermophysical Properties of Energy-Related Fluids. Annual Report, December 1, 1990--November 30, 1991.
DE94004399 02,470

Combustion of a Polymer (PMMA) Sphere in Microgravity.
N96-15569/2 01,354

LIQUID HYDROGEN
Cryogenic Research and Development (Quarterly Report Number 2 for Period Ending December 31, 1960).
AD-A280 398/9 01,454

Cryogenic Research and Development (Progress Report Number 4 for Period Ending December 31, 1961).
AD-A280 399/7 01,455

Progress Report to National Aeronautics and Space Administration on Cryogenic Research and Development.
AD-A286 612/7 01,458

Design and Construction of a Liquid Hydrogen Temperature Refrigeration System.
AD-A286 618/4 02,619

Helium Refrigeration and Liquefaction Using a Liquid Hydrogen Refrigerator for Precooling.
AD-A286 683/8 02,749

Liquid-Hydrogen Cold Neutron Source for the NBSR.
PB95-151619 03,729

Nuclear Heat Load Calculations for the NBSR Cold Neutron Source Using MCNP.
PB95-152955 03,730

LIQUID-IN-GLASS THERMOMETERS
Assessment of Uncertainties of Liquid-in-Glass Thermometer Calibrations at the National Institute of Standards and Technology.
PB94-142510 02,625

LIQUID METALS
Dynamic Measurements of Thermophysical Properties of Metals and Alloys at High Temperatures by Subsecond Pulse Heating Techniques.
N94-25124/6 03,309

Development in the Theory and Analysis of Eddy Current Sensing of Velocity in Liquid Metals.
PB94-212586 03,335

LIQUID OXYGEN
Vortex Shedding Flowmeters for SSME Ducts.
PB95-169215 01,453

Wear Mechanism Maps of 440C Martensitic Stainless Steel.
PB96-111810 *04,834*

LIQUID PHASE EPITAXY
RII Spectroscopy of Trap Levels in Bulk and LPE Hg1-xCdxTe.
PB96-160247 *04,084*

LIQUID PHASES
New Data and Correlations for the Custody Transfer of Natural Gas Liquids.
PB96-176664 *02,499*

LIQUID-SOLID INTERFACE
Effects of Elastic Stress on the Stability of a Solid-Liquid Interface.
PB95-163028 *03,350*

LIQUID-SOLID INTERFACES
Boundary Conforming Grid Generation System for Interface Tracking.
PB94-158268 *03,312*

Scanning Tunneling Microscopy and Fabrication of Nanometer Scale Structures at the Liquid-Gold Interface.
PB95-140414 *00,904*

Ultrasonic Method for Reconstructing the Two-Dimensional Liquid-Solid Interface in Solidifying Bodies.
PB95-161782 *03,349*

Boundary Conforming Grid Generation System for Interface Tracking.
PB96-103007 *03,357*

LIQUID-VAPOR EQUILIBRIUM
Modified Leung-Griffiths Model of Vapor-Liquid Equilibrium: Extended Scaling and Binary Mixtures of Dissimilar Fluids.
PB94-216108 *00,851*

Calculation of Enthalpy and Entropy Differences of Near-Critical Binary Mixtures with the Modified Leung-Griffiths Model.
PB95-108635 *00,885*

Vapor-Liquid Equilibria of Mixtures of Propane and Isomeric Hexanes.
PB95-175287 *00,995*

Critical Properties and Vapor-Liquid Equilibria of the Binary System Propane + Neopentane.
PB95-175683 *00,999*

LIQUID-VAPOR INTERFACES
Structure of the Vapor-Liquid Interface Near the Critical Point.
PB95-140174 *00,902*

Thermal Equilibration Near the Critical Point: Effects Due to Three Dimensions and Gravity.
PB95-152922 *03,919*

LIQUIDS
Density of Solids and Liquids.
AD-A278 517/8 *00,711*

Table of Dielectric Constants of Pure Liquids.
AD-A278 956/8 *00,712*

Near Critical Fluid Interfaces: A Comparison of Theory and Experiment.
PB95-140166 *00,901*

Length Scales for Fragile Glass-Forming Liquids.
PB96-102801 *01,065*

Intrinsic Viscosity and the Polarizability of Particles Having a Wide Range of Shapes.
PB96-119318 *03,170*

Long-Lived Structures in Fragile Glass-Forming Liquids.
PB96-119565 *04,212*

Simulation Studies of Supercooled and Glass Forming Liquids.
PB96-122627 *01,085*

LIQUIFIED AIR
Speed-of-Sound Measurements in Liquid and Gaseous Air.
PB95-151957 *04,186*

LITERATURE SURVEYS
Guide to Instrumentation Literature.
AD-A280 278/3 *02,617*

Irradiation Damage in Inorganic Insulation Materials for ITER Magnets: A Review.
PB95-147351 *03,705*

Robotics Application to Highway Transportation. Volume 2. Literature Search.
PB95-170551 *01,337*

Literature Review on Seismic Performance of Building Cladding Systems.
PB96-106901 *00,455*

LITHIUM
Angular Distributions for Near-Threshold (e,2e) Processes for Li and Mg.
PB94-185725 *00,778*

Regulation of Lithium and Boron Levels in Normal Human Blood: Environmental and Genetic Considerations.
PB94-198579 *03,491*

Determination of Boron and Lithium in Diverse Biological Matrices Using Neutron Activation - Mass Spectrometry (NA-MS).
PB94-212289 *00,554*

LITHIUM 6
Preparation and Characterization of (6)LiF and (10)B Reference Deposits for the Measurement of the Neutron Lifetime.
PB95-108692 *03,874*

LITHIUM ALLOYS
Recommended Changes in ASTM Test Methods D2512-82 and G86-84 for Oxygen-Compatibility Mechanical Impact Tests on Metals.
PB94-216694 *03,338*

Macro- and Microreactions in Mechanical-Impact Tests of Aluminum Alloys.
PB95-107348 *03,340*

Influence of Specimen Absorbed Energy in LOX Mechanical-Impact Tests.
PB95-107355 *03,341*

LITHIUM DEUTERIDES
FTS Infrared Measurements of the Rotational and Vibrational Spectrum of LiH and LiD.
PB94-216231 *00,856*

LITHIUM FLUORIDE
Colour Centres in LiF for Measurement of Absorbed Doses Up to 100 MGy.
PB97-118756 *04,169*

LITHIUM FLUORIDES
Preparation and Characterization of (6)LiF and (10)B Reference Deposits for the Measurement of the Neutron Lifetime.
PB95-108692 *03,874*

LITHIUM HYDRIDES
FTS Infrared Measurements of the Rotational and Vibrational Spectrum of LiH and LiD.
PB94-216231 *00,856*

LITHIUM-LIKE IONS
Laser-Produced and Tokamak Spectra of Lithiumlike Iron, Fe(23+).
PB95-180857 *04,314*

LITHOGRAPHY
Test Structures for the In-Plane Locations of Projected Features with Nanometer-Level Accuracy Traceable to a Coordinate Measurement System.
PB94-200565 *02,313*

Practical Photomask Linewidth Measurements.
PB95-108510 *02,324*

X-ray Mask Metrology: The Development of Linewidth Standards for X-ray Lithography.
PB95-162129 *02,348*

New Test Structure for Nanometer-Level Overlay and Feature-Placement Metrology.
PB95-175345 *02,363*

Microelectronic Test Structures for Feature Placement and Electrical Linewidth Metrology.
PB95-180568 *02,367*

Nanofabrication of a Two-Dimensional Array Using Laser-Focused Atomic Deposition.
PB96-119417 *04,732*

Use of Monte Carlo Modeling for Interpreting Scanning Electron Microscope Linewidth Measurements.
PB96-137807 *02,413*

Atom-Optical Properties of a Standing-Wave Light Field.
PB96-141072 *04,356*

New NIST/ARPA National Soft X-ray Reflectometry Facility.
PB96-158092 *04,080*

Improved Reflectometry Facility at the National Institute of Standards and Technology.
PB96-160338 *04,087*

NIST Metrology for Soft X-ray Multilayer Optics.
PB96-160379 *04,088*

Microlithography by Using Neutral Metastable Atoms and Self-Assembled Monolayers.
PB96-190038 *02,441*

LITHOGRAPHY MASKS
SEM Linewidth Metrology of X-ray Lithography Masks.
PB96-201108 *02,447*

LITIGATION
Using a Multi-Layered Approach to Representing Tort Law Cases for Case-Based Reasoning.
PB96-160874 *00,135*

LIVER
Nickel(II)-Mediated Oxidative DNA Base Damage in Renal and Hepatic Chromatin of Pregnant Rats and Their Fetuses. Possible Relevance to Carcinogenesis.
PB94-212628 *03,646*

Oxidative DNA Base Damage in Renal, Hepatic, and Pulmonary Chromatin of Rats After Intraperitoneal Injection of Cobalt (II) Acetate.
PB95-150025 *03,647*

DNA Base Damage Generated In vivo in Hepatic Chromatin of Mice upon Whole Body y-Irradiation.
PB95-161741 *03,627*

LIVERMORE LOOPS
Technique to Evaluate Benchmarks: A Case Study Using the Livermore Loops.
PB95-151320 *04,577*

LMR (LASER MAGNETIC RESONANCE)
Determination of the Molecular Parameters of NiH in Its (2)Delta Ground State by Laser Magnetic Resonance.
PB95-107116 *00,869*

LOADING RATE
Loading Device for Fracture Testing of Compact Tension Specimens in the Scanning Electron Microscope.
PB95-162434 *02,652*

LOCAL AREA NETWORKS
Guideline for the Analysis of Local Area Network Security. Category: Computer Security; Subcategory: Risk Analysis and Contingency Planning.
FIPS PUB 191 *01,799*

Planning for the Fiber Distributed Data Interface (FDDI).
PB94-135761 *01,621*

Local Area Networks in NAA: Advantages and Pitfalls.
PB94-172095 *00,527*

ISDN LAN Bridging.
PB95-154696 *01,477*

LOCAL OSCILLATORS
Ultra-High Stability Synthesizer for Diode Laser Pumped Rubidium.
PB94-216066 *01,527*

LOCALIZATION MODEL
Effect of Swelling on the Elasticity of Rubber: Localization Model Description.
PB94-211034 *01,216*

LOGIC DEVICES
Experimental Results on Single Flux Quantum Logic.
PB95-175071 *02,053*

LOGIC PROGRAMMING
Representing Designs with Logic Formulations of Spatial Relations.
PB97-111561 *02,792*

LOGISTICS MANAGEMENT
CALS-Department of Defense Computer Aided Acquisition Logistic Support (CALS).
PB94-962500 *03,662*

CALS-Department of Defense Computer Aided Acquisition Logistic Support (CALS).
PB95-962500 *03,671*

Federal Implementation Guideline for Electronic Data Interchange: ASC X12 003040 Transaction Set 838 Trading Partner Profile (Confirmation of Vendor Registration). Implementation Convention.
PB96-111190 *01,813*

LOMA PRIETA EARTHQUAKE
Assessment of Site Response Analysis Procedures.
PB95-210928 *00,450*

LORAN C
Using LORAN-C Broadcasts for Automated Frequency Calibrations.
PB94-216017 *01,526*

LOSS FREE COUNTING
Loss-Free Counting at IRI and NIST.
PB96-167119 *04,105*

LOSSY MEDIA
Aperture Excitation of Electrically Large, Lossy Cavities.
PB95-175675 *00,031*

LOW ALLOY STEELS
Characterization of the Hydrogen Induced Cold Cracking Susceptibility at Simulated Weld Zones in HSLA-100 Steel.
AD-A279 759/5 *03,200*

Apparent Bias in the X-Ray Fluorescence Determination of Titanium in Selected NIST SRM Low Alloy Steels.
PB95-108759 *03,212*

LOW FLOW PLUMBING FIXTURES
Water Efficient Plumbing Fixtures through Standards and Test Methods.
PB95-125951 *00,248*

LOW FREQUENCY
Noise Reduction in Low-Frequency SQUID Measurements with Laser-Driven Switching.
PB96-135165 *02,081*

Exploring the Low-Frequency Performance of Thermal Converters Using Circuit Models and a Digitally Synthesized Source.
PB97-112551 *02,848*

LOW FREQUENCY NOISE
Noise Characteristics Below 1 Hz of Zener Diode-Based Voltage Reference.
PB96-123476 *04,049*

LOW FREQUENCY VIBRATIONS
Measurement of Very Low Frequency Vibrations.
PB96-102660 *03,687*

LOW INDEX CONTRAST
Photonic Band-Structure Effects for Low-Index-Contrast Two-Dimensional Lattices in the Near Infrared.
PB97-122469 *04,401*

LOW-LEVEL RADIOACTIVE WASTES
Expansion of Cementitious Materials Exposed to Sulfate Solutions.
PB94-185782 *02,577*

Membrane Gas Separation for a Fluidized-Bed Incinerator.
PB95-169041 *02,550*

Prediction of Cracking in Reinforced Concrete Structures.
PB95-220448 *03,725*

4SIGHT Manual: A Computer Program for Modelling Degradation of Underground Low Level Waste Concrete Vaults.
PB95-231593 *03,726*

Long-Term Performance of Engineered Concrete Barriers.
PB95-260816 *03,727*

LOW-LOSS CAPACITORS
Capacitors with Very Low Loss: Cryogenic Vacuum-Gap Capacitors.
PB97-122600 *02,293*

LOW TEMPERATURE
Thermal Conductivity of Metals and Alloys at Low Temperatures. A Review of the Literature.
AD-A279 180/4 *03,302*

Design and Construction of a Liquid Hydrogen Temperature Refrigeration System.
AD-A286 618/4 *02,619*

Survey of the Literature on Heat Transfer from Solid Surfaces to Cryogenic Fluids.
AD-A286 680/4 *04,193*

LOW TEMPERATURE CELL
Simple and Efficient Low-Temperature Sample Cell for Infrared Spectrophotometry.
PB94-199197 *00,545*

LOW TEMPERATURE SCIENCE & ENGINEERING
Cryogenic Materials Data Handbook.
AD-A286 675/4 *03,303*

Helium Refrigeration and Liquefaction Using a Liquid Hydrogen Refrigerator for Precooling.
AD-A286 683/8 *02,749*

Cryogenic Blackbody Calibrations at the National Institute of Standards and Technology Low Background Infrared Calibration Facility.
PB94-169802 *02,117*

Effects of Critical Current Density, Equilibrium Magnetization and Surface Barrier on Magnetization of High Temperature Superconductors.
PB94-185162 *04,446*

Surface Barrier and Lower Critical Field in YBa2Cu3O7-delta Superconductors.
PB94-200128 *04,478*

High-Frequency Linear Response of Anisotropic Type-II Superconductors in the Mixed State.
PB94-200359 *04,483*

Nonlinear Response of Type-II Superconductors in the Mixed State in Slab Geometry.
PB94-200367 *04,484*

Cryogenic Properties of Silver.
PB94-203593 *03,330*

Critical Magnetic-Field Angle for High-Field Current Transport in YBa2Cu3O7 at 76 K.
PB94-211281 *04,490*

Superconducting Materials: Specification.
PB94-211299 *04,491*

Effect of Axial Strain on the Critical Current of Ag-Sheathed Bi-Based Superconductors in Magnetic Fields Up to 25 T.
PB94-211315 *04,493*

In situ Noble Metal YBa2Cu3O7 Thin-Film Contacts.
PB94-211323 *04,494*

YBa2Cu3O7-x to Si Interconnection for Hybrid Superconductor/Semiconductor Integration.
PB94-211711 *02,315*

Flux Expulsion at Intermediate Fields in Type-II Superconductors.
PB94-212230 *04,502*

Proposed High-Accuracy Superconducting Power Meter for Millimeter Waves.
PB94-212669 *02,034*

Effect of Thermal Noise on Shapiro Steps in High-Tc Josephson Weak Links.
PB94-212677 *04,506*

Self-Heating in the Coulomb-Blockade Electrometer.
PB94-212685 *04,507*

Cryogenic Precision Capacitance Bridge Using a Single Electron Tunneling Electrometer.
PB95-126074 *04,529*

Magnetic Measurement of Transport Critical Current Density of Granular Superconductors.
PB95-126199 *04,531*

n-Value and Second Derivative of the Superconductor Voltage-Current Characteristic.
PB95-126223 *04,533*

Thermally Activated Hopping of a Single Abrikosov Vortex.
PB95-140810 *04,548*

Micromagnetic Simulations of Tunneling Stabilized Magnetic Force Microscopy.
PB95-141073 *04,552*

Experimental Verification of a Micromagnetic Model of Dual-Layer Magnetic Films.
PB95-141081 *04,553*

Insulating Nanoparticles on YBa2Cu3O7-delta Thin Films Revealed by Comparison of Atomic Force and Scanning Tunneling Microscopy.
PB95-150843 *04,575*

Effects of Critical Current Density, Equilibrium Magnetization and Surface Barrier on Magnetization of High Temperature Superconductors.
PB95-153060 *04,588*

Even-Odd Asymmetry of a Superconductor Revealed by the Coulomb Blockade of Andreev Reflection.
PB95-153540 *04,593*

Preparation of Low Resistivity Contacts for High-Tc Superconductors.
PB95-153557 *02,258*

Improved Uniaxial Strain Tolerance of the Critical Current Measured in Ag-Sheathed Bi2Sr2Ca1Cu2O8+x Superconductors.
PB95-153565 *04,594*

Volume Magnetic Hysteresis Loss of Nb3Sn Superconductors as a Function of Wire Length.
PB95-153722 *04,597*

Tunneling Spectroscopy of Thallium-Based High-Temperature Superconductors.
PB95-161709 *04,606*

Magnetic Force Microscopy of Flux in Superconductors.
PB95-161733 *04,608*

Growth of Laser Ablated YBa2Cu3O7-delta Films as Examined by Rheed and Scanning Tunneling Microscopy.
PB95-162541 *04,614*

Critical Current Density, Irreversibility Line, and Flux Creep Activation Energy in Silver-Sheathed Bi2Sr2Ca2Cu2Ox Superconducting Tapes.
PB95-162749 *04,616*

Welding for Cryogenic Service.
PB95-162889 *02,852*

Combined Josephson and Charging Behavior of the Supercurrent in the Superconducting Single-Electron Transistor.
PB95-168522 *04,637*

High Current Pressure Contacts to Ag Pads on Thin Film Superconductors.
PB95-168621 *04,639*

Terahertz Detectors Based on Superconducting Kinetic Inductance.
PB95-168647 *02,160*

Optical Performance of Photoinductive Mixers at Terahertz Frequencies.
PB95-168662 *02,161*

Suitability of Metalorganic Chemical Vapor Deposition-Derived PrGaO3 Films as Buffer Layers for YBa2Cu3O7-x Pulsed Laser Deposition.
PB95-168670 *04,640*

Microwave Properties of YBa2Cu3O7-x Films at 35 GHz from Magnetotransmission and Magnetoreflection Measurements.
PB95-168977 *04,643*

Ultrasensitive-Hot-Electron Microbolometer.
PB95-168985 *02,163*

Hot-Electron Microcalorimeters for X-ray and Phonon Detection.
PB95-168993 *04,644*

Kinetic-Inductance Infrared Detector Based on an Antenna-Coupled High-Tc SQUID.
PB95-169116 *02,165*

High-Tc Superconducting Antenna-Coupled Microbolometer on Silicon.
PB95-169124 *02,166*

Terahertz Shapiro Steps in High Temperature SNS Josephson Junctions.
PB95-169140 *02,168*

Optical Detector Nonlinearity: A Comparison of Five Methods.
PB95-169355 *04,291*

Experimental Results on Single Flux Quantum Logic.
PB95-175071 *02,053*

Characterization of the Emission from 2D Array Josephson Oscillators.
PB95-175121 *02,054*

Emission Linewidth Measurements of Two-Dimensional Array Josephson Oscillators.
PB95-175139 *02,055*

Frequency Dependence of the Emission from 2D Array Josephson Oscillators.
PB95-175147 *02,056*

Aspects of a Deformable Superconductor Model for the Vortex Mass.
PB95-175303 *04,652*

Deformable Superconductor Model for the Fluxon Mass.
PB95-175311 *04,653*

Thermal Enhancement of Cotunneling in Ultra-Small Tunnel Junctions.
PB95-175436 *04,658*

Characterization of a Tunable Thin Film Microwave YBa2Cu3O7-x/SrTiO3 Coplanar Capacitor.
PB95-175527 *02,264*

Standard Reference Devices for High Temperature Superconductor Critical Current Measurements.
PB95-175543 *04,659*

Josephson Voltage Standard Based on Single-Flux-Quantum Voltage Multipliers.
PB95-175600 *02,058*

Experimental Aspects of Flux Expulsion in Type-II Superconductors.
PB95-175725 *04,660*

Effect in Environmental Noise on the Accuracy of Coulomb-Blockade Devices.
PB95-175865 *04,662*

Testing for Metrological Accuracy of the Electron Pump.
PB95-175873 *04,663*

dc Magnetic Force Microscopy Imaging of Thin-Film Recording Head.
PB95-176061 *04,665*

High Temperature Superconductor-Normal Metal-Superconductor Josephson Junctions with High Characteristic Voltages.
PB95-176079 *04,666*

Two-Stage Integrated SQUID Amplifier with Series Array Output.
PB95-176277 *02,061*

Noise in the Coulomb Blockade Electrometer.
PB95-176327 *04,670*

Increased Transition Temperature in In situ Coevaporated YBa2Cu3O7-delta Thin Films by Low Temperature Post-Annealing.
PB95-180071 *04,672*

Improved Eddy-Current Decay Method for Resistivity Characterization.
PB95-180451 *02,265*

Antenna-Coupled High-Tc Air-Bridge Microbolometer on Silicon.
PB95-180899 *04,315*

Comparison of Magnetic Fields of Thin-Film Heads and Their Corresponding Bit Patterns Using Magnetic Force Microscopy.
PB95-180907 *03,763*

Flexible-Diaphragm Force Microscope.
PB95-180915 *03,966*

Faraday Effect Current Sensor with Improved Sensitivity-Bandwidth Product.
PB95-203154 *02,180*

Step-Edge and Stacked-Heterostructure High-Tc Josephson Junctions for Voltage-Standard Arrays.
PB96-102066 *04,702*

Ferroelectric Thin Film Characterization Using Superconducting Microstrip Resonators.
PB96-102389 *02,270*

SUSAN: SUperconducting Systems ANalysis by Low Temperature Scanning Electron Microscopy (LTSEM).
PB96-112065 *04,728*

Thermal Isolation of High-Temperature Superconducting Thin Films Using Silicon Wafer Bonding and Micromachining.
PB96-135017 *02,408*

Noise Reduction in Low-Frequency SQUID Measurements with Laser-Driven Switching.
PB96-135165 *02,081*

Accuracy of the Electron Pump.
PB96-135223 *04,743*

Deep-UV Excimer Laser Measurements at NIST
PB96-141031 *04,355*

II-3: Critical Current Measurement Methods: Quantitative Evaluation.
PB96-147160 *04,767*

II-5: Thermal Contraction of Materials Used in Nb3Sn Critical Current Measurements.
PB96-147186 *04,769*

Microwave Noise in High-Tc Josephson Junctions.
PB96-148010 *04,771*

V-6: Effects of Temperature Variation.
PB96-148143 *04,772*

National Institute of Standards and Technology High-Accuracy Cryogenic Radiometer.
PB96-179585 *04,378*

High-Tc Multilayer Step-Edge Josephson Junctions and SQUIDs.
PB96-200183 *04,790*

Performance of the Electron Pump with Stray Capacitances.
PB96-200902 *01,976*

Novel Hot-Electron Microbolometer.
PB96-201025 *01,977*

LOW TEMPERATURE TESTS
V-6: Effects of Temperature Variation.
PB96-148143 *04,772*

LUBRICANTS
Development of Measurement Capabilities for the Thermophysical Properties of Energy-Related Fluids. Annual Report, December 1, 1990--November 30, 1991.
DE94004399 *02,470*

Tribochemical Reaction of Stearic Acid on Copper Surface Studied by Surface Enhanced Raman Spectroscopy.
PB94-212057 *02,964*

LUBRICATING OILS
New Method to Evaluate Deposit Forming Tendencies of Liquid Lubricants by Differential Scanning Calorimetry.
PB95-152120 *01,451*

Deposit Forming Tendencies of Diesel Engine Oils-Correlation between the Two-Peak Method and Engine Tests.
PB95-152138 *01,452*

LUBRICATION
Tribology Education: Present Status and Future Challenges.
PB94-212362 *02,965*

Lubrication Theory for Reactive Spreading of a Thin Drop.
PB95-189460 *02,865*

Silicon Nitride Boundary Lubrication: Lubrication Mechanism of Alcohols.
PB96-111703 *03,067*

Silicon Nitride Boundary Lubrication: Effect of Oxygenates.
PB96-111711 *03,068*

LUBRICATION THEORY
Lubrication Theory for Reactive Spreading of a Thin Drop.
PB96-123427 *04,214*

LUMBER
Voluntary Product Standard PS 20-94. American Softwood Lumber Standard.
PB94-162500 *03,402*

LUMINAIRES
Papers Presentations Shine.
PB94-200383 *00,244*

LUMINOSITY
Detector-Based Candela Scale and Related Photometric Calibration Procedures at NIST.
PB95-161949 *04,273*

LUMINOUS FLUX
Integrating Sphere Simulation: Application to Total Flux Scale Realization.
PB95-150173 *04,261*

New Method for Realizing a Luminous Flux Scale Using an Integrating Sphere with an External Source.
PB96-102843 *04,333*

Realization of NIST 1995 Luminous Flux Scale Using the Integrating Sphere Method.
PB96-176433 *04,374*

LUMINOUS INTENSITY
Performance of Compact Fluorescent Lamps at Different Ambient Temperatures.
PB95-175329 *00,258*

Intercomparison of Photometric Units Maintained at NIST (USA) and PTB (Germany), 1993.
PB95-261913 *04,329*

LUNAR EXPLORATION
In-Space Welding: Visions and Realities.
PB95-163234 *04,830*

LUNAR GRAVITATION
Integrated Laser Doppler Method for Measuring Planetary Gravity Fields.
PB94-198686 *03,681*

LUNAR RANGEFINDING
Lunar Laser Ranging: A Continuing Legacy of the Apollo Program.
PB95-202495 *03,683*

LUNG
Oxidative DNA Base Damage in Renal, Hepatic, and Pulmonary Chromatin of Rats After Intraperitoneal Injection of Cobalt (II) Acetate.
PB95-150025 *03,647*

LUNGS
Radon in the Lung.
PB97-110035 *03,638*

LUTETIUM
Enhanced Curie Temperatures and Magnetoelastic Domains in Dy/Lu Super Lattices and Films.
PB94-172665 *04,443*

Vibrations of Hydrogen and Deuterium in Solid Solution with Lutetium.
PB95-181038 *01,019*

LUTETIUM HYDRIDES
Neutron Spectroscopic Comparison of Rare-Earth/Hydrogen alpha-Phase Systems.
PB95-163523 *00,970*

LYASES
Thermodynamics of Enzyme-Catalyzed Reactions. Part 4. Lyases.
PB96-145941 *01,118*

LYMAN ALPHA RADIATION
Hydrogen Lyman-alpha Emission of Capella.
PB95-202263 *00,075*

New High-Redshift Damped Lyman-alpha Absorption Systems and the Redshift Evolution of Damped Absorbers.
PB95-203501 *00,083*

LYMPHOCYTES
DNA Base Damage in Lymphocytes of Cancer Patients Undergoing Radiation Therapy.
PB97-122444 *03,643*

M PROGRAMMING LANGUAGE
M (also known as MUMPS) Validation Test Suite, Version 8.3 (for Microcomputers).
PB94-502077 *01,699*

M1-TRANSITIONS
Magnetic Dipole Line from U LXXI Ground-Term Levels Predicted at 3200 Angstroms.
PB94-211497 *04,407*

MACHINE LEARNING
Effect of Training Dynamics on Neural Network Performance.
PB95-267845 *01,852*

MACHINE TOOLS
Open Architectures for Machine Control.
PB94-135621 *02,942*

Prediction of Geometric-Thermal Machine Tool Errors by Artificial Neural Networks.
PB94-186673 *02,943*

Displacement Method for Machine Geometry Calibration.
PB95-152088 *02,946*

Post-Process Control of Machine Tools.
PB95-203451 *02,952*

Machine Performance Standard Provides Opportunity to Improve Quality and Productivity.
PB96-154521 *02,837*

Development of a New Quality Control Strategy for Automated Manufacturing.
PB96-160486 *02,840*

Integrated Inspection System for Improved Machine Performance.
PB96-160569 *02,959*

New Concepts of Precision Dimensional Measurement for Modern Manufacturing.
PB96-160684 *02,924*

PIECS: A Software Program for Machine Tool Process-Intermittent Error Compensation.
PB96-165980 *02,842*

Compensation of Errors Detected by Process-Intermittent Gauging.
PB97-110472 *02,846*

Data Management for Error Compensation and Process Control.
PB97-110480 *02,847*

Static Structural Analysis of a Reconfigurable Rigid Platform Supported by Elastic Legs.
PB97-113898 *02,960*

MACHINE VISION
Hierarchical Interaction between Sensory Processing and World Modeling in Intelligent Systems.
PB94-198256 *01,580*

Physics-Based Vision: Principles and Practice, Shape Recovery (Book Review).
PB95-164075 *01,846*

MACHING
Evaluation of a Tapered Roller Bearing Spindle for High-Precision Hard Turning Applications.
PB96-160494 *02,700*

MACHINING
Issues Concerning Material Removal Shape Element Volumes (MRSEVs).
PB94-185493 *02,882*

Japan Technology Program Assessment: Precision Engineering/Precision Optics in Japan.
PB95-171112 *02,884*

Issues Concerning Material Removal Shape Element Volumes (MRSEVs).
PB95-210167 *02,885*

Evaluation of Thermal Wave Imaging for Detection of Machining Damage in Ceramics.
PB95-220547 *03,062*

Precision in Machining: Research Challenges.
PB95-242301 *02,953*

Effects of Spindle Dynamic Characteristics on Hard Turning.
PB96-122981 *02,699*

Machining Process Planning Activity Model for Systems Integration.
PB96-165428 *02,841*

Chip Morphology, Tool Wear and Cutting Mechanics in Finish Hard Turning.
PB97-112247 *03,106*

Standards Promote Credibility and Technology Transfer: The Need for Greater Industry Support of Technical Committees.
PB97-116206 *02,961*

MACHINING RATE
Chemical Effect in Ceramics Grinding.
PB97-122592 *03,113*

MACROMOLECULES
Book Review: Statistical Physics of Macromolecules.
PB96-123526 *01,280*

MAGENETIC PROPERTIES
Determining the Magnetic Properties of 1 kg Mass Standards.
PB95-261905 *04,016*

MAGNESIUM
Angular Distributions for Near-Threshold (e,2e) Processes for Li and Mg.
PB94-185725 *00,778*

Effect of Suppressants on Metal Fires.
PB96-109574 *01,402*

MAGNESIUM COMPOUNDS
Electric Field Effects on Crack Growth in a Lead Magnesium Niobate.
PB95-107322 *03,339*

MAGNESIUM HYDRIDES
Laboratory Measurements for the Astrophysical Identification of MgH.
PB95-152195 *00,073*

MAGNESIUM OXIDES
Reactive Coevaporation of DyBaCuO Superconducting Films: The Segregation of Bulk Impurities on Annealed MgO(100) Substrates.
PB95-164562 *04,635*

Dielectric Properties of Single Crystals of Al2O3, LaAlO3, SrTiO3, and MgO at Cryogenic Temperatures.
PB95-180477 *02,266*

MAGNETIC CORRELATION LENGTHS
Neutron-Scattering Studies of the Two Magnetic Correlation Lengths in Terbium.
PB95-152328 *04,586*

MAGNETIC DETECTION
Gradiometer Antennas for Detection of Long Subsurface Conductors.
PB95-175667 *01,862*

MAGNETIC DEVICES
Size and Self-Field Effects in Giant Magnetoresistive Thin-Film Devices.
PB95-180188 *04,674*

MAGNETIC DOMAINS
Micromagnetic Structure of Domains in Co/Pt Multilayers. 1. Investigations of Wall Structure.
PB95-162111 *04,610*

Magnetic Force Microscopy Images of Magnetic Garnet with Thin-Film Magnetic Tip.
PB95-176210 *04,669*

MAGNETIC ENERGY STORAGE EQUIPMENT
Composite Struts for SMES Plants.
PB95-155586 *02,507*

MAGNETIC EXCITATIONS
Polarization Analysis of the Magnetic Excitations in Fe65Ni35 Invar.
PB95-150082 *04,558*

Temperature Dependence of the Magnetic Excitations in Ordered and Disordered Fe72Pt28.
PB95-150223 *04,563*

MAGNETIC FIELD
NIST Watt Experiment: Monitoring the Kilogram.
PB97-122329 *01,997*

MAGNETIC FIELD SENSORS
Magneto-Optic Magnetic Field Sensor with 1.4pT/square root of 1(Hz) Minimum Detectable Field at 1 kHz.
PB94-199551 *02,125*

High Speed, High Sensitivity Magnetic Field Sensors Based on the Faraday Effect in Iron Garnets.
PB95-153391 *02,151*

Magneto-Optic Magnetic Field Sensors Based on Uniaxial Iron Garnet Films in Optical Waveguide Geometry.
PB95-153409 *02,152*

Magneto-Optic Magnetic Field Sensors Based on Uniaxial Iron Garnet Films in Optical Waveguide Geometry.
PB95-168498 *02,159*

Novel Bulk Iron Garnets for Magneto-Optic Magnetic Field Sensing.
PB95-180204 *04,675*

Domain Effects in Faraday Effect Sensors Based on Iron Garnets.
PB95-202461 *02,268*

High Frequency Magnetic Field Sensors Based on the Faraday Effect in Garnet Thick Films.
PB96-190384 *02,282*

Wideband Current and Magnetic Field Sensors Based on Iron Garnets.
PB96-200878 *01,975*

MAGNETIC FIELDS
Faraday Effect Sensors: A Review of Recent Progress.
PB94-200706 *02,128*

Three-Axis Coil Probe Dimensions and Uncertainties during Measurement of Magnetic Fields from Appliances.
PB94-219359 *01,885*

ELF Electric and Magnetic Field Measurement Methods.
PB95-161675 *04,423*

Comparison of Magnetic Fields of Thin-Film Heads and Their Corresponding Bit Patterns Using Magnetic Force Microscopy.
PB95-180907 *03,763*

Temperature Dependence and Magnetic Field Modulation of Critical Currents in Step-Edge SNS YBCO/Au Junctions.
PB96-111745 *04,723*

Magnetic Fields in Star-Forming Regions: Observations.
PB96-123005 *00,100*

Effect of Magnetic Field Orientation on the Critical Current of HTS Conductor and Coils.
PB96-141189 *02,956*

Novel Magnetic Field Characterization Techniques for Compound Semiconductor Materials and Devices.
PB96-176458 *02,433*

Distributions of Measurement Error for Three-Axis Magnetic Field Meters during Measurements Near Appliances.
PB96-180153 *02,110*

Measurement and Reduction of Alignment Errors of the NIST Watt Experiment.
PB97-111959 *01,987*

MAGNETIC FILMS
Brillouin Light Scattering Intensities for Thin Magnetic Films with Large Perpendicular Anisotropies.
PB94-211174 *04,488*

Micromagnetic Model of Dual-Layer Magnetic-Recording Thin Films.
PB95-141065 *04,551*

Experimental Verification of a Micromagnetic Model of Dual-Layer Magnetic Films.
PB95-141081 04,553

Magnetic and Magnetoresistive Properties of Inhomogeneous Magnetic Dual-Layer Films.
PB95-169025 04,646

X-ray Photoelectron and Auger Electron Forward Scattering: A Structural Diagnostic for Epitaxial Thin Films.
PB95-180220 04,676

MAGNETIC FLUX

Magnetic Force Microscopy of Flux in Superconductors.
PB95-161733 04,608

Relationship between Radiative and Magnetic Fluxes for Three Active Solar-Type Dwarfs.
PB96-119540 00,097

MAGNETIC FORCE MICROSCOPY

Micromagnetic Simulations of Tunneling Stabilized Magnetic Force Microscopy.
PB95-141073 04,552

Tunneling Stabilized Magnetic-Force Microscopy.
PB95-161717 04,607

Magnetic Force Microscopy of Flux in Superconductors.
PB95-161733 04,608

Proposed Antiferromagnetically Coupled Dual-Layer Magnetic Force Microscope Tips.
PB95-169017 04,645

Vortex Images in Thin Films of YBa2Cu3O(sub 7-x) and Bi2Sr2Ca1Cu2O(sub 8+x) Obtained by Low-Temperature Magnetic Force Microscopy.
PB97-119408 04,815

MAGNETIC FORCES

Methods for Aligning the NIST Watt-Balance.
PB96-123153 01,934

NIST Watt Balance: Progress Toward Monitoring the Kilogram.
PB97-113062 01,991

MAGNETIC HETEROSTRUCTURES

Exchange Coupling in Magnetic Heterostructures.
PB95-150314 04,566

MAGNETIC HYSTERESIS

Volume Magnetic Hysteresis Loss of Nb3Sn Superconductors as a Function of Wire Length.
PB95-153722 04,597

MAGNETIC MATERIALS

Surface Magnetic Microstructural Analysis Using Scanning Electron Microscopy with Polarization Analysis (SEMPA).
PB95-162657 03,938

Nanocomposite Magnetic Materials.
PB95-162780 04,617

MAGNETIC MEASUREMENT

Metrology for Electromagnetic Technology: A Bibliography of NIST Publications.
PB95-135588 02,143

Domain Effects in Faraday Effect Sensors Based on Iron Garnets.
PB95-202461 02,268

Distributions of Measurement Error for Three-Axis Magnetic Field Meters during Measurements Near Appliances.
PB96-180153 02,110

High Frequency Magnetic Field Sensors Based on the Faraday Effect in Garnet Thick Films.
PB96-190384 02,282

MAGNETIC MOMENTS

Magnetic Moments in Cr Thin Films on Fe(100).
PB95-108429 04,525

MAGNETIC MULTILAYERS

SEMPA Studies of Exchange Coupling in Magnetic Multilayers.
PB96-164074 04,780

Spin-Dependent Interface Transmission and Reflection in Magnetic Multilayers (Invited).
PB96-201173 04,130

MAGNETIC ORDER

Neutron Scattering Study of Antiferromagnetic Order in the Magnetic Superconductors RNi2B2C.
PB97-112411 04,812

MAGNETIC ORDERING

Incommensurate Magnetic Order in UPtGe.
PB95-140513 04,542

Magnetic Ordering of the Cu Spins in PrBa2Cu3O6+x.
PB95-140547 04,545

Crystal Structure and Magnetic Ordering of the Rare-Earth and Cu Moments in RBa2Cu2NbO8(R=Nd,Pr).
PB95-140554 04,546

Coupled-Bilayer Two-Dimensional Magnetic Order of the Dy Ions in Dy2Ba4Cu7O15.
PB95-152104 04,584

Neutron Powder Diffraction Study of the Nuclear and Magnetic Structures of the Oxygen-Deficient Perovskite YBaCuCoO5.
PB95-161097 00,954

Field Dependence of the Magnetic Ordering of Cu in R2CuO4 (R = Nd, Sm).
PB95-164521 04,633

Observation of Oscillatory Magnetic Order in the Antiferromagnetic Superconductor HoNi2B2C.
PB95-180303 04,679

MAGNETIC PERMEABILITY

Transmission/Reflection and Short-Circuit Line Methods for Measuring Permittivity and Permeability.
PB94-165537 02,211

MAGNETIC PROPERTIES

Monte Carlo and Mean-Field Calculations of the Magnetocaloric Effect of Ferromagnetically Interacting Clusters.
PB94-172087 03,201

Magnetocaloric Effect in Nanocomposites.
PB95-162798 04,618

Recent Results in Magnetic Force Microscopy.
PB96-103130 04,721

Magnetic Structure and Spin Dynamics of the Pr and Cu in Pr2CuO4.
PB96-111836 04,036

Preparation, Crystal Structure, Dielectric Properties, and Magnetic Behavior of Ba2Fe2Ti4O13.
PB96-186176 01,162

Dielectric and Magnetic Measurements from -50C to 200C and in the Frequency Band 50 MHz to 2 GHz.
PB96-191382 02,245

MAGNETIC RECORDING

Experimental Verification of a Vector Preisach Model.
PB95-163564 04,626

MAGNETIC RESONANCE

Atomic Iron in Its (5)D Ground State: A Direct Measurement of the J = 0 inverted arrow 1 and J = 1 inverted arrow 2 Fine-Structure Intervals (1.2).
PB96-141221 04,756

MAGNETIC SPECTROSCOPY

Binder Characterization and Evaluation by Nuclear Magnetic Resonance Spectroscopy.
PB94-193471 01,334

MAGNETIC STARS

Class of Radio-Emitting Magnetic B Stars and a Wind-Fed Magnetosphere Model.
PB94-213451 00,067

Radio Emission from Chemically Peculiar Stars.
PB94-213469 00,068

MAGNETIC STRUCTURE

Colossal Magnetoresistance without Mn(3+)/Mn(4-) Double Exchange in the Stoichiometric Pyrochlore Tl2Mn2O7.
PB97-113070 04,160

MAGNETIC SUSCEPTIBILITY

Alternating-Field Susceptometry and Magnetic Susceptibility of Supercondoctors. Presented at Office of Naval Research Workshop on Magnetic Susceptibility of Superconductors and Other Spin Systems. Held in Berkeley Springs, West Virginia on 20 May 1991.
PB94-145984 04,435

Harmonic and Static Susceptibilities of YBa2Cu3O7.
PB95-161139 04,599

Alternating-Field Susceptometry and Magnetic Susceptibility of Superconductors.
PB95-168613 04,638

Magnetic Susceptibility of Pr2-xCexCuO4 Monocrystals and Polycrystals.
PB95-180253 04,677

MAGNETIC TRAPS

Gravitational Sisyphus Cooling of (87)Rb in a Magnetic Trap.
PB96-200704 04,379

Stable, Tightly Confining Magnetic Trap for Evaporative Cooling of Neutral Atoms.
PB96-200720 04,126

MAGNETIORESISTANCE

Domain Structures in Magnetoresistive Granular Metals.
PB96-141346 04,760

MAGNETISM

Magnetic Neutron Scattering (Invited).
PB95-150074 04,557

Critical Current Density, Irreversibility Line, and Flux Creep Activation Energy in Silver-Sheathed Bi2Sr2Ca2Cu2Ox Superconducting Tapes.
PB95-162749 04,616

SEMPA Studies of Oscillatory Exchange Coupling.
PB95-163556 04,625

Influence of Thickness Fluctuations on Exchange Coupling in Fe/Cr/Fe Structures.
PB96-135371 04,745

Panel Discussion on Units in Magnetism.
PB96-137773 04,746

Isolated Spin Pairs and Two-Dimensional Magnetism in SrCr(sub 9p)Ga(sub 12-9p)O19.
PB97-112387 04,154

MAGNETIZATION

Effects of Critical Current Density, Equilibrium Magnetization and Surface Barrier on Magnetization of High Temperature Superconductors.
PB94-185162 04,446

Effects of Critical Current Density, Equilibrium Magnetization and Surface Barrier on Magnetization of High Temperature Superconductors.
PB95-153060 04,588

Simulating Device Size Effects on Magnetization Pinning Mechanisms in Spin Valves.
PB97-112593 04,158

MAGNETO-OPTIC

Dependence of Contrast on Probe/Sample Spacing with the Magneto-Optic Kerr-Effect Scanning Near-Field Optical Microscope (MOKE-SNOM).
PB96-138557 04,750

MAGNETO-OPTICAL EFFECTS

Theory of the Magneto-Optic Kerr Effect in the Near Field.
PB96-141387 04,761

MAGNETO OPTICS

Fiber-Optic Faraday-Effect Magnetic-Field Sensor Based on Flux Concentrators.
PB96-200308 02,201

MAGNETOABSORPTION

RII Spectroscopy of Trap Levels in Bulk and LPE Hg1-xCdxTe.
PB96-160247 04,084

MAGNETOCALORIC EFFECT

Monte Carlo and Mean-Field Calculations of the Magnetocaloric Effect of Ferromagnetically Interacting Clusters.
PB94-172087 03,201

Enhanced Magnetocaloric Effect in Gd3Ga5-xFexO12.
PB94-185659 04,450

Magnetocaloric Effect in Rapidly Solidified Nd-Fe-Al-B Materials.
PB94-185667 04,451

Magnetocaloric Effect of Ferromagnetic Particles.
PB94-185857 04,453

MAGNETOCONDUCTANCE

Measurement of the Weak-Localization Complex Conductivity at 1 Ghz in Disordered Ag Wires.
PB96-117239 04,731

MAGNETOMETERS

Faraday Effect Sensors: A Review of Recent Progress.
PB94-200706 02,128

Low Noise YBa2Cu3O7-x-SrTiO3-YBa2Cu3O7-x Mulitlayers for Improved Superconducting Magnetometers.
PB96-138417 04,747

Magnetometer Calibration Services.
PB97-113252 01,993

MAGNETOOPTICS

Magneto-Optical Trapping of Metastable Xenon: Isotope-Shift Measurements.
PB95-151254 03,905

Magnetooptic Effects.
PB96-119292 04,338

MAGNETORESISTANCE

Effects of Interfacial Roughness on the Magnetoresistance of Magnetic Metallic Multilayers.
PB95-150017 04,556

Transverse Magnetoresistance: A Novel Two-Terminal Method for Measuring the Carrier Density and Mobility of a Semiconductor Layer.
PB95-150066 02,332

Magnetic and Magnetoresistive Properties of Inhomogeneous Magnetic Dual-Layer Films.
PB95-169025 04,646

Micromagnetic Scanning Microprobe System.
PB95-176178 02,224

Size and Self-Field Effects in Giant Magnetoresistive Thin-Film Devices.
PB95-180188 04,674

Model for Determining the Density and Mobility of Carriers in Thin Semiconducting Layers with Only Two Contacts.
PB96-102702 02,378

Characterization of Liquid-Phase Epitaxially Grown HgCdTe Films by Magnetoresistance Measurements.
PB96-123617 04,738

Size Effects in Submicron NiFe/Ag GMR Devices.
PB96-155510 02,237

Novel Magnetic Field Characterization Techniques for Compound Semiconductor Materials and Devices.
PB96-176458 02,433

Magnetic Structure Determination for Annealed Ni80Fe20/Ag Multilayers Using Polarized-Neutron Reflectivity.
PB96-176615 03,739

Models of Granualr Giant Magnetoresistance Multilayer Thin Films.
PB96-190228 01,968

Size Effects and Giant Magnetoresistance in Unannealed NiFe/Ag Multilayer Stripes.
PB97-111306 04,145

Bias Current Dependent Resistance Peaks in NiFe/Ag Giant Magnetoresistance Multilayers.
PB97-112346 04,153

Modeling Effects of Temperature Annealing on Giant Magnetoresistive Response in Discontinuous Multilayer NiFe/Ag Films.
PB97-112585 04,157

Colossal Magnetoresistance without Mn(3+)/Mn(4-) Double Exchange in the Stoichiometric Pyrochlore Tl2Mn2O7.
PB97-113070 04,160

MAGNETORESISTIVITY
Magnetostriction and Giant Magnetoresistance in Annealed NiFe/Ag Multilayers.
PB96-102603 *04,716*

Low Magnetostriction in Annealed NiFe/Ag Giant Magnetoresistive Multilayers.
PB96-146691 *04,762*

Telegraph Noise in Silver-Permalloy Giant Magnetoresistance Test Structures.
PB96-146717 *04,763*

Magnetoresistance of Thin-Film NiFe Devices Exhibiting Single-Domain Behavior.
PB96-147087 *04,766*

MAGNETORESTRICTION
Low Magnetostriction in Annealed NiFe/Ag Giant Magnetoresistive Multilayers.
PB96-146691 *04,762*

MAGNETOSTATICS
Size Effects and Giant Magnetoresistance in Unannealed NiFe/Ag Multilayer Stripes.
PB97-111306 *04,145*

MAGNETOSTRICTION
Magnetoelasticity in Rare-Earth Multilayers and Films.
PB94-211356 *04,495*

Method for Determining Both Magnetostriction and Elastic Modulus by Ferromagnetic Resonance.
PB95-150108 *02,974*

Magnetostriction and Giant Magnetoresistance in Annealed NiFe/Ag Multilayers.
PB96-102603 *04,716*

MAGNIFICATION STANDARDS
Report on the NIST Low Accelerating Voltage SEM Magnification Standard Interlaboratory Study.
PB96-201074 *02,445*

MALEIMIDE/N-PHENYL
Thermal Behaviour of Methyl Methacrylate and N-Phenyl Maleimide Copolymers.
PB95-152237 *01,246*

Copolymerization of N-Phenyl Maleimide and gamma-Methacryloxypropyl Trimethoxysilane.
PB95-153144 *01,248*

MALTODEXTRIN
Protein Extraction in a Spray Column Using a Polyethylene Glycol Maltodextrin Two-Phase Polymer System.
PB95-162228 *00,595*

MAMMOGRAPHY
Noninvasive High-Voltage Measurement in Mammography by Crystal Diffraction Spectroscopy.
PB95-153417 *00,160*

Flat and Curved Crystal Spectrography for Mammographic X-ray Sources.
PB97-122246 *03,642*

MAN
Electron transport calculations with biomedical and environmental applications. Final report, December 23, 1992--January 31, 1994.
DE95007065 *03,613*

MAN COMPUTER INTERFACE
User Interface Component of the Applications Portability Profile Category: Software Standard; Subcategory: Application Program Interface.
FIPS PUB 158-1 *01,793*

Experimental Evaluation of Specification Techniques for Improving Functional Testing.
PB96-201009 *01,779*

MANAGEMENT
Models, Managing Models, Quality Models: An Example of Quality Management.
PB94-163466 *02,891*

Domain Analysis of the Alarm Surveillance Domain. Version 1.0. Conducted as Part of the Domain Analysis Case Study Project.
PB95-136339 *01,705*

Distributed Systems: Survey of Open Management Approaches.
PB96-128202 *01,746*

MANAGEMENT INFORMATION SYSTEMS
Integration Definition for Function Modeling (IDEF0); Category: Software Standard; Subcategory: Modeling Techniques.
FIPSPUB183 *02,800*

Fire Data Management System, FDMS 2.0, Technical Documentation.
PB94-164019 *01,358*

Production Management Information Model for Discrete Manufacturing.
PB96-112008 *02,830*

MANGANESE ADDITIONS
Effect of Mn Content on the Microstructure of Al-Mn Alloys Electrodeposited at 150C.
PB95-126355 *03,343*

MANGANESE ALLOYS
Electrochemical Synthesis of Metal and Intermetallic Composites.
AD-A294 088/0 *03,304*

MANIPULATORS
Evolution of the Flight Telerobotic Servicer.
PB94-216082 *04,832*

Three Dimensional Position Determination from Motion.
PB95-107108 *01,788*

MANOMETERS
Intercomparison of the Effective Areas of a Pneumatic Piston Gauge Determined by Different Techniques.
PB94-212370 *02,640*

MANUALS
ISO TC 184/SC4 Reference Manual.
PB95-242293 *02,663*

NIST ATM Network Simulator: Operation and Programming, Version 1.0.
PB96-106851 *01,487*

MANUFACTURED HOUSING
Controlling Moisture in the Walls of Manufactured Housing.
PB95-105136 *00,355*

MANUFACTURERS
Network Brokers Handbook: An Entrepreneurial Guide to Cooperative Strategies for Manufacturing Competitiveness.
PB95-219325 *00,490*

MANUFACTURING
Opportunities for Innovation: Advanced Manufacturing Technology.
PB94-100278 *02,801*

Applying Virtual Environments to Manufacturing.
PB94-142502 *02,803*

Learning to Change: Opportunities to Improve the Performance of Smaller Manufacturers.
PB94-166212 *00,010*

World Model Registration for Effective Off-Line Programming of Robots.
PB94-173010 *02,933*

Importance of Measurement in Technology-Based Competition.
PB94-211844 *02,929*

Program Requirements to Advance the Technology of Custom Footwear Manufacturing.
PB95-147906 *02,883*

Opportunities for Innovation: Software for Manufacturing.
PB95-155578 *02,851*

Optical Characterization in Microelectronics Manufacturing.
PB95-169397 *02,358*

Critical Issues in Scanning Electron Microscope Metrology.
PB95-169405 *02,359*

Apparel Manufacturing Glossary for Application Protocol Development.
PB95-198750 *02,755*

Proceedings of the Manufacturing Technology Needs and Issues: Establishing National Priorities and Strategies Conference. Held in Gaithersburg, Maryland on April 26-28, 1994.
PB95-206181 *02,930*

Network Brokers Handbook: An Entrepreneurial Guide to Cooperative Strategies for Manufacturing Competitiveness.
PB95-219325 *00,490*

Conceptual Design Plan for the National Advanced Manufacturing Testbed.
PB95-231866 *02,828*

Joint DoD/NIST Workshop on International Manufacturing Systems Research and Development. Held in Rockville, Maryland on November 3-5, 1992. Proceedings.
PB96-109491 *02,931*

Agile Manufacturing from a Statistical Perspective.
PB96-109525 *02,886*

Can Displays Deliver a Full Measure: Manufacturing.
PB96-111935 *02,185*

Proceedings of the Annual Manufacturing Technology Conference (2nd): Toward a Common Agenda. Held in Gaithersburg, Maryland on April 18-20, 1995.
PB96-112693 *02,887*

Scanning Electron Microscope Metrology.
PB96-201090 *02,446*

MANUFACTURING ENGINEERING LABORATORY
Publications of the Manufacturing Engineering Laboratory Covering the Period January 1989-September 1992.
PB94-165966 *02,750*

Program of the Manufacturing Engineering Laboratory, 1995. Infrastructural Technology, Measurements, and Standards for the U.S. Manufacturing Industries.
PB95-188835 *02,754*

MAPPING
Metrication.
PB94-172079 *03,676*

METRICATION: An Economic Wake-Up Call for Surveyors and Mappers.
PB96-159629 *03,680*

MARCH-DOLLASE
Texture Measurement of Sintered Alumina Using the March-Dollase Function.
PB96-179494 *04,784*

MARINE ANIMALS
Determination of PCBs and Chlorinated Hydrocarbons in Marine Mammal Tissues.
PB95-162640 *03,744*

MARINE ATMOSPHERES
Journal of Research of the National Institute of Standards and Technology, January/February 1996. Volume 101, Number 1.
PB96-175666 *00,113*

International Marine-Atmospheric (222)Rn Measurement Intercomparison in Bermuda. Part 1. NIST Calibration and Methodology for Standardized Sample Additions.
PB96-175674 *00,114*

International Marine-Atmospheric (222)Rn Measurement Intercomparison in Bermuda. Part 2. Results for the Participating Laboratories.
PB96-175682 *00,115*

MARINE CHEMISTRY
Atmospheric and Marine Trace Chemistry: Interfacial Biomediation and Monitoring.
PB94-199122 *03,752*

MARINE ENVIRONMENTS
Comparison of Methods for Gas Chromatographic Determination of PCBs and Chlorinated Pesticides in Marine Reference Materials.
PB95-140091 *02,584*

MARINE MAMMALS
Current Activities Within the National Biomonitoring Specimen Bank.
PB94-172806 *02,516*

Determination of Inorganic Constituents in Marine Mammal Tissues.
PB95-152047 *00,589*

Development of the National Marine Mammal Tissue Bank.
PB95-161402 *02,586*

Quality Assurance of Contaminant Measurements in Marine Mammal Tissues.
PB95-164034 *02,588*

Alaska Marine Mammal Tissue Archival Project: Specimen Inventory.
PB95-171344 *02,589*

Concentrations of Chlorinated Hydrocarbons, Heavy Metals and Other Elements in Tissues Banked by the Alaska Marine Mammal Tissue Archival Project.
PB95-209870 *02,590*

Quantitative Analysis of Selected PCB Congeners in Marine Matrix Reference Materials Using a Novel Cyanobiphenyl Stationary Phase.
PB96-111737 *02,591*

Trace Element Concentrations in Cetacean Liver Tissues Archived in the National Marine Mammal Tissue Bank.
PB96-167127 *02,595*

Relationship of Silver with Selenium and Mercury in the Liver of Two Species of Toothed Whales (Odontocetes).
PB96-167275 *02,596*

MARINE SEDIMENTS
Certification of Polycyclic Aromatic Hydrocarbons in a Marine Sediment Standard Reference Material.
PB96-111778 *02,592*

MARKET RESEARCH
India: Environmental Technologies Export Market Plan.
PB97-114359 *02,529*

MARKETING
Method of Sale for CNG Paves Way to Greater Public Acceptance.
PB95-168449 *02,489*

MARKOV ESTIMATORS
Compensation of Markov Estimator Errors in Time-Jittered Sampling of Nonmonotonic Signals.
PB95-150983 *01,590*

MARSHALL COMPACTION HAMMER
Field Evaluation of the System for Calibration of the Marshall Compaction Hammer.
PB95-190674 *01,323*

MARSHALL METHOD
System for Calibration of the Marshall Compaction Hammer.
PB94-145661 *01,303*

MARSHALL STABILITY
Precision of Marchall Stability and Flow Test Using 6-in. (152.4-mm) Diameter Specimens.
PB96-200910 *03,006*

MARTENSITIC STAINLESS STEELS
Wear Mechanism Maps of 440C Martensitic Stainless Steel.
PB96-111810 *04,834*

MARTENSITIC TRANSFORMATION
Structures of Sodium Metal.
PB94-198850 *03,319*

MARTENSITIC TRANSFORMATIONS
Shear-Induced Martensitic-Like Transformation in a Block Copolymer Melt.
PB96-119508 *01,277*

MASONRY
NIST Research Program on the Seismic Resistance of Partially-Grouted Masonry Shear Walls.
PB94-219052 *00,354*

MASS
Precision Laboratory Standards of Mass and Laboratory Weights.
AD-A280 562/0 *02,618*

Advanced Mass Calibration and Measurement Assurance Program for State Calibration Laboratories.
PB95-253571 *02,492*

Determining the Magnetic Properties of 1 kg Mass Standards.
PB95-261905 *04,016*

NIST Watt Experiment: Monitoring the Kilogram.
PB97-122329 *01,997*

MASS ATTENUATION COEFFICIENTS
Tables of X-ray Mass Attenuation Coefficients and Mass Energy-Absorption Coefficients 1 keV to 20 MeV for Elements Z = 1 to 92 and 48 Additional Substances of Dosimetric Interest.
PB95-220539 *04,013*

MASS ENERGY-ABSORPTION COEFFICIENTS
Tables of X-ray Mass Attenuation Coefficients and Mass Energy-Absorption Coefficients 1 keV to 20 MeV for Elements Z = 1 to 92 and 48 Additional Substances of Dosimetric Interest.
PB95-220539 *04,013*

MASS FLOW
Energy Flows in an Orifice Pulse Tube Refrigerator.
PB95-169082 *02,752*

MASS FLOW MEASUREMENT
Cryogenic Flow Calibration in NIST.
PB96-161930 *01,143*

MASS FRAGMENTOGRAPHY
Chemical Determination of Oxidative DNA Damage by Gas Chromatography-Mass Spectrometry.
PB95-175394 *03,540*

MASS MEASUREMENT
Use of the Electronic Balance for Highly Accurate Direct Mass Measurements Without the Use of External Mass Standards.
PB94-187713 *03,803*

Mass and Density Determinations.
PB94-200672 *00,504*

MASS SPECTROMETERS
Compositional Mapping of the Microstructure of Materials.
PB95-107199 *00,565*

Characteristics of Partial Pressure Analyzers.
PB95-150876 *00,582*

Electron-Ion-X-ray Spectrometer System.
PB95-176137 *03,958*

Isotope Dilution Mass Spectrometry as a Candidate Definitive Method for Determining Total Glycerides and Triglycerides in Serum.
PB96-102280 *03,519*

Analysis by a Combination of Gas Chromatography and Tandem Mass Spectrometry: Development of Quantitative Tandem-in-Time Ion Trap Mass Spectrometry: Isotope Dilution Quantification of 11-Nor-Delta-9-Tetrahydro cannabinol-9-Carboxylic Acid.
PB96-117221 *02,561*

Procedure for Measuring Trace Quantities of S2F10, S2OF10, and S2O2F10 in SF6 Using a Gas Chromatograph-Mass Spectrometer.
PB96-119755 *02,513*

MASS SPECTROMETRY
36Cl/Cl Accelerator-Mass-Spectrometry Standards: Verification of Their Serial-Dilution-Solution Preparations by Radioactivity Measurements.
PB94-140563 *00,524*

L-threo-beta-Hydroxyhistidine, an Unprecedented Iron(III) Ion-Binding Amino Acid in a Pyoverdine-type Siderophore from Pseudomonas fluorescens 244.
PB94-211620 *00,553*

Determination of Boron and Lithium in Diverse Biological Matrices Using Neutron Activation - Mass Spectrometry (NA-MS).
PB94-212289 *00,554*

MASS SPECTROSCOPY
National Institute of Standards and Technology Resonance Ionization Spectroscopy/Resonance Ionization Mass Spectroscopy Data Service.
PB94-172897 *03,793*

Comparative Strategies for Correction of Interferences in Isotope Dilution Mass Spectrometric Determination of Vanadium.
PB94-185261 *00,531*

Precision and Accuracy in Tandem Mass Spectrometry Measurements: A Kinetics-Based Protocol for Instrument-Independent Measurements of Collision-Activated Dissociation in RF-Only Quadrupoles.
PB94-216454 *00,858*

Use of Kinetic Energy Distributions to Determine the Relative Contributions of Gas Phase and Surface Fragmentation in KeV Ion Sputtering of a Quaternary Ammonium Salt.
PB95-126108 *00,570*

Molecular Ion Imaging and Dynamic Secondary Ion Mass Spectrometry of Organic Compounds.
PB95-126124 *00,571*

Factorial Design Techniques Applied to Optimization of AMS Graphite Target Preparation.
PB95-151197 *00,584*

Single-Photon Ionization and Detection of Ga, In, and As(sub n) Species in GaAs Growth.
PB95-152815 *00,591*

Reference Materials by Isotope Dilution Mass Spectrometry.
PB95-153383 *00,592*

Ionization Energy of Sulfur Pentafluoride and the Sulfur Pentafluoride-Fluorine Atom Bond Dissociation Energy.
PB95-162814 *00,966*

Using Secondary Ion Mass Spectrometry (SIMS) to Characterize Optical Waveguide Materials.
PB96-119599 *04,340*

MASS STANDARDS
Mass Unit Disseminated to Surrogated Laboratories Using the NIST Portable Mass Calibration Package.
PB94-142486 *03,781*

Examination of Parameters That Can Cause Error in Mass Determinations.
PB94-163037 *03,784*

Advanced Mass Calibration and Measurement Assurance Program for State Calibration Laboratories.
PB95-253571 *02,492*

MASS TRANSFER
Enzyme and Protein Mass Transfer Coefficient in Aqueous Two Phase Systems. 1. Spray Extraction Columns.
PB95-161162 *00,594*

Droplet Transfer Modes for a MIL 100S-1 GMAW Electrode.
PB95-209300 *02,867*

MASSIVELY PARALLEL PROCESSORS
Self-Organizing Neural Network Character Recognition on a Massively Parallel Computer.
PB95-163994 *01,845*

MATERIAL MODULES
Wire Bonding to Multichip Modules and Other Soft Substrates.
PB96-123583 *02,079*

Wire Bonding to Multichip Modules and Other Soft Substrates.
PB96-135207 *02,082*

MATERIAL REMOVAL SHAPE ELEMENT VOLUMES
Issues Concerning Material Removal Shape Element Volumes (MRSEVs).
PB94-185493 *02,882*

Issues Concerning Material Removal Shape Element Volumes (MRSEVs).
PB95-210167 *02,885*

MATERIAL STRENGTH
One-Sided beta-Content Tolerance Intervals for Mixed Models.
PB96-141171 *03,449*

MATERIALS
Preliminary Subject and Authors Index to Compilations of Data on Properties of Materials.
AD-A302 669/7 *03,242*

Preliminary List of References Containing Compilations of Data on Properties of Materials.
AD-A302 670/5 *03,243*

Intelligent Processing of Materials, Technical Activities 1993 (NAS-NRC Assessment Panel, April 21-22, 1994).
PB94-164183 *02,809*

Industry and Government-Laboratory Cooperative R and D: An Idea Whose Time Has Come.
PB94-172939 *02,970*

Fire Growth Models for Materials.
PB94-195856 *01,367*

Evaluation of Corrosion Data: A Review.
PB94-198348 *03,187*

Access Paths for Materials Databases: Approaches for Large Databases and Systems.
PB95-162525 *02,975*

Glimpse of Materials Research in China: A Report from an Interagency Study Team on Materials Visiting China from June 19, 1995 to June 30, 1995.
PB96-112677 *02,978*

Intelligent Processing of Materials, Technical Activities 1994 (NAS-NRC Assessment Panel, April 6-7, 1995).
PB96-115050 *03,359*

Beyond the Technology Roadmaps: An Assessment of Electronic Materials Research and Development.
PB96-165998 *01,961*

Materials Reliability. Technical Activities, 1995.
PB96-183082 *02,999*

Guide to Locating and Accessing Computerized Numeric Materials Databases.
PB96-204045 *03,007*

Conventional and Eccentric Uses of Crystallographic Databases in Practical Materials Identification Problems.
PB97-109102 *04,802*

MATERIALS CHARACTERIZATION
Design, Construction and Application of a Large Aperture Lens-Less Line-Focus PVDF Transducer.
PB97-122584 *02,765*

MATERIALS CHEMISTRY
Vapor Transport in Materials and Process Chemistry.
PB94-211745 *00,669*

MATERIALS RECOVERY
Vapor Transport in Materials and Process Chemistry.
PB94-211745 *00,669*

Bioleaching of Cobalt from Smelter Wastes by 'Thiobacillus ferrooxidans'.
PB95-140968 *02,582*

MATERIALS SCIENCE
Materials Science with SR Using X-Ray Imaging: Spatial-Resolution/Source Size.
PB94-213048 *04,510*

New Materials, Advanced Ceramics and Standards.
PB95-140208 *03,047*

Neutron Techniques in Materials Science and Related Disciplines.
PB96-119698 *02,980*

MATERIALS SCIENCE AND ENGINEERING LABORATORY
Materials Science and Engineering Laboratory Annual Report, 1993. NAS-NRC Assessment Panel, April 21-22, 1994.
PB94-162534 *02,969*

Materials Science and Engineering Laboratory Annual Report, 1994. NAS-NRC Assessment Panel, April 6-7, 1995.
PB95-196697 *02,976*

MATERIALS SCIENCE AND ENGINEERING LABORATORY (MSEL)
Materials Science and Engineering Laboratory Annual Report, 1995. Technical Activities.
PB96-214754 *03,009*

MATERIALS SUBSTITUTION
Fire Suppression System Performance of Alternative Agents in Aircraft Engine and Dry Bay Laboratory Simulations. SP890: Volume 1.
PB96-117775 *03,277*

Fire Suppression System Performance of Alternative Agents in Aircraft Engine and Dry Bay Laboratory Simulations. SP 890: Volume 2.
PB96-117783 *03,278*

MATERIALS TESTING
Assessment of Testing Methodology for Ceramic Matrix Composites.
PB94-200532 *03,139*

Proficiency Tests for the NIST Airborne Asbestos Program, 1993.
PB96-106463 *00,610*

MATHEMATICAL MODELS
Numerical Analysis Support for Compartment Fire Modeling and Incorporation of Heat Conduction into a Zone Fire Model.
PB94-156965 *01,357*

Replicate Measurements for Data Quality and Environmental Modeling.
PB94-172533 *02,515*

Scientific Protocols in Statistical Standards for Environmental Studies.
PB94-185527 *02,517*

Sulfate Attack of Cementitious Materials: Volumetric Relations and Expansions.
PB94-187317 *03,232*

Mathematical Modeling of Human Egress from Fires in Residential Buildings.
PB94-193778 *00,337*

Analysis of Moisture Accumulation in a Wood-Frame Wall Subjected to Winter Climate.
PB94-199320 *00,338*

Gas Phase Reactions Relevant to Chemical Vapor Deposition: Numerical Modeling.
PB94-199346 *03,117*

Statistical Thermodynamics of Phase Separation and Ion Partitioning in Aqueous Two-Phase Systems.
PB94-199387 *01,212*

Effect of Swelling on the Elasticity of Rubber: Localization Model Description.
PB94-211034 *01,216*

Wear Model for Alumina Sliding Wear.
PB95-163796 *03,239*

Outlier-Resistant Methods for Estimation and Model Fitting.
PB95-203436 *03,444*

New Mass Transport Elements and Components for the NIST IAQ Model.
PB95-255899 *02,558*

Comparison of a Fixed-Charge and a Polarizable Water Model.
PB96-111620 *01,072*

One-Dimensional Modeling Studies of the Gaseous Electronics Conference RF Reference Cell.
PB96-113428 *02,397*

Field Modeling: Simulating the Effect of Sloped Beamed Ceilings on Detector and Sprinkler Response.
PB96-122866 *01,406*

One-Sided beta-Content Tolerance Intervals for Mixed Models.
PB96-141171 *03,449*

Response to 'Draining in Dilute Polymer Solutions and Renormalization'.
PB96-146667 *01,283*

Stagnant Film Model of the Effect of Natural Convection on the Dendrite Operating State.
PB96-146832 *04,765*

Sensitivity Analysis for Mathematical Modeling of Fires in Residential Buildings.
PB96-154968 *00,215*

MATHEMATICAL PROGRAMMING
Guidelines for Reporting Results of Computational Experiments. Report of the Ad hoc Committee.
PB94-212347 *03,427*

MATHEMATICAL SOFTWARE

Software Libraries, Numerical and Statistical.
PB94-198967 *01,689*

Portable Vectorized Software for Bessel Function Evaluation.
PB94-198975 *01,690*

Virtual Software Repository System.
PB94-198983 *01,691*

MATHEMATICAL & STATISTICAL METHODS

Computing Effects and Error for Large Synthetic Perturbation Screenings.
PB94-139623 *01,675*

Assessment of Uncertainties of Calibration of Resistance Thermometers at the National Institute of Standards and Technology.
PB94-142478 *02,624*

Growth Surface for the Slopes at the Boundary of a Polygon.
PB94-152725 *03,408*

Boundary Conforming Grid Generation System for Interface Tracking.
PB94-158268 *03,312*

Computation of Dendrites Using a Phase Field Model.
PB94-160744 *04,436*

Comparison of Finite Element and Analytic Calculations of the Resonant Modes and Frequencies of a Thick Shell Sphere.
PB94-160785 *02,626*

Uncertainties in Dimensional Measurements Made at Nonstandard Temperatures.
PB94-169760 *02,893*

Derivation of the System Equation for Null-Balanced Total-Power Radiometer System NCS1.
PB94-169786 *02,022*

Evaluation of Uncertainties of the Null-Balanced Total-Power Radiometer System NCS1.
PB94-169794 *02,023*

Monte Carlo Approach to the Approximation of Invariant Measures.
PB94-172053 *03,409*

Infinite Divisibility and the Identification of Singular Waveforms.
PB94-172111 *02,701*

Complete Reduction of the Euler-Poinsot Problem.
PB94-172152 *03,788*

PC-Based Prototype Expert System for Data Management and Analysis of Creep and Fatigue of Selected Materials at Elevated Temperatures.
PB94-172251 *03,202*

Error Propagation Biases in the Calculation of Indentation Fracture Toughness for Ceramics.
PB94-172434 *03,032*

Replicate Measurements for Data Quality and Environmental Modeling.
PB94-172533 *02,515*

Process for Selecting Standard Reference Algorithms for Evaluating Coordinate Measurement Software.
PB94-173754 *02,629*

Anharmonic Oscillator Analysis Using Modified Airy Functions.
PB94-185311 *03,798*

Scientific Protocols in Statistical Standards for Environmental Studies.
PB94-185527 *02,517*

Experimental Optimization of Peak Shape with Application to Aerosol Generation.
PB94-185535 *00,501*

Modified Airy Function Method for the Analysis of Tunneling Problems in Optical Waveguides and Quantum Well Structures.
PB94-185824 *02,120*

Computing S(alpha) Using Symbolic Monte Carlo.
PB94-198660 *03,410*

Modeling Polarization Curves and Impedance Spectra for Simple Electrode Systems.
PB94-198876 *03,188*

Algorithmic Enhancements to the Method of Centers for Linear Programming Problems.
PB94-198959 *03,426*

Portable Vectorized Software for Bessel Function Evaluation.
PB94-198975 *01,690*

Statistical Quality Control Technology in Japan.
PB94-199064 *02,708*

Slowly Divergent Space Marching Schemes in the Inverse Heat Conduction Problem.
PB94-199486 *03,812*

Application of a Simple Technique for Estimating Errors of Finite-Element Solutions Using a General-Purpose Code.
PB94-200250 *04,818*

Analysis of Scattering Asymmetry Statistics When Background Corrected Counts Are Negative.
PB94-200334 *03,824*

Uncertainty Intervals for Polarized Beam Scattering Asymmetry Statistics.
PB94-200342 *03,825*

Hypercubic Lattice SAW Exponents nu and gamma : 3.99 Dimensions Revisited.
PB94-211026 *01,215*

Guidelines for Reporting Results of Computational Experiments. Report of the Ad hoc Committee.
PB94-212347 *03,427*

Chaos in a Computer-Animated Pendulum.
PB94-212651 *03,852*

Recent Approaches to Extreme Value Estimation with Application to Wind Speeds. Part 1. The Pickands Method.
PB94-213170 *00,019*

Statistical Analysis of Parameters Affecting the Measurement of Particle-Size Distribution of Silicon Nitride Powders by Sedigraph (Trade Name).
PB94-216249 *03,042*

Models and Interactions.
PB94-216306 *02,641*

Alternative Single Integral Equation for Scattering by a Dielectric.
PB94-216512 *04,422*

Autocorrelation Functions from Optical Scattering for One-Dimensionally Rough Surfaces.
PB94-216538 *04,244*

Boundary Integral Method for the Simulation of Two-Dimensional Particle Coarsening.
PB94-216744 *03,411*

Measurement and Uncertainty of a Calibration Standard for the Scanning Electron Microscope.
PB94-219250 *00,560*

New Expressions of Uncertainties for Humidity Calibrations at the National Institute of Standards and Technology.
PB95-103826 *02,645*

Extreme Value Theory and Applications: Proceedings of the Conference on Extreme Value Theory and Applications, Volume 3. Held in Gaithersburg, Maryland in May 1993.
PB95-104956 *03,432*

Capacity of the Lp Norm-Constrained Poisson Channel.
PB95-125753 *01,515*

Noise-Induced Chaos and Phase Space Flux.
PB95-125761 *03,433*

Complex Propagation Constants for Nonuniform Optical Waveguides: Calculations.
PB95-125910 *04,249*

Fiber Spot Size: A Simple Method of Calculation.
PB95-125936 *04,250*

Modal Properties of Circular and Noncircular Optical Waveguides.
PB95-125944 *04,251*

Development and Validation of Multicriteria Ratings: A Case Study.
PB95-126025 *00,004*

Constructing Invariant Tori for Two Weakly Coupled van der Pol Oscillators.
PB95-126165 *03,412*

Accuracy of Eigenvalues: A Comparison of Two Methods.
PB95-126249 *03,413*

Approximate Solution to the Scalar Wave Equation for Optical Waveguides.
PB95-126256 *04,254*

Sensitivity of Three-Point Circle Fitting.
PB95-136354 *02,901*

xi-Vector Formulation of Anisotropic Phase-Field Models: 3-D Asymptotics.
PB95-136628 *04,536*

Combining Data from Independent Chemical Analysis Methods.
PB95-140141 *00,572*

Micromagnetic Model of Dual-Layer Magnetic-Recording Thin Films.
PB95-141065 *04,551*

Guidelines for Evaluating and Expressing the Uncertainty of NIST Measurement Results. 1994 Edition.
PB95-143087 *02,649*

Phase-Field Model for Solidification of a Eutectic Alloy.
PB95-147914 *03,345*

Tolerance Intervals for the Distribution of True Values in the Presence of Measurement Errors.
PB95-150405 *03,434*

Approximate Confidence Intervals on Positive Linear Combinations of Expected Mean Squares.
PB95-151304 *03,436*

Ranges of Confidence Coefficients for Confiedence Intervals on Variance Components.
PB95-151312 *03,437*

Technique to Evaluate Benchmarks: A Case Study Using the Livermore Loops.
PB95-151320 *04,577*

Smart Clock: A New Time.
PB95-151445 *01,530*

Confidence on the Second Difference Estimation of Frequency Drift.
PB95-151460 *01,532*

Effect of Splitting on Estimation of Emission Rate Profiles from Neutron Depth Profiling Spectra.
PB95-152245 *03,916*

Representing a Large Collection of Curves: A Case for Principal Points.
PB95-152286 *03,438*

Image Restoration and Diffusion Processes.
PB95-153003 *01,843*

Constant-Width Calibration Intervals for Linear Regression.
PB95-153524 *03,439*

Assessment of 'Peaks Over Threshold' Methods for Estimating Extreme Value Distribution Tails.
PB95-161360 *00,441*

Underflow-Induced Graphics Failure Solved by SLI Arithmetic.
PB95-161444 *01,712*

Comparison of Elastic and Plastic Contact Models for the Prediction of Thermal Contact Conductance.
PB95-161659 *04,605*

New Exact Solution of the One-Dimensional Schrodinger Equation and Its Application to Polarized Neutron Reflectometry.
PB95-161832 *04,609*

Data-Parallel Algorithm for Three-Dimensional Delaunay Triangulation and Its Implementation.
PB95-163309 *01,714*

Confidence on the Three-Point Estimator of Frequency Drift.
PB95-163838 *01,539*

Look at Uncertainties over Twenty Decades of Pressure Measurement.
PB95-168506 *02,655*

Mode Coupling and Loss on Tapered Optical Waveguides.
PB95-168571 *04,282*

Symbolic Programming with Series Expansions: Applications to Optical Waveguides.
PB95-168589 *04,283*

Bending-Induced Loss in Dual-Mode Rectangular Waveguides.
PB95-168795 *04,288*

Bent Rectangular Core Waveguides: An Accurate Perturbation Approach.
PB95-168803 *04,289*

Design Equations and Scaling Laws for Linear Compressors with Flexure Springs.
PB95-168902 *02,948*

General Motion Model and Spatio-Temporal Filters for Computing Optical Flow.
PB95-171096 *01,847*

Fibre Splice Loss: A Simple Method of Calculation.
PB95-175519 *04,299*

Examination of the l/d Expansion Method from Exact Enumeration for a Self-Interacting Self-Avoiding Walk.
PB95-175733 *01,266*

Numerical Micromagnetic Techniques and Their Applications to Magnetic Force Microscopy Calculations.
PB95-175931 *04,664*

Interior-Point Method for Linear and Quadratic Programming Problems. (NIST Reprint).
PB95-180089 *03,429*

Convergence Properties of a Class of Rank-Two Updates. (NIST Reprint).
PB95-180097 *03,430*

Laplace's Equation and the Dirichlet-Neumann Map in Multiply Connected Domains. (NIST Reprint).
PB95-180295 *03,962*

Analytical Expressions for Barkhausen Jump Size Distributions.
PB95-180345 *04,680*

Existence and Nonexistence Theorems of Finite Diameter Sequential Confidence Regions for Errors-in-Variables Models.
PB95-180352 *03,441*

NIST Strategies for Reducing Testing Requirements.
PB95-180444 *01,909*

Cross-Correlation Analysis Improves Time Domain Measurements.
PB95-180535 *01,543*

Quantitative Measure of Efficiency of Monte Carlo Simulations.
PB95-180691 *01,011*

Improving Photomask Linewidth Measurement Accuracy via Emulated Stepper Aerial Image Measurement.
PB95-180816 *02,911*

Performance Characteristics of Fast Elliptic Solvers on Parallel Platforms.
PB95-180832 *01,723*

Calculation of the Thermal Conductivity and Gas Permeability in a Uniaxial Bundle of Fibers.
PB95-180931 *03,058*

Moments of the Quartic Assignment Statistic with an Application to Multiple Regression.
PB95-181103 *03,442*

Sifting Through Nine Years of NIST Clock Data with TA2.
PB95-181137 *01,547*

Analysis of Autocorrelations in Dynamic Processes.
PB95-181228 *02,826*

Thermal Modeling of Absolute Cryogenic Radiometers.
PB95-181236 *04,316*

MasPar MP-1 as a Computer Arithmetic Laboratory.
PB95-189437 *01,627*

Lubrication Theory for Reactive Spreading of a Thin Drop.
PB95-189460 *02,865*

Inserting Line Segments into Triangulations and Tetrahedralizations.
PB95-198933 *03,415*

Overcoming Hoelder Continuity in Ill-Posed Continuation Problems.
PB95-202354 *03,416*

Two Principal Points of Symmetric, Strongly Unimodal Distributions.
PB95-203360 *03,443*

Linking Anisotropic Sharp and Diffuse Surface Motion Laws via Gradient Flows.
PB95-203378 *04,698*

Outlier-Resistant Methods for Estimation and Model Fitting.
PB95-203436 *03,444*

Morphological Estimation of Tip Geometry for Scanned Probe Microscopy.
PB95-203444 *02,662*

Parallel and Serial Implementations of SLI Arithmetic.
PB95-242335 *01,732*

Expression Formatter for MACSYMA.
PB95-267829 *01,735*

Ceramic Powders Characterization: Results of an International Laboratory Study.
PB95-270039 *02,672*

Frozen Orbits for Satellites Close to an Earth-Like Planet.
PB96-102165 *04,839*

Self-Avoiding-Walk Contacts and Random-Walk Self-Intersections in Variable Dimensionality.
PB96-102231 *01,276*

Fluctuations in Probability Distribution on Chaotic Attractors.
PB96-102330 *04,022*

Probabilistic Computation of Poiseuille Flow Velocity Fields.
PB96-102520 *04,209*

Phase Locking in Two-Dimensional Arrays of Josephson Junctions: Effect of Critical-Current Nonuniformity.
PB96-102587 *04,714*

Measurement Methods and Algorithms for Comparison of Local and Remote Clocks.
PB96-102652 *01,549*

Conformance Testing for OSI Protocols.
PB96-102686 *01,631*

Analytical Method for Determining Thermal Conductivity from Dynamic Experiments.
PB96-102744 *04,024*

Boundary Conforming Grid Generation System for Interface Tracking.
PB96-103007 *03,357*

Agile Manufacturing from a Statistical Perspective.
PB96-109525 *02,886*

Error-Bounding in Level-Index Computer Arithmetic.
PB96-109582 *01,742*

Stable Phase Locking in a Two-Cell Ladder Array of Josephson Junctions.
PB96-111679 *04,722*

Taguchi's Parameter Design: A Panel Discussion.
PB96-111802 *03,445*

One-Dimensional Modeling Studies of the Gaseous Electronics Conference RF Reference Cell.
PB96-113428 *02,397*

Evolution Equations for Phase Separation and Ordering in Binary Alloys.
PB96-119243 *02,979*

Discussion: Statistical Signal Processing of Quasiperiodicities.
PB96-119532 *00,096*

Numerical Evaluation of Special Functions.
PB96-119557 *03,417*

Performance Measures for Geometric Fitting in the NIST Algorithm Testing and Evaluation Program for Coordinate Measurement Systems.
PB96-122122 *01,745*

Nonlinear Dynamics of Stiff Polymers.
PB96-122478 *01,278*

Parallel Monte Carlo Simulation of MBE Growth.
PB96-122841 *02,406*

Slow Evolution from the Boundary: A New Stabilizing Constraint in Ill-Posed Continuation Problems.
PB96-122858 *03,418*

Effects of Nonmodel Errors on Model-Based Testing.
PB96-123146 *02,604*

Lubrication Theory for Reactive Spreading of a Thin Drop.
PB96-123427 *04,214*

Anisotropy of Interfaces in an Ordered Alloy: A Multiple-Order-Parameter Model.
PB96-131594 *04,741*

Principal Points and Self-Consistent Points of Symmetric Multivariate Distributions.
PB96-135090 *03,446*

Proposed Changes to Charpy V-Notch Machine Certification Requirements.
PB96-135363 *02,955*

Test of a Slow Off-Axis Parabola at Its Center of Curvature.
PB96-138482 *04,352*

Thermal Modeling and Analysis of Laser Calorimeters.
PB96-140405 *04,354*

Anova Estimates of Variance Components for a Class of Mixed Models.
PB96-141163 *03,448*

One-Sided beta-Content Tolerance Intervals for Mixed Models.
PB96-141171 *03,449*

Response to 'Draining in Dilute Polymer Solutions and Renormalization'.
PB96-146667 *01,283*

Statistical Descriptors in Crystallography. 2. Report of a Working Group on Expression of Uncertainty in Measurement.
PB96-146824 *04,764*

Stagnant Film Model of the Effect of Natural Convection on the Dendrite Operating State.
PB96-146832 *04,765*

Collection of Results for the SPC/E Water Model.
PB96-147889 *01,127*

Effects of Nonmedel Errors on Model-Based Testing.
PB96-155577 *03,420*

Deterministic and Stochastic Chaos.
PB96-156138 *00,218*

Modeling Detector Response for Neutron Depth Profiling.
PB96-157813 *04,066*

Stochastic Modeling of a New Spectrometer.
PB96-157870 *04,068*

Exits in Multistable Systems Excited by Coin-Toss Square-Wave Dichotomous Noise: A Chaotic Dynamics Approach.
PB96-160650 *04,824*

Point Probe Decision Trees for Geometric Concept Classes.
PB96-160817 *01,612*

Nonequilibrium Statistical Mechanics.
PB96-161781 *04,097*

Optical Detector Nonlinearity: Simulation.
PB96-165378 *02,199*

Basic Linear Algebra Operations in SLI Arithmetic.
PB96-165931 *03,421*

Using S-Check, Alpha Release 1.0.
PB96-165964 *01,767*

MasPar MP-1 as a Computer Arithmetic Laboratory.
PB96-179155 *01,617*

Tree-Lookup for Partial Sums Or: How Can I Find This Stuff Quickly.
PB96-179411 *01,770*

Move-to-Root Rule for Self-Organizing Trees with Markov Dependent Requests.
PB96-179528 *03,431*

Distributions of Measurement Error for Three-Axis Magnetic Field Meters during Measurements Near Appliances.
PB96-180153 *02,110*

Tomographic Reconstruction of the Moments of Local Probability Density Functions in Turbulent Flow Fields.
PB96-180195 *04,219*

Wavelet Variance, Allan Variance, and Leakage.
PB96-190111 *01,509*

Confidence on the Modified Allan Variance and the Time Variance.
PB96-190376 *01,557*

SparseLib++ v. 1.5 Sparse Matrix Class Library. Reference Guide.
PB96-193636 *01,775*

Hybrid Gauss-Trapezoidal Quadrature Rules.
PB96-193750 *03,422*

Notion of a xi-Vector and a Stress Tensor for a General Class of Anisotropic Diffuse Interface Models.
PB96-193776 *04,788*

IML++ v.1.2 Iterative Methods Library Reference Guide.
PB96-195219 *01,776*

MV++ v. 1.5a Matrix/Vector Class Reference Guide.
PB96-195326 *01,777*

Shapiro Steps in Large-Area Metallic-Barrier Josephson Junctions.
PB96-200142 *02,090*

Accurate Modeling of Size and Strain Broadening in the Rietveld Refinement: The 'Double-Voigt' Approach.
PB96-200225 *00,664*

Data Evaluation of a Linear System by a Second-Order Transfer Function.
PB96-200282 *01,970*

Wavelet Analysis for Synchronization and Timekeeping.
PB96-200381 *01,558*

Self-Reciprocal Fourier Functions.
PB96-200852 *01,974*

Statistical Aspects of the Certification of Chemical Batch SRMs. Standard Reference Materials.
PB96-210877 *00,645*

Exact Series Solution to the Epstein-Hubbell Generalized Elliptic Type Integral Using Complex Variable Residue Theory.
PB97-110167 *03,423*

Hydrodynamic Friction of Arbitrarily Shaped Brownian Particles.
PB97-110191 *04,136*

Hypersingular Single Integral Equation and the Dielectric Wedge.
PB97-110274 *04,428*

Variances in the Measurement of Ceramic Powder Properties.
PB97-110316 *03,100*

Electron-Photon Monte Carlo Calculations: The ETRAN Code.
PB97-110407 *04,138*

Electromagnetic Scattering from a Dielectric Wedge and the Single Hypersingular Integral Equation.
PB97-110530 *04,430*

Numerical Evaluation of Hypersingular Integrals for Scattering by a Dielectric Wedge.
PB97-110555 *02,017*

Numerical Reference Models for Optical Metrology Simulation.
PB97-111330 *04,392*

Heap of Data.
PB97-111488 *03,424*

Representation of Axes for Geometric Fitting.
PB97-113799 *01,782*

Developing Measurement for Experimentation.
PB97-118707 *03,450*

Pilot Studies for Improving Sampling Protocols.
PB97-118715 *02,530*

Sources of Strain-Measurement Error in Flag-Based Extensometry.
PB97-118731 *03,108*

Making Connections.
PB97-119044 *01,785*

Application of the Collocation Method in Three Dimensions to a Model Semiconductor Problem.
PB97-122428 *02,457*

Xi-Vector Formulation of Anisotropic Phase-Field Models: 3-D Asymptotics.
PB97-122550 *04,816*

MATRICES (MATHEMATICS)

SparseLib++ v. 1.5 Sparse Matrix Class Library. Reference Guide.
PB96-193636 *01,775*

MATRIX ALGEBRA

MV++ v. 1.5a Matrix/Vector Class Reference Guide.
PB96-195326 *01,777*

MATRIX ISOLATION

Production and Spectroscopy of Small Polyatomic Molecular Ions Isolated in Solid Neon. (Reannouncement with New Availability Information).
AD-A234 043/8 *00,704*

Matrix Isolation Study of the Interaction of Excited Neon Atoms with O3: Infrared Spectrum of O((sub 3)(-)) and Evidence for the Stabilization of O2...O((sub 4)(+)).
PB97-112403 *04,155*

Matrix Isolation Study of the Interaction of Excited Neon Atoms with BCl3: Infrared Spectra of BCl(sub 3, sup +), BCl(sub 2, sup +), and BCl(sub 3, sup -).
PB97-119143 *01,187*

MATRIX TRANSFORMATION

Improving Color Measurements of Displays.
PB96-204441 *02,203*

MATRIX VESICLES

Membrane-Mediated Precipitation of Calcium Phosphate in Model Liposomes with Matrix Vesicle-Like Lipid Composition.
PB95-164547 *03,468*

MATURITY FUNCTIONS

Maturity Functions for Concrete Made with Various Cements and Admixtures.
PB94-199502 *01,314*

MATURITY METHOD

Maturity Method.
PB94-199494 *01,313*

MAUV PROJECT

Intelligent Control for Multiple Autonomous Undersea Vehicles.
PB94-211877 *03,747*

MEAN FREE PATH

Calculations of Electron Inelastic Mean Free Paths. 5. Data for 14 Organic Compounds over the 50-2000 eV Range.
PB95-150355 *00,916*

Calculations of Electron Inelastic Mean Free Paths (IMFPs). 4. Evaluation of Calculated IMFPs and of the Predictive IMFP Formula TPP-2 for Electron Energies between 50 and 2000 eV.
PB95-150728 *00,922*

MEASURE AND INTEGRATION

Numeric Data Distribution: The Vital Role of Data Exchange in Today's World.
N95-15937/2 *02,622*

MEASUREMENT
Report of the International Commission on Radiological Units and Measurements (ICRU), 1956.
AD-A279 120/0 *03,513*

Federal Basis for Weights and Measures: A Historical Review of Federal Legislative Effort, Statutes, and Administrative Action in the Field of Weights and Measures in the United States.
AD-A280 086/0 *02,616*

Voluntary Product Standard PS 20-94. American Softwood Lumber Standard.
PB94-162500 *03,402*

Importance of Measurement in Technology-Based Competition.
PB94-211844 *02,929*

Survey of the Components of Display-Measurement Standards.
PB96-122528 *02,188*

Accurate Computations of Radar Cross Sections of Simple Objects.
PB96-138474 *04,426*

New and Revised Half-Life Measurement Results.
PB96-160346 *00,695*

Methodology for Electromagnetic Interference Measurements.
PB96-200126 *02,014*

Comparison of Ultralow-Sidelobe-Antenna Far-Field Patterns Using the Planar-Near-Field Method and the Far-Field Method.
PB96-200373 *02,015*

Measurements of Properties of Materials in Electronic Packaging.
PB96-200837 *01,973*

Developing Measurement for Experimentation.
PB97-118707 *03,450*

Pilot Studies for Improving Sampling Protocols.
PB97-118715 *02,530*

Specular and Diffuse Reflection Measurements of Electronic Displays.
PB97-119200 *02,208*

Survey of the Components of Display-Measurement Standards.
PB97-122394 *02,209*

MEASUREMENT ACCURACY
Effects of Pipe Elbows and Tube Bundles on Selected Types of Flowmeters.
PB96-160999 *01,135*

MEASUREMENT ASSURANCE PROGRAM
NIST Measurement Assurance Program for Capacitance Standards at 1 kHz.
PB96-172333 *02,276*

MEASUREMENT ERRORS
Low Heat-Flux Measurements: Some Precautions.
PB96-201116 *02,685*

MEASUREMENT SCIENCE & TECHNOLOGY CALIBRATION
Mass Unit Disseminated to Surrogated Laboratories Using the NIST Portable Mass Calibration Package.
PB94-142486 *03,781*

Assessment of Uncertainties of Liquid-in-Glass Thermometer Calibrations at the National Institute of Standards and Technology.
PB94-142510 *02,625*

Assessment of Uncertainties of Thermocouple Calibrations at NIST.
PB94-152691 *03,782*

NIST Measurement Services: NIST Pressure Calibration Service.
PB94-164043 *02,892*

NIST Calibration of ASTM E127-Type Ultrasonic Reference Blocks.
PB94-191640 *02,702*

Development and Calibration of UV/VUV Radiometric Sources.
PB94-199098 *04,229*

Ensuring Accuracy and Traceability of Weighing Instruments.
PB94-211687 *02,638*

Summary of the Proceedings of the Workshop on Standard Phantoms for In-vivo Radioactivity Measurement.
PB94-212933 *03,622*

dc Method for the Absolute Determination of Conductivities of the Primary Standard KCl Solutions from 0C to 50C.
PB94-219342 *02,644*

Review of the USCEA/NIST Measurement Assurance Program for the Nuclear Power Industry.
PB95-126272 *03,712*

Calibration of GPS Equipment in Japan.
PB95-151452 *01,531*

Characterization of a Health Physics Instrument Calibration Range.
PB95-164554 *03,629*

Geometric Characterization of Rockwell Diamond Indenters.
PB95-203287 *02,950*

Standard Reference Materials: Polystyrene Films for Calibrating the Wavelength Scale of Infrared Spectrophotometers - SRM 1921.
PB95-226866 *03,386*

Energy Calibration of X-ray Photoelectron Spectrometers: Results of an Interlaboratory Comparison to Evaluate a Proposed Calibration Procedure.
PB96-102918 *04,027*

Long-Term Stability of Bayard-Alpert Gauge Performance: Results Obtained from Repeated Calibrations against the National Institute of Standards and Technology Primary Vacuum Standard.
PB96-123567 *02,676*

Comparison of NIST and Manufacturer Calibrations of (90)Sr+(90)Y Ophthalmic Applicators.
PB96-123708 *03,634*

Calorimeters for Calibration of High-Dose Dosimeters in High-Energy Electron Beams.
PB96-135272 *04,055*

Absolute Response Calibration of a Transfer Standard Cryogenic Bolometer.
PB96-147103 *04,358*

Direct Comparison Transfer of Microwave Power Sensor Calibrations.
PB96-158654 *02,086*

Calibration of Electret-Based Integral Radon Monitors Using NIST Polyethylene-Encapsulated (226)Ra/(222)Rn Emanation (PERE) Standards.
PB96-159223 *01,950*

Development of the NIST Transient Pressure and Temperature Calibration Facility.
PB96-160833 *00,626*

NIST Measurement Assurance of SPRT Calibrations on the ITS-90: A Quantitative Approach.
PB96-161336 *00,633*

Irradiance of Horizontal Quartz-Halogen Standard Lamps.
PB96-179130 *01,866*

Organization and Implementation of Calibration in the EOS Project. Part 1.
PB96-179437 *04,841*

Report on the NIST Low Accelerating Voltage SEM Magnification Standard Interlaboratory Study.
PB96-201074 *02,445*

Calibration in the Earth Observing System (EOS) Project. Part 2. Implementation.
PB97-112213 *04,842*

Empirical Linear Prediction Applied to a NIST Calibration Service.
PB97-112353 *02,287*

Realization of a Scale of Absolute Spectral Response Using the NIST High Accuracy Cryogenic Radiometer.
PB97-118640 *04,397*

MEASUREMENT SCIENCE & TECHNOLOGY: PHYSICAL STANDARDS & FUNDAMENTAL CONSTANTS
NIST Handbook 44, 1994: Specifications, Tolerances and Other Technical Requirements for Weighing and Measuring Devices as Adopted by the 78th National Conference on Weights and Measures 1993.
PB94-136009 *02,888*

Report of the National Conference on Weight and Measures (78th). Held in Kansas City, MO. on July 18-22, 1993.
PB94-138989 *02,623*

Examination of Parameters That Can Cause Error in Mass Determinations.
PB94-163037 *03,784*

Electronic Balance and Some Gravimetric Applications. (The Density of Solids and Liquids, Pycnometry and Mass).
PB94-163052 *03,785*

Piggyback Balance Experiment: An Illustration of Archimedes' Principles and Newton's Third Law.
PB94-163060 *03,786*

Determination of Density of Mass Standards: Requirement and Method.
PB94-163078 *03,787*

Realization of New NIST Radiation Temperature Scales for the 1000 K to 3000 K Region, Using Absolute Radiometric Techniques.
PB94-172905 *03,794*

Fine-Structure Constant.
PB94-172996 *03,795*

Design and Operation of Series-Array Josephson Voltage Standards.
PB94-185451 *02,030*

Effect of Curing History on Ultimate Glass Transition Temperature and Network Structure of Crosslinking Polymers.
PB94-200052 *01,214*

Report of Density Intercomparisons Undertaken by the Working Group on Density of the CCM.
PB94-200664 *00,503*

NIST Optically Pumped Cesium Frequency Standard.
PB94-211117 *03,835*

24 GHz Josephson Array Voltage Standard.
PB94-211588 *02,033*

Particle Size Standards and Their Certification at NIST.
PB94-211695 *02,639*

Development of a Temperature Scale below 0.5 K.
PB95-125639 *03,879*

International Intercomparison of Detector Responsivity at 1300 and 1550 nm.
PB95-126017 *02,141*

Frequency Stabilization of a Fiber Laser to Rubidium: A High-Accuracy 1.53 mu m Wavelength Standard.
PB95-126082 *04,252*

Precision High Temperature Blackbodies.
PB95-140059 *03,885*

Operational Mode and Gas Species Effects on Rotational Drag in Pneumatic Dead Weight Pressure Gages.
PB95-140182 *00,903*

New International Representations of the Volt and Ohm Effective January 1, 1990.
PB95-150777 *01,890*

Piezoelectric and Pyroelectric Polymers.
PB95-153367 *01,250*

NIST-7, the New US Primary Frequency Standard.
PB95-153458 *01,534*

Error Analysis of the NIST Optically Pumped Primary Frequency Standard.
PB95-153482 *01,535*

Practical Applications of the ITS-90: Inherent Uncertainties.
PB95-161527 *03,930*

Systematic Studies of the Effect of a Post-Detection Filter on a Josephson-Junction Noise Thermometer.
PB95-162988 *03,940*

Diode-Laser Pumped, Rubidium Cell Frequency Standards.
PB95-163218 *01,538*

How Accurate Are the Josephson and Quantum Hall Effects and QED.
PB95-163283 *03,942*

Criteria for Establishing Accurate Vapor Pressure Curves.
PB95-163812 *00,972*

Metrology.
PB95-164497 *03,946*

Superconductor Critical Current Standards for Fusion Applications. Final Progress Report, October 1993-July 1994.
PB95-169538 *02,222*

Improved Rubidium Frequency Standards Using Diode Lasers with AM and FM Noise Control.
PB95-176152 *04,303*

Traceability to the Mole: A New Initiative by CIPM.
PB95-180246 *00,605*

Early History and Future Outlook for the X-ray Crystal Density Method.
PB95-202487 *04,692*

Voltage-Standard Devices.
PB96-102496 *01,920*

Local Oscillator Requirements and Strategies for the Next Generation of High-Stability Frequency Standards.
PB96-112230 *01,551*

Measurement of the Weak-Localization Complex Conductivity at 1 Ghz in Disordered Ag Wires.
PB96-117239 *04,731*

Accurate Measurement of Time.
PB96-119482 *01,552*

Study of Technology for Detecting Pre-Ignition Conditions of Cooking-Related Fires Associated with Electric and Gas Ranges and Cooktops, Phase 1 Report.
PB96-128095 *00,303*

Metrology Issues in Terahertz Physics and Technology.
PB96-128277 *01,939*

Fiber Coating Diameter: Toward a Glass Artifact Standard.
PB96-140389 *02,234*

First VAMAS USA Interlaboratory Comparison of High Temperature Superconductor Critical Current Measurements.
PB96-147178 *04,768*

USA Interlaboratory Comparison of Superconductor Simulator Critical Current Measurements.
PB96-147194 *04,770*

Faraday Constant.
PB96-159793 *01,955*

Laser-Cooled Neutral Atom Frequency Standards.
PB96-160312 *04,086*

Q Branch Lineshape Functions for CARS Thermometry.
PB96-160643 *01,132*

Generating and Measuring Displacements Up to 0.1 m to an Accuracy of 0.1 nm: Is It Possible.
PB96-160700 *04,090*

Executive Summary: Proceedings of the Workshop on the Measurement of Transient Pressure and Temperature.
PB96-160841 *02,679*

ITS-90 Calibration Facility.
PB96-160916 *00,627*

Pressure Measurements with the Mercury Melting Line Referred to ITS-90.
PB96-161005 *01,136*

Direct Comparison of Three PTB Silver Fixed-Point Cells with the NIST Silver Fixed-Point Cell.
PB96-161286 *00,628*

Investigation of High-Temperature Platinum Resistance Thermometers at Temperatures Up to 962C, and, in Some Cases, 1064C.
PB96-161294 *00,629*

Investigation of the ITS-90 Subrange Inconsistencies for 25.5 Omega SPRTs.
PB96-161302 *00,630*

NIST Assessment of ITS-90 Non-Uniqueness for 25.5 Ohm SPRTs at Gallium, Indium and Cadmium Fixed Points.
PB96-161310 *00,631*

NIST Implementation and Realization of the ITS-90 Over the Range 83 K to 1235 K: Reproducibility, Stability, and Uncertainties.
PB96-161328 *00,632*

Length Metrology of Complimentary Small Plastic Rulers.
PB96-161724 *04,096*

Calibration Service for Coaxial Reference Standards for Microwave Power.
PB96-162722 *01,958*

Advances in the Measurement of Polymer CTE: Micrometer- to Atomic-Scale Measurements.
PB96-180229 *03,390*

Transient Creep Behaviour of Hot Isostatically Pressed Silicon Nitride.
PB96-180278 *03,086*

Introduction to Frequency Calibration. Part 1.
PB96-200654 *01,560*

Tensile Creep of Silicide Composites.
PB96-200803 *03,183*

National Measurement System for Radiometry, Photometry, and Pyrometry Base Upon Absolute Detectors.
PB97-108559 *04,382*

Current Status and Trends in Temperature Measurements at NIST, Cooperative Projects and New Mutual Agreement between NIST and IMGC.
PB97-110266 *02,691*

Comparisons of Some NIST Fixed-Point Cells with Similar Cells of Other Standards Laboratories.
PB97-119242 *00,655*

MEASUREMENT SCIENCE & TECHNOLOGY: POLICY & STATE-OF-THE-ART SURVEYS

Dielectric Properties Measurements and Data.
PB94-172186 *01,876*

Report on the Meeting of the CCU (10th) (of the International Committee of Weights and Measures). Held on July 10-11, 1990.
PB94-172889 *03,792*

Optical Fiber Sensors: Accelerating Applications in Navy Ships.
PB94-186848 *02,632*

Measurement of Diffusion in Supercritical Fluid Systems: A Review.
PB94-199189 *00,795*

Mass and Density Determinations.
PB94-200672 *00,504*

Comparison of Regular Transmittance Scales of Four National Standardizing Laboratories.
PB94-211232 *04,233*

National Quality Assurance Program for Personnel Radiation Dosimetry: A Case History.
PB94-211273 *03,620*

Lightwave Standards Development at NIST.
PB95-168563 *01,480*

Effect of Semiconductor Laser Characteristics on Optical Fiber Sensor Performance.
PB95-169132 *02,167*

Comparing NIST-B 50 mm Orifice Meter Gas Data to the ANSI Equation.
PB95-169207 *02,949*

Japan Technology Program Assessment: Precision Engineering/Precision Optics in Japan.
PB95-171112 *02,884*

Integrated-Optical Devices in Rare-Earth-Doped Glass.
PB95-202909 *02,179*

Guide for the Use of the International System of Units (SI).
PB95-226692 *02,747*

NBS/NIST Peltier-Effect Microcalorimeter: A Four-Decade Review.
PB96-102769 *01,064*

Metrology for Electromagnetic Technology: A Bibliography of NIST Publications, September 1995.
PB96-128269 *01,938*

Panel Discussion on Units in Magnetism.
PB96-137773 *04,746*

Optoelectronics at NIST.
PB96-200860 *02,202*

USCEA/NIST Measurement Assurance Programs for the Radiopharmaceutical and Nuclear Power Industries.
PB97-110514 *03,721*

MEASUREMENT SYSTEMS

Length Metrology of Complimentary Small Plastic Rulers.
PB96-161724 *04,096*

MEASUREMENT UNCERTAINTY

Assessment of Uncertainties of Calibration of Resistance Thermometers at the National Institute of Standards and Technology.
PB94-142478 *02,624*

Uncertainty Analysis of the NIST Nitrogen Flow Facility.
PB95-128906 *02,608*

Guidelines for Evaluating and Expressing the Uncertainty of NIST Measurement Results. 1994 Edition.
PB95-143087 *02,649*

MEASURING INSTRUMENTS

Methods of Measuring Humidity and Testing Hygrometers.
AD-A278 851/1 *00,123*

Technologic Papers of the Bureau of Standards: Number 170. Pyrometric Practice.
AD-A279 282/8 *03,766*

Guide to Instrumentation Literature.
AD-A280 278/3 *02,617*

Development of Measurement Capabilities for the Thermophysical Properties of Energy-Related Fluids. Annual Report, December 1, 1990--November 30, 1991.
DE94004399 *02,470*

Development of Measurement Capabilities for the Thermophysical Properties of Energy-Related Fluids. Annual Report, December 1, 1993--November 30, 1994.
DE94017738 *03,246*

Minutes of the CAALS Workshop on modularity and communications standards.
DE95005780 *02,621*

Partial Pressure Analysis in Space Testing.
N95-14084/4 *04,827*

NIST Handbook 44, 1994: Specifications, Tolerances and Other Technical Requirements for Weighing and Measuring Devices as Adopted by the 78th National Conference on Weights and Measures 1993.
PB94-136009 *02,888*

Transient Methods for Thermal Conductivity.
PB94-198405 *04,197*

Microanalysis to Nanoanalysis: Measuring Composition at High Spatial Resolution.
PB95-107173 *00,563*

NIST Handbook 44, 1995: Specifications, Tolerances and Other Technical Requirements for Weighing and Measuring Devices as Adopted by the 79th National Conference on Weights and Measures 1994.
PB95-146379 *02,903*

Airborne Smoke Sampling Package for Field Measurements of Fires.
PB95-150041 *01,381*

Two New Probes for a Coordinate Measuring Machine.
PB95-163093 *02,653*

Characterization of a Health Physics Instrument Calibration Range.
PB95-164554 *03,629*

High-Pressure Equilibrium Cell for Solubility Measurements in Supercritical Fluids.
PB95-175634 *00,998*

Interim Testing Artifact (ITA): A Performance Evaluation System for Coordinate Measuring Machines (CMMs). User Manual.
PB95-210589 *02,914*

Gage Block Handbook.
PB95-251716 *02,667*

NIST Handbook 44, 1996: Specifications, Tolerances, and Other Technical Requirements for Weighing and Measuring Devices as Adopted by the 80th National Conference on Weights and Measures, 1995.
PB96-166616 *02,926*

MEATS

Inter-Laboratory Trials of the EPR Method for the Detection of Irradiated Meats Containing Bone.
PB96-161690 *00,042*

MECC (MICELLAR ELECTROKINETIC CAPILLARY CHROMATOGRAPHY)

Separation and Identification of Organic Gunshot and Explosive Constituents by Micellar Electrokinetic Capillary Electrophoresis.
PB95-107249 *00,566*

MECHANICAL ENGINEERING

Tribology Education: Present Status and Future Challenges.
PB94-212362 *02,965*

Product Models and Virtual Prototypes in Mechanical Engineering.
PB95-253563 *02,783*

MECHANICAL PROPERTIES

Cryogenic Materials Data Handbook.
AD-A286 675/4 *03,303*

Effect of Backfill and Atomizing Gas on the Powder Porosity and Mechanical Properties of 304L Stainless Steel.
PB94-185394 *03,205*

Micro-Mechanical Aspects of Asperity-Controlled Friction in Fiber-Toughened Ceramic Composites.
PB94-199536 *03,136*

Assessment of Testing Methodology for Ceramic Matrix Composites.
PB94-200532 *03,139*

Tribological Characteristics of Alpha-Alumina at Elevated Temperatures.
PB94-211018 *02,963*

Fundamental Computer Simulation Models for Cement-Based Materials.
PB95-126009 *00,364*

Comparison of Fire Sprinkler Piping Materials: Steel, Copper, Chlorinated Polyvinyl Chloride and Polybutylene, in Residential and Light Hazard Installations.
PB95-182267 *00,299*

Low-Temperature Properties of Silver.
PB96-126198 *03,361*

MECHANICAL TESTS

Recent VAMAS Activity in Ceramics.
PB95-162681 *03,051*

MECHANICAL VIBRATION

Testing the Sensitivity of Accelerometers Using Mechanical Shock Pulses Under NIST Special Publication 250 Test No. 24040S.
PB96-179544 *02,683*

MECHANICS: DESIGN/TESTING/MEASUREMENT

Recommended Changes in ASTM Test Methods D2512-82 and G86-84 for Oxygen-Compatibility Mechanical Impact Tests on Metals.
PB94-216694 *03,338*

Ultrasonic Measurement of Residual Stress in Railroad Wheel Rims.
PB95-140430 *04,849*

Fundamental Mechanisms for CO and Soot Formation.
PB95-143160 *01,380*

Ultrasonic Technique for Sizing Voids Using Area Functions.
PB95-151916 *02,904*

Leady Axisymmetric Modes in Infinite Clad Rods. Part 1.
PB95-162905 *04,187*

Elastic Green's Function for a Bimaterial Composite Solid Containing a Free Surface Normal to the Interface.
PB95-163325 *03,162*

Green's Function for Generalized Hilbert Problem for Cracks and Free Surfaces in Composite Materials.
PB95-163333 *03,163*

Generalized Plane Strain Analysis of a Bimaterial Composite Containing a Free Surface Normal to the Interface.
PB95-163341 *03,164*

Stylus Flight in Surface Profiling.
PB96-123138 *02,675*

Ultrasonic Sensing of GMAW: Laser/EMAT Defect Detection System.
PB96-186028 *02,878*

Determination of Sheet Steel Formability Using Wide Band Electromagnetic-Acoustic Transducers.
PB96-186036 *02,279*

Effect of Liftoff on Accuracu of Phase Velocity Measurements Made with Electromagnetic-Acoustic Transducers.
PB96-186044 *02,280*

Methods to Improve the Accuracy of On-Line Ultrasonic Measurement of Steel Sheet Formability.
PB96-186051 *02,281*

Hemispherical Test Fixture for Measuring the Wavefields Generated in an Anisotropic Solid.
PB96-190087 *03,181*

Sensing Droplet Detachment and Electrode Extension for Control of Gas Metal Arc Welding.
PB96-190160 *03,297*

MEDIA

Dilemma-Preservation versus Access.
PB94-198488 *02,711*

MEDICAL IMPLANTS

International Standards and Reference Materials.
PB97-113120 *00,188*

MEDICAL RESEARCH

Publication and Presentation Abstracts, 1993. (Published by Paffenbarger Research Center and Center of Excellence for Materials Science Research).
PB95-153052 *03,562*

Publications and Presentation Abstracts, 1995. (Published by Paffenbarger Research Center and Center of Excellence for Materials Science Research).
PB96-119250 *03,568*

Publication and Presentation Abstracts, 1995.
PB96-164082 *03,576*

Publication and Presentation Abstracts, 1994.
PB96-176623 *03,577*

Publication and Presentation Abstracts, 1996.
PB97-122238 *03,585*

MEDICAL SUPPLIES

Polymers Technical Activities 1994. NAC-NRC Assessment Panel, April 6-7, 1995.
PB95-209896 *01,275*

Polymers Technical Activities, 1995.
PB96-193719 *01,291*

MEDICINAL PLANTS

Preliminary Investigation of Oleoresin Capsicum.
PB96-179486 *03,520*

MEDIUM-SIZED BUSINESSES

Opportunities for Innovation: Pollution Prevention.
PB95-147146 *02,520*

MEETINGS

Weatherability of Plastic Materials.
AD-A301 675/5 *02,968*

VAMAS interlaboratory comparisons of critical current vs. strain in Nb(sub 3)Sn.
DE95016656 *04,433*

Proceedings of the Digital Systems Reliability and Nuclear Safety Workshop. Held in Rockville, Maryland on September 13-14, 1993.
NUREG/CP-0136 *03,728*

Electroacoustics for Characterization of Particulates and Suspensions. Proceedings of a Workshop. Held in Gaithersburg, Maryland on February 3-4, 1993.
PB94-112695 *00,725*

Report of the NIST Workshop on Digital Signature Certificate Management. Held on December 10-11, 1992.
PB94-135001 *01,574*

Report of the National Conference on Weight and Measures (78th). Held in Kansas City, MO. on July 18-22, 1993.
PB94-138989 *02,623*

Report on Application Integration Architectures (AIA) Workshop. Held in Dallas, Texas on February 8-12, 1993.
PB94-142536 *01,803*

Photonic Materials: A Report on the Results of a Workshop. Held in Gaithersburg, Maryland on August 26-27, 1992, Volume 1.
PB94-152733 *02,114*

Report on the Workshop on Manufacturing Polymer Composites by Liquid Molding. Held in Gaithersburg, Maryland on September 20-22, 1993.
PB94-160066 *03,131*

Proceedings of the Workshop on the Federal Criteria for Information Technology Security. Held in Ellicot City, Maryland on June 2-3, 1993.
PB94-162583 *01,575*

Advanced Components for Electric and Hybrid Electric Vehicles. Workshop Proceedings. Held in Gaithersburg, Maryland on October 27-28, 1993.
PB94-177060 *04,858*

Second Text REtrieval Conference (TREC-2). Held in Gaithersburg, Maryland on August 31-September 2, 1993.
PB94-178407 *01,686*

International Institute of Welding: Report on 1992 Actions.
PB94-185873 *02,856*

International Institute of Welding: Report on 1993 Actions.
PB94-185881 *02,857*

Workshop on Characterizing Diamond Films (3rd). Held in Gaithersburg, Maryland on February 23-24, 1994.
PB94-187663 *04,456*

Second Census Optical Character Recognition Systems Conference.
PB94-188711 *01,832*

U.S. Green Building Conference, 1994.
PB94-206364 *02,519*

Technical Digest: Symposium on Optical Fiber Measurements (8th), 1994. Held in Boulder, Colorado on September 13-15, 1994.
PB94-207636 *04,231*

International Conference on Chemical Kinetics (2nd). Held in Gaithersburg, Maryland on July 24-27, 1989.
PB94-211901 *00,822*

Summary of the Proceedings of the Workshop on Standard Phantoms for In-vivo Radioactivity Measurement.
PB94-212933 *03,622*

Head Start on Assurance: Proceedings of an Invitational Workshop on Information Technology (IT) Assurance and Trustworthiness. Held in Williamsburg, Virginia on March 21-23, 1994.
PB94-215746 *01,586*

NIST Workshop on Nanostructured Material (1st): Report of an Industrial Workshop Conducted by the National Institute of Standards and Technology. Held in Gaithersburg, Maryland on May 14-15, 1992.
PB94-218567 *02,973*

Polymer Composites Workshop. Held in Winona, Minnesota on April 29-30, 1992 (Video).
PB94-780129 *03,147*

Report on the Workshop on Advanced Digital Video in the National Information Infrastructure. Held in Washington, D.C. on May 10-11, 1994.
PB95-103677 *01,472*

In Situ Burning Oil Spill Workshop Proceedings. Held in Orlando, Florida on January 26-28, 1994.
PB95-104907 *02,583*

Extreme Value Theory and Applications: Proceedings of the Conference on Extreme Value Theory and Applications, Volume 3. Held in Gaithersburg, Maryland in May 1993.
PB95-104956 *03,432*

Annual Conference on Fire Research: Book of Abstracts, October 17-20, 1994.
PB95-104964 *01,376*

Global Climatic Effects of Aerosols: The AAAR Symposium.
PB95-108791 *00,122*

NIST Workshop on the Computer Interface to Flat Panel Displays. Held in San Jose, California on January 13-14, 1994.
PB95-136388 *01,625*

Summary Report of NIST's Industry-Government Consortium Research Program on Flowmeter Installation Effects: The 45 Degree Elbow.
PB95-143061 *04,204*

Metrology and Data for Microelectronic Packaging and Interconnection: Results of a Joint Workshop on Materials Metrology and Data for Commercial Electrical and Optical Packaging and Interconnection Technologies. Held in Gaithersburg, Maryland on May 5-6, 1994. Volume 1. Results.
PB95-143111 *02,328*

Metrology and Data for Microelectronic Packaging and Interconnection: Results of a Joint Workshop on Materials Metrology and Data for Commercial Electrical and Optical Packaging and Interconnection Technologies. Held in Gaithersburg, Maryland on May 5-6, 1994. Volume 2. Presentation Material.
PB95-143327 *02,330*

Wind and Seismic Effects. Proceedings of the U.S.-Japan Cooperative Program in Natural Resources Panel on Wind and Seismic Effects (26th). Held in Gaithersburg, Maryland on May 17-20, 1994.
PB95-147385 *00,433*

Program Requirements to Advance the Technology of Custom Footwear Manufacturing.
PB95-147906 *02,883*

Journal of Research of the National Institute of Standards and Technology, July/August 1994. Volume 99, Number 4. Special Issue: Extreme Value Theory and Applications. Proceedings of the Conference on Extreme Value Theory and Applications, Volume 2. Held at Gaithersburg, Maryland, in May 1993.
PB95-160594 *03,440*

Forum for International Cooperation on Fire Research.
PB95-162939 *04,869*

Journal of Research of the National Institute of Standards and Technology, September/October 1994. Volume 99, Number 5.
PB95-169371 *04,293*

Report of the National Conference on Weights and Measures (79th). Held in San Diego, California on July 17-21, 1994.
PB95-169819 *02,656*

Workshop Summary Report: Industrial Applications of Scanned Probe Microscopy. A Workshop Co-sponsored by NIST, SEMATECH, ASTM, E42.14, and the American Vacuum Society. Held in Gaithersburg, Maryland on March 24-25, 1994.
PB95-170387 *00,506*

From Superconductivity to Supernovae: The Ginzburg Symposium. Report on the Symposium Held in Honor of Vitaly L. Ginzburg. Held in Gaithersburg, Maryland on May 22, 1992.
PB95-171963 *04,649*

Proceedings: Workshop on Research Needs in Wind Engineering. Held in Gaithersburg, Maryland on September 12-13, 1994.
PB95-189528 *00,448*

Proceedings of the Manufacturing Technology Needs and Issues: Establishing National Priorities and Strategies Conference. Held in Gaithersburg, Maryland on April 26-28, 1994.
PB95-206181 *02,930*

NIST Workshop on Gas Sensors: Strategies for Future Technologies. Proceedings of a Workshop. Held in Gaithersburg, Maryland on September 8-9, 1993.
PB95-210225 *00,507*

Overview of the Text REtrieval Conference (3rd) (TREC-3). Held in Gaithersburg, Maryland on November 2-4, 1994.
PB95-216883 *01,728*

Study of Potential Applications of Automation and Robotics Technology in Construction, Maintenance and Operation of Highway Systems: A Final Report. Volume 3.
PB95-251690 *01,342*

International Green Building Conference and Exposition (2nd). Held in Big Sky, Montana on August 13-15, 1995.
PB95-253605 *02,525*

Proceedings of the Applied Diamond Conference 1995: Applications of Diamond Films and Related Materials International Conference (3rd). Held in Gaithersburg, Maryland, on August 21-24, 1995.
PB95-255204 *04,701*

Applications of Diamond Films and Related Materials: International Conference (3rd). Held in Gaithersburg, Maryland on August 21-24, 1995. Supplement to NIST Special Publication 885.
PB95-256053 *03,063*

Proceedings of the 1995 Workshop on Fire Detector Research. Held on February 6-7, 1995.
PB95-270062 *02,611*

Joint DoD/NIST Workshop on International Manufacturing Systems Research and Development. Held in Rockville, Maryland on November 3-5, 1992. Proceedings.
PB96-109491 *02,931*

Composite Materials for Offshore Operations: Proceedings of the International Workshop (1st). Held in Houston, Texas on October 26-28, 1993.
PB96-109509 *03,169*

Proceedings of the Annual Manufacturing Technology Conference (2nd): Toward a Common Agenda. Held in Gaithersburg, Maryland on April 18-20, 1995.
PB96-112693 *02,887*

Journal of Research of the National Institute of Standards and Technology, July/August 1995. Volume 100, Number 4. Special Issue: The Gaseous Electronics Conference Radio-Frequency Reference Cell.
PB96-113311 *02,386*

Current and Voltage Measurements in the Gaseous Electronics Conference RF Reference Cell.
PB96-113337 *02,388*

Optical Emission Spectroscopy on the Gaseous Electronics Conference RF Reference Cell.
PB96-113345 *02,389*

Optical Diagnostics in the Gaseous Electronics Conference Reference Cell.
PB96-113352 *02,390*

Studies of Ion Kinetic-Energy Distributions in the Gaseous Electronics Conference RF Reference Cell.
PB96-113360 *02,391*

Microwave Diagnostic Results from the Gaseous Electronics Conference RF Reference Cell.
PB96-113378 *02,392*

Langmuir Probe Measurements in the Gaseous Electronics Conference RF Reference Cell.
PB96-113386 *02,393*

Inductively Coupled Plasma Source for the Gaseous Electronics Conference RF Reference Cell.
PB96-113394 *02,394*

Reactive Ion Etching in the Gaseous Electronics Conference RF Reference Cell.
PB96-113402 *02,395*

Dusty Plasma Studies in the Gaseous Electronics Conference Reference Cell.
PB96-113410 *02,396*

One-Dimensional Modeling Studies of the Gaseous Electronics Conference RF Reference Cell.
PB96-113428 *02,397*

Two-Dimensional Self-Consistent Radio Frequency Plasma Simulations Relevant to the Gaseous Electronics Conference RF Reference Cell.
PB96-113436 *02,398*

Post-Earthquake Fire and Lifelines Workshop. Held in Long Beach, California on January 30-31, 1995. Proceedings.
PB96-117916 *00,209*

Journal of Research of the National Institute of Standards and Technology, March/April 1995. Volume 100, Number 2.
PB96-126180 *04,349*

Metrology Issues in Terahertz Physics and Technology.
PB96-128277 *01,939*

Solid Propellant Gas Generators: Proceedings of the 1995 Workshop. Held in Gaithersburg, Maryland on June 28-29, 1995.
PB96-131479 *01,412*

Summary Report: Workshop on Industrial Applications of Scanned Probe Microscopy (2nd). A Workshop Co-Sponsored by NIST, SEMATECH, ASTM E42.14, and the American Vacuum Society. Held in Gaithersburg, Maryland on May 2-3, 1995.
PB96-131602 *00,509*

Computer-Aided Manufacturing Engineering Forum (1st). Technical Meeting Proceedings. Held in Gaithersburg, Maryland on March 21-22, 1995.
PB96-136965 *02,834*

Report on 1994 Actions of the International Institute of Welding.
PB96-138540 *02,873*

Summary and Results of the NIST Workshop on Proposed Guidelines for Testing and Evaluation of Seismic Isolation Systems. Held in San Francisco, California on July 25, 1994.
PB96-154901 *00,463*

Conference Proceedings: International Workshop on Instrumented Indentation. Held in San Diego, California on April 22-23, 1995.
PB96-158688 *01,948*

Executive Summary: Proceedings of the Workshop on the Measurement of Transient Pressure and Temperature.
PB96-160841 *02,679*

Response to Comments on the NIST Proposed Digital Signature Standard.
PB96-161815 *01,615*

Report of the National Conference on Weights and Measures (80th) as Adopted by the 80th National Conference on Weights and Measures, 1995. Held in Portland, Maine on July 16-20, 1995.
PB96-165840 *02,681*

Public Key Infrastructure Invitational Workshop. Held in McLean, Virginia on September 28, 1995.
PB96-166004 *01,616*

Unpredictable Certainty. Information Infrastructure through 2000.
PB96-182266 *00,016*

Workshop on Characterizing Diamond Films (4th). Held in Gaithersburg, Maryland on March 4-5, 1996.
PB96-183090 *04,786*

Proceedings of NIST Workshop: Industry Needs in Welding Research and Standards Development. Held on August 15-16, 1995.
PB96-183124 *02,877*

Hygrothermal Effects on the Performance of Polymers and Polymeric Composites: A Workshop Report. Held in Gaithersburg, Maryland on September 21-22, 1995.
PB96-183207 *03,180*

Financing Tomorrow's Infrastructure: Challenges and Issues. Proceedings of a Colloquium. Held in Washington, DC. on October 20, 1995.
PB96-189444 *00,481*

Computer-Aided Manufacturing Engineering Forum (2nd). Technical Meeting Proceedings. Held in Gaithersburg, Maryland on August 22-23, 1995.
PB96-195334 02,845

NIST Construction Automation Program Report No. 2. Proceedings of the NIST Construction Automation Workshop. Held in Gaithersburg, Maryland on March 30-31, 1995.
PB96-202239 00,413

Phase Separation in Thin Film Polymer Blends With and Without Block Copolymer Additives.
PB96-204482 01,294

Thermal Wave NDE of Advanced Materials Using Mirage Effect Detection.
PB96-204516 04,191

Report of a Workshop on Requalification of Tubular Steel Joints in Offshore Structures. Held in Houston, Texas on September 5-6, 1995.
PB96-210760 03,699

Wind and Seismic Effects: Proceedings of the Joint Meeting of the U.S.-Japan Cooperative Program in Natural Resources Panel on Wind and Seismic Effects (28th). Held in Gaithersburg, Maryland on May 14-17, 1996.
PB97-104376 00,476

Technical Digest: Symposium on Optical Fiber Measurements (9th), 1996. Held in Boulder, Colorado on October 1-3, 1996.
PB97-108583 04,383

Proceedings of a Workshop on Developing and Adopting Seismic Design and Construction Standards for Lifelines. Held in Denver, Colorado on September 25-27, 1991.
PB97-115794 01,302

Science, Technology, and Competitiveness: Retrospective on a Symposium in Celebration of NIST's 90th Anniversary and the 25th Anniversary of the Gaithersburg Laboratories, November 14-15, 1991.
PB97-121610 02,696

Text REtrieval Conference (4th) (TREC-4). Held in Gaithersburg, Maryland on November 1-3, 1995.
PB97-121636 01,786

International Green Building Conference and Exposition (3rd). Held in San Diego, California on November 17-19, 1996. (Reannouncement with new abstract).
PB97-121826 02,531

Conference Report: Calorimetry Conference (50th).
PB97-122279 03,722

MEISSNER EFFECT

Meissner, Shielding, and Flux Loss Behavior in Single-Crystal YBa2Cu3O6+x.
PB94-198744 04,464

MELNIKOV'S METHOD

Dynamics of Multi-DOF Stochastic Nonlinear Systems.
PB97-113245 00,477

MELTING

Shear-Induced Melting of Two-Dimensional Solids.
PB96-112057 01,075

MELTING LINE

Pressure Measurements with the Mercury Melting Line Referred to ITS-90.
PB96-161005 01,136

MELTING POINT

Radiance Temperature (in the Wavelength Range 519-906 nm) of Tungsten at Its Melting Point by a Pulse-Heating Technique.
PB94-172590 03,397

Wavelength Dependence of Normal Spectral Emissivity of High-Temperature Metals at Their Melting Point.
PB94-200011 03,398

MELTING POINT DEPRESSION

Melting Behavior of Organic Materials Confined in Porous Solids.
PB94-212313 00,834

MELTING POINTS

Melting Behavior of Organic Materials Confined in Porous Solids.
PB94-212313 00,834

Standard Reference Material 1744: Aluminum Freezing-Point Standard.
PB95-251732 01,055

Radiance Temperatures (in the Wavelength Range 523-907 nm) of Group IV B Transition Metals Titanium, Zirconium, and Hafnium at Their Melting Points by a Pulse-Heating Technique.
PB96-102207 03,356

Measurements of Thermophysical Properties of Nickel Near Its Melting Temperature by a Microsecond-Resolution Transient Technique.
PB96-102579 04,210

Radiance Temperatures (in the Wavelength Range 523-907 nm) of Group IVB Transition Metals Titanium, Zirconium, and Hafnium at Their Melting Points by a Pulse-Heating Technique.
PB96-135025 02,677

MELTS

Influence of Shear on the Ordering Temperature of a Triblock Copolymer Melt.
PB96-163753 01,288

MELTS (CRYSTAL GROWTH)

Fluorescence Anisotropy Measurements on a Polymer Melt as a Function of Applied Shear Stress.
PB94-199296 01,209

Observations of Shear Induced Molecular Orientation in a Polymer Melt Using Fluorescence Anisotropy Measurements.
PB94-199304 01,210

Observations of Shear Stress and Molecular Orientation Using Fluorescence Anisotropy Measurements.
PB94-199312 01,211

Shear-Induced Martensitic-Like Transformation in a Block Copolymer Melt.
PB96-119508 01,277

MEMBRANE LIPIDS

Membrane-Mediated Precipitation of Calcium Phosphate in Model Liposomes with Matrix Vesicle-Like Lipid Composition.
PB95-164547 03,468

Effect of 1-Hydroxyethylidene-1,1-Bisphosphonate on Membrane-Mediated Calcium Phosphate Formation in Model Liposomal Suspensions.
PB95-169223 03,469

MEMBRANE POTENTIAL

Electropermeabilization of Cell Membranes: Effect of the Resting Membrane Potential.
PB95-163291 03,537

MEMBRANES

Performance Approach to the Development of Criteria for Low-Sloped Roof Membranes.
PB94-160751 00,329

Application of Thermal Analysis Techniques to the Characterization of EPDM Roofing Membrane Materials.
PB95-125845 00,359

Use of Thermal Mechanical Analysis to Characterize Ethylene-Propylene-Diene Terpolymer (EPDM) Roofing Membrane Materials.
PB95-125852 00,360

Gas Transport Properties of Solution-Cast Perfluorosulfonic Acid Ionomer Films Containing Ionic Surfactants.
PB95-175998 01,267

Extending the Angular Range of Neutron Reflectivity Measurements from Planar Lipid Bilayers: Applications to a Model Biological Membrane.
PB96-122569 03,476

Swelling and Growth of Polymers, Membranes and Sponges.
PB97-118400 03,396

MEMORY FUNCTION

Memory Function Approach to the Shape of Pressure Broadened Molecular Bands.
PB95-152930 00,944

MEMS SYSTEMS

Directions in MEMS Research Application Development.
PB95-153797 02,106

MERCURY

Pressure Measurements with the Mercury Melting Line Referred to ITS-90.
PB96-161005 01,136

MERCURY BARIUM CALCIUM CUPRATES

Calibration of High-Energy Electron Beams by Use of Graphite Calorimeters.
PB95-161113 04,598

MERCURY CADMIUM TELLURIDES

Correlation of HgCdTe Epilayer Defects with Underlying Substrate Defects by Synchrotron X-Ray Topography.
PB94-200714 02,129

High-Spatial-Resolution Resistivity Mapping Applied to Mercury Cadmium Telluride.
PB94-212917 02,131

Review of Semiconductor Microelectronic Test Structures with Applications to Infrared Detector Materials and Processes.
PB94-212925 02,132

Investigation of Mercury Interstitials in Hg(1-x)CdxTe Alloys Using Resonant Impact-Ionization Spectroscopy.
PB94-213485 02,133

Heavily Accumulated Surfaces of Mercury Cadmium Telluride Detectors: Theory and Experiment.
PB94-216074 02,134

Hg1-xCdxTe Characterization Measurements: Current Practice and Future Needs.
PB95-164299 02,157

Electrical Characterization of Liquid-Phase Epitaxially Grown Single-Crystal Films of Mercury Cadmium Telluride by Variable-Magnetic-Field Hall Measurements.
PB95-175782 02,177

Magneto-Transport Properties of HgCdTe.
PB95-175840 04,661

Characterization of LPE HgCdTe Film by Magnetoresistance.
PB96-157961 02,197

MERCURY INTRUSION POROSIMETRY

Digitized Simulation of Mercury Intrusion Porosimetry.
PB94-172236 01,304

MERCURY IONS

Wavelengths and Isotope Shifts for Lines of Astrophysical Interest in the Spectrum of Doubly Ionized Mercury (Hg III).
PB95-140869 03,887

Progress on a Cryogenic Linear Trap for (199)Hg(+) Ions.
PB95-180790 03,965

MERCURY OXIDES

Oxygen Dependance of the Crystal Structure of HgBa2CuO4+ and Its Relation to Superconductivity.
PB96-102512 04,711

MERCURY PENCIL LAMP

Wavelengths of Spectral Lines in Mercury Pencil Lamps.
PB96-176474 04,376

MERCURY PENCIL LAMPS

Irradiances of Spectral Lines in Mercury Pencil Lamps.
PB96-176466 04,375

MERGED BEAMS

Merged-Beams Energy-Loss Technique for Electron-Ion Excitation: Absolute Total Cross Sections for O(5+) (2s yields 2p).
PB96-102058 04,017

MEROCYANINE 540

Radiation Chemistry of Cyanine Dyes: Oxidation and Reduction of Merocyanine 540.
PB94-211661 00,818

MESOSCOPIC

Mesoscopic Conductance Fluctuations in Large Devices.
PB96-119656 04,735

MESOSCOPICS

Observation of Hot-Electron Shot Noise in a Metallic Resistor.
PB97-112007 01,988

MESSAGE-PASSING INTERFACE

Experience with MPI: 'Converting Pvmmake to Mpimake under LAM' and 'MPI and Parallel Genetic Programming'.
PB96-141296 01,748

MESSAGE PROCESSING

Analysis of ANSI ASC X12 and UN/EDIFACT Electronic Data Interchange (EDI) Standards.
PB95-220554 01,729

National Voluntary Laboratory Accreditation Program. GOSIP: Government Open Systems Interconnection Profile.
PB95-267993 01,486

METABOLITES

Determination of 3-Quinuclidinyl Benzilate (Qnb) and Its Major Metabolites in Urine by Isotope Dilution Gas Chromatography Mass Spectrometry.
PB94-199379 03,492

METADATA

Application of Metadata Standards.
PB96-180187 01,771

METAL CARBONYLS

Photodecomposition of Mo(CO)6/Si(111) 7x7: CO State-Resolved Evidence for Excited State Relaxation and Quenching.
PB95-180154 01,009

METAL CLUSTERS

Characterization of the Interaction of Hydrogen with Iridium Clusters in Zeolites by Inelastic Neutron Scattering Spectroscopy.
PB95-180741 01,013

METAL COATINGS

In situ Measurements of Chloride Ion and Corrosion Potential at the Coating/Metal Interface.
PB95-140893 03,122

Aging Effects on XRF Measurements of Solder Coatings.
PB95-140927 03,123

METAL FILMS

Electrical Method for Determining the Thickness of Metal Films and the Cross-Sectional Area of Metal Lines.
PB95-203170 02,370

METAL IONS

Electrodeposition.
PB94-172517 00,760

METAL-LIGAND BINDING

Analysis of Protein Metal Binding Selectivity in a Cluster Model.
PB94-212990 00,845

METAL MATRIX COMPOSITES

Wear Mechanism Maps of Ceramics.
PB94-172368 03,229

Status of Electrocomposites.
PB94-212453 03,143

Thermal Expansion of an SiC Particle-Reinforced Aluminum Composite.
PB94-213204 03,144

Surface Energy Reduction in Fibrous Monotectic Structures.
PB95-140828 03,150

Residual Stresses in Aluminum-Mullite (alpha-Alumina) Composites.
PB95-152880 03,155

Elastic Properties of Al2O3/Al Composites: Measurements and Modeling.
PB95-161378 03,157

METAL PLATES

Determination of the Residual Stresses Near the Ends of Skip Welds Using Neutron Diffraction and X-ray Diffraction Procedures.
PB95-253589 02,868

METAL POWDER

Micromechanics of Densification and Distortion.
PB94-200326 03,327

Intelligent Control of an Inert Gas Atomization Process.
PB95-141057 03,344

METAL POWDERS
Development of Adaptive Control Strategies for Inert Gas Atomization.
PB95-162335 02,823

METAL SHEETS
Fracture Behavior of Large-Scale Thin-Sheet Aluminum Alloy.
N95-19494/0 03,311

Ultrasonic Measurement of Sheet Anisotropy and Formability.
PB95-153235 03,213

METAL SURFACES
Scanning Tunneling Microscopy and Fabrication of Nanometer Scale Structures at the Liquid-Gold Interface.
PB95-140414 00,904

METAL VAPORS
Vapor Transport in Materials and Process Chemistry.
PB94-211745 00,669

METALLIC IONS
Calorimetric Determination of the Standard Transformed Enthalpy of a Biochemical Reaction at Specified PH and pMg.
PB94-198249 03,454

METALLOIDS
Atmospheric and Marine Trace Chemistry: Interfacial Biomediation and Monitoring.
PB94-199122 03,752

METALLOPORPHYCENES
One-Electron Oxidation of Metalloporphycenes as Studied by Radiolytic Methods.
PB97-111967 01,179

METALLURGY
Fabrication of Platinum-Gold Alloys in Pre-Hispanic South America: Issues of Temperature and Microstructure Control.
PB94-211646 03,333

Metallurgy Technical Activities 1994 (NAS-NRC Assessment Panel, April 6-7, 1995).
PB96-136981 02,981

Metallurgy. Technical Activities, 1995.
PB96-195284 03,003

METALS
Standard Materials. A Descriptive List with Prices.
AD-A278 140/9 00,500

Thermal Conductivity of Metals and Alloys at Low Temperatures. A Review of the Literature.
AD-A279 180/4 03,302

High Temperature Reactions of Uranium Dioxide with Various Metal Oxides.
AD-A286 648/1 00,717

Intelligent Processing of Hot Isostatic Pressing.
PB94-172913 03,315

Calorimetric Determination of the Standard Transformed Enthalpy of a Biochemical Reaction at Specified PH and pMg.
PB94-198249 03,454

Atmospheric and Marine Trace Chemistry: Interfacial Biomediation and Monitoring.
PB94-199122 03,752

Investigation into a Practical Grain Growth Model for Hot Isostatic Pressing.
PB95-151684 03,347

Radiance Temperatures (in the Wavelength Range 523-907 nm) of Group IVB Transition Metals Titanium, Zirconium, and Hafnium at Their Melting Points by a Pulse-Heating Technique.
PB96-135025 02,677

Suppression of Ignition Over a Heated Metal Surface.
PB96-176425 03,291

Characterization of the Structure of YD3 by Neutron Powder Diffraction.
PB96-186150 01,161

CRYSTMET: The NRCC Metals Crystallographic Data File.
PB97-109029 04,799

Self-Consistent 'GW' and Higher-Order Calculations of Electron States in Metals.
PB97-119341 01,189

METAPHOSPHORIC ACID
Ascorbic and Dehydroascorbic Acids Measured in Plasma Preserved with Dithiothreitol or Metaphorphoric Acid.
PB94-216330 03,495

Measurement of Ascorbic Acid in Human Plasma and Serum: Stability, Intralaboratory Repeatability, and Interlaboratory Reproducibility.
PB97-112445 03,511

METASTABLE ATOMS
Microlithography by Using Neutral Metastable Atoms and Self-Assembled Monolayers.
PB96-190038 02,441

METEOR BURST COMMUNICATIONS
Comparison of Meteor Activity with Occurrence of Sporadic E Reflections.
AD-A292 039/5 00,116

METEORS
Comparison of Meteor Activity with Occurrence of Sporadic E Reflections.
AD-A292 039/5 00,116

METHACRYLATE/HYDROXYETHYL
Effects of Surface-Active Resins on Dentin/Composite Bonds.
PB95-140448 00,156

METHACRYLATES
Ring-Opening Polymerication of a 2-Methylene Spiro Orthocarbonate Bearing a Pendant Methacrylate Group.
PB95-176145 01,268

METHAMPHETAMINE
Determination of Amphetamine and Methamphetamine in a Lyophilized Human Urine Reference Material.
PB95-175444 03,597

METHANE
Thermodynamic Properties of the Methane-Ethane System.
PB95-125779 00,891

Chemical Inhibition of Methane-Air Diffusion Flame.
PB96-195532 01,431

Computations of Enhanced Soot Production in Time-Varying CH4/Air Diffusion Flames.
PB97-119218 01,440

NO Production and Destruction in a Methane/Air Diffusion Flame.
PB97-122519 01,443

METHANE/DIFLUORO
Thermodynamic Properties of Difluoromethane.
PB94-185204 00,772

METHANE-MARKER DEVICES
Simple and Efficient Methane-Marker Devices for Chromatographic Samples.
PB96-164041 00,635

METHANOL
Molecular-Beam Optothermal Spectrum of the OH Stretching Band of Methanol.
PB94-212826 00,839

Combustion of Methanol and Methanol/Dodecanol Spray Flames.
PB95-108544 02,478

Far Infrared Laser Frequencies of (13)CD3OH.
PB95-169363 04,292

Absolute Frequency Measurements of Methanol from 1.5 to 6.5 THz.
PB95-175881 04,300

METHANOL PEROXY RADICAL
Kinetics of the Self-Reaction of Hydroxymethylperoxyl Radicals.
PB94-212164 00,827

METHLACETYLENE
Rotational Spectra of CH3CCH-NH3, NCCCH-NH3, and NCCCH-OH2.
PB97-118798 04,170

METHOD OF CENTERS
Algorithmic Enhancements to the Method of Centers for Linear Programming Problems.
PB94-198959 03,426

METHOXY RADICALS
Observation of a Stable Methoxy Intermediate on Cr(110).
PB95-164422 00,981

METHOXYANISOLES
Thermal Decomposition of Hydroxy- and Methoxy-Substituted Anisoles.
PB94-173036 00,767

METHYL ALCOHOL
Far Infrared Laser Frequencies of (13)CD3OH.
PB95-169363 04,292

Effect of Dodecanol Content on the Combustion of Methanol Spray Flames.
PB95-176020 01,389

Far Infrared Laser Frequencies of CH3OD and N2H4.
PB96-119623 04,341

METHYL BROMIDE
Measurement of Atmospheric Methyl Bromide Using Gravimetric Gas Standards.
PB96-155494 02,497

METHYL METHACRYLATE
Thermal Behaviour of Methyl Methacrylate and N-Phenyl Maleimide Copolymers.
PB95-152237 01,246

METHYL PENDANT PBZT
Evidence of Crosslinking in Methyl Pendent PBZT Fiber.
PB97-112486 03,393

METHYL RADICALS
Laser Flash Photolysis/Time-Resolved FTIR Emission Study of a New Channel in the Reaction of CH3+O: Production of CO(v).
PB95-164281 00,974

METHYLENE LACTONES
Evaluation of Methylene Lactone Monomers in Dental Resins.
PB95-164661 00,164

METRIC SYSTEM
Report on the Meeting of the CCU (10th) (of the International Committee of Weights and Measures). Held on July 10-11, 1990.
PB94-172889 03,792

Metric for Success.
PB94-187630 02,633

Metric Path to Global Markets and New Jobs: A Question-and-Answer and Thematic Discussion.
PB94-206307 02,601

Think Metric.
PB95-151825 01,298

Guide for the Use of the International System of Units (SI).
PB95-226692 02,747

METRICATION: An Economic Wake-Up Call for Surveyors and Mappers.
PB96-159629 03,680

METRIC SYSTEMS
Federal Metric Progress in 1993.
PB94-196029 02,600

METRICATION
Metrication.
PB94-172079 03,676

Metric for Success.
PB94-187630 02,633

Federal Labs Have Key Role in Metrication.
PB96-123401 02,920

METROLOGY
NIST Handbook 44, 1994: Specifications, Tolerances and Other Technical Requirements for Weighing and Measuring Devices as Adopted by the 78th National Conference on Weights and Measures 1993.
PB94-136009 02,888

Report of the National Conference on Weight and Measures (78th). Held in Kansas City, MO. on July 18-22, 1993.
PB94-138989 02,623

Electronics and Electrical Engineering Laboratory Technical Progress Bulletin Covering Laboratory Programs, January to March 1991, with 1991 EEEL Events Calendar.
PB94-145968 02,113

Electronics and Electrical Engineering Laboratory Technical Progress Bulletin Covering Programs, October to December 1993, with 1994/1995 EEEL Events Calendar.
PB94-154341 02,115

Metrology for Electromagnetic Technology: A Bibliography of NIST Publications.
PB94-159761 02,116

Center for Electronics and Electrical Engineering Technical Progress Bulletin Covering Center Programs, October to December, with 1991 CEEE Events Calendar.
PB94-159787 02,296

National Type Evaluation Program: Index of Device Evaluations by Company. NCWM Publication 5 Part A (Second Edition).
PB94-160835 02,889

U.S. Navy Coordinate Measuring Machines: A Study of Needs.
PB94-162831 02,807

Electronics and Electrical Engineering Laboratory Technical Progress Bulletin Covering Laboratory Programs, October to December 1992, with 1992/1993 EEEL Events Calendar.
PB94-165958 02,299

Process for Selecting Standard Reference Algorithms for Evaluating Coordinate Measurement Software.
PB94-173754 02,629

NIST Response to the Fifth CORM Report on the Pressing Problems and Projected Needs in Optical Radiation Measurements.
PB94-188240 04,227

Electronics and Electrical Engineering Laboratory Technical Publication Announcements Covering Laboratory Programs, October to December 1993 with 1994/1995 EEEL Events Calendar.
PB94-193752 02,307

Electronics and Electrical Engineering Laboratory Technical Progress Bulletin Covering Laboratory Programs, January to March 1994 with 1994/1995 EEEL Events Calendar.
PB94-193810 02,308

Electronics and Electrical Engineering Laboratory Technical Progress Bulletin Covering Laboratory Programs, July to September 1993 with 1994 EEEL Events Calendar.
PB94-194354 02,309

Computer Vision Based Tool Setting Station.
PB94-199858 02,944

Metrological Measurement Accuracy: Discussion of 'Measurement Error Models' by Leon Jay Gleser.
PB94-200607 00,551

Advanced Angle Metrology System.
PB94-211364 02,637

Precision, Accuracy, Uncertainty and Traceability and Their Application to Submicrometer Dimensional Metrology.
PB94-213105 02,319

Electronics and Electrical Engineering Laboratory Technical Publication Announcements Covering Laboratory Programs, January to March 1994 with 1994/1995 EEEL Events Calendar.
PB94-213774 01,883

Metrology for Electromagnetic Technology: A Bibliography of NIST Publications.
PB95-135588 02,143

Sensitivity of Three-Point Circle Fitting.
PB95-136354 *02,901*

Metrology Requirements of Future Space Power Systems.
PB95-140984 *04,840*

Metrology and Data for Microelectronic Packaging and Interconnection: Results of a Joint Workshop on Materials Metrology and Data for Commercial Electrical and Optical Packaging and Interconnection Technologies. Held in Gaithersburg, Maryland on May 5-6, 1994. Volume 1. Results.
PB95-143111 *02,328*

Electronics and Electrical Engineering Laboratory Technical Progress Bulletin Covering Laboratory Programs, April to June 1994 with 1994/1995 EEEL Events Calendar.
PB95-143186 *02,329*

Electronics and Electrical Engineering Laboratory 1994 Technical Accomplishments Supporting Technology for U.S. Competitiveness in Electronics.
PB95-144309 *01,887*

Electronics and Electrical Engineering Laboratory 1995 Program Plan. Supporting Technology for U.S. Competitiveness in Electronics.
PB95-159885 *01,894*

Metrology.
PB95-164497 *03,946*

Report of the National Conference on Weights and Measures (79th). Held in San Diego, California on July 17-21, 1994.
PB95-169819 *02,656*

Electronics and Electrical Engineering Laboratory Technical Progress Bulletin Covering Laboratory Programs, July to September 1994 with 1994/1995 EEEL Events Calendar.
PB95-170395 *02,360*

Program of the Manufacturing Engineering Laboratory, 1995. Infrastructural Technology, Measurements, and Standards for the U.S. Manufacturing Industries.
PB95-188835 *02,754*

Electronics and Electrical Engineering Laboratory Technical Publication Announcements Covering Laboratory Programs, July to September 1994 with 1995 EEEL Events Calendar.
PB95-198925 *01,912*

Electronics and Electrical Engineering Laboratory Technical Progress Bulletin Covering Laboratory Programs, October to December 1994 with 1995 EEEL Events Calendar.
PB95-208724 *02,372*

Electronics and Electrical Engineering Laboratory Technical Progress Bulletin Covering Laboratory Programs, April to June 1991, with 1992 EEEL Events Calendar.
PB95-209821 *01,916*

Design, Specification and Tolerancing of Micrometer-Tolerance Assemblies.
PB95-209862 *02,913*

Electronics and Electrical Engineering Laboratory Technical Progress Bulletin Covering Laboratory Programs, January to March 1992, with 1992/1993 EEEL Events Calendar.
PB95-210480 *01,917*

Electronics and Electrical Engineering Laboratory Technical Publication Announcements Covering Laboratory Programs, January to March 1995 with 1995 EEEl Events Calendar.
PB95-242277 *02,373*

Algorithm Testing and Evaluation Program for Coordinate Measuring Systems: Testing Methods.
PB95-251658 *02,666*

Gage Block Handbook.
PB95-251716 *02,667*

Journal of Research of the National Institute of Standards and Technology, May/June 1995. Volume 100, Number 3.
PB95-261897 *02,670*

Determining the Magnetic Properties of 1 kg Mass Standards.
PB95-261905 *04,016*

High Accuracy Measurement of Aperture Area Relative to a Standard Known Aperture.
PB95-261954 *01,919*

Application of Single Electron Tunneling: Precision Capacitance Ratio Measurements.
PB96-102157 *04,703*

Journal of Research of the National Institute of Standards and Technology, July/August 1995. Volume 100, Number 4. Special Issue: The Gaseous Electronics Conference Radio-Frequency Reference Cell.
PB96-113311 *02,386*

Journal of Research of the National Institute of Standards and Technology, November/December 1994. Volume 99, Number 6.
PB96-113535 *04,336*

Semiconductor Measurement Technology: Test Structure Implementation Document: DC Parametric Test Structures and Test Methods for Monolithic Microwave Integrated Circuits (MMICs).
PB96-117692 *02,399*

Journal of Research of the National Institute of Standards and Technology, September/October 1995. Volume 100, Number 5.
PB96-117767 *01,927*

Electronics Packaging Materials Research at NIST.
PB96-122692 *02,405*

Electromagnetic Properties of Materials: The NIST Metrology Program.
PB96-122791 *01,933*

Bibliography of the NIST Optoelectronics Division.
PB96-128210 *02,193*

Metrology for Electromagnetic Technology: A Bibliography of NIST Publications, September 1995.
PB96-128269 *01,938*

Metrology Issues in Terahertz Physics and Technology.
PB96-128277 *01,939*

Metallurgy Technical Activities 1994 (NAS-NRC Assessment Panel, April 6-7, 1995).
PB96-136981 *02,981*

Progress Toward Accurate Metrology Using Atomic Force Microscopy.
PB96-146774 *02,417*

New NIST/ARPA National Soft X-ray Reflectometry Facility.
PB96-158092 *04,080*

Journal of Research of the National Institute of Standards and Technology, November/December 1995. Volume 100, Number 6.
PB96-159215 *01,949*

Calibration of Electret-Based Integral Radon Monitors Using NIST Polyethylene-Encapsulated (226)Ra/(222)Rn Emanation (PERE) Standards.
PB96-159223 *01,950*

Generating and Measuring Displacements Up to 0.1 m to an Accuracy of 0.1 nm: Is It Possible.
PB96-160700 *04,090*

Metrology Standards for Advanced Semiconductor Lithography Referenced to Atomic Spacings and Geometry.
PB96-160718 *02,424*

Nanometrology.
PB96-160726 *02,425*

Metrology.
PB96-160759 *02,925*

Scanned Probe Microscopies: Opportunities and Issues in Metrology.
PB96-160783 *02,426*

Residual Error Compensation of a Vision-Based Coordinate Measuring Machine.
PB96-161617 *04,091*

Length Metrology of Complimentary Small Plastic Rulers.
PB96-161724 *04,096*

Business and Manufacturing Motivations for the Developing of Analytical Technology and Metrology for Semiconductors.
PB96-161948 *04,778*

Enhanced Voltage-Dividing Potentiometer for High-Precision Feature Placement Metrology.
PB96-164025 *02,428*

Electronics and Electrical Engineering Laboratory 1995 Technical Accomplishments: Advancing Metrology for Electrotechnology to Support the U.S. Economy.
PB96-164520 *01,959*

Report of the National Conference on Weights and Measures (80th) as Adopted by the 80th National Conference on Weights and Measures, 1995. Held in Portland, Maine on July 16-20, 1995.
PB96-165840 *02,681*

Electronics and Electrical Engineering Laboratory: 1996 Program Plan. Supporting Technology for U.S. Competitiveness in Electronics.
PB96-175237 *01,962*

Improved Dose Metrology in Optical Lithography.
PB96-179510 *02,439*

Increasing the Value of Atomic Force Microscopy Process Metrology Using a High-Accuracy Scanner, Tip Characterization, and Morphological Image Analysis.
PB96-190293 *02,758*

Scanned Probe Microscope Tip Characterization Without Calibrated Tip Characterizers.
PB96-190368 *02,759*

National Semiconductor Metrology Program, Project Portfolio FY 1996.
PB96-195268 *04,789*

Program of the Manufacturing Engineering Laboratory, 1996. Infrastructural Technology, Measurements, and Standards for the U.S. Manufacturing Industries.
PB96-195276 *02,760*

Metallurgy. Technical Activities, 1995.
PB96-195284 *03,003*

Performance of the Electron Pump with Stray Capacitances.
PB96-200902 *01,976*

Monte Carlo Simulation of Scanning Electron Microscope Signals.
PB96-200969 *02,444*

SEM Linewidth Metrology of X-ray Lithography Masks.
PB96-201108 *02,447*

NIST/NCMS Program on Electronic Packaging: First Update.
PB96-204086 *03,008*

Present and Future Standard Specimens for Surface Finish Metrology.
PB97-110423 *02,928*

Results of Capacitance Ratio Measurements for the Single Electron Pump-Capacitor Charging Experiment.
PB97-113286 *04,813*

METROLOGY: PHYSICAL MEASUREMENTS

Density of Solids and Liquids.
AD-A278 517/8 *00,711*

Methods of Measuring Humidity and Testing Hygrometers.
AD-A278 851/1 *00,123*

Technologic Papers of the Bureau of Standards: Number 170. Pyrometric Practice.
AD-A279 282/8 *03,766*

Journal of Research of the National Institute of Standards and Technology, November-December 1993. Volume 98, Number 6.
PB94-140555 *04,223*

Journal of Research of the National Institute of Standards and Technology. January/February 1994. Volume 99, Number 1.
PB94-169737 *02,019*

Application of the Electronic Balance in High Precision Pycnometry.
PB94-187564 *00,534*

Use of the Electronic Balance for Highly Accurate Direct Mass Measurements Without the Use of External Mass Standards.
PB94-187713 *03,803*

Overview of Radiometric Program of the NIST Thermal Imaging Laboratory.
PB94-199163 *04,230*

Measuring the Stability of Three Copper Alloys.
PB94-199866 *03,326*

Characterization of Vertical-Cavity Semiconductor Structures.
PB94-200193 *02,126*

Faraday Effect Sensors: A Review of Recent Progress.
PB94-200706 *02,128*

Technical Digest: Symposium on Optical Fiber Measurements (8th), 1994. Held in Boulder, Colorado on September 13-15, 1994.
PB94-207636 *04,231*

Hybrid Undulator for the NIST-NRL Free-Electron Laser.
PB94-212529 *04,238*

Using LORAN-C Broadcasts for Automated Frequency Calibrations.
PB94-216017 *01,526*

Light Scattered by Coated Paper.
PB94-216546 *04,245*

Journal of Research of the National Institute of Standards and Technology. March/April 1994. Volume 99, Number 2.
PB94-219219 *02,000*

Journal of Research of the National Institute of Standards and Technology. May/June 1994. Volume 99, Number 3.
PB94-219326 *02,643*

Development of an Automated Part Inspection System Using the DMIS Standard.
PB95-108866 *02,899*

International Intercomparison of Detector Responsivity at 1300 and 1550 nm.
PB95-125928 *02,140*

Vacuum Gauges and Partial Pressure Analyzers.
PB95-150884 *02,650*

Optical Fiber Geometry: Accurate Measurement of Cladding Diameter.
PB95-151940 *04,266*

Journal of Research of the National Institute of Standards and Technology, July/August 1994. Volume 99, Number 4. Special Issue: Extreme Value Theory and Applications. Proceedings of the Conference on Extreme Value Theory and Applications, Volume 2. Held at Gaithersburg, Maryland, in May 1993.
PB95-160594 *03,440*

Satellite Two-Way Time Transfer: Fundamentals and Recent Progress.
PB95-161089 *01,536*

Optical Fiber Geometry by Gray-Scale Analysis with Robust Regression.
PB95-161519 *04,272*

Measurement of Surface Tension of Tantalum by a Dynamic Technique in a Microgravity Environment.
PB95-161667 *03,932*

Dimensional Characterization of Small Bores: A Survey.
PB95-162202 *02,651*

X-Ray Image Quality Indicator Designed for Easy Alignment.
PB95-164455 *02,907*

Comparison of UV-Induced Fluorescence and Bragg Grating Growth in Optical Fiber.
PB95-168597 *04,284*

Widths and Propagation of a Truncated Gaussian Beam.
PB95-168779 *04,287*

Metrological Accuracy of the Electron Pump.
PB95-168910 *03,951*

Journal of Research of the National Institute of Standards and Technology, September/October 1994. Volume 99, Number 5.
PB95-169371 *04,293*

Reduction of Interfilament Contact Loss in Nb3Sn Superconductor Wires.
PB95-175535 *02,223*

Photodetector Frequency Response Measurements at NIST, US, and NPL, UK: Preliminary Results of a Standards Laboratory Comparison.
PB95-175592 *02,175*

Time and Frequency: Bibliography of NIST Publications, March 1995.
PB95-220463 *01,548*

Reproducibility of the Temperature of the Ice Point in Routine Measurements.
PB95-255923 *04,015*

Journal of Research of the National Institute of Standards and Technology, May/June 1995. Volume 100, Number 3.
PB95-261897 *02,670*

High Accuracy Measurement of Aperture Area Relative to a Standard Known Aperture.
PB95-261954 *01,919*

Intracomparison Tests of the FG5 Absolute Gravity Meters.
PB96-102991 *03,688*

Contributions of Out-of-Plane Material to a Scanned-Beam Laminography Image.
PB96-111786 *02,704*

Comparison of Photodiode Frequency Response Measurements to 40 GHz between NPL and NIST.
PB96-111992 *04,038*

Journal of Research of the National Institute of Standards and Technology, July/August 1995. Volume 100, Number 4. Special Issue: The Gaseous Electronics Conference Radio-Frequency Reference Cell.
PB96-113311 *02,386*

Journal of Research of the National Institute of Standards and Technology, November/December 1994. Volume 99, Number 6.
PB96-113535 *04,336*

Journal of Research of the National Institute of Standards and Technology, September/October 1995. Volume 100, Number 5.
PB96-117767 *01,927*

Journal of Research of the National Institute of Standards and Technology, March/April 1995. Volume 100, Number 2.
PB96-126180 *04,349*

Apparatus for Resistance Measurement of Short, Small-Diameter Conductors.
PB96-141130 *04,417*

Metrology Approach to Unifying Rockwell C Hardness Scales.
PB96-155551 *02,957*

Liquid-Nitrogen-Cooled High Tc Electrical Substitution Radiometer as a Broadband IR Transfer Standard.
PB96-158704 *02,198*

Journal of Research of the National Institute of Standards and Technology, November/December 1995. Volume 100, Number 6.
PB96-159215 *01,949*

New Method for Achieving Accurate Thickness Control for Uniform and Graded Multilayer Coatings on Large Flat Substrates.
PB96-159744 *04,366*

New Concepts of Precision Dimensional Measurement for Modern Manufacturing.
PB96-160684 *02,924*

Nanometrology.
PB96-160726 *02,425*

Scanned Probe Microscopies: Opportunities and Issues in Metrology.
PB96-160783 *02,426*

Journal of Research of the National Institute of Standards and Technology, September/October 1993. Volume 98, Number 5.
PB96-169057 *03,368*

Transformation of BCC and B2 High Temperature Phases to HCP and Orthorhombic Structures in the Ti-Al-Nb System. Part 1. Microstructural Predictions Based on a Subgroup Relation between Phases.
PB96-169065 *03,370*

Transformation of BCC and B2 High Temperature Phases to HCP and Orthorhombic Structures in the Ti-Al-Nb System. Part 2. Experimental TEM Study of Microstructures.
PB96-169073 *03,371*

Corrosion Characteristics of Silicon Carbide and Silicon Nitride.
PB96-169081 *03,372*

Journal of Research of the National Institute of Standards and Technology, January/February 1996. Volume 101, Number 1.
PB96-175666 *00,113*

Journal of Research of the National Institute of Standards and Technology, March/April 1996. Volume 101, Number 2.
PB96-177381 *01,863*

NIST High Accuracy Scale for Absolute Spectral Response from 406 nm to 920 nm.
PB96-179122 *01,865*

Texture Measurement of Sintered Alumina Using the March-Dollase Function.
PB96-179494 *04,784*

Time and Frequency Metrology.
PB96-190319 *01,556*

Journal of Research of the National Institute of Standards and Technology, May/June 1996. Volume 101, Number 3. Special Issue: NIST Workshop on Crystallographic Databases.
PB97-109011 *04,798*

Model of an Optical Roughness-Measuring Instrument.
PB97-110209 *04,384*

Optical Scattering from Moderately Rough Surfaces.
PB97-110415 *04,385*

Present and Future Standard Specimens for Surface Finish Metrology.
PB97-110423 *02,928*

Light Scattering by Sinusoidal Surfaces: Illumination Windows and Harmonics in Standards.
PB97-110548 *04,387*

Characterization of Modified FEL Quartz-Halogen Lamps for Photometric Standards.
PB97-112544 *00,282*

Issues in High-Speed Pyrometry.
PB97-118368 *02,693*

METROPOLITAN AREAS

Metropolitan Areas (Including MSAs, CMSAs, PMASs, and NECMAs). Category: Data Standards and Guidelines; Subcategory: Representations and Codes.
FIPS PUB 8-6 *04,873*

FIPS PUB 8-6, Metropolitan Areas (for Microcomputers).
PB95-503280 *04,874*

MICA

Diffusion of Water along 'Closed' Mica Interfaces.
PB96-180039 *02,993*

MICELLAR ELECTROKINETIC CAPILLARY CHROMATOGRAPHY

Separation and Identification of Organic Gunshot and Explosive Constituents by Micellar Electrokinetic Capillary Electrophoresis.
PB95-107249 *00,566*

MICHAELIS-MENTEN EQUATION

Michaelis-Menten Equation for an Enzyme in an Oscillating Electric Field.
PB95-140489 *00,906*

MICHELSON INTERFEROMETERS

New Refractometer by Combining a Variable Length Vacuum Cell and a Double-Pass Michelson Interferometer.
PB97-111926 *01,986*

MICRO CALORIMETERS

Hot-Electron Microcalorimeter for X-ray Detection Using a Superconducting Transition Edge Sensor with Electrothermal Feedback.
PB96-200399 *04,792*

MICROACTUATORS

Test Structures for Determining Design Rules for Microelectromechanical-Based Sensors and Actuators.
PB95-150488 *02,105*

MICROALLOYING

Microstructure and Tensile Properties of Microalloyed Steel Forgings.
PB94-172715 *03,204*

MICROANALYSIS

Concentration Histogram Imaging: A Scatter Diagram Technique for Viewing Two or Three Related Images.
PB94-199114 *00,542*

Electron Probe X-Ray Microanalysis.
PB95-107165 *00,562*

Microanalysis to Nanoanalysis: Measuring Composition at High Spatial Resolution.
PB95-107173 *00,563*

Distribution of Fluoride in Saliva and Plaque Fluid After a 0.048 mol/L NaF Rinse.
PB95-151205 *03,561*

Micromagnetic Scanning Microprobe System.
PB95-176178 *02,224*

MICROBIAL DEGRADATION

Microbial Degradation of Polysulfides and Insights into Their Possible Occurrence in Coal.
PB95-163374 *02,488*

MICROBOLOMETER

Niobium Microbolometers for Far-Infrared Detection.
PB96-111729 *02,184*

MICROBOLOMETERS

Ultrasensitive-Hot-Electron Microbolometer.
PB95-168985 *02,163*

High-Tc Superconducting Antenna-Coupled Microbolometer on Silicon.
PB95-169124 *02,166*

Antenna-Coupled High-Tc Air-Bridge Microbolometer on Silicon.
PB95-180899 *04,315*

MICROCALORIMETERS

New Coaxial Microwave Microcalorimeter Evaluation Technique.
PB95-153227 *01,892*

Hot-Electron Microcalorimeters for X-ray and Phonon Detection.
PB95-168993 *04,644*

Method to Determine the Calorimetric Equivalence Correction for a Coaxial Microwave Microcalorimeter.
PB95-202404 *01,913*

Hot-Electron Microcalorimeters as High-Resolution X-ray Detectors.
PB96-123641 *04,739*

Hot-Electron-Microcalorimeters with 0.25 mm(2) Area.
PB96-200670 *04,793*

MICROCRACK

Model for Microcrack Initiation and Propagation beneath Hertzian Contacts in Polycrystalline Ceramics.
PB96-163704 *03,077*

MICROCRACKING

Asymmetric Tip Morphology of Creep Microcracks Growing Along Bimaterial Interfaces.
PB94-200243 *03,138*

MICROCRACKS

Elastic Constants and Microcracks in YBa2Cu3O7.
PB96-200761 *03,005*

MICRODOSIMETRY

Microdosimetry and Cellular Radiation Effects of Radon Progency in Human Bronchial Airways.
PB95-152344 *03,625*

MICROELECTROMECHANICS

Directions in MEMS Research Application Development.
PB95-153797 *02,106*

MEMS in Standard CMOS VLSI Technology.
PB96-102363 *02,377*

MICROELECTRONICS

Electronics and Electrical Engineering Laboratory Technical Progress Bulletin Covering Laboratory Programs, January to March 1991, with 1991 EEEL Events Calendar.
PB94-145968 *02,113*

Electronics and Electrical Engineering Laboratory Technical Progress Bulletin Covering Programs, October to December 1993, with 1994/1995 EEEL Events Calendar.
PB94-154341 *02,115*

Electronics and Electrical Engineering Laboratory Technical Publication Announcements Covering Laboratory Programs, October to December 1993 with 1994/1995 EEEL Events Calendar.
PB94-193752 *02,307*

Electronics and Electrical Engineering Laboratory Technical Progress Bulletin Covering Laboratory Programs, January to March 1994 with 1994/1995 EEEL Events Calendar.
PB94-193810 *02,308*

Electronics and Electrical Engineering Laboratory Technical Progress Bulletin Covering Laboratory Programs, July to September 1993 with 1994 EEEL Events Calendar.
PB94-194354 *02,309*

Test Structures for the In-Plane Locations of Projected Features with Nanometer-Level Accuracy Traceable to a Coordinate Measurement System.
PB94-200565 *02,313*

Wire Bond Testing.
PB94-211653 *02,314*

Electronics and Electrical Engineering Laboratory Technical Publication Announcements Covering Laboratory Programs, January to March 1994 with 1994/1995 EEEL Events Calendar.
PB94-213774 *01,883*

Metrology and Data for Microelectronic Packaging and Interconnection: Results of a Joint Workshop on Materials Metrology and Data for Commercial Electrical and Optical Packaging and Interconnection Technologies. Held in Gaithersburg, Maryland on May 5-6, 1994. Volume 1. Results.
PB95-143111 *02,328*

Electronics and Electrical Engineering Laboratory Technical Progress Bulletin Covering Laboratory Programs, April to June 1994 with 1994/1995 EEEL Events Calendar.
PB95-143186 *02,329*

Electronics and Electrical Engineering Laboratory Technical Progress Bulletin Covering Laboratory Programs, July to September 1994 with 1994/1995 EEEL Events Calendar.
PB95-170395 *02,360*

New Test Structure for Nanometer-Level Overlay and Feature-Placement Metrology.
PB95-175345 *02,363*

Microelectronic Test Structures for Feature Placement and Electrical Linewidth Metrology.
PB95-180568 *02,367*

Electronics and Electrical Engineering Laboratory Technical Publication Announcements Covering Laboratory Programs, July to September 1994 with 1995 EEEL Events Calendar.
PB95-198925 *01,912*

Electronics and Electrical Engineering Laboratory Technical Progress Bulletin Covering Laboratory Programs, April to June 1991, with 1992 EEEL Events Calendar.
PB95-209821 *01,916*

Electronics and Electrical Engineering Laboratory Technical Publication Announcements Covering Laboratory Programs, January to March 1995 with 1995 EEEI Events Calendar.
PB95-242277 *02,373*

Gaseous Electronics Conference RF Reference Cell: An Introduction.
PB96-113329 *02,387*

Current and Voltage Measurements in the Gaseous Electronics Conference RF Reference Cell.
PB96-113337 *02,388*

Optical Emission Spectroscopy on the Gaseous Electronics Conference RF Reference Cell.
PB96-113345 *02,389*

Optical Diagnostics in the Gaseous Electronics Conference Reference Cell.
PB96-113352 *02,390*

Studies of Ion Kinetic-Energy Distributions in the Gaseous Electronics Conference RF Reference Cell.
PB96-113360 *02,391*

Microwave Diagnostic Results from the Gaseous Electronics Conference RF Reference Cell.
PB96-113378 *02,392*

Langmuir Probe Measurements in the Gaseous Electronics Conference RF Reference Cell.
PB96-113386 *02,393*

Inductively Coupled Plasma Source for the Gaseous Electronics Conference RF Reference Cell.
PB96-113394 *02,394*

Reactive Ion Etching in the Gaseous Electronics Conference RF Reference Cell.
PB96-113402 *02,395*

Dusty Plasma Studies in the Gaseous Electronics Conference Reference Cell.
PB96-113410 *02,396*

One-Dimensional Modeling Studies of the Gaseous Electronics Conference RF Reference Cell.
PB96-113428 *02,397*

Two-Dimensional Self-Consistent Radio Frequency Plasma Simulations Relevant to the Gaseous Electronics Conference RF Reference Cell.
PB96-113436 *02,398*

Measurement of Patterned Film Linewidth for Interconnect Characterization.
PB96-148168 *02,420*

High-Speed Interconnection Characterization Using Time Domain Network Analysis.
PB96-148176 *04,061*

Microelectronic Test Structures for Overlay Metrology.
PB96-164249 *02,430*

Beyond the Technology Roadmaps: An Assessment of Electronic Materials Research and Development.
PB96-165998 *01,961*

MICROEMULSIONS

Flow of Microemulsions through Microscopic Pores.
PB95-140463 *00,905*

Structure of a Triglyceride Microemulsion: A Small Angle Neutron Scattering Study.
PB96-112255 *01,077*

MICROFORM

Microform Calibrations in Surface Metrology.
PB95-203295 *02,951*

MICROGRAVITY

Combustion of a Polymer (PMMA) Sphere in Microgravity.
N96-15569/2 *01,354*

Ignition and Subsequent Transition to Flame Spread in a Microgravity Environment.
N96-15584/1 *04,828*

Electric Field Effects on a Near-Critical Fluid in Microgravity.
PB96-161880 *04,217*

MICROINSTRUMENTATION

Integrated Thin-Film Micropotentiometers.
PB96-146709 *02,109*

MICROMACHINING

Realizing Suspended Structures on Chips Fabricated by CMOS Foundry Processes Through the MOSIS Service.
PB94-193984 *01,881*

High-Level CAD Melds Micromachined Devices with Foundries.
PB94-216413 *02,321*

Design and Machining of Copper Specimens with Micro Holes for Accurate Heat Transfer Measurements.
PB95-180428 *02,658*

Thermal Isolation of High-Temperature Superconducting Thin Films Using Silicon Wafer Bonding and Micromachining.
PB96-135017 *02,408*

Micromachined Display Output for a Cellular Neural Network.
PB96-156070 *02,422*

Micromachined Coplanar Waveguides in CMOS Technology.
PB97-119283 *02,456*

MICROMAGNETIC MODELS

Experimental Verification of a Micromagnetic Model of Dual-Layer Magnetic Films.
PB95-141081 *04,553*

MICROMAGNETICS

Numerical Micromagnetic Techniques and Their Applications to Magnetic Force Microscopy Calculations.
PB95-175931 *04,664*

MICROMECHANICS

Micromechanics of Fracture in Rubber-Toughened Epoxies.
PB94-212222 *03,011*

Hybrid Method for Determining Material Properties from Instrumented Micro-Indentation Experiments.
PB95-152229 *03,348*

MICROMETERS

Optical Fiber Geometry: Accurate Measurement of Cladding Diameter.
PB95-151940 *04,266*

MICROMINIATURIZATION

Directions in MEMS Research Application Development.
PB95-153797 *02,106*

MICROPHONES

Determination of Acoustic Center Correction for Type LS2aP Condensor Microphones.
PB96-204508 *04,190*

MICROSCOPE TIPS

Proposed Antiferromagnetically Coupled Dual-Layer Magnetic Force Microscope Tips.
PB95-169017 *04,645*

MICROSCOPES

Development of a Calibrated Atomic Force Microscope.
PB94-185683 *02,894*

Video Microscopy Applied to Optical Fiber Geometry Measurements.
PB95-173068 *04,295*

Flexible-Diaphragm Force Microscope.
PB95-180915 *03,966*

Standard Reference Materials for Optical Fibers and Connectors.
PB96-119805 *04,344*

MICROSCOPY

National Voluntary Laboratory Accreditation Program: Bulk Asbestos Analysis.
PB95-138129 *02,541*

Workshop Summary Report: Industrial Applications of Scanned Probe Microscopy. A Workshop Co-sponsored by NIST, SEMATECH, ASTM, E42.14, and the American Vacuum Society. Held in Gaithersburg, Maryland on March 24-25, 1994.
PB95-170387 *00,506*

Recent Results in Magnetic Force Microscopy.
PB96-103130 *04,721*

Summary Report: Workshop on Industrial Applications of Scanned Probe Microscopy (2nd). A Workshop Co-Sponsored by NIST, SEMATECH, ASTM E42.14, and the American Vacuum Society. Held in Gaithersburg, Maryland on May 2-3, 1995.
PB96-131602 *00,509*

Progress Toward Accurate Metrology Using Atomic Force Microscopy.
PB96-146774 *02,417*

Scanning Capacitance Microscopy Measurements and Modeling: Progress Towards Dopant Profiling of Silicon.
PB96-148150 *04,773*

2D-Scanning Capacitance Microscopy Measurements of Cross-Sectioned VLSI Teststructures.
PB96-163779 *04,104*

Scanning Capacitance Microscopy Measurements and Modeling for Dopant Profiling of Silicon.
PB96-164207 *04,781*

Morphology and Phase Separation Kinetics of a Compatibilized Blend.
PB97-119135 *01,297*

Vortex Images in Thin Films of YBa2Cu3O(sub 7-x) and Bi2Sr2Ca1Cu2O(sub 8+x) Obtained by Low-Temperature Magnetic Force Microscopy.
PB97-119408 *04,815*

MICROSENSORS

Test Structures for Determining Design Rules for Microelectromechanical-Based Sensors and Actuators.
PB95-150488 *02,105*

MICROSTRIP TRANSMISSION LINES

Crosstalk between Microstrip Transmission Lines.
PB94-135639 *02,210*

Crosstalk between Microstrip Transmission Lines. (NIST Reprint).
PB95-180337 *02,225*

Radiated Emissions and Immunity of Microstrip Transmission Lines: Theory and Measurements.
PB96-162649 *02,238*

MICROSTRIPS

Line-Reflect-Match Calibrations with Nonideal Microstrip Standards.
PB96-176599 *02,242*

MICROSTRUCTURAL DESIGN

Model for Toughness Curves in Two-Phase Ceramics. 2. Microstructural Variables.
PB96-163795 *03,078*

MICROSTRUCTURE

Microstructural Features of Some Low Water/Solids, Silica Fume Mortars Cured at Different Temperatures.
PB94-160777 *00,330*

Digitized Simulation of Mercury Intrusion Porosimetry.
PB94-172236 *01,304*

Microstructure and Tensile Properties of Microalloyed Steel Forgings.
PB94-172715 *03,204*

Energy and Migration of Grain Boundaries in Polycrystals.
PB94-211638 *03,332*

Fabrication of Platinum-Gold Alloys in Pre-Hispanic South America: Issues of Temperature and Microstructure Control.
PB94-211646 *03,333*

Effect of Microstructure on the Wear Transition of Zirconia-Toughened Alumina.
PB94-211778 *03,141*

Microstructural Evolution in Two-Dimensional Two-Phase Polycrystals.
PB94-211992 *04,498*

Compositional Mapping of the Microstructure of Materials.
PB95-107199 *00,565*

Computer Simulation of the Diffusivity of Cement-Based Materials.
PB95-125985 *00,362*

Fundamental Computer Simulation Models for Cement-Based Materials.
PB95-126009 *00,364*

Effect of Mn Content on the Microstructure of Al-Mn Alloys Electrodeposited at 150C.
PB95-126355 *03,343*

Rheology of Fresh Cement Paste.
PB95-163150 *00,378*

Wear Model for Alumina Sliding Wear.
PB95-163796 *03,239*

Cellular Automaton Simulations of Cement Hydration and Microstructure Development.
PB95-175055 *01,320*

Tensile Deformation-Induced Microstructures in Free-Standing Copper Thin Films.
PB96-102595 *04,715*

Low-Energy Vibrations and Octahedral Site Occupation in Nb95V5H(D)y.
PB96-160734 *01,133*

Neutron Spectroscopic Comparison of beta-Phase Rare Earth Hydrides.
PB96-160742 *01,134*

Phase Identification in a Scanning Electron Microscope Using Backscattered Electron Kikuchi Patterns.
PB97-109128 *04,804*

Multi-Scale Picture of Concrete and Its Transport Properties: Introduction for Non-Cement Researchers.
PB97-115802 *03,107*

MICROSTRUCTURE EFFECTS

Microstructure Effect on the Phase Behavior of Blends of Deuterated Polybutadiene and Protonated Polyisopene.
PB97-113146 *01,296*

MICROSTRUCTURES

Microlithography by Using Neutral Metastable Atoms and Self-Assembled Monolayers.
PB96-190038 *02,441*

MICROWAVE ABSORBERS

Bistatic Scattering of Absorbing Materials from 30 to 1000 MHz.
PB95-150934 *01,891*

MICROWAVE AMPLIFIERS

Comparison of Three Techniques for the Precision Measurement of Amplifier Noise.
PB95-163663 *02,349*

Measurement Accuracies for Various Techniques for Measuring Amplifier Noise.
PB95-163671 *02,350*

Investigations of AM and PM Noise in X-Band Devices.
PB95-180022 *02,062*

Origin of l/f PM and AM Noise in Bipolar Junction Transistor Amplifiers.
PB96-200787 *02,096*

Quest to Understand and Reduce l/f Noise in Amplifiers and Baw Quartz Oscillators.
PB96-200795 *02,097*

MICROWAVE CIRCUITS

Comments on 'Conversions between S, Z, Y, h, ABCD, and T Parameters Which Are Valid for Complex Source and Load Impedances'.
PB96-102785 *02,069*

Semiconductor Measurement Technology: Test Structure Implementation Document: DC Parametric Test Structures and Test Methods for Monolithic Microwave Integrated Circuits (MMICs).
PB96-117692 *02,399*

Microwave Characterization of Flip-Chip MMIC Components.
PB96-176722 *02,434*

Microwave Characterization of Flip-Chip MMIC Interconnections.
PB96-176730 *02,435*

Electrical Measurements of Microwave Flip-Chip Interconnections.
PB96-176748 *02,436*

30 MHz Comparison Receiver.
PB96-200407 *01,972*

MICROWAVE COMMUNITIES

NIST Metrology Program on Electromagnetic Characterization of Materials.
PB96-156062 *01,944*

MICROWAVE EQUIPMENT

Standard of Attenuation for Microwave Measurements.
AD-A297 905/2 *01,517*

NIST Model PM2 Power Measurement System for 1 mW at 1 GHz.
PB94-135803 02,018

Direct Comparison Transfer of Microwave Power Sensor Calibrations.
PB96-158654 02,086

MICROWAVE FREQUENCIES
Ferroelectric Thin Film Characterization Using Superconducting Microstrip Resonators.
PB96-102389 02,270

MICROWAVE OSCILLATORS
Investigations of AM and PM Noise in X-Band Devices.
PB95-180022 02,062

Phase Locking in Two-Dimensional Arrays of Josephson Junctions: Effect of Critical-Current Nonuniformity.
PB96-102587 04,714

Quest to Understand and Reduce I/f Noise in Amplifiers and Baw Quartz Oscillators.
PB96-200795 02,097

MICROWAVE POWER STANDARDS
New Coaxial Microwave Microcalorimeter Evaluation Technique.
PB95-153227 01,892

Method to Determine the Calorimetric Equivalence Correction for a Coaxial Microwave Microcalorimeter.
PB95-202404 01,913

Developing a NIST Coaxial Microwave Power Standard at 1 mW.
PB95-202412 01,914

Direct Comparison Transfer of Microwave Power Sensor Calibrations.
PB96-158654 02,086

MICROWAVE SENSORS
Performance of Commercial CMOS Foundry-Compatible Multijunction Thermal Converters.
PB95-153656 02,342

MICROWAVE SPECTRA
Tunneling-Rotation Spectrum of the Hydrogen Fluoride Dimer.
PB94-198678 00,793

2-Tunneling Path Internal-Axis-Method-Like Treatment of the Microwave Spectrum of Divinyl Ether.
PB94-200466 00,808

Microwave Spectra of van der Waals Complexes of Importance in Planetary Atmospheres.
PB95-150611 00,919

MICROWAVE SPECTROMETERS
Experimental Studies of Line Shapes from a Balle-Flygare Spectrometer.
PB94-199452 00,796

MICROWAVE SPECTROSCOPY
Microwave and Submillimeter Spectroscopy of Ar-NH3 States Correlating with Ar+NH3(j=1, k=1).
PB95-152211 00,942

MICROWAVE SPECTRUM
Microwave Spectrum and Structure of CH2O-H2O.
PB97-118723 04,168

MICROWAVE SUBSTRATES
Wire Bonding to Multichip Modules and Other Soft Substrates.
PB96-123583 02,079

Wire Bonding to Multichip Modules and Other Soft Substrates.
PB96-135207 02,082

MICROWAVE TRANSMISSION
Slant Path Atmospheric Refraction Calibrator: An Instrument to Measure the Microwave Propagation Delays Induced by Atmospheric Water Vapor.
PB95-151270 01,476

Microwave Diagnostic Results from the Gaseous Electronics Conference RF Reference Cell.
PB96-113378 02,392

MICROWAVES
Microwave Spectrum and Structure of CH3NO2-H20.
AD-A296 377/5 00,719

Molecular Microwave Spectra Tables.
AD-A296 498/9 00,720

Coaxial Reference Standard for Microwave Power.
PB94-193786 01,880

Hydrolysis of Proteins by Microwave Energy.
PB94-216322 03,528

Diffusion of Copper into Gold Plating.
PB95-162152 00,957

Microwave Characterization of Printed Circuit Transmission Lines.
PB96-122585 02,077

Calibration Service for Coaxial Reference Standards for Microwave Power.
PB96-162722 01,958

MICROWAVES POWER TRANSMISSION
Planar Near-Field Measurements of Low-Sidelobe Antennas.
PB94-219235 02,001

MICROZONATION
De Facto Microzonation through the Use of Soils Factors in Design Triggers.
PB96-141148 00,462

MIL-STD-1312
Review and Upgrading of Military Fastener Test Standard MIL-STD-1312.
PB95-154720 02,947

MILITARY FACILITIES
Present Worth Factors for Life-Cycle Cost Studies in the Department of Defense (1995).
PB95-105029 03,664

MILITARY STANDARDS
Review and Upgrading of Military Fastener Test Standard MIL-STD-1312.
PB95-154720 02,947

MILITARY VEHICLES
Ground Vehicle Control at NIST: From Teleoperation to Autonomy.
N94-34037/9 03,758

MILLIMETER WAVE EQUIPMENT
Dual-Frequency Millimeter-Wave Radiometer Antenna for Airborne Remote Sensing of Atmosphere and Ocean.
PB96-112289 02,009

MILLIMETER WAVES
Proposed High-Accuracy Superconducting Power Meter for Millimeter Waves.
PB94-212669 02,034

MIMD
Time-Perturbation Tuning of MIMD Programs.
PB94-164399 01,681

Time-Perturbation Tuning of MIMD Programs.
PB94-172566 01,684

Using Synthetic-Perturbation Techniques for Tuning Shared Memory Programs (Extended Abstract).
PB94-172657 01,685

MIMD (COMPUTERS)
Operating Principles of MultiKron II Performance Instrumentation for MIMD Computers.
PB95-189486 01,628

Scalability Test for Parallel Code.
PB96-146758 01,749

MIMD (MULTIPLE INSTRUCTION MULTIPLE DATA)
Synthetic-Perturbation Tuning of MIMD Programs.
PB94-185568 01,687

Simple Scalability Test for MIMD Code.
PB94-193638 01,688

MINERALIZATION
Calcium Phosphate Precipitation in Liposomal Suspensions.
PB94-172145 03,452

Critical Evaluation of the Purification of Biominerals by Hypochlorite Treatment.
PB95-150959 00,186

Remineralizing Dental Composites Based on Amorphous Calcium Phosphate.
PB96-147020 03,573

MINERALS
Procedure for the Study of Acidic Calcium Phosphate Precursor Phases in Enamel Mineral Formation.
PB95-164448 03,564

CRYSTMET: The NRCC Metals Crystallographic Data File.
PB97-109029 04,799

MINIMAL SURFACES
Singularities in Minimum Surface Energy Problems and Their Influence in Surface Motion.
PB94-199411 04,473

MINIMUM DETECTABLE ACTIVITY
Germanium Detector Optimization of MDA for Efficiency vs. Low Intrinsic Background.
PB94-199155 00,543

MINING EQUIPMENT
Environment Simulation for a Continuous Mining Machine.
PB94-203536 03,697

MIRAGE DETECTION
Thermal Wave NDE of Advanced Materials Using Mirage Effect Detection.
PB96-204516 04,191

MIRRORS
Simulations of Neutron Focusing with Curved Mirrors.
PB96-176649 02,200

MIS CAPACITORS
Development and Characterization of Insulating Layers on Silicon Carbide: Annual Report for February 14, 1988 to February 14, 1989.
PB94-155579 02,295

MIXERS
Milliwatt Mixer for Small Fluid Samples.
PB94-198819 02,634

MIXERS (ELECTRONICS)
Investigations of AM and PM Noise in X-Band Devices.
PB95-180022 02,062

Frequency Synthesis and Metrology at 10(-17) and Beyond.
PB97-113187 02,101

MIXING
Neutron Scattering Study of Shear Induced Turbidity in Polystyrene/Dioctyl Phthalate Solutions at High Shear Rates.
PB94-172624 01,197

MIXTURES
Prediction of the Thermal Conductivity of Refrigerants and Refrigerant Mixtures.
PB94-212107 03,258

Global Thermodynamic Behavior of Fluid Mixtures in the Critical Region.
PB94-212420 04,199

SANS and LS Studies of Polymer Mixtures Under Shear Flow.
PB95-107090 01,231

Thermophysical Property Computer Packages from NIST.
PB95-125787 04,203

Intrinsic Viscosity and the Polarizability of Particles Having a Wide Range of Shapes.
PB96-119318 03,170

MMIC (MONOLITHIC MICROWAVE INTEGRATED CIRCUITS)
Microwave Characterization of Flip-Chip MMIC Components.
PB96-176722 02,434

Microwave Characterization of Flip-Chip MMIC Interconnections.
PB96-176730 02,435

Electrical Measurements of Microwave Flip-Chip Interconnections.
PB96-176748 02,436

MOBILE COMMUNICATION SYSTEMS
Channel Coding for Code Excited Linear Prediction (CELP) Encoded Speech in Mobile Radio Applications.
PB95-143178 01,475

Error Protecting Characteristics of CDMA and Impacts on Speech.
PB96-122452 01,491

MOBILE HOMES
Wind Load Provisions of the Manufactured Home Construction and Safety Standards: A Review and Recommendations for Improvement.
PB94-206125 00,428

Manufactured Homes: Probability of Failure and the Need for Better Windstorm Protection through Improved Anchoring Systems.
PB95-143129 00,432

MOBILE PHASE COMPOSITIONS
Comparison of the Liquid Chromatographic Behavior of Selected Steroid Isomers Using Different Reversed-Phase Materials and Mobile Phase Compositions.
PB95-140976 00,574

MOBILE ROBOTS
Control System Architecture for a Remotely Operated Unmanned Land Vehicle.
PB95-163200 03,759

MODE COUPLING
Orientational Fluctuations, Diffuse Scattering, and Orientational Order in Solid C60.
PB97-119275 04,176

MODE LOCKED LASERS
Metrology Applications of Mode-Locked Erbium Fiber Lasers.
PB95-140158 04,256

Multiwavelength Birefringent-Cavity Mode-Locked Fibre Laser.
PB95-150496 04,262

MODEL TESTS
Model Precast Concrete Beam-to-Column Connections Subject to Cyclic Loading.
PB95-153094 00,438

Partially Prestressed and Debonded Precast Concrete Beam-Column Joints.
PB95-153102 00,439

Seismic Performance Behavior of Precast Concrete Beam-Column Joints.
PB95-153110 00,440

MODELS
Role of World Modeling and Value Judgment in Perception.
PB94-198264 01,581

Modelling the Leaching of Calcium Hydroxide from Cement Paste: Effects on Pore Space Percolation and Diffusivity.
PB94-198793 01,311

Simplified Cycle Simulation Model for the Performance Rating of Refrigerants and Refrigerant Mixtures.
PB94-199890 03,255

Product Models and Virtual Prototypes in Mechanical Engineering.
PB95-253563 02,783

Low-Frequency Model for Radio-Frequency Absorbers.
PB95-261939 04,424

Mapping Integration Definition for Function Modeling (IDEFO) Model into CASE Data Interchange Format (CDIF) Transfer File.
PB96-109533 01,741

Characterization of Two-Dimensional Dopant Profiles: Status and Review.
PB96-119300 02,400

Mechano-Chemical Model: Reaction Temperatures in a Concentrated Contact.
PB96-119466 03,227

Comparison of POSIX Open System Environment (OSE) and Open Distributed Processing (ODP) Reference Models.
PB96-131495 *01,820*

Machining Process Planning Activity Model for Systems Integration.
PB96-165428 *02,841*

Characterization of Two-Dimensional Dopant Profiles: Status and Review.
PB97-110134 *02,451*

MODEMS
High Resolution Time Interval Counter.
PB96-138607 *01,495*

MODERATORS
Experimental plan to determine the performance of the Oak Ridge National Laboratory Cold Neutron Moderator. Final report, September 1, 1993--November 30, 1993.
DE95011352 *03,778*

Thermal Hydraulic Tests of a Liquid Hydrogen Cold Neutron Source.
PB95-135570 *03,884*

Nuclear Heat Load Calculations for the NBSR Cold Neutron Source Using MCNP.
PB95-152955 *03,730*

MODERNIZATION
Learning to Change: Opportunities to Improve the Performance of Smaller Manufacturers.
PB94-166212 *00,010*

MODULATORS
Interdigitated Stacked P-I-N Multiple Quantum Well Modulator.
PB97-112296 *02,455*

MODULES
Integrating Automated Systems with Modular Architecture.
PB95-150231 *00,577*

MODULES OF ELASTICITY
Ultrasonic Measurement of Sheet Anisotropy and Formability.
PB95-153235 *03,213*

MODULUS OF ELASTICITY
Dynamic Shear Modulus Measurements with Four Independent Techniques in Nickel-Based Alloys.
PB94-198900 *03,320*

Dynamics vs. Static Young's Moduli: A Case Study.
PB94-213188 *03,210*

Hollow Clay Tile Prism Tests for Martin Marietta Energy Systems: Task 2 Testing.
PB94-217486 *00,352*

Method for Determining Both Magnetostriction and Elastic Modulus by Ferromagnetic Resonance.
PB95-150108 *02,974*

MOISTURE
Controlling Moisture in the Walls of Manufactured Housing.
PB95-105136 *00,355*

Measurements of Moisture Diffusivity for Porous Building Materials.
PB95-107397 *00,356*

Moisture and Water-Induced Crack Growth in Optical Materials.
PB95-153334 *04,267*

Sorption of Moisture on Epoxy and Alkyd Free Films and Coated Steel Panels.
PB95-162475 *03,192*

Water-Vapor Measurements of Low-Slope Roofing Materials.
PB95-251617 *00,399*

Water Adsorption at a Polyimide/Silicon Wafer Interface.
PB96-103197 *01,070*

Mathematical Analysis of Practices to Control Moisture in the Roof Cavities of Manufactured Houses.
PB97-106843 *00,278*

Experimental Verification of a Moisture and Heat Transfer Model in the Hygroscopic Regime.
PB97-111546 *00,309*

MOISTURE CONTENT
Analysis of Moisture Accumulation in a Wood-Frame Wall Subjected to Winter Climate.
PB94-199320 *00,338*

Heat and Moisture Transfer in Wood-Based Wall Construction: Measured versus Predicted.
PB95-200655 *00,391*

Amperometric Measurement of Moisture in Transformer Oil Using Karl Fischer Reagents.
PB96-146766 *00,623*

Empirical Validation of a Transient Computer Model for Combined Heat and Moisture Transfer.
PB97-111991 *00,416*

Parametric Study of Wall Moisture Contents Using a Revised Variable Indoor Relative Humidity Version of the 'Moist' Transient Heat and Moisture Transfer Model.
PB97-122535 *00,419*

MOISTURE TRANSFER
Manufactured Housing Walls That Provide Satisfactory Moisture Performance in All Climates.
PB95-178885 *00,383*

MOISTUREPROOFING
Manufactured Housing Walls That Provide Satisfactory Moisture Performance in All Climates.
PB95-178885 *00,383*

MOLAR ENTHALPY
Thermochemistry of the Hydrolysis of L-arginine to (L-citrulline + Ammonia) and of the Hydrolysis of L-arginine to (L-ornithine + Urea).
PB95-150801 *03,463*

MOLAR MASS
Adsorption of Polyacrylic Acids and Their Sodium Salts on Hydroxyapatite: Effect of Relative Molar Mass.
PB97-112510 *03,581*

MOLAR VOLUME
Apparent Molar Heat Capacities and Apparent Molar Volumes of Aqueous Glucose at Temperatures from 298.15 K to 327.01 K.
PB94-212800 *03,459*

MOLDING TECHNIQUES
Report on the Workshop on Manufacturing Polymer Composites by Liquid Molding. Held in Gaithersburg, Maryland on September 20-22, 1993.
PB94-160066 *03,131*

Effect of Heterogeneous Porous Media on Mold Filling in Resin Transfer Molding.
PB95-108676 *03,197*

MOLE FRACTION ERRORS
Nonlinear Correlation of High-Pressure Vapor-Liquid Equilibrium Data for Ethylene + n-Butane Showing Inconsistencies in Experimental Compositions.
PB96-161906 *01,141*

MOLECULAR ABSORPTION
Memory Function Approach to the Shape of Pressure Broadened Molecular Bands.
PB95-152930 *00,944*

MOLECULAR BEAM EPITAXY
Single-Photon Ionization and Detection of Ga, In, and As(sub n) Species in GaAs Growth.
PB95-152815 *00,591*

In-situ Monitoring of Molecular Beam Epitaxial Growth Using Single Photon Ionization.
PB95-202222 *01,023*

Laser Vacuum Ultraviolet Single Photon Ionization Probing of III-V Semiconductor Growth.
PB95-202370 *04,691*

Epitaxial Growth of Sb/GaSb Structures: An Example of V/III-V Heteroepitaxy.
PB95-202560 *04,693*

Single Photon Ionization, Laser Optical Probe Technique for Semiconductor Growth.
PB95-202776 *01,032*

Single-Photon Laser Ionization Time-of-Flight Mass Spectroscopy Detection in Molecular-Beam Epitaxy: Application to As4, As2, and Ga.
PB95-203337 *01,052*

Single Photon Laser Ionization as an In-situ Diagnostic for MBE growth.
PB96-102025 *01,059*

Stacked Series Arrays of High-Tc Trilayer Josephson Junctions.
PB96-102272 *04,705*

Buffer Layer Modulation-Doped Field-Effect-Transistor Interactions in the Al0.33Ga0.67As/GaAs Superlattice System.
PB96-102876 *02,380*

Laser Gas Ionization Technique Monitors MEB Crystal Growth.
PB96-112172 *01,076*

Parallel Monte Carlo Simulation of MBE Growth.
PB96-122841 *02,406*

In-situ Neutron Reflectivity of MBE Grown and Chemically Processed Surfaces and Interfaces.
PB96-146634 *02,416*

MOLECULAR BEAM SCATTERING
Dynamics of Hydrogen Interactions with Si(100) and Si(111) Surfaces.
PB96-159801 *04,082*

MOLECULAR BEAMS
Use of Extended Permutation-Inversion Groups in Constructing Hyperfine Hamiltonians for Symmetrical-Top Internal Rotor Molecules Like H3C-SiH3.
PB94-212032 *00,823*

MOLECULAR CHAINS
Molecular Weight Dependence of the Lamellar Domain Spacing of ABC Triblock Copolymers and Their Chain Conformation in Lamellar Domains.
PB95-161691 *01,254*

Small Angle Neutron Scattering Studies on Chain Asymmetry of Coextruded Poly(Vinyl Alcohol) Film.
PB95-164372 *01,262*

MOLECULAR CLOUDS
Extended CO(7 yields 6) Emission from Warm Gas in Orion.
PB96-102504 *00,090*

MOLECULAR CLUSTERS
High Resolution IR Studies of Polymolecular Clusters: Micromatrices and Unimolecular Ring Opening.
PB94-185691 *00,777*

High-Resolution Infrared Spectroscopy of DF Trimer: A Cyclic Ground State Structure and DF Stretch Induced Intramolecular Vibrational Coupling.
PB95-150678 *00,920*

Product State Correlations in the Reaction of O((1)D) and H2O in Bimolecular Collisions and in O3.H2O Clusters--Translation.
PB95-153011 *00,946*

MOLECULAR COLLISIONS
Three-Vector Correlation Theory for Orientation/Alignment Studies in Atomic and Molecular Collisions.
PB94-211109 *03,834*

N2(a'(sup 1)Sigma(sub g)(sup +)) Metastable Collisional Destruction and Rotational Excitation Transfer by N2.
PB95-151395 *00,933*

Product State Correlations in the Reaction of O((1)D) and H2O in Bimolecular Collisions and in O3.H2O Clusters--Translation.
PB95-153011 *00,946*

Collisional Alignment of CO2 Rotational Angular Momentum States in a Supersonic Expansion.
PB96-103171 *01,069*

MOLECULAR COMPOSITES
Phase Behavior of a Hydrogen Bonding Molecular Composite.
PB94-185188 *01,202*

MOLECULAR CONFORMATION
Molecular Weight Dependence of the Lamellar Domain Spacing of ABC Triblock Copolymers and Their Chain Conformation in Lamellar Domains.
PB95-161691 *01,254*

Small Angle Neutron Scattering Studies on Chain Asymmetry of Coextruded Poly(Vinyl Alcohol) Film.
PB95-164372 *01,262*

MOLECULAR DYNAMICS
Femtosecond Time-Resolved Wave Packet Motion in Molecular Multiphoton Ionization and Fragmentation.
PB94-198611 *00,790*

Neighbor Tables for Molecular Dynamics Simulations.
PB95-171948 *00,991*

Pulsed Laser Photolysis Time-Resolved FT-IR Emission Studies of Molecular Dynamics.
PB95-203162 *04,002*

Comparison of a Fixed-Charge and a Polarizable Water Model.
PB96-111620 *01,072*

Long-Lived Structures in Fragile Glass-Forming Liquids.
PB96-119565 *04,212*

Molecular Dynamics Investigation of the Surface/Bulk Equilibrium in an Ethanol-Water Solution.
PB97-113112 *01,183*

MOLECULAR EXCITATION
Electron Attachment to Excited Molecules(1).
PB96-122809 *01,087*

MOLECULAR IONS
Production and Spectroscopy of Small Polyatomic Molecular Ions Isolated in Solid Neon. (Reannouncement with New Availability Information).
AD-A234 043/8 *00,704*

Vibrational Spectra of Molecular Ions Isolated in Solid Neon. 6. CO4(-). (Reannouncement with New Availability Information).
AD-A238 415/4 *00,705*

Vibrational Spectra of Molecular Ions Isolated in Solid Neon. 7. CO(+), C2O2(+), and C2O2(-). (Reannouncement with New Availability Information).
AD-A239 729/7 *00,706*

Vibrational Spectra of Molecular Ions Isolated in Solid Neon: HCCH+ and HCC-. (Reannouncement with New Availability Information).
AD-A253 551/6 *00,707*

Vibrational Spectra of Molecular Ions Isolated in Solid Neon. 11. NO2(+), NO2(-), and NO3(-).
AD-A275 828/2 *00,708*

Vibrational Spectra of Molecular Ions Isolated in Solid Neon. X. H2O(+), HDO(+), and D2O(+).
PB95-125670 *00,889*

Vibrational Spectra of Molecular Ions Isolated in Solid Neon. XI. NO2(+), NO2(-), and NO3(-).
PB95-125688 *00,890*

Matrix Isolation Study of the Interaction of Excited Neon Atoms with BCl3: Infrared Spectra of BCl(sub 3, sup +), BCl(sub 2, sup +), and BCl(sub 3, sup -).
PB97-119143 *01,187*

Vibrational Spectra of Molecular Ions Isolated in Solid Neon. 13. Ions Derived from HBr and HI.
PB97-119234 *01,188*

MOLECULAR MEASURING MACHINE
Comparison of Finite Element and Analytic Calculations of the Resonant Modes and Frequencies of a Thick Shell Sphere.
PB94-160785 *02,626*

MOLECULAR MODELS
Effects of Variable Excluded Volume on the Dimensions of Off-Lattice Polymer Chains.
PB94-212941 *01,229*

MOLECULAR ORBITALS
Strong Hydrogen Bond in the Formic Acid-Formate Anion System.
PB94-198595 *00,788*

Analysis of Protein Metal Binding Selectivity in a Cluster Model.
PB94-212990 *00,845*

Molecular Orbital Calculations of Bond Rupture in Brittle Solids.
PB95-164059 *00,973*

Molecular Orbital Study of Water Enhanced Crack Growth Process.
PB95-164067 *03,240*

MOLECULAR PROPERTIES

Molecular Microwave Spectra Tables.
AD-A296 498/9 *00,720*

Collection of Results for the SPC/E Water Model.
PB96-147889 *01,127*

MOLECULAR SIEVES

Small Angle Neutron Scattering Study of the Structure and Formation of MCM-41 Mesoporous Molecular Sieves.
PB97-122337 *03,110*

MOLECULAR SPECTROSCOPY

Molecular Spectroscopy.
PB94-213337 *03,861*

Atomic, Molecular, and Optical Physics with X-rays.
PB94-213378 *03,863*

MOLECULAR STRUCTURE

Complementary Molecular Information on Phthalocyanine Compounds Derived from Laser Microprobe Mass Spectrometry and Micro-Raman Spectroscopy.
PB94-172269 *00,757*

Structure of Glycine-Water H-Bonded Complexes.
PB94-198603 *00,789*

Fluorescence Anisotropy Measurements on a Polymer Melt as a Function of Applied Shear Stress.
PB94-199296 *01,209*

Observations of Shear Induced Molecular Orientation in a Polymer Melt Using Fluorescence Anisotropy Measurements.
PB94-199304 *01,210*

Observations of Shear Stress and Molecular Orientation Using Fluorescence Anisotropy Measurements.
PB94-199312 *01,211*

Neutron Scattering by Multiblock Copolymers of Structure (A-B)N-A.
PB94-211547 *01,219*

Structure of Molecules on Surfaces as Determined Using Electron-Stimulated Desorption.
PB94-216165 *00,852*

Determination of the Molecular Parameters of NiH in Its (2)Delta Ground State by Laser Magnetic Resonance.
PB95-107116 *00,869*

Construction of Maximum-Entropy Density Maps, and Their Use in Phase Determination and Extension.
PB95-108593 *00,882*

Characterization of Chemically Modified Pore Surfaces by Small Angle Neutron Scattering.
PB95-126181 *00,898*

Structural Stabilization of Phase Separating PC/Polyester Blends through Interfacial Modification by Transesterification Reaction.
PB95-150454 *01,239*

Structural Heterogeneity in Epoxies.
PB95-151866 *01,243*

SANS Studies of Space-Time Organization of Structure in Polymer Blends.
PB95-153789 *01,251*

Octacalcium Phosphate Carboxylates. 2. Characterization and Structural Consideration.
PB95-161543 *00,955*

Localization of a Homopolymer Dissolved in a Lamellar Structure of a Block Copolymer Studied by Small-Angle Neutron Scattering.
PB95-161592 *01,253*

Elastic Scattering of Polymer Networks.
PB95-161816 *01,255*

Characterization of Molecular Network of Thermosets Using Neutron Scattering.
PB95-164109 *01,259*

Small-Angle Neutron Scattering of Poly(vinyl alcohol) Gels.
PB95-164117 *01,260*

Competition between Hydrodynamic Screening ('Draining') and Excluded Volume Interactions in an Isolated Polymer Chain.
PB95-175402 *01,265*

Comparison of a Fixed-Charge and a Polarizable Water Model.
PB96-111620 *01,072*

Long-Lived Structures in Fragile Glass-Forming Liquids.
PB96-119565 *04,212*

Slow Dynamics of Segregation in Hydrogen-Bonded Polymer Blends.
PB96-123591 *01,281*

Neutron Scattering Study of the Lattice Modes of Solid Cubane.
PB96-147152 *01,126*

New Generation of Fire Resistant Polymers. Part 1. Computer-Aided Molecular Design.
PB96-160593 *01,419*

Investigations of the Systematics of Crystal Packing Using the Cambridge Structural Database.
PB97-109144 *00,519*

MOLECULAR VIBRATION

Vibrational Spectra of Molecular Ions Isolated in Solid Neon. 6. CO4(-). (Reannouncement with New Availability Information).
AD-A238 415/4 *00,705*

High-Resolution IR Laser-Driven Vibrational Dynamics in Supersonic Jets: Weakly Bound Complexes and Intramolecular Energy Flow.
PB94-216751 *00,862*

Acceleration of Intramolecular Vibrational Redistribution by methyl Internal Rotation. A Chemical Timing Study of p-fluorotoluene and p-fluorotoluene-d3.
PB95-202982 *01,039*

MOLECULAR WEIGHT

Adsorption of Low-Molecular-Weight Sodium Polyacrylate on Hydroxyapatite.
PB94-172608 *00,139*

Effects of Molecular Weight and Thermal Stability on Polymer Gasification.
PB94-212610 *01,228*

Determination of the Weight Average Molecular Weight of Two Poly(Ethylene Oxides), SRM 1923 and SRM 1924.
PB94-217031 *01,230*

Molecular Weight Dependence of the Lamellar Domain Spacing of ABC Triblock Copolymers and Their Chain Conformation in Lamellar Domains.
PB95-161691 *01,254*

MOLECULE COLLISIONS

Energy Dependence of Collision Characteristics in Molecule-Surface Collisions.
PB94-198504 *00,786*

MOLECULE-MOLECULE COLLISIONS

Excitation Transfer in Barium by Collisions with Noble Gases.
PB96-200274 *01,163*

MOLYBDENUM

Texture Study of Two Molybdenum Shaped Charge Liners by Neutron Diffraction.
PB94-200177 *03,754*

Anomalous Odd- to Even-Mass Isotope Ratios in Resonance Ionization with Broad-Band Lasers.
PB94-211406 *03,839*

Analytical Method of Determining the Heat Capacity at High Temperatures from the Surface Temperature of a Cooling Sphere.
PB94-216124 *03,865*

Use of Sum Rules on the Energy-Loss Function for the Evaluation of Experimental Optical Data.
PB95-150736 *04,264*

Dynamic Technique for Measuring Normal Spectral Emissivity of Electrically Conducting Solids at High Temperatures with a High-Speed Spatial Scanning Pyrometer.
PB95-153045 *03,921*

Interfaces in Mo/Si Multilayers.
PB96-160668 *02,423*

MOLYBDENUM DISILICIDE

Creep Rupture of MoSi2/SiCp Composites.
PB95-152294 *03,154*

MOLYBDENUM DISULFIDE

Wear of Selected Materials and Composites Sliding against MoS2 Films.
PB94-172749 *03,231*

MOLYBDENUM-LANTHANUM

Atomic Energy Levels. As Derived From the Analyses of Optical Spectra. Volume 3.
AD-A280 279/1 *00,714*

MOLYBDENUM TO LANTHANUM

Ultraviolet Multiplet Table. Finding List for Spectra of the Elements Molybdenum to Lanthanum (Z = 42 to 57); Hafnium to Radium (Z = 72 to 88).
AD-A278 131/8 *00,709*

MOMENT PROBLEM

Distribution of Dielectric Relaxation Times and the Moment Problem.
PB96-112032 *04,727*

MONITORING

Through-the-Arc Sensing for Monitoring Arc Welding.
PB94-185899 *02,858*

Review of Cure Monitoring Techniques for On-Line Process Control.
PB94-216728 *03,145*

Guidance of the Legality of Keystroke Monitoring.
PB96-161237 *00,005*

Manager's Guide for Monitoring Data Integrity in Financial Systems.
PB96-165915 *00,003*

MONITORS

Monitoring Polymer Cure by Fluorescence Recovery After Photobleaching.
PB94-211422 *01,218*

MONOCHROMATOR

Soft X-ray Reflectometry Program at the National Institute of Standards and Technology.
PB96-160395 *04,368*

MONOCHROMATORS

Simple Variable Line Space Grating Monochromator for Synchrotron Light Source Beamlines.
PB96-156203 *04,065*

MONOLITHIC MICROWAVE INTEGRATED CIRCUITS

Microwave Characterization of Flip-Chip MMIC Components.
PB96-176722 *02,434*

Microwave Characterization of Flip-Chip MMIC Interconnections.
PB96-176730 *02,435*

Electrical Measurements of Microwave Flip-Chip Interconnections.
PB96-176748 *02,436*

MONOMERIZATION

DnaJ, DnaK, and GrpE Heat Shock Proteins are Required in 'ori'P1 DNA Replication Solely at the RepA Monomerization Step.
PB97-119382 *03,557*

MONOMERS

Neutron Reflectivity of End-Grafted Polymers: Concentration and Solvent Quality Dependence in Equilibrium Conditions.
PB94-185758 *01,206*

Modified Surface-Active Monomers for Adhesive Bonding to Dentin.
PB95-151163 *00,158*

Ring-Opening Dental Resin Systems Based on Cyclic Acetals.
PB95-162251 *00,162*

Synthesis and Polymerization of Difunctional and Multifunctional Monomers Capable of Cyclopolymerization.
PB95-163044 *01,257*

Evaluation of Methylene Lactone Monomers in Dental Resins.
PB95-164661 *00,164*

Ring-Opening Polymerication of a 2-Methylene Spiro Orthocarbonate Bearing a Pendant Methacrylate Group.
PB95-176145 *01,268*

MONOMOLECULAR FILMS

Silver Metalization of Octadecanethiol Monolayers Self-Assembled on Gold.
PB95-150744 *00,923*

UV-Photopatterning of Alkylthiolate Monolayers Self-Assembled on Gold and Silver.
PB95-150751 *C ,924*

Surface Geometry of BaO on W(100): A Surface-Extended X-Ray-Absorption Fine-Structure Study.
PB95-164414 *00,980*

Characterization of Cytochrome c/Alkanethiolate Structures Prepared by Self-Assembly on Gold.
PB95-164638 *00,987*

MONOPOLE ANTENNAS

Correction Factor for Nonplanar Incident Field in Monopole Calibrations.
PB95-108643 *02,002*

MONOTECTIC ALLOYS

Surface Energy Reduction in Fibrous Monotectic Structures.
PB95-140828 *03,150*

MONSEL-I COMPUTER CODE

MONSEL-II: Monte Carlo Simulation of SEM Signals for Linewidth Metrology.
PB96-102710 *02,379*

MONTE CARLO

Monte Carlo Simulation of Scanning Electron Microscope Signals.
PB96-200969 *02,444*

MONTE CARLO METHOD

Monte Carlo and Mean-Field Calculations of the Magnetocaloric Effect of Ferromagnetically Interacting Clusters.
PB94-172087 *03,201*

Effects of Variable Excluded Volume on the Dimensions of Off-Lattice Polymer Chains.
PB94-212941 *01,229*

Monte Carlo Electron Trajectory Simulation of X-Ray Emission from Films Supported on Substrates.
PB95-107207 *04,522*

Faster BKL Monte Carlo Simulations.
PB95-136370 *01,706*

Quantitative Measure of Efficiency of Monte Carlo Simulations.
PB95-180691 *01,011*

Faster Monte Carlo Simulations.
PB96-102074 *04,018*

Monte Carlo and Analytic Methods in the Transport of Electrons, Neutrons, and Alpha Particles.
PB96-111612 *04,033*

Parallel Monte Carlo Simulation of MBE Growth.
PB96-122841 *02,406*

Tree-Lookup for Partial Sums Or: How Can I Find This Stuff Quickly.
PB96-179411 *01,770*

MOONEY-RIVLIN EQUATION

Effect of Swelling on the Elasticity of Rubber: Localization Model Description.
PB94-211034 *01,216*

MORPHINE

Certification of Morphine and Codeine in a Human Urine Standard Reference Material.
PB95-176160 *03,499*

MORPHOLOGY
Shear-Excited Morphological States in a Triblock Copolymer.
PB94-172392 *01,196*

Temperature Dependence of the Morphology of Thin Diblock Copolymer Films as Revealed by Neutron Reflectivity.
PB94-172756 *01,199*

Morphology of Symmetric Diblock Copolymers as Revealed by Neutron Reflectivity.
PB95-140075 *01,234*

Morphological Estimation of Tip Geometry for Scanned Probe Microscopy.
PB95-203444 *02,662*

MORTALITY
Histopathology, Blood Chemistry, and Physiological Status of Normal and Moribund Striped Bass ('Morone saxatilis') Involved in Summer Mortality ('Die-Off') in the Sacramento-San Joaquin Delta of California.
PB94-198157 *00,034*

MORTARS (MATERIAL)
Water Permeability and Chloride Ion Diffusion in Portland Cement Mortars: Relationship to Sand Content and Critical Pore Diameter.
PB96-148036 *03,193*

MORTARS (MATERIALS)
Microstructural Features of Some Low Water/Solids, Silica Fume Mortars Cured at Different Temperatures.
PB94-160777 *00,330*

Interfacial Transport in Porous Media: Application to dc Electrical Conductivity of Mortars.
PB96-146816 *01,326*

MOS CAPACITORS
Development and Characterization of Insulating Layers on Silicon Carbide: Annual Report for February 14, 1988 to February 14, 1989.
PB94-155579 *02,295*

MOS GATE OXIDES
Assessing MOS Gate Oxide Reliability on Wafer Level with Ramped/Constant Voltage and Current Stress.
PB96-180112 *04,115*

MOSAIC
Approaches Using Virtual Environments with Mosaic.
PB95-169108 *01,599*

MOSAIC COMPUTER PROGRAM
Getting Started on Mosaic.
PB95-180360 *01,721*

MOSAIC SOFTWARE PACKAGE
World Wide Web and Mosaic: User's Guide.
PB94-207354 *02,722*

MOSFET
Numerical Simulation of Submicron Photolithographic Processing.
PB94-198561 *02,310*

Anomalous Behavior of a Quantized Hall Plateau in a High-Mobility Si Metal-Oxide-Semiconductor Field-Effect Transistor.
PB95-164174 *02,354*

MOTARS
Percolation and Pore Structure in Mortars and Concrete.
PB95-150439 *00,370*

MOTION
Adaptive, Predictive 2-D Feature Tracking Algorithm for Finding the Focus of Expansion.
PB94-218575 *01,588*

Three Dimensional Position Determination from Motion.
PB95-107108 *01,788*

Motion-Model-Based Boundary Extraction.
PB95-189502 *01,849*

MOTION SIMULATORS
Integration of Servo Control into a Large-Scale Control System Design: An Example from Coal Mining.
PB94-203429 *03,696*

Continuous Mining Machine Control Using the Real-Time Control System.
PB94-203528 *03,700*

Environment Simulation for a Continuous Mining Machine.
PB94-203536 *03,697*

MOUTHWASHES
Deposition of Loosely Bound and Firmly Bound Fluorides on Tooth Enamel by an Acidic Gel Containing Fluorosilicate and Monocalcium Phosphate Monohydrate.
PB95-150710 *03,559*

Interaction of Chlorhexidine Digluconate with and Adsorption of Chlorhexidine on Hydroxyapatite.
PB95-175907 *03,566*

MPI (MESSAGE-PASSING INTERFACE)
Experience with MPI: 'Converting Pvmmake to Mpimake under LAM' and 'MPI and Parallel Genetic Programming'.
PB96-141296 *01,748*

MRSEVS (MATERIAL REMOVAL SHAPE ELEMENT VOLUMES)
Issues Concerning Material Removal Shape Element Volumes (MRSEVs).
PB94-185493 *02,882*

MSEL
Materials Science and Engineering Laboratory Annual Report, 1993. NAS-NRC Assessment Panel, April 21-22, 1994.
PB94-162534 *02,969*

MSEL (MATERIALS SCIENCE AND ENGINEERING LABORATORY)
Materials Science and Engineering Laboratory Annual Report, 1994. NAS-NRC Assessment Panel, April 6-7, 1995.
PB95-196697 *02,976*

Materials Science and Engineering Laboratory Annual Report, 1995. Technical Activities.
PB96-214754 *03,009*

MULLITE
Crystal Structure and Compressibility of 3:2 Mullite.
PB95-175030 *03,682*

MULTI-ELEMENT ANALYSIS
Interpreting the Readings of Multi-Element Personnel Dosimeters in Terms of the Personal Dose Equivalent.
PB95-175428 *03,631*

MULTI-PHOTON PROCESSES
Resonance Enhanced Multiphoton Ionization Spectroscopy of the SnF Radical.
PB97-111223 *01,176*

MULTI-ZONE AIR FLOW
CONTAM88 Building Input Files for Multi-Zone Airflow and Contaminant Dispersal Modeling.
PB94-194388 *02,537*

MULTICHARGED IONS
Evaluation of Two-Photon Exchange Graphs for Highly-Charged Heliumlike Ions.
PB94-198918 *03,808*

Experimental Aspects and Z-Dependent Systematics in One- and Two-Electron Ions and Single Vacancy Systems.
PB94-199627 *03,815*

Relativistic and Quantum Electrodynamic Effects in Highly-Charged Ions.
PB94-212784 *03,854*

Atomic Branching Ratio Data for Carbon-Like Ions.
PB94-212842 *03,855*

Spectroscopic Data Tables for Highly-Ionized Atoms.
PB95-151585 *03,910*

Collisions of Electrons with Highly-Charged Ions.
PB96-200340 *04,791*

MULTICHIP MODULES
Wire Bonding to Multichip Modules and Other Soft Substrates.
PB96-123583 *02,079*

Wire Bonding to Multichip Modules and Other Soft Substrates.
PB96-135207 *02,082*

MULTICRITERIA
Development and Validation of Multicriteria Ratings: A Case Study.
PB95-126025 *00,004*

MULTIDIMENSIONAL SYSTEMS
Dynamics of Multi-DOF Stochastic Nonlinear Systems.
PB97-113245 *00,477*

MULTIJUNCTION THERMAL CONVERTERS
Development of Thin-Film Multijunction Thermal Converters at NIST.
PB97-112338 *02,286*

MULTIKRON II
Operating Principles of MultiKron II Performance Instrumentation for MIMD Computers.
PB95-189486 *01,628*

MULTILATERAL AGREEMENTS
GATT Standards Code Activities of the National Institute of Standards and Technology 1994.
PB96-106935 *00,497*

TBT Agreement Activities of the National Institute of Standards and Technology, 1995.
PB97-104178 *00,499*

MULTILAYER FILMS
Modeling Effects of Temperature Annealing on Giant Magnetoresistive Response in Discontinuous Multilayer NiFe/Ag Films.
PB97-112585 *04,157*

MULTILAYERS
Fracture in Multilayers.
PB96-163613 *02,988*

MULTIMEDIA
Porting Multimedia Applications to the Open System Environment.
PB94-172921 *02,721*

Preliminary Functional Specifications of a Prototype Electronic Research Notebook for NIST.
PB94-207750 *00,012*

Multimedia Tutorial on Phase Equilibria Diagrams.
PB96-200829 *03,088*

MULTIPATH TRANSMISSION
Analytical Estimation of Carrier Multipath Bias on GPS Position Measurements.
PB94-215712 *04,845*

MULTIPHOTON
Resonance Enhanced Multiphoton Ionization Spectroscopy of the PF Radical.
PB97-119119 *00,702*

MULTIPHOTON IONIZATION
Femtosecond Time-Resolved Wave Packet Motion in Molecular Multiphoton Ionization and Fragmentation.
PB94-198611 *00,790*

Electronic Spectra of CF2Cl and CFCl2 Radicals Observed by Resonance Enhanced Multiphoton Ionization.
PB95-151023 *00,927*

Femtosecond Time-Resolved Molecular Multiphoton Ionization: The Na2 System.
PB95-202305 *03,975*

Population Trapping in Short-Pulse Multiphoton Ionization.
PB96-164140 *04,371*

Resonance Enhanced Multiphoton Ionization Spectroscopy of the SnF Radical.
PB97-111223 *01,176*

MULTIPLE AUTONOMOUS UNDERSEA VEHICLES PROJECT
Intelligent Control for Multiple Autonomous Undersea Vehicles.
PB94-211877 *03,747*

MULTIPLE-INSTRUCTION MULTIPLE-DATA
Time-Perturbation Tuning of MIMD Programs.
PB94-164399 *01,681*

Time-Perturbation Tuning of MIMD Programs.
PB94-172566 *01,684*

Using Synthetic-Perturbation Techniques for Tuning Shared Memory Programs (Extended Abstract).
PB94-172657 *01,685*

Synthetic-Perturbation Tuning of MIMD Programs.
PB94-185568 *01,687*

MULTIPLE REFLECTION THEORY
Observation of the Transverse Second Harmonic Magneto-Optic Kerr Effect from Ni81Fe19 Thin Film Structures.
PB96-200332 *01,971*

MULTIPLE SCATTERING
Study of Multiple Scattering Background in Compton Scatter Imaging.
PB96-112222 *04,425*

MULTIPLET STRUCTURES
Charge-Transfer-Induced Multiplet Structure in the N4,5O2,3 Soft-X-ray Emission Spectrum of Lanthanum.
PB96-163746 *04,102*

MULTIPLET TABLE
Ultraviolet Multiplet Table. Finding List for Spectra of the Elements Molybdenum to Lanthanum (Z = 42 to 57); Hafnium to Radium (Z = 72 to 88).
AD-A278 131/8 *00,709*

Ultraviolet Multiplet Table.
AD-A278 446/0 *00,710*

MULTIPOINT COMMUNICATION
Strategy to Support Multipoint Communication Service Over Native ATM Service.
PB96-176672 *01,507*

MULTIPOLE EXCITATION
High-Order Multipole Excitation of a Bound Electron.
PB96-119789 *04,044*

MULTIPROCESSORS
Operating Principles of MultiKron Virtual Counter Performance Instrumentation for MIMD Computers.
PB96-131529 *01,632*

MULTIRANGE INSTRUMENTS
Modeling and Test Point Selection for a Thermal Transfer Standard.
PB95-161287 *01,896*

MULTIVARIATE DISTRIBUTIONS
Principal Points and Self-Consistent Points of Symmetric Multivariate Distributions.
PB96-135090 *03,446*

MULTIWAVE MIXING
Optical Sampling Using Nondegenerate Four-Wave Mixing in a Semiconductor Laser Amplifier.
PB96-123609 *04,348*

MULTIZONE ANALYSIS
Multizone Modeling of Three Residential Indoor Air Quality Control Options.
PB96-165782 *02,567*

MUMPS PROGRAMMING LANGUAGE
M (also known as MUMPS) Validation Test Suite, Version 8.3 (for Microcomputers).
PB94-502077 *01,699*

MUNICIPAL WASTES
Assessing the Credibility of the Calorific Content of Muncipal Solid Waste.
PB94-199882 *02,581*

MUON-CATALYZED FUSION
Comprehensive Theory of Nuclear Effects on the Intrinsic Sticking Probability. 1.
PB94-200623 *03,832*

Comprehensive Theory of Nuclear Effects on the Intrinsic Sticking Probability. 2.
PB94-200631 *03,833*

MUON SPIN ROTATIONS
Dynamics of Mu(+) in Sc and ScHx.
PB96-180021 *04,112*

MUTAGENESIS
Novel DNA N-Glycosylase Activity of E. coli T4 Endonuclease V That Excises 4,6-Diamino-5-Formamidopyrimidine from DNA, a UV-Radiation- and Hydroxyl Radical-Induced Product of Adenine.
PB96-160478 *03,549*

Pore-Forming Protein with a Metal-Actuated Switch.
PB96-176557 03,554

MUTAGENS
Tert-Butyl Hydroperoxide-Mediated DNA Base Damage in Cultured Mammalian Cells.
PB94-182003 03,644

Copper Ion-Mediated Modification of Bases in DNA in Vitro by Benzoyl Peroxide.
PB94-198231 03,645

Oxidative DNA Base Damage in Renal, Hepatic, and Pulmonary Chromatin of Rats After Intraperitoneal Injection of Cobalt (II) Acetate.
PB95-150025 03,647

MUTATION
Ionizing Radiation Causes Greater DNA Base Damage in Radiation-Sensitive Mutant M10 Cells That in Parent Mouse Lymphoma L5178Y Cells.
PB95-175915 03,632

N-GAS MODEL
Further Development of the N-Gas Mathematical Model: An Approach for Predicting the Toxic Potency of Complex Combustion Mixtures.
PB96-123260 03,650

N-HEXANE
Enhancement of R123 Pool Boiling by the Addition of N-Hexane.
PB96-165956 02,605

NACELLES
Flow of Alternative Agents in Piping.
PB95-202420 00,022

NANOANALYSIS
Microanalysis to Nanoanalysis: Measuring Composition at High Spatial Resolution.
PB95-107173 00,563

NANOCOMPOSITES
In situ Characterization of Vapor Phase Growth of Iron Oxide-Silica Nanocomposites: Part 1. 2-D Planar Laser-Induced Fluorescence and Mie Imaging.
PB97-112478 03,185

NANOCRYSTALLINE CERAMIC
Bulk Modulus and Young's Modulus of Nanocrystalline gamma-Alumina.
PB96-204185 03,092

NANOCRYSTALLINE MATERIALS
Small Angle Neutrons Scattering from Nanocrystalline Palladium as a Function of Annealing.
PB95-176103 03,354

Inelastic Neutron Scattering Study of Hydrogen in Nanocrystalline Pd.
PB96-146857 03,366

NANOCRYSTALS
Vibrational Excitations and the Position of Hydrogen in Nanocrystalline Palladium.
PB96-111828 04,035

NANOELECTRONICS
Integration of Scanning Tunneling Microscope Nanolithography and Electronics Device Processing.
PB95-153359 02,341

NANOHARDNESS
Force Calibrations in the Nanonewton Regime.
PB95-168696 03,949

NANOLITHOGRAPHY
Integration of Scanning Tunneling Microscope Nanolithography and Electronics Device Processing.
PB95-153359 02,341

NANOMATERIALS
Viewpoint: Nanocrystalline and Nanophase Materials.
PB94-185865 04,454

NIST Workshop on Nanostructured Material (1st): Report of an Industrial Workshop Conducted by the National Institute of Standards and Technology. Held in Gaithersburg, Maryland on May 14-15, 1992.
PB94-218567 02,973

X-ray Powder Diffraction from Carbon Nanotubes and Nanoparticles.
PB96-102975 03,064

NANOPARTICULATES
Growth and Nucleation of Hydrogenated Amorphous Silicon on Silicon (100) Surfaces.
PB96-176516 02,991

NANOSCALE PORES
Vitrification and Crystallization of Organic Liquids Confined to Nanoscale Pores.
PB97-112304 03,392

NANOSTRUCTURE
NIST Metrology for Soft X-ray Multilayer Optics.
PB96-160379 04,088

Nanostructure Fabrication via Laser-Focused Atomic Deposition (Invited).
PB96-204094 04,132

NANOSTRUCTURES
NIST Workshop on Nanostructured Material (1st): Report of an Industrial Workshop Conducted by the National Institute of Standards and Technology. Held in Gaithersburg, Maryland on May 14-15, 1992.
PB94-218567 02,973

Nanostructure Fabrication via Direct Writing with Atoms Focused in Laser Fields.
PB95-150272 04,564

Laser-Focused Atomic Deposition.
PB95-161618 04,604

Laser Focused Atomic Deposition.
PB95-180659 04,685

Construction of Silicon Nanocolumns with the Scanning Tunneling Microscope.
PB95-203063 04,696

Using Atom Optics to Fabricate Nanostructures.
PB96-141247 04,757

Excitons in Complex Quantum Nanostructures.
PB97-118343 01,184

NAPHTHALENE
Investigating the 3.3 Micron Infrared Fluorescence from Naphthalene Following Ultraviolet Excitation.
N95-15839/0 00,724

NASA STANDARD REFERENCE MODEL
Hierarchical Ada Robot Programming System (HARPS): A Complete and Working Telerobot Control System Based on the NASREM Model.
PB94-213162 02,934

NASREM (NASA STANDARD REFERENCE MODEL)
Hierarchical Ada Robot Programming System (HARPS): A Complete and Working Telerobot Control System Based on the NASREM Model.
PB94-213162 02,934

NATIONAL ARCHIVES AND RECORDS
Electronic Access: Blueprint for the National Archives and Records Administration.
PB95-219218 02,731

NATIONAL ARCHIVES AND RECORDS ADMINISTRATION
User Study: Informational Needs of Remote National Archives and Records Administration Customers.
PB95-154738 02,725

NATIONAL BUREAU OF STANDARDS
Standard Materials. A Descriptive List with Prices.
AD-A278 140/9 00,500

NATIONAL GOVERNMENT
Self Monitoring Accounting Systems.
PB95-216602 00,007

NATIONAL INFORMATION INFRASTRUCTURE
Information Infrastructure: Reaching Society's Goals. A Report of the Information Infrastructure Task Force Committee on Applications and Technology.
ED-376 823 00,131

Information Infrastructure: Reaching Society's Goals. Report of the Information Infrastructure Task Force Committee on Applications and Technology.
PB94-214756 01,469

Report on the Workshop on Advanced Digital Video in the National Information Infrastructure. Held in Washington, D.C. on May 10-11, 1994.
PB95-103677 01,472

Framework for National Information Infrastructure Services.
PB95-103719 02,723

Information Technology Engineering and Measurement Model: Adding Lane Markings to the Information Superhighway.
PB95-143145 01,474

Standards Policy and Information Infrastructure.
PB95-231882 01,485

Electronic Access to Standards on the Information Highway.
PB96-131578 01,494

NATIONAL INSTITUTE FOR STANDARDS AND TECHNOLOGY
Publications of the National Institute of Standards and Technology 1992 Catalog.
PB95-200747 00,014

NATIONAL INSTITUTE OF STANDARDS AND TECHNOLOGY
Abstract and Index Collection in the Research Information Center of the National Institute of Standards and Technology.
PB94-152204 02,744

Ceramics Technical Activities, 1993 (NAS-NRC Assessment Panel April 21-22, 1994).
PB94-162591 03,031

NIST Support to the Next Generation Controller Program: 1991 Final Technical Report.
PB94-163490 02,808

NIST Serial Holdings, 1994.
PB94-178068 02,745

Study of Federal Agency Needs for Information Technology Security.
PB94-193653 01,579

Graphical Analysis of the CCRL Portland Cement Proficiency Sample Database (Samples 1-72). (Part 1. Univariant Analysis of Portland Cement).
PB94-196557 01,308

National Voluntary Laboratory Accreditation Program 1995 Directory.
PB95-174454 00,483

Abstract and Index Collection in the Research Information Center of the National Institute of Standards and Technology.
PB95-232633 02,741

Electronics and Electrical Engineering Laboratory Technical Publication Announcements Covering Laboratory Programs, April to June 1995 with 1995 EEEL Events Calendar.
PB96-137187 01,941

Publications of the National Institute of Standards and Technology 1993 Catalog.
PB96-183215 00,017

Proposed Coating Technology Consortium. (National Coil Coaters Association Fall Conference). Held in Rosemont, Illinois in September 1992.
PB97-110431 03,129

NATIONAL INSTITUTE OF STANDARDS AND TECHNOLOGY (NIST)
Journal of Research of the National Institute of Standards and Technology, March/April 1995. Volume 100, Number 2.
PB96-126180 04,349

NATIONAL INSTITUTE OF STANDARDS AND TECHNOLOGY PRODUCT TESTING
National Voluntary Laboratory Accreditation Program 1996 Directory.
PB96-162714 00,485

NATIONAL INTERESTS
Putting the Information Infrastructure to Work: Report of the Information Infrastructure Task Force Committee on Applications and Technology.
PB94-163383 00,001

White Papers Prepared for the White House: Construction Industry Workshop on National Construction Goals. Held on December 14-16, 1994.
PB95-216891 01,299

NATIONAL MARINE MAMMAL TISSUE BANK
Development of the National Marine Mammal Tissue Bank.
PB95-161402 02,586

NATIONAL SECURITY
Impact of the FCC's Open Network Architecture on NS/NP Telecommunications Security.
PB95-189445 01,483

NATIONAL TYPE EVALUATION PROGRAM
National Type Evaluation Program: Index of Device Evaluations by Company. NCWM Publication 5 Part A (Second Edition).
PB94-160835 02,889

NATIONAL VOLUNTARY ACCREDITATION PROGRAM
Proficiency Tests for the NIST Airborne Asbestos Program, 1990.
PB94-188836 00,535

National Voluntary Laboratory Accreditation Program 1995 Directory.
PB95-174454 00,483

NATIONAL VOLUNTARY LABORATORY ACCREDITATION PROGRAM
NVLAP Procedures U.S. Code of Federal Regulations. Title 15, Subtitle A, Chapter 2, Part 7. (Effective December 1984; Amended September 1990).
PB94-160850 02,627

National Voluntary Laboratory Accreditation Program: Procedures and General Requirements.
PB94-178225 02,630

National Voluntary Laboratory Accreditation Program 1994 Directory.
PB94-178969 00,482

National Voluntary Laboratory Accreditation Program: Energy Efficient Lighting Products.
PB94-219060 02,642

National Voluntary Laboratory Accreditation Program: Ionizing Radiation Dosimetry.
PB95-128658 03,623

National Voluntary Laboratory Accreditation Program: POSIX. Portable Operating System Interface.
PB95-189478 02,661

Airborne Asbestos Analysis: National Voluntary Laboratory Accreditation Program.
PB96-147392 02,566

NATIONAL VOLUNTARY LABORATORY ACCREDITION PROGRAM (NVLAP)
National Voluntary Laboratory Accreditation Program 1996 Directory.
PB96-162714 00,485

NATURAL CONVECTION
Review of Flows Driven By Natural Convection in Adiabatic Shafts.
PB96-147897 01,416

Natural Convection from an Array of Electronic Packages Mounted on a Horizontal Board in a Narrow Aspect Ratio Enclosure.
PB96-164017 02,087

NATURAL EMISSIONS
Radiocarbon Measurements of Atmospheric Volatile Organic Compounds: Quantifying the Biogenic Contribution.
PB97-122352 02,574

NATURAL GAS
Low Temperature H(sub 2)S Separation Using Membrane Reactor with Redox Catalyst.
DE94008991 02,471

Thermophysical Properties of Fluids for the Gas Industry. Final Report, February 1, 1988-August 31, 1993.
PB94-146677 02,472

Constituents and Physical Properties of the C6+ Fraction of Natural Gas. Topical Report, April-June 1994.
PB95-136644 02,483

Sliding Vane Flow Conditioner Tests in a 100 Diameter Long 10 inch Natural Gas Orifice Meter at Pacific Gas and Electric. Topical Report, 1990-1992.
PB95-256335 *02,493*

Thermophysical Properties of Fluids for the Gas Industry.
PB96-122437 *02,494*

Development of Gas Standards from Solid 1,4-dichlorobenzene.
PB96-155486 *02,496*

NATURAL GAS LIQUIDS
New Data and Correlations for the Custody Transfer of Natural Gas Liquids.
PB96-176664 *02,499*

NATURAL GAS PIPELINES
Assessment of Technology for Detection of Stress Corrosion Cracking in Gas Pipelines. Final Report, July 1993-March 1994.
PB94-206646 *02,475*

NATURAL GAS WELLS
Investigation of Oil and Gas Well Fires and Flares.
PB94-193976 *03,695*

Development of Hazard Assessment and Suppression Technology for Oil and Gas Well Blowout and Diverter Fires.
PB96-122965 *01,408*

NATURAL LANGUAGE PROCESSING
Bringing Natural Language Information Retrieval Out of the Closet.
PB94-172335 *02,720*

Lab Report Special Section: Natural Language Processing and Information Retrieval Group Information Access and User Interfaces Division, National Institute of Standards and Technology.
PB97-118665 *02,742*

NATURAL RUBBER
Localization Model of Rubber Elasticity: Comparison with Torsional Data for Natural Rubber Networks in the Dry State.
PB95-107033 *03,195*

NAVAL VESSELS
Characterization of the Hydrogen Induced Cold Cracking Susceptibility at Simulated Weld Zones in HSLA-100 Steel.
PB94-174505 *03,746*

Optical Fiber Sensors: Accelerating Applications in Navy Ships.
PB94-186848 *02,632*

NAVIGATION SATELLITES
Preliminary Comparison of Time Transfers via LASSO, GPS and Two-Way Satellite.
PB95-151098 *01,529*

NAVY
NIST and the Navy: Past, Present and Future.
PB96-119649 *03,655*

NBSR REACTOR
NIST Reactor: Summary of Activities October 1992 through September 1993.
PB94-161502 *04,437*

Thermal Hydraulic Tests of a Liquid Hydrogen Cold Neutron Source.
PB95-135570 *03,884*

Liquid-Hydrogen Cold Neutron Source for the NBSR.
PB95-151619 *03,729*

Nuclear Heat Load Calculations for the NBSR Cold Neutron Source Using MCNP.
PB95-152955 *03,730*

Cold Neutron Gain Calculations for the NBSR Using MCNP.
PB95-163978 *03,731*

NIST Reactor: Summary of Activities, October 1993 through September 1994.
PB95-220430 *04,700*

MCNP Model of the National Bureau of Standards Reactor (NBSR) Core.
PB96-138599 *03,733*

NCS1 SYSTEM
Journal of Research of the National Institute of Standards and Technology. January/February 1994. Volume 99, Number 1.
PB94-169737 *02,019*

Null-Balanced Total-Power Radiometer System NCS1.
PB94-169778 *02,021*

Derivation of the System Equation for Null-Balanced Total-Power Radiometer System NCS1.
PB94-169786 *02,022*

Evaluation of Uncertainties of the Null-Balanced Total-Power Radiometer System NCS1.
PB94-169794 *02,023*

NEAR-AZEOTROPES
Role of Refrigerant Mixtures as Alternatives to CFCs.
PB94-199775 *03,252*

NEAR-CRITICAL DILUTE MIXTURE THEORY
Supercritical Solubility of Solids from Near-Critical Dilute-Mixture Theory.
PB94-211703 *00,819*

NEAR FIELD
Spherical-Wave Source-Scattering Matrix Analysis of Antennas and Antenna-Antenna Interactions.
PB96-111166 *02,008*

NEAR FIELDS
Development of Near-Field Test Procedures for Communication Satellite Antennas.
PB96-135082 *02,010*

NEAR INFRARED RADIATION
Infrared and Near-Infrared Spectra of HCC and DCC Trapped in Solid Neon.
AD-A295 578/9 *03,773*

High-Efficiency, High-Power Difference-Frequency Generation of 0.9-1.5 mu m Light in BBO.
PB95-202255 *04,317*

NEAR INFRARED SPECTROSCOPY
NIR-Spectroscopic Investigation of Water Sorption Characteristics of Dental Resins and Composites.
PB95-151171 *00,189*

NEIGHBOR TABLES
Neighbor Tables for Molecular Dynamics Simulations.
PB95-171948 *00,991*

NEODYMIUM BARIUM COPPER NIOBATES
Crystal Structure and Magnetic Ordering of the Rare-Earth and Cu Moments in RBa2Cu2NbO8(R=Nd,Pr).
PB95-140554 *04,546*

NEODYMIUM BARIUM TITANATES
Substitution-Induced Midgap States in the Mixed Oxides RxBa1-ChiTiO3-Delta, with R=Y, La, and Nd.
PB95-140505 *04,541*

NEODYMIUM CERIUM CUPRATES
Phonon Density of States in R2CuO4 and Superconducting R1.85Ce0.15CuO4 (R = Nd, Pr).
PB95-150686 *04,574*

NEODYMIUM CUPRATES
Phonon Density of States in R2CuO4 and Superconducting R1.85Ce0.15CuO4 (R = Nd, Pr).
PB95-150686 *04,574*

Field Dependence of the Magnetic Ordering of Cu in R2CuO4 (R = Nd, Sm).
PB95-164521 *04,633*

Observation of Noncollinear Magnetic Structure for the Cu Spins in Nd2CuO4-Type Systems.
PB95-164539 *04,634*

NEODYMIUM GALLATES
Dielectric Properties of Single Crystals of Al2O3, LaAlO3, SrTiO3, and MgO at Cryogenic Temperatures.
PB95-180477 *02,266*

NEODYMIUM IONS
Rb-Like Spectra: Pd X to Nd XXIV.
PB95-150645 *03,897*

NEODYMIUM LASERS
Integrated Optic Laser Emitting at 906, 1057, and 1358 nm.
PB94-216280 *02,135*

Integrated Optic Laser Emitting at 905, 1057, 1356 nm.
PB94-216298 *02,136*

Linewidth Narrowing in an Imbalanced Y-Branch Waveguide Laser.
PB95-140844 *04,258*

Nd:LiTaO3 Waveguide Laser.
PB95-140851 *04,259*

Passively Q-Switched Nd-Doped Waveguide Laser.
PB95-180048 *04,308*

NEON
Vibrational Spectra of Molecular Ions Isolated in Solid Neon. 7. CO(+), C2O2(+), and C2O2(-). (Reannouncement with New Availability Information).
AD-A239 729/7 *00,706*

Vibrational Spectra of Molecular Ions Isolated in Solid Neon: HCCH+ and HCC-. (Reannouncement with New Availability Information).
AD-A253 551/6 *00,707*

Vibrational Spectra of Molecular Ions Isolated in Solid Neon. 11. NO2(+), NO2(-), and NO3(-).
AD-A275 828/2 *00,708*

Infrared and Near-Infrared Spectra of HCC and DCC Trapped in Solid Neon.
AD-A295 578/9 *03,773*

Matrix Isolation Study of the Interaction of Excited Neon Atoms with BCl3: Infrared Spectra of BCl(sub 3, sup +), BCl(sub 2, sup +), and BCl(sub 3, sup -).
PB97-119143 *01,187*

NEON ATOMS
Matrix Isolation Study of the Interaction of Excited Neon Atoms with O3: Infrared Spectrum of O((sub 3)(-)) and Evidence for the Stabilization of O2...O((sub 4)(+)).
PB97-112403 *04,155*

NEON MATRICES
Vibrational Spectra of Molecular Ions Isolated in Solid Neon. 6. CO4(-). (Reannouncement with New Availability Information).
AD-A238 415/4 *00,705*

NEPHELOMETERS
Radiometric Model of the Transmission Cell-Reciprocal Nephelometer.
PB95-150132 *00,124*

NEPTUNIUM 237
Intercomparison Study of (237)Np Determination in Artificial Urine Samples.
PB96-102645 *03,633*

NETWORK ANALYSIS
Accuracy and Repeatability in Time Domain Network Analysis.
PB95-202644 *02,064*

Hardware Measurement Techniques for High-Speed Networks.
PB96-160551 *01,500*

NETWORK ANALYZERS
Multi-State Two-Port: An Alternative Transfer Standard.
PB95-168530 *02,049*

Time Domain Network Analysis Using the Multiline TRL Calibration.
PB95-202925 *02,065*

Two-Tier Multiline TRL for Calibration of Low-Cost Network Analyzers.
PB96-157888 *01,947*

NETWORK CONTROL
Context Analysis of the Network Management Domain. Conducted as Part of the Domain Analysis Case Study.
PB94-142528 *01,465*

NETWORK MANAGEMENT
Integrated Network Management.
PB94-199247 *01,583*

NETWORKS
Network Brokers Handbook: An Entrepreneurial Guide to Cooperative Strategies for Manufacturing Competitiveness.
PB95-219325 *00,490*

NEURAL NETS
Analysis of a Biologically Motivated Neural Network for Character Recognition.
PB94-172277 *00,182*

Prediction of Geometric-Thermal Machine Tool Errors by Artificial Neural Networks.
PB94-186673 *02,943*

Comparison of FFT Fingerprint Filtering Methods for Neural Network Classification.
PB95-136362 *01,840*

Self-Organizing Neural Network Character Recognition on a Massively Parallel Computer.
PB95-163994 *01,845*

Binary Decision Clustering for Neural Network Based Optical Character Recognition.
PB95-171971 *01,848*

Improving Neural Network Performance for Character and Fingerprint Classification by Altering Network Dynamics.
PB95-267803 *01,851*

Effect of Training Dynamics on Neural Network Performance.
PB95-267845 *01,852*

Improving Neural Network Performance for Character and Fingerprint Classification by Altering Network Dynamics.
PB96-123195 *01,856*

Binary Decision Clustering for Neural-Network-Based Optical Character Recognition.
PB96-186184 *01,857*

Fault Diagnosis of an Air-Handling Unit Using Artificial Neural Networks.
PB97-121321 *00,283*

NEURAL NETWORKS
Self-Organizing Neural Network Character Recognition Using Adaptive Filtering and Feature Extraction.
PB96-119797 *01,855*

Micromachined Display Output for a Cellular Neural Network.
PB96-156070 *02,422*

NEURON DIFFRACTION
Structure and Conductivity of Layered Oxides (Ba,Sr)n+1(Sn,Sb)nO3n+1.
PB96-102439 *04,707*

NEUTRON ACTIVATION ANALYSIS
Determination of Boron and Lithium in Diverse Biological Matrices Using Neutron Activation - Mass Spectrometry (NA-MS).
PB94-212289 *00,554*

High-Sensitivity Determination of Iodine Isotopic Ratios by Thermal and Fast Neutron Activation.
PB94-213386 *00,555*

Scattering and Absorption Effects in Neutron Beam Activation Analysis Experiments.
PB94-216140 *00,557*

Trace Elements Associated with Proteins. Neutron Activation Analysis Combined with Biological Isolation Techniques.
PB95-163101 *00,597*

Reactor Radiation Technical Activities, 1994. NAS-NRC Assessment Panel, April 6-7, 1995.
PB95-209888 *03,732*

Neutron Techniques in Materials Science and Related Disciplines.
PB96-119698 *02,980*

Determination of 21 Elements by INAA for Certification of SRM 1570a, Spinach.
PB96-167242 *00,698*

New NIST Rapid Pneumatic Tube System.
PB96-167259 *03,738*

Reactor Radiation Technical Activities, 1995.
PB96-193644 *03,741*

Unique Quality Assurance Aspects of INAA for Reference Material Homogeneity and Certification.
PB96-200811 *00,699*

NEUTRON BEAMS
Neutron Focusing Lens Using Polycapillary Fibers.
PB95-141206 *03,889*

Neutron Focusing Lens Using Polycapillary Fibers.
PB95-153078 *03,922*

Mass Assay and Uniformity Test of Boron Targets by Neutron Beam Methods.
PB97-119085 *04,175*

NEUTRON CAPTURE GAMMA RAYS
Grazing Incidence Prompt Gamma Emissions and Resonance-Enhanced Neutron Standing Waves in a Thin-Film.
PB95-150470 *03,892*

Use of Neutron Beams for Chemical Analysis at NIST.
PB97-112437 *00,652*

NEUTRON CROSS SECTIONS
Neutron Standard Cross Sections in Reactor Physics: Need and Status.
PB94-199510 *03,813*

Measurement of the (93)Nb(n,2n) (92m)Nb Cross Section in a (235)U Fission Spectrum.
PB95-163986 *03,945*

DETAN 95: Computer Code for Calculating Spectrum-Averaged Cross Sections and Detector Responses in Neutron Spectra.
PB95-242384 *04,014*

NEUTRON DECAY
Current Results and Future Prospects for a Neutron Lifetime Determination Using Trapped Protons.
PB94-199742 *03,817*

NEUTRON DEPTH PROFILING
Effect of Splitting on Estimation of Emission Rate Profiles from Neutron Depth Profiling Spectra.
PB95-152245 *03,916*

Modeling Detector Response for Neutron Depth Profiling.
PB96-157813 *04,066*

NEUTRON DIFFRACTION
Determination of the Residual Stresses Near the Ends of Skip Welds Using Neutron Diffraction and X-ray Diffraction Procedures.
PB95-253589 *02,868*

Characterization of the Structure of LaD2.50 by Neutron Powder Diffraction.
PB96-176797 *04,783*

Neutron Diffraction Texture Study of Deformed Uranium Plates.
PB97-111587 *03,010*

Colossal Magnetoresistance without Mn(3+)/Mn(4-) Double Exchange in the Stoichiometric Pyrochlore Tl2Mn2O7.
PB97-113070 *04,160*

NEUTRON DIFFRACTIONS
Determination of Anomalous Superexchange in MnCl2 and Its Graphite Intercalation Compound.
PB97-122568 *00,666*

NEUTRON DOSIMETRY
Measurement of Absorbed Dose of Neutrons, and of Mixtures of Neutrons and gamma rays.
AD-A286 647/3 *03,710*

Neutron Energy Deposition on the Nanometer Scale.
PB95-152260 *03,624*

NEUTRON ENERGY
Measurements of the (235)U(n,f) Cross Section in the 3 to 30 MeV Neutron Energy Region.
PB97-119051 *04,172*

NEUTRON FOCUSING
Neutron Focusing Lens Using Polycapillary Fibers.
PB95-141206 *03,889*

NEUTRON FOCUSING LENSES
Neutron Focusing Lens Using Polycapillary Fibers.
PB95-153078 *03,922*

NEUTRON GUIDES
Transmission Properties of Short Curved Neutron Guides. Part 1. Acceptance Diagram Analysis and Calculations.
PB96-102199 *04,021*

Analytical Applications of Guided Neutron Beams.
PB96-112347 *04,041*

NEUTRON INTERFEROMETRY
Multi-Stage, Position Stabilized Vibration Isolation System for Neutron Interferometry.
PB95-175022 *03,955*

NEUTRON LEAKAGE
Neutron Leakage Benchmark for Criticality Safety Research.
PB95-126132 *03,723*

NEUTRON LIFETIME
Current Results and Future Prospects for a Neutron Lifetime Determination Using Trapped Protons.
PB94-199742 *03,817*

Preparation and Characterization of (6)LiF and (10)B Reference Deposits for the Measurement of the Neutron Lifetime.
PB95-108692 *03,874*

NEUTRON MEASUREMENT
Neutron Measurement Intercomparisons Sponsored by CCEMRI, Section 3 (Neutron Measurements).
PB94-199916 *03,819*

NEUTRON MONOCHROMATORS
Acceptance Diagram Analysis of the Performance of Vertically Curved Neutron Monochromators.
PB94-200425 *03,827*

NEUTRON PHYSICS
Some Aspects of Fundamental Neutron Physics.
PB95-126298 *03,882*

NEUTRON POLARIZERS
Supermirror Transmission Polarizers for Neutrons.
PB94-216215 *03,866*

NEUTRON RADIOGRAPHY
Protection Against Neutron Radiation Up to 30 Million Electron Volts.
AD-A286 681/2 *03,611*

NEUTRON REACTIONS
Intermediate Structure in the Neutron-Induced Fission Cross Section of 236U.
PB94-185741 *03,802*

Neutron Standard Cross Sections in Reactor Physics: Need and Status.
PB94-199510 *03,813*

Measurement of the (235)U(n,f) Reaction from Thermal to 1 keV.
PB95-140422 *03,886*

Preparation of 2-Dimensional Ultra Thin Polystyrene Film by Water Casting Method.
PB95-162806 *04,619*

Measurement of the (93)Nb(n,2n) (92m)Nb Cross Section in a (235)U Fission Spectrum.
PB95-163986 *03,945*

NEUTRON REFLECTION
Analytic Calculation of Polarized Neutron Reflectivity from Superconductors.
PB95-164224 *04,629*

Simulations of Neutron Focusing with Curved Mirrors.
PB96-176649 *02,200*

NEUTRON REFLECTIVITY
Neutron Reflectivity Study of the Density Profile of a Model End-Grafted Polymer Brush: Influence of Solvent Quality.
PB95-202735 *01,274*

Extending the Angular Range of Neutron Reflectivity Measurements from Planar Lipid Bilayers: Applications to a Model Biological Membrane.
PB96-122569 *03,476*

Magnetic Structure Determination for Annealed Ni80Fe20/Ag Multilayers Using Polarized-Neutron Reflectivity.
PB96-176615 *03,739*

Compatibilization of Polymer Blends by Complexation. 2. Kinetics of Interfacial Mixing.
PB97-111900 *01,295*

NEUTRON SCATTERING
Small-Angle Neutron Scattering Characterization of Processing/Microstructure Relationships in the Sintering of Crystalline and Glassy Ceramics. (Reannouncement with New Availability Information).
AD-A249 510/9 *03,025*

Neutron Scattering Study of Shear Induced Turbidity in Polystyrene/Dioctyl Phthalate Solutions at High Shear Rates.
PB94-172624 *01,197*

Time Dependent Small Angle Neutron Scattering Behavior in Triblock Copolymers Under Steady Shear.
PB94-172632 *01,198*

Neutron Scattering by Multiblock Copolymers of Structure (A-B)N-A.
PB94-211547 *01,219*

Small-Angle X-Ray and Neutron Scattering Study of Block Copolymer/Homopolymer Mixtures.
PB94-211729 *01,221*

Crossover to Strong Shear in a Low-Molecular-Weight Critical Polymer Blend.
PB94-211976 *01,222*

Magnetic Neutron Scattering (Invited).
PB95-150074 *04,557*

SANS Study of the Plastic Deformation Mechanism in Polyethylene.
PB95-151841 *01,242*

Analysis of the Effectiveness of Oscillating Radial Collimators in Neutron Scattering Applications.
PB95-152252 *03,917*

Thermodynamic Interactions and Correlations in Mixtures of Two Homopolymers and a Block Copolymers by Small Angle Neutron Scattering.
PB95-152872 *01,247*

SANS Studies of Space-Time Organization of Structure in Polymer Blends.
PB95-153789 *01,251*

Time-Resolved Small-Angle Neutron Scattering Study of Spinodal Decomposition in Deuterated and Protonated Polybutadiene Blends. 1. Effect of Initial Thermal Fluctuations.
PB95-161196 *01,252*

Localization of a Homopolymer Dissolved in a Lamellar Structure of a Block Copolymer Studied by Small-Angle Neutron Scattering.
PB95-161592 *01,253*

Elastic Scattering of Polymer Networks.
PB95-161816 *01,255*

Neutron Scattering Study of Shear Induced Turbidity in Polystyrene Dissolved in Dioctyl Phthalate.
PB95-161865 *01,256*

Characterization of Molecular Network of Thermosets Using Neutron Scattering.
PB95-164109 *01,259*

Small-Angle Neutron Scattering of Poly(vinyl alcohol) Gels.
PB95-164117 *01,260*

Characterization of Polyquinoline Blends Using Small Angle Scattering.
PB95-164125 *01,261*

Small Angle Neutron Scattering Studies on Chain Asymmetry of Coextruded Poly(Vinyl Alcohol) Film.
PB95-164372 *01,262*

Small Angle Neutron Scattering Study on Poly(N-Isopropyl Acrylamide) Gels Near Their Volume-Phase Transition Temperature.
PB95-164380 *01,263*

Small-Angle Neutron Scattering Study on Weakly Charged Temperature Sensitive Polymer Gels.
PB95-164398 *01,264*

Partial Scattered Intensities from a Binary Suspension of Polystyrene and Silica.
PB95-175618 *00,996*

Neutron Scattering by Hydrogen in Cold Neutron Prompt Gamma-Activation Analysis.
PB95-175972 *00,603*

Small Angle Neutrons Scattering from Nanocrystalline Palladium as a Function of Annealing.
PB95-176103 *03,354*

Neutron Scattering Study of the Orientation of a Liquid Crystalline Polymer by Shear Flow.
PB95-180196 *01,270*

Water Adsorption at Polymer/Silicon Wafer Interfaces.
PB95-181178 *01,022*

Lattice Dynamics of Semiconducting, Metallic, and Superconducting Ba1-xKxBiO3 Studied by Inelastic Neutron Scattering.
PB96-102447 *04,708*

Small Angle Neutron Scattering Study of the Structure and Formation of Ordered Mesopores in Silica.
PB96-111919 *03,069*

Effects of Target Temperature on Analytical Sensitivities of Cold-Neutron Capture Prompt gamma-ray Activation Analysis.
PB96-112131 *00,616*

Structure of a Triglyceride Microemulsion: A Small Angle Neutron Scattering Study.
PB96-112255 *01,077*

Small Angle Neutron Scattering Studies of Structural Characteristics of Argarose Gels.
PB96-112305 *03,475*

Vortex Dynamics and Melting in Niobium.
PB96-112362 *02,073*

Anisotropy of the Surfaces of Pores in Plasma Sprayed Alumina Deposits.
PB96-123211 *03,126*

Slow Dynamics of Segregation in Hydrogen-Bonded Polymer Blends.
PB96-123591 *01,281*

Inelastic Neutron Scattering Study of Hydrogen in Nanocrystalline Pd.
PB96-146857 *03,366*

Neutron Scattering Study of the Lattice Modes of Solid Cubane.
PB96-147152 *01,126*

Analysis of Small-Angle Scattering Data Dominated by Multiple Scattering for Systems Containing Eccentrically Shaped Particles or Pores.
PB96-160411 *03,075*

Low-Energy Vibrations and Octahedral Site Occupation in Nb95V5H(D)y.
PB96-160734 *01,133*

Neutron Spectroscopic Comparison of beta-Phase Rare Earth Hydrides.
PB96-160742 *01,134*

Influence of Shear on the Ordering Temperature of a Triblock Copolymer Melt.
PB96-163753 *01,288*

Small-Angle Neutron Scattering (SANS) Study of Worm-Like Micelles Under Shear.
PB96-176698 *04,111*

Isolated Spin Pairs and Two-Dimensional Magnetism in SrCr(sub 9p)Ga(sub 12-9p)O19.
PB97-112387 *04,154*

Neutron Scattering Study of Antiferromagnetic Order in the Magnetic Superconductors RNi2B2C.
PB97-112411 *04,812*

Measurements of the (237)Np(n,f) Cross Section.
PB97-119069 *04,173*

Small Angle Neutron Scattering Study of the Structure and Formation of MCM-41 Mesoporous Molecular Sieves.
PB97-122337 *03,110*

NEUTRON SOURCES
Thermal Hydraulic Tests of a Liquid Hydrogen Cold Neutron Source.
PB95-135570 *03,884*

Liquid-Hydrogen Cold Neutron Source for the NBSR.
PB95-151619 03,729

Nuclear Heat Load Calculations for the NBSR Cold Neutron Source Using MCNP.
PB95-152955 03,730

Cold Neutron Gain Calculations for the NBSR Using MCNP.
PB95-163978 03,731

In-situ Neutron Reflectivity of MBE Grown and Chemically Processed Surfaces and Interfaces.
PB96-146634 02,416

NEUTRON SPECTRA
DETAN 95: Computer Code for Calculating Spectrum-Averaged Cross Sections and Detector Responses in Neutron Spectra.
PB95-242384 04,014

NEUTRON SPECTROSCOPY
Neutron and Raman Spectroscopies of 134 and 134a Hydrofluorocarbons Encaged in Na-X Zeolite.
PB96-186168 03,001

NEUTRON STANDARDS
Measurement of the (10)B(n, alpha1gamma)(7)Li Cross Section in the 0.3 to 4 MeV Neutron Energy Interval.
PB96-161799 04,098

NEUTRON STANDING WAVES
Grazing Incidence Prompt Gamma Emissions and Resonance-Enhanced Neutron Standing Waves in a Thin-Film.
PB95-150470 03,892

NEUTRON TRANSPORT
Slab Transmission and Reflection for Point Source and Point Detector.
PB94-211265 03,838

Neutron Focusing Lens Using Polycapillary Fibers.
PB95-153078 03,922

NEUTRON VELOCITY SELECTORS
Acceptance Diagram Analysis of the Performance of Multidisk Neutron Velocity Selectors.
PB94-200417 03,826

NEUTRONS
Polarizability of the Nucleon.
PB94-211760 03,846

Measurement of the Neutron Lifetime.
PB96-161708 04,094

Diffraction of Neutron Standing Waves in Thin Films with Resonance Enhancement.
PB97-113278 04,164

NICKEL
Temperature Dependence and Anharmonicity of Phonons on Ni(110) and Cu(110) Using Molecular Dynamics Simulations.
PB94-185477 04,449

Nickel(II)-Mediated Oxidative DNA Base Damage in Renal and Hepatic Chromatin of Pregnant Rats and Their Fetuses. Possible Relevance to Carcinogenesis.
PB94-212628 03,646

Measurements of Thermophysical Properties of Nickel Near Its Melting Temperature by a Microsecond-Resolution Transient Technique.
PB96-102579 04,210

NICKEL 63
63Ni Half-Life: A New Experimental Determination and Critical Review.
PB97-111603 00,700

Nickel-63 Standardization: 1968-1995.
PB97-111819 00,701

NICKEL ALLOYS
Dynamic Shear Modulus Measurements with Four Independent Techniques in Nickel-Based Alloys.
PB94-198900 03,320

Diagnosis and Treatment of an Oral Base-Metal Contact Lesion Following Negative Dermatologic Patch Tests.
PB95-180626 00,172

Chemical Aspects of Tool Wear in Single Point Diamond Turning.
PB97-112601 03,021

NICKEL ALUMINIDES
LMTO/CVM and LAPW/CVM Calculations of the Nickel Aluminide/Nickel Titanium Pseudobinary Phase Diagram.
PB94-199353 03,323

NICKEL ALUMINUM TITANIUM
LMTO/CVM and LAPW/CVM Calculations of the Nickel Aluminide/Nickel Titanium Pseudobinary Phase Diagram.
PB94-199353 03,323

NICKEL BASE ALLOYS
Evaluation of the Environmentally Induced Fracture Resistance of Ductile Nickel Aluminide. Technical Report Number 1, Final report. October-December 1990.
DE94017331 03,306

Evaluation of the Electrochemical Behavior of Ductile Nickel Aluminide and Nickel in a pH 7.9 Solution. Technical Report Number 3, April-June 1991.
DE94017351 03,307

NICKEL BASE SUPERALLOY
Fatigue Crack Thresholds of a Nickel-Iron Alloy for Superconductor Sheaths at 4 K.
PB96-190343 03,223

NICKEL-CADMIUM BATTERIES
Rechargeable Batteries for Personal/Portable.
PB96-164231 02,459

NICKEL COMPOUNDS
One-Electron Oxidation of Nickel Porphyrins. Effect of Structure and Medium on Formation of Nickel(III) Porphyrin or Nickel(II) Porphyrin pi-Radical Cation.
PB95-107058 00,865

Site of One-Electron Reduction of Ni(II) Porphyrins. Formation of Ni(I) Porphyrin of Ni(II) Porphyrin pi-Radical Anion.
PB95-107066 00,866

NICKEL HYDRIDES
Determination of the Molecular Parameters of NiH in Its (2)Delta Ground State by Laser Magnetic Resonance.
PB95-107116 00,869

NICKEL INTERMETALLICS
Disorder Trapping in Ni2TiAl.
PB94-198942 03,322

NICKEL MANGANESE ANTIMONIDES
Resonant-Photoemission Investigation of the Heusler Alloys Ni2MnSb and NiMnSb.
PB95-162384 04,612

NICKEL OXIDES
Structural and Magnetic Ordering in Iron Oxide/Nickel Oxide Multilayers by X-ray and Neutron Diffraction (Invited).
PB94-172558 04,442

NICKEL SILICIDES
Local Partial Densities of States in Ni and Co Silicides Studied by Soft X-Ray Emission Spectroscopy.
PB94-212412 04,504

NICKEL TITANIUM
LMTO/CVM and LAPW/CVM Calculations of the Nickel Aluminide/Nickel Titanium Pseudobinary Phase Diagram.
PB94-199353 03,323

NICKEL VANADIUM
Effects of Elastic Stress on Phase Equilibrium in the Ni-V System.
PB94-172707 03,313

NII (NATIONAL INFORMATION INFRASTRUCTURE)
Putting the Information Infrastructure to Work: Report of the Information Infrastructure Task Force Committee on Applications and Technology.
PB94-163383 00,001

Information Infrastructure: Reaching Society's Goals. Report of the Information Infrastructure Task Force Committee on Applications and Technology.
PB94-214756 01,469

Report on the Workshop on Advanced Digital Video in the National Information Infrastructure. Held in Washington, D.C. on May 10-11, 1994.
PB95-103677 01,472

Unpredictable Certainty. Information Infrastructure through 2000.
PB96-182266 00,016

NIOBATES
Electric Field Effects on Crack Growth in a Lead Magnesium Niobate.
PB95-107322 03,339

NIOBIUM
Intrinsic Stress in DC Sputtered Niobium.
PB94-199031 04,468

Effect of Microstructure on Phase Formation in the Reaction of Nb/Al Multilayer Thin Films.
PB95-168415 03,352

First Phase Formation Kinetics in the Reaction of Nb/Al.
PB95-168456 03,353

Niobium Microbolometers for Far-Infrared Detection.
PB96-111729 02,184

Vortex Dynamics and Melting in Niobium.
PB96-112362 02,073

Metallic-Barrier Junctions for Programmable Josephson Voltage Standards.
PB96-200134 02,089

Superconductor- Normal-Superconductor Junctions for Digital/Analog Converters.
PB96-200233 02,092

Superconductor- Normal-Superconductor Junctions for Programmable Voltage Standards.
PB96-200241 02,093

Radiance Temperatures at 1500 nm of Niobium and Molybdenum at Their Melting Points by a Pulse-Heating Technique.
PB97-118699 04,167

NIOBIUM 93 TARGET
Measurement of the (93)Nb(n,2n) (92m)Nb Cross Section in a (235)U Fission Spectrum.
PB95-163986 03,945

NIOBIUM ALLOYS
Magnetic Characteristics and Measurements of Filamentary Nb-Ti Wire for the Superconducting Super Collider.
DE94005988 03,775

Transverse stress effect on the critical current of internal tin and bronze process Nb(sub 3)Sn superconductors.
DE95016659 04,434

Thermodynamic Calculation of the Ternary Ti-Al-Nb System.
PB94-212636 03,336

Thin Film Reaction Kinetics of Niobium/Aluminum Multilayers.
PB95-175295 04,651

Journal of Research of the National Institute of Standards and Technology, September/October 1993. Volume 98, Number 5.
PB96-169057 03,368

NIOBIUM ALUMINIDES
Thin Film Reaction Kinetics of Niobium/Aluminum Multilayers.
PB95-175295 04,651

NIOBIUM BASE ALLOYS
VAMAS interlaboratory comparisons of critical current vs. strain in Nb(sub 3)Sn.
DE95016656 04,433

NIOBIUM COMPOUNDS
Low-Energy Vibrations and Octahedral Site Occupation in Nb95V5H(D)y.
PB96-160734 01,133

NIOBIUM INTERMETALLICS
Coherent Precipitates in the BCC/Orthorhombic Two Phase Field of the Ti-Al-Nb System.
PB94-198694 03,317

NIOBIUM IONS
Spectrum and Energy Levels of Five-Times-Ionized Niobium (Nb VI).
PB94-185246 04,226

NIOBIUM NITRIDES
Use of Ion Scattering Spectroscopy to Monitor the Nb Target Nitridation during Reactive Sputtering.
PB94-172525 00,761

NIOBIUM STANNIDES
Electromechanical Properties of Superconductors for DOE Fusion Applications.
PB94-139672 02,250

Flux Expulsion at Intermediate Fields in Type-II Superconductors.
PB94-212230 04,502

Volume Magnetic Hysteresis Loss of Nb3Sn Superconductors as a Function of Wire Length.
PB95-153722 04,597

Superconductor Critical Current Standards for Fusion Applications. Final Progress Report, October 1993-July 1994.
PB95-169538 02,222

Reduction of Interfilament Contact Loss in Nb3Sn Superconductor Wires.
PB95-175535 02,223

Experimental Aspects of Flux Expulsion in Type-II Superconductors.
PB95-175725 04,660

Simple and Repeatable Technique for Measuring the Critical Current of Nb3Sn Wires.
PB96-119409 02,229

VAMAS Intercomparison of Critical Current Measurements on NB3Sn Superconductors: A Summary Report.
PB96-119763 04,043

NIOBIUM STANNOIDES
II-5: Thermal Contraction of Materials Used in Nb3Sn Critical Current Measurements.
PB96-147186 04,769

NIOBIUM TEN
Volume Magnetic Hysteresis Loss of Nb3Sn Superconductors as a Function of Wire Length.
PB95-153722 04,597

NIST
NIST Serial Holdings, 1994.
PB94-178068 02,745

NIST-7 FREQUENCY STANDARD
Velocity Distribution of Atomic Beams by Gated Optical Pumping.
PB95-180519 01,542

Hybrid Digital/Analog Servo for the NIST-7 Frequency Standard.
PB95-180618 01,544

NIST-7 STANDARD
NIST-7, the New US Primary Frequency Standard.
PB95-153458 01,534

NIST REFERENCE MATERIALS
What Is a 'Standard Reference Material' - What Is Any Reference Material.
PB96-186135 03,000

NITRAMINES
Thermal Decomposition Pathways in Nitramine Propellants.
AD-A295 896/5 03,753

Spectroscopic Study of Reaction Intermediates and Mechanisms in Nitramine Decomposition and Combustion.
AD-A296 061/5 03,774

NITRATE IONS
Vibrational Spectra of Molecular Ions Isolated in Solid Neon. XI. NO2(+), NO2(-), and NO3(-).
PB95-125688 00,890

NITRIC OXIDE
Reaction of NO with Superoxide.
PB94-212198 00,830

Reaction of Nitric Oxide with Organic Peroxyl Radicals.
PB95-141107 00,910

Laser-Induced Desorption of NO from Si(111): Effects of Coverage on NO Vibrational Populations.
PB95-162319 00,959

NITRIC OXIDE COMPLEXES
Fragment State Correlations in the Dissociation of NO.HF(v=1).
PB95-164430 *00,982*

NITRITE IONS
Vibrational Spectra of Molecular Ions Isolated in Solid Neon. XI. NO2(+), NO2(-), and NO3(-).
PB95-125688 *00,890*

NITROANILINES
Inelastic Neutron Scattering Studies of Nonlinear Optical Materials: p-Nitroaniline Adsorbed in ALPO-5.
PB95-107223 *00,874*

NITROGEN
Beneficial Effects of Nitrogen Atomization on an Austenitic Stainless Steel.
PB94-212396 *03,209*

Reduction of Dinitrogen to Ammonia in Aqueous Solution Mediated by Colloidal Metals.
PB95-107074 *00,867*

Operational Mode and Gas Species Effects on Rotational Drag in Pneumatic Dead Weight Pressure Gages.
PB95-140182 *00,903*

N2(a'(sup 1)Sigma(sub g)(sup +)) Metastable Collisional Destruction and Rotational Excitation Transfer by N2.
PB95-151395 *00,933*

High Resolution Angle Resolved Photoelectron Spectroscopy Study of N2.
PB95-151494 *03,907*

Photoelectron Study of Electronic Autoionization in Rotationally Cooled N2: The n=6 Member of the Hopfield Series.
PB95-163531 *00,971*

Modified Effective Range Theory as an Alternative to Low-Energy Close-Coupling Calculations.
PB95-202701 *03,988*

Ion Kinetics and Symmetric Charge-Transfer Collisions in Low-Current, Diffuse (Townsend) Discharges in Argon and Nitrogen.
PB96-123658 *04,051*

NITROGEN COMPLEXES
Slit Jet Infrared Spectroscopy of Hydrogen Bonded N2HF Isotopomers: Rotational Rydberg-Klein-Rees Analysis and H/D Dependent Vibrational Predissociation Rates.
PB95-161873 *00,956*

Rotational-RKR Inversion of Intermolecular Stretching Potentials: Extension to Linear Hydrogen Bonded Complexes.
PB95-203014 *01,041*

NITROGEN COMPOUNDS
High-Resolution Infrared Overtone Spectroscopy of N2-HF: Vibrational Red Shifts and Predissociation Rate as a Function of HF Stretching Quanta.
PB96-102298 *01,061*

NITROGEN DIOXIDE
Vibrational Spectra of Molecular Ions Isolated in Solid Neon. XI. NO2(+), NO2(-), and NO3(-).
PB95-125688 *00,890*

Asymptotic and Numerical Analysis of a Premixed Laminar Nitrogen Dioxide-Hydrogen Flame.
PB96-164256 *01,422*

NITROGEN FLOW FACILITY
Uncertainty Analysis of the NIST Nitrogen Flow Facility.
PB95-128906 *02,608*

NITROGEN HETEROCYCLIC COMPOUNDS
Oxidation of 10-Methylacridan, a Synthetic Analogue of NADH and Deprotonation of Its Cation Radical. Convergent Application of Laser Flash Photolysis and Direct and Redox Catalyzed Electrochemistry to the Kinetics of Deprotonation of the Cation Radical.
PB94-198371 *00,785*

NITROGEN IONS
Selected Ion Flow Tube-Laser Induced Fluorescence Instrument for Vibrationally State-Specific Ion-Molecule Reactions.
PB94-185444 *00,774*

Fine-Structure Intervals of (14)N(+) By Far-Infrared Laser Magnetic Resonance.
PB95-175162 *00,993*

NITROGEN-LIKE IONS
Atomic Branching Ratio Data for Nitrogen-Like Species.
PB96-190152 *04,122*

NITROGEN OXIDES
P-Type Doubling in the Infrared Spectrum of NO-HF.
PB94-211463 *00,817*

NO Production and Destruction in a Methane/Air Diffusion Flame.
PB97-122519 *01,443*

NITROMETHANE
Microwave Spectrum and Structure of CH3NO2-H20.
AD-A296 377/5 *00,719*

NOBLE GASES
Excitation Transfer in Barium by Collisions with Noble Gases.
PB96-200274 *01,163*

NODULAR IRON
Application of ODF to the Rietveld Profile Refinement of Polycrystalline Solid.
PB95-202388 *03,401*

NOISE
New Model of 1/F Noise in Baw Quartz Resonators.
PB96-112248 *02,383*

Non-Gaussian Noise Effects on Reliability of Multistable Systems.
PB96-122726 *04,213*

Telegraph Noise in Silver-Permalloy Giant Magnetoresistance Test Structures.
PB96-146717 *04,763*

Transitions to Chaos Induced by Additive and Multiplicative Noise.
PB96-155759 *03,750*

Spectrum of the Stochastically Forced Duffing-Holmes Oscillator.
PB96-155767 *00,216*

Necessary Condition for Homoclinic Chaos Induces by Additive Noise.
PB96-155775 *04,063*

Noise-Induced Transitions to Chaos.
PB96-156120 *00,217*

Deterministic and Stochastic Chaos.
PB96-156138 *00,218*

Exits in Multistable Systems Excited by Coin-Toss Square-Wave Dichotomous Noise: A Chaotic Dynamics Approach.
PB96-160650 *04,824*

Observation of Hot-Electron Shot Noise in a Metallic Resistor.
PB97-112007 *01,988*

NOISE ANALYSIS
Current Noise Reveals Protonation Kinetics and Number of Ionizable Sites in an Open Protein Ion Channel.
PB96-161674 *04,092*

Noise Analysis of Ionization Kinetics in a Protein Ion Channel.
PB96-161682 *04,093*

Current Fluctuations Reveal Protonation Dynamics and Number of Ionizable Residues in the alpha-Toxin Channel.
PB96-161732 *03,588*

Protonation Dynamics of the alpha-Toxin Ion Channel from Spectral Analysis of pH-Dependent Current Fluctuations.
PB96-161740 *03,652*

Protonation Dynamics in an Ion Channel Pore.
PB96-161757 *03,589*

NOISE CALIBRATION SYSTEM
Journal of Research of the National Institute of Standards and Technology. January/February 1994. Volume 99, Number 1.
PB94-169737 *02,019*

Null-Balanced Total-Power Radiometer System NCS1.
PB94-169778 *02,021*

Derivation of the System Equation for Null-Balanced Total-Power Radiometer System NCS1.
PB94-169786 *02,022*

Evaluation of Uncertainties of the Null-Balanced Total-Power Radiometer System NCS1.
PB94-169794 *02,023*

NOISE CALIBRATION SYSTEMS
Uncertainties of the NIST Coaxial Noise Calibration System.
PB96-111984 *02,070*

NOISE MEASUREMENT
Relative Accuracy of Isolated and Unisolated Noise Comparison Radiometers.
PB96-111851 *01,924*

NOISE REDUCTION
Slow Evolution from the Boundary: A New Stabilizing Constraint in Ill-Posed Continuation Problems.
PB96-122858 *03,418*

Noise Reduction in Low-Frequency SQUID Measurements with Laser-Driven Switching.
PB96-135165 *02,081*

NOISE STANDARDS
Practical Standards for PM and AM Noise at 5, 10 and 100 MHz.
PB95-181129 *01,546*

NOISE TEMPERATURE
Systematic Studies of the Effect of a Bandpass Filter on a Josephson-Junction Noise Thermometer.
PB95-162970 *03,939*

Systematic Studies of the Effect of a Post-Detection Filter on a Josephson-Junction Noise Thermometer.
PB95-162988 *03,940*

NOISE THERMOMETERS
Systematic Studies of the Effect of a Bandpass Filter on a Josephson-Junction Noise Thermometer.
PB95-162970 *03,939*

Systematic Studies of the Effect of a Post-Detection Filter on a Josephson-Junction Noise Thermometer.
PB95-162988 *03,940*

NON-ABRASIVE WEAR TESTING
Critical Factors in Non-Lubricated, Non-Abrasive Wear Testing.
PB95-140588 *03,236*

NON-GAUSSIAN EFFECTS
Non-Gaussian Noise Effects on Reliability of Multistable Systems.
PB96-122726 *04,213*

NON-NEWTONIAN FLUIDS
Density Dependence of Fluid Properties and Non-Newtonian Flows: The Weisenberg Effect.
PB96-161898 *01,140*

NONAQUEOUS ELECTROLYTES
Susceptibility Critical Exponent for a Nonaqueous Ionic Binary Mixture Near a Consolute Point.
PB95-152112 *00,938*

NONDEGENERATE STARS
Volume-Limited ROSAT Survey of Extreme Ultraviolet Emission from all Nondegenerate Stars within 10 Parsecs.
PB96-103189 *00,093*

NONDESTRUCTIVE EVALUATION
Ultrasonic NDE of Sprayed Ceramic Coatings.
PB96-201157 *02,761*

NONDESTRUCTIVE TESTING
Intelligent Processing of Materials.
PB94-172780 *02,811*

Recent Development in Nondestructive Testing of Concrete.
PB96-122445 *01,325*

Classified Bibliography: Insulation Condition Monitoring Methods, 1989-1995.
PB96-131586 *02,232*

NONDESTRUCTIVE TESTS
Detection of Voids in Grouted Ducts Using the Impact-Echo Method.
PB94-185121 *01,306*

International Institute of Welding: Report on 1992 Actions.
PB94-185873 *02,856*

International Institute of Welding: Report on 1993 Actions.
PB94-185881 *02,857*

Dynamic Shear Modulus Measurements with Four Independent Techniques in Nickel-Based Alloys.
PB94-198900 *03,320*

Assessment of Technology for Detection of Stress Corrosion Cracking in Gas Pipelines. Final Report, July 1993-March 1994.
PB94-206646 *02,475*

Review of Cure Monitoring Techniques for On-Line Process Control.
PB94-216728 *03,145*

Potential Drop in the Center-Cracked Panel with Asymmetric Crack Extension.
PB95-107330 *04,819*

Ultrasonic Measurement of Residual Stress in Railroad Wheel Rims.
PB95-140430 *04,849*

Nondestructive Evaluation and Materials Processing.
PB95-140455 *02,902*

Critical Factors in Non-Lubricated, Non-Abrasive Wear Testing.
PB95-140588 *03,236*

Noncontact Ultrasonic Inspection of Train Rails for Stress.
PB95-162673 *04,851*

Determination of Hydrogen in Titanium Alloy Jet Engine Compressor Blades by Cold Neutron Capture Prompt Gamma-ray Activation Analysis.
PB95-175956 *01,448*

Nondestructive Testing of Concrete: History and Challenges.
PB95-180139 *00,385*

Reactor Radiation Technical Activities, 1994. NAS-NRC Assessment Panel, April 6-7, 1995.
PB95-209888 *03,732*

Comparison of Techniques for Nondestructive Composition Measurements in CdZnTe Substrates.
PB96-103098 *02,703*

Residual Stress in Induction-Heated Railroad Wheels: Ultrasonic and Saw Cut Measurements. Report No. 28.
PB96-106992 *04,854*

Contributions of Out-of-Plane Material to a Scanned-Beam Laminography Image.
PB96-111786 *02,704*

Open-Ended Coaxial Probes for Nondestructive Testing of Substrates and Circuit Boards.
PB96-122825 *02,078*

Report on 1994 Actions of the International Institute of Welding.
PB96-138540 *02,873*

Gas-Coupled, Pulse-Echo Ultrasonic Crack Detection and Thickness Gaging.
PB96-147129 *04,847*

International Institute of Welding: Report on 1995 Actions.
PB96-158076 *02,874*

Application of Electromagnetic-Acoustic Transducers for Nondestructive Evaluation of Stresses in Steel Bridge Structures.
PB96-167978 *01,301*

Dynamometer-Induced Residual Stress in Railroad Wheels: Ultrasonic and Saw Cut Measurements. Report No. 30.
PB96-183199 *04,857*

Reactor Radiation Technical Activities, 1995.
PB96-193644 *03,741*

Development of a Method for Measuring Water-Stripping Resistance of Asphalt/Siliceous Aggregate Mixtures.
PB96-197249 *01,348*

Development of a Method for Measuring Water-Stripping Resistance of Asphalt/Siliceous Aggregate Mixtures.
PB96-202296 *01,329*

NONEQUILIBRIUM ENTROPY
Nonequilibrium Statistical Mechanics.
PB96-161781 *04,097*

NONEQUILIBRIUM MOLECULAR DYNAMICS
Simulation and SANS Studies of Gelation Under Shear.
PB96-167176 *01,150*

NONIONIZING RADIATION
Bibliography of the NIST Electromagnetic Fields Division Publications.
PB94-165990 *01,875*

NONLINEAR ALGEBRAIC EQUATIONS
Algebraic Approximation of Attractors for Galloping Oscillators.
PB95-162897 *04,820*

NONLINEAR DIFFERENTIAL EQUATIONS
Melnikov Function and Homoclinic Chaos Induced by Weak Perturbations.
PB95-180923 *03,414*

NONLINEAR DYNAMICS
Nonlinear Dynamics of Stiff Polymers.
PB96-122478 *01,278*

NONLINEAR EQUATIONS
Foias-Temam Approximations of Attractors for Galloping Oscillators.
PB94-198298 *04,817*

NONLINEAR OPTICS
Scaling of the Nonlinear Optical Cross Sections of GaAs-AlGaAs Multiple Quantum-Well Hetero n-i-p-i's.
PB96-102793 *02,183*

Appearance Intensities for Multiply Charged Ions in a Strong Laser Field.
PB96-160445 *04,089*

NONLINEAR SYSTEMS
Exponentially Rapid Coarsening and Buckling in Coherently Self-Stressed Thin Plates.
PB95-202347 *04,821*

NONMODEL ERRORS
Effects of Nonmodel Errors on Model-Based Testing.
PB96-123146 *02,604*

NONPAIRWISE ADDITIVE FORCES
Pairwise and Nonpairwise Additive Forces in Weakly Bound Complexes: High Resolution Infrared Spectroscopy of ArnDF (n=1,2,3).
PB96-200357 *04,125*

NORDIC COUNTRIES
Forum for International Cooperation on Fire Research.
PB95-162939 *04,869*

NORTH AMERICA
ISO/IEC Workshop on Worldwide Recognition of OSI Test Results Regional Progress - North America.
PB94-172202 *02,719*

Status of Construction and Construction Technologies.
PB94-186004 *00,318*

NORTHERN HEMISPHERE
Modulation of Fossil Fuel Production by Global Temperature Variations, 2.
PB94-146636 *02,533*

NORTHRIDGE (CALIFORNIA)
Northridge Earthquake 1994: Performance of Structures, Lifelines, and Fire Protection Systems.
PB94-207461 *04,825*

NORTHRIDGE EARTHQUAKE
Performance of HUD-Affiliated Properties during the January 17, 1994 Northridge Earthquake.
PB95-174488 *00,443*

Survey of Steel Moment-Resisting Frame Buildings Affected by the 1994 Northridge Earthquake.
PB95-211918 *00,451*

Performance of Federal Buildings in the January 17, 1994 Northridge Earthquake.
PB95-231775 *00,453*

NUCLEAR COLLISIONS
Strangeness Flow Difference in Nuclear Collisions at 15A and 200A GeV.
PB96-119631 *04,042*

NUCLEAR MAGNETIC RESONANCE
Binder Characterization and Evaluation by Nuclear Magnetic Resonance Spectroscopy.
PB94-193471 *01,334*

Two-Dimensional POMMIE Carbon-Proton Chemical Shift Correlated (13)C NMR Spectrum Editing.
PB94-200508 *00,809*

L-threo-beta-Hydroxyhistidine, an Unprecedented Iron(III) Ion-Binding Amino Acid in a Pyoverdine-type Siderophore from Pseudomonas fluorescens 244.
PB94-211620 *00,553*

NMR Characterization of Injection-Moulded Alumina Green Compacts. Part 2. T2-Weighted Proton Imaging.
PB96-201181 *01,165*

NUCLEAR MEDICINE
Liquid-Scintillation Counting Techniques for the Standardization of Radionuclides Used in Therapy.
PB97-110084 *03,709*

Radioassays of Yttrium-90 Used in Nuclear Medicine.
PB97-110100 *03,522*

NUCLEAR PHYSICS & RADIATION TECHNOLOGY
Evolution of the Pore Size Distribution in Final-Stage Sintering of Alumina Measured by Small-Angle X-ray Scattering. (Reannouncement with New Availability Information).
AD-A249 178/5 *03,023*

Characterization of the Densification of Alumina by Multiple Small-Angle Neutron Scattering. (Reannouncement with New Availability Information).
AD-A249 179/3 *03,024*

Small-Angle Neutron Scattering Characterization of Processing/Microstructure Relationships in the Sintering of Crystalline and Glassy Ceramics. (Reannouncement with New Availability Information).
AD-A249 510/9 *03,025*

X-ray Attenuation Coefficients from 10 Kev to 100 Mev.
AD-A278 139/1 *03,765*

Ultraviolet Multiplet Table.
AD-A278 446/0 *00,710*

Report of the International Commission on Radiological Units and Measurements (ICRU), 1956.
AD-A279 120/0 *03,513*

X-ray Protection.
AD-A279 132/5 *03,605*

Recommendations for the Disposal of Carbon-14 Wastes.
AD-A279 133/3 *02,579*

X-ray Protection Design.
AD-A279 181/2 *03,606*

Protection Against Radiations from Radium, Cobalt-60, and Cesium-137.
AD-A279 261/2 *03,607*

Permissible Dose from External Sources of Ionizing Radiation.
AD-A279 281/0 *03,608*

X-Ray Attenuation Coefficients from 10 kev to 100 Mev.
AD-A279 289/3 *03,767*

Protection Against Neutron Radiation Up to 30 Million Electron Volts.
AD-A286 681/2 *03,611*

Penetration and Diffusion of Hard X-rays through Thick Barriers. III. Studies of Spectral Distributions.
AD-A292 502/2 *03,771*

Further Calculations of X-ray Diffusion in an Infinite Medium.
AD-A295 314/9 *03,772*

Experimental plan to determine the performance of the Oak Ridge National Laboratory Cold Neutron Moderator. Final report, September 1, 1993--November 30, 1993.
DE95011352 *03,778*

36Cl/Cl Accelerator-Mass-Spectrometry Standards: Verification of Their Serial-Dilution-Solution Preparations by Radioactivity Measurements.
PB94-140563 *00,524*

NIST Reactor: Summary of Activities October 1992 through September 1993.
PB94-161502 *04,437*

Characterization of the Binding of Gallium, Platinum, and Uranium to Pseudomonas Fluorescens by Small-Angle X-ray Scattering and Transmission Electron Microscopy.
PB94-172509 *03,453*

Neutron Scattering Study of Shear Induced Turbidity in Polystyrene/Dioctyl Phthalate Solutions at High Shear Rates.
PB94-172624 *01,197*

Time Dependent Small Angle Neutron Scattering Behavior in Triblock Copolymers Under Steady Shear.
PB94-172632 *01,198*

Measurement and Calibration of Large-Area Alpha-Particle Sources at NIST.
PB94-172855 *03,791*

Systematics of Alpha-Particle Energy Spectra and Lineal Energy (Y) Spectra for Radon Daughters.
PB94-185139 *03,615*

Intercomparison of Internal Proportional Gas Counting of (85)Kr and (3)H.
PB94-185576 *03,800*

Use of a Radiochromic Detector for the Determination of Stereotactic Radiosurgery Dose Characteristics.
PB94-185642 *03,514*

Intermediate Structure in the Neutron-Induced Fission Cross Section of 236U.
PB94-185741 *03,802*

Neutron Reflectivity of End-Grafted Polymers: Concentration and Solvent Quality Dependence in Equilibrium Conditions.
PB94-185758 *01,206*

Vibrational Distributions of As2 in the Cracking of As4 on Si(100) and Si(111).
PB94-198314 *00,784*

Combined Low- and High-Angle X-Ray Structural Refinement of a Co/Pt(111) Multilayer Exhibiting Perpendicular Magnetic Anisotropy.
PB94-198355 *04,457*

Characteristics of Light Emission After Low-Energy Electron Impact Excitation of Caesium Atoms.
PB94-198587 *03,806*

Femtosecond Time-Resolved Wave Packet Motion in Molecular Multiphoton Ionization and Fragmentation.
PB94-198611 *00,790*

Discovery of an X-Ray Selected, Radio-Loud Quasar at z=3.9.
PB94-198652 *00,052*

Integrated Laser Doppler Method for Measuring Planetary Gravity Fields.
PB94-198686 *03,681*

Germanium Detector Optimization of MDA for Efficiency vs. Low Intrinsic Background.
PB94-199155 *00,543*

IUE Observations of Solar-Type Stars in the Pleiades and the Hyades.
PB94-199437 *00,053*

Silicon Photodiodes Optimized for EUV and Soft X-Ray Regions.
PB94-199478 *02,124*

Neutron Standard Cross Sections in Reactor Physics: Need and Status.
PB94-199510 *03,813*

EPR Bone Dosimetry: A New Approach to Spectral Deconvolution Problems.
PB94-199643 *03,616*

Estimation of the Absorbed Dose in Radiation-Processed Food. 2. Test of the EPR Response Function by an Exponential Fitting Analysis.
PB94-199650 *00,036*

Experimental Validation of Radiopharmaceutical Absorbed Dose to Mineralized Bone Tissue.
PB94-199668 *03,617*

Radiation Doses.
PB94-199676 *03,618*

Estimation of the Absorbed Dose in Radiation-Processed Food. 3. The Effect of Time of Evaluation on the Accuracy of the Estimate.
PB94-199684 *00,037*

Estimation of the Absorbed Dose in Radiation-Processed Food. 4. EPR Measurements on Eggshell.
PB94-199692 *00,038*

New EPR Dosimeter Based on Polyvinylalcohol.
PB94-199700 *03,619*

Estimation of the Absorbed Dose in Radiation-Processed Food. 1. Test of the EPR Response Function by a Linear Regression Analysis.
PB94-199718 *00,039*

Current Results and Future Prospects for a Neutron Lifetime Determination Using Trapped Protons.
PB94-199742 *03,817*

Absolute Cross-Section Measurements for Electron-Impact Ionization of C1(+1).
PB94-199841 *03,818*

Neutron Measurement Intercomparisons Sponsored by CCEMRI, Section 3 (Neutron Measurements).
PB94-199916 *03,819*

Improvements in Computation of Form Factors.
PB94-200078 *03,820*

Photographic Response to X-Ray Irradiation. 1. Estimation of the Photographic Error Statistic and Development of Analytic Density-Intensity Equations.
PB94-200086 *03,821*

Photographic Response to X-Ray Irradiation. 2. Correlated Models.
PB94-200094 *03,822*

Photographic Response to X-Ray Irradiation. 3. Photographic Linearization of Beam-Foil Spectra.
PB94-200102 *03,823*

Textures of Tantalum Metal Sheets by Neutron Diffraction.
PB94-200169 *03,399*

Texture Study of Two Molybdenum Shaped Charge Liners by Neutron Diffraction.
PB94-200177 *03,754*

Neutron-Scattering Study of C60(n-) (n=3,6) Librations in Alkali-Metal Fullerides.
PB94-200219 *00,806*

Acceptance Diagram Analysis of the Performance of Multidisk Neutron Velocity Selectors.
PB94-200417 *03,826*

Acceptance Diagram Analysis of the Performance of Vertically Curved Neutron Monochromators.
PB94-200425 *03,827*

Joy of Acceptance Diagrams.
PB94-200433 *03,828*

Assay of the Eluent from the Alumina-Based Tungsten-188-Rhenium-188 Generator.
PB94-200482 *03,829*

Standardization and Decay Scheme of Rhenium-186.
PB94-200490 *03,830*

Accuracy-Weighted Variational Principle for Degenerate Continuum States.
PB94-200615 *03,831*

Comprehensive Theory of Nuclear Effects on the Intrinsic Sticking Probability. 1.
PB94-200623 *03,832*

Comprehensive Theory of Nuclear Effects on the Intrinsic Sticking Probability. 2.
PB94-200631 *03,833*

Measurement of Boron at Silicon Wafer Surfaces by Neutron Depth Profiling.
PB94-211059 *04,487*

Plasma Chemistry in Disilane Discharges.
PB94-211075 *02,514*

Radio Continuum and X-Ray Properties of the Coronae of RS Canum Venaticorum and Related Active Binary Systems.
PB94-211083 *00,057*

Three-Vector Correlation Theory for Orientation/Alignment Studies in Atomic and Molecular Collisions.
PB94-211109 *03,834*

Fine Structure of Negative Ions of Alkaline-Earth-Metal Atoms.
PB94-211182 *03,837*

Slab Transmission and Reflection for Point Source and Point Detector.
PB94-211265 *03,838*

Anomalous Odd- to Even-Mass Isotope Ratios in Resonance Ionization with Broad-Band Lasers.
PB94-211406 *03,839*

Earth-Based Gravitational Experiments.
PB94-211414 *03,840*

High-Resolution Infrared Overtone Spectroscopy of ArHF via Nd:YAG/Dye Laser Difference Frequency Generation.
PB94-211448 *00,816*

Dreams About the Next Generation of Super-Stable Lasers.
PB94-211570 *04,235*

Radiation Chemistry of Cyanine Dyes: Oxidation and Reduction of Merocyanine 540.
PB94-211661 *00,818*

Drill-Hearn-Gerasimov Sum Rule.
PB94-211752 *03,845*

Polarizability of the Nucleon.
PB94-211760 *03,846*

Interstellar Disk-Halo Connection in Galaxies: Review of Observational Aspects.
PB94-211802 *00,058*

Role of the Office of Radiation Measurement in Quality Assurance.
PB94-212255 *00,689*

Local Partial Densities of States in Ni and Co Silicides Studied by Soft X-Ray Emission Spectroscopy.
PB94-212412 *04,504*

NIST-NRL Free-Electron Laser Facility.
PB94-212511 *04,237*

Radiation-Driven Winds of Hot Luminous Stars X. The Determination of Stellar Masses Radii and Distances from Terminal Velocities and Mass-Loss Rates.
PB94-213022 *00,060*

Materials Science with SR Using X-Ray Imaging: Spatial-Resolution/Source Size.
PB94-213048 *04,510*

Laser-Induced Fluorescence Measurements of Rotationally Resolved Velocity Distributions for CO(+) Drifted in He.
PB94-213139 *00,848*

Astrophysical Aspects of Neutral Atom Line Broadening.
PB94-213287 *00,061*

Polarized X-Ray Emission Spectroscopy.
PB94-213360 *03,862*

High-Sensitivity Determination of Iodine Isotopic Ratios by Thermal and Fast Neutron Activation.
PB94-213386 *00,555*

Neutron Capture Prompt Gamma-Ray Activation Analysis at the NIST Cold Neutron Research Facility.
PB94-213394 *00,556*

Atomic Data Needed for Far Ultraviolet Astronomy with HUT and FUSE.
PB94-213402 *00,062*

FUSE: The Far Ultraviolet Spectrograph Explorer.
PB94-213410 *00,063*

Ultraviolet Observations of Stellar Coronae: Early Results from HST.
PB94-213428 *00,064*

X-rays from Stellar Flares.
PB94-213436 *00,065*

Goddard High-Resolution Spectrograph Observations of the Local Interstellar Medium and the Deuterium/Hydrogen Ratio along the Line of Sight Toward Capella.
PB94-213444 *00,066*

Radio Emission from Chemically Peculiar Stars.
PB94-213469 *00,068*

First Results from a Coordinated ROSAT, IUE, and VLA Study of RS CVn Systems.
PB94-213477 *00,069*

Rapid Decline in the Optical Emission from SN 1957D in M83.
PB94-216033 *00,070*

Spectroscopic Puzzle in ArHF Solved: The Test of a New Potential.
PB94-216058 *00,850*

Scattering and Absorption Effects in Neutron Beam Activation Analysis Experiments.
PB94-216140 *00,557*

Supermirror Transmission Polarizers for Neutrons.
PB94-216215 *03,866*

High-Resolution Measurements of the nu2 and 2nu2-nu2 Bands of (34)S(16)O2.
PB94-216223 *00,855*

Atomic Beam Splitters and Mirrors by Adiabatic Passage in Multilevel Systems.
PB94-216439 *03,867*

High-Resolution IR Laser-Driven Vibrational Dynamics in Supersonic Jets: Weakly Bound Complexes and Intramolecular Energy Flow.
PB94-216751 *00,862*

Sealed Water Calorimeter for Measuring Absorbed Dose.
PB94-219227 *03,517*

Intermolecular HF Motion in Ar(sub n)HF Micromatrices (n=1,2,3,4,): Classical and Quantum Calculations on a Pairwise Additive Potential Surface.
PB95-107025 *03,871*

SANS and LS Studies of Polymer Mixtures Under Shear Flow.
PB95-107090 *01,231*

Vibration, Rotation, and Parity Specific Predissociation Dynamics in Asymmetric OH Stretch Excited ArH2O: A Half Collision Study of Resonant V-V Energy Transfer in a Weakly Bound Complex.
PB95-107140 *00,872*

Monte Carlo Electron Trajectory Simulation of X-Ray Emission from Films Supported on Substrates.
PB95-107207 *04,522*

Thin Dyed-Plastic Dosimeter for Large Radiation Doses.
PB95-107363 *03,872*

Photoelectron Spectroscopy of Negatively Charged Bismuth Clusters: Bi(-)2, Bi(-)3, and Bi(-)4.
PB95-108494 *00,880*

Efficient Br(*) Laser Pumped by Frequency-Doubled Nd:YAG and Electronic-to-Vibrational Transfer-Pumped CO2 and HCN Lasers.
PB95-108684 *04,248*

Preparation and Characterization of (6)LiF and (10)B Reference Deposits for the Measurement of the Neutron Lifetime.
PB95-108692 *03,874*

Neutron Leakage Benchmark for Criticality Safety Research.
PB95-126132 *03,723*

Some Aspects of Fundamental Neutron Physics.
PB95-126298 *03,882*

Radiation Accident at an Industrial Accelerator Facility.
PB95-140117 *02,575*

Measurement of the (235)U(n,f) Reaction from Thermal to 1 keV.
PB95-140422 *03,886*

Neutron Focusing Lens Using Polycapillary Fibers.
PB95-141206 *03,889*

Grazing Incidence Prompt Gamma Emissions and Resonance-Enhanced Neutron Standing Waves in a Thin-Film.
PB95-150470 *03,892*

Excitation of Balmer Lines in Low-Current Discharges of Hydrogen and Deuterium.
PB95-150546 *03,893*

Fast Computer Evaluation of Radiative Properties of Hydrogenic Systems.
PB95-150553 *03,894*

Nanoscale Study of the As-Grown Hydrogenated Amorphous Silicon Surface.
PB95-150595 *04,573*

Laser Double Resonance Measurements of the Quenching Rates of Br((2)P1/2) with H20, D20, HDO, and O2.
PB95-150694 *00,921*

Standards for Corrected Fluorescence Spectra.
PB95-150835 *00,581*

Electron and Proton Dosimetry with Custom-Developed Radiochromic Dye Films.
PB95-151106 *03,713*

Electron-Impact Excitation of Si(3+)(3S yields 3P) Using a Merged-Beam Electron-Energy-Loss Technique.
PB95-151239 *03,904*

Slant Path Atmospheric Refraction Calibrator: An Instrument to Measure the Microwave Propagation Delays Induced by Atmospheric Water Vapor.
PB95-151270 *01,476*

Van der Waals Bond Lengths and Electronic Spectral Shifts of the Benzene-Kr and Benzene-Xe Complexes.
PB95-151387 *00,932*

N2(a'(sup 1)Sigma(sub g)(sup +)) Metastable Collisional Destruction and Rotational Excitation Transfer by N2.
PB95-151395 *00,933*

Nonadiabatic Effects in the Photoassociation of H2S.
PB95-151437 *00,934*

Liquid-Hydrogen Cold Neutron Source for the NBSR.
PB95-151619 *03,729*

Unusual Spin-Trap Chemistry for the Reaction of Hydroxyl Radical with the Carcinogen N-Nitrosodimethylamine.
PB95-151643 *00,692*

Photodissociation of Ammonia at 193.3nm: Rovibrational State Distribution of the NH2(A(2)A1) Fragment.
PB95-151775 *00,937*

Pattern-Recognition Analysis of Low-Resolution X-Ray Fluorescence Spectra.
PB95-151924 *00,588*

Tomographic Decoding Algorithm for a Nonoverlapping Redundant Array.
PB95-151932 *01,842*

IRAS Spectroscopic Observations of Young Planetary Nebulae.
PB95-152070 *00,072*

High-Precision Calculations of Cross Sections for Low-Energy Electron Scattering by Ground and Excited State of Sodium.
PB95-152161 *03,914*

Analysis of the Effectiveness of Oscillating Radial Collimators in Neutron Scattering Applications.
PB95-152252 *03,917*

Neutron Energy Deposition on the Nanometer Scale.
PB95-152260 *03,624*

Anomalous Dispersion and Thermal Expansion in Lightly-Doped KTa1-xNbxO3.
PB95-152302 *04,585*

Microdosimetry and Cellular Radiation Effects of Radon Progency in Human Bronchial Airways.
PB95-152344 *03,625*

Nuclear Heat Load Calculations for the NBSR Cold Neutron Source Using MCNP.
PB95-152955 *03,730*

Neutron Focusing Lens Using Polycapillary Fibers.
PB95-153078 *03,922*

Extrapolation Chamber Measurements on (90)Sr + (90)Y Beta-Particle Ophthalmic Applicator Dose Rates.
PB95-153375 *03,626*

Polarization Effects on Multiple Scattering Gamma Transport.
PB95-153615 *03,926*

Origin of the Second Length Scale Above the Magnetic Spiral Phase of Tb.
PB95-153698 *04,596*

Calibration of High-Energy Electron Beams by Use of Graphite Calorimeters.
PB95-161113 *04,598*

Time-Resolved Small-Angle Neutron Scattering Study of Spinodal Decomposition in Deuterated and Protonated Polybutadiene Blends. 1. Effect of Initial Thermal Fluctuations.
PB95-161196 *01,252*

Method of Realizing Spectral Irradiance Based on an Absolute Cryogenic Radiometer.
PB95-161204 *04,270*

ESR-Based Analysis in Radiation Processing.
PB95-161634 *03,931*

Detector-Based Candela Scale and Related Photometric Calibration Procedures at NIST.
PB95-161949 *04,273*

Vibronic Coupling and Other Many-Body Effects in the 4sigmag(-1) Photoionization Channel of CO2.
PB95-162509 *00,962*

Radiation Process Data: Collection, Analysis, and Interpretation.
PB95-162632 *03,628*

Dose Mapping of Radioactive Hot Particles Using Radiochromic Film.
PB95-162954 *03,714*

Problems Related to the Determination of Mass Densities of Evaporated Reference Deposits.
PB95-163226 *03,941*

Neutron Spectroscopic Comparison of Rare-Earth/Hydrogen alpha-Phase Systems.
PB95-163523 *00,970*

Cold Neutron Gain Calculations for the NBSR Using MCNP.
PB95-163978 *03,731*

Measurement of the (93)Nb(n,2n) (92m)Nb Cross Section in a (235)U Fission Spectrum.
PB95-163986 *03,945*

Analytic Calculation of Polarized Neutron Reflectivity from Superconductors.
PB95-164224 *04,629*

Thermal and Nonequilibrium Responses of Superconductors for Radiation Detectors.
PB95-164232 *02,156*

Laser Flash Photolysis/Time-Resolved FTIR Emission Study of a New Channel in the Reaction of CH3+O: Production of CO(v).
PB95-164281 *00,974*

Bonding in Doubly Charged Diatomics.
PB95-164315 *00,976*

Measurement of Radial Dose Distributions Around Small Beta Particle Emitters Using High Resolution Radiochromic Foil Dosimetry.
PB95-164604 *03,518*

Validation of the Inverse Square Law of Gravitation Using the Tower at Erie, Colorado, USA.
PB95-164646 *03,947*

Angular Variation of the Personal Dose Equivalent, Hp(0.07), for Beta Radiation and Nearly Monoenergetic Electron Beams: Preliminary Results.
PB95-168472 *03,630*

Updated Calculations for Routine Space-Shielding Radiation Dose Estimates: SHIELDOSE-2.
PB95-171039 *04,838*

Multi-Stage, Position Stabilized Vibration Isolation System for Neutron Interferometry.
PB95-175022 *03,955*

Interpreting the Readings of Multi-Element Personnel Dosimeters in Terms of the Personal Dose Equivalent.
PB95-175428 *03,631*

Grazing Incidence X-ray Photoemission and Its Implementation on Synchrotron Light Source X-ray Beamlines.
PB95-175766 *01,001*

Cold Neutron Prompt Gamma Activation Analysis at NIST: A Progress Report.
PB95-175964 *00,602*

Neutron Scattering by Hydrogen in Cold Neutron Prompt Gamma-Activation Analysis.
PB95-175972 *00,603*

Small Angle Neutrons Scattering from Nanocrystalline Palladium as a Function of Annealing.
PB95-176103 *03,354*

Electron-Ion-X-ray Spectrometer System.
PB95-176137 *03,958*

Polymerization Initiation by N-p-Tolylglycine: Free-Radical Reactions Studied by Pulse and Steady-State Radiolysis.
PB95-180014 *01,269*

Rayleigh Scattering Limits for Low-Level Bidirectional Reflectance Distribution Function Measurements.
PB95-180030 *04,307*

Neutron Scattering Study of the Orientation of a Liquid Crystalline Polymer by Shear Flow.
PB95-180196 *01,270*

Food Irradiation Dosimetry.
PB95-180675 *00,041*

Inelastic-Neutron-Scattering Studies of Poly(p-phenylene vinylene).
PB95-180766 *01,014*

High Resolution Inelastic Neutron Scattering Study of Phonon Self-Energy Effects in YBCO.
PB95-180881 *04,688*

Comparison of NIST and ISO Filtered Bremsstrahlung Calibration Beams.
PB95-180956 *03,967*

Calibration of Dosimeters for the Cryogenic Irradiation of Composite Materials Using an Electron Beam.
PB95-180964 *03,968*

Local-Mode Dynamics in YH2 and YD2 by Isotope-Dilution Neutron Spectroscopy.
PB95-181012 *01,017*

Roles of Local Classical Acceleration and Spatial Separation in the Neutral Particle Analogs of the Aharonov-Bohm Phases.
PB95-202362 *03,976*

Neutron Reflectivity Study of the Density Profile of a Model End-Grafted Polymer Brush: Influence of Solvent Quality.
PB95-202735 *01,274*

Hydration in Semicrystalline Polymers: Small-Angle Neutron Scattering Studies of the Effect of Drawing in Nylon-6 Fibers.
PB95-202990 *03,385*

Reactor Radiation Technical Activities, 1994. NAS-NRC Assessment Panel, April 6-7, 1995.
PB95-209888 *03,732*

NIST Reactor: Summary of Activities, October 1993 through September 1994.
PB95-220430 *04,700*

45 deg/0 deg Reflectance Factors of Pressed Polytetrafluoroethylene (PTFE) Powder.
PB95-260758 *04,328*

Intercomparison of Photometric Units Maintained at NIST (USA) and PTB (Germany), 1993.
PB95-261913 *04,329*

Transmission Properties of Short Curved Neutron Guides. Part 1. Acceptance Diagram Analysis and Calculations.
PB96-102199 *04,021*

Evolution of X-ray Resonance Raman Scattering into X-ray Fluorescence from the Excitation of Xenon Near the L3 Edge.
PB96-102751 *04,025*

Measuring Hydrogen by Cold-Neutron Prompt-Gamma Activation Analysis.
PB96-111877 *00,612*

Study of Multiple Scattering Background in Compton Scatter Imaging.
PB96-112222 *04,425*

Small Angle Neutron Scattering Studies of Structural Characteristics of Argarose Gels.
PB96-112305 *03,475*

Analytical Applications of Guided Neutron Beams.
PB96-112347 *04,041*

Strangeness Flow Difference in Nuclear Collisions at 15A and 200A GeV.
PB96-119631 *04,042*

Neutron Techniques in Materials Science and Related Disciplines.
PB96-119698 *02,980*

Extending the Angular Range of Neutron Reflectivity Measurements from Planar Lipid Bilayers: Applications to a Model Biological Membrane.
PB96-122569 *03,476*

Study of Laser Resonance Ionization Mass Spectrometry Using a Glow Discharge Source.
PB96-123203 *03,360*

Anionic Triphenylmethane Dye Solutions for Low-Dose Food Irradiation Dosimetry.
PB96-135173 *03,715*

Alcohol Solutions of Triphenyl-Tetrazolium Chloride as High-Dose Radiochromic Dosimeters.
PB96-135249 *03,716*

Oscillometric and Conductometric Analysis of Aqueous and Organic Dosimeter Solutions.
PB96-135256 *04,054*

Dosimetry Systems for Radiation Processing.
PB96-135280 *03,717*

Temperature and Relative Humidity Dependence of Radiochromic Film Dosimeter Response to Gamma and Electron Radiation.
PB96-135298 *03,718*

Real Time Monitoring of Electron Processors.
PB96-135306 *03,719*

Low-Frequency Excitations of Oriented DNA.
PB96-137799 *03,548*

MCNP Model of the National Bureau of Standards Reactor (NBSR) Core.
PB96-138599 *03,733*

Research and Development Activities in Electron Paramagnetic Resonance Dosimetry.
PB96-141288 *03,635*

Orientation Effects on ESR Analysis of Alanine-Polymer Dosimeters.
PB96-146725 *03,720*

Radiation-Chemical Reaction of 2,3,5-Triphenyl-Tetrazolium Chloride in Liquid and Solid State.
PB96-146733 *01,124*

Investigation of Applicability of Alanine and Radiochromic Detectors to Dosimetry of Proton Clinical Beams.
PB96-146782 *03,636*

Al L2,3 Core Excitons in AlxGa1-x as Studied by Soft-X-ray Reflection and Emission.
PB96-157839 *04,067*

Soft-X-ray-Emission Investigation of Cobalt Implanted Silicon Crystals.
PB96-157912 *04,069*

Soft-X-ray-Emission Spectra of Solid Kr and Xe.
PB96-157920 *04,070*

Soft-X-ray-Emission Studies of Bulk Fe3Si, FeSi, and FeSi2, and Implanted Iron Silicides.
PB96-157938 *04,071*

Cooper M(sub II,III) X-ray-Emission Spectra of Copper Oxides and the Bismuth Cuprate Superconductor.
PB96-158027 *04,077*

New NIST/ARPA National Soft X-ray Reflectometry Facility.
PB96-158092 *04,080*

Soft-X-ray Damage to p-terphenyl Coatings for Detectors.
PB96-159611 *04,364*

System for Intercomparing Standard Solutions of Beta-Particle Emitting Radionuclides.
PB96-159637 *03,707*

International Radon-in-Air Measurement Intercomparison Using a New Transfer Standard.
PB96-159751 *03,708*

External Gamma-ray Counting of Selected Tissues from a Thorotrast Patient.
PB96-160254 *03,637*

Phonon Relaxation in Soft-X-ray Emission of Insulators.
PB96-160296 *04,085*

New and Revised Half-Life Measurement Results.
PB96-160346 *00,695*

NIST Metrology for Soft X-ray Multilayer Optics.
PB96-160379 *04,088*

Soft X-ray Reflectometry Program at the National Institute of Standards and Technology.
PB96-160395 *04,368*

Instrumental Smearing Effects in Radially Symmetric Small-Angle Neutron Scattering by Numerical and Analytical Methods.
PB96-160429 *02,984*

Inter-Laboratory Trials of the EPR Method for the Detection of Irradiated Meats Containing Bone.
PB96-161690 *00,042*

Measurement of the Neutron Lifetime.
PB96-161708 *04,094*

Measurement of the (10)B(n, alpha1gamma)(7)Li Cross Section in the 0.3 to 4 MeV Neutron Energy Interval.
PB96-161799 *04,098*

Gas Absorption during Ion-Irradiation of a Polymer Target.
PB96-161864 *04,099*

Upgrade and Modernization Projects at the NBSR.
PB96-161872 *03,737*

International Marine-Atmospheric (222)Rn Measurement Intercomparison in Bermuda. Part 1. NIST Calibration and Methodology for Standardized Sample Additions.
PB96-175674 *00,114*

International Marine-Atmospheric (222)Rn Measurement Intercomparison in Bermuda. Part 2. Results for the Participating Laboratories.
PB96-175682 *00,115*

Realization of NIST 1995 Luminous Flux Scale Using the Integrating Sphere Method.
PB96-176433 *04,374*

Simulations of Neutron Focusing with Curved Mirrors.
PB96-176649 *02,200*

Design of a High-Flux Backscattering Spectrometer for Ultra-High Resolution Inelastic Neutron Measurements.
PB96-179577 *02,992*

Radiochromic Solid-State Polymerization Reaction.
PB96-180146 *01,290*

Alpha-Particle and Electron Capture Decay of (209)Po.
PB96-186085 *04,119*

Scattered Fractions of Dose from 18 and 25 MV X-ray Radiotherapy Linear Accelerators.
PB96-186101 *04,120*

Mode-Locked Lasers for High-Accuracy Radiometry.
PB96-204201 *04,134*

Radon in the Lung.
PB97-110035 *03,638*

Liquid-Scintillation Counting Techniques for the Standardization of Radionuclides Used in Therapy.
PB97-110084 *03,709*

Needs for Brachytherapy Source Calibrations in the United States.
PB97-110092 *03,521*

Radioassays of Yttrium-90 Used in Nuclear Medicine.
PB97-110100 *03,522*

Problem of Convection in the Water Absorbed Dose Calorimeter.
PB97-110159 *03,523*

Stable Silicon Photodiodes for Absolute Intensity Measurements in the VUV and Soft X-ray Regions.
PB97-110175 *04,135*

EPR Dosimetry of Cortical Bone and Tooth Enamel Irradiated with X and Gamma Rays: Study of Energy Dependence.
PB97-110373 *03,639*

Exposure-to-Absorbed-Dose Conversion for Human Adult Cortical Bone.
PB97-110381 *03,640*

Calculation of Photon Mass Energy-Transfer and Mass Energy-Absorption Coefficients.
PB97-110399 *04,137*

Neutron Diffraction Texture Study of Deformed Uranium Plates.
PB97-111587 *03,010*

63Ni Half-Life: A New Experimental Determination and Critical Review.
PB97-111603 *00,700*

Nickel-63 Standardization: 1968-1995.
PB97-111819 *00,701*

X-ray Reflectivity Determination of Interface Roughness Correlated with Transport Properties of (AlGa)As/GaAs High Electron Mobility Transistor Devices.
PB97-111868 *04,149*

Results of a NIST/VNIIOFI Comparison of Spectral-Radiance Measurements.
PB97-113021 *04,159*

Comparison of Filter Radiometer Spectral Responsivity with the NIST Spectral-Irradiance and Illuminance Scales.
PB97-113161 *04,162*

Diffraction of Neutron Standing Waves in Thin Films with Resonance Enhancement.
PB97-113278 *04,164*

Experimentally Measured Total X-ray Attenuation Coefficients Extracted from Previously Unprocessed Documents Held by the NIST Photon and Charged Particle Data Center.
PB97-114474 *04,165*

Simultaneous Measurement of Normal Spectral Emissivity by Spectral Radiometry and Laser Polarimetry at High Temperatures in Pulse-Heating Experiments: Application to Molybdenum and Tungsten.
PB97-118376 *02,694*

Colour Centres in LiF for Measurement of Absorbed Doses Up to 100 MGy.
PB97-118756 *04,169*

Effect of Formulation Changes on the Response to Ionizing Radiation of Radiochromic Dye Films.
PB97-119028 *04,171*

Results of the ASTM Nuclear Methods Intercomparison on NIST Apple and Peach Leaves Standard Reference Materials.
PB97-119036 *03,490*

Measurements of the (235)U(n,f) Cross Section in the 3 to 30 MeV Neutron Energy Region.
PB97-119051 *04,172*

Measurements of the (237)Np(n,f) Cross Section.
PB97-119069 *04,173*

Mass Assay and Uniformity Test of Boron Targets by Neutron Beam Methods.
PB97-119085 *04,175*

Novel Radiochromic Films for Clinical Dosimetry.
PB97-119259 *03,641*

Calibration and Performance of GafChromic DM-100 Radiochromic Dosemeters.
PB97-119291 *00,703*

Flat and Curved Crystal Spectrography for Mammographic X-ray Sources.
PB97-122246 *03,642*

Small Angle Neutron Scattering Study of the Structure and Formation of MCM-41 Mesoporous Molecular Sieves.
PB97-122337 *03,110*

Complex Time Dependence of the EPR Signal of Irradiated L-alpha-alanine.
PB97-122436 *04,180*

Overview of a Radiation Accident at an Industrial Accelerator Facility.
PB97-122485 *02,612*

Measuring Nondipolar Asymmetries of Photoelectron Angular Distributions.
PB97-122493 *01,193*

NUCLEAR POWER
Review of the USCEA/NIST Measurement Assurance Program for the Nuclear Power Industry.
PB95-126272 *03,712*

NUCLEAR POWER PLANTS
Proceedings of the Digital Systems Reliability and Nuclear Safety Workshop. Held in Rockville, Maryland on September 13-14, 1993.
NUREG/CP-0136 *03,728*

Assessing Functional Diversity by Program Slicing.
PB96-160890 *03,734*

Analysis of Standards for the Assurance of High Integrity Software.
PB96-161351 *03,735*

Control and Instrumentation: Standards for High-Integrity Software.
PB96-161369 *03,736*

Preliminary Processing of the Lotung LSST Data.
PB96-165972 *03,690*

Methodology for Developing and Implementing Alternative Temperature-Time Curves for Testing the Fire Resistance of Barriers for Nuclear Power Plant Applications.
PB96-193784 *03,742*

Estimation of System Damping at the Lotung Site by Application of System Identification.
PB96-214697 *01,351*

USCEA/NIST Measurement Assurance Programs for the Radiopharmaceutical and Nuclear Power Industries.
PB97-110514 *03,721*

NUCLEAR REACTORS
Reactor Radiation Technical Activities, 1994. NAS-NRC Assessment Panel, April 6-7, 1995.
PB95-209888 *03,732*

Upgrade and Modernization Projects at the NBSR.
PB96-161872 *03,737*

Reactor Radiation Technical Activities, 1995.
PB96-193644 *03,741*

NUCLEATE BOILING
Simultaneous Visual and Calorimetric Measurements of R11, R123, and R123/Alkylbenzene Nucleate Flow Boiling.
PB94-172426 *03,251*

Visual Measurement Technique for Analysis of Nucleate Flow Boiling.
PB95-143301 *03,262*

NUCLEATION
Controlled Nucleation in Aerosol Reactors for Supression of Agglomerate Formation.
PB95-151973 *00,672*

Surface Roughness Evaluation of Diamond Films Grown on Substrates with a High Density of Nucleation Sites.
PB95-162418 *03,018*

Growth and Nucleation of Hydrogenated Amorphous Silicon on Silicon (100) Surfaces.
PB96-176516 *02,991*

Epitaxial Nucleation and Growth of Chemically Derived Ba2YCu3O7-x Thin Films on (001) SrTiO3.
PB96-190186 *04,787*

NUCLEIC ACIDS
Salt-PEG Two-Phase Aqueous Systems to Purify Proteins and Nucleic Acid Mixtures.
PB94-200375 *03,527*

Nucleic Acid Database: Present and Future.
PB97-109078 *00,518*

NUCLEOTIDES
beta-D-Glucosyl-Hydroxymethyluracil: A Novel Modified Base Present in the DNA of the Parastic Protozoan T. brucei.
PB94-172319 *03,524*

NUETRON ATOMS
Gravitational Sisyphus Cooling of (87)Rb in a Magnetic Trap.
PB96-200704 *04,379*

NUETRON MEASUREMENTS
Design of a High-Flux Backscattering Spectrometer for Ultra-High Resolution Inelastic Neutron Measurements.
PB96-179577 *02,992*

NUMERICAL ANALYSIS
Convergence Properties of a Class of Rank-Two Updates. (NIST Reprint).
PB95-180097 *03,430*

Numerical Evaluation of Special Functions.
PB96-119557 *03,417*

NUMERICAL CONTROL
NIST RS274/NGC Interpreter Version 1.
PB94-187788 *02,814*

Issues Concerning Material Removal Shape Element Volumes (MRSEVs).
PB95-210167 *02,885*

NIST RS274KT Interpreter.
PB96-147954 *02,835*

NUMERICAL DATA BASES
Numeric Data Distribution: The Vital Role of Data Exchange in Today's World.
N95-15937/2 *02,622*

NUMERICAL SIMULATION
Gravity-Current Transport in Building Fires.
PB96-147046 *01,415*

NURSING HOMES
Evaluating Small Board and Care Homes: Sprinklered vs. Nonsprinklered Fire Protection.
PB94-206356 *00,195*

NUTRIENTS
Recently Developed NIST Food Related Standard Reference Materials.
PB94-198322 *00,035*

NUTRITION
Nutritional Status and Growth in Juvenile Rheumatoid Arthritis.
PB94-198470 *03,515*

NUTRITIVE VALUE
Mixed Diet Reference Materials for Nutrient Analysis of Foods: Preparation of SRM-1548 Total Diet.
PB95-151692 *03,593*

NVLAP (NATIONAL VOLUNTARY LABORATORY ACCREDITATION PROGRAM)
National Voluntary Laboratory Accreditation Program: Energy Efficient Lighting Products.
PB94-219060 *02,642*

National Voluntary Laboratory Accreditation Program: POSIX. Portable Operating System Interface.
PB95-189478 *02,661*

NVLAP (NATIONAL VOLUNTARY LABORATORY ACCREDITION PROGRAM)
National Voluntary Laboratory Accreditation Program 1996 Directory.
PB96-162714 *00,485*

NVLAP PROGRAM
National Voluntary Laboratory Accreditation Program: Ionizing Radiation Dosimetry.
PB95-128658 *03,623*

NVLAP SYSTEM
NVLAP Procedures U.S. Code of Federal Regulations. Title 15, Subtitle A, Chapter 2, Part 7. (Effective December 1984; Amended September 1990).
PB94-160850 *02,627*

NYLON 6
Hydration in Semicrystalline Polymers: Small-Angle Neutron Scattering Studies of the Effect of Drawing in Nylon-6 Fibers.
PB95-202990 *03,385*

NYLON FIBERS
Hydration in Semicrystalline Polymers: Small-Angle Neutron Scattering Studies of the Effect of Drawing in Nylon-6 Fibers.
PB95-202990 *03,385*

OBITUARIES
Churchill Eisenhart, 1913-1994.
PB96-137740 *03,447*

OBJECT DATABASE MANAGEMENT
Persistent Object Base System Testing and Evaluation.
PB95-220588 *01,730*

Interoperability Experiments with CORBA and Persistent Object Base Systems.
PB96-183140 *01,772*

OBJECT-ORIENTED PROGRAMMING
Object SQL: Language Extensions for Object Data Management.
PB95-125902 *01,704*

Object-Oriented Technology Research Areas.
PB95-199329 *01,726*

Testability of Object-Oriented Systems.
PB95-242418 *01,733*

Object-Oriented Tel/Tk Binding for Interpreted Control of the NIST EXPRESS Toolkit in the NIST STEP Application Protocol Development Environment.
PB96-141049 *02,785*

OBJECT ORIENTED PROGRAMS
Conformance Testing and Specification Management.
PB97-113781 *02,849*

OBJECT ORIENTED SYSTEMS
Roadmap for the Computer Integrated Manufacturing (CIM) Application Framework.
PB96-122759 *02,832*

OBJECT-ORIENTED TECHNOLOGY
Object-Oriented Technology Research Areas.
PB95-199329 *01,726*

OBJECT PROGRAMS
Associated Object Model for Distributed Systems.
PB94-212016 *01,694*

OBSERVATION
Developments in Stellar Coronae.
PB96-176706 *00,107*

OBSTACLE AVOIDANCE
New Method to Calculate Looming for Autonomous Obstacle Avoidance.
PB95-171435 *01,600*

Real-Time Obstacle Avoidance Using Central Flow Divergence and Peripheral Flow.
PB95-198677 *02,937*

OCCUPATIONAL EXPOSURE
Interpreting the Readings of Multi-Element Personnel Dosimeters in Terms of the Personal Dose Equivalent.
PB95-175428 *03,631*

OCCUPATIONAL SAFETY AND HEALTH
Documentation for Immediately Dangerous to Life or Health Concentrations (IDLHs).
PB94-195047 *03,602*

NIOSH Pocket Guide to Chemical Hazards.
PB95-100368 *03,603*

Radiation Accident at an Industrial Accelerator Facility.
PB95-140117 *02,575*

Characterization of a Health Physics Instrument Calibration Range.
PB95-164554 *03,629*

NIOSH Comments to DOL on Risk Estimates from the Cadmium Cohort Study by L. Stayner, February 7, 1992.
PB95-267779 *03,604*

Overview of a Radiation Accident at an Industrial Accelerator Facility.
PB97-122485 *02,612*

OCEAN ENGINEERING
Non-Gaussian Noise Effects on Reliability of Multistable Systems.
PB96-122726 *04,213*

OCTACALCIUM PHOSPHATE
Octacalcium Phosphate. 3. Infrared and Raman Vibrational Spectra.
PB94-172244 *00,756*

Procedure for the Study of Acidic Calcium Phosphate Precursor Phases in Enamel Mineral Formation.
PB95-164448 *03,564*

OCTACALCIUM PHOSPHATE CARBOXYLATES
Octacalcium Phosphate Carboxylates. 1. Preparation and Identification.
PB95-161535 *00,660*

Octacalcium Phosphate Carboxylates. 2. Characterization and Structural Consideration.
PB95-161543 *00,955*

OCTACALCIUM PHOSPHATE SUCCINATE
Octacalcium Phosphate Carboxylates IV. Kinetics of Formation and Solubility of Octacalcium Phosphate Succinate.
PB94-185600 *00,776*

Octacalcium Phosphate Carboxylates. 5. Incorporation of Excess Succinate and Ammonium Ions in the Octacalcium Phosphate Succinate Structure.
PB95-168894 *00,166*

OCTADECANETHIOL
Silver Metalization of Octadecanethiol Monolayers Self-Assembled on Gold.
PB95-150744 *00,923*

ODP (OPEN DISTRIBUTED PROCESSING)
Comparison of POSIX Open System Environment (OSE) and Open Distributed Processing (ODP) Reference Models.
PB96-131495 *01,820*

OFF-AXIS ASPHERICS
Test of a Slow Off-Axis Parabola at Its Center of Curvature.
PB96-138482 *04,352*

OFF LATTICE POLYMER CHAINS
Effects of Variable Excluded Volume on the Dimensions of Off-Lattice Polymer Chains.
PB94-212941 *01,229*

OFFICE BUILDINGS
Manual for Ventilation Assessment in Mechanically Ventilated Commercial Buildings.
PB94-145653 *00,239*

Source of Phenol Emissions Affecting the Indoor Air of an Office Building.
PB94-154382 *03,600*

Air Change Effectiveness Measurements in Two Modern Office Buildings.
PB94-185766 *00,243*

Environmental Evaluation of a New Federal Office Building.
PB94-199874 *02,538*

Fire Growth Analysis of the Fire of March 20, 1990, Pulaski Building, 20 Massachusetts Avenue, N.W., Washington, DC.
PB94-205952 *00,194*

Ventilation Rates in Office Buildings.
PB95-108825 *02,539*

Field Measurements of Ventilation and Ventilation Effectiveness in an Office/Library Building.
PB95-108833 *00,247*

Study of Ventilation and Carbon Dioxide in an Office Building.
PB95-150140 02,542

Assessing Ventilation Effectiveness in Mechanically Ventilated Office Buildings.
PB95-162079 00,255

Ventilation Effectiveness Measurements in Two Modern Office Buildings.
PB95-176012 02,553

Indoor Air Quality Commissioning of a New Office Building.
PB95-182309 00,262

Measurements of Outdoor Air Distribution in an Office Building.
PB95-210944 00,264

Workplan to Analyze the Energy Impacts of Envelope Airtightness in Office Buildings.
PB96-154463 00,273

Study of Ventilation Measurement in an Office Building.
PB96-155593 00,274

Development and Application of an Indoor Air Quality Commissioning Program in a New Office Building.
PB96-155601 00,275

Indoor Air Quality Commissioning of a New Office Building.
PB97-110142 00,279

Post-Occupancy Evaluation of the Forrestal Building.
PB97-111298 00,280

Survey of Fuel Loads in Contemporary Office Buildings.
PB97-114235 00,233

Evaluation of Survey Procedures for Determining Occupant Load Factors in Contemporary Office Buildings.
PB97-116222 00,238

Materials-Science Based Approach to Phenol Emissions from a Flooring Material in an Office Building.
PB97-118749 02,572

OFFICE EQUIPMENT

Office Work Station Heat Release Rate Study: Full Scale versus Bench Scale.
PB96-190178 01,428

OFFSET SUSCEPTIBILITY

Offset Susceptibility of Superconductors.
PB94-212263 04,503

OFFSHORE DRILLING

Composite Materials for Offshore Operations: Proceedings of the International Workshop (1st). Held in Houston, Texas on October 26-28, 1993.
PB96-109509 03,169

OFFSHORE STRUCTURES

Report of a Workshop on Requalification of Tubular Steel Joints in Offshore Structures. Held in Houston, Texas on September 5-6, 1995.
PB96-210760 03,699

OHM

New International Representations of the Volt and Ohm Effective January 1, 1990.
PB95-150777 01,890

OIL SPILLS

In situ Burning of Oil Spills: Mesoscale Experiments.
PB94-142973 01,355

In Situ Burning Oil Spill Workshop Proceedings. Held in Orlando, Florida on January 26-28, 1994.
PB95-104907 02,583

In situ Burning of Oil Spills: Mesoscale Experiments and Analysis.
PB95-163747 02,587

Smoke Emission from Burning Crude Oil.
PB96-122890 01,407

Smoke Plume Trajectory from In situ Burning of Crude Oil in Alaska: Field Experiments.
PB96-131560 02,594

Smoke Plume Trajectory from In situ Burning of Crude Oil: Field Experiments.
PB96-200993 02,597

OIL TANKERS

Stranding Experiments on Double Hull Tanker Structures.
PB96-123112 03,749

OIL WELLS

Ground-Based Smoke Sampling Techniques Training Course and Collaborative Local Smoke Sampling in Saudi Arabia.
PB94-143542 02,532

Investigation of Oil and Gas Well Fires and Flares.
PB94-193976 03,695

Flame Heights and Heat Release Rates of 1991 Kuwait Oil Field Fires.
PB96-119342 01,404

Development of Hazard Assessment and Suppression Technology for Oil and Gas Well Blowout and Diverter Fires.
PB96-122965 01,408

OILING POINT

Physical Properties of Some Purified Aliphatic Hydrocarbons.
AD-A297 265/1 00,657

OILS

National Standard Petroleum Oil Tables.
AD-A279 952/6 02,469

OLEORESINS

Preliminary Investigation of Oleoresin Capsicum.
PB96-179486 03,520

OLIGOMERS

Solid State (13)C NMR and Raman Studies of Cellulose Triacetate: Oligomers, Polymorphism, and Inferences about Chain Polarity.
PB96-176532 01,289

OLTIPRAZ

Determination of Oltipraz in Serum by High-Performanace Liquid Chromatography with Optical Absorbance and Mass Spectrometric Detection.
PB94-200201 03,493

OMEGA PHASE

Ordered omega-Derivatives in a Ti-37.5Al-2ONb at% Alloy.
PB94-211091 03,331

ON-LINE SYSTEMS

STEP On-Line Information Service (SOLIS). The IGES/PDES Organization.
PB95-137790 02,777

Electronic Access to Standards on the Information Highway.
PB96-131578 01,494

ONLINE SYSTEMS

Global Information Infrastructure: Agenda for Cooperation.
PB95-178604 01,482

OPEN CHANNEL FLOW

Probabilistic Computation of Poiseuille Flow Velocity Fields.
PB96-102520 04,209

OPEN DISTRIBUTED PROCESSING

Comparison of POSIX Open System Environment (OSE) and Open Distributed Processing (ODP) Reference Models.
PB96-131495 01,820

OPEN-ENDED PROBES

Open-Ended Coaxial Probes for Nondestructive Testing of Substrates and Circuit Boards.
PB96-122825 02,078

OPEN SYSTEM ENVIRONMENT

Porting Multimedia Applications to the Open System Environment.
PB94-172921 02,721

Guide on Open System Environment (OSE) Procurements.
PB95-169496 01,626

Comparison of POSIX Open System Environment (OSE) and Open Distributed Processing (ODP) Reference Models.
PB96-131495 01,820

Open System Environment (OSE): Architectural Framework for Information Infrastructure.
PB96-146360 00,002

Application Portability Profile (APP): The U.S. Government's Open System Environment Profile Version 3.0.
PB96-158712 01,753

OPEN SYSTEMS

Conference Report: International Conference on the Application of Standards for Open Systems (6th).
PB96-161211 01,762

OPEN SYSTEMS ENVIRONMENT

Open System Environment Implementors Workshop (OIW); Standardization Role Defined.
PB96-180047 01,828

OPEN SYSTEMS INTERCONNECTION

Formal Multi-Layer Test Methodology and Its Application to OSI.
PB94-172194 02,718

ISO/IEC Workshop on Worldwide Recognition of OSI Test Results Regional Progress - North America.
PB94-172202 02,719

IGOSS-Industry/Government Open Systems Specification.
PB94-207453 01,806

Conformance Testing for OSI Protocols.
PB96-102686 01,631

Lessons from the Establishment of the U.S. GOSIP Testing Program.
PB96-119359 01,817

Open Issues in OSI Protocol Development and Conformance Testing.
PB96-122908 01,818

Data Communications Strategy.
PB96-167846 02,738

OPEN SYSTEMS INTERCONNECTIONS

Supplement to Stable Implementation Agreements for Open Systems Interconnection Protocols. Version 3, September 1990. Change Page Index, Version 3, June 1990 (Stable) Change Pages Issued December 1990; Output from September 1990 OSI Workshop (NIST Special Publication 500-177).
PB94-164035 01,467

OPERATING SYSTEMS (COMPUTERS)

Portable Operating System Interface (POSIX). Part 2. Shell and Utilities. Category: Software Standard; Subcategory: Operating Systems.
FIPS PUB 189 01,797

Open Systems Software Standards in Concurrent Engineering.
PB96-160932 01,758

NIST POSIX Testing Program.
PB96-160973 01,821

OPERATIONS RESEARCH

Time Dependent Vector Dynamic Programming Algorithm for the Path Planning Problem.
PB94-215688 03,428

OPHTHALMIC APPLICATIONS

Comparison of NIST and Manufacturer Calibrations of (90)Sr+(90)Y Ophthalmic Applicators.
PB96-123708 03,634

OPHTHALMIC APPLICATORS

Extrapolation Chamber Measurements on (90)Sr + (90)Y Beta-Particle Ophthalmic Applicator Dose Rates.
PB95-153375 03,626

OPHTHALMOLOGY

Extrapolation Chamber Measurements on (90)Sr + (90)Y Beta-Particle Ophthalmic Applicator Dose Rates.
PB95-153375 03,626

Measurement of Radial Dose Distributions Around Small Beta Particle Emitters Using High Resolution Radiochromic Foil Dosimetry.
PB95-164604 03,518

OPTICAL ABSORPTION

Interdigitated Stacked P-I-N Multiple Quantum Well Modulator.
PB97-112296 02,455

OPTICAL BIOSENSORS

Optical Biosensor Using a Fluorescent, Swelling Sensing Element.
PB95-175899 03,541

OPTICAL CHARACTER RECOGNITION

Evaluating Form Designs for Optical Character Recognition.
PB94-168044 01,830

Second Census Optical Character Recognition Systems Conference.
PB94-188711 01,832

NIST Form-Based Handprint Recognition System.
PB94-217106 01,838

Binary Decision Clustering for Neural Network Based Optical Character Recognition.
PB95-171971 01,848

Method and Evaluation of Character Stroke Preservation on Handprint Recognition.
PB95-251724 01,850

Improving Neural Network Performance for Character and Fingerprint Classification by Altering Network Dynamics.
PB95-267803 01,851

Effect of Training Dynamics on Neural Network Performance.
PB95-267845 01,852

Improving Neural Network Performance for Character and Fingerprint Classification by Altering Network Dynamics.
PB96-123195 01,856

Binary Decision Clustering for Neural-Network-Based Optical Character Recognition.
PB96-186184 01,857

Generalized Form Registration Using Structure-Based Techniques.
PB96-191374 01,858

Component-Based Handprint Segmentation Using Adaptive Writing Style Model.
PB96-193669 01,859

OPTICAL CHARACTERIZATION

Optical Characterization of Materials and Devices for the Semiconductor Industry: Trends and Needs.
PB96-167192 02,431

OPTICAL COATINGS

XUV Characterization Comparison of Mo/Si Multilayer Coatings.
PB95-164000 04,278

OPTICAL COMMUNICATION

Lightwave Standards Development at NIST.
PB95-168563 01,480

Precise Laser-Based Measurements of Zero-Dispersion Wavelength in Single-Mode Fibers.
PB96-201124 01,511

OPTICAL CURRENT TRANSDUCERS

Optical Current Transducer for Calibration Studies.
PB94-185907 02,121

OPTICAL DATA

Use of Sum Rules on the Energy-Loss Function for the Evaluation of Experimental Optical Data.
PB95-150736 04,264

OPTICAL DATA STORAGE MATERIALS

Research on Methods for Determining Optical Disk Media Life Expectancy Estimates.
PB96-160304 01,633

OPTICAL DENSITY

Development of Neutral-Density Infrared Filters Using Metallic Thin Films.
PB96-180286 02,998

Optical Density Measurements of Laser Eye Protection Materials.
PB96-190301 00,190

OPTICAL DETECTION
Beamcon III, a Linearity Measurement Instrument for Optical Detectors.
PB96-113576 *04,337*

OPTICAL DETECTORS
Lightwave Standards Development at NIST.
PB95-168563 *01,480*

Spatial Uniformity of Optical Detector Responsivity.
PB95-168845 *02,162*

Optical Detector Nonlinearity: A Comparison of Five Methods.
PB95-169355 *04,291*

Accurate Measurement of Optical Detector Nonlinearity.
PB95-203576 *02,181*

Optical Detector Nonlinearity: Simulation.
PB96-165378 *02,199*

Precise Laser-Based Measurements of Zero-Dispersion Wavelength in Single-Mode Fibers.
PB96-201124 *01,511*

OPTICAL DISKS
Optical Storage Media Data Integrity Studies.
N95-24130/3 *01,620*

Design and Development of an Information Retrieval System for the EAMATE Data. Volume 2 of 2. Appendices.
PB94-168390 *00,487*

Standardization of Testing Methods for Optical Disk Media Characteristics and Related Activities at NIST.
PB95-108486 *01,624*

NIST Program for Investigating Error Reporting Capabilities of Optical Disk Drives.
PB96-160627 *01,635*

OPTICAL EQUIPMENT
Simple and Efficient Low-Temperature Sample Cell for Infrared Spectrophotometry.
PB94-199197 *00,545*

Video Microscopy Applied to Optical Fiber Geometry Measurements.
PB95-173068 *04,295*

OPTICAL FIBER SENSORS
Optical Fiber Sensors: Accelerating Applications in Navy Ships.
PB94-186848 *02,632*

Polarization Dependence of Response Functions in 3x3 Sagnac Optical Fiber Current Sensors.
PB95-162426 *02,154*

Effect of Semiconductor Laser Characteristics on Optical Fiber Sensor Performance.
PB95-169132 *02,167*

Self-Calibrating Fiber Optic Sensors: Potential Design Methods.
PB95-169298 *02,172*

Self Calibrating Fiber Optic Sensors: Potential Design Methods.
PB95-169306 *02,173*

Polarization Dependence of Response Functions in 3x3 Sagnac Optical Fiber Current Sensors.
PB96-122684 *02,189*

OPTICAL FIBERS
Technical Digest: Symposium on Optical Fiber Measurements (8th), 1994. Held in Boulder, Colorado on September 13-15, 1994.
PB94-207636 *04,231*

In situ On-Line Optical Fiber Sensor for Fluorescence Monitoring in Bioreactors.
PB94-212024 *03,587*

Complex Propagation Constants for Nonuniform Optical Waveguides: Calculations.
PB95-125910 *04,249*

Fiber Spot Size: A Simple Method of Calculation.
PB95-125936 *04,250*

LP11-Mode Leakage Loss in Coated Depressed Clad Fibers.
PB95-141115 *02,145*

Optical Fiber Geometry: Accurate Measurement of Cladding Diameter.
PB95-151940 *04,266*

Optical Fiber Geometry by Gray-Scale Analysis with Robust Regression.
PB95-161519 *04,272*

Bragg Gratings in Optical Fibers Produced by a Continuous-Wave Ultraviolet Source.
PB95-162020 *04,274*

Growth of Bragg Gratings Produced by Continuous-Wave Ultraviolet Light in Optical Fiber.
PB95-162038 *04,275*

Vector Theory of Diffraction by a Single-Mode Fiber: Application to Mode-Field Diameter Measurements.
PB95-164182 *04,279*

Interlaboratory Comparison of Polarization-Holding Parameter Measurements on High-Birefringence Optical Fiber.
PB95-168464 *04,280*

Low-Coherence Interferometric Measurement of Group Transit Times in Precision Optical Fibre Delay Lines.
PB95-168480 *02,158*

Lightwave Standards Development at NIST.
PB95-168563 *01,480*

Symbolic Programming with Series Expansions: Applications to Optical Waveguides.
PB95-168589 *04,283*

Comparison of UV-Induced Fluorescence and Bragg Grating Growth in Optical Fiber.
PB95-168597 *04,284*

Bent Rectangular Core Waveguides: An Accurate Perturbation Approach.
PB95-168803 *04,289*

Calculated Fiber Attenuation: A General Method Yielding Stationary Values.
PB95-175501 *04,298*

Fibre Splice Loss: A Simple Method of Calculation.
PB95-175519 *04,299*

Decrease of Fluorescence in Optical Fiber during Exposure to Pulsed or Continuous-Wave Ultraviolet Light.
PB95-203071 *04,320*

Polarization Insensitive 3x3 Sagnac Current Sensor Using Polarizing Spun High-Birefringence Fiber.
PB96-119276 *02,187*

Standard Reference Materials for Optical Fibers and Connectors.
PB96-119805 *04,344*

Decay of Bragg Gratings in Hydrogen-Loaded Optical Fibers.
PB96-122643 *04,345*

Fiber Coating Diameter: Toward a Glass Artifact Standard.
PB96-140389 *02,234*

Annealing of Bragg Gratings in Hydrogen-Loaded Optical Fiber.
PB96-155437 *04,361*

Comparison of UV Photosensitivity and Fluorescence during Fiber Grating Formation.
PB96-155445 *04,362*

Automated Measurement of Nonlinearity of Optical Fiber Power Meters.
PB96-176540 *04,110*

Precise Laser-Based Measurements of Zero-Dispersion Wavelength in Single-Mode Fibers.
PB96-201124 *01,511*

Technical Digest: Symposium on Optical Fiber Measurements (9th), 1996. Held in Boulder, Colorado on October 1-3, 1996.
PB97-108583 *04,383*

Anomalous Relation between Time and Frequency Domain PMD Measurements.
PB97-119390 *04,398*

OPTICAL FILTERS
Standard Reference Materials: Glass Filters as a Standard Reference Material for Spectrophotometry - Selection, Preparation, Certification, and Use of SRM 930 and SRM 1930.
PB94-188844 *00,536*

Determination of the Transmittance Uniformity of Optical Filter Standard Reference Materials.
PB95-261921 *02,182*

OPTICAL FLOW
Reliable Optical Flow Algorithm Using 3-D Hermite Polynomials.
PB94-145620 *01,829*

General Motion Model and Spatio-Temporal Filters for Computing Optical Flow.
PB95-171096 *01,847*

General Motion Model and Spatio-Temporal Filters for 3-D Motion Interpretations.
PB96-210703 *01,861*

OPTICAL FLOW (IMAGE ANALYSIS)
Visual-Motion Fixation Invariant.
PB94-206281 *01,836*

Real-Time Implementation of a Differential Range Finder.
PB95-108650 *01,839*

Real Time Differential Range Estimation Based on Time-Space Imagery Using PIPE.
PB95-161808 *01,844*

Calculating Time-to-Contact Using Real-Time Quantized Optical Flow.
PB95-210522 *01,604*

OPTICAL IMAGES
Greatly Enhanced Soot Scattering in Flickering Ch4/Air Diffusion Flames.
PB94-172988 *01,361*

OPTICAL INTERCONNECTIONS
Metrology and Data for Microelectronic Packaging and Interconnection: Results of a Joint Workshop on Materials Metrology and Data for Commercial Electrical and Optical Packaging and Interconnection Technologies. Held in Gaithersburg, Maryland on May 5-6, 1994. Volume 1. Results.
PB95-143111 *02,328*

OPTICAL INTERFERENCE
Interference in the Resonance Fluorescence of Two Trapped Atoms.
PB95-168514 *03,948*

Light Scattered from Two Atoms.
PB95-168753 *04,286*

OPTICAL INTERFEROMETERS
Test Optics Error Removal.
PB96-179536 *04,377*

Compensation for Errors Introduced by Nonzero Fringe Densities in Phase-Measuring Interferometers.
PB97-110506 *04,386*

OPTICAL LITHOGRAPHY
Improved Dose Metrology in Optical Lithography.
PB96-179510 *02,439*

OPTICAL MATERIALS
Moisture and Water-Induced Crack Growth in Optical Materials.
PB95-153334 *04,267*

OPTICAL MEASUREMENT
NIST Response to the Fifth CORM Report on the Pressing Problems and Projected Needs in Optical Radiation Measurements.
PB94-188240 *04,227*

Optical Metrology and More. Programs and Services of the Radiometric Physics Division, Physics Laboratory.
PB94-191707 *04,228*

Technical Digest: Symposium on Optical Fiber Measurements (8th), 1994. Held in Boulder, Colorado on September 13-15, 1994.
PB94-207636 *04,231*

Normal-Incidence Complex-Index Refractometry.
PB94-213097 *04,241*

Integrating Sphere Simulation: Application to Total Flux Scale Realization.
PB95-150173 *04,261*

Direct Dispersion Measurement of Highly-Erbium-Doped Optical Amplifiers Using a Low Coherence Reflectometer Coupled with Dispersive Fourier Spectroscopy.
PB95-150702 *04,263*

Guidelines for Refractive Index Measurements of Asbestos.
PB95-151189 *02,543*

Regimes of Surface Roughness Measurable with Light Scattering.
PB95-151213 *04,265*

Optical Fiber Geometry: Accurate Measurement of Cladding Diameter.
PB95-151940 *04,266*

Electrically Calibrated Pyroelectric Detector-Refinements for Improved Optical Power Measurements.
PB95-169066 *02,164*

Optical Power Meter Calibration Using Tunable Laser Diodes.
PB95-169256 *04,290*

New Method for Realizing a Luminous Flux Scale Using an Integrating Sphere with an External Source.
PB96-102843 *04,333*

Semiconductor Measurement Technology: Survey of Optical Characterization Methods for Materials, Processing, and Manufacturing in the Semiconductor Industry.
PB96-154596 *02,706*

Realization of NIST 1995 Luminous Flux Scale Using the Integrating Sphere Method.
PB96-176433 *04,374*

Technical Digest: Symposium on Optical Fiber Measurements (9th), 1996. Held in Boulder, Colorado on October 1-3, 1996.
PB97-108583 *04,383*

Numerical Reference Models for Optical Metrology Simulation.
PB97-111330 *04,392*

OPTICAL MEASURING INSTRUMENTS
Automated Optical Roughness Inspection.
PB95-152179 *02,905*

OPTICAL MEMORY (DATA STORAGE)
Optical Storage Media Data Integrity Studies.
N95-24130/3 *01,620*

OPTICAL METROLOGY
Model of an Optical Roughness-Measuring Instrument.
PB97-110209 *04,384*

OPTICAL MICROSCOPES
Optical Fiber Geometry: Accurate Measurement of Cladding Diameter.
PB95-151940 *04,266*

OPTICAL MOLASSES
Heterodyne Measurement of the Fluorescence Spectrum of Optical Molasses.
PB95-108411 *03,873*

Atoms in Optical Molasses.
PB95-108874 *03,875*

Atoms in Optical Molasses: Applications to Frequency Standards.
PB95-108882 *03,876*

Optical Molasses: Cold Atoms for Precision Measurements.
PB95-108890 *03,877*

Optical Molasses: The Coldest Atoms Ever.
PB95-108908 *03,878*

sigma+-sigma- Optical Molasses in a Longitudinal Magnetic Field.
PB95-161840 *03,934*

OPTICAL POWER
Electrically Calibrated Pyroelectric Detector-Refinements for Improved Optical Power Measurements.
PB95-169066 *02,164*

Optical Power Meter Calibration Using Tunable Laser Diodes.
PB95-169256 *04,290*

OPTICAL PROPERTIES
Lighting Quality and Light Source Size.
PB95-151783 *00,252*

Simultaneous Optical Measurement of Soot Volume Fraction, Temperature, and CO2 in Heptane Pool Fire.
PB96-102132 *01,397*

Mixing and Radiation Properties of Buoyant Luminous Flame Environments.
PB96-202254 *01,432*

OPTICAL PUMPING
Electronically Tunable Fiber Laser for Optical Pumping of (3)He and (4)He.
PB96-201165 *04,381*

OPTICAL PYROMETERS
Technologic Papers of the Bureau of Standards: Number 170. Pyrometric Practice.
AD-A279 282/8 *03,766*

OPTICAL RADAR
Model Minimum Performance Specifications for Lidar Speed Measurement Devices.
PB95-197455 *04,861*

Delivering the Same Optical Frequency at Two Places: Accurate Cancellation of Phase Noise Introduced by an Optical Fiber or Other Time-Varying Path.
PB96-102736 *04,332*

OPTICAL RANGE FINDERS
Real-Time Implementation of a Differential Range Finder.
PB95-108650 *01,839*

OPTICAL RETARDANCE
Standard Polarization Components: Progress Toward an Optical Retardance Standard.
PB96-119672 *04,342*

OPTICAL SAMPLING
High-Sensitivity Optical Sampling Using an Erbium-Doped Fiber Laser Strobe.
PB95-176111 *04,302*

Optical Sampling Using Nondegenerate Four-Wave Mixing in a Semiconductor Laser Amplifier.
PB96-122502 *02,076*

Millimeter-Resolution Optical Time-Domain Reflectometry Using a Four-Wave Mixing Sampling Gate.
PB96-122700 *02,190*

Optical Sampling Using Nondegenerate Four-Wave Mixing in a Semiconductor Laser Amplifier.
PB96-123609 *04,348*

OPTICAL SCATTERING
Optical Scattering from Moderately Rough Surfaces.
PB97-110415 *04,385*

OPTICAL SENSORS
Embossable Grating Couplers for Planar Waveguide Optical Sensors.
PB96-190277 *00,641*

OPTICAL STORAGE
Retinal-Protein Complexes as Optoelectronic Components.
PB95-150397 *02,146*

OPTICAL SURFACES
Rapid Post-Polishing of Diamond-Turned Optics.
PB95-175949 *04,301*

OPTICAL SYSTEMS
Glasses for Waveguide Lasers.
PB96-111950 *04,335*

OPTICAL TESTING
Visualization of Surface Figure by the Use of Zernike Polynomials.
PB96-137757 *04,351*

Test of a Slow Off-Axis Parabola at Its Center of Curvature.
PB96-138482 *04,352*

OPTICAL TESTS
Gas Phase Reactions Relevant to Chemical Vapor Deposition: Optical Diagnostics.
PB94-199338 *03,116*

OPTICAL THEOREMS
Generalized Optical Theorem for On-Axis Gaussian Beams.
PB97-122345 *04,177*

OPTICAL THERMOMETERS
Self-Calibrated Intelligent Optical Sensors and Systems.
PB96-200738 *04,380*

OPTICAL TRACKING
Adaptive, Predictive 2-D Feature Tracking Algorithm for Finding the Focus of Expansion.
PB94-218575 *01,588*

Visual Pursuit Systems.
PB95-143285 *01,841*

OPTICAL WAVEGUIDES
Modified Airy Function Method for the Analysis of Tunneling Problems in Optical Waveguides and Quantum Well Structures.
PB94-185824 *02,120*

Planar Waveguide Optical Sensors.
PB94-200185 *03,586*

Complex Propagation Constants for Nonuniform Optical Waveguides: Calculations.
PB95-125910 *04,249*

Modal Properties of Circular and Noncircular Optical Waveguides.
PB95-125944 *04,251*

Approximate Solution to the Scalar Wave Equation for Optical Waveguides.
PB95-126256 *04,254*

Bending-Induced Phase Shifts in Dual-Mode Planar Optical Waveguides.
PB95-161329 *04,271*

Mode Coupling and Loss on Tapered Optical Waveguides.
PB95-168571 *04,282*

Symbolic Programming with Series Expansions: Applications to Optical Waveguides.
PB95-168589 *04,283*

Improved Variational Analysis of Inhomogeneous Optical Waveguides Using Airy Functions.
PB95-168639 *04,285*

Bending-Induced Loss in Dual-Mode Rectangular Waveguides.
PB95-168795 *04,288*

Bent Rectangular Core Waveguides: An Accurate Perturbation Approach.
PB95-168803 *04,289*

Waveguide Polarizers Processed by Localized Plasma Etching.
PB95-169264 *02,171*

Modal Characteristics of Bent Dual Mode Planar Optical Waveguide.
PB95-180485 *04,311*

Using Secondary Ion Mass Spectrometry (SIMS) to Characterize Optical Waveguide Materials.
PB96-119599 *04,340*

Vector and Quasi-Vector Solutions for Optical Waveguide Modes Using Efficient Galerkin's Method with Hermite-Gauss Basis Functions.
PB96-141197 *04,357*

OPTICS
Atomic Energy Levels. As Derived From the Analyses of Optical Spectra. Volume 3.
AD-A280 279/1 *00,714*

Japan Technology Program Assessment: Precision Engineering/Precision Optics in Japan.
PB95-171112 *02,884*

Fabrication of Optics by Diamond Turning.
PB96-111695 *02,954*

Soft X-ray Reflectometry Program at the National Institute of Standards and Technology.
PB96-160395 *04,368*

OPTICS/NON-LINEAR OPTICS
Corrected Optical Pyrometer Readings.
AD-A279 949/2 *02,615*

Characterization of a Clipped Gaussian Beam.
PB96-102553 *04,331*

Planar Lenses for Field-Emitter Arrays.
PB96-103064 *02,112*

Optical Emission Spectroscopy on the Gaseous Electronics Conference RF Reference Cell.
PB96-113345 *02,389*

Optical Diagnostics in the Gaseous Electronics Conference Reference Cell.
PB96-113352 *02,390*

Millimeter-Resolution Optical Time-Domain Reflectometry Using a Four-Wave Mixing Sampling Gate.
PB96-122700 *02,190*

Growth Characteristics of Fiber Gratings.
PB96-122957 *04,346*

Optical Sampling Using Nondegenerate Four-Wave Mixing in a Semiconductor Laser Amplifier.
PB96-123609 *04,348*

Atom-Optical Properties of a Standing-Wave Light Field.
PB96-141072 *04,356*

Vector and Quasi-Vector Solutions for Optical Waveguide Modes Using Efficient Galerkin's Method with Hermite-Gauss Basis Functions.
PB96-141197 *04,357*

Theory of the Magneto-Optic Kerr Effect in the Near Field.
PB96-141387 *04,761*

Optical Fiber, Fiber Coating, and Connector Ferrule Geometry: Results of Interlaboratory Measurement Comparisons.
PB96-154422 *04,360*

Improved Dose Metrology in Optical Lithography.
PB96-179510 *02,439*

Test Optics Error Removal.
PB96-179536 *04,377*

Embossable Grating Couplers for Planar Waveguide Optical Sensors.
PB96-190277 *00,641*

Developing Quality System Documentation Based on ANSI/NCSL Z540-1-1994: The Optical Technology Division's Effort.
PB96-202122 *01,869*

Technical Digest: Symposium on Optical Fiber Measurements (9th), 1996. Held in Boulder, Colorado on October 1-3, 1996.
PB97-108583 *04,383*

Optical and Modeling Studies of Sodium/Halide Reactions for the Formation of Titanium and Boron Nanoparticles.
PB97-113054 *00,682*

Generalized Optical Theorem for On-Axis Gaussian Beams.
PB97-122345 *04,177*

OPTIMAL CONTROL
Optimal Control of Building and HVAC Systems.
PB96-141353 *00,272*

Modified Optimal Algorithm for Active Structural Control.
PB96-165949 *00,472*

OPTIMIZATION
Convergence Properties of a Class of Rank-Two Updates. (NIST Reprint).
PB95-180097 *03,430*

OPTOELECTRONIC DEVICES
Photonic Materials: A Report on the Results of a Workshop. Held in Gaithersburg, Maryland on August 26-27, 1992, Volume 1.
PB94-152733 *02,114*

Electronics and Electrical Engineering Laboratory Technical Progress Bulletin Covering Programs, October to December 1993, with 1994/1995 EEEL Events Calendar.
PB94-154341 *02,115*

Metrology for Electromagnetic Technology: A Bibliography of NIST Publications.
PB95-135588 *02,143*

Metrology and Data for Microelectronic Packaging and Interconnection: Results of a Joint Workshop on Materials Metrology and Data for Commercial Electrical and Optical Packaging and Interconnection Technologies. Held in Gaithersburg, Maryland on May 5-6, 1994. Volume 1. Results.
PB95-143111 *02,328*

Electronics and Electrical Engineering Laboratory Technical Progress Bulletin Covering Laboratory Programs, April to June 1994 with 1994/1995 EEEL Events Calendar.
PB95-143186 *02,329*

Metrology and Data for Microelectronic Packaging and Interconnection: Results of a Joint Workshop on Materials Metrology and Data for Commercial Electrical and Optical Packaging and Interconnection Technologies. Held in Gaithersburg, Maryland on May 5-6, 1994. Volume 2. Presentation Material.
PB95-143327 *02,330*

Integrated-Optical Devices in Rare-Earth-Doped Glass.
PB95-202909 *02,179*

Optoelectronics at NIST.
PB96-200860 *02,202*

OPTOELECTRONICS
Opportunities for Innovation: Optoelectronics.
PB96-118039 *01,928*

Optoelectronics and Optomechanics Manufacturing: An ATP Focused Program Development. Workshop Proceedings. Held in Gaithersburg, Maryland on February 15, 1995.
PB97-104186 *02,204*

Bibliography of the NIST Optoelectronics Division.
PB97-116040 *02,207*

ORDER-DISORDER TRANSFORMATIONS
Thermodynamic Constraints on Non-Equilibrium Solidification of Ordered Intermetallic Compounds.
PB94-198934 *03,321*

Fast-Ion Conduction and Disorder in Cation and Anion Arrays in Y2(ZryTi(1-y))2O7 Pyrochlores Induced by Zr Substitution: A Neutron Rietveld Analysis.
PB94-211869 *04,496*

Fast-Ion Conducting Y2(ZryTi1-y)2O7 Pyrochlores: Neutron Rietveld Analysis of Disorder Induced by Zr Substitution.
PB96-156104 *04,776*

ORDINARY DIFFERENTIAL EQUATIONS
Pressure Equations in Zone-Fire Modeling.
PB96-102967 *00,208*

ORGANIC COATINGS
Methodologies for Predicting the Service Lives of Coating Systems.
PB95-146387 *03,124*

ORGANIC COMPOUNDS
Interaction of Some Coupling Agents and Organic Compounds with Hydroxyapatite: Hydrogen Bonding, Adsorption and Adhesion.
PB94-172616 *00,140*

Glass Transition of Organic Liquids Confined to Small Pores.
PB94-212305 *00,833*

Melting Behavior of Organic Materials Confined in Porous Solids.
PB94-212313 *00,834*

Standard Reference Materials for the Determination of Trace Organic Constituents in Environmental Samples.
PB95-164026 *02,522*

Cambridge Structural Database (CSD): Current Activities and Future Plans.
PB97-109052 *00,516*

ORGANIC IONS
Temperature Dependence of the Rate Constants for Reactions of the Carbonate Radical with Organic and Inorganic Reductants.
PB94-212206 *00,831*

ORGANIC LIQUIDS
Glass Transition of Organic Liquids Confined to Small Pores.
PB94-212305 *00,833*

Melting Behavior of Organic Materials Confined in Porous Solids.
PB94-212313 *00,834*

Vitrification and Crystallization of Organic Liquids Confined to Nanoscale Pores.
PB97-112304 *03,392*

ORGANIZATIONS
Directory of Law Enforcement and Criminal Justice Associations and Research Centers.
PB96-178918 *04,872*

Standards Activities of Organizations in the United States.
PB97-124135 *00,006*

ORGANOMETALLIC COMPOUNDS
Liquid Chromatography: Laser-Enhanced Ionization Spectrometry for the Speciation of Organolead Compounds.
PB94-185253 *00,530*

Maximum Entropy as a Tool for the Determination of the C-Axis Profile of Layered Compounds.
PB94-199619 *00,800*

Total Surface Areas of Group IVA Organometallic Compounds: Predictors of Toxicity to Algae and Bacteria.
PB94-211331 *00,814*

Cambridge Structural Database (CSD): Current Activities and Future Plans.
PB97-109052 *00,516*

ORIENTATION
Fluorescence Anisotropy Measurements on a Polymer Melt as a Function of Applied Shear Stress.
PB94-199296 *01,209*

Observations of Shear Induced Molecular Orientation in a Polymer Melt Using Fluorescence Anisotropy Measurements.
PB94-199304 *01,210*

Observations of Shear Stress and Molecular Orientation Using Fluorescence Anisotropy Measurements.
PB94-199312 *01,211*

Neutron Scattering Study of the Orientation of a Liquid Crystalline Polymer by Shear Flow.
PB95-180196 *01,270*

ORIENTATIONAL DISORDER
Orientational Fluctuations, Diffuse Scattering, and Orientational Order in Solid C60.
PB97-119275 *04,176*

ORIFICE FLOW
Flow Conditioner Tests for Three Orifice Flowmeter Sizes.
PB95-105540 *04,201*

Flowmeter Installation Effects Due to a Generic Header.
PB96-210893 *02,606*

ORIFICE METERS
Comparing NIST-B 50 mm Orifice Meter Gas Data to the ANSI Equation.
PB95-169207 *02,949*

Sliding Vane Flow Conditioner Tests in a 100 Diameter Long 10 inch Natural Gas Orifice Meter at Pacific Gas and Electric. Topical Report, 1990-1992.
PB95-256335 *02,493*

ORIFICE PULSE TUBE REFRIGERATORS
Energy Flows in an Orifice Pulse Tube Refrigerator.
PB95-169082 *02,752*

ORIGIN OF REPLICATION
Function of DnaJ and DnaK as Chaperones in Origin-Specific DNA Binding by RepA.
PB95-151544 *03,533*

Deletion Analysis of the Mini-P1 Plasmid Origin of Replication and the Role of E.coli DnaA Protein.
PB95-163911 *03,539*

ORION NEBULA
Extended CO(7 yields 6) Emission from Warm Gas in Orion.
PB96-102504 *00,090*

Magnetic Fields in Star-Forming Regions: Observations.
PB96-123005 *00,100*

ORTHOPEDIC EQUIPMENT
Program Requirements to Advance the Technology of Custom Footwear Manufacturing.
PB95-147906 *02,883*

ORTHOPHOSPHACIDIUM ION
Crystal Structure of a New Monoclinic Form of Potassium Dihydrogen Phosphate Containing Orthophosphacidium Ion, (H4PO4)(sup+1).
PB96-111794 *04,725*

ORTHORHOMBIC LATTICES
Transformation of BCC and B2 High Temperature Phases to HCP and Orthorhombic Structures in the Ti-Al-Nb System. Part 1. Microstructural Predictions Based on a Subgroup Relation between Phases.
PB96-169065 *03,370*

Transformation of BCC and B2 High Temperature Phases to HCP and Orthorhombic Structures in the Ti-Al-Nb System. Part 2. Experimental TEM Study of Microstructures.
PB96-169073 *03,371*

OSCILLATING FLOW
Resistance Thermometers with Fast Response for Use in Rapidly Oscillating Gas Flows.
PB95-107298 *03,261*

Thermal Anemometry for Mass Flow Measurement in Oscillating Cryogenic Gas Flows.
PB96-176789 *04,218*

OSCILLATIONS
Foias-Temam Approximations of Attractors for Galloping Oscillators.
PB94-198298 *04,817*

High-Temperature High-Pressure Oscillating Tube Densimeter.
PB96-146618 *01,123*

Quadratic Response of a Chemical Reaction to External Oscillations.
PB96-161633 *01,138*

OSCILLATOR STRENGTH
Theory for Quantum-Dot Quantum Wells: Pair Correlation and Internal Quantum Confinement in Nanoheterostructures.
PB96-179445 *02,437*

OSCILLATOR STRENGTHS
Oscillator Strengths and Radiative Branching Ratios in Atomic Sr.
PB95-203493 *04,008*

OSCILLATORS
Precision Oscillators: Dependence of Frequency on Temperature, Humidity and Pressure.
PB94-198306 *02,031*

Algebraic Approximation of Attractors for Galloping Oscillators.
PB95-162897 *04,820*

Environmental Sensitivities of Quartz Oscillators.
PB96-103148 *02,271*

Noise Modeling and Reliability of Behavior Prediction for Multi-Stable Hydroelastic Systems.
PB96-111943 *04,822*

Local Oscillator Requirements and Strategies for the Next Generation of High-Stability Frequency Standards.
PB96-112230 *01,551*

Reducing Errors, Complexity, and Measurement Time of PM Noise Measurements.
PB96-119771 *02,075*

Chaotic Motions of Coupled Galloping Oscillators and Their Modeling as Diffusion Progresses.
PB96-122718 *04,823*

OSE
Porting Multimedia Applications to the Open System Environment.
PB94-172921 *02,721*

OSE (OPEN SYSTEM ENVIRONMENT)
Guide on Open System Environment (OSE) Procurements.
PB95-169496 *01,626*

Comparison of POSIX Open System Environment (OSE) and Open Distributed Processing (ODP) Reference Models.
PB96-131495 *01,820*

OSI
Formal Multi-Layer Test Methodology and Its Application to OSI.
PB94-172194 *02,718*

ISO/IEC Workshop on Worldwide Recognition of OSI Test Results Regional Progress - North America.
PB94-172202 *02,719*

OSI (OPEN SYSTEMS INTERCONNECTION)
IGOSS-Industry/Government Open Systems Specification.
PB94-207453 *01,806*

Conformance Testing for OSI Protocols.
PB96-102686 *01,631*

Lessons from the Establishment of the U.S. GOSIP Testing Program.
PB96-119359 *01,817*

Open Issues in OSI Protocol Development and Conformance Testing.
PB96-122908 *01,818*

OSMIUM
Analysis of the (5d(2)+5d6s)-5d6p Transition Arrays of Os VII and Ir VIII, and the 6s (2)S-6p (2)P Transitions of Ir IX.
PB96-159264 *01,954*

OSMOSIS
Non-Perturbative Relation between the Mutual Diffusion Coefficient, Suspension Viscosity, and Osmotic Compressibility: Application to Concentrated Protein Solutions.
PB96-102355 *01,062*

OSMOTIC PRESSURE
Determination of Osmotic Pressure and Fouling Resistances and Their Effects on Performance of Ultrafiltration Membranes.
PB94-212891 *00,841*

OTAVITE
Thermodynamic Properties of Synthetic Otavite, CdCO3(cr): Enthalpy Increment Measurements from 4.5 K to 350 K.
PB97-111447 *00,680*

OUT-OF-PLANE
Contributions of Out-of-Plane Material to a Scanned-Beam Laminography Image.
PB96-111786 *02,704*

OUTLIERS (STATISTICS)
Outlier-Resistant Methods for Estimation and Model Fitting.
PB95-203436 *03,444*

OVERCURRENT
Surging the Upside-Down House: Measurements and Modeling Results.
PB96-180138 *02,243*

OVERLAYS
Application of the Modified Voltage-Dividing Potentiometer to Overlay Metrology in a CMOS/Bulk Process.
PB94-181997 *02,302*

Electrical Test Structure for Overlay Metrology Referenced to Absolute Length Standards.
PB95-152278 *02,336*

New Test Structure for Nanometer-Level Overlay and Feature-Placement Metrology.
PB95-175345 *02,363*

Microelectronic Test Structures for Overlay Metrology.
PB96-164249 *02,430*

OVERVOLTAGE
Keeping Up with the Reality of Today's Surge Environment.
PB96-123633 *02,231*

OXAZOLE ORANGE
Enhanced Detection of PCR Products Through Use of TOTO and YOYO Intercalating Dyes with Laser Induced Fluorescence - Capillary Electrophoresis.
PB95-164653 *00,599*

OXIDATION
Oxidation of 10-Methylacridan, a Synthetic Analogue of NADH and Deprotonation of Its Cation Radical. Convergent Application of Laser Flash Photolysis and Direct and Redox Catalyzed Electrochemistry to the Kinetics of Deprotonation of the Cation Radical.
PB94-198371 *00,785*

X-Ray Photoelectron and Auger Electron Spectroscopy Study of Ultraviolet/Ozone Oxidized P2S5/(NH4)2S Treated GaAs(100) Surfaces.
PB94-200144 *04,479*

Changes in the Redox State of Iridium Oxide Clusters and Their Relation to Catalytic Water Oxidation: Radiolytic and Electrochemical Studies.
PB95-107017 *00,864*

One-Electron Oxidation of Nickel Porphyrins. Effect of Structure and Medium on Formation of Nickel(III) Porphyrin or Nickel(II) Porphyrin pi-Radical Cation.
PB95-107058 *00,865*

Metalloporphyrin Sensitized Photooxidation of Water to Oxygen on the Surface of Colloidal Iridium Oxides - Photochemical and Pulse Radiolytic Studies.
PB95-107082 *00,868*

Oxidation of Soot and Carbon Monoxide in Hydrocarbon Diffusion Flames.
PB95-150215 *01,382*

Neutron Reflectometry Studies of Surface Oxidation.
PB95-150421 *00,917*

Laser-Induced Fluorescence Measurements of OH. Concentrations in the Oxidation Region of Laminar, Hydrocarbon Diffusion Flames.
PB95-162160 *01,387*

Kinetics of the Reaction C2H + O2 from 193 to 350 K Using Laser Flash Kinetic Infrared Absorption Spectroscopy.
PB95-203055 *01,043*

Oxidation of SiC.
PB96-119516 *02,401*

Repair of Products of Oxidative DNA Base Damage in Human Cells.
PB96-190129 *03,555*

Oxidation of Caffeic Acid and Related Hydroxycinnamic Acids.
PB97-111975 *00,651*

Oxidation of Ferrous and Ferrocyanide Ions by Peroxyl Radicals.
PB97-122402 *01,191*

OXIDATION REDUCTION REACTIONS
Radiation Chemistry of Cyanine Dyes: Oxidation and Reduction of Merocyanine 540.
PB94-211661 *00,818*

Electron Transfer Reaction Rates and Equilibria of the Carbonate and Sulfate Radical Anions.
PB94-212180 *00,829*

OXIDE BREAKDOWN
Assessing MOS Gate Oxide Reliability on Wafer Level with Ramped/Constant Voltage and Current Stress.
PB96-180112 *04,115*

OXIDE FILMS
Spectroscopic Ellipsometry Determination of the Properties of the Thin Underlying Strained Si Layer and the Roughness at SiO2/Si Interface.
PB95-150157 *04,560*

Neutron Reflectometry Studies of Surface Oxidation.
PB95-150421 *00,917*

Optimization of ECR-Based PECVD Oxide Films for Superconducting Integrated Circuit Fabrication.
PB95-169165 02,051

Effects of Soxhlet Extraction on the Surface Oxide Layer of Silicon Nitride Powders.
PB95-175584 03,057

OXIDE REMOVAL
Effect of Annealing Ambient on the Removal of Oxide Precipitates in High-Dose Oxygen Implanted Silicon.
PB95-164356 02,356

OXIDES
High Temperature Reactions of Uranium Dioxide with Various Metal Oxides.
AD-A286 648/1 00,717

Description of Layered Structures: Applications to High Tc Superconductors.
PB95-162624 04,615

New Oxide Degradation Mechanism for Stresses in the Fowler-Nordheim Tunneling Regime.
PB96-200985 04,128

New Physics-Based Model for Time-Dependent- Dielectric-Breakdown.
PB96-201132 02,448

OXYGEN
Conductance Response of Pd/SnO2(110) Model Gas Sensors to H2 and O2.
PB95-125803 00,892

Product State Correlations in the Reaction of O((1)D) and H2O in Bimolecular Collisions and in O3.H2O Clusters--Translation.
PB95-153011 00,946

Development of a Standard Reference Material for Measurement of Interstitial Oxygen Concentration in Semiconductor Silicon by Infrared Absorption.
PB96-122668 02,404

Measurement of S2OF10, and S2O2F10 Production Rates from Spark and Negative Glow Corona Discharge in SF6/O2 Gas Mixtures.
PB96-123740 01,093

OXYGEN 17
Laser Magnetic-Resonance Measurement of the (3)P1 - (3)P2 Fine-Structure Splittings in (17)O and (18)O.
PB95-175170 00,994

OXYGEN 18
Laser Magnetic-Resonance Measurement of the (3)P1 - (3)P2 Fine-Structure Splittings in (17)O and (18)O.
PB95-175170 00,994

OXYGEN ATOMS
Atomic Oxygen Fine Structure Splittings with Tunable Far Infrared Spectroscopy.
PB95-152203 03,915

Laser Flash Photolysis/Time-Resolved FTIR Emission Study of a New Channel in the Reaction of CH3+O: Production of CO(v).
PB95-164281 00,974

Laser Magnetic-Resonance Measurement of the (3)P1 - (3)P2 Fine-Structure Splittings in (17)O and (18)O.
PB95-175170 00,994

OXYGEN COMPATIBILITY
Reaction Sensitivities of Al-Li Alloys and Alloy 2219 in Mechanical-Impact Tests.
PB94-172764 03,314

OXYGEN CONCENTRATION
Standard Reference Materials: Certification of a Standard Reference Material for the Determination of Interstitial Oxygen Concentration in Semiconductor Silicon by Infrared Spectrophotometry.
PB95-125076 02,326

OXYGEN IONS
Determination of Atomic Data Pertinent to the Fusion Energy Program. Progress Report for FY 92.
DE94004400 04,402

OXYGEN ISOTOPES
New IUPAC Guidelines for the Reporting of Stable Hydrogen, Carbon, and Oxygen Isotope-Ratio Data. Letter to the Editor.
PB95-261962 01,058

OXYGEN-LIKE IONS
Atomic Branching Ratio Data for Oxygen-Like Species.
PB95-180436 03,963

OZONE
Product State Correlations in the Reaction of O((1)D) and H2O in Bimolecular Collisions and in O3.H2O Clusters--Translation.
PB95-153011 00,946

OZONE DEPLETION
Thermodynamic Properties of Gas Phase Species of Importance to Ozone Depletion.
PB94-198215 00,126

P INVARIANCE
Long-Range Parity-Nonconserving Interaction.
PB95-202594 03,986

P-N JUNCTIONS
Junction Locations by Scanning Tunneling Microscopy: In-Air-Ambient Investigation of Passivated GaAs pn Junctions.
PB94-185964 02,306

PACKAGING
Performance of Plastic Packaging for Hazardous Materials Transportation. Part 1. Mechanical Properties.
AD-A301 258/0 02,580

Checking the Net Contents of Packaged Goods as Adopted by the 79th National Conference on Weights and Measures, 1994, Third Edition, Supplement 4.
PB95-182226 00,484

High-Speed Interconnection Characterization Using Time Domain Network Analysis.
PB96-148176 04,061

PACKED BEDS
Distributed measurements of tracer response on packed bed flows using a fiberoptic probe array. Final report.
DE95013079 00,667

PACKING MATERIALS
Volatile Corrosion Inhibitors.
AD-A310 087/2 03,114

PAFFENBARGER RESEARCH CENTER
Paffenbarger Research Center: The Cutting Edge of Dental Science.
PB94-216355 00,151

PALLADIUM
Magnetic Properties of Pd/Co Multilayers.
PB94-198751 04,465

Conductance Response of Pd/SnO2(110) Model Gas Sensors to H2 and O2.
PB95-125803 00,892

Fundamental Studies of Gas Sensor Response Mechanisms: Palladium on SnO2(110).
PB95-162731 00,963

Small Angle Neutrons Scattering from Nanocrystalline Palladium as a Function of Annealing.
PB95-176103 03,354

Vibrational Excitations and the Position of Hydrogen in Nanocrystalline Palladium.
PB96-111828 04,035

Inelastic Neutron Scattering Study of Hydrogen in Nanocrystalline Pd.
PB96-146857 03,366

PALLADIUM ALLOYS
New Alloys Show Extraordinary Resistance to Fracture and Wear.
PB95-151346 03,346

PALLADIUM IONS
Rb-Like Spectra: Pd X to Nd XXIV.
PB95-150645 03,897

PALLADIUM-LIKE IONS
Observation of Pd-Like Resonance Lines Through Pt(32+) and Zn-Like Resonance Lines of Er(38+) and Hf(42+).
PB95-150637 03,896

PANCREATIC RIBONUCLEASE
Crystal Packing Interactions of Two Different Crystal Forms of Bovine Ribonuclease A.
PB95-152823 00,943

PANELS
Test Procedures for Advanced Insulation Panels.
PB97-111892 00,415

PARAFFIN HYDROCARBONS
Physical Properties of Some Purified Aliphatic Hydrocarbons.
AD-A297 265/1 00,657

PARALLEL PROCESSING
Measuring Performance of Parallel Computers. Final Report.
DE94014586 01,665

Measuring Performance of Parallel Computers. Progress Report, 1989.
DE94014587 01,666

Distributed Supercomputing Software: Experiences with the Parallel Virtual Machine - PVM.
PB94-163086 01,680

Using Synthetic Perturbations and Statistical Screening to Assay Shared-Memory Programs.
PB96-103031 01,740

Parallel Monte Carlo Simulation of MBE Growth.
PB96-122841 02,406

Experience with MPI: 'Converting Pvmmake to Mpimake under LAM' and 'MPI and Parallel Genetic Programming'.
PB96-141296 01,748

Using S-Check, Alpha Release 1.0.
PB96-165964 01,767

Tree-Lookup for Partial Sums Or: How Can I Find This Stuff Quickly.
PB96-179411 01,770

Making Connections.
PB97-119044 01,785

PARALLEL PROCESSING (COMPUTERS)
Scalability Test for Parallel Code.
PB96-146758 01,749

PARALLEL PROGRAMMING
Computing Effects and Error for Large Synthetic Perturbation Screenings.
PB94-139623 01,675

Time-Perturbation Tuning of MIMD Programs.
PB94-164399 01,681

Using Synthetic-Perturbation Techniques for Tuning Shared Memory Programs (Extended Abstract).
PB94-172657 01,685

Synthetic-Perturbation Tuning of MIMD Programs.
PB94-185568 01,687

Simple Scalability Test for MIMD Code.
PB94-193638 01,688

PARALLEL VIRTUAL MACHINE
Performance Characteristics of Fast Elliptic Solvers on Parallel Platforms.
PB95-180832 01,723

PARAMETERS
Taguchi's Parameter Design: A Panel Discussion.
PB96-111802 03,445

PARAMETRIC PROCESSES
High-Order Multipole Excitation of a Bound Electron.
PB96-119789 04,044

PARITY
Long-Range Parity-Nonconserving Interaction.
PB95-202594 03,986

PARKING GARAGES
Diagnosis of Causes of Concrete Deterioration in the MLP-7A Parking Garage.
PB95-143095 01,318

PARSERS
SGML Parser Validation Procedures.
PB95-174959 01,717

Standard Generalized Markup Language Test Suite Evaluation Report.
PB96-154992 01,751

PARTIAL DIFFERENTIAL EQUATIONS
Overcoming Hoelder Continuity in Ill-Posed Continuation Problems.
PB95-202354 03,416

PARTIAL DISCHARGE
Behavior of Surface Partial Discharge on Aluminum Oxide Dielectrics.
PB96-123781 01,937

PARTIAL DISCHARGES
Performance Evaluation of a New Digital Partial Discharge Recording and Analysis System.
PB95-150389 01,888

Recent Developments at NIST on Optical Current Sensors and Partial Discharge Diagnostics.
PB95-151114 02,147

Observations of Partial Discharges in Hexane Under High Magnification.
PB95-163127 01,900

Importance of Unraveling Memory Propagation Effects in Interpreting Data on Partial Discharge Statistics.
PB95-163572 01,901

Nonstationary Behavior of Partial Discharge during Insulation Aging.
PB95-163580 01,902

Partial Discharge: Induced Aging of Cast Epoxies and Related Nonstationary Behavior of the Discharge Statistics.
PB95-163598 01,903

Physics and Chemistry of Partial Discharge and Corona: Recent Advances and Future Challenges.
PB95-181046 01,910

Continuous Recording and Stochastic Analysis of PD.
PB96-112156 01,925

Standardised Computer Data File Format for Storage, Transport, and Off-Line Processing of Partial Discharge Data.
PB96-122486 01,930

Physics and Chemistry of Partial Discharge and Corona - Recent Advances and Future Challenges.
PB96-123757 01,936

PARTIAL PRESSURE
Partial Pressure Analysis in Space Testing.
N95-14084/4 04,827

Characteristics of Partial Pressure Analyzers.
PB95-150876 00,582

Measurement of Very-Low Partial Pressures.
PB95-180998 02,659

Process Monitoring with Residual Gas Analyzers (RGAs): Limiting Factors.
PB95-181004 02,660

Partial Pressure Analysis in Space Testing.
PB96-103072 04,829

PARTIAL PRESSURE ANALYZERS
Characteristics of Partial Pressure Analyzers.
PB95-150876 00,582

PARTICLE ACCELERATOR TARGETS
Factorial Design Techniques Applied to Optimization of AMS Graphite Target Preparation.
PB95-151197 00,584

PARTICLE PRODUCTION
Modeling Ceramic Sub-Micron Particle Formation from the Vapor Using Detailed Chemical Kinetics: Comparison with In-situ Laser Diagnostics.
PB95-151965 00,671

Multiphoton Ionization Spectroscopy Measurements of Silicon Atoms during Vapor Phase Synthesis of Ceramic Particles.
PB95-151999 03,913

Experimental and Numerical Studies of Refractory Particle Formation in Flames: Application to Silica Growth.
PB95-152005 00,673

Simulation of Ceramic Particle Formation: Comparison with In-situ Measurements.
PB95-152013 *00,674*

PARTICLE SHAPE
Morphological Development of Second-Phase Particles in Elastically-Stressed Solids.
PB95-181111 *03,355*

PARTICLE SIZE
Particle Size Standards and Their Certification at NIST.
PB94-211695 *02,639*

Development of Adaptive Control Strategies for Inert Gas Atomization.
PB95-162335 *02,823*

Process Modeling and Control of Inert Gas Atomization.
PB95-162343 *02,824*

PARTICLE SIZE DISTRIBUTION
Experimental Optimization of Peak Shape with Application to Aerosol Generation.
PB94-185535 *00,501*

In-situ Fume Particle Size and Number Density Measurements from a Synthetic Smelt.
PB94-212040 *03,334*

Statistical Analysis of Parameters Affecting the Measurement of Particle-Size Distribution of Silicon Nitride Powders by Sedigraph (Trade Name).
PB94-216249 *03,042*

Parametric Investigation of Metal Powder Atomization Using Laser Diffraction.
PB95-108577 *03,342*

Modeling Ceramic Sub-Micron Particle Formation from the Vapor Using Detailed Chemical Kinetics: Comparison with In-situ Laser Diagnostics.
PB95-151965 *00,671*

PARTICLES
Airborne Asbestos Method: Standard Test Method for High Precision Counting of Asbestos Collected on Filters. Version 1.0.
PB94-163003 *00,525*

Environmental Scanning Electron Microscope Imaging Examples Related to Particle Analysis.
PB94-172822 *00,766*

Generation and Characterization of Acetylene Smokes.
PB94-200292 *01,372*

Characterization of Chemically Modified Pore Surfaces by Small Angle Neutron Scattering.
PB95-126181 *00,898*

Relativistic Quantum Mechanics of Interacting Particles.
PB97-110589 *04,141*

In-situ Studies of a Novel Sodium Flame Process for Synthesis of Fine Particles.
PB97-113047 *00,681*

PARTICULATE REINFORCED COMPOSITES
Residual Stresses in Aluminum-Mullite (alpha-Alumina) Composites.
PB95-152880 *03,155*

Elastic Properties of Al2O3/Al Composites: Measurements and Modeling.
PB95-161378 *03,157*

Fabrication of Flaw-Tolerant Aluminum-Titanate-Reinforced Alumina.
PB95-162533 *03,161*

PARTICULATES
Electroacoustics for Characterization of Particulates and Suspensions. Proceedings of a Workshop. Held in Gaithersburg, Maryland on February 3-4, 1993.
PB94-112695 *00,725*

Rare-Earth Isotopes as Tracers of Particulate Emissions: An Urban Scale Test.
PB94-161635 *02,535*

Computer Simulations of Binder Removal from 2-D and 3-D Model Particulate Bodies.
PB97-121339 *00,418*

PASCAL PROGRAMMING LANGUAGE
Validated Products List (Cobol, Fortran, ADA, Pascal, MUMPS, SQL).
PB94-937300 *01,700*

Validated Products List (Cobol, Fortran, ADA, Pascal, MUMPS, SQL).
PB95-937300 *01,738*

PASSENGERS
Fire Safety of Passenger Trains: A Review of Current Approaches and of New Concepts.
PB94-152006 *04,848*

PASSIVATION
Heavily Accumulated Surfaces of Mercury Cadmium Telluride Detectors: Theory and Experiment.
PB94-216074 *02,134*

PASSIVE CONTROL
Method of Estimating the Parameters of Tuned Mass Dampers for Seismic Applications.
PB96-167820 *00,473*

PATHS
Time Dependent Vector Dynamic Programming Algorithm for the Path Planning Problem.
PB94-215688 *03,428*

PATTERN RECOGNITION
Face Recognition Technology for Law Enforcement Applications.
PB94-207768 *01,837*

Pattern-Recognition Analysis of Low-Resolution X-Ray Fluorescence Spectra.
PB95-151924 *00,588*

PCASYS: A Pattern-Level Classification Automation System for Fingerprints.
PB95-267936 *01,853*

Human and Machine Recognition of Faces: A Survey.
PB96-111687 *01,854*

Using Logic to Specify Shapes and Spatial Relations in Design Grammars.
PB97-111579 *02,793*

PAVERS
Warping of Terrace Pavers at the U.S. Capitol Building.
PB96-193651 *00,411*

PDES (PRODUCT DATA EXCHANGE SPECIFICATION)
National PDES Testbed: An Overview.
PB95-125829 *02,775*

Capabilities for Product Data Exchange.
PB97-118764 *02,798*

PDES (PRODUCT DATA EXCHANGE USING STEP)
Security Considerations for SQL-Based Implementations of STEP.
PB94-139649 *02,766*

Guide to Configuration Management and the Revision Control System for Testbed Users.
PB94-150919 *01,678*

Summary and Notes of the Joint ISO/IGES/PDES Organization Technical Committee Meeting. Held in Albuquerque, New Mexico on October 15-20, 1989.
PB95-107314 *02,774*

Group 1 for the Process Engineering Data STEP Application Protocol.
PB97-116073 *02,797*

PEAKS OVER THRESHOLD METHOD
Estimates of Hurricane Wind Speeds by the 'Peaks Over Threshold' Method.
PB96-162540 *00,471*

Probabilistic Estimates of Design Load Factors for Wind-Sensitive Structures Using the 'Peaks Over Threshold' Approach.
PB96-183223 *00,474*

PEAKS OVER THRESHOLD METHODS
Extreme Wind Distribution Tails: A 'Peaks Over Threshold' Approach.
PB95-219416 *00,127*

PECULIAR STARS
Wavelengths and Isotope Shifts for Lines of Astrophysical Interest in the Spectrum of Doubly Ionized Mercury (Hg III).
PB95-140869 *03,887*

Search for Radio Emission from the 'Non-Magnetic' Chemically Peculiar Stars.
PB96-102249 *00,087*

X-ray Emission from Chemically Peculiar Stars.
PB96-102256 *00,088*

A-type and Chemically Peculiar Stars.
PB96-123286 *00,101*

Radio and X-ray Emissions from Chemically Peculiar B- and A-Type Stars: Observations and a Model.
PB96-123302 *00,103*

PEEL STRENGTH
Effects of Adhesive Thickness, Open Time, and Surface Cleanness on the Peel Strength of Adhesive-Bonded Seams of EPDM Rubber Roofing Membrane.
PB95-151338 *00,372*

PELTIER EFFECTS
NBS/NIST Peltier-Effect Microcalorimeter: A Four-Decade Review.
PB96-102769 *01,064*

PENDULUM IMPACT MACHINES
Proposed Changes to Charpy V-Notch Machine Certification Requirements.
PB96-135363 *02,955*

PENDULUMS
Chaos in a Computer-Animated Pendulum.
PB94-212651 *03,852*

PENICILLIN G
Thermodynamics of the Hydrolysis of Penicillin G and Ampicillin.
PB94-172467 *03,596*

PENS
Stylus Technique for the Direct Verification of Rockwell Diamond Intenders.
PB96-155569 *02,958*

PENTAFLUOROANILINE
Fluoride Elimination Upon Reaction of Pentafluoroaniline with e (sub eq')(sup -), H, and OH Radicals in Aqueous Solution.
PB97-111314 *01,177*

PENTAFLUORODIMETHYL ETHER
Vapor Pressure of Pentafluorodimethyl Ether.
PB96-201199 *00,677*

PENTAFLUOROETHANE
Viscosity of the Saturated Liquid Phase of Six Halogenated Compounds and Three Mixtures.
PB95-162368 *00,960*

Measurements of the Vapor Pressures of Difluoromethane, 1-Chloro-1,2,2,2-Tetrafluoroethane, and Pentafluoroethane.
PB95-169272 *03,270*

Vapour Pressures and Gas-Phase (p, rho n, T) Values for CF3CHF2(R125).
PB96-102090 *04,019*

PENTAFLUOROPROPANE
Vapor Pressure of 1,1,1,2,2-Pentafluoropropane.
PB97-113237 *00,684*

Thermodynamic Properties of CHF2-CF2-CHF, 1,1,2,2,3-Pentafluoropropane.
PB97-118392 *03,300*

PENTANES
Critical Properties and Vapor-Liquid Equilibria of the Binary System Propane + Neopentane.
PB95-175683 *00,999*

PEPPERS
Preliminary Investigation of Oleoresin Capsicum.
PB96-179486 *03,520*

PEPTIDES
Glucose Permease of Bacillus Subtilis Is a Single Polypeptide Chain That Functions to Energize the Sucrose Permease.
PB95-163192 *03,466*

PERCHLOROETHYLENE
Incinerability of Perchloroethylene and Chlorobenzene.
PB95-163457 *01,388*

Hydrogen Atom Attack on Perchloroethylene.
PB95-163473 *00,969*

PERCOLATION
Percolation and Pore Structure in Mortars and Concrete.
PB95-150439 *00,370*

Geometrical Percolation Threshold of Overlapping Ellipsoids.
PB96-102397 *03,167*

PERFORMANCE EVALUATION
Configuration and Performance Evaluation of a Real-Time Robot Control System: A Skeleton Approach.
PB95-163895 *01,598*

Performance of Compact Fluorescent Lamps at Different Ambient Temperatures.
PB95-175329 *00,258*

Interim Testing Artifact (ITA): A Performance Evaluation System for Coordinate Measuring Machines (CMMs). User Manual.
PB95-210589 *02,914*

Performance Testing of a Family of Type I Combination Appliance.
PB95-220521 *02,505*

4SIGHT Manual: A Computer Program for Modelling Degradation of Underground Low Level Waste Concrete Vaults.
PB95-231593 *03,726*

NIST SRM 9983 High-Rigidity Ball-Bar Stand. User Manual.
PB95-255840 *02,669*

Factors Affecting the Energy Consumption of Two Refrigerator-Freezers.
PB97-112312 *00,311*

Survey of the Components of Display-Measurement Standards.
PB97-122394 *02,209*

PERFORMANCE MEASUREMENT
Display-Measurement Round-Robin.
PB96-119227 *02,186*

PERFORMANCE STANDARDS
National Quality Assurance Program for Personnel Radiation Dosimetry: A Case History.
PB94-211273 *03,620*

Developing Rational Performance-Based Fire Safety Requirements in Model Building Codes.
PB95-175220 *00,200*

PERFORMANCE TESTING
Graded and Nongraded Regenerator Performance.
PB95-169090 *02,753*

Methodology for Developing and Implementing Alternative Temperature-Time Curves for Testing the Fire Resistance of Barriers for Nuclear Power Plant Applications.
PB96-193784 *03,742*

PERFORMANCE TESTS
Performance Standards: The Pro's and Con's.
PB94-216132 *02,896*

Using Emulators to Evaluate the Performance of Building Energy Management Systems.
PB95-175774 *00,259*

Reproducibility of Tests on Energy Management and Control Systems Using Building Emulators.
PB95-175980 *00,260*

Use of Building Emulators to Evaluate the Performance of Building Energy Management Systems.
PB96-111901 *00,269*

PERIODICALS
NIST Serial Holdings, 1994.
PB94-178068 *02,745*

Journal of Research of the National Institute of Standards and Technology, September/October 1994. Volume 99, Number 5.
PB95-169371 *04,293*

NIST Serial Holdings, 1995.
PB95-188926 *02,746*

Journal of Research of the National Institute of Standards and Technology, March/April 1995. Volume 100, Number 2.
PB96-126180 04,349

NIST Serial Holdings, 1996.
PB96-172523 02,748

PERMALLOYS (TRADEMARK)
Telegraph Noise in Silver-Permalloy Giant Magnetoresistance Test Structures.
PB96-146717 04,763

PERMANENT DENTAL RESTORATION
Properties and Interactions of Oral Structures and Restorative Materials. Annual Report for Period October 1, 1990 to September 30, 1991.
PB94-160843 03,558

PERMEABILITY
Controlling Moisture in the Walls of Manufactured Housing.
PB95-105136 00,355

Cross-Property Relations and Permeability Estimation in Model Porous Media.
PB95-150280 04,205

Calculation of the Thermal Conductivity and Gas Permeability in a Uniaxial Bundle of Fibers.
PB95-180931 03,058

Water-Vapor Measurements of Low-Slope Roofing Materials.
PB95-251617 00,399

PERMEATION
CO2/CH4 Transport in Polyperfluorosulfonate Ionomers: Effects of Polar Solvents on Permeation and Solubility.
PB96-163803 01,145

PERMEATION LEAKS
Commercial Helium Permeation Leak Standards: Their Properties and Reliability.
PB97-111413 04,146

PERMITTIVITY
Transmission/Reflection and Short-Circuit Line Methods for Measuring Permittivity and Permeability.
PB94-165537 02,211

Distribution of Dielectric Relaxation Times and the Moment Problem.
PB96-112032 04,727

PERMITTIVITY MEASUREMENTS
NIST 60-Millimeter Diameter Cylindrical Cavity Resonator: Performance Evaluation for Permittivity Measurements.
PB94-151776 02,251

PEROXIDASES
Potentiometric Enzyme-Amplified Flow Injection Analysis Detection System: Behavior of Free and Liposome-Released Peroxidase.
PB95-151833 03,534

PEROXY RADICALS
Kinetics of the Self-Reaction of Hydroxymethylperoxyl Radicals.
PB94-212164 00,827

PEROXYL RADICALS
Solvent Effects in the Reactions of Peroxyl Radicals with Organic Reductants. Evidence for Proton Transfer Mediated Electron Transfer.
PB95-107157 00,873

Reaction of Nitric Oxide with Organic Peroxyl Radicals.
PB95-141107 00,910

Oxidation of Ferrous and Ferrocyanide Ions by Peroxyl Radicals.
PB97-122402 01,191

PEROXYNITRITE RADICALS
Reaction of NO with Superoxide.
PB94-212198 00,830

PERSISTENCE LENGTH
Electrostatic Rigidity of Polyelectrolytes from Reparametrization Invariance.
PB96-180062 04,113

PERSONAL COMPUTERS
Vibration Laboratory Automation at NIST with Personal Computers.
PB95-108700 02,648

Keeping Time on Your PC.
PB95-161410 01,537

Precise Identification of Computer Viruses.
PB96-160825 01,613

PERSONAL DOSE EQUIVALENT
Angular Variation of the Personal Dose Equivalent, Hp(0.07), for Beta Radiation and Nearly Monoenergetic Electron Beams: Preliminary Results.
PB95-168472 03,630

PERSONNEL DOSIMETRY
National Quality Assurance Program for Personnel Radiation Dosimetry: A Case History.
PB94-211273 03,620

National Voluntary Laboratory Accreditation Program: Ionizing Radiation Dosimetry.
PB95-128658 03,623

Interpreting the Readings of Multi-Element Personnel Dosimeters in Terms of the Personal Dose Equivalent.
PB95-175428 03,631

PESTICIDES
Determination of Oltipraz in Serum by High-Performanace Liquid Chromatography with Optical Absorbance and Mass Spectrometric Detection.
PB94-200201 03,493

Comparison of Methods for Gas Chromatographic Determination of PCBs and Chlorinated Pesticides in Marine Reference Materials.
PB95-140091 02,584

NIST Standard Reference Materials (SRMs) for Polychlorinated Biphenyl (PCB) Determinations and Their Applicability to Toxaphene Measurements.
PB95-140109 02,585

Determination of PCBs and Chlorinated Hydrocarbons in Marine Mammal Tissues.
PB95-162640 03,744

Certification of Polychlorinated Biphenyl Congeners and Chlorinated Pesticides in a Whale Blubber Standard Reference Material.
PB96-103023 03,745

PETROCHEMISTRY
Framework for Information Technology Integration in Process Plant and Related Industries.
PB94-219086 02,772

PETROLEUM FRACTIONS
Viscosity of Defined and Undefined Hydrocarbon Liquids Calculated Using an Extended Corresponding-States Model.
PB96-167234 02,498

PF RADICALS
Resonance Enhanced Multiphoton Ionization Spectroscopy of the PF Radical.
PB97-119119 00,702

PH
Calorimetric Determination of the Standard Transformed Enthalpy of a Biochemical Reaction at Specified PH and pMg.
PB94-198249 03,454

PHARMACOLOGY
Modification of DNA Bases in Chromatin of Intact Target Human Cells by Activated Human Polymorphonuclear Leukocytes.
PB94-199833 03,526

Supercritical Fluid Extraction of Biological Products.
PB95-175204 00,040

PHASE DIAGRAMS
Effects of Elastic Stress on Phase Equilibrium in the Ni-V System.
PB94-172707 03,313

Statistical Thermodynamics of Phase Separation and Ion Partitioning in Aqueous Two-Phase Systems.
PB94-199387 01,212

Assessment of the Al-Sb System.
PB94-200474 03,329

Supercritical Solubility of Solids from Near-Critical Dilute-Mixture Theory.
PB94-211703 00,819

Inversion of the Phase Diagram from UCST to LCST in Deuterated Polybutadiene and Protonated Polybutadiene Blends.
PB94-212446 01,226

Crystal Chemistry and Phase Equilibria Studies of the BaO(BaCO3)-R2O3-CuO Systems. 4. Crystal Chemistry and Subsolidus Phase Relationship Studies of the CuO-Rich Region of the Ternary Diagrams, R=Lanthanides.
PB95-151759 00,936

Phase Composition, Viscosities, and Densities for Aqueous Two-Phase Systems Composed of Polyethylene Glycol and Various Salts at 25C.
PB95-164596 00,986

Vapor-Liquid Equilibria of Mixtures of Propane and Isomeric Hexanes.
PB95-175287 00,995

Critical Properties and Vapor-Liquid Equilibria of the Binary System Propane + Neopentane.
PB95-175683 00,999

Critical Lines for Type-III Aqueous Mixtures by Generalized Corresponding-States Models.
PB96-102371 01,063

Magnetic Dielectric Oxides: Subsolidus Phase Relations in the BaO: Fe2O3: TiO2 System.
PB96-176524 01,156

Multimedia Tutorial on Phase Equilibria Diagrams.
PB96-200829 03,088

PHASE EQUILIBRIA
Multimedia Tutorial on Phase Equilibria Diagrams.
PB96-200829 03,088

PHASE EQUILIBRIUM
Design of a High-Pressure Ebulliometer, with Vapor-Liquid Equilibrium Results for the Systems CHF2Cl + CF3-CH3 and CF3-CH2F + CH2F2.
PB97-113229 04,163

PHASE ERROR
Effect of Harmonic Distortion on Phase Errors in Frequency Distribution and Synthesis.
PB96-200779 01,563

PHASE FIELD MODELS
xi-Vector Formulation of Anisotropic Phase-Field Models: 3-D Asymptotics.
PB95-136628 04,536

Phase-Field Model for Solidification of a Eutectic Alloy.
PB95-147914 03,345

Xi-Vector Formulation of Anisotropic Phase-Field Models: 3-D Asymptotics.
PB97-122550 04,816

PHASE LOCKED SYSTEMS
Phase Locking in Two-Junction Systems of High-Temperature Superconductor-Normal Metal-Superconductor Junctions.
PB95-176053 02,060

Phase Locking in Two-Dimensional Arrays of Josephson Junctions: Effect of Critical-Current Nonuniformity.
PB96-102587 04,714

PHASE LOCKING
Stable Phase Locking in a Two-Cell Ladder Array of Josephson Junctions.
PB96-111679 04,722

Mutual Phase Locking in Systems of High-Tc Superconductor-Normal Metal-Superconductor Junctions.
PB96-135348 04,744

PHASE MODULATION
Investigations of AM and PM Noise in X-Band Devices.
PB95-180022 02,062

Practical Standards for PM and AM Noise at 5, 10 and 100 MHz.
PB95-181129 01,546

Secondary Standard for PM and AM Noise at 5, 10, and 100 MHz.
PB96-123187 01,554

Origin of l/f PM and AM Noise in Bipolar Junction Transistor Amplifiers.
PB96-200787 02,096

Reducing the 1/f AM and PM Noise in Electronics for Precision Frequency Metrology.
PB97-113195 02,102

PHASE MODULATORS
Ultralinear Small-Angle Phase Modulator.
PB95-168852 02,261

PHASE NOISE
Delivering the Same Optical Frequency at Two Places: Accurate Cancellation of Phase Noise Introduced by an Optical Fiber or Other Time-Varying Path.
PB96-102736 04,332

Reducing Errors, Complexity, and Measurement Time of PM Noise Measurements.
PB96-119771 02,075

Surface Transverse Wave Oscillators with Extremely Low Thermal Noise Floors.
PB96-186010 01,967

PHASE ORDERING
Evolution Equations for Phase Separation and Ordering in Binary Alloys.
PB96-119243 02,979

PHASE SEPARATION
Evolution Equations for Phase Separation and Ordering in Binary Alloys.
PB96-119243 02,979

Light-Scattering Studies on Phase Separation in a Binary Blend with Addition of Diblock Copolymers.
PB96-146865 01,286

Shear Suppression of Critical Fluctuations in a Diluted Polymer Blend.
PB96-204458 04,418

Dimensional Crossover in the Phase Separation Kinetics of Thin Polymer Blend Films.
PB97-113088 03,395

PHASE SEPARATION KINETICS
Phase Separation in Thin Film Polymer Blends With and Without Block Copolymer Additives.
PB96-204482 01,294

PHASE SEPARATION (MATERIALS)
Structural Stabilization of Phase Separating PC/Polyester Blends through Interfacial Modification by Transesterification Reaction.
PB95-150454 01,239

Anisotropic Phase Separation Kinetics in a Polymer Blend Solution Following Cessation of Shear Studied by Light Scattering.
PB95-151247 01,241

Real-Time Small-Angle X-Ray Scattering Study of the Early Stage of Phase Separation in the SiO2-BaO-K20 System.
PB95-163069 03,052

PHASE SHIFT
Phase Shifts and Intensity Dependence in Frequency-Modulation Spectroscopy.
PB96-103205 01,071

PHASE STABILITY (MATERIALS)
Convection and Morphological Stability During Directional Solidification.
N95-14548/8 03,310

PHASE STUDIES
Characterization of Phase and Surface Composition of Silicon Carbide Platelets.
PB94-216264 03,043

Crystal Structure of a New Sodium Zinc Arsenate Phase Solved by 'Simulated Annealing'.
PB95-107124 00,870

Thin Film Reaction Kinetics of Niobium/Aluminum Multilayers.
PB95-175295 04,651

Instrument for Evaluating Phase Behavior of Mixtures for Supercritical Fluid Experiments.
PB95-180758 00,606

PHASE TRANSFORMATIONS
Phase Behavior of a Hydrogen Bonding Molecular Composite.
PB94-185188 *01,202*

Effect of Transformation of Alloy on Transient and Residual Stresses in a Porcelain-Metal Strip.
PB94-198397 *00,143*

Phase-Field Model for Solidification of a Eutectic Alloy.
PB95-147914 *03,345*

Phase Transitions in Solid C70: Supercooling, Metastable Phases, and Impurity Effect.
PB95-150090 *00,914*

Comment on 'Phase Transitions in Antiferromagnetic Superlattices'.
PB95-152971 *04,587*

Small Angle Neutron Scattering Study on Poly(N-Isopropyl Acrylamide) Gels Near Their Volume-Phase Transition Temperature.
PB95-164380 *01,263*

New Data and Correlations for the Custody Transfer of Natural Gas Liquids.
PB96-176664 *02,499*

PHASE VELOCITY
Effect of Liftoff on Accuracu of Phase Velocity Measurements Made with Electromagnetic-Acoustic Transducers.
PB96-186044 *02,280*

PHENOLS
Source of Phenol Emissions Affecting the Indoor Air of an Office Building.
PB94-154382 *03,600*

Temperature Dependence of the Rate Constants for Reaction of Inorganic Radicals with Organic Reductants.
PB94-198280 *00,783*

Materials-Science Based Approach to Phenol Emissions from a Flooring Material in an Office Building.
PB97-118749 *02,572*

PHENYLALANINE/N-ACETYL- (ETHYL-ESTER)
Thermodynamics of the Hydrolysis of N-Acetyl-L-phenylalanine Ethyl Ester in Water and in Organic Solvents.
PB95-203386 *01,053*

PHENYLBUTADIENE
Lowest Excited Singlet State of Isolated 1-phenyl-1,3-butadiene and 1-phenyl-1,3,5-hexatriene.
PB95-202339 *01,026*

PHENYLHEXATRIENE
Lowest Excited Singlet State of Isolated 1-phenyl-1,3-butadiene and 1-phenyl-1,3,5-hexatriene.
PB95-202339 *01,026*

PHONETICS
Photonic Materials: A Report on the Results of a Workshop. Held in Gaithersburg, Maryland on August 26-27, 1992, Volume 1.
PB94-152733 *02,114*

PHONON DETECTORS
Hot-Electron Microcalorimeters for X-ray and Phonon Detection.
PB95-168993 *04,644*

Hot-Electron Microcalorimeters as High-Resolution X-ray Detectors.
PB96-123641 *04,739*

Hot-Electron Microcalorimeter for X-ray Detection Using a Superconducting Transition Edge Sensor with Electrothermal Feedback.
PB96-200399 *04,792*

PHONON DISPERSION
High-Energy Phonon Dispersion in La1.85Sr0.15CuO4.
PB96-138458 *04,748*

PHONON RESPONSE
Total-Dielectric-Function Approach to Electron and Phonon Response in Solids.
PB96-102884 *01,067*

PHONONS
Temperature Dependence and Anharmonicity of Phonons on Ni(110) and Cu(110) Using Molecular Dynamics Simulations.
PB94-185477 *04,449*

Anharmonic Phonons and the Isotope Effect in Superconductivity.
PB94-200557 *04,486*

Phonon Density of States in R2CuO4 and Superconducting R1.85Ce0.15CuO4 (R = Nd, Pr).
PB95-150686 *04,574*

High Resolution Inelastic Neutron Scattering Study of Phonon Self-Energy Effects in YBCO.
PB95-180881 *04,688*

Self-Biasing Cryogenic Particle Detector Utilizing Electrothermal Feedback and a SQUID Readout.
PB96-102538 *04,712*

Phonon Relaxation in Soft-X-ray Emission of Insulators.
PB96-160296 *04,085*

PHOSPHATE INORGANIC COMPOUNDS
Crystal Structure of a New Monoclinic Form of Potassium Dihydrogen Phosphate Containing Orthophosphacidium Ion, (H4PO4)(sup+1).
PB96-111794 *04,725*

PHOSPHATES
Modification of Deoxyribose-Phosphate Residues by Extracts of Ataxia Telangiectasia Cells.
PB94-212602 *03,458*

Cyclic Polyamine Ionophore for Use in a Dibasic Phosphate-Selective Electrode.
PB95-180121 *01,008*

PHOSPHOLIPIDS
Mixed Phospholipid Liposome Calcification.
PB94-211190 *03,457*

Self-Assembled Phospholipid/Alkanethiol Biomimetic Bilayers on Gold.
PB95-108460 *00,878*

Supported Phospholipid/Alkanthiol Biomimetic Membranes: Insulating Properties.
PB95-180782 *03,470*

Phospholipid/Alkanethiol Bilayers for Cell-Surface Receptor Studies by Surface Plasmon Resonance.
PB96-102900 *03,472*

PHOSPHOPROTEINS
Trace Elements Associated with Proteins. Neutron Activation Analysis Combined with Biological Isolation Techniques.
PB95-163101 *00,597*

PHOTOASSOCIATION
Nonadiabatic Effects in the Photoassociation of H2S.
PB95-151437 *00,934*

PHOTOCHEMICAL REACTIONS
Fragment Energy and Vector Correlations in the Overtone-Pumped Dissociation of HN3X(1)A'.
PB94-199908 *00,802*

Changes in the Redox State of Iridium Oxide Clusters and Their Relation to Catalytic Water Oxidation: Radiolytic and Electrochemical Studies.
PB95-107017 *00,864*

Bacteriorhodopsin Retains Its Light-Induced Proton-Pumping Function After Being Heated to 140C.
PB96-102728 *03,471*

PHOTOCHEMISTRY
Application of Photochemical Reaction in Electrochemical Detection of DNA Intercalation.
PB94-185733 *00,686*

PHOTODECOMPOSITION
Photodecomposition of Mo(CO)6/Si(111) 7x7: CO State-Resolved Evidence for Excited State Relaxation and Quenching.
PB95-180154 *01,009*

PHOTODESORPTION
Photodesorption Dynamics of CO from Si(111): The Role of Surface Defects.
PB96-111646 *03,066*

PHOTODETACHMENT
Resonant Two-Color Detachment of H(-) with Excitation of H(n=2).
PB95-202552 *03,984*

Relative Photoionization and Photodetachment Cross Sections for Particular Fine-Structure Transitions with Application to Cl 3s-subshell Photoionization.
PB95-203097 *03,998*

Short-Pulse Detachment of H(-) in the Presence of a Static Electric Field.
PB95-203477 *04,007*

PHOTODETECTORS
Accurate Characterization of High Speed Photodectors.
PB95-153763 *02,153*

Electrically Calibrated Pyroelectric Detector-Refinements for Improved Optical Power Measurements.
PB95-169066 *02,164*

Photodetector Frequency Response Measurements at NIST, US, and NPL, UK: Preliminary Results of a Standards Laboratory Comparison.
PB95-175592 *02,175*

PHOTODIODES
One Gigarad Passivating Nitrided Oxides for 100% Internal Quantum Efficiency Silicon Photodiodes.
PB94-185485 *02,119*

Silicon Photodiodes Optimized for EUV and Soft X-Ray Regions.
PB94-199478 *02,124*

Longterm Changes of Silicon Photodiodes and Their Use for Photometric Standardization.
PB94-211349 *04,234*

International Intercomparison of Detector Responsivity at 1300 and 1550 nm.
PB95-126017 *02,141*

Accurate Characterization of High Speed Photodectors.
PB95-153763 *02,153*

Photodetector Frequency Response Measurements at NIST, US, and NPL, UK: Preliminary Results of a Standards Laboratory Comparison.
PB95-175592 *02,175*

Comparison of Photodiode Frequency Response Measurements to 40 GHz between NPL and NIST.
PB96-111992 *04,038*

Stable Silicon Photodiodes for Absolute Intensity Measurements in the VUV and Soft X-ray Regions.
PB97-110175 *04,135*

PHOTODISSOCIATION
Multichannel Quantum Defect Half Collision Analysis of K2 Photodissociation Through the B1Pi(sub u) State.
PB94-211125 *00,812*

Asymptotic Wave Function Splitting Procedure for Propagating Spatially Extended Wave Functions: Application to Intense Field Photodissociation of H2(+).
PB94-211786 *03,847*

Vibrational Predissociation Dynamics of Overtone-Excited HN3.
PB95-125720 *00,691*

Nonadiabatic Effects in the Photoassociation of H2S.
PB95-151437 *00,934*

Photodissociation of Ammonia at 193.3nm: Rovibrational State Distribution of the NH2(A(2)A1) Fragment.
PB95-151775 *00,937*

PHOTOELECTRON SPECTROSCOPY
Photoelectron Spectroscopy of Negatively Charged Bismuth Clusters: Bi(-)2, Bi(-)3, and Bi(-)4.
PB95-108494 *00,880*

High Resolution Angle Resolved Photoelectron Spectroscopy Study of N2.
PB95-151494 *03,907*

Photoelectron Spectroscopy of Small Antimony Cluster Anions: Sb(-), Sb2(-), Sb3(-), and Sb4(-).
PB95-203139 *01,045*

PHOTOELECTRONS
Measuring Nondipolar Asymmetries of Photoelectron Angular Distributions.
PB97-122493 *01,193*

PHOTOEMISSION
Resonant-Photoemission Investigation of the Heusler Alloys Ni2MnSb and NiMnSb.
PB95-162384 *04,612*

Influence of Coadsorbed Potassium on the Electron-Stimulated Desorption of F(+), F(-), and F(*) from PF3 on Ru(0001).
PB96-157946 *04,072*

PHOTOGRAPHIC ANALYSIS
Photographic Response to X-Ray Irradiation. 1. Estimation of the Photographic Error Statistic and Development of Analytic Density-Intensity Equations.
PB94-200086 *03,821*

Photographic Response to X-Ray Irradiation. 2. Correlated Models.
PB94-200094 *03,822*

Photographic Response to X-Ray Irradiation. 3. Photographic Linearization of Beam-Foil Spectra.
PB94-200102 *03,823*

PHOTOGRAPHIC IMAGES
Human and Machine Recognition of Faces: A Survey.
PB96-111687 *01,854*

PHOTOIONIZATION
Vibrational Autoionization in H2: Vibrational Branching Ratios and Photoelectron Angular Distributions Near the v(+)=3 Threshold.
PB94-199577 *00,799*

Photoionization of Small Molecules Using Synchrotron Radiation.
PB94-211505 *03,841*

High-Energy Behavior of the Double Photoionization of Helium from 2 to 12 keV.
PB94-213279 *03,860*

High Resolution Angle Resolved Photoelectron Spectroscopy Study of N2.
PB95-151494 *03,907*

Vibronic Coupling and Other Many-Body Effects in the 4sigmag(-1) Photoionization Channel of CO2.
PB95-162509 *00,962*

Shape-Resonance-Enhanced Continuum-Continuum Coupling in Photoionization of CO2.
PB95-164471 *00,983*

Short-Range Correlation and Relaxation Effects on the (6p(2))(1)SO Autoionizing State of Atomic Barium.
PB95-202289 *03,973*

Relative Photoionization and Photodetachment Cross Sections for Particular Fine-Structure Transitions with Application to Cl 3s-subshell Photoionization.
PB95-203097 *03,998*

Intensity-Dependent Scattering Rings in High Order Above-Threshold Ionization.
PB96-110739 *04,032*

Experimental Determination of the Ionization Energy of IO(X(sup 2)II(sub 3/2)) and Estimations of Delta(sub f)H(sup deg)(sub 0)(IO(sup -)) and PA(IO).
PB96-146899 *00,694*

Ionization Energies, Appearance Energies and Thermochemistry of CF2O and FCO.
PB97-111538 *01,178*

PHOTOLITHOGRAPHY
Numerical Simulation of Submicron Photolithographic Processing.
PB94-198561 *02,310*

PHOTOLUMINESCENCE
Band-to-Band Photoluminescence and Luminescence Excitation in Extremely Heavily Carbon-Doped Epitaxial GaAs.
PB95-150413 *04,570*

Comparative Photoluminescence Measurement and Simulation of Vertical-Cavity Semiconductor Laser Structures.
PB95-169173 *02,169*

Measurement and Simulation of Photoluminescence Spectra from Vertical-Cavity Quantum-Well Laser Structures.
PB95-169181 *02,170*

Comparison of Techniques for Nondestructive Composition Measurements in CdZnTe Substrates.
PB96-103098 *02,703*

Cross-Sectional Photoluminescence and Its Application to Buried-Layer Semiconductor Structures.
PB96-141106 *02,415*

Photoluminescence Spectra of Epitaxial Single Crystal C60.
PB96-141205 *04,754*

PHOTOLYSIS

Metalloporphyrin Sensitized Photooxidation of Water to Oxygen on the Surface of Colloidal Iridium Oxides - Photochemical and Pulse Radiolytic Studies.
PB95-107082 *00,868*

PHOTOMASKS

Practical Photomask Linewidth Measurements.
PB95-108510 *02,324*

Accuracy in Integrated Circuit Dimensional Measurements.
PB95-180808 *02,368*

Improving Photomask Linewidth Measurement Accuracy via Emulated Stepper Aerial Image Measurement.
PB95-180816 *02,911*

PHOTOMETERS

Detector-Based Candela Scale and Related Photometric Calibration Procedures at NIST.
PB95-161949 *04,273*

Intercomparison of Photometric Units Maintained at NIST (USA) and PTB (Germany), 1993.
PB95-261913 *04,329*

Comparison of Filter Radiometer Spectral Responsivity with the NIST Spectral-Irradiance and Illuminance Scales.
PB97-113161 *04,162*

PHOTOMETRY

Longterm Changes of Silicon Photodiodes and Their Use for Photometric Standardization.
PB94-211349 *04,234*

National Measurement System for Radiometry, Photometry, and Pyrometry Base Upon Absolute Detectors.
PB97-108559 *04,382*

Characterization of Modified FEL Quartz-Halogen Lamps for Photometric Standards.
PB97-112544 *00,282*

PHOTON-ATOM COLLISIONS

Laser Assisted Collisions at Ultracold Temperatures.
PB95-161220 *03,929*

PHOTON-ATOM INTERACTIONS

Laser Focused Atomic Deposition.
PB95-180659 *04,685*

PHOTON BEAM EXCITATION

Barium Contributions to the Valence Electronic Structure of YBa2Cu3O7-delta, PrBa2Cu3O7-delta, and Other Barium-Containing Compounds.
PB96-158019 *04,076*

PHOTON CROSS SECTIONS

Bibliography of Photon Total Cross Section (Attenuation Coefficient) Measurements 10 eV to 13.5 GeV, 1907-1993.
PB94-193760 *03,804*

Experimentally Measured Total X-ray Attenuation Coefficients Extracted from Previously Unprocessed Documents Held by the NIST Photon and Charged Particle Data Center.
PB97-114474 *04,165*

PHOTON-ELECTRON COLLISIONS

Polarization Effects on Multiple Scattering Gamma Transport.
PB95-153615 *03,926*

PHOTON TRANSPORT

Slab Transmission and Reflection for Point Source and Point Detector.
PB94-211265 *03,838*

PHOTONIC BAND STRUCTURE

Photonic Band-Structure Effects for Low-Index-Contrast Two-Dimensional Lattices in the Near Infrared.
PB97-122469 *04,401*

PHOTONIC PROBES

Optically Linked Three-Loop Antenna System for Determining the Radiation Characteristics of an Electrically Small Source.
PB95-161915 *02,005*

PHOTONICS

Optically Sensed EM-Field Probes for Pulsed Fields.
PB94-212594 *02,130*

PHOTONS

Exposure-to-Absorbed-Dose Conversion for Human Adult Cortical Bone.
PB97-110381 *03,640*

Calculation of Photon Mass Energy-Transfer and Mass Energy-Absorption Coefficients.
PB97-110399 *04,137*

Electron-Photon Monte Carlo Calculations: The ETRAN Code.
PB97-110407 *04,138*

PHOTOOXIDATION

Ferric Ion Assisted Photooxidation of Halocetates.
PB97-112460 *00,521*

PHOTOPATTERNING

UV-Photopatterning of Alkylthiolate Monolayers Self-Assembled on Gold and Silver.
PB95-150751 *00,924*

PHOTOREFLECTANCE

Double-Modulation and Selective Excitation Photoreflectance for Wafer-Level Characterization of Quantum-Well Laser Structures.
PB96-167325 *04,372*

Double Modulation and Selective Excitation Photoreflectance for Characterizing Highly Luminescent Semiconductor Structures and Samples with Poor Surface Morphology.
PB97-111439 *02,452*

PHOTORESISTORS

Characterization of Interface Defects in Oxygen-Implanted Silicon Films.
PB94-216629 *02,322*

PHTHALIC ACID/ (DIOCTYL-ESTER)

Neutron Scattering Study of Shear Induced Turbidity in Polystyrene/Dioctyl Phthalate Solutions at High Shear Rates.
PB94-172624 *01,197*

PHTHALOCYANINES

Complementary Molecular Information on Phthalocyanine Compounds Derived from Laser Microprobe Mass Spectrometry and Micro-Raman Spectroscopy.
PB94-172269 *00,757*

PHYSICAL CHEMISTRY

Journal of Physical and Chemical Reference Data, Volume 22, No. 1, January/February 1993.
PB94-160975 *00,729*

Thermodynamic Properties of the Group IIA Elements.
PB94-160983 *00,730*

Spectroscopy and Structure of the Lithium Hydride Diatomic Molecules and Ions.
PB94-160991 *00,731*

Quantum Yields for the Photosensitized Formation of the Lowest Electronically Excited Singlet State of Molecular Oxygen in Solution.
PB94-161007 *00,732*

Journal of Physical and Chemical Reference Data, Volume 22, No. 2, March/April 1993.
PB94-162211 *00,733*

Wavelengths and Energy Level Classifications for the Spectra of Sulfur (S I through S XVI).
PB94-162229 *00,734*

Thermodynamic Properties of Alkenes (Mono-Olefins Larger Than C4).
PB94-162237 *00,735*

Thermodynamic Behavior of the CO2-H2O System from 400 to 1000 K, up to 100 MPa and 30% Mole Fraction of CO2.
PB94-162245 *00,736*

Thermodynamics of Enzyme-Catalyzed Reactions: Part 1. Oxidoreductases.
PB94-162252 *00,737*

Journal of Physical and Chemical Reference Data, Volume 22, No. 3, May/June 1993.
PB94-162260 *00,738*

Estimation of the Heat Capacities of Organic Liquids as a Function of Temperature Using Group Additivity. I. Hydrocarbon Compounds.
PB94-162278 *00,739*

Estimation of the Heat Capacities of Organic Liquids as a Function of Temperature Using Group Additivity. II. Compounds of Carbon, Hydrogen, Halogens, Nitrogen, Oxygen, and Sulfur.
PB94-162286 *00,740*

Thermodynamic and Thermophysical Properties of Organic Nitrogen Compounds. Part II. 1- and 2-Butanamine, 2-Methyl-1-Propanamine, 2-Methyl-2-Propanamine, Pyrrole, 1-, 2-, and 3-Methylpyrrole, Pyridine, 2-, 3-, and 4-Methylpyridine, Pyrrolidine, Piperidine, Indole, Quinoline, Isoquinoline, Acridine, Carbazole, Phenanthridine, 1- and 2-Naphthalenamine, and 9-Methylcarbazole.
PB94-162294 *00,741*

International Equations for the Saturation Properties of Ordinary Water Substance. Revised According to the International Temperature Scale of 1990. Addendum to Journal of Physical and Chemical Reference Data 16, 893 (1987).
PB94-162302 *00,742*

Journal of Physical and Chemical Reference Data, Volume 22, No. 4, July/August 1993.
PB94-162310 *00,743*

Estimation of the Thermodynamic Properties of C-H-N-O-S-Halogen Compounds at 298.15 K.
PB94-162328 *00,744*

Journal of Physical and Chemical Reference Data, Volume 22, No. 5, September/October 1993.
PB94-162336 *00,745*

Compilation of Energy Levels and Wavelengths for the Spectrum of Singly-Ionized Oxygen (O II).
PB94-162344 *00,746*

Energy Levels of Germanium, Ge I through Ge XXXII.
PB94-162351 *00,747*

Spectral Data and Grotrian Diagrams for Highly Ionized Chromium, Cr V through Cr XXIV.
PB94-162369 *00,748*

Journal of Physical and Chemical Reference Data, Volume 22, No. 6, November/December 1993.
PB94-168556 *00,749*

Thermodynamic Properties of Synthetic Sapphire (alpha-Al2O3), Standard Reference Material 720 and the Effect of Temperature-Scale Differences on Thermodynamic Properties.
PB94-168564 *00,750*

Thermodynamic Properties of Gaseous Silicon Monotelluride and the Bond Dissociation Enthalpy D(sub m)(SiTe) at T approaches 0.
PB94-168572 *00,751*

Disilicides of Tungsten, Molybdenum, Tantalum, Titanium, Cobalt, and Nickel, and Platinum Monosilicide: A Survey of Their Thermodynamic Properties.
PB94-168580 *00,752*

Evaluated Bimolecular Ion-Molecule Gas Phase Kinetics of Positive Ions for Use in Modeling Planetary Atmospheres, Cometary Comae, and Interstellar Clouds.
PB94-168598 *00,753*

Atomic Weights of the Elements 1991.
PB94-168606 *00,754*

PHYSICAL EQUILIBRIUM

Bibliography of the Physical Equilibria and Related Properties of Some Cryogenic Systems.
AD-A281 167/7 *03,769*

PHYSICAL PROPERTIES

Physical Properties of Some Purified Aliphatic Hydrocarbons.
AD-A297 265/1 *00,657*

Journal of Physical and Chemical Reference Data, Volume 22, No. 1, January/February 1993.
PB94-160975 *00,729*

Journal of Physical and Chemical Reference Data, Volume 22, No. 2, March/April 1993.
PB94-162211 *00,733*

Journal of Physical and Chemical Reference Data, Volume 22, No. 3, May/June 1993.
PB94-162260 *00,738*

Journal of Physical and Chemical Reference Data, Volume 22, No. 4, July/August 1993.
PB94-162310 *00,743*

Journal of Physical and Chemical Reference Data, Volume 22, No. 5, September/October 1993.
PB94-162336 *00,745*

Journal of Physical and Chemical Reference Data, Volume 22, No. 6, November/December 1993.
PB94-168556 *00,749*

Physicochemical Properties of Calcific Deposits Isolated from Porcine Bioprosthetic Heart Valves Removed from Patients Following 2-13 Years Function.
PB94-172863 *00,184*

Energy and Migration of Grain Boundaries in Polycrystals.
PB94-211638 *03,332*

Constituents and Physical Properties of the C6+ Fraction of Natural Gas. Topical Report, April-June 1994.
PB95-136644 *02,483*

Analysis of Physical Properties of Ceramic Powders in an International Interlaboratory Comparison Program.
PB95-161501 *03,050*

Physical and Chemical Properties of Resin-Reinforced Calcium Phosphate Cements.
PB95-180212 *00,171*

Compositional Analysis of Beneficiated Fly Ashes.
PB95-220497 *00,397*

Physical Properties of Alternatives to the Fully Halogenated Chlorofluorocarbons.
PB96-119573 *03,279*

Journal of Physical and Chemical Reference Data, Volume 24, No. 1, January/February 1995.
PB96-145560 *01,101*

Journal of Physical and Chemical Reference Data, Volume 24, No. 2, March/April 1995.
PB96-145818 *01,105*

Journal of Physical and Chemical Reference Data, Volume 24, No. 3, May/June 1995.
PB96-145842 *01,108*

Journal of Physical and Chemical Reference Data, Volume 24, No. 4, July/August 1995.
PB96-145883 *01,112*

Journal of Physical and Chemical Reference Data, Volume 24, No. 5, September/October 1995.
PB96-145925 *01,116*

Journal of Physical and Chemical Reference Data, Volume 24, No. 6, November/December 1995.
PB96-145966 *01,120*

Environmental Aspects of Halon Replacements: Considerations for Advanced Agents and the Ozone Depletion Potential of CF3I.
PB97-122261 *03,301*

PHYSICAL RADIATION EFFECTS

Decomposition of Sulfur Hexafluoride by X-rays.
PB96-135314 *01,095*

PHYSICOCHEMICAL PROPERTIES

Octacalcium Phosphate Carboxylates. 2. Characterization and Structural Consideration.
PB95-161543 *00,955*

Formation of Hydroxyapatite in Cement Systems.
PB95-175261 *00,170*

PHYSICS
Physics Laboratory Technical Activities, 1993.
PB94-176088 *03,796*

Metrology Issues in Terahertz Physics and Technology.
PB96-128277 *01,939*

PHYSIOLOGIC CALCIFICATION
Experimental Validation of Radiopharmaceutical Absorbed Dose to Mineralized Bone Tissue.
PB94-199668 *03,617*

PHYTOPLANKTON
High-Performance Liquid Chromatography of Phytoplankton Pigments Using a Polymeric Reversed-Phase C18 Column.
PB95-151130 *00,583*

PIEZOELECTRIC CERAMICS
High-Sensitivity Acoustic Emission Sensor/Preamplifier Subsystems.
PB95-125704 *02,900*

PIEZOELECTRICITY
Piezoelectric and Pyroelectric Polymers.
PB95-153367 *01,250*

PIGMENTS
Molar Absorptivities of Bilirubin (NIST SRM 916A) and Its Neutral and Alkaline Azopigments.
PB94-211042 *03,456*

High-Performance Liquid Chromatography of Phytoplankton Pigments Using a Polymeric Reversed-Phase C18 Column.
PB95-151130 *00,583*

PIPE BENDS
Summary Report of NIST's Industry-Government Consortium Research Program on Flowmeter Installation Effects: The 45 Degree Elbow.
PB95-143061 *04,204*

PIPE ELBOWS
Effects of Pipe Elbows and Tube Bundles on Selected Types of Flowmeters.
PB96-160999 *01,135*

PIPE FLOW
Summary Report of NIST's Industry-Government Consortium Research Program on Flowmeter Installation Effects with Emphasis on the Research Period, January-September 1991: The Reducer.
PB94-160736 *04,196*

Summary Report of NIST's Industry-Government Consortium Research Program on Flowmeter Installation Effects: The 45 Degree Elbow.
PB95-143061 *04,204*

PIPE JOINTS
Analysis of Failed Dry Pipe Fire Suppression System Couplings from the Filene Center at Wolf Trap Farm Park for the Performing Arts.
PB94-164407 *00,331*

PIPELINES
Earthquake Resistant Construction of Gas and Liquid Fuel Pipeline Systems Serving, or Regulated By, the Federal Government.
PB94-161999 *04,846*

PIPES
Polyvinyl Chloride (PVC) Plastic Drain, Waste, and Vent Pipe and Fittings.
AD-A310 426/2 *00,326*

Acrylonitrile-Butadiene-Styrene (ABS) Plastic Drain, Waste, and Vent Pipe and Fittings.
AD-A310 724/0 *00,327*

PIPING SYSTEMS
Water Efficient Plumbing Fixtures through Standards and Test Methods.
PB95-125951 *00,248*

Comparison of Fire Sprinkler Piping Materials: Steel, Copper, Chlorinated Polyvinyl Chloride and Polybutylene, in Residential and Light Hazard Installations.
PB95-182267 *00,299*

PISTON GAGES
NIST Measurement Services: NIST Pressure Calibration Service.
PB94-164043 *02,892*

Intercomparison of the Effective Areas of a Pneumatic Piston Gauge Determined by Different Techniques.
PB94-212370 *02,640*

PLANAR NEAR-FIELD METHOD
Planar Near-Field Measurements and Microwave Holography for Measuring Aperture Distribution on a 60 GHz Active Array Antenna.
PB96-167366 *03,762*

PLANAR STRUCTURES
Planar Lenses for Field-Emitter Arrays.
PB96-103064 *02,112*

PLANE OXYGEN VIBRATION
q Dependence of Self-Energy Effects of the Plane Oxygen Vibration in YBa2Cu3O7.
PB96-138516 *01,096*

PLANE WAVES
Spatial Correlation Function for Fields in a Reverberation Chamber.
PB96-148077 *04,427*

PLANETARY ATMOSPHERES
Infrared Spectra of van der Waals Complexes of Importance in Planetary Atmospheres.
PB95-125738 *00,071*

Microwave Spectra of van der Waals Complexes of Importance in Planetary Atmospheres.
PB95-150611 *00,919*

Experimental Determination of the Rate Constant for the Reaction of C2H3 with H2 and Implications for the Partitioning of Hydrocarbons in Atmospheres of the Outer Planets.
PB97-122295 *00,112*

PLANETARY GRAVITATION
Integrated Laser Doppler Method for Measuring Planetary Gravity Fields.
PB94-198686 *03,681*

PLANETARY NEBULAE
IRAS Spectroscopic Observations of Young Planetary Nebulae.
PB95-152070 *00,072*

PLANNING
Integration of Real-Time Process Planning for Small-Batch Flexible Manufacturing.
PB95-151908 *02,822*

Computer-Aided Manufacturing Engineering Forum (1st). Technical Meeting Proceedings. Held in Gaithersburg, Maryland on March 21-22, 1995.
PB96-136965 *02,834*

Machining Process Planning Activity Model for Systems Integration.
PB96-165428 *02,841*

PLASMA
Electrical Measurements for Monitoring and Control of rf Plasma Processing.
PB96-161963 *04,369*

PLASMA CHEMISTRY
Plasma Chemistry in Disilane Discharges.
PB94-211075 *02,514*

Plasma Chemical Model for Decomposition of SF6 in a Negative Glow Corona Discharge.
PB95-181053 *01,020*

Plasma Chemistry in Silane/Germane and Disilane/Germane Mixtures.
PB95-202537 *01,027*

PLASMA DIAGNOSTICS
Spectroscopic Data for Fusion Edge Plasmas.
PB95-151569 *04,410*

Spectroscopic Diagnostics of Low Temperature Plasmas: Techniques and Required Data.
PB95-151577 *04,411*

Visible and UV Light from Highly Charged Ions: Exotic Matter Advancing Technology.
PB96-119391 *04,414*

PLASMA EDGE
Electron-Ion Collisions in the Plasma Edge.
PB96-111885 *04,037*

PLASMA ETCHING
Waveguide Polarizers Processed by Localized Plasma Etching.
PB95-169264 *02,171*

PLASMA SHEATH
Electrical Sensors for Monitoring rf Plasma Sheaths.
PB95-162962 *04,412*

PLASMA SPRAY
Ultrasonic NDE of Sprayed Ceramic Coatings.
PB96-201157 *02,761*

Characterization and Processing of Spray-Dried Zirconia Powders for Plasma Spray Application.
PB97-111231 *04,419*

PLASMA SPRAYED ALUMINA
Anisotropy of the Surfaces of Pores in Plasma Sprayed Alumina Deposits.
PB96-123211 *03,126*

PLASMAS (PHYSICS)
Two-Dimensional Self-Consistent Radio Frequency Plasma Simulations Relevant to the Gaseous Electronics Conference RF Reference Cell.
PB96-113436 *02,398*

PLASMIDS
Deletion Analysis of the Mini-P1 Plasmid Origin of Replication and the Role of E.coli DnaA Protein.
PB95-163911 *03,539*

PLASTIC CONCRETE
Study on the Reuse of Plastic Concrete Using Extended Set-Retarding Admixtures.
PB96-122130 *00,402*

PLASTIC DEFORMATION
SANS Study of the Plastic Deformation Mechanism in Polyethylene.
PB95-151841 *01,242*

PLASTIC PROPERTIES
Simulation of C60 Through the Plastic Transition Temperatures.
PB96-102546 *04,713*

PLASTICALLY POLARIZABLE MATERIALS
Shielding of Cracks in a Plastically Polarizable Material.
PB95-164257 *04,631*

PLASTICS
Weatherability of Plastic Materials.
AD-A301 675/5 *02,968*

Polyvinyl Chloride (PVC) Plastic Drain, Waste, and Vent Pipe and Fittings.
AD-A310 426/2 *00,326*

PLATELETS (MATERIALS)
Characterization of Phase and Surface Composition of Silicon Carbide Platelets.
PB94-216264 *03,043*

PLATFORM INTEROPERABILITY
Interoperability Experiments with CORBA and Persistent Object Base Systems.
PB96-183140 *01,772*

PLATINUM
Characterization of the Binding of Gallium, Platinum, and Uranium to Pseudomonas Fluorescens by Small-Angle X-ray Scattering and Transmission Electron Microscopy.
PB94-172509 *03,453*

Combined Low- and High-Angle X-Ray Structural Refinement of a Co/Pt(111) Multilayer Exhibiting Perpendicular Magnetic Anisotropy.
PB94-198355 *04,457*

PLATINUM ALLOYS
Fabrication of Platinum-Gold Alloys in Pre-Hispanic South America: Issues of Temperature and Microstructure Control.
PB94-211646 *03,333*

PLATINUM CONTAINING ALLOYS
Temperature Dependence of the Magnetic Excitations in Ordered and Disordered Fe72Pt28.
PB95-150223 *04,563*

PLATINUM IONS
Observation of Pd-Like Resonance Lines Through Pt(32+) and Zn-Like Resonance Lines of Er(38+) and Hf(42+).
PB95-150637 *03,896*

Rh I Isoelectronic Sequence Observed from Er(23+) to Pt(33+).
PB95-150652 *03,898*

Spectra of Ag I Isoelectronic Sequence Observed from Er(21+) to Au(32+).
PB95-150660 *03,899*

PLEIADES CLUSTER
IUE Observations of Solar-Type Stars in the Pleiades and the Hyades.
PB94-199437 *00,053*

PLUMES
Computational Model for the Rise and Dispersion of Wind-Blown, Buoyancy-Driven Plumes. Part 2. Linearly Stratified Atmosphere.
PB94-143427 *00,119*

Dispersion and Deposition of Smoke Plumes Generated in Massive Fires.
PB95-126066 *02,540*

Airborne Smoke Sampling Package for Field Measurements of Fires.
PB95-150041 *01,381*

Fire-Plume-Generated Ceiling Jet Characteristics and Convective Heat Transfer to Ceiling and Wall Surfaces in a Two-Layer Fire Environment: Uniform Temperature Ceiling and Walls.
PB95-164711 *00,382*

Some Factors Affecting the Design of a Calorimeter Hood and Exhaust.
PB96-102181 *00,302*

Smoke Plume Trajectory from In situ Burning of Crude Oil in Alaska: Field Experiments.
PB96-131560 *02,594*

PLYWOOD
Voluntary Product Standard PS 1-95 Construction and Industrial Plywood.
PB96-178900 *03,406*

PMGDM
Modified Surface-Active Monomers for Adhesive Bonding to Dentin.
PB95-151163 *00,158*

PMMA
Fire Growth Models for Materials.
PB94-195856 *01,367*

Thermal Stability of Internal Electric Field and Polarization Distribution in Blend of Polyvinylidene Fluoride and Polymethylmethacrylate.
PB95-151072 *01,240*

PNEUMATIC EQUIPMENT
Intercomparison of the Effective Areas of a Pneumatic Piston Gauge Determined by Different Techniques.
PB94-212370 *02,640*

PNEUMATIC TUBE TERMINAL
New NIST Rapid Pneumatic Tube System.
PB96-167259 *03,738*

POB
Persistent Object Base System Testing and Evaluation.
PB95-220588 *01,730*

POB (PERSISTENT OBJECT BASED SYSTEMS)
Persistent Object Base System Testing and Evaluation.
PB95-220588 *01,730*

Interoperability Experiments with CORBA and Persistent Object Base Systems.
PB96-183140 *01,772*

POINT CHARGES
Point Charges, Radiation Reaction, and Quantum Mechanics.
PB97-110563 *04,139*

POISSON RATIO
Hollow Clay Tile Prism Tests for Martin Marietta Energy Systems: Task 2 Testing.
PB94-217486 *00,352*

POISSON'S EQUATION
Scanning Capacitance Microscopy Measurements and Modeling: Progress Towards Dopant Profiling of Silicon.
PB96-180070 *01,964*

POLAR GASES
Virial Coefficients of Five Binary Mixtures of Fluorinated Methanes and Ethanes.
PB96-156054 *01,128*

POLARIMETRY
Polarimetric Calibration of Reciprocal-Antenna Radars.
PB96-200696 *02,016*

POLARIZATION
Thermal Pulse Study of the Polarization Distributions Produced in Polyvinylidene Fluoride by Corona Poling at Constant Current.
PB94-172293 *01,195*

Surface Magnetic Microstructural Analysis Using Scanning Electron Microscopy with Polarization Analysis (SEMPA).
PB95-162657 *03,938*

Anisotropy of Polarized X-ray Emission from Atoms and Molecules.
PB95-163002 *04,621*

Vector and Quasi-Vector Solutions for Optical Waveguide Modes Using Efficient Galerkin's Method with Hermite-Gauss Basis Functions.
PB96-141197 *04,357*

Time-Resolved Measurements of the Polarization State of Four-Wave Mixing Signals from GaAs Multiple Quantum Wells.
PB96-201058 *04,796*

Polarization Measurements on a Magnetic Quadrupole Line in Ne-Like Barium.
PB97-113104 *04,161*

Integrated Optical Polarization-Discriminating Receiver in Glass.
PB97-113179 *02,206*

POLARIZATION (CHARGE SEPARATION)
Hysteresis Measurements of Remanent Polarization and Coercive Field in Polymers.
PB94-199767 *04,475*

Thermal Stability of Internal Electric Field and Polarization Distribution in Blend of Polyvinylidene Fluoride and Polymethylmethacrylate.
PB95-151072 *01,240*

Piezoelectric and Pyroelectric Polymers.
PB95-153367 *01,250*

POLARIZATION MODE DISPERSION
Anomalous Relation between Time and Frequency Domain PMD Measurements.
PB97-119390 *04,398*

POLARIZATION PROFILES
Thermal Pulse Study of the Polarization Distributions Produced in Polyvinylidene Fluoride by Corona Poling at Constant Current.
PB94-172293 *01,195*

POLARIZATION (WAVES)
Polarization Effects on Multiple Scattering Gamma Transport.
PB95-153615 *03,926*

POLARIZED BEAMS
Uncertainty Intervals for Polarized Beam Scattering Asymmetry Statistics.
PB94-200342 *03,825*

Connection between Superelastic and Inelastic Electron-Atom Collisions Involving Polarized Collision Partners.
PB95-202297 *03,974*

POLARIZED ELECTROMAGNETIC RADIATION
Resonance and Threshold Effects in Polarized X-Ray Emission from Atoms and Molecules.
PB95-150298 *03,891*

POLARIZED INTERFEROMETER
New Refractometer by Combining a Variable Length Vacuum Cell and a Double-Pass Michelson Interferometer.
PB97-111926 *01,986*

POLARIZED LIGHT
Characteristics of Light Emission After Low-Energy Electron Impact Excitation of Caesium Atoms.
PB94-198587 *03,806*

Polarization of Light Emitted After Positron Impact Excitation of Alkali Atoms.
PB94-199734 *03,816*

National Voluntary Laboratory Accreditation Program: Bulk Asbestos Analysis.
PB95-138129 *02,541*

POLARIZED NEUTRON REFLECTOMETRY
New Exact Solution of the One-Dimensional Schrodinger Equation and Its Application to Polarized Neutron Reflectometry.
PB95-161832 *04,609*

Analytic Calculation of Polarized Neutron Reflectivity from Superconductors.
PB95-164224 *04,629*

POLARIZERS
Supermirror Transmission Polarizers for Neutrons.
PB94-216215 *03,866*

Waveguide Polarizers Processed by Localized Plasma Etching.
PB95-169264 *02,171*

POLE FIGURES
Texture Measurement of Sintered Alumina Using the March-Dollase Function.
PB96-179494 *04,784*

POLICE PATROL CARS
AutoBid 2.0: The Microcomputer System for Police Patrol Vehicle Selection.
PB96-154570 *04,871*

POLICE VEHICLES
Evaluating Investments in Law Enforcement Equipment: An Annotated Bibliography.
PB95-151379 *04,867*

POLICY FORMATION
Information Infrastructure: Reaching Society's Goals. A Report of the Information Infrastructure Task Force Committee on Applications and Technology.
ED-376 823 *00,131*

POLICY MAKING
Standards Policy and Information Infrastructure.
PB95-231882 *01,485*

POLISHING
Rapid Post-Polishing of Diamond-Turned Optics.
PB95-175949 *04,301*

POLLUTANTS
Standard Reference Materials for Dioxins and Other Environmental Pollutants.
PB94-198330 *02,518*

POLLUTION ABATEMENT
Opportunities for Innovation: Pollution Prevention.
PB95-147146 *02,520*

International Green Building Conference and Exposition (2nd). Held in Big Sky, Montana on August 13-15, 1995.
PB95-253605 *02,525*

International Green Building Conference and Exposition (3rd). Held in San Diego, California on November 17-19, 1996. (Reannouncement with new abstract).
PB97-121826 *02,531*

POLLUTION CONTROL EQUIPMENT
India: Environmental Technologies Export Market Plan.
PB97-114359 *02,529*

POLLUTION SAMPLING
Standard Reference Materials for the Determination of Polycyclic Aromatic Hydrocarbons in Environmental Samples - Current Activities.
PB95-151668 *00,586*

POLONIUM 208
Long-Term Stability of Carrier-Free Polonium Solution Standards.
PB94-185170 *00,685*

POLY (AMIDE/N-PROPYLACRYL)
Small Angle Neutron Scattering Study on Poly(N-Isopropyl Acrylamide) Gels Near Their Volume-Phase Transition Temperature.
PB95-164380 *01,263*

Small-Angle Neutron Scattering Study on Weakly Charged Temperature Sensitive Polymer Gels.
PB95-164398 *01,264*

POLY (P-PHENYLENE VINYLENE)
Inelastic-Neutron-Scattering Studies of Poly(p-phenylene vinylene).
PB95-180766 *01,014*

POLY (SULFONIC ACID/TETRAFLUORO)
Gas Transport Properties of Solution-Cast Perfluorosulfonic Acid Ionomer Films Containing Ionic Surfactants.
PB95-175998 *01,267*

POLYACRYLAMIDE GEL ELECTROPHORESIS
Resolution of DNA in the Presence of Mobility Modifying Polar and Nonpolar Compounds by Discontinuous Electrophoresis on Rehydratable Polyacrylamide Gels.
PB95-152799 *00,590*

POLYACRYLATES
Adsorption of Low-Molecular-Weight Sodium Polyacrylate on Hydroxyapatite.
PB94-172608 *00,139*

POLYACRYLIC ACID
Small-Angle Neutron Scattering Study on Weakly Charged Temperature Sensitive Polymer Gels.
PB95-164398 *01,264*

POLYACRYLICS
Adsorption of Polyacrylic Acids and Their Sodium Salts on Hydroxyapatite: Effect of Relative Molar Mass.
PB97-112510 *03,581*

POLYAMINES
Cyclic Polyamine Ionophore for Use in a Dibasic Phosphate-Selective Electrode.
PB95-180121 *01,008*

POLYAROMATIC CARCINOGENS
New Method for the Detection and Measurement of Polyaromatic Carcinogens and Related Compounds by DNA Intercalation.
PB96-167382 *03,481*

POLYATOMIC MOLECULES
Doppler-Free Spectroscopy of Large Polyatomic Molecules and van der Waals Complexes.
PB96-119581 *04,339*

POLYBASIC ORGANIC ACIDS
Polymeric Calcium Phosphate Cements Derived from Poly(methyl vinyl ether-maleic acid).
PB96-164264 *00,180*

POLYBUTADIENE
Shear-Excited Morphological States in a Triblock Copolymer.
PB94-172392 *01,196*

Time Dependent Small Angle Neutron Scattering Behavior in Triblock Copolymers Under Steady Shear.
PB94-172632 *01,198*

Effect of Cross-Links on the Miscibility of a Deuterated Polybutadiene and Protonated Polybutadiene Blend.
PB94-212438 *01,225*

Inversion of the Phase Diagram from UCST to LCST in Deuterated Polybutadiene and Protonated Polybutadiene Blends.
PB94-212446 *01,226*

Dynamic Light-Scattering Study of a Diluted Polymer Blend Near Its Critical Point.
PB95-151890 *01,245*

SANS Studies of Space-Time Organization of Structure in Polymer Blends.
PB95-153789 *01,251*

Time-Resolved Small-Angle Neutron Scattering Study of Spinodal Decomposition in Deuterated and Protonated Polybutadiene Blends. 1. Effect of Initial Thermal Fluctuations.
PB95-161196 *01,252*

POLYBUTYLENE
Comparison of Fire Sprinkler Piping Materials: Steel, Copper, Chlorinated Polyvinyl Chloride and Polybutylene, in Residential and Light Hazard Installations.
PB95-182267 *00,299*

POLYCHLORINATED BIPHENYLS
Comparison of Methods for Gas Chromatographic Determination of PCBs and Chlorinated Pesticides in Marine Reference Materials.
PB95-140091 *02,584*

NIST Standard Reference Materials (SRMs) for Polychlorinated Biphenyl (PCB) Determinations and Their Applicability to Toxaphene Measurements.
PB95-140109 *02,585*

Certification of Polychlorinated Biphenyl Congeners and Chlorinated Pesticides in a Whale Blubber Standard Reference Material.
PB96-103023 *03,745*

Quantitative Analysis of Selected PCB Congeners in Marine Matrix Reference Materials Using a Novel Cyanobiphenyl Stationary Phase.
PB96-111737 *02,591*

POLYCRYSTALLINE
Unconventional Ferromagnetic Transition in La(sub 1-x)Ca(sub x)MnO3.
PB97-112429 *04,156*

POLYCRYSTALS
Energy and Migration of Grain Boundaries in Polycrystals.
PB94-211638 *03,332*

Microstructural Evolution in Two-Dimensional Two-Phase Polycrystals.
PB94-211992 *04,498*

POLYCYCLIC AROMATIC HYDROCARBONS
Determination of Polycyclic Aromatic Hydrocarbons by Liquid Chromatography.
PB95-151650 *00,585*

Standard Reference Materials for the Determination of Polycyclic Aromatic Hydrocarbons in Environmental Samples - Current Activities.
PB95-151668 *00,586*

Liquid Chromatographic Determination of Polycyclic Aromatic Hydrocarbon Isomers of Molecular Weight 278 and 302 in Environmental Standard Reference Materials.
PB95-164042 *02,523*

Certification of Polycyclic Aromatic Hydrocarbons in a Marine Sediment Standard Reference Material.
PB96-111778 *02,592*

POLYDIACETYLENES
Novel Polydiacetylenes Derived from Liquid Crystalline Monomers.
PB95-140125 *01,235*

POLYELECTROLYTES
Polyelectrolytes as Dispersants in Colloidal Processing of Silicon Nitride Ceramics.
PB95-175568 *03,055*

Surface Chemical Interactions of Si3N4 with Polyelectrolyte Deflocculants.
PB95-175576 *03,056*

Electrostatic Rigidity of Polyelectrolytes from Reparametrization Invariance.
PB96-180062 *04,113*

POLYENES
Lowest Excited Singlet State of Isolated 1-phenyl-1,3-butadiene and 1-phenyl-1,3,5-hexatriene.
PB95-202339 *01,026*

POLYETHLENES
Certification of the Standard Reference Material 1473a, a Low Density Polyethylene Resin.
PB96-128251 *01,282*

POLYETHYLENE
Polyethylene Crystallized from an Entangled Solution Observed by Scanning Tunneling Microscopy.
PB95-107389 *01,232*

SANS Study of the Plastic Deformation Mechanism in Polyethylene.
PB95-151841 *01,242*

POLYETHYLENE GLYCOL
Two Phase Aqueous Extraction: Rheological Properties of Dextran, Polyethylene Glycol, Bovine Serum Albumin and Their Mixtures.
PB95-161998 *00,676*

Protein Extraction in a Spray Column Using a Polyethylene Glycol Maltodextrin Two-Phase Polymer System.
PB95-162228 *00,595*

Phase Composition, Viscosities, and Densities for Aqueous Two-Phase Systems Composed of Polyethylene Glycol and Various Salts at 25C.
PB95-164596 *00,986*

POLYETHYLENE PLASTICS
Performance of Plastic Packaging for Hazardous Materials Transportation. Part 1. Mechanical Properties.
AD-A301 258/0 *02,580*

POLYETHYLENES
Recertification of the Standard Reference Material 1475A, a Linear Polyethylene Resin.
PB94-161932 *02,628*

POLYIMIDE
Gas Absorption during Ion-Irradiation of a Polymer Target.
PB96-161864 *04,099*

POLYIMIDES
Water Adsorption at a Polyimide/Silicon Wafer Interface.
PB96-103197 *01,070*

POLYISOCYANURATE
Effect of Environmentally Exposures on the Properties of Polyisocyanurate Foam Insulation: Thermal Conductivity Measurements.
PB95-181210 *00,388*

POLYISOPRENE
SANS Studies of Space-Time Organization of Structure in Polymer Blends.
PB95-153789 *01,251*

POLYMER BLENDS
Thermodynamic Interactions in Model Polyolefin Blends Obtained by Small-Angle Neutron Scattering.
PB94-198496 *01,208*

Statistical Thermodynamics of Phase Separation and Ion Partitioning in Aqueous Two-Phase Systems.
PB94-199387 *01,212*

How Far Is Far from Critical Point in Polymer Blends. Lattice Cluster Theory Computations for Structured Monomer, Compressible Systems.
PB94-211141 *01,217*

Crossover to Strong Shear in a Low-Molecular-Weight Critical Polymer Blend.
PB94-211976 *01,222*

Effect of Cross-Links on the Miscibility of a Deuterated Polybutadiene and Protonated Polybutadiene Blend.
PB94-212438 *01,225*

Inversion of the Phase Diagram from UCST to LCST in Deuterated Polybutadiene and Protonated Polybutadiene Blends.
PB94-212446 *01,226*

Glass Temperature of Polymer Blends: Comparison of Both the Free Volume and the Entropy Predictions with Data.
PB95-140190 *01,236*

Structural Stabilization of Phase Separating PC/Polyester Blends through Interfacial Modification by Transesterification Reaction.
PB95-150454 *01,239*

Thermal Stability of Internal Electric Field and Polarization Distribution in Blend of Polyvinylidene Fluoride and Polymethylmethacrylate.
PB95-151072 *01,240*

Anisotropic Phase Separation Kinetics in a Polymer Blend Solution Following Cessation of Shear Studied by Light Scattering.
PB95-151247 *01,241*

SANS Study of the Plastic Deformation Mechanism in Polyethylene.
PB95-151841 *01,242*

Dynamic Light-Scattering Study of a Diluted Polymer Blend Near Its Critical Point.
PB95-151890 *01,245*

Thermodynamic Interactions and Correlations in Mixtures of Two Homopolymers and a Block Copolymers by Small Angle Neutron Scattering.
PB95-152872 *01,247*

SANS Studies of Space-Time Organization of Structure in Polymer Blends.
PB95-153789 *01,251*

Time-Resolved Small-Angle Neutron Scattering Study of Spinodal Decomposition in Deuterated and Protonated Polybutadiene Blends. 1. Effect of Initial Thermal Fluctuations.
PB95-161196 *01,252*

Characterization of Polyquinoline Blends Using Small Angle Scattering.
PB95-164125 *01,261*

Polymers Technical Activities 1994. NAC-NRC Assessment Panel, April 6-7, 1995.
PB95-209896 *01,275*

Modification of the Phase Stability of Polymer Blends by Diblock Copolymer Additivies.
PB96-123542 *03,172*

Slow Dynamics of Segregation in Hydrogen-Bonded Polymer Blends.
PB96-123591 *01,281*

Light-Scattering Studies on Phase Separation in a Binary Blend with Addition of Diblock Copolymers.
PB96-146865 *01,286*

Phase Separation in Thin Film Polymer Blends With and Without Block Copolymer Additives.
PB96-204482 *01,294*

Lattice Model of a Hydrogen-Bonded Polymer Blend.
PB97-112262 *03,391*

Relaxation After a Temperature Jump Within the One Phase Region of a Polymer Mixture.
PB97-112494 *03,394*

Morphology and Phase Separation Kinetics of a Compatibilized Blend.
PB97-119135 *01,297*

POLYMER BRUSH
Neutron Reflectivity Study of the Density Profile of a Model End-Grafted Polymer Brush: Influence of Solvent Quality.
PB95-202735 *01,274*

POLYMER BRUSHES
Terminally Anchored Chain Interphases: Their Chromatographic Properties.
PB95-181061 *01,272*

Terminally Anchored Chain Interphases: The Effect of Multicomponent, Polydisperse Solvents on Their Equilibrium Properties.
PB95-181079 *01,273*

POLYMER CHEMISTRY
Fluorescence Anisotropy Measurements on a Polymer Melt as a Function of Applied Shear Stress.
PB94-199296 *01,209*

Observations of Shear Induced Molecular Orientation in a Polymer Melt Using Fluorescence Anisotropy Measurements.
PB94-199304 *01,210*

Observations of Shear Stress and Molecular Orientation Using Fluorescence Anisotropy Measurements.
PB94-199312 *01,211*

POLYMER COMPOSITES
Materials Aspects of Fiber-Reinforced Polymer Composites in Infrastructure.
PB96-210695 *03,184*

POLYMER FILMS
Advances in the Measurement of Polymer CTE: Micrometer- to Atomic-Scale Measurements.
PB96-180229 *03,390*

POLYMER INTERFACE
Compatibilization of Polymer Blends by Complexation. 2. Kinetics of Interfacial Mixing.
PB97-111900 *01,295*

POLYMER MATRIX COMPOSITES
Selection of Appropriate Ultrasonic System Components for NDE of Thick Polymer-Composites.
PB94-185279 *03,133*

Review of Cure Monitoring Techniques for On-Line Process Control.
PB94-216728 *03,145*

Polymer Composites Workshop. Held in Winona, Minnesota on April 29-30, 1992 (Video).
PB94-780129 *03,147*

Appropriate Ultrasonic System Components for NDE of Thick Polymer Composites.
PB95-125696 *03,148*

Thermoacoustic Technique for Determining the Interface and/or Interply Strength in Polymeric Composites.
PB95-161824 *03,158*

Environmental Durability of Glass-Fiber Composites.
PB95-203220 *03,166*

POLYMER NETWORKS
Synthesis of Hybrid Organic-Inorganic Materials from Interpenetrating Polymer Network Chemistry.
PB96-180054 *02,994*

POLYMER PHYSICS
Book Review: Statistical Physics of Macromolecules.
PB96-123526 *01,280*

POLYMERASE CHAIN REACTION
Electrophoretic Separations of Polymerase Chain Reaction: Amplified DNA Fragments in DNA Typing Using a Capillary Electrophoresis-Lased Induced Fluorescence System.
PB95-163036 *03,536*

Enhanced Detection of PCR Products Through Use of TOTO and YOYO Intercalating Dyes with Laser Induced Fluorescence - Capillary Electrophoresis.
PB95-164653 *00,599*

POLYMERIC FILMS
Diffusion of Cations Beneath Organic Coatings on Steel Substrate.
PB94-215704 *03,119*

Grazing Incidence Prompt Gamma Emissions and Resonance-Enhanced Neutron Standing Waves in a Thin-Film.
PB95-150470 *03,892*

Gas Transport Properties of Solution-Cast Perfluorosulfonic Acid Ionomer Films Containing Ionic Surfactants.
PB95-175998 *01,267*

Thermal Conductivity of Polypyromellitimide Film with Alumina Filler Particles from 4.2 to 300 K.
PB96-200753 *01,292*

POLYMERIZATION
Fluorescence Monitoring of Polarity Change and Gelation during Epoxy Cure.
PB94-185543 *01,204*

Effect of Curing History on Ultimate Glass Transition Temperature and Network Structure of Crosslinking Polymers.
PB94-200052 *01,214*

Thermal Behavior of 4-Maleimidophenyl Glycidyl Ether Resins.
PB95-153151 *01,249*

Ring-Opening Dental Resin Systems Based on Cyclic Acetals.
PB95-162251 *00,162*

Synthesis and Polymerization of Difunctional and Multifunctional Monomers Capable of Cyclopolymerization.
PB95-163044 *01,257*

Evaluation of Methylene Lactone Monomers in Dental Resins.
PB95-164661 *00,164*

Ring-Opening Polymerication of a 2-Methylene Spiro Orthocarbonate Bearing a Pendant Methacrylate Group.
PB95-176145 *01,268*

Polymerization Initiation by N-p-Tolylglycine: Free-Radical Reactions Studied by Pulse and Steady-State Radiolysis.
PB95-180014 *01,269*

Radiochromic Solid-State Polymerization Reaction.
PB95-180683 *01,271*

POLYMERS
Weatherability of Plastic Materials.
AD-A301 675/5 *02,968*

Combustion of a Polymer (PMMA) Sphere in Microgravity.
N96-15569/2 *01,354*

In-Line Optical Monitoring of Injection Molding.
PB94-185105 *01,201*

Influence of Surface Interaction and Chain Stiffness on Polymer-Induced Entropic Forces and the Dimensions of Confined Polymers.
PB94-185469 *01,203*

Neutron Reflectivity of End-Grafted Polymers: Concentration and Solvent Quality Dependence in Equilibrium Conditions.
PB94-185758 *01,206*

Hysteresis Measurements of Remanent Polarization and Coercive Field in Polymers.
PB94-199767 *04,475*

Peeling a Polymer from a Surface or from a Line.
PB94-199809 *01,213*

Hypercubic Lattice SAW Exponents nu and gamma : 3.99 Dimensions Revisited.
PB94-211026 *01,215*

Clinical Perspective on Dentin Adhesives.
PB94-211240 *00,146*

Monitoring Polymer Cure by Fluorescence Recovery After Photobleaching.
PB94-211422 *01,218*

Polymer Liquid Crystalline Materials.
PB94-212339 *01,224*

Topological Influences on Polymer Adsorption and Desorption Dynamics.
PB94-212479 *01,227*

Effects of Molecular Weight and Thermal Stability on Polymer Gasification.
PB94-212610 *01,228*

Effects of Variable Excluded Volume on the Dimensions of Off-Lattice Polymer Chains.
PB94-212941 *01,229*

Physics Required for Prediction of Long Term Performance of Polymers and Their Composites.
PB94-219243 *03,146*

SANS and LS Studies of Polymer Mixtures Under Shear Flow.
PB95-107090 *01,231*

Response of a Terminally Anchored Polymer Chain to Simple Shear Flow.
PB95-108668 *01,233*

Glass Temperature of Polymer Blends: Comparison of Both the Free Volume and the Entropy Predictions with Data.
PB95-140190 *01,236*

Effect of Hydrodynamic Interactions on a Terminally Anchored Bead-Rod Model Chain.
PB95-141156 *01,237*

Investigation into the Flammability Properties of Honeycomb Composites.
PB95-143293 *03,152*

Effect of Electrode-Polymer Interfacial Layers on Polymer Conduction. Part 2. Device Summary.
PB95-151155 02,335

Localization of a Homopolymer Dissolved in a Lamellar Structure of a Block Copolymer Studied by Small-Angle Neutron Scattering.
PB95-161592 01,253

Elastic Scattering of Polymer Networks.
PB95-161816 01,255

Applications of Fluorescence Spectroscopy in Polymer Science and Technology.
PB95-163770 01,258

Small Angle Neutron Scattering Study on Poly(N-Isopropyl Acrylamide) Gels Near Their Volume-Phase Transition Temperature.
PB95-164380 01,263

Small-Angle Neutron Scattering Study on Weakly Charged Temperature Sensitive Polymer Gels.
PB95-164398 01,264

Competition between Hydrodynamic Screening ('Draining') and Excluded Volume Interactions in an Isolated Polymer Chain.
PB95-175402 01,265

Examination of the l/d Expansion Method from Exact Enumeration for a Self-Interacting Self-Avoiding Walk.
PB95-175733 01,266

Optical Biosensor Using a Fluorescent, Swelling Sensing Element.
PB95-175899 03,541

Neutron Scattering Study of the Orientation of a Liquid Crystalline Polymer by Shear Flow.
PB95-180196 01,270

Formation of Hydroxyapatite in a Polymeric Calcium Phosphate Cement.
PB95-180642 00,173

Terminally Anchored Chain Interphases: Their Chromatographic Properties.
PB95-181061 01,272

Terminally Anchored Chain Interphases: The Effect of Multicomponent, Polydisperse Solvents on Their Equilibrium Properties.
PB95-181079 01,273

Polymers Technical Activities 1994. NAC-NRC Assessment Panel, April 6-7, 1995.
PB95-209896 01,275

Self-Avoiding-Walk Contacts and Random-Walk Self-Intersections in Variable Dimensionality.
PB96-102231 01,276

Nonlinear Dynamics of Stiff Polymers.
PB96-122478 01,278

Polymer Combustion and Flammability: Role of the Condensed Phase.
PB96-123245 01,279

Flow-Induced Structure in Polymer. Chapter 1. An Introduction to Flow-Induced Structures in Polymers.
PB96-123369 03,387

Flow-Induced Structure in Polymers. Chapter 17. Phase-Separation Kinetics of a Polymer Blend Solution Studied by a Two-Step Shear Quench.
PB96-123377 03,388

Response to 'Draining in Dilute Polymer Solutions and Renormalization'.
PB96-146667 01,283

Orientation Effects on ESR Analysis of Alanine-Polymer Dosimeters.
PB96-146725 03,720

Thermodynamic Properties of Dilute and Semidilute Solutions of Regular Star Polymers.
PB96-146808 01,284

Preparation and Characterization of Cyclopolymerizable Resin Formulations.
PB96-146840 01,285

Influence of an Impenetrable Interface on a Polymer Glass-Transition Temperature.
PB96-146873 03,175

Shear-Induced Mixing in Polymer Blends.
PB96-148085 01,287

NIST Metrology Program on Electromagnetic Characterization of Materials.
PB96-156062 01,944

Effects of Sample Mounting on Flammability Properties of Intumescent Polymers.
PB96-159777 03,389

Hygrothermal Effects on the Performance of Polymers and Polymeric Composites: A Workshop Report. Held in Gaithersburg, Maryland on September 21-22, 1995.
PB96-183207 03,180

Polymers Technical Activities, 1995.
PB96-193719 01,291

Gas Phase Oxygen Effect on Chain Scission and Monomer Content in Bulk Poly(methyl methacrylate) Degraded by External Thermal Radiation.
PB96-204078 01,293

Swelling and Growth of Polymers, Membranes and Sponges.
PB97-118400 03,396

Materials and Fire Threat.
PB97-122311 01,442

POLYMETHYL METHACRYLATE

Combustion of a Polymer (PMMA) Sphere in Microgravity.
N96-15569/2 01,354

Grafted Interpenetrating Polymer Networks.
PB94-185055 01,200

Investigation of the Thermal Stability and Char-Forming Tendency of Cross-linked Poly(methyl methacrylate).
PB94-213501 03,380

Morphology of Symmetric Diblock Copolymers as Revealed by Neutron Reflectivity.
PB95-140075 01,234

POLYOLEFINS

Thermodynamic Interactions in Model Polyolefin Blends Obtained by Small-Angle Neutron Scattering.
PB94-198496 01,208

Thermodynamic Interactions and Correlations in Mixtures of Two Homopolymers and a Block Copolymers by Small Angle Neutron Scattering.
PB95-152872 01,247

POLYOXYETHYLENE

Determination of the Weight Average Molecular Weight of Two Poly(Ethylene Oxides), SRM 1923 and SRM 1924.
PB94-217031 01,230

Two Phase Aqueous Extraction: Rheological Properties of Dextran, Polyethylene Glycol, Bovine Serum Albumin and Their Mixtures.
PB95-161998 00,676

Phase Composition, Viscosities, and Densities for Aqueous Two-Phase Systems Composed of Polyethylene Glycol and Various Salts at 25C.
PB95-164596 00,986

POLYOXYPROPYLENE

Influence of Physical Aging on the Yield Response of Model DGEBA + Poly(propylene oxide) Epoxy Glasses.
PB95-126363 03,381

POLYPERFLUOROSULFONATE IONOMER

CO2/CH4 Transport in Polyperfluorosulfonate Ionomers: Effects of Polar Solvents on Permeation and Solubility.
PB96-163803 01,145

POLYQUINOLINES

Characterization of Polyquinoline Block Copolymer Using Small Angle Scattering.
PB95-151882 01,244

Characterization of Polyquinoline Blends Using Small Angle Scattering.
PB95-164125 01,261

POLYSTYRENE

Shear-Excited Morphological States in a Triblock Copolymer.
PB94-172392 01,196

Neutron Scattering Study of Shear Induced Turbidity in Polystyrene/Dioctyl Phthalate Solutions at High Shear Rates.
PB94-172624 01,197

Time Dependent Small Angle Neutron Scattering Behavior in Triblock Copolymers Under Steady Shear.
PB94-172632 01,198

Shear Dependence of Critical Fluctuations in Binary Polymer Mixtures by Small Angle Neutron Scattering.
PB94-211612 01,220

Small-Angle X-Ray and Neutron Scattering Study of Block Copolymer/Homopolymer Mixtures.
PB94-211729 01,221

Morphology of Symmetric Diblock Copolymers as Revealed by Neutron Reflectivity.
PB95-140075 01,234

Dynamic Light-Scattering Study of a Diluted Polymer Blend Near Its Critical Point.
PB95-151890 01,245

Neutron Scattering Study of Shear Induced Turbidity in Polystyrene Dissolved in Dioctyl Phthalate.
PB95-161865 01,256

Preparation of 2-Dimensional Ultra Thin Polystyrene Film by Water Casting Method.
PB95-162806 04,619

Partial Scattered Intensities from a Binary Suspension of Polystyrene and Silica.
PB95-175618 00,996

Dielectric Properties of Materials at Cryogenic Temperatures and Microwave Frequencies.
PB95-202610 02,369

Standard Reference Materials: Polystyrene Films for Calibrating the Wavelength Scale of Infrared Spectrophotometers - SRM 1921.
PB95-226866 03,386

Room-Temperature Thermal Conductivity of Expanded Polystyrene Board for a Standard Reference Material.
PB96-193693 00,412

POLYSULFIDES

Microbial Degradation of Polysulfides and Insights into Their Possible Occurrence in Coal.
PB95-163374 02,488

POLYTETRAFLUOROETHYLENE

45 deg/0 deg Reflectance Factors of Pressed Polytetrafluoroethylene (PTFE) Powder.
PB95-260758 04,328

POLYURETHANE FOAM

New Approach for Reducing the Toxicity of the Combustion Products from Flexible Polyurethane Foam.
PB96-123625 01,411

POLYVINYL ALCOHOL

New EPR Dosimeter Based on Polyvinylalcohol.
PB94-199700 03,619

Small-Angle Neutron Scattering of Poly(vinyl alcohol) Gels.
PB95-164117 01,260

Small Angle Neutron Scattering Studies on Chain Asymmetry of Coextruded Poly(Vinyl Alcohol) Film.
PB95-164372 01,262

POLYVINYL CHLORIDE

Polyvinyl Chloride (PVC) Plastic Drain, Waste, and Vent Pipe and Fittings.
AD-A310 426/2 00,326

POLYVINYLIDENE FLUORIDE

Thermal Pulse Study of the Polarization Distributions Produced in Polyvinylidene Fluoride by Corona Poling at Constant Current.
PB94-172293 01,195

POLYVINYLIDENE FLUORIDES

Thermal Stability of Internal Electric Field and Polarization Distribution in Blend of Polyvinylidene Fluoride and Polymethylmethacrylate.
PB95-151072 01,240

POOL BOILING

Enhancement of R123 Pool Boiling by the Addition of N-Hexane.
PB96-165956 02,605

POOL BUILDING

Calorimetric and Visual Measurements of R123 Pool Boiling on Four Enhanced Surfaces.
PB96-128129 04,053

POOL FIRES

Structure and Radiation Properties of Pool Fires.
PB94-193802 02,473

Estimate of Flame Radiance via a Single Location Measurement in Liquid Pool Flames.
PB94-211596 02,476

Measurement of Radiative Feedback to the Fuel Surface of a Pool Fire.
PB94-211604 02,477

Estimate of the Effect of Scale on Radiative Heat Loss Fraction and Combustion Efficiency.
PB95-150447 02,486

PORCELAIN

Influence of Tempering Method on Residual Stress in Dental Porcelain.
PB94-172012 00,138

Evaluation of Fracture Toughness and Residual Stress in Dental Porcelain by Indentation-Microfracture Method.
PB95-125613 00,154

Evaluation of Fracture Toughness and Residual Stress in Dental Porcelain by Indentation-Microfracture Method.
PB95-152831 00,159

PORE SIZE DISTRIBUTION

Evolution of the Pore Size Distribution in Final-Stage Sintering of Alumina Measured by Small-Angle X-ray Scattering. (Reannouncement with New Availability Information).
AD-A249 178/5 03,023

PORE STRUCTURE

Percolation and Pore Structure in Mortars and Concrete.
PB95-150439 00,370

PORE SURFACE AREA

Anisotropy of the Surfaces of Pores in Plasma Sprayed Alumina Deposits.
PB96-123211 03,126

POROSITY

Effect of Backfill and Atomizing Gas on the Powder Porosity and Mechanical Properties of 304L Stainless Steel.
PB94-185394 03,205

Imaging of Fine Porosity in a Colloidal Silica: Potassium Silicate Gel by Defocus Contrast Microscopy.
PB94-212750 03,039

Water Permeability and Chloride Ion Diffusion in Portland Cement Mortars: Relationship to Sand Content and Critical Pore Diameter.
PB96-148036 03,193

POROUS CERAMICS

Analysis of Small-Angle Scattering Data Dominated by Multiple Scattering for Systems Containing Eccentrically Shaped Particles or Pores.
PB96-160411 03,075

POROUS MATERIALS

Digitized Simulation of Mercury Intrusion Porosimetry.
PB94-172236 01,304

Analysis of SANS from Controlled Pore Glasses.
PB94-198843 03,035

Glass Transition of Organic Liquids Confined to Small Pores.
PB94-212305 00,833

Melting Behavior of Organic Materials Confined in Porous Solids.
PB94-212313 00,834

Measurements of Moisture Diffusivity for Porous Building Materials.
PB95-107397 00,356

Cross-Property Relations and Permeability Estimation in Model Porous Media.
PB95-150280 04,205

Interaction between Micro and Macroscopic Flow in RTM Preforms.
PB95-162012 *03,159*

Transport and Diffusion in Three-Dimensional Composite Media.
PB95-176129 *04,668*

Small Angle Neutron Scattering Study of the Structure and Formation of Ordered Mesopores in Silica.
PB96-111919 *03,069*

Small Angle Neutron Scattering Study of the Structure and Formation of MCM-41 Mesoporous Molecular Sieves.
PB97-122337 *03,110*

POROUS MEDIA

Characterization of Chemically Modified Pore Surfaces by Small Angle Neutron Scattering.
PB95-126181 *00,898*

Hydraulic Radius and Transport in Reconstructed Model Three-Dimensional Porous Media.
PB96-123419 *00,403*

Analysis of Transverse Flow in Aligned Fibrous Porous Media.
PB96-167200 *03,177*

PORPHYRINS

One-Electron Oxidation of Nickel Porphyrins. Effect of Structure and Medium on Formation of Nickel(III) Porphyrin or Nickel(II) Porphyrin pi-Radical Cation.
PB95-107058 *00,865*

Site of One-Electron Reduction of Ni(II) Porphyrins. Formation of Ni(I) Porphyrin of Ni(II) Porphyrin pi-Radical Anion.
PB95-107066 *00,866*

Metalloporphyrin Sensitized Photooxidation of Water to Oxygen on the Surface of Colloidal Iridium Oxides - Photochemical and Pulse Radiolytic Studies.
PB95-107082 *00,868*

PORTABLE OPERATING SYSTEM INTERFACE

National Voluntary Laboratory Accreditation Program: POSIX. Portable Operating System Interface.
PB95-189478 *02,661*

PORTABLE OPERATING SYSTEM INTERFACE FOR COMPUTING ENVIRONMENTS

Comparison of POSIX Open System Environment (OSE) and Open Distributed Processing (ODP) Reference Models.
PB96-131495 *01,820*

PORTABLE OPERATING SYSTEMS INTERFACE FOR COMPUTER ENVIRONMENTS

IEEE's POSIX: Making Progress.
PB96-160924 *01,757*

NIST POSIX Testing Program.
PB96-160973 *01,821*

PORTLAND CEMENT

Interaction between Naphthalene Sulfonate and Silica Fume in Portland Cement Pastes.
PB94-199759 *01,315*

Computer Simulation of the Diffusivity of Cement-Based Materials.
PB95-125985 *00,362*

Cement and Concrete Characterization by Scanning Electron Microscopy.
PB95-163168 *00,379*

PORTLAND CEMENT CLINKER

Quantitative Phase Abundance Analysis of Three Cement Clinker Reference Materials by Scanning Electron Microscopy.
PB94-173051 *00,333*

PORTLAND CEMENTS

Optimization of Highway Concrete Technology.
PB94-182995 *01,333*

Graphical Analysis of the CCRL Portland Cement Proficiency Sample Database (Samples 1-72). (Part 1. Univariant Analysis of Portland Cement).
PB94-196557 *01,308*

Quantitative X-Ray Powder Diffraction Methods for Clinker and Cement.
PB95-143079 *01,317*

Water Permeability and Chloride Ion Diffusion in Portland Cement Mortars: Relationship to Sand Content and Critical Pore Diameter.
PB96-148036 *03,193*

POSITION FINDING

Analytical Estimation of Carrier Multipath Bias on GPS Position Measurements.
PB94-215712 *04,845*

Three Dimensional Position Determination from Motion.
PB95-107108 *01,788*

POSITION (LOCATION)

Spatial Data Transfer Standard (SDTS). Category: Software Standard; Subcategory: Information Interchange. (FIPS PUB 173-1A).
FIPS PUB 173-1A *01,795*

Spatial Data Transfer Standard (SDTS). Category: Software Standard; Subcategory: Information Interchange. (FIPS PUB 173-1B).
FIPS PUB 173-1B *01,796*

POSITION SENSING

Image Gradient Evolution: A Visual Cue for Danger.
PB96-154562 *02,939*

POSITIONING

Microelectronic Test Structures for Overlay Metrology.
PB96-164249 *02,430*

POSITRON-ATOM COLLISIONS

Polarization of Light Emitted After Positron Impact Excitation of Alkali Atoms.
PB94-199734 *03,816*

POSITRON SOURCES

Laser-Cooled Positron Source.
PB95-169348 *03,954*

POSITRONIUM

Positronium in Relativistic Quantum Mechanics.
PB97-110571 *04,140*

POSIX (PORTABLE OPERATING SYSTEM INTERFACE)

National Voluntary Laboratory Accreditation Program: POSIX. Portable Operating System Interface.
PB95-189478 *02,661*

POSIX (PORTABLE OPERATING SYSTEM INTERFACE FOR COMPUTING ENVIRONMENTS)

Comparison of POSIX Open System Environment (OSE) and Open Distributed Processing (ODP) Reference Models.
PB96-131495 *01,820*

POSIX (PORTABLE OPERATING SYSTEMS INTERFACE FOR COMPUTER ENVIRONMENTS)

IEEE's POSIX: Making Progress.
PB96-160924 *01,757*

NIST POSIX Testing Program.
PB96-160973 *01,821*

POTASSIUM

Frozen Human Serum Reference Material for Standardization of Sodium and Potassium Measurements in Serum or Plasma by Ion-Selective Electrode Analyzers.
PB94-185337 *00,532*

Multichannel Quantum Defect Half Collision Analysis of K2 Photodissociation Through the B1Pi(sub u) State.
PB94-211125 *00,812*

POTASSIUM BARIUM BISMUTHATES

Optical Conductivity of Single Crystals of Ba1-xMxBiO3(M=K, Rb, x=0.04, 0.37).
PB94-185329 *04,447*

POTASSIUM CHLORIDE

Absolute Determination of Electrolytic Conductivity for Primary Standard KC1 Solutions from 0 to 50C.
PB94-172798 *00,765*

dc Method for the Absolute Determination of Conductivities of the Primary Standard KCl Solutions from 0C to 50C.
PB94-219342 *02,644*

POTASSIUM DIHYDROGEN PHOSPHATE

Crystal Structure of a New Monoclinic Form of Potassium Dihydrogen Phosphate Containing Orthophosphacidium Ion, (H4PO4)(sup+1).
PB96-111794 *04,725*

POTASSIUM INORGANIC COMPOUNDS

Crystal Structure of a New Monoclinic Form of Potassium Dihydrogen Phosphate Containing Orthophosphacidium Ion, (H4PO4)(sup+1).
PB96-111794 *04,725*

POTASSIUM IONS

Kinetic-Energy Distributions of K(+) in Argon and Neon in Uniform Electric Fields.
PB95-151122 *03,902*

POTASSIUM PHOSPHATES

Crystal Structure of Dicalcium Potassium Trihydrogen Bis(pyrophosphate) Trihydrate.
PB94-216561 *00,152*

POTASSIUM SILICATES

Imaging of Fine Porosity in a Colloidal Silica: Potassium Silicate Gel by Defocus Contrast Microscopy.
PB94-212750 *03,039*

POTASSIUM TANTALATE NIOBATES

Anomalous Dispersion and Thermal Expansion in Lightly-Doped KTa1-xNbxO3.
PB95-152302 *04,585*

POTASSIUM TANTALATES

Anomalous Dispersion and Thermal Expansion in Lightly-Doped KTa1-xNbxO3.
PB95-152302 *04,585*

POTENTIAL ENERGY

Equilibrium Pair Distribution Function of a Gas: Aspects Associated with the Presence of Bound States.
PB95-176046 *01,004*

POTENTIAL FUNCTIONS

Equilibrium Pair Distribution Function of a Gas: Aspects Associated with the Presence of Bound States.
PB95-176046 *01,004*

POTENTIOMETER

Enhanced Voltage-Dividing Potentiometer for High-Precision Feature Placement Metrology.
PB96-164025 *02,428*

POTENTIOMETERS

Integrated Thin-Film Micropotentiometers.
PB96-146709 *02,109*

POTENTIOMETRIC ANALYSIS

Potentiometric Enzyme-Amplified Flow Injection Analysis Detection System: Behavior of Free and Liposome-Released Peroxidase.
PB95-151833 *03,534*

POWDER METALLURGY

Effect of Backfill and Atomizing Gas on the Powder Porosity and Mechanical Properties of 304L Stainless Steel.
PB94-185394 *03,205*

POWDER METALS

Crystal Structure of a New Sodium Zinc Arsenate Phase Solved by 'Simulated Annealing'.
PB95-107124 *00,870*

Parametric Investigation of Metal Powder Atomization Using Laser Diffraction.
PB95-108577 *03,342*

POWDER (PARTICLES)

Introduction of a NIST Instrument Sensitivity Standard Reference Material for X-Ray Powder Diffraction.
PB94-200318 *00,807*

Statistical Analysis of Parameters Affecting the Measurement of Particle-Size Distribution of Silicon Nitride Powders by Sedigraph (Trade Name).
PB94-216249 *03,042*

Rapid Hot Pressing of Ultra-Fine PSZ Powders.
PB94-216587 *03,045*

Analysis of Physical Properties of Ceramic Powders in an International Interlaboratory Comparison Program.
PB95-161501 *03,050*

Effects of Soxhlet Extraction on the Surface Oxide Layer of Silicon Nitride Powders.
PB95-175584 *03,057*

45 deg/0 deg Reflectance Factors of Pressed Polytetrafluoroethylene (PTFE) Powder.
PB95-260758 *04,328*

Ceramic Powders Characterization: Results of an International Laboratory Study.
PB95-270039 *02,672*

POWDERS

X-ray Powder Diffraction from Carbon Nanotubes and Nanoparticles.
PB96-102975 *03,064*

POWDERS (PARTICLES)

Surface Chemistry of Silicon Nitride Powder in the Presence of Dissolved Ions.
PB96-111760 *01,073*

Electroacoustic Characterization of Particle Size and Zeta Potential in Moderately Concentrated Suspensions.
PB96-119425 *01,079*

POWER

Power Characteristics in GMAW: Experimental and Numerical Investigation.
PB96-190145 *03,296*

DC-MHz Wattmeter Based on RMS Voltage Measurements.
PB97-113211 *01,992*

POWER AMPLIFIERS

100 Ampere, 100 kHZ Transconductance Amplifier.
PB96-102629 *02,068*

100 A, 100 kHz Transconductance Amplifier.
PB96-200936 *02,098*

POWER MEASUREMENT

NIST Model PM2 Power Measurement System for 1 mW at 1 GHz.
PB94-135803 *02,018*

Coaxial Reference Standard for Microwave Power.
PB94-193786 *01,880*

New Coaxial Microwave Microcalorimeter Evaluation Technique.
PB95-153227 *01,892*

Method to Determine the Calorimetric Equivalence Correction for a Coaxial Microwave Microcalorimeter.
PB95-202404 *01,913*

Developing a NIST Coaxial Microwave Power Standard at 1 mW.
PB95-202412 *01,914*

Direct Comparison Transfer of Microwave Power Sensor Calibrations.
PB96-158654 *02,086*

Calibration Service for Coaxial Reference Standards for Microwave Power.
PB96-162722 *01,958*

Ultrasound Power Measurement Techniques at NIST.
PB96-179569 *02,684*

POWER METERS

Proposed High-Accuracy Superconducting Power Meter for Millimeter Waves.
PB94-212669 *02,034*

Optical Power Meter Calibration Using Tunable Laser Diodes.
PB95-169256 *04,290*

Optical Detector Nonlinearity: A Comparison of Five Methods.
PB95-169355 *04,291*

Optical Detector Nonlinearity: Simulation.
PB96-165378 *02,199*

POWER OSCILLATOR

Surface Transverse Wave Oscillators with Extremely Low Thermal Noise Floors.
PB96-186010 *01,967*

POWER REFERENCE SOURCES

NIST Power Reference Source.
PB94-211513 *00,148*

PRASEODYMIUM
Magnetic Structure and Spin Dynamics of the Pr and Cu in Pr2CuO4.
PB96-111836 *04,036*

PRASEODYMIUM BARIUM COPPER NIOBATES
Crystal Structure and Magnetic Ordering of the Rare-Earth and Cu Moments in RBa2Cu2NbO8(R=Nd,Pr).
PB95-140554 *04,546*

PRASEODYMIUM BARIUM CUPRATES
Magnetic Ordering of the Cu Spins in PrBa2Cu3O6+x.
PB95-140547 *04,545*

PRASEODYMIUM CERIUM CUPRATES
Phonon Density of States in R2CuO4 and Superconducting R1.85Ce0.15CuO4 (R = Nd, Pr).
PB95-150686 *04,574*

Magnetic Susceptibility of Pr2-xCexCuO4 Monocrystals and Polycrystals.
PB95-180253 *04,677*

PRASEODYMIUM CUPRATES
Dispersions of Magnetic Excitations of the Pr Ions in Pr2CuO4.
PB94-173044 *04,444*

Phonon Density of States in R2CuO4 and Superconducting R1.85Ce0.15CuO4 (R = Nd, Pr).
PB95-150686 *04,574*

PRASEODYMIUM GALLATES
Suitability of Metalorganic Chemical Vapor Deposition-Derived PrGaO3 Films as Buffer Layers for YBa2Cu3O7-x Pulsed Laser Deposition.
PB95-168670 *04,640*

PRE-MAIN SEQUENCE STARS
High Sensitivity Survey of Radio Continuum Emission in Herbig Ae/Be Stars.
PB94-185915 *00,051*

PRECAST CONCRETE
Model Precast Concrete Beam-to-Column Connections Subject to Cyclic Loading.
PB95-153094 *00,438*

Partially Prestressed and Debonded Precast Concrete Beam-Column Joints.
PB95-153102 *00,439*

Seismic Performance Behavior of Precast Concrete Beam-Column Joints.
PB95-153110 *00,440*

Performance of 1/3-Scale Model Precast Concrete Beam-Column Connections Subjected to Cyclic Inelastic Loads. Report No. 4.
PB95-179024 *00,444*

Simplified Design Procedure for Hybrid Precast Concrete Connections.
PB96-154836 *00,405*

PRECIPITATION (CHEMISTRY)
Study of the Hydroxycarbonate Precursor Route to the YBa2Cu3O7-x High Tc Superconductor.
PB95-140471 *04,540*

Membrane-Mediated Precipitation of Calcium Phosphate in Model Liposomes with Matrix Vesicle-Like Lipid Composition.
PB95-164547 *03,468*

Dynamics of Calcium Phosphate Precipitation.
PB96-147095 *03,574*

PRECIPITATION HARDENING
Effects of Spindle Dynamic Characteristics on Hard Turning.
PB96-122981 *02,699*

PRECISION
Critical Issues in Scanning Electron Microscope Metrology.
PB95-169405 *02,359*

Japan Technology Program Assessment: Precision Engineering/Precision Optics in Japan.
PB95-171112 *02,884*

Precision in Machining: Research Challenges.
PB95-242301 *02,953*

Integrated Inspection System for Improved Machine Performance.
PB96-160569 *02,959*

New Concepts of Precision Dimensional Measurement for Modern Manufacturing.
PB96-160684 *02,924*

Scanning Electron Microscope Metrology.
PB96-201090 *02,446*

PRECOOLING
Helium Refrigeration and Liquefaction Using a Liquid Hydrogen Refrigerator for Precooling.
AD-A286 683/8 *02,749*

PRECURSORS
Study of the Hydroxycarbonate Precursor Route to the YBa2Cu3O7-x High Tc Superconductor.
PB95-140471 *04,540*

Diamond and Graphite Precursors: Comments.
PB95-163051 *00,967*

PREDICATE LOGIC
Predicate Differences and the Analysis of Dependencies in Formal Specifications.
PB96-160940 *01,759*

Technique for Analyzing the Effects of Changes in Formal Specifications.
PB96-160957 *01,760*

PREDICTIONS
Prediction of Cracking in Reinforced Concrete Structures.
PB95-220448 *03,725*

PREFABRICATED BUILDINGS
Wind Load Provisions of the Manufactured Home Construction and Safety Standards: A Review and Recommendations for Improvement.
PB94-206125 *00,428*

Manufactured Homes: Probability of Failure and the Need for Better Windstorm Protection through Improved Anchoring Systems.
PB95-143129 *00,432*

Manufactured Housing Walls That Provide Satisfactory Moisture Performance in All Climates.
PB95-178885 *00,383*

Recommended Performance-Based Criteria for the Design of Manufactured Home Foundation Systems to Resist Wind and Seismic Loads.
PB96-128285 *00,460*

Mathematical Analysis of Practices to Control Moisture in the Roof Cavities of Manufactured Houses.
PB97-106843 *00,278*

PREFERRED CIRCUITS
Handbook Preferred Circuits Navy Aeronautical Electronic Equipment. Supplement Number 3.
AD-A278 782/8 *00,026*

Handbook Preferred Circuits Navy Aeronautical Electronic Equipment. Supplement Number 2.
AD-A278 783/6 *00,027*

Handbook Preferred Circuits Navy Aeronautical Electronic Equipment. Supplement Number 1.
AD-A278 784/4 *00,028*

PREFORMS
Interaction between Micro and Macroscopic Flow in RTM Preforms.
PB95-162012 *03,159*

PREISACH MODEL
Experimental Verification of a Vector Preisach Model.
PB95-163564 *04,626*

PRESENT WORTH
Present Worth Factors for Life-Cycle Cost Studies in the Department of Defense (1995).
PB95-105029 *03,664*

PRESSES
Equipment for Investigation of Cryogenic Compaction of Nanosize Silicon Nitride Powders. 1993 Report.
DE94013593 *03,028*

PRESSURE
Pressure Dependencies of Standard Resistors.
PB95-153516 *02,257*

Intercomparison between NPL (India) and NIST (USA) Pressure Standards in the Hydraulic Pressure Region Up to 26 MPa.
PB96-113543 *04,211*

PRESSURE BROADENING
Memory Function Approach to the Shape of Pressure Broadened Molecular Bands.
PB95-152930 *00,944*

PRESSURE CALIBRATION SERVICE
NIST Measurement Services: NIST Pressure Calibration Service.
PB94-164043 *02,892*

PRESSURE CONTACTS
High Current Pressure Contacts to Ag Pads on Thin Film Superconductors.
PB95-168621 *04,639*

PRESSURE DEPENDENCE
Pressure Equations in Zone-Fire Modeling.
PB96-102967 *00,208*

PRESSURE GAGES
Intercomparison of the Effective Areas of a Pneumatic Piston Gauge Determined by Different Techniques.
PB94-212370 *02,640*

Operational Mode and Gas Species Effects on Rotational Drag in Pneumatic Dead Weight Pressure Gages.
PB95-140182 *00,903*

PRESSURE GRADIENTS
Characteristics of Turbulence in a Boundary Layer with Zero Pressure Gradient.
AD-A278 249/8 *04,192*

Single-Phase Heat Transfer and Pressure Drop Characteristics of an Integral-Spine-Fin Within an Annulus.
PB94-194073 *03,805*

Heat Transfer in Thin, Compact Heat Exchangers with Circular, Rectangular, or Pin-Fin Flow Passages.
PB95-140943 *02,751*

Single-Phase Heat Transfer and Pressure Drop Characteristics of an Integral-Spine Fin Within an Annulus.
PB97-122386 *04,179*

PRESSURE MEASUREMENT
NIST Measurement Services: NIST Pressure Calibration Service.
PB94-164043 *02,892*

Measurement of CO Pressures in the Ultrahigh Vacuum Regime Using Resonance-Enhanced Multiphoton-Ionization Time-of-Flight Mass Spectroscopy.
PB94-216041 *03,864*

Look at Uncertainties over Twenty Decades of Pressure Measurement.
PB95-168506 *02,655*

PC-Based Spinning Rotor Gage Controller.
PB95-175832 *02,609*

Laser Photoionization Measurements of Pressure in Vacuum.
PB95-180600 *03,964*

Measurement of Very-Low Partial Pressures.
PB95-180998 *02,659*

Process Monitoring with Residual Gas Analyzers (RGAs): Limiting Factors.
PB95-181004 *02,660*

Executive Summary: Proceedings of the Workshop on the Measurement of Transient Pressure and Temperature.
PB96-160841 *02,679*

PRESSURE VAPOR TEMPERATURE
Virial Coefficients of Five Binary Mixtures of Fluorinated Methanes and Ethanes.
PB96-156054 *01,128*

PRESTRESSING
Partially Prestressed and Debonded Precast Concrete Beam-Column Joints.
PB95-153102 *00,439*

Seismic Performance Behavior of Precast Concrete Beam-Column Joints.
PB95-153110 *00,440*

PRETREATMENTS
Effects of Aluminum Oxalate/Glycine Pretreatment Solutions on Dentin Permeability.
PB95-164505 *03,565*

PRICES
Energy Prices and Discount Factors for Life-Cycle Cost Analysis 1994. Annual Supplement to NIST Handbook 135 and NBS Special Publication 709.
PB94-206018 *02,508*

Energy Price Indices and Discount Factors for Life-Cycle Cost Analysis 1995. Annual Supplement to NIST Handbook 135 and NBS Special Publication 709. (Revised).
PB95-105011 *02,509*

Energy Price Indices and Discount Factors for Life-Cycle Cost Analysis 1996. Annual Supplement to NIST Handbook 135 and NBS Special Publication 709. (Revised).
PB96-162441 *02,510*

Energy Price Indices and Discount Factors for Life-Cycle Cost Analysis 1997. Annual Supplement to NIST Handbook 135 and NBS Special Publication 709. (Revised).
PB96-210745 *02,512*

PRIMARY STANDARDS
NIST Measurement Services: NIST Pressure Calibration Service.
PB94-164043 *02,892*

Absolute Determination of Electrolytic Conductivity for Primary Standard KC1 Solutions from 0 to 50C.
PB94-172798 *00,765*

Automated, High-Precision Coulometric Titrimetry. Part 1. Engineering and Implementation.
PB95-150199 *00,575*

NIST-7, the New US Primary Frequency Standard.
PB95-153458 *01,534*

Error Analysis of the NIST Optically Pumped Primary Frequency Standard.
PB95-153482 *01,535*

Design Challenges in a Commercial Quantum Hall Effect-Based Resistance Standard.
PB95-171419 *02,263*

PRINCIPAL ANGLE
High-Accuracy Principal-Angle Scanning Spectroscopic Ellipsometry of Semiconductor Interfaces.
PB96-163787 *02,427*

PRINCIPAL COMPONENTS ANALYSIS
Representing a Large Collection of Curves: A Case for Principal Points.
PB95-152286 *03,438*

PRINCIPAL POINTS
Two Principal Points of Symmetric, Strongly Unimodal Distributions.
PB95-203360 *03,443*

Principal Points and Self-Consistent Points of Symmetric Multivariate Distributions.
PB96-135090 *03,446*

PRINTED CIRCUIT BOARDS
Microwave Characterization of Printed Circuit Transmission Lines.
PB96-122585 *02,077*

PRIVACY
Optical Performance of Commercial Windows.
PB95-208757 *00,392*

PROBABILISTIC ESTIMATION
Probabilistic Estimates of Design Load Factors for Wind-Sensitive Structures Using the 'Peaks Over Threshold' Approach.
PB96-183223 *00,474*

PROBABILITY DENSITY FUNCTIONS
Tomographic Reconstruction of the Moments of Local Probability Density Functions in Turbulent Flow Fields.
PB96-180195 *04,219*

PROBABILITY DISTRIBUTION FUNCTIONS
Fluctuations in Probability Distribution on Chaotic Attractors.
PB96-102330 *04,022*

PROBABILITY THEORY
Three-Axis Coil Probe Dimensions and Uncertainties during Measurement of Magnetic Fields from Appliances.
PB94-219359 *01,885*

Bounds on Frequency Response Estimates Derived from Uncertain Step Response Data.
PB96-122874 *03,419*

PROBE-POSITION ERRORS
Comparison of k-Correction and Taylor-Series Correction for Probe-Position Errors in Planar Near-Field Scanning.
PB96-147137 *02,012*

PROBE TIP CALIBRATION
Verification of Commercial Probe-Tip Calibrations.
PB95-161576 *02,347*

Calibrating On-Wafer Probes to the Probe Tips.
PB95-163945 *02,352*

LRM Probe-Tip Calibrations with Imperfect Resistors and Lossy Lines.
PB95-163952 *02,353*

Compensation for Substrate Permittivity in Probe-Tip Calibration.
PB95-203519 *01,915*

LRM Probe-Tip Calibrations Using Nonideal Standards.
PB96-135389 *02,411*

PROBES
Measurement of the Thermal Properties of Electrically Conducting Fluids Using Coated Transient Hot Wires.
DE94017816 *00,722*

User's Guide to NIST SRM 2084: CMM Probe Performance Standard.
PB94-206109 *02,709*

Two New Probes for a Coordinate Measuring Machine.
PB95-163093 *02,653*

PROBES (ELECTROMAGNETIC)
Standard Probes for Electromagnetic Field Measurements.
PB94-185436 *01,999*

Optically Sensed EM-Field Probes for Pulsed Fields.
PB94-212594 *02,130*

General Order 'N' Analytic Correction of Probe-Position Errors in Planar Near-Field Measurements.
PB96-200688 *01,562*

PROCEEDINGS
Proceedings of the Annual Manufacturing Technology Conference (2nd): Toward a Common Agenda. Held in Gaithersburg, Maryland on April 18-20, 1995.
PB96-112693 *02,887*

PROCESS CONTROL
NIST Support to the Next Generation Controller Program: 1991 Final Technical Report.
PB94-163490 *02,808*

Intelligent Processing of Materials, Technical Activities 1993 (NAS-NRC Assessment Panel, April 21-22, 1994).
PB94-164183 *02,809*

Intelligent Processing of Materials.
PB94-172780 *02,811*

Intelligent Processing of Hot Isostatic Pressing.
PB94-172913 *03,315*

Integration of Real-Time Process Planning for Small-Batch Flexible Manufacturing.
PB95-151908 *02,822*

Development of Adaptive Control Strategies for Inert Gas Atomization.
PB95-162335 *02,823*

Process Modeling and Control of Inert Gas Atomization.
PB95-162343 *02,824*

Analysis of Autocorrelations in Dynamic Processes.
PB95-181228 *02,826*

Machine Performance Standard Provides Opportunity to Improve Quality and Productivity.
PB96-154521 *02,837*

Unified Process Specification Language: Requirements for Modeling Process.
PB97-116123 *02,850*

PROCESS CONTROL (INDUSTRY)
Review of Cure Monitoring Techniques for On-Line Process Control.
PB94-216728 *03,145*

PROCESS MODELS
Product Realization Process Modeling: A Study of Requirements, Methods and Research Issues.
PB96-147962 *02,836*

PROCESSES
State-of-the-Art Survey of Methodologies for Representing Manufacturing Process Capabilities.
PB94-187655 *02,812*

PROCESSING & PERFORMANCE OF MATERIALS
Reference Tables for Thermocouples.
AD-A279 948/4 *02,614*

Low-Temperature Performance of Radiosonde Electric Hygrometer Elements.
AD-A295 319/8 *00,121*

Electromechanical properties of superconductors for DOE fusion applications.
DE95015476 *04,432*

VAMAS interlaboratory comparisons of critical current vs. strain in Nb(sub 3)Sn.
DE95016656 *04,433*

Transverse stress effect on the critical current of internal tin and bronze process Nb(sub 3)Sn superconductors.
DE95016659 *04,434*

Measurement Methods and Standards for Processing and Application of Thermal Barrier Coatings.
N95-26123/6 *01,447*

Report on the Workshop on Manufacturing Polymer Composites by Liquid Molding. Held in Gaithersburg, Maryland on September 20-22, 1993.
PB94-160066 *03,131*

Cylinder Wipe Air-Drying Intaglio Ink Vehicles for U.S. Currency Inks.
PB94-160801 *03,115*

Electrodeposition.
PB94-172517 *00,760*

Intelligent Processing of Materials.
PB94-172780 *02,811*

Thermophysical Property Data for Supercritical Fluid Extraction Design.
PB94-199221 *00,668*

Stability, Microstructural Evolution, Grain Growth, and Coarsening in a Two-Dimensional Two-Phase Microstructure.
PB94-199429 *03,325*

Hot-Deformation Apparatus for Thermomechanical Processing Simulation.
PB94-200136 *03,207*

Effects of Crystalline Anisotropy and Buoyancy-Driven Convection on Morphological Stability.
PB94-200441 *03,328*

Status of Electrocomposites.
PB94-212453 *03,143*

Coating of Fibers by Colloidal Techniques in Ceramic Composites.
PB94-216256 *03,196*

Rapid Hot Pressing of Ultra-Fine PSZ Powders.
PB94-216587 *03,045*

Optimization of Inert Gas Atomization.
PB95-107405 *01,377*

Parametric Investigation of Metal Powder Atomization Using Laser Diffraction.
PB95-108577 *03,342*

Effect of Heterogeneous Porous Media on Mold Filling in Resin Transfer Molding.
PB95-108676 *03,197*

Novel Polydiacetylenes Derived from Liquid Crystalline Monomers.
PB95-140125 *01,235*

New Materials, Advanced Ceramics and Standards.
PB95-140208 *03,047*

Nondestructive Evaluation and Materials Processing.
PB95-140455 *02,902*

Study of the Hydroxycarbonate Precursor Route to the YBa2Cu3O7-x High Tc Superconductor.
PB95-140471 *04,540*

Influence of Deposition Parameters on Properties of Laser Ablated YBa2Cu3O7-Delta Films.
PB95-140539 *04,544*

UV-Photopatterning of Alkylthiolate Monolayers Self-Assembled on Gold and Silver.
PB95-150751 *00,924*

Regimes of Surface Roughness Measurable with Light Scattering.
PB95-151213 *04,265*

Investigation into a Practical Grain Growth Model for Hot Isostatic Pressing.
PB95-151684 *03,347*

Deposit Forming Tendencies of Diesel Engine Oils-Correlation between the Two-Peak Method and Engine Tests.
PB95-152138 *01,452*

Ultrasonic Method for Reconstructing the Two-Dimensional Liquid-Solid Interface in Solidifying Bodies.
PB95-161782 *03,349*

Process Modeling and Control of Inert Gas Atomization.
PB95-162343 *02,824*

Fabrication of Flaw-Tolerant Aluminum-Titanate-Reinforced Alumina.
PB95-162533 *03,161*

Through-the-Arc Sensing for Real-Time Measurement of Gas Metal Arc Weld Quality.
PB95-162871 *02,863*

In-Space Welding: Visions and Realities.
PB95-163234 *04,830*

Polyelectrolytes as Dispersants in Colloidal Processing of Silicon Nitride Ceramics.
PB95-175568 *03,055*

Process Monitoring with Residual Gas Analyzers (RGAs): Limiting Factors.
PB95-181004 *02,660*

Novel YBa2Cu3O7-x and YBa2Cu3O7-x/Y4Ba3O9 Multilayer Films by Bias-Masked 'On-Axis' Magnetron Sputtering.
PB95-181186 *04,690*

IIW Commission V Quality Control and Quality Assurance of Welded Products Annual Report 1994/95.
PB95-198743 *02,866*

Structural Ceramics Database. Topical Report, June 1989-May 1991.
PB95-203758 *03,060*

Determination of the Residual Stresses Near the Ends of Skip Welds Using Neutron Diffraction and X-ray Diffraction Procedures.
PB95-253589 *02,868*

Simulation of C60 Through the Plastic Transition Temperatures.
PB96-102546 *04,713*

Electronics Packaging Materials Research at NIST.
PB96-122692 *02,405*

Radiance Temperatures (in the Wavelength Range 523-907 nm) of Group IVB Transition Metals Titanium, Zirconium, and Hafnium at Their Melting Points by a Pulse-Heating Technique.
PB96-135025 *02,677*

High-Temperature Furnace for In situ Small-Angle Neutron Scattering during Ceramic Processing.
PB96-148127 *03,743*

Hygrothermal Effects on the Performance of Polymers and Polymeric Composites: A Workshop Report. Held in Gaithersburg, Maryland on September 21-22, 1995.
PB96-183207 *03,180*

Mapping the Droplet Transfer Modes for an ER100S-1 GMAW Electrode.
PB96-190095 *03,295*

Kinetic-Energy-Enhanced Neutral Etching.
PB96-200613 *00,665*

Need for Advanced Characterization Techniques in Product Manufacturing: A Case Study on Ceramic Matrix Composites.
PB96-204060 *03,089*

Data Management for Error Compensation and Process Control.
PB97-110480 *02,847*

Characterization and Processing of Spray-Dried Zirconia Powders for Plasma Spray Application.
PB97-111231 *04,419*

Vitrification and Crystallization of Organic Liquids Confined to Nanoscale Pores.
PB97-112304 *03,392*

In situ Characterization of Vapor Phase Growth of Iron Oxide-Silica Nanocomposites: Part 1. 2-D Planar Laser-Induced Fluorescence and Mie Imaging.
PB97-112478 *03,185*

In-situ Studies of a Novel Sodium Flame Process for Synthesis of Fine Particles.
PB97-113047 *00,681*

Segmental Concentration Profiles of End-Tethered Polymers with Excluded-Volume and Surface Interactions.
PB97-119002 *00,654*

PROCUREMENT
Videoconferencing Procurement and Usage Guide.
PB94-217023 *01,470*

Asynchronous Transfer Mode Procurement and Usage Guide.
PB95-174967 *01,481*

Federal Implementation Guideline for Electronic Data Interchange. ASC X12 003050 Transaction Set 850 Award Instrument. Implementation Convention.
PB96-114913 *01,814*

Federal Implementation Guideline for Electronic Data Interchange. ASC X12 003050 Transaction Set 860 Modifications to Award Instrument. Implementation Convention.
PB96-114921 *01,815*

Federal Implementation Guideline for Electronic Data Interchange. ASC X12 003050 Transaction Set 843 Response to Request for Quotation. Implementation Convention.
PB96-168984 *01,822*

Federal Implementation Guideline for Electronic Data Interchange. ASC X12 003050 Transaction Set 855 Purchase Order Acknowledgment: Implementation Convention.
PB96-172374 *01,823*

Federal Implementaion Guideline for Eletronic Data Interchange. ASC X12 003050 Transaction Set 865 Purchase Order Change Acknowledgement/Request - Seller Initiated. Implementation Convention.
PB96-172549 *01,825*

PRODUCT DATA EXCHANGE SPECIFICATIONS
Capabilities for Product Data Exchange.
PB97-118764 *02,798*

PRODUCT DATA EXCHANGE USING STEP
Summary and Notes of the Joint ISO/IGES/PDES Organization Technical Committee Meeting. Held in Albuquerque, New Mexico on October 15-20, 1989.
PB95-107314 *02,774*

PRODUCT DEVELOPMENT
Models, Managing Models, Quality Models: An Example of Quality Management.
PB94-163466 *02,891*

Formulation of Position on U.S. Standards Role in Enterprise Integration.
PB95-105052 *02,773*

Proceedings Report of the International Invitation Workshop on Development Assurance. Held in Ellicott City, Maryland on June 16-17, 1994.
PB95-189494 *02,912*

Product Models and Virtual Prototypes in Mechanical Engineering.
PB95-253563 *02,783*

Product Realization Process Modeling: A Study of Requirements, Methods and Research Issues.
PB96-147962 *02,836*

Improving the Design Process by Predicting Downstream Values of Design Attributes.
PB97-113096 *02,795*

PRODUCT INSPECTION

Directory of U.S. Private Sector Product Certification Programs.
PB96-215074 *02,688*

PRODUCT MODELS

Procedure for Product Data Exchange Using STEP Developed in the AutoSTEP Pilot.
PB96-183058 *02,843*

PRODUCTION ENGINEERING

Design Engineering Research at NIST.
PB95-267860 *02,784*

PRODUCTION MANAGEMENT

Production Management Information Model for Discrete Manufacturing.
PB96-112008 *02,830*

Roadmap for the Computer Integrated Manufacturing (CIM) Application Framework.
PB96-122759 *02,832*

Conformance Testing and Specification Management.
PB97-113781 *02,849*

PROFICIENCY TESTING

Proficiency Testing as a Component of Quality Assurance in Construction Materials Laboratories.
PB94-185774 *00,334*

PROFICIENCY TESTS

Proficiency Tests for the NIST Airborne Asbestos Program, 1990.
PB94-188836 *00,535*

Proficiency Tests for the NIST Airborne Asbestos Program - 1991.
PB94-193828 *00,537*

Proficiency Tests for the NIST Airborne Asbestos Program - 1992.
PB94-194362 *00,539*

Proficiency Tests for the NIST Airborne Asbestos Program, 1993.
PB96-106463 *00,610*

PROFILE

Stylus Flight in Surface Profiling.
PB96-123138 *02,675*

PROFILES

Thermal Pulse Study of the Polarization Distributions Produced in Polyvinylidene Fluoride by Corona Poling at Constant Current.
PB94-172293 *01,195*

PROFILOMETERS

Ultrasonic Measurements of Surface Roughness.
PB94-172137 *04,181*

Measuring Matching Wear Scars on Balls and Flats.
PB95-151528 *03,153*

PROGRAM SLICING

Software Safety and Program Slicing.
PB95-125894 *01,703*

Unravel: A CASE Tool to Assist Evaluation of High Integrity Software. Volume 1. Requirements and Design.
PB95-267886 *01,736*

Unravel: A CASE Tool to Assist Evaluation of High Integrity Software. Volume 2. User Manual.
PB95-267894 *01,737*

Slicing in the Presence of Parameter Aliasing.
PB96-160858 *01,755*

Assessing Functional Diversity by Program Slicing.
PB96-160890 *03,734*

Program Slicing.
PB96-160981 *01,761*

PROGRAMMING ENVIRONMENTS

SQL Environments. Category: Software Standard; Subcategory: Database.
FIPS PUB 193 *01,801*

Introduction to the P1003.1g and CPI-C Network Application Programming Interfaces.
PB95-231726 *01,731*

PROGRAMMING LANGUAGES

COBOL. Category: Software Standard; Subcategory: Programming Language. Includes ANSI'S X3.23-1985, X3.23A-1989 and X3.23B-1993.
FIPS PUB 21-4 *01,670*

COBOL. Category: Software Standard; Subcategory: Programming Language. Part A.
FIPS PUB 21-4A *01,671*

COBOL. Category: Software Standard; Subcategory: Programming Language. Part B.
FIPS PUB 21-4B *01,672*

Dynamic Objects and Meta-Level Programming of an EXPRESS Language Environment.
PB96-190053 *01,774*

PROGRAMMING MANUALS

DETAN 95: Computer Code for Calculating Spectrum-Averaged Cross Sections and Detector Responses in Neutron Spectra.
PB95-242384 *04,014*

PROJECT MANAGEMENT

Framework for the Development and Assurance of High Integrity Software.
PB95-173084 *01,716*

PROMETHIUM

Hyperfine Structure Investigations and Identification of New Energy Levels in the Ionic Spectrum of (147)Pm.
PB96-180203 *04,117*

PROMPT GAMMA RADIATION

Grazing Incidence Prompt Gamma Emissions and Resonance-Enhanced Neutron Standing Waves in a Thin-Film.
PB95-150470 *03,892*

PROPANE

Critical Properties and Vapor-Liquid Equilibria of the Binary System Propane + Neopentane.
PB95-175683 *00,999*

PROPANES

Vapor-Liquid Equilibria of Mixtures of Propane and Isomeric Hexanes.
PB95-175287 *00,995*

Viscosity of 1,1,1,2,3,3-Hexafluoropropane and 1,1,1,3,3,3-Hexafluoropropane at Saturated-Liquid Conditions from 262 K to 353 K.
PB96-176680 *03,292*

PROPELLANTS

Thermal Decomposition Pathways in Nitramine Propellants.
AD-A295 896/5 *03,753*

PROPER NAMES

Prototype Information Retrieval System to Perform a Best-Match Search for Names.
PB95-181152 *02,740*

PROPERTIES

Metallurgy Technical Activities 1994 (NAS-NRC Assessment Panel, April 6-7, 1995).
PB96-136981 *02,981*

Guide to a Format for Data on Chemical Admixtures in a Materials Property Database.
PB96-165394 *01,327*

Guide to a Format for Data on Chemical Admixtures in a Materials Property Database. (Reannouncement with new abstract).
PB96-186192 *01,328*

PROPERTIES OF MATERIALS: ELECTRONIC/MAGNETIC/OPTICAL

Magnetic Characteristics and Measurements of Filamentary Nb-Ti Wire for the Superconducting Super Collider.
DE94005988 *03,775*

Filter Transmittance Measurements in the Infrared.
PB94-140589 *04,224*

Alternating-Field Susceptometry and Magnetic Susceptibility of Supercondoctors. Presented at Office of Naval Research Workshop on Magnetic Susceptibility of Superconductors and Other Spin Systems. Held in Berkeley Springs, West Virginia on 20 May 1991.
PB94-145984 *04,435*

Photonic Materials: A Report on the Results of a Workshop. Held in Gaithersburg, Maryland on August 26-27, 1992, Volume 1.
PB94-152733 *02,114*

Monte Carlo and Mean-Field Calculations of the Magnetocaloric Effect of Ferromagnetically Interacting Clusters.
PB94-172087 *03,201*

Thermal Pulse Study of the Polarization Distributions Produced in Polyvinylidene Fluoride by Corona Poling at Constant Current.
PB94-172293 *01,195*

Structural and Magnetic Ordering in Iron Oxide/Nickel Oxide Multilayers by X-ray and Neutron Diffraction (Invited).
PB94-172558 *04,442*

Dispersions of Magnetic Excitations of the Pr Ions in Pr2CuO4.
PB94-173044 *04,444*

One Gigarad Passivating Nitrided Oxides for 100% Internal Quantum Efficiency Silicon Photodiodes.
PB94-185485 *02,119*

Enhanced Magnetocaloric Effect in Gd3Ga5-xFexO12.
PB94-185659 *04,450*

Magnetocaloric Effect in Rapidly Solidified Nd-Fe-Al-B Materials.
PB94-185667 *04,451*

Langevin Approach to Hysteresis and Barkhausen Modeling in Steel.
PB94-185675 *03,206*

Magnetocaloric Effect of Ferromagnetic Particles.
PB94-185857 *04,453*

PROPERTIES OF MATERIALS: ELECTRONIC/MAGNETIC/OPTICAL

NIST Response to the Fifth CORM Report on the Pressing Problems and Projected Needs in Optical Radiation Measurements.
PB94-188240 *04,227*

Magnetic Dead Layer in Fe/Si Multilayer: Profile Refinement of Polarized Neutron Reflectivity Data.
PB94-198363 *04,458*

Profile Fitting of X-Ray Diffraction Lines and Fourier Analysis of Broadening.
PB94-198512 *04,460*

Meissner, Shielding, and Flux Loss Behavior in Single-Crystal YBa2Cu3O6+x.
PB94-198744 *04,464*

Magnetic Properties of Pd/Co Multilayers.
PB94-198751 *04,465*

Concurrent Enhancement of Kerr Rotation and Antiferromagnetic Coupling in Epitaxial Fe/Cu/Fe Structures.
PB94-198769 *04,466*

Precision Nuclear Orientation Measurements for Determining Mixed Magnetic Dipole/Electric Quadrupole Hyperfine Interactions.
PB94-199080 *03,810*

Isotope Shifts and Hyperfine Splittings of the 398.8-nm Yb I Line.
PB94-199585 *03,814*

Hysteresis Measurements of Remanent Polarization and Coercive Field in Polymers.
PB94-199767 *04,475*

Electronic Correlations and Satellites in Superconducting Oxides.
PB94-200045 *04,477*

Correlation of HgCdTe Epilayer Defects with Underlying Substrate Defects by Synchrotron X-Ray Topography.
PB94-200714 *02,129*

Transport Critical Current of Aligned Polycrystalline Yttrium Barium Copper Oxide (YBa2Cu3O7-delta).
PB94-211307 *04,492*

Magnetoelasticity in Rare-Earth Multilayers and Films.
PB94-211356 *04,495*

Roles of Copper in Applied Superconductivity.
PB94-211521 *02,255*

Wire Bond Testing.
PB94-211653 *02,314*

Neutron Powder Diffraction Study of the Crystal Structure of YSr2AlCu2O7.
PB94-212073 *04,499*

Offset Susceptibility of Superconductors.
PB94-212263 *04,503*

Correlations of Modulation Noise with Magnetic Microstructure and Intergranular Interactions for CoCrTa and CoNi Thin Film Media.
PB94-212768 *04,509*

Normal-Incidence Complex-Index Refractometry.
PB94-213097 *04,241*

Magnetic and Structural Properties of Electrodeposited Copper-Nickel Microlayered Alloys.
PB94-213121 *04,512*

Polarization Analysis of the Magnetic Excitations in Invar and Non-Invar Amorphous Alloys.
PB94-216116 *04,516*

Refractive Indices of Fluids Related to Alternative Refrigerants.
PB94-219375 *03,260*

Comments on the Paper 'Wolf Shifts and Their Physical Interpretation under Laboratory Conditions'.
PB94-219391 *04,246*

Reply to Professor Wolf's Comments on My Paper on Wolf Shifts.
PB94-219409 *04,247*

Inelastic Neutron Scattering Studies of Nonlinear Optical Materials: p-Nitroaniline Adsorbed in ALPO-5.
PB95-107223 *00,874*

Magnetic Moments in Cr Thin Films on Fe(100).
PB95-108429 *04,525*

Asymmetry between Flux Penetration and Flux Expulsion in Tl-2212 Superconductors.
PB95-125647 *04,527*

Incommensurate Magnetic Order in UPtGe.
PB95-140513 *04,542*

Crystallographic and Magnetic Properties of UAuSn.
PB95-140521 *04,543*

Magnetic Ordering of the Cu Spins in PrBa2Cu3O6+x.
PB95-140547 *04,545*

Crystal Structure and Magnetic Ordering of the Rare-Earth and Cu Moments in RBa2Cu2NbO8(R=Nd,Pr).
PB95-140554 *04,546*

Quasielastic and Inelastic Neutron-Scattering Studies of ((CD3)3ND)FeCl3.2D2O: A One-Dimensional Ising Ferromagnet.
PB95-140562 *04,547*

Critical Current Behavior of Ag-Coated YBa2Cu3O7-x Thin Films.
PB95-141016 *04,549*

Magnetic Field Dependence of the Critical Current Anisotropy in Normal Metal-YBa2Cu3O7-delta Thin Film Bilayers.
PB95-141024 *04,550*

Trapped Vortices in a Superconducting Microbridge.
PB95-141149 *04,554*

Variation in Magnetic Properties of Cu/Fcc (001) Sandwich Structures.
PB95-141164 *04,555*

Effects of Interfacial Roughness on the Magnetoresistance of Magnetic Metallic Multilayers.
PB95-150017 *04,556*

Magnetic Neutron Scattering (Invited).
PB95-150074 *04,557*

Polarization Analysis of the Magnetic Excitations in Fe65Ni35 Invar.
PB95-150082 *04,558*

Method for Determining Both Magnetostriction and Elastic Modulus by Ferromagnetic Resonance.
PB95-150108 *02,974*

Temperature Dependence of the Magnetic Excitations in Ordered and Disordered Fe72Pt28.
PB95-150223 *04,563*

Use of Sum Rules on the Energy-Loss Function for the Evaluation of Experimental Optical Data.
PB95-150736 *04,264*

Studies of the Higher Order Smectic Phase of the Large Electroclinic Effect Material W317.
PB95-151601 *00,935*

Coupled-Bilayer Two-Dimensional Magnetic Order of the Dy Ions in Dy2Ba4Cu7O15.
PB95-152104 *04,584*

Neutron-Scattering Studies of the Two Magnetic Correlation Lengths in Terbium.
PB95-152328 *04,586*

Comment on 'Phase Transitions in Antiferromagnetic Superlattices'.
PB95-152971 *04,587*

Moisture and Water-Induced Crack Growth in Optical Materials.
PB95-153334 *04,267*

Neutron Powder Diffraction Study of the Nuclear and Magnetic Structures of the Oxygen-Deficient Perovskite YBaCuCoO5.
PB95-161097 *00,954*

Harmonic and Static Susceptibilities of YBa2Cu3O7.
PB95-161139 *04,599*

Micromagnetic Structure of Domains in Co/Pt Multilayers. 1. Investigations of Wall Structure.
PB95-162111 *04,610*

Magnetic Rare Earth Artificial Metallic Superlattices.
PB95-162293 *04,611*

Submicroampere-Per-Root-Hertz Current Sensor Based on the Faraday Effect in Ga: YIG.
PB95-162467 *02,155*

Surface Magnetic Microstructural Analysis Using Scanning Electron Microscopy with Polarization Analysis (SEMPA).
PB95-162657 *03,938*

Nanocomposite Magnetic Materials.
PB95-162780 *04,617*

Magnetocaloric Effect in Nanocomposites.
PB95-162798 *04,618*

Systematic Studies of the Effect of a Bandpass Filter on a Josephson-Junction Noise Thermometer.
PB95-162970 *03,939*

Observations of Partial Discharges in Hexane Under High Magnification.
PB95-163127 *01,900*

Determination of Thermoactivation Parameters of Vortex Mobility in YBa2Cu3O7 Using Only Magnetic Measurements.
PB95-163499 *04,624*

SEMPA Studies of Oscillatory Exchange Coupling.
PB95-163556 *04,625*

Experimental Verification of a Vector Preisach Model.
PB95-163564 *04,626*

High Critical Temperature Superconductor Tunneling Spectroscopy Using Squeezable Electron Tunneling Junctions.
PB95-163721 *04,627*

Tunneling Measurement of the Zero-Bias Conductance Peak and the Bi-Sr-Ca-Cu-O Thin-Film Energy Gap.
PB95-163739 *04,628*

Field Dependence of the Magnetic Ordering of Cu in R2CuO4 (R = Nd, Sm).
PB95-164521 *04,633*

Observation of Noncollinear Magnetic Structure for the Cu Spins in Nd2CuO4-Type Systems.
PB95-164539 *04,634*

Magneto-Optic Magnetic Field Sensors Based on Uniaxial Iron Garnet Films in Optical Waveguide Geometry.
PB95-168498 *02,159*

Alternating-Field Susceptometry and Magnetic Susceptibility of Superconductors.
PB95-168613 *04,638*

Magnetic and Magnetoresistive Properties of Inhomogeneous Magnetic Dual-Layer Films.
PB95-169025 *04,646*

Insulating Boundary Layer and Magnetic Scattering in YBa2Cu3O7-delta/Ag Interfaces Over a Contact Resistivity Range of 10(-8) - 10(-3) Omega cm(2).
PB95-169157 *04,648*

Tilt Effects in Optical Angle Measurements.
PB95-169389 *04,294*

Thermal Noise in High-Temperature Superconducting-Normal-Superconducting Step-Edge Josephson Junctions.
PB95-175089 *04,650*

Increased Pinning Energies and Critical Current Densities in Heavy-Ion-Irradiated Bi2Sr2CaCu2O8 Single Crystals.
PB95-175352 *04,654*

Determination of the Optical Constants of ZnSe Films by Spectroscopic Ellipsometry.
PB95-175378 *04,656*

Surface Degradation of Superconducting YBa2Cu3O7-delta Thin Films.
PB95-176095 *04,667*

Magnetic Force Microscopy Images of Magnetic Garnet with Thin-Film Magnetic Tip.
PB95-176210 *04,669*

Crossover in the Pinning Mechanism of Anisotropic Fluxon Cores.
PB95-180170 *04,673*

Size and Self-Field Effects in Giant Magnetoresistive Thin-Film Devices.
PB95-180188 *04,674*

Novel Bulk Iron Garnets for Magneto-Optic Magnetic Field Sensing.
PB95-180204 *04,675*

Magnetic Susceptibility of Pr2-xCexCuO4 Monocrystals and Polycrystals.
PB95-180253 *04,677*

Broadband High-Optical-Density Filters in the Infrared.
PB95-180261 *04,309*

Crystal Structure and Magnetic Properties of CuGeO3.
PB95-180287 *04,678*

Observation of Oscillatory Magnetic Order in the Antiferromagnetic Superconductor HoNi2B2C.
PB95-180303 *04,679*

Dependence of Tc on Debye Temperature Theta(sub D) for Various Cuprates.
PB95-180493 *04,683*

Magnetic Properties of Single-Crystalline UCu3Al2.
PB95-180717 *04,686*

Epitaxial Growth and Characterization of the Ordered Vacancy Compound CuIn3Se5 on GaAs (100) Fabricated by Molecular Beam Epitaxy.
PB95-180725 *04,687*

Terminally Anchored Chain Interphases: Their Chromatographic Properties.
PB95-181061 *01,272*

Dielectric Properties of Thin Film SrTiO3 Grown on LaAlO3 with YBa2Cu3O7-x Electodes.
PB95-181160 *02,267*

Domain Effects in Faraday Effect Sensors Based on Iron Garnets.
PB95-202461 *02,268*

Single Photon Ionization, Laser Optical Probe Technique for Semiconductor Growth.
PB95-202776 *01,032*

Determining the Magnetic Properties of 1 kg Mass Standards.
PB95-261905 *04,016*

Determination of the Transmittance Uniformity of Optical Filter Standard Reference Materials.
PB95-261921 *02,182*

30 THz Mixing Experiments on High Temperature Superconducting Josephson Junctions.
PB96-102462 *04,709*

Magnetostriction and Giant Magnetoresistance in Annealed NiFe/Ag Multilayers.
PB96-102603 *04,716*

Total-Dielectric-Function Approach to Electron and Phonon Response in Solids.
PB96-102884 *01,067*

Nanoscale Study of the Hydrogenated Amorphous Silicon Surface.
PB96-103056 *04,720*

Recent Results in Magnetic Force Microscopy.
PB96-103130 *04,721*

Magnetic Structure and Spin Dynamics of the Pr and Cu in Pr2CuO4.
PB96-111836 *04,036*

Temperature and Field Dependence of Flux Pinning in NbTi with Aritificial Pinning Centers.
PB96-112024 *04,726*

Current and Voltage Measurements in the Gaseous Electronics Conference RF Reference Cell.
PB96-113337 *02,388*

Magnetooptic Effects.
PB96-119292 *04,338*

Using Secondary Ion Mass Spectrometry (SIMS) to Characterize Optical Waveguide Materials.
PB96-119599 *04,340*

Structural and Magnetic Properties of CuCl2 Graphite Intercalation Compounds.
PB96-119748 *03,020*

Decay of Bragg Gratings in Hydrogen-Loaded Optical Fibers.
PB96-122643 *04,345*

Zimm Plot and Its Analogs as Indicators of Vesicle and Micelle Size Polydispersity.
PB96-123765 *01,094*

Low-Temperature Properties of Silver.
PB96-126198 *03,361*

Coexistence of Grains with Differing Orthorhombicity in High Quality YBa2Cu3O7-delta Thin Films.
PB96-135033 *04,742*

Growth of Epitaxial KNbO3 Thin Films.
PB96-135181 *02,409*

Effects of Etching on the Morphology and Surface Resistance of YBa2Cu3O7-delta Films.
PB96-135355 *02,410*

Dielectric Spectroscopic Determination of Temperature Behavior of Electroclinic Parameters in the Liquid Crystal W317.
PB96-140397 *01,098*

X-ray Observation of Electroclinic Layer Constriction and Rearrangement in a Chiral Smectic-A Liquid Crystal.
PB96-141080 *01,100*

Evidence for Tunneling and Magnetic Scatttering at 'In situ' YBCO/Noble-Metal Interfaces.
PB96-141098 *04,752*

Effect of Magnetic Field Orientation on the Critical Current of HTS Conductor and Coils.
PB96-141189 *02,956*

Quench Energy and Fatigue Degradation Properties of Cu- and Al/Cu-Stablized Nb-Ti Epoxy-Impregnated Superconductor Coils.
PB96-141213 *04,755*

Oxygen Annealing of Ex-situ YBCO/Ag Thin-Film Interfaces.
PB96-141312 *04,758*

Domain Structures in Magnetoresistive Granular Metals.
PB96-141346 *04,760*

Dielectric Measurements on Printed-Wiring and Circuit Boards, Thin Films, and Substrates: An Overview.
PB96-147038 *02,236*

Pinch Effect in Commensurate Vortex-Pin Lattices.
PB96-147079 *01,125*

Heterodyne Mixing and Direct Detection in High Temperature Josephson Junctions.
PB96-147202 *01,565*

Annealing of Bragg Gratings in Hydrogen-Loaded Optical Fiber.
PB96-155437 *04,361*

Comparison of UV Photosensitivity and Fluorescence during Fiber Grating Formation.
PB96-155445 *04,362*

Size Effects in Submicron NiFe/Ag GMR Devices.
PB96-155510 *02,237*

NIST Metrology Program on Electromagnetic Characterization of Materials.
PB96-156062 *01,944*

Applicability of Effective Medium Theory to Ferroelectric/Ferrimagnetic Composites with Composition and Frequency-Dependent Complex Permittivities and Permeabilities.
PB96-157854 *01,945*

Influence of Films' Thickness and Air Gaps in Surface Impedance Measurements of High Temperature Superconductors Using the Dielectric Resonator Technique.
PB96-157862 *01,946*

Influence of Electrical Isolation on the Structure and Reflectivity of Multilayer Coatings Deposited on Dielectric Substrates.
PB96-159736 *04,365*

Upgraded Facility for Multilayer Mirror Characterization at NIST.
PB96-160387 *04,367*

Elastic Scattering from Spheres under Non Plane-Wave Illumination.
PB96-163688 *04,370*

SEMPA Studies of Exchange Coupling in Magnetic Multilayers.
PB96-164074 *04,780*

Magnetic Dielectric Oxides: Subsolidus Phase Relations in the BaO: Fe2O3: TiO2 System.
PB96-176524 *01,156*

Magnetic Structure Determination for Annealed Ni80Fe20/Ag Multilayers Using Polarized-Neutron Reflectivity.
PB96-176615 *03,739*

Reference Relations for the Evaluation of the Materials Properties of Orthorhombic YBa2Cu3Ox Superconductors.
PB96-176763 *04,782*

Dielectric Behavior of a Polycarbonate/Polyester Mixture Upon Transesterification.
PB96-179551 *04,785*

Electrostatic Rigidity of Polyelectrolytes from Reparametrization Invariance.
PB96-180062 *04,113*

Preparation, Crystal Structure, Dielectric Properties, and Magnetic Behavior of Ba2Fe2Ti4O13.
PB96-186176 *01,162*

Models of Granualr Giant Magnetoresistance Multilayer Thin Films.
PB96-190228 *01,968*

High Frequency Magnetic Field Sensors Based on the Faraday Effect in Garnet Thick Films.
PB96-190384 *02,282*

Metallic-Barrier Junctions for Programmable Josephson Voltage Standards.
PB96-200134 *02,089*

Observation of the Transverse Second Harmonic Magneto-Optic Kerr Effect from Ni81Fe19 Thin Film Structures.
PB96-200332 *01,971*

Magnetic Flux Pinning in Epitaxial YBa2Cu3O7-delta Thin Films.
PB96-200746 *04,795*

Wideband Current and Magnetic Field Sensors Based on Iron Garnets.
PB96-200878 *01,975*

Spin-Dependent Interface Transmission and Reflection in Magnetic Multilayers (Invited).
PB96-201173 *04,130*

Windowing Effects on Light Scattering by Sinusoidal Surfaces.
PB97-111215 *04,389*

Size Effects and Giant Magnetoresistance in Unannealed NiFe/Ag Multilayer Stripes.
PB97-111306 *04,145*

Intrinsic Conductivity of Objects Having Arbitrary Shape and Conductivity.
PB97-111934 *04,150*

Observation of Two Length Scales Above (T sub N) in a Holmium Thin Film.
PB97-111942 *04,151*

Observation of Hot-Electron Shot Noise in a Metallic Resistor.
PB97-112007 *01,988*

Forward Scattering of a Gaussian Beam by a Nonabsorbing Sphere.
PB97-112288 *04,395*

Bias Current Dependent Resistance Peaks in NiFe/Ag Giant Magnetoresistance Multilayers.
PB97-112346 *04,153*

Isolated Spin Pairs and Two-Dimensional Magnetism in SrCr(sub 9p)Ga(sub 12-9p)O19.
PB97-112387 *04,154*

Neutron Scattering Study of Antiferromagnetic Order in the Magnetic Superconductors RNi2B2C.
PB97-112411 *04,812*

Unconventional Ferromagnetic Transition in La(sub 1-x)Ca(sub x)MnO3.
PB97-112429 *04,156*

Modeling Effects of Temperature Annealing on Giant Magnetoresistive Response in Discontinuous Multilayer NiFe/Ag Films.
PB97-112585 *04,157*

Simulating Device Size Effects on Magnetization Pinning Mechanisms in Spin Valves.
PB97-112593 *04,158*

Colossal Magnetoresistance without Mn(3+)/Mn(4-) Double Exchange in the Stoichiometric Pyrochlore Tl2Mn2O7.
PB97-113070 *04,160*

Radiance Temperatures at 1500 nm of Niobium and Molybdenum at Their Melting Points by a Pulse-Heating Technique.
PB97-118699 *04,167*

Vortex Images in Thin Films of YBa2Cu3O(sub 7-x) and Bi2Sr2Ca1Cu2O(sub 8+x) Obtained by Low-Temperature Magnetic Force Microscopy.
PB97-119408 *04,815*

Antiferromagnetic Interlayer Correlations in Annealed Ni80Fe20/Ag Multilayers.
PB97-122220 *03,109*

Large Local-Field Corrections in Optical Rotatory Power of Quartz and Selenium.
PB97-122378 *04,400*

Determination of Anomalous Superexchange in MnCl2 and Its Graphite Intercalation Compound.
PB97-122568 *00,666*

PROPERTIES OF MATERIALS: STRUCTURAL/ MECHANICAL

Effect of Green Density and the Role of Magnesium Oxide Additive on the Densification of Alumina Measured by Small-Angle Neutron Scattering. (Reannouncement with New Availability Information).
AD-A244 582/3 *03,022*

Electrochemical Synthesis of Metal and Intermetallic Composites.
AD-A294 088/0 *03,304*

Review of Corrosion Behavior of Ceramic Heat Exchanger Materals: Corrosion Characteristics of Silicon Carbide and Silicon Nitride. Final Report, September 11, 1992--March 11, 1993.
DE93041307 *03,228*

Low temperature fabrication from nano-size ceramic powders.
DE95013505 *03,029*

Electromechanical Properties of Superconductors for DOE Fusion Applications.
PB94-139672 *02,250*

Wavelengths and Energy Levels of Neutral Kr(84) and Level Shifts in All Kr Even Isotopes.
PB94-140605 *03,780*

Corrosion Resistance of Materials for Renovation of the United States Botanic Garden Conservatory.
PB94-154390 *00,032*

Precision Comparison of the Lattice Parameters of Silicon Monocrystals.
PB94-169745 *04,438*

RDFs and Fe-Fe Pair Correlations in an AlCuFe Icosahedral Alloy by Double Isotopic Substitution.
PB94-172129 *04,439*

Wear Mechanism Maps of Ceramics.
PB94-172368 *03,229*

Shear-Excited Morphological States in a Triblock Copolymer.
PB94-172392 *01,196*

Fracture Mechanics Analysis of Near-Surface Cracks.
PB94-172400 *03,230*

Nitrogen Effect on Elastic Constants of f.c.c. Fe-18Cr-19Mn Alloys.
PB94-172541 *03,203*

Enhanced Curie Temperatures and Magnetoelastic Domains in Dy/Lu Super Lattices and Films.
PB94-172665 *04,443*

Effects of Elastic Stress on Phase Equilibrium in the Ni-V System.
PB94-172707 *03,313*

Microstructure and Tensile Properties of Microalloyed Steel Forgings.
PB94-172715 *03,204*

Considerations on Data Requirements for Tribological Modeling.
PB94-172731 *02,962*

Wear of Selected Materials and Composites Sliding against MoS2 Films.
PB94-172749 *03,231*

Temperature Dependence of the Morphology of Thin Diblock Copolymer Films as Revealed by Neutron Reflectivity.
PB94-172756 *01,199*

Reaction Sensitivities of Al-Li Alloys and Alloy 2219 in Mechanical-Impact Tests.
PB94-172764 *03,314*

High Temperature Degradation of Structural Composites.
PB94-172848 *03,132*

Intelligent Processing of Hot Isostatic Pressing.
PB94-172913 *03,315*

Temperature Increases in Aluminum Alloys during Mechanical-Impact Tests for Oxygen Compatibility.
PB94-172962 *03,316*

Grafted Interpenetrating Polymer Networks.
PB94-185055 *01,200*

In-Line Optical Monitoring of Injection Molding.
PB94-185105 *01,201*

Phase Behavior of a Hydrogen Bonding Molecular Composite.
PB94-185188 *01,202*

Effect of Backfill and Atomizing Gas on the Powder Porosity and Mechanical Properties of 304L Stainless Steel.
PB94-185394 *03,205*

Influence of Surface Interaction and Chain Stiffness on Polymer-Induced Entropic Forces and the Dimensions of Confined Polymers.
PB94-185469 *01,203*

Fluorescence Monitoring of Polarity Change and Gelation during Epoxy Cure.
PB94-185543 *01,204*

Electron Beam Crosslinking of Poly(vinylmethyl ether).
PB94-185550 *01,205*

Viewpoint: Nanocrystalline and Nanophase Materials.
PB94-185865 *04,454*

Through-the-Arc Sensing for Monitoring Arc Welding.
PB94-185899 *02,858*

Evaluation of Corrosion Data: A Review.
PB94-198348 *03,187*

Facile Synthesis of Novel Fluorinated Multifunctional Acrylates.
PB94-198389 *01,207*

Effect of Transformation of Alloy on Transient and Residual Stresses in a Porcelain-Metal Strip.
PB94-198397 *00,143*

Weak-Link-Free Behavior of High Angle YBa2Cu3O7-x Grain Boundaries in High Magnetic Fields.
PB94-198421 *04,459*

Microstrains and Domain Sizes in Bi-Cu-O Superconductors: An X-Ray Diffraction Peak-Broadening Study.
PB94-198520 *04,461*

Experimental Constraints on Some Mechanisms for High-Temperature Superconductivity.
PB94-198553 *04,463*

Neutron Powder Diffraction Study of a Na, Cs-Rho Zeolite.
PB94-198629 *00,791*

Matrix Grain Bridging Contribution to the Toughness of Whisker Reinforced Ceramics.
PB94-198645 *03,134*

Coherent Precipitates in the BCC/Orthorhombic Two Phase Field of the Ti-Al-Nb System.
PB94-198694 *03,317*

Crystallographic Characterization of Some Intermetallic Compounds in the Al-Cr System.
PB94-198702 *03,318*

Analysis of SANS from Controlled Pore Glasses.
PB94-198843 *03,035*

Structures of Sodium Metal.
PB94-198850 *03,319*

Diffraction Imaging of Polycrystalline Materials.
PB94-198884 *02,971*

Dynamic Shear Modulus Measurements with Four Independent Techniques in Nickel-Based Alloys.
PB94-198900 *03,320*

Disorder Trapping in Ni2TiAl.
PB94-198942 *03,322*

Intrinsic Stress in DC Sputtered Niobium.
PB94-199031 *04,468*

Fluorescence Anisotropy Measurements on a Polymer Melt as a Function of Applied Shear Stress.
PB94-199296 *01,209*

Observations of Shear Induced Molecular Orientation in a Polymer Melt Using Fluorescence Anisotropy Measurements.
PB94-199304 *01,210*

Observations of Shear Stress and Molecular Orientation Using Fluorescence Anisotropy Measurements.
PB94-199312 *01,211*

LMTO/CVM and LAPW/CVM Calculations of the Nickel Aluminide/Nickel Titanium Pseudobinary Phase Diagram.
PB94-199353 *03,323*

Interface Properties for Ceramic Composites from a Single Fiber Pull-Out Test.
PB94-199361 *03,135*

Micro-Mechanical Aspects of Asperity-Controlled Friction in Fiber-Toughened Ceramic Composites.
PB94-199536 *03,136*

Peeling a Polymer from a Surface or from a Line.
PB94-199809 *01,213*

Cavitation Damage During Flexural Creep of SiAlON-YAG Ceramics.
PB94-200110 *03,036*

Crack Growth Resistance of Strain-Softening Materials under Flexural Loading.
PB94-200227 *02,972*

Generic Model for Creep Rupture Lifetime Estimation on Fibrous Ceramic Composites.
PB94-200235 *03,137*

Asymmetric Tip Morphology of Creep Microcracks Growing Along Bimaterial Interfaces.
PB94-200243 *03,138*

Analysis of Creep in a Si-SiC C-Ring by Finite Element Method.
PB94-200268 *03,037*

Incorporation of Gold into YBa2Cu3O7: Structure and Tc Enhancement.
PB94-200276 *04,481*

Unexpected Effects of Gold on the Structure, Superconductivity, and Normal State of YBa2Cu3O7.
PB94-200284 *04,482*

Introduction of a NIST Instrument Sensitivity Standard Reference Material for X-Ray Powder Diffraction.
PB94-200318 *00,807*

Micromechanics of Densification and Distortion.
PB94-200326 *03,327*

Neutron Scattering Structural Study of AlCuFe Quasicrystals Using Double Isotopic Substitution.
PB94-200458 *04,485*

Assessment of Testing Methodology for Ceramic Matrix Composites.
PB94-200532 *03,139*

Elastic Properties of Uniaxial-Fiber Reinforced Composites: General Features.
PB94-200649 *03,140*

Transient Subcritical Crack-Growth Behavior in Transformation-Toughened Ceramics.
PB94-200656 *03,038*

Tribological Characteristics of Alpha-Alumina at Elevated Temperatures.
PB94-211018 *02,963*

Effect of Swelling on the Elasticity of Rubber: Localization Model Description.
PB94-211034 *01,216*

Ordered omega-Derivatives in a Ti-37.5Al-2ONb at% Alloy.
PB94-211091 *03,331*

How Far Is Far from Critical Point in Polymer Blends. Lattice Cluster Theory Computations for Structured Monomer, Compressible Systems.
PB94-211141 *01,217*

Monitoring Polymer Cure by Fluorescence Recovery After Photobleaching.
PB94-211422 *01,218*

Neutron Scattering by Multiblock Copolymers of Structure (A-B)N-A.
PB94-211547 *01,219*

Shear Dependence of Critical Fluctuations in Binary Polymer Mixtures by Small Angle Neutron Scattering.
PB94-211612 *01,220*

Energy and Migration of Grain Boundaries in Polycrystals.
PB94-211638 *03,332*

Fabrication of Platinum-Gold Alloys in Pre-Hispanic South America: Issues of Temperature and Microstructure Control.
PB94-211646 *03,333*

Small-Angle X-Ray and Neutron Scattering Study of Block Copolymer/Homopolymer Mixtures.
PB94-211729 *01,221*

Effect of Microstructure on the Wear Transition of Zirconia-Toughened Alumina.
PB94-211778 *03,141*

Fast-Ion Conduction and Disorder in Cation and Anion Arrays in Y2(ZryTi(1-y))2O7 Pyrochlores Induced by Zr Substitution: A Neutron Rietveld Analysis.
PB94-211869 *04,496*

Determination of the Prior-Austenitic Grain Size of Selected Steels Using a Molten Glass Etch.
PB94-211927 *03,208*

Crossover to Strong Shear in a Low-Molecular-Weight Critical Polymer Blend.
PB94-211976 *01,222*

Tensile Creep of Whisker Reinforced Silicon Nitride.
PB94-211984 *03,142*

Microstructural Evolution in Two-Dimensional Two-Phase Polycrystals.
PB94-211992 *04,498*

Micromechanics of Fracture in Rubber-Toughened Epoxies.
PB94-212222 *03,011*

Glass Transition of Organic Liquids Confined to Small Pores.
PB94-212305 *00,833*

Melting Behavior of Organic Materials Confined in Porous Solids.
PB94-212313 *00,834*

Polymer Liquid Crystalline Materials.
PB94-212339 *01,224*

Mechanism of Mild to Severe Wear Transition in Alpha-Alumina.
PB94-212354 *03,233*

Tribology Education: Present Status and Future Challenges.
PB94-212362 *02,965*

Beneficial Effects of Nitrogen Atomization on an Austenitic Stainless Steel.
PB94-212396 *03,209*

Effect of Cross-Links on the Miscibility of a Deuterated Polybutadiene and Protonated Polybutadiene Blend.
PB94-212438 *01,225*

Inversion of the Phase Diagram from UCST to LCST in Deuterated Polybutadiene and Protonated Polybutadiene Blends.
PB94-212446 *01,226*

Topological Influences on Polymer Adsorption and Desorption Dynamics.
PB94-212479 *01,227*

Efficient Experiment to Study Superconducting Ceramics.
PB94-212578 *04,505*

Thermodynamic Assessment and Calculation of the Ti-Al System.
PB94-212644 *03,337*

Compositional Homogeneity in Processing Precursor Powders to the Ba2YCu3O7-x High Tc Superconductor.
PB94-212743 *04,508*

Imaging of Fine Porosity in a Colloidal Silica: Potassium Silicate Gel by Defocus Contrast Microscopy.
PB94-212750 *03,039*

Effects of Variable Excluded Volume on the Dimensions of Off-Lattice Polymer Chains.
PB94-212941 *01,229*

Observed and Theoretical Creep Rates for an Alumina Ceramic and a Silicon Nitride Ceramic in Flexure.
PB94-212958 *03,040*

Elastic Deformation of a Monolithic Perfect Crystal Interferometer: Implications for Gravitational Phase Shift Experiments.
PB94-213154 *03,858*

Dynamics vs. Static Young's Moduli: A Case Study.
PB94-213188 *03,210*

Elastic Constants of Polycrystalline Y1Ba2Cu3Ox.
PB94-213196 *04,513*

Cast-Iron Elastic Constants: Effect of Graphite Aspect Ratio.
PB94-213212 *03,211*

Correlation between Tc and Elastic Constants of (La-M)2CuO4.
PB94-213220 *04,514*

Elastic Constants and Debye Temperature of Y1Ba2Cu3Ox: Effect of Oxygen Content.
PB94-213352 *04,515*

Characterization of Phase and Surface Composition of Silicon Carbide Platelets.
PB94-216264 *03,043*

Crystal Structure of Pb2Sr2YCu3O8+delta with delta=1.32, 1.46, 1.61, 1.71, by Powder Neutron Diffraction.
PB94-216314 *04,518*

Non-Osmotic, Defect-Controlled Cathodic Disbondment of a Coating from a Steel Substrate.
PB94-216447 *03,120*

Atomic Theory of Fracture of Brittle Materials: Application to Covalent Semiconductors.
PB94-216553 *04,519*

Crystal Structure of Dicalcium Potassium Trihydrogen Bis(pyrophosphate) Trihydrate.
PB94-216561 *00,152*

Review of Cure Monitoring Techniques for On-Line Process Control.
PB94-216728 *03,145*

NIST Workshop on Nanostructured Material (1st): Report of an Industrial Workshop Conducted by the National Institute of Standards and Technology. Held in Gaithersburg, Maryland on May 14-15, 1992.
PB94-218567 *02,973*

Physics Required for Prediction of Long Term Performance of Polymers and Their Composites.
PB94-219243 *03,146*

Abrasive Wear by Diesel Engine Coal-Fuel and Related Particles.
PB95-104915 *01,450*

Localization Model of Rubber Elasticity: Comparison with Torsional Data for Natural Rubber Networks in the Dry State.
PB95-107033 *03,195*

Aging in Glasses Subjected to Large Stresses and Deformations.
PB95-107041 *03,235*

Crystal Structure of a New Sodium Zinc Arsenate Phase Solved by 'Simulated Annealing'.
PB95-107124 *00,870*

Improved Crystallographic Data for Aluminum Niobate (AlNbO4).
PB95-107306 *04,523*

Electric Field Effects on Crack Growth in a Lead Magnesium Niobate.
PB95-107322 *03,339*

Macro- and Microreactions in Mechanical-Impact Tests of Aluminum Alloys.
PB95-107348 *03,340*

Influence of Specimen Absorbed Energy in LOX Mechanical-Impact Tests.
PB95-107355 *03,341*

Rietveld Analysis of NaxWO3+x/2.yH2O, Which Has the Hexagonal Tungsten Bronze Structure.
PB95-107371 *04,524*

Polyethylene Crystallized from an Entangled Solution Observed by Scanning Tunneling Microscopy.
PB95-107389 *01,232*

1,4-Dinitrocubane and Cubane under High Pressure.
PB95-108437 *03,755*

Mathematical Aspects of Rietveld Refinement.
PB95-108601 *04,526*

Response of a Terminally Anchored Polymer Chain to Simple Shear Flow.
PB95-108668 *01,233*

Environmentally Enhanced Fracture of Ceramics.
PB95-125746 *03,046*

Determination of Fiber-Matrix Interfacial Properties of Importance to Ceramic Composite Toughening.
PB95-125811 *03,149*

Control of Friction and Wear of Alpha-Alumina with a Composite Solid-Lubricant Coating.
PB95-125969 *03,225*

Nature of (001) Tilt Grain Boundaries in YBa2Cu3O6+x.
PB95-126033 *04,528*

Characterization of Chemically Modified Pore Surfaces by Small Angle Neutron Scattering.
PB95-126181 *00,898*

Inelastic Neutron Scattering Measurements of Phonons in Icosahedral Al-Li-Cu.
PB95-126215 *04,532*

Ashland Tank Collapse Investigation.
PB95-126314 *02,481*

Effect of Mn Content on the Microstructure of Al-Mn Alloys Electrodeposited at 150C.
PB95-126355 *03,343*

Influence of Physical Aging on the Yield Response of Model DGEBA + Poly(propylene oxide) Epoxy Glasses.
PB95-126363 *03,381*

Volume Recovery in Epoxy Glasses Subjected to Torsional Deformations: The Question of Rejuvenation.
PB95-140018 *03,382*

Torsional Relaxation and Volume Response during Physical Aging in Epoxy Glasses Subjected to Large Torsional Deformations.
PB95-140026 *03,383*

Defective Structures of Barium Yttrium Copper Oxide (Ba2YCu3Ox) and Ba2YCu3-yMyOz (M=Fe, Co, Al, Ga, ..).
PB95-140034 *04,537*

Neutron Powder Diffraction Study of the Structures of La1.9Ca1.1Cu2O6 and La1.9Sr1.1Cu2O6+Delta.
PB95-140042 *04,538*

Normal Modes and Structure Factor for a Canted Spin System: The Generalized Villain Model.
PB95-140067 *04,539*

Morphology of Symmetric Diblock Copolymers as Revealed by Neutron Reflectivity.
PB95-140075 *01,234*

Determining Mobility from Homodyne ac Electrophoretic Light Scattering.
PB95-140497 *03,462*

Critical Factors in Non-Lubricated, Non-Abrasive Wear Testing.
PB95-140588 *03,236*

Tribological Data: Needs and Opportunities.
PB95-140596 *03,237*

In situ Measurements of Chloride Ion and Corrosion Potential at the Coating/Metal Interface.
PB95-140893 *03,122*

Using Torsional Dilatometry to Measure the Effects of Deformations on Physical Aging.
PB95-140901 *03,384*

Aging Effects on XRF Measurements of Solder Coatings.
PB95-140927 *03,123*

Ca4Bi6O13: A Compound Containing an Unusually Low Bismuth Coordination Number and Short Bi Bi Contacts.
PB95-141131 *00,911*

Irradiation Damage in Inorganic Insulation Materials for ITER Magnets: A Review.
PB95-147351 *03,705*

Observed Frustration in Confined Block Copolymers.
PB95-150033 *01,238*

Phase Transitions in Solid C70: Supercooling, Metastable Phases, and Impurity Effect.
PB95-150090 *00,914*

Effect of a Crystal Monochromator on the Local Angular Divergence of an X-Ray Beam.
PB95-150306 *04,565*

Structural Stabilization of Phase Separating PC/Polyester Blends through Interfacial Modification by Transesterification Reaction.
PB95-150454 *01,239*

Phonon Density of States in R2CuO4 and Superconducting R1.85Ce0.15CuO4 (R = Nd, Pr).
PB95-150686 *04,574*

Lattice Imperfections Studied by Use of Lattice Green's Functions.
PB95-150850 *04,576*

Thermal Stability of Internal Electric Field and Polarization Distribution in Blend of Polyvinylidene Fluoride and Polymethylmethacrylate.
PB95-151072 *01,240*

New Alloys Show Extraordinary Resistance to Fracture and Wear.
PB95-151346 *03,346*

Measuring Matching Wear Scars on Balls and Flats.
PB95-151528 *03,153*

X-Ray Characterization of the Crystallization Process of High-Tc Superconducting Oxides in the Sr-Bi-Pb-Ca-Cu-O System.
PB95-151700 *04,579*

X-Ray-Diffraction Study of a Thermomechanically Detwinned Single Crystal of YBa2Cu3O6+x.
PB95-151726 *04,581*

Crystal Chemistry and Phase Equilibria Studies of the BaO(BaCO3)-R2O3-CuO Systems. 4. Crystal Chemistry and Subsolidus Phase Relationship Studies of the CuO-Rich Region of the Ternary Diagrams, R=Lanthanides.
PB95-151759 *00,936*

X-Ray Powder Diffraction Data for BaCu(C2O4)2.6H2O.
PB95-151767 *04,583*

SANS Study of the Plastic Deformation Mechanism in Polyethylene.
PB95-151841 *01,242*

Structural Heterogeneity in Epoxies.
PB95-151866 *01,243*

Characterization of Polyquinoline Block Copolymer Using Small Angle Scattering.
PB95-151882 *01,244*

Dynamic Light-Scattering Study of a Diluted Polymer Blend Near Its Critical Point.
PB95-151890 *01,245*

Effects of Humidity and Elevated Temperature on the Density and Thermal Conductivity of a Rigid Polyisocyanurate Foam.
PB95-152021 *00,373*

Interaction between Dislocations and Intergranular Cracks.
PB95-152096 *03,190*

Hybrid Method for Determining Material Properties from Instrumented Micro-Indentation Experiments.
PB95-152229 *03,348*

Crystal Packing Interactions of Two Different Crystal Forms of Bovine Ribonuclease A.
PB95-152823 *00,943*

Residual Stresses in Aluminum-Mullite (alpha-Alumina) Composites.
PB95-152880 *03,155*

Copolymerization of N-Phenyl Maleimide and gamma-Methacryloxypropyl Trimethoxysilane.
PB95-153144 *01,248*

Structure and Dynamics of Buckyballs.
PB95-153292 *00,950*

Surface Topography and Ordering-Variant Segregation in GaInP2.
PB95-153649 *04,595*

SANS Studies of Space-Time Organization of Structure in Polymer Blends.
PB95-153789 *01,251*

Composite Struts for SMES Plants.
PB95-155586 *02,507*

Crystal Structure of Annealed and As-Prepared HgBa2CaCu2O6+delta Superconductors.
PB95-161105 *03,927*

Cryogenic Toughness of Austenitic Stainless Steel Weld Metals: Effect of Inclusions.
PB95-161261 *03,214*

Flat and Rising R-Curves for Elliptical Surface Cracks from Indentation and Superposed Flexure.
PB95-161295 *03,156*

Tensile Creep of a Silicon Nitride Ceramic.
PB95-161303 *03,049*

Sputtered High Temperature Thin Film Thermocouples.
PB95-161311 *02,259*

Elastic Properties of Al2O3/Al Composites: Measurements and Modeling.
PB95-161378 *03,157*

Analysis of Physical Properties of Ceramic Powders in an International Interlaboratory Comparison Program.
PB95-161501 *03,050*

Localization of a Homopolymer Dissolved in a Lamellar Structure of a Block Copolymer Studied by Small-Angle Neutron Scattering.
PB95-161592 *01,253*

Effects of Anneal Time and Cooling Rate on the Formation and Texture of Bi2Sr2CaCu2O8 Films.
PB95-161600 *04,603*

Molecular Weight Dependence of the Lamellar Domain Spacing of ABC Triblock Copolymers and Their Chain Conformation in Lamellar Domains.
PB95-161691 *01,254*

Neutron Scattering Study of Shear Induced Turbidity in Polystyrene Dissolved in Dioctyl Phthalate.
PB95-161865 *01,256*

Interaction between Micro and Macroscopic Flow in RTM Preforms.
PB95-162012 *03,159*

Evidence of Film-Induced Cleavage by Electrodeposited Rhodium.
PB95-162327 *03,191*

Surface Roughness Evaluation of Diamond Films Grown on Substrates with a High Density of Nucleation Sites.
PB95-162418 *03,018*

Temperature Dependence of Vortex Twin Boundary Interaction in Yttrium Barium Copper Oxide (YBa2Cu3O6+x).
PB95-162442 *04,613*

Introduction to ASTM 1199 'Wear Test Selection for Design and Application'.
PB95-162517 *03,238*

Description of Layered Structures: Applications to High Tc Superconductors.
PB95-162624 *04,615*

Recent VAMAS Activity in Ceramics.
PB95-162681 *03,051*

Ca1-xCuO2, a NaCuO2-Type Related Structure.
PB95-162822 *04,620*

Synthesis and Polymerization of Difunctional and Multifunctional Monomers Capable of Cyclopolymerization.
PB95-163044 *01,257*

Elastic Properties of Central-Force Networks with Bond-Length Mismatch.
PB95-163366 *04,623*

Wear Model for Alumina Sliding Wear.
PB95-163796 *03,239*

Creep and Creep Rupture of Ceramic Matrix Composites.
PB95-163929 *03,165*

Molecular Orbital Study of Water Enhanced Crack Growth Process.
PB95-164067 *03,240*

Characterization of Molecular Network of Thermosets Using Neutron Scattering.
PB95-164109 *01,259*

Small-Angle Neutron Scattering of Poly(vinyl alcohol) Gels.
PB95-164117 *01,260*

Characterization of Polyquinoline Blends Using Small Angle Scattering.
PB95-164125 *01,261*

Asperity-Asperity Contact Mechanisms Simulated by a Two-Ball Collision Apparatus.
PB95-164158 *02,966*

Dislocation Emission at Ledges on Cracks.
PB95-164240 *04,630*

Shielding of Cracks in a Plastically Polarizable Material.
PB95-164257 *04,631*

Small Angle Neutron Scattering Studies on Chain Asymmetry of Coextruded Poly(Vinyl Alcohol) Film.
PB95-164372 *01,262*

Small Angle Neutron Scattering Study on Poly(N-Isopropyl Acrylamide) Gels Near Their Volume-Phase Transition Temperature.
PB95-164380 *01,263*

Small-Angle Neutron Scattering Study on Weakly Charged Temperature Sensitive Polymer Gels.
PB95-164398 *01,264*

Influence of Lattice Mismatch on Indium Phosphide Based High Electron Mobility Transistor (HEMT) Structures Observed in High Resolution Monochromatic Synchrotron X-Radiation Diffraction Imaging.
PB95-164679 *02,357*

Low-Temperature Elastic Constants of Y1Ba2Cu3O7.
PB95-168837 *04,642*

Crystal Structure of Calcium Succinate Monohydrate.
PB95-168928 *00,167*

Ultrasonic Measurement of Residual Stress in Cast Steel Railroad Wheels.
PB95-169199 *04,852*

Crystal Structure and Compressibility of 3:2 Mullite.
PB95-175030 *03,682*

Competition between Hydrodynamic Screening ('Draining') and Excluded Volume Interactions in an Isolated Polymer Chain.
PB95-175402 *01,265*

Fabrication of Transparent gamma-Al2O3 from Nanosize Particles.
PB95-175493 *03,054*

Rapid Post-Polishing of Diamond-Turned Optics.
PB95-175949 *04,301*

Modified Surface Layers and Coatings.
PB95-176087 *03,125*

Elastic Constants of a Material with Orthorhombic Symmetry: An Alternative Measurement Approach.
PB95-180527 *04,684*

Structural and Chemical Investigations of Na3(ABO4)3.4H2O-Type Sodalite Phases.
PB95-180733 *01,012*

Powder Neutron Diffraction Investigation of Structure and Cation Ordering in Ba2+xBi2-xO6-y.
PB95-180865 *01,015*

Scanning Tunneling Microscopy of the Charge-Density-Wave Structure in 1T-TaS2.
PB95-180980 *04,689*

Morphological Development of Second-Phase Particles in Elastically-Stressed Solids.
PB95-181111 *03,355*

Evaluation of Wear Resistant Ceramic Valve Seats in Gas-Fueled Power Generation Engines. Topical Report, December 1991-April 1994.
PB95-200218 *02,466*

Application of ODF to the Rietveld Profile Refinement of Polycrystalline Solid.
PB95-202388 *03,401*

Microstructure Study of Molybdenum Liners by Neutron Diffraction.
PB95-202396 *03,756*

Off-Diagonal Orthorhombic-Symmetry Elastic Constants.
PB95-202768 *04,695*

Determination of Complex Structures from Powder Diffraction Data: The Crystal Structure of La3Ti5Al15O37.
PB95-202966 *01,038*

Boundary Lubrication of Silicon Nitride.
PB95-213583 *03,226*

Proceedings of the Applied Diamond Conference 1995: Applications of Diamond Films and Related Materials International Conference (3rd). Held in Gaithersburg, Maryland, on August 21-24, 1995.
PB95-255204 *04,701*

Applications of Diamond Films and Related Materials: International Conference (3rd). Held in Gaithersburg, Maryland on August 21-24, 1995. Supplement to NIST Special Publication 885.
PB95-256053 *03,063*

Degradation of Powder Epoxy Coated Panels Immersed in a Saturated Calcium Hydroxide Solution Containing Sodium Chloride.
PB96-101050 *01,344*

Lattice Dynamics of Ba1-xKxBiO3.
PB96-102421 *04,706*

Structure and Conductivity of Layered Oxides (Ba,Sr)n+1(Sn,Sb)nO3n+1.
PB96-102439 *04,707*

Lattice Dynamics of Semiconducting, Metallic, and Superconducting Ba1-xKxBiO3 Studied by Inelastic Neutron Scattering.
PB96-102447 *04,708*

Oxygen Dependance of the Crystal Structure of HgBa2CuO4+ and Its Relation to Superconductivity.
PB96-102512 *04,711*

Tensile Deformation-Induced Microstructures in Free-Standing Copper Thin Films.
PB96-102595 *04,715*

X-ray Powder Diffraction from Carbon Nanotubes and Nanoparticles.
PB96-102975 *03,064*

Damage Processes in Ceramics Resulting from Diamond Tool Indentation and Scratching in Various Environments.
PB96-102983 *03,065*

Wear Transitions in Monolithic Alumina and Zirconia-Alumina Composites.
PB96-103163 *03,168*

Residual Stress in Induction-Heated Railroad Wheels: Ultrasonic and Saw Cut Measurements. Report No. 28.
PB96-106992 *04,854*

Factors Significant to Precracking of Fracture Specimens.
PB96-109558 *03,358*

Silicon Nitride Boundary Lubrication: Lubrication Mechanism of Alcohols.
PB96-111703 *03,067*

Silicon Nitride Boundary Lubrication: Effect of Oxygenates.
PB96-111711 *03,068*

Wear Mechanism Maps of 440C Martensitic Stainless Steel.
PB96-111810 *04,834*

Crystal Structure of Calcium Glutarate Monohydrate.
PB96-111893 *01,074*

Small Angle Neutron Scattering Study of the Structure and Formation of Ordered Mesopores in Silica.
PB96-111919 *03,069*

Structure of a Triglyceride Microemulsion: A Small Angle Neutron Scattering Study.
PB96-112255 *01,077*

Torsion Modulus and Internal Friction of a Fiber-Reinforced Composite.
PB96-112339 *03,070*

Vortex Dynamics and Melting in Niobium.
PB96-112362 *02,073*

Intrinsic Viscosity and the Polarizability of Particles Having a Wide Range of Shapes.
PB96-119318 *03,170*

Effect of Sm2BaCuO5 on the Properties of Sintered (Bulk) YBa2Cu3O6+x.
PB96-119441 *04,733*

Mechano-Chemical Model: Reaction Temperatures in a Concentrated Contact.
PB96-119466 *03,227*

Shear-Induced Martensitic-Like Transformation in a Block Copolymer Melt.
PB96-119508 *01,277*

Long-Lived Structures in Fragile Glass-Forming Liquids.
PB96-119565 *04,212*

Tribological Behavior of 440/Diamond-Like-Carbon Film Couples.
PB96-119714 *03,019*

Optical Sampling Using Nondegenerate Four-Wave Mixing in a Semiconductor Laser Amplifier.
PB96-122502 *02,076*

Cavitation Contributes Substantially to Tensile Creep in Silicon Nitride.
PB96-122577 *03,171*

Chemically Assisted Machining of Si3N4.
PB96-122999 *03,072*

Properties and Mechanisms of Fast-Setting Calcium Phosphate Cements.
PB96-123229 *00,178*

Flow-Induced Structure in Polymers: Chapter 16. Shear-Induced Changes in the Order-Disorder Transition Temperature and the Morphology of a Triblock Copolymer.
PB96-123237 *03,127*

Flow-Induced Structure in Polymer. Chapter 1. An Introduction to Flow-Induced Structures in Polymers.
PB96-123369 *03,387*

Characterization of the Vibrational Dynamics in the Octahedral Sublattices of LaD2.25 and LaH2.25.
PB96-123724 *01,091*

Effects of Copper, Nickel and Boron on Mechanical Properties of Low-Alloy Steel Weld Metals Deposited at High Heat Input.
PB96-135231 *03,363*

Contact Tube Wear Detection in Gas Metal Arc Welding.
PB96-135330 *02,872*

Elastic Constants and Internal Friction of Polycrystalline Copper.
PB96-141015 *03,364*

Void Shape in Sintered Titanium.
PB96-141023 *02,705*

Crystal Structure of Decacalcium Tetrapotassium Hexakis (Pyrophosphate) Nonahydrate.
PB96-141064 *01,099*

Neutron-Powder-Diffraction Study of the Long-Range Order in the Octahedral Sublattice of LaD2.25.
PB96-141155 *04,753*

Ultrasonic-Resonance Spectroscopy of Bulk and Layered Solids.
PB96-141338 *04,759*

Artificial Crack in Steel: An Ultrasonic-Resonance-Spectroscopy and Modeling Study.
PB96-141395 *03,241*

Preparation and Characterization of Cyclopolymerizable Resin Formulations.
PB96-146840 *01,285*

Light-Scattering Studies on Phase Separation in a Binary Blend with Addition of Diblock Copolymers.
PB96-146865 *01,286*

Electrodeposited Cobalt-Tungsten as a Diffusion Barrier between Graphite Fibers and Nickel.
PB96-146881 *03,176*

Neutron Scattering Study of the Lattice Modes of Solid Cubane.
PB96-147152 *01,126*

Shear-Induced Mixing in Polymer Blends.
PB96-148085 *01,287*

Effects of Substrate Surface Steps on the Microstructure of Epitaxial Ba2YCu3O7-x Thin Films on (001) LaAlO3.
PB96-148184 *04,774*

International Institute of Welding: Report on 1995 Actions.
PB96-158076 *02,874*

Microstructural Characterization of Cobalt-Tungsten Coated Graphite Fibers.
PB96-159231 *01,951*

Analysis of Small-Angle Scattering Data Dominated by Multiple Scattering for Systems Containing Eccentrically Shaped Particles or Pores.
PB96-160411 *03,075*

Tetrahedral-Framework Lithium Zinc Phosphate Phases: Location of Light-Atom Positions in LiZnPO4 H2O by Powder Neutron Diffraction and Structure Determination of LiZnPO4 by ab Initio Methods.
PB96-160510 *01,129*

Characterization of the Structure of TbD2.25 at 70 K by Neutron Powder Diffraction.
PB96-160528 *01,130*

Neutron Spectroscopic Comparison of beta-Phase Rare Earth Hydrides.
PB96-160742 *01,134*

Powder X-ray Diffraction Data for Ca2Bi2O5 and C4Bi6O13.
PB96-161278 *04,777*

Friction Processes in Brittle Fracture.
PB96-161765 *03,076*

Nonlocal Effects of Existing Dislocations on Crack-Tip Emission and Cleavage.
PB96-161807 *03,367*

Fundamentals of Fracture: A 1993 Prologue, and Other Comments.
PB96-161971 *03,218*

Interfacial Crack in a Two-Dimensional Hexagonal Lattice.
PB96-161989 *04,100*

Whither Computational Materials Science. Some Thoughts from the Mechanical Properties Front.
PB96-161997 *02,987*

Fracture in Multilayers.
PB96-163613 *02,988*

Influence of Shear on the Ordering Temperature of a Triblock Copolymer Melt.
PB96-163753 *01,288*

Model for Toughness Curves in Two-Phase Ceramics. 2. Microstructural Variables.
PB96-163795 *03,078*

REFPROP Refrigerant Properties Database: Capabilities, Limitations, and Future Directions.
PB96-167150 *01,149*

Preparation and Crystal Structure of Sr5TiNb4O17.
PB96-167341 *04,107*

Solid State (13)C NMR and Raman Studies of Cellulose Triacetate: Oligomers, Polymorphism, and Inferences about Chain Polarity.
PB96-176532 *01,289*

Estimation of the Orientation Distribution of Short-Fiber Composites Using Ultrasonic Velocities.
PB96-176656 *03,178*

Objective Evaluation of Short-Crack Toughness Curves Using Indentation Flaws: Case Study on Alumina-Based Ceramics.
PB96-179429 *03,079*

Flaw Tolerance and Toughness Curves in Two-Phase Particulate Composites: SiC/Glass System.
PB96-179460 *03,081*

Effect of Grain Size on Hertzian Contact Damage in Alumina.
PB96-179601 *03,083*

Indentation Fatigue: A Simple Cyclic Hertzian Test for Measuring Damage Accumulation in Polycrystalline Ceramics.
PB96-180013 *03,084*

Diffusion of Water along 'Closed' Mica Interfaces.
PB96-180039 *02,993*

Model for Toughness Curves in Two-Phase Ceramics. 1. Basic Fracture Mechanics.
PB96-180088 *03,085*

Effect of Chemical Interaction on Barenblatt Crack Profiles in Brittle Solids.
PB96-180245 *02,996*

Pressurized Internal Lenticular Cracks at Healed Mica Interfaces.
PB96-180252 *02,997*

Characterization of the Structure of YD3 by Neutron Powder Diffraction.
PB96-186150 *01,161*

Power Characteristics in GMAW: Experimental and Numerical Investigation.
PB96-190145 *03,296*

Aluminum-Lithium Alloys: Evaluation of Fracture Toughness by Two Test Standards, ASTM Method E 813 and E 1304.
PB96-190236 *03,374*

Light-Weight Alloys for Aerospace Applications II.
PB96-190244 *03,375*

Temperature-Induced Transition in Ductile Fracture Appearance of a Nitrogen-Strengthened Austenitic Stainless Steel.
PB96-190269 *03,221*

Ductile Fracture and Tempered Martensite Embrittlement of 4140 Steel.
PB96-190285 *03,222*

Fatigue Crack Thresholds of a Nickel-Iron Alloy for Superconductor Sheaths at 4 K.
PB96-190343 *03,223*

Mechanical Properties and Warm Prestress of Ultra-Low Carbon Steel at 4 K.
PB96-190350 *03,224*

Orthotropic Elastic Constants of a Boron-Aluminum Fiber-Reinforced Composite: An Acoustic-Resonance-Spectroscopy Study.
PB96-200175 *03,182*

Elastic Constants and Microcracks in YBa2Cu3O7.
PB96-200761 *03,005*

Multimedia Tutorial on Phase Equilibria Diagrams.
PB96-200829 *03,088*

NMR Characterization of Injection-Moulded Alumina Green Compacts. Part 2. T2-Weighted Proton Imaging.
PB96-201181 *01,165*

Bulk Modulus and Young's Modulus of Nanocrystalline gamma-Alumina.
PB96-204185 *03,092*

Cavity Evolution during Tensil Creep of Si3N4.
PB96-204193 *03,376*

Shear Suppression of Critical Fluctuations in a Diluted Polymer Blend.
PB96-204458 *04,418*

Experimental Assessment of Crack-Tip Dislocation Emission Models for an Al67Cr8Ti25 Intermetallic Alloy.
PB96-204466 *03,377*

Alvin Van Valkenburg and the Diamond Anvil Cell.
PB96-204474 *04,797*

Phase Separation in Thin Film Polymer Blends With and Without Block Copolymer Additives.
PB96-204482 *01,294*

Thermal Wave NDE of Advanced Materials Using Mirage Effect Detection.
PB96-204516 *04,191*

Creep and Creep Rupture of Structural Ceramics.
PB96-204524 *03,093*

Fracture Mechanism Maps: Their Applicability to Silicon Nitride.
PB96-204532 *03,094*

Mathematical Analysis of Practices to Control Moisture in the Roof Cavities of Manufactured Houses.
PB97-106843 *00,278*

CRYSTMET: The NRCC Metals Crystallographic Data File.
PB97-109029 *04,799*

Inorganic Crystal Structure Database (ICSD) and Standardized Data and Crystal Chemical Characterization of Inorganic Structure Types (TYPIX): Two Tools for Inorganic Chemists and Crystallographers.
PB97-109037 *00,648*

Evaluation of Crystallographic Data with the Program DIAMOND.
PB97-109045 *00,649*

Cambridge Structural Database (CSD): Current Activities and Future Plans.
PB97-109052 *00,516*

Protein Data Bank: Current Status and Future Challenges.
PB97-109060 *00,517*

Nucleic Acid Database: Present and Future.
PB97-109078 *00,518*

Powder Diffraction File: Past, Present, and Future.
PB97-109086 *04,800*

NIST Crystallographic Databases for Research and Analysis.
PB97-109094 *04,801*

Conventional and Eccentric Uses of Crystallographic Databases in Practical Materials Identification Problems.
PB97-109102 *04,802*

Using NIST Crystal Data within Siemens Software for Four-Circle and SMART CCD Diffractometers.
PB97-109110 *04,803*

Phase Identification in a Scanning Electron Microscope Using Backscattered Electron Kikuchi Patterns.
PB97-109128 *04,804*

Biological Macromolecule Crystallization Database and NASA Protein Crystal Growth Archive.
PB97-109136 *01,171*

Investigations of the Systematics of Crystal Packing Using the Cambridge Structural Database.
PB97-109144 *00,519*

Troublesome Crystal Structures: Prevention, Detection, and Resolution.
PB97-109151 *01,172*

CIF Crystallographic Information File: A Standard for Crystallographic Data Interchange.
PB97-109169 *04,805*

Role of Journals in Maintaining Data Integrity: Checking of Crystal Structure Data in 'Acta Crystallographica'.
PB97-109177 *04,806*

Electronic Publishing and the Journals of the American Chemical Society.
PB97-109185 *04,807*

How the Cambridge Crystallographic Data Centre Obtains Its Information.
PB97-109193 *04,808*

Data Import and Validation in the Inorganic Crystal Structure Database.
PB97-109201 *04,809*

World Wide Web for Crystallography.
PB97-109219 *04,810*

Workshop Highlights.
PB97-109227 *04,811*

Flaw-Insensitive Ceramics.
PB97-110027 *03,095*

Tension/Compression Creep Asymmetry in Si3N4.
PB97-110258 *03,096*

Characterizing Materials Properties for Ceramic Matrix Composites.
PB97-110282 *03,097*

Database Development and Management (Project A.2.2): The Annual Report for 1992-1993.
PB97-110290 *03,098*

Role of Corrosion in a Material Selector Expert System for Advanced Structural Ceramics.
PB97-110308 *03,099*

Flaw-Tolerance and Crack-Resistance Properties of Alumina-Aluminum Titanate Composites with Tailored Microstructures.
PB97-110324 *03,101*

In situ-Toughened Silicon Carbide.
PB97-110332 *03,102*

High Temperature Structural Reliability of Silicon Nitride.
PB97-110456 *03,104*

Tensile Creep Testing of Structural Ceramics.
PB97-110464 *03,105*

Lattice Model of a Hydrogen-Bonded Polymer Blend.
PB97-112262 *03,391*

Evidence of Crosslinking in Methyl Pendent PBZT Fiber.
PB97-112486 *03,393*

Relaxation After a Temperature Jump Within the One Phase Region of a Polymer Mixture.
PB97-112494 *03,394*

Microstructure Effect on the Phase Behavior of Blends of Deuterated Polybutadiene and Protonated Polyisopene.
PB97-113146 *01,296*

Excitons in Complex Quantum Nanostructures.
PB97-118343 *01,184*

Swelling and Growth of Polymers, Membranes and Sponges.
PB97-118400 *03,396*

Effect of Beam Voltage on the Properties of Aluminum Nitride Prepared by Ion Beam Assisted Deposition.
PB97-118616 *01,995*

Shear-Induced Changes in the Order-Disorder Transition Temperature and the Morphology of a Triblock Copolymer.
PB97-118772 *03,130*

Influence of Envelopes Geometry on the Sensitivity of 'Nude' Ionization Gauges.
PB97-119077 *04,174*

Morphology and Phase Separation Kinetics of a Compatibilized Blend.
PB97-119135 *01,297*

Electronic Structure and Phase Equilibria in Ternary Substitutional Alloys.
PB97-119366 *03,378*

Nanoindentation and Instrumented Scratching Measurements on Hard Coatings.
PB97-122477 *03,111*

Wear Modeling of Si-Based Ceramics.
PB97-122501 *03,112*

PROPERTIES OF MATERIALS: THERMODYNAMIC/ TRANSPORT

Thermal Conductivity of Metals and Alloys at Low Temperatures. A Review of the Literature.
AD-A279 180/4 *03,302*

Pressure-Volume-Temperature Relations in Liquid and Solid Tritium.
PB94-140571 *00,726*

Thermophysical Properties of Fluids for the Gas Industry. Final Report, February 1, 1988-August 31, 1993.
PB94-146677 *02,472*

Rotational Dynamics of Solid C70: A Neutron-Scattering Study.
PB94-172178 *00,755*

Measurements of the Viscosities of Saturated and Compressed Fluid 1-chloro-1,2,2,2-tetrafluoroethane (R124) and Pentafluoroethane (R125) at Temperatures between 120 and 420 K.
PB94-199791 *03,254*

Assessment of the Al-Sb System.
PB94-200474 *03,329*

Conditions for Existence of a Reentrant Solid Phase in a Sheared Atomic Fluid.
PB94-211380 *04,198*

Analysis of Thermal Wave Propagation in Diamond Films.
PB94-211471 *03,014*

Thermal Wave Propagation in Diamond Films.
PB94-211489 *03,015*

Equation of State Formulation of the Thermodynamic Properties of R134a (1,1,1,2-Tetrafluoroethane).
PB94-212081 *03,256*

Prediction of Viscosity of Refrigerants and Refrigerant Mixtures.
PB94-212099 *03,257*

Prediction of the Thermal Conductivity of Refrigerants and Refrigerant Mixtures.
PB94-212107 *03,258*

Anomalous Freezing and Melting of Solvent Crystals in Swollen Gels of Natural Rubber.
PB94-212321 *01,223*

Thermal Conductivity of R134a.
PB94-213063 *03,857*

Modified Leung-Griffiths Model of Vapor-Liquid Equilibrium: Extended Scaling and Binary Mixtures of Dissimilar Fluids.
PB94-216108 *00,851*

Calculation of Enthalpy and Entropy Differences of Near-Critical Binary Mixtures with the Modified Leung-Griffiths Model.
PB95-108635 *00,885*

Polarized Transient Hot Wire Thermal Conductivity Measurements.
PB95-108817 *00,886*

Thermodynamic Properties of the Methane-Ethane System.
PB95-125779 *00,891*

Thermophysical Property Computer Packages from NIST.
PB95-125787 *04,203*

Effect of Hydrodynamic Interactions on a Terminally Anchored Bead-Rod Model Chain.
PB95-141156 *01,237*

Crystal Chemistry and Phase Equilibrium Studies of the BaO(BaCO3)-R2O3-CuO Systems. 5. Melting Relations in Ba2(Y,Nd,Eu)Cu3O6+x.
PB95-151718 *04,580*

Speed-of-Sound Measurements in Liquid and Gaseous Air.
PB95-151957 *04,186*

Single-Photon Ionization and Detection of Ga, In, and As(sub n) Species in GaAs Growth.
PB95-152815 *00,591*

Thermal Behavior of 4-Maleimidophenyl Glycidyl Ether Resins.
PB95-153151 *01,249*

Rotational Dynamics of Solid C70: A Neutron-Scattering Study.
PB95-153219 *00,949*

Grain Alignment and Transport Properties of Bi2Sr2CaCu2O8 Grown by Laser Heated Float Zone Method.
PB95-161451 *04,602*

Real-Time Small-Angle X-Ray Scattering Study of the Early Stage of Phase Separation in the SiO2-BaO-K20 System.
PB95-163069 *03,052*

Phase Composition, Viscosities, and Densities for Aqueous Two-Phase Systems Composed of Polyethylene Glycol and Various Salts at 25C.
PB95-164596 *00,986*

Reference Data for the Thermophysical Properties of Cryogenic Fluids.
PB95-168688 *03,263*

Thermodynamic Properties of R134a(1,1,1,2-Tetrafluoroethane).
PB95-168704 *00,988*

Relationship between Bulk-Modulus Temperature Dependence and Thermal Expansivity.
PB95-168829 *04,641*

High-Temperature Adiabatic Calorimeter for Constant-Volume Heat Capacity Measurements of Compressed Gases and Liquids.
PB95-168860 *00,989*

Measurements of Molar Heat Capacity at Constant Volume (Cv) for 1,1,1,2-Tetrafluoroethane (R134a).
PB95-168878 *03,264*

Development of a Dual-Sinker Densimeter for High-Accuracy Fluid P-V-T Measurements.
PB95-168951 *03,267*

Need for, and Availability of, Working Fluid Property Data: Results from Annexes XIII and XVIII.
PB95-168969 *03,268*

Enhanced Flux Pinning via Chemical Substitution in Bulk Superconducting T1-2212.
PB95-169033 *04,647*

Measurement of the Thermal Properties of Electrically Conducting Fluids Using Coated Transient Hot Wires.
PB95-169058 *03,269*

Measurement of Diffusion in Fluid Systems: Applications to the Supercritical Fluid Region.
PB95-175188 *02,490*

Supercritical Fluid Extraction of Biological Products.
PB95-175204 *00,040*

Fugacity Coefficients of Hydrogen in (Hydrogen + Butane).
PB95-175212 *02,491*

Vapor-Liquid Equilibria of Mixtures of Propane and Isomeric Hexanes.
PB95-175287 *00,995*

Thin Film Reaction Kinetics of Niobium/Aluminum Multilayers.
PB95-175295 *04,651*

Measurements of the Viscosities of Saturated and Compressed Liquid 1,1,1,2-Tetrafluoroethane (R134a), 2,2-Dichloro-1,1,1-Trifluoroethane (R123) and 1,1-Dichloro-1-Fluoroethane (R141b).
PB95-175386 *03,273*

Solubility Measurement by Direct Injection of Supercritical-Fluid Solutions into a HPLC System.
PB95-175626 *00,997*

Critical Properties and Vapor-Liquid Equilibria of the Binary System Propane + Neopentane.
PB95-175683 *00,999*

Coexisting Densities, Vapor Pressures and Critical Densities of Refrigerants R-32 and R-152a, at 300 - 385 K.
PB95-175691 *03,274*

Predictive Extended Corresponding States Model for Pure and Mixed Refrigerants Including an Equation of State for R134a.
PB95-175717 *03,275*

Correlation of the Ideal Gas Properties of Five Aromatic Hydrocarbons.
PB95-175816 *01,002*

Gas Transport Properties of Solution-Cast Perfluorosulfonic Acid Ionomer Films Containing Ionic Surfactants.
PB95-175998 *01,267*

Composition Dependence of a Field Variable Along the Binary Fluid Mixture Critical Locus.
PB95-176038 *01,003*

Transport and Diffusion in Three-Dimensional Composite Media.
PB95-176129 *04,668*

In-situ Monitoring of Molecular Beam Epitaxial Growth Using Single Photon Ionization.
PB95-202222 *01,023*

Direct Detection of Atomic Arsenic Desorption from Si(100).
PB95-202230 *01,024*

Laser Vacuum Ultraviolet Single Photon Ionization Probing of III-V Semiconductor Growth.
PB95-202370 *04,691*

Shear-Induced Melting of Two-Dimensional Solids.
PB96-112057 *01,075*

Physical Properties of Alternatives to the Fully Halogenated Chlorofluorocarbons.
PB96-119573 *03,279*

Mathematical Models of Transport Phenomena Associated with Arc-Welding Processes: A Survey.
PB96-135058 *02,870*

Vapor-Liquid Equilibria of Ternary Mixtures in the Critical Region on Paths of Constant Temperature and Overall Composition.
PB96-161856 *01,139*

Density Dependence of Fluid Properties and Non-Newtonian Flows: The Weisenberg Effect.
PB96-161898 *01,140*

Nonlinear Correlation of High-Pressure Vapor-Liquid Equilibrium Data for Ethylene + n-Butane Showing Inconsistencies in Experimental Compositions.
PB96-161906 *01,141*

Quantum Collisional Transfer Contributions to the Density Dependence of Gaseous Viscosity.
PB96-161914 *01,142*

Molar Heat Capacity at Constant Volume for Air from 67 to 300 K at Pressures to 35 MPa.
PB96-163738 *00,515*

Non-Newtonian Flow between Concentric Cylinders Calculated from Thermophysical Properties Obtained from Simulations.
PB96-163761 *04,103*

CO2/CH4 Transport in Polyperfluorosulfonate Ionomers: Effects of Polar Solvents on Permeation and Solubility.
PB96-163803 *01,145*

Solubilities of Copper(II) and Chromium(III) beta-Diketonates in Supercritical Carbon Dioxide.
PB96-164215 *01,147*

Molar Heat Capacity at Constant Volume for (xCO2 + (1-x)C2H6) from 220 to 340 K at Pressures to 35 MPa.
PB96-167135 *01,148*

Simulation and SANS Studies of Gelation Under Shear.
PB96-167176 *01,150*

Small-Angle Neutron-Scattering Study of Dense Sheared Silica Gels.
PB96-167184 *01,151*

Status of the Round Robin on the Transport Properties of R134a.
PB96-167218 *01,152*

Viscosity of Defined and Undefined Hydrocarbon Liquids Calculated Using an Extended Corresponding-States Model.
PB96-167234 *02,498*

Retention of Halocarbons on a Hexafluoropropylene Epoxide-Modified Graphitized Carbon Black. 3. Ethene-Based Compounds.
PB96-167309 *03,286*

Thermophysical Property Standard Reference Data from NIST.
PB96-167358 *01,153*

Small Angle Neutron Scattering Study of a Clay Suspension Under Shear.
PB96-167374 *00,663*

Isochoric (p-p-T) Measurements on Liquid and Gaseous Air from 67 to 400 K at Pressures to 35 MPa.
PB96-167390 *01,154*

New Data and Correlations for the Custody Transfer of Natural Gas Liquids.
PB96-176664 *02,499*

Viscosity of 1,1,1,2,3,3-Hexafluoropropane and 1,1,1,3,3,3-Hexafluoropropane at Saturated-Liquid Conditions from 262 K to 353 K.
PB96-176680 *03,292*

Small-Angle Neutron Scattering (SANS) Study of Worm-Like Micelles Under Shear.
PB96-176698 *04,111*

Report of the Refrigeration, Air Conditioning and Heat Pumps Technical Options Committee.
PB96-176755 *03,293*

International Standard Equation of State for the Thermodynamic Properties of Refrigerant 123 (2,2-Dichloro-1,1,1-Trifluoroethane).
PB96-176805 *03,294*

Thermal Conductivity of Polypyromellitimide Film with Alumina Filler Particles from 4.2 to 300 K.
PB96-200753 *01,292*

Internal Waves in Xenon Near the Critical Point.
PB97-111504 *04,221*

PROPERTY RIGHTS

Copyright and Information Services in the Context of the National Research and Education Network.
PB96-160536 *02,736*

Using Technology to Manage and Protect Intellectual Property.
PB97-112395 *01,513*

PROPULSION

Combustion of a Polymer (PMMA) Sphere in Microgravity.
N96-15569/2 *01,354*

PROPYNE

2nu9 Band of Propyne-d3.
PB95-164513 *00,985*

Sub-Doppler, Infrared Laser Spectroscopy of the Propyne 2nu1 Band: Evidence of z-Axis Coriolis Dominated Intramolecular State Mixing in the Acetylenic CH Stretch Overtone.
PB95-202941 *01,037*

PROPYNE COMPLEXES

Infrared and Microwave Spectroscopy of the Argon - Propyne Dimer.
PB94-198892 *00,794*

PROSTHESIS FAILURE

Physicochemical Properties of Calcific Deposits Isolated from Porcine Bioprosthetic Heart Valves Removed from Patients Following 2-13 Years Function.
PB94-172863 *00,184*

PROTECTION

Using Technology to Manage and Protect Intellectual Property.
PB97-112395 *01,513*

PROTECTIVE COATINGS

Sorption of Moisture on Epoxy and Alkyd Free Films and Coated Steel Panels.
PB95-162475 *03,192*

PROTECTIVE EQUIPMENT

Evaluating Investments in Law Enforcement Equipment: An Annotated Bibliography.
PB95-151379 *04,867*

PROTECTIVE EYEWEAR

Optical Density Measurements of Laser Eye Protection Materials.
PB96-190301 *00,190*

PROTEIN EXPRESSION

Mapping Domains in Proteins: Dissection and Expression of 'Escherichia coli' Adenylyl Cyclase.
PB96-155460 *03,478*

PROTEIN MUTANTS

Escherichis coli Cyclic AMP Receptor Protein Mutants Provide Evidence for Ligand Contacts Important in Activation.
PB96-201017 *03,592*

PROTEINS

Salt-PEG Two-Phase Aqueous Systems to Purify Proteins and Nucleic Acid Mixtures.
PB94-200375 *03,527*

Determination of Osmotic Pressure and Fouling Resistances and Their Effects on Performance of Ultrafiltration Membranes.
PB94-212891 *00,841*

Characterization of the Adsorption-Fouling Layer Using Globular Proteins on Ultrafiltration Membranes.
PB94-212909 *00,842*

Energy Transduction between a Concentration Gradient and an Alternating Electric Field.
PB94-216363 *03,461*

Preparation of Immobilized Proteins Covalently Coupled Through Silane Coupling Agents to Inorganic Supports.
PB95-151403 *03,530*

Enzyme and Protein Mass Transfer Coefficient in Aqueous Two Phase Systems. 1. Spray Extraction Columns.
PB95-161162 *00,594*

Continuous Counter-Current Two Phase Aqueous Extraction.
PB95-161212 *00,675*

Protein Extraction in a Spray Column Using a Polyethylene Glycol Maltodextrin Two-Phase Polymer System.
PB95-162228 *00,595*

Non-Perturbative Relation between the Mutual Diffusion Coefficient, Suspension Viscosity, and Osmotic Compressibility: Application to Concentrated Protein Solutions.
PB96-102355 *01,062*

Determination of Total Protein Adsorbed on Solid (Membrane) Surface by a Hydrolysis Technique: Single Protein Adsorption.
PB96-167093 *03,552*

Protein Data Bank: Current Status and Future Challenges.
PB97-109060 *00,517*

PROTEOGLYCANS

Proteoglycan Inhibition of Calcium Phosphate Precipitation in Liposomal Suspensions.
PB94-211208 *00,658*

PROTHESIS

Physicochemical Characterization of Natural and Bioprosthetic Heart Valve Calcific Deposits: Implications for Prevention.
PB96-156039 *00,187*

PROTOCOLS

Conformance Assessment of Transport Layer Security Implementations.
PB94-164373 *01,576*

RDI-SIM ECMA Inter-Domain Routing Protocol Simulation Tool.
PB94-172301 *01,683*

Conformance Testing of a Lower Layer Security Protocol.
PB94-185402 *01,577*

Scientific Protocols in Statistical Standards for Environmental Studies.
PB94-185527 *02,517*

ISDN Conformance Testing Guidelines: Guidelines for Implementors of ISDN Customer Premises Equipment to Conform to Both National ISDN-1 and North American ISDN Users' Forum Layer 3 Basic Rate Interface Basic Call Control Abstract Test Suites.
PB94-219094 *01,471*

Comparing Remote Procedure Calls: Open Network Computing, Distributed Computing Environment and International Organization for Standardization.
PB95-194205 *01,724*

Conformance Testing for OSI Protocols.
PB96-102686 *01,631*

Lessons from the Establishment of the U.S. GOSIP Testing Program.
PB96-119359 *01,817*

Open Issues in OSI Protocol Development and Conformance Testing.
PB96-122908 *01,818*

X Window System, Version 11, Release 5.
PB96-169099 *01,769*

Strategy to Support Multipoint Communication Service Over Native ATM Service.
PB96-176672 *01,507*

PROTON ACCELERATORS

Investigation of Applicability of Alanine and Radiochromic Detectors to Dosimetry of Proton Clinical Beams.
PB96-146782 *03,636*

PROTON AFFINITY

Proton Affinity Ladders from Variable-Temperature Equilibrium Measurements. 1. A Re-Evaluation of the Upper Proton Affinity Range.
PB94-216603 *00,861*

PROTON DOSIMETRY

Electron and Proton Dosimetry with Custom-Developed Radiochromic Dye Films.
PB95-151106 *03,713*

PROTON IMAGING

NMR Characterization of Injection-Moulded Alumina Green Compacts. Part 2. T2-Weighted Proton Imaging.
PB96-201181 *01,165*

PROTON TRANSPORT

Proton Affinity Ladders from Variable-Temperature Equilibrium Measurements. 1. A Re-Evaluation of the Upper Proton Affinity Range.
PB94-216603 *00,861*

PROTONS

Polarizability of the Nucleon.
PB94-211760 *03,846*

Bacteriorhodopsin Retains Its Light-Induced Proton-Pumping Function After Being Heated to 140C.
PB96-102728 *03,471*

PROTOTYPES

Draft Guidelines for Pre-Qualification and Prototype Testing of Seismic Isolation Systems.
PB94-161940 *01,331*

Product Models and Virtual Prototypes in Mechanical Engineering.
PB95-253563 *02,783*

Overview of the Manufacturing Engineering Toolkit Prototype.
PB96-128228 *02,833*

PROTOZOAN DNA

beta-D-Glucosyl-Hydroxymethyluracil: A Novel Modified Base Present in the DNA of the Parastic Protozoan T. brucei.
PB94-172319 *03,524*

PSES (PROJECT SUPPORT ENVIRONMENTS)

Next Generation Computer Resources: Reference Model for Project Support Environments (Version 2.0).
PB94-143401 *01,677*

PSEUDOMONAS FLUORESCENS

Characterization of the Binding of Gallium, Platinum, and Uranium to Pseudomonas Fluorescens by Small-Angle X-ray Scattering and Transmission Electron Microscopy.
PB94-172509 *03,453*

L-threo-beta-Hydroxyhistidine, an Unprecedented Iron(III) Ion-Binding Amino Acid in a Pyoverdine-type Siderophore from Pseudomonas fluorescens 244.
PB94-211620 *00,553*

PSN (PUBLIC SWITCHED NETWORK)

Telecommunications Security Guidelines for Telecommunications Management Network. Computer Security.
PB96-139415 *01,496*

PSYCHOLOGICAL EFFECTS

Psychological Aspects of Lighting: A Review of the Work of CIE TC 3.16.
PB94-172160 *00,241*

Psychological Aspects of Lighting: A Review of the Work of CIE TC 3.16.
PB95-153276 *00,254*

PUBLIC BUILDINGS

Administration Standard for the Telecommunications Infrastructure of Federal Buildings. Category: Telecommunications Standard; Subcategory: Telecommunications Administration.
FIPS PUB 187 *01,461*

Federal Building Grounding and Bonding Requirements for Telecommunications. Category: Telecommunications Standard; Subcategory: Grounding and Bonding.
FIPS PUB 195 *01,802*

Implementation of Executive Order 12699: Seismic Safety of Federal and Federally Assisted or Regulated New Building Construction.
PB95-151809 *00,436*

PUBLIC DOMAIN

Obtaining and Installing a Public Domain TEX.
PB95-175741 *01,719*

PUBLIC KEY CERTIFICATES

Public Key Infrastructure Invitational Workshop. Held in McLean, Virginia on September 28, 1995.
PB96-166004 *01,616*

PUBLIC POLICIES

Learning to Change: Opportunities to Improve the Performance of Smaller Manufacturers.
PB94-166212 *00,010*

PUBLIC POLICY

Information Infrastructure: Reaching Society's Goals. A Report of the Information Infrastructure Task Force Committee on Applications and Technology.
ED-376 823 *00,131*

PUBLIC-PRIVATE PARTNERSHIPS

Montgomery Education Connection and Resource Education Awareness Partnership Making Connections between Local Schools and NIST Volunteers.
PB96-159769 *00,134*

PUBLIC SWITCHED NETWORK

Telecommunications Security Guidelines for Telecommunications Management Network. Computer Security.
PB96-139415 *01,496*

PUBLIC WORKS

National Construction Sector Goals: Industry Strategies for Implementation.
PB95-269817 *00,204*

PUBLISHING

CALS-Markup Requirements and Generic Style Specifications for Electronic Printed Output and Exchange of Text.
PB94-962200 *03,659*

CALS-Markup Requirements and Generic Style Specifications for Electronic Printed Output and Exchange of Text.
PB95-962200 *03,668*

PULL-OUT TEST

Interface Properties for Ceramic Composites from a Single Fiber Pull-Out Test.
PB94-199361 *03,135*

PULSE-ECHO ULTRASONIC EVALUATION

Pulse-Echo Ultrasonic Evaluation of the Integrity of Seams of Single-Ply Roof Membranes.
PB95-163804 *00,381*

PULSE GENERATORS

Aging, Warm-Up Time and Retrace; Important Characteristics of Standard Frequency Generators.
PB96-103122 *04,031*

PULSE HEATING

Dynamic Measurements of Thermophysical Properties of Metals and Alloys at High Temperatures by Subsecond Pulse Heating Techniques.
N94-25124/6 *03,309*

Millisecond-Resolution Pulse Heating System for Specific-Heat Measurements at High Temperatures.
PB94-199999 *02,635*

Measurement of the Heat of Fusion of Tungsten by a Microsecond-Resolution Transient Technique.
PB94-216686 *03,400*

Radiance Temperatures (in the Wavelength Range 523-907 nm) of Group IV B Transition Metals Titanium, Zirconium, and Hafnium at Their Melting Points by a Pulse-Heating Technique.
PB96-102207 *03,356*

Radiance Temperatures (in the Wavelength Range 523-907 nm) of Group IVB Transition Metals Titanium, Zirconium, and Hafnium at Their Melting Points by a Pulse-Heating Technique.
PB96-135025 *02,677*

PULSE PILEUP

Dead Time, Pileup, and Accurate Gamma-Ray Spectrometry.
PB96-167101 *00,697*

PULSE RADIOLYSIS

Fluoride Elimination Upon Reaction of Pentafluoroaniline with e (sub eq')(sup -), H, and OH Radicals in Aqueous Solution.
PB97-111314 *01,177*

PULSE SYNCHRONIZATION

Laser-Synchrotron Hybrid Experiments: A Photon to Tickle, A Photon to Poke.
PB96-157847 *03,704*

PULSE TRANSFORMERS

Electrical Breakdown in Transformer Oil in Large Gaps.
PB95-150579 *01,889*

PULSE TUBE REFRIGERATORS

Graded and Nongraded Regenerator Performance.
PB95-169090 *02,753*

PULSED GAS METAL ARC WELDING

Through-the-Arc Sensing for Monitoring Arc Welding.
PB94-185899 *02,858*

PULSED LASER DEPOSITION

Coexistence of Grains with Differing Orthorhombicity in High Quality YBa2Cu3O7-delta Thin Films.
PB96-135033 *04,742*

PULSES

Comment and Discussion on Digital Processing of PD Pulses.
PB96-122775 *01,932*

Radiation-Chemical Reaction of 2,3,5-Triphenyl-Tetrazolium Chloride in Liquid and Solid State.
PB96-146733 *01,124*

PUNCTURE RESISTANCE

Study to Determine the Most Important Parameters for Evaluating the Resistance of Soft Body Armor to Penetration by Edged Weapons.
PB94-158573 *03,757*

PURIFICATION

Salt-PEG Two-Phase Aqueous Systems to Purify Proteins and Nucleic Acid Mixtures.
PB94-200375 *03,527*

Critical Evaluation of the Purification of Biominerals by Hypochlorite Treatment.
PB95-150959 *00,186*

High-Performance Liquid Chromatography of Phytoplankton Pigments Using a Polymeric Reversed-Phase C18 Column.
PB95-151130 *00,583*

Protein Extraction in a Spray Column Using a Polyethylene Glycol Maltodextrin Two-Phase Polymer System.
PB95-162228 *00,595*

All-Metal Collection System for Preparative-Scale Gas Chromatography: Purification of Low-Boiling-Point Compounds.
PB96-123435 *00,619*

PURPLE MEMBRANES

Optical Properties of Triton X-100-Treated Purple Membranes Embedded in Gelatin Films.
PB96-123500 *03,546*

PVDF TRANSDUCERS

Design, Construction and Application of a Large Aperture Lens-Less Line-Focus PVDF Transducer.
PB97-122584 *02,765*

PVM (PARALLEL VIRTUAL MACHINE)

Performance Characteristics of Fast Elliptic Solvers on Parallel Platforms.
PB95-180832 *01,723*

PYCNOMETERS

Application of the Electronic Balance in High Precision Pycnometry.
PB94-187564 *00,534*

PYROELECTRIC DETECTORS

Electrically Calibrated Pyroelectric Detector-Refinements for Improved Optical Power Measurements.
PB95-169066 *02,164*

PYROELECTRICITY
Piezoelectric and Pyroelectric Polymers.
PB95-153367 *01,250*

PYROLYSIS
Thermal Decomposition of Hydroxy- and Methoxy-Substituted Anisoles.
PB94-173036 *00,767*

Behavior of Charring Materials in Simulated Fire Environments.
PB94-196045 *01,368*

Upward Flame Spread along the Vertical Corner Walls (October 1993).
PB94-206299 *00,340*

PYROMELLITIC DIANHYDRIDE
Effects of Surface-Active Resins on Dentin/Composite Bonds.
PB95-140448 *00,156*

PYROMETERS
Corrected Optical Pyrometer Readings.
AD-A279 949/2 *02,615*

High-Speed Spatial Scanning Pyrometer.
PB94-200003 *02,636*

PYROMETRY
National Measurement System for Radiometry, Photometry, and Pyrometry Base Upon Absolute Detectors.
PB97-108559 *04,382*

Issues in High-Speed Pyrometry.
PB97-118368 *02,693*

PYROPHOSPHATES
Selective Inhibition of Crystal Growth on Octacalcium Phosphate and Nonstoichiometric Hydroxyapatite by Pyrophosphate at Physiological Concentration.
PB94-211257 *00,147*

Crystal Structure of Dicalcium Potassium Trihydrogen Bis(pyrophosphate) Trihydrate.
PB94-216561 *00,152*

Crystal Structure of Decacalcium Tetrapotassium Hexakis (Pyrophosphate) Nonahydrate.
PB96-141064 *01,099*

PYRUVATES
Equilibrium and Calorimetric Investigation of the Hydrolysis of L-Tryptophan to (Indole + Pyruvate + Ammonia).
PB95-163317 *00,661*

PZT
Microstructure and Ferroelectric Properties of Lead Zirconate-Titanate Films Produced by Laser Evaporation.
PB94-199148 *04,470*

QUADRATIC PROGRAMMING
Interior-Point Method for Linear and Quadratic Programming Problems. (NIST Reprint).
PB95-180089 *03,429*

QUADRATIC RESPONSE
Quadratic Response of a Chemical Reaction to External Oscillations.
PB96-161633 *01,138*

QUALITY
Models, Managing Models, Quality Models: An Example of Quality Management.
PB94-163466 *02,891*

QUALITY ASSURANCE
Proficiency Testing as a Component of Quality Assurance in Construction Materials Laboratories.
PB94-185774 *00,334*

International Institute of Welding: Report on 1992 Actions.
PB94-185873 *02,856*

International Institute of Welding: Report on 1993 Actions.
PB94-185881 *02,857*

Infratechnologies: Tools for Innovation.
PB94-185998 *00,317*

National Quality Assurance Program for Personnel Radiation Dosimetry: A Case History.
PB94-211273 *03,620*

Importance of Measurement in Technology-Based Competition.
PB94-211844 *02,929*

Role of the Office of Radiation Measurement in Quality Assurance.
PB94-212255 *00,689*

Questions and Answers on Quality, the ISO 9000 Standard Series, Quality System Registration, and Related Issues. More Questions and Answers on the ISO 9000 Standard Series and Related Issues.
PB95-103461 *00,495*

Certification, Development and Use of Standard Reference Materials.
PB95-107272 *00,567*

Software Safety and Program Slicing.
PB95-125894 *01,703*

Review of the USCEA/NIST Measurement Assurance Program for the Nuclear Power Industry.
PB95-126272 *03,712*

Quality Assurance of Contaminant Measurements in Marine Mammal Tissues.
PB95-164034 *02,588*

Proceedings Report of the International Invitation Workshop on Development Assurance. Held in Ellicott City, Maryland on June 16-17, 1994.
PB95-189494 *02,912*

IIW Commission V Quality Control and Quality Assurance of Welded Products Annual Report 1994/95.
PB95-198743 *02,866*

Overview of Reference Materials Prepared for Standardization of DNA Typing Procedures.
PB96-111653 *00,611*

Electrical Product Requirements (Especially Quality Requirements) in the United States.
PB96-119235 *01,929*

Dosimetry Systems for Radiation Processing.
PB96-135280 *03,717*

Report on 1994 Actions of the International Institute of Welding.
PB96-138540 *02,873*

Unique Quality Assurance Aspects of INAA for Reference Material Homogeneity and Certification.
PB96-200811 *00,699*

Developing Quality System Documentation Based on ANSI/NCSL Z540-1-1994: The Optical Technology Division's Effort.
PB96-202122 *01,869*

QUALITY CONTROL
Optical Storage Media Data Integrity Studies.
N95-24130/3 *01,620*

Draft Guidelines for Quality Control Testing of Sliding Seismic Isolation Systems.
PB94-161957 *01,332*

Through-the-Arc Sensing for Monitoring Arc Welding.
PB94-185899 *02,858*

Statistical Quality Control Technology in Japan.
PB94-199064 *02,708*

Program Handbook: Requirements for Obtaining NIST Approval/Recognition of a Laboratory Accreditation Body Under P.L. 101-592. The Fastener Quality Act.
PB94-210143 *02,859*

Through-the-Arc Sensing for Real-Time Measurement of Gas Metal Arc Weld Quality.
PB95-162871 *02,863*

Standards for Atmospheric Measurements.
PB95-163622 *02,547*

Through-the-Arc Sensing for Measuring Gas Metal Arc Weld Quality in Real Time.
PB95-164463 *02,908*

Optical Characterization in Microelectronics Manufacturing.
PB95-169397 *02,358*

IIW Commission V Quality Control and Quality Assurance of Welded Products Annual Report 1994/95.
PB95-198743 *02,866*

Defect Formation Mechanism Causing Increasing Defect Density during Decreasing Implant Dose in Low-Dose Simox.
PB96-119524 *02,402*

Development of a New Quality Control Strategy for Automated Manufacturing.
PB96-160486 *02,840*

Implementation of the Fastener Quality Act.
PB96-160676 *02,876*

IIW Commission V Quality Control and Quality Assurance of Welded Products, Annual Report 1995/96.
PB96-191366 *02,880*

NIST/NCMS Program on Electronic Packaging: First Update.
PB96-204086 *03,008*

National Voluntary Laboratory Accreditation Program (NVLAP): Fasteners and Metals.
PB97-114185 *02,881*

QUANTITATIVE ANALYSIS
Methods for Analysis of Cancer Chemopreventive Agents in Human Serum.
PB95-200648 *03,502*

Liquid Chromatographic Determination of Carotenoids in Human Serum Using an Engineered C30 and a C18 Stationary Phase.
PB97-119333 *03,512*

QUANTITATIVE CHEMICAL ANALYSIS
How to Verify Reference Materials.
PB95-151486 *03,497*

Determination of Polycyclic Aromatic Hydrocarbons by Liquid Chromatography.
PB95-151650 *00,585*

Development of a Gas Standard Reference Material Containing Eighteen Volatile Organic Compounds.
PB95-162277 *02,545*

Liquid Chromatographic Determination of Polycyclic Aromatic Hydrocarbon Isomers of Molecular Weight 278 and 302 in Environmental Standard Reference Materials.
PB95-164042 *02,523*

Interlaboratory Comparison Studies on the Analysis of Hair for Drugs of Abuse.
PB95-176251 *03,500*

Hair Analysis for Drugs of Abuse: Evaluation of Analytical Methods, Environmental Issues, and Development of Reference Materials.
PB95-176269 *03,501*

Quantitative Analysis of Selected PCB Congeners in Marine Matrix Reference Materials Using a Novel Cyanobiphenyl Stationary Phase.
PB96-111737 *02,591*

Hair Testing for Drugs of Abuse: International Research on Standards and Technology.
PB96-120555 *03,504*

NIST Reference Materials to Support Accuracy in Drug Testing.
PB96-123807 *03,505*

Certification of Phencyclidine in Lyophilized Human Urine Reference Materials.
PB96-160692 *03,508*

Interlaboratory Studies on the Analysis of Hair for Drugs of Abuse: Results from the Fifth Exercise.
PB97-110449 *03,509*

Interlaboratory Studies on the Analysis of Hair for Drugs of Abuse: Results from the Fourth Exercise.
PB97-111322 *03,510*

Use of Neutron Beams for Chemical Analysis at NIST.
PB97-112437 *00,652*

QUANTIZED DISSIPATION
Journal of Research of the National Institute of Standards and Technology, March/April 1996. Volume 101, Number 2.
PB96-177381 *01,863*

Evidence That Voltage Rather Than Resistance is Quantized in Breakdown of the Quantum Hall Effect.
PB96-179163 *01,868*

QUANTUM DOTS
Quantum Dots in Quantum Well Structures.
PB97-118350 *01,185*

QUANTUM ELECTRODYNAMICS
How Accurate Are the Josephson and Quantum Hall Effects and QED.
PB95-163283 *03,942*

QUANTUM ELECTRONICS
Using Quantized Breakdown Voltage Signals to Determine the Maximum Electric Fields in a Quantum Hall Effect Sample.
PB95-261947 *02,375*

QUANTUM HALL EFFECT
Quantized Dissipation of the Quantum Hall Effect at High Currents.
PB94-199395 *04,472*

How Accurate Are the Josephson and Quantum Hall Effects and QED.
PB95-163283 *03,942*

Anomalous Behavior of a Quantized Hall Plateau in a High-Mobility Si Metal-Oxide-Semiconductor Field-Effect Transistor.
PB95-164174 *02,354*

Design Challenges in a Commercial Quantum Hall Effect-Based Resistance Standard.
PB95-171419 *02,263*

Progress on the Quantized Hall Resistance Recommended Intrinsic/Derived Standards Practice.
PB96-122460 *02,403*

Precision Tests of a Quantum Hall Effect Device DC Equivalent Circuit Using Double-Series and Triple-Series Connections.
PB96-159256 *01,953*

Quantum Hall Effect-Based Resistance Standard: Capabilities and Implementation.
PB96-180096 *04,114*

Quantum Hall Effect-Based Resistance Standard (Quantum Hall Res).
PB96-200944 *04,127*

QUANTUM MEASUREMENTS
Quantum Measurements of Trapped Ions.
PB95-161147 *03,928*

QUANTUM MECHANICS
Quantum Projection Noise: Population Fluctuations in Two-Level Systems.
PB94-212271 *03,850*

Quantum Measurements of Trapped Ions.
PB95-161147 *03,928*

Quantum Mechanics of a Solid-State Bar Gravitational Antenna.
PB95-202628 *03,987*

Point Charges, Radiation Reaction, and Quantum Mechanics.
PB97-110563 *04,139*

Positronium in Relativistic Quantum Mechanics.
PB97-110571 *04,140*

Relativistic Quantum Mechanics of Interacting Particles.
PB97-110589 *04,141*

Spinor Equations in Relativistic Quantum Mechanics.
PB97-110605 *04,142*

QUANTUM THEORY
Potential and Current Distributions Calculated Across a Quantum Hall Effect Sample at Low and High Currents.
PB96-122106 *04,045*

QUANTUM-WELL
Use of Pressure for Quantum-Well Band-Structure Characterization.
PB96-164058 *04,779*

QUANTUM WELL LASERS
Comparative Photoluminescence Measurement and Simulation of Vertical-Cavity Semiconductor Laser Structures.
PB95-169173 *02,169*

Measurement and Simulation of Photoluminescence Spectra from Vertical-Cavity Quantum-Well Laser Structures.
PB95-169181 *02,170*

QUANTUM WELLS
Modified Airy Function Method for the Analysis of Tunneling Problems in Optical Waveguides and Quantum Well Structures.
PB94-185824 *02,120*

Determination of the Complex Refractive Index of Individual Quantum Wells from Distributed Reflectance.
PB95-175642 *02,176*

Scaling of the Nonlinear Optical Cross Sections of GaAs-AlGaAs Multiple Quantum-Well Hetero n-i-p-i's.
PB96-102793 *02,183*

Theory for Quantum-Dot Quantum Wells: Pair Correlation and Internal Quantum Confinement in Nanoheterostructures.
PB96-179445 *02,437*

Time-Resolved Measurements of the Polarization State of Four-Wave Mixing Signals from GaAs Multiple Quantum Wells.
PB96-201058 *04,796*

Interdigitated Stacked P-I-N Multiple Quantum Well Modulator.
PB97-112296 *02,455*

Excitons in Complex Quantum Nanostructures.
PB97-118343 *01,184*

QUARTZ
Fuzed-Quartz Fibers. A Survey of Properties, Applications and Production Methods.
AD-A286 620/0 *00,656*

Dielectric Properties of Materials at Cryogenic Temperatures and Microwave Frequencies.
PB95-202610 *02,369*

Environmental Sensitivities of Quartz Oscillators.
PB96-103148 *02,271*

Large Local-Field Corrections in Optical Rotatory Power of Quartz and Selenium.
PB97-122378 *04,400*

QUARTZ-HALOGEN LAMPS
Journal of Research of the National Institute of Standards and Technology, March/April 1996. Volume 101, Number 2.
PB96-177381 *01,863*

Irradiance of Horizontal Quartz-Halogen Standard Lamps.
PB96-179130 *01,866*

QUARTZ RESONATORS
Ultralinear Small-Angle Phase Modulator.
PB95-168852 *02,261*

Relationship of AM to PM Noise in Selected RF Oscillators.
PB95-169009 *02,262*

New Model of 1/F Noise in Baw Quartz Resonators.
PB96-112248 *02,383*

Quest to Understand and Reduce I/f Noise in Amplifiers and Baw Quartz Oscillators.
PB96-200795 *02,097*

QUASARS
Discovery of an X-Ray Selected, Radio-Loud Quasar at z=3.9.
PB94-198652 *00,052*

Observations of 3C 273 with the Goddard High Resolution Spectrograph on the Hubble Space Telescope.
PB95-202321 *00,076*

QUASICRYSTALS
RDFs and Fe-Fe Pair Correlations in an AlCuFe Icosahedral Alloy by Double Isotopic Substitution.
PB94-172129 *04,439*

Neutron Scattering Structural Study of AlCuFe Quasicrystals Using Double Isotopic Substitution.
PB94-200458 *04,485*

Inelastic Neutron Scattering Measurements of Phonons in Icosahedral Al-Li-Cu.
PB95-126215 *04,532*

QUASIELASTIC COMPONENT
Unconventional Ferromagnetic Transition in La(sub 1-x)Ca(sub x)MnO3.
PB97-112429 *04,156*

QUATERNARY AMMONIUM SALTS
Use of Kinetic Energy Distributions to Determine the Relative Contributions of Gas Phase and Surface Fragmentation in KeV Ion Sputtering of a Quaternary Ammonium Salt.
PB95-126108 *00,570*

QUENCHING (COOLING)
Hot-Deformation Apparatus for Thermomechanical Processing Simulation.
PB94-200136 *03,207*

QUERY LANGUAGES
Object SQL: Language Extensions for Object Data Management.
PB95-125902 *01,704*

Coping with Different Retrieval Methods in Next Generation Networks.
PB95-168555 *02,726*

QUINUCLIDINYL BENZILATE
Determination of 3-Quinuclidinyl Benzilate (Qnb) and Its Major Metabolites in Urine by Isotope Dilution Gas Chromatography Mass Spectrometry.
PB94-199379 *03,492*

R-123 REFRIGERANT
Enhancement of R123 Pool Boiling by the Addition of N-Hexane.
PB96-165956 *02,605*

R 22
Role of R22 in Refrigerating and Air Conditioning Equipment.
PB94-199783 *03,253*

R-CURVES
Flat and Rising R-Curves for Elliptical Surface Cracks from Indentation and Superposed Flexure.
PB95-161295 *03,156*

R123
Criteria for Establishing Accurate Vapor Pressure Curves.
PB95-163812 *00,972*

R124
Viscosity of the Saturated Liquid Phase of Six Halogenated Compounds and Three Mixtures.
PB95-162368 *00,960*

R125
Viscosity of the Saturated Liquid Phase of Six Halogenated Compounds and Three Mixtures.
PB95-162368 *00,960*

R134A
Equation of State Formulation of the Thermodynamic Properties of R134a (1,1,1,2-Tetrafluoroethane).
PB94-212081 *03,256*

Thermal Conductivity of R134a.
PB94-213063 *03,857*

Polarized Transient Hot Wire Thermal Conductivity Measurements.
PB95-108817 *00,886*

Viscosity of the Saturated Liquid Phase of Six Halogenated Compounds and Three Mixtures.
PB95-162368 *00,960*

Criteria for Establishing Accurate Vapor Pressure Curves.
PB95-163812 *00,972*

Thermodynamic Properties of R134a(1,1,1,2-Tetrafluoroethane).
PB95-168704 *00,988*

Measurements of Molar Heat Capacity at Constant Volume (Cv) for 1,1,1,2-Tetrafluoroethane (R134a).
PB95-168878 *03,264*

Vapour Pressure Measurements on 1,1,1,2-Tetrafluoroethane (R134a) from 180 to 350 K.
PB95-168886 *03,265*

Measurement of the Thermal Properties of Electrically Conducting Fluids Using Coated Transient Hot Wires.
PB95-169058 *03,269*

Predictive Extended Corresponding States Model for Pure and Mixed Refrigerants Including an Equation of State for R134a.
PB95-175717 *03,275*

R142B
Polarized Transient Hot Wire Thermal Conductivity Measurements.
PB95-108817 *00,886*

R236EA
Dielectric Studies of Fluids with Reentrant Resonators.
PB95-153730 *00,952*

R32
Ebulliometric Measurement of the Vapor Pressure of Difluoromethane.
PB95-151361 *00,931*

Viscosity of the Saturated Liquid Phase of Six Halogenated Compounds and Three Mixtures.
PB95-162368 *00,960*

RADAR CROSS SECTIONS
RangeCAD and the NIST RCS Uncertainty Analysis.
PB94-218591 *01,870*

Proposed Analysis of RCS Measurement Uncertainty.
PB95-203568 *01,871*

Polarimetric Calibration of Reciprocal-Antenna Radars.
PB95-216925 *01,872*

Accurate Computations of Radar Cross Sections of Simple Objects.
PB96-138474 *04,426*

Polarimetric Calibration of Reciprocal-Antenna Radars.
PB96-200696 *02,016*

RADAR POLARIMETRY
Polarimetric Calibration of Reciprocal-Antenna Radars.
PB95-216925 *01,872*

RADIANCE
Improved Automated Current Control for Standard Lamps.
PB94-219367 *00,246*

Intercomparison of the ITS-90 Radiance Temperature Scales of the National Physical Laboratory (U.K.) and the National Institute of Standards and Technology.
PB96-113550 *02,674*

RADIANCE TEMPERATURES
Radiance Temperatures (in the Wavelength Range 523-907 nm) of Group IVB Transition Metals Titanium, Zirconium, and Hafnium at Their Melting Points by a Pulse-Heating Technique.
PB96-135025 *02,677*

Radiance Temperatures at 1500 nm of Niobium and Molybdenum at Their Melting Points by a Pulse-Heating Technique.
PB97-118699 *04,167*

RADIANT COOLING
Analytical Method of Determining the Heat Capacity at High Temperatures from the Surface Temperature of a Cooling Sphere.
PB94-216124 *03,865*

RADIANT HEATING
Water Droplet Evaporation from Radiantly Heated Solids.
PB95-217147 *00,394*

RADIATION
Protection Against Neutron Radiation Up to 30 Million Electron Volts.
AD-A286 681/2 *03,611*

RADIATION ACCIDENTS
Radiation Accident at an Industrial Accelerator Facility.
PB95-140117 *02,575*

RADIATION ATTENUATION
X-ray Attenuation Coefficients from 10 Kev to 100 Mev.
AD-A278 139/1 *03,765*

RADIATION COUNTERS
Self-Biasing Cryogenic Particle Detector Utilizing Electrothermal Feedback and a SQUID Readout.
PB96-102538 *04,712*

RADIATION DAMAGE
Irradiation Damage in Inorganic Insulation Materials for ITER Magnets: A Review.
PB95-147351 *03,705*

Quantitative Determination of Oxidative Base Damage in DNA by Stable Isotope-Dilution Mass Spectrometry.
PB96-200886 *03,483*

Colour Centres in LiF for Measurement of Absorbed Doses Up to 100 MGy.
PB97-118756 *04,169*

RADIATION DETECTION
Unique Quality Assurance Aspects of INAA for Reference Material Homogeneity and Certification.
PB96-200811 *00,699*

RADIATION DETECTORS
Thermal and Nonequilibrium Responses of Superconductors for Radiation Detectors.
PB95-164232 *02,156*

RADIATION DOSAGE
Report of the International Commission on Radiological Units and Measurements (ICRU), 1956.
AD-A279 120/0 *03,513*

Radiation Doses.
PB94-199676 *03,618*

National Quality Assurance Program for Personnel Radiation Dosimetry: A Case History.
PB94-211273 *03,620*

Updated Calculations for Routine Space-Shielding Radiation Dose Estimates: SHIELDOSE-2.
PB95-171039 *04,838*

Food Irradiation Dosimetry.
PB95-180675 *00,041*

RADIATION DOSES
Journal of Research of the National Institute of Standards and Technology. March/April 1994. Volume 99, Number 2.
PB94-219219 *02,000*

Sealed Water Calorimeter for Measuring Absorbed Dose.
PB94-219227 *03,517*

Extrapolation Chamber Measurements on (90)Sr + (90)Y Beta-Particle Ophthalmic Applicator Dose Rates.
PB95-153375 *03,626*

Crystal Structure of Annealed and As-Prepared HgBa2CaCu2O6+delta Superconductors.
PB95-161105 *03,927*

Measurement of Radial Dose Distributions Around Small Beta Particle Emitters Using High Resolution Radiochromic Foil Dosimetry.
PB95-164604 *03,518*

Comparison of NIST and Manufacturer Calibrations of (90)Sr+(90)Y Ophthalmic Applicators.
PB96-123708 *03,634*

RADIATION EFFECTS
Increased Pinning Energies and Critical Current Densities in Heavy-Ion-Irradiated Bi2Sr2CaCu2O8 Single Crystals.
PB95-175352 *04,654*

Decrease of Fluorescence in Optical Fiber during Exposure to Pulsed or Continuous-Wave Ultraviolet Light.
PB95-203071 *04,320*

RADIATION HAZARDS
Electron transport calculations with biomedical and environmental applications. Final report, December 23, 1992--January 31, 1994.
DE95007065 *03,613*

RADIATION INJURIES
Radiation Accident at an Industrial Accelerator Facility.
PB95-140117 *02,575*

RADIATION MEASUREMENT
Review of the USCEA/NIST Measurement Assurance Program for the Nuclear Power Industry.
PB95-126272 *03,712*

USCEA/NIST Measurement Assurance Programs for the Radiopharmaceutical and Nuclear Power Industries.
PB97-110514 *03,721*

RADIATION MEASURING INSTRUMENTS
Report of the International Commission on Radiological Units and Measurements (ICRU), 1956.
AD-A279 120/0 *03,513*

RADIATION MONITORS
Dosimetry Systems for Radiation Processing.
PB96-135280 *03,717*

RADIATION PROCESSING
ESR-Based Analysis in Radiation Processing.
PB95-161634 *03,931*

RADIATION PROTECTION
X-ray Protection.
AD-A279 132/5 *03,605*

X-ray Protection Design.
AD-A279 181/2 *03,606*

Protection Against Radiations from Radium, Cobalt-60, and Cesium-137.
AD-A279 261/2 *03,607*

Maximum Permissible Body Burdens and Maximum Permissible Concentrations of Radionuclides in Air and in Water for Occupational Exposure.
AD-A280 282/5 *03,610*

Protection Against Neutron Radiation Up to 30 Million Electron Volts.
AD-A286 681/2 *03,611*

RADIATION PYROMETERS
Radiance Temperature (in the Wavelength Range 519-906 nm) of Tungsten at Its Melting Point by a Pulse-Heating Technique.
PB94-172590 *03,397*

RADIATION REACTIONS
Point Charges, Radiation Reaction, and Quantum Mechanics.
PB97-110563 *04,139*

RADIATION SCATTERING
Characterization of the Binding of Gallium, Platinum, and Uranium to Pseudomonas Fluorescens by Small-Angle X-ray Scattering and Transmission Electron Microscopy.
PB94-172509 *03,453*

RADIATION SHIELDING
New Method for Shielding Electron Beams Used for Head and Neck Cancer Treatment.
PB94-211430 *03,621*

RADIATION SOURCES
Precision High Temperature Blackbodies.
PB95-140059 *03,885*

RADIATION THERAPY
DNA Base Damage in Lymphocytes of Cancer Patients Undergoing Radiation Therapy.
PB97-122444 *03,643*

RADIATION TOLERANCE
Ionizing Radiation Causes Greater DNA Base Damage in Radiation-Sensitive Mutant M10 Cells That in Parent Mouse Lymphoma L5178Y Cells.
PB95-175915 *03,632*

RADIATION TRANSPORT
Electron transport calculations with biomedical and environmental applications. Final report, December 23, 1992--January 31, 1994.
DE95007065 *03,613*

RADIATIVE HEAT TRANSFER
Structure and Radiation Properties of Pool Fires.
PB94-193802 *02,473*

Investigation of Oil and Gas Well Fires and Flares.
PB94-193976 *03,695*

Estimate of Flame Radiance via a Single Location Measurement in Liquid Pool Flames.
PB94-211596 *02,476*

Measurement of Radiative Feedback to the Fuel Surface of a Pool Fire.
PB94-211604 *02,477*

Computing Radiative Heat Transfer Occurring in a Zone Fire Model.
PB96-102306 *01,399*

Flame Heights and Heat Release Rates of 1991 Kuwait Oil Field Fires.
PB96-119342 *01,404*

RADIATIVE TRANSFER
Opacity Project and the Practical Utilization of Atomic Data.
PB94-212214 *00,059*

Stars, Atmospheres, Radiative Transfer.
PB96-119474 *00,095*

Relationship between Radiative and Magnetic Fluxes for Three Active Solar-Type Dwarfs.
PB96-119540 *00,097*

RADIATORS
Screened-Room Measurements on the NIST Spherical-Dipole Standard Radiator.
PB96-113568 *01,926*

RADICALS
Solvent Effects in the Reactions of Peroxyl Radicals with Organic Reductants. Evidence for Proton Transfer Mediated Electron Transfer.
PB95-107157 *00,873*

Temperature Dependence of the Rate Constants for Reaction of Dihalide and Azide Radicals with Inorganic Reductants.
PB95-162756 *00,964*

RADIO EMISSION
Optically Linked Three-Loop Antenna System for Determining the Radiation Characteristics of an Electrically Small Source.
PB95-161915 *02,005*

Search for Radio Emission from the 'Non-Magnetic' Chemically Peculiar Stars.
PB96-102249 *00,087*

RADIO EQUIPMENT
Rechargeable Batteries for Personal/Portable.
PB96-164231 *02,459*

RADIO FREQUENCIES
Low-Frequency Model for Radio-Frequency Absorbers.
PB95-261939 *04,424*

RADIO FREQUENCY DETECTION
Quantum-Limited Cooling and Detection of Radio-Frequency Oscillations by Laser-Cooled Ions.
PB96-112073 *04,039*

RADIO FREQUENCY DISCHARGE
Gaseous Electronics Conference Radio-Frequency Reference Cell: A Defined Parallel-Plate Radio-Frequency System for Experimental and Theoretical Studies of Plasma-Processing Discharges.
PB94-172327 *04,404*

Plasma Chemistry in Disilane Discharges.
PB94-211075 *02,514*

Kinetic-Energy Distributions of Ions Sampled from Argon Plasmas in a Parallel-Plate, Radio-Frequency Reference Call.
PB95-161964 *03,935*

Electrical Characterization of Radio-Frequency Discharges in the Gaseous Electronics Conference Reference Call.
PB95-164612 *01,905*

Effect of Electrode Material on Measured Ion Energy Distributions in Radio-Frequency Discharges.
PB96-102850 *04,026*

Evidence for Inelastic Processes for N(+)3 and N(+)4 from Ion Energy Distributions in He/N2 Radio Frequency Glow Discharges.
PB96-146683 *04,059*

RADIO FREQUENCY DISCHARGES
Influence of Electrode Material on Measured Ion Kinetic-Energy Distributions in Radio-Frequency Discharges.
PB96-123179 *01,935*

Optical and Mass Spectrometric Investigations of Ions and Neutral Species in SF6 Radio-Frequency Discharges.
PB97-111918 *01,985*

RADIO SOURCES (ASTRONOMY)
Rotational Modulation and Flares on RS Canum Venaticorum and BY Draconis Stars. XVIII. Coordinated VLA, ROSAT, and IUE Observations of RS CVn Binaries.
PB96-102322 *00,089*

Developments in Stellar Coronae.
PB96-176706 *00,107*

RADIO STARS
Class of Radio-Emitting Magnetic B Stars and a Wind-Fed Magnetosphere Model.
PB94-213451 *00,067*

Radio Emission from Chemically Peculiar Stars.
PB94-213469 *00,068*

RADIO WAVES
Ionospheric Radio Propagation.
AD-A286 619/2 *01,459*

RADIOACTIVE AIR POLLUTANTS
Maximum Permissible Amounts of Radioisotopes in the Human Body and Maximum Permissible Concentrations in Air and Water.
AD-A280 281/7 *03,609*

Maximum Permissible Body Burdens and Maximum Permissible Concentrations of Radionuclides in Air and in Water for Occupational Exposure.
AD-A280 282/5 *03,610*

RADIOACTIVE WASTE DISPOSAL
Expansion of Cementitious Materials Exposed to Sulfate Solutions.
PB94-185782 *02,577*

4SIGHT Manual: A Computer Program for Modelling Degradation of Underground Low Level Waste Concrete Vaults.
PB95-231593 *03,726*

Long-Term Performance of Engineered Concrete Barriers.
PB95-260816 *03,727*

RADIOACTIVE WASTE STORAGE
Information Retrieval Using Key Words and a Structured Review.
PB95-161121 *03,724*

RADIOACTIVE WATER POLLUTANTS
Maximum Permissible Amounts of Radioisotopes in the Human Body and Maximum Permissible Concentrations in Air and Water.
AD-A280 281/7 *03,609*

Maximum Permissible Body Burdens and Maximum Permissible Concentrations of Radionuclides in Air and in Water for Occupational Exposure.
AD-A280 282/5 *03,610*

RADIOACTIVITY
Summary of the Proceedings of the Workshop on Standard Phantoms for In-vivo Radioactivity Measurement.
PB94-212933 *03,622*

Dose Mapping of Radioactive Hot Particles Using Radiochromic Film.
PB95-162954 *03,714*

NBS/NIST Peltier-Effect Microcalorimeter: A Four-Decade Review.
PB96-102769 *01,064*

RADIOASSAY
Intercomparison Study of (237)Np Determination in Artificial Urine Samples.
PB96-102645 *03,633*

RADIOASSAYS
Radioassays of Yttrium-90 Used in Nuclear Medicine.
PB97-110100 *03,522*

RADIOCHROMIC DOSIMETERS
Electron and Proton Dosimetry with Custom-Developed Radiochromic Dye Films.
PB95-151106 *03,713*

Alcohol Solutions of Triphenyl-Tetrazolium Chloride as High-Dose Radiochromic Dosimeters.
PB96-135249 *03,716*

RADIOCHROMIC DYES
Electron and Proton Dosimetry with Custom-Developed Radiochromic Dye Films.
PB95-151106 *03,713*

RADIOCHROMIC FILMS
Use of a Radiochromic Detector for the Determination of Stereotactic Radiosurgery Dose Characteristics.
PB94-185642 *03,514*

Radiochromic Solid-State Polymerization Reaction.
PB95-180683 *01,271*

Effect of Formulation Changes on the Response to Ionizing Radiation of Radiochromic Dye Films.
PB97-119028 *04,171*

Novel Radiochromic Films for Clinical Dosimetry.
PB97-119259 *03,641*

Calibration and Performance of GafChromic DM-100 Radiochromic Dosemeters.
PB97-119291 *00,703*

RADIOCHROMIC FOILS
Measurement of Radial Dose Distributions Around Small Beta Particle Emitters Using High Resolution Radiochromic Foil Dosimetry.
PB95-164604 *03,518*

RADIOFREQUENCIES
Electrical Sensors for Monitoring rf Plasma Sheaths.
PB95-162962 *04,412*

RADIOFREQUENCY CHARGES
Ion Kinetic-Energy Distributions and Balmer-alpha (Halpha) Excitation in Ar-H2 Radio-Frequency Discharges.
PB96-102959 *04,029*

RADIOFREQUENCY DISCHARGES
Time-Resolved Balmer-Alpha Emission from Fast Hydrogen Atoms in Low Pressure, Radio-Frequency Discharges in Hydrogen.
PB96-102942 *04,028*

RADIOFREQUENCY OSCILLATORS
Relationship of AM to PM Noise in Selected RF Oscillators.
PB95-169009 *02,262*

RADIOIMMUNOASSAY
Supercritical Fluid Extraction-Immunoassay for the Rapid Screening of Cocaine in Hair.
PB96-167168 *00,637*

RADIOISOTOPES
Maximum Permissible Amounts of Radioisotopes in the Human Body and Maximum Permissible Concentrations in Air and Water.
AD-A280 281/7 *03,609*

Maximum Permissible Body Burdens and Maximum Permissible Concentrations of Radionuclides in Air and in Water for Occupational Exposure.
AD-A280 282/5 *03,610*

System for Intercomparing Standard Solutions of Beta-Particle Emitting Radionuclides.
PB96-159637 *03,707*

New and Revised Half-Life Measurement Results.
PB96-160346 *00,695*

RADIOLOGY
Report of the International Commission on Radiological Units and Measurements (ICRU), 1956.
AD-A279 120/0 *03,513*

Noninvasive High-Voltage Measurement in Mammography by Crystal Diffraction Spectroscopy.
PB95-153417 *00,160*

RADIOLYSIS
Radiation Chemistry of Cyanine Dyes: Oxidation and Reduction of Merocyanine 540.
PB94-211661 *00,818*

Site of One-Electron Reduction of Ni(II) Porphyrins. Formation of Ni(I) Porphyrin of Ni(II) Porphyrin pi-Radical Anion.
PB95-107066 *00,866*

Solvent Effects in the Reactions of Peroxyl Radicals with Organic Reductants. Evidence for Proton Transfer Mediated Electron Transfer.
PB95-107157 *00,873*

Unusual Spin-Trap Chemistry for the Reaction of Hydroxyl Radical with the Carcinogen N-Nitrosodimethylamine.
PB95-151643 *00,692*

Temperature Dependence of the Rate Constants for Reaction of Dihalide and Azide Radicals with Inorganic Reductants.
PB95-162756 *00,964*

Iodine Atoms and Iodomethane Radical Cations: Their Formation in the Pulse Radiolysis of Iodomethane in Organic Solvents, Their Complexes, and Their Reactivity with Organic Reductants.
PB95-162764 *00,965*

Radiation-Chemical Reaction of 2,3,5-Triphenyl-Tetrazolium Chloride in Liquid and Solid State.
PB96-146733 *01,124*

One-Electron Oxidation of Metalloporphycenes as Studied by Radiolytic Methods.
PB97-111967 *01,179*

RADIOMETERS

Dual Frequency mm-Wave Radiometer Antenna for Airborne Remote Sensing of Atmosphere and Ocean.
PB95-180378 *02,006*

Thermal Modeling of Absolute Cryogenic Radiometers.
PB95-181236 *04,316*

Relative Accuracy of Isolated and Unisolated Noise Comparison Radiometers.
PB96-111851 *01,924*

Dual-Frequency Millimeter-Wave Radiometer Antenna for Airborne Remote Sensing of Atmosphere and Ocean.
PB96-112289 *02,009*

Radiometer Equation for Noise Comparison Radiometers.
PB96-140363 *02,195*

Single-Port Technique for Adaptor Efficiency Evaluation.
PB96-176441 *02,088*

Organization and Implementation of Calibration in the EOS Project. Part 1.
PB96-179437 *04,841*

National Measurement System for Radiometry, Photometry, and Pyrometry Base Upon Absolute Detectors.
PB97-108559 *04,382*

Calibration in the Earth Observing System (EOS) Project. Part 2. Implementation.
PB97-112213 *04,842*

Comparison of Filter Radiometer Spectral Responsivity with the NIST Spectral-Irradiance and Illuminance Scales.
PB97-113161 *04,162*

RADIOMETRIC CORRECTION

Radiometric Model of the Transmission Cell-Reciprocal Nephelometer.
PB95-150132 *00,124*

RADIOMETRIC PHYSICS DIVISION

Optical Metrology and More. Programs and Services of the Radiometric Physics Division, Physics Laboratory.
PB94-191707 *04,228*

RADIOMETRY

NIST Response to the Fifth CORM Report on the Pressing Problems and Projected Needs in Optical Radiation Measurements.
PB94-188240 *04,227*

Optical Metrology and More. Programs and Services of the Radiometric Physics Division, Physics Laboratory.
PB94-191707 *04,228*

Development and Calibration of UV/VUV Radiometric Sources.
PB94-199098 *04,229*

Overview of Radiometric Program of the NIST Thermal Imaging Laboratory.
PB94-199163 *04,230*

Theoretical Analysis of the Coherence-Induced Spectral Shift Experiments of Kandpal, Vaishya, and Joshi.
PB94-219383 *00,561*

National Institute of Standards and Technology High-Accuracy Cryogenic Radiometer.
PB96-179585 *04,378*

Mode-Locked Lasers for High-Accuracy Radiometry.
PB96-204201 *04,134*

Results of a NIST/VNIIOFI Comparison of Spectral-Radiance Measurements.
PB97-113021 *04,159*

Realization of a Scale of Absolute Spectral Response Using the NIST High Accuracy Cryogenic Radiometer.
PB97-118640 *04,397*

RADIONUCLIDE MIGRATION

Modeling Radon Transport in Multistory Residential Buildings.
PB95-162087 *00,256*

RADIONUCLIDES

Liquid-Scintillation Counting Techniques for the Standardization of Radionuclides Used in Therapy.
PB97-110084 *03,709*

RADIOPHARMACEUTICALS

Experimental Validation of Radiopharmaceutical Absorbed Dose to Mineralized Bone Tissue.
PB94-199668 *03,617*

Radiation Doses.
PB94-199676 *03,618*

USCEA/NIST Measurement Assurance Programs for the Radiopharmaceutical and Nuclear Power Industries.
PB97-110514 *03,721*

RADIOSONDES

Low-Temperature Performance of Radiosonde Electric Hygrometer Elements.
AD-A295 319/8 *00,121*

RADIOSURGERY

Use of a Radiochromic Detector for the Determination of Stereotactic Radiosurgery Dose Characteristics.
PB94-185642 *03,514*

RADIOTHERAPY

Standard Reference Materials (SRM's) for Measuring Genetic Damage.
PB94-198827 *03,516*

New Method for Shielding Electron Beams Used for Head and Neck Cancer Treatment.
PB94-211430 *03,621*

Scattered Fractions of Dose from 18 and 25 MV X-ray Radiotherapy Linear Accelerators.
PB96-186101 *04,120*

RADIOTHERAPY DOSAGE

Use of a Radiochromic Detector for the Determination of Stereotactic Radiosurgery Dose Characteristics.
PB94-185642 *03,514*

RADIUM

Protection Against Radiations from Radium, Cobalt-60, and Cesium-137.
AD-A279 261/2 *03,607*

RADIUM IONS

Fine Structure of Negative Ions of Alkaline-Earth-Metal Atoms.
PB94-211182 *03,837*

RADON

Measurement and Determination of Radon Source Potential: A Literature Review.
PB94-165602 *02,576*

Systematics of Alpha-Particle Energy Spectra and Lineal Energy (Y) Spectra for Radon Daughters.
PB94-185139 *03,615*

Microdosimetry and Cellular Radiation Effects of Radon Progency in Human Bronchial Airways.
PB95-152344 *03,625*

Modeling Radon Transport in Multistory Residential Buildings.
PB95-162087 *00,256*

Computer Simulations of Airflow and Radon Transport in Four Large Buildings.
PB95-220422 *02,557*

Radon in the Lung.
PB97-110035 *03,638*

RADON 222

International Radon-in-Air Measurement Intercomparison Using a New Transfer Standard.
PB96-159751 *03,708*

RAIL TRANSPORTATION

New Concepts for Fire Protection of Passenger Rail Transportation Vehicles.
PB95-162046 *04,850*

New Concepts for Fire Protection of Passenger Rail Transportation Vehicles. (NIST Reprint).
PB95-180774 *04,863*

RAILROAD CARS

Ultrasonic Measurement of Residual Stress in Cast Steel Railroad Wheels.
PB95-169199 *04,852*

RAILROAD PASSENGER SERVICE

Concepts for Fire Protection of Passenger Rail Transportation Vehicles: Past, Present, and Future.
PB96-102868 *04,853*

RAILROAD TRACKS

Noncontact Ultrasonic Inspection of Train Rails for Stress.
PB95-162673 *04,851*

RAILROAD TRAINS

Residual Stress in Induction-Heated Railroad Wheels: Ultrasonic and Saw Cut Measurements. Report No. 28.
PB96-106992 *04,854*

Dynamometer-Induced Residual Stress in Railroad Wheels: Ultrasonic and Saw Cut Measurements. Report No. 30.
PB96-183199 *04,857*

RAILROAD TRUCKS

Ultrasonic Measurement of Residual Stress in Railroad Wheel Rims.
PB95-140430 *04,849*

Safety Assessment of Railroad Wheels by Residual Stress Measurements.
PB96-141114 *04,855*

Safety Assessment of Railroad Wheels Through Roll-by Detection of Tread Cracks.
PB96-141254 *04,856*

RAMAN EFFECT

Frequency Shifting of Pulsed Narrow-Band Laser Light in a Multipass Raman Cell.
PB95-203352 *04,321*

RAMAN SPECTRA

Octacalcium Phosphate. 3. Infrared and Raman Vibrational Spectra.
PB94-172244 *00,756*

Simultaneous Forward-Backward Raman Scattering Studies of D2 Broadened by D2, He, and Ar.
PB95-162459 *00,961*

Evolution of X-ray Resonance Raman Scattering into X-ray Fluorescence from the Excitation of Xenon Near the L3 Edge.
PB96-102751 *04,025*

RAMAN SPECTROSCOPY

Measurement of the Self Broadening of the H2Q(0-5) Raman Transitions from 295 to 1000 K.
PB95-108627 *00,884*

Lineshape Analysis of the Raman Spectrum of Diamond Films Grown by Hot-Filament and Microwave-Plasma Chemical-Vapor Deposition.
PB95-162392 *03,016*

Studies of Defects in Diamond Films and Particles by Raman and Luminescence Spectroscopies.
PB95-162400 *03,017*

Q Branch Lineshape Functions for CARS Thermometry.
PB96-160643 *01,132*

Development of the NIST Transient Pressure and Temperature Calibration Facility.
PB96-160833 *00,626*

Structural Analysis of Heparin by Raman Spectroscopy.
PB96-167226 *03,480*

Neutron and Raman Spectroscopies of 134 and 134a Hydrofluorocarbons Encaged in Na-X Zeolite.
PB96-186168 *03,001*

RAMSAUER EFFECT

Semiclassical Explanation of the Generalized Ramsauer-Townsend Minima in Electron-Atom Scattering.
PB95-153532 *03,925*

RANDOM WALK

Book Review: Aspects and Applications of the Random Walk.
PB96-123534 *04,215*

RANDOM WALKS

Self-Avoiding-Walk Contacts and Random-Walk Self-Intersections in Variable Dimensionality.
PB96-102231 *01,276*

RAPID RESPONSE MANUFACTURING

Visualization Applications for Manufacturing: A State-of-the-Art Survey. Final Report.
PB94-194552 *02,816*

RARE EARTH COMPOUNDS

Crystal Chemistry and Phase Equilibrium Studies of the BaO-R2O3-CuO Systems. 2. X-Ray Characterization and Standard Patterns of BaR2CuO4, R=Lanthanides.
PB95-151734 *04,582*

Crystal Chemistry and Phase Equilibria Studies of the BaO(BaCO3)-R2O3-CuO Systems. 4. Crystal Chemistry and Subsolidus Phase Relationship Studies of the CuO-Rich Region of the Ternary Diagrams, R=Lanthanides.
PB95-151759 *00,936*

RARE EARTH ELEMENTS

Rare-Earth Isotopes as Tracers of Particulate Emissions: An Urban Scale Test.
PB94-161635 *02,535*

Magnetic Rare Earth Artificial Metallic Superlattices.
PB95-162293 *04,611*

Neutron Spectroscopic Comparison of beta-Phase Rare Earth Hydrides.
PB96-160742 *01,134*

RARE GAS SOLIDS

Soft-X-ray-Emission Spectra of Solid Kr and Xe.
PB96-157920 *04,070*

RARE GASES

Charge Transfer and Collision-Induced Dissociation Reactions of CF(2+) and CF2(2+) with the Rare Gases at a Laboratory Collision Energy of 49 eV.
PB94-185584 *00,775*

Collision-Induced Neutral Loss Reactions of Molecular Dications.
PB94-185808 *00,780*

Dipole Moments in Rare Gas Interactions.
PB94-212982 *00,844*

Optimization of Inert Gas Atomization.
PB95-107405 *01,377*

RATE CONSTANTS

Rate Constants for the Decay and Reactions of the Lowest Electronically Excited Singlet State of Molecular Oxygen in Solution. An Expanded and Revised Compilation.
PB96-145826 *01,106*

RATINGS

Development and Validation of Multicriteria Ratings: A Case Study.
PB95-126025 *00,004*

RAYLEIGH SCATTERING

Rayleigh Scattering Limits for Low-Level Bidirectional Reflectance Distribution Function Measurements.
PB95-180030 *04,307*

RAYLEIGH WAVES

Interaction of Rayleigh Waves with a Rib Attached to a Plate.
PB94-199023 *04,184*

RCS (REVISION CONTROL SYSTEM)
Guide to Configuration Management and the Revision Control System for Testbed Users.
PB94-150919 *01,678*

RE134
Viscosity of the Saturated Liquid Phase of Six Halogenated Compounds and Three Mixtures.
PB95-162368 *00,960*

RE245
Viscosity of the Saturated Liquid Phase of Six Halogenated Compounds and Three Mixtures.
PB95-162368 *00,960*

REACTION KINETICS
Tables of Chemical Kinetics Homogeneous Reactions.
AD-A280 293/2 *00,715*

Thermal Decomposition of Hydroxy- and Methoxy-Substituted Anisoles.
PB94-173036 *00,767*

Octacalcium Phosphate Carboxylates IV. Kinetics of Formation and Solubility of Octacalcium Phosphate Succinate.
PB94-185600 *00,776*

Temperature Dependence of the Rate Constants for Reaction of Inorganic Radicals with Organic Reductants.
PB94-198280 *00,783*

Oxidation of 10-Methylacridan, a Synthetic Analogue of NADH and Deprotonation of Its Cation Radical. Convergent Application of Laser Flash Photolysis and Direct and Redox Catalyzed Electrochemistry to the Kinetics of Deprotonation of the Cation Radical.
PB94-198371 *00,785*

Gas Phase Reactions Relevant to Chemical Vapor Deposition: Optical Diagnostics.
PB94-199338 *03,116*

Gas Phase Reactions Relevant to Chemical Vapor Deposition: Numerical Modeling.
PB94-199346 *03,117*

Rate Constants for Hydrogem Atom Attack on Some Chlorinated Benzenes at High Temperature.
PB94-200581 *00,810*

Reaction Rate Determinations of Vinyl Radical Reactions with Vinyl, Methyl, and Hydrogen Atoms.
PB94-211398 *00,815*

Radiation Chemistry of Cyanine Dyes: Oxidation and Reduction of Merocyanine 540.
PB94-211661 *00,818*

International Conference on Chemical Kinetics (2nd). Held in Gaithersburg, Maryland on July 24-27, 1989.
PB94-211901 *00,822*

Kinetics of the Reaction of CCl3-Br-2 and the Thermochemistry of CCl3 Radical and Cation.
PB94-212115 *00,824*

Kinetics of the Self-Reaction of Hydroxymethylperoxyl Radicals.
PB94-212164 *00,827*

Temperature Dependence of the Rate Constants for Reactions of the Sulfate Radical, SO4-, with Anions.
PB94-212172 *00,828*

Electron Transfer Reaction Rates and Equilibria of the Carbonate and Sulfate Radical Anions.
PB94-212180 *00,829*

Reaction of NO with Superoxide.
PB94-212198 *00,830*

Temperature Dependence of the Rate Constants for Reactions of the Carbonate Radical with Organic and Inorganic Reductants.
PB94-212206 *00,831*

Reaction of Nitric Oxide with Organic Peroxyl Radicals.
PB95-141107 *00,910*

Influence of Natural and Synthetic Inhibitors on the Crystallization of Calcium Oxalate Hydrates.
PB95-150967 *03,560*

Homogeneous Gas Phase Decyclization of Tetralin and Benzocyclobutene.
PB95-151049 *00,928*

Mechanism and Rate Constants for the Reactions of Hydrogen Atoms with Isobutene at High Temperatures.
PB95-151064 *00,929*

Modeling Ceramic Sub-Micron Particle Formation from the Vapor Using Detailed Chemical Kinetics: Comparison with In-situ Laser Diagnostics.
PB95-151965 *00,671*

Gas Phase Reactivity Study of OH Radicals with 1,1-Dichloroethene and cis-1,1-Dichloroethene and Trans-1,2-Dichloroethene over the Temperature Range 240-400 K.
PB95-152146 *00,939*

Rate Constants for the Gas Phase Reactions of the OH Radical with CF3CF2CHCl2 (HCFC-225ca) and CF2ClCF2CHClF (HCFC-225cb).
PB95-152153 *00,940*

Temperature Dependence of the Rate Constants for Reaction of Dihalide and Azide Radicals with Inorganic Reductants.
PB95-162756 *00,964*

Iodine Atoms and Iodomethane Radical Cations: Their Formation in the Pulse Radiolysis of Iodomethane in Organic Solvents, Their Complexes, and Their Reactivity with Organic Reductants.
PB95-162764 *00,965*

Shock Tube Techniques in Chemical Kinetics.
PB95-163465 *00,968*

Hydrogen Atom Attack on Perchloroethylene.
PB95-163473 *00,969*

Interaction of Chlorhexidine Digluconate with and Adsorption of Chlorhexidine on Hydroxyapatite.
PB95-175907 *03,566*

Kinetics of the Reaction C2H + O2 from 193 to 350 K Using Laser Flash Kinetic Infrared Absorption Spectroscopy.
PB95-203055 *01,043*

Thermochemical and Chemical Kinetic Data for Fluorinated Hydrocarbons.
PB95-260618 *01,056*

Kinetics and Dynamics of Vibrationally State Resolved Ion-Molecule Reactions: (14)N2(+)(v=1 and 2) and (15)N2(+)(v=0,1 and 2) with (14)N2.
PB96-102348 *04,023*

Radiation-Chemical Reaction of 2,3,5-Triphenyl-Tetrazolium Chloride in Liquid and Solid State.
PB96-146733 *01,124*

REACTION-TO-FIRE TESTS
Effects of Specimen Edge Conditions on Heat Release Rate.
PB95-152864 *00,375*

REACTIVITY
Reactivity of Product Gases Generated in Idealized Enclosure Fire Environments.
PB95-161790 *01,386*

REACTOR PHYSICS
Neutron Standard Cross Sections in Reactor Physics: Need and Status.
PB94-199510 *03,813*

REACTOR SAFETY
Proceedings of the Digital Systems Reliability and Nuclear Safety Workshop. Held in Rockville, Maryland on September 13-14, 1993.
NUREG/CP-0136 *03,728*

REACTORS
MCNP Model of the National Bureau of Standards Reactor (NBSR) Core.
PB96-138599 *03,733*

REAL TIME
Real-Time Implementation of a Differential Range Finder.
PB95-108650 *01,839*

Through-the-Arc Sensing for Measuring Gas Metal Arc Weld Quality in Real Time.
PB95-164463 *02,908*

REAL TIME CONTROL
Operator Experience with a Hierarchical Real-Time Control System (RCS).
PB96-195516 *03,751*

REAL-TIME CONTROL SYSTEMS
Integration of Servo Control into a Large-Scale Control System Design: An Example from Coal Mining.
PB94-203429 *03,696*

Continuous Mining Machine Control Using the Real-Time Control System.
PB94-203528 *03,700*

REAL TIME OPERATION
Ground Vehicle Control at NIST: From Teleoperation to Autonomy.
N94-34037/9 *03,758*

Utc Dissemination to the Real-Time User.
N19960042622 *01,521*

Continuous Mining Machine Control Using the Real-Time Control System.
PB94-203528 *03,700*

Real-Time Vision for Autonomous and Teleoperated Control of Unmanned Vehicles.
PB94-211885 *03,701*

Real-Time Vision for Unmanned Vehicles.
PB94-211893 *03,702*

Hierarchical Real-Time Control System for Use with Coal Mining Automation.
PB94-212065 *03,698*

Knowledge-Based Approach for Automating a Design Method for Concurrent and Real-Time Systems.
PB97-112502 *01,780*

REAL TIME OPERATIONS
Through-the-Arc Sensing for Real-Time Measurement of Gas Metal Arc Weld Quality.
PB95-162871 *02,863*

Outline of a Multiple Dimensional Reference Model Architecture and a Knowledge Engineering Methodology for Intelligent Systems Control.
PB95-220414 *03,703*

REAL TIME SYSTEMS
Toward a Reference Model Architecture for Real-Time Intelligent Control Systems (ARTICS).
PB94-172046 *02,932*

Reference Model Architecture for Intelligent Systems Design.
PB95-143137 *01,789*

RECEIVERS
Integrated Optical Polarization-Discriminating Receiver in Glass.
PB97-113179 *02,206*

RECEIVING TUBES
Tabulation of Data on Receiving Tubes. Handbook 68.
AD-A285 495/8 *02,111*

RECEPTOR PROTEINS
Escherichis coli Cyclic AMP Receptor Protein Mutants Provide Evidence for Ligand Contacts Important in Activation.
PB96-201017 *03,592*

RECHARGEABLE BATTERIES
Rechargeable Batteries for Personal/Portable.
PB96-164231 *02,459*

RECOIL LIMITS
Laser Cooling and the Recoil Limit.
PB97-111280 *04,391*

RECOMBINATION REACTIONS
Fluctuation Dominated Recombination Kinetics with Traps.
PB95-107264 *00,875*

RECONSTRUCTION
Dental Applications of Ceramics.
PB96-122940 *00,177*

RECORDING HEADS
dc Magnetic Force Microscopy Imaging of Thin-Film Recording Head.
PB95-176061 *04,665*

Comparison of Magnetic Fields of Thin-Film Heads and Their Corresponding Bit Patterns Using Magnetic Force Microscopy.
PB95-180907 *03,763*

RECORDS MANAGEMENT
Electronic Access: Blueprint for the National Archives and Records Administration.
PB95-219218 *02,731*

RECTILINEAR DIAMETER
Experimental Method for Obtaining Critical Densities of Binary Mixtures: Application to Ethane + n-Butane.
PB95-151148 *00,930*

RED GIANT STARS
Four Years of Monitoring alpha Orionis with the VLA: Where Have All the Flares Gone.
PB94-185212 *00,048*

RED SHIFT
Redshifts in Stellar Transition Regions.
PB96-123310 *00,104*

REDUCED CONDUCTIVITY TENSOR
Characterization of LPE HgCdTe Film by Magnetoresistance.
PB96-157961 *02,197*

REDUCED GRAVITY
Combustion of a Polymer (PMMA) Sphere in Microgravity.
N96-15569/2 *01,354*

Ignition and Subsequent Flame Spread Over a Thin Cellulosic Material.
PB96-160270 *04,836*

REDUCTION (CHEMISTRY)
Site of One-Electron Reduction of Ni(II) Porphyrins. Formation of Ni(I) Porphyrin of Ni(II) Porphyrin pi-Radical Anion.
PB95-107066 *00,866*

Reduction of Dinitrogen to Ammonia in Aqueous Solution Mediated by Colloidal Metals.
PB95-107074 *00,867*

REFERENCE DEPOSITS
Problems Related to the Determination of Mass Densities of Evaporated Reference Deposits.
PB95-163226 *03,941*

REFERENCE IMPEDANCE
Line-Reflect-Match Calibrations with Nonideal Microstrip Standards.
PB96-176599 *02,242*

REFERENCE MATERIALS
Journal of Physical and Chemical Reference Data, Volume 22, No. 1, January/February 1993.
PB94-160975 *00,729*

Journal of Physical and Chemical Reference Data, Volume 22, No. 2, March/April 1993.
PB94-162211 *00,733*

Journal of Physical and Chemical Reference Data, Volume 22, No. 3, May/June 1993.
PB94-162260 *00,738*

Journal of Physical and Chemical Reference Data, Volume 22, No. 4, July/August 1993.
PB94-162310 *00,743*

Journal of Physical and Chemical Reference Data, Volume 22, No. 5, September/October 1993.
PB94-162336 *00,745*

Journal of Physical and Chemical Reference Data, Volume 22, No. 6, November/December 1993.
PB94-168556 *00,749*

Quantitative Phase Abundance Analysis of Three Cement Clinker Reference Materials by Scanning Electron Microscopy.
PB94-173051 *00,333*

Quantitative X-Ray Powder Diffraction Methods for Clinker and Cement.
PB95-143079 *01,317*

Reference Materials by Isotope Dilution Mass Spectrometry.
PB95-153383 *00,592*

Reference Data for the Thermophysical Properties of Cryogenic Fluids.
PB95-168688 *03,263*

NIST Standard Reference Materials (Trade Name) Catalog 1995-1996.
PB95-232518 *00,508*

Journal of Physical and Chemical Reference Data, Volume 24, No. 1, January/February 1995.
PB96-145560 *01,101*

Journal of Physical and Chemical Reference Data, Volume 24, No. 2, March/April 1995.
PB96-145818 *01,105*

Journal of Physical and Chemical Reference Data, Volume 24, No. 4, July/August 1995.
PB96-145883 *01,112*

Journal of Physical and Chemical Reference Data, Volume 24, No. 5, September/October 1995.
PB96-145925 *01,116*

Journal of Physical and Chemical Reference Data, Volume 24, No. 6, November/December 1995.
PB96-145966 *01,120*

Interlaboratory Studies on the Analysis of Hair for Drugs of Abuse: Results from the Fourth Exercise.
PB97-111322 *03,510*

REFERENCE MODELS

Next Generation Computer Resources: Reference Model for Project Support Environments (Version 2.0).
PB94-143401 *01,677*

REFERENCE STANDARDS

Standard Samples and Reference Standards Issued by the National Bureau of Standards.
AD-A279 240/6 *02,613*

Coaxial Reference Standard for Microwave Power.
PB94-193786 *01,880*

How to Verify Reference Materials.
PB95-151486 *03,497*

Development of a Gas Standard Reference Material Containing Eighteen Volatile Organic Compounds.
PB95-162277 *02,545*

Standards for Atmospheric Measurements.
PB95-163622 *02,547*

Standard Reference Materials for the Determination of Trace Organic Constituents in Environmental Samples.
PB95-164026 *02,522*

Liquid Chromatographic Determination of Polycyclic Aromatic Hydrocarbon Isomers of Molecular Weight 278 and 302 in Environmental Standard Reference Materials.
PB95-164042 *02,523*

Alaska Marine Mammal Tissue Archival Project: Specimen Inventory.
PB95-171344 *02,589*

Determination of Amphetamine and Methamphetamine in a Lyophilized Human Urine Reference Material.
PB95-175444 *03,597*

Certification of Morphine and Codeine in a Human Urine Standard Reference Material.
PB95-176160 *03,499*

Hair Analysis for Drugs of Abuse: Evaluation of Analytical Methods, Environmental Issues, and Development of Reference Materials.
PB95-176269 *03,501*

Quantitative Analysis of Selected PCB Congeners in Marine Matrix Reference Materials Using a Novel Cyanobiphenyl Stationary Phase.
PB96-111737 *02,591*

Certification of Polycyclic Aromatic Hydrocarbons in a Marine Sediment Standard Reference Material.
PB96-111778 *02,592*

Considerations in the Design of an Environmental Specimen Bank: Experiences of the National Biomonitoring Specimen Bank Program.
PB96-112370 *02,527*

Long-Term Stability of Bayard-Alpert Gauge Performance: Results Obtained from Repeated Calibrations against the National Institute of Standards and Technology Primary Vacuum Standard.
PB96-123567 *02,676*

Certification of Standard Reference Material (SRM) 1941a, Organics in Marine Sediment.
PB96-123690 *02,593*

NIST Reference Materials to Support Accuracy in Drug Testing.
PB96-123807 *03,505*

Measurement Comparability, Traceability, and Measurement Assurance Programs.
PB97-111850 *02,692*

National Status and Trends Program Specimen Bank: Sampling Protocols, Analytical Methods, Results, and Archive Samples.
PB97-119226 *02,598*

REFERENCE SYSTEMS

Numeric Data Distribution: The Vital Role of Data Exchange in Today's World.
N95-15937/2 *02,622*

REFERENCES (STANDARDS)

Recertification of the Standard Reference Material 1475A, a Linear Polyethylene Resin.
PB94-161932 *02,628*

Standard Reference Materials: Glass Filters as a Standard Reference Material for Spectrophotometry - Selection, Preparation, Certification, and Use of SRM 930 and SRM 1930.
PB94-188844 *00,536*

REFLECTANCE

XUV Characterization Comparison of Mo/Si Multilayer Coatings.
PB95-164000 *04,278*

45 deg/0 deg Reflectance Factors of Pressed Polytetrafluoroethylene (PTFE) Powder.
PB95-260758 *04,328*

REFLECTANCE FACTORS

45 deg/0 deg Reflectance Factors of Pressed Polytetrafluoroethylene (PTFE) Powder.
PB95-260758 *04,328*

REFLECTION SPECTRA

Intermediate Coupling in L2-L3 Core Excitons of MgO, Al2O3, and SiO2.
PB96-158043 *04,079*

REFLECTIVE COATINGS

Interfaces in Mo/Si Multilayers.
PB96-160668 *02,423*

REFLECTIVITY

Near Critical Fluid Interfaces: A Comparison of Theory and Experiment.
PB95-140166 *00,901*

In-situ Neutron Reflectivity of MBE Grown and Chemically Processed Surfaces and Interfaces.
PB96-146634 *02,416*

REFLECTOMETERS

Improved Reflectometry Facility at the National Institute of Standards and Technology.
PB96-160338 *04,087*

Soft X-ray Reflectometry Program at the National Institute of Standards and Technology.
PB96-160395 *04,368*

REFLECTOMETRY

Upgraded Facility for Multilayer Mirror Characterization at NIST.
PB96-160387 *04,367*

REFRACTIVE INDEX

Physical Properties of Some Purified Aliphatic Hydrocarbons.
AD-A297 265/1 *00,657*

Normal-Incidence Complex-Index Refractometry.
PB94-213097 *04,241*

Formulation of the Refractive Index of Water and Steam.
PB95-140133 *00,900*

Guidelines for Refractive Index Measurements of Asbestos.
PB95-151189 *02,543*

Calculated Fiber Attenuation: A General Method Yielding Stationary Values.
PB95-175501 *04,298*

Determination of the Complex Refractive Index of Individual Quantum Wells from Distributed Reflectance.
PB95-175642 *02,176*

REFRACTIVE INDEXES

Verification of Revised Water Vapour Correction to the Index of Refraction of Air.
PB96-161666 *02,680*

REFRACTIVITY

Normal-Incidence Complex-Index Refractometry.
PB94-213097 *04,241*

Refractive Indices of Fluids Related to Alternative Refrigerants.
PB94-219375 *03,260*

REFRACTOMETERS

New Refractometer by Combining a Variable Length Vacuum Cell and a Double-Pass Michelson Interferometer.
PB97-111926 *01,986*

REFRACTORY METALS

Wavelength Dependence of Normal Spectral Emissivity of High-Temperature Metals at Their Melting Point.
PB94-200011 *03,398*

Measurement of the Heat of Fusion of Tungsten by a Microsecond-Resolution Transient Technique.
PB94-216686 *03,400*

REFRIGERANT COMPRESSORS

Design Equations and Scaling Laws for Linear Compressors with Flexure Springs.
PB95-168902 *02,948*

REFRIGERANT MIXTURES

Model for Calculating Virial Coefficients of Natural Gas Hydrocarbons with Impurities.
PB96-156047 *04,064*

Design of a High-Pressure Ebulliometer, with Vapor-Liquid Equilibrium Results for the Systems CHF2Cl + CF3-CH3 and CF3-CH2F + CH2F2.
PB97-113229 *04,163*

REFRIGERANTS

Properties of Working Fluids for Thermoacoustic Refrigerators.
AD-A297 420/2 *04,864*

Dielectric Studies of Fluids with Reentrant Resonators. Appendix B.
DE93019683 *03,244*

Thermophysical Properties of HFC-143a and HFC-152a. Quarterly Report, 1 July 1993--30 September 1993.
DE94004236 *03,245*

Development of Measurement Capabilities for the Thermophysical Properties of Energy-Related Fluids. Annual Report, December 1, 1990--November 30, 1991.
DE94004399 *02,470*

Development of Measurement Capabilities for the Thermophysical Properties of Energy-Related Fluids. Annual Report, December 1, 1993--November 30, 1994.
DE94017738 *03,246*

Thermophysical properties of HCFC alternatives. Quarterly report, 1 July 1994--30 September 1994.
DE95002261 *03,247*

Lean flammability limit as a fundamental refrigerant property. Phase 1, Interim technical report, 1 October 1994--31 March 1995.
DE95011238 *03,248*

Thermophysical properties of HCFC alternatives. Quarterly report, October 1--December 31, 1995.
DE96010433 *03,249*

Thermophysical properties of HCFC alternatives. Quarterly report, April 1--June 30, 1995.
DE96010579 *03,250*

Evaluation of GSA Maintenance Practices of Large Centrifugal Chillers and Review of GSA Refrigerant Management Practices.
PB94-143344 *02,502*

Simultaneous Visual and Calorimetric Measurements of R11, R123, and R123/Alkylbenzene Nucleate Flow Boiling.
PB94-172426 *03,251*

Thermodynamic Properties of CHF2-O-CHF2,Bis(difluoromethyl) Ether.
PB94-199569 *00,798*

Role of Refrigerant Mixtures as Alternatives to CFCs.
PB94-199775 *03,252*

Role of R22 in Refrigerating and Air Conditioning Equipment.
PB94-199783 *03,253*

Measurements of the Viscosities of Saturated and Compressed Fluid 1-chloro-1,2,2,2-tetrafluoroethane (R124) and Pentafluoroethane (R125) at Temperatures between 120 and 420 K.
PB94-199791 *03,254*

Simplified Cycle Simulation Model for the Performance Rating of Refrigerants and Refrigerant Mixtures.
PB94-199890 *03,255*

Equation of State Formulation of the Thermodynamic Properties of R134a (1,1,1,2-Tetrafluoroethane).
PB94-212081 *03,256*

Prediction of Viscosity of Refrigerants and Refrigerant Mixtures.
PB94-212099 *03,257*

Prediction of the Thermal Conductivity of Refrigerants and Refrigerant Mixtures.
PB94-212107 *03,258*

Causes of the Apparent Heat Transfer Degradation for Refrigerant Mixtures.
PB94-212701 *03,259*

Study of Heat Pump Performance Using Mixtures of R32/R134a and R32/R125/R134a as 'Drop-In' Working Fluids for R22 with and Without a Liquid-Suction Heat Exchanger.
PB94-218559 *02,503*

Refractive Indices of Fluids Related to Alternative Refrigerants.
PB94-219375 *03,260*

Vapor Pressure of 1,1-dichloro-2,2,2-trifluoroethane (R123).
PB95-126231 *00,899*

Visual Measurement Technique for Analysis of Nucleate Flow Boiling.
PB95-143301 *03,262*

Ebulliometric Measurement of the Vapor Pressure of Difluoromethane.
PB95-151361 *00,931*

Dielectric Studies of Fluids with Reentrant Resonators.
PB95-153730 *00,952*

Criteria for Establishing Accurate Vapor Pressure Curves.
PB95-163812 *00,972*

Ebulliometric Measurement of the Vapor Pressure of 1-Chloro-1,1-Difluoroethane and 1,1-Difluoroethane.
PB95-164489 *00,984*

Reference Data for the Thermophysical Properties of Cryogenic Fluids.
PB95-168688 *03,263*

Thermodynamic Properties of R134a(1,1,1,2-Tetrafluoroethane).
PB95-168704 *00,988*

Measurements of Molar Heat Capacity at Constant Volume (Cv) for 1,1,1,2-Tetrafluoroethane (R134a).
PB95-168878 *03,264*

Vapour Pressure Measurements on 1,1,1,2-Tetrafluoroethane (R134a) from 180 to 350 K.
PB95-168886 *03,265*

Annex 18: An International Study of Refrigerant Properties.
PB95-168936 *03,266*

Development of a Dual-Sinker Densimeter for High-Accuracy Fluid P-V-T Measurements.
PB95-168951 03,267

Measurements of the Vapor Pressures of Difluoromethane, 1-Chloro-1,2,2,2-Tetrafluoroethane, and Pentafluoroethane.
PB95-169272 03,270

Vapor Pressures and Gas-Phase PVT Data for 1-Chloro-1,2,2,2-Tetrafluoroethane (R124).
PB95-175154 03,271

Retention of Halocarbons on a Hexafluoropropylene Epoxide Modified Graphitized Carbon Black. Part 1. Methane-Based Compounds.
PB95-175196 03,272

Measurements of the Viscosities of Saturated and Compressed Liquid 1,1,1,2-Tetrafluoroethane (R134a), 2,2-Dichloro-1,1,1-Trifluoroethane (R123) and 1,1-Dichloro-1-Fluoroethane (R141b).
PB95-175386 03,273

Coexisting Densities, Vapor Pressures and Critical Densities of Refrigerants R-32 and R-152a, at 300 - 385 K.
PB95-175691 03,274

Predictive Extended Corresponding States Model for Pure and Mixed Refrigerants Including an Equation of State for R134a.
PB95-175717 03,275

Estimating the Virial Coefficients of Small Polar Molecules.
PB95-176236 03,276

Simple Method of Composition Shifting with a Distillation Column for a Heat Pump Employing a Zeotropic Refrigerant Mixture.
PB95-255824 02,603

Interaction Coefficients for 15 Mixtures of Flammable and Non-Flammable Components.
PB96-146626 03,281

Retention of Halocarbons on a Hexafluoropropylene Epoxide-Modified Graphitized Carbon Black. 4. Propane-Based Compounds.
PB96-164033 03,284

REFPROP Refrigerant Properties Database: Capabilities, Limitations, and Future Directions.
PB96-167150 01,149

Status of the Round Robin on the Transport Properties of R134a.
PB96-167218 01,152

Retention of Halocarbons on a Hexafluoropropylene Epoxide-Modified Graphitized Carbon Black. 3. Ethene-Based Compounds.
PB96-167309 03,286

Thermophysical Property Standard Reference Data from NIST.
PB96-167358 01,153

Study to Determine the Existence of an Azeotropic R-22 'Drop-In' Substitute.
PB96-167812 02,568

Viscosity of 1,1,1,2,3,3-Hexafluoropropane and 1,1,1,3,3,3-Hexafluoropropane at Saturated-Liquid Conditions from 262 K to 353 K.
PB96-176680 03,292

Report of the Refrigeration, Air Conditioning and Heat Pumps Technical Options Committee.
PB96-176755 03,293

International Standard Equation of State for the Thermodynamic Properties of Refrigerant 123 (2,2-Dichloro-1,1,1-Trifluoroethane).
PB96-176805 03,294

REFRIGERATING MACHINERY

Evaluation of GSA Maintenance Practices of Large Centrifugal Chillers and Review of GSA Refrigerant Management Practices.
PB94-143344 02,502

Role of R22 in Refrigerating and Air Conditioning Equipment.
PB94-199783 03,253

Effect of Inclination on the Performance of a Compact Brazed Plate Condenser and Evaporator.
PB96-136973 02,756

REFRIGERATION SYSTEMS

Design and Construction of a Liquid Hydrogen Temperature Refrigeration System.
AD-A286 618/4 02,619

Helium Refrigeration and Liquefaction Using a Liquid Hydrogen Refrigerator for Precooling.
AD-A286 683/8 02,749

Properties of Working Fluids for Thermoacoustic Refrigerators.
AD-A297 420/2 04,864

REFRIGERATORS

Resistance Thermometers with Fast Response for Use in Rapidly Oscillating Gas Flows.
PB95-107298 03,261

Electronic Microrefrigerator Based on a Normal-Insulator-Superconductor Tunnel Junction.
PB96-102827 04,718

Factors Affecting the Energy Consumption of Two Refrigerator-Freezers.
PB97-112312 00,311

REFUELING SYSTEM

Upgrade and Modernization Projects at the NBSR.
PB96-161872 03,737

REFUSE DERIVED FUELS

Sulfur Dioxide Capture in the Combustion of Mixtures of Lime, Refuse-Derived Fuel, and Coal.
PB94-155587 02,534

REGENERATORS

Graded and Nongraded Regenerator Performance.
PB95-169090 02,753

REGIONAL DEVELOPMENT

Aid for Smaller Businesses.
PB94-212461 00,492

REGISTRIES

SC4 Short Names Registry.
PB97-122410 02,799

REGULATIONS

National Center for Standards and Certification Information: Service and Programs.
N95-15938/0 02,717

Uniform Laws and Regulations in the Areas of Legal Metrology and Motor Fuel Quality, 1994 as Adopted by the 79th National Conference on Weights and Measures 1994.
PB95-174470 02,909

International Challenges in Defining the Public and Private Interest in Standards.
PB96-160361 00,498

REINFORCED CONCRETE

Corrosion Resistant Epoxy-Coated Reinforcing Steel.
PB94-185618 01,307

Strengthening Methodology for Lightly Reinforced Concrete Frames-II. Recommended Calculation Techniques for the Design of Infill Walls.
PB94-187648 00,426

Seismic Strengthening of Reinforced Concrete Frame Buildings.
PB95-108841 00,430

Enhancements to Program IDARC: Modeling Inelastic Behavior of Welded Connections in Steel Moment-Resisting Frames.
PB95-231601 00,452

Strengthening Methodology for Lightly Reinforced Concrete Frames: Recommended Design Guidelines for Strengthening with Infill Walls.
PB95-260725 00,454

Prediction of Potential Concrete Strength at Later Ages.
PB96-112180 01,324

REINFORCEMENT (STRUCTURAL)

Evaluation and Retrofit Standards for Existing Federally Owned and Leased Buildings.
PB95-150918 00,434

REINFORCEMENT (STRUCTURES)

Strengthening Methodology for Lightly Reinforced Concrete Frames-II. Recommended Calculation Techniques for the Design of Infill Walls.
PB94-187648 00,426

Seismic Strengthening of Reinforced Concrete Frame Buildings.
PB95-108841 00,430

Jacket Thickness Requirements for Seismic Retrofitting of Circular Bridge Columns.
PB95-163267 01,336

Seismic Safety of Federal Buildings. Initial Program: How Much Will It Cost.
PB95-182291 00,447

Strengthening Methodology for Lightly Reinforced Concrete Frames: Recommended Design Guidelines for Strengthening with Infill Walls.
PB95-260725 00,454

Strengthening Methodology for Lightly Reinforced Concrete Frames.
PB96-158050 00,466

REINFORCING FIBERS

Micro-Mechanical Aspects of Asperity-Controlled Friction in Fiber-Toughened Ceramic Composites.
PB94-199536 03,136

Elastic Properties of Uniaxial-Fiber Reinforced Composites: General Features.
PB94-200649 03,140

REINFORCING STEELS

Corrosion Resistant Epoxy-Coated Reinforcing Steel.
PB94-185618 01,307

Degradation of Powder Epoxy Coated Panels Immersed in a Saturated Calcium Hydroxide Solution Containing Sodium Chloride.
PB96-101050 01,344

REJUVENATION

Volume Recovery in Epoxy Glasses Subjected to Torsional Deformations: The Question of Rejuvenation.
PB95-140018 03,382

Torsional Relaxation and Volume Response during Physical Aging in Epoxy Glasses Subjected to Large Torsional Deformations.
PB95-140026 03,383

Using Torsional Dilatometry to Measure the Effects of Deformations on Physical Aging.
PB95-140901 03,384

RELATIVE HUMIDITY

Temperature and Relative Humidity Dependence of Radiochromic Film Dosimeter Response to Gamma and Electron Radiation.
PB96-135298 03,718

Parametric Study of Wall Moisture Contents Using a Revised Variable Indoor Relative Humidity Version of the 'Moist' Transient Heat and Moisture Transfer Model.
PB97-122535 00,419

RELAXATION (MECHANICS)

Operational Mode and Gas Species Effects on Rotational Drag in Pneumatic Dead Weight Pressure Gages.
PB95-140182 00,903

RELIABILITY

Numeric Data Distribution: The Vital Role of Data Exchange in Today's World.
N95-15937/2 02,622

Performance and Reliability of NIST 10-V Josephson Arrays.
PB96-148051 02,419

High Temperature Structural Reliability of Silicon Nitride.
PB97-110456 03,104

RELIABILITY ANALYSIS

Measurements of Properties of Materials in Electronic Packaging.
PB96-200837 01,973

REMANENT POLARIZATION

Hysteresis Measurements of Remanent Polarization and Coercive Field in Polymers.
PB94-199767 04,475

REMINERALIZATION

Remineralization of Root Lesions with Concentrated Calcium and Phosphate Solutions.
PB96-102140 03,567

Polymeric Calcium Phosphate Composites with Remineralization Potential.
PB96-155544 03,575

REMOTE CONSOLES

Concepts of the NIST EXPRESS Server.
PB95-180543 02,781

REMOTE PROCEDURE CALLS

Comparing Remote Procedure Calls: Open Network Computing, Distributed Computing Environment and International Organization for Standardization.
PB95-194205 01,724

REMOTE SENSORS

Activities of NIST (National Inst. Of Standards and Technology).
N94-23605/6 04,222

Dual-Frequency Millimeter-Wave Radiometer Antenna for Airborne Remote Sensing of Atmosphere and Ocean.
PB96-112289 02,009

REMOVAL

Computer Simulations of Binder Removal from 2-D and 3-D Model Particulate Bodies.
PB97-121339 00,418

RENOVATING

Corrosion Resistance of Materials for Renovation of the United States Botanic Garden Conservatory.
PB94-154390 00,032

REPARAMETRIZATION INVARIANCE

Electrostatic Rigidity of Polyelectrolytes from Reparametrization Invariance.
PB96-180062 04,113

REPLICATING

Replicate Measurements for Data Quality and Environmental Modeling.
PB94-172533 02,515

REPLICATION

DnaJ, DnaK, and GrpE Heat Shock Proteins are Required in 'ori'P1 DNA Replication Solely at the RepA Monomerization Step.
PB97-119382 03,557

REPORTING

Guidelines for Reporting Results of Computational Experiments. Report of the Ad hoc Committee.
PB94-212347 03,427

REPRESENTATIONS

Representing Designs with Logic Formulations of Spatial Relations.
PB97-111561 02,792

REQUIREMENTS

Validation Testing System Requirements. National PDES Testbed Report Series.
PB94-163482 02,771

CALS-Contractor Integrated Technical Information Service (CITIS), Functional Requirements.
PB94-962600 03,663

National Voluntary Laboratory Accreditation Program: POSIX. Portable Operating System Interface.
PB95-189478 02,661

CALS-Contractor Integrated Technical Information Service (CITIS), Functional Requirements.
PB95-962600 03,672

Standards Setting in the European Union: Standards Organization and Officials in EU Standards Activities.
PB96-115019 02,919

Defining Environment Integration Requirements.
PB96-131545 02,733

Copyright and Information Services in the Context of the National Research and Education Network.
PB96-160536 02,736

Addressing U.S. Government Security Requirements for OSI.
PB96-160577 *01,611*

Rechargeable Batteries for Personal/Portable.
PB96-164231 *02,459*

RESEARCH

Journal of Research of the National Institute of Standards and Technology, November-December 1993. Volume 98, Number 6.
PB94-140555 *04,223*

Thermodynamic Properties of the Group IIA Elements.
PB94-160983 *00,730*

Spectroscopy and Structure of the Lithium Hydride Diatomic Molecules and Ions.
PB94-160991 *00,731*

Quantum Yields for the Photosensitized Formation of the Lowest Electronically Excited Singlet State of Molecular Oxygen in Solution.
PB94-161007 *00,732*

Wavelengths and Energy Level Classifications for the Spectra of Sulfur (S I through S XVI).
PB94-162229 *00,734*

Thermodynamic Properties of Alkenes (Mono-Olefins Larger Than C4).
PB94-162237 *00,735*

Thermodynamic Behavior of the CO2-H2O System from 400 to 1000 K, up to 100 MPa and 30% Mole Fraction of CO2.
PB94-162245 *00,736*

Thermodynamics of Enzyme-Catalyzed Reactions: Part 1. Oxidoreductases.
PB94-162252 *00,737*

Estimation of the Heat Capacities of Organic Liquids as a Function of Temperature Using Group Additivity. I. Hydrocarbon Compounds.
PB94-162278 *00,739*

Estimation of the Heat Capacities of Organic Liquids as a Function of Temperature Using Group Additivity. II. Compounds of Carbon, Hydrogen, Halogens, Nitrogen, Oxygen, and Sulfur.
PB94-162286 *00,740*

Thermodynamic and Thermophysical Properties of Organic Nitrogen Compounds. Part II. 1- and 2-Butanamine, 2-Methyl-1-Propanamine, 2-Methyl-2-Propanamine, Pyrrole, 1-, 2-, and 3-Methylpyrrole, Pyridine, 2-, 3-, and 4-Methylpyridine, Pyrrolidine, Piperidine, Indole, Quinoline, Isoquinoline, Acridine, Carbazole, Phenanthridine, 1- and 2-Naphthalenamine, and 9-Methylcarbazole.
PB94-162294 *00,741*

International Equations for the Saturation Properties of Ordinary Water Substance. Revised According to the International Temperature Scale of 1990. Addendum to Journal of Physical and Chemical Reference Data 16, 893 (1987).
PB94-162302 *00,742*

Estimation of the Thermodynamic Properties of C-H-N-O-S-Halogen Compounds at 298.15 K.
PB94-162328 *00,744*

Compilation of Energy Levels and Wavelengths for the Spectrum of Singly-Ionized Oxygen (O II).
PB94-162344 *00,746*

Energy Levels of Germanium, Ge I through Ge XXXII.
PB94-162351 *00,747*

Spectral Data and Grotrian Diagrams for Highly Ionized Chromium, Cr V through Cr XXIV.
PB94-162369 *00,748*

Thermodynamic Properties of Synthetic Sapphire (alpha-Al2O3), Standard Reference Material 720 and the Effect of Temperature-Scale Differences on Thermodynamic Properties.
PB94-168564 *00,750*

Thermodynamic Properties of Gaseous Silicon Monotelluride and the Bond Dissociation Enthalpy D(sub m)(SiTe) at T approaches 0.
PB94-168572 *00,751*

Disilicides of Tungsten, Molybdenum, Tantalum, Titanium, Cobalt, and Nickel, and Platinum Monosilicide: A Survey of Their Thermodynamic Properties.
PB94-168580 *00,752*

Evaluated Bimolecular Ion-Molecule Gas Phase Kinetics of Positive Ions for Use in Modeling Planetary Atmospheres, Cometary Comae, and Interstellar Clouds.
PB94-168598 *00,753*

Atomic Weights of the Elements 1991.
PB94-168606 *00,754*

Growing Significance of CIB.
PB95-126306 *00,314*

Building and Fire Research Laboratory Publications, 1993.
PB95-143202 *00,369*

Rationale and Preliminary Plan for Federal Research for Construction and Building.
PB95-154704 *00,322*

Building and Fire Research Laboratory Publications, 1994.
PB95-226684 *00,398*

RESEARCH AND DEVELOPMENT

CSTL Technical Activities 1991.
PB94-160769 *00,728*

Industry and Government-Laboratory Cooperative R and D: An Idea Whose Time Has Come.
PB94-172939 *02,970*

Preliminary Functional Specifications of a Prototype Electronic Research Notebook for NIST.
PB94-207750 *00,012*

Program Requirements to Advance the Technology of Custom Footwear Manufacturing.
PB95-147906 *02,883*

CSTL Technical Activities, 1993.
PB95-160602 *00,953*

Encouraging Environmentally-Aware Inventions.
PB95-161394 *02,521*

Journal of Research of the National Institute of Standards and Technology, September/October 1994. Volume 99, Number 5.
PB95-169371 *04,293*

Materials Science and Engineering Laboratory Annual Report, 1994. NAS-NRC Assessment Panel, April 6-7, 1995.
PB95-196697 *02,976*

CSTL Technical Activities, 1994.
PB95-242319 *00,608*

Proceedings of the 1995 Workshop on Fire Detector Research. Held on February 6-7, 1995.
PB95-270062 *02,611*

Joint DoD/NIST Workshop on International Manufacturing Systems Research and Development. Held in Rockville, Maryland on November 3-5, 1992. Proceedings.
PB96-109491 *02,931*

Journal of Research of the National Institute of Standards and Technology, July/August 1995. Volume 100, Number 4. Special Issue: The Gaseous Electronics Conference Radio-Frequency Reference Cell.
PB96-113311 *02,386*

Journal of Research of the National Institute of Standards and Technology, November/December 1994. Volume 99, Number 6.
PB96-113535 *04,336*

Journal of Research of the National Institute of Standards and Technology, September/October 1995. Volume 100, Number 5.
PB96-117767 *01,927*

Journal of Research of the National Institute of Standards and Technology, March/April 1995. Volume 100, Number 2.
PB96-126180 *04,349*

National Planning for Construction and Building R and D.
PB96-137104 *00,324*

High-Temperature Furnace for In situ Small-Angle Neutron Scattering during Ceramic Processing.
PB96-148127 *03,743*

Journal of Research of the National Institute of Standards and Technology, November/December 1995. Volume 100, Number 6.
PB96-159215 *01,949*

Electronics and Electrical Engineering Laboratory 1995 Technical Accomplishments: Advancing Metrology for Electrotechnology to Support the U.S. Economy.
PB96-164520 *01,959*

Innovation in the Japanese Construction Industry: A 1995 Appraisal.
PB96-177373 *00,225*

CSTL Technical Activities, 1995.
PB96-214630 *00,647*

Materials Science and Engineering Laboratory Annual Report, 1995. Technical Activities.
PB96-214754 *03,009*

Summary of Federal Construction and Building R and D in 1994.
PB97-114250 *00,234*

Fire Safety Engineering in the Pursuit of Performance-Based Codes: Collected Papers.
PB97-114482 *00,235*

Science, Technology, and Competitiveness: Retrospective on a Symposium in Celebration of NIST's 90th Anniversary and the 25th Anniversary of the Gaithersburg Laboratories, November 14-15, 1991.
PB97-121610 *02,696*

RESEARCH COMMITTEE ON TRIBOLOGY

Tribology Education: Present Status and Future Challenges.
PB94-212362 *02,965*

RESEARCH FACILITIES

NIST-NRL Free-Electron Laser Facility.
PB94-212511 *04,237*

Automated Manufacturing Research Facility 1994 Annual Report.
PB95-209854 *00,015*

RESEARCH LABORATORIES

Publications 1995: NIST Building and Fire Research Laboratory.
PB96-183074 *00,226*

RESEARCH MANAGEMENT

Project Summaries 1994: NIST Building and Fire Research Laboratory.
PB94-207495 *00,343*

Survey of Recent Cementitious Materials Research in Western Europe.
PB94-218583 *00,353*

Project Summaries 1995: NIST Building and Fire Research Laboratory.
PB95-270047 *00,400*

Electronics and Electrical Engineering Laboratory Technical Publication Announcements Covering Laboratory Programs, April to June 1995 with 1995 EEEL Events Calendar.
PB96-137187 *01,941*

Benefits and Costs of Research: Two Case Studies in Building Technology.
PB96-202221 *00,230*

Benefits and Costs of Research: A Case Study of the Fire Safety Evaluation System.
PB96-202288 *00,232*

RESEARCH PROGRAMS

NIST Lighting and HVAC Interaction Test Facility.
PB95-151007 *00,251*

Glimpse of Materials Research in China: A Report from an Interagency Study Team on Materials Visiting China from June 19, 1995 to June 30, 1995.
PB96-112677 *02,978*

Electronics Packaging Materials Research at NIST.
PB96-122692 *02,405*

Internationalization of Fire Safety Engineering Research and Strategy.
PB96-156153 *00,220*

NIST Program for Investigating Error Reporting Capabilities of Optical Disk Drives.
PB96-160627 *01,635*

Optoelectronics at NIST.
PB96-200860 *02,202*

Optoelectronics and Optomechanics Manufacturing: An ATP Focused Program Development. Workshop Proceedings. Held in Gaithersburg, Maryland on February 15, 1995.
PB97-104186 *02,204*

RESEARCH PROJECTS

Ceramics Technical Activities, 1993 (NAS-NRC Assessment Panel April 21-22, 1994).
PB94-162591 *03,031*

Lighting Research and Theory Can Create Business Prospects.
PB95-151791 *00,253*

Publication and Presentation Abstracts, 1993. (Published by Paffenbarger Research Center and Center of Excellence for Materials Science Research).
PB95-153052 *03,562*

Structural Ceramics Database. Topical Report, June 1989-May 1991.
PB95-203758 *03,060*

Reactor Radiation Technical Activities, 1994. NAS-NRC Assessment Panel, April 6-7, 1995.
PB95-209888 *03,732*

Journal of Research of the National Institute of Standards and Technology, May/June 1995. Volume 100, Number 3.
PB95-261897 *02,670*

Electronics and Electrical Engineering Laboratory Technical Progress Bulletin Covering Laboratory Programs, April to June 1995 with 1995 EEEL Events Calendar.
PB96-106455 *01,923*

Publications and Presentation Abstracts, 1995. (Published by Paffenbarger Research Center and Center of Excellence for Materials Science Research).
PB96-119250 *03,568*

Metallurgy Technical Activities 1994 (NAS-NRC Assessment Panel, April 6-7, 1995).
PB96-136981 *02,981*

Electronics and Electrical Engineering Laboratory Technical Progress Bulletin Covering Laboratory Programs, July to September 1995 with 1996 EEEL Events Calendar.
PB96-147905 *01,942*

Publication and Presentation Abstracts, 1995.
PB96-164082 *03,576*

Publication and Presentation Abstracts, 1994.
PB96-176623 *03,577*

Electronics and Electrical Engineering Laboratory Technical Publication Announcements Covering Laboratory Programs, July to September 1995 with 1996 EEEL Events Calendar.
PB96-183066 *01,965*

Materials Reliability. Technical Activities, 1995.
PB96-183082 *02,999*

Electronics and Electrical Engineering Laboratory Technical Progress Bulletin Covering Laboratory Programs, October to December 1995 with 1996 EEEL Events Calendar.
PB96-183116 *01,966*

Electronics and Electrical Engineering Laboratory Technical Progress Bulletin Covering Laboratory Programs, January to March 1996, with 1996 EEEL Events Calendar.
PB96-191390 *01,969*

Reactor Radiation Technical Activities, 1995.
PB96-193644 *03,741*

Ceramics Technical Activities, 1995.
PB96-193677 *03,087*

Metallurgy. Technical Activities, 1995.
PB96-195284 *03,003*

Electronics and Electrical Engineering Laboratory Technical Publication Announcements Covering Laboratory Programs, October to December 1995, with 1996 EEEL Events Calendar.
PB96-202346 01,978

Electronics and Electrical Engineering Laboratory Technical Publication Announcements Covering Laboratory Programs, January to March 1996, with 1996 EEEL Events Calendar.
PB96-214622 01,981

Workshop Highlights.
PB97-109227 04,811

Electronics and Electrical Engineering Laboratory Technical Progress Bulletin Covering Laboratory Programs, April to June 1996 with 1996-1998 EEEL Events Calendar.
PB97-113880 01,994

Publication and Presentation Abstracts, 1996.
PB97-122238 03,585

RESIDENTIAL BUILDING

Carbon Monoxide Dispersion in Residential Buildings: Literature Review and Technical Analysis.
PB97-114227 02,571

RESIDENTIAL BUILDING FIRES

EXITT: A Simulation Model of Occupant Decisions and Actions in Residential Fires.
PB94-213261 00,351

RESIDENTIAL BUILDINGS

Mathematical Modeling of Human Egress from Fires in Residential Buildings.
PB94-193778 00,337

Studies Assess Performance of Residential Detectors.
PB94-199262 00,290

EXITT: A Simulation Model of Occupant Decisions and Actions in Residential Fires.
PB94-213261 00,351

Indoor Air Quality Impacts of Residential HVAC Systems, Phase 1 Report: Computer Simulation Plan.
PB95-135596 00,249

Modeling Radon Transport in Multistory Residential Buildings.
PB95-162087 00,256

Performance of HUD-Affiliated Properties during the January 17, 1994 Northridge Earthquake.
PB95-174488 00,443

Application of a Multizone Airflow and Contaminant Dispersal Model to Indoor Air Quality Control in Residential Buildings.
PB95-180238 02,555

Santa Ana Fire Department Experiment at 1315 South Bristol, July 14, 1994.
PB95-188868 00,389

Measurements of Indoor Pollutant Emissions from EPA Phase II Wood Stoves.
PB95-198735 02,556

National Construction Sector Goals: Industry Strategies for Implementation.
PB95-269817 00,204

Santa Ana Fire Department Experiment at 1315 South Bristol, July 14, 1994. (Reprint).
PB96-102934 00,207

Surging the Upside-Down House: Looking into Upsetting Reference Voltages.
PB96-112313 02,385

Effectiveness of a Heat Recovery Ventilator, an Outdoor Air Intake Damper and an Electrostatic Particulate Filter at Controlling Indoor Air Quality in Residential Buildings.
PB96-146642 02,564

Santa Ana Fire Department Experiments at South Bristol Street.
PB96-154810 00,305

Sensitivity Analysis for Mathematical Modeling of Fires in Residential Buildings.
PB96-154968 00,215

Protecting Your Family from Fire.
PB96-156187 00,307

Multizone Modeling of Three Residential Indoor Air Quality Control Options.
PB96-165782 02,567

Surging the Upside-Down House: Measurements and Modeling Results.
PB96-180138 02,243

Distributions of Measurement Error for Three-Axis Magnetic Field Meters during Measurements Near Appliances.
PB96-180153 02,110

Full-Scale Room Fire Experiments Conducted at the University of Maryland.
PB97-116081 00,236

RESIDUAL GAS

Measurement of Very-Low Partial Pressures.
PB95-180998 02,659

Process Monitoring with Residual Gas Analyzers (RGAs): Limiting Factors.
PB95-181004 02,660

RESIDUAL GAS ANALYZERS

Process Monitoring with Residual Gas Analyzers (RGAs): Limiting Factors.
PB95-181004 02,660

RESIDUAL STRENGTH

Fracture Behavior of Large-Scale Thin-Sheet Aluminum Alloy.
N95-19494/0 03,311

RESIDUAL STRESS

Influence of Tempering Method on Residual Stress in Dental Porcelain.
PB94-172012 00,138

Evaluation of Fracture Toughness and Residual Stress in Dental Porcelain by Indentation-Microfracture Method.
PB95-125613 00,154

Evaluation of Fracture Toughness and Residual Stress in Dental Porcelain by Indentation-Microfracture Method.
PB95-152831 00,159

Residual Stresses in Aluminum-Mullite (alpha-Alumina) Composites.
PB95-152880 03,155

Ultrasonic Measurement of Residual Stress in Cast Steel Railroad Wheels.
PB95-169199 04,852

Determination of the Residual Stresses Near the Ends of Skip Welds Using Neutron Diffraction and X-ray Diffraction Procedures.
PB95-253589 02,868

Ultrasonic Methods.
PB96-190327 02,707

RESIN TRANSFER MOLDING

Effect of Heterogeneous Porous Media on Mold Filling in Resin Transfer Molding.
PB95-108676 03,197

Comparison of the Unidirectional and Radial In-Plane Flow of Fluids Through Woven Composite Reinforcements.
PB95-162004 02,698

Interaction between Micro and Macroscopic Flow in RTM Preforms.
PB95-162012 03,159

RESISTANCE

Electrical Characterization of Narrow Gap n-Type Bulk HgCdTe Single Crystals by Variable-Magnetic-Field Hall Measurements and Reduced-Conductivity-Tensor Analyses.
PB96-164199 01,146

RESISTANCE BRIDGES

Leakage Current Detection in Cryogenic Current Comparator Bridges.
PB94-172228 02,024

RESISTANCE MEASUREMENTS

Resistance Measurements from 10 M Omega to 1 T Omega at NIST.
PB97-119168 02,290

RESISTANCE STANDARD

Quantum Hall Effect-Based Resistance Standard: Capabilities and Implementation.
PB96-180096 04,114

Quantum Hall Effect-Based Resistance Standard (Quantum Hall Res).
PB96-200944 04,127

RESISTANCE STANDARDS

New International Representations of the Volt and Ohm Effective January 1, 1990.
PB95-150777 01,890

Design Challenges in a Commercial Quantum Hall Effect-Based Resistance Standard.
PB95-171419 02,263

RESISTANCE THERMOMETERS

Assessment of Uncertainties of Calibration of Resistance Thermometers at the National Institute of Standards and Technology.
PB94-142478 02,624

RESISTIVE DIVIDERS

Transient Errors in a Precision Resistive Divider.
PB97-111512 01,983

RESISTIVITY MAPPING

High-Spatial-Resolution Resistivity Mapping Applied to Mercury Cadmium Telluride.
PB94-212917 02,131

RESISTORS

Journal of Research of the National Institute of Standards and Technology. May/June 1994. Volume 99, Number 3.
PB94-219326 02,643

Sources of Uncertainty in a DVM-Based Measurement System for a Quantized Hall Resistance Standard.
PB94-219334 01,884

Pressure Dependencies of Standard Resistors.
PB95-153516 02,257

Bonding Wires to Quantized Hall Resistors.
PB96-102637 01,921

Automated Resistance Measurements at NIST.
PB96-119326 02,274

Constant Temperature and Humidity Chamber for Standard Resistors.
PB96-122494 02,275

Resistors.
PB97-111876 02,284

Observation of Hot-Electron Shot Noise in a Metallic Resistor.
PB97-112007 01,988

Automated Guarded Bridge for Calibration of Multimegohm Standard Resistors.
PB97-119150 02,289

Resistance Measurements from 10 M Omega to 1 T Omega at NIST.
PB97-119168 02,290

RESOI

Electron and Hole Trapping in Irradiated SIMOX, ZMR and BESOI Buried Oxides.
PB96-160320 01,956

RESOLUTION FUNCTIONS

Instrumental Smearing Effects in Radially Symmetric Small-Angle Neutron Scattering by Numerical and Analytical Methods.
PB96-160429 02,984

RESONANCE

Resonances in Two-Dimensional Array Oscillator Circuits.
PB96-102082 02,066

RESONANCE FLUORESCENCE

Heterodyne Measurement of the Fluorescence Spectrum of Optical Molasses.
PB95-108411 03,873

Measurements of Fluorescence from Cold Atoms: Localization in Three-Dimensional Standing Waves.
PB95-163879 03,943

Interference in the Resonance Fluorescence of Two Trapped Atoms.
PB95-168514 03,948

Resonance Fluorescence with Squeezed-Light Excitation.
PB95-203469 04,322

RESONANCE IONIZATION MASS SPECTROSCOPY

Atom-counting standards and Doppler-free resonance ionization mass spectroscopy. (Progress report).
DE94018562 00,723

Improvement of Ultrasensitive Techniques Isotopic Biasing in the RIS Process Ionization Efficiencies and Selectivities.
DE94018563 00,522

I: Improvement of Resonance Ionization Spectroscopy (RIS) Techniques; II: Atomic Data for RIS; III: Standards for Ultratrace Analysis. Progress Report.
DE94018565 00,523

National Institute of Standards and Technology Resonance Ionization Spectroscopy/Resonance Ionization Mass Spectroscopy Data Service.
PB94-172897 03,793

Comparative Strategies for Correction of Interferences in Isotope Dilution Mass Spectrometric Determination of Vanadium.
PB94-185261 00,531

Laser Ablation of Thin Films as a Free Atom Source for Pulsed RIMS.
PB94-198710 00,540

RESONANCE IONIZATION SPECTROSCOPY

National Institute of Standards and Technology Resonance Ionization Spectroscopy/Resonance Ionization Mass Spectroscopy Data Service.
PB94-172897 03,793

RESONANCE LINES

Observation of Pd-Like Resonance Lines Through Pt(32+) and Zn-Like Resonance Lines of Er(38+) and Hf(42+).
PB95-150637 03,896

RESONANT FREQUENCY

Elastic Constants of Isotropic Cylinders Using Resonant Ultrasound.
PB94-211919 04,497

RESONANT TUNNELING

Single-Atom Point Source for Electrons: Field-Emission Resonance Tunneling in Scanning Tunneling Microscopy.
PB95-125860 00,893

RESONAT FREQUENCY

Ultrasonic-Resonance Spectroscopy of Bulk and Layered Solids.
PB96-141338 04,759

RESONATORS

Tunable High Temperature Superconductor Microstrip Resonators.
PB95-168423 02,048

Characterization of a Tunable Thin Film Microwave YBa2Cu3O7-x/SrTiO3 Coplanar Capacitor.
PB95-175527 02,264

Ferroelectric Thin Film Characterization Using Superconducting Microstrip Resonators.
PB96-102389 02,270

Measurements of Permittivity and the Dielectric Loss Tangent of Low Loss Dielectric Materials with a Dielectric Resonator Operating on the Higher Order Te(sub 0 gamma delta) Modes.
PB96-111869 02,273

New Model of 1/F Noise in Baw Quartz Resonators.
PB96-112248 02,383

RESPONSE TIME (COMPUTERS)

Scalability Test for Parallel Code.
PB96-146758 01,749

RETARDATION

Measurement of the Atomic Na(3P) Lifetime and of Retardation in the Interaction between Two Atoms Bound in a Molecule.
PB97-122360 04,178

RETARDING
Controlled Nucleation in Aerosol Reactors for Supression of Agglomerate Formation.
PB95-151973 *00,672*

RETENTION
Comparison of the Liquid Chromatographic Behavior of Selected Steroid Isomers Using Different Reversed-Phase Materials and Mobile Phase Compositions.
PB95-140976 *00,574*

RETINOIDS
Liquid Chromatographic Method for the Determination of Carotenoids, Retinoids, and Tocopherols in Human Serum and in Food.
PB95-153599 *00,593*

RETROFITTING
How-To Suggestions for Implementing Executive Order 12941 on Seismic Safety of Existing Federal Buildings, A Handbook.
PB96-131552 *00,461*

REVERBERATION
Spatial Correlation Function for Fields in a Reverberation Chamber.
PB96-148077 *04,427*

Rapid Evaluation of Mode-Stirred Chambers Using Impulsive Waveforms.
PB96-210026 *01,979*

REVERBERATION CHAMBERS
Electronic Mode Stirring for Reverberation Chambers.
PB95-180329 *01,908*

TEM/Reverberating Chamber Electromagnetic Radiation Test Facility at Rome Laboratory.
PB96-155023 *03,675*

Band-Limited, White Gaussian Noise Excitation for Reverberation Chambers and Applications to Radiated Susceptibility Testing.
PB96-165410 *01,960*

REVIEWS
Thermal Conductivity of Metals and Alloys at Low Temperatures. A Review of the Literature.
AD-A279 180/4 *03,302*

Shock Tube Techniques in Chemical Kinetics.
PB95-163465 *00,968*

RHENIUM 186
Standardization and Decay Scheme of Rhenium-186.
PB94-200490 *03,830*

RHENIUM 188
Assay of the Eluent from the Alumina-Based Tungsten-188-Rhenium-188 Generator.
PB94-200482 *03,829*

RHEOLOGICAL PROPERTIES
Measurement of Rheological Properties of High Performance Concrete: State of the Art Report.
PB96-202338 *00,414*

RHEOLOGY
Rheology of Fresh Cement Paste.
PB95-163150 *00,378*

Non-Newtonian Flow between Concentric Cylinders Calculated from Thermophysical Properties Obtained from Simulations.
PB96-163761 *04,103*

Structure and Rheology of Hard-Sphere Systems.
PB96-167333 *00,662*

RHODIUM
Preparation and Certification of a Rhodium Standard Reference Material Solution.
PB94-185071 *00,529*

Evidence of Film-Induced Cleavage by Electrodeposited Rhodium.
PB95-162327 *03,191*

RHODIUM-LIKE IONS
Rh I Isoelectronic Sequence Observed from Er(23+) to Pt(33+).
PB95-150652 *03,898*

RHODOPSIN
Retinal-Protein Complexes as Optoelectronic Components.
PB95-150397 *02,146*

RIETVELD METHOD
Mathematical Aspects of Rietveld Refinement.
PB95-108601 *04,526*

Application of ODF to the Rietveld Profile Refinement of Polycrystalline Solid.
PB95-202388 *03,401*

RIETVELD REFINEMENT
Accurate Modeling of Size and Strain Broadening in the Rietveld Refinement: The 'Double-Voigt' Approach.
PB96-200225 *00,664*

RIGID POLYISOCYANURATE FOAM
Effects of Humidity and Elevated Temperature on the Density and Thermal Conductivity of a Rigid Polyisocyanurate Foam Co-Blown with CCl3F and CO2.
PB95-150462 *00,371*

Effects of Humidity and Elevated Temperature on the Density and Thermal Conductivity of a Rigid Polyisocyanurate Foam.
PB95-152021 *00,373*

RING LASERS
Multiwavelength Birefringent-Cavity Mode-Locked Fibre Laser.
PB95-150496 *04,262*

Frequency-Stabilized LNA Laser at 1.083 mum: Application to the Manipulation of Helium 4 Atoms.
PB95-176186 *04,304*

RISK
Least-Cost Energy Decisions for Buildings: Part 2. Uncertainty and Risk Video Training Workbook.
PB94-165982 *00,240*

RISK ANALYSIS
Computer Virus Attacks.
PB95-163655 *01,715*

Earthquake and Fire in Japan: When the Threat Became a Reality.
PB95-175238 *00,201*

RISK ASSESSMENT
Fire Hazard and Risk: Evaluating Alternative Technologies.
PB94-173077 *00,242*

Fire Service and Fire Sciences: A Winning Combination.
PB95-150264 *01,383*

Quantitative Evaluation of Building Fire Safety: New Tools for Assessing Fire and Building Code Provisions.
PB95-164588 *00,199*

New Concepts for Fire Protection of Passenger Rail Transportation Vehicles. (NIST Reprint).
PB95-180774 *04,363*

NIOSH Comments to DOL on Risk Estimates from the Cadmium Cohort Study by L. Stayner, February 7, 1992.
PB95-267779 *03,604*

Concepts for Fire Protection of Passenger Rail Transportation Vehicles: Past, Present, and Future.
PB96-102868 *04,853*

Review of Internatioanl Fire Risk Predictions Methods.
PB96-156195 *00,222*

RMS VOLTAGE
Electro-Optic-Based RMS Voltage Measurement Technique.
PB96-138490 *02,194*

ROAD FOLLOWING
Visual Road Following without 3-D Reconstruction.
PB95-161030 *01,591*

Unified Approach to Camera Fixation and Vision-Based Road Following.
PB95-162244 *01,594*

ROBOT CONTROL
Overview of NASREM: The NASA/NBS Standard Reference Model for Telerobot Control System Architecture.
PB94-194560 *04,831*

Configuration and Performance Evaluation of a Real-Time Robot Control System: A Skeleton Approach.
PB95-163895 *01,598*

Unified Telerobotic Architecture Project (UTAP) Standard Interface Environment (SIE), May 1995.
PB95-242350 *02,938*

ROBOT DYNAMICS
Integrated Mobile Robot System for Testing Vision Algorithms.
PB95-164133 *02,936*

Real-Time Obstacle Avoidance Using Central Flow Divergence and Peripheral Flow.
PB95-198677 *02,937*

ROBOTICS
Toward a Reference Model Architecture for Real-Time Intelligent Control Systems (ARTICS).
PB94-172046 *02,932*

Integration of Servo Control into a Large-Scale Control System Design: An Example from Coal Mining.
PB94-203429 *03,696*

Certainty Grid to Object Boundary Algorithm.
PB94-203510 *01,835*

Continuous Mining Machine Control Using the Real-Time Control System.
PB94-203528 *03,700*

Environment Simulation for a Continuous Mining Machine.
PB94-203536 *03,697*

Publications of the Intelligent Systems Division (Previously Robot Systems Division) Covering the Period January 1971-April 1994.
PB94-217098 *02,935*

Unified Approach to Camera Fixation and Vision-Based Road Following.
PB95-162244 *01,594*

Vehicle-Command Center Communications in a Robotic Vehicle System.
PB95-162723 *03,665*

Robotics Application to Highway Transportation. Volume 2. Literature Search.
PB95-170551 *01,337*

Robotics Application to Highway Transportation. Volume 3. Proposed Research Topics and Cost/Benefit Evaluations by CERF.
PB95-171633 *01,338*

Robotics Application to Highway Transportation. Volume 4. Proposals for Potential Research.
PB95-193173 *01,339*

Unified Telerobotic Architecture Project (UTAP) Standard Interface Environment (SIE), May 1995.
PB95-242350 *02,938*

Study of Potential Applications of Automation and Robotics Technology in Construction, Maintenance and Operation of Highway Systems: A Final Report. Volume 4.
PB95-251641 *01,340*

Study of Potential Applications of Automation and Robotics Technology in Construction, Maintenance and Operation of Highway Systems: A Final Report. Volume 1.
PB95-251682 *01,341*

Study of Potential Applications of Automation and Robotics Technology in Construction, Maintenance and Operation of Highway Systems: A Final Report. Volume 3.
PB95-251690 *01,342*

Study of Potential Applications of Automation and Robotics Technology in Construction, Maintenance and Operation of Highway Systems: A Final Report. Volume 2.
PB95-255865 *01,343*

Scale-Space-Based Visual-Motion-Cue for Autonomous Navigation.
PB96-183173 *02,940*

NIST Construction Automation Program Report No. 2. Proceedings of the NIST Construction Automation Workshop. Held in Gaithersburg, Maryland on March 30-31, 1995.
PB96-202239 *00,413*

ROBOTS
AMRF Composite Fabrication Workstation.
PB94-172681 *02,810*

World Model Registration for Effective Off-Line Programming of Robots.
PB94-173010 *02,933*

Mapping Processes to Processors for Space-Based Robot Systems.
PB95-151510 *04,833*

Visual Road Following without 3-D Reconstruction.
PB95-161030 *01,591*

Reconstruction during Camera Fixation.
PB95-162236 *01,593*

Novel Active-Vision-Based Motion Cues for Local Navigation.
PB96-193727 *02,941*

ROCK MECHANICS
Temperature and Frequency Dependence of Anelasticity in a Nickel Oscillator.
PB96-137732 *03,689*

ROCKET ENGINES
Bibliography of Books and Published Reports on Gas Turbines, Jet Propulsion, and Rocket Power Plants.
AD-A278 138/3 *01,445*

Bibliography of Books and Published Reports on Gas Turbines, Jet Propulsion, and Rocket Power Plants, January 1950 through December 1953.
AD-A278 213/4 *01,446*

ROCKWELL HARDNESS
Microform Calibration Uncertainties of Rockwell Diamond Indenters.
PB96-122114 *03,280*

Metrology Approach to Unifying Rockwell C Hardness Scales.
PB96-155551 *02,957*

Stylus Technique for the Direct Verification of Rockwell Diamond Intenders.
PB96-155569 *02,958*

RODS
Leady Axisymmetric Modes in Infinite Clad Rods. Part 1.
PB95-162905 *04,187*

Analytical Method for Determining Thermal Conductivity from Dynamic Experiments.
PB96-102744 *04,024*

ROOFING
Effects of Adhesive Thickness, Open Time, and Surface Cleanness on the Peel Strength of Adhesive-Bonded Seams of EPDM Rubber Roofing Membrane.
PB95-151338 *00,372*

Characteristics of Adhesive-Bonded Seams Sampled from EPDM Roof Membranes.
PB95-162491 *00,377*

Pulse-Echo Ultrasonic Evaluation of the Integrity of Seams of Single-Ply Roof Membranes.
PB95-163804 *00,381*

Water-Vapor Measurements of Low-Slope Roofing Materials.
PB95-251617 *00,399*

ROOFS
Performance Approach to the Development of Criteria for Low-Sloped Roof Membranes.
PB94-160751 *00,329*

Application of Thermal Analysis Techniques to the Characterization of EPDM Roofing Membrane Materials.
PB95-125845 *00,359*

Use of Thermal Mechanical Analysis to Characterize Ethylene-Propylene-Diene Terpolymer (EPDM) Roofing Membrane Materials.
PB95-125852 *00,360*

Performance of Tape-Bonded Seams of EPDM Membranes: Comparison of the Peel Creep-Rupture Response of Tape-Bonded and Liquid-Adhesive-Bonded Seams.
PB96-183249 *03,012*

Mathematical Analysis of Practices to Control Moisture in the Roof Cavities of Manufactured Houses.
PB97-106843 *00,278*

ROOM FIRES
Verification of a Model of Fire and Smoke Transport.
PB95-108718 *00,357*

ROOMS
Application of Thermodynamic and Detailed Chemical Kinetic Modeling to Understanding Combustion Product Generation in Enclosure Fires.
PB96-135322 *01,413*

ROOT CANAL FILLING MATERIALS
Periapical Tissue Reactions to a Calcium Phosphate Cement in the Teeth of Monkeys.
PB94-212008 *00,149*

ROTARY POWERS
Large Local-Field Corrections in Optical Rotatory Power of Quartz and Selenium.
PB97-122378 *04,400*

ROTATING CYLINDERS
Density Dependence of Fluid Properties and Non-Newtonian Flows: The Weisenberg Effect.
PB96-161898 *01,140*

ROTATION
Operational Mode and Gas Species Effects on Rotational Drag in Pneumatic Dead Weight Pressure Gages.
PB95-140182 *00,903*

State-Resolved Rotational Energy Transfer in Open Shell Collisions: Cl((2)P3/2)+HCl.
PB96-176607 *01,157*

Internal Droplet Circulation Induced by Surface-Driven Rotation.
PB97-119267 *02,500*

ROTATIONAL DRAG
Operational Mode and Gas Species Effects on Rotational Drag in Pneumatic Dead Weight Pressure Gages.
PB95-140182 *00,903*

ROTATIONAL SPECTRA
Rotational Spectrum of Copper Hydride Using Tunable Far Infrared Radiation.
PB94-198637 *00,792*

Rotational Far Infrared Spectrum of (13)CO.
PB95-152187 *00,941*

Laboratory Measurements for the Astrophysical Identification of MgH.
PB95-152195 *00,073*

Rotational Spectroscopy of the CoH Radical in Its Ground (3)Phi State by Far-Infrared Laser Magnetic Resonance: Determination of Molecular Parameters.
PB95-175048 *00,992*

Pure Rotational Spectra of CuH and CuD in Their Ground States Measured by Tunable Far-Infrared Spectroscopy.
PB95-176194 *01,005*

Rotational Spectrum of OH in the v=0-3 Levels of Its Ground State.
PB95-176202 *01,006*

ROTATIONAL STATES
Reanalysis of the (010), (020), (100), and (001) Rotational Levels of (32)S(16)O2.
PB95-125621 *00,887*

ROTOR DYNAMICS
PC-Based Spinning Rotor Gage Controller.
PB95-175832 *02,609*

ROUGHNESS
Evolution of a Turbulent Boundary Layer Induced by a Three-Dimensional Roughness Element.
PB94-212818 *04,200*

ROUTING
RDI-SIM ECMA Inter-Domain Routing Protocol Simulation Tool.
PB94-172301 *01,683*

RPC (REMOTE PROCEDURE CALLS)
Comparing Remote Procedure Calls: Open Network Computing, Distributed Computing Environment and International Organization for Standardization.
PB95-194205 *01,724*

RS CVN STARS
First Results from a Coordinated ROSAT, IUE, and VLA Study of RS CVn Systems.
PB94-213477 *00,069*

RUBIDIUM
High-Resolution Spectroscopy of Laser-Cooled Rubidium in a Vapor-Cell Trap.
PB95-153714 *04,268*

Optical Probing of Cold Trapped Atoms.
PB95-175469 *04,296*

RUBIDIUM 87
Reduction of Light-Assisted Collisional Loss Rate from a Low-Pressure Vapor-Cell Trap.
PB95-202248 *03,971*

RUBIDIUM ATOMS
Temperature of Optical Molasses for Two Different Atomic Angular Momenta.
PB95-126058 *03,881*

RUBIDIUM BARIUM BISMUTHATES
Optical Conductivity of Single Crystals of Ba1-xMxBiO3(M=K, Rb, x=0.04, 0.37).
PB94-185329 *04,447*

RUBIDIUM FREQUENCY STANDARDS
Ultra-High Stability Synthesizer for Diode Laser Pumped Rubidium.
PB94-216066 *01,527*

Diode-Laser Pumped, Rubidium Cell Frequency Standards.
PB95-163218 *01,538*

Improved Rubidium Frequency Standards Using Diode Lasers with AM and FM Noise Control.
PB95-176152 *04,303*

RUBIDIUM-LIKE IONS
Rb-Like Spectra: Pd X to Nd XXIV.
PB95-150645 *03,897*

RUBIDIUM POTASSIUM FULLERIDES
Neutron-Scattering Study of Librations and Intramolecular Phonons in Rb2.6K0.4C60.
PB95-162269 *00,958*

RULERS
Length Metrology of Complimentary Small Plastic Rulers.
PB96-161724 *04,096*

RUN TIME (COMPUTERS)
Faster BKL Monte Carlo Simulations.
PB95-136370 *01,706*

RUSSIAN FEDERATION
Proceedings of the Meeting of the Intergovernmental U.S.-Russian Business Development Committee's Standard Working Group (4th). Held in New York City, New York on March 27-29, 1995 and in Northbrook, Illinois on March 30-31, 1995.
PB95-255881 *00,496*

RUTHENIUM ALLOYS
New Alloys Show Extraordinary Resistance to Fracture and Wear.
PB95-151346 *03,346*

RUTHENIUM OXIDE
Thin-Film Ruthenium Oxide - Iridium Oxide Thermocouples.
PB97-110225 *00,520*

RYDBERG ATOMS
RIS Measurements of the AC Stark Shift.
PB96-158035 *04,078*

RYDBERG STATES
Verification of the Ponderomotive Approximation for the ac Stark Shift in Xe Rydberg Levels.
PB94-185709 *03,801*

New Rydberg States of Aluminum Monofluoride Observed by Resonance-Enhanced Multiphoton Ionization Spectroscopy.
PB94-199544 *00,797*

Resonance Enhanced Multiphoton Ionization Detection of GeF and GeCl Radicals.
PB94-212123 *00,825*

Experimental and Abinitio Studies of Electronic Structures of the CCl3 Radical and Cation.
PB94-212131 *00,826*

Multiphoton Ionization of SiH3 and SiD3 Radicals. 2. Three Photon Resonance-Enhanced Spectra Observed between 460 and 610 nm.
PB94-212487 *00,835*

New Electronic States of NH and ND Observed from 258 to 288 nm by Resonance Enhanced Multiphoton Ionization Spectroscopy.
PB94-212495 *00,836*

Multiphoton Ionization of SiH3 and SiD3 Radicals: Electronic Spectra, Vibrational Analyses of the Ground and Rydberg States, and Ionization Potential.
PB94-212503 *00,837*

Electronic Spectra of CF2Cl and CFCl2 Radicals Observed by Resonance Enhanced Multiphoton Ionization.
PB95-151023 *00,927*

Alignment in Two-Step Pulsed Laser Excitation of Rydberg Levels in Light Atoms: The Example of Sodium.
PB95-202883 *03,993*

Alignment Probing of Rydberg States by Stimulated Emission.
PB96-200316 *04,124*

SACRAMENTO (CALIFORNIA)
Histopathology, Blood Chemistry, and Physiological Status of Normal and Moribund Striped Bass ('Morone saxatilis') Involved in Summer Mortality ('Die-Off') in the Sacramento-San Joaquin Delta of California.
PB94-198157 *00,034*

SAFETY
Software Safety and Program Slicing.
PB95-125894 *01,703*

NIST Workshop on Gas Sensors: Strategies for Future Technologies. Proceedings of a Workshop. Held in Gaithersburg, Maryland on September 8-9, 1993.
PB95-210225 *00,507*

SAFETY ENGINEERING
Some Basics on Who's Who and What's What in Seismic Safety.
PB95-150926 *00,435*

Implementation of Executive Order 12699: Seismic Safety of Federal and Federally Assisted or Regulated New Building Construction.
PB95-151809 *00,436*

Concepts for Fire Protection of Passenger Rail Transportation Vehicles: Past, Present, and Future.
PB96-102868 *04,853*

Fire Safety Engineering Research in the United States.
PB96-151394 *00,213*

Elements of a Framework for Fire Safety Engineering.
PB96-151402 *00,214*

C++ in Safety Critical Systems.
PB96-154588 *01,750*

Internationalization of Fire Safety Engineering Research and Strategy.
PB96-156153 *00,220*

International Organization for Standardization: Current Activities in Fire Safety Engineering.
PB96-159660 *00,223*

SAFETY FACTORS
Predicting the Fire Performance of Buildings: Establishing Appropriate Calculation Methods for Regulatory Applications.
PB96-141239 *00,316*

SAFETY PROGRAMS
Control and Instrumentation: Standards for High-Integrity Software.
PB96-161369 *03,736*

SAGNAC CURRENT SENSOR
Polarization Insensitive 3x3 Sagnac Current Sensor Using Polarizing Spun High-Birefringence Fiber.
PB96-119276 *02,187*

SAGNAC EFFECT
Polarization Dependence of Response Functions in 3x3 Sagnac Optical Fiber Current Sensors.
PB96-122684 *02,189*

SALES
Method of Sale for CNG Paves Way to Greater Public Acceptance.
PB95-168449 *02,489*

SALIVA
Distribution of Fluoride in Saliva and Plaque Fluid After a 0.048 mol/L NaF Rinse.
PB95-151205 *03,561*

SALIVATION
Effects on Whole Saliva of Chewing Gums Containing Calcium Phosphates.
PB95-153169 *03,563*

SAMARIUM CUPRATES
Field Dependence of the Magnetic Ordering of Cu in R2CuO4 (R = Nd, Sm).
PB95-164521 *04,633*

Observation of Noncollinear Magnetic Structure for the Cu Spins in Nd2CuO4-Type Systems.
PB95-164539 *04,634*

SAMPLE CONCENTRATORS
Simple, Inexpensive Apparatus for Sample Concentration.
PB94-199205 *00,546*

SAMPLE PREPARATION
Introduction of a NIST Instrument Sensitivity Standard Reference Material for X-Ray Powder Diffraction.
PB94-200318 *00,807*

SAMPLING
Wideband Sampling Voltmeter.
PB97-113039 *01,990*

Pilot Studies for Improving Sampling Protocols.
PB97-118715 *02,530*

SAN FRANCISCO AIRPORT
Assessment of Site Response Analysis Procedures.
PB95-210928 *00,450*

SAN FRANCISCO BAY
Histopathology, Blood Chemistry, and Physiological Status of Normal and Moribund Striped Bass ('Morone saxatilis') Involved in Summer Mortality ('Die-Off') in the Sacramento-San Joaquin Delta of California.
PB94-198157 *00,034*

SANTA ANA (CALIFORNIA)
Santa Ana Fire Department Experiment at 1315 South Bristol, July 14, 1994.
PB95-188868 *00,389*

Santa Ana Fire Department Experiment at 1315 South Bristol, July 14, 1994. (Reprint).
PB96-102934 *00,207*

SATELLITE ANTENNAS
Development of Near-Field Test Procedures for Communication Satellite Antennas.
PB96-135082 *02,010*

SATELLITE ATMOSPHERES
Laboratory Studies of Low-Temperature Reactions of C2H with C2H2 and Implications for Atmospheric Models of Titan.
PB95-108726 *00,690*

SATELLITE COMMUNICATION
Error Protecting Characteristics of CDMA and Impacts on Speech.
PB96-122452 *01,491*

SATELLITE INSTRUMENTS
Semiconductor Measurement Technology: Improved Characterization and Evaluation Measurements for HgCdTe Detector Materials, Processes, and Devices Used on the GOES and TIROS Satellites.
PB94-188810 *02,122*

SATELLITE ORBITS
Frozen Orbits for Satellites Close to an Earth-Like Planet.
PB96-102165 *04,839*

SATELLITE THEORY
Frozen Orbits for Satellites Close to an Earth-Like Planet.
PB96-102165 *04,839*

SATELLITE TRACKING
Comparison of GPS Broadcast and DMA Precise Ephemerides.
N94-30660/2 *01,523*

SATURATION (CHEMISTRY)
Measurements of the Viscosities of Saturated and Compressed Fluid 1-chloro-1,2,2,2-tetrafluoroethane (R124) and Pentafluoroethane (R125) at Temperatures between 120 and 420 K.
PB94-199791 *03,254*

Measurements of the Viscosities of Saturated and Compressed Liquid 1,1,1,2-Tetrafluoroethane (R134a), 2,2-Dichloro-1,1,1-Trifluoroethane (R123) and 1,1-Dichloro-1-Fluoroethane (R141b).
PB95-175386 *03,273*

SATURATION SPECTROSCOPY
Optically Stabilized Tunable Diode-Laser System for Saturation Spectroscopy.
PB96-102819 *04,717*

SCALAR APPROXIMATION
Vector and Quasi-Vector Solutions for Optical Waveguide Modes Using Efficient Galerkin's Method with Hermite-Gauss Basis Functions.
PB96-141197 *04,357*

SCALE ERROR STANDARDS
Length Metrology of Complimentary Small Plastic Rulers.
PB96-161724 *04,096*

SCALE MODELS
Scaling Compartment Fires: Reduced- and Full-Scale Enclosure Burns.
PB96-175708 *00,224*

SCALES
Comparison of Filter Radiometer Spectral Responsivity with the NIST Spectral-Irradiance and Illuminance Scales.
PB97-113161 *04,162*

SCALING
Simple Scalability Test for MIMD Code.
PB94-193638 *01,688*

SCALING FACTOR
Estimate of the Effect of Scale on Radiative Heat Loss Fraction and Combustion Efficiency.
PB95-150447 *02,486*

SCALING LAWS
Design Equations and Scaling Laws for Linear Compressors with Flexure Springs.
PB95-168902 *02,948*

Critical Scaling Laws and a Classical Equation of State.
PB95-169249 *00,990*

SCANDIUM HYDRIDES
Neutron Spectroscopic Comparison of Rare-Earth/Hydrogen alpha-Phase Systems.
PB95-163523 *00,970*

SCANDIUM IONS
Dielectronic Capture Processes in the Electron-Impact Ionization of Sc(2+).
PB95-203113 *04,000*

SCANNED PROBE MICROSCOPY
Summary Report: Workshop on Industrial Applications of Scanned Probe Microscopy (2nd). A Workshop Co-Sponsored by NIST, SEMATECH, ASTM E42.14, and the American Vacuum Society. Held in Gaithersburg, Maryland on May 2-3, 1995.
PB96-131602 *00,509*

SCANNING
Scanning Capacitance Microscopy Measurements and Modeling: Progress Towards Dopant Profiling of Silicon.
PB96-148150 *04,773*

Fabrication Issues for the Prototype National Institute of Standards and Technology SRM 2090A Scanning Electron Microscope Magnification Calibration Standard.
PB96-160585 *01,131*

Scanning Capacitance Microscopy Measurements and Modeling for Dopant Profiling of Silicon.
PB96-164207 *04,781*

Scanning Electron Microscope Magnification Calibration Interlaboratory Study.
PB96-201082 *01,164*

SCANNING CAPACITANCE MICROSCOPY
2D-Scanning Capacitance Microscopy Measurements of Cross-Sectioned VLSI Teststructures.
PB96-163779 *04,104*

Scanning Capacitance Microscopy Measurements and Modeling: Progress Towards Dopant Profiling of Silicon.
PB96-180070 *01,964*

SCANNING ELECTION MICROSCOPY
Phase Identification in a Scanning Electron Microscope Using Backscattered Electron Kikuchi Patterns.
PB97-109128 *04,804*

SCANNING ELECTRON MICROSCOPES
Scanning Electron Microscopy Observations of Misfit Dislocations in Epitaxial In0.25Ga0.75As on GaAs(001).
PB96-200159 *03,004*

Monte Carlo Simulation of Scanning Electron Microscope Signals.
PB96-200969 *02,444*

Modification of a Commercial SEM with a Computer Controlled Cathode Stabilized Power Supply.
PB96-201066 *04,129*

SCANNING ELECTRON MICROSCOPY
Environmental Scanning Electron Microscope Imaging Examples Related to Particle Analysis.
PB94-172822 *00,766*

Quantitative Phase Abundance Analysis of Three Cement Clinker Reference Materials by Scanning Electron Microscopy.
PB94-173051 *00,333*

Measurement and Uncertainty of a Calibration Standard for the Scanning Electron Microscope.
PB94-219250 *00,560*

Monte Carlo Model for SEM Linewidth Metrology.
PB95-150058 *02,331*

Loading Device for Fracture Testing of Compact Tension Specimens in the Scanning Electron Microscope.
PB95-162434 *02,652*

Cement and Concrete Characterization by Scanning Electron Microscopy.
PB95-163168 *00,379*

Micromagnetic Scanning Microprobe System.
PB95-176178 *02,224*

Use of Monte Carlo Modeling for Interpreting Scanning Electron Microscope Linewidth Measurements.
PB96-137807 *02,413*

SEMPA Studies of Exchange Coupling in Magnetic Multilayers.
PB96-164074 *04,780*

Report on the NIST Low Accelerating Voltage SEM Magnification Standard Interlaboratory Study.
PB96-201074 *02,445*

SEM Linewidth Metrology of X-ray Lithography Masks.
PB96-201108 *02,447*

SCANNING PROBE METHODS
Characterization of Two-Dimensional Dopant Profiles: Status and Review.
PB96-119300 *02,400*

SCANNING TUNNELING MICROSCOPY
Polyethylene Crystallized from an Entangled Solution Observed by Scanning Tunneling Microscopy.
PB95-107389 *01,232*

Single-Atom Point Source for Electrons: Field-Emission Resonance Tunneling in Scanning Tunneling Microscopy.
PB95-125860 *00,893*

Scanning Tunneling Microscopy and Fabrication of Nanometer Scale Structures at the Liquid-Gold Interface.
PB95-140414 *00,904*

Morphological Estimation of Tip Geometry for Scanned Probe Microscopy.
PB95-203444 *02,662*

SCATTERED FRACTIONS OF DOSE
Scattered Fractions of Dose from 18 and 25 MV X-ray Radiotherapy Linear Accelerators.
PB96-186101 *04,120*

SCATTERING
Scattering Properties of the Leveled-Wave Model of Random Morphologies.
PB94-198835 *03,807*

SCATTERING-PARAMETER MEASUREMENT
Line-Reflect-Match Calibrations with Nonideal Microstrip Standards.
PB96-176599 *02,242*

SCATTERING PARAMETERS
Verification of Scattering Parameter Measurements.
PB95-163960 *01,904*

Comments on 'Conversions between S, Z, Y, h, ABCD, and T Parameters Which Are Valid for Complex Source and Load Impedances'.
PB96-102785 *02,069*

Two-Tier Multiline TRL for Calibration of Low-Cost Network Analyzers.
PB96-157888 *01,947*

SCHRODINGER EQUATION
New Exact Solution of the One-Dimensional Schrodinger Equation and Its Application to Polarized Neutron Reflectometry.
PB95-161832 *04,609*

Numerical Solution of the Nonlinear Schroedinger Equation for Small Samples of Trapped Neutral Atoms.
PB95-202578 *03,985*

SCIENTIFIC LITERATURE
Standard Samples and Reference Standards Issued by the National Bureau of Standards.
AD-A279 240/6 *02,613*

Preliminary List of References Containing Compilations of Data on Properties of Materials.
AD-A302 670/5 *03,243*

SCIENTIFIC VISUALIZATION
Visualization Applications for Manufacturing: A State-of-the-Art Survey. Final Report.
PB94-194552 *02,816*

SCINTILLATION COUNTERS
Measurement of Absorbed Dose of Neutrons, and of Mixtures of Neutrons and gamma rays.
AD-A286 647/3 *03,710*

SCINTILLATION COUNTING
Liquid-Scintillation Counting Techniques for the Standardization of Radionuclides Used in Therapy.
PB97-110084 *03,709*

SCREW FIXATION
Reinforcement of Cancellous Bone Screws with Calcium Phosphate Cement.
PB96-158001 *00,179*

SCREW THREADS
Screw-Thread Standards for Federal Services, 1957. Part 3.
AD-A279 121/8 *02,854*

Screw-Thread Standards for Federal Services, 1957. Part 1.
AD-A279 290/1 *02,855*

Screw-Thread Standards for Federal Services, 1957. Handbook H28 (1957), Part 2. Revised.
AD-A280 082/9 *03,599*

1950 Supplement to Screw-Thread Standards for Federal Services. 1944.
AD-A280 223/9 *03,656*

Variations in Size Measurements by Indicating Gaging Systems.
PB95-163614 *02,864*

SDNS (SECURE DATA NETWORK SYSTEM)
SDNS Security Management.
PB95-161170 *01,592*

SEALING COMPOUNDS
Formation of Hydroxyapatite in Cement Systems.
PB95-175261 *00,170*

SEAMS (JOINTS)
Effects of Adhesive Thickness, Open Time, and Surface Cleanness on the Peel Strength of Adhesive-Bonded Seams of EPDM Rubber Roofing Membrane.
PB95-151338 *00,372*

Characteristics of Adhesive-Bonded Seams Sampled from EPDM Roof Membranes.
PB95-162491 *00,377*

Pulse-Echo Ultrasonic Evaluation of the Integrity of Seams of Single-Ply Roof Membranes.
PB95-163804 *00,381*

SEARCH PROFILES
Coping with Different Retrieval Methods in Next Generation Networks.
PB95-168555 *02,726*

Move-to-Root Rule for Self-Organizing Trees with Markov Dependent Requests.
PB96-179528 *03,431*

SEARCHING
Tree-Lookup for Partial Sums Or: How Can I Find This Stuff Quickly.
PB96-179411 *01,770*

SECONDARY ION MASS SPECTROSCOPY
Use of Kinetic Energy Distributions to Determine the Relative Contributions of Gas Phase and Surface Fragmentation in KeV Ion Sputtering of a Quaternary Ammonium Salt.
PB95-126108 *00,570*

Molecular Ion Imaging and Dynamic Secondary Ion Mass Spectrometry of Organic Compounds.
PB95-126124 *00,571*

SECTORAL ANALYSIS
Information Infrastructure: Reaching Society's Goals. Report of the Information Infrastructure Task Force Committee on Applications and Technology.
PB94-214756 *01,469*

SECURE COMMUNICATIONS
Data Encryption Standard.
PB95-162376 *01,595*

Telecommunications Security Guidelines for Telecommunications Management Network. Computer Security.
PB96-139415 *01,496*

Introduction to Secure Telephone Terminals.
PB97-110498 *01,512*

SECURE DATA NETWORK SYSTEM
SDNS Security Management.
PB95-161170 *01,592*

SECURITY
Impact of the FCC's Open Network Architecture on NS/NP Telecommunications Security.
PB95-189445 *01,483*

SECURITY LABELS
Standard Security Label for Information Transfer; Category: Computer Security; Subcategory: Security Labels.
FIPS PUB 188 *01,571*

SEDIGRAPH METHOD
Statistical Analysis of Parameters Affecting the Measurement of Particle-Size Distribution of Silicon Nitride Powders by Sedigraph (Trade Name).
PB94-216249 *03,042*

SEDIMENTS
National Status and Trends Program Specimen Bank: Sampling Protocols, Analytical Methods, Results, and Archive Samples.
PB97-119226 *02,598*

SEE (SOFTWARE ENGINEERING ENVIRONMENT)
Guide to Software Engineering Environment Assessment and Evaluation.
PB94-140167 *01,676*

SEES (SOFTWARE ENGINEERING ENVIRONMENTS)
Making Sense of Software Engineering Environment Framework Standards.
PB95-105037 *01,701*

SEGMENT INSERTION
Inserting Line Segments into Triangulations and Tetrahedralizations.
PB95-198933 *03,415*

SEISMIC DESIGN
Standards of Seismic Safety for Existing Federally Owned or Leased Buildings and Commentary.
PB95-130209 *00,431*

Implementation of Executive Order 12699: Seismic Safety of Federal and Federally Assisted or Regulated New Building Construction.
PB95-151809 *00,436*

World of Building Codes.
PB95-203428 *00,449*

ICSSC Guidance on Implementing Executive Order 12941 on Seismic Safety of Existing Federally Owned or Leased Buildings.
PB96-128103 *00,459*

De Facto Microzonation through the Use of Soils Factors in Design Triggers.
PB96-141148 *00,462*

Executive Order 12941. Seismic Safety of Existing Federally Owned or Leased Buildings: It's History, Content and Objectives.
PB96-156021 *00,465*

Proceedings of a Workshop on Developing and Adopting Seismic Design and Construction Standards for Lifelines. Held in Denver, Colorado on September 25-27, 1991.
PB97-115794 *01,302*

SEISMIC EFFECTS
Dynamic Characteristics of Five Tall Buildings during Strong and Low-Amplitude Motions.
PB94-199981 *00,427*

Wind and Seismic Effects. Proceedings of the U.S.-Japan Cooperative Program in Natural Resources Panel on Wind and Seismic Effects (26th). Held in Gaithersburg, Maryland on May 17-20, 1994.
PB95-147385 *00,433*

Performance of Federal Buildings in the January 17, 1994 Northridge Earthquake.
PB95-231775 *00,453*

Recommended Performance-Based Criteria for the Design of Manufactured Home Foundation Systems to Resist Wind and Seismic Loads.
PB96-128285 *00,460*

January 17, 1995 Hyogoken-Nanbu (Kobe) Earthquake. Performance of Structures, Lifelines and Fire Protection Systems. Executive Summary and Paper.
PB97-104160 *00,475*

Wind and Seismic Effects: Proceedings of the Joint Meeting of the U.S.-Japan Cooperative Program in Natural Resources Panel on Wind and Seismic Effects (28th). Held in Gaithersburg, Maryland on May 14-17, 1996.
PB97-104376 *00,476*

SEISMIC ISOLATION SYSTEMS
Draft Guideline for Testing and Evaluation of Seismic Isolation Systems.
PB94-172947 *00,423*

Summary and Results of the NIST Workshop on Proposed Guidelines for Testing and Evaluation of Seismic Isolation Systems. Held in San Francisco, California on July 25, 1994.
PB96-154901 *00,463*

SEISMIC RETROFITTING
Jacket Thickness Requirements for Seismic Retrofitting of Circular Bridge Columns.
PB95-163267 *01,336*

SEISMIC SAFETY
Evaluation and Retrofit Standards for Existing Federally Owned and Leased Buildings.
PB95-150918 *00,434*

Some Basics on Who's Who and What's What in Seismic Safety.
PB95-150926 *00,435*

Lessons from the Loma Prieta Earthquake.
PB95-164091 *00,442*

Seismic Safety of Federal Buildings. Initial Program: How Much Will It Cost.
PB95-182291 *00,447*

SEISMIC WAVES
Assessment of Site Response Analysis Procedures.
PB95-210928 *00,450*

Response of Buildings to Ambient Vibration and the Loma Prieta Earthquake: A Comparison.
PB96-119607 *00,457*

Estimation of System Damping at the Lotung Site by Application of System Identification.
PB96-214697 *01,351*

SELECTION RULES
Comparison of the Liquid Chromatographic Behavior of Selected Steroid Isomers Using Different Reversed-Phase Materials and Mobile Phase Compositions.
PB95-140976 *00,574*

SELECTIVE DISSEMINATION OF INFORMATION
Computer Security Management and Planning in the U.S. Federal Government.
PB95-163432 *01,596*

Guidance to Federal Agencies on the Use of Trusted Systems.
PB95-163440 *01,597*

SELECTIVE ELECTRODES
Cyclic Polyamine Ionophore for Use in a Dibasic Phosphate-Selective Electrode.
PB95-180121 *01,008*

SELECTIVITY
Developing Measurement for Experimentation.
PB97-118707 *03,450*

SELENIUM
Thermodynamics of (Germanium + Selenium): A Review and Critical Assessment.
PB97-112536 *01,182*

Large Local-Field Corrections in Optical Rotatory Power of Quartz and Selenium.
PB97-122378 *04,400*

SELENIUM IONS
Absolute Cross-Section Measurements for Electron-Impact Single Ionization of Se(+) and Te(+).
PB95-202503 *03,980*

SELF ASSEMBLED MONOLAYERS
Silver Metalization of Octadecanethiol Monolayers Self-Assembled on Gold.
PB95-150744 *00,923*

UV-Photopatterning of Alkylthiolate Monolayers Self-Assembled on Gold and Silver.
PB95-150751 *00,924*

Surface Plasmon Microscopy of Biotin-Streptavidin Binding Reactions on UV-Photopatterned Alkanethiol Self-Assembled Monolayers.
PB96-176771 *01,158*

SELF-AVOIDING SURFACES
Self-Avoiding Surfaces, Topology, and Lattice Animals.
PB95-150512 *04,571*

SELF-AVOIDING WALKS
Examination of the l/d Expansion Method from Exact Enumeration for a Self-Interacting Self-Avoiding Walk.
PB95-175733 *01,266*

Self-Avoiding-Walk Contacts and Random-Walk Self-Intersections in Variable Dimensionality.
PB96-102231 *01,276*

SELF CALIBRATION
Self-Calibrating Fiber Optic Sensors: Potential Design Methods.
PB95-169298 *02,172*

Self Calibrating Fiber Optic Sensors: Potential Design Methods.
PB95-169306 *02,173*

Self-Calibrated Intelligent Optical Sensors and Systems.
PB96-200738 *04,380*

SELF ORGANIZING SYSTEMS
Move-to-Root Rule for Self-Organizing Trees with Markov Dependent Requests.
PB96-179528 *03,431*

SELF-PRESERVATION BEHAVIOR
Global Density Effects on the Self-Preservation Behavior of Turbulent Free Jets.
PB95-162301 *04,207*

SELF RECIPROCAL FUNCTION
Self-Reciprocal Fourier Functions.
PB96-200852 *01,974*

SELF-SETTING
Physical and Chemical Properties of Resin-Reinforced Calcium Phosphate Cements.
PB95-180212 *00,171*

SELF TESTS
Self-Calibrating Fiber Optic Sensors: Potential Design Methods.
PB95-169298 *02,172*

Self Calibrating Fiber Optic Sensors: Potential Design Methods.
PB95-169306 *02,173*

SEMICONDUCTOR DEVICES
Development and Characterization of Insulating Layers on Silicon Carbide: Annual Report for February 14, 1988 to February 14, 1989.
PB94-155579 *02,295*

Wire Bond Testing.
PB94-211653 *02,314*

Precision, Accuracy, Uncertainty and Traceability and Their Application to Submicrometer Dimensional Metrology.
PB94-213105 *02,319*

Physics for Device Simulations and Its Verification by Measurements.
PB95-141172 *02,327*

Exact Solution of the Steady-State Surface Temperature for a General Multilayer Structure.
PB95-152773 *02,337*

Electrical Test Structure for Improved Measurement of Feature Placement and Overlay in Integrated Circuit Fabrication Processes.
PB95-164273 *02,355*

Optical Characterization in Microelectronics Manufacturing.
PB95-169397 *02,358*

Status and Trends in Power Semiconductor Devices.
PB95-175097 *02,361*

Correlation of Optical, X-ray, and Electron Microscopy Measurements of Semiconductor Multilayer Structures.
PB95-175279 *02,174*

Electronics and Electrical Engineering Laboratory Technical Progress Bulletin Covering Laboratory Programs, October to December 1994 with 1995 EEEL Events Calendar.
PB95-208724 *02,372*

Semiconductor Measurement Technology: HOTPAC. Programs for Thermal Analysis Including Version 3.0 of the TXYZ Program, TXYZ30, and the Thermal MultiLayer Program, TML.
PB95-260766 *02,374*

Exact Recursion Relation Solution for the Steady-State Surface Temperature of a General Multilayer Structure.
PB96-102017 *02,376*

Semiconductor Measurement Technology: Test Structure Implementation Document: DC Parametric Test Structures and Test Methods for Monolithic Microwave Integrated Circuits (MMICs).
PB96-117692 *02,399*

Millimeter-Resolution Optical Time-Domain Reflectometry Using a Four-Wave Mixing Sampling Gate.
PB96-122700 *02,190*

Scanning Capacitance Microscopy Measurements and Modeling: Progress Towards Dopant Profiling of Silicon.
PB96-148150 *04,773*

Semiconductor Measurement Technology: Survey of Optical Characterization Methods for Materials, Processing, and Manufacturing in the Semiconductor Industry.
PB96-154596 *02,706*

National Semiconductor Metrology Program, Project Portfolio FY 1996.
PB96-195268 *04,789*

SEMICONDUCTOR INTERFACES
High-Accuracy Principal-Angle Scanning Spectroscopic Ellipsometry of Semiconductor Interfaces.
PB96-163787 *02,427*

SEMICONDUCTOR JUNCTIONS
Junction Locations by Scanning Tunneling Microscopy: In-Air-Ambient Investigation of Passivated GaAs pn Junctions.
PB94-185964 *02,306*

SEMICONDUCTOR LASERS
Vertical-Cavity Optoelectronic Structures: CAD, Growth, and Structural Characterization.
PB95-153177 *02,148*

Vertical-Cavity Semiconductor Structures: Materials Characterization.
PB95-153185 *02,149*

Vertical-Cavity Semiconductor Lasers: Structural Characterization, CAD, and DFB Structures.
PB95-153193 *02,150*

Effect of Semiconductor Laser Characteristics on Optical Fiber Sensor Performance.
PB95-169132 *02,167*

High-Sensitivity Spectroscopy with Diode Lasers.
PB95-175477 *04,297*

Diode Laser as a Spectroscopic Tool.
PB95-175485 *00,600*

Stabilization of 3.3 and 5.1 m Lead-Salt Diode Lasers by Optical Feedback.
PB95-180709 *04,313*

Low-Noise High-Speed Diode Laser Current Controller.
PB95-202826 *02,178*

Narrow-Band Tunable Diode Laser System with Grating Feedback, and a Saturated Absorption Spectrometer for Cs and Rb.
PB95-202891 *04,319*

SEMICONDUCTOR MATERIALS
National Semiconductor Metrology Program, Project Portfolio FY 1996.
PB96-195268 *04,789*

SEMICONDUCTORS
Electronics and Electrical Engineering Laboratory Technical Publication Announcements Covering Laboratory Programs, October to December 1994 with 1995 EEEL Events Calendar.
PB95-231841 *01,918*

Nonequilibrium Total-Dielectric-Function Approach to the Electron Boltzmann Equation for Inelastic Scattering in Doped Polar Semiconductors.
PB96-138532 *04,416*

Cross-Sectional Photoluminescence and Its Application to Buried-Layer Semiconductor Structures.
PB96-141106 *02,415*

Methodology for the Certification of Reference Specimens for Determination of Oxygen Concentration in Semiconductor Silicon by Infrared Spectrophotometry.
PB96-155478 *02,421*

Soft-X-ray-Emission Investigation of Cobalt Implanted Silicon Crystals.
PB96-157912 *04,069*

Using Collocation in Three Dimensions and Solving a Model Semiconductor Problem.
PB96-159249 *01,952*

Business and Manufacturing Motivations for the Developing of Analytical Technology and Metrology for Semiconductors.
PB96-161948 *04,778*

President's Column 'Editorial'.
PB96-164090 *02,239*

Optical Characterization of Materials and Devices for the Semiconductor Industry: Trends and Needs.
PB96-167192 *02,431*

Novel Magnetic Field Characterization Techniques for Compound Semiconductor Materials and Devices.
PB96-176458 *02,433*

Hybrid Optical-Electrical Overlay Test Structure.
PB96-204136 *02,450*

Double Modulation and Selective Excitation Photoreflectance for Characterizing Highly Luminescent Semiconductor Structures and Samples with Poor Surface Morphology.
PB97-111439 *02,452*

Application of the Collocation Method in Three Dimensions to a Model Semiconductor Problem.
PB97-122428 *02,457*

SEMICONDUCTORS (MATERIALS)

Lattice Dynamics of Semiconducting, Metallic, and Superconducting Ba1-xKxBiO3 Studied by Inelastic Neutron Scattering.
PB96-102447 *04,708*

Development of a Standard Reference Material for Measurement of Interstitial Oxygen Concentration in Semiconductor Silicon by Infrared Absorption.
PB96-122668 *02,404*

SENICONDUCTOR DEVICES

Scanning Capacitance Microscopy Measurements and Modeling for Dopant Profiling of Silicon.
PB96-164207 *04,781*

SENSITIVITY

Influence of the Filament Potential Wave Form on the Sensitivity of Glass-Envelope Bayard-Alpert Gages.
PB95-175014 *02,657*

Environmental Sensitivities of Quartz Oscillators.
PB96-103148 *02,271*

Developing Measurement for Experimentation.
PB97-118707 *03,450*

SENSITIVITY ANALYSIS

Sensitivity Analysis for Mathematical Modeling of Fires in Residential Buildings.
PB96-154968 *00,215*

SENSORS

Intelligent Processing of Hot Isostatic Pressing.
PB94-172913 *03,315*

In-Line Optical Monitoring of Injection Molding.
PB94-185105 *01,201*

Polarization Insensitive 3x3 Sagnac Current Sensor Using Polarizing Spun High-Birefringence Fiber.
PB96-119276 *02,187*

Contact Tube Wear Detection in Gas Metal Arc Welding.
PB96-135330 *02,872*

SEPARATION MATRICES

Intercomparison of DNA Sizing Ladders in Electrophoretic Separation Matrices and Their Potential for Accurate Typing of the D1S80 Locus.
PB96-200928 *03,485*

SEPARATION PROCESSES

Low Temperature H(sub 2)S Separation Using Membrane Reactor with Redox Catalyst.
DE94008991 *02,471*

Development of Engineered Stationary Phases for the Separation of Carotenoid Isomers.
PB95-150249 *00,578*

Shape Selectivity Assessment of Stationary Phases in Gas Chromatography.
PB95-150256 *00,579*

Supercritical Fluid Extraction of Biological Products.
PB95-175204 *00,040*

SEQUENCE DELETION

Deletion Analysis of the Mini-P1 Plasmid Origin of Replication and the Role of E.coli DnaA Protein.
PB95-163911 *03,539*

SERIAL SECTIONING

Serial Sectioning of Hardened Cement Paste for Scanning Electron Microscopy.
PB94-172640 *01,305*

SERIES EXPANSION

Examination of the l/d Expansion Method from Exact Enumeration for a Self-Interacting Self-Avoiding Walk.
PB95-175733 *01,266*

Self-Avoiding-Walk Contacts and Random-Walk Self-Intersections in Variable Dimensionality.
PB96-102231 *01,276*

SERUM ALBUMIN

Two Phase Aqueous Extraction: Rheological Properties of Dextran, Polyethylene Glycol, Bovine Serum Albumin and Their Mixtures.
PB95-161998 *00,676*

SERUMS

Methods for Analysis of Cancer Chemopreventive Agents in Human Serum.
PB95-200648 *03,502*

Liquid Chromatographic Determination of Carotenoids in Human Serum Using an Engineered C30 and a C18 Stationary Phase.
PB97-119333 *03,512*

SERVICE LIFE

Suggestions for a Logically-Consistent Structure for Service Life Prediction Standards.
PB95-125795 *00,358*

Methodologies for Predicting the Service Lives of Coating Systems.
PB95-146387 *03,124*

Survey of Concrete Transport Properties and Their Measurement.
PB95-220489 *00,396*

SERVOCONTROL

Integration of Servo Control into a Large-Scale Control System Design: An Example from Coal Mining.
PB94-203429 *03,696*

SEWAGE

Water Efficient Plumbing Fixtures through Standards and Test Methods.
PB95-125951 *00,248*

SGML (STANDARD GENERALIZED MARKUP LANGUAGE)

SGML Environment for STEP.
PB95-143103 *02,778*

SGML Parser Validation Procedures.
PB95-174959 *01,717*

Standard Generalized Markup Language Test Suite Evaluation Report.
PB96-154992 *01,751*

SHAPE

Using Logic to Specify Shapes and Spatial Relations in Design Grammars.
PB97-111579 *02,793*

SHAPE RECOVERY

Physics-Based Vision: Principles and Practice, Shape Recovery (Book Review).
PB95-164075 *01,846*

SHAPE SELECTIVITY

Shape Selectivity Assessment of Stationary Phases in Gas Chromatography.
PB95-150256 *00,579*

Selectivity Trends in Packed Column Supercritical Fluid Chromatography with C18 Stationary Phases.
PB96-138581 *00,622*

SHAPED CHARGES

Texture Study of Two Molybdenum Shaped Charge Liners by Neutron Diffraction.
PB94-200177 *03,754*

Microstructure Study of Molybdenum Liners by Neutron Diffraction.
PB95-202396 *03,756*

SHAPIRO STEPS

Effect of Thermal Noise on Shapiro Steps in High-Tc Josephson Weak Links.
PB94-212677 *04,506*

Terahertz Shapiro Steps in High Temperature SNS Josephson Junctions.
PB95-169140 *02,168*

Large-Amplitude Shapiro Steps and Self-Field Effects in High-Tc Josephson Weak Links.
PB95-180410 *04,682*

SHARED MEMORY PROGRAMS

Using Synthetic Perturbations and Statistical Screening to Assay Shared-Memory Programs.
PB96-103031 *01,740*

SHEAR

Shear-Induced Martensitic-Like Transformation in a Block Copolymer Melt.
PB96-119508 *01,277*

Simulation and SANS Studies of Gelation Under Shear.
PB96-167176 *01,150*

Small-Angle Neutron-Scattering Study of Dense Sheared Silica Gels.
PB96-167184 *01,151*

SHEAR ALIGNMENT

Small-Angle Neutron Scattering (SANS) Study of Worm-Like Micelles Under Shear.
PB96-176698 *04,111*

SHEAR FLOW

Crossover to Strong Shear in a Low-Molecular-Weight Critical Polymer Blend.
PB94-211976 *01,222*

SANS and LS Studies of Polymer Mixtures Under Shear Flow.
PB95-107090 *01,231*

Response of a Terminally Anchored Polymer Chain to Simple Shear Flow.
PB95-108668 *01,233*

Anisotropic Phase Separation Kinetics in a Polymer Blend Solution Following Cessation of Shear Studied by Light Scattering.
PB95-151247 *01,241*

Neutron Scattering Study of the Orientation of a Liquid Crystalline Polymer by Shear Flow.
PB95-180196 *01,270*

Shear-Induced Mixing in Polymer Blends.
PB96-148085 *01,287*

SHEAR PROPERTIES

Dynamic Shear Modulus Measurements with Four Independent Techniques in Nickel-Based Alloys.
PB94-198900 *03,320*

SHEAR RATE

Shear-Excited Morphological States in a Triblock Copolymer.
PB94-172392 *01,196*

Shear Dependence of Critical Fluctuations in Binary Polymer Mixtures by Small Angle Neutron Scattering.
PB94-211612 *01,220*

SHEAR STRESS

Fluorescence Anisotropy Measurements on a Polymer Melt as a Function of Applied Shear Stress.
PB94-199296 *01,209*

Observations of Shear Induced Molecular Orientation in a Polymer Melt Using Fluorescence Anisotropy Measurements.
PB94-199304 *01,210*

Observations of Shear Stress and Molecular Orientation Using Fluorescence Anisotropy Measurements.
PB94-199312 *01,211*

SHEAR THINNING

Structure and Rheology of Hard-Sphere Systems.
PB96-167333 *00,662*

SHEET METAL

Determination of Sheet Steel Formability Using Wide Band Electromagnetic-Acoustic Transducers.
PB96-186036 *02,279*

SHEETS

Fracture Testing of Large-Scale Thin-Sheet Aluminum Alloy.
AD-A306 625/5 *03,305*

SHIELDING

Shielding of Cracks in a Plastically Polarizable Material.
PB95-164257 *04,631*

SHIELDOSE-2 COMPUTER PROGRAM

Updated Calculations for Routine Space-Shielding Radiation Dose Estimates: SHIELDOSE-2.
PB95-171039 *04,838*

SHIELDS

Standard Source Method for Reducing Antenna Factor Errors in Shielded Room Measurements.
PB96-183157 *02,013*

SHIP FIRES

Materials and Fire Threat.
PB97-122311 *01,442*

SHOCK TESTS

Testing the Sensitivity of Accelerometers Using Mechanical Shock Pulses Under NIST Special Publication 250 Test No. 24040S.
PB96-179544 *02,683*

SHOCK TUBES

Shock Tube Techniques in Chemical Kinetics.
PB95-163465 *00,968*

SHOT NOISE

Observation of Hot-Electron Shot Noise in a Metallic Resistor.
PB97-112007 *01,988*

SHRINKAGE

Reduction of Marginal Gaps in Composite Restorations by Use of Glass-Ceramic Inserts.
PB96-102405 *00,174*

Modelling Drying Shrinkage of Cement Paste and Mortar. Part 1. Structural Models from Angstroms to Millimeters.
PB96-135132 *03,074*

SIALON

Cavitation Damage During Flexural Creep of SiAlON-YAG Ceramics.
PB94-200110 *03,036*

SIDELOBES

Planar Near-Field Measurements of Low-Sidelobe Antennas.
PB94-219235 *02,001*

Comparison of Ultralow-Sidelobe-Antenna Far-Field Patterns Using the Planar-Near-Field Method and the Far-Field Method.
PB96-200373 *02,015*

SIGNAL CONDITIONING

Bounds on Least-Squares Four-Parameter Sine-Fit Errors Due to Harmonic Distortion and Noise.
PB96-141304 *01,609*

SIGNAL ESTIMATION

Compensation of Markov Estimator Errors in Time-Jittered Sampling of Nonmonotonic Signals.
PB95-150983 *01,590*

SIGNAL GENERATORS

Reducing Errors, Complexity, and Measurement Time of PM Noise Measurements.
PB96-119771 *02,075*

SIGNAL PROCESSING

Approach to Setting Performance Requirements for Automated Evaluation of the Parameters of High-Voltage Impulses.
PB94-185634 *01,878*

Analysis of Scattering Asymmetry Statistics When Background Corrected Counts Are Negative.
PB94-200334 *03,824*

Uncertainty Intervals for Polarized Beam Scattering Asymmetry Statistics.
PB94-200342 *03,825*

Satellite Two-Way Time Transfer: Fundamentals and Recent Progress.
PB95-161089 *01,536*

Comment and Discussion on Digital Processing of PD Pulses.
PB96-122775 *01,932*

SIGNAL RECONSTRUCTION
Casual Regularizing Deconvolution Filter for Optimal Waveform Reconstruction.
PB95-203089 *01,603*

SIGNAL-TO-NOISE RATIO
Perception of Clamp Noise in Television Receivers.
PB96-119433 *01,489*

SIGNAL TRANSDUCTION
Energy Transduction between a Concentration Gradient and an Alternating Electric Field.
PB94-216363 *03,461*

SIGNAL TRANSMISSION
Preliminary Comparison of Time Transfers via LASSO, GPS and Two-Way Satellite.
PB95-151098 *01,529*

SIGNALS
Procedures for Document Facsimile Transmission Issued by General Services Administration, April 14, 1982. Federal Standard 1063.
FIPS PUB 148 *01,516*

Electronics and Electrical Engineering Laboratory Technical Publication Announcements Covering Laboratory Programs, October to December 1994 with 1995 EEEL Events Calendar.
PB95-231841 *01,918*

Accuracy in Time Domain Transmission Line Measurements.
PB96-148069 *04,060*

SILANE
Preparation of Immobilized Proteins Covalently Coupled Through Silane Coupling Agents to Inorganic Supports.
PB95-151403 *03,530*

SILANE/METHACRYLOXYPROPHYL TRIMETHOXY
Copolymerization of N-Phenyl Maleimide and gamma-Methacryloxypropyl Trimethoxysilane.
PB95-153144 *01,248*

SILANES
Plasma Chemistry in Disilane Discharges.
PB94-211075 *02,514*

Plasma Chemistry in Silane/Germane and Disilane/Germane Mixtures.
PB95-202537 *01,027*

SILCON DIOXIDE
New Physics-Based Model for Time-Dependent- Dielectric-Breakdown.
PB96-186093 *02,440*

SILICA
Small Angle Neutron Scattering Study of the Structure and Formation of Ordered Mesopores in Silica.
PB96-111919 *03,069*

SILICA FUME
Evolution of Porosity and Calcium Hydroxide in Laboratory Concretes Containing Silica Fume.
PB95-175063 *01,321*

SILICATES
Real-Time Small-Angle X-Ray Scattering Study of the Early Stage of Phase Separation in the SiO2-BaO-K20 System.
PB95-163069 *03,052*

SILICIDES
Tensile Creep of Silicide Composites.
PB96-200803 *03,183*

SILICON
Precision Comparison of the Lattice Parameters of Silicon Monocrystals.
PB94-169745 *04,438*

Vibrational Distributions of As2 in the Cracking of As4 on Si(100) and Si(111).
PB94-198314 *00,784*

Magnetic Dead Layer in Fe/Si Multilayer: Profile Refinement of Polarized Neutron Reflectivity Data.
PB94-198363 *04,458*

Status of a Silicon Lattice Measurement and Dissemination Exercise.
PB94-199635 *04,474*

Measurement of Boron at Silicon Wafer Surfaces by Neutron Depth Profiling.
PB94-211059 *04,487*

Atomic Theory of Fracture of Brittle Materials: Application to Covalent Semiconductors.
PB94-216553 *04,519*

New Values for Silicon Reference Materials, Certified for Isotope Abundance Ratios. Letter to the Editor.
PB94-219268 *00,863*

Standard Reference Materials: Certification of a Standard Reference Material for the Determination of Interstitial Oxygen Concentration in Semiconductor Silicon by Infrared Spectrophotometry.
PB95-125076 *02,326*

Nanoscale Study of the As-Grown Hydrogenated Amorphous Silicon Surface.
PB95-150595 *04,573*

Use of Sum Rules on the Energy-Loss Function for the Evaluation of Experimental Optical Data.
PB95-150736 *04,264*

Multiphoton Ionization Spectroscopy Measurements of Silicon Atoms during Vapor Phase Synthesis of Ceramic Particles.
PB95-151999 *03,913*

Direct Detection of Atomic Arsenic Desorption from Si(100).
PB95-202230 *01,024*

Nanoscale Study of the Hydrogenated Amorphous Silicon Surface.
PB96-103056 *04,720*

Photodesorption Dynamics of CO from Si(111): The Role of Surface Defects.
PB96-111646 *03,066*

Effect of Anneal Temperature on Si/Buried Oxide Interface Roughness on SIMOX.
PB96-112206 *02,382*

Silicon Surface Chemistry by IR Spectroscopy in the Mid- to Far-IR Region: H2O and Ethanol on Si(100).
PB96-138565 *01,097*

Scanning Capacitance Microscopy Measurements and Modeling: Progress Towards Dopant Profiling of Silicon.
PB96-148150 *04,773*

Semiconductor Measurement Technology: Survey of Optical Characterization Methods for Materials, Processing, and Manufacturing in the Semiconductor Industry.
PB96-154596 *02,706*

Methodology for the Certification of Reference Specimens for Determination of Oxygen Concentration in Semiconductor Silicon by Infrared Spectrophotometry.
PB96-155478 *02,421*

Effect of Single versus Multiple Implant Processing on Defect Types and Densities in SIMOX.
PB96-160353 *01,957*

Interfaces in Mo/Si Multilayers.
PB96-160668 *02,423*

Scanning Capacitance Microscopy Measurements and Modeling for Dopant Profiling of Silicon.
PB96-164207 *04,781*

Kinetic-Energy-Enhanced Neutral Etching.
PB96-200613 *00,665*

Electrical Test Structures Replicated in Silicon-on-Insulator Material.
PB97-111827 *02,454*

SILICON 28
Measurement of the J=2 less than 1 Fine-Structure Interval for (28)Si and (29)Si in the Ground (3)P State.
PB94-185097 *00,771*

SILICON 29
Measurement of the J=2 less than 1 Fine-Structure Interval for (28)Si and (29)Si in the Ground (3)P State.
PB94-185097 *00,771*

SILICON ADDITIONS
Lattice Position of Si in GaAs Determined by X-Ray Standing Wave Measurements.
PB95-164406 *04,632*

SILICON ATOMS
Multiphoton Ionization Spectroscopy Measurements of Silicon Atoms during Vapor Phase Synthesis of Ceramic Particles.
PB95-151999 *03,913*

SILICON CARBIDE
In situ-Toughened Silicon Carbide.
PB97-110332 *03,102*

SILICON CARBIDES
Review of Corrosion Behavior of Ceramic Heat Exchanger Materals: Corrosion Characteristics of Silicon Carbide and Silicon Nitride. Final Report, September 11, 1992--March 11, 1993.
DE93041307 *03,228*

Ceramic Characterization.
DE94013170 *03,026*

Development and Characterization of Insulating Layers on Silicon Carbide: Annual Report for February 14, 1988 to February 14, 1989.
PB94-155579 *02,295*

Analysis of Creep in a Si-SiC C-Ring by Finite Element Method.
PB94-200268 *03,037*

Coating of Fibers by Colloidal Techniques in Ceramic Composites.
PB94-216256 *03,196*

Characterization of Phase and Surface Composition of Silicon Carbide Platelets.
PB94-216264 *03,043*

Interface Modification and Characterization of Silicon Carbide Platelets Coated with Alumina Particles.
PB95-108734 *03,121*

Creep Rupture of MoSi2/SiCp Composites.
PB95-152294 *03,154*

Flat and Rising R-Curves for Elliptical Surface Cracks from Indentation and Superposed Flexure.
PB95-161295 *03,156*

Oxidation of SiC.
PB96-119516 *02,401*

Journal of Research of the National Institute of Standards and Technology, September/October 1993. Volume 98, Number 5.
PB96-169057 *03,368*

Corrosion Characteristics of Silicon Carbide and Silicon Nitride.
PB96-169081 *03,372*

SILICON COMPOUNDS
Wear Modeling of Si-Based Ceramics.
PB97-122501 *03,112*

SILICON DEFECTS
Stacking Fault Pyramid Formation and Energetics in Silicon-on-Insulator Material Formed by Multiple Cycles of Oxygen Implantation and Annealing.
PB96-160221 *04,083*

SILICON DIODES
One Gigarad Passivating Nitrided Oxides for 100% Internal Quantum Efficiency Silicon Photodiodes.
PB94-185485 *02,119*

Silicon Photodiodes Optimized for EUV and Soft X-Ray Regions.
PB94-199478 *02,124*

SILICON DIOXIDE
Contact Electrification Induced by Monolayer Modification of a Surface and Relation to Acid-Base Interactions.
PB94-185378 *03,034*

Experimental Investigation of the Validity of TDDB Voltage Acceleration Models.
PB94-185949 *02,304*

Field and Temperature Acceleration of Time-Dependent Dielectric Breakdown in Intrinsic Thin SiO2.
PB94-185956 *02,305*

Imaging of Fine Porosity in a Colloidal Silica: Potassium Silicate Gel by Defocus Contrast Microscopy.
PB94-212750 *03,039*

Characterization of Chemically Modified Pore Surfaces by Small Angle Neutron Scattering.
PB95-126181 *00,898*

Spectroscopic Ellipsometry Determination of the Properties of the Thin Underlying Strained Si Layer and the Roughness at SiO2/Si Interface.
PB95-150157 *04,560*

High Temperature Reliability of Thin Film SiO2.
PB95-150348 *02,333*

Modeling Ceramic Sub-Micron Particle Formation from the Vapor Using Detailed Chemical Kinetics: Comparison with In-situ Laser Diagnostics.
PB95-151965 *00,671*

Experimental and Numerical Studies of Refractory Particle Formation in Flames: Application to Silica Growth.
PB95-152005 *00,673*

Simulation of Ceramic Particle Formation: Comparison with In-situ Measurements.
PB95-152013 *00,674*

Room Temperature Thermal Conductivity of Fumed-Silica Insulation for a Standard Reference Material.
PB95-152039 *00,374*

Molecular Orbital Study of Water Enhanced Crack Growth Process.
PB95-164067 *03,240*

Optimization of ECR-Based PECVD Oxide Films for Superconducting Integrated Circuit Fabrication.
PB95-169165 *02,051*

Partial Scattered Intensities from a Binary Suspension of Polystyrene and Silica.
PB95-175618 *00,996*

TDDB Characterization of Thin SiO2 Films with Bimodal Failure Populations.
PB96-102926 *02,381*

Alkali-Silica Reaction and High Performance Concrete.
PB96-131537 *01,345*

Time-Dependent Dielectric Breakdown of Intrinsic SiO2 Films under Dynamic Stress.
PB96-179478 *02,438*

Electric Field Dependent Dielectric Breakdown of Intrinsic SiO2 Films Under Dynamic Stress.
PB96-204102 *02,449*

Characterization of Time-Dependent Dielectric Breakdown in Intrinsic Thin SiO2.
PB97-122527 *02,458*

SILICON FILMS
Laser Melting of Thin Silicon Films.
PB94-199239 *04,471*

Characterization of Interface Defects in Oxygen-Implanted Silicon Films.
PB94-216629 *02,322*

SILICON IONS
Electron-Impact Excitation of Si(3+)(3S yields 3P) Using a Merged-Beam Electron-Energy-Loss Technique.
PB95-151239 *03,904*

Absolute Cross Sections for Electron-Impact Single Ionization of Si(+) and Si(2+).
PB95-202529 *03,982*

SILICON ISLANDS
Mechanism of Defect Formation in Low-Dose Oxygen Implanted Silicon-on-Insulator Material.
PB97-111462 *02,453*

SILICON MEMBRANES
Lithium-Drift Technique for Making Submicron Thick Silicon Membranes.
PB95-161386 *02,260*

SILICON NANOCOLUMNS
Construction of Silicon Nanocolumns with the Scanning Tunneling Microscope.
PB95-203063 *04,696*

SILICON NITRIDE
Cavitation Contributes Substantially to Tensile Creep in Silicon Nitride.
PB96-122577 *03,171*

Chemically Assisted Machining of Si3N4.
PB96-122999 *03,072*

Transient Creep Behaviour of Hot Isostatically Pressed Silicon Nitride.
PB96-180278 *03,086*

Cavity Evolution during Tensil Creep of Si3N4.
PB96-204193 *03,376*

Tension/Compression Creep Asymmetry in Si3N4.
PB97-110258 *03,096*

High Temperature Structural Reliability of Silicon Nitride.
PB97-110456 *03,104*

SILICON NITRIDES
Review of Corrosion Behavior of Ceramic Heat Exchanger Materals: Corrosion Characteristics of Silicon Carbide and Silicon Nitride. Final Report, September 11, 1992--March 11, 1993.
DE93041307 *03,228*

Densification of Nano-Size Powders. 1994 Report.
DE94013486 *03,027*

Equipment for Investigation of Cryogenic Compaction of Nanosize Silicon Nitride Powders. 1993 Report.
DE94013593 *03,028*

Low temperature fabrication from nano-size ceramic powders.
DE95013505 *03,029*

Tensile Creep of Whisker Reinforced Silicon Nitride.
PB94-211984 *03,142*

Observed and Theoretical Creep Rates for an Alumina Ceramic and a Silicon Nitride Ceramic in Flexure.
PB94-212958 *03,040*

Statistical Analysis of Parameters Affecting the Measurement of Particle-Size Distribution of Silicon Nitride Powders by Sedigraph (Trade Name).
PB94-216249 *03,042*

Deposition of Colloidal Sintering-Aid Particles on Silicon Nitride.
PB94-216272 *03,044*

Tensile Creep of a Silicon Nitride Ceramic.
PB95-161303 *03,049*

Polyelectrolytes as Dispersants in Colloidal Processing of Silicon Nitride Ceramics.
PB95-175568 *03,055*

Surface Chemical Interactions of Si3N4 with Polyelectrolyte Deflocculants.
PB95-175576 *03,056*

Effects of Soxhlet Extraction on the Surface Oxide Layer of Silicon Nitride Powders.
PB95-175584 *03,057*

Interaction of Stoichiometry, Mechanical Stress, and Interface Trap Density in LPCVD Si-rich SiNx-Si Structures.
PB95-176301 *02,366*

Boundary Lubrication of Silicon Nitride.
PB95-213583 *03,226*

Silicon Nitride Boundary Lubrication: Lubrication Mechanism of Alcohols.
PB96-111703 *03,067*

Silicon Nitride Boundary Lubrication: Effect of Oxygenates.
PB96-111711 *03,068*

Surface Chemistry of Silicon Nitride Powder in the Presence of Dissolved Ions.
PB96-111760 *01,073*

Electrokinetic Sonic Analysis of Silicon Nitride Suspensions.
PB96-123575 *03,073*

Journal of Research of the National Institute of Standards and Technology, September/October 1993. Volume 98, Number 5.
PB96-169057 *03,368*

Corrosion Characteristics of Silicon Carbide and Silicon Nitride.
PB96-169081 *03,372*

Fracture Mechanism Maps: Their Applicability to Silicon Nitride.
PB96-204532 *03,094*

SILICON ON INSULATOR
Effect of Intermediate Thermal Processing on Microstructural Changes of Oxygen Implanted Silicon-on-Insulator Material.
PB96-160213 *02,982*

Stacking Fault Pyramid Formation and Energetics in Silicon-on-Insulator Material Formed by Multiple Cycles of Oxygen Implantation and Annealing.
PB96-160221 *04,083*

SILICON SOLAR CELLS
Atomic-scale characterization of hydrogenated amorphous-silicon films and devices. Annual subcontract report, 14 February 1994--14 April 1995.
DE95009287 *02,294*

SILVER
Cryogenic Properties of Silver.
PB94-203593 *03,330*

Silver Metalization of Octadecanethiol Monolayers Self-Assembled on Gold.
PB95-150744 *00,923*

UV-Photopatterning of Alkylthiolate Monolayers Self-Assembled on Gold and Silver.
PB95-150751 *00,924*

Low-Temperature Properties of Silver.
PB96-126198 *03,361*

Direct Comparison of Three PTB Silver Fixed-Point Cells with the NIST Silver Fixed-Point Cell.
PB96-161286 *00,628*

SILVER DEPOSITION
Silver Metalization of Octadecanethiol Monolayers Self-Assembled on Gold.
PB95-150744 *00,923*

SILVER ELECTRODES
Conformational Alterations of Bovine Insulin Adsorbed on a Silver Electrode.
PB96-161773 *00,510*

SILVER-LIKE IONS
Spectra of Ag I Isoelectronic Sequence Observed from Er(21+) to Au(32+).
PB95-150660 *03,899*

SILVER SPRING (MARYLAND)
Source of Phenol Emissions Affecting the Indoor Air of an Office Building.
PB94-154382 *03,600*

SILYL RADICALS
Multiphoton Ionization of SiH3 and SiD3 Radicals. 2. Three Photon Resonance-Enhanced Spectra Observed between 460 and 610 nm.
PB94-212487 *00,835*

Multiphoton Ionization of SiH3 and SiD3 Radicals: Electronic Spectra, Vibrational Analyses of the Ground and Rydberg States, and Ionization Potential.
PB94-212503 *00,837*

SIMA (SYSTEMS INTEGRATED FOR MANUFACTURING APPLICATIONS)
NIST SIMA Interactive Management Workshop. Held in Fort Belvoir, Virginia on November 14-16, 1994.
PB96-154877 *02,838*

SIMA (SYSTEMS INTEGRATION FOR MANUFACTURING APPLICATIONS)
Technical Program Description Systems Integration for Manufacturing (SIMA).
PB94-213758 *02,819*

Requisite Elements, Rationale, and Technology Overview for the Systems Intergration for Manufacturing Applications (SIMA) Program. Background Study.
PB96-112685 *02,831*

Systems Integration for Manufacturing Applications Program 1995 Annual Report.
PB96-193735 *02,844*

SIMD (COMPUTERS)
MasPar MP-1 as a Computer Arithmetic Laboratory.
PB95-189437 *01,627*

SIMOX
Electron Traps, Structural Change, and Hydrogen Related SIMOX Defects.
PB94-200391 *02,312*

Charge Trapping and Breakdown Mechanism in SIMOX.
PB94-216637 *02,323*

Effect of Annealing Ambient on the Removal of Oxide Precipitates in High-Dose Oxygen Implanted Silicon.
PB95-164356 *02,356*

Evidence for a Deep Electron Trap and Charge Compensation in Separation by Implanted Oxygen Oxides.
PB95-175337 *02,362*

Defect Pair Formation by Implantation-Induced Stresses in High-Dose Oxygen Implanted Silicon-on-Insulator Material.
PB95-175824 *02,364*

Effect of Anneal Temperature on Si/Buried Oxide Interface Roughness on SIMOX.
PB96-112206 *02,382*

Nano-Defects in Commercial Bonded SOI and SIMOX.
PB96-123674 *02,407*

Effect of Intermediate Thermal Processing on Microstructural Changes of Oxygen Implanted Silicon-on-Insulator Material.
PB96-160213 *02,982*

Effect of Single versus Multiple Implant Processing on Defect Types and Densities in SIMOX.
PB96-160353 *01,957*

SIMULATION
Hot-Deformation Apparatus for Thermomechanical Processing Simulation.
PB94-200136 *03,207*

Cellular Automaton Simulations of Cement Hydration and Microstructure Development.
PB95-175055 *01,320*

Faster Monte Carlo Simulations.
PB96-102074 *04,018*

Two-Dimensional Self-Consistent Radio Frequency Plasma Simulations Relevant to the Gaseous Electronics Conference RF Reference Cell.
PB96-113436 *02,398*

Collection of Results for the SPC/E Water Model.
PB96-147889 *01,127*

SINGLE CRYSTALS
Environmentally Enhanced Fracture of Ceramics.
PB95-125746 *03,046*

Epitaxial Integration of Single Crystal C60.
PB95-153490 *04,592*

Photoluminescence Spectra of Epitaxial Single Crystal C60.
PB96-141205 *04,754*

SINGLE ELECTRON TRANSISTORS
Combined Josephson and Charging Behavior of the Supercurrent in the Superconducting Single-Electron Transistor.
PB95-168522 *04,637*

Voltage Gain in the Single-Electron Transistor.
PB95-176335 *04,671*

SINGLE ELECTRON TUNNELING
Proposed Tests to Evaluate the Frequency-Dependent Capacitor Ratio for Single Electron Tunneling Experiment.
PB97-111454 *01,982*

SINGLE FIBER PULL-OUT TEST
Determination of Fiber-Matrix Interfacial Properties of Importance to Ceramic Composite Toughening.
PB95-125811 *03,149*

SINGLE ION DETECTORS
Superconducting Resonator and a Cryogenic GaAs Field-Effect Transistor Amplifier as a Single-Ion Detection System.
PB95-202727 *03,990*

SINGLE-PLY ROOF MEMBRANES
Pulse-Echo Ultrasonic Evaluation of the Integrity of Seams of Single-Ply Roof Membranes.
PB95-163804 *00,381*

SINTERING
Evolution of the Pore Size Distribution in Final-Stage Sintering of Alumina Measured by Small-Angle X-ray Scattering. (Reannouncement with New Availability Information).
AD-A249 178/5 *03,023*

Small-Angle Neutron Scattering Characterization of Processing/Microstructure Relationships in the Sintering of Crystalline and Glassy Ceramics. (Reannouncement with New Availability Information).
AD-A249 510/9 *03,025*

Controlled Nucleation in Aerosol Reactors for Supression of Agglomerate Formation.
PB95-151973 *00,672*

Effect of Sm2BaCuO5 on the Properties of Sintered (Bulk) YBa2Cu3O6+x.
PB96-119441 *04,733*

SINUSOIDAL SURFACES
Light Scattering by Sinusoidal Surfaces: Illumination Windows and Harmonics in Standards.
PB97-110548 *04,387*

Sinusoidal Surfaces as Standards for BRDF Instruments.
PB97-110597 *04,388*

Windowing Effects on Light Scattering by Sinusoidal Surfaces.
PB97-111215 *04,389*

SITE CHARACTERIZATION
Assessment of Site Response Analysis Procedures.
PB95-210928 *00,450*

SIZE DETERMINATION
Bibliography on Apparel Sizing and Related Issues.
PB94-161924 *02,806*

Parametric Investigation of Metal Powder Atomization Using Laser Diffraction.
PB95-108577 *03,342*

Ultrasonic Technique for Sizing Voids Using Area Functions.
PB95-151916 *02,904*

Variations in Size Measurements by Indicating Gaging Systems.
PB95-163614 *02,864*

SIZE (DIMENSIONS)
Lighting Quality and Light Source Size.
PB95-151783 *00,252*

SKY SURVEYS (ASTRONOMY)
Volume-Limited ROSAT Survey of Extreme Ultraviolet Emission from all Nondegenerate Stars within 10 Parsecs.
PB96-103189 *00,093*

Efficient Way of Identifying New Active Stars: A VLA Survey of X-ray Selected Active Stellar Candidates.
PB96-122882 *00,099*

Scientific Rationale and Present Implementation Strategy for the Far Ultraviolet Spectrograph Explorer (FUSE).
PB96-123328 *00,045*

Riass Coronathon: Joint X-ray and Ultraviolet Observations of Normal F-K Stars.
PB96-200217 *00,109*

SLI ARITHMETRIC
Basic Linear Algebra Operations in SLI Arithmetic.
PB96-165931 *03,421*

SLIDING FRICTION
Wear Model for Alumina Sliding Wear.
PB95-163796 *03,239*

Friction and Oxidative Wear of 440C Ball Bearing Steels Under High Load and Extreme Bulk Temperatures.
PB95-175253 *03,215*

SLIDING VANES
Sliding Vane Flow Conditioner Tests in a 100 Diameter Long 10 inch Natural Gas Orifice Meter at Pacific Gas and Electric. Topical Report, 1990-1992.
PB95-256335 *02,493*

SLOW ELECTRONS
Electron Attachment to Excited Molecules(1).
PB96-122809 *01,087*

SMALL ANGLE NEUTRON SCATTERING
High-Temperature Furnace for In situ Small-Angle Neutron Scattering during Ceramic Processing.
PB96-148127 *03,743*

Instrumental Smearing Effects in Radially Symmetric Small-Angle Neutron Scattering by Numerical and Analytical Methods.
PB96-160429 *02,984*

Simulation and SANS Studies of Gelation Under Shear.
PB96-167176 *01,150*

Small-Angle Neutron-Scattering Study of Dense Sheared Silica Gels.
PB96-167184 *01,151*

Structure and Rheology of Hard-Sphere Systems.
PB96-167333 *00,662*

Small Angle Neutron Scattering Study of a Clay Suspension Under Shear.
PB96-167374 *00,663*

Small-Angle Neutron Scattering (SANS) Study of Worm-Like Micelles Under Shear.
PB96-176698 *04,111*

SMALL ANGLE SCATTERING
Neutron Scattering by Multiblock Copolymers of Structure (A-B)N-A.
PB94-211547 *01,219*

Shear Dependence of Critical Fluctuations in Binary Polymer Mixtures by Small Angle Neutron Scattering.
PB94-211612 *01,220*

Small-Angle X-Ray and Neutron Scattering Study of Block Copolymer/Homopolymer Mixtures.
PB94-211729 *01,221*

Crossover to Strong Shear in a Low-Molecular-Weight Critical Polymer Blend.
PB94-211976 *01,222*

Characterization of Chemically Modified Pore Surfaces by Small Angle Neutron Scattering.
PB95-126181 *00,898*

Characterization of Polyquinoline Block Copolymer Using Small Angle Scattering.
PB95-151882 *01,244*

Hydration in Semicrystalline Polymers: Small-Angle Neutron Scattering Studies of the Effect of Drawing in Nylon-6 Fibers.
PB95-202990 *03,385*

SMALL BUSINESSES
Learning to Change: Opportunities to Improve the Performance of Smaller Manufacturers.
PB94-166212 *00,010*

Opportunities for Innovation: Pollution Prevention.
PB95-147146 *02,520*

Network Brokers Handbook: An Entrepreneurial Guide to Cooperative Strategies for Manufacturing Competitiveness.
PB95-219325 *00,490*

SMALL POLAR MOLECULES
Estimating the Virial Coefficients of Small Polar Molecules.
PB95-176236 *03,276*

SMART CLOCK
Smart Clock: A New Time.
PB95-151445 *01,530*

SMELTING
In-situ Fume Particle Size and Number Density Measurements from a Synthetic Smelt.
PB94-212040 *03,334*

SMOKE
Two Numerical Techniques for Light Scattering by Dielectric Agglomerated Structures.
PB94-140597 *04,225*

Ground-Based Smoke Sampling Techniques Training Course and Collaborative Local Smoke Sampling in Saudi Arabia.
PB94-143542 *02,532*

Effective Measurement Techniques for Heat, Smoke, and Toxic Fire Gases.
PB94-198439 *01,369*

Ultrafine Combustion Aerosol Generator.
PB94-200300 *01,373*

Overview of Smoke Control Technology.
PB94-212867 *00,348*

Preview of ASHRAE's Revised Smoke Control Manual.
PB94-212875 *00,349*

Smoke Control Systems for Elevator Fire Evacuation.
PB94-212883 *00,291*

Development of a New Small-Scale Smoke Toxicity Test Method and Its Comparison with Real-Scale Fire Tests.
PB94-213253 *00,350*

Verification of a Model of Fire and Smoke Transport.
PB95-108718 *00,357*

Dispersion and Deposition of Smoke Plumes Generated in Massive Fires.
PB95-126066 *02,540*

Simulating Smoke Movement through Long Vertical Shafts in Zone-Type Compartment Fire Models.
PB95-143152 *00,368*

Method of Predicting Smoke Movement in Atria with Application to Smoke Management.
PB95-154746 *00,376*

Smoke Plume Trajectory from In situ Burning of Crude Oil in Alaska: Field Experiments.
PB96-131560 *02,594*

Large Eddy Simulations of Smoke Movement in Three Dimensions.
PB96-190012 *01,426*

SMOKE CONTROL
Full Scale Smoke Control Tests at the Plaza Hotel Building.
PB94-212859 *00,347*

Overview of Smoke Control Technology.
PB94-212867 *00,348*

Preview of ASHRAE's Revised Smoke Control Manual.
PB94-212875 *00,349*

Smoke Control Systems for Elevator Fire Evacuation.
PB94-212883 *00,291*

Fire and Smoke Control: An Historical Perspective.
PB95-175808 *00,202*

SMOKE DETECTORS
Measurement of Room Conditions and Response of Sprinklers and Smoke Detectors during a Simulated Two-Bed Hospital Patient Room Fire.
PB94-213717 *00,292*

Analysis of High Bay Hangar Facilities for Detector Sensitivity and Placement.
PB96-190210 *01,429*

SMOKE GENERATORS
Generation and Characterization of Acetylene Smokes.
PB94-200292 *01,372*

SMOKE MANAGEMENT
Method of Predicting Smoke Movement in Atria with Application to Smoke Management.
PB95-154746 *00,376*

SMOKE PROPAGATION
Improvement in Predicting Smoke Movement in Compartmented Structures.
PB94-172418 *00,332*

SMOKE TRANSPORT
Verification of a Model of Fire and Smoke Transport.
PB95-108718 *00,357*

SMOKE YIELD
Airborne Smoke Sampling Package for Field Measurements of Fires.
PB95-150041 *01,381*

SNS JUNCTIONS
Mutual Phase Locking in Systems of High-Tc Superconductor-Normal Metal-Superconductor Junctions.
PB96-135348 *04,744*

SODIUM
Electron-atom collision studies using optically state selected beams. Progress report, May 15, 1987--May 14, 1988.
DE95004446 *03,776*

Electron-atom collision studies using optically state selected beams. Progress report, May 15, 1988--May 14, 1991.
DE95004447 *03,777*

Can Quantum Mechanical Description of Electron-Sodium Collisions Be Considered Complete. Present Status and Future Prospects for 3s <-> 3p Transitions.
PB94-185014 *00,768*

Frozen Human Serum Reference Material for Standardization of Sodium and Potassium Measurements in Serum or Plasma by Ion-Selective Electrode Analyzers.
PB94-185337 *00,532*

Density Matrix Calculation of Population Transfer between Vibrational Levels of Na2 by Stimulated Raman Scattering with Temporally Shifted Laser Beams.
PB94-198546 *00,787*

Femtosecond Time-Resolved Wave Packet Motion in Molecular Multiphoton Ionization and Fragmentation.
PB94-198611 *00,790*

Structures of Sodium Metal.
PB94-198850 *03,319*

Determination of Complex Scattering Amplitudes in Low-Energy Elastic Electron-Sodium Scattering.
PB94-216652 *03,869*

Hyperfine Effects and Associative Ionization of Ultracold Sodium.
PB95-151221 *03,903*

High-Precision Calculations of Cross Sections for Low-Energy Electron Scattering by Ground and Excited State of Sodium.
PB95-152161 *03,914*

Spin-Resolved Elastic Scattering of Electrons from Sodium.
PB95-161774 *03,933*

Connection between Superelastic and Inelastic Electron-Atom Collisions Involving Polarized Collision Partners.
PB95-202297 *03,974*

Femtosecond Time-Resolved Molecular Multiphoton Ionization: The Na2 System.
PB95-202305 *03,975*

Three-Vector Correlation Study of Orientation and Coherence Effects in Na(3p, (2)P1/2 inversely maps (2)P3/2)+He: Semiclassical and Quantum Calculations.
PB95-202453 *03,979*

Alignment in Two-Step Pulsed Laser Excitation of Rydberg Levels in Light Atoms: The Example of Sodium.
PB95-202883 *03,993*

Threshold Electron Excitation of Na.
PB95-202917 *03,994*

Improved Hyperfine Measurements of the Na NP Excited State Through Frequency-Controlled Dopplerless Spectroscopy in a Zeeman Magneto-Optic Laser Trap.
PB95-203840 *04,012*

In-situ Studies of a Novel Sodium Flame Process for Synthesis of Fine Particles.
PB97-113047 *00,681*

Optical and Modeling Studies of Sodium/Halide Reactions for the Formation of Titanium and Boron Nanoparticles.
PB97-113054 *00,682*

SODIUM ATOMS
Associative Ionization in Collisions of Slowed and Trapped Sodium.
PB95-125886 *03,880*

Localization of Atoms in a Three-Dimensional Standing Wave.
PB95-163887 *03,944*

SODIUM BROMIDE
Isopiestic Investigation of the Osmotic and Activity Coefficients of Aqueous NaBr and the Solubility of NaBr2H2O(cr) at 298.15 K: Thermodynamic Properties of the NaBr + H2O System over Wide Ranges of Temperature and Pressure.
PB97-110365 *01,175*

SODIUM CARBONATES
Automated, High Precision Coulometric Titrimetry. Part 2. Strong and Weak Acids and Bases.
PB95-150207 *00,576*

SODIUM CHLORIDES
Comparison of the Corrosion Rates of FeAl, Fe(sub 3)Al and Steel in Distilled Water and 0.5 M Sodium Chloride. Technical Report Number 2, January--March 1991.
DE94017332 *03,186*

SODIUM RUBIDIUM FULLERIDES
Rotational Dynamics of C60 in Na2RbC60.
PB95-153201 *00,948*

SODIUM TUNGSTATES
Rietveld Analysis of NaxWO3+x/2.yH2O, Which Has the Hexagonal Tungsten Bronze Structure.
PB95-107371 *04,524*

SODIUM ZINC ARSENATE
Crystal Structure of a New Sodium Zinc Arsenate Phase Solved by 'Simulated Annealing'.
PB95-107124 *00,870*

SOFT X RAY
New NIST/ARPA National Soft X-ray Reflectometry Facility.
PB96-158092 *04,080*

Soft-X-ray Damage to p-terphenyl Coatings for Detectors.
PB96-159611 *04,364*

Influence of Electrical Isolation on the Structure and Reflectivity of Multilayer Coatings Deposited on Dielectric Substrates.
PB96-159736 *04,365*

New Method for Achieving Accurate Thickness Control for Uniform and Graded Multilayer Coatings on Large Flat Substrates.
PB96-159744 *04,366*

SOFT X-RAY EMISSION
Barium Contributions to the Valence Electronic Structure of YBa2Cu3O7-delta, PrBa2Cu3O7-delta, and Other Barium-Containing Compounds.
PB96-158019 *04,076*

SOFT X-RAY EMISSION SPECTRA
Charge-Transfer-Induced Multiplet Structure in the N4,5O2,3 Soft-X-ray Emission Spectrum of Lanthanum.
PB96-163746 *04,102*

SOFTWARE
FORTRAN Compiler Validation System, Version 2.1.
PB94-500691 *01,698*

HAZARD I Fire Hazard Assessment Method (Version 1.2) (for Microcomputers).
PB94-501988 *00,196*

HAZARD I Fire Hazard Assessment Method, Version 1.2 (Upgrade Package) (for Microcomputers).
PB94-501996 *00,197*

M (also known as MUMPS) Validation Test Suite, Version 8.3 (for Microcomputers).
PB94-502077 *01,699*

Building Life Cycle Cost Computer Program (BLCC), Version 4.2-95 (for Microcomputers).
PB95-501953 *00,266*

Building Life Cycle Cost Computer Program (BLCC) Version 4.21-95 (for Microcomputers).
PB95-502779 *00,267*

Building Life Cycle Cost Computer Program (BLCC) Version 4.22-95 (for Microcomputers).
PB95-503397 00,268

Building Life Cycle Cost Computer Program (BLCC) Version 4.22-95 (for Micrcomputers).
PB96-502794 00,277

Building Life Cycle Cost Computer Program (BLCC) Version 4.4-97 (for Microcomputers).
PB97-500342 00,284

SOFTWARE DEVELOPMENT

IEEE's POSIX: Making Progress.
PB96-160924 01,757

SOFTWARE ENGINEERING

User Interface Component of the Applications Portability Profile Category: Software Standard; Subcategory: Application Program Interface.
FIPS PUB 158-1 01,793

Guide to Software Engineering Environment Assessment and Evaluation.
PB94-140167 01,676

Next Generation Computer Resources: Reference Model for Project Support Environments (Version 2.0).
PB94-143401 01,677

Validation Testing System Requirements. National PDES Testbed Report Series.
PB94-163482 02,771

Time-Perturbation Tuning of MIMD Programs.
PB94-172566 01,684

Report on the Advanced Software Technology Workshop. Held on February 1, 1994.
PB95-136610 01,707

Information Technology Engineering and Measurement Model: Adding Lane Markings to the Information Superhighway.
PB95-143145 01,474

Use of an Environment Classification Model.
PB95-152062 01,709

Perspective on Software Engineering Standards.
PB95-171377 01,811

Framework for the Development and Assurance of High Integrity Software.
PB95-173084 01,716

Analysis of ANSI ASC X12 and UN/EDIFACT Electronic Data Interchange (EDI) Standards.
PB95-220554 01,729

Persistent Object Base System Testing and Evaluation.
PB95-220588 01,730

Unravel: A CASE Tool to Assist Evaluation of High Integrity Software. Volume 1. Requirements and Design.
PB95-267886 01,736

Unravel: A CASE Tool to Assist Evaluation of High Integrity Software. Volume 2. User Manual.
PB95-267894 01,737

Defining Environment Integration Requirements.
PB96-131545 02,733

Findings and Recommendations from a Software Reengineering Case Study.
PB96-155791 01,752

Slicing in the Presence of Parameter Aliasing.
PB96-160858 01,755

Assessing Functional Diversity by Program Slicing.
PB96-160890 03,734

Program Slicing.
PB96-160981 01,761

Verification and Validation.
PB96-161393 01,765

Interoperability Experiments with CORBA and Persistent Object Base Systems.
PB96-183140 01,772

Reference Information for the Software Verification and Validation Process.
PB96-188164 01,773

Measurement of Process Complexity.
PB97-113138 01,781

Experimental Models for Software Diagnosis.
PB97-113906 01,783

CSL View of Applications Portability, Scalability, and Interoperability.
PB97-122303 01,787

SOFTWARE ENGINEERING ENVIRONMENTS

Making Sense of Software Engineering Environment Framework Standards.
PB95-105037 01,701

SOFTWARE QUALITY ASSURANCE

SQA Standards and Total Quality Management.
PB96-111844 01,743

SQA and TQM in Software Quality Improvement.
PB96-160791 01,754

SOFTWARE REENGINEERING

Verification and Validation of Reengineered Software.
PB96-161401 01,766

SOFTWARE RELIABILITY

Quality Characteristics and Metrics for Reusable Software (Preliminary Report).
PB94-203437 01,693

Analysis of Selected Software Safety Standards.
PB95-151262 01,708

High Integrity Software Standards Activities at NIST.
PB96-112214 01,744

Control and Instrumentation: Standards for High-Integrity Software.
PB96-161369 03,736

Report of a Workshop on the Assurance of High Integrity Software.
PB96-161377 01,763

Standards for High Integrity Software.
PB96-161385 01,764

SOFTWARE REUSE

Context Analysis of the Network Management Domain. Conducted as Part of the Domain Analysis Case Study.
PB94-142528 01,465

Generic Manufacturing Controllers.
PB94-199940 02,818

Quality Characteristics and Metrics for Reusable Software (Preliminary Report).
PB94-203437 01,693

Domain Analysis of the Alarm Surveillance Domain. Version 1.0. Conducted as Part of the Domain Analysis Case Study Project.
PB95-136339 01,705

Glossary of Software Reuse Terms.
PB95-178992 01,720

Template-Driven Systems Development with IDEF: Enterprise Standards for Reuse.
PB96-160965 02,788

SOFTWARE TOOLS

RDI-SIM ECMA Inter-Domain Routing Protocol Simulation Tool.
PB94-172301 01,683

Retrieving Articles from the Internet (without a UNIX Workstation). Part 1. File Formats and Software Tools.
PB95-168720 02,728

Expert Control System Shell Version 1.0 User's Guide.
PB95-198859 01,790

PET and DINGO Tools for Deriving Distributed Implementations from Estelle.
PB95-203253 01,727

Unravel: A CASE Tool to Assist Evaluation of High Integrity Software. Volume 1. Requirements and Design.
PB95-267886 01,736

Unravel: A CASE Tool to Assist Evaluation of High Integrity Software. Volume 2. User Manual.
PB95-267894 01,737

Overview of the Manufacturing Engineering Toolkit Prototype.
PB96-128228 02,833

Method to Determine a Basis Set of Paths to Perform Program Testing.
PB96-131503 01,747

Object-Oriented Tel/Tk Binding for Interpreted Control of the NIST EXPRESS Toolkit in the NIST STEP Application Protocol Development Environment.
PB96-141049 02,785

Fire Protection Engineering Tools. Simple Tools: The Equations.
PB96-156179 00,221

Distributed Communication Methods and Role-Based Access Control for Use in Health Care Applications.
PB96-183165 01,508

Unified Process Specification Language: Requirements for Modeling Process.
PB97-116123 02,850

SC4 Short Names Registry.
PB97-122410 02,799

SOFTWEAR ENGINEERING

Making Sense of Software Engineering Environment Framework Standards.
PB95-105037 01,701

SOFTWOODS

Voluntary Product Standard PS 20-94. American Softwood Lumber Standard.
PB94-162500 03,402

SOI (SEMICONDUCTORS)

Efficient Method to Compute the Maximum Transient Drain Current Overshoot in Silicon on Insulator Devices.
PB94-172483 02,300

Electron Traps, Structural Change, and Hydrogen Related SIMOX Defects.
PB94-200391 02,312

Defect of Thermal Ramping and Annealing Conditions on Defect Formation in Oxygen Implanted Silicon-On-Insulator Material.
PB94-212966 02,318

Evidence for a Deep Electron Trap and Charge Compensation in Separation by Implanted Oxygen Oxides.
PB95-175337 02,362

Defect Pair Formation by Implantation-Induced Stresses in High-Dose Oxygen Implanted Silicon-on-Insulator Material.
PB95-175824 02,364

Nano-Defects in Commercial Bonded SOI and SIMOX.
PB96-123674 02,407

SOIL MECHANICS

Preliminary Processing of the Lotung LSST Data.
PB96-165972 03,690

Estimation of System Damping at the Lotung Site by Application of System Identification.
PB96-214697 01,351

SOIL STABILIZATION

Ground Improvement Techniques for Liquefaction Remediation Near Existing Lifelines.
PB96-128111 01,350

SOIL-STRUCTURE INTERACTIONS

Dynamic Characteristics of Five Tall Buildings during Strong and Low-Amplitude Motions.
PB94-199981 00,427

Assessment of Site Response Analysis Procedures.
PB95-210928 00,450

De Facto Microzonation through the Use of Soils Factors in Design Triggers.
PB96-141148 00,462

Preliminary Processing of the Lotung LSST Data.
PB96-165972 03,690

January 17, 1995 Hyogoken-Nanbu (Kobe) Earthquake. Performance of Structures, Lifelines and Fire Protection Systems. Executive Summary and Paper.
PB97-104160 00,475

SOL-GEL GLASS

Bacteriorhodopsin Immobilized in Sol-Gel Glass.
PB95-151429 03,532

SOLAR ACTIVITY

Distant Future of Solar Activity: A Case Study of Beta Hydri. 3. Transition Region, Corona, and Stellar Wind.
PB94-185220 00,049

Distant Future of Solar Activity: A Case Study of beta Hydri. 3. Transition Region, Corona, and Stellar Wind.
PB95-153441 00,074

SOLDER JOINTS

SPC Artifact for Automated Solder Joint Inspection.
PB96-161716 04,095

SOLDERING

Lubrication Theory for Reactive Spreading of a Thin Drop.
PB95-189460 02,865

SOLDERS

Aging Effects on XRF Measurements of Solder Coatings.
PB95-140927 03,123

SOLID CLUSTERS

Vibrational Relaxation Measurements of Carbon Monoxide on Metal Clusters.
PB94-211810 00,820

Cs Cluster Binding to a GaAs Surface.
PB94-213006 00,846

SOLID FUELS

Minimum Mass Flux Requirements to Suppress Burning Surfaces with Water Sprays.
PB96-183181 01,425

SOLID LUBRICANTS

Control of Friction and Wear of Alpha-Alumina with a Composite Solid-Lubricant Coating.
PB95-125969 03,225

SOLID NEON

Vibrational Spectra of Molecular Ions Isolated in Solid Neon. XI. NO2(+), NO2(-), and NO3(-).
PB95-125688 00,890

Vibrational Spectra of Molecular Ions Isolated in Solid Neon. 13. Ions Derived from HBr and HI.
PB97-119234 01,188

SOLID-PHASE ENTRAPMENT

Flow Immunoassay Using Solid-Phase Entrapment.
PB96-200951 00,642

SOLID PROPELLANT COMBUSTION

Solid Propellant Gas Generators: Proceedings of the 1995 Workshop. Held in Gaithersburg, Maryland on June 28-29, 1995.
PB96-131479 01,412

SOLID-SOLID INTERFACES

Generalized Plane Strain Analysis of a Bimaterial Composite Containing a Free Surface Normal to the Interface.
PB95-163341 03,164

Measuring Contact Charge Transfer at Interfaces: A New Experimental Technique.
PB95-164570 03,053

SOLID SOLUTIONS

Modeling the Evolution of Structure in Unstable Solid Solution Phases by Diffusional Mechanisms.
PB94-199403 03,324

Magnetic Dielectric Oxides: Subsolidus Phase Relations in the BaO: Fe2O3: TiO2 System.
PB96-176524 01,156

SOLIDIFICATION

Computation of Dendrites Using a Phase Field Model.
PB94-160744 04,436

In-Line Optical Monitoring of Injection Molding.
PB94-185105 01,201

Thermodynamic Constraints on Non-Equilibrium Solidification of Ordered Intermetallic Compounds.
PB94-198934 03,321

Disorder Trapping in Ni2TiAl.
PB94-198942 *03,322*

Asymptotic Behavior of Modulated Taylor-Couette Flows with a Crystalline Inner Cylinder.
PB94-199072 *04,469*

Effect of Modulated Taylor-Couette Flows on Crystal-Melt Interfaces: Theory and Initial Experiments.
PB94-216736 *04,521*

xi-Vector Formulation of Anisotropic Phase-Field Models: 3-D Asymptotics.
PB95-136628 *04,536*

Phase-Field Model for Solidification of a Eutectic Alloy.
PB95-147914 *03,345*

Morphological Stability.
PB95-153318 *04,591*

Ultrasonic Method for Reconstructing the Two-Dimensional Liquid-Solid Interface in Solidifying Bodies.
PB95-161782 *03,349*

Xi-Vector Formulation of Anisotropic Phase-Field Models: 3-D Asymptotics.
PB97-122550 *04,816*

SOLIDS

Vibrational Spectra of Molecular Ions Isolated in Solid Neon: HCCH+ and HCC-. (Reannouncement with New Availability Information).
AD-A253 551/6 *00,707*

Vibrational Spectra of Molecular Ions Isolated in Solid Neon. 11. NO2(+), NO2(-), and NO3(-).
AD-A275 828/2 *00,708*

Density of Solids and Liquids.
AD-A278 517/8 *00,711*

Survey of the Literature on Heat Transfer from Solid Surfaces to Cryogenic Fluids.
AD-A286 680/4 *04,193*

Infrared and Near-Infrared Spectra of HCC and DCC Trapped in Solid Neon.
AD-A295 578/9 *03,773*

Surface Forces and Adhesion between Dissimilar Materials Measured in Various Environments.
PB94-172970 *03,033*

Supercritical Solubility of Solids from Near-Critical Dilute-Mixture Theory.
PB94-211703 *00,819*

Observed Frustration in Confined Block Copolymers.
PB95-150033 *01,238*

Molecular Orbital Calculations of Bond Rupture in Brittle Solids.
PB95-164059 *00,973*

Water Droplet Evaporation from Radiantly Heated Solids.
PB95-217147 *00,394*

Total-Dielectric-Function Approach to Electron and Phonon Response in Solids.
PB96-102884 *01,067*

Shear-Induced Melting of Two-Dimensional Solids.
PB96-112057 *01,075*

Intrinsic Viscosity and the Polarizability of Particles Having a Wide Range of Shapes.
PB96-119318 *03,170*

Hemispherical Test Fixture for Measuring the Wavefields Generated in an Anisotropic Solid.
PB96-190087 *03,181*

SOLUBILITY

Octacalcium Phosphate Carboxylates IV. Kinetics of Formation and Solubility of Octacalcium Phosphate Succinate.
PB94-185600 *00,776*

Supercritical Solubility of Solids from Near-Critical Dilute-Mixture Theory.
PB94-211703 *00,819*

Effect of Ethanol on the Solubility of Dicalcium Phosphate Dihydrate in the System Ca(OH)2-H3PO4-H2O at 37C.
PB95-163507 *00,163*

Effect of Ethanol on the Solubility of Hydroxyapatite in the System Ca(OH)2-H3PO4-H2O at 25C and 33C.
PB95-169231 *00,169*

Solubility Measurement by Direct Injection of Supercritical-Fluid Solutions into a HPLC System.
PB95-175626 *00,997*

High-Pressure Equilibrium Cell for Solubility Measurements in Supercritical Fluids.
PB95-175634 *00,998*

CO2/CH4 Transport in Polyperfluorosulfonate Ionomers: Effects of Polar Solvents on Permeation and Solubility.
PB96-163803 *01,145*

Solubilities of Copper(II) and Chromium(III) beta-Diketonates in Supercritical Carbon Dioxide.
PB96-164215 *01,147*

SOLUBILITY PRODUCTS

Composition and Solubility Product of a Synthetic Calcium Hydroxyapatite.
PB96-180104 *02,995*

SOLUTES

Shape Selectivity in Reversed-Phase Liquid Chromatography for the Separation of Planar and Non-Planar Solutes.
PB95-162608 *00,596*

Solubility Measurement by Direct Injection of Supercritical-Fluid Solutions into a HPLC System.
PB95-175626 *00,997*

SOLUTIONS

Neutron Scattering Study of Shear Induced Turbidity in Polystyrene/Dioctyl Phthalate Solutions at High Shear Rates.
PB94-172624 *01,197*

Long-Term Stability of Carrier-Free Polonium Solution Standards.
PB94-185170 *00,685*

Neutron Scattering Study of Shear Induced Turbidity in Polystyrene Dissolved in Dioctyl Phthalate.
PB95-161865 *01,256*

Effects of Aluminum Oxalate/Glycine Pretreatment Solutions on Dentin Permeability.
PB95-164505 *03,565*

Competition between Hydrodynamic Screening ('Draining') and Excluded Volume Interactions in an Isolated Polymer Chain.
PB95-175402 *01,265*

SOLVENTS

Solvent Effects in the Reactions of Peroxyl Radicals with Organic Reductants. Evidence for Proton Transfer Mediated Electron Transfer.
PB95-107157 *00,873*

Terminally Anchored Chain Interphases: Their Chromatographic Properties.
PB95-181061 *01,272*

Terminally Anchored Chain Interphases: The Effect of Multicomponent, Polydisperse Solvents on Their Equilibrium Properties.
PB95-181079 *01,273*

Mixing Plate-Like and Rod-Like Molecules with Solvent: A Test of Flory-Huggins Lattice Statistics.
PB96-126206 *03,173*

SOMMERFELD CONSTANT

Fine-Structure Constant.
PB94-172996 *03,795*

SOOT

Greatly Enhanced Soot Scattering in Flickering Ch4/Air Diffusion Flames.
PB94-172988 *01,361*

Laser Imaging of Chemistry-Flowfield Interactions: Enhanced Soot Formation in Time-Varying Diffusion Flames.
PB94-185352 *01,364*

Fundamental Mechanisms for CO and Soot Formation.
PB95-143160 *01,380*

Oxidation of Soot and Carbon Monoxide in Hydrocarbon Diffusion Flames.
PB95-150215 *01,382*

Laser-Induced Fluorescence Measurements of OH. Concentrations in the Oxidation Region of Laminar, Hydrocarbon Diffusion Flames.
PB95-162160 *01,387*

Quantitative Measurements of Enhanced Soot Production in a Flickering Methane/Air Diffusion Flame.
PB95-203246 *01,393*

Simultaneous Optical Measurement of Soot Volume Fraction, Temperature, and CO2 in Heptane Pool Fire.
PB96-102132 *01,397*

Laser-Induced Fluorescence Measurements of OH in Laminar Diffusion Flames in the Presence of Soot Particles.
PB96-123120 *01,409*

Post-Flame Soot.
PB96-193701 *01,430*

Computations of Enhanced Soot Production in Time-Varying CH4/Air Diffusion Flames.
PB97-119218 *01,440*

SORPTION

Sorption of Moisture on Epoxy and Alkyd Free Films and Coated Steel Panels.
PB95-162475 *03,192*

SOUND VELOCITIES

Void Shape in Sintered Titanium.
PB96-141023 *02,705*

SOURCE LIST

Guide to Instrumentation Literature.
AD-A280 278/3 *02,617*

SOXHLET EXTRACTION

Effects of Soxhlet Extraction on the Surface Oxide Layer of Silicon Nitride Powders.
PB95-175584 *03,057*

SPACE

Partial Pressure Analysis in Space Testing.
PB96-103072 *04,829*

SPACE CHARGE

Effect of DC Tests on Induced Space Charge.
PB94-172350 *02,212*

Spatial Dependence of Electrical Fields Due to Space Charges in Films of Organic Dielectrics Used for Insulation of Power Cables.
PB94-199130 *02,214*

SPACE ENVIRONMENT SIMULATION

Partial Pressure Analysis in Space Testing.
N95-14084/4 *04,827*

SPACE GROUP SYMMETRY

Powder X-ray Diffraction Data for Ca2Bi2O5 and C4Bi6O13.
PB96-161278 *04,777*

SPACE HEATERS

Predicting the Energy Performance Ratings of a Family of Type I Combination Appliances.
PB95-105524 *02,504*

SPACE HVAC SYSTEMS

Computer Programs for Simulation of Lighting/HVAC Interactions.
PB94-140407 *02,501*

Lighting and HVAC.
PB95-150991 *00,250*

NIST Lighting and HVAC Interaction Test Facility.
PB95-151007 *00,251*

Using Emulators to Evaluate the Performance of Building Energy Management Systems.
PB95-175774 *00,259*

Reproducibility of Tests on Energy Management and Control Systems Using Building Emulators.
PB95-175980 *00,260*

Indoor Air Quality Impacts of Residential HVAC Systems. Phase 2.A Report: Baseline and Preliminary Simulations.
PB95-178893 *02,554*

Performance Testing of a Family of Type I Combination Appliance.
PB95-220521 *02,505*

Indoor Air Quality Impacts of Residential HVAC Systems Phase II.B Report: IAQ Control Retrofit Simulations and Analysis.
PB96-106877 *02,559*

Use of Building Emulators to Evaluate the Performance of Building Energy Management Systems.
PB96-111901 *00,269*

Optimal Control of Building and HVAC Systems.
PB96-141353 *00,272*

Multizone Modeling of Three Residential Indoor Air Quality Control Options.
PB96-146659 *02,565*

Workplan to Analyze the Energy Impacts of Envelope Airtightness in Office Buildings.
PB96-154463 *00,273*

HVAC CAD Layout Tools: A Case Study of University/Industry Collaboration.
PB97-112221 *00,281*

Fault Diagnosis of an Air-Handling Unit Using Artificial Neural Networks.
PB97-121321 *00,283*

SPACE INDUSTRIALIZATION

In-Space Welding: Visions and Realities.
PB95-163234 *04,830*

SPACE SHUTTLE

SSME LOX Duct Flowmeter Design and Test Results.
PB96-161955 *04,826*

SPACE SHUTTLE MAIN ENGINE

Vortex Shedding Flowmeters for SSME Ducts.
PB95-169215 *01,453*

Wear Mechanism Maps of 440C Martensitic Stainless Steel.
PB96-111810 *04,834*

SPACE STATION FREEDOM

Overview of NASREM: The NASA/NBS Standard Reference Model for Telerobot Control System Architecture.
PB94-194560 *04,831*

Evolution of the Flight Telerobotic Servicer.
PB94-216082 *04,832*

SPACE STATIONS

Mapping Processes to Processors for Space-Based Robot Systems.
PB95-151510 *04,833*

SPACE TESTINGS

Partial Pressure Analysis in Space Testing.
PB96-103072 *04,829*

SPACEBORNE ASTRONOMY

Goddard High Resolution Spectrograph: Instrument, Goals, and Science Results.
PB96-123278 *00,044*

SPACECRAFT CONSTRUCTION MATERIALS

Ignition and Subsequent Flame Spread Over a Thin Cellulosic Material.
PB96-160270 *04,836*

SPACECRAFT POWER SUPPLIES

Metrology Requirements of Future Space Power Systems.
PB95-140984 *04,840*

SPACECRAFT SHIELDING

Updated Calculations for Routine Space-Shielding Radiation Dose Estimates: SHIELDOSE-2.
PB95-171039 *04,838*

SPARC CALIBRATOR

Slant Path Atmospheric Refraction Calibrator: An Instrument to Measure the Microwave Propagation Delays Induced by Atmospheric Water Vapor.
PB95-151270 *01,476*

SPARK GAPS

Electrical Breakdown in Transformer Oil in Large Gaps.
PB95-150579 *01,889*

SPATIAL DISTRIBUTION

Effect of Swelling on the Elasticity of Rubber: Localization Model Description.
PB94-211034 *01,216*

Elastic Scattering of Polymer Networks.
PB95-161816 *01,255*

SPATIAL RELATIONS
Representing Designs with Logic Formulations of Spatial Relations.
PB97-111561 *02,792*

SPATIAL RESOLUTION
Microanalysis to Nanoanalysis: Measuring Composition at High Spatial Resolution.
PB95-107173 *00,563*

SPECIAL FUNCTIONS
Software Needs in Special Functions.
PB95-105045 *01,702*

Numerical Evaluation of Special Functions.
PB96-119557 *03,417*

SPECIAL FUNCTIONS (MATHEMATICS)
Software Needs in Special Functions.
PB96-200977 *01,778*

SPECIFIC HEAT
Millisecond-Resolution Pulse Heating System for Specific-Heat Measurements at High Temperatures.
PB94-199999 *02,635*

Apparent Molar Heat Capacities and Apparent Molar Volumes of Aqueous Glucose at Temperatures from 298.15 K to 327.01 K.
PB94-212800 *03,459*

Analytical Method of Determining the Heat Capacity at High Temperatures from the Surface Temperature of a Cooling Sphere.
PB94-216124 *03,865*

High-Temperature Adiabatic Calorimeter for Constant-Volume Heat Capacity Measurements of Compressed Gases and Liquids.
PB95-168860 *00,989*

Measurements of Molar Heat Capacity at Constant Volume (Cv) for 1,1,1,2-Tetrafluoroethane (R134a).
PB95-168878 *03,264*

Correlation of the Ideal Gas Properties of Five Aromatic Hydrocarbons.
PB95-175816 *01,002*

SPECIFICATIONS
Formal Multi-Layer Test Methodology and Its Application to OSI.
PB94-172194 *02,718*

Control Entity Interface Specification.
PB94-191715 *02,815*

Formal Specification and Verification of Control Software for Cryptographic Equipment.
PB94-213030 *01,585*

CALS-Automated Interchange of Technical Information.
PB94-962000 *03,657*

Model Minimum Performance Specifications for Lidar Speed Measurement Devices.
PB95-197455 *04,861*

CALS-Automated Interchange of Technical Information.
PB95-962000 *03,666*

Application Software Interface: ISDN Services for an Open Systems Environment.
PB96-131487 *01,492*

Development of Near-Field Test Procedures for Communication Satellite Antennas.
PB96-135082 *02,010*

Predicate Differences and the Analysis of Dependencies in Formal Specifications.
PB96-160940 *01,759*

Technique for Analyzing the Effects of Changes in Formal Specifications.
PB96-160957 *01,760*

Industry/Government Open Systems Specification: The Development of GOSIP Version 3.
PB96-161245 *01,505*

Experimental Evaluation of Specification Techniques for Improving Functional Testing.
PB96-201009 *01,779*

SPECTRA
Atomic Energy Levels. As Derived From the Analyses of Optical Spectra. Volume 3.
AD-A280 279/1 *00,714*

Microwave Spectrum and Structure of CH3NO2-H20.
AD-A296 377/5 *00,719*

Molecular Microwave Spectra Tables.
AD-A296 498/9 *00,720*

Energy Levels of Germanium, Ge I through Ge XXXII.
PB94-162351 *00,747*

SPECTRAL COMPARATOR
Comparison of Filter Radiometer Spectral Responsivity with the NIST Spectral-Irradiance and Illuminance Scales.
PB97-113161 *04,162*

SPECTRAL EMISSION
High-Speed Spatial Scanning Pyrometer.
PB94-200003 *02,636*

Standards for Corrected Fluorescence Spectra.
PB95-150835 *00,581*

Dynamic Technique for Measuring Normal Spectral Emissivity of Electrically Conducting Solids at High Temperatures with a High-Speed Spatial Scanning Pyrometer.
PB95-153045 *03,921*

SPECTRAL EMITTANCE
Wavelength Dependence of Normal Spectral Emissivity of High-Temperature Metals at Their Melting Point.
PB94-200011 *03,398*

SPECTRAL ENERGY DISTRIBUTION
Penetration and Diffusion of Hard X-rays through Thick Barriers. III. Studies of Spectral Distributions.
AD-A292 502/2 *03,771*

SPECTRAL INTERFERENCE
Spectral Interference in the Determination of Arsenic in High-Purity Lead and Lead-Base Alloys Using Electrothermal Atomic Absorption Spectrometry and Zeeman-Effect Background Correction.
PB96-112099 *00,614*

SPECTRAL LINES
Isotope Shifts and Hyperfine Splittings of the 398.8-nm Yb I Line.
PB94-199585 *03,814*

Sobolev Approximation for Line Formation with Partial Frequency Redistribution.
PB95-202669 *00,078*

Magnetic Fields in Star-Forming Regions: Observations.
PB96-123005 *00,100*

Irradiances of Spectral Lines in Mercury Pencil Lamps.
PB96-176466 *04,375*

SPECTRAL RADIANCE
Results of a NIST/VNIIOFI Comparison of Spectral-Radiance Measurements.
PB97-113021 *04,159*

SPECTRAL RADIOMETRY
Simultaneous Measurement of Normal Spectral Emissivity by Spectral Radiometry and Laser Polarimetry at High Temperatures in Pulse-Heating Experiments: Application to Molybdenum and Tungsten.
PB97-118376 *02,694*

SPECTRAL REFLECTANCE
Spectrally Smooth Reflectances That Match.
PB95-176319 *04,306*

SPECTRAL RESOLUTION
Observing Stellar Coronae with the Goddard High Resolution Spectrograph. I. The dMe Star AU Microscopii.
PB96-102777 *00,092*

Redshifts in Stellar Transition Regions.
PB96-123310 *00,104*

SPECTRAL SHIFT
Theoretical Analysis of the Coherence-Induced Spectral Shift Experiments of Kandpal, Vaishya, and Joshi.
PB94-219383 *00,561*

Comments on the Paper 'Wolf Shifts and Their Physical Interpretation under Laboratory Conditions'.
PB94-219391 *04,246*

Reply to Professor Wolf's Comments on My Paper on Wolf Shifts.
PB94-219409 *04,247*

Wavelengths and Isotope Shifts for Lines of Astrophysical Interest in the Spectrum of Doubly Ionized Mercury (Hg III).
PB95-140869 *03,887*

Van der Waals Bond Lengths and Electronic Spectral Shifts of the Benzene-Kr and Benzene-Xe Complexes.
PB95-151387 *00,932*

SPECTROCHEMISTRY ANALYSIS
Microanalysis to Nanoanalysis: Measuring Composition at High Spatial Resolution.
PB95-107173 *00,563*

SPECTROGRAPHS
Scientific Rationale and Present Implementation Strategy for the Far Ultraviolet Spectrograph Explorer (FUSE).
PB96-123328 *00,045*

SPECTROGRAPHY
Flat and Curved Crystal Spectrography for Mammographic X-ray Sources.
PB97-122246 *03,642*

SPECTROMETERS
Stabilization and Precise Calibration of a Continuous-Wave Difference Frequency Spectrometer by Use of a Simple Transfer Cavity.
PB95-162350 *04,276*

Electron-Ion-X-ray Spectrometer System.
PB95-176137 *03,958*

Narrow-Band Tunable Diode Laser System with Grating Feedback, and a Saturated Absorption Spectrometer for Cs and Rb.
PB95-202891 *04,319*

Energy Calibration of X-ray Photoelectron Spectrometers: Results of an Interlaboratory Comparison to Evaluate a Proposed Calibration Procedure.
PB96-102918 *04,027*

Simple Variable Line Space Grating Monochromator for Synchrotron Light Source Beamlines.
PB96-156203 *04,065*

SPECTROMETRY
Crystal Diffraction Spectrometry for Accurate, Non-Invasive kV/Spectral Measurement for Improvement of Mammographic Image Quality.
AD-A297 943/3 *00,721*

Spectral Interference in the Determination of Arsenic in High-Purity Lead and Lead-Base Alloys Using Electrothermal Atomic Absorption Spectrometry and Zeeman-Effect Background Correction.
PB96-112099 *00,614*

Quantitative Determination of Oxidative Base Damage in DNA by Stable Isotope-Dilution Mass Spectrometry.
PB96-200886 *03,483*

SPECTROPHOTOMETERS
Standard Reference Materials: Glass Filters as a Standard Reference Material for Spectrophotometry - Selection, Preparation, Certification, and Use of SRM 930 and SRM 1930.
PB94-188844 *00,536*

SPECTRORADIOMETERS
Report on USDA Ultraviolet Spectroradiometers.
PB96-214648 *00,125*

Interface-Filter Characterization of Spectraradiometers and Colorimeters.
PB97-122212 *04,399*

SPECTROSCOPIC ANALYSIS
Spectroscopic Data for Fusion Edge Plasmas.
PB95-151569 *04,410*

Spectroscopic Diagnostics of Low Temperature Plasmas: Techniques and Required Data.
PB95-151577 *04,411*

Diode Laser as a Spectroscopic Tool.
PB95-175485 *00,600*

Spectroscopic Study of Quantized Breakdown Voltage States of the Quantum Hall Effect.
PB96-113584 *04,730*

SPECTROSCOPIC COUPLING
Atomic Transition Probabilities and Tests of the Spectroscopic Coupling Scheme for N I.
PB96-138466 *04,057*

SPECTROSCOPIC DATA
Comprehensive Spectroscopic Data Tabulations and Progress in the Compilation of Atomic Transition Probabilities.
PB95-151551 *03,909*

Spectroscopic Data Tables for Highly-Ionized Atoms.
PB95-151585 *03,910*

SPECTROSCOPIC ELLIPSOMETRY
High-Accuracy Principal-Angle Scanning Spectroscopic Ellipsometry of Semiconductor Interfaces.
PB96-163787 *02,427*

SPECTROSCOPY
Spectroscopic Study of Reaction Intermediates and Mechanisms in Nitramine Decomposition and Combustion.
AD-A296 061/5 *03,774*

Theoretical Analysis of the Coherence-Induced Spectral Shift Experiments of Kandpal, Vaishya, and Joshi.
PB94-219383 *00,561*

Phase Shifts and Intensity Dependence in Frequency-Modulation Spectroscopy.
PB96-103205 *01,071*

In situ Fluorescence Cell Mass Measurements of 'Saccharomyces cerevisiae' Using Cellular Tryptophan.
PB96-135041 *03,547*

Artificial Crack in Steel: An Ultrasonic-Resonance-Spectroscopy and Modeling Study.
PB96-141395 *03,241*

RIS Measurements of the AC Stark Shift.
PB96-158035 *04,078*

Use of Pressure for Quantum-Well Band-Structure Characterization.
PB96-164058 *04,779*

Energy Distributions of Neutrons Scattered from Solid C60 by the Beryllium Detector Method.
PB96-176631 *03,740*

Pairwise and Nonpairwise Additive Forces in Weakly Bound Complexes: High Resolution Infrared Spectroscopy of ArnDF (n=1,2,3).
PB96-200357 *04,125*

Vibrationally Resolved Photoelectron Angular Distributions and Branching Ratios for the Carbon Dioxide Molecule in the Wavelength Region 685-795 Angstrom.
PB96-201207 *04,131*

Laser Bandwidth Effects in Quantitative Cavity Ring-Down Spectroscopy.
PB97-112254 *04,394*

Resonance Enhanced Multiphoton Ionization Spectroscopy of the PF Radical.
PB97-119119 *00,702*

SPECTRUM ANALYSIS
Complementary Molecular Information on Phthalocyanine Compounds Derived from Laser Microprobe Mass Spectrometry and Micro-Raman Spectroscopy.
PB94-172269 *00,757*

Thermodynamic Properties of Gas Phase Species of Importance to Ozone Depletion.
PB94-198215 *00,126*

Modeling Polarization Curves and Impedance Spectra for Simple Electrode Systems.
PB94-198876 *03,188*

2-Tunneling Path Internal-Axis-Method-Like Treatment of the Microwave Spectrum of Divinyl Ether.
PB94-200466 *00,808*

Two-Dimensional POMMIE Carbon-Proton Chemical Shift Correlated (13)C NMR Spectrum Editing.
PB94-200508 *00,809*

Resonance Enhanced Multiphoton Ionization Spectroscopy of 2-Butene-1-yl (C4H7) between 455-485 nm.
PB95-151031 *00,670*

Applications of Fluorescence Spectroscopy in Polymer Science and Technology.
PB95-163770 *01,258*

SPECULAR REFLECTION
Specular and Diffuse Reflection Measurements of Electronic Displays.
PB97-119200 *02,208*

SPEECH
Error Protecting Characteristics of CDMA and Impacts on Speech.
PB96-122452 *01,491*

SPEECH RECOGNITION
Benchmarks for the Evaluation of Speech Recognizers.
PB94-211539 *01,566*

SPEED INDICATORS
Model Minimum Performance Specifications for Lidar Speed Measurement Devices.
PB95-197455 *04,861*

SPHERES
Analytical Method of Determining the Heat Capacity at High Temperatures from the Surface Temperature of a Cooling Sphere.
PB94-216124 *03,865*

Brownian Diffusion of Hard Spheres at Finite Concentrations.
PB95-164307 *00,975*

Forward Scattering of a Gaussian Beam by a Nonabsorbing Sphere.
PB97-112288 *04,395*

SPI
Using Synthetic-Perturbation Techniques for Tuning Shared Memory Programs (Extended Abstract).
PB94-172657 *01,685*

SPIN DYNAMICS
Magnetic Structure and Spin Dynamics of the Pr and Cu in Pr2CuO4.
PB96-111836 *04,036*

SPIN TRAP
Unusual Spin-Trap Chemistry for the Reaction of Hydroxyl Radical with the Carcinogen N-Nitrosodimethylamine.
PB95-151643 *00,692*

SPIN VALVES
Simulating Device Size Effects on Magnetization Pinning Mechanisms in Spin Valves.
PB97-112593 *04,158*

SPINACH
Determination of 21 Elements by INAA for Certification of SRM 1570a, Spinach.
PB96-167242 *00,698*

SPINDLES
Evaluation of a Tapered Roller Bearing Spindle for High-Precision Hard Turning Applications.
PB96-160494 *02,700*

SPINDT CATHODES
Planar Lenses for Field-Emitter Arrays.
PB96-103064 *02,112*

SPINNING ROTOR GAGE CONTROLLERS
PC-Based Spinning Rotor Gage Controller.
PB95-175832 *02,609*

SPINODAL
Physical Limit to the Stability of Superheated and Stretched Water.
PB96-122551 *01,083*

SPINODAL DECOMPOSITION
Time-Resolved Small-Angle Neutron Scattering Study of Spinodal Decomposition in Deuterated and Protonated Polybutadiene Blends. 1. Effect of Initial Thermal Fluctuations.
PB95-161196 *01,252*

Relaxation After a Temperature Jump Within the One Phase Region of a Polymer Mixture.
PB97-112494 *03,394*

Dimensional Crossover in the Phase Separation Kinetics of Thin Polymer Blend Films.
PB97-113088 *03,395*

SPINOR EQUATIONS
Spinor Equations in Relativistic Quantum Mechanics.
PB97-110605 *04,142*

SPIRALLY-REINFORCED BRIDGE COLUMNS
Evaluating the Seismic Performance of Lightly-Reinforced Circular Concrete Bridge Columns.
PB95-163259 *01,335*

SPLICES
Fibre Splice Loss: A Simple Method of Calculation.
PB95-175519 *04,299*

SPONGES
Swelling and Growth of Polymers, Membranes and Sponges.
PB97-118400 *03,396*

SPRAY COMBUSTION
Role of Combustion on Droplet Transport in Pressure-Atomized Spray Flames.
PB96-204433 *01,434*

SPRAY COOLING
Transient Cooling of a Hot Surface by Droplets Evaporation.
PB94-156957 *03,783*

SPRAY DRIED POWDER
Characterization and Processing of Spray-Dried Zirconia Powders for Plasma Spray Application.
PB97-111231 *04,419*

SPRAY EXTRACTION COLUMNS
Enzyme and Protein Mass Transfer Coefficient in Aqueous Two Phase Systems. 1. Spray Extraction Columns.
PB95-161162 *00,594*

SPRAYING
Measurement Methods and Standards for Processing and Application of Thermal Barrier Coatings.
N95-26123/6 *01,447*

Combustion of Methanol and Methanol/Dodecanol Spray Flames.
PB95-108544 *02,478*

Study of Droplet Transport in Alcohol-Based Spray Flames Using Phase/Doppler Interferometry.
PB95-108551 *02,479*

Structure of a Swirl-Stabilized Kerosene Spray Flame.
PB95-108569 *02,480*

SPRAYS
Turbulent Spray Burner for Assessing Halon Alternative Fire Suppressants.
PB95-153748 *01,385*

Water Mist Fire Suppression Workshop Summary.
PB95-161907 *02,853*

SPRINKLER SYSTEMS
Analysis of Failed Dry Pipe Fire Suppression System Couplings from the Filene Center at Wolf Trap Farm Park for the Performing Arts.
PB94-164407 *00,331*

Field Modeling: Simulating the Effect of Sloped Beamed Ceilings on Detector and Sprinkler Response.
PB96-122866 *01,406*

Analysis of High Bay Hangar Facilities for Detector Sensitivity and Placement.
PB96-190210 *01,429*

State of the Art Report on Seismic Design Requirements for Nonstructural Building Components.
PB96-193800 *00,308*

Interaction of an Isolated Sprinkler Spray and a Two-Layer Compartment Fire Environment. Phenomena and Model Simulations.
PB97-110076 *01,437*

SPRINKLERS
Application of Boundary Element Methods to a Transient Axis-Symmetric Heat Conduction Problem.
PB94-212693 *01,375*

Measurement of Room Conditions and Response of Sprinklers and Smoke Detectors during a Simulated Two-Bed Hospital Patient Room Fire.
PB94-213717 *00,292*

Sprinkler Fire Suppression Algorithm.
PB94-216181 *00,293*

Comparison of Fire Sprinkler Piping Materials: Steel, Copper, Chlorinated Polyvinyl Chloride and Polybutylene, in Residential and Light Hazard Installations.
PB95-182267 *00,299*

Evaluation of Sprinkler Activation Prediction Methods.
PB96-141056 *00,304*

Computing the Effect of Sprinkler Sprays on Fire Induced Gas Flow.
PB96-147111 *00,404*

SPRINKLING
Protection of Data Processing Equipment with Fine Water Sprays.
PB95-174975 *02,610*

SPT (SYNTHETIC PERTURBATION TUNING)
Synthetic-Perturbation Tuning of MIMD Programs.
PB94-185568 *01,687*

SPUTTERING
Pure Element Sputtering Yield Data: Appendix 4.
PB94-200037 *00,805*

Deposition Rates in Direct Current Diode Sputtering.
PB95-203345 *04,697*

SQA (SOFTWARE QUALITY ASSURANCE)
SQA Standards and Total Quality Management.
PB96-111844 *01,743*

SQA and TQM in Software Quality Improvement.
PB96-160791 *01,754*

SQIDS (DETECTORS)
Self-Biasing Cryogenic Particle Detector Utilizing Electrothermal Feedback and a SQUID Readout.
PB96-102538 *04,712*

SQL DATABASE LANGUAGE
Object SQL: Language Extensions for Object Data Management.
PB95-125902 *01,704*

SQL (STRUCTURED QUERY LANGUAGE)
SQL Environments. Category: Software Standard; Subcategory: Database.
FIPS PUB 193 *01,801*

SQUEEZED STATES (QUANTUM THEORY)
Squeezed Atomic States and Projection Noise in Spectroscopy.
PB95-176293 *03,960*

SQUID AMPLIFIERS
Two-Stage Integrated SQUID Amplifier with Series Array Output.
PB95-176277 *02,061*

SQUID (DETECTORS)
Physical Basis for Half-Integral Shapiro Steps in a DC SQUID.
PB96-102264 *04,704*

SQUID DEVICES
Series Array of DC SQUIDs.
PB95-163861 *02,046*

Kinetic-Inductance Infrared Detector Based on an Antenna-Coupled High-Tc SQUID.
PB95-169116 *02,165*

Two-Stage Integrated SQUID Amplifier with Series Array Output.
PB95-176277 *02,061*

Noise Reduction in Low-Frequency SQUID Measurements with Laser-Driven Switching.
PB96-135165 *02,081*

SRA
Process for Selecting Standard Reference Algorithms for Evaluating Coordinate Measurement Software.
PB94-173754 *02,629*

SRM 1165
Apparent Bias in the X-Ray Fluorescence Determination of Titanium in Selected NIST SRM Low Alloy Steels.
PB95-108759 *03,212*

SRM 1264
Apparent Bias in the X-Ray Fluorescence Determination of Titanium in Selected NIST SRM Low Alloy Steels.
PB95-108759 *03,212*

SRM 1548
Mixed Diet Reference Materials for Nutrient Analysis of Foods: Preparation of SRM-1548 Total Diet.
PB95-151692 *03,593*

STABILITY
Long-Term Stability of Carrier-Free Polonium Solution Standards.
PB94-185170 *00,685*

Stability/Instability of Gas Mixtures Containing 1,3-Butadiene in Treated Aluminum Gas Cylinders.
PB95-162285 *02,546*

Stability and Surface Energies of Wetted Grain Boundaries in Aluminum Oxide.
PB95-202750 *03,059*

Comments on the Stability of Bayard-Alpert Ionization Gages.
PB96-103080 *02,673*

STADARDS
International Institute of Welding: Report on 1995 Actions.
PB96-158076 *02,874*

STAINLESS STEEL
PC-Based Prototype Expert System for Data Management and Analysis of Creep and Fatigue of Selected Materials at Elevated Temperatures.
PB94-172251 *03,202*

Temperature-Induced Transition in Ductile Fracture Appearance of a Nitrogen-Strengthened Austenitic Stainless Steel.
PB96-190269 *03,221*

STAINLESS STEEL-304L
Effect of Backfill and Atomizing Gas on the Powder Porosity and Mechanical Properties of 304L Stainless Steel.
PB94-185394 *03,205*

STANDARD CROSS SECTION
Measurements of the (235)U(n,f) Cross Section in the 3 to 30 MeV Neutron Energy Region.
PB97-119051 *04,172*

STANDARD FOR THE EXCHANGE OF PRODUCT MODEL DATA
Challenges to the National Information Infrastructure: The Barriers to Product Data Sharing. National PDES Testbed Report Series.
PB95-136347 *02,776*

STEP On-Line Information Service (SOLIS). The IGES/PDES Organization.
PB95-137790 *02,777*

SGML Environment for STEP.
PB95-143103 *02,778*

Initial NIST Testing Policy for STEP: Beta Testing Program for AP 203 Implementations. National PDES Testbed Report Series.
PB95-154688 *02,779*

Machining Process Planning Activity Model for Systems Integration.
PB96-165428 *02,841*

Procedure for Product Data Exchange Using STEP Developed in the AutoSTEP Pilot.
PB96-183058 *02,843*

Interoperability Requirements for CAD Data Transfer in the AutoSTEP Project.
PB97-114268 *02,796*

Capabilities for Product Data Exchange.
PB97-118764 *02,798*

STANDARD FOR THE EXCHANGE OF PRODUCT MODEL DATA (STEP)

Extensions of the Prototype Application Protocol of Ready-to-Wear Apparel Pattern Making.
PB96-128194 *03,198*

STANDARD GENERALIZED MARKUP LANGUAGE

SGML Environment for STEP.
PB95-143103 *02,778*

SGML Parser Validation Procedures.
PB95-174959 *01,717*

STANDARD RADIATORS

Screened-Room Measurements on the NIST Spherical-Dipole Standard Radiator.
PB96-113568 *01,926*

STANDARD REFERENCE ALGORITHM

Process for Selecting Standard Reference Algorithms for Evaluating Coordinate Measurement Software.
PB94-173754 *02,629*

STANDARD REFERENCE DATA

Numeric Data Distribution: The Vital Role of Data Exchange in Today's World.
N95-15937/2 *02,622*

Journal of Physical and Chemical Reference Data, Volume 22, No. 1, January/February 1993.
PB94-160975 *00,729*

Thermodynamic Properties of the Group IIA Elements.
PB94-160983 *00,730*

Spectroscopy and Structure of the Lithium Hydride Diatomic Molecules and Ions.
PB94-160991 *00,731*

Quantum Yields for the Photosensitized Formation of the Lowest Electronically Excited Singlet State of Molecular Oxygen in Solution.
PB94-161007 *00,732*

Journal of Physical and Chemical Reference Data, Volume 22, No. 2, March/April 1993.
PB94-162211 *00,733*

Wavelengths and Energy Level Classifications for the Spectra of Sulfur (S I through S XVI).
PB94-162229 *00,734*

Thermodynamic Properties of Alkenes (Mono-Olefins Larger Than C4).
PB94-162237 *00,735*

Thermodynamic Behavior of the CO2-H2O System from 400 to 1000 K, up to 100 MPa and 30% Mole Fraction of CO2.
PB94-162245 *00,736*

Thermodynamics of Enzyme-Catalyzed Reactions: Part 1. Oxidoreductases.
PB94-162252 *00,737*

Journal of Physical and Chemical Reference Data, Volume 22, No. 3, May/June 1993.
PB94-162260 *00,738*

Estimation of the Heat Capacities of Organic Liquids as a Function of Temperature Using Group Additivity. I. Hydrocarbon Compounds.
PB94-162278 *00,739*

Estimation of the Heat Capacities of Organic Liquids as a Function of Temperature Using Group Additivity. II. Compounds of Carbon, Hydrogen, Halogens, Nitrogen, Oxygen, and Sulfur.
PB94-162286 *00,740*

Thermodynamic and Thermophysical Properties of Organic Nitrogen Compounds. Part II. 1- and 2-Butanamine, 2-Methyl-1-Propanamine, 2-Methyl-2-Propanamine, Pyrrole, 1-, 2-, and 3-Methylpyrrole, Pyridine, 2-, 3-, and 4-Methylpyridine, Pyrrolidine, Piperidine, Indole, Quinoline, Isoquinoline, Acridine, Carbazole, Phenanthridine, 1- and 2-Naphthalenamine, and 9-Methylcarbazole.
PB94-162294 *00,741*

International Equations for the Saturation Properties of Ordinary Water Substance. Revised According to the International Temperature Scale of 1990. Addendum to Journal of Physical and Chemical Reference Data 16, 893 (1987).
PB94-162302 *00,742*

Journal of Physical and Chemical Reference Data, Volume 22, No. 4, July/August 1993.
PB94-162310 *00,743*

Estimation of the Thermodynamic Properties of C-H-N-O-S-Halogen Compounds at 298.15 K.
PB94-162328 *00,744*

Journal of Physical and Chemical Reference Data, Volume 22, No. 5, September/October 1993.
PB94-162336 *00,745*

Compilation of Energy Levels and Wavelengths for the Spectrum of Singly-Ionized Oxygen (O II).
PB94-162344 *00,746*

Energy Levels of Germanium, Ge I through Ge XXXII.
PB94-162351 *00,747*

Spectral Data and Grotrian Diagrams for Highly Ionized Chromium, Cr V through Cr XXIV.
PB94-162369 *00,748*

Journal of Physical and Chemical Reference Data, Volume 22, No. 6, November/December 1993.
PB94-168556 *00,749*

Thermodynamic Properties of Synthetic Sapphire (alpha-Al2O3), Standard Reference Material 720 and the Effect of Temperature-Scale Differences on Thermodynamic Properties.
PB94-168564 *00,750*

Thermodynamic Properties of Gaseous Silicon Monotelluride and the Bond Dissociation Enthalpy D(sub m)(SiTe) at T approaches 0.
PB94-168572 *00,751*

Disilicides of Tungsten, Molybdenum, Tantalum, Titanium, Cobalt, and Nickel, and Platinum Monosilicide: A Survey of Their Thermodynamic Properties.
PB94-168580 *00,752*

Evaluated Bimolecular Ion-Molecule Gas Phase Kinetics of Positive Ions for Use in Modeling Planetary Atmospheres, Cometary Comae, and Interstellar Clouds.
PB94-168598 *00,753*

Atomic Weights of the Elements 1991.
PB94-168606 *00,754*

Theoretical Analysis of the Coherence-Induced Spectral Shift Experiments of Kandpal, Vaishya, and Joshi.
PB94-219383 *00,561*

NIST Standard Reference Data Products Catalog, 1995-96. Achieve with Standard Reference Data.
PB95-260808 *01,057*

Building a Better Crycooler.
PB96-119615 *04,734*

Journal of Physical and Chemical Reference Data, Volume 24, No. 1, January/February 1995.
PB96-145560 *01,101*

Millimeter- and Submillimeter-Wave Spectrum of trans-Ethyl Alcohol.
PB96-145578 *01,102*

Database for the Static Dielectric Constant of Water and Steam.
PB96-145586 *01,103*

Theoretical Form Factor, Attenuation and Scattering Tabulation for Z=1-92 from E=1-10 eV to E=0.4-1.0 MeV.
PB96-145594 *01,104*

Journal of Physical and Chemical Reference Data, Volume 24, No. 2, March/April 1995.
PB96-145818 *01,105*

Rate Constants for the Decay and Reactions of the Lowest Electronically Excited Singlet State of Molecular Oxygen in Solution. An Expanded and Revised Compilation.
PB96-145826 *01,106*

Thermodynamic Properties of the Aqueous Ba(sup 2+) Ion and the Key Compounds of Barium.
PB96-145834 *01,107*

Journal of Physical and Chemical Reference Data, Volume 24, No. 3, May/June 1995.
PB96-145842 *01,108*

Critical Review of Rate Constants for Reactions of Transients from Metal Ions and Metal Complexes in Aqueous Solution.
PB96-145859 *01,109*

Ideal Gas Thermodynamic Properties of Sulphur Heterocyclic Compounds.
PB96-145867 *01,110*

Standard Reference Data for the Thermal Conductivity of Water.
PB96-145875 *01,111*

Journal of Physical and Chemical Reference Data, Volume 24, No. 4, July/August 1995.
PB96-145883 *01,112*

Summary of the Apparent Standard Partial Molal Gibbs Free Energies of Formation of Aqueous Species, Minerals, and Gases at Pressures 1 to 5000 Bars and Temperatures 25 to 1000C.
PB96-145891 *01,113*

Atomic Weights of the Elements, 1993.
PB96-145909 *01,114*

Spectral Data for Highly Ionized Krypton, Kr V through Kr XXXVI.
PB96-145917 *01,115*

Journal of Physical and Chemical Reference Data, Volume 24, No. 5, September/October 1995.
PB96-145925 *01,116*

Viscosity of Ammonia.
PB96-145933 *01,117*

Thermodynamics of Enzyme-Catalyzed Reactions. Part 4. Lyases.
PB96-145941 *01,118*

Thermodynamic Properties of the Aqueous Ions (2+ and 3+) of Iron and the Key Compounds of Iron.
PB96-145958 *01,119*

Journal of Physical and Chemical Reference Data, Volume 24, No. 6, November/December 1995.
PB96-145966 *01,120*

Thermodynamics of Enzyme-Catalyzed Reactions. Part 5. Isomerases and Ligases.
PB96-145974 *01,121*

Energy Levels of Zinc, Zn I through Zn XXX.
PB96-145982 *01,122*

STANDARD REFERENCE DEVICES

Standard Reference Devices for High Temperature Superconductor Critical Current Measurements.
PB95-175543 *04,659*

STANDARD REFERENCE MATERIAL

What Is a 'Standard Reference Material' - What Is Any Reference Material.
PB96-186135 *03,000*

STANDARD REFERENCE MATERIAL 1473A

Certification of the Standard Reference Material 1473a, a Low Density Polyethylene Resin.
PB96-128251 *01,282*

STANDARD REFERENCE MATERIAL 1475A

Recertification of the Standard Reference Material 1475A, a Linear Polyethylene Resin.
PB94-161932 *02,628*

STANDARD REFERENCE MATERIAL 1744

Standard Reference Material 1744: Aluminum Freezing-Point Standard.
PB95-251732 *01,055*

STANDARD REFERENCE MATERIALS

Standard Samples and Reference Standards Issued by the National Bureau of Standards.
AD-A279 240/6 *02,613*

NIST Standard Reference Data Products Catalog, 1994.
PB94-151842 *00,727*

Recertification of the Standard Reference Material 1475A, a Linear Polyethylene Resin.
PB94-161932 *02,628*

Preparation and Certification of a Rhodium Standard Reference Material Solution.
PB94-185071 *00,529*

Frozen Human Serum Reference Material for Standardization of Sodium and Potassium Measurements in Serum or Plasma by Ion-Selective Electrode Analyzers.
PB94-185337 *00,532*

Standard Reference Materials: Glass Filters as a Standard Reference Material for Spectrophotometry - Selection, Preparation, Certification, and Use of SRM 930 and SRM 1930.
PB94-188844 *00,536*

Recently Developed NIST Food Related Standard Reference Materials.
PB94-198322 *00,035*

Standard Reference Materials for Dioxins and Other Environmental Pollutants.
PB94-198330 *02,518*

Standard Reference Materials (SRM's) for Measuring Genetic Damage.
PB94-198827 *03,516*

Introduction of a NIST Instrument Sensitivity Standard Reference Material for X-Ray Powder Diffraction.
PB94-200318 *00,807*

Individual Carotenoid Content of SRM 1548 Total Diet and Influence of Storage Temperature, Lyophilization, and Irradiation on Dietary Carotenoids.
PB94-200524 *00,033*

User's Guide to NIST SRM 2084: CMM Probe Performance Standard.
PB94-206109 *02,709*

Molar Absorptivities of Bilirubin (NIST SRM 916A) and Its Neutral and Alkaline Azopigments.
PB94-211042 *03,456*

Determination of the Weight Average Molecular Weight of Two Poly(Ethylene Oxides), SRM 1923 and SRM 1924.
PB94-217031 *01,230*

New Values for Silicon Reference Materials, Certified for Isotope Abundance Ratios. Letter to the Editor.
PB94-219268 *00,863*

Certification, Development and Use of Standard Reference Materials.
PB95-107272 *00,567*

Apparent Bias in the X-Ray Fluorescence Determination of Titanium in Selected NIST SRM Low Alloy Steels.
PB95-108759 *03,212*

Standard Reference Materials: Certification of a Standard Reference Material for the Determination of Interstitial Oxygen Concentration in Semiconductor Silicon by Infrared Spectrophotometry.
PB95-125076 *02,326*

Dissolution Problems with Botanical Reference Materials.
PB95-126280 *03,487*

Comparison of Methods for Gas Chromatographic Determination of PCBs and Chlorinated Pesticides in Marine Reference Materials.
PB95-140091 *02,584*

NIST Standard Reference Materials (SRMs) for Polychlorinated Biphenyl (PCB) Determinations and Their Applicability to Toxaphene Measurements.
PB95-140109 *02,585*

Standards for Corrected Fluorescence Spectra.
PB95-150835 *00,581*

How to Verify Reference Materials.
PB95-151486 *03,497*

Standard Reference Materials for the Determination of Polycyclic Aromatic Hydrocarbons in Environmental Samples - Current Activities.
PB95-151668 *00,586*

Development of Frozen Whale Blubber and Liver Reference Materials for the Measurement of Organic and Inorganic Contaminants.
PB95-151676 *00,587*

Mixed Diet Reference Materials for Nutrient Analysis of Foods: Preparation of SRM-1548 Total Diet.
PB95-151692 *03,593*

Room Temperature Thermal Conductivity of Fumed-Silica Insulation for a Standard Reference Material.
PB95-152039 *00,374*

Reference Materials by Isotope Dilution Mass Spectrometry.
PB95-153383 *00,592*

Standards for Atmospheric Measurements.
PB95-163622 *02,547*

Standard Reference Materials for the Determination of Trace Organic Constituents in Environmental Samples.
PB95-164026 *02,522*

Liquid Chromatographic Determination of Polycyclic Aromatic Hydrocarbon Isomers of Molecular Weight 278 and 302 in Environmental Standard Reference Materials.
PB95-164042 *02,523*

Reference Data for the Thermophysical Properties of Cryogenic Fluids.
PB95-168688 *03,263*

Alaska Marine Mammal Tissue Archival Project: Specimen Inventory.
PB95-171344 *02,589*

Certification of Morphine and Codeine in a Human Urine Standard Reference Material.
PB95-176160 *03,499*

Hair Analysis for Drugs of Abuse: Evaluation of Analytical Methods, Environmental Issues, and Development of Reference Materials.
PB95-176269 *03,501*

NIST Standard Reference Materials (Trade Name) Catalog 1995-1996.
PB95-232518 *00,508*

Standard Reference Material 1744: Aluminum Freezing-Point Standard.
PB95-251732 *01,055*

NIST SRM 9983 High-Rigidity Ball-Bar Stand. User Manual.
PB95-255840 *02,669*

Standard Reference Material for the Measurement of Particle Mobility by Electrophoretic Light Scattering.
PB96-102488 *00,609*

Certification of Polychlorinated Biphenyl Congeners and Chlorinated Pesticides in a Whale Blubber Standard Reference Material.
PB96-103023 *03,745*

Certification of Polycyclic Aromatic Hydrocarbons in a Marine Sediment Standard Reference Material.
PB96-111778 *02,592*

History of NIST's Contributions to Development of Standard Reference Materials and Reference and Definitive Methods for Clinical Chemistry.
PB96-119706 *03,503*

Hair Testing for Drugs of Abuse: International Research on Standards and Technology.
PB96-120555 *03,504*

Development of a Standard Reference Material for Measurement of Interstitial Oxygen Concentration in Semiconductor Silicon by Infrared Absorption.
PB96-122668 *02,404*

Certification of Standard Reference Material (SRM) 1941a, Organics in Marine Sediment.
PB96-123690 *02,593*

NIST Reference Materials to Support Accuracy in Drug Testing.
PB96-123807 *03,505*

Certification of the Standard Reference Material 1473a, a Low Density Polyethylene Resin.
PB96-128251 *01,282*

Methodology for the Certification of Reference Specimens for Determination of Oxygen Concentration in Semiconductor Silicon by Infrared Spectrophotometry.
PB96-155478 *02,421*

System for Intercomparing Standard Solutions of Beta-Particle Emitting Radionuclides.
PB96-159637 *03,707*

Development of a Standard Reference Material for ISE Measurements of Sodium and Potassium.
PB96-159785 *03,507*

Certification of Phencyclidine in Lyophilized Human Urine Reference Materials.
PB96-160692 *03,508*

Determination of 21 Elements by INAA for Certification of SRM 1570a, Spinach.
PB96-167242 *00,698*

Recent Developments in NIST Botanical SRMs.
PB96-167267 *03,489*

Resolution of Discrepant Analytical Data in the Certification of Platinum in Two Automobile Catalyst SRMs.
PB96-167283 *00,638*

What Is a 'Standard Reference Material' - What Is Any Reference Material.
PB96-186135 *03,000*

Room-Temperature Thermal Conductivity of Expanded Polystyrene Board for a Standard Reference Material.
PB96-193693 *00,412*

Unique Quality Assurance Aspects of INAA for Reference Material Homogeneity and Certification.
PB96-200811 *00,699*

NIST Traceable Reference Material Program for Gas Standards: Standard Reference Materials.
PB96-210786 *00,644*

Statistical Aspects of the Certification of Chemical Batch SRMs. Standard Reference Materials.
PB96-210877 *00,645*

Present and Future Standard Specimens for Surface Finish Metrology.
PB97-110423 *02,928*

International Standards and Reference Materials.
PB97-113120 *00,188*

STANDARD RESISTORS

Automated Guarded Bridge for Calibration of Multimegohm Standard Resistors.
PB97-119150 *02,289*

Resistance Measurements from 10 M Omega to 1 T Omega at NIST.
PB97-119168 *02,290*

STANDARD SAMPLES

Standard Samples and Reference Standards Issued by the National Bureau of Standards.
AD-A279 240/6 *02,613*

STANDARDIZATION

Standard Materials. A Descriptive List with Prices.
AD-A278 140/9 *00,500*

Activities of NIST (National Inst. Of Standards and Technology).
N94-23605/6 *04,222*

Implementation of a Standard Format for GPS Common View Data.
N95-32323/4 *03,779*

International Institute of Welding: Report on 1992 Actions.
PB94-185873 *02,856*

International Institute of Welding: Report on 1993 Actions.
PB94-185881 *02,857*

Standardization of Formats and Presentation of Fire Data - The FDMS.
PB94-198462 *01,371*

Standardization of Testing Methods for Optical Disk Media Characteristics and Related Activities at NIST.
PB95-108486 *01,624*

Critical Factors in Non-Lubricated, Non-Abrasive Wear Testing.
PB95-140588 *03,236*

Think Metric.
PB95-151825 *01,298*

ISO Environmental Management Standardization Efforts.
PB95-220513 *02,524*

ISO TC 184/SC4 Reference Manual.
PB95-242293 *02,663*

Can Displays Deliver a Full Measure: Manufacturing.
PB96-111935 *02,185*

Comparison of POSIX Open System Environment (OSE) and Open Distributed Processing (ODP) Reference Models.
PB96-131495 *01,820*

Report on 1994 Actions of the International Institute of Welding.
PB96-138540 *02,873*

ISO Environmental Management Standardization Efforts.
PB96-158662 *02,528*

Implementation of a Standard Format for GPS Common View Data.
PB96-176581 *01,555*

Open System Environment Implementors Workshop (OIW); Standardization Role Defined.
PB96-180047 *01,828*

63Ni Half-Life: A New Experimental Determination and Critical Review.
PB97-111603 *00,700*

Nickel-63 Standardization: 1968-1995.
PB97-111819 *00,701*

SC4 Short Names Registry.
PB97-122410 *02,799*

Standards Activities of Organizations in the United States.
PB97-124135 *00,006*

STANDARDS

Screw-Thread Standards for Federal Services, 1957. Part 3.
AD-A279 121/8 *02,854*

Standard Samples and Reference Standards Issued by the National Bureau of Standards.
AD-A279 240/6 *02,613*

Technologic Papers of the Bureau of Standards: Number 170. Pyrometric Practice.
AD-A279 282/8 *03,766*

Screw-Thread Standards for Federal Services, 1957. Part 1.
AD-A279 290/1 *02,855*

National Standard Petroleum Oil Tables.
AD-A279 952/6 *02,469*

Screw-Thread Standards for Federal Services, 1957. Handbook H28 (1957), Part 2. Revised.
AD-A280 082/9 *03,599*

1950 Supplement to Screw-Thread Standards for Federal Services, 1944.
AD-A280 223/9 *03,656*

Precision Laboratory Standards of Mass and Laboratory Weights.
AD-A280 562/0 *02,618*

Standard of Attenuation for Microwave Measurements.
AD-A297 905/2 *01,517*

NIST Cooperative Laboratory for OSI Routing Technology.
DE94015308 *01,791*

COBOL. Category: Software Standard; Subcategory: Programming Language. Includes ANSI'S X3.23-1985, X3.23A-1989 and X3.23B-1993.
FIPS PUB 21-4 *01,670*

COBOL. Category: Software Standard; Subcategory: Programming Language. Part A.
FIPS PUB 21-4A *01,671*

COBOL. Category: Software Standard; Subcategory: Programming Language. Part B.
FIPS PUB 21-4B *01,672*

ADA; Category: Software Standard; Subcategory: Programming Language.
FIPS PUB 119-1 *01,667*

User Interface Component of the Applications Portability Profile Category: Software Standard; Subcategory: Application Program Interface.
FIPS PUB 158-1 *01,793*

Time and Frequency Technology at NIST.
N94-30641/2 *01,522*

Open System Environments.
N94-36857/8 *01,674*

Open System Environment Procurement.
N94-36858/6 *02,716*

Numeric Data Distribution: The Vital Role of Data Exchange in Today's World.
N95-15937/2 *02,622*

National Center for Standards and Certification Information: Service and Programs.
N95-15938/0 *02,717*

General Procedures for Registering Computer Security Objects.
PB94-134897 *01,573*

Open Architectures for Machine Control.
PB94-135621 *02,942*

Planning for the Fiber Distributed Data Interface (FDDI).
PB94-135761 *01,621*

36Cl/Cl Accelerator-Mass-Spectrometry Standards: Verification of Their Serial-Dilution-Solution Preparations by Radioactivity Measurements.
PB94-140563 *00,524*

Report on Application Integration Architectures (AIA) Workshop. Held in Dallas, Texas on February 8-12, 1993.
PB94-142536 *01,803*

Technical Program of the Factory Automation Systems Division 1993.
PB94-160819 *02,805*

Computer Graphics Metafile (CGM): Procedures for NIST CGM Validation Test Service.
PB94-161809 *01,804*

Voluntary Product Standard PS 20-94. American Softwood Lumber Standard.
PB94-162500 *03,402*

Models, Managing Models, Quality Models: An Example of Quality Management.
PB94-163466 *02,891*

Compatibility Analysis of the ANSI and ISO IRDS Services Interfaces.
PB94-163474 *01,805*

User's Guide for the PHIGS Validation Tests (Version 2.1).
PB94-165206 *01,682*

Preparation and Certification of a Rhodium Standard Reference Material Solution.
PB94-185071 *00,529*

Standards Development in North America for Performance of Whole Buildings and Facilities.
PB94-185196 *00,312*

Design and Operation of Series-Array Josephson Voltage Standards.
PB94-185451 *02,030*

Proficiency Tests for the NIST Airborne Asbestos Program, 1990.
PB94-188836 *00,535*

NIST Calibration of ASTM E127-Type Ultrasonic Reference Blocks.
PB94-191640 *02,702*

Coaxial Reference Standard for Microwave Power.
PB94-193786 *01,880*

Recommendations on Selection of Vehicle-to-Roadside Communications Standards for Commercial Vehicle Operations.
PB94-195914 *04,859*

Graphical Analysis of the CCRL Portland Cement Proficiency Sample Database (Samples 1-72). (Part 1. Univariant Analysis of Portland Cement).
PB94-196557 *01,308*

Neutron Standard Cross Sections in Reactor Physics: Need and Status.
PB94-199510 *03,813*

Graphical Conceptual Navigation as a Presentation Technique for a Graphics Standard.
PB94-200573 *01,692*

User's Guide to NIST SRM 2084: CMM Probe Performance Standard.
PB94-206109 *02,709*

IGOSS-Industry/Government Open Systems Specification.
PB94-207453 *01,806*

State Weights and Measures Laboratories: State Standards Program Description and Directory. 1994 Edition.
PB94-207727 *02,895*

24 GHz Josephson Array Voltage Standard.
PB94-211588 *02,033*

Summary of the Proceedings of the Workshop on Standard Phantoms for In-vivo Radioactivity Measurement.
PB94-212933 *03,622*

Technical Program Description Systems Integration for Manufacturing (SIMA).
PB94-213758 *02,819*

Performance Standards: The Pro's and Con's.
PB94-216132 *02,896*

Standards in Building Economics: Why We Need Them and How to Write Them.
PB94-216405 *00,320*

NIST-Coordinated Standard for Fingerprint Data Interchange.
PB94-216645 *01,808*

Journal of Research of the National Institute of Standards and Technology. May/June 1994. Volume 99, Number 3.
PB94-219326 *02,643*

Sources of Uncertainty in a DVM-Based Measurement System for a Quantized Hall Resistance Standard.
PB94-219334 *01,884*

dc Method for the Absolute Determination of Conductivities of the Primary Standard KCl Solutions from 0C to 50C.
PB94-219342 *02,644*

Improved Automated Current Control for Standard Lamps.
PB94-219367 *00,246*

CALS-Automated Interchange of Technical Information.
PB94-962000 *03,657*

Questions and Answers on Quality, the ISO 9000 Standard Series, Quality System Registration, and Related Issues. More Questions and Answers on the ISO 9000 Standard Series and Related Issues.
PB95-103461 *00,495*

Making Sense of Software Engineering Environment Framework Standards.
PB95-105037 *01,701*

Formulation of Position on U.S. Standards Role in Enterprise Integration.
PB95-105052 *02,773*

Certification, Development and Use of Standard Reference Materials.
PB95-107272 *00,567*

Summary and Notes of the Joint ISO/IGES/PDES Organization Technical Committee Meeting. Held in Albuquerque, New Mexico on October 15-20, 1989.
PB95-107314 *02,774*

Activities of the ASTM Committee E-42 on Surface Analysis.
PB95-108528 *00,881*

Suggestions for a Logically-Consistent Structure for Service Life Prediction Standards.
PB95-125795 *00,358*

National PDES Testbed: An Overview.
PB95-125829 *02,775*

Water Efficient Plumbing Fixtures through Standards and Test Methods.
PB95-125951 *00,248*

Information Resource Dictionary System (IRDS): A Status Report.
PB95-126207 *01,810*

Summaries of BFRL Fire Research In-House Projects and Grants, 1994.
PB95-130845 *00,366*

Challenges to the National Information Infrastructure: The Barriers to Product Data Sharing. National PDES Testbed Report Series.
PB95-136347 *02,776*

NIST Workshop on the Computer Interface to Flat Panel Displays. Held in San Jose, California on January 13-14, 1994.
PB95-136388 *01,625*

New Materials, Advanced Ceramics and Standards.
PB95-140208 *03,047*

SGML Environment for STEP.
PB95-143103 *02,778*

New International Representations of the Volt and Ohm Effective January 1, 1990.
PB95-150777 *01,890*

Standards for Corrected Fluorescence Spectra.
PB95-150835 *00,581*

Standards: A Cardinal Direction for Geographic Information Systems.
PB95-150942 *03,677*

Analysis of Selected Software Safety Standards.
PB95-151262 *01,708*

New Coaxial Microwave Microcalorimeter Evaluation Technique.
PB95-153227 *01,892*

Mapping Integration Definition for Information Modeling (IDEF1X) Model into CASE Data Interchange Format (CDIF) Transfer File.
PB95-154670 *01,711*

Frequency Extension of the NIST AC-DC Difference Calibration Service for Current.
PB95-161253 *01,895*

X-ray Mask Metrology: The Development of Linewidth Standards for X-ray Lithography.
PB95-162129 *02,348*

Introduction to ASTM 1199 'Wear Test Selection for Design and Application'.
PB95-162517 *03,238*

Recent VAMAS Activity in Ceramics.
PB95-162681 *03,051*

Geographic Information Systems Standards: A Federal Perspective.
PB95-163390 *03,678*

Accuracy Comparisons of Josephson Array Systems.
PB95-164687 *02,047*

Lightwave Standards Development at NIST.
PB95-168563 *01,480*

Measurements of the Characteristic Impedance of Coaxial Air Line Standards.
PB95-168787 *02,221*

Perspective on Software Engineering Standards.
PB95-171377 *01,811*

Design Challenges in a Commercial Quantum Hall Effect-Based Resistance Standard.
PB95-171419 *02,263*

Dimensional Inspection Planning Based on Product Data Standards.
PB95-175451 *02,910*

Taxonomy for Security Standards.
PB95-180386 *01,602*

Federal Government and Information Technology Standards: Building the National Information Infrastructure.
PB95-180840 *01,812*

Practical Standards for PM and AM Noise at 5, 10 and 100 MHz.
PB95-181129 *01,546*

Method to Determine the Calorimetric Equivalence Correction for a Coaxial Microwave Microcalorimeter.
PB95-202404 *01,913*

Developing a NIST Coaxial Microwave Power Standard at 1 mW.
PB95-202412 *01,914*

Survey of Concrete Transport Properties and Their Measurement.
PB95-220489 *00,396*

Analysis of ANSI ASC X12 and UN/EDIFACT Electronic Data Interchange (EDI) Standards.
PB95-220554 *01,729*

Standards Policy and Information Infrastructure.
PB95-231882 *01,485*

NIST Standard Reference Materials (Trade Name) Catalog 1995-1996.
PB95-232518 *00,508*

Operating Procedures and Life Cycle Documentation for the Initial Graphics Exchange Specification.
PB95-242285 *02,782*

Advanced Mass Calibration and Measurement Assurance Program for State Calibration Laboratories.
PB95-253571 *02,492*

Proceedings of the Meeting of the Intergovernmental U.S.-Russian Business Development Committee's Standard Working Group (4th). Held in New York City, New York on March 27-29, 1995 and in Northbrook, Illinois on March 30-31, 1995.
PB95-255881 *00,496*

45 deg/0 deg Reflectance Factors of Pressed Polytetrafluoroethylene (PTFE) Powder.
PB95-260758 *04,328*

Journal of Research of the National Institute of Standards and Technology, May/June 1995. Volume 100, Number 3.
PB95-261897 *02,670*

CALS-Automated Interchange of Technical Information.
PB95-962000 *03,666*

Ab initio Calculations for Helium: A Standard for Transport Property Measurements.
PB96-102041 *01,060*

Voltage-Standard Devices.
PB96-102496 *01,920*

Aging, Warm-Up Time and Retrace; Important Characteristics of Standard Frequency Generators.
PB96-103122 *04,031*

GATT Standards Code Activities of the National Institute of Standards and Technology 1994.
PB96-106935 *00,497*

Mapping Integration Definition for Function Modeling (IDEFO) Model into CASE Data Interchange Format (CDIF) Transfer File.
PB96-109533 *01,741*

Efficiency of Electric Motors. National Voluntary Lab. Accreditation Program (NVLAP).
PB96-111174 *02,107*

High Integrity Software Standards Activities at NIST.
PB96-112214 *01,744*

Local Oscillator Requirements and Strategies for the Next Generation of High-Stability Frequency Standards.
PB96-112230 *01,551*

Journal of Research of the National Institute of Standards and Technology, July/August 1995. Volume 100, Number 4. Special Issue: The Gaseous Electronics Conference Radio-Frequency Reference Cell.
PB96-113311 *02,386*

Gaseous Electronics Conference RF Reference Cell: An Introduction.
PB96-113329 *02,387*

Current and Voltage Measurements in the Gaseous Electronics Conference RF Reference Cell.
PB96-113337 *02,388*

Optical Emission Spectroscopy on the Gaseous Electronics Conference RF Reference Cell.
PB96-113345 *02,389*

Optical Diagnostics in the Gaseous Electronics Conference Reference Cell.
PB96-113352 *02,390*

Studies of Ion Kinetic-Energy Distributions in the Gaseous Electronics Conference RF Reference Cell.
PB96-113360 *02,391*

Langmuir Probe Measurements in the Gaseous Electronics Conference RF Reference Cell.
PB96-113386 *02,393*

Inductively Coupled Plasma Source for the Gaseous Electronics Conference RF Reference Cell.
PB96-113394 *02,394*

Reactive Ion Etching in the Gaseous Electronics Conference RF Reference Cell.
PB96-113402 *02,395*

Dusty Plasma Studies in the Gaseous Electronics Conference Reference Cell.
PB96-113410 *02,396*

One-Dimensional Modeling Studies of the Gaseous Electronics Conference RF Reference Cell.
PB96-113428 *02,397*

Two-Dimensional Self-Consistent Radio Frequency Plasma Simulations Relevant to the Gaseous Electronics Conference RF Reference Cell.
PB96-113436 *02,398*

Journal of Research of the National Institute of Standards and Technology, November/December 1994. Volume 99, Number 6.
PB96-113535 *04,336*

Intercomparison between NPL (India) and NIST (USA) Pressure Standards in the Hydraulic Pressure Region Up to 26 MPa.
PB96-113543 *04,211*

Screened-Room Measurements on the NIST Spherical-Dipole Standard Radiator.
PB96-113568 *01,926*

Federal Implementation Guideline for Electronic Data Interchange. ASC X12 003050 Transaction Set 850 Award Instrument. Implementation Convention.
PB96-114913 *01,814*

Federal Implementation Guideline for Electronic Data Interchange. ASC X12 003050 Transaction Set 860 Modifications to Award Instrument. Implementation Convention.
PB96-114921 *01,815*

Standards Setting in the European Union: Standards Organization and Officials in EU Standards Activities.
PB96-115019 *02,919*

Electrical Product Requirements (Especially Quality Requirements) in the United States.
PB96-119235 *01,929*

Making Displays Deliver a Full Measure.
PB96-122411 *01,490*

Survey of the Components of Display-Measurement Standards.
PB96-122528 *02,188*

Electromagnetic Properties of Materials: The NIST Metrology Program.
PB96-122791 *01,933*

EDI and EFT Security Standards.
PB96-122833 *01,605*

Database Management Standards: Status and Applicability.
PB96-122924 *01,819*

Proposed International Interactive Courseware Standard.
PB96-123161 *00,137*

Secondary Standard for PM and AM Noise at 5, 10, and 100 MHz.
PB96-123187 *01,554*

Electronic Access to Standards on the Information Highway.
PB96-131578 *01,494*

Spatial Information and Technology Standards Evolving.
PB96-135108 *03,679*

Frequency-Stabilized Lasers: A Driving Force for New Spectroscopies.
PB96-135199 *04,350*

Object-Oriented Tel/Tk Binding for Interpreted Control of the NIST EXPRESS Toolkit in the NIST STEP Application Protocol Development Environment.
PB96-141049 02,785

Summary Report on the Workshop on Advanced Digital Video in the National Information Infrastructure.
PB96-141320 01,497

Guidelines for the Development of Mapping Tables.
PB96-154539 02,786

Metrology and Regional Trade Pacts.
PB96-155429 02,923

Development of Computer-Based Models of Standards and Attendant Knowledge-Base and Procedural Systems.
PB96-155783 00,464

International Organization for Standardization: Current Activities in Fire Safety Engineering.
PB96-159660 00,223

U.S. Government Accreditation and Conformity Assessment System Evaluation.
PB96-160239 02,678

International Challenges in Defining the Public and Private Interest in Standards.
PB96-160361 00,498

Standardization for ATM and Related B-ISDN Technologies.
PB96-160460 01,499

ISDN in North America.
PB96-160767 01,502

North American Agreements on ISDN.
PB96-160775 01,503

Impact of Computer-Aided Acquisition and Logistic Support (CALS) in the Application of Standards.
PB96-160908 01,756

Conference Report: International Conference on the Application of Standards for Open Systems (6th).
PB96-161211 01,762

GOSIP Testing Program.
PB96-161229 01,504

Information Technology Standards in Federal Acquisitions.
PB96-161252 01,636

Using Information Technology Standards in Federal Acquisitions.
PB96-161260 01,637

Report of a Workshop on the Assurance of High Integrity Software.
PB96-161377 01,763

Standards for High Integrity Software.
PB96-161385 01,764

Group 1 for the Plant Spatial Configuration STEP Application Protocol.
PB96-165402 02,789

Federal Implementation Guideline for Electronic Data Interchange. ASC X12 003050 Transaction Set 843 Response to Request for Quotation. Implementation Convention.
PB96-168984 01,822

Federal Implementation Guideline for Electronic Data Interchange. ASC X12 003050 Transaction Set 855 Purchase Order Acknowledgment: Implementation Convention.
PB96-172374 01,823

Federal Implementation Guideline for Electronic Data Interchange. ASC X12 003050 Transaction Set 840 Request for Quotation. Implementation Convention.
PB96-172531 01,824

Federal Implementaion Guideline for Eletronic Data Interchange. ASC X12 003050 Transaction Set 865 Purchase Order Change Acknowledgement/Request - Seller Initiated. Implementation Convention.
PB96-172549 01,825

Voluntary Product Standard PS 1-95 Construction and Industrial Plywood.
PB96-178900 03,406

Specifications and Tolerances for Reference Standards and Field Standard Weights and Measures. 2. Specifications and Tolerances for Field Standard Measuring Flasks.
PB96-178926 02,682

Consensus Process in Standards Development.
PB96-179502 00,136

Application of Metadata Standards.
PB96-180187 01,771

Proceedings of NIST Workshop: Industry Needs in Welding Research and Standards Development. Held on August 15-16, 1995.
PB96-183124 02,877

What Is a 'Standard Reference Material' - What Is Any Reference Material.
PB96-186135 03,000

Helping to Reduce Technical Barriers to Trade.
PB96-190046 00,491

Room-Temperature Thermal Conductivity of Expanded Polystyrene Board for a Standard Reference Material.
PB96-193693 00,412

Systems Integration for Manufacturing Applications Program 1995 Annual Report.
PB96-193735 02,844

Report on the NIST Low Accelerating Voltage SEM Magnification Standard Interlaboratory Study.
PB96-201074 02,445

Precise Laser-Based Measurements of Zero-Dispersion Wavelength in Single-Mode Fibers.
PB96-201124 01,511

Application Protocol Information Base World Wide Web Gateway.
PB96-202320 02,791

Airborne Asbestos Method: Bootstrap Method for Determining the Uncertainty of Asbestos Concentration. Version 1.0.
PB96-214614 00,646

TBT Agreement Activities of the National Institute of Standards and Technology, 1995.
PB97-104178 00,499

CIF Crystallographic Information File: A Standard for Crystallographic Data Interchange.
PB97-109169 04,805

Role of Certified Reference Materials in Trace Analysis Quality Assurance.
PB97-110019 00,650

Examination Procedure Outlines: Keys to Solving the Handbook 44 Puzzle.
PB97-110217 02,690

Current Status and Trends in Temperature Measurements at NIST, Cooperative Projects and New Mutual Agreement between NIST and IMGC.
PB97-110266 02,691

Characterization of Modified FEL Quartz-Halogen Lamps for Photometric Standards.
PB97-112544 00,282

International Standards and Reference Materials.
PB97-113120 00,188

Standards Promote Credibility and Technology Transfer: The Need for Greater Industry Support of Technical Committees.
PB97-116206 02,961

STANDARDS REFERENCE MATERIALS

Role of Certified Reference Materials in Trace Analysis Quality Assurance.
PB97-110019 00,650

STANDING WAVES

Diffraction of Neutron Standing Waves in Thin Films with Resonance Enhancement.
PB97-113278 04,164

STAR PLOYMERS

Thermodynamic Properties of Dilute and Semidilute Solutions of Regular Star Polymers.
PB96-146808 01,284

STARK EFFECT

New Critical Review of Experimental Stark Widths and Shifts.
PB94-172830 03,790

Perturbative Calculation of the AC Stark Effect by the Complex Rotation Method.
PB95-141123 04,260

STATE SERVICES

State Weights and Measures Laboratories: State Standards Program Description and Directory. 1994 Edition.
PB94-207727 02,895

STATES (UNITED STATES)

State Weights and Measures Laboratories: Program Handbook.
PB96-214705 02,687

STATIC ANALYSIS

Application of the Pointer State Subgraph to Static Program Slicing.
PB96-167838 01,768

STATIC DIELECTRIC CONSTANTS

Database for the Static Dielectric Constant of Water and Steam.
PB96-145586 01,103

STATIC ELECTRICITY

Adhesion, Contact Electrification, and Acid-Base Properties of Surfaces.
PB96-204425 03,693

STATICS

Small-Angle Neutron Scattering Study on Weakly Charged Temperature Sensitive Polymer Gels.
PB95-164398 01,264

STATISTICAL ANALYSIS

Utc Dissemination to the Real-Time User.
N19960042622 01,521

Computing Effects and Error for Large Synthetic Perturbation Screenings.
PB94-139623 01,675

Statistical Analysis of Parameters Affecting the Measurement of Particle-Size Distribution of Silicon Nitride Powders by Sedigraph (Trade Name).
PB94-216249 03,042

Extreme Value Theory and Applications: Proceedings of the Conference on Extreme Value Theory and Applications, Volume 3. Held in Gaithersburg, Maryland in May 1993.
PB95-104956 03,432

Taguchi's Parameter Design: A Panel Discussion.
PB96-111802 03,445

Book Review: Statistical Physics of Macromolecules.
PB96-123526 01,280

Modeling of Extreme Loading by 'Peaks Over Threshold' Methods.
PB96-159694 00,469

Statistical Aspects of the Certification of Chemical Batch SRMs. Standard Reference Materials.
PB96-210877 00,645

Airborne Asbestos Method: Bootstrap Method for Determining the Uncertainty of Asbestos Concentration. Version 1.0.
PB96-214614 00,646

STATISTICAL DATA

Guide to Locating and Accessing Computerized Numeric Materials Databases.
PB96-204045 03,007

STATISTICAL DISTRIBUTIONS

Tolerance Intervals for the Distribution of True Values in the Presence of Measurement Errors.
PB95-150405 03,434

Two Principal Points of Symmetric, Strongly Unimodal Distributions.
PB95-203360 03,443

STATISTICAL INFERENCE

Scientific Protocols in Statistical Standards for Environmental Studies.
PB94-185527 02,517

STATISTICAL MECHANICS

Nonequilibrium Statistical Mechanics.
PB96-161781 04,097

STATISTICAL QUALITY CONTROL

Statistical Quality Control Technology in Japan.
PB94-199064 02,708

STATISTICS

Fracture of Silicon Nitride and Silicon Carbide at Elevated Temperatures.
PB96-180260 03,179

STEAM

Formulation of the Refractive Index of Water and Steam.
PB95-140133 00,900

Physical Limit to the Stability of Superheated and Stretched Water.
PB96-122551 01,083

Static Dielectric Constant of Water and Steam.
PB96-123559 01,090

Database for the Static Dielectric Constant of Water and Steam.
PB96-145586 01,103

STEARIC ACID

Tribochemical Reaction of Stearic Acid on Copper Surface Studied by Surface Enhanced Raman Spectroscopy.
PB94-212057 02,964

STEEL

Sensor System for Intelligent Processing of Hot-Rolled Steel.
PB96-186069 03,373

Ductile Fracture and Tempered Martensite Embrittlement of 4140 Steel.
PB96-190285 03,222

Mechanical Properties and Warm Prestress of Ultra-Low Carbon Steel at 4 K.
PB96-190350 03,224

STEEL-ASTM-A710

Hot-Deformation Apparatus for Thermomechanical Processing Simulation.
PB94-200136 03,207

STEEL JACKETING

Jacket Thickness Requirements for Seismic Retrofitting of Circular Bridge Columns.
PB95-163267 01,336

STEEL SHEET

Methods to Improve the Accuracy of On-Line Ultrasonic Measurement of Steel Sheet Formability.
PB96-186051 02,281

STEEL STRUCTURERS

Ashland Tank Collapse Investigation.
PB95-126314 02,481

STEEL STRUCTURES

Ashland Tank-Collapse Investigation: Closure by Authors.
PB95-126322 02,482

Fire Performance of an Interstitial Space Construction System.
PB95-188918 00,390

Survey of Steel Moment-Resisting Frame Buildings Affected by the 1994 Northridge Earthquake.
PB95-211918 00,451

Workgroup Summary Report: Plastic Hinge-Based Techniques for Advanced Analysis.
PB96-159702 00,470

STEELS

Microstructure and Tensile Properties of Microalloyed Steel Forgings.
PB94-172715 03,204

Relation between AC Impedance Data and Degradation of Coated Steel. 1. Effects of Surface Roughness and Contamination on the Corrosion Behavior of Epoxy Coated Steel.
PB94-213345 03,189

Diffusion of Cations Beneath Organic Coatings on Steel Substrate.
PB94-215704 *03,119*

Ashland Tank Collapse Investigation.
PB95-126314 *02,481*

Ashland Tank-Collapse Investigation: Closure by Authors.
PB95-126322 *02,482*

In situ Measurements of Chloride Ion and Corrosion Potential at the Coating/Metal Interface.
PB95-140893 *03,122*

Ultrasonic Measurement of Sheet Anisotropy and Formability.
PB95-153235 *03,213*

Sorption of Moisture on Epoxy and Alkyd Free Films and Coated Steel Panels.
PB95-162475 *03,192*

Friction and Oxidative Wear of 440C Ball Bearing Steels Under High Load and Extreme Bulk Temperatures.
PB95-175253 *03,215*

Comparison of Fire Sprinkler Piping Materials: Steel, Copper, Chlorinated Polyvinyl Chloride and Polybutylene in Residential and Light Hazard Installations.
PB95-182267 *00,299*

Factors Significant to Precracking of Fracture Specimens.
PB96-109558 *03,358*

Prediction of the Strength Properties for Plain-Carbon and Vanadium Micro-Alloyed Ferrite-Pearlite Steel.
PB96-123393 *03,216*

Artificial Crack in Steel: An Ultrasonic-Resonance-Spectroscopy and Modeling Study.
PB96-141395 *03,241*

STELLAR ATMOSPHERES

Aerodynamic Phenomena in Stellar Atmospheres - A Bibliography.
AD-A278 521/0 *00,046*

Opacity Project and the Practical Utilization of Atomic Data.
PB94-212214 *00,059*

Stars, Atmospheres, Radiative Transfer.
PB96-119474 *00,095*

Riass Coronathon: Joint X-ray and Ultraviolet Observations of Normal F-K Stars.
PB96-200217 *00,109*

STELLAR CHROMOSPHERES

First Results from the Goddard High-Resolution Spectrograph: The Chromosphere of Tauri.
PB94-199528 *00,054*

Transition Regions of Capella.
PB96-123336 *00,105*

Transition Regions of Capella (1995).
PB96-176714 *00,108*

STELLAR CORONAE

Radio Continuum and X-Ray Properties of the Coronae of RS Canum Venaticorum and Related Active Binary Systems.
PB94-211083 *00,057*

Ultraviolet Observations of Stellar Coronae: Early Results from HST.
PB94-213428 *00,064*

Distant Future of Solar Activity: A Case Study of beta Hydri. 3. Transition Region, Corona, and Stellar Wind.
PB95-153441 *00,074*

ROSAT All-Sky Survey of Active Binary Coronae. 1. Quiescent Fluxes for the RS Canum Venaticorum Systems.
PB95-202479 *00,077*

Stellar Coronal Structures.
PB95-202834 *00,080*

Observing Stellar Coronae with the Goddard High Resolution Spectrograph. I. The dMe Star AU Microscopii.
PB96-102777 *00,092*

STELLAR CORONAL

ROSAT All-Sky Survey of Active Binary Coronae. 2. Coronal Temperatures of the RS Canum Venaticorum Systems.
PB94-199601 *00,055*

STELLAR CORONAS

Developments in Stellar Coronae.
PB96-176706 *00,107*

STELLAR DISTANCES

Radiation-Driven Winds of Hot Luminous Stars X. The Determination of Stellar Masses Radii and Distances from Terminal Velocities and Mass-Loss Rates.
PB94-213022 *00,060*

STELLAR ENVELOPES

Opacity Project and the Practical Utilization of Atomic Data.
PB94-212214 *00,059*

STELLAR EVOLUTION

Distant Future of Solar Activity: A Case Study of Beta Hydri. 3. Transition Region, Corona, and Stellar Wind.
PB94-185220 *00,049*

Distant Future of Solar Activity: A Case Study of beta Hydri. 3. Transition Region, Corona, and Stellar Wind.
PB95-153441 *00,074*

STELLAR FLARES

Rotational Modulation and Flares on RS Canum Venaticorum and BY Draconis Stars. XVI. IUE Spectroscopy and VLA Observations of C1182(=V 1005 Orionis) in October 1983.
PB94-185626 *00,050*

Dynamic Phenomena on the RS Canum Venaticorum Binary II Pegasi in August 1989. 1. Observational Data.
PB94-211067 *00,056*

X-rays from Stellar Flares.
PB94-213436 *00,065*

Far-Ultraviolet Flare on a Pleiades G Dwarf.
PB96-102033 *00,086*

STELLAR MAGNETIC FIELDS

Search for Radio Emission from the 'Non-Magnetic' Chemically Peculiar Stars.
PB96-102249 *00,087*

X-ray Emission from Chemically Peculiar Stars.
PB96-102256 *00,088*

Relationship between Radiative and Magnetic Fluxes for Three Active Solar-Type Dwarfs.
PB96-119540 *00,097*

STELLAR MASS

Radiation-Driven Winds of Hot Luminous Stars X. The Determination of Stellar Masses Radii and Distances from Terminal Velocities and Mass-Loss Rates.
PB94-213022 *00,060*

STELLAR MASS ACCRETION

Discussion: Statistical Signal Processing of Quasiperiodicities.
PB96-119532 *00,096*

STELLAR MASS EJECTA

High Velocity Plasm in the Transition Region of Au Mic: A Stellar Analog of Solar Explosive Events.
PB96-123294 *00,102*

STELLAR RADIATION

Efficient Way of Identifying New Active Stars: A VLA Survey of X-ray Selected Active Stellar Candidates.
PB96-122882 *00,099*

STELLAR RADII

Radiation-Driven Winds of Hot Luminous Stars X. The Determination of Stellar Masses Radii and Distances from Terminal Velocities and Mass-Loss Rates.
PB94-213022 *00,060*

STELLAR SPECTRA

Observing Stellar Coronae with the Goddard High Resolution Spectrograph. I. The dMe Star AU Microscopii.
PB96-102777 *00,092*

GHRS Observations of Cool, Low-Gravity Stars. 1. The Far-Ultraviolet Spectrum of alpha Orions (M2 Iab).
PB96-112016 *00,094*

Sleuthing the Dynamo: HST/FOS Observations of UV Emissions of Solar-Type Stars in Young Clusters.
PB96-122817 *00,098*

Redshifts in Stellar Transition Regions.
PB96-123310 *00,104*

STELLAR TEMPERATURE

ROSAT All-Sky Survey of Active Binary Coronae. 2. Coronal Temperatures of the RS Canum Venaticorum Systems.
PB94-199601 *00,055*

A-type and Chemically Peculiar Stars.
PB96-123286 *00,101*

Radio and X-ray Emissions from Chemically Peculiar B- and A-Type Stars: Observations and a Model.
PB96-123302 *00,103*

STELLAR WINDS

Radiation-Driven Winds of Hot Luminous Stars X. The Determination of Stellar Masses Radii and Distances from Terminal Velocities and Mass-Loss Rates.
PB94-213022 *00,060*

STELLAR X-RAYS

X-rays from Stellar Flares.
PB94-213436 *00,065*

STELLER FLARES

Rotational Modulation and Flares on RS Canum Venaticorum and BY Draconis Stars. XVIII. Coordinated VLA, ROSAT, and IUE Observations of RS CVn Binaries.
PB96-102322 *00,089*

STEP RESPONSE

Uncertainties of Frequency Response Estimates Derived from Responses to Uncertain Step-Like Inputs.
PB97-111843 *01,984*

STEP (STANDARD FOR THE EXCHANGE OF PRODUCT MODEL DATA)

Structural EXPRESS Editor.
PB94-159795 *02,769*

Issues and Recommendations for a STEP Application Protocol Framework. National PDES Testbed.
PB94-160868 *02,770*

Challenges to the National Information Infrastructure: The Barriers to Product Data Sharing. National PDES Testbed Report Series.
PB95-136347 *02,776*

STEP On-Line Information Service (SOLIS). The IGES/PDES Organization.
PB95-137790 *02,777*

SGML Environment for STEP.
PB95-143103 *02,778*

Initial NIST Testing Policy for STEP: Beta Testing Program for AP 203 Implementations. National PDES Testbed Report Series.
PB95-154688 *02,779*

Extensions of the Prototype Application Protocol of Ready-to-Wear Apparel Pattern Making.
PB96-128194 *03,198*

Guidelines for the Development of Mapping Tables.
PB96-154539 *02,786*

STandard for the Exchange of Product Model Data (STEP): Procedures for NIST STEP Validation.
PB96-154976 *02,787*

Group 1 for the Plant Spatial Configuration STEP Application Protocol.
PB96-165402 *02,789*

Machining Process Planning Activity Model for Systems Integration.
PB96-165428 *02,841*

Procedure for Product Data Exchange Using STEP Developed in the AutoSTEP Pilot.
PB96-183058 *02,843*

Application Protocol Information Base World Wide Web Gateway.
PB96-202320 *02,791*

Interoperability Requirements for CAD Data Transfer in the AutoSTEP Project.
PB97-114268 *02,796*

Capabilities for Product Data Exchange.
PB97-118764 *02,798*

STEREOCHEMISTRY

Orbital Stereochemistry: Discovering the Symmetries of Collision Processes.
PB95-202800 *01,034*

Isolation and Structural Elucidation of the Predominant Geometrical Isomers of alpha-Carotene.
PB96-190061 *00,640*

STERILIZATION

Effect of Three Sterilization Techniques on Finger Pluggers.
PB94-216090 *00,150*

Radiation Process Data: Collection, Analysis, and Interpretation.
PB95-162632 *03,628*

STIFFNESS

Influence of Surface Interaction and Chain Stiffness on Polymer-Induced Entropic Forces and the Dimensions of Confined Polymers.
PB94-185469 *01,203*

STOCHASTIC ANALYSIS

Continuous Recording and Stochastic Analysis of PD.
PB96-112156 *01,925*

STOCHASTIC DIFFERENTIAL

Stochastic Modeling of a New Spectrometer.
PB96-157870 *04,068*

STOCHASTIC PROCESSES

Influence of Surface Charge on the Stochastic Behavior of Partial Discharge in Dielectrics.
PB96-122767 *01,931*

Exits in Multistable Systems Excited by Coin-Toss Square-Wave Dichotomous Noise: A Chaotic Dynamics Approach.
PB96-160650 *04,824*

STOICHIOMETRY

Effect of Stoichiometry on the Phases Present in Boron Nitride Thin Films.
PB96-102470 *04,710*

STOKES LAW (FLUID MECHANICS)

Cross-Property Relations and Permeability Estimation in Model Porous Media.
PB95-150280 *04,205*

STONES

Precision of Marchall Stability and Flow Test Using 6-in. (152.4-mm) Diameter Specimens.
PB96-200910 *03,006*

STOPPING POWER

Measured Stopping Powers of Hydrogen and Helium in Polystyrene Near Their Maximum Values.
PB96-112321 *04,729*

STORAGE TANKS

Earthquake Resistant Construction of Gas and Liquid Fuel Pipeline Systems Serving, or Regulated By, the Federal Government.
PB94-161999 *04,846*

Ashland Tank Collapse Investigation.
PB95-126314 *02,481*

Ashland Tank-Collapse Investigation: Closure by Authors.
PB95-126322 *02,482*

STOVES

Measurements of Indoor Pollutant Emissions from EPA Phase II Wood Stoves.
PB95-198735 *02,556*

STRAIN MEASUREMENT

Measurement and Interpretation of Tidal Tilts in a Small Array.
PB96-102611 *03,686*

Measurement of Very Low Frequency Vibrations.
PB96-102660 *03,687*

Sources of Strain-Measurement Error in Flag-Based Extensometry.
PB97-118731 *03,108*

STRAIN (MECHANICS)

Crack Growth Resistance of Strain-Softening Materials under Flexural Loading.
PB94-200227 *02,972*

STRANDINGS
Stranding Experiments on Double Hull Tanker Structures.
PB96-123112 *03,749*

STRANGE ATTRACTORS
Fluctuations in Probability Distribution on Chaotic Attractors.
PB96-102330 *04,022*

STRANGENESS FLOW
Strangeness Flow Difference in Nuclear Collisions at 15A and 200A GeV.
PB96-119631 *04,042*

STRATEGIC PLANNING
Electronic Access: Blueprint for the National Archives and Records Administration.
PB95-219218 *02,731*

STRATIFICATION
Reconstructing Stratified Fluid Flow from Reciprocal Scattering Measurements.
PB95-107256 *04,202*

STRESS ANALYSIS
Effects of Elastic Stress on Phase Equilibrium in the Ni-V System.
PB94-172707 *03,313*

Effect of Transformation of Alloy on Transient and Residual Stresses in a Porcelain-Metal Strip.
PB94-198397 *00,143*

Application of a Simple Technique for Estimating Errors of Finite-Element Solutions Using a General-Purpose Code.
PB94-200250 *04,818*

Generalized Plane Strain Analysis of a Bimaterial Composite Containing a Free Surface Normal to the Interface.
PB95-163341 *03,164*

Critical-Current Degradation in Nb3 Al Wires Due to Axial and Transverse Stress.
PB95-202784 *02,226*

Safety Assessment of Railroad Wheels by Residual Stress Measurements.
PB96-141114 *04,855*

STRESS CORROSION
Assessment of Technology for Detection of Stress Corrosion Cracking in Gas Pipelines. Final Report, July 1993-March 1994.
PB94-206646 *02,475*

Environmentally Enhanced Fracture of Ceramics.
PB95-125746 *03,046*

STRESS CORROSION CRACKING
Evidence of Film-Induced Cleavage by Electrodeposited Rhodium.
PB95-162327 *03,191*

STRESS MEASUREMENT
Ultrasonic Measurement of Residual Stress in Railroad Wheel Rims.
PB95-140430 *04,849*

Ultrasonic Methods.
PB96-190327 *02,707*

STRESS TENSORS
Notion of a xi-Vector and a Stress Tensor for a General Class of Anisotropic Diffuse Interface Models.
PB96-193776 *04,788*

STRESSES
Catastrophic Failures Propagate Field of Fracture Mechanics.
PB96-135140 *03,217*

STRIPED BASS
Histopathology, Blood Chemistry, and Physiological Status of Normal and Moribund Striped Bass ('Morone saxatilis') Involved in Summer Mortality ('Die-Off') in the Sacramento-San Joaquin Delta of California.
PB94-198157 *00,034*

STRONTIUM
Collisional Energy Transfer between Excited-State Strontium and Noble-Gas Atoms.
PB95-202958 *03,995*

Oscillator Strengths and Radiative Branching Ratios in Atomic Sr.
PB95-203493 *04,008*

STRONTIUM IONS
Fine Structure of Negative Ions of Alkaline-Earth-Metal Atoms.
PB94-211182 *03,837*

STRONTIUM TITANATES
Dielectric Properties of Single Crystals of Al2O3, LaAlO3, SrTiO3, and MgO at Cryogenic Temperatures.
PB95-180477 *02,266*

Dielectric Properties of Thin Film SrTiO3 Grown on LaAlO3 with YBa2Cu3O7-x Electodes.
PB95-181160 *02,267*

STRUCTURAL ANALYSIS
Foias-Temam Approximations of Attractors for Galloping Oscillators.
PB94-198298 *04,817*

Structural Analysis in Context.
PB95-151817 *00,437*

Model Precast Concrete Beam-to-Column Connections Subject to Cyclic Loading.
PB95-153094 *00,438*

Partially Prestressed and Debonded Precast Concrete Beam-Column Joints.
PB95-153102 *00,439*

Seismic Performance Behavior of Precast Concrete Beam-Column Joints.
PB95-153110 *00,440*

Assessment of 'Peaks Over Threshold' Methods for Estimating Extreme Value Distribution Tails.
PB95-161360 *00,441*

Gust Factors Applied to Hurricane Winds.
PB95-180469 *00,446*

Workgroup Summary Report: Plastic Hinge-Based Techniques for Advanced Analysis.
PB96-159702 *00,470*

STRUCTURAL CERAMICS
Database Development and Management (Project A.2.2): The Annual Report for 1992-1993.
PB97-110290 *03,098*

Role of Corrosion in a Material Selector Expert System for Advanced Structural Ceramics.
PB97-110308 *03,099*

STRUCTURAL CERAMICS DATABASE SYSTEM
Structural Ceramics Database. Topical Report, June 1989-May 1991.
PB95-203758 *03,060*

STRUCTURAL CHEMICAL ANALYSIS
Carbon Acidities of Aromatic Compounds. 1. Effects of In-Ring Aza and External Electron-Withdrawing Groups.
PB94-216595 *00,860*

STRUCTURAL COMPONENTS
High Temperature Degradation of Structural Composites.
PB94-172848 *03,132*

STRUCTURAL DESIGN
Strengthening Methodology for Lightly Reinforced Concrete Frames: Recommended Design Guidelines for Strengthening with Infill Walls.
PB95-260725 *00,454*

STRUCTURAL ENGINEERING
Wind and Seismic Effects. Proceedings of the U.S.-Japan Cooperative Program in Natural Resources Panel on Wind and Seismic Effects (26th). Held in Gaithersburg, Maryland on May 17-20, 1994.
PB95-147385 *00,433*

Think Metric.
PB95-151825 *01,298*

Algebraic Approximation of Attractors for Galloping Oscillators.
PB95-162897 *04,820*

Lessons from the Loma Prieta Earthquake.
PB95-164091 *00,442*

Structural Ceramics Database. Topical Report, June 1989-May 1991.
PB95-203758 *03,060*

Exits in Multistable Systems Excited by Coin-Toss Square-Wave Dichotomous Noise: A Chaotic Dynamics Approach.
PB96-160650 *04,824*

Wind and Seismic Effects: Proceedings of the Joint Meeting of the U.S.-Japan Cooperative Program in Natural Resources Panel on Wind and Seismic Effects (28th). Held in Gaithersburg, Maryland on May 14-17, 1996.
PB97-104376 *00,476*

STRUCTURAL FAILURE
Ashland Tank Collapse Investigation.
PB95-126314 *02,481*

Ashland Tank-Collapse Investigation: Closure by Authors.
PB95-126322 *02,482*

Proceedings: Workshop on Research Needs in Wind Engineering. Held in Gaithersburg, Maryland on September 12-13, 1994.
PB95-189528 *00,448*

STRUCTURAL PROPERTIES
Microwave Spectrum and Structure of CH3NO2-H20.
AD-A296 377/5 *00,719*

STRUCTURAL RESPONSE
Seismic Strengthening of Reinforced Concrete Frame Buildings.
PB95-108841 *00,430*

STRUCTURAL VIBRATION
Dynamic Characteristics of Five Tall Buildings during Strong and Low-Amplitude Motions.
PB94-199981 *00,427*

Response of Buildings to Ambient Vibration and the Loma Prieta Earthquake: A Comparison.
PB96-119607 *00,457*

Method of Estimating the Parameters of Tuned Mass Dampers for Seismic Applications.
PB96-167820 *00,473*

STRUCTURED QUERY LANGUAGE
SQL Environments. Category: Software Standard; Subcategory: Database.
FIPS PUB 193 *01,801*

STRUTS
Composite Struts for SMES Plants.
PB95-155586 *02,507*

STYRENES
Acrylonitrile-Butadiene-Styrene (ABS) Plastic Drain, Waste, and Vent Pipe and Fittings.
AD-A310 724/0 *00,327*

SUB-DOPPLER FREQUENCIES
Sub-Doppler Frequency Measurements on OCS at 87 THz (3.4 mu m) with the CO Overtone Laser.
PB96-102215 *04,330*

SUBAMBIENT TEMPERATURE CONTROL
Device for Subambient Temperature Control in Liquid Chromatography.
PB95-140604 *00,573*

SUBCRITICAL CRACK GROWTH
Transient Subcritical Crack-Growth Behavior in Transformation-Toughened Ceramics.
PB94-200656 *03,038*

SUBJECT INDEXING
Preliminary Subject and Authors Index to Compilations of Data on Properties of Materials.
AD-A302 669/7 *03,242*

SUBMARINES
Outline of a Multiple Dimensional Reference Model Architecture and a Knowledge Engineering Methodology for Intelligent Systems Control.
PB95-220414 *03,703*

Submarine Automation: Demonstration No. 5.
PB95-251633 *03,748*

Operator Experience with a Hierarchical Real-Time Control System (RCS).
PB96-195516 *03,751*

SUBMERGED ARC WELDING
Effects of Copper, Nickel and Boron on Mechanical Properties of Low-Alloy Steel Weld Metals Deposited at High Heat Input.
PB96-135231 *03,363*

SUBROUTINE LIBRARIES
Review of Mathematical Function Library for Microsoft-FORTRAN, John Wiley and Sons, 1989.
PB94-160793 *01,679*

Software Libraries, Numerical and Statistical.
PB94-198967 *01,689*

SUBROUTINES
VENTCF2: An Algorithm and Associated FORTRAN 77 Subroutine for Calculating Flow through a Horizontal Ceiling/Floor Vent in a Zone-Type Compartment Fire Model.
PB94-210127 *00,345*

SUBSTRATE SPECIFICITY
Substrate Specificity of the Escherichia coli Endonuclease III: Excision of Thymine- and Cytosine-Derived Lesions in DNA Produced by Radiation-Generated Free Radicals.
PB95-153425 *03,535*

SUBSTRATES
Substrate and Thin Film Measurements.
PB96-112297 *02,384*

SUBSURFACE CONDUCTORS
Gradiometer Antennas for Detection of Long Subsurface Conductors.
PB95-175667 *01,862*

SUBTILISINS
Analysis of Protein Metal Binding Selectivity in a Cluster Model.
PB94-212990 *00,845*

SUCROSE PERMEASE
Glucose Permease of Bacillus Subtilis Is a Single Polypeptide Chain That Functions to Energize the Sucrose Permease.
PB95-163192 *03,466*

SULFATE RADICALS
Temperature Dependence of the Rate Constants for Reactions of the Sulfate Radical, SO4-, with Anions.
PB94-212172 *00,828*

Electron Transfer Reaction Rates and Equilibria of the Carbonate and Sulfate Radical Anions.
PB94-212180 *00,829*

Kinetics of the Reaction of the Sulfate Radical with the Oxalate Anion.
PB97-119127 *01,186*

SULFATES
Expansion of Cementitious Materials Exposed to Sulfate Solutions.
PB94-185782 *02,577*

Sulfate Attack of Cementitious Materials: Volumetric Relations and Expansions.
PB94-187317 *03,232*

Temperature Dependence of the Rate Constants for Reactions of the Sulfate Radical, SO4-, with Anions.
PB94-212172 *00,828*

SULFIDES
Sub-Doppler Frequency Measurements on OCS at 87 THz (3.4 mu m) with the CO Overtone Laser.
PB96-102215 *04,330*

SULFUR
Determination of Sulfur in Fossil Fuels by Isotope Dilution Thermal Ionization Mass Spectrometry.
PB96-141379 *02,495*

Investigations of Sulfur Interferences in the Extraction of Methylmercury from Marine Tissues.
PB96-190020 *03,482*

SULFUR ATOMS
Atomic Sulfur: Frequency Measurement of the J=0 inversely maps 1 Fine-Structure Transition at 56.3 Microns by Laser Magnetic Resonance.
PB95-180105 *01,007*

SULFUR DIOXIDE
Sulfur Dioxide Capture in the Combustion of Mixtures of Lime, Refuse-Derived Fuel, and Coal.
PB94-155587 *02,534*

High-Resolution Measurements of the nu2 and 2nu2-nu2 Bands of (34)S(16)O2.
PB94-216223 *00,855*

Reanalysis of the (010), (020), (100), and (001) Rotational Levels of (32)S(16)O2.
PB95-125621 *00,887*

SULFUR FLUORIDES
Collision-Induced Neutral Loss Reactions of Molecular Dications.
PB94-185808 *00,780*

Investigation of S2F10 Production and Mitigation in Compressed SF6-Insulated Power Systems.
PB94-212388 *02,467*

Associative Electron Attachment to S2F10, S2OF10, and S2O2F10.
PB95-140992 *00,907*

Electron Scattering and Dissociative Attachment by SF6 and Its Electrical-Discharge By-Products.
PB95-151288 *02,256*

Investigation of S2F10 Production and Mitigation in Compressed SF6- Insulated Power Systems.
PB96-155528 *02,468*

SULFUR HEXAFLUORIDE
Operational Mode and Gas Species Effects on Rotational Drag in Pneumatic Dead Weight Pressure Gages.
PB95-140182 *00,903*

Plasma Chemical Model for Decomposition of SF6 in a Negative Glow Corona Discharge.
PB95-181053 *01,020*

SF6 Insulation: Possible Greenhouse Problems and Solutions.
PB95-251625 *02,269*

Gaseous Dielectrics Research: Possible SF6 Substitutes.
PB96-119268 *02,228*

Decomposition of SF6 and Production of S2F10 in Power Arcs.
PB96-122619 *01,084*

Decomposition of Sulfur Hexafluoride by X-rays.
PB96-135314 *01,095*

SULFUR INORGANIC COMPOUNDS
Chemical and Microbiological Problems Associated with Research on the Biodesulfurization of Coal.
PB95-140950 *02,484*

SULFUR IONS
Crossed-Beams Measurements of Absolute Cross Sections for Electron Impact Ionization of S(+).
PB95-202511 *03,981*

SULFUR-LIKE IONS
Labeling Conventions in Isoelectronic Sequences - Reply.
PB95-162574 *03,937*

SULFUR ORGANIC COMPOUNDS
Chemical and Microbiological Problems Associated with Research on the Biodesulfurization of Coal.
PB95-140950 *02,484*

SULFUR OXOFLUORIDES
Associative Electron Attachment to S2F10, S2OF10, and S2O2F10.
PB95-140992 *00,907*

SULPHUR HETEROCYCLIC COMPOUNDS
Ideal Gas Thermodynamic Properties of Sulphur Heterocyclic Compounds.
PB96-145867 *01,110*

SUM RULES
Drill-Hearn-Gerasimov Sum Rule.
PB94-211752 *03,845*

Use of Sum Rules on the Energy-Loss Function for the Evaluation of Experimental Optical Data.
PB95-150736 *04,264*

SUPERCOMPUTERS
Distributed Supercomputing Software: Experiences with the Parallel Virtual Machine - PVM.
PB94-163086 *01,680*

Nonlinear Color Transformations in Real Time Using a Video Supercomputer.
PB96-123021 *02,191*

SUPERCONDICTIVITY
Electrical Characterization of Narrow Gap n-Type Bulk HgCdTe Single Crystals by Variable-Magnetic-Field Hall Measurements and Reduced-Conductivity-Tensor Analyses.
PB96-164199 *01,146*

SUPERCONDUCTERS
Temperature and Field Dependence of Flux Pinning in NbTi with Aritificial Pinning Centers.
PB96-112024 *04,726*

SUPERCONDUCTING
High-Energy Phonon Dispersion in La1.85Sr0.15CuO4.
PB96-138458 *04,748*

SUPERCONDUCTING DEVICES
Roles of Copper in Applied Superconductivity.
PB94-211521 *02,255*

Far-Infrared Kinetic Inductance Detector.
PB95-126348 *02,142*

Superconducting Kinetic Inductance Radiometer.
PB95-140083 *02,144*

Thermal and Nonequilibrium Responses of Superconductors for Radiation Detectors.
PB95-164232 *02,156*

Terahertz Detectors Based on Superconducting Kinetic Inductance.
PB95-168647 *02,160*

Optical Performance of Photoinductive Mixers at Terahertz Frequencies.
PB95-168662 *02,161*

Ultrasensitive-Hot-Electron Microbolometer.
PB95-168985 *02,163*

Electronics and Electrical Engineering Laboratory Technical Progress Bulletin Covering Laboratory Programs, July to September 1994 with 1994/1995 EEEL Events Calendar.
PB95-170395 *02,360*

Experimental Results on Single Flux Quantum Logic.
PB95-175071 *02,053*

Characterization of a Tunable Thin Film Microwave YBa2Cu3O7-x/SrTiO3 Coplanar Capacitor.
PB95-175527 *02,264*

Electronics and Electrical Engineering Laboratory Technical Publication Announcements Covering Laboratory Programs, January to March 1995 with 1995 EEEl Events Calendar.
PB95-242277 *02,373*

SUPERCONDUCTING FILMS
YBa2Cu3O7-x to Si Interconnection for Hybrid Superconductor/Semiconductor Integration.
PB94-211711 *02,315*

Influence of Deposition Parameters on Properties of Laser Ablated YBa2Cu3O7-Delta Films.
PB95-140539 *04,544*

Critical Current Behavior of Ag-Coated YBa2Cu3O7-x Thin Films.
PB95-141016 *04,549*

Magnetic Field Dependence of the Critical Current Anisotropy in Normal Metal-YBa2Cu3O7-delta Thin Film Bilayers.
PB95-141024 *04,550*

Insulating Nanoparticles on YBa2Cu3O7-delta Thin Films Revealed by Comparison of Atomic Force and Scanning Tunneling Microscopy.
PB95-150843 *04,575*

Effects of Anneal Time and Cooling Rate on the Formation and Texture of Bi2Sr2CaCu2O8 Films.
PB95-161600 *04,603*

Growth of Laser Ablated YBa2Cu3O7-delta Films as Examined by Rheed and Scanning Tunneling Microscopy.
PB95-162541 *04,614*

Observation of Insulating Nanoparticles on YBCO Thin-Films by Atomic Force Microscopy.
PB95-163358 *04,622*

Tunneling Measurement of the Zero-Bias Conductance Peak and the Bi-Sr-Ca-Cu-O Thin-Film Energy Gap.
PB95-163739 *04,628*

Analytic Calculation of Polarized Neutron Reflectivity from Superconductors.
PB95-164224 *04,629*

Reactive Coevaporation of DyBaCuO Superconducting Films: The Segregation of Bulk Impurities on Annealed MgO(100) Substrates.
PB95-164562 *04,635*

High Current Pressure Contacts to Ag Pads on Thin Film Superconductors.
PB95-168621 *04,639*

Microwave Properties of YBa2Cu3O7-x Films at 35 GHz from Magnetotransmission and Magnetoreflection Measurements.
PB95-168977 *04,643*

Surface Degradation of Superconducting YBa2Cu3O7-delta Thin Films.
PB95-176095 *04,667*

Increased Transition Temperature in In situ Coevaporated YBa2Cu3O7-delta Thin Films by Low Temperature Post-Annealing.
PB95-180071 *04,672*

Novel YBa2Cu3O7-x and YBa2Cu3O7-x/Y4Ba3O9 Multilayer Films by Bias-Masked 'On-Axis' Magnetron Sputtering.
PB95-181186 *04,690*

Surface Modification of YBa2Cu3O7-delta Thin Films Using the Scanning Tunneling Microscope: Five Methods.
PB95-203394 *04,699*

SUPERCONDUCTING GRAVIMETERS
Calibration of a Superconducting Gravimeter Using Absolute Gravity Measurements.
PB95-202651 *03,684*

SUPERCONDUCTING JUNCTIONS
Half-Integral Constant Voltage Steps in High-Tc Grain Boundary Junctions.
PB94-211216 *04,489*

Tunneling Measurement of the Zero-Bias Conductance Peak and the Bi-Sr-Ca-Cu-O Thin-Film Energy Gap.
PB95-163739 *04,628*

Hot-Electron Microcalorimeters for X-ray and Phonon Detection.
PB95-168993 *04,644*

Hot-Electron Microcalorimeters as High-Resolution X-ray Detectors.
PB96-123641 *04,739*

Hot-Electron-Microcalorimeters with 0.25 mm(2) Area.
PB96-200670 *04,793*

SUPERCONDUCTING MAGNETIC ENERGY STORAGE PLANTS
Composite Struts for SMES Plants.
PB95-155586 *02,507*

SUPERCONDUCTING MAGNETS
Electromechanical properties of superconductors for DOE fusion applications.
DE95015476 *04,432*

Electromechanical Properties of Superconductors for DOE Fusion Applications.
PB94-139672 *02,250*

Irradiation Damage in Inorganic Insulation Materials for ITER Magnets: A Review.
PB95-147351 *03,705*

Cryogenic Properties of Inorganic Insulation Materials for ITER Magnets: A Review.
PB95-198768 *03,706*

SUSAN: SUperconducting Systems ANalysis by Low Temperature Scanning Electron Microscopy (LTSEM).
PB96-112065 *04,728*

SUPERCONDUCTING NETWORKS
Automated Josephson Integrated Circuit Test System.
PB95-175246 *02,057*

SUPERCONDUCTING SUPER COLLIDER
Magnetic Characteristics and Measurements of Filamentary Nb-Ti Wire for the Superconducting Super Collider.
DE94005988 *03,775*

SUPERCONDUCTING WIRES
Magnetic Characteristics and Measurements of Filamentary Nb-Ti Wire for the Superconducting Super Collider.
DE94005988 *03,775*

Volume Magnetic Hysteresis Loss of Nb3Sn Superconductors as a Function of Wire Length.
PB95-153722 *04,597*

Superconductor Critical Current Standards for Fusion Applications. Final Progress Report, October 1993-July 1994.
PB95-169538 *02,222*

Reduction of Interfilament Contact Loss in Nb3Sn Superconductor Wires.
PB95-175535 *02,223*

Critical-Current Degradation in Nb3 Al Wires Due to Axial and Transverse Stress.
PB95-202784 *02,226*

VAMAS Intercomparison of Critical Current Measurements on NB3Sn Superconductors: A Summary Report.
PB96-119763 *04,043*

Anomalous Switching Phenomenon in Critical-Current Measurements When Using Conductive Mandrels.
PB96-137781 *02,233*

SUPERCONDUCTIVITY
Roles of Copper in Applied Superconductivity.
PB94-211521 *02,255*

Systematic Studies of the Effect of a Bandpass Filter on a Josephson-Junction Noise Thermometer.
PB95-162970 *03,939*

Aspects of a Deformable Superconductor Model for the Vortex Mass.
PB95-175303 *04,652*

Deformable Superconductor Model for the Fluxon Mass.
PB95-175311 *04,653*

Lattice Dynamics of Ba1-xKxBiO3.
PB96-102421 *04,706*

Structure and Conductivity of Layered Oxides (Ba,Sr)n+1(Sn,Sb)nO3n+1.
PB96-102439 *04,707*

Oxygen Dependance of the Crystal Structure of HgBa2CuO4+ and Its Relation to Superconductivity.
PB96-102512 *04,711*

Shapiro Steps in Large-Area Metallic-Barrier Josephson Junctions.
PB96-200142 *02,090*

Metrology for Electromagnetic Technology: A Bibliography of NIST Publications.
PB97-116057 *04,396*

SUPERCONDUCTIVITY JUNCTIONS
Hot-Electron Microcalorimeter for X-ray Detection Using a Superconducting Transition Edge Sensor with Electrothermal Feedback.
PB96-200399 *04,792*

SUPERCONDUCTOR DEVICES
Metrology for Electromagnetic Technology: A Bibliography of NIST Publications.
PB95-135588 *02,143*

SUPERCONDUCTORS
Electromechanical properties of superconductors for DOE fusion applications.
DE95015476 *04,432*

Electromechanical Properties of Superconductors for DOE Fusion Applications.
PB94-139672 *02,250*

Alternating-Field Susceptometry and Magnetic Susceptibility of Supercondoctors. Presented at Office of Naval

Research Workshop on Magnetic Susceptibility of Superconductors and Other Spin Systems. Held in Berkeley Springs, West Virginia on 20 May 1991.
PB94-145984 *04,435*

Raman and Fluorescence Spectra Observed in Laser Microprobe Measurements of Several Compositions in the Ln-Ba-Cu-O System.
PB94-172210 *04,440*

Dispersions of Magnetic Excitations of the Pr Ions in Pr2CuO4.
PB94-173044 *04,444*

Neutron-Scattering Study of C60(n-) (n=3,6) Librations in Alkali-Metal Fullerides.
PB94-200219 *00,806*

High-Frequency Linear Response of Anisotropic Type-II Superconductors in the Mixed State.
PB94-200359 *04,483*

Nonlinear Response of Type-II Superconductors in the Mixed State in Slab Geometry.
PB94-200367 *04,484*

Superconducting Materials: Specification.
PB94-211299 *04,491*

Flux Expulsion at Intermediate Fields in Type-II Superconductors.
PB94-212230 *04,502*

Offset Susceptibility of Superconductors.
PB94-212263 *04,503*

Correlation between Tc and Elastic Constants of (La-M)2CuO4.
PB94-213220 *04,514*

n-Value and Second Derivative of the Superconductor Voltage-Current Characteristic.
PB95-126223 *04,533*

Superconducting Energy Gap of Bulk UBe13.
PB95-150116 *04,559*

Phonon Density of States in R2CuO4 and Superconducting R1.85Ce0.15CuO4 (R = Nd, Pr).
PB95-150686 *04,574*

Even-Odd Asymmetry of a Superconductor Revealed by the Coulomb Blockade of Andreev Reflection.
PB95-153540 *04,593*

Magnetic Force Microscopy of Flux in Superconductors.
PB95-161733 *04,608*

New Exact Solution of the One-Dimensional Schrodinger Equation and Its Application to Polarized Neutron Reflectometry.
PB95-161832 *04,609*

Description of Layered Structures: Applications to High Tc Superconductors.
PB95-162624 *04,615*

Critical Current Density, Irreversibility Line, and Flux Creep Activation Energy in Silver-Sheathed Bi2Sr2Ca2Cu2Ox Superconducting Tapes.
PB95-162749 *04,616*

Magnetocaloric Effect in Nanocomposites.
PB95-162798 *04,618*

Ca1-xCuO2, a NaCuO2-Type Related Structure.
PB95-162822 *04,620*

Analytic Calculation of Polarized Neutron Reflectivity from Superconductors.
PB95-164224 *04,629*

Alternating-Field Susceptometry and Magnetic Susceptibility of Superconductors.
PB95-168613 *04,638*

Crossover in the Pinning Mechanism of Anisotropic Fluxon Cores.
PB95-180170 *04,673*

Magnetic Susceptibility of Pr2-xCexCuO4 Monocrystals and Polycrystals.
PB95-180253 *04,677*

Observation of Oscillatory Magnetic Order in the Antiferromagnetic Superconductor HoNi2B2C.
PB95-180303 *04,679*

Lattice Dynamics of Semiconducting, Metallic, and Superconducting Ba1-xKxBiO3 Studied by Inelastic Neutron Scattering.
PB96-102447 *04,708*

30 THz Mixing Experiments on High Temperature Superconducting Josephson Junctions.
PB96-102462 *04,709*

Electronic Microrefrigerator Based on a Normal-Insulator-Superconductor Tunnel Junction.
PB96-102827 *04,718*

Superconducting Integrated Circuit Fabrication with Low Temperature ECR-Based PECVD SiO2 Dielectric Films.
PB96-103015 *04,719*

Comparing the Accuracy of Critical-Current Measurements Using the Voltage-Current Simulator.
PB96-119219 *02,227*

High-Temperature Superconductor Cryogenic Current Comparator.
PB96-119334 *02,074*

Simple and Repeatable Technique for Measuring the Critical Current of Nb3Sn Wires.
PB96-119409 *02,229*

Effect of Sm2BaCuO5 on the Properties of Sintered (Bulk) YBa2Cu3O6+x.
PB96-119441 *04,733*

Thermal Isolation of High-Temperature Superconducting Thin Films Using Silicon Wafer Bonding and Micromachining.
PB96-135017 *02,408*

Mutual Phase Locking in Systems of High-Tc Superconductor-Normal Metal-Superconductor Junctions.
PB96-135348 *04,744*

Quench Energy and Fatigue Degradation Properties of Cu- and Al/Cu-Stablized Nb-Ti Epoxy-Impregnated Superconductor Coils.
PB96-141213 *04,755*

II-3: Critical Current Measurement Methods: Quantitative Evaluation.
PB96-147160 *04,767*

II-5: Thermal Contraction of Materials Used in Nb3Sn Critical Current Measurements.
PB96-147186 *04,769*

USA Interlaboratory Comparison of Superconductor Simulator Critical Current Measurements.
PB96-147194 *04,770*

V-6: Effects of Temperature Variation.
PB96-148143 *04,772*

Metallic-Barrier Junctions for Programmable Josephson Voltage Standards.
PB96-200134 *02,089*

Superconductor- Normal-Superconductor Junctions for Digital/Analog Converters.
PB96-200233 *02,092*

Elastic Constants and Microcracks in YBa2Cu3O7.
PB96-200761 *03,005*

Neutron Scattering Study of Antiferromagnetic Order in the Magnetic Superconductors RNi2B2C.
PB97-112411 *04,812*

Vortex Images in Thin Films of YBa2Cu3O(sub 7-x) and Bi2Sr2Ca1Cu2O(sub 8+x) Obtained by Low-Temperature Magnetic Force Microscopy.
PB97-119408 *04,815*

SUPERCOOLED LIQUIDS

Simulations of Glass Forming Liquids: What Has Been Learned.
PB95-150124 *00,915*

Activated Dynamics, Loss of Ergodicity, and Transport in Supercooled Liquids.
PB95-150819 *00,925*

Simulation Studies of Supercooled and Glass Forming Liquids.
PB96-122627 *01,085*

SUPERCOOLING

Length Scales for Fragile Glass-Forming Liquids.
PB96-102801 *01,065*

Long-Lived Structures in Fragile Glass-Forming Liquids.
PB96-119565 *04,212*

Simulation Studies of Supercooled and Glass Forming Liquids.
PB96-122627 *01,085*

SUPERCRITICAL FLUID EXTRACTION

Thermophysical Property Data for Supercritical Fluid Extraction Design.
PB94-199221 *00,668*

Supercritical Fluid Extraction of Biological Products.
PB95-175204 *00,040*

SUPERCRITICAL FLUID SOLUTIONS

Measurement of Diffusion in Supercritical Fluid Systems: A Review.
PB94-199189 *00,795*

SUPERCRITICAL FLUIDS

Summary of the Patent Literature of Supercritical Fluid Technology.
PB94-199213 *00,502*

Supercritical Solubility of Solids from Near-Critical Dilute-Mixture Theory.
PB94-211703 *00,819*

Application of the Taylor Dispersion Method in Supercritical Fluids.
PB95-164323 *00,977*

Measurement of Diffusion in Fluid Systems: Applications to the Supercritical Fluid Region.
PB95-175188 *02,490*

Solubility Measurement by Direct Injection of Supercritical-Fluid Solutions into a HPLC System.
PB95-175626 *00,997*

High-Pressure Equilibrium Cell for Solubility Measurements in Supercritical Fluids.
PB95-175634 *00,998*

Instrument for Evaluating Phase Behavior of Mixtures for Supercritical Fluid Experiments.
PB95-180758 *00,606*

SUPERCRITICAL STATE

Measurement of Diffusion in Supercritical Fluid Systems: A Review.
PB94-199189 *00,795*

Thermophysical Property Data for Supercritical Fluid Extraction Design.
PB94-199221 *00,668*

SUPERGIANT STARS

Four Years of Monitoring alpha Orionis with the VLA: Where Have All the Flares Gone.
PB94-185212 *00,048*

SUPERLATTICES

Structural and Magnetic Ordering in Iron Oxide/Nickel Oxide Multilayers by X-ray and Neutron Diffraction (Invited).
PB94-172558 *04,442*

Enhanced Curie Temperatures and Magnetoelastic Domains in Dy/Lu Super Lattices and Films.
PB94-172665 *04,443*

Interface Roughness-Induced Changes in the Near-E(sub 0) Spectroscopic Behavior of Short-Period AlAs/GaAs Superlattices.
PB94-185154 *02,118*

Magnetic and Structural Properties of Electrodeposited Copper-Nickel Microlayered Alloys.
PB94-213121 *04,512*

Interface Roughness of Short-Period AlAs/GaAs Superlattices Studied by Spectroscopic Ellipsometry.
PB95-107215 *02,137*

Interface Sharpness in Low-Order III-V Superlattices.
PB95-108775 *02,138*

Interface Sharpness during the Initial Stages of Growth of Thin, Short-Period III-V Superlattices.
PB95-108783 *02,139*

Effects of Interfacial Roughness on the Magnetoresistance of Magnetic Metallic Multilayers.
PB95-150017 *04,556*

Comment on 'Phase Transitions in Antiferromagnetic Superlattices'.
PB95-152971 *04,587*

Magnetic Rare Earth Artificial Metallic Superlattices.
PB95-162293 *04,611*

SUPERMIRRORS

Supermirror Transmission Polarizers for Neutrons.
PB94-216215 *03,866*

SUPERNOVA 1957D

Rapid Decline in the Optical Emission from SN 1957D in M83.
PB94-216033 *00,070*

SUPERNOVA REMNANTS

Rapid Decline in the Optical Emission from SN 1957D in M83.
PB94-216033 *00,070*

CCD Mosaic Images of the Supernova Remnant 3C 400.2.
PB95-203527 *00,084*

G203.2-12.3: A New Optical Supernova Remnant in Orion.
PB95-203535 *00,085*

SUPERONDUCTORS

Reference Relations for the Evaluation of the Materials Properties of Orthorhombic YBa2Cu3Ox Superconductors.
PB96-176763 *04,782*

SUPEROXIDE RADICALS

Reaction of NO with Superoxide.
PB94-212198 *00,830*

SUPERPOSED FLEXURE

Flat and Rising R-Curves for Elliptical Surface Cracks from Indentation and Superposed Flexure.
PB95-161295 *03,156*

SUPERSTABLE LASERS

Introduction to Phase-Stable Optical Sources.
PB96-122973 *04,347*

SUPPORTS

Affinity Chromatography on Inorganic Support Materials.
PB95-163820 *03,467*

SURFACE ANALYSIS

Inelastic Interactions of Electrons with Surfaces: Application to Auger-Electron Spectroscopy and X-ray Photoelectron Spectroscopy.
PB94-172699 *00,764*

Compositional Analyses of Surfaces and Thin Films by Electron and Ion Spectroscopies.
PB94-185790 *00,779*

Reactivity of Pd and Sn Adsorbates on Plasma and Thermally Oxidized SnO2(110).
PB94-199973 *00,804*

Pure Element Sputtering Yield Data: Appendix 4.
PB94-200037 *00,805*

X-Ray Photoelectron and Auger Electron Spectroscopy Study of Ultraviolet/Ozone Oxidized P2S5/(NH4)2S Treated GaAs(100) Surfaces.
PB94-200144 *04,479*

Grazing-Incidence X-Ray Photoemission Spectroscopy Investigation of Oxidized GaAs(100): A Novel Approach to Nondestructive Depth Profiling.
PB94-200151 *04,480*

Formalism and Parameters for Quantitative Surface Analysis by Auger Electron Spectroscopy and X-Ray Photoelectron Spectroscopy.
PB94-212297 *00,832*

Analysis of Boron in CVD Diamond Surfaces Using Neutron Depth Profiling.
PB94-213089 *04,511*

Activities of the ASTM Committee E-42 on Surface Analysis.
PB95-108528 *00,881*

Formation of Technical Committee 201 on Surface Chemical Analysis by the International Organization for Standardization.
PB95-108536 *00,568*

Nanoscale Study of the As-Grown Hydrogenated Amorphous Silicon Surface.
PB95-150595 *04,573*

Grazing Angle X-Ray Photoemission System for Depth-Dependent Analysis.
PB95-161154 *04,600*

Observation of Insulating Nanoparticles on YBCO Thin-Films by Atomic Force Microscopy.
PB95-163358 *04,622*

Reactive Coevaporation of DyBaCuO Superconducting Films: The Segregation of Bulk Impurities on Annealed MgO(100) Substrates.
PB95-164562 *04,635*

SURFACE AREA

Total Surface Areas of Group IVA Organometallic Compounds: Predictors of Toxicity to Algae and Bacteria.
PB94-211331 *00,814*

SURFACE CHEMISTRY

Role of Adsorbed Alkalis in Desorption Induced by Electronic Transitions.
PB94-172574 *00,762*

Surface Forces and Adhesion between Dissimilar Materials Measured in Various Environments.
PB94-172970 *03,033*

Contact Electrification Induced by Monolayer Modification of a Surface and Relation to Acid-Base Interactions.
PB94-185378 *03,034*

Peeling a Polymer from a Surface or from a Line.
PB94-199809 *01,213*

Tribochemical Reaction of Stearic Acid on Copper Surface Studied by Surface Enhanced Raman Spectroscopy.
PB94-212057 *02,964*

Structure of Molecules on Surfaces as Determined Using Electron-Stimulated Desorption.
PB94-216165 *00,852*

Deposition of Colloidal Sintering-Aid Particles on Silicon Nitride.
PB94-216272 *03,044*

Interface Modification and Characterization of Silicon Carbide Platelets Coated with Alumina Particles.
PB95-108734 *03,121*

Characterization of Chemically Modified Pore Surfaces by Small Angle Neutron Scattering.
PB95-126181 *00,898*

Silver Metalization of Octadecanethiol Monolayers Self-Assembled on Gold.
PB95-150744 *00,923*

Time-Resolved Measurements of Energy Transfer at Surfaces.
PB95-153037 *00,947*

Fundamental Studies of Gas Sensor Response Mechanisms: Palladium on SnO2(110).
PB95-162731 *00,963*

Observation of a Stable Methoxy Intermediate on Cr(110).
PB95-164422 *00,981*

Surface Chemical Interactions of Si3N4 with Polyelectrolyte Deflocculants.
PB95-175576 *03,056*

Effects of Soxhlet Extraction on the Surface Oxide Layer of Silicon Nitride Powders.
PB95-175584 *03,057*

Activities of ISO Technical Committee 201 on Surface Chemical Analysis.
PB95-180824 *00,607*

Surface Chemistry of Silicon Nitride Powder in the Presence of Dissolved Ions.
PB96-111760 *01,073*

Mechano-Chemical Model: Reaction Temperatures in a Concentrated Contact.
PB96-119466 *03,227*

Silicon Surface Chemistry by IR Spectroscopy in the Mid- to Far-IR Region: H2O and Ethanol on Si(100).
PB96-138565 *01,097*

SURFACE CRACKS

Flat and Rising R-Curves for Elliptical Surface Cracks from Indentation and Superposed Flexure.
PB95-161295 *03,156*

SURFACE DEFECTS

Non-Osmotic, Defect-Controlled Cathodic Disbondment of a Coating from a Steel Substrate.
PB94-216447 *03,120*

Photodesorption Dynamics of CO from Si(111): The Role of Surface Defects.
PB96-111646 *03,066*

SURFACE DIFFUSION

Linking Anisotropic Sharp and Diffuse Surface Motion Laws via Gradient Flows.
PB95-203378 *04,698*

Notion of a xi-Vector and a Stress Tensor for a General Class of Anisotropic Diffuse Interface Models.
PB96-193776 *04,788*

SURFACE EMITTING LASERS

Characterization of Vertical-Cavity Semiconductor Structures.
PB94-200193 *02,126*

Comparative Photoluminescence Measurement and Simulation of Vertical-Cavity Semiconductor Laser Structures.
PB95-169173 *02,169*

Measurement and Simulation of Photoluminescence Spectra from Vertical-Cavity Quantum-Well Laser Structures.
PB95-169181 *02,170*

SURFACE ENERGY

Singularities in Minimum Surface Energy Problems and Their Influence in Surface Motion.
PB94-199411 *04,473*

Surface Energy Reduction in Fibrous Monotectic Structures.
PB95-140828 *03,150*

Measuring Contact Charge Transfer at Interfaces: A New Experimental Technique.
PB95-164570 *03,053*

SURFACE EXCHANGE

Interaction of Citric Acid with Hydroxyapatite: Surface Exchange of Ions and Precipitation of Calcium Citrate.
PB97-119309 *03,584*

SURFACE FIGURE

Upgraded Facility for Multilayer Mirror Characterization at NIST.
PB96-160387 *04,367*

SURFACE FINISHING

Opportunities for Innovation: Advanced Surface Engineering.
PB94-176666 *02,697*

SURFACE INTERACTION

Segmental Concentration Profiles of End-Tethered Polymers with Excluded-Volume and Surface Interactions.
PB97-119002 *00,654*

SURFACE MAGNETISM

Magnetic Moments in Cr Thin Films on Fe(100).
PB95-108429 *04,525*

SURFACE METROLOGY

Microform Calibrations in Surface Metrology.
PB95-203295 *02,951*

SURFACE MODIFICATION

Surface Modification of YBa2Cu3O7-delta Thin Films Using the Scanning Tunneling Microscope: Five Methods.
PB95-203394 *04,699*

SURFACE MORPHOLOGY

Coarsening of Unstable Surface Features during Fe(001) Homoepitaxy.
PB96-186127 *04,121*

SURFACE PLASMON RESONANCE

Surface Plasmon Microscopy of Biotin-Streptavidin Binding Reactions on UV-Photopatterned Alkanethiol Self-Assembled Monolayers.
PB96-176771 *01,158*

SURFACE PROFILING

Present and Future Standard Specimens for Surface Finish Metrology.
PB97-110423 *02,928*

SURFACE PROPERTIES

Temperature Dependence of the Morphology of Thin Diblock Copolymer Films as Revealed by Neutron Reflectivity.
PB94-172756 *01,199*

Interface Properties for Ceramic Composites from a Single Fiber Pull-Out Test.
PB94-199361 *03,135*

Active Site Ionicity and the Mechanism of Carbonic Anhydrase.
PB94-212974 *00,843*

Characterization of Phase and Surface Composition of Silicon Carbide Platelets.
PB94-216264 *03,043*

Observed Frustration in Confined Block Copolymers.
PB95-150033 *01,238*

Modified Surface Layers and Coatings.
PB95-176087 *03,125*

Influence of Surface Charge on the Stochastic Behavior of Partial Discharge in Dielectrics.
PB96-122767 *01,931*

Stylus Flight in Surface Profiling.
PB96-123138 *02,675*

SURFACE REACTIONS

Dynamics of Nonthermal Reactions: Femtosecond Surface Chemistry.
PB94-199965 *00,688*

Surface Degradation of Superconducting YBa2Cu3O7-delta Thin Films.
PB95-176095 *04,667*

Single Photon Ionization, Laser Optical Probe Technique for Semiconductor Growth.
PB95-202776 *01,032*

SURFACE RESISTANCE

Influence of Films' Thickness and Air Gaps in Surface Impedance Measurements of High Temperature Superconductors Using the Dielectric Resonator Technique.
PB96-157862 *01,946*

SURFACE ROUGHNESS

Ultrasonic Measurements of Surface Roughness.
PB94-172137 *04,181*

Light Scattering from Glossy Coatings on Paper.
PB94-213246 *04,242*

Relation between AC Impedance Data and Degradation of Coated Steel. 1. Effects of Surface Roughness and Contamination on the Corrosion Behavior of Epoxy Coated Steel.
PB94-213345 *03,189*

Determination of Surface Roughness from Scattered Light.
PB94-216520 *04,243*

Autocorrelation Functions from Optical Scattering for One-Dimensionally Rough Surfaces.
PB94-216538 *04,244*

Light Scattered by Coated Paper.
PB94-216546 *04,245*

Regimes of Surface Roughness Measurable with Light Scattering.
PB95-151213 *04,265*

Automated Optical Roughness Inspection.
PB95-152179 *02,905*

Surface Roughness Evaluation of Diamond Films Grown on Substrates with a High Density of Nucleation Sites.
PB95-162418 *03,018*

Surface Texture.
PB95-164620 *03,351*

Nanoscale Study of the Hydrogenated Amorphous Silicon Surface.
PB96-103056 *04,720*

Optical Scattering from Moderately Rough Surfaces.
PB97-110415 *04,385*

SURFACE ROUGHNESS INSTRUMENT CONTROLLERS

Automated Optical Roughness Inspection.
PB95-152179 *02,905*

SURFACE STATES

Tunneling Spectroscopy of bcc(001) Surface States.
PB96-155585 *04,775*

SURFACE TEMPERATURE

Analytical Method of Determining the Heat Capacity at High Temperatures from the Surface Temperature of a Cooling Sphere.
PB94-216124 *0^ 865*

Transient Cooling of a Hot Surface by Droplets Evaporation.
PB95-143194 *03,890*

Exact Solution of the Steady-State Surface Temperature for a General Multilayer Structure.
PB95-152773 *02,337*

SURFACE TENSION

Molecular Dynamics Investigation of the Surface/Bulk Equilibrium in an Ethanol-Water Solution.
PB97-113112 *01,183*

SURFACE TEXTURE

Surface Texture.
PB95-164620 *03,351*

SURFACE TOPOGRAPHY

Surface Topography and Ordering-Variant Segregation in GaInP2.
PB95-153649 *04,595*

SURFACE TRANSVERSE WAVE RESONATORS

Surface Transverse Wave Oscillators with Extremely Low Thermal Noise Floors.
PB96-186010 *01,967*

SURFACES

Survey of the Literature on Heat Transfer from Solid Surfaces to Cryogenic Fluids.
AD-A286 680/4 *04,193*

Transient Cooling of a Hot Surface by Droplets Evaporation.
PB94-156957 *03,783*

Influence of Surface Interaction and Chain Stiffness on Polymer-Induced Entropic Forces and the Dimensions of Confined Polymers.
PB94-185469 *01,203*

Measurement of Radiative Feedback to the Fuel Surface of a Pool Fire.
PB94-211604 *02,477*

Desorption Induced by Electronic Transitions.
PB94-216173 *00,853*

Neutron Scattering Studies of Surfaces and Interfaces.
PB94-216207 *04,517*

Polyethylene Crystallized from an Entangled Solution Observed by Scanning Tunneling Microscopy.
PB95-107389 *01,232*

Time-Resolved Measurements of Energy Transfer at Surfaces.
PB95-141198 *00,913*

Self-Avoiding Surfaces, Topology, and Lattice Animals.
PB95-150512 *04,571*

Evaluation of Fracture Toughness and Residual Stress in Dental Porcelain by Indentation-Microfracture Method.
PB95-152831 *00,159*

Stability and Surface Energies of Wetted Grain Boundaries in Aluminum Oxide.
PB95-202750 *03,059*

Suppression of Ignition Over a Heated Metal Surface.
PB96-176425 *03,291*

SURFACES & INTERFACES

Use of Ion Scattering Spectroscopy to Monitor the Nb Target Nitridation during Reactive Sputtering.
PB94-172525 *00,761*

Inelastic Interactions of Electrons with Surfaces: Application to Auger-Electron Spectroscopy and X-ray Photoelectron Spectroscopy.
PB94-172699 *00,764*

Environmental Scanning Electron Microscope Imaging Examples Related to Particle Analysis.
PB94-172822 *00,766*

Surface Forces and Adhesion between Dissimilar Materials Measured in Various Environments.
PB94-172970 *03,033*

Contact Electrification Induced by Monolayer Modification of a Surface and Relation to Acid-Base Interactions.
PB94-185378 *03,034*

Interfacial Free Energies from Substrate Curvature Measurements of the Creep of Multilayer Thin Films.
PB94-185428 *04,448*

High Temperature Silicide Thin-Film Thermocouples.
PB94-185501 *02,252*

Compositional Analyses of Surfaces and Thin Films by Electron and Ion Spectroscopies.
PB94-185790 *00,779*

Scaling of Diffusion-Mediated Island Growth in Iron-on-Iron Homoepitaxy.
PB94-185923 *04,455*

X-Ray Diffraction from Anodic TiO2 Films: In situ and Ex situ Comparison of the Ti(0001) Face.
PB94-185972 *00,782*

Workshop on Characterizing Diamond Films (3rd). Held in Gaithersburg, Maryland on February 23-24, 1994.
PB94-187663 *04,456*

Microstructure and Ferroelectric Properties of Lead Zirconate-Titanate Films Produced by Laser Evaporation.
PB94-199148 *04,470*

Laser Melting of Thin Silicon Films.
PB94-199239 *04,471*

Photodecomposition Dynamics of Mo(CO)6/Si(111) 7x7: CO Internal State and Translational Energy Distributions--Translation.
PB94-199288 *00,687*

Singularities in Minimum Surface Energy Problems and Their Influence in Surface Motion.
PB94-199411 *04,473*

Performance of a Reflectron Energy Compensating Mirror.
PB94-199460 *00,547*

Time-Resolved Probes of Surface Dynamics.
PB94-199957 *00,803*

Dynamics of Nonthermal Reactions: Femtosecond Surface Chemistry.
PB94-199965 *00,688*

Reactivity of Pd and Sn Adsorbates on Plasma and Thermally Oxidized SnO2(110).
PB94-199973 *00,804*

Pure Element Sputtering Yield Data: Appendix 4.
PB94-200037 *00,805*

X-Ray Photoelectron and Auger Electron Spectroscopy Study of Ultraviolet/Ozone Oxidized P2S5/(NH4)2S Treated GaAs(100) Surfaces.
PB94-200144 *04,479*

Grazing-Incidence X-Ray Photoemission Spectroscopy Investigation of Oxidized GaAs(100): A Novel Approach to Nondestructive Depth Profiling.
PB94-200151 *04,480*

Perspective on Fiber Coating Technology.
PB94-200540 *03,118*

Vibrational Relaxation Measurements of Carbon Monoxide on Metal Clusters.
PB94-211810 *00,820*

Tribochemical Reaction of Stearic Acid on Copper Surface Studied by Surface Enhanced Raman Spectroscopy.
PB94-212057 *02,964*

Surface Core-Level Shifts of Barium Observed in Photoemission of Vacuum-Fractured BaTiO3 (100).
PB94-212156 *04,501*

Formalism and Parameters for Quantitative Surface Analysis by Auger Electron Spectroscopy and X-Ray Photoelectron Spectroscopy.
PB94-212297 *00,832*

Cs Cluster Binding to a GaAs Surface.
PB94-213006 *00,846*

Iridium Oxide Thin-Film Stability in High-Temperature Corrosive Solutions.
PB94-213014 *03,234*

Analysis of Boron in CVD Diamond Surfaces Using Neutron Depth Profiling.
PB94-213089 *04,511*

Relation between AC Impedance Data and Degradation of Coated Steel. 1. Effects of Surface Roughness and Contamination on the Corrosion Behavior of Epoxy Coated Steel.
PB94-213345 *03,189*

Structures of Vapor-Deposited Yttria and Zirconia Thin Films.
PB94-216025 *03,041*

Structure of Molecules on Surfaces as Determined Using Electron-Stimulated Desorption.
PB94-216165 *00,852*

Desorption Induced by Electronic Transitions.
PB94-216173 *00,853*

Neutron Scattering Studies of Surfaces and Interfaces.
PB94-216207 *04,517*

Deposition of Colloidal Sintering-Aid Particles on Silicon Nitride.
PB94-216272 *03,044*

Effect of Modulated Taylor-Couette Flows on Crystal-Melt Interfaces: Theory and Initial Experiments.
PB94-216736 *04,521*

Activities of the ASTM Committee E-42 on Surface Analysis.
PB95-108528 *00,881*

Formation of Technical Committee 201 on Surface Chemical Analysis by the International Organization for Standardization.
PB95-108536 *00,568*

Interface Modification and Characterization of Silicon Carbide Platelets Coated with Alumina Particles.
PB95-108734 *03,121*

Picosecond Measurement of Substrate-to-Adsorbate Energy Transfer: The Frustrated Translation of CO/Pt(111)--Translation.
PB95-126041 *00,895*

Use of Kinetic Energy Distributions to Determine the Relative Contributions of Gas Phase and Surface Fragmentation in KeV Ion Sputtering of a Quaternary Ammonium Salt.
PB95-126108 *00,570*

Near Critical Fluid Interfaces: A Comparison of Theory and Experiment.
PB95-140166 *00,901*

Scanning Tunneling Microscopy and Fabrication of Nanometer Scale Structures at the Liquid-Gold Interface.
PB95-140414 *00,904*

Substitution-Induced Midgap States in the Mixed Oxides RxBa1-ChiTiO3-Delta, with R=Y, La, and Nd.
PB95-140505 *04,541*

Surface Energy Reduction in Fibrous Monotectic Structures.
PB95-140828 *03,150*

Time-Resolved Measurements of Energy Transfer at Surfaces.
PB95-141198 *00,913*

Spot-Profile-Analyzing LEED Study of the Epitaxial Growth of Fe, Co, and Cu on Cu(100).
PB95-150165 *04,561*

Influence of Cr Growth on Exchange Coupling in Fe/Cr/Fe(100).
PB95-150181 *04,562*

Exchange Coupling in Magnetic Heterostructures.
PB95-150314 *04,566*

Growth of Iron on Iron Whiskers.
PB95-150322 *04,567*

Scanning Tunneling Microscopy Study of the Growth of Cr/Fe(001): Correlation with Exchange Coupling of Magnetic Layers.
PB95-150330 *04,568*

Calculations of Electron Inelastic Mean Free Paths. 5. Data for 14 Organic Compounds over the 50-2000 eV Range.
PB95-150355 *00,916*

Oscillatory Exchange Coupling in Fe/Au/Fe(100).
PB95-150371 *04,569*

Neutron Reflectometry Studies of Surface Oxidation.
PB95-150421 *00,917*

Silver Metalization of Octadecanethiol Monolayers Self-Assembled on Gold.
PB95-150744 *00,923*

Manipulation of Adsorbed Atoms and Creation of New Structures on Room-Temperature Surfaces with a Scanning Tunneling Microscope.
PB95-151536 *04,578*

Time-Resolved Measurements of Energy Transfer at Surfaces.
PB95-153037 *00,947*

Grazing-Incidence X-Ray Photoelectron Spectroscopy: A Novel Approach to Thin Film Characterization.
PB95-153128 *04,589*

Epitaxial Integration of Single Crystal C60.
PB95-153490 *04,592*

Semiclassical Explanation of the Generalized Ramsauer-Townsend Minima in Electron-Atom Scattering.
PB95-153532 *03,925*

Laser-Focused Atomic Deposition.
PB95-161618 *04,604*

Tunneling Stabilized Magnetic-Force Microscopy.
PB95-161717 *04,607*

Thermoacoustic Technique for Determining the Interface and/or Interply Strength in Polymeric Composites.
PB95-161824 *03,158*

Production and Characterization of Ion Beam Sputtered Multilayers.
PB95-162053 *03,936*

Laser-Induced Desorption of NO from Si(111): Effects of Coverage on NO Vibrational Populations.
PB95-162319 *00,959*

Lineshape Analysis of the Raman Spectrum of Diamond Films Grown by Hot-Filament and Microwave-Plasma Chemical-Vapor Deposition.
PB95-162392 *03,016*

Studies of Defects in Diamond Films and Particles by Raman and Luminescence Spectroscopies.
PB95-162400 *03,017*

Sorption of Moisture on Epoxy and Alkyd Free Films and Coated Steel Panels.
PB95-162475 *03,192*

Fundamental Studies of Gas Sensor Response Mechanisms: Palladium on SnO2(110).
PB95-162731 *00,963*

Observation of Insulating Nanoparticles on YBCO Thin-Films by Atomic Force Microscopy.
PB95-163358 *04,622*

Observation of a Stable Methoxy Intermediate on Cr(110).
PB95-164422 *00,981*

Reactive Coevaporation of DyBaCuO Superconducting Films: The Segregation of Bulk Impurities on Annealed MgO(100) Substrates.
PB95-164562 *04,635*

Surface Texture.
PB95-164620 *03,351*

Characterization of the ZnSe/GaAs Interface Layer by TEM and Spectroscopic Ellipsometry.
PB95-175360 *04,655*

Surface Chemical Interactions of Si3N4 with Polyelectrolyte Deflocculants.
PB95-175576 *03,056*

Effects of Soxhlet Extraction on the Surface Oxide Layer of Silicon Nitride Powders.
PB95-175584 *03,057*

Micromagnetic Scanning Microprobe System.
PB95-176178 *02,224*

Photodecomposition of Mo(CO)6/Si(111) 7x7: CO State-Resolved Evidence for Excited State Relaxation and Quenching.
PB95-180154 *01,009*

X-ray Photoelectron and Auger Electron Forward Scattering: A Structural Diagnostic for Epitaxial Thin Films.
PB95-180220 *04,676*

Rayleigh Instability for a Cylindrical Crystal-Melt Interface.
PB95-180667 *01,010*

Activities of ISO Technical Committee 201 on Surface Chemical Analysis.
PB95-180824 *00,607*

Water Adsorption at Polymer/Silicon Wafer Interfaces.
PB95-181178 *01,022*

Stability and Surface Energies of Wetted Grain Boundaries in Aluminum Oxide.
PB95-202750 *03,059*

Microform Calibrations in Surface Metrology.
PB95-203295 *02,951*

Water Adsorption at a Polyimide/Silicon Wafer Interface.
PB96-103197 *01,070*

Photodesorption Dynamics of CO from Si(111): The Role of Surface Defects.
PB96-111646 *03,066*

Surface Chemistry of Silicon Nitride Powder in the Presence of Dissolved Ions.
PB96-111760 *01,073*

Epitaxial Growth of BaTiO3 Thin Films at 600C by Metalorganic Chemical Vapor Deposition.
PB96-122510 *03,071*

Anisotropy of the Surfaces of Pores in Plasma Sprayed Alumina Deposits.
PB96-123211 *03,126*

Ultrafast Time-Resolved Infrared Probing of Energy Transfer at Surfaces.
PB96-123443 *00,620*

Influence of Thickness Fluctuations on Exchange Coupling in Fe/Cr/Fe Structures.
PB96-135371 *04,745*

Silicon Surface Chemistry by IR Spectroscopy in the Mid- to Far-IR Region: H2O and Ethanol on Si(100).
PB96-138565 *01,097*

In-situ Neutron Reflectivity of MBE Grown and Chemically Processed Surfaces and Interfaces.
PB96-146634 *02,416*

Tunneling Spectroscopy of bcc(001) Surface States.
PB96-155585 *04,775*

Influence of Coadsorbed Potassium on the Electron-Stimulated Desorption of F(+), F(-), and F(*) from PF3 on Ru(0001).
PB96-157946 *04,072*

Dynamics of Hydrogen Interactions with Si(100) and Si(111) Surfaces.
PB96-159801 *04,082*

Interfaces in Mo/Si Multilayers.
PB96-160668 *02,423*

Growth and Nucleation of Hydrogenated Amorphous Silicon on Silicon (100) Surfaces.
PB96-176516 *02,991*

Surface Plasmon Microscopy of Biotin-Streptavidin Binding Reactions on UV-Photopatterned Alkanethiol Self-Assembled Monolayers.
PB96-176771 *01,158*

Workshop on Characterizing Diamond Films (4th). Held in Gaithersburg, Maryland on March 4-5, 1996.
PB96-183090 *04,786*

Coarsening of Unstable Surface Features during Fe(001) Homoepitaxy.
PB96-186127 *04,121*

Adhesion, Contact Electrification, and Acid-Base Properties of Surfaces.
PB96-204425 *03,693*

Thin-Film Ruthenium Oxide - Iridium Oxide Thermocouples.
PB97-110225 *00,520*

Molecular Dynamics Investigation of the Surface/Bulk Equilibrium in an Ethanol-Water Solution.
PB97-113112 *01,183*

SURFACTANTS
Effects of Surface-Active Resins on Dentin/Composite Bonds.
PB95-140448 *00,156*

SURGES
Coordinating Cascaded Surge Protection Devices: High-Low versus Low-High.
PB94-172061 *02,463*

Guarding Against Transients.
PB94-216470 *01,623*

Cascading Surge-Protective Devices: Options for Effective Implementation.
PB94-216488 *02,464*

Coordinating Cascaded Surge-Protective Devices: An Elusive Goal.
PB94-216496 *02,465*

Important Link in Entire-House Protection: Surge Reference Equalizers.
PB94-216504 *02,219*

Surging the Upside-Down House: Looking into Upsetting Reference Voltages.
PB96-112313 *02,385*

Keeping Up with the Reality of Today's Surge Environment.
PB96-123633 *02,231*

Surging the Upside-Down House: Measurements and Modeling Results.
PB96-180138 *02,243*

SURVEYING
METRICATION: An Economic Wake-Up Call for Surveyors and Mappers.
PB96-159629 *03,680*

SURVEYING (GEOGRAPHIC)
Metrication.
PB94-172079 *03,676*

SURVEYS
Survey of Standards for the U.S. Fiber/Textile/Apparel Industry.
PB96-193792 *03,199*

Post-Occupancy Evaluation of the Forrestal Building.
PB97-111298 *00,280*

SUSCEPTOMETERS
Alternating-Field Susceptometry and Magnetic Susceptibility of Supercondoctors. Presented at Office of Naval Research Workshop on Magnetic Susceptibility of Superconductors and Other Spin Systems. Held in Berkeley Springs, West Virginia on 20 May 1991.
PB94-145984 *04,435*

SUSPENSIONS
Contrast Matched Studies of a Sheared Binary Colloidal Suspension.
PB95-150561 *00,918*

Partial Scattered Intensities from a Binary Suspension of Polystyrene and Silica.
PB95-175618 *00,996*

Generalized Stokes-Einstein Equation for Spherical Particle Suspensions.
PB95-202743 *01,031*

SWEDEN
Ceramic Powders Characterization: Results of an International Laboratory Study.
PB95-270039 *02,672*

SWIMMING
Intensive Swimming: Can It Affect Your Patients' Smiles.
PB96-123666 *03,570*

SWIRLING
Structure of a Swirl-Stabilized Kerosene Spray Flame.
PB95-108569 *02,480*

SWITCHES
Noise Reduction in Low-Frequency SQUID Measurements with Laser-Driven Switching.
PB96-135165 *02,081*

SYMBOLIC PROGRAMMING
Symbolic Programming with Series Expansions: Applications to Optical Waveguides.
PB95-168589 *04,283*

SYNCHRONISM
Smart Clock: A New Time.
PB95-151445 *01,530*

Measurement Methods and Algorithms for Comparison of Local and Remote Clocks.
PB96-102652 *01,549*

Time Generation and Distribution.
PB96-103049 *01,550*

Wavelet Analysis for Synchronization and Timekeeping.
PB96-200381 *01,558*

SYNCHRONOUS SATELLITES
Satellite Two-Way Time Transfer: Fundamentals and Recent Progress.
PB95-161089 *01,536*

SYNCHROTRON RADIATION
Materials Science with SR Using X-Ray Imaging: Spatial-Resolution/Source Size.
PB94-213048 *04,510*

Atomic, Molecular, and Optical Physics with X-rays.
PB94-213378 *03,863*

SYNTHESIS (CHEMISTRY)
Cylinder Wipe Air-Drying Intaglio Ink Vehicles for U.S. Currency Inks.
PB94-160801 *03,115*

Thermal Behaviour of Methyl Methacrylate and N-Phenyl Maleimide Copolymers.
PB95-152237 *01,246*

Synthesis and Polymerization of Difunctional and Multifunctional Monomers Capable of Cyclopolymerization.
PB95-163044 *01,257*

Ambient Temperature Synthesis of Bulk Intermetallics.
PB95-169074 *00,168*

Ring-Opening Polymerication of a 2-Methylene Spiro Orthocarbonate Bearing a Pendant Methacrylate Group.
PB95-176145 *01,268*

SYNTHETIC PERTURBATION SCREENING
Computing Effects and Error for Large Synthetic Perturbation Screenings.
PB94-139623 *01,675*

Using Synthetic Perturbations and Statistical Screening to Assay Shared-Memory Programs.
PB96-103031 *01,740*

SYNTHETIC PERTURBATION TUNING
Using Synthetic-Perturbation Techniques for Tuning Shared Memory Programs (Extended Abstract).
PB94-172657 *01,685*

Synthetic-Perturbation Tuning of MIMD Programs.
PB94-185568 *01,687*

SYSTEM EFFECTIVENESS
Usability Engineering: Industry-Government Collaboration for System Effectiveness and Efficiency.
PB97-122287 *01,514*

SYSTEMATIC CORRECTIONS
Systematic Correction in Bragg X-ray Diffraction of Flat and Curved Crystals.
PB97-112239 *04,152*

SYSTEMS ANALYSIS
Configuration and Performance Evaluation of a Real-Time Robot Control System: A Skeleton Approach.
PB95-163895 *01,598*

Agile Manufacturing from a Statistical Perspective.
PB96-109525 *02,886*

SYSTEMS APPROACH
Template-Driven Systems Development with IDEF: Enterprise Standards for Reuse.
PB96-160965 *02,788*

SYSTEMS ARCHITECTURE
Control System Architecture for a Remotely Operated Unmanned Land Vehicle.
PB95-163200 *03,759*

SYSTEMS ENGINEERING
Integration Definition for Information Modeling (IDEF1X); Category: Software Standard; Subcategory: Modeling Techniques.
FIPSPUB184 *01,673*

Information Technology Engineering and Measurement Model: Adding Lane Markings to the Information Superhighway.
PB95-143145 *01,474*

Using Grafcet to Design Generic Controllers.
PB95-150827 *02,821*

Roadmap for the Computer Integrated Manufacturing (CIM) Application Framework.
PB96-122759 *02,832*

C++ in Safety Critical Systems.
PB96-154588 *01,750*

Usability Engineering: Industry-Government Collaboration for System Effectiveness and Efficiency.
PB97-122287 *01,514*

SYSTEMS INTEGRATED FOR MANUFACTURING APPLICATIONS
NIST SIMA Interactive Management Workshop. Held in Fort Belvoir, Virginia on November 14-16, 1994.
PB96-154877 *02,838*

SYSTEMS INTEGRATION
Integration of Servo Control into a Large-Scale Control System Design: An Example from Coal Mining.
PB94-203429 *03,696*

SYSTEMS INTEGRATION FOR MANUFACTURING APPLICATIONS
Technical Program Description Systems Integration for Manufacturing (SIMA).
PB94-213758 *02,819*

Requisite Elements, Rationale, and Technology Overview for the Systems Intergration for Manufacturing Applications (SIMA) Program. Background Study.
PB96-112685 *02,831*

SYSTEMS INTEGRATION FOR MANUFACTURING APPLICATIONS (SIMA)
Systems Integration for Manufacturing Applications Program 1995 Annual Report.
PB96-193735 *02,844*

SYSTEMS MANAGEMENT
Using Expect to Automate System Administration Tasks.
PB94-213329 *01,697*

Common Criteria: On the Road to International Harmonization.
PB96-123484 *01,606*

Functional Security Criteria for Distributed Systems.
PB96-123492 *01,607*

Open System Environment (OSE): Architectural Framework for Information Infrastructure.
PB96-146360 *00,002*

SYSTEMS SIMULATION
NIST ATM Network Simulator: Operation and Programming, Version 1.0.
PB96-106851 *01,487*

TA2 ALGORITHM
Promise into Practice: Implementing TA2 on Real Clocks at NIST.
PB95-151478 *01,533*

TABLES (DATA)
Tables of Chemical Kinetics Homogeneous Reactions.
AD-A280 293/2 *00,715*

Energy Levels of Germanium, Ge I through Ge XXXII.
PB94-162351 *00,747*

TABULATION PROCESSES
Tabulation of Data on Receiving Tubes. Handbook 68.
AD-A285 495/8 *02,111*

TACTILE SENSORS (ROBOTICS)
Integrated Vision Touch-Probe System for Dimensional Inspection Tasks.
PB95-255832 *02,917*

TAGGED PHOTON METHOD
Theoretical Aspects of Tagged Photon Facilities.
PB94-216611 *03,868*

TANTALUM
Textures of Tantalum Metal Sheets by Neutron Diffraction.
PB94-200169 *03,399*

Measurement of Surface Tension of Tantalum by a Dynamic Technique in a Microgravity Environment.
PB95-161667 *03,932*

TANTALUM SULFIDES
Scanning Tunneling Microscopy of the Charge-Density-Wave Structure in 1T-TaS2.
PB95-180980 *04,689*

TASK DECOMPOSITION
Task Decomposition Methodology for the Design of a Coal Mining Automation Hierarchical Real-Time Control System.
PB94-185386 *03,694*

TAXES
Evaluating Form Designs for Optical Character Recognition.
PB94-168044 *01,830*

TAXONOMY
Taxonomy for Security Standards.
PB95-180386 *01,602*

TAYLOR-COUETTE FLOW
Effect of Modulated Taylor-Couette Flows on Crystal-Melt Interfaces: Theory and Initial Experiments.
PB94-216736 *04,521*

TBT (TECHNICAL BARRIERS TO TRADE)
TBT Agreement Activities of the National Institute of Standards and Technology, 1995.
PB97-104178 *00,499*

TCL PROGRAMMING LANGUAGE
Debugger for Tcl Applications.
PB94-213303 *01,695*

TCL (TOOL COMMAND LANGUAGE) PROGRAMMING LANGUAGE
Debugger for Tcl Applications.
PB94-213303 *01,695*

TECHNICAL ASSISTANCE
NIST Industrial Impacts: A Sampling of Successful Partnerships.
PB95-111514 *00,488*

NIST Industrial Impacts: A Sampling of Successful Partnerships (Revision, March 1995).
PB95-209193 *00,489*

TECHNICAL BARRIERS
Helping to Reduce Technical Barriers to Trade.
PB96-190046 *00,491*

TECHNICAL BARRIERS TO TRADE (TBT)
TBT Agreement Activities of the National Institute of Standards and Technology, 1995.
PB97-104178 *00,499*

TECHNOLOGICAL ADVANCEMENT
Information Infrastructure: Reaching Society's Goals. A Report of the Information Infrastructure Task Force Committee on Applications and Technology.
ED-376 823 *00,131*

TECHNOLOGICAL INNOVATIONS
Technology Trends in Telecommunications: An Overview.
PB94-123080 *01,462*

TECHNOLOGY ASSESSMENT
Opportunities for Innovation: Advanced Manufacturing Technology.
PB94-100278 *02,801*

Visualization Applications for Manufacturing: A State-of-the-Art Survey. Final Report.
PB94-194552 *02,816*

Statistical Quality Control Technology in Japan.
PB94-199064 *02,708*

Benchmarks for the Evaluation of Speech Recognizers.
PB94-211539 *01,566*

Assessment of Technologies for Advanced Fire Detection.
PB95-126330 *00,294*

Report on the Advanced Software Technology Workshop. Held on February 1, 1994.
PB95-136610 *01,707*

Rationale and Preliminary Plan for Federal Research for Construction and Building.
PB95-154704 *00,322*

Robotics Application to Highway Transportation. Volume 2. Literature Search.
PB95-170551 *01,337*

Robotics Application to Highway Transportation. Volume 3. Proposed Research Topics and Cost/Benefit Evaluations by CERF.
PB95-171633 *01,338*

Robotics Application to Highway Transportation. Volume 4. Proposals for Potential Research.
PB95-193173 *01,339*

Object-Oriented Technology Research Areas.
PB95-199329 *01,726*

Proceedings of the Manufacturing Technology Needs and Issues: Establishing National Priorities and Strategies Conference. Held in Gaithersburg, Maryland on April 26-28, 1994.
PB95-206181 *02,930*

TECHNOLOGY INCENTIVES
Opportunities for Innovation: Advanced Manufacturing Technology.
PB94-100278 *02,801*

Transfer of Technology from Defense to Civilian Sectors.
PB94-185360 *00,011*

Network Brokers Handbook: An Entrepreneurial Guide to Cooperative Strategies for Manufacturing Competitiveness.
PB95-219325 *00,490*

TECHNOLOGY INNOVATION
Materials Science and Engineering Laboratory Annual Report, 1993. NAS-NRC Assessment Panel, April 21-22, 1994.
PB94-162534 *02,969*

Functions of Technology Infrastructure in a Competitive Economy.
PB94-173002 *00,478*

Opportunities for Innovation: Advanced Surface Engineering.
PB94-176666 *02,697*

Infratechnologies: Tools for Innovation.
PB94-185998 *00,317*

Program of the Subcommittee on Construction and Building.
PB94-193646 *00,319*

Differences in Competitive Strategies between the United States and Japan.
PB94-211836 *00,013*

Importance of Measurement in Technology-Based Competition.
PB94-211844 *02,929*

Paffenbarger Research Center: The Cutting Edge of Dental Science.
PB94-216355 *00,151*

Program of the Subcommittee on Construction and Building (July 1994).
PB95-122537 *00,321*

Publication and Presentation Abstracts, 1993. (Published by Paffenbarger Research Center and Center of Excellence for Materials Science Research).
PB95-153052 *03,562*

Fresh Look at Strategies for Fire Safety.
PB95-162947 *04,870*

Precision in Machining: Research Challenges.
PB95-242301 *02,953*

Publications and Presentation Abstracts, 1995. (Published by Paffenbarger Research Center and Center of Excellence for Materials Science Research).
PB96-119250 *03,568*

Publication and Presentation Abstracts, 1995.
PB96-164082 *03,576*

Publication and Presentation Abstracts, 1994.
PB96-176623 *03,577*

Working Conference on Global Growth of Technology: Is America Prepared. Held in Gaithersburg, Maryland on December 7, 1995.
PB96-210059 *00,018*

Publication and Presentation Abstracts, 1996.
PB97-122238 *03,585*

TECHNOLOGY INNOVATIONS
Opportunities for Innovation: Biotechnology.
PB94-157831 *00,009*

TECHNOLOGY TRANSFER
Transfer of Technology from Defense to Civilian Sectors.
PB94-185360 *00,011*

Lighting Research and Theory Can Create Business Prospects.
PB95-151791 *00,253*

Electronics and Electrical Engineering Laboratory 1995 Program Plan. Supporting Technology for U.S. Competitiveness in Electronics.
PB95-159885 *01,894*

Encouraging Environmentally-Aware Inventions.
PB95-161394 *02,521*

Japan Technology Program Assessment. Simulation: State-of the-Art in Japan.
PB95-217097 *02,827*

Electronics and Electrical Engineering Laboratory: 1996 Program Plan. Supporting Technology for U.S. Competitiveness in Electronics.
PB96-175237 *01,962*

Measurement of Process Complexity.
PB97-113138 *01,781*

Standards Promote Credibility and Technology Transfer: The Need for Greater Industry Support of Technical Committees.
PB97-116206 *02,961*

TECHNOLOGY UTILIZATION
Opportunities for Innovation: Advanced Manufacturing Technology.
PB94-100278 *02,801*

Catalog of National ISDN Solutions for Selected NIUF Applications.
PB94-166006 *01,468*

Workshop Summary Report: Industrial Applications of Scanned Probe Microscopy. A Workshop Co-sponsored by NIST, SEMATECH, ASTM, E42.14, and the American Vacuum Society. Held in Gaithersburg, Maryland on March 24-25, 1994.
PB95-170387 *00,506*

Applications of Diamond Films and Related Materials: International Conference (3rd). Held in Gaithersburg, Maryland on August 21-24, 1995. Supplement to NIST Special Publication 885.
PB95-256053 *03,063*

Opportunities for Innovation: Optoelectronics.
PB96-118039 *01,928*

Summary Report: Workshop on Industrial Applications of Scanned Probe Microscopy (2nd). A Workshop Co-Sponsored by NIST, SEMATECH, ASTM E42.14, and the American Vacuum Society. Held in Gaithersburg, Maryland on May 2-3, 1995.
PB96-131602 *00,509*

Survey of Standards for the U.S. Fiber/Textile/Apparel Industry.
PB96-193792 *03,199*

TEETH
Remineralization of Root Lesions with Concentrated Calcium and Phosphate Solutions.
PB96-102140 *03,567*

Intensive Swimming: Can It Affect Your Patients' Smiles.
PB96-123666 *03,570*

Polymeric Calcium Phosphate Composites with Remineralization Potential.
PB96-155544 *03,575*

Posterior Restorative Materials Research.
PB97-118624 *03,582*

TEFLON
Dielectric Properties of Materials at Cryogenic Temperatures and Microwave Frequencies.
PB95-202610 *02,369*

TELECOMMUNICATION
Administration Standard for the Telecommunications Infrastructure of Federal Buildings. Category: Telecommunications Standard; Subcategory: Telecommunications Administration.
FIPS PUB 187 *01,461*

Federal Building Grounding and Bonding Requirements for Telecommunications. Category: Telecommunications Standard; Subcategory: Grounding and Bonding.
FIPS PUB 195 *01,802*

Technology Trends in Telecommunications: An Overview.
PB94-123080 *01,462*

Earthquake Resistant Construction of Electric Transmission and Telecommunication Facilities Serving the Federal Government Report.
PB94-161817 *02,460*

Catalog of National ISDN Solutions for Selected NIUF Applications.
PB94-166006 *01,468*

Planning the Infrastructure for Global Electronic Commerce.
PB94-185832 *00,494*

ISDN Conformance Testing Guidelines: Guidelines for Implementors of ISDN Customer Premises Equipment to Conform to Both National ISDN-1 and North American ISDN Users' Forum Layer 3 Basic Rate Interface Basic Call Control Abstract Test Suites.
PB94-219094 *01,471*

Analyzing Electronic Commerce.
PB94-219102 *00,480*

Security in Open Systems.
PB95-105383 *01,473*

Impact of the FCC's Open Network Architecture on NS/NP Telecommunications Security.
PB95-189445 *01,483*

Electronic Implementors' Workshop.
PB95-210936 *01,484*

Summary Report on the Workshop on Advanced Digital Video in the National Information Infrastructure.
PB96-141320 *01,497*

Guidelines for the Evaluation of Electronic Data Interchange Products.
PB96-172325 *01,506*

Federal Implementation Guideline for Electronic Data Interchange: ASC X12 003050 Transaction Set 836 Procurement Notices. Implementation Convention.
PB96-178892 *01,827*

Unpredictable Certainty. Information Infrastructure through 2000.
PB96-182266 *00,016*

TELECONFERENCING
Videoconferencing Procurement and Usage Guide.
PB94-217023 *01,470*

TELEMEDICINE
Virtual Environments for Health Care. A White Paper for the Advanced Technology Program (ATP), the National Institute of Standards and Technology.
PB96-147814 *03,594*

TELEOPERATORS
Ground Vehicle Control at NIST: From Teleoperation to Autonomy.
N94-34037/9 *03,758*

Unified Telerobotic Architecture Project (UTAP) Standard Interface Environment (SIE), May 1995.
PB95-242350 *02,938*

TELEPHONE SYSTEMS
Introduction to Secure Telephone Terminals.
PB97-110498 *01,512*

TELEROBOTICS
Overview of NASREM: The NASA/NBS Standard Reference Model for Telerobot Control System Architecture.
PB94-194560 *04,831*

Real-Time Vision for Autonomous and Teleoperated Control of Unmanned Vehicles.
PB94-211885 *03,701*

Real-Time Vision for Unmanned Vehicles.
PB94-211893 *03,702*

Hierarchical Ada Robot Programming System (HARPS): A Complete and Working Telerobot Control System Based on the NASREM Model.
PB94-213162 *02,934*

TELEVISION SYSTEMS
Perception of Clamp Noise in Television Receivers.
PB96-119433 *01,489*

TELLURIUM IONS
Absolute Cross-Section Measurements for Electron-Impact Single Ionization of Se(+) and Te(+).
PB95-202503 *03,980*

TEM (TRANSMISSION ELECTRON MICROSCOPY)
Airborne Asbestos Method: Standard Practice for Recording Transmission Electron Microscopy Data for the Analysis of Asbestos Collected onto Filters. Version 1.0.
PB94-210168 *00,552*

TEMPERATURE
Fabrication of Platinum-Gold Alloys in Pre-Hispanic South America: Issues of Temperature and Microstructure Control.
PB94-211646 *03,333*

Temperature Dependence of the Rate Constants for Reaction of Dihalide and Azide Radicals with Inorganic Reductants.
PB95-162756 *00,964*

CMOS Circuit Design for Controlling Temperature in Micromachined Devices.
PB96-156088 *02,196*

Nonequilibrium Statistical Mechanics.
PB96-161781 *04,097*

TEMPERATURE COEFFICIENT OF RESISTANCE
JEDEC 'TCR' Interlaboratory Experiment: Lessons Learned.
PB95-203188 *02,371*

TEMPERATURE CONTROL
Device for Subambient Temperature Control in Liquid Chromatography.
PB95-140604 *00,573*

TEMPERATURE DEPENDENCE
Time Dependent Small Angle Neutron Scattering Behavior in Triblock Copolymers Under Steady Shear.
PB94-172632 *01,198*

Temperature Dependence of the Morphology of Thin Diblock Copolymer Films as Revealed by Neutron Reflectivity.
PB94-172756 *01,199*

Temperature Dependence of the Rate Constants for Reaction of Inorganic Radicals with Organic Reductants.
PB94-198280 *00,783*

Kinetics of the Reaction of CCl3-Br-2 and the Thermochemistry of CCl3 Radical and Cation.
PB94-212115 *00,824*

Temperature Dependence of the Rate Constants for Reactions of the Carbonate Radical with Organic and Inorganic Reductants.
PB94-212206 *00,831*

Small Angle Neutron Scattering Study on Poly(N-Isopropyl Acrylamide) Gels Near Their Volume-Phase Transition Temperature.
PB95-164380 *01,263*

Small-Angle Neutron Scattering Study on Weakly Charged Temperature Sensitive Polymer Gels.
PB95-164398 *01,264*

Cryogenics.
PB95-164703 *02,654*

Temperature Dependence and Magnetic Field Modulation of Critical Currents in Step-Edge SNS YBCO/Au Junctions.
PB96-111745 *04,723*

Effect of Anneal Temperature on Si/Buried Oxide Interface Roughness on SIMOX.
PB96-112206 *02,382*

Temperature Dependence of the Gas and Liquid Phase Ultraviolet Absorption Cross Sections of HCFC-123 (CF3CHCl2) and HCFC-142b (CH3CF2Cl).
PB96-201033 *03,298*

Temperature Dependence of the Ultraviolet Absorption Cross Section of CF3I.
PB96-204169 *01,168*

Temperature Dependent Ultraviolet Absorption Cross Sections of Propylene, Methylacetylene and Vinylacetylene.
PB96-204177 *01,169*

TEMPERATURE DISTRIBUTION

Comparison of Experimental and Computed Species Concentration and Temperature Profiles in Laminar, Two-Dimensional Methane/Air Diffusion Flames.
PB95-140919 *01,379*

TEMPERATURE EFFECTS

Performance of Compact Fluorescent Lamps at Different Ambient Temperatures.
PB95-175329 *00,258*

Room-Temperature Flexure Fixture for Advanced Ceramics.
PB95-210498 *03,061*

Temperature and Relative Humidity Dependence of Radiochromic Film Dosimeter Response to Gamma and Electron Radiation.
PB96-135298 *03,718*

TEMPERATURE FUNCTIONS

Correlation of the Ideal Gas Properties of Five Aromatic Hydrocarbons.
PB95-175816 *01,002*

TEMPERATURE GRADIENTS

Temperature Increases in Aluminum Alloys during Mechanical-Impact Tests for Oxygen Compatibility.
PB94-172962 *03,316*

TEMPERATURE MEASUREMENT

Technologic Papers of the Bureau of Standards: Number 170. Pyrometric Practice.
AD-A279 282/8 *03,766*

Corrected Optical Pyrometer Readings.
AD-A279 949/2 *02,615*

Ebulliometers for Measuring the Thermodynamic Properties of Fluids and Fluid Mixtures.
DE94017817 *04,195*

Assessment of Uncertainties of Liquid-in-Glass Thermometer Calibrations at the National Institute of Standards and Technology.
PB94-142510 *02,625*

High-Speed Spatial Scanning Pyrometer.
PB94-200003 *02,636*

Dynamic Technique for Measuring Normal Spectral Emissivity of Electrically Conducting Solids at High Temperatures with a High-Speed Spatial Scanning Pyrometer.
PB95-153045 *03,921*

Practical Applications of the ITS-90: Inherent Uncertainties.
PB95-161527 *03,930*

Design and Machining of Copper Specimens with Micro Holes for Accurate Heat Transfer Measurements.
PB95-180428 *02,658*

Reproducibility of the Temperature of the Ice Point in Routine Measurements.
PB95-255923 *04,015*

Radiance Temperatures (in the Wavelength Range 523-907 nm) of Group IVB Transition Metals Titanium, Zirconium, and Hafnium at Their Melting Points by a Pulse-Heating Technique.
PB96-135025 *02,677*

Q Branch Lineshape Functions for CARS Thermometry.
PB96-160643 *01,132*

Radiance Temperatures at 1500 nm of Niobium and Molybdenum at Their Melting Points by a Pulse-Heating Technique.
PB97-118699 *04,167*

Comparisons of Some NIST Fixed-Point Cells with Similar Cells of Other Standards Laboratories.
PB97-119242 *00,655*

TEMPERATURE MEASUREMENTS

Realization of New NIST Radiation Temperature Scales for the 1000 K to 3000 K Region, Using Absolute Radiometric Techniques.
PB94-172905 *03,794*

Current Status and Trends in Temperature Measurements at NIST, Cooperative Projects and New Mutual Agreement between NIST and IMGC.
PB97-110266 *02,691*

Issues in High-Speed Pyrometry.
PB97-118368 *02,693*

TEMPERATURE MEASURING INSTRUMENTS

Thermal Diffusivity of POCO AXM-5Q1 Graphite in the Range 1500 to 2500 K Measured by a Laser-Pulse Technique.
PB94-185022 *03,013*

High-Temperature Laser-Pulse Thermal Diffusivity Apparatus.
PB94-185147 *02,631*

TEMPERATURE SCALES

Realization of New NIST Radiation Temperature Scales for the 1000 K to 3000 K Region, Using Absolute Radiometric Techniques.
PB94-172905 *03,794*

Development of a Temperature Scale below 0.5 K.
PB95-125639 *03,879*

Intercomparison of the ITS-90 Radiance Temperature Scales of the National Physical Laboratory (U.K.) and the National Institute of Standards and Technology.
PB96-113550 *02,674*

TEMPERATURE SENSORS

Self-Calibrated Intelligent Optical Sensors and Systems.
PB96-200738 *04,380*

TEMPLATES

VLSI Architectures for Template Matching and Block Matching.
PB94-200029 *01,834*

TENSILE CREEP

Tensile Creep of Whisker Reinforced Silicon Nitride.
PB94-211984 *03,142*

Tensile Creep of a Silicon Nitride Ceramic.
PB95-161303 *03,049*

Cavitation Contributes Substantially to Tensile Creep in Silicon Nitride.
PB96-122577 *03,171*

TENSILE DEFORMATION

Tensile Deformation-Induced Microstructures in Free-Standing Copper Thin Films.
PB96-102595 *04,715*

TENSILE PROPERTIES

Microstructure and Tensile Properties of Microalloyed Steel Forgings.
PB94-172715 *03,204*

TERAHERTZ PHYSICS

Metrology Issues in Terahertz Physics and Technology.
PB96-128277 *01,939*

TERATOGENS

Nickel(II)-Mediated Oxidative DNA Base Damage in Renal and Hepatic Chromatin of Pregnant Rats and Their Fetuses. Possible Relevance to Carcinogenesis.
PB94-212628 *03,646*

TERBIUM

Neutron-Scattering Studies of the Two Magnetic Correlation Lengths in Terbium.
PB95-152328 *04,586*

Origin of the Second Length Scale Above the Magnetic Spiral Phase of Tb.
PB95-153698 *04,596*

TERBIUM 160

Precision Nuclear Orientation Measurements for Determining Mixed Magnetic Dipole/Electric Quadrupole Hyperfine Interactions.
PB94-199080 *03,810*

TERBIUM COMPOUNDS

Characterization of the Structure of TbD2.25 at 70 K by Neutron Powder Diffraction.
PB96-160528 *01,130*

TERBIUM HYDRIDES

Neutron Spectroscopic Evidence of Concentration-Dependent Hydrogen Ordering in the Octahedral Sublattice of beta-TbH2+x.
PB95-181020 *01,018*

TERMINOLOGY

Statistical Descriptors in Crystallography. 2. Report of a Working Group on Expression of Uncertainty in Measurement.
PB96-146824 *04,764*

TERNARY ALLOY SYSTEMS

Thermodynamic Calculation of the Ternary Ti-Al-Nb System.
PB94-212636 *03,336*

Electronic Structure and Phase Equilibria in Ternary Substitutional Alloys.
PB97-119366 *03,378*

TERNARY MIXTURES

Vapor-Liquid Equilibria of Mixtures of Propane and Isomeric Hexanes.
PB95-175287 *00,995*

TERT-BUTYL HYDROPEROXIDE

Tert-Butyl Hydroperoxide-Mediated DNA Base Damage in Cultured Mammalian Cells.
PB94-182003 *03,644*

TEST AND EVALUATION

Indoor Air Quality Commissioning of a New Office Building.
PB95-182309 *00,262*

TEST CHAMBERS

Constant Temperature and Humidity Chamber for Standard Resistors.
PB96-122494 *02,275*

Complicated Cases and Shielded Rooms: Audiometric Booths Shielded to Attenuate Electromagnetic Interference.
PB96-180179 *02,278*

TEST FACILITIES

Uncertainty Analysis of the NIST Nitrogen Flow Facility.
PB95-128906 *02,608*

NIST Lighting and HVAC Interaction Test Facility.
PB95-151007 *00,251*

New Extrapolation/Spherical/Cylindrical Measurement Facility at the National Institute of Standards and Technology.
PB95-153755 *02,004*

Characterization of a Health Physics Instrument Calibration Range.
PB95-164554 *03,629*

Room-Temperature Flexure Fixture for Advanced Ceramics.
PB95-210498 *03,061*

National Voluntary Laboratory Accreditation Program (NVLAP): Commercial Products Testing.
PB95-267944 *02,671*

Alternative EMC Compliance Test Facilities.
PB96-200324 *02,247*

TEST METHODS

Draft Guidelines for Pre-Qualification and Prototype Testing of Seismic Isolation Systems.
PB94-161940 *01,331*

Draft Guidelines for Quality Control Testing of Sliding Seismic Isolation Systems.
PB94-161957 *01,332*

Draft Guideline for Testing and Evaluation of Seismic Isolation Systems.
PB94-172947 *00,423*

Selection of Appropriate Ultrasonic System Components for NDE of Thick Polymer-Composites.
PB94-185279 *03,133*

Graphical Analysis of the CCRL Portland Cement Proficiency Sample Database (Samples 1-72). (Part 1. Univariant Analysis of Portland Cement).
PB94-196557 *01,308*

Effective Measurement Techniques for Heat, Smoke, and Toxic Fire Gases.
PB94-198439 *01,369*

Modern Test Methods for Flammability.
PB94-198447 *01,370*

Millisecond-Resolution Pulse Heating System for Specific-Heat Measurements at High Temperatures.
PB94-199999 *02,635*

Airborne Asbestos Method: Standard Practice for Recording Transmission Electron Microscopy Data for the Analysis of Asbestos Collected onto Filters. Version 1.0.
PB94-210168 *00,552*

Development of a New Small-Scale Smoke Toxicity Test Method and Its Comparison with Real-Scale Fire Tests.
PB94-213253 *00,350*

Recommended Changes in ASTM Test Methods D2512-82 and G86-84 for Oxygen-Compatibility Mechanical Impact Tests on Metals.
PB94-216694 *03,338*

Application of Thermal Analysis Techniques to the Characterization of EPDM Roofing Membrane Materials.
PB95-125845 *00,359*

Use of Thermal Mechanical Analysis to Characterize Ethylene-Propylene-Diene Terpolymer (EPDM) Roofing Membrane Materials.
PB95-125852 *00,360*

Water Efficient Plumbing Fixtures through Standards and Test Methods.
PB95-125951 *00,248*

Relating Bench-Scale and Full-Scale Toxicity Data.
PB95-125977 *00,361*

Comparison of Heat-Flow-Meter Tests from Four Laboratories.
PB95-126264 *00,365*

Nondestructive Evaluation and Materials Processing.
PB95-140455 *02,902*

Critical Factors in Non-Lubricated, Non-Abrasive Wear Testing.
PB95-140588 *03,236*

Review and Upgrading of Military Fastener Test Standard MIL-STD-1312.
PB95-154720 *02,947*

Introduction to ASTM 1199 'Wear Test Selection for Design and Application'.
PB95-162517 *03,238*

Asperity-Asperity Contact Mechanisms Simulated by a Two-Ball Collision Apparatus.
PB95-164158 *02,966*

Interlaboratory Comparison Studies on the Analysis of Hair for Drugs of Abuse.
PB95-176251 *03,500*

Effects of Testing Variables on the Measured Compressive Strength of High-Strength (90 MPa) Concrete.
PB95-179040 *00,445*

NIST Strategies for Reducing Testing Requirements.
PB95-180444 *01,909*

Effect of Environmentally Exposures on the Properties of Polyisocyanurate Foam Insulation: Thermal Conductivity Measurements.
PB95-181210 *00,388*

Effects of Testing Variables on the Strength of High-Strength (90 Mpa) Concrete Cylinders.
PB96-112198 *00,456*

Summary and Results of the NIST Workshop on Proposed Guidelines for Testing and Evaluation of Seismic Isolation Systems. Held in San Francisco, California on July 25, 1994.
PB96-154901 *00,463*

Development of a Test Method for Leaching of Lead from Lead-Based Paints Through Encapsulants.
PB96-154984 *03,128*

Rechargeable Batteries for Personal/Portable.
PB96-164231 *02,459*

Guidelines for Pre-Qualification, Prototype and Quality Control Testing of Seismic Isolation Systems.
PB96-193685 *01,347*

Airborne Asbestos Method: Bootstrap Method for Determining the Uncertainty of Asbestos Concentration. Version 1.0.
PB96-214614 *00,646*

Interlaboratory Studies on the Analysis of Hair for Drugs of Abuse: Results from the Fifth Exercise.
PB97-110449 *03,509*

Test Procedures for Advanced Insulation Panels.
PB97-111892 *00,415*

Structured Testing: A Testing Methodology Using the Cyclomatic Complexity Metric.
PB97-114169 *01,784*

TEST STRUCTURE

Hybrid Optical-Electrical Overlay Test Structure.
PB96-204136 *02,450*

TEST STRUCTURES

Review of Semiconductor Microelectronic Test Structures with Applications to Infrared Detector Materials and Processes.
PB94-212925 *02,132*

Test Structures for Determining Design Rules for Microelectromechanical-Based Sensors and Actuators.
PB95-150488 *02,105*

Electrical Test Structure for Overlay Metrology Referenced to Absolute Length Standards.
PB95-152278 *02,336*

Electrical Test Structure for Improved Measurement of Feature Placement and Overlay in Integrated Circuit Fabrication Processes.
PB95-164273 *02,355*

Microelectronic Test Structures for Feature Placement and Electrical Linewidth Metrology.
PB95-180568 *02,367*

Microelectronic Test Structures for Overlay Metrology.
PB96-164249 *02,430*

TESTIMONY

NIOSH Comments to DOL on Risk Estimates from the Cadmium Cohort Study by L. Stayner, February 7, 1992.
PB95-267779 *03,604*

TESTING

GOSIP Testing Program.
PB96-161229 *01,504*

TESTING LABORATORIES

Project Summaries 1994: NIST Building and Fire Research Laboratory.
PB94-207495 *00,343*

Project Summaries 1995: NIST Building and Fire Research Laboratory.
PB95-270047 *00,400*

Efficiency of Electric Motors. National Voluntary Lab. Accreditation Program (NVLAP).
PB96-111174 *02,107*

TESTS

Formal Multi-Layer Test Methodology and Its Application to OSI.
PB94-172194 *02,718*

ISO/IEC Workshop on Worldwide Recognition of OSI Test Results Regional Progress - North America.
PB94-172202 *02,719*

U.S. GOSIP Testing Program.
PB94-211455 *01,807*

Digital Techniques in HV Tests - Summary of 1989 Panel Session.
PB94-216702 *02,035*

National Voluntary Laboratory Accreditation Program: Energy Efficient Lighting Products.
PB94-219060 *02,642*

ISDN Conformance Testing Guidelines: Guidelines for Implementors of ISDN Customer Premises Equipment to Conform to Both National ISDN-1 and North American ISDN Users' Forum Layer 3 Basic Rate Interface Basic Call Control Abstract Test Suites.
PB94-219094 *01,471*

Industry/Government Open Systems Specification Testing Framework. Version 1.0.
PB94-219110 *01,809*

M (also known as MUMPS) Validation Test Suite, Version 8.3 (for Microcomputers).
PB94-502077 *01,699*

Standardization of Testing Methods for Optical Disk Media Characteristics and Related Activities at NIST.
PB95-108486 *01,624*

Some Considerations for Interim Testing of Coordinate Measuring Machine Performance Using a Specific Artifact.
PB95-108858 *02,898*

Developing Linear Error Models for Analog Devices.
PB95-150520 *02,037*

Initial NIST Testing Policy for STEP: Beta Testing Program for AP 203 Implementations. National PDES Testbed Report Series.
PB95-154688 *02,779*

Initial Graphics Exchange Specification (IGES): Procedures for the NIST IGES Validation Test Service.
PB95-171427 *02,780*

Testers Open Dialogue at Inaugural NIST Workshop.
PB95-175550 *01,718*

Testability of Object-Oriented Systems.
PB95-242418 *01,733*

Algorithm Testing and Evaluation Program for Coordinate Measuring Systems: Testing Methods.
PB95-251658 *02,666*

Partial Pressure Analysis in Space Testing.
PB96-103072 *04,829*

Development of Near-Field Test Procedures for Communication Satellite Antennas.
PB96-135082 *02,010*

STandard for the Exchange of Product Model Data (STEP): Procedures for NIST STEP Validation.
PB96-154976 *02,787*

TETRACHLOROETHYLENE

Incinerability of Perchloroethylene and Chlorobenzene.
PB95-163457 *01,388*

Hydrogen Atom Attack on Perchloroethylene.
PB95-163473 *00,969*

TETRACYANOQUINODIMETHANE

Amperometric Flow-Injection Analysis Biosensor for Glucose Based on Graphite Paste Modified with Tetracyanoquinodimethane.
PB95-161980 *03,498*

TETRACYCLINE

Fluorescence Measurements of Tetracycline in High Cell Mass for Fermentation Monitoring.
PB95-175709 *00,601*

Feasibility of Fluorescence Detection of Tetracycline in Media Mixtures Employing a Fiber Optic Probe.
PB96-163654 *00,511*

TETRADECANOYLPHORBOL ACETATE

Modification of DNA Bases in Chromatin of Intact Target Human Cells by Activated Human Polymorphonuclear Leukocytes.
PB94-199833 *03,526*

TETRAFLUOROETHANE

Equation of State Formulation of the Thermodynamic Properties of R134a (1,1,1,2-Tetrafluoroethane).
PB94-212081 *03,256*

Measurements of the Vapor Pressures of Difluoromethane, 1-Chloro-1,2,2,2-Tetrafluoroethane, and Pentafluoroethane.
PB95-169272 *03,270*

Predictive Extended Corresponding States Model for Pure and Mixed Refrigerants Including an Equation of State for R134a.
PB95-175717 *03,275*

TETRAFLUOROETHYLENE RESINS

Dielectric Properties of Materials at Cryogenic Temperatures and Microwave Frequencies.
PB95-202610 *02,369*

TETRAHEDRAL SITE VIBRATIONS

Characterization of the Vibrational Dynamics in the Octahedral Sublattices of LaD2.25 and LaH2.25.
PB96-123724 *01,091*

TETRAHEDRONS

Inserting Line Segments into Triangulations and Tetrahedralizations.
PB95-198933 *03,415*

TETRALIN

Homogeneous Gas Phase Decyclization of Tetralin and Benzocyclobutene.
PB95-151049 *00,928*

TEXT PROCESSING

Second Text REtrieval Conference (TREC-2). Held in Gaithersburg, Maryland on August 31-September 2, 1993.
PB94-178407 *01,686*

Important Papers in the History of Document Preparation Systems: Basic Sources.
PB95-125837 *02,712*

Obtaining and Installing a Public Domain TEX.
PB95-175741 *01,719*

Overview of the Text REtrieval Conference (3rd) (TREC-3). Held in Gaithersburg, Maryland on November 2-4, 1994.
PB95-216883 *01,728*

Lab Report Special Section: Natural Language Processing and Information Retrieval Group Information Access and User Interfaces Division, National Institute of Standards and Technology.
PB97-118665 *02,742*

Panel: Building and Using Test Collections.
PB97-118673 *02,743*

Text REtrieval Conference (4th) (TREC-4). Held in Gaithersburg, Maryland on November 1-3, 1995.
PB97-121636 *01,786*

TEXTILE INDUSTRY

Survey of Standards for the U.S. Fiber/Textile/Apparel Industry.
PB96-193792 *03,199*

THALLIUM

Arc Spectra of Gallium, Indium, and Thallium.
AD-A295 411/3 *00,718*

THALLIUM BARIUM CALCIUM CUPRATES

Asymmetry between Flux Penetration and Flux Expulsion in Tl-2212 Superconductors.
PB95-125647 *04,527*

Tunneling Spectroscopy of Thallium-Based High-Temperature Superconductors.
PB95-161709 *04,606*

Enhanced Flux Pinning via Chemical Substitution in Bulk Superconducting T1-2212.
PB95-169033 *04,647*

THALLIUM COMPOUNDS

Tunneling Spectroscopy of Thallium-Based High-Temperature Superconductors.
PB95-161709 *04,606*

THEOPHYLLINE

Planar Waveguide Optical Sensors.
PB94-200185 *03,586*

Liposome-Based Flow-Injection Immunoassay for Determining Theophyiline in Serum.
PB94-213493 *03,494*

THEORIES

Lighting Research and Theory Can Create Business Prospects.
PB95-151791 *00,253*

THERMAL ANALYSIS

Fire Induced Thermal Fields in Window Glass I: Theory.
PB94-139722 *00,328*

Application of Thermal Analysis Techniques to the Characterization of EPDM Roofing Membrane Materials.
PB95-125845 *00,359*

Simulating the Dynamic Electro Thermal Behavior of Power Electronic Circuits and Systems.
PB95-161014 *02,345*

Thermal Component Models for Electro-Thermal Network Simulation.
PB95-161022 *02,346*

Thermoacoustic Technique for Determining the Interface and/or Interply Strength in Polymeric Composites.
PB95-161824 *03,158*

Semiconductor Measurement Technology: HOTPAC. Programs for Thermal Analysis Including Version 3.0 of the TXYZ Program, TXYZ30, and the Thermal MultiLayer Program, TML.
PB95-260766 *02,374*

THERMAL COMFORT

Field Measurements of Ventilation and Ventilation Effectiveness in an Office/Library Building.
PB95-108833 *00,247*

THERMAL CONDUCTIONS

Thin Film Thermocouples for Measurement of Wall Temperatures in Internal Combustion Engines.
PB94-172103 *01,449*

THERMAL CONDUCTIVITY

Thermal Conductivity of Metals and Alloys at Low Temperatures. A Review of the Literature.
AD-A279 180/4 *03,302*

Measurement of the Thermal Properties of Electrically Conducting Fluids Using Coated Transient Hot Wires.
DE94017816 *00,722*

Transient Methods for Thermal Conductivity.
PB94-198405 *04,197*

Prediction of the Thermal Conductivity of Refrigerants and Refrigerant Mixtures.
PB94-212107 *03,258*

Thermal Conductivity of R134a.
PB94-213063 *03,857*

Polarized Transient Hot Wire Thermal Conductivity Measurements.
PB95-108817 *00,886*

Comparison of Heat-Flow-Meter Tests from Four Laboratories.
PB95-126264 *00,365*

Effects of Humidity and Elevated Temperature on the Density and Thermal Conductivity of a Rigid Polyisocyanurate Foam Co-Blown with CCl3F and CO2.
PB95-150462 *00,371*

Effects of Humidity and Elevated Temperature on the Density and Thermal Conductivity of a Rigid Polyisocyanurate Foam.
PB95-152021 *00,373*

Room Temperature Thermal Conductivity of Fumed-Silica Insulation for a Standard Reference Material.
PB95-152039 *00,374*

Measurement of the Thermal Properties of Electrically Conducting Fluids Using Coated Transient Hot Wires.
PB95-169058 *03,269*

Calculation of the Thermal Conductivity and Gas Permeability in a Uniaxial Bundle of Fibers.
PB95-180931 *03,058*

Intra-Laboratory Comparison of a Line-Heat-Source Guarded Hot Plate and Heat-Flow-Meter Apparatus.
PB95-181202 *00,387*

Effect of Environmentally Exposures on the Properties of Polyisocyanurate Foam Insulation: Thermal Conductivity Measurements.
PB95-181210 *00,388*

Analytical Method for Determining Thermal Conductivity from Dynamic Experiments.
PB96-102744 *04,024*

Standard Reference Data for the Thermal Conductivity of Water.
PB96-145875 *01,111*

Status of the Round Robin on the Transport Properties of R134a.
PB96-167218 *01,152*

Thermal Conductivity of Polypyromellitimide Film with Alumina Filler Particles from 4.2 to 300 K.
PB96-200753 *01,292*

THERMAL CONDUCTORS

Comparison of Elastic and Plastic Contact Models for the Prediction of Thermal Contact Conductance.
PB95-161659 *04,605*

THERMAL CONFORT

Ventilation Rates in Office Buildings.
PB95-108825 *02,539*

THERMAL CONTROL COATINGS

Measurement Methods and Standards for Processing and Application of Thermal Barrier Coatings.
N95-26123/6 *01,447*

THERMAL CONVERTERS

Intercomparison of NIST, NPL, PTB, and VSL Thermal Voltage Converters from 100 kHz to 1 MHz.
PB94-172442 *02,026*

Intercomparison of Thermal Converters at NIM, NIST, PTB, SIRI and VSL from 10 to 100 MHz.
PB94-172459 *02,027*

Performance of Commercial CMOS Foundry-Compatible Multijunction Thermal Converters.
PB95-153656 *02,342*

Multijunction Thermal Converters by Commercial CMOS Fabrication.
PB95-153664 *02,343*

High-Current Thin Film Multijunction Thermal Converters and Multi-Converter Modules.
PB97-112379 *01,989*

THERMAL DEGRADATION

High Temperature Degradation of Structural Composites.
PB94-172848 *03,132*

Causes of the Apparent Heat Transfer Degradation for Refrigerant Mixtures.
PB94-212701 *03,259*

Gas Phase Oxygen Effect on Chain Scission and Monomer Content in Bulk Poly(methyl methacrylate) Degraded by External Thermal Radiation.
PB96-204078 *01,293*

THERMAL DIFFUSIVITY

Thermal Diffusivity of POCO AXM-5Q1 Graphite in the Range 1500 to 2500 K Measured by a Laser-Pulse Technique.
PB94-185022 *03,013*

High-Temperature Laser-Pulse Thermal Diffusivity Apparatus.
PB94-185147 *02,631*

Analysis of Thermal Wave Propagation in Diamond Films.
PB94-211471 *03,014*

Thermal Wave Propagation in Diamond Films.
PB94-211489 *03,015*

THERMAL ELECTRONS

Dependence of the Thermal Electron Attachment Rate Constant in Gases and Liquids on the Energy Position of the Electron Attaching State.
PB97-122253 *01,996*

THERMAL EQUILIBRIUM

Thermal Equilibration Near the Critical Point: Effects Due to Three Dimensions and Gravity.
PB95-152922 *03,919*

THERMAL EXPANSION

Thermal Expansion of an SiC Particle-Reinforced Aluminum Composite.
PB94-213204 *03,144*

Anomalous Dispersion and Thermal Expansion in Lightly-Doped KTa1-xNbxO3.
PB95-152302 *04,585*

Relationship between Bulk-Modulus Temperature Dependence and Thermal Expansivity.
PB95-168829 *04,641*

THERMAL INSULATION

Comparison of Heat-Flow-Meter Tests from Four Laboratories.
PB95-126264 *00,365*

Effects of Humidity and Elevated Temperature on the Density and Thermal Conductivity of a Rigid Polyisocyanurate Foam Co-Blown with CCl3F and CO2.
PB95-150462 *00,371*

Effects of Humidity and Elevated Temperature on the Density and Thermal Conductivity of a Rigid Polyisocyanurate Foam.
PB95-152021 *00,373*

Room Temperature Thermal Conductivity of Fumed-Silica Insulation for a Standard Reference Material.
PB95-152039 *00,374*

Control Stability of a Heat-Flow-Meter Appartus.
PB95-181194 *00,386*

Intra-Laboratory Comparison of a Line-Heat-Source Guarded Hot Plate and Heat-Flow-Meter Apparatus.
PB95-181202 *00,387*

Effect of Environmentally Exposures on the Properties of Polyisocyanurate Foam Insulation: Thermal Conductivity Measurements.
PB95-181210 *00,388*

National Voluntary Laboratory Accreditation Program: Thermal Insulation Materials.
PB95-267985 *02,977*

Room-Temperature Thermal Conductivity of Expanded Polystyrene Board for a Standard Reference Material.
PB96-193693 *00,412*

Test Procedures for Advanced Insulation Panels.
PB97-111892 *00,415*

THERMAL IONIZATION MASS SPECTROSCOPY

Comparative Strategies for Correction of Interferences in Isotope Dilution Mass Spectrometric Determination of Vanadium.
PB94-185261 *00,531*

THERMAL MASS FLOW METERS

Critical Evaluation of Thermal Mass Flow Meters.
PB97-113153 *00,683*

THERMAL MECHANICAL ANALYSIS

Use of Thermal Mechanical Analysis to Characterize Ethylene-Propylene-Diene Terpolymer (EPDM) Roofing Membrane Materials.
PB95-125852 *00,360*

THERMAL NOISE

Null-Balanced Total-Power Radiometer System NCS1.
PB94-169778 *02,021*

Thermal Noise in High-Temperature Superconducting-Normal-Superconducting Step-Edge Josephson Junctions.
PB95-175089 *04,650*

THERMAL PROPERTIES

Cryogenic Materials Data Handbook.
AD-A286 675/4 *03,303*

Thermal Decomposition Pathways in Nitramine Propellants.
AD-A295 896/5 *03,753*

Temperature Dependence of the Gas and Liquid Phase Ultraviolet Absorption Cross Sections of HCFC-123 (CF3CHCl2) and HCFC-142b (CH3CF2Cl).
PB96-201033 *03,298*

THERMAL RADIATION

Estimate of the Effect of Scale on Radiative Heat Loss Fraction and Combustion Efficiency.
PB95-150447 *02,486*

THERMAL STABILITY

Synthesis of Thermally Stable Elastomers.
AD-A307 789/8 *03,194*

Effects of Molecular Weight and Thermal Stability on Polymer Gasification.
PB94-212610 *01,228*

Investigation of the Thermal Stability and Char-Forming Tendency of Cross-linked Poly(methyl methacrylate).
PB94-213501 *03,380*

Thermal Stability of Internal Electric Field and Polarization Distribution in Blend of Polyvinylidene Fluoride and Polymethylmethacrylate.
PB95-151072 *01,240*

Thermal Behaviour of Methyl Methacrylate and N-Phenyl Maleimide Copolymers.
PB95-152237 *01,246*

THERMAL TRANSFER STANDARDS

Modeling and Test Point Selection for a Thermal Transfer Standard.
PB95-161287 *01,896*

THERMAL VOLTAGE CONVERTERS

Intercomparison of NIST, NPL, PTB, and VSL Thermal Voltage Converters from 100 kHz to 1 MHz.
PB94-172442 *02,026*

Intercomparison of Thermal Converters at NIM, NIST, PTB, SIRI and VSL from 10 to 100 MHz.
PB94-172459 *02,027*

Exploring the Low-Frequency Performance of Thermal Converters Using Circuit Models and a Digitally Synthesized Source.
PB97-112551 *02,848*

Low Voltage Standards in the 10 Hz to 1 MHz Range.
PB97-112569 *02,100*

THERMAL WAVE IMAGING

Evaluation of Thermal Wave Imaging for Detection of Machining Damage in Ceramics.
PB95-220547 *03,062*

THERMAL WAVES

Thermal Wave NDE of Advanced Materials Using Mirage Effect Detection.
PB96-204516 *04,191*

THERMISTOR MOUNTS

Coaxial Reference Standard for Microwave Power.
PB94-193786 *01,880*

THERMOACOUSTICS

Properties of Working Fluids for Thermoacoustic Refrigerators.
AD-A297 420/2 *04,864*

THERMOCHEMISTRY

Recent Experimental and Modeling Developments in High Temperature Thermochemistry.
PB94-172343 *00,759*

Fluorinated Hydrocarbon Flame Suppression Chemistry.
PB94-185113 *01,362*

Assessment of the Al-Sb System.
PB94-200474 *03,329*

Thermochemistry of the Reactions between Adenosine, Adenosine 5'-monophosphate, Inosine, and Inosine 5'-monophosphate; the Conversion of L-histidine to (Urocanic Acid+Ammonia).
PB94-213113 *03,460*

Thermochemistry of the Hydrolysis of L-arginine to (L-citrulline + Ammonia) and of the Hydrolysis of L-arginine to (L-ornithine + Urea).
PB95-150801 *03,463*

Thermal Behavior of 4-Maleimidophenyl Glycidyl Ether Resins.
PB95-153151 *01,249*

Ionization Energy of Sulfur Pentafluoride and the Sulfur Pentafluoride-Fluorine Atom Bond Dissociation Energy.
PB95-162814 *00,966*

Thermochemical and Chemical Kinetic Data for Fluorinated Hydrocarbons.
PB95-260618 *01,056*

Halon Thermochemistry: 'Ab Initio' Calculations of the Enthalpies of Formation of Fluoromethanes.
PB96-175740 *03,289*

Chemical Inhibition of Methane-Air Diffusion Flame.
PB96-195532 *01,431*

Thermochemical Studies of Inorganic Chalocogenides by Fluorine-Combustion Calorimetry: Binary Compounds of Germanium and Silicon with Sulfur, Selenium and Tellurium.
PB97-112528 *01,181*

Thermodynamic Properties of Silicides. 5. Standard Molar Enthalpy of Formation at the Temperature 298.15 K of Trimolybdenum Monosilicide Mo3Si Determined by Fluorine-Combustion Calorimetry.
PB97-119358 *01,190*

THERMOCOUPLES

Reference Tables for Thermocouples.
AD-A279 948/4 *02,614*

Assessment of Uncertainties of Thermocouple Calibrations at NIST.
PB94-152691 *03,782*

Thin Film Thermocouples for Measurement of Wall Temperatures in Internal Combustion Engines.
PB94-172103 *01,449*

High Temperature Silicide Thin-Film Thermocouples.
PB94-185501 *02,252*

Thin Film Transparent Thermocouples.
PB94-185519 *02,253*

Sputtered High Temperature Thin Film Thermocouples.
PB95-161311 *02,259*

Cryogenics.
PB95-164703 *02,654*

Thin Film Thermocouple Research at NIST.
PB97-110233 *02,283*

THERMODYNAMIC EQUILIBRIUM

Proton Affinity Ladders from Variable-Temperature Equilibrium Measurements. 1. A Re-Evaluation of the Upper Proton Affinity Range.
PB94-216603 *00,861*

Nonequilibrium Thermodynamic Theory of Viscoplastic Materials.
PB96-111661 *04,034*

THERMODYNAMIC MODELING

Prediction of Strengthening Due to V Additions in Direct-Cooled Ferrite-Pearlite Forging Steels.
PB96-190251 *03,220*

THERMODYNAMIC PROPERTIES

Tabulation of the Thermodynamic Properties of Normal Hydrogen from Low Temperatures to 300K and from 1 to 100 Atmospheres.
AD-A279 951/8 *00,713*

Ebulliometers for Measuring the Thermodynamic Properties of Fluids and Fluid Mixtures.
DE94017817 *04,195*

Pressure-Volume-Temperature Relations in Liquid and Solid Tritium.
PB94-140571 *00,726*

Thermodynamic Properties of Difluoromethane.
PB94-185204 *00,772*

Thermodynamic Properties of Gas Phase Species of Importance to Ozone Depletion.
PB94-198215 *00,126*

Thermodynamic Properties of CHF2-O-CHF2,Bis(difluoromethyl) Ether.
PB94-199569 *00,798*

Simplified Cycle Simulation Model for the Performance Rating of Refrigerants and Refrigerant Mixtures.
PB94-199890 *03,255*

Assessment of the Al-Sb System.
PB94-200474 *03,329*

Equation of State Formulation of the Thermodynamic Properties of R134a (1,1,1,2-Tetrafluoroethane).
PB94-212081 *03,256*

Kinetics of the Reaction of CCl3-Br-2 and the Thermochemistry of CCl3 Radical and Cation.
PB94-212115 *00,824*

Global Thermodynamic Behavior of Fluid Mixtures in the Critical Region.
PB94-212420 *04,199*

Thermochemistry of the Reactions between Adenosine, Adenosine 5'-monophosphate, Inosine, and Inosine 5'-monophosphate; the Conversion of L-histidine to (Urocanic Acid+Ammonia).
PB94-213113 *03,460*

Progress in the Development of a Chemical Kinetic Database for Combustion Chemistry.
PB95-151056 *01,384*

Thermal Behavior of 4-Maleimidophenyl Glycidyl Ether Resins.
PB95-153151 *01,249*

Thermodynamic Properties of R134a(1,1,1,2-Tetrafluoroethane).
PB95-168704 *00,988*

Need for, and Availability of, Working Fluid Property Data: Results from Annexes XIII and XVIII.
PB95-168969 *03,268*

Vapor Pressures and Gas-Phase PVT Data for 1-Chloro-1,2,2,2-Tetrafluoroethane (R124).
PB95-175154 *03,271*

Retention of Halocarbons on a Hexafluoropropylene Epoxide Modified Graphitized Carbon Black. Part 1. Methane-Based Compounds.
PB95-175196 *03,272*

Coexisting Densities, Vapor Pressures and Critical Densities of Refrigerants R-32 and R-152a, at 300 - 385 K.
PB95-175691 *03,274*

Thermodynamic Study of the Reactions of Cyclodextrins with Primary and Secondary Aliphatic Alcohols, with D- and L-Phenylalanine, and with L-Phenylalanineamide.
PB95-180873 *01,016*

Thermodynamic Properties of Two Gaseous Halogenated Ethers from Speed-of-Sound Measurements: Difluoromethoxy-Difluoromethane and 2-Difluoromethoxy-1,1,1-Trifluoroethane.
PB96-102413 *04,189*

New Approach for Reducing the Toxicity of the Combustion Products from Flexible Polyurethane Foam.
PB96-123625 *01,411*

Ideal Gas Thermodynamic Properties of Sulphur Heterocyclic Compounds.
PB96-145867 *01,110*

Thermodynamics of Enzyme-Catalyzed Reactions. Part 4. Lyases.
PB96-145941 *01,118*

Thermodynamic Properties of the Aqueous Ions (2+ and 3+) of Iron and the Key Compounds of Iron.
PB96-145958 *01,119*

Interaction Coefficients for 15 Mixtures of Flammable and Non-Flammable Components.
PB96-146626 *03,281*

Thermodynamic Properties of Dilute and Semidilute Solutions of Regular Star Polymers.
PB96-146808 *01,284*

Retention of Halocarbons on a Hexafluoropropylene Epoxide-Modified Graphitized Carbon Black. 4. Propane-Based Compounds.
PB96-164033 *03,284*

Retention of Halocarbons on a Hexafluoropropylene Epoxide-Modified Graphitized Carbon Black. 3. Ethene-Based Compounds.
PB96-167309 *03,286*

Thermophysical Property Standard Reference Data from NIST.
PB96-167358 *01,153*

International Standard Equation of State for the Thermodynamic Properties of Refrigerant 123 (2,2-Dichloro-1,1,1-Trifluoroethane).
PB96-176805 *03,294*

Numerical Simulation of Rapid Combustion in an Underground Enclosure.
PB96-183132 *01,424*

Enthalpy Increment Measurements from 4.5 to 318 K for Bismuth(cr). Thermodynamic Properties from 0 K to the Melting Point.
PB96-204011 *01,166*

Enthalpy Increment Measurements from 4.5 to 350 K and the Thermodynamic Properties of Titanium Disilicide(cr) to 1700 K.
PB96-204029 *00,678*

Enthalpy Increment Measurements from 4.5 K to 350 K and the Thermodynamic Properties of the Titanium Silicide Ti5Si3(cr).
PB96-204037 *00,679*

Thermodynamics of (Germanium + Selenium): A Review and Critical Assessment.
PB97-112536 *01,182*

Thermodynamic Properties of CF3-CHF-CHF2, 1,1,1,2,3,3-Hexafluoropropane.
PB97-118384 *03,299*

Thermodynamic Properties of CHF2-CF2-CHF, 1,1,2,2,3-Pentafluoropropane.
PB97-118392 *03,300*

THERMODYNAMICS

Thermodynamics of the Hydrolysis of Penicillin G and Ampicillin.
PB94-172467 *03,596*

Octacalcium Phosphate Carboxylates IV. Kinetics of Formation and Solubility of Octacalcium Phosphate Succinate.
PB94-185600 *00,776*

Statistical Thermodynamics of Phase Separation and Ion Partitioning in Aqueous Two-Phase Systems.
PB94-199387 *01,212*

Thermodynamic Analysis of Heparin Binding to Human Antithrombin.
PB94-199593 *03,455*

Application of Thermodynamics to Biotechnology.
PB95-150793 *03,529*

Thermodynamic Interactions and Correlations in Mixtures of Two Homopolymers and a Block Copolymers by Small Angle Neutron Scattering.
PB95-152872 *01,247*

Biological Thermodynamic Data for the Calibration of Differential Scanning Calorimeters: Dynamic Temperature Data on the Gel to Liquid Crystal Phase Transition of Dialkylphosphatidylcholine in Water Suspensions.
PB95-162707 *03,464*

Thermodynamics of the Binding of Galactopyranoside Derivatives to the Basic Lectin from Winged Bean (Psophocarpus Tetrogonolobus).
PB95-162715 *03,465*

Thermodynamics of the Hydrolysis of N-Acetyl-L-phenylalanine Ethyl Ester in Water and in Organic Solvents.
PB95-203386 *01,053*

Generation Rate and Distribution of Products of Combustion in Two-Layer Fire Environments: A Model and Applications.
PB96-102173 *01,398*

Application of Thermodynamic and Detailed Chemical Kinetic Modeling to Understanding Combustion Product Generation in Enclosure Fires.
PB96-135322 *01,413*

Nonequilibrium Statistical Mechanics.
PB96-161781 *04,097*

Dynamics, Transport and Chemical Kinetics of Compartment Fire Exhaust Gases.
PB96-195508 *00,229*

Isopiestic Investigation of the Osmotic and Activity Coefficients of Aqueous NaBr and the Solubility of NaBr2H2O(cr) at 298.15 K: Thermodynamic Properties of the NaBr + H2O System over Wide Ranges of Temperature and Pressure.
PB97-110365 *01,175*

Thermodynamic Properties of Synthetic Otavite, CdCO3(cr): Enthalpy Increment Measurements from 4.5 K to 350 K.
PB97-111447 *00,680*

Conference Report: Calorimetry Conference (50th).
PB97-122279 *03,722*

THERMODYNAMICS & CHEMICAL KINETICS

Tabulation of the Thermodynamic Properties of Normal Hydrogen from Low Temperatures to 300K and from 1 to 100 Atmospheres.
AD-A279 951/8 *00,713*

Precise Measurement of Heat of Combustion with a Bomb Calorimeter.
AD-A286 701/8 *03,770*

Properties of Working Fluids for Thermoacoustic Refrigerators.
AD-A297 420/2 *04,864*

Thermophysical Properties of HFC-143a and HFC-152a. Quarterly Report, 1 July 1993--30 September 1993.
DE94004236 *03,245*

Development of Measurement Capabilities for the Thermophysical Properties of Energy-Related Fluids. Annual Report, December 1, 1990--November 30, 1991.
DE94004399 *02,470*

Thermophysical properties of HCFC alternatives. Quarterly report, 1 July 1994--30 September 1994.
DE95002261 *03,247*

Dynamic Measurements of Thermophysical Properties of Metals and Alloys at High Temperatures by Subsecond Pulse Heating Techniques.
N94-25124/6 *03,309*

Sulfur Dioxide Capture in the Combustion of Mixtures of Lime, Refuse-Derived Fuel, and Coal.
PB94-155587 *02,534*

Recent Experimental and Modeling Developments in High Temperature Thermochemistry.
PB94-172343 *00,759*

Thermodynamics of the Hydrolysis of Penicillin G and Ampicillin.
PB94-172467 *03,596*

Thermal Decomposition of Hydroxy- and Methoxy-Substituted Anisoles.
PB94-173036 *00,767*

Thermodynamic Properties of Difluoromethane.
PB94-185204 *00,772*

Thermodynamic and NMR Study of the Interactions of Cyclodextrins with Cyclohexane Derivatives.
PB94-185816 *00,781*

Thermodynamic Properties of Gas Phase Species of Importance to Ozone Depletion.
PB94-198215 *00,126*

Temperature Dependence of the Rate Constants for Reaction of Inorganic Radicals with Organic Reductants.
PB94-198280 *00,783*

Thermodynamic Interactions in Model Polyolefin Blends Obtained by Small-Angle Neutron Scattering.
PB94-198496 *01,208*

Non-Equilibrium Thermodynamic Theory of Viscoplastic Materials.
PB94-198868 *04,467*

Thermodynamic Constraints on Non-Equilibrium Solidification of Ordered Intermetallic Compounds.
PB94-198934 *03,321*

Calculation of Higher Heating Values of Biomass Materials and Waste Components from Elemental Analyses.
PB94-199254 *02,474*

Gas Phase Reactions Relevant to Chemical Vapor Deposition: Optical Diagnostics.
PB94-199338 *03,116*

Gas Phase Reactions Relevant to Chemical Vapor Deposition: Numerical Modeling.
PB94-199346 *03,117*

Statistical Thermodynamics of Phase Separation and Ion Partitioning in Aqueous Two-Phase Systems.
PB94-199387 *01,212*

Modeling the Evolution of Structure in Unstable Solid Solution Phases by Diffusional Mechanisms.
PB94-199403 *03,324*

Thermodynamic Properties of CHF2-O-CHF2,Bis(difluoromethyl) Ether.
PB94-199569 *00,798*

Maximum Entropy as a Tool for the Determination of the C-Axis Profile of Layered Compounds.
PB94-199619 *00,800*

Calibration Standards for Differential Scanning Calorimetry. 1. Zinc Absolute Calorimetric Measurement of Enthalpy of Fusion and Temperature of Fusion HM.
PB94-199817 *00,801*

Assessing the Credibility of the Calorific Content of Muncipal Solid Waste.
PB94-199882 *02,581*

Wavelength Dependence of Normal Spectral Emissivity of High-Temperature Metals at Their Melting Point.
PB94-200011 *03,398*

Rate Constants for Hydrogem Atom Attack on Some Chlorinated Benzenes at High Temperature.
PB94-200581 *00,810*

Supercritical Solubility of Solids from Near-Critical Dilute-Mixture Theory.
PB94-211703 *00,819*

Vapor Transport in Materials and Process Chemistry.
PB94-211745 *00,669*

International Conference on Chemical Kinetics (2nd). Held in Gaithersburg, Maryland on July 24-27, 1989.
PB94-211901 *00,822*

In-situ Fume Particle Size and Number Density Measurements from a Synthetic Smelt.
PB94-212040 *03,334*

Kinetics of the Reaction of CCl3-Br-2 and the Thermochemistry of CCl3 Radical and Cation.
PB94-212115 *00,824*

Resonance Enhanced Multiphoton Ionization Detection of GeF and GeCl Radicals.
PB94-212123 *00,825*

Kinetics of the Self-Reaction of Hydroxymethylperoxyl Radicals.
PB94-212164 *00,827*

Temperature Dependence of the Rate Constants for Reactions of the Sulfate Radical, SO4-, with Anions.
PB94-212172 *00,828*

Electron Transfer Reaction Rates and Equilibria of the Carbonate and Sulfate Radical Anions.
PB94-212180 *00,829*

Reaction of NO with Superoxide.
PB94-212198 *00,830*

Temperature Dependence of the Rate Constants for Reactions of the Carbonate Radical with Organic and Inorganic Reductants.
PB94-212206 *00,831*

Global Thermodynamic Behavior of Fluid Mixtures in the Critical Region.
PB94-212420 *04,199*

Thermodynamic Calculation of the Ternary Ti-Al-Nb System.
PB94-212636 *03,336*

Apparent Molar Heat Capacities and Apparent Molar Volumes of Aqueous Glucose at Temperatures from 298.15 K to 327.01 K.
PB94-212800 *03,459*

Thermochemistry of the Reactions between Adenosine, Adenosine 5'-monophosphate, Inosine, and Inosine 5'-monophosphate; the Conversion of L-histidine to (Urocanic Acid+Ammonia).
PB94-213113 *03,460*

Thermal Expansion of an SiC Particle-Reinforced Aluminum Composite.
PB94-213204 *03,144*

Analytical Method of Determining the Heat Capacity at High Temperatures from the Surface Temperature of a Cooling Sphere.
PB94-216124 *03,865*

Thermophysical Properties of CO2 and CO2-Rich Mixtures.
PB94-216199 *00,854*

Carbon Acidities of Aromatic Compounds. 1. Effects of In-Ring Aza and External Electron-Withdrawing Groups.
PB94-216595 *00,860*

Measurement of the Heat of Fusion of Tungsten by a Microsecond-Resolution Transient Technique.
PB94-216686 *03,400*

Changes in the Redox State of Iridium Oxide Clusters and Their Relation to Catalytic Water Oxidation: Radiolytic and Electrochemical Studies.
PB95-107017 *00,864*

Reduction of Dinitrogen to Ammonia in Aqueous Solution Mediated by Colloidal Metals.
PB95-107074 *00,867*

Solvent Effects in the Reactions of Peroxyl Radicals with Organic Reductants. Evidence for Proton Transfer Mediated Electron Transfer.
PB95-107157 *00,873*

Combustion of Methanol and Methanol/Dodecanol Spray Flames.
PB95-108544 *02,478*

Construction of Maximum-Entropy Density Maps, and Their Use in Phase Determination and Extension.
PB95-108593 *00,882*

Vibrational Energy Transfer in S1 p-Difluorobenzene. A Comparison of Low and Room Temperature Collisions.
PB95-108619 *00,883*

Laboratory Studies of Low-Temperature Reactions of C2H with C2H2 and Implications for Atmospheric Models of Titan.
PB95-108726 *00,690*

Vapor Pressure of 1,1-dichloro-2,2,2-trifluoroethane (R123).
PB95-126231 *00,899*

Formulation of the Refractive Index of Water and Steam.
PB95-140133 *00,900*

Glass Temperature of Polymer Blends: Comparison of Both the Free Volume and the Entropy Predictions with Data.
PB95-140190 *01,236*

Phase Equilibria in the Systems CaO-CuO and CaO-Bi2O3.
PB95-140570 *03,048*

Reaction of Nitric Oxide with Organic Peroxyl Radicals.
PB95-141107 *00,910*

Application of Thermodynamics to Biotechnology.
PB95-150793 *03,529*

Thermochemistry of the Hydrolysis of L-arginine to (L-citrulline + Ammonia) and of the Hydrolysis of L-arginine to (L-ornithine + Urea).
PB95-150801 *03,463*

Activated Dynamics, Loss of Ergodicity, and Transport in Supercooled Liquids.
PB95-150819 *00,925*

Resonance Enhanced Multiphoton Ionization Spectroscopy of 2-Butene-1-yl (C4H7) between 455-485 nm.
PB95-151031 *00,670*

Progress in the Development of a Chemical Kinetic Database for Combustion Chemistry.
PB95-151056 *01,384*

Mechanism and Rate Constants for the Reactions of Hydrogen Atoms with Isobutene at High Temperatures.
PB95-151064 *00,929*

Experimental Method for Obtaining Critical Densities of Binary Mixtures: Application to Ethane + n-Butane.
PB95-151148 *00,930*

Anisotropic Phase Separation Kinetics in a Polymer Blend Solution Following Cessation of Shear Studied by Light Scattering.
PB95-151247 *01,241*

Measurements of the Virial Coefficients and Equation of State of the Carbon Dioxide + Ethane System in the Supercritical Region.
PB95-151353 *03,906*

Ebulliometric Measurement of the Vapor Pressure of Difluoromethane.
PB95-151361 *00,931*

Crystal Chemistry and Phase Equilibrium Studies of the BaO-R2O3-CuO Systems. 2. X-Ray Characterization and Standard Patterns of BaR2CuO4, R=Lanthanides.
PB95-151734 *04,582*

Modeling Ceramic Sub-Micron Particle Formation from the Vapor Using Detailed Chemical Kinetics: Comparison with In-situ Laser Diagnostics.
PB95-151965 *00,671*

Susceptibility Critical Exponent for a Nonaqueous Ionic Binary Mixture Near a Consolute Point.
PB95-152112 *00,938*

Rate Constants for the Gas Phase Reactions of the OH Radical with CF3CF2CHCl2 (HCFC-225ca) and CF2ClCF2CHClF (HCFC-225cb).
PB95-152153 *00,940*

Thermodynamic Interactions and Correlations in Mixtures of Two Homopolymers and a Block Copolymers by Small Angle Neutron Scattering.
PB95-152872 *01,247*

Thermal Equilibration Near the Critical Point: Effects Due to Three Dimensions and Gravity.
PB95-152922 *03,919*

Dielectric Studies of Fluids with Reentrant Resonators.
PB95-153730 *00,952*

Viscosity of the Saturated Liquid Phase of Six Halogenated Compounds and Three Mixtures.
PB95-162368 *00,960*

Temperature Dependence of the Rate Constants for Reaction of Dihalide and Azide Radicals with Inorganic Reductants.
PB95-162756 *00,964*

Equilibrium and Calorimetric Investigation of the Hydrolysis of L-Tryptophan to (Indole + Pyruvate + Ammonia).
PB95-163317 *00,661*

Incinerability of Perchloroethylene and Chlorobenzene.
PB95-163457 *01,388*

Shock Tube Techniques in Chemical Kinetics.
PB95-163465 *00,968*

Application of the Taylor Dispersion Method in Supercritical Fluids.
PB95-164323 *00,977*

Standard States, Reference States and Finite-Concentration Effects in Near-Critical Mixtures with Applications to Aqueous Solutions.
PB95-164349 *00,979*

Ebulliometric Measurement of the Vapor Pressure of 1-Chloro-1,1-Difluoroethane and 1,1-Difluoroethane.
PB95-164489 *00,984*

Effect of Microstructure on Phase Formation in the Reaction of Nb/Al Multilayer Thin Films.
PB95-168415 *03,352*

Vapour Pressure Measurements on 1,1,1,2-Tetrafluoroethane (R134a) from 180 to 350 K.
PB95-168886 *03,265*

Critical Scaling Laws and a Classical Equation of State.
PB95-169249 *00,990*

Measurements of the Vapor Pressures of Difluoromethane, 1-Chloro-1,2,2,2-Tetrafluoroethane, and Pentafluoroethane.
PB95-169272 *03,270*

Neighbor Tables for Molecular Dynamics Simulations.
PB95-171948 *00,991*

Vapor Pressures and Gas-Phase PVT Data for 1-Chloro-1,2,2,2-Tetrafluoroethane (R124).
PB95-175154 *03,271*

Partial Scattered Intensities from a Binary Suspension of Polystyrene and Silica.
PB95-175618 *00,996*

Estimating the Virial Coefficients of Small Polar Molecules.
PB95-176236 *03,276*

Radiochromic Solid-State Polymerization Reaction.
PB95-180683 *01,271*

Thermodynamic Study of the Reactions of Cyclodextrins with Primary and Secondary Aliphatic Alcohols, with D- and L-Phenylalanine, and with L-Phenylalanineamide.
PB95-180873 *01,016*

Measurement of Very-Low Partial Pressures.
PB95-180998 *02,659*

Terminally Anchored Chain Interphases: The Effect of Multicomponent, Polydisperse Solvents on Their Equilibrium Properties.
PB95-181079 *01,273*

Thermodynamics of the Hydrolysis of N-Acetyl-L-phenylalanine Ethyl Ester in Water and in Organic Solvents.
PB95-203386 *01,053*

Thermochemical and Chemical Kinetic Data for Fluorinated Hydrocarbons.
PB95-260618 *01,056*

Vapour Pressures and Gas-Phase (p, rho n, T) Values for CF3CHF2(R125).
PB96-102090 *04,019*

Radiance Temperatures (in the Wavelength Range 523-907 nm) of Group IV B Transition Metals Titanium, Zirconium, and Hafnium at Their Melting Points by a Pulse-Heating Technique.
PB96-102207 *03,356*

Critical Lines for Type-III Aqueous Mixtures by Generalized Corresponding-States Models.
PB96-102371 *01,063*

Measurements of Thermophysical Properties of Nickel Near Its Melting Temperature by a Microsecond-Resolution Transient Technique.
PB96-102579 *04,210*

Principle of Congruence and Its Application to Compressible States.
PB96-102892 *01,068*

Comparison of a Fixed-Charge and a Polarizable Water Model.
PB96-111620 *01,072*

Nonequilibrium Thermodynamic Theory of Viscoplastic Materials.
PB96-111661 *04,034*

Physical Limit to the Stability of Superheated and Stretched Water.
PB96-122551 *01,083*

Flow-Induced Structure in Polymers. Chapter 17. Phase-Separation Kinetics of a Polymer Blend Solution Studied by a Two-Step Shear Quench.
PB96-123377 *03,388*

All-Metal Collection System for Preparative-Scale Gas Chromatography: Purification of Low-Boiling-Point Compounds.
PB96-123435 *00,619*

Static Dielectric Constant of Water and Steam.
PB96-123559 *01,090*

Slow Dynamics of Segregation in Hydrogen-Bonded Polymer Blends.
PB96-123591 *01,281*

Shape of the Temperature-Entropy Saturation Boundary.
PB96-135066 *02,506*

Interaction Coefficients for 15 Mixtures of Flammable and Non-Flammable Components.
PB96-146626 *03,281*

Thermodynamic Properties of Dilute and Semidilute Solutions of Regular Star Polymers.
PB96-146808 *01,284*

Experimental Determination of the Ionization Energy of IO(X(sup 2)II(sub 3/2)) and Estimations of Delta(sub f)H(sup deg)(sub 0)(IO(sup -)) and PA(IO).
PB96-146899 *00,694*

Model for Calculating Virial Coefficients of Natural Gas Hydrocarbons with Impurities.
PB96-156047 *04,064*

Virial Coefficients of Five Binary Mixtures of Fluorinated Methanes and Ethanes.
PB96-156054 *01,128*

Preliminary Results of a Comparison of Water Triple-Point Cells Prepared by Different Methods.
PB96-161344 *00,634*

Electric Field Effects on a Near-Critical Fluid in Microgravity.
PB96-161880 *04,217*

Dynamic Scaling in an Aggregating 2D Lennard-Jones System.
PB96-167317 *04,106*

Halon Thermochemistry: 'Ab Initio' Calculations of the Enthalpies of Formation of Fluoromethanes.
PB96-175740 *03,289*

Thermodynamics of the Hydrolysis of 3,4,5-Trihydroxybenzoic Acid Propyl Ester (n-Propylgallate) to 3,4,5-Trihydroxybenzoic Acid (Gallic Acid) and Propan-I-ol in Aqueous Media and in Toluene.
PB96-186143 *01,160*

Temperature Dependence of the Gas and Liquid Phase Ultraviolet Absorption Cross Sections of HCFC-123 (CF3CHCl2) and HCFC-142b (CH3CF2Cl).
PB96-201033 *03,298*

Vapor Pressure of Pentafluorodimethyl Ether.
PB96-201199 *00,677*

Enthalpy Increment Measurements from 4.5 to 318 K for Bismuth(cr). Thermodynamic Properties from 0 K to the Melting Point.
PB96-204011 *01,166*

Enthalpy Increment Measurements from 4.5 to 350 K and the Thermodynamic Properties of Titanium Disilicide(cr) to 1700 K.
PB96-204029 *00,678*

Enthalpy Increment Measurements from 4.5 K to 350 K and the Thermodynamic Properties of the Titanium Silicide Ti5Si3(cr).
PB96-204037 *00,679*

Deuterium Isotope Effect in Vinyl Radical Combination/Dispropor tionationReactions.
PB96-204151 *01,167*

Temperature Dependent Ultraviolet Absorption Cross Sections of Propylene, Methylacetylene and Vinylacetylene.
PB96-204177 *01,169*

Compressed Liquid Densities, Saturated Liquid Densities, and Vapor Pressures of 1,1-Difluoroethane.
PB97-110118 *01,173*

Isopiestic Investigation of the Osmotic and Activity Coefficients of Aqueous NaBr and the Solubility of NaBr2H2O(cr) at 298.15 K: Thermodynamic Properties of the NaBr + H2O System over Wide Ranges of Temperature and Pressure.
PB97-110365 *01,175*

Resonance Enhanced Multiphoton Ionization Spectroscopy of the SnF Radical.
PB97-111223 *01,176*

Fluoride Elimination Upon Reaction of Pentafluoroaniline with e (sub eq')(sup -), H, and OH Radicals in Aqueous Solution.
PB97-111314 *01,177*

Thermodynamic Properties of Synthetic Otavite, CdCO3(cr): Enthalpy Increment Measurements from 4.5 K to 350 K.
PB97-111447 *00,680*

Ionization Energies, Appearance Energies and Thermochemistry of CF2O and FCO.
PB97-111538 *01,178*

Compatibilization of Polymer Blends by Complexation. 2. Kinetics of Interfacial Mixing.
PB97-111900 *01,295*

One-Electron Oxidation of Metalloporphycenes as Studied by Radiolytic Methods.
PB97-111967 *01,179*

Oxidation of Caffeic Acid and Related Hydroxycinnamic Acids.
PB97-111975 *00,651*

Absorption Cross Sections, Kinetics of Formation, and Self-Reaction of the IO Radical Produced via the Laser Photolysis of N2O/I2/N2 Mixtures.
PB97-112361 *01,180*

Ferric Ion Assisted Photooxidation of Halocetates.
PB97-112460 *00,521*

Thermochemical Studies of Inorganic Chalocogenides by Fluorine-Combustion Calorimetry: Binary Compounds of Germanium and Silicon with Sulfur, Selenium and Tellurium.
PB97-112528 *01,181*

Thermodynamics of (Germanium + Selenium): A Review and Critical Assessment.
PB97-112536 *01,182*

Atmospheric Lifetimes of HFC-143a and HFC-245fa: Flash Photolysis Resonance Fluorescence Measurements of the OH Reaction Rate Constants.
PB97-112577 *00,118*

Dimensional Crossover in the Phase Separation Kinetics of Thin Polymer Blend Films.
PB97-113088 *03,395*

Vapor Pressure of 1,1,1,2,2-Pentafluoropropane.
PB97-113237 *00,684*

Thermodynamic Properties of CF3-CHF-CHF2, 1,1,1,2,3,3-Hexafluoropropane.
PB97-118384 *03,299*

Thermodynamic Properties of CHF2-CF2-CHF, 1,1,2,2,3-Pentafluoropropane.
PB97-118392 *03,300*

Kinetics of the Reaction of the Sulfate Radical with the Oxalate Anion.
PB97-119127 *01,186*

Thermodynamic Properties of Silicides. 5. Standard Molar Enthalpy of Formation at the Temperature 298.15 K of Trimolybdenum Monosilicide Mo3Si Determined by Fluorine-Combustion Calorimetry.
PB97-119358 *01,190*

Conference Report: Calorimetry Conference (50th).
PB97-122279 *03,722*

Experimental Determination of the Rate Constant for the Reaction of C2H3 with H2 and Implications for the Partitioning of Hydrocarbons in Atmospheres of the Outer Planets.
PB97-122295 *00,112*

Oxidation of Ferrous and Ferrocyanide Ions by Peroxyl Radicals.
PB97-122402 *01,191*

THERMOELECTRIC COOLERS

Device for Subambient Temperature Control in Liquid Chromatography.
PB95-140604 *00,573*

THERMOMAGNETIC EFFECTS

Transverse Thermomagnetic Effects in the Mixed State and Lower Critical Field of High-Tc Superconductors.
PB95-153250 *04,590*

THERMOMECHANICAL ANALYZER

Advances in the Measurement of Polymer CTE: Micrometer- to Atomic-Scale Measurements.
PB96-180229 *03,390*

THERMOMECHANICAL PROCESSING

Hot-Deformation Apparatus for Thermomechanical Processing Simulation.
PB94-200136 *03,207*

THERMOMECHANICAL TREATMENTS

Hot-Deformation Apparatus for Thermomechanical Processing Simulation.
PB94-200136 *03,207*

THERMOMETERS

Assessment of Uncertainties of Liquid-in-Glass Thermometer Calibrations at the National Institute of Standards and Technology.
PB94-142510 *02,625*

Resistance Thermometers with Fast Response for Use in Rapidly Oscillating Gas Flows.
PB95-107298 *03,261*

Systematic Studies of the Effect of a Post-Detection Filter on a Josephson-Junction Noise Thermometer.
PB95-162988 *03,940*

ITS-90 Calibration Facility.
PB96-160916 *00,627*

Direct Comparison of Three PTB Silver Fixed-Point Cells with the NIST Silver Fixed-Point Cell.
PB96-161286 *00,628*

Investigation of High-Temperature Platinum Resistance Thermometers at Temperatures Up to 962C, and, in Some Cases, 1064C.
PB96-161294 *00,629*

THERMOMETRY

Investigation of the ITS-90 Subrange Inconsistencies for 25.5 Omega SPRTs.
PB96-161302 *00,630*

NIST Assessment of ITS-90 Non-Uniqueness for 25.5 Ohm SPRTs at Gallium, Indium and Cadmium Fixed Points.
PB96-161310 *00,631*

NIST Implementation and Realization of the ITS-90 Over the Range 83 K to 1235 K: Reproducibility, Stability, and Uncertainties.
PB96-161328 *00,632*

NIST Measurement Assurance of SPRT Calibrations on the ITS-90: A Quantitative Approach.
PB96-161336 *00,633*

Preliminary Results of a Comparison of Water Triple-Point Cells Prepared by Different Methods.
PB96-161344 *00,634*

THERMONUCLEAR REACTOR MATERIALS

Electromechanical Properties of Superconductors for DOE Fusion Applications.
PB94-139672 *02,250*

Irradiation Damage in Inorganic Insulation Materials for ITER Magnets: A Review.
PB95-147351 *03,705*

Superconductor Critical Current Standards for Fusion Applications. Final Progress Report, October 1993-July 1994.
PB95-169538 *02,222*

THERMONUCLEAR REACTORS

Determination of Atomic Data Pertinent to the Fusion Energy Program. Progress Report for FY 92.
DE94004400 *04,402*

THERMOPHYSICAL PROPERTIES

Properties of Working Fluids for Thermoacoustic Refrigerators.
AD-A297 420/2 *04,864*

Thermophysical Properties of HFC-143a and HFC-152a. Quarterly Report, 1 July 1993--30 September 1993.
DE94004236 *03,245*

Development of Measurement Capabilities for the Thermophysical Properties of Energy-Related Fluids. Annual Report, December 1, 1990--November 30, 1991.
DE94004399 *02,470*

Development of Measurement Capabilities for the Thermophysical Properties of Energy-Related Fluids. Annual Report, December 1, 1993--November 30, 1994.
DE94017738 *03,246*

Thermophysical properties of HCFC alternatives. Quarterly report, 1 July 1994--30 September 1994.
DE95002261 *03,247*

Dynamic Measurements of Thermophysical Properties of Metals and Alloys at High Temperatures by Subsecond Pulse Heating Techniques.
N94-25124/6 *03,309*

Thermophysical Properties of Fluids for the Gas Industry. Final Report, February 1, 1988-August 31, 1993.
PB94-146677 *02,472*

Thermophysical Property Data for Supercritical Fluid Extraction Design.
PB94-199221 *00,668*

Thermophysical Properties of CO2 and CO2-Rich Mixtures.
PB94-216199 *00,854*

Thermodynamic Properties of the Methane-Ethane System.
PB95-125779 *00,891*

Thermophysical Property Computer Packages from NIST.
PB95-125787 *04,203*

Reference Data for the Thermophysical Properties of Cryogenic Fluids.
PB95-168688 *03,263*

Annex 18: An International Study of Refrigerant Properties.
PB95-168936 *03,266*

Development of a Dual-Sinker Densimeter for High-Accuracy Fluid P-V-T Measurements.
PB95-168951 *03,267*

Measurements of the Vapor Pressures of Difluoromethane, 1-Chloro-1,2,2,2-Tetrafluoroethane, and Pentafluoroethane.
PB95-169272 *03,270*

Predictive Extended Corresponding States Model for Pure and Mixed Refrigerants Including an Equation of State for R134a.
PB95-175717 *03,275*

Estimating the Virial Coefficients of Small Polar Molecules.
PB95-176236 *03,276*

Measurements of Thermophysical Properties of Nickel Near Its Melting Temperature by a Microsecond-Resolution Transient Technique.
PB96-102579 *04,210*

Physical Properties of Alternatives to the Fully Halogenated Chlorofluorocarbons.
PB96-119573 *03,279*

Thermophysical Properties of Fluids for the Gas Industry.
PB96-122437 *02,494*

New Data and Correlations for the Custody Transfer of Natural Gas Liquids.
PB96-176664 *02,499*

Report of the Refrigeration, Air Conditioning and Heat Pumps Technical Options Committee.
PB96-176755 *03,293*

THERMOPILES

Process Gas Chromatography Detector for Hydrocarbons Based on Catalytic Cracking.
PB95-141099 *02,485*

THERMOPLASTIC RESINS

Predicting the Ignition Time and Burning Rate of Thermoplastics in the Cone Calorimeter.
PB96-154794 *01,418*

Computer Simulations of Binder Removal from 2-D and 3-D Model Particulate Bodies.
PB97-121339 *00,418*

THERMOSETTING PLASTICS

AMRF Composite Fabrication Workstation.
PB94-172681 *02,810*

THERMOSETTING RESINS

Characterization of Molecular Network of Thermosets Using Neutron Scattering.
PB95-164109 *01,259*

THIAZOLE ORANGE

Enhanced Detection of PCR Products Through Use of TOTO and YOYO Intercalating Dyes with Laser Induced Fluorescence - Capillary Electrophoresis.
PB95-164653 *00,599*

THICKNESS

Jacket Thickness Requirements for Seismic Retrofitting of Circular Bridge Columns.
PB95-163267 *01,336*

THICKNESS GAGES

Gas-Coupled, Pulse-Echo Ultrasonic Crack Detection and Thickness Gaging.
PB96-147129 *04,847*

THIN DIELECTRIC RELIABILITY

New Physics-Based Model for Time-Dependent- Dielectric-Breakdown.
PB96-186093 *02,440*

THIN FILMS

Temperature Dependence of the Morphology of Thin Diblock Copolymer Films as Revealed by Neutron Reflectivity.
PB94-172756 *01,199*

Morphology of Symmetric Diblock Copolymers as Revealed by Neutron Reflectivity.
PB95-140075 *01,234*

Grazing-Incidence X-Ray Photoelectron Spectroscopy: A Novel Approach to Thin Film Characterization.
PB95-153128 *04,589*

Preparation of 2-Dimensional Ultra Thin Polystyrene Film by Water Casting Method.
PB95-162806 *04,619*

Micromagnetic Scanning Microprobe System.
PB95-176178 *02,224*

Proceedings of the Applied Diamond Conference 1995: Applications of Diamond Films and Related Materials International Conference (3rd). Held in Gaithersburg, Maryland, on August 21-24, 1995.
PB95-255204 *04,701*

Applications of Diamond Films and Related Materials: International Conference (3rd). Held in Gaithersburg, Maryland on August 21-24, 1995. Supplement to NIST Special Publication 885.
PB95-256053 *03,063*

Ferroelectric Thin Film Characterization Using Superconducting Microstrip Resonators.
PB96-102389 *02,270*

Effect of Stoichiometry on the Phases Present in Boron Nitride Thin Films.
PB96-102470 *04,710*

Tensile Deformation-Induced Microstructures in Free-Standing Copper Thin Films.
PB96-102595 *04,715*

Magnetostriction and Giant Magnetoresistance in Annealed NiFe/Ag Multilayers.
PB96-102603 *04,716*

Substrate and Thin Film Measurements.
PB96-112297 *02,384*

Holographic Properties of Triton X-100-Treated Bacteriorhodopsin Embedded in Gelatin Films.
PB96-119284 *03,761*

Novel Method for Determining Thin Film Density by Energy-Dispersive X-ray Reflectivity.
PB96-122783 *04,737*

Coexistence of Grains with Differing Orthorhombicity in High Quality YBa2Cu3O7-delta Thin Films.
PB96-135033 *04,742*

Growth of Epitaxial KNbO3 Thin Films.
PB96-135181 *02,409*

Effects of Etching on the Morphology and Surface Resistance of YBa2Cu3O7-delta Films.
PB96-135355 *02,410*

Low Magnetostriction in Annealed NiFe/Ag Giant Magnetoresistive Multilayers.
PB96-146691 *04,762*

Integrated Thin-Film Micropotentiometers.
PB96-146709 *02,109*

Magnetoresistance of Thin-Film NiFe Devices Exhibiting Single-Domain Behavior.
PB96-147087 *04,766*

Performance of Multilayer Thin-Film Multijunction Thermal Converters.
PB96-148135 *02,084*

Effects of Substrate Surface Steps on the Microstructure of Epitaxial Ba2YCu3O7-x Thin Films on (001) LaAlO3.
PB96-148184 *04,774*

Epitaxial Nucleation and Growth of Chemically Derived Ba2YCu3O7-x Thin Films on (001) SrTiO3.
PB96-190186 *04,787*

Models of Granualr Giant Magnetoresistance Multilayer Thin Films.
PB96-190228 *01,968*

Observation of the Transverse Second Harmonic Magneto-Optic Kerr Effect from Ni81Fe19 Thin Film Structures.
PB96-200332 *01,971*

Magnetic Flux Pinning in Epitaxial YBa2Cu3O7-delta Thin Films.
PB96-200746 *04,795*

Phase Separation in Thin Film Polymer Blends With and Without Block Copolymer Additives.
PB96-204482 *01,294*

Thin-Film Ruthenium Oxide - Iridium Oxide Thermocouples.
PB97-110225 *00,520*

Thin Film Thermocouple Research at NIST.
PB97-110233 *02,283*

Observation of Two Length Scales Above (T sub N) in a Holmium Thin Film.
PB97-111942 *04,151*

Development of Thin-Film Multijunction Thermal Converters at NIST.
PB97-112338 *02,286*

Bias Current Dependent Resistance Peaks in NiFe/Ag Giant Magnetoresistance Multilayers.
PB97-112346 *04,153*

High-Current Thin Film Multijunction Thermal Converters and Multi-Converter Modules.
PB97-112379 *01,989*

Dimensional Crossover in the Phase Separation Kinetics of Thin Polymer Blend Films.
PB97-113088 *03,395*

Diffraction of Neutron Standing Waves in Thin Films with Resonance Enhancement.
PB97-113278 *04,164*

Vortex Images in Thin Films of YBa2Cu3O(sub 7-x) and Bi2Sr2Ca1Cu2O(sub 8+x) Obtained by Low-Temperature Magnetic Force Microscopy.
PB97-119408 *04,815*

THIN PLATES
Exponentially Rapid Coarsening and Buckling in Coherently Self-Stressed Thin Plates.
PB95-202347 *04,821*

THINNESS
Fracture Testing of Large-Scale Thin-Sheet Aluminum Alloy.
AD-A306 625/5 *03,305*

THIOLS
Silver Metalization of Octadecanethiol Monolayers Self-Assembled on Gold.
PB95-150744 *00,923*

UV-Photopatterning of Alkylthiolate Monolayers Self-Assembled on Gold and Silver.
PB95-150751 *00,924*

THIOPHENES
Location of a (1)A(sub g) State in Bithiophene.
PB95-202313 *01,025*

THOMAS-FERMI MODEL
Appearance Intensities for Multiply Charged Ions in a Strong Laser Field.
PB96-160445 *04,089*

THOROTRAST
External Gamma-ray Counting of Selected Tissues from a Thorotrast Patient.
PB96-160254 *03,637*

THREAT EVALUATION
Computer Virus Attacks.
PB95-163655 *01,715*

THREE DIMENSIONAL MODELS
Data-Parallel Algorithm for Three-Dimensional Delaunay Triangulation and Its Implementation.
PB95-163309 *01,714*

THREE DIMENSIONAL MOTION
Visual-Motion Fixation Invariant.
PB94-206281 *01,836*

THROUGH-THE-ARC SENSING
Through-the-Arc Sensing for Monitoring Arc Welding.
PB94-185899 *02,858*

Through-the-Arc Sensing for Measuring Gas Metal Arc Weld Quality in Real Time.
PB95-164463 *02,908*

THYMINE
Substrate Specificity of the Escherichia coli Endonuclease III: Excision of Thymine- and Cytosine-Derived Lesions in DNA Produced by Radiation-Generated Free Radicals.
PB95-153425 *03,535*

TILES
Hollow Clay Tile Prism Tests for Martin Marietta Energy Systems: Task 2 Testing.
PB94-217486 *00,352*

TILTMETERS
Measurement and Interpretation of Tidal Tilts in a Small Array.
PB96-102611 *03,686*

Measurement of Very Low Frequency Vibrations.
PB96-102660 *03,687*

TIME
Accuracy in Time Domain Transmission Line Measurements.
PB96-148069 *04,060*

High-Speed Interconnection Characterization Using Time Domain Network Analysis.
PB96-148176 *04,061*

TIME-DEPENDENT DIELECTRIC BREAKDOWN
New Physics-Based Model for Time-Dependent- Dielectric-Breakdown.
PB96-186093 *02,440*

TIME DOMAIN
Accuracy in Time Domain Transmission Line Measurements.
PB96-148069 *04,060*

High-Speed Interconnection Characterization Using Time Domain Network Analysis.
PB96-148176 *04,061*

TIME DOMAIN NETWORK ANALYSIS
Optimizing Time-Domain Network Analysis.
PB96-157821 *02,085*

TIME INTERVAL ANALYZERS
High Resolution Time Interval Counter.
PB96-138607 *01,495*

TIME KEEPING
How to Get NIST-Traceable Time on Your Computer.
PB96-200647 *01,559*

TIME LAPSE
Evaluation of Sprinkler Activation Prediction Methods.
PB96-141056 *00,304*

Computing the Effect of Sprinkler Sprays on Fire Induced Gas Flow.
PB96-147111 *00,404*

TIME MEASUREMENT
Time and Frequency Technology at NIST.
N94-30641/2 *01,522*

Future of Time and Frequency Dissemination.
N94-30684/2 *01,524*

Utc Dissemination to the Real-Time User.
N19960042622 *01,521*

Time Scale Algorithm for Post-Processing: AT1 Plus Frequency Variance.
PB94-172772 *01,525*

TIME MEASUREMENTS
Accurate Measurement of Time.
PB96-119482 *01,552*

Atomic Clock.
PB96-119490 *01,553*

TIME MEASURING INSTRUMENTS
Calibration of GPS Equipment in Japan.
PB95-151452 *01,531*

Measurement Methods and Algorithms for Comparison of Local and Remote Clocks.
PB96-102652 *01,549*

TIME OF FLIGHT SPECTROMETERS
Speed-of-Sound Measurements in Liquid and Gaseous Air.
PB95-151957 *04,186*

TIME-PERTURBATION TUNING
Time-Perturbation Tuning of MIMD Programs.
PB94-164399 *01,681*

Time-Perturbation Tuning of MIMD Programs.
PB94-172566 *01,684*

TIME SCALE ALGORITHMS
Promise into Practice: Implementing TA2 on Real Clocks at NIST.
PB95-151478 *01,533*

TIME SERIES ANALYSIS
Wavelet Variance, Allan Variance, and Leakage.
PB96-190111 *01,509*

TIME SIGNALS
Implementation of a Standard Format for GPS Common View Data.
N95-32323/4 *03,779*

Utc Dissemination to the Real-Time User.
N19960042622 *01,521*

Preliminary Comparison of Time Transfers via LASSO, GPS and Two-Way Satellite.
PB95-151098 *01,529*

How to Get NIST-Traceable Time on Your Computer.
PB96-200647 *01,559*

TIME STANDARDS
NIST Internet Time Service.
AD-P009 132/2 *01,519*

Future of Time and Frequency Dissemination.
AD-P009 138/9 *01,520*

Atoms in Optical Molasses: Applications to Frequency Standards.
PB95-108882 *03,876*

Time and Frequency: Bibliography of NIST Publications, March 1995.
PB95-220463 *01,548*

Time Generation and Distribution.
PB96-103049 *01,550*

Time and Frequency Metrology.
PB96-190319 *01,556*

TIME-TO-CONTACT
Calculating Time-to-Contact Using Real-Time Quantized Optical Flow.
PB95-210522 *01,604*

TIME TRANSFER
Future of Time and Frequency Dissemination.
AD-P009 138/9 *01,520*

Preliminary Comparison of Time Transfers via LASSO, GPS and Two-Way Satellite.
PB95-151098 *01,529*

Smart Clock: A New Time.
PB95-151445 *01,530*

Calibration of GPS Equipment in Japan.
PB95-151452 *01,531*

Satellite Two-Way Time Transfer: Fundamentals and Recent Progress.
PB95-161089 *01,536*

Use of Ionospheric Data in GPS Time Transfer.
PB95-163853 *01,540*

Implementation of a Standard Format for GPS Common View Data.
PB96-176581 *01,555*

TIMEKEEPING
Wavelet Analysis for Synchronization and Timekeeping.
PB96-200381 *01,558*

TIMING DEVICES
Time and Frequency Technology at NIST.
N94-30641/2 *01,522*

TIMING ERRORS
Frequency Synthesis and Metrology at 10(-17) and Beyond.
PB97-113187 *02,101*

TIN
Anomalous Odd- to Even-Mass Isotope Ratios in Resonance Ionization with Broad-Band Lasers.
PB94-211406 *03,839*

TIN ALLOYS
VAMAS interlaboratory comparisons of critical current vs. strain in Nb(sub 3)Sn.
DE95016656 *04,433*

Transverse stress effect on the critical current of internal tin and bronze process Nb(sub 3)Sn superconductors.
DE95016659 *04,434*

TIN BASE ALLOYS
Effects of Crystalline Anisotropy and Buoyancy-Driven Convection on Morphological Stability.
PB94-200441 *03,328*

TIN MONOFLUORIDE
Resonance Enhanced Multiphoton Ionization Spectroscopy of the SnF Radical.
PB97-111223 *01,176*

TIN OXIDES
Reactivity of Pd and Sn Adsorbates on Plasma and Thermally Oxidized SnO2(110).
PB94-199973 *00,804*

Conductance Response of Pd/SnO2(110) Model Gas Sensors to H2 and O2.
PB95-125803 *00,892*

Tin Oxide Gas Sensor Fabricated Using CMOS Micro-Hotplates and In-situ Processing.
PB95-150603 *00,580*

Thin Film Thermocouple Research at NIST.
PB97-110233 *02,283*

TIPS
Morphological Estimation of Tip Geometry for Scanned Probe Microscopy.
PB95-203444 *02,662*

TIROS SATELLITES
Semiconductor Measurement Technology: Improved Characterization and Evaluation Measurements for HgCdTe Detector Materials, Processes, and Devices Used on the GOES and TIROS Satellites.
PB94-188810 *02,122*

TISSUE BANKS
Current Activities Within the National Biomonitoring Specimen Bank.
PB94-172806 *02,516*

Development of the National Marine Mammal Tissue Bank.
PB95-161402 *02,586*

Alaska Marine Mammal Tissue Archival Project: Specimen Inventory.
PB95-171344 *02,589*

Considerations in the Design of an Environmental Specimen Bank: Experiences of the National Biomonitoring Specimen Bank Program.
PB96-112370 *02,527*

National Status and Trends Program Specimen Bank: Sampling Protocols, Analytical Methods, Results, and Archive Samples.
PB97-119226 *02,598*

TITAN
Laboratory Studies of Low-Temperature Reactions of C2H with C2H2 and Implications for Atmospheric Models of Titan.
PB95-108726 *00,690*

TITANIUM
Apparent Bias in the X-Ray Fluorescence Determination of Titanium in Selected NIST SRM Low Alloy Steels.
PB95-108759 *03,212*

Use of Sum Rules on the Energy-Loss Function for the Evaluation of Experimental Optical Data.
PB95-150736 *04,264*

Factors Significant to Precracking of Fracture Specimens.
PB96-109558 *03,358*

Effect of Suppressants on Metal Fires.
PB96-109574 *01,402*

Void Shape in Sintered Titanium.
PB96-141023 *02,705*

Optical and Modeling Studies of Sodium/Halide Reactions for the Formation of Titanium and Boron Nanoparticles.
PB97-113054 *00,682*

TITANIUM ALLOYS
Magnetic Characteristics and Measurements of Filamentary Nb-Ti Wire for the Superconducting Super Collider.
DE94005988 *03,775*

Thermodynamic Calculation of the Ternary Ti-Al-Nb System.
PB94-212636 *03,336*

Thermodynamic Assessment and Calculation of the Ti-Al System.
PB94-212644 *03,337*

Determination of Hydrogen in Titanium Alloy Jet Engine Compressor Blades by Cold Neutron Capture Prompt Gamma-ray Activation Analysis.
PB95-175956 *01,448*

Journal of Research of the National Institute of Standards and Technology, September/October 1993. Volume 98, Number 5.
PB96-169057 *03,368*

Electronic Structure and Phase Equilibria in Ternary Substitutional Alloys.
PB97-119366 *03,378*

TITANIUM ALUMINUM NIOBIUM
Ordered omega-Derivatives in a Ti-37.5Al-2ONb at% Alloy.
PB94-211091 *03,331*

TITANIUM CONTAINING ALLOYS
Ordered omega-Derivatives in a Ti-37.5Al-2ONb at% Alloy.
PB94-211091 *03,331*

TITANIUM DIOXIDE
X-Ray Diffraction from Anodic TiO2 Films: In situ and Ex situ Comparison of the Ti(0001) Face.
PB94-185972 *00,782*

TITANIUM DISILICIDE
Enthalpy Increment Measurements from 4.5 to 350 K and the Thermodynamic Properties of Titanium Disilicide(cr) to 1700 K.
PB96-204029 *00,678*

TITANIUM INTERMETALLICS
Coherent Precipitates in the BCC/Orthorhombic Two Phase Field of the Ti-Al-Nb System.
PB94-198694 *03,317*

Ordered omega-Derivatives in a Ti-37.5Al-2ONb at% Alloy.
PB94-211091 *03,331*

TITANIUM OXIDES
Neutron Reflectometry Studies of Surface Oxidation.
PB95-150421 *00,917*

TITANIUM SILICIDES
Enthalpy Increment Measurements from 4.5 K to 350 K and the Thermodynamic Properties of the Titanium Silicide Ti5Si3(cr).
PB96-204037 *00,679*

TOCOPHEROL
Liquid Chromatographic Method for the Determination of Carotenoids, Retinoids, and Tocopherols in Human Serum and in Food.
PB95-153599 *00,593*

TOLERANCE INTERVALS
Tolerance Intervals for the Distribution of True Values in the Presence of Measurement Errors.
PB95-150405 *03,434*

TOLERANCES (MECHANICS)
NIST Handbook 44, 1994: Specifications, Tolerances and Other Technical Requirements for Weighing and Measuring Devices as Adopted by the 78th National Conference on Weights and Measures 1993.
PB94-136009 *02,888*

Design, Specification and Tolerancing of Micrometer-Tolerance Assemblies.
PB95-209862 *02,913*

TOLUENE
Correlation of the Ideal Gas Properties of Five Aromatic Hydrocarbons.
PB95-175816 *01,002*

TOMOGRAPHY
Tomographic Decoding Algorithm for a Nonoverlapping Redundant Array.
PB95-151932 *01,842*

TOOL COMMAND LANGUAGE
Debugger for Tcl Applications.
PB94-213303 *01,695*

TOOLS
Computer Vision Based Tool Setting Station.
PB94-199858 *02,944*

Fabrication of Optics by Diamond Turning.
PB96-111695 *02,954*

Combining Interactive Exploration and Optimization for Assembly Design.
PB97-112320 *02,794*

Chemical Aspects of Tool Wear in Single Point Diamond Turning.
PB97-112601 *03,021*

TOOTH ENAMEL
EPR Dosimetry of Cortical Bone and Tooth Enamel Irradiated with X and Gamma Rays: Study of Energy Dependence.
PB97-110373 *03,639*

TOOTH REMINERALIZATION
Effects on Whole Saliva of Chewing Gums Containing Calcium Phosphates.
PB95-153169 *03,563*

TORPEDOES
Assessment of Data by a Second-Order Transfer Function.
PB95-182390 *03,760*

TORSION
Torsional Dilatometer for Volume Change Measurements on Deformed Glasses: Instrument Description and Measurements on Equilibrated Glasses.
PB94-211166 *03,379*

TOTAL QUALITY MANAGEMENT
SQA Standards and Total Quality Management.
PB96-111844 *01,743*

SQA and TQM in Software Quality Improvement.
PB96-160791 *01,754*

TOUGHNESS
Cryogenic Toughness of Austenitic Stainless Steel Weld Metals: Effect of Inclusions.
PB95-161261 *03,214*

TOXAPHENE
NIST Standard Reference Materials (SRMs) for Polychlorinated Biphenyl (PCB) Determinations and Their Applicability to Toxaphene Measurements.
PB95-140109 *02,585*

TOXIC SUBSTANCES
Recently Developed NIST Food Related Standard Reference Materials.
PB94-198322 *00,035*

Investigation of S2F10 Production and Mitigation in Compressed SF6-Insulated Power Systems.
PB94-212388 *02,467*

Secondary Target X-Ray Excitation for In vivo Measurement of Lead in Bone.
PB95-108767 *03,496*

Analysis by a Combination of Gas Chromatography and Tandem Mass Spectrometry: Development of Quantitative Tandem-in-Time Ion Trap Mass Spectrometry: Isotope Dilution Quantification of 11-Nor-Delta-9-Tetrahydro cannabinol-9-Carboxylic Acid.
PB96-117221 *02,561*

TOXICITY
Documentation for Immediately Dangerous to Life or Health Concentrations (IDLHs).
PB94-195047 *03,602*

Effective Measurement Techniques for Heat, Smoke, and Toxic Fire Gases.
PB94-198439 *01,369*

Toxicity, Fire Hazard and Upholstered Furniture.
PB94-198454 *00,289*

Total Surface Areas of Group IVA Organometallic Compounds: Predictors of Toxicity to Algae and Bacteria.
PB94-211331 *00,814*

Development of a New Small-Scale Smoke Toxicity Test Method and Its Comparison with Real-Scale Fire Tests.
PB94-213253 *00,350*

Relating Bench-Scale and Full-Scale Toxicity Data.
PB95-125977 *00,361*

TPT
Time-Perturbation Tuning of MIMD Programs.
PB94-172566 *01,684*

TRACE ELEMENTS
Long-Term Stability of Carrier-Free Polonium Solution Standards.
PB94-185170 *00,685*

Establishing Quality Measurements for Inorganic Analysis of Biomaterials.
PB94-199726 *00,548*

Mixed Diet Reference Materials for Nutrient Analysis of Foods: Preparation of SRM-1548 Total Diet.
PB95-151692 *03,593*

Trace Elements Associated with Proteins. Neutron Activation Analysis Combined with Biological Isolation Techniques.
PB95-163101 *00,597*

Methods for Analysis of Cancer Chemopreventive Agents in Human Serum.
PB95-200648 *03,502*

Certifying the Chemical Composition of a Biological Material: A Case Study.
PB96-164272 *00,636*

Trace Element Concentrations in Cetacean Liver Tissues Archived in the National Marine Mammal Tissue Bank.
PB96-167127 *02,595*

Liquid Chromatographic Determination of Carotenoids in Human Serum Using an Engineered C30 and a C18 Stationary Phase.
PB97-119333 *03,512*

TRACE QUANTITIES
Procedure for Measuring Trace Quantities of S2F10, S2OF10, and S2O2F10 in SF6 Using a Gas Chromatograph-Mass Spectrometer.
PB96-119755 *02,513*

TRACER TECHNIQUES
Rare-Earth Isotopes as Tracers of Particulate Emissions: An Urban Scale Test.
PB94-161635 *02,535*

Air Change Effectiveness Measurements in Two Modern Office Buildings.
PB94-185766 *00,243*

Monitoring Polymer Cure by Fluorescence Recovery After Photobleaching.
PB94-211422 *01,218*

NIST Traceable Reference Material Program for Gas Standards: Standard Reference Materials.
PB96-210786 *00,644*

Measurement Comparability, Traceability, and Measurement Assurance Programs.
PB97-111850 *02,692*

TRADE
Helping to Reduce Technical Barriers to Trade.
PB96-190046 *00,491*

TRAFFIC MANAGEMENT
Introduction to Traffic Management for Broadband ISDN.
PB94-142494 *01,464*

TRAINING
Computer Security Training and Awareness Course Compendium.
PB95-130985 *01,589*

Life-Cycle Costing Workshop for Energy Conservation in Buildings: Student Manual.
PB95-175006 *00,257*

TRAINING AIDS
Proposed International Interactive Courseware Standard.
PB96-123161 *00,137*

TRAINS
Fire Safety of Passenger Trains: A Review of Current Approaches and of New Concepts.
PB94-152006 *04,848*

TRAJECTORIES
Dispersion and Deposition of Smoke Plumes Generated in Massive Fires.
PB95-126066 *02,540*

TRANSDUCERS
Material Characterization By a Time-Resolved and Polarization-Sensitive Ultrasonic Technique.
PB97-122576 *02,764*

Design, Construction and Application of a Large Aperture Lens-Less Line-Focus PVDF Transducer.
PB97-122584 *02,765*

TRANSESTERFICATION
Dielectric Behavior of a Polycarbonate/Polyester Mixture Upon Transesterification.
PB96-179551 *04,785*

TRANSFER FUNCTION
Stochastic Modeling of a New Spectrometer.
PB96-157870 *04,068*

TRANSFER STANDARDS
Multi-State Two-Port: An Alternative Transfer Standard.
PB95-168530 *02,049*

TRANSFORMERS
Wide Band Active Current Transformer and Shunt.
PB95-126371 *02,036*

Fabrication Issues in Optimizing YBa2Cu3O7-x Flux Transformers for Low l/f Noise.
PB95-175857 *02,059*

TRANSIENT ERRORS
Transient Errors in a Precision Resistive Divider.
PB97-111512 *01,983*

TRANSIENT ULTRASONIC WAVE
Transient Analysis of a Line-Focus Transducer Probing a Liquid/Solid Interface.
PB97-118681 *02,763*

TRANSIENTS
Transient Subcritical Crack-Growth Behavior in Transformation-Toughened Ceramics.
PB94-200656 *03,038*

TRANSISTORS
Handbook Preferred Circuits Navy Aeronautical Electronic Equipment. Supplement Number 2.
AD-A278 783/6 *00,027*

Physics for Device Simulations and Its Verification by Measurements.
PB95-152914 *02,339*

Characterization of Two-Dimensional Dopant Profiles: Status and Review.
PB96-119300 *02,400*

Characterization of Two-Dimensional Dopant Profiles: Status and Review.
PB97-110134 *02,451*

TRANSIT TIME
Utc Dissemination to the Real-Time User.
N19960042622 *01,521*

TRANSITION MANAGEMENT
Implementing a Transition Manager in the AMRF Cell Controller.
PB94-199932 *02,817*

TRANSITION METALS
Ultraviolet Multiplet Table. Finding List for Spectra of the Elements Molybdenum to Lanthanum (Z = 42 to 57); Hafnium to Radium (Z = 72 to 88).
AD-A278 131/8 *00,709*

Radiance Temperatures (in the Wavelength Range 523-907 nm) of Group IV B Transition Metals Titanium, Zirconium, and Hafnium at Their Melting Points by a Pulse-Heating Technique.
PB96-102207 *03,356*

TRANSITION PROBABILITIES
Comprehensive Spectroscopic Data Tabulations and Progress in the Compilation of Atomic Transition Probabilities.
PB95-151551 *03,909*

Stars, Atmospheres, Radiative Transfer.
PB96-119474 *00,095*

Transition Regions of Capella.
PB96-123336 *00,105*

Transition Regions of Capella (1995).
PB96-176714 *00,108*

TRANSITION TEMPERATURE
Step-Edge and Stacked-Heterostructure High-Tc Josephson Junctions for Voltage-Standard Arrays.
PB96-102066 *04,702*

Simulation of C60 Through the Plastic Transition Temperatures.
PB96-102546 *04,713*

TRANSMISSION ELECTRON MICROSCOPY
Proficiency Tests for the NIST Airborne Asbestos Program - 1991.
PB94-193828 *00,537*

Proficiency Tests for the NIST Airborne Asbestos Program - 1992.
PB94-194362 *00,539*

Airborne Asbestos Method: Bootstrap Method for Determining the Uncertainty of Asbestos Concentration. Version 1.0.
PB96-214614 *00,646*

TRANSMISSION LINES
Transmission/Reflection and Short-Circuit Line Methods for Measuring Permittivity and Permeability.
PB94-165537 *02,211*

Currents Induced on Multiconductor Transmission Lines by Radiation and Injection.
PB94-211943 *02,215*

Accurate Experimental Characterization of Interconnects: A Discussion of 'Experimental Electrical Characterization of Interconnects and Discontinuities in High-Speed Digital Systems'.
PB94-216389 *02,217*

Interconnection Transmission Line Parameter Characterization.
PB94-216397 *02,218*

Accurate Transmission Line Characterization.
PB95-151593 *02,220*

Accuracy in Time Domain Transmission Line Measurements.
PB96-148069 *04,060*

Accurate Electrical Characterization of High-Speed Interconnections.
PB96-167143 *02,240*

Dimensional Characterization of Precision Coaxial Transmission Line Standards.
PB96-176482 *02,241*

Dielectric and Magnetic Measurements from -50C to 200C and in the Frequency Band 50 MHz to 2 GHz.
PB96-191382 *02,245*

TRANSMISSION LOSS
LP11-Mode Leakage Loss in Coated Depressed Clad Fibers.
PB95-141115 *02,145*

Calculated Fiber Attenuation: A General Method Yielding Stationary Values.
PB95-175501 *04,298*

Fibre Splice Loss: A Simple Method of Calculation.
PB95-175519 *04,299*

TRANSMITTANCE
Comparison of Regular Transmittance Scales of Four National Standardizing Laboratories.
PB94-211232 *04,233*

Determination of the Transmittance Uniformity of Optical Filter Standard Reference Materials.
PB95-261921 *02,182*

Transmission Properties of Short Curved Neutron Guides. Part 1. Acceptance Diagram Analysis and Calculations.
PB96-102199 *04,021*

Partially Coherent Transmittance of Dielectric Lamellae.
PB96-148028 *04,359*

TRANSMITTER RECEIVERS
Electric-Field Strengths Measured Near Personal Transceivers.
PB94-172020 *01,564*

TRANSPORT
Study of Droplet Transport in Alcohol-Based Spray Flames Using Phase/Doppler Interferometry.
PB95-108551 *02,479*

Large Eddy Simulations of Smoke Movement in Three Dimensions.
PB96-190012 *01,426*

TRANSPORT CROSS SECTIONS
Absence of Quantum-Mechanical Effects on the Mobility of Argon Ions in Helium Gas at 4.35 K.
PB97-122543 *01,194*

TRANSPORT PROPERTIES
Transient Methods for Thermal Conductivity.
PB94-198405 *04,197*

Need for, and Availability of, Working Fluid Property Data: Results from Annexes XIII and XVIII.
PB95-168969 *03,268*

Transport and Diffusion in Three-Dimensional Composite Media.
PB95-176129 *04,668*

Mathematical Modeling and Computer Simulation of Fire Phenomena.
PB95-180063 *00,384*

Calculation of the Thermal Conductivity and Gas Permeability in a Uniaxial Bundle of Fibers.
PB95-180931 *03,058*

Survey of Concrete Transport Properties and Their Measurement.
PB95-220489 *00,396*

Ab initio Calculations for Helium: A Standard for Transport Property Measurements.
PB96-102041 *01,060*

Physical Characterization of Herparin by Light Scattering.
PB96-119383 *03,598*

Thermophysical Property Standard Reference Data from NIST.
PB96-167358 *01,153*

Greenspan Acoustic Viscometer for Gases.
PB96-204417 *04,220*

TRANSPORTATION SAFETY
New Concepts for Fire Protection of Passenger Rail Transportation Vehicles. (NIST Reprint).
PB95-180774 *04,863*

TRAPPED PARTICLES
Magneto-Optical Trapping of Metastable Xenon: Isotope-Shift Measurements.
PB95-151254 *03,905*

Trapped Atoms and Laser Cooling.
PB95-151627 *03,911*

Electrostatic Modes of Ion-Trap Plasmas.
PB95-152963 *03,920*

Trapped Ions and Laser Cooling 4: Selected Publications of the Ion Storage Group of the Time and Frequency Division, NIST, Boulder, Colorado.
PB96-172358 *04,108*

TRAPPING (CHARGED PARTICLES)
Infrared and Near-Infrared Spectra of HCC and DCC Trapped in Solid Neon.
AD-A295 578/9 *03,773*

Disorder Trapping in Ni2TiAl.
PB94-198942 *03,322*

Comment on <<A Dynamic Electric Trap for Ground-State Atoms>>.
PB96-200290 *04,123*

TREASURE ISLAND NAVAL STATION
Assessment of Site Response Analysis Procedures.
PB95-210928 *00,450*

TRENDS
Technology Trends in Telecommunications: An Overview.
PB94-123080 *01,462*

Scanned Probe Microscopies: Opportunities and Issues in Metrology.
PB96-160783 *02,426*

TRIACETYLOLEANDOMYCIN
Two-Dimensional POMMIE Carbon-Proton Chemical Shift Correlated (13)C NMR Spectrum Editing.
PB94-200508 *00,809*

TRIANGULATION
Data-Parallel Algorithm for Three-Dimensional Delaunay Triangulation and Its Implementation.
PB95-163309 *01,714*

Inserting Line Segments into Triangulations and Tetrahedralizations.
PB95-198933 *03,415*

TRIBLOCK COPOLYMER
Flow-Induced Structure in Polymers: Chapter 16. Shear-Induced Changes in the Order-Disorder Transition Temperature and the Morphology of a Triblock Copolymer.
PB96-123237 *03,127*

Shear-Induced Changes in the Order-Disorder Transition Temperature and the Morphology of a Triblock Copolymer.
PB97-118772 *03,130*

TRIBOLOGY
Wear Mechanism Maps of Ceramics.
PB94-172368 *03,229*

Considerations on Data Requirements for Tribological Modeling.
PB94-172731 *02,962*

Wear of Selected Materials and Composites Sliding against MoS2 Films.
PB94-172749 *03,231*

Tribological Characteristics of Alpha-Alumina at Elevated Temperatures.
PB94-211018 *02,963*

Tribochemical Reaction of Stearic Acid on Copper Surface Studied by Surface Enhanced Raman Spectroscopy.
PB94-212057 *02,964*

Tribology Education: Present Status and Future Challenges.
PB94-212362 *02,965*

Tribological Data: Needs and Opportunities.
PB95-140596 *03,237*

Modified Surface Layers and Coatings.
PB95-176087 *03,125*

Boundary Lubrication of Silicon Nitride.
PB95-213583 *03,226*

Wear Transitions in Monolithic Alumina and Zirconia-Alumina Composites.
PB96-103163 *03,168*

Wear Mechanism Maps of 440C Martensitic Stainless Steel.
PB96-111810 *04,834*

Mechano-Chemical Model. Reaction Temperatures in a Concentrated Contact.
PB96-119466 *03,227*

Tribological Behavior of 440/Diamond-Like-Carbon Film Couples.
PB96-119714 *03,019*

TRIBOMETERS
Tribometer for Measurements in Hostile Environments.
PB95-180949 *02,967*

TRICHLOROMETHYL RADICALS
Kinetics of the Reaction of CCl3-Br-2 and the Thermochemistry of CCl3 Radical and Cation.
PB94-212115 *00,824*

Experimental and Abinitio Studies of Electronic Structures of the CCl3 Radical and Cation.
PB94-212131 *00,826*

TRIFLUOROMETHYL IODIDE
Environmental Aspects of Halon Replacements: Considerations for Advanced Agents and the Ozone Depletion Potential of CF3I.
PB97-122261 *03,301*

TRIGLYCERIDES
Structure of a Triglyceride Microemulsion: A Small Angle Neutron Scattering Study.
PB96-112255 *01,077*

TRIMERS
Potential Surfaces and Dynamics of Weakly Bound Trimers: Perspectives from High Resolution IR Spectroscopy.
PB96-176508 *01,155*

TRIPHENYL TETRAZOLIUM CHLORIDE
Alcohol Solutions of Triphenyl-Tetrazolium Chloride as High-Dose Radiochromic Dosimeters.
PB96-135249 *03,716*

TRITIUM
Pressure-Volume-Temperature Relations in Liquid and Solid Tritium.
PB94-140571 *00,726*

Intercomparison of Internal Proportional Gas Counting of (85)Kr and (3)H.
PB94-185576 *03,800*

TRITON X-100
Holographic Properties of Triton X-100-Treated Bacteriorhodopsin Embedded in Gelatin Films.
PB96-119284 *03,761*

TRUSTED SYSTEMS
Guidance to Federal Agencies on the Use of Trusted Systems.
PB95-163440 *01,597*

Concept Paper: An Overview of the Proposed Trust Technology Assessment Program.
PB96-160882 *01,614*

TMACH Experiment Phase 1. Preliminary Developmental Evaluation.
PB96-195318 *01,618*

TRYPANOSOMA BRUCEI
beta-D-Glucosyl-Hydroxymethyluracil: A Novel Modified Base Present in the DNA of the Parastic Protozoan T. brucei.
PB94-172319 *03,524*

TRYPTOPHAN
Equilibrium and Calorimetric Investigation of the Hydrolysis of L-Tryptophan to (Indole + Pyruvate + Ammonia).
PB95-163317 *00,661*

TUNABLE LASERS
Narrow-Band Tunable Diode Laser System with Grating Feedback, and a Saturated Absorption Spectrometer for Cs and Rb.
PB95-202891 *04,319*

Doppler-Free Spectroscopy of Large Polyatomic Molecules and van der Waals Complexes.
PB96-119581 *04,339*

TUNGSTEN
Radiance Temperature (in the Wavelength Range 519-906 nm) of Tungsten at Its Melting Point by a Pulse-Heating Technique.
PB94-172590 *03,397*

Measurement of the Heat of Fusion of Tungsten by a Microsecond-Resolution Transient Technique.
PB94-216686 *03,400*

Use of Sum Rules on the Energy-Loss Function for the Evaluation of Experimental Optical Data.
PB95-150736 *04,264*

Application of ODF to the Rietveld Profile Refinement of Polycrystalline Solid.
PB95-202388 *03,401*

Analytical Method for Determining Thermal Conductivity from Dynamic Experiments.
PB96-102744 *04,024*

Microstructural Characterization of Cobalt-Tungsten Coated Graphite Fibers.
PB96-159231 *01,951*

TUNGSTEN IONS
Observation of Pd-Like Resonance Lines Through Pt(32+) and Zn-Like Resonance Lines of Er(38+) and Hf(42+).
PB95-150637 *03,896*

Rh I Isoelectronic Sequence Observed from Er(23+) to Pt(33+).
PB95-150652 *03,898*

Spectra of Ag I Isoelectronic Sequence Observed from Er(21+) to Au(32+).
PB95-150660 *03,899*

TUNGSTEN SILICIDE
UV Absorption Cross Sections of Methylchloroform: Temperature-Dependent Gas and Liquid Phase Measurements.
PB96-201041 *00,643*

TUNNEL JUNCTIONS
High Critical Temperature Superconductor Tunneling Spectroscopy Using Squeezable Electron Tunneling Junctions.
PB95-163721 *04,627*

TUNNELING
New Oxide Degradation Mechanism for Stresses in the Fowler-Nordheim Tunneling Regime.
PB96-200985 *04,128*

TUNNELING (ELECTRONICS)
Electronic Microrefrigerator Based on a Normal-Insulator-Superconductor Tunnel Junction.
PB96-102827 *04,718*

TUNNELING SPECTROSCOPY
Tunneling Spectroscopy of Thallium-Based High-Temperature Superconductors.
PB95-161709 *04,606*

Tunneling Spectroscopy of bcc(001) Surface States.
PB96-155585 *04,775*

TURBIDITY
Neutron Scattering Study of Shear Induced Turbidity in Polystyrene/Dioctyl Phthalate Solutions at High Shear Rates.
PB94-172624 *01,197*

Neutron Scattering Study of Shear Induced Turbidity in Polystyrene Dissolved in Dioctyl Phthalate.
PB95-161865 *01,256*

TURBINE PUMPS
Wear Mechanism Maps of 440C Martensitic Stainless Steel.
PB96-111810 *04,834*

TURBULENCE
Fire Propagation in Concurrent Flows.
PB94-193844 *01,365*

Mixing and Radiation Properties of Buoyant Turbulent Diffusion Flames.
PB95-242327 *01,396*

TURBULENT BOUNDARY LAYER
Characteristics of Turbulence in a Boundary Layer with Zero Pressure Gradient.
AD-A278 249/8 *04,192*

Evolution of a Turbulent Boundary Layer Induced by a Three-Dimensional Roughness Element.
PB94-212818 *04,200*

TURBULENT FLAMES
Turbulent Flame Spread on Vertical Corner Walls.
PB96-114764 *01,403*

Interaction of HFC-125, FC-218 and CF3I with High Speed Combustion Waves.
PB96-176417 *03,290*

TURBULENT FLOW
Turbulent Upward Flame Spread on a Vertical Wall under External Radiation.
PB94-207388 *00,341*

Experimental Study of the Stabilization Region of Lifted Turbulent-Jet Diffusion Flames.
PB96-122676 *01,405*

Review of Flows Driven By Natural Convection in Adiabatic Shafts.
PB96-147897 *01,416*

Tomographic Reconstruction of the Moments of Local Probability Density Functions in Turbulent Flow Fields.
PB96-180195 *04,219*

TURBULENT JETS
Global Density Effects on the Self-Preservation Behavior of Turbulent Free Jets.
PB95-162301 *04,207*

TURNING (MACHINING)
Real Time Compensation for Tool Form Errors in Turning Using Computer Vision.
PB95-107231 *02,945*

TWO-BALL COLLISION TEST APPARATUS
Asperity-Asperity Contact Mechanisms Simulated by a Two-Ball Collision Apparatus.
PB95-164158 *02,966*

TWO DIMENSIONAL FLOW
Adaptive, Predictive 2-D Feature Tracking Algorithm for Finding the Focus of Expansion.
PB94-218575 *01,588*

TWO-PEAK METHOD
New Method to Evaluate Deposit Forming Tendencies of Liquid Lubricants by Differential Scanning Calorimetry.
PB95-152120 *01,451*

Deposit Forming Tendencies of Diesel Engine Oils-Correlation between the Two-Peak Method and Engine Tests.
PB95-152138 *01,452*

TWO PHASE AQUEOUS EXTRACTION SYSTEMS
Continuous Counter-Current Two Phase Aqueous Extraction.
PB95-161212 *00,675*

TWO PHASE FLOW
Simulating Smoke Movement through Long Vertical Shafts in Zone-Type Compartment Fire Models.
PB95-143152 *00,368*

Generation Rate and Distribution of Products of Combustion in Two-Layer Fire Environments: A Model and Applications.
PB96-102173 *01,398*

TYPE 2 SUPERCONDUCTORS
High-Frequency Linear Response of Anisotropic Type-II Superconductors in the Mixed State.
PB94-200359 *04,483*

Nonlinear Response of Type-II Superconductors in the Mixed State in Slab Geometry.
PB94-200367 *04,484*

TYPE-III MIXTURES
Critical Lines for Type-III Aqueous Mixtures by Generalized Corresponding-States Models.
PB96-102371 *01,063*

ULTRACOLD ATOMS
Measurements of Fluorescence from Cold Atoms: Localization in Three-Dimensional Standing Waves.
PB95-163879 *03,943*

Laser Modification of Ultracold Collisions: Experiment.
PB96-157987 *04,075*

ULTRAFILTRATION
Determination of Osmotic Pressure and Fouling Resistances and Their Effects on Performance of Ultrafiltration Membranes.
PB94-212891 *00,841*

Characterization of the Adsorption-Fouling Layer Using Globular Proteins on Ultrafiltration Membranes.
PB94-212909 *00,842*

ULTRAHIGH VACUUM
Laser Photoionization Measurements of Pressure in Vacuum.
PB95-180600 *03,964*

Measurement of Very-Low Partial Pressures.
PB95-180998 *02,659*

ULTRASONIC FLAW DETECTION
Selection of Appropriate Ultrasonic System Components for NDE of Thick Polymer-Composites.
PB94-185279 *03,133*

ULTRASONIC FLOW DETECTION
Appropriate Ultrasonic System Components for NDE of Thick Polymer Composites.
PB95-125696 *03,148*

Examination of Objects Made of Wood Using Air-Coupled Ultrasound.
PB95-125712 *03,404*

Ultrasonic Measurement of Residual Stress in Railroad Wheel Rims.
PB95-140430 *04,849*

ULTRASONIC MICROSCOPY
Material Characterization By a Time-Resolved and Polarization-Sensitive Ultrasonic Technique.
PB97-122576 *02,764*

ULTRASONIC RADIATION
Absorption of Ultrasonic Waves in Air at High Frequencies (10-20 MHz).
PB94-199007 *04,182*

Absorption of Sound in Gases between 10 and 25 MHz: Argon.
PB94-199015 *04,183*

ULTRASONIC REFERENCE BLOCKS
NIST Calibration of ASTM E127-Type Ultrasonic Reference Blocks.
PB94-191640 *02,702*

ULTRASONIC-RESONANCE SPECTROSCOPY
Ultrasonic-Resonance Spectroscopy of Bulk and Layered Solids.
PB96-141338 *04,759*

ULTRASONIC SPECTROSCOPY
Ultrasonic Spectroscopy of Metallic Spheres Using Electromagnetic-Acoustic Transduction.
PB94-212537 *04,185*

ULTRASONIC TESTS
Infinite Divisibility and the Identification of Singular Waveforms.
PB94-172111 *02,701*

Ultrasonic Measurements of Surface Roughness.
PB94-172137 *04,181*

NIST Power Reference Source.
PB94-211513 *00,148*

Appropriate Ultrasonic System Components for NDE of Thick Polymer Composites.
PB95-125696 *03,148*

Ultrasonic Technique for Sizing Voids Using Area Functions.
PB95-151916 *02,904*

Ultrasonic Measurement of Sheet Anisotropy and Formability.
PB95-153235 *03,213*

Ultrasonic Method for Reconstructing the Two-Dimensional Liquid-Solid Interface in Solidifying Bodies.
PB95-161782 *03,349*

Pulse-Echo Ultrasonic Evaluation of the Integrity of Seams of Single-Ply Roof Membranes.
PB95-163804 *00,381*

Ultrasonic Measurement of Residual Stress in Cast Steel Railroad Wheels.
PB95-169199 *04,852*

Ultrasonic Methods.
PB96-190327 *02,707*

ULTRASONIC VELOCITIES
Estimation of the Orientation Distribution of Short-Fiber Composites Using Ultrasonic Velocities.
PB96-176656 *03,178*

ULTRASONIC WAVE TRANSDUCERS
High-Sensitivity Acoustic Emission Sensor/Preamplifier Subsystems.
PB95-125704 *02,900*

Ultrasound Power Measurement Techniques at NIST.
PB96-179569 *02,684*

ULTRASONICS
Well-Shielded EMAT for On-Line Ultrasonic Monitoring of GMA Welding.
PB96-186077 *02,879*

ULTRASONOGRAPHY
Ultrasonic Sensing of GMAW: Laser/EMAT Defect Detection System.
PB96-186028 *02,878*

ULTRAVIOLET
Temperature Dependent Ultraviolet Absorption Cross Sections of Propylene, Methylacetylene and Vinylacetylene.
PB96-204177 *01,169*

ULTRAVIOLET ABSORPTION
Temperature Dependence of the Gas and Liquid Phase Ultraviolet Absorption Cross Sections of HCFC-123 (CF3CHCl2) and HCFC-142b (CH3CF2Cl).
PB96-201033 *03,298*

ULTRAVIOLET ASTRONOMY
Atomic Data Needed for Far Ultraviolet Astronomy with HUT and FUSE.
PB94-213402 *00,062*

Peeking Through the Picket Fence: What Astrophysical Surprises May Be Present in the 100-1200 Angstrom Region.
PB95-202859 *00,082*

Goddard High Resolution Spectrograph: Instrument, Goals, and Science Results.
PB96-123278 *00,044*

Scientific Rationale and Present Implementation Strategy for the Far Ultraviolet Spectrograph Explorer (FUSE).
PB96-123328 *00,045*

Riass Coronathon: Joint X-ray and Ultraviolet Observations of Normal F-K Stars.
PB96-200217 *00,109*

ULTRAVIOLET DETECTORS
One Gigarad Passivating Nitrided Oxides for 100% Internal Quantum Efficiency Silicon Photodiodes.
PB94-185485 *02,119*

Silicon Photodiodes Optimized for EUV and Soft X-Ray Regions.
PB94-199478 02,124

ULTRAVIOLET RADIATION
Development and Calibration of UV/VUV Radiometric Sources.
PB94-199098 04,229

UV-Photopatterning of Alkylthiolate Monolayers Self-Assembled on Gold and Silver.
PB95-150751 00,924

Improved Dose Metrology in Optical Lithography.
PB96-179510 02,439

ULTRAVIOLET SPECTRA
Ultraviolet Multiplet Table. Finding List for Spectra of the Elements Molybdenum to Lanthanum (Z = 42 to 57); Hafnium to Radium (Z = 72 to 88).
AD-A278 131/8 00,709

Ultraviolet Multiplet Table.
AD-A278 446/0 00,710

Spectrum and Energy Levels of Five-Times-Ionized Niobium (Nb VI).
PB94-185246 04,226

Ultraviolet Observations of Stellar Coronae: Early Results from HST.
PB94-213428 00,064

Wavelengths and Isotope Shifts for Lines of Astrophysical Interest in the Spectrum of Doubly Ionized Mercury (Hg III).
PB95-140869 03,887

Spectrum and Energy Levels of Triply Ionized Barium (Ba IV).
PB95-140877 03,888

Improved Wavelengths for Prominent Lines of Cr XVI to Cr XXII.
PB95-150629 03,895

Rb-Like Spectra: Pd X to Nd XXIV.
PB95-150645 03,897

Spectra of Ag I Isoelectronic Sequence Observed from Er(21+) to Au(32+).
PB95-150660 03,899

Analysis of the 5s(2)5p(2)-(5s5p(3)+5s(2)5p5d+5s(2)5p6s) Transitions of Four-Times Ionized Xenon (Xe V).
PB95-150769 03,900

Laser-Produced and Tokamak Spectra of Lithiumlike Iron, Fe(23+).
PB95-180857 04,314

High-Velocity Plasma in the Transition Region of AU Microscopii: Evidence for Magnetic Reconnection and Saturated Heating during Quiescent and Flaring Conditions.
PB96-102694 00,091

GHRS Observations of Cool, Low-Gravity Stars. 1. The Far-Ultraviolet Spectrum of alpha Orions (M2 Iab).
PB96-112016 00,094

Sleuthing the Dynamo: HST/FOS Observations of UV Emissions of Solar-Type Stars in Young Clusters.
PB96-122817 00,098

High Velocity Plasm in the Transition Region of Au Mic: A Stellar Analog of Solar Explosive Events.
PB96-123294 00,102

Transition Regions of Capella.
PB96-123336 00,105

Recalibration for the Final Archive of the International Ultraviolet Explorer (IUE) Satellite.
PB96-135264 00,106

Transition Regions of Capella (1995).
PB96-176714 00,108

Temperature Dependence of the Ultraviolet Absorption Cross Section of CF3I.
PB96-204169 01,168

ULTRAVIOLET SPECTRORADIOMETERS
Report on USDA Ultraviolet Spectroradiometers.
PB96-214648 00,125

ULTRAVIOLET STAR
Deuterium and the Local Interstellar Medium: Properties for the Procyon and Capella Lines of Sight.
PB96-200639 00,111

ULTRAVIOLET STARS
Accurate Measurements of the Local Deuterium Abundance from HST Spectra.
PB96-200621 00,110

UNCERTAINTY
Look at Uncertainties over Twenty Decades of Pressure Measurement.
PB95-168506 02,655

UNCERTAINTY
RangeCAD and the NIST RCS Uncertainty Analysis.
PB94-218591 01,870

New Expressions of Uncertainties for Humidity Calibrations at the National Institute of Standards and Technology.
PB95-103826 02,645

UNCERTAINTY ANALYSIS
Statistical Descriptors in Crystallography. 2. Report of a Working Group on Expression of Uncertainty in Measurement.
PB96-146824 04,764

UNCERTAINTY BOUNDS
Bounds on Frequency Response Estimates Derived from Uncertain Step Response Data.
PB96-122874 03,419

UNCLASSIFIED SENSITIVE INFORMATION
Guidance to Federal Agencies on the Use of Trusted Systems.
PB95-163440 01,597

UNDERGROUND DISPOSAL
4SIGHT Manual: A Computer Program for Modelling Degradation of Underground Low Level Waste Concrete Vaults.
PB95-231593 03,726

UNDERGROUND SPACE
Numerical Simulation of Rapid Combustion in an Underground Enclosure.
PB96-183132 01,424

UNDERWATER NAVIGATION
Outline of a Multiple Dimensional Reference Model Architecture and a Knowledge Engineering Methodology for Intelligent Systems Control.
PB95-220414 03,703

UNDERWATER VEHICLES
Intelligent Control for Multiple Autonomous Undersea Vehicles.
PB94-211877 03,747

UNITED STATES
Differences in Competitive Strategies between the United States and Japan.
PB94-211836 00,013

Earthquake and Fire in Japan: When the Threat Became a Reality.
PB95-175238 00,201

Japan Technology Program Assessment. Simulation: State-of the-Art in Japan.
PB95-217097 02,827

Ceramic Powders Characterization: Results of an International Laboratory Study.
PB95-270039 02,672

Electrical Product Requirements (Especially Quality Requirements) in the United States.
PB96-119235 01,929

Working Conference on Global Growth of Technology: Is America Prepared. Held in Gaithersburg, Maryland on December 7, 1995.
PB96-210059 00,018

Directory of U.S. Private Sector Product Certification Programs.
PB96-215074 02,688

Standards Activities of Organizations in the United States.
PB97-124135 00,006

UNITED STATES AIR FORCE ACADEMY
Robotics Application to Highway Transportation. Volume 1. Final Report.
PB95-203790 03,654

UNITED STATES BOTANIC GARDEN
Corrosion Resistance of Materials for Renovation of the United States Botanic Garden Conservatory.
PB94-154390 00,032

UNITED STATES CAPITOL
Warping of Terrace Pavers at the U.S. Capitol Building.
PB96-193651 00,411

UNIVERSAL TIME
Utc Dissemination to the Real-Time User.
N19960042622 01,521

UNIX (OPERATING SYSTEM)
Using Expect to Automate System Administration Tasks.
PB94-213329 01,697

UNMANNED VEHICLES
Real-Time Vision for Autonomous and Teleoperated Control of Unmanned Vehicles.
PB94-211885 03,701

Real-Time Vision for Unmanned Vehicles.
PB94-211893 03,702

UPHOLSTERY
Toxicity, Fire Hazard and Upholstered Furniture.
PB94-198454 00,289

Influence of Ignition Source on the Flaming Fire Hazard of Upholstered Furniture. (NIST Reprint).
PB95-180162 00,297

UPWARD FLAME SPREAD
Wall Flame Heights with External Radiation.
PB95-163481 00,380

URACIL/5- ((BETA-D-GLYCOPYRANOSYL OXY)-METHYL)
beta-D-Glucosyl-Hydroxymethyluracil: A Novel Modified Base Present in the DNA of the Parastic Protozoan T. brucei.
PB94-172319 03,524

URANIUM
Characterization of the Binding of Gallium, Platinum, and Uranium to Pseudomonas Fluorescens by Small-Angle X-ray Scattering and Transmission Electron Microscopy.
PB94-172509 03,453

URANIUM 235
Measurement of the (235)U(n,f) Reaction from Thermal to 1 keV.
PB95-140422 03,886

URANIUM 236 TARGET
Intermediate Structure in the Neutron-Induced Fission Cross Section of 236U.
PB94-185741 03,802

URANIUM BERYLLIUM
Superconducting Energy Gap of Bulk UBe13.
PB95-150116 04,559

URANIUM COPPER ALUMINIDES
Magnetic Properties of Single-Crystalline UCu3Al2.
PB95-180717 04,686

URANIUM GOLD STANNIDES
Crystallographic and Magnetic Properties of UAuSn.
PB95-140521 04,543

URANIUM IONS
Magnetic Dipole Line from U LXXI Ground-Term Levels Predicted at 3200 Angstroms.
PB94-211497 04,407

URANIUM OXIDES
High Temperature Reactions of Uranium Dioxide with Various Metal Oxides.
AD-A286 648/1 00,717

URANIUM PLATES
Neutron Diffraction Texture Study of Deformed Uranium Plates.
PB97-111587 03,010

URANIUM PLATINUM GERMANIDES
Incommensurate Magnetic Order in UPtGe.
PB95-140513 04,542

URBAN AREAS
Sources of Urban Contemporary Carbon Aerosol.
PB95-175659 02,551

URINALYSIS
Determination of 3-Quinuclidinyl Benzilate (Qnb) and Its Major Metabolites in Urine by Isotope Dilution Gas Chromatography Mass Spectrometry.
PB94-199379 03,492

How to Verify Reference Materials.
PB95-151486 03,497

Certification of Morphine and Codeine in a Human Urine Standard Reference Material.
PB95-176160 03,499

URINE
Determination of Amphetamine and Methamphetamine in a Lyophilized Human Urine Reference Material.
PB95-175444 03,597

Intercomparison Study of (237)Np Determination in Artificial Urine Samples.
PB96-102645 03,633

Certification of Phencyclidine in Lyophilized Human Urine Reference Materials.
PB96-160692 03,508

US COUNCIL FOR ENERGY AWARENESS
Review of the USCEA/NIST Measurement Assurance Program for the Nuclear Power Industry.
PB95-126272 03,712

US DOD
Assessment of the DOD Goal Security Architecture (DGSA) for Non-Military Use.
PB95-189510 03,653

Present Worth Factors for Life-Cycle Cost Studies in the Department of Defense (1996).
PB96-106869 03,673

US HUD
Performance of HUD-Affiliated Properties during the January 17, 1994 Northridge Earthquake.
PB95-174488 00,443

US NBS
National Voluntary Laboratory Accreditation Program: Procedures and General Requirements.
PB94-178225 02,630

National Voluntary Laboratory Accreditation Program (NVLAP): Wood Based Products.
PB95-170429 03,405

Automated Resistance Measurements at NIST.
PB96-119326 02,274

US NIST
Opportunities for Innovation: Biotechnology.
PB94-157831 00,009

Electronics and Electrical Engineering Laboratory Technical Progress Bulletin Covering Laboratory Programs, October to December 1992, with 1992/1993 EEEL Events Calendar.
PB94-165958 02,299

Publications of the Manufacturing Engineering Laboratory Covering the Period January 1989-September 1992.
PB94-165966 02,750

Bibliography of the NIST Electromagnetic Fields Division Publications.
PB94-165990 01,875

Program Handbook: Requirements for Obtaining NIST Approval/Recognition of a Laboratory Accreditation Body Under P.L. 101-592. The Fastener Quality Act.
PB94-210143 02,859

NIST-Coordinated Standard for Fingerprint Data Interchange.
PB94-216645 01,808

NIST Industrial Impacts: A Sampling of Successful Partnerships.
PB95-111514 00,488

Review of the USCEA/NIST Measurement Assurance Program for the Nuclear Power Industry.
PB95-126272 *03,712*

Databases Available in the Research Information Center of the National Institute of Standards and Technology.
PB95-128641 *02,724*

Initial NIST Testing Policy for STEP: Beta Testing Program for AP 203 Implementations. National PDES Testbed Report Series.
PB95-154688 *02,779*

Automated Inspection: The Integration of National Standards and Commercial Products at NIST.
PB95-163077 *02,906*

Journal of Research of the National Institute of Standards and Technology, September/October 1994. Volume 99, Number 5.
PB95-169371 *04,293*

Concepts of the NIST EXPRESS Server.
PB95-180543 *02,781*

NIST Serial Holdings, 1995.
PB95-188926 *02,746*

Materials Science and Engineering Laboratory Annual Report, 1994. NAS-NRC Assessment Panel, April 6-7, 1995.
PB95-196697 *02,976*

NIST Industrial Impacts: A Sampling of Successful Partnerships (Revision, March 1995).
PB95-209193 *00,489*

Electronics and Electrical Engineering Laboratory Technical Progress Bulletin Covering Laboratory Programs, April to June 1991, with 1992 EEEL Events Calendar.
PB95-209821 *01,916*

Design, Specification and Tolerancing of Micrometer-Tolerance Assemblies.
PB95-209862 *02,913*

Electronics and Electrical Engineering Laboratory Technical Progress Bulletin Covering Laboratory Programs, January to March 1992, with 1992/1993 EEEL Events Calendar.
PB95-210480 *01,917*

Materials Science and Engineering Laboratory Annual Report, December 1993.
PB95-254439 *02,668*

Design Engineering Research at NIST.
PB95-267860 *02,784*

NIST and the Navy: Past, Present and Future.
PB96-119649 *03,655*

Databases Available in the Research Information Center of the National Institute of Standards and Technology (December 1995).
PB96-139407 *02,734*

Fire Hazard Model Developments and Research Efforts at NIST.
PB96-159652 *00,407*

Montgomery Education Connection and Resource Education Awareness Partnership Making Connections between Local Schools and NIST Volunteers.
PB96-159769 *00,134*

Uniform Laws and Regulations in the Areas of Legal Metrology and Motor Fuel Quality as Adopted by the 80th National Conference on Weights and Measures 1995. 1996 Edition.
PB96-172309 *02,927*

NIST Serial Holdings, 1996.
PB96-172523 *02,748*

NIST List of Publications, LP 103, March 1996. National Semiconductor Metrology Program.
PB96-175856 *02,432*

Publications 1995: NIST Building and Fire Research Laboratory.
PB96-183074 *00,226*

NIST Frequency Measurement Service.
PB96-200662 *01,561*

Optoelectronics at NIST.
PB96-200860 *02,202*

Bibliography of the NIST Electromagnetic Fields Division Publications.
PB96-210778 *01,980*

Materials Science and Engineering Laboratory Annual Report, 1995. Technical Activities.
PB96-214754 *03,009*

Science, Technology, and Competitiveness: Retrospective on a Symposium in Celebration of NIST's 90th Anniversary and the 25th Anniversary of the Gaithersburg Laboratories, November 14-15, 1991.
PB97-121610 *02,696*

USABILITY

Usability Engineering: Industry-Government Collaboration for System Effectiveness and Efficiency.
PB97-122287 *01,514*

USCEA (US COUNCIL FOR ENERGY AWARENESS)

Review of the USCEA/NIST Measurement Assurance Program for the Nuclear Power Industry.
PB95-126272 *03,712*

USER GUIDE

MV++ v. 1.5a Matrix/Vector Class Reference Guide.
PB96-195326 *01,777*

USER MANUALS

Fire Data Management System, FDMS 2.0, Technical Documentation.
PB94-164019 *01,358*

Reference Manual for the Algorithm Testing System Version 2.0.
PB96-128244 *02,922*

USER MANUALS (COMPUTER PROGRAMS)

CONTAM93 User Manual.
PB94-164381 *02,536*

FIREDOC Users Manual, 3rd Edition.
PB95-128674 *01,378*

USER NEEDS

User Profile for Researchers Studying Objects: Implications for Computer Systems.
PB94-188463 *00,133*

User Study: Informational Needs of Remote National Archives and Records Administration Customers.
PB95-154738 *02,725*

USER REQUIREMENTS

Information Technology Standards in a Changing World: The Rose of the Users.
PB96-160866 *02,737*

UTILIZATION

Asynchronous Transfer Mode Procurement and Usage Guide.
PB95-174967 *01,481*

VACUUM COATING

Wear of Selected Materials and Composites Sliding against MoS2 Films.
PB94-172749 *03,231*

VACUUM GAGES

Vacuum Gauges and Partial Pressure Analyzers.
PB95-150884 *02,650*

PC-Based Spinning Rotor Gage Controller.
PB95-175832 *02,609*

VACUUM-GAP CAPACITORS

Capacitors with Very Low Loss: Cryogenic Vacuum-Gap Capacitors.
PB97-122600 *02,293*

VACUUM ULTRAVIOLET RADIATION

Development and Calibration of UV/VUV Radiometric Sources.
PB94-199098 *04,229*

Photographic Response to X-Ray Irradiation. 1. Estimation of the Photographic Error Statistic and Development of Analytic Density-Intensity Equations.
PB94-200086 *03,821*

Photographic Response to X-Ray Irradiation. 2. Correlated Models.
PB94-200094 *03,822*

VALIDATION

Ada Compiler Validation Summary Report: Certificate Number 940902S1.11377 UNISYS Corporation. IntegrAda for Windows NT, Version 1.0. Intel Deskside Server with Intel 80486DX266 => Intel Deskside Server with Intel 80486DX266.
AD-A288 571/3 *01,658*

Ada Compiler Validation Summary Report: Certificate Number 940902S1.11376. UNISYS Corporation IntegrAda for Windows NT, Version 1.0. Intel Deskside Server for Intel Pentium 60 MHz =>. Intel Deskside Server with Intel Pentium 60 MHz.
AD-A288 572/1 *01,659*

Ada Compiler Validation Summary Report: Certificate Number 94101251.11379 TISOFT, Inc. Green Hills Optimizing Ada Compileer, Version 1.8.7 with PATCK ID 1 COMPAQ ProLiiant 2000 Model 55/66 => COMPAQ ProLiant 2000 Model 5/66.
AD-A288 573/9 *01,660*

Ada Complier Validation Summary Report: Certificate Number: 940929S1.11378. Digital Equipment Corporation DEC Ada for DEC OSF/1 AXP Systems, Version 3.2; DEC 3000 Model 400 AXP Workstation => DEC 3000 Model 400 AXP Workstation.
AD-A288 574/7 *01,661*

ADA Compiler Validation Summary Report, VC Number 950303S1.11381. Digital Equipment Corporation - Compiler Name: DEC Ada for OpenVMS Alpha Systems, Version 3.2.
AD-A293 709/2 *01,663*

Analysis of Standards for the Assurance of High Integrity Software.
PB96-161351 *03,735*

Verification and Validation.
PB96-161393 *01,765*

Verification and Validation of Reengineered Software.
PB96-161401 *01,766*

VALIDATION SUMMARY REPORTS

Ada Compiler Validation Summary Report: Certificate Number: 931029S1.11330, Digital Equipment Corporation, DEC Ada for DEC OSF/1 AXP Systems, Version 3.1, DEC 3000 Model 400 AXP Workstation, DEC 3000 Model 400 AXP Workstation.
AD-A274 872/1 *01,639*

Ada Compiler Validation Summary Report: Certificate Number: 931217S1.11336 Control Data Systems, Inc. NOS/VE Ada, Version 1.4 Cyber 180-930-31 => Cyber 180-930-31.
AD-A275 977/7 *01,640*

Ada Compiler Validation Summary Report. Certificate Number: 931119S1.11332, DDC-I, Inc. DACS MIPS R3000 Bare Ada Cross Compiler System, Version 4.7.1 Sun SPARCstation IPX => DACS Sun SPARC/SunOS to MIPS R3000 Bare Instruction Set Architecture Simulator, Version 4.7.1.
AD-A276 181/5 *01,641*

Ada Compiler Validation Summary Report: Certificate Number: 931119S1.11331 DDC-I, Inc. DACS Sun SPARC/SunOS to 80386 PM Bare Ada Cross Compiler System, Version 4.6.4 Sun Sparcstation 1+ => Bare Board iSBC 386/116.
AD-A276 283/9 *01,642*

Ada Compiler Validation Summary Report. Certificate Number: 930927S1.11328 Green Hills Software C Ada, Version 1.1 ZENY 386 => ZENY 386.
AD-A277 981/7 *01,643*

Ada Compiler Validation Summary Report: Certificate Number: 940325S1.11341 DDC-I, DACS Sun SPARC/SunOS to 80186 Bare Ada Cross Compiler System, Version 4.6.4 Sun SPARCstation IPX => Intel iSBC 186/100 (Bare Machine).
AD-A279 643/1 *01,645*

Ada Compiler Validation Summary Report: Certificate Number: 940325S1.11349 DDC-I, DACS Sun SPARC/Solaris to 80386 PM Bare Ada Cross Compiler System with Rate Monotonic Scheduling, Version 4.6.4 Sun SPARCclassic => Intel iSBC 386/116 (Bare Machine).
AD-A279 644/9 *01,646*

Ada Compiler Validation Summary Report: Certificate Number: 940325S1.11354 DDC-I, DACS Sun SPARC/Solaris Native Ada Compiler System, Version 4.6.2 Sun SPARCclassic => Sun SPARCclassic.
AD-A279 645/6 *01,647*

Ada Compiler Validation Summary Report: Certificate Number: 940325S1.11346 DDC-I, DACS Sun SPARC/SunOS to 680x0 Bare Ada Cross Compiler System (BASIC MODE), Version 4.6.9 Sun SPARCstation IPX => Lynwood j435TU (68030) (Bare Machine).
AD-A279 646/4 *01,648*

Ada Compiler Validation Summary Report: Certificate Number: 940325S1.11343 DDC-I, DACS Sun SPARC/Solaris to 80186 Bare Ada Cross Compiler System, Version 4.6.4 Sun SPARCclassic => Intel iSBC 186/100 (Bare Machine).
AD-A279 757/9 *01,649*

Ada Compiler Validation Summary Report: Certificate Number: 940325S1.11344 DDC-I, DACS Sun SPARC/Solaris to 80186 Bare Ada Cross Compiler System with Rate Monotonic Scheduling, Version 4.6.4 Sun SPARCclassic => Intel iSBC 186/100 (Bare Machine).
AD-A279 758/7 *01,650*

Ada Compiler Validation Summary Report: Certificate Number: 940325S1.11347 DDC-I, DACS Sun SPARC/SunOS to 680x0 Bare Ada Cross Compiler System (SECURE MODE), Version 4.6.9 Sun SPARCstation IPX => Lynwood j435TU (68030) (Bare Machine).
AD-A279 778/5 *01,651*

Ada Compiler Validation Summary Report: Certificate Number: 940325S1.11342 DDC-I, DACS Sun SPARC/SunOS to 80186 Bare Ada Cross Compiler System with Rate Monotonic Scheduling Version 4.6.4 Sun SPARCstation IPX => Intel iSBC 186/100 (Bare Machine).
AD-A279 779/3 *01,652*

Ada Compiler Validation Summary Report: Certificate Number: 940325S1.11351 DDC-I, DACS Sun SPARC/SunOS to Pentium PM Bare Ada Cross Compiler System with Rate Monotonic Scheduling, Version 4.6.4 Sun SPARCstation IPX => Intel Pentium (operated as Bare Machine) based in Xpress Desktop (Intel product number: XBASE6E4F-B).
AD-A279 804/9 *01,653*

Ada Compiler Validation Summary Report: Certificate Number: 940325S1.11350 DDC-I, DACS Sun SPARC/SunOS to Pentium PM Bare Ada Cross Compiler System, Version 4.6.4 Sun SPARCstation IPX => Intel Pentium (Operated as Bare Machine) Based in Xpress Desktop (Intel Product Number: XBASE6E4F-B).
AD-A279 864/3 *01,655*

Ada Compiler Validation Summary Report: Certificate Number 940325S1.11345 DDC-I. DACS Sun SPARC/SunOS to 680x0 Bare Ada Cross Compiler System, Version 4.6.9 Sun SPARCstation IPX => Motorola MVME143 68030/68882 (Bare Machine).
AD-A280 145/4 *01,656*

Ada Compiler Validation Summary Report: Certificate Number: 940325S1.11352 DDC-I DACS Sun SPARC/Solaries to Pentium PM Bare Ada Cross Compiler System, Version 4.6.4 Sun SPARCclassic => Intel Pentium (Operated as Bare Machine) Based in Xpress Desktop (Intel Product Number: XBASE6E4F-B).
AD-A280 295/7 *01,657*

Validated Products List (Cobol, Fortran, ADA, Pascal, MUMPS, SQL).
PB94-937300 *01,700*

Validated Products List (Cobol, Fortran, ADA, Pascal, MUMPS, SQL).
PB95-937300 *01,738*

VAN DER POL DIFFERENTIAL EQUATION

Constructing Invariant Tori for Two Weakly Coupled van der Pol Oscillators.
PB95-126165 *03,412*

VAN DER POL OSCILLATORS

Constructing Invariant Tori for Two Weakly Coupled van der Pol Oscillators.
PB95-126165 *03,412*

VAN DER WAALS COMPLEX
P-Type Doubling in the Infrared Spectrum of NO-HF.
PB94-211463 *00,817*

VANADIUM
Comparative Strategies for Correction of Interferences in Isotope Dilution Mass Spectrometric Determination of Vanadium.
PB94-185261 *00,531*

VANADIUM ALLOYS
Electronic Structure and Phase Equilibria in Ternary Substitutional Alloys.
PB97-119366 *03,378*

VAPOR COMPRESSION CYCLE
Theoretical Evaluation of the Vapor Compression Cycle with a Liquid-Line/Suction-Line Heat Exchanger, Economizer, and Ejector.
PB95-216917 *02,607*

VAPOR COMPRESSION REFRIGERATION CYCLE
Intracycle Evaporative Cooling in a Vapor Compression Cycle.
PB97-116107 *02,762*

VAPOR DEPOSITION
Measurement Methods and Standards for Processing and Application of Thermal Barrier Coatings.
N95-26123/6 *01,447*

Development and Characterization of Insulating Layers on Silicon Carbide: Annual Report for February 14, 1988 to February 14, 1989.
PB94-155579 *02,295*

Silver Metalization of Octadecanethiol Monolayers Self-Assembled on Gold.
PB95-150744 *00,923*

VAPOR LIQUID EQUILIBRIUM
Vapor-Liquid Equilibria of Ternary Mixtures in the Critical Region on Paths of Constant Temperature and Overall Composition.
PB96-161856 *01,139*

VAPOR PHASE
In situ Characterization of Vapor Phase Growth of Iron Oxide-Silica Nanocomposites: Part 1. 2-D Planar Laser-Induced Fluorescence and Mie Imaging.
PB97-112478 *03,185*

VAPOR PHASE EPITAXY
In situ Observation of Surface Morphology of InP Grown on Singular and Vicinal (001) Substrates.
PB95-168431 *04,636*

VAPOR PHASES
Thermodynamic Properties of Gas Phase Species of Importance to Ozone Depletion.
PB94-198215 *00,126*

Gas Phase Reactions Relevant to Chemical Vapor Deposition: Optical Diagnostics.
PB94-199338 *03,116*

Gas Phase Reactions Relevant to Chemical Vapor Deposition: Numerical Modeling.
PB94-199346 *03,117*

Homogeneous Gas Phase Decyclization of Tetralin and Benzocyclobutene.
PB95-151049 *00,928*

Multiphoton Ionization Spectroscopy Measurements of Silicon Atoms during Vapor Phase Synthesis of Ceramic Particles.
PB95-151999 *03,913*

Simulation of Ceramic Particle Formation: Comparison with In-situ Measurements.
PB95-152013 *00,674*

Gas Phase Reactivity Study of OH Radicals with 1,1-Dichloroethene and cis-1,1-Dichloroethene and Trans-1,2-Dichloroethene over the Temperature Range 240-400 K.
PB95-152146 *00,939*

Rate Constants for the Gas Phase Reactions of the OH Radical with CF3CF2CHCl2 (HCFC-225ca) and CF2ClCF2CHClF (HCFC-225cb).
PB95-152153 *00,940*

VAPOR PRESSURE
Vapor Pressure of 1,1-dichloro-2,2,2-trifluoroethane (R123).
PB95-126231 *00,899*

Ebulliometric Measurement of the Vapor Pressure of Difluoromethane.
PB95-151361 *00,931*

Criteria for Establishing Accurate Vapor Pressure Curves.
PB95-163812 *00,972*

Ebulliometric Measurement of the Vapor Pressure of 1-Chloro-1,1-Difluoroethane and 1,1-Difluoroethane.
PB95-164489 *00,984*

Vapour Pressure Measurements on 1,1,1,2-Tetrafluoroethane (R134a) from 180 to 350 K.
PB95-168886 *03,265*

Coexisting Densities, Vapor Pressures and Critical Densities of Refrigerants R-32 and R-152a, at 300 - 385 K.
PB95-175691 *03,274*

Vapour Pressures and Gas-Phase (p, rho n, T) Values for CF3CHF2(R125).
PB96-102090 *04,019*

Vapor Pressure of Pentafluorodimethyl Ether.
PB96-201199 *00,677*

Vapor Pressure of 1,1,1,2,2-Pentafluoropropane.
PB97-113237 *00,684*

VAPOR PRESSURES
Compressed Liquid Densities, Saturated Liquid Densities, and Vapor Pressures of 1,1-Difluoroethane.
PB97-110118 *01,173*

VAPOR TRANSPORT
Vapor Transport in Materials and Process Chemistry.
PB94-211745 *00,669*

VARIANCE ESTIMATES
Anova Estimates of Variance Components for a Class of Mixed Models.
PB96-141163 *03,448*

VARIANCE (STATISTICS)
Approximate Confidence Intervals on Linear Combinations of Expected Mean Squares.
PB95-151296 *03,435*

Approximate Confidence Intervals on Positive Linear Combinations of Expected Mean Squares.
PB95-151304 *03,436*

VARIANCES
Variances in the Measurement of Ceramic Powder Properties.
PB97-110316 *03,100*

VARIANT DESIGN
Variant Design for Mechanical Artifacts-A State of the Art Survey.
PB94-154358 *02,768*

VARIATIONS
Fluctuations in Probability Distribution on Chaotic Attractors.
PB96-102330 *04,022*

VECTOR FIELDS
MV++ v. 1.5a Matrix/Vector Class Reference Guide.
PB96-195326 *01,777*

VELOCITY DISTRIBUTION
Velocity Distribution of Atomic Beams by Gated Optical Pumping.
PB95-180519 *01,542*

VELOCITY MEASUREMENT
Development in the Theory and Analysis of Eddy Current Sensing of Velocity in Liquid Metals.
PB94-212586 *03,335*

VENTCF2 COMPUTER PROGRAM
VENTCF2: An Algorithm and Associated FORTRAN 77 Subroutine for Calculating Flow through a Horizontal Ceiling/Floor Vent in a Zone-Type Compartment Fire Model.
PB94-210127 *00,345*

VENTILATION
Manual for Ventilation Assessment in Mechanically Ventilated Commercial Buildings.
PB94-145653 *00,239*

Air Change Effectiveness Measurements in Two Modern Office Buildings.
PB94-185766 *00,243*

Ventilation Rates in Office Buildings.
PB95-108825 *02,539*

Field Measurements of Ventilation and Ventilation Effectiveness in an Office/Library Building.
PB95-108833 *00,247*

Study of Ventilation and Carbon Dioxide in an Office Building.
PB95-150140 *02,542*

Ventilation, Carbon Dioxide and ASHRAE Standard 62-1989.
PB95-162095 *02,544*

Fire and Smoke Control: An Historical Perspective.
PB95-175808 *00,202*

Limits of CO2 Monitoring in Determining Ventilation Rates.
PB95-176004 *02,552*

Ventilation Effectiveness Measurements in Two Modern Office Buildings.
PB95-176012 *02,553*

Measurements of Outdoor Air Distribution in an Office Building.
PB95-210944 *00,264*

Study of Ventilation Measurement in an Office Building.
PB96-155593 *00,274*

NASA Fire Detector Study.
PB96-183108 *01,423*

VENTILATION SYSTEMS
Assessing Ventilation Effectiveness in Mechanically Ventilated Office Buildings.
PB95-162079 *00,255*

Indoor Air Quality Commissioning of a New Office Building.
PB95-182309 *00,262*

Improving the Evaluation of Building Ventilation.
PB96-138508 *00,271*

Effectiveness of a Heat Recovery Ventilator, an Outdoor Air Intake Damper and an Electrostatic Particulate Filter at Controlling Indoor Air Quality in Residential Buildings.
PB96-146642 *02,564*

Workplan to Analyze the Energy Impacts of Envelope Airtightness in Office Buildings.
PB96-154463 *00,273*

VENTS
Polyvinyl Chloride (PVC) Plastic Drain, Waste, and Vent Pipe and Fittings.
AD-A310 426/2 *00,326*

Acrylonitrile-Butadiene-Styrene (ABS) Plastic Drain, Waste, and Vent Pipe and Fittings.
AD-A310 724/0 *00,327*

Combined Buoyancy- and Pressure-Driven Flow Through a Shallow, Horizontal, Circular Vent.
PB94-210077 *00,344*

VENTCF2: An Algorithm and Associated FORTRAN 77 Subroutine for Calculating Flow through a Horizontal Ceiling/Floor Vent in a Zone-Type Compartment Fire Model.
PB94-210127 *00,345*

Calculating Combined Buoyancy- and Pressure-Driven Flow Through a Shallow, Horizontal, Circular Vent; Application to Problem of Steady Burning in a Ceiling-Vented Enclosure.
PB96-164108 *00,409*

Combined Buoyancy and Pressure-Driven Flow Through a Shallow, Horizontal, Circular Vent.
PB96-164116 *00,410*

VERIFICATION
How to Verify Reference Materials.
PB95-151486 *03,497*

VERIFICATION INSPECTION
User's Guide for the Algorithm Testing System Version 2.0.
PB95-251666 *02,916*

Integrated Vision Touch-Probe System for Dimensional Inspection Tasks.
PB95-255832 *02,917*

VERIFIED ANALYSIS
Airborne Asbestos Method: Standard Test Method for Verified Analysis of Asbestos by Transmission Electron Microscopy. Version 2.0.
PB94-163045 *00,526*

VERTICAL SURFACES
Heat Flux from Flames to Vertical Surfaces.
PB97-110357 *01,438*

VERY LARGE SCALE INTEGRATION
Design Guide for CMOS-On-SIMOX. Test Chips NIST3 and NIST4.
PB94-163458 *02,297*

Color Supplement to NIST Special Publication 400-93: Semiconductor Measurement Technology: Design and Testing Guides for the CMOS and Lateral Bipolar-on-SOI Test Library.
PB94-164316 *02,298*

Semiconductor Measurement Technology: Design and Testing Guides for the CMOS and Lateral Bipolar-on-SOI Test Library.
PB94-178019 *02,301*

Application of the Modified Voltage-Dividing Potentiometer to Overlay Metrology in a CMOS/Bulk Process.
PB94-181997 *02,302*

Electrical Test Structure for Overlay Metrology Referenced to Absolute Length Standards.
PB95-152278 *02,336*

Comparisons of Measured Linewidths of Sub-Micrometer Lines Using Optical, Electrical, and SEM Metrologies.
PB95-152807 *02,338*

Operating Principles of MultiKron II Performance Instrumentation for MIMD Computers.
PB95-189486 *01,628*

Operating Principles of the SBus MultiKron Interface Board.
PB95-231783 *01,630*

MEMS in Standard CMOS VLSI Technology.
PB96-102363 *02,377*

Hardware Measurement Techniques for High-Speed Networks.
PB96-160551 *01,500*

VESICLES
Optical Control of Enzymatic Conversion of Sucrose to Glucose by Bacteriorhodopsin Incorporated into Self-Assembled Phosphatidylcholine Vesicles.
PB96-123344 *03,477*

Zimm Plot and Its Analogs as Indicators of Vesicle and Micelle Size Polydispersity.
PB96-123765 *01,094*

VIBRATION
Vibrational Spectra of Molecular Ions Isolated in Solid Neon. 11. NO2(+), NO2(-), and NO3(-).
AD-A275 828/2 *00,708*

VIBRATION DAMPING
Method of Estimating the Parameters of Tuned Mass Dampers for Seismic Applications.
PB96-167820 *00,473*

VIBRATION ISOLATORS
Draft Guidelines for Quality Control Testing of Elastomeric Seismic Isolation Systems.
PB94-161734 *00,422*

Draft Guidelines for Pre-Qualification and Prototype Testing of Seismic Isolation Systems.
PB94-161940 *01,331*

Draft Guidelines for Quality Control Testing of Sliding Seismic Isolation Systems.
PB94-161957 *01,332*

Draft Guideline for Testing and Evaluation of Seismic Isolation Systems.
PB94-172947 *00,423*

Multi-Stage, Position Stabilized Vibration Isolation System for Neutron Interferometry.
PB95-175022 03,955

Low-Frequency, Active Vibration Isolation System.
PB95-203303 02,710

Summary and Results of the NIST Workshop on Proposed Guidelines for Testing and Evaluation of Seismic Isolation Systems. Held in San Francisco, California on July 25, 1994.
PB96-154901 00,463

Guidelines for Pre-Qualification, Prototype and Quality Control Testing of Seismic Isolation Systems.
PB96-193685 01,347

VIBRATION MEASUREMENT

Electro-Optical Sensor for Surface Displacement Measurements of Compliant Coatings.
PB94-198223 02,123

Vibration Laboratory Automation at NIST with Personal Computers.
PB95-108700 02,648

VIBRATION TESTS

Dynamic Shear Modulus Measurements with Four Independent Techniques in Nickel-Based Alloys.
PB94-198900 03,320

VIBRATIONAL PREDISSOCIATION

Fragment State Correlations in the Dissociation of NO.HF(v=1).
PB95-164430 00,982

VIBRATIONAL SPECTRA

Vibrational Spectra of Molecular Ions Isolated in Solid Neon. 6. CO4(-). (Reannouncement with New Availability Information).
AD-A238 415/4 00,705

Vibrational Spectra of Molecular Ions Isolated in Solid Neon. 7. CO(+), C2O2(+), and C2O2(-). (Reannouncement with New Availability Information).
AD-A239 729/7 00,706

Vibrational Spectra of Molecular Ions Isolated in Solid Neon: HCCH+ and HCC-. (Reannouncement with New Availability Information).
AD-A253 551/6 00,707

Vibrational Spectra of Molecular Ions Isolated in Solid Neon. 11. NO2(+), NO2(-), and NO3(-).
AD-A275 828/2 00,708

Octacalcium Phosphate. 3. Infrared and Raman Vibrational Spectra.
PB94-172244 00,756

New Rydberg States of Aluminum Monofluoride Observed by Resonance-Enhanced Multiphoton Ionization Spectroscopy.
PB94-199544 00,797

Inelastic Neutron Scattering Studies of Nonlinear Optical Materials: p-Nitroaniline Adsorbed in ALPO-5.
PB95-107223 00,874

Vibrational Spectra of Molecular Ions Isolated in Solid Neon. X. H2O(+), HDO(+), and D2O(+).
PB95-125670 00,889

Vibrational Spectra of Molecular Ions Isolated in Solid Neon. XI. NO2(+), NO2(-), and NO3(-).
PB95-125688 00,890

Neutron Spectroscopic Comparison of Rare-Earth/Hydrogen alpha-Phase Systems.
PB95-163523 00,970

Vibrations of Hydrogen and Deuterium in Solid Solution with Lutetium.
PB95-181038 01,019

Vibrations of S1((1)B2u) p-Difluorobenzene - d4. S1-S0 Fluorescence Spectroscopy and ab Initio Calculations.
PB95-202586 01,028

Matrix Isolation Study of the Interaction of Excited Neon Atoms with BCl3: Infrared Spectra of BCl(sub 3, sup +), BCl(sub 2, sup +), and BCl(sub 3, sup -).
PB97-119143 01,187

Vibrational Spectra of Molecular Ions Isolated in Solid Neon. 13. Ions Derived from HBr and HI.
PB97-119234 01,188

VIBRATIONAL SPECTROSCOPY

Vibrational Excitations and the Position of Hydrogen in Nanocrystalline Palladium.
PB96-111828 04,035

Characterization of the Vibrational Dynamics in the Octahedral Sublattices of LaD2.25 and LaH2.25.
PB96-123724 01,091

VIBRATIONAL STATES

Electronic Spectra of CF2Cl and CFCl2 Radicals Observed by Resonance Enhanced Multiphoton Ionization.
PB95-151023 00,927

VIBRATIONS

q Dependence of Self-Energy Effects of the Plane Oxygen Vibration in YBa2Cu3O7.
PB96-138516 01,096

VIDEO COMMUNICATION

Videoconferencing Procurement and Usage Guide.
PB94-217023 01,470

VIDEO COMPRESSION

Nonlinear Color Transformations in Real Time Using a Video Supercomputer.
PB96-123021 02,191

VIDEO DATA

Report on the Workshop on Advanced Digital Video in the National Information Infrastructure. Held in Washington, D.C. on May 10-11, 1994.
PB95-103677 01,472

National Information Infrastructure and Advanced Digital Video.
PB96-119367 01,488

Summary Report on the Workshop on Advanced Digital Video in the National Information Infrastructure.
PB96-141320 01,497

VIDEO MICROSCOPE

Video Microscopy Applied to Optical Fiber Geometry Measurements.
PB95-173068 04,295

VIDEO RECORDING

Proposed International Interactive Courseware Standard.
PB96-123161 00,137

Development of an Economical Video Based Fire Detection and Location System.
PB96-193743 00,228

VILLAIN MODEL

Normal Modes and Structure Factor for a Canted Spin System: The Generalized Villain Model.
PB95-140067 04,539

VINYL COPOLYMERS

Piezoelectric and Pyroelectric Polymers.
PB95-153367 01,250

VINYL ETHER RESINS

Electron Beam Crosslinking of Poly(vinylmethyl ether).
PB94-185550 01,205

VINYL PLASTICS

Comparison of Fire Sprinkler Piping Materials: Steel, Copper, Chlorinated Polyvinyl Chloride and Polybutylene, in Residential and Light Hazard Installations.
PB95-182267 00,299

VINYL RADICAL

Deuterium Isotope Effect in Vinyl Radical Combination/ Dispropor tionationReactions.
PB96-204151 01,167

VINYL RADICALS

Reaction Rate Determinations of Vinyl Radical Reactions with Vinyl, Methyl, and Hydrogen Atoms.
PB94-211398 00,815

VINYL RESINS

Thermal Pulse Study of the Polarization Distributions Produced in Polyvinylidene Fluoride by Corona Poling at Constant Current.
PB94-172293 01,195

VIRIAL COEFFICIENTS

Estimating the Virial Coefficients of Small Polar Molecules.
PB95-176236 03,276

Thermodynamic Properties of Dilute and Semidilute Solutions of Regular Star Polymers.
PB96-146808 01,284

VIRIAL EQUATION

Measurements of the Virial Coefficients and Equation of State of the Carbon Dioxide + Ethane System in the Supercritical Region.
PB95-151353 03,906

VIRTUAL ENVIRONMENTS

Applying Virtual Environments to Manufacturing.
PB94-142502 02,803

VIRTUAL REALITY

Approaches Using Virtual Environments with Mosaic.
PB95-169108 01,599

Workshop on the Application of Virtual Reality to Manufacturing. Final Report. Held in Gaithersburg, Maryland on August 9, 1994.
PB95-173555 02,825

Virtual Environments for Health Care. A White Paper for the Advanced Technology Program (ATP), the National Institute of Standards and Technology.
PB96-147814 03,594

VISCOELASTICITY

Physics Required for Prediction of Long Term Performance of Polymers and Their Composites.
PB94-219243 03,146

VISCOMETERS

Hydrodynamic Similarity in an Oscillating-Body Viscometer.
PB96-122429 01,082

Greenspan Acoustic Viscometer for Gases.
PB96-204417 04,220

VISCOPLASTICITY

Non-Equilibrium Thermodynamic Theory of Viscoplastic Materials.
PB94-198868 04,467

VISCOSITY

Measurements of the Viscosities of Saturated and Compressed Fluid 1-chloro-1,2,2,2-tetrafluoroethane (R124) and Pentafluoroethane (R125) at Temperatures between 120 and 420 K.
PB94-199791 03,254

Prediction of Viscosity of Refrigerants and Refrigerant Mixtures.
PB94-212099 03,257

Flow of Microemulsions through Microscopic Pores.
PB95-140463 00,905

Two Phase Aqueous Extraction: Rheological Properties of Dextran, Polyethylene Glycol, Bovine Serum Albumin and Their Mixtures.
PB95-161998 00,676

Brownian Diffusion of Hard Spheres at Finite Concentrations.
PB95-164307 00,975

Measurements of the Viscosities of Saturated and Compressed Liquid 1,1,1,2-Tetrafluoroethane (R134a), 2,2-Dichloro-1,1,1-Trifluoroethane (R123) and 1,1-Dichloro-1-Fluoroethane (R141b).
PB95-175386 03,273

Non-Perturbative Relation between the Mutual Diffusion Coefficient, Suspension Viscosity, and Osmotic Compressibility: Application to Concentrated Protein Solutions.
PB96-102355 01,062

Viscosity of Ammonia.
PB96-145933 01,117

Viscosity of 1,1,1,2,3,3-Hexafluoropropane and 1,1,1,3,3,3-Hexafluoropropane at Saturated-Liquid Conditions from 262 K to 353 K.
PB96-176680 03,292

VISCOSITY PREDICTION

Viscosity of Defined and Undefined Hydrocarbon Liquids Calculated Using an Extended Corresponding-States Model.
PB96-167234 02,498

VISUAL DISCRIMINATION

Nonlinear Color Transformations in Real Time Using a Video Supercomputer.
PB96-123021 02,191

VISUAL LOOMING

New Method to Calculate Looming for Autonomous Obstacle Avoidance.
PB95-171435 01,600

VISUAL MEASUREMENT

Visual Measurement Technique for Analysis of Nucleate Flow Boiling.
PB95-143301 03,262

VISUAL PERCEPTION

Human and Machine Recognition of Faces: A Survey.
PB96-111687 01,854

VISUAL PURSUIT SYSTEMS

Visual Pursuit Systems.
PB95-143285 01,841

VITAMIN K

Determination of Vitamin K1 in Serum Using Catalytic-Reduction Liquid Chromatography with Fluorescence Detection.
PB96-138425 03,506

VITAMINS

Population Distributions and Intralaboratory Reproducibility for Fat-Soluble Vitamin-Related Compounds in Human Serum.
PB96-155536 00,624

VOICE COMMUNICATIONS

Telecommunications Security Guidelines for Telecommunications Management Network. Computer Security.
PB96-139415 01,496

VOID SHAPES

Void Shape in Sintered Titanium.
PB96-141023 02,705

VOIDS

Detection of Voids in Grouted Ducts Using the Impact-Echo Method.
PB94-185121 01,306

Ultrasonic Technique for Sizing Voids Using Area Functions.
PB95-151916 02,904

VOIGHT FUNCTION

Accurate Modeling of Size and Strain Broadening in the Rietveld Refinement: The 'Double-Voigt' Approach.
PB96-200225 00,664

VOIGHT FUNCTIONS

Voigt-Function Modeling in Fourier Analysis of Size- and Strain-Broadened X-Ray Diffraction Peaks.
PB94-198538 04,462

VOLATILE ORGANIC COMPOUNDS

Development of a Gas Standard Reference Material Containing Eighteen Volatile Organic Compounds.
PB95-162277 02,545

Stability of Compressed Gas Mixtures Containing Low Level Volatile Organic Compounds in Aluminum Cylinders.
PB96-111968 00,613

Issues in the Field Measurement of VOC Emission Rates.
PB97-118806 02,573

Radiocarbon Measurements of Atmospheric Volatile Organic Compounds: Quantifying the Biogenic Contribution.
PB97-122352 02,574

VOLATILITY

Volatile Corrosion Inhibitors.
AD-A310 087/2 03,114

VOLT

New International Representations of the Volt and Ohm Effective January 1, 1990.
PB95-150777 01,890

VOLTAGE
NIST Watt Experiment: Monitoring the Kilogram.
PB97-122329 *01,997*

VOLTAGE AMPLIFIERS
100 Ampere, 100 kHZ Transconductance Amplifier.
PB96-102629 *02,068*

100 A, 100 kHz Transconductance Amplifier.
PB96-200936 *02,098*

VOLTAGE CURRENT SIMULATION
Comparing the Accuracy of Critical-Current Measurements Using the Voltage-Current Simulator.
PB96-119219 *02,227*

VOLTAGE DIVIDERS
Automatic Inductive Voltage Divider Bridge Operates from 10 Hz to 100 kHz.
PB94-198413 *02,032*

Automatic Calibration of Inductive Voltage Dividers for the NASA Zeno Experiment.
PB95-152849 *02,041*

Inductive Voltage Divider Calibration for the NASA Flight Experiment.
PB95-152856 *02,042*

10 kV DC Resistive Divider Calibration.
PB95-198685 *02,063*

Binary versus Decade Inductive Voltage Divider Comparison and Error Decomposition.
PB96-112263 *02,071*

Active High Voltage Divider with 20-PPM Uncertainty.
PB97-119317 *02,104*

VOLTAGE MEASUREMENT
Voltage Ratio Measurements of a Zener Reference Using a Digital Voltmeter.
PB95-164695 *01,906*

Electro-Optic-Based RMS Voltage Measurement Technique.
PB96-138490 *02,194*

VOLTAGE MEASURING INSTRUMENTS
Performance of Commercial CMOS Foundry-Compatible Multijunction Thermal Converters.
PB95-153656 *02,342*

VOLTAGE REFERENCE
Noise Characteristics Below 1 Hz of Zener Diode-Based Voltage Reference.
PB96-123476 *04,049*

VOLTAGE REGULATIONS
Surging the Upside-Down House: Looking into Upsetting Reference Voltages.
PB96-112313 *02,385*

VOLTAGE STANDARDS
Design and Operation of Series-Array Josephson Voltage Standards.
PB94-185451 *02,030*

24 GHz Josephson Array Voltage Standard.
PB94-211588 *02,033*

New International Representations of the Volt and Ohm Effective January 1, 1990.
PB95-150777 *01,890*

Accuracy Comparisons of Josephson Array Systems.
PB95-164687 *02,047*

Josephson Voltage Standard Based on Single-Flux-Quantum Voltage Multipliers.
PB95-175600 *02,058*

Pulse-Driven Programmable Josephson Voltage Standard.
PB97-111496 *04,148*

Low Voltage Standards in the 10 Hz to 1 MHz Range.
PB97-112569 *02,100*

VOLTMETERS
Wideband Sampling Voltmeter.
PB97-113039 *01,990*

VOLUME
Torsional Dilatometer for Volume Change Measurements on Deformed Glasses: Instrument Description and Measurements on Equilibrated Glasses.
PB94-211166 *03,379*

Apparent Molar Heat Capacities and Apparent Molar Volumes of Aqueous Glucose at Temperatures from 298.15 K to 327.01 K.
PB94-212800 *03,459*

Glass Temperature of Polymer Blends: Comparison of Both the Free Volume and the Entropy Predictions with Data.
PB95-140190 *01,236*

VORONOI DIAGRAMS
Submissions to a Planned Encyclopedia of Operations Research on Computational Geometry and the Voronoi/Delaunay Construct.
PB94-152709 *03,425*

VORTEX
SSME LOX Duct Flowmeter Design and Test Results.
PB96-161955 *04,826*

VORTEX GENERATORS
Evolution of a Turbulent Boundary Layer Induced by a Three-Dimensional Roughness Element.
PB94-212818 *04,200*

VORTEX SHEDDING FLOWMETERS
Vortex Shedding Flowmeters for SSME Ducts.
PB95-169215 *01,453*

VORTEX TUBES
Applications of the Vortex Tube in Chemical Analysis.
PB94-199171 *00,544*

Applications of the Vortex Tube in Chemical Analysis. Part 2. Applications.
PB96-112107 *00,615*

VORTICES
Direct Observation of Vortex Dynamics in Two-Dimensional Josephson-Junction Arrays.
PB96-102223 *02,067*

Novel Vortex Dynamics in Two-Dimensional Josephson Arrays.
PB96-200167 *02,091*

VTS (VALIDATION TESTING SYSTEM)
Validation Testing System Requirements. National PDES Testbed Report Series.
PB94-163482 *02,771*

W317 LIQUID CRYSTAL
Studies of the Higher Order Smectic Phase of the Large Electroclinic Effect Material W317.
PB95-151601 *00,935*

WAFER BONDING
Thermal Isolation of High-Temperature Superconducting Thin Films Using Silicon Wafer Bonding and Micromachining.
PB96-135017 *02,408*

WAFER PROBE STATIONS
Verification of Commercial Probe-Tip Calibrations.
PB95-161576 *02,347*

Planar Resistors for Probe Station Calibration.
PB95-163697 *02,351*

Calibrating On-Wafer Probes to the Probe Tips.
PB95-163945 *02,352*

LRM Probe-Tip Calibrations with Imperfect Resistors and Lossy Lines.
PB95-163952 *02,353*

LRM Probe-Tip Calibrations Using Nonideal Standards.
PB96-135389 *02,411*

WAFERS
Water Adsorption at Polymer/Silicon Wafer Interfaces.
PB95-181178 *01,022*

Water Adsorption at a Polyimide/Silicon Wafer Interface.
PB96-103197 *01,070*

WAGES
Design and Development of an Information Retrieval System for the EAMATE Data. Volume 2 of 2. Appendices.
PB94-168390 *00,487*

WALL FIRES
Algorithm to Describe the Spread of a Wall Fire under a Ceiling.
PB95-182259 *00,261*

WALLBOARDS
Empirical Validation of a Transient Computer Model for Combined Heat and Moisture Transfer.
PB97-111991 *00,416*

WALLS
Analysis of Moisture Accumulation in a Wood-Frame Wall Subjected to Winter Climate.
PB94-199320 *00,338*

Upward Flame Spread along the Vertical Corner Walls (October 1993).
PB94-206299 *00,340*

Turbulent Upward Flame Spread on a Vertical Wall under External Radiation.
PB94-207388 *00,341*

Comparison of Wall-Fire Behavior With and Without a Ceiling.
PB94-207404 *00,342*

NIST Research Program on the Seismic Resistance of Partially-Grouted Masonry Shear Walls.
PB94-219052 *00,354*

Controlling Moisture in the Walls of Manufactured Housing.
PB95-105136 *00,355*

Wall Flame Heights with External Radiation.
PB95-163481 *00,380*

Fire-Plume-Generated Ceiling Jet Characteristics and Convective Heat Transfer to Ceiling and Wall Surfaces in a Two-Layer Fire Environment: Uniform Temperature Ceiling and Walls.
PB95-164711 *00,382*

Manufactured Housing Walls That Provide Satisfactory Moisture Performance in All Climates.
PB95-178885 *00,383*

Heat and Moisture Transfer in Wood-Based Wall Construction: Measured versus Predicted.
PB95-200655 *00,391*

Turbulent Flame Spread on Vertical Corner Walls.
PB96-114764 *01,403*

Heights of Wall-Fire Flames.
PB96-148192 *00,212*

Parametric Study of Wall Moisture Contents Using a Revised Variable Indoor Relative Humidity Version of the 'Moist' Transient Heat and Moisture Transfer Model.
PB97-122535 *00,419*

WARPING
Warping of Terrace Pavers at the U.S. Capitol Building.
PB96-193651 *00,411*

WASTE CONSUMPTION
Water Efficient Plumbing Fixtures through Standards and Test Methods.
PB95-125951 *00,248*

WASTE DISPOSAL
Recommendations for the Disposal of Carbon-14 Wastes.
AD-A279 133/3 *02,579*

Opportunities for Innovation: Pollution Prevention.
PB95-147146 *02,520*

WASTE RECYCLING
Opportunities for Innovation: Pollution Prevention.
PB95-147146 *02,520*

WASTE TREATMENT
Bioleaching of Cobalt from Smelter Wastes by 'Thiobacillus ferrooxidans'.
PB95-140968 *02,582*

WASTE UTILIZATION
Calculation of Higher Heating Values of Biomass Materials and Waste Components from Elemental Analyses.
PB94-199254 *02,474*

WASTES
Acrylonitrile-Butadiene-Styrene (ABS) Plastic Drain, Waste, and Vent Pipe and Fittings.
AD-A310 724/0 *00,327*

WATER
Structure of Glycine-Water H-Bonded Complexes.
PB94-198603 *00,789*

Journal of Research of the National Institute of Standards and Technology. March/April 1994. Volume 99, Number 2.
PB94-219219 *02,000*

Sealed Water Calorimeter for Measuring Absorbed Dose.
PB94-219227 *03,517*

Changes in the Redox State of Iridium Oxide Clusters and Their Relation to Catalytic Water Oxidation: Radiolytic and Electrochemical Studies.
PB95-107017 *00,864*

Metalloporphyrin Sensitized Photooxidation of Water to Oxygen on the Surface of Colloidal Iridium Oxides - Photochemical and Pulse Radiolytic Studies.
PB95-107082 *00,868*

Vibration, Rotation, and Parity Specific Predissociation Dynamics in Asymmetric OH Stretch Excited ArH2O: A Half Collision Study of Resonant V-V Energy Transfer in a Weakly Bound Complex.
PB95-107140 *00,872*

Mid- and Near-Infrared Spectra of Water and Water Dimer Isolated in Solid Neon.
PB95-125662 *00,888*

Vibrational Spectra of Molecular Ions Isolated in Solid Neon. X. H2O(+), HDO(+), and D2O(+).
PB95-125670 *00,889*

Formulation of the Refractive Index of Water and Steam.
PB95-140133 *00,900*

NIR-Spectroscopic Investigation of Water Sorption Characteristics of Dental Resins and Composites.
PB95-151171 *00,189*

Product State Correlations in the Reaction of O((1)D) and H2O in Bimolecular Collisions and in O3.H2O Clusters--Translation.
PB95-153011 *00,946*

Water Adsorption at Polymer/Silicon Wafer Interfaces.
PB95-181178 *01,022*

Reproducibility of the Temperature of the Ice Point in Routine Measurements.
PB95-255923 *04,015*

Comparison of a Fixed-Charge and a Polarizable Water Model.
PB96-111620 *01,072*

Measurements of the Relative Permittivity of Liquid Water at Frequencies in the Range of 0.1 to 10 kHz and at Temperatures between 273.1 and 373.2 K at Ambient Pressure.
PB96-119375 *01,078*

Static Dielectric Constant of Water and Steam.
PB96-123559 *01,090*

Database for the Static Dielectric Constant of Water and Steam.
PB96-145586 *01,103*

Standard Reference Data for the Thermal Conductivity of Water.
PB96-145875 *01,111*

Collection of Results for the SPC/E Water Model.
PB96-147889 *01,127*

WATER ANALYSIS
Bacterial Enumeration in Storage Water.
PB96-163647 *03,591*

WATER COMPLEXES
Slit-Jet Near-Infrared Spectroscopy and Internal Rotor Dynamics of the ArH2O van der Waals Complex: An Angular Potential-Energy Surface for Internal H2O Rotation.
PB95-202792 *01,033*

Photodissociation Dynamics in Quantum State-Selected Clusters: A Test of the One-Atom Cage Effect in Ar-H2O.
PB95-203121 *01,044*

WATER DIMERS
Microwave Spectra of van der Waals Complexes of Importance in Planetary Atmospheres.
PB95-150611 *00,919*

WATER DISTRIBUTION
NMR Characterization of Injection-Moulded Alumina Green Compacts. Part 2. T2-Weighted Proton Imaging.
PB96-201181 *01,165*

WATER EFFECTS
Development of a Method for Measuring Water-Stripping Resistance of Asphalt/Siliceous Aggregate Mixtures.
PB96-202296 *01,329*

WATER EROSION
Moisture and Water-Induced Crack Growth in Optical Materials.
PB95-153334 *04,267*

WATER HEATERS
Predicting the Energy Performance Ratings of a Family of Type I Combination Appliances.
PB95-105524 *02,504*

WATER IMMERSION
Molecular Orbital Study of Water Enhanced Crack Growth Process.
PB95-164067 *03,240*

WATER MIST
Water Mist Fire Suppression Workshop Summary.
PB95-161907 *02,853*

WATER POLLUTION CONTROL
In Situ Burning Oil Spill Workshop Proceedings. Held in Orlando, Florida on January 26-28, 1994.
PB95-104907 *02,583*

WATER POLLUTION DETECTION
Comparison of Methods for Gas Chromatographic Determination of PCBs and Chlorinated Pesticides in Marine Reference Materials.
PB95-140091 *02,584*

NIST Standard Reference Materials (SRMs) for Polychlorinated Biphenyl (PCB) Determinations and Their Applicability to Toxaphene Measurements.
PB95-140109 *02,585*

WATER POLLUTION EFFECTS
Certification of Standard Reference Material (SRM) 1941a, Organics in Marine Sediment.
PB96-123690 *02,593*

WATER POLLUTION EFFECTS (ANIMALS)
Current Activities Within the National Biomonitoring Specimen Bank.
PB94-172806 *02,516*

Development of Frozen Whale Blubber and Liver Reference Materials for the Measurement of Organic and Inorganic Contaminants.
PB95-151676 *00,587*

Determination of Inorganic Constituents in Marine Mammal Tissues.
PB95-152047 *00,589*

Alaska Marine Mammal Tissue Archival Project: Specimen Inventory.
PB95-171344 *02,589*

Relationship of Silver with Selenium and Mercury in the Liver of Two Species of Toothed Whales (Odontocetes).
PB96-167275 *02,596*

WATER RESISTANCE
Development of a Method for Measuring Water-Stripping Resistance of Asphalt/Siliceous Aggregate Mixtures.
PB96-197249 *01,348*

WATER STRUCTURE
Physical Limit to the Stability of Superheated and Stretched Water.
PB96-122551 *01,083*

WATER TEMPERATURE
Lake Erie Water Temperature Data, Put-in-Bay, Ohio, 1918-1992.
PB96-202452 *03,692*

WATER TRIPLE POINT CELLS
Investigation of the ITS-90 Subrange Inconsistencies for 25.5 Omega SPRTs.
PB96-161302 *00,630*

WATER VAPOR
Formulation of the Refractive Index of Water and Steam.
PB95-140133 *00,900*

Slant Path Atmospheric Refraction Calibrator: An Instrument to Measure the Microwave Propagation Delays Induced by Atmospheric Water Vapor.
PB95-151270 *01,476*

WATERPROOFING
Performance Approach to the Development of Criteria for Low-Sloped Roof Membranes.
PB94-160751 *00,329*

WATT BALANCE METHOD
Measurement and Reduction of Alignment Errors of the NIST Watt Experiment.
PB97-111959 *01,987*

WATT MEASUREMENT
Methods for Aligning the NIST Watt-Balance.
PB96-123153 *01,934*

NIST Watt Balance: Progress Toward Monitoring the Kilogram.
PB97-113062 *01,991*

WATTMETERS
NIST High-Accuracy Sampling Wattmeter.
PB97-108575 *02,689*

DC-MHz Wattmeter Based on RMS Voltage Measurements.
PB97-113211 *01,992*

WAVE DIFFRACTION
Vector Theory of Diffraction by a Single-Mode Fiber: Application to Mode-Field Diameter Measurements.
PB95-164182 *04,279*

WAVE EQUATIONS
Approximate Solution to the Scalar Wave Equation for Optical Waveguides.
PB95-126256 *04,254*

WAVE PROPAGATION
Interaction of Rayleigh Waves with a Rib Attached to a Plate.
PB94-199023 *04,184*

Hemispherical Test Fixture for Measuring the Wavefields Generated in an Anisotropic Solid.
PB96-190087 *03,181*

WAVE SPECTRUMS
Millimeter- and Submillimeter-Wave Spectrum of trans-Ethyl Alcohol.
PB96-145578 *01,102*

WAVEFORM RECONSTRUCTION
Casual Regularizing Deconvolution Filter for Optimal Waveform Reconstruction.
PB95-203089 *01,603*

WAVEFORMS
Approach to Setting Performance Requirements for Automated Evaluation of the Parameters of High-Voltage Impulses.
PB94-185634 *01,878*

Influence of the Filament Potential Wave Form on the Sensitivity of Glass-Envelope Bayard-Alpert Gages.
PB95-175014 *02,657*

WAVEGUIDE BENDS
Modal Characteristics of Bent Dual Mode Planar Optical Waveguide.
PB95-180485 *04,311*

WAVEGUIDE JUNCTIONS
Reciprocity Relations in Waveguide Junctions.
PB94-172814 *02,213*

WAVEGUIDE LASERS
Rare-Earth-Doped Waveguide Devices: The Potential for Compact Blue-Green Lasers.
PB95-140836 *04,257*

Linewidth Narrowing in an Imbalanced Y-Branch Waveguide Laser.
PB95-140844 *04,258*

Nd:LiTaO3 Waveguide Laser.
PB95-140851 *04,259*

Passively Q-Switched Nd-Doped Waveguide Laser.
PB95-180048 *04,308*

WAVEGUIDE POLARIZERS
Waveguide Polarizers Processed by Localized Plasma Etching.
PB95-169264 *02,171*

WAVEGUIDES
Microwave Properties of Voltage-Tunable YBa2Cu3O7-delta/SrTiO3 Coplanar Waveguide Transmission Lines.
PB96-141262 *02,235*

Micromachined Coplanar Waveguides in CMOS Technology.
PB97-119283 *02,456*

WAVELENGTH STANDARDS
Frequency Stabilization of a Fiber Laser to Rubidium: A High-Accuracy 1.53 mu m Wavelength Standard.
PB95-126082 *04,252*

WAVELENGTHS
Wavelength Dependence of Normal Spectral Emissivity of High-Temperature Metals at Their Melting Point.
PB94-200011 *03,398*

Improved Wavelengths for Prominent Lines of Fe XX to Fe XXIII.
PB96-111638 *04,334*

Wavelengths of Spectral Lines in Mercury Pencil Lamps.
PB96-176474 *04,376*

WAVELET ANALYSIS
Wavelet Analysis for Synchronization and Timekeeping.
PB96-200381 *01,558*

WAVES
Leady Axisymmetric Modes in Infinite Clad Rods. Part 1.
PB95-162905 *04,187*

Wavelet Variance, Allan Variance, and Leakage.
PB96-190111 *01,509*

WEAK LOCALIZATION
Measurement of the Weak-Localization Complex Conductivity at 1 Ghz in Disordered Ag Wires.
PB96-117239 *04,731*

WEAPON SYSTEMS
U.S. Navy Coordinate Measuring Machines: A Study of Needs.
PB94-162831 *02,807*

WEAPONS SYSTEM
CALS-Department of Defense Computer Aided Acquisition Logistic Support (CALS).
PB94-962500 *03,662*

CALS-Department of Defense Computer Aided Acquisition Logistic Support (CALS).
PB95-962500 *03,671*

WEAR
Mechanism of Mild to Severe Wear Transition in Alpha-Alumina.
PB94-212354 *03,233*

Asperity-Asperity Contact Mechanisms Simulated by a Two-Ball Collision Apparatus.
PB95-164158 *02,966*

Friction and Oxidative Wear of 440C Ball Bearing Steels Under High Load and Extreme Bulk Temperatures.
PB95-175253 *03,215*

Wear Mechanism Maps of 440C Martensitic Stainless Steel.
PB96-111810 *04,834*

Wear of Enamel against Glass-Ceramic, Porcelain, and Amalgam.
PB96-179593 *03,082*

Chip Morphology, Tool Wear and Cutting Mechanics in Finish Hard Turning.
PB97-112247 *03,106*

Chemical Aspects of Tool Wear in Single Point Diamond Turning.
PB97-112601 *03,021*

WEAR MECHANICS
Wear Modeling of Si-Based Ceramics.
PB97-122501 *03,112*

WEAR RESISTANCE
Control of Friction and Wear of Alpha-Alumina with a Composite Solid-Lubricant Coating.
PB95-125969 *03,225*

New Alloys Show Extraordinary Resistance to Fracture and Wear.
PB95-151346 *03,346*

Evaluation of Wear Resistant Ceramic Valve Seats in Gas-Fueled Power Generation Engines. Topical Report, December 1991-April 1994.
PB95-200218 *02,466*

WEAR SCARS
Measuring Matching Wear Scars on Balls and Flats.
PB95-151528 *03,153*

WEAR TESTS
Wear Mechanism Maps of Ceramics.
PB94-172368 *03,229*

Fracture Mechanics Analysis of Near-Surface Cracks.
PB94-172400 *03,230*

Wear of Selected Materials and Composites Sliding against MoS2 Films.
PB94-172749 *03,231*

Effect of Microstructure on the Wear Transition of Zirconia-Toughened Alumina.
PB94-211778 *03,141*

Abrasive Wear by Diesel Engine Coal-Fuel and Related Particles.
PB95-104915 *01,450*

Critical Factors in Non-Lubricated, Non-Abrasive Wear Testing.
PB95-140588 *03,236*

Measuring Matching Wear Scars on Balls and Flats.
PB95-151528 *03,153*

Wear of Human Enamel against a Commercial Castable Ceramic Restorative Material.
PB95-161972 *00,161*

Introduction to ASTM 1199 'Wear Test Selection for Design and Application'.
PB95-162517 *03,238*

Wear Model for Alumina Sliding Wear.
PB95-163796 *03,239*

Tribometer for Measurements in Hostile Environments.
PB95-180949 *02,967*

Silicon Nitride Boundary Lubrication: Lubrication Mechanism of Alcohols.
PB96-111703 *03,067*

Silicon Nitride Boundary Lubrication: Effect of Oxygenates.
PB96-111711 *03,068*

Mechano-Chemical Model: Reaction Temperatures in a Concentrated Contact.
PB96-119466 *03,227*

Contact Tube Wear Detection in Gas Metal Arc Welding.
PB96-135330 *02,872*

WEATHERING
Weatherability of Plastic Materials.
AD-A301 675/5 *02,968*

WEATHERPROOFING
Weatherability of Plastic Materials.
AD-A301 675/5 *02,968*

WEIBULL MODULUS
Correlations between Flaw Tolerance and Reliability in Zirconia.
PB96-161922 *02,986*

WEIGHT
Precision Laboratory Standards of Mass and Laboratory Weights.
AD-A280 562/0 *02,618*

WEIGHT INDICATORS
Application of the Electronic Balance in High Precision Pycnometry.
PB94-187564 *00,534*

Ensuring Accuracy and Traceability of Weighing Instruments.
PB94-211687 *02,638*

WEIGHT MEASUREMENT
NIST Handbook 44, 1994: Specifications, Tolerances and Other Technical Requirements for Weighing and Measuring Devices as Adopted by the 78th National Conference on Weights and Measures 1993.
PB94-136009 *02,888*

Report of the National Conference on Weight and Measures (78th). Held in Kansas City, MO. on July 18-22, 1993.
PB94-138989 *02,623*

NIST Handbook 44, 1995: Specifications, Tolerances and Other Technical Requirements for Weighing and Measuring Devices as Adopted by the 79th National Conference on Weights and Measures 1994.
PB95-146379 *02,903*

Report of the National Conference on Weights and Measures (79th). Held in San Diego, California on July 17-21, 1994.
PB95-169819 *02,656*

Uniform Laws and Regulations in the Areas of Legal Metrology and Motor Fuel Quality, 1994 as Adopted by the 79th National Conference on Weights and Measures 1994.
PB95-174470 *02,909*

Report of the National Conference on Weights and Measures (80th) as Adopted by the 80th National Conference on Weights and Measures, 1995. Held in Portland, Maine on July 16-20, 1995.
PB96-165840 *02,681*

NIST Handbook 44, 1996: Specifications, Tolerances, and Other Technical Requirements for Weighing and Measuring Devices as Adopted by the 80th National Conference on Weights and Measures, 1995.
PB96-166616 *02,926*

Uniform Laws and Regulations in the Areas of Legal Metrology and Motor Fuel Quality as Adopted by the 80th National Conference on Weights and Measures 1995. 1996 Edition.
PB96-172309 *02,927*

Examination Procedure Outlines: Keys to Solving the Handbook 44 Puzzle.
PB97-110217 *02,690*

WEIGHTLESSNESS SIMULATION
Measurement of Surface Tension of Tantalum by a Dynamic Technique in a Microgravity Environment.
PB95-161667 *03,932*

WEIGHTS AND MEASURES
Federal Basis for Weights and Measures: A Historical Review of Federal Legislative Effort, Statutes, and Administrative Action in the Field of Weights and Measures in the United States.
AD-A280 086/0 *02,616*

State Weights and Measures Laboratories: State Standards Program Description and Directory. 1994 Edition.
PB94-207727 *02,895*

WEISSENBERG EFFECT
Density Dependence of Fluid Properties and Non-Newtonian Flows: The Weisenberg Effect.
PB96-161898 *01,140*

WELD METAL
Effects of Copper, Nickel and Boron on Mechanical Properties of Low-Alloy Steel Weld Metals Deposited at High Heat Input.
PB96-135231 *03,363*

WELD TESTS
IIW Commission V Quality Control and Quality Assurance of Welded Products Annual Report 1994/95.
PB95-198743 *02,866*

WELDED JOINTS
Cryogenic Toughness of Austenitic Stainless Steel Weld Metals: Effect of Inclusions.
PB95-161261 *03,214*

X-Ray Image Quality Indicator Designed for Easy Alignment.
PB95-164455 *02,907*

IIW Commission V Quality Control and Quality Assurance of Welded Products Annual Report 1994/95.
PB95-198743 *02,866*

WELDED STEEL TANKS
Ashland Tank Collapse Investigation.
PB95-126314 *02,481*

Ashland Tank-Collapse Investigation: Closure by Authors.
PB95-126322 *02,482*

WELDING
Characterization of the Hydrogen Induced Cold Cracking Susceptibility at Simulated Weld Zones in HSLA-100 Steel.
AD-A279 759/5 *03,200*

Characterization of the Hydrogen Induced Cold Cracking Susceptibility at Simulated Weld Zones in HSLA-100 Steel.
PB94-174505 *03,746*

International Institute of Welding: Report on 1992 Actions.
PB94-185873 *02,856*

International Institute of Welding: Report on 1993 Actions.
PB94-185881 *02,857*

Computers in Welding: A Primer.
PB95-162863 *02,862*

Welding for Cryogenic Service.
PB95-162889 *02,852*

In-Space Welding: Visions and Realities.
PB95-163234 *04,830*

Mathematical Models of Transport Phenomena Associated with Arc-Welding Processes: A Survey.
PB96-135058 *02,870*

Electrode Extension Model for Gas Metal Arc Welding.
PB96-135074 *02,871*

Report on 1994 Actions of the International Institute of Welding.
PB96-138540 *02,873*

International Institute of Welding: Report on 1995 Actions.
PB96-158076 *02,874*

What's Available in Welding Software.
PB96-158084 *02,875*

Proceedings of NIST Workshop: Industry Needs in Welding Research and Standards Development. Held on August 15-16, 1995.
PB96-183124 *02,877*

Well-Shielded EMAT for On-Line Ultrasonic Monitoring of GMA Welding.
PB96-186077 *02,879*

IIW Commission V Quality Control and Quality Assurance of Welded Products, Annual Report 1995/96.
PB96-191366 *02,880*

WELDING CURRENT
Contact Tube Wear Detection in Gas Metal Arc Welding.
PB96-135330 *02,872*

WELDING ELECTRODES
Droplet Transfer Modes for a MIL 100S-1 GMAW Electrode.
PB95-209300 *02,867*

WELL FIRES
Investigation of Oil and Gas Well Fires and Flares.
PB94-193976 *03,695*

WELL FLARES
Investigation of Oil and Gas Well Fires and Flares.
PB94-193976 *03,695*

WHALES
Development of Frozen Whale Blubber and Liver Reference Materials for the Measurement of Organic and Inorganic Contaminants.
PB95-151676 *00,587*

Certification of Polychlorinated Biphenyl Congeners and Chlorinated Pesticides in a Whale Blubber Standard Reference Material.
PB96-103023 *03,745*

WHEELS
Ultrasonic Measurement of Residual Stress in Railroad Wheel Rims.
PB95-140430 *04,849*

Ultrasonic Measurement of Residual Stress in Cast Steel Railroad Wheels.
PB95-169199 *04,852*

Residual Stress in Induction-Heated Railroad Wheels: Ultrasonic and Saw Cut Measurements. Report No. 28.
PB96-106992 *04,854*

Safety Assessment of Railroad Wheels by Residual Stress Measurements.
PB96-141114 *04,855*

Safety Assessment of Railroad Wheels Through Roll-by Detection of Tread Cracks.
PB96-141254 *04,856*

Dynamometer-Induced Residual Stress in Railroad Wheels: Ultrasonic and Saw Cut Measurements. Report No. 30.
PB96-183199 *04,857*

WHISKER COMPOSITES
Matrix Grain Bridging Contribution to the Toughness of Whisker Reinforced Ceramics.
PB94-198645 *03,134*

Tensile Creep of Whisker Reinforced Silicon Nitride.
PB94-211984 *03,142*

Flat and Rising R-Curves for Elliptical Surface Cracks from Indentation and Superposed Flexure.
PB95-161295 *03,156*

WIDE AREA NETWORKS
Comparison of FDDI Asynchronous Mode and DQDB Queue Arbitrated Mode Data Transmission for Metropolitan Area Network Applications.
PB96-160452 *01,498*

WIDEBAND
Wideband Sampling Voltmeter.
PB97-113039 *01,990*

WIGGLER MAGNETS
Hybrid Undulator for the NIST-NRL Free-Electron Laser.
PB94-212529 *04,238*

WIND DIRECTION
Computational Model for the Rise and Dispersion of Wind-Blown, Buoyancy-Driven Plumes. Part 2. Linearly Stratified Atmosphere.
PB94-143427 *00,119*

WIND EFFECTS
Wind and Seismic Effects. Proceedings of the U.S.-Japan Cooperative Program in Natural Resources Panel on Wind and Seismic Effects (26th). Held in Gaithersburg, Maryland on May 17-20, 1994.
PB95-147385 *00,433*

Assessment of 'Peaks Over Threshold' Methods for Estimating Extreme Value Distribution Tails.
PB95-161360 *00,441*

Proceedings: Workshop on Research Needs in Wind Engineering. Held in Gaithersburg, Maryland on September 12-13, 1994.
PB95-189528 *00,448*

Recommended Performance-Based Criteria for the Design of Manufactured Home Foundation Systems to Resist Wind and Seismic Loads.
PB96-128285 *00,460*

Wind and Seismic Effects: Proceedings of the Joint Meeting of the U.S.-Japan Cooperative Program in Natural Resources Panel on Wind and Seismic Effects (28th). Held in Gaithersburg, Maryland on May 14-17, 1996.
PB97-104376 *00,476*

WIND LOADS
Wind Load Provisions of the Manufactured Home Construction and Safety Standards: A Review and Recommendations for Improvement.
PB94-206125 *00,428*

Manufactured Homes: Probability of Failure and the Need for Better Windstorm Protection through Improved Anchoring Systems.
PB95-143129 *00,432*

Gust Factors Applied to Hurricane Winds.
PB95-180469 *00,446*

Extreme Winds Estimation by 'Peaks Over Threshold' and Epochal Methods.
PB96-159686 *00,468*

Modeling of Extreme Loading by 'Peaks Over Threshold' Methods.
PB96-159694 *00,469*

WIND PRESSURE
Recent Approaches to Extreme Value Estimation with Application to Wind Speeds. Part 1. The Pickands Method.
PB94-213170 *00,019*

Lessons Learned by a Wing Engineer.
PB94-216421 *00,429*

Proceedings: Workshop on Research Needs in Wind Engineering. Held in Gaithersburg, Maryland on September 12-13, 1994.
PB95-189528 *00,448*

WIND TUNNELS
Measurement of the Uniformity of Particle Deposition of Filter Cassette Sampling in a Low Velocity Wind Tunnel.
PB95-163754 *02,549*

WIND VELOCITY
Recent Approaches to Extreme Value Estimation with Application to Wind Speeds. Part 1. The Pickands Method.
PB94-213170 *00,019*

Extreme Wind Distribution Tails: A 'Peaks Over Threshold' Approach.
PB95-219416 *00,127*

Extreme Wind Estimates by the Conditional Mean Exceedance Procedure.
PB95-220471 *00,120*

Some Notable Hurricanes Revisited.
PB96-122601 *00,458*

Estimates of Hurricane Wind Speeds by the 'Peaks Over Threshold' Method.
PB96-162540 *00,471*

Probabilistic Estimates of Design Load Factors for Wind-Sensitive Structures Using the 'Peaks Over Threshold' Approach.
PB96-183223 *00,474*

WINDOW FUNCTIONS
Windowing Effects on Light Scattering by Sinusoidal Surfaces.
PB97-111215 *04,389*

WINDOWING
User Interface Component of the Applications Portability Profile Category: Software Standard; Subcategory: Application Program Interface.
FIPS PUB 158-1 *01,793*

WINDOWS
Fire Induced Thermal Fields in Window Glass I: Theory.
PB94-139722 *00,328*

Optical Performance of Commercial Windows.
PB95-208757 *00,392*

WIRE
Simple and Repeatable Technique for Measuring the Critical Current of Nb3Sn Wires.
PB96-119409 *02,229*

WIRE BONDING
Bonding Wires to Quantized Hall Resistors.
PB96-102637 *01,921*

Wire Bonding to Multichip Modules and Other Soft Substrates.
PB96-123583 *02,079*

Wire Bonding to Multichip Modules and Other Soft Substrates.
PB96-135207 *02,082*

WIRE BONDS
Wire Bond Testing.
PB94-211653 *02,314*

WIREWOUND RESISTORS
Precision Resistors and Their Measurement.
AD-A284 623/6 *02,249*

WOLF SHIFTS
Comments on the Paper 'Wolf Shifts and Their Physical Interpretation under Laboratory Conditions'.
PB94-219391 *04,246*

Reply to Professor Wolf's Comments on My Paper on Wolf Shifts.
PB94-219409 *04,247*

WOOD
Rate of Heat Release of Wood Products.
PB94-212404 *03,403*

Examination of Objects Made of Wood Using Air-Coupled Ultrasound.
PB95-125712 *03,404*

Heat and Moisture Transfer in Wood-Based Wall Construction: Measured versus Predicted.
PB95-200655 *00,391*

WOOD BURNING APPLIANCES
Measurements of Indoor Pollutant Emissions from EPA Phase II Wood Stoves.
PB95-198735 *02,556*

WOOD PRODUCTS
Analysis of Moisture Accumulation in a Wood-Frame Wall Subjected to Winter Climate.
PB94-199320 *00,338*

National Voluntary Laboratory Accreditation Program (NVLAP): Wood Based Products.
PB95-170429 *03,405*

WORD RECOGNITION
Unconstrained Handprint Recognition Using a Limited Lexicon.
PB94-168051 *01,831*

WORK ENVIRONMENTS
Post-Occupancy Evaluation of the Forrestal Building.
PB97-111298 *00,280*

WORKING FLUIDS
Development of Measurement Capabilities for the Thermophysical Properties of Energy-Related Fluids. Annual Report, December 1, 1990--November 30, 1991.
DE94004399 *02,470*

Role of Refrigerant Mixtures as Alternatives to CFCs.
PB94-199775 *03,252*

Study of Heat Pump Performance Using Mixtures of R32/R134a and R32/R125/R134a as 'Drop-In' Working Fluids for R22 with and Without a Liquid-Suction Heat Exchanger.
PB94-218559 *02,503*

Resistance Thermometers with Fast Response for Use in Rapidly Oscillating Gas Flows.
PB95-107298 *03,261*

Need for, and Availability of, Working Fluid Property Data: Results from Annexes XIII and XVIII.
PB95-168969 *03,268*

WORKPLACE LAYOUT
Psychological Aspects of Lighting: A Review of the Work of CIE TC 3.16.
PB95-153276 *00,254*

WORKSHOPS
NIST SIMA Interactive Management Workshop. Held in Fort Belvoir, Virginia on November 14-16, 1994.
PB96-154877 *02,838*

WORKSTATIONS
AMRF Composite Fabrication Workstation.
PB94-172681 *02,810*

Portsmouth Fastener Manufacturing Workstation. User's Manual.
PB95-147922 *02,860*

WORLD MODELS
World Model Registration for Effective Off-Line Programming of Robots.
PB94-173010 *02,933*

Role of World Modeling and Value Judgment in Perception.
PB94-198264 *01,581*

WORLD WIDE WEB
World Wide Web and Mosaic: User's Guide.
PB94-207354 *02,722*

WOVEN COMPOSITES
Comparison of the Unidirectional and Radial In-Plane Flow of Fluids Through Woven Composite Reinforcements.
PB95-162004 *02,698*

WWW (WORLD WIDE WEB)
World Wide Web and Mosaic: User's Guide.
PB94-207354 *02,722*

X BAND
High Spectral Purity X-Band Source.
PB95-163713 *02,045*

X RAY
Flat and Curved Crystal Spectrography for Mammographic X-ray Sources.
PB97-122246 *03,642*

X-RAY ABSORPTION ANALYSIS
X-Ray Attenuation Coefficients from 10 KEV to 100 MEV.
AD-A280 290/8 *03,768*

X-RAY ANALYSIS
Design of a Protocol for an Electron Probe Microanalyzer k-Value Round Robin.
PB95-107181 *00,564*

Monte Carlo Electron Trajectory Simulation of X-Ray Emission from Films Supported on Substrates.
PB95-107207 *04,522*

Secondary Target X-Ray Excitation for In vivo Measurement of Lead in Bone.
PB95-108767 *03,496*

X-RAY ANLAYSIS
Electron Probe X-Ray Microanalysis.
PB95-107165 *00,562*

X RAY ASTRONOMY
Riass Coronathon: Joint X-ray and Ultraviolet Observations of Normal F-K Stars.
PB96-200217 *00,109*

X RAY DENSITY MEASUREMENT
Novel Method for Determining Thin Film Density by Energy-Dispersive X-ray Reflectivity.
PB96-122783 *04,737*

X-RAY DETECTION
Silicon Photodiodes Optimized for EUV and Soft X-Ray Regions.
PB94-199478 *02,124*

X RAY DETECTORS
Hot-Electron Microcalorimeters for X-ray and Phonon Detection.
PB95-168993 *04,644*

Hot-Electron Microcalorimeters as High-Resolution X-ray Detectors.
PB96-123641 *04,739*

Hot-Electron Microcalorimeter for X-ray Detection Using a Superconducting Transition Edge Sensor with Electrothermal Feedback.
PB96-200399 *04,792*

Hot-Electron-Microcalorimeters with 0.25 mm(2) Area.
PB96-200670 *04,793*

X-RAY DIFFRACTION
Profile Fitting of X-Ray Diffraction Lines and Fourier Analysis of Broadening.
PB94-198512 *04,460*

Voigt-Function Modeling in Fourier Analysis of Size- and Strain-Broadened X-Ray Diffraction Peaks.
PB94-198538 *04,462*

Diffraction Imaging of Polycrystalline Materials.
PB94-198884 *02,971*

Diffraction of X-rays at the Far Tails of the Bragg Peaks.
PB94-199924 *04,476*

Introduction of a NIST Instrument Sensitivity Standard Reference Material for X-Ray Powder Diffraction.
PB94-200318 *00,807*

X-Ray Powder Diffraction Data for BaCu(C2O4)2.6H2O.
PB95-151767 *04,583*

Residual Stresses in Aluminum-Mullite (alpha-Alumina) Composites.
PB95-152880 *03,155*

Determination of the Residual Stresses Near the Ends of Skip Welds Using Neutron Diffraction and X-ray Diffraction Procedures.
PB95-253589 *02,868*

Crystal Structure of a New Monoclinic Form of Potassium Dihydrogen Phosphate Containing Orthophosphacidium Ion, (H4PO4)(sup+1).
PB96-111794 *04,725*

Coexistence of Grains with Differing Orthorhombicity in High Quality YBa2Cu3O7-delta Thin Films.
PB96-135033 *04,742*

Powder X-ray Diffraction Data for Ca2Bi2O5 and C4Bi6O13.
PB96-161278 *04,777*

Preparation and Crystal Structure of Sr5TiNb4O17.
PB96-167341 *04,107*

Accurate Modeling of Size and Strain Broadening in the Rietveld Refinement: The 'Double-Voigt' Approach.
PB96-200225 *00,664*

Biological Macromolecule Crystallization Database and NASA Protein Crystal Growth Archive.
PB97-109136 *01,171*

X-RAY DIFFRACTOMETERS
Using NIST Crystal Data within Siemens Software for Four-Circle and SMART CCD Diffractometers.
PB97-109110 *04,803*

X RAY DIFFRACTOMETRY
Interface Roughness, Composition, and Alloying of Low-Order AlAs/GaAs Superlattices Studies by X-ray Diffraction.
PB96-160262 *02,983*

X-RAY EMISSION
Resonance and Threshold Effects in Polarized X-Ray Emission from Atoms and Molecules.
PB95-150298 *03,891*

X-ray Emission from Chemically Peculiar Stars.
PB96-102256 *00,088*

Al L2,3 Core Excitons in AlxGa1-x as Studied by Soft-X-ray Reflection and Emission.
PB96-157839 *04,067*

X RAY EMISSIONS
Soft-X-ray-Emission Investigation of Cobalt Implanted Silicon Crystals.
PB96-157912 *04,069*

Soft-X-ray-Emission Spectra of Solid Kr and Xe.
PB96-157920 *04,070*

Soft-X-ray-Emission Studies of Bulk Fe3Si, FeSi, and FeSi2, and Implanted Iron Silicides.
PB96-157938 *04,071*

X-RAY FLUORESCENCE
Polarized X-Ray Emission Spectroscopy.
PB94-213360 *03,862*

Apparent Bias in the X-Ray Fluorescence Determination of Titanium in Selected NIST SRM Low Alloy Steels.
PB95-108759 *03,212*

Image Information Transfer Properties of X-Ray Intensifying Screens in the Energy Range from 17 to 320 keV.
PB95-126173 *00,155*

Aging Effects on XRF Measurements of Solder Coatings.
PB95-140927 *03,123*

Evolution of X-ray Resonance Raman Scattering into X-ray Fluorescence from the Excitation of Xenon Near the L3 Edge.
PB96-102751 *04,025*

Cooper M(sub II,III) X-ray-Emission Spectra of Copper Oxides and the Bismuth Cuprate Superconductor.
PB96-158027 *04,077*

X-RAY FLUORESCENCE ANALYSIS
Addition of M and L-Series Lines to NIST Algorithm for Calculation of X-Ray Tube Output Spectral Distributions.
PB95-108742 *00,569*

Pattern-Recognition Analysis of Low-Resolution X-Ray Fluorescence Spectra.
PB95-151924 *00,588*

X-RAY IMAGERY
Materials Science with SR Using X-Ray Imaging: Spatial-Resolution/Source Size.
PB94-213048 *04,510*

X-Ray Image Quality Indicator Designed for Easy Alignment.
PB95-164455 *02,907*

X-RAY INSPECTION
Evaluation and Qualification Standards for an X-Ray Laminography System.
PB94-172954 *02,029*

X-Ray Image Quality Indicator Designed for Easy Alignment.
PB95-164455 *02,907*

Contributions of Out-of-Plane Material to a Scanned-Beam Laminography Image.
PB96-111786 *02,704*

X-RAY LAMINOGRAPHY
Evaluation and Qualification Standards for an X-Ray Laminography System.
PB94-172954 *02,029*

Contributions of Out-of-Plane Material to a Scanned-Beam Laminography Image.
PB96-111786 *02,704*

X RAY LITHOGRAPHY
X-ray Mask Metrology: The Development of Linewidth Standards for X-ray Lithography.
PB95-162129 *02,348*

Use of Monte Carlo Modeling for Interpreting Scanning Electron Microscope Linewidth Measurements.
PB96-137807 *02,413*

X RAY MASKS
X-ray Mask Metrology: The Development of Linewidth Standards for X-ray Lithography.
PB95-162129 *02,348*

X-RAY MICROSCOPES
High Resolution Hard X-Ray Microscope.
PB94-213055 *03,856*

X RAY MICROTOMOGRAPHY
Transport and Diffusion in Three-Dimensional Composite Media.
PB95-176129 *04,668*

X-RAY MONOCHROMATORS
Effect of a Crystal Monochromator on the Local Angular Divergence of an X-Ray Beam.
PB95-150306 *04,565*

X-RAY OPTICS
Design and Characterization of X-Ray Multilayer Analyzers for the 50 - 1000 eV Region.
PB94-211851 *03,848*

Effect of a Crystal Monochromator on the Local Angular Divergence of an X-Ray Beam.
PB95-150306 *04,565*

Production and Characterization of Ion Beam Sputtered Multilayers.
PB95-162053 *03,936*

NIST Metrology for Soft X-ray Multilayer Optics.
PB96-160379 *04,088*

X RAY PHOTOELECTRON SPECTROSCOPY
Inelastic Interactions of Electrons with Surfaces: Application to Auger-Electron Spectroscopy and X-ray Photoelectron Spectroscopy.
PB94-172699 *00,764*

Grazing-Incidence X-Ray Photoelectron Spectroscopy: A Novel Approach to Thin Film Characterization.
PB95-153128 *04,589*

Grazing Angle X-Ray Photoemission System for Depth-Dependent Analysis.
PB95-161154 *04,600*

Elastic-Electron-Scattering Effects on Angular Distributions in X-ray Photoelectron Spectroscopy.
PB95-175758 *01,000*

Grazing Incidence X-ray Photoemission and Its Implementation on Synchrotron Light Source X-ray Beamlines.
PB95-175766 *01,001*

X-ray Photoelectron and Auger Electron Forward Scattering: A Structural Diagnostic for Epitaxial Thin Films.
PB95-180220 *04,676*

X-RAY POWDER DIFFRACTION

Powder Diffraction File: Past, Present, and Future.
PB97-109086 *04,800*

X RAY REFLECTIVITY

X-ray Reflectivity Determination of Interface Roughness Correlated with Transport Properties of (AlGa)As/GaAs High Electron Mobility Transistor Devices.
PB97-111868 *04,149*

X RAY SCATTERING

Evolution of the Pore Size Distribution in Final-Stage Sintering of Alumina Measured by Small-Angle X-ray Scattering. (Reannouncement with New Availability Information).
AD-A249 178/5 *03,023*

Further Calculations of X-ray Diffusion in an Infinite Medium.
AD-A295 314/9 *03,772*

Small-Angle X-Ray and Neutron Scattering Study of Block Copolymer/Homopolymer Mixtures.
PB94-211729 *01,221*

Polarization Effects on Multiple Scattering Gamma Transport.
PB95-153615 *03,926*

Molecular Weight Dependence of the Lamellar Domain Spacing of ABC Triblock Copolymers and Their Chain Conformation in Lamellar Domains.
PB95-161691 *01,254*

Real-Time Small-Angle X-Ray Scattering Study of the Early Stage of Phase Separation in the SiO2-BaO-K20 System.
PB95-163069 *03,052*

Characterization of Polyquinoline Blends Using Small Angle Scattering.
PB95-164125 *01,261*

Analysis of Small-Angle Scattering Data Dominated by Multiple Scattering for Systems Containing Eccentrically Shaped Particles or Pores.
PB96-160411 *03,075*

X-RAY SOURCES

Discovery of an X-Ray Selected, Radio-Loud Quasar at z=3.9.
PB94-198652 *00,052*

Rotational Modulation and Flares on RS Canum Venaticorum and BY Draconis Stars. XVIII. Coordinated VLA, ROSAT, and IUE Observations of RS CVn Binaries.
PB96-102322 *00,089*

Efficient Way of Identifying New Active Stars: A VLA Survey of X-ray Selected Active Stellar Candidates.
PB96-122882 *00,099*

Developments in Stellar Coronae.
PB96-176706 *00,107*

X-RAY SPECTRA

Experimental Aspects and Z-Dependent Systematics in One- and Two-Electron Ions and Single Vacancy Systems.
PB94-199627 *03,815*

Resonance and Threshold Effects in Polarized X-Ray Emission from Atoms and Molecules.
PB95-150298 *03,891*

Improved Wavelengths for Prominent Lines of Cr XVI to Cr XXII.
PB95-150629 *03,895*

Rh I Isoelectronic Sequence Observed from Er(23+) to Pt(33+).
PB95-150652 *03,898*

Spectra of Ag I Isoelectronic Sequence Observed from Er(21+) to Au(32+).
PB95-150660 *03,899*

Discussion: Statistical Signal Processing of Quasiperiodicities.
PB96-119532 *00,096*

X-RAY SPECTROMETERS

Noninvasive High-Voltage Measurement in Mammography by Crystal Diffraction Spectroscopy.
PB95-153417 *00,160*

Grazing Angle X-Ray Photoemission System for Depth-Dependent Analysis.
PB95-161154 *04,600*

Electron-Ion-X-ray Spectrometer System.
PB95-176137 *03,958*

X-RAY SPECTROSCOPY

Polarized X-Ray Emission Spectroscopy.
PB94-213360 *03,862*

Design of a Protocol for an Electron Probe Microanalyzer k-Value Round Robin.
PB95-107181 *00,564*

Polarization Measurements on a Magnetic Quadrupole Line in Ne-Like Barium.
PB97-113104 *04,161*

X-RAY TUBES

Addition of M and L-Series Lines to NIST Algorithm for Calculation of X-Ray Tube Output Spectral Distributions.
PB95-108742 *00,569*

X RAYS

X-ray Attenuation Coefficients from 10 Kev to 100 Mev.
AD-A278 139/1 *03,765*

X-ray Protection.
AD-A279 132/5 *03,605*

X-ray Protection Design.
AD-A279 181/2 *03,606*

X-Ray Attenuation Coefficients from 10 kev to 100 Mev.
AD-A279 289/3 *03,767*

Bibliography of Photon Total Cross Section (Attenuation Coefficient) Measurements 10 eV to 13.5 GeV, 1907-1993.
PB94-193760 *03,804*

Photographic Response to X-Ray Irradiation. 1. Estimation of the Photographic Error Statistic and Development of Analytic Density-Intensity Equations.
PB94-200086 *03,821*

Photographic Response to X-Ray Irradiation. 2. Correlated Models.
PB94-200094 *03,822*

Photographic Response to X-Ray Irradiation. 3. Photographic Linearization of Beam-Foil Spectra.
PB94-200102 *03,823*

Anisotropy of Polarized X-ray Emission from Atoms and Molecules.
PB95-163002 *04,621*

Tables of X-ray Mass Attenuation Coefficients and Mass Energy-Absorption Coefficients 1 keV to 20 MeV for Elements Z = 1 to 92 and 48 Additional Substances of Dosimetric Interest.
PB95-220539 *04,013*

Decomposition of Sulfur Hexafluoride by X-rays.
PB96-135314 *01,095*

Stable Silicon Photodiodes for Absolute Intensity Measurements in the VUV and Soft X-ray Regions.
PB97-110175 *04,135*

EPR Dosimetry of Cortical Bone and Tooth Enamel Irradiated with X and Gamma Rays: Study of Energy Dependence.
PB97-110373 *03,639*

Experimentally Measured Total X-ray Attenuation Coefficients Extracted from Previously Unprocessed Documents Held by the NIST Photon and Charged Particle Data Center.
PB97-114474 *04,165*

Measuring Nondipolar Asymmetries of Photoelectron Angular Distributions.
PB97-122493 *01,193*

X WINDOW SYSTEM

X Window System, Version 11, Release 5.
PB96-169099 *01,769*

X500 DIRECTORY

Guidelines for the Evaluation of X.500 Directory Products.
PB95-231908 *02,732*

X.500 Directory Schema Design Handbook.
PB96-183041 *02,739*

XENON

Verification of the Ponderomotive Approximation for the ac Stark Shift in Xe Rydberg Levels.
PB94-185709 *03,801*

Evolution of X-ray Resonance Raman Scattering into X-ray Fluorescence from the Excitation of Xenon Near the L3 Edge.
PB96-102751 *04,025*

Intensity-Dependent Scattering Rings in High Order Above-Threshold Ionization.
PB96-110739 *04,032*

XENON COMPLEXES

Van der Waals Bond Lengths and Electronic Spectral Shifts of the Benzene-Kr and Benzene-Xe Complexes.
PB95-151387 *00,932*

XENON IONS

Electron-Impact Ionization of In(+) and Xe(+).
PB94-185089 *00,770*

Analysis of the 5s(2)5p(2)-(5s5p(3)+5s(2)5p5d+5s(2)5p6s) Transitions of Four-Times Ionized Xenon (Xe V).
PB95-150769 *03,900*

Electron-Impact Ionization of In(+) and Xe(+).
PB95-152906 *03,918*

XENON ISOTOPES

Magneto-Optical Trapping of Metastable Xenon: Isotope-Shift Measurements.
PB95-151254 *03,905*

XYLENES

Correlation of the Ideal Gas Properties of Five Aromatic Hydrocarbons.
PB95-175816 *01,002*

Y SPECTRA

Systematics of Alpha-Particle Energy Spectra and Lineal Energy (Y) Spectra for Radon Daughters.
PB94-185139 *03,615*

YBCO

q Dependence of Self-Energy Effects of the Plane Oxygen Vibration in YBa2Cu3O7.
PB96-138516 *01,096*

YBCO SUPERCONDUCTORS

Neutron-Spectroscopy Study of the Hydrogen Vibrations in Hydrogen-Doped YBa2Cu3Ox.
PB94-172475 *04,441*

Weak-Link-Free Behavior of High Angle YBa2Cu3O7-x Grain Boundaries in High Magnetic Fields.
PB94-198421 *04,459*

Electronic Correlations and Satellites in Superconducting Oxides.
PB94-200045 *04,477*

Surface Barrier and Lower Critical Field in YBa2Cu3O7-delta Superconductors.
PB94-200128 *04,478*

Incorporation of Gold into YBa2Cu3O7: Structure and Tc Enhancement.
PB94-200276 *04,481*

Unexpected Effects of Gold on the Structure, Superconductivity, and Normal State of YBa2Cu3O7.
PB94-200284 *04,482*

Critical Magnetic-Field Angle for High-Field Current Transport in YBa2Cu3O7 at 76 K.
PB94-211281 *04,490*

Transport Critical Current of Aligned Polycrystalline Yttrium Barium Copper Oxide (YBa2Cu3O7-delta).
PB94-211307 *04,492*

In situ Noble Metal YBa2Cu3O7 Thin-Film Contacts.
PB94-211323 *04,494*

Flux Expulsion at Intermediate Fields in Type-II Superconductors.
PB94-212230 *04,502*

Offset Susceptibility of Superconductors.
PB94-212263 *04,503*

Compositional Homogeneity in Processing Precursor Powders to the Ba2YCu3O7-x High Tc Superconductor.
PB94-212743 *04,508*

Elastic Constants of Polycrystalline Y1Ba2Cu3Ox.
PB94-213196 *04,513*

Elastic Constants and Debye Temperature of Y1Ba2Cu3Ox: Effect of Oxygen Content.
PB94-213352 *04,515*

Nature of (001) Tilt Grain Boundaries in YBa2Cu3O6+x.
PB95-126033 *04,528*

Image Depth Profiling SIMS: An Evaluation for the Analysis of Light Element Diffusion in YBa2Cu3O7-x Single Crystal Superconductors.
PB95-126116 *04,530*

Defective Structures of Barium Yttrium Copper Oxide (Ba2YCu3Ox) and Ba2YCu3-yMyOz (M=Fe, Co, Al, Ga, ..).
PB95-140034 *04,537*

Study of the Hydroxycarbonate Precursor Route to the YBa2Cu3O7-x High Tc Superconductor.
PB95-140471 *04,540*

Influence of Deposition Parameters on Properties of Laser Ablated YBa2Cu3O7-Delta Films.
PB95-140539 *04,544*

Critical Current Behavior of Ag-Coated YBa2Cu3O7-x Thin Films.
PB95-141016 *04,549*

Magnetic Field Dependence of the Critical Current Anisotropy in Normal Metal-YBa2Cu3O7-delta Thin Film Bilayers.
PB95-141024 *04,550*

Insulating Nanoparticles on YBa2Cu3O7-delta Thin Films Revealed by Comparison of Atomic Force and Scanning Tunneling Microscopy.
PB95-150843 *04,575*

Crystal Chemistry and Phase Equilibrium Studies of the BaO(BaCO3)-R2O3-CuO Systems. 5. Melting Relations in Ba2(Y,Nd,Eu)Cu3O6+x.
PB95-151718 *04,580*

X-Ray-Diffraction Study of a Thermomechanically Detwinned Single Crystal of YBa2Cu3O6+x.
PB95-151726 *04,581*

Flame Synthesis of High Tc Superconductors.
PB95-151981 *00,659*

Harmonic and Static Susceptibilities of YBa2Cu3O7.
PB95-161139 *04,599*

Hydrogen in YBa2Cu3Ox: A Neutron Spectroscopy and a Nuclear Magnetic Resonance Study.
PB95-161279 *04,601*

Temperature Dependence of Vortex Twin Boundary Interaction in Yttrium Barium Copper Oxide (YBa2Cu3O6+x).
PB95-162442 *04,613*

Growth of Laser Ablated YBa2Cu3O7-delta Films as Examined by Rheed and Scanning Tunneling Microscopy.
PB95-162541 *04,614*

Observation of Insulating Nanoparticles on YBCO Thin-Films by Atomic Force Microscopy.
PB95-163358 *04,622*

Determination of Thermoactivation Parameters of Vortex Mobility in YBa2Cu3O7 Using Only Magnetic Measurements.
PB95-163499 04,624

High Current Pressure Contacts to Ag Pads on Thin Film Superconductors.
PB95-168621 04,639

Suitability of Metalorganic Chemical Vapor Deposition-Derived PrGaO3 Films as Buffer Layers for YBa2Cu3O7-x Pulsed Laser Deposition.
PB95-168670 04,640

Low-Temperature Elastic Constants of Y1Ba2Cu3O7.
PB95-168837 04,642

Microwave Properties of YBa2Cu3O7-x Films at 35 GHz from Magnetotransmission and Magnetoreflection Measurements.
PB95-168977 04,643

Insulating Boundary Layer and Magnetic Scattering in YBa2Cu3O7-delta/Ag Interfaces Over a Contact Resistivity Range of 10(-8) - 10(-3) Omega cm(2).
PB95-169157 04,648

Experimental Aspects of Flux Expulsion in Type-II Superconductors.
PB95-175725 04,660

Surface Degradation of Superconducting YBa2Cu3O7-delta Thin Films.
PB95-176095 04,667

Increased Transition Temperature in In situ Coevaporated YBa2Cu3O7-delta Thin Films by Low Temperature Post-Annealing.
PB95-180071 04,672

High Resolution Inelastic Neutron Scattering Study of Phonon Self-Energy Effects in YBCO.
PB95-180881 04,688

Novel YBa2Cu3O7-x and YBa2Cu3O7-x/Y4Ba3O9 Multilayer Films by Bias-Masked 'On-Axis' Magnetron Sputtering.
PB95-181186 04,690

Surface Modification of YBa2Cu3O7-delta Thin Films Using the Scanning Tunneling Microscope: Five Methods.
PB95-203394 04,699

Effect of Sm2BaCuO5 on the Properties of Sintered (Bulk) YBa2Cu3O6+x.
PB96-119441 04,733

Evidence for Tunneling and Magnetic Scatttering at 'In situ' YBCO/Noble-Metal Interfaces.
PB96-141098 04,752

Oxygen Annealing of Ex-situ YBCO/Ag Thin-Film Interfaces.
PB96-141312 04,758

Microwave Noise in High-Tc Josephson Junctions.
PB96-148010 04,771

Effects of Substrate Surface Steps on the Microstructure of Epitaxial Ba2YCu3O7-x Thin Films on (001) LaAlO3.
PB96-148184 04,774

Epitaxial Nucleation and Growth of Chemically Derived Ba2YCu3O7-x Thin Films on (001) SrTiO3.
PB96-190186 04,787

YOUNG'S MODULUS

Bulk Modulus and Young's Modulus of Nanocrystalline gamma-Alumina.
PB96-204185 03,092

YTTERBIUM

Isotope Shifts and Hyperfine Splittings of the 398.8-nm Yb I Line.
PB94-199585 03,814

YTTERBIUM COMPOUNDS

Meissner, Shielding, and Flux Loss Behavior in Single-Crystal YBa2Cu3O6+x.
PB94-198744 04,464

YTTERBIUM IONS

Observation of Pd-Like Resonance Lines Through Pt(32+) and Zn-Like Resonance Lines of Er(38+) and Hf(42+).
PB95-150637 03,896

Rh I Isoelectronic Sequence Observed from Er(23+) to Pt(33+).
PB95-150652 03,898

Spectra of Ag I Isoelectronic Sequence Observed from Er(21+) to Au(32+).
PB95-150660 03,899

YTTRIUM

Magnetoelasticity in Rare-Earth Multilayers and Films.
PB94-211356 04,495

YTTRIUM-90

Radioassays of Yttrium-90 Used in Nuclear Medicine.
PB97-110100 03,522

YTTRIUM BARIUM COPPER OXIDES

High-Tc Multilayer Step-Edge Josephson Junctions and SQUIDs.
PB96-200183 04,790

YTTRIUM BARIUM CUPRATE COBALTATES

Neutron Powder Diffraction Study of the Nuclear and Magnetic Structures of the Oxygen-Deficient Perovskite YBaCuCoO5.
PB95-161097 00,954

YTTRIUM BARIUM CUPRATES

Weak-Link-Free Behavior of High Angle YBa2Cu3O7-x Grain Boundaries in High Magnetic Fields.
PB94-198421 04,459

Electronic Correlations and Satellites in Superconducting Oxides.
PB94-200045 04,477

Surface Barrier and Lower Critical Field in YBa2Cu3O7-delta Superconductors.
PB94-200128 04,478

Incorporation of Gold into YBa2Cu3O7: Structure and Tc Enhancement.
PB94-200276 04,481

Unexpected Effects of Gold on the Structure, Superconductivity, and Normal State of YBa2Cu3O7.
PB94-200284 04,482

Critical Magnetic-Field Angle for High-Field Current Transport in YBa2Cu3O7 at 76 K.
PB94-211281 04,490

In situ Noble Metal YBa2Cu3O7 Thin-Film Contacts.
PB94-211323 04,494

Flux Expulsion at Intermediate Fields in Type-II Superconductors.
PB94-212230 04,502

Offset Susceptibility of Superconductors.
PB94-212263 04,503

Compositional Homogeneity in Processing Precursor Powders to the Ba2YCu3O7-x High Tc Superconductor.
PB94-212743 04,508

Elastic Constants of Polycrystalline Y1Ba2Cu3Ox.
PB94-213196 04,513

Elastic Constants and Debye Temperature of Y1Ba2Cu3Ox: Effect of Oxygen Content.
PB94-213352 04,515

Nature of (001) Tilt Grain Boundaries in YBa2Cu3O6+x.
PB95-126033 04,528

Image Depth Profiling SIMS: An Evaluation for the Analysis of Light Element Diffusion in YBa2Cu3O7-x Single Crystal Superconductors.
PB95-126116 04,530

Defective Structures of Barium Yttrium Copper Oxide (Ba2YCu3Ox) and Ba2YCu3-yMyOz (M=Fe, Co, Al, Ga, ..).
PB95-140034 04,537

Study of the Hydroxycarbonate Precursor Route to the YBa2Cu3O7-x High Tc Superconductor.
PB95-140471 04,540

Influence of Deposition Parameters on Properties of Laser Ablated YBa2Cu3O7-Delta Films.
PB95-140539 04,544

Critical Current Behavior of Ag-Coated YBa2Cu3O7-x Thin Films.
PB95-141016 04,549

Magnetic Field Dependence of the Critical Current Anisotropy in Normal Metal-YBa2Cu3O7-delta Thin Film Bilayers.
PB95-141024 04,550

Insulating Nanoparticles on YBa2Cu3O7-delta Thin Films Revealed by Comparison of Atomic Force and Scanning Tunneling Microscopy.
PB95-150843 04,575

X-Ray-Diffraction Study of a Thermomechanically Detwinned Single Crystal of YBa2Cu3O6+x.
PB95-151726 04,581

Flame Synthesis of High Tc Superconductors.
PB95-151981 00,659

Harmonic and Static Susceptibilities of YBa2Cu3O7.
PB95-161139 04,599

Hydrogen in YBa2Cu3Ox: A Neutron Spectroscopy and a Nuclear Magnetic Resonance Study.
PB95-161279 04,601

Temperature Dependence of Vortex Twin Boundary Interaction in Yttrium Barium Copper Oxide (YBa2Cu3O6+x).
PB95-162442 04,613

Growth of Laser Ablated YBa2Cu3O7-delta Films as Examined by Rheed and Scanning Tunneling Microscopy.
PB95-162541 04,614

Observation of Insulating Nanoparticles on YBCO Thin-Films by Atomic Force Microscopy.
PB95-163358 04,622

Determination of Thermoactivation Parameters of Vortex Mobility in YBa2Cu3O7 Using Only Magnetic Measurements.
PB95-163499 04,624

High Current Pressure Contacts to Ag Pads on Thin Film Superconductors.
PB95-168621 04,639

Suitability of Metalorganic Chemical Vapor Deposition-Derived PrGaO3 Films as Buffer Layers for YBa2Cu3O7-x Pulsed Laser Deposition.
PB95-168670 04,640

Low-Temperature Elastic Constants of Y1Ba2Cu3O7.
PB95-168837 04,642

Insulating Boundary Layer and Magnetic Scattering in YBa2Cu3O7-delta/Ag Interfaces Over a Contact Resistivity Range of 10(-8) - 10(-3) Omega cm(2).
PB95-169157 04,648

Experimental Aspects of Flux Expulsion in Type-II Superconductors.
PB95-175725 04,660

Surface Degradation of Superconducting YBa2Cu3O7-delta Thin Films.
PB95-176095 04,667

Increased Transition Temperature in In situ Coevaporated YBa2Cu3O7-delta Thin Films by Low Temperature Post-Annealing.
PB95-180071 04,672

High Resolution Inelastic Neutron Scattering Study of Phonon Self-Energy Effects in YBCO.
PB95-180881 04,688

Novel YBa2Cu3O7-x and YBa2Cu3O7-x/Y4Ba3O9 Multilayer Films by Bias-Masked 'On-Axis' Magnetron Sputtering.
PB95-181186 04,690

Surface Modification of YBa2Cu3O7-delta Thin Films Using the Scanning Tunneling Microscope: Five Methods.
PB95-203394 04,699

YTTRIUM BARIUM TITANATES

Substitution-Induced Midgap States in the Mixed Oxides RxBa1-ChiTiO3-Delta, with R=Y, La, and Nd.
PB95-140505 04,541

YTTRIUM DEUTERIDES

Local-Mode Dynamics in YH2 and YD2 by Isotope-Dilution Neutron Spectroscopy.
PB95-181012 01,017

YTTRIUM HYDRIDES

Neutron Spectroscopic Comparison of Rare-Earth/Hydrogen alpha-Phase Systems.
PB95-163523 00,970

Local-Mode Dynamics in YH2 and YD2 by Isotope-Dilution Neutron Spectroscopy.
PB95-181012 01,017

YTTRIUM IRON GARNETS

Submicroampere-Per-Root-Hertz Current Sensor Based on the Faraday Effect in Ga: YIG.
PB95-162467 02,155

YTTRIUM OXIDES

Structures of Vapor-Deposited Yttria and Zirconia Thin Films.
PB94-216025 03,041

Rapid Hot Pressing of Ultra-Fine PSZ Powders.
PB94-216587 03,045

Crystal Chemistry and Phase Equilibria Studies of the BaO(BaCO3)-R2O3-CuO Systems. 4. Crystal Chemistry and Subsolidus Phase Relationship Studies of the CuO-Rich Region of the Ternary Diagrams, R=Lanthanides.
PB95-151759 00,936

Effects of Etching on the Morphology and Surface Resistance of YBa2Cu3O7-delta Films.
PB96-135355 02,410

YTTRIUM STRONTIUM ALUMINUM CUPRATES

Neutron Powder Diffraction Study of the Crystal Structure of YSr2AlCu2O7.
PB94-212073 04,499

ZEOLITES

Neutron Powder Diffraction Study of a Na, Cs-Rho Zeolite.
PB94-198629 00,791

ZEOTROPES

Role of Refrigerant Mixtures as Alternatives to CFCs.
PB94-199775 03,252

ZERNIKE POLYNOMIALS

Test of a Slow Off-Axis Parabola at Its Center of Curvature.
PB96-138482 04,352

ZERO-FIELD ORDERED MOMENT

Magnetic Structure and Spin Dynamics of the Pr and Cu in Pr2CuO4.
PB96-111836 04,036

ZINC

Calibration Standards for Differential Scanning Calorimetry. 1. Zinc Absolute Calorimetric Measurement of Enthalpy of Fusion and Temperature of Fusion HM.
PB94-199817 00,801

Energy Levels of Zinc, Zn I through Zn XXX.
PB96-145982 01,122

ZINC SELENIDES

Characterization of the ZnSe/GaAs Interface Layer by TEM and Spectroscopic Ellipsometry.
PB95-175360 04,655

Determination of the Optical Constants of ZnSe Films by Spectroscopic Ellipsometry.
PB95-175378 04,656

ZIRCONIA

Correlations between Flaw Tolerance and Reliability in Zirconia.
PB96-161922 02,986

ZIRCONIA POWDER

Characterization and Processing of Spray-Dried Zirconia Powders for Plasma Spray Application.
PB97-111231 04,419

ZIRCONIUM ALLOYS

New Alloys Show Extraordinary Resistance to Fracture and Wear.
PB95-151346 03,346

ZIRCONIUM IONS

Hyperfine-Structure Studies of Zr II: Experimental and Relativistic Configuration-Interaction Results.
PB95-203824 04,011

ZIRCONIUM OXIDES

Effect of Microstructure on the Wear Transition of Zirconia-Toughened Alumina.
PB94-211778 03,141

Structures of Vapor-Deposited Yttria and Zirconia Thin Films.
PB94-216025 *03,041*
Rapid Hot Pressing of Ultra-Fine PSZ Powders.
PB94-216587 *03,045*
Wear Transitions in Monolithic Alumina and Zirconia-Alumina Composites.
PB96-103163 *03,168*

ZONE-TYPE COMPARTMENT FIRE MODELS

Simulating Smoke Movement through Long Vertical Shafts in Zone-Type Compartment Fire Models.
PB95-143152 *00,368*

TITLE INDEX

SAMPLE ENTRY

Performance Parameters of Fire Detection Systems | Title
PB94-194339 *00,123* PC **A03**/MF **A01** | NTIS order number *Abstract number* Availability **Price Code**

1,4-Dinitrocubane and Cubane under High Pressure.
PB95-108437 *03,755* Not available NTIS

2D-Scanning Capacitance Microscopy Measurements of Cross-Sectioned VLSI Teststructures.
PB96-163779 *04,104* Not available NTIS

2nu9 Band of Propyne-d3.
PB95-164513 *00,985* Not available NTIS

2-Tunneling Path Internal-Axis-Method-Like Treatment of the Microwave Spectrum of Divinyl Ether.
PB94-200466 *00,808* Not available NTIS

4SIGHT Manual: A Computer Program for Modelling Degradation of Underground Low Level Waste Concrete Vaults.
PB95-231593 *03,726* PC A05/MF A01

10 kV DC Resistive Divider Calibration.
PB95-198685 *02,063* PC A04/MF A01

24 GHz Josephson Array Voltage Standard.
PB94-211588 *02,033* Not available NTIS

30 MHz Comparison Receiver.
PB96-200407 *01,972* Not available NTIS

30 THz Mixing Experiments on High Temperature Superconducting Josephson Junctions.
PB96-102462 *04,709* Not available NTIS

36Cl/Cl Accelerator-Mass-Spectrometry Standards: Verification of Their Serial-Dilution-Solution Preparations by Radioactivity Measurements.
PB94-140563 *00,524*
(Order as PB94-140555, PC A06/MF A02)

45 deg/0 deg Reflectance Factors of Pressed Polytetrafluoroethylene (PTFE) Powder.
PB95-260758 *04,328* PC A06/MF A02

63Ni Half-Life: A New Experimental Determination and Critical Review.
PB97-111603 *00,700* Not available NTIS

100 A, 100 kHz Transconductance Amplifier.
PB96-200936 *02,098* Not available NTIS

100 Ampere, 100 kHZ Transconductance Amplifier.
PB96-102629 *02,068* Not available NTIS

1950 Supplement to Screw-Thread Standards for Federal Services. 1944.
AD-A280 223/9 *03,656* PC A06/MF A02

Ab initio Calculations for Helium: A Standard for Transport Property Measurements.
PB96-102041 *01,060* Not available NTIS

Abrasive Wear by Diesel Engine Coal-Fuel and Related Particles.
PB95-104915 *01,450* PC A04/MF A01

Absence of Quantum-Mechanical Effects on the Mobility of Argon Ions in Helium Gas at 4.35 K.
PB97-122543 *01,194* Not available NTIS

Absolute Cross-Section Measurements for Electron-Impact Ionization of C1(+1).
PB94-199841 *03,818* Not available NTIS

Absolute Cross-Section Measurements for Electron-Impact Single Ionization of Se(+) and Te(+).
PB95-202503 *03,980* Not available NTIS

Absolute Cross Sections for Electron-Impact Single Ionization of Si(+) and Si(2+).
PB95-202529 *03,982* Not available NTIS

Absolute Determination of Electrolytic Conductivity for Primary Standard KC1 Solutions from 0 to 50C.
PB94-172798 *00,765* Not available NTIS

Absolute Frequency Measurements of Methanol from 1.5 to 6.5 THz.
PB95-175881 *04,300* Not available NTIS

Absolute Response Calibration of a Transfer Standard Cryogenic Bolometer.
PB96-147103 *04,358* Not available NTIS

Absorption Cross Sections, Kinetics of Formation, and Self-Reaction of the IO Radical Produced via the Laser Photolysis of N2O/I2/N2 Mixtures.
PB97-112361 *01,180* Not available NTIS

Absorption of Sound in Gases between 10 and 25 MHz: Argon.
PB94-199015 *04,183* Not available NTIS

Absorption of Ultrasonic Waves in Air at High Frequencies (10-20 MHz).
PB94-199007 *04,182* Not available NTIS

Abstract and Index Collection in the Research Information Center of the National Institute of Standards and Technology.
PB94-152204 *02,744* PC A03/MF A01

Abstract and Index Collection in the Research Information Center of the National Institute of Standards and Technology.
PB95-232633 *02,741* PC A03/MF A01

AC-DC Difference Characteristics of High-Voltage Thermal Converters.
PB96-148093 *02,083* Not available NTIS

Acceleration of Intramolecular Vibrational Redistribution by methyl Internal Rotation. A Chemical Timing Study of p-fluorotoluene and p-fluorotoluene-d3.
PB95-202982 *01,039* Not available NTIS

Acceptance Diagram Analysis of the Performance of Multidisk Neutron Velocity Selectors.
PB94-200417 *03,826* Not available NTIS

Acceptance Diagram Analysis of the Performance of Vertically Curved Neutron Monochromators.
PB94-200425 *03,827* Not available NTIS

Access Paths for Materials Databases: Approaches for Large Databases and Systems.
PB95-162525 *02,975* Not available NTIS

Accuracy and Repeatability in Time Domain Network Analysis.
PB95-202644 *02,064* Not available NTIS

Accuracy Comparisons of Josephson Array Systems.
PB95-164687 *02,047* Not available NTIS

Accuracy in Integrated Circuit Dimensional Measurements.
PB95-180808 *02,368* Not available NTIS

TITLE INDEX

Accuracy in Time Domain Transmission Line Measurements.
PB96-148069 *04,060* Not available NTIS

Accuracy of Eigenvalues: A Comparison of Two Methods.
PB95-126249 *03,413* Not available NTIS

Accuracy of the Electron Pump.
PB96-135223 *04,743* Not available NTIS

Accuracy-Weighted Variational Principle for Degenerate Continuum States.
PB94-200615 *03,831* Not available NTIS

Accurate Characterization of High Speed Photodectors.
PB95-153763 *02,153* Not available NTIS

Accurate Computations of Radar Cross Sections of Simple Objects.
PB96-138474 *04,426* Not available NTIS

Accurate Electrical Characterization of High-Speed Interconnections.
PB96-167143 *02,240* Not available NTIS

Accurate Experimental Characterization of Interconnects: A Discussion of 'Experimental Electrical Characterization of Interconnects and Discontinuities in High-Speed Digital Systems'.
PB94-216389 *02,217* Not available NTIS

Accurate Measurement of Optical Detector Nonlinearity.
PB95-203576 *02,181* Not available NTIS

Accurate Measurement of Time.
PB96-119482 *01,552* Not available NTIS

Accurate Measurements of the Local Deuterium Abundance from HST Spectra.
PB96-200621 *00,110* Not available NTIS

Accurate Modeling of Size and Strain Broadening in the Rietveld Refinement: The 'Double-Voigt' Approach.
PB96-200225 *00,664* Not available NTIS

Accurate Transmission Line Characterization.
PB95-151593 *02,220* Not available NTIS

Acid Gas Production in Inhibited Diffusion Flames.
PB95-180576 *01,390* Not available NTIS

Acoustic Emission of Structural Materials Exposed to Open Flames.
PB95-164810 *00,296* Not available NTIS

Acrylonitrile-Butadiene-Styrene (ABS) Plastic Drain, Waste, and Vent Pipe and Fittings.
AD-A310 724/0 *00,327* PC A03/MF A01

Activated Dynamics, Loss of Ergodicity, and Transport in Supercooled Liquids.
PB95-150819 *00,925* Not available NTIS

Active High Voltage Divider with 20-PPM Uncertainty.
PB97-119317 *02,104* Not available NTIS

Active Site Ionicity and the Mechanism of Carbonic Anhydrase.
PB94-212974 *00,843* Not available NTIS

Activities of ISO Technical Committee 201 on Surface Chemical Analysis.
PB95-180824 *00,607* Not available NTIS

Activities of NIST (National Inst. Of Standards and Technology).
N94-23605/6 *04,222*
(Order as N94-23595/9, PC A21/MF A04)

Activities of the ASTM Committee E-42 on Surface Analysis.
PB95-108528 *00,881* Not available NTIS

ADA; Category: Software Standard; Subcategory: Programming Language.
FIPS PUB 119-1 *01,667* PC$278.00

Ada Compiler Validation Summary Report. Certificate Number: 930927S1.11328 Green Hills Software C Ada, Version 1.1 ZENY 386 => ZENY 386.
AD-A277 981/7 *01,643* PC A03/MF A01

Ada Compiler Validation Summary Report: Certificate Number: 931029S1.11330, Digital Equipment Corporation, DEC Ada for DEC OSF/1 AXP Systems, Version 3.1, DEC 3000 Model 400 AXP Workstation, DEC 3000 Model 400 AXP Workstation.
AD-A274 872/1 *01,639* PC A04/MF A01

Ada Compiler Validation Summary Report: Certificate Number: 931119S1.11331 DDC-I, Inc. DACS Sun SPARC/SunOS to 80386 PM Bare Ada Cross Compiler System, Version 4.6.4 Sun Sparcstation 1+ => Bare Board iSBC 386/116.
AD-A276 283/9 *01,642* PC A08/MF A02

Ada Compiler Validation Summary Report. Certificate Number: 931119S1.11332, DDC-I, Inc. DACS MIPS R3000 Bare Ada Cross Compiler System, Version 4.7.1 Sun SPARCstation IPX => DACS Sun SPARC/SunOS to MIPS R3000 Bare Instruction Set Architecture Simulator, Version 4.7.1.
AD-A276 181/5 *01,641* PC A04/MF A01

Ada Compiler Validation Summary Report: Certificate Number: 931217S1.11336 Control Data Systems, Inc. NOS/VE Ada, Version 1.4 Cyber 180-930-31 => Cyber 180-930-31.
AD-A275 977/7 *01,640* PC A03/MF A01

Ada Compiler Validation Summary Report: Certificate Number: 940325S1.11341 DDC-I, DACS Sun SPARC/SunOS to 80186 Bare Ada Cross Compiler System, Version 4.6.4 Sun SPARCstation IPX => Intel iSBC 186/100 (Bare Machine).
AD-A279 643/1 *01,645* PC A06/MF A02

Ada Compiler Validation Summary Report: Certificate Number: 940325S1.11342 DDC-I, DACS Sun SPARC/SunOS to 80186 Bare Ada Cross Compiler System with Rate Monotonic Scheduling Version 4.6.4 Sun SPARCstation IPX => Intel iSBC 186/100 (Bare Machine).
AD-A279 779/3 *01,652* PC A06/MF A02

Ada Compiler Validation Summary Report: Certificate Number: 940325S1.11343 DDC-I, DACS Sun SPARC/Solaris to 80186 Bare Ada Cross Compiler System, Version 4.6.4 Sun SPARCclassic => Intel iSBC 186/100 (Bare Machine).
AD-A279 757/9 *01,649* PC A06/MF A02

Ada Compiler Validation Summary Report: Certificate Number: 940325S1.11344 DDC-I, DACS Sun SPARC/Solaris to 80186 Bare Ada Cross Compiler System with Rate Monotonic Scheduling, Version 4.6.4 Sun SPARCclassic => Intel iSBC 186/100 (Bare Machine).
AD-A279 758/7 *01,650* PC A06/MF A02

Ada Compiler Validation Summary Report: Certificate Number 940325S1.11345 DDC-I. DACS Sun SPARC/SunOS to 680x0 Bare Ada Cross Compiler System, Version 4.6.9 Sun SPARCstation IPX => Motorola MVME143 68030/68882 (Bare Machine).
AD-A280 145/4 *01,656* PC A05/MF A02

Ada Compiler Validation Summary Report: Certificate Number: 940325S1.11346 DDC-I, DACS Sun SPARC/SunOS to 680x0 Bare Ada Cross Compiler System (BASIC MODE), Version 4.6.9 Sun SPARCstation IPX => Lynwood j435TU (68030) (Bare Machine).
AD-A279 646/4 *01,648* PC A05/MF A02

Ada Compiler Validation Summary Report: Certificate Number: 940325S1.11347 DDC-I, DACS Sun SPARC/SunOS to 680x0 Bare Ada Cross Compiler System (SECURE MODE), Version 4.6.9 Sun SPARCstation IPX => Lynwood j435TU (68030) (Bare Machine).
AD-A279 778/5 *01,651* PC A06/MF A02

Ada Compiler Validation Summary Report: Certificate Number: 940325S1.11348 DDC-I, DACS Sun SPARC/Solaris to 80386 PM Bare Ada Cross Compiler System, Version 4.6.4 Sun SPARCclassic => Intel iSBC 386/116 (Bare Machine).
AD-A279 642/3 *01,644* PC A06/MF A02

Ada Compiler Validation Summary Report: Certificate Number: 940325S1.11349 DDC-I, DACS Sun SPARC/Solaris to 80386 PM Bare Ada Cross Compiler System with Rate Monotonic Scheduling, Version 4.6.4 Sun SPARCclassic => Intel iSBC 386/116 (Bare Machine).
AD-A279 644/9 *01,646* PC A06/MF A02

Ada Compiler Validation Summary Report: Certificate Number: 940325S1.11350 DDC-I, DACS Sun SPARC/SunOS to Pentium PM Bare Ada Cross Compiler System, Version 4.6.4 Sun SPARCstation IPX => Intel Pentium (Operated as Bare Machine) Based in Xpress Desktop (Intel Product Number: XBASE6E4F-B).
AD-A279 864/3 *01,655* PC A06/MF A02

Ada Compiler Validation Summary Report: Certificate Number: 940325S1.11351 DDC-I, DACS Sun SPARC/SunOS to Pentium PM Bare Ada Cross Compiler System with Rate Monotonic Scheduling, Version 4.6.4 Sun SPARCstation IPX => Intel Pentium (operated as Bare Machine) based in Xpress Desktop (Intel product number: XBASE6E4F-B).
AD-A279 804/9 *01,653* PC A06/MF A02

Ada Compiler Validation Summary Report: Certificate Number: 940325S1.11352 DDC-I DACS Sun SPARC/Solaries to Pentium PM Bare Ada Cross Compiler System, Version 4.6.4 Sun SPARCclassic => Intel Pentium (Operated as Bare Machine) Based in Xpress Desktop (Intel Product Number: XBASE6E4F-B).
AD-A280 295/7 *01,657* PC A06/MF A02

Ada Compiler Validation Summary Report: Certificate Number: 940325S1.11353 DDC-I, DACS Sun SPARC/Solaris to Pentium PM Bare Ada Cross Compiler System with Rate Monotonic Scheduling, Version 4.6.4 Sun SPARCclassic => Intel Pentium (operated as Bare Machine) based in Xpress Desktop (Intel product number: XBASE6E4F-B).
AD-A279 805/6 *01,654* PC A06/MF A02

Ada Compiler Validation Summary Report: Certificate Number: 940325S1.11354 DDC-I, DACS Sun SPARC/Solaris Native Ada Compiler System, Version 4.6.2 Sun SPARCclassic => Sun SPARCclassic.
AD-A279 645/6 *01,647* PC A04/MF A01

Ada Compiler Validation Summary Report: Certificate Number 940902S1.11376. UNISYS Corporation IntegrAda for Windows NT, Version 1.0. Intel Deskside Server for Intel Pentium 60 MHz =>. Intel Deskside Server with Intel Pentium 60 MHz.
AD-A288 572/1 *01,659* PC A03/MF A01

Ada Compiler Validation Summary Report: Certificate Number 940902S1.11377 UNISYS Corporation. IntegrAda for Windows NT, Version 1.0. Intel Deskside Server with Intel 80486DX266 => Intel Deskside Server with Intel 80486DX266.
AD-A288 571/3 *01,658* PC A03/MF A01

Ada Compiler Validation Summary Report. Certificate Number 941117S1.11380. Electronic Data Systems Corp. Compiler: OC Systems Legacy Ada/370, Release 1.4.1 (without optimization).
AD-A289 895/5 *01,662* PC A05/MF A01

Ada Compiler Validation Summary Report: Certificate Number 94101251.11379 TISOFT, Inc. Green Hills Optimizing Ada Compileer, Version 1.8.7 with PATCK ID 1 COMPAQ ProLiiant 2000 Model 55/66 => COMPAQ ProLiant 2000 Model 5/66.
AD-A288 573/9 *01,660* PC A03/MF A01

Ada Compiler Validation Summary Report, VC No. 950609S1.11390 Digital Equipment Corporation - Compiler Name: DEC Ada Version 3.2 for OpenVMS VAX Systems.
AD-A296 794/1 *01,664* PC A05/MF A01

ADA Compiler Validation Summary Report, VC Number 950303S1.11381. Digital Equipment Corporation - Compiler Name: DEC Ada for OpenVMS Alpha Systems, Version 3.2.
AD-A293 709/2 *01,663* PC A05/MF A01

Ada Complier Validation Summary Report: Certificate Number: 940929S1.11378. Digital Equipment Corporation DEC Ada for DEC OSF/1 AXP Systems, Version 3.2; DEC 3000 Model 400 AXP Workstation => DEC 3000 Model 400 AXP Workstation.
AD-A288 574/7 *01,661* PC A05/MF A01

Adaptive, Predictive 2-D Feature Tracking Algorithm for Finding the Focus of Expansion.
PB94-218575 *01,588* PC A03/MF A01

Addition of M and L-Series Lines to NIST Algorithm for Calculation of X-Ray Tube Output Spectral Distributions.
PB95-108742 *00,569* Not available NTIS

Addressing U.S. Government Security Requirements for OSI.
PB96-160577 *01,611* Not available NTIS

Adhesion, Contact Electrification, and Acid-Base Properties of Surfaces.
PB96-204425 *03,693* Not available NTIS

Adhesion of Composites to Dentin and Enamel.
PB94-199049 *00,144* Not available NTIS

Administration Standard for the Telecommunications Infrastructure of Federal Buildings. Category: Telecommunications Standard; Subcategory: Telecommunications Administration.
FIPS PUB 187 *01,461* PC A02/MF A01

Adsorption of Low-Molecular-Weight Sodium Polyacrylate on Hydroxyapatite.
PB94-172608 *00,139* Not available NTIS

Adsorption of Polyacrylic Acids and Their Sodium Salts on Hydroxyapatite: Effect of Relative Molar Mass.
PB97-112510 *03,581* Not available NTIS

Adsorption of Potassium N-phenylglycinate on Hydroxyapatite: Role of Solvents and Ionic Charge.
PB96-180161 *01,159* Not available NTIS

Advanced Angle Metrology System.
PB94-211364 *02,637* Not available NTIS

Advanced Components for Electric and Hybrid Electric Vehicles. Workshop Proceedings. Held in Gaithersburg, Maryland on October 27-28, 1993.
PB94-177060 *04,858* PC A10/MF A03

Advanced Mass Calibration and Measurement Assurance Program for State Calibration Laboratories.
PB95-253571 *02,492* PC A03/MF A01

Advances in the Measurement of Polymer CTE: Micrometer- to Atomic-Scale Measurements.
PB96-180229 *03,390* Not available NTIS

Aerodynamic Phenomena in Stellar Atmospheres - A Bibliography.
AD-A278 521/0 *00,046* PC A05/MF A02

Affinity Chromatography on Inorganic Support Materials.
PB95-163820 *03,467* Not available NTIS

Agent Screening for Halon 1301 Aviation Replacement.
PB96-159710 *03,282* Not available NTIS

Aggregation Kinetics of Colloidal Particles Destabilized by Enzymes.
PB95-125878 *00,894* Not available NTIS

Agile Manufacturing from a Statistical Perspective.
PB96-109525 *02,886* PC A03/MF A01

Aging Effects on XRF Measurements of Solder Coatings.
PB95-140927 *03,123* Not available NTIS

Aging in Glasses Subjected to Large Stresses and Deformations.
PB95-107041 *03,235* Not available NTIS

Aging, Warm-Up Time and Retrace; Important Characteristics of Standard Frequency Generators.
PB96-103122 *04,031* Not available NTIS

TITLE INDEX

Aid for Smaller Businesses.
PB94-212461 *00,492* Not available NTIS

Air Change Effectiveness Measurements in Two Modern Office Buildings.
PB94-185766 *00,243* Not available NTIS

Air Flow in the Boundary Layer of an Elliptic Cylinder.
AD-A297 391/5 *04,194* PC A03/MF A01

Airborne Asbestos Analysis: National Voluntary Laboratory Accreditation Program.
PB96-147392 *02,566* PC A05/MF A01

Airborne Asbestos Method: Bootstrap Method for Determining the Uncertainty of Asbestos Concentration. Version 1.0.
PB96-214614 *00,646* PC A04/MF A01

Airborne Asbestos Method: Standard Practice for Recording Transmission Electron Microscopy Data for the Analysis of Asbestos Collected onto Filters. Version 1.0.
PB94-210168 *00,552* PC A03/MF A03

Airborne Asbestos Method: Standard Test Method for High Precision Counting of Asbestos Collected on Filters. Version 1.0.
PB94-163003 *00,525* PC A02/MF A01

Airborne Asbestos Method: Standard Test Method for Verified Analysis of Asbestos by Transmission Electron Microscopy. Version 2.0.
PB94-163045 *00,526* PC A03/MF A01

Airborne Smoke Sampling Package for Field Measurements of Fires.
PB95-150041 *01,381* Not available NTIS

Al L2,3 Core Excitons in AlxGa1-x as Studied by Soft-X-ray Reflection and Emission.
PB96-157839 *04,067* Not available NTIS

Alaska Marine Mammal Tissue Archival Project: Specimen Inventory.
PB95-171344 *02,589* PC A05/MF A01

Alcohol Solutions of Triphenyl-Tetrazolium Chloride as High-Dose Radiochromic Dosimeters.
PB96-135249 *03,716* Not available NTIS

Algebraic Approximation of Attractors for Galloping Oscillators.
PB95-162897 *04,820* Not available NTIS

Algorithm Testing and Evaluation Program for Coordinate Measuring Systems: Long Range Plan.
PB95-231833 *02,915* PC A03/MF A01

Algorithm Testing and Evaluation Program for Coordinate Measuring Systems: Testing Methods.
PB95-251658 *02,666* PC A03/MF A01

Algorithm to Describe the Spread of a Wall Fire under a Ceiling.
PB95-182259 *00,261* PC A04/MF A01

Algorithmic Enhancements to the Method of Centers for Linear Programming Problems.
PB94-198959 *03,426* Not available NTIS

Alignment in Two-Step Pulsed Laser Excitation of Rydberg Levels in Light Atoms: The Example of Sodium.
PB95-202883 *03,993* Not available NTIS

Alignment Probing of Rydberg States by Stimulated Emission.
PB96-200316 *04,124* Not available NTIS

Alkali-Silica Reaction and High Performance Concrete.
PB96-131537 *01,345* PC A03/MF A01

All-Metal Collection System for Preparative-Scale Gas Chromatography: Purification of Low-Boiling-Point Compounds.
PB96-123435 *00,619* Not available NTIS

Alpha-Particle and Electron Capture Decay of (209)Po.
PB96-186085 *04,119* Not available NTIS

Alternating-Field Susceptometry and Magnetic Susceptibility of Supercondoctors. Presented at Office of Naval Research Workshop on Magnetic Susceptibility of Superconductors and Other Spin Systems. Held in Berkeley Springs, West Virginia on 20 May 1991.
PB94-145984 *04,435* PC A01/MF A01

Alternating-Field Susceptometry and Magnetic Susceptibility of Superconductors.
PB95-168613 *04,638* Not available NTIS

Alternative Contour Technique for the Efficient Computation of the Effective Length of an Antenna.
PB96-141361 *02,011* Not available NTIS

Alternative EMC Compliance Test Facilities.
PB96-200324 *02,247* Not available NTIS

Alternative Single Integral Equation for Scattering by a Dielectric.
PB94-216512 *04,422* Not available NTIS

Aluminum-Lithium Alloys: Evaluation of Fracture Toughness by Two Test Standards, ASTM Method E 813 and E 1304.
PB96-190236 *03,374* Not available NTIS

Alvin Van Valkenburg and the Diamond Anvil Cell.
PB96-204474 *04,797* Not available NTIS

Ambient Temperature Synthesis of Bulk Intermetallics.
PB95-169074 *00,168* Not available NTIS

Amperometric Flow-Injection Analysis Biosensor for Glucose Based on Graphite Paste Modified with Tetracyanoquinodimethane.
PB95-161980 *03,498* Not available NTIS

Amperometric Measurement of Moisture in Transformer Oil Using Karl Fischer Reagents.
PB96-146766 *00,623* Not available NTIS

AMRF Composite Fabrication Workstation.
PB94-172681 *02,810* Not available NTIS

Analyses of Recent Experimental and Theoretical Determinations of e-H2 Vibrational Excitation Cross Sections: Assessing a Long-Standing Controversy.
PB95-202438 *03,977* Not available NTIS

Analysis by a Combination of Gas Chromatography and Tandem Mass Spectrometry: Development of Quantitative Tandem-in-Time Ion Trap Mass Spectrometry: Isotope Dilution Quantification of 11-Nor-Delta-9-Tetrahydro cannabinol-9-Carboxylic Acid.
PB96-117221 *02,561* Not available NTIS

Analysis of a Biologically Motivated Neural Network for Character Recognition.
PB94-172277 *00,182* Not available NTIS

Analysis of an Open-Ended Coaxial Probe with Lift-Off for Nondestructive Testing.
PB96-135116 *01,940* Not available NTIS

Analysis of ANSI ASC X12 and UN/EDIFACT Electronic Data Interchange (EDI) Standards.
PB95-220554 *01,729* PC A03/MF A01

Analysis of Autocorrelations in Dynamic Processes.
PB95-181228 *02,826* Not available NTIS

Analysis of Boron in CVD Diamond Surfaces Using Neutron Depth Profiling.
PB94-213089 *04,511* Not available NTIS

Analysis of Creep in a Si-SiC C-Ring by Finite Element Method.
PB94-200268 *03,037* Not available NTIS

Analysis of Droplet Arrival Statistics in a Pressure-Atomized Spray Flame.
PB97-112270 *01,352* Not available NTIS

Analysis of Failed Dry Pipe Fire Suppression System Couplings from the Filene Center at Wolf Trap Farm Park for the Performing Arts.
PB94-164407 *00,331* PC A03/MF A01

Analysis of High Bay Hangar Facilities for Detector Sensitivity and Placement.
PB96-190210 *01,429* Not available NTIS

Analysis of Moisture Accumulation in a Wood-Frame Wall Subjected to Winter Climate.
PB94-199320 *00,338* Not available NTIS

Analysis of Physical Properties of Ceramic Powders in an International Interlaboratory Comparison Program.
PB95-161501 *03,050* Not available NTIS

Analysis of Protein Metal Binding Selectivity in a Cluster Model.
PB94-212990 *00,845* Not available NTIS

Analysis of SANS from Controlled Pore Glasses.
PB94-198843 *03,035* Not available NTIS

Analysis of Scattering Asymmetry Statistics When Background Corrected Counts Are Negative.
PB94-200334 *03,824* Not available NTIS

Analysis of Selected Software Safety Standards.
PB95-151262 *01,708* Not available NTIS

Analysis of Small-Angle Scattering Data Dominated by Multiple Scattering for Systems Containing Eccentrically Shaped Particles or Pores.
PB96-160411 *03,075* Not available NTIS

Analysis of Standards for the Assurance of High Integrity Software.
PB96-161351 *03,735* Not available NTIS

Analysis of the Effectiveness of Oscillating Radial Collimators in Neutron Scattering Applications.
PB95-152252 *03,917* Not available NTIS

Analysis of the Happyland Social Club Fire with HAZARD I.
PB94-199270 *00,193* Not available NTIS

Analysis of the (5d(2)+5d6s)-5d6p Transition Arrays of Os VII and Ir VIII, and the 6s (2)S-6p (2)P Transitions of Ir IX.
PB96-159264 *01,954*
(Order as PB96-159215, PC A07/MF A02)

Analysis of the 5s(2)5p(2)-(5s5p(3)+5s(2)5p5d+5s(2)5p6s) Transitions of Four-Times Ionized Xenon (Xe V).
PB95-150769 *03,900* Not available NTIS

Analysis of Thermal Wave Propagation in Diamond Films.
PB94-211471 *03,014* Not available NTIS

Analysis of Transverse Flow in Aligned Fibrous Porous Media.
PB96-167200 *03,177* Not available NTIS

Analytic Calculation of Polarized Neutron Reflectivity from Superconductors.
PB95-164224 *04,629* Not available NTIS

Analytical Applications of Guided Neutron Beams.
PB96-112347 *04,041* Not available NTIS

Analytical Estimation of Carrier Multipath Bias on GPS Position Measurements.
PB94-215712 *04,845* PC A04/MF A01

Analytical Expressions for Barkhausen Jump Size Distributions.
PB95-180345 *04,680* Not available NTIS

Analytical Method for Determining Thermal Conductivity from Dynamic Experiments.
PB96-102744 *04,024* Not available NTIS

Analytical Method of Determining the Heat Capacity at High Temperatures from the Surface Temperature of a Cooling Sphere.
PB94-216124 *03,865* Not available NTIS

Analyzing and Exploiting Numerical Characteristics of Zone Fire Models.
PB96-102314 *01,400* Not available NTIS

Analyzing Electronic Commerce.
PB94-219102 *00,480* PC A03/MF A01

Angle-Differential and Momentum-Transfer Cross Sections for Low-Energy Electron-Cs Scattering.
PB95-203402 *04,005* Not available NTIS

Angular Distributions for Near-Threshold (e,2e) Processes for Li and Mg.
PB94-185725 *00,778* Not available NTIS

Angular Variation of the Personal Dose Equivalent, Hp(0.07), for Beta Radiation and Nearly Monoenergetic Electron Beams: Preliminary Results.
PB95-168472 *03,630* Not available NTIS

Anharmonic Oscillator Analysis Using Modified Airy Functions.
PB94-185311 *03,798* Not available NTIS

Anharmonic Phonons and the Isotope Effect in Superconductivity.
PB94-200557 *04,486* Not available NTIS

Anionic Triphenylmethane Dye Solutions for Low-Dose Food Irradiation Dosimetry.
PB96-135173 *03,715* Not available NTIS

Anisotropic Phase Separation Kinetics in a Polymer Blend Solution Following Cessation of Shear Studied by Light Scattering.
PB95-151247 *01,241* Not available NTIS

Anisotropy of Interfaces in an Ordered Alloy: A Multiple-Order-Parameter Model.
PB96-131594 *04,741* PC A04/MF A01

Anisotropy of Polarized X-ray Emission from Atoms and Molecules.
PB95-163002 *04,621* Not available NTIS

Anisotropy of the Surfaces of Pores in Plasma Sprayed Alumina Deposits.
PB96-123211 *03,126* Not available NTIS

Annealing of Bragg Gratings in Hydrogen-Loaded Optical Fiber.
PB96-155437 *04,361* Not available NTIS

Annex 18: An International Study of Refrigerant Properties.
PB95-168936 *03,266* Not available NTIS

Annual Conference on Fire Research: Book of Abstracts, October 17-20, 1994.
PB95-104964 *01,376* PC A09/MF A02

Anomalous Behavior of a Quantized Hall Plateau in a High-Mobility Si Metal-Oxide-Semiconductor Field-Effect Transistor.
PB95-164174 *02,354* Not available NTIS

Anomalous Dispersion and Thermal Expansion in Lightly-Doped KTa1-xNbxO3.
PB95-152302 *04,585* Not available NTIS

Anomalous Freezing and Melting of Solvent Crystals in Swollen Gels of Natural Rubber.
PB94-212321 *01,223* Not available NTIS

Anomalous Odd- to Even-Mass Isotope Ratios in Resonance Ionization with Broad-Band Lasers.
PB94-211406 *03,839* Not available NTIS

Anomalous Relation between Time and Frequency Domain PMD Measurements.
PB97-119390 *04,398* Not available NTIS

TITLE INDEX

Anomalous Switching Phenomenon in Critical-Current Measurements When Using Conductive Mandrels.
PB96-137781 *02,233* Not available NTIS

Anova Estimates of Variance Components for a Class of Mixed Models.
PB96-141163 *03,448* Not available NTIS

Antenna-Coupled High-Tc Air-Bridge Microbolometer on Silicon.
PB95-180899 *04,315* Not available NTIS

Antiferromagnetic Interlayer Correlations in Annealed Ni80Fe20/Ag Multilayers.
PB97-122220 *03,109* Not available NTIS

APDE Demonstration System Architecture. National PDES Testbed Report Series.
PB94-154325 *02,767* PC A03/MF A01

Aperture Coupling to a Coaxial Air Line: Theory and Experiment.
PB94-211968 *02,216* Not available NTIS

Aperture Excitation of Electrically Large, Lossy Cavities.
PB94-145711 *00,029* PC A05/MF A01

Aperture Excitation of Electrically Large, Lossy Cavities.
PB95-175675 *00,031* Not available NTIS

Apparatus for Resistance Measurement of Short, Small-Diameter Conductors.
PB96-141130 *04,417* Not available NTIS

Apparel Manufacturing Glossary for Application Protocol Development.
PB95-198750 *02,755* PC A04/MF A01

Apparent Bias in the X-Ray Fluorescence Determination of Titanium in Selected NIST SRM Low Alloy Steels.
PB95-108759 *03,212* Not available NTIS

Apparent Molar Heat Capacities and Apparent Molar Volumes of Aqueous Glucose at Temperatures from 298.15 K to 327.01 K.
PB94-212800 *03,459* Not available NTIS

Appearance Intensities for Multiply Charged Ions in a Strong Laser Field.
PB96-160445 *04,089* Not available NTIS

Appearance Potentials of Ions Produced by Electron-Impact Induced Dissociative Ionization of SF6, SF4, SF5Cl, S2F10, SO2, SO2F2, SOF2, and SOF4.
PB96-119730 *01,080* Not available NTIS

Applicability of Effective Medium Theory to Ferroelectric/Ferrimagnetic Composites with Composition and Frequency-Dependent Complex Permittivities and Permeabilities.
PB96-157854 *01,945* Not available NTIS

Application of a Multizone Airflow and Contaminant Dispersal Model to Indoor Air Quality Control in Residential Buildings.
PB95-180238 *02,555* Not available NTIS

Application of a Novel Slurry Furnace AAS Protocol for Rapid Assessment of Lead Environmental Contamination.
PB96-112354 *02,526* Not available NTIS

Application of a Simple Technique for Estimating Errors of Finite-Element Solutions Using a General-Purpose Code.
PB94-200250 *04,818* Not available NTIS

Application of Boundary Element Methods to a Transient Axis-Symmetric Heat Conduction Problem.
PB94-212693 *01,375* Not available NTIS

Application of Digital-Image-Based Models to Microstructure, Transport Properties, and Degradation of Cement-Based Materials.
PB96-156161 *00,406* Not available NTIS

Application of Electromagnetic-Acoustic Transducers for Nondestructive Evaluation of Stresses in Steel Bridge Structures.
PB96-167978 *01,301* PC A04/MF A01

Application of Expert System to Select Data Sources from Chemical Information Databases.
PB95-125654 *00,505* Not available NTIS

Application of Metadata Standards.
PB96-180187 *01,771* Not available NTIS

Application of ODF to the Rietveld Profile Refinement of Polycrystalline Solid.
PB95-202388 *03,401* Not available NTIS

Application of Photochemical Reaction in Electrochemical Detection of DNA Intercalation.
PB94-185733 *00,686* Not available NTIS

Application of Single Electron Tunneling: Precision Capacitance Ratio Measurements.
PB96-102157 *04,703* Not available NTIS

Application of the Collocation Method in Three Dimensions to a Model Semiconductor Problem.
PB97-122428 *02,457* Not available NTIS

Application of the Electronic Balance in High Precision Pycnometry.
PB94-187564 *00,534* PC A03/MF A01

Application of the Modified Voltage-Dividing Potentiometer to Overlay Metrology in a CMOS/Bulk Process.
PB94-181997 *02,302* Not available NTIS

Application of the Pointer State Subgraph to Static Program Slicing.
PB96-167838 *01,768* PC A03/MF A01

Application of the Taylor Dispersion Method in Supercritical Fluids.
PB95-164323 *00,977* Not available NTIS

Application of Thermal Analysis Techniques to the Characterization of EPDM Roofing Membrane Materials.
PB95-125845 *00,359* Not available NTIS

Application of Thermodynamic and Detailed Chemical Kinetic Modeling to Understanding Combustion Product Generation in Enclosure Fires.
PB96-135322 *01,413* Not available NTIS

Application of Thermodynamics to Biotechnology.
PB95-150793 *03,529* Not available NTIS

Application Portability Profile (APP): The U.S. Government's Open System Environment Profile Version 3.0.
PB96-158712 *01,753* PC A07/MF A02

Application Profile for ISDN.
PB95-163689 *01,479* Not available NTIS

Application Profile for the Government Information Locator Service (GILS). Category: Software Standard; Subcategory: Information Interchange.
FIPS PUB 192 *01,800* PC A03/MF A01

Application Protocol Information Base World Wide Web Gateway.
PB96-202320 *02,791* PC A03/MF A01

Application Software Interface: ISDN Services for an Open Systems Environment.
PB96-131487 *01,492* PC A03/MF A01

Applications of Diamond Films and Related Materials: International Conference (3rd). Held in Gaithersburg, Maryland on August 21-24, 1995. Supplement to NIST Special Publication 885.
PB95-256053 *03,063* PC A04/MF A01

Applications of Fluorescence Spectroscopy in Polymer Science and Technology.
PB95-163770 *01,258* Not available NTIS

Applications of the Vortex Tube in Chemical Analysis.
PB94-199171 *00,544* Not available NTIS

Applications of the Vortex Tube in Chemical Analysis. Part 2. Applications.
PB96-112107 *00,615* Not available NTIS

Applying Virtual Environments to Manufacturing.
PB94-142502 *02,803* PC A03/MF A01

Approach to Setting Performance Requirements for Automated Evaluation of the Parameters of High-Voltage Impulses.
PB94-185634 *01,878* Not available NTIS

Approaches Using Virtual Environments with Mosaic.
PB95-169108 *01,599* Not available NTIS

Appropriate Ultrasonic System Components for NDE of Thick Polymer Composites.
PB95-125696 *03,148* Not available NTIS

Approximate Confidence Intervals on Linear Combinations of Expected Mean Squares.
PB95-151296 *03,435* Not available NTIS

Approximate Confidence Intervals on Positive Linear Combinations of Expected Mean Squares.
PB95-151304 *03,436* Not available NTIS

Approximate Solution to the Scalar Wave Equation for Optical Waveguides.
PB95-126256 *04,254* Not available NTIS

Arc Spectra of Gallium, Indium, and Thallium.
AD-A295 411/3 *00,718* PC A03/MF A01

Artificial Crack in Steel: An Ultrasonic-Resonance-Spectroscopy and Modeling Study.
PB96-141395 *03,241* Not available NTIS

Ascorbic and Dehydroascorbic Acids Measured in Plasma Preserved with Dithiothreitol or Metaphorphoric Acid.
PB94-216330 *03,495* Not available NTIS

Ashland Tank Collapse Investigation.
PB95-126314 *02,481* Not available NTIS

Ashland Tank-Collapse Investigation: Closure by Authors.
PB95-126322 *02,482* Not available NTIS

Aspects of a Deformable Superconductor Model for the Vortex Mass.
PB95-175303 *04,652* Not available NTIS

Aspects of a Product Model Supporting Apparel Virtual Enterprises.
PB96-183231 *02,790* PC A03/MF A01

Asperity-Asperity Contact Mechanisms Simulated by a Two-Ball Collision Apparatus.
PB95-164158 *02,966* Not available NTIS

Assay of the Eluent from the Alumina-Based Tungsten-188-Rhenium-188 Generator.
PB94-200482 *03,829* Not available NTIS

Assessing Functional Diversity by Program Slicing.
PB96-160890 *03,734* Not available NTIS

Assessing Halon Alternatives for Aircraft Engine Nacelle Fire Suppression.
PB96-102454 *01,401* Not available NTIS

Assessing MOS Gate Oxide Reliability on Wafer Level with Ramped/Constant Voltage and Current Stress.
PB96-180112 *04,115* Not available NTIS

Assessing the Credibility of the Calorific Content of Muncipal Solid Waste.
PB94-199882 *02,581* Not available NTIS

Assessing Ventilation Effectiveness in Mechanically Ventilated Office Buildings.
PB95-162079 *00,255* Not available NTIS

Assessment of Data by a Second-Order Transfer Function.
PB95-182390 *03,760* PC A05/MF A01

Assessment of 'Peaks Over Threshold' Methods for Estimating Extreme Value Distribution Tails.
PB95-161360 *00,441* Not available NTIS

Assessment of Site Response Analysis Procedures.
PB95-210928 *00,450* PC A07/MF A02

Assessment of Technologies for Advanced Fire Detection.
PB95-126330 *00,294* Not available NTIS

Assessment of Technology for Detection of Stress Corrosion Cracking in Gas Pipelines. Final Report, July 1993-March 1994.
PB94-206646 *02,475* PC A05/MF A02

Assessment of Testing Methodology for Ceramic Matrix Composites.
PB94-200532 *03,139* Not available NTIS

Assessment of the Al-Sb System.
PB94-200474 *03,329* Not available NTIS

Assessment of the DOD Goal Security Architecture (DGSA) for Non-Military Use.
PB95-189510 *03,653* PC A03/MF A01

Assessment of Uncertainties of Calibration of Resistance Thermometers at the National Institute of Standards and Technology.
PB94-142478 *02,624* PC A03/MF A01

Assessment of Uncertainties of Liquid-in-Glass Thermometer Calibrations at the National Institute of Standards and Technology.
PB94-142510 *02,625* PC A03/MF A01

Assessment of Uncertainties of Thermocouple Calibrations at NIST.
PB94-152691 *03,782* PC A03/MF A01

Associated Object Model for Distributed Systems.
PB94-212016 *01,694* Not available NTIS

Associative Electron Attachment to S2F10, S2OF10, and S2O2F10.
PB95-140992 *00,907* Not available NTIS

Associative Ionization in Collisions of Slowed and Trapped Sodium.
PB95-125886 *03,880* Not available NTIS

Astrophysical Aspects of Neutral Atom Line Broadening.
PB94-213287 *00,061* Not available NTIS

Asymmetric Tip Morphology of Creep Microcracks Growing Along Bimaterial Interfaces.
PB94-200243 *03,138* Not available NTIS

Asymmetry between Flux Penetration and Flux Expulsion in Tl-2212 Superconductors.
PB95-125647 *04,527* Not available NTIS

Asymptotic and Numerical Analysis of a Premixed Laminar Nitrogen Dioxide-Hydrogen Flame.
PB96-164256 *01,422* Not available NTIS

Asymptotic Behavior of Modulated Taylor-Couette Flows with a Crystalline Inner Cylinder.
PB94-199072 *04,469* Not available NTIS

Asymptotic Wave Function Splitting Procedure for Propagating Spatially Extended Wave Functions: Application to Intense Field Photodissociation of H2(+).
PB94-211786 *03,847* Not available NTIS

Asynchronous Transfer Mode Procurement and Usage Guide.
PB95-174967 *01,481* PC A03/MF A01

Atmospheric and Marine Trace Chemistry: Interfacial Biomediation and Monitoring.
PB94-199122 *03,752* Not available NTIS

Atmospheric Lifetimes of HFC-143a and HFC-245fa: Flash Photolysis Resonance Fluorescence Measurements of the OH Reaction Rate Constants.
PB97-112577 *00,118* Not available NTIS

Atmospheric Reactivity of alpha-Methyl-Tetrahydrofuran.
PB95-163705 *02,548* Not available NTIS

Atom Cooling and Trapping, and Collisions of Trapped Atoms.
PB96-122916 *04,048* Not available NTIS

Atom-counting standards and Doppler-free resonance ionization mass spectroscopy. (Progress report).
DE94018562 *00,723* PC A02/MF A01

Atom-Optical Properties of a Standing-Wave Light Field.
PB96-141072 *04,356* Not available NTIS

Atomic Beam Splitters and Mirrors by Adiabatic Passage in Multilevel Systems.
PB94-216439 *03,867* Not available NTIS

Atomic Branching Ratio Data for Carbon-Like Ions.
PB94-212842 *03,855* Not available NTIS

Atomic Branching Ratio Data for Nitrogen-Like Species.
PB96-190152 *04,122* Not available NTIS

Atomic Branching Ratio Data for Oxygen-Like Species.
PB95-180436 *03,963* Not available NTIS

Atomic Clock.
PB96-119490 *01,553* Not available NTIS

Atomic Data Needed for Far Ultraviolet Astronomy with HUT and FUSE.
PB94-213402 *00,062* Not available NTIS

Atomic Energy Levels As Derived from the Analyses of Optical Spectra. Volume 1. Section 1. The Spectra of Hydrogen, Deuterium, Helium, Lithium Beryllium, Boron, Carbon, Nitrogen, Oxygen, and Fluorine.
AD-A278 130/0 *03,764* PC A05/MF A01

Atomic Energy Levels. As Derived From the Analyses of Optical Spectra. Volume 3.
AD-A280 279/1 *00,714* PC A13/MF A03

Atomic Energy Levels in Crystals.
AD-A280 150/4 *04,431* PC A05/MF A01

Atomic Iron in Its (5)D Ground State: A Direct Measurement of the J = 0 inverted arrow 1 and J = 1 inverted arrow 2 Fine-Structure Intervals (1.2).
PB96-141221 *04,756* Not available NTIS

Atomic Manipulation of Polarizable Atoms by Electric Field Directional Diffusion.
PB95-150587 *04,572* Not available NTIS

Atomic, Molecular, and Optical Physics with X-rays.
PB94-213378 *03,863* Not available NTIS

Atomic Oxygen Fine Structure Splittings with Tunable Far Infrared Spectroscopy.
PB95-152203 *03,915* Not available NTIS

Atomic-scale characterization of hydrogenated amorphous-silicon films and devices. Annual subcontract report, 14 February 1994--14 April 1995.
DE95009287 *02,294* PC A03/MF A01

Atomic Sulfur: Frequency Measurement of the J=0 inversely maps 1 Fine-Structure Transition at 56.3 Microns by Laser Magnetic Resonance.
PB95-180105 *01,007* Not available NTIS

Atomic Theory of Fracture of Brittle Materials: Application to Covalent Semiconductors.
PB94-216553 *04,519* Not available NTIS

Atomic Transition Probabilities and Tests of the Spectroscopic Coupling Scheme for N I.
PB96-138466 *04,057* Not available NTIS

Atomic Transition Probability Ratios between Some Ar I 4s-4p and 4s-5p Transitions.
PB94-211554 *03,842* Not available NTIS

Atomic Weights of the Elements 1991.
PB94-168606 *00,754* Not available NTIS

Atomic Weights of the Elements, 1993.
PB96-145909 *01,114* Not available NTIS

Atoms in Optical Molasses.
PB95-108874 *03,875* Not available NTIS

Atoms in Optical Molasses: Applications to Frequency Standards.
PB95-108882 *03,876* Not available NTIS

Attempts at Extending the Unified Theory to Include Many-Body Effects.
PB94-212719 *04,408* Not available NTIS

AutoBid 2.0: The Microcomputer System for Police Patrol Vehicle Selection.
PB96-154570 *04,871* PC A03/MF A01

Autocorrelation Functions from Optical Scattering for One-Dimensionally Rough Surfaces.
PB94-216538 *04,244* Not available NTIS

Autofluorescence Detection of 'Escherichia coli' on Silver Membrane Filters.
PB96-163639 *03,590* Not available NTIS

Autoionizing Resonances in Electric Fields.
PB94-212727 *03,853* Not available NTIS

Automated Guarded Bridge for Calibration of Multimegohm Standard Resistors.
PB97-119150 *02,289* Not available NTIS

Automated, High-Precision Coulometric Titrimetry. Part 1. Engineering and Implementation.
PB95-150199 *00,575* Not available NTIS

Automated, High Precision Coulometric Titrimetry. Part 2. Strong and Weak Acids and Bases.
PB95-150207 *00,576* Not available NTIS

Automated Inspection: The Integration of National Standards and Commercial Products at NIST.
PB95-163077 *02,906* Not available NTIS

Automated Josephson Integrated Circuit Test System.
PB95-175246 *02,057* Not available NTIS

Automated Manufacturing Research Facility 1994 Annual Report.
PB95-209854 *00,015* PC A05/MF A01

Automated Measurement of Nonlinearity of Optical Fiber Power Meters.
PB96-176540 *04,110* Not available NTIS

Automated Optical Roughness Inspection.
PB95-152179 *02,905* Not available NTIS

Automated Resistance Measurements at NIST.
PB96-119326 *02,274* Not available NTIS

Automatic Calibration of Inductive Voltage Dividers for the NASA Zeno Experiment.
PB95-152849 *02,041* Not available NTIS

Automatic Inductive Voltage Divider Bridge Operates from 10 Hz to 100 kHz.
PB94-198413 *02,032* Not available NTIS

Backdraft Phenomena.
PB94-193927 *01,366* PC A11/MF A03

Backscattering in Electron-Impact Excitation of Multiply Charged Ions.
PB94-185345 *03,799* Not available NTIS

Bacterial Enumeration in Storage Water.
PB96-163647 *03,591* Not available NTIS

Bacteriorhodopsin Immobilized in Sol-Gel Glass.
PB95-151429 *03,532* Not available NTIS

Bacteriorhodopsin Retains Its Light-Induced Proton-Pumping Function After Being Heated to 140C
PB96-102728 *03,471* Not available NTIS

Band-Limited, White Gaussian Noise Excitation for Reverberation Chambers and Applications to Radiated Susceptibility Testing.
PB96-165410 *01,960* PC A07/MF A02

Band-to-Band Photoluminescence and Luminescence Excitation in Extremely Heavily Carbon-Doped Epitaxial GaAs.
PB95-150413 *04,570* Not available NTIS

Barium Contributions to the Valence Electronic Structure of YBa2Cu3O7-delta, PrBa2Cu3O7-delta, and Other Barium-Containing Compounds.
PB96-158019 *04,076* Not available NTIS

Basic Linear Algebra Operations in SLI Arithmetic.
PB96-165931 *03,421* PC A03/MF A01

Beam Analysis Round Robin.
PB94-212545 *04,239* Not available NTIS

Beam Line for Highly Charged Ions.
PB97-111256 *04,143* Not available NTIS

Beamcon III, a Linearity Measurement Instrument for Optical Detectors.
PB96-113576 *04,337*
(Order as PB96-113535, PC A05/MF A01)

Behavior of a Calcium Phosphate Cement in Simulated Blood Plasma In vitro.
PB95-168712 *00,165* Not available NTIS

Behavior of Atoms in a Compressed Magneto-Optical Trap.
PB95-203105 *03,999* Not available NTIS

Behavior of Charring Materials in Simulated Fire Environments.
PB94-196045 *01,368* PC A99/MF A06

Behavior of Mock-Ups in the California Technical Bulletin 133 Test Protocol: Fabric and Barrier Effects.
PB95-231585 *00,301* PC A05/MF A01

Behavior of Surface Partial Discharge on Aluminum Oxide Dielectrics.
PB96-123781 *01,937* Not available NTIS

Benchmarks for the Evaluation of Speech Recognizers.
PB94-211539 *01,566* Not available NTIS

Bending-Induced Loss in Dual-Mode Rectangular Waveguides.
PB95-168795 *04,288* Not available NTIS

Bending-Induced Phase Shifts in Dual-Mode Planar Optical Waveguides.
PB95-161329 *04,271* Not available NTIS

Beneficial Effects of Nitrogen Atomization on an Austenitic Stainless Steel.
PB94-212396 *03,209* Not available NTIS

Benefits and Costs of Research: A Case Study of the Fire Safety Evaluation System.
PB96-202288 *00,232* PC A06/MF A01

Benefits and Costs of Research: Two Case Studies in Building Technology.
PB96-202221 *00,230* PC A07/MF A02

Bent Rectangular Core Waveguides: An Accurate Perturbation Approach.
PB95-168803 *04,289* Not available NTIS

beta-D-Glucosyl-Hydroxymethyluracil: A Novel Modified Base Present in the DNA of the Parastic Protozoan T. brucei.
PB94-172319 *03,524* Not available NTIS

Beyond the Technology Roadmaps: An Assessment of Electronic Materials Research and Development.
PB96-165998 *01,961* PC A05/MF A01

BFRL Fire Publications, 1993.
PB94-164191 *00,192* PC A03/MF A01

Bias Current Dependent Resistance Peaks in NiFe/Ag Giant Magnetoresistance Multilayers.
PB97-112346 *04,153* Not available NTIS

Bibliography of Books and Published Reports on Gas Turbines, Jet Propulsion, and Rocket Power Plants.
AD-A278 138/3 *01,445* PC A04/MF A01

Bibliography of Books and Published Reports on Gas Turbines, Jet Propulsion, and Rocket Power Plants, January 1950 through December 1953.
AD-A278 213/4 *01,446* PC A06/MF A02

Bibliography of Computer Security Glossaries.
PB94-216710 *01,587* Not available NTIS

Bibliography of Photon Total Cross Section (Attenuation Coefficient) Measurements 10 eV to 13.5 GeV, 1907-1993.
PB94-193760 *03,804* PC A06/MF A02

Bibliography of the NIST Electromagnetic Fields Division Publications.
PB94-165990 *01,875* PC A06/MF A02

Bibliography of the NIST Electromagnetic Fields Division Publications.
PB95-135562 *01,886* PC A06/MF A02

Bibliography of the NIST Electromagnetic Fields Division Publications.
PB96-210778 *01,980* PC A08/MF A02

Bibliography of the NIST Optoelectronics Division.
PB96-128210 *02,193* PC A04/MF A01

Bibliography of the NIST Optoelectronics Division.
PB97-116040 *02,207* PC A06/MF A01

Bibliography of the Physical Equilibria and Related Properties of Some Cryogenic Systems.
AD-A281 167/7 *03,769* PC A07/MF A02

Bibliography on Apparel Sizing and Related Issues.
PB94-161924 *02,806* PC A03/MF A01

Bimolecular Interactions in (Et)3SiOH:Base:CCl4 Hydrogen-Bonded Solutions Studied by Deactivation of the Free OH-Stretch Vibration.
PB97-118657 *04,166* Not available NTIS

Binary Decision Clustering for Neural Network Based Optical Character Recognition.
PB95-171971 *01,848* PC A03/MF A01

Binary Decision Clustering for Neural-Network-Based Optical Character Recognition.
PB96-186184 *01,857* Not available NTIS

Binary versus Decade Inductive Voltage Divider Comparison and Error Decomposition.
PB96-112263 *02,071* Not available NTIS

Binder Characterization and Evaluation by Nuclear Magnetic Resonance Spectroscopy.
PB94-193471 *01,334* PC A08/MF A02

Bioactive Polymeric Dental Materials Based on Amorphous Calcium Phosphate.
PB96-147012 *03,572* Not available NTIS

Bioleaching of Cobalt from Smelter Wastes by 'Thiobacillus ferrooxidans'.
PB95-140968 *02,582* Not available NTIS

Biological Macromolecular Crystallization Database: A Tool for Developing Crystallization Strategies.
PB95-126157 *00,897* Not available NTIS

Biological Macromolecule Crystallization Database and NASA Protein Crystal Growth Archive.
PB97-109136 *01,171*
(Order as PB97-109011, PC A11/MF A03)

Biological Thermodynamic Data for the Calibration of Differential Scanning Calorimeters: Dynamic Temperature Data on the Gel to Liquid Crystal Phase Transition of Dialkylphosphatidylcholine in Water Suspensions.
PB95-162707 *03,464* Not available NTIS

Bistatic Scattering of Absorbing Materials from 30 to 1000 MHz.
PB95-150934 *01,891* Not available NTIS

BLCC: The NIST 'Building Life-Cycle Cost' Program, Version 4.21. User's Guide and Reference Manual.
PB95-190682 *00,263* PC A06/MF A02

Body Dimensions for Apparel.
PB94-187739 *02,813* PC A03/MF A01

Bonding in Doubly Charged Diatomics.
PB95-164315 *00,976* Not available NTIS

Bonding Wires to Quantized Hall Resistors.
PB96-102637 *01,921* Not available NTIS

Book Review: Aspects and Applications of the Random Walk.
PB96-123534 *04,215* Not available NTIS

Book Review: Statistical Physics of Macromolecules.
PB96-123526 *01,280* Not available NTIS

Boron-Implanted 6H-SiC Diodes.
PB96-159678 *04,081* Not available NTIS

Boundary Conforming Grid Generation System for Interface Tracking.
PB94-158268 *03,312* PC A03/MF A01

Boundary Conforming Grid Generation System for Interface Tracking.
PB96-103007 *03,357* Not available NTIS

Boundary Integral Method for the Simulation of Two-Dimensional Particle Coarsening.
PB94-216744 *03,411* Not available NTIS

Boundary Lubrication of Silicon Nitride.
PB95-213583 *03,226* PC A18/MF A04

Bounds on Frequency Response Estimates Derived from Uncertain Step Response Data.
PB96-122874 *03,419* Not available NTIS

Bounds on Least-Squares Four-Parameter Sine-Fit Errors Due to Harmonic Distortion and Noise.
PB96-141304 *01,609* Not available NTIS

Bragg Gratings in Optical Fibers Produced by a Continuous-Wave Ultraviolet Source.
PB95-162020 *04,274* Not available NTIS

Brillouin Light Scattering Intensities for Thin Magnetic Films with Large Perpendicular Anisotropies.
PB94-211174 *04,488* Not available NTIS

Bringing Natural Language Information Retrieval Out of the Closet.
PB94-172335 *02,720* Not available NTIS

Broadband High-Optical-Density Filters in the Infrared.
PB95-180261 *04,309* Not available NTIS

Broadband Mismatch Error in Noise Measurement Systems.
PB95-162061 *02,044* Not available NTIS

Brownian Diffusion of Hard Spheres at Finite Concentrations.
PB95-164307 *00,975* Not available NTIS

Buffer Layer Modulation-Doped Field-Effect-Transistor Interactions in the Al0.33Ga0.67As/GaAs Superlattice System.
PB96-102876 *02,380* Not available NTIS

Building a Better Crycooler.
PB96-119615 *04,734* Not available NTIS

Building and Fire Research Laboratory Publications, 1993.
PB95-143202 *00,369* PC A06/MF A02

Building and Fire Research Laboratory Publications, 1994.
PB95-226684 *00,398* PC A07/MF A02

Building Life Cycle Cost Computer Program (BLCC), Version 4.2-95 (for Microcomputers).
PB95-501953 *00,266* CP D02

Building Life Cycle Cost Computer Program (BLCC) Version 4.4-97 (for Microcomputers).
PB97-500342 *00,284* CP D02

Building Life Cycle Cost Computer Program (BLCC) Version 4.21-95 (for Microcomputers).
PB95-502779 *00,267* CP D02

Building Life Cycle Cost Computer Program (BLCC) Version 4.22-95 (for Mircomputers).
PB96-502794 *00,277* CP D02

Building Life Cycle Cost Computer Program (BLCC) Version 4.22-95 (for Microcomputers).
PB95-503397 *00,268* CP D02

Bulk Modulus and Young's Modulus of Nanocrystalline gamma-Alumina.
PB96-204185 *03,092* Not available NTIS

Burning Rate and Flame Heat Flux For PMMA in the Cone Calorimeter.
PB95-216990 *00,393* PC A07/MF A02

Burning Rate of Premixed Methane-Air Flames Inhibited by Fluorinated Hydrocarbons.
PB95-180584 *01,391* Not available NTIS

Business and Manufacturing Motivations for the Developing of Analytical Technology and Metrology for Semiconductors.
PB96-161948 *04,778* Not available NTIS

C++ in Safety Critical Systems.
PB96-154588 *01,750* PC A04/MF A01

Ca1-xCuO2, a NaCuO2-Type Related Structure.
PB95-162822 *04,620* Not available NTIS

Ca4Bi6O13: A Compound Containing an Unusually Low Bismuth Coordination Number and Short Bi Bi Contacts.
PB95-141131 *00,911* Not available NTIS

Calcium Phosphate Cements.
PB97-111595 *03,580* Not available NTIS

Calcium Phosphate Precipitation in Liposomal Suspensions.
PB94-172145 *03,452* Not available NTIS

Calculated Fiber Attenuation: A General Method Yielding Stationary Values.
PB95-175501 *04,298* Not available NTIS

Calculating Combined Buoyancy- and Pressure-Driven Flow Through a Shallow, Horizontal, Circular Vent; Application to Problem of Steady Burning in a Ceiling-Vented Enclosure.
PB96-164108 *00,409* Not available NTIS

Calculating Flame Spread on Horizontal and Vertical Surfaces.
PB94-187283 *00,335* PC A04/MF A01

Calculating Time-to-Contact Using Real-Time Quantized Optical Flow.
PB95-210522 *01,604* PC A03/MF A01

Calculation of Enthalpy and Entropy Differences of Near-Critical Binary Mixtures with the Modified Leung-Griffiths Model.
PB95-108635 *00,885* Not available NTIS

Calculation of Higher Heating Values of Biomass Materials and Waste Components from Elemental Analyses.
PB94-199254 *02,474* Not available NTIS

Calculation of Photon Mass Energy-Transfer and Mass Energy-Absorption Coefficients.
PB97-110399 *04,137* Not available NTIS

Calculation of the Thermal Conductivity and Gas Permeability in a Uniaxial Bundle of Fibers.
PB95-180931 *03,058* Not available NTIS

Calculations of Electron Inelastic Mean Free Paths (IMFPs). 4. Evaluation of Calculated IMFPs and of the Predictive IMFP Formula TPP-2 for Electron Energies between 50 and 2000 eV.
PB95-150728 *00,922* Not available NTIS

Calculations of Electron Inelastic Mean Free Paths. 5. Data for 14 Organic Compounds over the 50-2000 eV Range.
PB95-150355 *00,916* Not available NTIS

Calibrating On-Wafer Probes to the Probe Tips.
PB95-163945 *02,352* Not available NTIS

Calibration and Performance of GafChromic DM-100 Radiochromic Dosemeters.
PB97-119291 *00,703* Not available NTIS

Calibration in the Earth Observing System (EOS) Project. Part 2. Implementation.
PB97-112213 *04,842* Not available NTIS

Calibration of a Superconducting Gravimeter Using Absolute Gravity Measurements.
PB95-202651 *03,684* Not available NTIS

Calibration of Dosimeters for the Cryogenic Irradiation of Composite Materials Using an Electron Beam.
PB95-180964 *03,968* Not available NTIS

Calibration of Electret-Based Integral Radon Monitors Using NIST Polyethylene-Encapsulated (226)Ra/(222)Rn Emanation (PERE) Standards.
PB96-159223 *01,950*
(Order as PB96-159215, PC A07/MF A02)

Calibration of GPS Equipment in Japan.
PB95-151452 *01,531* Not available NTIS

Calibration of High-Energy Electron Beams by Use of Graphite Calorimeters.
PB95-161113 *04,598* Not available NTIS

Calibration Service for Coaxial Reference Standards for Microwave Power.
PB96-162722 *01,958* PC A07/MF A02

Calibration Standards for Differential Scanning Calorimetry. 1. Zinc Absolute Calorimetric Measurement of Enthalpy of Fusion and Temperature of Fusion HM.
PB94-199817 *00,801* Not available NTIS

Calorimeters for Calibration of High-Dose Dosimeters in High-Energy Electron Beams.
PB96-135272 *04,055* Not available NTIS

Calorimetric and Visual Measurements of R123 Pool Boiling on Four Enhanced Surfaces.
PB96-128129 *04,053* PC A04/MF A01

Calorimetric Determination of the Standard Transformed Enthalpy of a Biochemical Reaction at Specified PH and pMg.
PB94-198249 *03,454* Not available NTIS

CALS-Automated Interchange of Technical Information.
PB94-962000 *03,657* Standing Order

CALS-Automated Interchange of Technical Information.
PB95-962000 *03,666* Standing Order

CALS-Contractor Integrated Technical Information Service (CITIS), Functional Requirements.
PB94-962600 *03,663* Standing Order

CALS-Contractor Integrated Technical Information Service (CITIS), Functional Requirements.
PB95-962600 *03,672* Standing Order

CALS-Department of Defense Computer Aided Acquisition Logistic Support (CALS).
PB94-962500 *03,662* Standing Order

CALS-Department of Defense Computer Aided Acquisition Logistic Support (CALS).
PB95-962500 *03,671* Standing Order

CALS-Digital Representation for Communication of Illustration Date: CGM Application Profile.
PB94-962400 *03,661* Standing Order

CALS-Digital Representation for Communication of Illustration Date: CGM Application Profile.
PB95-962400 *03,670* Standing Order

CALS-Digital Representation for Communication of Product Data: IGES Application Subsets.
PB94-962100 *03,658* Standing Order

CALS-Digital Representation for Communication of Product Data: IGES Application Subsets.
PB95-962100 *03,667* Standing Order

CALS-Markup Requirements and Generic Style Specifications for Electronic Printed Output and Exchange of Text.
PB94-962200 *03,659* Standing Order

CALS-Markup Requirements and Generic Style Specifications for Electronic Printed Output and Exchange of Text.
PB95-962200 *03,668* Standing Order

CALS-Raster Graphics Representation Binary Format Requirements.
PB94-962300 *03,660* Standing Order

CALS-Raster Graphics Representation Binary Format Requirements.
PB95-962300 *03,669* Standing Order

Cambridge Structural Database (CSD): Current Activities and Future Plans.
PB97-109052 *00,516*
(Order as PB97-109011, PC A11/MF A03)

Can Displays Deliver a Full Measure: Manufacturing.
PB96-111935 *02,185* Not available NTIS

Can Quantum Mechanical Description of Electron-Sodium Collisions Be Considered Complete. Present Status and Future Prospects for 3s <-> 3p Transitions.
PB94-185014 *00,768* Not available NTIS

Capabilities for Product Data Exchange.
PB97-118764 *02,798* Not available NTIS

Capacitors with Very Low Loss: Cryogenic Vacuum-Gap Capacitors.
PB97-122600 *02,293* Not available NTIS

Capacity of the Lp Norm-Constrained Poisson Channel.
PB95-125753 *01,515* Not available NTIS

Carbon Acidities of Aromatic Compounds. 1. Effects of In-Ring Aza and External Electron-Withdrawing Groups.
PB94-216595 *00,860* Not available NTIS

Carbon Monoxide Dispersion in Residential Buildings: Literature Review and Technical Analysis.
PB97-114227 *02,571* PC A05/MF A01

TITLE INDEX

Carbon Monoxide Production in Compartment Fires: Reduced-Scale Enclosure Test Facility.
PB95-231700 *01,394* PC A10/MF A03

Carotenoid Reversed-Phase High-Performance Liquid Chromatography Methods: Reference Compendium.
PB94-200516 *00,549* Not available NTIS

Cascading Surge-Protective Devices: Options for Effective Implementation.
PB94-216488 *02,464* Not available NTIS

Cast-Iron Elastic Constants: Effect of Graphite Aspect Ratio.
PB94-213212 *03,211* Not available NTIS

Casual Regularizing Deconvolution Filter for Optimal Waveform Reconstruction.
PB95-203089 *01,603* Not available NTIS

Catalog of National ISDN Solutions for Selected NIUF Applications.
PB94-166006 *01,468* PC A99/MF A06

Catalogue of Electromagnetic Environment Measurements, 30-300 Hz.
PB96-155452 *01,943* Not available NTIS

Catastrophic Failures Propagate Field of Fracture Mechanics.
PB96-135140 *03,217* Not available NTIS

Causality and Maxwell's Equations.
PB97-110522 *04,429* Not available NTIS

Causes of the Apparent Heat Transfer Degradation for Refrigerant Mixtures.
PB94-212701 *03,259* Not available NTIS

Cavitation Contributes Substantially to Tensile Creep in Silicon Nitride.
PB96-122577 *03,171* Not available NTIS

Cavitation Damage During Flexural Creep of SiAlON-YAG Ceramics.
PB94-200110 *03,036* Not available NTIS

Cavity Evolution during Tensil Creep of Si3N4.
PB96-204193 *03,376* Not available NTIS

CCD Mosaic Images of the Supernova Remnant 3C 400.2.
PB95-203527 *00,084* Not available NTIS

Cellular Automaton Simulations of Cement Hydration and Microstructure Development.
PB95-175055 *01,320* Not available NTIS

Cement and Concrete Characterization by Scanning Electron Microscopy.
PB95-163168 *00,379* Not available NTIS

Center for Electronics and Electrical Engineering Technical Progress Bulletin Covering Center Programs, October to December, with 1991 CEEE Events Calendar.
PB94-159787 *02,296* PC A03/MF A01

Center for High Integrity Software System Assurance: Initial Goals and Activities.
PB95-251674 *01,734* PC A03/MF A01

Ceramic Characterization.
DE94013170 *03,026* PC A02/MF A01

Ceramic Powders Characterization: Results of an International Laboratory Study.
PB95-270039 *02,672* PC A22/MF A04

Ceramics Technical Activities, 1993 (NAS-NRC Assessment Panel April 21-22, 1994).
PB94-162591 *03,031* PC A10/MF A03

Ceramics Technical Activities, 1995.
PB96-193677 *03,087* PC A11/MF A03

Certainty Grid to Object Boundary Algorithm.
PB94-203510 *01,835* PC A03/MF A01

Certification, Development and Use of Standard Reference Materials.
PB95-107272 *00,567* Not available NTIS

Certification of Morphine and Codeine in a Human Urine Standard Reference Material.
PB95-176160 *03,499* Not available NTIS

Certification of Phencyclidine in Lyophilized Human Urine Reference Materials.
PB96-160692 *03,508* Not available NTIS

Certification of Polychlorinated Biphenyl Congeners and Chlorinated Pesticides in a Whale Blubber Standard Reference Material.
PB96-103023 *03,745* Not available NTIS

Certification of Polycyclic Aromatic Hydrocarbons in a Marine Sediment Standard Reference Material.
PB96-111778 *02,592* Not available NTIS

Certification of Standard Reference Material (SRM) 1941a, Organics in Marine Sediment.
PB96-123690 *02,593* Not available NTIS

Certification of the Standard Reference Material 1473a, a Low Density Polyethylene Resin.
PB96-128251 *01,282* PC A03/MF A01

Certifying the Chemical Composition of a Biological Material: A Case Study.
PB96-164272 *00,636* Not available NTIS

CFAST Output Comparison Method and Its Use in Comparing Different CFAST Versions.
PB96-109541 *00,401* PC A04/MF A01

Challenges to the National Information Infrastructure: The Barriers to Product Data Sharing. National PDES Testbed Report Series.
PB95-136347 *02,776* PC A03/MF A01

Changes in the Redox State of Iridium Oxide Clusters and Their Relation to Catalytic Water Oxidation: Radiolytic and Electrochemical Studies.
PB95-107017 *00,864* Not available NTIS

Channel Coding for Code Excited Linear Prediction (CELP) Encoded Speech in Mobile Radio Applications.
PB95-143178 *01,475* PC A03/MF A01

Chaos in a Computer-Animated Pendulum.
PB94-212651 *03,852* Not available NTIS

Chaotic Motions of Coupled Galloping Oscillators and Their Modeling as Diffusion Progresses.
PB96-122718 *04,823* Not available NTIS

Characteristics of Adhesive-Bonded Seams Sampled from EPDM Roof Membranes.
PB95-162491 *00,377* Not available NTIS

Characteristics of Light Emission After Low-Energy Electron Impact Excitation of Caesium Atoms.
PB94-198587 *03,806* Not available NTIS

Characteristics of Partial Pressure Analyzers.
PB95-150876 *00,582* Not available NTIS

Characteristics of Turbulence in a Boundary Layer with Zero Pressure Gradient.
AD-A278 249/8 *04,192* PC A03/MF A01

Characterization and Processing of Spray-Dried Zirconia Powders for Plasma Spray Application.
PB97-111231 *04,419* Not available NTIS

Characterization of a Clipped Gaussian Beam.
PB96-102553 *04,331* Not available NTIS

Characterization of a Health Physics Instrument Calibration Range.
PB95-164554 *03,629* Not available NTIS

Characterization of a Tunable Thin Film Microwave YBa2Cu3O7-x/SrTiO3 Coplanar Capacitor.
PB95-175527 *02,264* Not available NTIS

Characterization of Chemically Modified Pore Surfaces by Small Angle Neutron Scattering.
PB95-126181 *00,898* Not available NTIS

Characterization of Cytochrome c/Alkanethiolate Structures Prepared by Self-Assembly on Gold.
PB95-164638 *00,987* Not available NTIS

Characterization of Interface Defects in Oxygen-Implanted Silicon Films.
PB94-216629 *02,322* Not available NTIS

Characterization of Liquid-Phase Epitaxially Grown HgCdTe Films by Magnetoresistance Measurements.
PB96-123617 *04,738* Not available NTIS

Characterization of LPE HgCdTe Film by Magnetoresistance.
PB96-157961 *02,197* Not available NTIS

Characterization of Modified FEL Quartz-Halogen Lamps for Photometric Standards.
PB97-112544 *00,282* Not available NTIS

Characterization of Molecular Network of Thermosets Using Neutron Scattering.
PB95-164109 *01,259* Not available NTIS

Characterization of Phase and Surface Composition of Silicon Carbide Platelets.
PB94-216264 *03,043* Not available NTIS

Characterization of Polyquinoline Blends Using Small Angle Scattering.
PB95-164125 *01,261* Not available NTIS

Characterization of Polyquinoline Block Copolymer Using Small Angle Scattering.
PB95-151882 *01,244* Not available NTIS

Characterization of the Adsorption-Fouling Layer Using Globular Proteins on Ultrafiltration Membranes.
PB94-212909 *00,842* Not available NTIS

Characterization of the Binding of Gallium, Platinum, and Uranium to Pseudomonas Fluorescens by Small-Angle X-ray Scattering and Transmission Electron Microscopy.
PB94-172509 *03,453* Not available NTIS

Characterization of the Densification of Alumina by Multiple Small-Angle Neutron Scattering. (Reannouncement with New Availability Information).
AD-A249 179/3 *03,024* PC A02/MF A01

Characterization of the Emission from 2D Array Josephson Oscillators.
PB95-175121 *02,054* Not available NTIS

Characterization of the Hydrogen Induced Cold Cracking Susceptibility at Simulated Weld Zones in HSLA-100 Steel.
AD-A279 759/5 *03,200* PC A04/MF A01

Characterization of the Hydrogen Induced Cold Cracking Susceptibility at Simulated Weld Zones in HSLA-100 Steel.
PB94-174505 *03,746* PC A04/MF A01

Characterization of the Interaction of Hydrogen with Iridium Clusters in Zeolites by Inelastic Neutron Scattering Spectroscopy.
PB95-180741 *01,013* Not available NTIS

Characterization of the Structure of LaD2.50 by Neutron Powder Diffraction.
PB96-176797 *04,783* Not available NTIS

Characterization of the Structure of TbD2.25 at 70 K by Neutron Powder Diffraction.
PB96-160528 *01,130* Not available NTIS

Characterization of the Structure of YD3 by Neutron Powder Diffraction.
PB96-186150 *01,161* Not available NTIS

Characterization of the Vibrational Dynamics in the Octahedral Sublattices of LaD2.25 and LaH2.25.
PB96-123724 *01,091* Not available NTIS

Characterization of the ZnSe/GaAs Interface Layer by TEM and Spectroscopic Ellipsometry.
PB95-175360 *04,655* Not available NTIS

Characterization of Time-Dependent Dielectric Breakdown in Intrinsic Thin SiO2.
PB97-122527 *02,458* Not available NTIS

Characterization of Two-Dimensional Dopant Profiles: Status and Review.
PB96-119300 *02,400* Not available NTIS

Characterization of Two-Dimensional Dopant Profiles: Status and Review.
PB97-110134 *02,451* Not available NTIS

Characterization of Unknown Linear Systems Based on Measured CW Amplitude.
PB95-161485 *01,897* Not available NTIS

Characterization of Vertical-Cavity Semiconductor Structures.
PB94-200193 *02,126* Not available NTIS

Characterizing Materials Properties for Ceramic Matrix Composites.
PB97-110282 *03,097* Not available NTIS

Charge Cloud Distribution of Heavy Atoms After Excitation by Polarized Electrons.
PB95-203147 *04,001* Not available NTIS

Charge Transfer and Collision-Induced Dissociation Reactions of CF(2+) and CF2(2+) with the Rare Gases at a Laboratory Collision Energy of 49 eV.
PB94-185584 *00,775* Not available NTIS

Charge-Transfer-Induced Multiplet Structure in the N4,5O2,3 Soft-X-ray Emission Spectrum of Lanthanum.
PB96-163746 *04,102* Not available NTIS

Charge Trapping and Breakdown Mechanism in SIMOX.
PB94-216637 *02,323* Not available NTIS

Charpy Impact Test as an Evaluation of 4 K Fracture Toughness.
PB96-190194 *03,219* Not available NTIS

Charpy Specimen Tests at 4 K.
PB96-190335 *03,002* Not available NTIS

Checking the Net Contents of Packaged Goods as Adopted by the 79th National Conference on Weights and Measures, 1994, Third Edition, Supplement 4.
PB95-182226 *00,484* PC A04/MF A01

Chemical and Microbiological Problems Associated with Research on the Biodesulfurization of Coal.
PB95-140950 *02,484* Not available NTIS

Chemical Aspects of Tool Wear in Single Point Diamond Turning.
PB97-112601 *03,021* Not available NTIS

Chemical Determination of Oxidative DNA Damage by Gas Chromatography-Mass Spectrometry.
PB95-175394 *03,540* Not available NTIS

Chemical Effect in Ceramics Grinding.
PB97-122592 *03,113* Not available NTIS

Chemical Inhibition of Methane-Air Diffusion Flame.
PB96-195532 *01,431* PC A04/MF A01

Chemical Stability of Upper-Layer Fire Gases.
PB96-123385 *01,410* Not available NTIS

Chemically Assisted Machining of Si3N4.
PB96-122999 *03,072* Not available NTIS

Chip Morphology, Tool Wear and Cutting Mechanics in Finish Hard Turning.
PB97-112247 *03,106* Not available NTIS

Chromatographic Cryofocusing and Cryotrapping with the Vortex Tube.
PB95-180113 *00,604* Not available NTIS

Churchill Eisenhart, 1913-1994.
PB96-137740 *03,447* Not available NTIS

CIF Crystallographic Information File: A Standard for Crystallographic Data Interchange.
PB97-109169 *04,805*
(Order as PB97-109011, PC A11/MF A03)

Class of Radio-Emitting Magnetic B Stars and a Wind-Fed Magnetosphere Model.
PB94-213451 *00,067* Not available NTIS

Classical Analysis: A Look at the Past, Present, and Future.
PB94-185063 *00,528* Not available NTIS

Classification of Advanced Technical Ceramics.
N94-35335/6 *03,030* PC A07/MF A02

Classified Bibliography: Insulation Condition Monitoring Methods, 1989-1995.
PB96-131586 *02,232* PC A05/MF A01

Clinical Perspective on Dentin Adhesives.
PB94-211240 *00,146* Not available NTIS

Closed Loop Controller for Electron-Beam Evaporators.
PB97-111470 *04,393* Not available NTIS

CMOS Circuit Design for Controlling Temperature in Micromachined Devices.
PB96-156088 *02,196* Not available NTIS

CO2/CH4 Transport in Polyperfluorosulfonate Ionomers: Effects of Polar Solvents on Permeation and Solubility.
PB96-163803 *01,145* Not available NTIS

Coarsening of Unstable Surface Features during Fe(001) Homoepitaxy.
PB96-186127 *04,121* Not available NTIS

Coating of Fibers by Colloidal Techniques in Ceramic Composites.
PB94-216256 *03,196* Not available NTIS

Coaxial Line-Reflect-Match Calibration.
PB96-200118 *02,246* Not available NTIS

Coaxial Reference Standard for Microwave Power.
PB94-193786 *01,880* PC A04/MF A01

COBOL. Category: Software Standard; Subcategory: Programming Language. Includes ANSI'S X3.23-1985, X3.23A-1989 and X3.23B-1993.
FIPS PUB 21-4 *01,670* PC E99

COBOL. Category: Software Standard; Subcategory: Programming Language. Part A.
FIPS PUB 21-4A *01,671* PC E99

COBOL. Category: Software Standard; Subcategory: Programming Language. Part B.
FIPS PUB 21-4B *01,672* PC E99

Codes for Named Populated Places, Primary County Divisions, and Other Locational Entities of the United States (FIPS PUB 55-3) (on Magnetic Tape).
PB95-502563 *00,129* CP T05

Coexistence of Grains with Differing Orthorhombicity in High Quality YBa2Cu3O7-delta Thin Films.
PB96-135033 *04,742* Not available NTIS

Coexisting Densities, Vapor Pressures and Critical Densities of Refrigerants R-32 and R-152a, at 300 - 385 K.
PB95-175691 *03,274* Not available NTIS

Coherent Precipitates in the BCC/Orthorhombic Two Phase Field of the Ti-Al-Nb System.
PB94-198694 *03,317* Not available NTIS

Cold Neutron Gain Calculations for the NBSR Using MCNP.
PB95-163978 *03,731* Not available NTIS

Cold Neutron Prompt Gamma Activation Analysis at NIST: A Progress Report.
PB95-175964 *00,602* Not available NTIS

Collection of Results for the SPC/E Water Model.
PB96-147889 *01,127* PC A03/MF A01

Collision-Induced Emission in the Fundamental Vibration-Rotation Band of H2.
PB94-199445 *03,811* Not available NTIS

Collision-Induced Neutral Loss Reactions of Molecular Dications.
PB94-185808 *00,780* Not available NTIS

Collisional Alignment of CO2 Rotational Angular Momentum States in a Supersonic Expansion.
PB96-103171 *01,069* Not available NTIS

Collisional Energy Transfer between Excited-State Strontium and Noble-Gas Atoms.
PB95-202958 *03,995* Not available NTIS

Collisions of Electrons with Highly-Charged Ions.
PB96-200340 *04,791* Not available NTIS

Color Supplement to NIST Special Publication 400-93: Semiconductor Measurement Technology: Design and Testing Guides for the CMOS and Lateral Bipolar-on-SOI Test Library.
PB94-164316 *02,298* PC A03/MF A01

Colossal Magnetoresistance without Mn(3+)/Mn(4-) Double Exchange in the Stoichiometric Pyrochlore Tl2Mn2O7.
PB97-113070 *04,160* Not available NTIS

Colour Centres in LiF for Measurement of Absorbed Doses Up to 100 MGy.
PB97-118756 *04,169* Not available NTIS

Combined Buoyancy- and Pressure-Driven Flow Through a Shallow, Horizontal, Circular Vent.
PB94-210077 *00,344* PC A03/MF A01

Combined Buoyancy and Pressure-Driven Flow Through a Shallow, Horizontal, Circular Vent.
PB96-164116 *00,410* Not available NTIS

Combined Josephson and Charging Behavior of the Supercurrent in the Superconducting Single-Electron Transistor.
PB95-168522 *04,637* Not available NTIS

Combined Low- and High-Angle X-Ray Structural Refinement of a Co/Pt(111) Multilayer Exhibiting Perpendicular Magnetic Anisotropy.
PB94-198355 *04,457* Not available NTIS

Combining Data from Independent Chemical Analysis Methods.
PB95-140141 *00,572* Not available NTIS

Combining Interactive Exploration and Optimization for Assembly Design.
PB97-112320 *02,794* Not available NTIS

Combustion of a Polymer (PMMA) Sphere in Microgravity.
N96-15569/2 *01,354*
(Order as N96-15552, PC A20/MF A04)

Combustion of Methanol and Methanol/Dodecanol Spray Flames.
PB95-108544 *02,478* Not available NTIS

Comment and Discussion on Digital Processing of PD Pulses.
PB96-122775 *01,932* Not available NTIS

Comment on <<A Dynamic Electric Trap for Ground-State Atoms>>.
PB96-200290 *04,123* Not available NTIS

Comment on 'Phase Transitions in Antiferromagnetic Superlattices'.
PB95-152971 *04,587* Not available NTIS

Comment On: Two-Photon Absorption Series of Calcium.
PB96-157979 *04,074* Not available NTIS

Commentary on 'Optimization of Experimental Parameters for the EPR Detection of the Cellulosic Radical in Irradiated Foodstuffs'.
PB96-164124 *00,043* Not available NTIS

Commentary: The Measurement of Oxidative Damage to DNA by HPLC and GC/MS Techniques.
PB96-200894 *03,484* Not available NTIS

Comments on 'Conversions between S, Z, Y, h, ABCD, and T Parameters Which Are Valid for Complex Source and Load Impedances'.
PB96-102785 *02,069* Not available NTIS

Comments on 'Protecting EFIE-Based Scattering Computations from Effects of Internal Resonances'.
PB95-161568 *01,898* Not available NTIS

Comments on the Paper 'Wolf Shifts and Their Physical Interpretation under Laboratory Conditions'.
PB94-219391 *04,246*
(Order as PB94-219326, PC A05/MF A02)

Comments on the Stability of Bayard-Alpert Ionization Gages.
PB96-103080 *02,673* Not available NTIS

Commercial Helium Permeation Leak Standards: Their Properties and Reliability.
PB97-111413 *04,146* Not available NTIS

Common Criteria: On the Road to International Harmonization.
PB96-123484 *01,606* Not available NTIS

Comparative Measurements of High-Voltage Impulses Using a Kerr Cell and a Resistor Divider.
PB94-172582 *02,028* Not available NTIS

Comparative Photoluminescence Measurement and Simulation of Vertical-Cavity Semiconductor Laser Structures.
PB95-169173 *02,169* Not available NTIS

Comparative Strategies for Correction of Interferences in Isotope Dilution Mass Spectrometric Determination of Vanadium.
PB94-185261 *00,531* Not available NTIS

Comparative Study of Fe-C Bead and Graphite Target Performance with the National Ocean Sciences AMS (NOSAMS) Facility Recombinator Ion Source.
PB95-175790 *00,693* Not available NTIS

Comparing NIST-B 50 mm Orifice Meter Gas Data to the ANSI Equation.
PB95-169207 *02,949* Not available NTIS

Comparing Remote Procedure Calls: Open Network Computing, Distributed Computing Environment and International Organization for Standardization.
PB95-194205 *01,724* PC A03/MF A01

Comparing the Accuracy of Critical-Current Measurements Using the Voltage-Current Simulator.
PB96-119219 *02,227* Not available NTIS

Comparison of a Fixed-Charge and a Polarizable Water Model.
PB96-111620 *01,072* Not available NTIS

Comparison of Elastic and Plastic Contact Models for the Prediction of Thermal Contact Conductance.
PB95-161659 *04,605* Not available NTIS

Comparison of Experimental and Computed Species Concentration and Temperature Profiles in Laminar, Two-Dimensional Methane/Air Diffusion Flames.
PB95-140919 *01,379* Not available NTIS

Comparison of FDDI Asynchronous Mode and DQDB Queue Arbitrated Mode Data Transmission for Metropolitan Area Network Applications.
PB96-160452 *01,498* Not available NTIS

Comparison of FFT Fingerprint Filtering Methods for Neural Network Classification.
PB95-136362 *01,840* PC A03/MF A01

Comparison of Filter Radiometer Spectral Responsivity with the NIST Spectral-Irradiance and Illuminance Scales.
PB97-113161 *04,162* Not available NTIS

Comparison of Finite Element and Analytic Calculations of the Resonant Modes and Frequencies of a Thick Shell Sphere.
PB94-160785 *02,626* PC A03/MF A01

Comparison of Fire Sprinkler Piping Materials: Steel, Copper, Chlorinated Polyvinyl Chloride and Polybutylene, in Residential and Light Hazard Installations.
PB95-182267 *00,299* PC A03/MF A01

Comparison of GPS Broadcast and DMA Precise Ephemerides.
AD-P009 114/0 *01,518* PC A03/MF A01

Comparison of GPS Broadcast and DMA Precise Ephemerides.
N94-30660/2 *01,523*
(Order as N94-30639/6, PC A25/MF A06)

Comparison of Heat-Flow-Meter Tests from Four Laboratories.
PB95-126264 *00,365* Not available NTIS

Comparison of k-Correction and Taylor-Series Correction for Probe-Position Errors in Planar Near-Field Scanning.
PB96-147137 *02,012* Not available NTIS

Comparison of Magnetic Fields of Thin-Film Heads and Their Corresponding Bit Patterns Using Magnetic Force Microscopy.
PB95-180907 *03,763* Not available NTIS

Comparison of Meteor Activity with Occurrence of Sporadic E Reflections.
AD-A292 039/5 *00,116* PC A01/MF A01

Comparison of Methods for Gas Chromatographic Determination of PCBs and Chlorinated Pesticides in Marine Reference Materials.
PB95-140091 *02,584* Not available NTIS

Comparison of NIST and ISO Filtered Bremsstrahlung Calibration Beams.
PB95-180956 *03,967* Not available NTIS

Comparison of NIST and Manufacturer Calibrations of (90)Sr+(90)Y Ophthalmic Applicators.
PB96-123708 *03,634* Not available NTIS

Comparison of Photodiode Frequency Response Measurements to 40 GHz between NPL and NIST.
PB96-111992 *04,038* Not available NTIS

Comparison of POSIX Open System Environment (OSE) and Open Distributed Processing (ODP) Reference Models.
PB96-131495 *01,820* PC A03/MF A01

Comparison of Regular Transmittance Scales of Four National Standardizing Laboratories.
PB94-211232 *04,233* Not available NTIS

Comparison of Responses of a Select Number of Buildings to the 10/17/1989 Loma Prieta (California) Earthquake and Low-Level Amplitude Test Results.
PB96-159645 *00,467* Not available NTIS

TITLE INDEX

Comparison of Selectivities for PCBs in Gas Chromatography for a Series of Cyanobiphenyl Stationary Phases.
PB96-119458 *00,618* Not available NTIS

Comparison of Techniques for Nondestructive Composition Measurements in CdZnTe Substrates.
PB96-103098 *02,703* Not available NTIS

Comparison of the Corrosion Rates of FeAl, Fe(sub 3)Al and Steel in Distilled Water and 0.5 M Sodium Chloride. Technical Report Number 2, January--March 1991.
DE94017332 *03,186* PC A02/MF A01

Comparison of the Liquid Chromatographic Behavior of Selected Steroid Isomers Using Different Reversed-Phase Materials and Mobile Phase Compositions.
PB95-140976 *00,574* Not available NTIS

Comparison of the Seismic Provisions of Model Building Codes and Standards to the 1991 NEHRP Recommended Provisions.
PB95-231858 *00,315* PC A05/MF A02

Comparison of the Unidirectional and Radial In-Plane Flow of Fluids Through Woven Composite Reinforcements.
PB95-162004 *02,698* Not available NTIS

Comparison of Three Techniques for the Precision Measurement of Amplifier Noise.
PB95-163663 *02,349* Not available NTIS

Comparison of Ultralow-Sidelobe-Antenna Far-Field Patterns Using the Planar-Near-Field Method and the Far-Field Method.
PB96-200373 *02,015* Not available NTIS

Comparison of UV-Induced Fluorescence and Bragg Grating Growth in Optical Fiber.
PB95-168597 *04,284* Not available NTIS

Comparison of UV Photosensitivity and Fluorescence during Fiber Grating Formation.
PB96-155445 *04,362* Not available NTIS

Comparison of Wall-Fire Behavior With and Without a Ceiling.
PB94-207404 *00,342* PC A03/MF A01

Comparisons of Measured Linewidths of Sub-Micrometer Lines Using Optical, Electrical, and SEM Metrologies.
PB95-152807 *02,338* Not available NTIS

Comparisons of Some NIST Fixed-Point Cells with Similar Cells of Other Standards Laboratories.
PB97-119242 *00,655* Not available NTIS

Compartment Fire Combustion Dynamics. Annual Report, September 1, 1993-September 1, 1994.
PB95-217162 *00,203* PC A04/MF A01

Compatibility Analysis of the ANSI and ISO IRDS Services Interfaces.
PB94-163474 *01,805* PC A06/MF A02

Compatibilization of Polymer Blends by Complexation. 2. Kinetics of Interfacial Mixing.
PB97-111900 *01,295* Not available NTIS

Compensation for Errors Introduced by Nonzero Fringe Densities in Phase-Measuring Interferometers.
PB97-110506 *04,386* Not available NTIS

Compensation for Substrate Permittivity in Probe-Tip Calibration.
PB95-203519 *01,915* Not available NTIS

Compensation of Errors Detected by Process-Intermittent Gauging.
PB97-110472 *02,846* Not available NTIS

Compensation of Markov Estimator Errors in Time-Jittered Sampling of Nonmonotonic Signals.
PB95-150983 *01,590* Not available NTIS

Competition between Hydrodynamic Screening ('Draining') and Excluded Volume Interactions in an Isolated Polymer Chain.
PB95-175402 *01,265* Not available NTIS

Compilation of Energy Levels and Wavelengths for the Spectrum of Singly-Ionized Oxygen (O II).
PB94-162344 *00,746* Not available NTIS

Compilation of the Physical Equilibria and Related Properties of the Hydrogen-Carbon Monoxide System.
AD-A286 603/6 *00,716* PC A05/MF A01

Complementary Molecular Information on Phthalocyanine Compounds Derived from Laser Microprobe Mass Spectrometry and Micro-Raman Spectroscopy.
PB94-172269 *00,757* Not available NTIS

Complete Reduction of the Euler-Poinsot Problem.
PB94-172152 *03,788* Not available NTIS

Complex Propagation Constants for Nonuniform Optical Waveguides: Calculations.
PB95-125910 *04,249* Not available NTIS

Complex Time Dependence of the EPR Signal of Irradiated L-alpha-alanine.
PB97-122436 *04,180* Not available NTIS

Complicated Cases and Shielded Rooms: Audiometric Booths Shielded to Attenuate Electromagnetic Interference.
PB96-180179 *02,278* Not available NTIS

Component-Based Handprint Segmentation Using Adaptive Writing Style Model.
PB96-193669 *01,859* PC A03/MF A01

Composite Materials for Offshore Operations: Proceedings of the International Workshop (1st). Held in Houston, Texas on October 26-28, 1993.
PB96-109509 *03,169* PC A17/MF A04

Composite Struts for SMES Plants.
PB95-155586 *02,507* PC A99/MF A06

Composition and Solubility Product of a Synthetic Calcium Hydroxyapatite.
PB96-180104 *02,995* Not available NTIS

Composition Dependence of a Field Variable Along the Binary Fluid Mixture Critical Locus.
PB95-176038 *01,003* Not available NTIS

Compositional Analyses of Surfaces and Thin Films by Electron and Ion Spectroscopies.
PB94-185790 *00,779* Not available NTIS

Compositional Analysis of Beneficiated Fly Ashes.
PB95-220497 *00,397* PC A03/MF A01

Compositional Homogeneity in Processing Precursor Powders to the Ba2YCu3O7-x High Tc Superconductor.
PB94-212743 *04,508* Not available NTIS

Compositional Mapping of the Microstructure of Materials.
PB95-107199 *00,565* Not available NTIS

Comprehensive Spectroscopic Data Tabulations and Progress in the Compilation of Atomic Transition Probabilities.
PB95-151551 *03,909* Not available NTIS

Comprehensive Theory of Nuclear Effects on the Intrinsic Sticking Probability. 1.
PB94-200623 *03,832* Not available NTIS

Comprehensive Theory of Nuclear Effects on the Intrinsic Sticking Probability. 2.
PB94-200631 *03,833* Not available NTIS

Compressed Liquid Densities, Saturated Liquid Densities, and Vapor Pressures of 1,1-Difluoroethane.
PB97-110118 *01,173* Not available NTIS

Compressibility of Polycrystal and Monocrystal Copper: Acoustic-Resonance Spectroscopy.
PB96-164223 *02,990* Not available NTIS

Computation of Dendrites Using a Phase Field Model.
PB94-160744 *04,436* PC A03/MF A01

Computational Model for the Rise and Dispersion of Wind-Blown, Buoyancy-Driven Plumes. Part 2. Linearly Stratified Atmosphere.
PB94-143427 *00,119* PC A03/MF A01

Computations of Enhanced Soot Production in Time-Varying CH4/Air Diffusion Flames.
PB97-119218 *01,440* Not available NTIS

Computer-Aided Manufacturing Engineering Forum (1st). Technical Meeting Proceedings. Held in Gaithersburg, Maryland on March 21-22, 1995.
PB96-136965 *02,834* PC A10/MF A03

Computer-Aided Manufacturing Engineering Forum (2nd). Technical Meeting Proceedings. Held in Gaithersburg, Maryland on August 22-23, 1995.
PB96-195334 *02,845* PC A11/MF A03

Computer-Aided Molecular Design of Fire Resistant Aircraft Materials.
PB96-160601 *00,025* Not available NTIS

Computer Graphics Metafile (CGM): Procedures for NIST CGM Validation Test Service.
PB94-161809 *01,804* PC A03/MF A01

Computer Programs for Simulation of Lighting/HVAC Interactions.
PB94-140407 *02,501* PC A08/MF A02

Computer Security: An Introduction to Computer Security. The NIST Handbook.
PB96-131610 *01,608* PC A13/MF A03

Computer Security: Generally Accepted Principles and Practices for Securing Information Technology Systems.
PB97-110811 *01,619* PC A05/MF A01

Computer Security Management and Planning in the U.S. Federal Government.
PB95-163432 *01,596* Not available NTIS

Computer Security Training and Awareness Course Compendium.
PB95-130985 *01,589* PC A09/MF A02

Computer Simulation of the Diffusivity of Cement-Based Materials.
PB95-125985 *00,362* Not available NTIS

Computer Simulations of Airflow and Radon Transport in Four Large Buildings.
PB95-220422 *02,557* PC A03/MF A01

Computer Simulations of Binder Removal from 2-D and 3-D Model Particulate Bodies.
PB97-121339 *00,418* Not available NTIS

Computer Systems Laboratory Annual Report, 1993.
PB94-162518 *01,622* PC A05/MF A02

Computer Systems Laboratory Annual Report 1994.
PB95-209920 *01,629* PC A07/MF A02

Computer Systems Laboratory Computing and Applied Mathematics Laboratory Technical Accomplishments, October 1994-March 1996.
PB96-193768 *01,638* PC A05/MF A01

Computer Virus Attacks.
PB95-163655 *01,715* Not available NTIS

Computer Vision Based Tool Setting Station.
PB94-199858 *02,944* Not available NTIS

Computers in Welding: A Primer.
PB95-162863 *02,862* Not available NTIS

Computing Effects and Error for Large Synthetic Perturbation Screenings.
PB94-139623 *01,675* PC A03/MF A01

Computing Radiative Heat Transfer Occurring in a Zone Fire Model.
PB96-102306 *01,399* Not available NTIS

Computing S(alpha) Using Symbolic Monte Carlo.
PB94-198660 *03,410* Not available NTIS

Computing the Effect of Sprinkler Sprays on Fire Induced Gas Flow.
PB96-147111 *00,404* Not available NTIS

Concentration Histogram Imaging: A Scatter Diagram Technique for Viewing Two or Three Related Images.
PB94-199114 *00,542* Not available NTIS

Concentrations of Chlorinated Hydrocarbons, Heavy Metals and Other Elements in Tissues Banked by the Alaska Marine Mammal Tissue Archival Project.
PB95-209870 *02,590* PC A06/MF A02

Concept for an Algorithm Testing and Evaluation Program at NIST.
PB94-163029 *02,890* PC A03/MF A01

Concept Paper: An Overview of the Proposed Trust Technology Assessment Program.
PB96-160882 *01,614* Not available NTIS

Concepts for Fire Protection of Passenger Rail Transportation Vehicles: Past, Present, and Future.
PB96-102868 *04,853* Not available NTIS

Concepts of the NIST EXPRESS Server.
PB95-180543 *02,781* Not available NTIS

Conceptual Design Plan for the National Advanced Manufacturing Testbed.
PB95-231866 *02,828* PC A05/MF A01

Concurrent Enhancement of Kerr Rotation and Antiferromagnetic Coupling in Epitaxial Fe/Cu/Fe Structures.
PB94-198769 *04,466* Not available NTIS

Concurrent Flow Flame Spread Study.
PB94-156866 *01,356* PC A08/MF A02

Condensed Catalogue of Electromagnetic Environment Measurements, 30 - 300 Hz.
PB95-162210 *01,899* Not available NTIS

Conditions for Existence of a Reentrant Solid Phase in a Sheared Atomic Fluid.
PB94-211380 *04,198* Not available NTIS

Conductance Response of Pd/SnO2(110) Model Gas Sensors to H2 and O2.
PB95-125803 *00,892* Not available NTIS

Cone Emission from Laser-Pumped Two-Level Atoms. 1. Quantum Theory of Resonant Light Propagation.
PB95-203584 *04,325* Not available NTIS

Cone Emission from Laser-Pumped Two-Level Atoms. 2. Analytical Model Studies.
PB95-203592 *04,326* Not available NTIS

Conference Proceedings: International Workshop on Instrumented Indentation. Held in San Diego, California on April 22-23, 1995.
PB96-158688 *01,948* PC A06/MF A01

Conference Report: Calorimetry Conference (50th).
PB97-122279 *03,722* Not available NTIS

Conference Report: International Conference on the Application of Standards for Open Systems (6th).
PB96-161211 *01,762* Not available NTIS

Confidence on the Modified Allan Variance and the Time Variance.
PB96-190376 *01,557* Not available NTIS

Confidence on the Second Difference Estimation of Frequency Drift.
PB95-151460 *01,532* Not available NTIS

Confidence on the Three-Point Estimator of Frequency Drift.
PB95-163838 *01,539* Not available NTIS

Configuration and Performance Evaluation of a Real-Time Robot Control System: A Skeleton Approach.
PB95-163895 *01,598* Not available NTIS

Configuration-Dependent AC Stark Shifts in Calcium.
PB96-157995 *04,363* Not available NTIS

Conformance Assessment of Transport Layer Security Implementations.
PB94-164373 *01,576* PC A03/MF A01

Conformance Testing and Specification Management.
PB97-113781 *02,849* PC A03/MF A01

Conformance Testing for OSI Protocols.
PB96-102686 *01,631* Not available NTIS

Conformance Testing of a Lower Layer Security Protocol.
PB94-185402 *01,577* Not available NTIS

Conformational Alterations of Bovine Insulin Adsorbed on a Silver Electrode.
PB96-161773 *00,510* Not available NTIS

Connection between Superelastic and Inelastic Electron-Atom Collisions Involving Polarized Collision Partners.
PB95-202297 *03,974* Not available NTIS

Consensus Process in Standards Development.
PB96-179502 *00,136* Not available NTIS

Considerations in the Design of an Environmental Specimen Bank: Experiences of the National Biomonitoring Specimen Bank Program.
PB96-112370 *02,527* Not available NTIS

Considerations on Data Requirements for Tribological Modeling.
PB94-172731 *02,962* Not available NTIS

Constant Temperature and Humidity Chamber for Standard Resistors.
PB96-122494 *02,275* Not available NTIS

Constant-Width Calibration Intervals for Linear Regression.
PB95-153524 *03,439* Not available NTIS

Constituents and Physical Properties of the C6+ Fraction of Natural Gas. Topical Report, April-June 1994.
PB95-136644 *02,483* PC A03/MF A01

Constructing Invariant Tori for Two Weakly Coupled van der Pol Oscillators.
PB95-126165 *03,412* Not available NTIS

Construction of Maximum-Entropy Density Maps, and Their Use in Phase Determination and Extension.
PB95-108593 *00,882* Not available NTIS

Construction of Silicon Nanocolumns with the Scanning Tunneling Microscope.
PB95-203063 *04,696* Not available NTIS

Contact Electrification Induced by Monolayer Modification of a Surface and Relation to Acid-Base Interactions.
PB94-185378 *03,034* Not available NTIS

Contact Tube Wear Detection in Gas Metal Arc Welding.
PB96-135330 *02,872* Not available NTIS

CONTAM88 Building Input Files for Multi-Zone Airflow and Contaminant Dispersal Modeling.
PB94-194388 *02,537* PC A04/MF A01

CONTAM93 User Manual.
PB94-164381 *02,536* PC A05/MF A01

CONTAM94: A Multizone Airflow and Contaminant Dispersal Model with a Graphic User Interface.
PB97-113203 *02,570* Not available NTIS

Context Analysis of the Network Management Domain. Conducted as Part of the Domain Analysis Case Study.
PB94-142528 *01,465* PC A05/MF A01

Continuous Counter-Current Two Phase Aqueous Extraction.
PB95-161212 *00,675* Not available NTIS

Continuous Gravity Observations Using Joint Institute for Laboratory Astrophysics Absolute Gravimeters.
PB95-203048 *03,685* Not available NTIS

Continuous Mining Machine Control Using the Real-Time Control System.
PB94-203528 *03,700* PC A02/MF A01

Continuous Recording and Stochastic Analysis of PD.
PB96-112156 *01,925* Not available NTIS

Contrast Matched Studies of a Sheared Binary Colloidal Suspension.
PB95-150561 *00,918* Not available NTIS

Contributions of Out-of-Plane Material to a Scanned-Beam Laminography Image.
PB96-111786 *02,704* Not available NTIS

Control and Instrumentation: Standards for High-Integrity Software.
PB96-161369 *03,736* Not available NTIS

Control Entity Interface Specification.
PB94-191715 *02,815* PC A06/MF A02

Control of Friction and Wear of Alpha-Alumina with a Composite Solid-Lubricant Coating.
PB95-125969 *03,225* Not available NTIS

Control of Gas-Metal-Arc Welding Using Arc-Light Sensing.
PB96-131461 *02,869* PC A06/MF A02

Control Stability of a Heat-Flow-Meter Appartus.
PB95-181194 *00,386* Not available NTIS

Control System Architecture for a Remotely Operated Unmanned Land Vehicle.
PB95-163200 *03,759* Not available NTIS

Controlled Nucleation in Aerosol Reactors for Supression of Agglomerate Formation.
PB95-151973 *00,672* Not available NTIS

Controlling Moisture in the Walls of Manufactured Housing.
PB95-105136 *00,355* PC A03/MF A01

Controlling the Critical Current Density of High-Temperature SNS Josephson Junctions.
PB96-200712 *04,794* Not available NTIS

Convection and Morphological Stability During Directional Solidification.
N95-14548/8 *03,310*
(Order as N95-14522/3, PC A20/MF A04)

Convective Stability in the Rayleigh-Benard and Directional Solidification Problems: High-Frequency Gravity Modulation.
PB95-181145 *04,208* Not available NTIS

Conventional and Eccentric Uses of Crystallographic Databases in Practical Materials Identification Problems.
PB97-109102 *04,802*
(Order as PB97-109011, PC A11/MF A03)

Convergence Properties of a Class of Rank-Two Updates. (NIST Reprint).
PB95-180097 *03,430* Not available NTIS

Conversion of a 2-Terminal-Pair Bridge to a 4-Terminal-Pair Bridge for Increased Range and Precision in Impedance Measurements.
PB97-119176 *02,103* Not available NTIS

Cooper M(sub II,III) X-ray-Emission Spectra of Copper Oxides and the Bismuth Cuprate Superconductor.
PB96-158027 *04,077* Not available NTIS

Coordinating Cascaded Surge Protection Devices: High-Low versus Low-High.
PB94-172061 *02,463* Not available NTIS

Coordinating Cascaded Surge-Protective Devices: An Elusive Goal.
PB94-216496 *02,465* Not available NTIS

Coping with Different Retrieval Methods in Next Generation Networks.
PB95-168555 *02,726* Not available NTIS

Copolymerization of N-Phenyl Maleimide and gamma-Methacryloxypropyl Trimethoxysilane.
PB95-153144 *01,248* Not available NTIS

Copper Ion-Mediated Modification of Bases in DNA in Vitro by Benzoyl Peroxide.
PB94-198231 *03,645* Not available NTIS

Copyright and Information Services in the Context of the National Research and Education Network.
PB96-160536 *02,736* Not available NTIS

Core Potentials for Quasi-One-Electron Systems.
PB95-202214 *03,970* Not available NTIS

Corrected Optical Pyrometer Readings.
AD-A279 949/2 *02,615* PC A05/MF A01

Correction Factor for Nonplanar Incident Field in Monopole Calibrations.
PB95-108643 *02,002* Not available NTIS

Correction to the Decay Rate of Nonequilibrium Carrier Distributions Due to Scattering-in Processes.
PB94-185840 *04,452* Not available NTIS

Correlation between Tc and Elastic Constants of (La-M)2CuO4.
PB94-213220 *04,514* Not available NTIS

Correlation of HgCdTe Epilayer Defects with Underlying Substrate Defects by Synchrotron X-Ray Topography.
PB94-200714 *02,129* Not available NTIS

Correlation of Optical, X-ray, and Electron Microscopy Measurements of Semiconductor Multilayer Structures.
PB95-175279 *02,174* Not available NTIS

Correlation of the Ideal Gas Properties of Five Aromatic Hydrocarbons.
PB95-175816 *01,002* Not available NTIS

Correlations between Electrical and Acoustic Detection of Partial Discharge in Liquids and Implications for Continuous Data Recording.
PB96-204490 *02,248* Not available NTIS

Correlations between Flaw Tolerance and Reliability in Zirconia.
PB96-161922 *02,986* Not available NTIS

Correlations of Modulation Noise with Magnetic Microstructure and Intergranular Interactions for CoCrTa and CoNi Thin Film Media.
PB94-212768 *04,509* Not available NTIS

Corrosion Characteristics of Silicon Carbide and Silicon Nitride.
PB96-169081 *03,372*
(Order as PB96-169057, PC A05/MF A01)

Corrosion Resistance of Materials for Renovation of the United States Botanic Garden Conservatory.
PB94-154390 *00,032* PC A03/MF A01

Corrosion Resistant Epoxy-Coated Reinforcing Steel.
PB94-185618 *01,307* Not available NTIS

Countries, Dependencies, Areas of Special Sovereignty, and Their Principal Administrative Divisions. Category: Data Standards and Guidelines; Subcategory: Representation and Codes.
FIPS PUB 10-4 *00,128* PC E05

Countries, Dependencies, Areas of Special Sovereignty, and Their Principal Administrative Divisions (for Microcomputers).
PB95-503504 *00,130* Diskette $30.00

Coupled-Bilayer Two-Dimensional Magnetic Order of the Dy Ions in Dy2Ba4Cu7O15.
PB95-152104 *04,584* Not available NTIS

Crack Growth Resistance of Strain-Softening Materials under Flexural Loading.
PB94-200227 *02,972* Not available NTIS

Cracks and Dislocations in Face-Centered Cubic Metallic Multilayers.
PB96-163696 *02,989* Not available NTIS

Creep and Creep Rupture of Ceramic Matrix Composites.
PB95-163929 *03,165* Not available NTIS

Creep and Creep Rupture of Structural Ceramics.
PB96-204524 *03,093* Not available NTIS

Creep Rupture of MoSi2/SiCp Composites.
PB95-152294 *03,154* Not available NTIS

Criteria for Establishing Accurate Vapor Pressure Curves.
PB95-163812 *00,972* Not available NTIS

Critical Behavior of Ionic Fluids
PB95-164331 *00,978* Not available NTIS

Critical Current and Normal Resistance of High-Tc Step-Edge SNS Junctions.
PB96-111752 *04,724* Not available NTIS

Critical Current Behavior of Ag-Coated YBa2Cu3O7-x Thin Films.
PB95-141016 *04,549* Not available NTIS

Critical-Current Degradation in Nb3 Al Wires Due to Axial and Transverse Stress.
PB95-202784 *02,226* Not available NTIS

Critical Current Density, Irreversibility Line, and Flux Creep Activation Energy in Silver-Sheathed Bi2Sr2Ca2Cu2Ox Superconducting Tapes.
PB95-162749 *04,616* Not available NTIS

Critical Evaluation of the Purification of Biominerals by Hypochlorite Treatment.
PB95-150959 *00,186* Not available NTIS

Critical Evaluation of Thermal Mass Flow Meters.
PB97-113153 *00,683* Not available NTIS

Critical Factors in Non-Lubricated, Non-Abrasive Wear Testing.
PB95-140588 *03,236* Not available NTIS

Critical Issues in Scanning Electron Microscope Metrology.
PB95-169405 *02,359*
(Order as PB95-169371, PC A07/MF A02)

Critical Lines for Type-III Aqueous Mixtures by Generalized Corresponding-States Models.
PB96-102371 *01,063* Not available NTIS

Critical Magnetic-Field Angle for High-Field Current Transport in YBa2Cu3O7 at 76 K.
PB94-211281 *04,490* Not available NTIS

Critical Properties and Vapor-Liquid Equilibria of the Binary System Propane + Neopentane.
PB95-175683 *00,999* Not available NTIS

Critical Review of Rate Constants for Reactions of Transients from Metal Ions and Metal Complexes in Aqueous Solution.
PB96-145859 *01,109* Not available NTIS

TITLE INDEX

Critical Scaling Laws and a Classical Equation of State.
PB95-169249 *00,990* Not available NTIS

Cross-Correlation Analysis Improves Time Domain Measurements.
PB95-180535 *01,543* Not available NTIS

Cross-Property Relations and Permeability Estimation in Model Porous Media.
PB95-150280 *04,205* Not available NTIS

Cross-Sectional Photoluminescence and Its Application to Buried-Layer Semiconductor Structures.
PB96-141106 *02,415* Not available NTIS

Crossed-Beams Measurements of Absolute Cross Sections for Electron Impact Ionization of S(+).
PB95-202511 *03,981* Not available NTIS

Crossover in the Pinning Mechanism of Anisotropic Fluxon Cores.
PB95-180170 *04,673* Not available NTIS

Crossover to Strong Shear in a Low-Molecular-Weight Critical Polymer Blend.
PB94-211976 *01,222* Not available NTIS

Crosstalk between Microstrip Transmission Lines.
PB94-135639 *02,210* PC A03/MF A01

Crosstalk between Microstrip Transmission Lines. (NIST Reprint).
PB95-180337 *02,225* Not available NTIS

Cryogenic Blackbody Calibrations at the National Institute of Standards and Technology Low Background Infrared Calibration Facility.
PB94-169802 *02,117* Not available NTIS

Cryogenic Flow Calibration in NIST.
PB96-161930 *01,143* Not available NTIS

Cryogenic Materials Data Handbook.
AD-A286 675/4 *03,303* PC A04/MF A01

Cryogenic Precision Capacitance Bridge Using a Single Electron Tunneling Electrometer.
PB95-126074 *04,529* Not available NTIS

Cryogenic Precision Capacitance Bridge Using a Single Electron Tunneling Electrometer.
PB95-152310 *02,040* Not available NTIS

Cryogenic Precision Capacitance Bridge Using a Single Electron Tunneling Electrometer.
PB96-112271 *02,072* Not available NTIS

Cryogenic Properties of Inorganic Insulation Materials for ITER Magnets: A Review.
PB95-198768 *03,706* PC A10/MF A03

Cryogenic Properties of Silver.
PB94-203593 *03,330* PC A03

Cryogenic Research and Development (June 30, 1961).
AD-A280 679/2 *01,457* PC A04/MF A01

Cryogenic Research and Development (Progress Report Number 4 for Period Ending December 31, 1961).
AD-A280 399/7 *01,455* PC A04/MF A01

Cryogenic Research and Development (Quarterly Report Number 1 for Period Ending September 30, 1960).
AD-A280 401/1 *01,456* PC A04/MF A01

Cryogenic Research and Development (Quarterly Report Number 2 for Period Ending December 31, 1960).
AD-A280 398/9 *01,454* PC A05/MF A01

Cryogenic Toughness of Austenitic Stainless Steel Weld Metals: Effect of Inclusions.
PB95-161261 *03,214* Not available NTIS

Cryogenics.
PB95-164703 *02,654* Not available NTIS

Crystal Chemistry and Phase Equilibria Studies of the BaO(BaCO3)-R2O3-CuO Systems. 4. Crystal Chemistry and Subsolidus Phase Relationship Studies of the CuO-Rich Region of the Ternary Diagrams, R=Lanthanides.
PB95-151759 *00,936* Not available NTIS

Crystal Chemistry and Phase Equilibrium Studies of the BaO(BaCO3)-R2O3-CuO Systems. 5. Melting Relations in Ba2(Y,Nd,Eu)Cu3O6+x.
PB95-151718 *04,580* Not available NTIS

Crystal Chemistry and Phase Equilibrium Studies of the BaO-R2O3-CuO Systems. 2. X-Ray Characterization and Standard Patterns of BaR2CuO4, R=Lanthanides.
PB95-151734 *04,582* Not available NTIS

Crystal Diffraction Spectrometry for Accurate, Non-Invasive kV/Spectral Measurement for Improvement of Mammographic Image Quality.
AD-A297 943/3 *00,721* PC A03/MF A01

Crystal Packing Interactions of Two Different Crystal Forms of Bovine Ribonuclease A.
PB95-152823 *00,943* Not available NTIS

Crystal Structure and Compressibility of 3:2 Mullite.
PB95-175030 *03,682* Not available NTIS

Crystal Structure and Magnetic Ordering of the Rare-Earth and Cu Moments in RBa2Cu2NbO8(R=Nd,Pr).
PB95-140554 *04,546* Not available NTIS

Crystal Structure and Magnetic Properties of CuGeO3.
PB95-180287 *04,678* Not available NTIS

Crystal Structure of a New Monoclinic Form of Potassium Dihydrogen Phosphate Containing Orthophosphacidium Ion, (H4PO4)(sup+1).
PB96-111794 *04,725* Not available NTIS

Crystal Structure of a New Sodium Zinc Arsenate Phase Solved by 'Simulated Annealing'.
PB95-107124 *00,870* Not available NTIS

Crystal Structure of Annealed and As-Prepared HgBa2CaCu2O6+delta Superconductors.
PB95-161105 *03,927* Not available NTIS

Crystal Structure of Calcium Adipate Monohydrate.
PB94-216579 *00,153* Not available NTIS

Crystal Structure of Calcium Glutarate Monohydrate.
PB96-111893 *01,074* Not available NTIS

Crystal Structure of Calcium Succinate Monohydrate.
PB95-168928 *00,167* Not available NTIS

Crystal Structure of Decacalcium Tetrapotassium Hexakis (Pyrophosphate) Nonahydrate.
PB96-141064 *01,099* Not available NTIS

Crystal Structure of Dicalcium Potassium Trihydrogen Bis(pyrophosphate) Trihydrate.
PB94-216561 *00,152* Not available NTIS

Crystal Structure of Pb2Sr2YCu3O8+delta with delta=1.32, 1.46, 1.61, 1.71, by Powder Neutron Diffraction.
PB94-216314 *04,518* Not available NTIS

Crystallographic and Magnetic Properties of UAuSn.
PB95-140521 *04,543* Not available NTIS

Crystallographic Characterization of Some Intermetallic Compounds in the Al-Cr System.
PB94-198702 *03,318* Not available NTIS

CRYSTMET: The NRCC Metals Crystallographic Data File.
PB97-109029 *04,799*
(Order as PB97-109011, PC A11/MF A03)

Cs Cluster Binding to a GaAs Surface.
PB94-213006 *00,846* Not available NTIS

CSL View of Applications Portability, Scalability, and Interoperability.
PB97-122303 *01,787* Not available NTIS

CSTL Technical Activities 1991.
PB94-160769 *00,728* PC A16/MF A03

CSTL Technical Activities, 1993.
PB95-160602 *00,953* PC A17/MF A04

CSTL Technical Activities, 1994.
PB95-242319 *00,608* PC A16/MF A03

CSTL Technical Activities, 1995.
PB96-214630 *00,647* PC A10/MF A03

Current Activities Within the National Biomonitoring Specimen Bank.
PB94-172806 *02,516* Not available NTIS

Current and Voltage Measurements in the Gaseous Electronics Conference RF Reference Cell.
PB96-113337 *02,388*
(Order as PB96-113311, PC A09/MF A03)

Current Fluctuations Reveal Protonation Dynamics and Number of Ionizable Residues in the alpha-Toxin Channel.
PB96-161732 *03,588* Not available NTIS

Current Noise Reveals Protonation Kinetics and Number of Ionizable Sites in an Open Protein Ion Channel.
PB96-161674 *04,092* Not available NTIS

Current Results and Future Prospects for a Neutron Lifetime Determination Using Trapped Protons.
PB94-199742 *03,817* Not available NTIS

Current Status and Trends in Temperature Measurements at NIST, Cooperative Projects and New Mutual Agreement between NIST and IMGC.
PB97-110266 *02,691* Not available NTIS

Currents Induced on Multiconductor Transmission Lines by Radiation and Injection.
PB94-211943 *02,215* Not available NTIS

Custom Integrated Circuit Comparator for High-Performance Sampling Applications.
PB94-213147 *02,320* Not available NTIS

Cyclic Polyamine Ionophore for Use in a Dibasic Phosphate-Selective Electrode.
PB95-180121 *01,008* Not available NTIS

Cylinder Wipe Air-Drying Intaglio Ink Vehicles for U.S. Currency Inks.
PB94-160801 *03,115* PC A03/MF A01

Damage Processes in Ceramics Resulting from Diamond Tool Indentation and Scratching in Various Environments.
PB96-102983 *03,065* Not available NTIS

Data Communications Strategy.
PB96-167846 *02,738* PC A05/MF A01

Data Encryption Standard.
PB95-162376 *01,595* Not available NTIS

Data Encryption Standard (DES); Category: Computer Security; Subcategory: Cryptography.
FIPS PUB 46-2 *01,572* PC E04

Data Evaluation of a Linear System by a Second-Order Transfer Function.
PB96-200282 *01,970* Not available NTIS

Data Import and Validation in the Inorganic Crystal Structure Database.
PB97-109201 *04,809*
(Order as PB97-109011, PC A11/MF A03)

Data Management for Error Compensation and Process Control.
PB97-110480 *02,847* Not available NTIS

Data-Parallel Algorithm for Three-Dimensional Delaunay Triangulation and Its Implementation.
PB95-163309 *01,714* Not available NTIS

Database Development and Management (Project A.2.2): The Annual Report for 1992-1993.
PB97-110290 *03,098* Not available NTIS

Database for the Static Dielectric Constant of Water and Steam.
PB96-145586 *01,103* Not available NTIS

Database Management Standards: Status and Applicability.
PB96-122924 *01,819* Not available NTIS

Databases Available in the Research Information Center of the National Institute of Standards and Technology.
PB95-128641 *02,724* PC A08/MF A01

Databases Available in the Research Information Center of the National Institute of Standards and Technology (December 1995).
PB96-139407 *02,734* PC A07/MF A02

dc Magnetic Force Microscopy Imaging of Thin-Film Recording Head.
PB95-176061 *04,665* Not available NTIS

dc Method for the Absolute Determination of Conductivities of the Primary Standard KCl Solutions from 0C to 50C.
PB94-219342 *02,644*
(Order as PB94-219326, PC A05/MF A02)

DC-MHz Wattmeter Based on RMS Voltage Measurements.
PB97-113211 *01,992* Not available NTIS

De Facto Microzonation through the Use of Soils Factors in Design Triggers.
PB96-141148 *00,462* Not available NTIS

Dead Time, Pileup, and Accurate Gamma-Ray Spectrometry.
PB96-167101 *00,697* Not available NTIS

Debugger for Tcl Applications.
PB94-213303 *01,695* Not available NTIS

Decay of Bragg Gratings in Hydrogen-Loaded Optical Fibers.
PB96-122643 *04,345* Not available NTIS

Decomposition of SF6 and Production of S2F10 in Power Arcs.
PB96-122619 *01,084* Not available NTIS

Decomposition of Sulfur Hexafluoride by X-rays.
PB96-135314 *01,095* Not available NTIS

Decoupling in the Line Mixing of Acetylene Infrared Q Branches.
PB95-108452 *00,877* Not available NTIS

Decrease of Fluorescence in Optical Fiber during Exposure to Pulsed or Continuous-Wave Ultraviolet Light.
PB95-203071 *04,320* Not available NTIS

Deep-UV Excimer Laser Measurements at NIST.
PB96-141031 *04,355* Not available NTIS

Defect Formation Mechanism Causing Increasing Defect Density during Decreasing Implant Dose in Low-Dose Simox.
PB96-119524 *02,402* Not available NTIS

Defect of Thermal Ramping and Annealing Conditions on Defect Formation in Oxygen Implanted Silicon-On-Insulator Material.
PB94-212966 *02,318* Not available NTIS

Defect Pair Formation by Implantation-Induced Stresses in High-Dose Oxygen Implanted Silicon-on-Insulator Material.
PB95-175824 *02,364* Not available NTIS

Defective Structures of Barium Yttrium Copper Oxide (Ba2YCu3Ox) and Ba2YCu3-yMyOz (M=Fe, Co, Al, Ga, ..).
PB95-140034 *04,537* Not available NTIS

Defining Environment Integration Requirements.
PB96-131545 *02,733* PC A03/MF A01

Deformable Superconductor Model for the Fluxon Mass.
PB95-175311 *04,653* Not available NTIS

Deformation and Fracture of Mica-Containing Glass-Ceramics in Hertzian Contacts.
PB96-179452 *03,080* Not available NTIS

Degradation of Powder Epoxy Coated Panels Immersed in a Saturated Calcium Hydroxide Solution Containing Sodium Chloride.
PB96-101050 *01,344* PC A03/MF A01

Deletion Analysis of the Mini-P1 Plasmid Origin of Replication and the Role of E.coli DnaA Protein.
PB95-163911 *03,539* Not available NTIS

Delivering the Same Optical Frequency at Two Places: Accurate Cancellation of Phase Noise Introduced by an Optical Fiber or Other Time-Varying Path.
PB96-102736 *04,332* Not available NTIS

Densification of Nano-Size Powders. 1994 Report.
DE94013486 *03,027* PC A03/MF A01

Density Dependence of Fluid Properties and Non-Newtonian Flows: The Weisenberg Effect.
PB96-161898 *01,140* Not available NTIS

Density Matrix Calculation of Population Transfer between Vibrational Levels of Na2 by Stimulated Raman Scattering with Temporally Shifted Laser Beams.
PB94-198546 *00,787* Not available NTIS

Density of Solids and Liquids.
AD-A278 517/8 *00,711* PC A03/MF A01

Dental Applications of Ceramics.
PB96-122940 *00,177* Not available NTIS

Dental Materials.
PB94-172871 *00,142* Not available NTIS

Dependence of Contrast on Probe/Sample Spacing with the Magneto-Optic Kerr-Effect Scanning Near-Field Optical Microscope (MOKE-SNOM).
PB96-138557 *04,750* Not available NTIS

Dependence of Tc on Debye Temperature Theta(sub D) for Various Cuprates.
PB95-180493 *04,683* Not available NTIS

Dependence of the Thermal Electron Attachment Rate Constant in Gases and Liquids on the Energy Position of the Electron Attaching State.
PB97-122253 *01,996* Not available NTIS

Deposit Forming Tendencies of Diesel Engine Oils-Correlation between the Two-Peak Method and Engine Tests.
PB95-152138 *01,452* Not available NTIS

Deposition of Colloidal Sintering-Aid Particles on Silicon Nitride.
PB94-216272 *03,044* Not available NTIS

Deposition of Loosely Bound and Firmly Bound Fluorides on Tooth Enamel by an Acidic Gel Containing Fluorosilicate and Monocalcium Phosphate Monohydrate.
PB95-150710 *03,559* Not available NTIS

Deposition Rates in Direct Current Diode Sputtering.
PB95-203345 *04,697* Not available NTIS

Derivation of the System Equation for Null-Balanced Total-Power Radiometer System NCS1.
PB94-169786 *02,022* Not available NTIS

Description of Layered Structures: Applications to High Tc Superconductors.
PB95-162624 *04,615* Not available NTIS

Design and Characterization of X-Ray Multilayer Analyzers for the 50 - 1000 eV Region.
PB94-211851 *03,848* Not available NTIS

Design and Construction of a Liquid Hydrogen Temperature Refrigeration System.
AD-A286 618/4 *02,619* PC A03/MF A01

Design and Development of an Information Retrieval System for the EAMATE Data. Volume 2 of 2. Appendices.
PB94-168390 *00,487* PC A19/MF A04

Design and Machining of Copper Specimens with Micro Holes for Accurate Heat Transfer Measurements.
PB95-180428 *02,658* Not available NTIS

Design and Operation of Series-Array Josephson Voltage Standards.
PB94-185451 *02,030* Not available NTIS

Design Challenges in a Commercial Quantum Hall Effect-Based Resistance Standard.
PB95-171419 *02,263* PC A03/MF A01

Design, Construction and Application of a Large Aperture Lens-Less Line-Focus PVDF Transducer.
PB97-122584 *02,765* Not available NTIS

Design Criteria for BJT Amplifiers with Low l/f AM and PM Noise.
PB96-200365 *02,442* Not available NTIS

Design Engineering Research at NIST.
PB95-267860 *02,784* PC A03/MF A01

Design Equations and Scaling Laws for Linear Compressors with Flexure Springs.
PB95-168902 *02,948* Not available NTIS

Design Guide for CMOS-On-SIMOX. Test Chips NIST3 and NIST4.
PB94-163458 *02,297* PC A05/MF A01

Design of a High-Flux Backscattering Spectrometer for Ultra-High Resolution Inelastic Neutron Measurements.
PB96-179577 *02,992* Not available NTIS

Design of a High-Pressure Ebulliometer, with Vapor-Liquid Equilibrium Results for the Systems CHF2Cl + CF3-CH3 and CF3-CH2F + CH2F2.
PB97-113229 *04,163* Not available NTIS

Design of a Protocol for an Electron Probe Microanalyzer k-Value Round Robin.
PB95-107181 *00,564* Not available NTIS

Design of High-Frequency, High-Power Oscillators Using Josephson-Junction Arrays.
PB96-200258 *02,094* Not available NTIS

Design of Technically Complex Facilities.
PB97-119101 *02,695* Not available NTIS

Design, Specification and Tolerancing of Micrometer-Tolerance Assemblies.
PB95-209862 *02,913* PC A03/MF A01

Designations of ds(2)p Energy Levels in Neutral Zirconium, Hafnium, and Rutherfordium (Z=104).
PB96-180120 *04,116* Not available NTIS

Desorption Induced by Electronic Transitions.
PB94-216173 *00,853* Not available NTIS

DETAN 95: Computer Code for Calculating Spectrum-Averaged Cross Sections and Detector Responses in Neutron Spectra.
PB95-242384 *04,014* PC A04/MF A01

Detection of Aromatic Compounds Based on DNA Intercalation Using an Evanescent Wave Biosensor.
PB96-111976 *03,473* Not available NTIS

Detection of OH+ in Its a(1)Delta State by Far Infrared Laser Magnetic Resonance.
PB95-181087 *01,021* Not available NTIS

Detection of Voids in Grouted Ducts Using the Impact-Echo Method.
PB94-185121 *01,306* Not available NTIS

Detector-Based Candela Scale and Related Photometric Calibration Procedures at NIST.
PB95-161949 *04,273* Not available NTIS

Determination of Acoustic Center Correction for Type LS2aP Condensor Microphones.
PB96-204508 *04,190* Not available NTIS

Determination of Amphetamine and Methamphetamine in a Lyophilized Human Urine Reference Material.
PB95-175444 *03,597* Not available NTIS

Determination of Anomalous Superexchange in MnCl2 and Its Graphite Intercalation Compound.
PB97-122568 *00,666* Not available NTIS

Determination of Atomic Data Pertinent to the Fusion Energy Program. Progress Report for FY 92.
DE94004400 *04,402* PC A02/MF A01

Determination of Boron and Lithium in Diverse Biological Matrices Using Neutron Activation - Mass Spectrometry (NA-MS).
PB94-212289 *00,554* Not available NTIS

Determination of Complex Scattering Amplitudes in Low-Energy Elastic Electron-Sodium Scattering.
PB94-216652 *03,869* Not available NTIS

Determination of Complex Structures from Powder Diffraction Data: The Crystal Structure of La3Ti5Al15O37.
PB95-202966 *01,038* Not available NTIS

Determination of Density of Mass Standards: Requirement and Method.
PB94-163078 *03,787* PC A03/MF A01

Determination of Fiber-Matrix Interfacial Properties of Importance to Ceramic Composite Toughening.
PB95-125811 *03,149* Not available NTIS

Determination of Hydrogen in Titanium Alloy Jet Engine Compressor Blades by Cold Neutron Capture Prompt Gamma-ray Activation Analysis.
PB95-175956 *01,448* Not available NTIS

Determination of Inorganic Constituents in Marine Mammal Tissues.
PB95-152047 *00,589* Not available NTIS

Determination of Oltipraz in Serum by High-Performanace Liquid Chromatography with Optical Absorbance and Mass Spectrometric Detection.
PB94-200201 *03,493* Not available NTIS

Determination of Osmotic Pressure and Fouling Resistances and Their Effects on Performance of Ultrafiltration Membranes.
PB94-212891 *00,841* Not available NTIS

Determination of PCBs and Chlorinated Hydrocarbons in Marine Mammal Tissues.
PB95-162640 *03,744* Not available NTIS

Determination of Polycyclic Aromatic Hydrocarbons by Liquid Chromatography.
PB95-151650 *00,585* Not available NTIS

Determination of Sheet Steel Formability Using Wide Band Electromagnetic-Acoustic Transducers.
PB96-186036 *02,279* Not available NTIS

Determination of Sulfur in Fossil Fuels by Isotope Dilution Thermal Ionization Mass Spectrometry.
PB96-141379 *02,495* Not available NTIS

Determination of Surface Roughness from Scattered Light.
PB94-216520 *04,243* Not available NTIS

Determination of the Complex Refractive Index of Individual Quantum Wells from Distributed Reflectance.
PB95-175642 *02,176* Not available NTIS

Determination of the Molecular Parameters of NiH in Its (2)Delta Ground State by Laser Magnetic Resonance.
PB95-107116 *00,869* Not available NTIS

Determination of the Optical Constants of ZnSe Films by Spectroscopic Ellipsometry.
PB95-175378 *04,656* Not available NTIS

Determination of the Prior-Austenitic Grain Size of Selected Steels Using a Molten Glass Etch.
PB94-211927 *03,208* Not available NTIS

Determination of the Residual Stresses Near the Ends of Skip Welds Using Neutron Diffraction and X-ray Diffraction Procedures.
PB95-253589 *02,868* PC A03/MF A01

Determination of the Transmittance Uniformity of Optical Filter Standard Reference Materials.
PB95-261921 *02,182*
(Order as PB95-261897, PC A07/MF A02)

Determination of the Weight Average Molecular Weight of Two Poly(Ethylene Oxides), SRM 1923 and SRM 1924.
PB94-217031 *01,230* PC A03/MF A01

Determination of Thermoactivation Parameters of Vortex Mobility in YBa2Cu3O7 Using Only Magnetic Measurements.
PB95-163499 *04,624* Not available NTIS

Determination of Total Protein Adsorbed on Solid (Membrane) Surface by a Hydrolysis Technique: Single Protein Adsorption.
PB96-167093 *03,552* Not available NTIS

Determination of Vitamin K1 in Serum Using Catalytic-Reduction Liquid Chromatography with Fluorescence Detection.
PB96-138425 *03,506* Not available NTIS

Determination of 3-Quinuclidinyl Benzilate (Qnb) and Its Major Metabolites in Urine by Isotope Dilution Gas Chromatography Mass Spectrometry.
PB94-199379 *03,492* Not available NTIS

Determination of 21 Elements by INAA for Certification of SRM 1570a, Spinach.
PB96-167242 *00,698* Not available NTIS

Determining Mobility from Homodyne ac Electrophoretic Light Scattering.
PB95-140497 *03,462* Not available NTIS

Determining the Magnetic Properties of 1 kg Mass Standards.
PB95-261905 *04,016*
(Order as PB95-261897, PC A07/MF A02)

Deterministic and Stochastic Chaos.
PB96-156138 *00,218* Not available NTIS

Deuterium and the Local Interstellar Medium: Properties for the Procyon and Capella Lines of Sight.
PB96-200639 *00,111* Not available NTIS

Deuterium in the Local Interstellar Medium: Its Cosmological Significance.
PB95-202842 *00,081* Not available NTIS

Deuterium Isotope Effect in Vinyl Radical Combination/Dispropor tionationReactions.
PB96-204151 *01,167* Not available NTIS

Developing a NIST Coaxial Microwave Power Standard at 1 mW.
PB95-202412 *01,914* Not available NTIS

Developing Linear Error Models for Analog Devices.
PB95-150520 *02,037* Not available NTIS

Developing Measurement for Experimentation.
PB97-118707 *03,450* Not available NTIS

Developing Quality System Documentation Based on ANSI/ NCSL Z540-1-1994: The Optical Technology Division's Effort.
PB96-202122 *01,869* PC A05/MF A01

Developing Rational Performance-Based Fire Safety Requirements in Model Building Codes.
PB95-175220 *00,200* Not available NTIS

Development and Application of an Indoor Air Quality Commissioning Program in a New Office Building.
PB96-155601 *00,275* Not available NTIS

Development and Calibration of UV/VUV Radiometric Sources.
PB94-199098 *04,229* Not available NTIS

Development and Characterization of Insulating Layers on Silicon Carbide: Annual Report for February 14, 1988 to February 14, 1989.
PB94-155579 *02,295* PC A03/MF A01

Development and Validation of Multicriteria Ratings: A Case Study.
PB95-126025 *00,004* Not available NTIS

Development in the Theory and Analysis of Eddy Current Sensing of Velocity in Liquid Metals.
PB94-212586 *03,335* Not available NTIS

Development of a Calibrated Atomic Force Microscope.
PB94-185683 *02,894* Not available NTIS

Development of a Dual-Sinker Densimeter for High-Accuracy Fluid P-V-T Measurements.
PB95-168951 *03,267* Not available NTIS

Development of a Dual-Sinker Densimeter for High-Accuracy Fluid P-V-T Measurements. Appendix A.
DE93019682 *02,620* PC A02/MF A01

Development of a Gas Standard Reference Material Containing Eighteen Volatile Organic Compounds.
PB95-162277 *02,545* Not available NTIS

Development of a Method for Measuring Water-Stripping Resistance of Asphalt/Siliceous Aggregate Mixtures.
PB96-197249 *01,348* PC A04/MF A01

Development of a Method for Measuring Water-Stripping Resistance of Asphalt/Siliceous Aggregate Mixtures.
PB96-202296 *01,329* PC A09/MF A02

Development of a New Quality Control Strategy for Automated Manufacturing.
PB96-160486 *02,840* Not available NTIS

Development of a New Small-Scale Smoke Toxicity Test Method and Its Comparison with Real-Scale Fire Tests.
PB94-213253 *00,350* Not available NTIS

Development of a Standard Reference Material for ISE Measurements of Sodium and Potassium.
PB96-159785 *03,507* Not available NTIS

Development of a Standard Reference Material for Measurement of Interstitial Oxygen Concentration in Semiconductor Silicon by Infrared Absorption.
PB96-122668 *02,404* Not available NTIS

Development of a Temperature Scale below 0.5 K.
PB95-125639 *03,879* Not available NTIS

Development of a Test Method for Leaching of Lead from Lead-Based Paints Through Encapsulants.
PB96-154984 *03,128* PC A04/MF A01

Development of Adaptive Control Strategies for Inert Gas Atomization.
PB95-162335 *02,823* Not available NTIS

Development of an Adhesive Bonding System.
PB94-199056 *00,145* Not available NTIS

Development of an Automated Part Inspection System Using the DMIS Standard.
PB95-108866 *02,899* Not available NTIS

Development of an Economical Video Based Fire Detection and Location System.
PB96-193743 *00,228* PC A05/MF A01

Development of Computer-Based Models of Standards and Attendant Knowledge-Base and Procedural Systems.
PB96-155783 *00,464* Not available NTIS

Development of Engineered Stationary Phases for the Separation of Carotenoid Isomers.
PB95-150249 *00,578* Not available NTIS

Development of Frozen Whale Blubber and Liver Reference Materials for the Measurement of Organic and Inorganic Contaminants.
PB95-151676 *00,587* Not available NTIS

Development of Gas Standards from Solid 1,4-dichlorobenzene.
PB96-155486 *02,496* Not available NTIS

Development of Hazard Assessment and Suppression Technology for Oil and Gas Well Blowout and Diverter Fires.
PB96-122965 *01,408* Not available NTIS

Development of Highly Conductive Cantilevers for Atomic Force Microscopy Point Contact Measurements.
PB96-138573 *04,751* Not available NTIS

Development of Measurement Capabilities for the Thermophysical Properties of Energy-Related Fluids. Annual Report, December 1, 1990--November 30, 1991.
DE94004399 *02,470* PC A02/MF A01

Development of Measurement Capabilities for the Thermophysical Properties of Energy-Related Fluids. Annual Report, December 1, 1993--November 30, 1994.
DE94017738 *03,246* PC A03/MF A01

Development of Near-Field Test Procedures for Communication Satellite Antennas.
PB96-135082 *02,010* Not available NTIS

Development of Neutral-Density Infrared Filters Using Metallic Thin Films.
PB96-180286 *02,998* Not available NTIS

Development of the Fire Data Management System.
PB94-206091 *00,339* PC A03/MF A01

Development of the Ion Exchange-Gravimetric Method for Sodium in Serum as a Definitive Method.
PB96-179148 *01,867*
(Order as PB96-177381, PC A07/MF A02)

Development of the National Marine Mammal Tissue Bank.
PB95-161402 *02,586* Not available NTIS

Development of the NIST Transient Pressure and Temperature Calibration Facility.
PB96-160833 *00,626* Not available NTIS

Development of Thin-Film Multijunction Thermal Converters at NIST.
PB97-112338 *02,286* Not available NTIS

Developments in Stellar Coronae.
PB96-176706 *00,107* Not available NTIS

Device for Subambient Temperature Control in Liquid Chromatography.
PB95-140604 *00,573* Not available NTIS

Diagnosis and Treatment of an Oral Base-Metal Contact Lesion Following Negative Dermatologic Patch Tests.
PB95-180626 *00,172* Not available NTIS

Diagnosis of Causes of Concrete Deterioration in the MLP-7A Parking Garage.
PB95-143095 *01,318* PC A03/MF A01

Diakoptic and Large Change Sensitivity Analysis.
PB95-150538 *02,038* Not available NTIS

Diamond and Graphite Precursors: Comments.
PB95-163051 *00,967* Not available NTIS

Dielectric and Magnetic Measurements from -50C to 200C and in the Frequency Band 50 MHz to 2 GHz.
PB96-191382 *02,245* PC A03/MF A01

Dielectric Behavior of a Polycarbonate/Polyester Mixture Upon Transesterification.
PB96-179551 *04,785* Not available NTIS

Dielectric Measurements on Printed-Wiring and Circuit Boards, Thin Films, and Substrates: An Overview.
PB96-147038 *02,236* Not available NTIS

Dielectric Properties Measurements and Data.
PB94-172186 *01,876* Not available NTIS

Dielectric Properties of Materials at Cryogenic Temperatures and Microwave Frequencies.
PB95-202610 *02,369* Not available NTIS

Dielectric Properties of Single Crystals of Al2O3, LaAlO3, SrTiO3, and MgO at Cryogenic Temperatures.
PB95-180477 *02,266* Not available NTIS

Dielectric Properties of Thin Film SrTiO3 Grown on LaAlO3 with YBa2Cu3O7-x Electodes.
PB95-181160 *02,267* Not available NTIS

Dielectric Spectroscopic Determination of Temperature Behavior of Electroclinic Parameters in the Liquid Crystal W317.
PB96-140397 *01,098* Not available NTIS

Dielectric Studies of Fluids with Reentrant Resonators.
PB95-153730 *00,952* Not available NTIS

Dielectric Studies of Fluids with Reentrant Resonators. Appendix B.
DE93019683 *03,244* PC A02/MF A01

Dielectronic Capture Processes in the Electron-Impact Ionization of Sc(2+).
PB95-203113 *04,000* Not available NTIS

Differences in Competitive Strategies between the United States and Japan.
PB94-211836 *00,013* Not available NTIS

Diffraction Imaging of Polycrystalline Materials.
PB94-198884 *02,971* Not available NTIS

Diffraction of Neutron Standing Waves in Thin Films with Resonance Enhancement.
PB97-113278 *04,164* Not available NTIS

Diffraction of X-rays at the Far Tails of the Bragg Peaks.
PB94-199924 *04,476* Not available NTIS

Diffuse-Interface Description of Fluid Systems.
PB96-210711 *01,170* PC A04/MF A01

Diffusion of Cations Beneath Organic Coatings on Steel Substrate.
PB94-215704 *03,119* PC A03/MF A01

Diffusion of Copper into Gold Plating.
PB95-162152 *00,957* Not available NTIS

Diffusion of Water along 'Closed' Mica Interfaces.
PB96-180039 *02,993* Not available NTIS

Diffusion Studies in a Digital-Image-Based Cement Paste Microstructural Model.
PB94-198801 *01,312* Not available NTIS

Diffusive Crack Growth at a Bimaterial Interface.
PB96-204110 *03,090* Not available NTIS

Digital Impedance Bridge.
PB96-103155 *02,272* Not available NTIS

Digital Signature Standard (DSS). Category: Computer Security; Subcategory: Cryptography.
FIPS PUB 186 *01,570* PC E04

Digital Simulation of the Aggregate-Cement Paste Interfacial Zone in Concrete.
PB95-125993 *00,363* Not available NTIS

Digital Techniques in HV Tests - Summary of 1989 Panel Session.
PB94-216702 *02,035* Not available NTIS

Digitized Direct Simulation Model of the Microstructural Development of Cement Paste.
PB94-198777 *01,309* Not available NTIS

Digitized Simulation Model for Microstructural Development.
PB94-198785 *01,310* Not available NTIS

Digitized Simulation of Mercury Intrusion Porosimetry.
PB94-172236 *01,304* Not available NTIS

Dilemma-Preservation versus Access.
PB94-198488 *02,711* Not available NTIS

Dimensional Characterization of Precision Coaxial Transmission Line Standards.
PB96-176482 *02,241* Not available NTIS

Dimensional Characterization of Small Bores: A Survey.
PB95-162202 *02,651* Not available NTIS

Dimensional Crossover in the Phase Separation Kinetics of Thin Polymer Blend Films.
PB97-113088 *03,395* Not available NTIS

Dimensional Inspection Planning Based on Product Data Standards.
PB95-175451 *02,910* Not available NTIS

Diode Laser as a Spectroscopic Tool.
PB95-175485 *00,600* Not available NTIS

Diode-Laser Pumped, Rubidium Cell Frequency Standards.
PB95-163218 *01,538* Not available NTIS

Dipole Moments in Rare Gas Interactions.
PB94-212982 *00,844* Not available NTIS

Direct Comparison of Three PTB Silver Fixed-Point Cells with the NIST Silver Fixed-Point Cell.
PB96-161286 *00,628* Not available NTIS

Direct Comparison Transfer of Microwave Power Sensor Calibrations.
PB96-158654 *02,086* PC A03/MF A01

Direct Detection of Atomic Arsenic Desorption from Si(100).
PB95-202230 *01,024* Not available NTIS

Direct Dispersion Measurement of Highly-Erbium-Doped Optical Amplifiers Using a Low Coherence Reflectometer Coupled with Dispersive Fourier Spectroscopy.
PB95-150702 *04,263* Not available NTIS

Direct Observation of Vortex Dynamics in Two-Dimensional Josephson-Junction Arrays.
PB96-102223 *02,067* Not available NTIS

Directions in MEMS Research Application Development.
PB95-153797 *02,106* Not available NTIS

Directory of Law Enforcement and Criminal Justice Associations and Research Centers.
PB96-178918 *04,872* PC A05/MF A01

Directory of U.S. Private Sector Product Certification Programs.
PB96-215074 *02,688* PC A20/MF A04

Discontinuous Volume Change at the Orientational-Ordering Transition in Solid C60.
PB94-211828 *00,821* Not available NTIS

Discovery of an X-Ray Selected, Radio-Loud Quasar at z=3.9.
PB94-198652 *00,052* Not available NTIS

Discussion: Statistical Signal Processing of Quasiperiodicities.
PB96-119532 *00,096* Not available NTIS

Disilicides of Tungsten, Molybdenum, Tantalum, Titanium, Cobalt, and Nickel, and Platinum Monosilicide: A Survey of Their Thermodynamic Properties.
PB94-168580 *00,752* Not available NTIS

Dislocation Core-Core Interaction and Peierls Stress in a Model Hexagonal Lattice.
PB96-162003 *04,101* Not available NTIS

Dislocation Emission at Ledges on Cracks.
PB95-164240 *04,630* Not available NTIS

Disorder Trapping in Ni2TiAl.
PB94-198942 *03,322* Not available NTIS

Dispersion and Deposition of Smoke Plumes Generated in Massive Fires.
PB95-126066 *02,540* Not available NTIS

Dispersions of Magnetic Excitations of the Pr Ions in Pr2CuO4.
PB94-173044 *04,444* Not available NTIS

Displacement Method for Machine Geometry Calibration.
PB95-152088 *02,946* Not available NTIS

Display-Measurement Round-Robin.
PB96-119227 *02,186* Not available NTIS

Dissolution Problems with Botanical Reference Materials.
PB95-126280 *03,487* Not available NTIS

Distant Future of Solar Activity: A Case Study of Beta Hydri. 3. Transition Region, Corona, and Stellar Wind.
PB94-185220 *00,049* Not available NTIS

Distant Future of Solar Activity: A Case Study of beta Hydri. 3. Transition Region, Corona, and Stellar Wind.
PB95-153441 *00,074* Not available NTIS

Distinguishing the Contributions of Residential Wood Combustion and Mobile Source Emissions Using Relative Concentrations of Dimethylphenanthrene Isomers.
PB96-135124 *02,563* Not available NTIS

Distributed Architecture for Standards Processing.
PB96-164181 *00,276* Not available NTIS

Distributed Communication Methods and Role-Based Access Control for Use in Health Care Applications.
PB96-183165 *01,508* PC A05/MF A01

Distributed Feedback Lasers in Rare-Earth-Doped Phosphate Glass.
PB96-123773 *04,740* Not available NTIS

Distributed measurements of tracer response on packed bed flows using a fiberoptic probe array. Final report.
DE95013079 *00,667* PC A03/MF A01

Distributed Supercomputing Software: Experiences with the Parallel Virtual Machine - PVM.
PB94-163086 *01,680* PC A03/MF A01

Distributed Systems: Survey of Open Management Approaches.
PB96-128202 *01,746* PC A03/MF A01

Distribution of Dielectric Relaxation Times and the Moment Problem.
PB96-112032 *04,727* Not available NTIS

Distribution of Fluoride in Saliva and Plaque Fluid After a 0.048 mol/L NaF Rinse.
PB95-151205 *03,561* Not available NTIS

Distributions of Measurement Error for Three-Axis Magnetic Field Meters during Measurements Near Appliances.
PB96-180153 *02,110* Not available NTIS

DNA Base Damage Generated In vivo in Hepatic Chromatin of Mice upon Whole Body y-Irradiation.
PB95-161741 *03,627* Not available NTIS

DNA Base Damage in Lymphocytes of Cancer Patients Undergoing Radiation Therapy.
PB97-122444 *03,643* Not available NTIS

DNA Base Modifications in Renal Chromatin of Wistar Rats Treated with a Renal Carcinogen, Ferric Nitrilotriacetate.
PB95-150363 *03,648* Not available NTIS

DNA Damage and DNA Sequence Retrieval from Ancient Tissues.
PB97-111983 *03,556* Not available NTIS

DnaJ, DnaK, and GrpE Heat Shock Proteins are Required in 'ori'P1 DNA Replication Solely at the RepA Monomerization Step.
PB97-119382 *03,557* Not available NTIS

Documentation for Immediately Dangerous to Life or Health Concentrations (IDLHs).
PB94-195047 *03,602* PC A22/MF A04

Domain Analysis of the Alarm Surveillance Domain. Version 1.0. Conducted as Part of the Domain Analysis Case Study Project.
PB95-136339 *01,705* PC A10/MF A03

Domain Effects in Faraday Effect Sensors Based on Iron Garnets.
PB95-202461 *02,268* Not available NTIS

Domain Structures in Magnetoresistive Granular Metals.
PB96-141346 *04,760* Not available NTIS

Doppler-Free Spectroscopy of Large Polyatomic Molecules and van der Waals Complexes.
PB96-119581 *04,339* Not available NTIS

Dose Mapping of Radioactive Hot Particles Using Radiochromic Film.
PB95-162954 *03,714* Not available NTIS

Dosimetry Systems for Radiation Processing.
PB96-135280 *03,717* Not available NTIS

Double Modulation and Selective Excitation Photoreflectance for Characterizing Highly Luminescent Semiconductor Structures and Samples with Poor Surface Morphology.
PB97-111439 *02,452* Not available NTIS

Double-Modulation and Selective Excitation Photoreflectance for Wafer-Level Characterization of Quantum-Well Laser Structures.
PB96-167325 *04,372* Not available NTIS

Draft Guideline for Testing and Evaluation of Seismic Isolation Systems.
PB94-172947 *00,423* Not available NTIS

Draft Guidelines for Pre-Qualification and Prototype Testing of Seismic Isolation Systems.
PB94-161940 *01,331* PC A06/MF A01

Draft Guidelines for Quality Control Testing of Elastomeric Seismic Isolation Systems.
PB94-161734 *00,422* PC A03/MF A01

Draft Guidelines for Quality Control Testing of Sliding Seismic Isolation Systems.
PB94-161957 *01,332* PC A03/MF A01

Dreams About the Next Generation of Super-Stable Lasers.
PB94-211570 *04,235* Not available NTIS

Drill-Hearn-Gerasimov Sum Rule.
PB94-211752 *03,845* Not available NTIS

Droplet Transfer Modes for a MIL 100S-1 GMAW Electrode.
PB95-209300 *02,867* PC A04/MF A01

Dual-Frequency Millimeter-Wave Radiometer Antenna for Airborne Remote Sensing of Atmosphere and Ocean.
PB96-112289 *02,009* Not available NTIS

Dual Frequency mm-Wave Radiometer Antenna for Airborne Remote Sensing of Atmosphere and Ocean.
PB95-180378 *02,006* Not available NTIS

Ductile Fracture and Tempered Martensite Embrittlement of 4140 Steel.
PB96-190285 *03,222* Not available NTIS

Dusty Plasma Studies in the Gaseous Electronics Conference Reference Cell.
PB96-113410 *02,396*
(Order as PB96-113311, PC A09/MF A03)

Dynamic Characteristics of Five Tall Buildings during Strong and Low-Amplitude Motions.
PB94-199981 *00,427* Not available NTIS

Dynamic Light-Scattering Study of a Diluted Polymer Blend Near Its Critical Point.
PB95-151890 *01,245* Not available NTIS

Dynamic Measurements of Thermophysical Properties of Metals and Alloys at High Temperatures by Subsecond Pulse Heating Techniques.
N94-25124/6 *03,309*
(Order as N94-25120/4, PC A11/MF A03)

Dynamic Objects and Meta-Level Programming of an EXPRESS Language Environment.
PB96-190053 *01,774* Not available NTIS

Dynamic Phenomena on the RS Canum Venaticorum Binary II Pegasi in August 1989. 1. Observational Data.
PB94-211067 *00,056* Not available NTIS

Dynamic Scaling in an Aggregating 2D Lennard-Jones System.
PB96-167317 *04,106* Not available NTIS

Dynamic Shear Modulus Measurements with Four Independent Techniques in Nickel-Based Alloys.
PB94-198900 *03,320* Not available NTIS

Dynamic Technique for Measuring Normal Spectral Emissivity of Electrically Conducting Solids at High Temperatures with a High-Speed Spatial Scanning Pyrometer.
PB95-153045 *03,921* Not available NTIS

Dynamics of Calcium Phosphate Precipitation.
PB96-147095 *03,574* Not available NTIS

Dynamics of Hydrogen Interactions with Si(100) and Si(111) Surfaces.
PB96-159801 *04,082* Not available NTIS

Dynamics of Mu(+) in Sc and ScHx.
PB96-180021 *04,112* Not available NTIS

Dynamics of Multi-DOF Stochastic Nonlinear Systems.
PB97-113245 *00,477* Not available NTIS

Dynamics of Nonthermal Reactions: Femtosecond Surface Chemistry.
PB94-199965 *00,688* Not available NTIS

Dynamics, Transport and Chemical Kinetics of Compartment Fire Exhaust Gases.
PB96-195508 *00,229* PC A06/MF A01

Dynamics vs. Static Young's Moduli: A Case Study.
PB94-213188 *03,210* Not available NTIS

Dynamometer-Induced Residual Stress in Railroad Wheels: Ultrasonic and Saw Cut Measurements. Report No. 30.
PB96-183199 *04,857* PC A04/MF A01

Early Detection of Room Fires Through Acoustic Emission. (NIST Reprint).
PB95-180311 *00,298* Not available NTIS

Early Dielectronic Recombination Measurements: Singly Charged Ions.
PB94-211158 *03,836* Not available NTIS

Early History and Future Outlook for the X-ray Crystal Density Method.
PB95-202487 *04,692* Not available NTIS

Earth-Based Gravitational Experiments.
PB94-211414 *03,840* Not available NTIS

Earthquake and Fire in Japan: When the Threat Became a Reality.
PB95-175238 *00,201* Not available NTIS

Earthquake Resistant Construction of Electric Transmission and Telecommunication Facilities Serving the Federal Government Report.
PB94-161817 *02,460* PC A03/MF A01

Earthquake Resistant Construction of Gas and Liquid Fuel Pipeline Systems Serving, or Regulated By, the Federal Government.
PB94-161999 *04,846* PC A05/MF A01

Ebulliometers for Measuring the Thermodynamic Properties of Fluids and Fluid Mixtures.
DE94017817 *04,195* PC A02/MF A01

Ebulliometric Measurement of the Vapor Pressure of Difluoromethane.
PB95-151361 *00,931* Not available NTIS

Ebulliometric Measurement of the Vapor Pressure of 1-Chloro-1,1-Difluoroethane and 1,1-Difluoroethane.
PB95-164489 *00,984* Not available NTIS

Economic, Energy, and Environmental Impacts of the Energy-Related Inventions Program.
DE94-017162 *00,008* PC A05/MF A02

Economic Methods and Risk Analysis Techniques for Evaluating Building Investments: A Survey.
PB96-122593 *00,323* Not available NTIS

Economics of New-Technology Materials: A Case Study of FRP Bridge Decking.
PB96-202353 *01,349* PC A06/MF A01

EDI and EFT Security Standards.
PB96-122833 *01,605* Not available NTIS

Effect in Environmental Noise on the Accuracy of Coulomb-Blockade Devices.
PB95-175865 *04,662* Not available NTIS

Effect of a Crystal Monochromator on the Local Angular Divergence of an X-Ray Beam.
PB95-150306 *04,565* Not available NTIS

Effect of Anneal Temperature on Si/Buried Oxide Interface Roughness on SIMOX.
PB96-112206 *02,382* Not available NTIS

Effect of Annealing Ambient on the Removal of Oxide Precipitates in High-Dose Oxygen Implanted Silicon.
PB95-164356 *02,356* Not available NTIS

Effect of Axial Strain on the Critical Current of Ag-Sheathed Bi-Based Superconductors in Magnetic Fields Up to 25 T.
PB94-211315 *04,493* Not available NTIS

Effect of Backfill and Atomizing Gas on the Powder Porosity and Mechanical Properties of 304L Stainless Steel.
PB94-185394 *03,205* Not available NTIS

Effect of Beam Voltage on the Properties of Aluminum Nitride Prepared by Ion Beam Assisted Deposition.
PB97-118616 *01,995* Not available NTIS

Effect of CF3H and CF3Br on Laminar Diffusion Flames in Normal and Microgravity.
PB96-161831 *01,420* Not available NTIS

TITLE INDEX

Effect of CF3H and CF3Br on Laminar Diffusion Flames in Normal and Microgravity.
PB96-161849 *01,421* Not available NTIS

Effect of Charpy V-Notch Striker Radii on the Absorbed Energy.
PB96-141122 *03,365* Not available NTIS

Effect of Chemical Interaction on Barenblatt Crack Profiles in Brittle Solids.
PB96-180245 *02,996* Not available NTIS

Effect of Cross-Links on the Miscibility of a Deuterated Polybutadiene and Protonated Polybutadiene Blend.
PB94-212438 *01,225* Not available NTIS

Effect of Curing History on Ultimate Glass Transition Temperature and Network Structure of Crosslinking Polymers.
PB94-200052 *01,214* Not available NTIS

Effect of DC Tests on Induced Space Charge.
PB94-172350 *02,212* Not available NTIS

Effect of Dodecanol Content on the Combustion of Methanol Spray Flames.
PB95-176020 *01,389* Not available NTIS

Effect of Electrode Material on Measured Ion Energy Distributions in Radio-Frequency Discharges.
PB96-102850 *04,026* Not available NTIS

Effect of Electrode-Polymer Interfacial Layers on Polymer Conduction. Part 2. Device Summary.
PB95-151155 *02,335* Not available NTIS

Effect of Environmentally Exposures on the Properties of Polyisocyanurate Foam Insulation: Thermal Conductivity Measurements.
PB95-181210 *00,388* Not available NTIS

Effect of Ethanol on the Solubility of Dicalcium Phosphate Dihydrate in the System Ca(OH)2-H3PO4-H2O at 37C.
PB95-163507 *00,163* Not available NTIS

Effect of Ethanol on the Solubility of Hydroxyapatite in the System Ca(OH)2-H3PO4-H2O at 25C and 33C.
PB95-169231 *00,169* Not available NTIS

Effect of Finite Beam Width on Elastic Light Scattering from Droplets.
PB96-163670 *01,144* Not available NTIS

Effect of Formulation Changes on the Response to Ionizing Radiation of Radiochromic Dye Films.
PB97-119028 *04,171* Not available NTIS

Effect of Fuel Tank Rupture Mode on the Ignitability of Expelled Fuel.
PB97-110043 *01,444* Not available NTIS

Effect of Grain Size on Hertzian Contact Damage in Alumina.
PB96-179601 *03,083* Not available NTIS

Effect of Green Density and the Role of Magnesium Oxide Additive on the Densification of Alumina Measured by Small-Angle Neutron Scattering. (Reannouncement with New Availability Information).
AD-A244 582/3 *03,022* PC A02/MF A01

Effect of Harmonic Distortion on Phase Errors in Frequency Distribution and Synthesis.
PB96-200779 *01,563* Not available NTIS

Effect of Heterogeneous Porous Media on Mold Filling in Resin Transfer Molding.
PB95-108676 *03,197* Not available NTIS

Effect of Hydrodynamic Interactions on a Terminally Anchored Bead-Rod Model Chain.
PB95-141156 *01,237* Not available NTIS

Effect of Inclination on the Performance of a Compact Brazed Plate Condenser and Evaporator.
PB96-136973 *02,756* PC A03/MF A01

Effect of Intermediate Thermal Processing on Microstructural Changes of Oxygen Implanted Silicon-on-Insulator Material.
PB96-160213 *02,982* Not available NTIS

Effect of Liftoff on Accuracu of Phase Velocity Measurements Made with Electromagnetic-Acoustic Transducers.
PB96-186044 *02,280* Not available NTIS

Effect of Magnetic Field Orientation on the Critical Current of HTS Conductor and Coils.
PB96-141189 *02,956* Not available NTIS

Effect of Microstructure on Phase Formation in the Reaction of Nb/Al Multilayer Thin Films.
PB95-168415 *03,352* Not available NTIS

Effect of Microstructure on the Wear Transition of Zirconia-Toughened Alumina.
PB94-211778 *03,141* Not available NTIS

Effect of Mn Content on the Microstructure of Al-Mn Alloys Electrodeposited at 150C.
PB95-126355 *03,343* Not available NTIS

Effect of Modulated Taylor-Couette Flows on Crystal-Melt Interfaces: Theory and Initial Experiments.
PB94-216736 *04,521* Not available NTIS

Effect of Semiconductor Laser Characteristics on Optical Fiber Sensor Performance.
PB95-169132 *02,167* Not available NTIS

Effect of Single versus Multiple Implant Processing on Defect Types and Densities in SIMOX.
PB96-160353 *01,957* Not available NTIS

Effect of Sm2BaCuO5 on the Properties of Sintered (Bulk) YBa2Cu3O6+x.
PB96-119441 *04,733* Not available NTIS

Effect of Splitting on Estimation of Emission Rate Profiles from Neutron Depth Profiling Spectra.
PB95-152245 *03,916* Not available NTIS

Effect of Stoichiometry on the Phases Present in Boron Nitride Thin Films.
PB96-102470 *04,710* Not available NTIS

Effect of Supersaturation on Apatite Crystal Formation in Aqueous Solutions at Physiologic pH and Temperature.
PB96-135215 *03,571* Not available NTIS

Effect of Suppressants on Metal Fires.
PB96-109574 *01,402* PC A03/MF A01

Effect of Swelling on the Elasticity of Rubber: Localization Model Description.
PB94-211034 *01,216* Not available NTIS

Effect of Thermal Noise on Shapiro Steps in High-Tc Josephson Weak Links.
PB94-212677 *04,506* Not available NTIS

Effect of Three Sterilization Techniques on Finger Pluggers.
PB94-216090 *00,150* Not available NTIS

Effect of Training Dynamics on Neural Network Performance.
PB95-267845 *01,852* PC A03/MF A01

Effect of Transformation of Alloy on Transient and Residual Stresses in a Porcelain-Metal Strip.
PB94-198397 *00,143* Not available NTIS

Effect of Two Initiator/Stabilizer Concentrations in a Metal Primer on Bond Strengths of a Composite to a Base Metal Alloy.
PB94-172723 *00,141* Not available NTIS

Effect of 1-Hydroxyethylidene-1,1-Bisphosphonate on Membrane-Mediated Calcium Phosphate Formation in Model Liposomal Suspensions.
PB95-169223 *03,469* Not available NTIS

Effective Measurement Techniques for Heat, Smoke, and Toxic Fire Gases.
PB94-198439 *01,369* Not available NTIS

Effective Medium Theory for Ferrite-Loaded Materials.
PB95-154662 *01,893* PC A03/MF A01

Effectiveness of a Heat Recovery Ventilator, an Outdoor Air Intake Damper and an Electrostatic Particulate Filter at Controlling Indoor Air Quality in Residential Buildings.
PB96-146642 *02,564* Not available NTIS

Effectiveness of Halon Alternatives in Suppressing Dynamic Combustion Process.
PB96-175732 *03,288* Not available NTIS

Effects of Adhesive Thickness, Open Time, and Surface Cleanness on the Peel Strength of Adhesive-Bonded Seams of EPDM Rubber Roofing Membrane.
PB95-151338 *00,372* Not available NTIS

Effects of Aluminum Oxalate/Glycine Pretreatment Solutions on Dentin Permeability.
PB95-164505 *03,565* Not available NTIS

Effects of Anneal Time and Cooling Rate on the Formation and Texture of Bi2Sr2CaCu2O8 Films.
PB95-161600 *04,603* Not available NTIS

Effects of Calcium Phosphate Solutions on Dentin Permeability.
PB95-151080 *00,157* Not available NTIS

Effects of Copper, Nickel and Boron on Mechanical Properties of Low-Alloy Steel Weld Metals Deposited at High Heat Input.
PB96-135231 *03,363* Not available NTIS

Effects of Critical Current Density, Equilibrium Magnetization and Surface Barrier on Magnetization of High Temperature Superconductors.
PB94-185162 *04,446* Not available NTIS

Effects of Critical Current Density, Equilibrium Magnetization and Surface Barrier on Magnetization of High Temperature Superconductors.
PB95-153060 *04,588* Not available NTIS

Effects of Crystalline Anisotropy and Buoyancy-Driven Convection on Morphological Stability.
PB94-200441 *03,328* Not available NTIS

Effects of Elastic Stress on Phase Equilibrium in the Ni-V System.
PB94-172707 *03,313* Not available NTIS

Effects of Elastic Stress on the Stability of a Solid-Liquid Interface.
PB95-163028 *03,350* Not available NTIS

Effects of Etching on the Morphology and Surface Resistance of YBa2Cu3O7-delta Films.
PB96-135355 *02,410* Not available NTIS

Effects of Heavy Doping on Numerical Simulations of Gallium Arsenide Bipolar Transistors.
PB95-150975 *02,334* Not available NTIS

Effects of Humidity and Elevated Temperature on the Density and Thermal Conductivity of a Rigid Polyisocyanurate Foam.
PB95-152021 *00,373* Not available NTIS

Effects of Humidity and Elevated Temperature on the Density and Thermal Conductivity of a Rigid Polyisocyanurate Foam Co-Blown with CCl3F and CO2.
PB95-150462 *00,371* Not available NTIS

Effects of Interfacial Roughness on the Magnetoresistance of Magnetic Metallic Multilayers.
PB95-150017 *04,556* Not available NTIS

Effects of Molecular Weight and Thermal Stability on Polymer Gasification.
PB94-212610 *01,228* Not available NTIS

Effects of Nonmedel Errors on Model-Based Testing.
PB96-155577 *03,420* Not available NTIS

Effects of Nonmodel Errors on Model-Based Testing.
PB96-123146 *02,604* Not available NTIS

Effects of Pipe Elbows and Tube Bundles on Selected Types of Flowmeters.
PB96-160999 *01,135* Not available NTIS

Effects of Sample Mounting on Flammability Properties of Intumescent Polymers.
PB96-159777 *03,389* Not available NTIS

Effects of Soxhlet Extraction on the Surface Oxide Layer of Silicon Nitride Powders.
PB95-175584 *03,057* Not available NTIS

Effects of Specimen Edge Conditions on Heat Release Rate.
PB95-152864 *00,375* Not available NTIS

Effects of Spindle Dynamic Characteristics on Hard Turning.
PB96-122981 *02,699* Not available NTIS

Effects of Substrate Surface Steps on the Microstructure of Epitaxial Ba2YCu3O7-x Thin Films on (001) LaAlO3.
PB96-148184 *04,774* Not available NTIS

Effects of Surface-Active Resins on Dentin/Composite Bonds.
PB95-140448 *00,156* Not available NTIS

Effects of Target Shape and Neutron Scattering on Element Sensitivities for Neutron-Capture Prompt Gamma-ray Activation Analysis.
PB94-216157 *00,558* Not available NTIS

Effects of Target Temperature on Analytical Sensitivities of Cold-Neutron Capture Prompt gamma-ray Activation Analysis.
PB96-112131 *00,616* Not available NTIS

Effects of Testing Variables on the Measured Compressive Strength of High-Strength (90 MPa) Concrete.
PB95-179040 *00,445* PC A07/MF A02

Effects of Testing Variables on the Strength of High-Strength (90 Mpa) Concrete Cylinders.
PB96-112198 *00,456* Not available NTIS

Effects of Variable Excluded Volume on the Dimensions of Off-Lattice Polymer Chains.
PB94-212941 *01,229* Not available NTIS

Effects on Whole Saliva of Chewing Gums Containing Calcium Phosphates.
PB95-153169 *03,563* Not available NTIS

Efficiency of Electric Motors. National Voluntary Lab. Accreditation Program (NVLAP).
PB96-111174 *02,107* PC A05/MF A01

Efficient Br(*) Laser Pumped by Frequency-Doubled Nd: YAG and Electronic-to-Vibrational Transfer-Pumped CO2 and HCN Lasers.
PB95-108684 *04,248* Not available NTIS

Efficient Experiment to Study Superconducting Ceramics.
PB94-212578 *04,505* Not available NTIS

Efficient Method to Compute the Maximum Transient Drain Current Overshoot in Silicon on Insulator Devices.
PB94-172483 *02,300* Not available NTIS

Efficient Way of Identifying New Active Stars: A VLA Survey of X-ray Selected Active Stellar Candidates.
PB96-122882 *00,099* Not available NTIS

Elastic Constants and Debye Temperature of Y1Ba2Cu3Ox: Effect of Oxygen Content.
PB94-213352 *04,515* Not available NTIS

Elastic Constants and Internal Friction of Polycrystalline Copper.
PB96-141015 *03,364* Not available NTIS

Elastic Constants and Microcracks in YBa2Cu3O7.
PB96-200761 *03,005* Not available NTIS

Elastic Constants of a Material with Orthorhombic Symmetry: An Alternative Measurement Approach.
PB95-180527 *04,684* Not available NTIS

Elastic Constants of Isotropic Cylinders Using Resonant Ultrasound.
PB94-211919 *04,497* Not available NTIS

Elastic Constants of Polycrystalline Y1Ba2Cu3Ox.
PB94-213196 *04,513* Not available NTIS

Elastic Deformation of a Monolithic Perfect Crystal Interferometer: Implications for Gravitational Phase Shift Experiments.
PB94-213154 *03,858* Not available NTIS

Elastic-Electron-Scattering Effects on Angular Distributions in X-ray Photoelectron Spectroscopy.
PB95-175758 *01,000* Not available NTIS

Elastic Green's Function for a Bimaterial Composite Solid Containing a Free Surface Normal to the Interface.
PB95-163325 *03,162* Not available NTIS

Elastic Properties of Al2O3/Al Composites: Measurements and Modeling.
PB95-161378 *03,157* Not available NTIS

Elastic Properties of Central-Force Networks with Bond-Length Mismatch.
PB95-163366 *04,623* Not available NTIS

Elastic Properties of Uniaxial-Fiber Reinforced Composites: General Features.
PB94-200649 *03,140* Not available NTIS

Elastic Scattering from Spheres under Non Plane-Wave Illumination.
PB96-163688 *04,370* Not available NTIS

Elastic Scattering of Polymer Networks.
PB95-161816 *01,255* Not available NTIS

Electric Dipole Excitation of a Long Conductor in a Lossy Medium.
PB96-146675 *04,058* Not available NTIS

Electric Field Dependent Dielectric Breakdown of Intrinsic SiO2 Films Under Dynamic Stress.
PB96-204102 *02,449* Not available NTIS

Electric Field Effects on a Near-Critical Fluid in Microgravity.
PB96-161880 *04,217* Not available NTIS

Electric Field Effects on Crack Growth in a Lead Magnesium Niobate.
PB95-107322 *03,339* Not available NTIS

Electric-Field Strengths Measured Near Personal Transceivers.
PB94-172020 *01,564* Not available NTIS

Electrical Breakdown in Transformer Oil in Large Gaps.
PB95-150579 *01,889* Not available NTIS

Electrical Characteristics of Argon Radio Frequency Glow Discharges in an Asymmetric Cell.
PB96-176490 *04,109* Not available NTIS

Electrical Characterization of Integrated Circuit Metal Line Thickness.
PB96-138433 *02,414* Not available NTIS

Electrical Characterization of Liquid-Phase Epitaxially Grown Single-Crystal Films of Mercury Cadmium Telluride by Variable-Magnetic-Field Hall Measurements.
PB95-175782 *02,177* Not available NTIS

Electrical Characterization of Narrow Gap n-Type Bulk HgCdTe Single Crystals by Variable-Magnetic-Field Hall Measurements and Reduced-Conductivity-Tensor Analyses.
PB96-164199 *01,146* Not available NTIS

Electrical Characterization of Radio-Frequency Discharges in the Gaseous Electronics Conference Reference Cell.
PB95-164612 *01,905* Not available NTIS

Electrical Measurements for Monitoring and Control of rf Plasma Processing.
PB96-161963 *04,369* Not available NTIS

Electrical Measurements of Microwave Flip-Chip Interconnections.
PB96-176748 *02,436* Not available NTIS

Electrical Method for Determining the Thickness of Metal Films and the Cross-Sectional Area of Metal Lines.
PB95-203170 *02,370* Not available NTIS

Electrical Product Requirements (Especially Quality Requirements) in the United States.
PB96-119235 *01,929* Not available NTIS

Electrical Sensors for Monitoring rf Plasma Sheaths.
PB95-162962 *04,412* Not available NTIS

Electrical Test Structure for Improved Measurement of Feature Placement and Overlay in Integrated Circuit Fabrication Processes.
PB95-164273 *02,355* Not available NTIS

Electrical Test Structure for Overlay Metrology Referenced to Absolute Length Standards.
PB95-152278 *02,336* Not available NTIS

Electrical Test Structures Replicated in Silicon-on-Insulator Material.
PB97-111827 *02,454* Not available NTIS

Electrically Calibrated Pyroelectric Detector-Refinements for Improved Optical Power Measurements.
PB95-169066 *02,164* Not available NTIS

Electro-Optic-Based RMS Voltage Measurement Technique.
PB96-138490 *02,194* Not available NTIS

Electro-Optical Sensor for Surface Displacement Measurements of Compliant Coatings.
PB94-198223 *02,123* Not available NTIS

Electro-Thermal Simulation of an IGBT PWM Inverter.
PB94-185592 *02,303* Not available NTIS

Electroacoustic Characterization of Particle Size and Zeta Potential in Moderately Concentrated Suspensions.
PB96-119425 *01,079* Not available NTIS

Electroacoustics for Characterization of Particulates and Suspensions. Proceedings of a Workshop. Held in Gaithersburg, Maryland on February 3-4, 1993.
PB94-112695 *00,725* PC A15/MF A03

Electrochemical Synthesis of Metal and Intermetallic Composites.
AD-A294 088/0 *03,304* PC A04/MF A01

Electrode Extension Model for Gas Metal Arc Welding.
PB96-135074 *02,871* Not available NTIS

Electrodeposited Cobalt-Tungsten as a Diffusion Barrier between Graphite Fibers and Nickel.
PB96-146881 *03,176* Not available NTIS

Electrodeposition.
PB94-172517 *00,760* Not available NTIS

Electrohydrodynamic Instability and Electrical Discharge Initiation in Hexane.
PB96-186119 *02,244* Not available NTIS

Electrokinetic Sonic Analysis of Silicon Nitride Suspensions.
PB96-123575 *03,073* Not available NTIS

Electrolytes Constrained on Fractal Structures: Debye-Huckel Theory.
PB97-110241 *01,174* Not available NTIS

Electromagnetic Coupling Character of (001) Twist Boundaries in Sintered Bi2Sr2CaCu2O8+x Bicrystals.
PB96-176573 *01,963* Not available NTIS

Electromagnetic Properties of Materials: The NIST Metrology Program.
PB96-122791 *01,933* Not available NTIS

Electromagnetic Scattering by a Periodic Surface with a Wedge Profile.
PB94-211950 *04,421* Not available NTIS

Electromagnetic Scattering from a Dielectric Wedge and the Single Hypersingular Integral Equation.
PB97-110530 *04,430* Not available NTIS

Electromagnetic Shielding Characterization of Gaskets.
PB95-198917 *01,911* PC A03/MF A01

Electromechanical properties of superconductors for DOE fusion applications.
DE95015476 *04,432* PC A04/MF A01

Electromechanical Properties of Superconductors for DOE Fusion Applications.
PB94-139672 *02,250* PC A06/MF A02

Electron and Hole Trapping in Irradiated SIMOX, ZMR and BESOI Buried Oxides.
PB96-160320 *01,956* Not available NTIS

Electron and Proton Dosimetry with Custom-Developed Radiochromic Dye Films.
PB95-151106 *03,713* Not available NTIS

Electron-atom collision studies using optically state selected beams. Progress report, May 15, 1987--May 14, 1988.
DE95004446 *03,776* PC A03/MF A01

Electron-atom collision studies using optically state selected beams. Progress report, May 15, 1988--May 14, 1991.
DE95004447 *03,777* PC A03/MF A01

Electron Attachment to Excited Molecules(1).
PB96-122809 *01,087* Not available NTIS

Electron Beam Crosslinking of Poly(vinylmethyl ether).
PB94-185550 *01,205* Not available NTIS

Electron-electron Interactions, Coupled-Plasmon-Phonon Modes, and Mobility in n-Type GaAs.
PB96-138524 *04,749* Not available NTIS

Electron-Impact Excitation of Si(3+)(3S yields 3P) Using a Merged-Beam Electron-Energy-Loss Technique.
PB95-151239 *03,904* Not available NTIS

Electron-Impact Ionization of In(+) and Xe(+).
PB94-185089 *00,770* Not available NTIS

Electron-Impact Ionization of In(+) and Xe(+).
PB95-152906 *03,918* Not available NTIS

Electron-Ion Collisions in the Plasma Edge.
PB96-111885 *04,037* Not available NTIS

Electron-Ion-X-ray Spectrometer System.
PB95-176137 *03,958* Not available NTIS

Electron-Photon Monte Carlo Calculations: The ETRAN Code.
PB97-110407 *04,138* Not available NTIS

Electron Probe X-Ray Microanalysis.
PB95-107165 *00,562* Not available NTIS

Electron Scattering and Dissociative Attachment by SF6 and Its Electrical-Discharge By-Products.
PB95-151288 *02,256* Not available NTIS

Electron Screening Correction to the Self Energy in High-Z Atoms.
PB94-172376 *03,789* Not available NTIS

Electron Transfer Reaction Rates and Equilibria of the Carbonate and Sulfate Radical Anions.
PB94-212180 *00,829* Not available NTIS

Electron transport calculations with biomedical and environmental applications. Final report, December 23, 1992--January 31, 1994.
DE95007065 *03,613* PC A01/MF A01

Electron Traps, Structural Change, and Hydrogen Related SIMOX Defects.
PB94-200391 *02,312* Not available NTIS

Electronic Access: Blueprint for the National Archives and Records Administration.
PB95-219218 *02,731* PC A04/MF A01

Electronic Access to Standards on the Information Highway.
PB96-131578 *01,494* PC A03/MF A01

Electronic Balance and Some Gravimetric Applications. (The Density of Solids and Liquids, Pycnometry and Mass).
PB94-163052 *03,785* PC A03/MF A01

Electronic Correlations and Satellites in Superconducting Oxides.
PB94-200045 *04,477* Not available NTIS

Electronic Implementors' Workshop.
PB95-210936 *01,484* PC A03/MF A01

Electronic Microrefrigerator Based on a Normal-Insulator-Superconductor Tunnel Junction.
PB96-102827 *04,718* Not available NTIS

Electronic Mode Stirring for Reverberation Chambers.
PB95-180329 *01,908* Not available NTIS

Electronic Publishing and the Journals of the American Chemical Society.
PB97-109185 *04,807*
(Order as PB97-109011, PC A11/MF A03)

Electronic Spectra of CF2Cl and CFCl2 Radicals Observed by Resonance Enhanced Multiphoton Ionization.
PB95-151023 *00,927* Not available NTIS

Electronic Structure and Phase Equilibria in Ternary Substitutional Alloys.
PB97-119366 *03,378* Not available NTIS

Electronically Tunable Fiber Laser for Optical Pumping of (3)He and (4)He.
PB96-201165 *04,381* Not available NTIS

Electronics and Electrical Engineering Laboratory Technical Progress Bulletin Covering Laboratory Programs, April to June 1991, with 1992 EEEL Events Calendar.
PB95-209821 *01,916* PC A03/MF A01

Electronics and Electrical Engineering Laboratory Technical Progress Bulletin Covering Laboratory Programs, April to June 1994 with 1994/1995 EEEL Events Calendar.
PB95-143186 *02,329* PC A03/MF A01

Electronics and Electrical Engineering Laboratory Technical Progress Bulletin Covering Laboratory Programs, April to June 1995 with 1995 EEEL Events Calendar.
PB96-106455 *01,923* PC A03/MF A01

Electronics and Electrical Engineering Laboratory Technical Progress Bulletin Covering Laboratory Programs, April to June 1996 with 1996-1998 EEEL Events Calendar.
PB97-113880 *01,994* PC A04/MF A01

Electronics and Electrical Engineering Laboratory Technical Progress Bulletin Covering Laboratory Programs, January to March 1991, with 1991 EEEL Events Calendar.
PB94-145968 *02,113* PC A03/MF A01

TITLE INDEX

Electronics and Electrical Engineering Laboratory Technical Progress Bulletin Covering Laboratory Programs, January to March 1992, with 1992/1993 EEEL Events Calendar.
PB95-210480 *01,917* PC A03/MF A01

Electronics and Electrical Engineering Laboratory Technical Progress Bulletin Covering Laboratory Programs, January to March 1994 with 1994/1995 EEEL Events Calendar.
PB94-193810 *02,308* PC A03/MF A01

Electronics and Electrical Engineering Laboratory Technical Progress Bulletin Covering Laboratory Programs, January to March 1996, with 1996 EEEL Events Calendar.
PB96-191390 *01,969* PC A04/MF A01

Electronics and Electrical Engineering Laboratory Technical Progress Bulletin Covering Laboratory Programs, July to September 1993 with 1994 EEEL Events Calendar.
PB94-194354 *02,309* PC A03/MF A01

Electronics and Electrical Engineering Laboratory Technical Progress Bulletin Covering Laboratory Programs, July to September 1994 with 1994/1995 EEEL Events Calendar.
PB95-170395 *02,360* PC A03/MF A01

Electronics and Electrical Engineering Laboratory Technical Progress Bulletin Covering Laboratory Programs, July to September 1995 with 1996 EEEL Events Calendar.
PB96-147905 *01,942* PC A04/MF A01

Electronics and Electrical Engineering Laboratory Technical Progress Bulletin Covering Laboratory Programs, October to December 1992, with 1992/1993 EEEL Events Calendar.
PB94-165958 *02,299* PC A03/MF A01

Electronics and Electrical Engineering Laboratory Technical Progress Bulletin Covering Laboratory Programs, October to December 1994 with 1995 EEEL Events Calendar.
PB95-208724 *02,372* PC A04/MF A01

Electronics and Electrical Engineering Laboratory Technical Progress Bulletin Covering Laboratory Programs, October to December 1995 with 1996 EEEL Events Calendar.
PB96-183116 *01,966* PC A04/MF A01

Electronics and Electrical Engineering Laboratory Technical Progress Bulletin Covering Programs, October to December 1993, with 1994/1995 EEEL Events Calendar.
PB94-154341 *02,115* PC A03/MF A01

Electronics and Electrical Engineering Laboratory Technical Publication Announcements Covering Laboratory Programs, April to June 1995 with 1995 EEEL Events Calendar.
PB96-137187 *01,941* PC A03/MF A01

Electronics and Electrical Engineering Laboratory Technical Publication Announcements Covering Laboratory Programs, January to March 1994 with 1994/1995 EEEL Events Calendar.
PB94-213774 *01,883* PC A03/MF A01

Electronics and Electrical Engineering Laboratory Technical Publication Announcements Covering Laboratory Programs, January to March 1995 with 1995 EEEl Events Calendar.
PB95-242277 *02,373* PC A03/MF A01

Electronics and Electrical Engineering Laboratory Technical Publication Announcements Covering Laboratory Programs, January to March 1996, with 1996 EEEL Events Calendar.
PB96-214622 *01,981* PC A03/MF A01

Electronics and Electrical Engineering Laboratory Technical Publication Announcements Covering Laboratory Programs, July to September 1994 with 1995 EEEL Events Calendar.
PB95-198925 *01,912* PC A03/MF A01

Electronics and Electrical Engineering Laboratory Technical Publication Announcements Covering Laboratory Programs, July to September 1995 with 1996 EEEL Events Calendar.
PB96-183066 *01,965* PC A03/MF A01

Electronics and Electrical Engineering Laboratory Technical Publication Announcements Covering Laboratory Programs, October to December 1993 with 1994/1995 EEEL Events Calendar.
PB94-193752 *02,307* PC A03/MF A01

Electronics and Electrical Engineering Laboratory Technical Publication Announcements Covering Laboratory Programs, October to December 1994 with 1995 EEEL Events Calendar.
PB95-231841 *01,918* PC A03/MF A01

Electronics and Electrical Engineering Laboratory Technical Publication Announcements Covering Laboratory Programs, October to December 1995, with 1996 EEEL Events Calendar.
PB96-202346 *01,978* PC A04/MF A01

Electronics and Electrical Engineering Laboratory 1994 Program Plan: Supporting Technology for U.S. Competitiveness in Electronics.
PB94-126901 *01,873* PC A09/MF A02

Electronics and Electrical Engineering Laboratory: 1994 Strategic Plan. Supporting Technology for U.S. Competitiveness in Electronics.
PB94-161320 *01,874* PC A04/MF A01

Electronics and Electrical Engineering Laboratory 1994 Technical Accomplishments Supporting Technology for U.S. Competitiveness in Electronics.
PB95-144309 *01,887* PC A06/MF A02

Electronics and Electrical Engineering Laboratory 1995 Program Plan. Supporting Technology for U.S. Competitiveness in Electronics.
PB95-159885 *01,894* PC A09/MF A03

Electronics and Electrical Engineering Laboratory 1995 Technical Accomplishments: Advancing Metrology for Electrotechnology to Support the U.S. Economy.
PB96-164520 *01,959* PC A05/MF A01

Electronics and Electrical Engineering Laboratory: 1996 Program Plan. Supporting Technology for U.S. Competitiveness in Electronics.
PB96-175237 *01,962* PC A10/MF A03

Electronics Packaging Materials Research at NIST.
PB96-122692 *02,405* Not available NTIS

Electropermeabilization of Cell Membranes: Effect of the Resting Membrane Potential.
PB95-163291 *03,537* Not available NTIS

Electrophoretic Separations of Polymerase Chain Reaction: Amplified DNA Fragments in DNA Typing Using a Capillary Electrophoresis-Lased Induced Fluorescence System.
PB95-163036 *03,536* Not available NTIS

Electrostatic Modes as a Diagnostic in Penning-Trap Experiments.
PB95-176244 *03,959* Not available NTIS

Electrostatic Modes of Ion-Trap Plasmas.
PB95-152963 *03,920* Not available NTIS

Electrostatic Rigidity of Polyelectrolytes from Reparametrization Invariance.
PB96-180062 *04,113* Not available NTIS

Elements of a Framework for Fire Safety Engineering.
PB96-151402 *00,214* Not available NTIS

ELF Electric and Magnetic Field Measurement Methods.
PB95-161675 *04,423* Not available NTIS

Embossable Grating Couplers for Planar Waveguide Optical Sensors.
PB96-190277 *00,641* Not available NTIS

EMISS: A Program for Estimating Local Air Pollution Emission Factors Related to Energy Use in Buildings: User's Guide and Reference Manual.
PB96-109566 *02,560* PC A03/MF A01

Emission Linewidth Measurements of Two-Dimensional Array Josephson Oscillators.
PB95-175139 *02,055* Not available NTIS

Empirical Linear Prediction Applied to a NIST Calibration Service.
PB97-112353 *02,287* Not available NTIS

Empirical Validation of a Transient Computer Model for Combined Heat and Moisture Transfer.
PB97-111991 *00,416* Not available NTIS

Encouraging Environmentally-Aware Inventions.
PB95-161394 *02,521* Not available NTIS

Energy and Migration of Grain Boundaries in Polycrystals.
PB94-211638 *03,332* Not available NTIS

Energy-Based Method for Liquefaction Potential Evaluation. Phase 1. Feasibility Study.
PB96-214747 *03,691* PC A13/MF A03

Energy Calibration of X-ray Photoelectron Spectrometers: Results of an Interlaboratory Comparison to Evaluate a Proposed Calibration Procedure.
PB96-102918 *04,027* Not available NTIS

Energy Dependence of Collision Characteristics in Molecule-Surface Collisions.
PB94-198504 *00,786* Not available NTIS

Energy Dependences of Absorption in Beryllium Windows and Argon Gas.
PB96-102124 *04,020* Not available NTIS

Energy Distributions of Neutrons Scattered from Solid C60 by the Beryllium Detector Method.
PB96-176631 *03,740* Not available NTIS

Energy Flows in an Orifice Pulse Tube Refrigerator.
PB95-169082 *02,752* Not available NTIS

Energy Levels of Germanium, Ge I through Ge XXXII.
PB94-162351 *00,747* Not available NTIS

Energy Levels of Zinc, Zn I through Zn XXX.
PB96-145982 *01,122* Not available NTIS

Energy-Pooling Collisions in Barium.
PB95-203030 *03,997* Not available NTIS

Energy Price Indices and Discount Factors for Life-Cycle Cost Analysis 1995. Annual Supplement to NIST Handbook 135 and NBS Special Publication 709. (Revised).
PB95-105011 *02,509* PC A04/MF A01

Energy Price Indices and Discount Factors for Life-Cycle Cost Analysis 1996. Annual Supplement to NIST Handbook 135 and NBS Special Publication 709. (Revised).
PB96-162441 *02,510* PC A05/MF A01

Energy Price Indices and Discount Factors for Life-Cycle Cost Analysis 1997. Annual Supplement to NIST Handbook 135 and NBS Special Publication 709. (Revised).
PB96-210745 *02,512* PC A05/MF A01

Energy Prices and Discount Factors for Life-Cycle Cost Analysis 1994. Annual Supplement to NIST Handbook 135 and NBS Special Publication 709.
PB94-206018 *02,508* PC A04/MF A01

Energy Transduction between a Concentration Gradient and an Alternating Electric Field.
PB94-216363 *03,461* Not available NTIS

Enhanced Curie Temperatures and Magnetoelastic Domains in Dy/Lu Super Lattices and Films.
PB94-172665 *04,443* Not available NTIS

Enhanced Detection of PCR Products Through Use of TOTO and YOYO Intercalating Dyes with Laser Induced Fluorescence - Capillary Electrophoresis.
PB95-164653 *00,599* Not available NTIS

Enhanced Flux Pinning via Chemical Substitution in Bulk Superconducting T1-2212.
PB95-169033 *04,647* Not available NTIS

Enhanced Machine Controller Architecture Overview.
PB94-142460 *02,802* PC A03/MF A01

Enhanced Magnetocaloric Effect in Gd3Ga5-xFexO12.
PB94-185659 *04,450* Not available NTIS

Enhanced Voltage-Dividing Potentiometer for High-Precision Feature Placement Metrology.
PB96-164025 *02,428* Not available NTIS

Enhancement of EXIT89 and Analysis of World Trade Center Data.
PB96-202247 *00,231* PC A04/MF A01

Enhancement of R123 Pool Boiling by the Addition of N-Hexane.
PB96-165956 *02,605* PC A04/MF A01

Enhancements to Program IDARC: Modeling Inelastic Behavior of Welded Connections in Steel Moment-Resisting Frames.
PB95-231601 *00,452* PC A05/MF A01

Ensuring Accuracy and Traceability of Weighing Instruments.
PB94-211687 *02,638* Not available NTIS

Enthalpy Increment Measurements from 4.5 K to 350 K and the Thermodynamic Properties of the Titanium Silicide Ti5Si3(cr).
PB96-204037 *00,679* Not available NTIS

Enthalpy Increment Measurements from 4.5 to 318 K for Bismuth(cr). Thermodynamic Properties from 0 K to the Melting Point.
PB96-204011 *01,166* Not available NTIS

Enthalpy Increment Measurements from 4.5 to 350 K and the Thermodynamic Properties of Titanium Disilicide(cr) to 1700 K.
PB96-204029 *00,678* Not available NTIS

Environment Simulation for a Continuous Mining Machine.
PB94-203536 *03,697* PC A03/MF A01

Environmental Aspects of Halon Replacements: Considerations for Advanced Agents and the Ozone Depletion Potential of CF3I.
PB97-122261 *03,301* Not available NTIS

Environmental Durability of Glass-Fiber Composites.
PB95-203220 *03,166* Not available NTIS

Environmental Evaluation of a New Federal Office Building.
PB94-199874 *02,538* Not available NTIS

Environmental Scanning Electron Microscope Imaging Examples Related to Particle Analysis.
PB94-172822 *00,766* Not available NTIS

Environmental Sensitivities of Quartz Oscillators.
PB96-103148 *02,271* Not available NTIS

Environmentally Enhanced Fracture of Ceramics.
PB95-125746 *03,046* Not available NTIS

Enzyme and Protein Mass Transfer Coefficient in Aqueous Two Phase Systems. 1. Spray Extraction Columns.
PB95-161162 *00,594* Not available NTIS

Epitaxial Growth and Characterization of the Ordered Vacancy Compound CuIn3Se5 on GaAs (100) Fabricated by Molecular Beam Epitaxy.
PB95-180725 *04,687* Not available NTIS

Epitaxial Growth of BaTiO3 Thin Films at 600C by Metalorganic Chemical Vapor Deposition.
PB96-122510 *03,071* Not available NTIS

Epitaxial Growth of Sb/GaSb Structures: An Example of V/III-V Heteroepitaxy.
PB95-202560 *04,693* Not available NTIS

Epitaxial Integration of Single Crystal C60.
PB95-153490 *04,592* Not available NTIS

Epitaxial Nucleation and Growth of Chemically Derived Ba2YCu3O7-x Thin Films on (001) SrTiO3.
PB96-190186 *04,787* Not available NTIS

EPR Bone Dosimetry: A New Approach to Spectral Deconvolution Problems.
PB94-199643 *03,616* Not available NTIS

EPR Dosimetry of Cortical Bone and Tooth Enamel Irradiated with X and Gamma Rays: Study of Energy Dependence.
PB97-110373 *03,639* Not available NTIS

Equation of State Formulation of the Thermodynamic Properties of R134a (1,1,1,2-Tetrafluoroethane).
PB94-212081 *03,256* Not available NTIS

Equilibrium and Calorimetric Investigation of the Hydrolysis of L-Tryptophan to (Indole + Pyruvate + Ammonia).
PB95-163317 *00,661* Not available NTIS

Equilibrium Pair Distribution Function of a Gas: Aspects Associated with the Presence of Bound States.
PB95-176046 *01,004* Not available NTIS

Equipment for Investigation of Cryogenic Compaction of Nanosize Silicon Nitride Powders. 1993 Report.
DE94013593 *03,028* PC A03/MF A01

Error Analysis of the NIST Optically Pumped Primary Frequency Standard.
PB95-153482 *01,535* Not available NTIS

Error-Bounding in Level-Index Computer Arithmetic.
PB96-109582 *01,742* PC A02/MF A01

Error Propagation Biases in the Calculation of Indentation Fracture Toughness for Ceramics.
PB94-172434 *03,032* Not available NTIS

Error Propagation in Laser Beam Spatial Parameters.
PB95-180394 *04,310* Not available NTIS

Error Protecting Characteristics of CDMA and Impacts on Speech.
PB96-122452 *01,491* Not available NTIS

Escherichis coli Cyclic AMP Receptor Protein Mutants Provide Evidence for Ligand Contacts Important in Activation.
PB96-201017 *03,592* Not available NTIS

Escrowed Encryption Standard (EES); Category: Computer Security; Subcategory: Cryptography.
FIPS PUB 185 *01,569* PC E03

ESR-Based Analysis in Radiation Processing.
PB95-161634 *03,931* Not available NTIS

Establishing Quality Measurements for Inorganic Analysis of Biomaterials.
PB94-199726 *00,548* Not available NTIS

Estimate of Flame Radiance via a Single Location Measurement in Liquid Pool Flames.
PB94-211596 *02,476* Not available NTIS

Estimate of the Effect of Scale on Radiative Heat Loss Fraction and Combustion Efficiency.
PB95-150447 *02,486* Not available NTIS

Estimates of Hurricane Wind Speeds by the 'Peaks Over Threshold' Method.
PB96-162540 *00,471* PC A04/MF A01

Estimating the Virial Coefficients of Small Polar Molecules.
PB95-176236 *03,276* Not available NTIS

Estimation of Measurement Uncertainty of Small Circular Features Measured by CMMs.
PB95-267928 *02,918* PC A03/MF A01

Estimation of System Damping at the Lotung Site by Application of System Identification.
PB96-214697 *01,351* PC A10/MF A03

Estimation of the Absorbed Dose in Radiation-Processed Food. 1. Test of the EPR Response Function by a Linear Regression Analysis.
PB94-199718 *00,039* Not available NTIS

Estimation of the Absorbed Dose in Radiation-Processed Food. 2. Test of the EPR Response Function by an Exponential Fitting Analysis.
PB94-199650 *00,036* Not available NTIS

Estimation of the Absorbed Dose in Radiation-Processed Food. 3. The Effect of Time of Evaluation on the Accuracy of the Estimate.
PB94-199684 *00,037* Not available NTIS

Estimation of the Absorbed Dose in Radiation-Processed Food. 4. EPR Measurements on Eggshell.
PB94-199692 *00,038* Not available NTIS

Estimation of the Heat Capacities of Organic Liquids as a Function of Temperature Using Group Additivity. I. Hydrocarbon Compounds.
PB94-162278 *00,739* Not available NTIS

Estimation of the Heat Capacities of Organic Liquids as a Function of Temperature Using Group Additivity. II. Compounds of Carbon, Hydrogen, Halogens, Nitrogen, Oxygen, and Sulfur.
PB94-162286 *00,740* Not available NTIS

Estimation of the Orientation Distribution of Short-Fiber Composites Using Ultrasonic Velocities.
PB96-176656 *03,178* Not available NTIS

Estimation of the Thermodynamic Properties of C-H-N-O-S-Halogen Compounds at 298.15 K.
PB94-162328 *00,744* Not available NTIS

Evaluated Bimolecular Ion-Molecule Gas Phase Kinetics of Positive Ions for Use in Modeling Planetary Atmospheres, Cometary Comae, and Interstellar Clouds.
PB94-168598 *00,753* Not available NTIS

Evaluating Form Designs for Optical Character Recognition.
PB94-168044 *01,830* PC A06/MF A02

Evaluating Investments in Law Enforcement Equipment: An Annotated Bibliography.
PB95-151379 *04,867* Not available NTIS

Evaluating Small Board and Care Homes: Sprinklered vs. Nonsprinklered Fire Protection.
PB94-206356 *00,195* PC A04/MF A01

Evaluating the Seismic Performance of Lightly-Reinforced Circular Concrete Bridge Columns.
PB95-163259 *01,335* Not available NTIS

Evaluation and Accreditation of State Calibration Laboratories.
PB97-110183 *00,486* Not available NTIS

Evaluation and Qualification Standards for an X-Ray Laminography System.
PB94-172954 *02,029* Not available NTIS

Evaluation and Retrofit Standards for Existing Federally Owned and Leased Buildings.
PB95-150918 *00,434* Not available NTIS

Evaluation and Strengthening Guidelines for Federal Buildings: Assessment of Current Federal Agency Evaluation Programs and Rehabilitation Criteria and Development of Typical Costs for Seismic Rehabilitation.
PB94-181856 *00,425* PC A08/MF A02

Evaluation and Strengthening Guidelines for Federal Buildings: Identification of Current Federal Agency Programs.
PB94-176278 *00,424* PC A08/MF A02

Evaluation of a Tapered Roller Bearing Spindle for High-Precision Hard Turning Applications.
PB96-160494 *02,700* Not available NTIS

Evaluation of Alternative In-Flight Fire Suppressants for Full-Scale Testing in Simulated Aircraft Engine Nacelles and Dry Bays.
PB94-203403 *00,023* PC A99/MF E08

Evaluation of Corrosion Data: A Review.
PB94-198348 *03,187* Not available NTIS

Evaluation of Crystallographic Data with the Program DIAMOND.
PB97-109045 *00,649*
(Order as PB97-109011, PC A11/MF A03)

Evaluation of Fracture Toughness and Residual Stress in Dental Porcelain by Indentation-Microfracture Method.
PB95-125613 *00,154* Not available NTIS

Evaluation of Fracture Toughness and Residual Stress in Dental Porcelain by Indentation-Microfracture Method.
PB95-152831 *00,159* Not available NTIS

Evaluation of GSA Maintenance Practices of Large Centrifugal Chillers and Review of GSA Refrigerant Management Practices.
PB94-143344 *02,502* PC A04/MF A01

Evaluation of Methylene Lactone Monomers in Dental Resins.
PB95-164661 *00,164* Not available NTIS

Evaluation of Sprinkler Activation Prediction Methods.
PB96-141056 *00,304* Not available NTIS

Evaluation of Survey Procedures for Determining Occupant Load Factors in Contemporary Office Buildings.
PB97-116222 *00,238* PC A03/MF A01

Evaluation of the Economic Impacts Associated with the NIST Power and Energy Calibration Services.
PB95-188850 *02,461* PC A03/MF A01

Evaluation of the Electrochemical Behavior of Ductile Nickel Aluminide and Nickel in a pH 7.9 Solution. Technical Report Number 3, April-June 1991.
DE94017351 *03,307* PC A02/MF A01

Evaluation of the Environmentally Induced Fracture Resistance of Ductile Nickel Aluminide. Technical Report Number 1, Final report. October-December 1990.
DE94017331 *03,306* PC A03/MF A01

Evaluation of Thermal Wave Imaging for Detection of Machining Damage in Ceramics.
PB95-220547 *03,062* PC A05/MF A02

Evaluation of Two-Photon Exchange Graphs for Highly-Charged Heliumlike Ions.
PB94-198918 *03,808* Not available NTIS

Evaluation of Uncertainties of the Null-Balanced Total-Power Radiometer System NCS1.
PB94-169794 *02,023* Not available NTIS

Evaluation of Wear Resistant Ceramic Valve Seats in Gas-Fueled Power Generation Engines. Topical Report, December 1991-April 1994.
PB95-200218 *02,466* PC A07/MF A02

Even-Odd Asymmetry of a Superconductor Revealed by the Coulomb Blockade of Andreev Reflection.
PB95-153540 *04,593* Not available NTIS

Evidence for a Deep Electron Trap and Charge Compensation in Separation by Implanted Oxygen Oxides.
PB95-175337 *02,362* Not available NTIS

Evidence for Inelastic Processes for N(+)3 and N(+)4 from Ion Energy Distributions in He/N2 Radio Frequency Glow Discharges.
PB96-146683 *04,059* Not available NTIS

Evidence for Parallel Junctions Within High-Tc Grain-Boundary Junctions.
PB95-175410 *04,657* Not available NTIS

Evidence for Significant Backscattering in Near-Threshold Electron-Impact Excitation of Ar(7+)(3s yields 3p).
PB95-126405 *03,883* Not available NTIS

Evidence for Tunneling and Magnetic Scatttering at 'In situ' YBCO/Noble-Metal Interfaces.
PB96-141098 *04,752* Not available NTIS

Evidence of Crosslinking in Methyl Pendent PBZT Fiber.
PB97-112486 *03,393* Not available NTIS

Evidence of Film-Induced Cleavage by Electrodeposited Rhodium.
PB95-162327 *03,191* Not available NTIS

Evidence That Voltage Rather Than Resistance is Quantized in Breakdown of the Quantum Hall Effect.
PB96-179163 *01,868*
(Order as PB96-177381, PC A07/MF A02)

Evolution Equations for Phase Separation and Ordering in Binary Alloys.
PB96-119243 *02,979* Not available NTIS

Evolution of a Turbulent Boundary Layer Induced by a Three-Dimensional Roughness Element.
PB94-212818 *04,200* Not available NTIS

Evolution of a United States Information System.
PB96-157896 *02,713* Not available NTIS

Evolution of Automatic Line Scale Measurement at the National Institute of Standards and Technology.
PB95-108809 *02,897* Not available NTIS

Evolution of Porosity and Calcium Hydroxide in Laboratory Concretes Containing Silica Fume.
PB95-175063 *01,321* Not available NTIS

Evolution of the Flight Telerobotic Servicer.
PB94-216082 *04,832* Not available NTIS

Evolution of the Pore Size Distribution in Final-Stage Sintering of Alumina Measured by Small-Angle X-ray Scattering. (Reannouncement with New Availability Information).
AD-A249 178/5 *03,023* PC A03/MF A01

Evolution of X-ray Resonance Raman Scattering into X-ray Fluorescence from the Excitation of Xenon Near the L3 Edge.
PB96-102751 *04,025* Not available NTIS

Exact Recursion Relation Solution for the Steady-State Surface Temperature of a General Multilayer Structure.
PB96-102017 *02,376* Not available NTIS

Exact Series Solution to the Epstein-Hubbell Generalized Eliiptic Type Integral Using Complex Variable Residue Theory.
PB97-110167 *03,423* Not available NTIS

Exact Solution of the Steady-State Surface Temperature for a General Multilayer Structure.
PB95-152773 *02,337* Not available NTIS

Examination of Objects Made of Wood Using Air-Coupled Ultrasound.
PB95-125712 *03,404* Not available NTIS

Examination of Parameters That Can Cause Error in Mass Determinations.
PB94-163037 *03,784* PC A03/MF A01

Examination of the Correlation between Cone Calorimeter Data and Full-Scale Furniture Mock-Up Fires.
PB96-148200 *01,417* Not available NTIS

Examination of the l/d Expansion Method from Exact Enumeration for a Self-Interacting Self-Avoiding Walk.
PB95-175733 *01,266* Not available NTIS

Examination Procedure Outlines: Keys to Solving the Handbook 44 Puzzle.
PB97-110217 *02,690* Not available NTIS

Exchange Coupling in Magnetic Heterostructures.
PB95-150314 *04,566* Not available NTIS

TITLE INDEX

Excitation of Balmer Lines in Low-Current Discharges of Hydrogen and Deuterium.
PB95-150546 *03,893* Not available NTIS

Excitation Transfer in Barium by Collisions with Noble Gases.
PB96-200274 *01,163* Not available NTIS

Excitons in Complex Quantum Nanostructures.
PB97-118343 *01,184* Not available NTIS

Executive Order 12941. Seismic Safety of Existing Federally Owned or Leased Buildings: It's History, Content and Objectives.
PB96-156021 *00,465* Not available NTIS

Executive Summary: Proceedings of the Workshop on the Measurement of Transient Pressure and Temperature.
PB96-160841 *02,679* Not available NTIS

Existence and Nonexistence Theorems of Finite Diameter Sequential Confidence Regions for Errors-in-Variables Models.
PB95-180352 *03,441* Not available NTIS

Exits in Multistable Systems Excited by Coin-Toss Square-Wave Dichotomous Noise: A Chaotic Dynamics Approach.
PB96-160650 *04,824* Not available NTIS

EXITT: A Simulation Model of Occupant Decisions and Actions in Residential Fires.
PB94-213261 *00,351* Not available NTIS

Expansion of Cementitious Materials Exposed to Sulfate Solutions.
PB94-185782 *02,577* Not available NTIS

Experience with MPI: 'Converting Pvmmake to Mpimake under LAM' and 'MPI and Parallel Genetic Programming'.
PB96-141296 *01,748* Not available NTIS

Experimental and Abinitio Studies of Electronic Structures of the CCI3 Radical and Cation.
PB94-212131 *00,826* Not available NTIS

Experimental and Numerical Burning Rates of Premixed Methane-Air Inhibited by Fluoromethanes.
PB95-180592 *01,392* Not available NTIS

Experimental and Numerical Chaos in Continuous Systems: Two Case Studies.
PB96-156146 *00,219* Not available NTIS

Experimental and Numerical Studies of Refractory Particle Formation in Flames: Application to Silica Growth.
PB95-152005 *00,673* Not available NTIS

Experimental and Numerical Studies on Two-Dimensional Gravity Currents in a Horizontal Channel.
PB94-165941 *01,359* PC A12/MF A03

Experimental Aspects and Z-Dependent Systematics in One- and Two-Electron Ions and Single Vacancy Systems.
PB94-199627 *03,815* Not available NTIS

Experimental Aspects of Flux Expulsion in Type-II Superconductors.
PB95-175725 *04,660* Not available NTIS

Experimental assessment of absorbed dose to mineralized bone tissue from internal emitters: An electron paramagnetic resonance study.
DE96007979 *03,614* PC A02/MF A01

Experimental Assessment of Crack-Tip Dislocation Emission Models for an Al67Cr8Ti25 Intermetallic Alloy.
PB96-204466 *03,377* Not available NTIS

Experimental Constraints on Some Mechanisms for High-Temperature Superconductivity.
PB94-198553 *04,463* Not available NTIS

Experimental Data and Theoretical Modeling of Gas Flows Through Metal Capillary Leaks.
PB95-150892 *04,206* Not available NTIS

Experimental Determination of the Ionization Energy of IO(X(sup 2)II(sub 3/2)) and Estimations of Delta(sub f)H(sup deg)(sub 0)(IO(sup -)) and PA(IO).
PB96-146899 *00,694* Not available NTIS

Experimental Determination of the Rate Constant for the Reaction of C2H3 with H2 and Implications for the Partitioning of Hydrocarbons in Atmospheres of the Outer Planets.
PB97-122295 *00,112* Not available NTIS

Experimental Evaluation of Specification Techniques for Improving Functional Testing.
PB96-201009 *01,779* Not available NTIS

Experimental Investigation of the Validity of TDDB Voltage Acceleration Models.
PB94-185949 *02,304* Not available NTIS

Experimental Method for Obtaining Critical Densities of Binary Mixtures: Application to Ethane + n-Butane.
PB95-151148 *00,930* Not available NTIS

Experimental Models for Software Diagnosis.
PB97-113906 *01,783* PC A04/MF A01

Experimental Optimization of Peak Shape with Application to Aerosol Generation.
PB94-185535 *00,501* Not available NTIS

Experimental plan to determine the performance of the Oak Ridge National Laboratory Cold Neutron Moderator. Final report, September 1, 1993--November 30, 1993.
DE95011352 *03,778* PC A03/MF A01

Experimental Results on Normal Modes in Cold, Pure Ion Plasmas.
PB95-175105 *03,956* Not available NTIS

Experimental Results on Single Flux Quantum Logic.
PB95-175071 *02,053* Not available NTIS

Experimental Studies of Line Shapes from a Balle-Flygare Spectrometer.
PB94-199452 *00,796* Not available NTIS

Experimental Study of Reverse-Bias Failure Mechanisms in Bipolar Mode JFET (BMFET).
PB95-152997 *02,340* Not available NTIS

Experimental Study of the Stabilization Region of Lifted Turbulent-Jet Diffusion Flames.
PB96-122676 *01,405* Not available NTIS

Experimental Validation of Radiopharmaceutical Absorbed Dose to Mineralized Bone Tissue.
PB94-199668 *03,617* Not available NTIS

Experimental Verification of a Micromagnetic Model of Dual-Layer Magnetic Films.
PB95-141081 *04,553* Not available NTIS

Experimental Verification of a Moisture and Heat Transfer Model in the Hygroscopic Regime.
PB97-111546 *00,309* Not available NTIS

Experimental Verification of a Vector Preisach Model.
PB95-163564 *04,626* Not available NTIS

Experimentally Measured Total X-ray Attenuation Coefficients Extracted from Previously Unprocessed Documents Held by the NIST Photon and Charged Particle Data Center.
PB97-114474 *04,165* PC A04/MF A01

Expert Control System Shell Version 1.0 User's Guide.
PB95-198859 *01,790* PC A03/MF A01

Exploring the Low-Frequency Performance of Thermal Converters Using Circuit Models and a Digitally Synthesized Source.
PB97-112551 *02,848* Not available NTIS

Exponentially Rapid Coarsening and Buckling in Coherently Self-Stressed Thin Plates.
PB95-202347 *04,821* Not available NTIS

Exposure: An Expert System Fire Code.
PB95-162913 *04,868* Not available NTIS

Exposure-to-Absorbed-Dose Conversion for Human Adult Cortical Bone.
PB97-110381 *03,640* Not available NTIS

Expression Formatter for MACSYMA.
PB95-267829 *01,735* PC A03/MF A01

Extended CO(7 yields 6) Emission from Warm Gas in Orion.
PB96-102504 *00,090* Not available NTIS

Extending the Angular Range of Neutron Reflectivity Measurements from Planar Lipid Bilayers: Applications to a Model Biological Membrane.
PB96-122569 *03,476* Not available NTIS

Extension of Heterodyne Frequency Measurements on OCS to 87 THz (2900 cm(-1)).
PB94-200680 *00,811* Not available NTIS

Extensions of the Prototype Application Protocol of Ready-to-Wear Apparel Pattern Making.
PB96-128194 *03,198* PC A03/MF A01

External Gamma-ray Counting of Selected Tissues from a Thorotrast Patient.
PB96-160254 *03,637* Not available NTIS

Extrapolation Chamber Measurements on (90)Sr + (90)Y Beta-Particle Ophthalmic Applicator Dose Rates.
PB95-153375 *03,626* Not available NTIS

Extrapolation of the Heat Capacity in Liquid and Amorphous Phases.
PB97-111421 *04,147* Not available NTIS

Extreme Value Theory and Applications: Proceedings of the Conference on Extreme Value Theory and Applications, Volume 3. Held in Gaithersburg, Maryland in May 1993.
PB95-104956 *03,432* PC A11/MF A03

Extreme Wind Distribution Tails: A 'Peaks Over Threshold' Approach.
PB95-219416 *00,127* PC A05/MF A01

Extreme Wind Estimates by the Conditional Mean Exceedance Procedure.
PB95-220471 *00,120* PC A03/MF A01

Extreme Winds Estimation by 'Peaks Over Threshold' and Epochal Methods.
PB96-159686 *00,468* Not available NTIS

Fabrication Issues for the Prototype National Institute of Standards and Technology SRM 2090A Scanning Electron Microscope Magnification Calibration Standard.
PB96-160585 *01,131* Not available NTIS

Fabrication Issues in Optimizing YBa2Cu3O7-x Flux Transformers for Low I/f Noise.
PB95-175857 *02,059* Not available NTIS

Fabrication of Flaw-Tolerant Aluminum-Titanate-Reinforced Alumina.
PB95-162533 *03,161* Not available NTIS

Fabrication of Optics by Diamond Turning.
PB96-111695 *02,954* Not available NTIS

Fabrication of Platinum-Gold Alloys in Pre-Hispanic South America: Issues of Temperature and Microstructure Control.
PB94-211646 *03,333* Not available NTIS

Fabrication of Transparent gamma-Al2O3 from Nanosize Particles.
PB95-175493 *03,054* Not available NTIS

Face Recognition Technology for Law Enforcement Applications.
PB94-207768 *01,837* PC A05/MF A01

Facile Synthesis of Novel Fluorinated Multifunctional Acrylates.
PB94-198389 *01,207* Not available NTIS

Factorial Design Techniques Applied to Optimization of AMS Graphite Target Preparation.
PB95-151197 *00,584* Not available NTIS

Factors Affecting the Energy Consumption of Two Refrigerator-Freezers.
PB97-112312 *00,311* Not available NTIS

Factors Significant to Precracking of Fracture Specimens.
PB96-109558 *03,358* PC A06/MF A02

Failure of All-Ceramic Fixed Partial Dentures 'In vitro' and 'In vivo': Analysis and Modeling.
PB96-122536 *00,175* Not available NTIS

Failures of the Four-Wave Mixing Model for Cone Emission.
PB95-202636 *04,318* Not available NTIS

Far-Infrared Kinetic Inductance Detector.
PB95-126348 *02,142* Not available NTIS

Far Infrared Laser Frequencies of CH3OD and N2H4.
PB96-119623 *04,341* Not available NTIS

Far Infrared Laser Frequencies of (13)CD3OH.
PB95-169363 *04,292* Not available NTIS

Far-Ultraviolet Flare on a Pleiades G Dwarf.
PB96-102033 *00,086* Not available NTIS

Faraday Constant.
PB96-159793 *01,955* Not available NTIS

Faraday Effect Current Sensor with Improved Sensitivity-Bandwidth Product.
PB95-203154 *02,180* Not available NTIS

Faraday Effect Current Sensors.
PB94-200698 *02,127* Not available NTIS

Faraday Effect Sensors: A Review of Recent Progress.
PB94-200706 *02,128* Not available NTIS

Faraday Effect Sensors for Magnet Field and Electric Current.
PB96-119664 *04,736* Not available NTIS

Fast Computer Evaluation of Radiative Properties of Hydrogenic Systems.
PB95-150553 *03,894* Not available NTIS

Fast-Ion Conducting Y2(ZryTi1-y)2O7 Pyrochlores: Neutron Rietveld Analysis of Disorder Induced by Zr Substitution.
PB96-156104 *04,776* Not available NTIS

Fast-Ion Conduction and Disorder in Cation and Anion Arrays in Y2(ZryTi(1-y))2O7 Pyrochlores Induced by Zr Substitution: A Neutron Rietveld Analysis.
PB94-211869 *04,496* Not available NTIS

Faster BKL Monte Carlo Simulations.
PB95-136370 *01,706* PC A03/MF A01

Faster Monte Carlo Simulations.
PB96-102074 *04,018* Not available NTIS

Fatigue Crack Thresholds of a Nickel-Iron Alloy for Superconductor Sheaths at 4 K.
PB96-190343 *03,223* Not available NTIS

Fault Diagnosis of an Air-Handling Unit Using Artificial Neural Networks.
PB97-121321 *00,283* Not available NTIS

Feasibility and Design Considerations of Emergency Evacuation by Elevators.
PB94-163441 *00,287* PC A07/MF A02

Feasibility of Fire Evacuation by Elevators at FAA Control Towers.
PB94-213857 *04,844* PC A06/MF A02

Feasibility of Fluorescence Detection of Tetracycline in Media Mixtures Employing a Fiber Optic Probe.
PB96-163654 *00,511* Not available NTIS

Feasibility Study: Reference Architecture for Machine Control Systems Integration.
PB94-142791 *02,804* PC A12/MF A03

Federal Basis for Weights and Measures: A Historical Review of Federal Legislative Effort, Statutes, and Administrative Action in the Field of Weights and Measures in the United States.
AD-A280 086/0 *02,616* PC A03/MF A01

Federal Building Grounding and Bonding Requirements for Telecommunications. Category: Telecommunications Standard; Subcategory: Grounding and Bonding.
FIPS PUB 195 *01,802* PC E18

Federal Certification Authority Liability and Policy: Law and Policy of Certificate-Based Public Key and Digital Signatures.
PB94-191202 *01,578* PC A21/MF A04

Federal Government and Information Technology Standards: Building the National Information Infrastructure.
PB95-180840 *01,812* Not available NTIS

Federal Implementaion Guideline for Eletronic Data Interchange. ASC X12 003050 Transaction Set 865 Purchase Order Change Acknowledgement/Request - Seller Initiated. Implementation Convention.
PB96-172549 *01,825* PC A09/MF A02

Federal Implementation Guideline for Electronic Data Interchange: ASC X12 003040 Transaction Set 838 Trading Partner Profile (Confirmation of Vendor Registration). Implementation Convention.
PB96-111190 *01,813* PC A03/MF A01

Federal Implementation Guideline for Electronic Data Interchange: ASC X12 003040 Transaction Set 838 Trading Partner Profile (Vendor Registration), Implementation Convention.
PB96-112651 *03,674* PC A04/MF A01

Federal Implementation Guideline for Electronic Data Interchange: ASC X12 003050 Transaction Set 836 Procurement Notices. Implementation Convention.
PB96-178892 *01,827* PC A04/MF A01

Federal Implementation Guideline for Electronic Data Interchange. ASC X12 003050 Transaction Set 840 Request for Quotation. Implementation Convention.
PB96-172531 *01,824* PC A10/MF A03

Federal Implementation Guideline for Electronic Data Interchange. ASC X12 003050 Transaction Set 843 Response to Request for Quotation. Implementation Convention.
PB96-168984 *01,822* PC A09/MF A02

Federal Implementation Guideline for Electronic Data Interchange. ASC X12 003050 Transaction Set 850 Award Instrument. Implementation Convention.
PB96-114913 *01,814* PC A11/MF A03

Federal Implementation Guideline for Electronic Data Interchange. ASC X12 003050 Transaction Set 855 Purchase Order Acknowledgment: Implementation Convention.
PB96-172374 *01,823* PC A04/MF A01

Federal Implementation Guideline for Electronic Data Interchange. ASC X12 003050 Transaction Set 860 Modifications to Award Instrument. Implementation Convention.
PB96-114921 *01,815* PC A11/MF A03

Federal Labs Have Key Role in Metrication.
PB96-123401 *02,920* Not available NTIS

Federal Metric Progress in 1993.
PB94-196029 *02,600* PC A03/MF A01

Femtosecond Time-Resolved Molecular Multiphoton Ionization: The Na2 System.
PB95-202305 *03,975* Not available NTIS

Femtosecond Time-Resolved Wave Packet Motion in Molecular Multiphoton Ionization and Fragmentation.
PB94-198611 *00,790* Not available NTIS

Ferric Ion Assisted Photooxidation of Halocetates.
PB97-112460 *00,521* Not available NTIS

Ferroelectric Thin Film Characterization Using Superconducting Microstrip Resonators.
PB96-102389 *02,270* Not available NTIS

Few Caveats on Carbon Dioxide Monitoring.
PB96-122650 *02,562* Not available NTIS

Fiber Coating Diameter: Toward a Glass Artifact Standard.
PB96-140389 *02,234* Not available NTIS

Fiber-Optic Faraday-Effect Magnetic-Field Sensor Based on Flux Concentrators.
PB96-200308 *02,201* Not available NTIS

Fiber Spot Size: A Simple Method of Calculation.
PB95-125936 *04,250* Not available NTIS

Fibre Splice Loss: A Simple Method of Calculation.
PB95-175519 *04,299* Not available NTIS

Field and Temperature Acceleration of Time-Dependent Dielectric Breakdown in Intrinsic Thin SiO2.
PB94-185956 *02,305* Not available NTIS

Field Dependence of the Magnetic Ordering of Cu in R2CuO4 (R = Nd, Sm).
PB95-164521 *04,633* Not available NTIS

Field Evaluation of the System for Calibration of the Marshall Compaction Hammer.
PB95-190674 *01,323* PC A05/MF A01

Field Measurements of Ventilation and Ventilation Effectiveness in an Office/Library Building.
PB95-108833 *00,247* Not available NTIS

Field Modeling: Simulating the Effect of Sloped Beamed Ceilings on Detector and Sprinkler Response.
PB96-122866 *01,406* Not available NTIS

Filter Transmittance Measurements in the Infrared.
PB94-140589 *04,224*
(Order as PB94-140555, PC A06/MF A02)

Financing Tomorrow's Infrastructure: Challenges and Issues. Proceedings of a Colloquium. Held in Washington, DC. on October 20, 1995.
PB96-189444 *00,481* PC A07/MF A02

Findings and Recommendations from a Software Reengineering Case Study.
PB96-155791 *01,752* Not available NTIS

Fine-Structure Constant.
PB94-172996 *03,795* Not available NTIS

Fine-Structure Intervals of (14)N(+) By Far-Infrared Laser Magnetic Resonance.
PB95-175162 *00,993* Not available NTIS

Fine Structure of Negative Ions of Alkaline-Earth-Metal Atoms.
PB94-211182 *03,837* Not available NTIS

FIPS PUB 8-6, Metropolitan Areas (for Microcomputers).
PB95-503280 *04,874* Diskette $59.00

Fire and Smoke Control: An Historical Perspective.
PB95-175808 *00,202* Not available NTIS

Fire Codes for Global Practice.
PB96-102108 *00,205* Not available NTIS

Fire Data Management System, FDMS 2.0, Technical Documentation.
PB94-164019 *01,358* PC A05/MF A01

Fire Growth Analysis of the Fire of March 20, 1990, Pulaski Building, 20 Massachusetts Avenue, N.W., Washington, DC.
PB94-205952 *00,194* PC A03/MF A01

Fire Growth Models for Materials.
PB94-195856 *01,367* PC A03/MF A01

Fire Hazard and Risk: Evaluating Alternative Technologies.
PB94-173077 *00,242* Not available NTIS

Fire Hazard Model Developments and Research Efforts at NIST.
PB96-159652 *00,407* Not available NTIS

Fire Induced Thermal Fields in Window Glass I: Theory.
PB94-139722 *00,328* PC A03/MF A01

Fire Performance of an Interstitial Space Construction System.
PB95-188918 *00,390* PC A04/MF A01

Fire-Plume-Generated Ceiling Jet Characteristics and Convective Heat Transfer to Ceiling and Wall Surfaces in a Two-Layer Fire Environment: Uniform Temperature Ceiling and Walls.
PB95-164711 *00,382* Not available NTIS

Fire Propagation in Concurrent Flows.
PB94-193844 *01,365* PC A04/MF A01

Fire Protection Engineering Tools. Simple Tools: The Equations.
PB96-156179 *00,221* Not available NTIS

Fire Protection Foam Behavior in a Radiative Environment.
PB97-116131 *00,237* PC A10/MF A02

Fire Safety Engineering in the Pursuit of Performance-Based Codes: Collected Papers.
PB97-114482 *00,235* PC A07/MF A02

Fire Safety Engineering Research in the United States.
PB96-151394 *00,213* Not available NTIS

Fire Safety of Passenger Trains: A Review of Current Approaches and of New Concepts.
PB94-152006 *04,848* PC A11/MF A03

Fire Service and Fire Sciences: A Winning Combination.
PB95-150264 *01,383* Not available NTIS

Fire Suppression System Performance of Alternative Agents in Aircraft Engine and Dry Bay Laboratory Simulations. SP890: Volume 1.
PB96-117775 *03,277* PC A99/MF E08

Fire Suppression System Performance of Alternative Agents in Aircraft Engine and Dry Bay Laboratory Simulations. SP 890: Volume 2.
PB96-117783 *03,278* PC A99/MF A06

FIREDOC Users Manual, 3rd Edition.
PB95-128674 *01,378* PC A03/MF A01

First Phase Formation Kinetics in the Reaction of Nb/Al.
PB95-168456 *03,353* Not available NTIS

First Results from a Coordinated ROSAT, IUE, and VLA Study of RS CVn Systems.
PB94-213477 *00,069* Not available NTIS

First Results from the Goddard High-Resolution Spectrograph: The Chromosphere of Tauri.
PB94-199528 *00,054* Not available NTIS

First VAMAS USA Interlaboratory Comparison of High Temperature Superconductor Critical Current Measurements.
PB96-147178 *04,768* Not available NTIS

Five Q's (Cues) of the U.S. GOSIP Testing Program.
PB96-175716 *01,826* Not available NTIS

Flame Heights and Heat Release Rates of 1991 Kuwait Oil Field Fires.
PB96-119342 *01,404* Not available NTIS

Flame Retardants - Overview.
PB94-185287 *01,363* Not available NTIS

Flame Synthesis of High Tc Superconductors.
PB95-151981 *00,659* Not available NTIS

Flammability Characterization with the Lift Apparatus and the Cone Calorimeter.
PB97-110050 *01,435* Not available NTIS

Flat and Curved Crystal Spectrography for Mammographic X-ray Sources.
PB97-122246 *03,642* Not available NTIS

Flat and Rising R-Curves for Elliptical Surface Cracks from Indentation and Superposed Flexure.
PB95-161295 *03,156* Not available NTIS

Flaw-Insensitive Ceramics.
PB97-110027 *03,095* Not available NTIS

Flaw-Tolerance and Crack-Resistance Properties of Alumina-Aluminum Titanate Composites with Tailored Microstructures.
PB97-110324 *03,101* Not available NTIS

Flaw Tolerance and Toughness Curves in Two-Phase Particulate Composites: SiC/Glass System.
PB96-179460 *03,081* Not available NTIS

Flexible-Diaphragm Force Microscope.
PB95-180915 *03,966* Not available NTIS

Flow Conditioner Tests for Three Orifice Flowmeter Sizes.
PB95-105540 *04,201* PC A05/MF A01

Flow Immunoassay Using Solid-Phase Entrapment.
PB96-200951 *00,642* Not available NTIS

Flow-Induced Structure in Polymer. Chapter 1. An Introduction to Flow-Induced Structures in Polymers.
PB96-123369 *03,387* Not available NTIS

Flow-Induced Structure in Polymers: Chapter 16. Shear-Induced Changes in the Order-Disorder Transition Temperature and the Morphology of a Triblock Copolymer.
PB96-123237 *03,127* Not available NTIS

Flow-Induced Structure in Polymers. Chapter 17. Phase-Separation Kinetics of a Polymer Blend Solution Studied by a Two-Step Shear Quench.
PB96-123377 *03,388* Not available NTIS

Flow of Alternative Agents in Piping.
PB95-202420 *00,022* Not available NTIS

Flow of Microemulsions through Microscopic Pores.
PB95-140463 *00,905* Not available NTIS

Flowmeter Installation Effects Due to a Generic Header.
PB96-210893 *02,606* PC A07/MF A02

Fluctuation Dominated Recombination Kinetics with Traps.
PB95-107264 *00,875* Not available NTIS

Fluctuations in Probability Distribution on Chaotic Attractors.
PB96-102330 *04,022* Not available NTIS

Fluorescence Anisotropy Measurements on a Polymer Melt as a Function of Applied Shear Stress.
PB94-199296 *01,209* Not available NTIS

Fluorescence Measurements of Tetracycline in High Cell Mass for Fermentation Monitoring.
PB95-175709 *00,601* Not available NTIS

Fluorescence Monitoring of Polarity Change and Gelation during Epoxy Cure.
PB94-185543 *01,204* Not available NTIS

Fluoride Analytical Methods.
PB96-180237 *03,578* Not available NTIS

TITLE INDEX

Fluoride Elimination Upon Reaction of Pentafluoroaniline with e (sub eq')(sup -), H, and OH Radicals in Aqueous Solution.
PB97-111314 *01,177* Not available NTIS

Fluorinated Hydrocarbon Flame Suppression Chemistry.
PB94-185113 *01,362* Not available NTIS

Flux Expulsion at Intermediate Fields in Type-II Superconductors.
PB94-212230 *04,502* Not available NTIS

Flux-Locked Current Source Reference.
PB95-150785 *02,039* Not available NTIS

Foias-Temam Approximations of Attractors for Galloping Oscillators.
PB94-198298 *04,817* PC A01

Fokker-Planck Description of Multivalent Interactions.
PB95-108478 *00,879* Not available NTIS

Food Irradiation Dosimetry.
PB95-180675 *00,041* Not available NTIS

Force Calibrations in the Nanonewton Regime.
PB95-168696 *03,949* Not available NTIS

Formal Methods in Conformance Testing: Result and Perspectives.
PB95-153029 *01,710* Not available NTIS

Formal Multi-Layer Test Methodology and Its Application to OSI.
PB94-172194 *02,718* Not available NTIS

Formal Specification and Verification of Control Software for Cryptographic Equipment.
PB94-213030 *01,585* Not available NTIS

Formalism and Parameters for Quantitative Surface Analysis by Auger Electron Spectroscopy and X-Ray Photoelectron Spectroscopy.
PB94-212297 *00,832* Not available NTIS

Formation of DNA-Protein Cross-Links in Cultured Mammalian Cells Upon Treatment with Iron Ions.
PB96-137724 *03,651* Not available NTIS

Formation of Hydroxyapatite in a Polymeric Calcium Phosphate Cement.
PB95-180642 *00,173* Not available NTIS

Formation of Hydroxyapatite in Cement Systems.
PB95-175261 *00,170* Not available NTIS

Formation of Technical Committee 201 on Surface Chemical Analysis by the International Organization for Standardization.
PB95-108536 *00,568* Not available NTIS

Formulation of Position on U.S. Standards Role in Enterprise Integration.
PB95-105052 *02,773* PC A03/MF A01

Formulation of the Refractive Index of Water and Steam.
PB95-140133 *00,900* Not available NTIS

FORTRAN Compiler Validation System, Version 2.1.
PB94-500691 *01,698* CP T99

Forum for International Cooperation on Fire Research.
PB95-162939 *04,869* Not available NTIS

Forward Scattering of a Gaussian Beam by a Nonabsorbing Sphere.
PB97-112288 *04,395* Not available NTIS

Four Years of Monitoring alpha Orionis with the VLA: Where Have All the Flares Gone.
PB94-185212 *00,048* Not available NTIS

Fourier Transform Atomic Emission Studies Using a Glow Discharge as the Emission Source.
PB94-185980 *00,533* Not available NTIS

FPETOOL: Fire Protection Tools for Hazard Estimation. An Overview of Features.
PB95-140885 *00,367* Not available NTIS

Fracture Behavior of Large-Scale Thin-Sheet Aluminum Alloy.
N95-19494/0 *03,311*
(Order as N95-19468/4, PC A24/MF A04)

Fracture in Multilayers.
PB96-163613 *02,988* Not available NTIS

Fracture Mechanics Analysis of Near-Surface Cracks.
PB94-172400 *03,230* Not available NTIS

Fracture Mechanism Maps: Their Applicability to Silicon Nitride.
PB96-204532 *03,094* Not available NTIS

Fracture of Silicon Nitride and Silicon Carbide at Elevated Temperatures.
PB96-180260 *03,179* Not available NTIS

Fracture Testing of Large-Scale Thin-Sheet Aluminum Alloy.
AD-A306 625/5 *03,305* PC A04/MF A01

Fracture Testing of Large-Scale Thin-Sheet Aluminum Alloy.
PB95-242368 *00,024* PC A03/MF A01

Fracture Toughness of Advanced Ceramics at Room Temperature: A Vamas Round-Robin.
PB95-162194 *03,160* Not available NTIS

Fragment Energy and Vector Correlations in the Overtone-Pumped Dissociation of HN3X(1)A'.
PB94-199908 *00,802* Not available NTIS

Fragment State Correlations in the Dissociation of NO.HF(v=1).
PB95-164430 *00,982* Not available NTIS

Framework for Information Technology Integration in Process Plant and Related Industries.
PB94-219086 *02,772* PC A04/MF A01

Framework for National Information Infrastructure Services.
PB95-103719 *02,723* PC A07/MF A02

Framework for the Development and Assurance of High Integrity Software.
PB95-173084 *01,716* PC A05/MF A01

Free Radical Chemistry of the Atmospheric Aqueous Phase.
PB96-148101 *00,117* Not available NTIS

Frequency Dependence of the Emission from 2D Array Josephson Oscillators.
PB95-175147 *02,056* Not available NTIS

Frequency Extension of the NIST AC-DC Difference Calibration Service for Current.
PB95-161253 *01,895* Not available NTIS

Frequency Shifting of Pulsed Narrow-Band Laser Light in a Multipass Raman Cell.
PB95-203352 *04,321* Not available NTIS

Frequency Stabilization of a Fiber Laser to Rubidium: A High-Accuracy 1.53 mu m Wavelength Standard.
PB95-126082 *04,252* Not available NTIS

Frequency-Stabilized Lasers: A Driving Force for New Spectroscopies.
PB96-135199 *04,350* Not available NTIS

Frequency Stabilized Lasers: A Parochial Review.
PB95-153771 *04,269* Not available NTIS

Frequency-Stabilized LNA Laser at 1.083 mum: Application to the Manipulation of Helium 4 Atoms.
PB95-176186 *04,304* Not available NTIS

Frequency Synthesis and Metrology at 10(-17) and Beyond.
PB97-113187 *02,101* Not available NTIS

Fresh Look at Strategies for Fire Safety.
PB95-162947 *04,870* Not available NTIS

Friction and Oxidative Wear of 440C Ball Bearing Steels Under High Load and Extreme Bulk Temperatures.
PB95-175253 *03,215* Not available NTIS

Friction Processes in Brittle Fracture.
PB96-161765 *03,076* Not available NTIS

From Superconductivity to Supernovae: The Ginzburg Symposium. Report on the Symposium Held in Honor of Vitaly L. Ginzburg. Held in Gaithersburg, Maryland on May 22, 1992.
PB95-171963 *04,649* PC A05/MF A01

Frozen Human Serum Reference Material for Standardization of Sodium and Potassium Measurements in Serum or Plasma by Ion-Selective Electrode Analyzers.
PB94-185337 *00,532* Not available NTIS

Frozen Orbits for Satellites Close to an Earth-Like Planet.
PB96-102165 *04,839* Not available NTIS

FTS Infrared Measurements of the Rotational and Vibrational Spectrum of LiH and LiD.
PB94-216231 *00,856* Not available NTIS

Fugacity Coefficients of Hydrogen in (Hydrogen + Butane).
PB95-175212 *02,491* Not available NTIS

Full-Scale Room Fire Experiments Conducted at the University of Maryland.
PB97-116081 *00,236* PC A04/MF A01

Full Scale Smoke Control Tests at the Plaza Hotel Building.
PB94-212859 *00,347* Not available NTIS

Function of DnaJ and DnaK as Chaperones in Origin-Specific DNA Binding by RepA.
PB95-151544 *03,533* Not available NTIS

Functional Security Criteria for Distributed Systems.
PB96-123492 *01,607* Not available NTIS

Functions of Technology Infrastructure in a Competitive Economy.
PB94-173002 *00,478* Not available NTIS

Fundamental Computer Simulation Models for Cement-Based Materials.
PB95-126009 *00,364* Not available NTIS

Fundamental Limits on the Frequency Stabilities of Crystal Oscillators.
PB96-176565 *02,277* Not available NTIS

Fundamental Mechanisms for CO and Soot Formation.
PB95-143160 *01,380* PC A08/MF A02

Fundamental Processes in Gas Discharges.
PB96-123450 *01,089* Not available NTIS

Fundamental Studies of Gas Sensor Response Mechanisms: Palladium on SnO2(110).
PB95-162731 *00,963* Not available NTIS

Fundamental Torsion Band in Acetaldehyde.
PB94-212834 *00,840* Not available NTIS

Fundamentals and Problems of Fiber Current Sensors.
PB97-111835 *02,205* Not available NTIS

Fundamentals of Fracture: A 1993 Prologue, and Other Comments.
PB96-161971 *03,218* Not available NTIS

Further Calculations of X-ray Diffusion in an Infinite Medium.
AD-A295 314/9 *03,772* PC A01/MF A01

Further Development of the N-Gas Mathematical Model: An Approach for Predicting the Toxic Potency of Complex Combustion Mixtures.
PB96-123260 *03,650* Not available NTIS

FUSE: The Far Ultraviolet Spectrograph Explorer.
PB94-213410 *00,063* Not available NTIS

Future of Time and Frequency Dissemination.
AD-P009 138/9 *01,520* PC A02/MF A01

Future of Time and Frequency Dissemination.
N94-30684/2 *01,524*
(Order as N94-30639/6, PC A25/MF A06)

Fuzed-Quartz Fibers. A Survey of Properties, Applications and Production Methods.
AD-A286 620/0 *00,656* PC A03/MF A01

G203.2-12.3: A New Optical Supernova Remnant in Orion.
PB95-203535 *00,085* Not available NTIS

Gage Block Handbook.
PB95-251716 *02,667* PC A08/MF A02

Gage Block Standards, Measurement Capabilities and Laboratory Accreditation.
PB96-163621 *02,757* Not available NTIS

Gas Absorption during Ion-Irradiation of a Polymer Target.
PB96-161864 *04,099* Not available NTIS

Gas-Coupled, Pulse-Echo Ultrasonic Crack Detection and Thickness Gaging.
PB96-147129 *04,847* Not available NTIS

Gas Phase Oxygen Effect on Chain Scission and Monomer Content in Bulk Poly(methyl methacrylate) Degraded by External Thermal Radiation.
PB96-204078 *01,293* Not available NTIS

Gas Phase Reactions Relevant to Chemical Vapor Deposition: Numerical Modeling.
PB94-199346 *03,117* Not available NTIS

Gas Phase Reactions Relevant to Chemical Vapor Deposition: Optical Diagnostics.
PB94-199338 *03,116* Not available NTIS

Gas Phase Reactivity Study of OH Radicals with 1,1-Dichloroethene and cis-1,1-Dichloroethene and Trans-1,2-Dichloroethene over the Temperature Range 240-400 K.
PB95-152146 *00,939* Not available NTIS

Gas Transport Properties of Solution-Cast Perfluorosulfonic Acid Ionomer Films Containing Ionic Surfactants.
PB95-175998 *01,267* Not available NTIS

Gaseous Dielectrics Research: Possible SF6 Substitutes.
PB96-119268 *02,228* Not available NTIS

Gaseous Electronics Conference Radio-Frequency Reference Cell: A Defined Parallel-Plate Radio-Frequency System for Experimental and Theoretical Studies of Plasma-Processing Discharges.
PB94-172327 *04,404* Not available NTIS

Gaseous Electronics Conference RF Reference Cell: An Introduction.
PB96-113329 *02,387*
(Order as PB96-113311, PC A09/MF A03)

GATT Standards Code Activities of the National Institute of Standards and Technology 1994.
PB96-106935 *00,497* PC A03/MF A01

General Motion Model and Spatio-Temporal Filters for Computing Optical Flow.
PB95-171096 *01,847* PC A03/MF A01

General Motion Model and Spatio-Temporal Filters for 3-D Motion Interpretations.
PB96-210703 *01,861* PC A07/MF A02

General Order 'N' Analytic Correction of Probe-Position Errors in Planar Near-Field Measurements.
PB96-200688 *01,562* Not available NTIS

General Procedures for Registering Computer Security Objects.
PB94-134897 *01,573* PC A03/MF A01

General Types of Information Services.
PB96-147053 *02,735* Not available NTIS

Generalized Form Registration Using Structure-Based Techniques.
PB96-191374 *01,858* PC A03/MF A01

Generalized Optical Theorem for On-Axis Gaussian Beams.
PB97-122345 *04,177* Not available NTIS

Generalized Plane Strain Analysis of a Bimaterial Composite Containing a Free Surface Normal to the Interface.
PB95-163341 *03,164* Not available NTIS

Generalized Stokes-Einstein Equation for Spherical Particle Suspensions.
PB95-202743 *01,031* Not available NTIS

Generating and Measuring Displacements Up to 0.1 m to an Accuracy of 0.1 nm: Is It Possible.
PB96-160700 *04,090* Not available NTIS

Generation and Characterization of Acetylene Smokes.
PB94-200292 *01,372* Not available NTIS

Generation Rate and Distribution of Products of Combustion in Two-Layer Fire Environments: A Model and Applications.
PB96-102173 *01,398* Not available NTIS

Generic Manufacturing Controllers.
PB94-199940 *02,818* Not available NTIS

Generic Model for Creep Rupture Lifetime Estimation on Fibrous Ceramic Composites.
PB94-200235 *03,137* Not available NTIS

Genetically Engineered Pore as a Metal Ion Biosensor.
PB96-161658 *03,551* Not available NTIS

Genetically Engineered Pores as Metal Ion Biosensors.
PB96-167408 *03,553* Not available NTIS

Genetically Engineered Pores for New Materials.
PB96-161641 *03,550* Not available NTIS

Geographic Information Systems Standards: A Federal Perspective.
PB95-163390 *03,678* Not available NTIS

Geometric Characterization of Rockwell Diamond Indenters.
PB95-203287 *02,950* Not available NTIS

Geometrical Percolation Threshold of Overlapping Ellipsoids.
PB96-102397 *03,167* Not available NTIS

Germanium Detector Optimization of MDA for Efficiency vs. Low Intrinsic Background.
PB94-199155 *00,543* Not available NTIS

Getting Started on Mosaic.
PB95-180360 *01,721* Not available NTIS

GHRS Observations of Cool, Low-Gravity Stars. 1. The Far-Ultraviolet Spectrum of alpha Orions (M2 Iab).
PB96-112016 *00,094* Not available NTIS

Glass Temperature of Polymer Blends: Comparison of Both the Free Volume and the Entropy Predictions with Data.
PB95-140190 *01,236* Not available NTIS

Glass Transition of Organic Liquids Confined to Small Pores.
PB94-212305 *00,833* Not available NTIS

Glasses for Waveguide Lasers.
PB96-111950 *04,335* Not available NTIS

Glimpse of Materials Research in China: A Report from an Interagency Study Team on Materials Visiting China from June 19, 1995 to June 30, 1995.
PB96-112677 *02,978* PC A11/MF A03

Global Climatic Effects of Aerosols: The AAAR Symposium.
PB95-108791 *00,122* Not available NTIS

Global Density Effects on the Self-Preservation Behavior of Turbulent Free Jets.
PB95-162301 *04,207* Not available NTIS

Global Equivalence Ratio Concept and the Formation Mechanisms of Carbon Monoxide in Enclosure Fires.
PB96-146790 *00,210* Not available NTIS

Global Equivalence Ratio Concept and the Prediction of Carbon Monoxide Formation in Enclosure Fires.
PB94-207511 *00,313* PC A08/MF A02

Global Information Infrastructure: Agenda for Cooperation.
PB95-178604 *01,482* PC$9.00

Global Thermodynamic Behavior of Fluid Mixtures in the Critical Region.
PB94-212420 *04,199* Not available NTIS

Glossary of Software Reuse Terms.
PB95-178992 *01,720* PC A03/MF A01

Glucose Permease of Bacillus Subtilis Is a Single Polypeptide Chain That Functions to Energize the Sucrose Permease.
PB95-163192 *03,466* Not available NTIS

Goddard High Resolution Spectrograph: Instrument, Goals, and Science Results.
PB96-123278 *00,044* Not available NTIS

Goddard High-Resolution Spectrograph Observations of the Local Interstellar Medium and the Deuterium/Hydrogen Ratio along the Line of Sight Toward Capella.
PB94-213444 *00,066* Not available NTIS

Good Security Practices for Electronic Commerce, Including Electronic Data Interchange.
PB94-139045 *01,463* PC A04/MF A01

Gordon Research Conference on the Physics and Chemistry of Laser Diagnostics in Combustion Held in Plymouth, New Hampshire on 12-16 July 1993.
AD-A274 609/7 *01,353* PC A03/MF A01

GOSIP Testing Program.
PB96-161229 *01,504* Not available NTIS

Graded and Nongraded Regenerator Performance.
PB95-169090 *02,753* Not available NTIS

Gradiometer Antennas for Detection of Long Subsurface Conductors.
PB95-175667 *01,862* Not available NTIS

Grafted Interpenetrating Polymer Networks.
PB94-185055 *01,200* Not available NTIS

Grain Alignment and Transport Properties of Bi2Sr2CaCu2O8 Grown by Laser Heated Float Zone Method.
PB95-161451 *04,602* Not available NTIS

Graphical Analysis of the CCRL Portland Cement Proficiency Sample Database (Samples 1-72). (Part 1. Univariant Analysis of Portland Cement).
PB94-196557 *01,308* PC A06/MF A02

Graphical Conceptual Navigation as a Presentation Technique for a Graphics Standard.
PB94-200573 *01,692* Not available NTIS

Graphical Kernel System (GKS). Category: Software Standard. Subcategory: Graphics. International Standard: Information Technology; Computer Graphics; Graphical Kernel System (GKS) Language Bindings. Part 4: C.
FIPS PUB 120-1C *01,792* PC A06/MF A02

Gravitational Sisyphus Cooling of (87)Rb in a Magnetic Trap.
PB96-200704 *04,379* Not available NTIS

Gravity-Current Transport in Building Fires.
PB96-147046 *01,415* Not available NTIS

Gravity Dependent Processes and Intracellular Motion.
PB95-163382 *03,538* Not available NTIS

Grazing Angle X-Ray Photoemission System for Depth-Dependent Analysis.
PB95-161154 *04,600* Not available NTIS

Grazing Incidence Prompt Gamma Emissions and Resonance-Enhanced Neutron Standing Waves in a Thin-Film.
PB95-150470 *03,892* Not available NTIS

Grazing-Incidence X-Ray Photoelectron Spectroscopy: A Novel Approach to Thin Film Characterization.
PB95-153128 *04,589* Not available NTIS

Grazing Incidence X-ray Photoemission and Its Implementation on Synchrotron Light Source X-ray Beamlines.
PB95-175766 *01,001* Not available NTIS

Grazing-Incidence X-Ray Photoemission Spectroscopy Investigation of Oxidized GaAs(100): A Novel Approach to Nondestructive Depth Profiling.
PB94-200151 *04,480* Not available NTIS

Greatly Enhanced Soot Scattering in Flickering Ch4/Air Diffusion Flames.
PB94-172988 *01,361* Not available NTIS

Green's Function for Generalized Hilbert Problem for Cracks and Free Surfaces in Composite Materials.
PB95-163333 *03,163* Not available NTIS

Greenspan Acoustic Viscometer for Gases.
PB96-204417 *04,220* Not available NTIS

Ground-Based Smoke Sampling Techniques Training Course and Collaborative Local Smoke Sampling in Saudi Arabia.
PB94-143542 *02,532* PC A05/MF A01

Ground Improvement Techniques for Liquefaction Remediation Near Existing Lifelines.
PB96-128111 *01,350* PC A05/MF A01

Ground Vehicle Control at NIST: From Teleoperation to Autonomy.
N94-34037/9 *03,758*
(Order as N94-34019/7, PC A21/MF A04)

Group 1 for the Plant Spatial Configuration STEP Application Protocol.
PB96-165402 *02,789* PC A11/MF A03

Group 1 for the Process Engineering Data STEP Application Protocol.
PB97-116073 *02,797* PC A99/MF A06

Growing Significance of CIB.
PB95-126306 *00,314* Not available NTIS

Growth and Nucleation of Hydrogenated Amorphous Silicon on Silicon (100) Surfaces.
PB96-176516 *02,991* Not available NTIS

Growth Characteristics of Fiber Gratings.
PB96-122957 *04,346* Not available NTIS

Growth of Bragg Gratings Produced by Continuous-Wave Ultraviolet Light in Optical Fiber.
PB95-162038 *04,275* Not available NTIS

Growth of Epitaxial KNbO3 Thin Films.
PB96-135181 *02,409* Not available NTIS

Growth of Iron on Iron Whiskers.
PB95-150322 *04,567* Not available NTIS

Growth of Laser Ablated YBa2Cu3O7-delta Films as Examined by Rheed and Scanning Tunneling Microscopy.
PB95-162541 *04,614* Not available NTIS

Growth Surface for the Slopes at the Boundary of a Polygon.
PB94-152725 *03,408* PC A03/MF A01

Guarding Against Transients.
PB94-216470 *01,623* Not available NTIS

Guidance of the Legality of Keystroke Monitoring.
PB96-161237 *00,005* Not available NTIS

Guidance to Federal Agencies on the Use of Trusted Systems.
PB95-163440 *01,597* Not available NTIS

Guide for the Use of the International System of Units (SI).
PB95-226692 *02,747* PC A05/MF A01

Guide on Open System Environment (OSE) Procurements.
PB95-169496 *01,626* PC A08/MF A02

Guide to a Format for Data on Chemical Admixtures in a Materials Property Database.
PB96-165394 *01,327* PC A04/MF A01

Guide to a Format for Data on Chemical Admixtures in a Materials Property Database. (Reannouncement with new abstract).
PB96-186192 *01,328* PC A04/MF A01

Guide to Configuration Management and the Revision Control System for Testbed Users.
PB94-150919 *01,678* PC A03/MF A01

Guide to Instrumentation Literature.
AD-A280 278/3 *02,617* PC A08/MF A02

Guide to Locating and Accessing Computerized Numeric Materials Databases.
PB96-204045 *03,007* Not available NTIS

Guide to Software Engineering Environment Assessment and Evaluation.
PB94-140167 *01,676* PC A04/MF A01

Guideline: Codes for Named Populatd Places, Primary County Divisions, and Other Locational Entities of the United States, Puerto Rico, and the Outlying Areas. Category: Data Standards and Guidelines; Subcategory: Representation and Codes.
FIPS PUB 55-DC3 *04,866* PC E99

Guideline: Codes for Named Populated Places, Primary County Divisions, and Other Locational Entities of the United States, Puerto Rico, and the Outlying Areas. Category: Data Standards and Guidelines. Subcategory: Representations and Codes.
FIPS PUB 55-3 *04,865* PC E04

Guideline for the Analysis of Local Area Network Security. Category: Computer Security; Subcategory: Risk Analysis and Contingency Planning.
FIPS PUB 191 *01,799* PC A04/MF A01

Guideline for the Use of Advanced Authentication Technology Alternatives. Category: Computer Security. Subcategory: Access Control.
FIPS PUB 190 *01,798* PC A04/MF A01

Guidelines for Evaluating and Expressing the Uncertainty of NIST Measurement Results. 1994 Edition.
PB95-143087 *02,649* PC A03/MF A01

Guidelines for Pre-Qualification, Prototype and Quality Control Testing of Seismic Isolation Systems.
PB96-193685 *01,347* PC A08/MF A02

Guidelines for Refractive Index Measurements of Asbestos.
PB95-151189 *02,543* Not available NTIS

Guidelines for Reporting Results of Computational Experiments. Report of the Ad hoc Committee.
PB94-212347 *03,427* Not available NTIS

Guidelines for the Development of Mapping Tables.
PB96-154539 *02,786* PC A03/MF A01

Guidelines for the Evaluation of Electronic Data Interchange Products.
PB96-172325 *01,506* PC A05/MF A01

Guidelines for the Evaluation of X.500 Directory Products.
PB95-231908 *02,732* PC A04/MF A01

Gust Factors Applied to Hurricane Winds.
PB95-180469 *00,446* Not available NTIS

Hair Analysis for Drugs of Abuse: Evaluation of Analytical Methods, Environmental Issues, and Development of Reference Materials.
PB95-176269 *03,501* Not available NTIS

Hair Testing for Drugs of Abuse: International Research on Standards and Technology.
PB96-120555 *03,504* PC A18/MF A04

Half-Integral Constant Voltage Steps in High-Tc Grain Boundary Junctions.
PB94-211216 *04,489* Not available NTIS

Halon Thermochemistry: 'Ab Initio'. Calculations of the Enthalpies of Formation of Fluoromethanes.
PB96-175740 *03,289* Not available NTIS

Handbook Preferred Circuits Navy Aeronautical Electronic Equipment. Supplement Number 1.
AD-A278 784/4 *00,028* PC A05/MF A01

Handbook Preferred Circuits Navy Aeronautical Electronic Equipment. Supplement Number 2.
AD-A278 783/6 *00,027* PC A03/MF A01

Handbook Preferred Circuits Navy Aeronautical Electronic Equipment. Supplement Number 3.
AD-A278 782/8 *00,026* PC A03/MF A01

Handling Passwords with Security and Reliability in Background Processes.
PB95-180550 *01,722* Not available NTIS

Hardware Measurement Techniques for High-Speed Networks.
PB96-160551 *01,500* Not available NTIS

Harmonic and Static Susceptibilities of YBa2Cu3O7.
PB95-161139 *04,599* Not available NTIS

HAZARD I Fire Hazard Assessment Method (Version 1.2) (for Microcomputers).
PB94-501988 *00,196* Diskette $250.00

HAZARD I Fire Hazard Assessment Method, Version 1.2 (Upgrade Package) (for Microcomputers).
PB94-501996 *00,197* CP D99

Head Start on Assurance: Proceedings of an Invitational Workshop on Information Technology (IT) Assurance and Trustworthiness. Held in Williamsburg, Virginia on March 21-23, 1994.
PB94-215746 *01,586* PC A05/MF A01

Heap of Data.
PB97-111488 *03,424* Not available NTIS

Heat and Moisture Transfer in Wood-Based Wall Construction: Measured versus Predicted.
PB95-200655 *00,391* PC A05/MF A01

Heat Flux from Flames to Vertical Surfaces.
PB97-110357 *01,438* Not available NTIS

Heat Transfer in an Intumescent Material Using a Three-Dimensional Lagrangian Model.
PB96-164066 *00,408* Not available NTIS

Heat Transfer in Thin, Compact Heat Exchangers with Circular, Rectangular, or Pin-Fin Flow Passages.
PB95-140943 *02,751* Not available NTIS

Heavily Accumulated Surfaces of Mercury Cadmium Telluride Detectors: Theory and Experiment.
PB94-216074 *02,134* Not available NTIS

Heights of Wall-Fire Flames.
PB96-148192 *00,212* Not available NTIS

Helium Refrigeration and Liquefaction Using a Liquid Hydrogen Refrigerator for Precooling.
AD-A286 683/8 *02,749* PC A03/MF A01

Helping to Reduce Technical Barriers to Trade.
PB96-190046 *00,491* Not available NTIS

Hemispherical Test Fixture for Measuring the Wavefields Generated in an Anisotropic Solid.
PB96-190087 *03,181* Not available NTIS

Heterodyne Measurement of the Fluorescence Spectrum of Optical Molasses.
PB95-108411 *03,873* Not available NTIS

Heterodyne Mixing and Direct Detection in High Temperature Josephson Junctions.
PB96-147202 *01,565* Not available NTIS

Hg1-xCdxTe Characterization Measurements: Current Practice and Future Needs.
PB95-164299 *02,157* Not available NTIS

Hierarchical Ada Robot Programming System (HARPS): A Complete and Working Telerobot Control System Based on the NASREM Model.
PB94-213162 *02,934* Not available NTIS

Hierarchical Interaction between Sensory Processing and World Modeling in Intelligent Systems.
PB94-198256 *01,580* Not available NTIS

Hierarchical Real-Time Control System for Use with Coal Mining Automation.
PB94-212065 *03,698* Not available NTIS

High Accuracy Measurement of Aperture Area Relative to a Standard Known Aperture.
PB95-261954 *01,919*
(Order as PB95-261897, PC A07/MF A02)

High-Accuracy Principal-Angle Scanning Spectroscopic Ellipsometry of Semiconductor Interfaces.
PB96-163787 *02,427* Not available NTIS

High Critical Temperature Superconductor Tunneling Spectroscopy Using Squeezable Electron Tunneling Junctions.
PB95-163721 *04,627* Not available NTIS

High Current Pressure Contacts to Ag Pads on Thin Film Superconductors.
PB95-168621 *04,639* Not available NTIS

High-Current Thin Film Multijunction Thermal Converters and Multi-Converter Modules.
PB97-112379 *01,989* Not available NTIS

High-Efficiency, High-Power Difference-Frequency Generation of 0.9-1.5 mu m Light in BBO.
PB95-202255 *04,317* Not available NTIS

High-Energy Behavior of the Double Photoionization of Helium from 2 to 12 keV.
PB94-213279 *03,860* Not available NTIS

High-Energy Phonon Dispersion in La1.85Sr0.15CuO4.
PB96-138458 *04,748* Not available NTIS

High-Frequency Linear Response of Anisotropic Type-II Superconductors in the Mixed State.
PB94-200359 *04,483* Not available NTIS

High Frequency Magnetic Field Sensors Based on the Faraday Effect in Garnet Thick Films.
PB96-190384 *02,282* Not available NTIS

High-Frequency Oscillators Using Phase-Locked Arrays of Josephson Junctions.
PB96-135157 *02,080* Not available NTIS

High Integrity Software Standards Activities at NIST.
PB96-112214 *01,744* Not available NTIS

High-Level CAD Melds Micromachined Devices with Foundries.
PB94-216413 *02,321* Not available NTIS

High-Order Harmonic Mixing with GaAs Schottky Diodes.
PB95-108585 *01,528* Not available NTIS

High-Order Multipole Excitation of a Bound Electron.
PB96-119789 *04,044* Not available NTIS

High-Performance Concrete: Research Needs to Enhance Its Use.
PB95-180147 *01,322* Not available NTIS

High-Performance Liquid Chromatography of Phytoplankton Pigments Using a Polymeric Reversed-Phase C18 Column.
PB95-151130 *00,583* Not available NTIS

High Power Generation with Distributed Josephson-Junction Arrays.
PB97-111520 *02,099* Not available NTIS

High-Power, High-Frequency Oscillators Using Distributed Josephson-Junction Arrays.
PB96-200266 *02,095* Not available NTIS

High-Precision Calculations of Cross Sections for Low-Energy Electron Scattering by Ground and Excited State of Sodium.
PB95-152161 *03,914* Not available NTIS

High-Pressure Equilibrium Cell for Solubility Measurements in Supercritical Fluids.
PB95-175634 *00,998* Not available NTIS

High Resolution Angle Resolved Photoelectron Spectroscopy Study of N2.
PB95-151494 *03,907* Not available NTIS

High-Resolution Atomic Spectroscopy of Laser-Cooled Ions.
PB95-169330 *03,953* Not available NTIS

High-Resolution Diode-Laser Spectroscopy of Calcium.
PB95-181244 *03,969* Not available NTIS

High-Resolution, Direct Infrared Laser Absorption Spectroscopy in Slit Supersonic Jets: Intermolecular Forces and Unimolecular Vibrational Dynamics in Clusters.
PB95-203006 *01,040* Not available NTIS

High Resolution Hard X-Ray Microscope.
PB94-213055 *03,856* Not available NTIS

High Resolution Inelastic Neutron Scattering Study of Phonon Self-Energy Effects in YBCO.
PB95-180881 *04,688* Not available NTIS

High-Resolution Infrared Overtone Spectroscopy of ArHF via Nd:YAG/Dye Laser Difference Frequency Generation.
PB94-211448 *00,816* Not available NTIS

High-Resolution Infrared Overtone Spectroscopy of N2-HF: Vibrational Red Shifts and Predissociation Rate as a Function of HF Stretching Quanta.
PB96-102298 *01,061* Not available NTIS

High-Resolution Infrared Spectroscopy of DF Trimer: A Cyclic Ground State Structure and DF Stretch Induced Intramolecular Vibrational Coupling.
PB95-150678 *00,920* Not available NTIS

High-Resolution IR Laser-Driven Vibrational Dynamics in Supersonic Jets: Weakly Bound Complexes and Intramolecular Energy Flow.
PB94-216751 *00,862* Not available NTIS

High Resolution IR Studies of Polymolecular Clusters: Micromatrices and Unimolecular Ring Opening.
PB94-185691 *00,777* Not available NTIS

High Resolution, Jet-Cooled Infrared Spectroscopy of (HCl)2: Analysis of nu1 and nu2 HCl Stretching Fundamentals, Interconversion Tunneling, and Mode-Specific Predissociation Lifetimes.
PB95-203196 *01,046* Not available NTIS

High-Resolution Measurements of the nu2 and 2nu2-nu2 Bands of (34)S(16)O2.
PB94-216223 *00,855* Not available NTIS

High Resolution Near Infrared Spectroscopy of HCl-DCl and DCl-HCl: Relative Binding Energies, Isomer Interconversion Rates, and Mode Specific Vibrational Predissociation.
PB95-203212 *01,048* Not available NTIS

High-Resolution Optical Multiplex Spectroscopy.
PB95-203543 *04,323* Not available NTIS

High-Resolution Spectroscopy of Laser-Cooled Rubidium in a Vapor-Cell Trap.
PB95-153714 *04,268* Not available NTIS

High Resolution Time Interval Counter.
PB96-138607 *01,495* Not available NTIS

High-Sensitivity Acoustic Emission Sensor/Preamplifier Subsystems.
PB95-125704 *02,900* Not available NTIS

High-Sensitivity Determination of Iodine Isotopic Ratios by Thermal and Fast Neutron Activation.
PB94-213386 *00,555* Not available NTIS

High-Sensitivity Optical Sampling Using an Erbium-Doped Fiber Laser Strobe.
PB95-176111 *04,302* Not available NTIS

High-Sensitivity Spectroscopy with Diode Lasers.
PB95-175477 *04,297* Not available NTIS

High Sensitivity Survey of Radio Continuum Emission in Herbig Ae/Be Stars.
PB94-185915 *00,051* Not available NTIS

High-Spatial-Resolution Resistivity Mapping Applied to Mercury Cadmium Telluride.
PB94-212917 *02,131* Not available NTIS

High Spectral Purity X-Band Source.
PB95-163713 *02,045* Not available NTIS

High Speed, High Sensitivity Magnetic Field Sensors Based on the Faraday Effect in Iron Garnets.
PB95-153391 *02,151* Not available NTIS

High-Speed Interconnection Characterization Using Time Domain Network Analysis.
PB96-148176 *04,061* Not available NTIS

High-Speed Spatial Scanning Pyrometer.
PB94-200003 *02,636* Not available NTIS

High-Tc Multilayer Step-Edge Josephson Junctions and SQUIDs.
PB96-200183 *04,790* Not available NTIS

High-Tc Superconducting Antenna-Coupled Microbolometer on Silicon.
PB95-169124 *02,166* Not available NTIS

High Temperature.
PB94-211737 *03,844* Not available NTIS

High-Temperature Adiabatic Calorimeter for Constant-Volume Heat Capacity Measurements of Compressed Gases and Liquids.
PB95-168860 *00,989* Not available NTIS

High Temperature Degradation of Structural Composites.
PB94-172848 *03,132* Not available NTIS

High-Temperature Furnace for In situ Small-Angle Neutron Scattering during Ceramic Processing.
PB96-148127 *03,743* Not available NTIS

High-Temperature High-Pressure Oscillating Tube Densimeter.
PB96-146618 *01,123* Not available NTIS

High-Temperature Laser-Pulse Thermal Diffusivity Apparatus.
PB94-185147 *02,631* Not available NTIS

High Temperature Reactions of Uranium Dioxide with Various Metal Oxides.
AD-A286 648/1 *00,717* PC A03/MF A01

High Temperature Reliability of Thin Film SiO2.
PB95-150348 *02,333* Not available NTIS

High Temperature Silicide Thin-Film Thermocouples.
PB94-185501 *02,252* Not available NTIS

High Temperature Structural Reliability of Silicon Nitride.
PB97-110456 *03,104* Not available NTIS

High-Temperature Superconductor Cryogenic Current Comparator.
PB96-119334 *02,074* Not available NTIS

High Temperature Superconductor-Normal Metal-Superconductor Josephson Junctions with High Characteristic Voltages.
PB95-176079 *04,666* Not available NTIS

High Velocity Plasm in the Transition Region of Au Mic: A Stellar Analog of Solar Explosive Events.
PB96-123294 *00,102* Not available NTIS

High-Velocity Plasma in the Transition Region of AU Microscopii: Evidence for Magnetic Reconnection and Saturated Heating during Quiescent and Flaring Conditions.
PB96-102694 *00,091* Not available NTIS

Higher-Order Approximations in Ionospheric Wave-Propagation.
AD-A292 471/0 *04,420* PC A02/MF A01

Highway Concrete (HWYCON) Expert System User Reference and Enhancement Guide.
PB94-215670 *01,316* PC A08/MF A02

Histopathology, Blood Chemistry, and Physiological Status of Normal and Moribund Striped Bass ('Morone saxatilis') Involved in Summer Mortality ('Die-Off') in the Sacramento-San Joaquin Delta of California.
PB94-198157 *00,034* PC A03/MF A01

History of NIST's Contributions to Development of Standard Reference Materials and Reference and Definitive Methods for Clinical Chemistry.
PB96-119706 *03,503* Not available NTIS

Hole Dispersion and Enhancement of Antiferromagnetic Interaction of Localized Spins in High-Tc Superconductors.
PB95-202602 *04,694* Not available NTIS

Hollow Clay Tile Prism Tests for Martin Marietta Energy Systems: Task 2 Testing.
PB94-217486 *00,352* PC A14/MF A03

Holographic Properties of Triton X-100-Treated Bacteriorhodopsin Embedded in Gelatin Films.
PB96-119284 *03,761* Not available NTIS

Homoepitaxial Growth of Iron and a Real Space View of Reflection-High-Energy-Electron Diffraction.
PB94-173069 *04,445* Not available NTIS

Homogeneous Gas Phase Decyclization of Tetralin and Benzocyclobutene.
PB95-151049 *00,928* Not available NTIS

Hot Carrier Excitation of Adlayers: Time-Resolved Measurement of Adsorbate-Lattice Coupling.
PB94-172285 *00,758* Not available NTIS

Hot-Deformation Apparatus for Thermomechanical Processing Simulation.
PB94-200136 *03,207* Not available NTIS

Hot-Electron Microcalorimeter for X-ray Detection Using a Superconducting Transition Edge Sensor with Electrothermal Feedback.
PB96-200399 *04,792* Not available NTIS

Hot-Electron Microcalorimeters as High-Resolution X-ray Detectors.
PB96-123641 *04,739* Not available NTIS

Hot-Electron Microcalorimeters for X-ray and Phonon Detection.
PB95-168993 *04,644* Not available NTIS

Hot-Electron-Microcalorimeters with 0.25 mm(2) Area.
PB96-200670 *04,793* Not available NTIS

How Accurate Are the Josephson and Quantum Hall Effects and QED.
PB95-163283 *03,942* Not available NTIS

How Far Is Far from Critical Point in Polymer Blends. Lattice Cluster Theory Computations for Structured Monomer, Compressible Systems.
PB94-211141 *01,217* Not available NTIS

How the Cambridge Crystallographic Data Centre Obtains Its Information.
PB97-109193 *04,808*
(Order as PB97-109011, PC A11/MF A03)

How to Evaluate Alternative Designs Based on Fire Modeling.
PB96-102116 *00,206* Not available NTIS

How to Get NIST-Traceable Time on Your Computer.
PB96-200647 *01,559* Not available NTIS

How-To Suggestions for Implementing Executive Order 12941 on Seismic Safety of Existing Federal Buildings, A Handbook.
PB96-131552 *00,461* PC A10/MF A03

How to Verify Reference Materials.
PB95-151486 *03,497* Not available NTIS

Human and Machine Recognition of Faces: A Survey.
PB96-111687 *01,854* Not available NTIS

Human Factors Considerations for the Potential Use of Elevators for Fire Evacuation of FAA Air Traffic Control Towers.
PB94-217163 *01,300* PC A03/MF A01

HVAC CAD Layout Tools: A Case Study of University/Industry Collaboration.
PB97-112221 *00,281* Not available NTIS

Hybrid Digital/Analog Servo for the NIST-7 Frequency Standard.
PB95-180618 *01,544* Not available NTIS

Hybrid Gauss-Trapezoidal Quadrature Rules.
PB96-193750 *03,422* PC A04/MF A01

Hybrid Method for Determining Material Properties from Instrumented Micro-Indentation Experiments.
PB95-152229 *03,348* Not available NTIS

Hybrid Optical-Electrical Overlay Test Structure.
PB96-204136 *02,450* Not available NTIS

Hybrid Undulator for the NIST-NRL Free-Electron Laser.
PB94-212529 *04,238* Not available NTIS

Hydration in Semicrystalline Polymers: Small-Angle Neutron Scattering Studies of the Effect of Drawing in Nylon-6 Fibers.
PB95-202990 *03,385* Not available NTIS

Hydraulic Radius and Transport in Reconstructed Model Three-Dimensional Porous Media.
PB96-123419 *00,403* Not available NTIS

Hydrodynamic Friction of Arbitrarily Shaped Brownian Particles.
PB97-110191 *04,136* Not available NTIS

Hydrodynamic Similarity in an Oscillating-Body Viscometer.
PB96-122429 *01,082* Not available NTIS

Hydrogen Atom Attack on Perchloroethylene.
PB95-163473 *00,969* Not available NTIS

Hydrogen Balmer Alpha Line Shapes for Hydrogen-Argon Mixtures in a Low-Pressure rf Discharge.
PB95-153433 *03,924* Not available NTIS

Hydrogen in YBa2Cu3Ox: A Neutron Spectroscopy and a Nuclear Magnetic Resonance Study.
PB95-161279 *04,601* Not available NTIS

Hydrogen Lyman-alpha Emission of Capella.
PB95-202263 *00,075* Not available NTIS

Hydrolysis of Proteins by Microwave Energy.
PB94-216322 *03,528* Not available NTIS

Hygrothermal Effects on the Performance of Polymers and Polymeric Composites: A Workshop Report. Held in Gaithersburg, Maryland on September 21-22, 1995.
PB96-183207 *03,180* PC A04/MF A01

Hypercubic Lattice SAW Exponents nu and gamma : 3.99 Dimensions Revisited.
PB94-211026 *01,215* Not available NTIS

Hyperfine Effects and Associative Ionization of Ultracold Sodium.
PB95-151221 *03,903* Not available NTIS

Hyperfine Structure Investigations and Identification of New Energy Levels in the Ionic Spectrum of (147)Pm.
PB96-180203 *04,117* Not available NTIS

Hyperfine-Structure Studies of Zr II: Experimental and Relativistic Configuration-Interaction Results.
PB95-203824 *04,011* Not available NTIS

Hypersingular Single Integral Equation and the Dielectric Wedge.
PB97-110274 *04,428* Not available NTIS

Hysteresis Measurements of Remanent Polarization and Coercive Field in Polymers.
PB94-199767 *04,475* Not available NTIS

I: Improvement of Resonance Ionization Spectroscopy (RIS) Techniques; II: Atomic Data for RIS; III: Standards for Ultratrace Analysis. Progress Report.
DE94018565 *00,523* PC A02/MF A01

ICSSC Guidance on Implementing Executive Order 12941 on Seismic Safety of Existing Federally Owned or Leased Buildings.
PB96-128103 *00,459* PC A03/MF A01

Ideal Gas Thermodynamic Properties of Sulphur Heterocyclic Compounds.
PB96-145867 *01,110* Not available NTIS

IEEE's POSIX: Making Progress.
PB96-160924 *01,757* Not available NTIS

Ignition and Subsequent Flame Spread Over a Thin Cellulosic Material.
PB96-160270 *04,836* Not available NTIS

Ignition and Subsequent Transition to Flame Spread in a Microgravity Environment.
N96-15584/1 *04,828*
(Order as N96-15552, PC A20/MF A04)

Ignition and Transition to Flame Spread Over a Thermally Thin Cellulosic Sheet in a Microgravity Environment.
PB96-160288 *04,837* Not available NTIS

IGOSS-Industry/Government Open Systems Specification.
PB94-207453 *01,806* PC A07/MF A02

II-3: Critical Current Measurement Methods: Quantitative Evaluation.
PB96-147160 *04,767* Not available NTIS

II-5: Thermal Contraction of Materials Used in Nb3Sn Critical Current Measurements.
PB96-147186 *04,769* Not available NTIS

IIW Commission V Quality Control and Quality Assurance of Welded Products Annual Report 1994/95.
PB95-198743 *02,866* PC A03/MF A01

IIW Commission V Quality Control and Quality Assurance of Welded Products, Annual Report 1995/96.
PB96-191366 *02,880* PC A04/MF A01

Image Depth Profiling SIMS: An Evaluation for the Analysis of Light Element Diffusion in YBa2Cu3O7-x Single Crystal Superconductors.
PB95-126116 *04,530* Not available NTIS

Image Gradient Evolution: A Visual Cue for Danger.
PB96-154562 *02,939* PC A03/MF A01

Image Information Transfer Properties of X-Ray Intensifying Screens in the Energy Range from 17 to 320 keV.
PB95-126173 *00,155* Not available NTIS

Image Restoration and Diffusion Processes.
PB95-153003 *01,843* Not available NTIS

Imaging of Fine Porosity in a Colloidal Silica: Potassium Silicate Gel by Defocus Contrast Microscopy.
PB94-212750 *03,039* Not available NTIS

IML++ v.1.2 Iterative Methods Library Reference Guide.
PB96-195219 *01,776* PC A04/MF A01

Impact of Computer-Aided Acquisition and Logistic Support (CALS) in the Application of Standards.
PB96-160908 *01,756* Not available NTIS

Impact of the FCC's Open Network Architecture on NS/NP Telecommunications Security.
PB95-189445 *01,483* PC A03/MF A01

Implementation of a Standard Format for GPS Common View Data.
N95-32323/4 *03,779*
(Order as N95-32319, PC A20/MF A04)

Implementation of a Standard Format for GPS Common View Data.
PB96-176581 *01,555* Not available NTIS

Implementation of Executive Order 12699: Seismic Safety of Federal and Federally Assisted or Regulated New Building Construction.
PB95-151809 *00,436* Not available NTIS

Implementation of the Fastener Quality Act.
PB96-160676 *02,876* Not available NTIS

Implementing a Transition Manager in the AMRF Cell Controller.
PB94-199932 *02,817* Not available NTIS

Importance of Bound-Free Correlation Effects for Vibrational Excitation of Molecules by Electron Impact: A Sensitivity Analysis.
PB95-202974 *03,996* Not available NTIS

Importance of Chemometrics in Biomedical Measurements.
PB94-200599 *00,550* Not available NTIS

Importance of Measurement in Technology-Based Competition.
PB94-211844 *02,929* Not available NTIS

Importance of Unraveling Memory Propagation Effects in Interpreting Data on Partial Discharge Statistics.
PB95-163572 *01,901* Not available NTIS

TITLE INDEX

Important Link in Entire-House Protection: Surge Reference Equalizers.
PB94-216504 *02,219* Not available NTIS

Important Papers in the History of Document Preparation Systems: Basic Sources.
PB95-125837 *02,712* Not available NTIS

Imposed Oscillations of Kinetic Barriers Can Cause an Enzyme to Drive a Chemical Reaction Away from Equilibrium.
PB96-161625 *01,137* Not available NTIS

Improved Annealing Technique for Optical Fiber.
PB96-119680 *04,343* Not available NTIS

Improved Automated Current Control for Standard Lamps.
PB94-219367 *00,246*
(Order as PB94-219326, PC A05/MF A02)

Improved Crystallographic Data for Aluminum Niobate (AlNbO4).
PB95-107306 *04,523* Not available NTIS

Improved Dose Metrology in Optical Lithography.
PB96-179510 *02,439* Not available NTIS

Improved Eddy-Current Decay Method for Resistivity Characterization.
PB95-180451 *02,265* Not available NTIS

Improved Gas Flow Measurements for Next-Generation Processes.
PB96-156013 *04,216* Not available NTIS

Improved Hyperfine Measurements of the Na NP Excited State Through Frequency-Controlled Dopplerless Spectroscopy in a Zeeman Magneto-Optic Laser Trap.
PB95-203840 *04,012* Not available NTIS

Improved Molecular Constants and Frequencies for the CO2 Laser from New High-J Regular and Hot-Band Frequency Measurements.
PB95-180634 *04,312* Not available NTIS

Improved Reflectometry Facility at the National Institute of Standards and Technology.
PB96-160338 *04,087* Not available NTIS

Improved Rubidium Frequency Standards Using Diode Lasers with AM and FM Noise Control.
PB95-176152 *04,303* Not available NTIS

Improved Uniaxial Strain Tolerance of the Critical Current Measured in Ag-Sheathed Bi2Sr2Ca1Cu2O8+x Superconductors.
PB95-153565 *04,594* Not available NTIS

Improved Variational Analysis of Inhomogeneous Optical Waveguides Using Airy Functions.
PB95-168639 *04,285* Not available NTIS

Improved Wavelengths for Prominent Lines of Cr XVI to Cr XXII.
PB95-150629 *03,895* Not available NTIS

Improved Wavelengths for Prominent Lines of Fe XX to Fe XXIII.
PB96-111638 *04,334* Not available NTIS

Improvement in Predicting Smoke Movement in Compartmented Structures.
PB94-172418 *00,332* Not available NTIS

Improvement of Ultrasensitive Techniques Isotopic Biasing in the RIS Process Ionization Efficiencies and Selectivities.
DE94018563 *00,522* PC A02/MF A01

Improvements in Computation of Form Factors.
PB94-200078 *03,820* Not available NTIS

Improving Color Measurements of Displays.
PB96-204441 *02,203* Not available NTIS

Improving measurement quality assurance for photon irradiations at Department of Energy facilities. Final technical report.
DE96010065 *03,711* PC A03/MF A01

Improving Neural Network Performance for Character and Fingerprint Classification by Altering Network Dynamics.
PB95-267803 *01,851* PC A03/MF A01

Improving Neural Network Performance for Character and Fingerprint Classification by Altering Network Dynamics.
PB96-123195 *01,856* Not available NTIS

Improving Photomask Linewidth Measurement Accuracy via Emulated Stepper Aerial Image Measurement.
PB95-180816 *02,911* Not available NTIS

Improving the Design Process by Predicting Downstream Values of Design Attributes.
PB97-113096 *02,795* Not available NTIS

Improving the Evaluation of Building Ventilation.
PB96-138508 *00,271* Not available NTIS

In-Line Optical Monitoring of Injection Molding.
PB94-185105 *01,201* Not available NTIS

In Search of Alternative Fire Suppressants.
PB96-164165 *03,285* Not available NTIS

In situ Burning of Oil Spills: Mesoscale Experiments.
PB94-142973 *01,355* PC A04/MF A01

In situ Burning of Oil Spills: Mesoscale Experiments and Analysis.
PB95-163747 *02,587* Not available NTIS

In Situ Burning Oil Spill Workshop Proceedings. Held in Orlando, Florida on January 26-28, 1994.
PB95-104907 *02,583* PC A06/MF A02

In situ Characterization of Vapor Phase Growth of Iron Oxide-Silica Nanocomposites: Part 1. 2-D Planar Laser-Induced Fluorescence and Mie Imaging.
PB97-112478 *03,185* Not available NTIS

In situ Fluorescence Cell Mass Measurements of 'Saccharomyces cerevisiae' Using Cellular Tryptophan.
PB96-135041 *03,547* Not available NTIS

In-situ Fume Particle Size and Number Density Measurements from a Synthetic Smelt.
PB94-212040 *03,334* Not available NTIS

In situ Measurements of Chloride Ion and Corrosion Potential at the Coating/Metal Interface.
PB95-140893 *03,122* Not available NTIS

In-situ Monitoring of Molecular Beam Epitaxial Growth Using Single Photon Ionization.
PB95-202222 *01,023* Not available NTIS

In-situ Neutron Reflectivity of MBE Grown and Chemically Processed Surfaces and Interfaces.
PB96-146634 *02,416* Not available NTIS

In situ Noble Metal YBa2Cu3O7 Thin-Film Contacts.
PB94-211323 *04,494* Not available NTIS

In situ Observation of Surface Morphology of InP Grown on Singular and Vicinal (001) Substrates.
PB95-168431 *04,636* Not available NTIS

In situ On-Line Optical Fiber Sensor for Fluorescence Monitoring in Bioreactors.
PB94-212024 *03,587* Not available NTIS

In-situ Studies of a Novel Sodium Flame Process for Synthesis of Fine Particles.
PB97-113047 *00,681* Not available NTIS

In situ-Toughened Silicon Carbide.
PB97-110332 *03,102* Not available NTIS

In-Space Welding: Visions and Realities.
PB95-163234 *04,830* Not available NTIS

In vitro Fracture Behavior of Ceramic and Metal-Ceramic Restorations.
PB96-119722 *03,569* Not available NTIS

In vitro Inhibition of Membrane-Mediated Calcification by Novel Phosphonates.
PB96-201140 *03,595* Not available NTIS

Incinerability of Perchloroethylene and Chlorobenzene.
PB95-163457 *01,388* Not available NTIS

Incommensurate Magnetic Order in UPtGe.
PB95-140513 *04,542* Not available NTIS

Incorporation of Gold into YBa2Cu3O7: Structure and Tc Enhancement.
PB94-200276 *04,481* Not available NTIS

Increased Pinning Energies and Critical Current Densities in Heavy-Ion-Irradiated Bi2Sr2CaCu2O8 Single Crystals.
PB95-175352 *04,654* Not available NTIS

Increased Transition Temperature in In situ Coevaporated YBa2Cu3O7-delta Thin Films by Low Temperature Post-Annealing.
PB95-180071 *04,672* Not available NTIS

Increasing the Value of Atomic Force Microscopy Process Metrology Using a High-Accuracy Scanner, Tip Characterization, and Morphological Image Analysis.
PB96-190293 *02,758* Not available NTIS

Indentation Fatigue: A Simple Cyclic Hertzian Test for Measuring Damage Accumulation in Polycrystalline Ceramics.
PB96-180013 *03,084* Not available NTIS

India: Environmental Technologies Export Market Plan.
PB97-114359 *02,529* PC A05/MF A01

Individual Carotenoid Content of SRM 1548 Total Diet and Influence of Storage Temperature, Lyophilization, and Irradiation on Dietary Carotenoids.
PB94-200524 *00,033* Not available NTIS

Indoor Air Quality Commissioning of a New Office Building.
PB95-182309 *00,262* PC A04/MF A01

Indoor Air Quality Commissioning of a New Office Building.
PB97-110142 *00,279* Not available NTIS

Indoor Air Quality Impacts of Residential HVAC Systems Phase II.B Report: IAQ Control Retrofit Simulations and Analysis.
PB96-106877 *02,559* PC A05/MF A01

Indoor Air Quality Impacts of Residential HVAC Systems, Phase 1 Report: Computer Simulation Plan.
PB95-135596 *00,249* PC A06/MF A02

Indoor Air Quality Impacts of Residential HVAC Systems. Phase 2.A Report: Baseline and Preliminary Simulations.
PB95-178893 *02,554* PC A05/MF A01

Inductive Voltage Divider Calibration for the NASA Flight Experiment.
PB95-152856 *02,042* Not available NTIS

Inductively Coupled Plasma Source for the Gaseous Electronics Conference RF Reference Cell.
PB96-113394 *02,394*
(Order as PB96-113311, PC A09/MF A03)

Industry and Government-Laboratory Cooperative R and D: An Idea Whose Time Has Come.
PB94-172939 *02,970* Not available NTIS

Industry/Government Open Systems Specification Testing Framework. Version 1.0.
PB94-219110 *01,809* PC A06/MF A02

Industry/Government Open Systems Specification: The Development of GOSIP Version 3.
PB96-161245 *01,505* Not available NTIS

Inelastic Interactions of Electrons with Surfaces: Application to Auger-Electron Spectroscopy and X-ray Photoelectron Spectroscopy.
PB94-172699 *00,764* Not available NTIS

Inelastic Neutron Scattering Measurements of Phonons in Icosahedral Al-Li-Cu.
PB95-126215 *04,532* Not available NTIS

Inelastic Neutron Scattering Studies of Nonlinear Optical Materials: p-Nitroaniline Adsorbed in ALPO-5.
PB95-107223 *00,874* Not available NTIS

Inelastic-Neutron-Scattering Studies of Poly(p-phenylene vinylene).
PB95-180766 *01,014* Not available NTIS

Inelastic Neutron Scattering Studies of Rotational Excitations and the Orientational Potential in C60 and A3C60 Compounds.
PB94-172673 *00,763* Not available NTIS

Inelastic Neutron Scattering Study of Hydrogen in Nanocrystalline Pd.
PB96-146857 *03,366* Not available NTIS

Inexpensive Laser Cooling and Trapping Experiment for Undergraduate Laboratories.
PB96-140371 *04,353* Not available NTIS

Infinite Divisibility and the Identification of Singular Waveforms.
PB94-172111 *02,701* Not available NTIS

Influence of an Impenetrable Interface on a Polymer Glass-Transition Temperature.
PB96-146873 *03,175* Not available NTIS

Influence of Coadsorbed Potassium on the Electron-Stimulated Desorption of F(+), F(-), and F(*) from PF3 on Ru(0001).
PB96-157946 *04,072* Not available NTIS

Influence of Cr Growth on Exchange Coupling in Fe/Cr/Fe(100).
PB95-150181 *04,562* Not available NTIS

Influence of Deposition Parameters on Properties of Laser Ablated YBa2Cu3O7-Delta Films.
PB95-140539 *04,544* Not available NTIS

Influence of Electrical Isolation on the Structure and Reflectivity of Multilayer Coatings Deposited on Dielectric Substrates.
PB96-159736 *04,365* Not available NTIS

Influence of Electrode Material on Measured Ion Kinetic-Energy Distributions in Radio-Frequency Discharges.
PB96-123179 *01,935* Not available NTIS

Influence of Envelopes Geometry on the Sensitivity of 'Nude' Ionization Gauges.
PB97-119077 *04,174* Not available NTIS

Influence of Films' Thickness and Air Gaps in Surface Impedance Measurements of High Temperature Superconductors Using the Dielectric Resonator Technique.
PB96-157862 *01,946* Not available NTIS

Influence of Ignition Source on the Flaming Fire Hazard of Upholstered Furniture. (NIST Reprint).
PB95-180162 *00,297* Not available NTIS

Influence of Lattice Mismatch on Indium Phosphide Based High Electron Mobility Transistor (HEMT) Structures Observed in High Resolution Monochromatic Synchrotron X-Radiation Diffraction Imaging.
PB95-164679 *02,357* Not available NTIS

Influence of Natural and Synthetic Inhibitors on the Crystallization of Calcium Oxalate Hydrates.
PB95-150967 *03,560* Not available NTIS

Influence of Physical Aging on the Yield Response of Model DGEBA + Poly(propylene oxide) Epoxy Glasses.
PB95-126363 *03,381* Not available NTIS

Influence of Shear on the Ordering Temperature of a Triblock Copolymer Melt.
PB96-163753 *01,288* Not available NTIS

Influence of Specimen Absorbed Energy in LOX Mechanical-Impact Tests.
PB95-107355 *03,341* Not available NTIS

Influence of Stationary Phase Chemistry on Shape Recognition in Liquid Chromatography.
PB96-123682 *00,621* Not available NTIS

Influence of Surface Charge on the Stochastic Behavior of Partial Discharge in Dielectrics.
PB96-122767 *01,931* Not available NTIS

Influence of Surface Interaction and Chain Stiffness on Polymer-Induced Entropic Forces and the Dimensions of Confined Polymers.
PB94-185469 *01,203* Not available NTIS

Influence of Tempering Method on Residual Stress in Dental Porcelain.
PB94-172012 *00,138* Not available NTIS

Influence of the Filament Potential Wave Form on the Sensitivity of Glass-Envelope Bayard-Alpert Gages.
PB95-175014 *02,657* Not available NTIS

Influence of Thickness Fluctuations on Exchange Coupling in Fe/Cr/Fe Structures.
PB96-135371 *04,745* Not available NTIS

Information Infrastructure: Reaching Society's Goals. A Report of the Information Infrastructure Task Force Committee on Applications and Technology.
ED-376 823 *00,131* Not available NTIS

Information Infrastructure: Reaching Society's Goals. Report of the Information Infrastructure Task Force Committee on Applications and Technology.
PB94-214756 *01,469* PC A08/MF A02

Information Resource Dictionary System (IRDS): A Status Report.
PB95-126207 *01,810* Not available NTIS

Information Resources for the Fire Community.
PB96-148119 *00,211* Not available NTIS

Information Retrieval Using Key Words and a Structured Review.
PB95-161121 *03,724* Not available NTIS

Information Technologies Make Business Sense for the Custom Therapeutic Footwear Industry.
PB95-251708 *02,829* PC A03/MF A01

Information Technology Engineering and Measurement Model: Adding Lane Markings to the Information Superhighway.
PB95-143145 *01,474* PC A03/MF A01

Information Technology Standards in a Changing World: The Rose of the Users.
PB96-160866 *02,737* Not available NTIS

Information Technology Standards in Federal Acquisitions.
PB96-161252 *01,636* Not available NTIS

Information Transfer in the 21st Century.
PB96-157904 *02,714* Not available NTIS

Infrared and Microwave Spectroscopy of the Argon - Propyne Dimer.
PB94-198892 *00,794* Not available NTIS

Infrared and Near-Infrared Spectra of HCC and DCC Trapped in Solid Neon.
AD-A295 578/9 *03,773* PC A03/MF A01

Infrared Spectra of van der Waals Complexes of Importance in Planetary Atmospheres.
PB95-125738 *00,071* Not available NTIS

Infrared Spectrum of OCIO in the 2000/cm(-1) Region: The 2(nu sub 1) and (nu sub 1 + nu sub 3) Bands.
PB95-141032 *00,908* Not available NTIS

Infratechnologies: Tools for Innovation.
PB94-185998 *00,317* Not available NTIS

Inhibition of Premixed Methane-Air Flames by Halon Alternatives.
PB96-146741 *01,414* Not available NTIS

Inhibition of Premixed Methane-Air Flames by Iron Pentacarbonyl.
PB96-163712 *00,513* Not available NTIS

Initial and Final Orbital Alignment Probing of the Fine-Structure-Changing Collisions among the Ca (4s)(1)(4p)(1), (3)PJ States with He: Determination of Coherence and Conventional Cross-Sections.
PB95-203279 *04,004* Not available NTIS

Initial Graphics Exchange Specification (IGES): Procedures for the NIST IGES Validation Test Service.
PB95-171427 *02,780* PC A03/MF A01

Initial NIST Testing Policy for STEP: Beta Testing Program for AP 203 Implementations. National PDES Testbed Report Series.
PB95-154688 *02,779* PC A03/MF A01

Inner-Valence States CO(+) between 22 eV and 46 eV Studied by High Resolution Photoelectron Spectroscopy and ab Initio CI Calculations.
PB95-180055 *03,961* Not available NTIS

Innovation in the Japanese Construction Industry: A 1995 Appraisal.
PB96-177373 *00,225* PC A13/MF A03

Inorganic Crystal Structure Database (ICSD) and Standardized Data and Crystal Chemical Characterization of Inorganic Structure Types (TYPIX): Two Tools for Inorganic Chemists and Crystallographers.
PB97-109037 *00,648*
(Order as PB97-109011, PC A11/MF A03)

Inserting Line Segments into Triangulations and Tetrahedralizations.
PB95-198933 *03,415* PC A03/MF A01

Instrument for Evaluating Phase Behavior of Mixtures for Supercritical Fluid Experiments.
PB95-180758 *00,606* Not available NTIS

Instrumental Smearing Effects in Radially Symmetric Small-Angle Neutron Scattering by Numerical and Analytical Methods.
PB96-160429 *02,984* Not available NTIS

Insulating Boundary Layer and Magnetic Scattering in YBa2Cu3O7-delta/Ag Interfaces Over a Contact Resistivity Range of 10(-8) - 10(-3) Omega cm(2).
PB95-169157 *04,648* Not available NTIS

Insulating Nanoparticles on YBa2Cu3O7-delta Thin Films Revealed by Comparison of Atomic Force and Scanning Tunneling Microscopy.
PB95-150843 *04,575* Not available NTIS

Integral Occurring in Coherence Theory.
PB95-203550 *04,324* Not available NTIS

Integrated Inspection System for Improved Machine Performance.
PB96-160569 *02,959* Not available NTIS

Integrated Laser Doppler Method for Measuring Planetary Gravity Fields.
PB94-198686 *03,681* Not available NTIS

Integrated Mobile Robot System for Testing Vision Algorithms.
PB95-164133 *02,936* Not available NTIS

Integrated Network Management.
PB94-199247 *01,583* Not available NTIS

Integrated Optic Laser Emitting at 905, 1057, 1356 nm.
PB94-216298 *02,136* Not available NTIS

Integrated Optic Laser Emitting at 906, 1057, and 1358 nm.
PB94-216280 *02,135* Not available NTIS

Integrated-Optical Devices in Rare-Earth-Doped Glass.
PB95-202909 *02,179* Not available NTIS

Integrated Optical Polarization-Discriminating Receiver in Glass.
PB97-113179 *02,206* Not available NTIS

Integrated Services Digital Network (ISDN); Category: Telecommunications Standard; Subcategory: Integrated Services Digital Network.
FIPS PUB 182 *01,460* PC E03

Integrated Thin-Film Micropotentiometers.
PB96-146709 *02,109* Not available NTIS

Integrated Vision Touch-Probe System for Dimensional Inspection Tasks.
PB95-255832 *02,917* PC A03/MF A01

Integrating Automated Systems with Modular Architecture.
PB95-150231 *00,577* Not available NTIS

Integrating Sphere Simulation: Application to Total Flux Scale Realization.
PB95-150173 *04,261* Not available NTIS

Integration Definition for Function Modeling (IDEF0); Category: Software Standard; Subcategory: Modeling Techniques.
FIPSPUB183 *02,800* PC E07

Integration Definition for Information Modeling (IDEF1X); Category: Software Standard; Subcategory: Modeling Techniques.
FIPSPUB184 *01,673* PC E10

Integration of Real-Time Process Planning for Small-Batch Flexible Manufacturing.
PB95-151908 *02,822* Not available NTIS

Integration of Scanning Tunneling Microscope Nanolithography and Electronics Device Processing.
PB95-153359 *02,341* Not available NTIS

Integration of Servo Control into a Large-Scale Control System Design: An Example from Coal Mining.
PB94-203429 *03,696* PC A02/MF A01

Intelligent Control for Multiple Autonomous Undersea Vehicles.
PB94-211877 *03,747* Not available NTIS

Intelligent Control of an Inert Gas Atomization Process.
PB95-141057 *03,344* Not available NTIS

Intelligent Processing of Hot Isostatic Pressing.
PB94-172913 *03,315* Not available NTIS

Intelligent Processing of Materials.
PB94-172780 *02,811* Not available NTIS

Intelligent Processing of Materials, Technical Activities 1993 (NAS-NRC Assessment Panel, April 21-22, 1994).
PB94-164183 *02,809* PC A04/MF A01

Intelligent Processing of Materials, Technical Activities 1994 (NAS-NRC Assessment Panel, April 6-7, 1995).
PB96-115050 *03,359* PC A04/MF A01

Intensities and Dipole Moment Derivatives of the Fundamental Bands of (35)ClO2 and an Intensity Analysis of the nu1 Band.
PB95-141040 *00,909* Not available NTIS

Intensity-Dependent Scattering Rings in High Order Above-Threshold Ionization.
PB96-110739 *04,032* Not available NTIS

Intensive Swimming: Can It Affect Your Patients' Smiles.
PB96-123666 *03,570* Not available NTIS

Inter-Laboratory Trials of the EPR Method for the Detection of Irradiated Meats Containing Bone.
PB96-161690 *00,042* Not available NTIS

Interaction between Dislocations and Intergranular Cracks.
PB95-152096 *03,190* Not available NTIS

Interaction between Micro and Macroscopic Flow in RTM Preforms.
PB95-162012 *03,159* Not available NTIS

Interaction between Naphthalene Sulfonate and Silica Fume in Portland Cement Pastes.
PB94-199759 *01,315* Not available NTIS

Interaction Coefficients for 15 Mixtures of Flammable and Non-Flammable Components.
PB96-146626 *03,281* Not available NTIS

Interaction of an Isolated Sprinkler Spray and a Two-Layer Compartment Fire Environment. Phenomena and Model Simulations.
PB97-110076 *01,437* Not available NTIS

Interaction of Chlorhexidine Digluconate with and Adsorption of Chlorhexidine on Hydroxyapatite.
PB95-175907 *03,566* Not available NTIS

Interaction of Citric Acid with Hydroxyapatite: Surface Exchange of Ions and Precipitation of Calcium Citrate.
PB97-119309 *03,584* Not available NTIS

Interaction of HFC-125, FC-218 and CF3I with High Speed Combustion Waves.
PB96-176417 *03,290* Not available NTIS

Interaction of Rayleigh Waves with a Rib Attached to a Plate.
PB94-199023 *04,184* Not available NTIS

Interaction of Some Coupling Agents and Organic Compounds with Hydroxyapatite: Hydrogen Bonding, Adsorption and Adhesion.
PB94-172616 *00,140* Not available NTIS

Interaction of Stoichiometry, Mechanical Stress, and Interface Trap Density in LPCVD Si-rich SiNx-Si Structures.
PB95-176301 *02,366* Not available NTIS

Interatomic Potential of Argon.
PB95-141180 *00,912* Not available NTIS

Interatomic Potential of Argon.
PB95-152989 *00,945* Not available NTIS

Intercomparison between NPL (India) and NIST (USA) Pressure Standards in the Hydraulic Pressure Region Up to 26 MPa.
PB96-113543 *04,211*
(Order as PB96-113535, PC A05/MF A01)

Intercomparison of DNA Sizing Ladders in Electrophoretic Separation Matrices and Their Potential for Accurate Typing of the D1S80 Locus.
PB96-200928 *03,485* Not available NTIS

Intercomparison of Internal Proportional Gas Counting of (85)Kr and (3)H.
PB94-185576 *03,800* Not available NTIS

Intercomparison of NIST, NPL, PTB, and VSL Thermal Voltage Converters from 100 kHz to 1 MHz.
PB94-172442 *02,026* Not available NTIS

Intercomparison of Photometric Units Maintained at NIST (USA) and PTB (Germany), 1993.
PB95-261913 *04,329*

(Order as PB95-261897, PC A07/MF A02)

Intercomparison of the Effective Areas of a Pneumatic Piston Gauge Determined by Different Techniques.
PB94-212370 *02,640* Not available NTIS

Intercomparison of the ITS-90 Radiance Temperature Scales of the National Physical Laboratory (U.K.) and the National Institute of Standards and Technology.
PB96-113550 *02,674*
(Order as PB96-113535, PC A05/MF A01)

Intercomparison of Thermal Converters at NIM, NIST, PTB, SIRI and VSL from 10 to 100 MHz.
PB94-172459 *02,027* Not available NTIS

Intercomparison Study of (237)Np Determination in Artificial Urine Samples.
PB96-102645 *03,633* Not available NTIS

Interconnection Transmission Line Parameter Characterization.
PB94-216397 *02,218* Not available NTIS

Interdigitated Stacked P-I-N Multiple Quantum Well Modulator.
PB97-112296 *02,455* Not available NTIS

Interface-Filter Characterization of Spectraradiometers and Colorimeters.
PB97-122212 *04,399* Not available NTIS

Interface Modification and Characterization of Silicon Carbide Platelets Coated with Alumina Particles.
PB95-108734 *03,121* Not available NTIS

Interface Properties for Ceramic Composites from a Single Fiber Pull-Out Test.
PB94-199361 *03,135* Not available NTIS

Interface Roughness, Composition, and Alloying of Low-Order AlAs/GaAs Superlattices Studies by X-ray Diffraction.
PB96-160262 *02,983* Not available NTIS

Interface Roughness-Induced Changes in the Near-E(sub 0) Spectroscopic Behavior of Short-Period AlAs/GaAs Superlattices.
PB94-185154 *02,118* Not available NTIS

Interface Roughness of Short-Period AlAs/GaAs Superlattices Studied by Spectroscopic Ellipsometry.
PB95-107215 *02,137* Not available NTIS

Interface Sharpness during the Initial Stages of Growth of Thin, Short-Period III-V Superlattices.
PB95-108783 *02,139* Not available NTIS

Interface Sharpness in Low-Order III-V Superlattices.
PB95-108775 *02,138* Not available NTIS

Interfaces in Mo/Si Multilayers.
PB96-160668 *02,423* Not available NTIS

Interfacial Crack in a Two-Dimensional Hexagonal Lattice.
PB96-161989 *04,100* Not available NTIS

Interfacial Free Energies from Substrate Curvature Measurements of the Creep of Multilayer Thin Films.
PB94-185428 *04,448* Not available NTIS

Interfacial Transport in Porous Media: Application to dc Electrical Conductivity of Mortars.
PB96-146816 *01,326* Not available NTIS

Interference in the Resonance Fluorescence of Two Trapped Atoms.
PB95-168514 *03,948* Not available NTIS

Interim Testing Artifact (ITA): A Performance Evaluation System for Coordinate Measuring Machines (CMMs). User Manual.
PB95-210589 *02,914* PC A04/MF A01

Interior-Point Method for Linear and Quadratic Programming Problems. (NIST Reprint).
PB95-180089 *03,429* Not available NTIS

Interlaboratory Comparison of Autoradiographic DNA Profiling Measurements. 1. Data and Summary Statistics.
PB95-175923 *03,542* Not available NTIS

Interlaboratory Comparison of Autoradiographic DNA Profiling Measurements. 2. Measurement Uncertainty and Its Propagation.
PB96-112123 *03,545* Not available NTIS

Interlaboratory Comparison of Polarization-Holding Parameter Measurements on High-Birefringence Optical Fiber.
PB95-168464 *04,280* Not available NTIS

Interlaboratory Comparison Studies on the Analysis of Hair for Drugs of Abuse.
PB95-176251 *03,500* Not available NTIS

Interlaboratory Studies on the Analysis of Hair for Drugs of Abuse: Results from the Fifth Exercise.
PB97-110449 *03,509* Not available NTIS

Interlaboratory Studies on the Analysis of Hair for Drugs of Abuse: Results from the Fourth Exercise.
PB97-111322 *03,510* Not available NTIS

Intermediate Coupling in L2-L3 Core Excitons of MgO, Al2O3, and SiO2.
PB96-158043 *04,079* Not available NTIS

Intermediate Structure in the Neutron-Induced Fission Cross Section of 236U.
PB94-185741 *03,802* Not available NTIS

Intermolecular HF Motion in Ar(sub n)HF Micromatrices (n=1,2,3,4,): Classical and Quantum Calculations on a Pairwise Additive Potential Surface.
PB95-107025 *03,871* Not available NTIS

Internal Droplet Circulation Induced by Surface-Driven Rotation.
PB97-119267 *02,500* Not available NTIS

Internal Waves in Xenon Near the Critical Point.
PB97-111504 *04,221* Not available NTIS

International Challenges in Defining the Public and Private Interest in Standards.
PB96-160361 *00,498* Not available NTIS

International Conference on Chemical Kinetics (2nd). Held in Gaithersburg, Maryland on July 24-27, 1989.
PB94-211901 *00,822* Not available NTIS

International Equations for the Saturation Properties of Ordinary Water Substance. Revised According to the International Temperature Scale of 1990. Addendum to Journal of Physical and Chemical Reference Data 16, 893 (1987).
PB94-162302 *00,742* Not available NTIS

International Green Building Conference and Exposition (2nd). Held in Big Sky, Montana on August 13-15, 1995.
PB95-253605 *02,525* PC A04/MF A01

International Green Building Conference and Exposition (3rd). Held in San Diego, California on November 17-19, 1996. (Reannouncement with new abstract).
PB97-121826 *02,531* PC A12/MF A03

International Institute of Welding: Report on 1992 Actions.
PB94-185873 *02,856* Not available NTIS

International Institute of Welding: Report on 1993 Actions.
PB94-185881 *02,857* Not available NTIS

International Institute of Welding: Report on 1995 Actions.
PB96-158076 *02,874* Not available NTIS

International Intercomparison of Detector Responsivity at 1300 and 1550 nm.
PB95-125928 *02,140* Not available NTIS

International Intercomparison of Detector Responsivity at 1300 and 1550 nm.
PB95-126017 *02,141* Not available NTIS

International Marine-Atmospheric (222)Rn Measurement Intercomparison in Bermuda. Part 1. NIST Calibration and Methodology for Standardized Sample Additions.
PB96-175674 *00,114*
(Order as PB96-175666, PC A07/MF A02)

International Marine-Atmospheric (222)Rn Measurement Intercomparison in Bermuda. Part 2. Results for the Participating Laboratories.
PB96-175682 *00,115*
(Order as PB96-175666, PC A07/MF A02)

International Organization for Standardization: Current Activities in Fire Safety Engineering.
PB96-159660 *00,223* Not available NTIS

International Radon-in-Air Measurement Intercomparison Using a New Transfer Standard.
PB96-159751 *03,708* Not available NTIS

International Standard Equation of State for the Thermodynamic Properties of Refrigerant 123 (2,2-Dichloro- 1,1,1-Trifluoroethane).
PB96-176805 *03,294* Not available NTIS

International Standards and Reference Materials.
PB97-113120 *00,188* Not available NTIS

Internationalization of Fire Safety Engineering Research and Strategy.
PB96-156153 *00,220* Not available NTIS

Interoperability Experiments with CORBA and Persistent Object Base Systems.
PB96-183140 *01,772* PC A04/MF A01

Interoperability Requirements for CAD Data Transfer in the AutoSTEP Project.
PB97-114268 *02,796* PC A03/MF A01

Interpreting the Readings of Multi-Element Personnel Dosimeters in Terms of the Personal Dose Equivalent.
PB95-175428 *03,631* Not available NTIS

Interstellar Disk-Halo Connection in Galaxies: Review of Observational Aspects.
PB94-211802 *00,058* Not available NTIS

Intersystem Crossing in Collisions of Aligned Ca(4s5p (1)P) + He: A Half Collision Analysis Using Multichannel Quantum Defect Theory.
PB94-211133 *00,813* Not available NTIS

Intra-Laboratory Comparison of a Line-Heat-Source Guarded Hot Plate and Heat-Flow-Meter Apparatus.
PB95-181202 *00,387* Not available NTIS

Intracomparison Tests of the FG5 Absolute Gravity Meters.
PB96-102991 *03,688* Not available NTIS

Intracycle Evaporative Cooling in a Vapor Compression Cycle.
PB97-116107 *02,762* PC A03/MF A01

Intrinsic Conductivity of Objects Having Arbitrary Shape and Conductivity.
PB97-111934 *04,150* Not available NTIS

Intrinsic Stress in DC Sputtered Niobium.
PB94-199031 *04,468* Not available NTIS

Intrinsic Viscosity and the Polarizability of Particles Having a Wide Range of Shapes.
PB96-119318 *03,170* Not available NTIS

Introduction of a NIST Instrument Sensitivity Standard Reference Material for X-Ray Powder Diffraction.
PB94-200318 *00,807* Not available NTIS

Introduction to ASTM 1199 'Wear Test Selection for Design and Application'.
PB95-162517 *03,238* Not available NTIS

Introduction to Frequency Calibration. Part 1.
PB96-200654 *01,560* Not available NTIS

Introduction to Phase-Stable Optical Sources.
PB96-122973 *04,347* Not available NTIS

Introduction to Secure Telephone Terminals.
PB97-110498 *01,512* Not available NTIS

Introduction to the P1003.1g and CPI-C Network Application Programming Interfaces.
PB95-231726 *01,731* PC A03/MF A01

Introduction to Traffic Management for Broadband ISDN.
PB94-142494 *01,464* PC A03/MF A01

Inversion of the Phase Diagram from UCST to LCST in Deuterated Polybutadiene and Protonated Polybutadiene Blends.
PB94-212446 *01,226* Not available NTIS

Investigating the 3.3 Micron Infrared Fluorescence from Naphthalene Following Ultraviolet Excitation.
N95-15839/0 *00,724*
(Order as N95-15827/5, PC A07/MF A02)

Investigation into a Practical Grain Growth Model for Hot Isostatic Pressing.
PB95-151684 *03,347* Not available NTIS

Investigation into the Flammability Properties of Honeycomb Composites.
PB95-143293 *03,152* PC A03/MF A01

Investigation of Applicability of Alanine and Radiochromic Detectors to Dosimetry of Proton Clinical Beams.
PB96-146782 *03,636* Not available NTIS

Investigation of High-Temperature Platinum Resistance Thermometers at Temperatures Up to 962C, and, in Some Cases, 1064C.
PB96-161294 *00,629* Not available NTIS

Investigation of LS Coupling in Boronlike Ions.
PB94-185295 *03,797* Not available NTIS

Investigation of Mercury Interstitials in Hg(1-x)CdxTe Alloys Using Resonant Impact-Ionization Spectroscopy.
PB94-213485 *02,133* Not available NTIS

Investigation of Oil and Gas Well Fires and Flares.
PB94-193976 *03,695* PC A04/MF A01

Investigation of S2F10 Production and Mitigation in Compressed SF6-Insulated Power Systems.
PB94-212388 *02,467* Not available NTIS

Investigation of S2F10 Production and Mitigation in Compressed SF6- Insulated Power Systems.
PB96-155528 *02,468* Not available NTIS

Investigation of the Drive Circuit Requirements for the Power Insulated Gate Bipolar Transistor (IGBT).
PB94-211794 *02,316* Not available NTIS

Investigation of the Effects of Aging on the Calibration of a Kerr-Cell Measuring System for High Voltage Impulses.
PB94-172384 *02,025* Not available NTIS

Investigation of the ITS-90 Subrange Inconsistencies for 25.5 Omega SPRTs.
PB96-161302 *00,630* Not available NTIS

Investigation of the Thermal Stability and Char-Forming Tendency of Cross-linked Poly(methyl methacrylate).
PB94-213501 *03,380* Not available NTIS

Investigations of AM and PM Noise in X-Band Devices.
PB95-180022 *02,062* Not available NTIS

Investigations of Sulfur Interferences in the Extraction of Methylmercury from Marine Tissues.
PB96-190020 *03,482* Not available NTIS

Investigations of the Systematics of Crystal Packing Using the Cambridge Structural Database.
PB97-109144 *00,519*
(Order as PB97-109011, PC A11/MF A03)

Investing in Education to Meet a National Need for a Technical-Professional Workforce in a Post-Industrial Economy.
PB94-173028 *00,132* Not available NTIS

Iodine Atoms and Iodomethane Radical Cations: Their Formation in the Pulse Radiolysis of Iodomethane in Organic Solvents, Their Complexes, and Their Reactivity with Organic Reductants.
PB95-162764 *00,965* Not available NTIS

Ion Broadening Parameters for Several Argon and Carbon Lines.
PB94-211562 *03,843* Not available NTIS

Ion Kinetic-Energy Distributions and Balmer-alpha (Halpha) Excitation in Ar-H2 Radio-Frequency Discharges.
PB96-102959 *04,029* Not available NTIS

Ion Kinetic-Energy Distributions in Argon rf Glow Discharges.
PB95-141008 *04,409* Not available NTIS

Ion Kinetics and Symmetric Charge-Transfer Collisions in Low-Current, Diffuse (Townsend) Discharges in Argon and Nitrogen.
PB96-123658 *04,051* Not available NTIS

Ionization Energies, Appearance Energies and Thermochemistry of CF2O and FCO.
PB97-111538 *01,178* Not available NTIS

Ionization Energy of Sulfur Pentafluoride and the Sulfur Pentafluoride-Fluorine Atom Bond Dissociation Energy.
PB95-162814 *00,966* Not available NTIS

Ionizing Radiation Causes Greater DNA Base Damage in Radiation-Sensitive Mutant M10 Cells That in Parent Mouse Lymphoma L5178Y Cells.
PB95-175915 *03,632* Not available NTIS

Ionizing radiation-induced DNA damage and its repair in human cells. Progress report, (April 1, 1993--February 28, 1994).
DE94014709 *03,612* PC A01/MF A01

Ionospheric Radio Propagation.
AD-A286 619/2 *01,459* PC A10/MF A03

IRAS Spectroscopic Observations of Young Planetary Nebulae.
PB95-152070 *00,072* Not available NTIS

Iridium Oxide Thin-Film Stability in High-Temperature Corrosive Solutions.
PB94-213014 *03,234* Not available NTIS

Irradiance of Horizontal Quartz-Halogen Standard Lamps.
PB96-179130 *01,866*
(Order as PB96-177381, PC A07/MF A02)

Irradiances of Spectral Lines in Mercury Pencil Lamps.
PB96-176466 *04,375* Not available NTIS

Irradiation Damage in Inorganic Insulation Materials for ITER Magnets: A Review.
PB95-147351 *03,705* PC A18/MF A04

ISDN Conformance Testing.
PB95-163176 *01,478* Not available NTIS

ISDN Conformance Testing Guidelines: Guidelines for Implementors of ISDN Customer Premises Equipment to Conform to Both National ISDN-1 and North American ISDN Users' Forum Layer 3 Basic Rate Interface Basic Call Control Abstract Test Suites.
PB94-219094 *01,471* PC A03/MF A01

ISDN in North America.
PB96-160767 *01,502* Not available NTIS

ISDN LAN Bridging.
PB95-154696 *01,477* PC A03/MF A01

ISO Environmental Management Standardization Efforts.
PB95-220513 *02,524* PC A03/MF A01

ISO Environmental Management Standardization Efforts.
PB96-158662 *02,528* PC A03/MF A01

ISO/IEC Workshop on Worldwide Recognition of OSI Test Results Regional Progress - North America.
PB94-172202 *02,719* Not available NTIS

ISO TC 184/SC4 Reference Manual.
PB95-242293 *02,663* PC A04/MF A01

Isochoric (p-p-T) Measurements on Liquid and Gaseous Air from 67 to 400 K at Pressures to 35 MPa.
PB96-167390 *01,154* Not available NTIS

Isolated Spin Pairs and Two-Dimensional Magnetism in SrCr(sub 9p)Ga(sub 12-9p)O19.
PB97-112387 *04,154* Not available NTIS

Isolation and Structural Elucidation of the Predominant Geometrical Isomers of alpha-Carotene.
PB96-190061 *00,640* Not available NTIS

Isopiestic Investigation of the Osmotic and Activity Coefficients of Aqueous NaBr and the Solubility of NaBr2H2O(cr) at 298.15 K: Thermodynamic Properties of the NaBr + H2O System over Wide Ranges of Temperature and Pressure.
PB97-110365 *01,175* Not available NTIS

Isotope Dilution Mass Spectrometry as a Candidate Definitive Method for Determining Total Glycerides and Triglycerides in Serum.
PB96-102280 *03,519* Not available NTIS

Isotope Shifts and Hyperfine Splittings of the 398.8-nm Yb I Line.
PB94-199585 *03,814* Not available NTIS

Isotopic and Nuclear Analytical Techniques in Biological Systems: A Critical Study. 10. Elemental Isotopic Dilution Analysis with Radioactive and Stable Isotopes (Technical Report).
PB96-164157 *00,696* Not available NTIS

Issues and Recommendations for a STEP Application Protocol Framework. National PDES Testbed.
PB94-160868 *02,770* PC A05/MF A01

Issues Concerning Material Removal Shape Element Volumes (MRSEVs).
PB94-185493 *02,882* Not available NTIS

Issues Concerning Material Removal Shape Element Volumes (MRSEVs).
PB95-210167 *02,885* PC A03/MF A01

Issues in High-Speed Pyrometry.
PB97-118368 *02,693* Not available NTIS

Issues in the Field Measurement of VOC Emission Rates.
PB97-118806 *02,573* Not available NTIS

ITS-90 Calibration Facility.
PB96-160916 *00,627* Not available NTIS

IUE Observations of Solar-Type Stars in the Pleiades and the Hyades.
PB94-199437 *00,053* Not available NTIS

Jacket Thickness Requirements for Seismic Retrofitting of Circular Bridge Columns.
PB95-163267 *01,336* Not available NTIS

January 17, 1995 Hyogoken-Nanbu (Kobe) Earthquake. Performance of Structures, Lifelines and Fire Protection Systems. Executive Summary and Paper.
PB97-104160 *00,475* PC A99/MF A06

Japan Technology Program Assessment: Precision Engineering/Precision Optics in Japan.
PB95-171112 *02,884* PC A03/MF A01

Japan Technology Program Assessment. Simulation: State-of the-Art in Japan.
PB95-217097 *02,827* PC A03/MF A01

JEDEC 'TCR' Interlaboratory Experiment: Lessons Learned.
PB95-203188 *02,371* Not available NTIS

Joint DoD/NIST Workshop on International Manufacturing Systems Research and Development. Held in Rockville, Maryland on November 3-5, 1992. Proceedings.
PB96-109491 *02,931* PC A11/MF A03

Josephson D/A Converter with Fundamental Accuracy.
PB96-148044 *02,418* Not available NTIS

Josephson Voltage Standard Based on Single-Flux-Quantum Voltage Multipliers.
PB95-175600 *02,058* Not available NTIS

Journal of Physical and Chemical Reference Data, Volume 22, No. 1, January/February 1993.
PB94-160975 *00,729* Not available NTIS

Journal of Physical and Chemical Reference Data, Volume 22, No. 2, March/April 1993.
PB94-162211 *00,733* Not available NTIS

Journal of Physical and Chemical Reference Data, Volume 22, No. 3, May/June 1993.
PB94-162260 *00,738* Not available NTIS

Journal of Physical and Chemical Reference Data, Volume 22, No. 4, July/August 1993.
PB94-162310 *00,743* Not available NTIS

Journal of Physical and Chemical Reference Data, Volume 22, No. 5, September/October 1993.
PB94-162336 *00,745* Not available NTIS

Journal of Physical and Chemical Reference Data, Volume 22, No. 6, November/December 1993.
PB94-168556 *00,749* Not available NTIS

Journal of Physical and Chemical Reference Data, Volume 24, No. 1, January/February 1995.
PB96-145560 *01,101* Not available NTIS

Journal of Physical and Chemical Reference Data, Volume 24, No. 2, March/April 1995.
PB96-145818 *01,105* Not available NTIS

Journal of Physical and Chemical Reference Data, Volume 24, No. 3, May/June 1995.
PB96-145842 *01,108* Not available NTIS

Journal of Physical and Chemical Reference Data, Volume 24, No. 4, July/August 1995.
PB96-145883 *01,112* Not available NTIS

Journal of Physical and Chemical Reference Data, Volume 24, No. 5, September/October 1995.
PB96-145925 *01,116* Not available NTIS

Journal of Physical and Chemical Reference Data, Volume 24, No. 6, November/December 1995.
PB96-145966 *01,120* Not available NTIS

Journal of Research of the National Institute of Standards and Technology. January/February 1994. Volume 99, Number 1.
PB94-169737 *02,019* PC A07/MF A02

Journal of Research of the National Institute of Standards and Technology, January/February 1996. Volume 101, Number 1.
PB96-175666 *00,113* PC A07/MF A02

Journal of Research of the National Institute of Standards and Technology, July/August 1994. Volume 99, Number 4. Special Issue: Extreme Value Theory and Applications. Proceedings of the Conference on Extreme Value Theory and Applications, Volume 2. Held at Gaithersburg, Maryland, in May 1993.
PB95-160594 *03,440* PC A13/MF A03

Journal of Research of the National Institute of Standards and Technology, July/August 1995. Volume 100, Number 4. Special Issue: The Gaseous Electronics Conference Radio-Frequency Reference Cell.
PB96-113311 *02,386* PC A09/MF A03

Journal of Research of the National Institute of Standards and Technology. March/April 1994. Volume 99, Number 2.
PB94-219219 *02,000* PC A06/MF A02

Journal of Research of the National Institute of Standards and Technology, March/April 1995. Volume 100, Number 2.
PB96-126180 *04,349* PC A05/MF A01

Journal of Research of the National Institute of Standards and Technology, March/April 1996. Volume 101, Number 2.
PB96-177381 *01,863* PC A07/MF A02

Journal of Research of the National Institute of Standards and Technology. May/June 1994. Volume 99, Number 3.
PB94-219326 *02,643* PC A05/MF A02

Journal of Research of the National Institute of Standards and Technology, May/June 1995. Volume 100, Number 3.
PB95-261897 *02,670* PC A07/MF A02

Journal of Research of the National Institute of Standards and Technology, May/June 1996. Volume 101, Number 3. Special Issue: NIST Workshop on Crystallographic Databases.
PB97-109011 *04,798* PC A11/MF A03

Journal of Research of the National Institute of Standards and Technology, November-December 1993. Volume 98, Number 6.
PB94-140555 *04,223* PC A06/MF A02

Journal of Research of the National Institute of Standards and Technology, November/December 1994. Volume 99, Number 6.
PB96-113535 *04,336* PC A05/MF A01

Journal of Research of the National Institute of Standards and Technology, November/December 1995. Volume 100, Number 6.
PB96-159215 *01,949* PC A08/MF A02

Journal of Research of the National Institute of Standards and Technology, September-October 1993. Volume 98, Number 5.
PB96-134954 *03,362* PC A05/MF A01

Journal of Research of the National Institute of Standards and Technology, September/October 1993. Volume 98, Number 5.
PB96-169057 *03,368* PC A06/MF A01

Journal of Research of the National Institute of Standards and Technology, September/October 1994. Volume 99, Number 5.
PB95-169371 *04,293* PC A07/MF A02

Journal of Research of the National Institute of Standards and Technology, September/October 1995. Volume 100, Number 5.
PB96-117767 *01,927* PC A08/MF A02

Joy of Acceptance Diagrams.
PB94-200433 *03,828* Not available NTIS

Junction Locations by Scanning Tunneling Microscopy: In-Air-Ambient Investigation of Passivated GaAs pn Junctions.
PB94-185964 *02,306* Not available NTIS

K alpha Transitions in Few-Electron Ions and in Atoms.
PB94-212248 *03,849* Not available NTIS

Keeping Time on Your PC.
PB95-161410 *01,537* Not available NTIS

Keeping Up with the Reality of Today's Surge Environment.
PB96-123633 *02,231* Not available NTIS

Keeping Your Site Comfortably Secure: An Introduction to Internet Firewalls.
PB95-182275 *02,730* PC A05/MF A01

Kibitz-Connecting Multiple Interactive Programs Together.
PB94-213311 *01,696* Not available NTIS

Kinetic Energy Distribution of Ions Produced from Townsend Discharges in Neon and Argon.
PB96-111927 *04,413* Not available NTIS

Kinetic Energy Distributions of H(+), H2(+), and H3(+) from a Diffuse Townsend Discharge in H2 at High E/N.
PB96-123351 *04,415* Not available NTIS

Kinetic-Energy Distributions of Ions Sampled from Argon Plasmas in a Parallel-Plate, Radio-Frequency Reference Cell.
PB95-161964 *03,935* Not available NTIS

Kinetic-Energy Distributions of Ions Sampled from Radio-Frequency Discharges in Helium, Nitrogen, and Oxygen.
PB96-123732 *01,092* Not available NTIS

Kinetic-Energy Distributions of K(+) in Argon and Neon in Uniform Electric Fields.
PB95-151122 *03,902* Not available NTIS

Kinetic-Energy-Enhanced Neutral Etching.
PB96-200613 *00,665* Not available NTIS

Kinetic-Inductance Infrared Detector Based on an Antenna-Coupled High-Tc SQUID.
PB95-169116 *02,165* Not available NTIS

Kinetics and Dynamics of Vibrationally State Resolved Ion-Molecule Reactions: (14)N2(+)(v=1 and 2) and (15)N2(+)(v=0,1 and 2) with (14)N2.
PB96-102348 *04,023* Not available NTIS

Kinetics and Mechanism of the Collision-Activated Dissociation of the Acetone Cation.
PB94-216462 *00,859* Not available NTIS

Kinetics of the Reaction C2H + O2 from 193 to 350 K Using Laser Flash Kinetic Infrared Absorption Spectroscopy.
PB95-203055 *01,043* Not available NTIS

Kinetics of the Reaction of CCl3-Br-2 and the Thermochemistry of CCl3 Radical and Cation.
PB94-212115 *00,824* Not available NTIS

Kinetics of the Reaction of the Sulfate Radical with the Oxalate Anion.
PB97-119127 *01,186* Not available NTIS

Kinetics of the Self-Reaction of Hydroxymethylperoxyl Radicals.
PB94-212164 *00,827* Not available NTIS

Knowledge-Based Approach for Automating a Design Method for Concurrent and Real-Time Systems.
PB97-112502 *01,780* Not available NTIS

L-threo-beta-Hydroxyhistidine, an Unprecedented Iron(III) Ion-Binding Amino Acid in a Pyoverdine-type Siderophore from Pseudomonas fluorescens 244.
PB94-211620 *00,553* Not available NTIS

Lab Report Special Section: Natural Language Processing and Information Retrieval Group Information Access and User Interfaces Division, National Institute of Standards and Technology.
PB97-118665 *02,742* Not available NTIS

Labeling Conventions in Isoelectronic Sequences - Reply.
PB95-162574 *03,937* Not available NTIS

Laboratory Accreditation for Testing Energy Efficient Lighting.
PB96-122932 *00,270* Not available NTIS

Laboratory Measurements for the Astrophysical Identification of MgH.
PB95-152195 *00,073* Not available NTIS

Laboratory Studies of Low-Temperature Reactions of C2H with C2H2 and Implications for Atmospheric Models of Titan.
PB95-108726 *00,690* Not available NTIS

Lake Erie Water Temperature Data, Put-in-Bay, Ohio, 1918-1992.
PB96-202452 *03,692* PC A04/MF A01

Langevin Approach to Hysteresis and Barkhausen Modeling in Steel.
PB94-185675 *03,206* Not available NTIS

Langmuir Probe Measurements in the Gaseous Electronics Conference RF Reference Cell.
PB96-113386 *02,393*
(Order as PB96-113311, PC A09/MF A03)

Laplace's Equation and the Dirichlet-Neumann Map in Multiply Connected Domains. (NIST Reprint).
PB95-180295 *03,962* Not available NTIS

Large-Amplitude Shapiro Steps and Self-Field Effects in High-Tc Josephson Weak Links.
PB95-180410 *04,682* Not available NTIS

Large Amplitude Skeletal Isomerization as a Promoter of Intramolecular Vibrational Relaxation in CH Stretch Excited Hydrocarbons.
PB95-202933 *01,036* Not available NTIS

Large Eddy Simulations of Smoke Movement in Three Dimensions.
PB96-190012 *01,426* Not available NTIS

Large Fire Experiments for Fire Model Evaluations.
PB96-190079 *01,427* Not available NTIS

Large Local-Field Corrections in Optical Rotatory Power of Quartz and Selenium.
PB97-122378 *04,400* Not available NTIS

Laser Ablation of Thin Films as a Free Atom Source for Pulsed RIMS.
PB94-198710 *00,540* Not available NTIS

Laser Assisted Collisions at Ultracold Temperatures.
PB95-161220 *03,929* Not available NTIS

Laser Bandwidth Effects in Quantitative Cavity Ring-Down Spectroscopy.
PB97-112254 *04,394* Not available NTIS

Laser-Beam Analysis Pinpoints Critical Parameters.
PB94-212552 *04,240* Not available NTIS

Laser-Cooled Neutral Atom Frequency Standards.
PB96-160312 *04,086* Not available NTIS

Laser-Cooled Positron Source.
PB95-169348 *03,954* Not available NTIS

Laser Cooling.
PB95-151502 *03,908* Not available NTIS

Laser Cooling and the Recoil Limit.
PB97-111280 *04,391* Not available NTIS

Laser Cooling and Trapping for the Masses.
PB95-126090 *04,253* Not available NTIS

Laser Cooling of Trapped Ions.
PB95-168746 *03,950* Not available NTIS

Laser Doppler Velocimeter Studies of the Pipeflow Produced by a Generic Header.
PB95-226916 *02,602* PC A05/MF A01

Laser Double Resonance Measurements of the Quenching Rates of Br((2)P1/2) with H20, D20, HDO, and O2.
PB95-150694 *00,921* Not available NTIS

Laser Flash Photolysis, Time-Resolved Fourier Transform Infrared Emission Study of the Reaction Cl + C2H5 yields HCl(v) + C2H4.
PB95-203238 *01,049* Not available NTIS

Laser Flash Photolysis/Time-Resolved FTIR Emission Study of a New Channel in the Reaction of CH3+O: Production of CO(v).
PB95-164281 *00,974* Not available NTIS

Laser-Focused Atomic Deposition.
PB95-161618 *04,604* Not available NTIS

Laser Focused Atomic Deposition.
PB95-180659 *04,685* Not available NTIS

Laser Focusing of Atoms: A Particle Optics Approach.
PB94-216660 *03,870* Not available NTIS

Laser Gas Ionization Technique Monitors MEB Crystal Growth.
PB96-112172 *01,076* Not available NTIS

Laser Imaging of Chemistry-Flowfield Interactions: Enhanced Soot Formation in Time-Varying Diffusion Flames.
PB94-185352 *01,364* Not available NTIS

Laser-Induced Desorption of In and Ga from Si(100) and Adsorbate Enhanced Surface Damage.
PB95-203311 *01,050* Not available NTIS

Laser-Induced Desorption of NO from Si(111): Effects of Coverage on NO Vibrational Populations.
PB95-162319 *00,959* Not available NTIS

Laser-Induced Fluorescence Measurements of Formaldehyde in a Methane/Air Diffusion Flame.
PB94-211679 *01,374* Not available NTIS

Laser-Induced Fluorescence Measurements of OH. Concentrations in the Oxidation Region of Laminar, Hydrocarbon Diffusion Flames.
PB95-162160 *01,387* Not available NTIS

Laser-Induced Fluorescence Measurements of OH in Laminar Diffusion Flames in the Presence of Soot Particles.
PB96-123120 *01,409* Not available NTIS

Laser-Induced Fluorescence Measurements of Rotationally Resolved Velocity Distributions for CO(+) Drifted in He.
PB94-213139 *00,848* Not available NTIS

Laser Magnetic-Resonance Measurement of the (3)P1 - (3)P2 Fine-Structure Splittings in (17)O and (18)O.
PB95-175170 *00,994* Not available NTIS

Laser Melting of Thin Silicon Films.
PB94-199239 *04,471* Not available NTIS

Laser Modification of Ultracold Collisions: Experiment.
PB96-157987 *04,075* Not available NTIS

Laser Photoionization Measurements of Pressure in Vacuum.
PB95-180600 *03,964* Not available NTIS

Laser Preparation and Probing of Initial and Final Orbital Alignment in Collision-Induced Energy Transfer Ca(4s5p,(1)P1) + He yields Ca(4s5p,(3)P2) + He.
PB95-203261 *04,003* Not available NTIS

Laser-Produced and Tokamak Spectra of Lithiumlike Iron, Fe(23+).
PB95-180857 *04,314* Not available NTIS

Laser Spectroscopy of Carbon Monoxide: A Frequency Reference for the Far Infrared.
PB95-163606 *04,277* Not available NTIS

Laser-Synchrotron Hybrid Experiments: A Photon to Tickle, A Photon to Poke.
PB96-157847 *03,704* Not available NTIS

Laser Vacuum Ultraviolet Single Photon Ionization Probing of III-V Semiconductor Growth.
PB95-202370 *04,691* Not available NTIS

Lattice Dynamics of Ba1-xKxBiO3.
PB96-102421 *04,706* Not available NTIS

Lattice Dynamics of Semiconducting, Metallic, and Superconducting Ba1-xKxBiO3 Studied by Inelastic Neutron Scattering.
PB96-102447 *04,708* Not available NTIS

Lattice Imperfections Studied by Use of Lattice Green's Functions.
PB95-150850 *04,576* Not available NTIS

Lattice Model of a Hydrogen-Bonded Polymer Blend.
PB97-112262 *03,391* Not available NTIS

Lattice Position of Si in GaAs Determined by X-Ray Standing Wave Measurements.
PB95-164406 *04,632* Not available NTIS

Lattice Statics of Interfaces and Interfacial Cracks in Bimaterial Solids.
PB96-161823 *02,985* Not available NTIS

Lead Abatement in Buildings and Related Structures.
PB94-172038 *03,601* Not available NTIS

Leady Axisymmetric Modes in Infinite Clad Rods. Part 1.
PB95-162905 *04,187* Not available NTIS

Leakage Current Detection in Cryogenic Current Comparator Bridges.
PB94-172228 *02,024* Not available NTIS

Lean flammability limit as a fundamental refrigerant property. Phase 1, Interim technical report, 1 October 1994--31 March 1995.
DE95011238 *03,248* PC A03/MF A01

Learning to Change: Opportunities to Improve the Performance of Smaller Manufacturers.
PB94-166212 *00,010* PC A08/MF A02

Least-Cost Energy Decisions for Buildings: Part 2. Uncertainty and Risk Video Training Workbook.
PB94-165982 *00,240* PC A04/MF A01

Least-Cost Energy Decisions for Buildings. Part 3. Choosing Economic Evaluation Methods. Video Training Workbook.
PB95-253597 *00,265* PC A04/MF A01

Length Metrology of Complimentary Small Plastic Rulers.
PB96-161724 *04,096* Not available NTIS

Length Scales for Fragile Glass-Forming Liquids.
PB96-102801 *01,065* Not available NTIS

Lessons from the Establishment of the U.S. GOSIP Testing Program.
PB96-119359 *01,817* Not available NTIS

Lessons from the Loma Prieta Earthquake.
PB95-164091 *00,442* Not available NTIS

Lessons Learned by a Wing Engineer.
PB94-216421 *00,429* Not available NTIS

Letter Report on Flame Spread Testing of a Composite Material.
PB97-110068 *01,436* Not available NTIS

Life-Cycle Costing Manual for the Federal Energy Management Program. 1995 Edition.
PB96-172317 *02,511* PC A10/MF A02

Life-Cycle Costing Workshop for Energy Conservation in Buildings: Student Manual.
PB95-175006 *00,257* PC A11/MF A03

Life Prediction of a Continuous Fiber Reinforced Ceramic Composite Under Creep Conditions.
PB96-204128 *03,091* Not available NTIS

Light Scattered by Coated Paper.
PB94-216546 *04,245* Not available NTIS

Light Scattered from Two Atoms.
PB95-168753 *04,286* Not available NTIS

Light Scattering by Sinusoidal Surfaces: Illumination Windows and Harmonics in Standards.
PB97-110548 *04,387* Not available NTIS

Light Scattering from Glossy Coatings on Paper.
PB94-213246 *04,242* Not available NTIS

Light-Scattering Studies on Phase Separation in a Binary Blend with Addition of Diblock Copolymers.
PB96-146865 *01,286* Not available NTIS

Light-Weight Alloys for Aerospace Applications II.
PB96-190244 *03,375* Not available NTIS

Lighting and HVAC.
PB95-150991 *00,250* Not available NTIS

Lighting Quality and Light Source Size.
PB95-151783 *00,252* Not available NTIS

Lighting Research and Theory Can Create Business Prospects.
PB95-151791 *00,253* Not available NTIS

Lightwave Standards Development at NIST.
PB95-168563 *01,480* Not available NTIS

Limits of CO2 Monitoring in Determining Ventilation Rates.
PB95-176004 *02,552* Not available NTIS

Line-Heat-Source Guarded-Hot-Plate Apparatus.
PB97-118996 *00,417* Not available NTIS

Line-Reflect-Match Calibrations with Nonideal Microstrip Standards.
PB96-176599 *02,242* Not available NTIS

Lineshape Analysis of the Raman Spectrum of Diamond Films Grown by Hot-Filament and Microwave-Plasma Chemical-Vapor Deposition.
PB95-162392 *03,016* Not available NTIS

Linewidth Narrowing in an Imbalanced Y-Branch Waveguide Laser.
PB95-140844 *04,258* Not available NTIS

Linking Anisotropic Sharp and Diffuse Surface Motion Laws via Gradient Flows.
PB95-203378 *04,698* Not available NTIS

Liposome-Based Flow-Injection Immunoassay for Determining Theophylline in Serum.
PB94-213493 *03,494* Not available NTIS

Liquid and Solid Atomic Ion Plasmas.
PB94-198991 *03,809* Not available NTIS

Liquid Chromatographic Determination of Carotenoids in Human Serum Using an Engineered C30 and a C18 Stationary Phase.
PB97-119333 *03,512* Not available NTIS

Liquid Chromatographic Determination of Polycyclic Aromatic Hydrocarbon Isomers of Molecular Weight 278 and 302 in Environmental Standard Reference Materials.
PB95-164042 *02,523* Not available NTIS

Liquid Chromatographic Method for the Determination of Carotenoids, Retinoids, and Tocopherols in Human Serum and in Food.
PB95-153599 *00,593* Not available NTIS

Liquid Chromatography: Laser-Enhanced Ionization Spectrometry for the Speciation of Organolead Compounds.
PB94-185253 *00,530* Not available NTIS

Liquid-Hydrogen Cold Neutron Source for the NBSR.
PB95-151619 *03,729* Not available NTIS

Liquid-Nitrogen-Cooled High Tc Electrical Substitution Radiometer as a Broadband IR Transfer Standard.
PB96-158704 *02,198* PC A03/MF A01

Liquid-Scintillation Counting Techniques for the Standardization of Radionuclides Used in Therapy.
PB97-110084 *03,709* Not available NTIS

Literature Review on Seismic Performance of Building Cladding Systems.
PB96-106901 *00,455* PC A09/MF A02

Lithium-Drift Technique for Making Submicron Thick Silicon Membranes.
PB95-161386 *02,260* Not available NTIS

LMTO/CVM and LAPW/CVM Calculations of the Nickel Aluminide/Nickel Titanium Pseudobinary Phase Diagram.
PB94-199353 *03,323* Not available NTIS

Loading Device for Fracture Testing of Compact Tension Specimens in the Scanning Electron Microscope.
PB95-162434 *02,652* Not available NTIS

Loading Effects in Resistance Scaling.
PB97-111884 *02,285* Not available NTIS

Local Area Networks in NAA: Advantages and Pitfalls.
PB94-172095 *00,527* Not available NTIS

Local-Mode Dynamics in YH2 and YD2 by Isotope-Dilution Neutron Spectroscopy.
PB95-181012 *01,017* Not available NTIS

Local Oscillator Requirements and Strategies for the Next Generation of High-Stability Frequency Standards.
PB96-112230 *01,551* Not available NTIS

Local Partial Densities of States in Ni and Co Silicides Studied by Soft X-Ray Emission Spectroscopy.
PB94-212412 *04,504* Not available NTIS

Localization Model of Rubber Elasticity: Comparison with Torsional Data for Natural Rubber Networks in the Dry State.
PB95-107033 *03,195* Not available NTIS

Localization of a Homopolymer Dissolved in a Lamellar Structure of a Block Copolymer Studied by Small-Angle Neutron Scattering.
PB95-161592 *01,253* Not available NTIS

Localization of Atoms in a Three-Dimensional Standing Wave.
PB95-163887 *03,944* Not available NTIS

Locating Fire Engineering Information.
PB95-161188 *00,198* Not available NTIS

Locating Fire Information.
PB96-190137 *00,227* Not available NTIS

Location of a (1)A(sub g) State in Bithiophene.
PB95-202313 *01,025* Not available NTIS

Long-Lived Structures in Fragile Glass-Forming Liquids.
PB96-119565 *04,212* Not available NTIS

Long-Range Parity-Nonconserving Interaction.
PB95-202594 *03,986* Not available NTIS

Long-Term Performance of Engineered Concrete Barriers.
PB95-260816 *03,727* PC A03/MF A01

Long-Term Stability of Bayard-Alpert Gauge Performance: Results Obtained from Repeated Calibrations against the National Institute of Standards and Technology Primary Vacuum Standard.
PB96-123567 *02,676* Not available NTIS

Long-Term Stability of Carrier-Free Polonium Solution Standards.
PB94-185170 *00,685* Not available NTIS

Longterm Changes of Silicon Photodiodes and Their Use for Photometric Standardization.
PB94-211349 *04,234* Not available NTIS

Look at Uncertainties over Twenty Decades of Pressure Measurement.
PB95-168506 *02,655* Not available NTIS

Loss-Free Counting at IRI and NIST.
PB96-167119 *04,105* Not available NTIS

Low-Coherence Interferometric Measurement of Group Transit Times in Precision Optical Fibre Delay Lines.
PB95-168480 *02,158* Not available NTIS

Low Electrolytic Conductivity Standards.
PB96-122098 *01,081*
(Order as PB96-117767, PC A08/MF A02)

Low-Energy-Electron Collisions with Sodium: Elastic and Inelastic Scattering from the Ground State.
PB96-103106 *04,030* Not available NTIS

Low-Energy Electron Scattering from Caesium Atoms: Comparison of a Semirelativistic Breit-Pauli and a Full Relativistic Direc Treatment.
PB94-185030 *00,769* Not available NTIS

Low-Energy Vibrations and Octahedral Site Occupation in Nb95V5H(D)y.
PB96-160734 *01,133* Not available NTIS

Low-Frequency, Active Vibration Isolation System.
PB95-203303 *02,710* Not available NTIS

Low-Frequency Excitations of Oriented DNA.
PB96-137799 *03,548* Not available NTIS

Low-Frequency Model for Radio-Frequency Absorbers.
PB95-261939 *04,424*
(Order as PB95-261897, PC A07/MF A02)

Low Heat-Flux Measurements: Some Precautions.
PB96-201116 *02,685* Not available NTIS

Low Magnetostriction in Annealed NiFe/Ag Giant Magnetoresistive Multilayers.
PB96-146691 *04,762* Not available NTIS

Low-Noise High-Speed Diode Laser Current Controller.
PB95-202826 *02,178* Not available NTIS

Low Noise YBa2Cu3O7-x-SrTiO3-YBa2Cu3O7-x Mulitlayers for Improved Superconducting Magnetometers.
PB96-138417 *04,747* Not available NTIS

Low-Temperature Elastic Constants of Y1Ba2Cu3O7.
PB95-168837 *04,642* Not available NTIS

Low temperature fabrication from nano-size ceramic powders.
DE95013505 *03,029* PC A05/MF A01

Low Temperature H(sub 2)S Separation Using Membrane Reactor with Redox Catalyst.
DE94008991 *02,471* PC A02/MF A01

Low-Temperature Performance of Radiosonde Electric Hygrometer Elements.
AD-A295 319/8 *00,121* PC A02/MF A01

Low-Temperature Properties of Silver.
PB96-126198 *03,361*
(Order as PB96-126180, PC A05/MF A01)

Low Thermal Guarded Scanner for High Resistance Measurement Systems.
PB97-112452 *02,288* Not available NTIS

Low Voltage Standards in the 10 Hz to 1 MHz Range.
PB97-112569 *02,100* Not available NTIS

Lowest Excited Singlet State of Isolated 1-phenyl-1,3-butadiene and 1-phenyl-1,3,5-hexatriene.
PB95-202339 *01,026* Not available NTIS

LP11-Mode Leakage Loss in Coated Depressed Clad Fibers.
PB95-141115 *02,145* Not available NTIS

LRM Probe-Tip Calibrations Using Nonideal Standards.
PB96-135389 *02,411* Not available NTIS

LRM Probe-Tip Calibrations with Imperfect Resistors and Lossy Lines.
PB95-163952 *02,353* Not available NTIS

Lubrication Theory for Reactive Spreading of a Thin Drop.
PB95-189460 *02,865* PC A03/MF A01

Lubrication Theory for Reactive Spreading of a Thin Drop.
PB96-123427 *04,214* Not available NTIS

Lunar Laser Ranging: A Continuing Legacy of the Apollo Program.
PB95-202495 *03,683* Not available NTIS

M (also known as MUMPS) Validation Test Suite, Version 8.3 (for Microcomputers).
PB94-502077 *01,699* Diskette $250.00

Machine Performance Standard Provides Opportunity to Improve Quality and Productivity.
PB96-154521 *02,837* PC A02/MF A01

Machining Process Planning Activity Model for Systems Integration.
PB96-165428 *02,841* PC A03/MF A01

Macro- and Microreactions in Mechanical-Impact Tests of Aluminum Alloys.
PB95-107348 *03,340* Not available NTIS

Magnetic and Magnetoresistive Properties of Inhomogeneous Magnetic Dual-Layer Films.
PB95-169025 *04,646* Not available NTIS

Magnetic and Structural Properties of Electrodeposited Copper-Nickel Microlayered Alloys.
PB94-213121 *04,512* Not available NTIS

Magnetic Characteristics and Measurements of Filamentary Nb-Ti Wire for the Superconducting Super Collider.
DE94005988 *03,775* PC A02/MF A01

Magnetic Dead Layer in Fe/Si Multilayer: Profile Refinement of Polarized Neutron Reflectivity Data.
PB94-198363 *04,458* Not available NTIS

Magnetic Dielectric Oxides: Subsolidus Phase Relations in the BaO: Fe2O3: TiO2 System.
PB96-176524 *01,156* Not available NTIS

Magnetic Dipole Line from U LXXI Ground-Term Levels Predicted at 3200 Angstroms.
PB94-211497 *04,407* Not available NTIS

Magnetic Field Dependence of the Critical Current Anisotropy in Normal Metal-YBa2Cu3O7-delta Thin Film Bilayers.
PB95-141024 *04,550* Not available NTIS

Magnetic Fields in Star-Forming Regions: Observations.
PB96-123005 *00,100* Not available NTIS

Magnetic Flux Pinning in Epitaxial YBa2Cu3O7-delta Thin Films.
PB96-200746 *04,795* Not available NTIS

Magnetic Force Microscopy Images of Magnetic Garnet with Thin-Film Magnetic Tip.
PB95-176210 *04,669* Not available NTIS

Magnetic Force Microscopy of Flux in Superconductors.
PB95-161733 *04,608* Not available NTIS

Magnetic Measurement of Transport Critical Current Density of Granular Superconductors.
PB95-126199 *04,531* Not available NTIS

Magnetic Moments in Cr Thin Films on Fe(100).
PB95-108429 *04,525* Not available NTIS

Magnetic Neutron Scattering (Invited).
PB95-150074 *04,557* Not available NTIS

Magnetic Ordering of the Cu Spins in PrBa2Cu3O6+x.
PB95-140547 *04,545* Not available NTIS

Magnetic Properties of Pd/Co Multilayers.
PB94-198751 *04,465* Not available NTIS

Magnetic Properties of Single-Crystalline UCu3Al2.
PB95-180717 *04,686* Not available NTIS

Magnetic Rare Earth Artificial Metallic Superlattices.
PB95-162293 *04,611* Not available NTIS

Magnetic Structure and Spin Dynamics of the Pr and Cu in Pr2CuO4.
PB96-111836 *04,036* Not available NTIS

Magnetic Structure Determination for Annealed Ni80Fe20/Ag Multilayers Using Polarized-Neutron Reflectivity.
PB96-176615 *03,739* Not available NTIS

Magnetic Susceptibility of Pr2-xCexCuO4 Monocrystals and Polycrystals.
PB95-180253 *04,677* Not available NTIS

Magneto-Optic Magnetic Field Sensor with 1.4pT/square root of 1(Hz) Minimum Detectable Field at 1 kHz.
PB94-199551 *02,125* Not available NTIS

Magneto-Optic Magnetic Field Sensors Based on Uniaxial Iron Garnet Films in Optical Waveguide Geometry.
PB95-153409 *02,152* Not available NTIS

Magneto-Optic Magnetic Field Sensors Based on Uniaxial Iron Garnet Films in Optical Waveguide Geometry.
PB95-168498 *02,159* Not available NTIS

Magneto-Optic Rotation Sensor Using a Laser Diode as Both Source and Detector.
PB97-111272 *04,390* Not available NTIS

Magneto-Optical Trapping of Metastable Xenon: Isotope-Shift Measurements.
PB95-151254 *03,905* Not available NTIS

Magneto-Transport Properties of HgCdTe.
PB95-175840 *04,661* Not available NTIS

Magnetocaloric Effect in Nanocomposites.
PB95-162798 *04,618* Not available NTIS

Magnetocaloric Effect in Rapidly Solidified Nd-Fe-Al-B Materials.
PB94-185667 *04,451* Not available NTIS

Magnetocaloric Effect of Ferromagnetic Particles.
PB94-185857 *04,453* Not available NTIS

Magnetoelasticity in Rare-Earth Multilayers and Films.
PB94-211356 *04,495* Not available NTIS

Magnetometer Calibration Services.
PB97-113252 *01,993* Not available NTIS

Magnetooptic Effects.
PB96-119292 *04,338* Not available NTIS

Magnetoresistance of Thin-Film NiFe Devices Exhibiting Single-Domain Behavior.
PB96-147087 *04,766* Not available NTIS

Magnetostriction and Giant Magnetoresistance in Annealed NiFe/Ag Multilayers.
PB96-102603 *04,716* Not available NTIS

Majority and Minority Electron and Hole Mobilities in Heavily Doped Gallium Aluminum Arsenide.
PB97-118335 *04,814* Not available NTIS

Majority and Minority Mobilities in Heavily Doped Silicon for Device Simulations.
PB94-198728 *02,311* Not available NTIS

Making Connections.
PB97-119044 *01,785* Not available NTIS

Making Displays Deliver a Full Measure.
PB96-122411 *01,490* Not available NTIS

Making Sense of Software Engineering Environment Framework Standards.
PB95-105037 *01,701* PC A03/MF A01

Manager's Guide for Monitoring Data Integrity in Financial Systems.
PB96-165915 *00,003* PC A05/MF A01

Manipulation of Adsorbed Atoms and Creation of New Structures on Room-Temperature Surfaces with a Scanning Tunneling Microscope.
PB95-151536 *04,578* Not available NTIS

Manual for Ventilation Assessment in Mechanically Ventilated Commercial Buildings.
PB94-145653 *00,239* PC A07/MF A02

Manufactured Homes: Probability of Failure and the Need for Better Windstorm Protection through Improved Anchoring Systems.
PB95-143129 *00,432* PC A04/MF A01

Manufactured Housing Walls That Provide Satisfactory Moisture Performance in All Climates.
PB95-178885 *00,383* PC A03/MF A01

Mapping Domains in Proteins: Dissection and Expression of 'Escherichia coli' Adenylyl Cyclase.
PB96-155460 *03,478* Not available NTIS

Mapping Integration Definition for Function Modeling (IDEFO) Model into CASE Data Interchange Format (CDIF) Transfer File.
PB96-109533 *01,741* PC A07/MF A02

Mapping Integration Definition for Information Modeling (IDEF1X) Model into CASE Data Interchange Format (CDIF) Transfer File.
PB95-154670 *01,711* PC A06/MF A02

Mapping Processes to Processors for Space-Based Robot Systems.
PB95-151510 *04,833* Not available NTIS

Mapping the Droplet Transfer Modes for an ER100S-1 GMAW Electrode.
PB96-190095 *03,295* Not available NTIS

MasPar MP-1 as a Computer Arithmetic Laboratory.
PB95-189437 *01,627* PC A03/MF A01

MasPar MP-1 as a Computer Arithmetic Laboratory.
PB96-179155 *01,617*
(Order as PB96-177381, PC A07/MF A02)

Mass and Density Determinations.
PB94-200672 *00,504* Not available NTIS

Mass Assay and Uniformity Test of Boron Targets by Neutron Beam Methods.
PB97-119085 *04,175* Not available NTIS

Mass Unit Disseminated to Surrogated Laboratories Using the NIST Portable Mass Calibration Package.
PB94-142486 *03,781* PC A03/MF A01

Material Characterization By a Time-Resolved and Polarization-Sensitive Ultrasonic Technique.
PB97-122576 *02,764* Not available NTIS

Materials and Fire Threat.
PB97-122311 *01,442* Not available NTIS

Materials Aspects of Fiber-Reinforced Polymer Composites in Infrastructure.
PB96-210695 *03,184* PC A04/MF A01

Materials Reliability. Technical Activities, 1995.
PB96-183082 *02,999* PC A07/MF A02

Materials Science and Engineering Laboratory Annual Report, December 1993.
PB95-254439 *02,668* PC A03/MF A01

Materials Science and Engineering Laboratory Annual Report, 1993. NAS-NRC Assessment Panel, April 21-22, 1994.
PB94-162534 *02,969* PC A05/MF A01

Materials Science and Engineering Laboratory Annual Report, 1994. NAS-NRC Assessment Panel, April 6-7, 1995.
PB95-196697 *02,976* PC A06/MF A02

Materials Science and Engineering Laboratory Annual Report, 1995. Technical Activities.
PB96-214754 *03,009* PC A05/MF A01

Materials-Science Based Approach to Phenol Emissions from a Flooring Material in an Office Building.
PB97-118749 *02,572* Not available NTIS

Materials Science with SR Using X-Ray Imaging: Spatial-Resolution/Source Size.
PB94-213048 *04,510* Not available NTIS

Mathematical Analysis of Practices to Control Moisture in the Roof Cavities of Manufactured Houses.
PB97-106843 *00,278* PC A05/MF A01

Mathematical Aspects of Rietveld Refinement.
PB95-108601 *04,526* Not available NTIS

Mathematical Modeling and Computer Simulation of Fire Phenomena.
PB95-180063 *00,384* Not available NTIS

Mathematical Modeling of Human Egress from Fires in Residential Buildings.
PB94-193778 *00,337* PC A05/MF A02

Mathematical Models of Transport Phenomena Associated with Arc-Welding Processes: A Survey.
PB96-135058 *02,870* Not available NTIS

Matrix Grain Bridging Contribution to the Toughness of Whisker Reinforced Ceramics.
PB94-198645 *03,134* Not available NTIS

Matrix Isolation Study of the Interaction of Excited Neon Atoms with BCl3: Infrared Spectra of BCl(sub 3, sup +), BCl(sub 2, sup +), and BCl(sub 3, sup -).
PB97-119143 *01,187* Not available NTIS

Matrix Isolation Study of the Interaction of Excited Neon Atoms with O3: Infrared Spectrum of O((sub 3)(-)) and Evidence for the Stabilization of O2...O((sub 4)(+)).
PB97-112403 *04,155* Not available NTIS

Maturity Functions for Concrete Made with Various Cements and Admixtures.
PB94-199502 *01,314* Not available NTIS

Maturity Method.
PB94-199494 *01,313* Not available NTIS

Maximum Entropy as a Tool for the Determination of the C-Axis Profile of Layered Compounds.
PB94-199619 *00,800* Not available NTIS

Maximum Permissible Amounts of Radioisotopes in the Human Body and Maximum Permissible Concentrations in Air and Water.
AD-A280 281/7 *03,609* PC A04/MF A01

Maximum Permissible Body Burdens and Maximum Permissible Concentrations of Radionuclides in Air and in Water for Occupational Exposure.
AD-A280 282/5 *03,610* PC A06/MF A02

MCNP Model of the National Bureau of Standards Reactor (NBSR) Core.
PB96-138599 *03,733* Not available NTIS

Measured Stopping Powers of Hydrogen and Helium in Polystyrene Near Their Maximum Values.
PB96-112321 *04,729* Not available NTIS

Measurement Accuracies for Various Techniques for Measuring Amplifier Noise.
PB95-163671 *02,350* Not available NTIS

Measurement and Calibration of Large-Area Alpha-Particle Sources at NIST.
PB94-172855 *03,791* Not available NTIS

Measurement and Determination of Radon Source Potential: A Literature Review.
PB94-165602 *02,576* PC A09/MF A03

Measurement and Interpretation of Tidal Tilts in a Small Array.
PB96-102611 *03,686* Not available NTIS

Measurement and Reduction of Alignment Errors of the NIST Watt Experiment.
PB97-111959 *01,987* Not available NTIS

Measurement and Simulation of Photoluminescence Spectra from Vertical-Cavity Quantum-Well Laser Structures.
PB95-169181 *02,170* Not available NTIS

Measurement and Uncertainty of a Calibration Standard for the Scanning Electron Microscope.
PB94-219250 *00,560*
(Order as PB94-219219, PC A06/MF A02)

Measurement Comparability, Traceability, and Measurement Assurance Programs.
PB97-111850 *02,692* Not available NTIS

Measurement Methods and Algorithms for Comparison of Local and Remote Clocks.
PB96-102652 *01,549* Not available NTIS

Measurement Methods and Standards for Processing and Application of Thermal Barrier Coatings.
N95-26123/6 *01,447*
(Order as N95-26119, PC A03/MF A01)

Measurement of Absorbed Dose of Neutrons, and of Mixtures of Neutrons and gamma rays.
AD-A286 647/3 *03,710* PC A05/MF A01

Measurement of Ascorbic Acid in Human Plasma and Serum: Stability, Intralaboratory Repeatability, and Interlaboratory Reproducibility.
PB97-112445 *03,511* Not available NTIS

Measurement of Atmospheric Methyl Bromide Using Gravimetric Gas Standards.
PB96-155494 *02,497* Not available NTIS

Measurement of Boron at Silicon Wafer Surfaces by Neutron Depth Profiling.
PB94-211059 *04,487* Not available NTIS

Measurement of CO Pressures in the Ultrahigh Vacuum Regime Using Resonance-Enhanced Multiphoton-Ionization Time-of-Flight Mass Spectroscopy.
PB94-216041 *03,864* Not available NTIS

Measurement of Diffusion in Fluid Systems: Applications to the Supercritical Fluid Region.
PB95-175188 *02,490* Not available NTIS

Measurement of Diffusion in Supercritical Fluid Systems: A Review.
PB94-199189 *00,795* Not available NTIS

Measurement of Patterned Film Linewidth for Interconnect Characterization.
PB96-148168 *02,420* Not available NTIS

Measurement of Process Complexity.
PB97-113138 *01,781* Not available NTIS

Measurement of Radial Dose Distributions Around Small Beta Particle Emitters Using High Resolution Radiochromic Foil Dosimetry.
PB95-164604 *03,518* Not available NTIS

Measurement of Radiative Feedback to the Fuel Surface of a Pool Fire.
PB94-211604 *02,477* Not available NTIS

Measurement of Rheological Properties of High Performance Concrete: State of the Art Report.
PB96-202338 *00,414* PC A04/MF A01

Measurement of Room Conditions and Response of Sprinklers and Smoke Detectors during a Simulated Two-Bed Hospital Patient Room Fire.
PB94-213717 *00,292* PC A07/MF A02

Measurement of S2OF10, and S2O2F10 Production Rates from Spark and Negative Glow Corona Discharge in SF6/O2 Gas Mixtures.
PB96-123740 *01,093* Not available NTIS

Measurement of Surface Tension of Tantalum by a Dynamic Technique in a Microgravity Environment.
PB95-161667 *03,932* Not available NTIS

Measurement of the Atomic Na(3P) Lifetime and of Retardation in the Interaction between Two Atoms Bound in a Molecule.
PB97-122360 *04,178* Not available NTIS

Measurement of the Heat of Fusion of Tungsten by a Microsecond-Resolution Transient Technique.
PB94-216686 *03,400* Not available NTIS

Measurement of the J=2 less than 1 Fine-Structure Interval for (28)Si and (29)Si in the Ground (3)P State.
PB94-185097 *00,771* Not available NTIS

Measurement of the Neutron Lifetime.
PB96-161708 *04,094* Not available NTIS

Measurement of the Self Broadening of the H2Q(0-5) Raman Transitions from 295 to 1000 K.
PB95-108627 *00,884* Not available NTIS

Measurement of the Thermal Properties of Electrically Conducting Fluids Using Coated Transient Hot Wires.
DE94017816 *00,722* PC A02/MF A01

Measurement of the Thermal Properties of Electrically Conducting Fluids Using Coated Transient Hot Wires.
PB95-169058 *03,269* Not available NTIS

Measurement of the Uniformity of Particle Deposition of Filter Cassette Sampling in a Low Velocity Wind Tunnel.
PB95-163754 *02,549* Not available NTIS

Measurement of the Weak-Localization Complex Conductivity at 1 Ghz in Disordered Ag Wires.
PB96-117239 *04,731* Not available NTIS

Measurement of the (10)B(n, alpha1gamma)(7)Li Cross Section in the 0.3 to 4 MeV Neutron Energy Interval.
PB96-161799 *04,098* Not available NTIS

Measurement of the (93)Nb(n,2n) (92m)Nb Cross Section in a (235)U Fission Spectrum.
PB95-163986 *03,945* Not available NTIS

Measurement of the (235)U(n,f) Reaction from Thermal to 1 keV.
PB95-140422 *03,886* Not available NTIS

Measurement of Very Low Frequency Vibrations.
PB96-102660 *03,687* Not available NTIS

Measurement of Very-Low Partial Pressures.
PB95-180998 *02,659* Not available NTIS

Measurements of Fluorescence from Cold Atoms: Localization in Three-Dimensional Standing Waves.
PB95-163879 *03,943* Not available NTIS

Measurements of Indoor Pollutant Emissions from EPA Phase II Wood Stoves.
PB95-198735 *02,556* PC A04/MF A01

Measurements of Moisture Diffusivity for Porous Building Materials.
PB95-107397 *00,356* Not available NTIS

Measurements of Molar Heat Capacity at Constant Volume (Cv) for 1,1,1,2-Tetrafluoroethane (R134a).
PB95-168878 *03,264* Not available NTIS

Measurements of Outdoor Air Distribution in an Office Building.
PB95-210944 *00,264* PC A04/MF A01

Measurements of Permittivity and the Dielectric Loss Tangent of Low Loss Dielectric Materials with a Dielectric Resonator Operating on the Higher Order Te(sub 0 gamma delta) Modes.
PB96-111869 *02,273* Not available NTIS

Measurements of Properties of Materials in Electronic Packaging.
PB96-200837 *01,973* Not available NTIS

Measurements of quantum electrodynamic sensitive transitions in Na-like and Cu-like ions: Final report, 1 October 1993--29 September 1994.
DE95011593 *04,403* PC A02/MF A01

Measurements of Shielding Effectiveness and Cavity Characteristics of Airplanes.
PB94-210051 *00,030* PC A04/MF A01

Measurements of the Characteristic Impedance of Coaxial Air Line Standards.
PB95-168787 *02,221* Not available NTIS

Measurements of the Relative Permittivity of Liquid Water at Frequencies in the Range of 0.1 to 10 kHz and at Temperatures between 273.1 and 373.2 K at Ambient Pressure.
PB96-119375 *01,078* Not available NTIS

Measurements of the Resonance Lines of (6)Li and (7)Li by Doppler-Free Frequency-Modulation Spectroscopy.
PB96-180211 *04,118* Not available NTIS

Measurements of the Vapor Pressures of Difluoromethane, 1-Chloro-1,2,2,2-Tetrafluoroethane, and Pentafluoroethane.
PB95-169272 *03,270* Not available NTIS

Measurements of the Virial Coefficients and Equation of State of the Carbon Dioxide + Ethane System in the Supercritical Region.
PB95-151353 *03,906* Not available NTIS

Measurements of the Viscosities of Saturated and Compressed Fluid 1-chloro-1,2,2,2-tetrafluoroethane (R124) and Pentafluoroethane (R125) at Temperatures between 120 and 420 K.
PB94-199791 *03,254* Not available NTIS

Measurements of the Viscosities of Saturated and Compressed Liquid 1,1,1,2-Tetrafluoroethane (R134a), 2,2-Dichloro-1,1,1-Trifluoroethane (R123) and 1,1-Dichloro-1-Fluoroethane (R141b).
PB95-175386 *03,273* Not available NTIS

Measurements of the (235)U(n,f) Cross Section in the 3 to 30 MeV Neutron Energy Region.
PB97-119051 *04,172* Not available NTIS

Measurements of the (237)Np(n,f) Cross Section.
PB97-119069 *04,173* Not available NTIS

Measurements of Thermophysical Properties of Nickel Near Its Melting Temperature by a Microsecond-Resolution Transient Technique.
PB96-102579 *04,210* Not available NTIS

Measuring Contact Charge Transfer at Interfaces: A New Experimental Technique.
PB95-164570 *03,053* Not available NTIS

Measuring Hydrogen by Cold-Neutron Prompt-Gamma Activation Analysis.
PB96-111877 *00,612* Not available NTIS

Measuring Long Gage Blocks with the NIST Line Scale Interferometer.
PB95-242400 *02,665* PC A03/MF A01

Measuring Matching Wear Scars on Balls and Flats.
PB95-151528 *03,153* Not available NTIS

Measuring Nondipolar Asymmetries of Photoelectron Angular Distributions.
PB97-122493 *01,193* Not available NTIS

Measuring Performance of Parallel Computers. Final Report.
DE94014586 *01,665* PC A03/MF A01

Measuring Performance of Parallel Computers. Progress Report, 1989.
DE94014587 *01,666* PC A03/MF A01

Measuring the Stability of Three Copper Alloys.
PB94-199866 *03,326* Not available NTIS

Mechanical Properties and Warm Prestress of Ultra-Low Carbon Steel at 4 K.
PB96-190350 *03,224* Not available NTIS

Mechanism and Rate Constants for the Reactions of Hydrogen Atoms with Isobutene at High Temperatures.
PB95-151064 *00,929* Not available NTIS

Mechanism of Defect Formation in Low-Dose Oxygen Implanted Silicon-on-Insulator Material.
PB97-111462 *02,453* Not available NTIS

Mechanism of Mild to Severe Wear Transition in Alpha-Alumina.
PB94-212354 *03,233* Not available NTIS

Mechano-Chemical Model: Reaction Temperatures in a Concentrated Contact.
PB96-119466 *03,227* Not available NTIS

Meissner, Shielding, and Flux Loss Behavior in Single-Crystal YBa2Cu3O6+x.
PB94-198744 *04,464* Not available NTIS

Melnikov Function and Homoclinic Chaos Induced by Weak Perturbations.
PB95-180923 *03,414* Not available NTIS

Melting Behavior of Organic Materials Confined in Porous Solids.
PB94-212313 *00,834* Not available NTIS

Membrane Gas Separation for a Fluidized-Bed Incinerator.
PB95-169041 *02,550* Not available NTIS

Membrane-Mediated Precipitation of Calcium Phosphate in Model Liposomes with Matrix Vesicle-Like Lipid Composition.
PB95-164547 *03,468* Not available NTIS

Memory Function Approach to the Shape of Pressure Broadened Molecular Bands.
PB95-152930 *00,944* Not available NTIS

MEMS in Standard CMOS VLSI Technology.
PB96-102363 *02,377* Not available NTIS

Merged-Beams Energy-Loss Technique for Electron-Ion Excitation: Absolute Total Cross Sections for O(5+) (2s yields 2p).
PB96-102058 *04,017* Not available NTIS

Mesoscopic Conductance Fluctuations in Large Devices.
PB96-119656 *04,735* Not available NTIS

Metallic-Barrier Junctions for Programmable Josephson Voltage Standards.
PB96-200134 *02,089* Not available NTIS

Metalloporphyrin Sensitized Photooxidation of Water to Oxygen on the Surface of Colloidal Iridium Oxides - Photochemical and Pulse Radiolytic Studies.
PB95-107082 *00,868* Not available NTIS

Metallurgy Technical Activities 1994 (NAS-NRC Assessment Panel, April 6-7, 1995).
PB96-136981 *02,981* PC A08/MF A02

Metallurgy. Technical Activities, 1995.
PB96-195284 *03,003* PC A09/MF A02

Method and Evaluation of Character Stroke Preservation on Handprint Recognition.
PB95-251724 *01,850* PC A03/MF A01

Method for Determining Both Magnetostriction and Elastic Modulus by Ferromagnetic Resonance.
PB95-150108 *02,974* Not available NTIS

Method for the Assay of Hydrolytic Enzymes Using Dynamic Light Scattering.
PB95-151411 *03,531* Not available NTIS

Method of Estimating the Parameters of Tuned Mass Dampers for Seismic Applications.
PB96-167820 *00,473* PC A04/MF A01

Method of Predicting Smoke Movement in Atria with Application to Smoke Management.
PB95-154746 *00,376* PC A05/MF A01

Method of Realizing Spectral Irradiance Based on an Absolute Cryogenic Radiometer.
PB95-161204 *04,270* Not available NTIS

Method of Sale for CNG Paves Way to Greater Public Acceptance.
PB95-168449 *02,489* Not available NTIS

Method to Determine a Basis Set of Paths to Perform Program Testing.
PB96-131503 *01,747* PC A03/MF A01

Method to Determine the Calorimetric Equivalence Correction for a Coaxial Microwave Microcalorimeter.
PB95-202404 *01,913* Not available NTIS

Methodologies for Predicting the Service Lives of Coating Systems.
PB95-146387 *03,124* PC A05/MF A01

Methodology for Developing and Implementing Alternative Temperature-Time Curves for Testing the Fire Resistance of Barriers for Nuclear Power Plant Applications.
PB96-193784 *03,742* PC A07/MF A02

Methodology for Electromagnetic Interference Measurements.
PB96-200126 *02,014* Not available NTIS

Methodology for the Certification of Reference Specimens for Determination of Oxygen Concentration in Semiconductor Silicon by Infrared Spectrophotometry.
PB96-155478 *02,421* Not available NTIS

Methods for Aligning the NIST Watt-Balance.
PB96-123153 *01,934* Not available NTIS

Methods for Analysis of Cancer Chemopreventive Agents in Human Serum.
PB95-200648 *03,502* PC A07/MF A02

Methods of Measuring Humidity and Testing Hygrometers.
AD-A278 851/1 *00,123* PC A03/MF A01

Methods to Improve the Accuracy of On-Line Ultrasonic Measurement of Steel Sheet Formability.
PB96-186051 *02,281* Not available NTIS

Methyl Torsional Levels of Solid Acetonitrile (CH3CN): A Neutron Scattering Study.
PB95-151015 *00,926* Not available NTIS

Metric for Success.
PB94-187630 *02,633* PC A03/MF A01

Metric Path to Global Markets and New Jobs: A Question-and-Answer and Thematic Discussion.
PB94-206307 *02,601* PC A02/MF A01

Metrication.
PB94-172079 *03,676* Not available NTIS

METRICATION: An Economic Wake-Up Call for Surveyors and Mappers.
PB96-159629 *03,680* Not available NTIS

Metrological Accuracy of the Electron Pump.
PB95-168910 *03,951* Not available NTIS

Metrological Measurement Accuracy: Discussion of 'Measurement Error Models' by Leon Jay Gleser.
PB94-200607 *00,551* Not available NTIS

Metrology.
PB95-164497 *03,946* Not available NTIS

Metrology.
PB96-160759 *02,925* Not available NTIS

Metrology and Data for Microelectronic Packaging and Interconnection: Results of a Joint Workshop on Materials Metrology and Data for Commercial Electrical and Optical Packaging and Interconnection Technologies. Held in Gaithersburg, Maryland on May 5-6, 1994. Volume 1. Results.
PB95-143111 *02,328* PC A05/MF A01

Metrology and Data for Microelectronic Packaging and Interconnection: Results of a Joint Workshop on Materials Metrology and Data for Commercial Electrical and Optical Packaging and Interconnection Technologies. Held in Gaithersburg, Maryland on May 5-6, 1994. Volume 2. Presentation Material.
PB95-143327 *02,330* PC A08/MF A02

Metrology and Regional Trade Pacts.
PB96-155429 *02,923* Not available NTIS

Metrology Applications of Mode-Locked Erbium Fiber Lasers.
PB95-140158 *04,256* Not available NTIS

Metrology Approach to Unifying Rockwell C Hardness Scales.
PB96-155551 *02,957* Not available NTIS

Metrology for Electromagnetic Technology: A Bibliography of NIST Publications.
PB94-159761 *02,116* PC A04/MF A01

Metrology for Electromagnetic Technology: A Bibliography of NIST Publications.
PB95-135588 *02,143* PC A05/MF A01

Metrology for Electromagnetic Technology: A Bibliography of NIST Publications.
PB97-116057 *04,396* PC A06/MF A01

Metrology for Electromagnetic Technology: A Bibliography of NIST Publications, September 1995.
PB96-128269 *01,938* PC A05/MF A01

Metrology Issues in Terahertz Physics and Technology.
PB96-128277 *01,939* PC A08/MF A02

Metrology Model for Submicrometer Dimensional Measurements.
PB95-108502 *02,647* Not available NTIS

Metrology Requirements of Future Space Power Systems.
PB95-140984 *04,840* Not available NTIS

Metrology Standards for Advanced Semiconductor Lithography Referenced to Atomic Spacings and Geometry.
PB96-160718 *02,424* Not available NTIS

Metropolitan Areas (Including MSAs, CMSAs, PMASs, and NECMAs). Category: Data Standards and Guidelines; Subcategory: Representations and Codes.
FIPS PUB 8-6 *04,873* PC E09

Michaelis-Menten Equation for an Enzyme in an Oscillating Electric Field.
PB95-140489 *00,906* Not available NTIS

Micro-Mechanical Aspects of Asperity-Controlled Friction in Fiber-Toughened Ceramic Composites.
PB94-199536 *03,136* Not available NTIS

Microanalysis to Nanoanalysis: Measuring Composition at High Spatial Resolution.
PB95-107173 *00,563* Not available NTIS

Microbial Degradation of Polysulfides and Insights into Their Possible Occurrence in Coal.
PB95-163374 *02,488* Not available NTIS

Microdosimetry and Cellular Radiation Effects of Radon Progency in Human Bronchial Airways.
PB95-152344 *03,625* Not available NTIS

Microelectronic Test Structures for Feature Placement and Electrical Linewidth Metrology.
PB95-180568 *02,367* Not available NTIS

Microelectronic Test Structures for Overlay Metrology.
PB96-164249 *02,430* Not available NTIS

Microform Calibration Uncertainties of Rockwell Diamond Indenters.
PB96-122114 *03,280*
(Order as PB96-117767, PC A08/MF A02)

Microform Calibrations in Surface Metrology.
PB95-203295 *02,951* Not available NTIS

Microlithography by Using Neutral Metastable Atoms and Self-Assembled Monolayers.
PB96-190038 *02,441* Not available NTIS

Micromachined Coplanar Waveguides in CMOS Technology.
PB97-119283 *02,456* Not available NTIS

Micromachined Display Output for a Cellular Neural Network.
PB96-156070 *02,422* Not available NTIS

Micromagnetic Model of Dual-Layer Magnetic-Recording Thin Films.
PB95-141065 *04,551* Not available NTIS

Micromagnetic Scanning Microprobe System.
PB95-176178 *02,224* Not available NTIS

Micromagnetic Simulations of Tunneling Stabilized Magnetic Force Microscopy.
PB95-141073 *04,552* Not available NTIS

Micromagnetic Structure of Domains in Co/Pt Multilayers. 1. Investigations of Wall Structure.
PB95-162111 *04,610* Not available NTIS

Micromechanics of Densification and Distortion.
PB94-200326 *03,327* Not available NTIS

Micromechanics of Fracture in Rubber-Toughened Epoxies.
PB94-212222 *03,011* Not available NTIS

Microstrains and Domain Sizes in Bi-Cu-O Superconductors: An X-Ray Diffraction Peak-Broadening Study.
PB94-198520 *04,461* Not available NTIS

Microstructural Characterization of Cobalt-Tungsten Coated Graphite Fibers.
PB96-159231 *01,951*
(Order as PB96-159215, PC A07/MF A02)

Microstructural Evolution in Two-Dimensional Two-Phase Polycrystals.
PB94-211992 *04,498* Not available NTIS

Microstructural Features of Some Low Water/Solids, Silica Fume Mortars Cured at Different Temperatures.
PB94-160777 *00,330* PC A03/MF A01

Microstructure and Ferroelectric Properties of Lead Zirconate-Titanate Films Produced by Laser Evaporation.
PB94-199148 *04,470* Not available NTIS

Microstructure and Tensile Properties of Microalloyed Steel Forgings.
PB94-172715 *03,204* Not available NTIS

Microstructure Effect on the Phase Behavior of Blends of Deuterated Polybutadiene and Protonated Polyisopene.
PB97-113146 *01,296* Not available NTIS

Microstructure Study of Molybdenum Liners by Neutron Diffraction.
PB95-202396 *03,756* Not available NTIS

Microwave and Submillimeter Spectroscopy of Ar-NH3 States Correlating with Ar+NH3(j=1, k=1).
PB95-152211 *00,942* Not available NTIS

Microwave Characterization of Flip-Chip MMIC Components.
PB96-176722 *02,434* Not available NTIS

Microwave Characterization of Flip-Chip MMIC Interconnections.
PB96-176730 *02,435* Not available NTIS

Microwave Characterization of Printed Circuit Transmission Lines.
PB96-122585 *02,077* Not available NTIS

Microwave Diagnostic Results from the Gaseous Electronics Conference RF Reference Cell.
PB96-113378 *02,392*
(Order as PB96-113311, PC A09/MF A03)

Microwave Dielectric Properties of Anisotropic Materials at Cryogenic Temperatures.
PB96-137765 *02,412* Not available NTIS

Microwave Leakage as a Source of Frequency Error and Long-Term Instability in Cesium Atomic-Beam Frequency Standards.
PB95-180501 *01,541* Not available NTIS

Microwave Noise in High-Tc Josephson Junctions.
PB96-148010 *04,771* Not available NTIS

Microwave Properties of Voltage-Tunable YBa2Cu3O7-delta/SrTiO3 Coplanar Waveguide Transmission Lines.
PB96-141262 *02,235* Not available NTIS

Microwave Properties of YBa2Cu3O7-x Films at 35 GHz from Magnetotransmission and Magnetoreflection Measurements.
PB95-168977 *04,643* Not available NTIS

Microwave Spectra of van der Waals Complexes of Importance in Planetary Atmospheres.
PB95-150611 *00,919* Not available NTIS

Microwave Spectrum and Structure of CH2O-H2O.
PB97-118723 *04,168* Not available NTIS

Microwave Spectrum and Structure of CH3NO2-H2O.
AD-A296 377/5 *00,719* PC A03/MF A01

Mid- and Near-Infrared Spectra of Water and Water Dimer Isolated in Solid Neon.
PB95-125662 *00,888* Not available NTIS

Millimeter- and Submillimeter-Wave Spectrum of trans-Ethyl Alcohol.
PB96-145578 *01,102* Not available NTIS

Millimeter-Resolution Optical Time-Domain Reflectometry Using a Four-Wave Mixing Sampling Gate.
PB96-122700 *02,190* Not available NTIS

Millisecond-Resolution Pulse Heating System for Specific-Heat Measurements at High Temperatures.
PB94-199999 *02,635* Not available NTIS

Milliwatt Mixer for Small Fluid Samples.
PB94-198819 *02,634* Not available NTIS

Minimum Mass Flux Requirements to Suppress Burning Surfaces with Water Sprays.
PB96-183181 *01,425* PC A05/MF A01

Minutes of the CAALS Workshop on modularity and communications standards.
DE95005780 *02,621* PC A03/MF A01

Mixed Diet Reference Materials for Nutrient Analysis of Foods: Preparation of SRM-1548 Total Diet.
PB95-151692 *03,593* Not available NTIS

Mixed Phospholipid Liposome Calcification.
PB94-211190 *03,457* Not available NTIS

Mixing and Radiation Properties of Buoyant Luminous Flame Environments.
PB96-202254 *01,432* PC A06/MF A01

Mixing and Radiation Properties of Buoyant Turbulent Diffusion Flames.
PB95-242327 *01,396* PC A05/MF A02

Mixing Plate-Like and Rod-Like Molecules with Solvent: A Test of Flory-Huggins Lattice Statistics.
PB96-126206 *03,173*
(Order as PB96-126180, PC A05/MF A01)

Modal Characteristics of Bent Dual Mode Planar Optical Waveguide.
PB95-180485 *04,311* Not available NTIS

Modal Properties of Circular and Noncircular Optical Waveguides.
PB95-125944 *04,251* Not available NTIS

Mode Coupling and Loss on Tapered Optical Waveguides.
PB95-168571 *04,282* Not available NTIS

Mode-Locked Lasers for High-Accuracy Radiometry.
PB96-204201 *04,134* Not available NTIS

Mode Specific Vibrational Predissociation Dynamics in Fragile Molecules.
PB95-107132 *00,871* Not available NTIS

Model for Calculating Virial Coefficients of Natural Gas Hydrocarbons with Impurities.
PB96-156047 *04,064* Not available NTIS

Model for Determining the Density and Mobility of Carriers in Thin Semiconducting Layers with Only Two Contacts.
PB96-102702 *02,378* Not available NTIS

Model for Microcrack Initiation and Propagation beneath Hertzian Contacts in Polycrystalline Ceramics.
PB96-163704 *03,077* Not available NTIS

Model for Toughness Curves in Two-Phase Ceramics. 1. Basic Fracture Mechanics.
PB96-180088 *03,085* Not available NTIS

Model for Toughness Curves in Two-Phase Ceramics. 2. Microstructural Variables.
PB96-163795 *03,078* Not available NTIS

Model Minimum Performance Specifications for Lidar Speed Measurement Devices.
PB95-197455 *04,861* PC A03/MF A01

Model of an Optical Roughness-Measuring Instrument.
PB97-110209 *04,384* Not available NTIS

Model Precast Concrete Beam-to-Column Connections Subject to Cyclic Loading.
PB95-153094 *00,438* Not available NTIS

Modeling and Test Point Selection for a Thermal Transfer Standard.
PB95-161287 *01,896* Not available NTIS

Modeling Buffer Layer IGBT's for Circuit Simulation.
PB96-164173 *02,429* Not available NTIS

Modeling Buffer Layer IGBTs for Circuit Simulation.
PB95-153805 *02,344* Not available NTIS

Modeling Ceramic Sub-Micron Particle Formation from the Vapor Using Detailed Chemical Kinetics: Comparison with In-situ Laser Diagnostics.
PB95-151965 *00,671* Not available NTIS

Modeling Detector Response for Neutron Depth Profiling.
PB96-157813 *04,066* Not available NTIS

Modeling Effects of Temperature Annealing on Giant Magnetoresistive Response in Discontinuous Multilayer NiFe/Ag Films.
PB97-112585 *04,157* Not available NTIS

Modeling of Extreme Loading by 'Peaks Over Threshold' Methods.
PB96-159694 *00,469* Not available NTIS

Modeling Polarization Curves and Impedance Spectra for Simple Electrode Systems.
PB94-198876 *03,188* Not available NTIS

Modeling Radon Transport in Multistory Residential Buildings.
PB95-162087 *00,256* Not available NTIS

Modeling the Evolution of Structure in Unstable Solid Solution Phases by Diffusional Mechanisms.
PB94-199403 *03,324* Not available NTIS

Modelling Drying Shrinkage of Cement Paste and Mortar. Part 1. Structural Models from Angstroms to Millimeters.
PB96-135132 *03,074* Not available NTIS

Modelling the Leaching of Calcium Hydroxide from Cement Paste: Effects on Pore Space Percolation and Diffusivity.
PB94-198793 *01,311* Not available NTIS

Models and Interactions.
PB94-216306 *02,641* Not available NTIS

Models, Managing Models, Quality Models: An Example of Quality Management.
PB94-163466 *02,891* PC A03/MF A01

Models of Granualr Giant Magnetoresistance Multilayer Thin Films.
PB96-190228 *01,968* Not available NTIS

Modern Test Methods for Flammability.
PB94-198447 *01,370* Not available NTIS

Modification of a Commercial SEM with a Computer Controlled Cathode Stabilized Power Supply.
PB96-201066 *04,129* Not available NTIS

Modification of Cast Epoxy Resin Surfaces during Exposure to Partial Discharges.
PB96-122734 *01,086* Not available NTIS

Modification of Deoxyribose-Phosphate Residues by Extracts of Ataxia Telangiectasia Cells.
PB94-212602 *03,458* Not available NTIS

Modification of DNA Bases in Chromatin of Intact Target Human Cells by Activated Human Polymorphonuclear Leukocytes.
PB94-199833 *03,526* Not available NTIS

Modification of the Phase Stability of Polymer Blends by Diblock Copolymer Additivies.
PB96-123542 *03,172* Not available NTIS

Modified Airy Function Method for the Analysis of Tunneling Problems in Optical Waveguides and Quantum Well Structures.
PB94-185824 *02,120* Not available NTIS

Modified Effective Range Theory as an Alternative to Low-Energy Close-Coupling Calculations.
PB95-202701 *03,988* Not available NTIS

Modified Leung-Griffiths Model of Vapor-Liquid Equilibrium: Extended Scaling and Binary Mixtures of Dissimilar Fluids.
PB94-216108 *00,851* Not available NTIS

Modified Optimal Algorithm for Active Structural Control.
PB96-165949 *00,472* PC A04/MF A01

Modified Surface-Active Monomers for Adhesive Bonding to Dentin.
PB95-151163 *00,158* Not available NTIS

Modified Surface Layers and Coatings.
PB95-176087 *03,125* Not available NTIS

Modulation of Fossil Fuel Production by Global Temperature Variations, 2.
PB94-146636 *02,533* PC A04/MF A01

Moisture and Water-Induced Crack Growth in Optical Materials.
PB95-153334 *04,267* Not available NTIS

Molar Absorptivities of Bilirubin (NIST SRM 916A) and Its Neutral and Alkaline Azopigments.
PB94-211042 *03,456* Not available NTIS

Molar Heat Capacity at Constant Volume for Air from 67 to 300 K at Pressures to 35 MPa.
PB96-163738 *00,515* Not available NTIS

Molar Heat Capacity at Constant Volume for (xCO2 + (1-x)C2H6) from 220 to 340 K at Pressures to 35 MPa.
PB96-167135 *01,148* Not available NTIS

Molecular-Beam Optothermal Spectrum of the OH Stretching Band of Methanol.
PB94-212826 *00,839* Not available NTIS

Molecular Dynamics Investigation of the Surface/Bulk Equilibrium in an Ethanol-Water Solution.
PB97-113112 *01,183* Not available NTIS

Molecular Ion Imaging and Dynamic Secondary Ion Mass Spectrometry of Organic Compounds.
PB95-126124 *00,571* Not available NTIS

Molecular Microwave Spectra Tables.
AD-A296 498/9 *00,720* PC A03/MF A01

Molecular Orbital Calculations of Bond Rupture in Brittle Solids.
PB95-164059 *00,973* Not available NTIS

Molecular Orbital Study of Water Enhanced Crack Growth Process.
PB95-164067 *03,240* Not available NTIS

Molecular Spectroscopy.
PB94-213337 *03,861* Not available NTIS

Molecular Weight Dependence of the Lamellar Domain Spacing of ABC Triblock Copolymers and Their Chain Conformation in Lamellar Domains.
PB95-161691 *01,254* Not available NTIS

Moments of the Quartic Assignment Statistic with an Application to Multiple Regression.
PB95-181103 *03,442* Not available NTIS

Monitoring Polymer Cure by Fluorescence Recovery After Photobleaching.
PB94-211422 *01,218* Not available NTIS

MONSEL-II: Monte Carlo Simulation of SEM Signals for Linewidth Metrology.
PB96-102710 *02,379* Not available NTIS

Monte Carlo and Analytic Methods in the Transport of Electrons, Neutrons, and Alpha Particles.
PB96-111612 *04,033* Not available NTIS

Monte Carlo and Mean-Field Calculations of the Magnetocaloric Effect of Ferromagnetically Interacting Clusters.
PB94-172087 *03,201* Not available NTIS

Monte Carlo Approach to the Approximation of Invariant Measures.
PB94-172053 *03,409* Not available NTIS

Monte Carlo Electron Trajectory Simulation of X-Ray Emission from Films Supported on Substrates.
PB95-107207 *04,522* Not available NTIS

Monte Carlo Model for SEM Linewidth Metrology.
PB95-150058 *02,331* Not available NTIS

Monte Carlo Simulation of Scanning Electron Microscope Signals.
PB96-200969 *02,444* Not available NTIS

Montgomery Education Connection and Resource Education Awareness Partnership Making Connections between Local Schools and NIST Volunteers.
PB96-159769 *00,134* Not available NTIS

Morphological Development of Second-Phase Particles in Elastically-Stressed Solids.
PB95-181111 *03,355* Not available NTIS

Morphological Estimation of Tip Geometry for Scanned Probe Microscopy.
PB95-203444 *02,662* Not available NTIS

Morphological Stability.
PB95-153318 *04,591* Not available NTIS

Morphology and Phase Separation Kinetics of a Compatibilized Blend.
PB97-119135 *01,297* Not available NTIS

Morphology of Symmetric Diblock Copolymers as Revealed by Neutron Reflectivity.
PB95-140075 *01,234* Not available NTIS

Motion-Model-Based Boundary Extraction.
PB95-189502 *01,849* PC A03/MF A01

Move-to-Root Rule for Self-Organizing Trees with Markov Dependent Requests.
PB96-179528 *03,431* Not available NTIS

Multi-Agency Certification and Accreditation (C and A) Process: A Worked Example.
PB95-171955 *01,601* PC A05/MF A01

Multi-Scale Picture of Concrete and Its Transport Properties: Introduction for Non-Cement Researchers.
PB97-115802 *03,107* PC A05/MF A01

Multi-Stage, Position Stabilized Vibration Isolation System for Neutron Interferometry.
PB95-175022 *03,955* Not available NTIS

Multi-State Two-Port: An Alternative Transfer Standard.
PB95-168530 *02,049* Not available NTIS

Multiattribute Decision Analysis Method for Evaluating Buildings and Building Systems.
PB96-158670 *00,325* PC A06/MF A01

Multicarrier Characterization Method for Extracting Mobilities and Carrier Densities of Semiconductors from Variable Magnetic Field Measurements.
PB94-212776 *02,317* Not available NTIS

Multichannel Quantum Defect Half Collision Analysis of K2 Photodissociation Through the B1Pi(sub u) State.
PB94-211125 *00,812* Not available NTIS

Multijunction Thermal Converters by Commercial CMOS Fabrication.
PB95-153664 *02,343* Not available NTIS

Multimedia Tutorial on Phase Equilibria Diagrams.
PB96-200829 *03,088* Not available NTIS

Multiphoton Ionization of SiH3 and SiD3 Radicals: Electronic Spectra, Vibrational Analyses of the Ground and Rydberg States, and Ionization Potential.
PB94-212503 *00,837* Not available NTIS

Multiphoton Ionization of SiH3 and SiD3 Radicals. 2. Three Photon Resonance-Enhanced Spectra Observed between 460 and 610 nm.
PB94-212487 *00,835* Not available NTIS

Multiphoton Ionization Spectroscopy Measurements of Silicon Atoms during Vapor Phase Synthesis of Ceramic Particles.
PB95-151999 *03,913* Not available NTIS

Multiwavelength Birefringent-Cavity Mode-Locked Fibre Laser.
PB95-150496 *04,262* Not available NTIS

Multizone Modeling of Three Residential Indoor Air Quality Control Options.
PB96-146659 *02,565* Not available NTIS

Multizone Modeling of Three Residential Indoor Air Quality Control Options.
PB96-165782 *02,567* PC A08/MF A02

Mutual Phase Locking in Systems of High-Tc Superconductor-Normal Metal-Superconductor Junctions.
PB96-135348 *04,744* Not available NTIS

MV++ v. 1.5a Matrix/Vector Class Reference Guide.
PB96-195326 *01,777* PC A03/MF A01

n-Value and Second Derivative of the Superconductor Voltage-Current Characteristic.
PB95-126223 *04,533* Not available NTIS

n-Vector Correlations in Collision Dynamics with Atomic Orbital Alignment: The Importance of Coherence Denoting Azimuthal Structure for n (greater than or equal to) 3.
PB95-202545 *03,983* Not available NTIS

N2(a'(sup 1)Sigma(sub g)(sup +)) Metastable Collisional Destruction and Rotational Excitation Transfer by N2.
PB95-151395 *00,933* Not available NTIS

Nano-Defects in Commercial Bonded SOI and SIMOX.
PB96-123674 *02,407* Not available NTIS

Nanocomposite Magnetic Materials.
PB95-162780 *04,617* Not available NTIS

Nanofabrication of a Two-Dimensional Array Using Laser-Focused Atomic Deposition.
PB96-119417 *04,732* Not available NTIS

Nanoindentation and Instrumented Scratching Measurements on Hard Coatings.
PB97-122477 *03,111* Not available NTIS

Nanometrology.
PB96-160726 *02,425* Not available NTIS

Nanoscale Study of the As-Grown Hydrogenated Amorphous Silicon Surface.
PB95-150595 *04,573* Not available NTIS

Nanoscale Study of the Hydrogenated Amorphous Silicon Surface.
PB96-103056 *04,720* Not available NTIS

Nanostructure Fabrication via Direct Writing with Atoms Focused in Laser Fields.
PB95-150272 *04,564* Not available NTIS

Nanostructure Fabrication via Laser-Focused Atomic Deposition (Invited).
PB96-204094 *04,132* Not available NTIS

Narrow-Band Tunable Diode Laser System with Grating Feedback, and a Saturated Absorption Spectrometer for Cs and Rb.
PB95-202891 *04,319* Not available NTIS

NASA Fire Detector Study.
PB96-183108 *01,423* PC A04/MF A01

National Center for Standards and Certification Information: Service and Programs.
N95-15938/0 *02,717*

(Order as N95-15919/0, PC A11/MF A03)

National Construction Sector Goals: Industry Strategies for Implementation.
PB95-269817 *00,204* PC A03/MF A01

National Information Infrastructure and Advanced Digital Video.
PB96-119367 *01,488* Not available NTIS

National Institute of Standards and Technology High-Accuracy Cryogenic Radiometer.
PB96-179585 *04,378* Not available NTIS

National Institute of Standards and Technology Resonance Ionization Spectroscopy/Resonance Ionization Mass Spectroscopy Data Service.
PB94-172897 *03,793* Not available NTIS

National Measurement System for Radiometry, Photometry, and Pyrometry Base Upon Absolute Detectors.
PB97-108559 *04,382* PC A04/MF A01

National PDES Testbed: An Overview.
PB95-125829 *02,775* Not available NTIS

National Planning for Construction and Building R and D.
PB96-137104 *00,324* PC A06/MF A02

National Quality Assurance Program for Personnel Radiation Dosimetry: A Case History.
PB94-211273 *03,620* Not available NTIS

National Semiconductor Metrology Program, Project Portfolio FY 1996.
PB96-195268 *04,789* PC A03/MF A01

National Standard Petroleum Oil Tables.
AD-A279 952/6 *02,469* PC A09/MF A02

National Status and Trends Program Specimen Bank: Sampling Protocols, Analytical Methods, Results, and Archive Samples.
PB97-119226 *02,598* Not available NTIS

National Type Evaluation Program: Index of Device Evaluations by Company. NCWM Publication 5 Part A (Second Edition).
PB94-160835 *02,889* PC A05/MF A01

National Voluntary Laboratory Accreditation Program Acoustical Testing Services.
PB95-182234 *04,188* PC A05/MF A01

National Voluntary Laboratory Accreditation Program: Bulk Asbestos Analysis.
PB95-138129 *02,541* PC A04/MF A01

National Voluntary Laboratory Accreditation Program: Carpet and Carpet Cushion.
PB95-155560 *00,295* PC A04/MF A01

National Voluntary Laboratory Accreditation Program: Construction Materials Testing.
PB95-155552 *01,319* PC A05/MF A01

National Voluntary Laboratory Accreditation Program: Electromagnetic Compatibility and Telecommunications. FCC Methods.
PB95-242376 *02,664* PC A06/MF A02

National Voluntary Laboratory Accreditation Program: Energy Efficient Lighting Products.
PB94-219060 *02,642* PC A04/MF A01

National Voluntary Laboratory Accreditation Program. GOSIP: Government Open Systems Interconnection Profile.
PB95-267993 *01,486* PC A06/MF A02

National Voluntary Laboratory Accreditation Program: Ionizing Radiation Dosimetry.
PB95-128658 *03,623* PC A06/MF A02

National Voluntary Laboratory Accreditation Program (NVLAP): Commercial Products Testing.
PB95-267944 *02,671* PC A02/MF A01

National Voluntary Laboratory Accreditation Program (NVLAP): Fasteners and Metals.
PB97-114185 *02,881* PC A06/MF A01

National Voluntary Laboratory Accreditation Program (NVLAP): Wood Based Products.
PB95-170429 *03,405* PC A04/MF A01

National Voluntary Laboratory Accreditation Program: POSIX. Portable Operating System Interface.
PB95-189478 *02,661* PC A05/MF A01

National Voluntary Laboratory Accreditation Program: Procedures and General Requirements.
PB94-178225 *02,630* PC A03/MF A01

National Voluntary Laboratory Accreditation Program: Thermal Insulation Materials.
PB95-267985 *02,977* PC A05/MF A01

National Voluntary Laboratory Accreditation Program 1994 Directory.
PB94-178969 *00,482* PC A08/MF A02

National Voluntary Laboratory Accreditation Program 1995 Directory.
PB95-174454 *00,483* PC A08/MF A02

National Voluntary Laboratory Accreditation Program 1996 Directory.
PB96-162714 *00,485* PC A10/MF A03

Natural Convection from an Array of Electronic Packages Mounted on a Horizontal Board in a Narrow Aspect Ratio Enclosure.
PB96-164017 *02,087* Not available NTIS

Nature of (001) Tilt Grain Boundaries in YBa2Cu3O6+x.
PB95-126033 *04,528* Not available NTIS

NBS/NIST Peltier-Effect Microcalorimeter: A Four-Decade Review.
PB96-102769 *01,064* Not available NTIS

Nd:LiTaO3 Waveguide Laser.
PB95-140851 *04,259* Not available NTIS

Near Critical Fluid Interfaces: A Comparison of Theory and Experiment.
PB95-140166 *00,901* Not available NTIS

Necessary Condition for Homoclinic Chaos Induces by Additive Noise.
PB96-155775 *04,063* Not available NTIS

Need for Advanced Characterization Techniques in Product Manufacturing: A Case Study on Ceramic Matrix Composites.
PB96-204060 *03,089* Not available NTIS

Need for, and Availability of, Working Fluid Property Data: Results from Annexes XIII and XVIII.
PB95-168969 *03,268* Not available NTIS

Needs for Brachytherapy Source Calibrations in the United States.
PB97-110092 *03,521* Not available NTIS

Neighbor Tables for Molecular Dynamics Simulations.
PB95-171948 *00,991* PC A03/MF A01

Network Brokers Handbook: An Entrepreneurial Guide to Cooperative Strategies for Manufacturing Competitiveness.
PB95-219325 *00,490* PC A08/MF A02

Neutron and Raman Spectroscopies of 134 and 134a Hydrofluorocarbons Encaged in Na-X Zeolite.
PB96-186168 *03,001* Not available NTIS

Neutron and X-Ray Scattering Cross Sections of Orientationally Disordered Soild C60.
PB95-153300 *00,951* Not available NTIS

Neutron Capture Prompt Gamma-Ray Activation Analysis at the NIST Cold Neutron Research Facility.
PB94-213394 *00,556* Not available NTIS

Neutron Diffraction Texture Study of Deformed Uranium Plates.
PB97-111587 *03,010* Not available NTIS

Neutron Energy Deposition on the Nanometer Scale.
PB95-152260 *03,624* Not available NTIS

Neutron Focusing Lens Using Polycapillary Fibers.
PB95-141206 *03,889* Not available NTIS

Neutron Focusing Lens Using Polycapillary Fibers.
PB95-153078 *03,922* Not available NTIS

Neutron Leakage Benchmark for Criticality Safety Research.
PB95-126132 *03,723* Not available NTIS

Neutron Measurement Intercomparisons Sponsored by CCEMRI, Section 3 (Neutron Measurements).
PB94-199916 *03,819* Not available NTIS

Neutron Powder Diffraction Study of a Na, Cs-Rho Zeolite.
PB94-198629 *00,791* Not available NTIS

Neutron Powder Diffraction Study of the Crystal Structure of YSr2AlCu2O7.
PB94-212073 *04,499* Not available NTIS

Neutron-Powder-Diffraction Study of the Long-Range Order in the Octahedral Sublattice of LaD2.25.
PB96-141155 *04,753* Not available NTIS

Neutron Powder Diffraction Study of the Nuclear and Magnetic Structures of the Oxygen-Deficient Perovskite YBaCuCoO5.
PB95-161097 *00,954* Not available NTIS

Neutron Powder Diffraction Study of the Structures of La1.9Ca1.1Cu2O6 and La1.9Sr1.1Cu2O6+Delta.
PB95-140042 *04,538* Not available NTIS

Neutron Reflectivity of End-Grafted Polymers: Concentration and Solvent Quality Dependence in Equilibrium Conditions.
PB94-185758 *01,206* Not available NTIS

Neutron Reflectivity Study of the Density Profile of a Model End-Grafted Polymer Brush: Influence of Solvent Quality.
PB95-202735 *01,274* Not available NTIS

Neutron Reflectometry Studies of Surface Oxidation.
PB95-150421 *00,917* Not available NTIS

Neutron Scattering by Hydrogen in Cold Neutron Prompt Gamma-Activation Analysis.
PB95-175972 *00,603* Not available NTIS

Neutron Scattering by Multiblock Copolymers of Structure (A-B)N-A.
PB94-211547 *01,219* Not available NTIS

Neutron Scattering Structural Study of AlCuFe Quasicrystals Using Double Isotopic Substitution.
PB94-200458 *04,485* Not available NTIS

Neutron Scattering Studies of Surfaces and Interfaces.
PB94-216207 *04,517* Not available NTIS

Neutron-Scattering Studies of the Two Magnetic Correlation Lengths in Terbium.
PB95-152328 *04,586* Not available NTIS

Neutron Scattering Study of Antiferromagnetic Order in the Magnetic Superconductors RNi2B2C.
PB97-112411 *04,812* Not available NTIS

Neutron-Scattering Study of C60(n-) (n=3,6) Librations in Alkali-Metal Fullerides.
PB94-200219 *00,806* Not available NTIS

Neutron-Scattering Study of Librations and Intramolecular Phonons in Rb2.6K0.4C60.
PB95-162269 *00,958* Not available NTIS

Neutron Scattering Study of Shear Induced Turbidity in Polystyrene/Dioctyl Phthalate Solutions at High Shear Rates.
PB94-172624 *01,197* Not available NTIS

Neutron Scattering Study of Shear Induced Turbidity in Polystyrene Dissolved in Dioctyl Phthalate.
PB95-161865 *01,256* Not available NTIS

Neutron Scattering Study of the Lattice Modes of Solid Cubane.
PB96-147152 *01,126* Not available NTIS

Neutron Scattering Study of the Orientation of a Liquid Crystalline Polymer by Shear Flow.
PB95-180196 *01,270* Not available NTIS

Neutron Spectroscopic Comparison of beta-Phase Rare Earth Hydrides.
PB96-160742 *01,134* Not available NTIS

Neutron Spectroscopic Comparison of Rare-Earth/Hydrogen alpha-Phase Systems.
PB95-163523 *00,970* Not available NTIS

Neutron Spectroscopic Evidence of Concentration-Dependent Hydrogen Ordering in the Octahedral Sublattice of beta-TbH2+x.
PB95-181020 *01,018* Not available NTIS

Neutron-Spectroscopy Study of the Hydrogen Vibrations in Hydrogen-Doped YBa2Cu3Ox.
PB94-172475 *04,441* Not available NTIS

Neutron Standard Cross Sections in Reactor Physics: Need and Status.
PB94-199510 *03,813* Not available NTIS

Neutron Techniques in Materials Science and Related Disciplines.
PB96-119698 *02,980* Not available NTIS

New Alloys Show Extraordinary Resistance to Fracture and Wear.
PB95-151346 *03,346* Not available NTIS

New and Revised Half-Life Measurement Results.
PB96-160346 *00,695* Not available NTIS

New Approach for Reducing the Toxicity of the Combustion Products from Flexible Polyurethane Foam.
PB96-123625 *01,411* Not available NTIS

New Coaxial Microwave Microcalorimeter Evaluation Technique.
PB95-153227 *01,892* Not available NTIS

New Concepts for Fire Protection of Passenger Rail Transportation Vehicles.
PB95-162046 *04,850* Not available NTIS

New Concepts for Fire Protection of Passenger Rail Transportation Vehicles. (NIST Reprint).
PB95-180774 *04,863* Not available NTIS

New Concepts of Precision Dimensional Measurement for Modern Manufacturing.
PB96-160684 *02,924* Not available NTIS

New Critical Review of Experimental Stark Widths and Shifts.
PB94-172830 *03,790* Not available NTIS

New cw CO2 Laser Lines: The 9-mu m Hot Band.
PB95-168548 *04,281* Not available NTIS

New Data and Correlations for the Custody Transfer of Natural Gas Liquids.
PB96-176664 *02,499* Not available NTIS

New Electronic States of NH and ND Observed from 258 to 288 nm by Resonance Enhanced Multiphoton Ionization Spectroscopy.
PB94-212495 *00,836* Not available NTIS

New EPR Dosimeter Based on Polyvinylalcohol.
PB94-199700 *03,619* Not available NTIS

New Exact Solution of the One-Dimensional Schrodinger Equation and Its Application to Polarized Neutron Reflectometry.
PB95-161832 *04,609* Not available NTIS

New Expressions of Uncertainties for Humidity Calibrations at the National Institute of Standards and Technology.
PB95-103826 *02,645* PC A02/MF A01

New Extrapolation/Spherical/Cylindrical Measurement Facility at the National Institute of Standards and Technology.
PB95-153755 *02,004* Not available NTIS

New Generation of Fire Resistant Polymers. Part 1. Computer-Aided Molecular Design.
PB96-160593 *01,419* Not available NTIS

New High-Redshift Damped Lyman-alpha Absorption Systems and the Redshift Evolution of Damped Absorbers.
PB95-203501 *00,083* Not available NTIS

New International Representations of the Volt and Ohm Effective January 1, 1990.
PB95-150777 *01,890* Not available NTIS

New IUPAC Guidelines for the Reporting of Stable Hydrogen, Carbon, and Oxygen Isotope-Ratio Data. Letter to the Editor.
PB95-261962 *01,058*
(Order as PB95-261897, PC A07/MF A02)

New Mass Transport Elements and Components for the NIST IAQ Model.
PB95-255899 *02,558* PC A05/MF A01

New Materials, Advanced Ceramics and Standards.
PB95-140208 *03,047* Not available NTIS

New Mechanisms for Laser Cooling.
PB95-153268 *03,923* Not available NTIS

New Method for Achieving Accurate Thickness Control for Uniform and Graded Multilayer Coatings on Large Flat Substrates.
PB96-159744 *04,366* Not available NTIS

New Method for Realizing a Luminous Flux Scale Using an Integrating Sphere with an External Source.
PB96-102843 *04,333* Not available NTIS

New Method for Shielding Electron Beams Used for Head and Neck Cancer Treatment.
PB94-211430 *03,621* Not available NTIS

New Method for the Detection and Measurement of Polyaromatic Carcinogens and Related Compounds by DNA Intercalation.
PB96-167382 *03,481* Not available NTIS

New Method to Calculate Looming for Autonomous Obstacle Avoidance.
PB95-171435 *01,600* PC A03/MF A01

New Method to Evaluate Deposit Forming Tendencies of Liquid Lubricants by Differential Scanning Calorimetry.
PB95-152120 *01,451* Not available NTIS

New Model of 1/F Noise in Baw Quartz Resonators.
PB96-112248 *02,383* Not available NTIS

New NIST/ARPA National Soft X-ray Reflectometry Facility.
PB96-158092 *04,080* Not available NTIS

New NIST Rapid Pneumatic Tube System.
PB96-167259 *03,738* Not available NTIS

New Oxide Degradation Mechanism for Stresses in the Fowler-Nordheim Tunneling Regime.
PB96-200985 *04,128* Not available NTIS

New Physics-Based Model for Time-Dependent- Dielectric-Breakdown.
PB96-186093 *02,440* Not available NTIS

New Physics-Based Model for Time-Dependent- Dielectric-Breakdown.
PB96-201132 *02,448* Not available NTIS

New Refractometer by Combining a Variable Length Vacuum Cell and a Double-Pass Michelson Interferometer.
PB97-111926 *01,986* Not available NTIS

New Rydberg States of Aluminum Monofluoride Observed by Resonance-Enhanced Multiphoton Ionization Spectroscopy.
PB94-199544 *00,797* Not available NTIS

New Surface-Active Comonomer for Adhesive Bonding.
PB96-204052 *03,579* Not available NTIS

New Test Structure for Nanometer-Level Overlay and Feature-Placement Metrology.
PB95-175345 *02,363* Not available NTIS

New Values for Silicon Reference Materials, Certified for Isotope Abundance Ratios. Letter to the Editor.
PB94-219268 *00,863*
(Order as PB94-219219, PC A06/MF A02)

New 5 and 10 MHz High Isolation Distribution Amplifier.
PB96-190202 *01,510* Not available NTIS

Next Generation Computer Resources: Reference Model for Project Support Environments (Version 2.0).
PB94-143401 *01,677* PC A06/MF A02

Nickel(II)-Mediated Oxidative DNA Base Damage in Renal and Hepatic Chromatin of Pregnant Rats and Their Fetuses. Possible Relevance to Carcinogenesis.
PB94-212628 *03,646* Not available NTIS

Nickel-63 Standardization: 1968-1995.
PB97-111819 *00,701* Not available NTIS

Niobium Microbolometers for Far-Infrared Detection.
PB96-111729 *02,184* Not available NTIS

NIOSH Comments to DOL on Risk Estimates from the Cadmium Cohort Study by L. Stayner, February 7, 1992.
PB95-267779 *03,604* PC A02/MF A01

NIOSH Pocket Guide to Chemical Hazards.
PB95-100368 *03,603* PC$14.00/MF A04

NIR-Spectroscopic Investigation of Water Sorption Characteristics of Dental Resins and Composites.
PB95-151171 *00,189* Not available NTIS

NIST and the Navy: Past, Present and Future.
PB96-119649 *03,655* Not available NTIS

NIST Assessment of ITS-90 Non-Uniqueness for 25.5 Ohm SPRTs at Gallium, Indium and Cadmium Fixed Points.
PB96-161310 *00,631* Not available NTIS

NIST ATM Network Simulator: Operation and Programming, Version 1.0.
PB96-106851 *01,487* PC A04/MF A01

NIST Calibration of ASTM E127-Type Ultrasonic Reference Blocks.
PB94-191640 *02,702* PC A03/MF A01

NIST Capacitance Measurement Assurance Program (MAP).
PB94-200060 *02,254* Not available NTIS

NIST Comparison of the Quantized Hall Resistance and the Realization of the SI Ohm Through the Calculable Capacitor.
PB97-119184 *02,291* Not available NTIS

NIST Comparison of the Quantized Hall Resistance and the Realization of the SI Ohm Through the Calculable Capacitor. Conference Proceedings, June 17-20, 1996.
PB97-119192 *02,292* Not available NTIS

NIST Construction Automation Program Report No. 2. Proceedings of the NIST Construction Automation Workshop. Held in Gaithersburg, Maryland on March 30-31, 1995.
PB96-202239 *00,413* PC A09/MF A02

NIST Cooperative Laboratory for OSI Routing Technology.
DE94015308 *01,791* PC A03/MF A01

NIST-Coordinated Standard for Fingerprint Data Interchange.
PB94-216645 *01,808* Not available NTIS

NIST Crystallographic Databases for Research and Analysis.
PB97-109094 *04,801*
(Order as PB97-109011, PC A11/MF A03)

NIST Detector-Based Luminous Intensity Scale.
PB96-179114 *01,864*
(Order as PB96-177381, PC A07/MF A02)

NIST Form-Based Handprint Recognition System.
PB94-217106 *01,838* PC A04/MF A01

NIST Frequency Measurement Service.
PB96-200662 *01,561* Not available NTIS

NIST Handbook 44, 1994: Specifications, Tolerances and Other Technical Requirements for Weighing and Measuring Devices as Adopted by the 78th National Conference on Weights and Measures 1993.
PB94-136009 *02,888* PC A11/MF A03

NIST Handbook 44, 1995: Specifications, Tolerances and Other Technical Requirements for Weighing and Measuring Devices as Adopted by the 79th National Conference on Weights and Measures 1994.
PB95-146379 *02,903* PC A11/MF A03

NIST Handbook 44, 1996: Specifications, Tolerances, and Other Technical Requirements for Weighing and Measuring Devices as Adopted by the 80th National Conference on Weights and Measures, 1995.
PB96-166616 *02,926* PC A13/MF A03

NIST High-Accuracy Sampling Wattmeter.
PB97-108575 *02,689* PC A04/MF A01

NIST High Accuracy Scale for Absolute Spectral Response from 406 nm to 920 nm.
PB96-179122 *01,865*
(Order as PB96-177381, PC A07/MF A02)

NIST Implementation and Realization of the ITS-90 Over the Range 83 K to 1235 K: Reproducibility, Stability, and Uncertainties.
PB96-161328 *00,632* Not available NTIS

NIST Industrial Impacts: A Sampling of Successful Partnerships.
PB95-111514 *00,488* PC A05/MF A01

NIST Industrial Impacts: A Sampling of Successful Partnerships (Revision, March 1995).
PB95-209193 *00,489* PC A05/MF A01

NIST Internet Time Service.
AD-P009 132/2 *01,519* PC A02/MF A01

NIST Lighting and HVAC Interaction Test Facility.
PB95-151007 *00,251* Not available NTIS

NIST List of Publications, LP 103, March 1996. National Semiconductor Metrology Program.
PB96-175856 *02,432* PC A07/MF A02

NIST Measurement Assurance of SPRT Calibrations on the ITS-90: A Quantitative Approach.
PB96-161336 *00,633* Not available NTIS

NIST Measurement Assurance Program for Capacitance Standards at 1 kHz.
PB96-172333 *02,276* PC A03/MF A01

NIST Measurement Services: NIST Pressure Calibration Service.
PB94-164043 *02,892* PC A06/MF A02

NIST Metrology for Soft X-ray Multilayer Optics.
PB96-160379 *04,088* Not available NTIS

NIST Metrology Program on Electromagnetic Characterization of Materials.
PB96-156062 *01,944* Not available NTIS

NIST Model PM2 Power Measurement System for 1 mW at 1 GHz.
PB94-135803 *02,018* PC A03/MF A01

NIST/NCMS Program on Electronic Packaging: First Update.
PB96-204086 *03,008* Not available NTIS

NIST-NRL Free-Electron Laser Facility.
PB94-212511 *04,237* Not available NTIS

NIST Optically Pumped Cesium Frequency Standard.
PB94-211117 *03,835* Not available NTIS

NIST POSIX Testing Program.
PB96-160973 *01,821* Not available NTIS

NIST Power Reference Source.
PB94-211513 *00,148* Not available NTIS

NIST Program for Investigating Error Reporting Capabilities of Optical Disk Drives.
PB96-160627 *01,635* Not available NTIS

NIST Reactor: Summary of Activities October 1992 through September 1993.
PB94-161502 *04,437* PC A08/MF A02

NIST Reactor: Summary of Activities, October 1993 through September 1994.
PB95-220430 *04,700* PC A09/MF A02

NIST Reference Materials to Support Accuracy in Drug Testing.
PB96-123807 *03,505* Not available NTIS

NIST Research on Less-Flammable Materials.
PB97-118632 *01,439* Not available NTIS

NIST Research Program on the Seismic Resistance of Partially-Grouted Masonry Shear Walls.
PB94-219052 *00,354* PC A06/MF A02

NIST Response to the Fifth CORM Report on the Pressing Problems and Projected Needs in Optical Radiation Measurements.
PB94-188240 *04,227* PC A03/MF A01

NIST RS274KT Interpreter.
PB96-147954 *02,835* PC A05/MF A01

NIST RS274/NGC Interpreter Version 1.
PB94-187788 *02,814* PC A03/MF A01

NIST Serial Holdings, 1994.
PB94-178068 *02,745* PC A12/MF A03

NIST Serial Holdings, 1995.
PB95-188926 *02,746* PC A12/MF A03

NIST Serial Holdings, 1996.
PB96-172523 *02,748* PC A13/MF A03

NIST SIMA Interactive Management Workshop. Held in Fort Belvoir, Virginia on November 14-16, 1994.
PB96-154877 *02,838* PC A08/MF A02

NIST SRM 9983 High-Rigidity Ball-Bar Stand. User Manual.
PB95-255840 *02,669* PC A03/MF A01

NIST Standard Reference Data Products Catalog, 1994.
PB94-151842 *00,727* PC A06/MF A02

NIST Standard Reference Data Products Catalog, 1995-96. Achieve with Standard Reference Data.
PB95-260808 *01,057* PC A03/MF A01

TITLE INDEX

NIST Standard Reference Materials (SRMs) for Polychlorinated Biphenyl (PCB) Determinations and Their Applicability to Toxaphene Measurements.
PB95-140109 *02,585* Not available NTIS

NIST Standard Reference Materials (Trade Name) Catalog 1995-1996.
PB95-232518 *00,508* PC A03/MF A01

NIST Strategies for Reducing Testing Requirements.
PB95-180444 *01,909* Not available NTIS

NIST Support to the Next Generation Controller Program: 1991 Final Technical Report.
PB94-163490 *02,808* PC A09/MF A02

NIST Thermal Infrared Transfer Standard Radiometer for the Earth Observing System (EOS) Program.
PB97-113013 *04,843* Not available NTIS

NIST Traceable Reference Material Program for Gas Standards: Standard Reference Materials.
PB96-210786 *00,644* PC A04/MF A01

NIST Watt Balance: Progress Toward Monitoring the Kilogram.
PB97-113062 *01,991* Not available NTIS

NIST Watt Experiment: Monitoring the Kilogram.
PB97-122329 *01,997* Not available NTIS

NIST Workshop on Gas Sensors: Strategies for Future Technologies. Proceedings of a Workshop. Held in Gaithersburg, Maryland on September 8-9, 1993.
PB95-210225 *00,507* PC A08/MF A02

NIST Workshop on Nanostructured Material (1st): Report of an Industrial Workshop Conducted by the National Institute of Standards and Technology. Held in Gaithersburg, Maryland on May 14-15, 1992.
PB94-218567 *02,973* PC A04/MF A01

NIST Workshop on the Computer Interface to Flat Panel Displays. Held in San Jose, California on January 13-14, 1994.
PB95-136388 *01,625* PC A11/MF A03

NIST-7, the New US Primary Frequency Standard.
PB95-153458 *01,534* Not available NTIS

NIST 30 MHz Linear Measurement System.
PB94-169752 *02,020* Not available NTIS

NIST 60-Millimeter Diameter Cylindrical Cavity Resonator: Performance Evaluation for Permittivity Measurements.
PB94-151776 *02,251* PC A11/MF A03

Nitrogen Effect on Elastic Constants of f.c.c. Fe-18Cr-19Mn Alloys.
PB94-172541 *03,203* Not available NTIS

NMR Characterization of Injection-Moulded Alumina Green Compacts. Part 2. T2-Weighted Proton Imaging.
PB96-201181 *01,165* Not available NTIS

NO Production and Destruction in a Methane/Air Diffusion Flame.
PB97-122519 *01,443* Not available NTIS

Noise Analysis of Ionization Kinetics in a Protein Ion Channel.
PB96-161682 *04,093* Not available NTIS

Noise Characteristics Below 1 Hz of Zener Diode-Based Voltage Reference.
PB96-123476 *04,049* Not available NTIS

Noise in the Coulomb Blockade Electrometer.
PB95-176327 *04,670* Not available NTIS

Noise-Induced Chaos and Phase Space Flux.
PB95-125761 *03,433* Not available NTIS

Noise-Induced Transitions to Chaos.
PB96-156120 *00,217* Not available NTIS

Noise Modeling and Reliability of Behavior Prediction for Multi-Stable Hydroelastic Systems.
PB96-111943 *04,822* Not available NTIS

Noise Reduction in Low-Frequency SQUID Measurements with Laser-Driven Switching.
PB96-135165 *02,081* Not available NTIS

Non-Equilibrium Thermodynamic Theory of Viscoplastic Materials.
PB94-198868 *04,467* Not available NTIS

Non-Gaussian Noise Effects on Reliability of Multistable Systems.
PB96-122726 *04,213* Not available NTIS

Non-Neutral Ion Plasmas and Crystals, Laser Cooling, and Atomic Clocks.
PB95-175113 *03,957* Not available NTIS

Non-Newtonian Flow between Concentric Cylinders Calculated from Thermophysical Properties Obtained from Simulations.
PB96-163761 *04,103* Not available NTIS

Non-Osmotic, Defect-Controlled Cathodic Disbondment of a Coating from a Steel Substrate.
PB94-216447 *03,120* Not available NTIS

Non-Perturbative Relation between the Mutual Diffusion Coefficient, Suspension Viscosity, and Osmotic Compressibility: Application to Concentrated Protein Solutions.
PB96-102355 *01,062* Not available NTIS

Nonadiabatic Effects in the Photoassociation of H2S.
PB95-151437 *00,934* Not available NTIS

Noncontact Ultrasonic Inspection of Train Rails for Stress.
PB95-162673 *04,851* Not available NTIS

Nondestructive Evaluation and Materials Processing.
PB95-140455 *02,902* Not available NTIS

Nondestructive Testing of Concrete: History and Challenges.
PB95-180139 *00,385* Not available NTIS

Nonequilibrium Statistical Mechanics.
PB96-161781 *04,097* Not available NTIS

Nonequilibrium Thermodynamic Theory of Viscoplastic Materials.
PB96-111661 *04,034* Not available NTIS

Nonequilibrium Total-Dielectric-Function Approach to the Electron Boltzmann Equation for Inelastic Scattering in Doped Polar Semiconductors.
PB96-138532 *04,416* Not available NTIS

Noninvasive High-Voltage Measurement in Mammography by Crystal Diffraction Spectroscopy.
PB95-153417 *00,160* Not available NTIS

Nonlinear Color Transformations in Real Time Using a Video Supercomputer.
PB96-123021 *02,191* Not available NTIS

Nonlinear Correlation of High-Pressure Vapor-Liquid Equilibrium Data for Ethylene + n-Butane Showing Inconsistencies in Experimental Compositions.
PB96-161906 *01,141* Not available NTIS

Nonlinear Dynamics of Stiff Polymers.
PB96-122478 *01,278* Not available NTIS

Nonlinear Response of Type-II Superconductors in the Mixed State in Slab Geometry.
PB94-200367 *04,484* Not available NTIS

Nonlocal Effects of Existing Dislocations on Crack-Tip Emission and Cleavage.
PB96-161807 *03,367* Not available NTIS

Nonstationary Behavior of Partial Discharge during Insulation Aging.
PB95-163580 *01,902* Not available NTIS

Nonstationary Behaviour of Partial Discharge during Discharge Induced Ageing of Dielectrics.
PB96-103114 *01,922* Not available NTIS

Normal-Incidence Complex-Index Refractometry.
PB94-213097 *04,241* Not available NTIS

Normal Modes and Structure Factor for a Canted Spin System: The Generalized Villain Model.
PB95-140067 *04,539* Not available NTIS

North American Agreements on ISDN.
PB96-160775 *01,503* Not available NTIS

North American ISDN Users' Forum Agreements on Integrated Services Digital Network.
PB94-162559 *01,466* PC A16/MF A03

Northridge Earthquake, 1994. Performance of Structures, Lifelines and Fire Protection Systems.
PB94-161114 *00,421* PC A09/MF A02

Northridge Earthquake 1994: Performance of Structures, Lifelines, and Fire Protection Systems.
PB94-207461 *04,825* PC A09/MF A02

Notion of a xi-Vector and a Stress Tensor for a General Class of Anisotropic Diffuse Interface Models.
PB96-193776 *04,788* PC A03/MF A01

Novel Active-Vision-Based Motion Cues for Local Navigation.
PB96-193727 *02,941* PC A05/MF A01

Novel Activities of Human Uracil DNA N-glycosylase for Cytosine-Derived Products of Oxidative DNA Damage.
PB96-164132 *03,479* Not available NTIS

Novel Activity of E. coli uracil DNA N-glycosylase Excision of Isodialuric Acid (5,6-dihydroxyuracil), a Major Product of Oxidative DNA Damage, from DNA.
PB96-110747 *03,543* Not available NTIS

Novel Amperometric Immunosensor for Procainamide Employing Light Activated Labels.
PB96-163662 *00,512* Not available NTIS

Novel Bulk Iron Garnets for Magneto-Optic Magnetic Field Sensing.
PB95-180204 *04,675* Not available NTIS

Novel DNA N-Glycosylase Activity of E. coli T4 Endonuclease V That Excises 4,6-Diamino-5-Formamidopyrimidine from DNA, a UV-Radiation- and Hydroxyl Radical-Induced Product of Adenine.
PB96-160478 *03,549* Not available NTIS

Novel Hot-Electron Microbolometer.
PB96-201025 *01,977* Not available NTIS

Novel Magnetic Field Characterization Techniques for Compound Semiconductor Materials and Devices.
PB96-176458 *02,433* Not available NTIS

Novel Method for Determining Thin Film Density by Energy-Dispersive X-ray Reflectivity.
PB96-122783 *04,737* Not available NTIS

Novel Polydiacetylenes Derived from Liquid Crystalline Monomers.
PB95-140125 *01,235* Not available NTIS

Novel Radiochromic Films for Clinical Dosimetry.
PB97-119259 *03,641* Not available NTIS

Novel Vortex Dynamics in Two-Dimensional Josephson Arrays.
PB96-200167 *02,091* Not available NTIS

Novel YBa2Cu3O7-x and YBa2Cu3O7-x/Y4Ba3O9 Multilayer Films by Bias-Masked 'On-Axis' Magnetron Sputtering.
PB95-181186 *04,690* Not available NTIS

Nuclear Heat Load Calculations for the NBSR Cold Neutron Source Using MCNP.
PB95-152955 *03,730* Not available NTIS

Nucleic Acid Database: Present and Future.
PB97-109078 *00,518*
(Order as PB97-109011, PC A11/MF A03)

Null-Balanced Total-Power Radiometer System NCS1.
PB94-169778 *02,021* Not available NTIS

Numeric Data Distribution: The Vital Role of Data Exchange in Today's World.
N95-15937/2 *02,622*
(Order as N95-15919/0, PC A11/MF A03)

Numerical Analysis Support for Compartment Fire Modeling and Incorporation of Heat Conduction into a Zone Fire Model.
PB94-156965 *01,357* PC A04/MF A01

Numerical Evaluation of Hypersingular Integrals for Scattering by a Dielectric Wedge.
PB97-110555 *02,017* Not available NTIS

Numerical Evaluation of Special Functions.
PB96-119557 *03,417* Not available NTIS

Numerical Micromagnetic Techniques and Their Applications to Magnetic Force Microscopy Calculations.
PB95-175931 *04,664* Not available NTIS

Numerical Reference Models for Optical Metrology Simulation.
PB97-111330 *04,392* Not available NTIS

Numerical Simulation of Rapid Combustion in an Underground Enclosure.
PB96-183132 *01,424* PC A03/MF A01

Numerical Simulation of Submicron Photolithographic Processing.
PB94-198561 *02,310* Not available NTIS

Numerical Solution of the Nonlinear Schroedinger Equation for Small Samples of Trapped Neutral Atoms.
PB95-202578 *03,985* Not available NTIS

Nutritional Status and Growth in Juvenile Rheumatoid Arthritis.
PB94-198470 *03,515* Not available NTIS

NVLAP Procedures U.S. Code of Federal Regulations. Title 15, Subtitle A, Chapter 2, Part 7. (Effective December 1984; Amended September 1990).
PB94-160850 *02,627* PC A03/MF A01

Object Finder for Digital Images Based on Multiple Thresholds, Connectivity, and Internal Structures.
PB94-199106 *01,833* Not available NTIS

Object-Oriented Technology Research Areas.
PB95-199329 *01,726* PC A03/MF A01

Object-Oriented Tel/Tk Binding for Interpreted Control of the NIST EXPRESS Toolkit in the NIST STEP Application Protocol Development Environment.
PB96-141049 *02,785* Not available NTIS

Object SQL: Language Extensions for Object Data Management.
PB95-125902 *01,704* Not available NTIS

Objective Evaluation of Short-Crack Toughness Curves Using Indentation Flaws: Case Study on Alumina-Based Ceramics.
PB96-179429 *03,079* Not available NTIS

Observation and Visible and uv Magnetic Dipole Transitions in Highly Charged Xenon and Barium.
PB96-138441 *04,056* Not available NTIS

Observation of a Stable Methoxy Intermediate on Cr(110).
PB95-164422 *00,981* Not available NTIS

Observation of Hot-Electron Shot Noise in a Metallic Resistor.
PB97-112007 *01,988* Not available NTIS

Observation of Insulating Nanoparticles on YBCO Thin-Films by Atomic Force Microscopy.
PB95-163358 *04,622* Not available NTIS

Observation of Noncollinear Magnetic Structure for the Cu Spins in Nd2CuO4-Type Systems.
PB95-164539 *04,634* Not available NTIS

Observation of Oscillatory Magnetic Order in the Antiferromagnetic Superconductor HoNi2B2C.
PB95-180303 *04,679* Not available NTIS

Observation of Pd-Like Resonance Lines Through Pt(32+) and Zn-Like Resonance Lines of Er(38+) and Hf(42+).
PB95-150637 *03,896* Not available NTIS

Observation of the Transverse Second Harmonic Magneto-Optic Kerr Effect from Ni81Fe19 Thin Film Structures.
PB96-200332 *01,971* Not available NTIS

Observation of Two Length Scales Above (T sub N) in a Holmium Thin Film.
PB97-111942 *04,151* Not available NTIS

Observation of Vortex Dynamics in Two-Dimensional Josephson-Junction Arrays.
PB95-168811 *02,050* Not available NTIS

Observations of Partial Discharges in Hexane Under High Magnification.
PB95-163127 *01,900* Not available NTIS

Observations of Shear Induced Molecular Orientation in a Polymer Melt Using Fluorescence Anisotropy Measurements.
PB94-199304 *01,210* Not available NTIS

Observations of Shear Stress and Molecular Orientation Using Fluorescence Anisotropy Measurements.
PB94-199312 *01,211* Not available NTIS

Observations of 3C 273 with the Goddard High Resolution Spectrograph on the Hubble Space Telescope.
PB95-202321 *00,076* Not available NTIS

Observed and Theoretical Creep Rates for an Alumina Ceramic and a Silicon Nitride Ceramic in Flexure.
PB94-212958 *03,040* Not available NTIS

Observed Frustration in Confined Block Copolymers.
PB95-150033 *01,238* Not available NTIS

Observing Stellar Coronae with the Goddard High Resolution Spectrograph. I. The dMe Star AU Microscopii.
PB96-102777 *00,092* Not available NTIS

Obtaining and Installing a Public Domain TEX.
PB95-175741 *01,719* Not available NTIS

Octacalcium Phosphate Carboxylates IV. Kinetics of Formation and Solubility of Octacalcium Phosphate Succinate.
PB94-185600 *00,776* Not available NTIS

Octacalcium Phosphate Carboxylates. 1. Preparation and Identification.
PB95-161535 *00,660* Not available NTIS

Octacalcium Phosphate Carboxylates. 2. Characterization and Structural Consideration.
PB95-161543 *00,955* Not available NTIS

Octacalcium Phosphate Carboxylates. 5. Incorporation of Excess Succinate and Ammonium Ions in the Octacalcium Phosphate Succinate Structure.
PB95-168894 *00,166* Not available NTIS

Octacalcium Phosphate. 3. Infrared and Raman Vibrational Spectra.
PB94-172244 *00,756* Not available NTIS

Off-Diagonal Orthorhombic-Symmetry Elastic Constants.
PB95-202768 *04,695* Not available NTIS

Office Work Station Heat Release Rate Study: Full Scale versus Bench Scale.
PB96-190178 *01,428* Not available NTIS

Offset Susceptibility of Superconductors.
PB94-212263 *04,503* Not available NTIS

On-Wafer Impedance Measurement on Lossy Substrates.
PB95-176285 *02,365* Not available NTIS

One- and Two-Sided Burning of Thermally Thin Materials.
PB95-140935 *03,151* Not available NTIS

One-Dimensional Modeling Studies of the Gaseous Electronics Conference RF Reference Cell.
PB96-113428 *02,397*
(Order as PB96-113311, PC A09/MF A03)

One-Electron Oxidation of Metalloporphycenes as Studied by Radiolytic Methods.
PB97-111967 *01,179* Not available NTIS

One-Electron Oxidation of Nickel Porphyrins. Effect of Structure and Medium on Formation of Nickel(III) Porphyrin or Nickel(II) Porphyrin pi-Radical Cation.
PB95-107058 *00,865* Not available NTIS

One Gigarad Passivating Nitrided Oxides for 100% Internal Quantum Efficiency Silicon Photodiodes.
PB94-185485 *02,119* Not available NTIS

One-Sided beta-Content Tolerance Intervals for Mixed Models.
PB96-141171 *03,449* Not available NTIS

Opacity Project and the Practical Utilization of Atomic Data.
PB94-212214 *00,059* Not available NTIS

Open Architectures for Machine Control.
PB94-135621 *02,942* PC A03/MF A01

Open Document Architecture (ODA) Raster Document Application Profile (DAP). Category: Software Standard; Subcategory: Graphics.
FIPS PUB 194 *01,669* PC E04

Open-Ended Coaxial Probes for Nondestructive Testing of Substrates and Circuit Boards.
PB96-122825 *02,078* Not available NTIS

Open Issues in OSI Protocol Development and Conformance Testing.
PB96-122908 *01,818* Not available NTIS

Open System Environment Implementors Workshop (OIW); Standardization Role Defined.
PB96-180047 *01,828* Not available NTIS

Open System Environment (OSE): Architectural Framework for Information Infrastructure.
PB96-146360 *00,002* PC A04/MF A01

Open System Environment Procurement.
N94-36858/6 *02,716*
(Order as N94-36853/7, PC A10/MF A03)

Open System Environments.
N94-36857/8 *01,674*
(Order as N94-36853/7, PC A10/MF A03)

Open Systems Software Standards in Concurrent Engineering.
PB96-160932 *01,758* Not available NTIS

Operating Principles of MultiKron II Performance Instrumentation for MIMD Computers.
PB95-189486 *01,628* PC A03/MF A01

Operating Principles of MultiKron Virtual Counter Performance Instrumentation for MIMD Computers.
PB96-131529 *01,632* PC A03/MF A01

Operating Principles of the SBus MultiKron Interface Board.
PB95-231783 *01,630* PC A03/MF A01

Operating Procedures and Life Cycle Documentation for the Initial Graphics Exchange Specification.
PB95-242285 *02,782* PC A04/MF A01

Operational Mode and Gas Species Effects on Rotational Drag in Pneumatic Dead Weight Pressure Gages.
PB95-140182 *00,903* Not available NTIS

Operator Experience with a Hierarchical Real-Time Control System (RCS).
PB96-195516 *03,751* PC A03/MF A01

Opportunities for Innovation: Advanced Manufacturing Technology.
PB94-100278 *02,801* PC A07/MF A02

Opportunities for Innovation: Advanced Surface Engineering.
PB94-176666 *02,697* PC A09/MF A02

Opportunities for Innovation: Biotechnology.
PB94-157831 *00,009* PC A12/MF A03

Opportunities for Innovation: Optoelectronics.
PB96-118039 *01,928* PC A19/MF A04

Opportunities for Innovation: Pollution Prevention.
PB95-147146 *02,520* PC A09/MF A02

Opportunities for Innovation: Software for Manufacturing.
PB95-155578 *02,851* PC A09/MF A03

Optical and Mass Spectrometric Investigations of Ions and Neutral Species in SF6 Radio-Frequency Discharges.
PB97-111918 *01,985* Not available NTIS

Optical and Modeling Studies of Sodium/Halide Reactions for the Formation of Titanium and Boron Nanoparticles.
PB97-113054 *00,682* Not available NTIS

Optical Biosensor Using a Fluorescent, Swelling Sensing Element.
PB95-175899 *03,541* Not available NTIS

Optical Characterization in Microelectronics Manufacturing.
PB95-169397 *02,358*
(Order as PB95-169371, PC A07/MF A02)

Optical Characterization of Materials and Devices for the Semiconductor Industry: Trends and Needs.
PB96-167192 *02,431* Not available NTIS

Optical Conductivity of Single Crystals of Ba1-xMxBiO3(M=K, Rb, x=0.04, 0.37).
PB94-185329 *04,447* Not available NTIS

Optical Control of Enzymatic Conversion of Sucrose to Glucose by Bacteriorhodopsin Incorporated into Self-Assembled Phosphatidylcholine Vesicles.
PB96-123344 *03,477* Not available NTIS

Optical Current Transducer for Calibration Studies.
PB94-185907 *02,121* Not available NTIS

Optical Density Measurements of Laser Eye Protection Materials.
PB96-190301 *00,190* Not available NTIS

Optical Detector Nonlinearity: A Comparison of Five Methods.
PB95-169355 *04,291* Not available NTIS

Optical Detector Nonlinearity: Simulation.
PB96-165378 *02,199* PC A04/MF A01

Optical Diagnostics in the Gaseous Electronics Conference Reference Cell.
PB96-113352 *02,390*
(Order as PB96-113311, PC A09/MF A03)

Optical Emission Spectroscopy on the Gaseous Electronics Conference RF Reference Cell.
PB96-113345 *02,389*
(Order as PB96-113311, PC A09/MF A03)

Optical Fiber, Fiber Coating, and Connector Ferrule Geometry: Results of Interlaboratory Measurement Comparisons.
PB96-154422 *04,360* PC A05/MF A01

Optical Fiber Geometry: Accurate Measurement of Cladding Diameter.
PB95-151940 *04,266* Not available NTIS

Optical Fiber Geometry by Gray-Scale Analysis with Robust Regression.
PB95-161519 *04,272* Not available NTIS

Optical Fiber Sensors: Accelerating Applications in Navy Ships.
PB94-186848 *02,632* PC A06/MF A02

Optical Measurements of Atomic Hydrogen, Hydroxyl, and Carbon Monoxide in Hydrocarbon Diffusion Flames.
PB95-150900 *02,487* Not available NTIS

Optical Metrology and More. Programs and Services of the Radiometric Physics Division, Physics Laboratory.
PB94-191707 *04,228* PC A03/MF A01

Optical Molasses: Cold Atoms for Precision Measurements.
PB95-108890 *03,877* Not available NTIS

Optical Molasses: The Coldest Atoms Ever.
PB95-108908 *03,878* Not available NTIS

Optical Performance of Commercial Windows.
PB95-208757 *00,392* PC A09/MF A02

Optical Performance of Photoinductive Mixers at Terahertz Frequencies.
PB95-168662 *02,161* Not available NTIS

Optical Power Meter Calibration Using Tunable Laser Diodes.
PB95-169256 *04,290* Not available NTIS

Optical Probing of Cold Trapped Atoms.
PB95-175469 *04,296* Not available NTIS

Optical Properties of Triton X-100-Treated Purple Membranes Embedded in Gelatin Films.
PB96-123500 *03,546* Not available NTIS

Optical Sampling Using Nondegenerate Four-Wave Mixing in a Semiconductor Laser Amplifier.
PB96-122502 *02,076* Not available NTIS

Optical Sampling Using Nondegenerate Four-Wave Mixing in a Semiconductor Laser Amplifier.
PB96-123609 *04,348* Not available NTIS

Optical Scattering from Moderately Rough Surfaces.
PB97-110415 *04,385* Not available NTIS

Optical Storage Media Data Integrity Studies.
N95-24130/3 *01,620*
(Order as N95-24108, PC A17/MF A04)

Optically Linked Three-Loop Antenna System for Determining the Radiation Characteristics of an Electrically Small Source.
PB95-161915 *02,005* Not available NTIS

Optically Sensed EM-Field Probes for Pulsed Fields.
PB94-212594 *02,130* Not available NTIS

Optically Stabilized Tunable Diode-Laser System for Saturation Spectroscopy.
PB96-102819 *04,717* Not available NTIS

Optimal Control of Building and HVAC Systems.
PB96-141353 *00,272* Not available NTIS

Optimization of ECR-Based PECVD Oxide Films for Superconducting Integrated Circuit Fabrication.
PB95-169165 *02,051* Not available NTIS

Optimization of Highway Concrete Technology.
PB94-182995 *01,333* PC A13/MF A03

Optimization of Inert Gas Atomization.
PB95-107405 *01,377* Not available NTIS

Optimizing Time-Domain Network Analysis.
PB96-157821 *02,085* Not available NTIS

Optoelectronics and Optomechanics Manufacturing: An ATP Focused Program Development. Workshop Proceedings. Held in Gaithersburg, Maryland on February 15, 1995.
PB97-104186 *02,204* PC A11/MF A03

Optoelectronics at NIST.
PB96-200860 *02,202* Not available NTIS

Orbital Alignment and Vector Correlations in Inelastic Atomic Collisions.
PB96-122742 *04,047* Not available NTIS

Orbital Stereochemistry: Discovering the Symmetries of Collision Processes.
PB95-202800 *01,034* Not available NTIS

Ordered omega-Derivatives in a Ti-37.5Al-2ONb at% Alloy.
PB94-211091 *03,331* Not available NTIS

Organization and Implementation of Calibration in the EOS Project. Part 1.
PB96-179437 *04,841* Not available NTIS

Orientation Effects on ESR Analysis of Alanine-Polymer Dosimeters.
PB96-146725 *03,720* Not available NTIS

Orientational Fluctuations, Diffuse Scattering, and Orientational Order in Solid C60.
PB97-119275 *04,176* Not available NTIS

Origin of I/f PM and AM Noise in Bipolar Junction Transistor Amplifiers.
PB96-200787 *02,096* Not available NTIS

Origin of the Second Length Scale Above the Magnetic Spiral Phase of Tb.
PB95-153698 *04,596* Not available NTIS

Orthotropic Elastic Constants of a Boron-Aluminum Fiber-Reinforced Composite: An Acoustic-Resonance-Spectroscopy Study.
PB96-200175 *03,182* Not available NTIS

Oscillator Strengths and Radiative Branching Ratios in Atomic Sr.
PB95-203493 *04,008* Not available NTIS

Oscillatory Exchange Coupling in Fe/Au/Fe(100).
PB95-150371 *04,569* Not available NTIS

Oscillometric and Conductometric Analysis of Aqueous and Organic Dosimeter Solutions.
PB96-135256 *04,054* Not available NTIS

Ouch Those Programs are Painful.
PB96-102678 *01,739* Not available NTIS

Outlier-Resistant Methods for Estimation and Model Fitting.
PB95-203436 *03,444* Not available NTIS

Outline of a Multiple Dimensional Reference Model Architecture and a Knowledge Engineering Methodology for Intelligent Systems Control.
PB95-220414 *03,703* PC A03/MF A01

Overcoming Hoelder Continuity in Ill-Posed Continuation Problems.
PB95-202354 *03,416* Not available NTIS

Overview of a Radiation Accident at an Industrial Accelerator Facility.
PB97-122485 *02,612* Not available NTIS

Overview of Bioelectrical Impedance Analyzers.
PB96-122635 *00,176* Not available NTIS

Overview of Bioelectrical Impedance Analyzers.
PB97-118780 *00,181* Not available NTIS

Overview of NASREM: The NASA/NBS Standard Reference Model for Telerobot Control System Architecture.
PB94-194560 *04,831* PC A03/MF A01

Overview of Radiometric Program of the NIST Thermal Imaging Laboratory.
PB94-199163 *04,230* Not available NTIS

Overview of Reference Materials Prepared for Standardization of DNA Typing Procedures.
PB96-111653 *00,611* Not available NTIS

Overview of Smoke Control Technology.
PB94-212867 *00,348* Not available NTIS

Overview of the Manufacturing Engineering Toolkit Prototype.
PB96-128228 *02,833* PC A03/MF A01

Overview of the Text REtrieval Conference (3rd) (TREC-3). Held in Gaithersburg, Maryland on November 2-4, 1994.
PB95-216883 *01,728* PC A25/MF A06

Overview of U.S. Government Advanced Packaging Programs.
PB96-200845 *02,443* Not available NTIS

Oxidation of Caffeic Acid and Related Hydroxycinnamic Acids.
PB97-111975 *00,651* Not available NTIS

Oxidation of Ferrous and Ferrocyanide Ions by Peroxyl Radicals.
PB97-122402 *01,191* Not available NTIS

Oxidation of SiC.
PB96-119516 *02,401* Not available NTIS

Oxidation of Soot and Carbon Monoxide in Hydrocarbon Diffusion Flames.
PB95-150215 *01,382* Not available NTIS

Oxidation of 10-Methylacridan, a Synthetic Analogue of NADH and Deprotonation of Its Cation Radical. Convergent Application of Laser Flash Photolysis and Direct and Redox Catalyzed Electrochemistry to the Kinetics of Deprotonation of the Cation Radical.
PB94-198371 *00,785* Not available NTIS

Oxidative Damage to DNA in Mammalian Chromatin.
PB94-199825 *03,525* Not available NTIS

Oxidative DNA Base Damage in Renal, Hepatic, and Pulmonary Chromatin of Rats After Intraperitoneal Injection of Cobalt (II) Acetate.
PB95-150025 *03,647* Not available NTIS

Oxygen Annealing of Ex-situ YBCO/Ag Thin-Film Interfaces.
PB96-141312 *04,758* Not available NTIS

Oxygen Dependance of the Crystal Structure of HgBa2CuO4+ and Its Relation to Superconductivity.
PB96-102512 *04,711* Not available NTIS

P-Type Doubling in the Infrared Spectrum of NO-HF.
PB94-211463 *00,817* Not available NTIS

Paffenbarger Research Center: The Cutting Edge of Dental Science.
PB94-216355 *00,151* Not available NTIS

Pairwise and Nonpairwise Additive Forces in Weakly Bound Complexes: High Resolution Infrared Spectroscopy of ArnDF (n=1,2,3).
PB96-200357 *04,125* Not available NTIS

Panel: Building and Using Test Collections.
PB97-118673 *02,743* Not available NTIS

Panel Discussion on Units in Magnetism.
PB96-137773 *04,746* Not available NTIS

Papers on the Symposium on Collision Phenomena in Astrophysics, Geophysics, and Masers.
AD-A280 291/6 *00,047* PC A03/MF A01

Papers Presentations Shine.
PB94-200383 *00,244* Not available NTIS

Parallel and Serial Implementations of SLI Arithmetic.
PB95-242335 *01,732* PC A03/MF A01

Parallel Monte Carlo Simulation of MBE Growth.
PB96-122841 *02,406* Not available NTIS

Parametric Investigation of Metal Powder Atomization Using Laser Diffraction.
PB95-108577 *03,342* Not available NTIS

Parametric Study of Hydrogen Fluoride Formation in Suppressed Fires.
PB96-163720 *00,514* Not available NTIS

Parametric Study of Wall Moisture Contents Using a Revised Variable Indoor Relative Humidity Version of the 'Moist' Transient Heat and Moisture Transfer Model.
PB97-122535 *00,419* Not available NTIS

Partial Discharge: Induced Aging of Cast Epoxies and Related Nonstationary Behavior of the Discharge Statistics.
PB95-163598 *01,903* Not available NTIS

Partial Pressure Analysis in Space Testing.
N95-14084/4 *04,827*
(Order as N95-14062/0, PC A20/MF A04)

Partial Pressure Analysis in Space Testing.
PB96-103072 *04,829* Not available NTIS

Partial Scattered Intensities from a Binary Suspension of Polystyrene and Silica.
PB95-175618 *00,996* Not available NTIS

Partially Coherent Transmittance of Dielectric Lamellae.
PB96-148028 *04,359* Not available NTIS

Partially Prestressed and Debonded Precast Concrete Beam-Column Joints.
PB95-153102 *00,439* Not available NTIS

Particle Size Standards and Their Certification at NIST.
PB94-211695 *02,639* Not available NTIS

Passively Q-Switched Nd-Doped Waveguide Laser.
PB95-180048 *04,308* Not available NTIS

Pattern-Recognition Analysis of Low-Resolution X-Ray Fluorescence Spectra.
PB95-151924 *00,588* Not available NTIS

PC-Based Prototype Expert System for Data Management and Analysis of Creep and Fatigue of Selected Materials at Elevated Temperatures.
PB94-172251 *03,202* Not available NTIS

PC-Based Spinning Rotor Gage Controller.
PB95-175832 *02,609* Not available NTIS

PCASYS: A Pattern-Level Classification Automation System for Fingerprints.
PB95-267936 *01,853* PC A03/MF A01

Peeking Through the Picket Fence: What Astrophysical Surprises May Be Present in the 100-1200 Angstrom Region.
PB95-202859 *00,082* Not available NTIS

Peeling a Polymer from a Surface or from a Line.
PB94-199809 *01,213* Not available NTIS

Penetration and Diffusion of Hard X-rays through Thick Barriers. III. Studies of Spectral Distributions.
AD-A292 502/2 *03,771* PC A01/MF A01

Perception of Clamp Noise in Television Receivers.
PB96-119433 *01,489* Not available NTIS

Percolation and Pore Structure in Mortars and Concrete.
PB95-150439 *00,370* Not available NTIS

Performance and Reliability of NIST 10-V Josephson Arrays.
PB96-148051 *02,419* Not available NTIS

Performance Approach to the Development of Criteria for Low-Sloped Roof Membranes.
PB94-160751 *00,329* PC A03/MF A01

Performance Characteristics of Fast Elliptic Solvers on Parallel Platforms.
PB95-180832 *01,723* Not available NTIS

Performance Evaluation of a New Digital Partial Discharge Recording and Analysis System.
PB95-150389 *01,888* Not available NTIS

Performance Measures for Geometric Fitting in the NIST Algorithm Testing and Evaluation Program for Coordinate Measurement Systems.
PB96-122122 *01,745*
(Order as PB96-117767, PC A08/MF A02)

Performance of a Reflectron Energy Compensating Mirror.
PB94-199460 *00,547* Not available NTIS

Performance of Commercial CMOS Foundry-Compatible Multijunction Thermal Converters.
PB95-153656 *02,342* Not available NTIS

Performance of Compact Fluorescent Lamps at Different Ambient Temperatures.
PB95-175329 *00,258* Not available NTIS

Performance of Federal Buildings in the January 17, 1994 Northridge Earthquake.
PB95-231775 *00,453* PC A03/MF A01

Performance of HUD-Affiliated Properties during the January 17, 1994 Northridge Earthquake.
PB95-174488 *00,443* PC A04/MF A01

Performance of Multilayer Thin-Film Multijunction Thermal Converters.
PB96-148135 *02,084* Not available NTIS

Performance of Plastic Packaging for Hazardous Materials Transportation. Part 1. Mechanical Properties.
AD-A301 258/0 *02,580* PC A04/MF A01

Performance of Tape-Bonded Seams of EPDM Membranes: Comparison of the Peel Creep-Rupture Response of Tape-Bonded and Liquid-Adhesive-Bonded Seams.
PB96-183249 *03,012* PC A05/MF A01

Performance of the Electron Pump with Stray Capacitances.
PB96-200902 *01,976* Not available NTIS

Performance of 1/3-Scale Model Precast Concrete Beam-Column Connections Subjected to Cyclic Inelastic Loads. Report No. 4.
PB95-179024 *00,444* PC A04/MF A01

Performance Parameters of Fire Detection Systems.
PB94-194339 *00,288* PC A03/MF A01

Performance Standards: The Pro's and Con's.
PB94-216132 *02,896* Not available NTIS

Performance Testing of a Family of Type I Combination Appliance.
PB95-220521 *02,505* PC A03/MF A01

Periapical Tissue Reactions to a Calcium Phosphate Cement in the Teeth of Monkeys.
PB94-212008 *00,149* Not available NTIS

Permeation Tube Approach to Long-Term Use of Automatic Sampler Retention Index Standards.
PB96-167291 *00,639* Not available NTIS

Permissible Dose from External Sources of Ionizing Radiation.
AD-A279 281/0 *03,608* PC A05/MF A01

Perpendicular C-H Stretching Band nu9/nu13 and the Torsional Potential of Dimethylacetylene.
PB97-122451 *01,192* Not available NTIS

Persistent Object Base System Testing and Evaluation.
PB95-220588 *01,730* PC A05/MF A01

Perspective on Fiber Coating Technology.
PB94-200540 *03,118* Not available NTIS

Perspective on Software Engineering Standards.
PB95-171377 *01,811* PC A03/MF A01

Perturbative Calculation of the AC Stark Effect by the Complex Rotation Method.
PB95-141123 *04,260* Not available NTIS

PET and DINGO Tools for Deriving Distributed Implementations from Estelle.
PB95-203253 *01,727* Not available NTIS

Phase Behavior of a Hydrogen Bonding Molecular Composite.
PB94-185188 *01,202* Not available NTIS

Phase Composition, Viscosities, and Densities for Aqueous Two-Phase Systems Composed of Polyethylene Glycol and Various Salts at 25C.
PB95-164596 *00,986* Not available NTIS

Phase Equilibria in the Systems CaO-CuO and CaO-Bi2O3.
PB95-140570 *03,048* Not available NTIS

Phase-Field Model for Solidification of a Eutectic Alloy.
PB95-147914 *03,345* PC A04/MF A01

Phase Identification in a Scanning Electron Microscope Using Backscattered Electron Kikuchi Patterns.
PB97-109128 *04,804*
(Order as PB97-109011, PC A11/MF A03)

Phase-Locked Oscillator Optimization for Arrays of Josephson Junctions.
PB95-169314 *02,052* Not available NTIS

Phase Locking in Two-Dimensional Arrays of Josephson Junctions: Effect of Critical-Current Nonuniformity.
PB96-102587 *04,714* Not available NTIS

Phase Locking in Two-Junction Systems of High-Temperature Superconductor-Normal Metal-Superconductor Junctions.
PB95-176053 *02,060* Not available NTIS

Phase Separation in Thin Film Polymer Blends With and Without Block Copolymer Additives.
PB96-204482 *01,294* Not available NTIS

Phase Shifts and Intensity Dependence in Frequency-Modulation Spectroscopy.
PB96-103205 *01,071* Not available NTIS

Phase Transitions in Solid C70: Supercooling, Metastable Phases, and Impurity Effect.
PB95-150090 *00,914* Not available NTIS

Phonon Density of States in R2CuO4 and Superconducting R1.85Ce0.15CuO4 (R = Nd, Pr).
PB95-150686 *04,574* Not available NTIS

Phonon Relaxation in Soft-X-ray Emission of Insulators.
PB96-160296 *04,085* Not available NTIS

Phospholipid/Alkanethiol Bilayers for Cell-Surface Receptor Studies by Surface Plasmon Resonance.
PB96-102900 *03,472* Not available NTIS

Photodecomposition Dynamics of Mo(CO)6/Si(111) 7x7: CO Internal State and Translational Energy Distributions--Translation.
PB94-199288 *00,687* Not available NTIS

Photodecomposition of Mo(CO)6/Si(111) 7x7: CO State-Resolved Evidence for Excited State Relaxation and Quenching.
PB95-180154 *01,009* Not available NTIS

Photodesorption Dynamics of CO from Si(111): The Role of Surface Defects.
PB96-111646 *03,066* Not available NTIS

Photodetector Frequency Response Measurements at NIST, US, and NPL, UK: Preliminary Results of a Standards Laboratory Comparison.
PB95-175592 *02,175* Not available NTIS

Photodissociation Dynamics in Quantum State-Selected Clusters: A Test of the One-Atom Cage Effect in Ar-H2O.
PB95-203121 *01,044* Not available NTIS

Photodissociation of Ammonia at 193.3nm: Rovibrational State Distribution of the NH2(A(2)A1) Fragment.
PB95-151775 *00,937* Not available NTIS

Photoelectron Spectroscopic Study of the Valence and Core-Level Electronic Structure of BaTiO3.
PB94-212149 *04,500* Not available NTIS

Photoelectron Spectroscopy of Negatively Charged Bismuth Clusters: Bi(-)2, Bi(-)3, and Bi(-)4.
PB95-108494 *00,880* Not available NTIS

Photoelectron Spectroscopy of Small Antimony Cluster Anions: Sb(-), Sb2(-), Sb3(-), and Sb4(-).
PB95-203139 *01,045* Not available NTIS

Photoelectron Study of Electronic Autoionization in Rotationally Cooled N2: The n=6 Member of the Hopfield Series.
PB95-163531 *00,971* Not available NTIS

Photographic Response to X-Ray Irradiation. 1. Estimation of the Photographic Error Statistic and Development of Analytic Density-Intensity Equations.
PB94-200086 *03,821* Not available NTIS

Photographic Response to X-Ray Irradiation. 2. Correlated Models.
PB94-200094 *03,822* Not available NTIS

Photographic Response to X-Ray Irradiation. 3. Photographic Linearization of Beam-Foil Spectra.
PB94-200102 *03,823* Not available NTIS

Photoionization of Small Molecules Using Synchrotron Radiation.
PB94-211505 *03,841* Not available NTIS

Photoluminescence Spectra of Epitaxial Single Crystal C60.
PB96-141205 *04,754* Not available NTIS

Photonic Band-Structure Effects for Low-Index-Contrast Two-Dimensional Lattices in the Near Infrared.
PB97-122469 *04,401* Not available NTIS

Photonic Materials: A Report on the Results of a Workshop. Held in Gaithersburg, Maryland on August 26-27, 1992, Volume 1.
PB94-152733 *02,114* PC A05/MF A01

Physical and Chemical Properties of Resin-Reinforced Calcium Phosphate Cements.
PB95-180212 *00,171* Not available NTIS

Physical Basis for Half-Integral Shapiro Steps in a DC SQUID.
PB96-102264 *04,704* Not available NTIS

Physical Characterization of Herparin by Light Scattering.
PB96-119383 *03,598* Not available NTIS

Physical Limit to the Stability of Superheated and Stretched Water.
PB96-122551 *01,083* Not available NTIS

Physical Properties of Alternatives to the Fully Halogenated Chlorofluorocarbons.
PB96-119573 *03,279* Not available NTIS

Physical Properties of Some Purified Aliphatic Hydrocarbons.
AD-A297 265/1 *00,657* PC A03/MF A01

Physicochemical Characterization of Low Molecular Weight Heparin.
PB96-112040 *03,474* Not available NTIS

Physicochemical Characterization of Natural and Bioprosthetic Heart Valve Calcific Deposits: Implications for Prevention.
PB96-156039 *00,187* Not available NTIS

Physicochemical Properties of Calcific Deposits Isolated from Porcine Bioprosthetic Heart Valves Removed from Patients Following 2-13 Years Function.
PB94-172863 *00,184* Not available NTIS

Physics and Chemistry of Partial Discharge and Corona: Recent Advances and Future Challenges.
PB95-181046 *01,910* Not available NTIS

Physics and Chemistry of Partial Discharge and Corona - Recent Advances and Future Challenges.
PB96-123757 *01,936* Not available NTIS

Physics and Prospects of Inertial Confinement Fusion.
PB94-185048 *04,405* Not available NTIS

Physics-Based Vision: Principles and Practice, Shape Recovery (Book Review).
PB95-164075 *01,846* Not available NTIS

Physics for Device Simulations and Its Verification by Measurements.
PB95-141172 *02,327* Not available NTIS

Physics for Device Simulations and Its Verification by Measurements.
PB95-152914 *02,339* Not available NTIS

Physics Laboratory Technical Activities, 1993.
PB94-176088 *03,796* PC A10/MF A03

Physics Required for Prediction of Long Term Performance of Polymers and Their Composites.
PB94-219243 *03,146*
(Order as PB94-219219, PC A06/MF A02)

Picosecond Measurement of Substrate-to-Adsorbate Energy Transfer: The Frustrated Translation of CO/Pt(111)--Translation.
PB95-126041 *00,895* Not available NTIS

PIECS: A Software Program for Machine Tool Process-Intermittent Error Compensation.
PB96-165980 *02,842* PC A08/MF A02

Piezoelectric and Pyroelectric Polymers.
PB95-153367 *01,250* Not available NTIS

Piggyback Balance Experiment: An Illustration of Archimedes' Principles and Newton's Third Law.
PB94-163060 *03,786* PC A03/MF A01

Pilot Studies for Improving Sampling Protocols.
PB97-118715 *02,530* Not available NTIS

Pinch Effect in Commensurate Vortex-Pin Lattices.
PB96-147079 *01,125* Not available NTIS

Planar Lenses for Field-Emitter Arrays.
PB96-103064 *02,112* Not available NTIS

Planar Near-Field Alignment.
PB94-172491 *01,998* Not available NTIS

Planar Near-Field Measurements and Microwave Holography for Measuring Aperture Distribution on a 60 GHz Active Array Antenna.
PB96-167366 *03,762* Not available NTIS

Planar Near-Field Measurements of Low-Sidelobe Antennas.
PB94-219235 *02,001*
(Order as PB94-219219, PC A06/MF A02)

Planar Resistors for Probe Station Calibration.
PB95-163697 *02,351* Not available NTIS

Planar Waveguide Optical Sensors.
PB94-200185 *03,586* Not available NTIS

Planning for the Fiber Distributed Data Interface (FDDI).
PB94-135761 *01,621* PC A06/MF A02

Planning the Infrastructure for Global Electronic Commerce.
PB94-185832 *00,494* Not available NTIS

Plasma Chemical Model for Decomposition of SF6 in a Negative Glow Corona Discharge.
PB95-181053 *01,020* Not available NTIS

Plasma Chemistry in Disilane Discharges.
PB94-211075 *02,514* Not available NTIS

Plasma Chemistry in Silane/Germane and Disilane/Germane Mixtures.
PB95-202537 *01,027* Not available NTIS

Point Charges, Radiation Reaction, and Quantum Mechanics.
PB97-110563 *04,139* Not available NTIS

Point Probe Decision Trees for Geometric Concept Classes.
PB96-160817 *01,612* Not available NTIS

Polarimetric Calibration of Reciprocal-Antenna Radars.
PB95-216925 *01,872* PC A03/MF A01

Polarimetric Calibration of Reciprocal-Antenna Radars.
PB96-200696 *02,016* Not available NTIS

Polarizability of the Nucleon.
PB94-211760 *03,846* Not available NTIS

Polarization Analysis of the Magnetic Excitations in Fe65Ni35 Invar.
PB95-150082 *04,558* Not available NTIS

Polarization Analysis of the Magnetic Excitations in Invar and Non-Invar Amorphous Alloys.
PB94-216116 *04,516* Not available NTIS

Polarization Dependence of Response Functions in 3x3 Sagnac Optical Fiber Current Sensors.
PB95-162426 *02,154* Not available NTIS

Polarization Dependence of Response Functions in 3x3 Sagnac Optical Fiber Current Sensors.
PB96-122684 *02,189* Not available NTIS

Polarization Effects on Multiple Scattering Gamma Transport.
PB95-153615 *03,926* Not available NTIS

Polarization Insensitive 3x3 Sagnac Current Sensor Using Polarizing Spun High-Birefringence Fiber.
PB96-119276 *02,187* Not available NTIS

Polarization Measurements on a Magnetic Quadrupole Line in Ne-Like Barium.
PB97-113104 *04,161* Not available NTIS

Polarization of Light Emitted After Positron Impact Excitation of Alkali Atoms.
PB94-199734 *03,816* Not available NTIS

Polarized Transient Hot Wire Thermal Conductivity Measurements.
PB95-108817 *00,886* Not available NTIS

Polarized X-Ray Emission Spectroscopy.
PB94-213360 *03,862* Not available NTIS

Polyelectrolytes as Dispersants in Colloidal Processing of Silicon Nitride Ceramics.
PB95-175568 *03,055* Not available NTIS

Polyethylene Crystallized from an Entangled Solution Observed by Scanning Tunneling Microscopy.
PB95-107389 *01,232* Not available NTIS

Polymer Combustion and Flammability: Role of the Condensed Phase.
PB96-123245 *01,279* Not available NTIS

Polymer Composites Workshop. Held in Winona, Minnesota on April 29-30, 1992 (Video).
PB94-780129 *03,147* AV E99

Polymer Liquid Crystalline Materials.
PB94-212339 *01,224* Not available NTIS

Polymeric Calcium Phosphate Cements Derived from Poly(methyl vinyl ether-maleic acid).
PB96-164264 *00,180* Not available NTIS

Polymeric Calcium Phosphate Composites with Remineralization Potential.
PB96-155544 *03,575* Not available NTIS

Polymerization Initiation by N-p-Tolylglycine: Free-Radical Reactions Studied by Pulse and Steady-State Radiolysis.
PB95-180014 *01,269* Not available NTIS

Polymers Technical Activities 1994. NAC-NRC Assessment Panel, April 6-7, 1995.
PB95-209896 *01,275* PC A07/MF A02

Polymers Technical Activities, 1995.
PB96-193719 *01,291* PC A10/MF A02

Polyvinyl Chloride (PVC) Plastic Drain, Waste, and Vent Pipe and Fittings.
AD-A310 426/2 *00,326* PC A03/MF A01

Population Distributions and Intralaboratory Reproducibility for Fat-Soluble Vitamin-Related Compounds in Human Serum.
PB96-155536 *00,624* Not available NTIS

Population Trapping in Short-Pulse Multiphoton Ionization.
PB96-164140 *04,371* Not available NTIS

Pore-Forming Protein with a Metal-Actuated Switch.
PB96-176557 *03,554* Not available NTIS

Portable Operating System Interface (POSIX). Part 2. Shell and Utilities. Category: Software Standard; Subcategory: Operating Systems.
FIPS PUB 189 *01,797* PC A03/MF A01

Portable Vectorized Software for Bessel Function Evaluation.
PB94-198975 *01,690* Not available NTIS

Porting Multimedia Applications to the Open System Environment.
PB94-172921 *02,721* Not available NTIS

Portsmouth Fastener Manufacturing Workstation. User's Manual.
PB95-147922 *02,860* PC A06/MF A02

Positive and Negative Cooperativities at Subsequent Steps of Oxygenation Regulate the Allosteric Behavior of Multistate Sebacylhemoglobin.
PB97-119374 *03,486* Not available NTIS

Positronium in Relativistic Quantum Mechanics.
PB97-110571 *04,140* Not available NTIS

Post-Earthquake Fire and Lifelines Workshop. Held in Long Beach, California on January 30-31, 1995. Proceedings.
PB96-117916 *00,209* PC A04/MF A01

Post-Flame Soot.
PB96-193701 *01,430* PC A04/MF A01

Post-Occupancy Evaluation of the Forrestal Building.
PB97-111298 *00,280* Not available NTIS

Post-Process Control of Machine Tools.
PB95-203451 *02,952* Not available NTIS

Posterior Restorative Materials Research.
PB97-118624 *03,582* Not available NTIS

Postfailure Subsidiary Cracking from Indentation Flaws in Brittle Materials.
PB97-110340 *03,103* Not available NTIS

Potential and Current Distributions Calculated Across a Quantum Hall Effect Sample at Low and High Currents.
PB96-122106 *04,045*
(Order as PB96-117767, PC A08/MF A02)

Potential Drop in the Center-Cracked Panel with Asymmetric Crack Extension.
PB95-107330 *04,819* Not available NTIS

Potential Surfaces and Dynamics of Weakly Bound Trimers: Perspectives from High Resolution IR Spectroscopy.
PB96-176508 *01,155* Not available NTIS

Potentiometric Enzyme-Amplified Flow Injection Analysis Detection System: Behavior of Free and Liposome-Released Peroxidase.
PB95-151833 *03,534* Not available NTIS

Powder Diffraction File: Past, Present, and Future.
PB97-109086 *04,800*
(Order as PB97-109011, PC A11/MF A03)

Powder Neutron Diffraction Investigation of Structure and Cation Ordering in Ba2+xBi2-xO6-y.
PB95-180865 *01,015* Not available NTIS

Powder X-ray Diffraction Data for Ca2Bi2O5 and C4Bi6O13.
PB96-161278 *04,777* Not available NTIS

Power Characteristics in GMAW: Experimental and Numerical Investigation.
PB96-190145 *03,296* Not available NTIS

Practical Applications of the ITS-90: Inherent Uncertainties.
PB95-161527 *03,930* Not available NTIS

Practical Photomask Linewidth Measurements.
PB95-108510 *02,324* Not available NTIS

Practical Standards for PM and AM Noise at 5, 10 and 100 MHz.
PB95-181129 *01,546* Not available NTIS

Precise Identification of Computer Viruses.
PB96-160825 *01,613* Not available NTIS

Precise Laser-Based Measurements of Zero-Dispersion Wavelength in Single-Mode Fibers.
PB96-201124 *01,511* Not available NTIS

Precise Measurement of Heat of Combustion with a Bomb Calorimeter.
AD-A286 701/8 *03,770* PC A03/MF A01

Precise Optical Frequency References and Difference Frequency Measurements with Diode Lasers.
PB95-176228 *04,305* Not available NTIS

Precise Spectroscopy for Fundamental Physics.
PB96-112164 *04,040* Not available NTIS

Precision, Accuracy, Uncertainty and Traceability and Their Application to Submicrometer Dimensional Metrology.
PB94-213105 *02,319* Not available NTIS

Precision and Accuracy in Tandem Mass Spectrometry Measurements: A Kinetics-Based Protocol for Instrument-Independent Measurements of Collision-Activated Dissociation in RF-Only Quadrupoles.
PB94-216454 *00,858* Not available NTIS

Precision Comparison of the Lattice Parameters of Silicon Monocrystals.
PB94-169745 *04,438* Not available NTIS

Precision High Temperature Blackbodies.
PB95-140059 *03,885* Not available NTIS

Precision in Machining: Research Challenges.
PB95-242301 *02,953* PC A04/MF A01

Precision Laboratory Standards of Mass and Laboratory Weights.
AD-A280 562/0 *02,618* PC A03/MF A01

Precision Lifetime Measurements of Cs 6p (2)P1/2 and 6p (2)P3/2 Levels by Single-Photon Counting.
PB95-203816 *04,010* Not available NTIS

Precision Nuclear Orientation Measurements for Determining Mixed Magnetic Dipole/Electric Quadrupole Hyperfine Interactions.
PB94-199080 *03,810* Not available NTIS

Precision of Marchall Stability and Flow Test Using 6-in. (152.4-mm) Diameter Specimens.
PB96-200910 *03,006* Not available NTIS

Precision Oscillators: Dependence of Frequency on Temperature, Humidity and Pressure.
PB94-198306 *02,031* PC A03

Precision Resistors and Their Measurement.
AD-A284 623/6 *02,249* PC A03/MF A01

Precision Tests of a Quantum Hall Effect Device DC Equivalent Circuit Using Double-Series and Triple-Series Connections.
PB96-159256 *01,953*
(Order as PB96-159215, PC A07/MF A02)

Predicate Differences and the Analysis of Dependencies in Formal Specifications.
PB96-160940 *01,759* Not available NTIS

Predicting the Energy Performance Ratings of a Family of Type I Combination Appliances.
PB95-105524 *02,504* PC A03/MF A01

Predicting the Fire Performance of Buildings: Establishing Appropriate Calculation Methods for Regulatory Applications.
PB96-141239 *00,316* Not available NTIS

Predicting the Ignition Time and Burning Rate of Thermoplastics in the Cone Calorimeter.
PB96-154794 *01,418* PC A10/MF A03

Prediction of Cracking in Reinforced Concrete Structures.
PB95-220448 *03,725* PC A04/MF A01

Prediction of Fire Dynamics.
PB94-193620 *00,336* PC A03/MF A01

Prediction of Geometric-Thermal Machine Tool Errors by Artificial Neural Networks.
PB94-186673 *02,943* PC A07/MF A02

Prediction of Potential Concrete Strength at Later Ages.
PB96-112180 *01,324* Not available NTIS

Prediction of Strengthening Due to V Additions in Direct-Cooled Ferrite-Pearlite Forging Steels.
PB96-190251 *03,220* Not available NTIS

Prediction of the Strength Properties for Plain-Carbon and Vanadium Micro-Alloyed Ferrite-Pearlite Steel.
PB96-123393 *03,216* Not available NTIS

Prediction of the Thermal Conductivity of Refrigerants and Refrigerant Mixtures.
PB94-212107 *03,258* Not available NTIS

Prediction of Viscosity of Refrigerants and Refrigerant Mixtures.
PB94-212099 *03,257* Not available NTIS

Predictive Extended Corresponding States Model for Pure and Mixed Refrigerants Including an Equation of State for R134a.
PB95-175717 *03,275* Not available NTIS

Preferential In-Plane Rotational Excitation of H2O (001) by Translational-to-Vibrational Transfer from 2.2 eV H Atoms.
PB95-202875 *01,035* Not available NTIS

Preliminary Comparison of Time Transfers via LASSO, GPS and Two-Way Satellite.
PB95-151098 *01,529* Not available NTIS

Preliminary Functional Specifications of a Prototype Electronic Research Notebook for NIST.
PB94-207750 *00,012* PC A04/MF A01

Preliminary Investigation of Oleoresin Capsicum.
PB96-179486 *03,520* Not available NTIS

Preliminary List of References Containing Compilations of Data on Properties of Materials.
AD-A302 670/5 *03,243* PC A05/MF A01

Preliminary Processing of the Lotung LSST Data.
PB96-165972 *03,690* PC A05/MF A01

Preliminary Results of a Comparison of Water Triple-Point Cells Prepared by Different Methods.
PB96-161344 *00,634* Not available NTIS

Preliminary Subject and Authors Index to Compilations of Data on Properties of Materials.
AD-A302 669/7 *03,242* PC A04/MF A01

Preparation and Certification of a Rhodium Standard Reference Material Solution.
PB94-185071 *00,529* Not available NTIS

Preparation and Characterization of Cyclopolymerizable Resin Formulations.
PB96-146840 *01,285* Not available NTIS

Preparation and Characterization of (6)LiF and (10)B Reference Deposits for the Measurement of the Neutron Lifetime.
PB95-108692 *03,874* Not available NTIS

Preparation and Crystal Structure of Sr5TiNb4O17.
PB96-167341 *04,107* Not available NTIS

Preparation and Monitoring of Lead Acetate Containing Drinking Water Solutions for Toxicity Studies.
PB94-193885 *00,538* PC A03/MF A01

Preparation, Crystal Structure, Dielectric Properties, and Magnetic Behavior of Ba2Fe2Ti4O13.
PB96-186176 *01,162* Not available NTIS

Preparation of Immobilized Proteins Covalently Coupled Through Silane Coupling Agents to Inorganic Supports.
PB95-151403 *03,530* Not available NTIS

Preparation of Low Resistivity Contacts for High-Tc Superconductors.
PB95-153557 *02,258* Not available NTIS

Preparation of 2-Dimensional Ultra Thin Polystyrene Film by Water Casting Method.
PB95-162806 *04,619* Not available NTIS

Present and Future Standard Specimens for Surface Finish Metrology.
PB97-110423 *02,928* Not available NTIS

Present Worth Factors for Life-Cycle Cost Studies in the Department of Defense (1995).
PB95-105029 *03,664* PC A04/MF A01

Present Worth Factors for Life-Cycle Cost Studies in the Department of Defense (1996).
PB96-106869 *03,673* PC A04/MF A01

President's Column 'Editorial'.
PB96-164090 *02,239* Not available NTIS

President's Column for Dielectrics and Electrical Insulation Society Newsletter.
PB94-200409 *01,882* Not available NTIS

Pressure Dependencies of Standard Resistors.
PB95-153516 *02,257* Not available NTIS

Pressure Equations in Zone-Fire Modeling.
PB96-102967 *00,208* Not available NTIS

Pressure Measurements with the Mercury Melting Line Referred to ITS-90.
PB96-161005 *01,136* Not available NTIS

Pressure-Volume-Temperature Relations in Liquid and Solid Tritium.
PB94-140571 *00,726*
(Order as PB94-140555, PC A06/MF A02)

Pressurized Internal Lenticular Cracks at Healed Mica Interfaces.
PB96-180252 *02,997* Not available NTIS

Preview of ASHRAE's Revised Smoke Control Manual.
PB94-212875 *00,349* Not available NTIS

Principal Points and Self-Consistent Points of Symmetric Multivariate Distributions.
PB96-135090 *03,446* Not available NTIS

Principle of Congruence and Its Application to Compressible States.
PB96-102892 *01,068* Not available NTIS

Probabilistic Computation of Poiseuille Flow Velocity Fields.
PB96-102520 *04,209* Not available NTIS

Probabilistic Estimates of Design Load Factors for Wind-Sensitive Structures Using the 'Peaks Over Threshold' Approach.
PB96-183223 *00,474* PC A04/MF A01

Probing Bose-Einstein Condensed Atoms with Short Laser Pulses.
PB95-202818 *03,991* Not available NTIS

Probing Potential-Energy Surfaces via High-Resolution IR Laser Spectroscopy.
PB96-102835 *01,066* Not available NTIS

Problem of Convection in the Water Absorbed Dose Calorimeter.
PB97-110159 *03,523* Not available NTIS

Problems Related to the Determination of Mass Densities of Evaporated Reference Deposits.
PB95-163226 *03,941* Not available NTIS

Procedure for Measuring Trace Quantities of S2F10, S2OF10, and S2O2F10 in SF6 Using a Gas Chromatograph-Mass Spectrometer.
PB96-119755 *02,513* Not available NTIS

Procedure for Product Data Exchange Using STEP Developed in the AutoSTEP Pilot.
PB96-183058 *02,843* PC A04/MF A01

Procedure for the Study of Acidic Calcium Phosphate Precursor Phases in Enamel Mineral Formation.
PB95-164448 *03,564* Not available NTIS

Procedures for Document Facsimile Transmission Issued by General Services Administration, April 14, 1982. Federal Standard 1063.
FIPS PUB 148 *01,516* PC E99

Proceedings of a Workshop on Developing and Adopting Seismic Design and Construction Standards for Lifelines. Held in Denver, Colorado on September 25-27, 1991.
PB97-115794 *01,302* PC A16/MF A03

Proceedings of NIST Workshop: Industry Needs in Welding Research and Standards Development. Held on August 15-16, 1995.
PB96-183124 *02,877* PC A04/MF A01

Proceedings of the Annual Manufacturing Technology Conference (2nd): Toward a Common Agenda. Held in Gaithersburg, Maryland on April 18-20, 1995.
PB96-112693 *02,887* PC A99/MF E08

Proceedings of the Applied Diamond Conference 1995: Applications of Diamond Films and Related Materials International Conference (3rd). Held in Gaithersburg, Maryland, on August 21-24, 1995.
PB95-255204 *04,701* PC A99/MF E11

Proceedings of the Digital Systems Reliability and Nuclear Safety Workshop. Held in Rockville, Maryland on September 13-14, 1993.
NUREG/CP-0136 *03,728* PC A16/MF A03

Proceedings of the Manufacturing Technology Needs and Issues: Establishing National Priorities and Strategies Conference. Held in Gaithersburg, Maryland on April 26-28, 1994.
PB95-206181 *02,930* PC A22/MF A04

Proceedings of the Meeting of the Intergovernmental U.S.-Russian Business Development Committee's Standard Working Group (4th). Held in New York City, New York on March 27-29, 1995 and in Northbrook, Illinois on March 30-31, 1995.
PB95-255881 *00,496* PC A11/MF A03

Proceedings of the Open Forum on Laboratory Accreditation at the National Institute of Standards and Technology, October 13, 1995.
PB96-210141 *02,686* PC A10/MF A03

Proceedings of the Workshop on the Federal Criteria for Information Technology Security. Held in Ellicot City, Maryland on June 2-3, 1993.
PB94-162583 *01,575* PC A04/MF A01

Proceedings of the 1995 Workshop on Fire Detector Research. Held on February 6-7, 1995.
PB95-270062 *02,611* PC A03/MF A01

Proceedings Report of the International Invitation Workshop on Development Assurance. Held in Ellicott City, Maryland on June 16-17, 1994.
PB95-189494 *02,912* PC A03/MF A01

Proceedings: Workshop on Research Needs in Wind Engineering. Held in Gaithersburg, Maryland on September 12-13, 1994.
PB95-189528 *00,448* PC A05/MF A01

Process for Selecting Standard Reference Algorithms for Evaluating Coordinate Measurement Software.
PB94-173754 *02,629* PC A03/MF A01

Process Gas Chromatography Detector for Hydrocarbons Based on Catalytic Cracking.
PB95-141099 *02,485* Not available NTIS

Process Modeling and Control of Inert Gas Atomization.
PB95-162343 *02,824* Not available NTIS

Process Monitoring with Residual Gas Analyzers (RGAs): Limiting Factors.
PB95-181004 *02,660* Not available NTIS

Product Kinetic Energies, Correlations, and Scattering Anisotropy in the Bimolecular Reactor O((1)D)+H2O yields 2OH.
PB94-212792 *00,838* Not available NTIS

Product Models and Virtual Prototypes in Mechanical Engineering.
PB95-253563 *02,783* PC A03/MF A01

Product Realization Process Modeling: A Study of Requirements, Methods and Research Issues.
PB96-147962 *02,836* PC A04/MF A01

Product State Correlations in the Reaction of O((1)D) and H2O in Bimolecular Collisions and in O3.H2O Clusters--Translation.
PB95-153011 *00,946* Not available NTIS

Production and Characterization of Ion Beam Sputtered Multilayers.
PB95-162053 *03,936* Not available NTIS

Production and Spectroscopy of Small Polyatomic Molecular Ions Isolated in Solid Neon. (Reannouncement with New Availability Information).
AD-A234 043/8 *00,704* PC A03/MF A01

Production Management Information Model for Discrete Manufacturing.
PB96-112008 *02,830* Not available NTIS

Proficiency Testing as a Component of Quality Assurance in Construction Materials Laboratories.
PB94-185774 *00,334* Not available NTIS

Proficiency Tests for the NIST Airborne Asbestos Program, 1990.
PB94-188836 *00,535* PC A07/MF A02

Proficiency Tests for the NIST Airborne Asbestos Program - 1991.
PB94-193828 *00,537* PC A04/MF A01

Proficiency Tests for the NIST Airborne Asbestos Program - 1992.
PB94-194362 *00,539* PC A03/MF A01

Proficiency Tests for the NIST Airborne Asbestos Program, 1993.
PB96-106463 *00,610* PC A03/MF A01

Profile Fitting of X-Ray Diffraction Lines and Fourier Analysis of Broadening.
PB94-198512 *04,460* Not available NTIS

Program Handbook: Requirements for Obtaining NIST Approval/Recognition of a Laboratory Accreditation Body Under P.L. 101-592. The Fastener Quality Act.
PB94-210143 *02,859* PC A03/MF A01

Program of the Manufacturing Engineering Laboratory, 1995. Infrastructural Technology, Measurements, and Standards for the U.S. Manufacturing Industries.
PB95-188835 *02,754* PC A11/MF A02

Program of the Manufacturing Engineering Laboratory, 1996. Infrastructural Technology, Measurements, and Standards for the U.S. Manufacturing Industries.
PB96-195276 *02,760* PC A11/MF A03

Program of the Subcommittee on Construction and Building.
PB94-193646 *00,319* PC A03/MF A01

Program of the Subcommittee on Construction and Building (July 1994).
PB95-122537 *00,321* PC A03/MF A01

Program Requirements to Advance the Technology of Custom Footwear Manufacturing.
PB95-147906 *02,883* PC A04/MF A01

Program Slicing.
PB96-160981 *01,761* Not available NTIS

Programmable Guarded Coaxial Connector Panel.
PB96-122544 *02,108* Not available NTIS

Programmer's Hierarchical Interactive Graphics System (PHIGS). Category: Software Standard; Subcategory: Graphics.
FIPS PUB 153-1 *01,668* PC E99

Progress in the Development of a Chemical Kinetic Database for Combustion Chemistry.
PB95-151056 *01,384* Not available NTIS

Progress on a Cryogenic Linear Trap for (199)Hg(+) Ions.
PB95-180790 *03,965* Not available NTIS

Progress on the Quantized Hall Resistance Recommended Intrinsic/Derived Standards Practice.
PB96-122460 *02,403* Not available NTIS

Progress Report to National Aeronautics and Space Administration on Cryogenic Research and Development.
AD-A286 612/7 *01,458* PC A05/MF A01

Progress Toward Accurate Metrology Using Atomic Force Microscopy.
PB96-146774 *02,417* Not available NTIS

Project Summaries 1994: NIST Building and Fire Research Laboratory.
PB94-207495 *00,343* PC A08/MF A02

Project Summaries 1995: NIST Building and Fire Research Laboratory.
PB95-270047 *00,400* PC A10/MF A03

Promise into Practice: Implementing TA2 on Real Clocks at NIST.
PB95-151478 *01,533* Not available NTIS

Properties and Interactions of Oral Structures and Restorative Materials. Annual Report for Period October 1, 1990 to September 30, 1991.
PB94-160843 *03,558* PC A06/MF A01

Properties and Mechanisms of Fast-Setting Calcium Phosphate Cements.
PB96-123229 *00,178* Not available NTIS

Properties of a Bose-Einstein Condensate in an Anisotropic Harmonic Potential.
PB96-204144 *04,133* Not available NTIS

Properties of Working Fluids for Thermoacoustic Refrigerators.
AD-A297 420/2 *04,864* PC A06/MF A02

Proposed Analysis of RCS Measurement Uncertainty.
PB95-203568 *01,871* Not available NTIS

Proposed Antiferromagnetically Coupled Dual-Layer Magnetic Force Microscope Tips.
PB95-169017 *04,645* Not available NTIS

Proposed Changes to Charpy V-Notch Machine Certification Requirements.
PB96-135363 *02,955* Not available NTIS

Proposed Coating Technology Consortium. (National Coil Coaters Association Fall Conference). Held in Rosemont, Illinois in September 1992.
PB97-110431 *03,129* Not available NTIS

Proposed High-Accuracy Superconducting Power Meter for Millimeter Waves.
PB94-212669 *02,034* Not available NTIS

Proposed International Interactive Courseware Standard.
PB96-123161 *00,137* Not available NTIS

Proposed Tests to Evaluate the Frequency-Dependent Capacitor Ratio for Single Electron Tunneling Experiment.
PB97-111454 *01,982* Not available NTIS

Protecting Your Family from Fire.
PB96-156187 *00,307* Not available NTIS

Protection Against Neutron Radiation Up to 30 Million Electron Volts.
AD-A286 681/2 *03,611* PC A05/MF A01

Protection Against Radiations from Radium, Cobalt-60, and Cesium-137.
AD-A279 261/2 *03,607* PC A04/MF A01

Protection of Data Processing Equipment with Fine Water Sprays.
PB95-174975 *02,610* PC A04/MF A01

Protein Data Bank: Current Status and Future Challenges.
PB97-109060 *00,517*
(Order as PB97-109011, PC A11/MF A03)

Protein Extraction in a Spray Column Using a Polyethylene Glycol Maltodextrin Two-Phase Polymer System.
PB95-162228 *00,595* Not available NTIS

Proteoglycan Inhibition of Calcium Phosphate Precipitation in Liposomal Suspensions.
PB94-211208 *00,658* Not available NTIS

Proton Affinity Ladders from Variable-Temperature Equilibrium Measurements. 1. A Re-Evaluation of the Upper Proton Affinity Range.
PB94-216603 *00,861* Not available NTIS

Protonation Dynamics in an Ion Channel Pore.
PB96-161757 *03,589* Not available NTIS

Protonation Dynamics of the alpha-Toxin Ion Channel from Spectral Analysis of pH-Dependent Current Fluctuations.
PB96-161740 *03,652* Not available NTIS

Prototype Information Retrieval System to Perform a Best-Match Search for Names.
PB95-181152 *02,740* Not available NTIS

Prototyping a Graphical User Interface for DHCP.
PB96-160544 *02,599* Not available NTIS

Provision of Isochronous Service on IEEE 802.6.
PB96-160635 *01,501* Not available NTIS

Psychological Aspects of Lighting: A Review of the Work of CIE TC 3.16.
PB94-172160 *00,241* Not available NTIS

Psychological Aspects of Lighting: A Review of the Work of CIE TC 3.16.
PB95-153276 *00,254* Not available NTIS

Public Key Infrastructure Invitational Workshop. Held in McLean, Virginia on September 28, 1995.
PB96-166004 *01,616* PC A08/MF A02

Publication and Presentation Abstracts, 1993. (Published by Paffenbarger Research Center and Center of Excellence for Materials Science Research).
PB95-153052 *03,562* Not available NTIS

Publication and Presentation Abstracts, 1994.
PB96-176623 *03,577* Not available NTIS

Publication and Presentation Abstracts, 1995.
PB96-164082 *03,576* Not available NTIS

Publication and Presentation Abstracts, 1996.
PB97-122238 *03,585* Not available NTIS

Publications and Presentation Abstracts, 1995. (Published by Paffenbarger Research Center and Center of Excellence for Materials Science Research).
PB96-119250 *03,568* Not available NTIS

Publications of the Intelligent Systems Division (Previously Robot Systems Division) Covering the Period January 1971-April 1994.
PB94-217098 *02,935* PC A05/MF A01

Publications of the Manufacturing Engineering Laboratory Covering the Period January 1989-September 1992.
PB94-165966 *02,750* PC A06/MF A02

Publications of the National Institute of Standards and Technology 1992 Catalog.
PB95-200747 *00,014* PC A17/MF A04

Publications of the National Institute of Standards and Technology 1993 Catalog.
PB96-183215 *00,017* PC A11/MF A03

Publications 1995: NIST Building and Fire Research Laboratory.
PB96-183074 *00,226* PC A08/MF A02

Pulse-Driven Programmable Josephson Voltage Standard.
PB97-111496 *04,148* Not available NTIS

Pulse-Echo Ultrasonic Evaluation of the Integrity of Seams of Single-Ply Roof Membranes.
PB95-163804 *00,381* Not available NTIS

Pulsed Laser Irradiation at 532 nm of In and Ga Adsorbed on Si(100): Desorption, Incorporation, and Damage.
PB95-203329 *01,051* Not available NTIS

Pulsed Laser Photolysis Time-Resolved FT-IR Emission Studies of Molecular Dynamics.
PB95-203162 *04,002* Not available NTIS

Pump-Induced Dispersion of Erbium-Doped Fiber Measured by Fourier-Transform Spectroscopy.
PB94-211935 *04,236* Not available NTIS

Pure Element Sputtering Yield Data: Appendix 4.
PB94-200037 *00,805* Not available NTIS

Pure Rotational Spectra of CuH and CuD in Their Ground States Measured by Tunable Far-Infrared Spectroscopy.
PB95-176194 *01,005* Not available NTIS

Putting the Information Infrastructure to Work: Report of the Information Infrastructure Task Force Committee on Applications and Technology.
N94-31228/7 *02,715* PC A06/MF A02

Putting the Information Infrastructure to Work: Report of the Information Infrastructure Task Force Committee on Applications and Technology.
PB94-163383 *00,001* PC A06/MF A02

Q Branch Lineshape Functions for CARS Thermometry.
PB96-160643 *01,132* Not available NTIS

q Dependence of Self-Energy Effects of the Plane Oxygen Vibration in YBa2Cu3O7.
PB96-138516 *01,096* Not available NTIS

Quadratic Response of a Chemical Reaction to External Oscillations.
PB96-161633 *01,138* Not available NTIS

Quality Assurance of Contaminant Measurements in Marine Mammal Tissues.
PB95-164034 *02,588* Not available NTIS

Quality Characteristics and Metrics for Reusable Software (Preliminary Report).
PB94-203437 *01,693* PC A03/MF A01

Quality in Automated Manufacturing.
PB96-160437 *02,839* Not available NTIS

Quantifying the Ignition Propensity of Cigarettes.
PB96-155411 *00,306* Not available NTIS

Quantitative Analysis of Selected PCB Congeners in Marine Matrix Reference Materials Using a Novel Cyanobiphenyl Stationary Phase.
PB96-111737 *02,591* Not available NTIS

Quantitative Determination of Oxidative Base Damage in DNA by Stable Isotope-Dilution Mass Spectrometry.
PB96-200886 *03,483* Not available NTIS

Quantitative Evaluation of Building Fire Safety: New Tools for Assessing Fire and Building Code Provisions.
PB95-164588 *00,199* Not available NTIS

Quantitative Measure of Efficiency of Monte Carlo Simulations.
PB95-180691 *01,011* Not available NTIS

Quantitative Measurements of Enhanced Soot Production in a Flickering Methane/Air Diffusion Flame.
PB95-203246 *01,393* Not available NTIS

Quantitative Phase Abundance Analysis of Three Cement Clinker Reference Materials by Scanning Electron Microscopy.
PB94-173051 *00,333* Not available NTIS

Quantitative X-Ray Powder Diffraction Methods for Clinker and Cement.
PB95-143079 *01,317* PC A03/MF A01

Quantized Dissipation of the Quantum Hall Effect at High Currents.
PB94-199395 *04,472* Not available NTIS

Quantum Collisional Transfer Contributions to the Density Dependence of Gaseous Viscosity.
PB96-161914 *01,142* Not available NTIS

Quantum Conductance Fluctuations in the Larger-Size-Scale Regime.
PB97-111264 *04,144* Not available NTIS

Quantum Dots in Quantum Well Structures.
PB97-118350 *01,185* Not available NTIS

Quantum Dynamics of Renner-Teller Vibronic Coupling: The Predissociation HCO.
PB94-185303 *00,773* Not available NTIS

Quantum Hall Effect-Based Resistance Standard: Capabilities and Implementation.
PB96-180096 *04,114* Not available NTIS

Quantum Hall Effect-Based Resistance Standard (Quantum Hall Res).
PB96-200944 *04,127* Not available NTIS

Quantum-Limited Cooling and Detection of Radio-Frequency Oscillations by Laser-Cooled Ions.
PB96-112073 *04,039* Not available NTIS

Quantum Measurements of Trapped Ions.
PB95-161147 *03,928* Not available NTIS

Quantum Mechanics of a Solid-State Bar Gravitational Antenna.
PB95-202628 *03,987* Not available NTIS

Quantum Projection Noise: Population Fluctuations in Two-Level Systems.
PB94-212271 *03,850* Not available NTIS

Quantum Yields for the Photosensitized Formation of the Lowest Electronically Excited Singlet State of Molecular Oxygen in Solution.
PB94-161007 *00,732* Not available NTIS

Quasielastic and Inelastic Neutron-Scattering Studies of ((CD3)3ND)FeCl3.2D2O: A One-Dimensional Ising Ferromagnet.
PB95-140562 *04,547* Not available NTIS

Quasipotential and the Stability of Phase Lock in Nonhysteretic Josephson Junctions.
PB95-180402 *04,681* Not available NTIS

Quench Energy and Fatigue Degradation Properties of Cu- and Al/Cu-Stablized Nb-Ti Epoxy-Impregnated Superconductor Coils.
PB96-141213 *04,755* Not available NTIS

Quest to Understand and Reduce I/f Noise in Amplifiers and Baw Quartz Oscillators.
PB96-200795 *02,097* Not available NTIS

Questions and Answers on Quality, the ISO 9000 Standard Series, Quality System Registration, and Related Issues. More Questions and Answers on the ISO 9000 Standard Series and Related Issues.
PB95-103461 *00,495* PC A03/MF A01

Radiance Temperature (in the Wavelength Range 519-906 nm) of Tungsten at Its Melting Point by a Pulse-Heating Technique.
PB94-172500 *03,397* Not available NTIS

Radiance Temperatures at 1500 nm of Niobium and Molybdenum at Their Melting Points by a Pulse-Heating Technique.
PB97-118699 *04,167* Not available NTIS

Radiance Temperatures (in the Wavelength Range 523-907 nm) of Group IV B Transition Metals Titanium, Zirconium, and Hafnium at Their Melting Points by a Pulse-Heating Technique.
PB96-102207 *03,356* Not available NTIS

Radiance Temperatures (in the Wavelength Range 523-907 nm) of Group IVB Transition Metals Titanium, Zirconium, and Hafnium at Their Melting Points by a Pulse-Heating Technique.
PB96-135025 *02,677* Not available NTIS

Radiated Emissions and Immunity of Microstrip Transmission Lines: Theory and Measurements.
PB96-162649 *02,238* PC A04/MF A01

Radiation Accident at an Industrial Accelerator Facility.
PB95-140117 *02,575* Not available NTIS

Radiation and Mixing Properties of Buoyant Turbulent Diffusion Flames.
PB94-165974 *01,360* PC A04/MF A01

Radiation-Chemical Reaction of 2,3,5-Triphenyl-Tetrazolium Chloride in Liquid and Solid State.
PB96-146733 *01,124* Not available NTIS

Radiation Chemistry of Cyanine Dyes: Oxidation and Reduction of Merocyanine 540.
PB94-211661 *00,818* Not available NTIS

Radiation Doses.
PB94-199676 *03,618* Not available NTIS

Radiation-Driven Winds of Hot Luminous Stars X. The Determination of Stellar Masses Radii and Distances from Terminal Velocities and Mass-Loss Rates.
PB94-213022 *00,060* Not available NTIS

Radiation Process Data: Collection, Analysis, and Interpretation.
PB95-162632 *03,628* Not available NTIS

Radio and X-ray Emissions from Chemically Peculiar B- and A-Type Stars: Observations and a Model.
PB96-123302 *00,103* Not available NTIS

Radio Continuum and X-Ray Properties of the Coronae of RS Canum Venaticorum and Related Active Binary Systems.
PB94-211083 *00,057* Not available NTIS

Radio Emission from Chemically Peculiar Stars.
PB94-213469 *00,068* Not available NTIS

Radioassays of Yttrium-90 Used in Nuclear Medicine.
PB97-110100 *03,522* Not available NTIS

Radiocarbon Measurements of Atmospheric Volatile Organic Compounds: Quantifying the Biogenic Contribution.
PB97-122352 *02,574* Not available NTIS

Radiochromic Solid-State Polymerization Reaction.
PB95-180683 *01,271* Not available NTIS

Radiochromic Solid-State Polymerization Reaction.
PB96-180146 *01,290* Not available NTIS

Radiometer Equation for Noise Comparison Radiometers.
PB96-140363 *02,195* Not available NTIS

Radiometric Model of the Transmission Cell-Reciprocal Nephelometer.
PB95-150132 *00,124* Not available NTIS

Radon in the Lung.
PB97-110035 *03,638* Not available NTIS

Raman and Fluorescence Spectra Observed in Laser Microprobe Measurements of Several Compositions in the Ln-Ba-Cu-O System.
PB94-172210 *04,440* Not available NTIS

Range Statistics and Rutherford Backscattering Studies on Fe-Implanted In0.53Ga0.47As.
PB95-126397 *04,535* Not available NTIS

RangeCAD and the NIST RCS Uncertainty Analysis.
PB94-218591 *01,870* PC A03/MF A01

Ranges of Confidence Coefficients for Confiedence Intervals on Variance Components.
PB95-151312 *03,437* Not available NTIS

Rapid Decline in the Optical Emission from SN 1957D in M83.
PB94-216033 *00,070* Not available NTIS

Rapid Evaluation of Mode-Stirred Chambers Using Impulsive Waveforms.
PB96-210026 *01,979* PC A04/MF A01

Rapid Hot Pressing of Ultra-Fine PSZ Powders.
PB94-216587 *03,045* Not available NTIS

Rapid Method for the Isolation of Genomic DNA from 'Aspergillus fumigatus'.
PB96-147061 *03,488* Not available NTIS

Rapid pH Change Due to Bacteriorhodopsin Measured with a Tin-Oxide Electrode.
PB96-112081 *03,544* Not available NTIS

Rapid Post-Polishing of Diamond-Turned Optics.
PB95-175949 *04,301* Not available NTIS

Rare-Earth-Doped Waveguide Devices: The Potential for Compact Blue-Green Lasers.
PB95-140836 *04,257* Not available NTIS

Rare-Earth Isotopes as Tracers of Particulate Emissions: An Urban Scale Test.
PB94-161635 *02,535* PC A03/MF A01

Rate Constants for Hydrogem Atom Attack on Some Chlorinated Benzenes at High Temperature.
PB94-200581 *00,810* Not available NTIS

Rate Constants for the Decay and Reactions of the Lowest Electronically Excited Singlet State of Molecular Oxygen in Solution. An Expanded and Revised Compilation.
PB96-145826 *01,106* Not available NTIS

Rate Constants for the Gas Phase Reactions of the OH Radical with CF3CF2CHCl2 (HCFC-225ca) and CF2ClCF2CHClF (HCFC-225cb).
PB95-152153 *00,940* Not available NTIS

Rate of Heat Release of Wood Products.
PB94-212404 *03,403* Not available NTIS

Rationale and Preliminary Plan for Federal Research for Construction and Building.
PB95-154704 *00,322* PC A07/MF A02

Rayleigh Instability for a Cylindrical Crystal-Melt Interface.
PB95-180667 *01,010* Not available NTIS

Rayleigh Scattering Limits for Low-Level Bidirectional Reflectance Distribution Function Measurements.
PB95-180030 *04,307* Not available NTIS

Rb-Like Spectra: Pd X to Nd XXIV.
PB95-150645 *03,897* Not available NTIS

RDFs and Fe-Fe Pair Correlations in an AlCuFe Icosahedral Alloy by Double Isotopic Substitution.
PB94-172129 *04,439* Not available NTIS

RDI-SIM ECMA Inter-Domain Routing Protocol Simulation Tool.
PB94-172301 *01,683* Not available NTIS

Reaction of Nitric Oxide with Organic Peroxyl Radicals.
PB95-141107 *00,910* Not available NTIS

Reaction of NO with Superoxide.
PB94-212198 *00,830* Not available NTIS

Reaction Rate Determinations of Vinyl Radical Reactions with Vinyl, Methyl, and Hydrogen Atoms.
PB94-211398 *00,815* Not available NTIS

Reaction Sensitivities of Al-Li Alloys and Alloy 2219 in Mechanical-Impact Tests.
PB94-172764 *03,314* Not available NTIS

Reactive Coevaporation of DyBaCuO Superconducting Films: The Segregation of Bulk Impurities on Annealed MgO(100) Substrates.
PB95-164562 *04,635* Not available NTIS

Reactive Ion Etching in the Gaseous Electronics Conference RF Reference Cell.
PB96-113402 *02,395*
(Order as PB96-113311, PC A09/MF A03)

Reactivity of Pd and Sn Adsorbates on Plasma and Thermally Oxidized SnO2(110).
PB94-199973 *00,804* Not available NTIS

Reactivity of Product Gases Generated in Idealized Enclosure Fire Environments.
PB95-161790 *01,386* Not available NTIS

Reactor Radiation Technical Activities, 1994. NAS-NRC Assessment Panel, April 6-7, 1995.
PB95-209888 *03,732* PC A08/MF A02

Reactor Radiation Technical Activities, 1995.
PB96-193644 *03,741* PC A07/MF A02

Real Time Compensation for Tool Form Errors in Turning Using Computer Vision.
PB95-107231 *02,945* Not available NTIS

Real Time Differential Range Estimation Based on Time-Space Imagery Using PIPE.
PB95-161808 *01,844* Not available NTIS

Real-Time Implementation of a Differential Range Finder.
PB95-108650 *01,839* Not available NTIS

Real Time Monitoring of Electron Processors.
PB96-135306 *03,719* Not available NTIS

Real-Time Obstacle Avoidance Using Central Flow Divergence and Peripheral Flow.
PB95-198677 *02,937* PC A03/MF A01

Real-Time Small-Angle X-Ray Scattering Study of the Early Stage of Phase Separation in the SiO2-BaO-K20 System.
PB95-163069 *03,052* Not available NTIS

Real-Time Vision for Autonomous and Teleoperated Control of Unmanned Vehicles.
PB94-211885 *03,701* Not available NTIS

Real-Time Vision for Unmanned Vehicles.
PB94-211893 *03,702* Not available NTIS

Realization of a Scale of Absolute Spectral Response Using the NIST High Accuracy Cryogenic Radiometer.
PB97-118640 *04,397* Not available NTIS

Realization of New NIST Radiation Temperature Scales for the 1000 K to 3000 K Region, Using Absolute Radiometric Techniques.
PB94-172905 *03,794* Not available NTIS

Realization of NIST 1995 Luminous Flux Scale Using the Integrating Sphere Method.
PB96-176433 *04,374* Not available NTIS

Realizing Suspended Structures on Chips Fabricated by CMOS Foundry Processes Through the MOSIS Service.
PB94-193984 *01,881* PC A04/MF A01

Reanalysis of the (010), (020), (100), and (001) Rotational Levels of (32)S(16)O2.
PB95-125621 *00,887* Not available NTIS

Recalibration for the Final Archive of the International Ultraviolet Explorer (IUE) Satellite.
PB96-135264 *00,106* Not available NTIS

Recent Approaches to Extreme Value Estimation with Application to Wind Speeds. Part 1. The Pickands Method.
PB94-213170 *00,019* Not available NTIS

Recent Development in Nondestructive Testing of Concrete.
PB96-122445 *01,325* Not available NTIS

Recent Developments at NIST on Optical Current Sensors and Partial Discharge Diagnostics.
PB95-151114 *02,147* Not available NTIS

Recent Developments in NIST Botanical SRMs.
PB96-167267 *03,489* Not available NTIS

Recent Experimental and Modeling Developments in High Temperature Thermochemistry.
PB94-172343 *00,759* Not available NTIS

Recent Experiments on Trapped Ions at the National Institute of Standards and Technology.
PB95-169322 *03,952* Not available NTIS

Recent Results in Magnetic Force Microscopy.
PB96-103130 *04,721* Not available NTIS

Recent VAMAS Activity in Ceramics.
PB95-162681 *03,051* Not available NTIS

Recently Developed NIST Food Related Standard Reference Materials.
PB94-198322 *00,035* Not available NTIS

Recertification of the Standard Reference Material 1475A, a Linear Polyethylene Resin.
PB94-161932 *02,628* PC A03/MF A01

Rechargeable Batteries for Personal/Portable.
PB96-164231 *02,459* Not available NTIS

Reciprocity Relations in Waveguide Junctions.
PB94-172814 *02,213* Not available NTIS

Recombination Line Intensities for Hydrogenic Ions-III. Effects of Finite Optical Depth and Dust.
PB95-202677 *00,079* Not available NTIS

Recommendations for the Disposal of Carbon-14 Wastes.
AD-A279 133/3 *02,579* PC A03/MF A01

Recommendations on Selection of Vehicle-to-Roadside Communications Standards for Commercial Vehicle Operations.
PB94-195914 *04,859* PC A05/MF A01

Recommended Changes in ASTM Test Methods D2512-82 and G86-84 for Oxygen-Compatibility Mechanical Impact Tests on Metals.
PB94-216694 *03,338* Not available NTIS

Recommended Performance-Based Criteria for the Design of Manufactured Home Foundation Systems to Resist Wind and Seismic Loads.
PB96-128285 *00,460* PC A05/MF A01

Reconstructing Stratified Fluid Flow from Reciprocal Scattering Measurements.
PB95-107256 *04,202* Not available NTIS

Reconstruction during Camera Fixation.
PB95-162236 *01,593* Not available NTIS

Redshifts in Stellar Transition Regions.
PB96-123310 *00,104* Not available NTIS

Reducing Errors, Complexity, and Measurement Time of PM Noise Measurements.
PB96-119771 *02,075* Not available NTIS

Reducing the Effect of Local Oscillator Phase Noise on the Frequency Stability of Passive Frequency Standards.
PB95-180972 *01,545* Not available NTIS

Reducing the 1/f AM and PM Noise in Electronics for Precision Frequency Metrology.
PB97-113195 *02,102* Not available NTIS

Reduction of Dinitrogen to Ammonia in Aqueous Solution Mediated by Colloidal Metals.
PB95-107074 *00,867* Not available NTIS

Reduction of Interfilament Contact Loss in Nb3Sn Superconductor Wires.
PB95-175535 *02,223* Not available NTIS

Reduction of Light-Assisted Collisional Loss Rate from a Low-Pressure Vapor-Cell Trap.
PB95-202248 *03,971* Not available NTIS

Reduction of Marginal Gaps in Composite Restorations by Use of Glass-Ceramic Inserts.
PB96-102405 *00,174* Not available NTIS

Reference Architecture for Machine Control Systems Integration: Interim Report.
PB95-144549 *02,820* PC A06/MF A02

Reference Data for the Thermophysical Properties of Cryogenic Fluids.
PB95-168688 *03,263* Not available NTIS

Reference Information for the Software Verification and Validation Process.
PB96-188164 *01,773* PC A06/MF A01

Reference Manual for the Algorithm Testing System Version 2.0.
PB96-128244 *02,922* PC A03/MF A01

Reference Materials by Isotope Dilution Mass Spectrometry.
PB95-153383 *00,592* Not available NTIS

Reference Model Architecture for Intelligent Systems Design.
PB95-143137 *01,789* PC A03/MF A01

Reference Relations for the Evaluation of the Materials Properties of Orthorhombic YBa2Cu3Ox Superconductors.
PB96-176763 *04,782* Not available NTIS

Reference Tables for Thermocouples.
AD-A279 948/4 *02,614* PC A05/MF A01

REFPROP Refrigerant Properties Database: Capabilities, Limitations, and Future Directions.
PB96-167150 *01,149* Not available NTIS

Refraction of Light by Graded Birefringent Media.
PB96-123716 *02,192* Not available NTIS

Refractive Indices of Fluids Related to Alternative Refrigerants.
PB94-219375 *03,260*
(Order as PB94-219326, PC A05/MF A02)

Regimes of Surface Roughness Measurable with Light Scattering.
PB95-151213 *04,265* Not available NTIS

Regulation of Lithium and Boron Levels in Normal Human Blood: Environmental and Genetic Considerations.
PB94-198579 *03,491* Not available NTIS

Reinforcement of Cancellous Bone Screws with Calcium Phosphate Cement.
PB96-158001 *00,179* Not available NTIS

Relating Bench-Scale and Full-Scale Toxicity Data.
PB95-125977 *00,361* Not available NTIS

Relation between AC Impedance Data and Degradation of Coated Steel. 1. Effects of Surface Roughness and Contamination on the Corrosion Behavior of Epoxy Coated Steel.
PB94-213345 *03,189* Not available NTIS

Relationship between Bulk-Modulus Temperature Dependence and Thermal Expansivity.
PB95-168829 *04,641* Not available NTIS

Relationship between Indoor Air Quality and Carbon Dioxide.
PB97-111249 *02,569* Not available NTIS

Relationship between Radiative and Magnetic Fluxes for Three Active Solar-Type Dwarfs.
PB96-119540 *00,097* Not available NTIS

Relationship of AM to PM Noise in Selected RF Oscillators.
PB95-169009 *02,262* Not available NTIS

Relationship of Silver with Selenium and Mercury in the Liver of Two Species of Toothed Whales (Odontocetes).
PB96-167275 *02,596* Not available NTIS

Relative Accuracy of Isolated and Unisolated Noise Comparison Radiometers.
PB96-111851 *01,924* Not available NTIS

Relative Photoionization and Photodetachment Cross Sections for Particular Fine-Structure Transitions with Application to Cl 3s-subshell Photoionization.
PB95-203097 *03,998* Not available NTIS

Relative Sensitivity Factors and Useful Yields for a Microfocused Gallium Ion Beam and Time-of-Flight Secondary Ion Mass Spectrometer.
PB94-198736 *00,541* Not available NTIS

Relativistic and Quantum Electrodynamic Effects in Highly-Charged Ions.
PB94-212784 *03,854* Not available NTIS

Relativistic Effects in Spin-Polarization Parameters for Low-Energy Electron-Cs Scattering.
PB95-150868 *03,901* Not available NTIS

Relativistic Modifications of Charge Expansion Theory.
PB96-123799 *04,052* Not available NTIS

Relativistic Quantum Mechanics of Interacting Particles.
PB97-110589 *04,141* Not available NTIS

Relativistic R-Matrix Calculations for Electron - Alkali-Metal-Atom Scattering: Cs as a Test Case.
PB95-203410 *04,006* Not available NTIS

Relaxation After a Temperature Jump Within the One Phase Region of a Polymer Mixture.
PB97-112494 *03,394* Not available NTIS

Reliable Optical Flow Algorithm Using 3-D Hermite Polynomials.
PB94-145620 *01,829* PC A03/MF A01

Remineralization of Root Lesions with Concentrated Calcium and Phosphate Solutions.
PB96-102140 *03,567* Not available NTIS

Remineralizing Dental Composites Based on Amorphous Calcium Phosphate.
PB96-147020 *03,573* Not available NTIS

Repair of Products of Oxidative DNA Base Damage in Human Cells.
PB96-190129 *03,555* Not available NTIS

Replicate Measurements for Data Quality and Environmental Modeling.
PB94-172533 *02,515* Not available NTIS

Reply to Professor Wolf's Comments on My Paper on Wolf Shifts.
PB94-219409 *04,247*
(Order as PB94-219326, PC A05/MF A02)

Report of a Workshop on Requalification of Tubular Steel Joints in Offshore Structures. Held in Houston, Texas on September 5-6, 1995.
PB96-210760 *03,699* PC A07/MF A02

Report of a Workshop on the Assurance of High Integrity Software.
PB96-161377 *01,763* Not available NTIS

Report of Density Intercomparisons Undertaken by the Working Group on Density of the CCM.
PB94-200664 *00,503* Not available NTIS

Report of the Federal Internetworking Requirements Panel.
DE95017761 *03,407* PC A03/MF A01

Report of the International Commission on Radiological Units and Measurements (ICRU), 1956.
AD-A279 120/0 *03,513* PC A04/MF A01

Report of the National Conference on Weight and Measures (78th). Held in Kansas City, MO. on July 18-22, 1993.
PB94-138989 *02,623* PC A18/MF A04

Report of the National Conference on Weights and Measures (79th). Held in San Diego, California on July 17-21, 1994.
PB95-169819 *02,656* PC A20/MF A04

Report of the National Conference on Weights and Measures (80th) as Adopted by the 80th National Conference on Weights and Measures, 1995. Held in Portland, Maine on July 16-20, 1995.
PB96-165840 *02,681* PC A15/MF A03

Report of the NIST Workshop on Digital Signature Certificate Management. Held on December 10-11, 1992.
PB94-135001 *01,574* PC A09/MF A02

Report of the NIST Workshop on Key Escrow Encryption. Held in Gaithersburg, Maryland on June 8-10, 1994.
PB94-209459 *01,584* PC A08/MF A02

Report of the Refrigeration, Air Conditioning and Heat Pumps Technical Options Committee.
PB96-176755 *03,293* Not available NTIS

Report on Application Integration Architectures (AIA) Workshop. Held in Dallas, Texas on February 8-12, 1993.
PB94-142536 *01,803* PC A07/MF A02

Report on the Advanced Software Technology Workshop. Held on February 1, 1994.
PB95-136610 *01,707* PC A03/MF A01

Report on the Meeting of the CCU (10th) (of the International Committee of Weights and Measures). Held on July 10-11, 1990.
PB94-172889 *03,792* Not available NTIS

Report on the NIST Low Accelerating Voltage SEM Magnification Standard Interlaboratory Study.
PB96-201074 *02,445* Not available NTIS

Report on the Workshop on Advanced Digital Video in the National Information Infrastructure. Held in Washington, D.C. on May 10-11, 1994.
PB95-103677 *01,472* PC A09/MF A03

Report on the Workshop on Manufacturing Polymer Composites by Liquid Molding. Held in Gaithersburg, Maryland on September 20-22, 1993.
PB94-160066 *03,131* PC A13/MF A03

Report on USDA Ultraviolet Spectroradiometers.
PB96-214648 *00,125* PC A04/MF A01

Report on 1994 Actions of the International Institute of Welding.
PB96-138540 *02,873* Not available NTIS

Representation of Axes for Geometric Fitting.
PB97-113799 *01,782* PC A03/MF A01

Representing a Large Collection of Curves: A Case for Principal Points.
PB95-152286 *03,438* Not available NTIS

Representing Designs with Logic Formulations of Spatial Relations.
PB97-111561 *02,792* Not available NTIS

Reproducibility of JEDEC Standard Current and Voltage Ramp Test Procedures for Thin-Dielectric Breakdown Characterization.
PB94-185931 *01,879* Not available NTIS

Reproducibility of Tests on Energy Management and Control Systems Using Building Emulators.
PB95-175980 *00,260* Not available NTIS

Reproducibility of the Temperature of the Ice Point in Routine Measurements.
PB95-255923 *04,015* PC A03/MF A01

Requisite Elements, Rationale, and Technology Overview for the Systems Intergration for Manufacturing Applications (SIMA) Program. Background Study.
PB96-112685 *02,831* PC A07/MF A02

Research and Development Activities in Electron Paramagnetic Resonance Dosimetry.
PB96-141288 *03,635* Not available NTIS

Research on Methods for Determining Optical Disk Media Life Expectancy Estimates.
PB96-160304 *01,633* Not available NTIS

Residual Error Compensation of a Vision-Based Coordinate Measuring Machine.
PB96-161617 *04,091* Not available NTIS

Residual Stress in Induction-Heated Railroad Wheels: Ultrasonic and Saw Cut Measurements. Report No. 28.
PB96-106992 *04,854* PC A04/MF A01

Residual Stresses in Aluminum-Mullite (alpha-Alumina) Composites.
PB95-152880 *03,155* Not available NTIS

Resistance Measurements from 10 M Omega to 1 T Omega at NIST.
PB97-119168 *02,290* Not available NTIS

Resistance Thermometers with Fast Response for Use in Rapidly Oscillating Gas Flows.
PB95-107298 *03,261* Not available NTIS

Resistors.
PB97-111876 *02,284* Not available NTIS

Resolution of Discrepant Analytical Data in the Certification of Platinum in Two Automobile Catalyst SRMs.
PB96-167283 *00,638* Not available NTIS

Resolution of DNA in the Presence of Mobility Modifying Polar and Nonpolar Compounds by Discontinuous Electrophoresis on Rehydratable Polyacrylamide Gels.
PB95-152799 *00,590* Not available NTIS

Resonance and Threshold Effects in Polarized X-Ray Emission from Atoms and Molecules.
PB95-150298 *03,891* Not available NTIS

Resonance Enhanced Multiphoton Ionization Detection of GeF and GeCl Radicals.
PB94-212123 *00,825* Not available NTIS

Resonance Enhanced Multiphoton Ionization Spectroscopy of the PF Radical.
PB97-119119 *00,702* Not available NTIS

Resonance Enhanced Multiphoton Ionization Spectroscopy of the SnF Radical.
PB97-111223 *01,176* Not available NTIS

Resonance Enhanced Multiphoton Ionization Spectroscopy of 2-Butene-1-yl (C4H7) between 455-485 nm.
PB95-151031 *00,670* Not available NTIS

Resonance Fluorescence with Squeezed-Light Excitation.
PB95-203469 *04,322* Not available NTIS

Resonance Ionization Spectroscopy/Resonance Ionization Mass Spectrometry Data Service. V-Data Sheets for Ga, Mn, Sc, and Tl.
PB96-158068 *00,625* Not available NTIS

Resonance Structure and Absolute Cross Sections in Near-Threshold Electron-Impact Excitation of the 4s(2) (1)S yields 4s4p (3)P Intercombination Transition in Kr(6+).
PB95-202271 *03,972* Not available NTIS

Resonances in Two-Dimensional Array Oscillator Circuits.
PB96-102082 *02,066* Not available NTIS

Resonant-Photoemission Investigation of the Heusler Alloys Ni2MnSb and NiMnSb.
PB95-162384 *04,612* Not available NTIS

Resonant Two-Color Detachment of H(-) with Excitation of H(n=2).
PB95-202552 *03,984* Not available NTIS

Response Comparison of Electret Ion Chambers, LiF TLD, and HPIC.
PB96-190103 *02,578* Not available NTIS

Response of a Terminally Anchored Polymer Chain to Simple Shear Flow.
PB95-108668 *01,233* Not available NTIS

Response of Buildings to Ambient Vibration and the Loma Prieta Earthquake: A Comparison.
PB96-119607 *00,457* Not available NTIS

Response to Comments on the NIST Proposed Digital Signature Standard.
PB96-161815 *01,615* Not available NTIS

Response to 'Draining in Dilute Polymer Solutions and Renormalization'.
PB96-146667 *01,283* Not available NTIS

Results of a NIST/VNIIOFI Comparison of Spectral-Radiance Measurements.
PB97-113021 *04,159* Not available NTIS

Results of Capacitance Ratio Measurements for the Single Electron Pump-Capacitor Charging Experiment.
PB97-113286 *04,813* Not available NTIS

Results of the ASTM Nuclear Methods Intercomparison on NIST Apple and Peach Leaves Standard Reference Materials.
PB97-119036 *03,490* Not available NTIS

Retention of Halocarbons on a Hexafluoropropylene Epoxide Modified Graphitized Carbon Black. Part 1. Methane-Based Compounds.
PB95-175196 *03,272* Not available NTIS

Retention of Halocarbons on a Hexafluoropropylene Epoxide-Modified Graphitized Carbon Black. 3. Ethene-Based Compounds.
PB96-167309 *03,286* Not available NTIS

Retention of Halocarbons on a Hexafluoropropylene Epoxide-Modified Graphitized Carbon Black. 4. Propane-Based Compounds.
PB96-164033 *03,284* Not available NTIS

Retinal-Protein Complexes as Optoelectronic Components.
PB95-150397 *02,146* Not available NTIS

Retrieving Articles from the Internet (without a UNIX Workstation). Part 1. File Formats and Software Tools.
PB95-168720 *02,728* Not available NTIS

Retrieving Articles from the Internet (without a UNIX Workstation). Part 2. An Example.
PB95-168738 *02,729* Not available NTIS

Review and Upgrading of Military Fastener Test Standard MIL-STD-1312.
PB95-154720 *02,947* PC A07/MF A02

Review of Corrosion Behavior of Ceramic Heat Exchanger Materals: Corrosion Characteristics of Silicon Carbide and Silicon Nitride. Final Report, September 11, 1992--March 11, 1993.
DE93041307 *03,228* PC A06/MF A02

Review of Cure Monitoring Techniques for On-Line Process Control.
PB94-216728 *03,145* Not available NTIS

Review of Flows Driven By Natural Convection in Adiabatic Shafts.
PB96-147897 *01,416* PC A04/MF A01

Review of Internatioanl Fire Risk Predictions Methods.
PB96-156195 *00,222* Not available NTIS

Review of Mathematical Function Library for Microsoft-FORTRAN, John Wiley and Sons, 1989.
PB94-160793 *01,679* PC A03/MF A01

Review of Measurements and Candidate Signatures for Early Fire Detection.
PB95-189452 *00,300* PC A03/MF A01

Review of Semiconductor Microelectronic Test Structures with Applications to Infrared Detector Materials and Processes.
PB94-212925 *02,132* Not available NTIS

Review of the USCEA/NIST Measurement Assurance Program for the Nuclear Power Industry.
PB95-126272 *03,712* Not available NTIS

Revised Uncertainty Analysis for the NIST 30-MHz Attenuation Calibration System.
PB95-168761 *01,907* Not available NTIS

Rh I Isoelectronic Sequence Observed from Er(23+) to Pt(33+).
PB95-150652 *03,898* Not available NTIS

Rheology of Fresh Cement Paste.
PB95-163150 *00,378* Not available NTIS

Riass Coronathon: Joint X-ray and Ultraviolet Observations of Normal F-K Stars.
PB96-200217 *00,109* Not available NTIS

Rietveld Analysis of NaxWO3+x/2.yH2O, Which Has the Hexagonal Tungsten Bronze Structure.
PB95-107371 *04,524* Not available NTIS

Rigid Bender Analysis of van der Waals Complexes: The Intermolecular Bending Potential of a Hydrogen Bond.
PB95-203022 *01,042* Not available NTIS

RII Spectroscopy of Trap Levels in Bulk and LPE Hg1-xCdxTe.
PB96-160247 *04,084* Not available NTIS

Ring-Opening Dental Resin Systems Based on Cyclic Acetals.
PB95-162251 *00,162* Not available NTIS

Ring-Opening Polymerication of a 2-Methylene Spiro Orthocarbonate Bearing a Pendant Methacrylate Group.
PB95-176145 *01,268* Not available NTIS

RIS Measurement of AC Stark Shifts and Photoionization Cross Sections in Calcium.
PB96-157953 *04,073* Not available NTIS

RIS Measurements of the AC Stark Shift.
PB96-158035 *04,078* Not available NTIS

RIS Studies of Autoionization in Calcium.
PB94-213295 *00,849* Not available NTIS

Risk Analysis for the Fire Safety of Airline Passengers.
PB94-194065 *04,862* PC A03/MF A01

Roadmap for the Computer Integrated Manufacturing (CIM) Application Framework.
PB96-122759 *02,832* Not available NTIS

Robotics Application to Highway Transportation. Volume 1. Final Report.
PB95-203790 *03,654* PC A03/MF A01

Robotics Application to Highway Transportation. Volume 2. Literature Search.
PB95-170551 *01,337* PC A06/MF A02

Robotics Application to Highway Transportation. Volume 3. Proposed Research Topics and Cost/Benefit Evaluations by CERF.
PB95-171633 *01,338* PC A20/MF A04

Robotics Application to Highway Transportation. Volume 4. Proposals for Potential Research.
PB95-193173 *01,339* PC A07/MF A02

Role of Adsorbed Alkalis in Desorption Induced by Electronic Transitions.
PB94-172574 *00,762* Not available NTIS

Role of Certified Reference Materials in Trace Analysis Quality Assurance.
PB97-110019 *00,650* Not available NTIS

Role of Combustion on Droplet Transport in Pressure-Atomized Spray Flames.
PB96-204433 *01,434* Not available NTIS

Role of Corrosion in a Material Selector Expert System for Advanced Structural Ceramics.
PB97-110308 *03,099* Not available NTIS

Role of Journals in Maintaining Data Integrity: Checking of Crystal Structure Data in 'Acta Crystallographica'.
PB97-109177 *04,806*
(Order as PB97-109011, PC A11/MF A03)

Role of R22 in Refrigerating and Air Conditioning Equipment.
PB94-199783 *03,253* Not available NTIS

Role of Refrigerant Mixtures as Alternatives to CFCs.
PB94-199775 *03,252* Not available NTIS

Role of the Office of Radiation Measurement in Quality Assurance.
PB94-212255 *00,689* Not available NTIS

Role of World Modeling and Value Judgment in Perception.
PB94-198264 *01,581* Not available NTIS

Roles of Copper in Applied Superconductivity.
PB94-211521 *02,255* Not available NTIS

Roles of Local Classical Acceleration and Spatial Separation in the Neutral Particle Analogs of the Aharonov-Bohm Phases.
PB95-202362 *03,976* Not available NTIS

Room-Temperature Flexure Fixture for Advanced Ceramics.
PB95-210498 *03,061* PC A03/MF A01

Room-Temperature Thermal Conductivity of Expanded Polystyrene Board for a Standard Reference Material.
PB96-193693 *00,412* PC A04/MF A01

Room Temperature Thermal Conductivity of Fumed-Silica Insulation for a Standard Reference Material.
PB95-152039 *00,374* Not available NTIS

ROSAT All-Sky Survey of Active Binary Coronae. 1. Quiescent Fluxes for the RS Canum Venaticorum Systems.
PB95-202479 *00,077* Not available NTIS

ROSAT All-Sky Survey of Active Binary Coronae. 2. Coronal Temperatures of the RS Canum Venaticorum Systems.
PB94-199601 *00,055* Not available NTIS

Rotational Dynamics of C60 in Na2RbC60.
PB95-153201 *00,948* Not available NTIS

Rotational Dynamics of Solid C70: A Neutron-Scattering Study.
PB94-172178 *00,755* Not available NTIS

Rotational Dynamics of Solid C70: A Neutron-Scattering Study.
PB95-153219 *00,949* Not available NTIS

Rotational Far Infrared Spectrum of (13)CO.
PB95-152187 *00,941* Not available NTIS

Rotational Modulation and Flares on RS Canum Venaticorum and BY Draconis Stars. XVI. IUE Spectroscopy and VLA Observations of C1182(=V 1005 Orionis) in October 1983.
PB94-185626 *00,050* Not available NTIS

Rotational Modulation and Flares on RS Canum Venaticorum and BY Draconis Stars. XVIII. Coordinated VLA, ROSAT, and IUE Observations of RS CVn Binaries.
PB96-102322 *00,089* Not available NTIS

Rotational-RKR Inversion of Intermolecular Stretching Potentials: Extension to Linear Hydrogen Bonded Complexes.
PB95-203014 *01,041* Not available NTIS

Rotational Spectra of CH3CCH-NH3, NCCCH-NH3, and NCCCH-OH2.
PB97-118798 *04,170* Not available NTIS

Rotational Spectroscopy of the CoH Radical in Its Ground (3)Phi State by Far-Infrared Laser Magnetic Resonance: Determination of Molecular Parameters.
PB95-175048 *00,992* Not available NTIS

Rotational Spectrum and Structure of a Weakly Bound Complex of Ketene and Acetylene.
PB95-126140 *00,896* Not available NTIS

Rotational Spectrum of Copper Hydride Using Tunable Far Infrared Radiation.
PB94-198637 *00,792* Not available NTIS

Rotational Spectrum of OH in the v=0-3 Levels of Its Ground State.
PB95-176202 *01,006* Not available NTIS

Safety Assessment of Railroad Wheels by Residual Stress Measurements.
PB96-141114 *04,855* Not available NTIS

Safety Assessment of Railroad Wheels Through Roll-by Detection of Tread Cracks.
PB96-141254 *04,856* Not available NTIS

Salt-PEG Two-Phase Aqueous Systems to Purify Proteins and Nucleic Acid Mixtures.
PB94-200375 *03,527* Not available NTIS

SANS and LS Studies of Polymer Mixtures Under Shear Flow.
PB95-107090 *01,231* Not available NTIS

SANS Studies of Space-Time Organization of Structure in Polymer Blends.
PB95-153789 *01,251* Not available NTIS

SANS Study of the Plastic Deformation Mechanism in Polyethylene.
PB95-151841 *01,242* Not available NTIS

Santa Ana Fire Department Experiment at 1315 South Bristol, July 14, 1994.
PB95-188868 *00,389* PC A03/MF A01

Santa Ana Fire Department Experiment at 1315 South Bristol, July 14, 1994. (Reprint).
PB96-102934 *00,207* Not available NTIS

Santa Ana Fire Department Experiments at South Bristol Street.
PB96-154810 *00,305* PC A11/MF A03

Satellite Two-Way Time Transfer: Fundamentals and Recent Progress.
PB95-161089 *01,536* Not available NTIS

SC4 Short Names Registry.
PB97-122410 *02,799* Not available NTIS

Scalability Test for Parallel Code.
PB96-146758 *01,749* Not available NTIS

Scale-Space-Based Visual-Motion-Cue for Autonomous Navigation.
PB96-183173 *02,940* PC A06/MF A01

Scaling Compartment Fires: Reduced- and Full-Scale Enclosure Burns.
PB96-175708 *00,224* Not available NTIS

Scaling of Diffusion-Mediated Island Growth in Iron-on-Iron Homoepitaxy.
PB94-185923 *04,455* Not available NTIS

Scaling of the Nonlinear Optical Cross Sections of GaAs-AlGaAs Multiple Quantum-Well Hetero n-i-p-i's.
PB96-102793 *02,183* Not available NTIS

Scanned Probe Microscope Tip Characterization Without Calibrated Tip Characterizers.
PB96-190368 *02,759* Not available NTIS

Scanned Probe Microscopies: Opportunities and Issues in Metrology.
PB96-160783 *02,426* Not available NTIS

Scanning Capacitance Microscopy Measurements and Modeling for Dopant Profiling of Silicon.
PB96-164207 *04,781* Not available NTIS

Scanning Capacitance Microscopy Measurements and Modeling: Progress Towards Dopant Profiling of Silicon.
PB96-148150 *04,773* Not available NTIS

Scanning Capacitance Microscopy Measurements and Modeling: Progress Towards Dopant Profiling of Silicon.
PB96-180070 *01,964* Not available NTIS

Scanning Electron Microscope Magnification Calibration Interlaboratory Study.
PB96-201082 *01,164* Not available NTIS

Scanning Electron Microscope Metrology.
PB96-201090 *02,446* Not available NTIS

Scanning Electron Microscopy Observations of Misfit Dislocations in Epitaxial In0.25Ga0.75As on GaAs(001).
PB96-200159 *03,004* Not available NTIS

Scanning Tunneling Microscopy and Fabrication of Nanometer Scale Structures at the Liquid-Gold Interface.
PB95-140414 *00,904* Not available NTIS

Scanning Tunneling Microscopy of the Charge-Density-Wave Structure in 1T-TaS2.
PB95-180980 *04,689* Not available NTIS

Scanning Tunneling Microscopy Study of the Growth of Cr/Fe(001): Correlation with Exchange Coupling of Magnetic Layers.
PB95-150330 *04,568* Not available NTIS

Scattered Fractions of Dose from 18 and 25 MV X-ray Radiotherapy Linear Accelerators.
PB96-186101 *04,120* Not available NTIS

Scattering and Absorption Effects in Neutron Beam Activation Analysis Experiments.
PB94-216140 *00,557* Not available NTIS

Scattering Properties of the Leveled-Wave Model of Random Morphologies.
PB94-198835 *03,807* Not available NTIS

Science, Technology, and Competitiveness: Retrospective on a Symposium in Celebration of NIST's 90th Anniversary and the 25th Anniversary of the Gaithersburg Laboratories, November 14-15, 1991.
PB97-121610 *02,696* PC A08/MF A02

Scientific Protocols in Statistical Standards for Environmental Studies.
PB94-185527 *02,517* Not available NTIS

Scientific Rationale and Present Implementation Strategy for the Far Ultraviolet Spectrograph Explorer (FUSE).
PB96-123328 *00,045* Not available NTIS

Screened-Room Measurements on the NIST Spherical-Dipole Standard Radiator.
PB96-113568 *01,926*
(Order as PB96-113535, PC A05/MF A01)

TITLE INDEX

Screw-Thread Standards for Federal Services, 1957. Handbook H28 (1957), Part 2. Revised.
AD-A280 082/9 *03,599* PC A06/MF A02

Screw-Thread Standards for Federal Services, 1957. Part 1.
AD-A279 290/1 *02,855* PC A10/MF A03

Screw-Thread Standards for Federal Services, 1957. Part 3.
AD-A279 121/8 *02,854* PC A04/MF A01

SDNS Security Management.
PB95-161170 *01,592* Not available NTIS

Sealed Water Calorimeter for Measuring Absorbed Dose.
PB94-219227 *03,517*
(Order as PB94-219219, PC A06/MF A02)

Search for Radio Emission from the 'Non-Magnetic' Chemically Peculiar Stars.
PB96-102249 *00,087* Not available NTIS

Search for Small Violations of the Symmetrization Postulate in an Excited State of Helium.
PB96-123518 *04,050* Not available NTIS

Second Census Optical Character Recognition Systems Conference.
PB94-188711 *01,832* PC A12/MF A03

Second Text REtrieval Conference (TREC-2). Held in Gaithersburg, Maryland on August 31-September 2, 1993.
PB94-178407 *01,686* PC A21/MF A04

Secondary Standard for PM and AM Noise at 5, 10, and 100 MHz.
PB96-123187 *01,554* Not available NTIS

Secondary Target X-Ray Excitation for In vivo Measurement of Lead in Bone.
PB95-108767 *03,496* Not available NTIS

Secure Hash Standard. Category: Computer Security.
FIPS PUB 180-1 *01,568* PC E04

Security Considerations for SQL-Based Implementations of STEP.
PB94-139649 *02,766* PC A03/MF A01

Security in Open Systems.
PB95-105383 *01,473* PC A13/MF A03

Security Program Management.
PB96-156112 *01,610* Not available NTIS

Security Requirements for Cryptographic Modules; Category: Computer Security; Subcategory: Cryptography.
FIPS PUB 140-1 *01,567* PC E05

Segmental Concentration Profiles of End-Tethered Polymers with Excluded-Volume and Surface Interactions.
PB97-119002 *00,654* Not available NTIS

Seismic Instrumentation of Existing Buildings.
PB94-159779 *00,420* PC A04/MF A01

Seismic Performance Behavior of Precast Concrete Beam-Column Joints.
PB95-153110 *00,440* Not available NTIS

Seismic Performance of Circular Bridge Columns Designed in Accordance with AASHTO/CALTRANS Standards.
PB96-146352 *01,346* PC A07/MF A02

Seismic Safety of Federal Buildings. Initial Program: How Much Will It Cost.
PB95-182291 *00,447* PC A03/MF A01

Seismic Strengthening of Reinforced Concrete Frame Buildings.
PB95-108841 *00,430* Not available NTIS

Selected Ion Flow Tube-Laser Induced Fluorescence Instrument for Vibrationally State-Specific Ion-Molecule Reactions.
PB94-185444 *00,774* Not available NTIS

Selection of Appropriate Ultrasonic System Components for NDE of Thick Polymer-Composites.
PB94-185279 *03,133* Not available NTIS

Selective Inhibition of Crystal Growth on Octacalcium Phosphate and Nonstoichiometric Hydroxyapatite by Pyrophosphate at Physiological Concentration.
PB94-211257 *00,147* Not available NTIS

Selectivity Trends in Packed Column Supercritical Fluid Chromatography with C18 Stationary Phases.
PB96-138581 *00,622* Not available NTIS

Self-Assembled Phospholipid/Alkanethiol Biomimetic Bilayers on Gold.
PB95-108460 *00,878* Not available NTIS

Self-Avoiding Surfaces, Topology, and Lattice Animals.
PB95-150512 *04,571* Not available NTIS

Self-Avoiding-Walk Contacts and Random-Walk Self-Intersections in Variable Dimensionality.
PB96-102231 *01,276* Not available NTIS

Self-Biasing Cryogenic Particle Detector Utilizing Electrothermal Feedback and a SQUID Readout.
PB96-102538 *04,712* Not available NTIS

Self Broadening in the nu1 Band of NH3.
PB94-216371 *00,857* Not available NTIS

Self-Calibrated Intelligent Optical Sensors and Systems.
PB96-200738 *04,380* Not available NTIS

Self-Calibrating Fiber Optic Sensors: Potential Design Methods.
PB95-169298 *02,172* Not available NTIS

Self Calibrating Fiber Optic Sensors: Potential Design Methods.
PB95-169306 *02,173* Not available NTIS

Self-Consistent 'GW' and Higher-Order Calculations of Electron States in Metals.
PB97-119341 *01,189* Not available NTIS

Self-Heating in the Coulomb-Blockade Electrometer.
PB94-212685 *04,507* Not available NTIS

Self Monitoring Accounting Systems.
PB95-216602 *00,007* PC A03/MF A01

Self-, N2- and Ar-Broadening and Line Mixing in HCN and C2H2.
PB95-108445 *00,876* Not available NTIS

Self-Organizing Neural Network Character Recognition on a Massively Parallel Computer.
PB95-163994 *01,845* Not available NTIS

Self-Organizing Neural Network Character Recognition Using Adaptive Filtering and Feature Extraction.
PB96-119797 *01,855* Not available NTIS

Self-Reciprocal Fourier Functions.
PB96-200852 *01,974* Not available NTIS

SEM Linewidth Metrology of X-ray Lithography Masks.
PB96-201108 *02,447* Not available NTIS

Semiclassical Explanation of the Generalized Ramsauer-Townsend Minima in Electron-Atom Scattering.
PB95-153532 *03,925* Not available NTIS

Semiconductor Measurement Technology: Design and Testing Guides for the CMOS and Lateral Bipolar-on-SOI Test Library.
PB94-178019 *02,301* PC A07/MF A02

Semiconductor Measurement Technology: HOTPAC. Programs for Thermal Analysis Including Version 3.0 of the TXYZ Program, TXYZ30, and the Thermal MultiLayer Program, TML.
PB95-260766 *02,374* PC A05/MF A01

Semiconductor Measurement Technology: Improved Characterization and Evaluation Measurements for HgCdTe Detector Materials, Processes, and Devices Used on the GOES and TIROS Satellites.
PB94-188810 *02,122* PC A09/MF A02

Semiconductor Measurement Technology: Survey of Optical Characterization Methods for Materials, Processing, and Manufacturing in the Semiconductor Industry.
PB96-154596 *02,706* PC A05/MF A01

Semiconductor Measurement Technology: Test Structure Implementation Document: DC Parametric Test Structures and Test Methods for Monolithic Microwave Integrated Circuits (MMICs).
PB96-117692 *02,399* PC A05/MF A01

SEMPA Studies of Exchange Coupling in Magnetic Multilayers.
PB96-164074 *04,780* Not available NTIS

SEMPA Studies of Oscillatory Exchange Coupling.
PB95-163556 *04,625* Not available NTIS

Sensing Droplet Detachment and Electrode Extension for Control of Gas Metal Arc Welding.
PB96-190160 *03,297* Not available NTIS

Sensitivity Analysis for Mathematical Modeling of Fires in Residential Buildings.
PB96-154968 *00,215* PC A03/MF A01

Sensitivity of Three-Point Circle Fitting.
PB95-136354 *02,901* PC A03/MF A01

Sensor System for Intelligent Processing of Hot-Rolled Steel.
PB96-186069 *03,373* Not available NTIS

Separation and Identification of Organic Gunshot and Explosive Constituents by Micellar Electrokinetic Capillary Electrophoresis.
PB95-107249 *00,566* Not available NTIS

Serial Sectioning of Hardened Cement Paste for Scanning Electron Microscopy.
PB94-172640 *01,305* Not available NTIS

Series Array of DC SQUIDs.
PB95-163861 *02,046* Not available NTIS

SF6 Insulation: Possible Greenhouse Problems and Solutions.
PB95-251625 *02,269* PC A03/MF A01

SF6/N2 Mixtures: Basic and High-Voltage-Insulation Properties.
PB96-123468 *02,230* Not available NTIS

SGML Environment for STEP.
PB95-143103 *02,778* PC A03/MF A01

SGML Parser Validation Procedures.
PB95-174959 *01,717* PC A03/MF A01

Shape of the Temperature-Entropy Saturation Boundary.
PB96-135066 *02,506* Not available NTIS

Shape-Resonance-Enhanced Continuum-Continuum Coupling in Photoionization of CO2.
PB95-164471 *00,983* Not available NTIS

Shape Selectivity Assessment of Stationary Phases in Gas Chromatography.
PB95-150256 *00,579* Not available NTIS

Shape Selectivity in Reversed-Phase Liquid Chromatography for the Separation of Planar and Non-Planar Solutes.
PB95-162608 *00,596* Not available NTIS

Shapiro Steps in Large-Area Metallic-Barrier Josephson Junctions.
PB96-200142 *02,090* Not available NTIS

Sharing Information via the Internet: An Infoserver Case Study.
PB96-131511 *01,493* PC A03/MF A01

Shear Dependence of Critical Fluctuations in Binary Polymer Mixtures by Small Angle Neutron Scattering.
PB94-211612 *01,220* Not available NTIS

Shear Design of High-Strength Concrete Beams: A Review of the State-of-the-Art.
PB96-214713 *01,330* PC A11/MF A03

Shear-Excited Morphological States in a Triblock Copolymer.
PB94-172392 *01,196* Not available NTIS

Shear-Induced Changes in the Order-Disorder Transition Temperature and the Morphology of a Triblock Copolymer.
PB97-118772 *03,130* Not available NTIS

Shear-Induced Martensitic-Like Transformation in a Block Copolymer Melt.
PB96-119508 *01,277* Not available NTIS

Shear-Induced Melting of Two-Dimensional Solids.
PB96-112057 *01,075* Not available NTIS

Shear-Induced Mixing in Polymer Blends.
PB96-148085 *01,287* Not available NTIS

Shear Suppression of Critical Fluctuations in a Diluted Polymer Blend.
PB96-204458 *04,418* Not available NTIS

Shielding of Cracks in a Plastically Polarizable Material.
PB95-164257 *04,631* Not available NTIS

Shock Tube Techniques in Chemical Kinetics.
PB95-163465 *00,968* Not available NTIS

Short-Pulse Detachment of H(-) in the Presence of a Static Electric Field.
PB95-203477 *04,007* Not available NTIS

Short-Range Correlation and Relaxation Effects on the (6p(2))(1)SO Autoionizing State of Atomic Barium.
PB95-202289 *03,973* Not available NTIS

Should NIST Accredit U.S. Calibration Laboratories.
PB95-107280 *02,646* Not available NTIS

Sifting Through Nine Years of NIST Clock Data with TA2.
PB95-181137 *01,547* Not available NTIS

sigma+-sigma- Optical Molasses in a Longitudinal Magnetic Field.
PB95-161840 *03,934* Not available NTIS

Signatures of Large Amplitude Motion in a Weakly Bound Complex: High-Resolution IR Spectroscopy and Quantum Calculations for HeCO2.
PB95-203485 *01,054* Not available NTIS

Significant Contributions of IAPWS to the Power Industry, Science and Technology.
PB96-123252 *01,088* Not available NTIS

Silicon Nitride Boundary Lubrication: Effect of Oxygenates.
PB96-111711 *03,068* Not available NTIS

Silicon Nitride Boundary Lubrication: Lubrication Mechanism of Alcohols.
PB96-111703 *03,067* Not available NTIS

Silicon Photodiodes Optimized for EUV and Soft X-Ray Regions.
PB94-199478 *02,124* Not available NTIS

Silicon Surface Chemistry by IR Spectroscopy in the Mid- to Far-IR Region: H2O and Ethanol on Si(100).
PB96-138565 *01,097* Not available NTIS

Silver Metalization of Octadecanethiol Monolayers Self-Assembled on Gold.
PB95-150744 *00,923* Not available NTIS

Simple and Efficient Low-Temperature Sample Cell for Infrared Spectrophotometry.
PB94-199197 *00,545* Not available NTIS

Simple and Efficient Methane-Marker Devices for Chromatographic Samples.
PB96-164041 *00,635* Not available NTIS

Simple and Repeatable Technique for Measuring the Critical Current of Nb3Sn Wires.
PB96-119409 *02,229* Not available NTIS

Simple, Compact, High-Purity Cr Evaporator for Ultrahigh Vacuum.
PB94-216678 *04,520* Not available NTIS

Simple, Inexpensive Apparatus for Sample Concentration.
PB94-199205 *00,546* Not available NTIS

Simple Method of Composition Shifting with a Distillation Column for a Heat Pump Employing a Zeotropic Refrigerant Mixture.
PB95-255824 *02,603* PC A03/MF A01

Simple Scalability Test for MIMD Code.
PB94-193638 *01,688* PC A03/MF A01

Simple Variable Line Space Grating Monochromator for Synchrotron Light Source Beamlines.
PB96-156203 *04,065* Not available NTIS

Simplified Cycle Simulation Model for the Performance Rating of Refrigerants and Refrigerant Mixtures.
PB94-199890 *03,255* Not available NTIS

Simplified Design Procedure for Hybrid Precast Concrete Connections.
PB96-154836 *00,405* PC A06/MF A01

Simulating Device Size Effects on Magnetization Pinning Mechanisms in Spin Valves.
PB97-112593 *04,158* Not available NTIS

Simulating Smoke Movement through Long Vertical Shafts in Zone-Type Compartment Fire Models.
PB95-143152 *00,368* PC A03/MF A01

Simulating the Dynamic Electro Thermal Behavior of Power Electronic Circuits and Systems.
PB95-161014 *02,345* Not available NTIS

Simulation and SANS Studies of Gelation Under Shear.
PB96-167176 *01,150* Not available NTIS

Simulation of C60 Through the Plastic Transition Temperatures.
PB96-102546 *04,713* Not available NTIS

Simulation of Ceramic Particle Formation: Comparison with In-situ Measurements.
PB95-152013 *00,674* Not available NTIS

Simulation Studies of Supercooled and Glass Forming Liquids.
PB96-122627 *01,085* Not available NTIS

Simulations of Glass Forming Liquids: What Has Been Learned.
PB95-150124 *00,915* Not available NTIS

Simulations of Neutron Focusing with Curved Mirrors.
PB96-176649 *02,200* Not available NTIS

Simultaneous Forward-Backward Raman Scattering Studies of D2 Broadened by D2, He, and Ar.
PB95-162459 *00,961* Not available NTIS

Simultaneous Laser-Diode Emission and Detection for Fiber-Optic Sensor Applications.
PB96-155502 *04,062* Not available NTIS

Simultaneous Measurement of Normal Spectral Emissivity by Spectral Radiometry and Laser Polarimetry at High Temperatures in Pulse-Heating Experiments: Application to Molybdenum and Tungsten.
PB97-118376 *02,694* Not available NTIS

Simultaneous Optical Measurement of Soot Volume Fraction, Temperature, and CO2 in Heptane Pool Fire.
PB96-102132 *01,397* Not available NTIS

Simultaneous Visual and Calorimetric Measurements of R11, R123, and R123/Alkylbenzene Nucleate Flow Boiling.
PB94-172426 *03,251* Not available NTIS

Single-Atom Point Source for Electrons: Field-Emission Resonance Tunneling in Scanning Tunneling Microscopy.
PB95-125860 *00,893* Not available NTIS

Single-Phase Heat Transfer and Pressure Drop Characteristics of an Integral-Spine-Fin Within an Annulus.
PB94-194073 *03,805* PC A03/MF A01

Single-Phase Heat Transfer and Pressure Drop Characteristics of an Integral-Spine Fin Within an Annulus.
PB97-122386 *04,179* Not available NTIS

Single-Photon Ionization and Detection of Ga, In, and As(sub n) Species in GaAs Growth.
PB95-152815 *00,591* Not available NTIS

Single Photon Ionization, Laser Optical Probe Technique for Semiconductor Growth.
PB95-202776 *01,032* Not available NTIS

Single Photon Laser Ionization as an In-situ Diagnostic for MBE growth.
PB96-102025 *01,059* Not available NTIS

Single-Photon Laser Ionization Time-of-Flight Mass Spectroscopy Detection in Molecular-Beam Epitaxy: Application to As4, As2, and Ga.
PB95-203337 *01,052* Not available NTIS

Single-Port Technique for Adaptor Efficiency Evaluation.
PB96-176441 *02,088* Not available NTIS

Singularities in Minimum Surface Energy Problems and Their Influence in Surface Motion.
PB94-199411 *04,473* Not available NTIS

Sinusoidal Surfaces as Standards for BRDF Instruments.
PB97-110597 *04,388* Not available NTIS

Site of One-Electron Reduction of Ni(II) Porphyrins. Formation of Ni(I) Porphyrin of Ni(II) Porphyrin pi-Radical Anion.
PB95-107066 *00,866* Not available NTIS

Size and Self-Field Effects in Giant Magnetoresistive Thin-Film Devices.
PB95-180188 *04,674* Not available NTIS

Size Effects and Giant Magnetoresistance in Unannealed NiFe/Ag Multilayer Stripes.
PB97-111306 *04,145* Not available NTIS

Size Effects in Submicron NiFe/Ag GMR Devices.
PB96-155510 *02,237* Not available NTIS

Slab Transmission and Reflection for Point Source and Point Detector.
PB94-211265 *03,838* Not available NTIS

Slant Path Atmospheric Refraction Calibrator: An Instrument to Measure the Microwave Propagation Delays Induced by Atmospheric Water Vapor.
PB95-151270 *01,476* Not available NTIS

Sleuthing the Dynamo: HST/FOS Observations of UV Emissions of Solar-Type Stars in Young Clusters.
PB96-122817 *00,098* Not available NTIS

Slicing in the Presence of Parameter Aliasing.
PB96-160858 *01,755* Not available NTIS

Sliding Vane Flow Conditioner Tests in a 100 Diameter Long 10 inch Natural Gas Orifice Meter at Pacific Gas and Electric. Topical Report, 1990-1992.
PB95-256335 *02,493* PC A04/MF A01

Slit Jet Infrared Spectroscopy of Hydrogen Bonded N2HF Isotopomers: Rotational Rydberg-Klein-Rees Analysis and H/D Dependent Vibrational Predissociation Rates.
PB95-161873 *00,956* Not available NTIS

Slit-Jet Near-Infrared Diode Laser Spectroscopy of (DCl)2: nu1, nu2 DCl Stretching Fundamentals, Tunneling Dynamics, and the Influence of Large Amplitude 'Geared' Intermolecular Rotation.
PB95-203204 *01,047* Not available NTIS

Slit-Jet Near-Infrared Spectroscopy and Internal Rotor Dynamics of the ArH2O van der Waals Complex: An Angular Potential-Energy Surface for Internal H2O Rotation.
PB95-202792 *01,033* Not available NTIS

Slow Dynamics of Segregation in Hydrogen-Bonded Polymer Blends.
PB96-123591 *01,281* Not available NTIS

Slow-Electron Collisions with CO Molecules in an Exact-Exchange Plus Parameter-Free Polarization Model.
PB95-202719 *03,989* Not available NTIS

Slow Evolution from the Boundary: A New Stabilizing Constraint in Ill-Posed Continuation Problems.
PB96-122858 *03,418* Not available NTIS

Slowly Divergent Space Marching Schemes in the Inverse Heat Conduction Problem.
PB94-199486 *03,812* Not available NTIS

Small-Angle Neutron Scattering Characterization of Processing/Microstructure Relationships in the Sintering of Crystalline and Glassy Ceramics. (Reannouncement with New Availability Information).
AD-A249 510/9 *03,025* PC A03/MF A01

Small-Angle Neutron Scattering of Poly(vinyl alcohol) Gels.
PB95-164117 *01,260* Not available NTIS

Small-Angle Neutron Scattering (SANS) Study of Worm-Like Micelles Under Shear.
PB96-176698 *04,111* Not available NTIS

Small Angle Neutron Scattering Studies of Structural Characteristics of Argarose Gels.
PB96-112305 *03,475* Not available NTIS

Small Angle Neutron Scattering Studies on Chain Asymmetry of Coextruded Poly(Vinyl Alcohol) Film.
PB95-164372 *01,262* Not available NTIS

Small Angle Neutron Scattering Study of a Clay Suspension Under Shear.
PB96-167374 *00,663* Not available NTIS

Small-Angle Neutron-Scattering Study of Dense Sheared Silica Gels.
PB96-167184 *01,151* Not available NTIS

Small Angle Neutron Scattering Study of the Structure and Formation of MCM-41 Mesoporous Molecular Sieves.
PB97-122337 *03,110* Not available NTIS

Small Angle Neutron Scattering Study of the Structure and Formation of Ordered Mesopores in Silica.
PB96-111919 *03,069* Not available NTIS

Small Angle Neutron Scattering Study on Poly(N-Isopropyl Acrylamide) Gels Near Their Volume-Phase Transition Temperature.
PB95-164380 *01,263* Not available NTIS

Small-Angle Neutron Scattering Study on Weakly Charged Temperature Sensitive Polymer Gels.
PB95-164398 *01,264* Not available NTIS

Small Angle Neutrons Scattering from Nanocrystalline Palladium as a Function of Annealing.
PB95-176103 *03,354* Not available NTIS

Small-Angle X-Ray and Neutron Scattering Study of Block Copolymer/Homopolymer Mixtures.
PB94-211729 *01,221* Not available NTIS

Small genomes: New initiatives in mapping and sequencing. Workshop summary report.
DE96014476 *03,451* PC A05/MF A01

Smart Clock: A New Time.
PB95-151445 *01,530* Not available NTIS

Smoke Control Systems for Elevator Fire Evacuation.
PB94-212883 *00,291* Not available NTIS

Smoke Emission from Burning Crude Oil.
PB96-122890 *01,407* Not available NTIS

Smoke Plume Trajectory from In situ Burning of Crude Oil: Field Experiments.
PB96-200993 *02,597* Not available NTIS

Smoke Plume Trajectory from In situ Burning of Crude Oil in Alaska: Field Experiments.
PB96-131560 *02,594* PC A03/MF A01

Sobolev Approximation for Line Formation with Partial Frequency Redistribution.
PB95-202669 *00,078* Not available NTIS

Soft-X-ray Damage to p-terphenyl Coatings for Detectors.
PB96-159611 *04,364* Not available NTIS

Soft-X-ray-Emission Investigation of Cobalt Implanted Silicon Crystals.
PB96-157912 *04,069* Not available NTIS

Soft-X-ray-Emission Spectra of Solid Kr and Xe.
PB96-157920 *04,070* Not available NTIS

Soft-X-ray-Emission Studies of Bulk Fe3Si, FeSi, and FeSi2, and Implanted Iron Silicides.
PB96-157938 *04,071* Not available NTIS

Soft X-ray Reflectometry Program at the National Institute of Standards and Technology.
PB96-160395 *04,368* Not available NTIS

Software Libraries, Numerical and Statistical.
PB94-198967 *01,689* Not available NTIS

Software Needs in Special Functions.
PB95-105045 *01,702* PC A03/MF A01

Software Needs in Special Functions.
PB96-200977 *01,778* Not available NTIS

Software Safety and Program Slicing.
PB95-125894 *01,703* Not available NTIS

Solid Propellant Gas Generators: Proceedings of the 1995 Workshop. Held in Gaithersburg, Maryland on June 28-29, 1995.
PB96-131479 *01,412* PC A11/MF A03

Solid State (13)C NMR and Raman Studies of Cellulose Triacetate: Oligomers, Polymorphism, and Inferences about Chain Polarity.
PB96-176532 *01,289* Not available NTIS

Solubilities of Copper(II) and Chromium(III) beta-Diketonates in Supercritical Carbon Dioxide.
PB96-164215 *01,147* Not available NTIS

Solubility Measurement by Direct Injection of Supercritical-Fluid Solutions into a HPLC System.
PB95-175626 *00,997* Not available NTIS

Solvent Effects in the Reactions of Peroxyl Radicals with Organic Reductants. Evidence for Proton Transfer Mediated Electron Transfer.
PB95-107157 *00,873* Not available NTIS

Some Aspects of Fundamental Neutron Physics.
PB95-126298 *03,882* Not available NTIS

TITLE INDEX

Some Basics on Who's Who and What's What in Seismic Safety.
PB95-150926 *00,435* Not available NTIS

Some Considerations for Interim Testing of Coordinate Measuring Machine Performance Using a Specific Artifact.
PB95-108858 *02,898* Not available NTIS

Some Factors Affecting Design of a Furniture Calorimeter Hood and Exhaust.
PB94-139193 *00,285* PC A03/MF A01

Some Factors Affecting the Design of a Calorimeter Hood and Exhaust.
PB96-102181 *00,302* Not available NTIS

Some Notable Hurricanes Revisited.
PB96-122601 *00,458* Not available NTIS

Sorption of Moisture on Epoxy and Alkyd Free Films and Coated Steel Panels.
PB95-162475 *03,192* Not available NTIS

Source of Phenol Emissions Affecting the Indoor Air of an Office Building.
PB94-154382 *03,600* PC A04/MF A01

Sources of Strain-Measurement Error in Flag-Based Extensometry.
PB97-118731 *03,108* Not available NTIS

Sources of Uncertainty in a DVM-Based Measurement System for a Quantized Hall Resistance Standard.
PB94-219334 *01,884*
(Order as PB94-219326, PC A05/MF A02)

Sources of Urban Contemporary Carbon Aerosol.
PB95-175659 *02,551* Not available NTIS

Sparse Water Sprays in Fire Protection.
PB96-202304 *01,433* PC A13/MF A03

SparseLib++ v. 1.5 Sparse Matrix Class Library. Reference Guide.
PB96-193636 *01,775* PC A03/MF A01

Spatial Correlation Function for Fields in a Reverberation Chamber.
PB96-148077 *04,427* Not available NTIS

Spatial Data Transfer Standard (SDTS): Category: Software Standard; Subcategory: Information Interchange.
FIPS PUB 173-1 *01,794* PC A04/MF A01

Spatial Data Transfer Standard (SDTS). Category: Software Standard; Subcategory: Information Interchange. (FIPS PUB 173-1A).
FIPS PUB 173-1A *01,795* PC$44.50

Spatial Data Transfer Standard (SDTS). Category: Software Standard; Subcategory: Information Interchange. (FIPS PUB 173-1B).
FIPS PUB 173-1B *01,796* PC E99

Spatial Dependence of Electrical Fields Due to Space Charges in Films of Organic Dielectrics Used for Insulation of Power Cables.
PB94-199130 *02,214* Not available NTIS

Spatial Information and Technology Standards Evolving.
PB96-135108 *03,679* Not available NTIS

Spatial Uniformity of Optical Detector Responsivity.
PB95-168845 *02,162* Not available NTIS

SPC Artifact for Automated Solder Joint Inspection.
PB96-161716 *04,095* Not available NTIS

Specification for Interoperability between Ballistic Imaging Systems. Part 1. Cartridge Cases.
PB96-195524 *01,860* PC A04/MF A01

Specifications and Tolerances for Reference Standards and Field Standard Weights and Measures. 2. Specifications and Tolerances for Field Standard Measuring Flasks.
PB96-178926 *02,682* PC A03/MF A01

Spectra of Ag I Isoelectronic Sequence Observed from Er(21+) to Au(32+).
PB95-150660 *03,899* Not available NTIS

Spectral Data and Grotrian Diagrams for Highly Ionized Chromium, Cr V through Cr XXIV.
PB94-162369 *00,748* Not available NTIS

Spectral Data for Highly Ionized Krypton, Kr V through Kr XXXVI.
PB96-145917 *01,115* Not available NTIS

Spectral Interference in the Determination of Arsenic in High-Purity Lead and Lead-Base Alloys Using Electrothermal Atomic Absorption Spectrometry and Zeeman-Effect Background Correction.
PB96-112099 *00,614* Not available NTIS

Spectrally Smooth Reflectances That Match.
PB95-176319 *04,306* Not available NTIS

Spectroscopic Constants for the 2.5 and 3.0 micrometer Bands of Acetylene.
PB94-213071 *00,847* Not available NTIS

Spectroscopic Data for Fusion Edge Plasmas.
PB95-151569 *04,410* Not available NTIS

Spectroscopic Data Tables for Highly-Ionized Atoms.
PB95-151585 *03,910* Not available NTIS

Spectroscopic Diagnostics of Low Temperature Plasmas: Techniques and Required Data.
PB95-151577 *04,411* Not available NTIS

Spectroscopic Ellipsometry Determination of the Properties of the Thin Underlying Strained Si Layer and the Roughness at SiO2/Si Interface.
PB95-150157 *04,560* Not available NTIS

Spectroscopic Puzzle in ArHF Solved: The Test of a New Potential.
PB94-216058 *00,850* Not available NTIS

Spectroscopic Study of Quantized Breakdown Voltage States of the Quantum Hall Effect.
PB96-113584 *04,730*
(Order as PB96-113535, PC A05/MF A01)

Spectroscopic Study of Reaction Intermediates and Mechanisms in Nitramine Decomposition and Combustion.
AD-A296 061/5 *03,774* PC A03/MF A01

Spectroscopy and Structure of the Lithium Hydride Diatomic Molecules and Ions.
PB94-160991 *00,731* Not available NTIS

Spectrum and Energy Levels of Five-Times-Ionized Niobium (Nb VI).
PB94-185246 *04,226* Not available NTIS

Spectrum and Energy Levels of Triply Ionized Barium (Ba IV).
PB95-140877 *03,888* Not available NTIS

Spectrum of the Stochastically Forced Duffing-Holmes Oscillator.
PB96-155767 *00,216* Not available NTIS

Specular and Diffuse Reflection Measurements of Electronic Displays.
PB97-119200 *02,208* Not available NTIS

Speed-of-Sound Measurements in Liquid and Gaseous Air.
PB95-151957 *04,186* Not available NTIS

Spherical-Wave Source-Scattering Matrix Analysis of Antennas and Antenna-Antenna Interactions.
PB96-111166 *02,008* PC A08/MF A02

Spin-Dependent Interface Transmission and Reflection in Magnetic Multilayers (Invited).
PB96-201173 *04,130* Not available NTIS

Spin-Resolved Elastic Scattering of Electrons from Sodium.
PB95-161774 *03,933* Not available NTIS

Spin Squeezing and Reduced Quantum Noise in Spectroscopy.
PB95-151635 *03,912* Not available NTIS

Spinor Equations in Relativistic Quantum Mechanics.
PB97-110605 *04,142* Not available NTIS

Spot-Profile-Analyzing LEED Study of the Epitaxial Growth of Fe, Co, and Cu on Cu(100).
PB95-150165 *04,561* Not available NTIS

Sprinkler Fire Suppression Algorithm.
PB94-216181 *00,293* Not available NTIS

Sputtered High Temperature Thin Film Thermocouples.
PB95-161311 *02,259* Not available NTIS

SQA and TQM in Software Quality Improvement.
PB96-160791 *01,754* Not available NTIS

SQA Standards and Total Quality Management.
PB96-111844 *01,743* Not available NTIS

SQL Environments. Category: Software Standard; Subcategory: Database.
FIPS PUB 193 *01,801* PC A04/MF A01

Squeezed Atomic States and Projection Noise in Spectroscopy.
PB95-176293 *03,960* Not available NTIS

SSME LOX Duct Flowmeter Design and Test Results.
PB96-161955 *04,826* Not available NTIS

Stability and Surface Energies of Wetted Grain Boundaries in Aluminum Oxide.
PB95-202750 *03,059* Not available NTIS

Stability/Instability of Gas Mixtures Containing 1,3-Butadiene in Treated Aluminum Gas Cylinders.
PB95-162285 *02,546* Not available NTIS

Stability, Microstructural Evolution, Grain Growth, and Coarsening in a Two-Dimensional Two-Phase Microstructure.
PB94-199429 *03,325* Not available NTIS

Stability of Compressed Gas Mixtures Containing Low Level Volatile Organic Compounds in Aluminum Cylinders.
PB96-111968 *00,613* Not available NTIS

Stabilization and Precise Calibration of a Continuous-Wave Difference Frequency Spectrometer by Use of a Simple Transfer Cavity.
PB95-162350 *04,276* Not available NTIS

Stabilization of Optical Phase/Frequency of a Laser System: Application to a Commercial Dye Laser with an External Stabilizer.
PB95-203832 *04,327* Not available NTIS

Stabilization of 3.3 and 5.1 m Lead-Salt Diode Lasers by Optical Feedback.
PB95-180709 *04,313* Not available NTIS

Stable Phase Locking in a Two-Cell Ladder Array of Josephson Junctions.
PB96-111679 *04,722* Not available NTIS

Stable Silicon Photodiodes for Absolute Intensity Measurements in the VUV and Soft X-ray Regions.
PB97-110175 *04,135* Not available NTIS

Stable, Tightly Confining Magnetic Trap for Evaporative Cooling of Neutral Atoms.
PB96-200720 *04,126* Not available NTIS

Stacked Series Arrays of High-Tc Trilayer Josephson Junctions.
PB96-102272 *04,705* Not available NTIS

Stacking Fault Pyramid Formation and Energetics in Silicon-on-Insulator Material Formed by Multiple Cycles of Oxygen Implantation and Annealing.
PB96-160221 *04,083* Not available NTIS

Stacking the Cards in Europe: One Company's Story.
PB97-110126 *00,493* Not available NTIS

Stagnant Film Model of the Effect of Natural Convection on the Dendrite Operating State.
PB96-146832 *04,765* Not available NTIS

Standard Antennas for Electromagnetic Interference Measurements and Methods to Calibrate Them.
PB96-102561 *02,007* Not available NTIS

STandard for the Exchange of Product Model Data (STEP): Procedures for NIST STEP Validation.
PB96-154976 *02,787* PC A03/MF A01

Standard Generalized Markup Language Test Suite Evaluation Report.
PB96-154992 *01,751* PC A03/MF A01

Standard Materials. A Descriptive List with Prices.
AD-A278 140/9 *00,500* PC A03/MF A01

Standard of Attenuation for Microwave Measurements.
AD-A297 905/2 *01,517* PC A02/MF A01

Standard Polarization Components: Progress Toward an Optical Retardance Standard.
PB96-119672 *04,342* Not available NTIS

Standard Probes for Electromagnetic Field Measurements.
PB94-185436 *01,999* Not available NTIS

Standard Reference Data for the Thermal Conductivity of Water.
PB96-145875 *01,111* Not available NTIS

Standard Reference Devices for High Temperature Superconductor Critical Current Measurements.
PB95-175543 *04,659* Not available NTIS

Standard Reference Material for the Measurement of Particle Mobility by Electrophoretic Light Scattering.
PB96-102488 *00,609* Not available NTIS

Standard Reference Material 1744: Aluminum Freezing-Point Standard.
PB95-251732 *01,055* PC A03/MF A01

Standard Reference Materials: Certification of a Standard Reference Material for the Determination of Interstitial Oxygen Concentration in Semiconductor Silicon by Infrared Spectrophotometry.
PB95-125076 *02,326* PC A05/MF A01

Standard Reference Materials for Dioxins and Other Environmental Pollutants.
PB94-198330 *02,518* Not available NTIS

Standard Reference Materials for Optical Fibers and Connectors.
PB96-119805 *04,344* Not available NTIS

Standard Reference Materials for the Determination of Polycyclic Aromatic Hydrocarbons in Environmental Samples - Current Activities.
PB95-151668 *00,586* Not available NTIS

Standard Reference Materials for the Determination of Trace Organic Constituents in Environmental Samples.
PB95-164026 *02,522* Not available NTIS

Standard Reference Materials: Glass Filters as a Standard Reference Material for Spectrophotometry - Selection, Preparation, Certification, and Use of SRM 930 and SRM 1930.
PB94-188844 *00,536* PC A10/MF A03

Standard Reference Materials: Polystyrene Films for Calibrating the Wavelength Scale of Infrared Spectrophotometers - SRM 1921.
PB95-226866 *03,386* PC A03/MF A01

Standard Reference Materials (SRM's) for Measuring Genetic Damage.
PB94-198827 *03,516* Not available NTIS

Standard Samples and Reference Standards Issued by the National Bureau of Standards.
AD-A279 240/6 *02,613* PC A03/MF A01

Standard Security Label for Information Transfer; Category: Computer Security; Subcategory: Security Labels.
FIPS PUB 188 *01,571* PC E04

Standard Source Method for Reducing Antenna Factor Errors in Shielded Room Measurements.
PB96-183157 *02,013* PC A04/MF A01

Standard States, Reference States and Finite-Concentration Effects in Near-Critical Mixtures with Applications to Aqueous Solutions.
PB95-164349 *00,979* Not available NTIS

Standardised Computer Data File Format for Storage, Transport, and Off-Line Processing of Partial Discharge Data.
PB96-122486 *01,930* Not available NTIS

Standardization and Decay Scheme of Rhenium-186.
PB94-200490 *03,830* Not available NTIS

Standardization for ATM and Related B-ISDN Technologies.
PB96-160460 *01,499* Not available NTIS

Standardization of Formats and Presentation of Fire Data - The FDMS.
PB94-198462 *01,371* Not available NTIS

Standardization of Testing Methods for Optical Disk Media Characteristics and Related Activities at NIST.
PB95-108486 *01,624* Not available NTIS

Standards: A Cardinal Direction for Geographic Information Systems.
PB95-150942 *03,677* Not available NTIS

Standards Activities of Organizations in the United States.
PB97-124135 *00,006* PC A99/MF E08

Standards and Linkages: What Data Sharing Needs.
PB95-161881 *01,713* Not available NTIS

Standards Development in North America for Performance of Whole Buildings and Facilities.
PB94-185196 *00,312* Not available NTIS

Standards for Atmospheric Measurements.
PB95-163622 *02,547* Not available NTIS

Standards for Corrected Fluorescence Spectra.
PB95-150835 *00,581* Not available NTIS

Standards for High Integrity Software.
PB96-161385 *01,764* Not available NTIS

Standards in Building Economics: Why We Need Them and How to Write Them.
PB94-216405 *00,320* Not available NTIS

Standards of Seismic Safety for Existing Federally Owned or Leased Buildings and Commentary.
PB95-130209 *00,431* PC A06/MF A02

Standards Policy and Information Infrastructure.
PB95-231882 *01,485* PC A20/MF A04

Standards Promote Credibility and Technology Transfer: The Need for Greater Industry Support of Technical Committees.
PB97-116206 *02,961* PC A03/MF A01

Standards Setting in the European Union: Standards Organization and Officials in EU Standards Activities.
PB96-115019 *02,919* PC A04/MF A01

Stars, Atmospheres, Radiative Transfer.
PB96-119474 *00,095* Not available NTIS

State of the Art Report on Seismic Design Requirements for Nonstructural Building Components.
PB96-193800 *00,308* PC A06/MF A01

State-of-the-Art Survey of Methodologies for Representing Manufacturing Process Capabilities.
PB94-187655 *02,812* PC A03/MF A01

State-Resolved Rotational Energy Transfer in Open Shell Collisions: Cl((2)P3/2)+HCl.
PB96-176607 *01,157* Not available NTIS

State Weights and Measures Laboratories: Program Handbook.
PB96-214705 *02,687* PC A07/MF A02

State Weights and Measures Laboratories: State Standards Program Description and Directory. 1994 Edition.
PB94-207727 *02,895* PC A07/MF A02

Static Dielectric Constant of Water and Steam.
PB96-123559 *01,090* Not available NTIS

Static Structural Analysis of a Reconfigurable Rigid Platform Supported by Elastic Legs.
PB97-113898 *02,960* PC A05/MF A01

Statistical Analysis of Parameters Affecting the Measurement of Particle-Size Distribution of Silicon Nitride Powders by Sedigraph (Trade Name).
PB94-216249 *03,042* Not available NTIS

Statistical Aspects of the Certification of Chemical Batch SRMs. Standard Reference Materials.
PB96-210877 *00,645* PC A05/MF A01

Statistical Descriptors in Crystallography. 2. Report of a Working Group on Expression of Uncertainty in Measurement.
PB96-146824 *04,764* Not available NTIS

Statistical Quality Control Technology in Japan.
PB94-199064 *02,708* Not available NTIS

Statistical Thermodynamics of Phase Separation and Ion Partitioning in Aqueous Two-Phase Systems.
PB94-199387 *01,212* Not available NTIS

Status and Trends in Power Semiconductor Devices.
PB95-175097 *02,361* Not available NTIS

Status of a Silicon Lattice Measurement and Dissemination Exercise.
PB94-199635 *04,474* Not available NTIS

Status of Construction and Construction Technologies.
PB94-186004 *00,318* Not available NTIS

Status of Electrocomposites.
PB94-212453 *03,143* Not available NTIS

Status of Emerging Standards for Removable Computer Storage Media and Related Contributions of NIST.
PB96-160619 *01,634* Not available NTIS

Status of the Round Robin on the Transport Properties of R134a.
PB96-167218 *01,152* Not available NTIS

Status Report: AWS Standards for Identifying Arc Welds (A91.1) and Recording Weld Data (A9.2).
PB95-162855 *02,861* Not available NTIS

Stellar Coronal Structures.
PB95-202834 *00,080* Not available NTIS

Step-Edge and Stacked-Heterostructure High-Tc Josephson Junctions for Voltage-Standard Arrays.
PB96-102066 *04,702* Not available NTIS

STEP On-Line Information Service (SOLIS). The IGES/PDES Organization.
PB95-137790 *02,777* PC A02/MF A01

Stochastic Modeling of a New Spectrometer.
PB96-157870 *04,068* Not available NTIS

Stranding Experiments on Double Hull Tanker Structures.
PB96-123112 *03,749* Not available NTIS

Strangeness Flow Difference in Nuclear Collisions at 15A and 200A GeV.
PB96-119631 *04,042* Not available NTIS

Strategy to Support Multipoint Communication Service Over Native ATM Service.
PB96-176672 *01,507* Not available NTIS

Strengthening Methodology for Lightly Reinforced Concrete Frames.
PB96-158050 *00,466* Not available NTIS

Strengthening Methodology for Lightly Reinforced Concrete Frames-II. Recommended Calculation Techniques for the Design of Infill Walls.
PB94-187648 *00,426* PC A03/MF A01

Strengthening Methodology for Lightly Reinforced Concrete Frames: Recommended Design Guidelines for Strengthening with Infill Walls.
PB95-260725 *00,454* PC A04/MF A01

Strong Hydrogen Bond in the Formic Acid-Formate Anion System.
PB94-198595 *00,788* Not available NTIS

Structural Analysis in Context.
PB95-151817 *00,437* Not available NTIS

Structural Analysis of Heparin by Raman Spectroscopy.
PB96-167226 *03,480* Not available NTIS

Structural and Chemical Investigations of Na3(ABO4)3.4H2O-Type Sodalite Phases.
PB95-180733 *01,012* Not available NTIS

Structural and Magnetic Ordering in Iron Oxide/Nickel Oxide Multilayers by X-ray and Neutron Diffraction (Invited).
PB94-172558 *04,442* Not available NTIS

Structural and Magnetic Properties of CuCl2 Graphite Intercalation Compounds.
PB96-119748 *03,020* Not available NTIS

Structural Ceramics Database. Topical Report, June 1989-May 1991.
PB95-203758 *03,060* PC A04/MF A01

Structural EXPRESS Editor.
PB94-159795 *02,769* PC A04/MF A01

Structural Heterogeneity in Epoxies.
PB95-151866 *01,243* Not available NTIS

Structural Stabilization of Phase Separating PC/Polyester Blends through Interfacial Modification by Transesterification Reaction.
PB95-150454 *01,239* Not available NTIS

Structure and Conductivity of Layered Oxides (Ba,Sr)n+1(Sn,Sb)nO3n+1.
PB96-102439 *04,707* Not available NTIS

Structure and Dynamics of Buckyballs.
PB95-153292 *00,950* Not available NTIS

Structure and Radiation Properties of Pool Fires.
PB94-193802 *02,473* PC A08/MF A02

Structure and Rheology of Hard-Sphere Systems.
PB96-167333 *00,662* Not available NTIS

Structure of a Swirl-Stabilized Kerosene Spray Flame.
PB95-108569 *02,480* Not available NTIS

Structure of a Triglyceride Microemulsion: A Small Angle Neutron Scattering Study.
PB96-112255 *01,077* Not available NTIS

Structure of Glycine-Water H-Bonded Complexes.
PB94-198603 *00,789* Not available NTIS

Structure of Molecules on Surfaces as Determined Using Electron-Stimulated Desorption.
PB94-216165 *00,852* Not available NTIS

Structure of the Vapor-Liquid Interface Near the Critical Point.
PB95-140174 *00,902* Not available NTIS

Structured Testing: A Testing Methodology Using the Cyclomatic Complexity Metric.
PB97-114169 *01,784* PC A07/MF A02

Structures of Sodium Metal.
PB94-198850 *03,319* Not available NTIS

Structures of Vapor-Deposited Yttria and Zirconia Thin Films.
PB94-216025 *03,041* Not available NTIS

Studies Assess Performance of Residential Detectors.
PB94-199262 *00,290* Not available NTIS

Studies of Defects in Diamond Films and Particles by Raman and Luminescence Spectroscopies.
PB95-162400 *03,017* Not available NTIS

Studies of Ion Kinetic-Energy Distributions in the Gaseous Electronics Conference RF Reference Cell.
PB96-113360 *02,391*
(Order as PB96-113311, PC A09/MF A03)

Studies of the Higher Order Smectic Phase of the Large Electroclinic Effect Material W317.
PB95-151601 *00,935* Not available NTIS

Study of Diffusion Zones with Electron Microprobe Compositional Mapping.
PB94-216348 *00,559* Not available NTIS

Study of Droplet Transport in Alcohol-Based Spray Flames Using Phase/Doppler Interferometry.
PB95-108551 *02,479* Not available NTIS

Study of Federal Agency Needs for Information Technology Security.
PB94-193653 *01,579* PC A07/MF A02

Study of Heat Pump Performance Using Mixtures of R32/R134a and R32/R125/R134a as 'Drop-In' Working Fluids for R22 with and Without a Liquid-Suction Heat Exchanger.
PB94-218559 *02,503* PC A04/MF A01

Study of Laser Resonance Ionization Mass Spectrometry Using a Glow Discharge Source.
DE94018566 *03,308* PC A01/MF A01

Study of Laser Resonance Ionization Mass Spectrometry Using a Glow Discharge Source.
PB96-123203 *03,360* Not available NTIS

Study of Multiple Scattering Background in Compton Scatter Imaging.
PB96-112222 *04,425* Not available NTIS

Study of Potential Applications of Automation and Robotics Technology in Construction, Maintenance and Operation of Highway Systems: A Final Report. Volume 1.
PB95-251682 *01,341* PC A06/MF A02

Study of Potential Applications of Automation and Robotics Technology in Construction, Maintenance and Operation of Highway Systems: A Final Report. Volume 2.
PB95-255865 *01,343* PC A19/MF A04

Study of Potential Applications of Automation and Robotics Technology in Construction, Maintenance and Operation of Highway Systems: A Final Report. Volume 3.
PB95-251690 *01,342* PC A15/MF A03

Study of Potential Applications of Automation and Robotics Technology in Construction, Maintenance and Operation of Highway Systems: A Final Report. Volume 4.
PB95-251641 *01,340* PC A06/MF A02

Study of Technology for Detecting Pre-Ignition Conditions of Cooking-Related Fires Associated with Electric and Gas Ranges and Cooktops, Phase 1 Report.
PB96-128095 *00,303* PC A06/MF A02

Study of the Hydroxycarbonate Precursor Route to the YBa2Cu3O7-x High Tc Superconductor.
PB95-140471 *04,540* Not available NTIS

Study of Ventilation and Carbon Dioxide in an Office Building.
PB95-150140 *02,542* Not available NTIS

Study of Ventilation Measurement in an Office Building.
PB96-155593 *00,274* Not available NTIS

Study on Hazard Analysis in High Integrity Software Standards and Guidelines.
PB95-198727 *01,725* PC A04/MF A01

Study on the Reuse of Plastic Concrete Using Extended Set-Retarding Admixtures.
PB96-122130 *00,402*
(Order as PB96-117767, PC A08/MF A02)

Study to Determine the Existence of an Azeotropic R-22 'Drop-In' Substitute.
PB96-167812 *02,568* PC A04/MF A01

Study to Determine the Most Important Parameters for Evaluating the Resistance of Soft Body Armor to Penetration by Edged Weapons.
PB94-158573 *03,757* PC A03/MF A01

Stylus Flight in Surface Profiling.
PB96-123138 *02,675* Not available NTIS

Stylus Technique for the Direct Verification of Rockwell Diamond Intenders.
PB96-155569 *02,958* Not available NTIS

Sub-Doppler Frequency Measurements on OCS at 87 Thz (3.4 micrometers) with the CO Overtone Laser: Considerations and Details.
PB95-128633 *04,255* PC A03/MF A01

Sub-Doppler Frequency Measurements on OCS at 87 THz (3.4 mu m) with the CO Overtone Laser.
PB96-102215 *04,330* Not available NTIS

Sub-Doppler, Infrared Laser Spectroscopy of the Propyne 2nu1 Band: Evidence of z-Axis Coriolis Dominated Intramolecular State Mixing in the Acetylenic CH Stretch Overtone.
PB95-202941 *01,037* Not available NTIS

Submarine Automation: Demonstration No. 5.
PB95-251633 *03,748* PC A03/MF A01

Submicroampere-Per-Root-Hertz Current Sensor Based on the Faraday Effect in Ga: YIG.
PB95-162467 *02,155* Not available NTIS

Submissions to a Planned Encyclopedia of Operations Research on Computational Geometry and the Voronoi/Delaunay Construct.
PB94-152709 *03,425* PC A03/MF A01

Substitution-Induced Midgap States in the Mixed Oxides RxBa1-ChiTiO3-Delta, with R=Y, La, and Nd.
PB95-140505 *04,541* Not available NTIS

Substrate and Thin Film Measurements.
PB96-112297 *02,384* Not available NTIS

Substrate Specificity of the Escherichia coli Endonuclease III: Excision of Thymine- and Cytosine-Derived Lesions in DNA Produced by Radiation-Generated Free Radicals.
PB95-153425 *03,535* Not available NTIS

Suggestions for a Logically-Consistent Structure for Service Life Prediction Standards.
PB95-125795 *00,358* Not available NTIS

Suitability of Metalorganic Chemical Vapor Deposition-Derived PrGaO3 Films as Buffer Layers for YBa2Cu3O7-x Pulsed Laser Deposition.
PB95-168670 *04,640* Not available NTIS

Sulfate Attack of Cementitious Materials: Volumetric Relations and Expansions.
PB94-187317 *03,232* PC A03/MF A01

Sulfur Dioxide Capture in the Combustion of Mixtures of Lime, Refuse-Derived Fuel, and Coal.
PB94-155587 *02,534* PC A04/MF A01

SUM and MEAN: Standard Programs for Activation Analysis.
PB96-112149 *00,617* Not available NTIS

Summaries of BFRL Fire Research In-House Projects and Grants, 1994.
PB95-130845 *00,366* PC A10/MF A03

Summaries of Center for Fire Research In-House Projects and Grants: 1990.
PB94-160876 *00,286* PC A10/MF A03

Summary and Notes of the Joint ISO/IGES/PDES Organization Technical Committee Meeting. Held in Albuquerque, New Mexico on October 15-20, 1989.
PB95-107314 *02,774* Not available NTIS

Summary and Results of the NIST Workshop on Proposed Guidelines for Testing and Evaluation of Seismic Isolation Systems. Held in San Francisco, California on July 25, 1994.
PB96-154901 *00,463* PC A04/MF A01

Summary of Federal Construction and Building R and D in 1994.
PB97-114250 *00,234* PC A04/MF A01

Summary of the Apparent Standard Partial Molal Gibbs Free Energies of Formation of Aqueous Species, Minerals, and Gases at Pressures 1 to 5000 Bars and Temperatures 25 to 1000C.
PB96-145891 *01,113* Not available NTIS

Summary of the Patent Literature of Supercritical Fluid Technology.
PB94-199213 *00,502* Not available NTIS

Summary of the Proceedings of the Workshop on Standard Phantoms for In-vivo Radioactivity Measurement.
PB94-212933 *03,622* Not available NTIS

Summary Report of NIST's Industry-Government Consortium Research Program on Flowmeter Installation Effects: The 45 Degree Elbow.
PB95-143061 *04,204* PC A06/MF A02

Summary Report of NIST's Industry-Government Consortium Research Program on Flowmeter Installation Effects with Emphasis on the Research Period, January-September 1991: The Reducer.
PB94-160736 *04,196* PC A04/MF A01

Summary Report on the Workshop on Advanced Digital Video in the National Information Infrastructure.
PB96-141320 *01,497* Not available NTIS

Summary Report: Workshop on Industrial Applications of Scanned Probe Microscopy (2nd). A Workshop Co-Sponsored by NIST, SEMATECH, ASTM E42.14, and the American Vacuum Society. Held in Gaithersburg, Maryland on May 2-3, 1995.
PB96-131602 *00,509* PC A07/MF A02

Superconducting Energy Gap of Bulk UBe13.
PB95-150116 *04,559* Not available NTIS

Superconducting Integrated Circuit Fabrication with Low Temperature ECR-Based PECVD SiO2 Dielectric Films.
PB96-103015 *04,719* Not available NTIS

Superconducting Kinetic Inductance Radiometer.
PB95-140083 *02,144* Not available NTIS

Superconducting Materials: Specification.
PB94-211299 *04,491* Not available NTIS

Superconducting Resonator and a Cryogenic GaAs Field-Effect Transistor Amplifier as a Single-Ion Detection System.
PB95-202727 *03,990* Not available NTIS

Superconductor Critical Current Standards for Fusion Applications. Final Progress Report, October 1993-July 1994.
PB95-169538 *02,222* PC A05/MF A02

Superconductor- Normal-Superconductor Junctions for Digital/Analog Converters.
PB96-200233 *02,092* Not available NTIS

Superconductor- Normal-Superconductor Junctions for Programmable Voltage Standards.
PB96-200241 *02,093* Not available NTIS

Supercritical Fluid Extraction-Immunoassay for the Rapid Screening of Cocaine in Hair.
PB96-167168 *00,637* Not available NTIS

Supercritical Fluid Extraction of Biological Products.
PB95-175204 *00,040* Not available NTIS

Supercritical Solubility of Solids from Near-Critical Dilute-Mixture Theory.
PB94-211703 *00,819* Not available NTIS

Supermirror Transmission Polarizers for Neutrons.
PB94-216215 *03,866* Not available NTIS

Supplement to Stable Implementation Agreements for Open Systems Interconnection Protocols. Version 3, September 1990. Change Page Index, Version 3, June 1990 (Stable) Change Pages Issued December 1990; Output from September 1990 OSI Workshop (NIST Special Publication 500-177).
PB94-164035 *01,467* PC A06/MF A02

Supported Phospholipid/Alkanthiol Biomimetic Membranes: Insulating Properties.
PB95-180782 *03,470* Not available NTIS

Suppression Effectiveness of Extinguishing Agents under Highly Dynamic Conditions.
PB95-180279 *00,020* Not available NTIS

Suppression of Elevated Temperature Hydraulic Fluid and JP-8 Spray Flames.
PB95-181095 *00,021* Not available NTIS

Suppression of High-Speed C2H4/Air Flames with C1-Halocarbons.
PB96-175724 *03,287* Not available NTIS

Suppression of High Speed Turbulent Flames in a Detonation/Deflagration Tube.
PB95-231817 *01,395* PC A04/MF A01

Suppression of Ignition Over a Heated Metal Surface.
PB96-176425 *03,291* Not available NTIS

Suppression of Ionization in One- and Two-Dimensional Model Calculations.
PB95-203600 *04,009* Not available NTIS

Suppression Research: Strategies.
PB94-211372 *00,346* Not available NTIS

Surface Barrier and Lower Critical Field in YBa2Cu3O7-delta Superconductors.
PB94-200128 *04,478* Not available NTIS

Surface Chemical Interactions of Si3N4 with Polyelectrolyte Deflocculants.
PB95-175576 *03,056* Not available NTIS

Surface Chemistry of Silicon Nitride Powder in the Presence of Dissolved Ions.
PB96-111760 *01,073* Not available NTIS

Surface Core-Level Shifts of Barium Observed in Photoemission of Vacuum-Fractured BaTiO3 (100).
PB94-212156 *04,501* Not available NTIS

Surface Degradation of Superconducting YBa2Cu3O7-delta Thin Films.
PB95-176095 *04,667* Not available NTIS

Surface Energy Reduction in Fibrous Monotectic Structures.
PB95-140828 *03,150* Not available NTIS

Surface Forces and Adhesion between Dissimilar Materials Measured in Various Environments.
PB94-172970 *03,033* Not available NTIS

Surface Geometry of BaO on W(100): A Surface-Extended X-Ray-Absorption Fine-Structure Study.
PB95-164414 *00,980* Not available NTIS

Surface Magnetic Microstructural Analysis Using Scanning Electron Microscopy with Polarization Analysis (SEMPA).
PB95-162657 *03,938* Not available NTIS

Surface Modification of YBa2Cu3O7-delta Thin Films Using the Scanning Tunneling Microscope: Five Methods.
PB95-203394 *04,699* Not available NTIS

Surface Plasmon Microscopy of Biotin-Streptavidin Binding Reactions on UV-Photopatterned Alkanethiol Self-Assembled Monolayers.
PB96-176771 *01,158* Not available NTIS

Surface Roughness Evaluation of Diamond Films Grown on Substrates with a High Density of Nucleation Sites.
PB95-162418 *03,018* Not available NTIS

Surface Roughness of Glass-Ceramic Insert. Composite Restorations: Assessing Several Polishing Techniques.
PB97-119010 *03,583* Not available NTIS

Surface Texture.
PB95-164620 *03,351* Not available NTIS

Surface Topography and Ordering-Variant Segregation in GaInP2.
PB95-153649 *04,595* Not available NTIS

Surface Transverse Wave Oscillators with Extremely Low Thermal Noise Floors.
PB96-186010 *01,967* Not available NTIS

Surging the Upside-Down House: Looking into Upsetting Reference Voltages.
PB96-112313 *02,385* Not available NTIS

Surging the Upside-Down House: Measurements and Modeling Results.
PB96-180138 *02,243* Not available NTIS

Survey of Concrete Transport Properties and Their Measurement.
PB95-220489 *00,396* PC A04/MF A01

Survey of Fuel Loads in Contemporary Office Buildings.
PB97-114235 *00,233* PC A04/MF A01

Survey of Recent Cementitious Materials Research in Western Europe.
PB94-218583 *00,353* PC A03/MF A01

Survey of Standards for the U.S. Fiber/Textile/Apparel Industry.
PB96-193792 *03,199* PC A06/MF A01

Survey of Steel Moment-Resisting Frame Buildings Affected by the 1994 Northridge Earthquake.
PB95-211918 *00,451* PC A09/MF A02

Survey of the Components of Display-Measurement Standards.
PB96-122528 *02,188* Not available NTIS

Survey of the Components of Display-Measurement Standards.
PB97-122394 *02,209* Not available NTIS

Survey of the Literature on Heat Transfer from Solid Surfaces to Cryogenic Fluids.
AD-A286 680/4 *04,193* PC A04/MF A01

Survey on the Implementation of ISO/IEC Guide 25 by National Laboratory Accreditation Programs.
PB94-210150 *00,479* PC A04/MF A01

SUSAN: SUperconducting Systems ANalysis by Low Temperature Scanning Electron Microscopy (LTSEM).
PB96-112065 *04,728* Not available NTIS

Susceptibility Critical Exponent for a Nonaqueous Ionic Binary Mixture Near a Consolute Point.
PB95-152112 *00,938* Not available NTIS

Swelling and Growth of Polymers, Membranes and Sponges.
PB97-118400 *03,396* Not available NTIS

Symbolic Programming with Series Expansions: Applications to Optical Waveguides.
PB95-168589 *04,283* Not available NTIS

Synthesis and Polymerization of Difunctional and Multifunctional Monomers Capable of Cyclopolymerization.
PB95-163044 *01,257* Not available NTIS

Synthesis of Hybrid Organic-Inorganic Materials from Interpenetrating Polymer Network Chemistry.
PB96-180054 *02,994* Not available NTIS

Synthesis of Thermally Stable Elastomers.
AD-A307 789/8 *03,194* PC A03/MF A01

Synthetic-Perturbation Tuning of MIMD Programs.
PB94-185568 *01,687* Not available NTIS

System for Calibration of the Marshall Compaction Hammer.
PB94-145661 *01,303* PC A08/MF A02

System for Intercomparing Standard Solutions of Beta-Particle Emitting Radionuclides.
PB96-159637 *03,707* Not available NTIS

Systematic Correction in Bragg X-ray Diffraction of Flat and Curved Crystals.
PB97-112239 *04,152* Not available NTIS

Systematic Studies of the Effect of a Bandpass Filter on a Josephson-Junction Noise Thermometer.
PB95-162970 *03,939* Not available NTIS

Systematic Studies of the Effect of a Post-Detection Filter on a Josephson-Junction Noise Thermometer.
PB95-162988 *03,940* Not available NTIS

Systematics of Alpha-Particle Energy Spectra and Lineal Energy (Y) Spectra for Radon Daughters.
PB94-185139 *03,615* Not available NTIS

Systems Integration for Manufacturing Applications Program 1995 Annual Report.
PB96-193735 *02,844* PC A05/MF A01

Table of Dielectric Constants of Pure Liquids.
AD-A278 956/8 *00,712* PC A04/MF A01

Tables of Chemical Kinetics Homogeneous Reactions.
AD-A280 293/2 *00,715* PC A20/MF A04

Tables of X-ray Mass Attenuation Coefficients and Mass Energy-Absorption Coefficients 1 keV to 20 MeV for Elements Z = 1 to 92 and 48 Additional Substances of Dosimetric Interest.
PB95-220539 *04,013* PC A06/MF A02

Tabulation of Data on Receiving Tubes. Handbook 68.
AD-A285 495/8 *02,111* PC A06/MF A02

Tabulation of the Thermodynamic Properties of Normal Hydrogen from Low Temperatures to 300K and from 1 to 100 Atmospheres.
AD-A279 951/8 *00,713* PC A05/MF A01

Taguchi's Parameter Design: A Panel Discussion.
PB96-111802 *03,445* Not available NTIS

Tapered Cross-Pin Attachments for Fixed Bridges.
PB94-185238 *00,185* Not available NTIS

Task Decomposition Methodology for the Design of a Coal Mining Automation Hierarchical Real-Time Control System.
PB94-185386 *03,694* Not available NTIS

Taxonomy for Security Standards.
PB95-180386 *01,602* Not available NTIS

TBT Agreement Activities of the National Institute of Standards and Technology, 1995.
PB97-104178 *00,499* PC A04/MF A01

TDDB Characterization of Thin SiO2 Films with Bimodal Failure Populations.
PB96-102926 *02,381* Not available NTIS

Technical Digest: Symposium on Optical Fiber Measurements (8th), 1994. Held in Boulder, Colorado on September 13-15, 1994.
PB94-207636 *04,231* PC A10/MF A03

Technical Digest: Symposium on Optical Fiber Measurements (9th), 1996. Held in Boulder, Colorado on October 1-3, 1996.
PB97-108583 *04,383* PC A12/MF A03

Technical Impact of the NIST Calibration Service for Electrical Power and Energy.
PB96-147913 *02,462* PC A05/MF A01

Technical Program Description Systems Integration for Manufacturing (SIMA).
PB94-213758 *02,819* PC A05/MF A01

Technical Program of the Factory Automation Systems Division 1993.
PB94-160819 *02,805* PC A03/MF A01

Technique for Analyzing the Effects of Changes in Formal Specifications.
PB96-160957 *01,760* Not available NTIS

Technique to Evaluate Benchmarks: A Case Study Using the Livermore Loops.
PB95-151320 *04,577* Not available NTIS

Technologic Papers of the Bureau of Standards: Number 170. Pyrometric Practice.
AD-A279 282/8 *03,766* PC A15/MF A03

Technology Trends in Telecommunications: An Overview.
PB94-123080 *01,462* PC A03/MF A01

Telecommunications Security Guidelines for Telecommunications Management Network. Computer Security.
PB96-139415 *01,496* PC A03/MF A01

Telegraph Noise in Silver-Permalloy Giant Magnetoresistance Test Structures.
PB96-146717 *04,763* Not available NTIS

TEM/Reverberating Chamber Electromagnetic Radiation Test Facility at Rome Laboratory.
PB96-155023 *03,675* PC A05/MF A01

Temperature and Field Dependence of Flux Pinning in NbTi with Artificial Pinning Centers.
PB96-112024 *04,726* Not available NTIS

Temperature and Frequency Dependence of Anelasticity in a Nickel Oscillator.
PB96-137732 *03,689* Not available NTIS

Temperature and Relative Humidity Dependence of Radiochromic Film Dosimeter Response to Gamma and Electron Radiation.
PB96-135298 *03,718* Not available NTIS

Temperature Dependence and Anharmonicity of Phonons on Ni(110) and Cu(110) Using Molecular Dynamics Simulations.
PB94-185477 *04,449* Not available NTIS

Temperature Dependence and Magnetic Field Modulation of Critical Currents in Step-Edge SNS YBCO/Au Junctions.
PB96-111745 *04,723* Not available NTIS

Temperature Dependence of the Gas and Liquid Phase Ultraviolet Absorption Cross Sections of HCFC-123 (CF3CHCl2) and HCFC-142b (CH3CF2Cl).
PB96-201033 *03,298* Not available NTIS

Temperature Dependence of the Magnetic Excitations in Ordered and Disordered Fe72Pt28.
PB95-150223 *04,563* Not available NTIS

Temperature Dependence of the Morphology of Thin Diblock Copolymer Films as Revealed by Neutron Reflectivity.
PB94-172756 *01,199* Not available NTIS

Temperature Dependence of the Rate Constants for Reaction of Dihalide and Azide Radicals with Inorganic Reductants.
PB95-162756 *00,964* Not available NTIS

Temperature Dependence of the Rate Constants for Reaction of Inorganic Radicals with Organic Reductants.
PB94-198280 *00,783* PC A02

Temperature Dependence of the Rate Constants for Reactions of the Carbonate Radical with Organic and Inorganic Reductants.
PB94-212206 *00,831* Not available NTIS

Temperature Dependence of the Rate Constants for Reactions of the Sulfate Radical, SO4-, with Anions.
PB94-212172 *00,828* Not available NTIS

Temperature Dependence of the Ultraviolet Absorption Cross Section of CF3I.
PB96-204169 *01,168* Not available NTIS

Temperature Dependence of Vortex Twin Boundary Interaction in Yttrium Barium Copper Oxide (YBa2Cu3O6+x).
PB95-162442 *04,613* Not available NTIS

Temperature Dependent Ultraviolet Absorption Cross Sections of Propylene, Methylacetylene and Vinylacetylene.
PB96-204177 *01,169* Not available NTIS

Temperature Increases in Aluminum Alloys during Mechanical-Impact Tests for Oxygen Compatibility.
PB94-172962 *03,316* Not available NTIS

Temperature-Induced Transition in Ductile Fracture Appearance of a Nitrogen-Strengthened Austenitic Stainless Steel.
PB96-190269 *03,221* Not available NTIS

Temperature of Optical Molasses for Two Different Atomic Angular Momenta.
PB95-126058 *03,881* Not available NTIS

Template-Driven Systems Development with IDEF: Enterprise Standards for Reuse.
PB96-160965 *02,788* Not available NTIS

Tensile Creep of a Silicon Nitride Ceramic.
PB95-161303 *03,049* Not available NTIS

Tensile Creep of Silicide Composites.
PB96-200803 *03,183* Not available NTIS

Tensile Creep of Whisker Reinforced Silicon Nitride.
PB94-211984 *03,142* Not available NTIS

Tensile Creep Testing of Structural Ceramics.
PB97-110464 *03,105* Not available NTIS

Tensile Deformation-Induced Microstructures in Free-Standing Copper Thin Films.
PB96-102595 *04,715* Not available NTIS

Tension/Compression Creep Asymmetry in Si3N4.
PB97-110258 *03,096* Not available NTIS

Terahertz Detectors Based on Superconducting Kinetic Inductance.
PB95-168647 *02,160* Not available NTIS

Terahertz Shapiro Steps in High Temperature SNS Josephson Junctions.
PB95-169140 *02,168* Not available NTIS

Terminal Invariant Description of Amplifier Noise.
PB95-153573 *02,043* Not available NTIS

Terminally Anchored Chain Interphases: The Effect of Multicomponent, Polydisperse Solvents on Their Equilibrium Properties.
PB95-181079 *01,273* Not available NTIS

Terminally Anchored Chain Interphases: Their Chromatographic Properties.
PB95-181061 *01,272* Not available NTIS

Tert-Butyl Hydroperoxide-Mediated DNA Base Damage in Cultured Mammalian Cells.
PB94-182003 *03,644* Not available NTIS

Test of a Slow Off-Axis Parabola at Its Center of Curvature.
PB96-138482 *04,352* Not available NTIS

Test of Newton's Inverse Square Law of Gravitation Using the 300-m Tower at Erie, Colorado.
PB95-202446 *03,978* Not available NTIS

Test Optics Error Removal.
PB96-179536 *04,377* Not available NTIS

Test Procedures for Advanced Insulation Panels.
PB97-111892 *00,415* Not available NTIS

Test Structures for Determining Design Rules for Microelectromechanical-Based Sensors and Actuators.
PB95-150488 *02,105* Not available NTIS

Test Structures for the In-Plane Locations of Projected Features with Nanometer-Level Accuracy Traceable to a Coordinate Measurement System.
PB94-200565 *02,313* Not available NTIS

Testability of Object-Oriented Systems.
PB95-242418 *01,733* PC A05/MF A01

Testers Open Dialogue at Inaugural NIST Workshop.
PB95-175550 *01,718* Not available NTIS

Testing Conformance and Interoperability of BACnet (Trade Name) Building Automation Products.
PB97-111553 *00,310* Not available NTIS

Testing for Metrological Accuracy of the Electron Pump.
PB95-175873 *04,663* Not available NTIS

Testing of Selected Self-Leveling Compounds for Floors.
PB95-220455 *00,395* PC A03/MF A01

Testing the Sensitivity of Accelerometers Using Mechanical Shock Pulses Under NIST Special Publication 250 Test No. 24040S.
PB96-179544 *02,683* Not available NTIS

Tetrahedral-Framework Lithium Zinc Phosphate Phases: Location of Light-Atom Positions in LiZnPO4 H2O by Powder Neutron Diffraction and Structure Determination of LiZnPO4 by ab Initio Methods.
PB96-160510 *01,129* Not available NTIS

Text REtrieval Conference (4th) (TREC-4). Held in Gaithersburg, Maryland on November 1-3, 1995.
PB97-121636 *01,786* PC A99/MF E08

Texture-Independent Vision-Based Closed-Loop Fuzzy Controllers for Navigation Tasks.
PB95-220505 *00,183* PC A03/MF A01

TITLE INDEX

Texture Measurement of Sintered Alumina Using the March-Dollase Function.
PB96-179494 *04,784* Not available NTIS

Texture Study of Two Molybdenum Shaped Charge Liners by Neutron Diffraction.
PB94-200177 *03,754* Not available NTIS

Textures of Tantalum Metal Sheets by Neutron Diffraction.
PB94-200169 *03,399* Not available NTIS

Theoretical Analysis of the Coherence-Induced Spectral Shift Experiments of Kandpal, Vaishya, and Joshi.
PB94-219383 *00,561*
(Order as PB94-219326, PC A05/MF A02)

Theoretical Aspects of Tagged Photon Facilities.
PB94-216611 *03,868* Not available NTIS

Theoretical Evaluation of the Vapor Compression Cycle with a Liquid-Line/Suction-Line Heat Exchanger, Economizer, and Ejector.
PB95-216917 *02,607* PC A03/MF A01

Theoretical Form Factor, Attenuation and Scattering Tabulation for Z=1-92 from E=1-10 eV to E=0.4-1.0 MeV.
PB96-145594 *01,104* Not available NTIS

Theory for Quantum-Dot Quantum Wells: Pair Correlation and Internal Quantum Confinement in Nanoheterostructures.
PB96-179445 *02,437* Not available NTIS

Theory of Atomic Collisions at Ultracold Temperatures.
PB94-212560 *03,851* Not available NTIS

Theory of Electron Beam Moire.
PB96-175690 *04,373*
(Order as PB96-175666, PC A07/MF A02)

Theory of Intelligent Systems.
PB94-198272 *01,582* PC A02

Theory of the Magneto-Optic Kerr Effect in the Near Field.
PB96-141387 *04,761* Not available NTIS

Thermal and Nonequilibrium Responses of Superconductors for Radiation Detectors.
PB95-164232 *02,156* Not available NTIS

Thermal Anemometry for Mass Flow Measurement in Oscillating Cryogenic Gas Flows.
PB96-176789 *04,218* Not available NTIS

Thermal Behavior of 4-Maleimidophenyl Glycidyl Ether Resins.
PB95-153151 *01,249* Not available NTIS

Thermal Behaviour of Methyl Methacrylate and N-Phenyl Maleimide Copolymers.
PB95-152237 *01,246* Not available NTIS

Thermal Component Models for Electro-Thermal Network Simulation.
PB95-161022 *02,346* Not available NTIS

Thermal Conductivity of Metals and Alloys at Low Temperatures. A Review of the Literature.
AD-A279 180/4 *03,302* PC A04/MF A01

Thermal Conductivity of Polypyromellitimide Film with Alumina Filler Particles from 4.2 to 300 K.
PB96-200753 *01,292* Not available NTIS

Thermal Conductivity of R134a.
PB94-213063 *03,857* Not available NTIS

Thermal Decomposition of Hydroxy- and Methoxy-Substituted Anisoles.
PB94-173036 *00,767* Not available NTIS

Thermal Decomposition Pathways in Nitramine Propellants.
AD-A295 896/5 *03,753* PC A03/MF A01

Thermal Diffusivity of POCO AXM-5Q1 Graphite in the Range 1500 to 2500 K Measured by a Laser-Pulse Technique.
PB94-185022 *03,013* Not available NTIS

Thermal Enhancement of Cotunneling in Ultra-Small Tunnel Junctions.
PB95-175436 *04,658* Not available NTIS

Thermal Equilibration Near the Critical Point: Effects Due to Three Dimensions and Gravity.
PB95-152922 *03,919* Not available NTIS

Thermal Expansion of an SiC Particle-Reinforced Aluminum Composite.
PB94-213204 *03,144* Not available NTIS

Thermal Hydraulic Tests of a Liquid Hydrogen Cold Neutron Source.
PB95-135570 *03,884* PC A03/MF A01

Thermal Isolation of High-Temperature Superconducting Thin Films Using Silicon Wafer Bonding and Micromachining.
PB96-135017 *02,408* Not available NTIS

Thermal Modeling and Analysis of Laser Calorimeters.
PB96-140405 *04,354* Not available NTIS

Thermal Modeling of Absolute Cryogenic Radiometers.
PB95-181236 *04,316* Not available NTIS

Thermal Noise in High-Temperature Superconducting-Normal-Superconducting Step-Edge Josephson Junctions.
PB95-175089 *04,650* Not available NTIS

Thermal Pulse Study of the Polarization Distributions Produced in Polyvinylidene Fluoride by Corona Poling at Constant Current.
PB94-172293 *01,195* Not available NTIS

Thermal Stability of Internal Electric Field and Polarization Distribution in Blend of Polyvinylidene Fluoride and Polymethylmethacrylate.
PB95-151072 *01,240* Not available NTIS

Thermal Wave NDE of Advanced Materials Using Mirage Effect Detection.
PB96-204516 *04,191* Not available NTIS

Thermal Wave Propagation in Diamond Films.
PB94-211489 *03,015* Not available NTIS

Thermally Activated Hopping of a Single Abrikosov Vortex.
PB95-140810 *04,548* Not available NTIS

Thermoacoustic Technique for Determining the Interface and/or Interply Strength in Polymeric Composites.
PB95-161824 *03,158* Not available NTIS

Thermochemical and Chemical Kinetic Data for Fluorinated Hydrocarbons.
PB95-260618 *01,056* PC A09/MF A02

Thermochemical Studies of Inorganic Chalocogenides by Fluorine-Combustion Calorimetry: Binary Compounds of Germanium and Silicon with Sulfur, Selenium and Tellurium.
PB97-112528 *01,181* Not available NTIS

Thermochemistry of the Hydrolysis of L-arginine to (L-citrulline + Ammonia) and of the Hydrolysis of L-arginine to (L-ornithine + Urea).
PB95-150801 *03,463* Not available NTIS

Thermochemistry of the Reactions between Adenosine, Adenosine 5'-monophosphate, Inosine, and Inosine 5'-monophosphate; the Conversion of L-histidine to (Urocanic Acid+Ammonia).
PB94-213113 *03,460* Not available NTIS

Thermodynamic Analysis of Heparin Binding to Human Antithrombin.
PB94-199593 *03,455* Not available NTIS

Thermodynamic and NMR Study of the Interactions of Cyclodextrins with Cyclohexane Derivatives.
PB94-185816 *00,781* Not available NTIS

Thermodynamic and Thermophysical Properties of Organic Nitrogen Compounds. Part II. 1- and 2-Butanamine, 2-Methyl-1-Propanamine, 2-Methyl-2-Propanamine, Pyrrole, 1-, 2-, and 3-Methylpyrrole, Pyridine, 2-, 3-, and 4-Methylpyridine, Pyrrolidine, Piperidine, Indole, Quinoline, Isoquinoline, Acridine, Carbazole, Phenanthridine, 1- and 2-Naphthalenamine, and 9-Methylcarbazole.
PB94-162294 *00,741* Not available NTIS

Thermodynamic Assessment and Calculation of the Ti-Al System.
PB94-212644 *03,337* Not available NTIS

Thermodynamic Behavior of the CO2-H2O System from 400 to 1000 K, up to 100 MPa and 30% Mole Fraction of CO2.
PB94-162245 *00,736* Not available NTIS

Thermodynamic Calculation of the Ternary Ti-Al-Nb System.
PB94-212636 *03,336* Not available NTIS

Thermodynamic Constraints on Non-Equilibrium Solidification of Ordered Intermetallic Compounds.
PB94-198934 *03,321* Not available NTIS

Thermodynamic Interactions and Correlations in Mixtures of Two Homopolymers and a Block Copolymers by Small Angle Neutron Scattering.
PB95-152872 *01,247* Not available NTIS

Thermodynamic Interactions in Model Polyolefin Blends Obtained by Small-Angle Neutron Scattering.
PB94-198496 *01,208* Not available NTIS

Thermodynamic Properties of Alkenes (Mono-Olefins Larger Than C4).
PB94-162237 *00,735* Not available NTIS

Thermodynamic Properties of CF3-CHF-CHF2, 1,1,1,2,3,3-Hexafluoropropane.
PB97-118384 *03,299* Not available NTIS

Thermodynamic Properties of CHF2-CF2-CHF, 1,1,2,2,3-Pentafluoropropane.
PB97-118392 *03,300* Not available NTIS

Thermodynamic Properties of CHF2-O-CHF2,Bis(difluoromethyl) Ether.
PB94-199569 *00,798* Not available NTIS

Thermodynamic Properties of Difluoromethane.
PB94-185204 *00,772* Not available NTIS

Thermodynamic Properties of Dilute and Semidilute Solutions of Regular Star Polymers.
PB96-146808 *01,284* Not available NTIS

Thermodynamic Properties of Gas Phase Species of Importance to Ozone Depletion.
PB94-198215 *00,126* Not available NTIS

Thermodynamic Properties of Gaseous Silicon Monotelluride and the Bond Dissociation Enthalpy D(sub m)(SiTe) at T approaches 0.
PB94-168572 *00,751* Not available NTIS

Thermodynamic Properties of R134a(1,1,1,2-Tetrafluoroethane).
PB95-168704 *00,988* Not available NTIS

Thermodynamic Properties of Silicides. 5. Standard Molar Enthalpy of Formation at the Temperature 298.15 K of Trimolybdenum Monosilicide Mo3Si Determined by Fluorine-Combustion Calorimetry.
PB97-119358 *01,190* Not available NTIS

Thermodynamic Properties of Synthetic Otavite, CdCO3(cr): Enthalpy Increment Measurements from 4.5 K to 350 K.
PB97-111447 *00,680* Not available NTIS

Thermodynamic Properties of Synthetic Sapphire (alpha-Al2O3), Standard Reference Material 720 and the Effect of Temperature-Scale Differences on Thermodynamic Properties.
PB94-168564 *00,750* Not available NTIS

Thermodynamic Properties of the Aqueous Ba(sup 2+) Ion and the Key Compounds of Barium.
PB96-145834 *01,107* Not available NTIS

Thermodynamic Properties of the Aqueous Ions (2+ and 3+) of Iron and the Key Compounds of Iron.
PB96-145958 *01,119* Not available NTIS

Thermodynamic Properties of the Group IIA Elements.
PB94-160983 *00,730* Not available NTIS

Thermodynamic Properties of the Methane-Ethane System.
PB95-125779 *00,891* Not available NTIS

Thermodynamic Properties of Two Gaseous Halogenated Ethers from Speed-of-Sound Measurements: Difluoromethoxy-Difluoromethane and 2-Difluoromethoxy-1,1,1-Trifluoroethane.
PB96-102413 *04,189* Not available NTIS

Thermodynamic Study of the Reactions of Cyclodextrins with Primary and Secondary Aliphatic Alcohols, with D- and L-Phenylalanine, and with L-Phenylalanineamide.
PB95-180873 *01,016* Not available NTIS

Thermodynamics of Enzyme-Catalyzed Reactions: Part 1. Oxidoreductases.
PB94-162252 *00,737* Not available NTIS

Thermodynamics of Enzyme-Catalyzed Reactions. Part 4. Lyases.
PB96-145941 *01,118* Not available NTIS

Thermodynamics of Enzyme-Catalyzed Reactions. Part 5. Isomerases and Ligases.
PB96-145974 *01,121* Not available NTIS

Thermodynamics of (Germanium + Selenium): A Review and Critical Assessment.
PB97-112536 *01,182* Not available NTIS

Thermodynamics of the Binding of Galactopyranoside Derivatives to the Basic Lectin from Winged Bean (Psophocarpus Tetrogonolobus).
PB95-162715 *03,465* Not available NTIS

Thermodynamics of the Hydrolysis of N-Acetyl-L-phenylalanine Ethyl Ester in Water and in Organic Solvents.
PB95-203386 *01,053* Not available NTIS

Thermodynamics of the Hydrolysis of Penicillin G and Ampicillin.
PB94-172467 *03,596* Not available NTIS

Thermodynamics of the Hydrolysis of 3,4,5-Trihydroxybenzoic Acid Propyl Ester (n-Propylgallate) to 3,4,5-Trihydroxybenzoic Acid (Gallic Acid) and Propan-I-ol in Aqueous Media and in Toluene.
PB96-186143 *01,160* Not available NTIS

Thermophysical Properties of CO2 and CO2-Rich Mixtures.
PB94-216199 *00,854* Not available NTIS

Thermophysical Properties of Fluids for the Gas Industry.
PB96-122437 *02,494* Not available NTIS

Thermophysical Properties of Fluids for the Gas Industry. Final Report, February 1, 1988-August 31, 1993.
PB94-146677 *02,472* PC A03/MF A01

Thermophysical properties of HCFC alternatives. Quarterly report, April 1--June 30, 1995.
DE96010579 *03,250* PC A05/MF A01

Thermophysical properties of HCFC alternatives. Quarterly report, October 1--December 31, 1995.
DE96010433 *03,249* PC A04/MF A01

Thermophysical properties of HCFC alternatives. Quarterly report, 1 July 1994--30 September 1994.
DE95002261 *03,247* PC A02/MF A01

Thermophysical Properties of HFC-143a and HFC-152a. Quarterly Report, 1 July 1993--30 September 1993.
DE94004236 *03,245* PC A03/MF A01

Thermophysical Property Computer Packages from NIST.
PB95-125787 *04,203* Not available NTIS

Thermophysical Property Data for Supercritical Fluid Extraction Design.
PB94-199221 *00,668* Not available NTIS

Thermophysical Property Standard Reference Data from NIST.
PB96-167358 *01,153* Not available NTIS

Thin Dyed-Plastic Dosimeter for Large Radiation Doses.
PB95-107363 *03,872* Not available NTIS

Thin Film Reaction Kinetics of Niobium/Aluminum Multilayers.
PB95-175295 *04,651* Not available NTIS

Thin-Film Ruthenium Oxide - Iridium Oxide Thermocouples.
PB97-110225 *00,520* Not available NTIS

Thin Film Thermocouple Research at NIST.
PB97-110233 *02,283* Not available NTIS

Thin Film Thermocouples for Measurement of Wall Temperatures in Internal Combustion Engines.
PB94-172103 *01,449* Not available NTIS

Thin Film Transparent Thermocouples.
PB94-185519 *02,253* Not available NTIS

Think Metric.
PB95-151825 *01,298* Not available NTIS

Third Generation Water Bath Based Blackbody Source.
PB96-122148 *04,046*
(Order as PB96-117767, PC A08/MF A02)

Three-Axis Coil Probe Dimensions and Uncertainties during Measurement of Magnetic Fields from Appliances.
PB94-219359 *01,885*
(Order as PB94-219326, PC A05/MF A02)

Three Dimensional Position Determination from Motion.
PB95-107108 *01,788* Not available NTIS

Three-Vector Correlation Study of Orientation and Coherence Effects in Na(3p, (2)P1/2 inversely maps (2)P3/2)+He: Semiclassical and Quantum Calculations.
PB95-202453 *03,979* Not available NTIS

Three-Vector Correlation Theory for Orientation/Alignment Studies in Atomic and Molecular Collisions.
PB94-211109 *03,834* Not available NTIS

Threshold Electron Excitation of Na.
PB95-202917 *03,994* Not available NTIS

Through-the-Arc Sensing for Measuring Gas Metal Arc Weld Quality in Real Time.
PB95-164463 *02,908* Not available NTIS

Through-the-Arc Sensing for Monitoring Arc Welding.
PB94-185899 *02,858* Not available NTIS

Through-the-Arc Sensing for Real-Time Measurement of Gas Metal Arc Weld Quality.
PB95-162871 *02,863* Not available NTIS

Tilt Effects in Optical Angle Measurements.
PB95-169389 *04,294*
(Order as PB95-169371, PC A07/MF A02)

Time and Frequency: Bibliography of NIST Publications, March 1995.
PB95-220463 *01,548* PC A06/MF A02

Time and Frequency Metrology.
PB96-190319 *01,556* Not available NTIS

Time and Frequency Technology at NIST.
N94-30641/2 *01,522*
(Order as N94-30639/6, PC A25/MF A06)

Time-Dependent Dielectric Breakdown of Intrinsic SiO2 Films under Dynamic Stress.
PB96-179478 *02,438* Not available NTIS

Time Dependent Small Angle Neutron Scattering Behavior in Triblock Copolymers Under Steady Shear.
PB94-172632 *01,198* Not available NTIS

Time Dependent Vector Dynamic Programming Algorithm for the Path Planning Problem.
PB94-215688 *03,428* PC A04/MF A01

Time-Domain Antenna Characterizations.
PB95-152781 *02,003* Not available NTIS

Time-Domain Measurements of the Electromagnetic Backscatter of Pyramidal Absorbers and Metallic Plates.
PB94-185410 *01,877* Not available NTIS

Time Domain Network Analysis Using the Multiline TRL Calibration.
PB95-202925 *02,065* Not available NTIS

Time Generation and Distribution.
PB96-103049 *01,550* Not available NTIS

Time-Perturbation Tuning of MIMD Programs.
PB94-164399 *01,681* PC A03/MF A01

Time-Perturbation Tuning of MIMD Programs.
PB94-172566 *01,684* Not available NTIS

Time-Resolved Balmer-Alpha Emission from Fast Hydrogen Atoms in Low Pressure, Radio-Frequency Discharges in Hydrogen.
PB96-102942 *04,028* Not available NTIS

Time-Resolved Measurements of Energy Transfer at Surfaces.
PB95-141198 *00,913* Not available NTIS

Time-Resolved Measurements of Energy Transfer at Surfaces.
PB95-153037 *00,947* Not available NTIS

Time-Resolved Measurements of the Polarization State of Four-Wave Mixing Signals from GaAs Multiple Quantum Wells.
PB96-201058 *04,796* Not available NTIS

Time-Resolved Probes of Surface Dynamics.
PB94-199957 *00,803* Not available NTIS

Time-Resolved Small-Angle Neutron Scattering Study of Spinodal Decomposition in Deuterated and Protonated Polybutadiene Blends. 1. Effect of Initial Thermal Fluctuations.
PB95-161196 *01,252* Not available NTIS

Time Scale Algorithm for Post-Processing: AT1 Plus Frequency Variance.
PB94-172772 *01,525* Not available NTIS

Tin Oxide Gas Sensor Fabricated Using CMOS Micro-Hotplates and In-situ Processing.
PB95-150603 *00,580* Not available NTIS

TMACH Experiment Phase 1. Preliminary Developmental Evaluation.
PB96-195318 *01,618* PC A03/MF A01

Tolerance Intervals for the Distribution of True Values in the Presence of Measurement Errors.
PB95-150405 *03,434* Not available NTIS

Tomographic Decoding Algorithm for a Nonoverlapping Redundant Array.
PB95-151932 *01,842* Not available NTIS

Tomographic Reconstruction of the Moments of Local Probability Density Functions in Turbulent Flow Fields.
PB96-180195 *04,219* Not available NTIS

Topological Influences on Polymer Adsorption and Desorption Dynamics.
PB94-212479 *01,227* Not available NTIS

Torsion Modulus and Internal Friction of a Fiber-Reinforced Composite.
PB96-112339 *03,070* Not available NTIS

Torsional Dilatometer for Volume Change Measurements on Deformed Glasses: Instrument Description and Measurements on Equilibrated Glasses.
PB94-211166 *03,379* Not available NTIS

Torsional Relaxation and Volume Response during Physical Aging in Epoxy Glasses Subjected to Large Torsional Deformations.
PB95-140026 *03,383* Not available NTIS

Total-Dielectric-Function Approach to Electron and Phonon Response in Solids.
PB96-102884 *01,067* Not available NTIS

Total Surface Areas of Group IVA Organometallic Compounds: Predictors of Toxicity to Algae and Bacteria.
PB94-211331 *00,814* Not available NTIS

Toward a Reference Model Architecture for Real-Time Intelligent Control Systems (ARTICS).
PB94-172046 *02,932* Not available NTIS

Toxicity, Fire Hazard and Upholstered Furniture.
PB94-198454 *00,289* Not available NTIS

Trace Detection in Conducting Solids Using Laser-Induced Fluorescence in a Cathodic Sputtering Cell.
PB95-163424 *00,598* Not available NTIS

Trace Element Concentrations in Cetacean Liver Tissues Archived in the National Marine Mammal Tissue Bank.
PB96-167127 *02,595* Not available NTIS

Trace Elements Associated with Proteins. Neutron Activation Analysis Combined with Biological Isolation Techniques.
PB95-163101 *00,597* Not available NTIS

Traceability to the Mole: A New Initiative by CIPM.
PB95-180246 *00,605* Not available NTIS

Transfer of Technology from Defense to Civilian Sectors.
PB94-185360 *00,011* Not available NTIS

Transformation of BCC and B2 High Tempera[illegible] Phases to HCP and Orthorhombic Structures in the [illegible]b System. Part 1. Microstructural Predictions Based on a Subgroup Relation between Phases.
PB96-169065 *03,370*
(Order as PB96-169057, PC A05/MF A01)

Transformation of BCC and B2 High Temperature Phases to HCP and Orthorhombic Structures in the Ti-Al-Nb System. Part 2. Experimental TEM Study of Microstructures.
PB96-169073 *03,371*
(Order as PB96-169057, PC A05/MF A01)

Transient Analysis of a Line-Focus Transducer Probing a Liquid/Solid Interface.
PB97-118681 *02,763* Not available NTIS

Transient Cooling of a Hot Surface by Droplets Evaporation.
PB94-156957 *03,783* PC A08/MF A02

Transient Cooling of a Hot Surface by Droplets Evaporation.
PB95-143194 *03,890* PC A09/MF A02

Transient Creep Behaviour of Hot Isostatically Pressed Silicon Nitride.
PB96-180278 *03,086* Not available NTIS

Transient Errors in a Precision Resistive Divider.
PB97-111512 *01,983* Not available NTIS

Transient Methods for Thermal Conductivity.
PB94-198405 *04,197* Not available NTIS

Transient Subcritical Crack-Growth Behavior in Transformation-Toughened Ceramics.
PB94-200656 *03,038* Not available NTIS

Transition from Localized Ignition to Flame Spread Over a Thin Cellulosic Material in Microgravity.
PB96-155809 *04,835* Not available NTIS

Transition Metal Implants in In0.53GA0.47As.
PB95-126389 *04,534* Not available NTIS

Transition Regions of Capella.
PB96-123336 *00,105* Not available NTIS

Transition Regions of Capella (1995).
PB96-176714 *00,108* Not available NTIS

Transitions to Chaos Induced by Additive and Multiplicative Noise.
PB96-155759 *03,750* Not available NTIS

Transmission Properties of Short Curved Neutron Guides. Part 1. Acceptance Diagram Analysis and Calculations.
PB96-102199 *04,021* Not available NTIS

Transmission/Reflection and Short-Circuit Line Methods for Measuring Permittivity and Permeability.
PB94-165537 *02,211* PC A06/MF A02

Transport and Diffusion in Three-Dimensional Composite Media.
PB95-176129 *04,668* Not available NTIS

Transport by Gravity Currents in Building Fires.
PB97-119325 *01,441* Not available NTIS

Transport Critical Current of Aligned Polycrystalline Yttrium Barium Copper Oxide (YBa2Cu3O7-delta).
PB94-211307 *04,492* Not available NTIS

Transverse Magnetoresistance: A Novel Two-Terminal Method for Measuring the Carrier Density and Mobility of a Semiconductor Layer.
PB95-150066 *02,332* Not available NTIS

Transverse stress effect on the critical current of internal tin and bronze process Nb(sub 3)Sn superconductors.
DE95016659 *04,434* PC A01/MF A01

Transverse Thermomagnetic Effects in the Mixed State and Lower Critical Field of High-Tc Superconductors.
PB95-153250 *04,590* Not available NTIS

Trapped Atoms and Laser Cooling.
PB95-151627 *03,911* Not available NTIS

Trapped Ions and Laser Cooling 4: Selected Publications of the Ion Storage Group of the Time and Frequency Division, NIST, Boulder, Colorado.
PB96-172358 *04,108* PC A11/MF A03

Trapped Vortices in a Superconducting Microbridge.
PB95-141149 *04,554* Not available NTIS

Treatment of Wistar Rats with a Renal Carcinogen, Ferric Nitrilotriacetate, Causes DNA-Protein Cross-Linking between Thymine and Tyrosine in Their Renal Chromatin.
PB96-112115 *03,649* Not available NTIS

Tree-Lookup for Partial Sums Or: How Can I Find This Stuff Quickly.
PB96-179411 *01,770* Not available NTIS

Tribochemical Reaction of Stearic Acid on Copper Surface Studied by Surface Enhanced Raman Spectroscopy.
PB94-212057 *02,964* Not available NTIS

Tribological Behavior of 440/Diamond-Like-Carbon Film Couples.
PB96-119714 *03,019* Not available NTIS

TITLE INDEX

Tribological Characteristics of Alpha-Alumina at Elevated Temperatures.
PB94-211018 *02,963* Not available NTIS

Tribological Data: Needs and Opportunities.
PB95-140596 *03,237* Not available NTIS

Tribology Education: Present Status and Future Challenges.
PB94-212362 *02,965* Not available NTIS

Tribometer for Measurements in Hostile Environments.
PB95-180949 *02,967* Not available NTIS

Troublesome Crystal Structures: Prevention, Detection, and Resolution.
PB97-109151 *01,172*
(Order as PB97-109011, PC A11/MF A03)

Tunable High Temperature Superconductor Microstrip Resonators.
PB95-168423 *02,048* Not available NTIS

Tunneling Measurement of the Zero-Bias Conductance Peak and the Bi-Sr-Ca-Cu-O Thin-Film Energy Gap.
PB95-163739 *04,628* Not available NTIS

Tunneling-Rotation Spectrum of the Hydrogen Fluoride Dimer.
PB94-198678 *00,793* Not available NTIS

Tunneling Spectroscopy of bcc(001) Surface States.
PB96-155585 *04,775* Not available NTIS

Tunneling Spectroscopy of Thallium-Based High-Temperature Superconductors.
PB95-161709 *04,606* Not available NTIS

Tunneling Stabilized Magnetic-Force Microscopy.
PB95-161717 *04,607* Not available NTIS

Turbulent Flame Spread on Vertical Corner Walls.
PB96-114764 *01,403* PC A08/MF A02

Turbulent Spray Burner for Assessing Halon Alternative Fire Suppressants.
PB95-153748 *01,385* Not available NTIS

Turbulent Upward Flame Spread on a Vertical Wall under External Radiation.
PB94-207388 *00,341* PC A05/MF A01

Two-Dimensional POMMIE Carbon-Proton Chemical Shift Correlated (13)C NMR Spectrum Editing.
PB94-200508 *00,809* Not available NTIS

Two-Dimensional Self-Consistent Radio Frequency Plasma Simulations Relevant to the Gaseous Electronics Conference RF Reference Cell.
PB96-113436 *02,398*
(Order as PB96-113311, PC A09/MF A03)

Two New Probes for a Coordinate Measuring Machine.
PB95-163093 *02,653* Not available NTIS

Two Numerical Techniques for Light Scattering by Dielectric Agglomerated Structures.
PB94-140597 *04,225*
(Order as PB94-140555, PC A06/MF A02)

Two Phase Aqueous Extraction: Rheological Properties of Dextran, Polyethylene Glycol, Bovine Serum Albumin and Their Mixtures.
PB95-161998 *00,676* Not available NTIS

Two Principal Points of Symmetric, Strongly Unimodal Distributions.
PB95-203360 *03,443* Not available NTIS

Two-Stage Integrated SQUID Amplifier with Series Array Output.
PB95-176277 *02,061* Not available NTIS

Two-Tier Multiline TRL for Calibration of Low-Cost Network Analyzers.
PB96-157888 *01,947* Not available NTIS

A-type and Chemically Peculiar Stars.
PB96-123286 *00,101* Not available NTIS

U.S. GOSIP Testing Program.
PB94-211455 *01,807* Not available NTIS

U.S. Government Accreditation and Conformity Assessment System Evaluation.
PB96-160239 *02,678* Not available NTIS

U.S. Green Building Conference, 1994.
PB94-206364 *02,519* PC A08/MF A02

U.S. Navy Coordinate Measuring Machines: A Study of Needs.
PB94-162831 *02,807* PC A04/MF A01

Ultra-High Stability Synthesizer for Diode Laser Pumped Rubidium.
PB94-216066 *01,527* Not available NTIS

Ultracold Collisions: Associative Ionization in a Laser Trap.
PB94-213238 *03,859* Not available NTIS

Ultrafast Time-Resolved Infrared Probing of Energy Transfer at Surfaces.
PB96-123443 *00,620* Not available NTIS

Ultrafine Combustion Aerosol Generator.
PB94-200300 *01,373* Not available NTIS

Ultralinear Small-Angle Phase Modulator.
PB95-168852 *02,261* Not available NTIS

Ultrasensitive-Hot-Electron Microbolometer.
PB95-168985 *02,163* Not available NTIS

Ultrasonic Measurement of Residual Stress in Cast Steel Railroad Wheels.
PB95-169199 *04,852* Not available NTIS

Ultrasonic Measurement of Residual Stress in Railroad Wheel Rims.
PB95-140430 *04,849* Not available NTIS

Ultrasonic Measurement of Sheet Anisotropy and Formability.
PB95-153235 *03,213* Not available NTIS

Ultrasonic Measurements of Surface Roughness.
PB94-172137 *04,181* Not available NTIS

Ultrasonic Method for Reconstructing the Two-Dimensional Liquid-Solid Interface in Solidifying Bodies.
PB95-161782 *03,349* Not available NTIS

Ultrasonic Methods.
PB96-190327 *02,707* Not available NTIS

Ultrasonic NDE of Sprayed Ceramic Coatings.
PB96-201157 *02,761* Not available NTIS

Ultrasonic-Resonance Spectroscopy of Bulk and Layered Solids.
PB96-141338 *04,759* Not available NTIS

Ultrasonic Sensing of GMAW: Laser/EMAT Defect Detection System.
PB96-186028 *02,878* Not available NTIS

Ultrasonic Spectroscopy of Metallic Spheres Using Electromagnetic-Acoustic Transduction.
PB94-212537 *04,185* Not available NTIS

Ultrasonic Technique for Sizing Voids Using Area Functions.
PB95-151916 *02,904* Not available NTIS

Ultrasound Power Measurement Techniques at NIST.
PB96-179569 *02,684* Not available NTIS

Ultraviolet Multiplet Table.
AD-A278 446/0 *00,710* PC A08/MF A02

Ultraviolet Multiplet Table. Finding List for Spectra of the Elements Molybdenum to Lanthanum (Z = 42 to 57); Hafnium to Radium (Z = 72 to 88).
AD-A278 131/8 *00,709* PC A03/MF A01

Ultraviolet Observations of Stellar Coronae: Early Results from HST.
PB94-213428 *00,064* Not available NTIS

Uncertainties in Dimensional Measurements Made at Nonstandard Temperatures.
PB94-169760 *02,893* Not available NTIS

Uncertainties of Frequency Response Estimates Derived from Responses to Uncertain Step-Like Inputs.
PB97-111843 *01,984* Not available NTIS

Uncertainties of the NIST Coaxial Noise Calibration System.
PB96-111984 *02,070* Not available NTIS

Uncertainty Analysis of the NIST Nitrogen Flow Facility.
PB95-128906 *02,608* PC A04/MF A01

Uncertainty Intervals for Polarized Beam Scattering Asymmetry Statistics.
PB94-200342 *03,825* Not available NTIS

Unconstrained Handprint Recognition Using a Limited Lexicon.
PB94-168051 *01,831* PC A03/MF A01

Unconventional Ferromagnetic Transition in La(sub 1-x)Ca(sub x)MnO3.
PB97-112429 *04,156* Not available NTIS

Underflow-Induced Graphics Failure Solved by SLI Arithmetic.
PB95-161444 *01,712* Not available NTIS

Unexpected Effects of Gold on the Structure, Superconductivity, and Normal State of YBa2Cu3O7.
PB94-200284 *04,482* Not available NTIS

Unified Approach to Camera Fixation and Vision-Based Road Following.
PB95-162244 *01,594* Not available NTIS

Unified Process Specification Language: Requirements for Modeling Process.
PB97-116123 *02,850* PC A06/MF A01

Unified Telerobotic Architecture Project (UTAP) Standard Interface Environment (SIE), May 1995.
PB95-242350 *02,938* PC A09/MF A02

Uniform Laws and Regulations in the Areas of Legal Metrology and Motor Fuel Quality as Adopted by the 80th National Conference on Weights and Measures 1995. 1996 Edition.
PB96-172309 *02,927* PC A12/MF A03

Uniform Laws and Regulations in the Areas of Legal Metrology and Motor Fuel Quality, 1994 as Adopted by the 79th National Conference on Weights and Measures 1994.
PB95-174470 *02,909* PC A09/MF A02

Unique Quality Assurance Aspects of INAA for Reference Material Homogeneity and Certification.
PB96-200811 *00,699* Not available NTIS

Unpredictable Certainty. Information Infrastructure through 2000.
PB96-182266 *00,016* PC A14/MF A03

Unravel: A CASE Tool to Assist Evaluation of High Integrity Software. Volume 1. Requirements and Design.
PB95-267886 *01,736* PC A05/MF A01

Unravel: A CASE Tool to Assist Evaluation of High Integrity Software. Volume 2. User Manual.
PB95-267894 *01,737* PC A04/MF A01

Unreacted Cement Content in Macro-Defect-Free Composites: Impact on Processing-Structure-Property Relations.
PB96-141270 *03,174* Not available NTIS

Unusual Spin-Trap Chemistry for the Reaction of Hydroxyl Radical with the Carcinogen N-Nitrosodimethylamine.
PB95-151643 *00,692* Not available NTIS

Update on the Low Background IR Calibration Facility at the National Institute of Standards and Technology.
PB94-211224 *04,232* Not available NTIS

Updated Calculations for Routine Space-Shielding Radiation Dose Estimates: SHIELDOSE-2.
PB95-171039 *04,838* PC A04/MF A01

Upgrade and Modernization Projects at the NBSR.
PB96-161872 *03,737* Not available NTIS

Upgraded Facility for Multilayer Mirror Characterization at NIST.
PB96-160387 *04,367* Not available NTIS

Upward Flame Spread along the Vertical Corner Walls (October 1993).
PB94-206299 *00,340* PC A03/MF A01

USA Interlaboratory Comparison of Superconductor Simulator Critical Current Measurements.
PB96-147194 *04,770* Not available NTIS

Usability Engineering: Industry-Government Collaboration for System Effectiveness and Efficiency.
PB97-122287 *01,514* Not available NTIS

USCEA/NIST Measurement Assurance Programs for the Radiopharmaceutical and Nuclear Power Industries.
PB97-110514 *03,721* Not available NTIS

Use of a Naphthylethylcarbamoylated- beta-Cyclodextrin Chiral Stationary Phase for the Separation of Drug Enantiomers and Related Compounds by Sub- and Supercritical Fluid Chromatography.
PB97-113260 *00,653* Not available NTIS

Use of a Radiochromic Detector for the Determination of Stereotactic Radiosurgery Dose Characteristics.
PB94-185642 *03,514* Not available NTIS

Use of an Environment Classification Model.
PB95-152062 *01,709* Not available NTIS

Use of an Ion Energy Analyzer: Mass Spectrometer to Measure Ion Kinetic-Energy Distributions from RF Discharges in Argon-Helium Gas Mixtures.
PB94-185717 *04,406* Not available NTIS

Use of Building Emulators to Evaluate the Performance of Building Energy Management Systems.
PB96-111901 *00,269* Not available NTIS

Use of Computer Models to Predict Temperature and Smoke Movement in High Bay Spaces.
PB94-145976 *00,191* PC A04/MF A01

Use of Extended Permutation-Inversion Groups in Constructing Hyperfine Hamiltonians for Symmetrical-Top Internal Rotor Molecules Like H3C-SiH3.
PB94-212032 *00,823* Not available NTIS

Use of Ion Scattering Spectroscopy to Monitor the Nb Target Nitridation during Reactive Sputtering.
PB94-172525 *00,761* Not available NTIS

Use of Ionospheric Data in GPS Time Transfer.
PB95-163853 *01,540* Not available NTIS

Use of Kinetic Energy Distributions to Determine the Relative Contributions of Gas Phase and Surface Fragmentation in KeV Ion Sputtering of a Quaternary Ammonium Salt.
PB95-126108 *00,570* Not available NTIS

Use of Monte Carlo Modeling for Interpreting Scanning Electron Microscope Linewidth Measurements.
PB96-137807 *02,413* Not available NTIS

Use of Neutron Beams for Chemical Analysis at NIST.
PB97-112437 *00,652* Not available NTIS

Use of Pressure for Quantum-Well Band-Structure Characterization.
PB96-164058 *04,779* Not available NTIS

Use of Sum Rules on the Energy-Loss Function for the Evaluation of Experimental Optical Data.
PB95-150736 *04,264* Not available NTIS

Use of the Electronic Balance for Highly Accurate Direct Mass Measurements Without the Use of External Mass Standards.
PB94-187713 *03,803* PC A03/MF A01

Use of Thermal Mechanical Analysis to Characterize Ethylene-Propylene-Diene Terpolymer (EPDM) Roofing Membrane Materials.
PB95-125852 *00,360* Not available NTIS

User Interface Component of the Applications Portability Profile Category: Software Standard; Subcategory: Application Program Interface.
FIPS PUB 158-1 *01,793* PC E01

User Profile for Researchers Studying Objects: Implications for Computer Systems.
PB94-188463 *00,133* PC A03/MF A01

User's Guide for the Algorithm Testing System Version 2.0.
PB95-251666 *02,916* PC A03/MF A01

User's Guide for the PHIGS Validation Tests (Version 2.1).
PB94-165206 *01,682* PC A08/MF A02

User's Guide to NIST SRM 2084: CMM Probe Performance Standard.
PB94-206109 *02,709* PC A03/MF A01

User's Guide to 'SuperFit' Modeling Software for CMM Probe Lobing.
PB96-128236 *02,921* PC A03/MF A01

User's Manual for the Program MONSEL-1: Monte Carlo Simulation of SEM Signals for Linewidth Metrology.
PB95-111522 *02,325* PC A03/MF A01

User Study: Informational Needs of Remote National Archives and Records Administration Customers.
PB95-154738 *02,725* PC A06/MF A02

Using a Multi-Layered Approach to Representing Tort Law Cases for Case-Based Reasoning.
PB96-160874 *00,135* Not available NTIS

Using Archie to Find Files on the INTERNET.
PB95-168605 *02,727* Not available NTIS

Using Atom Optics to Fabricate Nanostructures.
PB96-141247 *04,757* Not available NTIS

Using Collocation in Three Dimensions and Solving a Model Semiconductor Problem.
PB96-159249 *01,952*
(Order as PB96-159215, PC A07/MF A02)

Using Emulator/Testers for Commissioning EMCS Software, Operator Training, Algorithm Development, and Tuning Local Control Loops.
PB94-212735 *00,245* Not available NTIS

Using Emulators to Evaluate the Performance of Building Energy Management Systems.
PB95-175774 *00,259* Not available NTIS

Using Expect to Automate System Administration Tasks.
PB94-213329 *01,697* Not available NTIS

Using Grafcet to Design Generic Controllers.
PB95-150827 *02,821* Not available NTIS

Using Information Technology Standards in Federal Acquisitions.
PB96-161260 *01,637* Not available NTIS

Using Logic to Specify Shapes and Spatial Relations in Design Grammars.
PB97-111579 *02,793* Not available NTIS

Using LORAN-C Broadcasts for Automated Frequency Calibrations.
PB94-216017 *01,526* Not available NTIS

Using NIST Crystal Data within Siemens Software for Four-Circle and SMART CCD Diffractometers.
PB97-109110 *04,803*
(Order as PB97-109011, PC A11/MF A03)

Using Quantized Breakdown Voltage Signals to Determine the Maximum Electric Fields in a Quantum Hall Effect Sample.
PB95-261947 *02,375*
(Order as PB95-261897, PC A07/MF A02)

Using S-Check, Alpha Release 1.0.
PB96-165964 *01,767* PC A05/MF A01

Using Secondary Ion Mass Spectrometry (SIMS) to Characterize Optical Waveguide Materials.
PB96-119599 *04,340* Not available NTIS

Using Synthetic-Perturbation Techniques for Tuning Shared Memory Programs (Extended Abstract).
PB94-172657 *01,685* Not available NTIS

Using Synthetic Perturbations and Statistical Screening to Assay Shared-Memory Programs.
PB96-103031 *01,740* Not available NTIS

Using Technology to Manage and Protect Intellectual Property.
PB97-112395 *01,513* Not available NTIS

Using Torsional Dilatometry to Measure the Effects of Deformations on Physical Aging.
PB95-140901 *03,384* Not available NTIS

Utc Dissemination to the Real-Time User.
N19960042622 *01,521*
(Order as N19960042616, PC A20/MF A04)

UV Absorption Cross Sections of Methylchloroform: Temperature-Dependent Gas and Liquid Phase Measurements.
PB96-201041 *00,643* Not available NTIS

UV-Photopatterning of Alkylthiolate Monolayers Self-Assembled on Gold and Silver.
PB95-150751 *00,924* Not available NTIS

V-6: Effects of Temperature Variation.
PB96-148143 *04,772* Not available NTIS

Vacuum Gauges and Partial Pressure Analyzers.
PB95-150884 *02,650* Not available NTIS

Validated Products List (Cobol, Fortran, ADA, Pascal, MUMPS, SQL).
PB94-937300 *01,700* Standing Order

Validated Products List (Cobol, Fortran, ADA, Pascal, MUMPS, SQL).
PB95-937300 *01,738* Standing Order

Validation of a Turbulent Spray Flame Facility for the Assessment of Halon Alternatives.
PB96-159728 *03,283* Not available NTIS

Validation of the Inverse Square Law of Gravitation Using the Tower at Erie, Colorado, USA.
PB95-164646 *03,947* Not available NTIS

Validation Testing System Requirements. National PDES Testbed Report Series.
PB94-163482 *02,771* PC A03/MF A01

VAMAS Intercomparison of Critical Current Measurements on NB3Sn Superconductors: A Summary Report.
PB96-119763 *04,043* Not available NTIS

VAMAS interlaboratory comparisons of critical current vs. strain in Nb(sub 3)Sn.
DE95016656 *04,433* PC A01/MF A01

Van der Waals Bond Lengths and Electronic Spectral Shifts of the Benzene-Kr and Benzene-Xe Complexes.
PB95-151387 *00,932* Not available NTIS

Vapor-Liquid Equilibria of Mixtures of Propane and Isomeric Hexanes.
PB95-175287 *00,995* Not available NTIS

Vapor-Liquid Equilibria of Ternary Mixtures in the Critical Region on Paths of Constant Temperature and Overall Composition.
PB96-161856 *01,139* Not available NTIS

Vapor Pressure of Pentafluorodimethyl Ether.
PB96-201199 *00,677* Not available NTIS

Vapor Pressure of 1,1,1,2,2-Pentafluoropropane.
PB97-113237 *00,684* Not available NTIS

Vapor Pressure of 1,1-dichloro-2,2,2-trifluoroethane (R123).
PB95-126231 *00,899* Not available NTIS

Vapor Pressures and Gas-Phase PVT Data for 1-Chloro-1,2,2,2-Tetrafluoroethane (R124).
PB95-175154 *03,271* Not available NTIS

Vapor Transport in Materials and Process Chemistry.
PB94-211745 *00,669* Not available NTIS

Vapour Pressure Measurements on 1,1,1,2-Tetrafluoroethane (R134a) from 180 to 350 K.
PB95-168886 *03,265* Not available NTIS

Vapour Pressures and Gas-Phase (p, rho n, T) Values for CF3CHF2(R125).
PB96-102090 *04,019* Not available NTIS

Variances in the Measurement of Ceramic Powder Properties.
PB97-110316 *03,100* Not available NTIS

Variant Design for Mechanical Artifacts-A State of the Art Survey.
PB94-154358 *02,768* PC A03/MF A01

Variation in Magnetic Properties of Cu/Fcc (001) Sandwich Structures.
PB95-141164 *04,555* Not available NTIS

Variationally Stable Treatment of Two- and Three-Photon Detachment of H(-) Including Electron-Correlation Effects.
PB95-202867 *03,992* Not available NTIS

Variations in Size Measurements by Indicating Gaging Systems.
PB95-163614 *02,864* Not available NTIS

Vector and Quasi-Vector Solutions for Optical Waveguide Modes Using Efficient Galerkin's Method with Hermite-Gauss Basis Functions.
PB96-141197 *04,357* Not available NTIS

Vector Theory of Diffraction by a Single-Mode Fiber: Application to Mode-Field Diameter Measurements.
PB95-164182 *04,279* Not available NTIS

Vehicle-Command Center Communications in a Robotic Vehicle System.
PB95-162723 *03,665* Not available NTIS

Vehicle-to-Roadside Communications for Commercial Vehicle Operations: Requirements and Approaches.
PB95-188827 *04,860* PC A05/MF A01

Velocity Distribution of Atomic Beams by Gated Optical Pumping.
PB95-180519 *01,542* Not available NTIS

VENTCF2: An Algorithm and Associated FORTRAN 77 Subroutine for Calculating Flow through a Horizontal Ceiling/Floor Vent in a Zone-Type Compartment Fire Model.
PB94-210127 *00,345* PC A04/MF A01

Ventilation, Carbon Dioxide and ASHRAE Standard 62-1989.
PB95-162095 *02,544* Not available NTIS

Ventilation Effectiveness Measurements in Two Modern Office Buildings.
PB95-176012 *02,553* Not available NTIS

Ventilation Rates in Office Buildings.
PB95-108825 *02,539* Not available NTIS

Verification and Validation.
PB96-161393 *01,765* Not available NTIS

Verification and Validation of Reengineered Software.
PB96-161401 *01,766* Not available NTIS

Verification of a Model of Fire and Smoke Transport.
PB95-108718 *00,357* Not available NTIS

Verification of Commercial Probe-Tip Calibrations.
PB95-161576 *02,347* Not available NTIS

Verification of Revised Water Vapour Correction to the Index of Refraction of Air.
PB96-161666 *02,680* Not available NTIS

Verification of Scattering Parameter Measurements.
PB95-163960 *01,904* Not available NTIS

Verification of the Ponderomotive Approximation for the ac Stark Shift in Xe Rydberg Levels.
PB94-185709 *03,801* Not available NTIS

Vertical-Cavity Optoelectronic Structures: CAD, Growth, and Structural Characterization.
PB95-153177 *02,148* Not available NTIS

Vertical-Cavity Semiconductor Lasers: Structural Characterization, CAD, and DFB Structures.
PB95-153193 *02,150* Not available NTIS

Vertical-Cavity Semiconductor Structures: Materials Characterization.
PB95-153185 *02,149* Not available NTIS

Vibration Laboratory Automation at NIST with Personal Computers.
PB95-108700 *02,648* Not available NTIS

Vibration, Rotation, and Parity Specific Predissociation Dynamics in Asymmetric OH Stretch Excited ArH2O: A Half Collision Study of Resonant V-V Energy Transfer in a Weakly Bound Complex.
PB95-107140 *00,872* Not available NTIS

Vibrational Autoionization in H2: Vibrational Branching Ratios and Photoelectron Angular Distributions Near the v(+)=3 Threshold.
PB94-199577 *00,799* Not available NTIS

Vibrational Dependence of the Anisotropic Intermolecular Potential of Ar-HCl.
PB95-202685 *01,029* Not available NTIS

Vibrational Dependence of the Anisotropic Intermolecular Potential of Ar-HF.
PB95-202693 *01,030* Not available NTIS

Vibrational Distributions of As2 in the Cracking of As4 on Si(100) and Si(111).
PB94-198314 *00,784* Not available NTIS

Vibrational Energy Transfer in S1 p-Difluorobenzene. A Comparison of Low and Room Temperature Collisions.
PB95-108619 *00,883* Not available NTIS

Vibrational Excitations and the Position of Hydrogen in Nanocrystalline Palladium.
PB96-111828 *04,035* Not available NTIS

Vibrational Predissociation Dynamics of Overtone-Excited HN3.
PB95-125720 *00,691* Not available NTIS

Vibrational Relaxation Measurements of Carbon Monoxide on Metal Clusters.
PB94-211810 *00,820* Not available NTIS

Vibrational Spectra of Molecular Ions Isolated in Solid Neon: HCCH+ and HCC-. (Reannouncement with New Availability Information).
AD-A253 551/6 *00,707* PC A03/MF A01

Vibrational Spectra of Molecular Ions Isolated in Solid Neon. X. H2O(+), HDO(+), and D2O(+).
PB95-125670 *00,889* Not available NTIS

Vibrational Spectra of Molecular Ions Isolated in Solid Neon. XI. NO2(+), NO2(-), and NO3(-).
PB95-125688 *00,890* Not available NTIS

Vibrational Spectra of Molecular Ions Isolated in Solid Neon. 6. CO4(-). (Reannouncement with New Availability Information).
AD-A238 415/4 *00,705* PC A02/MF A01

Vibrational Spectra of Molecular Ions Isolated in Solid Neon. 7. CO(+), C2O2(+), and C2O2(-). (Reannouncement with New Availability Information).
AD-A239 729/7 *00,706* PC A03/MF A01

Vibrational Spectra of Molecular Ions Isolated in Solid Neon. 11. NO2(+), NO2(-), and NO3(-).
AD-A275 828/2 *00,708* Not available NTIS

Vibrational Spectra of Molecular Ions Isolated in Solid Neon. 13. Ions Derived from HBr and HI.
PB97-119234 *01,188* Not available NTIS

Vibrationally Resolved Photoelectron Angular Distributions and Branching Ratios for the Carbon Dioxide Molecule in the Wavelength Region 685-795 Angstrom.
PB96-201207 *04,131* Not available NTIS

Vibrations of Hydrogen and Deuterium in Solid Solution with Lutetium.
PB95-181038 *01,019* Not available NTIS

Vibrations of S1((1)B2u) p-Difluorobenzene - d4. S1-S0 Fluorescence Spectroscopy and ab Initio Calculations.
PB95-202586 *01,028* Not available NTIS

Vibronic Coupling and Other Many-Body Effects in the 4sigmag(-1) Photoionization Channel of CO2.
PB95-162509 *00,962* Not available NTIS

Video Microscopy Applied to Optical Fiber Geometry Measurements.
PB95-173068 *04,295* PC A04/MF A01

Videoconferencing Procurement and Usage Guide.
PB94-217023 *01,470* PC A04/MF A01

Viewpoint: Nanocrystalline and Nanophase Materials.
PB94-185865 *04,454* Not available NTIS

Virial Coefficients of Five Binary Mixtures of Fluorinated Methanes and Ethanes.
PB96-156054 *01,128* Not available NTIS

Virtual Environments for Health Care. A White Paper for the Advanced Technology Program (ATP), the National Institute of Standards and Technology.
PB96-147814 *03,594* PC A05/MF A01

Virtual Software Repository System.
PB94-198983 *01,691* Not available NTIS

Viscosity of Ammonia.
PB96-145933 *01,117* Not available NTIS

Viscosity of Defined and Undefined Hydrocarbon Liquids Calculated Using an Extended Corresponding-States Model.
PB96-167234 *02,498* Not available NTIS

Viscosity of the Saturated Liquid Phase of Six Halogenated Compounds and Three Mixtures.
PB95-162368 *00,960* Not available NTIS

Viscosity of 1,1,1,2,3,3-Hexafluoropropane and 1,1,1,3,3,3-Hexafluoropropane at Saturated-Liquid Conditions from 262 K to 353 K.
PB96-176680 *03,292* Not available NTIS

Visible and UV Light from Highly Charged Ions: Exotic Matter Advancing Technology.
PB96-119391 *04,414* Not available NTIS

Visual Measurement Technique for Analysis of Nucleate Flow Boiling.
PB95-143301 *03,262* PC A05/MF A02

Visual-Motion Fixation Invariant.
PB94-206281 *01,836* PC A03/MF A01

Visual Pursuit Systems.
PB95-143285 *01,841* PC A03/MF A01

Visual Road Following without 3-D Reconstruction.
PB95-161030 *01,591* Not available NTIS

Visualization Applications for Manufacturing: A State-of-the-Art Survey. Final Report.
PB94-194552 *02,816* PC A03/MF A01

Visualization of Surface Figure by the Use of Zernike Polynomials.
PB96-137757 *04,351* Not available NTIS

Vitrification and Crystallization of Organic Liquids Confined to Nanoscale Pores.
PB97-112304 *03,392* Not available NTIS

VLSI Architectures for Template Matching and Block Matching.
PB94-200029 *01,834* Not available NTIS

Void Shape in Sintered Titanium.
PB96-141023 *02,705* Not available NTIS

Voigt-Function Modeling in Fourier Analysis of Size- and Strain-Broadened X-Ray Diffraction Peaks.
PB94-198538 *04,462* Not available NTIS

Volatile Corrosion Inhibitors.
AD-A310 087/2 *03,114* PC A03/MF A01

Voltage Gain in the Single-Electron Transistor.
PB95-176335 *04,671* Not available NTIS

Voltage Ratio Measurements of a Zener Reference Using a Digital Voltmeter.
PB95-164695 *01,906* Not available NTIS

Voltage-Standard Devices.
PB96-102496 *01,920* Not available NTIS

Volume-Limited ROSAT Survey of Extreme Ultraviolet Emission from all Nondegenerate Stars within 10 Parsecs.
PB96-103189 *00,093* Not available NTIS

Volume Magnetic Hysteresis Loss of Nb3Sn Superconductors as a Function of Wire Length.
PB95-153722 *04,597* Not available NTIS

Volume Recovery in Epoxy Glasses Subjected to Torsional Deformations: The Question of Rejuvenation.
PB95-140018 *03,382* Not available NTIS

Voluntary Product Standard PS 1-95 Construction and Industrial Plywood.
PB96-178900 *03,406* PC A04/MF A01

Voluntary Product Standard PS 20-94. American Softwood Lumber Standard.
PB94-162500 *03,402* PC A03/MF A01

Vortex Dynamics and Melting in Niobium.
PB96-112362 *02,073* Not available NTIS

Vortex Images in Thin Films of YBa2Cu3O(sub 7-x) and Bi2Sr2Ca1Cu2O(sub 8+x) Obtained by Low-Temperature Magnetic Force Microscopy.
PB97-119408 *04,815* Not available NTIS

Vortex Shedding Flowmeters for SSME Ducts.
PB95-169215 *01,453* Not available NTIS

Wall Flame Heights with External Radiation.
PB95-163481 *00,380* Not available NTIS

Warping of Terrace Pavers at the U.S. Capitol Building.
PB96-193651 *00,411* PC A03/MF A01

Water Adsorption at a Polyimide/Silicon Wafer Interface.
PB96-103197 *01,070* Not available NTIS

Water Adsorption at Polymer/Silicon Wafer Interfaces.
PB95-181178 *01,022* Not available NTIS

Water Droplet Evaporation from Radiantly Heated Solids.
PB95-217147 *00,394* PC A08/MF A02

Water Efficient Plumbing Fixtures through Standards and Test Methods.
PB95-125951 *00,248* Not available NTIS

Water Mist Fire Suppression Workshop Summary.
PB95-161907 *02,853* Not available NTIS

Water Permeability and Chloride Ion Diffusion in Portland Cement Mortars: Relationship to Sand Content and Critical Pore Diameter.
PB96-148036 *03,193* Not available NTIS

Water-Vapor Measurements of Low-Slope Roofing Materials.
PB95-251617 *00,399* PC A03/MF A01

Waveguide Polarizers Processed by Localized Plasma Etching.
PB95-169264 *02,171* Not available NTIS

Wavelength Dependence of Normal Spectral Emissivity of High-Temperature Metals at Their Melting Point.
PB94-200011 *03,398* Not available NTIS

Wavelengths and Energy Level Classifications for the Spectra of Sulfur (S I through S XVI).
PB94-162229 *00,734* Not available NTIS

Wavelengths and Energy Levels of Neutral Kr(84) and Level Shifts in All Kr Even Isotopes.
PB94-140605 *03,780*
(Order as PB94-140555, PC A06/MF A02)

Wavelengths and Isotope Shifts for Lines of Astrophysical Interest in the Spectrum of Doubly Ionized Mercury (Hg III).
PB95-140869 *03,887* Not available NTIS

Wavelengths of Spectral Lines in Mercury Pencil Lamps.
PB96-176474 *04,376* Not available NTIS

Wavelet Analysis for Synchronization and Timekeeping.
PB96-200381 *01,558* Not available NTIS

Wavelet Variance, Allan Variance, and Leakage.
PB96-190111 *01,509* Not available NTIS

Weak-Link-Free Behavior of High Angle YBa2Cu3O7-x Grain Boundaries in High Magnetic Fields.
PB94-198421 *04,459* Not available NTIS

Wear Mechanism Maps of Ceramics.
PB94-172368 *03,229* Not available NTIS

Wear Mechanism Maps of 440C Martensitic Stainless Steel.
PB96-111810 *04,834* Not available NTIS

Wear Model for Alumina Sliding Wear.
PB95-163796 *03,239* Not available NTIS

Wear Modeling of Si-Based Ceramics.
PB97-122501 *03,112* Not available NTIS

Wear of Enamel against Glass-Ceramic, Porcelain, and Amalgam.
PB96-179593 *03,082* Not available NTIS

Wear of Human Enamel against a Commercial Castable Ceramic Restorative Material.
PB95-161972 *00,161* Not available NTIS

Wear of Selected Materials and Composites Sliding against MoS2 Films.
PB94-172749 *03,231* Not available NTIS

Wear Transitions in Monolithic Alumina and Zirconia-Alumina Composites.
PB96-103163 *03,168* Not available NTIS

Weatherability of Plastic Materials.
AD-A301 675/5 *02,968* PC A14/MF A03

Welding for Cryogenic Service.
PB95-162889 *02,852* Not available NTIS

Well-Shielded EMAT for On-Line Ultrasonic Monitoring of GMA Welding.
PB96-186077 *02,879* Not available NTIS

What Is a 'Standard Reference Material' - What Is Any Reference Material.
PB96-186135 *03,000* Not available NTIS

What's Available in Welding Software.
PB96-158084 *02,875* Not available NTIS

White Papers Prepared for the White House: Construction Industry Workshop on National Construction Goals. Held on December 14-16, 1994.
PB95-216891 *01,299* PC A08/MF A02

Whither Computational Materials Science. Some Thoughts from the Mechanical Properties Front.
PB96-161997 *02,987* Not available NTIS

Wide Band Active Current Transformer and Shunt.
PB95-126371 *02,036* Not available NTIS

Wideband Current and Magnetic Field Sensors Based on Iron Garnets.
PB96-200878 *01,975* Not available NTIS

Wideband Sampling Voltmeter.
PB97-113039 *01,990* Not available NTIS

Widths and Propagation of a Truncated Gaussian Beam.
PB95-168779 *04,287* Not available NTIS

Wind and Seismic Effects: Proceedings of the Joint Meeting of the U.S.-Japan Cooperative Program in Natural Resources Panel on Wind and Seismic Effects (28th). Held in Gaithersburg, Maryland on May 14-17, 1996.
PB97-104376 *00,476* PC A99/MF A06

Wind and Seismic Effects. Proceedings of the U.S.-Japan Cooperative Program in Natural Resources Panel on Wind and Seismic Effects (26th). Held in Gaithersburg, Maryland on May 17-20, 1994.
PB95-147385 *00,433* PC A99/MF A06

Wind Load Provisions of the Manufactured Home Construction and Safety Standards: A Review and Recommendations for Improvement.
PB94-206125 *00,428* PC A06/MF A02

Windowing Effects on Light Scattering by Sinusoidal Surfaces.
PB97-111215 *04,389* Not available NTIS

Wire Bond Testing.
PB94-211653 *02,314* Not available NTIS

Wire Bonding to Multichip Modules and Other Soft Substrates.
PB96-123583 *02,079* Not available NTIS

Wire Bonding to Multichip Modules and Other Soft Substrates.
PB96-135207 *02,082* Not available NTIS

Workgroup Summary Report: Plastic Hinge-Based Techniques for Advanced Analysis.
PB96-159702 *00,470* Not available NTIS

Working Conference on Global Growth of Technology: Is America Prepared. Held in Gaithersburg, Maryland on December 7, 1995.
PB96-210059 *00,018* PC A07/MF A02

Workplan to Analyze the Energy Impacts of Envelope Airtightness in Office Buildings.
PB96-154463 *00,273* PC A04/MF A01

Workshop Highlights.
PB97-109227 *04,811*
(Order as PB97-109011, PC A11/MF A03)

Workshop on Characterizing Diamond Films (3rd). Held in Gaithersburg, Maryland on February 23-24, 1994.
PB94-187663 *04,456* PC A04/MF A01

Workshop on Characterizing Diamond Films (4th). Held in Gaithersburg, Maryland on March 4-5, 1996.
PB96-183090 *04,786* PC A04/MF A01

Workshop on the Application of Virtual Reality to Manufacturing. Final Report. Held in Gaithersburg, Maryland on August 9, 1994.
PB95-173555 *02,825* PC A11/MF A03

Workshop Summary Report: Industrial Applications of Scanned Probe Microscopy. A Workshop Co-sponsored by NIST, SEMATECH, ASTM, E42.14, and the American Vacuum Society. Held in Gaithersburg, Maryland on March 24-25, 1994.
PB95-170387 *00,506* PC A07/MF A02

World Model Registration for Effective Off-Line Programming of Robots.
PB94-173010 *02,933* Not available NTIS

World of Building Codes.
PB95-203428 *00,449* Not available NTIS

World Wide Web and Mosaic: User's Guide.
PB94-207354 *02,722* PC A03/MF A01

World Wide Web for Crystallography.
PB97-109219 *04,810*
(Order as PB97-109011, PC A11/MF A03)

X-ray Attenuation Coefficients from 10 Kev to 100 Mev.
AD-A278 139/1 *03,765* PC A04/MF A01

X-Ray Attenuation Coefficients from 10 kev to 100 Mev.
AD-A279 289/3 *03,767* PC A03/MF A01

X-Ray Attenuation Coefficients from 10 KEV to 100 MEV.
AD-A280 290/8 *03,768* PC A04/MF A01

X-Ray Characterization of the Crystallization Process of High-Tc Superconducting Oxides in the Sr-Bi-Pb-Ca-Cu-O System.
PB95-151700 *04,579* Not available NTIS

X-Ray Diffraction from Anodic TiO2 Films: In situ and Ex situ Comparison of the Ti(0001) Face.
PB94-185972 *00,782* Not available NTIS

X-Ray-Diffraction Study of a Thermomechanically Detwinned Single Crystal of YBa2Cu3O6+x.
PB95-151726 *04,581* Not available NTIS

X-ray Emission from Chemically Peculiar Stars.
PB96-102256 *00,088* Not available NTIS

X-Ray Image Quality Indicator Designed for Easy Alignment.
PB95-164455 *02,907* Not available NTIS

X-ray Mask Metrology: The Development of Linewidth Standards for X-ray Lithography.
PB95-162129 *02,348* Not available NTIS

X-ray Observation of Electroclinic Layer Constriction and Rearrangement in a Chiral Smectic-A Liquid Crystal.
PB96-141080 *01,100* Not available NTIS

X-ray Photoelectron and Auger Electron Forward Scattering: A Structural Diagnostic for Epitaxial Thin Films.
PB95-180220 *04,676* Not available NTIS

X-Ray Photoelectron and Auger Electron Spectroscopy Study of Ultraviolet/Ozone Oxidized P2S5/(NH4)2S Treated GaAs(100) Surfaces.
PB94-200144 *04,479* Not available NTIS

X-Ray Powder Diffraction Data for BaCu(C2O4)2.6H2O.
PB95-151767 *04,583* Not available NTIS

X-ray Powder Diffraction from Carbon Nanotubes and Nanoparticles.
PB96-102975 *03,064* Not available NTIS

X-ray Protection.
AD-A279 132/5 *03,605* PC A03/MF A01

X-ray Protection Design.
AD-A279 181/2 *03,606* PC A03/MF A01

X-ray Reflectivity Determination of Interface Roughness Correlated with Transport Properties of (AlGa)As/GaAs High Electron Mobility Transistor Devices.
PB97-111868 *04,149* Not available NTIS

X-rays from Stellar Flares.
PB94-213436 *00,065* Not available NTIS

X Window System, Version 11, Release 5.
PB96-169099 *01,769* PC E99

X.500 Directory Schema Design Handbook.
PB96-183041 *02,739* PC A03/MF A01

xi-Vector Formulation of Anisotropic Phase-Field Models: 3-D Asymptotics.
PB95-136628 *04,536* PC A03/MF A01

Xi-Vector Formulation of Anisotropic Phase-Field Models: 3-D Asymptotics.
PB97-122550 *04,816* Not available NTIS

XUV Characterization Comparison of Mo/Si Multilayer Coatings.
PB95-164000 *04,278* Not available NTIS

YBa2Cu3O7-x to Si Interconnection for Hybrid Superconductor/Semiconductor Integration.
PB94-211711 *02,315* Not available NTIS

Z39.50 Implementation Experiences.
PB96-114939 *01,816* PC A07/MF A02

Zimm Plot and Its Analogs as Indicators of Vesicle and Micelle Size Polydispersity.
PB96-123765 *01,094* Not available NTIS

NTIS ORDER/REPORT NUMBER INDEX

SAMPLE ENTRY

NISTIR-5439
Performance Parameters of Fire Detection Systems
PB94-194339 *00,123* PC **A03**/MF **A01**

PB94-194339
Performance Parameters of Fire Detection Systems
PB94-194339 *00,123* PC **A03**/MF **A01**

Report or series number
Title
NTIS order number *Abstract number* Availability **Price Code**

Report or series number
Title
NTIS order number *Abstract number* Availability **Price code**

AD-A234 043/8
Production and Spectroscopy of Small Polyatomic Molecular Ions Isolated in Solid Neon. (Reannouncement with New Availability Information).
AD-A234 043/8 *00,704* PC A03/MF A01

AD-A238 415/4
Vibrational Spectra of Molecular Ions Isolated in Solid Neon. 6. CO4(-). (Reannouncement with New Availability Information).
AD-A238 415/4 *00,705* PC A02/MF A01

AD-A239 729/7
Vibrational Spectra of Molecular Ions Isolated in Solid Neon. 7. CO(+), C2O2(+), and C2O2(-). (Reannouncement with New Availability Information).
AD-A239 729/7 *00,706* PC A03/MF A01

AD-A244 582/3
Effect of Green Density and the Role of Magnesium Oxide Additive on the Densification of Alumina Measured by Small-Angle Neutron Scattering. (Reannouncement with New Availability Information).
AD-A244 582/3 *03,022* PC A02/MF A01

AD-A249 178/5
Evolution of the Pore Size Distribution in Final-Stage Sintering of Alumina Measured by Small-Angle X-ray Scattering. (Reannouncement with New Availability Information).
AD-A249 178/5 *03,023* PC A03/MF A01

AD-A249 179/3
Characterization of the Densification of Alumina by Multiple Small-Angle Neutron Scattering. (Reannouncement with New Availability Information).
AD-A249 179/3 *03,024* PC A02/MF A01

AD-A249 510/9
Small-Angle Neutron Scattering Characterization of Processing/Microstructure Relationships in the Sintering of Crystalline and Glassy Ceramics. (Reannouncement with New Availability Information).
AD-A249 510/9 *03,025* PC A03/MF A01

AD-A253 551/6
Vibrational Spectra of Molecular Ions Isolated in Solid Neon: HCCH+ and HCC-. (Reannouncement with New Availability Information).
AD-A253 551/6 *00,707* PC A03/MF A01

AD-A274 609/7
Gordon Research Conference on the Physics and Chemistry of Laser Diagnostics in Combustion Held in Plymouth, New Hampshire on 12-16 July 1993.
AD-A274 609/7 *01,353* PC A03/MF A01

AD-A274 872/1
Ada Compiler Validation Summary Report: Certificate Number: 931029S1.11330, Digital Equipment Corporation, DEC Ada for DEC OSF/1 AXP Systems, Version 3.1, DEC 3000 Model 400 AXP Workstation, DEC 3000 Model 400 AXP Workstation.
AD-A274 872/1 *01,639* PC A04/MF A01

AD-A275 828/2
Vibrational Spectra of Molecular Ions Isolated in Solid Neon. 11. NO2(+), NO2(-), and NO3(-).
AD-A275 828/2 *00,708* Not available NTIS

AD-A275 977/7
Ada Compiler Validation Summary Report: Certificate Number: 931217S1.11336 Control Data Systems, Inc. NOS/VE Ada, Version 1.4 Cyber 180-930-31 => Cyber 180-930-31.
AD-A275 977/7 *01,640* PC A03/MF A01

AD-A276 181/5
Ada Compiler Validation Summary Report. Certificate Number: 931119S1.11332, DDC-I, Inc. DACS MIPS R3000 Bare Ada Cross Compiler System, Version 4.7.1 Sun SPARCstation IPX => DACS Sun SPARC/SunOS to MIPS R3000 Bare Instruction Set Architecture Simulator, Version 4.7.1.
AD-A276 181/5 *01,641* PC A04/MF A01

AD-A276 283/9
Ada Compiler Validation Summary Report: Certificate Number: 931119S1.11331 DDC-I, Inc. DACS Sun SPARC/SunOS to 80386 PM Bare Ada Cross Compiler System, Version 4.6.4 Sun Sparcstation 1+ => Bare Board iSBC 386/116.
AD-A276 283/9 *01,642* PC A08/MF A02

AD-A277 981/7
Ada Compiler Validation Summary Report. Certificate Number: 930927S1.11328 Green Hills Software C Ada, Version 1.1 ZENY 386 => ZENY 386.
AD-A277 981/7 *01,643* PC A03/MF A01

AD-A278 130/0

Atomic Energy Levels As Derived from the Analyses of Optical Spectra. Volume 1. Section 1. The Spectra of Hydrogen, Deuterium, Helium, Lithium Beryllium, Boron, Carbon, Nitrogen, Oxygen, and Fluorine.
AD-A278 130/0 *03,764* PC A05/MF A01

AD-A278 131/8

Ultraviolet Multiplet Table. Finding List for Spectra of the Elements Molybdenum to Lanthanum (Z = 42 to 57); Hafnium to Radium (Z = 72 to 88).
AD-A278 131/8 *00,709* PC A03/MF A01

AD-A278 138/3

Bibliography of Books and Published Reports on Gas Turbines, Jet Propulsion, and Rocket Power Plants.
AD-A278 138/3 *01,445* PC A04/MF A01

AD-A278 139/1

X-ray Attenuation Coefficients from 10 Kev to 100 Mev.
AD-A278 139/1 *03,765* PC A04/MF A01

AD-A278 140/9

Standard Materials. A Descriptive List with Prices.
AD-A278 140/9 *00,500* PC A03/MF A01

AD-A278 213/4

Bibliography of Books and Published Reports on Gas Turbines, Jet Propulsion, and Rocket Power Plants, January 1950 through December 1953.
AD-A278 213/4 *01,446* PC A06/MF A02

AD-A278 249/8

Characteristics of Turbulence in a Boundary Layer with Zero Pressure Gradient.
AD-A278 249/8 *04,192* PC A03/MF A01

AD-A278 446/0

Ultraviolet Multiplet Table.
AD-A278 446/0 *00,710* PC A08/MF A02

AD-A278 517/8

Density of Solids and Liquids.
AD-A278 517/8 *00,711* PC A03/MF A01

AD-A278 521/0

Aerodynamic Phenomena in Stellar Atmospheres - A Bibliography.
AD-A278 521/0 *00,046* PC A05/MF A02

AD-A278 782/8

Handbook Preferred Circuits Navy Aeronautical Electronic Equipment. Supplement Number 3.
AD-A278 782/8 *00,026* PC A03/MF A01

AD-A278 783/6

Handbook Preferred Circuits Navy Aeronautical Electronic Equipment. Supplement Number 2.
AD-A278 783/6 *00,027* PC A03/MF A01

AD-A278 784/4

Handbook Preferred Circuits Navy Aeronautical Electronic Equipment. Supplement Number 1.
AD-A278 784/4 *00,028* PC A05/MF A01

AD-A278 851/1

Methods of Measuring Humidity and Testing Hygrometers.
AD-A278 851/1 *00,123* PC A03/MF A01

AD-A278 956/8

Table of Dielectric Constants of Pure Liquids.
AD-A278 956/8 *00,712* PC A04/MF A01

AD-A279 120/0

Report of the International Commission on Radiological Units and Measurements (ICRU), 1956.
AD-A279 120/0 *03,513* PC A04/MF A01

AD-A279 121/8

Screw-Thread Standards for Federal Services, 1957. Part 3.
AD-A279 121/8 *02,854* PC A04/MF A01

AD-A279 132/5

X-ray Protection.
AD-A279 132/5 *03,605* PC A03/MF A01

AD-A279 133/3

Recommendations for the Disposal of Carbon-14 Wastes.
AD-A279 133/3 *02,579* PC A03/MF A01

AD-A279 180/4

Thermal Conductivity of Metals and Alloys at Low Temperatures. A Review of the Literature.
AD-A279 180/4 *03,302* PC A04/MF A01

AD-A279 181/2

X-ray Protection Design.
AD-A279 181/2 *03,606* PC A03/MF A01

AD-A279 240/6

Standard Samples and Reference Standards Issued by the National Bureau of Standards.
AD-A279 240/6 *02,613* PC A03/MF A01

AD-A279 261/2

Protection Against Radiations from Radium, Cobalt-60, and Cesium-137.
AD-A279 261/2 *03,607* PC A04/MF A01

AD-A279 281/0

Permissible Dose from External Sources of Ionizing Radiation.
AD-A279 281/0 *03,608* PC A05/MF A01

AD-A279 282/8

Technologic Papers of the Bureau of Standards: Number 170. Pyrometric Practice.
AD-A279 282/8 *03,766* PC A15/MF A03

AD-A279 289/3

X-Ray Attenuation Coefficients from 10 kev to 100 Mev.
AD-A279 289/3 *03,767* PC A03/MF A01

AD-A279 290/1

Screw-Thread Standards for Federal Services, 1957. Part 1.
AD-A279 290/1 *02,855* PC A10/MF A03

AD-A279 642/3

Ada Compiler Validation Summary Report: Certificate Number: 940325S1.11348 DDC-I, DACS Sun SPARC/Solaris to 80386 PM Bare Ada Cross Compiler System, Version 4.6.4 Sun SPARCclassic => Intel iSBC 386/116 (Bare Machine).
AD-A279 642/3 *01,644* PC A06/MF A02

AD-A279 643/1

Ada Compiler Validation Summary Report: Certificate Number: 940325S1.11341 DDC-I, DACS Sun SPARC/SunOS to 80186 Bare Ada Cross Compiler System, Version 4.6.4 Sun SPARCstation IPX => Intel iSBC 186/100 (Bare Machine).
AD-A279 643/1 *01,645* PC A06/MF A02

AD-A279 644/9

Ada Compiler Validation Summary Report: Certificate Number: 940325S1.11349 DDC-I, DACS Sun SPARC/Solaris to 80386 PM Bare Ada Cross Compiler System with Rate Monotonic Scheduling, Version 4.6.4 Sun SPARCclassic => Intel iSBC 386/116 (Bare Machine).
AD-A279 644/9 *01,646* PC A06/MF A02

AD-A279 645/6

Ada Compiler Validation Summary Report: Certificate Number: 940325S1.11354 DDC-I, DACS Sun SPARC/Solaris Native Ada Compiler System, Version 4.6.2 Sun SPARCclassic => Sun SPARCclassic.
AD-A279 645/6 *01,647* PC A04/MF A01

AD-A279 646/4

Ada Compiler Validation Summary Report: Certificate Number: 940325S1.11346 DDC-I, DACS Sun SPARC/SunOS to 680x0 Bare Ada Cross Compiler System (BASIC MODE), Version 4.6.9 Sun SPARCstation IPX => Lynwood j435TU (68030) (Bare Machine).
AD-A279 646/4 *01,648* PC A05/MF A02

AD-A279 757/9

Ada Compiler Validation Summary Report: Certificate Number: 940325S1.11343 DDC-I, DACS Sun SPARC/Solaris to 80186 Bare Ada Cross Compiler System, Version 4.6.4 Sun SPARCclassic => Intel iSBC 186/100 (Bare Machine).
AD-A279 757/9 *01,649* PC A06/MF A02

AD-A279 758/7

Ada Compiler Validation Summary Report: Certificate Number: 940325S1.11344 DDC-I, DACS Sun SPARC/Solaris to 80186 Bare Ada Cross Compiler System with Rate Monotonic Scheduling, Version 4.6.4 Sun SPARCclassic => Intel iSBC 186/100 (Bare Machine).
AD-A279 758/7 *01,650* PC A06/MF A02

AD-A279 759/5

Characterization of the Hydrogen Induced Cold Cracking Susceptibility at Simulated Weld Zones in HSLA-100 Steel.
AD-A279 759/5 *03,200* PC A04/MF A01

AD-A279 778/5

Ada Compiler Validation Summary Report: Certificate Number: 940325S1.11347 DDC-I, DACS Sun SPARC/SunOS to 680x0 Bare Ada Cross Compiler System (SECURE MODE), Version 4.6.9 Sun SPARCstation IPX => Lynwood j435TU (68030) (Bare Machine).
AD-A279 778/5 *01,651* PC A06/MF A02

AD-A279 779/3

Ada Compiler Validation Summary Report: Certificate Number: 940325S1.11342 DDC-I, DACS Sun SPARC/SunOS to 80186 Bare Ada Cross Compiler System with Rate Monotonic Scheduling Version 4.6.4 Sun SPARCstation IPX => Intel iSBC 186/100 (Bare Machine).
AD-A279 779/3 *01,652* PC A06/MF A02

AD-A279 804/9

Ada Compiler Validation Summary Report: Certificate Number: 940325S1.11351 DDC-I, DACS Sun SPARC/SunOS to Pentium PM Bare Ada Cross Compiler System with Rate Monotonic Scheduling, Version 4.6.4 Sun SPARCstation IPX => Intel Pentium (operated as Bare Machine) based in Xpress Desktop (Intel product number: XBASE6E4F-B).
AD-A279 804/9 *01,653* PC A06/MF A02

AD-A279 805/6

Ada Compiler Validation Summary Report: Certificate Number: 940325S1.11353 DDC-I, DACS Sun SPARC/Solaris to Pentium PM Bare Ada Cross Compiler System with Rate Monotonic Scheduling, Version 4.6.4 Sun SPARCclassic => Intel Pentium (operated as Bare Machine) based in Xpress Desktop (Intel product number: XBASE6E4F-B).
AD-A279 805/6 *01,654* PC A06/MF A02

AD-A279 864/3

Ada Compiler Validation Summary Report: Certificate Number: 940325S1.11350 DDC-I, DACS Sun SPARC/SunOS to Pentium PM Bare Ada Cross Compiler System, Version 4.6.4 Sun SPARCstation IPX => Intel Pentium (Operated as Bare Machine) Based in Xpress Desktop (Intel Product Number: XBASE6E4F-B).
AD-A279 864/3 *01,655* PC A06/MF A02

AD-A279 948/4

Reference Tables for Thermocouples.
AD-A279 948/4 *02,614* PC A05/MF A01

AD-A279 949/2

Corrected Optical Pyrometer Readings.
AD-A279 949/2 *02,615* PC A05/MF A01

AD-A279 951/8

Tabulation of the Thermodynamic Properties of Normal Hydrogen from Low Temperatures to 300K and from 1 to 100 Atmospheres.
AD-A279 951/8 *00,713* PC A05/MF A01

AD-A279 952/6

National Standard Petroleum Oil Tables.
AD-A279 952/6 *02,469* PC A09/MF A02

AD-A280 082/9

Screw-Thread Standards for Federal Services, 1957. Handbook H28 (1957), Part 2. Revised.
AD-A280 082/9 *03,599* PC A06/MF A02

AD-A280 086/0

Federal Basis for Weights and Measures: A Historical Review of Federal Legislative Effort, Statutes, and Administrative Action in the Field of Weights and Measures in the United States.
AD-A280 086/0 *02,616* PC A03/MF A01

AD-A280 145/4

Ada Compiler Validation Summary Report: Certificate Number 940325S1.11345 DDC-I. DACS Sun SPARC/SunOS to 680x0 Bare Ada Cross Compiler System, Version 4.6.9 Sun SPARCstation IPX => Motorola MVME143 68030/68882 (Bare Machine).
AD-A280 145/4 *01,656* PC A05/MF A02

AD-A280 150/4

Atomic Energy Levels in Crystals.
AD-A280 150/4 *04,431* PC A05/MF A01

AD-A280 223/9

1950 Supplement to Screw-Thread Standards for Federal Services. 1944.
AD-A280 223/9 *03,656* PC A06/MF A02

AD-A280 278/3

Guide to Instrumentation Literature.
AD-A280 278/3 *02,617* PC A08/MF A02

AD-A280 279/1

Atomic Energy Levels. As Derived From the Analyses of Optical Spectra. Volume 3.
AD-A280 279/1 *00,714* PC A13/MF A03

AD-A280 281/7

Maximum Permissible Amounts of Radioisotopes in the Human Body and Maximum Permissible Concentrations in Air and Water.
AD-A280 281/7 *03,609* PC A04/MF A01

AD-A280 282/5

Maximum Permissible Body Burdens and Maximum Permissible Concentrations of Radionuclides in Air and in Water for Occupational Exposure.
AD-A280 282/5 *03,610* PC A06/MF A02

AD-A280 290/8

X-Ray Attenuation Coefficients from 10 KEV to 100 MEV.
AD-A280 290/8 *03,768* PC A04/MF A01

AD-A280 291/6

Papers on the Symposium on Collision Phenomena in Astrophysics, Geophysics, and Masers.
AD-A280 291/6 *00,047* PC A03/MF A01

AD-A280 293/2

Tables of Chemical Kinetics Homogeneous Reactions.
AD-A280 293/2 *00,715* PC A20/MF A04

AD-A280 295/7

Ada Compiler Validation Summary Report: Certificate Number: 940325S1.11352 DDC-I DACS Sun SPARC/Solaries to Pentium PM Bare Ada Cross Compiler System, Version 4.6.4 Sun SPARCclassic => Intel Pentium (Operated as Bare Machine) Based in Xpress Desktop (Intel Product Number: XBASE6E4F-B).
AD-A280 295/7 *01,657* PC A06/MF A02

AD-A280 398/9

Cryogenic Research and Development (Quarterly Report Number 2 for Period Ending December 31, 1960).
AD-A280 398/9 *01,454* PC A05/MF A01

AD-A280 399/7

Cryogenic Research and Development (Progress Report Number 4 for Period Ending December 31, 1961).
AD-A280 399/7 *01,455* PC A04/MF A01

AD-A280 401/1

Cryogenic Research and Development (Quarterly Report Number 1 for Period Ending September 30, 1960).
AD-A280 401/1 *01,456* PC A04/MF A01

AD-A280 562/0

Precision Laboratory Standards of Mass and Laboratory Weights.
AD-A280 562/0 *02,618* PC A03/MF A01

AD-A280 679/2

Cryogenic Research and Development (June 30, 1961).
AD-A280 679/2 *01,457* PC A04/MF A01

AD-A281 167/7

Bibliography of the Physical Equilibria and Related Properties of Some Cryogenic Systems.
AD-A281 167/7 *03,769* PC A07/MF A02

AD-A284 623/6

Precision Resistors and Their Measurement.
AD-A284 623/6 *02,249* PC A03/MF A01

AD-A285 495/8

Tabulation of Data on Receiving Tubes. Handbook 68.
AD-A285 495/8 *02,111* PC A06/MF A02

AD-A286 603/6

Compilation of the Physical Equilibria and Related Properties of the Hydrogen-Carbon Monoxide System.
AD-A286 603/6 *00,716* PC A05/MF A01

AD-A286 612/7

Progress Report to National Aeronautics and Space Administration on Cryogenic Research and Development.
AD-A286 612/7 *01,458* PC A05/MF A01

AD-A286 618/4

Design and Construction of a Liquid Hydrogen Temperature Refrigeration System.
AD-A286 618/4 *02,619* PC A03/MF A01

AD-A286 619/2
Ionospheric Radio Propagation.
AD-A286 619/2 *01,459* PC A10/MF A03

AD-A286 620/0
Fuzed-Quartz Fibers. A Survey of Properties, Applications and Production Methods.
AD-A286 620/0 *00,656* PC A03/MF A01

AD-A286 647/3
Measurement of Absorbed Dose of Neutrons, and of Mixtures of Neutrons and gamma rays.
AD-A286 647/3 *03,710* PC A05/MF A01

AD-A286 648/1
High Temperature Reactions of Uranium Dioxide with Various Metal Oxides.
AD-A286 648/1 *00,717* PC A03/MF A01

AD-A286 675/4
Cryogenic Materials Data Handbook.
AD-A286 675/4 *03,303* PC A04/MF A01

AD-A286 680/4
Survey of the Literature on Heat Transfer from Solid Surfaces to Cryogenic Fluids.
AD-A286 680/4 *04,193* PC A04/MF A01

AD-A286 681/2
Protection Against Neutron Radiation Up to 30 Million Electron Volts.
AD-A286 681/2 *03,611* PC A05/MF A01

AD-A286 683/8
Helium Refrigeration and Liquefaction Using a Liquid Hydrogen Refrigerator for Precooling.
AD-A286 683/8 *02,749* PC A03/MF A01

AD-A286 701/8
Precise Measurement of Heat of Combustion with a Bomb Calorimeter.
AD-A286 701/8 *03,770* PC A03/MF A01

AD-A288 571/3
Ada Compiler Validation Summary Report: Certificate Number 940902S1.11377 UNISYS Corporation. IntegrAda for Windows NT, Version 1.0. Intel Deskside Server with Intel 80486DX266 => Intel Deskside Server with Intel 80486DX266.
AD-A288 571/3 *01,658* PC A03/MF A01

AD-A288 572/1
Ada Compiler Validation Summary Report: Certificate Number 940902S1.11376. UNISYS Corporation IntegrAda for Windows NT, Version 1.0. Intel Deskside Server for Intel Pentium 60 MHz =>. Intel Deskside Server with Intel Pentium 60 MHz.
AD-A288 572/1 *01,659* PC A03/MF A01

AD-A288 573/9
Ada Compiler Validation Summary Report: Certificate Number 94101251.11379 TISOFT, Inc. Green Hills Optimizing Ada Compileer, Version 1.8.7 with PATCK ID 1 COMPAQ ProLiant 2000 Model 55/66 => COMPAQ ProLiant 2000 Model 5/66.
AD-A288 573/9 *01,660* PC A03/MF A01

AD-A288 574/7
Ada Complier Validation Summary Report: Certificate Number: 940929S1.11378. Digital Equipment Corporation DEC Ada for DEC OSF/1 AXP Systems, Version 3.2; DEC 3000 Model 400 AXP Workstation => DEC 3000 Model 400 AXP Workstation.
AD-A288 574/7 *01,661* PC A05/MF A01

AD-A289 895/5
Ada Compiler Validation Summary Report. Certificate Number 941117S1.11380. Electronic Data Systems Corp. Compiler: OC Systems Legacy Ada/370, Release 1.4.1 (without optimization).
AD-A289 895/5 *01,662* PC A05/MF A01

AD-A292 039/5
Comparison of Meteor Activity with Occurrence of Sporadic E Reflections.
AD-A292 039/5 *00,116* PC A01/MF A01

AD-A292 471/0
Higher-Order Approximations in Ionospheric Wave-Propagation.
AD-A292 471/0 *04,420* PC A02/MF A01

AD-A292 502/2
Penetration and Diffusion of Hard X-rays through Thick Barriers. III. Studies of Spectral Distributions.
AD-A292 502/2 *03,771* PC A01/MF A01

AD-A293 709/2
ADA Compiler Validation Summary Report, VC Number 950303S1.11381. Digital Equipment Corporation - Compiler Name: DEC Ada for OpenVMS Alpha Systems, Version 3.2.
AD-A293 709/2 *01,663* PC A05/MF A01

AD-A294 088/0
Electrochemical Synthesis of Metal and Intermetallic Composites.
AD-A294 088/0 *03,304* PC A04/MF A01

AD-A295 314/9
Further Calculations of X-ray Diffusion in an Infinite Medium.
AD-A295 314/9 *03,772* PC A01/MF A01

AD-A295 319/8
Low-Temperature Performance of Radiosonde Electric Hygrometer Elements.
AD-A295 319/8 *00,121* PC A02/MF A01

AD-A295 411/3
Arc Spectra of Gallium, Indium, and Thallium.
AD-A295 411/3 *00,718* PC A03/MF A01

AD-A295 578/9
Infrared and Near-Infrared Spectra of HCC and DCC Trapped in Solid Neon.
AD-A295 578/9 *03,773* PC A03/MF A01

AD-A295 896/5
Thermal Decomposition Pathways in Nitramine Propellants.
AD-A295 896/5 *03,753* PC A03/MF A01

AD-A296 061/5
Spectroscopic Study of Reaction Intermediates and Mechanisms in Nitramine Decomposition and Combustion.
AD-A296 061/5 *03,774* PC A03/MF A01

AD-A296 377/5
Microwave Spectrum and Structure of CH3NO2-H20.
AD-A296 377/5 *00,719* PC A03/MF A01

AD-A296 498/9
Molecular Microwave Spectra Tables.
AD-A296 498/9 *00,720* PC A03/MF A01

AD-A296 794/1
Ada Compiler Validation Summary Report, VC No. 950609S1.11390 Digital Equipment Corporation - Compiler Name: DEC Ada Version 3.2 for OpenVMS VAX Systems.
AD-A296 794/1 *01,664* PC A05/MF A01

AD-A297 265/1
Physical Properties of Some Purified Aliphatic Hydrocarbons.
AD-A297 265/1 *00,657* PC A03/MF A01

AD-A297 391/5
Air Flow in the Boundary Layer of an Elliptic Cylinder.
AD-A297 391/5 *04,194* PC A03/MF A01

AD-A297 420/2
Properties of Working Fluids for Thermoacoustic Refrigerators.
AD-A297 420/2 *04,864* PC A06/MF A02

AD-A297 905/2
Standard of Attenuation for Microwave Measurements.
AD-A297 905/2 *01,517* PC A02/MF A01

AD-A297 943/3
Crystal Diffraction Spectrometry for Accurate, Non-Invasive kV/Spectral Measurement for Improvement of Mammographic Image Quality.
AD-A297 943/3 *00,721* PC A03/MF A01

AD-A301 258/0
Performance of Plastic Packaging for Hazardous Materials Transportation. Part 1. Mechanical Properties.
AD-A301 258/0 *02,580* PC A04/MF A01

AD-A301 675/5
Weatherability of Plastic Materials.
AD-A301 675/5 *02,968* PC A14/MF A03

AD-A302 669/7
Preliminary Subject and Authors Index to Compilations of Data on Properties of Materials.
AD-A302 669/7 *03,242* PC A04/MF A01

AD-A302 670/5
Preliminary List of References Containing Compilations of Data on Properties of Materials.
AD-A302 670/5 *03,243* PC A05/MF A01

AD-A306 625/5
Fracture Testing of Large-Scale Thin-Sheet Aluminum Alloy.
AD-A306 625/5 *03,305* PC A04/MF A01

AD-A307 789/8
Synthesis of Thermally Stable Elastomers.
AD-A307 789/8 *03,194* PC A03/MF A01

AD-A310 087/2
Volatile Corrosion Inhibitors.
AD-A310 087/2 *03,114* PC A03/MF A01

AD-A310 426/2
Polyvinyl Chloride (PVC) Plastic Drain, Waste, and Vent Pipe and Fittings.
AD-A310 426/2 *00,326* PC A03/MF A01

AD-A310 724/0
Acrylonitrile-Butadiene-Styrene (ABS) Plastic Drain, Waste, and Vent Pipe and Fittings.
AD-A310 724/0 *00,327* PC A03/MF A01

AD-P009 114/0
Comparison of GPS Broadcast and DMA Precise Ephemerides.
AD-P009 114/0 *01,518* PC A03/MF A01

AD-P009 132/2
NIST Internet Time Service.
AD-P009 132/2 *01,519* PC A02/MF A01

AD-P009 138/9
Future of Time and Frequency Dissemination.
AD-P009 138/9 *01,520* PC A02/MF A01

ANSI/ISO/IEC-8652-1995
ADA; Category: Software Standard; Subcategory: Programming Language.
FIPS PUB 119-1 *01,667* PC$278.00

ARO-25664.2-CH
Production and Spectroscopy of Small Polyatomic Molecular Ions Isolated in Solid Neon. (Reannouncement with New Availability Information).
AD-A234 043/8 *00,704* PC A03/MF A01

ARO-25664.9-CH
Vibrational Spectra of Molecular Ions Isolated in Solid Neon. 6. CO4(-). (Reannouncement with New Availability Information).
AD-A238 415/4 *00,705* PC A02/MF A01

ARO-25664.10-CH
Vibrational Spectra of Molecular Ions Isolated in Solid Neon. 7. CO(+), C2O2(+), and C2O2(-). (Reannouncement with New Availability Information).
AD-A239 729/7 *00,706* PC A03/MF A01

ARO-25664.12-CH
Vibrational Spectra of Molecular Ions Isolated in Solid Neon: HCCH+ and HCC-. (Reannouncement with New Availability Information).
AD-A253 551/6 *00,707* PC A03/MF A01

ARO-26123.2-MS
Characterization of the Densification of Alumina by Multiple Small-Angle Neutron Scattering. (Reannouncement with New Availability Information).
AD-A249 179/3 *03,024* PC A02/MF A01

ARO-26123.3-MS
Effect of Green Density and the Role of Magnesium Oxide Additive on the Densification of Alumina Measured by Small-Angle Neutron Scattering. (Reannouncement with New Availability Information).
AD-A244 582/3 *03,022* PC A02/MF A01

ARO-26123.4-MS
Evolution of the Pore Size Distribution in Final-Stage Sintering of Alumina Measured by Small-Angle X-ray Scattering. (Reannouncement with New Availability Information).
AD-A249 178/5 *03,023* PC A03/MF A01

ARO-26123.5-MS
Small-Angle Neutron Scattering Characterization of Processing/Microstructure Relationships in the Sintering of Crystalline and Glassy Ceramics. (Reannouncement with New Availability Information).
AD-A249 510/9 *03,025* PC A03/MF A01

ARO-29596.1-CH
Microwave Spectrum and Structure of CH3NO2-H20.
AD-A296 377/5 *00,719* PC A03/MF A01

ARO-29596.2-CH
Thermal Decomposition Pathways in Nitramine Propellants.
AD-A295 896/5 *03,753* PC A03/MF A01

ARO-30094.3-CH
Vibrational Spectra of Molecular Ions Isolated in Solid Neon. 11. NO2(+), NO2(-), and NO3(-).
AD-A275 828/2 *00,708* Not available NTIS

ARO-30094.4-CH
Infrared and Near-Infrared Spectra of HCC and DCC Trapped in Solid Neon.
AD-A295 578/9 *03,773* PC A03/MF A01

ARO-30094.5-CH
Spectroscopic Study of Reaction Intermediates and Mechanisms in Nitramine Decomposition and Combustion.
AD-A296 061/5 *03,774* PC A03/MF A01

ARPA-7829-2
Submarine Automation: Demonstration No. 5.
PB95-251633 *03,748* PC A03/MF A01

BUAER-16-1-519-SUPP-1
Handbook Preferred Circuits Navy Aeronautical Electronic Equipment. Supplement Number 1.
AD-A278 784/4 *00,028* PC A05/MF A01

BUAER-16-1-519-SUPP-2
Handbook Preferred Circuits Navy Aeronautical Electronic Equipment. Supplement Number 2.
AD-A278 783/6 *00,027* PC A03/MF A01

CAM-9201
Structural Ceramics Database. Topical Report, June 1989-May 1991.
PB95-203758 *03,060* PC A04/MF A01

CBRM-TR-91-2
Rare-Earth Isotopes as Tracers of Particulate Emissions: An Urban Scale Test.
PB94-161635 *02,535* PC A03/MF A01

CONF-890701-32
Magnetic Characteristics and Measurements of Filamentary Nb-Ti Wire for the Superconducting Super Collider.
DE94005988 *03,775* PC A02/MF A01

CONF-931156-41
Low Temperature H(sub 2)S Separation Using Membrane Reactor with Redox Catalyst.
DE94008991 *02,471* PC A02/MF A01

CONF-8710535
Ceramic Characterization.
DE94013170 *03,026* PC A02/MF A01

CONF-8902131-2
Transverse stress effect on the critical current of internal tin and bronze process Nb(sub 3)Sn superconductors.
DE95016659 *04,434* PC A01/MF A01

CONF-8902131-3
VAMAS interlaboratory comparisons of critical current vs. strain in Nb(sub 3)Sn.
DE95016656 *04,433* PC A01/MF A01

CONF-9305134-3-APP.A
Development of a Dual-Sinker Densimeter for High-Accuracy Fluid P-V-T Measurements. Appendix A.
DE93019682 *02,620* PC A02/MF A01

CONF-9305134-4-APP.B
Dielectric Studies of Fluids with Reentrant Resonators. Appendix B.
DE93019683 *03,244* PC A02/MF A01

CONF-9307232-SUMM
Small genomes: New initiatives in mapping and sequencing. Workshop summary report.
DE96014476 *03,451* PC A05/MF A01

CONF-9404137-5
Ebulliometers for Measuring the Thermodynamic Properties of Fluids and Fluid Mixtures.
DE94017817 *04,195* PC A02/MF A01

CONF-9404137-6
Measurement of the Thermal Properties of Electrically Conducting Fluids Using Coated Transient Hot Wires.
DE94017816 *00,722* PC A02/MF A01

CRPL-9-8
Standard of Attenuation for Microwave Measurements.
AD-A297 905/2 *01,517* PC A02/MF A01

CS270-65
Acrylonitrile-Butadiene-Styrene (ABS) Plastic Drain, Waste, and Vent Pipe and Fittings.
AD-A310 724/0 *00,327* PC A03/MF A01

DE94-017162
Economic, Energy, and Environmental Impacts of the Energy-Related Inventions Program.
DE94-017162 *00,008* PC A05/MF A02

DE93019682
Development of a Dual-Sinker Densimeter for High-Accuracy Fluid P-V-T Measurements. Appendix A.
DE93019682 *02,620* PC A02/MF A01

DE93019683
Dielectric Studies of Fluids with Reentrant Resonators. Appendix B.
DE93019683 *03,244* PC A02/MF A01

DE93041307
Review of Corrosion Behavior of Ceramic Heat Exchanger Materals: Corrosion Characteristics of Silicon Carbide and Silicon Nitride. Final Report, September 11, 1992--March 11, 1993.
DE93041307 *03,228* PC A06/MF A02

DE94004236
Thermophysical Properties of HFC-143a and HFC-152a. Quarterly Report, 1 July 1993--30 September 1993.
DE94004236 *03,245* PC A03/MF A01

DE94004399
Development of Measurement Capabilities for the Thermophysical Properties of Energy-Related Fluids. Annual Report, December 1, 1990--November 30, 1991.
DE94004399 *02,470* PC A02/MF A01

DE94004400
Determination of Atomic Data Pertinent to the Fusion Energy Program. Progress Report for FY 92.
DE94004400 *04,402* PC A02/MF A01

DE94005988
Magnetic Characteristics and Measurements of Filamentary Nb-Ti Wire for the Superconducting Super Collider.
DE94005988 *03,775* PC A02/MF A01

DE94008991
Low Temperature H(sub 2)S Separation Using Membrane Reactor with Redox Catalyst.
DE94008991 *02,471* PC A02/MF A01

DE94013170
Ceramic Characterization.
DE94013170 *03,026* PC A02/MF A01

DE94013486
Densification of Nano-Size Powders. 1994 Report.
DE94013486 *03,027* PC A03/MF A01

DE94013593
Equipment for Investigation of Cryogenic Compaction of Nanosize Silicon Nitride Powders. 1993 Report.
DE94013593 *03,028* PC A03/MF A01

DE94014586
Measuring Performance of Parallel Computers. Final Report.
DE94014586 *01,665* PC A03/MF A01

DE94014587
Measuring Performance of Parallel Computers. Progress Report, 1989.
DE94014587 *01,666* PC A03/MF A01

DE94014709
Ionizing radiation-induced DNA damage and its repair in human cells. Progress report, (April 1, 1993--February 28, 1994).
DE94014709 *03,612* PC A01/MF A01

DE94015308
NIST Cooperative Laboratory for OSI Routing Technology.
DE94015308 *01,791* PC A03/MF A01

DE94017331
Evaluation of the Environmentally Induced Fracture Resistance of Ductile Nickel Aluminide. Technical Report Number 1, Final report. October-December 1990.
DE94017331 *03,306* PC A03/MF A01

DE94017332
Comparison of the Corrosion Rates of FeAl, Fe(sub 3)Al and Steel in Distilled Water and 0.5 M Sodium Chloride. Technical Report Number 2, January--March 1991.
DE94017332 *03,186* PC A02/MF A01

DE94017351
Evaluation of the Electrochemical Behavior of Ductile Nickel Aluminide and Nickel in a pH 7.9 Solution. Technical Report Number 3, April-June 1991.
DE94017351 *03,307* PC A02/MF A01

DE94017738
Development of Measurement Capabilities for the Thermophysical Properties of Energy-Related Fluids. Annual Report, December 1, 1993--November 30, 1994.
DE94017738 *03,246* PC A03/MF A01

DE94017816
Measurement of the Thermal Properties of Electrically Conducting Fluids Using Coated Transient Hot Wires.
DE94017816 *00,722* PC A02/MF A01

DE94017817
Ebulliometers for Measuring the Thermodynamic Properties of Fluids and Fluid Mixtures.
DE94017817 *04,195* PC A02/MF A01

DE94018562
Atom-counting standards and Doppler-free resonance ionization mass spectroscopy. (Progress report).
DE94018562 *00,723* PC A02/MF A01

DE94018563
Improvement of Ultrasensitive Techniques Isotopic Biasing in the RIS Process Ionization Efficiencies and Selectivities.
DE94018563 *00,522* PC A02/MF A01

DE94018565
I: Improvement of Resonance Ionization Spectroscopy (RIS) Techniques; II: Atomic Data for RIS; III: Standards for Ultratrace Analysis. Progress Report.
DE94018565 *00,523* PC A02/MF A01

DE94018566
Study of Laser Resonance Ionization Mass Spectrometry Using a Glow Discharge Source.
DE94018566 *03,308* PC A01/MF A01

DE95002261
Thermophysical properties of HCFC alternatives. Quarterly report, 1 July 1994--30 September 1994.
DE95002261 *03,247* PC A02/MF A01

DE95004446
Electron-atom collision studies using optically state selected beams. Progress report, May 15, 1987--May 14, 1988.
DE95004446 *03,776* PC A03/MF A01

DE95004447
Electron-atom collision studies using optically state selected beams. Progress report, May 15, 1988--May 14, 1991.
DE95004447 *03,777* PC A03/MF A01

DE95005780
Minutes of the CAALS Workshop on modularity and communications standards.
DE95005780 *02,621* PC A03/MF A01

DE95007065
Electron transport calculations with biomedical and environmental applications. Final report, December 23, 1992--January 31, 1994.
DE95007065 *03,613* PC A01/MF A01

DE95009287
Atomic-scale characterization of hydrogenated amorphous-silicon films and devices. Annual subcontract report, 14 February 1994--14 April 1995.
DE95009287 *02,294* PC A03/MF A01

DE95011238
Lean flammability limit as a fundamental refrigerant property. Phase 1, Interim technical report, 1 October 1994--31 March 1995.
DE95011238 *03,248* PC A03/MF A01

DE95011352
Experimental plan to determine the performance of the Oak Ridge National Laboratory Cold Neutron Moderator. Final report, September 1, 1993--November 30, 1993.
DE95011352 *03,778* PC A03/MF A01

DE95011593
Measurements of quantum electrodynamic sensitive transitions in Na-like and Cu-like ions: Final report, 1 October 1993--29 September 1994.
DE95011593 *04,403* PC A02/MF A01

DE95013079
Distributed measurements of tracer response on packed bed flows using a fiberoptic probe array. Final report.
DE95013079 *00,667* PC A03/MF A01

DE95013505
Low temperature fabrication from nano-size ceramic powders.
DE95013505 *03,029* PC A05/MF A01

DE95015476
Electromechanical properties of superconductors for DOE fusion applications.
DE95015476 *04,432* PC A04/MF A01

DE95016656
VAMAS interlaboratory comparisons of critical current vs. strain in Nb(sub 3)Sn.
DE95016656 *04,433* PC A01/MF A01

DE95016659
Transverse stress effect on the critical current of internal tin and bronze process Nb(sub 3)Sn superconductors.
DE95016659 *04,434* PC A01/MF A01

DE95017761
Report of the Federal Internetworking Requirements Panel.
DE95017761 *03,407* PC A03/MF A01

DE96007979
Experimental assessment of absorbed dose to mineralized bone tissue from internal emitters: An electron paramagnetic resonance study.
DE96007979 *03,614* PC A02/MF A01

DE96010065
Improving measurement quality assurance for photon irradiations at Department of Energy facilities. Final technical report.
DE96010065 *03,711* PC A03/MF A01

DE96010433
Thermophysical properties of HCFC alternatives. Quarterly report, October 1--December 31, 1995.
DE96010433 *03,249* PC A04/MF A01

DE96010579
Thermophysical properties of HCFC alternatives. Quarterly report, April 1--June 30, 1995.
DE96010579 *03,250* PC A05/MF A01

DE96014476
Small genomes: New initiatives in mapping and sequencing. Workshop summary report.
DE96014476 *03,451* PC A05/MF A01

DOE/CE/23810-22A
Thermophysical Properties of HFC-143a and HFC-152a. Quarterly Report, 1 July 1993--30 September 1993.
DE94004236 *03,245* PC A03/MF A01

DOE/CE/23810-48A
Thermophysical properties of HCFC alternatives. Quarterly report, 1 July 1994--30 September 1994.
DE95002261 *03,247* PC A02/MF A01

DOE/CE/23810-58
Lean flammability limit as a fundamental refrigerant property. Phase 1, Interim technical report, 1 October 1994--31 March 1995.
DE95011238 *03,248* PC A03/MF A01

DOE/CE/23810-61A
Thermophysical properties of HCFC alternatives. Quarterly report, April 1--June 30, 1995.
DE96010579 *03,250* PC A05/MF A01

DOE/CE/23810-66A
Thermophysical properties of HCFC alternatives. Quarterly report, October 1--December 31, 1995.
DE96010433 *03,249* PC A04/MF A01

DOE/EH/89321-T1
Improving measurement quality assurance for photon irradiations at Department of Energy facilities. Final technical report.
DE96010065 *03,711* PC A03/MF A01

DOE/EH/89334-T1
Experimental assessment of absorbed dose to mineralized bone tissue from internal emitters: An electron paramagnetic resonance study.
DE96007979 *03,614* PC A02/MF A01

DOE/ER/13520-T1
Electron-atom collision studies using optically state selected beams. Progress report, May 15, 1987--May 14, 1988.
DE95004446 *03,776* PC A03/MF A01

DOE/ER/13520-T2
Electron-atom collision studies using optically state selected beams. Progress report, May 15, 1988--May 14, 1991.
DE95004447 *03,777* PC A03/MF A01

DOE/ER/13770-T3
Distributed measurements of tracer response on packed bed flows using a fiberoptic probe array. Final report.
DE95013079 *00,667* PC A03/MF A01

DOE/ER/13823-T2
Development of Measurement Capabilities for the Thermophysical Properties of Energy-Related Fluids. Annual Report, December 1, 1990--November 30, 1991.
DE94004399 *02,470* PC A02/MF A01

DOE/ER/13823-T3
Development of Measurement Capabilities for the Thermophysical Properties of Energy-Related Fluids. Annual Report, December 1, 1993--November 30, 1994.
DE94017738 *03,246* PC A03/MF A01

DOE/ER/25046-T1
Measuring Performance of Parallel Computers. Final Report.
DE94014586 *01,665* PC A03/MF A01

DOE/ER/25046-T2
Measuring Performance of Parallel Computers. Progress Report, 1989.
DE94014587 *01,666* PC A03/MF A01

DOE/ER/25114-1
NIST Cooperative Laboratory for OSI Routing Technology.
DE94015308 *01,791* PC A03/MF A01

DOE/ER/25188-T1
Report of the Federal Internetworking Requirements Panel.
DE95017761 *03,407* PC A03/MF A01

DOE/ER/53237-T1
Determination of Atomic Data Pertinent to the Fusion Energy Program. Progress Report for FY 92.
DE94004400 *04,402* PC A02/MF A01

DOE/ER/60447-T2
Atom-counting standards and Doppler-free resonance ionization mass spectroscopy. (Progress report).
DE94018562 *00,723* PC A02/MF A01

DOE/ER/60447-T3
Improvement of Ultrasensitive Techniques Isotopic Biasing in the RIS Process Ionization Efficiencies and Selectivities.
DE94018563 *00,522* PC A02/MF A01

DOE/ER/60447-T5
I: Improvement of Resonance Ionization Spectroscopy (RIS) Techniques; II: Atomic Data for RIS; III: Standards for Ultratrace Analysis. Progress Report.
DE94018565 *00,523* PC A02/MF A01

DOE/ER/60447-T6
Study of Laser Resonance Ionization Mass Spectrometry Using a Glow Discharge Source.
DE94018566 *03,308* PC A01/MF A01

DOE/ER/60826-T1

Ionizing radiation-induced DNA damage and its repair in human cells. Progress report, (April 1, 1993--February 28, 1994).
DE94014709 *03,612* PC A01/MF A01

DOE/ER/61529-T1

Electron transport calculations with biomedical and environmental applications. Final report, December 23, 1992--January 31, 1994.
DE95007065 *03,613* PC A01/MF A01

DOE/EW/50009-T2

Minutes of the CAALS Workshop on modularity and communications standards.
DE95005780 *02,621* PC A03/MF A01

DOE/OR/21941-T1

Evaluation of the Environmentally Induced Fracture Resistance of Ductile Nickel Aluminide. Technical Report Number 1, Final report. October-December 1990.
DE94017331 *03,306* PC A03/MF A01

DOE/OR/21941-T2

Comparison of the Corrosion Rates of FeAl, Fe(sub 3)Al and Steel in Distilled Water and 0.5 M Sodium Chloride. Technical Report Number 2, January--March 1991.
DE94017332 *03,186* PC A02/MF A01

DOE/OR/21941-T3

Evaluation of the Electrochemical Behavior of Ductile Nickel Aluminide and Nickel in a pH 7.9 Solution. Technical Report Number 3, April-June 1991.
DE94017351 *03,307* PC A02/MF A01

DOE/OR/22041-2

Densification of Nano-Size Powders. 1994 Report.
DE94013486 *03,027* PC A03/MF A01

DOE/OR/22041-T1

Equipment for Investigation of Cryogenic Compaction of Nanosize Silicon Nitride Powders. 1993 Report.
DE94013593 *03,028* PC A03/MF A01

DOE/OR/22041-T2

Low temperature fabrication from nano-size ceramic powders.
DE95013505 *03,029* PC A05/MF A01

DOE/OR/22121-T1

Experimental plan to determine the performance of the Oak Ridge National Laboratory Cold Neutron Moderator. Final report, September 1, 1993--November 30, 1993.
DE95011352 *03,778* PC A03/MF A01

DOE/PC/92179-T1

Review of Corrosion Behavior of Ceramic Heat Exchanger Materals: Corrosion Characteristics of Silicon Carbide and Silicon Nitride. Final Report, September 11, 1992--March 11, 1993.
DE93041307 *03,228* PC A06/MF A02

DOE/SF/20143-T2

Measurements of quantum electrodynamic sensitive transitions in Na-like and Cu-like ions: Final report, 1 October 1993--29 September 1994.
DE95011593 *04,403* PC A02/MF A01

DOT/FAA/AR-95/11

Fracture Testing of Large-Scale Thin-Sheet Aluminum Alloy.
AD-A306 625/5 *03,305* PC A04/MF A01

DOT-HS-808 214

Model Minimum Performance Specifications for Lidar Speed Measurement Devices.
PB95-197455 *04,861* PC A03/MF A01

DOT/MTB/OHMO-76/4

Performance of Plastic Packaging for Hazardous Materials Transportation. Part 1. Mechanical Properties.
AD-A301 258/0 *02,580* PC A04/MF A01

ED-376 823

Information Infrastructure: Reaching Society's Goals. A Report of the Information Infrastructure Task Force Committee on Applications and Technology.
ED-376 823 *00,131* Not available NTIS

EIA-RS-466

Procedures for Document Facsimile Transmission Issued by General Services Administration, April 14, 1982. Federal Standard 1063.
FIPS PUB 148 *01,516* PC E99

EPA/600/J-94/339

Histopathology, Blood Chemistry, and Physiological Status of Normal and Moribund Striped Bass ('Morone saxatilis') Involved in Summer Mortality ('Die-Off') in the Sacramento-San Joaquin Delta of California.
PB94-198157 *00,034* PC A03/MF A01

FEMA-202

Earthquake Resistant Construction of Electric Transmission and Telecommunication Facilities Serving the Federal Government Report.
PB94-161817 *02,460* PC A03/MF A01

FEMA-233

Earthquake Resistant Construction of Gas and Liquid Fuel Pipeline Systems Serving, or Regulated By, the Federal Government.
PB94-161999 *04,846* PC A05/MF A01

FHWA/RD-94/002

System for Calibration of the Marshall Compaction Hammer.
PB94-145661 *01,303* PC A08/MF A02

FHWA/RD-94/053

Robotics Application to Highway Transportation. Volume 1. Final Report.
PB95-203790 *03,654* PC A03/MF A01

FHWA/RD-94/054

Robotics Application to Highway Transportation. Volume 2. Literature Search.
PB95-170551 *01,337* PC A06/MF A02

FHWA/RD-94/094

Robotics Application to Highway Transportation. Volume 3. Proposed Research Topics and Cost/Benefit Evaluations by CERF.
PB95-171633 *01,338* PC A20/MF A04

FHWA/RD-94/095

Robotics Application to Highway Transportation. Volume 4. Proposals for Potential Research.
PB95-193173 *01,339* PC A07/MF A02

FHWA/RD-94/174

Degradation of Powder Epoxy Coated Panels Immersed in a Saturated Calcium Hydroxide Solution Containing Sodium Chloride.
PB96-101050 *01,344* PC A03/MF A01

FHWA/RD-95/063

Field Evaluation of the System for Calibration of the Marshall Compaction Hammer.
PB95-190674 *01,323* PC A05/MF A01

FIPS PUB 8-6

Metropolitan Areas (Including MSAs, CMSAs, PMASs, and NECMAs). Category: Data Standards and Guidelines; Subcategory: Representations and Codes.
FIPS PUB 8-6 *04,873* PC E09

FIPS PUB 10-4

Countries, Dependencies, Areas of Special Sovereignty, and Their Principal Administrative Divisions. Category: Data Standards and Guidelines; Subcategory: Representation and Codes.
FIPS PUB 10-4 *00,128* PC E05

FIPS PUB 21-4

COBOL. Category: Software Standard; Subcategory: Programming Language. Includes ANSI'S X3.23-1985, X3.23A-1989 and X3.23B-1993.
FIPS PUB 21-4 *01,670* PC E99

FIPS PUB 21-4A

COBOL. Category: Software Standard; Subcategory: Programming Language. Part A.
FIPS PUB 21-4A *01,671* PC E99

FIPS PUB 21-4B

COBOL. Category: Software Standard; Subcategory: Programming Language. Part B.
FIPS PUB 21-4B *01,672* PC E99

FIPS PUB 46-2

Data Encryption Standard (DES); Category: Computer Security; Subcategory: Cryptography.
FIPS PUB 46-2 *01,572* PC E04

FIPS PUB 55-3

Guideline: Codes for Named Populated Places, Primary County Divisions, and Other Locational Entities of the United States, Puerto Rico, and the Outlying Areas. Category: Data Standards and Guidelines. Subcategory: Representations and Codes.
FIPS PUB 55-3 *04,865* PC E04

FIPS PUB 55-DC3

Guideline: Codes for Named Populatd Places, Primary County Divisions, and Other Locational Entities of the United States, Puerto Rico, and the Outlying Areas. Category: Data Standards and Guidelines; Subcategory: Representation and Codes.
FIPS PUB 55-DC3 *04,866* PC E99

FIPS PUB 119-1

ADA; Category: Software Standard; Subcategory: Programming Language.
FIPS PUB 119-1 *01,667* PC$278.00

FIPS PUB 120-1C

Graphical Kernel System (GKS). Category: Software Standard. Subcategory: Graphics. International Standard: Information Technology; Computer Graphics; Graphical Kernel System (GKS) Language Bindings. Part 4: C.
FIPS PUB 120-1C *01,792* PC A06/MF A02

FIPS PUB 140-1

Security Requirements for Cryptographic Modules; Category: Computer Security; Subcategory: Cryptography.
FIPS PUB 140-1 *01,567* PC E05

FIPS PUB 148

Procedures for Document Facsimile Transmission Issued by General Services Administration, April 14, 1982. Federal Standard 1063.
FIPS PUB 148 *01,516* PC E99

FIPS PUB 153-1

Programmer's Hierarchical Interactive Graphics System (PHIGS). Category: Software Standard; Subcategory: Graphics.
FIPS PUB 153-1 *01,668* PC E99

FIPS PUB 158-1

User Interface Component of the Applications Portability Profile Category: Software Standard; Subcategory: Application Program Interface.
FIPS PUB 158-1 *01,793* PC E01

FIPS PUB 173-1

Spatial Data Transfer Standard (SDTS): Category: Software Standard; Subcategory: Information Interchange.
FIPS PUB 173-1 *01,794* PC A04/MF A01

FIPS PUB 173-1A

Spatial Data Transfer Standard (SDTS). Category: Software Standard; Subcategory: Information Interchange. (FIPS PUB 173-1A).
FIPS PUB 173-1A *01,795* PC$44.50

FIPS PUB 173-1B

Spatial Data Transfer Standard (SDTS). Category: Software Standard; Subcategory: Information Interchange. (FIPS PUB 173-1B).
FIPS PUB 173-1B *01,796* PC E99

FIPS PUB 180-1

Secure Hash Standard. Category: Computer Security.
FIPS PUB 180-1 *01,568* PC E04

FIPS PUB 182

Integrated Services Digital Network (ISDN); Category: Telecommunications Standard; Subcategory: Integrated Services Digital Network.
FIPS PUB 182 *01,460* PC E03

FIPS PUB 185

Escrowed Encryption Standard (EES); Category: Computer Security; Subcategory: Cryptography.
FIPS PUB 185 *01,569* PC E03

FIPS PUB 186

Digital Signature Standard (DSS). Category: Computer Security; Subcategory: Cryptography.
FIPS PUB 186 *01,570* PC E04

FIPS PUB 187

Administration Standard for the Telecommunications Infrastructure of Federal Buildings. Category: Telecommunications Standard; Subcategory: Telecommunications Administration.
FIPS PUB 187 *01,461* PC A02/MF A01

FIPS PUB 188

Standard Security Label for Information Transfer; Category: Computer Security; Subcategory: Security Labels.
FIPS PUB 188 *01,571* PC E04

FIPS PUB 189

Portable Operating System Interface (POSIX). Part 2. Shell and Utilities. Category: Software Standard; Subcategory: Operating Systems.
FIPS PUB 189 *01,797* PC A03/MF A01

FIPS PUB 190

Guideline for the Use of Advanced Authentication Technology Alternatives. Category: Computer Security. Subcategory: Access Control.
FIPS PUB 190 *01,798* PC A04/MF A01

FIPS PUB 191

Guideline for the Analysis of Local Area Network Security. Category: Computer Security; Subcategory: Risk Analysis and Contingency Planning.
FIPS PUB 191 *01,799* PC A04/MF A01

FIPS PUB 192

Application Profile for the Government Information Locator Service (GILS). Category: Software Standard; Subcategory: Information Interchange.
FIPS PUB 192 *01,800* PC A03/MF A01

FIPS PUB 193

SQL Environments. Category: Software Standard; Subcategory: Database.
FIPS PUB 193 *01,801* PC A04/MF A01

FIPS PUB 194

Open Document Architecture (ODA) Raster Document Application Profile (DAP). Category: Software Standard; Subcategory: Graphics.
FIPS PUB 194 *01,669* PC E04

FIPS PUB 195

Federal Building Grounding and Bonding Requirements for Telecommunications. Category: Telecommunications Standard; Subcategory: Grounding and Bonding.
FIPS PUB 195 *01,802* PC E18

FIPSPUB183

Integration Definition for Function Modeling (IDEF0); Category: Software Standard; Subcategory: Modeling Techniques.
FIPSPUB183 *02,800* PC E07

FIPSPUB184

Integration Definition for Information Modeling (IDEF1X); Category: Software Standard; Subcategory: Modeling Techniques.
FIPSPUB184 *01,673* PC E10

FR-3995

Santa Ana Fire Department Experiment at 1315 South Bristol, July 14, 1994.
PB95-188868 *00,389* PC A03/MF A01

GDL/GMF-95-02

Mixing and Radiation Properties of Buoyant Luminous Flame Environments.
PB96-202254 *01,432* PC A06/MF A01

GRI-92/0042

Structural Ceramics Database. Topical Report, June 1989-May 1991.
PB95-203758 *03,060* PC A04/MF A01

GRI-92/0576

Sliding Vane Flow Conditioner Tests in a 100 Diameter Long 10 inch Natural Gas Orifice Meter at Pacific Gas and Electric. Topical Report, 1990-1992.
PB95-256335 *02,493* PC A04/MF A01

GRI-93/0396

Thermophysical Properties of Fluids for the Gas Industry. Final Report, February 1, 1988-August 31, 1993.
PB94-146677 *02,472* PC A03/MF A01

GRI-94/0145

Assessment of Technology for Detection of Stress Corrosion Cracking in Gas Pipelines. Final Report, July 1993-March 1994.
PB94-206646 *02,475* PC A05/MF A02

GRI-94/0274
Constituents and Physical Properties of the C6+ Fraction of Natural Gas. Topical Report, April-June 1994.
PB95-136644 *02,483* PC A03/MF A01

GRI-94/0411
Evaluation of Wear Resistant Ceramic Valve Seats in Gas-Fueled Power Generation Engines. Topical Report, December 1991-April 1994.
PB95-200218 *02,466* PC A07/MF A02

HANDBOOK-52
Maximum Permissible Amounts of Radioisotopes in the Human Body and Maximum Permissible Concentrations in Air and Water.
AD-A280 281/7 *03,609* PC A04/MF A01

HANDBOOK-69
Maximum Permissible Body Burdens and Maximum Permissible Concentrations of Radionuclides in Air and in Water for Occupational Exposure.
AD-A280 282/5 *03,610* PC A06/MF A02

HUD-0006080
Controlling Moisture in the Walls of Manufactured Housing.
PB95-105136 *00,355* PC A03/MF A01

IIW-V-1046-95
IIW Commission V Quality Control and Quality Assurance of Welded Products Annual Report 1994/95.
PB95-198743 *02,866* PC A03/MF A01

IIW-V-1059-96
IIW Commission V Quality Control and Quality Assurance of Welded Products, Annual Report 1995/96.
PB96-191366 *02,880* PC A04/MF A01

ISBN-0-16-043188-3
Putting the Information Infrastructure to Work: Report of the Information Infrastructure Task Force Committee on Applications and Technology.
N94-31228/7 *02,715* PC A06/MF A02
Putting the Information Infrastructure to Work: Report of the Information Infrastructure Task Force Committee on Applications and Technology.
PB94-163383 *00,001* PC A06/MF A02

ISBN-0-16-045384-4
Checking the Net Contents of Packaged Goods as Adopted by the 79th National Conference on Weights and Measures, 1994, Third Edition, Supplement 4.
PB95-182226 *00,484* PC A04/MF A01

ISBN-0-309-04982-2
Learning to Change: Opportunities to Improve the Performance of Smaller Manufacturers.
PB94-166212 *00,010* PC A08/MF A02

ISBN-0-309-05252-1
Binder Characterization and Evaluation by Nuclear Magnetic Resonance Spectroscopy.
PB94-193471 *01,334* PC A08/MF A02

ISBN-0-309-05432-X
Unpredictable Certainty. Information Infrastructure through 2000.
PB96-182266 *00,016* PC A14/MF A03

ISBN-0-309-05543-1
Financing Tomorrow's Infrastructure: Challenges and Issues. Proceedings of a Colloquium. Held in Washington, DC. on October 20, 1995.
PB96-189444 *00,481* PC A07/MF A02

ISBN-0-309-05751-5
Optimization of Highway Concrete Technology.
PB94-182995 *01,333* PC A13/MF A03

ISBN-1-886843-01-5
Proceedings of the Applied Diamond Conference 1995: Applications of Diamond Films and Related Materials International Conference (3rd). Held in Gaithersburg, Maryland, on August 21-24, 1995.
PB95-255204 *04,701* PC A99/MF E11

N94-23605/6
Activities of NIST (National Inst. Of Standards and Technology).
N94-23605/6 *04,222*
(Order as N94-23595/9, PC A21/MF A04)

N94-25124/6
Dynamic Measurements of Thermophysical Properties of Metals and Alloys at High Temperatures by Subsecond Pulse Heating Techniques.
N94-25124/6 *03,309*
(Order as N94-25120/4, PC A11/MF A03)

N94-30641/2
Time and Frequency Technology at NIST.
N94-30641/2 *01,522*
(Order as N94-30639/6, PC A25/MF A06)

N94-30660/2
Comparison of GPS Broadcast and DMA Precise Ephemerides.
N94-30660/2 *01,523*
(Order as N94-30639/6, PC A25/MF A06)

N94-30684/2
Future of Time and Frequency Dissemination.
N94-30684/2 *01,524*
(Order as N94-30639/6, PC A25/MF A06)

N94-31228/7
Putting the Information Infrastructure to Work: Report of the Information Infrastructure Task Force Committee on Applications and Technology.
N94-31228/7 *02,715* PC A06/MF A02

N94-34037/9
Ground Vehicle Control at NIST: From Teleoperation to Autonomy.
N94-34037/9 *03,758*
(Order as N94-34019/7, PC A21/MF A04)

N94-35335/6
Classification of Advanced Technical Ceramics.
N94-35335/6 *03,030* PC A07/MF A02

N94-36857/8
Open System Environments.
N94-36857/8 *01,674*
(Order as N94-36853/7, PC A10/MF A03)

N94-36858/6
Open System Environment Procurement.
N94-36858/6 *02,716*
(Order as N94-36853/7, PC A10/MF A03)

N95-14084/4
Partial Pressure Analysis in Space Testing.
N95-14084/4 *04,827*
(Order as N95-14062/0, PC A20/MF A04)

N95-14548/8
Convection and Morphological Stability During Directional Solidification.
N95-14548/8 *03,310*
(Order as N95-14522/3, PC A20/MF A04)

N95-15839/0
Investigating the 3.3 Micron Infrared Fluorescence from Naphthalene Following Ultraviolet Excitation.
N95-15839/0 *00,724*
(Order as N95-15827/5, PC A07/MF A02)

N95-15937/2
Numeric Data Distribution: The Vital Role of Data Exchange in Today's World.
N95-15937/2 *02,622*
(Order as N95-15919/0, PC A11/MF A03)

N95-15938/0
National Center for Standards and Certification Information: Service and Programs.
N95-15938/0 *02,717*
(Order as N95-15919/0, PC A11/MF A03)

N95-19494/0
Fracture Behavior of Large-Scale Thin-Sheet Aluminum Alloy.
N95-19494/0 *03,311*
(Order as N95-19468/4, PC A24/MF A04)

N95-24130/3
Optical Storage Media Data Integrity Studies.
N95-24130/3 *01,620*
(Order as N95-24108, PC A17/MF A04)

N95-26123/6
Measurement Methods and Standards for Processing and Application of Thermal Barrier Coatings.
N95-26123/6 *01,447*
(Order as N95-26119, PC A03/MF A01)

N95-32323/4
Implementation of a Standard Format for GPS Common View Data.
N95-32323/4 *03,779*
(Order as N95-32319, PC A20/MF A04)

N96-15569/2
Combustion of a Polymer (PMMA) Sphere in Microgravity.
N96-15569/2 *01,354*
(Order as N96-15552, PC A20/MF A04)

N96-15584/1
Ignition and Subsequent Transition to Flame Spread in a Microgravity Environment.
N96-15584/1 *04,828*
(Order as N96-15552, PC A20/MF A04)

N19960042622
Utc Dissemination to the Real-Time User.
N19960042622 *01,521*
(Order as N19960042616, PC A20/MF A04)

NASA-L-1247
Characteristics of Turbulence in a Boundary Layer with Zero Pressure Gradient.
AD-A278 249/8 *04,192* PC A03/MF A01

NBS-CIRC-487
Density of Solids and Liquids.
AD-A278 517/8 *00,711* PC A03/MF A01

NBS-CIRC-509-SUPPL
Bibliography of Books and Published Reports on Gas Turbines, Jet Propulsion, and Rocket Power Plants, January 1950 through December 1953.
AD-A278 213/4 *01,446* PC A06/MF A02

NBS-CIRC-552
Standard Samples and Reference Standards Issued by the National Bureau of Standards.
AD-A279 240/6 *02,613* PC A03/MF A01

NBS-CIRC-568
High Temperature Reactions of Uranium Dioxide with Various Metal Oxides.
AD-A286 648/1 *00,717* PC A03/MF A01

NBS-CIRC-583-SUPP
X-Ray Attenuation Coefficients from 10 kev to 100 Mev.
AD-A279 289/3 *03,767* PC A03/MF A01

NBS-CIRCULAR-467
Atomic Energy Levels As Derived from the Analyses of Optical Spectra. Volume 1. Section 1. The Spectra of Hydrogen, Deuterium, Helium, Lithium Beryllium, Boron, Carbon, Nitrogen, Oxygen, and Fluorine.
AD-A278 130/0 *03,764* PC A05/MF A01

NBS-CIRCULAR-509
Bibliography of Books and Published Reports on Gas Turbines, Jet Propulsion, and Rocket Power Plants.
AD-A278 138/3 *01,445* PC A04/MF A01

NBS-CIRCULAR-583
X-ray Attenuation Coefficients from 10 Kev to 100 Mev.
AD-A278 139/1 *03,765* PC A04/MF A01

NBS-HB-H28-PT-1
Screw-Thread Standards for Federal Services, 1957. Part 1.
AD-A279 290/1 *02,855* PC A10/MF A03

NBS-HB-54
Protection Against Radiations from Radium, Cobalt-60, and Cesium-137.
AD-A279 261/2 *03,607* PC A04/MF A01

NBS-HB-75
Measurement of Absorbed Dose of Neutrons, and of Mixtures of Neutrons and gamma rays.
AD-A286 647/3 *03,710* PC A05/MF A01

NBS-MR-241
Standard Materials. A Descriptive List with Prices.
AD-A278 140/9 *00,500* PC A03/MF A01

NBS-RP-2107
Molecular Microwave Spectra Tables.
AD-A296 498/9 *00,720* PC A03/MF A01

NBS-TN-56
Bibliography of the Physical Equilibria and Related Properties of Some Cryogenic Systems.
AD-A281 167/7 *03,769* PC A07/MF A02

NBS-TN-124
Papers on the Symposium on Collision Phenomena in Astrophysics, Geophysics, and Masers.
AD-A280 291/6 *00,047* PC A03/MF A01

NBS-34
Tables of Chemical Kinetics Homogeneous Reactions.
AD-A280 293/2 *00,715* PC A20/MF A04

NBS-462
Ionospheric Radio Propagation.
AD-A286 619/2 *01,459* PC A10/MF A03

NBS-470
Precision Resistors and Their Measurement.
AD-A284 623/6 *02,249* PC A03/MF A01

NBS-512
Methods of Measuring Humidity and Testing Hygrometers.
AD-A278 851/1 *00,123* PC A03/MF A01

NBS-514
Table of Dielectric Constants of Pure Liquids.
AD-A278 956/8 *00,712* PC A04/MF A01

NBS-567
Guide to Instrumentation Literature.
AD-A280 278/3 *02,617* PC A08/MF A02

NBS-569
Fuzed-Quartz Fibers. A Survey of Properties, Applications and Production Methods.
AD-A286 620/0 *00,656* PC A03/MF A01

NBS-652
Air Flow in the Boundary Layer of an Elliptic Cylinder.
AD-A297 391/5 *04,194* PC A03/MF A01

NBS-6728
Cryogenic Research and Development (Quarterly Report Number 1 for Period Ending September 30, 1960).
AD-A280 401/1 *01,456* PC A04/MF A01

NBS-6736
Cryogenic Research and Development (Quarterly Report Number 2 for Period Ending December 31, 1960).
AD-A280 398/9 *01,454* PC A05/MF A01

NBS-6785
Cryogenic Research and Development (June 30, 1961).
AD-A280 679/2 *01,457* PC A04/MF A01

NBS-7219
Cryogenic Research and Development (Progress Report Number 4 for Period Ending December 31, 1961).
AD-A280 399/7 *01,455* PC A04/MF A01
Progress Report to National Aeronautics and Space Administration on Cryogenic Research and Development.
AD-A286 612/7 *01,458* PC A05/MF A01

NBS-9057
Preliminary List of References Containing Compilations of Data on Properties of Materials.
AD-A302 670/5 *03,243* PC A05/MF A01

NBS-9058
Preliminary Subject and Authors Index to Compilations of Data on Properties of Materials.
AD-A302 669/7 *03,242* PC A04/MF A01

NCRP-25
Measurement of Absorbed Dose of Neutrons, and of Mixtures of Neutrons and gamma rays.
AD-A286 647/3 *03,710* PC A05/MF A01

NIH/PUB-95-3727
Hair Testing for Drugs of Abuse: International Research on Standards and Technology.
PB96-120555 *03,504* PC A18/MF A04

NIST/BSS-170
Seismic Performance of Circular Bridge Columns Designed in Accordance with AASHTO/CALTRANS Standards.
PB96-146352 *01,346* PC A07/MF A02

NIST/BSS-172
Methodologies for Predicting the Service Lives of Coating Systems.
PB95-146387 *03,124* PC A05/MF A01

NIST/BSS-173
Heat and Moisture Transfer in Wood-Based Wall Construction: Measured versus Predicted.
PB95-200655 *00,391* PC A05/MF A01

NIST/BSS-175
Performance of Tape-Bonded Seams of EPDM Membranes: Comparison of the Peel Creep-Rupture Response of Tape-Bonded and Liquid-Adhesive-Bonded Seams.
PB96-183249 *03,012* PC A05/MF A01

NIST/GCR-92/603
Concurrent Flow Flame Spread Study.
PB94-156866 *01,356* PC A08/MF A02

NIST/GCR-92/605
Numerical Analysis Support for Compartment Fire Modeling and Incorporation of Heat Conduction into a Zone Fire Model.
PB94-156965 *01,357* PC A04/MF A01

NIST/GCR-92/610-1
Opportunities for Innovation: Advanced Manufacturing Technology.
PB94-100278 *02,801* PC A07/MF A02

NIST/GCR-93/623
Transient Cooling of a Hot Surface by Droplets Evaporation.
PB94-156957 *03,783* PC A08/MF A02

NIST/GCR-93/630
Experimental and Numerical Studies on Two-Dimensional Gravity Currents in a Horizontal Channel.
PB94-165941 *01,359* PC A12/MF A03

NIST/GCR-93/631
Radiation and Mixing Properties of Buoyant Turbulent Diffusion Flames.
PB94-165974 *01,360* PC A04/MF A01

NIST/GCR-93/633
Opportunities for Innovation: Biotechnology.
PB94-157831 *00,009* PC A12/MF A03

NIST-GCR-93-634
Fire Induced Thermal Fields in Window Glass I: Theory.
PB94-139722 *00,328* PC A03/MF A01

NIST/GCR-93/636
Time Dependent Vector Dynamic Programming Algorithm for the Path Planning Problem.
PB94-215688 *03,428* PC A04/MF A01

NIST-GCR-93-637
Computational Model for the Rise and Dispersion of Wind-Blown, Buoyancy-Driven Plumes. Part 2. Linearly Stratified Atmosphere.
PB94-143427 *00,119* PC A03/MF A01

NIST/GCR-93/659
Opportunities for Innovation: Pollution Prevention.
PB95-147146 *02,520* PC A09/MF A02

NIST/GCR-94/638
Turbulent Upward Flame Spread on a Vertical Wall under External Radiation.
PB94-207388 *00,341* PC A05/MF A01

NIST/GCR-94/639
Development of the Fire Data Management System.
PB94-206091 *00,339* PC A03/MF A01

NIST/GCR-94/640-1
Opportunities for Innovation: Advanced Surface Engineering.
PB94-176666 *02,697* PC A09/MF A02

NIST/GCR-94/642
Prediction of Fire Dynamics.
PB94-193620 *00,336* PC A03/MF A01

NIST/GCR-94/643
Mathematical Modeling of Human Egress from Fires in Residential Buildings.
PB94-193778 *00,337* PC A05/MF A02

NIST/GCR-94/644
Fire Propagation in Concurrent Flows.
PB94-193844 *01,365* PC A04/MF A01

NIST/GCR-94/645
Behavior of Charring Materials in Simulated Fire Environments.
PB94-196045 *01,368* PC A99/MF A06

NIST/GCR-94/646
Backdraft Phenomena.
PB94-193927 *01,366* PC A11/MF A03

NIST/GCR-94/647
Fire Growth Models for Materials.
PB94-195856 *01,367* PC A03/MF A01

NIST/GCR-94/648
Upward Flame Spread along the Vertical Corner Walls (October 1993).
PB94-206299 *00,340* PC A03/MF A01

NIST/GCR-94/649
Evaluation and Strengthening Guidelines for Federal Buildings: Identification of Current Federal Agency Programs.
PB94-176278 *00,424* PC A08/MF A02

NIST/GCR-94/650
Evaluation and Strengthening Guidelines for Federal Buildings: Assessment of Current Federal Agency Evaluation Programs and Rehabilitation Criteria and Development of Typical Costs for Seismic Rehabilitation.
PB94-181856 *00,425* PC A08/MF A02

NIST/GCR-94/651
Structure and Radiation Properties of Pool Fires.
PB94-193802 *02,473* PC A08/MF A02

NIST/GCR-94/653
Investigation of Oil and Gas Well Fires and Flares.
PB94-193976 *03,695* PC A04/MF A01

NIST/GCR-94/654
Federal Certification Authority Liability and Policy: Law and Policy of Certificate-Based Public Key and Digital Signatures.
PB94-191202 *01,578* PC A21/MF A04

NIST/GCR-94/656
Human Factors Considerations for the Potential Use of Elevators for Fire Evacuation of FAA Air Traffic Control Towers.
PB94-217163 *01,300* PC A03/MF A01

NIST/GCR-94/657
Framework for Information Technology Integration in Process Plant and Related Industries.
PB94-219086 *02,772* PC A04/MF A01

NIST/GCR-94/658
Opportunities for Innovation: Software for Manufacturing.
PB95-155578 *02,851* PC A09/MF A03

NIST/GCR-94/661
Fundamental Mechanisms for CO and Soot Formation.
PB95-143160 *01,380* PC A08/MF A02

NIST/GCR-94/662
Transient Cooling of a Hot Surface by Droplets Evaporation.
PB95-143194 *03,890* PC A09/MF A02

NIST/GCR-94/663
Network Brokers Handbook: An Entrepreneurial Guide to Cooperative Strategies for Manufacturing Competitiveness.
PB95-219325 *00,490* PC A08/MF A02

NIST/GCR-95/664
Burning Rate and Flame Heat Flux For PMMA in the Cone Calorimeter.
PB95-216990 *00,393* PC A07/MF A02

NIST/GCR-95/665
Water Droplet Evaporation from Radiantly Heated Solids.
PB95-217147 *00,394* PC A08/MF A02

NIST/GCR-95/666
Compartment Fire Combustion Dynamics. Annual Report, September 1, 1993-September 1, 1994.
PB95-217162 *00,203* PC A04/MF A01

NIST/GCR-95/667
Assessment of Site Response Analysis Procedures.
PB95-210928 *00,450* PC A07/MF A02

NIST/GCR-95/669
Turbulent Flame Spread on Vertical Corner Walls.
PB96-114764 *01,403* PC A08/MF A02

NIST/GCR-95/670
Standards Policy and Information Infrastructure.
PB95-231882 *01,485* PC A20/MF A04

NIST/GCR-95/671
Mixing and Radiation Properties of Buoyant Turbulent Diffusion Flames.
PB95-242327 *01,396* PC A05/MF A02

NIST/GCR-95/672
Opportunities for Innovation: Optoelectronics.
PB96-118039 *01,928* PC A19/MF A04

NIST/GCR-95/673
Enhancements to Program IDARC: Modeling Inelastic Behavior of Welded Connections in Steel Moment-Resisting Frames.
PB95-231601 *00,452* PC A05/MF A01

NIST/GCR-95/674
Comparison of the Seismic Provisions of Model Building Codes and Standards to the 1991 NEHRP Recommended Provisions.
PB95-231858 *00,315* PC A05/MF A02

NIST/GCR-95/675
Testability of Object-Oriented Systems.
PB95-242418 *01,733* PC A05/MF A01

NIST/GCR-95/676
New Mass Transport Elements and Components for the NIST IAQ Model.
PB95-255899 *02,558* PC A05/MF A01

NIST/GCR-95/677
Predicting the Ignition Time and Burning Rate of Thermoplastics in the Cone Calorimeter.
PB96-154794 *01,418* PC A10/MF A03

NIST/GCR-95/679
Review of Flows Driven By Natural Convection in Adiabatic Shafts.
PB96-147897 *01,416* PC A04/MF A01

NIST/GCR-95/681
Literature Review on Seismic Performance of Building Cladding Systems.
PB96-106901 *00,455* PC A09/MF A02

NIST/GCR-95/683
Sensitivity Analysis for Mathematical Modeling of Fires in Residential Buildings.
PB96-154968 *00,215* PC A03/MF A01

NIST/GCR-95/684
Enhancement of EXIT89 and Analysis of World Trade Center Data.
PB96-202247 *00,231* PC A04/MF A01

NIST/GCR-95/685
Chemical Inhibition of Methane-Air Diffusion Flame.
PB96-195532 *01,431* PC A04/MF A01

NIST/GCR-96/687
Sparse Water Sprays in Fire Protection.
PB96-202304 *01,433* PC A13/MF A03

NIST/GCR-96/688
Dynamics, Transport and Chemical Kinetics of Compartment Fire Exhaust Gases.
PB96-195508 *00,229* PC A06/MF A01

NIST/GCR-96/690
Preliminary Processing of the Lotung LSST Data.
PB96-165972 *03,690* PC A05/MF A01

NIST/GCR-96/691
Mixing and Radiation Properties of Buoyant Luminous Flame Environments.
PB96-202254 *01,432* PC A06/MF A01

NIST/GCR-96/694
Post-Flame Soot.
PB96-193701 *01,430* PC A04/MF A01

NIST/GCR-96/695
Development of an Economical Video Based Fire Detection and Location System.
PB96-193743 *00,228* PC A05/MF A01

NIST/GCR-96/697
Survey of Fuel Loads in Contemporary Office Buildings.
PB97-114235 *00,233* PC A04/MF A01

NIST/GCR-96/698
Evaluation of Survey Procedures for Determining Occupant Load Factors in Contemporary Office Buildings.
PB97-116222 *00,238* PC A03/MF A01

NIST/GCR-96/700
Estimation of System Damping at the Lotung Site by Application of System Identification.
PB96-214697 *01,351* PC A10/MF A03

NIST/GCR-96/701
Energy-Based Method for Liquefaction Potential Evaluation. Phase 1. Feasibility Study.
PB96-214747 *03,691* PC A13/MF A03

NIST/GCR-96/702
Fire Protection Foam Behavior in a Radiative Environment.
PB97-116131 *00,237* PC A10/MF A02

NIST/GCR-96/703
Full-Scale Room Fire Experiments Conducted at the University of Maryland.
PB97-116081 *00,236* PC A04/MF A01

NIST/HB-44
NIST Handbook 44, 1994: Specifications, Tolerances and Other Technical Requirements for Weighing and Measuring Devices as Adopted by the 78th National Conference on Weights and Measures 1993.
PB94-136009 *02,888* PC A11/MF A03
NIST Handbook 44, 1995: Specifications, Tolerances and Other Technical Requirements for Weighing and Measuring Devices as Adopted by the 79th National Conference on Weights and Measures 1994.
PB95-146379 *02,903* PC A11/MF A03

NIST/HB-105/2
Specifications and Tolerances for Reference Standards and Field Standard Weights and Measures. 2. Specifications and Tolerances for Field Standard Measuring Flasks.
PB96-178926 *02,682* PC A03/MF A01

NIST/HB-130-1995
Uniform Laws and Regulations in the Areas of Legal Metrology and Motor Fuel Quality, 1994 as Adopted by the 79th National Conference on Weights and Measures 1994.
PB95-174470 *02,909* PC A09/MF A02

NIST/HB-130-1996
Uniform Laws and Regulations in the Areas of Legal Metrology and Motor Fuel Quality as Adopted by the 80th National Conference on Weights and Measures 1995. 1996 Edition.
PB96-172309 *02,927* PC A12/MF A03

NIST/HB-133-ED-3-SUP-4
Checking the Net Contents of Packaged Goods as Adopted by the 79th National Conference on Weights and Measures, 1994, Third Edition, Supplement 4.
PB95-182226 *00,484* PC A04/MF A01

NIST/HB-135
Life-Cycle Costing Manual for the Federal Energy Management Program. 1995 Edition.
PB96-172317 *02,511* PC A10/MF A02

NIST/HB-143
State Weights and Measures Laboratories: Program Handbook.
PB96-214705 *02,687* PC A07/MF A02

NIST/HB-150
National Voluntary Laboratory Accreditation Program: Procedures and General Requirements.
PB94-178225 *02,630* PC A03/MF A01

NIST/HB-150/1
National Voluntary Laboratory Accreditation Program: Energy Efficient Lighting Products.
PB94-219060 *02,642* PC A04/MF A01

NIST/HB-150/3
National Voluntary Laboratory Accreditation Program: Bulk Asbestos Analysis.
PB95-138129 *02,541* PC A04/MF A01

NIST/HB-150-4
National Voluntary Laboratory Accreditation Program: Ionizing Radiation Dosimetry.
PB95-128658 *03,623* PC A06/MF A02

NIST/HB-150/5
National Voluntary Laboratory Accreditation Program: Construction Materials Testing.
PB95-155552 *01,319* PC A05/MF A01

NIST/HB-150/6
National Voluntary Laboratory Accreditation Program: Carpet and Carpet Cushion.
PB95-155560 *00,295* PC A04/MF A01

NIST/HB-150/7
National Voluntary Laboratory Accreditation Program: POSIX. Portable Operating System Interface.
PB95-189478 *02,661* PC A05/MF A01

NIST/HB-150-8
National Voluntary Laboratory Accreditation Program Acoustical Testing Services.
PB95-182234 *04,188* PC A05/MF A01

NIST/HB-150-9
National Voluntary Laboratory Accreditation Program (NVLAP): Wood Based Products.
PB95-170429 *03,405* PC A04/MF A01

NIST/HB-150/10
Efficiency of Electric Motors. National Voluntary Lab. Accreditation Program (NVLAP).
PB96-111174 *02,107* PC A05/MF A01

NIST/HB-150-11
National Voluntary Laboratory Accreditation Program: Electromagnetic Compatibility and Telecommunications. FCC Methods.
PB95-242376 *02,664* PC A06/MF A02

NIST/HB-150/12
National Voluntary Laboratory Accreditation Program. GOSIP: Government Open Systems Interconnection Profile.
PB95-267993 *01,486* PC A06/MF A02

NIST/HB-150-13
Airborne Asbestos Analysis: National Voluntary Laboratory Accreditation Program.
PB96-147392 *02,566* PC A05/MF A01

NIST/HB-150-15
National Voluntary Laboratory Accreditation Program: Thermal Insulation Materials.
PB95-267985 *02,977* PC A05/MF A01

NIST/HB-150/16
National Voluntary Laboratory Accreditation Program (NVLAP): Commercial Products Testing.
PB95-267944 *02,671* PC A02/MF A01

NIST/HB-150-18
National Voluntary Laboratory Accreditation Program (NVLAP): Fasteners and Metals.
PB97-114185 *02,881* PC A06/MF A01

NIST/MONO-179
Global Equivalence Ratio Concept and the Prediction of Carbon Monoxide Formation in Enclosure Fires.
PB94-207511 *00,313* PC A08/MF A02

NIST/MONO-180
Gage Block Handbook.
PB95-251716 *02,667* PC A08/MF A02

NIST/PS-20/94
Voluntary Product Standard PS 20-94. American Softwood Lumber Standard.
PB94-162500 *03,402* PC A03/MF A01

NIST-S-PUB-868
Information Infrastructure: Reaching Society's Goals. A Report of the Information Infrastructure Task Force Committee on Applications and Technology.
ED-376 823 *00,131* Not available NTIS

NIST-SP-250-39
NIST Measurement Services: NIST Pressure Calibration Service.
PB94-164043 *02,892* PC A06/MF A02

NIST/SP-260
NIST Standard Reference Materials (Trade Name) Catalog 1995-1996.
PB95-232518 *00,508* PC A03/MF A01

NIST/SP-260/116
Standard Reference Materials: Glass Filters as a Standard Reference Material for Spectrophotometry - Selection, Preparation, Certification, and Use of SRM 930 and SRM 1930.
PB94-188844 *00,536* PC A10/MF A03

NIST-SP-260-120
User's Guide to NIST SRM 2084: CMM Probe Performance Standard.
PB94-206109 *02,709* PC A03/MF A01

NIST/SP-260/121
Standard Reference Materials: Certification of a Standard Reference Material for the Determination of Interstitial Oxygen Concentration in Semiconductor Silicon by Infrared Spectrophotometry.
PB95-125076 *02,326* PC A05/MF A01

NIST/SP-260-122
Standard Reference Materials: Polystyrene Films for Calibrating the Wavelength Scale of Infrared Spectrophotometers - SRM 1921.
PB95-226866 *03,386* PC A03/MF A01

NIST/SP-260-124
Standard Reference Material 1744: Aluminum Freezing-Point Standard.
PB95-251732 *01,055* PC A03/MF A01

NIST-SP-260-125
Statistical Aspects of the Certification of Chemical Batch SRMs. Standard Reference Materials.
PB96-210877 *00,645* PC A05/MF A01

NIST-SP-260-126
NIST Traceable Reference Material Program for Gas Standards: Standard Reference Materials.
PB96-210786 *00,644* PC A04/MF A01

NIST/SP-305/24
Publications of the National Institute of Standards and Technology 1992 Catalog.
PB95-200747 *00,014* PC A17/MF A04

NIST/SP-305/25
Publications of the National Institute of Standards and Technology 1993 Catalog.
PB96-183215 *00,017* PC A11/MF A03

NIST/SP-400-93
Semiconductor Measurement Technology: Design and Testing Guides for the CMOS and Lateral Bipolar-on-SOI Test Library.
PB94-178019 *02,301* PC A07/MF A02

NIST/SP-400-94
Semiconductor Measurement Technology: Improved Characterization and Evaluation Measurements for HgCdTe Detector Materials, Processes, and Devices Used on the GOES and TIROS Satellites.
PB94-188810 *02,122* PC A09/MF A02

NIST/SP-400-95
User's Manual for the Program MONSEL-1: Monte Carlo Simulation of SEM Signals for Linewidth Metrology.
PB95-111522 *02,325* PC A03/MF A01

NIST/SP-400-96
Semiconductor Measurement Technology: HOTPAC. Programs for Thermal Analysis Including Version 3.0 of the TXYZ Program, TXYZ30, and the Thermal MultiLayer Program, TML.
PB95-260766 *02,374* PC A05/MF A01

NIST/SP-400-97
Semiconductor Measurement Technology: Test Structure Implementation Document: DC Parametric Test Structures and Test Methods for Monolithic Microwave Integrated Circuits (MMICs).
PB96-117692 *02,399* PC A05/MF A01

NIST/SP-400-98
Semiconductor Measurement Technology: Survey of Optical Characterization Methods for Materials, Processing, and Manufacturing in the Semiconductor Industry.
PB96-154596 *02,706* PC A05/MF A01

NIST/SP-480/20-ED-1996
Directory of Law Enforcement and Criminal Justice Associations and Research Centers.
PB96-178918 *04,872* PC A05/MF A01

NIST/SP-500/212
Planning for the Fiber Distributed Data Interface (FDDI).
PB94-135761 *01,621* PC A06/MF A02

NIST/SP-500/213
Next Generation Computer Resources: Reference Model for Project Support Environments (Version 2.0).
PB94-143401 *01,677* PC A06/MF A02

NIST/SP-500-215
Second Text REtrieval Conference (TREC-2). Held in Gaithersburg, Maryland on August 31-September 2, 1993.
PB94-178407 *01,686* PC A21/MF A04

NIST-SP-500-216
Proceedings of the Digital Systems Reliability and Nuclear Safety Workshop. Held in Rockville, Maryland on September 13-14, 1993.
NUREG/CP-0136 *03,728* PC A16/MF A03

NIST/SP-500/217
IGOSS-Industry/Government Open Systems Specification.
PB94-207453 *01,806* PC A07/MF A02

NIST/SP-500/218
Analyzing Electronic Commerce.
PB94-219102 *00,480* PC A03/MF A01

NIST/SP-500/219
NIST Workshop on the Computer Interface to Flat Panel Displays. Held in San Jose, California on January 13-14, 1994.
PB95-136388 *01,625* PC A11/MF A03

NIST/SP-500/220
Guide on Open System Environment (OSE) Procurements.
PB95-169496 *01,626* PC A08/MF A02

NIST/SP-500/221
User Study: Informational Needs of Remote National Archives and Records Administration Customers.
PB95-154738 *02,725* PC A06/MF A02

NIST/SP-500/222
Glossary of Software Reuse Terms.
PB95-178992 *01,720* PC A03/MF A01

NIST/SP-500/223
Framework for the Development and Assurance of High Integrity Software.
PB95-173084 *01,716* PC A05/MF A01

NIST/SP-500/225
Overview of the Text REtrieval Conference (3rd) (TREC-3). Held in Gaithersburg, Maryland on November 2-4, 1994.
PB95-216883 *01,728* PC A25/MF A06

NIST/SP-500/226
Self Monitoring Accounting Systems.
PB95-216602 *00,007* PC A03/MF A01

NIST/SP-500/227
Electronic Access: Blueprint for the National Archives and Records Administration.
PB95-219218 *02,731* PC A04/MF A01

NIST/SP-500/228
Guidelines for the Evaluation of X.500 Directory Products.
PB95-231908 *02,732* PC A04/MF A01

NIST/SP-500/229
Z39.50 Implementation Experiences.
PB96-114939 *01,816* PC A07/MF A02

NIST/SP-500/230
Application Portability Profile (APP): The U.S. Government's Open System Environment Profile Version 3.0.
PB96-158712 *01,753* PC A07/MF A02

NIST/SP-500/231
Guidelines for the Evaluation of Electronic Data Interchange Products.
PB96-172325 *01,506* PC A05/MF A01

NIST/SP-500/232
Open System Environment (OSE): Architectural Framework for Information Infrastructure.
PB96-146360 *00,002* PC A04/MF A01

NIST/SP-500-233
Manager's Guide for Monitoring Data Integrity in Financial Systems.
PB96-165915 *00,003* PC A05/MF A01

NIST/SP-500-234
Reference Information for the Software Verification and Validation Process.
PB96-188164 *01,773* PC A06/MF A01

NIST/SP-500/235
Structured Testing: A Testing Methodology Using the Cyclomatic Complexity Metric.
PB97-114169 *01,784* PC A07/MF A02

NIST/SP-500-236
Text REtrieval Conference (4th) (TREC-4). Held in Gaithersburg, Maryland on November 1-3, 1995.
PB97-121636 *01,786* PC A99/MF E08

NIST/SP-777-94-ED
NIST Serial Holdings, 1994.
PB94-178068 *02,745* PC A12/MF A03

NIST/SP-777-95
NIST Serial Holdings, 1995.
PB95-188926 *02,746* PC A12/MF A03

NIST/SP-782
NIST Standard Reference Data Products Catalog, 1995-96. Achieve with Standard Reference Data.
PB95-260808 *01,057* PC A03/MF A01

NIST/SP-782-1994ED
NIST Standard Reference Data Products Catalog, 1994.
PB94-151842 *00,727* PC A06/MF A02

NIST/SP-791
State Weights and Measures Laboratories: State Standards Program Description and Directory. 1994 Edition.
PB94-207727 *02,895* PC A07/MF A02

NIST/SP-800/7
Security in Open Systems.
PB95-105383 *01,473* PC A13/MF A03

NIST/SP-800/9
Good Security Practices for Electronic Commerce, Including Electronic Data Interchange.
PB94-139045 *01,463* PC A04/MF A01

NIST/SP-800/10
Keeping Your Site Comfortably Secure: An Introduction to Internet Firewalls.
PB95-182275 *02,730* PC A05/MF A01

NIST/SP-800/11
Impact of the FCC's Open Network Architecture on NS/NP Telecommunications Security.
PB95-189445 *01,483* PC A03/MF A01

NIST/SP-800/12
Computer Security: An Introduction to Computer Security. The NIST Handbook.
PB96-131610 *01,608* PC A13/MF A03

NIST/SP-800/13
Telecommunications Security Guidelines for Telecommunications Management Network. Computer Security.
PB96-139415 *01,496* PC A03/MF A01

NIST/SP-800/14
Computer Security: Generally Accepted Principles and Practices for Securing Information Technology Systems.
PB97-110811 *01,619* PC A05/MF A01

NIST/SP-810-ED-1994
National Voluntary Laboratory Accreditation Program 1994 Directory.
PB94-178969 *00,482* PC A08/MF A02

NIST/SP-810-ED-1995
National Voluntary Laboratory Accreditation Program 1995 Directory.
PB95-174454 *00,483* PC A08/MF A02

NIST/SP-810-ED-1996
National Voluntary Laboratory Accreditation Program 1996 Directory.
PB96-162714 *00,485* PC A10/MF A03

NIST-SP-811

Guide for the Use of the International System of Units (SI).
PB95-226692 *02,747* PC A05/MF A01

NIST/SP-823/5

North American ISDN Users' Forum Agreements on Integrated Services Digital Network.
PB94-162559 *01,466* PC A16/MF A03

NIST/SP-823/6

ISDN Conformance Testing Guidelines: Guidelines for Implementors of ISDN Customer Premises Equipment to Conform to Both National ISDN-1 and North American ISDN Users' Forum Layer 3 Basic Rate Interface Basic Call Control Abstract Test Suites.
PB94-219094 *01,471* PC A03/MF A01

NIST/SP-837

Science, Technology, and Competitiveness: Retrospective on a Symposium in Celebration of NIST's 90th Anniversary and the 25th Anniversary of the Gaithersburg Laboratories, November 14-15, 1991.
PB97-121610 *02,696* PC A08/MF A02

NIST/SP-838/5

Project Summaries 1994: NIST Building and Fire Research Laboratory.
PB94-207495 *00,343* PC A08/MF A02

NIST/SP-838/6

Building and Fire Research Laboratory Publications, 1993.
PB95-143202 *00,369* PC A06/MF A02

NIST/SP-838/7

Building and Fire Research Laboratory Publications, 1994.
PB95-226684 *00,398* PC A07/MF A02

NIST/SP-838/8

Project Summaries 1995: NIST Building and Fire Research Laboratory.
PB95-270047 *00,400* PC A10/MF A03

NIST/SP-838/9

Publications 1995: NIST Building and Fire Research Laboratory.
PB96-183074 *00,226* PC A08/MF A02

NIST/SP-854

Report of the National Conference on Weight and Measures (78th). Held in Kansas City, MO. on July 18-22, 1993.
PB94-138989 *02,623* PC A18/MF A04

NIST/SP-856

Electroacoustics for Characterization of Particulates and Suspensions. Proceedings of a Workshop. Held in Gaithersburg, Maryland on February 3-4, 1993.
PB94-112695 *00,725* PC A15/MF A03

NIST/SP-857

Putting the Information Infrastructure to Work: Report of the Information Infrastructure Task Force Committee on Applications and Technology.
N94-31228/7 *02,715* PC A06/MF A02
Putting the Information Infrastructure to Work: Report of the Information Infrastructure Task Force Committee on Applications and Technology.
PB94-163383 *00,001* PC A06/MF A02

NIST-SP-859

Abstract and Index Collection in the Research Information Center of the National Institute of Standards and Technology.
PB94-152204 *02,744* PC A03/MF A01

NIST/SP-860

Advanced Components for Electric and Hybrid Electric Vehicles. Workshop Proceedings. Held in Gaithersburg, Maryland on October 27-28, 1993.
PB94-177060 *04,858* PC A10/MF A03

NIST/SP-861

Evaluation of Alternative In-Flight Fire Suppressants for Full-Scale Testing in Simulated Aircraft Engine Nacelles and Dry Bays.
PB94-203403 *00,023* PC A99/MF E08

NIST/SP-862

Northridge Earthquake 1994: Performance of Structures, Lifelines, and Fire Protection Systems.
PB94-207461 *04,825* PC A09/MF A02

NIST/SP-863

U.S. Green Building Conference, 1994.
PB94-206364 *02,519* PC A08/MF A02

NIST/SP-864

Technical Digest: Symposium on Optical Fiber Measurements (8th), 1994. Held in Boulder, Colorado on September 13-15, 1994.
PB94-207636 *04,231* PC A10/MF A03

NIST/SP-865

NIST Workshop on Gas Sensors: Strategies for Future Technologies. Proceedings of a Workshop. Held in Gaithersburg, Maryland on September 8-9, 1993.
PB95-210225 *00,507* PC A08/MF A02

NIST/SP-866

Extreme Value Theory and Applications: Proceedings of the Conference on Extreme Value Theory and Applications, Volume 3. Held in Gaithersburg, Maryland in May 1993.
PB95-104956 *03,432* PC A11/MF A03

NIST/SP-867

In Situ Burning Oil Spill Workshop Proceedings. Held in Orlando, Florida on January 26-28, 1994.
PB95-104907 *02,583* PC A06/MF A02

NIST/SP-868

Information Infrastructure: Reaching Society's Goals. Report of the Information Infrastructure Task Force Committee on Applications and Technology.
PB94-214756 *01,469* PC A08/MF A02

NIST/SP-869

Databases Available in the Research Information Center of the National Institute of Standards and Technology.
PB95-128641 *02,724* PC A08/MF A01

NIST/SP-870

Report of the National Conference on Weights and Measures (79th). Held in San Diego, California on July 17-21, 1994.
PB95-169819 *02,656* PC A20/MF A04

NIST/SP-871

Wind and Seismic Effects. Proceedings of the U.S.-Japan Cooperative Program in Natural Resources Panel on Wind and Seismic Effects (26th). Held in Gaithersburg, Maryland on May 17-20, 1994.
PB95-147385 *00,433* PC A99/MF A06

NIST/SP-872

NIST Industrial Impacts: A Sampling of Successful Partnerships.
PB95-111514 *00,488* PC A05/MF A01

NIST/SP-872-REV-1-95

NIST Industrial Impacts: A Sampling of Successful Partnerships (Revision, March 1995).
PB95-209193 *00,489* PC A05/MF A01

NIST/SP-873

Joint DoD/NIST Workshop on International Manufacturing Systems Research and Development. Held in Rockville, Maryland on November 3-5, 1992. Proceedings.
PB96-109491 *02,931* PC A11/MF A03

NIST/SP-874

Methods for Analysis of Cancer Chemopreventive Agents in Human Serum.
PB95-200648 *03,502* PC A07/MF A02

NIST/SP-876

Boundary Lubrication of Silicon Nitride.
PB95-213583 *03,226* PC A18/MF A04

NIST/SP-877

Proceedings of the Manufacturing Technology Needs and Issues: Establishing National Priorities and Strategies Conference. Held in Gaithersburg, Maryland on April 26-28, 1994.
PB95-206181 *02,930* PC A22/MF A04

NIST/SP-879

Ceramic Powders Characterization: Results of an International Laboratory Study.
PB95-270039 *02,672* PC A22/MF A04

NIST/SP-881/1

Federal Implementation Guideline for Electronic Data Interchange: ASC X12 003040 Transaction Set 838 Trading Partner Profile (Vendor Registration), Implementation Convention.
PB96-112651 *03,674* PC A04/MF A01

NIST/SP-881/2

Federal Implementation Guideline for Electronic Data Interchange: ASC X12 003040 Transaction Set 838 Trading Partner Profile (Confirmation of Vendor Registration). Implementation Convention.
PB96-111190 *01,813* PC A03/MF A01

NIST/SP-881/3

Federal Implementation Guideline for Electronic Data Interchange. ASC X12 003050 Transaction Set 850 Award Instrument. Implementation Convention.
PB96-114913 *01,814* PC A11/MF A03

NIST/SP-881-4

Federal Implementation Guideline for Electronic Data Interchange. ASC X12 003050 Transaction Set 860 Modifications to Award Instrument. Implementation Convention.
PB96-114921 *01,815* PC A11/MF A03

NIST/SP-881-5

Federal Implementaion Guideline for Eletronic Data Interchange. ASC X12 003050 Transaction Set 865 Purchase Order Change Acknowledgement/Request - Seller Initiated. Implementation Convention.
PB96-172549 *01,825* PC A09/MF A02

NIST/SP-881/6

Federal Implementation Guideline for Electronic Data Interchange. ASC X12 003050 Transaction Set 855 Purchase Order Acknowledgment: Implementation Convention.
PB96-172374 *01,823* PC A04/MF A01

NIST/SP-881-7

Federal Implementation Guideline for Electronic Data Interchange. ASC X12 003050 Transaction Set 843 Response to Request for Quotation. Implementation Convention.
PB96-168984 *01,822* PC A09/MF A02

NIST/SP-881-8

Federal Implementation Guideline for Electronic Data Interchange. ASC X12 003050 Transaction Set 840 Request for Quotation. Implementation Convention.
PB96-172531 *01,824* PC A10/MF A03

NIST/SP-881/9

Federal Implementation Guideline for Electronic Data Interchange: ASC X12 003050 Transaction Set 836 Procurement Notices. Implementation Convention.
PB96-178892 *01,827* PC A04/MF A01

NIST/SP-882

Conceptual Design Plan for the National Advanced Manufacturing Testbed.
PB95-231866 *02,828* PC A05/MF A01

NIST/SP-884

Abstract and Index Collection in the Research Information Center of the National Institute of Standards and Technology.
PB95-232633 *02,741* PC A03/MF A01

NIST/SP-885

Proceedings of the Applied Diamond Conference 1995: Applications of Diamond Films and Related Materials International Conference (3rd). Held in Gaithersburg, Maryland, on August 21-24, 1995.
PB95-255204 *04,701* PC A99/MF E11

NIST/SP-886

Proceedings of the Annual Manufacturing Technology Conference (2nd): Toward a Common Agenda. Held in Gaithersburg, Maryland on April 18-20, 1995.
PB96-112693 *02,887* PC A99/MF E08

NIST/SP-887

Composite Materials for Offshore Operations: Proceedings of the International Workshop (1st). Held in Houston, Texas on October 26-28, 1993.
PB96-109509 *03,169* PC A17/MF A04

NIST/SP-888

International Green Building Conference and Exposition (2nd). Held in Big Sky, Montana on August 13-15, 1995.
PB95-253605 *02,525* PC A04/MF A01

NIST/SP-889

Post-Earthquake Fire and Lifelines Workshop. Held in Long Beach, California on January 30-31, 1995. Proceedings.
PB96-117916 *00,209* PC A04/MF A01

NIST/SP-890-V1

Fire Suppression System Performance of Alternative Agents in Aircraft Engine and Dry Bay Laboratory Simulations. SP890: Volume 1.
PB96-117775 *03,277* PC A99/MF E08

NIST/SP-890-V2

Fire Suppression System Performance of Alternative Agents in Aircraft Engine and Dry Bay Laboratory Simulations. SP 890: Volume 2.
PB96-117783 *03,278* PC A99/MF A06

NIST/SP-891

Standards Setting in the European Union: Standards Organization and Officials in EU Standards Activities.
PB96-115019 *02,919* PC A04/MF A01

NIST/SP-893

Glimpse of Materials Research in China: A Report from an Interagency Study Team on Materials Visiting China from June 19, 1995 to June 30, 1995.
PB96-112677 *02,978* PC A11/MF A03

NIST/SP-894

Report of the National Conference on Weights and Measures (80th) as Adopted by the 80th National Conference on Weights and Measures, 1995. Held in Portland, Maine on July 16-20, 1995.
PB96-165840 *02,681* PC A15/MF A03

NIST/SP-895

Databases Available in the Research Information Center of the National Institute of Standards and Technology (December 1995).
PB96-139407 *02,734* PC A07/MF A02

NIST/SP-896

Conference Proceedings: International Workshop on Instrumented Indentation. Held in San Diego, California on April 22-23, 1995.
PB96-158688 *01,948* PC A06/MF A01

NIST/SP-897

Working Conference on Global Growth of Technology: Is America Prepared. Held in Gaithersburg, Maryland on December 7, 1995.
PB96-210059 *00,018* PC A07/MF A02

NIST/SP-898

Innovation in the Japanese Construction Industry: A 1995 Appraisal.
PB96-177373 *00,225* PC A13/MF A03

NIST/SP-901

January 17, 1995 Hyogoken-Nanbu (Kobe) Earthquake. Performance of Structures, Lifelines and Fire Protection Systems. Executive Summary and Paper.
PB97-104160 *00,475* PC A99/MF A06

NIST/SP-902

Proceedings of the Open Forum on Laboratory Accreditation at the National Institute of Standards and Technology, October 13, 1995.
PB96-210141 *02,686* PC A10/MF A03

NIST/SP-903

Directory of U.S. Private Sector Product Certification Programs.
PB96-215074 *02,688* PC A20/MF A04

NIST/SP-904

Wind and Seismic Effects: Proceedings of the Joint Meeting of the U.S.-Japan Cooperative Program in Natural Resources Panel on Wind and Seismic Effects (28th). Held in Gaithersburg, Maryland on May 14-17, 1996.
PB97-104376 *00,476* PC A99/MF A06

NIST/SP-905

Technical Digest: Symposium on Optical Fiber Measurements (9th), 1996. Held in Boulder, Colorado on October 1-3, 1996.
PB97-108583 *04,383* PC A12/MF A03

NIST/SP-908

International Green Building Conference and Exposition (3rd). Held in San Diego, California on November 17-19, 1996. (Reannouncement with new abstract).
PB97-121826 *02,531* PC A12/MF A03

NIST/SW/DK-94/001

HAZARD I Fire Hazard Assessment Method (Version 1.2) (for Microcomputers).
PB94-501988 *00,196* Diskette $250.00

NIST/SW/DK-94/002
HAZARD I Fire Hazard Assessment Method, Version 1.2 (Upgrade Package) (for Microcomputers).
PB94-501996 *00,197* CP D99

NIST/SW/DK-94/003
Building Life Cycle Cost Computer Program (BLCC), Version 4.2-95 (for Microcomputers).
PB95-501953 *00,266* CP D02

NIST/SW/DK-95/002
Building Life Cycle Cost Computer Program (BLCC) Version 4.21-95 (for Microcomputers).
PB95-502779 *00,267* CP D02
Building Life Cycle Cost Computer Program (BLCC) Version 4.22-95 (for Microcomputers).
PB95-503397 *00,268* CP D02

NIST/SW/MT-93/008
FORTRAN Compiler Validation System, Version 2.1.
PB94-500691 *01,698* CP T99

NIST/TN-1297
Guidelines for Evaluating and Expressing the Uncertainty of NIST Measurement Results. 1994 Edition.
PB95-143087 *02,649* PC A03/MF A01

NIST/TN-1354
NIST 60-Millimeter Diameter Cylindrical Cavity Resonator: Performance Evaluation for Permittivity Measurements.
PB94-151776 *02,251* PC A11/MF A03

NIST/TN-1355-R
Transmission/Reflection and Short-Circuit Line Methods for Measuring Permittivity and Permeability.
PB94-165537 *02,211* PC A06/MF A02

NIST/TN-1357
Coaxial Reference Standard for Microwave Power.
PB94-193786 *01,880* PC A04/MF A01

NIST/TN-1361
Aperture Excitation of Electrically Large, Lossy Cavities.
PB94-145711 *00,029* PC A05/MF A01

NIST/TN-1363
Cryogenic Properties of Silver.
PB94-203593 *03,330* PC A03

NIST/TN-1364
Uncertainty Analysis of the NIST Nitrogen Flow Facility.
PB95-128906 *02,608* PC A04/MF A01

NIST/TN-1365
Sub-Doppler Frequency Measurements on OCS at 87 Thz (3.4 micrometers) with the CO Overtone Laser: Considerations and Details.
PB95-128633 *04,255* PC A03/MF A01

NIST/TN-1366
Analytical Estimation of Carrier Multipath Bias on GPS Position Measurements
PB94-215712 *04,845* PC A04/MF A01

NIST/TN-1367
Flow Conditioner Tests for Three Orifice Flowmeter Sizes.
PB95-105540 *04,201* PC A05/MF A01

NIST/TN-1369
Video Microscopy Applied to Optical Fiber Geometry Measurements.
PB95-173068 *04,295* PC A04/MF A01

NIST/TN-1371
Effective Medium Theory for Ferrite-Loaded Materials.
PB95-154662 *01,893* PC A03/MF A01

NIST/TN-1372
Assessment of Data by a Second-Order Transfer Function.
PB95-182390 *03,760* PC A05/MF A01

NIST/TN-1373
Spherical-Wave Source-Scattering Matrix Analysis of Antennas and Antenna-Antenna Interactions.
PB96-111166 *02,008* PC A08/MF A02

NIST/TN-1374
Calibration Service for Coaxial Reference Standards for Microwave Power.
PB96-162722 *01,958* PC A07/MF A02

NIST/TN-1375
Band-Limited, White Gaussian Noise Excitation for Reverberation Chambers and Applications to Radiated Susceptibility Testing.
PB96-165410 *01,960* PC A07/MF A02

NIST/TN-1376
Optical Detector Nonlinearity: Simulation.
PB96-165378 *02,199* PC A04/MF A01

NIST/TN-1377
Radiated Emissions and Immunity of Microstrip Transmission Lines: Theory and Measurements.
PB96-162649 *02,238* PC A04/MF A01

NIST/TN-1378
Optical Fiber, Fiber Coating, and Connector Ferrule Geometry: Results of Interlaboratory Measurement Comparisons.
PB96-154422 *04,360* PC A05/MF A01

NIST/TN-1379
Direct Comparison Transfer of Microwave Power Sensor Calibrations.
PB96-158654 *02,086* PC A03/MF A01

NIST/TN-1380
Trapped Ions and Laser Cooling 4: Selected Publications of the Ion Storage Group of the Time and Frequency Division, NIST, Boulder, Colorado.
PB96-172358 *04,108* PC A11/MF A03

NIST/TN-1381
Rapid Evaluation of Mode-Stirred Chambers Using Impulsive Waveforms.
PB96-210026 *01,979* PC A04/MF A01

NIST/TN-1382
Standard Source Method for Reducing Antenna Factor Errors in Shielded Room Measurements.
PB96-183157 *02,013* PC A04/MF A01

NIST/TN-1406
Fire Safety of Passenger Trains: A Review of Current Approaches and of New Concepts.
PB94-152006 *04,848* PC A11/MF A03

NIST/TN-1407
Fire Data Management System, FDMS 2.0, Technical Documentation.
PB94-164019 *01,358* PC A05/MF A01

NIST/TN-1408
Summary Report of NIST's Industry-Government Consortium Research Program on Flowmeter Installation Effects: The 45 Degree Elbow.
PB95-143061 *04,204* PC A06/MF A02

NIST/TN-1409
Laser Doppler Velocimeter Studies of the Pipeflow Produced by a Generic Header.
PB95-226916 *02,602* PC A05/MF A01

NIST/TN-1410
Measuring Long Gage Blocks with the NIST Line Scale Interferometer.
PB95-242400 *02,665* PC A03/MF A01

NIST/TN-1411
Reproducibility of the Temperature of the Ice Point in Routine Measurements.
PB95-255923 *04,015* PC A03/MF A01

NIST/TN-1412
Thermochemical and Chemical Kinetic Data for Fluorinated Hydrocarbons.
PB95-260618 *01,056* PC A09/MF A02

NIST/TN-1413
45 deg/0 deg Reflectance Factors of Pressed Polytetrafluoroethylene (PTFE) Powder.
PB95-260758 *04,328* PC A06/MF A02

NIST/TN-1414
Liquid-Nitrogen-Cooled High Tc Electrical Substitution Radiometer as a Broadband IR Transfer Standard.
PB96-158704 *02,198* PC A03/MF A01

NIST/TN-1416
Estimates of Hurricane Wind Speeds by the 'Peaks Over Threshold' Method.
PB96-162540 *00,471* PC A04/MF A01

NIST/TN-1417
NIST Measurement Assurance Program for Capacitance Standards at 1 kHz.
PB96-172333 *02,276* PC A03/MF A01

NIST/TN-1418
Probabilistic Estimates of Design Load Factors for Wind-Sensitive Structures Using the 'Peaks Over Threshold' Approach.
PB96-183223 *00,474* PC A04/MF A01

NIST/TN-1419
Flowmeter Installation Effects Due to a Generic Header.
PB96-210893 *02,606* PC A07/MF A02

NIST/TN-1420
NIST High-Accuracy Sampling Wattmeter.
PB97-108575 *02,689* PC A04/MF A01

NIST/TN-1421
National Measurement System for Radiometry, Photometry, and Pyrometry Base Upon Absolute Detectors.
PB97-108559 *04,382* PC A04/MF A01

NIST92DDI510-5-1.11
Ada Compiler Validation Summary Report. Certificate Number: 931119S1.11332, DDC-I, Inc. DACS MIPS R3000 Bare Ada Cross Compiler System, Version 4.7.1 Sun SPARCstation IPX => DACS Sun SPARC/SunOS to MIPS R3000 Bare Instruction Set Architecture Simulator, Version 4.7.1.
AD-A276 181/5 *01,641* PC A04/MF A01

NISTIR/GCR-95/680
National Construction Sector Goals: Industry Strategies for Implementation.
PB95-269817 *00,204* PC A03/MF A01

NISTIR-85-3273-8
Energy Prices and Discount Factors for Life-Cycle Cost Analysis 1994. Annual Supplement to NIST Handbook 135 and NBS Special Publication 709.
PB94-206018 *02,508* PC A04/MF A01

NISTIR-85/3273-9
Energy Price Indices and Discount Factors for Life-Cycle Cost Analysis 1995. Annual Supplement to NIST Handbook 135 and NBS Special Publication 709. (Revised).
PB95-105011 *02,509* PC A04/MF A01

NISTIR-85/3273-10
Energy Price Indices and Discount Factors for Life-Cycle Cost Analysis 1996. Annual Supplement to NIST Handbook 135 and NBS Special Publication 709. (Revised).
PB96-162441 *02,510* PC A05/MF A01

NISTIR-85-3273-11
Energy Price Indices and Discount Factors for Life-Cycle Cost Analysis 1997. Annual Supplement to NIST Handbook 135 and NBS Special Publication 709. (Revised).
PB96-210745 *02,512* PC A05/MF A01

NISTIR-89-4157
Development and Characterization of Insulating Layers on Silicon Carbide: Annual Report for February 14, 1988 to February 14, 1989.
PB94-155579 *02,295* PC A03/MF A01

NISTIR-89/4213
Earthquake Resistant Construction of Electric Transmission and Telecommunication Facilities Serving the Federal Government Report.
PB94-161817 *02,460* PC A03/MF A01

NISTIR-89/4214
Factors Significant to Precracking of Fracture Specimens.
PB96-109558 *03,358* PC A06/MF A02

NISTIR-3976
Droplet Transfer Modes for a MIL 100S-1 GMAW Electrode.
PB95-209300 *02,867* PC A04/MF A01

NISTIR-3977
Alternating-Field Susceptometry and Magnetic Susceptibility of Supercondoctors. Presented at Office of Naval Research Workshop on Magnetic Susceptibility of Superconductors and Other Spin Systems. Held in Berkeley Springs, West Virginia on 20 May 1991.
PB94-145984 *04,435* PC A01/MF A01

NISTIR-3993
Bibliography of the NIST Electromagnetic Fields Division Publications.
PB94-165990 *01,875* PC A06/MF A02

NISTIR-3994
Metrology for Electromagnetic Technology: A Bibliography of NIST Publications.
PB94-159761 *02,116* PC A04/MF A01

NISTIR-4333
National Type Evaluation Program: Index of Device Evaluations by Company. NCWM Publication 5 Part A (Second Edition).
PB94-160835 *02,889* PC A05/MF A01

NISTIR-4419
Seismic Instrumentation of Existing Buildings.
PB94-159779 *00,420* PC A04/MF A01

NISTIR-4440
Summaries of Center for Fire Research In-House Projects and Grants: 1990.
PB94-160876 *00,286* PC A10/MF A03

NISTIR-4443
Sulfur Dioxide Capture in the Combustion of Mixtures of Lime, Refuse-Derived Fuel, and Coal.
PB94-155587 *02,534* PC A04/MF A01

NISTIR-4489
Fire Growth Analysis of the Fire of March 20, 1990, Pulaski Building, 20 Massachusetts Avenue, N.W., Washington, DC.
PB94-205952 *00,194* PC A03/MF A01

NISTIR-4490
Review of Mathematical Function Library for Microsoft-FORTRAN, John Wiley and Sons, 1989.
PB94-160793 *01,679* PC A03/MF A01

NISTIR-4493
NVLAP Procedures U.S. Code of Federal Regulations. Title 15, Subtitle A, Chapter 2, Part 7. (Effective December 1984; Amended September 1990).
PB94-160850 *02,627* PC A03/MF A01

NISTIR-4498
Cylinder Wipe Air-Drying Intaglio Ink Vehicles for U.S. Currency Inks.
PB94-160801 *03,115* PC A03/MF A01

NISTIR-4548
Center for Electronics and Electrical Engineering Technical Progress Bulletin Covering Center Programs, October to December, with 1991 CEEE Events Calendar.
PB94-159787 *02,296* PC A03/MF A01

NISTIR-4568
Comparison of Finite Element and Analytic Calculations of the Resonant Modes and Frequencies of a Thick Shell Sphere.
PB94-160785 *02,626* PC A03/MF A01

NISTIR-4621
Electronics and Electrical Engineering Laboratory Technical Progress Bulletin Covering Laboratory Programs, January to March 1991, with 1991 EEEL Events Calendar.
PB94-145968 *02,113* PC A03/MF A01

NISTIR-4638
Performance Approach to the Development of Criteria for Low-Sloped Roof Membranes.
PB94-160751 *00,329* PC A03/MF A01

NISTIR-4646
Guide to Configuration Management and the Revision Control System for Testbed Users.
PB94-150919 *01,678* PC A03/MF A01

NISTIR-4670
Electronics and Electrical Engineering Laboratory Technical Progress Bulletin Covering Laboratory Programs, April to June 1991, with 1992 EEEL Events Calendar.
PB95-209821 *01,916* PC A03/MF A01

NISTIR-4676
Validation Testing System Requirements. National PDES Testbed Report Series.
PB94-163482 *02,771* PC A03/MF A01

NISTIR-4711
Optical Performance of Commercial Windows.
PB95-208757 *00,392* PC A09/MF A02

NISTIR-4721
Questions and Answers on Quality, the ISO 9000 Standard Series, Quality System Registration, and Related Issues. More Questions and Answers on the ISO 9000 Standard Series and Related Issues.
PB95-103461 *00,495* PC A03/MF A01

NISTIR-4738
Models, Managing Models, Quality Models: An Example of Quality Management.
PB94-163466 *02,891* PC A03/MF A01

NISTIR-4755
Issues and Recommendations for a STEP Application Protocol Framework. National PDES Testbed.
PB94-160868 *02,770* PC A05/MF A01

NISTIR-4779
Summary Report of NIST's Industry-Government Consortium Research Program on Flowmeter Installation Effects with Emphasis on the Research Period, January-September 1991: The Reducer.
PB94-160736 *04,196* PC A04/MF A01

NISTIR-4790
Microstructural Features of Some Low Water/Solids, Silica Fume Mortars Cured at Different Temperatures.
PB94-160777 *00,330* PC A03/MF A01

NISTIR-4795
Earthquake Resistant Construction of Gas and Liquid Fuel Pipeline Systems Serving, or Regulated By, the Federal Government.
PB94-161999 *04,846* PC A05/MF A01

NISTIR-4804
Issues Concerning Material Removal Shape Element Volumes (MRSEVs).
PB95-210167 *02,885* PC A03/MF A01

NISTIR-4841
Properties and Interactions of Oral Structures and Restorative Materials. Annual Report for Period October 1, 1990 to September 30, 1991.
PB94-160843 *03,558* PC A06/MF A01

NISTIR-4859
Time-Perturbation Tuning of MIMD Programs.
PB94-164399 *01,681* PC A03/MF A01

NISTIR-4870
Feasibility and Design Considerations of Emergency Evacuation by Elevators.
PB94-163441 *00,287* PC A07/MF A02

NISTIR-4877
Room-Temperature Flexure Fixture for Advanced Ceramics.
PB95-210498 *03,061* PC A03/MF A01

NISTIR-4888
NIST Support to the Next Generation Controller Program: 1991 Final Technical Report.
PB94-163490 *02,808* PC A09/MF A02

NISTIR-4889
Design Guide for CMOS-On-SIMOX. Test Chips NIST3 and NIST4.
PB94-163458 *02,297* PC A05/MF A01

NISTIR-4894
Computation of Dendrites Using a Phase Field Model.
PB94-160744 *04,436* PC A03/MF A01

NISTIR-4895
Study to Determine the Most Important Parameters for Evaluating the Resistance of Soft Body Armor to Penetration by Edged Weapons.
PB94-158573 *03,757* PC A03/MF A01

NISTIR-4901
Electronics and Electrical Engineering Laboratory Technical Progress Bulletin Covering Laboratory Programs, January to March 1992, with 1992/1993 EEEL Events Calendar.
PB95-210480 *01,917* PC A03/MF A01

NISTIR-4903
Structural EXPRESS Editor.
PB94-159795 *02,769* PC A04/MF A01

NISTIR-4904
Compatibility Analysis of the ANSI and ISO IRDS Services Interfaces.
PB94-163474 *01,805* PC A06/MF A02

NISTIR-4942-2
Present Worth Factors for Life-Cycle Cost Studies in the Department of Defense (1995).
PB95-105029 *03,664* PC A04/MF A01

NISTIR-4942-3
Present Worth Factors for Life-Cycle Cost Studies in the Department of Defense (1996).
PB96-106869 *03,673* PC A04/MF A01

NISTIR-4974
Publications of the Manufacturing Engineering Laboratory Covering the Period January 1989-September 1992.
PB94-165966 *02,750* PC A06/MF A02

NISTIR-4981
Controlling Moisture in the Walls of Manufactured Housing.
PB95-105136 *00,355* PC A03/MF A01

NISTIR-5002
TEM/Reverberating Chamber Electromagnetic Radiation Test Facility at Rome Laboratory.
PB96-155023 *03,675* PC A05/MF A01

NISTIR-5013
Electromechanical properties of superconductors for DOE fusion applications.
DE95015476 *04,432* PC A04/MF A01
Electromechanical Properties of Superconductors for DOE Fusion Applications.
PB94-139672 *02,250* PC A06/MF A02

NISTIR-5015
Crosstalk between Microstrip Transmission Lines.
PB94-135639 *02,210* PC A03/MF A01

NISTIR-5016
NIST Model PM2 Power Measurement System for 1 mW at 1 GHz.
PB94-135803 *02,018* PC A03/MF A01

NISTIR-5018
Optical Fiber Sensors: Accelerating Applications in Navy Ships.
PB94-186848 *02,632* PC A06/MF A02

NISTIR-5022
RangeCAD and the NIST RCS Uncertainty Analysis.
PB94-218591 *01,870* PC A03/MF A01

NISTIR-5023
Measurements of Shielding Effectiveness and Cavity Characteristics of Airplanes.
PB94-210051 *00,030* PC A04/MF A01

NISTIR-5024
Composite Struts for SMES Plants.
PB95-155586 *02,507* PC A99/MF A06

NISTIR-5025
Irradiation Damage in Inorganic Insulation Materials for ITER Magnets: A Review.
PB95-147351 *03,705* PC A18/MF A04

NISTIR-5026
Thermal Hydraulic Tests of a Liquid Hydrogen Cold Neutron Source.
PB95-135570 *03,884* PC A03/MF A01

NISTIR-5027
Superconductor Critical Current Standards for Fusion Applications. Final Progress Report, October 1993-July 1994.
PB95-169538 *02,222* PC A05/MF A02

NISTIR-5028
Bibliography of the NIST Electromagnetic Fields Division Publications.
PB95-135562 *01,886* PC A06/MF A02

NISTIR-5029
Metrology for Electromagnetic Technology: A Bibliography of NIST Publications.
PB95-135588 *02,143* PC A05/MF A01

NISTIR-5030
Cryogenic Properties of Inorganic Insulation Materials for ITER Magnets: A Review.
PB95-198768 *03,706* PC A10/MF A03

NISTIR-5032
Electromagnetic Shielding Characterization of Gaskets
PB95-198917 *01,911* PC A03/MF A01

NISTIR-5033
Polarimetric Calibration of Reciprocal-Antenna Radars.
PB95-216925 *01,872* PC A03/MF A01

NISTIR-5034
IIW Commission V Quality Control and Quality Assurance of Welded Products Annual Report 1994/95.
PB95-198743 *02,866* PC A03/MF A01

NISTIR-5035
Time and Frequency: Bibliography of NIST Publications, March 1995.
PB95-220463 *01,548* PC A06/MF A02

NISTIR-5037
Control of Gas-Metal-Arc Welding Using Arc-Light Sensing.
PB96-131461 *02,869* PC A06/MF A02

NISTIR-5038
Residual Stress in Induction-Heated Railroad Wheels: Ultrasonic and Saw Cut Measurements. Report No. 28.
PB96-106992 *04,854* PC A04/MF A01

NISTIR-5040
Metrology for Electromagnetic Technology: A Bibliography of NIST Publications, September 1995.
PB96-128269 *01,938* PC A05/MF A01

NISTIR-5041
Bibliography of the NIST Optoelectronics Division.
PB96-128210 *02,193* PC A04/MF A01

NISTIR-5043
Dynamometer-Induced Residual Stress in Railroad Wheels: Ultrasonic and Saw Cut Measurements. Report No. 30.
PB96-183199 *04,857* PC A04/MF A01

NISTIR-5044
IIW Commission V Quality Control and Quality Assurance of Welded Products, Annual Report 1995/96.
PB96-191366 *02,880* PC A04/MF A01

NISTIR-5045
Dielectric and Magnetic Measurements from -50C to 200C and in the Frequency Band 50 MHz to 2 GHz.
PB96-191382 *02,245* PC A03/MF A01

NISTIR-5048
Hybrid Gauss-Trapezoidal Quadrature Rules.
PB96-193750 *03,422* PC A04/MF A01

NISTIR-5050
Bibliography of the NIST Electromagnetic Fields Division Publications.
PB96-210778 *01,980* PC A08/MF A02

NISTIR-5051
Metrology for Electromagnetic Technology: A Bibliography of NIST Publications.
PB97-116057 *04,396* PC A06/MF A01

NISTIR-5052
Bibliography of the NIST Optoelectronics Division.
PB97-116040 *02,207* PC A06/MF A01

NISTIR-5102
Diffusion of Cations Beneath Organic Coatings on Steel Substrate.
PB94-215704 *03,119* PC A03/MF A01

NISTIR-5122
Questions and Answers on Quality, the ISO 9000 Standard Series, Quality System Registration, and Related Issues. More Questions and Answers on the ISO 9000 Standard Series and Related Issues.
PB95-103461 *00,495* PC A03/MF A01

NISTIR-5145
Electronics and Electrical Engineering Laboratory Technical Progress Bulletin Covering Laboratory Programs, October to December 1992, with 1992/1993 EEEL Events Calendar.
PB94-165958 *02,299* PC A03/MF A01

NISTIR-5165
Life-Cycle Costing Workshop for Energy Conservation in Buildings: Student Manual.
PB95-175006 *00,257* PC A11/MF A03

NISTIR-5178
Least-Cost Energy Decisions for Buildings: Part 2. Uncertainty and Risk Video Training Workbook.
PB94-165982 *00,240* PC A04/MF A01

NISTIR-5184
Highway Concrete (HWYCON) Expert System User Reference and Enhancement Guide.
PB94-215670 *01,316* PC A08/MF A02

NISTIR-5185-2
BLCC: The NIST 'Building Life-Cycle Cost' Program, Version 4.21. User's Guide and Reference Manual.
PB95-190682 *00,263* PC A06/MF A02

NISTIR-5189
Wind Load Provisions of the Manufactured Home Construction and Safety Standards: A Review and Recommendations for Improvement.
PB94-206125 *00,428* PC A06/MF A02

NISTIR-5199
Recertification of the Standard Reference Material 1475A, a Linear Polyethylene Resin.
PB94-161932 *02,628* PC A03/MF A01

NISTIR-5212
Constituents and Physical Properties of the C6+ Fraction of Natural Gas. Topical Report, April-June 1994.
PB95-136644 *02,483* PC A03/MF A01

NISTIR-5214
Introduction to Traffic Management for Broadband ISDN.
PB94-142494 *01,464* PC A03/MF A01

NISTIR-5225
Technical Program of the Factory Automation Systems Division 1993.
PB94-160819 *02,805* PC A03/MF A01

NISTIR-5234
Report of the NIST Workshop on Digital Signature Certificate Management. Held on December 10-11, 1992.
PB94-135001 *01,574* PC A09/MF A02

NISTIR-5240
Measurement of Room Conditions and Response of Sprinklers and Smoke Detectors during a Simulated Two-Bed Hospital Patient Room Fire.
PB94-213717 *00,292* PC A07/MF A02

NISTIR-5250
Predicting the Energy Performance Ratings of a Family of Type I Combination Appliances.
PB95-105524 *02,504* PC A03/MF A01

NISTIR-5266
In situ Burning of Oil Spills: Mesoscale Experiments.
PB94-142973 *01,355* PC A04/MF A01

NISTIR-5272
Control Entity Interface Specification.
PB94-191715 *02,815* PC A06/MF A02

NISTIR-5277
Comparing Remote Procedure Calls: Open Network Computing, Distributed Computing Environment and International Organization for Standardization.
PB95-194205 *01,724* PC A03/MF A01

NISTIR-5282
Technology Trends in Telecommunications: An Overview.
PB94-123080 *01,462* PC A03/MF A01

NISTIR-5283
Security Considerations for SQL-Based Implementations of STEP.
PB94-139649 *02,766* PC A03/MF A01

NISTIR-5286
Determination of the Weight Average Molecular Weight of Two Poly(Ethylene Oxides), SRM 1923 and SRM 1924.
PB94-217031 *01,230* PC A03/MF A01

NISTIR-5288
Electronics and Electrical Engineering Laboratory Technical Progress Bulletin Covering Laboratory Programs, July to September 1993 with 1994 EEEL Events Calendar.
PB94-194354 *02,309* PC A03/MF A01

NISTIR-5290
Mass Unit Disseminated to Surrogated Laboratories Using the NIST Portable Mass Calibration Package.
PB94-142486 *03,781* PC A03/MF A01

NISTIR-5295
Guide to Software Engineering Environment Assessment and Evaluation.
PB94-140167 *01,676* PC A04/MF A01

NISTIR-5296
Computing Effects and Error for Large Synthetic Perturbation Screenings.
PB94-139623 *01,675* PC A03/MF A01

NISTIR-5297
Feasibility Study: Reference Architecture for Machine Control Systems Integration.
PB94-142791 *02,804* PC A12/MF A03

NISTIR-5298
Some Factors Affecting Design of a Furniture Calorimeter Hood and Exhaust.
PB94-139193 *00,285* PC A03/MF A01

NISTIR-5299
Photonic Materials: A Report on the Results of a Workshop. Held in Gaithersburg, Maryland on August 26-27, 1992, Volume 1.
PB94-152733 *02,114* PC A05/MF A01

NISTIR-5302
Evaluating Small Board and Care Homes: Sprinklered vs. Nonsprinklered Fire Protection.
PB94-206356 *00,195* PC A04/MF A01

NISTIR-5303
CSTL Technical Activities, 1993.
PB95-160602 *00,953* PC A17/MF A04

NISTIR-5304
Use of Computer Models to Predict Temperature and Smoke Movement in High Bay Spaces.
PB94-145976 *00,191* PC A04/MF A01

NISTIR-5305
FIREDOC Users Manual, 3rd Edition.
PB95-128674 *01,378* PC A03/MF A01

NISTIR-5306
Ground-Based Smoke Sampling Techniques Training Course and Collaborative Local Smoke Sampling in Saudi Arabia.
PB94-143542 *02,532* PC A05/MF A01

NISTIR-5307
Open Architectures for Machine Control.
PB94-135621 *02,942* PC A03/MF A01

NISTIR-5308
General Procedures for Registering Computer Security Objects.
PB94-134897 *01,573* PC A03/MF A01

NISTIR-5309
Context Analysis of the Network Management Domain. Conducted as Part of the Domain Analysis Case Study.
PB94-142528 *01,465* PC A05/MF A01

NISTIR-5310
Unconstrained Handprint Recognition Using a Limited Lexicon.
PB94-168051 *01,831* PC A03/MF A01

NISTIR-5311
Materials Science and Engineering Laboratory Annual Report, 1993. NAS-NRC Assessment Panel, April 21-22, 1994.
PB94-162534 *02,969* PC A05/MF A01

NISTIR-5312
Intelligent Processing of Materials, Technical Activities 1993 (NAS-NRC Assessment Panel, April 21-22, 1994).
PB94-164183 *02,809* PC A04/MF A01

NISTIR-5313
Ceramics Technical Activities, 1993 (NAS-NRC Assessment Panel April 21-22, 1994).
PB94-162591 *03,031* PC A10/MF A03

NISTIR-5318
APDE Demonstration System Architecture. National PDES Testbed Report Series.
PB94-154325 *02,767* PC A03/MF A01

NISTIR-5319
Assessment of Uncertainties of Calibration of Resistance Thermometers at the National Institute of Standards and Technology.
PB94-142478 *02,624* PC A03/MF A01

NISTIR-5320
Measurements of Outdoor Air Distribution in an Office Building.
PB95-210944 *00,264* PC A04/MF A01

NISTIR-5321
Study of Heat Pump Performance Using Mixtures of R32/R134a and R32/R125/R134a as 'Drop-In' Working Fluids for R22 with and Without a Liquid-Suction Heat Exchanger.
PB94-218559 *02,503* PC A04/MF A01

NISTIR-5322
Computer Programs for Simulation of Lighting/HVAC Interactions.
PB94-140407 *02,501* PC A08/MF A02

NISTIR-5324
Color Supplement to NIST Special Publication 400-93: Semiconductor Measurement Technology: Design and Testing Guides for the CMOS and Lateral Bipolar-on-SOI Test Library.
PB94-164316 *02,298* PC A03/MF A01

NISTIR-5325
Conformance Assessment of Transport Layer Security Implementations.
PB94-164373 *01,576* PC A03/MF A01

NISTIR-5326
Report on Application Integration Architectures (AIA) Workshop. Held in Dallas, Texas on February 8-12, 1993.
PB94-142536 *01,803* PC A07/MF A02

NISTIR-5328
Hollow Clay Tile Prism Tests for Martin Marietta Energy Systems: Task 2 Testing.
PB94-217486 *00,352* PC A14/MF A03

NISTIR-5329
Manual for Ventilation Assessment in Mechanically Ventilated Commercial Buildings.
PB94-145653 *00,239* PC A07/MF A02

NISTIR-5331
Enhanced Machine Controller Architecture Overview.
PB94-142460 *02,802* PC A03/MF A01

NISTIR-5332
Modulation of Fossil Fuel Production by Global Temperature Variations, 2.
PB94-146636 *02,533* PC A04/MF A01

NISTIR-5333
Reliable Optical Flow Algorithm Using 3-D Hermite Polynomials.
PB94-145620 *01,829* PC A03/MF A01

NISTIR-5336
Evaluation of GSA Maintenance Practices of Large Centrifugal Chillers and Review of GSA Refrigerant Management Practices.
PB94-143344 *02,502* PC A04/MF A01

NISTIR-5337
Electronics and Electrical Engineering Laboratory 1994 Program Plan: Supporting Technology for U.S. Competitiveness in Electronics.
PB94-126901 *01,873* PC A09/MF A02

NISTIR-5338
System for Calibration of the Marshall Compaction Hammer.
PB94-145661 *01,303* PC A08/MF A02

NISTIR-5339
Comparison of Fire Sprinkler Piping Materials: Steel, Copper, Chlorinated Polyvinyl Chloride and Polybutylene, in Residential and Light Hazard Installations.
PB95-182267 *00,299* PC A03/MF A01

NISTIR-5340
Assessment of Uncertainties of Thermocouple Calibrations at NIST.
PB94-152691 *03,782* PC A03/MF A01

NISTIR-5341
Assessment of Uncertainties of Liquid-in-Glass Thermometer Calibrations at the National Institute of Standards and Technology.
PB94-142510 *02,625* PC A03/MF A01

NISTIR-5342
Computer Systems Laboratory Annual Report, 1993.
PB94-162518 *01,622* PC A05/MF A02

NISTIR-5343
Applying Virtual Environments to Manufacturing.
PB94-142502 *02,803* PC A03/MF A01

NISTIR-5344
Growth Surface for the Slopes at the Boundary of a Polygon.
PB94-152725 *03,408* PC A03/MF A01

NISTIR-5345
Draft Guidelines for Quality Control Testing of Elastomeric Seismic Isolation Systems.
PB94-161734 *00,422* PC A03/MF A01

NISTIR-5346
Indoor Air Quality Impacts of Residential HVAC Systems, Phase 1 Report: Computer Simulation Plan.
PB95-135596 *00,249* PC A06/MF A02

NISTIR-5349
Submissions to a Planned Encyclopedia of Operations Research on Computational Geometry and the Voronoi/Delaunay Construct.
PB94-152709 *03,425* PC A03/MF A01

NISTIR-5350
Airborne Asbestos Method: Standard Test Method for High Precision Counting of Asbestos Collected on Filters. Version 1.0.
PB94-163003 *00,525* PC A02/MF A01

NISTIR-5351
Airborne Asbestos Method: Standard Test Method for Verified Analysis of Asbestos by Transmission Electron Microscopy. Version 2.0.
PB94-163045 *00,526* PC A03/MF A01

NISTIR-5352
Boundary Conforming Grid Generation System for Interface Tracking.
PB94-158268 *03,312* PC A03/MF A01

NISTIR-5353
Source of Phenol Emissions Affecting the Indoor Air of an Office Building.
PB94-154382 *03,600* PC A04/MF A01

NISTIR-5356
Variant Design for Mechanical Artifacts-A State of the Art Survey.
PB94-154358 *02,768* PC A03/MF A01

NISTIR-5357
Electronics and Electrical Engineering Laboratory Technical Progress Bulletin Covering Programs, October to December 1993, with 1994/1995 EEEL Events Calendar.
PB94-154341 *02,115* PC A03/MF A01

NISTIR-5358
Airborne Asbestos Method: Standard Practice for Recording Transmission Electron Microscopy Data for the Analysis of Asbestos Collected onto Filters. Version 1.0.
PB94-210168 *00,552* PC A03/MF A03

NISTIR-5359
Draft Guidelines for Pre-Qualification and Prototype Testing of Seismic Isolation Systems.
PB94-161940 *01,331* PC A06/MF A01

NISTIR-5360
Corrosion Resistance of Materials for Renovation of the United States Botanic Garden Conservatory.
PB94-154390 *00,032* PC A03/MF A01

NISTIR-5362
NIST Reactor: Summary of Activities October 1992 through September 1993.
PB94-161502 *04,437* PC A08/MF A02

NISTIR-5363
Physics Laboratory Technical Activities, 1993.
PB94-176088 *03,796* PC A10/MF A03

NISTIR-5364
Evaluating Form Designs for Optical Character Recognition.
PB94-168044 *01,830* PC A06/MF A02

NISTIR-5365
Bibliography on Apparel Sizing and Related Issues.
PB94-161924 *02,806* PC A03/MF A01

NISTIR-5366
Concept for an Algorithm Testing and Evaluation Program at NIST.
PB94-163029 *02,890* PC A03/MF A01

NISTIR-5367
Prediction of Geometric-Thermal Machine Tool Errors by Artificial Neural Networks.
PB94-186673 *02,943* PC A07/MF A02

NISTIR-5370
Manufactured Homes: Probability of Failure and the Need for Better Windstorm Protection through Improved Anchoring Systems.
PB95-143129 *00,432* PC A04/MF A01

NISTIR-5371
Draft Guidelines for Quality Control Testing of Sliding Seismic Isolation Systems.
PB94-161957 *01,332* PC A03/MF A01

NISTIR-5372
Computer Graphics Metafile (CGM): Procedures for NIST CGM Validation Test Service.
PB94-161809 *01,804* PC A03/MF A01

NISTIR-5373
Report on the Workshop on Manufacturing Polymer Composites by Liquid Molding. Held in Gaithersburg, Maryland on September 20-22, 1993.
PB94-160066 *03,131* PC A13/MF A03

NISTIR-5374
Process for Selecting Standard Reference Algorithms for Evaluating Coordinate Measurement Software.
PB94-173754 *02,629* PC A03/MF A01

NISTIR-5375
Electronic Balance and Some Gravimetric Applications. (The Density of Solids and Liquids, Pycnometry and Mass).
PB94-163052 *03,785* PC A03/MF A01

NISTIR-5376
Examination of Parameters That Can Cause Error in Mass Determinations.
PB94-163037 *03,784* PC A03/MF A01

NISTIR-5377
Piggyback Balance Experiment: An Illustration of Archimedes' Principles and Newton's Third Law.
PB94-163060 *03,786* PC A03/MF A01

NISTIR-5378
Determination of Density of Mass Standards: Requirement and Method.
PB94-163078 *03,787* PC A03/MF A01

NISTIR-5379
U.S. Navy Coordinate Measuring Machines: A Study of Needs.
PB94-162831 *02,807* PC A04/MF A01

NISTIR-5380
Comparison of Wall-Fire Behavior With and Without a Ceiling.
PB94-207404 *00,342* PC A03/MF A01

NISTIR-5381
Distributed Supercomputing Software: Experiences with the Parallel Virtual Machine - PVM.
PB94-163086 *01,680* PC A03/MF A01

NISTIR-5382
Standards of Seismic Safety for Existing Federally Owned or Leased Buildings and Commentary.
PB95-130209 *00,431* PC A06/MF A02

NISTIR-5384
Combined Buoyancy- and Pressure-Driven Flow Through a Shallow, Horizontal, Circular Vent.
PB94-210077 *00,344* PC A03/MF A01

NISTIR-5385
CONTAM93 User Manual.
PB94-164381 *02,536* PC A05/MF A01

NISTIR-5386
Proceedings of the Workshop on the Federal Criteria for Information Technology Security. Held in Ellicot City, Maryland on June 2-3, 1993.
PB94-162583 *01,575* PC A04/MF A01

NISTIR-5387
Graphical Analysis of the CCRL Portland Cement Proficiency Sample Database (Samples 1-72). (Part 1. Univariant Analysis of Portland Cement).
PB94-196557 *01,308* PC A06/MF A02

NISTIR-5388
Preparation and Monitoring of Lead Acetate Containing Drinking Water Solutions for Toxicity Studies.
PB94-193885 *00,538* PC A03/MF A01

NISTIR-5389
Analysis of Failed Dry Pipe Fire Suppression System Couplings from the Filene Center at Wolf Trap Farm Park for the Performing Arts.
PB94-164407 *00,331* PC A03/MF A01

NISTIR-5390
Sulfate Attack of Cementitious Materials: Volumetric Relations and Expansions.
PB94-187317 *03,232* PC A03/MF A01

NISTIR-5391
State-of-the-Art Survey of Methodologies for Representing Manufacturing Process Capabilities.
PB94-187655 *02,812* PC A03/MF A01

NISTIR-5392
Calculating Flame Spread on Horizontal and Vertical Surfaces.
PB94-187283 *00,335* PC A04/MF A01

NISTIR-5394
Design and Development of an Information Retrieval System for the EAMATE Data. Volume 2 of 2. Appendices.
PB94-168390 *00,487* PC A19/MF A04

NISTIR-5395
Preliminary Functional Specifications of a Prototype Electronic Research Notebook for NIST.
PB94-207750 *00,012* PC A04/MF A01

NISTIR-5396
Northridge Earthquake, 1994. Performance of Structures, Lifelines and Fire Protection Systems.
PB94-161114 *00,421* PC A09/MF A02

NISTIR-5397
BFRL Fire Publications, 1993.
PB94-164191 *00,192* PC A03/MF A01

NISTIR-5398
User's Guide for the PHIGS Validation Tests (Version 2.1).
PB94-165206 *01,682* PC A08/MF A02

NISTIR-5399
Measurement and Determination of Radon Source Potential: A Literature Review.
PB94-165602 *02,576* PC A09/MF A03

NISTIR-5402
Realizing Suspended Structures on Chips Fabricated by CMOS Foundry Processes Through the MOSIS Service.
PB94-193984 *01,881* PC A04/MF A01

NISTIR-5403
Quantitative X-Ray Powder Diffraction Methods for Clinker and Cement.
PB95-143079 *01,317* PC A03/MF A01

NISTIR-5405
Effects of Testing Variables on the Measured Compressive Strength of High-Strength (90 MPa) Concrete.
PB95-179040 *00,445* PC A07/MF A02

NISTIR-5408
Characterization of the Hydrogen Induced Cold Cracking Susceptibility at Simulated Weld Zones in HSLA-100 Steel.
AD-A279 759/5 *03,200* PC A04/MF A01
Characterization of the Hydrogen Induced Cold Cracking Susceptibility at Simulated Weld Zones in HSLA-100 Steel.
PB94-174505 *03,746* PC A04/MF A01

NISTIR-5409
Electronics and Electrical Engineering Laboratory: 1994 Strategic Plan. Supporting Technology for U.S. Competitiveness in Electronics.
PB94-161320 *01,874* PC A04/MF A01

NISTIR-5411
Body Dimensions for Apparel.
PB94-187739 *02,813* PC A03/MF A01

NISTIR-5412
Overview of NASREM: The NASA/NBS Standard Reference Model for Telerobot Control System Architecture.
PB94-194560 *04,831* PC A03/MF A01

NISTIR-5413
Federal Metric Progress in 1993.
PB94-196029 *02,600* PC A03/MF A01

NISTIR-5415
User Profile for Researchers Studying Objects: Implications for Computer Systems.
PB94-188463 *00,133* PC A03/MF A01

NISTIR-5416
NIST RS274/NGC Interpreter Version 1.
PB94-187788 *02,814* PC A03/MF A01

NISTIR-5417
Simple Scalability Test for MIMD Code.
PB94-193638 *01,688* PC A03/MF A01

NISTIR-5418
Workshop on Characterizing Diamond Films (3rd). Held in Gaithersburg, Maryland on February 23-24, 1994.
PB94-187663 *04,456* PC A04/MF A01

NISTIR-5419
Seismic Safety of Federal Buildings. Initial Program: How Much Will It Cost.
PB95-182291 *00,447* PC A03/MF A01

NISTIR-5420
NIST Response to the Fifth CORM Report on the Pressing Problems and Projected Needs in Optical Radiation Measurements.
PB94-188240 *04,227* PC A03/MF A01

NISTIR-5421
Strengthening Methodology for Lightly Reinforced Concrete Frames-II. Recommended Calculation Techniques for the Design of Infill Walls.
PB94-187648 *00,426* PC A03/MF A01

NISTIR-5422
Application of the Electronic Balance in High Precision Pycnometry.
PB94-187564 *00,534* PC A03/MF A01

NISTIR-5423
Use of the Electronic Balance for Highly Accurate Direct Mass Measurements Without the Use of External Mass Standards.
PB94-187713 *03,803* PC A03/MF A01

NISTIR-5424
Study of Federal Agency Needs for Information Technology Security.
PB94-193653 *01,579* PC A07/MF A02

NISTIR-5425
Metric for Success.
PB94-187630 *02,633* PC A03/MF A01

NISTIR-5427
Visualization Applications for Manufacturing: A State-of-the-Art Survey. Final Report.
PB94-194552 *02,816* PC A03/MF A01

NISTIR-5428
Program Handbook: Requirements for Obtaining NIST Approval/Recognition of a Laboratory Accreditation Body Under P.L. 101-592. The Fastener Quality Act.
PB94-210143 *02,859* PC A03/MF A01

NISTIR-5429
Optical Metrology and More. Programs and Services of the Radiometric Physics Division, Physics Laboratory.
PB94-191707 *04,228* PC A03/MF A01

NISTIR-5430
NIST Calibration of ASTM E127-Type Ultrasonic Reference Blocks.
PB94-191640 *02,702* PC A03/MF A01

NISTIR-5431
Proficiency Tests for the NIST Airborne Asbestos Program, 1990.
PB94-188836 *00,535* PC A07/MF A02

NISTIR-5432
Proficiency Tests for the NIST Airborne Asbestos Program - 1991.
PB94-193828 *00,537* PC A04/MF A01

NISTIR-5433
Proficiency Tests for the NIST Airborne Asbestos Program - 1992.
PB94-194362 *00,539* PC A03/MF A01

NISTIR-5434
Electronics and Electrical Engineering Laboratory Technical Progress Bulletin Covering Laboratory Programs, January to March 1994 with 1994/1995 EEEL Events Calendar.
PB94-193810 *02,308* PC A03/MF A01

NISTIR-5435
Electronics and Electrical Engineering Laboratory Technical Publication Announcements Covering Laboratory Programs, October to December 1993 with 1994/1995 EEEL Events Calendar.
PB94-193752 *02,307* PC A03/MF A01

NISTIR-5436
Performance of 1/3-Scale Model Precast Concrete Beam-Column Connections Subjected to Cyclic Inelastic Loads. Report No. 4.
PB95-179024 *00,444* PC A04/MF A01

NISTIR-5437
Bibliography of Photon Total Cross Section (Attenuation Coefficient) Measurements 10 eV to 13.5 GeV, 1907-1993.
PB94-193760 *03,804* PC A06/MF A02

NISTIR-5438
Industry/Government Open Systems Specification Testing Framework. Version 1.0.
PB94-219110 *01,809* PC A06/MF A02

NISTIR-5439
Performance Parameters of Fire Detection Systems.
PB94-194339 *00,288* PC A03/MF A01

NISTIR-5440
CONTAM88 Building Input Files for Multi-Zone Airflow and Contaminant Dispersal Modeling.
PB94-194388 *02,537* PC A04/MF A01

NISTIR-5441
Risk Analysis for the Fire Safety of Airline Passengers.
PB94-194065 *04,862* PC A03/MF A01

NISTIR-5442
Visual-Motion Fixation Invariant.
PB94-206281 *01,836* PC A03/MF A01

NISTIR-5443
Program of the Subcommittee on Construction and Building.
PB94-193646 *00,319* PC A03/MF A01

NISTIR-5443-A
Program of the Subcommittee on Construction and Building (July 1994).
PB95-122537 *00,321* PC A03/MF A01

NISTIR-5444
Recommendations on Selection of Vehicle-to-Roadside Communications Standards for Commercial Vehicle Operations.
PB94-195914 *04,859* PC A05/MF A01

NISTIR-5445
Feasibility of Fire Evacuation by Elevators at FAA Control Towers.
PB94-213857 *04,844* PC A06/MF A02

NISTIR-5446
Integration of Servo Control into a Large-Scale Control System Design: An Example from Coal Mining.
PB94-203429 *03,696* PC A02/MF A01

NISTIR-5447
Certainty Grid to Object Boundary Algorithm.
PB94-203510 *01,835* PC A03/MF A01

NISTIR-5448
Continuous Mining Machine Control Using the Real-Time Control System.
PB94-203528 *03,700* PC A02/MF A01

NISTIR-5449
Environment Simulation for a Continuous Mining Machine.
PB94-203536 *03,697* PC A03/MF A01

NISTIR-5452
Second Census Optical Character Recognition Systems Conference.
PB94-188711 *01,832* PC A12/MF A03

NISTIR-5453
World Wide Web and Mosaic: User's Guide.
PB94-207354 *02,722* PC A03/MF A01

NISTIR-5454
Single-Phase Heat Transfer and Pressure Drop Characteristics of an Integral-Spine-Fin Within an Annulus.
PB94-194073 *03,805* PC A03/MF A01

NISTIR-5455
New Expressions of Uncertainties for Humidity Calibrations at the National Institute of Standards and Technology.
PB95-103826 *02,645* PC A02/MF A01

NISTIR-5456
NIST Workshop on Nanostructured Material (1st): Report of an Industrial Workshop Conducted by the National Institute of Standards and Technology. Held in Gaithersburg, Maryland on May 14-15, 1992.
PB94-218567 *02,973* PC A04/MF A01

NISTIR-5457
Report on the Workshop on Advanced Digital Video in the National Information Infrastructure. Held in Washington, D.C. on May 10-11, 1994.
PB95-103677 *01,472* PC A09/MF A03

NISTIR-5459
Quality Characteristics and Metrics for Reusable Software (Preliminary Report).
PB94-203437 *01,693* PC A03/MF A01

NISTIR-5460
Adaptive, Predictive 2-D Feature Tracking Algorithm for Finding the Focus of Expansion.
PB94-218575 *01,588* PC A03/MF A01

NISTIR-5461
Abrasive Wear by Diesel Engine Coal-Fuel and Related Particles.
PB95-104915 *01,450* PC A04/MF A01

NISTIR-5462
Alaska Marine Mammal Tissue Archival Project: Specimen Inventory.
PB95-171344 *02,589* PC A05/MF A01

NISTIR-5463
Metric Path to Global Markets and New Jobs: A Question-and-Answer and Thematic Discussion.
PB94-206307 *02,601* PC A02/MF A01

NISTIR-5464
Design Engineering Research at NIST.
PB95-267860 *02,784* PC A03/MF A01

NISTIR-5465
Face Recognition Technology for Law Enforcement Applications.
PB94-207768 *01,837* PC A05/MF A01

NISTIR-5468
Report of the NIST Workshop on Key Escrow Encryption. Held in Gaithersburg, Maryland on June 8-10, 1994.
PB94-209459 *01,584* PC A08/MF A02

NISTIR-5469
NIST Form-Based Handprint Recognition System.
PB94-217106 *01,838* PC A04/MF A01

NISTIR-5470
VENTCF2: An Algorithm and Associated FORTRAN 77 Subroutine for Calculating Flow through a Horizontal Ceiling/Floor Vent in a Zone-Type Compartment Fire Model.
PB94-210127 *00,345* PC A04/MF A01

NISTIR-5471
Electronics and Electrical Engineering Laboratory Technical Publication Announcements Covering Laboratory Programs, January to March 1994 with 1994/1995 EEEL Events Calendar.
PB94-213774 *01,883* PC A03/MF A01

NISTIR-5472
Head Start on Assurance: Proceedings of an Invitational Workshop on Information Technology (IT) Assurance and

Trustworthiness. Held in Williamsburg, Virginia on March 21-23, 1994.
PB94-215746 *01,586* PC A05/MF A01

NISTIR-5473
Survey on the Implementation of ISO/IEC Guide 25 by National Laboratory Accreditation Programs.
PB94-210150 *00,479* PC A04/MF A01

NISTIR-5474
Publications of the Intelligent Systems Division (Previously Robot Systems Division) Covering the Period January 1971-April 1994.
PB94-217098 *02,935* PC A05/MF A01

NISTIR-5476
Technical Program Description Systems Integration for Manufacturing (SIMA).
PB94-213758 *02,819* PC A05/MF A01

NISTIR-5477
Updated Calculations for Routine Space-Shielding Radiation Dose Estimates: SHIELDOSE-2.
PB95-171039 *04,838* PC A04/MF A01

NISTIR-5478
Framework for National Information Infrastructure Services.
PB95-103719 *02,723* PC A07/MF A02

NISTIR-5480
Survey of Recent Cementitious Materials Research in Western Europe.
PB94-218583 *00,353* PC A03/MF A01

NISTIR-5481
NIST Research Program on the Seismic Resistance of Partially-Grouted Masonry Shear Walls.
PB94-219052 *00,354* PC A06/MF A02

NISTIR-5483
Electronics and Electrical Engineering Laboratory Technical Progress Bulletin Covering Laboratory Programs, April to June 1994 with 1994/1995 EEEL Events Calendar.
PB95-143186 *02,329* PC A03/MF A01

NISTIR-5484
Formulation of Position on U.S. Standards Role in Enterprise Integration.
PB95-105052 *02,773* PC A03/MF A01

NISTIR-5485
Videoconferencing Procurement and Usage Guide.
PB94-217023 *01,470* PC A04/MF A01

NISTIR-5487
Making Sense of Software Engineering Environment Framework Standards.
PB95-105037 *01,701* PC A03/MF A01

NISTIR-5488
Performance of HUD-Affiliated Properties during the January 17, 1994 Northridge Earthquake.
PB95-174488 *00,443* PC A04/MF A01

NISTIR-5489
Faster BKL Monte Carlo Simulations.
PB95-136370 *01,706* PC A03/MF A01

NISTIR-5490
Software Needs in Special Functions.
PB95-105045 *01,702* PC A03/MF A01

NISTIR-5491
Japan Technology Program Assessment: Precision Engineering/Precision Optics in Japan.
PB95-171112 *02,884* PC A03/MF A01

NISTIR-5492
Diagnosis of Causes of Concrete Deterioration in the MLP-7A Parking Garage.
PB95-143095 *01,318* PC A03/MF A01

NISTIR-5493
Comparison of FFT Fingerprint Filtering Methods for Neural Network Classification.
PB95-136362 *01,840* PC A03/MF A01

NISTIR-5494
Domain Analysis of the Alarm Surveillance Domain. Version 1.0. Conducted as Part of the Domain Analysis Case Study Project.
PB95-136339 *01,705* PC A10/MF A03

NISTIR-5495
Computer Security Training and Awareness Course Compendium.
PB95-130985 *01,589* PC A09/MF A02

NISTIR-5498
Challenges to the National Information Infrastructure: The Barriers to Product Data Sharing. National PDES Testbed Report Series.
PB95-136347 *02,776* PC A03/MF A01

NISTIR-5499
Annual Conference on Fire Research: Book of Abstracts, October 17-20, 1994.
PB95-104964 *01,376* PC A09/MF A02

NISTIR-5500
Report on the Advanced Software Technology Workshop. Held on February 1, 1994.
PB95-136610 *01,707* PC A03/MF A01

NISTIR-5501
Sensitivity of Three-Point Circle Fitting.
PB95-136354 *02,901* PC A03/MF A01

NISTIR-5502
Reference Model Architecture for Intelligent Systems Design.
PB95-143137 *01,789* PC A03/MF A01

NISTIR-5503
Channel Coding for Code Excited Linear Prediction (CELP) Encoded Speech in Mobile Radio Applications.
PB95-143178 *01,475* PC A03/MF A01

NISTIR-5504
Summaries of BFRL Fire Research In-House Projects and Grants, 1994.
PB95-130845 *00,366* PC A10/MF A03

NISTIR-5505
xi-Vector Formulation of Anisotropic Phase-Field Models: 3-D Asymptotics.
PB95-136628 *04,536* PC A03/MF A01

NISTIR-5507
Portsmouth Fastener Manufacturing Workstation. User's Manual.
PB95-147922 *02,860* PC A06/MF A02

NISTIR-5509
Investigation into the Flammability Properties of Honeycomb Composites.
PB95-143293 *03,152* PC A03/MF A01

NISTIR-5511
STEP On-Line Information Service (SOLIS). The IGES/PDES Organization.
PB95-137790 *02,777* PC A02/MF A01

NISTIR-5512
New Method to Calculate Looming for Autonomous Obstacle Avoidance.
PB95-171435 *01,600* PC A03/MF A01

NISTIR-5513
Visual Pursuit Systems.
PB95-143285 *01,841* PC A03/MF A01

NISTIR-5514
Protection of Data Processing Equipment with Fine Water Sprays.
PB95-174975 *02,610* PC A04/MF A01

NISTIR-5515
SGML Environment for STEP.
PB95-143103 *02,778* PC A03/MF A01

NISTIR-5516
Method of Predicting Smoke Movement in Atria with Application to Smoke Management.
PB95-154746 *00,376* PC A05/MF A01

NISTIR-5517
Reference Architecture for Machine Control Systems Integration: Interim Report.
PB95-144549 *02,820* PC A06/MF A02

NISTIR-5519
Visual Measurement Technique for Analysis of Nucleate Flow Boiling.
PB95-143301 *03,262* PC A05/MF A02

NISTIR-5520
Metrology and Data for Microelectronic Packaging and Interconnection: Results of a Joint Workshop on Materials Metrology and Data for Commercial Electrical and Optical Packaging and Interconnection Technologies. Held in Gaithersburg, Maryland on May 5-6, 1994. Volume 1. Results.
PB95-143111 *02,328* PC A05/MF A01

NISTIR-5520-V2
Metrology and Data for Microelectronic Packaging and Interconnection: Results of a Joint Workshop on Materials Metrology and Data for Commercial Electrical and Optical Packaging and Interconnection Technologies. Held in Gaithersburg, Maryland on May 5-6, 1994. Volume 2. Presentation Material.
PB95-143327 *02,330* PC A08/MF A02

NISTIR-5521
Program Requirements to Advance the Technology of Custom Footwear Manufacturing.
PB95-147906 *02,883* PC A04/MF A01

NISTIR-5522
Information Technology Engineering and Measurement Model: Adding Lane Markings to the Information Superhighway.
PB95-143145 *01,474* PC A03/MF A01

NISTIR-5523
Phase-Field Model for Solidification of a Eutectic Alloy.
PB95-147914 *03,345* PC A04/MF A01

NISTIR-5524
Review and Upgrading of Military Fastener Test Standard MIL-STD-1312.
PB95-154720 *02,947* PC A07/MF A02

NISTIR-5526
Simulating Smoke Movement through Long Vertical Shafts in Zone-Type Compartment Fire Models.
PB95-143152 *00,368* PC A03/MF A01

NISTIR-5529
Electronics and Electrical Engineering Laboratory Technical Progress Bulletin Covering Laboratory Programs, July to September 1994 with 1994/1995 EEEL Events Calendar.
PB95-170395 *02,360* PC A03/MF A01

NISTIR-5530
Mapping Integration Definition for Information Modeling (IDEF1X) Model into CASE Data Interchange Format (CDIF) Transfer File.
PB95-154670 *01,711* PC A06/MF A02

NISTIR-5531
Extreme Wind Estimates by the Conditional Mean Exceedance Procedure.
PB95-220471 *00,120* PC A03/MF A01

NISTIR-5532
ISDN LAN Bridging.
PB95-154696 *01,477* PC A03/MF A01

NISTIR-5533
Design Challenges in a Commercial Quantum Hall Effect-Based Resistance Standard.
PB95-171419 *02,263* PC A03/MF A01

NISTIR-5535
Initial NIST Testing Policy for STEP: Beta Testing Program for AP 203 Implementations. National PDES Testbed Report Series.
PB95-154688 *02,779* PC A03/MF A01

NISTIR-5536
Rationale and Preliminary Plan for Federal Research for Construction and Building.
PB95-154704 *00,322* PC A07/MF A02

NISTIR-5538
SGML Parser Validation Procedures.
PB95-174959 *01,717* PC A03/MF A01

NISTIR-5539
General Motion Model and Spatio-Temporal Filters for Computing Optical Flow.
PB95-171096 *01,847* PC A03/MF A01

NISTIR-5540
Multi-Agency Certification and Accreditation (C and A) Process: A Worked Example.
PB95-171955 *01,601* PC A05/MF A01

NISTIR-5541
Initial Graphics Exchange Specification (IGES): Procedures for the NIST IGES Validation Test Service.
PB95-171427 *02,780* PC A03/MF A01

NISTIR-5542
Binary Decision Clustering for Neural Network Based Optical Character Recognition.
PB95-171971 *01,848* PC A03/MF A01

NISTIR-5543
Workshop on the Application of Virtual Reality to Manufacturing. Final Report. Held in Gaithersburg, Maryland on August 9, 1994.
PB95-173555 *02,825* PC A11/MF A03

NISTIR-5545
Neighbor Tables for Molecular Dynamics Simulations.
PB95-171948 *00,991* PC A03/MF A01

NISTIR-5546
Perspective on Software Engineering Standards.
PB95-171377 *01,811* PC A03/MF A01

NISTIR-5547
Algorithm to Describe the Spread of a Wall Fire under a Ceiling.
PB95-182259 *00,261* PC A04/MF A01

NISTIR-5550
Workshop Summary Report: Industrial Applications of Scanned Probe Microscopy. A Workshop Co-sponsored by NIST, SEMATECH, ASTM, E42.14, and the American Vacuum Society. Held in Gaithersburg, Maryland on March 24-25, 1994.
PB95-170387 *00,506* PC A07/MF A02

NISTIR-5551
Electronics and Electrical Engineering Laboratory 1994 Technical Accomplishments Supporting Technology for U.S. Competitiveness in Electronics.
PB95-144309 *01,887* PC A06/MF A02

NISTIR-5553
Field Evaluation of the System for Calibration of the Marshall Compaction Hammer.
PB95-190674 *01,323* PC A05/MF A01

NISTIR-5555
Review of Measurements and Candidate Signatures for Early Fire Detection.
PB95-189452 *00,300* PC A03/MF A01

NISTIR-5556
From Superconductivity to Supernovae: The Ginzburg Symposium. Report on the Symposium Held in Honor of Vitaly L. Ginzburg. Held in Gaithersburg, Maryland on May 22, 1992.
PB95-171963 *04,649* PC A05/MF A01

NISTIR-5557
Lubrication Theory for Reactive Spreading of a Thin Drop.
PB95-189460 *02,865* PC A03/MF A01

NISTIR-5558
Manufactured Housing Walls That Provide Satisfactory Moisture Performance in All Climates.
PB95-178885 *00,383* PC A03/MF A01

NISTIR-5559
Indoor Air Quality Impacts of Residential HVAC Systems. Phase 2.A Report: Baseline and Preliminary Simulations.
PB95-178893 *02,554* PC A05/MF A01

NISTIR-5560
Fire Performance of an Interstitial Space Construction System.
PB95-188918 *00,390* PC A04/MF A01

NISTIR-5561
Asynchronous Transfer Mode Procurement and Usage Guide.
PB95-174967 *01,481* PC A03/MF A01

NISTIR-5563
Electronics and Electrical Engineering Laboratory 1995 Program Plan. Supporting Technology for U.S. Competitiveness in Electronics.
PB95-159885 *01,894* PC A09/MF A03

NISTIR-5564
Technical Impact of the NIST Calibration Service for Electrical Power and Energy.
PB96-147913 *02,462* PC A05/MF A01

NISTIR-5565
Evaluation of the Economic Impacts Associated with the NIST Power and Energy Calibration Services.
PB95-188850 *02,461* PC A03/MF A01

NISTIR-5566
10 kV DC Resistive Divider Calibration.
PB95-198685 *02,063* PC A04/MF A01

NISTIR-5568
Carbon Monoxide Production in Compartment Fires: Reduced-Scale Enclosure Test Facility.
PB95-231700 *01,394* PC A10/MF A03

NISTIR-5569
MasPar MP-1 as a Computer Arithmetic Laboratory.
PB95-189437 *01,627* PC A03/MF A01

NISTIR-5570
Assessment of the DOD Goal Security Architecture (DGSA) for Non-Military Use.
PB95-189510 *03,653* PC A03/MF A01

NISTIR-5571
Operating Principles of MultiKron II Performance Instrumentation for MIMD Computers.
PB95-189486 *01,628* PC A03/MF A01

NISTIR-5572
Apparel Manufacturing Glossary for Application Protocol Development.
PB95-198750 *02,755* PC A04/MF A01

NISTIR-5573
Agile Manufacturing from a Statistical Perspective.
PB96-109525 *02,886* PC A03/MF A01

NISTIR-5574
Performance of Federal Buildings in the January 17, 1994 Northridge Earthquake.
PB95-231775 *00,453* PC A03/MF A01

NISTIR-5575
Measurements of Indoor Pollutant Emissions from EPA Phase II Wood Stoves.
PB95-198735 *02,556* PC A04/MF A01

NISTIR-5576
Computer Systems Laboratory Annual Report 1994.
PB95-209920 *01,629* PC A07/MF A02

NISTIR-5577
Materials Science and Engineering Laboratory Annual Report, 1994. NAS-NRC Assessment Panel, April 6-7, 1995.
PB95-196697 *02,976* PC A06/MF A02

NISTIR-5578
Intelligent Processing of Materials, Technical Activities 1994 (NAS-NRC Assessment Panel, April 6-7, 1995).
PB96-115050 *03,359* PC A04/MF A01

NISTIR-5581
Polymers Technical Activities 1994. NAC-NRC Assessment Panel, April 6-7, 1995.
PB95-209896 *01,275* PC A07/MF A02

NISTIR-5582
Metallurgy Technical Activities 1994 (NAS-NRC Assessment Panel, April 6-7, 1995).
PB96-136981 *02,981* PC A08/MF A02

NISTIR-5583
Reactor Radiation Technical Activities, 1994. NAS-NRC Assessment Panel, April 6-7, 1995.
PB95-209888 *03,732* PC A08/MF A02

NISTIR-5584
CSTL Technical Activities, 1994.
PB95-242319 *00,608* PC A16/MF A03

NISTIR-5586
Indoor Air Quality Commissioning of a New Office Building.
PB95-182309 *00,262* PC A04/MF A01

NISTIR-5587
Motion-Model-Based Boundary Extraction.
PB95-189502 *01,849* PC A03/MF A01

NISTIR-5589
Study on Hazard Analysis in High Integrity Software Standards and Guidelines.
PB95-198727 *01,725* PC A04/MF A01

NISTIR-5590
Proceedings Report of the International Invitation Workshop on Development Assurance. Held in Ellicott City, Maryland on June 16-17, 1994
PB95-189494 *02,912* PC A03/MF A01

NISTIR-5592
Survey of Concrete Transport Properties and Their Measurement.
PB95-220489 *00,396* PC A04/MF A01

NISTIR-5593
Vehicle-to-Roadside Communications for Commercial Vehicle Operations: Requirements and Approaches.
PB95-188827 *04,860* PC A05/MF A01

NISTIR-5594
NIST Reactor: Summary of Activities, October 1993 through September 1994.
PB95-220430 *04,700* PC A09/MF A02

NISTIR-5595
Application Software Interface: ISDN Services for an Open Systems Environment.
PB96-131487 *01,492* PC A03/MF A01

NISTIR-5596
Inserting Line Segments into Triangulations and Tetrahedralizations.
PB95-198933 *03,415* PC A03/MF A01

NISTIR-5597
Proceedings: Workshop on Research Needs in Wind Engineering. Held in Gaithersburg, Maryland on September 12-13, 1994.
PB95-189528 *00,448* PC A05/MF A01

NISTIR-5598
Compositional Analysis of Beneficiated Fly Ashes.
PB95-220497 *00,397* PC A03/MF A01

NISTIR-5599
Program of the Manufacturing Engineering Laboratory, 1995. Infrastructural Technology, Measurements, and Standards for the U.S. Manufacturing Industries.
PB95-188835 *02,754* PC A11/MF A02

NISTIR-5600
Object-Oriented Technology Research Areas.
PB95-199329 *01,726* PC A03/MF A01

NISTIR-5601
Expert Control System Shell Version 1.0 User's Guide.
PB95-198859 *01,790* PC A03/MF A01

NISTIR-5602
Interim Testing Artifact (ITA): A Performance Evaluation System for Coordinate Measuring Machines (CMMs). User Manual.
PB95-210589 *02,914* PC A04/MF A01

NISTIR-5604
Least-Cost Energy Decisions for Buildings. Part 3. Choosing Economic Evaluation Methods. Video Training Workbook.
PB95-253597 *00,265* PC A04/MF A01

NISTIR-5605
Real-Time Obstacle Avoidance Using Central Flow Divergence and Peripheral Flow.
PB95-198677 *02,937* PC A03/MF A01

NISTIR-5606
Theoretical Evaluation of the Vapor Compression Cycle with a Liquid-Line/Suction-Line Heat Exchanger, Economizer, and Ejector.
PB95-216917 *02,607* PC A03/MF A01

NISTIR-5607
Electronics and Electrical Engineering Laboratory Technical Publication Announcements Covering Laboratory Programs, July to September 1994 with 1995 EEEL Events Calendar.
PB95-198925 *01,912* PC A03/MF A01

NISTIR-5608
Electronics and Electrical Engineering Laboratory Technical Progress Bulletin Covering Laboratory Programs, October to December 1994 with 1995 EEEL Events Calendar.
PB95-208724 *02,372* PC A04/MF A01

NISTIR-5609
Calculating Time-to-Contact Using Real-Time Quantized Optical Flow.
PB95-210522 *01,604* PC A03/MF A01

NISTIR-5610
White Papers Prepared for the White House: Construction Industry Workshop on National Construction Goals. Held on December 14-16, 1994.
PB95-216891 *01,299* PC A08/MF A02

NISTIR-5611
Computer Simulations of Airflow and Radon Transport in Four Large Buildings.
PB95-220422 *02,557* PC A03/MF A01

NISTIR-5612
4SIGHT Manual: A Computer Program for Modelling Degradation of Underground Low Level Waste Concrete Vaults.
PB95-231593 *03,726* PC A05/MF A01

NISTIR-5613
Automated Manufacturing Research Facility 1994 Annual Report.
PB95-209854 *00,015* PC A05/MF A01

NISTIR-5614
Japan Technology Program Assessment. Simulation: State-of-the-Art in Japan.
PB95-217097 *02,827* PC A03/MF A01

NISTIR-5615
Design, Specification and Tolerancing of Micrometer-Tolerance Assemblies.
PB95-209862 *02,913* PC A03/MF A01

NISTIR-5618
Expression Formatter for MACSYMA.
PB95-267829 *01,735* PC A03/MF A01

NISTIR-5620
Concentrations of Chlorinated Hydrocarbons, Heavy Metals and Other Elements in Tissues Banked by the Alaska Marine Mammal Tissue Archival Project.
PB95-209870 *02,590* PC A06/MF A02

NISTIR-5622
DETAN 95: Computer Code for Calculating Spectrum-Averaged Cross Sections and Detector Responses in Neutron Spectra.
PB95-242384 *04,014* PC A04/MF A01

NISTIR-5623
Electronic Implementors' Workshop.
PB95-210936 *01,484* PC A03/MF A01

NISTIR-5625
Survey of Steel Moment-Resisting Frame Buildings Affected by the 1994 Northridge Earthquake.
PB95-211918 *00,451* PC A09/MF A02

NISTIR-5626
Performance Testing of a Family of Type I Combination Appliance.
PB95-220521 *02,505* PC A03/MF A01

NISTIR-5628
Precision in Machining: Research Challenges.
PB95-242301 *02,953* PC A04/MF A01

NISTIR-5631
Analysis of ANSI ASC X12 and UN/EDIFACT Electronic Data Interchange (EDI) Standards.
PB95-220554 *01,729* PC A03/MF A01

NISTIR-5632
Tables of X-ray Mass Attenuation Coefficients and Mass Energy-Absorption Coefficients 1 keV to 20 MeV for Elements Z = 1 to 92 and 48 Additional Substances of Dosimetric Interest.
PB95-220539 *04,013* PC A06/MF A02

NISTIR-5633
Testing of Selected Self-Leveling Compounds for Floors.
PB95-220455 *00,395* PC A03/MF A01

NISTIR-5634
Prediction of Cracking in Reinforced Concrete Structures.
PB95-220448 *03,725* PC A04/MF A01

NISTIR-5636
Persistent Object Base System Testing and Evaluation.
PB95-220588 *01,730* PC A05/MF A01

NISTIR-5637
Texture-Independent Vision-Based Closed-Loop Fuzzy Controllers for Navigation Tasks.
PB95-220505 *00,183* PC A03/MF A01

NISTIR-5638
ISO Environmental Management Standardization Efforts.
PB95-220513 *02,524* PC A03/MF A01

NISTIR-5638-1
ISO Environmental Management Standardization Efforts.
PB96-158662 *02,528* PC A03/MF A01

NISTIR-5639
Certification of the Standard Reference Material 1473a, a Low Density Polyethylene Resin.
PB96-128251 *01,282* PC A03/MF A01

NISTIR-5641
Anisotropy of Interfaces in an Ordered Alloy: A Multiple-Order-Parameter Model.
PB96-131594 *04,741* PC A04/MF A01

NISTIR-5642
Suppression of High Speed Turbulent Flames in a Detonation/Deflagration Tube.
PB95-231817 *01,395* PC A04/MF A01

NISTIR-5643
Outline of a Multiple Dimensional Reference Model Architecture and a Knowledge Engineering Methodology for Intelligent Systems Control.
PB95-220414 *03,703* PC A03/MF A01

NISTIR-5645
Evaluation of Thermal Wave Imaging for Detection of Machining Damage in Ceramics.
PB95-220547 *03,062* PC A05/MF A02

NISTIR-5647
PCASYS: A Pattern-Level Classification Automation System for Fingerprints.
PB95-267936 *01,853* PC A03/MF A01

NISTIR-5649
Electronics and Electrical Engineering Laboratory Technical Publication Announcements Covering Laboratory Programs, October to December 1994 with 1995 EEEL Events Calendar.
PB95-231841 *01,918* PC A03/MF A01

NISTIR-5650
Product Models and Virtual Prototypes in Mechanical Engineering.
PB95-253563 *02,783* PC A03/MF A01

NISTIR-5651
Algorithm Testing and Evaluation Program for Coordinate Measuring Systems: Long Range Plan.
PB95-231833 *02,915* PC A03/MF A01

NISTIR-5652
Operating Principles of the SBus MultiKron Interface Board.
PB95-231783 *01,630* PC A03/MF A01

NISTIR-5653
Behavior of Mock-Ups in the California Technical Bulletin 133 Test Protocol: Fabric and Barrier Effects.
PB95-231585 *00,301* PC A05/MF A01

NISTIR-5654
Defining Environment Integration Requirements.
PB96-131545 *02,733* PC A03/MF A01

NISTIR-5657
Introduction to the P1003.1g and CPI-C Network Application Programming Interfaces.
PB95-231726 *01,731* PC A03/MF A01

NISTIR-5658
Unified Telerobotic Architecture Project (UTAP) Standard Interface Environment (SIE), May 1995.
PB95-242350 *02,938* PC A09/MF A02

NISTIR-5659
NIST SRM 9983 High-Rigidity Ball-Bar Stand. User Manual.
PB95-255840 *02,669* PC A03/MF A01

NISTIR-5660
Parallel and Serial Implementations of SLI Arithmetic.
PB95-242335 *01,732* PC A03/MF A01

NISTIR-5661
Fracture Testing of Large-Scale Thin-Sheet Aluminum Alloy.
PB95-242368 *00,024* PC A03/MF A01

NISTIR-5662
Requisite Elements, Rationale, and Technology Overview for the Systems Intergration for Manufacturing Applications (SIMA) Program. Background Study.
PB96-112685 *02,831* PC A07/MF A02

NISTIR-5663
Multiattribute Decision Analysis Method for Evaluating Buildings and Building Systems.
PB96-158670 *00,325* PC A06/MF A01

NISTIR-5664
Recommended Performance-Based Criteria for the Design of Manufactured Home Foundation Systems to Resist Wind and Seismic Loads.
PB96-128285 *00,460* PC A05/MF A01

NISTIR-5665
ISO TC 184/SC4 Reference Manual.
PB95-242293 *02,663* PC A04/MF A01

NISTIR-5666
Operating Procedures and Life Cycle Documentation for the Initial Graphics Exchange Specification.
PB95-242285 *02,782* PC A04/MF A01

NISTIR-5667-V1
Study of Potential Applications of Automation and Robotics Technology in Construction, Maintenance and Operation of Highway Systems: A Final Report. Volume 1.
PB95-251682 *01,341* PC A06/MF A02

NISTIR-5667-V2
Study of Potential Applications of Automation and Robotics Technology in Construction, Maintenance and Operation of Highway Systems: A Final Report. Volume 2.
PB95-255865 *01,343* PC A19/MF A04

NISTIR-5667-V3
Study of Potential Applications of Automation and Robotics Technology in Construction, Maintenance and Operation of Highway Systems: A Final Report. Volume 3.
PB95-251690 *01,342* PC A15/MF A03

NISTIR-5667-V4
Study of Potential Applications of Automation and Robotics Technology in Construction, Maintenance and Operation of Highway Systems: A Final Report. Volume 4.
PB95-251641 *01,340* PC A06/MF A02

NISTIR-5669
Electronics and Electrical Engineering Laboratory Technical Publication Announcements Covering Laboratory Programs, January to March 1995 with 1995 EEEI Events Calendar.
PB95-242277 *02,373* PC A03/MF A01

NISTIR-5671
Determination of the Residual Stresses Near the Ends of Skip Welds Using Neutron Diffraction and X-ray Diffraction Procedures.
PB95-253589 *02,868* PC A03/MF A01

NISTIR-5672
Advanced Mass Calibration and Measurement Assurance Program for State Calibration Laboratories.
PB95-253571 *02,492* PC A03/MF A01

NISTIR-5673
Information Technologies Make Business Sense for the Custom Therapeutic Footwear Industry.
PB95-251708 *02,829* PC A03/MF A01

NISTIR-5674
User's Guide for the Algorithm Testing System Version 2.0.
PB95-251666 *02,916* PC A03/MF A01

NISTIR-5675
Group 1 for the Plant Spatial Configuration STEP Application Protocol.
PB96-165402 *02,789* PC A11/MF A03

NISTIR-5676
Submarine Automation: Demonstration No. 5.
PB95-251633 *03,748* PC A03/MF A01

NISTIR-5677
Center for High Integrity Software System Assurance: Initial Goals and Activities.
PB95-251674 *01,734* PC A03/MF A01

NISTIR-5678
Integrated Vision Touch-Probe System for Dimensional Inspection Tasks.
PB95-255832 *02,917* PC A03/MF A01

NISTIR-5680
Proficiency Tests for the NIST Airborne Asbestos Program, 1993.
PB96-106463 *00,610* PC A03/MF A01

NISTIR-5681
Water-Vapor Measurements of Low-Slope Roofing Materials.
PB95-251617 *00,399* PC A03/MF A01

NISTIR-5682
Strengthening Methodology for Lightly Reinforced Concrete Frames: Recommended Design Guidelines for Strengthening with Infill Walls.
PB95-260725 *00,454* PC A04/MF A01

NISTIR-5685
SF6 Insulation: Possible Greenhouse Problems and Solutions.
PB95-251625 *02,269* PC A03/MF A01

NISTIR-5686
Algorithm Testing and Evaluation Program for Coordinate Measuring Systems: Testing Methods.
PB95-251658 *02,666* PC A03/MF A01

NISTIR-5687
Method and Evaluation of Character Stroke Preservation on Handprint Recognition.
PB95-251724 *01,850* PC A03/MF A01

NISTIR-5688
Proceedings of the Meeting of the Intergovernmental U.S.-Russian Business Development Committee's Standard Working Group (4th). Held in New York City, New York on March 27-29, 1995 and in Northbrook, Illinois on March 30-31, 1995.
PB95-255881 *00,496* PC A11/MF A03

NISTIR-5689
Simple Method of Composition Shifting with a Distillation Column for a Heat Pump Employing a Zeotropic Refrigerant Mixture.
PB95-255824 *02,603* PC A03/MF A01

NISTIR-5690
Long-Term Performance of Engineered Concrete Barriers.
PB95-260816 *03,727* PC A03/MF A01

NISTIR-5691-V1
Unravel: A CASE Tool to Assist Evaluation of High Integrity Software. Volume 1. Requirements and Design.
PB95-267886 *01,736* PC A05/MF A01

NISTIR-5691-V2
Unravel: A CASE Tool to Assist Evaluation of High Integrity Software. Volume 2. User Manual.
PB95-267894 *01,737* PC A04/MF A01

NISTIR-5692-SUP
Applications of Diamond Films and Related Materials: International Conference (3rd). Held in Gaithersburg, Maryland on August 21-24, 1995. Supplement to NIST Special Publication 885.
PB95-256053 *03,063* PC A04/MF A01

NISTIR-5695
Improving Neural Network Performance for Character and Fingerprint Classification by Altering Network Dynamics.
PB95-267803 *01,851* PC A03/MF A01

NISTIR-5696
Effect of Training Dynamics on Neural Network Performance.
PB95-267845 *01,852* PC A03/MF A01

NISTIR-5697
GATT Standards Code Activities of the National Institute of Standards and Technology 1994.
PB96-106935 *00,497* PC A03/MF A01

NISTIR-5698
Estimation of Measurement Uncertainty of Small Circular Features Measured by CMMs.
PB95-267928 *02,918* PC A03/MF A01

NISTIR-5699
Computer-Aided Manufacturing Engineering Forum (1st). Technical Meeting Proceedings. Held in Gaithersburg, Maryland on March 21-22, 1995.
PB96-136965 *02,834* PC A10/MF A03

NISTIR-5700
Proceedings of the 1995 Workshop on Fire Detector Research. Held on February 6-7, 1995.
PB95-270062 *02,611* PC A03/MF A01

NISTIR-5701
Metrology Issues in Terahertz Physics and Technology.
PB96-128277 *01,939* PC A08/MF A02

NISTIR-5703
NIST ATM Network Simulator: Operation and Programming, Version 1.0.
PB96-106851 *01,487* PC A04/MF A01

NISTIR-5704
EMISS: A Program for Estimating Local Air Pollution Emission Factors Related to Energy Use in Buildings: User's Guide and Reference Manual.
PB96-109566 *02,560* PC A03/MF A01

NISTIR-5705
CFAST Output Comparison Method and Its Use in Comparing Different CFAST Versions.
PB96-109541 *00,401* PC A04/MF A01

NISTIR-5708
Electronic Access to Standards on the Information Highway.
PB96-131578 *01,494* PC A03/MF A01

NISTIR-5709
Electronics and Electrical Engineering Laboratory Technical Progress Bulletin Covering Laboratory Programs, April to June 1995 with 1995 EEEL Events Calendar.
PB96-106455 *01,923* PC A03/MF A01

NISTIR-5710
Effect of Suppressants on Metal Fires.
PB96-109574 *01,402* PC A03/MF A01

NISTIR-5712
Indoor Air Quality Impacts of Residential HVAC Systems Phase II.B Report: IAQ Control Retrofit Simulations and Analysis.
PB96-106877 *02,559* PC A05/MF A01

NISTIR-5714
Ground Improvement Techniques for Liquefaction Remediation Near Existing Lifelines.
PB96-128111 *01,350* PC A05/MF A01

NISTIR-5715
Optoelectronics and Optomechanics Manufacturing: An ATP Focused Program Development. Workshop Proceedings. Held in Gaithersburg, Maryland on February 15, 1995.
PB97-104186 *02,204* PC A11/MF A03

NISTIR-5716
Guidelines for the Development of Mapping Tables.
PB96-154539 *02,786* PC A03/MF A01

NISTIR-5717
NIST SIMA Interactive Management Workshop. Held in Fort Belvoir, Virginia on November 14-16, 1994.
PB96-154877 *02,838* PC A08/MF A02

NISTIR-5719
Mapping Integration Definition for Function Modeling (IDEFO) Model into CASE Data Interchange Format (CDIF) Transfer File.
PB96-109533 *01,741* PC A07/MF A02

NISTIR-5720
User's Guide to 'SuperFit' Modeling Software for CMM Probe Lobing.
PB96-128236 *02,921* PC A03/MF A01

NISTIR-5722
Reference Manual for the Algorithm Testing System Version 2.0.
PB96-128244 *02,922* PC A03/MF A01

NISTIR-5723
Airborne Asbestos Method: Bootstrap Method for Determining the Uncertainty of Asbestos Concentration. Version 1.0.
PB96-214614 *00,646* PC A04/MF A01

NISTIR-5724
Error-Bounding in Level-Index Computer Arithmetic.
PB96-109582 *01,742* PC A02/MF A01

NISTIR-5726
Generalized Form Registration Using Structure-Based Techniques.
PB96-191374 *01,858* PC A03/MF A01

NISTIR-5727
Extensions of the Prototype Application Protocol of Ready-to-Wear Apparel Pattern Making.
PB96-128194 *03,198* PC A03/MF A01

NISTIR-5728
Image Gradient Evolution: A Visual Cue for Danger.
PB96-154562 *02,939* PC A03/MF A01

NISTIR-5729
Study of Technology for Detecting Pre-Ignition Conditions of Cooking-Related Fires Associated with Electric and Gas Ranges and Cooktops, Phase 1 Report.
PB96-128095 *00,303* PC A06/MF A02

NISTIR-5730
Overview of the Manufacturing Engineering Toolkit Prototype.
PB96-128228 *02,833* PC A03/MF A01

NISTIR-5732
Calorimetric and Visual Measurements of R123 Pool Boiling on Four Enhanced Surfaces.
PB96-128129 *04,053* PC A04/MF A01

NISTIR-5734
ICSSC Guidance on Implementing Executive Order 12941 on Seismic Safety of Existing Federally Owned or Leased Buildings.
PB96-128103 *00,459* PC A03/MF A01

NISTIR-5735
Distributed Systems: Survey of Open Management Approaches.
PB96-128202 *01,746* PC A03/MF A01

NISTIR-5736
Comparison of POSIX Open System Environment (OSE) and Open Distributed Processing (ODP) Reference Models.
PB96-131495 *01,820* PC A03/MF A01

NISTIR-5737
Method to Determine a Basis Set of Paths to Perform Program Testing.
PB96-131503 *01,747* PC A03/MF A01

NISTIR-5738
NIST RS274KT Interpreter.
PB96-147954 *02,835* PC A05/MF A01

NISTIR-5740
Virtual Environments for Health Care. A White Paper for the Advanced Technology Program (ATP), the National Institute of Standards and Technology.
PB96-147814 *03,594* PC A05/MF A01

NISTIR-5742
Alkali-Silica Reaction and High Performance Concrete.
PB96-131537 *01,345* PC A03/MF A01

NISTIR-5743
Operating Principles of MultiKron Virtual Counter Performance Instrumentation for MIMD Computers.
PB96-131529 *01,632* PC A03/MF A01

NISTIR-5745
Product Realization Process Modeling: A Study of Requirements, Methods and Research Issues.
PB96-147962 *02,836* PC A04/MF A01

NISTIR-5746
Materials Science and Engineering Laboratory Annual Report, 1995. Technical Activities.
PB96-214754 *03,009* PC A05/MF A01

NISTIR-5747
Ceramics Technical Activities, 1995.
PB96-193677 *03,087* PC A11/MF A03

NISTIR-5748
Materials Reliability. Technical Activities, 1995.
PB96-183082 *02,999* PC A07/MF A02

NISTIR-5749
Polymers Technical Activities, 1995.
PB96-193719 *01,291* PC A10/MF A02

NISTIR-5750
Metallurgy. Technical Activities, 1995.
PB96-195284 *03,003* PC A09/MF A02

NISTIR-5751
Reactor Radiation Technical Activities, 1995.
PB96-193644 *03,741* PC A07/MF A02

NISTIR-5752
Summary Report: Workshop on Industrial Applications of Scanned Probe Microscopy (2nd). A Workshop Co-Sponsored by NIST, SEMATECH, ASTM E42.14, and the American Vacuum Society. Held in Gaithersburg, Maryland on May 2-3, 1995.
PB96-131602 *00,509* PC A07/MF A02

NISTIR-5757
Sharing Information via the Internet: An Infoserver Case Study.
PB96-131511 *01,493* PC A03/MF A01

NISTIR-5758
Workplan to Analyze the Energy Impacts of Envelope Airtightness in Office Buildings.
PB96-154463 *00,273* PC A04/MF A01

NISTIR-5759
National Planning for Construction and Building R and D.
PB96-137104 *00,324* PC A06/MF A02

NISTIR-5760
Classified Bibliography: Insulation Condition Monitoring Methods, 1989-1995.
PB96-131586 *02,232* PC A05/MF A01

NISTIR-5762
Standard Generalized Markup Language Test Suite Evaluation Report.
PB96-154992 *01,751* PC A03/MF A01

NISTIR-5763
General Motion Model and Spatio-Temporal Filters for 3-D Motion Interpretations.
PB96-210703 *01,861* PC A07/MF A02

NISTIR-5764
Smoke Plume Trajectory from In situ Burning of Crude Oil in Alaska: Field Experiments.
PB96-131560 *02,594* PC A03/MF A01

NISTIR-5765
Simplified Design Procedure for Hybrid Precast Concrete Connections.
PB96-154836 *00,405* PC A06/MF A01

NISTIR-5766
Solid Propellant Gas Generators: Proceedings of the 1995 Workshop. Held in Gaithersburg, Maryland on June 28-29, 1995.
PB96-131479 *01,412* PC A11/MF A03

NISTIR-5767
Effect of Inclination on the Performance of a Compact Brazed Plate Condenser and Evaporator.
PB96-136973 *02,756* PC A03/MF A01

NISTIR-5769
C++ in Safety Critical Systems.
PB96-154588 *01,750* PC A04/MF A01

NISTIR-5770
How-To Suggestions for Implementing Executive Order 12941 on Seismic Safety of Existing Federal Buildings, A Handbook.
PB96-131552 *00,461* PC A10/MF A03

NISTIR-5771
STandard for the Exchange of Product Model Data (STEP): Procedures for NIST STEP Validation.
PB96-154976 *02,787* PC A03/MF A01

NISTIR-5773
Electronics and Electrical Engineering Laboratory Technical Publication Announcements Covering Laboratory Programs, April to June 1995 with 1995 EEEL Events Calendar.
PB96-137187 *01,941* PC A03/MF A01

NISTIR-5774
Electronics and Electrical Engineering Laboratory Technical Progress Bulletin Covering Laboratory Programs, July to September 1995 with 1996 EEEL Events Calendar.
PB96-147905 *01,942* PC A04/MF A01

NISTIR-5775
Machine Performance Standard Provides Opportunity to Improve Quality and Productivity.
PB96-154521 *02,837* PC A02/MF A01

NISTIR-5776
Santa Ana Fire Department Experiments at South Bristol Street.
PB96-154810 *00,305* PC A11/MF A03

NISTIR-5777
Beyond the Technology Roadmaps: An Assessment of Electronic Materials Research and Development.
PB96-165998 *01,961* PC A05/MF A01

NISTIR-5778
Collection of Results for the SPC/E Water Model.
PB96-147889 *01,127* PC A03/MF A01

NISTIR-5780
Enhancement of R123 Pool Boiling by the Addition of N-Hexane.
PB96-165956 *02,605* PC A04/MF A01

NISTIR-5782
Modified Optimal Algorithm for Active Structural Control.
PB96-165949 *00,472* PC A04/MF A01

NISTIR-5783
Development of a Test Method for Leaching of Lead from Lead-Based Paints Through Encapsulants.
PB96-154984 *03,128* PC A04/MF A01

NISTIR-5784
Study to Determine the Existence of an Azeotropic R-22 'Drop-In' Substitute.
PB96-167812 *02,568* PC A04/MF A01

NISTIR-5785
Summary and Results of the NIST Workshop on Proposed Guidelines for Testing and Evaluation of Seismic Isolation Systems. Held in San Francisco, California on July 25, 1994.
PB96-154901 *00,463* PC A04/MF A01

NISTIR-5787
AutoBid 2.0: The Microcomputer System for Police Patrol Vehicle Selection.
PB96-154570 *04,871* PC A03/MF A01

NISTIR-5788
Public Key Infrastructure Invitational Workshop. Held in McLean, Virginia on September 28, 1995.
PB96-166004 *01,616* PC A08/MF A02

NISTIR-5789
Using S-Check, Alpha Release 1.0.
PB96-165964 *01,767* PC A05/MF A01

NISTIR-5790
Scale-Space-Based Visual-Motion-Cue for Autonomous Navigation.
PB96-183173 *02,940* PC A06/MF A01

NISTIR-5791
Novel Active-Vision-Based Motion Cues for Local Navigation.
PB96-193727 *02,941* PC A05/MF A01

NISTIR-5793
Data Communications Strategy.
PB96-167846 *02,738* PC A05/MF A01

NISTIR-5795
Minimum Mass Flux Requirements to Suppress Burning Surfaces with Water Sprays.
PB96-183181 *01,425* PC A05/MF A01

NISTIR-5796
Guide to a Format for Data on Chemical Admixtures in a Materials Property Database.
PB96-165394 *01,327* PC A04/MF A01
Guide to a Format for Data on Chemical Admixtures in a Materials Property Database. (Reannouncement with new abstract).
PB96-186192 *01,328* PC A04/MF A01

NISTIR-5797
PIECS: A Software Program for Machine Tool Process-Intermittent Error Compensation.
PB96-165980 *02,842* PC A08/MF A02

NISTIR-5798
NASA Fire Detector Study.
PB96-183108 *01,423* PC A04/MF A01

NISTIR-5799
Application of the Pointer State Subgraph to Static Program Slicing.
PB96-167838 *01,768* PC A03/MF A01

NISTIR-5800
Guidelines for Pre-Qualification, Prototype and Quality Control Testing of Seismic Isolation Systems.
PB96-193685 *01,347* PC A08/MF A02

NISTIR-5801
Multizone Modeling of Three Residential Indoor Air Quality Control Options.
PB96-165782 *02,567* PC A08/MF A02

NISTIR-5806
Method of Estimating the Parameters of Tuned Mass Dampers for Seismic Applications.
PB96-167820 *00,473* PC A04/MF A01

NISTIR-5808
Machining Process Planning Activity Model for Systems Integration.
PB96-165428 *02,841* PC A03/MF A01

NISTIR-5809
Numerical Simulation of Rapid Combustion in an Underground Enclosure.
PB96-183132 *01,424* PC A03/MF A01

NISTIR-5810
TMACH Experiment Phase 1. Preliminary Developmental Evaluation.
PB96-195318 *01,618* PC A03/MF A01

NISTIR-5811
Basic Linear Algebra Operations in SLI Arithmetic.
PB96-165931 *03,421* PC A03/MF A01

NISTIR-5815
Electronics and Electrical Engineering Laboratory Technical Progress Bulletin Covering Laboratory Programs, October to December 1995 with 1996 EEEL Events Calendar.
PB96-183116 *01,966* PC A04/MF A01

NISTIR-5816
Electronics and Electrical Engineering Laboratory Technical Publication Announcements Covering Laboratory Programs, July to September 1995 with 1996 EEEL Events Calendar.
PB96-183066 *01,965* PC A03/MF A01

NISTIR-5818
Electronics and Electrical Engineering Laboratory 1995 Technical Accomplishments: Advancing Metrology for Electrotechnology to Support the U.S. Economy.
PB96-164520 *01,959* PC A05/MF A01

NISTIR-5819
X.500 Directory Schema Design Handbook.
PB96-183041 *02,739* PC A03/MF A01

NISTIR-5820
Distributed Communication Methods and Role-Based Access Control for Use in Health Care Applications.
PB96-183165 *01,508* PC A05/MF A01

NISTIR-5821
Aspects of a Product Model Supporting Apparel Virtual Enterprises.
PB96-183231 *02,790* PC A03/MF A01

NISTIR-5822
Proceedings of NIST Workshop: Industry Needs in Welding Research and Standards Development. Held on August 15-16, 1995.
PB96-183124 *02,877* PC A04/MF A01

NISTIR-5823
Survey of Standards for the U.S. Fiber/Textile/Apparel Industry.
PB96-193792 *03,199* PC A06/MF A01

NISTIR-5824
Interoperability Experiments with CORBA and Persistent Object Base Systems.
PB96-183140 *01,772* PC A04/MF A01

NISTIR-5826
Hygrothermal Effects on the Performance of Polymers and Polymeric Composites: A Workshop Report. Held in Gaithersburg, Maryland on September 21-22, 1995.
PB96-183207 *03,180* PC A04/MF A01

NISTIR-5828
CSTL Technical Activities, 1995.
PB96-214630 *00,647* PC A10/MF A03

NISTIR-5832
Electronics and Electrical Engineering Laboratory: 1996 Program Plan. Supporting Technology for U.S. Competitiveness in Electronics.
PB96-175237 *01,962* PC A10/MF A03

NISTIR-5833
Procedure for Product Data Exchange Using STEP Developed in the AutoSTEP Pilot.
PB96-183058 *02,843* PC A04/MF A01

NISTIR-5837
Workshop on Characterizing Diamond Films (4th). Held in Gaithersburg, Maryland on March 4-5, 1996.
PB96-183090 *04,786* PC A04/MF A01

NISTIR-5838
Room-Temperature Thermal Conductivity of Expanded Polystyrene Board for a Standard Reference Material.
PB96-193693 *00,412* PC A04/MF A01

NISTIR-5839
Systems Integration for Manufacturing Applications Program 1995 Annual Report.
PB96-193735 *02,844* PC A05/MF A01

NISTIR-5840
Benefits and Costs of Research: Two Case Studies in Building Technology.
PB96-202221 *00,230* PC A07/MF A02

NISTIR-5842
Methodology for Developing and Implementing Alternative Temperature-Time Curves for Testing the Fire Resistance of Barriers for Nuclear Power Plant Applications.
PB96-193784 *03,742* PC A07/MF A02

NISTIR-5843
Component-Based Handprint Segmentation Using Adaptive Writing Style Model.
PB96-193669 *01,859* PC A03/MF A01

NISTIR-5844
Interoperability Requirements for CAD Data Transfer in the AutoSTEP Project.
PB97-114268 *02,796* PC A03/MF A01

NISTIR-5845
Program of the Manufacturing Engineering Laboratory, 1996. Infrastructural Technology, Measurements, and Standards for the U.S. Manufacturing Industries.
PB96-195276 *02,760* PC A11/MF A03

NISTIR-5846
Computer-Aided Manufacturing Engineering Forum (2nd). Technical Meeting Proceedings. Held in Gaithersburg, Maryland on August 22-23, 1995.
PB96-195334 *02,845* PC A11/MF A03

NISTIR-5847
Warping of Terrace Pavers at the U.S. Capitol Building.
PB96-193651 *00,411* PC A03/MF A01

NISTIR-5848
Notion of a xi-Vector and a Stress Tensor for a General Class of Anisotropic Diffuse Interface Models.
PB96-193776 *04,788* PC A03/MF A01

NISTIR-5849
Summary of Federal Construction and Building R and D in 1994.
PB97-114250 *00,234* PC A04/MF A01

NISTIR-5851
National Semiconductor Metrology Program, Project Portfolio FY 1996.
PB96-195268 *04,789* PC A03/MF A01

NISTIR-5853
Electronics and Electrical Engineering Laboratory Technical Progress Bulletin Covering Laboratory Programs, January to March 1996, with 1996 EEEL Events Calendar.
PB96-191390 *01,969* PC A04/MF A01

NISTIR-5854
Computer Systems Laboratory Computing and Applied Mathematics Laboratory Technical Accomplishments, October 1994-March 1996.
PB96-193768 *01,638* PC A05/MF A01

NISTIR-5855
Specification for Interoperability between Ballistic Imaging Systems. Part 1. Cartridge Cases.
PB96-195524 *01,860* PC A04/MF A01

NISTIR-5856
NIST Construction Automation Program Report No. 2. Proceedings of the NIST Construction Automation Workshop. Held in Gaithersburg, Maryland on March 30-31, 1995.
PB96-202239 *00,413* PC A09/MF A02

NISTIR-5857
State of the Art Report on Seismic Design Requirements for Nonstructural Building Components.
PB96-193800 *00,308* PC A06/MF A01

NISTIR-5859
MV++ v. 1.5a Matrix/Vector Class Reference Guide.
PB96-195326 *01,777* PC A03/MF A01

NISTIR-5860
IML++ v.1.2 Iterative Methods Library Reference Guide.
PB96-195219 *01,776* PC A04/MF A01

NISTIR-5861
SparseLib++ v. 1.5 Sparse Matrix Class Library. Reference Guide.
PB96-193636 *01,775* PC A03/MF A01

NISTIR-5862
Operator Experience with a Hierarchical Real-Time Control System (RCS).
PB96-195516 *03,751* PC A03/MF A01

NISTIR-5863
Benefits and Costs of Research: A Case Study of the Fire Safety Evaluation System.
PB96-202288 *00,232* PC A06/MF A01

NISTIR-5864
Economics of New-Technology Materials: A Case Study of FRP Bridge Decking.
PB96-202353 *01,349* PC A06/MF A01

NISTIR-5865
Development of a Method for Measuring Water-Stripping Resistance of Asphalt/Siliceous Aggregate Mixtures.
PB96-202296 *01,329* PC A09/MF A02

NISTIR-5866
Developing Quality System Documentation Based on ANSI/NCSL Z540-1-1994: The Optical Technology Division's Effort.
PB96-202122 *01,869* PC A05/MF A01

NISTIR-5868
Application Protocol Information Base World Wide Web Gateway.
PB96-202320 *02,791* PC A03/MF A01

NISTIR-5869
Measurement of Rheological Properties of High Performance Concrete: State of the Art Report.
PB96-202338 *00,414* PC A04/MF A01

NISTIR-5870
Shear Design of High-Strength Concrete Beams: A Review of the State-of-the-Art.
PB96-214713 *01,330* PC A11/MF A03

NISTIR-5871
Report on USDA Ultraviolet Spectroradiometers.
PB96-214648 *00,125* PC A04/MF A01

NISTIR-5872
Electronics and Electrical Engineering Laboratory Technical Publication Announcements Covering Laboratory Programs, October to December 1995, with 1996 EEEL Events Calendar.
PB96-202346 *01,978* PC A04/MF A01

NISTIR-5873
Intracycle Evaporative Cooling in a Vapor Compression Cycle.
PB97-116107 *02,762* PC A03/MF A01

NISTIR-5877
Report of a Workshop on Requalification of Tubular Steel Joints in Offshore Structures. Held in Houston, Texas on September 5-6, 1995.
PB96-210760 *03,699* PC A07/MF A02

NISTIR-5878
Fire Safety Engineering in the Pursuit of Performance-Based Codes: Collected Papers.
PB97-114482 *00,235* PC A07/MF A02

NISTIR-5879
Conformance Testing and Specification Management.
PB97-113781 *02,849* PC A03/MF A01

NISTIR-5880
Mathematical Analysis of Practices to Control Moisture in the Roof Cavities of Manufactured Houses.
PB97-106843 *00,278* PC A05/MF A01

NISTIR-5885
Static Structural Analysis of a Reconfigurable Rigid Platform Supported by Elastic Legs.
PB97-113898 *02,960* PC A05/MF A01

NISTIR-5887
Diffuse-Interface Description of Fluid Systems.
PB96-210711 *01,170* PC A04/MF A01

NISTIR-5888
Materials Aspects of Fiber-Reinforced Polymer Composites in Infrastructure.
PB96-210695 *03,184* PC A04/MF A01

NISTIR-5889
Experimental Models for Software Diagnosis.
PB97-113906 *01,783* PC A04/MF A01

NISTIR-5892
Electronics and Electrical Engineering Laboratory Technical Publication Announcements Covering Laboratory Programs, January to March 1996, with 1996 EEEL Events Calendar.
PB96-214622 *01,981* PC A03/MF A01

NISTIR-5893
Experimentally Measured Total X-ray Attenuation Coefficients Extracted from Previously Unprocessed Documents Held by the NIST Photon and Charged Particle Data Center.
PB97-114474 *04,165* PC A04/MF A01

NISTIR-5895
Electronics and Electrical Engineering Laboratory Technical Progress Bulletin Covering Laboratory Programs, April to June 1996 with 1996-1998 EEEL Events Calendar.
PB97-113880 *01,994* PC A04/MF A01

NISTIR-5897
Representation of Axes for Geometric Fitting.
PB97-113799 *01,782* PC A03/MF A01

NISTIR-5898
TBT Agreement Activities of the National Institute of Standards and Technology, 1995.
PB97-104178 *00,499* PC A04/MF A01

NISTIR-5899
Standards Promote Credibility and Technology Transfer: The Need for Greater Industry Support of Technical Committees.
PB97-116206 *02,961* PC A03/MF A01

NISTIR-5900
Multi-Scale Picture of Concrete and Its Transport Properties: Introduction for Non-Cement Researchers.
PB97-115802 *03,107* PC A05/MF A01

NISTIR-5906
Carbon Monoxide Dispersion in Residential Buildings: Literature Review and Technical Analysis.
PB97-114227 *02,571* PC A05/MF A01

NISTIR-5907
Proceedings of a Workshop on Developing and Adopting Seismic Design and Construction Standards for Lifelines. Held in Denver, Colorado on September 25-27, 1991.
PB97-115794 *01,302* PC A16/MF A03

NISTIR-5909
Group 1 for the Process Engineering Data STEP Application Protocol.
PB97-116073 *02,797* PC A99/MF A06

NISTIR-5910
Unified Process Specification Language: Requirements for Modeling Process.
PB97-116123 *02,850* PC A06/MF A01

NOAA-TM-ERL-GLERL-97
Lake Erie Water Temperature Data, Put-in-Bay, Ohio, 1918-1992.
PB96-202452 *03,692* PC A04/MF A01

NREL/TP-411-8246
Atomic-scale characterization of hydrogenated amorphous-silicon films and devices. Annual subcontract report, 14 February 1994--14 April 1995.
DE95009287 *02,294* PC A03/MF A01

NUREG/CP-0136
Proceedings of the Digital Systems Reliability and Nuclear Safety Workshop. Held in Rockville, Maryland on September 13-14, 1993.
NUREG/CP-0136 *03,728* PC A16/MF A03

ORNL/CON-381
Economic, Energy, and Environmental Impacts of the Energy-Related Inventions Program.
DE94-017162 *00,008* PC A05/MF A02

ORNL/SUB/83-21322/03
Abrasive Wear by Diesel Engine Coal-Fuel and Related Particles.
PB95-104915 *01,450* PC A04/MF A01

PB94-100278
Opportunities for Innovation: Advanced Manufacturing Technology.
PB94-100278 *02,801* PC A07/MF A02

PB94-112695
Electroacoustics for Characterization of Particulates and Suspensions. Proceedings of a Workshop. Held in Gaithersburg, Maryland on February 3-4, 1993.
PB94-112695 *00,725* PC A15/MF A03

PB94-123080
Technology Trends in Telecommunications: An Overview.
PB94-123080 *01,462* PC A03/MF A01

PB94-126901
Electronics and Electrical Engineering Laboratory 1994 Program Plan: Supporting Technology for U.S. Competitiveness in Electronics.
PB94-126901 *01,873* PC A09/MF A02

PB94-134897
General Procedures for Registering Computer Security Objects.
PB94-134897 *01,573* PC A03/MF A01

PB94-135001
Report of the NIST Workshop on Digital Signature Certificate Management. Held on December 10-11, 1992.
PB94-135001 *01,574* PC A09/MF A02

PB94-135621
Open Architectures for Machine Control.
PB94-135621 *02,942* PC A03/MF A01

PB94-135639
Crosstalk between Microstrip Transmission Lines.
PB94-135639 *02,210* PC A03/MF A01

PB94-135761
Planning for the Fiber Distributed Data Interface (FDDI).
PB94-135761 *01,621* PC A06/MF A02

PB94-135803
NIST Model PM2 Power Measurement System for 1 mW at 1 GHz.
PB94-135803 *02,018* PC A03/MF A01

PB94-136009
NIST Handbook 44, 1994: Specifications, Tolerances and Other Technical Requirements for Weighing and Measuring Devices as Adopted by the 78th National Conference on Weights and Measures 1993.
PB94-136009 *02,888* PC A11/MF A03

PB94-138989
Report of the National Conference on Weight and Measures (78th). Held in Kansas City, MO. on July 18-22, 1993.
PB94-138989 *02,623* PC A18/MF A04

PB94-139045
Good Security Practices for Electronic Commerce, Including Electronic Data Interchange.
PB94-139045 *01,463* PC A04/MF A01

PB94-139193
Some Factors Affecting Design of a Furniture Calorimeter Hood and Exhaust.
PB94-139193 *00,285* PC A03/MF A01

PB94-139623
Computing Effects and Error for Large Synthetic Perturbation Screenings.
PB94-139623 *01,675* PC A03/MF A01

PB94-139649
Security Considerations for SQL-Based Implementations of STEP.
PB94-139649 *02,766* PC A03/MF A01

PB94-139672
Electromechanical Properties of Superconductors for DOE Fusion Applications.
PB94-139672 *02,250* PC A06/MF A02

PB94-139722
Fire Induced Thermal Fields in Window Glass I: Theory.
PB94-139722 *00,328* PC A03/MF A01

PB94-140167
Guide to Software Engineering Environment Assessment and Evaluation.
PB94-140167 *01,676* PC A04/MF A01

PB94-140407
Computer Programs for Simulation of Lighting/HVAC Interactions.
PB94-140407 *02,501* PC A08/MF A02

PB94-140555
Journal of Research of the National Institute of Standards and Technology, November-December 1993. Volume 98, Number 6.
PB94-140555 *04,223* PC A06/MF A02

PB94-140563
36Cl/Cl Accelerator-Mass-Spectrometry Standards: Verification of Their Serial-Dilution-Solution Preparations by Radioactivity Measurements.
PB94-140563 *00,524*
(Order as PB94-140555, PC A06/MF A02)

PB94-140571
Pressure-Volume-Temperature Relations in Liquid and Solid Tritium.
PB94-140571 *00,726*
(Order as PB94-140555, PC A06/MF A02)

PB94-140589
Filter Transmittance Measurements in the Infrared.
PB94-140589 *04,224*
(Order as PB94-140555, PC A06/MF A02)

PB94-140597
Two Numerical Techniques for Light Scattering by Dielectric Agglomerated Structures.
PB94-140597 *04,225*
(Order as PB94-140555, PC A06/MF A02)

PB94-140605
Wavelengths and Energy Levels of Neutral Kr(84) and Level Shifts in All Kr Even Isotopes.
PB94-140605 *03,780*
(Order as PB94-140555, PC A06/MF A02)

PB94-142460
Enhanced Machine Controller Architecture Overview.
PB94-142460 *02,802* PC A03/MF A01

PB94-142478
Assessment of Uncertainties of Calibration of Resistance Thermometers at the National Institute of Standards and Technology.
PB94-142478 *02,624* PC A03/MF A01

PB94-142486
Mass Unit Disseminated to Surrogated Laboratories Using the NIST Portable Mass Calibration Package.
PB94-142486 *03,781* PC A03/MF A01

PB94-142494
Introduction to Traffic Management for Broadband ISDN.
PB94-142494 *01,464* PC A03/MF A01

PB94-142502
Applying Virtual Environments to Manufacturing.
PB94-142502 *02,803* PC A03/MF A01

PB94-142510
Assessment of Uncertainties of Liquid-in-Glass Thermometer Calibrations at the National Institute of Standards and Technology.
PB94-142510 *02,625* PC A03/MF A01

PB94-142528
Context Analysis of the Network Management Domain. Conducted as Part of the Domain Analysis Case Study.
PB94-142528 *01,465* PC A05/MF A01

PB94-142536
Report on Application Integration Architectures (AIA) Workshop. Held in Dallas, Texas on February 8-12, 1993.
PB94-142536 *01,803* PC A07/MF A02

PB94-142791
Feasibility Study: Reference Architecture for Machine Control Systems Integration.
PB94-142791 *02,804* PC A12/MF A03

PB94-142973
In situ Burning of Oil Spills: Mesoscale Experiments.
PB94-142973 *01,355* PC A04/MF A01

PB94-143344
Evaluation of GSA Maintenance Practices of Large Centrifugal Chillers and Review of GSA Refrigerant Management Practices.
PB94-143344 *02,502* PC A04/MF A01

PB94-143401
Next Generation Computer Resources: Reference Model for Project Support Environments (Version 2.0).
PB94-143401 *01,677* PC A06/MF A02

PB94-143427
Computational Model for the Rise and Dispersion of Wind-Blown, Buoyancy-Driven Plumes. Part 2. Linearly Stratified Atmosphere.
PB94-143427 *00,119* PC A03/MF A01

PB94-143542
Ground-Based Smoke Sampling Techniques Training Course and Collaborative Local Smoke Sampling in Saudi Arabia.
PB94-143542 *02,532* PC A05/MF A01

PB94-145620
Reliable Optical Flow Algorithm Using 3-D Hermite Polynomials.
PB94-145620 *01,829* PC A03/MF A01

PB94-145653
Manual for Ventilation Assessment in Mechanically Ventilated Commercial Buildings.
PB94-145653 *00,239* PC A07/MF A02

PB94-145661
System for Calibration of the Marshall Compaction Hammer.
PB94-145661 *01,303* PC A08/MF A02

PB94-145711
Aperture Excitation of Electrically Large, Lossy Cavities.
PB94-145711 *00,029* PC A05/MF A01

PB94-145968
Electronics and Electrical Engineering Laboratory Technical Progress Bulletin Covering Laboratory Programs, January to March 1991, with 1991 EEEL Events Calendar.
PB94-145968 *02,113* PC A03/MF A01

PB94-145976
Use of Computer Models to Predict Temperature and Smoke Movement in High Bay Spaces.
PB94-145976 *00,191* PC A04/MF A01

PB94-145984
Alternating-Field Susceptometry and Magnetic Susceptibility of Supercondoctors. Presented at Office of Naval Research Workshop on Magnetic Susceptibility of Superconductors and Other Spin Systems. Held in Berkeley Springs, West Virginia on 20 May 1991.
PB94-145984 *04,435* PC A01/MF A01

PB94-146636
Modulation of Fossil Fuel Production by Global Temperature Variations, 2.
PB94-146636 *02,533* PC A04/MF A01

PB94-146677
Thermophysical Properties of Fluids for the Gas Industry. Final Report, February 1, 1988-August 31, 1993.
PB94-146677 *02,472* PC A03/MF A01

PB94-150919
Guide to Configuration Management and the Revision Control System for Testbed Users.
PB94-150919 *01,678* PC A03/MF A01

PB94-151776
NIST 60-Millimeter Diameter Cylindrical Cavity Resonator: Performance Evaluation for Permittivity Measurements.
PB94-151776 *02,251* PC A11/MF A03

PB94-151842
NIST Standard Reference Data Products Catalog, 1994.
PB94-151842 *00,727* PC A06/MF A02

PB94-152006
Fire Safety of Passenger Trains: A Review of Current Approaches and of New Concepts.
PB94-152006 *04,848* PC A11/MF A03

PB94-152204
Abstract and Index Collection in the Research Information Center of the National Institute of Standards and Technology.
PB94-152204 *02,744* PC A03/MF A01

PB94-152691
Assessment of Uncertainties of Thermocouple Calibrations at NIST.
PB94-152691 *03,782* PC A03/MF A01

PB94-152709
Submissions to a Planned Encyclopedia of Operations Research on Computational Geometry and the Voronoi/Delaunay Construct.
PB94-152709 *03,425* PC A03/MF A01

PB94-152725
Growth Surface for the Slopes at the Boundary of a Polygon.
PB94-152725 *03,408* PC A03/MF A01

PB94-152733
Photonic Materials: A Report on the Results of a Workshop. Held in Gaithersburg, Maryland on August 26-27, 1992, Volume 1.
PB94-152733 *02,114* PC A05/MF A01

PB94-154325
APDE Demonstration System Architecture. National PDES Testbed Report Series.
PB94-154325 *02,767* PC A03/MF A01

PB94-154341
Electronics and Electrical Engineering Laboratory Technical Progress Bulletin Covering Programs, October to December 1993, with 1994/1995 EEEL Events Calendar.
PB94-154341 *02,115* PC A03/MF A01

PB94-154358
Variant Design for Mechanical Artifacts-A State of the Art Survey.
PB94-154358 *02,768* PC A03/MF A01

PB94-154382
Source of Phenol Emissions Affecting the Indoor Air of an Office Building.
PB94-154382 *03,600* PC A04/MF A01

PB94-154390
Corrosion Resistance of Materials for Renovation of the United States Botanic Garden Conservatory.
PB94-154390 *00,032* PC A03/MF A01

PB94-155579
Development and Characterization of Insulating Layers on Silicon Carbide: Annual Report for February 14, 1988 to February 14, 1989.
PB94-155579 *02,295* PC A03/MF A01

PB94-155587
Sulfur Dioxide Capture in the Combustion of Mixtures of Lime, Refuse-Derived Fuel, and Coal.
PB94-155587 *02,534* PC A04/MF A01

PB94-156866
Concurrent Flow Flame Spread Study.
PB94-156866 *01,356* PC A08/MF A02

PB94-156957
Transient Cooling of a Hot Surface by Droplets Evaporation.
PB94-156957 *03,783* PC A08/MF A02

PB94-156965
Numerical Analysis Support for Compartment Fire Modeling and Incorporation of Heat Conduction into a Zone Fire Model.
PB94-156965 *01,357* PC A04/MF A01

PB94-157831
Opportunities for Innovation: Biotechnology.
PB94-157831 *00,009* PC A12/MF A03

PB94-158268
Boundary Conforming Grid Generation System for Interface Tracking.
PB94-158268 *03,312* PC A03/MF A01

PB94-158573
Study to Determine the Most Important Parameters for Evaluating the Resistance of Soft Body Armor to Penetration by Edged Weapons.
PB94-158573 *03,757* PC A03/MF A01

PB94-159761
Metrology for Electromagnetic Technology: A Bibliography of NIST Publications.
PB94-159761 *02,116* PC A04/MF A01

PB94-159779
Seismic Instrumentation of Existing Buildings.
PB94-159779 *00,420* PC A04/MF A01

PB94-159787
Center for Electronics and Electrical Engineering Technical Progress Bulletin Covering Center Programs, October to December, with 1991 CEEE Events Calendar.
PB94-159787 *02,296* PC A03/MF A01

PB94-159795
Structural EXPRESS Editor.
PB94-159795 *02,769* PC A04/MF A01

PB94-160066
Report on the Workshop on Manufacturing Polymer Composites by Liquid Molding. Held in Gaithersburg, Maryland on September 20-22, 1993.
PB94-160066 *03,131* PC A13/MF A03

PB94-160736
Summary Report of NIST's Industry-Government Consortium Research Program on Flowmeter Installation Effects with Emphasis on the Research Period, January-September 1991: The Reducer.
PB94-160736 *04,196* PC A04/MF A01

PB94-160744
Computation of Dendrites Using a Phase Field Model.
PB94-160744 *04,436* PC A03/MF A01

PB94-160751
Performance Approach to the Development of Criteria for Low-Sloped Roof Membranes.
PB94-160751 *00,329* PC A03/MF A01

PB94-160769
CSTL Technical Activities 1991.
PB94-160769 *00,728* PC A16/MF A03

PB94-160777
Microstructural Features of Some Low Water/Solids, Silica Fume Mortars Cured at Different Temperatures.
PB94-160777 *00,330* PC A03/MF A01

PB94-160785
Comparison of Finite Element and Analytic Calculations of the Resonant Modes and Frequencies of a Thick Shell Sphere.
PB94-160785 *02,626* PC A03/MF A01

PB94-160793
Review of Mathematical Function Library for Microsoft-FORTRAN, John Wiley and Sons, 1989.
PB94-160793 *01,679* PC A03/MF A01

PB94-160801
Cylinder Wipe Air-Drying Intaglio Ink Vehicles for U.S. Currency Inks.
PB94-160801 *03,115* PC A03/MF A01

PB94-160819
Technical Program of the Factory Automation Systems Division 1993.
PB94-160819 *02,805* PC A03/MF A01

PB94-160835
National Type Evaluation Program: Index of Device Evaluations by Company. NCWM Publication 5 Part A (Second Edition).
PB94-160835 *02,889* PC A05/MF A01

PB94-160843
Properties and Interactions of Oral Structures and Restorative Materials. Annual Report for Period October 1, 1990 to September 30, 1991.
PB94-160843 *03,558* PC A06/MF A01

PB94-160850
NVLAP Procedures U.S. Code of Federal Regulations. Title 15, Subtitle A, Chapter 2, Part 7. (Effective December 1984; Amended September 1990).
PB94-160850 *02,627* PC A03/MF A01

PB94-160868
Issues and Recommendations for a STEP Application Protocol Framework. National PDES Testbed.
PB94-160868 *02,770* PC A05/MF A01

PB94-160876
Summaries of Center for Fire Research In-House Projects and Grants: 1990.
PB94-160876 *00,286* PC A10/MF A03

PB94-160975
Journal of Physical and Chemical Reference Data, Volume 22, No. 1, January/February 1993.
PB94-160975 *00,729* Not available NTIS

PB94-160983
Thermodynamic Properties of the Group IIA Elements.
PB94-160983 *00,730* Not available NTIS

PB94-160991
Spectroscopy and Structure of the Lithium Hydride Diatomic Molecules and Ions.
PB94-160991 *00,731* Not available NTIS

PB94-161007
Quantum Yields for the Photosensitized Formation of the Lowest Electronically Excited Singlet State of Molecular Oxygen in Solution.
PB94-161007 *00,732* Not available NTIS

PB94-161114
Northridge Earthquake, 1994. Performance of Structures, Lifelines and Fire Protection Systems.
PB94-161114 *00,421* PC A09/MF A02

PB94-161320
Electronics and Electrical Engineering Laboratory: 1994 Strategic Plan. Supporting Technology for U.S. Competitiveness in Electronics.
PB94-161320 *01,874* PC A04/MF A01

PB94-161502
NIST Reactor: Summary of Activities October 1992 through September 1993.
PB94-161502 *04,437* PC A08/MF A02

PB94-161635
Rare-Earth Isotopes as Tracers of Particulate Emissions: An Urban Scale Test.
PB94-161635 *02,535* PC A03/MF A01

PB94-161734
Draft Guidelines for Quality Control Testing of Elastomeric Seismic Isolation Systems.
PB94-161734 *00,422* PC A03/MF A01

PB94-161809
Computer Graphics Metafile (CGM): Procedures for NIST CGM Validation Test Service.
PB94-161809 *01,804* PC A03/MF A01

PB94-161817
Earthquake Resistant Construction of Electric Transmission and Telecommunication Facilities Serving the Federal Government Report.
PB94-161817 *02,460* PC A03/MF A01

PB94-161924
Bibliography on Apparel Sizing and Related Issues.
PB94-161924 *02,806* PC A03/MF A01

PB94-161932
Recertification of the Standard Reference Material 1475A, a Linear Polyethylene Resin.
PB94-161932 *02,628* PC A03/MF A01

PB94-161940
Draft Guidelines for Pre-Qualification and Prototype Testing of Seismic Isolation Systems.
PB94-161940 *01,331* PC A06/MF A01

PB94-161957
Draft Guidelines for Quality Control Testing of Sliding Seismic Isolation Systems.
PB94-161957 *01,332* PC A03/MF A01

PB94-161999
Earthquake Resistant Construction of Gas and Liquid Fuel Pipeline Systems Serving, or Regulated By, the Federal Government.
PB94-161999 *04,846* PC A05/MF A01

PB94-162211
Journal of Physical and Chemical Reference Data, Volume 22, No. 2, March/April 1993.
PB94-162211 *00,733* Not available NTIS

PB94-162229
Wavelengths and Energy Level Classifications for the Spectra of Sulfur (S I through S XVI).
PB94-162229 *00,734* Not available NTIS

PB94-162237
Thermodynamic Properties of Alkenes (Mono-Olefins Larger Than C4).
PB94-162237 *00,735* Not available NTIS

PB94-162245
Thermodynamic Behavior of the CO2-H2O System from 400 to 1000 K, up to 100 MPa and 30% Mole Fraction of CO2.
PB94-162245 *00,736* Not available NTIS

PB94-162252
Thermodynamics of Enzyme-Catalyzed Reactions: Part 1. Oxidoreductases.
PB94-162252 *00,737* Not available NTIS

PB94-162260
Journal of Physical and Chemical Reference Data, Volume 22, No. 3, May/June 1993.
PB94-162260 *00,738* Not available NTIS

PB94-162278
Estimation of the Heat Capacities of Organic Liquids as a Function of Temperature Using Group Additivity. I. Hydrocarbon Compounds.
PB94-162278 *00,739* Not available NTIS

PB94-162286
Estimation of the Heat Capacities of Organic Liquids as a Function of Temperature Using Group Additivity. II. Compounds of Carbon, Hydrogen, Halogens, Nitrogen, Oxygen, and Sulfur.
PB94-162286 *00,740* Not available NTIS

PB94-162294
Thermodynamic and Thermophysical Properties of Organic Nitrogen Compounds. Part II. 1- and 2-Butanamine, 2-Methyl-1-Propanamine, 2-Methyl-2-Propanamine, Pyrrole, 1-, 2-, and 3-Methylpyrrole, Pyridine, 2-, 3-, and 4-Methylpyridine, Pyrrolidine, Piperidine, Indole, Quinoline, Isoquinoline, Acridine, Carbazole, Phenanthridine, 1- and 2-Naphthalenamine, and 9-Methylcarbazole.
PB94-162294 *00,741* Not available NTIS

PB94-162302
International Equations for the Saturation Properties of Ordinary Water Substance. Revised According to the International Temperature Scale of 1990. Addendum to Journal of Physical and Chemical Reference Data 16, 893 (1987).
PB94-162302 *00,742* Not available NTIS

PB94-162310
Journal of Physical and Chemical Reference Data, Volume 22, No. 4, July/August 1993.
PB94-162310 *00,743* Not available NTIS

PB94-162328
Estimation of the Thermodynamic Properties of C-H-N-O-S-Halogen Compounds at 298.15 K.
PB94-162328 *00,744* Not available NTIS

PB94-162336
Journal of Physical and Chemical Reference Data, Volume 22, No. 5, September/October 1993.
PB94-162336 *00,745* Not available NTIS

PB94-162344
Compilation of Energy Levels and Wavelengths for the Spectrum of Singly-Ionized Oxygen (O II).
PB94-162344 *00,746* Not available NTIS

PB94-162351
Energy Levels of Germanium, Ge I through Ge XXXII.
PB94-162351 *00,747* Not available NTIS

PB94-162369
Spectral Data and Grotrian Diagrams for Highly Ionized Chromium, Cr V through Cr XXIV.
PB94-162369 *00,748* Not available NTIS

PB94-162500
Voluntary Product Standard PS 20-94. American Softwood Lumber Standard.
PB94-162500 *03,402* PC A03/MF A01

PB94-162518
Computer Systems Laboratory Annual Report, 1993.
PB94-162518 *01,622* PC A05/MF A02

PB94-162534
Materials Science and Engineering Laboratory Annual Report, 1993. NAS-NRC Assessment Panel, April 21-22, 1994.
PB94-162534 *02,969* PC A05/MF A01

PB94-162559
North American ISDN Users' Forum Agreements on Integrated Services Digital Network.
PB94-162559 *01,466* PC A16/MF A03

PB94-162583
Proceedings of the Workshop on the Federal Criteria for Information Technology Security. Held in Ellicot City, Maryland on June 2-3, 1993.
PB94-162583 *01,575* PC A04/MF A01

PB94-162591
Ceramics Technical Activities, 1993 (NAS-NRC Assessment Panel April 21-22, 1994).
PB94-162591 *03,031* PC A10/MF A03

PB94-162831
U.S. Navy Coordinate Measuring Machines: A Study of Needs.
PB94-162831 *02,807* PC A04/MF A01

PB94-163003
Airborne Asbestos Method: Standard Test Method for High Precision Counting of Asbestos Collected on Filters. Version 1.0.
PB94-163003 *00,525* PC A02/MF A01

PB94-163029
Concept for an Algorithm Testing and Evaluation Program at NIST.
PB94-163029 *02,890* PC A03/MF A01

PB94-163037
Examination of Parameters That Can Cause Error in Mass Determinations.
PB94-163037 *03,784* PC A03/MF A01

PB94-163045
Airborne Asbestos Method: Standard Test Method for Verified Analysis of Asbestos by Transmission Electron Microscopy. Version 2.0.
PB94-163045 *00,526* PC A03/MF A01

PB94-163052
Electronic Balance and Some Gravimetric Applications. (The Density of Solids and Liquids, Pycnometry and Mass).
PB94-163052 *03,785* PC A03/MF A01

PB94-163060
Piggyback Balance Experiment: An Illustration of Archimedes' Principles and Newton's Third Law.
PB94-163060 *03,786* PC A03/MF A01

PB94-163078
Determination of Density of Mass Standards: Requirement and Method.
PB94-163078 *03,787* PC A03/MF A01

PB94-163086
Distributed Supercomputing Software: Experiences with the Parallel Virtual Machine - PVM.
PB94-163086 *01,680* PC A03/MF A01

PB94-163383
Putting the Information Infrastructure to Work: Report of the Information Infrastructure Task Force Committee on Applications and Technology.
PB94-163383 *00,001* PC A06/MF A02

PB94-163441
Feasibility and Design Considerations of Emergency Evacuation by Elevators.
PB94-163441 *00,287* PC A07/MF A02

PB94-163458
Design Guide for CMOS-On-SIMOX. Test Chips NIST3 and NIST4.
PB94-163458 *02,297* PC A05/MF A01

PB94-163466
Models, Managing Models, Quality Models: An Example of Quality Management.
PB94-163466 *02,891* PC A03/MF A01

PB94-163474
Compatibility Analysis of the ANSI and ISO IRDS Services Interfaces.
PB94-163474 *01,805* PC A06/MF A02

PB94-163482
Validation Testing System Requirements. National PDES Testbed Report Series.
PB94-163482 *02,771* PC A03/MF A01

PB94-163490
NIST Support to the Next Generation Controller Program: 1991 Final Technical Report.
PB94-163490 *02,808* PC A09/MF A02

PB94-164019
Fire Data Management System, FDMS 2.0, Technical Documentation.
PB94-164019 *01,358* PC A05/MF A01

PB94-164035
Supplement to Stable Implementation Agreements for Open Systems Interconnection Protocols. Version 3, September 1990. Change Page Index, Version 3, June 1990 (Stable) Change Pages Issued December 1990; Output from September 1990 OSI Workshop (NIST Special Publication 500-177).
PB94-164035 *01,467* PC A06/MF A02

PB94-164043
NIST Measurement Services: NIST Pressure Calibration Service.
PB94-164043 *02,892* PC A06/MF A02

PB94-164183
Intelligent Processing of Materials, Technical Activities 1993 (NAS-NRC Assessment Panel, April 21-22, 1994).
PB94-164183 *02,809* PC A04/MF A01

PB94-164191
BFRL Fire Publications, 1993.
PB94-164191 *00,192* PC A03/MF A01

PB94-164316
Color Supplement to NIST Special Publication 400-93: Semiconductor Measurement Technology: Design and Testing Guides for the CMOS and Lateral Bipolar-on-SOI Test Library.
PB94-164316 *02,298* PC A03/MF A01

PB94-164373
Conformance Assessment of Transport Layer Security Implementations.
PB94-164373 *01,576* PC A03/MF A01

PB94-164381
CONTAM93 User Manual.
PB94-164381 *02,536* PC A05/MF A01

PB94-164399
Time-Perturbation Tuning of MIMD Programs.
PB94-164399 *01,681* PC A03/MF A01

PB94-164407
Analysis of Failed Dry Pipe Fire Suppression System Couplings from the Filene Center at Wolf Trap Farm Park for the Performing Arts.
PB94-164407 *00,331* PC A03/MF A01

PB94-165206
User's Guide for the PHIGS Validation Tests (Version 2.1).
PB94-165206 *01,682* PC A08/MF A02

PB94-165537
Transmission/Reflection and Short-Circuit Line Methods for Measuring Permittivity and Permeability.
PB94-165537 *02,211* PC A06/MF A02

PB94-165602
Measurement and Determination of Radon Source Potential: A Literature Review.
PB94-165602 *02,576* PC A09/MF A03

PB94-165941
Experimental and Numerical Studies on Two-Dimensional Gravity Currents in a Horizontal Channel.
PB94-165941 *01,359* PC A12/MF A03

PB94-165958
Electronics and Electrical Engineering Laboratory Technical Progress Bulletin Covering Laboratory Programs, October to December 1992, with 1992/1993 EEEL Events Calendar.
PB94-165958 *02,299* PC A03/MF A01

PB94-165966
Publications of the Manufacturing Engineering Laboratory Covering the Period January 1989-September 1992.
PB94-165966 *02,750* PC A06/MF A02

PB94-165974
Radiation and Mixing Properties of Buoyant Turbulent Diffusion Flames.
PB94-165974 *01,360* PC A04/MF A01

PB94-165982
Least-Cost Energy Decisions for Buildings: Part 2. Uncertainty and Risk Video Training Workbook.
PB94-165982 *00,240* PC A04/MF A01

PB94-165990
Bibliography of the NIST Electromagnetic Fields Division Publications.
PB94-165990 *01,875* PC A06/MF A02

PB94-166006
Catalog of National ISDN Solutions for Selected NIUF Applications.
PB94-166006 *01,468* PC A99/MF A06

PB94-166212
Learning to Change: Opportunities to Improve the Performance of Smaller Manufacturers.
PB94-166212 *00,010* PC A08/MF A02

PB94-168044
Evaluating Form Designs for Optical Character Recognition.
PB94-168044 *01,830* PC A06/MF A02

PB94-168051
Unconstrained Handprint Recognition Using a Limited Lexicon.
PB94-168051 *01,831* PC A03/MF A01

PB94-168390
Design and Development of an Information Retrieval System for the EAMATE Data. Volume 2 of 2. Appendices.
PB94-168390 *00,487* PC A19/MF A04

PB94-168556
Journal of Physical and Chemical Reference Data, Volume 22, No. 6, November/December 1993.
PB94-168556 *00,749* Not available NTIS

PB94-168564
Thermodynamic Properties of Synthetic Sapphire (alpha-Al2O3), Standard Reference Material 720 and the Effect of

Temperature-Scale Differences on Thermodynamic Properties.
PB94-168564 *00,750* Not available NTIS

PB94-168572
Thermodynamic Properties of Gaseous Silicon Monotelluride and the Bond Dissociation Enthalpy D(sub m)(SiTe) at T approaches 0.
PB94-168572 *00,751* Not available NTIS

PB94-168580
Disilicides of Tungsten, Molybdenum, Tantalum, Titanium, Cobalt, and Nickel, and Platinum Monosilicide: A Survey of Their Thermodynamic Properties.
PB94-168580 *00,752* Not available NTIS

PB94-168598
Evaluated Bimolecular Ion-Molecule Gas Phase Kinetics of Positive Ions for Use in Modeling Planetary Atmospheres, Cometary Comae, and Interstellar Clouds.
PB94-168598 *00,753* Not available NTIS

PB94-168606
Atomic Weights of the Elements 1991.
PB94-168606 *00,754* Not available NTIS

PB94-169737
Journal of Research of the National Institute of Standards and Technology. January/February 1994. Volume 99, Number 1.
PB94-169737 *02,019* PC A07/MF A02

PB94-169745
Precision Comparison of the Lattice Parameters of Silicon Monocrystals.
PB94-169745 *04,438* Not available NTIS

PB94-169752
NIST 30 MHz Linear Measurement System.
PB94-169752 *02,020* Not available NTIS

PB94-169760
Uncertainties in Dimensional Measurements Made at Nonstandard Temperatures.
PB94-169760 *02,893* Not available NTIS

PB94-169778
Null-Balanced Total-Power Radiometer System NCS1.
PB94-169778 *02,021* Not available NTIS

PB94-169786
Derivation of the System Equation for Null-Balanced Total-Power Radiometer System NCS1.
PB94-169786 *02,022* Not available NTIS

PB94-169794
Evaluation of Uncertainties of the Null-Balanced Total-Power Radiometer System NCS1.
PB94-169794 *02,023* Not available NTIS

PB94-169802
Cryogenic Blackbody Calibrations at the National Institute of Standards and Technology Low Background Infrared Calibration Facility.
PB94-169802 *02,117* Not available NTIS

PB94-172012
Influence of Tempering Method on Residual Stress in Dental Porcelain.
PB94-172012 *00,138* Not available NTIS

PB94-172020
Electric-Field Strengths Measured Near Personal Transceivers.
PB94-172020 *01,564* Not available NTIS

PB94-172038
Lead Abatement in Buildings and Related Structures.
PB94-172038 *03,601* Not available NTIS

PB94-172046
Toward a Reference Model Architecture for Real-Time Intelligent Control Systems (ARTICS).
PB94-172046 *02,932* Not available NTIS

PB94-172053
Monte Carlo Approach to the Approximation of Invariant Measures.
PB94-172053 *03,409* Not available NTIS

PB94-172061
Coordinating Cascaded Surge Protection Devices: High-Low versus Low-High.
PB94-172061 *02,463* Not available NTIS

PB94-172079
Metrication.
PB94-172079 *03,676* Not available NTIS

PB94-172087
Monte Carlo and Mean-Field Calculations of the Magnetocaloric Effect of Ferromagnetically Interacting Clusters.
PB94-172087 *03,201* Not available NTIS

PB94-172095
Local Area Networks in NAA: Advantages and Pitfalls.
PB94-172095 *00,527* Not available NTIS

PB94-172103
Thin Film Thermocouples for Measurement of Wall Temperatures in Internal Combustion Engines.
PB94-172103 *01,449* Not available NTIS

PB94-172111
Infinite Divisibility and the Identification of Singular Waveforms.
PB94-172111 *02,701* Not available NTIS

PB94-172129
RDFs and Fe-Fe Pair Correlations in an AlCuFe Icosahedral Alloy by Double Isotopic Substitution.
PB94-172129 *04,439* Not available NTIS

PB94-172137
Ultrasonic Measurements of Surface Roughness.
PB94-172137 *04,181* Not available NTIS

PB94-172145
Calcium Phosphate Precipitation in Liposomal Suspensions.
PB94-172145 *03,452* Not available NTIS

PB94-172152
Complete Reduction of the Euler-Poinsot Problem.
PB94-172152 *03,788* Not available NTIS

PB94-172160
Psychological Aspects of Lighting: A Review of the Work of CIE TC 3.16.
PB94-172160 *00,241* Not available NTIS

PB94-172178
Rotational Dynamics of Solid C70: A Neutron-Scattering Study.
PB94-172178 *00,755* Not available NTIS

PB94-172186
Dielectric Properties Measurements and Data.
PB94-172186 *01,876* Not available NTIS

PB94-172194
Formal Multi-Layer Test Methodology and Its Application to OSI.
PB94-172194 *02,718* Not available NTIS

PB94-172202
ISO/IEC Workshop on Worldwide Recognition of OSI Test Results Regional Progress - North America.
PB94-172202 *02,719* Not available NTIS

PB94-172210
Raman and Fluorescence Spectra Observed in Laser Microprobe Measurements of Several Compositions in the Ln-Ba-Cu-O System.
PB94-172210 *04,440* Not available NTIS

PB94-172228
Leakage Current Detection in Cryogenic Current Comparator Bridges.
PB94-172228 *02,024* Not available NTIS

PB94-172236
Digitized Simulation of Mercury Intrusion Porosimetry.
PB94-172236 *01,304* Not available NTIS

PB94-172244
Octacalcium Phosphate. 3. Infrared and Raman Vibrational Spectra.
PB94-172244 *00,756* Not available NTIS

PB94-172251
PC-Based Prototype Expert System for Data Management and Analysis of Creep and Fatigue of Selected Materials at Elevated Temperatures.
PB94-172251 *03,202* Not available NTIS

PB94-172269
Complementary Molecular Information on Phthalocyanine Compounds Derived from Laser Microprobe Mass Spectrometry and Micro-Raman Spectroscopy.
PB94-172269 *00,757* Not available NTIS

PB94-172277
Analysis of a Biologically Motivated Neural Network for Character Recognition.
PB94-172277 *00,182* Not available NTIS

PB94-172285
Hot Carrier Excitation of Adlayers: Time-Resolved Measurement of Adsorbate-Lattice Coupling.
PB94-172285 *00,758* Not available NTIS

PB94-172293
Thermal Pulse Study of the Polarization Distributions Produced in Polyvinylidene Fluoride by Corona Poling at Constant Current.
PB94-172293 *01,195* Not available NTIS

PB94-172301
RDI-SIM ECMA Inter-Domain Routing Protocol Simulation Tool.
PB94-172301 *01,683* Not available NTIS

PB94-172319
beta-D-Glucosyl-Hydroxymethyluracil: A Novel Modified Base Present in the DNA of the Parastic Protozoan T. brucei.
PB94-172319 *03,524* Not available NTIS

PB94-172327
Gaseous Electronics Conference Radio-Frequency Reference Cell: A Defined Parallel-Plate Radio-Frequency System for Experimental and Theoretical Studies of Plasma-Processing Discharges.
PB94-172327 *04,404* Not available NTIS

PB94-172335
Bringing Natural Language Information Retrieval Out of the Closet.
PB94-172335 *02,720* Not available NTIS

PB94-172343
Recent Experimental and Modeling Developments in High Temperature Thermochemistry.
PB94-172343 *00,759* Not available NTIS

PB94-172350
Effect of DC Tests on Induced Space Charge.
PB94-172350 *02,212* Not available NTIS

PB94-172368
Wear Mechanism Maps of Ceramics.
PB94-172368 *03,229* Not available NTIS

PB94-172376
Electron Screening Correction to the Self Energy in High-Z Atoms.
PB94-172376 *03,789* Not available NTIS

PB94-172384
Investigation of the Effects of Aging on the Calibration of a Kerr-Cell Measuring System for High Voltage Impulses.
PB94-172384 *02,025* Not available NTIS

PB94-172392
Shear-Excited Morphological States in a Triblock Copolymer.
PB94-172392 *01,196* Not available NTIS

PB94-172400
Fracture Mechanics Analysis of Near-Surface Cracks.
PB94-172400 *03,230* Not available NTIS

PB94-172418
Improvement in Predicting Smoke Movement in Compartmented Structures.
PB94-172418 *00,332* Not available NTIS

PB94-172426
Simultaneous Visual and Calorimetric Measurements of R11, R123, and R123/Alkylbenzene Nucleate Flow Boiling.
PB94-172426 *03,251* Not available NTIS

PB94-172434
Error Propagation Biases in the Calculation of Indentation Fracture Toughness for Ceramics.
PB94-172434 *03,032* Not available NTIS

PB94-172442
Intercomparison of NIST, NPL, PTB, and VSL Thermal Voltage Converters from 100 kHz to 1 MHz.
PB94-172442 *02,026* Not available NTIS

PB94-172459
Intercomparison of Thermal Converters at NIM, NIST, PTB, SIRI and VSL from 10 to 100 MHz.
PB94-172459 *02,027* Not available NTIS

PB94-172467
Thermodynamics of the Hydrolysis of Penicillin G and Ampicillin.
PB94-172467 *03,596* Not available NTIS

PB94-172475
Neutron-Spectroscopy Study of the Hydrogen Vibrations in Hydrogen-Doped YBa2Cu3Ox.
PB94-172475 *04,441* Not available NTIS

PB94-172483
Efficient Method to Compute the Maximum Transient Drain Current Overshoot in Silicon on Insulator Devices.
PB94-172483 *02,300* Not available NTIS

PB94-172491
Planar Near-Field Alignment.
PB94-172491 *01,998* Not available NTIS

PB94-172509
Characterization of the Binding of Gallium, Platinum, and Uranium to Pseudomonas Fluorescens by Small-Angle X-ray Scattering and Transmission Electron Microscopy.
PB94-172509 *03,453* Not available NTIS

PB94-172517
Electrodeposition.
PB94-172517 *00,760* Not available NTIS

PB94-172525
Use of Ion Scattering Spectroscopy to Monitor the Nb Target Nitridation during Reactive Sputtering.
PB94-172525 *00,761* Not available NTIS

PB94-172533
Replicate Measurements for Data Quality and Environmental Modeling.
PB94-172533 *02,515* Not available NTIS

PB94-172541
Nitrogen Effect on Elastic Constants of f.c.c. Fe-18Cr-19Mn Alloys.
PB94-172541 *03,203* Not available NTIS

PB94-172558
Structural and Magnetic Ordering in Iron Oxide/Nickel Oxide Multilayers by X-ray and Neutron Diffraction (Invited).
PB94-172558 *04,442* Not available NTIS

PB94-172566
Time-Perturbation Tuning of MIMD Programs.
PB94-172566 *01,684* Not available NTIS

PB94-172574
Role of Adsorbed Alkalis in Desorption Induced by Electronic Transitions.
PB94-172574 *00,762* Not available NTIS

PB94-172582
Comparative Measurements of High-Voltage Impulses Using a Kerr Cell and a Resistor Divider.
PB94-172582 *02,028* Not available NTIS

PB94-172590
Radiance Temperature (in the Wavelength Range 519-906 nm) of Tungsten at Its Melting Point by a Pulse-Heating Technique.
PB94-172590 *03,397* Not available NTIS

PB94-172608
Adsorption of Low-Molecular-Weight Sodium Polyacrylate on Hydroxyapatite.
PB94-172608 *00,139* Not available NTIS

PB94-172616
Interaction of Some Coupling Agents and Organic Compounds with Hydroxyapatite: Hydrogen Bonding, Adsorption and Adhesion.
PB94-172616 *00,140* Not available NTIS

PB94-172624
Neutron Scattering Study of Shear Induced Turbidity in Polystyrene/Dioctyl Phthalate Solutions at High Shear Rates.
PB94-172624 *01,197* Not available NTIS

PB94-172632
Time Dependent Small Angle Neutron Scattering Behavior in Triblock Copolymers Under Steady Shear.
PB94-172632 *01,198* Not available NTIS

PB94-172640
Serial Sectioning of Hardened Cement Paste for Scanning Electron Microscopy.
PB94-172640 *01,305* Not available NTIS

PB94-172657
Using Synthetic-Perturbation Techniques for Tuning Shared Memory Programs (Extended Abstract).
PB94-172657 *01,685* Not available NTIS

PB94-172665
Enhanced Curie Temperatures and Magnetoelastic Domains in Dy/Lu Super Lattices and Films.
PB94-172665 *04,443* Not available NTIS

PB94-172673
Inelastic Neutron Scattering Studies of Rotational Excitations and the Orientational Potential in C60 and A3C60 Compounds.
PB94-172673 *00,763* Not available NTIS

PB94-172681
AMRF Composite Fabrication Workstation.
PB94-172681 *02,810* Not available NTIS

PB94-172699
Inelastic Interactions of Electrons with Surfaces: Application to Auger-Electron Spectroscopy and X-ray Photoelectron Spectroscopy.
PB94-172699 *00,764* Not available NTIS

PB94-172707
Effects of Elastic Stress on Phase Equilibrium in the Ni-V System.
PB94-172707 *03,313* Not available NTIS

PB94-172715
Microstructure and Tensile Properties of Microalloyed Steel Forgings.
PB94-172715 *03,204* Not available NTIS

PB94-172723
Effect of Two Initiator/Stabilizer Concentrations in a Metal Primer on Bond Strengths of a Composite to a Base Metal Alloy.
PB94-172723 *00,141* Not available NTIS

PB94-172731
Considerations on Data Requirements for Tribological Modeling.
PB94-172731 *02,962* Not available NTIS

PB94-172749
Wear of Selected Materials and Composites Sliding against MoS2 Films.
PB94-172749 *03,231* Not available NTIS

PB94-172756
Temperature Dependence of the Morphology of Thin Diblock Copolymer Films as Revealed by Neutron Reflectivity.
PB94-172756 *01,199* Not available NTIS

PB94-172764
Reaction Sensitivities of Al-Li Alloys and Alloy 2219 in Mechanical-Impact Tests.
PB94-172764 *03,314* Not available NTIS

PB94-172772
Time Scale Algorithm for Post-Processing: AT1 Plus Frequency Variance.
PB94-172772 *01,525* Not available NTIS

PB94-172780
Intelligent Processing of Materials.
PB94-172780 *02,811* Not available NTIS

PB94-172798
Absolute Determination of Electrolytic Conductivity for Primary Standard KC1 Solutions from 0 to 50C.
PB94-172798 *00,765* Not available NTIS

PB94-172806
Current Activities Within the National Biomonitoring Specimen Bank.
PB94-172806 *02,516* Not available NTIS

PB94-172814
Reciprocity Relations in Waveguide Junctions.
PB94-172814 *02,213* Not available NTIS

PB94-172822
Environmental Scanning Electron Microscope Imaging Examples Related to Particle Analysis.
PB94-172822 *00,766* Not available NTIS

PB94-172830
New Critical Review of Experimental Stark Widths and Shifts.
PB94-172830 *03,790* Not available NTIS

PB94-172848
High Temperature Degradation of Structural Composites.
PB94-172848 *03,132* Not available NTIS

PB94-172855
Measurement and Calibration of Large-Area Alpha-Particle Sources at NIST.
PB94-172855 *03,791* Not available NTIS

PB94-172863
Physicochemical Properties of Calcific Deposits Isolated from Porcine Bioprosthetic Heart Valves Removed from Patients Following 2-13 Years Function.
PB94-172863 *00,184* Not available NTIS

PB94-172871
Dental Materials.
PB94-172871 *00,142* Not available NTIS

PB94-172889
Report on the Meeting of the CCU (10th) (of the International Committee of Weights and Measures). Held on July 10-11, 1990.
PB94-172889 *03,792* Not available NTIS

PB94-172897
National Institute of Standards and Technology Resonance Ionization Spectroscopy/Resonance Ionization Mass Spectroscopy Data Service.
PB94-172897 *03,793* Not available NTIS

PB94-172905
Realization of New NIST Radiation Temperature Scales for the 1000 K to 3000 K Region, Using Absolute Radiometric Techniques.
PB94-172905 *03,794* Not available NTIS

PB94-172913
Intelligent Processing of Hot Isostatic Pressing.
PB94-172913 *03,315* Not available NTIS

PB94-172921
Porting Multimedia Applications to the Open System Environment.
PB94-172921 *02,721* Not available NTIS

PB94-172939
Industry and Government-Laboratory Cooperative R and D: An Idea Whose Time Has Come.
PB94-172939 *02,970* Not available NTIS

PB94-172947
Draft Guideline for Testing and Evaluation of Seismic Isolation Systems.
PB94-172947 *00,423* Not available NTIS

PB94-172954
Evaluation and Qualification Standards for an X-Ray Laminography System.
PB94-172954 *02,029* Not available NTIS

PB94-172962
Temperature Increases in Aluminum Alloys during Mechanical-Impact Tests for Oxygen Compatibility.
PB94-172962 *03,316* Not available NTIS

PB94-172970
Surface Forces and Adhesion between Dissimilar Materials Measured in Various Environments.
PB94-172970 *03,033* Not available NTIS

PB94-172988
Greatly Enhanced Soot Scattering in Flickering Ch4/Air Diffusion Flames.
PB94-172988 *01,361* Not available NTIS

PB94-172996
Fine-Structure Constant.
PB94-172996 *03,795* Not available NTIS

PB94-173002
Functions of Technology Infrastructure in a Competitive Economy.
PB94-173002 *00,478* Not available NTIS

PB94-173010
World Model Registration for Effective Off-Line Programming of Robots.
PB94-173010 *02,933* Not available NTIS

PB94-173028
Investing in Education to Meet a National Need for a Technical-Professional Workforce in a Post-Industrial Economy.
PB94-173028 *00,132* Not available NTIS

PB94-173036
Thermal Decomposition of Hydroxy- and Methoxy-Substituted Anisoles.
PB94-173036 *00,767* Not available NTIS

PB94-173044
Dispersions of Magnetic Excitations of the Pr Ions in Pr2CuO4.
PB94-173044 *04,444* Not available NTIS

PB94-173051
Quantitative Phase Abundance Analysis of Three Cement Clinker Reference Materials by Scanning Electron Microscopy.
PB94-173051 *00,333* Not available NTIS

PB94-173069
Homoepitaxial Growth of Iron and a Real Space View of Reflection-High-Energy-Electron Diffraction.
PB94-173069 *04,445* Not available NTIS

PB94-173077
Fire Hazard and Risk: Evaluating Alternative Technologies.
PB94-173077 *00,242* Not available NTIS

PB94-173754
Process for Selecting Standard Reference Algorithms for Evaluating Coordinate Measurement Software.
PB94-173754 *02,629* PC A03/MF A01

PB94-174505
Characterization of the Hydrogen Induced Cold Cracking Susceptibility at Simulated Weld Zones in HSLA-100 Steel.
PB94-174505 *03,746* PC A04/MF A01

PB94-176088
Physics Laboratory Technical Activities, 1993.
PB94-176088 *03,796* PC A10/MF A03

PB94-176278
Evaluation and Strengthening Guidelines for Federal Buildings: Identification of Current Federal Agency Programs.
PB94-176278 *00,424* PC A08/MF A02

PB94-176666
Opportunities for Innovation: Advanced Surface Engineering.
PB94-176666 *02,697* PC A09/MF A02

PB94-177060
Advanced Components for Electric and Hybrid Electric Vehicles. Workshop Proceedings. Held in Gaithersburg, Maryland on October 27-28, 1993.
PB94-177060 *04,858* PC A10/MF A03

PB94-178019
Semiconductor Measurement Technology: Design and Testing Guides for the CMOS and Lateral Bipolar-on-SOI Test Library.
PB94-178019 *02,301* PC A07/MF A02

PB94-178068
NIST Serial Holdings, 1994.
PB94-178068 *02,745* PC A12/MF A03

PB94-178225
National Voluntary Laboratory Accreditation Program: Procedures and General Requirements.
PB94-178225 *02,630* PC A03/MF A01

PB94-178407
Second Text REtrieval Conference (TREC-2). Held in Gaithersburg, Maryland on August 31-September 2, 1993.
PB94-178407 *01,686* PC A21/MF A04

PB94-178969
National Voluntary Laboratory Accreditation Program 1994 Directory.
PB94-178969 *00,482* PC A08/MF A02

PB94-181856
Evaluation and Strengthening Guidelines for Federal Buildings: Assessment of Current Federal Agency Evaluation Programs and Rehabilitation Criteria and Development of Typical Costs for Seismic Rehabilitation.
PB94-181856 *00,425* PC A08/MF A02

PB94-181997
Application of the Modified Voltage-Dividing Potentiometer to Overlay Metrology in a CMOS/Bulk Process.
PB94-181997 *02,302* Not available NTIS

PB94-182003
Tert-Butyl Hydroperoxide-Mediated DNA Base Damage in Cultured Mammalian Cells.
PB94-182003 *03,644* Not available NTIS

PB94-182995
Optimization of Highway Concrete Technology.
PB94-182995 *01,333* PC A13/MF A03

PB94-185014
Can Quantum Mechanical Description of Electron-Sodium Collisions Be Considered Complete. Present Status and Future Prospects for 3s <-> 3p Transitions.
PB94-185014 *00,768* Not available NTIS

PB94-185022
Thermal Diffusivity of POCO AXM-5Q1 Graphite in the Range 1500 to 2500 K Measured by a Laser-Pulse Technique.
PB94-185022 *03,013* Not available NTIS

PB94-185030
Low-Energy Electron Scattering from Caesium Atoms: Comparison of a Semirelativistic Breit-Pauli and a Full Relativistic Direc Treatment.
PB94-185030 *00,769* Not available NTIS

PB94-185048
Physics and Prospects of Inertial Confinement Fusion.
PB94-185048 *04,405* Not available NTIS

PB94-185055
Grafted Interpenetrating Polymer Networks.
PB94-185055 *01,200* Not available NTIS

PB94-185063
Classical Analysis: A Look at the Past, Present, and Future.
PB94-185063 *00,528* Not available NTIS

PB94-185071
Preparation and Certification of a Rhodium Standard Reference Material Solution.
PB94-185071 *00,529* Not available NTIS

PB94-185089
Electron-Impact Ionization of In(+) and Xe(+).
PB94-185089 *00,770* Not available NTIS

PB94-185097
Measurement of the J=2 less than 1 Fine-Structure Interval for (28)Si and (29)Si in the Ground (3)P State.
PB94-185097 *00,771* Not available NTIS

PB94-185105
In-Line Optical Monitoring of Injection Molding.
PB94-185105 *01,201* Not available NTIS

PB94-185113
Fluorinated Hydrocarbon Flame Suppression Chemistry.
PB94-185113 *01,362* Not available NTIS

PB94-185121
Detection of Voids in Grouted Ducts Using the Impact-Echo Method.
PB94-185121 *01,306* Not available NTIS

PB94-185139
Systematics of Alpha-Particle Energy Spectra and Lineal Energy (Y) Spectra for Radon Daughters.
PB94-185139 *03,615* Not available NTIS

PB94-185147
High-Temperature Laser-Pulse Thermal Diffusivity Apparatus.
PB94-185147 *02,631* Not available NTIS

PB94-185154
Interface Roughness-Induced Changes in the Near-E(sub 0) Spectroscopic Behavior of Short-Period AlAs/GaAs Superlattices.
PB94-185154 *02,118* Not available NTIS

PB94-185162
Effects of Critical Current Density, Equilibrium Magnetization and Surface Barrier on Magnetization of High Temperature Superconductors.
PB94-185162 *04,446* Not available NTIS

PB94-185170
Long-Term Stability of Carrier-Free Polonium Solution Standards.
PB94-185170 *00,685* Not available NTIS

PB94-185188
Phase Behavior of a Hydrogen Bonding Molecular Composite.
PB94-185188 *01,202* Not available NTIS

PB94-185196
Standards Development in North America for Performance of Whole Buildings and Facilities.
PB94-185196 *00,312* Not available NTIS

PB94-185204
Thermodynamic Properties of Difluoromethane.
PB94-185204 *00,772* Not available NTIS

PB94-185212
Four Years of Monitoring alpha Orionis with the VLA: Where Have All the Flares Gone.
PB94-185212 *00,048* Not available NTIS

PB94-185220
Distant Future of Solar Activity: A Case Study of Beta Hydri. 3. Transition Region, Corona, and Stellar Wind.
PB94-185220 *00,049* Not available NTIS

PB94-185238
Tapered Cross-Pin Attachments for Fixed Bridges.
PB94-185238 *00,185* Not available NTIS

PB94-185246
Spectrum and Energy Levels of Five-Times-Ionized Niobium (Nb VI).
PB94-185246 *04,226* Not available NTIS

PB94-185253
Liquid Chromatography: Laser-Enhanced Ionization Spectrometry for the Speciation of Organolead Compounds.
PB94-185253 *00,530* Not available NTIS

PB94-185261
Comparative Strategies for Correction of Interferences in Isotope Dilution Mass Spectrometric Determination of Vanadium.
PB94-185261 *00,531* Not available NTIS

PB94-185279
Selection of Appropriate Ultrasonic System Components for NDE of Thick Polymer-Composites.
PB94-185279 *03,133* Not available NTIS

PB94-185287
Flame Retardants - Overview.
PB94-185287 *01,363* Not available NTIS

PB94-185295
Investigation of LS Coupling in Boronlike Ions.
PB94-185295 *03,797* Not available NTIS

PB94-185303
Quantum Dynamics of Renner-Teller Vibronic Coupling: The Predissociation HCO.
PB94-185303 *00,773* Not available NTIS

PB94-185311
Anharmonic Oscillator Analysis Using Modified Airy Functions.
PB94-185311 *03,798* Not available NTIS

PB94-185329
Optical Conductivity of Single Crystals of Ba1-xMxBiO3(M=K, Rb, x=0.04, 0.37).
PB94-185329 *04,447* Not available NTIS

PB94-185337
Frozen Human Serum Reference Material for Standardization of Sodium and Potassium Measurements in Serum or Plasma by Ion-Selective Electrode Analyzers.
PB94-185337 *00,532* Not available NTIS

PB94-185345
Backscattering in Electron-Impact Excitation of Multiply Charged Ions.
PB94-185345 *03,799* Not available NTIS

PB94-185352
Laser Imaging of Chemistry-Flowfield Interactions: Enhanced Soot Formation in Time-Varying Diffusion Flames.
PB94-185352 *01,364* Not available NTIS

PB94-185360
Transfer of Technology from Defense to Civilian Sectors.
PB94-185360 *00,011* Not available NTIS

PB94-185378
Contact Electrification Induced by Monolayer Modification of a Surface and Relation to Acid-Base Interactions.
PB94-185378 *03,034* Not available NTIS

PB94-185386
Task Decomposition Methodology for the Design of a Coal Mining Automation Hierarchical Real-Time Control System.
PB94-185386 *03,694* Not available NTIS

PB94-185394
Effect of Backfill and Atomizing Gas on the Powder Porosity and Mechanical Properties of 304L Stainless Steel.
PB94-185394 *03,205* Not available NTIS

PB94-185402
Conformance Testing of a Lower Layer Security Protocol.
PB94-185402 *01,577* Not available NTIS

PB94-185410
Time-Domain Measurements of the Electromagnetic Backscatter of Pyramidal Absorbers and Metallic Plates.
PB94-185410 *01,877* Not available NTIS

PB94-185428
Interfacial Free Energies from Substrate Curvature Measurements of the Creep of Multilayer Thin Films.
PB94-185428 *04,448* Not available NTIS

PB94-185436
Standard Probes for Electromagnetic Field Measurements.
PB94-185436 *01,999* Not available NTIS

PB94-185444
Selected Ion Flow Tube-Laser Induced Fluorescence Instrument for Vibrationally State-Specific Ion-Molecule Reactions.
PB94-185444 *00,774* Not available NTIS

PB94-185451
Design and Operation of Series-Array Josephson Voltage Standards.
PB94-185451 *02,030* Not available NTIS

PB94-185469
Influence of Surface Interaction and Chain Stiffness on Polymer-Induced Entropic Forces and the Dimensions of Confined Polymers.
PB94-185469 *01,203* Not available NTIS

PB94-185477
Temperature Dependence and Anharmonicity of Phonons on Ni(110) and Cu(110) Using Molecular Dynamics Simulations.
PB94-185477 *04,449* Not available NTIS

PB94-185485
One Gigarad Passivating Nitrided Oxides for 100% Internal Quantum Efficiency Silicon Photodiodes.
PB94-185485 *02,119* Not available NTIS

PB94-185493
Issues Concerning Material Removal Shape Element Volumes (MRSEVs).
PB94-185493 *02,882* Not available NTIS

PB94-185501
High Temperature Silicide Thin-Film Thermocouples.
PB94-185501 *02,252* Not available NTIS

PB94-185519
Thin Film Transparent Thermocouples.
PB94-185519 *02,253* Not available NTIS

PB94-185527
Scientific Protocols in Statistical Standards for Environmental Studies.
PB94-185527 *02,517* Not available NTIS

PB94-185535
Experimental Optimization of Peak Shape with Application to Aerosol Generation.
PB94-185535 *00,501* Not available NTIS

PB94-185543
Fluorescence Monitoring of Polarity Change and Gelation during Epoxy Cure.
PB94-185543 *01,204* Not available NTIS

PB94-185550
Electron Beam Crosslinking of Poly(vinylmethyl ether).
PB94-185550 *01,205* Not available NTIS

PB94-185568
Synthetic-Perturbation Tuning of MIMD Programs.
PB94-185568 *01,687* Not available NTIS

PB94-185576
Intercomparison of Internal Proportional Gas Counting of (85)Kr and (3)H.
PB94-185576 *03,800* Not available NTIS

PB94-185584
Charge Transfer and Collision-Induced Dissociation Reactions of CF(2+) and CF2(2+) with the Rare Gases at a Laboratory Collision Energy of 49 eV.
PB94-185584 *00,775* Not available NTIS

PB94-185592
Electro-Thermal Simulation of an IGBT PWM Inverter.
PB94-185592 *02,303* Not available NTIS

PB94-185600
Octacalcium Phosphate Carboxylates IV. Kinetics of Formation and Solubility of Octacalcium Phosphate Succinate.
PB94-185600 *00,776* Not available NTIS

PB94-185618
Corrosion Resistant Epoxy-Coated Reinforcing Steel.
PB94-185618 *01,307* Not available NTIS

PB94-185626
Rotational Modulation and Flares on RS Canum Venaticorum and BY Draconis Stars. XVI. IUE Spectroscopy and VLA Observations of C1182(=V 1005 Orionis) in October 1983.
PB94-185626 *00,050* Not available NTIS

PB94-185634
Approach to Setting Performance Requirements for Automated Evaluation of the Parameters of High-Voltage Impulses.
PB94-185634 *01,878* Not available NTIS

PB94-185642
Use of a Radiochromic Detector for the Determination of Stereotactic Radiosurgery Dose Characteristics.
PB94-185642 *03,514* Not available NTIS

PB94-185659
Enhanced Magnetocaloric Effect in Gd3Ga5-xFexO12.
PB94-185659 *04,450* Not available NTIS

PB94-185667
Magnetocaloric Effect in Rapidly Solidified Nd-Fe-Al-B Materials.
PB94-185667 *04,451* Not available NTIS

PB94-185675
Langevin Approach to Hysteresis and Barkhausen Modeling in Steel.
PB94-185675 *03,206* Not available NTIS

PB94-185683
Development of a Calibrated Atomic Force Microscope.
PB94-185683 *02,894* Not available NTIS

PB94-185691
High Resolution IR Studies of Polymolecular Clusters: Micromatrices and Unimolecular Ring Opening.
PB94-185691 *00,777* Not available NTIS

PB94-185709
Verification of the Ponderomotive Approximation for the ac Stark Shift in Xe Rydberg Levels.
PB94-185709 *03,801* Not available NTIS

PB94-185717
Use of an Ion Energy Analyzer: Mass Spectrometer to Measure Ion Kinetic-Energy Distributions from RF Discharges in Argon-Helium Gas Mixtures.
PB94-185717 *04,406* Not available NTIS

PB94-185725
Angular Distributions for Near-Threshold (e,2e) Processes for Li and Mg.
PB94-185725 *00,778* Not available NTIS

PB94-185733
Application of Photochemical Reaction in Electrochemical Detection of DNA Intercalation.
PB94-185733 *00,686* Not available NTIS

PB94-185741
Intermediate Structure in the Neutron-Induced Fission Cross Section of 236U.
PB94-185741 *03,802* Not available NTIS

PB94-185758
Neutron Reflectivity of End-Grafted Polymers: Concentration and Solvent Quality Dependence in Equilibrium Conditions.
PB94-185758 *01,206* Not available NTIS

PB94-185766
Air Change Effectiveness Measurements in Two Modern Office Buildings.
PB94-185766 *00,243* Not available NTIS

PB94-185774
Proficiency Testing as a Component of Quality Assurance in Construction Materials Laboratories.
PB94-185774 *00,334* Not available NTIS

PB94-185782
Expansion of Cementitious Materials Exposed to Sulfate Solutions.
PB94-185782 *02,577* Not available NTIS

PB94-185790
Compositional Analyses of Surfaces and Thin Films by Electron and Ion Spectroscopies.
PB94-185790 *00,779* Not available NTIS

PB94-185808
Collision-Induced Neutral Loss Reactions of Molecular Dications.
PB94-185808 *00,780* Not available NTIS

PB94-185816
Thermodynamic and NMR Study of the Interactions of Cyclodextrins with Cyclohexane Derivatives.
PB94-185816 *00,781* Not available NTIS

PB94-185824
Modified Airy Function Method for the Analysis of Tunneling Problems in Optical Waveguides and Quantum Well Structures.
PB94-185824 *02,120* Not available NTIS

PB94-185832
Planning the Infrastructure for Global Electronic Commerce.
PB94-185832 *00,494* Not available NTIS

PB94-185840
Correction to the Decay Rate of Nonequilibrium Carrier Distributions Due to Scattering-in Processes.
PB94-185840 *04,452* Not available NTIS

PB94-185857
Magnetocaloric Effect of Ferromagnetic Particles.
PB94-185857 *04,453* Not available NTIS

PB94-185865
Viewpoint: Nanocrystalline and Nanophase Materials.
PB94-185865 *04,454* Not available NTIS

PB94-185873
International Institute of Welding: Report on 1992 Actions.
PB94-185873 *02,856* Not available NTIS

PB94-185881
International Institute of Welding: Report on 1993 Actions.
PB94-185881 *02,857* Not available NTIS

PB94-185899
Through-the-Arc Sensing for Monitoring Arc Welding.
PB94-185899 *02,858* Not available NTIS

PB94-185907
Optical Current Transducer for Calibration Studies.
PB94-185907 *02,121* Not available NTIS

PB94-185915
High Sensitivity Survey of Radio Continuum Emission in Herbig Ae/Be Stars.
PB94-185915 *00,051* Not available NTIS

PB94-185923
Scaling of Diffusion-Mediated Island Growth in Iron-on-Iron Homoepitaxy.
PB94-185923 *04,455* Not available NTIS

PB94-185931
Reproducibility of JEDEC Standard Current and Voltage Ramp Test Procedures for Thin-Dielectric Breakdown Characterization.
PB94-185931 *01,879* Not available NTIS

PB94-185949
Experimental Investigation of the Validity of TDDB Voltage Acceleration Models.
PB94-185949 *02,304* Not available NTIS

PB94-185956
Field and Temperature Acceleration of Time-Dependent Dielectric Breakdown in Intrinsic Thin SiO2.
PB94-185956 *02,305* Not available NTIS

PB94-185964
Junction Locations by Scanning Tunneling Microscopy: In-Air-Ambient Investigation of Passivated GaAs pn Junctions.
PB94-185964 *02,306* Not available NTIS

PB94-185972
X-Ray Diffraction from Anodic TiO2 Films: In situ and Ex situ Comparison of the Ti(0001) Face.
PB94-185972 *00,782* Not available NTIS

PB94-185980
Fourier Transform Atomic Emission Studies Using a Glow Discharge as the Emission Source.
PB94-185980 *00,533* Not available NTIS

PB94-185998
Infratechnologies: Tools for Innovation.
PB94-185998 *00,317* Not available NTIS

PB94-186004
Status of Construction and Construction Technologies.
PB94-186004 *00,318* Not available NTIS

PB94-186673
Prediction of Geometric-Thermal Machine Tool Errors by Artificial Neural Networks.
PB94-186673 *02,943* PC A07/MF A02

PB94-186848
Optical Fiber Sensors: Accelerating Applications in Navy Ships.
PB94-186848 *02,632* PC A06/MF A02

PB94-187283
Calculating Flame Spread on Horizontal and Vertical Surfaces.
PB94-187283 *00,335* PC A04/MF A01

PB94-187317
Sulfate Attack of Cementitious Materials: Volumetric Relations and Expansions.
PB94-187317 *03,232* PC A03/MF A01

PB94-187564
Application of the Electronic Balance in High Precision Pycnometry.
PB94-187564 *00,534* PC A03/MF A01

PB94-187630
Metric for Success.
PB94-187630 *02,633* PC A03/MF A01

PB94-187648
Strengthening Methodology for Lightly Reinforced Concrete Frames-II. Recommended Calculation Techniques for the Design of Infill Walls.
PB94-187648 *00,426* PC A03/MF A01

PB94-187655
State-of-the-Art Survey of Methodologies for Representing Manufacturing Process Capabilities.
PB94-187655 *02,812* PC A03/MF A01

PB94-187663
Workshop on Characterizing Diamond Films (3rd). Held in Gaithersburg, Maryland on February 23-24, 1994.
PB94-187663 *04,456* PC A04/MF A01

PB94-187713
Use of the Electronic Balance for Highly Accurate Direct Mass Measurements Without the Use of External Mass Standards.
PB94-187713 *03,803* PC A03/MF A01

PB94-187739
Body Dimensions for Apparel.
PB94-187739 *02,813* PC A03/MF A01

PB94-187788
NIST RS274/NGC Interpreter Version 1.
PB94-187788 *02,814* PC A03/MF A01

PB94-188240
NIST Response to the Fifth CORM Report on the Pressing Problems and Projected Needs in Optical Radiation Measurements.
PB94-188240 *04,227* PC A03/MF A01

PB94-188463
User Profile for Researchers Studying Objects: Implications for Computer Systems.
PB94-188463 *00,133* PC A03/MF A01

PB94-188711
Second Census Optical Character Recognition Systems Conference.
PB94-188711 *01,832* PC A12/MF A03

PB94-188810
Semiconductor Measurement Technology: Improved Characterization and Evaluation Measurements for HgCdTe Detector Materials, Processes, and Devices Used on the GOES and TIROS Satellites.
PB94-188810 *02,122* PC A09/MF A02

PB94-188836
Proficiency Tests for the NIST Airborne Asbestos Program, 1990.
PB94-188836 *00,535* PC A07/MF A02

PB94-188844
Standard Reference Materials: Glass Filters as a Standard Reference Material for Spectrophotometry - Selection, Preparation, Certification, and Use of SRM 930 and SRM 1930.
PB94-188844 *00,536* PC A10/MF A03

PB94-191202
Federal Certification Authority Liability and Policy: Law and Policy of Certificate-Based Public Key and Digital Signatures.
PB94-191202 *01,578* PC A21/MF A04

PB94-191640
NIST Calibration of ASTM E127-Type Ultrasonic Reference Blocks.
PB94-191640 *02,702* PC A03/MF A01

PB94-191707
Optical Metrology and More. Programs and Services of the Radiometric Physics Division, Physics Laboratory.
PB94-191707 *04,228* PC A03/MF A01

PB94-191715
Control Entity Interface Specification.
PB94-191715 *02,815* PC A06/MF A02

PB94-193471
Binder Characterization and Evaluation by Nuclear Magnetic Resonance Spectroscopy.
PB94-193471 *01,334* PC A08/MF A02

PB94-193620
Prediction of Fire Dynamics.
PB94-193620 *00,336* PC A03/MF A01

PB94-193638
Simple Scalability Test for MIMD Code.
PB94-193638 *01,688* PC A03/MF A01

PB94-193646
Program of the Subcommittee on Construction and Building.
PB94-193646 *00,319* PC A03/MF A01

PB94-193653
Study of Federal Agency Needs for Information Technology Security.
PB94-193653 *01,579* PC A07/MF A02

PB94-193752
Electronics and Electrical Engineering Laboratory Technical Publication Announcements Covering Laboratory Programs, October to December 1993 with 1994/1995 EEEL Events Calendar.
PB94-193752 *02,307* PC A03/MF A01

PB94-193760
Bibliography of Photon Total Cross Section (Attenuation Coefficient) Measurements 10 eV to 13.5 GeV, 1907-1993.
PB94-193760 *03,804* PC A06/MF A02

PB94-193778
Mathematical Modeling of Human Egress from Fires in Residential Buildings.
PB94-193778 *00,337* PC A05/MF A02

PB94-193786
Coaxial Reference Standard for Microwave Power.
PB94-193786 *01,880* PC A04/MF A01

PB94-193802
Structure and Radiation Properties of Pool Fires.
PB94-193802 *02,473* PC A08/MF A02

PB94-193810
Electronics and Electrical Engineering Laboratory Technical Progress Bulletin Covering Laboratory Programs, January to March 1994 with 1994/1995 EEEL Events Calendar.
PB94-193810 *02,308* PC A03/MF A01

PB94-193828
Proficiency Tests for the NIST Airborne Asbestos Program - 1991.
PB94-193828 *00,537* PC A04/MF A01

PB94-193844
Fire Propagation in Concurrent Flows.
PB94-193844 *01,365* PC A04/MF A01

PB94-193885
Preparation and Monitoring of Lead Acetate Containing Drinking Water Solutions for Toxicity Studies.
PB94-193885 *00,538* PC A03/MF A01

PB94-193927
Backdraft Phenomena.
PB94-193927 *01,366* PC A11/MF A03

PB94-193976
Investigation of Oil and Gas Well Fires and Flares.
PB94-193976 *03,695* PC A04/MF A01

PB94-193984
Realizing Suspended Structures on Chips Fabricated by CMOS Foundry Processes Through the MOSIS Service.
PB94-193984 *01,881* PC A04/MF A01

PB94-194065
Risk Analysis for the Fire Safety of Airline Passengers.
PB94-194065 *04,862* PC A03/MF A01

PB94-194073
Single-Phase Heat Transfer and Pressure Drop Characteristics of an Integral-Spine-Fin Within an Annulus.
PB94-194073 *03,805* PC A03/MF A01

PB94-194339
Performance Parameters of Fire Detection Systems.
PB94-194339 *00,288* PC A03/MF A01

PB94-194354
Electronics and Electrical Engineering Laboratory Technical Progress Bulletin Covering Laboratory Programs, July to September 1993 with 1994 EEEL Events Calendar.
PB94-194354 *02,309* PC A03/MF A01

PB94-194362
Proficiency Tests for the NIST Airborne Asbestos Program - 1992.
PB94-194362 *00,539* PC A03/MF A01

PB94-194388
CONTAM88 Building Input Files for Multi-Zone Airflow and Contaminant Dispersal Modeling.
PB94-194388 *02,537* PC A04/MF A01

PB94-194552
Visualization Applications for Manufacturing: A State-of-the-Art Survey. Final Report.
PB94-194552 *02,816* PC A03/MF A01

PB94-194560
Overview of NASREM: The NASA/NBS Standard Reference Model for Telerobot Control System Architecture.
PB94-194560 *04,831* PC A03/MF A01

PB94-195047
Documentation for Immediately Dangerous to Life or Health Concentrations (IDLHs).
PB94-195047 *03,602* PC A22/MF A04

PB94-195856
Fire Growth Models for Materials.
PB94-195856 *01,367* PC A03/MF A01

PB94-195914
Recommendations on Selection of Vehicle-to-Roadside Communications Standards for Commercial Vehicle Operations.
PB94-195914 *04,859* PC A05/MF A01

PB94-196029
Federal Metric Progress in 1993.
PB94-196029 *02,600* PC A03/MF A01

PB94-196045
Behavior of Charring Materials in Simulated Fire Environments.
PB94-196045 *01,368* PC A99/MF A06

PB94-196557
Graphical Analysis of the CCRL Portland Cement Proficiency Sample Database (Samples 1-72). (Part 1. Univariant Analysis of Portland Cement).
PB94-196557 *01,308* PC A06/MF A02

PB94-198157
Histopathology, Blood Chemistry, and Physiological Status of Normal and Moribund Striped Bass ('Morone saxatilis') Involved in Summer Mortality ('Die-Off') in the Sacramento-San Joaquin Delta of California.
PB94-198157 *00,034* PC A03/MF A01

PB94-198215
Thermodynamic Properties of Gas Phase Species of Importance to Ozone Depletion.
PB94-198215 *00,126* Not available NTIS

PB94-198223
Electro-Optical Sensor for Surface Displacement Measurements of Compliant Coatings.
PB94-198223 *02,123* Not available NTIS

PB94-198231
Copper Ion-Mediated Modification of Bases in DNA in Vitro by Benzoyl Peroxide.
PB94-198231 *03,645* Not available NTIS

PB94-198249
Calorimetric Determination of the Standard Transformed Enthalpy of a Biochemical Reaction at Specified PH and pMg.
PB94-198249 *03,454* Not available NTIS

PB94-198256
Hierarchical Interaction between Sensory Processing and World Modeling in Intelligent Systems.
PB94-198256 *01,580* Not available NTIS

PB94-198264
Role of World Modeling and Value Judgment in Perception.
PB94-198264 *01,581* Not available NTIS

PB94-198272
Theory of Intelligent Systems.
PB94-198272 *01,582* PC A02

PB94-198280
Temperature Dependence of the Rate Constants for Reaction of Inorganic Radicals with Organic Reductants.
PB94-198280 *00,783* PC A02

PB94-198298
Foias-Temam Approximations of Attractors for Galloping Oscillators.
PB94-198298 *04,817* PC A01

PB94-198306
Precision Oscillators: Dependence of Frequency on Temperature, Humidity and Pressure.
PB94-198306 *02,031* PC A03

PB94-198314
Vibrational Distributions of As2 in the Cracking of As4 on Si(100) and Si(111).
PB94-198314 *00,784* Not available NTIS

PB94-198322
Recently Developed NIST Food Related Standard Reference Materials.
PB94-198322 *00,035* Not available NTIS

PB94-198330
Standard Reference Materials for Dioxins and Other Environmental Pollutants.
PB94-198330 *02,518* Not available NTIS

PB94-198348
Evaluation of Corrosion Data: A Review.
PB94-198348 *03,187* Not available NTIS

PB94-198355
Combined Low- and High-Angle X-Ray Structural Refinement of a Co/Pt(111) Multilayer Exhibiting Perpendicular Magnetic Anisotropy.
PB94-198355 *04,457* Not available NTIS

PB94-198363
Magnetic Dead Layer in Fe/Si Multilayer: Profile Refinement of Polarized Neutron Reflectivity Data.
PB94-198363 *04,458* Not available NTIS

PB94-198371
Oxidation of 10-Methylacridan, a Synthetic Analogue of NADH and Deprotonation of Its Cation Radical. Convergent Application of Laser Flash Photolysis and Direct and Redox Catalyzed Electrochemistry to the Kinetics of Deprotonation of the Cation Radical.
PB94-198371 *00,785* Not available NTIS

PB94-198389
Facile Synthesis of Novel Fluorinated Multifunctional Acrylates.
PB94-198389 *01,207* Not available NTIS

PB94-198397
Effect of Transformation of Alloy on Transient and Residual Stresses in a Porcelain-Metal Strip.
PB94-198397 *00,143* Not available NTIS

PB94-198405
Transient Methods for Thermal Conductivity.
PB94-198405 *04,197* Not available NTIS

PB94-198413
Automatic Inductive Voltage Divider Bridge Operates from 10 Hz to 100 kHz.
PB94-198413 *02,032* Not available NTIS

PB94-198421
Weak-Link-Free Behavior of High Angle YBa2Cu3O7-x Grain Boundaries in High Magnetic Fields.
PB94-198421 *04,459* Not available NTIS

PB94-198439
Effective Measurement Techniques for Heat, Smoke, and Toxic Fire Gases.
PB94-198439 *01,369* Not available NTIS

PB94-198447
Modern Test Methods for Flammability.
PB94-198447 *01,370* Not available NTIS

PB94-198454
Toxicity, Fire Hazard and Upholstered Furniture.
PB94-198454 *00,289* Not available NTIS

PB94-198462
Standardization of Formats and Presentation of Fire Data - The FDMS.
PB94-198462 *01,371* Not available NTIS

PB94-198470
Nutritional Status and Growth in Juvenile Rheumatoid Arthritis.
PB94-198470 *03,515* Not available NTIS

PB94-198488
Dilemma-Preservation versus Access.
PB94-198488 *02,711* Not available NTIS

PB94-198496
Thermodynamic Interactions in Model Polyolefin Blends Obtained by Small-Angle Neutron Scattering.
PB94-198496 *01,208* Not available NTIS

PB94-198504
Energy Dependence of Collision Characteristics in Molecule-Surface Collisions.
PB94-198504 *00,786* Not available NTIS

PB94-198512
Profile Fitting of X-Ray Diffraction Lines and Fourier Analysis of Broadening.
PB94-198512 *04,460* Not available NTIS

PB94-198520
Microstrains and Domain Sizes in Bi-Cu-O Superconductors: An X-Ray Diffraction Peak-Broadening Study.
PB94-198520 *04,461* Not available NTIS

PB94-198538
Voigt-Function Modeling in Fourier Analysis of Size- and Strain-Broadened X-Ray Diffraction Peaks.
PB94-198538 *04,462* Not available NTIS

PB94-198546
Density Matrix Calculation of Population Transfer between Vibrational Levels of Na2 by Stimulated Raman Scattering with Temporally Shifted Laser Beams.
PB94-198546 *00,787* Not available NTIS

PB94-198553
Experimental Constraints on Some Mechanisms for High-Temperature Superconductivity.
PB94-198553 *04,463* Not available NTIS

PB94-198561
Numerical Simulation of Submicron Photolithographic Processing.
PB94-198561 *02,310* Not available NTIS

PB94-198579
Regulation of Lithium and Boron Levels in Normal Human Blood: Environmental and Genetic Considerations.
PB94-198579 *03,491* Not available NTIS

PB94-198587
Characteristics of Light Emission After Low-Energy Electron Impact Excitation of Caesium Atoms.
PB94-198587 *03,806* Not available NTIS

PB94-198595
Strong Hydrogen Bond in the Formic Acid-Formate Anion System.
PB94-198595 *00,788* Not available NTIS

PB94-198603
Structure of Glycine-Water H-Bonded Complexes.
PB94-198603 *00,789* Not available NTIS

PB94-198611
Femtosecond Time-Resolved Wave Packet Motion in Molecular Multiphoton Ionization and Fragmentation.
PB94-198611 *00,790* Not available NTIS

PB94-198629
Neutron Powder Diffraction Study of a Na, Cs-Rho Zeolite.
PB94-198629 *00,791* Not available NTIS

PB94-198637
Rotational Spectrum of Copper Hydride Using Tunable Far Infrared Radiation.
PB94-198637 *00,792* Not available NTIS

PB94-198645
Matrix Grain Bridging Contribution to the Toughness of Whisker Reinforced Ceramics.
PB94-198645 *03,134* Not available NTIS

PB94-198652
Discovery of an X-Ray Selected, Radio-Loud Quasar at z=3.9.
PB94-198652 *00,052* Not available NTIS

PB94-198660
Computing S(alpha) Using Symbolic Monte Carlo.
PB94-198660 *03,410* Not available NTIS

PB94-198678
Tunneling-Rotation Spectrum of the Hydrogen Fluoride Dimer.
PB94-198678 *00,793* Not available NTIS

PB94-198686
Integrated Laser Doppler Method for Measuring Planetary Gravity Fields.
PB94-198686 *03,681* Not available NTIS

PB94-198694
Coherent Precipitates in the BCC/Orthorhombic Two Phase Field of the Ti-Al-Nb System.
PB94-198694 *03,317* Not available NTIS

PB94-198702
Crystallographic Characterization of Some Intermetallic Compounds in the Al-Cr System.
PB94-198702 *03,318* Not available NTIS

PB94-198710
Laser Ablation of Thin Films as a Free Atom Source for Pulsed RIMS.
PB94-198710 *00,540* Not available NTIS

PB94-198728
Majority and Minority Mobilities in Heavily Doped Silicon for Device Simulations.
PB94-198728 *02,311* Not available NTIS

PB94-198736
Relative Sensitivity Factors and Useful Yields for a Microfocused Gallium Ion Beam and Time-of-Flight Secondary Ion Mass Spectrometer.
PB94-198736 *00,541* Not available NTIS

PB94-198744
Meissner, Shielding, and Flux Loss Behavior in Single-Crystal YBa2Cu3O6+x.
PB94-198744 *04,464* Not available NTIS

PB94-198751
Magnetic Properties of Pd/Co Multilayers.
PB94-198751 *04,465* Not available NTIS

PB94-198769
Concurrent Enhancement of Kerr Rotation and Antiferromagnetic Coupling in Epitaxial Fe/Cu/Fe Structures.
PB94-198769 *04,466* Not available NTIS

PB94-198777
Digitized Direct Simulation Model of the Microstructural Development of Cement Paste.
PB94-198777 *01,309* Not available NTIS

PB94-198785
Digitized Simulation Model for Microstructural Development.
PB94-198785 *01,310* Not available NTIS

PB94-198793
Modelling the Leaching of Calcium Hydroxide from Cement Paste: Effects on Pore Space Percolation and Diffusivity.
PB94-198793 *01,311* Not available NTIS

PB94-198801
Diffusion Studies in a Digital-Image-Based Cement Paste Microstructural Model.
PB94-198801 *01,312* Not available NTIS

PB94-198819
Milliwatt Mixer for Small Fluid Samples.
PB94-198819 *02,634* Not available NTIS

PB94-198827
Standard Reference Materials (SRM's) for Measuring Genetic Damage.
PB94-198827 *03,516* Not available NTIS

PB94-198835
Scattering Properties of the Leveled-Wave Model of Random Morphologies.
PB94-198835 *03,807* Not available NTIS

PB94-198843
Analysis of SANS from Controlled Pore Glasses.
PB94-198843 *03,035* Not available NTIS

PB94-198850
Structures of Sodium Metal.
PB94-198850 *03,319* Not available NTIS

PB94-198868
Non-Equilibrium Thermodynamic Theory of Viscoplastic Materials.
PB94-198868 *04,467* Not available NTIS

PB94-198876
Modeling Polarization Curves and Impedance Spectra for Simple Electrode Systems.
PB94-198876 *03,188* Not available NTIS

PB94-198884
Diffraction Imaging of Polycrystalline Materials.
PB94-198884 *02,971* Not available NTIS

PB94-198892
Infrared and Microwave Spectroscopy of the Argon - Propyne Dimer.
PB94-198892 *00,794* Not available NTIS

PB94-198900
Dynamic Shear Modulus Measurements with Four Independent Techniques in Nickel-Based Alloys.
PB94-198900 *03,320* Not available NTIS

PB94-198918
Evaluation of Two-Photon Exchange Graphs for Highly-Charged Heliumlike Ions.
PB94-198918 *03,808* Not available NTIS

PB94-198934
Thermodynamic Constraints on Non-Equilibrium Solidification of Ordered Intermetallic Compounds.
PB94-198934 *03,321* Not available NTIS

PB94-198942
Disorder Trapping in Ni2TiAl.
PB94-198942 *03,322* Not available NTIS

PB94-198959
Algorithmic Enhancements to the Method of Centers for Linear Programming Problems.
PB94-198959 *03,426* Not available NTIS

PB94-198967
Software Libraries, Numerical and Statistical.
PB94-198967 *01,689* Not available NTIS

PB94-198975
Portable Vectorized Software for Bessel Function Evaluation.
PB94-198975 *01,690* Not available NTIS

PB94-198983
Virtual Software Repository System.
PB94-198983 *01,691* Not available NTIS

PB94-198991
Liquid and Solid Atomic Ion Plasmas.
PB94-198991 *03,809* Not available NTIS

PB94-199007
Absorption of Ultrasonic Waves in Air at High Frequencies (10-20 MHz).
PB94-199007 *04,182* Not available NTIS

PB94-199015
Absorption of Sound in Gases between 10 and 25 MHz: Argon.
PB94-199015 *04,183* Not available NTIS

PB94-199023
Interaction of Rayleigh Waves with a Rib Attached to a Plate.
PB94-199023 *04,184* Not available NTIS

PB94-199031
Intrinsic Stress in DC Sputtered Niobium.
PB94-199031 *04,468* Not available NTIS

PB94-199049
Adhesion of Composites to Dentin and Enamel.
PB94-199049 *00,144* Not available NTIS

PB94-199056
Development of an Adhesive Bonding System.
PB94-199056 *00,145* Not available NTIS

PB94-199064
Statistical Quality Control Technology in Japan.
PB94-199064 *02,708* Not available NTIS

PB94-199072
Asymptotic Behavior of Modulated Taylor-Couette Flows with a Crystalline Inner Cylinder.
PB94-199072 *04,469* Not available NTIS

PB94-199080
Precision Nuclear Orientation Measurements for Determining Mixed Magnetic Dipole/Electric Quadrupole Hyperfine Interactions.
PB94-199080 *03,810* Not available NTIS

PB94-199098
Development and Calibration of UV/VUV Radiometric Sources.
PB94-199098 *04,229* Not available NTIS

PB94-199106
Object Finder for Digital Images Based on Multiple Thresholds, Connectivity, and Internal Structures.
PB94-199106 *01,833* Not available NTIS

PB94-199114
Concentration Histogram Imaging: A Scatter Diagram Technique for Viewing Two or Three Related Images.
PB94-199114 *00,542* Not available NTIS

PB94-199122
Atmospheric and Marine Trace Chemistry: Interfacial Biomediation and Monitoring.
PB94-199122 *03,752* Not available NTIS

PB94-199130
Spatial Dependence of Electrical Fields Due to Space Charges in Films of Organic Dielectrics Used for Insulation of Power Cables.
PB94-199130 *02,214* Not available NTIS

PB94-199148
Microstructure and Ferroelectric Properties of Lead Zirconate-Titanate Films Produced by Laser Evaporation.
PB94-199148 *04,470* Not available NTIS

PB94-199155
Germanium Detector Optimization of MDA for Efficiency vs. Low Intrinsic Background.
PB94-199155 *00,543* Not available NTIS

PB94-199163
Overview of Radiometric Program of the NIST Thermal Imaging Laboratory.
PB94-199163 *04,230* Not available NTIS

PB94-199171
Applications of the Vortex Tube in Chemical Analysis.
PB94-199171 *00,544* Not available NTIS

PB94-199189
Measurement of Diffusion in Supercritical Fluid Systems: A Review.
PB94-199189 *00,795* Not available NTIS

PB94-199197
Simple and Efficient Low-Temperature Sample Cell for Infrared Spectrophotometry.
PB94-199197 *00,545* Not available NTIS

PB94-199205
Simple, Inexpensive Apparatus for Sample Concentration.
PB94-199205 *00,546* Not available NTIS

PB94-199213
Summary of the Patent Literature of Supercritical Fluid Technology.
PB94-199213 *00,502* Not available NTIS

PB94-199221
Thermophysical Property Data for Supercritical Fluid Extraction Design.
PB94-199221 *00,668* Not available NTIS

PB94-199239
Laser Melting of Thin Silicon Films.
PB94-199239 *04,471* Not available NTIS

PB94-199247
Integrated Network Management.
PB94-199247 *01,583* Not available NTIS

PB94-199254
Calculation of Higher Heating Values of Biomass Materials and Waste Components from Elemental Analyses.
PB94-199254 *02,474* Not available NTIS

PB94-199262
Studies Assess Performance of Residential Detectors.
PB94-199262 *00,290* Not available NTIS

PB94-199270
Analysis of the Happyland Social Club Fire with HAZARD I.
PB94-199270 *00,193* Not available NTIS

PB94-199288
Photodecomposition Dynamics of Mo(CO)6/Si(111) 7x7: CO Internal State and Translational Energy Distributions--Translation.
PB94-199288 *00,687* Not available NTIS

PB94-199296
Fluorescence Anisotropy Measurements on a Polymer Melt as a Function of Applied Shear Stress.
PB94-199296 *01,209* Not available NTIS

PB94-199304
Observations of Shear Induced Molecular Orientation in a Polymer Melt Using Fluorescence Anisotropy Measurements.
PB94-199304 *01,210* Not available NTIS

PB94-199312
Observations of Shear Stress and Molecular Orientation Using Fluorescence Anisotropy Measurements.
PB94-199312 *01,211* Not available NTIS

PB94-199320
Analysis of Moisture Accumulation in a Wood-Frame Wall Subjected to Winter Climate.
PB94-199320 *00,338* Not available NTIS

PB94-199338
Gas Phase Reactions Relevant to Chemical Vapor Deposition: Optical Diagnostics.
PB94-199338 *03,116* Not available NTIS

PB94-199346
Gas Phase Reactions Relevant to Chemical Vapor Deposition: Numerical Modeling.
PB94-199346 *03,117* Not available NTIS

PB94-199353
LMTO/CVM and LAPW/CVM Calculations of the Nickel Aluminide/Nickel Titanium Pseudobinary Phase Diagram.
PB94-199353 *03,323* Not available NTIS

PB94-199361
Interface Properties for Ceramic Composites from a Single Fiber Pull-Out Test.
PB94-199361 *03,135* Not available NTIS

PB94-199379
Determination of 3-Quinuclidinyl Benzilate (Qnb) and Its Major Metabolites in Urine by Isotope Dilution Gas Chromatography Mass Spectrometry.
PB94-199379 *03,492* Not available NTIS

PB94-199387
Statistical Thermodynamics of Phase Separation and Ion Partitioning in Aqueous Two-Phase Systems.
PB94-199387 *01,212* Not available NTIS

PB94-199395
Quantized Dissipation of the Quantum Hall Effect at High Currents.
PB94-199395 *04,472* Not available NTIS

PB94-199403
Modeling the Evolution of Structure in Unstable Solid Solution Phases by Diffusional Mechanisms.
PB94-199403 *03,324* Not available NTIS

PB94-199411
Singularities in Minimum Surface Energy Problems and Their Influence in Surface Motion.
PB94-199411 *04,473* Not available NTIS

PB94-199429
Stability, Microstructural Evolution, Grain Growth, and Coarsening in a Two-Dimensional Two-Phase Microstructure.
PB94-199429 *03,325* Not available NTIS

PB94-199437
IUE Observations of Solar-Type Stars in the Pleiades and the Hyades.
PB94-199437 *00,053* Not available NTIS

PB94-199445
Collision-Induced Emission in the Fundamental Vibration-Rotation Band of H2.
PB94-199445 *03,811* Not available NTIS

PB94-199452
Experimental Studies of Line Shapes from a Balle-Flygare Spectrometer.
PB94-199452 *00,796* Not available NTIS

PB94-199460
Performance of a Reflectron Energy Compensating Mirror.
PB94-199460 *00,547* Not available NTIS

PB94-199478
Silicon Photodiodes Optimized for EUV and Soft X-Ray Regions.
PB94-199478 *02,124* Not available NTIS

PB94-199486
Slowly Divergent Space Marching Schemes in the Inverse Heat Conduction Problem.
PB94-199486 *03,812* Not available NTIS

PB94-199494
Maturity Method.
PB94-199494 *01,313* Not available NTIS

PB94-199502
Maturity Functions for Concrete Made with Various Cements and Admixtures.
PB94-199502 *01,314* Not available NTIS

PB94-199510
Neutron Standard Cross Sections in Reactor Physics: Need and Status.
PB94-199510 *03,813* Not available NTIS

PB94-199528
First Results from the Goddard High-Resolution Spectrograph: The Chromosphere of Tauri.
PB94-199528 *00,054* Not available NTIS

PB94-199536
Micro-Mechanical Aspects of Asperity-Controlled Friction in Fiber-Toughened Ceramic Composites.
PB94-199536 *03,136* Not available NTIS

PB94-199544
New Rydberg States of Aluminum Monofluoride Observed by Resonance-Enhanced Multiphoton Ionization Spectroscopy.
PB94-199544 *00,797* Not available NTIS

PB94-199551
Magneto-Optic Magnetic Field Sensor with 1.4pT/square root of 1(Hz) Minimum Detectable Field at 1 kHz.
PB94-199551 *02,125* Not available NTIS

PB94-199569
Thermodynamic Properties of CHF2-O-CHF2,Bis(difluoromethyl) Ether.
PB94-199569 *00,798* Not available NTIS

PB94-199577
Vibrational Autoionization in H2: Vibrational Branching Ratios and Photoelectron Angular Distributions Near the v(+)=3 Threshold.
PB94-199577 *00,799* Not available NTIS

PB94-199585
Isotope Shifts and Hyperfine Splittings of the 398.8-nm Yb I Line.
PB94-199585 *03,814* Not available NTIS

PB94-199593
Thermodynamic Analysis of Heparin Binding to Human Antithrombin.
PB94-199593 *03,455* Not available NTIS

PB94-199601
ROSAT All-Sky Survey of Active Binary Coronae. 2. Coronal Temperatures of the RS Canum Venaticorum Systems.
PB94-199601 *00,055* Not available NTIS

PB94-199619
Maximum Entropy as a Tool for the Determination of the C-Axis Profile of Layered Compounds.
PB94-199619 *00,800* Not available NTIS

PB94-199627
Experimental Aspects and Z-Dependent Systematics in One- and Two-Electron Ions and Single Vacancy Systems.
PB94-199627 *03,815* Not available NTIS

PB94-199635
Status of a Silicon Lattice Measurement and Dissemination Exercise.
PB94-199635 *04,474* Not available NTIS

PB94-199643
EPR Bone Dosimetry: A New Approach to Spectral Deconvolution Problems.
PB94-199643 *03,616* Not available NTIS

PB94-199650
Estimation of the Absorbed Dose in Radiation-Processed Food. 2. Test of the EPR Response Function by an Exponential Fitting Analysis.
PB94-199650 *00,036* Not available NTIS

PB94-199668
Experimental Validation of Radiopharmaceutical Absorbed Dose to Mineralized Bone Tissue.
PB94-199668 *03,617* Not available NTIS

PB94-199676
Radiation Doses.
PB94-199676 *03,618* Not available NTIS

PB94-199684
Estimation of the Absorbed Dose in Radiation-Processed Food. 3. The Effect of Time of Evaluation on the Accuracy of the Estimate.
PB94-199684 *00,037* Not available NTIS

PB94-199692
Estimation of the Absorbed Dose in Radiation-Processed Food. 4. EPR Measurements on Eggshell.
PB94-199692 *00,038* Not available NTIS

PB94-199700
New EPR Dosimeter Based on Polyvinylalcohol.
PB94-199700 *03,619* Not available NTIS

PB94-199718
Estimation of the Absorbed Dose in Radiation-Processed Food. 1. Test of the EPR Response Function by a Linear Regression Analysis.
PB94-199718 *00,039* Not available NTIS

PB94-199726
Establishing Quality Measurements for Inorganic Analysis of Biomaterials.
PB94-199726 *00,548* Not available NTIS

PB94-199734
Polarization of Light Emitted After Positron Impact Excitation of Alkali Atoms.
PB94-199734 *03,816* Not available NTIS

PB94-199742
Current Results and Future Prospects for a Neutron Lifetime Determination Using Trapped Protons.
PB94-199742 *03,817* Not available NTIS

PB94-199759
Interaction between Naphthalene Sulfonate and Silica Fume in Portland Cement Pastes.
PB94-199759 *01,315* Not available NTIS

PB94-199767
Hysteresis Measurements of Remanent Polarization and Coercive Field in Polymers.
PB94-199767 *04,475* Not available NTIS

PB94-199775
Role of Refrigerant Mixtures as Alternatives to CFCs.
PB94-199775 *03,252* Not available NTIS

PB94-199783
Role of R22 in Refrigerating and Air Conditioning Equipment.
PB94-199783 *03,253* Not available NTIS

PB94-199791
Measurements of the Viscosities of Saturated and Compressed Fluid 1-chloro-1,2,2,2-tetrafluoroethane (R124) and Pentafluoroethane (R125) at Temperatures between 120 and 420 K.
PB94-199791 *03,254* Not available NTIS

PB94-199809
Peeling a Polymer from a Surface or from a Line.
PB94-199809 *01,213* Not available NTIS

PB94-199817
Calibration Standards for Differential Scanning Calorimetry. 1. Zinc Absolute Calorimetric Measurement of Enthalpy of Fusion and Temperature of Fusion HM.
PB94-199817 *00,801* Not available NTIS

PB94-199825
Oxidative Damage to DNA in Mammalian Chromatin.
PB94-199825 *03,525* Not available NTIS

PB94-199833
Modification of DNA Bases in Chromatin of Intact Target Human Cells by Activated Human Polymorphonuclear Leukocytes.
PB94-199833 *03,526* Not available NTIS

PB94-199841
Absolute Cross-Section Measurements for Electron-Impact Ionization of C1(+1).
PB94-199841 *03,818* Not available NTIS

PB94-199858
Computer Vision Based Tool Setting Station.
PB94-199858 *02,944* Not available NTIS

PB94-199866
Measuring the Stability of Three Copper Alloys.
PB94-199866 *03,326* Not available NTIS

PB94-199874
Environmental Evaluation of a New Federal Office Building.
PB94-199874 *02,538* Not available NTIS

PB94-199882
Assessing the Credibility of the Calorific Content of Muncipal Solid Waste.
PB94-199882 *02,581* Not available NTIS

PB94-199890
Simplified Cycle Simulation Model for the Performance Rating of Refrigerants and Refrigerant Mixtures.
PB94-199890 *03,255* Not available NTIS

PB94-199908
Fragment Energy and Vector Correlations in the Overtone-Pumped Dissociation of HN3X(1)A'.
PB94-199908 *00,802* Not available NTIS

PB94-199916
Neutron Measurement Intercomparisons Sponsored by CCEMRI, Section 3 (Neutron Measurements).
PB94-199916 *03,819* Not available NTIS

PB94-199924
Diffraction of X-rays at the Far Tails of the Bragg Peaks.
PB94-199924 *04,476* Not available NTIS

PB94-199932
Implementing a Transition Manager in the AMRF Cell Controller.
PB94-199932 *02,817* Not available NTIS

PB94-199940
Generic Manufacturing Controllers.
PB94-199940 *02,818* Not available NTIS

PB94-199957
Time-Resolved Probes of Surface Dynamics.
PB94-199957 *00,803* Not available NTIS

PB94-199965
Dynamics of Nonthermal Reactions: Femtosecond Surface Chemistry.
PB94-199965 *00,688* Not available NTIS

PB94-199973
Reactivity of Pd and Sn Adsorbates on Plasma and Thermally Oxidized SnO2(110).
PB94-199973 *00,804* Not available NTIS

PB94-199981
Dynamic Characteristics of Five Tall Buildings during Strong and Low-Amplitude Motions.
PB94-199981 *00,427* Not available NTIS

PB94-199999
Millisecond-Resolution Pulse Heating System for Specific-Heat Measurements at High Temperatures.
PB94-199999 *02,635* Not available NTIS

PB94-200003
High-Speed Spatial Scanning Pyrometer.
PB94-200003 *02,636* Not available NTIS

PB94-200011
Wavelength Dependence of Normal Spectral Emissivity of High-Temperature Metals at Their Melting Point.
PB94-200011 *03,398* Not available NTIS

PB94-200029
VLSI Architectures for Template Matching and Block Matching.
PB94-200029 *01,834* Not available NTIS

PB94-200037
Pure Element Sputtering Yield Data: Appendix 4.
PB94-200037 *00,805* Not available NTIS

PB94-200045
Electronic Correlations and Satellites in Superconducting Oxides.
PB94-200045 *04,477* Not available NTIS

PB94-200052
Effect of Curing History on Ultimate Glass Transition Temperature and Network Structure of Crosslinking Polymers.
PB94-200052 *01,214* Not available NTIS

PB94-200060
NIST Capacitance Measurement Assurance Program (MAP).
PB94-200060 *02,254* Not available NTIS

PB94-200078
Improvements in Computation of Form Factors.
PB94-200078 *03,820* Not available NTIS

PB94-200086
Photographic Response to X-Ray Irradiation. 1. Estimation of the Photographic Error Statistic and Development of Analytic Density-Intensity Equations.
PB94-200086 *03,821* Not available NTIS

PB94-200094
Photographic Response to X-Ray Irradiation. 2. Correlated Models.
PB94-200094 *03,822* Not available NTIS

PB94-200102
Photographic Response to X-Ray Irradiation. 3. Photographic Linearization of Beam-Foil Spectra.
PB94-200102 *03,823* Not available NTIS

PB94-200110
Cavitation Damage During Flexural Creep of SiAlON-YAG Ceramics.
PB94-200110 *03,036* Not available NTIS

PB94-200128
Surface Barrier and Lower Critical Field in YBa2Cu3O7-delta Superconductors.
PB94-200128 *04,478* Not available NTIS

PB94-200136
Hot-Deformation Apparatus for Thermomechanical Processing Simulation.
PB94-200136 *03,207* Not available NTIS

PB94-200144
X-Ray Photoelectron and Auger Electron Spectroscopy Study of Ultraviolet/Ozone Oxidized P2S5/(NH4)2S Treated GaAs(100) Surfaces.
PB94-200144 *04,479* Not available NTIS

PB94-200151
Grazing-Incidence X-Ray Photoemission Spectroscopy Investigation of Oxidized GaAs(100): A Novel Approach to Nondestructive Depth Profiling.
PB94-200151 *04,480* Not available NTIS

PB94-200169
Textures of Tantalum Metal Sheets by Neutron Diffraction.
PB94-200169 *03,399* Not available NTIS

PB94-200177
Texture Study of Two Molybdenum Shaped Charge Liners by Neutron Diffraction.
PB94-200177 *03,754* Not available NTIS

PB94-200185
Planar Waveguide Optical Sensors.
PB94-200185 *03,586* Not available NTIS

PB94-200193
Characterization of Vertical-Cavity Semiconductor Structures.
PB94-200193 *02,126* Not available NTIS

PB94-200201
Determination of Oltipraz in Serum by High-Performanace Liquid Chromatography with Optical Absorbance and Mass Spectrometric Detection.
PB94-200201 *03,493* Not available NTIS

PB94-200219
Neutron-Scattering Study of C60(n-) (n=3,6) Librations in Alkali-Metal Fullerides.
PB94-200219 *00,806* Not available NTIS

PB94-200227
Crack Growth Resistance of Strain-Softening Materials under Flexural Loading.
PB94-200227 *02,972* Not available NTIS

PB94-200235
Generic Model for Creep Rupture Lifetime Estimation on Fibrous Ceramic Composites.
PB94-200235 *03,137* Not available NTIS

PB94-200243
Asymmetric Tip Morphology of Creep Microcracks Growing Along Bimaterial Interfaces.
PB94-200243 *03,138* Not available NTIS

PB94-200250
Application of a Simple Technique for Estimating Errors of Finite-Element Solutions Using a General-Purpose Code.
PB94-200250 *04,818* Not available NTIS

PB94-200268
Analysis of Creep in a Si-SiC C-Ring by Finite Element Method.
PB94-200268 *03,037* Not available NTIS

PB94-200276
Incorporation of Gold into YBa2Cu3O7: Structure and Tc Enhancement.
PB94-200276 *04,481* Not available NTIS

PB94-200284
Unexpected Effects of Gold on the Structure, Superconductivity, and Normal State of YBa2Cu3O7.
PB94-200284 *04,482* Not available NTIS

PB94-200292
Generation and Characterization of Acetylene Smokes.
PB94-200292 *01,372* Not available NTIS

PB94-200300
Ultrafine Combustion Aerosol Generator.
PB94-200300 *01,373* Not available NTIS

PB94-200318
Introduction of a NIST Instrument Sensitivity Standard Reference Material for X-Ray Powder Diffraction.
PB94-200318 *00,807* Not available NTIS

PB94-200326
Micromechanics of Densification and Distortion.
PB94-200326 *03,327* Not available NTIS

PB94-200334
Analysis of Scattering Asymmetry Statistics When Background Corrected Counts Are Negative.
PB94-200334 *03,824* Not available NTIS

PB94-200342
Uncertainty Intervals for Polarized Beam Scattering Asymmetry Statistics.
PB94-200342 *03,825* Not available NTIS

PB94-200359
High-Frequency Linear Response of Anisotropic Type-II Superconductors in the Mixed State.
PB94-200359 *04,483* Not available NTIS

PB94-200367
Nonlinear Response of Type-II Superconductors in the Mixed State in Slab Geometry.
PB94-200367 *04,484* Not available NTIS

PB94-200375
Salt-PEG Two-Phase Aqueous Systems to Purify Proteins and Nucleic Acid Mixtures.
PB94-200375 *03,527* Not available NTIS

PB94-200383
Papers Presentations Shine.
PB94-200383 *00,244* Not available NTIS

PB94-200391
Electron Traps, Structural Change, and Hydrogen Related SIMOX Defects.
PB94-200391 *02,312* Not available NTIS

PB94-200409
President's Column for Dielectrics and Electrical Insulation Society Newsletter.
PB94-200409 *01,882* Not available NTIS

PB94-200417
Acceptance Diagram Analysis of the Performance of Multidisk Neutron Velocity Selectors.
PB94-200417 *03,826* Not available NTIS

PB94-200425
Acceptance Diagram Analysis of the Performance of Vertically Curved Neutron Monochromators.
PB94-200425 *03,827* Not available NTIS

PB94-200433
Joy of Acceptance Diagrams.
PB94-200433 *03,828* Not available NTIS

PB94-200441
Effects of Crystalline Anisotropy and Buoyancy-Driven Convection on Morphological Stability.
PB94-200441 *03,328* Not available NTIS

PB94-200458
Neutron Scattering Structural Study of AlCuFe Quasicrystals Using Double Isotopic Substitution.
PB94-200458 *04,485* Not available NTIS

PB94-200466
2-Tunneling Path Internal-Axis-Method-Like Treatment of the Microwave Spectrum of Divinyl Ether.
PB94-200466 *00,808* Not available NTIS

PB94-200474
Assessment of the Al-Sb System.
PB94-200474 *03,329* Not available NTIS

PB94-200482
Assay of the Eluent from the Alumina-Based Tungsten-188-Rhenium-188 Generator.
PB94-200482 *03,829* Not available NTIS

PB94-200490
Standardization and Decay Scheme of Rhenium-186.
PB94-200490 *03,830* Not available NTIS

PB94-200508
Two-Dimensional POMMIE Carbon-Proton Chemical Shift Correlated (13)C NMR Spectrum Editing.
PB94-200508 *00,809* Not available NTIS

PB94-200516
Carotenoid Reversed-Phase High-Performance Liquid Chromatography Methods: Reference Compendium.
PB94-200516 *00,549* Not available NTIS

PB94-200524
Individual Carotenoid Content of SRM 1548 Total Diet and Influence of Storage Temperature, Lyophilization, and Irradiation on Dietary Carotenoids.
PB94-200524 *00,033* Not available NTIS

PB94-200532
Assessment of Testing Methodology for Ceramic Matrix Composites.
PB94-200532 *03,139* Not available NTIS

PB94-200540
Perspective on Fiber Coating Technology.
PB94-200540 *03,118* Not available NTIS

PB94-200557
Anharmonic Phonons and the Isotope Effect in Superconductivity.
PB94-200557 *04,486* Not available NTIS

PB94-200565
Test Structures for the In-Plane Locations of Projected Features with Nanometer-Level Accuracy Traceable to a Coordinate Measurement System.
PB94-200565 *02,313* Not available NTIS

PB94-200573
Graphical Conceptual Navigation as a Presentation Technique for a Graphics Standard.
PB94-200573 *01,692* Not available NTIS

PB94-200581
Rate Constants for Hydrogem Atom Attack on Some Chlorinated Benzenes at High Temperature.
PB94-200581 *00,810* Not available NTIS

PB94-200599
Importance of Chemometrics in Biomedical Measurements.
PB94-200599 *00,550* Not available NTIS

PB94-200607
Metrological Measurement Accuracy: Discussion of 'Measurement Error Models' by Leon Jay Gleser.
PB94-200607 *00,551* Not available NTIS

PB94-200615
Accuracy-Weighted Variational Principle for Degenerate Continuum States.
PB94-200615 *03,831* Not available NTIS

PB94-200623
Comprehensive Theory of Nuclear Effects on the Intrinsic Sticking Probability. 1.
PB94-200623 *03,832* Not available NTIS

PB94-200631
Comprehensive Theory of Nuclear Effects on the Intrinsic Sticking Probability. 2.
PB94-200631 *03,833* Not available NTIS

PB94-200649
Elastic Properties of Uniaxial-Fiber Reinforced Composites: General Features.
PB94-200649 *03,140* Not available NTIS

PB94-200656
Transient Subcritical Crack-Growth Behavior in Transformation-Toughened Ceramics.
PB94-200656 *03,038* Not available NTIS

PB94-200664
Report of Density Intercomparisons Undertaken by the Working Group on Density of the CCM.
PB94-200664 *00,503* Not available NTIS

PB94-200672
Mass and Density Determinations.
PB94-200672 *00,504* Not available NTIS

PB94-200680
Extension of Heterodyne Frequency Measurements on OCS to 87 THz (2900 cm(-1)).
PB94-200680 *00,811* Not available NTIS

PB94-200698
Faraday Effect Current Sensors.
PB94-200698 *02,127* Not available NTIS

PB94-200706
Faraday Effect Sensors: A Review of Recent Progress.
PB94-200706 *02,128* Not available NTIS

PB94-200714
Correlation of HgCdTe Epilayer Defects with Underlying Substrate Defects by Synchrotron X-Ray Topography.
PB94-200714 *02,129* Not available NTIS

PB94-203403
Evaluation of Alternative In-Flight Fire Suppressants for Full-Scale Testing in Simulated Aircraft Engine Nacelles and Dry Bays.
PB94-203403 *00,023* PC A99/MF E08

PB94-203429
Integration of Servo Control into a Large-Scale Control System Design: An Example from Coal Mining.
PB94-203429 *03,696* PC A02/MF A01

PB94-203437
Quality Characteristics and Metrics for Reusable Software (Preliminary Report).
PB94-203437 *01,693* PC A03/MF A01

PB94-203510
Certainty Grid to Object Boundary Algorithm.
PB94-203510 *01,835* PC A03/MF A01

PB94-203528
Continuous Mining Machine Control Using the Real-Time Control System.
PB94-203528 *03,700* PC A02/MF A01

PB94-203536
Environment Simulation for a Continuous Mining Machine.
PB94-203536 *03,697* PC A03/MF A01

PB94-203593
Cryogenic Properties of Silver.
PB94-203593 *03,330* PC A03

PB94-205952
Fire Growth Analysis of the Fire of March 20, 1990, Pulaski Building, 20 Massachusetts Avenue, N.W., Washington, DC.
PB94-205952 *00,194* PC A03/MF A01

PB94-206018
Energy Prices and Discount Factors for Life-Cycle Cost Analysis 1994. Annual Supplement to NIST Handbook 135 and NBS Special Publication 709.
PB94-206018 *02,508* PC A04/MF A01

PB94-206091
Development of the Fire Data Management System.
PB94-206091 *00,339* PC A03/MF A01

PB94-206109
User's Guide to NIST SRM 2084: CMM Probe Performance Standard.
PB94-206109 *02,709* PC A03/MF A01

PB94-206125
Wind Load Provisions of the Manufactured Home Construction and Safety Standards: A Review and Recommendations for Improvement.
PB94-206125 *00,428* PC A06/MF A02

PB94-206281
Visual-Motion Fixation Invariant.
PB94-206281 *01,836* PC A03/MF A01

PB94-206299
Upward Flame Spread along the Vertical Corner Walls (October 1993).
PB94-206299 *00,340* PC A03/MF A01

PB94-206307
Metric Path to Global Markets and New Jobs: A Question-and-Answer and Thematic Discussion.
PB94-206307 *02,601* PC A02/MF A01

PB94-206356
Evaluating Small Board and Care Homes: Sprinklered vs. Nonsprinklered Fire Protection.
PB94-206356 *00,195* PC A04/MF A01

PB94-206364
U.S. Green Building Conference, 1994.
PB94-206364 *02,519* PC A08/MF A02

PB94-206646
Assessment of Technology for Detection of Stress Corrosion Cracking in Gas Pipelines. Final Report, July 1993-March 1994.
PB94-206646 *02,475* PC A05/MF A02

PB94-207354
World Wide Web and Mosaic: User's Guide.
PB94-207354 *02,722* PC A03/MF A01

PB94-207388
Turbulent Upward Flame Spread on a Vertical Wall under External Radiation.
PB94-207388 *00,341* PC A05/MF A01

PB94-207404
Comparison of Wall-Fire Behavior With and Without a Ceiling.
PB94-207404 *00,342* PC A03/MF A01

PB94-207453
IGOSS-Industry/Government Open Systems Specification.
PB94-207453 *01,806* PC A07/MF A02

PB94-207461
Northridge Earthquake 1994: Performance of Structures, Lifelines, and Fire Protection Systems.
PB94-207461 *04,825* PC A09/MF A02

PB94-207495
Project Summaries 1994: NIST Building and Fire Research Laboratory.
PB94-207495 *00,343* PC A08/MF A02

PB94-207511
Global Equivalence Ratio Concept and the Prediction of Carbon Monoxide Formation in Enclosure Fires.
PB94-207511 *00,313* PC A08/MF A02

PB94-207636
Technical Digest: Symposium on Optical Fiber Measurements (8th), 1994. Held in Boulder, Colorado on September 13-15, 1994.
PB94-207636 *04,231* PC A10/MF A03

PB94-207727
State Weights and Measures Laboratories: State Standards Program Description and Directory. 1994 Edition.
PB94-207727 *02,895* PC A07/MF A02

PB94-207750
Preliminary Functional Specifications of a Prototype Electronic Research Notebook for NIST.
PB94-207750 *00,012* PC A04/MF A01

PB94-207768
Face Recognition Technology for Law Enforcement Applications.
PB94-207768 *01,837* PC A05/MF A01

PB94-209459
Report of the NIST Workshop on Key Escrow Encryption. Held in Gaithersburg, Maryland on June 8-10, 1994.
PB94-209459 *01,584* PC A08/MF A02

PB94-210051
Measurements of Shielding Effectiveness and Cavity Characteristics of Airplanes.
PB94-210051 *00,030* PC A04/MF A01

PB94-210077
Combined Buoyancy- and Pressure-Driven Flow Through a Shallow, Horizontal, Circular Vent.
PB94-210077 *00,344* PC A03/MF A01

PB94-210127
VENTCF2: An Algorithm and Associated FORTRAN 77 Subroutine for Calculating Flow through a Horizontal Ceiling/Floor Vent in a Zone-Type Compartment Fire Model.
PB94-210127 *00,345* PC A04/MF A01

PB94-210143
Program Handbook: Requirements for Obtaining NIST Approval/Recognition of a Laboratory Accreditation Body Under P.L. 101-592. The Fastener Quality Act.
PB94-210143 *02,859* PC A03/MF A01

PB94-210150
Survey on the Implementation of ISO/IEC Guide 25 by National Laboratory Accreditation Programs.
PB94-210150 *00,479* PC A04/MF A01

PB94-210168
Airborne Asbestos Method: Standard Practice for Recording Transmission Electron Microscopy Data for the Analysis of Asbestos Collected onto Filters. Version 1.0.
PB94-210168 *00,552* PC A03/MF A03

PB94-211018
Tribological Characteristics of Alpha-Alumina at Elevated Temperatures.
PB94-211018 *02,963* Not available NTIS

PB94-211026
Hypercubic Lattice SAW Exponents nu and gamma : 3.99 Dimensions Revisited.
PB94-211026 *01,215* Not available NTIS

PB94-211034
Effect of Swelling on the Elasticity of Rubber: Localization Model Description.
PB94-211034 *01,216* Not available NTIS

PB94-211042
Molar Absorptivities of Bilirubin (NIST SRM 916A) and Its Neutral and Alkaline Azopigments.
PB94-211042 *03,456* Not available NTIS

PB94-211059
Measurement of Boron at Silicon Wafer Surfaces by Neutron Depth Profiling.
PB94-211059 *04,487* Not available NTIS

PB94-211067
Dynamic Phenomena on the RS Canum Venaticorum Binary II Pegasi in August 1989. 1. Observational Data.
PB94-211067 *00,056* Not available NTIS

PB94-211075
Plasma Chemistry in Disilane Discharges.
PB94-211075 *02,514* Not available NTIS

PB94-211083
Radio Continuum and X-Ray Properties of the Coronae of RS Canum Venaticorum and Related Active Binary Systems.
PB94-211083 *00,057* Not available NTIS

PB94-211091
Ordered omega-Derivatives in a Ti-37.5Al-2ONb at% Alloy.
PB94-211091 *03,331* Not available NTIS

PB94-211109
Three-Vector Correlation Theory for Orientation/Alignment Studies in Atomic and Molecular Collisions.
PB94-211109 *03,834* Not available NTIS

PB94-211117
NIST Optically Pumped Cesium Frequency Standard.
PB94-211117 *03,835* Not available NTIS

PB94-211125
Multichannel Quantum Defect Half Collision Analysis of K2 Photodissociation Through the B1Pi(sub u) State.
PB94-211125 *00,812* Not available NTIS

PB94-211133
Intersystem Crossing in Collisions of Aligned Ca(4s5p (1)P) + He: A Half Collision Analysis Using Multichannel Quantum Defect Theory.
PB94-211133 *00,813* Not available NTIS

PB94-211141
How Far Is Far from Critical Point in Polymer Blends. Lattice Cluster Theory Computations for Structured Monomer, Compressible Systems.
PB94-211141 *01,217* Not available NTIS

PB94-211158
Early Dielectronic Recombination Measurements: Singly Charged Ions.
PB94-211158 *03,836* Not available NTIS

PB94-211166
Torsional Dilatometer for Volume Change Measurements on Deformed Glasses: Instrument Description and Measurements on Equilibrated Glasses.
PB94-211166 *03,379* Not available NTIS

PB94-211174
Brillouin Light Scattering Intensities for Thin Magnetic Films with Large Perpendicular Anisotropies.
PB94-211174 *04,488* Not available NTIS

PB94-211182
Fine Structure of Negative Ions of Alkaline-Earth-Metal Atoms.
PB94-211182 *03,837* Not available NTIS

PB94-211190
Mixed Phospholipid Liposome Calcification.
PB94-211190 *03,457* Not available NTIS

PB94-211208
Proteoglycan Inhibition of Calcium Phosphate Precipitation in Liposomal Suspensions.
PB94-211208 *00,658* Not available NTIS

PB94-211216
Half-Integral Constant Voltage Steps in High-Tc Grain Boundary Junctions.
PB94-211216 *04,489* Not available NTIS

PB94-211224
Update on the Low Background IR Calibration Facility at the National Institute of Standards and Technology.
PB94-211224 *04,232* Not available NTIS

PB94-211232
Comparison of Regular Transmittance Scales of Four National Standardizing Laboratories.
PB94-211232 *04,233* Not available NTIS

PB94-211240
Clinical Perspective on Dentin Adhesives.
PB94-211240 *00,146* Not available NTIS

PB94-211257
Selective Inhibition of Crystal Growth on Octacalcium Phosphate and Nonstoichiometric Hydroxyapatite by Pyrophosphate at Physiological Concentration.
PB94-211257 *00,147* Not available NTIS

PB94-211265
Slab Transmission and Reflection for Point Source and Point Detector.
PB94-211265 *03,838* Not available NTIS

PB94-211273
National Quality Assurance Program for Personnel Radiation Dosimetry: A Case History.
PB94-211273 *03,620* Not available NTIS

PB94-211281
Critical Magnetic-Field Angle for High-Field Current Transport in YBa2Cu3O7 at 76 K.
PB94-211281 *04,490* Not available NTIS

PB94-211299
Superconducting Materials: Specification.
PB94-211299 *04,491* Not available NTIS

PB94-211307
Transport Critical Current of Aligned Polycrystalline Yttrium Barium Copper Oxide (YBa2Cu3O7-delta).
PB94-211307 *04,492* Not available NTIS

PB94-211315
Effect of Axial Strain on the Critical Current of Ag-Sheathed Bi-Based Superconductors in Magnetic Fields Up to 25 T.
PB94-211315 *04,493* Not available NTIS

PB94-211323
In situ Noble Metal YBa2Cu3O7 Thin-Film Contacts.
PB94-211323 *04,494* Not available NTIS

PB94-211331
Total Surface Areas of Group IVA Organometallic Compounds: Predictors of Toxicity to Algae and Bacteria.
PB94-211331 *00,814* Not available NTIS

PB94-211349
Longterm Changes of Silicon Photodiodes and Their Use for Photometric Standardization.
PB94-211349 *04,234* Not available NTIS

PB94-211356
Magnetoelasticity in Rare-Earth Multilayers and Films.
PB94-211356 *04,495* Not available NTIS

PB94-211364
Advanced Angle Metrology System.
PB94-211364 *02,637* Not available NTIS

PB94-211372
Suppression Research: Strategies.
PB94-211372 *00,346* Not available NTIS

PB94-211380
Conditions for Existence of a Reentrant Solid Phase in a Sheared Atomic Fluid.
PB94-211380 *04,198* Not available NTIS

PB94-211398
Reaction Rate Determinations of Vinyl Radical Reactions with Vinyl, Methyl, and Hydrogen Atoms.
PB94-211398 *00,815* Not available NTIS

PB94-211406
Anomalous Odd- to Even-Mass Isotope Ratios in Resonance Ionization with Broad-Band Lasers.
PB94-211406 *03,839* Not available NTIS

PB94-211414
Earth-Based Gravitational Experiments.
PB94-211414 *03,840* Not available NTIS

PB94-211422
Monitoring Polymer Cure by Fluorescence Recovery After Photobleaching.
PB94-211422 *01,218* Not available NTIS

PB94-211430
New Method for Shielding Electron Beams Used for Head and Neck Cancer Treatment.
PB94-211430 *03,621* Not available NTIS

PB94-211448
High-Resolution Infrared Overtone Spectroscopy of ArHF via Nd:YAG/Dye Laser Difference Frequency Generation.
PB94-211448 *00,816* Not available NTIS

PB94-211455
U.S. GOSIP Testing Program.
PB94-211455 *01,807* Not available NTIS

PB94-211463
P-Type Doubling in the Infrared Spectrum of NO-HF.
PB94-211463 *00,817* Not available NTIS

PB94-211471
Analysis of Thermal Wave Propagation in Diamond Films.
PB94-211471 *03,014* Not available NTIS

PB94-211489
Thermal Wave Propagation in Diamond Films.
PB94-211489 *03,015* Not available NTIS

PB94-211497
Magnetic Dipole Line from U LXXI Ground-Term Levels Predicted at 3200 Angstroms.
PB94-211497 *04,407* Not available NTIS

PB94-211505
Photoionization of Small Molecules Using Synchrotron Radiation.
PB94-211505 *03,841* Not available NTIS

PB94-211513
NIST Power Reference Source.
PB94-211513 *00,148* Not available NTIS

PB94-211521
Roles of Copper in Applied Superconductivity.
PB94-211521 *02,255* Not available NTIS

PB94-211539
Benchmarks for the Evaluation of Speech Recognizers.
PB94-211539 *01,566* Not available NTIS

PB94-211547
Neutron Scattering by Multiblock Copolymers of Structure (A-B)N-A.
PB94-211547 *01,219* Not available NTIS

PB94-211554
Atomic Transition Probability Ratios between Some Ar I 4s-4p and 4s-5p Transitions.
PB94-211554 *03,842* Not available NTIS

PB94-211562
Ion Broadening Parameters for Several Argon and Carbon Lines.
PB94-211562 *03,843* Not available NTIS

PB94-211570
Dreams About the Next Generation of Super-Stable Lasers.
PB94-211570 *04,235* Not available NTIS

PB94-211588
24 GHz Josephson Array Voltage Standard.
PB94-211588 *02,033* Not available NTIS

PB94-211596
Estimate of Flame Radiance via a Single Location Measurement in Liquid Pool Flames.
PB94-211596 *02,476* Not available NTIS

PB94-211604
Measurement of Radiative Feedback to the Fuel Surface of a Pool Fire.
PB94-211604 *02,477* Not available NTIS

PB94-211612
Shear Dependence of Critical Fluctuations in Binary Polymer Mixtures by Small Angle Neutron Scattering.
PB94-211612 *01,220* Not available NTIS

PB94-211620
L-threo-beta-Hydroxyhistidine, an Unprecedented Iron(III) Ion-Binding Amino Acid in a Pyoverdine-type Siderophore from Pseudomonas fluorescens 244.
PB94-211620 *00,553* Not available NTIS

PB94-211638
Energy and Migration of Grain Boundaries in Polycrystals.
PB94-211638 *03,332* Not available NTIS

PB94-211646
Fabrication of Platinum-Gold Alloys in Pre-Hispanic South America: Issues of Temperature and Microstructure Control.
PB94-211646 *03,333* Not available NTIS

PB94-211653
Wire Bond Testing.
PB94-211653 *02,314* Not available NTIS

PB94-211661
Radiation Chemistry of Cyanine Dyes: Oxidation and Reduction of Merocyanine 540.
PB94-211661 *00,818* Not available NTIS

PB94-211679
Laser-Induced Fluorescence Measurements of Formaldehyde in a Methane/Air Diffusion Flame.
PB94-211679 *01,374* Not available NTIS

PB94-211687
Ensuring Accuracy and Traceability of Weighing Instruments.
PB94-211687 *02,638* Not available NTIS

PB94-211695
Particle Size Standards and Their Certification at NIST.
PB94-211695 *02,639* Not available NTIS

PB94-211703
Supercritical Solubility of Solids from Near-Critical Dilute-Mixture Theory.
PB94-211703 *00,819* Not available NTIS

PB94-211711
YBa2Cu3O7-x to Si Interconnection for Hybrid Superconductor/Semiconductor Integration.
PB94-211711 *02,315* Not available NTIS

PB94-211729
Small-Angle X-Ray and Neutron Scattering Study of Block Copolymer/Homopolymer Mixtures.
PB94-211729 *01,221* Not available NTIS

PB94-211737
High Temperature.
PB94-211737 *03,844* Not available NTIS

PB94-211745
Vapor Transport in Materials and Process Chemistry.
PB94-211745 *00,669* Not available NTIS

PB94-211752
Drill-Hearn-Gerasimov Sum Rule.
PB94-211752 *03,845* Not available NTIS

PB94-211760
Polarizability of the Nucleon.
PB94-211760 *03,846* Not available NTIS

PB94-211778
Effect of Microstructure on the Wear Transition of Zirconia-Toughened Alumina.
PB94-211778 *03,141* Not available NTIS

PB94-211786
Asymptotic Wave Function Splitting Procedure for Propagating Spatially Extended Wave Functions: Application to Intense Field Photodissociation of H2(+).
PB94-211786 *03,847* Not available NTIS

PB94-211794
Investigation of the Drive Circuit Requirements for the Power Insulated Gate Bipolar Transistor (IGBT).
PB94-211794 *02,316* Not available NTIS

PB94-211802
Interstellar Disk-Halo Connection in Galaxies: Review of Observational Aspects.
PB94-211802 *00,058* Not available NTIS

PB94-211810
Vibrational Relaxation Measurements of Carbon Monoxide on Metal Clusters.
PB94-211810 *00,820* Not available NTIS

PB94-211828
Discontinuous Volume Change at the Orientational-Ordering Transition in Solid C60.
PB94-211828 *00,821* Not available NTIS

PB94-211836
Differences in Competitive Strategies between the United States and Japan.
PB94-211836 *00,013* Not available NTIS

PB94-211844
Importance of Measurement in Technology-Based Competition.
PB94-211844 *02,929* Not available NTIS

PB94-211851
Design and Characterization of X-Ray Multilayer Analyzers for the 50 - 1000 eV Region.
PB94-211851 *03,848* Not available NTIS

PB94-211869
Fast-Ion Conduction and Disorder in Cation and Anion Arrays in Y2(ZryTi(1-y))2O7 Pyrochlores Induced by Zr Substitution: A Neutron Rietveld Analysis.
PB94-211869 *04,496* Not available NTIS

PB94-211877
Intelligent Control for Multiple Autonomous Undersea Vehicles.
PB94-211877 *03,747* Not available NTIS

PB94-211885
Real-Time Vision for Autonomous and Teleoperated Control of Unmanned Vehicles.
PB94-211885 *03,701* Not available NTIS

PB94-211893
Real-Time Vision for Unmanned Vehicles.
PB94-211893 *03,702* Not available NTIS

PB94-211901
International Conference on Chemical Kinetics (2nd). Held in Gaithersburg, Maryland on July 24-27, 1989.
PB94-211901 *00,822* Not available NTIS

PB94-211919
Elastic Constants of Isotropic Cylinders Using Resonant Ultrasound.
PB94-211919 *04,497* Not available NTIS

PB94-211927
Determination of the Prior-Austenitic Grain Size of Selected Steels Using a Molten Glass Etch.
PB94-211927 *03,208* Not available NTIS

PB94-211935
Pump-Induced Dispersion of Erbium-Doped Fiber Measured by Fourier-Transform Spectroscopy.
PB94-211935 *04,236* Not available NTIS

PB94-211943
Currents Induced on Multiconductor Transmission Lines by Radiation and Injection.
PB94-211943 *02,215* Not available NTIS

PB94-211950
Electromagnetic Scattering by a Periodic Surface with a Wedge Profile.
PB94-211950 *04,421* Not available NTIS

PB94-211968
Aperture Coupling to a Coaxial Air Line: Theory and Experiment.
PB94-211968 *02,216* Not available NTIS

PB94-211976
Crossover to Strong Shear in a Low-Molecular-Weight Critical Polymer Blend.
PB94-211976 *01,222* Not available NTIS

PB94-211984
Tensile Creep of Whisker Reinforced Silicon Nitride.
PB94-211984 *03,142* Not available NTIS

PB94-211992
Microstructural Evolution in Two-Dimensional Two-Phase Polycrystals.
PB94-211992 *04,498* Not available NTIS

PB94-212008
Periapical Tissue Reactions to a Calcium Phosphate Cement in the Teeth of Monkeys.
PB94-212008 *00,149* Not available NTIS

PB94-212016
Associated Object Model for Distributed Systems.
PB94-212016 *01,694* Not available NTIS

PB94-212024
In situ On-Line Optical Fiber Sensor for Fluorescence Monitoring in Bioreactors.
PB94-212024 *03,587* Not available NTIS

PB94-212032
Use of Extended Permutation-Inversion Groups in Constructing Hyperfine Hamiltonians for Symmetrical-Top Internal Rotor Molecules Like H3C-SiH3.
PB94-212032 *00,823* Not available NTIS

PB94-212040
In-situ Fume Particle Size and Number Density Measurements from a Synthetic Smelt.
PB94-212040 *03,334* Not available NTIS

PB94-212057
Tribochemical Reaction of Stearic Acid on Copper Surface Studied by Surface Enhanced Raman Spectroscopy.
PB94-212057 *02,964* Not available NTIS

PB94-212065
Hierarchical Real-Time Control System for Use with Coal Mining Automation.
PB94-212065 *03,698* Not available NTIS

PB94-212073
Neutron Powder Diffraction Study of the Crystal Structure of YSr2AlCu2O7.
PB94-212073 *04,499* Not available NTIS

PB94-212081
Equation of State Formulation of the Thermodynamic Properties of R134a (1,1,1,2-Tetrafluoroethane).
PB94-212081 *03,256* Not available NTIS

PB94-212099
Prediction of Viscosity of Refrigerants and Refrigerant Mixtures.
PB94-212099 *03,257* Not available NTIS

PB94-212107
Prediction of the Thermal Conductivity of Refrigerants and Refrigerant Mixtures.
PB94-212107 *03,258* Not available NTIS

PB94-212115
Kinetics of the Reaction of CCl3-Br-2 and the Thermochemistry of CCl3 Radical and Cation.
PB94-212115 *00,824* Not available NTIS

PB94-212123
Resonance Enhanced Multiphoton Ionization Detection of GeF and GeCl Radicals.
PB94-212123 *00,825* Not available NTIS

PB94-212131
Experimental and Abinitio Studies of Electronic Structures of the CCl3 Radical and Cation.
PB94-212131 *00,826* Not available NTIS

PB94-212149
Photoelectron Spectroscopic Study of the Valence and Core-Level Electronic Structure of BaTiO3.
PB94-212149 *04,500* Not available NTIS

PB94-212156
Surface Core-Level Shifts of Barium Observed in Photoemission of Vacuum-Fractured BaTiO3 (100).
PB94-212156 *04,501* Not available NTIS

PB94-212164
Kinetics of the Self-Reaction of Hydroxymethylperoxyl Radicals.
PB94-212164 *00,827* Not available NTIS

PB94-212172
Temperature Dependence of the Rate Constants for Reactions of the Sulfate Radical, SO4-, with Anions.
PB94-212172 *00,828* Not available NTIS

PB94-212180
Electron Transfer Reaction Rates and Equilibria of the Carbonate and Sulfate Radical Anions.
PB94-212180 *00,829* Not available NTIS

PB94-212198
Reaction of NO with Superoxide.
PB94-212198 *00,830* Not available NTIS

PB94-212206
Temperature Dependence of the Rate Constants for Reactions of the Carbonate Radical with Organic and Inorganic Reductants.
PB94-212206 *00,831* Not available NTIS

PB94-212214
Opacity Project and the Practical Utilization of Atomic Data.
PB94-212214 *00,059* Not available NTIS

PB94-212222
Micromechanics of Fracture in Rubber-Toughened Epoxies.
PB94-212222 *03,011* Not available NTIS

PB94-212230
Flux Expulsion at Intermediate Fields in Type-II Superconductors.
PB94-212230 *04,502* Not available NTIS

PB94-212248
K alpha Transitions in Few-Electron Ions and in Atoms.
PB94-212248 *03,849* Not available NTIS

PB94-212255
Role of the Office of Radiation Measurement in Quality Assurance.
PB94-212255 *00,689* Not available NTIS

PB94-212263
Offset Susceptibility of Superconductors.
PB94-212263 *04,503* Not available NTIS

PB94-212271
Quantum Projection Noise: Population Fluctuations in Two-Level Systems.
PB94-212271 *03,850* Not available NTIS

PB94-212289
Determination of Boron and Lithium in Diverse Biological Matrices Using Neutron Activation - Mass Spectrometry (NA-MS).
PB94-212289 *00,554* Not available NTIS

PB94-212297
Formalism and Parameters for Quantitative Surface Analysis by Auger Electron Spectroscopy and X-Ray Photoelectron Spectroscopy.
PB94-212297 *00,832* Not available NTIS

PB94-212305
Glass Transition of Organic Liquids Confined to Small Pores.
PB94-212305 *00,833* Not available NTIS

PB94-212313
Melting Behavior of Organic Materials Confined in Porous Solids.
PB94-212313 *00,834* Not available NTIS

PB94-212321
Anomalous Freezing and Melting of Solvent Crystals in Swollen Gels of Natural Rubber.
PB94-212321 *01,223* Not available NTIS

PB94-212339
Polymer Liquid Crystalline Materials.
PB94-212339 *01,224* Not available NTIS

PB94-212347
Guidelines for Reporting Results of Computational Experiments. Report of the Ad hoc Committee.
PB94-212347 *03,427* Not available NTIS

PB94-212354
Mechanism of Mild to Severe Wear Transition in Alpha-Alumina.
PB94-212354 *03,233* Not available NTIS

PB94-212362
Tribology Education: Present Status and Future Challenges.
PB94-212362 *02,965* Not available NTIS

PB94-212370
Intercomparison of the Effective Areas of a Pneumatic Piston Gauge Determined by Different Techniques.
PB94-212370 *02,640* Not available NTIS

PB94-212388
Investigation of S2F10 Production and Mitigation in Compressed SF6-Insulated Power Systems.
PB94-212388 *02,467* Not available NTIS

PB94-212396
Beneficial Effects of Nitrogen Atomization on an Austenitic Stainless Steel.
PB94-212396 *03,209* Not available NTIS

PB94-212404
Rate of Heat Release of Wood Products.
PB94-212404 *03,403* Not available NTIS

PB94-212412
Local Partial Densities of States in Ni and Co Silicides Studied by Soft X-Ray Emission Spectroscopy.
PB94-212412 *04,504* Not available NTIS

PB94-212420
Global Thermodynamic Behavior of Fluid Mixtures in the Critical Region.
PB94-212420 *04,199* Not available NTIS

PB94-212438
Effect of Cross-Links on the Miscibility of a Deuterated Polybutadiene and Protonated Polybutadiene Blend.
PB94-212438 *01,225* Not available NTIS

PB94-212446
Inversion of the Phase Diagram from UCST to LCST in Deuterated Polybutadiene and Protonated Polybutadiene Blends.
PB94-212446 *01,226* Not available NTIS

PB94-212453
Status of Electrocomposites.
PB94-212453 *03,143* Not available NTIS

PB94-212461
Aid for Smaller Businesses.
PB94-212461 *00,492* Not available NTIS

PB94-212479
Topological Influences on Polymer Adsorption and Desorption Dynamics.
PB94-212479 *01,227* Not available NTIS

PB94-212487
Multiphoton Ionization of SiH3 and SiD3 Radicals. 2. Three Photon Resonance-Enhanced Spectra Observed between 460 and 610 nm.
PB94-212487 *00,835* Not available NTIS

PB94-212495
New Electronic States of NH and ND Observed from 258 to 288 nm by Resonance Enhanced Multiphoton Ionization Spectroscopy.
PB94-212495 *00,836* Not available NTIS

PB94-212503
Multiphoton Ionization of SiH3 and SiD3 Radicals: Electronic Spectra, Vibrational Analyses of the Ground and Rydberg States, and Ionization Potential.
PB94-212503 *00,837* Not available NTIS

PB94-212511
NIST-NRL Free-Electron Laser Facility.
PB94-212511 *04,237* Not available NTIS

PB94-212529
Hybrid Undulator for the NIST-NRL Free-Electron Laser.
PB94-212529 *04,238* Not available NTIS

PB94-212537
Ultrasonic Spectroscopy of Metallic Spheres Using Electromagnetic-Acoustic Transduction.
PB94-212537 *04,185* Not available NTIS

PB94-212545
Beam Analysis Round Robin.
PB94-212545 *04,239* Not available NTIS

PB94-212552
Laser-Beam Analysis Pinpoints Critical Parameters.
PB94-212552 *04,240* Not available NTIS

PB94-212560
Theory of Atomic Collisions at Ultracold Temperatures.
PB94-212560 *03,851* Not available NTIS

PB94-212578
Efficient Experiment to Study Superconducting Ceramics.
PB94-212578 *04,505* Not available NTIS

PB94-212586
Development in the Theory and Analysis of Eddy Current Sensing of Velocity in Liquid Metals.
PB94-212586 *03,335* Not available NTIS

PB94-212594
Optically Sensed EM-Field Probes for Pulsed Fields.
PB94-212594 *02,130* Not available NTIS

PB94-212602
Modification of Deoxyribose-Phosphate Residues by Extracts of Ataxia Telangiectasia Cells.
PB94-212602 *03,458* Not available NTIS

PB94-212610
Effects of Molecular Weight and Thermal Stability on Polymer Gasification.
PB94-212610 *01,228* Not available NTIS

PB94-212628
Nickel(II)-Mediated Oxidative DNA Base Damage in Renal and Hepatic Chromatin of Pregnant Rats and Their Fetuses. Possible Relevance to Carcinogenesis.
PB94-212628 *03,646* Not available NTIS

PB94-212636
Thermodynamic Calculation of the Ternary Ti-Al-Nb System.
PB94-212636 *03,336* Not available NTIS

PB94-212644
Thermodynamic Assessment and Calculation of the Ti-Al System.
PB94-212644 *03,337* Not available NTIS

PB94-212651
Chaos in a Computer-Animated Pendulum.
PB94-212651 *03,852* Not available NTIS

PB94-212669
Proposed High-Accuracy Superconducting Power Meter for Millimeter Waves.
PB94-212669 *02,034* Not available NTIS

PB94-212677
Effect of Thermal Noise on Shapiro Steps in High-Tc Josephson Weak Links.
PB94-212677 *04,506* Not available NTIS

PB94-212685
Self-Heating in the Coulomb-Blockade Electrometer.
PB94-212685 *04,507* Not available NTIS

PB94-212693
Application of Boundary Element Methods to a Transient Axis-Symmetric Heat Conduction Problem.
PB94-212693 *01,375* Not available NTIS

PB94-212701
Causes of the Apparent Heat Transfer Degradation for Refrigerant Mixtures.
PB94-212701 *03,259* Not available NTIS

PB94-212719
Attempts at Extending the Unified Theory to Include Many-Body Effects.
PB94-212719 *04,408* Not available NTIS

PB94-212727
Autoionizing Resonances in Electric Fields.
PB94-212727 *03,853* Not available NTIS

PB94-212735
Using Emulator/Testers for Commissioning EMCS Software, Operator Training, Algorithm Development, and Tuning Local Control Loops.
PB94-212735 *00,245* Not available NTIS

PB94-212743
Compositional Homogeneity in Processing Precursor Powders to the Ba2YCu3O7-x High Tc Superconductor.
PB94-212743 *04,508* Not available NTIS

PB94-212750
Imaging of Fine Porosity in a Colloidal Silica: Potassium Silicate Gel by Defocus Contrast Microscopy.
PB94-212750 *03,039* Not available NTIS

PB94-212768
Correlations of Modulation Noise with Magnetic Microstructure and Intergranular Interactions for CoCrTa and CoNi Thin Film Media.
PB94-212768 *04,509* Not available NTIS

PB94-212776
Multicarrier Characterization Method for Extracting Mobilities and Carrier Densities of Semiconductors from Variable Magnetic Field Measurements.
PB94-212776 *02,317* Not available NTIS

PB94-212784
Relativistic and Quantum Electrodynamic Effects in Highly-Charged Ions.
PB94-212784 *03,854* Not available NTIS

PB94-212792
Product Kinetic Energies, Correlations, and Scattering Anisotropy in the Bimolecular Reactor O((1)D)+H2O yields 2OH.
PB94-212792 *00,838* Not available NTIS

PB94-212800
Apparent Molar Heat Capacities and Apparent Molar Volumes of Aqueous Glucose at Temperatures from 298.15 K to 327.01 K.
PB94-212800 *03,459* Not available NTIS

PB94-212818
Evolution of a Turbulent Boundary Layer Induced by a Three-Dimensional Roughness Element.
PB94-212818 *04,200* Not available NTIS

PB94-212826
Molecular-Beam Optothermal Spectrum of the OH Stretching Band of Methanol.
PB94-212826 *00,839* Not available NTIS

PB94-212834
Fundamental Torsion Band in Acetaldehyde.
PB94-212834 *00,840* Not available NTIS

PB94-212842
Atomic Branching Ratio Data for Carbon-Like Ions.
PB94-212842 *03,855* Not available NTIS

PB94-212859
Full Scale Smoke Control Tests at the Plaza Hotel Building.
PB94-212859 *00,347* Not available NTIS

PB94-212867
Overview of Smoke Control Technology.
PB94-212867 *00,348* Not available NTIS

PB94-212875
Preview of ASHRAE's Revised Smoke Control Manual.
PB94-212875 *00,349* Not available NTIS

PB94-212883
Smoke Control Systems for Elevator Fire Evacuation.
PB94-212883 *00,291* Not available NTIS

PB94-212891
Determination of Osmotic Pressure and Fouling Resistances and Their Effects on Performance of Ultrafiltration Membranes.
PB94-212891 *00,841* Not available NTIS

PB94-212909
Characterization of the Adsorption-Fouling Layer Using Globular Proteins on Ultrafiltration Membranes.
PB94-212909 *00,842* Not available NTIS

PB94-212917
High-Spatial-Resolution Resistivity Mapping Applied to Mercury Cadmium Telluride.
PB94-212917 *02,131* Not available NTIS

PB94-212925
Review of Semiconductor Microelectronic Test Structures with Applications to Infrared Detector Materials and Processes.
PB94-212925 *02,132* Not available NTIS

PB94-212933
Summary of the Proceedings of the Workshop on Standard Phantoms for In-vivo Radioactivity Measurement.
PB94-212933 *03,622* Not available NTIS

PB94-212941
Effects of Variable Excluded Volume on the Dimensions of Off-Lattice Polymer Chains.
PB94-212941 *01.229* Not available NTIS

PB94-212958
Observed and Theoretical Creep Rates for an Alumina Ceramic and a Silicon Nitride Ceramic in Flexure.
PB94-212958 *03,040* Not available NTIS

PB94-212966
Defect of Thermal Ramping and Annealing Conditions on Defect Formation in Oxygen Implanted Silicon-On-Insulator Material.
PB94-212966 *02,318* Not available NTIS

PB94-212974
Active Site Ionicity and the Mechanism of Carbonic Anhydrase.
PB94-212974 *00,843* Not available NTIS

PB94-212982
Dipole Moments in Rare Gas Interactions.
PB94-212982 *00,844* Not available NTIS

PB94-212990
Analysis of Protein Metal Binding Selectivity in a Cluster Model.
PB94-212990 *00,845* Not available NTIS

PB94-213006
Cs Cluster Binding to a GaAs Surface.
PB94-213006 *00,846* Not available NTIS

PB94-213014
Iridium Oxide Thin-Film Stability in High-Temperature Corrosive Solutions.
PB94-213014 *03,234* Not available NTIS

PB94-213022
Radiation-Driven Winds of Hot Luminous Stars X. The Determination of Stellar Masses Radii and Distances from Terminal Velocities and Mass-Loss Rates.
PB94-213022 *00,060* Not available NTIS

PB94-213030
Formal Specification and Verification of Control Software for Cryptographic Equipment.
PB94-213030 *01,585* Not available NTIS

PB94-213048
Materials Science with SR Using X-Ray Imaging: Spatial-Resolution/Source Size.
PB94-213048 *04,510* Not available NTIS

PB94-213055
High Resolution Hard X-Ray Microscope.
PB94-213055 *03,856* Not available NTIS

PB94-213063
Thermal Conductivity of R134a.
PB94-213063 *03,857* Not available NTIS

PB94-213071
Spectroscopic Constants for the 2.5 and 3.0 micrometer Bands of Acetylene.
PB94-213071 *00,847* Not available NTIS

PB94-213089
Analysis of Boron in CVD Diamond Surfaces Using Neutron Depth Profiling.
PB94-213089 *04,511* Not available NTIS

PB94-213097
Normal-Incidence Complex-Index Refractometry.
PB94-213097 *04,241* Not available NTIS

PB94-213105
Precision, Accuracy, Uncertainty and Traceability and Their Application to Submicrometer Dimensional Metrology.
PB94-213105 *02,319* Not available NTIS

PB94-213113
Thermochemistry of the Reactions between Adenosine, Adenosine 5'-monophosphate, Inosine, and Inosine 5'-monophosphate; the Conversion of L-histidine to (Urocanic Acid+Ammonia).
PB94-213113 *03,460* Not available NTIS

PB94-213121
Magnetic and Structural Properties of Electrodeposited Copper-Nickel Microlayered Alloys.
PB94-213121 *04,512* Not available NTIS

PB94-213139
Laser-Induced Fluorescence Measurements of Rotationally Resolved Velocity Distributions for CO(+) Drifted in He.
PB94-213139 *00,848* Not available NTIS

PB94-213147
Custom Integrated Circuit Comparator for High-Performance Sampling Applications.
PB94-213147 *02,320* Not available NTIS

PB94-213154
Elastic Deformation of a Monolithic Perfect Crystal Interferometer: Implications for Gravitational Phase Shift Experiments.
PB94-213154 *03,858* Not available NTIS

PB94-213162
Hierarchical Ada Robot Programming System (HARPS): A Complete and Working Telerobot Control System Based on the NASREM Model.
PB94-213162 *02,934* Not available NTIS

PB94-213170
Recent Approaches to Extreme Value Estimation with Application to Wind Speeds. Part 1. The Pickands Method.
PB94-213170 *00,019* Not available NTIS

PB94-213188
Dynamics vs. Static Young's Moduli: A Case Study.
PB94-213188 *03,210* Not available NTIS

PB94-213196
Elastic Constants of Polycrystalline Y1Ba2Cu3Ox.
PB94-213196 *04,513* Not available NTIS

PB94-213204
Thermal Expansion of an SiC Particle-Reinforced Aluminum Composite.
PB94-213204 *03,144* Not available NTIS

PB94-213212
Cast-Iron Elastic Constants: Effect of Graphite Aspect Ratio.
PB94-213212 *03,211* Not available NTIS

PB94-213220
Correlation between Tc and Elastic Constants of (La-M)2CuO4.
PB94-213220 *04,514* Not available NTIS

PB94-213238
Ultracold Collisions: Associative Ionization in a Laser Trap.
PB94-213238 *03,859* Not available NTIS

PB94-213246
Light Scattering from Glossy Coatings on Paper.
PB94-213246 *04,242* Not available NTIS

PB94-213253
Development of a New Small-Scale Smoke Toxicity Test Method and Its Comparison with Real-Scale Fire Tests.
PB94-213253 *00,350* Not available NTIS

PB94-213261
EXITT: A Simulation Model of Occupant Decisions and Actions in Residential Fires.
PB94-213261 *00,351* Not available NTIS

PB94-213279
High-Energy Behavior of the Double Photoionization of Helium from 2 to 12 keV.
PB94-213279 *03,860* Not available NTIS

PB94-213287
Astrophysical Aspects of Neutral Atom Line Broadening.
PB94-213287 *00,061* Not available NTIS

PB94-213295
RIS Studies of Autoionization in Calcium.
PB94-213295 *00,849* Not available NTIS

PB94-213303
Debugger for Tcl Applications.
PB94-213303 *01,695* Not available NTIS

PB94-213311
Kibitz-Connecting Multiple Interactive Programs Together.
PB94-213311 *01,696* Not available NTIS

PB94-213329
Using Expect to Automate System Administration Tasks.
PB94-213329 *01,697* Not available NTIS

PB94-213337
Molecular Spectroscopy.
PB94-213337 *03,861* Not available NTIS

PB94-213345
Relation between AC Impedance Data and Degradation of Coated Steel. 1. Effects of Surface Roughness and Contamination on the Corrosion Behavior of Epoxy Coated Steel.
PB94-213345 *03,189* Not available NTIS

PB94-213352
Elastic Constants and Debye Temperature of Y1Ba2Cu3Ox: Effect of Oxygen Content.
PB94-213352 *04,515* Not available NTIS

PB94-213360
Polarized X-Ray Emission Spectroscopy.
PB94-213360 *03,862* Not available NTIS

PB94-213378
Atomic, Molecular, and Optical Physics with X-rays.
PB94-213378 *03,863* Not available NTIS

PB94-213386
High-Sensitivity Determination of Iodine Isotopic Ratios by Thermal and Fast Neutron Activation.
PB94-213386 *00,555* Not available NTIS

PB94-213394
Neutron Capture Prompt Gamma-Ray Activation Analysis at the NIST Cold Neutron Research Facility.
PB94-213394 *00,556* Not available NTIS

PB94-213402
Atomic Data Needed for Far Ultraviolet Astronomy with HUT and FUSE.
PB94-213402 *00,062* Not available NTIS

PB94-213410
FUSE: The Far Ultraviolet Spectrograph Explorer.
PB94-213410 *00,063* Not available NTIS

PB94-213428
Ultraviolet Observations of Stellar Coronae: Early Results from HST.
PB94-213428 *00,064* Not available NTIS

PB94-213436
X-rays from Stellar Flares.
PB94-213436 *00,065* Not available NTIS

PB94-213444
Goddard High-Resolution Spectrograph Observations of the Local Interstellar Medium and the Deuterium/Hydrogen Ratio along the Line of Sight Toward Capella.
PB94-213444 *00,066* Not available NTIS

PB94-213451
Class of Radio-Emitting Magnetic B Stars and a Wind-Fed Magnetosphere Model.
PB94-213451 *00,067* Not available NTIS

PB94-213469
Radio Emission from Chemically Peculiar Stars.
PB94-213469 *00,068* Not available NTIS

PB94-213477
First Results from a Coordinated ROSAT, IUE, and VLA Study of RS CVn Systems.
PB94-213477 *00,069* Not available NTIS

PB94-213485
Investigation of Mercury Interstitials in Hg(1-x)CdxTe Alloys Using Resonant Impact-Ionization Spectroscopy.
PB94-213485 *02,133* Not available NTIS

PB94-213493
Liposome-Based Flow-Injection Immunoassay for Determining Theophylline in Serum.
PB94-213493 *03,494* Not available NTIS

PB94-213501
Investigation of the Thermal Stability and Char-Forming Tendency of Cross-linked Poly(methyl methacrylate).
PB94-213501 *03,380* Not available NTIS

PB94-213717
Measurement of Room Conditions and Response of Sprinklers and Smoke Detectors during a Simulated Two-Bed Hospital Patient Room Fire.
PB94-213717 *00,292* PC A07/MF A02

PB94-213758
Technical Program Description Systems Integration for Manufacturing (SIMA).
PB94-213758 *02,819* PC A05/MF A01

PB94-213774
Electronics and Electrical Engineering Laboratory Technical Publication Announcements Covering Laboratory Programs,

January to March 1994 with 1994/1995 EEEL Events Calendar.
PB94-213774 *01,883* PC A03/MF A01

PB94-213857
Feasibility of Fire Evacuation by Elevators at FAA Control Towers.
PB94-213857 *04,844* PC A06/MF A02

PB94-214756
Information Infrastructure: Reaching Society's Goals. Report of the Information Infrastructure Task Force Committee on Applications and Technology.
PB94-214756 *01,469* PC A08/MF A02

PB94-215670
Highway Concrete (HWYCON) Expert System User Reference and Enhancement Guide.
PB94-215670 *01,316* PC A08/MF A02

PB94-215688
Time Dependent Vector Dynamic Programming Algorithm for the Path Planning Problem.
PB94-215688 *03,428* PC A04/MF A01

PB94-215704
Diffusion of Cations Beneath Organic Coatings on Steel Substrate.
PB94-215704 *03,119* PC A03/MF A01

PB94-215712
Analytical Estimation of Carrier Multipath Bias on GPS Position Measurements.
PB94-215712 *04,845* PC A04/MF A01

PB94-215746
Head Start on Assurance: Proceedings of an Invitational Workshop on Information Technology (IT) Assurance and Trustworthiness. Held in Williamsburg, Virginia on March 21-23, 1994.
PB94-215746 *01,586* PC A05/MF A01

PB94-216017
Using LORAN-C Broadcasts for Automated Frequency Calibrations.
PB94-216017 *01,526* Not available NTIS

PB94-216025
Structures of Vapor-Deposited Yttria and Zirconia Thin Films.
PB94-216025 *03,041* Not available NTIS

PB94-216033
Rapid Decline in the Optical Emission from SN 1957D in M83.
PB94-216033 *00,070* Not available NTIS

PB94-216041
Measurement of CO Pressures in the Ultrahigh Vacuum Regime Using Resonance-Enhanced Multiphoton-Ionization Time-of-Flight Mass Spectroscopy.
PB94-216041 *03,864* Not available NTIS

PB94-216058
Spectroscopic Puzzle in ArHF Solved: The Test of a New Potential.
PB94-216058 *00,850* Not available NTIS

PB94-216066
Ultra-High Stability Synthesizer for Diode Laser Pumped Rubidium.
PB94-216066 *01,527* Not available NTIS

PB94-216074
Heavily Accumulated Surfaces of Mercury Cadmium Telluride Detectors: Theory and Experiment.
PB94-216074 *02,134* Not available NTIS

PB94-216082
Evolution of the Flight Telerobotic Servicer.
PB94-216082 *04,832* Not available NTIS

PB94-216090
Effect of Three Sterilization Techniques on Finger Pluggers.
PB94-216090 *00,150* Not available NTIS

PB94-216108
Modified Leung-Griffiths Model of Vapor-Liquid Equilibrium: Extended Scaling and Binary Mixtures of Dissimilar Fluids.
PB94-216108 *00,851* Not available NTIS

PB94-216116
Polarization Analysis of the Magnetic Excitations in Invar and Non-Invar Amorphous Alloys.
PB94-216116 *04,516* Not available NTIS

PB94-216124
Analytical Method of Determining the Heat Capacity at High Temperatures from the Surface Temperature of a Cooling Sphere.
PB94-216124 *03,865* Not available NTIS

PB94-216132
Performance Standards: The Pro's and Con's.
PB94-216132 *02,896* Not available NTIS

PB94-216140
Scattering and Absorption Effects in Neutron Beam Activation Analysis Experiments.
PB94-216140 *00,557* Not available NTIS

PB94-216157
Effects of Target Shape and Neutron Scattering on Element Sensitivities for Neutron-Capture Prompt Gamma-ray Activation Analysis.
PB94-216157 *00,558* Not available NTIS

PB94-216165
Structure of Molecules on Surfaces as Determined Using Electron-Stimulated Desorption.
PB94-216165 *00,852* Not available NTIS

PB94-216173
Desorption Induced by Electronic Transitions.
PB94-216173 *00,853* Not available NTIS

PB94-216181
Sprinkler Fire Suppression Algorithm.
PB94-216181 *00,293* Not available NTIS

PB94-216199
Thermophysical Properties of CO2 and CO2-Rich Mixtures.
PB94-216199 *00,854* Not available NTIS

PB94-216207
Neutron Scattering Studies of Surfaces and Interfaces.
PB94-216207 *04,517* Not available NTIS

PB94-216215
Supermirror Transmission Polarizers for Neutrons.
PB94-216215 *03,866* Not available NTIS

PB94-216223
High-Resolution Measurements of the nu2 and 2nu2-nu2 Bands of (34)S(16)O2.
PB94-216223 *00,855* Not available NTIS

PB94-216231
FTS Infrared Measurements of the Rotational and Vibrational Spectrum of LiH and LiD.
PB94-216231 *00,856* Not available NTIS

PB94-216249
Statistical Analysis of Parameters Affecting the Measurement of Particle-Size Distribution of Silicon Nitride Powders by Sedigraph (Trade Name).
PB94-216249 *03,042* Not available NTIS

PB94-216256
Coating of Fibers by Colloidal Techniques in Ceramic Composites.
PB94-216256 *03,196* Not available NTIS

PB94-216264
Characterization of Phase and Surface Composition of Silicon Carbide Platelets.
PB94-216264 *03,043* Not available NTIS

PB94-216272
Deposition of Colloidal Sintering-Aid Particles on Silicon Nitride.
PB94-216272 *03,044* Not available NTIS

PB94-216280
Integrated Optic Laser Emitting at 906, 1057, and 1358 nm.
PB94-216280 *02,135* Not available NTIS

PB94-216298
Integrated Optic Laser Emitting at 905, 1057, 1356 nm.
PB94-216298 *02,136* Not available NTIS

PB94-216306
Models and Interactions.
PB94-216306 *02,641* Not available NTIS

PB94-216314
Crystal Structure of Pb2Sr2YCu3O8+delta with delta=1.32, 1.46, 1.61, 1.71, by Powder Neutron Diffraction.
PB94-216314 *04,518* Not available NTIS

PB94-216322
Hydrolysis of Proteins by Microwave Energy.
PB94-216322 *03,528* Not available NTIS

PB94-216330
Ascorbic and Dehydroascorbic Acids Measured in Plasma Preserved with Dithiothreitol or Metaphorphoric Acid.
PB94-216330 *03,495* Not available NTIS

PB94-216348
Study of Diffusion Zones with Electron Microprobe Compositional Mapping.
PB94-216348 *00,559* Not available NTIS

PB94-216355
Paffenbarger Research Center: The Cutting Edge of Dental Science.
PB94-216355 *00,151* Not available NTIS

PB94-216363
Energy Transduction between a Concentration Gradient and an Alternating Electric Field.
PB94-216363 *03,461* Not available NTIS

PB94-216371
Self Broadening in the nu1 Band of NH3.
PB94-216371 *00,857* Not available NTIS

PB94-216389
Accurate Experimental Characterization of Interconnects: A Discussion of 'Experimental Electrical Characterization of Interconnects and Discontinuities in High-Speed Digital Systems'.
PB94-216389 *02,217* Not available NTIS

PB94-216397
Interconnection Transmission Line Parameter Characterization.
PB94-216397 *02,218* Not available NTIS

PB94-216405
Standards in Building Economics: Why We Need Them and How to Write Them.
PB94-216405 *00,320* Not available NTIS

PB94-216413
High-Level CAD Melds Micromachined Devices with Foundries.
PB94-216413 *02,321* Not available NTIS

PB94-216421
Lessons Learned by a Wing Engineer.
PB94-216421 *00,429* Not available NTIS

PB94-216439
Atomic Beam Splitters and Mirrors by Adiabatic Passage in Multilevel Systems.
PB94-216439 *03,867* Not available NTIS

PB94-216447
Non-Osmotic, Defect-Controlled Cathodic Disbondment of a Coating from a Steel Substrate.
PB94-216447 *03,120* Not available NTIS

PB94-216454
Precision and Accuracy in Tandem Mass Spectrometry Measurements: A Kinetics-Based Protocol for Instrument-Independent Measurements of Collision-Activated Dissociation in RF-Only Quadrupoles.
PB94-216454 *00,858* Not available NTIS

PB94-216462
Kinetics and Mechanism of the Collision-Activated Dissociation of the Acetone Cation.
PB94-216462 *00,859* Not available NTIS

PB94-216470
Guarding Against Transients.
PB94-216470 *01,623* Not available NTIS

PB94-216488
Cascading Surge-Protective Devices: Options for Effective Implementation.
PB94-216488 *02,464* Not available NTIS

PB94-216496
Coordinating Cascaded Surge-Protective Devices: An Elusive Goal.
PB94-216496 *02,465* Not available NTIS

PB94-216504
Important Link in Entire-House Protection: Surge Reference Equalizers.
PB94-216504 *02,219* Not available NTIS

PB94-216512
Alternative Single Integral Equation for Scattering by a Dielectric.
PB94-216512 *04,422* Not available NTIS

PB94-216520
Determination of Surface Roughness from Scattered Light.
PB94-216520 *04,243* Not available NTIS

PB94-216538
Autocorrelation Functions from Optical Scattering for One-Dimensionally Rough Surfaces.
PB94-216538 *04,244* Not available NTIS

PB94-216546
Light Scattered by Coated Paper.
PB94-216546 *04,245* Not available NTIS

PB94-216553
Atomic Theory of Fracture of Brittle Materials: Application to Covalent Semiconductors.
PB94-216553 *04,519* Not available NTIS

PB94-216561
Crystal Structure of Dicalcium Potassium Trihydrogen Bis(pyrophosphate) Trihydrate.
PB94-216561 *00,152* Not available NTIS

PB94-216579
Crystal Structure of Calcium Adipate Monohydrate.
PB94-216579 *00,153* Not available NTIS

PB94-216587
Rapid Hot Pressing of Ultra-Fine PSZ Powders.
PB94-216587 *03,045* Not available NTIS

PB94-216595
Carbon Acidities of Aromatic Compounds. 1. Effects of In-Ring Aza and External Electron-Withdrawing Groups.
PB94-216595 *00,860* Not available NTIS

PB94-216603
Proton Affinity Ladders from Variable-Temperature Equilibrium Measurements. 1. A Re-Evaluation of the Upper Proton Affinity Range.
PB94-216603 *00,861* Not available NTIS

PB94-216611
Theoretical Aspects of Tagged Photon Facilities.
PB94-216611 *03,868* Not available NTIS

PB94-216629
Characterization of Interface Defects in Oxygen-Implanted Silicon Films.
PB94-216629 *02,322* Not available NTIS

PB94-216637
Charge Trapping and Breakdown Mechanism in SIMOX.
PB94-216637 *02,323* Not available NTIS

PB94-216645
NIST-Coordinated Standard for Fingerprint Data Interchange.
PB94-216645 *01,808* Not available NTIS

PB94-216652
Determination of Complex Scattering Amplitudes in Low-Energy Elastic Electron-Sodium Scattering.
PB94-216652 *03,869* Not available NTIS

PB94-216660
Laser Focusing of Atoms: A Particle Optics Approach.
PB94-216660 *03,870* Not available NTIS

PB94-216678
Simple, Compact, High-Purity Cr Evaporator for Ultrahigh Vacuum.
PB94-216678 *04,520* Not available NTIS

PB94-216686
Measurement of the Heat of Fusion of Tungsten by a Microsecond-Resolution Transient Technique.
PB94-216686 *03,400* Not available NTIS

PB94-216694
Recommended Changes in ASTM Test Methods D2512-82 and G86-84 for Oxygen-Compatibility Mechanical Impact Tests on Metals.
PB94-216694 *03,338* Not available NTIS

PB94-216702
Digital Techniques in HV Tests - Summary of 1989 Panel Session.
PB94-216702 *02,035* Not available NTIS

PB94-216710
Bibliography of Computer Security Glossaries.
PB94-216710 *01,587* Not available NTIS

PB94-216728
Review of Cure Monitoring Techniques for On-Line Process Control.
PB94-216728 *03,145* Not available NTIS

PB94-216736
Effect of Modulated Taylor-Couette Flows on Crystal-Melt Interfaces: Theory and Initial Experiments.
PB94-216736 *04,521* Not available NTIS

PB94-216744
Boundary Integral Method for the Simulation of Two-Dimensional Particle Coarsening.
PB94-216744 *03;411* Not available NTIS

PB94-216751
High-Resolution IR Laser-Driven Vibrational Dynamics in Supersonic Jets: Weakly Bound Complexes and Intramolecular Energy Flow.
PB94-216751 *00,862* Not available NTIS

PB94-217023
Videoconferencing Procurement and Usage Guide.
PB94-217023 *01,470* PC A04/MF A01

PB94-217031
Determination of the Weight Average Molecular Weight of Two Poly(Ethylene Oxides), SRM 1923 and SRM 1924.
PB94-217031 *01,230* PC A03/MF A01

PB94-217098
Publications of the Intelligent Systems Division (Previously Robot Systems Division) Covering the Period January 1971-April 1994.
PB94-217098 *02,935* PC A05/MF A01

PB94-217106
NIST Form-Based Handprint Recognition System.
PB94-217106 *01,838* PC A04/MF A01

PB94-217163
Human Factors Considerations for the Potential Use of Elevators for Fire Evacuation of FAA Air Traffic Control Towers.
PB94-217163 *01,300* PC A03/MF A01

PB94-217486
Hollow Clay Tile Prism Tests for Martin Marietta Energy Systems: Task 2 Testing.
PB94-217486 *00,352* PC A14/MF A03

PB94-218559
Study of Heat Pump Performance Using Mixtures of R32/R134a and R32/R125/R134a as 'Drop-In' Working Fluids for R22 with and Without a Liquid-Suction Heat Exchanger.
PB94-218559 *02,503* PC A04/MF A01

PB94-218567
NIST Workshop on Nanostructured Material (1st): Report of an Industrial Workshop Conducted by the National Institute of Standards and Technology. Held in Gaithersburg, Maryland on May 14-15, 1992.
PB94-218567 *02,973* PC A04/MF A01

PB94-218575
Adaptive, Predictive 2-D Feature Tracking Algorithm for Finding the Focus of Expansion.
PB94-218575 *01,588* PC A03/MF A01

PB94-218583
Survey of Recent Cementitious Materials Research in Western Europe.
PB94-218583 *00,353* PC A03/MF A01

PB94-218591
RangeCAD and the NIST RCS Uncertainty Analysis.
PB94-218591 *01,870* PC A03/MF A01

PB94-219052
NIST Research Program on the Seismic Resistance of Partially-Grouted Masonry Shear Walls.
PB94-219052 *00,354* PC A06/MF A02

PB94-219060
National Voluntary Laboratory Accreditation Program: Energy Efficient Lighting Products.
PB94-219060 *02,642* PC A04/MF A01

PB94-219086
Framework for Information Technology Integration in Process Plant and Related Industries.
PB94-219086 *02,772* PC A04/MF A01

PB94-219094
ISDN Conformance Testing Guidelines: Guidelines for Implementors of ISDN Customer Premises Equipment to Conform to Both National ISDN-1 and North American ISDN Users' Forum Layer 3 Basic Rate Interface Basic Call Control Abstract Test Suites.
PB94-219094 *01,471* PC A03/MF A01

PB94-219102
Analyzing Electronic Commerce.
PB94-219102 *00,480* PC A03/MF A01

PB94-219110
Industry/Government Open Systems Specification Testing Framework. Version 1.0.
PB94-219110 *01,809* PC A06/MF A02

PB94-219219
Journal of Research of the National Institute of Standards and Technology. March/April 1994. Volume 99, Number 2.
PB94-219219 *02,000* PC A06/MF A02

PB94-219227
Sealed Water Calorimeter for Measuring Absorbed Dose.
PB94-219227 *03,517*
(Order as PB94-219219, PC A06/MF A02)

PB94-219235
Planar Near-Field Measurements of Low-Sidelobe Antennas.
PB94-219235 *02,001*
(Order as PB94-219219, PC A06/MF A02)

PB94-219243
Physics Required for Prediction of Long Term Performance of Polymers and Their Composites.
PB94-219243 *03,146*
(Order as PB94-219219, PC A06/MF A02)

PB94-219250
Measurement and Uncertainty of a Calibration Standard for the Scanning Electron Microscope.
PB94-219250 *00,560*
(Order as PB94-219219, PC A06/MF A02)

PB94-219268
New Values for Silicon Reference Materials, Certified for Isotope Abundance Ratios. Letter to the Editor.
PB94-219268 *00,863*
(Order as PB94-219219, PC A06/MF A02)

PB94-219326
Journal of Research of the National Institute of Standards and Technology. May/June 1994. Volume 99, Number 3.
PB94-219326 *02,643* PC A05/MF A02

PB94-219334
Sources of Uncertainty in a DVM-Based Measurement System for a Quantized Hall Resistance Standard.
PB94-219334 *01,884*
(Order as PB94-219326, PC A05/MF A02)

PB94-219342
dc Method for the Absolute Determination of Conductivities of the Primary Standard KCl Solutions from 0C to 50C.
PB94-219342 *02,644*
(Order as PB94-219326, PC A05/MF A02)

PB94-219359
Three-Axis Coil Probe Dimensions and Uncertainties during Measurement of Magnetic Fields from Appliances.
PB94-219359 *01,885*
(Order as PB94-219326, PC A05/MF A02)

PB94-219367
Improved Automated Current Control for Standard Lamps.
PB94-219367 *00,246*
(Order as PB94-219326, PC A05/MF A02)

PB94-219375
Refractive Indices of Fluids Related to Alternative Refrigerants.
PB94-219375 *03,260*
(Order as PB94-219326, PC A05/MF A02)

PB94-219383
Theoretical Analysis of the Coherence-Induced Spectral Shift Experiments of Kandpal, Vaishya, and Joshi.
PB94-219383 *00,561*
(Order as PB94-219326, PC A05/MF A02)

PB94-219391
Comments on the Paper 'Wolf Shifts and Their Physical Interpretation under Laboratory Conditions'.
PB94-219391 *04,246*
(Order as PB94-219326, PC A05/MF A02)

PB94-219409
Reply to Professor Wolf's Comments on My Paper on Wolf Shifts.
PB94-219409 *04,247*
(Order as PB94-219326, PC A05/MF A02)

PB94-500691
FORTRAN Compiler Validation System, Version 2.1.
PB94-500691 *01,698* CP T99

PB94-501988
HAZARD I Fire Hazard Assessment Method (Version 1.2) (for Microcomputers).
PB94-501988 *00,196* Diskette $250.00

PB94-501996
HAZARD I Fire Hazard Assessment Method, Version 1.2 (Upgrade Package) (for Microcomputers).
PB94-501996 *00,197* CP D99

PB94-502077
M (also known as MUMPS) Validation Test Suite, Version 8.3 (for Microcomputers).
PB94-502077 *01,699* Diskette $250.00

PB94-780129
Polymer Composites Workshop. Held in Winona, Minnesota on April 29-30, 1992 (Video).
PB94-780129 *03,147* AV E99

PB94-937300
Validated Products List (Cobol, Fortran, ADA, Pascal, MUMPS, SQL).
PB94-937300 *01,700* Standing Order

PB94-962000
CALS-Automated Interchange of Technical Information.
PB94-962000 *03,657* Standing Order

PB94-962100
CALS-Digital Representation for Communication of Product Data: IGES Application Subsets.
PB94-962100 *03,658* Standing Order

PB94-962200
CALS-Markup Requirements and Generic Style Specifications for Electronic Printed Output and Exchange of Text.
PB94-962200 *03,659* Standing Order

PB94-962300
CALS-Raster Graphics Representation Binary Format Requirements.
PB94-962300 *03,660* Standing Order

PB94-962400
CALS-Digital Representation for Communication of Illustration Date: CGM Application Profile.
PB94-962400 *03,661* Standing Order

PB94-962500
CALS-Department of Defense Computer Aided Acquisition Logistic Support (CALS).
PB94-962500 *03,662* Standing Order

PB94-962600
CALS-Contractor Integrated Technical Information Service (CITIS), Functional Requirements.
PB94-962600 *03,663* Standing Order

PB95-100368
NIOSH Pocket Guide to Chemical Hazards.
PB95-100368 *03,603* PC$14.00/MF A04

PB95-103461
Questions and Answers on Quality, the ISO 9000 Standard Series, Quality System Registration, and Related Issues. More Questions and Answers on the ISO 9000 Standard Series and Related Issues.
PB95-103461 *00,495* PC A03/MF A01

PB95-103677
Report on the Workshop on Advanced Digital Video in the National Information Infrastructure. Held in Washington, D.C. on May 10-11, 1994.
PB95-103677 *01,472* PC A09/MF A03

PB95-103719
Framework for National Information Infrastructure Services.
PB95-103719 *02,723* PC A07/MF A02

PB95-103826
New Expressions of Uncertainties for Humidity Calibrations at the National Institute of Standards and Technology.
PB95-103826 *02,645* PC A02/MF A01

PB95-104907
In Situ Burning Oil Spill Workshop Proceedings. Held in Orlando, Florida on January 26-28, 1994.
PB95-104907 *02,583* PC A06/MF A02

PB95-104915
Abrasive Wear by Diesel Engine Coal-Fuel and Related Particles.
PB95-104915 *01,450* PC A04/MF A01

PB95-104956
Extreme Value Theory and Applications: Proceedings of the Conference on Extreme Value Theory and Applications, Volume 3. Held in Gaithersburg, Maryland in May 1993.
PB95-104956 *03,432* PC A11/MF A03

PB95-104964
Annual Conference on Fire Research: Book of Abstracts, October 17-20, 1994.
PB95-104964 *01,376* PC A09/MF A02

PB95-105011
Energy Price Indices and Discount Factors for Life-Cycle Cost Analysis 1995. Annual Supplement to NIST Handbook 135 and NBS Special Publication 709. (Revised).
PB95-105011 *02,509* PC A04/MF A01

PB95-105029
Present Worth Factors for Life-Cycle Cost Studies in the Department of Defense (1995).
PB95-105029 *03,664* PC A04/MF A01

PB95-105037
Making Sense of Software Engineering Environment Framework Standards.
PB95-105037 *01,701* PC A03/MF A01

PB95-105045
Software Needs in Special Functions.
PB95-105045 *01,702* PC A03/MF A01

PB95-105052
Formulation of Position on U.S. Standards Role in Enterprise Integration.
PB95-105052 *02,773* PC A03/MF A01

PB95-105136
Controlling Moisture in the Walls of Manufactured Housing.
PB95-105136 *00,355* PC A03/MF A01

PB95-105383
Security in Open Systems.
PB95-105383 *01,473* PC A13/MF A03

PB95-105524
Predicting the Energy Performance Ratings of a Family of Type I Combination Appliances.
PB95-105524 *02,504* PC A03/MF A01

PB95-105540
Flow Conditioner Tests for Three Orifice Flowmeter Sizes.
PB95-105540 *04,201* PC A05/MF A01

PB95-107017
Changes in the Redox State of Iridium Oxide Clusters and Their Relation to Catalytic Water Oxidation: Radiolytic and Electrochemical Studies.
PB95-107017 *00,864* Not available NTIS

PB95-107025
Intermolecular HF Motion in Ar(sub n)HF Micromatrices (n=1,2,3,4,): Classical and Quantum Calculations on a Pairwise Additive Potential Surface.
PB95-107025 *03,871* Not available NTIS

PB95-107033
Localization Model of Rubber Elasticity: Comparison with Torsional Data for Natural Rubber Networks in the Dry State.
PB95-107033 *03,195* Not available NTIS

PB95-107041
Aging in Glasses Subjected to Large Stresses and Deformations.
PB95-107041 *03,235* Not available NTIS

PB95-107058
One-Electron Oxidation of Nickel Porphyrins. Effect of Structure and Medium on Formation of Nickel(III) Porphyrin or Nickel(II) Porphyrin pi-Radical Cation.
PB95-107058 *00,865* Not available NTIS

PB95-107066
Site of One-Electron Reduction of Ni(II) Porphyrins. Formation of Ni(I) Porphyrin of Ni(II) Porphyrin pi-Radical Anion.
PB95-107066 *00,866* Not available NTIS

PB95-107074
Reduction of Dinitrogen to Ammonia in Aqueous Solution Mediated by Colloidal Metals.
PB95-107074 *00,867* Not available NTIS

PB95-107082
Metalloporphyrin Sensitized Photooxidation of Water to Oxygen on the Surface of Colloidal Iridium Oxides - Photochemical and Pulse Radiolytic Studies.
PB95-107082 *00,868* Not available NTIS

PB95-107090
SANS and LS Studies of Polymer Mixtures Under Shear Flow.
PB95-107090 *01,231* Not available NTIS

PB95-107108
Three Dimensional Position Determination from Motion.
PB95-107108 *01,788* Not available NTIS

PB95-107116
Determination of the Molecular Parameters of NiH in Its (2)Delta Ground State by Laser Magnetic Resonance.
PB95-107116 *00,869* Not available NTIS

PB95-107124
Crystal Structure of a New Sodium Zinc Arsenate Phase Solved by 'Simulated Annealing'.
PB95-107124 *00,870* Not available NTIS

PB95-107132
Mode Specific Vibrational Predissociation Dynamics in Fragile Molecules.
PB95-107132 *00,871* Not available NTIS

PB95-107140
Vibration, Rotation, and Parity Specific Predissociation Dynamics in Asymmetric OH Stretch Excited ArH2O: A Half Collision Study of Resonant V-V Energy Transfer in a Weakly Bound Complex.
PB95-107140 *00,872* Not available NTIS

PB95-107157
Solvent Effects in the Reactions of Peroxyl Radicals with Organic Reductants. Evidence for Proton Transfer Mediated Electron Transfer.
PB95-107157 *00,873* Not available NTIS

PB95-107165
Electron Probe X-Ray Microanalysis.
PB95-107165 *00,562* Not available NTIS

PB95-107173
Microanalysis to Nanoanalysis: Measuring Composition at High Spatial Resolution.
PB95-107173 *00,563* Not available NTIS

PB95-107181
Design of a Protocol for an Electron Probe Microanalyzer k-Value Round Robin.
PB95-107181 *00,564* Not available NTIS

PB95-107199
Compositional Mapping of the Microstructure of Materials.
PB95-107199 *00,565* Not available NTIS

PB95-107207
Monte Carlo Electron Trajectory Simulation of X-Ray Emission from Films Supported on Substrates.
PB95-107207 *04,522* Not available NTIS

PB95-107215
Interface Roughness of Short-Period AlAs/GaAs Superlattices Studied by Spectroscopic Ellipsometry.
PB95-107215 *02,137* Not available NTIS

PB95-107223
Inelastic Neutron Scattering Studies of Nonlinear Optical Materials: p-Nitroaniline Adsorbed in ALPO-5.
PB95-107223 *00,874* Not available NTIS

PB95-107231
Real Time Compensation for Tool Form Errors in Turning Using Computer Vision.
PB95-107231 *02,945* Not available NTIS

PB95-107249
Separation and Identification of Organic Gunshot and Explosive Constituents by Micellar Electrokinetic Capillary Electrophoresis.
PB95-107249 *00,566* Not available NTIS

PB95-107256
Reconstructing Stratified Fluid Flow from Reciprocal Scattering Measurements.
PB95-107256 *04,202* Not available NTIS

PB95-107264
Fluctuation Dominated Recombination Kinetics with Traps.
PB95-107264 *00,875* Not available NTIS

PB95-107272
Certification, Development and Use of Standard Reference Materials.
PB95-107272 *00,567* Not available NTIS

PB95-107280
Should NIST Accredit U.S. Calibration Laboratories.
PB95-107280 *02,646* Not available NTIS

PB95-107298
Resistance Thermometers with Fast Response for Use in Rapidly Oscillating Gas Flows.
PB95-107298 *03,261* Not available NTIS

PB95-107306
Improved Crystallographic Data for Aluminum Niobate (AlNbO4).
PB95-107306 *04,523* Not available NTIS

PB95-107314
Summary and Notes of the Joint ISO/IGES/PDES Organization Technical Committee Meeting. Held in Albuquerque, New Mexico on October 15-20, 1989.
PB95-107314 *02,774* Not available NTIS

PB95-107322
Electric Field Effects on Crack Growth in a Lead Magnesium Niobate.
PB95-107322 *03,339* Not available NTIS

PB95-107330
Potential Drop in the Center-Cracked Panel with Asymmetric Crack Extension.
PB95-107330 *04,819* Not available NTIS

PB95-107348
Macro- and Microreactions in Mechanical-Impact Tests of Aluminum Alloys.
PB95-107348 *03,340* Not available NTIS

PB95-107355
Influence of Specimen Absorbed Energy in LOX Mechanical-Impact Tests.
PB95-107355 *03,341* Not available NTIS

PB95-107363
Thin Dyed-Plastic Dosimeter for Large Radiation Doses.
PB95-107363 *03,872* Not available NTIS

PB95-107371
Rietveld Analysis of NaxWO3+x/2.yH2O, Which Has the Hexagonal Tungsten Bronze Structure.
PB95-107371 *04,524* Not available NTIS

PB95-107389
Polyethylene Crystallized from an Entangled Solution Observed by Scanning Tunneling Microscopy.
PB95-107389 *01,232* Not available NTIS

PB95-107397
Measurements of Moisture Diffusivity for Porous Building Materials.
PB95-107397 *00,356* Not available NTIS

PB95-107405
Optimization of Inert Gas Atomization.
PB95-107405 *01,377* Not available NTIS

PB95-108411
Heterodyne Measurement of the Fluorescence Spectrum of Optical Molasses.
PB95-108411 *03,873* Not available NTIS

PB95-108429
Magnetic Moments in Cr Thin Films on Fe(100).
PB95-108429 *04,525* Not available NTIS

PB95-108437
1,4-Dinitrocubane and Cubane under High Pressure.
PB95-108437 *03,755* Not available NTIS

PB95-108445
Self-, N2- and Ar-Broadening and Line Mixing in HCN and C2H2.
PB95-108445 *00,876* Not available NTIS

PB95-108452
Decoupling in the Line Mixing of Acetylene Infrared Q Branches.
PB95-108452 *00,877* Not available NTIS

PB95-108460
Self-Assembled Phospholipid/Alkanethiol Biomimetic Bilayers on Gold.
PB95-108460 *00,878* Not available NTIS

PB95-108478
Fokker-Planck Description of Multivalent Interactions.
PB95-108478 *00,879* Not available NTIS

PB95-108486
Standardization of Testing Methods for Optical Disk Media Characteristics and Related Activities at NIST.
PB95-108486 *01,624* Not available NTIS

PB95-108494
Photoelectron Spectroscopy of Negatively Charged Bismuth Clusters: Bi(-)2, Bi(-)3, and Bi(-)4.
PB95-108494 *00,880* Not available NTIS

PB95-108502
Metrology Model for Submicrometer Dimensional Measurements.
PB95-108502 *02,647* Not available NTIS

PB95-108510
Practical Photomask Linewidth Measurements.
PB95-108510 *02,324* Not available NTIS

PB95-108528
Activities of the ASTM Committee E-42 on Surface Analysis.
PB95-108528 *00,881* Not available NTIS

PB95-108536
Formation of Technical Committee 201 on Surface Chemical Analysis by the International Organization for Standardization.
PB95-108536 *00,568* Not available NTIS

PB95-108544
Combustion of Methanol and Methanol/Dodecanol Spray Flames.
PB95-108544 *02,478* Not available NTIS

PB95-108551
Study of Droplet Transport in Alcohol-Based Spray Flames Using Phase/Doppler Interferometry.
PB95-108551 *02,479* Not available NTIS

PB95-108569
Structure of a Swirl-Stabilized Kerosene Spray Flame.
PB95-108569 *02,480* Not available NTIS

PB95-108577
Parametric Investigation of Metal Powder Atomization Using Laser Diffraction.
PB95-108577 *03,342* Not available NTIS

PB95-108585
High-Order Harmonic Mixing with GaAs Schottky Diodes.
PB95-108585 *01,528* Not available NTIS

PB95-108593
Construction of Maximum-Entropy Density Maps, and Their Use in Phase Determination and Extension.
PB95-108593 *00,882* Not available NTIS

PB95-108601
Mathematical Aspects of Rietveld Refinement.
PB95-108601 *04,526* Not available NTIS

PB95-108619
Vibrational Energy Transfer in S1 p-Difluorobenzene. A Comparison of Low and Room Temperature Collisions.
PB95-108619 *00,883* Not available NTIS

PB95-108627
Measurement of the Self Broadening of the H2Q(0-5) Raman Transitions from 295 to 1000 K.
PB95-108627 *00,884* Not available NTIS

PB95-108635
Calculation of Enthalpy and Entropy Differences of Near-Critical Binary Mixtures with the Modified Leung-Griffiths Model.
PB95-108635 *00,885* Not available NTIS

PB95-108643
Correction Factor for Nonplanar Incident Field in Monopole Calibrations.
PB95-108643 *02,002* Not available NTIS

PB95-108650
Real-Time Implementation of a Differential Range Finder.
PB95-108650 *01,839* Not available NTIS

PB95-108668
Response of a Terminally Anchored Polymer Chain to Simple Shear Flow.
PB95-108668 *01,233* Not available NTIS

PB95-108676
Effect of Heterogeneous Porous Media on Mold Filling in Resin Transfer Molding.
PB95-108676 *03,197* Not available NTIS

PB95-108684
Efficient Br(*) Laser Pumped by Frequency-Doubled Nd:YAG and Electronic-to-Vibrational Transfer-Pumped CO2 and HCN Lasers.
PB95-108684 *04,248* Not available NTIS

PB95-108692
Preparation and Characterization of (6)LiF and (10)B Reference Deposits for the Measurement of the Neutron Lifetime.
PB95-108692 *03,874* Not available NTIS

PB95-108700
Vibration Laboratory Automation at NIST with Personal Computers.
PB95-108700 *02,648* Not available NTIS

PB95-108718
Verification of a Model of Fire and Smoke Transport.
PB95-108718 *00,357* Not available NTIS

PB95-108726
Laboratory Studies of Low-Temperature Reactions of C2H with C2H2 and Implications for Atmospheric Models of Titan.
PB95-108726 *00,690* Not available NTIS

PB95-108734
Interface Modification and Characterization of Silicon Carbide Platelets Coated with Alumina Particles.
PB95-108734 *03,121* Not available NTIS

PB95-108742
Addition of M and L-Series Lines to NIST Algorithm for Calculation of X-Ray Tube Output Spectral Distributions.
PB95-108742 *00,569* Not available NTIS

PB95-108759
Apparent Bias in the X-Ray Fluorescence Determination of Titanium in Selected NIST SRM Low Alloy Steels.
PB95-108759 *03,212* Not available NTIS

PB95-108767
Secondary Target X-Ray Excitation for In vivo Measurement of Lead in Bone.
PB95-108767 *03,496* Not available NTIS

PB95-108775
Interface Sharpness in Low-Order III-V Superlattices.
PB95-108775 *02,138* Not available NTIS

PB95-108783
Interface Sharpness during the Initial Stages of Growth of Thin, Short-Period III-V Superlattices.
PB95-108783 *02,139* Not available NTIS

PB95-108791
Global Climatic Effects of Aerosols: The AAAR Symposium.
PB95-108791 *00,122* Not available NTIS

PB95-108809
Evolution of Automatic Line Scale Measurement at the National Institute of Standards and Technology.
PB95-108809 *02,897* Not available NTIS

PB95-108817
Polarized Transient Hot Wire Thermal Conductivity Measurements.
PB95-108817 *00,886* Not available NTIS

PB95-108825
Ventilation Rates in Office Buildings.
PB95-108825 *02,539* Not available NTIS

PB95-108833
Field Measurements of Ventilation and Ventilation Effectiveness in an Office/Library Building.
PB95-108833 *00,247* Not available NTIS

PB95-108841
Seismic Strengthening of Reinforced Concrete Frame Buildings.
PB95-108841 *00,430* Not available NTIS

PB95-108858
Some Considerations for Interim Testing of Coordinate Measuring Machine Performance Using a Specific Artifact.
PB95-108858 *02,898* Not available NTIS

PB95-108866
Development of an Automated Part Inspection System Using the DMIS Standard.
PB95-108866 *02,899* Not available NTIS

PB95-108874
Atoms in Optical Molasses.
PB95-108874 *03,875* Not available NTIS

PB95-108882
Atoms in Optical Molasses: Applications to Frequency Standards.
PB95-108882 *03,876* Not available NTIS

PB95-108890
Optical Molasses: Cold Atoms for Precision Measurements.
PB95-108890 *03,877* Not available NTIS

PB95-108908
Optical Molasses: The Coldest Atoms Ever.
PB95-108908 *03,878* Not available NTIS

PB95-111514
NIST Industrial Impacts: A Sampling of Successful Partnerships.
PB95-111514 *00,488* PC A05/MF A01

PB95-111522
User's Manual for the Program MONSEL-1: Monte Carlo Simulation of SEM Signals for Linewidth Metrology.
PB95-111522 *02,325* PC A03/MF A01

PB95-122537
Program of the Subcommittee on Construction and Building (July 1994).
PB95-122537 *00,321* PC A03/MF A01

PB95-125076
Standard Reference Materials: Certification of a Standard Reference Material for the Determination of Interstitial Oxygen Concentration in Semiconductor Silicon by Infrared Spectrophotometry.
PB95-125076 *02,326* PC A05/MF A01

PB95-125613
Evaluation of Fracture Toughness and Residual Stress in Dental Porcelain by Indentation-Microfracture Method.
PB95-125613 *00,154* Not available NTIS

PB95-125621
Reanalysis of the (010), (020), (100), and (001) Rotational Levels of (32)S(16)O2.
PB95-125621 *00,887* Not available NTIS

PB95-125639
Development of a Temperature Scale below 0.5 K.
PB95-125639 *03,879* Not available NTIS

PB95-125647
Asymmetry between Flux Penetration and Flux Expulsion in Tl-2212 Superconductors.
PB95-125647 *04,527* Not available NTIS

PB95-125654
Application of Expert System to Select Data Sources from Chemical Information Databases.
PB95-125654 *00,505* Not available NTIS

PB95-125662
Mid- and Near-Infrared Spectra of Water and Water Dimer Isolated in Solid Neon.
PB95-125662 *00,888* Not available NTIS

PB95-125670
Vibrational Spectra of Molecular Ions Isolated in Solid Neon. X. H2O(+), HDO(+), and D2O(+).
PB95-125670 *00,889* Not available NTIS

PB95-125688
Vibrational Spectra of Molecular Ions Isolated in Solid Neon. XI. NO2(+), NO2(-), and NO3(-).
PB95-125688 *00,890* Not available NTIS

PB95-125696
Appropriate Ultrasonic System Components for NDE of Thick Polymer Composites.
PB95-125696 *03,148* Not available NTIS

PB95-125704
High-Sensitivity Acoustic Emission Sensor/Preamplifier Subsystems.
PB95-125704 *02,900* Not available NTIS

PB95-125712
Examination of Objects Made of Wood Using Air-Coupled Ultrasound.
PB95-125712 *03,404* Not available NTIS

PB95-125720
Vibrational Predissociation Dynamics of Overtone-Excited HN3.
PB95-125720 *00,691* Not available NTIS

PB95-125738
Infrared Spectra of van der Waals Complexes of Importance in Planetary Atmospheres.
PB95-125738 *00,071* Not available NTIS

PB95-125746
Environmentally Enhanced Fracture of Ceramics.
PB95-125746 *03,046* Not available NTIS

PB95-125753
Capacity of the Lp Norm-Constrained Poisson Channel.
PB95-125753 *01,515* Not available NTIS

PB95-125761
Noise-Induced Chaos and Phase Space Flux.
PB95-125761 *03,433* Not available NTIS

PB95-125779
Thermodynamic Properties of the Methane-Ethane System.
PB95-125779 *00,891* Not available NTIS

PB95-125787
Thermophysical Property Computer Packages from NIST.
PB95-125787 *04,203* Not available NTIS

PB95-125795
Suggestions for a Logically-Consistent Structure for Service Life Prediction Standards.
PB95-125795 *00,358* Not available NTIS

PB95-125803
Conductance Response of Pd/SnO2(110) Model Gas Sensors to H2 and O2.
PB95-125803 *00,892* Not available NTIS

PB95-125811
Determination of Fiber-Matrix Interfacial Properties of Importance to Ceramic Composite Toughening.
PB95-125811 *03,149* Not available NTIS

PB95-125829
National PDES Testbed: An Overview.
PB95-125829 *02,775* Not available NTIS

PB95-125837
Important Papers in the History of Document Preparation Systems: Basic Sources.
PB95-125837 *02,712* Not available NTIS

PB95-125845
Application of Thermal Analysis Techniques to the Characterization of EPDM Roofing Membrane Materials.
PB95-125845 *00,359* Not available NTIS

PB95-125852
Use of Thermal Mechanical Analysis to Characterize Ethylene-Propylene-Diene Terpolymer (EPDM) Roofing Membrane Materials.
PB95-125852 *00,360* Not available NTIS

PB95-125860
Single-Atom Point Source for Electrons: Field-Emission Resonance Tunneling in Scanning Tunneling Microscopy.
PB95-125860 *00,893* Not available NTIS

PB95-125878
Aggregation Kinetics of Colloidal Particles Destabilized by Enzymes.
PB95-125878 *00,894* Not available NTIS

PB95-125886
Associative Ionization in Collisions of Slowed and Trapped Sodium.
PB95-125886 *03,880* Not available NTIS

PB95-125894
Software Safety and Program Slicing.
PB95-125894 *01,703* Not available NTIS

PB95-125902
Object SQL: Language Extensions for Object Data Management.
PB95-125902 *01,704* Not available NTIS

PB95-125910
Complex Propagation Constants for Nonuniform Optical Waveguides: Calculations.
PB95-125910 *04,249* Not available NTIS

PB95-125928
International Intercomparison of Detector Responsivity at 1300 and 1550 nm.
PB95-125928 *02,140* Not available NTIS

PB95-125936
Fiber Spot Size: A Simple Method of Calculation.
PB95-125936 *04,250* Not available NTIS

PB95-125944
Modal Properties of Circular and Noncircular Optical Waveguides.
PB95-125944 *04,251* Not available NTIS

PB95-125951
Water Efficient Plumbing Fixtures through Standards and Test Methods.
PB95-125951 *00,248* Not available NTIS

PB95-125969
Control of Friction and Wear of Alpha-Alumina with a Composite Solid-Lubricant Coating.
PB95-125969 *03,225* Not available NTIS

PB95-125977
Relating Bench-Scale and Full-Scale Toxicity Data.
PB95-125977 *00,361* Not available NTIS

PB95-125985
Computer Simulation of the Diffusivity of Cement-Based Materials.
PB95-125985 *00,362* Not available NTIS

PB95-125993
Digital Simulation of the Aggregate-Cement Paste Interfacial Zone in Concrete.
PB95-125993 *00,363* Not available NTIS

PB95-126009
Fundamental Computer Simulation Models for Cement-Based Materials.
PB95-126009 *00,364* Not available NTIS

PB95-126017
International Intercomparison of Detector Responsivity at 1300 and 1550 nm.
PB95-126017 *02,141* Not available NTIS

PB95-126025
Development and Validation of Multicriteria Ratings: A Case Study.
PB95-126025 *00,004* Not available NTIS

PB95-126033
Nature of (001) Tilt Grain Boundaries in YBa2Cu3O6+x.
PB95-126033 *04,528* Not available NTIS

PB95-126041
Picosecond Measurement of Substrate-to-Adsorbate Energy Transfer: The Frustrated Translation of CO/Pt(111)--Translation.
PB95-126041 *00,895* Not available NTIS

PB95-126058
Temperature of Optical Molasses for Two Different Atomic Angular Momenta.
PB95-126058 *03,881* Not available NTIS

PB95-126066
Dispersion and Deposition of Smoke Plumes Generated in Massive Fires.
PB95-126066 *02,540* Not available NTIS

PB95-126074
Cryogenic Precision Capacitance Bridge Using a Single Electron Tunneling Electrometer.
PB95-126074 *04,529* Not available NTIS

PB95-126082
Frequency Stabilization of a Fiber Laser to Rubidium: A High-Accuracy 1.53 mu m Wavelength Standard.
PB95-126082 *04,252* Not available NTIS

PB95-126090
Laser Cooling and Trapping for the Masses.
PB95-126090 *04,253* Not available NTIS

PB95-126108
Use of Kinetic Energy Distributions to Determine the Relative Contributions of Gas Phase and Surface Fragmentation in KeV Ion Sputtering of a Quaternary Ammonium Salt.
PB95-126108 *00,570* Not available NTIS

PB95-126116
Image Depth Profiling SIMS: An Evaluation for the Analysis of Light Element Diffusion in YBa2Cu3O7-x Single Crystal Superconductors.
PB95-126116 *04,530* Not available NTIS

PB95-126124
Molecular Ion Imaging and Dynamic Secondary Ion Mass Spectrometry of Organic Compounds.
PB95-126124 *00,571* Not available NTIS

PB95-126132
Neutron Leakage Benchmark for Criticality Safety Research.
PB95-126132 *03,723* Not available NTIS

PB95-126140
Rotational Spectrum and Structure of a Weakly Bound Complex of Ketene and Acetylene.
PB95-126140 *00,896* Not available NTIS

PB95-126157
Biological Macromolecular Crystallization Database: A Tool for Developing Crystallization Strategies.
PB95-126157 *00,897* Not available NTIS

PB95-126165
Constructing Invariant Tori for Two Weakly Coupled van der Pol Oscillators.
PB95-126165 *03,412* Not available NTIS

PB95-126173
Image Information Transfer Properties of X-Ray Intensifying Screens in the Energy Range from 17 to 320 keV.
PB95-126173 *00,155* Not available NTIS

PB95-126181
Characterization of Chemically Modified Pore Surfaces by Small Angle Neutron Scattering.
PB95-126181 *00,898* Not available NTIS

PB95-126199
Magnetic Measurement of Transport Critical Current Density of Granular Superconductors.
PB95-126199 *04,531* Not available NTIS

PB95-126207
Information Resource Dictionary System (IRDS): A Status Report.
PB95-126207 *01,810* Not available NTIS

PB95-126215
Inelastic Neutron Scattering Measurements of Phonons in Icosahedral Al-Li-Cu.
PB95-126215 *04,532* Not available NTIS

PB95-126223
n-Value and Second Derivative of the Superconductor Voltage-Current Characteristic.
PB95-126223 *04,533* Not available NTIS

PB95-126231
Vapor Pressure of 1,1-dichloro-2,2,2-trifluoroethane (R123).
PB95-126231 *00,899* Not available NTIS

PB95-126249
Accuracy of Eigenvalues: A Comparison of Two Methods.
PB95-126249 *03,413* Not available NTIS

PB95-126256
Approximate Solution to the Scalar Wave Equation for Optical Waveguides.
PB95-126256 *04,254* Not available NTIS

PB95-126264
Comparison of Heat-Flow-Meter Tests from Four Laboratories.
PB95-126264 *00,365* Not available NTIS

PB95-126272
Review of the USCEA/NIST Measurement Assurance Program for the Nuclear Power Industry.
PB95-126272 *03,712* Not available NTIS

PB95-126280
Dissolution Problems with Botanical Reference Materials.
PB95-126280 *03,487* Not available NTIS

PB95-126298
Some Aspects of Fundamental Neutron Physics.
PB95-126298 *03,882* Not available NTIS

PB95-126306
Growing Significance of CIB.
PB95-126306 *00,314* Not available NTIS

PB95-126314
Ashland Tank Collapse Investigation.
PB95-126314 *02,481* Not available NTIS

PB95-126322
Ashland Tank-Collapse Investigation: Closure by Authors.
PB95-126322 *02,482* Not available NTIS

PB95-126330
Assessment of Technologies for Advanced Fire Detection.
PB95-126330 *00,294* Not available NTIS

PB95-126348
Far-Infrared Kinetic Inductance Detector.
PB95-126348 *02,142* Not available NTIS

PB95-126355
Effect of Mn Content on the Microstructure of Al-Mn Alloys Electrodeposited at 150C.
PB95-126355 *03,343* Not available NTIS

PB95-126363
Influence of Physical Aging on the Yield Response of Model DGEBA + Poly(propylene oxide) Epoxy Glasses.
PB95-126363 *03,381* Not available NTIS

PB95-126371
Wide Band Active Current Transformer and Shunt.
PB95-126371 *02,036* Not available NTIS

PB95-126389
Transition Metal Implants in In0.53GA0.47As.
PB95-126389 *04,534* Not available NTIS

PB95-126397
Range Statistics and Rutherford Backscattering Studies on Fe-Implanted In0.53Ga0.47As.
PB95-126397 *04,535* Not available NTIS

PB95-126405
Evidence for Significant Backscattering in Near-Threshold Electron-Impact Excitation of Ar(7+)(3s yields 3p).
PB95-126405 *03,883* Not available NTIS

PB95-128633
Sub-Doppler Frequency Measurements on OCS at 87 Thz (3.4 micrometers) with the CO Overtone Laser: Considerations and Details.
PB95-128633 *04,255* PC A03/MF A01

PB95-128641
Databases Available in the Research Information Center of the National Institute of Standards and Technology.
PB95-128641 *02,724* PC A08/MF A01

PB95-128658
National Voluntary Laboratory Accreditation Program: Ionizing Radiation Dosimetry.
PB95-128658 *03,623* PC A06/MF A02

PB95-128674
FIREDOC Users Manual, 3rd Edition.
PB95-128674 *01,378* PC A03/MF A01

PB95-128906
Uncertainty Analysis of the NIST Nitrogen Flow Facility.
PB95-128906 *02,608* PC A04/MF A01

PB95-130209
Standards of Seismic Safety for Existing Federally Owned or Leased Buildings and Commentary.
PB95-130209 *00,431* PC A06/MF A02

PB95-130845
Summaries of BFRL Fire Research In-House Projects and Grants, 1994.
PB95-130845 *00,366* PC A10/MF A03

PB95-130985
Computer Security Training and Awareness Course Compendium.
PB95-130985 *01,589* PC A09/MF A02

PB95-135562
Bibliography of the NIST Electromagnetic Fields Division Publications.
PB95-135562 *01,886* PC A06/MF A02

PB95-135570
Thermal Hydraulic Tests of a Liquid Hydrogen Cold Neutron Source.
PB95-135570 *03,884* PC A03/MF A01

PB95-135588
Metrology for Electromagnetic Technology: A Bibliography of NIST Publications.
PB95-135588 *02,143* PC A05/MF A01

PB95-135596
Indoor Air Quality Impacts of Residential HVAC Systems, Phase 1 Report: Computer Simulation Plan.
PB95-135596 *00,249* PC A06/MF A02

PB95-136339
Domain Analysis of the Alarm Surveillance Domain. Version 1.0. Conducted as Part of the Domain Analysis Case Study Project.
PB95-136339 *01,705* PC A10/MF A03

PB95-136347
Challenges to the National Information Infrastructure: The Barriers to Product Data Sharing. National PDES Testbed Report Series.
PB95-136347 *02,776* PC A03/MF A01

PB95-136354
Sensitivity of Three-Point Circle Fitting.
PB95-136354 *02,901* PC A03/MF A01

PB95-136362
Comparison of FFT Fingerprint Filtering Methods for Neural Network Classification.
PB95-136362 *01,840* PC A03/MF A01

PB95-136370
Faster BKL Monte Carlo Simulations.
PB95-136370 *01,706* PC A03/MF A01

PB95-136388
NIST Workshop on the Computer Interface to Flat Panel Displays. Held in San Jose, California on January 13-14, 1994.
PB95-136388 *01,625* PC A11/MF A03

PB95-136610
Report on the Advanced Software Technology Workshop. Held on February 1, 1994.
PB95-136610 *01,707* PC A03/MF A01

PB95-136628
xi-Vector Formulation of Anisotropic Phase-Field Models: 3-D Asymptotics.
PB95-136628 *04,536* PC A03/MF A01

PB95-136644
Constituents and Physical Properties of the C6+ Fraction of Natural Gas. Topical Report, April-June 1994.
PB95-136644 *02,483* PC A03/MF A01

PB95-137790
STEP On-Line Information Service (SOLIS). The IGES/PDES Organization.
PB95-137790 *02,777* PC A02/MF A01

PB95-138129
National Voluntary Laboratory Accreditation Program: Bulk Asbestos Analysis.
PB95-138129 *02,541* PC A04/MF A01

PB95-140018
Volume Recovery in Epoxy Glasses Subjected to Torsional Deformations: The Question of Rejuvenation.
PB95-140018 *03,382* Not available NTIS

PB95-140026
Torsional Relaxation and Volume Response during Physical Aging in Epoxy Glasses Subjected to Large Torsional Deformations.
PB95-140026 *03,383* Not available NTIS

PB95-140034
Defective Structures of Barium Yttrium Copper Oxide (Ba2YCu3Ox) and Ba2YCu3-yMyOz (M=Fe, Co, Al, Ga, ..).
PB95-140034 *04,537* Not available NTIS

PB95-140042
Neutron Powder Diffraction Study of the Structures of La1.9Ca1.1Cu2O6 and La1.9Sr1.1Cu2O6+Delta.
PB95-140042 *04,538* Not available NTIS

PB95-140059
Precision High Temperature Blackbodies.
PB95-140059 *03,885* Not available NTIS

PB95-140067
Normal Modes and Structure Factor for a Canted Spin System: The Generalized Villain Model.
PB95-140067 *04,539* Not available NTIS

PB95-140075
Morphology of Symmetric Diblock Copolymers as Revealed by Neutron Reflectivity.
PB95-140075 *01,234* Not available NTIS

PB95-140083
Superconducting Kinetic Inductance Radiometer.
PB95-140083 *02,144* Not available NTIS

PB95-140091
Comparison of Methods for Gas Chromatographic Determination of PCBs and Chlorinated Pesticides in Marine Reference Materials.
PB95-140091 *02,584* Not available NTIS

PB95-140109
NIST Standard Reference Materials (SRMs) for Polychlorinated Biphenyl (PCB) Determinations and Their Applicability to Toxaphene Measurements.
PB95-140109 *02,585* Not available NTIS

PB95-140117
Radiation Accident at an Industrial Accelerator Facility.
PB95-140117 *02,575* Not available NTIS

PB95-140125
Novel Polydiacetylenes Derived from Liquid Crystalline Monomers.
PB95-140125 *01,235* Not available NTIS

PB95-140133
Formulation of the Refractive Index of Water and Steam.
PB95-140133 *00,900* Not available NTIS

PB95-140141
Combining Data from Independent Chemical Analysis Methods.
PB95-140141 *00,572* Not available NTIS

PB95-140158
Metrology Applications of Mode-Locked Erbium Fiber Lasers.
PB95-140158 *04,256* Not available NTIS

PB95-140166
Near Critical Fluid Interfaces: A Comparison of Theory and Experiment.
PB95-140166 *00,901* Not available NTIS

PB95-140174
Structure of the Vapor-Liquid Interface Near the Critical Point.
PB95-140174 *00,902* Not available NTIS

PB95-140182
Operational Mode and Gas Species Effects on Rotational Drag in Pneumatic Dead Weight Pressure Gages.
PB95-140182 *00,903* Not available NTIS

PB95-140190
Glass Temperature of Polymer Blends: Comparison of Both the Free Volume and the Entropy Predictions with Data.
PB95-140190 *01,236* Not available NTIS

PB95-140208
New Materials, Advanced Ceramics and Standards.
PB95-140208 *03,047* Not available NTIS

PB95-140414
Scanning Tunneling Microscopy and Fabrication of Nanometer Scale Structures at the Liquid-Gold Interface.
PB95-140414 *00,904* Not available NTIS

PB95-140422
Measurement of the (235)U(n,f) Reaction from Thermal to 1 keV.
PB95-140422 *03,886* Not available NTIS

PB95-140430
Ultrasonic Measurement of Residual Stress in Railroad Wheel Rims.
PB95-140430 *04,849* Not available NTIS

PB95-140448
Effects of Surface-Active Resins on Dentin/Composite Bonds.
PB95-140448 *00,156* Not available NTIS

PB95-140455
Nondestructive Evaluation and Materials Processing.
PB95-140455 *02,902* Not available NTIS

PB95-140463
Flow of Microemulsions through Microscopic Pores.
PB95-140463 *00,905* Not available NTIS

PB95-140471
Study of the Hydroxycarbonate Precursor Route to the YBa2Cu3O7-x High Tc Superconductor.
PB95-140471 *04,540* Not available NTIS

PB95-140489
Michaelis-Menten Equation for an Enzyme in an Oscillating Electric Field.
PB95-140489 *00,906* Not available NTIS

PB95-140497
Determining Mobility from Homodyne ac Electrophoretic Light Scattering.
PB95-140497 *03,462* Not available NTIS

PB95-140505
Substitution-Induced Midgap States in the Mixed Oxides RxBa1-ChiTiO3-Delta, with R=Y, La, and Nd.
PB95-140505 *04,541* Not available NTIS

PB95-140513
Incommensurate Magnetic Order in UPtGe.
PB95-140513 *04,542* Not available NTIS

PB95-140521
Crystallographic and Magnetic Properties of UAuSn.
PB95-140521 *04,543* Not available NTIS

PB95-140539
Influence of Deposition Parameters on Properties of Laser Ablated YBa2Cu3O7-Delta Films.
PB95-140539 *04,544* Not available NTIS

PB95-140547
Magnetic Ordering of the Cu Spins in PrBa2Cu3O6+x.
PB95-140547 *04,545* Not available NTIS

PB95-140554
Crystal Structure and Magnetic Ordering of the Rare-Earth and Cu Moments in RBa2Cu2NbO8(R=Nd,Pr).
PB95-140554 *04,546* Not available NTIS

PB95-140562
Quasielastic and Inelastic Neutron-Scattering Studies of ((CD3)3ND)FeCl3.2D2O: A One-Dimensional Ising Ferromagnet.
PB95-140562 *04,547* Not available NTIS

PB95-140570
Phase Equilibria in the Systems CaO-CuO and CaO-Bi2O3.
PB95-140570 *03,048* Not available NTIS

PB95-140588
Critical Factors in Non-Lubricated, Non-Abrasive Wear Testing.
PB95-140588 *03,236* Not available NTIS

PB95-140596
Tribological Data: Needs and Opportunities.
PB95-140596 *03,237* Not available NTIS

PB95-140604
Device for Subambient Temperature Control in Liquid Chromatography.
PB95-140604 *00,573* Not available NTIS

PB95-140810
Thermally Activated Hopping of a Single Abrikosov Vortex.
PB95-140810 *04,548* Not available NTIS

PB95-140828
Surface Energy Reduction in Fibrous Monotectic Structures.
PB95-140828 *03,150* Not available NTIS

PB95-140836
Rare-Earth-Doped Waveguide Devices: The Potential for Compact Blue-Green Lasers.
PB95-140836 *04,257* Not available NTIS

PB95-140844
Linewidth Narrowing in an Imbalanced Y-Branch Waveguide Laser.
PB95-140844 *04,258* Not available NTIS

PB95-140851
Nd:LiTaO3 Waveguide Laser.
PB95-140851 *04,259* Not available NTIS

PB95-140869
Wavelengths and Isotope Shifts for Lines of Astrophysical Interest in the Spectrum of Doubly Ionized Mercury (Hg III).
PB95-140869 *03,887* Not available NTIS

PB95-140877
Spectrum and Energy Levels of Triply Ionized Barium (Ba IV).
PB95-140877 *03,888* Not available NTIS

PB95-140885
FPETOOL: Fire Protection Tools for Hazard Estimation. An Overview of Features.
PB95-140885 *00,367* Not available NTIS

PB95-140893
In situ Measurements of Chloride Ion and Corrosion Potential at the Coating/Metal Interface.
PB95-140893 *03,122* Not available NTIS

PB95-140901
Using Torsional Dilatometry to Measure the Effects of Deformations on Physical Aging.
PB95-140901 *03,384* Not available NTIS

PB95-140919
Comparison of Experimental and Computed Species Concentration and Temperature Profiles in Laminar, Two-Dimensional Methane/Air Diffusion Flames.
PB95-140919 *01,379* Not available NTIS

PB95-140927
Aging Effects on XRF Measurements of Solder Coatings.
PB95-140927 *03,123* Not available NTIS

PB95-140935
One- and Two-Sided Burning of Thermally Thin Materials.
PB95-140935 *03,151* Not available NTIS

PB95-140943
Heat Transfer in Thin, Compact Heat Exchangers with Circular, Rectangular, or Pin-Fin Flow Passages.
PB95-140943 *02,751* Not available NTIS

PB95-140950
Chemical and Microbiological Problems Associated with Research on the Biodesulfurization of Coal.
PB95-140950 *02,484* Not available NTIS

PB95-140968
Bioleaching of Cobalt from Smelter Wastes by 'Thiobacillus ferrooxidans'.
PB95-140968 *02,582* Not available NTIS

PB95-140976
Comparison of the Liquid Chromatographic Behavior of Selected Steroid Isomers Using Different Reversed-Phase Materials and Mobile Phase Compositions.
PB95-140976 *00,574* Not available NTIS

PB95-140984
Metrology Requirements of Future Space Power Systems.
PB95-140984 *04,840* Not available NTIS

PB95-140992
Associative Electron Attachment to S2F10, S2OF10, and S2O2F10.
PB95-140992 *00,907* Not available NTIS

PB95-141008
Ion Kinetic-Energy Distributions in Argon rf Glow Discharges.
PB95-141008 *04,409* Not available NTIS

PB95-141016
Critical Current Behavior of Ag-Coated YBa2Cu3O7-x Thin Films.
PB95-141016 *04,549* Not available NTIS

PB95-141024
Magnetic Field Dependence of the Critical Current Anisotropy in Normal Metal-YBa2Cu3O7-delta Thin Film Bilayers.
PB95-141024 *04,550* Not available NTIS

PB95-141032
Infrared Spectrum of OClO in the 2000/cm(-1) Region: The 2(nu sub 1) and (nu sub 1 + nu sub 3) Bands.
PB95-141032 *00,908* Not available NTIS

PB95-141040
Intensities and Dipole Moment Derivatives of the Fundamental Bands of (35)ClO2 and an Intensity Analysis of the nu1 Band.
PB95-141040 *00,909* Not available NTIS

PB95-141057
Intelligent Control of an Inert Gas Atomization Process.
PB95-141057 *03,344* Not available NTIS

PB95-141065
Micromagnetic Model of Dual-Layer Magnetic-Recording Thin Films.
PB95-141065 *04,551* Not available NTIS

PB95-141073
Micromagnetic Simulations of Tunneling Stabilized Magnetic Force Microscopy.
PB95-141073 *04,552* Not available NTIS

PB95-141081
Experimental Verification of a Micromagnetic Model of Dual-Layer Magnetic Films.
PB95-141081 *04,553* Not available NTIS

PB95-141099
Process Gas Chromatography Detector for Hydrocarbons Based on Catalytic Cracking.
PB95-141099 *02,485* Not available NTIS

PB95-141107
Reaction of Nitric Oxide with Organic Peroxyl Radicals.
PB95-141107 *00,910* Not available NTIS

PB95-141115
LP11-Mode Leakage Loss in Coated Depressed Clad Fibers.
PB95-141115 *02,145* Not available NTIS

PB95-141123
Perturbative Calculation of the AC Stark Effect by the Complex Rotation Method.
PB95-141123 *04,260* Not available NTIS

PB95-141131
Ca4Bi6O13: A Compound Containing an Unusually Low Bismuth Coordination Number and Short Bi Bi Contacts.
PB95-141131 *00,911* Not available NTIS

PB95-141149
Trapped Vortices in a Superconducting Microbridge.
PB95-141149 *04,554* Not available NTIS

PB95-141156
Effect of Hydrodynamic Interactions on a Terminally Anchored Bead-Rod Model Chain.
PB95-141156 *01,237* Not available NTIS

PB95-141164
Variation in Magnetic Properties of Cu/Fcc (001) Sandwich Structures.
PB95-141164 *04,555* Not available NTIS

PB95-141172
Physics for Device Simulations and Its Verification by Measurements.
PB95-141172 *02,327* Not available NTIS

PB95-141180
Interatomic Potential of Argon.
PB95-141180 *00,912* Not available NTIS

PB95-141198
Time-Resolved Measurements of Energy Transfer at Surfaces.
PB95-141198 *00,913* Not available NTIS

PB95-141206
Neutron Focusing Lens Using Polycapillary Fibers.
PB95-141206 *03,889* Not available NTIS

PB95-143061
Summary Report of NIST's Industry-Government Consortium Research Program on Flowmeter Installation Effects: The 45 Degree Elbow.
PB95-143061 *04,204* PC A06/MF A02

PB95-143079
Quantitative X-Ray Powder Diffraction Methods for Clinker and Cement.
PB95-143079 *01,317* PC A03/MF A01

PB95-143087
Guidelines for Evaluating and Expressing the Uncertainty of NIST Measurement Results. 1994 Edition.
PB95-143087 *02,649* PC A03/MF A01

PB95-143095
Diagnosis of Causes of Concrete Deterioration in the MLP-7A Parking Garage.
PB95-143095 *01,318* PC A03/MF A01

PB95-143103
SGML Environment for STEP.
PB95-143103 *02,778* PC A03/MF A01

PB95-143111
Metrology and Data for Microelectronic Packaging and Interconnection: Results of a Joint Workshop on Materials Metrology and Data for Commercial Electrical and Optical Packaging and Interconnection Technologies. Held in Gaithersburg, Maryland on May 5-6, 1994. Volume 1. Results.
PB95-143111 *02,328* PC A05/MF A01

PB95-143129
Manufactured Homes: Probability of Failure and the Need for Better Windstorm Protection through Improved Anchoring Systems.
PB95-143129 *00,432* PC A04/MF A01

PB95-143137
Reference Model Architecture for Intelligent Systems Design.
PB95-143137 *01,789* PC A03/MF A01

PB95-143145
Information Technology Engineering and Measurement Model: Adding Lane Markings to the Information Superhighway.
PB95-143145 *01,474* PC A03/MF A01

PB95-143152
Simulating Smoke Movement through Long Vertical Shafts in Zone-Type Compartment Fire Models.
PB95-143152 *00,368* PC A03/MF A01

PB95-143160
Fundamental Mechanisms for CO and Soot Formation.
PB95-143160 *01,380* PC A08/MF A02

PB95-143178
Channel Coding for Code Excited Linear Prediction (CELP) Encoded Speech in Mobile Radio Applications.
PB95-143178 *01,475* PC A03/MF A01

PB95-143186
Electronics and Electrical Engineering Laboratory Technical Progress Bulletin Covering Laboratory Programs, April to June 1994 with 1994/1995 EEEL Events Calendar.
PB95-143186 *02,329* PC A03/MF A01

PB95-143194
Transient Cooling of a Hot Surface by Droplets Evaporation.
PB95-143194 *03,890* PC A09/MF A02

PB95-143202
Building and Fire Research Laboratory Publications, 1993.
PB95-143202 *00,369* PC A06/MF A02

PB95-143285
Visual Pursuit Systems.
PB95-143285 *01,841* PC A03/MF A01

PB95-143293
Investigation into the Flammability Properties of Honeycomb Composites.
PB95-143293 *03,152* PC A03/MF A01

PB95-143301
Visual Measurement Technique for Analysis of Nucleate Flow Boiling.
PB95-143301 *03,262* PC A05/MF A02

PB95-143327
Metrology and Data for Microelectronic Packaging and Interconnection: Results of a Joint Workshop on Materials Metrology and Data for Commercial Electrical and Optical Packaging and Interconnection Technologies. Held in Gaithersburg, Maryland on May 5-6, 1994. Volume 2. Presentation Material.
PB95-143327 *02,330* PC A08/MF A02

PB95-144309
Electronics and Electrical Engineering Laboratory 1994 Technical Accomplishments Supporting Technology for U.S. Competitiveness in Electronics.
PB95-144309 *01,887* PC A06/MF A02

PB95-144549
Reference Architecture for Machine Control Systems Integration: Interim Report.
PB95-144549 *02,820* PC A06/MF A02

PB95-146379
NIST Handbook 44, 1995: Specifications, Tolerances and Other Technical Requirements for Weighing and Measuring Devices as Adopted by the 79th National Conference on Weights and Measures 1994.
PB95-146379 *02,903* PC A11/MF A03

PB95-146387
Methodologies for Predicting the Service Lives of Coating Systems.
PB95-146387 *03,124* PC A05/MF A01

PB95-147146
Opportunities for Innovation: Pollution Prevention.
PB95-147146 *02,520* PC A09/MF A02

PB95-147351
Irradiation Damage in Inorganic Insulation Materials for ITER Magnets: A Review.
PB95-147351 *03,705* PC A18/MF A04

PB95-147385
Wind and Seismic Effects. Proceedings of the U.S.-Japan Cooperative Program in Natural Resources Panel on Wind and Seismic Effects (26th). Held in Gaithersburg, Maryland on May 17-20, 1994.
PB95-147385 *00,433* PC A99/MF A06

PB95-147906
Program Requirements to Advance the Technology of Custom Footwear Manufacturing.
PB95-147906 *02,883* PC A04/MF A01

PB95-147914
Phase-Field Model for Solidification of a Eutectic Alloy.
PB95-147914 *03,345* PC A04/MF A01

PB95-147922
Portsmouth Fastener Manufacturing Workstation. User's Manual.
PB95-147922 *02,860* PC A06/MF A02

PB95-150017
Effects of Interfacial Roughness on the Magnetoresistance of Magnetic Metallic Multilayers.
PB95-150017 *04,556* Not available NTIS

PB95-150025
Oxidative DNA Base Damage in Renal, Hepatic, and Pulmonary Chromatin of Rats After Intraperitoneal Injection of Cobalt (II) Acetate.
PB95-150025 *03,647* Not available NTIS

PB95-150033
Observed Frustration in Confined Block Copolymers.
PB95-150033 *01,238* Not available NTIS

PB95-150041
Airborne Smoke Sampling Package for Field Measurements of Fires.
PB95-150041 *01,381* Not available NTIS

PB95-150058
Monte Carlo Model for SEM Linewidth Metrology.
PB95-150058 *02,331* Not available NTIS

PB95-150066
Transverse Magnetoresistance: A Novel Two-Terminal Method for Measuring the Carrier Density and Mobility of a Semiconductor Layer.
PB95-150066 *02,332* Not available NTIS

PB95-150074
Magnetic Neutron Scattering (Invited).
PB95-150074 *04,557* Not available NTIS

PB95-150082
Polarization Analysis of the Magnetic Excitations in Fe65Ni35 Invar.
PB95-150082 *04,558* Not available NTIS

PB95-150090
Phase Transitions in Solid C70: Supercooling, Metastable Phases, and Impurity Effect.
PB95-150090 *00,914* Not available NTIS

PB95-150108
Method for Determining Both Magnetostriction and Elastic Modulus by Ferromagnetic Resonance.
PB95-150108 *02,974* Not available NTIS

PB95-150116
Superconducting Energy Gap of Bulk UBe13.
PB95-150116 *04,559* Not available NTIS

PB95-150124
Simulations of Glass Forming Liquids: What Has Been Learned.
PB95-150124 *00,915* Not available NTIS

PB95-150132
Radiometric Model of the Transmission Cell-Reciprocal Nephelometer.
PB95-150132 *00,124* Not available NTIS

PB95-150140
Study of Ventilation and Carbon Dioxide in an Office Building.
PB95-150140 *02,542* Not available NTIS

PB95-150157
Spectroscopic Ellipsometry Determination of the Properties of the Thin Underlying Strained Si Layer and the Roughness at SiO2/Si Interface.
PB95-150157 *04,560* Not available NTIS

PB95-150165
Spot-Profile-Analyzing LEED Study of the Epitaxial Growth of Fe, Co, and Cu on Cu(100).
PB95-150165 *04,561* Not available NTIS

PB95-150173
Integrating Sphere Simulation: Application to Total Flux Scale Realization.
PB95-150173 *04,261* Not available NTIS

PB95-150181
Influence of Cr Growth on Exchange Coupling in Fe/Cr/Fe(100).
PB95-150181 *04,562* Not available NTIS

PB95-150199
Automated, High-Precision Coulometric Titrimetry. Part 1. Engineering and Implementation.
PB95-150199 *00,575* Not available NTIS

PB95-150207
Automated, High Precision Coulometric Titrimetry. Part 2. Strong and Weak Acids and Bases.
PB95-150207 *00,576* Not available NTIS

PB95-150215
Oxidation of Soot and Carbon Monoxide in Hydrocarbon Diffusion Flames.
PB95-150215 *01,382* Not available NTIS

PB95-150223
Temperature Dependence of the Magnetic Excitations in Ordered and Disordered Fe72Pt28.
PB95-150223 *04,563* Not available NTIS

PB95-150231
Integrating Automated Systems with Modular Architecture.
PB95-150231 *00,577* Not available NTIS

PB95-150249
Development of Engineered Stationary Phases for the Separation of Carotenoid Isomers.
PB95-150249 *00,578* Not available NTIS

PB95-150256
Shape Selectivity Assessment of Stationary Phases in Gas Chromatography.
PB95-150256 *00,579* Not available NTIS

PB95-150264
Fire Service and Fire Sciences: A Winning Combination.
PB95-150264 *01,383* Not available NTIS

PB95-150272
Nanostructure Fabrication via Direct Writing with Atoms Focused in Laser Fields.
PB95-150272 *04,564* Not available NTIS

PB95-150280
Cross-Property Relations and Permeability Estimation in Model Porous Media.
PB95-150280 *04,205* Not available NTIS

PB95-150298
Resonance and Threshold Effects in Polarized X-Ray Emission from Atoms and Molecules.
PB95-150298 *03,891* Not available NTIS

PB95-150306
Effect of a Crystal Monochromator on the Local Angular Divergence of an X-Ray Beam.
PB95-150306 *04,565* Not available NTIS

PB95-150314
Exchange Coupling in Magnetic Heterostructures.
PB95-150314 *04,566* Not available NTIS

PB95-150322
Growth of Iron on Iron Whiskers.
PB95-150322 *04,567* Not available NTIS

PB95-150330
Scanning Tunneling Microscopy Study of the Growth of Cr/Fe(001): Correlation with Exchange Coupling of Magnetic Layers.
PB95-150330 *04,568* Not available NTIS

PB95-150348
High Temperature Reliability of Thin Film SiO2.
PB95-150348 *02,333* Not available NTIS

PB95-150355
Calculations of Electron Inelastic Mean Free Paths. 5. Data for 14 Organic Compounds over the 50-2000 eV Range.
PB95-150355 *00,916* Not available NTIS

PB95-150363
DNA Base Modifications in Renal Chromatin of Wistar Rats Treated with a Renal Carcinogen, Ferric Nitrilotriacetate.
PB95-150363 *03,648* Not available NTIS

PB95-150371
Oscillatory Exchange Coupling in Fe/Au/Fe(100).
PB95-150371 *04,569* Not available NTIS

PB95-150389
Performance Evaluation of a New Digital Partial Discharge Recording and Analysis System.
PB95-150389 *01,888* Not available NTIS

PB95-150397
Retinal-Protein Complexes as Optoelectronic Components.
PB95-150397 *02,146* Not available NTIS

PB95-150405
Tolerance Intervals for the Distribution of True Values in the Presence of Measurement Errors.
PB95-150405 *03,434* Not available NTIS

PB95-150413
Band-to-Band Photoluminescence and Luminescence Excitation in Extremely Heavily Carbon-Doped Epitaxial GaAs.
PB95-150413 *04,570* Not available NTIS

PB95-150421
Neutron Reflectometry Studies of Surface Oxidation.
PB95-150421 *00,917* Not available NTIS

PB95-150439
Percolation and Pore Structure in Mortars and Concrete.
PB95-150439 *00,370* Not available NTIS

PB95-150447
Estimate of the Effect of Scale on Radiative Heat Loss Fraction and Combustion Efficiency.
PB95-150447 *02,486* Not available NTIS

PB95-150454
Structural Stabilization of Phase Separating PC/Polyester Blends through Interfacial Modification by Transesterification Reaction.
PB95-150454 *01,239* Not available NTIS

PB95-150462
Effects of Humidity and Elevated Temperature on the Density and Thermal Conductivity of a Rigid Polyisocyanurate Foam Co-Blown with CCl3F and CO2.
PB95-150462 *00,371* Not available NTIS

PB95-150470
Grazing Incidence Prompt Gamma Emissions and Resonance-Enhanced Neutron Standing Waves in a Thin-Film.
PB95-150470 *03,892* Not available NTIS

PB95-150488
Test Structures for Determining Design Rules for Microelectromechanical-Based Sensors and Actuators.
PB95-150488 *02,105* Not available NTIS

PB95-150496
Multiwavelength Birefringent-Cavity Mode-Locked Fibre Laser.
PB95-150496 *04,262* Not available NTIS

PB95-150512
Self-Avoiding Surfaces, Topology, and Lattice Animals.
PB95-150512 *04,571* Not available NTIS

PB95-150520
Developing Linear Error Models for Analog Devices.
PB95-150520 *02,037* Not available NTIS

PB95-150538
Diakoptic and Large Change Sensitivity Analysis.
PB95-150538 *02,038* Not available NTIS

PB95-150546
Excitation of Balmer Lines in Low-Current Discharges of Hydrogen and Deuterium.
PB95-150546 *03,893* Not available NTIS

PB95-150553
Fast Computer Evaluation of Radiative Properties of Hydrogenic Systems.
PB95-150553 *03,894* Not available NTIS

PB95-150561
Contrast Matched Studies of a Sheared Binary Colloidal Suspension.
PB95-150561 *00,918* Not available NTIS

PB95-150579
Electrical Breakdown in Transformer Oil in Large Gaps.
PB95-150579 *01,889* Not available NTIS

PB95-150587
Atomic Manipulation of Polarizable Atoms by Electric Field Directional Diffusion.
PB95-150587 *04,572* Not available NTIS

PB95-150595
Nanoscale Study of the As-Grown Hydrogenated Amorphous Silicon Surface.
PB95-150595 *04,573* Not available NTIS

PB95-150603
Tin Oxide Gas Sensor Fabricated Using CMOS Micro-Hotplates and In-situ Processing.
PB95-150603 *00,580* Not available NTIS

PB95-150611
Microwave Spectra of van der Waals Complexes of Importance in Planetary Atmospheres.
PB95-150611 *00,919* Not available NTIS

PB95-150629
Improved Wavelengths for Prominent Lines of Cr XVI to Cr XXII.
PB95-150629 *03,895* Not available NTIS

PB95-150637
Observation of Pd-Like Resonance Lines Through Pt(32+) and Zn-Like Resonance Lines of Er(38+) and Hf(42+).
PB95-150637 *03,896* Not available NTIS

PB95-150645
Rb-Like Spectra: Pd X to Nd XXIV.
PB95-150645 *03,897* Not available NTIS

PB95-150652
Rh I Isoelectronic Sequence Observed from Er(23+) to Pt(33+).
PB95-150652 *03,898* Not available NTIS

PB95-150660
Spectra of Ag I Isoelectronic Sequence Observed from Er(21+) to Au(32+).
PB95-150660 *03,899* Not available NTIS

PB95-150678
High-Resolution Infrared Spectroscopy of DF Trimer: A Cyclic Ground State Structure and DF Stretch Induced Intramolecular Vibrational Coupling.
PB95-150678 *00,920* Not available NTIS

PB95-150686
Phonon Density of States in R2CuO4 and Superconducting R1.85Ce0.15CuO4 (R = Nd, Pr).
PB95-150686 *04,574* Not available NTIS

PB95-150694
Laser Double Resonance Measurements of the Quenching Rates of Br((2)P1/2) with H20, D20, HDO, and O2.
PB95-150694 *00,921* Not available NTIS

PB95-150702
Direct Dispersion Measurement of Highly-Erbium-Doped Optical Amplifiers Using a Low Coherence Reflectometer Coupled with Dispersive Fourier Spectroscopy.
PB95-150702 *04,263* Not available NTIS

PB95-150710
Deposition of Loosely Bound and Firmly Bound Fluorides on Tooth Enamel by an Acidic Gel Containing Fluorosilicate and Monocalcium Phosphate Monohydrate.
PB95-150710 *03,559* Not available NTIS

PB95-150728
Calculations of Electron Inelastic Mean Free Paths (IMFPs). 4. Evaluation of Calculated IMFPs and of the Predictive IMFP Formula TPP-2 for Electron Energies between 50 and 2000 eV.
PB95-150728 *00,922* Not available NTIS

PB95-150736
Use of Sum Rules on the Energy-Loss Function for the Evaluation of Experimental Optical Data.
PB95-150736 *04,264* Not available NTIS

PB95-150744
Silver Metalization of Octadecanethiol Monolayers Self-Assembled on Gold.
PB95-150744 *00,923* Not available NTIS

PB95-150751
UV-Photopatterning of Alkylthiolate Monolayers Self-Assembled on Gold and Silver.
PB95-150751 *00,924* Not available NTIS

PB95-150769
Analysis of the 5s(2)5p(2)-(5s5p(3)+5s(2)5p5d+5s(2)5p6s) Transitions of Four-Times Ionized Xenon (Xe V).
PB95-150769 *03,900* Not available NTIS

PB95-150777
New International Representations of the Volt and Ohm Effective January 1, 1990.
PB95-150777 *01,890* Not available NTIS

PB95-150785
Flux-Locked Current Source Reference.
PB95-150785 *02,039* Not available NTIS

PB95-150793
Application of Thermodynamics to Biotechnology.
PB95-150793 *03,529* Not available NTIS

PB95-150801
Thermochemistry of the Hydrolysis of L-arginine to (L-citrulline + Ammonia) and of the Hydrolysis of L-arginine to (L-ornithine + Urea).
PB95-150801 *03,463* Not available NTIS

PB95-150819
Activated Dynamics, Loss of Ergodicity, and Transport in Supercooled Liquids.
PB95-150819 *00,925* Not available NTIS

PB95-150827
Using Grafcet to Design Generic Controllers.
PB95-150827 *02,821* Not available NTIS

PB95-150835
Standards for Corrected Fluorescence Spectra.
PB95-150835 *00,581* Not available NTIS

PB95-150843
Insulating Nanoparticles on YBa2Cu3O7-delta Thin Films Revealed by Comparison of Atomic Force and Scanning Tunneling Microscopy.
PB95-150843 *04,575* Not available NTIS

PB95-150850
Lattice Imperfections Studied by Use of Lattice Green's Functions.
PB95-150850 *04,576* Not available NTIS

PB95-150868
Relativistic Effects in Spin-Polarization Parameters for Low-Energy Electron-Cs Scattering.
PB95-150868 *03,901* Not available NTIS

PB95-150876
Characteristics of Partial Pressure Analyzers.
PB95-150876 *00,582* Not available NTIS

PB95-150884
Vacuum Gauges and Partial Pressure Analyzers.
PB95-150884 *02,650* Not available NTIS

PB95-150892
Experimental Data and Theoretical Modeling of Gas Flows Through Metal Capillary Leaks.
PB95-150892 *04,206* Not available NTIS

PB95-150900
Optical Measurements of Atomic Hydrogen, Hydroxyl, and Carbon Monoxide in Hydrocarbon Diffusion Flames.
PB95-150900 *02,487* Not available NTIS

PB95-150918
Evaluation and Retrofit Standards for Existing Federally Owned and Leased Buildings.
PB95-150918 *00,434* Not available NTIS

PB95-150926
Some Basics on Who's Who and What's What in Seismic Safety.
PB95-150926 *00,435* Not available NTIS

PB95-150934
Bistatic Scattering of Absorbing Materials from 30 to 1000 MHz.
PB95-150934 *01,891* Not available NTIS

PB95-150942
Standards: A Cardinal Direction for Geographic Information Systems.
PB95-150942 *03,677* Not available NTIS

PB95-150959
Critical Evaluation of the Purification of Biominerals by Hypochlorite Treatment.
PB95-150959 *00,186* Not available NTIS

PB95-150967
Influence of Natural and Synthetic Inhibitors on the Crystallization of Calcium Oxalate Hydrates.
PB95-150967 *03,560* Not available NTIS

PB95-150975
Effects of Heavy Doping on Numerical Simulations of Gallium Arsenide Bipolar Transistors.
PB95-150975 *02,334* Not available NTIS

PB95-150983
Compensation of Markov Estimator Errors in Time-Jittered Sampling of Nonmonotonic Signals.
PB95-150983 *01,590* Not available NTIS

PB95-150991
Lighting and HVAC.
PB95-150991 *00,250* Not available NTIS

PB95-151007
NIST Lighting and HVAC Interaction Test Facility.
PB95-151007 *00,251* Not available NTIS

PB95-151015
Methyl Torsional Levels of Solid Acetonitrile (CH3CN): A Neutron Scattering Study.
PB95-151015 *00,926* Not available NTIS

PB95-151023
Electronic Spectra of CF2Cl and CFCl2 Radicals Observed by Resonance Enhanced Multiphoton Ionization.
PB95-151023 *00,927* Not available NTIS

PB95-151031
Resonance Enhanced Multiphoton Ionization Spectroscopy of 2-Butene-1-yl (C4H7) between 455-485 nm.
PB95-151031 *00,670* Not available NTIS

PB95-151049
Homogeneous Gas Phase Decyclization of Tetralin and Benzocyclobutene.
PB95-151049 *00,928* Not available NTIS

PB95-151056
Progress in the Development of a Chemical Kinetic Database for Combustion Chemistry.
PB95-151056 *01,384* Not available NTIS

PB95-151064
Mechanism and Rate Constants for the Reactions of Hydrogen Atoms with Isobutene at High Temperatures.
PB95-151064 *00,929* Not available NTIS

PB95-151072
Thermal Stability of Internal Electric Field and Polarization Distribution in Blend of Polyvinylidene Fluoride and Polymethylmethacrylate.
PB95-151072 *01,240* Not available NTIS

PB95-151080
Effects of Calcium Phosphate Solutions on Dentin Permeability.
PB95-151080 *00,157* Not available NTIS

PB95-151098
Preliminary Comparison of Time Transfers via LASSO, GPS and Two-Way Satellite.
PB95-151098 *01,529* Not available NTIS

PB95-151106
Electron and Proton Dosimetry with Custom-Developed Radiochromic Dye Films.
PB95-151106 *03,713* Not available NTIS

PB95-151114
Recent Developments at NIST on Optical Current Sensors and Partial Discharge Diagnostics.
PB95-151114 *02,147* Not available NTIS

PB95-151122
Kinetic-Energy Distributions of K(+) in Argon and Neon in Uniform Electric Fields.
PB95-151122 *03,902* Not available NTIS

PB95-151130
High-Performance Liquid Chromatography of Phytoplankton Pigments Using a Polymeric Reversed-Phase C18 Column.
PB95-151130 *00,583* Not available NTIS

PB95-151148
Experimental Method for Obtaining Critical Densities of Binary Mixtures: Application to Ethane + n-Butane.
PB95-151148 *00,930* Not available NTIS

PB95-151155
Effect of Electrode-Polymer Interfacial Layers on Polymer Conduction. Part 2. Device Summary.
PB95-151155 *02,335* Not available NTIS

PB95-151163
Modified Surface-Active Monomers for Adhesive Bonding to Dentin.
PB95-151163 *00,158* Not available NTIS

PB95-151171
NIR-Spectroscopic Investigation of Water Sorption Characteristics of Dental Resins and Composites.
PB95-151171 *00,189* Not available NTIS

PB95-151189
Guidelines for Refractive Index Measurements of Asbestos.
PB95-151189 *02,543* Not available NTIS

PB95-151197
Factorial Design Techniques Applied to Optimization of AMS Graphite Target Preparation.
PB95-151197 *00,584* Not available NTIS

PB95-151205
Distribution of Fluoride in Saliva and Plaque Fluid After a 0.048 mol/L NaF Rinse.
PB95-151205 *03,561* Not available NTIS

PB95-151213
Regimes of Surface Roughness Measurable with Light Scattering.
PB95-151213 *04,265* Not available NTIS

PB95-151221
Hyperfine Effects and Associative Ionization of Ultracold Sodium.
PB95-151221 *03,903* Not available NTIS

PB95-151239
Electron-Impact Excitation of Si(3+)(3S yields 3P) Using a Merged-Beam Electron-Energy-Loss Technique.
PB95-151239 *03,904* Not available NTIS

PB95-151247
Anisotropic Phase Separation Kinetics in a Polymer Blend Solution Following Cessation of Shear Studied by Light Scattering.
PB95-151247 *01,241* Not available NTIS

PB95-151254
Magneto-Optical Trapping of Metastable Xenon: Isotope-Shift Measurements.
PB95-151254 *03,905* Not available NTIS

PB95-151262
Analysis of Selected Software Safety Standards.
PB95-151262 *01,708* Not available NTIS

PB95-151270
Slant Path Atmospheric Refraction Calibrator: An Instrument to Measure the Microwave Propagation Delays Induced by Atmospheric Water Vapor.
PB95-151270 *01,476* Not available NTIS

PB95-151288
Electron Scattering and Dissociative Attachment by SF6 and Its Electrical-Discharge By-Products.
PB95-151288 *02,256* Not available NTIS

PB95-151296
Approximate Confidence Intervals on Linear Combinations of Expected Mean Squares.
PB95-151296 *03,435* Not available NTIS

PB95-151304
Approximate Confidence Intervals on Positive Linear Combinations of Expected Mean Squares.
PB95-151304 *03,436* Not available NTIS

PB95-151312
Ranges of Confidence Coefficients for Confiedence Intervals on Variance Components.
PB95-151312 *03,437* Not available NTIS

PB95-151320
Technique to Evaluate Benchmarks: A Case Study Using the Livermore Loops.
PB95-151320 *04,577* Not available NTIS

PB95-151338
Effects of Adhesive Thickness, Open Time, and Surface Cleanness on the Peel Strength of Adhesive-Bonded Seams of EPDM Rubber Roofing Membrane.
PB95-151338 *00,372* Not available NTIS

PB95-151346
New Alloys Show Extraordinary Resistance to Fracture and Wear.
PB95-151346 *03,346* Not available NTIS

PB95-151353
Measurements of the Virial Coefficients and Equation of State of the Carbon Dioxide + Ethane System in the Supercritical Region.
PB95-151353 *03,906* Not available NTIS

PB95-151361
Ebulliometric Measurement of the Vapor Pressure of Difluoromethane.
PB95-151361 *00,931* Not available NTIS

PB95-151379
Evaluating Investments in Law Enforcement Equipment: An Annotated Bibliography.
PB95-151379 *04,867* Not available NTIS

PB95-151387
Van der Waals Bond Lengths and Electronic Spectral Shifts of the Benzene-Kr and Benzene-Xe Complexes.
PB95-151387 *00,932* Not available NTIS

PB95-151395
N2(a'(sup 1)Sigma(sub g)(sup +)) Metastable Collisional Destruction and Rotational Excitation Transfer by N2.
PB95-151395 *00,933* Not available NTIS

PB95-151403
Preparation of Immobilized Proteins Covalently Coupled Through Silane Coupling Agents to Inorganic Supports.
PB95-151403 *03,530* Not available NTIS

PB95-151411
Method for the Assay of Hydrolytic Enzymes Using Dynamic Light Scattering.
PB95-151411 *03,531* Not available NTIS

PB95-151429
Bacteriorhodopsin Immobilized in Sol-Gel Glass.
PB95-151429 *03,532* Not available NTIS

PB95-151437
Nonadiabatic Effects in the Photoassociation of H2S.
PB95-151437 *00,934* Not available NTIS

PB95-151445
Smart Clock: A New Time.
PB95-151445 *01,530* Not available NTIS

PB95-151452
Calibration of GPS Equipment in Japan.
PB95-151452 *01,531* Not available NTIS

PB95-151460
Confidence on the Second Difference Estimation of Frequency Drift.
PB95-151460 *01,532* Not available NTIS

PB95-151478
Promise into Practice: Implementing TA2 on Real Clocks at NIST.
PB95-151478 *01,533* Not available NTIS

PB95-151486
How to Verify Reference Materials.
PB95-151486 *03,497* Not available NTIS

PB95-151494
High Resolution Angle Resolved Photoelectron Spectroscopy Study of N2.
PB95-151494 *03,907* Not available NTIS

PB95-151502
Laser Cooling.
PB95-151502 *03,908* Not available NTIS
PB95-151510
Mapping Processes to Processors for Space-Based Robot Systems.
PB95-151510 *04,833* Not available NTIS
PB95-151528
Measuring Matching Wear Scars on Balls and Flats.
PB95-151528 *03,153* Not available NTIS
PB95-151536
Manipulation of Adsorbed Atoms and Creation of New Structures on Room-Temperature Surfaces with a Scanning Tunneling Microscope.
PB95-151536 *04,578* Not available NTIS
PB95-151544
Function of DnaJ and DnaK as Chaperones in Origin-Specific DNA Binding by RepA.
PB95-151544 *03,533* Not available NTIS
PB95-151551
Comprehensive Spectroscopic Data Tabulations and Progress in the Compilation of Atomic Transition Probabilities.
PB95-151551 *03,909* Not available NTIS
PB95-151569
Spectroscopic Data for Fusion Edge Plasmas.
PB95-151569 *04,410* Not available NTIS
PB95-151577
Spectroscopic Diagnostics of Low Temperature Plasmas: Techniques and Required Data.
PB95-151577 *04,411* Not available NTIS
PB95-151585
Spectroscopic Data Tables for Highly-Ionized Atoms.
PB95-151585 *03,910* Not available NTIS
PB95-151593
Accurate Transmission Line Characterization.
PB95-151593 *02,220* Not available NTIS
PB95-151601
Studies of the Higher Order Smectic Phase of the Large Electroclinic Effect Material W317.
PB95-151601 *00,935* Not available NTIS
PB95-151619
Liquid-Hydrogen Cold Neutron Source for the NBSR.
PB95-151619 *03,729* Not available NTIS
PB95-151627
Trapped Atoms and Laser Cooling.
PB95-151627 *03,911* Not available NTIS
PB95-151635
Spin Squeezing and Reduced Quantum Noise in Spectroscopy.
PB95-151635 *03,912* Not available NTIS
PB95-151643
Unusual Spin-Trap Chemistry for the Reaction of Hydroxyl Radical with the Carcinogen N-Nitrosodimethylamine.
PB95-151643 *00,692* Not available NTIS
PB95-151650
Determination of Polycyclic Aromatic Hydrocarbons by Liquid Chromatography.
PB95-151650 *00,585* Not available NTIS
PB95-151668
Standard Reference Materials for the Determination of Polycyclic Aromatic Hydrocarbons in Environmental Samples - Current Activities.
PB95-151668 *00,586* Not available NTIS
PB95-151676
Development of Frozen Whale Blubber and Liver Reference Materials for the Measurement of Organic and Inorganic Contaminants.
PB95-151676 *00,587* Not available NTIS
PB95-151684
Investigation into a Practical Grain Growth Model for Hot Isostatic Pressing.
PB95-151684 *03,347* Not available NTIS
PB95-151692
Mixed Diet Reference Materials for Nutrient Analysis of Foods: Preparation of SRM-1548 Total Diet.
PB95-151692 *03,593* Not available NTIS
PB95-151700
X-Ray Characterization of the Crystallization Process of High-Tc Superconducting Oxides in the Sr-Bi-Pb-Ca-Cu-O System.
PB95-151700 *04,579* Not available NTIS
PB95-151718
Crystal Chemistry and Phase Equilibrium Studies of the BaO(BaCO3)-R2O3-CuO Systems. 5. Melting Relations in Ba2(Y,Nd,Eu)Cu3O6+x.
PB95-151718 *04,580* Not available NTIS
PB95-151726
X-Ray-Diffraction Study of a Thermomechanically Detwinned Single Crystal of YBa2Cu3O6+x.
PB95-151726 *04,581* Not available NTIS
PB95-151734
Crystal Chemistry and Phase Equilibrium Studies of the BaO-R2O3-CuO Systems. 2. X-Ray Characterization and Standard Patterns of BaR2CuO4, R=Lanthanides.
PB95-151734 *04,582* Not available NTIS
PB95-151759
Crystal Chemistry and Phase Equilibria Studies of the BaO(BaCO3)-R2O3-CuO Systems. 4. Crystal Chemistry and Subsolidus Phase Relationship Studies of the CuO-Rich Region of the Ternary Diagrams, R=Lanthanides.
PB95-151759 *00,936* Not available NTIS
PB95-151767
X-Ray Powder Diffraction Data for BaCu(C2O4)2.6H2O.
PB95-151767 *04,583* Not available NTIS
PB95-151775
Photodissociation of Ammonia at 193.3nm: Rovibrational State Distribution of the NH2(A(2)A1) Fragment.
PB95-151775 *00,937* Not available NTIS
PB95-151783
Lighting Quality and Light Source Size.
PB95-151783 *00,252* Not available NTIS
PB95-151791
Lighting Research and Theory Can Create Business Prospects.
PB95-151791 *00,253* Not available NTIS
PB95-151809
Implementation of Executive Order 12699: Seismic Safety of Federal and Federally Assisted or Regulated New Building Construction.
PB95-151809 *00,436* Not available NTIS
PB95-151817
Structural Analysis in Context.
PB95-151817 *00,437* Not available NTIS
PB95-151825
Think Metric.
PB95-151825 *01,298* Not available NTIS
PB95-151833
Potentiometric Enzyme-Amplified Flow Injection Analysis Detection System: Behavior of Free and Liposome-Released Peroxidase.
PB95-151833 *03,534* Not available NTIS
PB95-151841
SANS Study of the Plastic Deformation Mechanism in Polyethylene.
PB95-151841 *01,242* Not available NTIS
PB95-151866
Structural Heterogeneity in Epoxies.
PB95-151866 *01,243* Not available NTIS
PB95-151882
Characterization of Polyquinoline Block Copolymer Using Small Angle Scattering.
PB95-151882 *01,244* Not available NTIS
PB95-151890
Dynamic Light-Scattering Study of a Diluted Polymer Blend Near Its Critical Point.
PB95-151890 *01,245* Not available NTIS
PB95-151908
Integration of Real-Time Process Planning for Small-Batch Flexible Manufacturing.
PB95-151908 *02,822* Not available NTIS
PB95-151916
Ultrasonic Technique for Sizing Voids Using Area Functions.
PB95-151916 *02,904* Not available NTIS
PB95-151924
Pattern-Recognition Analysis of Low-Resolution X-Ray Fluorescence Spectra.
PB95-151924 *00,588* Not available NTIS
PB95-151932
Tomographic Decoding Algorithm for a Nonoverlapping Redundant Array.
PB95-151932 *01,842* Not available NTIS
PB95-151940
Optical Fiber Geometry: Accurate Measurement of Cladding Diameter.
PB95-151940 *04,266* Not available NTIS
PB95-151957
Speed-of-Sound Measurements in Liquid and Gaseous Air.
PB95-151957 *04,186* Not available NTIS
PB95-151965
Modeling Ceramic Sub-Micron Particle Formation from the Vapor Using Detailed Chemical Kinetics: Comparison with In-situ Laser Diagnostics.
PB95-151965 *00,671* Not available NTIS
PB95-151973
Controlled Nucleation in Aerosol Reactors for Supression of Agglomerate Formation.
PB95-151973 *00,672* Not available NTIS
PB95-151981
Flame Synthesis of High Tc Superconductors.
PB95-151981 *00,659* Not available NTIS
PB95-151999
Multiphoton Ionization Spectroscopy Measurements of Silicon Atoms during Vapor Phase Synthesis of Ceramic Particles.
PB95-151999 *03,913* Not available NTIS
PB95-152005
Experimental and Numerical Studies of Refractory Particle Formation in Flames: Application to Silica Growth.
PB95-152005 *00,673* Not available NTIS
PB95-152013
Simulation of Ceramic Particle Formation: Comparison with In-situ Measurements.
PB95-152013 *00,674* Not available NTIS
PB95-152021
Effects of Humidity and Elevated Temperature on the Density and Thermal Conductivity of a Rigid Polyisocyanurate Foam.
PB95-152021 *00,373* Not available NTIS
PB95-152039
Room Temperature Thermal Conductivity of Fumed-Silica Insulation for a Standard Reference Material.
PB95-152039 *00,374* Not available NTIS
PB95-152047
Determination of Inorganic Constituents in Marine Mammal Tissues.
PB95-152047 *00,589* Not available NTIS
PB95-152062
Use of an Environment Classification Model.
PB95-152062 *01,709* Not available NTIS
PB95-152070
IRAS Spectroscopic Observations of Young Planetary Nebulae.
PB95-152070 *00,072* Not available NTIS
PB95-152088
Displacement Method for Machine Geometry Calibration.
PB95-152088 *02,946* Not available NTIS
PB95-152096
Interaction between Dislocations and Intergranular Cracks.
PB95-152096 *03,190* Not available NTIS
PB95-152104
Coupled-Bilayer Two-Dimensional Magnetic Order of the Dy Ions in Dy2Ba4Cu7O15.
PB95-152104 *04,584* Not available NTIS
PB95-152112
Susceptibility Critical Exponent for a Nonaqueous Ionic Binary Mixture Near a Consolute Point.
PB95-152112 *00,938* Not available NTIS
PB95-152120
New Method to Evaluate Deposit Forming Tendencies of Liquid Lubricants by Differential Scanning Calorimetry.
PB95-152120 *01,451* Not available NTIS
PB95-152138
Deposit Forming Tendencies of Diesel Engine Oils-Correlation between the Two-Peak Method and Engine Tests.
PB95-152138 *01,452* Not available NTIS
PB95-152146
Gas Phase Reactivity Study of OH Radicals with 1,1-Dichloroethene and cis-1,1-Dichloroethene and Trans-1,2-Dichloroethene over the Temperature Range 240-400 K.
PB95-152146 *00,939* Not available NTIS
PB95-152153
Rate Constants for the Gas Phase Reactions of the OH Radical with CF3CF2CHCl2 (HCFC-225ca) and CF2ClCF2CHClF (HCFC-225cb).
PB95-152153 *00,940* Not available NTIS
PB95-152161
High-Precision Calculations of Cross Sections for Low-Energy Electron Scattering by Ground and Excited State of Sodium.
PB95-152161 *03,914* Not available NTIS
PB95-152179
Automated Optical Roughness Inspection.
PB95-152179 *02,905* Not available NTIS
PB95-152187
Rotational Far Infrared Spectrum of (13)CO.
PB95-152187 *00,941* Not available NTIS
PB95-152195
Laboratory Measurements for the Astrophysical Identification of MgH.
PB95-152195 *00,073* Not available NTIS
PB95-152203
Atomic Oxygen Fine Structure Splittings with Tunable Far Infrared Spectroscopy.
PB95-152203 *03,915* Not available NTIS
PB95-152211
Microwave and Submillimeter Spectroscopy of Ar-NH3 States Correlating with Ar+NH3(j=1, k=1).
PB95-152211 *00,942* Not available NTIS
PB95-152229
Hybrid Method for Determining Material Properties from Instrumented Micro-Indentation Experiments.
PB95-152229 *03,348* Not available NTIS
PB95-152237
Thermal Behaviour of Methyl Methacrylate and N-Phenyl Maleimide Copolymers.
PB95-152237 *01,246* Not available NTIS
PB95-152245
Effect of Splitting on Estimation of Emission Rate Profiles from Neutron Depth Profiling Spectra.
PB95-152245 *03,916* Not available NTIS
PB95-152252
Analysis of the Effectiveness of Oscillating Radial Collimators in Neutron Scattering Applications.
PB95-152252 *03,917* Not available NTIS
PB95-152260
Neutron Energy Deposition on the Nanometer Scale.
PB95-152260 *03,624* Not available NTIS
PB95-152278
Electrical Test Structure for Overlay Metrology Referenced to Absolute Length Standards.
PB95-152278 *02,336* Not available NTIS
PB95-152286
Representing a Large Collection of Curves: A Case for Principal Points.
PB95-152286 *03,438* Not available NTIS

PB95-152294
Creep Rupture of MoSi2/SiCp Composites.
PB95-152294 *03,154* Not available NTIS

PB95-152302
Anomalous Dispersion and Thermal Expansion in Lightly-Doped KTa1-xNbxO3.
PB95-152302 *04,585* Not available NTIS

PB95-152310
Cryogenic Precision Capacitance Bridge Using a Single Electron Tunneling Electrometer.
PB95-152310 *02,040* Not available NTIS

PB95-152328
Neutron-Scattering Studies of the Two Magnetic Correlation Lengths in Terbium.
PB95-152328 *04,586* Not available NTIS

PB95-152344
Microdosimetry and Cellular Radiation Effects of Radon Progency in Human Bronchial Airways.
PB95-152344 *03,625* Not available NTIS

PB95-152773
Exact Solution of the Steady-State Surface Temperature for a General Multilayer Structure.
PB95-152773 *02,337* Not available NTIS

PB95-152781
Time-Domain Antenna Characterizations.
PB95-152781 *02,003* Not available NTIS

PB95-152799
Resolution of DNA in the Presence of Mobility Modifying Polar and Nonpolar Compounds by Discontinuous Electrophoresis on Rehydratable Polyacrylamide Gels.
PB95-152799 *00,590* Not available NTIS

PB95-152807
Comparisons of Measured Linewidths of Sub-Micrometer Lines Using Optical, Electrical, and SEM Metrologies.
PB95-152807 *02,338* Not available NTIS

PB95-152815
Single-Photon Ionization and Detection of Ga, In, and As(sub n) Species in GaAs Growth.
PB95-152815 *00,591* Not available NTIS

PB95-152823
Crystal Packing Interactions of Two Different Crystal Forms of Bovine Ribonuclease A.
PB95-152823 *00,943* Not available NTIS

PB95-152831
Evaluation of Fracture Toughness and Residual Stress in Dental Porcelain by Indentation-Microfracture Method.
PB95-152831 *00,159* Not available NTIS

PB95-152849
Automatic Calibration of Inductive Voltage Dividers for the NASA Zeno Experiment.
PB95-152849 *02,041* Not available NTIS

PB95-152856
Inductive Voltage Divider Calibration for the NASA Flight Experiment.
PB95-152856 *02,042* Not available NTIS

PB95-152864
Effects of Specimen Edge Conditions on Heat Release Rate.
PB95-152864 *00,375* Not available NTIS

PB95-152872
Thermodynamic Interactions and Correlations in Mixtures of Two Homopolymers and a Block Copolymers by Small Angle Neutron Scattering.
PB95-152872 *01,247* Not available NTIS

PB95-152880
Residual Stresses in Aluminum-Mullite (alpha-Alumina) Composites.
PB95-152880 *03,155* Not available NTIS

PB95-152906
Electron-Impact Ionization of In(+) and Xe(+).
PB95-152906 *03,918* Not available NTIS

PB95-152914
Physics for Device Simulations and Its Verification by Measurements.
PB95-152914 *02,339* Not available NTIS

PB95-152922
Thermal Equilibration Near the Critical Point: Effects Due to Three Dimensions and Gravity.
PB95-152922 *03,919* Not available NTIS

PB95-152930
Memory Function Approach to the Shape of Pressure Broadened Molecular Bands.
PB95-152930 *00,944* Not available NTIS

PB95-152955
Nuclear Heat Load Calculations for the NBSR Cold Neutron Source Using MCNP.
PB95-152955 *03,730* Not available NTIS

PB95-152963
Electrostatic Modes of Ion-Trap Plasmas.
PB95-152963 *03,920* Not available NTIS

PB95-152971
Comment on 'Phase Transitions in Antiferromagnetic Superlattices'.
PB95-152971 *04,587* Not available NTIS

PB95-152989
Interatomic Potential of Argon.
PB95-152989 *00,945* Not available NTIS

PB95-152997
Experimental Study of Reverse-Bias Failure Mechanisms in Bipolar Mode JFET (BMFET).
PB95-152997 *02,340* Not available NTIS

PB95-153003
Image Restoration and Diffusion Processes.
PB95-153003 *01,843* Not available NTIS

PB95-153011
Product State Correlations in the Reaction of O((1)D) and H2O in Bimolecular Collisions and in O3.H2O Clusters--Translation.
PB95-153011 *00,946* Not available NTIS

PB95-153029
Formal Methods in Conformance Testing: Result and Perspectives.
PB95-153029 *01,710* Not available NTIS

PB95-153037
Time-Resolved Measurements of Energy Transfer at Surfaces.
PB95-153037 *00,947* Not available NTIS

PB95-153045
Dynamic Technique for Measuring Normal Spectral Emissivity of Electrically Conducting Solids at High Temperatures with a High-Speed Spatial Scanning Pyrometer.
PB95-153045 *03,921* Not available NTIS

PB95-153052
Publication and Presentation Abstracts, 1993. (Published by Paffenbarger Research Center and Center of Excellence for Materials Science Research).
PB95-153052 *03,562* Not available NTIS

PB95-153060
Effects of Critical Current Density, Equilibrium Magnetization and Surface Barrier on Magnetization of High Temperature Superconductors.
PB95-153060 *04,588* Not available NTIS

PB95-153078
Neutron Focusing Lens Using Polycapillary Fibers.
PB95-153078 *03,922* Not available NTIS

PB95-153094
Model Precast Concrete Beam-to-Column Connections Subject to Cyclic Loading.
PB95-153094 *00,438* Not available NTIS

PB95-153102
Partially Prestressed and Debonded Precast Concrete Beam-Column Joints.
PB95-153102 *00,439* Not available NTIS

PB95-153110
Seismic Performance Behavior of Precast Concrete Beam-Column Joints.
PB95-153110 *00,440* Not available NTIS

PB95-153128
Grazing-Incidence X-Ray Photoelectron Spectroscopy: A Novel Approach to Thin Film Characterization.
PB95-153128 *04,589* Not available NTIS

PB95-153144
Copolymerization of N-Phenyl Maleimide and gamma-Methacryloxypropyl Trimethoxysilane.
PB95-153144 *01,248* Not available NTIS

PB95-153151
Thermal Behavior of 4-Maleimidophenyl Glycidyl Ether Resins.
PB95-153151 *01,249* Not available NTIS

PB95-153169
Effects on Whole Saliva of Chewing Gums Containing Calcium Phosphates.
PB95-153169 *03,563* Not available NTIS

PB95-153177
Vertical-Cavity Optoelectronic Structures: CAD, Growth, and Structural Characterization.
PB95-153177 *02,148* Not available NTIS

PB95-153185
Vertical-Cavity Semiconductor Structures: Materials Characterization.
PB95-153185 *02,149* Not available NTIS

PB95-153193
Vertical-Cavity Semiconductor Lasers: Structural Characterization, CAD, and DFB Structures.
PB95-153193 *02,150* Not available NTIS

PB95-153201
Rotational Dynamics of C60 in Na2RbC60.
PB95-153201 *00,948* Not available NTIS

PB95-153219
Rotational Dynamics of Solid C70: A Neutron-Scattering Study.
PB95-153219 *00,949* Not available NTIS

PB95-153227
New Coaxial Microwave Microcalorimeter Evaluation Technique.
PB95-153227 *01,892* Not available NTIS

PB95-153235
Ultrasonic Measurement of Sheet Anisotropy and Formability.
PB95-153235 *03,213* Not available NTIS

PB95-153250
Transverse Thermomagnetic Effects in the Mixed State and Lower Critical Field of High-Tc Superconductors.
PB95-153250 *04,590* Not available NTIS

PB95-153268
New Mechanisms for Laser Cooling.
PB95-153268 *03,923* Not available NTIS

PB95-153276
Psychological Aspects of Lighting: A Review of the Work of CIE TC 3.16.
PB95-153276 *00,254* Not available NTIS

PB95-153292
Structure and Dynamics of Buckyballs.
PB95-153292 *00,950* Not available NTIS

PB95-153300
Neutron and X-Ray Scattering Cross Sections of Orientationally Disordered Soild C60.
PB95-153300 *00,951* Not available NTIS

PB95-153318
Morphological Stability.
PB95-153318 *04,591* Not available NTIS

PB95-153334
Moisture and Water-Induced Crack Growth in Optical Materials.
PB95-153334 *04,267* Not available NTIS

PB95-153359
Integration of Scanning Tunneling Microscope Nanolithography and Electronics Device Processing.
PB95-153359 *02,341* Not available NTIS

PB95-153367
Piezoelectric and Pyroelectric Polymers.
PB95-153367 *01,250* Not available NTIS

PB95-153375
Extrapolation Chamber Measurements on (90)Sr + (90)Y Beta-Particle Ophthalmic Applicator Dose Rates.
PB95-153375 *03,626* Not available NTIS

PB95-153383
Reference Materials by Isotope Dilution Mass Spectrometry.
PB95-153383 *00,592* Not available NTIS

PB95-153391
High Speed, High Sensitivity Magnetic Field Sensors Based on the Faraday Effect in Iron Garnets.
PB95-153391 *02,151* Not available NTIS

PB95-153409
Magneto-Optic Magnetic Field Sensors Based on Uniaxial Iron Garnet Films in Optical Waveguide Geometry.
PB95-153409 *02,152* Not available NTIS

PB95-153417
Noninvasive High-Voltage Measurement in Mammography by Crystal Diffraction Spectroscopy.
PB95-153417 *00,160* Not available NTIS

PB95-153425
Substrate Specificity of the Escherichia coli Endonuclease III: Excision of Thymine- and Cytosine-Derived Lesions in DNA Produced by Radiation-Generated Free Radicals.
PB95-153425 *03,535* Not available NTIS

PB95-153433
Hydrogen Balmer Alpha Line Shapes for Hydrogen-Argon Mixtures in a Low-Pressure rf Discharge.
PB95-153433 *03,924* Not available NTIS

PB95-153441
Distant Future of Solar Activity: A Case Study of beta Hydri. 3. Transition Region, Corona, and Stellar Wind.
PB95-153441 *00,074* Not available NTIS

PB95-153458
NIST-7, the New US Primary Frequency Standard.
PB95-153458 *01,534* Not available NTIS

PB95-153482
Error Analysis of the NIST Optically Pumped Primary Frequency Standard.
PB95-153482 *01,535* Not available NTIS

PB95-153490
Epitaxial Integration of Single Crystal C60.
PB95-153490 *04,592* Not available NTIS

PB95-153516
Pressure Dependencies of Standard Resistors.
PB95-153516 *02,257* Not available NTIS

PB95-153524
Constant-Width Calibration Intervals for Linear Regression.
PB95-153524 *03,439* Not available NTIS

PB95-153532
Semiclassical Explanation of the Generalized Ramsauer-Townsend Minima in Electron-Atom Scattering.
PB95-153532 *03,925* Not available NTIS

PB95-153540
Even-Odd Asymmetry of a Superconductor Revealed by the Coulomb Blockade of Andreev Reflection.
PB95-153540 *04,593* Not available NTIS

PB95-153557
Preparation of Low Resistivity Contacts for High-Tc Superconductors.
PB95-153557 *02,258* Not available NTIS

PB95-153565
Improved Uniaxial Strain Tolerance of the Critical Current Measured in Ag-Sheathed Bi2Sr2Ca1Cu2O8+x Superconductors.
PB95-153565 *04,594* Not available NTIS

PB95-153573
Terminal Invariant Description of Amplifier Noise.
PB95-153573 *02,043* Not available NTIS

PB95-153599
Liquid Chromatographic Method for the Determination of Carotenoids, Retinoids, and Tocopherols in Human Serum and in Food.
PB95-153599 *00,593* Not available NTIS

PB95-153615
Polarization Effects on Multiple Scattering Gamma Transport.
PB95-153615 *03,926* Not available NTIS

PB95-153649
Surface Topography and Ordering-Variant Segregation in GaInP2.
PB95-153649 *04,595* Not available NTIS

PB95-153656
Performance of Commercial CMOS Foundry-Compatible Multijunction Thermal Converters.
PB95-153656 *02,342* Not available NTIS

PB95-153664
Multijunction Thermal Converters by Commercial CMOS Fabrication.
PB95-153664 *02,343* Not available NTIS

PB95-153698
Origin of the Second Length Scale Above the Magnetic Spiral Phase of Tb.
PB95-153698 *04,596* Not available NTIS

PB95-153714
High-Resolution Spectroscopy of Laser-Cooled Rubidium in a Vapor-Cell Trap.
PB95-153714 *04,268* Not available NTIS

PB95-153722
Volume Magnetic Hysteresis Loss of Nb3Sn Superconductors as a Function of Wire Length.
PB95-153722 *04,597* Not available NTIS

PB95-153730
Dielectric Studies of Fluids with Reentrant Resonators.
PB95-153730 *00,952* Not available NTIS

PB95-153748
Turbulent Spray Burner for Assessing Halon Alternative Fire Suppressants.
PB95-153748 *01,385* Not available NTIS

PB95-153755
New Extrapolation/Spherical/Cylindrical Measurement Facility at the National Institute of Standards and Technology.
PB95-153755 *02,004* Not available NTIS

PB95-153763
Accurate Characterization of High Speed Photodectors.
PB95-153763 *02,153* Not available NTIS

PB95-153771
Frequency Stabilized Lasers: A Parochial Review.
PB95-153771 *04,269* Not available NTIS

PB95-153789
SANS Studies of Space-Time Organization of Structure in Polymer Blends.
PB95-153789 *01,251* Not available NTIS

PB95-153797
Directions in MEMS Research Application Development.
PB95-153797 *02,106* Not available NTIS

PB95-153805
Modeling Buffer Layer IGBTs for Circuit Simulation.
PB95-153805 *02,344* Not available NTIS

PB95-154662
Effective Medium Theory for Ferrite-Loaded Materials.
PB95-154662 *01,893* PC A03/MF A01

PB95-154670
Mapping Integration Definition for Information Modeling (IDEF1X) Model into CASE Data Interchange Format (CDIF) Transfer File.
PB95-154670 *01,711* PC A06/MF A02

PB95-154688
Initial NIST Testing Policy for STEP: Beta Testing Program for AP 203 Implementations. National PDES Testbed Report Series.
PB95-154688 *02,779* PC A03/MF A01

PB95-154696
ISDN LAN Bridging.
PB95-154696 *01,477* PC A03/MF A01

PB95-154704
Rationale and Preliminary Plan for Federal Research for Construction and Building.
PB95-154704 *00,322* PC A07/MF A02

PB95-154720
Review and Upgrading of Military Fastener Test Standard MIL-STD-1312.
PB95-154720 *02,947* PC A07/MF A02

PB95-154738
User Study: Informational Needs of Remote National Archives and Records Administration Customers.
PB95-154738 *02,725* PC A06/MF A02

PB95-154746
Method of Predicting Smoke Movement in Atria with Application to Smoke Management.
PB95-154746 *00,376* PC A05/MF A01

PB95-155552
National Voluntary Laboratory Accreditation Program: Construction Materials Testing.
PB95-155552 *01,319* PC A05/MF A01

PB95-155560
National Voluntary Laboratory Accreditation Program: Carpet and Carpet Cushion.
PB95-155560 *00,295* PC A04/MF A01

PB95-155578
Opportunities for Innovation: Software for Manufacturing.
PB95-155578 *02,851* PC A09/MF A03

PB95-155586
Composite Struts for SMES Plants.
PB95-155586 *02,507* PC A99/MF A06

PB95-159885
Electronics and Electrical Engineering Laboratory 1995 Program Plan. Supporting Technology for U.S. Competitiveness in Electronics.
PB95-159885 *01,894* PC A09/MF A03

PB95-160594
Journal of Research of the National Institute of Standards and Technology, July/August 1994. Volume 99, Number 4. Special Issue: Extreme Value Theory and Applications. Proceedings of the Conference on Extreme Value Theory and Applications, Volume 2. Held at Gaithersburg, Maryland, in May 1993.
PB95-160594 *03,440* PC A13/MF A03

PB95-160602
CSTL Technical Activities, 1993.
PB95-160602 *00,953* PC A17/MF A04

PB95-161014
Simulating the Dynamic Electro Thermal Behavior of Power Electronic Circuits and Systems.
PB95-161014 *02,345* Not available NTIS

PB95-161022
Thermal Component Models for Electro-Thermal Network Simulation.
PB95-161022 *02,346* Not available NTIS

PB95-161030
Visual Road Following without 3-D Reconstruction.
PB95-161030 *01,591* Not available NTIS

PB95-161089
Satellite Two-Way Time Transfer: Fundamentals and Recent Progress.
PB95-161089 *01,536* Not available NTIS

PB95-161097
Neutron Powder Diffraction Study of the Nuclear and Magnetic Structures of the Oxygen-Deficient Perovskite YBaCuCoO5.
PB95-161097 *00,954* Not available NTIS

PB95-161105
Crystal Structure of Annealed and As-Prepared HgBa2CaCu2O6+delta Superconductors.
PB95-161105 *03,927* Not available NTIS

PB95-161113
Calibration of High-Energy Electron Beams by Use of Graphite Calorimeters.
PB95-161113 *04,598* Not available NTIS

PB95-161121
Information Retrieval Using Key Words and a Structured Review.
PB95-161121 *03,724* Not available NTIS

PB95-161139
Harmonic and Static Susceptibilities of YBa2Cu3O7.
PB95-161139 *04,599* Not available NTIS

PB95-161147
Quantum Measurements of Trapped Ions.
PB95-161147 *03,928* Not available NTIS

PB95-161154
Grazing Angle X-Ray Photoemission System for Depth-Dependent Analysis.
PB95-161154 *04,600* Not available NTIS

PB95-161162
Enzyme and Protein Mass Transfer Coefficient in Aqueous Two Phase Systems. 1. Spray Extraction Columns.
PB95-161162 *00,594* Not available NTIS

PB95-161170
SDNS Security Management.
PB95-161170 *01,592* Not available NTIS

PB95-161188
Locating Fire Engineering Information.
PB95-161188 *00,198* Not available NTIS

PB95-161196
Time-Resolved Small-Angle Neutron Scattering Study of Spinodal Decomposition in Deuterated and Protonated Polybutadiene Blends. 1. Effect of Initial Thermal Fluctuations.
PB95-161196 *01,252* Not available NTIS

PB95-161204
Method of Realizing Spectral Irradiance Based on an Absolute Cryogenic Radiometer.
PB95-161204 *04,270* Not available NTIS

PB95-161212
Continuous Counter-Current Two Phase Aqueous Extraction.
PB95-161212 *00,675* Not available NTIS

PB95-161220
Laser Assisted Collisions at Ultracold Temperatures.
PB95-161220 *03,929* Not available NTIS

PB95-161253
Frequency Extension of the NIST AC-DC Difference Calibration Service for Current.
PB95-161253 *01,895* Not available NTIS

PB95-161261
Cryogenic Toughness of Austenitic Stainless Steel Weld Metals: Effect of Inclusions.
PB95-161261 *03,214* Not available NTIS

PB95-161279
Hydrogen in YBa2Cu3Ox: A Neutron Spectroscopy and a Nuclear Magnetic Resonance Study.
PB95-161279 *04,601* Not available NTIS

PB95-161287
Modeling and Test Point Selection for a Thermal Transfer Standard.
PB95-161287 *01,896* Not available NTIS

PB95-161295
Flat and Rising R-Curves for Elliptical Surface Cracks from Indentation and Superposed Flexure.
PB95-161295 *03,156* Not available NTIS

PB95-161303
Tensile Creep of a Silicon Nitride Ceramic.
PB95-161303 *03,049* Not available NTIS

PB95-161311
Sputtered High Temperature Thin Film Thermocouples.
PB95-161311 *02,259* Not available NTIS

PB95-161329
Bending-Induced Phase Shifts in Dual-Mode Planar Optical Waveguides.
PB95-161329 *04,271* Not available NTIS

PB95-161360
Assessment of 'Peaks Over Threshold' Methods for Estimating Extreme Value Distribution Tails.
PB95-161360 *00,441* Not available NTIS

PB95-161378
Elastic Properties of Al2O3/Al Composites: Measurements and Modeling.
PB95-161378 *03,157* Not available NTIS

PB95-161386
Lithium-Drift Technique for Making Submicron Thick Silicon Membranes.
PB95-161386 *02,260* Not available NTIS

PB95-161394
Encouraging Environmentally-Aware Inventions.
PB95-161394 *02,521* Not available NTIS

PB95-161402
Development of the National Marine Mammal Tissue Bank.
PB95-161402 *02,586* Not available NTIS

PB95-161410
Keeping Time on Your PC.
PB95-161410 *01,537* Not available NTIS

PB95-161444
Underflow-Induced Graphics Failure Solved by SLI Arithmetic.
PB95-161444 *01,712* Not available NTIS

PB95-161451
Grain Alignment and Transport Properties of Bi2Sr2CaCu2O8 Grown by Laser Heated Float Zone Method.
PB95-161451 *04,602* Not available NTIS

PB95-161485
Characterization of Unknown Linear Systems Based on Measured CW Amplitude.
PB95-161485 *01,897* Not available NTIS

PB95-161501
Analysis of Physical Properties of Ceramic Powders in an International Interlaboratory Comparison Program.
PB95-161501 *03,050* Not available NTIS

PB95-161519
Optical Fiber Geometry by Gray-Scale Analysis with Robust Regression.
PB95-161519 *04,272* Not available NTIS

PB95-161527
Practical Applications of the ITS-90: Inherent Uncertainties.
PB95-161527 *03,930* Not available NTIS

PB95-161535
Octacalcium Phosphate Carboxylates. 1. Preparation and Identification.
PB95-161535 *00,660* Not available NTIS

PB95-161543
Octacalcium Phosphate Carboxylates. 2. Characterization and Structural Consideration.
PB95-161543 *00,955* Not available NTIS

PB95-161568
Comments on 'Protecting EFIE-Based Scattering Computations from Effects of Internal Resonances'.
PB95-161568 *01,898* Not available NTIS

PB95-161576
Verification of Commercial Probe-Tip Calibrations.
PB95-161576 *02,347* Not available NTIS

PB95-161592
Localization of a Homopolymer Dissolved in a Lamellar Structure of a Block Copolymer Studied by Small-Angle Neutron Scattering.
PB95-161592 *01,253* Not available NTIS

PB95-161600
Effects of Anneal Time and Cooling Rate on the Formation and Texture of Bi2Sr2CaCu2O8 Films.
PB95-161600 *04,603* Not available NTIS

PB95-161618
Laser-Focused Atomic Deposition.
PB95-161618 *04,604* Not available NTIS

PB95-161634
ESR-Based Analysis in Radiation Processing.
PB95-161634 *03,931* Not available NTIS

PB95-161659
Comparison of Elastic and Plastic Contact Models for the Prediction of Thermal Contact Conductance.
PB95-161659 *04,605* Not available NTIS

PB95-161667
Measurement of Surface Tension of Tantalum by a Dynamic Technique in a Microgravity Environment.
PB95-161667 *03,932* Not available NTIS

PB95-161675
ELF Electric and Magnetic Field Measurement Methods.
PB95-161675 *04,423* Not available NTIS

PB95-161691
Molecular Weight Dependence of the Lamellar Domain Spacing of ABC Triblock Copolymers and Their Chain Conformation in Lamellar Domains.
PB95-161691 *01,254* Not available NTIS

PB95-161709
Tunneling Spectroscopy of Thallium-Based High-Temperature Superconductors.
PB95-161709 *04,606* Not available NTIS

PB95-161717
Tunneling Stabilized Magnetic-Force Microscopy.
PB95-161717 *04,607* Not available NTIS

PB95-161733
Magnetic Force Microscopy of Flux in Superconductors.
PB95-161733 *04,608* Not available NTIS

PB95-161741
DNA Base Damage Generated In vivo in Hepatic Chromatin of Mice upon Whole Body y-Irradiation.
PB95-161741 *03,627* Not available NTIS

PB95-161774
Spin-Resolved Elastic Scattering of Electrons from Sodium.
PB95-161774 *03,933* Not available NTIS

PB95-161782
Ultrasonic Method for Reconstructing the Two-Dimensional Liquid-Solid Interface in Solidifying Bodies.
PB95-161782 *03,349* Not available NTIS

PB95-161790
Reactivity of Product Gases Generated in Idealized Enclosure Fire Environments.
PB95-161790 *01,386* Not available NTIS

PB95-161808
Real Time Differential Range Estimation Based on Time-Space Imagery Using PIPE.
PB95-161808 *01,844* Not available NTIS

PB95-161816
Elastic Scattering of Polymer Networks.
PB95-161816 *01,255* Not available NTIS

PB95-161824
Thermoacoustic Technique for Determining the Interface and/or Interply Strength in Polymeric Composites.
PB95-161824 *03,158* Not available NTIS

PB95-161832
New Exact Solution of the One-Dimensional Schrodinger Equation and Its Application to Polarized Neutron Reflectometry.
PB95-161832 *04,609* Not available NTIS

PB95-161840
sigma+-sigma- Optical Molasses in a Longitudinal Magnetic Field.
PB95-161840 *03,934* Not available NTIS

PB95-161865
Neutron Scattering Study of Shear Induced Turbidity in Polystyrene Dissolved in Dioctyl Phthalate.
PB95-161865 *01,256* Not available NTIS

PB95-161873
Slit Jet Infrared Spectroscopy of Hydrogen Bonded N2HF Isotopomers: Rotational Rydberg-Klein-Rees Analysis and H/D Dependent Vibrational Predissociation Rates.
PB95-161873 *00,956* Not available NTIS

PB95-161881
Standards and Linkages: What Data Sharing Needs.
PB95-161881 *01,713* Not available NTIS

PB95-161907
Water Mist Fire Suppression Workshop Summary.
PB95-161907 *02,853* Not available NTIS

PB95-161915
Optically Linked Three-Loop Antenna System for Determining the Radiation Characteristics of an Electrically Small Source.
PB95-161915 *02,005* Not available NTIS

PB95-161949
Detector-Based Candela Scale and Related Photometric Calibration Procedures at NIST.
PB95-161949 *04,273* Not available NTIS

PB95-161964
Kinetic-Energy Distributions of Ions Sampled from Argon Plasmas in a Parallel-Plate, Radio-Frequency Reference Cell.
PB95-161964 *03,935* Not available NTIS

PB95-161972
Wear of Human Enamel against a Commercial Castable Ceramic Restorative Material.
PB95-161972 *00,161* Not available NTIS

PB95-161980
Amperometric Flow-Injection Analysis Biosensor for Glucose Based on Graphite Paste Modified with Tetracyanoquinodimethane.
PB95-161980 *03,498* Not available NTIS

PB95-161998
Two Phase Aqueous Extraction: Rheological Properties of Dextran, Polyethylene Glycol, Bovine Serum Albumin and Their Mixtures.
PB95-161998 *00,676* Not available NTIS

PB95-162004
Comparison of the Unidirectional and Radial In-Plane Flow of Fluids Through Woven Composite Reinforcements.
PB95-162004 *02,698* Not available NTIS

PB95-162012
Interaction between Micro and Macroscopic Flow in RTM Preforms.
PB95-162012 *03,159* Not available NTIS

PB95-162020
Bragg Gratings in Optical Fibers Produced by a Continuous-Wave Ultraviolet Source.
PB95-162020 *04,274* Not available NTIS

PB95-162038
Growth of Bragg Gratings Produced by Continuous-Wave Ultraviolet Light in Optical Fiber.
PB95-162038 *04,275* Not available NTIS

PB95-162046
New Concepts for Fire Protection of Passenger Rail Transportation Vehicles.
PB95-162046 *04,850* Not available NTIS

PB95-162053
Production and Characterization of Ion Beam Sputtered Multilayers.
PB95-162053 *03,936* Not available NTIS

PB95-162061
Broadband Mismatch Error in Noise Measurement Systems.
PB95-162061 *02,044* Not available NTIS

PB95-162079
Assessing Ventilation Effectiveness in Mechanically Ventilated Office Buildings.
PB95-162079 *00,255* Not available NTIS

PB95-162087
Modeling Radon Transport in Multistory Residential Buildings.
PB95-162087 *00,256* Not available NTIS

PB95-162095
Ventilation, Carbon Dioxide and ASHRAE Standard 62-1989.
PB95-162095 *02,544* Not available NTIS

PB95-162111
Micromagnetic Structure of Domains in Co/Pt Multilayers. 1. Investigations of Wall Structure.
PB95-162111 *04,610* Not available NTIS

PB95-162129
X-ray Mask Metrology: The Development of Linewidth Standards for X-ray Lithography.
PB95-162129 *02,348* Not available NTIS

PB95-162152
Diffusion of Copper into Gold Plating.
PB95-162152 *00,957* Not available NTIS

PB95-162160
Laser-Induced Fluorescence Measurements of OH. Concentrations in the Oxidation Region of Laminar, Hydrocarbon Diffusion Flames.
PB95-162160 *01,387* Not available NTIS

PB95-162194
Fracture Toughness of Advanced Ceramics at Room Temperature: A Vamas Round-Robin.
PB95-162194 *03,160* Not available NTIS

PB95-162202
Dimensional Characterization of Small Bores: A Survey.
PB95-162202 *02,651* Not available NTIS

PB95-162210
Condensed Catalogue of Electromagnetic Environment Measurements, 30 - 300 Hz.
PB95-162210 *01,899* Not available NTIS

PB95-162228
Protein Extraction in a Spray Column Using a Polyethylene Glycol Maltodextrin Two-Phase Polymer System.
PB95-162228 *00,595* Not available NTIS

PB95-162236
Reconstruction during Camera Fixation.
PB95-162236 *01,593* Not available NTIS

PB95-162244
Unified Approach to Camera Fixation and Vision-Based Road Following.
PB95-162244 *01,594* Not available NTIS

PB95-162251
Ring-Opening Dental Resin Systems Based on Cyclic Acetals.
PB95-162251 *00,162* Not available NTIS

PB95-162269
Neutron-Scattering Study of Librations and Intramolecular Phonons in Rb2.6K0.4C60.
PB95-162269 *00,958* Not available NTIS

PB95-162277
Development of a Gas Standard Reference Material Containing Eighteen Volatile Organic Compounds.
PB95-162277 *02,545* Not available NTIS

PB95-162285
Stability/Instability of Gas Mixtures Containing 1,3-Butadiene in Treated Aluminum Gas Cylinders.
PB95-162285 *02,546* Not available NTIS

PB95-162293
Magnetic Rare Earth Artificial Metallic Superlattices.
PB95-162293 *04,611* Not available NTIS

PB95-162301
Global Density Effects on the Self-Preservation Behavior of Turbulent Free Jets.
PB95-162301 *04,207* Not available NTIS

PB95-162319
Laser-Induced Desorption of NO from Si(111): Effects of Coverage on NO Vibrational Populations.
PB95-162319 *00,959* Not available NTIS

PB95-162327
Evidence of Film-Induced Cleavage by Electrodeposited Rhodium.
PB95-162327 *03,191* Not available NTIS

PB95-162335
Development of Adaptive Control Strategies for Inert Gas Atomization.
PB95-162335 *02,823* Not available NTIS

PB95-162343
Process Modeling and Control of Inert Gas Atomization.
PB95-162343 *02,824* Not available NTIS

PB95-162350
Stabilization and Precise Calibration of a Continuous-Wave Difference Frequency Spectrometer by Use of a Simple Transfer Cavity.
PB95-162350 *04,276* Not available NTIS

PB95-162368
Viscosity of the Saturated Liquid Phase of Six Halogenated Compounds and Three Mixtures.
PB95-162368 *00,960* Not available NTIS

PB95-162376
Data Encryption Standard.
PB95-162376 *01,595* Not available NTIS

PB95-162384
Resonant-Photoemission Investigation of the Heusler Alloys Ni2MnSb and NiMnSb.
PB95-162384 *04,612* Not available NTIS

PB95-162392
Lineshape Analysis of the Raman Spectrum of Diamond Films Grown by Hot-Filament and Microwave-Plasma Chemical-Vapor Deposition.
PB95-162392 *03,016* Not available NTIS

PB95-162400
Studies of Defects in Diamond Films and Particles by Raman and Luminescence Spectroscopies.
PB95-162400 *03,017* Not available NTIS

PB95-162418
Surface Roughness Evaluation of Diamond Films Grown on Substrates with a High Density of Nucleation Sites.
PB95-162418 *03,018* Not available NTIS

PB95-162426
Polarization Dependence of Response Functions in 3x3 Sagnac Optical Fiber Current Sensors.
PB95-162426 *02,154* Not available NTIS

PB95-162434
Loading Device for Fracture Testing of Compact Tension Specimens in the Scanning Electron Microscope.
PB95-162434 *02,652* Not available NTIS

PB95-162442
Temperature Dependence of Vortex Twin Boundary Interaction in Yttrium Barium Copper Oxide (YBa2Cu3O6+x).
PB95-162442 *04,613* Not available NTIS

PB95-162459
Simultaneous Forward-Backward Raman Scattering Studies of D2 Broadened by D2, He, and Ar.
PB95-162459 *00,961* Not available NTIS

PB95-162467
Submicroampere-Per-Root-Hertz Current Sensor Based on the Faraday Effect in Ga: YIG.
PB95-162467 *02,155* Not available NTIS

PB95-162475
Sorption of Moisture on Epoxy and Alkyd Free Films and Coated Steel Panels.
PB95-162475 *03,192* Not available NTIS

PB95-162491
Characteristics of Adhesive-Bonded Seams Sampled from EPDM Roof Membranes.
PB95-162491 *00,377* Not available NTIS

PB95-162509
Vibronic Coupling and Other Many-Body Effects in the 4sigmag(-1) Photoionization Channel of CO2.
PB95-162509 *00,962* Not available NTIS

PB95-162517
Introduction to ASTM 1199 'Wear Test Selection for Design and Application'.
PB95-162517 *03,238* Not available NTIS

PB95-162525
Access Paths for Materials Databases: Approaches for Large Databases and Systems.
PB95-162525 *02,975* Not available NTIS

PB95-162533
Fabrication of Flaw-Tolerant Aluminum-Titanate-Reinforced Alumina.
PB95-162533 *03,161* Not available NTIS

PB95-162541
Growth of Laser Ablated YBa2Cu3O7-delta Films as Examined by Rheed and Scanning Tunneling Microscopy.
PB95-162541 *04,614* Not available NTIS

PB95-162574
Labeling Conventions in Isoelectronic Sequences - Reply.
PB95-162574 *03,937* Not available NTIS

PB95-162608
Shape Selectivity in Reversed-Phase Liquid Chromatography for the Separation of Planar and Non-Planar Solutes.
PB95-162608 *00,596* Not available NTIS

PB95-162624
Description of Layered Structures: Applications to High Tc Superconductors.
PB95-162624 *04,615* Not available NTIS

PB95-162632
Radiation Process Data: Collection, Analysis, and Interpretation.
PB95-162632 *03,628* Not available NTIS

PB95-162640
Determination of PCBs and Chlorinated Hydrocarbons in Marine Mammal Tissues.
PB95-162640 *03,744* Not available NTIS

PB95-162657
Surface Magnetic Microstructural Analysis Using Scanning Electron Microscopy with Polarization Analysis (SEMPA).
PB95-162657 *03,938* Not available NTIS

PB95-162673
Noncontact Ultrasonic Inspection of Train Rails for Stress.
PB95-162673 *04,851* Not available NTIS

PB95-162681
Recent VAMAS Activity in Ceramics.
PB95-162681 *03,051* Not available NTIS

PB95-162707
Biological Thermodynamic Data for the Calibration of Differential Scanning Calorimeters: Dynamic Temperature Data on the Gel to Liquid Crystal Phase Transition of Dialkylphosphatidylcholine in Water Suspensions.
PB95-162707 *03,464* Not available NTIS

PB95-162715
Thermodynamics of the Binding of Galactopyranoside Derivatives to the Basic Lectin from Winged Bean (Psophocarpus Tetrogonolobus).
PB95-162715 *03,465* Not available NTIS

PB95-162723
Vehicle-Command Center Communications in a Robotic Vehicle System.
PB95-162723 *03,665* Not available NTIS

PB95-162731
Fundamental Studies of Gas Sensor Response Mechanisms: Palladium on SnO2(110).
PB95-162731 *00,963* Not available NTIS

PB95-162749
Critical Current Density, Irreversibility Line, and Flux Creep Activation Energy in Silver-Sheathed Bi2Sr2Ca2Cu2Ox Superconducting Tapes.
PB95-162749 *04,616* Not available NTIS

PB95-162756
Temperature Dependence of the Rate Constants for Reaction of Dihalide and Azide Radicals with Inorganic Reductants.
PB95-162756 *00,964* Not available NTIS

PB95-162764
Iodine Atoms and Iodomethane Radical Cations: Their Formation in the Pulse Radiolysis of Iodomethane in Organic Solvents, Their Complexes, and Their Reactivity with Organic Reductants.
PB95-162764 *00,965* Not available NTIS

PB95-162780
Nanocomposite Magnetic Materials.
PB95-162780 *04,617* Not available NTIS

PB95-162798
Magnetocaloric Effect in Nanocomposites.
PB95-162798 *04,618* Not available NTIS

PB95-162806
Preparation of 2-Dimensional Ultra Thin Polystyrene Film by Water Casting Method.
PB95-162806 *04,619* Not available NTIS

PB95-162814
Ionization Energy of Sulfur Pentafluoride and the Sulfur Pentafluoride-Fluorine Atom Bond Dissociation Energy.
PB95-162814 *00,966* Not available NTIS

PB95-162822
Ca1-xCuO2, a NaCuO2-Type Related Structure.
PB95-162822 *04,620* Not available NTIS

PB95-162855
Status Report: AWS Standards for Identifying Arc Welds (A91.1) and Recording Weld Data (A9.2).
PB95-162855 *02,861* Not available NTIS

PB95-162863
Computers in Welding: A Primer.
PB95-162863 *02,862* Not available NTIS

PB95-162871
Through-the-Arc Sensing for Real-Time Measurement of Gas Metal Arc Weld Quality.
PB95-162871 *02,863* Not available NTIS

PB95-162889
Welding for Cryogenic Service.
PB95-162889 *02,852* Not available NTIS

PB95-162897
Algebraic Approximation of Attractors for Galloping Oscillators.
PB95-162897 *04,820* Not available NTIS

PB95-162905
Leady Axisymmetric Modes in Infinite Clad Rods. Part 1.
PB95-162905 *04,187* Not available NTIS

PB95-162913
Exposure: An Expert System Fire Code.
PB95-162913 *04,868* Not available NTIS

PB95-162939
Forum for International Cooperation on Fire Research.
PB95-162939 *04,869* Not available NTIS

PB95-162947
Fresh Look at Strategies for Fire Safety.
PB95-162947 *04,870* Not available NTIS

PB95-162954
Dose Mapping of Radioactive Hot Particles Using Radiochromic Film.
PB95-162954 *03,714* Not available NTIS

PB95-162962
Electrical Sensors for Monitoring rf Plasma Sheaths.
PB95-162962 *04,412* Not available NTIS

PB95-162970
Systematic Studies of the Effect of a Bandpass Filter on a Josephson-Junction Noise Thermometer.
PB95-162970 *03,939* Not available NTIS

PB95-162988
Systematic Studies of the Effect of a Post-Detection Filter on a Josephson-Junction Noise Thermometer.
PB95-162988 *03,940* Not available NTIS

PB95-163002
Anisotropy of Polarized X-ray Emission from Atoms and Molecules.
PB95-163002 *04,621* Not available NTIS

PB95-163028
Effects of Elastic Stress on the Stability of a Solid-Liquid Interface.
PB95-163028 *03,350* Not available NTIS

PB95-163036
Electrophoretic Separations of Polymerase Chain Reaction: Amplified DNA Fragments in DNA Typing Using a Capillary Electrophoresis-Lased Induced Fluorescence System.
PB95-163036 *03,536* Not available NTIS

PB95-163044
Synthesis and Polymerization of Difunctional and Multifunctional Monomers Capable of Cyclopolymerization.
PB95-163044 *01,257* Not available NTIS

PB95-163051
Diamond and Graphite Precursors: Comments.
PB95-163051 *00,967* Not available NTIS

PB95-163069
Real-Time Small-Angle X-Ray Scattering Study of the Early Stage of Phase Separation in the SiO2-BaO-K20 System.
PB95-163069 *03,052* Not available NTIS

PB95-163077
Automated Inspection: The Integration of National Standards and Commercial Products at NIST.
PB95-163077 *02,906* Not available NTIS

PB95-163093
Two New Probes for a Coordinate Measuring Machine.
PB95-163093 *02,653* Not available NTIS

PB95-163101
Trace Elements Associated with Proteins. Neutron Activation Analysis Combined with Biological Isolation Techniques.
PB95-163101 *00,597* Not available NTIS

PB95-163127
Observations of Partial Discharges in Hexane Under High Magnification.
PB95-163127 *01,900* Not available NTIS

PB95-163150
Rheology of Fresh Cement Paste.
PB95-163150 *00,378* Not available NTIS

PB95-163168
Cement and Concrete Characterization by Scanning Electron Microscopy.
PB95-163168 *00,379* Not available NTIS

PB95-163176
ISDN Conformance Testing.
PB95-163176 *01,478* Not available NTIS

PB95-163192
Glucose Permease of Bacillus Subtilis Is a Single Polypeptide Chain That Functions to Energize the Sucrose Permease.
PB95-163192 *03,466* Not available NTIS

PB95-163200
Control System Architecture for a Remotely Operated Unmanned Land Vehicle.
PB95-163200 *03,759* Not available NTIS

PB95-163218
Diode-Laser Pumped, Rubidium Cell Frequency Standards.
PB95-163218 *01,538* Not available NTIS

PB95-163226
Problems Related to the Determination of Mass Densities of Evaporated Reference Deposits.
PB95-163226 *03,941* Not available NTIS

PB95-163234
In-Space Welding: Visions and Realities.
PB95-163234 *04,830* Not available NTIS

PB95-163259
Evaluating the Seismic Performance of Lightly-Reinforced Circular Concrete Bridge Columns.
PB95-163259 *01,335* Not available NTIS

PB95-163267
Jacket Thickness Requirements for Seismic Retrofitting of Circular Bridge Columns.
PB95-163267 *01,336* Not available NTIS

PB95-163283
How Accurate Are the Josephson and Quantum Hall Effects and QED.
PB95-163283 *03,942* Not available NTIS

PB95-163291
Electropermeabilization of Cell Membranes: Effect of the Resting Membrane Potential.
PB95-163291 *03,537* Not available NTIS

PB95-163309
Data-Parallel Algorithm for Three-Dimensional Delaunay Triangulation and Its Implementation.
PB95-163309 *01,714* Not available NTIS

PB95-163317
Equilibrium and Calorimetric Investigation of the Hydrolysis of L-Tryptophan to (Indole + Pyruvate + Ammonia).
PB95-163317 *00,661* Not available NTIS

PB95-163325
Elastic Green's Function for a Bimaterial Composite Solid Containing a Free Surface Normal to the Interface.
PB95-163325 *03,162* Not available NTIS

PB95-163333
Green's Function for Generalized Hilbert Problem for Cracks and Free Surfaces in Composite Materials.
PB95-163333 *03,163* Not available NTIS

PB95-163341
Generalized Plane Strain Analysis of a Bimaterial Composite Containing a Free Surface Normal to the Interface.
PB95-163341 *03,164* Not available NTIS

PB95-163358
Observation of Insulating Nanoparticles on YBCO Thin-Films by Atomic Force Microscopy.
PB95-163358 *04,622* Not available NTIS

PB95-163366
Elastic Properties of Central-Force Networks with Bond-Length Mismatch.
PB95-163366 *04,623* Not available NTIS

PB95-163374
Microbial Degradation of Polysulfides and Insights into Their Possible Occurrence in Coal.
PB95-163374 *02,488* Not available NTIS

PB95-163382
Gravity Dependent Processes and Intracellular Motion.
PB95-163382 *03,538* Not available NTIS

PB95-163390
Geographic Information Systems Standards: A Federal Perspective.
PB95-163390 *03,678* Not available NTIS

PB95-163424
Trace Detection in Conducting Solids Using Laser-Induced Fluorescence in a Cathodic Sputtering Cell.
PB95-163424 *00,598* Not available NTIS

PB95-163432
Computer Security Management and Planning in the U.S. Federal Government.
PB95-163432 *01,596* Not available NTIS

PB95-163440
Guidance to Federal Agencies on the Use of Trusted Systems.
PB95-163440 *01,597* Not available NTIS

PB95-163457
Incinerability of Perchloroethylene and Chlorobenzene.
PB95-163457 *01,388* Not available NTIS

PB95-163465
Shock Tube Techniques in Chemical Kinetics.
PB95-163465 *00,968* Not available NTIS

PB95-163473
Hydrogen Atom Attack on Perchloroethylene.
PB95-163473 *00,969* Not available NTIS

PB95-163481
Wall Flame Heights with External Radiation.
PB95-163481 *00,380* Not available NTIS

PB95-163499
Determination of Thermoactivation Parameters of Vortex Mobility in YBa2Cu3O7 Using Only Magnetic Measurements.
PB95-163499 *04,624* Not available NTIS

PB95-163507
Effect of Ethanol on the Solubility of Dicalcium Phosphate Dihydrate in the System Ca(OH)2-H3PO4-H2O at 37C.
PB95-163507 *00,163* Not available NTIS

PB95-163523
Neutron Spectroscopic Comparison of Rare-Earth/Hydrogen alpha-Phase Systems.
PB95-163523 *00,970* Not available NTIS

PB95-163531
Photoelectron Study of Electronic Autoionization in Rotationally Cooled N2: The n=6 Member of the Hopfield Series.
PB95-163531 *00,971* Not available NTIS

PB95-163556
SEMPA Studies of Oscillatory Exchange Coupling.
PB95-163556 *04,625* Not available NTIS

PB95-163564
Experimental Verification of a Vector Preisach Model.
PB95-163564 *04,626* Not available NTIS

PB95-163572
Importance of Unraveling Memory Propagation Effects in Interpreting Data on Partial Discharge Statistics.
PB95-163572 *01,901* Not available NTIS

PB95-163580
Nonstationary Behavior of Partial Discharge during Insulation Aging.
PB95-163580 *01,902* Not available NTIS

PB95-163598
Partial Discharge: Induced Aging of Cast Epoxies and Related Nonstationary Behavior of the Discharge Statistics.
PB95-163598 *01,903* Not available NTIS

PB95-163606
Laser Spectroscopy of Carbon Monoxide: A Frequency Reference for the Far Infrared.
PB95-163606 *04,277* Not available NTIS

PB95-163614
Variations in Size Measurements by Indicating Gaging Systems.
PB95-163614 *02,864* Not available NTIS

PB95-163622
Standards for Atmospheric Measurements.
PB95-163622 *02,547* Not available NTIS

PB95-163655
Computer Virus Attacks.
PB95-163655 *01,715* Not available NTIS

PB95-163663
Comparison of Three Techniques for the Precision Measurement of Amplifier Noise.
PB95-163663 *02,349* Not available NTIS

PB95-163671
Measurement Accuracies for Various Techniques for Measuring Amplifier Noise.
PB95-163671 *02,350* Not available NTIS

PB95-163689
Application Profile for ISDN.
PB95-163689 *01,479* Not available NTIS

PB95-163697
Planar Resistors for Probe Station Calibration.
PB95-163697 *02,351* Not available NTIS

PB95-163705
Atmospheric Reactivity of alpha-Methyl-Tetrahydrofuran.
PB95-163705 *02,548* Not available NTIS

PB95-163713
High Spectral Purity X-Band Source.
PB95-163713 *02,045* Not available NTIS

PB95-163721
High Critical Temperature Superconductor Tunneling Spectroscopy Using Squeezable Electron Tunneling Junctions.
PB95-163721 *04,627* Not available NTIS

PB95-163739
Tunneling Measurement of the Zero-Bias Conductance Peak and the Bi-Sr-Ca-Cu-O Thin-Film Energy Gap.
PB95-163739 *04,628* Not available NTIS

PB95-163747
In situ Burning of Oil Spills: Mesoscale Experiments and Analysis.
PB95-163747 *02,587* Not available NTIS

PB95-163754
Measurement of the Uniformity of Particle Deposition of Filter Cassette Sampling in a Low Velocity Wind Tunnel.
PB95-163754 *02,549* Not available NTIS

PB95-163770
Applications of Fluorescence Spectroscopy in Polymer Science and Technology.
PB95-163770 *01,258* Not available NTIS

PB95-163796
Wear Model for Alumina Sliding Wear.
PB95-163796 *03,239* Not available NTIS

PB95-163804
Pulse-Echo Ultrasonic Evaluation of the Integrity of Seams of Single-Ply Roof Membranes.
PB95-163804 *00,381* Not available NTIS

PB95-163812
Criteria for Establishing Accurate Vapor Pressure Curves.
PB95-163812 *00,972* Not available NTIS

PB95-163820
Affinity Chromatography on Inorganic Support Materials.
PB95-163820 *03,467* Not available NTIS

PB95-163838
Confidence on the Three-Point Estimator of Frequency Drift.
PB95-163838 *01,539* Not available NTIS

PB95-163853
Use of Ionospheric Data in GPS Time Transfer.
PB95-163853 *01,540* Not available NTIS

PB95-163861
Series Array of DC SQUIDs.
PB95-163861 *02,046* Not available NTIS

PB95-163879
Measurements of Fluorescence from Cold Atoms: Localization in Three-Dimensional Standing Waves.
PB95-163879 *03,943* Not available NTIS

PB95-163887
Localization of Atoms in a Three-Dimensional Standing Wave.
PB95-163887 *03,944* Not available NTIS

PB95-163895
Configuration and Performance Evaluation of a Real-Time Robot Control System: A Skeleton Approach.
PB95-163895 *01,598* Not available NTIS

PB95-163911
Deletion Analysis of the Mini-P1 Plasmid Origin of Replication and the Role of E.coli DnaA Protein.
PB95-163911 *03,539* Not available NTIS

PB95-163929
Creep and Creep Rupture of Ceramic Matrix Composites.
PB95-163929 *03,165* Not available NTIS

PB95-163945
Calibrating On-Wafer Probes to the Probe Tips.
PB95-163945 *02,352* Not available NTIS

PB95-163952
LRM Probe-Tip Calibrations with Imperfect Resistors and Lossy Lines.
PB95-163952 *02,353* Not available NTIS

PB95-163960
Verification of Scattering Parameter Measurements.
PB95-163960 *01,904* Not available NTIS

PB95-163978
Cold Neutron Gain Calculations for the NBSR Using MCNP.
PB95-163978 *03,731* Not available NTIS

PB95-163986
Measurement of the (93)Nb(n,2n) (92m)Nb Cross Section in a (235)U Fission Spectrum.
PB95-163986 *03,945* Not available NTIS

PB95-163994
Self-Organizing Neural Network Character Recognition on a Massively Parallel Computer.
PB95-163994 *01,845* Not available NTIS

PB95-164000
XUV Characterization Comparison of Mo/Si Multilayer Coatings.
PB95-164000 *04,278* Not available NTIS

PB95-164026
Standard Reference Materials for the Determination of Trace Organic Constituents in Environmental Samples.
PB95-164026 *02,522* Not available NTIS

PB95-164034
Quality Assurance of Contaminant Measurements in Marine Mammal Tissues.
PB95-164034 *02,588* Not available NTIS

PB95-164042
Liquid Chromatographic Determination of Polycyclic Aromatic Hydrocarbon Isomers of Molecular Weight 278 and 302 in Environmental Standard Reference Materials.
PB95-164042 *02,523* Not available NTIS

PB95-164059
Molecular Orbital Calculations of Bond Rupture in Brittle Solids.
PB95-164059 *00,973* Not available NTIS

PB95-164067
Molecular Orbital Study of Water Enhanced Crack Growth Process.
PB95-164067 *03,240* Not available NTIS

PB95-164075
Physics-Based Vision: Principles and Practice, Shape Recovery (Book Review).
PB95-164075 *01,846* Not available NTIS

PB95-164091
Lessons from the Loma Prieta Earthquake.
PB95-164091 *00,442* Not available NTIS

PB95-164109
Characterization of Molecular Network of Thermosets Using Neutron Scattering.
PB95-164109 *01,259* Not available NTIS

PB95-164117
Small-Angle Neutron Scattering of Poly(vinyl alcohol) Gels.
PB95-164117 *01,260* Not available NTIS

PB95-164125
Characterization of Polyquinoline Blends Using Small Angle Scattering.
PB95-164125 *01,261* Not available NTIS

PB95-164133
Integrated Mobile Robot System for Testing Vision Algorithms.
PB95-164133 *02,936* Not available NTIS

PB95-164158
Asperity-Asperity Contact Mechanisms Simulated by a Two-Ball Collision Apparatus.
PB95-164158 *02,966* Not available NTIS

PB95-164174
Anomalous Behavior of a Quantized Hall Plateau in a High-Mobility Si Metal-Oxide-Semiconductor Field-Effect Transistor.
PB95-164174 *02,354* Not available NTIS

PB95-164182
Vector Theory of Diffraction by a Single-Mode Fiber: Application to Mode-Field Diameter Measurements.
PB95-164182 *04,279* Not available NTIS

PB95-164224
Analytic Calculation of Polarized Neutron Reflectivity from Superconductors.
PB95-164224 *04,629* Not available NTIS

PB95-164232
Thermal and Nonequilibrium Responses of Superconductors for Radiation Detectors.
PB95-164232 *02,156* Not available NTIS

PB95-164240
Dislocation Emission at Ledges on Cracks.
PB95-164240 *04,630* Not available NTIS

PB95-164257
Shielding of Cracks in a Plastically Polarizable Material.
PB95-164257 *04,631* Not available NTIS

PB95-164273
Electrical Test Structure for Improved Measurement of Feature Placement and Overlay in Integrated Circuit Fabrication Processes.
PB95-164273 *02,355* Not available NTIS

PB95-164281
Laser Flash Photolysis/Time-Resolved FTIR Emission Study of a New Channel in the Reaction of CH3+O: Production of CO(v).
PB95-164281 *00,974* Not available NTIS

PB95-164299
Hg1-xCdxTe Characterization Measurements: Current Practice and Future Needs.
PB95-164299 *02,157* Not available NTIS

PB95-164307
Brownian Diffusion of Hard Spheres at Finite Concentrations.
PB95-164307 *00,975* Not available NTIS

PB95-164315
Bonding in Doubly Charged Diatomics.
PB95-164315 *00,976* Not available NTIS

PB95-164323
Application of the Taylor Dispersion Method in Supercritical Fluids.
PB95-164323 *00,977* Not available NTIS

PB95-164331
Critical Behavior of Ionic Fluids.
PB95-164331 *00,978* Not available NTIS

PB95-164349
Standard States, Reference States and Finite-Concentration Effects in Near-Critical Mixtures with Applications to Aqueous Solutions.
PB95-164349 *00,979* Not available NTIS

PB95-164356
Effect of Annealing Ambient on the Removal of Oxide Precipitates in High-Dose Oxygen Implanted Silicon.
PB95-164356 *02,356* Not available NTIS

PB95-164372
Small Angle Neutron Scattering Studies on Chain Asymmetry of Coextruded Poly(Vinyl Alcohol) Film.
PB95-164372 *01,262* Not available NTIS

PB95-164380
Small Angle Neutron Scattering Study on Poly(N-Isopropyl Acrylamide) Gels Near Their Volume-Phase Transition Temperature.
PB95-164380 *01,263* Not available NTIS

PB95-164398
Small-Angle Neutron Scattering Study on Weakly Charged Temperature Sensitive Polymer Gels.
PB95-164398 *01,264* Not available NTIS

PB95-164406
Lattice Position of Si in GaAs Determined by X-Ray Standing Wave Measurements.
PB95-164406 *04,632* Not available NTIS

PB95-164414
Surface Geometry of BaO on W(100): A Surface-Extended X-Ray-Absorption Fine-Structure Study.
PB95-164414 *00,980* Not available NTIS

PB95-164422
Observation of a Stable Methoxy Intermediate on Cr(110).
PB95-164422 *00,981* Not available NTIS

PB95-164430
Fragment State Correlations in the Dissociation of NO.HF(v=1).
PB95-164430 *00,982* Not available NTIS

PB95-164448
Procedure for the Study of Acidic Calcium Phosphate Precursor Phases in Enamel Mineral Formation.
PB95-164448 *03,564* Not available NTIS

PB95-164455
X-Ray Image Quality Indicator Designed for Easy Alignment.
PB95-164455 *02,907* Not available NTIS

PB95-164463
Through-the-Arc Sensing for Measuring Gas Metal Arc Weld Quality in Real Time.
PB95-164463 *02,908* Not available NTIS

PB95-164471
Shape-Resonance-Enhanced Continuum-Continuum Coupling in Photoionization of CO2.
PB95-164471 *00,983* Not available NTIS

PB95-164489
Ebulliometric Measurement of the Vapor Pressure of 1-Chloro-1,1-Difluoroethane and 1,1-Difluoroethane.
PB95-164489 *00,984* Not available NTIS

PB95-164497
Metrology.
PB95-164497 *03,946* Not available NTIS

PB95-164505
Effects of Aluminum Oxalate/Glycine Pretreatment Solutions on Dentin Permeability.
PB95-164505 *03,565* Not available NTIS

PB95-164513
2nu9 Band of Propyne-d3.
PB95-164513 *00,985* Not available NTIS

PB95-164521
Field Dependence of the Magnetic Ordering of Cu in R2CuO4 (R = Nd, Sm).
PB95-164521 *04,633* Not available NTIS

PB95-164539
Observation of Noncollinear Magnetic Structure for the Cu Spins in Nd2CuO4-Type Systems.
PB95-164539 *04,634* Not available NTIS

PB95-164547
Membrane-Mediated Precipitation of Calcium Phosphate in Model Liposomes with Matrix Vesicle-Like Lipid Composition.
PB95-164547 *03,468* Not available NTIS

PB95-164554
Characterization of a Health Physics Instrument Calibration Range.
PB95-164554 *03,629* Not available NTIS

PB95-164562
Reactive Coevaporation of DyBaCuO Superconducting Films: The Segregation of Bulk Impurities on Annealed MgO(100) Substrates.
PB95-164562 *04,635* Not available NTIS

PB95-164570
Measuring Contact Charge Transfer at Interfaces: A New Experimental Technique.
PB95-164570 *03,053* Not available NTIS

PB95-164588
Quantitative Evaluation of Building Fire Safety: New Tools for Assessing Fire and Building Code Provisions.
PB95-164588 *00,199* Not available NTIS

PB95-164596
Phase Composition, Viscosities, and Densities for Aqueous Two-Phase Systems Composed of Polyethylene Glycol and Various Salts at 25C.
PB95-164596 *00,986* Not available NTIS

PB95-164604
Measurement of Radial Dose Distributions Around Small Beta Particle Emitters Using High Resolution Radiochromic Foil Dosimetry.
PB95-164604 *03,518* Not available NTIS

PB95-164612
Electrical Characterization of Radio-Frequency Discharges in the Gaseous Electronics Conference Reference Call.
PB95-164612 *01,905* Not available NTIS

PB95-164620
Surface Texture.
PB95-164620 *03,351* Not available NTIS

PB95-164638
Characterization of Cytochrome c/Alkanethiolate Structures Prepared by Self-Assembly on Gold.
PB95-164638 *00,987* Not available NTIS

PB95-164646
Validation of the Inverse Square Law of Gravitation Using the Tower at Erie, Colorado, USA.
PB95-164646 *03,947* Not available NTIS

PB95-164653
Enhanced Detection of PCR Products Through Use of TOTO and YOYO Intercalating Dyes with Laser Induced Fluorescence - Capillary Electrophoresis.
PB95-164653 *00,599* Not available NTIS

PB95-164661
Evaluation of Methylene Lactone Monomers in Dental Resins.
PB95-164661 *00,164* Not available NTIS

PB95-164679
Influence of Lattice Mismatch on Indium Phosphide Based High Electron Mobility Transistor (HEMT) Structures Observed in High Resolution Monochromatic Synchrotron X-Radiation Diffraction Imaging.
PB95-164679 *02,357* Not available NTIS

PB95-164687
Accuracy Comparisons of Josephson Array Systems.
PB95-164687 *02,047* Not available NTIS

PB95-164695
Voltage Ratio Measurements of a Zener Reference Using a Digital Voltmeter.
PB95-164695 *01,906* Not available NTIS

PB95-164703
Cryogenics.
PB95-164703 *02,654* Not available NTIS

PB95-164711
Fire-Plume-Generated Ceiling Jet Characteristics and Convective Heat Transfer to Ceiling and Wall Surfaces in a Two-Layer Fire Environment: Uniform Temperature Ceiling and Walls.
PB95-164711 *00,382* Not available NTIS

PB95-164810
Acoustic Emission of Structural Materials Exposed to Open Flames.
PB95-164810 *00,296* Not available NTIS

PB95-168415
Effect of Microstructure on Phase Formation in the Reaction of Nb/Al Multilayer Thin Films.
PB95-168415 *03,352* Not available NTIS

PB95-168423
Tunable High Temperature Superconductor Microstrip Resonators.
PB95-168423 *02,048* Not available NTIS

PB95-168431
In situ Observation of Surface Morphology of InP Grown on Singular and Vicinal (001) Substrates.
PB95-168431 *04,636* Not available NTIS

PB95-168449
Method of Sale for CNG Paves Way to Greater Public Acceptance.
PB95-168449 *02,489* Not available NTIS

PB95-168456
First Phase Formation Kinetics in the Reaction of Nb/Al.
PB95-168456 *03,353* Not available NTIS

PB95-168464
Interlaboratory Comparison of Polarization-Holding Parameter Measurements on High-Birefringence Optical Fiber.
PB95-168464 *04,280* Not available NTIS

PB95-168472
Angular Variation of the Personal Dose Equivalent, Hp(0.07), for Beta Radiation and Nearly Monoenergetic Electron Beams: Preliminary Results.
PB95-168472 *03,630* Not available NTIS

PB95-168480
Low-Coherence Interferometric Measurement of Group Transit Times in Precision Optical Fibre Delay Lines.
PB95-168480 *02,158* Not available NTIS

PB95-168498
Magneto-Optic Magnetic Field Sensors Based on Uniaxial Iron Garnet Films in Optical Waveguide Geometry.
PB95-168498 *02,159* Not available NTIS

PB95-168506
Look at Uncertainties over Twenty Decades of Pressure Measurement.
PB95-168506 *02,655* Not available NTIS

PB95-168514
Interference in the Resonance Fluorescence of Two Trapped Atoms.
PB95-168514 *03,948* Not available NTIS

PB95-168522
Combined Josephson and Charging Behavior of the Supercurrent in the Superconducting Single-Electron Transistor.
PB95-168522 *04,637* Not available NTIS

PB95-168530
Multi-State Two-Port: An Alternative Transfer Standard.
PB95-168530 *02,049* Not available NTIS

PB95-168548
New cw CO2 Laser Lines: The 9-mu m Hot Band.
PB95-168548 *04,281* Not available NTIS

PB95-168555
Coping with Different Retrieval Methods in Next Generation Networks.
PB95-168555 *02,726* Not available NTIS

PB95-168563
Lightwave Standards Development at NIST.
PB95-168563 *01,480* Not available NTIS

PB95-168571
Mode Coupling and Loss on Tapered Optical Waveguides.
PB95-168571 *04,282* Not available NTIS

PB95-168589
Symbolic Programming with Series Expansions: Applications to Optical Waveguides.
PB95-168589 *04,283* Not available NTIS

PB95-168597
Comparison of UV-Induced Fluorescence and Bragg Grating Growth in Optical Fiber.
PB95-168597 *04,284* Not available NTIS

PB95-168605
Using Archie to Find Files on the INTERNET.
PB95-168605 *02,727* Not available NTIS

PB95-168613
Alternating-Field Susceptometry and Magnetic Susceptibility of Superconductors.
PB95-168613 *04,638* Not available NTIS

PB95-168621
High Current Pressure Contacts to Ag Pads on Thin Film Superconductors.
PB95-168621 *04,639* Not available NTIS

PB95-168639
Improved Variational Analysis of Inhomogeneous Optical Waveguides Using Airy Functions.
PB95-168639 *04,285* Not available NTIS

PB95-168647
Terahertz Detectors Based on Superconducting Kinetic Inductance.
PB95-168647 *02,160* Not available NTIS

PB95-168662
Optical Performance of Photoinductive Mixers at Terahertz Frequencies.
PB95-168662 *02,161* Not available NTIS

PB95-168670
Suitability of Metalorganic Chemical Vapor Deposition-Derived PrGaO3 Films as Buffer Layers for YBa2Cu3O7-x Pulsed Laser Deposition.
PB95-168670 *04,640* Not available NTIS

PB95-168688
Reference Data for the Thermophysical Properties of Cryogenic Fluids.
PB95-168688 *03,263* Not available NTIS

PB95-168696
Force Calibrations in the Nanonewton Regime.
PB95-168696 *03,949* Not available NTIS

PB95-168704
Thermodynamic Properties of R134a(1,1,1,2-Tetrafluoroethane).
PB95-168704 *00,988* Not available NTIS

PB95-168712
Behavior of a Calcium Phosphate Cement in Simulated Blood Plasma In vitro.
PB95-168712 *00,165* Not available NTIS

PB95-168720
Retrieving Articles from the Internet (without a UNIX Workstation). Part 1. File Formats and Software Tools.
PB95-168720 *02,728* Not available NTIS

PB95-168738
Retrieving Articles from the Internet (without a UNIX Workstation). Part 2. An Example.
PB95-168738 *02,729* Not available NTIS

PB95-168746
Laser Cooling of Trapped Ions.
PB95-168746 *03,950* Not available NTIS

PB95-168753
Light Scattered from Two Atoms.
PB95-168753 *04,286* Not available NTIS

PB95-168761
Revised Uncertainty Analysis for the NIST 30-MHz Attenuation Calibration System.
PB95-168761 *01,907* Not available NTIS

PB95-168779
Widths and Propagation of a Truncated Gaussian Beam.
PB95-168779 *04,287* Not available NTIS

PB95-168787
Measurements of the Characteristic Impedance of Coaxial Air Line Standards.
PB95-168787 *02,221* Not available NTIS

PB95-168795
Bending-Induced Loss in Dual-Mode Rectangular Waveguides.
PB95-168795 *04,288* Not available NTIS

PB95-168803
Bent Rectangular Core Waveguides: An Accurate Perturbation Approach.
PB95-168803 *04,289* Not available NTIS

PB95-168811
Observation of Vortex Dynamics in Two-Dimensional Josephson-Junction Arrays.
PB95-168811 *02,050* Not available NTIS

PB95-168829
Relationship between Bulk-Modulus Temperature Dependence and Thermal Expansivity.
PB95-168829 *04,641* Not available NTIS

PB95-168837
Low-Temperature Elastic Constants of Y1Ba2Cu3O7.
PB95-168837 *04,642* Not available NTIS

PB95-168845
Spatial Uniformity of Optical Detector Responsivity.
PB95-168845 *02,162* Not available NTIS

PB95-168852
Ultralinear Small-Angle Phase Modulator.
PB95-168852 *02,261* Not available NTIS

PB95-168860
High-Temperature Adiabatic Calorimeter for Constant-Volume Heat Capacity Measurements of Compressed Gases and Liquids.
PB95-168860 *00,989* Not available NTIS

PB95-168878
Measurements of Molar Heat Capacity at Constant Volume (Cv) for 1,1,1,2-Tetrafluoroethane (R134a).
PB95-168878 *03,264* Not available NTIS

PB95-168886
Vapour Pressure Measurements on 1,1,1,2-Tetrafluoroethane (R134a) from 180 to 350 K.
PB95-168886 *03,265* Not available NTIS

PB95-168894
Octacalcium Phosphate Carboxylates. 5. Incorporation of Excess Succinate and Ammonium Ions in the Octacalcium Phosphate Succinate Structure.
PB95-168894 *00,166* Not available NTIS

PB95-168902
Design Equations and Scaling Laws for Linear Compressors with Flexure Springs.
PB95-168902 *02,948* Not available NTIS

PB95-168910
Metrological Accuracy of the Electron Pump.
PB95-168910 *03,951* Not available NTIS

PB95-168928
Crystal Structure of Calcium Succinate Monohydrate.
PB95-168928 *00,167* Not available NTIS

PB95-168936
Annex 18: An International Study of Refrigerant Properties.
PB95-168936 *03,266* Not available NTIS

PB95-168951
Development of a Dual-Sinker Densimeter for High-Accuracy Fluid P-V-T Measurements.
PB95-168951 *03,267* Not available NTIS

PB95-168969
Need for, and Availability of, Working Fluid Property Data: Results from Annexes XIII and XVIII.
PB95-168969 *03,268* Not available NTIS

PB95-168977
Microwave Properties of YBa2Cu3O7-x Films at 35 GHz from Magnetotransmission and Magnetoreflection Measurements.
PB95-168977 *04,643* Not available NTIS

PB95-168985
Ultrasensitive-Hot-Electron Microbolometer.
PB95-168985 *02,163* Not available NTIS

PB95-168993
Hot-Electron Microcalorimeters for X-ray and Phonon Detection.
PB95-168993 *04,644* Not available NTIS

PB95-169009
Relationship of AM to PM Noise in Selected RF Oscillators.
PB95-169009 *02,262* Not available NTIS

PB95-169017
Proposed Antiferromagnetically Coupled Dual-Layer Magnetic Force Microscope Tips.
PB95-169017 *04,645* Not available NTIS

PB95-169025
Magnetic and Magnetoresistive Properties of Inhomogeneous Magnetic Dual-Layer Films.
PB95-169025 *04,646* Not available NTIS

PB95-169033
Enhanced Flux Pinning via Chemical Substitution in Bulk Superconducting T1-2212.
PB95-169033 *04,647* Not available NTIS

PB95-169041
Membrane Gas Separation for a Fluidized-Bed Incinerator.
PB95-169041 *02,550* Not available NTIS

PB95-169058
Measurement of the Thermal Properties of Electrically Conducting Fluids Using Coated Transient Hot Wires.
PB95-169058 *03,269* Not available NTIS

PB95-169066
Electrically Calibrated Pyroelectric Detector-Refinements for Improved Optical Power Measurements.
PB95-169066 *02,164* Not available NTIS

PB95-169074
Ambient Temperature Synthesis of Bulk Intermetallics.
PB95-169074 *00,168* Not available NTIS

PB95-169082
Energy Flows in an Orifice Pulse Tube Refrigerator.
PB95-169082 *02,752* Not available NTIS

PB95-169090
Graded and Nongraded Regenerator Performance.
PB95-169090 *02,753* Not available NTIS

PB95-169108
Approaches Using Virtual Environments with Mosaic.
PB95-169108 *01,599* Not available NTIS

PB95-169116
Kinetic-Inductance Infrared Detector Based on an Antenna-Coupled High-Tc SQUID.
PB95-169116 *02,165* Not available NTIS

PB95-169124
High-Tc Superconducting Antenna-Coupled Microbolometer on Silicon.
PB95-169124 *02,166* Not available NTIS

PB95-169132
Effect of Semiconductor Laser Characteristics on Optical Fiber Sensor Performance.
PB95-169132 *02,167* Not available NTIS

PB95-169140
Terahertz Shapiro Steps in High Temperature SNS Josephson Junctions.
PB95-169140 *02,168* Not available NTIS

PB95-169157
Insulating Boundary Layer and Magnetic Scattering in YBa2Cu3O7-delta/Ag Interfaces Over a Contact Resistivity Range of 10(-8) - 10(-3) Omega cm(2).
PB95-169157 *04,648* Not available NTIS

PB95-169165
Optimization of ECR-Based PECVD Oxide Films for Superconducting Integrated Circuit Fabrication.
PB95-169165 *02,051* Not available NTIS

PB95-169173
Comparative Photoluminescence Measurement and Simulation of Vertical-Cavity Semiconductor Laser Structures.
PB95-169173 *02,169* Not available NTIS

PB95-169181
Measurement and Simulation of Photoluminescence Spectra from Vertical-Cavity Quantum-Well Laser Structures.
PB95-169181 *02,170* Not available NTIS

PB95-169199
Ultrasonic Measurement of Residual Stress in Cast Steel Railroad Wheels.
PB95-169199 *04,852* Not available NTIS

PB95-169207
Comparing NIST-B 50 mm Orifice Meter Gas Data to the ANSI Equation.
PB95-169207 *02,949* Not available NTIS

PB95-169215
Vortex Shedding Flowmeters for SSME Ducts.
PB95-169215 *01,453* Not available NTIS

PB95-169223
Effect of 1-Hydroxyethylidene-1,1-Bisphosphonate on Membrane-Mediated Calcium Phosphate Formation in Model Liposomal Suspensions.
PB95-169223 *03,469* Not available NTIS

PB95-169231
Effect of Ethanol on the Solubility of Hydroxyapatite in the System Ca(OH)2-H3PO4-H2O at 25C and 33C.
PB95-169231 *00,169* Not available NTIS

PB95-169249
Critical Scaling Laws and a Classical Equation of State.
PB95-169249 *00,990* Not available NTIS

PB95-169256
Optical Power Meter Calibration Using Tunable Laser Diodes.
PB95-169256 *04,290* Not available NTIS

PB95-169264
Waveguide Polarizers Processed by Localized Plasma Etching.
PB95-169264 *02,171* Not available NTIS

PB95-169272
Measurements of the Vapor Pressures of Difluoromethane, 1-Chloro-1,2,2,2-Tetrafluoroethane, and Pentafluoroethane.
PB95-169272 *03,270* Not available NTIS

PB95-169298
Self-Calibrating Fiber Optic Sensors: Potential Design Methods.
PB95-169298 *02,172* Not available NTIS

PB95-169306
Self Calibrating Fiber Optic Sensors: Potential Design Methods.
PB95-169306 *02,173* Not available NTIS

PB95-169314
Phase-Locked Oscillator Optimization for Arrays of Josephson Junctions.
PB95-169314 *02,052* Not available NTIS

PB95-169322
Recent Experiments on Trapped Ions at the National Institute of Standards and Technology.
PB95-169322 *03,952* Not available NTIS

PB95-169330
High-Resolution Atomic Spectroscopy of Laser-Cooled Ions.
PB95-169330 *03,953* Not available NTIS

PB95-169348
Laser-Cooled Positron Source.
PB95-169348 *03,954* Not available NTIS

PB95-169355
Optical Detector Nonlinearity: A Comparison of Five Methods.
PB95-169355 *04,291* Not available NTIS

PB95-169363
Far Infrared Laser Frequencies of (13)CD3OH.
PB95-169363 *04,292* Not available NTIS

PB95-169371
Journal of Research of the National Institute of Standards and Technology, September/October 1994. Volume 99, Number 5.
PB95-169371 *04,293* PC A07/MF A02

PB95-169389
Tilt Effects in Optical Angle Measurements.
PB95-169389 *04,294*
(Order as PB95-169371, PC A07/MF A02)

PB95-169397
Optical Characterization in Microelectronics Manufacturing.
PB95-169397 *02,358*
(Order as PB95-169371, PC A07/MF A02)

PB95-169405
Critical Issues in Scanning Electron Microscope Metrology.
PB95-169405 *02,359*
(Order as PB95-169371, PC A07/MF A02)

PB95-169496
Guide on Open System Environment (OSE) Procurements.
PB95-169496 *01,626* PC A08/MF A02

PB95-169538
Superconductor Critical Current Standards for Fusion Applications. Final Progress Report, October 1993-July 1994.
PB95-169538 *02,222* PC A05/MF A02

PB95-169819
Report of the National Conference on Weights and Measures (79th). Held in San Diego, California on July 17-21, 1994.
PB95-169819 *02,656* PC A20/MF A04

PB95-170387
Workshop Summary Report: Industrial Applications of Scanned Probe Microscopy. A Workshop Co-sponsored by NIST, SEMATECH, ASTM, E42.14, and the American Vacuum Society. Held in Gaithersburg, Maryland on March 24-25, 1994.
PB95-170387 *00,506* PC A07/MF A02

PB95-170395
Electronics and Electrical Engineering Laboratory Technical Progress Bulletin Covering Laboratory Programs, July to September 1994 with 1994/1995 EEEL Events Calendar.
PB95-170395 *02,360* PC A03/MF A01

PB95-170429
National Voluntary Laboratory Accreditation Program (NVLAP): Wood Based Products.
PB95-170429 *03,405* PC A04/MF A01

PB95-170551
Robotics Application to Highway Transportation. Volume 2. Literature Search.
PB95-170551 *01,337* PC A06/MF A02

PB95-171039
Updated Calculations for Routine Space-Shielding Radiation Dose Estimates: SHIELDOSE-2.
PB95-171039 *04,838* PC A04/MF A01

PB95-171096
General Motion Model and Spatio-Temporal Filters for Computing Optical Flow.
PB95-171096 *01,847* PC A03/MF A01

PB95-171112
Japan Technology Program Assessment: Precision Engineering/Precision Optics in Japan.
PB95-171112 *02,884* PC A03/MF A01

PB95-171344
Alaska Marine Mammal Tissue Archival Project: Specimen Inventory.
PB95-171344 *02,589* PC A05/MF A01

PB95-171377
Perspective on Software Engineering Standards.
PB95-171377 *01,811* PC A03/MF A01

PB95-171419
Design Challenges in a Commercial Quantum Hall Effect-Based Resistance Standard.
PB95-171419 *02,263* PC A03/MF A01

PB95-171427
Initial Graphics Exchange Specification (IGES): Procedures for the NIST IGES Validation Test Service.
PB95-171427 *02,780* PC A03/MF A01

PB95-171435
New Method to Calculate Looming for Autonomous Obstacle Avoidance.
PB95-171435 *01,600* PC A03/MF A01

PB95-171633
Robotics Application to Highway Transportation. Volume 3. Proposed Research Topics and Cost/Benefit Evaluations by CERF.
PB95-171633 *01,338* PC A20/MF A04

PB95-171948
Neighbor Tables for Molecular Dynamics Simulations.
PB95-171948 *00,991* PC A03/MF A01

PB95-171955
Multi-Agency Certification and Accreditation (C and A) Process: A Worked Example.
PB95-171955 *01,601* PC A05/MF A01

PB95-171963
From Superconductivity to Supernovae: The Ginzburg Symposium. Report on the Symposium Held in Honor of Vitaly L. Ginzburg. Held in Gaithersburg, Maryland on May 22, 1992.
PB95-171963 *04,649* PC A05/MF A01

PB95-171971
Binary Decision Clustering for Neural Network Based Optical Character Recognition.
PB95-171971 *01,848* PC A03/MF A01

PB95-173068
Video Microscopy Applied to Optical Fiber Geometry Measurements.
PB95-173068 *04,295* PC A04/MF A01

PB95-173084
Framework for the Development and Assurance of High Integrity Software.
PB95-173084 *01,716* PC A05/MF A01

PB95-173555
Workshop on the Application of Virtual Reality to Manufacturing. Final Report. Held in Gaithersburg, Maryland on August 9, 1994.
PB95-173555 *02,825* PC A11/MF A03

PB95-174454
National Voluntary Laboratory Accreditation Program 1995 Directory.
PB95-174454 *00,483* PC A08/MF A02

PB95-174470
Uniform Laws and Regulations in the Areas of Legal Metrology and Motor Fuel Quality, 1994 as Adopted by the 79th National Conference on Weights and Measures 1994.
PB95-174470 *02,909* PC A09/MF A02

PB95-174488
Performance of HUD-Affiliated Properties during the January 17, 1994 Northridge Earthquake.
PB95-174488 *00,443* PC A04/MF A01

PB95-174959
SGML Parser Validation Procedures.
PB95-174959 *01,717* PC A03/MF A01

PB95-174967
Asynchronous Transfer Mode Procurement and Usage Guide.
PB95-174967 *01,481* PC A03/MF A01

PB95-174975
Protection of Data Processing Equipment with Fine Water Sprays.
PB95-174975 *02,610* PC A04/MF A01

PB95-175006
Life-Cycle Costing Workshop for Energy Conservation in Buildings: Student Manual.
PB95-175006 *00,257* PC A11/MF A03

PB95-175014
Influence of the Filament Potential Wave Form on the Sensitivity of Glass-Envelope Bayard-Alpert Gages.
PB95-175014 *02,657* Not available NTIS

PB95-175022
Multi-Stage, Position Stabilized Vibration Isolation System for Neutron Interferometry.
PB95-175022 *03,955* Not available NTIS

PB95-175030
Crystal Structure and Compressibility of 3:2 Mullite.
PB95-175030 *03,682* Not available NTIS

PB95-175048
Rotational Spectroscopy of the CoH Radical in Its Ground (3)Phi State by Far-Infrared Laser Magnetic Resonance: Determination of Molecular Parameters.
PB95-175048 *00,992* Not available NTIS

PB95-175055
Cellular Automaton Simulations of Cement Hydration and Microstructure Development.
PB95-175055 *01,320* Not available NTIS

PB95-175063
Evolution of Porosity and Calcium Hydroxide in Laboratory Concretes Containing Silica Fume.
PB95-175063 *01,321* Not available NTIS

PB95-175071
Experimental Results on Single Flux Quantum Logic.
PB95-175071 *02,053* Not available NTIS

PB95-175089
Thermal Noise in High-Temperature Superconducting-Normal-Superconducting Step-Edge Josephson Junctions.
PB95-175089 *04,650* Not available NTIS

PB95-175097
Status and Trends in Power Semiconductor Devices.
PB95-175097 *02,361* Not available NTIS

PB95-175105
Experimental Results on Normal Modes in Cold, Pure Ion Plasmas.
PB95-175105 *03,956* Not available NTIS

PB95-175113
Non-Neutral Ion Plasmas and Crystals, Laser Cooling, and Atomic Clocks.
PB95-175113 *03,957* Not available NTIS

PB95-175121
Characterization of the Emission from 2D Array Josephson Oscillators.
PB95-175121 *02,054* Not available NTIS

PB95-175139
Emission Linewidth Measurements of Two-Dimensional Array Josephson Oscillators.
PB95-175139 *02,055* Not available NTIS

PB95-175147
Frequency Dependence of the Emission from 2D Array Josephson Oscillators.
PB95-175147 *02,056* Not available NTIS

PB95-175154
Vapor Pressures and Gas-Phase PVT Data for 1-Chloro-1,2,2,2-Tetrafluoroethane (R124).
PB95-175154 *03,271* Not available NTIS

PB95-175162
Fine-Structure Intervals of (14)N(+) By Far-Infrared Laser Magnetic Resonance.
PB95-175162 *00,993* Not available NTIS

PB95-175170
Laser Magnetic-Resonance Measurement of the (3)P1 - (3)P2 Fine-Structure Splittings in (17)O and (18)O.
PB95-175170 *00,994* Not available NTIS

PB95-175188
Measurement of Diffusion in Fluid Systems: Applications to the Supercritical Fluid Region.
PB95-175188 *02,490* Not available NTIS

PB95-175196
Retention of Halocarbons on a Hexafluoropropylene Epoxide Modified Graphitized Carbon Black. Part 1. Methane-Based Compounds.
PB95-175196 *03,272* Not available NTIS

PB95-175204
Supercritical Fluid Extraction of Biological Products.
PB95-175204 *00,040* Not available NTIS

PB95-175212
Fugacity Coefficients of Hydrogen in (Hydrogen + Butane).
PB95-175212 *02,491* Not available NTIS

PB95-175220
Developing Rational Performance-Based Fire Safety Requirements in Model Building Codes.
PB95-175220 *00,200* Not available NTIS

PB95-175238
Earthquake and Fire in Japan: When the Threat Became a Reality.
PB95-175238 *00,201* Not available NTIS

PB95-175246
Automated Josephson Integrated Circuit Test System.
PB95-175246 *02,057* Not available NTIS

PB95-175253
Friction and Oxidative Wear of 440C Ball Bearing Steels Under High Load and Extreme Bulk Temperatures.
PB95-175253 *03,215* Not available NTIS

PB95-175261
Formation of Hydroxyapatite in Cement Systems.
PB95-175261 *00,170* Not available NTIS

PB95-175279
Correlation of Optical, X-ray, and Electron Microscopy Measurements of Semiconductor Multilayer Structures.
PB95-175279 *02,174* Not available NTIS

PB95-175287
Vapor-Liquid Equilibria of Mixtures of Propane and Isomeric Hexanes.
PB95-175287 *00,995* Not available NTIS

PB95-175295
Thin Film Reaction Kinetics of Niobium/Aluminum Multilayers.
PB95-175295 *04,651* Not available NTIS

PB95-175303
Aspects of a Deformable Superconductor Model for the Vortex Mass.
PB95-175303 *04,652* Not available NTIS

PB95-175311
Deformable Superconductor Model for the Fluxon Mass.
PB95-175311 *04,653* Not available NTIS

PB95-175329
Performance of Compact Fluorescent Lamps at Different Ambient Temperatures.
PB95-175329 *00,258* Not available NTIS

PB95-175337
Evidence for a Deep Electron Trap and Charge Compensation in Separation by Implanted Oxygen Oxides.
PB95-175337 *02,362* Not available NTIS

PB95-175345
New Test Structure for Nanometer-Level Overlay and Feature-Placement Metrology.
PB95-175345 *02,363* Not available NTIS

PB95-175352
Increased Pinning Energies and Critical Current Densities in Heavy-Ion-Irradiated Bi2Sr2CaCu2O8 Single Crystals.
PB95-175352 *04,654* Not available NTIS

PB95-175360
Characterization of the ZnSe/GaAs Interface Layer by TEM and Spectroscopic Ellipsometry.
PB95-175360 *04,655* Not available NTIS

PB95-175378
Determination of the Optical Constants of ZnSe Films by Spectroscopic Ellipsometry.
PB95-175378 *04,656* Not available NTIS

PB95-175386
Measurements of the Viscosities of Saturated and Compressed Liquid 1,1,1,2-Tetrafluoroethane (R134a), 2,2-Dichloro-1,1,1-Trifluoroethane (R123) and 1,1-Dichloro-1-Fluoroethane (R141b).
PB95-175386 *03,273* Not available NTIS

PB95-175394
Chemical Determination of Oxidative DNA Damage by Gas Chromatography-Mass Spectrometry.
PB95-175394 *03,540* Not available NTIS

PB95-175402
Competition between Hydrodynamic Screening ('Draining') and Excluded Volume Interactions in an Isolated Polymer Chain.
PB95-175402 *01,265* Not available NTIS

PB95-175410
Evidence for Parallel Junctions Within High-Tc Grain-Boundary Junctions.
PB95-175410 *04,657* Not available NTIS

PB95-175428
Interpreting the Readings of Multi-Element Personnel Dosimeters in Terms of the Personal Dose Equivalent.
PB95-175428 *03,631* Not available NTIS

PB95-175436
Thermal Enhancement of Cotunneling in Ultra-Small Tunnel Junctions.
PB95-175436 *04,658* Not available NTIS

PB95-175444
Determination of Amphetamine and Methamphetamine in a Lyophilized Human Urine Reference Material.
PB95-175444 *03,597* Not available NTIS

PB95-175451
Dimensional Inspection Planning Based on Product Data Standards.
PB95-175451 *02,910* Not available NTIS

PB95-175469
Optical Probing of Cold Trapped Atoms.
PB95-175469 *04,296* Not available NTIS

PB95-175477
High-Sensitivity Spectroscopy with Diode Lasers.
PB95-175477 *04,297* Not available NTIS

PB95-175485
Diode Laser as a Spectroscopic Tool.
PB95-175485 *00,600* Not available NTIS

PB95-175493
Fabrication of Transparent gamma-Al2O3 from Nanosize Particles.
PB95-175493 *03,054* Not available NTIS

PB95-175501
Calculated Fiber Attenuation: A General Method Yielding Stationary Values.
PB95-175501 *04,298* Not available NTIS

PB95-175519
Fibre Splice Loss: A Simple Method of Calculation.
PB95-175519 *04,299* Not available NTIS

PB95-175527
Characterization of a Tunable Thin Film Microwave YBa2Cu3O7-x/SrTiO3 Coplanar Capacitor.
PB95-175527 *02,264* Not available NTIS

PB95-175535
Reduction of Interfilament Contact Loss in Nb3Sn Superconductor Wires.
PB95-175535 *02,223* Not available NTIS

PB95-175543
Standard Reference Devices for High Temperature Superconductor Critical Current Measurements.
PB95-175543 *04,659* Not available NTIS

PB95-175550
Testers Open Dialogue at Inaugural NIST Workshop.
PB95-175550 *01,718* Not available NTIS

PB95-175568
Polyelectrolytes as Dispersants in Colloidal Processing of Silicon Nitride Ceramics.
PB95-175568 *03,055* Not available NTIS

PB95-175576
Surface Chemical Interactions of Si3N4 with Polyelectrolyte Deflocculants.
PB95-175576 *03,056* Not available NTIS

PB95-175584
Effects of Soxhlet Extraction on the Surface Oxide Layer of Silicon Nitride Powders.
PB95-175584 *03,057* Not available NTIS

PB95-175592
Photodetector Frequency Response Measurements at NIST, US, and NPL, UK: Preliminary Results of a Standards Laboratory Comparison.
PB95-175592 *02,175* Not available NTIS

PB95-175600
Josephson Voltage Standard Based on Single-Flux-Quantum Voltage Multipliers.
PB95-175600 *02,058* Not available NTIS

PB95-175618
Partial Scattered Intensities from a Binary Suspension of Polystyrene and Silica.
PB95-175618 *00,996* Not available NTIS

PB95-175626
Solubility Measurement by Direct Injection of Supercritical-Fluid Solutions into a HPLC System.
PB95-175626 *00,997* Not available NTIS

PB95-175634
High-Pressure Equilibrium Cell for Solubility Measurements in Supercritical Fluids.
PB95-175634 *00,998* Not available NTIS

PB95-175642
Determination of the Complex Refractive Index of Individual Quantum Wells from Distributed Reflectance.
PB95-175642 *02,176* Not available NTIS

PB95-175659
Sources of Urban Contemporary Carbon Aerosol.
PB95-175659 *02,551* Not available NTIS

PB95-175667
Gradiometer Antennas for Detection of Long Subsurface Conductors.
PB95-175667 *01,862* Not available NTIS

PB95-175675
Aperture Excitation of Electrically Large, Lossy Cavities.
PB95-175675 *00,031* Not available NTIS

PB95-175683
Critical Properties and Vapor-Liquid Equilibria of the Binary System Propane + Neopentane.
PB95-175683 *00,999* Not available NTIS

PB95-175691
Coexisting Densities, Vapor Pressures and Critical Densities of Refrigerants R-32 and R-152a, at 300 - 385 K.
PB95-175691 *03,274* Not available NTIS

PB95-175709
Fluorescence Measurements of Tetracycline in High Cell Mass for Fermentation Monitoring.
PB95-175709 *00,601* Not available NTIS

PB95-175717
Predictive Extended Corresponding States Model for Pure and Mixed Refrigerants Including an Equation of State for R134a.
PB95-175717 *03,275* Not available NTIS

PB95-175725
Experimental Aspects of Flux Expulsion in Type-II Superconductors.
PB95-175725 *04,660* Not available NTIS

PB95-175733
Examination of the I/d Expansion Method from Exact Enumeration for a Self-Interacting Self-Avoiding Walk.
PB95-175733 *01,266* Not available NTIS

PB95-175741
Obtaining and Installing a Public Domain TEX.
PB95-175741 *01,719* Not available NTIS

PB95-175758
Elastic-Electron-Scattering Effects on Angular Distributions in X-ray Photoelectron Spectroscopy.
PB95-175758 *01,000* Not available NTIS

PB95-175766
Grazing Incidence X-ray Photoemission and Its Implementation on Synchrotron Light Source X-ray Beamlines.
PB95-175766 *01,001* Not available NTIS

PB95-175774
Using Emulators to Evaluate the Performance of Building Energy Management Systems.
PB95-175774 *00,259* Not available NTIS

PB95-175782
Electrical Characterization of Liquid-Phase Epitaxially Grown Single-Crystal Films of Mercury Cadmium Telluride by Variable-Magnetic-Field Hall Measurements.
PB95-175782 *02,177* Not available NTIS

PB95-175790
Comparative Study of Fe-C Bead and Graphite Target Performance with the National Ocean Sciences AMS (NOSAMS) Facility Recombinator Ion Source.
PB95-175790 *00,693* Not available NTIS

PB95-175808
Fire and Smoke Control: An Historical Perspective.
PB95-175808 *00,202* Not available NTIS

PB95-175816
Correlation of the Ideal Gas Properties of Five Aromatic Hydrocarbons.
PB95-175816 *01,002* Not available NTIS

PB95-175824
Defect Pair Formation by Implantation-Induced Stresses in High-Dose Oxygen Implanted Silicon-on-Insulator Material.
PB95-175824 *02,364* Not available NTIS

PB95-175832
PC-Based Spinning Rotor Gage Controller.
PB95-175832 *02,609* Not available NTIS

PB95-175840
Magneto-Transport Properties of HgCdTe.
PB95-175840 *04,661* Not available NTIS

PB95-175857
Fabrication Issues in Optimizing YBa2Cu3O7-x Flux Transformers for Low I/f Noise.
PB95-175857 *02,059* Not available NTIS

PB95-175865
Effect in Environmental Noise on the Accuracy of Coulomb-Blockade Devices.
PB95-175865 *04,662* Not available NTIS

PB95-175873
Testing for Metrological Accuracy of the Electron Pump.
PB95-175873 *04,663* Not available NTIS

PB95-175881
Absolute Frequency Measurements of Methanol from 1.5 to 6.5 THz.
PB95-175881 *04,300* Not available NTIS

PB95-175899
Optical Biosensor Using a Fluorescent, Swelling Sensing Element.
PB95-175899 *03,541* Not available NTIS

PB95-175907
Interaction of Chlorhexidine Digluconate with and Adsorption of Chlorhexidine on Hydroxyapatite.
PB95-175907 *03,566* Not available NTIS

PB95-175915
Ionizing Radiation Causes Greater DNA Base Damage in Radiation-Sensitive Mutant M10 Cells That in Parent Mouse Lymphoma L5178Y Cells.
PB95-175915 *03,632* Not available NTIS

PB95-175923
Interlaboratory Comparison of Autoradiographic DNA Profiling Measurements. 1. Data and Summary Statistics.
PB95-175923 *03,542* Not available NTIS

PB95-175931
Numerical Micromagnetic Techniques and Their Applications to Magnetic Force Microscopy Calculations.
PB95-175931 *04,664* Not available NTIS

PB95-175949
Rapid Post-Polishing of Diamond-Turned Optics.
PB95-175949 *04,301* Not available NTIS

PB95-175956
Determination of Hydrogen in Titanium Alloy Jet Engine Compressor Blades by Cold Neutron Capture Prompt Gamma-ray Activation Analysis.
PB95-175956 *01,448* Not available NTIS

PB95-175964
Cold Neutron Prompt Gamma Activation Analysis at NIST: A Progress Report.
PB95-175964 *00,602* Not available NTIS

PB95-175972
Neutron Scattering by Hydrogen in Cold Neutron Prompt Gamma-Activation Analysis.
PB95-175972 *00,603* Not available NTIS

PB95-175980
Reproducibility of Tests on Energy Management and Control Systems Using Building Emulators.
PB95-175980 *00,260* Not available NTIS

PB95-175998
Gas Transport Properties of Solution-Cast Perfluorosulfonic Acid Ionomer Films Containing Ionic Surfactants.
PB95-175998 *01,267* Not available NTIS

PB95-176004
Limits of CO2 Monitoring in Determining Ventilation Rates.
PB95-176004 *02,552* Not available NTIS

PB95-176012
Ventilation Effectiveness Measurements in Two Modern Office Buildings.
PB95-176012 *02,553* Not available NTIS

PB95-176020
Effect of Dodecanol Content on the Combustion of Methanol Spray Flames.
PB95-176020 *01,389* Not available NTIS

PB95-176038
Composition Dependence of a Field Variable Along the Binary Fluid Mixture Critical Locus.
PB95-176038 *01,003* Not available NTIS

PB95-176046
Equilibrium Pair Distribution Function of a Gas: Aspects Associated with the Presence of Bound States.
PB95-176046 *01,004* Not available NTIS

PB95-176053
Phase Locking in Two-Junction Systems of High-Temperature Superconductor-Normal Metal-Superconductor Junctions.
PB95-176053 *02,060* Not available NTIS

PB95-176061
dc Magnetic Force Microscopy Imaging of Thin-Film Recording Head.
PB95-176061 *04,665* Not available NTIS

PB95-176079
High Temperature Superconductor-Normal Metal-Superconductor Josephson Junctions with High Characteristic Voltages.
PB95-176079 *04,666* Not available NTIS

PB95-176087
Modified Surface Layers and Coatings.
PB95-176087 *03,125* Not available NTIS

PB95-176095
Surface Degradation of Superconducting YBa2Cu3O7-delta Thin Films.
PB95-176095 *04,667* Not available NTIS

PB95-176103
Small Angle Neutrons Scattering from Nanocrystalline Palladium as a Function of Annealing.
PB95-176103 *03,354* Not available NTIS

PB95-176111
High-Sensitivity Optical Sampling Using an Erbium-Doped Fiber Laser Strobe.
PB95-176111 *04,302* Not available NTIS

PB95-176129
Transport and Diffusion in Three-Dimensional Composite Media.
PB95-176129 *04,668* Not available NTIS

PB95-176137
Electron-Ion-X-ray Spectrometer System.
PB95-176137 *03,958* Not available NTIS

PB95-176145
Ring-Opening Polymerication of a 2-Methylene Spiro Orthocarbonate Bearing a Pendant Methacrylate Group.
PB95-176145 *01,268* Not available NTIS

PB95-176152
Improved Rubidium Frequency Standards Using Diode Lasers with AM and FM Noise Control.
PB95-176152 *04,303* Not available NTIS

PB95-176160
Certification of Morphine and Codeine in a Human Urine Standard Reference Material.
PB95-176160 *03,499* Not available NTIS

PB95-176178
Micromagnetic Scanning Microprobe System.
PB95-176178 *02,224* Not available NTIS

PB95-176186
Frequency-Stabilized LNA Laser at 1.083 mum: Application to the Manipulation of Helium 4 Atoms.
PB95-176186 *04,304* Not available NTIS

PB95-176194
Pure Rotational Spectra of CuH and CuD in Their Ground States Measured by Tunable Far-Infrared Spectroscopy.
PB95-176194 *01,005* Not available NTIS

PB95-176202
Rotational Spectrum of OH in the v=0-3 Levels of Its Ground State.
PB95-176202 *01,006* Not available NTIS

PB95-176210
Magnetic Force Microscopy Images of Magnetic Garnet with Thin-Film Magnetic Tip.
PB95-176210 *04,669* Not available NTIS

PB95-176228
Precise Optical Frequency References and Difference Frequency Measurements with Diode Lasers.
PB95-176228 *04,305* Not available NTIS

PB95-176236
Estimating the Virial Coefficients of Small Polar Molecules.
PB95-176236 *03,276* Not available NTIS

PB95-176244
Electrostatic Modes as a Diagnostic in Penning-Trap Experiments.
PB95-176244 *03,959* Not available NTIS

PB95-176251
Interlaboratory Comparison Studies on the Analysis of Hair for Drugs of Abuse.
PB95-176251 *03,500* Not available NTIS

PB95-176269
Hair Analysis for Drugs of Abuse: Evaluation of Analytical Methods, Environmental Issues, and Development of Reference Materials.
PB95-176269 *03,501* Not available NTIS

PB95-176277
Two-Stage Integrated SQUID Amplifier with Series Array Output.
PB95-176277 *02,061* Not available NTIS

PB95-176285
On-Wafer Impedance Measurement on Lossy Substrates.
PB95-176285 *02,365* Not available NTIS

PB95-176293
Squeezed Atomic States and Projection Noise in Spectroscopy.
PB95-176293 *03,960* Not available NTIS

PB95-176301
Interaction of Stoichiometry, Mechanical Stress, and Interface Trap Density in LPCVD Si-rich SiNx-Si Structures.
PB95-176301 *02,366* Not available NTIS

PB95-176319
Spectrally Smooth Reflectances That Match.
PB95-176319 *04,306* Not available NTIS

PB95-176327
Noise in the Coulomb Blockade Electrometer.
PB95-176327 *04,670* Not available NTIS

PB95-176335
Voltage Gain in the Single-Electron Transistor.
PB95-176335 *04,671* Not available NTIS

PB95-178604
Global Information Infrastructure: Agenda for Cooperation.
PB95-178604 *01,482* PC$9.00

PB95-178885
Manufactured Housing Walls That Provide Satisfactory Moisture Performance in All Climates.
PB95-178885 *00,383* PC A03/MF A01

PB95-178893
Indoor Air Quality Impacts of Residential HVAC Systems. Phase 2.A Report: Baseline and Preliminary Simulations.
PB95-178893 *02,554* PC A05/MF A01

PB95-178992
Glossary of Software Reuse Terms.
PB95-178992 *01,720* PC A03/MF A01

PB95-179024
Performance of 1/3-Scale Model Precast Concrete Beam-Column Connections Subjected to Cyclic Inelastic Loads. Report No. 4.
PB95-179024 *00,444* PC A04/MF A01

PB95-179040
Effects of Testing Variables on the Measured Compressive Strength of High-Strength (90 MPa) Concrete.
PB95-179040 *00,445* PC A07/MF A02

PB95-180014
Polymerization Initiation by N-p-Tolylglycine: Free-Radical Reactions Studied by Pulse and Steady-State Radiolysis.
PB95-180014 *01,269* Not available NTIS

PB95-180022
Investigations of AM and PM Noise in X-Band Devices.
PB95-180022 *02,062* Not available NTIS

PB95-180030
Rayleigh Scattering Limits for Low-Level Bidirectional Reflectance Distribution Function Measurements.
PB95-180030 *04,307* Not available NTIS

PB95-180048
Passively Q-Switched Nd-Doped Waveguide Laser.
PB95-180048 *04,308* Not available NTIS

PB95-180055
Inner-Valence States CO(+) between 22 eV and 46 eV Studied by High Resolution Photoelectron Spectroscopy and ab Initio CI Calculations.
PB95-180055 *03,961* Not available NTIS

PB95-180063
Mathematical Modeling and Computer Simulation of Fire Phenomena.
PB95-180063 *00,384* Not available NTIS

PB95-180071
Increased Transition Temperature in In situ Coevaporated YBa2Cu3O7-delta Thin Films by Low Temperature Post-Annealing.
PB95-180071 *04,672* Not available NTIS

PB95-180089
Interior-Point Method for Linear and Quadratic Programming Problems. (NIST Reprint).
PB95-180089 *03,429* Not available NTIS

PB95-180097
Convergence Properties of a Class of Rank-Two Updates. (NIST Reprint).
PB95-180097 *03,430* Not available NTIS

PB95-180105
Atomic Sulfur: Frequency Measurement of the J=0 inversely maps 1 Fine-Structure Transition at 56.3 Microns by Laser Magnetic Resonance.
PB95-180105 *01,007* Not available NTIS

PB95-180113
Chromatographic Cryofocusing and Cryotrapping with the Vortex Tube.
PB95-180113 *00,604* Not available NTIS

PB95-180121
Cyclic Polyamine Ionophore for Use in a Dibasic Phosphate-Selective Electrode.
PB95-180121 *01,008* Not available NTIS

PB95-180139
Nondestructive Testing of Concrete: History and Challenges.
PB95-180139 *00,385* Not available NTIS

PB95-180147
High-Performance Concrete: Research Needs to Enhance Its Use.
PB95-180147 *01,322* Not available NTIS

PB95-180154
Photodecomposition of Mo(CO)6/Si(111) 7x7: CO State-Resolved Evidence for Excited State Relaxation and Quenching.
PB95-180154 *01,009* Not available NTIS

PB95-180162
Influence of Ignition Source on the Flaming Fire Hazard of Upholstered Furniture. (NIST Reprint).
PB95-180162 *00,297* Not available NTIS

PB95-180170
Crossover in the Pinning Mechanism of Anisotropic Fluxon Cores.
PB95-180170 *04,673* Not available NTIS

PB95-180188
Size and Self-Field Effects in Giant Magnetoresistive Thin-Film Devices.
PB95-180188 *04,674* Not available NTIS

PB95-180196
Neutron Scattering Study of the Orientation of a Liquid Crystalline Polymer by Shear Flow.
PB95-180196 *01,270* Not available NTIS

PB95-180204
Novel Bulk Iron Garnets for Magneto-Optic Magnetic Field Sensing.
PB95-180204 *04,675* Not available NTIS

PB95-180212
Physical and Chemical Properties of Resin-Reinforced Calcium Phosphate Cements.
PB95-180212 *00,171* Not available NTIS

PB95-180220
X-ray Photoelectron and Auger Electron Forward Scattering: A Structural Diagnostic for Epitaxial Thin Films.
PB95-180220 *04,676* Not available NTIS

PB95-180238
Application of a Multizone Airflow and Contaminant Dispersal Model to Indoor Air Quality Control in Residential Buildings.
PB95-180238 *02,555* Not available NTIS

PB95-180246
Traceability to the Mole: A New Initiative by CIPM.
PB95-180246 *00,605* Not available NTIS

PB95-180253
Magnetic Susceptibility of Pr2-xCexCuO4 Monocrystals and Polycrystals.
PB95-180253 *04,677* Not available NTIS

PB95-180261
Broadband High-Optical-Density Filters in the Infrared.
PB95-180261 *04,309* Not available NTIS

PB95-180279
Suppression Effectiveness of Extinguishing Agents under Highly Dynamic Conditions.
PB95-180279 *00,020* Not available NTIS

PB95-180287
Crystal Structure and Magnetic Properties of CuGeO3.
PB95-180287 *04,678* Not available NTIS

PB95-180295
Laplace's Equation and the Dirichlet-Neumann Map in Multiply Connected Domains. (NIST Reprint).
PB95-180295 *03,962* Not available NTIS

PB95-180303
Observation of Oscillatory Magnetic Order in the Antiferromagnetic Superconductor HoNi2B2C.
PB95-180303 *04,679* Not available NTIS

PB95-180311
Early Detection of Room Fires Through Acoustic Emission. (NIST Reprint).
PB95-180311 *00,298* Not available NTIS

PB95-180329
Electronic Mode Stirring for Reverberation Chambers.
PB95-180329 *01,908* Not available NTIS

PB95-180337
Crosstalk between Microstrip Transmission Lines. (NIST Reprint).
PB95-180337 *02,225* Not available NTIS

PB95-180345
Analytical Expressions for Barkhausen Jump Size Distributions.
PB95-180345 *04,680* Not available NTIS

PB95-180352
Existence and Nonexistence Theorems of Finite Diameter Sequential Confidence Regions for Errors-in-Variables Models.
PB95-180352 *03,441* Not available NTIS

PB95-180360
Getting Started on Mosaic.
PB95-180360 *01,721* Not available NTIS

PB95-180378
Dual Frequency mm-Wave Radiometer Antenna for Airborne Remote Sensing of Atmosphere and Ocean.
PB95-180378 *02,006* Not available NTIS

PB95-180386
Taxonomy for Security Standards.
PB95-180386 *01,602* Not available NTIS

PB95-180394
Error Propagation in Laser Beam Spatial Parameters.
PB95-180394 *04,310* Not available NTIS

PB95-180402
Quasipotential and the Stability of Phase Lock in Nonhysteretic Josephson Junctions.
PB95-180402 *04,681* Not available NTIS

PB95-180410
Large-Amplitude Shapiro Steps and Self-Field Effects in High-Tc Josephson Weak Links.
PB95-180410 *04,682* Not available NTIS

PB95-180428
Design and Machining of Copper Specimens with Micro Holes for Accurate Heat Transfer Measurements.
PB95-180428 *02,658* Not available NTIS

PB95-180436
Atomic Branching Ratio Data for Oxygen-Like Species.
PB95-180436 *03,963* Not available NTIS

PB95-180444
NIST Strategies for Reducing Testing Requirements.
PB95-180444 *01,909* Not available NTIS

PB95-180451
Improved Eddy-Current Decay Method for Resistivity Characterization.
PB95-180451 *02,265* Not available NTIS

PB95-180469
Gust Factors Applied to Hurricane Winds.
PB95-180469 *00,446* Not available NTIS

PB95-180477
Dielectric Properties of Single Crystals of Al2O3, LaAlO3, SrTiO3, and MgO at Cryogenic Temperatures.
PB95-180477 *02,266* Not available NTIS

PB95-180485
Modal Characteristics of Bent Dual Mode Planar Optical Waveguide.
PB95-180485 *04,311* Not available NTIS

PB95-180493
Dependence of Tc on Debye Temperature Theta(sub D) for Various Cuprates.
PB95-180493 *04,683* Not available NTIS

PB95-180501
Microwave Leakage as a Source of Frequency Error and Long-Term Instability in Cesium Atomic-Beam Frequency Standards.
PB95-180501 *01,541* Not available NTIS

PB95-180519
Velocity Distribution of Atomic Beams by Gated Optical Pumping.
PB95-180519 *01,542* Not available NTIS

PB95-180527
Elastic Constants of a Material with Orthorhombic Symmetry: An Alternative Measurement Approach.
PB95-180527 *04,684* Not available NTIS

PB95-180535
Cross-Correlation Analysis Improves Time Domain Measurements.
PB95-180535 *01,543* Not available NTIS

PB95-180543
Concepts of the NIST EXPRESS Server.
PB95-180543 *02,781* Not available NTIS

PB95-180550
Handling Passwords with Security and Reliability in Background Processes.
PB95-180550 *01,722* Not available NTIS

PB95-180568
Microelectronic Test Structures for Feature Placement and Electrical Linewidth Metrology.
PB95-180568 *02,367* Not available NTIS

PB95-180576
Acid Gas Production in Inhibited Diffusion Flames.
PB95-180576 *01,390* Not available NTIS

PB95-180584
Burning Rate of Premixed Methane-Air Flames Inhibited by Fluorinated Hydrocarbons.
PB95-180584 *01,391* Not available NTIS

PB95-180592
Experimental and Numerical Burning Rates of Premixed Methane-Air Inhibited by Fluoromethanes.
PB95-180592 *01,392* Not available NTIS

PB95-180600
Laser Photoionization Measurements of Pressure in Vacuum.
PB95-180600 *03,964* Not available NTIS

PB95-180618
Hybrid Digital/Analog Servo for the NIST-7 Frequency Standard.
PB95-180618 *01,544* Not available NTIS

PB95-180626
Diagnosis and Treatment of an Oral Base-Metal Contact Lesion Following Negative Dermatologic Patch Tests.
PB95-180626 *00,172* Not available NTIS

PB95-180634
Improved Molecular Constants and Frequencies for the CO2 Laser from New High-J Regular and Hot-Band Frequency Measurements.
PB95-180634 *04,312* Not available NTIS

PB95-180642
Formation of Hydroxyapatite in a Polymeric Calcium Phosphate Cement.
PB95-180642 *00,173* Not available NTIS

PB95-180659
Laser Focused Atomic Deposition.
PB95-180659 *04,685* Not available NTIS

PB95-180667
Rayleigh Instability for a Cylindrical Crystal-Melt Interface.
PB95-180667 *01,010* Not available NTIS

PB95-180675
Food Irradiation Dosimetry.
PB95-180675 *00,041* Not available NTIS

PB95-180683
Radiochromic Solid-State Polymerization Reaction.
PB95-180683 *01,271* Not available NTIS

PB95-180691
Quantitative Measure of Efficiency of Monte Carlo Simulations.
PB95-180691 *01,011* Not available NTIS

PB95-180709
Stabilization of 3.3 and 5.1 m Lead-Salt Diode Lasers by Optical Feedback.
PB95-180709 *04,313* Not available NTIS

PB95-180717
Magnetic Properties of Single-Crystalline UCu3Al2.
PB95-180717 *04,686* Not available NTIS

PB95-180725
Epitaxial Growth and Characterization of the Ordered Vacancy Compound CuIn3Se5 on GaAs (100) Fabricated by Molecular Beam Epitaxy.
PB95-180725 *04,687* Not available NTIS

PB95-180733
Structural and Chemical Investigations of Na3(ABO4)3.4H2O-Type Sodalite Phases.
PB95-180733 *01,012* Not available NTIS

PB95-180741
Characterization of the Interaction of Hydrogen with Iridium Clusters in Zeolites by Inelastic Neutron Scattering Spectroscopy.
PB95-180741 *01,013* Not available NTIS

PB95-180758
Instrument for Evaluating Phase Behavior of Mixtures for Supercritical Fluid Experiments.
PB95-180758 *00,606* Not available NTIS

PB95-180766
Inelastic-Neutron-Scattering Studies of Poly(p-phenylene vinylene).
PB95-180766 *01,014* Not available NTIS

PB95-180774
New Concepts for Fire Protection of Passenger Rail Transportation Vehicles. (NIST Reprint).
PB95-180774 *04,863* Not available NTIS

PB95-180782
Supported Phospholipid/Alkanthiol Biomimetic Membranes: Insulating Properties.
PB95-180782 *03,470* Not available NTIS

PB95-180790
Progress on a Cryogenic Linear Trap for (199)Hg(+) Ions.
PB95-180790 *03,965* Not available NTIS

PB95-180808
Accuracy in Integrated Circuit Dimensional Measurements.
PB95-180808 *02,368* Not available NTIS

PB95-180816
Improving Photomask Linewidth Measurement Accuracy via Emulated Stepper Aerial Image Measurement.
PB95-180816 *02,911* Not available NTIS

PB95-180824
Activities of ISO Technical Committee 201 on Surface Chemical Analysis.
PB95-180824 *00,607* Not available NTIS

PB95-180832
Performance Characteristics of Fast Elliptic Solvers on Parallel Platforms.
PB95-180832 *01,723* Not available NTIS

PB95-180840
Federal Government and Information Technology Standards: Building the National Information Infrastructure.
PB95-180840 *01,812* Not available NTIS

PB95-180857
Laser-Produced and Tokamak Spectra of Lithiumlike Iron, Fe(23+).
PB95-180857 *04,314* Not available NTIS

PB95-180865
Powder Neutron Diffraction Investigation of Structure and Cation Ordering in Ba2+xBi2-xO6-y.
PB95-180865 *01,015* Not available NTIS

PB95-180873
Thermodynamic Study of the Reactions of Cyclodextrins with Primary and Secondary Aliphatic Alcohols, with D- and L-Phenylalanine, and with L-Phenylalanineamide.
PB95-180873 *01,016* Not available NTIS

PB95-180881
High Resolution Inelastic Neutron Scattering Study of Phonon Self-Energy Effects in YBCO.
PB95-180881 *04,688* Not available NTIS

PB95-180899
Antenna-Coupled High-Tc Air-Bridge Microbolometer on Silicon.
PB95-180899 *04,315* Not available NTIS

PB95-180907
Comparison of Magnetic Fields of Thin-Film Heads and Their Corresponding Bit Patterns Using Magnetic Force Microscopy.
PB95-180907 *03,763* Not available NTIS

PB95-180915
Flexible-Diaphragm Force Microscope.
PB95-180915 *03,966* Not available NTIS

PB95-180923
Melnikov Function and Homoclinic Chaos Induced by Weak Perturbations.
PB95-180923 *03,414* Not available NTIS

PB95-180931
Calculation of the Thermal Conductivity and Gas Permeability in a Uniaxial Bundle of Fibers.
PB95-180931 *03,058* Not available NTIS

PB95-180949
Tribometer for Measurements in Hostile Environments.
PB95-180949 *02,967* Not available NTIS

PB95-180956
Comparison of NIST and ISO Filtered Bremsstrahlung Calibration Beams.
PB95-180956 *03,967* Not available NTIS

PB95-180964
Calibration of Dosimeters for the Cryogenic Irradiation of Composite Materials Using an Electron Beam.
PB95-180964 *03,968* Not available NTIS

PB95-180972
Reducing the Effect of Local Oscillator Phase Noise on the Frequency Stability of Passive Frequency Standards.
PB95-180972 *01,545* Not available NTIS

PB95-180980
Scanning Tunneling Microscopy of the Charge-Density-Wave Structure in 1T-TaS2.
PB95-180980 *04,689* Not available NTIS

PB95-180998
Measurement of Very-Low Partial Pressures.
PB95-180998 *02,659* Not available NTIS

PB95-181004
Process Monitoring with Residual Gas Analyzers (RGAs): Limiting Factors.
PB95-181004 *02,660* Not available NTIS

PB95-181012
Local-Mode Dynamics in YH2 and YD2 by Isotope-Dilution Neutron Spectroscopy.
PB95-181012 *01,017* Not available NTIS

PB95-181020
Neutron Spectroscopic Evidence of Concentration-Dependent Hydrogen Ordering in the Octahedral Sublattice of beta-TbH2+x.
PB95-181020 *01,018* Not available NTIS

PB95-181038
Vibrations of Hydrogen and Deuterium in Solid Solution with Lutetium.
PB95-181038 *01,019* Not available NTIS

PB95-181046
Physics and Chemistry of Partial Discharge and Corona: Recent Advances and Future Challenges.
PB95-181046 *01,910* Not available NTIS

PB95-181053
Plasma Chemical Model for Decomposition of SF6 in a Negative Glow Corona Discharge.
PB95-181053 *01,020* Not available NTIS

PB95-181061
Terminally Anchored Chain Interphases: Their Chromatographic Properties.
PB95-181061 *01,272* Not available NTIS

PB95-181079
Terminally Anchored Chain Interphases: The Effect of Multicomponent, Polydisperse Solvents on Their Equilibrium Properties.
PB95-181079 *01,273* Not available NTIS

PB95-181087
Detection of OH+ in Its a(1)Delta State by Far Infrared Laser Magnetic Resonance.
PB95-181087 *01,021* Not available NTIS

PB95-181095
Suppression of Elevated Temperature Hydraulic Fluid and JP-8 Spray Flames.
PB95-181095 *00,021* Not available NTIS

PB95-181103
Moments of the Quartic Assignment Statistic with an Application to Multiple Regression.
PB95-181103 *03,442* Not available NTIS

PB95-181111
Morphological Development of Second-Phase Particles in Elastically-Stressed Solids.
PB95-181111 *03,355* Not available NTIS

PB95-181129
Practical Standards for PM and AM Noise at 5, 10 and 100 MHz.
PB95-181129 *01,546* Not available NTIS

PB95-181137
Sifting Through Nine Years of NIST Clock Data with TA2.
PB95-181137 *01,547* Not available NTIS

PB95-181145
Convective Stability in the Rayleigh-Benard and Directional Solidification Problems: High-Frequency Gravity Modulation.
PB95-181145 *04,208* Not available NTIS

PB95-181152
Prototype Information Retrieval System to Perform a Best-Match Search for Names.
PB95-181152 *02,740* Not available NTIS

PB95-181160
Dielectric Properties of Thin Film SrTiO3 Grown on LaAlO3 with YBa2Cu3O7-x Electodes.
PB95-181160 *02,267* Not available NTIS

PB95-181178
Water Adsorption at Polymer/Silicon Wafer Interfaces.
PB95-181178 *01,022* Not available NTIS

PB95-181186
Novel YBa2Cu3O7-x and YBa2Cu3O7-x/Y4Ba3O9 Multilayer Films by Bias-Masked 'On-Axis' Magnetron Sputtering.
PB95-181186 *04,690* Not available NTIS

PB95-181194
Control Stability of a Heat-Flow-Meter Appartus.
PB95-181194 *00,386* Not available NTIS

PB95-181202
Intra-Laboratory Comparison of a Line-Heat-Source Guarded Hot Plate and Heat-Flow-Meter Apparatus.
PB95-181202 *00,387* Not available NTIS

PB95-181210
Effect of Environmentally Exposures on the Properties of Polyisocyanurate Foam Insulation: Thermal Conductivity Measurements.
PB95-181210 *00,388* Not available NTIS

PB95-181228
Analysis of Autocorrelations in Dynamic Processes.
PB95-181228 *02,826* Not available NTIS

PB95-181236
Thermal Modeling of Absolute Cryogenic Radiometers.
PB95-181236 *04,316* Not available NTIS

PB95-181244
High-Resolution Diode-Laser Spectroscopy of Calcium.
PB95-181244 *03,969* Not available NTIS

PB95-182226
Checking the Net Contents of Packaged Goods as Adopted by the 79th National Conference on Weights and Measures, 1994, Third Edition, Supplement 4.
PB95-182226 *00,484* PC A04/MF A01

PB95-182234
National Voluntary Laboratory Accreditation Program Acoustical Testing Services.
PB95-182234 *04,188* PC A05/MF A01

PB95-182259
Algorithm to Describe the Spread of a Wall Fire under a Ceiling.
PB95-182259 *00,261* PC A04/MF A01

PB95-182267
Comparison of Fire Sprinkler Piping Materials: Steel, Copper, Chlorinated Polyvinyl Chloride and Polybutylene, in Residential and Light Hazard Installations.
PB95-182267 *00,299* PC A03/MF A01

PB95-182275
Keeping Your Site Comfortably Secure: An Introduction to Internet Firewalls.
PB95-182275 *02,730* PC A05/MF A01

PB95-182291
Seismic Safety of Federal Buildings. Initial Program: How Much Will It Cost.
PB95-182291 *00,447* PC A03/MF A01

PB95-182309
Indoor Air Quality Commissioning of a New Office Building.
PB95-182309 *00,262* PC A04/MF A01

PB95-182390
Assessment of Data by a Second-Order Transfer Function.
PB95-182390 *03,760* PC A05/MF A01

PB95-188827
Vehicle-to-Roadside Communications for Commercial Vehicle Operations: Requirements and Approaches.
PB95-188827 *04,860* PC A05/MF A01

PB95-188835
Program of the Manufacturing Engineering Laboratory, 1995. Infrastructural Technology, Measurements, and Standards for the U.S. Manufacturing Industries.
PB95-188835 *02,754* PC A11/MF A02

PB95-188850
Evaluation of the Economic Impacts Associated with the NIST Power and Energy Calibration Services.
PB95-188850 *02,461* PC A03/MF A01

PB95-188868
Santa Ana Fire Department Experiment at 1315 South Bristol, July 14, 1994.
PB95-188868 *00,389* PC A03/MF A01

PB95-188918
Fire Performance of an Interstitial Space Construction System.
PB95-188918 *00,390* PC A04/MF A01

PB95-188926
NIST Serial Holdings, 1995.
PB95-188926 *02,746* PC A12/MF A03

PB95-189437
MasPar MP-1 as a Computer Arithmetic Laboratory.
PB95-189437 *01,627* PC A03/MF A01

PB95-189445
Impact of the FCC's Open Network Architecture on NS/NP Telecommunications Security.
PB95-189445 *01,483* PC A03/MF A01

PB95-189452
Review of Measurements and Candidate Signatures for Early Fire Detection.
PB95-189452 *00,300* PC A03/MF A01

PB95-189460
Lubrication Theory for Reactive Spreading of a Thin Drop.
PB95-189460 *02,865* PC A03/MF A01

PB95-189478
National Voluntary Laboratory Accreditation Program: POSIX. Portable Operating System Interface.
PB95-189478 *02,661* PC A05/MF A01

PB95-189486
Operating Principles of MultiKron II Performance Instrumentation for MIMD Computers.
PB95-189486 *01,628* PC A03/MF A01

PB95-189494
Proceedings Report of the International Invitation Workshop on Development Assurance. Held in Ellicott City, Maryland on June 16-17, 1994.
PB95-189494 *02,912* PC A03/MF A01

PB95-189502
Motion-Model-Based Boundary Extraction.
PB95-189502 *01,849* PC A03/MF A01

PB95-189510
Assessment of the DOD Goal Security Architecture (DGSA) for Non-Military Use.
PB95-189510 *03,653* PC A03/MF A01

PB95-189528
Proceedings: Workshop on Research Needs in Wind Engineering. Held in Gaithersburg, Maryland on September 12-13, 1994.
PB95-189528 *00,448* PC A05/MF A01

PB95-190674
Field Evaluation of the System for Calibration of the Marshall Compaction Hammer.
PB95-190674 *01,323* PC A05/MF A01

PB95-190682
BLCC: The NIST 'Building Life-Cycle Cost' Program, Version 4.21. User's Guide and Reference Manual.
PB95-190682 *00,263* PC A06/MF A02

PB95-193173
Robotics Application to Highway Transportation. Volume 4. Proposals for Potential Research.
PB95-193173 *01,339* PC A07/MF A02

PB95-194205
Comparing Remote Procedure Calls: Open Network Computing, Distributed Computing Environment and International Organization for Standardization.
PB95-194205 *01,724* PC A03/MF A01

PB95-196697
Materials Science and Engineering Laboratory Annual Report, 1994. NAS-NRC Assessment Panel, April 6-7, 1995.
PB95-196697 *02,976* PC A06/MF A02

PB95-197455
Model Minimum Performance Specifications for Lidar Speed Measurement Devices.
PB95-197455 *04,861* PC A03/MF A01

PB95-198677
Real-Time Obstacle Avoidance Using Central Flow Divergence and Peripheral Flow.
PB95-198677 *02,937* PC A03/MF A01

PB95-198685
10 kV DC Resistive Divider Calibration.
PB95-198685 *02,063* PC A04/MF A01

PB95-198727
Study on Hazard Analysis in High Integrity Software Standards and Guidelines.
PB95-198727 *01,725* PC A04/MF A01

PB95-198735
Measurements of Indoor Pollutant Emissions from EPA Phase II Wood Stoves.
PB95-198735 *02,556* PC A04/MF A01

PB95-198743
IIW Commission V Quality Control and Quality Assurance of Welded Products Annual Report 1994/95.
PB95-198743 *02,866* PC A03/MF A01

PB95-198750
Apparel Manufacturing Glossary for Application Protocol Development.
PB95-198750 *02,755* PC A04/MF A01

PB95-198768
Cryogenic Properties of Inorganic Insulation Materials for ITER Magnets: A Review.
PB95-198768 *03,706* PC A10/MF A03

PB95-198859
Expert Control System Shell Version 1.0 User's Guide.
PB95-198859 *01,790* PC A03/MF A01

PB95-198917
Electromagnetic Shielding Characterization of Gaskets.
PB95-198917 *01,911* PC A03/MF A01

PB95-198925
Electronics and Electrical Engineering Laboratory Technical Publication Announcements Covering Laboratory Programs, July to September 1994 with 1995 EEEL Events Calendar.
PB95-198925 *01,912* PC A03/MF A01

PB95-198933
Inserting Line Segments into Triangulations and Tetrahedralizations.
PB95-198933 *03,415* PC A03/MF A01

PB95-199329
Object-Oriented Technology Research Areas.
PB95-199329 *01,726* PC A03/MF A01

PB95-200218
Evaluation of Wear Resistant Ceramic Valve Seats in Gas-Fueled Power Generation Engines. Topical Report, December 1991-April 1994.
PB95-200218 *02,466* PC A07/MF A02

PB95-200648
Methods for Analysis of Cancer Chemopreventive Agents in Human Serum.
PB95-200648 *03,502* PC A07/MF A02

PB95-200655
Heat and Moisture Transfer in Wood-Based Wall Construction: Measured versus Predicted.
PB95-200655 *00,391* PC A05/MF A01

PB95-200747
Publications of the National Institute of Standards and Technology 1992 Catalog.
PB95-200747 *00,014* PC A17/MF A04

PB95-202214
Core Potentials for Quasi-One-Electron Systems.
PB95-202214 *03,970* Not available NTIS

PB95-202222
In-situ Monitoring of Molecular Beam Epitaxial Growth Using Single Photon Ionization.
PB95-202222 *01,023* Not available NTIS

PB95-202230
Direct Detection of Atomic Arsenic Desorption from Si(100).
PB95-202230 *01,024* Not available NTIS

PB95-202248
Reduction of Light-Assisted Collisional Loss Rate from a Low-Pressure Vapor-Cell Trap.
PB95-202248 *03,971* Not available NTIS

PB95-202255
High-Efficiency, High-Power Difference-Frequency Generation of 0.9-1.5 mu m Light in BBO.
PB95-202255 *04,317* Not available NTIS

PB95-202263
Hydrogen Lyman-alpha Emission of Capella.
PB95-202263 *00,075* Not available NTIS

PB95-202271
Resonance Structure and Absolute Cross Sections in Near-Threshold Electron-Impact Excitation of the 4s(2) (1)S yields 4s4p (3)P Intercombination Transition in Kr(6+).
PB95-202271 *03,972* Not available NTIS

PB95-202289
Short-Range Correlation and Relaxation Effects on the (6p(2))(1)SO Autoionizing State of Atomic Barium.
PB95-202289 *03,973* Not available NTIS

PB95-202297
Connection between Superelastic and Inelastic Electron-Atom Collisions Involving Polarized Collision Partners.
PB95-202297 *03,974* Not available NTIS

PB95-202305
Femtosecond Time-Resolved Molecular Multiphoton Ionization: The Na2 System.
PB95-202305 *03,975* Not available NTIS

PB95-202313
Location of a (1)A(sub g) State in Bithiophene.
PB95-202313 *01,025* Not available NTIS

PB95-202321
Observations of 3C 273 with the Goddard High Resolution Spectrograph on the Hubble Space Telescope.
PB95-202321 *00,076* Not available NTIS

PB95-202339
Lowest Excited Singlet State of Isolated 1-phenyl-1,3-butadiene and 1-phenyl-1,3,5-hexatriene.
PB95-202339 *01,026* Not available NTIS

PB95-202347
Exponentially Rapid Coarsening and Buckling in Coherently Self-Stressed Thin Plates.
PB95-202347 *04,821* Not available NTIS

PB95-202354
Overcoming Hoelder Continuity in Ill-Posed Continuation Problems.
PB95-202354 *03,416* Not available NTIS

PB95-202362
Roles of Local Classical Acceleration and Spatial Separation in the Neutral Particle Analogs of the Aharonov-Bohm Phases.
PB95-202362 *03,976* Not available NTIS

PB95-202370
Laser Vacuum Ultraviolet Single Photon Ionization Probing of III-V Semiconductor Growth.
PB95-202370 *04,691* Not available NTIS

PB95-202388
Application of ODF to the Rietveld Profile Refinement of Polycrystalline Solid.
PB95-202388 *03,401* Not available NTIS

PB95-202396
Microstructure Study of Molybdenum Liners by Neutron Diffraction.
PB95-202396 *03,756* Not available NTIS

PB95-202404
Method to Determine the Calorimetric Equivalence Correction for a Coaxial Microwave Microcalorimeter.
PB95-202404 *01,913* Not available NTIS

PB95-202412
Developing a NIST Coaxial Microwave Power Standard at 1 mW.
PB95-202412 *01,914* Not available NTIS

PB95-202420
Flow of Alternative Agents in Piping.
PB95-202420 *00,022* Not available NTIS

PB95-202438
Analyses of Recent Experimental and Theoretical Determinations of e-H2 Vibrational Excitation Cross Sections: Assessing a Long-Standing Controversy.
PB95-202438 *03,977* Not available NTIS

PB95-202446
Test of Newton's Inverse Square Law of Gravitation Using the 300-m Tower at Erie, Colorado.
PB95-202446 *03,978* Not available NTIS

PB95-202453
Three-Vector Correlation Study of Orientation and Coherence Effects in Na(3p, (2)P1/2 inversely maps (2)P3/2)+He: Semiclassical and Quantum Calculations.
PB95-202453 *03,979* Not available NTIS

PB95-202461
Domain Effects in Faraday Effect Sensors Based on Iron Garnets.
PB95-202461 *02,268* Not available NTIS

PB95-202479
ROSAT All-Sky Survey of Active Binary Coronae. 1. Quiescent Fluxes for the RS Canum Venaticorum Systems.
PB95-202479 *00,077* Not available NTIS

PB95-202487
Early History and Future Outlook for the X-ray Crystal Density Method.
PB95-202487 *04,692* Not available NTIS

PB95-202495
Lunar Laser Ranging: A Continuing Legacy of the Apollo Program.
PB95-202495 *03,683* Not available NTIS

PB95-202503
Absolute Cross-Section Measurements for Electron-Impact Single Ionization of Se(+) and Te(+).
PB95-202503 *03,980* Not available NTIS

PB95-202511
Crossed-Beams Measurements of Absolute Cross Sections for Electron Impact Ionization of S(+).
PB95-202511 *03,981* Not available NTIS

PB95-202529
Absolute Cross Sections for Electron-Impact Single Ionization of Si(+) and Si(2+).
PB95-202529 *03,982* Not available NTIS

PB95-202537
Plasma Chemistry in Silane/Germane and Disilane/Germane Mixtures.
PB95-202537 *01,027* Not available NTIS

PB95-202545
n-Vector Correlations in Collision Dynamics with Atomic Orbital Alignment: The Importance of Coherence Denoting Azimuthal Structure for n (greater than or equal to) 3.
PB95-202545 *03,983* Not available NTIS

PB95-202552
Resonant Two-Color Detachment of H(-) with Excitation of H(n=2).
PB95-202552 *03,984* Not available NTIS

PB95-202560
Epitaxial Growth of Sb/GaSb Structures: An Example of V/III-V Heteroepitaxy.
PB95-202560 *04,693* Not available NTIS

PB95-202578
Numerical Solution of the Nonlinear Schroedinger Equation for Small Samples of Trapped Neutral Atoms.
PB95-202578 *03,985* Not available NTIS

PB95-202586
Vibrations of S1((1)B2u) p-Difluorobenzene - d4. S1-S0 Fluorescence Spectroscopy and ab Initio Calculations.
PB95-202586 *01,028* Not available NTIS

PB95-202594
Long-Range Parity-Nonconserving Interaction.
PB95-202594 *03,986* Not available NTIS

PB95-202602
Hole Dispersion and Enhancement of Antiferromagnetic Interaction of Localized Spins in High-Tc Superconductors.
PB95-202602 *04,694* Not available NTIS

PB95-202610
Dielectric Properties of Materials at Cryogenic Temperatures and Microwave Frequencies.
PB95-202610 *02,369* Not available NTIS

PB95-202628
Quantum Mechanics of a Solid-State Bar Gravitational Antenna.
PB95-202628 *03,987* Not available NTIS

PB95-202636
Failures of the Four-Wave Mixing Model for Cone Emission.
PB95-202636 *04,318* Not available NTIS

PB95-202644
Accuracy and Repeatability in Time Domain Network Analysis.
PB95-202644 *02,064* Not available NTIS

PB95-202651
Calibration of a Superconducting Gravimeter Using Absolute Gravity Measurements.
PB95-202651 *03,684* Not available NTIS

PB95-202669
Sobolev Approximation for Line Formation with Partial Frequency Redistribution.
PB95-202669 *00,078* Not available NTIS

PB95-202677
Recombination Line Intensities for Hydrogenic Ions-III. Effects of Finite Optical Depth and Dust.
PB95-202677 *00,079* Not available NTIS

PB95-202685
Vibrational Dependence of the Anisotropic Intermolecular Potential of Ar-HCl.
PB95-202685 *01,029* Not available NTIS

PB95-202693
Vibrational Dependence of the Anisotropic Intermolecular Potential of Ar-HF.
PB95-202693 *01,030* Not available NTIS

PB95-202701
Modified Effective Range Theory as an Alternative to Low-Energy Close-Coupling Calculations.
PB95-202701 *03,988* Not available NTIS

PB95-202719
Slow-Electron Collisions with CO Molecules in an Exact-Exchange Plus Parameter-Free Polarization Model.
PB95-202719 *03,989* Not available NTIS

PB95-202727
Superconducting Resonator and a Cryogenic GaAs Field-Effect Transistor Amplifier as a Single-Ion Detection System.
PB95-202727 *03,990* Not available NTIS

PB95-202735
Neutron Reflectivity Study of the Density Profile of a Model End-Grafted Polymer Brush: Influence of Solvent Quality.
PB95-202735 *01,274* Not available NTIS

PB95-202743
Generalized Stokes-Einstein Equation for Spherical Particle Suspensions.
PB95-202743 *01,031* Not available NTIS

PB95-202750
Stability and Surface Energies of Wetted Grain Boundaries in Aluminum Oxide.
PB95-202750 *03,059* Not available NTIS

PB95-202768
Off-Diagonal Orthorhombic-Symmetry Elastic Constants.
PB95-202768 *04,695* Not available NTIS

PB95-202776
Single Photon Ionization, Laser Optical Probe Technique for Semiconductor Growth.
PB95-202776 *01,032* Not available NTIS

PB95-202784
Critical-Current Degradation in Nb3 Al Wires Due to Axial and Transverse Stress.
PB95-202784 *02,226* Not available NTIS

PB95-202792
Slit-Jet Near-Infrared Spectroscopy and Internal Rotor Dynamics of the ArH2O van der Waals Complex: An Angular Potential-Energy Surface for Internal H2O Rotation.
PB95-202792 *01,033* Not available NTIS

PB95-202800
Orbital Stereochemistry: Discovering the Symmetries of Collision Processes.
PB95-202800 *01,034* Not available NTIS

PB95-202818
Probing Bose-Einstein Condensed Atoms with Short Laser Pulses.
PB95-202818 *03,991* Not available NTIS

PB95-202826
Low-Noise High-Speed Diode Laser Current Controller.
PB95-202826 *02,178* Not available NTIS

PB95-202834
Stellar Coronal Structures.
PB95-202834 *00,080* Not available NTIS

PB95-202842
Deuterium in the Local Interstellar Medium: Its Cosmological Significance.
PB95-202842 *00,081* Not available NTIS

PB95-202859
Peeking Through the Picket Fence: What Astrophysical Surprises May Be Present in the 100-1200 Angstrom Region.
PB95-202859 *00,082* Not available NTIS

PB95-202867
Variationally Stable Treatment of Two- and Three-Photon Detachment of H(-) Including Electron-Correlation Effects.
PB95-202867 *03,992* Not available NTIS

PB95-202875
Preferential In-Plane Rotational Excitation of H2O (001) by Translational-to-Vibrational Transfer from 2.2 eV H Atoms.
PB95-202875 *01,035* Not available NTIS

PB95-202883
Alignment in Two-Step Pulsed Laser Excitation of Rydberg Levels in Light Atoms: The Example of Sodium.
PB95-202883 *03,993* Not available NTIS

PB95-202891
Narrow-Band Tunable Diode Laser System with Grating Feedback, and a Saturated Absorption Spectrometer for Cs and Rb.
PB95-202891 *04,319* Not available NTIS

PB95-202909
Integrated-Optical Devices in Rare-Earth-Doped Glass.
PB95-202909 *02,179* Not available NTIS

PB95-202917
Threshold Electron Excitation of Na.
PB95-202917 *03,994* Not available NTIS

PB95-202925
Time Domain Network Analysis Using the Multiline TRL Calibration.
PB95-202925 *02,065* Not available NTIS

PB95-202933
Large Amplitude Skeletal Isomerization as a Promoter of Intramolecular Vibrational Relaxation in CH Stretch Excited Hydrocarbons.
PB95-202933 *01,036* Not available NTIS

PB95-202941
Sub-Doppler, Infrared Laser Spectroscopy of the Propyne 2nu1 Band: Evidence of z-Axis Coriolis Dominated Intramolecular State Mixing in the Acetylenic CH Stretch Overtone.
PB95-202941 *01,037* Not available NTIS

PB95-202958
Collisional Energy Transfer between Excited-State Strontium and Noble-Gas Atoms.
PB95-202958 *03,995* Not available NTIS

PB95-202966
Determination of Complex Structures from Powder Diffraction Data: The Crystal Structure of La3Ti5Al15O37.
PB95-202966 *01,038* Not available NTIS

PB95-202974
Importance of Bound-Free Correlation Effects for Vibrational Excitation of Molecules by Electron Impact: A Sensitivity Analysis.
PB95-202974 *03,996* Not available NTIS

PB95-202982
Acceleration of Intramolecular Vibrational Redistribution by methyl Internal Rotation. A Chemical Timing Study of p-fluorotoluene and p-fluorotoluene-d3.
PB95-202982 *01,039* Not available NTIS

PB95-202990
Hydration in Semicrystalline Polymers: Small-Angle Neutron Scattering Studies of the Effect of Drawing in Nylon-6 Fibers.
PB95-202990 *03,385* Not available NTIS

PB95-203006
High-Resolution, Direct Infrared Laser Absorption Spectroscopy in Slit Supersonic Jets: Intermolecular Forces and Unimolecular Vibrational Dynamics in Clusters.
PB95-203006 *01,040* Not available NTIS

PB95-203014
Rotational-RKR Inversion of Intermolecular Stretching Potentials: Extension to Linear Hydrogen Bonded Complexes.
PB95-203014 *01,041* Not available NTIS

PB95-203022
Rigid Bender Analysis of van der Waals Complexes: The Intermolecular Bending Potential of a Hydrogen Bond.
PB95-203022 *01,042* Not available NTIS

PB95-203030
Energy-Pooling Collisions in Barium.
PB95-203030 *03,997* Not available NTIS

PB95-203048
Continuous Gravity Observations Using Joint Institute for Laboratory Astrophysics Absolute Gravimeters.
PB95-203048 *03,685* Not available NTIS

PB95-203055
Kinetics of the Reaction C2H + O2 from 193 to 350 K Using Laser Flash Kinetic Infrared Absorption Spectroscopy.
PB95-203055 *01,043* Not available NTIS

PB95-203063
Construction of Silicon Nanocolumns with the Scanning Tunneling Microscope.
PB95-203063 *04,696* Not available NTIS

PB95-203071
Decrease of Fluorescence in Optical Fiber during Exposure to Pulsed or Continuous-Wave Ultraviolet Light.
PB95-203071 *04,320* Not available NTIS

PB95-203089
Casual Regularizing Deconvolution Filter for Optimal Waveform Reconstruction.
PB95-203089 *01,603* Not available NTIS

PB95-203097
Relative Photoionization and Photodetachment Cross Sections for Particular Fine-Structure Transitions with Application to Cl 3s-subshell Photoionization.
PB95-203097 *03,998* Not available NTIS

PB95-203105
Behavior of Atoms in a Compressed Magneto-Optical Trap.
PB95-203105 *03,999* Not available NTIS

PB95-203113
Dielectronic Capture Processes in the Electron-Impact Ionization of Sc(2+).
PB95-203113 *04,000* Not available NTIS

PB95-203121
Photodissociation Dynamics in Quantum State-Selected Clusters: A Test of the One-Atom Cage Effect in Ar-H2O.
PB95-203121 *01,044* Not available NTIS

PB95-203139
Photoelectron Spectroscopy of Small Antimony Cluster Anions: Sb(-), Sb2(-), Sb3(-), and Sb4(-).
PB95-203139 *01,045* Not available NTIS

PB95-203147
Charge Cloud Distribution of Heavy Atoms After Excitation by Polarized Electrons.
PB95-203147 *04,001* Not available NTIS

PB95-203154
Faraday Effect Current Sensor with Improved Sensitivity-Bandwidth Product.
PB95-203154 *02,180* Not available NTIS

PB95-203162
Pulsed Laser Photolysis Time-Resolved FT-IR Emission Studies of Molecular Dynamics.
PB95-203162 *04,002* Not available NTIS

PB95-203170
Electrical Method for Determining the Thickness of Metal Films and the Cross-Sectional Area of Metal Lines.
PB95-203170 *02,370* Not available NTIS

PB95-203188
JEDEC 'TCR' Interlaboratory Experiment: Lessons Learned.
PB95-203188 *02,371* Not available NTIS

PB95-203196
High Resolution, Jet-Cooled Infrared Spectroscopy of (HCl)2: Analysis of nu1 and nu2 HCl Stretching Fundamentals, Interconversion Tunneling, and Mode-Specific Predissociation Lifetimes.
PB95-203196 *01,046* Not available NTIS

PB95-203204
Slit-Jet Near-Infrared Diode Laser Spectroscopy of (DCl)2: nu1, nu2 DCl Stretching Fundamentals, Tunneling Dynamics, and the Influence of Large Amplitude 'Geared' Intermolecular Rotation.
PB95-203204 *01,047* Not available NTIS

PB95-203212
High Resolution Near Infrared Spectroscopy of HCl-DCl and DCl-HCl: Relative Binding Energies, Isomer Interconversion Rates, and Mode Specific Vibrational Predissociation.
PB95-203212 *01,048* Not available NTIS

PB95-203220
Environmental Durability of Glass-Fiber Composites.
PB95-203220 *03,166* Not available NTIS

PB95-203238
Laser Flash Photolysis, Time-Resolved Fourier Transform Infrared Emission Study of the Reaction Cl + C2H5 yields HCl(v) + C2H4.
PB95-203238 *01,049* Not available NTIS

PB95-203246
Quantitative Measurements of Enhanced Soot Production in a Flickering Methane/Air Diffusion Flame.
PB95-203246 *01,393* Not available NTIS

PB95-203253
PET and DINGO Tools for Deriving Distributed Implementations from Estelle.
PB95-203253 *01,727* Not available NTIS

PB95-203261
Laser Preparation and Probing of Initial and Final Orbital Alignment in Collision-Induced Energy Transfer Ca(4s5p,(1)P1) + He yields Ca(4s5p,(3)P2) + He.
PB95-203261 *04,003* Not available NTIS

PB95-203279
Initial and Final Orbital Alignment Probing of the Fine-Structure-Changing Collisions among the Ca (4s)(1)(4p)(1), (3)PJ States with He: Determination of Coherence and Conventional Cross-Sections.
PB95-203279 *04,004* Not available NTIS

PB95-203287
Geometric Characterization of Rockwell Diamond Indenters.
PB95-203287 *02,950* Not available NTIS

PB95-203295
Microform Calibrations in Surface Metrology.
PB95-203295 *02,951* Not available NTIS

PB95-203303
Low-Frequency, Active Vibration Isolation System.
PB95-203303 *02,710* Not available NTIS

PB95-203311
Laser-Induced Desorption of In and Ga from Si(100) and Adsorbate Enhanced Surface Damage.
PB95-203311 *01,050* Not available NTIS

PB95-203329
Pulsed Laser Irradiation at 532 nm of In and Ga Adsorbed on Si(100): Desorption, Incorporation, and Damage.
PB95-203329 *01,051* Not available NTIS

PB95-203337
Single-Photon Laser Ionization Time-of-Flight Mass Spectroscopy Detection in Molecular-Beam Epitaxy: Application to As4, As2, and Ga.
PB95-203337 *01,052* Not available NTIS

PB95-203345
Deposition Rates in Direct Current Diode Sputtering.
PB95-203345 *04,697* Not available NTIS

PB95-203352
Frequency Shifting of Pulsed Narrow-Band Laser Light in a Multipass Raman Cell.
PB95-203352 *04,321* Not available NTIS

PB95-203360
Two Principal Points of Symmetric, Strongly Unimodal Distributions.
PB95-203360 *03,443* Not available NTIS

PB95-203378
Linking Anisotropic Sharp and Diffuse Surface Motion Laws via Gradient Flows.
PB95-203378 *04,698* Not available NTIS

PB95-203386
Thermodynamics of the Hydrolysis of N-Acetyl-L-phenylalanine Ethyl Ester in Water and in Organic Solvents.
PB95-203386 *01,053* Not available NTIS

PB95-203394
Surface Modification of YBa2Cu3O7-delta Thin Films Using the Scanning Tunneling Microscope: Five Methods.
PB95-203394 *04,699* Not available NTIS

PB95-203402
Angle-Differential and Momentum-Transfer Cross Sections for Low-Energy Electron-Cs Scattering.
PB95-203402 *04,005* Not available NTIS

PB95-203410
Relativistic R-Matrix Calculations for Electron - Alkali-Metal-Atom Scattering: Cs as a Test Case.
PB95-203410 *04,006* Not available NTIS

PB95-203428
World of Building Codes.
PB95-203428 *00,449* Not available NTIS

PB95-203436
Outlier-Resistant Methods for Estimation and Model Fitting.
PB95-203436 *03,444* Not available NTIS

PB95-203444
Morphological Estimation of Tip Geometry for Scanned Probe Microscopy.
PB95-203444 *02,662* Not available NTIS

PB95-203451
Post-Process Control of Machine Tools.
PB95-203451 *02,952* Not available NTIS

PB95-203469
Resonance Fluorescence with Squeezed-Light Excitation.
PB95-203469 *04,322* Not available NTIS

PB95-203477
Short-Pulse Detachment of H(-) in the Presence of a Static Electric Field.
PB95-203477 *04,007* Not available NTIS

PB95-203485
Signatures of Large Amplitude Motion in a Weakly Bound Complex: High-Resolution IR Spectroscopy and Quantum Calculations for HeCO2.
PB95-203485 *01,054* Not available NTIS

PB95-203493
Oscillator Strengths and Radiative Branching Ratios in Atomic Sr.
PB95-203493 *04,008* Not available NTIS

PB95-203501
New High-Redshift Damped Lyman-alpha Absorption Systems and the Redshift Evolution of Damped Absorbers.
PB95-203501 *00,083* Not available NTIS

PB95-203519
Compensation for Substrate Permittivity in Probe-Tip Calibration.
PB95-203519 *01,915* Not available NTIS

PB95-203527
CCD Mosaic Images of the Supernova Remnant 3C 400.2.
PB95-203527 *00,084* Not available NTIS

PB95-203535
G203.2-12.3: A New Optical Supernova Remnant in Orion.
PB95-203535 *00,085* Not available NTIS

PB95-203543
High-Resolution Optical Multiplex Spectroscopy.
PB95-203543 *04,323* Not available NTIS

PB95-203550
Integral Occurring in Coherence Theory.
PB95-203550 *04,324* Not available NTIS

PB95-203568
Proposed Analysis of RCS Measurement Uncertainty.
PB95-203568 *01,871* Not available NTIS

PB95-203576
Accurate Measurement of Optical Detector Nonlinearity.
PB95-203576 *02,181* Not available NTIS

PB95-203584
Cone Emission from Laser-Pumped Two-Level Atoms. 1. Quantum Theory of Resonant Light Propagation.
PB95-203584 *04,325* Not available NTIS

PB95-203592
Cone Emission from Laser-Pumped Two-Level Atoms. 2. Analytical Model Studies.
PB95-203592 *04,326* Not available NTIS

PB95-203600
Suppression of Ionization in One- and Two-Dimensional Model Calculations.
PB95-203600 *04,009* Not available NTIS

PB95-203758
Structural Ceramics Database. Topical Report, June 1989-May 1991.
PB95-203758 *03,060* PC A04/MF A01

PB95-203790
Robotics Application to Highway Transportation. Volume 1. Final Report.
PB95-203790 *03,654* PC A03/MF A01

PB95-203816
Precision Lifetime Measurements of Cs 6p (2)P1/2 and 6p (2)P3/2 Levels by Single-Photon Counting.
PB95-203816 *04,010* Not available NTIS

PB95-203824
Hyperfine-Structure Studies of Zr II: Experimental and Relativistic Configuration-Interaction Results.
PB95-203824 *04,011* Not available NTIS

PB95-203832
Stabilization of Optical Phase/Frequency of a Laser System: Application to a Commercial Dye Laser with an External Stabilizer.
PB95-203832 *04,327* Not available NTIS

PB95-203840
Improved Hyperfine Measurements of the Na NP Excited State Through Frequency-Controlled Dopplerless Spectroscopy in a Zeeman Magneto-Optic Laser Trap.
PB95-203840 *04,012* Not available NTIS

PB95-206181
Proceedings of the Manufacturing Technology Needs and Issues: Establishing National Priorities and Strategies Conference. Held in Gaithersburg, Maryland on April 26-28, 1994.
PB95-206181 *02,930* PC A22/MF A04

PB95-208724
Electronics and Electrical Engineering Laboratory Technical Progress Bulletin Covering Laboratory Programs, October to December 1994 with 1995 EEEL Events Calendar.
PB95-208724 *02,372* PC A04/MF A01

PB95-208757
Optical Performance of Commercial Windows.
PB95-208757 *00,392* PC A09/MF A02

PB95-209193
NIST Industrial Impacts: A Sampling of Successful Partnerships (Revision, March 1995).
PB95-209193 *00,489* PC A05/MF A01

PB95-209300
Droplet Transfer Modes for a MIL 100S-1 GMAW Electrode.
PB95-209300 *02,867* PC A04/MF A01

PB95-209821
Electronics and Electrical Engineering Laboratory Technical Progress Bulletin Covering Laboratory Programs, April to June 1991, with 1992 EEEL Events Calendar.
PB95-209821 *01,916* PC A03/MF A01

PB95-209854
Automated Manufacturing Research Facility 1994 Annual Report.
PB95-209854 *00,015* PC A05/MF A01

PB95-209862
Design, Specification and Tolerancing of Micrometer-Tolerance Assemblies.
PB95-209862 *02,913* PC A03/MF A01

PB95-209870
Concentrations of Chlorinated Hydrocarbons, Heavy Metals and Other Elements in Tissues Banked by the Alaska Marine Mammal Tissue Archival Project.
PB95-209870 *02,590* PC A06/MF A02

PB95-209888
Reactor Radiation Technical Activities, 1994. NAS-NRC Assessment Panel, April 6-7, 1995.
PB95-209888 *03,732* PC A08/MF A02

PB95-209896
Polymers Technical Activities 1994. NAC-NRC Assessment Panel, April 6-7, 1995.
PB95-209896 *01,275* PC A07/MF A02

PB95-209920
Computer Systems Laboratory Annual Report 1994.
PB95-209920 *01,629* PC A07/MF A02

PB95-210167
Issues Concerning Material Removal Shape Element Volumes (MRSEVs).
PB95-210167 *02,885* PC A03/MF A01

PB95-210225
NIST Workshop on Gas Sensors: Strategies for Future Technologies. Proceedings of a Workshop. Held in Gaithersburg, Maryland on September 8-9, 1993.
PB95-210225 *00,507* PC A08/MF A02

PB95-210480
Electronics and Electrical Engineering Laboratory Technical Progress Bulletin Covering Laboratory Programs, January to March 1992, with 1992/1993 EEEL Events Calendar.
PB95-210480 *01,917* PC A03/MF A01

PB95-210498
Room-Temperature Flexure Fixture for Advanced Ceramics.
PB95-210498 *03,061* PC A03/MF A01

PB95-210522
Calculating Time-to-Contact Using Real-Time Quantized Optical Flow.
PB95-210522 *01,604* PC A03/MF A01

PB95-210589
Interim Testing Artifact (ITA): A Performance Evaluation System for Coordinate Measuring Machines (CMMs). User Manual.
PB95-210589 *02,914* PC A04/MF A01

PB95-210928
Assessment of Site Response Analysis Procedures.
PB95-210928 *00,450* PC A07/MF A02

PB95-210936
Electronic Implementors' Workshop.
PB95-210936 *01,484* PC A03/MF A01

PB95-210944
Measurements of Outdoor Air Distribution in an Office Building.
PB95-210944 *00,264* PC A04/MF A01

PB95-211918
Survey of Steel Moment-Resisting Frame Buildings Affected by the 1994 Northridge Earthquake.
PB95-211918 *00,451* PC A09/MF A02

PB95-213583
Boundary Lubrication of Silicon Nitride.
PB95-213583 *03,226* PC A18/MF A04

PB95-216602
Self Monitoring Accounting Systems.
PB95-216602 *00,007* PC A03/MF A01

PB95-216883
Overview of the Text REtrieval Conference (3rd) (TREC-3). Held in Gaithersburg, Maryland on November 2-4, 1994.
PB95-216883 *01,728* PC A25/MF A06

PB95-216891
White Papers Prepared for the White House: Construction Industry Workshop on National Construction Goals. Held on December 14-16, 1994.
PB95-216891 *01,299* PC A08/MF A02

PB95-216917
Theoretical Evaluation of the Vapor Compression Cycle with a Liquid-Line/Suction-Line Heat Exchanger, Economizer, and Ejector.
PB95-216917 *02,607* PC A03/MF A01

PB95-216925
Polarimetric Calibration of Reciprocal-Antenna Radars.
PB95-216925 *01,872* PC A03/MF A01

PB95-216990
Burning Rate and Flame Heat Flux For PMMA in the Cone Calorimeter.
PB95-216990 *00,393* PC A07/MF A02

PB95-217097
Japan Technology Program Assessment. Simulation: State-of the-Art in Japan.
PB95-217097 *02,827* PC A03/MF A01

PB95-217147
Water Droplet Evaporation from Radiantly Heated Solids.
PB95-217147 *00,394* PC A08/MF A02

PB95-217162
Compartment Fire Combustion Dynamics. Annual Report, September 1, 1993-September 1, 1994.
PB95-217162 *00,203* PC A04/MF A01

PB95-219218
Electronic Access: Blueprint for the National Archives and Records Administration.
PB95-219218 *02,731* PC A04/MF A01

PB95-219325
Network Brokers Handbook: An Entrepreneurial Guide to Cooperative Strategies for Manufacturing Competitiveness.
PB95-219325 *00,490* PC A08/MF A02

PB95-219416
Extreme Wind Distribution Tails: A 'Peaks Over Threshold' Approach.
PB95-219416 *00,127* PC A05/MF A01

PB95-220414
Outline of a Multiple Dimensional Reference Model Architecture and a Knowledge Engineering Methodology for Intelligent Systems Control.
PB95-220414 *03,703* PC A03/MF A01

PB95-220422
Computer Simulations of Airflow and Radon Transport in Four Large Buildings.
PB95-220422 *02,557* PC A03/MF A01

PB95-220430
NIST Reactor: Summary of Activities, October 1993 through September 1994.
PB95-220430 *04,700* PC A09/MF A02

PB95-220448
Prediction of Cracking in Reinforced Concrete Structures.
PB95-220448 *03,725* PC A04/MF A01

PB95-220455
Testing of Selected Self-Leveling Compounds for Floors.
PB95-220455 *00,395* PC A03/MF A01

PB95-220463
Time and Frequency: Bibliography of NIST Publications, March 1995.
PB95-220463 *01,548* PC A06/MF A02

PB95-220471
Extreme Wind Estimates by the Conditional Mean Exceedance Procedure.
PB95-220471 *00,120* PC A03/MF A01

PB95-220489
Survey of Concrete Transport Properties and Their Measurement.
PB95-220489 *00,396* PC A04/MF A01

PB95-220497
Compositional Analysis of Beneficiated Fly Ashes.
PB95-220497 *00,397* PC A03/MF A01

PB95-220505
Texture-Independent Vision-Based Closed-Loop Fuzzy Controllers for Navigation Tasks.
PB95-220505 *00,183* PC A03/MF A01

PB95-220513
ISO Environmental Management Standardization Efforts.
PB95-220513 *02,524* PC A03/MF A01

PB95-220521
Performance Testing of a Family of Type I Combination Appliance.
PB95-220521 *02,505* PC A03/MF A01

PB95-220539
Tables of X-ray Mass Attenuation Coefficients and Mass Energy-Absorption Coefficients 1 keV to 20 MeV for Elements Z = 1 to 92 and 48 Additional Substances of Dosimetric Interest.
PB95-220539 *04,013* PC A06/MF A02

PB95-220547
Evaluation of Thermal Wave Imaging for Detection of Machining Damage in Ceramics.
PB95-220547 *03,062* PC A05/MF A02

PB95-220554
Analysis of ANSI ASC X12 and UN/EDIFACT Electronic Data Interchange (EDI) Standards.
PB95-220554 *01,729* PC A03/MF A01

PB95-220588
Persistent Object Base System Testing and Evaluation.
PB95-220588 *01,730* PC A05/MF A01

PB95-226684
Building and Fire Research Laboratory Publications, 1994.
PB95-226684 *00,398* PC A07/MF A02

PB95-226692
Guide for the Use of the International System of Units (SI).
PB95-226692 *02,747* PC A05/MF A01

PB95-226866
Standard Reference Materials: Polystyrene Films for Calibrating the Wavelength Scale of Infrared Spectrophotometers - SRM 1921.
PB95-226866 *03,386* PC A03/MF A01

PB95-226916
Laser Doppler Velocimeter Studies of the Pipeflow Produced by a Generic Header.
PB95-226916 *02,602* PC A05/MF A01

PB95-231585
Behavior of Mock-Ups in the California Technical Bulletin 133 Test Protocol: Fabric and Barrier Effects.
PB95-231585 *00,301* PC A05/MF A01

PB95-231593
4SIGHT Manual: A Computer Program for Modelling Degradation of Underground Low Level Waste Concrete Vaults.
PB95-231593 *03,726* PC A05/MF A01

PB95-231601
Enhancements to Program IDARC: Modeling Inelastic Behavior of Welded Connections in Steel Moment-Resisting Frames.
PB95-231601 *00,452* PC A05/MF A01

PB95-231700
Carbon Monoxide Production in Compartment Fires: Reduced-Scale Enclosure Test Facility.
PB95-231700 *01,394* PC A10/MF A03

PB95-231726
Introduction to the P1003.1g and CPI-C Network Application Programming Interfaces.
PB95-231726 *01,731* PC A03/MF A01

PB95-231775
Performance of Federal Buildings in the January 17, 1994 Northridge Earthquake.
PB95-231775 *00,453* PC A03/MF A01

PB95-231783
Operating Principles of the SBus MultiKron Interface Board.
PB95-231783 *01,630* PC A03/MF A01

PB95-231817
Suppression of High Speed Turbulent Flames in a Detonation/Deflagration Tube.
PB95-231817 *01,395* PC A04/MF A01

PB95-231833
Algorithm Testing and Evaluation Program for Coordinate Measuring Systems: Long Range Plan.
PB95-231833 *02,915* PC A03/MF A01

PB95-231841
Electronics and Electrical Engineering Laboratory Technical Publication Announcements Covering Laboratory Programs, October to December 1994 with 1995 EEEL Events Calendar.
PB95-231841 *01,918* PC A03/MF A01

PB95-231858
Comparison of the Seismic Provisions of Model Building Codes and Standards to the 1991 NEHRP Recommended Provisions.
PB95-231858 *00,315* PC A05/MF A02

PB95-231866
Conceptual Design Plan for the National Advanced Manufacturing Testbed.
PB95-231866 *02,828* PC A05/MF A01

PB95-231882
Standards Policy and Information Infrastructure.
PB95-231882 *01,485* PC A20/MF A04

PB95-231908
Guidelines for the Evaluation of X.500 Directory Products.
PB95-231908 *02,732* PC A04/MF A01

PB95-232518
NIST Standard Reference Materials (Trade Name) Catalog 1995-1996.
PB95-232518 *00,508* PC A03/MF A01

PB95-232633
Abstract and Index Collection in the Research Information Center of the National Institute of Standards and Technology.
PB95-232633 *02,741* PC A03/MF A01

PB95-242277
Electronics and Electrical Engineering Laboratory Technical Publication Announcements Covering Laboratory Programs, January to March 1995 with 1995 EEEI Events Calendar.
PB95-242277 *02,373* PC A03/MF A01

PB95-242285
Operating Procedures and Life Cycle Documentation for the Initial Graphics Exchange Specification.
PB95-242285 *02,782* PC A04/MF A01

PB95-242293
ISO TC 184/SC4 Reference Manual.
PB95-242293 *02,663* PC A04/MF A01

PB95-242301
Precision in Machining: Research Challenges.
PB95-242301 *02,953* PC A04/MF A01

PB95-242319
CSTL Technical Activities, 1994.
PB95-242319 *00,608* PC A16/MF A03

PB95-242327
Mixing and Radiation Properties of Buoyant Turbulent Diffusion Flames.
PB95-242327 *01,396* PC A05/MF A02

PB95-242335
Parallel and Serial Implementations of SLI Arithmetic.
PB95-242335 *01,732* PC A03/MF A01

PB95-242350
Unified Telerobotic Architecture Project (UTAP) Standard Interface Environment (SIE), May 1995.
PB95-242350 *02,938* PC A09/MF A02

PB95-242368
Fracture Testing of Large-Scale Thin-Sheet Aluminum Alloy.
PB95-242368 *00,024* PC A03/MF A01

PB95-242376
National Voluntary Laboratory Accreditation Program: Electromagnetic Compatibility and Telecommunications. FCC Methods.
PB95-242376 *02,664* PC A06/MF A02

PB95-242384
DETAN 95: Computer Code for Calculating Spectrum-Averaged Cross Sections and Detector Responses in Neutron Spectra.
PB95-242384 *04,014* PC A04/MF A01

PB95-242400
Measuring Long Gage Blocks with the NIST Line Scale Interferometer.
PB95-242400 *02,665* PC A03/MF A01

PB95-242418
Testability of Object-Oriented Systems.
PB95-242418 *01,733* PC A05/MF A01

PB95-251617
Water-Vapor Measurements of Low-Slope Roofing Materials.
PB95-251617 *00,399* PC A03/MF A01

PB95-251625
SF6 Insulation: Possible Greenhouse Problems and Solutions.
PB95-251625 *02,269* PC A03/MF A01

PB95-251633
Submarine Automation: Demonstration No. 5.
PB95-251633 *03,748* PC A03/MF A01

PB95-251641
Study of Potential Applications of Automation and Robotics Technology in Construction, Maintenance and Operation of Highway Systems: A Final Report. Volume 4.
PB95-251641 *01,340* PC A06/MF A02

PB95-251658
Algorithm Testing and Evaluation Program for Coordinate Measuring Systems: Testing Methods.
PB95-251658 *02,666* PC A03/MF A01

PB95-251666
User's Guide for the Algorithm Testing System Version 2.0.
PB95-251666 *02,916* PC A03/MF A01

PB95-251674
Center for High Integrity Software System Assurance: Initial Goals and Activities.
PB95-251674 *01,734* PC A03/MF A01

PB95-251682
Study of Potential Applications of Automation and Robotics Technology in Construction, Maintenance and Operation of Highway Systems: A Final Report. Volume 1.
PB95-251682 *01,341* PC A06/MF A02

PB95-251690
Study of Potential Applications of Automation and Robotics Technology in Construction, Maintenance and Operation of Highway Systems: A Final Report. Volume 3.
PB95-251690 *01,342* PC A15/MF A03

PB95-251708
Information Technologies Make Business Sense for the Custom Therapeutic Footwear Industry.
PB95-251708 *02,829* PC A03/MF A01

PB95-251716
Gage Block Handbook.
PB95-251716 *02,667* PC A08/MF A02

PB95-251724
Method and Evaluation of Character Stroke Preservation on Handprint Recognition.
PB95-251724 *01,850* PC A03/MF A01

PB95-251732
Standard Reference Material 1744: Aluminum Freezing-Point Standard.
PB95-251732 *01,055* PC A03/MF A01

PB95-253563
Product Models and Virtual Prototypes in Mechanical Engineering.
PB95-253563 *02,783* PC A03/MF A01

PB95-253571
Advanced Mass Calibration and Measurement Assurance Program for State Calibration Laboratories.
PB95-253571 *02,492* PC A03/MF A01

PB95-253589
Determination of the Residual Stresses Near the Ends of Skip Welds Using Neutron Diffraction and X-ray Diffraction Procedures.
PB95-253589 *02,868* PC A03/MF A01

PB95-253597
Least-Cost Energy Decisions for Buildings. Part 3. Choosing Economic Evaluation Methods. Video Training Workbook.
PB95-253597 *00,265* PC A04/MF A01

PB95-253605
International Green Building Conference and Exposition (2nd). Held in Big Sky, Montana on August 13-15, 1995.
PB95-253605 *02,525* PC A04/MF A01

PB95-254439
Materials Science and Engineering Laboratory Annual Report, December 1993.
PB95-254439 *02,668* PC A03/MF A01

PB95-255204
Proceedings of the Applied Diamond Conference 1995: Applications of Diamond Films and Related Materials International Conference (3rd). Held in Gaithersburg, Maryland, on August 21-24, 1995.
PB95-255204 *04,701* PC A99/MF E11

PB95-255824
Simple Method of Composition Shifting with a Distillation Column for a Heat Pump Employing a Zeotropic Refrigerant Mixture.
PB95-255824 *02,603* PC A03/MF A01

PB95-255832
Integrated Vision Touch-Probe System for Dimensional Inspection Tasks.
PB95-255832 *02,917* PC A03/MF A01

PB95-255840
NIST SRM 9983 High-Rigidity Ball-Bar Stand. User Manual.
PB95-255840 *02,669* PC A03/MF A01

PB95-255865
Study of Potential Applications of Automation and Robotics Technology in Construction, Maintenance and Operation of Highway Systems: A Final Report. Volume 2.
PB95-255865 *01,343* PC A19/MF A04

PB95-255881
Proceedings of the Meeting of the Intergovernmental U.S.-Russian Business Development Committee's Standard Working Group (4th). Held in New York City, New York on March 27-29, 1995 and in Northbrook, Illinois on March 30-31, 1995.
PB95-255881 *00,496* PC A11/MF A03

PB95-255899
New Mass Transport Elements and Components for the NIST IAQ Model.
PB95-255899 *02,558* PC A05/MF A01

PB95-255923
Reproducibility of the Temperature of the Ice Point in Routine Measurements.
PB95-255923 *04,015* PC A03/MF A01

PB95-256053
Applications of Diamond Films and Related Materials: International Conference (3rd). Held in Gaithersburg, Maryland on August 21-24, 1995. Supplement to NIST Special Publication 885.
PB95-256053 *03,063* PC A04/MF A01

PB95-256335
Sliding Vane Flow Conditioner Tests in a 100 Diameter Long 10 inch Natural Gas Orifice Meter at Pacific Gas and Electric. Topical Report, 1990-1992.
PB95-256335 *02,493* PC A04/MF A01

PB95-260618
Thermochemical and Chemical Kinetic Data for Fluorinated Hydrocarbons.
PB95-260618 *01,056* PC A09/MF A02

PB95-260725
Strengthening Methodology for Lightly Reinforced Concrete Frames: Recommended Design Guidelines for Strengthening with Infill Walls.
PB95-260725 *00,454* PC A04/MF A01

PB95-260758
45 deg/0 deg Reflectance Factors of Pressed Polytetrafluoroethylene (PTFE) Powder.
PB95-260758 *04,328* PC A06/MF A02

PB95-260766
Semiconductor Measurement Technology: HOTPAC. Programs for Thermal Analysis Including Version 3.0 of the TXYZ Program, TXYZ30, and the Thermal MultiLayer Program, TML.
PB95-260766 *02,374* PC A05/MF A01

PB95-260808
NIST Standard Reference Data Products Catalog, 1995-96. Achieve with Standard Reference Data.
PB95-260808 *01,057* PC A03/MF A01

PB95-260816
Long-Term Performance of Engineered Concrete Barriers.
PB95-260816 *03,727* PC A03/MF A01

PB95-261897
Journal of Research of the National Institute of Standards and Technology, May/June 1995. Volume 100, Number 3.
PB95-261897 *02,670* PC A07/MF A02

PB95-261905
Determining the Magnetic Properties of 1 kg Mass Standards.
PB95-261905 *04,016*
(Order as PB95-261897, PC A07/MF A02)

PB95-261913
Intercomparison of Photometric Units Maintained at NIST (USA) and PTB (Germany), 1993.
PB95-261913 *04,329*
(Order as PB95-261897, PC A07/MF A02)

PB95-261921
Determination of the Transmittance Uniformity of Optical Filter Standard Reference Materials.
PB95-261921 *02,182*
(Order as PB95-261897, PC A07/MF A02)

PB95-261939
Low-Frequency Model for Radio-Frequency Absorbers.
PB95-261939 *04,424*
(Order as PB95-261897, PC A07/MF A02)

PB95-261947
Using Quantized Breakdown Voltage Signals to Determine the Maximum Electric Fields in a Quantum Hall Effect Sample.
PB95-261947 *02,375*
(Order as PB95-261897, PC A07/MF A02)

PB95-261954
High Accuracy Measurement of Aperture Area Relative to a Standard Known Aperture.
PB95-261954 *01,919*
(Order as PB95-261897, PC A07/MF A02)

PB95-261962
New IUPAC Guidelines for the Reporting of Stable Hydrogen, Carbon, and Oxygen Isotope-Ratio Data. Letter to the Editor.
PB95-261962 *01,058*
(Order as PB95-261897, PC A07/MF A02)

PB95-267779
NIOSH Comments to DOL on Risk Estimates from the Cadmium Cohort Study by L. Stayner, February 7, 1992.
PB95-267779 *03,604* PC A02/MF A01

PB95-267803
Improving Neural Network Performance for Character and Fingerprint Classification by Altering Network Dynamics.
PB95-267803 *01,851* PC A03/MF A01

PB95-267829
Expression Formatter for MACSYMA.
PB95-267829 *01,735* PC A03/MF A01

PB95-267845
Effect of Training Dynamics on Neural Network Performance.
PB95-267845 *01,852* PC A03/MF A01

PB95-267860
Design Engineering Research at NIST.
PB95-267860 *02,784* PC A03/MF A01

PB95-267886
Unravel: A CASE Tool to Assist Evaluation of High Integrity Software. Volume 1. Requirements and Design.
PB95-267886 *01,736* PC A05/MF A01

PB95-267894
Unravel: A CASE Tool to Assist Evaluation of High Integrity Software. Volume 2. User Manual.
PB95-267894 *01,737* PC A04/MF A01

PB95-267928
Estimation of Measurement Uncertainty of Small Circular Features Measured by CMMs.
PB95-267928 *02,918* PC A03/MF A01

PB95-267936
PCASYS: A Pattern-Level Classification Automation System for Fingerprints.
PB95-267936 *01,853* PC A03/MF A01

PB95-267944
National Voluntary Laboratory Accreditation Program (NVLAP): Commercial Products Testing.
PB95-267944 *02,671* PC A02/MF A01

PB95-267985
National Voluntary Laboratory Accreditation Program: Thermal Insulation Materials.
PB95-267985 *02,977* PC A05/MF A01

PB95-267993
National Voluntary Laboratory Accreditation Program. GOSIP: Government Open Systems Interconnection Profile.
PB95-267993 *01,486* PC A06/MF A02

PB95-269817
National Construction Sector Goals: Industry Strategies for Implementation.
PB95-269817 *00,204* PC A03/MF A01

PB95-270039
Ceramic Powders Characterization: Results of an International Laboratory Study.
PB95-270039 *02,672* PC A22/MF A04

PB95-270047
Project Summaries 1995: NIST Building and Fire Research Laboratory.
PB95-270047 *00,400* PC A10/MF A03

PB95-270062
Proceedings of the 1995 Workshop on Fire Detector Research. Held on February 6-7, 1995.
PB95-270062 *02,611* PC A03/MF A01

PB95-501953
Building Life Cycle Cost Computer Program (BLCC), Version 4.2-95 (for Microcomputers).
PB95-501953 *00,266* CP D02

PB95-502563
Codes for Named Populated Places, Primary County Divisions, and Other Locational Entities of the United States (FIPS PUB 55-3) (on Magnetic Tape).
PB95-502563 *00,129* CP T05

PB95-502779
Building Life Cycle Cost Computer Program (BLCC) Version 4.21-95 (for Microcomputers).
PB95-502779 *00,267* CP D02

PB95-503280
FIPS PUB 8-6, Metropolitan Areas (for Microcomputers).
PB95-503280 *04,874* Diskette $59.00

PB95-503397
Building Life Cycle Cost Computer Program (BLCC) Version 4.22-95 (for Microcomputers).
PB95-503397 *00,268* CP D02

PB95-503504
Countries, Dependencies, Areas of Special Sovereignty, and Their Principal Administrative Divisions (for Microcomputers).
PB95-503504 *00,130* Diskette $30.00

PB95-937300
Validated Products List (Cobol, Fortran, ADA, Pascal, MUMPS, SQL).
PB95-937300 *01,738* Standing Order

PB95-962000
CALS-Automated Interchange of Technical Information.
PB95-962000 *03,666* Standing Order

PB95-962100
CALS-Digital Representation for Communication of Product Data: IGES Application Subsets.
PB95-962100 *03,667* Standing Order

PB95-962200
CALS-Markup Requirements and Generic Style Specifications for Electronic Printed Output and Exchange of Text.
PB95-962200 *03,668* Standing Order

PB95-962300
CALS-Raster Graphics Representation Binary Format Requirements.
PB95-962300 *03,669* Standing Order

PB95-962400
CALS-Digital Representation for Communication of Illustration Date: CGM Application Profile.
PB95-962400 *03,670* Standing Order

PB95-962500
CALS-Department of Defense Computer Aided Acquisition Logistic Support (CALS).
PB95-962500 *03,671* Standing Order

PB95-962600
CALS-Contractor Integrated Technical Information Service (CITIS), Functional Requirements.
PB95-962600 *03,672* Standing Order

PB96-101050
Degradation of Powder Epoxy Coated Panels Immersed in a Saturated Calcium Hydroxide Solution Containing Sodium Chloride.
PB96-101050 *01,344* PC A03/MF A01

PB96-102017
Exact Recursion Relation Solution for the Steady-State Surface Temperature of a General Multilayer Structure.
PB96-102017 *02,376* Not available NTIS

PB96-102025
Single Photon Laser Ionization as an In-situ Diagnostic for MBE growth.
PB96-102025 *01,059* Not available NTIS

PB96-102033
Far-Ultraviolet Flare on a Pleiades G Dwarf.
PB96-102033 *00,086* Not available NTIS

PB96-102041
Ab initio Calculations for Helium: A Standard for Transport Property Measurements.
PB96-102041 *01,060* Not available NTIS

PB96-102058
Merged-Beams Energy-Loss Technique for Electron-Ion Excitation: Absolute Total Cross Sections for O(5+) (2s yields 2p).
PB96-102058 *04,017* Not available NTIS

PB96-102066
Step-Edge and Stacked-Heterostructure High-Tc Josephson Junctions for Voltage-Standard Arrays.
PB96-102066 *04,702* Not available NTIS

PB96-102074
Faster Monte Carlo Simulations.
PB96-102074 *04,018* Not available NTIS

PB96-102082
Resonances in Two-Dimensional Array Oscillator Circuits.
PB96-102082 *02,066* Not available NTIS

PB96-102090
Vapour Pressures and Gas-Phase (p, rho n, T) Values for CF3CHF2(R125).
PB96-102090 *04,019* Not available NTIS

PB96-102108
Fire Codes for Global Practice.
PB96-102108 *00,205* Not available NTIS

PB96-102116
How to Evaluate Alternative Designs Based on Fire Modeling.
PB96-102116 *00,206* Not available NTIS

PB96-102124
Energy Dependences of Absorption in Beryllium Windows and Argon Gas.
PB96-102124 *04,020* Not available NTIS

PB96-102132
Simultaneous Optical Measurement of Soot Volume Fraction, Temperature, and CO2 in Heptane Pool Fire.
PB96-102132 *01,397* Not available NTIS

PB96-102140
Remineralization of Root Lesions with Concentrated Calcium and Phosphate Solutions.
PB96-102140 *03,567* Not available NTIS

PB96-102157
Application of Single Electron Tunneling: Precision Capacitance Ratio Measurements.
PB96-102157 *04,703* Not available NTIS

PB96-102165
Frozen Orbits for Satellites Close to an Earth-Like Planet.
PB96-102165 *04,839* Not available NTIS

PB96-102173
Generation Rate and Distribution of Products of Combustion in Two-Layer Fire Environments: A Model and Applications.
PB96-102173 *01,398* Not available NTIS

PB96-102181
Some Factors Affecting the Design of a Calorimeter Hood and Exhaust.
PB96-102181 *00,302* Not available NTIS

PB96-102199
Transmission Properties of Short Curved Neutron Guides. Part 1. Acceptance Diagram Analysis and Calculations.
PB96-102199 *04,021* Not available NTIS

PB96-102207
Radiance Temperatures (in the Wavelength Range 523-907 nm) of Group IV B Transition Metals Titanium, Zirconium, and Hafnium at Their Melting Points by a Pulse-Heating Technique.
PB96-102207 *03,356* Not available NTIS

PB96-102215
Sub-Doppler Frequency Measurements on OCS at 87 THz (3.4 mu m) with the CO Overtone Laser.
PB96-102215 *04,330* Not available NTIS

PB96-102223
Direct Observation of Vortex Dynamics in Two-Dimensional Josephson-Junction Arrays.
PB96-102223 *02,067* Not available NTIS

PB96-102231
Self-Avoiding-Walk Contacts and Random-Walk Self-Intersections in Variable Dimensionality.
PB96-102231 *01,276* Not available NTIS

PB96-102249
Search for Radio Emission from the 'Non-Magnetic' Chemically Peculiar Stars.
PB96-102249 *00,087* Not available NTIS

PB96-102256
X-ray Emission from Chemically Peculiar Stars.
PB96-102256 *00,088* Not available NTIS

PB96-102264
Physical Basis for Half-Integral Shapiro Steps in a DC SQUID.
PB96-102264 *04,704* Not available NTIS

PB96-102272
Stacked Series Arrays of High-Tc Trilayer Josephson Junctions.
PB96-102272 *04,705* Not available NTIS

PB96-102280
Isotope Dilution Mass Spectrometry as a Candidate Definitive Method for Determining Total Glycerides and Triglycerides in Serum.
PB96-102280 *03,519* Not available NTIS

PB96-102298
High-Resolution Infrared Overtone Spectroscopy of N2-HF: Vibrational Red Shifts and Predissociation Rate as a Function of HF Stretching Quanta.
PB96-102298 *01,061* Not available NTIS

PB96-102306
Computing Radiative Heat Transfer Occurring in a Zone Fire Model.
PB96-102306 *01,399* Not available NTIS

PB96-102314
Analyzing and Exploiting Numerical Characteristics of Zone Fire Models.
PB96-102314 *01,400* Not available NTIS

PB96-102322
Rotational Modulation and Flares on RS Canum Venaticorum and BY Draconis Stars. XVIII. Coordinated VLA, ROSAT, and IUE Observations of RS CVn Binaries.
PB96-102322 *00,089* Not available NTIS

PB96-102330
Fluctuations in Probability Distribution on Chaotic Attractors.
PB96-102330 *04,022* Not available NTIS

PB96-102348
Kinetics and Dynamics of Vibrationally State Resolved Ion-Molecule Reactions: (14)N2(+)(v=1 and 2) and (15)N2(+)(v=0,1 and 2) with (14)N2.
PB96-102348 *04,023* Not available NTIS

PB96-102355
Non-Perturbative Relation between the Mutual Diffusion Coefficient, Suspension Viscosity, and Osmotic Compressibility: Application to Concentrated Protein Solutions.
PB96-102355 *01,062* Not available NTIS

PB96-102363
MEMS in Standard CMOS VLSI Technology.
PB96-102363 *02,377* Not available NTIS

PB96-102371
Critical Lines for Type-III Aqueous Mixtures by Generalized Corresponding-States Models.
PB96-102371 *01,063* Not available NTIS

PB96-102389
Ferroelectric Thin Film Characterization Using Superconducting Microstrip Resonators.
PB96-102389 *02,270* Not available NTIS

PB96-102397
Geometrical Percolation Threshold of Overlapping Ellipsoids.
PB96-102397 *03,167* Not available NTIS

PB96-102405
Reduction of Marginal Gaps in Composite Restorations by Use of Glass-Ceramic Inserts.
PB96-102405 *00,174* Not available NTIS

PB96-102413
Thermodynamic Properties of Two Gaseous Halogenated Ethers from Speed-of-Sound Measurements: Difluoromethoxy-Difluoromethane and 2-Difluoromethoxy-1,1,1-Trifluoroethane.
PB96-102413 *04,189* Not available NTIS

PB96-102421
Lattice Dynamics of Ba1-xKxBiO3.
PB96-102421 *04,706* Not available NTIS

PB96-102439
Structure and Conductivity of Layered Oxides (Ba,Sr)n+1(Sn,Sb)nO3n+1.
PB96-102439 *04,707* Not available NTIS

PB96-102447
Lattice Dynamics of Semiconducting, Metallic, and Superconducting Ba1-xKxBiO3 Studied by Inelastic Neutron Scattering.
PB96-102447 *04,708* Not available NTIS

PB96-102454
Assessing Halon Alternatives for Aircraft Engine Nacelle Fire Suppression.
PB96-102454 *01,401* Not available NTIS

PB96-102462
30 THz Mixing Experiments on High Temperature Superconducting Josephson Junctions.
PB96-102462 *04,709* Not available NTIS

PB96-102470
Effect of Stoichiometry on the Phases Present in Boron Nitride Thin Films.
PB96-102470 *04,710* Not available NTIS

PB96-102488
Standard Reference Material for the Measurement of Particle Mobility by Electrophoretic Light Scattering.
PB96-102488 *00,609* Not available NTIS

PB96-102496
Voltage-Standard Devices.
PB96-102496 *01,920* Not available NTIS

PB96-102504
Extended CO(7 yields 6) Emission from Warm Gas in Orion.
PB96-102504 *00,090* Not available NTIS

PB96-102512
Oxygen Dependance of the Crystal Structure of HgBa2CuO4+ and Its Relation to Superconductivity.
PB96-102512 *04,711* Not available NTIS

PB96-102520
Probabilistic Computation of Poiseuille Flow Velocity Fields.
PB96-102520 *04,209* Not available NTIS

PB96-102538
Self-Biasing Cryogenic Particle Detector Utilizing Electrothermal Feedback and a SQUID Readout.
PB96-102538 *04,712* Not available NTIS

PB96-102546
Simulation of C60 Through the Plastic Transition Temperatures.
PB96-102546 *04,713* Not available NTIS

PB96-102553
Characterization of a Clipped Gaussian Beam.
PB96-102553 *04,331* Not available NTIS

PB96-102561
Standard Antennas for Electromagnetic Interference Measurements and Methods to Calibrate Them.
PB96-102561 *02,007* Not available NTIS

PB96-102579
Measurements of Thermophysical Properties of Nickel Near Its Melting Temperature by a Microsecond-Resolution Transient Technique.
PB96-102579 *04,210* Not available NTIS

PB96-102587
Phase Locking in Two-Dimensional Arrays of Josephson Junctions: Effect of Critical-Current Nonuniformity.
PB96-102587 *04,714* Not available NTIS

PB96-102595
Tensile Deformation-Induced Microstructures in Free-Standing Copper Thin Films.
PB96-102595 *04,715* Not available NTIS

PB96-102603
Magnetostriction and Giant Magnetoresistance in Annealed NiFe/Ag Multilayers.
PB96-102603 *04,716* Not available NTIS

PB96-102611
Measurement and Interpretation of Tidal Tilts in a Small Array.
PB96-102611 *03,686* Not available NTIS

PB96-102629
100 Ampere, 100 kHZ Transconductance Amplifier.
PB96-102629 *02,068* Not available NTIS

PB96-102637
Bonding Wires to Quantized Hall Resistors.
PB96-102637 *01,921* Not available NTIS

PB96-102645
Intercomparison Study of (237)Np Determination in Artificial Urine Samples.
PB96-102645 *03,633* Not available NTIS

PB96-102652
Measurement Methods and Algorithms for Comparison of Local and Remote Clocks.
PB96-102652 *01,549* Not available NTIS

PB96-102660
Measurement of Very Low Frequency Vibrations.
PB96-102660 *03,687* Not available NTIS

PB96-102678
Ouch Those Programs are Painful.
PB96-102678 *01,739* Not available NTIS

PB96-102686
Conformance Testing for OSI Protocols.
PB96-102686 *01,631* Not available NTIS

PB96-102694
High-Velocity Plasma in the Transition Region of AU Microscopii: Evidence for Magnetic Reconnection and Saturated Heating during Quiescent and Flaring Conditions.
PB96-102694 *00,091* Not available NTIS

PB96-102702
Model for Determining the Density and Mobility of Carriers in Thin Semiconducting Layers with Only Two Contacts.
PB96-102702 *02,378* Not available NTIS

PB96-102710
MONSEL-II: Monte Carlo Simulation of SEM Signals for Linewidth Metrology.
PB96-102710 *02,379* Not available NTIS

PB96-102728
Bacteriorhodopsin Retains Its Light-Induced Proton-Pumping Function After Being Heated to 140C.
PB96-102728 *03,471* Not available NTIS

PB96-102736
Delivering the Same Optical Frequency at Two Places: Accurate Cancellation of Phase Noise Introduced by an Optical Fiber or Other Time-Varying Path.
PB96-102736 *04,332* Not available NTIS

PB96-102744
Analytical Method for Determining Thermal Conductivity from Dynamic Experiments.
PB96-102744 *04,024* Not available NTIS

PB96-102751
Evolution of X-ray Resonance Raman Scattering into X-ray Fluorescence from the Excitation of Xenon Near the L3 Edge.
PB96-102751 *04,025* Not available NTIS

PB96-102769
NBS/NIST Peltier-Effect Microcalorimeter: A Four-Decade Review.
PB96-102769 *01,064* Not available NTIS

PB96-102777
Observing Stellar Coronae with the Goddard High Resolution Spectrograph. I. The dMe Star AU Microscopii.
PB96-102777 *00,092* Not available NTIS

PB96-102785
Comments on 'Conversions between S, Z, Y, h, ABCD, and T Parameters Which Are Valid for Complex Source and Load Impedances'.
PB96-102785 *02,069* Not available NTIS

PB96-102793
Scaling of the Nonlinear Optical Cross Sections of GaAs-AlGaAs Multiple Quantum-Well Hetero n-i-p-i's.
PB96-102793 *02,183* Not available NTIS

PB96-102801
Length Scales for Fragile Glass-Forming Liquids.
PB96-102801 *01,065* Not available NTIS

PB96-102819
Optically Stabilized Tunable Diode-Laser System for Saturation Spectroscopy.
PB96-102819 *04,717* Not available NTIS

PB96-102827
Electronic Microrefrigerator Based on a Normal-Insulator-Superconductor Tunnel Junction.
PB96-102827 *04,718* Not available NTIS

PB96-102835
Probing Potential-Energy Surfaces via High-Resolution IR Laser Spectroscopy.
PB96-102835 *01,066* Not available NTIS

PB96-102843
New Method for Realizing a Luminous Flux Scale Using an Integrating Sphere with an External Source.
PB96-102843 *04,333* Not available NTIS

PB96-102850
Effect of Electrode Material on Measured Ion Energy Distributions in Radio-Frequency Discharges.
PB96-102850 *04,026* Not available NTIS

PB96-102868
Concepts for Fire Protection of Passenger Rail Transportation Vehicles: Past, Present, and Future.
PB96-102868 *04,853* Not available NTIS

PB96-102876
Buffer Layer Modulation-Doped Field-Effect-Transistor Interactions in the Al0.33Ga0.67As/GaAs Superlattice System.
PB96-102876 *02,380* Not available NTIS

PB96-102884
Total-Dielectric-Function Approach to Electron and Phonon Response in Solids.
PB96-102884 *01,067* Not available NTIS

PB96-102892
Principle of Congruence and Its Application to Compressible States.
PB96-102892 *01,068* Not available NTIS

PB96-102900
Phospholipid/Alkanethiol Bilayers for Cell-Surface Receptor Studies by Surface Plasmon Resonance.
PB96-102900 *03,472* Not available NTIS

PB96-102918
Energy Calibration of X-ray Photoelectron Spectrometers: Results of an Interlaboratory Comparison to Evaluate a Proposed Calibration Procedure.
PB96-102918 *04,027* Not available NTIS

PB96-102926
TDDB Characterization of Thin SiO2 Films with Bimodal Failure Populations.
PB96-102926 *02,381* Not available NTIS

PB96-102934
Santa Ana Fire Department Experiment at 1315 South Bristol, July 14, 1994. (Reprint).
PB96-102934 *00,207* Not available NTIS

PB96-102942
Time-Resolved Balmer-Alpha Emission from Fast Hydrogen Atoms in Low Pressure, Radio-Frequency Discharges in Hydrogen.
PB96-102942 *04,028* Not available NTIS

PB96-102959
Ion Kinetic-Energy Distributions and Balmer-alpha (Halpha) Excitation in Ar-H2 Radio-Frequency Discharges.
PB96-102959 *04,029* Not available NTIS

PB96-102967
Pressure Equations in Zone-Fire Modeling.
PB96-102967 *00,208* Not available NTIS

PB96-102975
X-ray Powder Diffraction from Carbon Nanotubes and Nanoparticles.
PB96-102975 *03,064* Not available NTIS

PB96-102983
Damage Processes in Ceramics Resulting from Diamond Tool Indentation and Scratching in Various Environments.
PB96-102983 *03,065* Not available NTIS

PB96-102991
Intracomparison Tests of the FG5 Absolute Gravity Meters.
PB96-102991 *03,688* Not available NTIS

PB96-103007
Boundary Conforming Grid Generation System for Interface Tracking.
PB96-103007 *03,357* Not available NTIS

PB96-103015
Superconducting Integrated Circuit Fabrication with Low Temperature ECR-Based PECVD SiO2 Dielectric Films.
PB96-103015 *04,719* Not available NTIS

PB96-103023
Certification of Polychlorinated Biphenyl Congeners and Chlorinated Pesticides in a Whale Blubber Standard Reference Material.
PB96-103023 *03,745* Not available NTIS

PB96-103031
Using Synthetic Perturbations and Statistical Screening to Assay Shared-Memory Programs.
PB96-103031 *01,740* Not available NTIS

PB96-103049
Time Generation and Distribution.
PB96-103049 *01,550* Not available NTIS

PB96-103056
Nanoscale Study of the Hydrogenated Amorphous Silicon Surface.
PB96-103056 *04,720* Not available NTIS

PB96-103064
Planar Lenses for Field-Emitter Arrays.
PB96-103064 *02,112* Not available NTIS

PB96-103072
Partial Pressure Analysis in Space Testing.
PB96-103072 *04,829* Not available NTIS

PB96-103080
Comments on the Stability of Bayard-Alpert Ionization Gages.
PB96-103080 *02,673* Not available NTIS

PB96-103098
Comparison of Techniques for Nondestructive Composition Measurements in CdZnTe Substrates.
PB96-103098 *02,703* Not available NTIS

PB96-103106
Low-Energy-Electron Collisions with Sodium: Elastic and Inelastic Scattering from the Ground State.
PB96-103106 *04,030* Not available NTIS

PB96-103114
Nonstationary Behaviour of Partial Discharge during Discharge Induced Ageing of Dielectrics.
PB96-103114 *01,922* Not available NTIS

PB96-103122
Aging, Warm-Up Time and Retrace; Important Characteristics of Standard Frequency Generators.
PB96-103122 *04,031* Not available NTIS

PB96-103130
Recent Results in Magnetic Force Microscopy.
PB96-103130 *04,721* Not available NTIS

PB96-103148
Environmental Sensitivities of Quartz Oscillators.
PB96-103148 *02,271* Not available NTIS

PB96-103155
Digital Impedance Bridge.
PB96-103155 *02,272* Not available NTIS

PB96-103163
Wear Transitions in Monolithic Alumina and Zirconia-Alumina Composites.
PB96-103163 *03,168* Not available NTIS

PB96-103171
Collisional Alignment of CO2 Rotational Angular Momentum States in a Supersonic Expansion.
PB96-103171 *01,069* Not available NTIS

PB96-103189
Volume-Limited ROSAT Survey of Extreme Ultraviolet Emission from all Nondegenerate Stars within 10 Parsecs.
PB96-103189 *00,093* Not available NTIS

PB96-103197
Water Adsorption at a Polyimide/Silicon Wafer Interface.
PB96-103197 *01,070* Not available NTIS

PB96-103205
Phase Shifts and Intensity Dependence in Frequency-Modulation Spectroscopy.
PB96-103205 *01,071* Not available NTIS

PB96-106455
Electronics and Electrical Engineering Laboratory Technical Progress Bulletin Covering Laboratory Programs, April to June 1995 with 1995 EEEL Events Calendar.
PB96-106455 *01,923* PC A03/MF A01

PB96-106463
Proficiency Tests for the NIST Airborne Asbestos Program, 1993.
PB96-106463 *00,610* PC A03/MF A01

PB96-106851
NIST ATM Network Simulator: Operation and Programming, Version 1.0.
PB96-106851 *01,487* PC A04/MF A01

PB96-106869
Present Worth Factors for Life-Cycle Cost Studies in the Department of Defense (1996).
PB96-106869 *03,673* PC A04/MF A01

PB96-106877
Indoor Air Quality Impacts of Residential HVAC Systems Phase II.B Report: IAQ Control Retrofit Simulations and Analysis.
PB96-106877 *02,559* PC A05/MF A01

PB96-106901
Literature Review on Seismic Performance of Building Cladding Systems.
PB96-106901 *00,455* PC A09/MF A02

PB96-106935
GATT Standards Code Activities of the National Institute of Standards and Technology 1994.
PB96-106935 *00,497* PC A03/MF A01

PB96-106992
Residual Stress in Induction-Heated Railroad Wheels: Ultrasonic and Saw Cut Measurements. Report No. 28.
PB96-106992 *04,854* PC A04/MF A01

PB96-109491
Joint DoD/NIST Workshop on International Manufacturing Systems Research and Development. Held in Rockville, Maryland on November 3-5, 1992. Proceedings.
PB96-109491 *02,931* PC A11/MF A03

PB96-109509
Composite Materials for Offshore Operations: Proceedings of the International Workshop (1st). Held in Houston, Texas on October 26-28, 1993.
PB96-109509 *03,169* PC A17/MF A04

PB96-109525
Agile Manufacturing from a Statistical Perspective.
PB96-109525 *02,886* PC A03/MF A01

PB96-109533
Mapping Integration Definition for Function Modeling (IDEFO) Model into CASE Data Interchange Format (CDIF) Transfer File.
PB96-109533 *01,741* PC A07/MF A02

PB96-109541
CFAST Output Comparison Method and Its Use in Comparing Different CFAST Versions.
PB96-109541 *00,401* PC A04/MF A01

PB96-109558
Factors Significant to Precracking of Fracture Specimens.
PB96-109558 *03,358* PC A06/MF A02

PB96-109566
EMISS: A Program for Estimating Local Air Pollution Emission Factors Related to Energy Use in Buildings: User's Guide and Reference Manual.
PB96-109566 *02,560* PC A03/MF A01

PB96-109574
Effect of Suppressants on Metal Fires.
PB96-109574 *01,402* PC A03/MF A01

PB96-109582
Error-Bounding in Level-Index Computer Arithmetic.
PB96-109582 *01,742* PC A02/MF A01

PB96-110739
Intensity-Dependent Scattering Rings in High Order Above-Threshold Ionization.
PB96-110739 *04,032* Not available NTIS

PB96-110747
Novel Activity of E. coli uracil DNA N-glycosylase Excision of Isodialuric Acid (5,6-dihydroxyuracil), a Major Product of Oxidative DNA Damage, from DNA.
PB96-110747 *03,543* Not available NTIS

PB96-111166
Spherical-Wave Source-Scattering Matrix Analysis of Antennas and Antenna-Antenna Interactions.
PB96-111166 *02,008* PC A08/MF A02

PB96-111174
Efficiency of Electric Motors. National Voluntary Lab. Accreditation Program (NVLAP).
PB96-111174 *02,107* PC A05/MF A01

PB96-111190
Federal Implementation Guideline for Electronic Data Interchange: ASC X12 003040 Transaction Set 838 Trading Partner Profile (Confirmation of Vendor Registration). Implementation Convention.
PB96-111190 *01,813* PC A03/MF A01

PB96-111612
Monte Carlo and Analytic Methods in the Transport of Electrons, Neutrons, and Alpha Particles.
PB96-111612 *04,033* Not available NTIS

PB96-111620
Comparison of a Fixed-Charge and a Polarizable Water Model.
PB96-111620 *01,072* Not available NTIS

PB96-111638
Improved Wavelengths for Prominent Lines of Fe XX to Fe XXIII.
PB96-111638 *04,334* Not available NTIS

PB96-111646
Photodesorption Dynamics of CO from Si(111): The Role of Surface Defects.
PB96-111646 *03,066* Not available NTIS

PB96-111653
Overview of Reference Materials Prepared for Standardization of DNA Typing Procedures.
PB96-111653 *00,611* Not available NTIS

PB96-111661
Nonequilibrium Thermodynamic Theory of Viscoplastic Materials.
PB96-111661 *04,034* Not available NTIS

PB96-111679
Stable Phase Locking in a Two-Cell Ladder Array of Josephson Junctions.
PB96-111679 *04,722* Not available NTIS

PB96-111687
Human and Machine Recognition of Faces: A Survey.
PB96-111687 *01,854* Not available NTIS

PB96-111695
Fabrication of Optics by Diamond Turning.
PB96-111695 *02,954* Not available NTIS

PB96-111703
Silicon Nitride Boundary Lubrication: Lubrication Mechanism of Alcohols.
PB96-111703 *03,067* Not available NTIS

PB96-111711
Silicon Nitride Boundary Lubrication: Effect of Oxygenates.
PB96-111711 *03,068* Not available NTIS

PB96-111729
Niobium Microbolometers for Far-Infrared Detection.
PB96-111729 *02,184* Not available NTIS

PB96-111737
Quantitative Analysis of Selected PCB Congeners in Marine Matrix Reference Materials Using a Novel Cyanobiphenyl Stationary Phase.
PB96-111737 *02,591* Not available NTIS

PB96-111745
Temperature Dependence and Magnetic Field Modulation of Critical Currents in Step-Edge SNS YBCO/Au Junctions.
PB96-111745 *04,723* Not available NTIS

PB96-111752
Critical Current and Normal Resistance of High-Tc Step-Edge SNS Junctions.
PB96-111752 *04,724* Not available NTIS

PB96-111760
Surface Chemistry of Silicon Nitride Powder in the Presence of Dissolved Ions.
PB96-111760 *01,073* Not available NTIS

PB96-111778
Certification of Polycyclic Aromatic Hydrocarbons in a Marine Sediment Standard Reference Material.
PB96-111778 *02,592* Not available NTIS

PB96-111786
Contributions of Out-of-Plane Material to a Scanned-Beam Laminography Image.
PB96-111786 *02,704* Not available NTIS

PB96-111794
Crystal Structure of a New Monoclinic Form of Potassium Dihydrogen Phosphate Containing Orthophosphacidium Ion, (H4PO4)(sup+1).
PB96-111794 *04,725* Not available NTIS

PB96-111802
Taguchi's Parameter Design: A Panel Discussion.
PB96-111802 *03,445* Not available NTIS

PB96-111810
Wear Mechanism Maps of 440C Martensitic Stainless Steel.
PB96-111810 *04,834* Not available NTIS

PB96-111828
Vibrational Excitations and the Position of Hydrogen in Nanocrystalline Palladium.
PB96-111828 *04,035* Not available NTIS

PB96-111836
Magnetic Structure and Spin Dynamics of the Pr and Cu in Pr2CuO4.
PB96-111836 *04,036* Not available NTIS

PB96-111844
SQA Standards and Total Quality Management.
PB96-111844 *01,743* Not available NTIS

PB96-111851
Relative Accuracy of Isolated and Unisolated Noise Comparison Radiometers.
PB96-111851 *01,924* Not available NTIS

PB96-111869
Measurements of Permittivity and the Dielectric Loss Tangent of Low Loss Dielectric Materials with a Dielectric Resonator Operating on the Higher Order Te(sub 0 gamma delta) Modes.
PB96-111869 *02,273* Not available NTIS

PB96-111877
Measuring Hydrogen by Cold-Neutron Prompt-Gamma Activation Analysis.
PB96-111877 *00,612* Not available NTIS

PB96-111885
Electron-Ion Collisions in the Plasma Edge.
PB96-111885 *04,037* Not available NTIS

PB96-111893
Crystal Structure of Calcium Glutarate Monohydrate.
PB96-111893 *01,074* Not available NTIS

PB96-111901
Use of Building Emulators to Evaluate the Performance of Building Energy Management Systems.
PB96-111901 *00,269* Not available NTIS

PB96-111919
Small Angle Neutron Scattering Study of the Structure and Formation of Ordered Mesopores in Silica.
PB96-111919 *03,069* Not available NTIS

PB96-111927
Kinetic Energy Distribution of Ions Produced from Townsend Discharges in Neon and Argon.
PB96-111927 *04,413* Not available NTIS

PB96-111935
Can Displays Deliver a Full Measure: Manufacturing.
PB96-111935 *02,185* Not available NTIS

PB96-111943
Noise Modeling and Reliability of Behavior Prediction for Multi-Stable Hydroelastic Systems.
PB96-111943 *04,822* Not available NTIS

PB96-111950
Glasses for Waveguide Lasers.
PB96-111950 *04,335* Not available NTIS

PB96-111968
Stability of Compressed Gas Mixtures Containing Low Level Volatile Organic Compounds in Aluminum Cylinders.
PB96-111968 *00,613* Not available NTIS

PB96-111976
Detection of Aromatic Compounds Based on DNA Intercalation Using an Evanescent Wave Biosensor.
PB96-111976 *03,473* Not available NTIS

PB96-111984
Uncertainties of the NIST Coaxial Noise Calibration System.
PB96-111984 *02,070* Not available NTIS

PB96-111992
Comparison of Photodiode Frequency Response Measurements to 40 GHz between NPL and NIST.
PB96-111992 *04,038* Not available NTIS

PB96-112008
Production Management Information Model for Discrete Manufacturing.
PB96-112008 *02,830* Not available NTIS

PB96-112016
GHRS Observations of Cool, Low-Gravity Stars. 1. The Far-Ultraviolet Spectrum of alpha Orions (M2 Iab).
PB96-112016 *00,094* Not available NTIS

PB96-112024
Temperature and Field Dependence of Flux Pinning in NbTi with Aritificial Pinning Centers.
PB96-112024 *04,726* Not available NTIS

PB96-112032
Distribution of Dielectric Relaxation Times and the Moment Problem.
PB96-112032 *04,727* Not available NTIS

PB96-112040
Physicochemical Characterization of Low Molecular Weight Heparin.
PB96-112040 *03,474* Not available NTIS

PB96-112057
Shear-Induced Melting of Two-Dimensional Solids.
PB96-112057 *01,075* Not available NTIS

PB96-112065
SUSAN: SUperconducting Systems ANalysis by Low Temperature Scanning Electron Microscopy (LTSEM).
PB96-112065 *04,728* Not available NTIS

PB96-112073
Quantum-Limited Cooling and Detection of Radio-Frequency Oscillations by Laser-Cooled Ions.
PB96-112073 *04,039* Not available NTIS

PB96-112081
Rapid pH Change Due to Bacteriorhodopsin Measured with a Tin-Oxide Electrode.
PB96-112081 *03,544* Not available NTIS

PB96-112099
Spectral Interference in the Determination of Arsenic in High-Purity Lead and Lead-Base Alloys Using Electrothermal Atomic Absorption Spectrometry and Zeeman-Effect Background Correction.
PB96-112099 *00,614* Not available NTIS

PB96-112107
Applications of the Vortex Tube in Chemical Analysis. Part 2. Applications.
PB96-112107 *00,615* Not available NTIS

PB96-112115
Treatment of Wistar Rats with a Renal Carcinogen, Ferric Nitrilotriacetate, Causes DNA-Protein Cross-Linking between Thymine and Tyrosine in Their Renal Chromatin.
PB96-112115 *03,649* Not available NTIS

PB96-112123
Interlaboratory Comparison of Autoradiographic DNA Profiling Measurements. 2. Measurement Uncertainty and Its Propagation.
PB96-112123 *03,545* Not available NTIS

PB96-112131
Effects of Target Temperature on Analytical Sensitivities of Cold-Neutron Capture Prompt gamma-ray Activation Analysis.
PB96-112131 *00,616* Not available NTIS

PB96-112149
SUM and MEAN: Standard Programs for Activation Analysis.
PB96-112149 *00,617* Not available NTIS

PB96-112156
Continuous Recording and Stochastic Analysis of PD.
PB96-112156 *01,925* Not available NTIS

PB96-112164
Precise Spectroscopy for Fundamental Physics.
PB96-112164 *04,040* Not available NTIS

PB96-112172
Laser Gas Ionization Technique Monitors MEB Crystal Growth.
PB96-112172 *01,076* Not available NTIS

PB96-112180
Prediction of Potential Concrete Strength at Later Ages.
PB96-112180 *01,324* Not available NTIS

PB96-112198
Effects of Testing Variables on the Strength of High-Strength (90 Mpa) Concrete Cylinders.
PB96-112198 *00,456* Not available NTIS

PB96-112206
Effect of Anneal Temperature on Si/Buried Oxide Interface Roughness on SIMOX.
PB96-112206 *02,382* Not available NTIS

PB96-112214
High Integrity Software Standards Activities at NIST.
PB96-112214 *01,744* Not available NTIS

PB96-112222
Study of Multiple Scattering Background in Compton Scatter Imaging.
PB96-112222 *04,425* Not available NTIS

PB96-112230
Local Oscillator Requirements and Strategies for the Next Generation of High-Stability Frequency Standards.
PB96-112230 *01,551* Not available NTIS

PB96-112248
New Model of 1/F Noise in Baw Quartz Resonators.
PB96-112248 *02,383* Not available NTIS

PB96-112255
Structure of a Triglyceride Microemulsion: A Small Angle Neutron Scattering Study.
PB96-112255 *01,077* Not available NTIS

PB96-112263
Binary versus Decade Inductive Voltage Divider Comparison and Error Decomposition.
PB96-112263 *02,071* Not available NTIS

PB96-112271
Cryogenic Precision Capacitance Bridge Using a Single Electron Tunneling Electrometer.
PB96-112271 *02,072* Not available NTIS

PB96-112289
Dual-Frequency Millimeter-Wave Radiometer Antenna for Airborne Remote Sensing of Atmosphere and Ocean.
PB96-112289 *02,009* Not available NTIS

PB96-112297
Substrate and Thin Film Measurements.
PB96-112297 *02,384* Not available NTIS

PB96-112305
Small Angle Neutron Scattering Studies of Structural Characteristics of Argarose Gels.
PB96-112305 *03,475* Not available NTIS

PB96-112313
Surging the Upside-Down House: Looking into Upsetting Reference Voltages.
PB96-112313 *02,385* Not available NTIS

PB96-112321
Measured Stopping Powers of Hydrogen and Helium in Polystyrene Near Their Maximum Values.
PB96-112321 *04,729* Not available NTIS

PB96-112339
Torsion Modulus and Internal Friction of a Fiber-Reinforced Composite.
PB96-112339 *03,070* Not available NTIS

PB96-112347
Analytical Applications of Guided Neutron Beams.
PB96-112347 *04,041* Not available NTIS

PB96-112354
Application of a Novel Slurry Furnace AAS Protocol for Rapid Assessment of Lead Environmental Contamination.
PB96-112354 *02,526* Not available NTIS

PB96-112362
Vortex Dynamics and Melting in Niobium.
PB96-112362 *02,073* Not available NTIS

PB96-112370
Considerations in the Design of an Environmental Specimen Bank: Experiences of the National Biomonitoring Specimen Bank Program.
PB96-112370 *02,527* Not available NTIS

PB96-112651
Federal Implementation Guideline for Electronic Data Interchange: ASC X12 003040 Transaction Set 838 Trading Partner Profile (Vendor Registration), Implementation Convention.
PB96-112651 *03,674* PC A04/MF A01

PB96-112677
Glimpse of Materials Research in China: A Report from an Interagency Study Team on Materials Visiting China from June 19, 1995 to June 30, 1995.
PB96-112677 *02,978* PC A11/MF A03

PB96-112685
Requisite Elements, Rationale, and Technology Overview for the Systems Intergration for Manufacturing Applications (SIMA) Program. Background Study.
PB96-112685 *02,831* PC A07/MF A02

PB96-112693
Proceedings of the Annual Manufacturing Technology Conference (2nd): Toward a Common Agenda. Held in Gaithersburg, Maryland on April 18-20, 1995.
PB96-112693 *02,887* PC A99/MF E08

PB96-113311
Journal of Research of the National Institute of Standards and Technology, July/August 1995. Volume 100, Number 4. Special Issue: The Gaseous Electronics Conference Radio-Frequency Reference Cell.
PB96-113311 *02,386* PC A09/MF A03

PB96-113329
Gaseous Electronics Conference RF Reference Cell: An Introduction.
PB96-113329 *02,387*
(Order as PB96-113311, PC A09/MF A03)

PB96-113337
Current and Voltage Measurements in the Gaseous Electronics Conference RF Reference Cell.
PB96-113337 *02,388*
(Order as PB96-113311, PC A09/MF A03)

PB96-113345
Optical Emission Spectroscopy on the Gaseous Electronics Conference RF Reference Cell.
PB96-113345 *02,389*
(Order as PB96-113311, PC A09/MF A03)

PB96-113352
Optical Diagnostics in the Gaseous Electronics Conference Reference Cell.
PB96-113352 *02,390*
(Order as PB96-113311, PC A09/MF A03)

PB96-113360
Studies of Ion Kinetic-Energy Distributions in the Gaseous Electronics Conference RF Reference Cell.
PB96-113360 *02,391*
(Order as PB96-113311, PC A09/MF A03)

PB96-113378
Microwave Diagnostic Results from the Gaseous Electronics Conference RF Reference Cell.
PB96-113378 *02,392*
(Order as PB96-113311, PC A09/MF A03)

PB96-113386
Langmuir Probe Measurements in the Gaseous Electronics Conference RF Reference Cell.
PB96-113386 *02,393*
(Order as PB96-113311, PC A09/MF A03)

PB96-113394
Inductively Coupled Plasma Source for the Gaseous Electronics Conference RF Reference Cell.
PB96-113394 *02,394*
(Order as PB96-113311, PC A09/MF A03)

PB96-113402
Reactive Ion Etching in the Gaseous Electronics Conference RF Reference Cell.
PB96-113402 *02,395*
(Order as PB96-113311, PC A09/MF A03)

PB96-113410
Dusty Plasma Studies in the Gaseous Electronics Conference Reference Cell.
PB96-113410 *02,396*
(Order as PB96-113311, PC A09/MF A03)

PB96-113428
One-Dimensional Modeling Studies of the Gaseous Electronics Conference RF Reference Cell.
PB96-113428 *02,397*
(Order as PB96-113311, PC A09/MF A03)

PB96-113436
Two-Dimensional Self-Consistent Radio Frequency Plasma Simulations Relevant to the Gaseous Electronics Conference RF Reference Cell.
PB96-113436 *02,398*
(Order as PB96-113311, PC A09/MF A03)

PB96-113535
Journal of Research of the National Institute of Standards and Technology, November/December 1994. Volume 99, Number 6.
PB96-113535 *04,336* PC A05/MF A01

PB96-113543
Intercomparison between NPL (India) and NIST (USA) Pressure Standards in the Hydraulic Pressure Region Up to 26 MPa.
PB96-113543 *04,211*
(Order as PB96-113535, PC A05/MF A01)

PB96-113550
Intercomparison of the ITS-90 Radiance Temperature Scales of the National Physical Laboratory (U.K.) and the National Institute of Standards and Technology.
PB96-113550 *02,674*
(Order as PB96-113535, PC A05/MF A01)

PB96-113568
Screened-Room Measurements on the NIST Spherical-Dipole Standard Radiator.
PB96-113568 *01,926*
(Order as PB96-113535, PC A05/MF A01)

PB96-113576
Beamcon III, a Linearity Measurement Instrument for Optical Detectors.
PB96-113576 *04,337*
(Order as PB96-113535, PC A05/MF A01)

PB96-113584
Spectroscopic Study of Quantized Breakdown Voltage States of the Quantum Hall Effect.
PB96-113584 *04,730*
(Order as PB96-113535, PC A05/MF A01)

PB96-114764
Turbulent Flame Spread on Vertical Corner Walls.
PB96-114764 *01,403* PC A08/MF A02

PB96-114913
Federal Implementation Guideline for Electronic Data Interchange. ASC X12 003050 Transaction Set 850 Award Instrument. Implementation Convention.
PB96-114913 *01,814* PC A11/MF A03

PB96-114921
Federal Implementation Guideline for Electronic Data Interchange. ASC X12 003050 Transaction Set 860 Modifications to Award Instrument. Implementation Convention.
PB96-114921 *01,815* PC A11/MF A03

PB96-114939
Z39.50 Implementation Experiences.
PB96-114939 *01,816* PC A07/MF A02

PB96-115019
Standards Setting in the European Union: Standards Organization and Officials in EU Standards Activities.
PB96-115019 *02,919* PC A04/MF A01

PB96-115050
Intelligent Processing of Materials, Technical Activities 1994 (NAS-NRC Assessment Panel, April 6-7, 1995).
PB96-115050 *03,359* PC A04/MF A01

PB96-117221
Analysis by a Combination of Gas Chromatography and Tandem Mass Spectrometry: Development of Quantitative Tandem-in-Time Ion Trap Mass Spectrometry: Isotope Dilution Quantification of 11-Nor-Delta-9-Tetrahydro cannabinol-9-Carboxylic Acid.
PB96-117221 *02,561* Not available NTIS

PB96-117239
Measurement of the Weak-Localization Complex Conductivity at 1 Ghz in Disordered Ag Wires.
PB96-117239 *04,731* Not available NTIS

PB96-117692
Semiconductor Measurement Technology: Test Structure Implementation Document: DC Parametric Test Structures and Test Methods for Monolithic Microwave Integrated Circuits (MMICs).
PB96-117692 *02,399* PC A05/MF A01

PB96-117767
Journal of Research of the National Institute of Standards and Technology, September/October 1995. Volume 100, Number 5.
PB96-117767 *01,927* PC A08/MF A02

PB96-117775
Fire Suppression System Performance of Alternative Agents in Aircraft Engine and Dry Bay Laboratory Simulations. SP890: Volume 1.
PB96-117775 *03,277* PC A99/MF E08

PB96-117783
Fire Suppression System Performance of Alternative Agents in Aircraft Engine and Dry Bay Laboratory Simulations. SP 890: Volume 2.
PB96-117783 *03,278* PC A99/MF A06

PB96-117916
Post-Earthquake Fire and Lifelines Workshop. Held in Long Beach, California on January 30-31, 1995. Proceedings.
PB96-117916 *00,209* PC A04/MF A01

PB96-118039
Opportunities for Innovation: Optoelectronics.
PB96-118039 *01,928* PC A19/MF A04

PB96-119219
Comparing the Accuracy of Critical-Current Measurements Using the Voltage-Current Simulator.
PB96-119219 *02,227* Not available NTIS

PB96-119227
Display-Measurement Round-Robin.
PB96-119227 *02,186* Not available NTIS

PB96-119235
Electrical Product Requirements (Especially Quality Requirements) in the United States.
PB96-119235 *01,929* Not available NTIS

PB96-119243
Evolution Equations for Phase Separation and Ordering in Binary Alloys.
PB96-119243 *02,979* Not available NTIS

PB96-119250
Publications and Presentation Abstracts, 1995. (Published by Paffenbarger Research Center and Center of Excellence for Materials Science Research).
PB96-119250 *03,568* Not available NTIS

PB96-119268
Gaseous Dielectrics Research: Possible SF6 Substitutes.
PB96-119268 *02,228* Not available NTIS

PB96-119276
Polarization Insensitive 3x3 Sagnac Current Sensor Using Polarizing Spun High-Birefringence Fiber.
PB96-119276 *02,187* Not available NTIS

PB96-119284
Holographic Properties of Triton X-100-Treated Bacteriorhodopsin Embedded in Gelatin Films.
PB96-119284 *03,761* Not available NTIS

PB96-119292
Magnetooptic Effects.
PB96-119292 *04,338* Not available NTIS

PB96-119300
Characterization of Two-Dimensional Dopant Profiles: Status and Review.
PB96-119300 *02,400* Not available NTIS

PB96-119318
Intrinsic Viscosity and the Polarizability of Particles Having a Wide Range of Shapes.
PB96-119318 *03,170* Not available NTIS

PB96-119326
Automated Resistance Measurements at NIST.
PB96-119326 *02,274* Not available NTIS

PB96-119334
High-Temperature Superconductor Cryogenic Current Comparator.
PB96-119334 *02,074* Not available NTIS

PB96-119342
Flame Heights and Heat Release Rates of 1991 Kuwait Oil Field Fires.
PB96-119342 *01,404* Not available NTIS

PB96-119359
Lessons from the Establishment of the U.S. GOSIP Testing Program.
PB96-119359 *01,817* Not available NTIS

PB96-119367
National Information Infrastructure and Advanced Digital Video.
PB96-119367 *01,488* Not available NTIS

PB96-119375
Measurements of the Relative Permittivity of Liquid Water at Frequencies in the Range of 0.1 to 10 kHz and at Temperatures between 273.1 and 373.2 K at Ambient Pressure.
PB96-119375 *01,078* Not available NTIS

PB96-119383
Physical Characterization of Herparin by Light Scattering.
PB96-119383 *03,598* Not available NTIS

PB96-119391
Visible and UV Light from Highly Charged Ions: Exotic Matter Advancing Technology.
PB96-119391 *04,414* Not available NTIS

PB96-119409
Simple and Repeatable Technique for Measuring the Critical Current of Nb3Sn Wires.
PB96-119409 *02,229* Not available NTIS

PB96-119417
Nanofabrication of a Two-Dimensional Array Using Laser-Focused Atomic Deposition.
PB96-119417 *04,732* Not available NTIS

PB96-119425
Electroacoustic Characterization of Particle Size and Zeta Potential in Moderately Concentrated Suspensions.
PB96-119425 *01,079* Not available NTIS

PB96-119433
Perception of Clamp Noise in Television Receivers.
PB96-119433 *01,489* Not available NTIS

PB96-119441
Effect of Sm2BaCuO5 on the Properties of Sintered (Bulk) YBa2Cu3O6+x.
PB96-119441 *04,733* Not available NTIS

PB96-119458
Comparison of Selectivities for PCBs in Gas Chromatography for a Series of Cyanobiphenyl Stationary Phases.
PB96-119458 *00,618* Not available NTIS

PB96-119466
Mechano-Chemical Model: Reaction Temperatures in a Concentrated Contact.
PB96-119466 *03,227* Not available NTIS

PB96-119474
Stars, Atmospheres, Radiative Transfer.
PB96-119474 *00,095* Not available NTIS

PB96-119482
Accurate Measurement of Time.
PB96-119482 *01,552* Not available NTIS

PB96-119490
Atomic Clock.
PB96-119490 *01,553* Not available NTIS

PB96-119508
Shear-Induced Martensitic-Like Transformation in a Block Copolymer Melt.
PB96-119508 *01,277* Not available NTIS

PB96-119516
Oxidation of SiC.
PB96-119516 *02,401* Not available NTIS

PB96-119524
Defect Formation Mechanism Causing Increasing Defect Density during Decreasing Implant Dose in Low-Dose Simox.
PB96-119524 *02,402* Not available NTIS

PB96-119532
Discussion: Statistical Signal Processing of Quasiperiodicities.
PB96-119532 *00,096* Not available NTIS

PB96-119540
Relationship between Radiative and Magnetic Fluxes for Three Active Solar-Type Dwarfs.
PB96-119540 *00,097* Not available NTIS

PB96-119557
Numerical Evaluation of Special Functions.
PB96-119557 *03,417* Not available NTIS

PB96-119565
Long-Lived Structures in Fragile Glass-Forming Liquids.
PB96-119565 *04,212* Not available NTIS

PB96-119573
Physical Properties of Alternatives to the Fully Halogenated Chlorofluorocarbons.
PB96-119573 *03,279* Not available NTIS

PB96-119581
Doppler-Free Spectroscopy of Large Polyatomic Molecules and van der Waals Complexes.
PB96-119581 *04,339* Not available NTIS

PB96-119599
Using Secondary Ion Mass Spectrometry (SIMS) to Characterize Optical Waveguide Materials.
PB96-119599 *04,340* Not available NTIS

PB96-119607
Response of Buildings to Ambient Vibration and the Loma Prieta Earthquake: A Comparison.
PB96-119607 *00,457* Not available NTIS

PB96-119615
Building a Better Crycooler.
PB96-119615 *04,734* Not available NTIS

PB96-119623
Far Infrared Laser Frequencies of CH3OD and N2H4.
PB96-119623 *04,341* Not available NTIS

PB96-119631
Strangeness Flow Difference in Nuclear Collisions at 15A and 200A GeV.
PB96-119631 *04,042* Not available NTIS

PB96-119649
NIST and the Navy: Past, Present and Future.
PB96-119649 *03,655* Not available NTIS

PB96-119656
Mesoscopic Conductance Fluctuations in Large Devices.
PB96-119656 *04,735* Not available NTIS

PB96-119664
Faraday Effect Sensors for Magnet Field and Electric Current.
PB96-119664 *04,736* Not available NTIS

PB96-119672
Standard Polarization Components: Progress Toward an Optical Retardance Standard.
PB96-119672 *04,342* Not available NTIS

PB96-119680
Improved Annealing Technique for Optical Fiber.
PB96-119680 *04,343* Not available NTIS

PB96-119698
Neutron Techniques in Materials Science and Related Disciplines.
PB96-119698 *02,980* Not available NTIS

PB96-119706
History of NIST's Contributions to Development of Standard Reference Materials and Reference and Definitive Methods for Clinical Chemistry.
PB96-119706 *03,503* Not available NTIS

PB96-119714
Tribological Behavior of 440/Diamond-Like-Carbon Film Couples.
PB96-119714 *03,019* Not available NTIS

PB96-119722
In vitro Fracture Behavior of Ceramic and Metal-Ceramic Restorations.
PB96-119722 *03,569* Not available NTIS

PB96-119730
Appearance Potentials of Ions Produced by Electron-Impact Induced Dissociative Ionization of SF6, SF4, SF5Cl, S2F10, SO2, SO2F2, SOF2, and SOF4.
PB96-119730 *01,080* Not available NTIS

PB96-119748
Structural and Magnetic Properties of CuCl2 Graphite Intercalation Compounds.
PB96-119748 *03,020* Not available NTIS

PB96-119755
Procedure for Measuring Trace Quantities of S2F10, S2OF10, and S2O2F10 in SF6 Using a Gas Chromatograph-Mass Spectrometer.
PB96-119755 *02,513* Not available NTIS

PB96-119763
VAMAS Intercomparison of Critical Current Measurements on NB3Sn Superconductors: A Summary Report.
PB96-119763 *04,043* Not available NTIS

PB96-119771
Reducing Errors, Complexity, and Measurement Time of PM Noise Measurements.
PB96-119771 *02,075* Not available NTIS

PB96-119789
High-Order Multipole Excitation of a Bound Electron.
PB96-119789 *04,044* Not available NTIS

PB96-119797
Self-Organizing Neural Network Character Recognition Using Adaptive Filtering and Feature Extraction.
PB96-119797 *01,855* Not available NTIS

PB96-119805
Standard Reference Materials for Optical Fibers and Connectors.
PB96-119805 *04,344* Not available NTIS

PB96-120555
Hair Testing for Drugs of Abuse: International Research on Standards and Technology.
PB96-120555 *03,504* PC A18/MF A04

PB96-122098
Low Electrolytic Conductivity Standards.
PB96-122098 *01,081*
(Order as PB96-117767, PC A08/MF A02)

PB96-122106
Potential and Current Distributions Calculated Across a Quantum Hall Effect Sample at Low and High Currents.
PB96-122106 *04,045*
(Order as PB96-117767, PC A08/MF A02)

PB96-122114
Microform Calibration Uncertainties of Rockwell Diamond Indenters.
PB96-122114 *03,280*
(Order as PB96-117767, PC A08/MF A02)

PB96-122122
Performance Measures for Geometric Fitting in the NIST Algorithm Testing and Evaluation Program for Coordinate Measurement Systems.
PB96-122122 *01,745*
(Order as PB96-117767, PC A08/MF A02)

PB96-122130
Study on the Reuse of Plastic Concrete Using Extended Set-Retarding Admixtures.
PB96-122130 *00,402*
(Order as PB96-117767, PC A08/MF A02)

PB96-122148
Third Generation Water Bath Based Blackbody Source.
PB96-122148 *04,046*
(Order as PB96-117767, PC A08/MF A02)

PB96-122411
Making Displays Deliver a Full Measure.
PB96-122411 *01,490* Not available NTIS

PB96-122429
Hydrodynamic Similarity in an Oscillating-Body Viscometer.
PB96-122429 *01,082* Not available NTIS

PB96-122437
Thermophysical Properties of Fluids for the Gas Industry.
PB96-122437 *02,494* Not available NTIS

PB96-122445
Recent Development in Nondestructive Testing of Concrete.
PB96-122445 *01,325* Not available NTIS

PB96-122452
Error Protecting Characteristics of CDMA and Impacts on Speech.
PB96-122452 *01,491* Not available NTIS

PB96-122460
Progress on the Quantized Hall Resistance Recommended Intrinsic/Derived Standards Practice.
PB96-122460 *02,403* Not available NTIS

PB96-122478
Nonlinear Dynamics of Stiff Polymers.
PB96-122478 *01,278* Not available NTIS

PB96-122486
Standardised Computer Data File Format for Storage, Transport, and Off-Line Processing of Partial Discharge Data.
PB96-122486 *01,930* Not available NTIS

PB96-122494
Constant Temperature and Humidity Chamber for Standard Resistors.
PB96-122494 *02,275* Not available NTIS

PB96-122502
Optical Sampling Using Nondegenerate Four-Wave Mixing in a Semiconductor Laser Amplifier.
PB96-122502 *02,076* Not available NTIS

PB96-122510
Epitaxial Growth of BaTiO3 Thin Films at 600C by Metalorganic Chemical Vapor Deposition.
PB96-122510 *03,071* Not available NTIS

PB96-122528
Survey of the Components of Display-Measurement Standards.
PB96-122528 *02,188* Not available NTIS

PB96-122536
Failure of All-Ceramic Fixed Partial Dentures 'In vitro' and 'In vivo': Analysis and Modeling.
PB96-122536 *00,175* Not available NTIS

PB96-122544
Programmable Guarded Coaxial Connector Panel.
PB96-122544 *02,108* Not available NTIS

PB96-122551
Physical Limit to the Stability of Superheated and Stretched Water.
PB96-122551 *01,083* Not available NTIS

PB96-122569
Extending the Angular Range of Neutron Reflectivity Measurements from Planar Lipid Bilayers: Applications to a Model Biological Membrane.
PB96-122569 *03,476* Not available NTIS

PB96-122577
Cavitation Contributes Substantially to Tensile Creep in Silicon Nitride.
PB96-122577 *03,171* Not available NTIS

PB96-122585
Microwave Characterization of Printed Circuit Transmission Lines.
PB96-122585 *02,077* Not available NTIS

PB96-122593
Economic Methods and Risk Analysis Techniques for Evaluating Building Investments: A Survey.
PB96-122593 *00,323* Not available NTIS

PB96-122601
Some Notable Hurricanes Revisited.
PB96-122601 *00,458* Not available NTIS

PB96-122619
Decomposition of SF6 and Production of S2F10 in Power Arcs.
PB96-122619 *01,084* Not available NTIS

PB96-122627
Simulation Studies of Supercooled and Glass Forming Liquids.
PB96-122627 *01,085* Not available NTIS

PB96-122635
Overview of Bioelectrical Impedance Analyzers.
PB96-122635 *00,176* Not available NTIS

PB96-122643
Decay of Bragg Gratings in Hydrogen-Loaded Optical Fibers.
PB96-122643 *04,345* Not available NTIS

PB96-122650
Few Caveats on Carbon Dioxide Monitoring.
PB96-122650 *02,562* Not available NTIS

PB96-122668
Development of a Standard Reference Material for Measurement of Interstitial Oxygen Concentration in Semiconductor Silicon by Infrared Absorption.
PB96-122668 *02,404* Not available NTIS

PB96-122676
Experimental Study of the Stabilization Region of Lifted Turbulent-Jet Diffusion Flames.
PB96-122676 *01,405* Not available NTIS

PB96-122684
Polarization Dependence of Response Functions in 3x3 Sagnac Optical Fiber Current Sensors.
PB96-122684 *02,189* Not available NTIS

PB96-122692
Electronics Packaging Materials Research at NIST.
PB96-122692 *02,405* Not available NTIS

PB96-122700
Millimeter-Resolution Optical Time-Domain Reflectometry Using a Four-Wave Mixing Sampling Gate.
PB96-122700 *02,190* Not available NTIS

PB96-122718
Chaotic Motions of Coupled Galloping Oscillators and Their Modeling as Diffusion Progresses.
PB96-122718 *04,823* Not available NTIS

PB96-122726
Non-Gaussian Noise Effects on Reliability of Multistable Systems.
PB96-122726 *04,213* Not available NTIS

PB96-122734
Modification of Cast Epoxy Resin Surfaces during Exposure to Partial Discharges.
PB96-122734 *01,086* Not available NTIS

PB96-122742
Orbital Alignment and Vector Correlations in Inelastic Atomic Collisions.
PB96-122742 *04,047* Not available NTIS

PB96-122759
Roadmap for the Computer Integrated Manufacturing (CIM) Application Framework.
PB96-122759 *02,832* Not available NTIS

PB96-122767
Influence of Surface Charge on the Stochastic Behavior of Partial Discharge in Dielectrics.
PB96-122767 *01,931* Not available NTIS

PB96-122775
Comment and Discussion on Digital Processing of PD Pulses.
PB96-122775 *01,932* Not available NTIS

PB96-122783
Novel Method for Determining Thin Film Density by Energy-Dispersive X-ray Reflectivity.
PB96-122783 *04,737* Not available NTIS

PB96-122791
Electromagnetic Properties of Materials: The NIST Metrology Program.
PB96-122791 *01,933* Not available NTIS

PB96-122809
Electron Attachment to Excited Molecules(1).
PB96-122809 *01,087* Not available NTIS

PB96-122817
Sleuthing the Dynamo: HST/FOS Observations of UV Emissions of Solar-Type Stars in Young Clusters.
PB96-122817 *00,098* Not available NTIS

PB96-122825
Open-Ended Coaxial Probes for Nondestructive Testing of Substrates and Circuit Boards.
PB96-122825 *02,078* Not available NTIS

PB96-122833
EDI and EFT Security Standards.
PB96-122833 *01,605* Not available NTIS

PB96-122841
Parallel Monte Carlo Simulation of MBE Growth.
PB96-122841 *02,406* Not available NTIS

PB96-122858
Slow Evolution from the Boundary: A New Stabilizing Constraint in Ill-Posed Continuation Problems.
PB96-122858 *03,418* Not available NTIS

PB96-122866
Field Modeling: Simulating the Effect of Sloped Beamed Ceilings on Detector and Sprinkler Response.
PB96-122866 *01,406* Not available NTIS

PB96-122874
Bounds on Frequency Response Estimates Derived from Uncertain Step Response Data.
PB96-122874 *03,419* Not available NTIS

PB96-122882
Efficient Way of Identifying New Active Stars: A VLA Survey of X-ray Selected Active Stellar Candidates.
PB96-122882 *00,099* Not available NTIS

PB96-122890
Smoke Emission from Burning Crude Oil.
PB96-122890 *01,407* Not available NTIS

PB96-122908
Open Issues in OSI Protocol Development and Conformance Testing.
PB96-122908 *01,818* Not available NTIS

PB96-122916
Atom Cooling and Trapping, and Collisions of Trapped Atoms.
PB96-122916 *04,048* Not available NTIS

PB96-122924
Database Management Standards: Status and Applicability.
PB96-122924 *01,819* Not available NTIS

PB96-122932
Laboratory Accreditation for Testing Energy Efficient Lighting.
PB96-122932 *00,270* Not available NTIS

PB96-122940
Dental Applications of Ceramics.
PB96-122940 *00,177* Not available NTIS

PB96-122957
Growth Characteristics of Fiber Gratings.
PB96-122957 *04,346* Not available NTIS

PB96-122965
Development of Hazard Assessment and Suppression Technology for Oil and Gas Well Blowout and Diverter Fires.
PB96-122965 *01,408* Not available NTIS

PB96-122973
Introduction to Phase-Stable Optical Sources.
PB96-122973 *04,347* Not available NTIS

PB96-122981
Effects of Spindle Dynamic Characteristics on Hard Turning.
PB96-122981 *02,699* Not available NTIS

PB96-122999
Chemically Assisted Machining of Si3N4.
PB96-122999 *03,072* Not available NTIS

PB96-123005
Magnetic Fields in Star-Forming Regions: Observations.
PB96-123005 *00,100* Not available NTIS

PB96-123021
Nonlinear Color Transformations in Real Time Using a Video Supercomputer.
PB96-123021 *02,191* Not available NTIS

PB96-123112
Stranding Experiments on Double Hull Tanker Structures.
PB96-123112 *03,749* Not available NTIS

PB96-123120
Laser-Induced Fluorescence Measurements of OH in Laminar Diffusion Flames in the Presence of Soot Particles.
PB96-123120 *01,409* Not available NTIS

PB96-123138
Stylus Flight in Surface Profiling.
PB96-123138 *02,675* Not available NTIS

PB96-123146
Effects of Nonmodel Errors on Model-Based Testing.
PB96-123146 *02,604* Not available NTIS

PB96-123153
Methods for Aligning the NIST Watt-Balance.
PB96-123153 *01,934* Not available NTIS

PB96-123161
Proposed International Interactive Courseware Standard.
PB96-123161 *00,137* Not available NTIS

PB96-123179
Influence of Electrode Material on Measured Ion Kinetic-Energy Distributions in Radio-Frequency Discharges.
PB96-123179 *01,935* Not available NTIS

PB96-123187
Secondary Standard for PM and AM Noise at 5, 10, and 100 MHz.
PB96-123187 *01,554* Not available NTIS

PB96-123195
Improving Neural Network Performance for Character and Fingerprint Classification by Altering Network Dynamics.
PB96-123195 *01,856* Not available NTIS

PB96-123203
Study of Laser Resonance Ionization Mass Spectrometry Using a Glow Discharge Source.
PB96-123203 *03,360* Not available NTIS

PB96-123211
Anisotropy of the Surfaces of Pores in Plasma Sprayed Alumina Deposits.
PB96-123211 *03,126* Not available NTIS

PB96-123229
Properties and Mechanisms of Fast-Setting Calcium Phosphate Cements.
PB96-123229 *00,178* Not available NTIS

PB96-123237
Flow-Induced Structure in Polymers: Chapter 16. Shear-Induced Changes in the Order-Disorder Transition Temperature and the Morphology of a Triblock Copolymer.
PB96-123237 *03,127* Not available NTIS

PB96-123245
Polymer Combustion and Flammability: Role of the Condensed Phase.
PB96-123245 *01,279* Not available NTIS

PB96-123252
Significant Contributions of IAPWS to the Power Industry, Science and Technology.
PB96-123252 *01,088* Not available NTIS

PB96-123260
Further Development of the N-Gas Mathematical Model: An Approach for Predicting the Toxic Potency of Complex Combustion Mixtures.
PB96-123260 *03,650* Not available NTIS

PB96-123278
Goddard High Resolution Spectrograph: Instrument, Goals, and Science Results.
PB96-123278 *00,044* Not available NTIS

PB96-123286
A-type and Chemically Peculiar Stars.
PB96-123286 *00,101* Not available NTIS

PB96-123294
High Velocity Plasm in the Transition Region of Au Mic: A Stellar Analog of Solar Explosive Events.
PB96-123294 *00,102* Not available NTIS

PB96-123302
Radio and X-ray Emissions from Chemically Peculiar B- and A-Type Stars: Observations and a Model.
PB96-123302 *00,103* Not available NTIS

PB96-123310
Redshifts in Stellar Transition Regions.
PB96-123310 *00,104* Not available NTIS

PB96-123328
Scientific Rationale and Present Implementation Strategy for the Far Ultraviolet Spectrograph Explorer (FUSE).
PB96-123328 *00,045* Not available NTIS

PB96-123336
Transition Regions of Capella.
PB96-123336 *00,105* Not available NTIS

PB96-123344
Optical Control of Enzymatic Conversion of Sucrose to Glucose by Bacteriorhodopsin Incorporated into Self-Assembled Phosphatidylcholine Vesicles.
PB96-123344 *03,477* Not available NTIS

PB96-123351
Kinetic Energy Distributions of H(+), H2(+), and H3(+) from a Diffuse Townsend Discharge in H2 at High E/N.
PB96-123351 *04,415* Not available NTIS

PB96-123369
Flow-Induced Structure in Polymer. Chapter 1. An Introduction to Flow-Induced Structures in Polymers.
PB96-123369 *03,387* Not available NTIS

PB96-123377
Flow-Induced Structure in Polymers. Chapter 17. Phase-Separation Kinetics of a Polymer Blend Solution Studied by a Two-Step Shear Quench.
PB96-123377 *03,388* Not available NTIS

PB96-123385
Chemical Stability of Upper-Layer Fire Gases.
PB96-123385 *01,410* Not available NTIS

PB96-123393
Prediction of the Strength Properties for Plain-Carbon and Vanadium Micro-Alloyed Ferrite-Pearlite Steel.
PB96-123393 *03,216* Not available NTIS

PB96-123401
Federal Labs Have Key Role in Metrication.
PB96-123401 *02,920* Not available NTIS

PB96-123419
Hydraulic Radius and Transport in Reconstructed Model Three-Dimensional Porous Media.
PB96-123419 *00,403* Not available NTIS

PB96-123427
Lubrication Theory for Reactive Spreading of a Thin Drop.
PB96-123427 *04,214* Not available NTIS

PB96-123435
All-Metal Collection System for Preparative-Scale Gas Chromatography: Purification of Low-Boiling-Point Compounds.
PB96-123435 *00,619* Not available NTIS

PB96-123443
Ultrafast Time-Resolved Infrared Probing of Energy Transfer at Surfaces.
PB96-123443 *00,620* Not available NTIS

PB96-123450
Fundamental Processes in Gas Discharges.
PB96-123450 *01,089* Not available NTIS

PB96-123468
SF6/N2 Mixtures: Basic and High-Voltage-Insulation Properties.
PB96-123468 *02,230* Not available NTIS

PB96-123476
Noise Characteristics Below 1 Hz of Zener Diode-Based Voltage Reference.
PB96-123476 *04,049* Not available NTIS

PB96-123484
Common Criteria: On the Road to International Harmonization.
PB96-123484 *01,606* Not available NTIS

PB96-123492
Functional Security Criteria for Distributed Systems.
PB96-123492 *01,607* Not available NTIS

PB96-123500
Optical Properties of Triton X-100-Treated Purple Membranes Embedded in Gelatin Films.
PB96-123500 *03,546* Not available NTIS

PB96-123518
Search for Small Violations of the Symmetrization Postulate in an Excited State of Helium.
PB96-123518 *04,050* Not available NTIS

PB96-123526
Book Review: Statistical Physics of Macromolecules.
PB96-123526 *01,280* Not available NTIS

PB96-123534
Book Review: Aspects and Applications of the Random Walk.
PB96-123534 *04,215* Not available NTIS

PB96-123542
Modification of the Phase Stability of Polymer Blends by Diblock Copolymer Additivies.
PB96-123542 *03,172* Not available NTIS

PB96-123559
Static Dielectric Constant of Water and Steam.
PB96-123559 *01,090* Not available NTIS

PB96-123567
Long-Term Stability of Bayard-Alpert Gauge Performance: Results Obtained from Repeated Calibrations against the National Institute of Standards and Technology Primary Vacuum Standard.
PB96-123567 *02,676* Not available NTIS

PB96-123575
Electrokinetic Sonic Analysis of Silicon Nitride Suspensions.
PB96-123575 *03,073* Not available NTIS

PB96-123583
Wire Bonding to Multichip Modules and Other Soft Substrates.
PB96-123583 *02,079* Not available NTIS

PB96-123591
Slow Dynamics of Segregation in Hydrogen-Bonded Polymer Blends.
PB96-123591 *01,281* Not available NTIS

PB96-123609
Optical Sampling Using Nondegenerate Four-Wave Mixing in a Semiconductor Laser Amplifier.
PB96-123609 *04,348* Not available NTIS

PB96-123617
Characterization of Liquid-Phase Epitaxially Grown HgCdTe Films by Magnetoresistance Measurements.
PB96-123617 *04,738* Not available NTIS

PB96-123625
New Approach for Reducing the Toxicity of the Combustion Products from Flexible Polyurethane Foam.
PB96-123625 *01,411* Not available NTIS

PB96-123633
Keeping Up with the Reality of Today's Surge Environment.
PB96-123633 *02,231* Not available NTIS

PB96-123641
Hot-Electron Microcalorimeters as High-Resolution X-ray Detectors.
PB96-123641 *04,739* Not available NTIS

PB96-123658
Ion Kinetics and Symmetric Charge-Transfer Collisions in Low-Current, Diffuse (Townsend) Discharges in Argon and Nitrogen.
PB96-123658 *04,051* Not available NTIS

PB96-123666
Intensive Swimming: Can It Affect Your Patients' Smiles.
PB96-123666 *03,570* Not available NTIS

PB96-123674
Nano-Defects in Commercial Bonded SOI and SIMOX.
PB96-123674 *02,407* Not available NTIS

PB96-123682
Influence of Stationary Phase Chemistry on Shape Recognition in Liquid Chromatography.
PB96-123682 *00,621* Not available NTIS

PB96-123690
Certification of Standard Reference Material (SRM) 1941a, Organics in Marine Sediment.
PB96-123690 *02,593* Not available NTIS

PB96-123708
Comparison of NIST and Manufacturer Calibrations of (90)Sr+(90)Y Ophthalmic Applicators.
PB96-123708 *03,634* Not available NTIS

PB96-123716
Refraction of Light by Graded Birefringent Media.
PB96-123716 *02,192* Not available NTIS

PB96-123724
Characterization of the Vibrational Dynamics in the Octahedral Sublattices of LaD2.25 and LaH2.25.
PB96-123724 *01,091* Not available NTIS

PB96-123732
Kinetic-Energy Distributions of Ions Sampled from Radio-Frequency Discharges in Helium, Nitrogen, and Oxygen.
PB96-123732 *01,092* Not available NTIS

PB96-123740
Measurement of S2OF10, and S2O2F10 Production Rates from Spark and Negative Glow Corona Discharge in SF6/O2 Gas Mixtures.
PB96-123740 *01,093* Not available NTIS

PB96-123757
Physics and Chemistry of Partial Discharge and Corona - Recent Advances and Future Challenges.
PB96-123757 *01,936* Not available NTIS

PB96-123765
Zimm Plot and Its Analogs as Indicators of Vesicle and Micelle Size Polydispersity.
PB96-123765 *01,094* Not available NTIS

PB96-123773
Distributed Feedback Lasers in Rare-Earth-Doped Phosphate Glass.
PB96-123773 *04,740* Not available NTIS

PB96-123781
Behavior of Surface Partial Discharge on Aluminum Oxide Dielectrics.
PB96-123781 *01,937* Not available NTIS

PB96-123799
Relativistic Modifications of Charge Expansion Theory.
PB96-123799 *04,052* Not available NTIS

PB96-123807
NIST Reference Materials to Support Accuracy in Drug Testing.
PB96-123807 *03,505* Not available NTIS

PB96-126180
Journal of Research of the National Institute of Standards and Technology, March/April 1995. Volume 100, Number 2.
PB96-126180 *04,349* PC A05/MF A01

PB96-126198
Low-Temperature Properties of Silver.
PB96-126198 *03,361*
(Order as PB96-126180, PC A05/MF A01)

PB96-126206
Mixing Plate-Like and Rod-Like Molecules with Solvent: A Test of Flory-Huggins Lattice Statistics.
PB96-126206 *03,173*
(Order as PB96-126180, PC A05/MF A01)

PB96-128095
Study of Technology for Detecting Pre-Ignition Conditions of Cooking-Related Fires Associated with Electric and Gas Ranges and Cooktops, Phase 1 Report.
PB96-128095 *00,303* PC A06/MF A02

PB96-128103
ICSSC Guidance on Implementing Executive Order 12941 on Seismic Safety of Existing Federally Owned or Leased Buildings.
PB96-128103 *00,459* PC A03/MF A01

PB96-128111
Ground Improvement Techniques for Liquefaction Remediation Near Existing Lifelines.
PB96-128111 *01,350* PC A05/MF A01

PB96-128129
Calorimetric and Visual Measurements of R123 Pool Boiling on Four Enhanced Surfaces.
PB96-128129 *04,053* PC A04/MF A01

PB96-128194
Extensions of the Prototype Application Protocol of Ready-to-Wear Apparel Pattern Making.
PB96-128194 *03,198* PC A03/MF A01

PB96-128202
Distributed Systems: Survey of Open Management Approaches.
PB96-128202 *01,746* PC A03/MF A01

PB96-128210
Bibliography of the NIST Optoelectronics Division.
PB96-128210 *02,193* PC A04/MF A01

PB96-128228
Overview of the Manufacturing Engineering Toolkit Prototype.
PB96-128228 *02,833* PC A03/MF A01

PB96-128236
User's Guide to 'SuperFit' Modeling Software for CMM Probe Lobing.
PB96-128236 *02,921* PC A03/MF A01

PB96-128244
Reference Manual for the Algorithm Testing System Version 2.0.
PB96-128244 *02,922* PC A03/MF A01

PB96-128251
Certification of the Standard Reference Material 1473a, a Low Density Polyethylene Resin.
PB96-128251 *01,282* PC A03/MF A01

PB96-128269
Metrology for Electromagnetic Technology: A Bibliography of NIST Publications, September 1995.
PB96-128269 *01,938* PC A05/MF A01

PB96-128277
Metrology Issues in Terahertz Physics and Technology.
PB96-128277 *01,939* PC A08/MF A02

PB96-128285
Recommended Performance-Based Criteria for the Design of Manufactured Home Foundation Systems to Resist Wind and Seismic Loads.
PB96-128285 *00,460* PC A05/MF A01

PB96-131461
Control of Gas-Metal-Arc Welding Using Arc-Light Sensing.
PB96-131461 *02,869* PC A06/MF A02

PB96-131479
Solid Propellant Gas Generators: Proceedings of the 1995 Workshop. Held in Gaithersburg, Maryland on June 28-29, 1995.
PB96-131479 *01,412* PC A11/MF A03

PB96-131487
Application Software Interface: ISDN Services for an Open Systems Environment.
PB96-131487 *01,492* PC A03/MF A01

PB96-131495
Comparison of POSIX Open System Environment (OSE) and Open Distributed Processing (ODP) Reference Models.
PB96-131495 *01,820* PC A03/MF A01

PB96-131503
Method to Determine a Basis Set of Paths to Perform Program Testing.
PB96-131503 *01,747* PC A03/MF A01

PB96-131511
Sharing Information via the Internet: An Infoserver Case Study.
PB96-131511 *01,493* PC A03/MF A01

PB96-131529
Operating Principles of MultiKron Virtual Counter Performance Instrumentation for MIMD Computers.
PB96-131529 *01,632* PC A03/MF A01

PB96-131537
Alkali-Silica Reaction and High Performance Concrete.
PB96-131537 *01,345* PC A03/MF A01

PB96-131545
Defining Environment Integration Requirements.
PB96-131545 *02,733* PC A03/MF A01

PB96-131552
How-To Suggestions for Implementing Executive Order 12941 on Seismic Safety of Existing Federal Buildings, A Handbook.
PB96-131552 *00,461* PC A10/MF A03

PB96-131560
Smoke Plume Trajectory from In situ Burning of Crude Oil in Alaska: Field Experiments.
PB96-131560 *02,594* PC A03/MF A01

PB96-131578
Electronic Access to Standards on the Information Highway.
PB96-131578 *01,494* PC A03/MF A01

PB96-131586
Classified Bibliography: Insulation Condition Monitoring Methods, 1989-1995.
PB96-131586 *02,232* PC A05/MF A01

PB96-131594
Anisotropy of Interfaces in an Ordered Alloy: A Multiple-Order-Parameter Model.
PB96-131594 *04,741* PC A04/MF A01

PB96-131602
Summary Report: Workshop on Industrial Applications of Scanned Probe Microscopy (2nd). A Workshop Co-Sponsored by NIST, SEMATECH, ASTM E42.14, and the American Vacuum Society. Held in Gaithersburg, Maryland on May 2-3, 1995.
PB96-131602 *00,509* PC A07/MF A02

PB96-131610
Computer Security: An Introduction to Computer Security. The NIST Handbook.
PB96-131610 *01,608* PC A13/MF A03

PB96-134954
Journal of Research of the National Institute of Standards and Technology, September-October 1993. Volume 98, Number 5.
PB96-134954 *03,362* PC A05/MF A01

PB96-135017
Thermal Isolation of High-Temperature Superconducting Thin Films Using Silicon Wafer Bonding and Micromachining.
PB96-135017 *02,408* Not available NTIS

PB96-135025
Radiance Temperatures (in the Wavelength Range 523-907 nm) of Group IVB Transition Metals Titanium, Zirconium, and Hafnium at Their Melting Points by a Pulse-Heating Technique.
PB96-135025 *02,677* Not available NTIS

PB96-135033
Coexistence of Grains with Differing Orthorhombicity in High Quality YBa2Cu3O7-delta Thin Films.
PB96-135033 *04,742* Not available NTIS

PB96-135041
In situ Fluorescence Cell Mass Measurements of 'Saccharomyces cerevisiae' Using Cellular Tryptophan.
PB96-135041 *03,547* Not available NTIS

PB96-135058
Mathematical Models of Transport Phenomena Associated with Arc-Welding Processes: A Survey.
PB96-135058 *02,870* Not available NTIS

PB96-135066
Shape of the Temperature-Entropy Saturation Boundary.
PB96-135066 *02,506* Not available NTIS

PB96-135074
Electrode Extension Model for Gas Metal Arc Welding.
PB96-135074 *02,871* Not available NTIS

PB96-135082
Development of Near-Field Test Procedures for Communication Satellite Antennas.
PB96-135082 *02,010* Not available NTIS

PB96-135090
Principal Points and Self-Consistent Points of Symmetric Multivariate Distributions.
PB96-135090 *03,446* Not available NTIS

PB96-135108
Spatial Information and Technology Standards Evolving.
PB96-135108 *03,679* Not available NTIS

PB96-135116
Analysis of an Open-Ended Coaxial Probe with Lift-Off for Nondestructive Testing.
PB96-135116 *01,940* Not available NTIS

PB96-135124
Distinguishing the Contributions of Residential Wood Combustion and Mobile Source Emissions Using Relative Concentrations of Dimethylphenanthrene Isomers.
PB96-135124 *02,563* Not available NTIS

PB96-135132
Modelling Drying Shrinkage of Cement Paste and Mortar. Part 1. Structural Models from Angstroms to Millimeters.
PB96-135132 *03,074* Not available NTIS

PB96-135140
Catastrophic Failures Propagate Field of Fracture Mechanics.
PB96-135140 *03,217* Not available NTIS

PB96-135157
High-Frequency Oscillators Using Phase-Locked Arrays of Josephson Junctions.
PB96-135157 *02,080* Not available NTIS

PB96-135165
Noise Reduction in Low-Frequency SQUID Measurements with Laser-Driven Switching.
PB96-135165 *02,081* Not available NTIS

PB96-135173
Anionic Triphenylmethane Dye Solutions for Low-Dose Food Irradiation Dosimetry.
PB96-135173 *03,715* Not available NTIS

PB96-135181
Growth of Epitaxial KNbO3 Thin Films.
PB96-135181 *02,409* Not available NTIS

PB96-135199
Frequency-Stabilized Lasers: A Driving Force for New Spectroscopies.
PB96-135199 *04,350* Not available NTIS

PB96-135207
Wire Bonding to Multichip Modules and Other Soft Substrates.
PB96-135207 *02,082* Not available NTIS

PB96-135215
Effect of Supersaturation on Apatite Crystal Formation in Aqueous Solutions at Physiologic pH and Temperature.
PB96-135215 *03,571* Not available NTIS

PB96-135223
Accuracy of the Electron Pump.
PB96-135223 *04,743* Not available NTIS

PB96-135231
Effects of Copper, Nickel and Boron on Mechanical Properties of Low-Alloy Steel Weld Metals Deposited at High Heat Input.
PB96-135231 *03,363* Not available NTIS

PB96-135249
Alcohol Solutions of Triphenyl-Tetrazolium Chloride as High-Dose Radiochromic Dosimeters.
PB96-135249 *03,716* Not available NTIS

PB96-135256
Oscillometric and Conductometric Analysis of Aqueous and Organic Dosimeter Solutions.
PB96-135256 *04,054* Not available NTIS

PB96-135264
Recalibration for the Final Archive of the International Ultraviolet Explorer (IUE) Satellite.
PB96-135264 *00,106* Not available NTIS

PB96-135272
Calorimeters for Calibration of High-Dose Dosimeters in High-Energy Electron Beams.
PB96-135272 *04,055* Not available NTIS

PB96-135280
Dosimetry Systems for Radiation Processing.
PB96-135280 *03,717* Not available NTIS

PB96-135298
Temperature and Relative Humidity Dependence of Radiochromic Film Dosimeter Response to Gamma and Electron Radiation.
PB96-135298 *03,718* Not available NTIS

PB96-135306
Real Time Monitoring of Electron Processors.
PB96-135306 *03,719* Not available NTIS

PB96-135314
Decomposition of Sulfur Hexafluoride by X-rays.
PB96-135314 *01,095* Not available NTIS

PB96-135322
Application of Thermodynamic and Detailed Chemical Kinetic Modeling to Understanding Combustion Product Generation in Enclosure Fires.
PB96-135322 *01,413* Not available NTIS

PB96-135330
Contact Tube Wear Detection in Gas Metal Arc Welding.
PB96-135330 *02,872* Not available NTIS

PB96-135348
Mutual Phase Locking in Systems of High-Tc Superconductor-Normal Metal-Superconductor Junctions.
PB96-135348 *04,744* Not available NTIS

PB96-135355
Effects of Etching on the Morphology and Surface Resistance of YBa2Cu3O7-delta Films.
PB96-135355 *02,410* Not available NTIS

PB96-135363
Proposed Changes to Charpy V-Notch Machine Certification Requirements.
PB96-135363 *02,955* Not available NTIS

PB96-135371
Influence of Thickness Fluctuations on Exchange Coupling in Fe/Cr/Fe Structures.
PB96-135371 *04,745* Not available NTIS

PB96-135389
LRM Probe-Tip Calibrations Using Nonideal Standards.
PB96-135389 *02,411* Not available NTIS

PB96-136965
Computer-Aided Manufacturing Engineering Forum (1st). Technical Meeting Proceedings. Held in Gaithersburg, Maryland on March 21-22, 1995.
PB96-136965 *02,834* PC A10/MF A03

PB96-136973
Effect of Inclination on the Performance of a Compact Brazed Plate Condenser and Evaporator.
PB96-136973 *02,756* PC A03/MF A01

PB96-136981
Metallurgy Technical Activities 1994 (NAS-NRC Assessment Panel, April 6-7, 1995).
PB96-136981 *02,981* PC A08/MF A02

PB96-137104
National Planning for Construction and Building R and D.
PB96-137104 *00,324* PC A06/MF A02

PB96-137187
Electronics and Electrical Engineering Laboratory Technical Publication Announcements Covering Laboratory Programs, April to June 1995 with 1995 EEEL Events Calendar.
PB96-137187 *01,941* PC A03/MF A01

PB96-137724
Formation of DNA-Protein Cross-Links in Cultured Mammalian Cells Upon Treatment with Iron Ions.
PB96-137724 *03,651* Not available NTIS

PB96-137732
Temperature and Frequency Dependence of Anelasticity in a Nickel Oscillator.
PB96-137732 *03,689* Not available NTIS

PB96-137740
Churchill Eisenhart, 1913-1994.
PB96-137740 *03,447* Not available NTIS

PB96-137757
Visualization of Surface Figure by the Use of Zernike Polynomials.
PB96-137757 *04,351* Not available NTIS

PB96-137765
Microwave Dielectric Properties of Anisotropic Materials at Cryogenic Temperatures.
PB96-137765 *02,412* Not available NTIS

PB96-137773
Panel Discussion on Units in Magnetism.
PB96-137773 *04,746* Not available NTIS

PB96-137781
Anomalous Switching Phenomenon in Critical-Current Measurements When Using Conductive Mandrels.
PB96-137781 *02,233* Not available NTIS

PB96-137799
Low-Frequency Excitations of Oriented DNA.
PB96-137799 *03,548* Not available NTIS

PB96-137807
Use of Monte Carlo Modeling for Interpreting Scanning Electron Microscope Linewidth Measurements.
PB96-137807 *02,413* Not available NTIS

PB96-138417
Low Noise YBa2Cu3O7-x-SrTiO3-YBa2Cu3O7-x Mulitlayers for Improved Superconducting Magnetometers.
PB96-138417 *04,747* Not available NTIS

PB96-138425
Determination of Vitamin K1 in Serum Using Catalytic-Reduction Liquid Chromatography with Fluorescence Detection.
PB96-138425 *03,506* Not available NTIS

PB96-138433
Electrical Characterization of Integrated Circuit Metal Line Thickness.
PB96-138433 *02,414* Not available NTIS

PB96-138441
Observation and Visible and uv Magnetic Dipole Transitions in Highly Charged Xenon and Barium.
PB96-138441 *04,056* Not available NTIS

PB96-138458
High-Energy Phonon Dispersion in La1.85Sr0.15CuO4.
PB96-138458 *04,748* Not available NTIS

PB96-138466
Atomic Transition Probabilities and Tests of the Spectroscopic Coupling Scheme for N I.
PB96-138466 *04,057* Not available NTIS

PB96-138474
Accurate Computations of Radar Cross Sections of Simple Objects.
PB96-138474 *04,426* Not available NTIS

PB96-138482
Test of a Slow Off-Axis Parabola at Its Center of Curvature.
PB96-138482 *04,352* Not available NTIS

PB96-138490
Electro-Optic-Based RMS Voltage Measurement Technique.
PB96-138490 *02,194* Not available NTIS

PB96-138508
Improving the Evaluation of Building Ventilation.
PB96-138508 *00,271* Not available NTIS

PB96-138516
q Dependence of Self-Energy Effects of the Plane Oxygen Vibration in YBa2Cu3O7.
PB96-138516 *01,096* Not available NTIS

PB96-138524
Electron-electron Interactions, Coupled-Plasmon-Phonon Modes, and Mobility in n-Type GaAs.
PB96-138524 *04,749* Not available NTIS

PB96-138532
Nonequilibrium Total-Dielectric-Function Approach to the Electron Boltzmann Equation for Inelastic Scattering in Doped Polar Semiconductors.
PB96-138532 *04,416* Not available NTIS

PB96-138540
Report on 1994 Actions of the International Institute of Welding.
PB96-138540 *02,873* Not available NTIS

PB96-138557
Dependence of Contrast on Probe/Sample Spacing with the Magneto-Optic Kerr-Effect Scanning Near-Field Optical Microscope (MOKE-SNOM).
PB96-138557 *04,750* Not available NTIS

PB96-138565
Silicon Surface Chemistry by IR Spectroscopy in the Mid- to Far-IR Region: H2O and Ethanol on Si(100).
PB96-138565 *01,097* Not available NTIS

PB96-138573
Development of Highly Conductive Cantilevers for Atomic Force Microscopy Point Contact Measurements.
PB96-138573 *04,751* Not available NTIS

PB96-138581
Selectivity Trends in Packed Column Supercritical Fluid Chromatography with C18 Stationary Phases.
PB96-138581 *00,622* Not available NTIS

PB96-138599
MCNP Model of the National Bureau of Standards Reactor (NBSR) Core.
PB96-138599 *03,733* Not available NTIS

PB96-138607
High Resolution Time Interval Counter.
PB96-138607 *01,495* Not available NTIS

PB96-139407
Databases Available in the Research Information Center of the National Institute of Standards and Technology (December 1995).
PB96-139407 *02,734* PC A07/MF A02

PB96-139415
Telecommunications Security Guidelines for Telecommunications Management Network. Computer Security.
PB96-139415 *01,496* PC A03/MF A01

PB96-140363
Radiometer Equation for Noise Comparison Radiometers.
PB96-140363 *02,195* Not available NTIS

PB96-140371
Inexpensive Laser Cooling and Trapping Experiment for Undergraduate Laboratories.
PB96-140371 *04,353* Not available NTIS

PB96-140389
Fiber Coating Diameter: Toward a Glass Artifact Standard.
PB96-140389 *02,234* Not available NTIS

PB96-140397
Dielectric Spectroscopic Determination of Temperature Behavior of Electroclinic Parameters in the Liquid Crystal W317.
PB96-140397 *01,098* Not available NTIS

PB96-140405
Thermal Modeling and Analysis of Laser Calorimeters.
PB96-140405 *04,354* Not available NTIS

PB96-141015
Elastic Constants and Internal Friction of Polycrystalline Copper.
PB96-141015 *03,364* Not available NTIS

PB96-141023
Void Shape in Sintered Titanium.
PB96-141023 *02,705* Not available NTIS

PB96-141031
Deep-UV Excimer Laser Measurements at NIST.
PB96-141031 *04,355* Not available NTIS

PB96-141049
Object-Oriented Tel/Tk Binding for Interpreted Control of the NIST EXPRESS Toolkit in the NIST STEP Application Protocol Development Environment.
PB96-141049 *02,785* Not available NTIS

PB96-141056
Evaluation of Sprinkler Activation Prediction Methods.
PB96-141056 *00,304* Not available NTIS

PB96-141064
Crystal Structure of Decacalcium Tetrapotassium Hexakis (Pyrophosphate) Nonahydrate.
PB96-141064 *01,099* Not available NTIS

PB96-141072
Atom-Optical Properties of a Standing-Wave Light Field.
PB96-141072 *04,356* Not available NTIS

PB96-141080
X-ray Observation of Electroclinic Layer Constriction and Rearrangement in a Chiral Smectic-A Liquid Crystal.
PB96-141080 *01,100* Not available NTIS

PB96-141098
Evidence for Tunneling and Magnetic Scatttering at 'In situ' YBCO/Noble-Metal Interfaces.
PB96-141098 *04,752* Not available NTIS

PB96-141106
Cross-Sectional Photoluminescence and Its Application to Buried-Layer Semiconductor Structures.
PB96-141106 *02,415* Not available NTIS

PB96-141114
Safety Assessment of Railroad Wheels by Residual Stress Measurements.
PB96-141114 *04,855* Not available NTIS

PB96-141122
Effect of Charpy V-Notch Striker Radii on the Absorbed Energy.
PB96-141122 *03,365* Not available NTIS

PB96-141130
Apparatus for Resistance Measurement of Short, Small-Diameter Conductors.
PB96-141130 *04,417* Not available NTIS

PB96-141148
De Facto Microzonation through the Use of Soils Factors in Design Triggers.
PB96-141148 *00,462* Not available NTIS

PB96-141155
Neutron-Powder-Diffraction Study of the Long-Range Order in the Octahedral Sublattice of LaD2.25.
PB96-141155 *04,753* Not available NTIS

PB96-141163
Anova Estimates of Variance Components for a Class of Mixed Models.
PB96-141163 *03,448* Not available NTIS

PB96-141171
One-Sided beta-Content Tolerance Intervals for Mixed Models.
PB96-141171 *03,449* Not available NTIS

PB96-141189
Effect of Magnetic Field Orientation on the Critical Current of HTS Conductor and Coils.
PB96-141189 *02,956* Not available NTIS

PB96-141197
Vector and Quasi-Vector Solutions for Optical Waveguide Modes Using Efficient Galerkin's Method with Hermite-Gauss Basis Functions.
PB96-141197 *04,357* Not available NTIS

PB96-141205
Photoluminescence Spectra of Epitaxial Single Crystal C60.
PB96-141205 *04,754* Not available NTIS

PB96-141213
Quench Energy and Fatigue Degradation Properties of Cu- and Al/Cu-Stablized Nb-Ti Epoxy-Impregnated Superconductor Coils.
PB96-141213 *04,755* Not available NTIS

PB96-141221
Atomic Iron in Its (5)D Ground State: A Direct Measurement of the J = 0 inverted arrow 1 and J = 1 inverted arrow 2 Fine-Structure Intervals (1.2).
PB96-141221 *04,756* Not available NTIS

PB96-141239
Predicting the Fire Performance of Buildings: Establishing Appropriate Calculation Methods for Regulatory Applications.
PB96-141239 *00,316* Not available NTIS

PB96-141247
Using Atom Optics to Fabricate Nanostructures.
PB96-141247 *04,757* Not available NTIS

PB96-141254
Safety Assessment of Railroad Wheels Through Roll-by Detection of Tread Cracks.
PB96-141254 *04,856* Not available NTIS

PB96-141262
Microwave Properties of Voltage-Tunable YBa2Cu3O7-delta/SrTiO3 Coplanar Waveguide Transmission Lines.
PB96-141262 *02,235* Not available NTIS

PB96-141270
Unreacted Cement Content in Macro-Defect-Free Composites: Impact on Processing-Structure-Property Relations.
PB96-141270 *03,174* Not available NTIS

PB96-141288
Research and Development Activities in Electron Paramagnetic Resonance Dosimetry.
PB96-141288 *03,635* Not available NTIS

PB96-141296
Experience with MPI: 'Converting Pvmmake to Mpimake under LAM' and 'MPI and Parallel Genetic Programming'.
PB96-141296 *01,748* Not available NTIS

PB96-141304
Bounds on Least-Squares Four-Parameter Sine-Fit Errors Due to Harmonic Distortion and Noise.
PB96-141304 *01,609* Not available NTIS

PB96-141312
Oxygen Annealing of Ex-situ YBCO/Ag Thin-Film Interfaces.
PB96-141312 *04,758* Not available NTIS

PB96-141320
Summary Report on the Workshop on Advanced Digital Video in the National Information Infrastructure.
PB96-141320 *01,497* Not available NTIS

PB96-141338
Ultrasonic-Resonance Spectroscopy of Bulk and Layered Solids.
PB96-141338 *04,759* Not available NTIS

PB96-141346
Domain Structures in Magnetoresistive Granular Metals.
PB96-141346 *04,760* Not available NTIS

PB96-141353
Optimal Control of Building and HVAC Systems.
PB96-141353 *00,272* Not available NTIS

PB96-141361
Alternative Contour Technique for the Efficient Computation of the Effective Length of an Antenna.
PB96-141361 *02,011* Not available NTIS

PB96-141379
Determination of Sulfur in Fossil Fuels by Isotope Dilution Thermal Ionization Mass Spectrometry.
PB96-141379 *02,495* Not available NTIS

PB96-141387
Theory of the Magneto-Optic Kerr Effect in the Near Field.
PB96-141387 *04,761* Not available NTIS

PB96-141395
Artificial Crack in Steel: An Ultrasonic-Resonance-Spectroscopy and Modeling Study.
PB96-141395 *03,241* Not available NTIS

PB96-145560
Journal of Physical and Chemical Reference Data, Volume 24, No. 1, January/February 1995.
PB96-145560 *01,101* Not available NTIS

PB96-145578
Millimeter- and Submillimeter-Wave Spectrum of trans-Ethyl Alcohol.
PB96-145578 *01,102* Not available NTIS

PB96-145586
Database for the Static Dielectric Constant of Water and Steam.
PB96-145586 *01,103* Not available NTIS

PB96-145594
Theoretical Form Factor, Attenuation and Scattering Tabulation for Z=1-92 from E=1-10 eV to E=0.4-1.0 MeV.
PB96-145594 *01,104* Not available NTIS

PB96-145818
Journal of Physical and Chemical Reference Data, Volume 24, No. 2, March/April 1995.
PB96-145818 *01,105* Not available NTIS

PB96-145826
Rate Constants for the Decay and Reactions of the Lowest Electronically Excited Singlet State of Molecular Oxygen in Solution. An Expanded and Revised Compilation.
PB96-145826 *01,106* Not available NTIS

PB96-145834
Thermodynamic Properties of the Aqueous Ba(sup 2+) Ion and the Key Compounds of Barium.
PB96-145834 *01,107* Not available NTIS

PB96-145842
Journal of Physical and Chemical Reference Data, Volume 24, No. 3, May/June 1995.
PB96-145842 *01,108* Not available NTIS

PB96-145859
Critical Review of Rate Constants for Reactions of Transients from Metal Ions and Metal Complexes in Aqueous Solution.
PB96-145859 *01,109* Not available NTIS

PB96-145867
Ideal Gas Thermodynamic Properties of Sulphur Heterocyclic Compounds.
PB96-145867 *01,110* Not available NTIS

PB96-145875
Standard Reference Data for the Thermal Conductivity of Water.
PB96-145875 *01,111* Not available NTIS

PB96-145883
Journal of Physical and Chemical Reference Data, Volume 24, No. 4, July/August 1995.
PB96-145883 *01,112* Not available NTIS

PB96-145891
Summary of the Apparent Standard Partial Molal Gibbs Free Energies of Formation of Aqueous Species, Minerals, and Gases at Pressures 1 to 5000 Bars and Temperatures 25 to 1000C.
PB96-145891 *01,113* Not available NTIS

PB96-145909
Atomic Weights of the Elements, 1993.
PB96-145909 *01,114* Not available NTIS

PB96-145917
Spectral Data for Highly Ionized Krypton, Kr V through Kr XXXVI.
PB96-145917 *01,115* Not available NTIS

PB96-145925
Journal of Physical and Chemical Reference Data, Volume 24, No. 5, September/October 1995.
PB96-145925 *01,116* Not available NTIS

PB96-145933
Viscosity of Ammonia.
PB96-145933 *01,117* Not available NTIS

PB96-145941
Thermodynamics of Enzyme-Catalyzed Reactions. Part 4. Lyases.
PB96-145941 *01,118* Not available NTIS

PB96-145958
Thermodynamic Properties of the Aqueous Ions (2+ and 3+) of Iron and the Key Compounds of Iron.
PB96-145958 *01,119* Not available NTIS

PB96-145966
Journal of Physical and Chemical Reference Data, Volume 24, No. 6, November/December 1995.
PB96-145966 *01,120* Not available NTIS

PB96-145974
Thermodynamics of Enzyme-Catalyzed Reactions. Part 5. Isomerases and Ligases.
PB96-145974 *01,121* Not available NTIS

PB96-145982
Energy Levels of Zinc, Zn I through Zn XXX.
PB96-145982 *01,122* Not available NTIS

PB96-146352
Seismic Performance of Circular Bridge Columns Designed in Accordance with AASHTO/CALTRANS Standards.
PB96-146352 *01,346* PC A07/MF A02

PB96-146360
Open System Environment (OSE): Architectural Framework for Information Infrastructure.
PB96-146360 *00,002* PC A04/MF A01

PB96-146618
High-Temperature High-Pressure Oscillating Tube Densimeter.
PB96-146618 *01,123* Not available NTIS

PB96-146626
Interaction Coefficients for 15 Mixtures of Flammable and Non-Flammable Components.
PB96-146626 *03,281* Not available NTIS

PB96-146634
In-situ Neutron Reflectivity of MBE Grown and Chemically Processed Surfaces and Interfaces.
PB96-146634 *02,416* Not available NTIS

PB96-146642
Effectiveness of a Heat Recovery Ventilator, an Outdoor Air Intake Damper and an Electrostatic Particulate Filter at Controlling Indoor Air Quality in Residential Buildings.
PB96-146642 *02,564* Not available NTIS

PB96-146659
Multizone Modeling of Three Residential Indoor Air Quality Control Options.
PB96-146659 *02,565* Not available NTIS

PB96-146667
Response to 'Draining in Dilute Polymer Solutions and Renormalization'.
PB96-146667 *01,283* Not available NTIS

PB96-146675
Electric Dipole Excitation of a Long Conductor in a Lossy Medium.
PB96-146675 *04,058* Not available NTIS

PB96-146683
Evidence for Inelastic Processes for N(+)3 and N(+)4 from Ion Energy Distributions in He/N2 Radio Frequency Glow Discharges.
PB96-146683 *04,059* Not available NTIS

PB96-146691
Low Magnetostriction in Annealed NiFe/Ag Giant Magnetoresistive Multilayers.
PB96-146691 *04,762* Not available NTIS

PB96-146709
Integrated Thin-Film Micropotentiometers.
PB96-146709 *02,109* Not available NTIS

PB96-146717
Telegraph Noise in Silver-Permalloy Giant Magnetoresistance Test Structures.
PB96-146717 *04,763* Not available NTIS

PB96-146725
Orientation Effects on ESR Analysis of Alanine-Polymer Dosimeters.
PB96-146725 *03,720* Not available NTIS

PB96-146733
Radiation-Chemical Reaction of 2,3,5-Triphenyl-Tetrazolium Chloride in Liquid and Solid State.
PB96-146733 *01,124* Not available NTIS

PB96-146741
Inhibition of Premixed Methane-Air Flames by Halon Alternatives.
PB96-146741 *01,414* Not available NTIS

PB96-146758
Scalability Test for Parallel Code.
PB96-146758 *01,749* Not available NTIS

PB96-146766
Amperometric Measurement of Moisture in Transformer Oil Using Karl Fischer Reagents.
PB96-146766 *00,623* Not available NTIS

PB96-146774
Progress Toward Accurate Metrology Using Atomic Force Microscopy.
PB96-146774 *02,417* Not available NTIS

PB96-146782
Investigation of Applicability of Alanine and Radiochromic Detectors to Dosimetry of Proton Clinical Beams.
PB96-146782 *03,636* Not available NTIS

PB96-146790
Global Equivalence Ratio Concept and the Formation Mechanisms of Carbon Monoxide in Enclosure Fires.
PB96-146790 *00,210* Not available NTIS

PB96-146808
Thermodynamic Properties of Dilute and Semidilute Solutions of Regular Star Polymers.
PB96-146808 *01,284* Not available NTIS

PB96-146816
Interfacial Transport in Porous Media: Application to dc Electrical Conductivity of Mortars.
PB96-146816 *01,326* Not available NTIS

PB96-146824
Statistical Descriptors in Crystallography. 2. Report of a Working Group on Expression of Uncertainty in Measurement.
PB96-146824 *04,764* Not available NTIS

PB96-146832
Stagnant Film Model of the Effect of Natural Convection on the Dendrite Operating State.
PB96-146832 *04,765* Not available NTIS

PB96-146840
Preparation and Characterization of Cyclopolymerizable Resin Formulations.
PB96-146840 *01,285* Not available NTIS

PB96-146857
Inelastic Neutron Scattering Study of Hydrogen in Nanocrystalline Pd.
PB96-146857 *03,366* Not available NTIS

PB96-146865
Light-Scattering Studies on Phase Separation in a Binary Blend with Addition of Diblock Copolymers.
PB96-146865 *01,286* Not available NTIS

PB96-146873
Influence of an Impenetrable Interface on a Polymer Glass-Transition Temperature.
PB96-146873 *03,175* Not available NTIS

PB96-146881
Electrodeposited Cobalt-Tungsten as a Diffusion Barrier between Graphite Fibers and Nickel.
PB96-146881 *03,176* Not available NTIS

PB96-146899
Experimental Determination of the Ionization Energy of IO(X(sup 2)II(sub 3/2)) and Estimations of Delta(sub f)H(sup deg)(sub 0)(IO(sup -)) and PA(IO).
PB96-146899 *00,694* Not available NTIS

PB96-147012
Bioactive Polymeric Dental Materials Based on Amorphous Calcium Phosphate.
PB96-147012 *03,572* Not available NTIS

PB96-147020
Remineralizing Dental Composites Based on Amorphous Calcium Phosphate.
PB96-147020 *03,573* Not available NTIS

PB96-147038
Dielectric Measurements on Printed-Wiring and Circuit Boards, Thin Films, and Substrates: An Overview.
PB96-147038 *02,236* Not available NTIS

PB96-147046
Gravity-Current Transport in Building Fires.
PB96-147046 *01,415* Not available NTIS

PB96-147053
General Types of Information Services.
PB96-147053 *02,735* Not available NTIS

PB96-147061
Rapid Method for the Isolation of Genomic DNA from 'Aspergillus fumigatus'.
PB96-147061 *03,488* Not available NTIS

PB96-147079
Pinch Effect in Commensurate Vortex-Pin Lattices.
PB96-147079 *01,125* Not available NTIS

PB96-147087
Magnetoresistance of Thin-Film NiFe Devices Exhibiting Single-Domain Behavior.
PB96-147087 *04,766* Not available NTIS

PB96-147095
Dynamics of Calcium Phosphate Precipitation.
PB96-147095 *03,574* Not available NTIS

PB96-147103
Absolute Response Calibration of a Transfer Standard Cryogenic Bolometer.
PB96-147103 *04,358* Not available NTIS

PB96-147111
Computing the Effect of Sprinkler Sprays on Fire Induced Gas Flow.
PB96-147111 *00,404* Not available NTIS

PB96-147129
Gas-Coupled, Pulse-Echo Ultrasonic Crack Detection and Thickness Gaging.
PB96-147129 *04,847* Not available NTIS

PB96-147137
Comparison of k-Correction and Taylor-Series Correction for Probe-Position Errors in Planar Near-Field Scanning.
PB96-147137 *02,012* Not available NTIS

PB96-147152
Neutron Scattering Study of the Lattice Modes of Solid Cubane.
PB96-147152 *01,126* Not available NTIS

PB96-147160
II-3: Critical Current Measurement Methods: Quantitative Evaluation.
PB96-147160 *04,767* Not available NTIS

PB96-147178
First VAMAS USA Interlaboratory Comparison of High Temperature Superconductor Critical Current Measurements.
PB96-147178 *04,768* Not available NTIS

PB96-147186
II-5: Thermal Contraction of Materials Used in Nb3Sn Critical Current Measurements.
PB96-147186 *04,769* Not available NTIS

PB96-147194
USA Interlaboratory Comparison of Superconductor Simulator Critical Current Measurements.
PB96-147194 *04,770* Not available NTIS

PB96-147202
Heterodyne Mixing and Direct Detection in High Temperature Josephson Junctions.
PB96-147202 *01,565* Not available NTIS

PB96-147392
Airborne Asbestos Analysis: National Voluntary Laboratory Accreditation Program.
PB96-147392 *02,566* PC A05/MF A01

PB96-147814
Virtual Environments for Health Care. A White Paper for the Advanced Technology Program (ATP), the National Institute of Standards and Technology.
PB96-147814 *03,594* PC A05/MF A01

PB96-147889
Collection of Results for the SPC/E Water Model.
PB96-147889 *01,127* PC A03/MF A01

PB96-147897
Review of Flows Driven By Natural Convection in Adiabatic Shafts.
PB96-147897 *01,416* PC A04/MF A01

PB96-147905
Electronics and Electrical Engineering Laboratory Technical Progress Bulletin Covering Laboratory Programs, July to September 1995 with 1996 EEEL Events Calendar.
PB96-147905 *01,942* PC A04/MF A01

PB96-147913
Technical Impact of the NIST Calibration Service for Electrical Power and Energy.
PB96-147913 *02,462* PC A05/MF A01

PB96-147954
NIST RS274KT Interpreter.
PB96-147954 *02,835* PC A05/MF A01

PB96-147962
Product Realization Process Modeling: A Study of Requirements, Methods and Research Issues.
PB96-147962 *02,836* PC A04/MF A01

PB96-148010
Microwave Noise in High-Tc Josephson Junctions.
PB96-148010 *04,771* Not available NTIS

PB96-148028
Partially Coherent Transmittance of Dielectric Lamellae.
PB96-148028 *04,359* Not available NTIS

PB96-148036
Water Permeability and Chloride Ion Diffusion in Portland Cement Mortars: Relationship to Sand Content and Critical Pore Diameter.
PB96-148036 *03,193* Not available NTIS

PB96-148044
Josephson D/A Converter with Fundamental Accuracy.
PB96-148044 *02,418* Not available NTIS

PB96-148051
Performance and Reliability of NIST 10-V Josephson Arrays.
PB96-148051 *02,419* Not available NTIS

PB96-148069
Accuracy in Time Domain Transmission Line Measurements.
PB96-148069 *04,060* Not available NTIS

PB96-148077
Spatial Correlation Function for Fields in a Reverberation Chamber.
PB96-148077 *04,427* Not available NTIS

PB96-148085
Shear-Induced Mixing in Polymer Blends.
PB96-148085 *01,287* Not available NTIS

PB96-148093
AC-DC Difference Characteristics of High-Voltage Thermal Converters.
PB96-148093 *02,083* Not available NTIS

PB96-148101
Free Radical Chemistry of the Atmospheric Aqueous Phase.
PB96-148101 *00,117* Not available NTIS

PB96-148119
Information Resources for the Fire Community.
PB96-148119 *00,211* Not available NTIS

PB96-148127
High-Temperature Furnace for In situ Small-Angle Neutron Scattering during Ceramic Processing.
PB96-148127 *03,743* Not available NTIS

PB96-148135
Performance of Multilayer Thin-Film Multijunction Thermal Converters.
PB96-148135 *02,084* Not available NTIS

PB96-148143
V-6: Effects of Temperature Variation.
PB96-148143 *04,772* Not available NTIS

PB96-148150
Scanning Capacitance Microscopy Measurements and Modeling: Progress Towards Dopant Profiling of Silicon.
PB96-148150 *04,773* Not available NTIS

PB96-148168
Measurement of Patterned Film Linewidth for Interconnect Characterization.
PB96-148168 *02,420* Not available NTIS

PB96-148176
High-Speed Interconnection Characterization Using Time Domain Network Analysis.
PB96-148176 *04,061* Not available NTIS

PB96-148184
Effects of Substrate Surface Steps on the Microstructure of Epitaxial Ba2YCu3O7-x Thin Films on (001) LaAlO3.
PB96-148184 *04,774* Not available NTIS

PB96-148192
Heights of Wall-Fire Flames.
PB96-148192 *00,212* Not available NTIS

PB96-148200
Examination of the Correlation between Cone Calorimeter Data and Full-Scale Furniture Mock-Up Fires.
PB96-148200 *01,417* Not available NTIS

PB96-151394
Fire Safety Engineering Research in the United States.
PB96-151394 *00,213* Not available NTIS

PB96-151402
Elements of a Framework for Fire Safety Engineering.
PB96-151402 *00,214* Not available NTIS

PB96-154422
Optical Fiber, Fiber Coating, and Connector Ferrule Geometry: Results of Interlaboratory Measurement Comparisons.
PB96-154422 *04,360* PC A05/MF A01

PB96-154463
Workplan to Analyze the Energy Impacts of Envelope Airtightness in Office Buildings.
PB96-154463 *00,273* PC A04/MF A01

PB96-154521
Machine Performance Standard Provides Opportunity to Improve Quality and Productivity.
PB96-154521 *02,837* PC A02/MF A01

PB96-154539
Guidelines for the Development of Mapping Tables.
PB96-154539 *02,786* PC A03/MF A01

PB96-154562
Image Gradient Evolution: A Visual Cue for Danger.
PB96-154562 *02,939* PC A03/MF A01

PB96-154570
AutoBid 2.0: The Microcomputer System for Police Patrol Vehicle Selection.
PB96-154570 *04,871* PC A03/MF A01

PB96-154588
C++ in Safety Critical Systems.
PB96-154588 *01,750* PC A04/MF A01

PB96-154596
Semiconductor Measurement Technology: Survey of Optical Characterization Methods for Materials, Processing, and Manufacturing in the Semiconductor Industry.
PB96-154596 *02,706* PC A05/MF A01

PB96-154794
Predicting the Ignition Time and Burning Rate of Thermoplastics in the Cone Calorimeter.
PB96-154794 *01,418* PC A10/MF A03

PB96-154810
Santa Ana Fire Department Experiments at South Bristol Street.
PB96-154810 *00,305* PC A11/MF A03

PB96-154836
Simplified Design Procedure for Hybrid Precast Concrete Connections.
PB96-154836 *00,405* PC A06/MF A01

PB96-154877
NIST SIMA Interactive Management Workshop. Held in Fort Belvoir, Virginia on November 14-16, 1994.
PB96-154877 *02,838* PC A08/MF A02

PB96-154901
Summary and Results of the NIST Workshop on Proposed Guidelines for Testing and Evaluation of Seismic Isolation Systems. Held in San Francisco, California on July 25, 1994.
PB96-154901 *00,463* PC A04/MF A01

PB96-154968
Sensitivity Analysis for Mathematical Modeling of Fires in Residential Buildings.
PB96-154968 *00,215* PC A03/MF A01

PB96-154976
STandard for the Exchange of Product Model Data (STEP): Procedures for NIST STEP Validation.
PB96-154976 *02,787* PC A03/MF A01

PB96-154984
Development of a Test Method for Leaching of Lead from Lead-Based Paints Through Encapsulants.
PB96-154984 *03,128* PC A04/MF A01

PB96-154992
Standard Generalized Markup Language Test Suite Evaluation Report.
PB96-154992 *01,751* PC A03/MF A01

PB96-155023
TEM/Reverberating Chamber Electromagnetic Radiation Test Facility at Rome Laboratory.
PB96-155023 *03,675* PC A05/MF A01

PB96-155411
Quantifying the Ignition Propensity of Cigarettes.
PB96-155411 *00,306* Not available NTIS

PB96-155429
Metrology and Regional Trade Pacts.
PB96-155429 *02,923* Not available NTIS

PB96-155437
Annealing of Bragg Gratings in Hydrogen-Loaded Optical Fiber.
PB96-155437 *04,361* Not available NTIS

PB96-155445
Comparison of UV Photosensitivity and Fluorescence during Fiber Grating Formation.
PB96-155445 *04,362* Not available NTIS

PB96-155452
Catalogue of Electromagnetic Environment Measurements, 30-300 Hz.
PB96-155452 *01,943* Not available NTIS

PB96-155460
Mapping Domains in Proteins: Dissection and Expression of 'Escherichia coli' Adenylyl Cyclase.
PB96-155460 *03,478* Not available NTIS

PB96-155478
Methodology for the Certification of Reference Specimens for Determination of Oxygen Concentration in Semiconductor Silicon by Infrared Spectrophotometry.
PB96-155478 *02,421* Not available NTIS

PB96-155486
Development of Gas Standards from Solid 1,4-dichlorobenzene.
PB96-155486 *02,496* Not available NTIS

PB96-155494
Measurement of Atmospheric Methyl Bromide Using Gravimetric Gas Standards.
PB96-155494 *02,497* Not available NTIS

PB96-155502
Simultaneous Laser-Diode Emission and Detection for Fiber-Optic Sensor Applications.
PB96-155502 *04,062* Not available NTIS

PB96-155510
Size Effects in Submicron NiFe/Ag GMR Devices.
PB96-155510 *02,237* Not available NTIS

PB96-155528
Investigation of S2F10 Production and Mitigation in Compressed SF6- Insulated Power Systems.
PB96-155528 *02,468* Not available NTIS

PB96-155536
Population Distributions and Intralaboratory Reproducibility for Fat-Soluble Vitamin-Related Compounds in Human Serum.
PB96-155536 *00,624* Not available NTIS

PB96-155544
Polymeric Calcium Phosphate Composites with Remineralization Potential.
PB96-155544 *03,575* Not available NTIS

PB96-155551
Metrology Approach to Unifying Rockwell C Hardness Scales.
PB96-155551 *02,957* Not available NTIS

PB96-155569
Stylus Technique for the Direct Verification of Rockwell Diamond Intenders.
PB96-155569 *02,958* Not available NTIS

PB96-155577
Effects of Nonmedel Errors on Model-Based Testing.
PB96-155577 *03,420* Not available NTIS

PB96-155585
Tunneling Spectroscopy of bcc(001) Surface States.
PB96-155585 *04,775* Not available NTIS

PB96-155593
Study of Ventilation Measurement in an Office Building.
PB96-155593 *00,274* Not available NTIS

PB96-155601
Development and Application of an Indoor Air Quality Commissioning Program in a New Office Building.
PB96-155601 *00,275* Not available NTIS

PB96-155759
Transitions to Chaos Induced by Additive and Multiplicative Noise.
PB96-155759 *03,750* Not available NTIS

PB96-155767
Spectrum of the Stochastically Forced Duffing-Holmes Oscillator.
PB96-155767 *00,216* Not available NTIS

PB96-155775
Necessary Condition for Homoclinic Chaos Induces by Additive Noise.
PB96-155775 *04,063* Not available NTIS

PB96-155783
Development of Computer-Based Models of Standards and Attendant Knowledge-Base and Procedural Systems.
PB96-155783 *00,464* Not available NTIS

PB96-155791
Findings and Recommendations from a Software Reengineering Case Study.
PB96-155791 *01,752* Not available NTIS

PB96-155809
Transition from Localized Ignition to Flame Spread Over a Thin Cellulosic Material in Microgravity.
PB96-155809 *04,835* Not available NTIS

PB96-156013
Improved Gas Flow Measurements for Next-Generation Processes.
PB96-156013 *04,216* Not available NTIS

PB96-156021
Executive Order 12941. Seismic Safety of Existing Federally Owned or Leased Buildings: It's History, Content and Objectives.
PB96-156021 *00,465* Not available NTIS

PB96-156039
Physicochemical Characterization of Natural and Bioprosthetic Heart Valve Calcific Deposits: Implications for Prevention.
PB96-156039 *00,187* Not available NTIS

PB96-156047
Model for Calculating Virial Coefficients of Natural Gas Hydrocarbons with Impurities.
PB96-156047 *04,064* Not available NTIS

PB96-156054
Virial Coefficients of Five Binary Mixtures of Fluorinated Methanes and Ethanes.
PB96-156054 *01,128* Not available NTIS

PB96-156062
NIST Metrology Program on Electromagnetic Characterization of Materials.
PB96-156062 *01,944* Not available NTIS

PB96-156070
Micromachined Display Output for a Cellular Neural Network.
PB96-156070 *02,422* Not available NTIS

PB96-156088
CMOS Circuit Design for Controlling Temperature in Micromachined Devices.
PB96-156088 *02,196* Not available NTIS

PB96-156104
Fast-Ion Conducting Y2(ZryTi1-y)2O7 Pyrochlores: Neutron Rietveld Analysis of Disorder Induced by Zr Substitution.
PB96-156104 *04,776* Not available NTIS

PB96-156112
Security Program Management.
PB96-156112 *01,610* Not available NTIS

PB96-156120
Noise-Induced Transitions to Chaos.
PB96-156120 *00,217* Not available NTIS

PB96-156138
Deterministic and Stochastic Chaos.
PB96-156138 *00,218* Not available NTIS

PB96-156146
Experimental and Numerical Chaos in Continuous Systems: Two Case Studies.
PB96-156146 *00,219* Not available NTIS

PB96-156153
Internationalization of Fire Safety Engineering Research and Strategy.
PB96-156153 *00,220* Not available NTIS

PB96-156161
Application of Digital-Image-Based Models to Microstructure, Transport Properties, and Degradation of Cement-Based Materials.
PB96-156161 *00,406* Not available NTIS

PB96-156179
Fire Protection Engineering Tools. Simple Tools: The Equations.
PB96-156179 *00,221* Not available NTIS

PB96-156187
Protecting Your Family from Fire.
PB96-156187 *00,307* Not available NTIS

PB96-156195
Review of Internatioanl Fire Risk Predictions Methods.
PB96-156195 *00,222* Not available NTIS

PB96-156203
Simple Variable Line Space Grating Monochromator for Synchrotron Light Source Beamlines.
PB96-156203 *04,065* Not available NTIS

PB96-157813
Modeling Detector Response for Neutron Depth Profiling.
PB96-157813 *04,066* Not available NTIS

PB96-157821
Optimizing Time-Domain Network Analysis.
PB96-157821 *02,085* Not available NTIS

PB96-157839
Al L2,3 Core Excitons in AlxGa1-x as Studied by Soft-X-ray Reflection and Emission.
PB96-157839 *04,067* Not available NTIS

PB96-157847
Laser-Synchrotron Hybrid Experiments: A Photon to Tickle, A Photon to Poke.
PB96-157847 *03,704* Not available NTIS

PB96-157854
Applicability of Effective Medium Theory to Ferroelectric/Ferrimagnetic Composites with Composition and Frequency-Dependent Complex Permittivities and Permeabilities.
PB96-157854 *01,945* Not available NTIS

PB96-157862
Influence of Films' Thickness and Air Gaps in Surface Impedance Measurements of High Temperature Superconductors Using the Dielectric Resonator Technique.
PB96-157862 *01,946* Not available NTIS

PB96-157870
Stochastic Modeling of a New Spectrometer.
PB96-157870 *04,068* Not available NTIS

PB96-157888
Two-Tier Multiline TRL for Calibration of Low-Cost Network Analyzers.
PB96-157888 *01,947* Not available NTIS

PB96-157896
Evolution of a United States Information System.
PB96-157896 *02,713* Not available NTIS

PB96-157904
Information Transfer in the 21st Century.
PB96-157904 *02,714* Not available NTIS

PB96-157912
Soft-X-ray-Emission Investigation of Cobalt Implanted Silicon Crystals.
PB96-157912 *04,069* Not available NTIS

PB96-157920
Soft-X-ray-Emission Spectra of Solid Kr and Xe.
PB96-157920 *04,070* Not available NTIS

PB96-157938
Soft-X-ray-Emission Studies of Bulk Fe3Si, FeSi, and FeSi2, and Implanted Iron Silicides.
PB96-157938 *04,071* Not available NTIS

PB96-157946
Influence of Coadsorbed Potassium on the Electron-Stimulated Desorption of F(+), F(-), and F(*) from PF3 on Ru(0001).
PB96-157946 *04,072* Not available NTIS

PB96-157953
RIS Measurement of AC Stark Shifts and Photoionization Cross Sections in Calcium.
PB96-157953 *04,073* Not available NTIS

PB96-157961
Characterization of LPE HgCdTe Film by Magnetoresistance.
PB96-157961 *02,197* Not available NTIS

PB96-157979
Comment On: Two-Photon Absorption Series of Calcium.
PB96-157979 *04,074* Not available NTIS

PB96-157987
Laser Modification of Ultracold Collisions: Experiment.
PB96-157987 *04,075* Not available NTIS

PB96-157995
Configuration-Dependent AC Stark Shifts in Calcium.
PB96-157995 *04,363* Not available NTIS

PB96-158001
Reinforcement of Cancellous Bone Screws with Calcium Phosphate Cement.
PB96-158001 *00,179* Not available NTIS

PB96-158019
Barium Contributions to the Valence Electronic Structure of YBa2Cu3O7-delta, PrBa2Cu3O7-delta, and Other Barium-Containing Compounds.
PB96-158019 *04,076* Not available NTIS

PB96-158027
Cooper M(sub II,III) X-ray-Emission Spectra of Copper Oxides and the Bismuth Cuprate Superconductor.
PB96-158027 *04,077* Not available NTIS

PB96-158035
RIS Measurements of the AC Stark Shift.
PB96-158035 *04,078* Not available NTIS

PB96-158043
Intermediate Coupling in L2-L3 Core Excitons of MgO, Al2O3, and SiO2.
PB96-158043 *04,079* Not available NTIS

PB96-158050
Strengthening Methodology for Lightly Reinforced Concrete Frames.
PB96-158050 *00,466* Not available NTIS

PB96-158068
Resonance Ionization Spectroscopy/Resonance Ionization Mass Spectrometry Data Service. V-Data Sheets for Ga, Mn, Sc, and Tl.
PB96-158068 *00,625* Not available NTIS

PB96-158076
International Institute of Welding: Report on 1995 Actions.
PB96-158076 *02,874* Not available NTIS

PB96-158084
What's Available in Welding Software.
PB96-158084 *02,875* Not available NTIS

PB96-158092
New NIST/ARPA National Soft X-ray Reflectometry Facility.
PB96-158092 *04,080* Not available NTIS

PB96-158654
Direct Comparison Transfer of Microwave Power Sensor Calibrations.
PB96-158654 *02,086* PC A03/MF A01

PB96-158662
ISO Environmental Management Standardization Efforts.
PB96-158662 *02,528* PC A03/MF A01

PB96-158670
Multiattribute Decision Analysis Method for Evaluating Buildings and Building Systems.
PB96-158670 *00,325* PC A06/MF A01

PB96-158688
Conference Proceedings: International Workshop on Instrumented Indentation. Held in San Diego, California on April 22-23, 1995.
PB96-158688 *01,948* PC A06/MF A01

PB96-158704
Liquid-Nitrogen-Cooled High Tc Electrical Substitution Radiometer as a Broadband IR Transfer Standard.
PB96-158704 *02,198* PC A03/MF A01

PB96-158712
Application Portability Profile (APP): The U.S. Government's Open System Environment Profile Version 3.0.
PB96-158712 *01,753* PC A07/MF A02

PB96-159215
Journal of Research of the National Institute of Standards and Technology, November/December 1995. Volume 100, Number 6.
PB96-159215 *01,949* PC A08/MF A02

PB96-159223
Calibration of Electret-Based Integral Radon Monitors Using NIST Polyethylene-Encapsulated (226)Ra/(222)Rn Emanation (PERE) Standards.
PB96-159223 *01,950*
(Order as PB96-159215, PC A07/MF A02)

PB96-159231
Microstructural Characterization of Cobalt-Tungsten Coated Graphite Fibers.
PB96-159231 *01,951*
(Order as PB96-159215, PC A07/MF A02)

PB96-159249
Using Collocation in Three Dimensions and Solving a Model Semiconductor Problem.
PB96-159249 *01,952*
(Order as PB96-159215, PC A07/MF A02)

PB96-159256
Precision Tests of a Quantum Hall Effect Device DC Equivalent Circuit Using Double-Series and Triple-Series Connections.
PB96-159256 *01,953*
(Order as PB96-159215, PC A07/MF A02)

PB96-159264
Analysis of the (5d(2)+5d6s)-5d6p Transition Arrays of Os VII and Ir VIII, and the 6s (2)S-6p (2)P Transitions of Ir IX.
PB96-159264 *01,954*
(Order as PB96-159215, PC A07/MF A02)

PB96-159611
Soft-X-ray Damage to p-terphenyl Coatings for Detectors.
PB96-159611 *04,364* Not available NTIS

PB96-159629
METRICATION: An Economic Wake-Up Call for Surveyors and Mappers.
PB96-159629 *03,680* Not available NTIS

PB96-159637
System for Intercomparing Standard Solutions of Beta-Particle Emitting Radionuclides.
PB96-159637 *03,707* Not available NTIS

PB96-159645
Comparison of Responses of a Select Number of Buildings to the 10/17/1989 Loma Prieta (California) Earthquake and Low-Level Amplitude Test Results.
PB96-159645 *00,467* Not available NTIS

PB96-159652
Fire Hazard Model Developments and Research Efforts at NIST.
PB96-159652 *00,407* Not available NTIS

PB96-159660
International Organization for Standardization: Current Activities in Fire Safety Engineering.
PB96-159660 *00,223* Not available NTIS

PB96-159678
Boron-Implanted 6H-SiC Diodes.
PB96-159678 *04,081* Not available NTIS

PB96-159686
Extreme Winds Estimation by 'Peaks Over Threshold' and Epochal Methods.
PB96-159686 *00,468* Not available NTIS

PB96-159694
Modeling of Extreme Loading by 'Peaks Over Threshold' Methods.
PB96-159694 *00,469* Not available NTIS

PB96-159702
Workgroup Summary Report: Plastic Hinge-Based Techniques for Advanced Analysis.
PB96-159702 *00,470* Not available NTIS

PB96-159710
Agent Screening for Halon 1301 Aviation Replacement.
PB96-159710 *03,282* Not available NTIS

PB96-159728
Validation of a Turbulent Spray Flame Facility for the Assessment of Halon Alternatives.
PB96-159728 *03,283* Not available NTIS

PB96-159736
Influence of Electrical Isolation on the Structure and Reflectivity of Multilayer Coatings Deposited on Dielectric Substrates.
PB96-159736 *04,365* Not available NTIS

PB96-159744
New Method for Achieving Accurate Thickness Control for Uniform and Graded Multilayer Coatings on Large Flat Substrates.
PB96-159744 *04,366* Not available NTIS

PB96-159751
International Radon-in-Air Measurement Intercomparison Using a New Transfer Standard.
PB96-159751 *03,708* Not available NTIS

PB96-159769
Montgomery Education Connection and Resource Education Awareness Partnership Making Connections between Local Schools and NIST Volunteers.
PB96-159769 *00,134* Not available NTIS

PB96-159777
Effects of Sample Mounting on Flammability Properties of Intumescent Polymers.
PB96-159777 *03,389* Not available NTIS

PB96-159785
Development of a Standard Reference Material for ISE Measurements of Sodium and Potassium.
PB96-159785 *03,507* Not available NTIS

PB96-159793
Faraday Constant.
PB96-159793 *01,955* Not available NTIS

PB96-159801
Dynamics of Hydrogen Interactions with Si(100) and Si(111) Surfaces.
PB96-159801 *04,082* Not available NTIS

PB96-160213
Effect of Intermediate Thermal Processing on Microstructural Changes of Oxygen Implanted Silicon-on-Insulator Material.
PB96-160213 *02,982* Not available NTIS

PB96-160221
Stacking Fault Pyramid Formation and Energetics in Silicon-on-Insulator Material Formed by Multiple Cycles of Oxygen Implantation and Annealing.
PB96-160221 *04,083* Not available NTIS

PB96-160239
U.S. Government Accreditation and Conformity Assessment System Evaluation.
PB96-160239 *02,678* Not available NTIS

PB96-160247
RII Spectroscopy of Trap Levels in Bulk and LPE Hg1-xCdxTe.
PB96-160247 *04,084* Not available NTIS

PB96-160254
External Gamma-ray Counting of Selected Tissues from a Thorotrast Patient.
PB96-160254 *03,637* Not available NTIS

PB96-160262
Interface Roughness, Composition, and Alloying of Low-Order AlAs/GaAs Superlattices Studies by X-ray Diffraction.
PB96-160262 *02,983* Not available NTIS

PB96-160270
Ignition and Subsequent Flame Spread Over a Thin Cellulosic Material.
PB96-160270 *04,836* Not available NTIS

PB96-160288
Ignition and Transition to Flame Spread Over a Thermally Thin Cellulosic Sheet in a Microgravity Environment.
PB96-160288 *04,837* Not available NTIS

PB96-160296
Phonon Relaxation in Soft-X-ray Emission of Insulators.
PB96-160296 *04,085* Not available NTIS

PB96-160304
Research on Methods for Determining Optical Disk Media Life Expectancy Estimates.
PB96-160304 *01,633* Not available NTIS

PB96-160312
Laser-Cooled Neutral Atom Frequency Standards.
PB96-160312 *04,086* Not available NTIS

PB96-160320
Electron and Hole Trapping in Irradiated SIMOX, ZMR and BESOI Buried Oxides.
PB96-160320 *01,956* Not available NTIS

PB96-160338
Improved Reflectometry Facility at the National Institute of Standards and Technology.
PB96-160338 *04,087* Not available NTIS

PB96-160346
New and Revised Half-Life Measurement Results.
PB96-160346 *00,695* Not available NTIS

PB96-160353
Effect of Single versus Multiple Implant Processing on Defect Types and Densities in SIMOX.
PB96-160353 *01,957* Not available NTIS

PB96-160361
International Challenges in Defining the Public and Private Interest in Standards.
PB96-160361 *00,498* Not available NTIS

PB96-160379
NIST Metrology for Soft X-ray Multilayer Optics.
PB96-160379 *04,088* Not available NTIS

PB96-160387
Upgraded Facility for Multilayer Mirror Characterization at NIST.
PB96-160387 *04,367* Not available NTIS

PB96-160395
Soft X-ray Reflectometry Program at the National Institute of Standards and Technology.
PB96-160395 *04,368* Not available NTIS

PB96-160411
Analysis of Small-Angle Scattering Data Dominated by Multiple Scattering for Systems Containing Eccentrically Shaped Particles or Pores.
PB96-160411 *03,075* Not available NTIS

PB96-160429
Instrumental Smearing Effects in Radially Symmetric Small-Angle Neutron Scattering by Numerical and Analytical Methods.
PB96-160429 *02,984* Not available NTIS

PB96-160437
Quality in Automated Manufacturing.
PB96-160437 *02,839* Not available NTIS

PB96-160445
Appearance Intensities for Multiply Charged Ions in a Strong Laser Field.
PB96-160445 *04,089* Not available NTIS

PB96-160452
Comparison of FDDI Asynchronous Mode and DQDB Queue Arbitrated Mode Data Transmission for Metropolitan Area Network Applications.
PB96-160452 *01,498* Not available NTIS

PB96-160460
Standardization for ATM and Related B-ISDN Technologies.
PB96-160460 *01,499* Not available NTIS

PB96-160478
Novel DNA N-Glycosylase Activity of E. coli T4 Endonuclease V That Excises 4,6-Diamino-5-Formamidopyrimidine from DNA, a UV-Radiation- and Hydroxyl Radical-Induced Product of Adenine.
PB96-160478 *03,549* Not available NTIS

PB96-160486
Development of a New Quality Control Strategy for Automated Manufacturing.
PB96-160486 *02,840* Not available NTIS

PB96-160494
Evaluation of a Tapered Roller Bearing Spindle for High-Precision Hard Turning Applications.
PB96-160494 *02,700* Not available NTIS

PB96-160510
Tetrahedral-Framework Lithium Zinc Phosphate Phases: Location of Light-Atom Positions in LiZnPO4 H2O by Powder Neutron Diffraction and Structure Determination of LiZnPO4 by ab Initio Methods.
PB96-160510 *01,129* Not available NTIS

PB96-160528
Characterization of the Structure of TbD2.25 at 70 K by Neutron Powder Diffraction.
PB96-160528 *01,130* Not available NTIS

PB96-160536
Copyright and Information Services in the Context of the National Research and Education Network.
PB96-160536 *02,736* Not available NTIS

PB96-160544
Prototyping a Graphical User Interface for DHCP.
PB96-160544 *02,599* Not available NTIS

PB96-160551
Hardware Measurement Techniques for High-Speed Networks.
PB96-160551 *01,500* Not available NTIS

PB96-160569
Integrated Inspection System for Improved Machine Performance.
PB96-160569 *02,959* Not available NTIS

PB96-160577
Addressing U.S. Government Security Requirements for OSI.
PB96-160577 *01,611* Not available NTIS

PB96-160585
Fabrication Issues for the Prototype National Institute of Standards and Technology SRM 2090A Scanning Electron Microscope Magnification Calibration Standard.
PB96-160585 *01,131* Not available NTIS

PB96-160593
New Generation of Fire Resistant Polymers. Part 1. Computer-Aided Molecular Design.
PB96-160593 *01,419* Not available NTIS

PB96-160601
Computer-Aided Molecular Design of Fire Resistant Aircraft Materials.
PB96-160601 *00,025* Not available NTIS

PB96-160619
Status of Emerging Standards for Removable Computer Storage Media and Related Contributions of NIST.
PB96-160619 *01,634* Not available NTIS

PB96-160627
NIST Program for Investigating Error Reporting Capabilities of Optical Disk Drives.
PB96-160627 *01,635* Not available NTIS

PB96-160635
Provision of Isochronous Service on IEEE 802.6.
PB96-160635 *01,501* Not available NTIS

PB96-160643
Q Branch Lineshape Functions for CARS Thermometry.
PB96-160643 *01,132* Not available NTIS

PB96-160650
Exits in Multistable Systems Excited by Coin-Toss Square-Wave Dichotomous Noise: A Chaotic Dynamics Approach.
PB96-160650 *04,824* Not available NTIS

PB96-160668
Interfaces in Mo/Si Multilayers.
PB96-160668 *02,423* Not available NTIS

PB96-160676
Implementation of the Fastener Quality Act.
PB96-160676 *02,876* Not available NTIS

PB96-160684
New Concepts of Precision Dimensional Measurement for Modern Manufacturing.
PB96-160684 *02,924* Not available NTIS

PB96-160692
Certification of Phencyclidine in Lyophilized Human Urine Reference Materials.
PB96-160692 *03,508* Not available NTIS

PB96-160700
Generating and Measuring Displacements Up to 0.1 m to an Accuracy of 0.1 nm: Is It Possible.
PB96-160700 *04,090* Not available NTIS

PB96-160718
Metrology Standards for Advanced Semiconductor Lithography Referenced to Atomic Spacings and Geometry.
PB96-160718 *02,424* Not available NTIS

PB96-160726
Nanometrology.
PB96-160726 *02,425* Not available NTIS

PB96-160734
Low-Energy Vibrations and Octahedral Site Occupation in Nb95V5H(D)y.
PB96-160734 *01,133* Not available NTIS

PB96-160742
Neutron Spectroscopic Comparison of beta-Phase Rare Earth Hydrides.
PB96-160742 *01,134* Not available NTIS

PB96-160759
Metrology.
PB96-160759 *02,925* Not available NTIS

PB96-160767
ISDN in North America.
PB96-160767 *01,502* Not available NTIS

PB96-160775
North American Agreements on ISDN.
PB96-160775 *01,503* Not available NTIS

PB96-160783
Scanned Probe Microscopies: Opportunities and Issues in Metrology.
PB96-160783 *02,426* Not available NTIS

PB96-160791
SQA and TQM in Software Quality Improvement.
PB96-160791 *01,754* Not available NTIS

PB96-160817
Point Probe Decision Trees for Geometric Concept Classes.
PB96-160817 *01,612* Not available NTIS

PB96-160825
Precise Identification of Computer Viruses.
PB96-160825 *01,613* Not available NTIS

PB96-160833
Development of the NIST Transient Pressure and Temperature Calibration Facility.
PB96-160833 *00,626* Not available NTIS

PB96-160841
Executive Summary: Proceedings of the Workshop on the Measurement of Transient Pressure and Temperature.
PB96-160841 *02,679* Not available NTIS

PB96-160858
Slicing in the Presence of Parameter Aliasing.
PB96-160858 *01,755* Not available NTIS

PB96-160866
Information Technology Standards in a Changing World: The Rose of the Users.
PB96-160866 *02,737* Not available NTIS

PB96-160874
Using a Multi-Layered Approach to Representing Tort Law Cases for Case-Based Reasoning.
PB96-160874 *00,135* Not available NTIS

PB96-160882
Concept Paper: An Overview of the Proposed Trust Technology Assessment Program.
PB96-160882 *01,614* Not available NTIS

PB96-160890
Assessing Functional Diversity by Program Slicing.
PB96-160890 *03,734* Not available NTIS

PB96-160908
Impact of Computer-Aided Acquisition and Logistic Support (CALS) in the Application of Standards.
PB96-160908 *01,756* Not available NTIS

PB96-160916
ITS-90 Calibration Facility.
PB96-160916 *00,627* Not available NTIS

PB96-160924
IEEE's POSIX: Making Progress.
PB96-160924 *01,757* Not available NTIS

PB96-160932
Open Systems Software Standards in Concurrent Engineering.
PB96-160932 *01,758* Not available NTIS

PB96-160940
Predicate Differences and the Analysis of Dependencies in Formal Specifications.
PB96-160940 *01,759* Not available NTIS

PB96-160957
Technique for Analyzing the Effects of Changes in Formal Specifications.
PB96-160957 *01,760* Not available NTIS

PB96-160965
Template-Driven Systems Development with IDEF: Enterprise Standards for Reuse.
PB96-160965 *02,788* Not available NTIS

PB96-160973
NIST POSIX Testing Program.
PB96-160973 *01,821* Not available NTIS

PB96-160981
Program Slicing.
PB96-160981 *01,761* Not available NTIS

PB96-160999
Effects of Pipe Elbows and Tube Bundles on Selected Types of Flowmeters.
PB96-160999 *01,135* Not available NTIS

PB96-161005
Pressure Measurements with the Mercury Melting Line Referred to ITS-90.
PB96-161005 *01,136* Not available NTIS

PB96-161211
Conference Report: International Conference on the Application of Standards for Open Systems (6th).
PB96-161211 *01,762* Not available NTIS

PB96-161229
GOSIP Testing Program.
PB96-161229 *01,504* Not available NTIS

PB96-161237
Guidance of the Legality of Keystroke Monitoring.
PB96-161237 *00,005* Not available NTIS

PB96-161245
Industry/Government Open Systems Specification: The Development of GOSIP Version 3.
PB96-161245 *01,505* Not available NTIS

PB96-161252
Information Technology Standards in Federal Acquisitions.
PB96-161252 *01,636* Not available NTIS

PB96-161260
Using Information Technology Standards in Federal Acquisitions.
PB96-161260 *01,637* Not available NTIS

PB96-161278
Powder X-ray Diffraction Data for Ca2Bi2O5 and C4Bi6O13.
PB96-161278 *04,777* Not available NTIS

PB96-161286
Direct Comparison of Three PTB Silver Fixed-Point Cells with the NIST Silver Fixed-Point Cell.
PB96-161286 *00,628* Not available NTIS

PB96-161294
Investigation of High-Temperature Platinum Resistance Thermometers at Temperatures Up to 962C, and, in Some Cases, 1064C.
PB96-161294 *00,629* Not available NTIS

PB96-161302
Investigation of the ITS-90 Subrange Inconsistencies for 25.5 Omega SPRTs.
PB96-161302 *00,630* Not available NTIS

PB96-161310
NIST Assessment of ITS-90 Non-Uniqueness for 25.5 Ohm SPRTs at Gallium, Indium and Cadmium Fixed Points.
PB96-161310 *00,631* Not available NTIS

PB96-161328
NIST Implementation and Realization of the ITS-90 Over the Range 83 K to 1235 K: Reproducibility, Stability, and Uncertainties.
PB96-161328 *00,632* Not available NTIS

PB96-161336
NIST Measurement Assurance of SPRT Calibrations on the ITS-90: A Quantitative Approach.
PB96-161336 *00,633* Not available NTIS

PB96-161344
Preliminary Results of a Comparison of Water Triple-Point Cells Prepared by Different Methods.
PB96-161344 *00,634* Not available NTIS

PB96-161351
Analysis of Standards for the Assurance of High Integrity Software.
PB96-161351 *03,735* Not available NTIS

PB96-161369
Control and Instrumentation: Standards for High-Integrity Software.
PB96-161369 *03,736* Not available NTIS

PB96-161377
Report of a Workshop on the Assurance of High Integrity Software.
PB96-161377 *01,763* Not available NTIS

PB96-161385
Standards for High Integrity Software.
PB96-161385 *01,764* Not available NTIS

PB96-161393
Verification and Validation.
PB96-161393 *01,765* Not available NTIS

PB96-161401
Verification and Validation of Reengineered Software.
PB96-161401 *01,766* Not available NTIS

PB96-161617
Residual Error Compensation of a Vision-Based Coordinate Measuring Machine.
PB96-161617 *04,091* Not available NTIS

PB96-161625
Imposed Oscillations of Kinetic Barriers Can Cause an Enzyme to Drive a Chemical Reaction Away from Equilibrium.
PB96-161625 *01,137* Not available NTIS

PB96-161633
Quadratic Response of a Chemical Reaction to External Oscillations.
PB96-161633 *01,138* Not available NTIS

PB96-161641
Genetically Engineered Pores for New Materials.
PB96-161641 *03,550* Not available NTIS

PB96-161658
Genetically Engineered Pore as a Metal Ion Biosensor.
PB96-161658 *03,551* Not available NTIS

PB96-161666
Verification of Revised Water Vapour Correction to the Index of Refraction of Air.
PB96-161666 *02,680* Not available NTIS

PB96-161674
Current Noise Reveals Protonation Kinetics and Number of Ionizable Sites in an Open Protein Ion Channel.
PB96-161674 *04,092* Not available NTIS

PB96-161682
Noise Analysis of Ionization Kinetics in a Protein Ion Channel.
PB96-161682 *04,093* Not available NTIS

PB96-161690
Inter-Laboratory Trials of the EPR Method for the Detection of Irradiated Meats Containing Bone.
PB96-161690 *00,042* Not available NTIS

PB96-161708
Measurement of the Neutron Lifetime.
PB96-161708 *04,094* Not available NTIS

PB96-161716
SPC Artifact for Automated Solder Joint Inspection.
PB96-161716 *04,095* Not available NTIS

PB96-161724
Length Metrology of Complimentary Small Plastic Rulers.
PB96-161724 *04,096* Not available NTIS

PB96-161732
Current Fluctuations Reveal Protonation Dynamics and Number of Ionizable Residues in the alpha-Toxin Channel.
PB96-161732 *03,588* Not available NTIS

PB96-161740
Protonation Dynamics of the alpha-Toxin Ion Channel from Spectral Analysis of pH-Dependent Current Fluctuations.
PB96-161740 *03,652* Not available NTIS

PB96-161757
Protonation Dynamics in an Ion Channel Pore.
PB96-161757 *03,589* Not available NTIS

PB96-161765
Friction Processes in Brittle Fracture.
PB96-161765 *03,076* Not available NTIS

PB96-161773
Conformational Alterations of Bovine Insulin Adsorbed on a Silver Electrode.
PB96-161773 *00,510* Not available NTIS

PB96-161781
Nonequilibrium Statistical Mechanics.
PB96-161781 *04,097* Not available NTIS

PB96-161799
Measurement of the (10)B(n, alpha1gamma)(7)Li Cross Section in the 0.3 to 4 MeV Neutron Energy Interval.
PB96-161799 *04,098* Not available NTIS

PB96-161807
Nonlocal Effects of Existing Dislocations on Crack-Tip Emission and Cleavage.
PB96-161807 *03,367* Not available NTIS

PB96-161815
Response to Comments on the NIST Proposed Digital Signature Standard.
PB96-161815 *01,615* Not available NTIS

PB96-161823
Lattice Statics of Interfaces and Interfacial Cracks in Bimaterial Solids.
PB96-161823 *02,985* Not available NTIS

PB96-161831
Effect of CF3H and CF3Br on Laminar Diffusion Flames in Normal and Microgravity.
PB96-161831 *01,420* Not available NTIS

PB96-161849
Effect of CF3H and CF3Br on Laminar Diffusion Flames in Normal and Microgravity.
PB96-161849 *01,421* Not available NTIS

PB96-161856
Vapor-Liquid Equilibria of Temary Mixtures in the Critical Region on Paths of Constant Temperature and Overall Composition.
PB96-161856 *01,139* Not available NTIS

PB96-161864
Gas Absorption during Ion-Irradiation of a Polymer Target.
PB96-161864 *04,099* Not available NTIS

PB96-161872
Upgrade and Modernization Projects at the NBSR.
PB96-161872 *03,737* Not available NTIS

PB96-161880
Electric Field Effects on a Near-Critical Fluid in Microgravity.
PB96-161880 *04,217* Not available NTIS

PB96-161898
Density Dependence of Fluid Properties and Non-Newtonian Flows: The Weisenberg Effect.
PB96-161898 *01,140* Not available NTIS

PB96-161906
Nonlinear Correlation of High-Pressure Vapor-Liquid Equilibrium Data for Ethylene + n-Butane Showing Inconsistencies in Experimental Compositions.
PB96-161906 *01,141* Not available NTIS

PB96-161914
Quantum Collisional Transfer Contributions to the Density Dependence of Gaseous Viscosity.
PB96-161914 *01,142* Not available NTIS

PB96-161922
Correlations between Flaw Tolerance and Reliability in Zirconia.
PB96-161922 *02,986* Not available NTIS

PB96-161930
Cryogenic Flow Calibration in NIST.
PB96-161930 *01,143* Not available NTIS

PB96-161948
Business and Manufacturing Motivations for the Developing of Analytical Technology and Metrology for Semiconductors.
PB96-161948 *04,778* Not available NTIS

PB96-161955
SSME LOX Duct Flowmeter Design and Test Results.
PB96-161955 *04,826* Not available NTIS

PB96-161963
Electrical Measurements for Monitoring and Control of rf Plasma Processing.
PB96-161963 *04,369* Not available NTIS

PB96-161971
Fundamentals of Fracture: A 1993 Prologue, and Other Comments.
PB96-161971 *03,218* Not available NTIS

PB96-161989
Interfacial Crack in a Two-Dimensional Hexagonal Lattice.
PB96-161989 *04,100* Not available NTIS

PB96-161997
Whither Computational Materials Science. Some Thoughts from the Mechanical Properties Front.
PB96-161997 *02,987* Not available NTIS

PB96-162003
Dislocation Core-Core Interaction and Peierls Stress in a Model Hexagonal Lattice.
PB96-162003 *04,101* Not available NTIS

PB96-162441
Energy Price Indices and Discount Factors for Life-Cycle Cost Analysis 1996. Annual Supplement to NIST Handbook 135 and NBS Special Publication 709. (Revised).
PB96-162441 *02,510* PC A05/MF A01

PB96-162540
Estimates of Hurricane Wind Speeds by the 'Peaks Over Threshold' Method.
PB96-162540 *00,471* PC A04/MF A01

PB96-162649
Radiated Emissions and Immunity of Microstrip Transmission Lines: Theory and Measurements.
PB96-162649 *02,238* PC A04/MF A01

PB96-162714
National Voluntary Laboratory Accreditation Program 1996 Directory.
PB96-162714 *00,485* PC A10/MF A03

PB96-162722
Calibration Service for Coaxial Reference Standards for Microwave Power.
PB96-162722 *01,958* PC A07/MF A02

PB96-163613
Fracture in Multilayers.
PB96-163613 *02,988* Not available NTIS

PB96-163621
Gage Block Standards, Measurement Capabilities and Laboratory Accreditation.
PB96-163621 *02,757* Not available NTIS

PB96-163639
Autofluorescence Detection of 'Escherichia coli' on Silver Membrane Filters.
PB96-163639 *03,590* Not available NTIS

PB96-163647
Bacterial Enumeration in Storage Water.
PB96-163647 *03,591* Not available NTIS

PB96-163654
Feasibility of Fluorescence Detection of Tetracycline in Media Mixtures Employing a Fiber Optic Probe.
PB96-163654 *00,511* Not available NTIS

PB96-163662
Novel Amperometric Immunosensor for Procainamide Employing Light Activated Labels.
PB96-163662 *00,512* Not available NTIS

PB96-163670
Effect of Finite Beam Width on Elastic Light Scattering from Droplets.
PB96-163670 *01,144* Not available NTIS

PB96-163688
Elastic Scattering from Spheres under Non Plane-Wave Illumination.
PB96-163688 *04,370* Not available NTIS

PB96-163696
Cracks and Dislocations in Face-Centered Cubic Metallic Multilayers.
PB96-163696 *02,989* Not available NTIS

PB96-163704
Model for Microcrack Initiation and Propagation beneath Hertzian Contacts in Polycrystalline Ceramics.
PB96-163704 *03,077* Not available NTIS

PB96-163712
Inhibition of Premixed Methane-Air Flames by Iron Pentacarbonyl.
PB96-163712 *00,513* Not available NTIS

PB96-163720
Parametric Study of Hydrogen Fluoride Formation in Suppressed Fires.
PB96-163720 *00,514* Not available NTIS

PB96-163738
Molar Heat Capacity at Constant Volume for Air from 67 to 300 K at Pressures to 35 MPa.
PB96-163738 *00,515* Not available NTIS

PB96-163746
Charge-Transfer-Induced Multiplet Structure in the N4,5O2,3 Soft-X-ray Emission Spectrum of Lanthanum.
PB96-163746 *04,102* Not available NTIS

PB96-163753
Influence of Shear on the Ordering Temperature of a Triblock Copolymer Melt.
PB96-163753 *01,288* Not available NTIS

PB96-163761
Non-Newtonian Flow between Concentric Cylinders Calculated from Thermophysical Properties Obtained from Simulations.
PB96-163761 *04,103* Not available NTIS

PB96-163779
2D-Scanning Capacitance Microscopy Measurements of Cross-Sectioned VLSI Teststructures.
PB96-163779 *04,104* Not available NTIS

PB96-163787
High-Accuracy Principal-Angle Scanning Spectroscopic Ellipsometry of Semiconductor Interfaces.
PB96-163787 *02,427* Not available NTIS

PB96-163795
Model for Toughness Curves in Two-Phase Ceramics. 2. Microstructural Variables.
PB96-163795 *03,078* Not available NTIS

PB96-163803
CO2/CH4 Transport in Polyperfluorosulfonate Ionomers: Effects of Polar Solvents on Permeation and Solubility.
PB96-163803 *01,145* Not available NTIS

PB96-164017
Natural Convection from an Array of Electronic Packages Mounted on a Horizontal Board in a Narrow Aspect Ratio Enclosure.
PB96-164017 *02,087* Not available NTIS

PB96-164025
Enhanced Voltage-Dividing Potentiometer for High-Precision Feature Placement Metrology.
PB96-164025 *02,428* Not available NTIS

PB96-164033
Retention of Halocarbons on a Hexafluoropropylene Epoxide-Modified Graphitized Carbon Black. 4. Propane-Based Compounds.
PB96-164033 *03,284* Not available NTIS

PB96-164041
Simple and Efficient Methane-Marker Devices for Chromatographic Samples.
PB96-164041 *00,635* Not available NTIS

PB96-164058
Use of Pressure for Quantum-Well Band-Structure Characterization.
PB96-164058 *04,779* Not available NTIS

PB96-164066
Heat Transfer in an Intumescent Material Using a Three-Dimensional Lagrangian Model.
PB96-164066 *00,408* Not available NTIS

PB96-164074
SEMPA Studies of Exchange Coupling in Magnetic Multilayers.
PB96-164074 *04,780* Not available NTIS

PB96-164082
Publication and Presentation Abstracts, 1995.
PB96-164082 *03,576* Not available NTIS

PB96-164090
President's Column 'Editorial'.
PB96-164090 *02,239* Not available NTIS

PB96-164108
Calculating Combined Buoyancy- and Pressure-Driven Flow Through a Shallow, Horizontal, Circular Vent; Application to Problem of Steady Burning in a Ceiling-Vented Enclosure.
PB96-164108 *00,409* Not available NTIS

PB96-164116
Combined Buoyancy and Pressure-Driven Flow Through a Shallow, Horizontal, Circular Vent.
PB96-164116 *00,410* Not available NTIS

PB96-164124
Commentary on 'Optimization of Experimental Parameters for the EPR Detection of the Cellulosic Radical in Irradiated Foodstuffs'.
PB96-164124 *00,043* Not available NTIS

PB96-164132
Novel Activities of Human Uracil DNA N-glycosylase for Cytosine-Derived Products of Oxidative DNA Damage.
PB96-164132 *03,479* Not available NTIS

PB96-164140
Population Trapping in Short-Pulse Multiphoton Ionization.
PB96-164140 *04,371* Not available NTIS

PB96-164157
Isotopic and Nuclear Analytical Techniques in Biological Systems: A Critical Study. 10. Elemental Isotopic Dilution Analysis with Radioactive and Stable Isotopes (Technical Report).
PB96-164157 *00,696* Not available NTIS

PB96-164165
In Search of Alternative Fire Suppressants.
PB96-164165 *03,285* Not available NTIS

PB96-164173
Modeling Buffer Layer IGBT's for Circuit Simulation.
PB96-164173 *02,429* Not available NTIS

PB96-164181
Distributed Architecture for Standards Processing.
PB96-164181 *00,276* Not available NTIS

PB96-164199
Electrical Characterization of Narrow Gap n-Type Bulk HgCdTe Single Crystals by Variable-Magnetic-Field Hall Measurements and Reduced-Conductivity-Tensor Analyses.
PB96-164199 *01,146* Not available NTIS

PB96-164207
Scanning Capacitance Microscopy Measurements and Modeling for Dopant Profiling of Silicon.
PB96-164207 *04,781* Not available NTIS

PB96-164215
Solubilities of Copper(II) and Chromium(III) beta-Diketonates in Supercritical Carbon Dioxide.
PB96-164215 *01,147* Not available NTIS

PB96-164223
Compressibility of Polycrystal and Monocrystal Copper: Acoustic-Resonance Spectroscopy.
PB96-164223 *02,990* Not available NTIS

PB96-164231
Rechargeable Batteries for Personal/Portable.
PB96-164231 *02,459* Not available NTIS

PB96-164249
Microelectronic Test Structures for Overlay Metrology.
PB96-164249 *02,430* Not available NTIS

PB96-164256
Asymptotic and Numerical Analysis of a Premixed Laminar Nitrogen Dioxide-Hydrogen Flame.
PB96-164256 *01,422* Not available NTIS

PB96-164264
Polymeric Calcium Phosphate Cements Derived from Poly(methyl vinyl ether-maleic acid).
PB96-164264 *00,180* Not available NTIS

PB96-164272
Certifying the Chemical Composition of a Biological Material: A Case Study.
PB96-164272 *00,636* Not available NTIS

PB96-164520
Electronics and Electrical Engineering Laboratory 1995 Technical Accomplishments: Advancing Metrology for Electrotechnology to Support the U.S. Economy.
PB96-164520 *01,959* PC A05/MF A01

PB96-165378
Optical Detector Nonlinearity: Simulation.
PB96-165378 *02,199* PC A04/MF A01

PB96-165394
Guide to a Format for Data on Chemical Admixtures in a Materials Property Database.
PB96-165394 *01,327* PC A04/MF A01

PB96-165402
Group 1 for the Plant Spatial Configuration STEP Application Protocol.
PB96-165402 *02,789* PC A11/MF A03

PB96-165410
Band-Limited, White Gaussian Noise Excitation for Reverberation Chambers and Applications to Radiated Susceptibility Testing.
PB96-165410 *01,960* PC A07/MF A02

PB96-165428
Machining Process Planning Activity Model for Systems Integration.
PB96-165428 *02,841* PC A03/MF A01

PB96-165782
Multizone Modeling of Three Residential Indoor Air Quality Control Options.
PB96-165782 *02,567* PC A08/MF A02

PB96-165840
Report of the National Conference on Weights and Measures (80th) as Adopted by the 80th National Conference on Weights and Measures, 1995. Held in Portland, Maine on July 16-20, 1995.
PB96-165840 *02,681* PC A15/MF A03

PB96-165915
Manager's Guide for Monitoring Data Integrity in Financial Systems.
PB96-165915 *00,003* PC A05/MF A01

PB96-165931
Basic Linear Algebra Operations in SLI Arithmetic.
PB96-165931 *03,421* PC A03/MF A01

PB96-165949
Modified Optimal Algorithm for Active Structural Control.
PB96-165949 *00,472* PC A04/MF A01

PB96-165956
Enhancement of R123 Pool Boiling by the Addition of N-Hexane.
PB96-165956 *02,605* PC A04/MF A01

PB96-165964
Using S-Check, Alpha Release 1.0.
PB96-165964 *01,767* PC A05/MF A01

PB96-165972
Preliminary Processing of the Lotung LSST Data.
PB96-165972 *03,690* PC A05/MF A01

PB96-165980
PIECS: A Software Program for Machine Tool Process-Intermittent Error Compensation.
PB96-165980 *02,842* PC A08/MF A02

PB96-165998
Beyond the Technology Roadmaps: An Assessment of Electronic Materials Research and Development.
PB96-165998 *01,961* PC A05/MF A01

PB96-166004
Public Key Infrastructure Invitational Workshop. Held in McLean, Virginia on September 28, 1995.
PB96-166004 *01,616* PC A08/MF A02

PB96-166616
NIST Handbook 44, 1996: Specifications, Tolerances, and Other Technical Requirements for Weighing and Measuring Devices as Adopted by the 80th National Conference on Weights and Measures, 1995.
PB96-166616 *02,926* PC A13/MF A03

PB96-167093
Determination of Total Protein Adsorbed on Solid (Membrane) Surface by a Hydrolysis Technique: Single Protein Adsorption.
PB96-167093 *03,552* Not available NTIS

PB96-167101
Dead Time, Pileup, and Accurate Gamma-Ray Spectrometry.
PB96-167101 *00,697* Not available NTIS

PB96-167119
Loss-Free Counting at IRI and NIST.
PB96-167119 *04,105* Not available NTIS

PB96-167127
Trace Element Concentrations in Cetacean Liver Tissues Archived in the National Marine Mammal Tissue Bank.
PB96-167127 *02,595* Not available NTIS

PB96-167135
Molar Heat Capacity at Constant Volume for (xCO2 + (1-x)C2H6) from 220 to 340 K at Pressures to 35 MPa.
PB96-167135 *01,148* Not available NTIS

PB96-167143
Accurate Electrical Characterization of High-Speed Interconnections.
PB96-167143 *02,240* Not available NTIS

PB96-167150
REFPROP Refrigerant Properties Database: Capabilities, Limitations, and Future Directions.
PB96-167150 *01,149* Not available NTIS

PB96-167168
Supercritical Fluid Extraction-Immunoassay for the Rapid Screening of Cocaine in Hair.
PB96-167168 *00,637* Not available NTIS

PB96-167176
Simulation and SANS Studies of Gelation Under Shear.
PB96-167176 *01,150* Not available NTIS

PB96-167184
Small-Angle Neutron-Scattering Study of Dense Sheared Silica Gels.
PB96-167184 *01,151* Not available NTIS

PB96-167192
Optical Characterization of Materials and Devices for the Semiconductor Industry: Trends and Needs.
PB96-167192 *02,431* Not available NTIS

PB96-167200
Analysis of Transverse Flow in Aligned Fibrous Porous Media.
PB96-167200 *03,177* Not available NTIS

PB96-167218
Status of the Round Robin on the Transport Properties of R134a.
PB96-167218 *01,152* Not available NTIS

PB96-167226
Structural Analysis of Heparin by Raman Spectroscopy.
PB96-167226 *03,480* Not available NTIS

PB96-167234
Viscosity of Defined and Undefined Hydrocarbon Liquids Calculated Using an Extended Corresponding-States Model.
PB96-167234 *02,498* Not available NTIS

PB96-167242
Determination of 21 Elements by INAA for Certification of SRM 1570a, Spinach.
PB96-167242 *00,698* Not available NTIS

PB96-167259
New NIST Rapid Pneumatic Tube System.
PB96-167259 *03,738* Not available NTIS

PB96-167267
Recent Developments in NIST Botanical SRMs.
PB96-167267 *03,489* Not available NTIS

PB96-167275
Relationship of Silver with Selenium and Mercury in the Liver of Two Species of Toothed Whales (Odontocetes).
PB96-167275 *02,596* Not available NTIS

PB96-167283
Resolution of Discrepant Analytical Data in the Certification of Platinum in Two Automobile Catalyst SRMs.
PB96-167283 *00,638* Not available NTIS

PB96-167291
Permeation Tube Approach to Long-Term Use of Automatic Sampler Retention Index Standards.
PB96-167291 *00,639* Not available NTIS

PB96-167309
Retention of Halocarbons on a Hexafluoropropylene Epoxide-Modified Graphitized Carbon Black. 3. Ethene-Based Compounds.
PB96-167309 *03,286* Not available NTIS

PB96-167317
Dynamic Scaling in an Aggregating 2D Lennard-Jones System.
PB96-167317 *04,106* Not available NTIS

PB96-167325
Double-Modulation and Selective Excitation Photoreflectance for Wafer-Level Characterization of Quantum-Well Laser Structures.
PB96-167325 *04,372* Not available NTIS

PB96-167333
Structure and Rheology of Hard-Sphere Systems.
PB96-167333 *00,662* Not available NTIS

PB96-167341
Preparation and Crystal Structure of Sr5TiNb4O17.
PB96-167341 *04,107* Not available NTIS

PB96-167358
Thermophysical Property Standard Reference Data from NIST.
PB96-167358 *01,153* Not available NTIS

PB96-167366
Planar Near-Field Measurements and Microwave Holography for Measuring Aperture Distribution on a 60 GHz Active Array Antenna.
PB96-167366 *03,762* Not available NTIS

PB96-167374
Small Angle Neutron Scattering Study of a Clay Suspension Under Shear.
PB96-167374 *00,663* Not available NTIS

PB96-167382
New Method for the Detection and Measurement of Polyaromatic Carcinogens and Related Compounds by DNA Intercalation.
PB96-167382 *03,481* Not available NTIS

PB96-167390
Isochoric (p-p-T) Measurements on Liquid and Gaseous Air from 67 to 400 K at Pressures to 35 MPa.
PB96-167390 *01,154* Not available NTIS

PB96-167408
Genetically Engineered Pores as Metal Ion Biosensors.
PB96-167408 *03,553* Not available NTIS

PB96-167812
Study to Determine the Existence of an Azeotropic R-22 'Drop-In' Substitute.
PB96-167812 *02,568* PC A04/MF A01

PB96-167820
Method of Estimating the Parameters of Tuned Mass Dampers for Seismic Applications.
PB96-167820 *00,473* PC A04/MF A01

PB96-167838
Application of the Pointer State Subgraph to Static Program Slicing.
PB96-167838 *01,768* PC A03/MF A01

PB96-167846
Data Communications Strategy.
PB96-167846 *02,738* PC A05/MF A01

PB96-167978
Application of Electromagnetic-Acoustic Transducers for Nondestructive Evaluation of Stresses in Steel Bridge Structures.
PB96-167978 *01,301* PC A04/MF A01

PB96-168984
Federal Implementation Guideline for Electronic Data Interchange. ASC X12 003050 Transaction Set 843 Response to Request for Quotation. Implementation Convention.
PB96-168984 *01,822* PC A09/MF A02

PB96-169057
Journal of Research of the National Institute of Standards and Technology, September/October 1993. Volume 98, Number 5.
PB96-169057 *03,368* PC A06/MF A01

PB96-169065
Transformation of BCC and B2 High Temperature Phases to HCP and Orthorhombic Structures in the Ti-Al-Nb System. Part 1. Microstructural Predictions Based on a Subgroup Relation between Phases.
PB96-169065 *03,370*
(Order as PB96-169057, PC A05/MF A01)

PB96-169073
Transformation of BCC and B2 High Temperature Phases to HCP and Orthorhombic Structures in the Ti-Al-Nb System. Part 2. Experimental TEM Study of Microstructures.
PB96-169073 *03,371*
(Order as PB96-169057, PC A05/MF A01)

PB96-169081
Corrosion Characteristics of Silicon Carbide and Silicon Nitride.
PB96-169081 *03,372*
(Order as PB96-169057, PC A05/MF A01)

PB96-169099
X Window System, Version 11, Release 5.
PB96-169099 *01,769* PC E99

PB96-172309
Uniform Laws and Regulations in the Areas of Legal Metrology and Motor Fuel Quality as Adopted by the 80th National Conference on Weights and Measures 1995. 1996 Edition.
PB96-172309 *02,927* PC A12/MF A03

PB96-172317
Life-Cycle Costing Manual for the Federal Energy Management Program. 1995 Edition.
PB96-172317 *02,511* PC A10/MF A02

PB96-172325
Guidelines for the Evaluation of Electronic Data Interchange Products.
PB96-172325 *01,506* PC A05/MF A01

PB96-172333
NIST Measurement Assurance Program for Capacitance Standards at 1 kHz.
PB96-172333 *02,276* PC A03/MF A01

PB96-172358
Trapped Ions and Laser Cooling 4: Selected Publications of the Ion Storage Group of the Time and Frequency Division, NIST, Boulder, Colorado.
PB96-172358 *04,108* PC A11/MF A03

PB96-172374
Federal Implementation Guideline for Electronic Data Interchange. ASC X12 003050 Transaction Set 855 Purchase Order Acknowledgment: Implementation Convention.
PB96-172374 *01,823* PC A04/MF A01

PB96-172523
NIST Serial Holdings, 1996.
PB96-172523 *02,748* PC A13/MF A03

PB96-172531
Federal Implementation Guideline for Electronic Data Interchange. ASC X12 003050 Transaction Set 840 Request for Quotation. Implementation Convention.
PB96-172531 *01,824* PC A10/MF A03

PB96-172549
Federal Implementaion Guideline for Eletronic Data Interchange. ASC X12 003050 Transaction Set 865 Purchase Order Change Acknowledgement/Request - Seller Initiated. Implementation Convention.
PB96-172549 *01,825* PC A09/MF A02

PB96-175237
Electronics and Electrical Engineering Laboratory: 1996 Program Plan. Supporting Technology for U.S. Competitiveness in Electronics.
PB96-175237 *01,962* PC A10/MF A03

PB96-175666
Journal of Research of the National Institute of Standards and Technology, January/February 1996. Volume 101, Number 1.
PB96-175666 *00,113* PC A07/MF A02

PB96-175674

International Marine-Atmospheric (222)Rn Measurement Intercomparison in Bermuda. Part 1. NIST Calibration and Methodology for Standardized Sample Additions.
PB96-175674 *00,114*
(Order as PB96-175666, PC A07/MF A02)

PB96-175682

International Marine-Atmospheric (222)Rn Measurement Intercomparison in Bermuda. Part 2. Results for the Participating Laboratories.
PB96-175682 *00,115*
(Order as PB96-175666, PC A07/MF A02)

PB96-175690

Theory of Electron Beam Moire.
PB96-175690 *04,373*
(Order as PB96-175666, PC A07/MF A02)

PB96-175708

Scaling Compartment Fires: Reduced- and Full-Scale Enclosure Burns.
PB96-175708 *00,224* Not available NTIS

PB96-175716

Five Q's (Cues) of the U.S. GOSIP Testing Program.
PB96-175716 *01,826* Not available NTIS

PB96-175724

Suppression of High-Speed C2H4/Air Flames with C1-Halocarbons.
PB96-175724 *03,287* Not available NTIS

PB96-175732

Effectiveness of Halon Alternatives in Suppressing Dynamic Combustion Process.
PB96-175732 *03,288* Not available NTIS

PB96-175740

Halon Thermochemistry: 'Ab Initio' Calculations of the Enthalpies of Formation of Fluoromethanes.
PB96-175740 *03,289* Not available NTIS

PB96-175856

NIST List of Publications, LP 103, March 1996. National Semiconductor Metrology Program.
PB96-175856 *02,432* PC A07/MF A02

PB96-176417

Interaction of HFC-125, FC-218 and CF3I with High Speed Combustion Waves.
PB96-176417 *03,290* Not available NTIS

PB96-176425

Suppression of Ignition Over a Heated Metal Surface.
PB96-176425 *03,291* Not available NTIS

PB96-176433

Realization of NIST 1995 Luminous Flux Scale Using the Integrating Sphere Method.
PB96-176433 *04,374* Not available NTIS

PB96-176441

Single-Port Technique for Adaptor Efficiency Evaluation.
PB96-176441 *02,088* Not available NTIS

PB96-176458

Novel Magnetic Field Characterization Techniques for Compound Semiconductor Materials and Devices.
PB96-176458 *02,433* Not available NTIS

PB96-176466

Irradiances of Spectral Lines in Mercury Pencil Lamps.
PB96-176466 *04,375* Not available NTIS

PB96-176474

Wavelengths of Spectral Lines in Mercury Pencil Lamps.
PB96-176474 *04,376* Not available NTIS

PB96-176482

Dimensional Characterization of Precision Coaxial Transmission Line Standards.
PB96-176482 *02,241* Not available NTIS

PB96-176490

Electrical Characteristics of Argon Radio Frequency Glow Discharges in an Asymmetric Cell.
PB96-176490 *04,109* Not available NTIS

PB96-176508

Potential Surfaces and Dynamics of Weakly Bound Trimers: Perspectives from High Resolution IR Spectroscopy.
PB96-176508 *01,155* Not available NTIS

PB96-176516

Growth and Nucleation of Hydrogenated Amorphous Silicon on Silicon (100) Surfaces.
PB96-176516 *02,991* Not available NTIS

PB96-176524

Magnetic Dielectric Oxides: Subsolidus Phase Relations in the BaO: Fe2O3: TiO2 System.
PB96-176524 *01,156* Not available NTIS

PB96-176532

Solid State (13)C NMR and Raman Studies of Cellulose Triacetate: Oligomers, Polymorphism, and Inferences about Chain Polarity.
PB96-176532 *01,289* Not available NTIS

PB96-176540

Automated Measurement of Nonlinearity of Optical Fiber Power Meters.
PB96-176540 *04,110* Not available NTIS

PB96-176557

Pore-Forming Protein with a Metal-Actuated Switch.
PB96-176557 *03,554* Not available NTIS

PB96-176565

Fundamental Limits on the Frequency Stabilities of Crystal Oscillators.
PB96-176565 *02,277* Not available NTIS

PB96-176573

Electromagnetic Coupling Character of (001) Twist Boundaries in Sintered Bi2Sr2CaCu2O8+x Bicrystals.
PB96-176573 *01,963* Not available NTIS

PB96-176581

Implementation of a Standard Format for GPS Common View Data.
PB96-176581 *01,555* Not available NTIS

PB96-176599

Line-Reflect-Match Calibrations with Nonideal Microstrip Standards.
PB96-176599 *02,242* Not available NTIS

PB96-176607

State-Resolved Rotational Energy Transfer in Open Shell Collisions: Cl((2)P3/2)+HCl.
PB96-176607 *01,157* Not available NTIS

PB96-176615

Magnetic Structure Determination for Annealed Ni80Fe20/Ag Multilayers Using Polarized-Neutron Reflectivity.
PB96-176615 *03,739* Not available NTIS

PB96-176623

Publication and Presentation Abstracts, 1994.
PB96-176623 *03,577* Not available NTIS

PB96-176631

Energy Distributions of Neutrons Scattered from Solid C60 by the Beryllium Detector Method.
PB96-176631 *03,740* Not available NTIS

PB96-176649

Simulations of Neutron Focusing with Curved Mirrors.
PB96-176649 *02,200* Not available NTIS

PB96-176656

Estimation of the Orientation Distribution of Short-Fiber Composites Using Ultrasonic Velocities.
PB96-176656 *03,178* Not available NTIS

PB96-176664

New Data and Correlations for the Custody Transfer of Natural Gas Liquids.
PB96-176664 *02,499* Not available NTIS

PB96-176672

Strategy to Support Multipoint Communication Service Over Native ATM Service.
PB96-176672 *01,507* Not available NTIS

PB96-176680

Viscosity of 1,1,1,2,3,3-Hexafluoropropane and 1,1,1,3,3,3-Hexafluoropropane at Saturated-Liquid Conditions from 262 K to 353 K.
PB96-176680 *03,292* Not available NTIS

PB96-176698

Small-Angle Neutron Scattering (SANS) Study of Worm-Like Micelles Under Shear.
PB96-176698 *04,111* Not available NTIS

PB96-176706

Developments in Stellar Coronae.
PB96-176706 *00,107* Not available NTIS

PB96-176714

Transition Regions of Capella (1995).
PB96-176714 *00,108* Not available NTIS

PB96-176722

Microwave Characterization of Flip-Chip MMIC Components.
PB96-176722 *02,434* Not available NTIS

PB96-176730

Microwave Characterization of Flip-Chip MMIC Interconnections.
PB96-176730 *02,435* Not available NTIS

PB96-176748

Electrical Measurements of Microwave Flip-Chip Interconnections.
PB96-176748 *02,436* Not available NTIS

PB96-176755

Report of the Refrigeration, Air Conditioning and Heat Pumps Technical Options Committee.
PB96-176755 *03,293* Not available NTIS

PB96-176763

Reference Relations for the Evaluation of the Materials Properties of Orthorhombic YBa2Cu3Ox Superconductors.
PB96-176763 *04,782* Not available NTIS

PB96-176771

Surface Plasmon Microscopy of Biotin-Streptavidin Binding Reactions on UV-Photopatterned Alkanethiol Self-Assembled Monolayers.
PB96-176771 *01,158* Not available NTIS

PB96-176789

Thermal Anemonetry for Mass Flow Measurement in Oscillating Cryogenic Gas Flows.
PB96-176789 *04,218* Not available NTIS

PB96-176797

Characterization of the Structure of LaD2.50 by Neutron Powder Diffraction.
PB96-176797 *04,783* Not available NTIS

PB96-176805

International Standard Equation of State for the Thermodynamic Properties of Refrigerant 123 (2,2-Dichloro- 1,1,1-Trifluoroethane).
PB96-176805 *03,294* Not available NTIS

PB96-177373

Innovation in the Japanese Construction Industry: A 1995 Appraisal.
PB96-177373 *00,225* PC A13/MF A03

PB96-177381

Journal of Research of the National Institute of Standards and Technology, March/April 1996. Volume 101, Number 2.
PB96-177381 *01,863* PC A07/MF A02

PB96-178892

Federal Implementation Guideline for Electronic Data Interchange: ASC X12 003050 Transaction Set 836 Procurement Notices. Implementation Convention.
PB96-178892 *01,827* PC A04/MF A01

PB96-178900

Voluntary Product Standard PS 1-95 Construction and Industrial Plywood.
PB96-178900 *03,406* PC A04/MF A01

PB96-178918

Directory of Law Enforcement and Criminal Justice Associations and Research Centers.
PB96-178918 *04,872* PC A05/MF A01

PB96-178926

Specifications and Tolerances for Reference Standards and Field Standard Weights and Measures. 2. Specifications and Tolerances for Field Standard Measuring Flasks.
PB96-178926 *02,682* PC A03/MF A01

PB96-179114

NIST Detector-Based Luminous Intensity Scale.
PB96-179114 *01,864*
(Order as PB96-177381, PC A07/MF A02)

PB96-179122

NIST High Accuracy Scale for Absolute Spectral Response from 406 nm to 920 nm.
PB96-179122 *01,865*
(Order as PB96-177381, PC A07/MF A02)

PB96-179130

Irradiance of Horizontal Quartz-Halogen Standard Lamps.
PB96-179130 *01,866*
(Order as PB96-177381, PC A07/MF A02)

PB96-179148

Development of the Ion Exchange-Gravimetric Method for Sodium in Serum as a Definitive Method.
PB96-179148 *01,867*
(Order as PB96-177381, PC A07/MF A02)

PB96-179155

MasPar MP-1 as a Computer Arithmetic Laboratory.
PB96-179155 *01,617*
(Order as PB96-177381, PC A07/MF A02)

PB96-179163

Evidence That Voltage Rather Than Resistance is Quantized in Breakdown of the Quantum Hall Effect.
PB96-179163 *01,868*
(Order as PB96-177381, PC A07/MF A02)

PB96-179411

Tree-Lookup for Partial Sums Or: How Can I Find This Stuff Quickly.
PB96-179411 *01,770* Not available NTIS

PB96-179429

Objective Evaluation of Short-Crack Toughness Curves Using Indentation Flaws: Case Study on Alumina-Based Ceramics.
PB96-179429 *03,079* Not available NTIS

PB96-179437

Organization and Implementation of Calibration in the EOS Project. Part 1.
PB96-179437 *04,841* Not available NTIS

PB96-179445

Theory for Quantum-Dot Quantum Wells: Pair Correlation and Internal Quantum Confinement in Nanoheterostructures.
PB96-179445 *02,437* Not available NTIS

PB96-179452

Deformation and Fracture of Mica-Containing Glass-Ceramics in Hertzian Contacts.
PB96-179452 *03,080* Not available NTIS

PB96-179460

Flaw Tolerance and Toughness Curves in Two-Phase Particulate Composites: SiC/Glass System.
PB96-179460 *03,081* Not available NTIS

PB96-179478

Time-Dependent Dielectric Breakdown of Intrinsic SiO2 Films under Dynamic Stress.
PB96-179478 *02,438* Not available NTIS

PB96-179486

Preliminary Investigation of Oleoresin Capsicum.
PB96-179486 *03,520* Not available NTIS

PB96-179494

Texture Measurement of Sintered Alumina Using the March-Dollase Function.
PB96-179494 *04,784* Not available NTIS

PB96-179502

Consensus Process in Standards Development.
PB96-179502 *00,136* Not available NTIS

PB96-179510

Improved Dose Metrology in Optical Lithography.
PB96-179510 *02,439* Not available NTIS

PB96-179528

Move-to-Root Rule for Self-Organizing Trees with Markov Dependent Requests.
PB96-179528 *03,431* Not available NTIS

PB96-179536

Test Optics Error Removal.
PB96-179536 *04,377* Not available NTIS

PB96-179544
Testing the Sensitivity of Accelerometers Using Mechanical Shock Pulses Under NIST Special Publication 250 Test No. 24040S.
PB96-179544 *02,683* Not available NTIS

PB96-179551
Dielectric Behavior of a Polycarbonate/Polyester Mixture Upon Transesterification.
PB96-179551 *04,785* Not available NTIS

PB96-179569
Ultrasound Power Measurement Techniques at NIST.
PB96-179569 *02,684* Not available NTIS

PB96-179577
Design of a High-Flux Backscattering Spectrometer for Ultra-High Resolution Inelastic Neutron Measurements.
PB96-179577 *02,992* Not available NTIS

PB96-179585
National Institute of Standards and Technology High-Accuracy Cryogenic Radiometer.
PB96-179585 *04,378* Not available NTIS

PB96-179593
Wear of Enamel against Glass-Ceramic, Porcelain, and Amalgam.
PB96-179593 *03,082* Not available NTIS

PB96-179601
Effect of Grain Size on Hertzian Contact Damage in Alumina.
PB96-179601 *03,083* Not available NTIS

PB96-180013
Indentation Fatigue: A Simple Cyclic Hertzian Test for Measuring Damage Accumulation in Polycrystalline Ceramics.
PB96-180013 *03,084* Not available NTIS

PB96-180021
Dynamics of Mu(+) in Sc and ScHx.
PB96-180021 *04,112* Not available NTIS

PB96-180039
Diffusion of Water along 'Closed' Mica Interfaces.
PB96-180039 *02,993* Not available NTIS

PB96-180047
Open System Environment Implementors Workshop (OIW); Standardization Role Defined.
PB96-180047 *01,828* Not available NTIS

PB96-180054
Synthesis of Hybrid Organic-Inorganic Materials from Interpenetrating Polymer Network Chemistry.
PB96-180054 *02,994* Not available NTIS

PB96-180062
Electrostatic Rigidity of Polyelectrolytes from Reparametrization Invariance.
PB96-180062 *04,113* Not available NTIS

PB96-180070
Scanning Capacitance Microscopy Measurements and Modeling: Progress Towards Dopant Profiling of Silicon.
PB96-180070 *01,964* Not available NTIS

PB96-180088
Model for Toughness Curves in Two-Phase Ceramics. 1. Basic Fracture Mechanics.
PB96-180088 *03,085* Not available NTIS

PB96-180096
Quantum Hall Effect-Based Resistance Standard: Capabilities and Implementation.
PB96-180096 *04,114* Not available NTIS

PB96-180104
Composition and Solubility Product of a Synthetic Calcium Hydroxyapatite.
PB96-180104 *02,995* Not available NTIS

PB96-180112
Assessing MOS Gate Oxide Reliability on Wafer Level with Ramped/Constant Voltage and Current Stress.
PB96-180112 *04,115* Not available NTIS

PB96-180120
Designations of ds(2)p Energy Levels in Neutral Zirconium, Hafnium, and Rutherfordium (Z=104).
PB96-180120 *04,116* Not available NTIS

PB96-180138
Surging the Upside-Down House: Measurements and Modeling Results.
PB96-180138 *02,243* Not available NTIS

PB96-180146
Radiochromic Solid-State Polymerization Reaction.
PB96-180146 *01,290* Not available NTIS

PB96-180153
Distributions of Measurement Error for Three-Axis Magnetic Field Meters during Measurements Near Appliances.
PB96-180153 *02,110* Not available NTIS

PB96-180161
Adsorption of Potassium N-phenylglycinate on Hydroxyapatite: Role of Solvents and Ionic Charge.
PB96-180161 *01,159* Not available NTIS

PB96-180179
Complicated Cases and Shielded Rooms: Audiometric Booths Shielded to Attenuate Electromagnetic Interference.
PB96-180179 *02,278* Not available NTIS

PB96-180187
Application of Metadata Standards.
PB96-180187 *01,771* Not available NTIS

PB96-180195
Tomographic Reconstruction of the Moments of Local Probability Density Functions in Turbulent Flow Fields.
PB96-180195 *04,219* Not available NTIS

PB96-180203
Hyperfine Structure Investigations and Identification of New Energy Levels in the Ionic Spectrum of (147)Pm.
PB96-180203 *04,117* Not available NTIS

PB96-180211
Measurements of the Resonance Lines of (6)Li and (7)Li by Doppler-Free Frequency-Modulation Spectroscopy.
PB96-180211 *04,118* Not available NTIS

PB96-180229
Advances in the Measurement of Polymer CTE: Micrometer- to Atomic-Scale Measurements.
PB96-180229 *03,390* Not available NTIS

PB96-180237
Fluoride Analytical Methods.
PB96-180237 *03,578* Not available NTIS

PB96-180245
Effect of Chemical Interaction on Barenblatt Crack Profiles in Brittle Solids.
PB96-180245 *02,996* Not available NTIS

PB96-180252
Pressurized Internal Lenticular Cracks at Healed Mica Interfaces.
PB96-180252 *02,997* Not available NTIS

PB96-180260
Fracture of Silicon Nitride and Silicon Carbide at Elevated Temperatures.
PB96-180260 *03,179* Not available NTIS

PB96-180278
Transient Creep Behaviour of Hot Isostatically Pressed Silicon Nitride.
PB96-180278 *03,086* Not available NTIS

PB96-180286
Development of Neutral-Density Infrared Filters Using Metallic Thin Films.
PB96-180286 *02,998* Not available NTIS

PB96-182266
Unpredictable Certainty. Information Infrastructure through 2000.
PB96-182266 *00,016* PC A14/MF A03

PB96-183041
X.500 Directory Schema Design Handbook.
PB96-183041 *02,739* PC A03/MF A01

PB96-183058
Procedure for Product Data Exchange Using STEP Developed in the AutoSTEP Pilot.
PB96-183058 *02,843* PC A04/MF A01

PB96-183066
Electronics and Electrical Engineering Laboratory Technical Publication Announcements Covering Laboratory Programs, July to September 1995 with 1996 EEEL Events Calendar.
PB96-183066 *01,965* PC A03/MF A01

PB96-183074
Publications 1995: NIST Building and Fire Research Laboratory.
PB96-183074 *00,226* PC A08/MF A02

PB96-183082
Materials Reliability. Technical Activities, 1995.
PB96-183082 *02,999* PC A07/MF A02

PB96-183090
Workshop on Characterizing Diamond Films (4th). Held in Gaithersburg, Maryland on March 4-5, 1996.
PB96-183090 *04,786* PC A04/MF A01

PB96-183108
NASA Fire Detector Study.
PB96-183108 *01,423* PC A04/MF A01

PB96-183116
Electronics and Electrical Engineering Laboratory Technical Progress Bulletin Covering Laboratory Programs, October to December 1995 with 1996 EEEL Events Calendar.
PB96-183116 *01,966* PC A04/MF A01

PB96-183124
Proceedings of NIST Workshop: Industry Needs in Welding Research and Standards Development. Held on August 15-16, 1995.
PB96-183124 *02,877* PC A04/MF A01

PB96-183132
Numerical Simulation of Rapid Combustion in an Underground Enclosure.
PB96-183132 *01,424* PC A03/MF A01

PB96-183140
Interoperability Experiments with CORBA and Persistent Object Base Systems.
PB96-183140 *01,772* PC A04/MF A01

PB96-183157
Standard Source Method for Reducing Antenna Factor Errors in Shielded Room Measurements.
PB96-183157 *02,013* PC A04/MF A01

PB96-183165
Distributed Communication Methods and Role-Based Access Control for Use in Health Care Applications.
PB96-183165 *01,508* PC A05/MF A01

PB96-183173
Scale-Space-Based Visual-Motion-Cue for Autonomous Navigation.
PB96-183173 *02,940* PC A06/MF A01

PB96-183181
Minimum Mass Flux Requirements to Suppress Burning Surfaces with Water Sprays.
PB96-183181 *01,425* PC A05/MF A01

PB96-183199
Dynamometer-Induced Residual Stress in Railroad Wheels: Ultrasonic and Saw Cut Measurements. Report No. 30.
PB96-183199 *04,857* PC A04/MF A01

PB96-183207
Hygrothermal Effects on the Performance of Polymers and Polymeric Composites: A Workshop Report. Held in Gaithersburg, Maryland on September 21-22, 1995.
PB96-183207 *03,180* PC A04/MF A01

PB96-183215
Publications of the National Institute of Standards and Technology 1993 Catalog.
PB96-183215 *00,017* PC A11/MF A03

PB96-183223
Probabilistic Estimates of Design Load Factors for Wind-Sensitive Structures Using the 'Peaks Over Threshold' Approach.
PB96-183223 *00,474* PC A04/MF A01

PB96-183231
Aspects of a Product Model Supporting Apparel Virtual Enterprises.
PB96-183231 *02,790* PC A03/MF A01

PB96-183249
Performance of Tape-Bonded Seams of EPDM Membranes: Comparison of the Peel Creep-Rupture Response of Tape-Bonded and Liquid-Adhesive-Bonded Seams.
PB96-183249 *03,012* PC A05/MF A01

PB96-186010
Surface Transverse Wave Oscillators with Extremely Low Thermal Noise Floors.
PB96-186010 *01,967* Not available NTIS

PB96-186028
Ultrasonic Sensing of GMAW: Laser/EMAT Defect Detection System.
PB96-186028 *02,878* Not available NTIS

PB96-186036
Determination of Sheet Steel Formability Using Wide Band Electromagnetic-Acoustic Transducers.
PB96-186036 *02,279* Not available NTIS

PB96-186044
Effect of Liftoff on Accuracu of Phase Velocity Measurements Made with Electromagnetic-Acoustic Transducers.
PB96-186044 *02,280* Not available NTIS

PB96-186051
Methods to Improve the Accuracy of On-Line Ultrasonic Measurement of Steel Sheet Formability.
PB96-186051 *02,281* Not available NTIS

PB96-186069
Sensor System for Intelligent Processing of Hot-Rolled Steel.
PB96-186069 *03,373* Not available NTIS

PB96-186077
Well-Shielded EMAT for On-Line Ultrasonic Monitoring of GMA Welding.
PB96-186077 *02,879* Not available NTIS

PB96-186085
Alpha-Particle and Electron Capture Decay of (209)Po.
PB96-186085 *04,119* Not available NTIS

PB96-186093
New Physics-Based Model for Time-Dependent- Dielectric-Breakdown.
PB96-186093 *02,440* Not available NTIS

PB96-186101
Scattered Fractions of Dose from 18 and 25 MV X-ray Radiotherapy Linear Accelerators.
PB96-186101 *04,120* Not available NTIS

PB96-186119
Electrohydrodynamic Instability and Electrical Discharge Initiation in Hexane.
PB96-186119 *02,244* Not available NTIS

PB96-186127
Coarsening of Unstable Surface Features during Fe(001) Homoepitaxy.
PB96-186127 *04,121* Not available NTIS

PB96-186135
What Is a 'Standard Reference Material' - What Is Any Reference Material.
PB96-186135 *03,000* Not available NTIS

PB96-186143
Thermodynamics of the Hydrolysis of 3,4,5-Trihydroxybenzoic Acid Propyl Ester (n-Propylgallate) to 3,4,5-Trihydroxybenzoic Acid (Gallic Acid) and Propan-I-ol in Aqueous Media and in Toluene.
PB96-186143 *01,160* Not available NTIS

PB96-186150
Characterization of the Structure of YD3 by Neutron Powder Diffraction.
PB96-186150 *01,161* Not available NTIS

PB96-186168
Neutron and Raman Spectroscopies of 134 and 134a Hydrofluorocarbons Encaged in Na-X Zeolite.
PB96-186168 *03,001* Not available NTIS

PB96-186176
Preparation, Crystal Structure, Dielectric Properties, and Magnetic Behavior of Ba2Fe2Ti4O13.
PB96-186176 *01,162* Not available NTIS

PB96-186184
Binary Decision Clustering for Neural-Network-Based Optical Character Recognition.
PB96-186184 *01,857* Not available NTIS

PB96-186192
Guide to a Format for Data on Chemical Admixtures in a Materials Property Database. (Reannouncement with new abstract).
PB96-186192 *01,328* PC A04/MF A01

PB96-188164
Reference Information for the Software Verification and Validation Process.
PB96-188164 *01,773* PC A06/MF A01

PB96-189444
Financing Tomorrow's Infrastructure: Challenges and Issues. Proceedings of a Colloquium. Held in Washington, DC. on October 20, 1995.
PB96-189444 *00,481* PC A07/MF A02

PB96-190012
Large Eddy Simulations of Smoke Movement in Three Dimensions.
PB96-190012 *01,426* Not available NTIS

PB96-190020
Investigations of Sulfur Interferences in the Extraction of Methylmercury from Marine Tissues.
PB96-190020 *03,482* Not available NTIS

PB96-190038
Microlithography by Using Neutral Metastable Atoms and Self-Assembled Monolayers.
PB96-190038 *02,441* Not available NTIS

PB96-190046
Helping to Reduce Technical Barriers to Trade.
PB96-190046 *00,491* Not available NTIS

PB96-190053
Dynamic Objects and Meta-Level Programming of an EXPRESS Language Environment.
PB96-190053 *01,774* Not available NTIS

PB96-190061
Isolation and Structural Elucidation of the Predominant Geometrical Isomers of alpha-Carotene.
PB96-190061 *00,640* Not available NTIS

PB96-190079
Large Fire Experiments for Fire Model Evaluations.
PB96-190079 *01,427* Not available NTIS

PB96-190087
Hemispherical Test Fixture for Measuring the Wavefields Generated in an Anisotropic Solid.
PB96-190087 *03,181* Not available NTIS

PB96-190095
Mapping the Droplet Transfer Modes for an ER100S-1 GMAW Electrode.
PB96-190095 *03,295* Not available NTIS

PB96-190103
Response Comparison of Electret Ion Chambers, LiF TLD, and HPIC.
PB96-190103 *02,578* Not available NTIS

PB96-190111
Wavelet Variance, Allan Variance, and Leakage.
PB96-190111 *01,509* Not available NTIS

PB96-190129
Repair of Products of Oxidative DNA Base Damage in Human Cells.
PB96-190129 *03,555* Not available NTIS

PB96-190137
Locating Fire Information.
PB96-190137 *00,227* Not available NTIS

PB96-190145
Power Characteristics in GMAW: Experimental and Numerical Investigation.
PB96-190145 *03,296* Not available NTIS

PB96-190152
Atomic Branching Ratio Data for Nitrogen-Like Species.
PB96-190152 *04,122* Not available NTIS

PB96-190160
Sensing Droplet Detachment and Electrode Extension for Control of Gas Metal Arc Welding.
PB96-190160 *03,297* Not available NTIS

PB96-190178
Office Work Station Heat Release Rate Study: Full Scale versus Bench Scale.
PB96-190178 *01,428* Not available NTIS

PB96-190186
Epitaxial Nucleation and Growth of Chemically Derived Ba2YCu3O7-x Thin Films on (001) SrTiO3.
PB96-190186 *04,787* Not available NTIS

PB96-190194
Charpy Impact Test as an Evaluation of 4 K Fracture Toughness.
PB96-190194 *03,219* Not available NTIS

PB96-190202
New 5 and 10 MHz High Isolation Distribution Amplifier.
PB96-190202 *01,510* Not available NTIS

PB96-190210
Analysis of High Bay Hangar Facilities for Detector Sensitivity and Placement.
PB96-190210 *01,429* Not available NTIS

PB96-190228
Models of Granualr Giant Magnetoresistance Multilayer Thin Films.
PB96-190228 *01,968* Not available NTIS

PB96-190236
Aluminum-Lithium Alloys: Evaluation of Fracture Toughness by Two Test Standards, ASTM Method E 813 and E 1304.
PB96-190236 *03,374* Not available NTIS

PB96-190244
Light-Weight Alloys for Aerospace Applications II.
PB96-190244 *03,375* Not available NTIS

PB96-190251
Prediction of Strengthening Due to V Additions in Direct-Cooled Ferrite-Pearlite Forging Steels.
PB96-190251 *03,220* Not available NTIS

PB96-190269
Temperature-Induced Transition in Ductile Fracture Appearance of a Nitrogen-Strengthened Austenitic Stainless Steel.
PB96-190269 *03,221* Not available NTIS

PB96-190277
Embossable Grating Couplers for Planar Waveguide Optical Sensors.
PB96-190277 *00,641* Not available NTIS

PB96-190285
Ductile Fracture and Tempered Martensite Embrittlement of 4140 Steel.
PB96-190285 *03,222* Not available NTIS

PB96-190293
Increasing the Value of Atomic Force Microscopy Process Metrology Using a High-Accuracy Scanner, Tip Characterization, and Morphological Image Analysis.
PB96-190293 *02,758* Not available NTIS

PB96-190301
Optical Density Measurements of Laser Eye Protection Materials.
PB96-190301 *00,190* Not available NTIS

PB96-190319
Time and Frequency Metrology.
PB96-190319 *01,556* Not available NTIS

PB96-190327
Ultrasonic Methods.
PB96-190327 *02,707* Not available NTIS

PB96-190335
Charpy Specimen Tests at 4 K.
PB96-190335 *03,002* Not available NTIS

PB96-190343
Fatigue Crack Thresholds of a Nickel-Iron Alloy for Superconductor Sheaths at 4 K.
PB96-190343 *03,223* Not available NTIS

PB96-190350
Mechanical Properties and Warm Prestress of Ultra-Low Carbon Steel at 4 K.
PB96-190350 *03,224* Not available NTIS

PB96-190368
Scanned Probe Microscope Tip Characterization Without Calibrated Tip Characterizers.
PB96-190368 *02,759* Not available NTIS

PB96-190376
Confidence on the Modified Allan Variance and the Time Variance.
PB96-190376 *01,557* Not available NTIS

PB96-190384
High Frequency Magnetic Field Sensors Based on the Faraday Effect in Garnet Thick Films.
PB96-190384 *02,282* Not available NTIS

PB96-191366
IIW Commission V Quality Control and Quality Assurance of Welded Products, Annual Report 1995/96.
PB96-191366 *02,880* PC A04/MF A01

PB96-191374
Generalized Form Registration Using Structure-Based Techniques.
PB96-191374 *01,858* PC A03/MF A01

PB96-191382
Dielectric and Magnetic Measurements from -50C to 200C and in the Frequency Band 50 MHz to 2 GHz.
PB96-191382 *02,245* PC A03/MF A01

PB96-191390
Electronics and Electrical Engineering Laboratory Technical Progress Bulletin Covering Laboratory Programs, January to March 1996, with 1996 EEEL Events Calendar.
PB96-191390 *01,969* PC A04/MF A01

PB96-193636
SparseLib++ v. 1.5 Sparse Matrix Class Library. Reference Guide.
PB96-193636 *01,775* PC A03/MF A01

PB96-193644
Reactor Radiation Technical Activities, 1995.
PB96-193644 *03,741* PC A07/MF A02

PB96-193651
Warping of Terrace Pavers at the U.S. Capitol Building.
PB96-193651 *00,411* PC A03/MF A01

PB96-193669
Component-Based Handprint Segmentation Using Adaptive Writing Style Model.
PB96-193669 *01,859* PC A03/MF A01

PB96-193677
Ceramics Technical Activities, 1995.
PB96-193677 *03,087* PC A11/MF A03

PB96-193685
Guidelines for Pre-Qualification, Prototype and Quality Control Testing of Seismic Isolation Systems.
PB96-193685 *01,347* PC A08/MF A02

PB96-193693
Room-Temperature Thermal Conductivity of Expanded Polystyrene Board for a Standard Reference Material.
PB96-193693 *00,412* PC A04/MF A01

PB96-193701
Post-Flame Soot.
PB96-193701 *01,430* PC A04/MF A01

PB96-193719
Polymers Technical Activities, 1995.
PB96-193719 *01,291* PC A10/MF A02

PB96-193727
Novel Active-Vision-Based Motion Cues for Local Navigation.
PB96-193727 *02,941* PC A05/MF A01

PB96-193735
Systems Integration for Manufacturing Applications Program 1995 Annual Report.
PB96-193735 *02,844* PC A05/MF A01

PB96-193743
Development of an Economical Video Based Fire Detection and Location System.
PB96-193743 *00,228* PC A05/MF A01

PB96-193750
Hybrid Gauss-Trapezoidal Quadrature Rules.
PB96-193750 *03,422* PC A04/MF A01

PB96-193768
Computer Systems Laboratory Computing and Applied Mathematics Laboratory Technical Accomplishments, October 1994-March 1996.
PB96-193768 *01,638* PC A05/MF A01

PB96-193776
Notion of a xi-Vector and a Stress Tensor for a General Class of Anisotropic Diffuse Interface Models.
PB96-193776 *04,788* PC A03/MF A01

PB96-193784
Methodology for Developing and Implementing Alternative Temperature-Time Curves for Testing the Fire Resistance of Barriers for Nuclear Power Plant Applications.
PB96-193784 *03,742* PC A07/MF A02

PB96-193792
Survey of Standards for the U.S. Fiber/Textile/Apparel Industry.
PB96-193792 *03,199* PC A06/MF A01

PB96-193800
State of the Art Report on Seismic Design Requirements for Nonstructural Building Components.
PB96-193800 *00,308* PC A06/MF A01

PB96-195219
IML++ v.1.2 Iterative Methods Library Reference Guide.
PB96-195219 *01,776* PC A04/MF A01

PB96-195268
National Semiconductor Metrology Program, Project Portfolio FY 1996.
PB96-195268 *04,789* PC A03/MF A01

PB96-195276
Program of the Manufacturing Engineering Laboratory, 1996. Infrastructural Technology, Measurements, and Standards for the U.S. Manufacturing Industries.
PB96-195276 *02,760* PC A11/MF A03

PB96-195284
Metallurgy. Technical Activities, 1995.
PB96-195284 *03,003* PC A09/MF A02

PB96-195318
TMACH Experiment Phase 1. Preliminary Developmental Evaluation.
PB96-195318 *01,618* PC A03/MF A01

PB96-195326
MV++ v. 1.5a Matrix/Vector Class Reference Guide.
PB96-195326 *01,777* PC A03/MF A01

PB96-195334
Computer-Aided Manufacturing Engineering Forum (2nd). Technical Meeting Proceedings. Held in Gaithersburg, Maryland on August 22-23, 1995.
PB96-195334 *02,845* PC A11/MF A03

PB96-195508
Dynamics, Transport and Chemical Kinetics of Compartment Fire Exhaust Gases.
PB96-195508 *00,229* PC A06/MF A01

PB96-195516
Operator Experience with a Hierarchical Real-Time Control System (RCS).
PB96-195516 *03,751* PC A03/MF A01

PB96-195524
Specification for Interoperability between Ballistic Imaging Systems. Part 1. Cartridge Cases.
PB96-195524 *01,860* PC A04/MF A01

PB96-195532
Chemical Inhibition of Methane-Air Diffusion Flame.
PB96-195532 *01,431* PC A04/MF A01

PB96-197249
Development of a Method for Measuring Water-Stripping Resistance of Asphalt/Siliceous Aggregate Mixtures.
PB96-197249 *01,348* PC A04/MF A01

PB96-200118
Coaxial Line-Reflect-Match Calibration.
PB96-200118 *02,246* Not available NTIS

PB96-200126
Methodology for Electromagnetic Interference Measurements.
PB96-200126 *02,014* Not available NTIS

PB96-200134
Metallic-Barrier Junctions for Programmable Josephson Voltage Standards.
PB96-200134 *02,089* Not available NTIS

PB96-200142
Shapiro Steps in Large-Area Metallic-Barrier Josephson Junctions.
PB96-200142 *02,090* Not available NTIS

PB96-200159
Scanning Electron Microscopy Observations of Misfit Dislocations in Epitaxial In0.25Ga0.75As on GaAs(001).
PB96-200159 *03,004* Not available NTIS

PB96-200167
Novel Vortex Dynamics in Two-Dimensional Josephson Arrays.
PB96-200167 *02,091* Not available NTIS

PB96-200175
Orthotropic Elastic Constants of a Boron-Aluminum Fiber-Reinforced Composite: An Acoustic-Resonance-Spectroscopy Study.
PB96-200175 *03,182* Not available NTIS

PB96-200183
High-Tc Multilayer Step-Edge Josephson Junctions and SQUIDs.
PB96-200183 *04,790* Not available NTIS

PB96-200217
Riass Coronathon: Joint X-ray and Ultraviolet Observations of Normal F-K Stars.
PB96-200217 *00,109* Not available NTIS

PB96-200225
Accurate Modeling of Size and Strain Broadening in the Rietveld Refinement: The 'Double-Voigt' Approach.
PB96-200225 *00,664* Not available NTIS

PB96-200233
Superconductor- Normal-Superconductor Junctions for Digital/Analog Converters.
PB96-200233 *02,092* Not available NTIS

PB96-200241
Superconductor- Normal-Superconductor Junctions for Programmable Voltage Standards.
PB96-200241 *02,093* Not available NTIS

PB96-200258
Design of High-Frequency, High-Power Oscillators Using Josephson-Junction Arrays.
PB96-200258 *02,094* Not available NTIS

PB96-200266
High-Power, High-Frequency Oscillators Using Distributed Josephson-Junction Arrays.
PB96-200266 *02,095* Not available NTIS

PB96-200274
Excitation Transfer in Barium by Collisions with Noble Gases.
PB96-200274 *01,163* Not available NTIS

PB96-200282
Data Evaluation of a Linear System by a Second-Order Transfer Function.
PB96-200282 *01,970* Not available NTIS

PB96-200290
Comment on <<A Dynamic Electric Trap for Ground-State Atoms>>.
PB96-200290 *04,123* Not available NTIS

PB96-200308
Fiber-Optic Faraday-Effect Magnetic-Field Sensor Based on Flux Concentrators.
PB96-200308 *02,201* Not available NTIS

PB96-200316
Alignment Probing of Rydberg States by Stimulated Emission.
PB96-200316 *04,124* Not available NTIS

PB96-200324
Alternative EMC Compliance Test Facilities.
PB96-200324 *02,247* Not available NTIS

PB96-200332
Observation of the Transverse Second Harmonic Magneto-Optic Kerr Effect from Ni81Fe19 Thin Film Structures.
PB96-200332 *01,971* Not available NTIS

PB96-200340
Collisions of Electrons with Highly-Charged Ions.
PB96-200340 *04,791* Not available NTIS

PB96-200357
Pairwise and Nonpairwise Additive Forces in Weakly Bound Complexes: High Resolution Infrared Spectroscopy of ArnDF (n=1,2,3).
PB96-200357 *04,125* Not available NTIS

PB96-200365
Design Criteria for BJT Amplifiers with Low I/f AM and PM Noise.
PB96-200365 *02,442* Not available NTIS

PB96-200373
Comparison of Ultralow-Sidelobe-Antenna Far-Field Patterns Using the Planar-Near-Field Method and the Far-Field Method.
PB96-200373 *02,015* Not available NTIS

PB96-200381
Wavelet Analysis for Synchronization and Timekeeping.
PB96-200381 *01,558* Not available NTIS

PB96-200399
Hot-Electron Microcalorimeter for X-ray Detection Using a Superconducting Transition Edge Sensor with Electrothermal Feedback.
PB96-200399 *04,792* Not available NTIS

PB96-200407
30 MHz Comparison Receiver.
PB96-200407 *01,972* Not available NTIS

PB96-200613
Kinetic-Energy-Enhanced Neutral Etching.
PB96-200613 *00,665* Not available NTIS

PB96-200621
Accurate Measurements of the Local Deuterium Abundance from HST Spectra.
PB96-200621 *00,110* Not available NTIS

PB96-200639
Deuterium and the Local Interstellar Medium: Properties for the Procyon and Capella Lines of Sight.
PB96-200639 *00,111* Not available NTIS

PB96-200647
How to Get NIST-Traceable Time on Your Computer.
PB96-200647 *01,559* Not available NTIS

PB96-200654
Introduction to Frequency Calibration. Part 1.
PB96-200654 *01,560* Not available NTIS

PB96-200662
NIST Frequency Measurement Service.
PB96-200662 *01,561* Not available NTIS

PB96-200670
Hot-Electron-Microcalorimeters with 0.25 mm(2) Area.
PB96-200670 *04,793* Not available NTIS

PB96-200688
General Order 'N' Analytic Correction of Probe-Position Errors in Planar Near-Field Measurements.
PB96-200688 *01,562* Not available NTIS

PB96-200696
Polarimetric Calibration of Reciprocal-Antenna Radars.
PB96-200696 *02,016* Not available NTIS

PB96-200704
Gravitational Sisyphus Cooling of (87)Rb in a Magnetic Trap.
PB96-200704 *04,379* Not available NTIS

PB96-200712
Controlling the Critical Current Density of High-Temperature SNS Josephson Junctions.
PB96-200712 *04,794* Not available NTIS

PB96-200720
Stable, Tightly Confining Magnetic Trap for Evaporative Cooling of Neutral Atoms.
PB96-200720 *04,126* Not available NTIS

PB96-200738
Self-Calibrated Intelligent Optical Sensors and Systems.
PB96-200738 *04,380* Not available NTIS

PB96-200746
Magnetic Flux Pinning in Epitaxial YBa2Cu3O7-delta Thin Films.
PB96-200746 *04,795* Not available NTIS

PB96-200753
Thermal Conductivity of Polypyromellitimide Film with Alumina Filler Particles from 4.2 to 300 K.
PB96-200753 *01,292* Not available NTIS

PB96-200761
Elastic Constants and Microcracks in YBa2Cu3O7.
PB96-200761 *03,005* Not available NTIS

PB96-200779
Effect of Harmonic Distortion on Phase Errors in Frequency Distribution and Synthesis.
PB96-200779 *01,563* Not available NTIS

PB96-200787
Origin of I/f PM and AM Noise in Bipolar Junction Transistor Amplifiers.
PB96-200787 *02,096* Not available NTIS

PB96-200795
Quest to Understand and Reduce I/f Noise in Amplifiers and Baw Quartz Oscillators.
PB96-200795 *02,097* Not available NTIS

PB96-200803
Tensile Creep of Silicide Composites.
PB96-200803 *03,183* Not available NTIS

PB96-200811
Unique Quality Assurance Aspects of INAA for Reference Material Homogeneity and Certification.
PB96-200811 *00,699* Not available NTIS

PB96-200829
Multimedia Tutorial on Phase Equilibria Diagrams.
PB96-200829 *03,088* Not available NTIS

PB96-200837
Measurements of Properties of Materials in Electronic Packaging.
PB96-200837 *01,973* Not available NTIS

PB96-200845
Overview of U.S. Government Advanced Packaging Programs.
PB96-200845 *02,443* Not available NTIS

PB96-200852
Self-Reciprocal Fourier Functions.
PB96-200852 *01,974* Not available NTIS

PB96-200860
Optoelectronics at NIST.
PB96-200860 *02,202* Not available NTIS

PB96-200878
Wideband Current and Magnetic Field Sensors Based on Iron Garnets.
PB96-200878 *01,975* Not available NTIS

PB96-200886
Quantitative Determination of Oxidative Base Damage in DNA by Stable Isotope-Dilution Mass Spectrometry.
PB96-200886 *03,483* Not available NTIS

PB96-200894
Commentary: The Measurement of Oxidative Damage to DNA by HPLC and GC/MS Techniques.
PB96-200894 *03,484* Not available NTIS

PB96-200902
Performance of the Electron Pump with Stray Capacitances.
PB96-200902 *01,976* Not available NTIS

PB96-200910
Precision of Marchall Stability and Flow Test Using 6-in. (152.4-mm) Diameter Specimens.
PB96-200910 *03,006* Not available NTIS

PB96-200928
Intercomparison of DNA Sizing Ladders in Electrophoretic Separation Matrices and Their Potential for Accurate Typing of the D1S80 Locus.
PB96-200928 *03,485* Not available NTIS

PB96-200936
100 A, 100 kHz Transconductance Amplifier.
PB96-200936 *02,098* Not available NTIS

PB96-200944
Quantum Hall Effect-Based Resistance Standard (Quantum Hall Res).
PB96-200944 *04,127* Not available NTIS

PB96-200951
Flow Immunoassay Using Solid-Phase Entrapment.
PB96-200951 *00,642* Not available NTIS

PB96-200969
Monte Carlo Simulation of Scanning Electron Microscope Signals.
PB96-200969 *02,444* Not available NTIS

PB96-200977
Software Needs in Special Functions.
PB96-200977 *01,778* Not available NTIS

PB96-200985
New Oxide Degradation Mechanism for Stresses in the Fowler-Nordheim Tunneling Regime.
PB96-200985 *04,128* Not available NTIS

PB96-200993
Smoke Plume Trajectory from In situ Burning of Crude Oil: Field Experiments.
PB96-200993 *02,597* Not available NTIS

PB96-201009
Experimental Evaluation of Specification Techniques for Improving Functional Testing.
PB96-201009 *01,779* Not available NTIS

PB96-201017
Escherichis coli Cyclic AMP Receptor Protein Mutants Provide Evidence for Ligand Contacts Important in Activation.
PB96-201017 *03,592* Not available NTIS

PB96-201025
Novel Hot-Electron Microbolometer.
PB96-201025 *01,977* Not available NTIS

PB96-201033
Temperature Dependence of the Gas and Liquid Phase Ultraviolet Absorption Cross Sections of HCFC-123 (CF3CHCl2) and HCFC-142b (CH3CF2Cl).
PB96-201033 *03,298* Not available NTIS

PB96-201041
UV Absorption Cross Sections of Methylchloroform: Temperature-Dependent Gas and Liquid Phase Measurements.
PB96-201041 *00,643* Not available NTIS

PB96-201058
Time-Resolved Measurements of the Polarization State of Four-Wave Mixing Signals from GaAs Multiple Quantum Wells.
PB96-201058 *04,796* Not available NTIS

PB96-201066
Modification of a Commercial SEM with a Computer Controlled Cathode Stabilized Power Supply.
PB96-201066 *04,129* Not available NTIS

PB96-201074
Report on the NIST Low Accelerating Voltage SEM Magnification Standard Interlaboratory Study.
PB96-201074 *02,445* Not available NTIS

PB96-201082
Scanning Electron Microscope Magnification Calibration Interlaboratory Study.
PB96-201082 *01,164* Not available NTIS

PB96-201090
Scanning Electron Microscope Metrology.
PB96-201090 *02,446* Not available NTIS

PB96-201108
SEM Linewidth Metrology of X-ray Lithography Masks.
PB96-201108 *02,447* Not available NTIS

PB96-201116
Low Heat-Flux Measurements: Some Precautions.
PB96-201116 *02,685* Not available NTIS

PB96-201124
Precise Laser-Based Measurements of Zero-Dispersion Wavelength in Single-Mode Fibers.
PB96-201124 *01,511* Not available NTIS

PB96-201132
New Physics-Based Model for Time-Dependent- Dielectric-Breakdown.
PB96-201132 *02,448* Not available NTIS

PB96-201140
In vitro Inhibition of Membrane-Mediated Calcification by Novel Phosphonates.
PB96-201140 *03,595* Not available NTIS

PB96-201157
Ultrasonic NDE of Sprayed Ceramic Coatings.
PB96-201157 *02,761* Not available NTIS

PB96-201165
Electronically Tunable Fiber Laser for Optical Pumping of (3)He and (4)He.
PB96-201165 *04,381* Not available NTIS

PB96-201173
Spin-Dependent Interface Transmission and Reflection in Magnetic Multilayers (Invited).
PB96-201173 *04,130* Not available NTIS

PB96-201181
NMR Characterization of Injection-Moulded Alumina Green Compacts. Part 2. T2-Weighted Proton Imaging.
PB96-201181 *01,165* Not available NTIS

PB96-201199
Vapor Pressure of Pentafluorodimethyl Ether.
PB96-201199 *00,677* Not available NTIS

PB96-201207
Vibrationally Resolved Photoelectron Angular Distributions and Branching Ratios for the Carbon Dioxide Molecule in the Wavelength Region 685-795 Angstrom.
PB96-201207 *04,131* Not available NTIS

PB96-202122
Developing Quality System Documentation Based on ANSI/NCSL Z540-1-1994: The Optical Technology Division's Effort.
PB96-202122 *01,869* PC A05/MF A01

PB96-202221
Benefits and Costs of Research: Two Case Studies in Building Technology.
PB96-202221 *00,230* PC A07/MF A02

PB96-202239
NIST Construction Automation Program Report No. 2. Proceedings of the NIST Construction Automation Workshop. Held in Gaithersburg, Maryland on March 30-31, 1995.
PB96-202239 *00,413* PC A09/MF A02

PB96-202247
Enhancement of EXIT89 and Analysis of World Trade Center Data.
PB96-202247 *00,231* PC A04/MF A01

PB96-202254
Mixing and Radiation Properties of Buoyant Luminous Flame Environments.
PB96-202254 *01,432* PC A06/MF A01

PB96-202288
Benefits and Costs of Research: A Case Study of the Fire Safety Evaluation System.
PB96-202288 *00,232* PC A06/MF A01

PB96-202296
Development of a Method for Measuring Water-Stripping Resistance of Asphalt/Siliceous Aggregate Mixtures.
PB96-202296 *01,329* PC A09/MF A02

PB96-202304
Sparse Water Sprays in Fire Protection.
PB96-202304 *01,433* PC A13/MF A03

PB96-202320
Application Protocol Information Base World Wide Web Gateway.
PB96-202320 *02,791* PC A03/MF A01

PB96-202338
Measurement of Rheological Properties of High Performance Concrete: State of the Art Report.
PB96-202338 *00,414* PC A04/MF A01

PB96-202346
Electronics and Electrical Engineering Laboratory Technical Publication Announcements Covering Laboratory Programs, October to December 1995, with 1996 EEEL Events Calendar.
PB96-202346 *01,978* PC A04/MF A01

PB96-202353
Economics of New-Technology Materials: A Case Study of FRP Bridge Decking.
PB96-202353 *01,349* PC A06/MF A01

PB96-202452
Lake Erie Water Temperature Data, Put-in-Bay, Ohio, 1918-1992.
PB96-202452 *03,692* PC A04/MF A01

PB96-204011
Enthalpy Increment Measurements from 4.5 to 318 K for Bismuth(cr). Thermodynamic Properties from 0 K to the Melting Point.
PB96-204011 *01,166* Not available NTIS

PB96-204029
Enthalpy Increment Measurements from 4.5 to 350 K and the Thermodynamic Properties of Titanium Disilicide(cr) to 1700 K.
PB96-204029 *00,678* Not available NTIS

PB96-204037
Enthalpy Increment Measurements from 4.5 K to 350 K and the Thermodynamic Properties of the Titanium Silicide Ti5Si3(cr).
PB96-204037 *00,679* Not available NTIS

PB96-204045
Guide to Locating and Accessing Computerized Numeric Materials Databases.
PB96-204045 *03,007* Not available NTIS

PB96-204052
New Surface-Active Comonomer for Adhesive Bonding.
PB96-204052 *03,579* Not available NTIS

PB96-204060
Need for Advanced Characterization Techniques in Product Manufacturing: A Case Study on Ceramic Matrix Composites.
PB96-204060 *03,089* Not available NTIS

PB96-204078
Gas Phase Oxygen Effect on Chain Scission and Monomer Content in Bulk Poly(methyl methacrylate) Degraded by External Thermal Radiation.
PB96-204078 *01,293* Not available NTIS

PB96-204086
NIST/NCMS Program on Electronic Packaging: First Update.
PB96-204086 *03,008* Not available NTIS

PB96-204094
Nanostructure Fabrication via Laser-Focused Atomic Deposition (Invited).
PB96-204094 *04,132* Not available NTIS

PB96-204102
Electric Field Dependent Dielectric Breakdown of Intrinsic SiO2 Films Under Dynamic Stress.
PB96-204102 *02,449* Not available NTIS

PB96-204110
Diffusive Crack Growth at a Bimaterial Interface.
PB96-204110 *03,090* Not available NTIS

PB96-204128
Life Prediction of a Continuous Fiber Reinforced Ceramic Composite Under Creep Conditions.
PB96-204128 *03,091* Not available NTIS

PB96-204136
Hybrid Optical-Electrical Overlay Test Structure.
PB96-204136 *02,450* Not available NTIS

PB96-204144
Properties of a Bose-Einstein Condensate in an Anisotropic Harmonic Potential.
PB96-204144 *04,133* Not available NTIS

PB96-204151
Deuterium Isotope Effect in Vinyl Radical Combination/Dispropor tionationReactions.
PB96-204151 *01,167* Not available NTIS

PB96-204169
Temperature Dependence of the Ultraviolet Absorption Cross Section of CF3I.
PB96-204169 *01,168* Not available NTIS

PB96-204177
Temperature Dependent Ultraviolet Absorption Cross Sections of Propylene, Methylacetylene and Vinylacetylene.
PB96-204177 *01,169* Not available NTIS

PB96-204185
Bulk Modulus and Young's Modulus of Nanocrystalline gamma-Alumina.
PB96-204185 *03,092* Not available NTIS

PB96-204193
Cavity Evolution during Tensil Creep of Si3N4.
PB96-204193 *03,376* Not available NTIS

PB96-204201
Mode-Locked Lasers for High-Accuracy Radiometry.
PB96-204201 *04,134* Not available NTIS

PB96-204417
Greenspan Acoustic Viscometer for Gases.
PB96-204417 *04,220* Not available NTIS

PB96-204425
Adhesion, Contact Electrification, and Acid-Base Properties of Surfaces.
PB96-204425 *03,693* Not available NTIS

PB96-204433
Role of Combustion on Droplet Transport in Pressure-Atomized Spray Flames.
PB96-204433 *01,434* Not available NTIS

PB96-204441
Improving Color Measurements of Displays.
PB96-204441 *02,203* Not available NTIS

PB96-204458
Shear Suppression of Critical Fluctuations in a Diluted Polymer Blend.
PB96-204458 *04,418* Not available NTIS

PB96-204466
Experimental Assessment of Crack-Tip Dislocation Emission Models for an Al67Cr8Ti25 Intermetallic Alloy.
PB96-204466 *03,377* Not available NTIS

PB96-204474
Alvin Van Valkenburg and the Diamond Anvil Cell.
PB96-204474 *04,797* Not available NTIS

PB96-204482
Phase Separation in Thin Film Polymer Blends With and Without Block Copolymer Additives.
PB96-204482 *01,294* Not available NTIS

PB96-204490
Correlations between Electrical and Acoustic Detection of Partial Discharge in Liquids and Implications for Continuous Data Recording.
PB96-204490 *02,248* Not available NTIS

PB96-204508
Determination of Acoustic Center Correction for Type LS2aP Condensor Microphones.
PB96-204508 *04,190* Not available NTIS

PB96-204516
Thermal Wave NDE of Advanced Materials Using Mirage Effect Detection.
PB96-204516 *04,191* Not available NTIS

PB96-204524
Creep and Creep Rupture of Structural Ceramics.
PB96-204524 *03,093* Not available NTIS

PB96-204532
Fracture Mechanism Maps: Their Applicability to Silicon Nitride.
PB96-204532 *03,094* Not available NTIS

PB96-210026
Rapid Evaluation of Mode-Stirred Chambers Using Impulsive Waveforms.
PB96-210026 *01,979* PC A04/MF A01

PB96-210059
Working Conference on Global Growth of Technology: Is America Prepared. Held in Gaithersburg, Maryland on December 7, 1995.
PB96-210059 *00,018* PC A07/MF A02

PB96-210141
Proceedings of the Open Forum on Laboratory Accreditation at the National Institute of Standards and Technology, October 13, 1995.
PB96-210141 *02,686* PC A10/MF A03

PB96-210695
Materials Aspects of Fiber-Reinforced Polymer Composites in Infrastructure.
PB96-210695 *03,184* PC A04/MF A01

PB96-210703
General Motion Model and Spatio-Temporal Filters for 3-D Motion Interpretations.
PB96-210703 *01,861* PC A07/MF A02

PB96-210711
Diffuse-Interface Description of Fluid Systems.
PB96-210711 *01,170* PC A04/MF A01

PB96-210745
Energy Price Indices and Discount Factors for Life-Cycle Cost Analysis 1997. Annual Supplement to NIST Handbook 135 and NBS Special Publication 709. (Revised).
PB96-210745 *02,512* PC A05/MF A01

PB96-210760
Report of a Workshop on Requalification of Tubular Steel Joints in Offshore Structures. Held in Houston, Texas on September 5-6, 1995.
PB96-210760 *03,699* PC A07/MF A02

PB96-210778
Bibliography of the NIST Electromagnetic Fields Division Publications.
PB96-210778 *01,980* PC A08/MF A02

PB96-210786
NIST Traceable Reference Material Program for Gas Standards: Standard Reference Materials.
PB96-210786 *00,644* PC A04/MF A01

PB96-210877
Statistical Aspects of the Certification of Chemical Batch SRMs. Standard Reference Materials.
PB96-210877 *00,645* PC A05/MF A01

PB96-210893
Flowmeter Installation Effects Due to a Generic Header.
PB96-210893 *02,606* PC A07/MF A02

PB96-214614
Airborne Asbestos Method: Bootstrap Method for Determining the Uncertainty of Asbestos Concentration. Version 1.0.
PB96-214614 *00,646* PC A04/MF A01

PB96-214622
Electronics and Electrical Engineering Laboratory Technical Publication Announcements Covering Laboratory Programs, January to March 1996, with 1996 EEEL Events Calendar.
PB96-214622 *01,981* PC A03/MF A01

PB96-214630
CSTL Technical Activities, 1995.
PB96-214630 *00,647* PC A10/MF A03

PB96-214648
Report on USDA Ultraviolet Spectroradiometers.
PB96-214648 *00,125* PC A04/MF A01

PB96-214697
Estimation of System Damping at the Lotung Site by Application of System Identification.
PB96-214697 *01,351* PC A10/MF A03

PB96-214705
State Weights and Measures Laboratories: Program Handbook.
PB96-214705 *02,687* PC A07/MF A02

PB96-214713
Shear Design of High-Strength Concrete Beams: A Review of the State-of-the-Art.
PB96-214713 *01,330* PC A11/MF A03

PB96-214747
Energy-Based Method for Liquefaction Potential Evaluation. Phase 1. Feasibility Study.
PB96-214747 *03,691* PC A13/MF A03

PB96-214754
Materials Science and Engineering Laboratory Annual Report, 1995. Technical Activities.
PB96-214754 *03,009* PC A05/MF A01

PB96-215074
Directory of U.S. Private Sector Product Certification Programs.
PB96-215074 *02,688* PC A20/MF A04

PB96-502794
Building Life Cycle Cost Computer Program (BLCC) Version 4.22-95 (for Micrcomputers).
PB96-502794 *00,277* CP D02

PB97-104160
January 17, 1995 Hyogoken-Nanbu (Kobe) Earthquake. Performance of Structures, Lifelines and Fire Protection Systems. Executive Summary and Paper.
PB97-104160 *00,475* PC A99/MF A06

PB97-104178
TBT Agreement Activities of the National Institute of Standards and Technology, 1995.
PB97-104178 *00,499* PC A04/MF A01

PB97-104186
Optoelectronics and Optomechanics Manufacturing: An ATP Focused Program Development. Workshop Proceedings. Held in Gaithersburg, Maryland on February 15, 1995.
PB97-104186 *02,204* PC A11/MF A03

PB97-104376
Wind and Seismic Effects: Proceedings of the Joint Meeting of the U.S.-Japan Cooperative Program in Natural Resources Panel on Wind and Seismic Effects (28th). Held in Gaithersburg, Maryland on May 14-17, 1996.
PB97-104376 *00,476* PC A99/MF A06

PB97-106843
Mathematical Analysis of Practices to Control Moisture in the Roof Cavities of Manufactured Houses.
PB97-106843 *00,278* PC A05/MF A01

PB97-108559
National Measurement System for Radiometry, Photometry, and Pyrometry Base Upon Absolute Detectors.
PB97-108559 *04,382* PC A04/MF A01

PB97-108575
NIST High-Accuracy Sampling Wattmeter.
PB97-108575 *02,689* PC A04/MF A01

PB97-108583
Technical Digest: Symposium on Optical Fiber Measurements (9th), 1996. Held in Boulder, Colorado on October 1-3, 1996.
PB97-108583 *04,383* PC A12/MF A03

PB97-109011
Journal of Research of the National Institute of Standards and Technology, May/June 1996. Volume 101, Number 3. Special Issue: NIST Workshop on Crystallographic Databases.
PB97-109011 *04,798* PC A11/MF A03

PB97-109029
CRYSTMET: The NRCC Metals Crystallographic Data File.
PB97-109029 *04,799*
(Order as PB97-109011, PC A11/MF A03)

PB97-109037
Inorganic Crystal Structure Database (ICSD) and Standardized Data and Crystal Chemical Characterization of Inorganic Structure Types (TYPIX): Two Tools for Inorganic Chemists and Crystallographers.
PB97-109037 *00,648*
(Order as PB97-109011, PC A11/MF A03)

PB97-109045
Evaluation of Crystallographic Data with the Program DIAMOND.
PB97-109045 *00,649*
(Order as PB97-109011, PC A11/MF A03)

PB97-109052
Cambridge Structural Database (CSD): Current Activities and Future Plans.
PB97-109052 *00,516*
(Order as PB97-109011, PC A11/MF A03)

PB97-109060
Protein Data Bank: Current Status and Future Challenges.
PB97-109060 *00,517*
(Order as PB97-109011, PC A11/MF A03)

PB97-109078
Nucleic Acid Database: Present and Future.
PB97-109078 *00,518*
(Order as PB97-109011, PC A11/MF A03)

PB97-109086
Powder Diffraction File: Past, Present, and Future.
PB97-109086 *04,800*
(Order as PB97-109011, PC A11/MF A03)

PB97-109094
NIST Crystallographic Databases for Research and Analysis.
PB97-109094 *04,801*
(Order as PB97-109011, PC A11/MF A03)

PB97-109102
Conventional and Eccentric Uses of Crystallographic Databases in Practical Materials Identification Problems.
PB97-109102 *04,802*
(Order as PB97-109011, PC A11/MF A03)

PB97-109110
Using NIST Crystal Data within Siemens Software for Four-Circle and SMART CCD Diffractometers.
PB97-109110 *04,803*
(Order as PB97-109011, PC A11/MF A03)

PB97-109128
Phase Identification in a Scanning Electron Microscope Using Backscattered Electron Kikuchi Patterns.
PB97-109128 *04,804*
(Order as PB97-109011, PC A11/MF A03)

PB97-109136
Biological Macromolecule Crystallization Database and NASA Protein Crystal Growth Archive.
PB97-109136 *01,171*
(Order as PB97-109011, PC A11/MF A03)

PB97-109144
Investigations of the Systematics of Crystal Packing Using the Cambridge Structural Database.
PB97-109144 *00,519*
(Order as PB97-109011, PC A11/MF A03)

PB97-109151
Troublesome Crystal Structures: Prevention, Detection, and Resolution.
PB97-109151 *01,172*
(Order as PB97-109011, PC A11/MF A03)

PB97-109169
CIF Crystallographic Information File: A Standard for Crystallographic Data Interchange.
PB97-109169 *04,805*
(Order as PB97-109011, PC A11/MF A03)

PB97-109177
Role of Journals in Maintaining Data Integrity: Checking of Crystal Structure Data in 'Acta Crystallographica'.
PB97-109177 *04,806*
(Order as PB97-109011, PC A11/MF A03)

PB97-109185
Electronic Publishing and the Journals of the American Chemical Society.
PB97-109185 *04,807*
(Order as PB97-109011, PC A11/MF A03)

PB97-109193
How the Cambridge Crystallographic Data Centre Obtains Its Information.
PB97-109193 *04,808*
(Order as PB97-109011, PC A11/MF A03)

PB97-109201
Data Import and Validation in the Inorganic Crystal Structure Database.
PB97-109201 *04,809*
(Order as PB97-109011, PC A11/MF A03)

PB97-109219
World Wide Web for Crystallography.
PB97-109219 *04,810*
(Order as PB97-109011, PC A11/MF A03)

PB97-109227
Workshop Highlights.
PB97-109227 *04,811*
(Order as PB97-109011, PC A11/MF A03)

PB97-110019
Role of Certified Reference Materials in Trace Analysis Quality Assurance.
PB97-110019 *00,650* Not available NTIS

PB97-110027
Flaw-Insensitive Ceramics.
PB97-110027 *03,095* Not available NTIS

PB97-110035
Radon in the Lung.
PB97-110035 *03,638* Not available NTIS

PB97-110043
Effect of Fuel Tank Rupture Mode on the Ignitability of Expelled Fuel.
PB97-110043 *01,444* Not available NTIS

PB97-110050
Flammability Characterization with the Lift Apparatus and the Cone Calorimeter.
PB97-110050 *01,435* Not available NTIS

PB97-110068
Letter Report on Flame Spread Testing of a Composite Material.
PB97-110068 *01,436* Not available NTIS

PB97-110076
Interaction of an Isolated Sprinkler Spray and a Two-Layer Compartment Fire Environment. Phenomena and Model Simulations.
PB97-110076 *01,437* Not available NTIS

PB97-110084
Liquid-Scintillation Counting Techniques for the Standardization of Radionuclides Used in Therapy.
PB97-110084 *03,709* Not available NTIS

PB97-110092
Needs for Brachytherapy Source Calibrations in the United States.
PB97-110092 *03,521* Not available NTIS

PB97-110100
Radioassays of Yttrium-90 Used in Nuclear Medicine.
PB97-110100 *03,522* Not available NTIS

PB97-110118
Compressed Liquid Densities, Saturated Liquid Densities, and Vapor Pressures of 1,1-Difluoroethane.
PB97-110118 *01,173* Not available NTIS

PB97-110126
Stacking the Cards in Europe: One Company's Story.
PB97-110126 *00,493* Not available NTIS

PB97-110134
Characterization of Two-Dimensional Dopant Profiles: Status and Review.
PB97-110134 *02,451* Not available NTIS

PB97-110142
Indoor Air Quality Commissioning of a New Office Building.
PB97-110142 *00,279* Not available NTIS

PB97-110159
Problem of Convection in the Water Absorbed Dose Calorimeter.
PB97-110159 *03,523* Not available NTIS

PB97-110167
Exact Series Solution to the Epstein-Hubbell Generalized Elliptic Type Integral Using Complex Variable Residue Theory.
PB97-110167 *03,423* Not available NTIS

PB97-110175
Stable Silicon Photodiodes for Absolute Intensity Measurements in the VUV and Soft X-ray Regions.
PB97-110175 *04,135* Not available NTIS

PB97-110183
Evaluation and Accreditation of State Calibration Laboratories.
PB97-110183 *00,486* Not available NTIS

PB97-110191
Hydrodynamic Friction of Arbitrarily Shaped Brownian Particles.
PB97-110191 *04,136* Not available NTIS

PB97-110209
Model of an Optical Roughness-Measuring Instrument.
PB97-110209 *04,384* Not available NTIS

PB97-110217
Examination Procedure Outlines: Keys to Solving the Handbook 44 Puzzle.
PB97-110217 *02,690* Not available NTIS

PB97-110225
Thin-Film Ruthenium Oxide - Iridium Oxide Thermocouples.
PB97-110225 *00,520* Not available NTIS

PB97-110233
Thin Film Thermocouple Research at NIST.
PB97-110233 *02,283* Not available NTIS

PB97-110241
Electrolytes Constrained on Fractal Structures: Debye-Huckel Theory.
PB97-110241 *01,174* Not available NTIS

PB97-110258
Tension/Compression Creep Asymmetry in Si3N4.
PB97-110258 *03,096* Not available NTIS

PB97-110266
Current Status and Trends in Temperature Measurements at NIST, Cooperative Projects and New Mutual Agreement between NIST and IMGC.
PB97-110266 *02,691* Not available NTIS

PB97-110274
Hypersingular Single Integral Equation and the Dielectric Wedge.
PB97-110274 *04,428* Not available NTIS

PB97-110282
Characterizing Materials Properties for Ceramic Matrix Composites.
PB97-110282 *03,097* Not available NTIS

PB97-110290
Database Development and Management (Project A.2.2): The Annual Report for 1992-1993.
PB97-110290 *03,098* Not available NTIS

PB97-110308
Role of Corrosion in a Material Selector Expert System for Advanced Structural Ceramics.
PB97-110308 *03,099* Not available NTIS

PB97-110316
Variances in the Measurement of Ceramic Powder Properties.
PB97-110316 *03,100* Not available NTIS

PB97-110324
Flaw-Tolerance and Crack-Resistance Properties of Alumina-Aluminum Titanate Composites with Tailored Microstructures.
PB97-110324 *03,101* Not available NTIS

PB97-110332
In situ-Toughened Silicon Carbide.
PB97-110332 *03,102* Not available NTIS

PB97-110340
Postfailure Subsidiary Cracking from Indentation Flaws in Brittle Materials.
PB97-110340 *03,103* Not available NTIS

PB97-110357
Heat Flux from Flames to Vertical Surfaces.
PB97-110357 *01,438* Not available NTIS

PB97-110365
Isopiestic Investigation of the Osmotic and Activity Coefficients of Aqueous NaBr and the Solubility of NaBr2H2O(cr) at 298.15 K: Thermodynamic Properties of the NaBr + H2O System over Wide Ranges of Temperature and Pressure.
PB97-110365 *01,175* Not available NTIS

PB97-110373
EPR Dosimetry of Cortical Bone and Tooth Enamel Irradiated with X and Gamma Rays: Study of Energy Dependence.
PB97-110373 *03,639* Not available NTIS

PB97-110381
Exposure-to-Absorbed-Dose Conversion for Human Adult Cortical Bone.
PB97-110381 *03,640* Not available NTIS

PB97-110399
Calculation of Photon Mass Energy-Transfer and Mass Energy-Absorption Coefficients.
PB97-110399 *04,137* Not available NTIS

PB97-110407
Electron-Photon Monte Carlo Calculations: The ETRAN Code.
PB97-110407 *04,138* Not available NTIS

PB97-110415
Optical Scattering from Moderately Rough Surfaces.
PB97-110415 *04,385* Not available NTIS

PB97-110423
Present and Future Standard Specimens for Surface Finish Metrology.
PB97-110423 *02,928* Not available NTIS

PB97-110431
Proposed Coating Technology Consortium. (National Coil Coaters Association Fall Conference). Held in Rosemont, Illinois in September 1992.
PB97-110431 *03,129* Not available NTIS

PB97-110449
Interlaboratory Studies on the Analysis of Hair for Drugs of Abuse: Results from the Fifth Exercise.
PB97-110449 *03,509* Not available NTIS

PB97-110456
High Temperature Structural Reliability of Silicon Nitride.
PB97-110456 *03,104* Not available NTIS

PB97-110464
Tensile Creep Testing of Structural Ceramics.
PB97-110464 *03,105* Not available NTIS

PB97-110472
Compensation of Errors Detected by Process-Intermittent Gauging.
PB97-110472 *02,846* Not available NTIS

PB97-110480
Data Management for Error Compensation and Process Control.
PB97-110480 *02,847* Not available NTIS

PB97-110498
Introduction to Secure Telephone Terminals.
PB97-110498 *01,512* Not available NTIS

PB97-110506
Compensation for Errors Introduced by Nonzero Fringe Densities in Phase-Measuring Interferometers.
PB97-110506 *04,386* Not available NTIS

PB97-110514
USCEA/NIST Measurement Assurance Programs for the Radiopharmaceutical and Nuclear Power Industries.
PB97-110514 *03,721* Not available NTIS

PB97-110522
Causality and Maxwell's Equations.
PB97-110522 *04,429* Not available NTIS

PB97-110530
Electromagnetic Scattering from a Dielectric Wedge and the Single Hypersingular Integral Equation.
PB97-110530 *04,430* Not available NTIS

PB97-110548
Light Scattering by Sinusoidal Surfaces: Illumination Windows and Harmonics in Standards.
PB97-110548 *04,387* Not available NTIS

PB97-110555
Numerical Evaluation of Hypersingular Integrals for Scattering by a Dielectric Wedge.
PB97-110555 *02,017* Not available NTIS

PB97-110563
Point Charges, Radiation Reaction, and Quantum Mechanics.
PB97-110563 *04,139* Not available NTIS

PB97-110571
Positronium in Relativistic Quantum Mechanics.
PB97-110571 *04,140* Not available NTIS

PB97-110589
Relativistic Quantum Mechanics of Interacting Particles.
PB97-110589 *04,141* Not available NTIS

PB97-110597
Sinusoidal Surfaces as Standards for BRDF Instruments.
PB97-110597 *04,388* Not available NTIS

PB97-110605
Spinor Equations in Relativistic Quantum Mechanics.
PB97-110605 *04,142* Not available NTIS

PB97-110811
Computer Security: Generally Accepted Principles and Practices for Securing Information Technology Systems.
PB97-110811 *01,619* PC A05/MF A01

PB97-111215
Windowing Effects on Light Scattering by Sinusoidal Surfaces.
PB97-111215 *04,389* Not available NTIS

PB97-111223
Resonance Enhanced Multiphoton Ionization Spectroscopy of the SnF Radical.
PB97-111223 *01,176* Not available NTIS

PB97-111231
Characterization and Processing of Spray-Dried Zirconia Powders for Plasma Spray Application.
PB97-111231 *04,419* Not available NTIS

PB97-111249
Relationship between Indoor Air Quality and Carbon Dioxide.
PB97-111249 *02,569* Not available NTIS

PB97-111256
Beam Line for Highly Charged Ions.
PB97-111256 *04,143* Not available NTIS

PB97-111264
Quantum Conductance Fluctuations in the Larger-Size-Scale Regime.
PB97-111264 *04,144* Not available NTIS

PB97-111272
Magneto-Optic Rotation Sensor Using a Laser Diode as Both Source and Detector.
PB97-111272 *04,390* Not available NTIS

PB97-111280
Laser Cooling and the Recoil Limit.
PB97-111280 *04,391* Not available NTIS

PB97-111298
Post-Occupancy Evaluation of the Forrestal Building.
PB97-111298 *00,280* Not available NTIS

PB97-111306
Size Effects and Giant Magnetoresistance in Unannealed NiFe/Ag Multilayer Stripes.
PB97-111306 *04,145* Not available NTIS

PB97-111314
Fluoride Elimination Upon Reaction of Pentafluoroaniline with e (sub eq')(sup -), H, and OH Radicals in Aqueous Solution.
PB97-111314 *01,177* Not available NTIS

PB97-111322
Interlaboratory Studies on the Analysis of Hair for Drugs of Abuse: Results from the Fourth Exercise.
PB97-111322 *03,510* Not available NTIS

PB97-111330
Numerical Reference Models for Optical Metrology Simulation.
PB97-111330 *04,392* Not available NTIS

PB97-111413
Commercial Helium Permeation Leak Standards: Their Properties and Reliability.
PB97-111413 *04,146* Not available NTIS

PB97-111421
Extrapolation of the Heat Capacity in Liquid and Amorphous Phases.
PB97-111421 *04,147* Not available NTIS

PB97-111439
Double Modulation and Selective Excitation Photoreflectance for Characterizing Highly Luminescent Semiconductor Structures and Samples with Poor Surface Morphology.
PB97-111439 *02,452* Not available NTIS

PB97-111447
Thermodynamic Properties of Synthetic Otavite, CdCO3(cr): Enthalpy Increment Measurements from 4.5 K to 350 K.
PB97-111447 *00,680* Not available NTIS

PB97-111454
Proposed Tests to Evaluate the Frequency-Dependent Capacitor Ratio for Single Electron Tunneling Experiment.
PB97-111454 *01,982* Not available NTIS

PB97-111462
Mechanism of Defect Formation in Low-Dose Oxygen Implanted Silicon-on-Insulator Material.
PB97-111462 *02,453* Not available NTIS

PB97-111470
Closed Loop Controller for Electron-Beam Evaporators.
PB97-111470 *04,393* Not available NTIS

PB97-111488
Heap of Data.
PB97-111488 *03,424* Not available NTIS

PB97-111496
Pulse-Driven Programmable Josephson Voltage Standard.
PB97-111496 *04,148* Not available NTIS

PB97-111504
Internal Waves in Xenon Near the Critical Point.
PB97-111504 *04,221* Not available NTIS

PB97-111512
Transient Errors in a Precision Resistive Divider.
PB97-111512 *01,983* Not available NTIS

PB97-111520
High Power Generation with Distributed Josephson-Junction Arrays.
PB97-111520 *02,099* Not available NTIS

PB97-111538
Ionization Energies, Appearance Energies and Thermochemistry of CF2O and FCO.
PB97-111538 *01,178* Not available NTIS

PB97-111546
Experimental Verification of a Moisture and Heat Transfer Model in the Hygroscopic Regime.
PB97-111546 *00,309* Not available NTIS

PB97-111553
Testing Conformance and Interoperability of BACnet (Trade Name) Building Automation Products.
PB97-111553 *00,310* Not available NTIS

PB97-111561
Representing Designs with Logic Formulations of Spatial Relations.
PB97-111561 *02,792* Not available NTIS

PB97-111579
Using Logic to Specify Shapes and Spatial Relations in Design Grammars
PB97-111579 *02,793* Not available NTIS

PB97-111587
Neutron Diffraction Texture Study of Deformed Uranium Plates.
PB97-111587 *03,010* Not available NTIS

PB97-111595
Calcium Phosphate Cements.
PB97-111595 *03,580* Not available NTIS

PB97-111603
63Ni Half-Life: A New Experimental Determination and Critical Review.
PB97-111603 *00,700* Not available NTIS

PB97-111819
Nickel-63 Standardization: 1968-1995.
PB97-111819 *00,701* Not available NTIS

PB97-111827
Electrical Test Structures Replicated in Silicon-on-Insulator Material.
PB97-111827 *02,454* Not available NTIS

PB97-111835
Fundamentals and Problems of Fiber Current Sensors.
PB97-111835 *02,205* Not available NTIS

PB97-111843
Uncertainties of Frequency Response Estimates Derived from Responses to Uncertain Step-Like Inputs.
PB97-111843 *01,984* Not available NTIS

PB97-111850
Measurement Comparability, Traceability, and Measurement Assurance Programs.
PB97-111850 *02,692* Not available NTIS

PB97-111868
X-ray Reflectivity Determination of Interface Roughness Correlated with Transport Properties of (AlGa)As/GaAs High Electron Mobility Transistor Devices.
PB97-111868 *04,149* Not available NTIS

PB97-111876
Resistors.
PB97-111876 *02,284* Not available NTIS

PB97-111884
Loading Effects in Resistance Scaling.
PB97-111884 *02,285* Not available NTIS

PB97-111892
Test Procedures for Advanced Insulation Panels.
PB97-111892 *00,415* Not available NTIS

PB97-111900
Compatibilization of Polymer Blends by Complexation. 2. Kinetics of Interfacial Mixing.
PB97-111900 *01,295* Not available NTIS

PB97-111918
Optical and Mass Spectrometric Investigations of Ions and Neutral Species in SF6 Radio-Frequency Discharges.
PB97-111918 *01,985* Not available NTIS

PB97-111926
New Refractometer by Combining a Variable Length Vacuum Cell and a Double-Pass Michelson Interferometer.
PB97-111926 *01,986* Not available NTIS

PB97-111934
Intrinsic Conductivity of Objects Having Arbitrary Shape and Conductivity.
PB97-111934 *04,150* Not available NTIS

PB97-111942
Observation of Two Length Scales Above (T sub N) in a Holmium Thin Film.
PB97-111942 *04,151* Not available NTIS

PB97-111959
Measurement and Reduction of Alignment Errors of the NIST Watt Experiment.
PB97-111959 *01,987* Not available NTIS

PB97-111967
One-Electron Oxidation of Metalloporphycenes as Studied by Radiolytic Methods.
PB97-111967 *01,179* Not available NTIS

PB97-111975
Oxidation of Caffeic Acid and Related Hydroxycinnamic Acids.
PB97-111975 *00,651* Not available NTIS

PB97-111983
DNA Damage and DNA Sequence Retrieval from Ancient Tissues.
PB97-111983 *03,556* Not available NTIS

PB97-111991
Empirical Validation of a Transient Computer Model for Combined Heat and Moisture Transfer.
PB97-111991 *00,416* Not available NTIS

PB97-112007
Observation of Hot-Electron Shot Noise in a Metallic Resistor.
PB97-112007 *01,988* Not available NTIS

PB97-112213
Calibration in the Earth Observing System (EOS) Project. Part 2. Implementation.
PB97-112213 *04,842* Not available NTIS

PB97-112221
HVAC CAD Layout Tools: A Case Study of University/Industry Collaboration.
PB97-112221 *00,281* Not available NTIS

PB97-112239
Systematic Correction in Bragg X-ray Diffraction of Flat and Curved Crystals.
PB97-112239 *04,152* Not available NTIS

PB97-112247
Chip Morphology, Tool Wear and Cutting Mechanics in Finish Hard Turning.
PB97-112247 *03,106* Not available NTIS

PB97-112254
Laser Bandwidth Effects in Quantitative Cavity Ring-Down Spectroscopy.
PB97-112254 *04,394* Not available NTIS

PB97-112262
Lattice Model of a Hydrogen-Bonded Polymer Blend.
PB97-112262 *03,391* Not available NTIS

PB97-112270
Analysis of Droplet Arrival Statistics in a Pressure-Atomized Spray Flame.
PB97-112270 *01,352* Not available NTIS

PB97-112288
Forward Scattering of a Gaussian Beam by a Nonabsorbing Sphere.
PB97-112288 *04,395* Not available NTIS

PB97-112296
Interdigitated Stacked P-I-N Multiple Quantum Well Modulator.
PB97-112296 *02,455* Not available NTIS

PB97-112304
Vitrification and Crystallization of Organic Liquids Confined to Nanoscale Pores.
PB97-112304 *03,392* Not available NTIS

PB97-112312
Factors Affecting the Energy Consumption of Two Refrigerator-Freezers.
PB97-112312 *00,311* Not available NTIS

PB97-112320
Combining Interactive Exploration and Optimization for Assembly Design.
PB97-112320 *02,794* Not available NTIS

PB97-112338
Development of Thin-Film Multijunction Thermal Converters at NIST.
PB97-112338 *02,286* Not available NTIS

PB97-112346
Bias Current Dependent Resistance Peaks in NiFe/Ag Giant Magnetoresistance Multilayers.
PB97-112346 *04,153* Not available NTIS

PB97-112353
Empirical Linear Prediction Applied to a NIST Calibration Service.
PB97-112353 *02,287* Not available NTIS

PB97-112361
Absorption Cross Sections, Kinetics of Formation, and Self-Reaction of the IO Radical Produced via the Laser Photolysis of N2O/I2/N2 Mixtures.
PB97-112361 *01,180* Not available NTIS

PB97-112379
High-Current Thin Film Multijunction Thermal Converters and Multi-Converter Modules.
PB97-112379 *01,989* Not available NTIS

PB97-112387
Isolated Spin Pairs and Two-Dimensional Magnetism in SrCr(sub 9p)Ga(sub 12-9p)O19.
PB97-112387 *04,154* Not available NTIS

PB97-112395
Using Technology to Manage and Protect Intellectual Property.
PB97-112395 *01,513* Not available NTIS

PB97-112403
Matrix Isolation Study of the Interaction of Excited Neon Atoms with O3: Infrared Spectrum of O((sub 3)(-)) and Evidence for the Stabilization of O2...O((sub 4)(+)).
PB97-112403 *04,155* Not available NTIS

PB97-112411
Neutron Scattering Study of Antiferromagnetic Order in the Magnetic Superconductors RNi2B2C.
PB97-112411 *04,812* Not available NTIS

PB97-112429
Unconventional Ferromagnetic Transition in La(sub 1-x)Ca(sub x)MnO3.
PB97-112429 *04,156* Not available NTIS

PB97-112437
Use of Neutron Beams for Chemical Analysis at NIST.
PB97-112437 *00,652* Not available NTIS

PB97-112445
Measurement of Ascorbic Acid in Human Plasma and Serum: Stability, Intralaboratory Repeatability, and Interlaboratory Reproducibility.
PB97-112445 *03,511* Not available NTIS

PB97-112452
Low Thermal Guarded Scanner for High Resistance Measurement Systems.
PB97-112452 *02,288* Not available NTIS

PB97-112460
Ferric Ion Assisted Photooxidation of Halocetates.
PB97-112460 *00,521* Not available NTIS

PB97-112478
In situ Characterization of Vapor Phase Growth of Iron Oxide-Silica Nanocomposites: Part 1. 2-D Planar Laser-Induced Fluorescence and Mie Imaging.
PB97-112478 *03,185* Not available NTIS

PB97-112486
Evidence of Crosslinking in Methyl Pendent PBZT Fiber.
PB97-112486 *03,393* Not available NTIS

PB97-112494
Relaxation After a Temperature Jump Within the One Phase Region of a Polymer Mixture.
PB97-112494 *03,394* Not available NTIS

PB97-112502
Knowledge-Based Approach for Automating a Design Method for Concurrent and Real-Time Systems.
PB97-112502 *01,780* Not available NTIS

PB97-112510
Adsorption of Polyacrylic Acids and Their Sodium Salts on Hydroxyapatite: Effect of Relative Molar Mass.
PB97-112510 *03,581* Not available NTIS

PB97-112528
Thermochemical Studies of Inorganic Chalocogenides by Fluorine-Combustion Calorimetry: Binary Compounds of Germanium and Silicon with Sulfur, Selenium and Tellurium.
PB97-112528 *01,181* Not available NTIS

PB97-112536
Thermodynamics of (Germanium + Selenium): A Review and Critical Assessment.
PB97-112536 *01,182* Not available NTIS

PB97-112544
Characterization of Modified FEL Quartz-Halogen Lamps for Photometric Standards.
PB97-112544 *00,282* Not available NTIS

PB97-112551
Exploring the Low-Frequency Performance of Thermal Converters Using Circuit Models and a Digitally Synthesized Source.
PB97-112551 *02,848* Not available NTIS

PB97-112569
Low Voltage Standards in the 10 Hz to 1 MHz Range.
PB97-112569 *02,100* Not available NTIS

PB97-112577
Atmospheric Lifetimes of HFC-143a and HFC-245fa: Flash Photolysis Resonance Fluorescence Measurements of the OH Reaction Rate Constants.
PB97-112577 *00,118* Not available NTIS

PB97-112585
Modeling Effects of Temperature Annealing on Giant Magnetoresistive Response in Discontinuous Multilayer NiFe/Ag Films.
PB97-112585 *04,157* Not available NTIS

PB97-112593
Simulating Device Size Effects on Magnetization Pinning Mechanisms in Spin Valves.
PB97-112593 *04,158* Not available NTIS

PB97-112601
Chemical Aspects of Tool Wear in Single Point Diamond Turning.
PB97-112601 *03,021* Not available NTIS

PB97-113013
NIST Thermal Infrared Transfer Standard Radiometer for the Earth Observing System (EOS) Program.
PB97-113013 *04,843* Not available NTIS

PB97-113021
Results of a NIST/VNIIOFI Comparison of Spectral-Radiance Measurements.
PB97-113021 *04,159* Not available NTIS

PB97-113039
Wideband Sampling Voltmeter.
PB97-113039 *01,990* Not available NTIS

PB97-113047
In-situ Studies of a Novel Sodium Flame Process for Synthesis of Fine Particles.
PB97-113047 *00,681* Not available NTIS

PB97-113054
Optical and Modeling Studies of Sodium/Halide Reactions for the Formation of Titanium and Boron Nanoparticles.
PB97-113054 *00,682* Not available NTIS

PB97-113062
NIST Watt Balance: Progress Toward Monitoring the Kilogram.
PB97-113062 *01,991* Not available NTIS

PB97-113070
Colossal Magnetoresistance without Mn(3+)/Mn(4-) Double Exchange in the Stoichiometric Pyrochlore Tl2Mn2O7.
PB97-113070 *04,160* Not available NTIS

PB97-113088
Dimensional Crossover in the Phase Separation Kinetics of Thin Polymer Blend Films.
PB97-113088 *03,395* Not available NTIS

PB97-113096
Improving the Design Process by Predicting Downstream Values of Design Attributes.
PB97-113096 *02,795* Not available NTIS

PB97-113104
Polarization Measurements on a Magnetic Quadrupole Line in Ne-Like Barium.
PB97-113104 *04,161* Not available NTIS

PB97-113112
Molecular Dynamics Investigation of the Surface/Bulk Equilibrium in an Ethanol-Water Solution.
PB97-113112 *01,183* Not available NTIS

PB97-113120
International Standards and Reference Materials.
PB97-113120 *00,188* Not available NTIS

PB97-113138
Measurement of Process Complexity.
PB97-113138 *01,781* Not available NTIS

PB97-113146
Microstructure Effect on the Phase Behavior of Blends of Deuterated Polybutadiene and Protonated Polyisopene.
PB97-113146 *01,296* Not available NTIS

PB97-113153
Critical Evaluation of Thermal Mass Flow Meters.
PB97-113153 *00,683* Not available NTIS

PB97-113161
Comparison of Filter Radiometer Spectral Responsivity with the NIST Spectral-Irradiance and Illuminance Scales.
PB97-113161 *04,162* Not available NTIS

PB97-113179
Integrated Optical Polarization-Discriminating Receiver in Glass.
PB97-113179 *02,206* Not available NTIS

PB97-113187
Frequency Synthesis and Metrology at 10(-17) and Beyond.
PB97-113187 *02,101* Not available NTIS

PB97-113195
Reducing the 1/f AM and PM Noise in Electronics for Precision Frequency Metrology.
PB97-113195 *02,102* Not available NTIS

PB97-113203
CONTAM94: A Multizone Airflow and Contaminant Dispersal Model with a Graphic User Interface.
PB97-113203 *02,570* Not available NTIS

PB97-113211
DC-MHz Wattmeter Based on RMS Voltage Measurements.
PB97-113211 *01,992* Not available NTIS

PB97-113229
Design of a High-Pressure Ebulliometer, with Vapor-Liquid Equilibrium Results for the Systems CHF2Cl + CF3-CH3 and CF3-CH2F + CH2F2.
PB97-113229 *04,163* Not available NTIS

PB97-113237
Vapor Pressure of 1,1,1,2,2-Pentafluoropropane.
PB97-113237 *00,684* Not available NTIS

PB97-113245
Dynamics of Multi-DOF Stochastic Nonlinear Systems.
PB97-113245 *00,477* Not available NTIS

PB97-113252
Magnetometer Calibration Services.
PB97-113252 *01,993* Not available NTIS

PB97-113260
Use of a Naphthylethylcarbamoylated- beta-Cyclodextrin Chiral Stationary Phase for the Separation of Drug Enantiomers and Related Compounds by Sub- and Supercritical Fluid Chromatography.
PB97-113260 *00,653* Not available NTIS

PB97-113278
Diffraction of Neutron Standing Waves in Thin Films with Resonance Enhancement.
PB97-113278 *04,164* Not available NTIS

PB97-113286
Results of Capacitance Ratio Measurements for the Single Electron Pump-Capacitor Charging Experiment.
PB97-113286 *04,813* Not available NTIS

PB97-113781
Conformance Testing and Specification Management.
PB97-113781 *02,849* PC A03/MF A01

PB97-113799
Representation of Axes for Geometric Fitting.
PB97-113799 *01,782* PC A03/MF A01

PB97-113880
Electronics and Electrical Engineering Laboratory Technical Progress Bulletin Covering Laboratory Programs, April to June 1996 with 1996-1998 EEEL Events Calendar.
PB97-113880 *01,994* PC A04/MF A01

PB97-113898
Static Structural Analysis of a Reconfigurable Rigid Platform Supported by Elastic Legs.
PB97-113898 *02,960* PC A05/MF A01

PB97-113906
Experimental Models for Software Diagnosis.
PB97-113906 *01,783* PC A04/MF A01

PB97-114169
Structured Testing: A Testing Methodology Using the Cyclomatic Complexity Metric.
PB97-114169 *01,784* PC A07/MF A02

PB97-114185
National Voluntary Laboratory Accreditation Program (NVLAP): Fasteners and Metals.
PB97-114185 *02,881* PC A06/MF A01

PB97-114227
Carbon Monoxide Dispersion in Residential Buildings: Literature Review and Technical Analysis.
PB97-114227 *02,571* PC A05/MF A01

PB97-114235
Survey of Fuel Loads in Contemporary Office Buildings.
PB97-114235 *00,233* PC A04/MF A01

PB97-114250
Summary of Federal Construction and Building R and D in 1994.
PB97-114250 *00,234* PC A04/MF A01

PB97-114268
Interoperability Requirements for CAD Data Transfer in the AutoSTEP Project.
PB97-114268 *02,796* PC A03/MF A01

PB97-114359
India: Environmental Technologies Export Market Plan.
PB97-114359 *02,529* PC A05/MF A01

PB97-114474
Experimentally Measured Total X-ray Attenuation Coefficients Extracted from Previously Unprocessed Documents Held by the NIST Photon and Charged Particle Data Center.
PB97-114474 *04,165* PC A04/MF A01

PB97-114482
Fire Safety Engineering in the Pursuit of Performance-Based Codes: Collected Papers.
PB97-114482 *00,235* PC A07/MF A02

PB97-115794
Proceedings of a Workshop on Developing and Adopting Seismic Design and Construction Standards for Lifelines. Held in Denver, Colorado on September 25-27, 1991.
PB97-115794 *01,302* PC A16/MF A03

PB97-115802
Multi-Scale Picture of Concrete and Its Transport Properties: Introduction for Non-Cement Researchers.
PB97-115802 *03,107* PC A05/MF A01

PB97-116040
Bibliography of the NIST Optoelectronics Division.
PB97-116040 *02,207* PC A06/MF A01

PB97-116057
Metrology for Electromagnetic Technology: A Bibliography of NIST Publications.
PB97-116057 *04,396* PC A06/MF A01

PB97-116073
Group 1 for the Process Engineering Data STEP Application Protocol.
PB97-116073 *02,797* PC A99/MF A06

PB97-116081
Full-Scale Room Fire Experiments Conducted at the University of Maryland.
PB97-116081 *00,236* PC A04/MF A01

PB97-116107
Intracycle Evaporative Cooling in a Vapor Compression Cycle.
PB97-116107 *02,762* PC A03/MF A01

PB97-116123
Unified Process Specification Language: Requirements for Modeling Process.
PB97-116123 *02,850* PC A06/MF A01

PB97-116131
Fire Protection Foam Behavior in a Radiative Environment.
PB97-116131 *00,237* PC A10/MF A02

PB97-116206
Standards Promote Credibility and Technology Transfer: The Need for Greater Industry Support of Technical Committees.
PB97-116206 *02,961* PC A03/MF A01

PB97-116222
Evaluation of Survey Procedures for Determining Occupant Load Factors in Contemporary Office Buildings.
PB97-116222 *00,238* PC A03/MF A01

PB97-118335
Majority and Minority Electron and Hole Mobilities in Heavily Doped Gallium Aluminum Arsenide.
PB97-118335 *04,814* Not available NTIS

PB97-118343
Excitons in Complex Quantum Nanostructures.
PB97-118343 *01,184* Not available NTIS

PB97-118350
Quantum Dots in Quantum Well Structures.
PB97-118350 *01,185* Not available NTIS

PB97-118368
Issues in High-Speed Pyrometry.
PB97-118368 *02,693* Not available NTIS

PB97-118376
Simultaneous Measurement of Normal Spectral Emissivity by Spectral Radiometry and Laser Polarimetry at High Temperatures in Pulse-Heating Experiments: Application to Molybdenum and Tungsten.
PB97-118376 *02,694* Not available NTIS

PB97-118384
Thermodynamic Properties of CF3-CHF-CHF2, 1,1,1,2,3,3-Hexafluoropropane.
PB97-118384 *03,299* Not available NTIS

PB97-118392
Thermodynamic Properties of CHF2-CF2-CHF, 1,1,2,2,3-Pentafluoropropane.
PB97-118392 *03,300* Not available NTIS

PB97-118400
Swelling and Growth of Polymers, Membranes and Sponges.
PB97-118400 *03,396* Not available NTIS

PB97-118616
Effect of Beam Voltage on the Properties of Aluminum Nitride Prepared by Ion Beam Assisted Deposition.
PB97-118616 *01,995* Not available NTIS

PB97-118624
Posterior Restorative Materials Research.
PB97-118624 *03,582* Not available NTIS

PB97-118632
NIST Research on Less-Flammable Materials.
PB97-118632 *01,439* Not available NTIS

PB97-118640
Realization of a Scale of Absolute Spectral Response Using the NIST High Accuracy Cryogenic Radiometer.
PB97-118640 *04,397* Not available NTIS

PB97-118657
Bimolecular Interactions in (Et)3SiOH:Base:CCl4 Hydrogen-Bonded Solutions Studied by Deactivation of the Free OH-Stretch Vibration.
PB97-118657 *04,166* Not available NTIS

PB97-118665
Lab Report Special Section: Natural Language Processing and Information Retrieval Group Information Access and User Interfaces Division, National Institute of Standards and Technology.
PB97-118665 *02,742* Not available NTIS

PB97-118673
Panel: Building and Using Test Collections.
PB97-118673 *02,743* Not available NTIS

PB97-118681
Transient Analysis of a Line-Focus Transducer Probing a Liquid/Solid Interface.
PB97-118681 *02,763* Not available NTIS

PB97-118699
Radiance Temperatures at 1500 nm of Niobium and Molybdenum at Their Melting Points by a Pulse-Heating Technique.
PB97-118699 *04,167* Not available NTIS

PB97-118707
Developing Measurement for Experimentation.
PB97-118707 *03,450* Not available NTIS

PB97-118715
Pilot Studies for Improving Sampling Protocols.
PB97-118715 *02,530* Not available NTIS

PB97-118723
Microwave Spectrum and Structure of CH2O-H2O.
PB97-118723 *04,168* Not available NTIS

PB97-118731
Sources of Strain-Measurement Error in Flag-Based Extensometry.
PB97-118731 *03,108* Not available NTIS

PB97-118749
Materials-Science Based Approach to Phenol Emissions from a Flooring Material in an Office Building.
PB97-118749 *02,572* Not available NTIS

PB97-118756
Colour Centres in LiF for Measurement of Absorbed Doses Up to 100 MGy.
PB97-118756 *04,169* Not available NTIS

PB97-118764
Capabilities for Product Data Exchange.
PB97-118764 *02,798* Not available NTIS

PB97-118772
Shear-Induced Changes in the Order-Disorder Transition Temperature and the Morphology of a Triblock Copolymer.
PB97-118772 *03,130* Not available NTIS

PB97-118780
Overview of Bioelectrical Impedance Analyzers.
PB97-118780 *00,181* Not available NTIS

PB97-118798
Rotational Spectra of CH3CCH-NH3, NCCCH-NH3, and NCCCH-OH2.
PB97-118798 *04,170* Not available NTIS

PB97-118806
Issues in the Field Measurement of VOC Emission Rates.
PB97-118806 *02,573* Not available NTIS

PB97-118996
Line-Heat-Source Guarded-Hot-Plate Apparatus.
PB97-118996 *00,417* Not available NTIS

PB97-119002
Segmental Concentration Profiles of End-Tethered Polymers with Excluded-Volume and Surface Interactions.
PB97-119002 *00,654* Not available NTIS

PB97-119010
Surface Roughness of Glass-Ceramic Insert. Composite Restorations: Assessing Several Polishing Techniques.
PB97-119010 *03,583* Not available NTIS

PB97-119028
Effect of Formulation Changes on the Response to Ionizing Radiation of Radiochromic Dye Films.
PB97-119028 *04,171* Not available NTIS

PB97-119036
Results of the ASTM Nuclear Methods Intercomparison on NIST Apple and Peach Leaves Standard Reference Materials.
PB97-119036 *03,490* Not available NTIS

PB97-119044
Making Connections.
PB97-119044 *01,785* Not available NTIS

PB97-119051
Measurements of the (235)U(n,f) Cross Section in the 3 to 30 MeV Neutron Energy Region.
PB97-119051 *04,172* Not available NTIS

PB97-119069
Measurements of the (237)Np(n,f) Cross Section.
PB97-119069 *04,173* Not available NTIS

PB97-119077
Influence of Envelopes Geometry on the Sensitivity of 'Nude' Ionization Gauges.
PB97-119077 *04,174* Not available NTIS

PB97-119085
Mass Assay and Uniformity Test of Boron Targets by Neutron Beam Methods.
PB97-119085 *04,175* Not available NTIS

PB97-119101
Design of Technically Complex Facilities.
PB97-119101 *02,695* Not available NTIS

PB97-119119
Resonance Enhanced Multiphoton Ionization Spectroscopy of the PF Radical.
PB97-119119 *00,702* Not available NTIS

PB97-119127
Kinetics of the Reaction of the Sulfate Radical with the Oxalate Anion.
PB97-119127 *01,186* Not available NTIS

PB97-119135
Morphology and Phase Separation Kinetics of a Compatibilized Blend.
PB97-119135 *01,297* Not available NTIS

PB97-119143
Matrix Isolation Study of the Interaction of Excited Neon Atoms with BCl3: Infrared Spectra of BCl(sub 3, sup +), BCl(sub 2, sup +), and BCl(sub 3, sup -).
PB97-119143 *01,187* Not available NTIS

PB97-119150
Automated Guarded Bridge for Calibration of Multimegohm Standard Resistors.
PB97-119150 *02,289* Not available NTIS

PB97-119168
Resistance Measurements from 10 M Omega to 1 T Omega at NIST.
PB97-119168 *02,290* Not available NTIS

PB97-119176
Conversion of a 2-Terminal-Pair Bridge to a 4-Terminal-Pair Bridge for Increased Range and Precision in Impedance Measurements.
PB97-119176 *02,103* Not available NTIS

PB97-119184
NIST Comparison of the Quantized Hall Resistance and the Realization of the SI Ohm Through the Calculable Capacitor.
PB97-119184 *02,291* Not available NTIS

PB97-119192
NIST Comparison of the Quantized Hall Resistance and the Realization of the SI Ohm Through the Calculable Capacitor. Conference Proceedings, June 17-20, 1996.
PB97-119192 *02,292* Not available NTIS

PB97-119200
Specular and Diffuse Reflection Measurements of Electronic Displays.
PB97-119200 *02,208* Not available NTIS

PB97-119218
Computations of Enhanced Soot Production in Time-Varying CH4/Air Diffusion Flames.
PB97-119218 *01,440* Not available NTIS

PB97-119226
National Status and Trends Program Specimen Bank: Sampling Protocols, Analytical Methods, Results, and Archive Samples.
PB97-119226 *02,598* Not available NTIS

PB97-119234
Vibrational Spectra of Molecular Ions Isolated in Solid Neon. 13. Ions Derived from HBr and HI.
PB97-119234 *01,188* Not available NTIS

PB97-119242
Comparisons of Some NIST Fixed-Point Cells with Similar Cells of Other Standards Laboratories.
PB97-119242 *00,655* Not available NTIS

PB97-119259
Novel Radiochromic Films for Clinical Dosimetry.
PB97-119259 *03,641* Not available NTIS

PB97-119267
Internal Droplet Circulation Induced by Surface-Driven Rotation.
PB97-119267 *02,500* Not available NTIS

PB97-119275
Orientational Fluctuations, Diffuse Scattering, and Orientational Order in Solid C60.
PB97-119275 *04,176* Not available NTIS

PB97-119283
Micromachined Coplanar Waveguides in CMOS Technology.
PB97-119283 *02,456* Not available NTIS

PB97-119291
Calibration and Performance of GafChromic DM-100 Radiochromic Dosemeters.
PB97-119291 *00,703* Not available NTIS

PB97-119309
Interaction of Citric Acid with Hydroxyapatite: Surface Exchange of Ions and Precipitation of Calcium Citrate.
PB97-119309 *03,584* Not available NTIS

PB97-119317
Active High Voltage Divider with 20-PPM Uncertainty.
PB97-119317 *02,104* Not available NTIS

PB97-119325
Transport by Gravity Currents in Building Fires.
PB97-119325 *01,441* Not available NTIS

PB97-119333
Liquid Chromatographic Determination of Carotenoids in Human Serum Using an Engineered C30 and a C18 Stationary Phase.
PB97-119333 *03,512* Not available NTIS

PB97-119341
Self-Consistent 'GW' and Higher-Order Calculations of Electron States in Metals.
PB97-119341 *01,189* Not available NTIS

PB97-119358
Thermodynamic Properties of Silicides. 5. Standard Molar Enthalpy of Formation at the Temperature 298.15 K of Trimolybdenum Monosilicide Mo3Si Determined by Fluorine-Combustion Calorimetry.
PB97-119358 *01,190* Not available NTIS

PB97-119366
Electronic Structure and Phase Equilibria in Ternary Substitutional Alloys.
PB97-119366 *03,378* Not available NTIS

PB97-119374
Positive and Negative Cooperativities at Subsequent Steps of Oxygenation Regulate the Allosteric Behavior of Multistate Sebacylhemoglobin.
PB97-119374 *03,486* Not available NTIS

PB97-119382
DnaJ, DnaK, and GrpE Heat Shock Proteins are Required in 'ori'P1 DNA Replication Solely at the RepA Monomerization Step.
PB97-119382 *03,557* Not available NTIS

PB97-119390
Anomalous Relation between Time and Frequency Domain PMD Measurements.
PB97-119390 *04,398* Not available NTIS

PB97-119408
Vortex Images in Thin Films of YBa2Cu3O(sub 7-x) and Bi2Sr2Ca1Cu2O(sub 8+x) Obtained by Low-Temperature Magnetic Force Microscopy.
PB97-119408 *04,815* Not available NTIS

PB97-121321
Fault Diagnosis of an Air-Handling Unit Using Artificial Neural Networks.
PB97-121321 *00,283* Not available NTIS

PB97-121339
Computer Simulations of Binder Removal from 2-D and 3-D Model Particulate Bodies.
PB97-121339 *00,418* Not available NTIS

PB97-121610
Science, Technology, and Competitiveness: Retrospective on a Symposium in Celebration of NIST's 90th Anniversary and the 25th Anniversary of the Gaithersburg Laboratories, November 14-15, 1991.
PB97-121610 *02,696* PC A08/MF A02

PB97-121636
Text REtrieval Conference (4th) (TREC-4). Held in Gaithersburg, Maryland on November 1-3, 1995.
PB97-121636 *01,786* PC A99/MF E08

PB97-121826
International Green Building Conference and Exposition (3rd). Held in San Diego, California on November 17-19, 1996. (Reannouncement with new abstract).
PB97-121826 *02,531* PC A12/MF A03

PB97-122212
Interface-Filter Characterization of Spectraradiometers and Colorimeters.
PB97-122212 *04,399* Not available NTIS

PB97-122220
Antiferromagnetic Interlayer Correlations in Annealed Ni80Fe20/Ag Multilayers.
PB97-122220 *03,109* Not available NTIS

PB97-122238
Publication and Presentation Abstracts, 1996.
PB97-122238 *03,585* Not available NTIS

PB97-122246
Flat and Curved Crystal Spectrography for Mammographic X-ray Sources.
PB97-122246 *03,642* Not available NTIS

PB97-122253
Dependence of the Thermal Electron Attachment Rate Constant in Gases and Liquids on the Energy Position of the Electron Attaching State.
PB97-122253 *01,996* Not available NTIS

PB97-122261
Environmental Aspects of Halon Replacements: Considerations for Advanced Agents and the Ozone Depletion Potential of CF3I.
PB97-122261 *03,301* Not available NTIS

PB97-122279
Conference Report: Calorimetry Conference (50th).
PB97-122279 *03,722* Not available NTIS

PB97-122287
Usability Engineering: Industry-Government Collaboration for System Effectiveness and Efficiency.
PB97-122287 *01,514* Not available NTIS

PB97-122295
Experimental Determination of the Rate Constant for the Reaction of C2H3 with H2 and Implications for the Partitioning of Hydrocarbons in Atmospheres of the Outer Planets.
PB97-122295 *00,112* Not available NTIS

PB97-122303
CSL View of Applications Portability, Scalability, and Interoperability.
PB97-122303 *01,787* Not available NTIS

PB97-122311
Materials and Fire Threat.
PB97-122311 *01,442* Not available NTIS

PB97-122329
NIST Watt Experiment: Monitoring the Kilogram.
PB97-122329 *01,997* Not available NTIS

PB97-122337
Small Angle Neutron Scattering Study of the Structure and Formation of MCM-41 Mesoporous Molecular Sieves.
PB97-122337 *03,110* Not available NTIS

PB97-122345
Generalized Optical Theorem for On-Axis Gaussian Beams.
PB97-122345 *04,177* Not available NTIS

PB97-122352
Radiocarbon Measurements of Atmospheric Volatile Organic Compounds: Quantifying the Biogenic Contribution.
PB97-122352 *02,574* Not available NTIS

PB97-122360
Measurement of the Atomic Na(3P) Lifetime and of Retardation in the Interaction between Two Atoms Bound in a Molecule.
PB97-122360 *04,178* Not available NTIS

PB97-122378
Large Local-Field Corrections in Optical Rotatory Power of Quartz and Selenium.
PB97-122378 *04,400* Not available NTIS

PB97-122386
Single-Phase Heat Transfer and Pressure Drop Characteristics of an Integral-Spine Fin Within an Annulus.
PB97-122386 *04,179* Not available NTIS

PB97-122394
Survey of the Components of Display-Measurement Standards.
PB97-122394 *02,209* Not available NTIS

PB97-122402
Oxidation of Ferrous and Ferrocyanide Ions by Peroxyl Radicals.
PB97-122402 *01,191* Not available NTIS

PB97-122410
SC4 Short Names Registry.
PB97-122410 *02,799* Not available NTIS

PB97-122428
Application of the Collocation Method in Three Dimensions to a Model Semiconductor Problem.
PB97-122428 *02,457* Not available NTIS

PB97-122436
Complex Time Dependence of the EPR Signal of Irradiated L-alpha-alanine.
PB97-122436 *04,180* Not available NTIS

PB97-122444
DNA Base Damage in Lymphocytes of Cancer Patients Undergoing Radiation Therapy.
PB97-122444 *03,643* Not available NTIS

PB97-122451
Perpendicular C-H Stretching Band nu9/nu13 and the Torsional Potential of Dimethylacetylene.
PB97-122451 *01,192* Not available NTIS

PB97-122469
Photonic Band-Structure Effects for Low-Index-Contrast Two-Dimensional Lattices in the Near Infrared.
PB97-122469 *04,401* Not available NTIS

PB97-122477
Nanoindentation and Instrumented Scratching Measurements on Hard Coatings.
PB97-122477 *03,111* Not available NTIS

PB97-122485
Overview of a Radiation Accident at an Industrial Accelerator Facility.
PB97-122485 *02,612* Not available NTIS

PB97-122493
Measuring Nondipolar Asymmetries of Photoelectron Angular Distributions.
PB97-122493 *01,193* Not available NTIS

PB97-122501
Wear Modeling of Si-Based Ceramics.
PB97-122501 *03,112* Not available NTIS

PB97-122519
NO Production and Destruction in a Methane/Air Diffusion Flame.
PB97-122519 *01,443* Not available NTIS

PB97-122527
Characterization of Time-Dependent Dielectric Breakdown in Intrinsic Thin SiO2.
PB97-122527 *02,458* Not available NTIS

PB97-122535
Parametric Study of Wall Moisture Contents Using a Revised Variable Indoor Relative Humidity Version of the 'Moist' Transient Heat and Moisture Transfer Model.
PB97-122535 *00,419* Not available NTIS

PB97-122543
Absence of Quantum-Mechanical Effects on the Mobility of Argon Ions in Helium Gas at 4.35 K.
PB97-122543 *01,194* Not available NTIS

PB97-122550
Xi-Vector Formulation of Anisotropic Phase-Field Models: 3-D Asymptotics.
PB97-122550 *04,816* Not available NTIS

PB97-122568
Determination of Anomalous Superexchange in MnCl2 and Its Graphite Intercalation Compound.
PB97-122568 *00,666* Not available NTIS

PB97-122576
Material Characterization By a Time-Resolved and Polarization-Sensitive Ultrasonic Technique.
PB97-122576 *02,764* Not available NTIS

PB97-122584
Design, Construction and Application of a Large Aperture Lens-Less Line-Focus PVDF Transducer.
PB97-122584 *02,765* Not available NTIS

PB97-122592
Chemical Effect in Ceramics Grinding.
PB97-122592 *03,113* Not available NTIS

PB97-122600
Capacitors with Very Low Loss: Cryogenic Vacuum-Gap Capacitors.
PB97-122600 *02,293* Not available NTIS

PB97-124135
Standards Activities of Organizations in the United States.
PB97-124135 *00,006* PC A99/MF E08

PB97-500342
Building Life Cycle Cost Computer Program (BLCC) Version 4.4-97 (for Microcomputers).
PB97-500342 *00,284* CP D02

RP2003
Low-Temperature Performance of Radiosonde Electric Hygrometer Elements.
AD-A295 319/8 *00,121* PC A02/MF A01

SHRP-A-335
Binder Characterization and Evaluation by Nuclear Magnetic Resonance Spectroscopy.
PB94-193471 *01,334* PC A08/MF A02

SHRP-C-373
Optimization of Highway Concrete Technology.
PB94-182995 *01,333* PC A13/MF A03

SWRI-4770
Evaluation of Wear Resistant Ceramic Valve Seats in Gas-Fueled Power Generation Engines. Topical Report, December 1991-April 1994.
PB95-200218 *02,466* PC A07/MF A02

TN-38
Design and Construction of a Liquid Hydrogen Temperature Refrigeration System.
AD-A286 618/4 *02,619* PC A03/MF A01

TRB/NCHRP-ID002
Development of a Method for Measuring Water-Stripping Resistance of Asphalt/Siliceous Aggregate Mixtures.
PB96-197249 *01,348* PC A04/MF A01

VTRC-96-R30
Application of Electromagnetic-Acoustic Transducers for Nondestructive Evaluation of Stresses in Steel Bridge Structures.
PB96-167978 *01,301* PC A04/MF A01

APPENDIX A
List of Depository Libraries in the United States

ALABAMA

Auburn

Auburn University Ralph Draughon Library

Birmingham

Birmingham Public Library
Birmingham–Southern College Library
Jefferson State Community College James B. Allen Library
Samford University Harwell G. Davis Library

Enterprise

Enterprise State Junior College Learning Resources Center

Fayette

Bevill State Community College at Brewer Learning Resources Center

Florence

University of North Alabama Collier Library

Gadsden

Gadsden Public Library

Huntsville

University of Alabama in Huntsville Library

Jacksonville

Jacksonville State University Houston Cole Library

Maxwell Air Base

Air University Library/LSAS

Mobile

Mobile Public Library
Spring Hill College Thomas Byrne Memorial Library
University of South Alabama University Library

Montgomery

Alabama Public Library Service
Alabama Supreme Court and State Law Library
Auburn University at Montgomery Library REGIONAL

Normal

Alabama Agricultural and Mechanical University J. F. Drake Memorial Library

Troy

Troy State University Library

Tuscaloosa

University of Alabama Amelia Gayle Gorgas Library REGIONAL
University of Alabama School of Law Library

Tuskegee

Tuskegee University Hollis Burke Frissell Library

ALASKA

Anchorage

Anchorage Law Library
Anchorage Municipal Libraries Z. J. Loussac Public Library
Department of the Interior Alaska Resources Library
University of Alaska at Anchorage Consortium Library

Fairbanks

University of Alaska Elmer E. Rasmuson Library

Juneau

Alaska State Library
University of Alaska Southeast William A. Egan Library

Ketchikan

University of Alaska Southeast Ketchikan College Library

AMERICAN SAMOA

Pago Pago

American Samoa Community College Learning Resources Center

ARIZONA

Apache Junction

Apache Junction Public Library

Coolidge

Central Arizona College Learning Resources Center

Flagstaff

Northern Arizona University Cline Library

Glendale

Glendale Public LIbrary

Mesa

Mesa Public Library

Phoenix

Arizona Department of Library Archives and Public Records REGIONAL
Grand Canyon University Fleming Library
Maricopa County Library District
Phoenix Public Library

Prescott

Yavapai College Library

Tempe

Arizona State University Hayden Library/Government Documents
Arizona State University Ross-Blakley Law Library

Tucson

Tucson-Pima Public Library
University of Arizona College of Law Library
University of Arizona Main Library

Winslow

Northland Pioneer College Winslow Center Learning Resources Center

Yuma

Yuma County District Library

ARKANSAS

Arkadelphia

Ouachita Baptist University Riley-Hickingbotham Library

Batesville

Lyon College Mabee-Simpson Library

Clarksville

University of the Ozarks Dobson Memorial Library

Conway

University of Central Arkansas Torreyson Library

Fayetteville

University of Arkansas Library
University of Arkansas School of Law Young Law Library

Little Rock

Arkansas State Library REGIONAL
Arkansas Supreme Court Library
Central Arkansas Library System Main Library
University of Arkansas at Little Rock Ottenheimer Library
University of Arkansas at Little Rock Pulaski County Law Library

Magnolia

Southern Arkansas University Magale Library

Monticello

University of Arkansas at Monticello Library

Pine Bluff

University of Arkansas at Pine Bluff Watson Memorial Library

Russellville

Arkansas Technical University Tomlinson Library

Searcy

Harding University Brackett Library

State University

Arkansas State University–Jonesboro Dean B. Ellis Library

Walnut Ridge

Williams Baptist College Felix Goodson Library

CALIFORNIA

Anaheim

Anaheim Public Library

Arcadia

Arcadia Public Library

Arcata

Humboldt State University Library

Bakersfield

California State University Walter W. Stiern Library
Kern County, Beale Memorial Library

Berkeley

University of California Main Library
University of California School of Law Library

Carson

California State University at Dominguez Library
Carson Regional Library Los Angeles County Public Library

Chico

California State University at Chico Meriam Library

Claremont

Claremont Colleges Honnold/Mouth Library

Culver City

Culver City Library Los Angeles County Public Library

Davis

University of California at Davis Shields Library
University of California at Davis Law Library

Downey

Downey City Library

Fresno

California State University at Fresno Henry Madden Library
Fresno County Free Library

Fullerton

California State University at Fullerton University Library

Garden Grove

Orange County Public Library

Hayward

California State University at Hayward Library

Inglewood

Inglewood Public Library

Irvine

University of California at Irvine Main Library

La Jolla

University of California at San Diego Geisel Library

Lakewood

Angelo M. Iacoboni Public Library·Los Angeles County Public Library

Lancaster

Lancaster Public Library

La Verne

University of La Verne College of Law Library

Long Beach

California State University at Long Beach Library
Long Beach Public Library

Los Angeles

California State University at Los Angeles Kennedy Memorial Library
Los Angeles County Law Library
Los Angeles Public Library
Loyola Law School William M. Rains Law Library
Occidental College Mary Norton Clapp Library
Southwestern University School of Law Library
University of California at Los Angeles University Research Library
University of California at Los Angeles Hugh & Hazel Darling Law Library
University of Southern California Doheny Memorial Library
University of Southern California Law Library
U.S. Court of Appeals Ninth Circuit Library
Whittier College School of Law Library

Malibu

Pepperdine University Payson Library

Menlo Park

U.S. Geological Survey Library

Montebello

Montebello Regional Library

Monterey

U.S. Naval Postgraduate School Dudley Knox Library

Monterey Park

Bruggemeyer Memorial Library

Northridge

California State University at Northridge Delmar T. Oviatt Library

Norwalk

Norwalk Regional Library Los Angeles County Public Library

Oakland

Oakland Public Library

Ontario

Ontario City Library

Palm Springs

Palm Springs Public Library

Pasadena

California Institute of Technology Millikan Memorial Library
Pasadena Public Library

Pleasant Hill

Contra Costa County Public Library

Redding

Shasta County Library

Redlands

University of Redlands Armacost Library

Redwood City

Redwood City Public Library

Reseda

West Valley Regional Branch Library Los Angeles Public Library

Richmond

Richmond Public Library

Riverside

Riverside City and County Public Library
University of California at Riverside Library/Government Publications

Sacramento

California State Library/Government Publications REGIONAL
California State University at Sacramento Library
Sacramento County Law Library
Sacramento Public Library Central Library/Federal Documents
University of the Pacific Schaber Law Library

San Bernardino

San Bernardino County Law Library
San Bernardino County Library

San Diego

San Diego County Law Library
San Diego County Library
San Diego Public Library Central Library
San Diego State University Library
University of San Diego Malcolm A. Love Library School of Law Library

San Francisco

California Supreme Court Library
Golden Gate University Law Library
San Francisco Public Library/Government Document Department
San Francisco State University J. Paul Leonard Library
University of California Hastings College of Law
University of San Francisco Richard A. Gleeson Library
U.S. Court of Appeals Ninth Circuit Library

San Jose

San Jose State University Clark Library

San Leandro

San Leandro Public Library Community Library Center

San Luis Obispo

California Polytechnic State University Robert F. Kennedy Library

San Marcos

California State University at San Marcos Library & Information Services

San Mateo

College of San Mateo Library

San Rafael

Marin County Free Library

Santa Ana

Orange County Law Library
Santa Ana Public Library

Santa Barbara

University of California at Santa Barbara Davidson Library

Santa Clara

Santa Clara University Orradre Library

Santa Cruz

University of California at Santa Cruz McHenry Library

Santa Rosa

Sonoma County Public Library

Stanford

Stanford University Jonsson Library (1895)
Stanford University Robert Crown Law Library

Stockton

Public Library of Stockton and San Joaquin County

Thousand Oaks

California Lutheran University Pearson Library

Torrance

Torrance Public Library

Turlock

California State University, Stanislaus Library

Valencia

Valencia Library Los Angeles County Public Library

Vallejo

Solano County Library System John F. Kennedy Library

Ventura

Ventura County Library E. P. Foster Library

Visalia

Tulare County Free Library

Walnut

Mount San Antonio College Learning Resources Library

West Covina

West Covina Regional Library

Whittier

Whittier College Wardman Library

COLORADO

Alamosa

Adams State College Library

Aurora

Aurora Public Library

Boulder

University of Colorado at Boulder Libraries Government Publications REGIONAL
University of Colorado at Boulder School of Law Library

Broomfield

Mamie Doud Eisenhower Public Library

Colorado Springs

Colorado College Tutt Library
University of Colorado at Colorado Springs Library

Denver

Auraria Library
Colorado Supreme Court Library
Denver Public Library REGIONAL
Regis University Dayton Memorial Library
University of Denver College of Law Library Westminister Law Library
University of Denver Penrose Library
U.S. Courts Library

Fort Collins

Colorado State University Libraries/Documents Department

Golden

Colorado School of Mines Arthur Lakes Library

Grand Junction

Mesa County Public Library District
Mesa State College John U. Tomlinson Library

Greeley

University of Northern Colorado James A. Michener Library

Gunnison

Western State College Leslie J. Savage Library

La Junta

Otero Junior College Wheeler Library

Lakewood

Jefferson County Public Library Lakewood Branch

Pueblo

Pueblo Library District McClelland Library
University of Southern Colorado Library

USAF Academy

U.S. Air Force Academy Library

CONNECTICUT

Bridgeport

Bridgeport Public Library/Reference Department

Danbury

Western Connecticut State University Ruth A. Haas Library

Hamden

Quinnipiac College School of Law Library

Hartford

Connecticut State Library REGIONAL
Hartford Public Library

Trinity College Library
University of Connecticut School of Law Library

Middletown

Wesleyan University Olin Library

New Britain

Central Connecticut State University Elihu Burritt Library

New Haven

Southern Connecticut State University Hilton C. Buley Library
Yale University Lillian Goldman Law Library
Yale University Seeley G. Mudd Library

New London

Connecticut College C. E. Shain Library
U.S. Coast Guard Academy Library

Stamford

Ferguson Library

Storrs

University of Connecticut Homer Babbidge Library

Waterbury

Silas Bronson Public Library
Teikyo Post University Traurig Library

West Haven

University of New Haven Marvin K. Peterson Library

Willimantic

Eastern Connecticut State University J. Eugene Smith Library

DELAWARE

Dover

Delaware Division of Libraries/Government Documents
Delaware State University William C. Jason Library

Georgetown

Delaware Technical and Community College Stephen J. Betez Library

Newark

University of Delaware Library

Wilmington

Widener University School of Law Library

DISTRICT OF COLUMBIA

Washington

American University Washington College of Law Library
Board of Governors of the Federal Reserve System Law Library
Catholic University of America Judge Kathryn J. Dufour Law Library
Comptroller of the Currency Library
Department of Commerce Library
Department of Education National Library of Education
Department of Housing and Urban Development Library
Department of Justice Main Library
Department of Labor Library
Department of State Law Library
Department of State Library
Department of the Army Pentagon Library
Department of the Interior Departmental Library
Department of the Navy Library Naval Historical Center
Department of the Treasury Library
Department of Transportation Main Library
Department of Transportation U.S. Coast Guard Law Library
Department of Veterans' Headquarters Library
District of Columbia Court of Appeals Library
District of Columbia Public Library/Document Department
Equal Employment Opportunity Library
Executive Office of the President Library
Federal Election Commission Law Library
Federal Energy Regulatory Commission Library
Federal Mine Safety, Health Review Library
General Accounting Office Information Services Center
General Services Administration Library
George Washington University Melvin Gelman Library
George Washington University National Law Center Jacob Burns Law Library
Georgetown University Law Center E. B. Williams Law Library
Georgetown University Lavinger Library
Library of Congress Congressional Research Service
Library of Congress Serial and Government Publications
National Defense University Library Fort Lesley J. McNair
Pension Benefit Guaranty Corporation Office of General Counsel Library
U.S. Court of Appeals Federal Circuit Library
U.S. Court of Appeals Judges' Library
U.S. Information Agency Information Resource Center
U.S. Postal Service Library
U.S. Senate Library
U.S. Supreme Court Library

FLORIDA

Boca Raton

Florida Atlantic University S. E. Wimberly Library

Bradenton

Manatee County Public Library Information Service Department

Clearwater

Clearwater Public Library System U.S. Government Documents

Cocoa

Brevard County Library System Central Brevard Library

Coral Gables

University of Miami Otto G. Richter Library

Daytona Beach

Volusia County Public Library Volusia County Library Center

De Land

Stetson University duPont-Ball Library

Fort Lauderdale

Broward County Main Library/Government Documents
Nova Southeastern University Shepard Broad Law Center Library

Fort Pierce

Indian River Community College Miley Learning Resource Center

Gainesville

University of Florida College of Law Library
University of Florida Libraries REGIONAL

Jacksonville

Jacksonville Public Library
Jacksonville University Carl S. Swisher Library
University of North Florida Thomas G. Carpenter Library

Key West

Florida Keys Community College Key West Campus Learning Resources Center

Lakeland

Lakeland Public Library

Leesburg

Lake-Sumter Community College Library

Melbourne

Florida Institute of Technology Evans Library

Miami

Florida International University University Park Campus Library
Miami-Dade Public Library Documents Division
St. Thomas University Library Documents Department

North Miami

Florida International University North Miami Campus Library

Orlando

University of Central Florida Library/Documents

Palatka

Saint Johns River Community College Library B. C. Pearce Learning Resources

Panama City

Bay County Public Library

Pensacola

University of West Florida John C. Pace Library

Saint Petersburg

Saint Petersburg Public Library Reference Department
Stetson University College of Law Charles A. Dana Law Library

Sarasota

Selby Public Library
University of South Florida at Sarasota Jane Bancroft Cook Library

Tallahassee

Florida Agricultural and Mechanical University Coleman Memorial Library
Florida State University College of Law Library
Florida State University Strozier Library
Florida Supreme Court Library
State Library of Florida

Tampa

Tampa-Hillsborough County Public Library
University of South Florida Library
University of Tampa Merl Kelce Library

Winter Park

Rollins College Olin Library

GEORGIA

Albany

Dougherty County Public Library

Americus

Georgia Southwestern College James Earl Carter Library

Athens

University of Georgia Libraries/Government Documents REGIONAL
University of Georgia School of Law Library

Atlanta

Atlanta University Center Robert W. Woodruff Library
Atlanta-Fulton Public Library (1880)
Emory University Robert W. Woodruff Library
Emory University School of Law McMillan Law Library
Georgia Institute of Technology Library and Information Center
Georgia State Law Library
Georgia State University College of Law Library
Georgia State University William Russell Pullen Library
U.S. Court of Appeals Eleventh Circuit Library

Augusta

Augusta College Reese Library
Medical College of Georgia Greenblatt Library

Brunswick

Brunswick-Glynn County Regional Library

Carrollton

State University of West Georgia Irvine Sullivan Ingram Library

Columbus

Columbus State University Simon Schwob Memorial Library

Dahlonega

North Georgia College Stewart Library

Dalton

Dalton College Library Resources Center

Kennesaw

Kennesaw State University Horace W. Sturgis Library

Macon

Mercer University Main Library
Mercer University School of Law Library

Milledgeville

Georgia College Ina Dillard Russell Library

Mount Berry

Berry College Memorial Library

Savannah

Chatham-Effingham-Liberty Regional Library

Smyrna

Smyrna Public Library

Statesboro

Georgia Southern University Zoch S. Henderson Library (1939)

Valdosta

Valdosta State University Odum Library

GUAM

Agana

Nieves M. Flores Memorial Library

Mangilao

University of Guam Kennedy Memorial Library

HAWAII

Hilo

University of Hawaii at Hilo Edwin H. Mookini Library

Honolulu

Hawaii Medical Library Incorporated
Hawaii State Library/Federal Documents
Municipal Reference & Records Center
Supreme Court Law Library (1973)
University of Hawaii Hamilton Library REGIONAL
University of Hawaii School of Law Library

Laie

Brigham Young University Hawaii Campus Joseph F. Smith Library

Lihue

Lihue Public Library

Pearl City

Leeward Community College Library

Wailuku

Wailuku Public Library

IDAHO

Boise

Boise Public Library
Boise State University Albertsons Library
Idaho State Library
Idaho Supreme Court State Law Library

Caldwell

Albertson College of Idaho N. L. Terteling Library

Lewiston

Lewis-Clark State College The Library

Moscow

University of Idaho College of Law Library
University of Idaho Library/Government Documents Department
REGIONAL

Nampa

Northwest Nazarene College John E. Riley Library

Pocatello

Idaho State University Eli Oboler Library

Rexburg

Ricks College David O. McKay Learning Resources Center

Twin Falls

College of Southern Idaho Library

ILLINOIS

Bloomington

Illinois Wesleyan University Sheean Library

Bourbonnais

Olivet Nazarene University Benner Library and Resource Center

Carbondale

Southern Illinois University at Carbondale Morris Library
Southern Illinois University at Carbondale School of Law Library

Carlinville

Blackburn College Lumpkin Library

Carterville

John A. Logan College Learning Resources Center

Champaign

University of Illinois Law Library

Charleston

Eastern Illinois University Booth Library/Documents

Chicago

Chicago Public Library Harold Washington Library/Government Publications Department
Chicago State University Paul and Emily Douglas Library
DePaul University Law Library
Field Museum of Natural History Library
Illinois Institute of Technology Chicago-Kent College of Law Library
Illinois Institute of Technology Paul V. Galvin Library
John Marshall Law School Library
Loyola University of Chicago E. M. Cudahy Memorial Library
Loyola University of Chicago School of Law Library
Northeastern Illinois University Ronald Williams Library
Northwestern University School of Law Library
University of Chicago D'Angelo Law Library
University of Chicago Regenstein Library
University of Illinois at Chicago Library/Documents and Maps
William J. Campbell Library of the U.S. Courts

Decatur

Decatur Public Library/Government Documents

De Kalb

Northern Illinois University College of Law Library
Northern Illinois University Founders' Memorial Library

Des Plaines

Oakton Community College Library

Edwardsville

Southern Illinois University at Edwardsville Lovejoy Memorial Library

Elsah

Principia College Marshall Brooks Library

Evanston

Northwestern University Library/Government Publications

Freeport

Freeport Public Library

Galesburg

Galesburg Public Library

Jacksonville

MacMurray College Henry Pfeiffer Library

Lake Forest

Lake Forest College Donnelley Library

Lebanon

McKendree College Holman Library

Lisle

Illinois Benedictine College Theodore F. Lownik Library

Macomb

Western Illinois University Library/Government Publications

Moline

Black Hawk College Library (1970)

Monmouth

Monmouth College Hewes Library

Mount Carmel

Wabash Valley College Bauer Media Center

Mount Prospect

Mount Prospect Public Library/Government Information Center

Normal

Illinois State University Milner Library

Oak Park

Oak Park Public Library

Oglesby

Illinois Valley Community College Jacobs Library

Palos Hills

Moraine Valley Community College Robert E. Turner Library

Peoria

Bradley University Cullom-Davis Library
Peoria Public Library

River Forest

Rosary College Rebecca Crown Library

Rockford

Rockford Public Library

Romeoville

Lewis University Library

South Holland

South Suburban College Library

Springfield

Illinois State Library/Federal Documents Department REGIONAL

Streamwood

Poplar Creek Public Library District

University Park

Governors State University Library

Urbana

University of Illinois/Documents Library

Wheaton

Wheaton College Buswell Memorial Library

Woodstock

Woodstock Public Library

INDIANA

Anderson

Anderson Public Library/Government Publications
Anderson University Robert A. Nicholson Library

Bloomington

Indiana University Library
Indiana University School of Law Library

Crawfordsville

Wabash College Lilly Library

Evansville

Evansville-Vanderburgh County Public Library
University of Southern Indiana David L. Rice Library

Fort Wayne

Allen County Public Library
Indiana University-Purdue University at Fort Wayne Helmke Library

Franklin

Franklin College Library

Gary

Gary Public Library Main Library
Indiana University Northwest Campus Library

Greencastle

DePauw University Roy O. West Library

Hammond

Hammond Public Library

Hanover

Hanover College Duggan Library

Huntington

Huntington College Richlyn Library

Indianapolis

Butler University Irwin Library–Serials/Documents Section
Indiana State Library REGIONAL
Indiana Supreme Court Law Library
Indiana University at Indianapolis School of Law Library
Indiana University-Purdue University Libraries
Indianapolis-Marion County Public Central Library

Kokomo

Indiana University Kokomo Learning Resource Center

Muncie

Ball State University Alexander M. Bracken Library
Muncie Public Library

New Albany

Indiana University Southeast Library

Notre Dame

University of Notre Dame Kresge Law Library
University of Notre Dame Theodore M. Hesburgh Library

Rensselaer

Saint Joseph's College Robinson Memorial Library

Richmond

Earlham College Lilly Library
Morrisson-Reeves Library

South Bend

Indiana University at South Bend Franklin D. Schurz Library

Terre Haute

Indiana State University Cunningham Memorial Library

Valparaiso

Valparaiso University Law Library
Valparaiso University Moellering Memorial Library

West Lafayette

Purdue University HSSE Library

IOWA

Ames

Iowa State University Parks Library

Cedar Falls

University of Northern Iowa Donald O. Rod Library

Cedar Rapids

Cedar Rapids Public Library

Council Bluffs

Council Bluffs Public Library

Davenport

Davenport Public Library

Des Moines

Drake University Cowles Library
Drake University Law Library
Public Library of Des Moines/Documents Department
State Library of Iowa/Documents Section

Dubuque

Carnegie-Stout Public Library
Loras College Wahlert Memorial Library

Fayette

Upper Iowa University Henderson-Wilder Library

Grinnell

Grinnell College Burling Library

Iowa City

University of Iowa College of Law Library
University of Iowa Libraries/Government Publications REGIONAL

Lamoni

Graceland College Frederick Madison Smith Library

Mason City

North Iowa Area Community College Library

Mount Vernon

Cornell College Russell D. Cole Library

Orange City

Northwestern College Ramaker Library

Sioux City

Sioux City Public Library Wilbur Aalfs Library

KANSAS

Atchison

Benedictine College Library

Baldwin City

Baker University Collins Library

Colby

Colby Community College H. F. Davis Memorial Library

Dodge City

Dodge City Community College Learning Resources Center

Emporia

Emporia State University William Allen White Library

Hays

Fort Hays State University Forsyth Library

Hutchinson

Hutchinson Public Library/Depository Section

Kansas City

Kansas City Community College Library

Lawrence

University of Kansas Government Documents and Maps Library REGIONAL
University of Kansas Law School Library

Manhattan

Kansas State University Farrell Library

Overland Park

Johnson County Library/Documents Department

Pittsburg

Pittsburg State University Leonard H. Axe Library

Salina

Kansas Wesleyan University Memorial Library

Topeka

Kansas State Historical Society Library/Government Documents
Kansas State Library
Kansas Supreme Court Law Library
Washburn University of Topeka School of Law Library

Wichita

Wichita State University Ablah Library (1901)

KENTUCKY

Ashland

Ashland Community College Library

Barbourville

Union College Weeks-Townsend Memorial Library

Bowling Green

Western Kentucky University Helm-Cravens Library

Columbia

Lindsey Wilson College Katie Murrell Library

Crestview Hills

Thomas More College Library

Danville

Centre College Grace Doherty Library

Frankfort

Kentucky Department of Libraries State Library Service Division
Kentucky State Law Library
Kentucky State University Paul G. Blazer Library

Hazard

Hazard Community College Library

Highland Heights

Northern Kentucky University W. Frank Steely Library

Lexington

University of Kentucky King Library South REGIONAL
University of Kentucky Law Library

Louisville

Louisville Free Public Library/Government Publications
University of Louisville Belknap Campus Ekstrom Library
University of Louisville School of Law Library

Morehead

Morehead State University Camden-Carroll Library

Murray

Murray State University Waterfield Library

Owensboro

Kentucky-Wesleyan College Library Learning Center

Richmond

Eastern Kentucky University John Grant Crabbe Library

Williamsburg

Cumberland College Hagan Memorial Library

LOUISIANA

Baton Rouge

Louisiana State University Middleton Library REGIONAL
Louisiana State University Paul M. Herbert Law Center Library

Southern University John B. Cade Library
Southern University Law Center Library
State Library of Louisiana

Eunice

Louisiana State University at Eunice Arnold LeDoux Library

Hammond

Southeastern Louisiana University Sims Memorial Library

Lafayette

University of Southwestern Louisiana Edith Garland Dupre Library

Lake Charles

McNeese State University Lether E. Frazar Memorial Library

Leesville

Vernon Parish Library

Monroe

Northeast Louisiana University Sandel Library

Natchitoches

Northwestern State University Watson Memorial Library

New Orleans

Law Library of Louisiana
Loyola University Law Library
Loyola University Library
New Orleans Public Library/Government Documents
Our Lady of Holy Cross College Blaine S. Kern Library
Southern University at New Orleans Leonard S. Washington Library
Tulane University Howard-Tilton Memorial Library
Tulane University School of Law Library
U.S. Court of Appeals Fifth Circuit Library
University of New Orleans Earl K. Long Library
Xavier University Library

Pineville

Louisiana College Norton Memorial Library

Ruston

Louisiana Tech University Prescott Memorial Library REGIONAL

Shreveport

Louisiana State University in Shreveport Noel Memorial Library
Shreve Memorial Library

Thibodaux

Nicholls State University Ellender Memorial Library

MAINE

Augusta

Maine Law and Legislative Reference Library
Maine State Library/Documents

Bangor

Bangor Public Library

Brunswick

Bowdoin College Hawthorne-Longfellow Library

Castine

Maine Maritime Academy Nutting Memorial Library

Lewiston

Bates College George and Helen Ladd Library

Orono

University of Maine Raymond H. Fogler Library REGIONAL

Portland

Portland Public Library
University of Maine School of Law Garbrecht Law Library

Presque Isle

University of Maine at Presque Isle Library

Sanford

Louis B. Goodall Memorial Library

Waterville

Colby College Miller Library

MARYLAND

Annapolis

Maryland State Law Library
U.S. Naval Academy Nimitz Library

Baltimore

Enoch Pratt Free Library/Documents Division
Goucher College Julia Rogers Library
Johns Hopkins University Government/Publication/Maps Law Library
Morgan State University Soper Library
University of Baltimore Langsdale Library
University of Baltimore Law Library
University of Maryland School of Law Thurgood Marshall Law Library
U.S. Court of Appeals Fourth Circuit Library

Bel Air

Harford Community College Library

Beltsville

Department of Agriculture National Agricultural Library

Bethesda

Department of Health and Human Services National Library of Medicine
Uniformed Services University of Health Sciences Learning Resources Center

Catonsville

University of Maryland Baltimore County Albin O. Kuhn Library & Gallery

Chestertown

Washington College Clifton M. Miller Library

College Park

University of Maryland at College Park McKeldin Library REGIONAL

Cumberland

Allegany College of Maryland Library

Frostburg

Frostburg State University Lewis J. Ort Library

Patuxent River

Naval Air Warfare Center Central Library

Rockville

Montgomery County Department of Public Libraries Rockville Regional Library

Salisbury

Salisbury State University Blackwell Library

Silver Spring

Department of Commerce NOAA Central Library

Towson

Towson State University Albert S. Cook Library

Westminster

Western Maryland College Hoover Library

MASSACHUSETTS

Amherst

Amherst College Robert Frost Library
University of Massachusetts at Amherst University Library

Boston

Boston Athenaeum Library
Boston Public Library/Government Documents REGIONAL
Boston University School of Law Pappas Law Library
Northeastern University Snell Library
State Library of Massachusetts/Documents Department
Suffolk University Law Library
Supreme Judicial Court Social Law Library
U.S. Court of Appeals First Circuit Library

Brookline

Public Library of Brookline

Cambridge

Harvard College Lamont Library
Harvard Law School Library
Massachusetts Institute of Technology Libraries

Chestnut Hill

Boston College Thomas P. O'Neill Jr. Library

Chicopee

College of Our Lady of the Elms Alumnae Library

Lowell

University of Massachusetts South Campus Lowell O'Leary Library

Medford

Tufts University Tisch Library

Milton

Curry College Levin Library

New Bedford

New Bedford Free Public Library

Newton Center

Boston College Law School Library

North Dartmouth

University of Massachusetts Dartmouth Library/Government Publications

North Easton

Stonehill College Cushing-Martin Library

Springfield

Massachusetts Trial Court Hampden Law Library
Springfield City Library/Documents Section
Western New England College School of Law Library

Waltham

Brandeis University Goldfarb Library

Wellesley

Wellesley College Margaret Clapp Library

Wenham

Gordon College Jenks Learning Resource Center

Williamstown

Williams College Sawyer Library

Worcester

American Antiquarian Society Library
University of Massachusetts Medical Center Lamar Soutter Medical Library
Worcester Public Library

MICHIGAN

Albion

Albion College Stockwell-Mudd Library

Allendale

Grand Valley State University Zumberge Library

Alma

Alma College Monteith Library

Ann Arbor

University of Michigan Harlan Hatcher Graduate Library
University of Michigan Law Library

Benton Harbor

Benton Harbor Public Library

Clinton Township

Macomb County Library

Dearborn

Henry Ford Community College Eshleman Library

Detroit

Detroit College of Law Library
Detroit Public Library REGIONAL
Marygrove College Library
University of Detroit Mercy School of Law Library
University of Detroit Mercy McNichols Campus Library
Wayne State University Purdy/Kresge Library
Wayne State University Arthur Neef Law Library

Dowagiac

Southwestern Michigan College Fred L. Mathews Library

East Lansing

Michigan State University Main Library

Farmington Hills

Oakland Community College M. L. King Learning Resources Center

Flint

Flint Public Library (1967)
University of Michigan at Flint Francis Wilson Thompson Library

Grand Rapids

Calvin College & Theological Seminary Heckman Library
Grand Rapids Public Library/Government Documents

Houghton

Michigan Technological University J. Robert Van Pelt Library

Jackson

Jackson District Library

Kalamazoo

Kalamazoo Public Library
Western Michigan University Dwight B. Waldo Library

Lansing

Library of Michigan/Government Documents REGIONAL
Thomas M. Cooley Law School Library

Livonia

Livonia Public Library
Schoolcraft College Eric J. Bradner Library

Madison Heights

Madison Heights Public Library

Marquette

Northern Michigan University Lydia M. Olson Library

Monroe

Monroe County Library System

Mount Pleasant

Central Michigan University Charles V. Park Library

Muskegon

Hackley Public Library

Petoskey

North Central Michigan College Library

Pontiac

Oakland County Research Library/Reference

Port Huron

Saint Clair County Library

Rochester

Oakland University Kresge Library

Royal Oak

Royal Oak Public Library/Reference Department

Saginaw

Hoyt Public Library

Sault Ste. Marie

Lake Superior State University Kenneth Shouldice Library

Traverse City

Northwestern Michigan College Osterlin Library

University Center

Delta College Library

Warren

Warren Public Library Arthur J. Miller Branch

Ypsilanti

Eastern Michigan University Library

MINNESOTA

Bemidji

Bemidji State University A. C. Clark Library

Blaine

Anoka County Library

Collegeville

Saint John's University Alcuin Library

Duluth

Duluth Public Library/Documents Section
University of Minnesota at Duluth Library

Eagan

Dakota County Library—Westcott Branch

Edina

Hennepin County Library Southdale-Hennepin Library

Mankato

Mankato State University Memorial Library

Marshall

Southwest State University Library

Minneapolis

Minneapolis Public Library/Technology/Science/Government
University of Minnesota Law School Library
University of Minnesota Wilson Library REGIONAL

Moorhead

Moorhead State University Livingston Lord Library

Morris

University of Minnesota at Morris Rodney A. Briggs Library

Northfield

Carleton College The Library
Saint Olaf College Rolvaag Memorial Library

Roseville

Ramsey County Public Library Roseville Library

Saint Cloud

Saint Cloud State University, Learning Resources Center

Saint Paul

Hamline University School of Law Library
Minnesota State Law Library
Saint Paul Public Library/Government Publications
University of Minnesota Saint Paul Campus Library
William Mitchell College of Law Library Warren E. Burger Library

Saint Peter

Gustavus Adolphus College Folke Bernadotte Memorial Library

Winona

Winona State University Maxwell Library

MISSISSIPPI

Cleveland

Delta State University W. B. Roberts Library

Columbus

Mississippi University for Women Fant Memorial Library

Hattiesburg

University of Southern Mississippi Cook Memorial Library

Jackson

Jackson State University Henry Thomas Sampson Library
Millsaps College Millsaps-Wilson Library
Mississippi College School of Law Library
Mississippi Library Commission/Documents Section
Supreme Court of Mississippi State Law Library

Lorman

Alcorn State University J. D. Boyd Library

Mississippi State

Mississippi State University Mitchell Memorial Library

University

University of Mississippi J. D. Williams Library REGIONAL
University of Mississippi James O. Eastland Law Library

MISSOURI

Cape Girardeau

Southeast Missouri State University Kent Library

Columbia

University of Missouri at Columbia Ellis Library REGIONAL
University of Missouri at Columbia School of Law Library

Fulton

Westminster College Reeves Library

Hillsboro

Jefferson College Library (1984)

Jefferson City

Lincoln University Inman E. Page Library
Missouri State Library
Missouri Supreme Court Library

Joplin

Missouri Southern State College George A. Spiva Library

Kansas City

Kansas City Missouri Public Library/Documents Division
Rockhurst College Greenlease Library
University of Missouri at Kansas City Leon E. Bloch Law Library
University of Missouri at Kansas City Miller Nichols Library

Kirksville

Truman State University Pickler Memorial Library

Liberty

William Jewell College Charles F. Curry Library

Maryville

Northwest Missouri State University B. D. Owens Library

O'Fallon

Saint Charles City Middendorf-Kredell Branch County Library

Rolla

University of Missouri at Rolla Curtis Laws Wilson Library

Saint Charles

Lindenwood College Butler Library
Saint Charles City/County Library District Kisker Road Branch Library

Saint Joseph

River Bluffs Regional Library Central Library

Saint Louis

Maryville University Library
Saint Louis County Library
Saint Louis Public Library/Government Information Department
Saint Louis University Law Library
Saint Louis University Pius XII Memorial Library
U.S. Court of Appeals Eighth Circuit Library
University of Missouri at Saint Louis Thomas Jefferson Library
Washington University John M. Olin Library
Washington University Freund Law Library

Springfield

Drury College F. W. Olin Library
Southwest Missouri State University Duane G. Meyer Library

Warrensburg

Central Missouri State University Ward Edwards Library

MONTANA

Billings

Montana State University Billings Library

Bozeman

Montana State University at Bozeman Renne Library

Butte

Montana Tech of the University of Montana Library

Havre

Montana State University at Havre Northern Vande Bogart Library

Helena

Carroll College Corette Library
Montana State Library
State Law Library of Montana

Missoula

University of Montana Mansfield Library REGIONAL

NEBRASKA

Blair

Dana College C. A. Dana Life Library

Crete

Doane College Perkins Library

Fremont

Midland Lutheran College Luther Library

Kearney

University of Nebraska at Kearney Calvin T. Ryan Library

Lincoln

Nebraska Library Commission
Nebraska State Library
University of Nebraska at Lincoln D. L. Love Memorial Library REGIONAL
University of Nebraska at Lincoln Schmid Law Library

Omaha

Creighton University Reinert/Alumni Library
Creighton University Klutznick Law Library
Omaha Public Library W. Dale Clark Library
University of Nebraska at Omaha University Library

Scottsbluff

Scottsbluff Public Library

Wayne

Wayne State College Conn Library

NEVADA

Carson City

Nevada State Library and Archives
Nevada Supreme Court Library

Elko

Elko County Library
Great Basin College Learning Resources Center

Las Vegas

Clark County Law Library
Las Vegas-Clark County Library District
University of Nevada at Las Vegas James R. Dickinson Library

Reno

University of Nevada National Judicial College Law Library
Nevada Historical Society Library
University of Nevada at Reno Getchell Library REGIONAL
Washoe County Library/Government Documents Department

NEW HAMPSHIRE

Concord

Franklin Pierce Law Center Library
New Hampshire Law Library
New Hampshire State Library/Reference and Information

Durham

University of New Hampshire Dimond Library

Hanover

Dartmouth College Baker Library

Henniker

New England College Danforth Library

Manchester

Manchester City Library
New Hampshire College Shapiro Memorial Library
Saint Anselm College Geisel Library

Nashua

Nashua Public Library

NEW JERSEY

Bayonne

Bayonne Free Public Library/Government Documents Department

Bridgeton

Cumberland County Library

Camden

Rutgers University Law School Library
Rutgers University Paul Robeson Library

East Brunswick

East Brunswick Public Library

East Orange

East Orange Public Library

Elizabeth

Free Public Library of Elizabeth

Glassboro

Rowan College of New Jersey Savitz Library

Hackensack

Johnson Free Public Library

Irvington

Irvington Public Library

Jersey City

Jersey City Public Library/U.S. Documents Department
Jersey City State College Forrest A. Irwin Library

Lawrenceville

Rider University Franklin F. Moore Library

Madison

Drew University Library

Mahwah

Ramapo College George T. Potter Library

Morristown

College of Saint Elizabeth Mahoney Library

Mount Holly

Burlington County Library

New Brunswick

Rutgers University Alexander Library

Newark

Newark Public Library/U.S. Documents REGIONAL
Rutgers University John Cotton Dana Library
Rutgers University Ackerson Law Library
Seton Hall University School of Law Peter W. Rodino Jr. Law Library

Newton

Sussex County Library

Phillipsburg

Phillipsburg Free Public Library

Plainfield

Plainfield Public Library

Pomona

Stockton State College of New Jersey Library/Documents

Princeton

Princeton University Firestone Library

Randolph

County College of Morris Masten Learning Resources Center

Shrewsbury

Monmouth County Library–Eastern Branch

South Orange

Seton Hall University Walsh Library

Teaneck

Fairleigh Dickinson University Weiner Library

Toms River

Ocean County College Library

Trenton

New Jersey State Library/U.S. Documents
Trenton Free Public Library

Upper Montclair

Montclair State College Harry A. Sprague Library

West Long Branch

Monmouth College Guggenheim Memorial Library

Woodbridge

Free Public Library of Woodbridge Main Library

NEW MEXICO

Albuquerque

University of New Mexico Health Science Center Library
University of New Mexico School of Law Library
University of New Mexico General Library REGIONAL

Hobbs

New Mexico Junior College Pannell Library

Las Cruces

New Mexico State University Branson Library

Las Vegas

New Mexico Highlands University Thomas C. Donnelly Library

Portales

Eastern New Mexico University Golden Library

Santa Fe

New Mexico State Library REGIONAL
New Mexico Supreme Court Law Library

Silver City

Western New Mexico University Miller Library

Socorro

New Mexico Institute of Mining and Technology Library

NEW YORK

Albany

Albany Law School Schaffer Law Library
New York State Library/Cultural Education Center REGIONAL
State University of New York at Albany University Library (1964)

Binghamton

Binghamton University Glenn G. Bartle Library

Brockport

State University of New York at Brockport Drake Memorial Library

Bronx

Fordham University Library/Public Documents Section
Herbert H. Lehman College Library
State University of New York Maritime College Stephen B. Luce Library

Bronxville

Sarah Lawrence College Esther Raushenbush Library

Brooklyn

Brooklyn College Library/Government Documents Division
Brooklyn Law School Library
Brooklyn Public Library Business Library
Brooklyn Public Library Central Library
Pratt Institute Library

Brookville

Long Island University Schwartz Memorial Library

Buffalo

Buffalo and Erie County Public Library/Documents Division
State University of New York at Buffalo Charles B. Sears Law Library
State University of New York at Buffalo Lockwood Memorial Library

Canton

Saint Lawrence University Owen D. Young Library

Corning

Corning Community College Arthur A. Houghton Jr. Library

Cortland

State University College Cortland Memorial Library

Delhi

State University of New York College of Technology Resnick Library

East Islip

East Islip Public Library Suffolk Cooperative Library System

Elmira

Elmira College Gannett-Tripp Library

Farmingdale

State University of New York at Farmingdale Greenley Library

Flushing

Queens College Benjamin S. Rosenthal Library
Queens College of City University of New York Law School Library

Garden City

Adelphi University Swirbul Library

Geneseo

State University of New York at Geneseo Milne Library

Hamilton

Colgate University Everett Needham Case Library

Hempstead

Hofstra University Axinn Library
Hofstra University School of Law Library

Huntington

Touro College School of Law Library

Ithaca

Cornell University Albert R. Mann Library
Cornell University Law School Library
Cornell University Olin Library

Jamaica

Queens Borough Public Library/Magazine Documents Department
Saint John's University Library St. Augustine Hall
Saint John's University School of Law Library

Kings Point

U.S. Merchant Marine Academy Bland Memorial Library

Long Island City

LaGuardia Community College Library

Middletown

Middletown Thrall Library

Mount Vernon

Mount Vernon Public Library

New Paltz

State University College at New Paltz Sojourner Truth Library

New York City

City College of City University of New York Cohen Library
College of Insurance Library
Columbia University Lehman Library
Columbia University School of Law Library
Cooper Union for the Advancement of Science and Arts Library
Fordham University Leo T. Kissam Memorial Law Library
Medical Library Center of New York/Technical Services
New York Law Institute Library
New York Law School Library
New York Public Library Astor Branch
New York Public Library Hunt's Points Regional Branch
New York Public Library Lenox Branch
New York University Elmer Holmes Bobst Library
New York University Law Library
U.S. Court of Appeals Second Circuit Library
Yeshiva University Chutick Law Library
Yeshiva University Pollack Library

Newburgh

Newburgh Free Library

Niagara Falls

Niagara Falls Public Library

Oakdale

Dowling College Library/Government Documents

Oneonta

State University College at Oneonta James M. Milne Library

Oswego

State University of New York at Oswego Penfield Library

Plattsburgh

State University College at Plattsburgh Benjamin F. Feinberg Library

Potsdam

Clarkson University Burnap Memorial Library/Schuler Educational Resources Center
State University College at Potsdam Crumb Memorial Library

Poughkeepsie

Vassar College Thompson Library

Purchase

State University of New York at Purchase Library

Rochester

Rochester/Monroe County Public Library
University of Rochester Rush Rhees Library

Saint Bonaventure

Saint Bonaventure University Friedsam Memorial Library

Saratoga Springs

Skidmore College Lucy Scribner Library

Schenectady

Union College Schaffer Library

Southampton

Long Island University Southhampton Campus Library

Sparkill

St. Thomas Aquinas College Lougheed Library

Staten Island

Wagner College Horrmann Library

Stony Brook

State University of New York at Stony Brook Melville Library

Syracuse

Onondaga County Public Library/The Galleries of Syracuse
Syracuse University E. S. Byrd Library
Syracuse University College of Law H. Douglas Barclay Law Library

Troy

Troy Public Library/Government Documents

Uniondale

Nassau Library System/Documents Collections

Utica

State University of New York, Institute of Technology at Utica Library
Utica Public Library

West Point

U.S. Military Academy Library

White Plains

Pace University School of Law Library

Yonkers

Yonkers Public Library Getty Square Branch

Yorktown Heights

Mercy College Library Yorktown Branch Campus

NORTH CAROLINA

Asheville

University of North Carolina at Asheville D. Hiden Ramsey Library

Boiling Springs

Gardner-Webb University Dover Memorial Library

Boone

Appalachian State University Carol Grotnes Belk Library

Buies Creek

Campbell University Carrie Rich Memorial Library

Chapel Hill

University of North Carolina at Chapel Hill Everel Law Library/ Documents
University of North Carolina at Chapel Hill Walter Royal Davis Library REGIONAL

Charlotte

Public Library of Charlotte and Mecklenburg County
Queens College Everett Library
University of North Carolina at Charlotte J. Murrey Atkins Library

Cullowhee

Western Carolina University Hunter Library

Davidson

Davidson College E. H. Little Library

Durham

Duke University School of Law Library
Duke University William R. Perkins Library
North Carolina Central University Law School Library
North Carolina Central University James E. Shepard Library

Elon College

Elon College Iris Holt McEwen Library

Fayetteville

Fayetteville State University Charles W. Chesnutt Library

Greensboro

North Carolina Agricultural and Technical State University F. D. Bluford Library
University of North Carolina at Greensboro Walter Clinton Jackson Library

Greenville

East Carolina University J. Y. Joyner Library

Laurinburg

Saint Andrews Presbyterian College DeTamble Library

Lexington

Davidson County Public Library

Mount Olive

Mount Olive College Moye Library

Pembroke

Pembroke State University Mary Livermore Library

Raleigh

North Carolina State University D. H. Hill Library
North Carolina Supreme Court Library
State Library of North Carolina/Department of Cultural Resources

Rocky Mount

North Carolina Wesleyan College Pearsall Library

Salisbury

Catawba College Corriher-Linn-Black Library

Wilmington

University of North Carolina at Wilmington William M. Randall Library

Wilson

Barton College Hackney Library

Winston-Salem

Forsyth County Public Library Main Library
Wake Forest University Professional Center Library
Wake Forest University Z. Smith Reynolds Library

NORTH DAKOTA

Bismarck

Bismarck Veterans' Memorial Public Library
North Dakota State Library
North Dakota Supreme Court Law Library
State Historical Society of North Dakota State Archives & Historical Research Library

Dickinson

Dickinson State University Stoxen Library

Fargo

North Dakota State University Libraries REGIONAL

Grand Forks

University of North Dakota Chester Fritz Library REGIONAL

Minot

Minot State University Gordon B. Olson Library

Valley City

Valley City State University Allen Memorial Library

NORTHERN MARIANA ISLANDS

Saipan

Northern Marianas College Borja Memorial Library

OHIO

Ada

Ohio Northern University Jay P. Taggart Law Library

Akron

Akron-Summit County Public Library
University of Akron Bierce Library
University of Akron School of Law Library

Alliance

Mount Union College Library

Ashland

Ashland University Library

Athens

Ohio University Alden Library

Bluffton

Bluffton College Musselman Library

Bowling Green

Bowling Green State University Jerome Library

Canton

Malone College Everett L. Cattel Library

Chardon

Chardon Public Library

Cincinnati

Public Library of Cincinnati and Hamilton County Main Library
University of Cincinnati College of Law Robert Marx Law Library
University of Cincinnati Langsam Library
U.S. Court of Appeals Sixth Circuit Library

Cleveland

Case Western Reserve University Kelvin Smith Library
Case Western Reserve University School of Law Library
Cleveland Public Library/Government Documents
Cleveland State University Joseph W. Bartunek III Law Library
Cleveland State University University Library
Municipal Reference Library (1970)

Columbus

Capital University Law School Library
Capital University Library
Columbus Metropolitan Main Library
Ohio State University College of Law Library
Ohio State University Main Library
Ohio Supreme Court Law Library
State Library of Ohio/Documents Department REGIONAL

Dayton

Dayton and Montgomery County Public Library
University of Dayton Roesch Library
Wright State University Paul Laurence Dunbar Library

Delaware

Ohio Wesleyan University L. A. Beeghly Library

Elyria

Elyria Public Library

Findlay

University of Findlay Shafer Library

Gambier

Kenyon College Olin/Chalmers Libraries

Granville

Denison University William Howard Doane Library

Hiram

Hiram College Teachout-Price Memorial Library

Kent

Kent State University Libraries and Media Services

Marietta

Marietta College Dawes Memorial Library

Marion

Marion Public Library/Federal Documents

Middletown

Miami University Middletown Gardner-Harvey Library

New Concord

Muskingum College Library/Documents

Oberlin

Oberlin College Library/Documents Department

Oxford

Miami University King Library

Portsmouth

Shawnee State University Library

Rio Grande

University of Rio Grande Jeanette Albiez Davis Library

Springfield

Clark County Public Library/Government Documents

Steubenville

Franciscan University of Steubenville John Paul II Library
Public Library of Steubenville and Jefferson County

Tiffin

Heidelberg College Beeghly Library

Toledo

Toledo-Lucus County Public Library/Social Sciences Department
University of Toledo College of Law Library
University of Toledo William S. Carlson Library

University Heights

John Carroll University Grasselli Library

Westerville

Otterbein College Courtright Memorial Library

Westlake

Westlake Porter Public Library

Wilmington

Wilmington College S. Arthur Watson Library

Wooster

College of Wooster Andrews Library

Worthington

Worthington Public Library

Youngstown

Public Library of Youngstown and Mahoning County Main Library
Youngstown State University William F. Maag Library

OKLAHOMA

Ada

East Central University Linscheid Library

Alva

Northwestern Oklahoma State University J. W. Martin Library

Bethany

Southern Nazarene University Williams Learning Resources Center

Durant

Southeastern Oklahoma State University Henry G. Bennett Memorial Library

Edmond

University of Central Oklahoma Chambers Library

Enid

Public Library of Enid and Garfield County

Langston

Langston University G. Lamar Harrison Library

Lawton

Lawton Public Library

Norman

University of Oklahoma Bizzell Memorial Library
University of Oklahoma Law Library

Oklahoma City

Metropolitan Library System Downtown Library
Oklahoma City University Dulaney Browne Library
Oklahoma Department of Libraries–U.S. Government Information Division REGIONAL

Shawnee

Oklahoma Baptist University Mabee Learning Center

Stillwater

Oklahoma State University Edmon Low Library REGIONAL

Tahlequah

Northeastern State University John Vaughan Library

Tulsa

Tulsa City-County Library System
University of Tulsa College of Law Library
University of Tulsa McFarlin Library

Weatherford

Southwestern Oklahoma State University Al Harris Library

OREGON

Ashland

Southern Oregon State College Library

Bend

Central Oregon Community College Library/Media Center

Corvallis

Oregon State University Kerr Library

Eugene

University of Oregon Law Library
University of Oregon Library

Forest Grove

Pacific University Harvey Scott Memorial Library

Klamath Falls

Oregon Institute of Technology Library

La Grande

Eastern Oregon State College Walter M. Pierce Library

McMinnville

Linfield College Northup Library

Monmouth

Western Oregon State College Library

Pendleton

Blue Mountain Community College Library

Portland

Lewis and Clark College Aubrey R. Watzek Library
Multnomah County Library/Science and Business Section
Northwestern School of Law Paul L. Boley Law Library
Portland State University Branford P. Millar Library REGIONAL
Reed College Eric V. Houser Library
U.S. Department of Energy Bonneville Power Administration (BPA) Library

Salem

Oregon State Library
Oregon Supreme Court Law Library
Willamette University College of Law Library
Willamette University Mark O. Hatfield Library

PANAMA CANAL

Balboa Heights

Panama Canal Commission Technical Resources Center

PENNSYLVANIA

Allentown

Muhlenberg College Trexler Library

Altoona

Altoona Area Public Library

Bethel Park

Bethel Park Public Library/Depository Library Office

Bethlehem

Lehigh University Fairchild-Martindale Library

Bloomsburg

Bloomsburg University of Pennsylvania Harvey A. Andruss Library

Blue Bell

Montgomery County Community College Learning Resources Center

Bradford

University of Pittsburgh at Bradford Hanley Library

Broomall

Marple Public Library

California

California University of Pennsylvania Louis L. Manderino Library

Carlisle

Dickinson College Boyd Lee Spahr Library
Dickinson School of Law Sheeley-Lee Law Library

Cheyney

Cheyney University Leslie Pinckney Hill Library

Collegeville

Ursinus College Myrin Library

Coraopolis

Robert Morris College Library

Doylestown

Bucks County Free Library/Bucks County Library Center

East Stroudsburg

East Stroudsburg University Kemp Library

Erie

Erie County Library System

Greenville

Thiel College Langenheim Memorial Library

Harrisburg

State Library of Pennsylvania/Law-Government Publications REGIONAL
Widener University Harrisburg Campus School of Law Library

Haverford

Haverford College Magill Library

Indiana

Indiana University of Pennsylvania Stapleton Library

Johnstown

Cambria County Library System Glosser Memorial Library

Lancaster

Franklin and Marshall College Shadek-Fackenthal Library

Lewisburg

Bucknell University Ellen Clarke Bertrand Library

Mansfield

Mansfield University Library

Meadville

Allegheny College Lawrence Lee Pelletier Library

Millersville

Millersville University Helen A. Ganser Library

Monessen

Monessen Public Library

New Castle

New Castle Public Library

Newton

Bucks County Community College Library

Norristown

Montgomery County-Norristown Public Library

Philadelphia

Free Library of Philadelphia/Government Publications Department
Saint Joseph's University Francis A. Drexel Library
Temple University Paley Library
Temple University School of Law Library
U.S. Court of Appeals Third Circuit Library
University of Pennsylvania Biddle Law Library
University of Pennsylvania Library

Pittsburgh

Allegheny County Law Library
Carnegie Library of Pittsburgh Allegheny Regional Branch
Carnegie Library of Pittsburgh/Government Documents Department
Duquesne University School of Law Library
La Roche College John J. Wright Library
University of Pittsburgh Hillman Library
University of Pittsburgh School of Law Barco Law Library
U.S. Department of Energy Bureau of Mines Pittsburgh Research Center Library

Pottsville

Pottsville Free Public Library

Reading

Reading Public Library/Government Documents Department

Scranton

Scranton Public Library

Shippensburg

Shippensburg University Ezra Lehman Memorial Library

Slippery Rock

Slippery Rock University Bailey Library

Swarthmore

Swarthmore College McCabe Library

University Park

Pennsylvania State University Pattee Library

Villanova

Villanova University Law School Library

Warren

Warren Library Association Warren Public Library

West Chester

West Chester University Francis Harvey Green Library

Williamsport

Lycoming College Snowden Memorial Library

Youngwood

Westmoreland County Community College/Learning Resources Center

PUERTO RICO

Mayaguez

University of Puerto Rico Mayaguez Campus Library

Ponce

Pontifical Catholic University of Puerto Rico/Encarnacion Valdes Library
Pontifical Catholic University of Puerto Rico/School of Law Library

San Juan

University of Puerto Rico Jose M. Lazaro Library
University of Puerto Rico Law Library

RHODE ISLAND

Barrington

Barrington Public Library

Kingston

University of Rhode Island Library

Newport

U.S. Naval War College Library

Providence

Brown University John D. Rockefeller Jr. Library
Providence College Phillips Memorial Library
Providence Public Library
Rhode Island College James P. Adams Library
Rhode Island State Law Library
Rhode Island State Library

Warwick

Warwick Public Library

Westerly

Westerly Public Library

Woonsocket

Woonsocket Harris Public Library

SOUTH CAROLINA

Aiken

University of South Carolina at Aiken–Gregg-Graniteville Library

Charleston

Charleston Southern University L. Mendel Rivers Library
The Citadel Military College Daniel Library
College of Charleston Robert Scott Small Library

Clemson

Clemson University Robert Muldrow Cooper Library REGIONAL

Columbia

Benedict College Payton Learning Resources Center
South Carolina State Library/Documents Department
University of South Carolina Coleman Karesh Law Library
University of South Carolina Thomas Cooper Library REGIONAL

Conway

Coastal Carolina University Kimbel Library

Due West

Erskine College McCain Library

Florence

Florence County Library
Francis Marion University James A. Rogers Library

Greenville

Furman University James B. Duke Library
Greenville County Library

Greenwood

Lander University Jackson Library

Lancaster

University of South Carolina at Lancaster Medford Library

Orangeburg

South Carolina State University Miller F. Whittaker Library

Rock Hill

Winthrop University Dacus Library

Spartanburg

Spartanburg County Public Library

SOUTH DAKOTA

Aberdeen

Northern State University Williams Library

Brookings

South Dakota State University Hilton M. Briggs Library

Pierre

South Dakota State Library/Federal Documents Department
South Dakota Supreme Court Library

Rapid City

Rapid City Public Library
South Dakota School of Mines and Technology Devereaux Library

Sioux Falls

Augustana College Mikkelsen Library
Sioux Falls Public Library Siouxland Libraries

Spearfish

Black Hills State University E. Y. Berry Library

Vermillion

University of South Dakota I. D. Weeks Library

TENNESSEE

Bristol

King College E. W. King Library

Chattanooga

Chattanooga-Hamilton County Bicentennial Library
U.S. Tennessee Valley Authority Corporate Library

Clarksville

Austin Peay State University Felix G. Woodward Library

Cleveland

Cleveland State Community College Library

Columbia

Columbia State Community College John Finney Memorial Library

Cookeville

Tennessee Technological University Library

Jackson

Lambuth University Luther L. Gobbel Library

Jefferson City

Carson-Newman College Stephens-Burnett Library

Johnson City

East Tennessee State University Sherrod Library

Knoxville

Knox County Public Library System Lawson-McGhee Library
University of Tennessee at Knoxville John C. Hodges Library
University of Tennessee at Knoxville Law Library

Martin

University of Tennessee at Martin Paul Meek Library

Memphis

Memphis-Shelby County Public Library
University of Memphis Humphreys School of Law Library
University of Memphis University Libraries

Murfreesboro

Middle Tennessee State University Andrew L. Todd Library

Nashville

Fisk University Library
Public Library of Nashville and Davidson County Ben West Library
Tennessee State Library and Archives/State Library Division
Tennessee State University Brown-Daniel Library
Vanderbilt University Massey Law Library
Vanderbilt University Central Library

Sewanee

University of the South Jessie Ball duPont Library

TEXAS

Abilene

Abilene Christian University Brown Library
Hardin-Simmons University Richardson Library

Arlington

Arlington Public Library
University of Texas at Arlington Library

Austin

Texas State Law Library
Texas State Library/United States Documents REGIONAL
University of Texas at Austin Wasserman Library
University of Texas at Austin Perry-Castaneda Library
University of Texas at Austin Tarlton Law Library (1965)

Baytown

Lee College Carlson Learning Resources Center

Beaumont

Lamar University Gray Library

Brownwood

Howard Payne University Walker Memorial Library

Canyon

West Texas A&M University Cornette Library/Documents

College Station

Texas A&M University Sterling C. Evans Library

Commerce

East Texas State University James Gilliam Gee Library

Corpus Christi

Texas A&M University at Corpus Christi Jeff and Mary Bell Library

Corsicana

Navarro College Learning Resources Center

Dallas

Dallas Baptist University Vance Memorial Library
Dallas Public Library/Government Publications Department
Southern Methodist University Fondren Library

Denton

University of North Texas Libraries

Edinburg

University of Texas Pan American Library

El Paso

El Paso Public Library/Government Documents Section
University of Texas at El Paso Library

Fort Worth

Fort Worth Public Library
Texas Christian University Mary Couts Burnett Library

Galveston

Rosenberg Library

Garland

Nicholson Memorial Library System

Houston

Houston Public Library/Government Documents Section
North Harris College Learning Resources Center
Rice University Fondren Library
South Texas College of Law Library/Government Documents Department
Texas Southern University Marshall School of Law Library
University of Houston at Clear Lake Alfred R. Neumann Library
University of Houston O'Quinn Law Library
University of Houston M. D. Anderson Library

Huntsville

Sam Houston State University Newton Gresham Library

Irving

Irving Public Library System

Kingsville

Texas A&M University at Kingsville James C. Jernigan Library

Laredo

Laredo Community College Harold R. Yeary Library

Longview

Longview Public Library

Lubbock

Texas Tech University Libraries REGIONAL
Texas Tech University School of Law Library

Nacogdoches

Stephen F. Austin State University Steen Library

Richardson

University of Texas at Dallas Eugene McDermott Library

San Angelo

Angelo State University Porter Henderson Library

San Antonio

Palo Alto College Learning Resources Center
Saint Mary's University Academic Library
Saint Mary's University Sarita Kenedy East Law Library
San Antonio College Library
San Antonio Public Library Central Library
Trinity University Maddux Library
University of Texas at San Antonio Library

San Marcos

Southwest Texas State University Albert B. Alkek Library

Seguin

Texas Lutheran College Blumberg Memorial Library

Sherman

Austin College Gladys Abell Library Center

Texarkana

Texarkana College Palmer Memorial Library

Victoria

University of Houston at Victoria Library

Waco

Baylor University Caston Law Library
Baylor University Moody Memorial Library

Wichita Falls

Midwestern State University Moffett Library

UTAH

Cedar City

Southern Utah University Library

Ephraim

Snow College Lucy A. Phillips Library

Logan

Utah State University Merrill Library REGIONAL

Ogden

Weber State University Stewart Library

Provo

Brigham Young University Harold B. Lee Library
Brigham Young University Howard W. Hunter Law Library

Salt Lake City

University of Utah Eccles Health Science Library
University of Utah Law Library
University of Utah Marriott Library
Utah State Library
Utah State Supreme Court Law Library

VERMONT

Burlington

University of Vermont Bailey/Howe Library

Castleton

Castleton State College Calvin Coolidge Library

Johnson

Johnson State College John Dewey Library

Lyndonville

Lyndon State College Samuel Reed Hall Library

Middlebury

Middlebury College Egbert Starr Library

Montpelier

Vermont Department of Libraries/Reference and Law Services

Northfield

Norwich University Kreitzberg Library

South Royalton

Vermont Law School Cornell Library

VIRGIN ISLANDS

Saint Croix

Virgin Islands Division of LIbraries c/o Florence Williams Public Library

Saint Thomas

University of the Virgin Islands Ralph M. Paiewonsky Library

VIRGINIA

Alexandria

Dept. of the Navy Office of Judge Advocate General Law Library

Arlington

George Mason University School of Law Library
U.S. Patent & Trademark Office Scientific Technology Library

Blacksburg

Virginia Polytechnic Institute and State University Newman Library

Bridgewater

Bridgewater College Alexander Mack Memorial Library

Charlottesville

University of Virginia Alderman Library REGIONAL
University of Virginia Arthur J. Morris Law Library

Chesapeake

Chesapeake Public Library System Chesapeake Central Library

Danville

Danville Community College Learning Resources Center

Emory

Emory and Henry College Kelly Library

Fairfax

George Mason University Fenwick Library

Fredericksburg

Mary Washington College Simpson Library

Hampden-Sydney

Hampden-Sydney College Eggleston Library

Hampton

Hampton University Harvey Library

Harrisonburg

James Madison University Carrier Library

Lexington

Virginia Military Institute Preston Library
Washington and Lee University James B. Leyburn Library
Washington and Lee University Wilbur C. Hall Law Library

Martinsville

Patrick Henry Community College Learning Resources Center

Norfolk

Norfolk Public Library System Kirn Memorial Library
Old Dominion University Library
U.S. Armed Forces Staff College Library

Petersburg

Virginia State University Johnston Memorial Library

Quantico

Federal Bureau of Investigation FBI Academy Library
Marine Corps Research Center Marine Corps University Library

Reston

Department of the Interior U.S. Geological Survey Library

Richmond

Library of Virginia
University of Richmond Boatwright Memorial Library
University of Richmond Law School Library
U.S. Court of Appeals Fourth Circuit Library
Virginia Commonwealth University James Branch Cabell Library
Virginia State Law Library

Roanoke

Hollins College Fishburn Library

Salem

Roanoke College Fintel Library

Williamsburg

College of William and Mary Earl Gregg Swem Library
College of William and Mary Marshall-Wythe Law Library

Wise

Clinch Valley College John Cook Wyllie Library

WASHINGTON

Bellevue

King County Library System Bellevue Regional Library

Bellingham

Western Washington University Mable Zoe Wilson Library

Cheney

Eastern Washington University John F. Kennedy Memorial Library

Des Moines

Highline Community College Library

Ellensburg

Central Washington University Library

Everett

Everett Public Library/Documents Section

Olympia

Evergreen State College Daniel J. Evans Library
Washington State Law Library
Washington State Library/Government Publications REGIONAL

Port Angeles

North Olympic Library System Port Angeles Branch

Pullman

Washington State University Holland Library TSD

Seattle

Seattle Public Library/Government Publications
University of Washington Gallagher Law Library
University of Washington Suzzallo Library
U.S. Court of Appeals Ninth Circuit Library

Spokane

Gonzaga University School of Law Library
Spokane Public Library/Documents Department

Tacoma

Tacoma Public Library/Documents Division
University of Puget Sound Collins Memorial Library
Seattle University School of Law Library

Vancouver

Fort Vancouver Regional Library

Walla Walla

Whitman College Penrose Memorial Library

WEST VIRGINIA

Athens

Concord College J. Frank Marsh Library

Bluefield

Bluefield State College Hardway Library

Charleston

Kanawha County Public Library
West Virginia Library Commission/Reference Library
West Virginia Supreme Court Law Library

Elkins

Davis and Elkins College Booth Library

Fairmont

Fairmont State College Musick Library

Huntington

Marshall University James E. Morrow Library

Institute

West Virginia State College Drain-Jordan Library

Montgomery

West Virginia Institute of Technology Vining Library

Morgantown

West Virginia University Library/Government Documents REGIONAL

Salem

Salem-Teikyo University Benedum Library

Shepherdstown

Shepherd College Ruth Scarborough Library

Weirton

Mary H. Weir Public Library

Wheeling

Wheeling Jesuit College Hodges Library

WISCONSIN

Appleton

Lawrence University Seeley G. Mudd Library

Beloit

Beloit College Col. Robert H. Morse Library

Eau Claire

University of Wisconsin-Eau Claire William D. McIntyre Library

Fond du Lac

Fond du Lac Public Library

Green Bay

University of Wisconsin at Green Bay Cofrin Library

La Crosse

La Crosse Public Library
University of Wisconsin at La Crosse Murphy Library

Madison

Madison Public Library/Adult Services Division
State Historical Society of Wisconsin Library/Government Publications REGIONAL
University of Wisconsin at Madison Law Library
University of Wisconsin at Madison Memorial Library
Wisconsin State Law Library

Milwaukee

Alverno College Library/Media Center
Marquette University Law Library
Medical College of Wisconsin Libraries Todd Wehr Library
Milwaukee Public Library/Documents Division REGIONAL
Mount Mary College Haggerty Library
University of Wisconsin at Milwaukee Golda Meir Library

Oshkosh

University of Wisconsin at Oshkosh Polk Memorial Library

Platteville

University of Wisconsin at Platteville Karrmann Library

Racine

Racine Public Library/Documents

Ripon

Ripon College Lane Library

River Falls

University of Wisconsin at River Falls Chalmer Davee Library

Sheboygan

Mead Public Library

Stevens Point

University of Wisconsin at Stevens Point Learning Resources Center

Superior

Superior Public Library
University of Wisconsin at Superior Jim Dan Hill Library

Waukesha

Waukesha Public Library

Wausau

Marathon County Public Library

Whitewater

University of Wisconsin at Whitewater Harold G. Anderson Library

WYOMING

Casper

Natrona County Public Library

Cheyenne

Wyoming State Law Library
Wyoming State Library

Gillette

Campbell County Public Library/Documents Division

Laramie

University of Wyoming Coe Library
University of Wyoming George W. Hopper Law Library

Powell

Northwest College John Taggart Hinckley Library

Riverton

Central Wyoming College Library

Rock Springs

Western Wyoming Community College Library

Sheridan

Sheridan College Griffith Memorial Library

APPENDIX B
Export Assistance Center Directory of the U.S. Department of Commerce

ALABAMA

Birmingham–Medical Forum Building, 7th Floor, 950 22nd Street North, 35203, Area Code 205 Tel 731–1331, FAX 205-731-0076

ALASKA

Anchorage–421 W. First Street, World Trade Center, 99501, Area Code 907 Tel 271–6237, FAX 907-271–6242

ARIZONA

Phoenix–Phoenix Plaza, Suite 970, 2901 N. Central Avenue, 85012, Area Code 602 Tel 640–2513, FAX 602-640–2518

ARKANSAS

Little Rock–TCBY Tower Building, Suite 700, 425 W. Capitol Avenue, 72201, Area Code 501 Tel 324–5794, FAX 501-324–7380

CALIFORNIA

Long Beach–One World Trade Center, Suite 1670, 90831, Area Code 310 Tel 980-4550, FAX 310-980-4561

Los Angeles–11000 Wilshire Blvd., Room 9200, 90024, Area Code 310 Tel 235–7104, FAX 310-235–7220

Monterey–c/o Center for Trade and Commercial Diplomacy, 411 Pacific Street, Suite 200, 93940, Area Code 408 Tel 641-9850, FAX 408-641-9849

Newport Beach–3300 Irvine Avenue, Suite 305, 92660, Area Code 714 Tel 660-1688, FAX 714-660-8039

Novato–330 Ignacio Boulevard, Suite 102, 94949, Area Code 415 Tel 883-1966, FAX 415-883-2711

Oakland–530 Water Street, Suite 740, 94607, Area Code 510 Tel 273-7350, FAX 510-251-7352

Ontario–2940 Inland Empire Boulevard, Suite 121, 91764, Area Code 909 Tel 466-4134, FAX 909-466-4140

Oxnard–300 Esplanade Drive, Suite 290, 93030, Area Code 805 Tel 988-4106, FAX 805-988-1862

Sacramento–917 7th Street, 2nd Floor, 95814, Area Code 916 Tel 498-5155, FAX 916-498-5923

San Diego–6363 Greenwich Drive, Suite 230, 92122, Area Code 619 Tel 557-5395, FAX 619-557-6176

San Francisco–250 Montgomery Street, 14th Floor, 94104, Area Code 415 Tel 705–2300, FAX 415-705-2297

San Jose–101 Park Center Plaza, Suite 1001, 95113, Area Code 408 Tel 271-7300, FAX 408-271-7307

Santa Clara–5201 Great American Parkway, #456, 95054, Area Code 408 Tel 970–4610, FAX 408-970-4618

COLORADO

Denver–1625 Broadway, Suite 680, 80202, Area Code 303 Tel 844–6622, FAX 303-844-5651

CONNECTICUT

Middletown–213 Court Street, Suite 903, 06457-3346, Area Code 860 Tel 638-6950, FAX 860-638-6970

DELAWARE

Served by the Philadelphia, PA, Export Assistance Center

DISTRICT OF COLUMBIA

Served by the Baltimore, MD, EAC

FLORIDA

Clearwater–128 N. Osceola Avenue, 34615, Area Code 813 Tel 461–0011, FAX 813-449-2889

Miami–P.O. Box 590570, 5600 Northwest 36th Street, Suite 617, 33159, Area Code 305 Tel 526–7425, FAX 305-526-7434

Orlando–Eola Park Centre, 200 E. Robinson Street, Suite 1270, 32801, Area Code 407 Tel 648–6235, FAX 407-648-6756

Tallahassee–107 W. Gaines Street, Room G-01, 32399, Area Code 904 Tel 488–6469, FAX 904-487-1407

GEORGIA

Atlanta–Marquis Two Tower, 285 Peachtree Center Avenue, N.E., Suite 200, 30303-1229, Area Code 404 Tel 657–1900, FAX 404-657-1970

Savannah–120 Barnard Street, Room A–107, 31401, Area Code 912 Tel 652–4204, FAX 912-652-4241

HAWAII

Honolulu–P.O. Box 50026, 300 Ala Moana Blvd., Room 4106, 96850, Area Code 808 Tel 541–1782, FAX 808-541-3435

IDAHO

Boise–700 W. State Street, 2nd Floor, 83720, Area Code 208 Tel 334–3857, FAX 208-334-2783

ILLINOIS

Chicago–Xerox Center, 55 W. Monroe Street, Suite 2440, 60603, Area Code 312 Tel 353–8040, FAX 312-353-8098

Highland Park–610 Central Avenue, Suite 150, 60035, Area Code 847 Tel 681-8010, FAX 847-681-8012

Rockford–P.O. Box 1747, 515 N. Court Street, 61110, Area Code 815 Tel 987–8123, FAX 815-963-7943

Wheaton–Illinois Institute of Technology, 201 E. Loop Road, 60187, Area Code 312 Tel 353-4332, FAX 312-353-4336

INDIANA

Indianapolis–Penwood One, Suite 106, 11405 N. Pennsylvania Street, Carmel, IN, 46032, Area Code 317 Tel 582-2300, FAX 317-582-2301

IOWA

Des Moines–Room 817, Federal Building, 210 Walnut Street, 50309, Area Code 515 Tel 284–4222, FAX 515-284-4021

KANSAS

Wichita–151 North Volutsia, 67214, Area Code 316 Tel 269–6160, FAX 316-683-7326

KENTUCKY

Louisville–601 W. Broadway, Room 634B, 40202, Area Code 502 Tel 582–5066, FAX 502-582-6573

Somerset–2292 S. Highway 27, Suite 320, 42501, Area Code 606 Tel 677-6160, FAX 606-677-6161

LOUISIANA

New Orleans–One Canal Place, 365 Canal Street, Suite 2150, 70130, Area Code 504 Tel 589–6546, FAX 504-589-2337

MAINE

Portland–511 Congress Street, 04104, Area Code 207 Tel 541-7430, FAX 207-541-7420

MARYLAND

Baltimore–World Trade Center, 401 E. Pratt Street, Suite 2432, 21202, Area Code 410 Tel 962–4539, FAX 410-962-4529

MASSACHUSETTS

Boston–World Trade Center, 164 Northern Avenue, Suite 307, 02210, Area Code 617 Tel 424–5990, FAX 617-424-5992

Marlborough–100 Granger Boulevard, Unit 102, 01752, Area Code 508 Tel 624-6000, FAX 508-624-7145

MICHIGAN

Ann Arbor–425 S. Main Street, Suite 103, 48104, Area Code 313 Tel 741-2430, FAX 313-741-2432

Detroit–211 W. Fort Street, Suite 2220, 48226, Area Code 313 Tel 226–3650, FAX 313-226-3657

Grand Rapids–301 W. Fulton Street, Suite 718-S, 49504, Area Code 616 Tel 458–3564, FAX 616-458-3872

Pontiac–Oakland Pointe Office Building, 250 Elizabeth Lake Road, 48341, Area Code 810 Tel 975-9600, FAX 810-975-9606

MINNESOTA

Minneapolis–110 South 4th Street, Room 108, 55401, Area Code 612 Tel 348–1638, FAX 612-348-1650

MISSISSIPPI

Jackson–201 W. Capitol Street, Suite 310, 39201, Area Code 601 Tel 965–4388, FAX 601-965-5386

MISSOURI

Kansas City–601 E. 12th Street, Room 635, 64106, Area Code 816 Tel 426–3141, FAX 816-426-3140

St. Louis–8182 Maryland Avenue, Suite 303, 63105, Area Code 314 Tel 425–3302, FAX 314-425-3381

MONTANA

Served by the Boise, ID, Export Assistance Center

NEBRASKA

Omaha–11135 "O" Street, 68137, Area Code 402 Tel 221–3664, FAX 402-221-3668

NEVADA

Reno–1755 E. Plumb Lane, Suite 152, 89502, Area Code 702 Tel 784–5203, FAX 702-784-5343

NEW HAMPSHIRE

Portsmouth–601 Spaulding Turnpike, Suite 29, 03801, Area Code 603 Tel 334-6074, FAX 603-334-6110

NEW JERSEY

Newark–7-45 Raymond Plaza, W., 9th Floor, 07102, Area Code 201 Tel 645-4682, FAX 201-645-4783

Trenton–3131 Princeton Pike, Building #6, Suite 100, 08648, Area Code 609 Tel 989–2100, FAX 609-989-2395

NEW MEXICO

Santa Fe–c/o New Mexico Dept. of Economic Development, P.O. Box 20003, 87504-5003, Area Code 505 Tel 827-0350, FAX 505-827-0263

NEW YORK

Buffalo–111 W. Huron Street, Room 1304, 14202, Area Code 716 Tel 551–4191 FAX 716-551-5290

Harlem–163 W. 125th Street, Suite 904, New York, New York, 10027, Area Code 212 Tel 860-6200, FAX 212-860-6203

Long Island–1550 Franklin Avenue, Room 207, Mineola, 11501, Area Code 516 Tel 739-1765, FAX 516-571-4161

New York–6 World Trade Center, Room 635, 10048, Area Code 212 Tel 264–0635, FAX 212-264-1356

Rochester–111 E. Avenue, Suite 220, 14604, Area Code 716 Tel 263–6480, FAX 716-325-6505

Westchester–707 West Chester Avenue, White Plains, 10604, Area Code 914 Tel 682-6218 FAX 914-682-6698

NORTH CAROLINA

Carolinas–521 E. Morehead Street, Suite 435, Charlotte, 28202, Area Code 704 Tel 333-4886, FAX 704-332-2681

Greensboro–400 W. Market Street, Suite 400, 27401, Area Code 910 Tel 333–5345, FAX 910-333-5158

NORTH DAKOTA

Served by the Minneapolis, MN, Export Assistance Center

OHIO

Cincinnati–36 E. 7th Street, Suite 2650, 45202, Area Code 513 Tel 684–2944, FAX 513-684-3227

Cleveland–Bank One Center, 600 Superior Avenue, E., Suite 700, 44114, Area Code 216 Tel 522–4750, FAX 216-522-2235

Columbus–37 N. High Street, 4th Floor, 43215, Area Code 614 Tel 365-9510, FAX 614-365-9598

Toledo–300 Madison Avenue, 43604, Area Code 419 Tel 241-0683, FAX 419-241-0684

OKLAHOMA

Oklahoma City–301 Northwest 63rd Street, Suite 330, 73116, Area Code 405 Tel 231–5302, FAX 405-231-4211

Tulsa–440 S. Houston Steet, Room 505, 74127, Area Code 918 Tel 581–7650, FAX 918-581-2844

OREGON

Eugene–1401 Willamette Street, 97401-4003, Area Code 541 Tel 465-6575, FAX 541-465-6704

Portland–One World Trade Center, 121 S.W. Salmon Street, Suite 242, 97204, Area Code 503 Tel 326–3001, FAX 503-326-6351

PENNSYLVANIA

Harrisburg–One Commerce Square, 417 Walnut Street, 3rd Floor, 17101, Area Code 717 Tel 232-0051, FAX 717-232-0054

Philadelphia–615 Chestnut Street, Suite 1501, 19106, Area Code 215 Tel 597–6101, FAX 215-597-6123

Pittsburgh–2002 Federal Building, 1000 Liberty Avenue, 15222, Area Code 412 Tel 644–2850, FAX 412-644-4875

Scranton–One Montage Mountain Road, Suite B, 18507, Area Code 717 Tel 969-2530, FAX 717-969-2539

PUERTO RICO

San Juan (Hato Rey)–Federal Building, Chardon Avenue, Room G-55, 00918, Area Code 787 Tel 766–5555, FAX 787-766-5692

RHODE ISLAND

Providence–One West Exchange Street, 02903, Area Code 401 Tel 528–5104, FAX 401-528-5067

SOUTH CAROLINA

Charleston–P.O. Box 975, 29402 or 81 Mary Street, 29403, Area Code 803 Tel 727–4051, FAX 803-727-4052

Columbia–Strom Thurmond Federal Building, 1835 Assembly Street, Suite 172, 29201, Area Code 803 Tel 765–5345, FAX 803-253-3614

Upstate—Park Central Office Park, 555 N. Pleasantburg Drive, Building 1, Suite 109, Greenville, SC 29607, Area Code 864 Tel 271-1976, FAX 864-271-4171

SOUTH DAKOTA

Siouxland–Augustana College, 2001 S. Summit Avenue, Room SS-29A, Sioux Falls, 57197, Area Code 605 Tel 330-4264, FAX 605-330-4266

TENNESSEE

Knoxville–301 E. Church Avenue, 37915, Area Code 423 Tel 545-4637, FAX 615-545-4435

Memphis–22 N. Front Street, Suite 200, 38103, Area Code 901 Tel 544–4137, FAX 901-544-3646

Nashville–Parkway Towers, 404 James Robertson Parkway, Suite 114, 37219, Area Code 615 Tel 736–5161, FAX 615-736-2454

TEXAS

Austin–P.O. Box 12728, 1700 Congress, 2nd Floor, Suite 300R, 78701, Area Code 512 Tel 916–5939, FAX 512-916-5940

Dallas–P.O. Box 420069, 2050 N. Stemmons Freeway, Suite 170, 75207, Area Code 214 Tel 767–0542, FAX 214-767-8240

Houston–#1 Allen Center, 500 Dallas, Suite 1160, 77002, Area Code 713 Tel 718–3062, FAX 713-718-3060

San Antonio–1222 N. Main, Suite 450, 78212, Area Code 210 Tel 228-9878, FAX 210-228-9874

UTAH

Salt Lake City–324 S. State Street, Suite 105, 84111, Area Code 801 Tel 524–5116, FAX 801-524-5886

VERMONT

Montpelier–109 State Street, 4th Floor, 05609, Area Code 802 Tel 828-4508, FAX 802-828-3258

VIRGINIA

Richmond–700 Centre, 704 E. Franklin Street, Suite 550, 23219, Area Code 804 Tel 771–2246, FAX 804-771-2390

WASHINGTON

Seattle–Westin Building, 2001 6th Avenue, Suite 650, 98121, Area Code 206 Tel 553–5615, FAX 206-553-7253

Spokane–1020 W. Riverside, 99210, Area Code 509 Tel 459-4125, FAX 509-747-0077

WEST VIRGINIA

Charleston–405 Capitol Street, Suite 807, 25301, Area Code 304 Tel 347–5123, FAX 304-347-5408

Wheeling—1310 Market Street, 2nd Floor, 26003, Area Code 304 Tel 233-7472, FAX 304-233-7492

WISCONSIN

Milwaukee–517 E. Wisconsin Avenue, Room 596, 53202, Area Code 414 Tel 297–3473, FAX 414-297-3470

WYOMING

Served by the Denver, CO, Export Assistance Center

☆U.S. GOVERNMENT PRINTING OFFICE: 1997-417-392/72671

Order Processing Code:
*6870

Superintendent of Documents **Publications and Subscriptions** Order Form

PS

Charge your order. It's Easy!

To fax your orders (202) 512–2250

Publications

Please Type or Print (Form is aligned for typewriter use.)

Qty.	Stock Number	Title	Price Each	Total Price
			Total for Publications	

Subscriptions

Qty.	(List ID)	Title	Price Each	Total Price
			Total for Subscriptions	
			Total Cost of Order	

NOTE: Prices include regular domestic postage and handling and are subject to change. International customers please add 25%.

(Company or Personal Name) (Please type or print)

(Additional address/attention line)

(Street address)

(City, State, ZIP Code)

(Daytime phone including area code)

(Purchase Order No.)

May we make your name/address available to other mailers? YES ☐ NO ☐

Please Choose Method of Payment:

☐ Check Payable to the Superintendent of Documents

☐ GPO Deposit Account ☐☐☐☐☐☐☐☐ – ☐

☐ VISA or MasterCard Account

☐☐☐☐☐☐☐☐☐☐☐☐☐☐☐☐

☐☐☐☐ (Credit card expiration date)

Thank you for your order!

(Authorizing Signature)

Mail To: New Orders, Superintendent of Documents
P.O. Box 371954, Pittsburgh, PA 15250–7954

U.S. DEPARTMENT OF COMMERCE
TECHNOLOGY ADMINISTRATION
NATIONAL TECHNICAL INFORMATION SERVICE

ORDER FORM

NTIS Information is our business.

NTIS Web Site — http://www.ntis.gov

SHIP TO ADDRESS (please print or type)

CUSTOMER MASTER NUMBER (IF KNOWN) | DATE

ATTENTION/NAME

ORGANIZATION | DIVISION / ROOM NUMBER

STREET ADDRESS

CITY | STATE | ZIP CODE

PROVINCE / TERRITORY | INTERNATIONAL POSTAL CODE

COUNTRY

PHONE NUMBER ( ) | FAX NUMBER ( )

CONTACT NAME | INTERNET E-MAIL ADDRESS

METHOD OF PAYMENT (please print or type)

❑ VISA ❑ MasterCard ❑ American Express

CREDIT CARD NUMBER | EXPIRATION DATE

CARDHOLDER'S NAME

❑ NTIS Deposit Account Number:

❑ Check / Money Order enclosed for $ (PAYABLE TO NTIS IN U.S. DOLLARS)

ORDER BY PHONE (ELIMINATE MAIL TIME)
8:30 a.m. - 5:00 p.m. Eastern Time, M – F.
Sales Desk: (703) 487-4650
TDD: (703) 487-4639

ORDER BY FAX
24 hours/7 days a week: (703) 321-8547
To verify receipt of fax: call (703) 487-4679
7:00 a.m. – 5:00 p.m., Eastern Time, M – F.

ORDER BY MAIL
National Technical Information Service
5285 Port Royal Road
Springfield, VA 22161

RUSH SERVICE
RUSH service is available for an additional fee.
1-800-553-NTIS

NTIS ORDERNOW™ ONLINE
Order the most recent additions to the NTIS collection at NTIS Web site **http://www.ntis.gov/ordernow**.

ORDER VIA E-MAIL
Order via E-mail 24 hours a day.
orders@ntis.fedworld.gov
If concerned about Internet security, you may register your credit card at NTIS. Simply call (703) 487-4682.

BILL ME
(U.S., Canada, and Mexico only.)
NTIS will gladly bill your order, for an additional fee of $7.50. A request to be billed must be on a purchase order or company letterhead. An authorizing signature, contact name, and telephone number should be included with this request. Requests may be mailed or faxed.

PRODUCT SELECTION (please print or type)

NTIS PRODUCT NUMBER	INTERNAL CUSTOMER ROUTING (OPTIONAL) UP TO 8 CHARACTERS	UNIT PRICE	QUANTITY: PAPER COPY	MICRO-FICHE	MAGNETIC TAPE *	DISKETTE	CD-ROM	OTHER	TOTAL PRICE
		$							$
		$							$
		$							$
		$							$
		$							$
		$							$

* CIRCLE REQUIREMENTS	3480 CARTRIDGE	1600 BPI	6250 BPI	LABELING: STANDARD	NONLABELED	FORMAT: EBCDIC	ASCII

TOTAL	$
HANDLING FEE PER TOTAL ORDER	$ 4.00
Outside North America–$8	$
GRAND TOTAL	$

PLEASE NOTE
Unless microfiche or other is specified, paper copy will be sent.

Please call the Sales Desk at (703) 487-4650 for information on multiple copy discounts available for certain documents.

Out-Of-Print Surcharge
A 25% out-of-print surcharge will be added to titles acquired by NTIS more than three years prior to the current calendar year.

Thank you for your order!

NIST Technical Publications

Periodical

Journal of Research of the National Institute of Standards and Technology—Reports NIST research and development in those disciplines of the physical and engineering sciences in which the Institute is active. These include physics, chemistry, engineering, mathematics, and computer sciences. Papers cover a broad range of subjects, with major emphasis on measurement methodology and the basic technology underlying standardization. Also included from time to time are survey articles on topics closely related to the Institute's technical and scientific programs. Issued six times a year.

Nonperiodicals

Monographs—Major contributions to the technical literature on various subjects related to the Institute's scientific and technical activities.

Handbooks—Recommended codes of engineering and industrial practice (including safety codes) developed in cooperation with interested industries, professional organizations, and regulatory bodies.

Special Publications—Include proceedings of conferences sponsored by NIST, NIST annual reports, and other special publications appropriate to this grouping such as wall charts, pocket cards, and bibliographies.

National Standard Reference Data Series—Provides quantitative data on the physical and chemical properties of materials, compiled from the world's literature and critically evaluated. Developed under a worldwide program coordinated by NIST under the authority of the National Standard Data Act (Public Law 90-396). NOTE: The Journal of Physical and Chemical Reference Data (JPCRD) is published bimonthly for NIST by the American Chemical Society (ACS) and the American Institute of Physics (AIP). Subscriptions, reprints, and supplements are available from ACS, 1155 Sixteenth St., NW, Washington, DC 20056.

Building Science Series—Disseminates technical information developed at the Institute on building materials, components, systems, and whole structures. The series presents research results, test methods, and performance criteria related to the structural and environmental functions and the durability and safety characteristics of building elements and systems.

Technical Notes—Studies or reports which are complete in themselves but restrictive in their treatment of a subject. Analogous to monographs but not so comprehensive in scope or definitive in treatment of the subject area. Often serve as a vehicle for final reports of work performed at NIST under the sponsorship of other government agencies.

Voluntary Product Standards—Developed under procedures published by the Department of Commerce in Part 10, Title 15, of the Code of Federal Regulations. The standards establish nationally recognized requirements for products, and provide all concerned interests with a basis for common understanding of the characteristics of the products. NIST administers this program in support of the efforts of private-sector standardizing organizations.

Order the **following** *NIST publications—FIPS and NISTIRs—from the National Technical Information Service, Springfield, VA 22161.*

Federal Information Processing Standards Publications (FIPS PUB)—Publications in this series collectively constitute the Federal Information Processing Standards Register. The Register serves as the official source of information in the Federal Government regarding standards issued by NIST pursuant to the Federal Property and Administrative Services Act of 1949 as amended, Public Law 89-306 (79 Stat. 1127), and as implemented by Executive Order 11717 (38 FR 12315, dated May 11, 1973) and Part 6 of Title 15 CFR (Code of Federal Regulations).

NIST Interagency Reports (NISTIR)—A special series of interim or final reports on work performed by NIST for outside sponsors (both government and nongovernment). In general, initial distribution is handled by the sponsor; public distribution is by the National Technical Information Service, Springfield, VA 22161, in paper copy or microfiche form.

ADMINISTRATION & MANAGEMENT

AERONAUTICS & AERODYNAMICS

AGRICULTURE & FOOD

ASTRONOMY & ASTROPHYSICS

ATMOSPHERIC SCIENCES

BEHAVIOR & SOCIETY

BIOMEDICAL TECHNOLOGY & HUMAN FACTORS ENGINEERING

BUILDING INDUSTRY TECHNOLOGY

BUSINESS & ECONOMICS

CHEMISTRY

CIVIL ENGINEERING

COMBUSTION, ENGINES, & PROPELLANTS

COMMUNICATION

COMPUTERS, CONTROL & INFORMATION THEORY

DETECTION & COUNTERMEASURES

ELECTROTECHNOLOGY

ENERGY

ENVIRONMENTAL POLLUTION & CONTROL

HEALTH CARE

INDUSTRIAL & MECHANICAL ENGINEERING

LIBRARY & INFORMATION SCIENCES

MANUFACTURING TECHNOLOGY

MATERIALS SCIENCES

MATHEMATICAL SCIENCES

MEDICINE & BIOLOGY

MILITARY SCIENCES

NATURAL RESOURCES & EARTH SCIENCES

NAVIGATION, GUIDANCE, & CONTROL

NUCLEAR SCIENCE & TECHNOLOGY

OCEAN SCIENCES & TECHNOLOGY

ORDNANCE

PHOTOGRAPHY & RECORDING DEVICES

PHYSICS

PROBLEM-SOLVING INFORMATION FOR STATE & LOCAL GOVERNMENTS

SPACE TECHNOLOGY

TRANSPORTATION

URBAN & REGIONAL TECHNOLOGY & DEVELOPMENT

